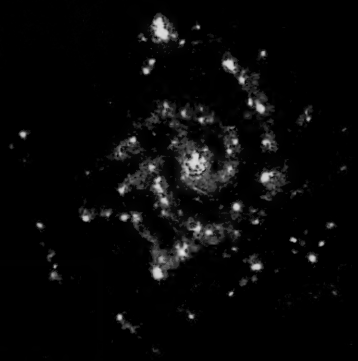
Annual Index
1994



Part Two
SUBJECT
LET-Z

NASA

Volume 32
1994
N94-10001 to N94-37856

The NASA STI Office ... in Profile

Since its founding, NASA has been dedicated to the advancement of aeronautics and space science. The NASA Scientific and Technical Information (STI) Office plays a key part in helping NASA maintain this important role.

The NASA STI Office provides access to the NASA STI Database, the largest collection of aeronautical and space science STI in the world. The Office is also NASA's institutional mechanism for disseminating the results of its research and development activities.

Specialized services that help round out the Office's diverse offerings include creating custom thesauri, translating material to or from 34 foreign languages, building customized databases, organizing and publishing research results ... even providing videos.

For more information about the NASA STI Office, you can:

- **Phone** the NASA Access Help Desk at (301) 621-0390
- **Fax** your question to the NASA Access Help Desk at (301) 621-0134
- **E-mail** your question via the **Internet** to help@sti.nasa.gov
- **Write** to:

NASA Access Help Desk
NASA Center for AeroSpace Information
800 Elkridge Landing Road
Linthicum Heights, MD 21090-2934

Scientific and Technical Aerospace Reports



Scientific and Technical Aerospace Reports (STAR), is published each month as a major product of the NASA Scientific and Technical Information (STI) Office.

Inside this issue you will find:

- **Front Matter** containing a typical citation and abstract sample explaining the standard format, including codes for ordering reports
- **An Abstract Section** containing citations and abstracts of reports and publications that provide comprehensive coverage of worldwide aerospace-related topics including aeronautics and space science technology. *STAR* lists published and publicly available reports entered into the NASA STI Database during the four weeks preceding publication of this issue. These citations and abstracts are listed by subject categories.
- **An Index Section**
  - Subject
  - Personal author
  - Corporate source
  - Contract number
  - Report number
- **An Appendix** containing a guide for ordering cited reports, registering with the NASA STI Office, and using the available products and services. Additionally, price schedules, phone numbers, and addresses are included in this information packed section.

NASA also sponsors the companion journal, *NASA Open Volumes on Aerospace (NOVA)*, which lists abstracts of the open literature on aerospace subjects available worldwide. *NOVA* is for internal NASA use only, available from the NASA Center for AeroSpace Information (CASI).

Entries found in *STAR* are available through the NASA online retrieval service, RECON, and through DIALOG as the Aerospace Database.

The NASA STI Office gathers information through national and international agreements and exchanges and makes this information available to the NASA community and to the public in many forms through various outlets.

For additional information on the NASA STI Office, call the NASA Access Help Desk at (301) 621-0390, or write to:

NASA Center for AeroSpace Information
800 Elkridge Landing Road
Linthicum Heights, Maryland 21090-2934

US ISSN 0036-8741

SPECIAL NOTICE

The abstract sections of the monthly *STAR* journals can be bound separately. Individual abstracts can be located readily by means of the page numbers given at each entry, e.g., p 3181. To assist the user in binding *STAR* Volume 32, two (2) title pages are included in the back of Part Two.

This publication was prepared by the NASA Center for AeroSpace Information,
800 Elkridge Landing Road, Linthicum Heights, MD 21090-2934, (301) 621-0390.

VOLUME 32 NUMBERS 1-12

Scientific and Technical Aerospace Reports

Annual Index (Part Two) January – December 1994

TABLE OF CONTENTS

Part One Page
Introduction v
Subject Index (A-LES) A-1

Part Two Page
Introduction v
Subject Index (LET-Z) A-822

Part Three
Introduction v
Personal Author Index B-1

Part Four Page
Introduction v
Corporate Source Index C-1
Contract Number Index D-1
Report Number Index E-1

LETHALITY
Current directions in the vulnerability/lethality process structure
[AD-A272836] 05 p1964 N94-21175
Space radiation health research, 1991-1992
[NASA-TM-109721] 07 p2932 N94-27556
Supernovae and mass extinctions
07 p2891 N94-28314
LETTERS (SYMBOLS)
U SYMBOLS
LEUKOCYTES
NT LYMPHOCYTES
LEVEL (HORIZONTAL)
NT LIQUID LEVELS
LEVEL (QUANTITY)
NT ATOMIC ENERGY LEVELS
NT EFFECTIVE PERCEIVED NOISE LEVELS
NT ELECTRON STATES
NT ENERGY LEVELS
NT GROUND STATE
NT INTERMOLECULAR FORCES
NT MOLECULAR ENERGY LEVELS
NT ROTATIONAL STATES
NT VIBRATIONAL STATES
LEVELING
Alignment of the Amsterdam Pulse Stretcher (AmPS)
[MTG-93-02] 07 p2809 N94-25637
LEVITATION
NT ACOUSTIC LEVITATION
Gas film levitator for containerless processing of glasses in microgravity conditions: Early concept and technology demonstration 01 p0108 N94-10122
TEMPUS: An electromagnetic levitation facility for containerless processing under micro-g in Spacelab
01 p0109 N94-10125
Force and power efficiency of micro-g electromagnetic levitation coils 01 p0110 N94-10129
Development of passive superconducting bearings. Phase 3
[AD-A266050] 01 p0180 N94-10706
Improvement of azimuthal homogeneity in permanent-magnet bearing rotors
[DE93-009954] 01 p0144 N94-11607
Effects of levitated dust on astronomical observations from the lunar surface 03 p1239 N94-16433
Six degree of freedom fine motion positioning stage based on magnetic levitation
[DE93-017651] 04 p1446 N94-19547
Processing of YBCO superconductors for improved levitation force
[DE94-001326] 06 p2559 N94-22994
Performance analysis of the combined EDS maglev propulsion, levitation, and guidance system
[DE94-001346] 06 p2352 N94-22996
Electrostatic levitation technology for thermophysical properties of molten materials 06 p2238 N94-25135
Basic research on levitation fusing/solidification technology 07 p2723 N94-25552
Nearly time-optimal feedback control of a magnetically levitated photolithography positioning system
[DE94-005288] 08 p3266 N94-30055
Neural network based time-optimal control of a magnetically levitated precision positioning system
[DE94-006573] 08 p3437 N94-30250
Measurement and characterization of force dynamics in high T(sub c) superconductors
11 p4214 N94-35844
Superconducting Electromagnetic Suspension (EMS) system for Grumman Maglev concept
11 p4215 N94-35849
Six degree of freedom fine motion positioning stage based on magnetic levitation 11 p4225 N94-35916
Future ultra-speed tube-flight
11 p4225 N94-35918
Maglev crude oil pipeline 11 p4226 N94-35919
Melt-processing of Y-Ba-Cu-O superconductors for improved levitation
[DE94-011503] 12 p4537 N94-37377
LEVITATION MELTING
Force and power efficiency of micro-g electromagnetic levitation coils 01 p0110 N94-10129
Microstructure and associated properties of YB2Cu3O(x) superconductors prepared by melt processing techniques
[DE93-010675] 01 p0398 N94-11004
Basic research on levitation fusing/solidification technology 07 p2723 N94-25552
Plasma heating for containerless and microgravity materials processing
[NASA-CASE-NPO-18819-1-CU]
08 p3229 N94-29371
LEWIS BASE
Synthesis and structural characterization of new light molecular weight inorganic oxidizers and relative derivatives, volume 1
[AD-A271437] 05 p2012 N94-19842
Volatile CVD precursors based on copper alkoxides and mixed group 2A-copper alkoxides
[AD-D015930] 05 p1701 N94-20349
LIABILITIES
NT LEGAL LIABILITY
LIAPUNOV FUNCTIONS
Construction of the Courant-Snyder invariants for the non-linear equations of motion under presence of the linear coupling
[DE93-017565] 02 p0788 N94-14872
Fast-training algorithm for hidden-layer forward-feed neural networks
[AD-A269253] 04 p1540 N94-18263
The optimal projection equations for finite-dimensional fixed-order H2-optimal control of infinite-dimensional discrete-time systems
[REPT-93-11] 04 p1542 N94-19085
The fixed, finite-order L(sup 2)-optimal control of infinite-dimensional time-varying discrete-time systems
[REPT-93-23] 04 p1542 N94-19138
Control of a serpentine manipulator with collision avoidance 06 p2368 N94-23232
Continuous gust response and sensitivity derivatives using state-space models 06 p2161 N94-24287
Neural network-based control using Lyapunov functions 06 p2477 N94-24433
Liapunov stability in chemical engineering
[MATHS-REPT-A-184] 06 p2236 N94-25427
Stability of large scale interconnected dynamical systems
[DE94-601536] 07 p2993 N94-26408
On the phi(sub 0)-stability of perturbed nonlinear differential systems
[DE93-634304] 07 p2993 N94-26441
Cone-valued Lyapunov functions and the stability of stochastic differential equations
[DE94-601504] 07 p2994 N94-26458
On the (Phi)(sub 0)-stability of functional differential equations
[DE94-601507] 07 p3006 N94-26460
Lyapunov exponents for some quasi-periodic cocycles
[PB94-124377] 07 p2997 N94-26994
Impulsive control and stabilization
[ISBN-0-315-84563-5] 07 p2988 N94-27271
On the linear stability of Verkley's modons
08 p3324 N94-28695
Stability of dynamical systems in the presence of noise
[AD-A275383] 08 p3243 N94-29072
Existence of quantum characteristic exponents
[PB94-138161] 08 p3523 N94-29146
Significant figures and Lyapunov exponents in chaos and constrained divergence of chaotic orbits
08 p3467 N94-29910
Dynamics and control of tethered satellite systems
08 p3170 N94-30864
A Hyland-Bernstein approach to the digital control of Pritchard-Salamon systems
[REPT-93-76] 09 p3844 N94-31693
Decoherence, chaos, the quantum and the classical
[DE94-009317] 10 p4149 N94-34099
LIBRARIES
Portable programming on parallel/networked computers using the Application Portable Parallel Library (APPL)
[NASA-TM-106238] 01 p0327 N94-11232
Guidelines for the establishment and operation of an RFP (Request for proposal) library
[AD-A265894] 01 p0417 N94-12360
Satellite technology for environmental monitoring in developing countries 02 p0692 N94-14236
Public census data on CD-ROM at Lawrence Berkeley Laboratory
[DE93-015273] 02 p0825 N94-14433
A TRALINET guide to the Internet
[AD-A266946] 03 p1229 N94-15178
Managing information as a corporate asset: Key strategies for information professionals to remain competitive
[DE93-015515] 03 p1232 N94-16875
Application of new technologies in the virtual library: Seminars in Turkey, Portugal, and Spain
[NASA-TM-109718] 04 p1611 N94-19131
Cesar user library
[FFI-93/7021] 04 p1529 N94-19378
CVL: A C vector library manual. Version 2
[AD-A270614] 04 p1531 N94-19592
Research in image management and access
[NASA-CR-194797] 05 p1907 N94-20376
Experiments on technology mapping using different cell libraries 05 p1758 N94-21118
The three-dimensional Event-Driven Graphics Environment (3D-EDGE) 05 p1922 N94-21342
Assessment of the organizational structure and services of DOE National Laboratory Libraries
[DE93-040697] 05 p2045 N94-21750
NASA/DOD Aerospace Knowledge Diffusion Research Project. Report number 21: US aerospace industry librarians and technical information specialists as information intermediaries: Results of the phase 2 survey
[AD-A276020] 06 p2593 N94-24709
Factors influencing perceived usability and utility of LIBERTAS at Cranfield: Implications for system modification and user education
[CRANFIELD-AERO-9212] 06 p2594 N94-25485
NACA collections: A directory of significant collections of the documents of the National Advisory Committee for Aeronautics
[NASA-CR-195686] 06 p2594 N94-25541
Full-text information services at the desktop
[DE94-003728] 07 p3096 N94-25813
Index to BROND-2, CENDL-2, ENDF/B-6, JEF-2, JENDL-3
[DE93-634500] 07 p3016 N94-26034
TRADOC library and information network (TRALINET). Union list of periodicals (TULIP)
[AD-A275263] 08 p3529 N94-28903
Evaluation of the Resource Library System in Finland
[PB94-137734] 08 p3532 N94-29682
Information center assessment
08 p3533 N94-29855
NASA/DOD Aerospace Knowledge Diffusion Research Project. Report 22: US academic librarians and technical information specialists as information intermediaries: Results of the phase 3 survey
[NASA-TM-109067] 08 p3534 N94-30150
Marketing tools for increasing proactivity in technical information centers
[AGARD-AR-326] 08 p3528 N94-30934
Texture library for 3-dimensional visualization systems
[AD-A276125] 09 p3917 N94-31829
A high-speed linear algebra library with automatic parallelism 09 p3828 N94-32440
NASA/DOD Aerospace Knowledge Diffusion Research Project. Paper 5: Aerospace librarians and technical information specialists as information intermediaries: A report of phase 2 activities of the NASA/DOD Aerospace Knowledge Diffusion Research Project
[NASA-TM-109777] 09 p3921 N94-32829
MDFF HELP library, version 2: On-line documentation for the map data formatting facility
[AD-A277763] 09 p3922 N94-32987
Toward a digital library strategy for a National Information Infrastructure 10 p4151 N94-33793
A petabyte size electronic library using the N-Gram memory engine 10 p4153 N94-33802
Using magnetic tape technology for data migration
10 p4154 N94-33812
Issues for bringing digital libraries into public use
10 p4156 N94-33821
A practical large scale/high speed data distribution system using 8 mm libraries 10 p4157 N94-33825
TILDA for Windows: A system for registration of journals in the library at NDRE NBC-Defence
[PB94-149168] 10 p4158 N94-34161
The impact of HPF data layout on the design of efficient and maintainable parallel linear algebra libraries
[DE94-012382] 12 p4504 N94-37246
International High Speed Networks for Scientific and Technical Information
[AGARD-CP-544] 12 p4543 N94-37333
An introduction to the Internet and its services
12 p4543 N94-37334
The virtual library: Coming of age
12 p4544 N94-37338
Electronic document delivery: Towards the virtual library 12 p4544 N94-37340
Bulletin boards, electronic mail, conferencing, current use by scientists and engineers: Effects on libraries and information centres: Do they have a role?
12 p4544 N94-37343
LIBRATION
Molecular structure of low temperature form of triaminoguanidinium nitrate (TAGN)
[AD-A270409] 04 p1377 N94-18708
Forced libration of Mercury and geodetic determination of a possible fluid core 09 p3774 N94-32493
LICENSING
Intergovernmental decisionmaking for environmental protection and public works
[PB93-176824] 01 p0266 N94-11584
Industrial Hygiene Laboratory accreditation: The JSC experience 03 p1125 N94-16623
Setting the global thermostat with an exhaustible tradeable permit system
[DE93-012911] 04 p1472 N94-17891
LIDAR
U OPTICAL RADAR
LIE GROUPS
NT SPINOR GROUPS

One-loop quantum gravity on de Sitter space
[DE92-641349] 01 p0425 N94-11152
Gauging the octonion algebra
[DE93-622864] 02 p0775 N94-12843
Soliton equations and self-dual gauge fields
[DE93-626620] 02 p0818 N94-14887
Quantum Heisenberg groups and Sklyanin algebras
[DE93-628590] 03 p1175 N94-17643
Further on the current algebra of WZNW models at and away from criticality
[DE93-624809] 04 p1545 N94-17686
Multidimensional geometric quantization and U(1)-covering
[DE93-624770] 04 p1546 N94-17795
Finite-dimensional singletons of the quantum anti de Sitter algebra
[DE93-624771] 04 p1546 N94-17810
A reduction of the globalization and U(1)-covering
[DE93-624769] 04 p1546 N94-17817
Functional analysis of subelliptic operators on lie groups
[PB93-194793] 04 p1547 N94-18077
Paragrassmann analysis and quantum groups
[DE93-628593] 04 p1561 N94-18168
On paragrassmann differential calculus
[DE93-628594] 04 p1548 N94-18169
On a possible algebra morphism of U(sub q)(osp1/2) onto the deformed oscillator algebra W(sub q)(N)
[DE93-629857] 04 p1548 N94-18176
About symmetry of the gravitational action
[DE93-629955] 04 p1608 N94-18252
Extensions of 2D gravity
[DE93-018525] 04 p1485 N94-18929
L(sub p)-regularity of subelliptic operators on Lie groups
[PB93-194785] 04 p1549 N94-18948
Group-invariant solutions of hydrodynamics and radiation hydrodynamics
[DE93-018373] 04 p1423 N94-19604
Production and test of pseudo random elements
[ETN-93-95070] 04 p1559 N94-19610
Explicit results on gl(lambda) and sl(lambda)
[MEMO-1075] 05 p1953 N94-21072
A working algorithm to isolate integrable surfaces in E cubed
[SSCL-PREPRINT-761] 06 p2452 N94-23518
Coadjoint orbits and conformal field theory
[DE94-002285] 06 p2523 N94-24658
On BRST quantization of constrained systems
[ETN-94-95386] 06 p2570 N94-25258
The massless representations of the conformal quantum algebra
[DE94-601555] 07 p3006 N94-26413
Affine algebras on the torus
[DE94-601556] 07 p3006 N94-26414
Higher spin extensions of the Virasoro algebra, area-preserving algebras and the matrix algebra a-bar(sub (infinity))
[DE94-601557] 07 p3006 N94-26415
Finite dimensional representations of the quantum superalgebra U(sub q)(gl(3/2))
[DE93-634303] 07 p2993 N94-26440
Quantum Hamiltonian differential geometry: How does quantization affect space?
[DE93-634306] 07 p2993 N94-26442
The extensions of space-time. Physics in the 8-dimensional homogeneous space D is equal to SU(2,2)/K
[DE93-634336] 07 p3072 N94-26551
String hypothesis and characters of coset CFTs
[DE93-634337] 07 p3007 N94-26552
Deformation of the exterior algebra and the GL(sub q)(r, included in) algebra
[DE94-602558] 07 p2996 N94-26898
Poisson-lie group of pseudodifferential symbols
[PB94-124393] 07 p2997 N94-26996
Q - difference intertwining operators for a Lorentz quantum algebra
[DE94-602559] 07 p2997 N94-27023
The gl(n/m) and related q-identitiesematics and computer science ends in nuclear and related q-identities
[DE94-603653] 07 p3001 N94-27839
Extended nonabelian symmetries for free fermionic model
[DE94-601554] 08 p3481 N94-28470
Path integral for coherent states of the dynamical U(sub 2) group and U(sub 2/1) supergroup
[DE94-606382] 08 p3466 N94-28785
On wavelet representations of differential equations
[RR-482] 09 p3842 N94-31412
On a connection between the Yang-Mills equations in dimension greater than four and the classical Yang-Baxter equations
[DE94-611115] 10 p4131 N94-33883
Recent progress in irrational conformal field theory
[DE94-011908] 11 p4317 N94-36234
N = 4 supersymmetry from the quantum affine algebra U(sub q)(A-circumflex(sup 1)(sub 3))
[DE94-611145] 11 p4317 N94-36307
Representations of the q-deformed algebras U(q)(so(2,1)) and U(q) (so(3,1)
[DE94-616619] 12 p4505 N94-37483

LIF (FLUORESCENCE)
U LASER INDUCED FLUORESCENCE

LIFE (BIOLOGY)
U LIFE SCIENCES

LIFE (DURABILITY)
NT CARRIER LIFETIME
NT FATIGUE LIFE
NT HALF LIFE
NT SATELLITE LIFETIME
NT SERVICE LIFE
NT STORAGE STABILITY
Environmental Protection Agency's life cycle methodology: Guidelines for use in development of packaging
[PB93-194199] 01 p0265 N94-10841
Model of optical scatter from microimpacts on the Hubble Telescope 01 p0384 N94-12189
A hot dynamic seal rig for measuring hypersonic engine seal durability and flow performance
[NASA-TM-106294] 02 p0664 N94-14727
Multiaxial deformation and life prediction model and experimental data for advanced silicon nitride ceramics
[DE93-015450] 03 p0967 N94-16067
Software Engineering Guidebook
[NASA-CR-177625] 03 p1150 N94-16656
Development of a constitutive model for creep and life prediction of advanced silicon nitride ceramics
[DE93-015894] 03 p0968 N94-16813
The Ceramic Technology Project: Ten years of progress
[DE93-015991] 03 p0968 N94-16843
Environment enhanced fatigue crack propagation in metals: Inputs to fracture mechanics life prediction models
[NASA-CR-191538] 03 p0942 N94-17638
Measurement of the B(+) and B(0) lifetimes
[DE93-019906] 05 p1969 N94-19814
Computational Methods for Failure Analysis and Life Prediction
[NASA-CP-3230] 05 p1833 N94-22608
Nonlinear and progressive failure aspects of transport composite fuselage damage tolerance 05 p1834 N94-22609
NASA Langley developments in response calculations needed for failure and life prediction 05 p1836 N94-22621
Small rocket research and technology 06 p2211 N94-23038
Strength and life of pressure vessels subjected to impacts and thermomechanical GFRP loading
[VTT-JULK-771] 06 p2379 N94-25418
Study on high temperature damage control and life improvement 07 p2729 N94-25580
Composite raw materials for the building industry
[VTT-TIED-1433] 07 p2708 N94-26544
MSOFC development status
[DE94-003192] 07 p2858 N94-26792
Space Station Freedom NiH2 cell testing program 07 p2861 N94-28108
Process guide for the Domain-Specific Software Architectures (DSSA) process life cycle
[AD-A275642] 08 p3407 N94-28648
Service life prediction of composite structures through fiber testing
[AD-A275661] 08 p3176 N94-28654
Novel techniques applied to polymer lifetime predictions
[DE94-005095] 08 p3218 N94-30102
The development of an auxiliary power unit for a fighter aircraft 10 p4001 N94-34442
Rotorcraft fatigue life-prediction: Past, present, and future 10 p4072 N94-34590
Damage tolerance management of the X-29 vertical tail 10 p3996 N94-34595
Developing software for ease of change: Metrics from later in the TRALAB system life cycle
[AD-A278759] 11 p4302 N94-35490
Propulsion system technologies for long range and long endurance aircraft 11 p4195 N94-36334
Characterisation of Fibre Reinforced Titanium Matrix Composites
[AGARD-R-796] 12 p4400 N94-36649
The life cycles of intense cyclonic and anticyclonic circulation systems observed over oceans
[NASA-CR-196271] 12 p4473 N94-37294

LIFE CYCLE COSTS
ACARA user's manual
[NASA-TM-106277] 01 p0183 N94-11167
In-flight aircraft structure health monitoring based on smart structures technology 01 p0022 N94-11333
Life-cycle cost analysis of conventional and fuel cell/battery powered urban passenger vehicles
[DE93-010770] 01 p0182 N94-11438
Chip-level testability requirements guidelines
[AD-A262583] 02 p0619 N94-12967
Optimal maintenance policies of a Markovian system
[ITN-93-85216] 02 p0774 N94-14502
The automated ground network system 05 p1932 N94-21330
US Department of Energy phaseout of CFC-refrigerants
[DE94-001668] 06 p2397 N94-23016
Life cycle cost modeling of conceptual space vehicles
[NASA-CR-194813] 06 p2203 N94-23329
National Institute of Standards and Technology Conference on Reducing the Cost of Space Infrastructure and Operations. Part 2: Topical papers
[PB94-113487] 06 p2194 N94-23819
New Technologies for Space Avionics, 1993
[NASA-CR-188272] 06 p2272 N94-25193
MSOFC development status
[DE94-003192] 07 p2858 N94-26792
Interdisciplinary technology 07 p2686 N94-27363
Automation life-cycle cost model
[NASA-CR-195695] 07 p3095 N94-27866
Aircraft age impact on individual operating and support cost elements
[AD-A275739] 08 p3121 N94-28732
Demonstration of improved software support labor estimation for Air Force operational flight programs through functional orientation
[AD-A275789] 08 p3121 N94-28743
Towards an information model and mechanisms for design rationale capture and use
[AD-A275060] 08 p3530 N94-29138
An analysis of non-integerizing the aircraft engines Cost Effectiveness Analysis Spreadsheet Model (CEAMOD version 2.0)
[AD-A276251] 09 p3583 N94-31290
Software reuse case study: TRILLIUM
[AD-A276108] 09 p3811 N94-31465
The development of an auxiliary power unit for a fighter aircraft 10 p4001 N94-34442
LNG vehicle technology, economics, and safety assessment
[PB94-165487] 12 p4450 N94-36721
Space Shuttle: Incomplete data and funding approach increase cost risk for upgrade program. Report to Congressional Requesters
[GAO/NSIAD-94-23] 12 p4392 N94-37026
Operations and support cost modeling of conceptual space vehicles
[NASA-CR-196299] 12 p4397 N94-37580

LIFE RAFTS
AN/APS-137 Forward Looking Airborne Radar (FLAR) evaluation Spring 1992 experiment
[AD-A268899] 04 p1384 N94-18228
Survival suit for submarine personnel: Summary of evaluation studies
[PB93-204634] 06 p2430 N94-23743

LIFE SCIENCES
NT EXTRATERRESTRIAL LIFE
NT MOLECULAR BIOLOGY
The International Microgravity Laboratory, a Spacelab for materials and life sciences 01 p0125 N94-10249
Aerospace medicine and biology: A continuing bibliography with indexes (supplement 375)
[NASA-SP-7011(375)] 01 p0303 N94-10398
Aerospace medicine and biology: A continuing bibliography with indexes (supplement 376)
[NASA-SP-7011(376)] 01 p0303 N94-10399
Proceedings of the Symposium on Radiation Research in Life Science
[DE93-754137] 01 p0300 N94-10888
Five biomedical experiments flown in an Earth orbiting laboratory: Lessons learned from developing these experiments on the first international microgravity mission from concept to landing 01 p0302 N94-11556
Aerospace medicine and biology: A continuing bibliography with indexes (supplement 374)
[NASA-SP-7011(374)] 01 p0304 N94-11689
Aerospace medicine and biology: A continuing bibliography with indexes (supplement 379)
[NASA-SP-7011(379)] 02 p0733 N94-14412
Cellular responses to low-gravity: Pilot studies on suborbital rockets and orbiting spacecraft
[NASA-CR-194402] 02 p0729 N94-14494
STS-40 crew during spacelab Sim
[NASA-TM-109493] 03 p0876 N94-15452
Canadian microgravity experiments flown in 1989-1990 03 p0977 N94-16075
Statistical techniques for study design of microgravity life sciences experiments 03 p0980 N94-16094

Aerospace medicine and biology: A continuing bibliography with indexes (supplement 378)
[NASA-SP-7011(378)] 03 p1122 N94-16478
Aerospace medicine and biology: A continuing bibliography with indexes (supplement 380)
[NASA-SP-7011(380)] 03 p1122 N94-16479
Looking at science on board Eureca
[ESA-BR-80] 03 p0874 N94-16584
Design of an experiment hardware for the ESA space facility BIOPAN
[DLR-FB-93-06] 03 p0876 N94-17548
Interdisciplinary training in life science (FY 1991 ASSERT)
[AD-A269220] 04 p1512 N94-18886
Aerospace medicine and biology: A continuing bibliography with indexes (supplement 382)
[NASA-SP-7011(382)] 04 p1507 N94-18936
Aerospace medicine and biology: A continuing bibliography with indexes (supplement 381)
[NASA-SP-7011(381)] 04 p1507 N94-19069
Guide to programs, fiscal year 1993
[NSF-92-78] 04 p1633 N94-19620
Aerospace medicine and biology: A continuing bibliography with indexes (supplement 383)
[NASA-SP-7011(383)] 05 p1892 N94-21288
Asteroid exploration and utilization
07 p3080 N94-25697
The 27th Annual Meeting of the Israel Society for Microscopy and the 12th Annual Meeting of the Israel Society for Histochemistry and Cytochemistry
[DE93-632416] 07 p2716 N94-26519
Spacelab life sciences 2 post mission report
[NASA-CR-188279] 07 p2942 N94-27410
Aerospace medicine and biology: A continuing bibliography with indexes (supplement 386)
[NASA-SP-7011(386)] 07 p2933 N94-28208
Aerospace medicine and biology: A continuing bibliography with indexes (supplement 387)
[NASA-SP-7011(387)] 07 p2933 N94-28213
A general theory of impacts and mass extinctions, and the consequences of large-body impact on the Earth
07 p2891 N94-28310
Research and technology, 1992
[NASA-TM-103996] 08 p3555 N94-29891
Aerospace medicine and biology: A continuing bibliography with indexes (supplement 388)
[NASA-SP-7011(388)] 09 p3795 N94-31414
Aerospace medicine and biology: A continuing bibliography with indexes (supplement 389)
[NASA-SP-7011(389)] 09 p3797 N94-32347
Aerospace medicine and biology: A continuing bibliography with indexes (supplement 385)
[NASA-SP-7011(385)] 09 p3797 N94-32348
Aerospace medicine and biology: A continuing bibliography with indexes (supplement 390)
[NASA-SP-7011(390)] 10 p4095 N94-34602
Johnson Space Center (JSC) research and technology
[NASA-TM-104788] 10 p4187 N94-34677
JPRS report: Science and technology. Central Eurasia
[JPRS-UST-94-001] 11 p4229 N94-35340
JPRS report: Science and technology. Central Eurasia
[JPRS-UST-94-004] 11 p4249 N94-35341
JPRS report: Science and technology. Central Eurasia
[JPRS-UST-94-005] 11 p4249 N94-35342
Aerospace medicine and biology: A continuing bibliography with indexes (supplement 391)
[NASA-SP-7011(391)] 11 p4297 N94-35345
Director's discretionary fund
[NASA-TM-103997] 11 p4376 N94-35370
JPRS report: Science and technology. Central Eurasia
[JPRS-UST-94-010] 11 p4250 N94-35385
JPRS report: Science and technology. Central Eurasia
[JPRS-UST-94-011] 11 p4250 N94-35386
JPRS report: Science and technology. Central Eurasia
[JPRS-UST-94-012] 11 p4250 N94-35387
Research and technology, 1993
[NASA-TM-108816] 11 p4380 N94-36117
JPRS report: Science and technology. Central Eurasia
[JPRS-UST-94-013] 12 p4509 N94-37006
Aerospace medicine and biology: A continuing bibliography with indexes (supplement 392)
[NASA-SP-7011(392)] 12 p4482 N94-37445

LIFE SPAN
Single crystal faceplate evaluation
[AD-A277922] 10 p4038 N94-33399

LIFE SUPPORT SYSTEMS
NT CLOSED ECOLOGICAL SYSTEMS
NT EMERGENCY LIFE SUSTAINING SYSTEMS
NT PORTABLE LIFE SUPPORT SYSTEMS
Aerospace medicine and biology: A continuing bibliography with indexes (supplement 375)
[NASA-SP-7011(375)] 01 p0303 N94-10398
Aerospace medicine and biology: A continuing bibliography with indexes (supplement 376)
[NASA-SP-7011(376)] 01 p0303 N94-10399
Aerospace medicine and biology: A continuing bibliography with indexes (supplement 374)
[NASA-SP-7011(374)] 01 p0304 N94-11689
Space Life Support Engineering Program
[NASA-CR-193474] 01 p0316 N94-12365
Systems analysis of a closed loop ECLSS using the ASPEN simulation tool. Thermodynamic efficiency analysis of ECLSS components 01 p0316 N94-12366
Modifications to an interactive model of the human body during exercise: With special emphasis on thermoregulation 01 p0317 N94-12368
An estimate of the second law thermodynamic efficiency of the various units comprising an Environmental Control and Life Support System (ECLSS)
01 p0317 N94-12369
Medical evaluations on the KC-135 1991 flight report summary
[NASA-TM-104755] 02 p0731 N94-12832
Life support and habitability manual, volume 1
[ESA-PSS-03-406-ISSUE-1-VOL-1]
02 p0737 N94-13901
Life support and habitability manual, volume 2
[ESA-PSS-03-406-ISSUE-1-VOL-2]
02 p0738 N94-13902
Aerospace medicine and biology: A continuing bibliography with indexes (supplement 379)
[NASA-SP-7011(379)] 02 p0733 N94-14412
Aerospace medicine and biology: A continuing bibliography with indexes (supplement 378)
[NASA-SP-7011(378)] 03 p1122 N94-16478
Aerospace medicine and biology: A continuing bibliography with indexes (supplement 380)
[NASA-SP-7011(380)] 03 p1122 N94-16479
Illness/injury pattern complex 40 (Titan)
03 p1125 N94-16625
Aircrew/groundcrew life support systems research. Volume 1: CLIN 0001 research requirements
[AD-A268229] 03 p1139 N94-17563
Aircrew/groundcrew life support systems research. Volume 2: CLIN 0002 task order requirements
[AD-A268230] 03 p1139 N94-17564
Analysis of seating and restraint limitations restricting total body weight for aircrew and passengers on US Army helicopters
[AD-A269117] 04 p1511 N94-18296
Aircrew life support, AFSC 122X0(1T1X1)
[AD-A268998] 04 p1511 N94-18394
Aerospace medicine and biology: A continuing bibliography with indexes (supplement 382)
[NASA-SP-7011(382)] 04 p1507 N94-18936
Aerospace medicine and biology: A continuing bibliography with indexes (supplement 381)
[NASA-SP-7011(381)] 04 p1507 N94-19069
Environmental control and life support
[ESA-PSS-03-40-ISSUE-1] 04 p1513 N94-19442
Quinoa: An emerging new crop with potential for CELSS
[NASA-TP-3422] 05 p1895 N94-20137
Characterization of Minnesota lunar simulant for plant growth 05 p1897 N94-20665
Aerospace medicine and biology: A continuing bibliography with indexes (supplement 383)
[NASA-SP-7011(383)] 05 p1892 N94-21288
Chemical characterization of some aerobic liquids in CELSS 06 p2422 N94-23241
Weld joint concepts for on-orbit repair of Space Station Freedom fluid system tube assemblies
06 p2371 N94-24427
Bioregenerative system components for microgravity
07 p2903 N94-25673
Enabler operator station 07 p2943 N94-25679
Automation of closed environments in space for human comfort and safety 07 p2943 N94-25684
Design and development of the second generation Mars Habitat 07 p2943 N94-25693
Pressurized Lunar Rover (PLR)
07 p2833 N94-25704
Designing for human presence in space: An introduction to environmental control and life support systems
[NASA-RP-1324] 07 p2942 N94-27437
Aerospace medicine and biology: A continuing bibliography with indexes (supplement 386)
[NASA-SP-7011(386)] 07 p2933 N94-28208
Aerospace medicine and biology: A continuing bibliography with indexes (supplement 387)
[NASA-SP-7011(387)] 07 p2933 N94-28213
Evaluation of life support equipment during an unsupported North Pole expedition
08 p3379 N94-28422
Advanced seal delivery system life support parameters
[AD-A275304] 08 p3401 N94-29184
Technical assessment of Mir-1 life support hardware for the international space station
[NASA-TM-108441] 09 p3803 N94-31380
Design of a logistics model for building and supporting a lunar station
[ILR-MITT-282(1993)] 09 p3803 N94-31852
Aerospace medicine and biology: A continuing bibliography with indexes (supplement 389)
[NASA-SP-7011(389)] 09 p3797 N94-32347
Aerospace medicine and biology: A continuing bibliography with indexes (supplement 385)
[NASA-SP-7011(385)] 09 p3797 N94-32348
Catalytic methods using molecular oxygen for treatment of PMMS and ECLSS waste streams, volume 2
[NASA-CR-190299] 09 p3804 N94-32697
Characterization and utilization of opiate-like hibernation factors
[AD-A278136] 09 p3794 N94-33098
Seventh Annual Workshop on Space Operations Applications and Research (SOAR 1993), volume 2
[AD-A278178] 10 p4167 N94-33612
Gravity, the third dimension of life support in space
10 p4101 N94-33635
Current and future issues in USAF full pressure suit research and development 10 p4102 N94-33656
Advanced integrated life support system update
10 p4102 N94-33657
Seventh Annual Workshop on Space Operations Applications and Research (SOAR 1993), volume 1
[NASA-CP-3240-VOL-1] 10 p4179 N94-34019
Aerospace medicine and biology: A continuing bibliography with indexes (supplement 390)
[NASA-SP-7011(390)] 10 p4095 N94-34602
Aerospace medicine and biology: A continuing bibliography with indexes (supplement 391)
[NASA-SP-7011(391)] 11 p4297 N94-35345
Aerospace medicine and biology: A continuing bibliography with indexes (supplement 392)
[NASA-SP-7011(392)] 12 p4482 N94-37445

LIFETIME (DURABILITY)
U LIFE (DURABILITY)

LIFT
NT INTERFERENCE LIFT
NT JET LIFT
NT ROTOR LIFT
In-flight simulation of backside operating models using direct lift controller
[NAL-TR-1152] 01 p0030 N94-10734
Experimental studies of vortex flaps and vortex plates. Part 1: 0.53 m span 60 deg delta wing
[DE93-767969] 02 p0505 N94-14059
Numerical simulation of dynamic stall of NACA0012 airfoil oscillating near static stall angle using the Navier-Stokes equations
[DE93-767970] 02 p0505 N94-14061
Numerical simulation of a powered-lift landing, tracking flow features using overset grids, and simulation of high lift devices on a fighter-lift-and-control wing
[NASA-CR-194260] 02 p0527 N94-14322
High-Lift System Aerodynamics
[AGARD-CP-515] 04 p1305 N94-18415
Calculation of maximum and high lift characteristics of multi element aerofoils 04 p1305 N94-18419
Navier-Stokes computations of turbulent flow around high-lift configurations 04 p1306 N94-18420
Efficient simulation of incompressible viscous flow over multi-element airfoils 04 p1306 N94-18421
High Reynolds number configuration development of a high-lift airfoil 04 p1306 N94-18424
Numerical calculations of high lift flows using structured and unstructured methods 04 p1307 N94-18428
Navier-Stokes simulation of flow field around a blown-flap high-lift system 04 p1307 N94-18429
An experimental investigation of the optimum slat setting on a combat aircraft model 04 p1308 N94-18431
Viscous phenomena affecting high-lift systems and suggestions for future CFD development
04 p1308 N94-18433
A study of the use of half-models in high-lift wind-tunnel testing 04 p1308 N94-18434
High lift and the forward swept wing
04 p1308 N94-18436
Wake structure and aerodynamic behavior of high lift aircraft configurations during unsteady maneuvers in ground effect 04 p1309 N94-18439
Viscous-inviscid calculation of high-lift separated compressible flows over airfoils and wings
04 p1309 N94-18440
Forty years of high-lift R/D: An aircraft manufacturer's experience 04 p1309 N94-18441
High-lift research: Application to the design of the ATR72 flap 04 p1309 N94-18442
High-lift design for large civil aircraft
04 p1310 N94-18445
High lift systems for transport aircraft with advanced airfoils 04 p1310 N94-18446
Lift and pitching moment induced on jet STOVL aircraft by the ground vortex
[AD-A269816] 04 p1318 N94-18733

Nonlinear aerodynamics and the design of wing tips
[NASA-CR-194732] 05 p1638 N94-21833
A numerical study of airplanes flying in proximity
[AD-A273373] 06 p2173 N94-24718
Active control of oscillatory lift forces on a circular cylinder
[AD-A273243] 06 p2338 N94-25140
High lift aerodynamics
[NASA-CR-195183] 06 p2184 N94-25268
An investigation into the aerodynamic effects of wing patches
[ISBN-0-315-84121-4] 07 p2646 N94-26672
High-lift system analysis method using unstructured meshes
[NLR-TP-92351-U] 07 p2647 N94-27554
Numerical simulation of a powered-lift landing 07 p2671 N94-28033
Program for calculation of maximum lift coefficient of plain aerofoils and wings at subsonic speeds
[ESDU-93015] 07 p2649 N94-28076
Preliminary assessment of aerodynamic effects of wing repair patches 07 p2657 N94-28346
Unsteady aerodynamic computations around NACA0012 at high angles of attack 08 p3126 N94-28969
Aerodynamic characteristics of a propeller-powered high-lift semispan wing
[NASA-TM-4541] 08 p3132 N94-29937
Computation of wind tunnel wall effects for complex models using a low-order panel method
[NASA-TM-104019] 08 p3132 N94-30151
Aerodynamic analysis of slipstream/wing/nacelle interference for preliminary design of aircraft configurations
[AD-B173651] 08 p3135 N94-30916
First Annual High-Speed Research Workshop, part 4
[NASA-CP-10087-PT-4] 10 p3979 N94-33517
Overview of NASA HSR high-lift program 10 p3979 N94-33518
Status of LaRC HSCT high-lift research 10 p3979 N94-33519
Status of CFD for LaRC's HSR high-lift program 10 p3980 N94-33520
HSR high lift research program: Status and plans 10 p3980 N94-33521
HSCT high lift system aerodynamic requirements 10 p3980 N94-33522
HSCT high-lift technology requirements 10 p3980 N94-33523
Lift enhancement by trapped vortex 10 p3980 N94-33524
Supersonic HLFC: Potential benefits and technology development requirements 10 p3982 N94-33531
Icing test results on an advanced two-dimensional high-lift multi-element airfoil
[NASA-TM-106620] 10 p3982 N94-33705

LIFT AUGMENTATION
Lift augmentation on a delta wing via leading edge fences and the Gurney flap
[NASA-CR-194793] 06 p2168 N94-24103
Numerical study of the trailing vortex of a wing with wing-tip blowing
[NASA-CR-195803] 08 p3130 N94-29760
Aerodynamic characteristics of a propeller-powered high-lift semispan wing
[NASA-TM-4541] 08 p3132 N94-29937
STOVL
[NASA-TM-109845] 10 p3989 N94-33790
Concepts and application of dynamic separation for agility and super-maneuverability of aircraft: An assessment 10 p3997 N94-34988

LIFT COEFFICIENTS
U AERODYNAMIC COEFFICIENTS
U LIFT

LIFT DEVICES
Lift enhancement device
[AD-D015868] 04 p1317 N94-17704
High-Lift System Aerodynamics
[AGARD-CP-515] 04 p1305 N94-18415
Where is high-lift today? A review of past UK research programmes 04 p1305 N94-18416
A design procedure for slotted flaps 04 p1305 N94-18418
Navier-Stokes computations of turbulent flow around high-lift configurations 04 p1306 N94-18420
Navier-Stokes calculations on multi-element airfoils using a chimera-based solver 04 p1306 N94-18422
Numerical solution of the Navier-Stokes equations for high-lift configurations on structured composite grids 04 p1306 N94-18423
High Reynolds number configuration development of a high-lift airfoil 04 p1306 N94-18424
A viscous-inviscid solver for high-lift incompressible flows over multi-element airfoils at deep separation conditions 04 p1306 N94-18425
High-lift system analysis method using unstructured meshes 04 p1307 N94-18426
Prediction of the high-lift performance of multi-element aerofoils using an unstructured Navier-Stokes solver 04 p1307 N94-18427
Numerical calculations of high lift flows using structured and unstructured methods 04 p1307 N94-18428
Navier-Stokes simulation of flow field around a blown-flap high-lift system 04 p1307 N94-18429
The GARTEUR high lift research programme 04 p1307 N94-18430
An experimental investigation of the optimum slat setting on a combat aircraft model 04 p1308 N94-18431
An experimental investigation of attachment-line transition on the slat of a combat aircraft model 04 p1308 N94-18432
Viscous phenomena affecting high-lift systems and suggestions for future CFD development 04 p1308 N94-18433
In-flight pressure distributions and skin-friction measurements on a subsonic transport high-lift wing section 04 p1308 N94-18435
High lift and the forward swept wing 04 p1308 N94-18436
A fast computing method for the flow over high-lift wings 04 p1308 N94-18437
Calculation of multielement airfoils and wings at high lift 04 p1309 N94-18438
Wake structure and aerodynamic behavior of high lift aircraft configurations during unsteady maneuvers in ground effect 04 p1309 N94-18439
Forty years of high-lift R/D: An aircraft manufacturer's experience 04 p1309 N94-18441
High-lift research: Application to the design of the ATR72 flap 04 p1309 N94-18442
The aero-mechanical design of a novel Fowler flap mechanism 04 p1309 N94-18443
High-lift design for large civil aircraft 04 p1310 N94-18445
High lift systems for transport aircraft with advanced airfoils 04 p1310 N94-18446
Choice and optimization of a high-lift system for an advanced amphibious aircraft 04 p1310 N94-18447
Eagle RTS: A design of a regional transport 07 p2671 N94-25709
Role of computational fluid dynamics in aeronautical engineering. Part 10: Numerical analysis of flow around 2-D multi-element HLD 08 p3125 N94-28964
Aeroservoelastic tailoring with piezoelectric materials: Actuator optimization studies
[AD-A278640] 11 p4199 N94-36384

LIFT DISTRIBUTION
U FORCE DISTRIBUTION
U LIFT

LIFT DRAG RATIO
Optimization and performance analysis of a supersonic conical-flow waverider for a deck-launched intercept mission
[AD-A272498] 05 p1648 N94-21433
The Triton: Design concepts and methods
[NASA-CR-195542] 06 p2184 N94-25004
Numerical analysis of supersonic transport wings 08 p3124 N94-28959
Improvement of endurance performance by periodic optimal control of variable camber 11 p4194 N94-36329
Numerical investigation of multi-element airfoils
[NASA-CR-194592] 11 p4191 N94-36394

LIFT FANS
The lift-fan powered-lift aircraft concept: Lessons learned
[NASA-CR-177616] 03 p0866 N94-15718
Lift-fan aircraft: Lessons learned-the pilot's perspective
[NASA-CR-177620] 03 p0867 N94-15950
Survey of lift-fan aerodynamic technology
[NASA-CR-177615] 05 p1646 N94-21592
Summary of lift and lift/cruise fan powered lift concept technology
[NASA-CR-177619] 06 p2176 N94-23489

LIFT FORCES
U LIFT

LIFTING BODIES
NT HL-10 REENTRY VEHICLE
NT LIFTING REENTRY VEHICLES
HL-20 personnel launch system
[NASA-TM-109292] 02 p0504 N94-13632
The 1966 highlights --- NASA research programs
[NASA-TM-109444] 03 p1302 N94-15343
The 1968 highlights --- NASA programs and research
[NASA-TM-109627] 03 p1302 N94-15413
Subsonic aerodynamic characteristics of the HL-20 lifting-body configuration
[NASA-TM-4515] 03 p0861 N94-17284
Users manual for the NASA Lewis three-dimensional ice accretion code (LEWICE 3D)
[NASA-TM-105974] 05 p1642 N94-21590
Experimental and theoretical study of aerodynamic characteristics of some lifting bodies at angles of attack from -10 degrees to 53 degrees at Mach numbers from 2.30 to 4.62
[NASA-TM-4528] 07 p2646 N94-26693
Prediction of leading-edge transition and relaminarization phenomena on a subsonic multi-element high-lift system 07 p2659 N94-27929
Aeroelastic vibrations of lifting surfaces
[ECL-91-01] 09 p3585 N94-31677
Launch-pad abort capabilities of the HL-20 lifting body
[NASA-TM-4550] 10 p4007 N94-34687
Optimal control theory determination of feasible return-to-launch-site aborts for the HL-20 Personnel Launch System vehicle
[NASA-TP-3449] 12 p4396 N94-37260

LIFTING REENTRY VEHICLES
NT HL-10 REENTRY VEHICLE
HL-20 personnel launch system
[NASA-TM-109292] 02 p0504 N94-13632

LIFTING ROTORS
The ISL rotor bench
[ISL-R-108/92] 06 p2185 N94-25301
A design of third-generation airfoils for helicopter rotor blades using Navier-Stokes 08 p3124 N94-28957

LIFTING SURFACES
U LIFT DEVICES
U LIFTING BODIES
U SURFACES

LIGAMENTS
Carpal tunnel syndrome and other cumulative trauma disorders of the arm and hand and occupation in US Navy enlisted personnel
[AD-A267747] 03 p1129 N94-17374
Direct observation of fracture of CAS-glass/SiC composites and processing of toughened alumina
[AD-A268275] 03 p0941 N94-17457

LIGANDS
Publications/Patents/Presentations/Honors/Student eport
[AD-A265136] 01 p0078 N94-11873
Synthesis and properties of novel cluster phases
[DE93-017056] 02 p0577 N94-13072
Thermochemistry of transition metal clusters
[DE93-016201] 02 p0571 N94-13977
Synthesis of organic ligands for f-element separations
[DE93-012915] 02 p0554 N94-14290
Binding of carbon dioxide to metal macrocycles: Toward a mechanistic understanding of electrochemical and photochemical carbon dioxide reduction
[DE93-016244] 03 p0949 N94-16870
Pulsed laser kinetic studies of liquids under high pressure
[DE93-017826] 03 p1041 N94-16998
Synthesis, reactivity, and characterization of (-hexacarbocyclic) manganese dicarbonyl complexes with sulfur and phosphorus ligands
[AD-A267592] 03 p0930 N94-17192
Oligomer and mixed-metal compounds, potential multielectron transfer catalysts
[DE93-019592] 04 p1350 N94-19017
Synthesis and structural characterization of new light molecular weight inorganic oxidizers and relative derivatives, volume 1
[AD-A271437] 05 p2012 N94-19842
Catalytic hydrogenation of carbon monoxide
[DE94-000881] 05 p1678 N94-20103
Low temperature absorption spectra and ground state electronic structure of tetrakis(2,6-di-tert-butylphenoxide)uranium(IV)
[DE94-000774] 05 p2035 N94-22387
Transition metal activation and functionalization of carbon-hydrogen bonds
[DE94-003650] 07 p2715 N94-26369
Radiochemistry Division annual progress report : 1991
[DE94-600652] 07 p2715 N94-26392
Property enchancement of polyimide films by way of the incorporation of lanthanide metal ions 07 p2758 N94-27926
Development of novel switchable protein surfaces
[AD-A275510] 08 p3384 N94-28667
Anodization of copper in chloride media
[AD-A275565] 08 p3202 N94-28793
Silicone grease as a precursor to a pseudo crown-ether ligand: Crystal structure of (K(+)K(Me2SiO)7(+))(HIn(CH2CMe3)3(-))4)
[AD-A276343] 09 p3895 N94-31327
Combinatorial ion sensors
[AD-A276567] 09 p3825 N94-32032
A genetic algorithm based method for docking flexible molecules
[DE94-007525] 09 p3793 N94-32269

Laser flash photolysis, EPR and Raman studies of liquids at elevated pressures
[DE94-008351] 09 p3718 N94-32413
Ligand intermediates in metal-catalyzed reactions
[DE94-008713] 09 p3638 N94-32887
Method of determining the concentration of a chemical of interest in a solution
[AD-D016165] 10 p4021 N94-33765
Development of immobilized ligands for actinide separations
[DE94-012714] 12 p4410 N94-37284

LIGHT (VISIBLE RADIATION)
NT AIRGLOW
NT COHERENT LIGHT
NT DAYGLOW
NT GEOCORONAL EMISSIONS
NT NIGHTGLOW
NT POLARIZED LIGHT
NT SKY RADIATION
NT SUNLIGHT
NT TWILIGHT GLOW
NT ZODIACAL LIGHT
Optical transfer operator of the atmosphere-ocean system 01 p0225 N94-12742
The Large Area Pulsed Solar Simulator (LAPSS)
[NASA-CR-194507] 02 p0703 N94-13940
Photovoltaic advanced research and development project: Solar radiation research
[DE92-016430] 02 p0704 N94-14350
Visible light photon counters for astronomy 03 p0902 N94-15043
Method and apparatus for performing scanning tunneling optical absorption spectroscopy
[AD-D015796] 03 p0948 N94-16539
Using controlled daylight exposure and sleep timing in the prevention of shift lag during night operations
[AD-A269304] 04 p1504 N94-17824
Rosat and optical observations of two X-ray transients: MX 0836-42 and GS 0834-430
[MPE-PREPRINT-237] 04 p1622 N94-19451
Optical and Gamma Ray Space Observations
[NASA-TM-109389] 05 p2149 N94-20602
Simultaneous optical/gamma ray observations of GRB's 05 p2149 N94-20603
Estimation of the net production of moss community at Langhovde, East Antarctica 08 p3358 N94-29081
Deployable reflector structure
[NASA-CASE-LAR-14513-1-SB] 08 p3245 N94-29360
Optical field ionization of atoms and ions using ultrashort laser pulses
[DE94-006643] 08 p3488 N94-29845
Correlation analysis on optical and radio light curves for a large sample of active galactic nuclei 08 p3546 N94-29992
Circadian countermeasures for shiftworkers during USMP-2: A report to mission management
[NASA-CR-195260] 08 p3402 N94-30188
Implementing bright light treatment for MSFC payload operations shiftworkers 10 p4098 N94-33623
Ives-Stilwell experiment and relativistic length
[DE94-611076] 10 p4142 N94-33903
Visible and infrared (1.54 micrometers) LED based on Er-doped porous Si
[AD-A278528] 10 p4042 N94-34295
About mid-infrared optical spectrum of high-Tc superconducting compounds
[DE94-615646] 11 p4340 N94-36030
Ground and space flight experiments of the effects of light, sound and/or temperature on animals
[NASA-CR-196102] 12 p4478 N94-36986

LIGHT ABSORPTION
U ELECTROMAGNETIC ABSORPTION

LIGHT ADAPTATION
DCT quantization matrices visually optimized for individual images 06 p2442 N94-25509

LIGHT AIRCRAFT
NT FIREBEE 2 TARGET DRONE AIRCRAFT
NT LIGHT HELICOPTERS
NT MYSTERE 20 AIRCRAFT
NT OH-6 HELICOPTER
NT PIPER AIRCRAFT
Design project: Viper
[NASA-CR-195484] 06 p2184 N94-25021
Solar powered multipurpose remotely powered aircraft 07 p2671 N94-25719
EGADS: A microcomputer program for estimating the aerodynamic performance of general aviation aircraft
[NASA-TM-104013] 07 p2667 N94-26091
Investigation of the aerodynamic environment for an advanced lightweight rotor in forward flight. Volume 4: Laser velocimeter wake data, advance ratio of 0.037
[NASA-TM-109040-VOL-4] 07 p2645 N94-26483
Investigation of the aerodynamic environment for an advanced lightweight rotor in forward flight. Volume 1: Laser velocimeter inflow data, advance ratio of 0.37, thrust coefficient of 0.0081 and hover tip speed of 603 feet/second
[NASA-TM-109040-VOL-1] 07 p2645 N94-26489
Investigation of the aerodynamic environment for an advanced lightweight rotor in forward flight. Volume 2: Laser velocimeter inflow data, advance ratio of 0.37, thrust coefficient of 0.0064 and hover tip speed of 710 feet/second
[NASA-TM-109040-VOL-2] 07 p2645 N94-26492
Investigation of the aerodynamic environment for an advanced lightweight rotor in forward flight. Volume 3: Laser velocimeter inflow data, advance ratio of 0.37, thrust coefficient of 0.0064 and hover tip speed of 603 feet/second
[NASA-TM-109040-VOL-3] 07 p2645 N94-26497
Perseus: Global watcher
[NASA-TM-109813] 10 p3989 N94-33565
Crash impact survival in light planes
[NASA-TM-109799] 10 p3987 N94-33749
High Altitude Long Endurance aircraft design studies 11 p4193 N94-36322

LIGHT ALLOYS
NT ALUMINUM ALLOYS
NT ALUMINUM-LITHIUM ALLOYS
NT BERYLLIUM ALLOYS
NT MAGNESIUM ALLOYS

LIGHT AMPLIFIERS
Method and apparatus for polarization-maintaining fiber optical amplification with orthogonal polarization output
[AD-D015756] 01 p0374 N94-10372
Horizontal-cavity surface-emitting lasers, superluminescent LEDs, and amplifiers, and parabolic gain unstable resonator semiconductor lasers 02 p0656 N94-13573
Design, development and characterization studies of a large aperture high power Nd: Glass rod amplifier stage
[DE93-624944] 03 p1042 N94-17630
X-ray laser oscillator-amplifier experiments
[DE93-017165] 04 p1436 N94-17868
Integrated photonics research volume 10. Conference edition
[AD-A269298] 04 p1577 N94-18298
Applications of nonlinear optic effects in new specialty fibers
[AD-A268890] 04 p1578 N94-18457
Quantum Optoelectronics. Organization of the 1993 photonics science topical meetings. Technical digest series, volume 8
[AD-A269026] 04 p1578 N94-18488
Advanced Solid-State Lasers/Compact Blue-Green Lasers. 1993 technical digest series. Volume 2: Organization of the 1993 photonics science topical meetings
[AD-A269058] 04 p1438 N94-18492
Photonics in Switching: Organization of the 1993 photonics science topical meetings. Technical digest
[AD-A269024] 04 p1578 N94-18528
Integrated Photonics Research: Post-deadline papers
[AD-A269232] 04 p1609 N94-18908
Pulsed power supply for Nova Upgrade
[DE93-019626] 04 p1441 N94-19307
A study of the amplification of laser and VLF waves using a simple pendulum model
[AD-A270857] 04 p1442 N94-19770
Laser amplifier developments at Mercury
[DE93-040103] 05 p1814 N94-19867
Compact lightweight CO2 laser for SDIO application
[AD-A273010] 05 p1817 N94-21284
Investigation of Raman beam cleanup and phase conjugation
[AD-A273157] 06 p2545 N94-24672
Design and testing of ubitron amplifier tubes
[AD-A273297] 06 p2311 N94-24818
Improvement of system properties of a pulsed laser Doppler anemometer with respect to an optical amplifier
[DLR-FB-93-19] 06 p2547 N94-25305
Theory and modeling of stimulated Raman scattering
[AD-A273755] 07 p3033 N94-25721
All-optical gain switching of erbium-doped fibre amplifiers
[ISBN-0-315-84120-6] 07 p2784 N94-26704
Fiber laser amplifiers and oscillators
[AD-A274231] 07 p2820 N94-28068
Photonic devices and systems for optical signal processing
[AD-A275818] 08 p3498 N94-28804
Short-pulse, high-intensity lasers at Los Alamos
[DE94-007545] 09 p3720 N94-32760
Concepts for UV-FEL optics
[DE94-008996] 10 p4142 N94-33982
U-turn alternative to the large aperture switch
[DE94-011541] 12 p4524 N94-37112
Sensitivity and signal to noise ratio improvement of a one micron ladar system incorporating a neodymium doped optical fiber preamplifier. Laser radar testbed
[AD-A280235] 12 p4447 N94-37137

LIGHT BEAMS
NT LASER BEAMS
A compact, four-way image splitter
[AD-A266107] 01 p0382 N94-11656
Development of the one-component diode-array velocimeter
[AD-A265552] 01 p0171 N94-12533
Plume primary smoke 03 p0923 N94-15218
Linear encoding device
[NASA-CASE-GSC-13562-1] 03 p1147 N94-15703
Rotary encoding device
[NASA-CASE-GSC-13556-1] 03 p1148 N94-15943
Controlling chaotic behavior in CO2 and other lasers
[AD-A266431] 03 p1040 N94-16546
Frequency resolution of an acousto-optical spectrometer
[AD-A267822] 03 p1035 N94-17401
Study of high speed interference photography with two-dimensional acousto-optical lattice deflection
[AD-A267823] 03 p1035 N94-17402
High spatial resolution, range gated, underwater imaging method and apparatus
[AD-D015882] 04 p1430 N94-18530
Direct solar pumping of semiconductor lasers: A feasibility study
[NASA-CR-193760] 04 p1440 N94-18834
Rotary encoding device using polygonal mirror with diffraction gratings on each facet
[NASA-CASE-GSC-13543-1] 05 p1985 N94-20240
Study of possible energy upgrade for the ALS and modeling of the real lattice for the diagnosis of lattice problems
[DE93-040286] 05 p2016 N94-20323
System for solving Boolean equations using optical lookup tables
[AD-D015962] 05 p1951 N94-20358
Optical beam forming techniques for phased array antennas 05 p1727 N94-20442
Effects of stimulated Raman scattering on light beam properties during high-power laser beam long-path propagation
[AD-A273109] 05 p1818 N94-21509
Particle image velocimetry
[DE93-040657] 05 p1804 N94-21748
Parametric instabilities in picosecond time scales
[DE94-000384] 05 p1966 N94-21958
Output optics for laser velocimeters
[NASA-CASE-ARC-11889-1-SB] 06 p2543 N94-23309
Method and apparatus for the non-invasive measurement of pressure inside pipes using a fiber optic interferometer sensor
[AD-D016013] 06 p2344 N94-24734
Three-wave nonlinear interactions in KTiOPO4 (KTP) and KTP isomorphs
[AD-A274079] 07 p3052 N94-25993
Spectral and temporal correlations of multifrequency waves in the turbulent atmosphere
[ITN-94-85229] 07 p2774 N94-27233
Advances in tunable powerful lasers: The advanced free-electron laser
[DE94-004997] 08 p3294 N94-29934
Studies of optical beam phase conjugation and electromagnetic scattering process
[AD-A278389] 09 p3884 N94-33145
Method and apparatus for imaging an object in or through a scattering medium by using multiple-wave mixing
[AD-D016212] 11 p4334 N94-36368

LIGHT BULBS
U LUMINAIRES

LIGHT COMMUNICATION
U OPTICAL COMMUNICATION

LIGHT CURVE
A method to determine asteroid poles 01 p0431 N94-12205
Yohkoh Bragg Crystal Spectrometer light curves for Ca XIX (3.1631-3.1912A): 1 October 1991 - 30 September 1992
[AD-A266090] 01 p0483 N94-12414
The soft x ray transient Cen X-4 in quiescence
[NASA-CR-194033] 02 p0833 N94-14406
Analysis of the IUE spectra of the strongly interacting binary beta Lyrae
[NASA-CR-194118] 02 p0833 N94-14493
X ray emission from Wolf-Rayet stars with recurrent dust formation
[NASA-CR-189321] 03 p1300 N94-15533
Variability of the Seyfert galaxy MKN 766 in the Rosat all sky survey
[MPE-PREPRINT-221] 03 p1240 N94-17591
Computational astrophysics: Pulsating stars
[DE93-018369] 04 p1627 N94-18857

Detection of a long-duration solar gamma-ray flare on Jun. 11, 1991 with EGRET on Compton-GRO
04 p1623 N94-19463
SO2 on Venus: A final cross-calibration with Pioneer Venus
[NASA-CR-195162] 06 p2599 N94-24988
On observing neutron star oscillations
08 p3538 N94-29795
Correlation analysis on optical and radio light curves for a large sample of active galactic nuclei
08 p3546 N94-29992

LIGHT DURATION
U PULSE DURATION

LIGHT ELEMENTS
Cometary interplanetary dust particles? An update on carbon in anhydrous IDPS 05 p2084 N94-20828
Asbestos characterization using scanning electron microscopy/light element x ray spectrometry
[AD-A271611] 05 p1681 N94-21241
Zr-rich corner of the Zr-Sn-O diagram
[DE93-633764] 07 p2734 N94-26161
Strongly coupled ionic mixtures and the H/He EOS
[DE94-006391] 09 p3934 N94-31782
Determination of interface structure and bonding at atomic resolution in the stem
[DE94-011466] 12 p4517 N94-37238

LIGHT EMISSION
NT BIOLUMINESCENCE
NT CATHODOLUMINESCENCE
NT CHEMILUMINESCENCE
NT ELECTROLUMINESCENCE
NT FLUORESCENCE
NT LASER INDUCED FLUORESCENCE
NT LUMINESCENCE
NT LUNAR LUMINESCENCE
NT OPTICAL RESONANCE
NT PHOSPHORESCENCE
NT PHOTOLUMINESCENCE
NT RESONANCE FLUORESCENCE
NT SONOLUMINESCENCE
NT SPACECRAFT GLOW
NT THERMOLUMINESCENCE
NT X RAY FLUORESCENCE
Journal of Research of the National Institute of Standards and Technology, volume 98, number 2, March - April 1993
[PB93-196228] 01 p0485 N94-10850
Thermographic properties of eight blue-emitting phosphors
[DE93-011459] 01 p0078 N94-11622
Observations of optical counterparts of Gamma-Ray bursts
[NASA-CR-193573] 01 p0485 N94-12589
Studies of gas in cooling flow clusters
[NASA-CR-193597] 02 p0628 N94-12959
Fabrication of AlGaAs/GaAs-light-emitting devices by selective MOCVD using dialkylmetalchloride
02 p0627 N94-13433
Extending bandwidth of optical emitters using active matching technique
[AD-D015875] 04 p1394 N94-17707
Rapid analysis of mixed waste samples via the optical emission from laser initiated microplasmas
[DE93-014563] 04 p1582 N94-17727
Compact free electron lasers for medical applications
[AD-A271272] 04 p1442 N94-19729
Polarized optical emission due to decay or recombination of spin-polarized injected carriers
[AD-D015907] 04 p1408 N94-19763
Collisional processes involving atmospheric gases
[AD-A270729] 05 p1854 N94-19954
Radio and optical emission: Spectral shapes and breaks in GRB
[NASA-CR-194763] 05 p2150 N94-21781
Stationary plasma thruster plume emissions
[NASA-CR-194471] 07 p2701 N94-26209
Researches of the Electrotechnical Laboratory. No. 53: Spectral emission from combustion gas containing scattering media
[JTN-94-80603] 07 p2717 N94-27246
Observation of stimulated emission from an MBE grown GaN film on sapphire
[DE94-003638] 07 p3068 N94-27724
Energy parameters of the incident auroral electrons derived by the intensity ratio of auroral emissions
07 p2779 N94-27964
A study of white dwarf radiative accretion shocks
08 p3544 N94-29731
A multiwavelength study of two prototypical supernova remnants
08 p3540 N94-29833
Matter-radiation interactions in the atmosphere
09 p3776 N94-30998
Growth, characterization, and device development in monocrystalline diamond films
[AD-A277863] 10 p4146 N94-33774
Visible and infrared (1.54 micrometers) LED based on Er-doped porous Si
[AD-A278528] 10 p4042 N94-34295

LIGHT EMITTING DIODES
Improved super luminescent light source specification
[AD-D015746] 01 p0176 N94-12329
Horizontal-cavity surface-emitting lasers, superluminescent LEDs, and amplifiers, and parabolic gain unstable resonator semiconductor lasers
02 p0656 N94-13573
Laser with optically driven Q-switch
[NASA-CASE-NPO-18470-1-CU] 03 p1038 N94-15932
JSEP fellowship
[AD-A266568] 03 p1211 N94-16800
Extending bandwidth of optical emitters using active matching technique
[AD-D015875] 04 p1394 N94-17707
Polarized optical emission due to decay or recombination of spin-polarized injected carriers
[AD-D015907] 04 p1408 N94-19763
Analytical study of beam handling and emittance control
[AD-A274412] 07 p3033 N94-27078
Visible light emitting materials and injection devices
[AD-A274418] 07 p2786 N94-27079
Temperature dependence of the exciton-exciton annihilation rate constant in poly(di-n-hexylsilane)
[DE94-005584] 09 p3655 N94-32102
Visible and infrared (1.54 micrometers) LED based on Er-doped porous Si
[AD-A278528] 10 p4042 N94-34295

LIGHT GAS GUNS
Experimental technique to simulate orbital-debris impact on space shields at impact velocities over 10 km/s
[DE93-011619] 02 p0539 N94-12909
Calibration of a magnetic induction system for measurement of hypervelocities
[DE93-013949] 02 p0652 N94-14578
Intact capture of hypervelocity particles on Shuttle
05 p2085 N94-20837
Shock compression of low-density foams
[DE93-040545] 05 p1707 N94-21546
High-speed repetitive pellet injector for plasma fueling of magnetic confinement fusion devices
[DE94-002792] 07 p3042 N94-26140
Energy and technology review, July 1993
[DE94-004219] 07 p3118 N94-27566
Transient internal probe
[AD-A275054] 08 p3505 N94-29134
Experimental investigation of nozzle/plume aerodynamics at hypersonic speeds
[NASA-CR-195829] 12 p4382 N94-36687

LIGHT HELICOPTERS
NT OH-6 HELICOPTER
Noise measurement flight test of five light helicopters
[AD-A268566] 03 p1179 N94-17599
Planning German Army helicopter maintenance and mission assignment
[AD-A280483] 12 p4381 N94-37352

LIGHT INTENSITY
U LUMINOUS INTENSITY

LIGHT IONS
Physics of gas breakdown for ion beam transport in gas
[DE93-015646] 02 p0801 N94-14349
Calculations of cosmic-ray helium transport in shielding materials
[NASA-TP-3354] 03 p1301 N94-17666
Electron stripping cross sections for light impurity ions in colliding with atomic hydrogens relevant to fusion research
[DE93-788476] 04 p1566 N94-18158
Development and characterization of a time-, position- and energy-resolved x ray diagnostic for PBFA 2 target experiments
[DE93-019429] 05 p1808 N94-20297
Ion channeling peculiarities in YBa2Cu3 O7 monocrystal
[DE94-606885] 08 p3512 N94-28787
Kinetics of surface roughening and smoothing during ion sputtering
[DE94-006358] 08 p3219 N94-30263
Beam transport
[DE94-010755] 11 p4331 N94-36199

LIGHT MODULATION
Smart spatial light modulator research and development
[AD-A264928] 01 p0382 N94-11286
Spatial light modulator having photosensitive and ferroelectric layers
[AD-D015731] 01 p0404 N94-12400
Optical residue processing module
[AD-A267721] 03 p1188 N94-14940
Velocity matched millimeterwave electro-optic modulator
[AD-A267264] 03 p1188 N94-14957
An optically modulated scatterer for microwave antenna metrology
[NPL-DES-126] 03 p0986 N94-15020
Two-dimensional acousto-optical interaction theory and experimental analysis
[AD-A267761] 03 p1193 N94-17254
Measurements of microlens performance
03 p1197 N94-17355
CO2 laser with modulated losses: Theoretical models and experiments in the chaotic regime
[DE93-624901] 04 p1435 N94-17771
Evaluation of a liquid crystal spatial light modulator capable of amplitude- and phase-modulating modes
[AD-A269252] 04 p1577 N94-18262
Spatial light modulators and applications: Summaries of papers presented at the Spatial Light Modulators and Applications Topical Meeting
[AD-A269452] 04 p1577 N94-18283
Kinetic aspects of lattice mismatch in molecular beam epitaxial growth on planar and patterned substrates
[AD-A270424] 04 p1597 N94-18506
Photonics in Switching: Organization of the 1993 photonics science topical meetings. Technical digest
[AD-A269024] 04 p1578 N94-18528
Integration of ferroelectric/semiconductor thin films for SLM and photorefractive applications
[AD-A268645] 04 p1598 N94-18633
Photodetector array having high pixel density
[AD-D015859] 04 p1432 N94-18731
Direct solar pumping of semiconductor lasers: A feasibility study
[NASA-CR-193760] 04 p1440 N94-18834
Optoelectronic associative memory
[NASA-CASE-NPO-18278-1-CU] 05 p1985 N94-20303
System for solving Boolean equations using optical lookup tables
[AD-D015962] 05 p1951 N94-20358
Optical beam forming techniques for phased array antennas 05 p1727 N94-20442
Center for the integration of optical computing
[AD-A271874] 05 p1899 N94-20469
Simulations of spectral broadening by cross-phase modulation (XPM) with chaotic light pulses
[DE93-019623] 05 p1819 N94-21872
Effect of bandwidth on beam smoothing and frequency conversion at the third harmonic of the Nova laser
[DE93-019917] 05 p1819 N94-21920
A fully automated stage for optical waveguide measurements
[AD-A273042] 06 p2542 N94-22915
Characterization of an LCD for use as a programmable phase shifter to produce a single-lobed far-field pattern in a phased array
[AD-A273883] 07 p3034 N94-25729
Optoelectronic Technology Consortium
[AD-A274909] 07 p2782 N94-26344
Micro-electron deflector
[AD-D016055] 07 p2787 N94-27672
Spatial light modulators with arbitrary quantum wells profiles
[AD-A275023] 08 p3499 N94-29114
Reconfigurable optical interconnections via dynamic computer-generated holograms
[NASA-CASE-NPO-19039-1-CU] 08 p3499 N94-29491
Optical Chopper Assembly for the Mars Observer
08 p3162 N94-29639
Optical techniques for time and frequency transfer
08 p3469 N94-30647
Optical and image transmission through desert atmospheres
[AD-A276022] 09 p3742 N94-31496
Correlation filter synthesis using neural networks
[AD-A278124] 09 p3836 N94-33043
Organosilicon polymeric nonlinear optical materials for optical switching and modulation
[AD-A278245] 10 p4140 N94-33381
Phase-only 128x128 spatial light modulator based on LASLM technology
[AD-A277901] 10 p4141 N94-33591
Two-micron modelocked laser system
[AD-D016219] 12 p4448 N94-37481
Design of a composite filter realizable on practical spatial light modulators
[NASA-CR-196297] 12 p4525 N94-37579

LIGHT PRESSURE
U ILLUMINANCE

LIGHT PROBES
U LIGHT BEAMS

LIGHT SCATTERING
NT HALOS

Optimization of a CO2 laser Thomson scattering alpha particle diagnostic
[DE93-012782] 01 p0173 N94-10160
Phasing operator for two oscillators in classical field 01 p0370 N94-10579
Flowfield structure of swept shock wave/turbulent boundary-layer interactions 01 p0149 N94-10899
Advanced diagnostics for in situ measurement of particle formation and deposition in thermally stressed jet fuels
[DE93-009798] 01 p0098 N94-11366
Bi-directional reflectance by oceanic waters studied via Monte-Carlo simulations 01 p0203 N94-11971
Dust in the Martian atmosphere: Polarimetric sensing 01 p0473 N94-12223
Light scattering from a spherical particle on a conducting plane. Part 1: Normal incidence
[AD-A265920] 01 p0383 N94-12341
Limitations to the quality of optical phase conjugation by stimulated Brillouin scattering
[AD-A266006] 01 p0383 N94-12389
Remote sensing of light scattering coefficient of sea water vertical distribution by the means of airborne lidar 01 p0224 N94-12736
Experimental determination of droplets local mean diameter of a sprag from impinging jets
[INPE-5469-TDI/500] 02 p0631 N94-13365
Image processing and analysis of airborne POLDER data 02 p0689 N94-14219
Brillouin scattering from fluctuations produced by stimulated Raman scattering
[DE93-016531] 02 p0792 N94-14438
Image reconstruction for x ray holographic microscopy
[DE93-013094] 02 p0653 N94-14772
Secondary smoke 03 p0924 N94-15220
Convective flow effects on protein crystal growth
[NASA-CR-194560] 03 p1206 N94-15476
Spatial and frequency diversity in lidar systems
[AD-A266192] 03 p1039 N94-16124
A test of the applicability of independent scattering to high albedo planetary regoliths 03 p1250 N94-16187
Effects of levitated dust on astronomical observations from the lunar surface 03 p1239 N94-16433
Maximum likelihood techniques applied to quasi-elastic light scattering
[NASA-CR-193550] 03 p1192 N94-16718
Speckles statistics and decorrelation effects in complex ABCD optical systems
[AD-A267843] 03 p1193 N94-17012
Scattering from binary optics 03 p1195 N94-17341
Elastic properties of a polyimide film determined by Brillouin scattering and mechanical techniques
[DE93-017404] 04 p1368 N94-18098
High spatial resolution, range gated, underwater imaging method and apparatus
[AD-D015882] 04 p1430 N94-18530
Millimeter wave reflectivity measurement system
[AD-A270008] 04 p1387 N94-18601
Effects of the Mount Pinatubo eruption on solar insolation: Four case studies
[DE93-018454] 04 p1475 N94-18817
Study of electromagnetic wave scattering from characterized rough surfaces
[AD-A270931] 05 p1716 N94-19934
Oceanic in situ Fraunhofer-line characteristics: Fraunhofer-line underwater experiment (FLUX)
[AD-A270659] 05 p1881 N94-19952
Development of a technique to determine the morphology and dynamics of agglomerates in chemically reacting flows
[AD-A271160] 05 p1678 N94-20000
Light scattering studies of an electrorheological fluid
[DE93-019419] 05 p1700 N94-20315
Intensity and polarization of light scattered by size distributions of randomly oriented nonspherical particles 05 p1721 N94-20416
Obtaining surface optical properties from space-based lidar systems
[AD-A272831] 05 p1987 N94-21172
Documentation for PCDIST, a FORTRAN subroutine to calculate Pollack-Cuzzi scattering
[AD-A273070] 05 p1988 N94-21491
Surface and subsurface defect detection in Si3N4 components by laser scattering
[DE93-040829] 05 p1832 N94-21772
Laser diagnostics for small rockets 06 p2210 N94-23032
Laser light scattering instrument advanced technology development
[NASA-CR-194803] 06 p2349 N94-23286
Flight solar calibrations using the Mirror Attenuator Mosaic (MAM): Low scattering mirror 06 p2384 N94-23602
Particle size measurement for the control of industrial crystallizers
[PB94-119104] 06 p2562 N94-23766
Measuring the dynamics of structural changes in biological macromolecules from light scattering data 06 p2422 N94-24426
LRAT: Lightning Radiative Transfer 06 p2416 N94-24443
The chemistry of particulate formation in fluorocarbon plasmas
[DE94-001500] 06 p2552 N94-24546
Investigation of Raman beam cleanup and phase conjugation
[AD-A273157] 06 p2545 N94-24672
Ultrastructure processing of macromolecular materials
[AD-A273413] 06 p2258 N94-24782
Numerical simulation and analysis of experimental results on stimulated Raman scattering in laser-plasma Hohlraum targets
[DE93-613719] 06 p2554 N94-25330
Theory and modeling of stimulated Raman scattering
[AD-A273755] 07 p3033 N94-25721
A numerical solution to the one and two dimensional line radiative transfer equation
[ISBN-0-315-84258-X] 07 p2994 N94-26640
Researches of the Electrotechnical Laboratory. No. 53: Spectral emission from combustion gas containing scattering media
[JTN-94-80603] 07 p2717 N94-27246
Analytic approximation to randomly oriented spheroid extinction
[DREV-4712-93] 07 p3038 N94-27598
Report of the National Research Institute for Earth Science and Disaster Prevention, No. 51
[JTN-94-80509] 07 p2886 N94-27985
Detection of water on road surface by the polarized light 07 p2886 N94-27989
Experimental and theoretical studies of molecular solids
[AD-A275511] 08 p3485 N94-28668
CBSD: The celestial background scene descriptor
[AD-A275521] 08 p3538 N94-28671
Backscatter haze device for measurement of haze in aircraft transparencies
[AD-A275127] 08 p3146 N94-29042
Deformed ellipsoidal diffraction grating blank
[NASA-CR-189334] 08 p3289 N94-29872
The enhancement of compressible turbulent mixing via streamwise vorticity 08 p3280 N94-30487
Single scattering of light by ensembles of particles with various shapes
[ETN-94-96016] 09 p3878 N94-31550
Methods for SBS threshold reduction
[AD-A276554] 09 p3717 N94-31936
Multiple size scale structures in silica/siloxane composites studied by small-angle scattering
[DE94-007300] 09 p3625 N94-32642
Light scattering studies of a model electrorheological fluid
[DE94-007860] 09 p3883 N94-32818
Multiple scattering of light in a comet atmosphere 10 p4163 N94-33388
The modelling of the ocean surface image in optical remote sensing 10 p4078 N94-34369
Fiber optic probes for laser light scattering: Ground based evaluation for micgrogravity flight experimentation. Integrated coherent imaging fiber optic systems for laser light scattering and other applications
[NASA-CR-194377] 10 p4144 N94-34914
Lunar horizon glow and the Clementine mission 11 p4366 N94-35478
Analysis of regional visibility in the eastern United States using aerosol models
[PB94-158698] 11 p4332 N94-35584
Application of GaSe and AgGaSe2 crystal growth to non-linear optics
[PB94-170552] 11 p4341 N94-36212
Efficient light propagation for multiple anisotropic volume scattering
[DE94-006474] 11 p4334 N94-36356
Method and apparatus for imaging an object in or through a scattering medium by using multiple-wave mixing
[AD-D016212] 11 p4334 N94-36368
United States Air Force Summer Research Program, 1993. Volume 13: Phillips Laboratory
[AD-A278657] 12 p4550 N94-36977
Time-gated imaging through defense-scattering materials using stimulated Raman amplification
[AD-D016305] 12 p4440 N94-37775

LIGHT SCATTERING METERS

Laser light scattering instrument advanced technology development
[NASA-CR-194803] 06 p2349 N94-23286
Granulometry in environments with very small particle concentrations 08 p3259 N94-30511

LIGHT SOURCES

NT ILLUMINATORS

LCLS optics: Selected technological issues and scientific opportunities
[DE93-010953] 01 p0175 N94-11468
Improved super luminescent light source specification
[AD-D015746] 01 p0176 N94-12329
Fundamentals and techniques of nonimaging optics
[DE93-013145] 02 p0791 N94-13015
Applications of the Advanced Light Source to problems in the earth, soil, and environmental sciences
[DE93-015258] 02 p0710 N94-14477
Validation of an inexpensive illuminant for aeromedical color vision screening
[DOT/FAA/AM-93/16] 02 p0736 N94-14854
Velocity matched millimeterwave electro-optic modulator
[AD-A267264] 03 p1188 N94-14957
An improved light source for laser ranging 03 p0913 N94-15567
Linear encoding device
[NASA-CASE-GSC-13562-1] 03 p1147 N94-15703
Laser with optically driven Q-switch
[NASA-CASE-NPO-18470-1-CU] 03 p1038 N94-15932
Acousto-optical classifier
[AD-D015894] 03 p1000 N94-16921
Developmental testing of a prototype all-reflection Michelson interferometer
[AD-A269064] 04 p1430 N94-18406
Magnetic field measurements of a superconducting undulator for a Harmonic Generation FEL experiment at the NSLS
[DE93-017621] 04 p1438 N94-18504
Simulation of the ALS longitudinal multibunch feedback system
[DE93-019227] 04 p1575 N94-19152
Study of coupled-bunch collective effects in the ALS
[DE93-019236] 04 p1575 N94-19558
The 1982 to 1992 decade of research on the vacuum ultraviolet ring at National Synchrotron Light Source
[DE93-019469] 04 p1603 N94-19564
Robust photo-topography by fusing shape-from-shading and stereo
[NASA-CR-194697] 05 p1806 N94-19920
ALE project
[AD-A271080] 05 p2014 N94-19980
Study of transverse coupled bunch instabilities by using non-linear Taylor maps for the Advanced Light Source (ALS)
[DE93-040287] 05 p1979 N94-19989
Emittance measurement and modeling of the ALS 50 MeV LINAC to booster line
[DE93-040116] 05 p1979 N94-20273
Measurement and computation of the higher order modes of the ALS 500 MHz accelerating cavities
[DE93-019256] 05 p1980 N94-20292
Study of possible energy upgrade for the ALS and modeling of the real lattice for the diagnosis of lattice problems
[DE93-040286] 05 p2016 N94-20323
System for solving Boolean equations using optical lookup tables
[AD-D015962] 05 p1951 N94-20358
Survey and alignment analysis for the ALS storage ring using computer spreadsheets
[DE93-019254] 05 p1917 N94-21917
Laser energized high voltage direct current power supply
[AD-D015977] 06 p2312 N94-25036
Object-oriented software construction at ALS
[DE94-003418] 07 p2967 N94-27049
Laser phase induced intensity noise in fiber-optic signal processing and sensing systems
[ITN-94-85234] 07 p2819 N94-27179
Opportunities for High Aspect Ratio Micro-Electro-Magnetic-Mechanical Systems (HAR-MEMMS) at Lawrence Berkeley Laboratory
[DE94-003499] 07 p2827 N94-27722
MODIS airborne simulator visible and near-infrared calibration, 1992 ASTEX field experiment. Calibration version: ASTEX King 1.0
[NASA-TM-104599] 07 p2897 N94-28179
Linac Coherent Light Source (LCLS) at 2-4 nm using the SLAC linac
[DE94-005235] 08 p3292 N94-28481
Backscatter haze device for measurement of haze in aircraft transparencies
[AD-A275127] 08 p3146 N94-29042
Light in Thermal Environments (LITE) Workshop
[NASA-CR-195851] 09 p3790 N94-32981
New light sources and concepts for electro-optic sampling
[AD-A278533] 10 p4141 N94-33672
The measurement of three-dimensional geometric parameter 10 p4057 N94-34358

Color center laser with transverse auxiliary illumination
[AD-D016201] 11 p4273 N94-36365
Time-gated imaging through defense-scattering materials using stimulated Raman amplification
[AD-D016305] 12 p4440 N94-37775

LIGHT SPEED
On the importance of the Michelson-Morley experiment
[DE94-606298] 08 p3523 N94-28620

LIGHT TRANSMISSION
NT HALOS
NT LIGHT SCATTERING
Smoothly deformed light 01 p0375 N94-10566
Non classical effects in planar waveguides 01 p0376 N94-10574
Nonperturbative methods in the problem of multiphoton excitation of atom by squeezed light 01 p0376 N94-10575
Wigner functions for nonclassical states of a collection of two-level atoms 01 p0379 N94-10603
Radiation defect production in InAs crystals under electron irradiation
[DE93-617202] 01 p0397 N94-10845
Plans to improve the experimental limit in the comparison of the east-west and west-east one-way light propagation times on the rotating earth 01 p0351 N94-10971
A development on estimation method of undersea light 01 p0204 N94-11974
Propagation of light pulses through a three-layer medium (cloud, pure air, and ocean water) 01 p0222 N94-12725
Trajectory curving in underwater propagation of light 01 p0226 N94-12748
Gathering and exchange information on atmospheric chemistry and polluted atmospheres
[DE93-009940] 02 p0705 N94-12869
Optical propagation through atmospheric turbulence. Model analysis of anisoplanatism and application to adaptive optics
[ONERA-P-1992-4] 02 p0716 N94-14192
A method of detecting and locating electrical current imbalances
[NASA-CASE-LEW-15407-1] 03 p1009 N94-15706
Optical properties and surface morphology studies of palladium contacts on mercuric iodide single crystals
[DE93-012510] 03 p1207 N94-15973
Method and apparatus for performing scanning tunneling optical absorption spectroscopy
[AD-D015796] 03 p0948 N94-16539
Detection of subsurface defects in machined silicon nitride ceramics by optical scattering methods
[DE93-015554] 03 p0968 N94-16658
Transmission of light through a turbulent mixing layer
[AD-A267266] 03 p1193 N94-17264
An ultraviolet faraday rotator glass
[AD-D015879] 04 p1371 N94-18529
Photonic electromagnetic field sensor apparatus
[AD-D015939] 05 p1718 N94-20334
Optical and transport properties of metallic and semiconductor nanostructures
[AD-A271716] 05 p2018 N94-20554
X ray reflection masks: Manufacturing, characterization and first tests
[BONN-IR-92-31] 05 p1986 N94-21043
Photonics and nonlinear optics with molecular materials and polymers
[AD-A271747] 05 p1988 N94-21457
Effects of stimulated Raman scattering on light beam properties during high-power laser beam long-path propagation
[AD-A273109] 05 p1818 N94-21509
OTDR strain gauge for smart skins
[DE93-041043] 05 p1810 N94-21953
Dual frequency optical carrier technique for transmission of reference frequencies in dispersive media
[NASA-CASE-NPO-18007-2-CU] 06 p2543 N94-23270
Design and implementation issues of end-to-end protocols in high-speed networks
[PB94-110905] 06 p2467 N94-23752
Analytic approximation to randomly oriented spheroid extinction
[DREV-4712-93] 07 p3038 N94-27598
UV laser long-path absorption spectroscopy 08 p3343 N94-28595
Optical modeling of visibility and visibility instrumentation using stratified Mie theory 08 p3348 N94-29750
Developing a diode array spectrometer for tropospheric chemistry studies 08 p3362 N94-29752
Characterization of thermally annealed Sb implanted fused silica
[DE94-005464] 08 p3219 N94-30335
Estimation of transmittance from satellite imagery 08 p3257 N94-30500
Calculation of turbulence degraded point spread function of an imaging system 08 p3260 N94-30514
Near resonant absorption by atoms in intense fluctuating laser fields
[DE94-005873] 09 p3714 N94-31200
Optical and image transmission through desert atmospheres
[AD-A276022] 09 p3742 N94-31496
Optimization of Y junctions in integrated optics
[ISBN-0-315-86782-5] 09 p3879 N94-31751
Fast acting optical deflection
[AD-A276630] 09 p3879 N94-32037
Statistics of time averaged atmospheric scintillation
[DE94-006998] 09 p3747 N94-32249
Ocean optics, ocean imaging and optical tomography
[AD-A277010] 09 p3789 N94-32402
Mathematical nonlinear optics
[AD-A277320] 09 p3882 N94-32510
Femtosecond probe-probe transmission studies of LT-grown GaAs near the band edge
[DE94-006660] 09 p3904 N94-32634
Structural studies of photoinduced intramolecular electron transfer in cyclopentadienylnickelnitrosyl
[DE94-008467] 09 p3874 N94-32876
Strain sensing using optical fibers
[NASA-CR-195807] 09 p3740 N94-32940
Studies of optical beam phase conjugation and electromagnetic scattering process
[AD-A278389] 09 p3884 N94-33145
Guiding hard x rays with glass polycapillary fiber
[DE94-004949] 12 p4525 N94-37258

LIGHT TRANSPORT AIRCRAFT
SRISTI: The NAL method for the design and analysis of Natural Laminar Flow (NLF) airfoils 02 p0516 N94-14615

LIGHT VALVES
A full-color, high-resolution laser projector for a flight simulator visual display
[AD-A270578] 05 p1651 N94-20108

LIGHT WATER
Nuclear thermal propulsion engine based on particle bed reactor using light water steam as a propellant
[DE93-014336] 02 p0552 N94-14111

LIGHT WATER REACTORS
Radiation hardening and radiation-induced chromium depletion effects on intergranular stress corrosion cracking of austenitic stainless steels
[DE93-011602] 02 p0572 N94-14058
Fundamental study on monitoring technology on local surface damages 07 p2724 N94-25555
Theoretical study of reactions at the electrode-electrolyte interface
[DE94-009658] 10 p4138 N94-34100
A coarse-mesh nodal method-diffusive-mesh finite difference method
[DE94-010809] 12 p4502 N94-36455

LIGHT-CONE EXPANSION
On spontaneous symmetry breaking mechanism in light-front quantized field theory
[DE93-633211] 06 p2568 N94-22968

LIGHTHILL GAS MODEL
Computation of the sound generated by isotropic turbulence
[NASA-CR-191543] 05 p1804 N94-21880
Sound radiation due to boundary layer transition 06 p2332 N94-24163

LIGHTING
U ILLUMINATING

LIGHTING EQUIPMENT
NT AIRCRAFT LIGHTS
NT ARC LAMPS
NT FLASH LAMPS
NT ILLUMINATORS
NT LUMINAIRES
NT MERCURY LAMPS
NT QUARTZ LAMPS
NT RUNWAY LIGHTS
Cockpit/NVG visual integration issues 06 p2432 N94-23983
Implementing bright light treatment for MSFC payload operations shiftworkers 10 p4098 N94-33623
US manufacturers of commercially available stand-alone photovoltaic lighting systems
[DE94-006917] 12 p4462 N94-37407

LIGHTNING
Oxidation state of the Earth's upper mantle during the last 3800 million years: Implications for the origin of life 01 p0283 N94-12210
Primordial lightning: Evidence preserved in chondrites 01 p0432 N94-12230
Lightning simulation and determination of expected striking points
[ITN-93-85202] 02 p0719 N94-13188
Mesoscale lightning
[NASA-TM-109655] 03 p1105 N94-15226
Venus lightning
[NASA-TM-109644] 03 p1105 N94-15430
Middle atmospheric electric fields over thunderstorms
[NASA-CR-194619] 03 p1106 N94-16493
Remote sensing of precipitation and electrification with a dual-polarization, coherent, wideband radar system
[AD-A267479] 03 p1004 N94-17364
Analysis of high contact resistances associated with hermetic and lightning arrestor connectors
[DE93-014850] 04 p1395 N94-17783
Studies of enhanced radar backscatter
[AD-A269544] 04 p1385 N94-18288
Predicting lightning events in the KSC area: A feasibility study using single station data
[AD-A271440] 05 p1864 N94-20088
Lightning studies using LDAR and LLP data 06 p2416 N94-23238
Lightning, atmospheric electricity, and climate change
[DE94-002003] 06 p2408 N94-23471
CAPE for CaPE 06 p2416 N94-24409
LRAT: Lightning Radiative Transfer 06 p2416 N94-24443
Lightning tests and analyses of tunnel bond straps and shielded cables on the Space Shuttle solid rocket booster
[NASA-CR-193921] 06 p2200 N94-24801
Catalog of absolutely calibrated, range normalized, wideband, electric field waveforms from triggered lightning flashes in Florida
[AD-A273793] 07 p2892 N94-25873
FNAS lightning detection
[NASA-CR-193927] 07 p2893 N94-26134
Thunderstorm Hypothesis Reasoner
[NASA-CR-195714] 07 p2897 N94-27884
MUSIC for localization of thunderstorm cells
[DE94-004985] 07 p2897 N94-28146
A space-based classification system for RF transients
[DE94-003933] 08 p3240 N94-28522
A study of cloud-to-ground lightning processes with emphasis on data analysis and modeling of the return stroke 08 p3372 N94-29802
Lightning-induced coupling of the radiation belts to geomagnetically conjugate ionospheric regions 09 p3772 N94-31773
A numerical study of thunderstorm electrification
[AD-A277531] 10 p4089 N94-33709
Kinetic theory of runaway air breakdown and the implications for lightning initiation
[DE94-001683] 11 p4295 N94-36240
Three flights into thunderstorms with the revised Rocket Electric Field Sounding (REFS) payload
[AD-A280424] 12 p4473 N94-37217

LIGHTS
U LUMINAIRES

LIGNIN
A linear spectral matching technique for retrieving equivalent water thickness and biochemical constituents of green vegetation 03 p1068 N94-16678
Towards a detailed understanding of the structural variability in lignins: A new approach
[DE94-007449] 09 p3793 N94-32267

LIKELIHOOD RATIO
Generalized multichannel signal detection
[AD-A271385] 04 p1391 N94-19587
Stochastic optimization by simulation: Convergence proofs for the G1/G/1 queue in steady-state
[AD-A271141] 05 p1962 N94-19999
Asymptotics of the GLRT for the disorder problem in diffusion processes
[INRIA-RR-1735] 05 p1951 N94-20227
Area-interaction point processes
[CWI-BS-R9318] 09 p3847 N94-32197

LIMB DARKENING
Atmospheric corrections for TIMS estimated emittance 03 p1064 N94-16602
Wavelength dependence of limb-darkening of Mars from visible and near-IR telescopic spectral imaging 05 p2101 N94-20685

LIMBS (ANATOMY)
NT ARM (ANATOMY)
NT ELBOW (ANATOMY)
NT FEET (ANATOMY)
NT FINGERS
NT FOREARM
NT HAND (ANATOMY)
NT KNEE (ANATOMY)
NT LEG (ANATOMY)

LIME
U CALCIUM OXIDES

LIMESTONE
Earth's partial pressure of CO2 over the past 100-500 Ma; evidence from Ce anomalies in mostly shallow seas (less than 200 m) as recorded in carbonate sediments, 2 03 p1104 N94-16360
CO2 production by impact in carbonates? An ATEM and stable isotope (C,O) study 03 p0954 N94-16383

Effects of slot on rock surface for percussive rock excavation: Water jet assisted percussive rock excavation
07 p2871 N94-28155

Influence of clearance and rake angles on the cutting force of rock
08 p3368 N94-29520

LIMITATIONS
U CONSTRAINTS

LIMITER CIRCUITS
Assessment of the impact of HTSC's on superconducting fault-current limiters
[DE93-009986] 01 p0143 N94-11454

LIMITERS (FUSION REACTORS)
A two-dimensional kinetic model of the scrape-off layer
[DE94-001235] 05 p1999 N94-22562

Temporal behavior of the electron density profile during limiter biasing in the HYBTOK-2 tokamak
[NIFS-257] 06 p2552 N94-24456

Initial report on calorimetry for the Tore Supra Outboard pump Limiter
[DE94-011244] 12 p4531 N94-37626

LIMITS (MATHEMATICS)
Automatic differentiation of limit functions
[DE93-016376] 03 p1168 N94-14928

Setting test limits under prescribed consumer loss
[MEMO-1107] 06 p2478 N94-22725

Infinite divisible and stable distributions modulo 1
[PB94-110640] 06 p2495 N94-23815

Uniform limit theorems for marked point processes
[PB94-118726] 06 p2488 N94-24526

Limit theorems for functionals of Markov processes and renormalizable stable fields
[AD-A274645] 07 p3004 N94-27106

On wavelet representations of differential equations
[RR-482] 09 p3842 N94-31412

Stirling's formula and approximations for n(factorial) and the middle ratio
[REPT-93-73] 09 p3843 N94-31642

Qualitative properties of two-dimensional predator-prey systems
[REPT-93-75] 09 p3844 N94-31644

A predator-prey model with Ivlev's functional response
[REPT-93-79] 09 p3844 N94-31696

Kaplan-Meier estimators of interpoint distance distributions for spatial point processes
[CWI-BS-R9315] 09 p3846 N94-32107

Multiserver queues with impatient customers
[CWI-BS-R9319] 09 p3835 N94-32198

LINE CURRENT
Response of transmission line systems to pulse excitation by radiation and injection methods
[DE93-015112] 04 p1384 N94-18210

Transient analysis of conducting half-plane problem with noncausal scattering image
[PB93-225027] 06 p2524 N94-23110

Image theory for DC problems involving a conducting half space bounded by the general anisotropic impedance surface
[PB94-132917] 07 p2779 N94-28390

LINE OF SIGHT
Hypervelocity orbital intercept guidance using certainty control
[AD-A267297] 03 p1174 N94-17219

Sporadic-E observations during LoVHF transionospheric direction finder measurements
[AD-A270619] 05 p1716 N94-19951

A new procedure for orbit determination based on three lines of sight: Angles only
[AD-A272937] 05 p1652 N94-21224

Gaze orientation under G(z)-load. Methodological aspects: Preliminary results
12 p4485 N94-37274

LINE OF SIGHT COMMUNICATION
Laser-based communication link
[FFI-93/7023] 07 p2817 N94-26203

LINE SHAPE
Implementation and use of a computational ray-tracing program for the design and analysis of complex optical systems
[AD-A265075] 01 p0382 N94-11653

Experimental measurements of selenium x-ray laser spectral line profiles
[DE93-016543] 02 p0659 N94-14595

Photoemission and the electronic properties of heavy fermions: Limitations of the Kondo model
[DE93-040191] 05 p1974 N94-21553

Laser phase induced intensity noise in fiber-optic signal processing and sensing systems
[ITN-94-85234] 07 p2819 N94-27179

LINE SPECTRA
NT BALMER SERIES
NT D LINES
NT ELECTRONIC SPECTRA
NT FRAUNHOFER LINES
NT H ALPHA LINE
NT H LINES
NT K LINES
NT LYMAN SPECTRA
NT RYDBERG SERIES

NMR spectroscopy of experimentally shocked single crystal quartz: A reexamination of the NMR shock barometer
01 p0081 N94-12258

Studies of gas in cooling flow clusters
[NASA-CR-193597] 02 p0628 N94-12959

Basic research in solar physics
[NASA-CR-193632] 02 p0844 N94-13234

The infrared solar spectrum
[COMMUNICATIONS-SER-B-159]
02 p0844 N94-13502

Submillimeter, millimeter, and microwave spectral line catalogue, revision 3
[NASA-CR-194501] 02 p0602 N94-13813

Emission line variability in active galactic nuclei
[ITN-93-85209] 02 p0849 N94-14553

Background suppression techniques in germanium detectors
03 p0899 N94-15026

CdTe array detectors for high energy astronomy
03 p0899 N94-15029

Optical fiber spectroscopy: A study of the luminescent properties of the europium ion for thermal sensors
[NASA-CR-194576] 03 p1189 N94-15647

The pressure broadening of HDO by O2, N2, H2, and He between 100 K and 600 K
[AD-A267118] 03 p0946 N94-15684

Spectroscopic and computer modeling investigations of a laser-sustained plasma
[IFTR-30/1991] 03 p1204 N94-17066

The formation process of the He I lambda 10830 line in cool giant stars
[NASA-CR-194648] 03 p1240 N94-17094

Unified NLTE model atmospheres including spherical extension and stellar winds, 4: Improved line transfer and wind contamination of H, He profiles
[MPA-905] 04 p1624 N94-17736

Detection of accreting gas toward HD 45677: A newly recognized, Herbig Be proto-planetary system
[NASA-CR-189312] 04 p1621 N94-19288

Suitability of infrared spectroscopy for remote sensing of tropospheric trace gases
[KFK-5183] 04 p1479 N94-19507

Interactive Spectral Analysis and Computation (ISAAC)
05 p1926 N94-22505

Adaptive filtering of Echelle spectra of distant Quasars
05 p2072 N94-22520

Factor analysis as a tool for spectral line component separation 21cm emission in the direction of L1780
05 p1965 N94-22536

Molecular abundances in the envelopes around evolved stars
[PB94-104916] 06 p2602 N94-23812

UV laser long-path absorption spectroscopy
08 p3343 N94-28595

Camera artifacts in IUE spectra
[NASA-CR-189337] 08 p3198 N94-29857

Spectral and temporal behavior of low mass x ray binaries observed with the Einstein SSS and MPC, and the Broad Band X Ray Telescope
08 p3542 N94-30862

Line-strength gradients and kinematic profiles in elliptical galaxies
09 p3934 N94-31788

Airborne astronomy with a 150 micrometer - 500 micrometer heterodyne spectrometer
[NASA-CR-195940] 10 p4162 N94-34705

Detection of the 267 GHz J = 1-0 rotational transition of PH3 in Saturn with a new Fourier transform spectrometer
[NASA-CR-194364] 10 p4162 N94-34718

Far-infrared emission line spectroscopy of planetary nebulae from the KAO
[NASA-CR-196289] 12 p4547 N94-37825

LINEAMENT
U STRUCTURAL PROPERTIES (GEOLOGY)

LINEAR AC ALTERNATORS
U LINEAR ALTERNATORS

LINEAR ACCELERATORS
Nonlinear space charge effect of bunched beam in linac
[DE93-612176] 01 p0371 N94-10409

DILUTE: A code for studying beam evolution under RF noise
[DE93-011605] 01 p0133 N94-10960

Experimental investigation of wake field excitation in plasma by a periodic succession of relativistic particle clots
[DE93-621655] 01 p0391 N94-11211

LCLS optics: Selected technological issues and scientific opportunities
[DE93-010953] 01 p0175 N94-11468

Operational characteristics of a 100-mA, 2-MeV radio-frequency quadrupole
[DE93-014474] 01 p0374 N94-12786

Evolution of high-repetition-rate induction accelerators through advancements in switching
[DE93-012599] 02 p0654 N94-12963

Beam halo formation from space-charge dominated beams in uniform focusing channels
[DE93-014458] 02 p0789 N94-13209

Design for low beam loss in accelerators for intense neutron source applications
[DE93-014557] 02 p0789 N94-13327

Beam halo in high-intensity beams
[DE93-014565] 02 p0789 N94-13328

Longitudinal beam dynamics for heavy ion fusion
[DE93-013850] 02 p0789 N94-13727

The standing wave FEL/TBA: Realistic cavity geometry and energy extraction
[DE93-016972] 02 p0659 N94-14520

Advanced methods for the computation of particle beam transport and the computation of electromagnetic fields and beam-cavity interactions
[DE93-018160] 04 p1573 N94-17807

Alternating-phase focusing with amplitude modulation
[DE93-018618] 04 p1574 N94-18273

Experimental research in high energy physics
[DE93-011912] 04 p1574 N94-18916

Spice modeling of a FET-switched induction accelerator cell
[DE93-018662] 04 p1575 N94-18996

Induction accelerator development for heavy ion fusion
[DE93-019228] 04 p1591 N94-19479

Transverse beam combiner for ILSE
[DE93-019239] 04 p1591 N94-19559

The ILSE Experimental Program
[DE93-019247] 04 p1576 N94-19560

Method to evaluate steering and alignment algorithms for controlling emittance growth
[DE93-041004] 05 p1978 N94-19856

Emittance measurement and modeling of the ALS 50 MeV LINAC to booster line
[DE93-040116] 05 p1979 N94-20273

Performance of the high brightness linac for the Advanced Free Electron Laser Initiative at Los Alamos
[DE93-040141] 05 p1816 N94-20277

Longitudinal instability of an induction linac with acceleration
[DE93-019249] 05 p1980 N94-20290

Low emittance 0.8A K(+) ion source for the LBL Induction Linac System Experiment (ILSE)
[DE93-019237] 05 p1981 N94-21439

Demonstration of ultraviolet lasing with a low energy electron beam
[DE93-040192] 05 p1818 N94-21554

A high-intensity He-jet production source for radioactive beams
[DE93-040247] 05 p1981 N94-21767

The preservation of low emittance flat beams
[DE93-040964] 05 p1981 N94-21773

A FET-switched induction accelerator cell
[DE93-019604] 05 p1769 N94-21838

A system for managing information at ATLAS
[DE94-001337] 06 p2590 N94-23190

The CEBAF beam loss sensors
[CEBAF-PR-93-032] 06 p2540 N94-24662

Activities of Academia Sinica
[DE93-614529] 06 p2541 N94-25335

JLC-1
[DE93-520380] 07 p3031 N94-26113

Proceedings of the Second EGS4 User's Meeting in Japan
[DE93-520383] 07 p3032 N94-26543

Fluid dynamic linear accelerometer
[AD-D016042] 07 p2678 N94-27112

Linac Coherent Light Source (LCLS) at 2-4 nm using the SLAC linac
[DE94-005235] 08 p3292 N94-28481

Towards short wavelengths FELs workshop
[DE94-004346] 08 p3296 N94-30688

Experiment studies of electron-positron interactions at the Stanford Linear Accelerator Center
[DE94-005877] 08 p3491 N94-30702

A transmission-loss monitor using current transformers
[DE94-003974] 08 p3267 N94-30716

Atomic physics with highly charged ions
[DE94-003397] 08 p3492 N94-30837

Free electrons as a versatile source of coherent radiation
[ETN-94-96011] 09 p3715 N94-31545

Selected applications of planar permanent magnet multipoles in FEL insertion device design
[DE94-009014] 09 p3721 N94-32845

10-GW CO2 laser system at the Brookhaven Accelerator Test Facility
[DE94-009001] 10 p4058 N94-34374

Elastic charge form factors for K mesons
[DE94-010014] 11 p4325 N94-36086

Spin dynamics in storage rings and linear accelerators
[DE94-010320] 11 p4330 N94-36106
ILSE combiner study
[DE94-011009] 11 p4331 N94-36202
High Energy Physics Division of research activities
[DE93-019681] 12 p4521 N94-36694
Activities of the Photon Factory
[DE94-748682] 12 p4522 N94-37236
Recent progress of the Los Alamos advanced free electron laser
[DE94-011654] 12 p4449 N94-37733

LINEAR ALTERNATORS
Lightweight linear alternators with and without capacitive tuning
[NASA-CR-185273] 01 p0140 N94-10505
SPDE/SPRE final summary report
[NASA-CR-187086] 03 p0924 N94-15482

LINEAR AMPLIFIERS
Quantum noise studies with superconducting tunnel junction mixers
[AD-A270897] 05 p2012 N94-19897
Ultralinear wideband integrated circuit design
[ISBN-0-315-84130-3] 07 p2784 N94-26675

LINEAR ARRAYS
NT YAGI ANTENNAS
A 12.5 micron infrared detector for Earth observation
03 p0903 N94-15052
A linear monolithic 4-6 on silicon IR detector array
03 p0910 N94-15098
Sensor modelling for the Cyclops focal plane detector array based technology demonstrator
[AD-A267172] 03 p1190 N94-15846
Rotary encoding device using polygonal mirror with diffraction gratings on each facet
[NASA-CASE-GSC-13543-1] 05 p1985 N94-20240
Probe compensation in cylindrical near-field scanning: A novel simulation methodology
05 p1718 N94-20404
Analysis of microstrip dipoles and slots transversely coupled to a microstrip line using the FDTD method
05 p1718 N94-20405
Optimal sorting in linear arrays with minimum global control
[CWI-CS-R9244] 05 p1908 N94-21024
Analyzing adaptive beamformer performance in a stable multipath environment
[AD-A274029] 07 p2766 N94-25766
Analysis of spark-induced bubble experiments using CALE
[DE94-003667] 08 p3270 N94-28476
Broadband EUV survey spectrometer for short-timescale experiments
[DE94-005459] 08 p3498 N94-28534
Physical interpretation and development of ultrasonic nondestructive evaluation techniques applied to the quantitative characterization of textile composite materials
[NASA-CR-195766] 08 p3183 N94-30016
Comparative semantics for linear arrays of communicating processes
[CWI-CS-R9336] 08 p3426 N94-30491
A monolithic Si bolometer array for the Caltech Submillimeter Observatory
[NASA-TM-109402] 10 p4056 N94-34719

LINEAR CIRCUITS
Using crosscorrelation techniques to determine the impulse response of linear systems
05 p1759 N94-21122
APLAC: An object-oriented analog circuit simulator and design tool. 6.1 system simulations manual
[PB93-224871] 06 p2450 N94-23226
Digitally programmable composite operational amplifier applications
[AD-A275081] 08 p3262 N94-28842
Analysis and synthesis of MOS translinear circuits
[ISBN-9-09-005495-2] 09 p3690 N94-31616

LINEAR ENERGY TRANSFER (LET)
Nonperturbative methods in HZE ion transport
[NASA-TP-3363] 01 p0484 N94-10759
Single event effects and laser simulation studies
[NASA-CR-194506] 02 p0657 N94-13812
Single Event Upset (SEU) testing of semiconductor components at the McMaster Accelerator Laboratory
[DSIS-93-00071] 02 p0823 N94-13834
Approximate Green's function methods for HZE transport in multilayered materials
[NASA-TM-4519] 03 p1300 N94-17084
Energy deposition fluctuations induced by ions in microvolumes and nanovolumes: An analytic approach. 1: Theory
[AD-A267959] 03 p1173 N94-17495
The LET spectrum and its uncertainty during the CRRES mission
[AD-A269977] 04 p1630 N94-18676
To perform a proof-of-concept study on the use of superheated drop detectors for the measurement of LET spectra in space environments
[BTI-92/3-31] 06 p2629 N94-24695
Adaption of the bubble detector for use as a LET spectrometer 08 p3291 N94-30216
Using Cf-252 for single event upset testing
08 p3496 N94-30219
Effects of isotope selection on solution convergence in HZE transport
[NASA-TP-3445] 10 p4167 N94-33686
LET spectra of fragmented 600-MeV/A iron beam on aluminum and polyethylene: A preliminary analysis
[NASA-TP-3436] 12 p4416 N94-36993

LINEAR EQUATIONS
NT LINEAR EVOLUTION EQUATIONS
NT RICCATI EQUATION
The solving of equations by the method of boundary elements 01 p0326 N94-11182
Formally biorthogonal polynomials and a look-ahead Levinson algorithm for general Toeplitz systems
[NASA-CR-194297] 02 p0748 N94-13586
EDF tests for normality in linear models after a Box-Cox transformation
[AD-A269068] 04 p1557 N94-18517
Implementation of the turn function method in KIVA-F90
[DE93-018394] 04 p1419 N94-19027
On the numerical stability of quasi-definite systems
[DE93-019404] 05 p1950 N94-20217
Classical and generalized solutions of time-dependent linear differential algebraic equations
[AD-A272834] 05 p1954 N94-21173
Finite difference methods for time-dependent, linear differential algebraic equations
[AD-A272835] 05 p1954 N94-21174
A retrieval error analysis technique for passive infrared atmospheric sounders
[AD-A272618] 05 p1867 N94-21212
Derivation of a model of the exciter of a brushless synchronous machine
[EUT-92-E-258] 05 p1761 N94-21538
Universality in blow-up for non linear heat equations
[PB93-215465] 05 p2038 N94-22095
Multigrid method for integral equations and automatic programs 06 p2464 N94-23696
Nested Krylov methods based on GCR
[PB94-125317] 07 p2995 N94-26818
Ma42: A new frontal code for solving sparse unsymmetric systems
[PB94-124302] 07 p2998 N94-27115
Review and analysis of dense linear system solver package for distributed memory machines
07 p2978 N94-27916
Frequency-domain transfer-function identification using Chebyshev polynomials
[DE94-004777] 08 p3451 N94-28739
Solution of augmented systems
[PB94-138211] 08 p3452 N94-29111
An introduction to the conjugate gradient method that even an idiot can understand
[AD-A277565] 10 p4128 N94-33392
Time-dependent, linear DAE's with discontinuous inputs
[AD-A277839] 10 p4128 N94-33834
Boundary layer transition: Predictions based on linear theory 10 p4045 N94-33886
Pseudospectral collocation methods for fourth order differential equations
[AD-A281653] 10 p4129 N94-34260

LINEAR EVOLUTION EQUATIONS
Curvature effects in three-dimensional boundary layers
01 p0164 N94-12623

LINEAR FILTERS
NT KALMAN FILTERS
NT REDUCED ORDER FILTERS
A comparative robustness evaluation of feedforward neurofilters
[NASA-TM-106440] 05 p1650 N94-21742
Imaging vector fields using line integral convolution
[DE93-019922] 05 p1917 N94-21841
An adaptive method for group delay compensation using switched capacitor filters 05 p1793 N94-22248
Equalization and cancellation of nonlinear intersymbol interference in a dispersive satellite communication channel
[ISBN-0-315-85147-3] 07 p2775 N94-27274
A novel approach to noise-filtering based on a gain-scheduling neural network architecture
[NASA-TM-106563] 08 p3155 N94-30204
Contact level fusion of radar and IRST contacts on almost electromagnetically silent platform
12 p4395 N94-36634

LINEAR INTEGRATED CIRCUITS
Ultralinear wideband integrated circuit design
[ISBN-0-315-84130-3] 07 p2784 N94-26675

LINEAR OPERATORS
Parameter estimation with cost function of second order in output-error-problem
[DLR-FB-92-38] 05 p1964 N94-21139
Classification of linear differential operators with an invariant subspace in monomials
[PB94-126620] 07 p2996 N94-26915
Hessenberg matrices in Krylov subspaces and the computation of the spectrum
[PB94-133170] 07 p3001 N94-28389

LINEAR POLARIZATION
A test of the applicability of independent scattering to high albedo planetary regoliths
03 p1250 N94-16187
Intensity and polarization of light scattered by size distributions of randomly oriented nonspherical particles
05 p1721 N94-20416
The Brewster angle effect in SAR polarimetry
05 p1731 N94-20456
The coherent backscattering opposition effect
05 p1991 N94-20646
Magellan vertical polarization radar observations
05 p1744 N94-20691
SLD results from the study of polarized Z(sup 0) produced at the SLC
[DE93-041020] 05 p1982 N94-21952
Fiber optic Faraday flux transformer specification
[AD-D016058] 07 p3039 N94-27674
Infrared polarization signatures
08 p3258 N94-30506
High-resolution synthetic aperture radar observations of the Moon 09 p3676 N94-31952
Post-calibration correction for rotating-analyzer ellipsometer with optical fiber bundle detection system
[AD-A277329] 09 p3881 N94-32280
On the ULF waves in the Earth's dayside magnetosphere 10 p4085 N94-33416

LINEAR PREDICTION
Linear parameter identification methods for ARMA models with periodic coefficients
[REPT-92-070] 04 p1556 N94-17938
Algorithms for speech coding systems based on linear prediction
[EUT-92-E-260] 06 p2447 N94-22731
Psychophysical and signal-processing aspects of speech representation
[ETN-94-95292] 06 p2302 N94-25077

LINEAR PROGRAMMING
A simplicial approach to integer programming
[REPT-93-06] 01 p0322 N94-10355
Progress in multidisciplinary design optimization at NASA Langley
[NASA-TM-107754] 01 p0318 N94-10814
Gate assignment using linear programming
[LR-698] 02 p0775 N94-13987
Finding stable orientations of assemblies with linear programming
[AD-A266990] 03 p1143 N94-15212
Planning under uncertainty solving large-scale stochastic linear programs
[DE93-013920] 04 p1516 N94-17701
A model and an execution mechanism for active data bases
[ETN-93-94404] 04 p1614 N94-17979
A teaching tool for linear programming
[AD-A270240] 04 p1523 N94-18905
The theory of linear programming: Skew symmetric self-dual problems and the central path
[REPT-93-15] 04 p1524 N94-19089
Interior-point methodology for linear programming: Duality, sensitivity analysis and computational aspects
[PB94-149663] 04 p1525 N94-19143
A polynomial primal-dual Dikin-type algorithm for linear programming
[REPT-93-36] 04 p1525 N94-19156
Optimal sorting in linear arrays with minimum global control
[CWI-CS-R9244] 05 p1908 N94-21024
Multigrid approach to solving the long transportation problem on a regular grid in cost space
[AD-A272323] 05 p1909 N94-21038
Linear programming for standard and nonstandard Markovian control problems. A survey
[PB93-191948] 05 p1963 N94-21066
A neural network approach to the maximum flow problem 05 p1783 N94-22183
Algorithmic advances in stochastic programming
[DE94-001160] 05 p1921 N94-22406
The Third Twente Workshop on Graphs and Combinatorial Optimization
[PB94-110947] 06 p2486 N94-23722
A note on central cutting plane methods for convex programming
[REPT-93-44] 07 p2958 N94-25762

Research on primal-dual interior point algorithms for mathematical programming
[DE94-003982] 07 p2959 N94-25821
A linear description of the discrete lot-sizing and scheduling problem
[MEMO-COSOR-92-47] 07 p2992 N94-26227
Polyhedral characterization of the economic lot-sizing problem with start-up costs
[MEMO-COSOR-92-46] 07 p2969 N94-27396
Weighted and unweighted maximum clique algorithms with upper bounds from fractional coloring
[AD-A275326] 08 p3409 N94-28917
Solution of augmented systems
[PB94-138211] 08 p3452 N94-29111
Center for Parallel Optimization
[AD-A274988] 08 p3431 N94-29127
Natural deduction for intuitionistic linear logic
[ML-93-09] 08 p3457 N94-30385
Parallel structured optimization algorithms for inverse problems
[AD-A276053] 09 p3811 N94-31443
Perfect 0, +/- matrices
[AD-A277387] 09 p3848 N94-32286
A simple model for determining photoelectron-generated radiation scaling laws
[DE94-006130] 09 p3761 N94-32660
Optimal planning of residential photovoltaic systems under various rate structure
[DE94-757272] 09 p3762 N94-32919
An investigation of simulated annealing applied to structural optimization problems
[AD-A278461] 10 p4068 N94-33541
Enhanced algorithms for stochastic programming
[DE94-009423] 10 p4106 N94-33912
Stopping rules for a class of sampling-based stochastic programming algorithms
[AD-A278654] 11 p4303 N94-35577
A scalable parallel algorithm for multiple objective linear programs
[NASA-CR-194920] 12 p4495 N94-37539

LINEAR QUADRATIC GAUSSIAN CONTROL

Project of an attitude control system (three axis) of a satellite using the LQG/LTR methodology
[INPE-5473-TDI/504] 01 p0044 N94-12356
On comparison and extensions of control methods for narrow-band disturbance rejection
[REPT-93-015] 04 p1540 N94-17922
Acceleration-augmented LQG control of an active magnetic bearing 05 p1757 N94-21112
A new eddy current model for magnetic bearing control system design 05 p1763 N94-21698
Balancing for unstable nonlinear systems
[MEMO-1118] 06 p2469 N94-22705
A homotopy algorithm for digital optimal projection control GASD-HADOC
[NASA-CR-193881] 06 p2456 N94-24470
Flight controller design using mixed H2/H infinity optimization with a singular H infinity constraint
[AD-A273831] 06 p2191 N94-25525
Necessary and sufficient conditions for the existence of the stabilizing solution of the Riccati equation in a Hilbert space: A Popov function approach
[PB94-125341] 07 p2997 N94-26999
Multiple model adaptive control of a large flexible space structure with purposeful dither for enhanced identifiability
[AD-A274132] 07 p2987 N94-27122
Dynamics and robust control for uncertain flexible space systems
[INPE-5510-TAE/020] 07 p2696 N94-27357
A stochastic control approach to flight path monitoring
[AD-B174630] 08 p3143 N94-30853
A Hyland-Bernstein approach to the digital control of Pritchard-Salamon systems
[REPT-93-76] 09 p3844 N94-31693
Synthesis of model reference LQG optimal systems 10 p4114 N94-34310
Control of the SCOLE configuration using distributed parameter models 11 p4221 N94-35885
CSI, optimal control, and accelerometers: Trials and tribulations 11 p4221 N94-35888
Robustness properties of LQG optimized compensators for collocated rate sensors 11 p4221 N94-35890
LQG optimal compensator transfer function for the NASA LaRC CSI Evolutionary Model 11 p4221 N94-35891
Rational positive real approximations for LQG optimal compensators arising in active stabilization of flexible structures 11 p4222 N94-35892
A note on the regularity of solutions of infinite dimensional Riccati equations
[NASA-CR-194898] 12 p4502 N94-36562

LINEAR QUADRATIC REGULATOR

NT LINEAR QUADRATIC GAUSSIAN CONTROL

Active control of acoustic pressure fields using smart material technologies
[NASA-CR-191480] 02 p0768 N94-13354
Robust synthesis of discrete-time multivariable control systems with induced delays 02 p0862 N94-13642
The digital linear quadratic control problem for Pritchard-Salamon systems
[REPT-93-27] 04 p1542 N94-19142
Digital control of Pritchard-Salamon systems
[REPT-93-33] 04 p1543 N94-19286
Operating the Daisy facility to perform control experiments
[ISBN-0-315-83554-0] 06 p2196 N94-22889
Solving the linear quadratic optimal control problem for infinite-dimensional systems
[ISBN-0-315-84562-7] 07 p2999 N94-27405
Approximation theory and computational methods for the identification and control of distributed parameter systems
[AD-A277335] 09 p3848 N94-32244
Microgravity isolation system design: A modern control synthesis framework 11 p4215 N94-35851
Maneuvering and control of flexible space robots 11 p4218 N94-35867
Semigroup approximation and robust stabilization of distributed parameter systems 11 p4222 N94-35894
A note on the regularity of solutions of infinite dimensional Riccati equations
[NASA-CR-194898] 12 p4502 N94-36562

LINEAR REGULATOR

U LINEAR QUADRATIC REGULATOR

LINEAR SYSTEMS

Sample-data and discrete-time H2 optimal control
[MEMO-COSOR-92-53] 01 p0339 N94-10869
The Nehari problem for the Pritchard-Salamon class of infinite-dimensional linear systems: A direct approach
[CS-9216] 01 p0344 N94-10905
Discrete Kalman filtering equations of second-order form for control-structure interaction simulations
[NASA-CR-193723] 01 p0331 N94-11522
Computational algorithms or identification of distributed parameter systems
[AD-A265252] 01 p0331 N94-11680
Calculation of the required sensor accuracy to obtain a specified state estimation accuracy
[NAL-TR-1173] 02 p0649 N94-13343
Decentralized control of uncertain systems via sensitivity models
[DE93-012963] 02 p0766 N94-14568
Simulation of linear mechanical systems 02 p0680 N94-14641
Optimization-based controller design for rotorcraft 02 p0527 N94-14642
A rational interpolation method to compute frequency response 02 p0681 N94-14644
A new treatment of periodic systems with applications to helicopter rotor blade dynamics
[AD-A266770] 02 p0510 N94-14784
Efficiency effects of variation in controlled experimental variables
[DE93-014345] 03 p1169 N94-15979
Invariance of slip movements with respect to the control matrix
[IFTR-43/1991] 03 p1170 N94-17045
A modified direct preconditioner for indefinite symmetric Toeplitz systems
[DE93-015234] 04 p1516 N94-17800
A noniterative improvement of Guyan reduction 04 p1449 N94-17833
An extension of Wolovich's definition of equivalence of linear systems
[MATHS-REPT-A-183] 04 p1547 N94-18069
Advances in the identification of transfer function models using Prony analysis
[DE93-017980] 04 p1548 N94-18094
Generalization of optimal control theory: Linear and nonlinear structures
[PB93-188621] 04 p1540 N94-18125
An ab initio study of the weakly bonded CO-Cl2 complex
[AD-A269000] 04 p1349 N94-18395
A multigrid acceleration technique for computing steady solutions to the equations of compressible flow 04 p1412 N94-18559
New insights in GMRES-like methods with variable preconditioners
[REPT-93-10] 04 p1524 N94-19084
Deadbeat control by measurement feedback: A two sided approach
[REPT-93-20] 04 p1542 N94-19091
Stabilization of time-delay systems: An overview of the algebraic approach
[PB93-191989] 04 p1553 N94-19556
Convex set and linear mixing model 05 p1844 N94-20688
Using crosscorrelation techniques to determine the impulse response of linear systems 05 p1759 N94-21122
An automatic multigrid method for the solution of sparse linear systems 05 p1957 N94-21478
Hybrid finite element/waveguide mode analysis of passive RF devices
[AD-A273074] 05 p1740 N94-21518
Using parallel banded linear system solvers in generalized eigenvalue problems
[NASA-CR-191540] 05 p1915 N94-21584
Reduced-order modelling and control of a class of systems for which balanced truncation is Hankel-norm optimal
[OUEL-1922/92] 06 p2472 N94-23163
Nested Krylov methods and preserving the orthogonality 06 p2483 N94-23681
Coordinate-free interpretations of the optimal costs for Lq problems subject to implicit systems
[PB94-118700] 06 p2473 N94-23760
Neural network-based control using Lyapunov functions 06 p2477 N94-24433
The state space method for integro-differential equations of convolution type with rational matrix symbols
[ETN-94-95379] 06 p2491 N94-25244
From circuit to signal: Development of a piecewise linear simulator
[ISBN-9-09-005713-7] 06 p2462 N94-25263
Arbitrary-order numerical schemes for linear hyperbolic systems
[CRANFIELD-AERO-9211] 06 p2523 N94-25480
Enumeration of n-fold tangent hyperplanes to a surface
[DE94-601544] 07 p2993 N94-26412
Review and analysis of dense linear system solver package for distributed memory machines 07 p2978 N94-27916
Parameter estimation of linear systems from frequency response measurements (computer program)
[ESDU-93016] 07 p2976 N94-28137
Design and analysis of a low-loss linear analog phase modulator for deep space spacecraft X-band transponder applications 08 p3248 N94-29625
Microgravity compatible drive system-rider. New technologies
[PB94-138583] 08 p3229 N94-29996
Robust control of robots via linear estimated state-feedback
[MEMO-1153] 08 p3449 N94-30963
Structural properties of inverse linear systems
[MATHS-REPT-A-200] 09 p3840 N94-31156
Wavevector-frequency analysis with applications to acoustics
[AD-A276618] 09 p3861 N94-32125
Parameter estimation of the vibrational model for the SCOLE experimental facility 11 p4219 N94-35878
Numerical method to study the stability of periodic solutions of particle motion in nonlinear magnetic fields
[DE94-610740] 11 p4325 N94-36088
Estimation with multisensor/multiscan detection fusion
[AD-A278753] 11 p4256 N94-36092
A Galerkin method for linear PDE systems in circular geometries with structural acoustic applications
[NASA-CR-194925] 12 p4503 N94-36923
Robust stabilization of marginally stable positive-real systems
[NASA-TM-109136] 12 p4500 N94-37058

LINEAR TRANSFORMATIONS

Stability by linear processes
[NASA-CR-194131] 01 p0323 N94-10862
The alignment-distribution graph
[NASA-CR-194292] 03 p1168 N94-15112
Reducing data dimension to lower signal processing computational requirements and maximize performance
[AD-A266606] 03 p0999 N94-16728
Robust control of uncertain nonlinear systems
[AD-A268056] 03 p1167 N94-17506
Enumerative geometry of Del Pezzo Surfaces
[DE93-624768] 04 p1546 N94-17816
A parallel and pipelined architecture for estimation of direction of arrival using a bilinear transformation method, volume 3
[AD-A270137] 04 p1389 N94-18897
On geometric and algebraic aspects of 3D affine and projective structures from perspective 2D views
[AD-A270520] 05 p1983 N94-19968
Orbit spaces over commutative rings and projectives as semi-isomorphisms
[DE93-616822] 06 p2493 N94-25473
Satellite attitude determination using linear combination of models
[AD-A274082] 07 p2694 N94-25996
Path integral for coherent states of the dynamical U(sub 2) group and U(sub 2/1) supergroup
[DE94-606382] 08 p3466 N94-28785

Line transects, covariance functions and set approximation
[CWI-BS-R9311] 09 p3846 N94-32084

LINEAR VIBRATION
Acoustic radiation damping of flat rectangular plates subjected to subsonic flows
[NASA-TM-109382] 05 p1967 N94-20211

LINEARITY
On the linearity of fast atomic oxygen effects 09 p3594 N94-31027

LINEARIZATION
On output linearization of observable dynamics
[MEMO-1105] 01 p0341 N94-10276
Wait-free linearization with an assertional proof
[CS-9208] 01 p0323 N94-10878
Computational algorithms or identification of distributed parameter systems
[AD-A265252] 01 p0331 N94-11680
Nonlinear random response prediction using MSC/NASTRAN
[NASA-TM-109029] 03 p1179 N94-17650
Continuum modeling of materials that can undergo martensitic phase transitions
[AD-A268767] 04 p1360 N94-18386
Nonlinear disturbance decoupling and linearization: A partial interpretation of integral feedback
[PB93-197515] 04 p1543 N94-19328
Decoupling problems around a trajectory: From linearity to nonlinearity
[MEMO-1115] 06 p2469 N94-22703
On dynamic input-output linearization of discrete-time nonlinear systems
[MEMO-1123] 06 p2447 N94-22711
Feedback linearization of parametrized nonlinear time-varying systems
[MEMO-1126] 06 p2470 N94-22714
Broadband linearisation of high-efficiency power amplifiers 06 p2275 N94-22747
The structure of exponentials: Uncovering the dynamics of linear logic proofs
[ML-93-10] 08 p3430 N94-30973
Modeling and control of nonlinear systems
[AD-A277377] 09 p3834 N94-32095

LINERS
U LININGS

LINES (GEOMETRY)
NT CHORDS (GEOMETRY)
NT GEODESIC LINES

LINES OF FORCE
New evidence for flux cutting in type II superconductors
[ISBN-0-315-85830-3] 08 p3515 N94-30032

LINGUISTICS
NT MACHINE TRANSLATION
NT PHONEMES
NT PHONEMICS
NT PSYCHOLINGUISTICS
NT SEMANTICS
NT SENTENCES
NT SYLLABLES
NT SYNTAX
NT WORDS (LANGUAGE)
Automatic word categorization: An information-theoretic approach
[CS-9209] 01 p0419 N94-10903
Proceedings of the Seventh International Symposium on Methodologies for Intelligent Systems (poster session)
[DE93-013470] 01 p0340 N94-12428
Using multiple adaptively-weighted strategies for the resolution of demonstratives
[AD-A266463] 03 p1150 N94-16585
Monads and comonads in intensional semantics
[AD-A266522] 03 p1151 N94-16790
Activities of the Research Laboratory of Electronics
[AD-A266730] 03 p1304 N94-17651
A real-time spoken-language system for interactive problem-solving, combining linguistic and statistical technology for improved spoken language understanding
[AD-A270901] 04 p1392 N94-19749
Connectionism and Natural Language Processing
[MEMO-INF-92-64] 05 p1940 N94-20242
Representation of idioms in connectionist models 05 p1940 N94-20247
Neural data oriented parsing 05 p1940 N94-20248
Hopfield models as neural-network acceptors 05 p1941 N94-20250
Recognizing hesitation phenomena in continuous, spontaneous speech 05 p1746 N94-22210
An architecturally-based theory of human sentence comprehension
[AD-A275380] 08 p3398 N94-29313
Interrogatives and adverbs of quantification
[LP-92-14] 08 p3456 N94-30372
Commutative Lambek categorial grammars
[ML-93-01] 08 p3457 N94-30395
The interpretation of free focus
[CL-93-01] 09 p3855 N94-31390
An exploratory study of neuro linguistic programming and communication anxiety
[AD-A277756] 09 p3682 N94-32986
Dialog structure and plan recognition in spontaneous spoken dialog
[AD-A277566] 10 p4032 N94-33393
A linguistic geometry for space applications 10 p4123 N94-35050
Using International English to prepare technical text for translation
[DE94-002628] 11 p4347 N94-36102
An error-resistant linguistic protocol for air traffic control
[NASA-CR-196098] 12 p4385 N94-37013

LININGS
Spin-rolling, welding, and heat treatment of aluminium 2219 for Ariane 5 GAM high pressure vessel liners 01 p0062 N94-10045
A repair patching system for aircraft cargo liners 01 p0017 N94-10771
Ceramics technology project database
[DE93-012431] 01 p0091 N94-11672
Studies of dynamic contact of ceramics and alloys for advanced heat engines
[DE93-016366] 04 p1368 N94-18110
Evaluation of life support equipment during an unsupported North Pole expedition 08 p3379 N94-28422
Combustor technology for future small gas turbine aircraft 10 p4002 N94-34452
Composite matrix experimental combustor
[AD-280344] 10 p4005 N94-34679

LINKAGES
The design of chain links and slings
[NPL-DMM(A)-94] 02 p0662 N94-13808
A robust adaptive control design for flexible joint manipulators 05 p1790 N94-22230
Robot link and contact surface dynamic interaction: An experimental study of contact instability
[ISBN-0-315-83439-0] 05 p1827 N94-22578
Docking mechanisms: An overview of different systems 06 p2357 N94-24004
High precision double four bar linkage mechanism for interferometric linear scanning 06 p2359 N94-24013
Motion planning for serial manipulators with many degrees of freedom: Implementation of a sequential search strategy
[ISBN-0-315-83682-2] 07 p2822 N94-26642
Implementation of integral manifold control on a two degree of freedom flexible joint manipulator: Theory and experiments
[ISBN-0-315-83572-9] 07 p2823 N94-26658
Simulation dynamics of a multibody chain: Recursion based on chain modal coordinates
[ISBN-0-315-83555-9] 07 p2994 N94-26659
Simplified and symmetrical five-bar linkage driver for manipulating a six-degree-of-freedom parallel minimanipulator with three inextensible limbs
[NASA-CASE-GSC-13485-2] 08 p3301 N94-29556
Lock-up failure of a four-bar linkage deployment mechanism 08 p3163 N94-29646

LINKING
U JOINING

LINKS
A design methodology for synthesizing low-order robust controllers for flexible structures 08 p3302 N94-29870

LIOUVILLE EQUATIONS
Stochastic solution to quantum dynamics
[NASA-TP-3408] 07 p3114 N94-26550
A general stochastic Liouville theory for sequential and superexchange electron-transfer reactions involving three Marcus potential surfaces
[DE94-007695] 09 p3869 N94-32141

LIOUVILLE THEOREM
Classical gravity coupled to Liouville theory
[DE93-613049] 01 p0275 N94-10798
On the twisted N=2 superconformal structure in 2d gravity coupled to matter
[DE93-628627] 05 p2037 N94-20178
The generalized spin-boson model for electron-transfer reactions involving two harmonic potentials with a different force constant
[DE94-005470] 08 p3482 N94-28509
Theory for electron-transfer reactions involving two Marcus surfaces with a different force constant
[DE94-005925] 08 p3493 N94-30874

LIPID METABOLISM
Lipid metabolism in cold-exposed humans 09 p3796 N94-31741

LIPIDS
NT CHOLESTEROL
NT PROSTAGLANDINS
NT RETINENE
NT STEROIDS
NT TOCOPHEROL
Probability of alamethicin conductance states varies with nonlamellar tendency of bilayer phospholipids
[AD-A264957] 01 p0301 N94-11648
Biodiesel/aquatic species project report, FY 1992
[DE93-010024] 02 p0709 N94-14087
Structures and shear response of lipid monolayers
[DE93-015076] 02 p0730 N94-14802
Encapsulation of hemoglobin in non-phospholipid vesicles
[AD-A266505] 03 p1128 N94-16785
Polymerizable lipids in the development of controlled release carriers
[AD-D015789] 04 p1368 N94-17982
Morphology of polymerized membranes on an amorphous substrate at molecular resolution by AFM
[AD-A268760] 04 p1370 N94-18403
Lateral distribution of lipids in membranes at high pressure
[AD-A271183] 05 p1700 N94-20299
Primary prevention of coronary heart disease 06 p2423 N94-23317
Synthesis and in-vivo detection of boronated compounds for use in BNCT
[DE94-001899] 06 p2233 N94-23780
Biodiesel from aquatic species
[DE94-000275] 08 p3225 N94-30038
Effect of barbiturates and hyperoxia on lipid peroxidation in hypoxic neurons
[AD-A278467] 10 p4094 N94-33545
Adhesion of phospholipid monolayers to planar supports deposited with the Langmuir-Blodgett technique
[PB94-148699] 10 p4029 N94-34102

LIPSCHITZ CONDITION
Complicated problem solution techniques in optimal parameter searching
[DE94-608007] 08 p3421 N94-30077

LIQUEFACTION
NT COAL LIQUEFACTION
Condensation phenomena 01 p0162 N94-12550
Reverse micelle synthesis of nanoscale metal containing catalysts
[DE93-012869] 02 p0572 N94-14184
Ionic conductivity of alkali halides and their mixtures near liquid-solid phase transition
[ITN-93-85222] 02 p0566 N94-14558
Report of National Institute for Resources and Environment. No. 5: Study on direct liquefaction of woody biomass
[JTN-94-80551] 07 p2859 N94-27204
Oil production from buckwheat stillage by thermochemical liquefaction 07 p2871 N94-28154

LIQUEFIED GASES
NT LIQUEFIED NATURAL GAS
NT LIQUID AIR
NT LIQUID HELIUM
NT LIQUID HELIUM 2
NT LIQUID HYDROGEN
NT LIQUID NITROGEN
NT LIQUID OXYGEN
Statistical mechanical theory of liquid entropy
[DE93-016524] 02 p0817 N94-14593
Structure, thermodynamics, and dynamical properties of supercooled liquids
[DE93-788387] 04 p1607 N94-18211
Evaluation of aftermarket LPG conversion kits in light-duty vehicle applications
[DE93-010035] 04 p1377 N94-18617
Thermal information regarding the cooldown and operation of liquid argon calorimeters
[DE93-019391] 05 p1807 N94-19987
A High Resolution Liquid Xenon Imaging Telescope for 0.3-10 MeV Gamma Ray Astrophysics: Construction and Initial Balloon Flights
[NASA-CR-194709] 05 p2056 N94-22281
The polarization sensitivity of the liquid xenon imaging telescope 05 p2056 N94-22282
Physical characteristics of polymethylmethacrylate scintillator SOFG-120
[DE93-634184] 07 p2810 N94-26395
On possibility to create the scintillation trigger for liquid-argon neutrino detector
[DE94-607844] 08 p3489 N94-30050
Ionization EM calorimetry with accordion electrodes and liquid krypton or argon
[DE94-009082] 09 p3713 N94-32821
Beam tests of a prototype level-1 calorimeter trigger for LHC experiments
[PB94-170495] 11 p4269 N94-35599

Alternative fuel information: Facts about CNG and LPG conversion
[DE94-006888] 12 p4429 N94-37402
Technical evaluation and assessment of CNG/LPG bi-fuel and flex-fuel vehicle viability
[DE94-006925] 12 p4451 N94-37408

LIQUEFIED NATURAL GAS
Assessment of costs and benefits of flexible and alternative fuel use in the US transportation sector
[DE94-006100] 08 p3226 N94-30885
LNG vehicle technology, economics, and safety assessment
[PB94-165487] 12 p4450 N94-36721

LIQUID AIR
An experimental study of plunging liquid jet induced air carryunder and dispersion
[AD-A274414] 07 p2794 N94-26979

LIQUID ALLOYS
Solidification of eutectic system alloys in space (M-19) 02 p0589 N94-13751
Optical properties and emissivities of liquid metals and alloys 06 p2248 N94-25129
Structural ordering in liquid K-Te alloys
[DE94-008477] 09 p3645 N94-32514

LIQUID ATOMIZATION
A computer model for liquid jet atomization in rocket thrust chambers
[NASA-CR-194194] 02 p0627 N94-12803
Mechanism of intermittent atomization
[AD-A266625] 03 p1021 N94-15770
Measurement of intact-core length of atomizing liquid jets by image deconvolution 06 p2210 N94-23029
A theoretical evaluation of aluminum gel propellant two-phase flow losses on vehicle performance 06 p2210 N94-23031
Spray formation processes of impinging jet injectors 06 p2212 N94-23042
Modeling of the phase liquidates in combustion chambers 08 p3195 N94-29278
Investigation of the two-phase flow in a research combustor under reacting and non-reacting conditions 08 p3196 N94-29282
Liquid atomization in supersonic flows 08 p3276 N94-29839
Spray combustion model improvement study, 1
[NASA-CR-196122] 12 p4410 N94-37250

LIQUID BEARINGS
Cryogenic fluid film bearing tester development study
[NASA-CR-192586] 02 p0660 N94-12791
A test apparatus and facility to identify the rotordynamic coefficients of high-speed hydrostatic bearings 10 p4065 N94-34199

LIQUID BRIDGES
Axial response of differently excited anchored viscous liquid bridges in zero-gravity
[LRT-WE-9-FB-1-1992] 04 p1379 N94-19489
Free fall liquid column dynamics in a droptower
[LRT-WE-9-FB-6-1992] 04 p1379 N94-19491
Transient response of a viscous and anchored liquid bridge to an axial pulse
[LRT-WE-9-FB-7-1992] 04 p1379 N94-19492
Stability limits and dynamics of nonaxisymmetric liquid bridges
[NASA-CR-194706] 05 p1797 N94-20037

LIQUID CHROMATOGRAPHY
Chromatographic assessment of hydrogen-bond donating ability
[AD-A265292] 01 p0369 N94-11826
Characterization of dissolved organic matter in the ocean by using the fluorescence excitation-emission matrix 01 p0211 N94-12659
Linear and nonlinear spectroscopic probing of solute interactions with chemically modified silica surface
[DE93-014648] 02 p0562 N94-13001
Direct probing of chromatography columns by laser-induced fluorescence
[DE93-015206] 02 p0654 N94-13022
Reactor studies of metal ions associated with chromatographic silica
[AD-A266675] 02 p0573 N94-14779
Capillary electrokinetic separations with optical detection
[DE94-001639] 06 p2233 N94-23716
Analytical method for estimation of the total amount of aromatic and poly aromatic compounds in diesel fuel
[PB94-123692] 07 p2759 N94-25907
Measurement of elemental speciation by liquid chromatography: Inductively coupled plasma mass spectrometry (LC-ICP-MS) with the Direct Injection Nebulizer (DIN)
[DE94-005261] 08 p3187 N94-28483
Chemically modified polymeric resins for separation of cations, organic acids, and small polar molecules by high performance liquid chromatography
[DE94-005548] 08 p3211 N94-28516
Structural analysis of amorphous phosphates using high performance liquid chromatography
[DE94-004791] 08 p3199 N94-30723
Chemical and structural characterization of nitroaromatic adducts with hemoglobins
[AD-A280533] 12 p4480 N94-37089

LIQUID COOLED REACTORS
NT HEAVY WATER REACTORS
NT LIGHT WATER REACTORS
NT LIQUID METAL COOLED REACTORS
NT PRESSURIZED WATER REACTORS
NT WATER COOLED REACTORS

LIQUID COOLING
NT FILM COOLING
Liquid Cooled Heat Sink with through Vias (LCHS)
[AD-A266008] 01 p0073 N94-12344
Boiling heat-transfer processes and their application in the cooling of high heat flux devices
[AD-A266086] 01 p0413 N94-12535
Hot-gas-side heat transfer characteristics of subscale, plug-nozzle rocket calorimeter chamber
[NASA-TP-3380] 01 p0055 N94-12569
Test apparatus for ITER blanket cooling water distribution design
[DE93-753157] 02 p0795 N94-12944
Description of cooling water calorimetry and wall thermometry diagnostic at tokamak ASDEX-Upgrade
[IPP-5/46] 03 p1200 N94-14966
USAF physiological studies of personal microclimate cooling: A review
[AD-A267203] 03 p1022 N94-15858
Preliminary design of a water cooled avionics cooling rack
[AD-A268826] 04 p1320 N94-18536
A laboratory model of a cooled continental shelf
[AD-A270862] 04 p1500 N94-19792
Cold-start minidiesel engine development
[AD-A271064] 05 p1823 N94-20567
A dc Penning surface-plasma source
[DE93-040126] 05 p1997 N94-21989
The use of liquid and air microclimate conditioning systems to alleviate heat stress in helicopter NBC operations 08 p3384 N94-28453
A review of microclimate cooling systems in the chemical, biological, radiological environment
[AD-A276446] 09 p3802 N94-31302
Heat transfer studies on a rectangular channel with offset plate fins
[AD-A277300] 09 p3912 N94-32043
Evaluation of a liquid cooling garment as a component of the Launch and Entry Suit (LES) 10 p4101 N94-33653
Active cooling from the sixties to NASP
[NASA-TM-109079] 12 p4456 N94-37541

LIQUID CRYSTALS
Vectra insulative support structures within spacecraft 01 p0062 N94-10050
Solidification from supercooled melt under microgravity 01 p0113 N94-10176
Physical properties of injection molded liquid crystal polymers and high temperature engineering polymers
[AD-A264912] 01 p0087 N94-10508
Stability and dynamics of spatio-temporal structures
[DE93-011374] 01 p0401 N94-11610
Spatial light modulator having photosensitive and ferroelectric layers
[AD-D015731] 01 p0404 N94-12400
Colorimetric qualification of shear sensitive liquid crystal coatings
[NASA-CR-194126] 02 p0806 N94-13291
A continuum theory for liquid crystals describing different degrees of orientational order
[ETN-93-94392] 02 p0807 N94-13590
Suppression of bright objects using a spatial light modulator when imaging with CCD- and image intensified cameras
[FFI-93/7008] 02 p0650 N94-13665
Workshop on Formation of Supermolecular Structures in Composite Fluid: Phase Rule and Dynamics
[DE93-782887] 02 p0581 N94-14421
Phases and phase transitions of polymeric liquid crystals: A high resolution x ray diffraction and light scattering study
[ITN-93-85218] 02 p0816 N94-14826
Unidirectional solidification of liquid-crystal material 03 p0945 N94-15167
Electrically controlled liquid-crystal heat valve
[AD-D015872] 04 p1443 N94-17705
Molecular composites from liquid crystalline polymers and liquid crystalline thermosets
[DE93-016608] 04 p1368 N94-18096
Evaluation of a liquid crystal spatial light modulator capable of amplitude- and phase-modulating modes
[AD-A269252] 04 p1577 N94-18262
Spatial light modulators and applications: Summaries of papers presented at the Spatial Light Modulators and Applications Topical Meeting
[AD-A269452] 04 p1577 N94-18283
Measurement Techniques
[VKI-LS-1993-05] 04 p1430 N94-18643
Liquid crystal heat transfer measurements 04 p1432 N94-18653
The application of liquid crystal techniques to determine heat transfer rates 04 p1432 N94-18654
Polymer technology publication. Series no. 14, 1993
[PB93-195964] 04 p1372 N94-19052
Complex and stereoregular nonlinear optical materials
[AD-A271067] 05 p1983 N94-19846
Optically induced rotation diffusion in polymer liquid crystals: Phenomenological theory and experimental verification
[ETN-93-95068] 05 p2014 N94-20026
A full-color, high-resolution laser projector for a flight simulator visual display
[AD-A270578] 05 p1651 N94-20108
Molecular and atomic arrays in nano- and mesoporous materials synthesis
[AD-A271500] 05 p2017 N94-20544
Liquid crystal displays 05 p1752 N94-20634
LCD display tests 05 p1752 N94-20635
Miniature color display, phase 4
[AD-A272920] 05 p1760 N94-21221
Recent developments in aromatic azo polymers research
[AD-A272966] 05 p1705 N94-21259
Fluorescent microthermographic imaging
[DE93-040332] 05 p1810 N94-22000
Method of determining shear stress employing a monomer-polymer laminate structure
[NASA-CASE-LAR-14654-2] 06 p2375 N94-23308
Application of multigrid methods to the solution of liquid crystal equations on a SIMD computer 06 p2484 N94-23686
Ultrastructure processing of macromolecular materials
[AD-A273413] 06 p2258 N94-24782
Center for advanced electrical and structural polymers
[AD-A273415] 06 p2259 N94-24783
Surface-induced static undulations in multilayer films of liquid-crystalline polymers
[AD-A273517] 06 p2262 N94-25159
Structure of cholesteryl-4-vinylbenzoate
[AD-A273686] 06 p2567 N94-25441
Characterization of an LCD for use as a programmable phase shifter to produce a single-lobed far-field pattern in a phased array
[AD-A273883] 07 p3034 N94-25729
Microtubules for nonlinear optical limiting
[AD-A273940] 07 p3035 N94-25941
Color head down display program
[AD-A274807] 07 p2672 N94-26340
Octahedral metallomesogens: Liquid crystallinity in low aspect ratio materials
[AD-A274830] 07 p3059 N94-26571
Ferroelectricity in a Langmuir-Blodgett multilayer film of a liquid crystalline side-chain polymer
[AD-A274477] 07 p2754 N94-27033
Liquid crystalline side-chain polysiloxanes with 4-amino-4'-stilbene-carboxylic ester mesogens
[AD-A274510] 07 p2754 N94-27036
Research and development within nonlinear optics for protection of optical sensors against laser irradiation on of optical sensors against laser irradiation. Quarterannual report 1 (april 1993))
[PB94-124245] 07 p3037 N94-27046
Ultrastructure processing of macromolecular materials
[AD-A274460] 07 p2754 N94-27086
Controlled thermal expansion printed wiring boards based on liquid crystal polymer dielectrics
[NASA-CR-189338] 08 p3287 N94-29400
Active matrix liquid crystal display. Industry survey results
[AD-A276415] 09 p3895 N94-31329
Thermotropic liquid crystals: A variable Clo material 09 p3796 N94-31739
The sol-gel-xerogel transition
[AD-A276647] 09 p3616 N94-32038
Mathematical nonlinear optics
[AD-A277320] 09 p3882 N94-32510
Development of large area, tiled, liquid crystal display
[AD-A277564] 10 p4039 N94-33588
Smart IR-camera: Description of a simulator
[PB94-149010] 10 p4143 N94-34127
Liquid crystalline thermosetting polyimides
[DE94-009939] 11 p4244 N94-35768

LIQUID DROPS
U DROPS (LIQUIDS)

LIQUID FILLED SHELLS
Spin-up in a rectangular cylinder
[AD-A275465] 08 p3271 N94-28738

LIQUID FLOW
NT OPEN CHANNEL FLOW
NT WATER FLOW
Stability of oscillatory two phase Couette flow
[NASA-CR-191501] 02 p0636 N94-13817
Microchannel cooled heatsinks for high average power laser diode arrays
[DE93-016533] 02 p0658 N94-14442
A study of thin liquid sheet flows
[NASA-TM-106323] 02 p0642 N94-14732
Coaxial airblast atomizers
[NASA-CR-193845] 03 p1016 N94-15109
Contribution to the study of a symmetric film flow (with or without tensio-active elements)
[ECL-93-13] 04 p1421 N94-19461
Ejectors and jet pumps: Computer program for design and performance for liquid flow
[ESDU-93022] 07 p2832 N94-28093
Spin-up in a rectangular cylinder
[AD-A275465] 08 p3271 N94-28738
Transient body force effects on the dryout and rewet of a heated capillary structure
[AD-A278677] 11 p4264 N94-35690

LIQUID FUELS
NT AIRCRAFT FUELS
NT AUTOMOBILE FUELS
NT DIESEL FUELS
NT GASOLINE
NT HYDROGEN FUELS
NT JET ENGINE FUELS
NT JP-8 JET FUEL
NT KEROSENE
A computer model for liquid jet atomization in rocket thrust chambers
[NASA-CR-194194] 02 p0627 N94-12803
Conversion of light hydrocarbon gases to metal carbides for production of liquid fuels and chemicals
[DE93-014962] 02 p0583 N94-13002
Status and future opportunities for conversion of synthesis gas to liquid energy fuels
[DE93-010025] 02 p0584 N94-14089
Publications of the Oak Ridge National Laboratory Fossil Energy Program, 1 October 1991 - 31 March 1993
[DE93-014643] 03 p1232 N94-16967
Liquid rocket propulsion. Theory
05 p1667 N94-20069
Cryogenic propellant rocket engine problems
05 p1668 N94-20076
Electro-rheology fluids and liquid fuel flow
[AD-A273640] 06 p2337 N94-25032
An apparatus for measurement of ignition and burning characteristics of metallic particles
[AD-A274815] 07 p2716 N94-26487
Liquid monopropellants
[AD-D016074] 07 p2760 N94-28226
Impact study on the use of biomass-derived fuels in gas turbines for power generation
[DE94-000261] 08 p3224 N94-28502
Ultra low NO(x) ultra lean gas turbine primary zones with liquid fuels 08 p3154 N94-29267
Research and development of ramjets/ramrockets. Part 1: Integral solid propellant ramrockets
08 p3151 N94-29294
Biodiesel from aquatic species
[DE94-000275] 08 p3225 N94-30038
Heterogeneous catalytic process for alcohol fuels from syngas
[DE94-008729] 09 p3667 N94-32583
Gasoline from natural gas by sulfur processing
[DE94-011130] 11 p4248 N94-36035
Heterogeneous catalytic process for alcohol fuels from syngas
[DE94-010263] 11 p4248 N94-36299

LIQUID HELIUM
NT LIQUID HELIUM 2
Quantum dynamics of helium clusters
[AD-A266060] 01 p0411 N94-10874
Development of commercially viable high-T(sub c) Bi-2223 superconductor tapes
[DE93-009966] 01 p0142 N94-10951
Superfluid turbulence 01 p0158 N94-12307
Three-stage linear, split-Stirling cryocooler for 1 to 2K magnetic cold stage
[NASA-CR-4538] 02 p0776 N94-13897
Cryogenic measurements of aerojet GaAs n-JFETs
[NASA-TM-103972] 03 p1009 N94-15765
Superfluid Helium On-Orbit Transfer (SHOOT) flight demonstration 04 p1327 N94-19185
Two-dimensional turbulent nonstationary superfluid counterflows: Numerical simulations, qualitative effects
[MPIS-23/1992] 04 p1422 N94-19510
Acoustic microscopy and nonlinear effects in pressurized superfluid helium
[AD-A270598] 05 p1967 N94-19949
Neutron and PIMC determination of the longitudinal momentum distribution of HCP, BCC and normal liquid He-4
[DE93-019009] 05 p1972 N94-20187
Growth of small fatigue cracks in Incoloy-908
[DE94-003406] 07 p2836 N94-26129
Argon frost continuous cryopump for fusion applications
[DE94-004478] 08 p3230 N94-29017
Acoustic and optical investigations of superfluid (3)He
[PB94-135415] 08 p3477 N94-29186
Spatio-temporal properties of centrifugal instabilities: Abstracts of 8th Couette-Taylor Meeting
[PB94-150240] 11 p4266 N94-35981
Josephson acoustic radiation in superfluid helium
[AD-A280208] 12 p4533 N94-36742

LIQUID HELIUM 2
Sloshing dynamics on rotating helium dewar tank
[NASA-CR-194403] 02 p0637 N94-13959
Examinations of converging cylindrically symmetric second sound propagation in He2
[MPIS-9/1992] 04 p1564 N94-19715
A numerical study of quantized vortices in HeII
[ISBN-9-03-860232-4] 07 p2792 N94-26479
Superfluid helium sloshing dynamics induced oscillations and fluctuations of angular momentum, force and moment actuated on spacecraft driven by gravity gradient or jitter acceleration associated with slew motion
[NASA-CR-193928] 07 p2799 N94-27931
Josephson acoustic radiation in superfluid helium
[AD-A280208] 12 p4533 N94-36742

LIQUID HYDROGEN
An environmental study of the National Aerospace Plane
[AD-A266071] 01 p0025 N94-10945
Preprints of the 13th Hydrogen Energy System Symposium
[DE93-781115] 01 p0099 N94-11444
CFM technologies for space transportation: Multipurpose hydrogen testbed system definition and tank procurement
[NASA-CR-194355] 02 p0539 N94-12827
Semiempirical fragmentation models on galactic cosmic ray transport calculations with hydrogen target
[NASA-TP-3350] 02 p0847 N94-13263
Liquid hydrogen and liquid oxygen feedline passive recirculation analysis
[TABES PAPER 93-620] 03 p1031 N94-16145
Power Reactant Storage Assembly (PRSA) (Space Shuttle). PRSA hydrogen and oxygen DVT tank refurbishment
[NASA-CR-188262] 03 p0926 N94-16922
ALS liquid hydrogen turbopump
[NASA-CR-194646] 03 p0927 N94-17016
Project WISH: The Emerald City
07 p2703 N94-25690
Orbital transfer vehicle engine technology high velocity ratio diffusing crossover
[AD-A277180] 07 p2703 N94-27212
Inertial electrostatic confinement as a power source for electric propulsion 07 p2688 N94-27373
Computational modeling of convective heat transfer to liquid hydrogen coolant 09 p3707 N94-32485
Experimental investigation of jet-induced mixing of a large liquid hydrogen storage tank
[NASA-TM-106629] 10 p4044 N94-33607
Experimental results of hydrogen slosh in a 62 cubic foot (1750 liter) tank
[NASA-TM-106625] 11 p4263 N94-35250
Fluids at high shock pressures and temperatures and some thoughts about future possibilities
[DE94-003625] 12 p4407 N94-36458
Cryogenic fluid management technologies for space transportation. Zero G thermodynamic vent system
[NASA-CR-193981] 12 p4430 N94-36806

LIQUID INJECTION
NT WATER INJECTION
Atomization characteristics of a prefilming airblast atomizer
[NAL-TM-644] 01 p0148 N94-10727
Analysis of gas turbine engines using water and oxygen injection to achieve high Mach numbers and high thrust
[NASA-TM-106270] 02 p0518 N94-13143
Mechanism of intermittent atomization
[AD-A266625] 03 p1021 N94-15770
Combustion instability phenomena of importance to liquid propellant engines
[AD-A268800] 04 p1348 N94-18389
Inherent stability of central element coaxial liquid-liquid injectors 06 p2212 N94-23043
Investigation of the two-phase flow in a research combustor under reacting and non-reacting conditions
08 p3196 N94-29282
Liquid atomization in supersonic flows
08 p3276 N94-29839
Analysis of strong acoustic excitation on the breakup and dispersion of a liquid jet
[ONERA-NT-1993-9] 09 p3701 N94-31422

LIQUID LASERS
Proof of the feasibility of coherent and incoherent schemes for pumping a gamma ray laser
[AD-A269173] 04 p1440 N94-18880

LIQUID LEVELS
Temperature and pressure effects on capacitance probe cryogenic liquid level measurement accuracy
[NASA-CR-190763] 03 p1034 N94-16521
Thermodynamic models for bounding pressurant mass requirements of cryogenic tanks
[NASA-TM-106476] 06 p2346 N94-25202
Method of measuring liquid level
[AD-D016049] 07 p3038 N94-27153

LIQUID LITHIUM
Development of intermetallic coatings for fusion power applications
[DE94-012647] 12 p4419 N94-37442

LIQUID MERCURY
U MERCURY (METAL)

LIQUID METAL COOLED REACTORS
Scoping calculations of power sources for nuclear electric propulsion
[NASA-CR-191133] 10 p4017 N94-34211

LIQUID METAL FAST BREEDER REACTORS
Nonswelling behavior of HT9 alloy irradiated to high exposure
[DE94-003502] 07 p2736 N94-26522
An overview of the current status of resonance theory in reactor physics applications
[DE94-010465] 12 p4521 N94-37194

LIQUID METALS
NT LIQUID LITHIUM
NT LIQUID SODIUM
NT MERCURY (METAL)
Measurement of the thermal conductivity of molten InSb in a drop shaft 01 p0105 N94-10102
Experimental approach to non-contact calorimetry in space 01 p0112 N94-10143
Thermophysical properties of undercooled liquid metals 01 p0086 N94-10190
Ostwald ripening of solid cobalt particles in liquid copper 01 p0087 N94-10202
Measurements of heat capacity in undercooled metals 01 p0087 N94-10231
The reaction between titanium carbide and aluminium carbide in liquid aluminium; a microgravity study 01 p0123 N94-10238
Shear flow control of gas jets in liquids
[AD-A264673] 01 p0152 N94-11448
Performance aspects of de Laval spray-forming nozzles
[DE93-013671] 01 p0163 N94-12604
Diffusion in liquid state and solidification of binary system (M-7) 02 p0587 N94-13739
Liquid metal drop ejection
[NASA-CR-193718] 02 p0572 N94-14133
Statistical mechanical theory of liquid entropy
[DE93-016524] 02 p0817 N94-14593
First on-sun test of NaK pool-boiler solar receiver
[DE93-015003] 04 p1466 N94-18208
Structure, thermodynamics, and dynamical properties of supercooled liquids
[DE93-788387] 04 p1607 N94-18211
Metal slurry droplet and spray combustion
[AD-A269648] 04 p1349 N94-18736
Bench-scale screening tests for a boiling sodium-potassium alloy solar receiver
[DE93-018512] 04 p1469 N94-19040
SP-100 heat transport technology development
[DE94-000769] 06 p2218 N94-23452
Workshop on the Thermophysical Properties of Molten Materials
[NASA-CP-10121] 06 p2246 N94-25120
Detection of velocity in high temperature liquid metals 06 p2247 N94-25127
Optical properties and emissivities of liquid metals and alloys 06 p2248 N94-25129
Thermophysical properties of simple liquid metals: A brief review of theory 06 p2248 N94-25130
Surface chemistry of liquid metals 06 p2249 N94-25133
Liquid metal MHD research and development in Israel 07 p2854 N94-26055
Modelling the mass migration phenomena in partially frozen heat pipes
[DE94-002716] 07 p2797 N94-27709
Liquid metal MHD and heat transfer in a tokamak blanket slotted coolant channel
[DE94-004622] 08 p3506 N94-29510
Electromagnetic effect on turbulent transport in liquid metals and electrolytes (bath)
[PB94-138450] 08 p3206 N94-29946

On the structure and atomic motions in liquid sodium
[DE94-608386] 08 p3490 N94-30182
Near-net-shape manufacturing: Spray-formed metal matrix composites and tooling 08 p3186 N94-30447
Nature of dissolution of binary tantalum-titanium alloys by molten plutonium
[DE94-005090] 08 p3210 N94-30776
Solidification structure synthesis in undercooled liquids
[AD-A276166] 09 p3910 N94-31054
Metal induced embrittlement
[DE94-007450] 09 p3640 N94-31325
Control experiments in liquid metal combustion
[AD-A276918] 09 p3635 N94-32234
Molten metal analysis by laser produced plasmas
[DE94-007014] 09 p3646 N94-32782
The logic behind thick, liquid-walled, fusion concepts
[DE94-012678] 12 p4528 N94-37307

LIQUID NITROGEN
Development of commercially viable high-T(sub c) Bi-2223 superconductor tapes
[DE93-009966] 01 p0142 N94-10951
Liquid Oxygen (LO2) propellant conditioning concept testing
[TABES PAPER 93-621] 03 p0976 N94-16146
Cryogenic spray vaporization in high-velocity helium, argon and nitrogen gasflows
[NASA-TM-106363] 03 p1035 N94-17446
Temperature lowering in cryogenic chemical-synthesis techniques and system
[DE93-018348] 04 p1562 N94-18810
Thermal stresses in the microchannel heatsink cooled by liquid nitrogen
[DE93-018660] 04 p1418 N94-18995
Design of microchannels for cryostabilization of high temperature superconducting magnets
[DE94-001324] 06 p2559 N94-22993
Experimental and analytical study of cryogenic propellant boiloff to develop and verify alternate pressurization concepts for Space Shuttle external tank using a scaled down tank 06 p2266 N94-23657
Tribological behaviour of fluorinated resins and polyimide resins sliding over a metallic surface in liquid nitrogen 06 p2355 N94-23991
The cryogenic tunnel Cologne at DLR
[DLR-MITT-93-10] 07 p2681 N94-27587
An alternate method for achieving temperature control in the -160 to +90 C range
[NASA-CASE-NPO-18995-1-CU] 08 p3288 N94-29497
Characteristics of vaporizing cryogenic sprays for rocket combustion modeling
[NASA-TM-106615] 10 p4055 N94-33605
Characterization of lithium niobate electro-optic modulators at cryogenic temperatures
[DE94-010059] 11 p4333 N94-35697
A precise passive narrow-beam filter infrared radiometer and its use with LIDAR in the ARM program
[DE94-004167] 11 p4269 N94-36085
Fluids at high shock pressures and temperatures and some thoughts about future possibilities
[DE94-003625] 12 p4407 N94-36458

LIQUID OXYGEN
Shear coaxial injector atomization phenomena for combusting and non-combusting conditions
[NASA-CR-193339] 01 p0152 N94-11526
Thermodynamics of lunar ilmenite reduction 01 p0415 N94-12028
Effects of hydrogen addition on combustion performance of a LOX/kerosene rocket
[NAL-TR-1177] 02 p0548 N94-12945
Liquid hydrogen and liquid oxygen feedline passive recirculation analysis
[TABES PAPER 93-620] 03 p1031 N94-16145
Liquid Oxygen (LO2) propellant conditioning concept testing
[TABES PAPER 93-621] 03 p0976 N94-16146
Power Reactant Storage Assembly (PRSA) (Space Shuttle). PRSA hydrogen and oxygen DVT tank refurbishment
[NASA-CR-188262] 03 p0926 N94-16922
Actively controlled shaft seals for aerospace applications
[NASA-CR-194759] 05 p1823 N94-20538
Production of O2 on the Moon: A lab-top demonstration of ilmenite reduction with hydrogen 05 p2126 N94-20821
Detailed study of oxidation/wear mechanism in lox turbopump bearings
[NASA-TM-108434] 05 p1825 N94-21580
LOX droplet vaporization in a supercritical forced convective environment 06 p2211 N94-23034
Evaporation and combustion of LOX under supercritical and subcritical conditions 06 p2211 N94-23035
Axisymmetric single shear element combustion instability experiment 06 p2213 N94-23044
Shear coaxial injector instability mechanisms 06 p2213 N94-23047
Computational Fluid Dynamics (CFD) applications in rocket propulsion analysis and design 06 p2214 N94-23054
Features of a SINDA/FLUINT model of a liquid oxygen supply line 06 p2322 N94-23649
Design considerations of hybrid rockets 06 p2156 N94-24254
Validation of a nonintrusive optical technique for the measurement of liquid mass distribution in a two-phase spray 06 p2548 N94-24420
Advanced launch system. Advanced development oxidizer turbopump program
[NASA-CR-193920] 06 p2367 N94-25174
Liquid-oxygen droplet vaporization and combustion: Analysis of transcritical behavior and application to liquid-rocket combustion instability 08 p3197 N94-29592

LIQUID PHASE EPITAXY
Effect of gravity on the dissolution and liquid phase epitaxial growth processes in a horizontal sandwich system 01 p0118 N94-10208
Liquid phase epitaxy of gallium arsenide: A review
[DE93-622212] 02 p0804 N94-12893
Activities of the optoelectronics laboratory
[PB94-171196] 11 p4334 N94-36190
Study and fabrication of GaSb-based laser heterostructures
[PB94-170677] 11 p4273 N94-36218

LIQUID PHASE SINTERING
Liquid phase sintering of tungsten composites under microgravity. Effect of matrix composition 01 p0118 N94-10207
Study on the mechanism of liquid phase sintering (M-12) 02 p0588 N94-13744
Army P/M research and development overview
[AD-A266921] 03 p0954 N94-15104
Liquid phase sintering of tungsten composites under microgravity. Effect of matrix composition 03 p0945 N94-15171
Recent advances in high density tungsten composite processing
[AD-A270764] 04 p1344 N94-19576
High performance heavy alloys by alloying and process control
[AD-A271129] 05 p1689 N94-20019
Innovative processing of composites for ultra-high temperature applications, book 3
[AD-A275599] 08 p3177 N94-28731

LIQUID PHASES
The stability of hibonite and other aluminous phases in silicate melts: Implications for the origin of hibonite-bearing inclusions 01 p0080 N94-12052
Multiphase equation of state for iron
[DE93-013956] 02 p0568 N94-12977
Growth of samarskite crystal under microgravity conditions (M-20) 02 p0590 N94-13752
The influence of microstructure on the mechanical behavior of silicon nitride ceramics
[DE93-015363] 03 p0966 N94-16018
Process of shaping an electrorheological solid
[AD-D015885] 03 p1012 N94-16914
Ceramic fiber coatings development and demonstration
[AD-A267286] 03 p0972 N94-17242
A basic principles description of liquid vapor phase transitions
[AD-A268331] 03 p1176 N94-17581
A new multiphase equation of state for iron
[DE93-017629] 04 p1357 N94-17819
Molecular nonlinear optical susceptibilities in condensed phases
[AD-A270200] 04 p1568 N94-18784
Neutron and PIMC determination of the longitudinal momentum distribution of HCP, BCC and normal liquid He-4
[DE93-019009] 05 p1972 N94-20187
High strain rate superplasticity in metals and composites
[DE94-001521] 06 p2229 N94-24547
Development of liquid membrane separation processes 07 p2717 N94-27386
Energy Dispersive X ray Diffraction (EDXD) apparatus for liquids at high temperature 07 p2721 N94-28159
Modeling of the phase liquidates in combustion chambers 08 p3195 N94-29278
Development of a catalytic system for gasification of wet biomass
[DE94-006216] 09 p3759 N94-31762
Liquid crystalline thermosetting polyimides
[DE94-009939] 11 p4244 N94-35768
Preliminary results of sulfide melt/silicate wetting experiments in a partially melted ordinary chondrite 11 p4353 N94-36147
Mineralogy and metallurgical properties of iron ore sinter based on magnetite fines
[DE94-763309] 12 p4414 N94-36525

LIQUID PROPELLANT ROCKET ENGINES
NT HYDRAZINE ENGINES
NT HYDROGEN OXYGEN ENGINES
NT J-2 ENGINE
NT RL-10 ENGINES
NT SPACE SHUTTLE MAIN ENGINE
Axisymmetric single shear element combustion instability experiment
[NASA-TM-106327] 01 p0046 N94-10763
Combustion chamber analysis code
[NASA-CR-192585] 01 p0046 N94-10934
Energy and technology review, March 1993
[DE93-013941] 02 p0849 N94-13019
Numerical studies of spray combustion in liquid-fueled engines 02 p0564 N94-13685
Computational analysis of Variable Thrust Engine (VTE) performance
[NASA-CR-193852] 03 p0928 N94-17442
CPIA/M5 liquid propellant engine manual
[AD-A268062] 03 p0929 N94-17589
Combustion instability phenomena of importance to liquid propellant engines
[AD-A268800] 04 p1348 N94-18389
A tutorial on the aero/thermodynamical design of liquid-propellant rocket engine nozzles 05 p1668 N94-20074
Liquid fuel injection elements for rocket engines
[NASA-CASE-MFS-28547-1] 05 p1669 N94-20370
Method of fabricating a rocket engine combustion chamber
[NASA-CASE-MFS-28569-1] 05 p1703 N94-20541
Advanced transportation system studies, technical area 3. Alternate propulsion subsystem concepts: J-2S restart study
[NASA-CR-193874] 05 p1670 N94-21271
NASA Propulsion Engineering Research Center, volume 1
[NASA-CR-194721-VOL-1] 05 p1671 N94-22428
Measurement of intact-core length of atomizing liquid jets by image deconvolution 06 p2210 N94-23029
LOX droplet vaporization in a supercritical forced convective environment 06 p2211 N94-23034
Droplet turbulence interactions under subcritical and supercritical conditions 06 p2211 N94-23036
Fundamental rocket injector/spray programs at the Phillips Laboratory 06 p2211 N94-23039
Numerical parametric studies of spray combustion instability 06 p2212 N94-23041
Spray formation processes of impinging jet injectors 06 p2212 N94-23042
Inherent stability of central element coaxial liquid-liquid injectors 06 p2212 N94-23043
Flow visualization study in high aspect ratio cooling channels for rocket engines 06 p2213 N94-23049
Heat transfer in rocket combustion chambers 06 p2214 N94-23051
Computational Fluid Dynamics (CFD) applications in rocket propulsion analysis and design 06 p2214 N94-23054
Liquid rocket propulsion: Retrospective and prospects 06 p2154 N94-24243
Heat transfer in rocket engine combustion chambers and regeneratively cooled nozzles
[NASA-CR-193949] 06 p2220 N94-24471
Ignition and combustion characteristics of metallized propellants, phase 2
[NASA-CR-195107] 06 p2266 N94-24700
Integrated model development for liquid fueled rocket propulsion systems
[NASA-CR-195253] 07 p2702 N94-27166
AFOSR Contractors Propulsion Meeting
[AD-A279028] 11 p4198 N94-35746
Space and transatmospheric propulsion technology 11 p4229 N94-36047

LIQUID ROCKET PROPELLANTS
NT CRYOGENIC ROCKET PROPELLANTS
NT GELLED ROCKET PROPELLANTS
NT MONOPROPELLANTS
NT SLURRY PROPELLANTS
NT SLUSH HYDROGEN
Development of a high specific 1.5 to 5 kW thermal arcjet
[NASA-CR-193133] 01 p0047 N94-11354
Shear coaxial injector atomization phenomena for combusting and non-combusting conditions
[NASA-CR-193339] 01 p0152 N94-11526
A computer model for liquid jet atomization in rocket thrust chambers
[NASA-CR-194194] 02 p0627 N94-12803
Numerical studies of spray combustion in liquid-fueled engines 02 p0564 N94-13685

Nuclear thermal propulsion engine based on particle bed reactor using light water steam as a propellant
[DE93-014336] 02 p0552 N94-14111
Liquid Oxygen (LO2) propellant conditioning concept testing
[TABES PAPER 93-621] 03 p0976 N94-16146
Lunar lander and return propulsion system trade study
[NASA-TP-3388] 03 p0925 N94-16496
Liquid rocket propulsion. Theory
05 p1667 N94-20069
Cryogenic propellant rocket engine problems
05 p1668 N94-20076
The Vulcain cryogenic engine
05 p1668 N94-20077
Development of a computational testbed for numerical simulation of combustion instability
06 p2213 N94-23046
Recent advances in SPE (tm) water electrolyzer
06 p2393 N94-23362
Assessment of an SP-100 bi-modal propulsion and power system
[DE94-000889] 06 p2218 N94-23433
Hydrogen-oxygen torch ignitor
[NASA-TM-106493] 07 p2691 N94-27424
Liquid monopropellants
[AD-D016074] 07 p2760 N94-28226
Introduction and overview of research and development of solid propellant ramrockets, liquid fuel ramjets and experimental hydrogen ram combustors
08 p3151 N94-29292
Research and development of ramjets/ramrockets. Part 2: Integral liquid fuel ramjets 08 p3152 N94-29297
Catalytic ignitor for regenerative propellant gun
[NASA-CASE-NPO-18987-1-CU]
08 p3225 N94-29490
Aspects of model-based rocket engine condition monitoring and control
[NASA-CR-195116] 08 p3173 N94-29848
The 30th JANNAF Combustion Subcommittee Meeting, volume 1
[AD-A278793] 11 p4247 N94-35655

LIQUID ROTATION
U ROTATING LIQUIDS

LIQUID SLOSHING
Sloshing dynamics on rotating helium dewar tank
[NASA-CR-194403] 02 p0637 N94-13959
Report of three microgravity experiments by the drop shaft
[JTN-94-80579] 07 p2761 N94-27341
Superfluid helium sloshing dynamics induced oscillations and fluctuations of angular momentum, force and moment actuated on spacecraft driven by gravity gradient or jitter acceleration associated with slew motion
[NASA-CR-193928] 07 p2799 N94-27931
Determination of acceleration field parameters with linear accelerometers
[PB94-125606] 08 p3290 N94-30742
Experimental results of hydrogen slosh in a 62 cubic foot (1750 liter) tank
[NASA-TM-106625] 11 p4263 N94-35250

LIQUID SODIUM
On the structure and atomic motions in liquid sodium
[DE94-608386] 08 p3490 N94-30182

LIQUID SURFACES
NT MENISCI
Thermocapillary instabilities in cylindrical liquid bridges: Mechanisms and transition boundaries
01 p0101 N94-10077
Evaporation under microgravity conditions
01 p0102 N94-10086
Boundary layers along horizontal free surfaces due to combined effects of temperature and concentration gradients 01 p0106 N94-10108
Description of the liquid structure facility architecture and experimental demonstration of the diagnostic capabilities
01 p0039 N94-10118
Instability of thermocapillary convection in multiple superposed immiscible liquid layers
01 p0120 N94-10218
Convective motion in a multi-layered system with a free surface 01 p0120 N94-10219
Capillary surfaces in a wedge: Differing contact angles
[DE93-013903] 02 p0631 N94-13244
Measurement of intact-core length of atomizing liquid jets by image deconvolution 06 p2210 N94-23029
Response of an anchored annular cylindrical liquid layer to various axial excitations in zero-gravity
[LRT-WE-9-FB-3-1992] 06 p2266 N94-23195
Design of a surface deformation measuring instrument for the Surface Tension Driven Convection Experiment (STDCE-2)
[NASA-CR-194758] 06 p2343 N94-23285
Method of measuring liquid level
[AD-D016049] 07 p3038 N94-27153
Liquid atomization in supersonic flows
08 p3276 N94-29839
Hydrogen storage for vehicular applications: Technology status and key development areas
[DE94-011626] 12 p4428 N94-37243

LIQUID WASTES
NT URINE
NT WASTE WATER

LIQUID-GAS MIXTURES
NT AEROSOLS
NT FOG
Studies of momentum and energy transfer across wavy gas-liquid interfaces
[AD-A266432] 02 p0635 N94-13699
Measurement of viscosity, density, and gas solubility of refrigerant blends in selected synthetic lubricants
[DE93-040221] 04 p1350 N94-18977
Film condensation in a shock wave
[MPIS-22/1992] 04 p1422 N94-19509
Hydrodynamics of stirred gas-liquid dispersions
[ETN-94-95368] 06 p2339 N94-25254
Interface configuration experiment: Preliminary results
[NASA-TM-109684] 07 p2760 N94-25849
Report of three microgravity experiments by the drop shaft
[JTN-94-80579] 07 p2761 N94-27341

LIQUID-LIQUID INTERFACES
Proceedings of the 8th European Symposium on Materials and Fluid Sciences in Microgravity, volume 1
[ESA-SP-333-VOL-1] 01 p0099 N94-10070
The formation and breakage of liquid bridges under microgravity 01 p0100 N94-10071
Non-linear liquid bridge dynamics
01 p0100 N94-10074
Dielectric liquid bridge stabilization in microgravity by means of electric fields 01 p0100 N94-10075
Thermocapillary instabilities in cylindrical liquid bridges: Mechanisms and transition boundaries
01 p0101 N94-10077
Stability of liquid bridges between parallel plates
01 p0101 N94-10078
Transient three-dimensional numerical simulation of Marangoni flow in a liquid column under microgravity
01 p0101 N94-10079
Coupled thermovibrational and thermocapillary convection in liquid bridge (floating zone system)
01 p0101 N94-10082
Effects of axial and centrifugal forces on the stability of liquid bridges 01 p0102 N94-10083
High Prandtl number fluids in a multilayered system under 1-g or micro-g environment
01 p0104 N94-10096
Benard and Marangoni convection in multiple liquid layers 01 p0105 N94-10100
Coupled thermogravitational and thermocapillary convection in a two-layer fluid system
01 p0105 N94-10101
Thermocapillary slug flow in a capillary tube
01 p0105 N94-10104
Proceedings of the 8th European Symposium on Materials and Fluid Sciences in Microgravity, volume 2
[ESA-SP-333-VOL-2] 01 p0112 N94-10171
Transient effects in the Benard instabilities: Coupling between capillary and gravity effects
01 p0119 N94-10216
Numerical investigations on Marangoni-Benard instability in multi layer systems
01 p0120 N94-10217
Instability of thermocapillary convection in multiple superposed immiscible liquid layers
01 p0120 N94-10218
Convective motion in a multi-layered system with a free surface 01 p0120 N94-10219
Appearance of convective instabilities caused by liquid-liquid phase separation under small buoyancy forces 01 p0120 N94-10221
Surface tension and adsorption kinetics in immiscible liquid systems at microgravity 01 p0121 N94-10225
Fluid-fluid interfacial instabilities induced by gravity
01 p0121 N94-10229
Use of inert immiscible liquid for crystal separation out of its feeding solution in weightlessness
01 p0124 N94-10242
The application of front tracking to the simulation of shock refractions and shock accelerated interface mixing
[DE93-018342] 04 p1419 N94-19025
Multigrid for a groundwater flow problem
[PB94-149655] 04 p1420 N94-19144
Electrochemically mediated polymerization of 2-pentadecylaniline confined to a planar liquid-liquid interface
[AD-A273541] 06 p2259 N94-24792
The hydrodynamics of a moving fluid-liquid contact line
[ETN-94-95352] 06 p2339 N94-25247
Mapping of seawater intrusion into the coastal aquifer of Israel (the seawater-freshwater interface) by TDEM (Time Domain Electromagnetic) method
[ITN-94-85238] 07 p2850 N94-27331
Steady thermal convection in multiple liquid layers
09 p3705 N94-31844

LIQUID-SOLID INTERFACES
Proceedings of the 8th European Symposium on Materials and Fluid Sciences in Microgravity, volume 1
[ESA-SP-333-VOL-1] 01 p0099 N94-10070
The formation and breakage of liquid bridges under microgravity 01 p0100 N94-10071
Experimental study of axisymmetric thermocapillary flows 01 p0100 N94-10072
Non-linear liquid bridge dynamics
01 p0100 N94-10074
Dielectric liquid bridge stabilization in microgravity by means of electric fields 01 p0100 N94-10075
Thermocapillary instabilities in cylindrical liquid bridges: Mechanisms and transition boundaries
01 p0101 N94-10077
Stability of liquid bridges between parallel plates
01 p0101 N94-10078
Effects of axial and centrifugal forces on the stability of liquid bridges 01 p0102 N94-10083
Liquid bridges and floating zones
01 p0102 N94-10085
Separation of gravitational effects on the flow of suspension in tubes by measurements in weightlessness
01 p0105 N94-10105
On the role of Soret effect in concentration distribution in crystals growing from the melt
01 p0112 N94-10173
TEXUS 28 experiment: Convections and crystal growth of Ge:Ga. Analysis of temperature measurements
01 p0114 N94-10184
Convection related radial segregation in an idealized horizontal Bridgman configuration
01 p0115 N94-10185
Ground results of the Mephisto program: Benefits and space experiments orientation 01 p0086 N94-10197
Transient effects in the Benard instabilities: Coupling between capillary and gravity effects
01 p0119 N94-10216
The physics of pattern formation of liquid interfaces
[DE93-013333] 01 p0154 N94-11814
An analytical investigation of transient effects on rewetting of heated thin flat plates
[NASA-TM-106120] 02 p0628 N94-12968
Thermodynamic status of static and dynamic contact angles
[ISBN-0-315-73844-8] 02 p0817 N94-13554
Immiscible phase incorporation during directional solidification of hypermonotectics
[NASA-CR-194412] 02 p0565 N94-14480
Unidirectional solidification of liquid-crystal material
03 p0945 N94-15167
Liquidus equilibria of lunar analogs at high pressure
03 p1283 N94-16364
Particle Engulfment and Pushing by Solidifying Interfaces (PEPSI)
[NASA-CR-193856] 03 p0960 N94-17079
Axial response of differently excited anchored viscous liquid bridges in zero-gravity
[LRT-WE-9-FB-1-1992] 04 p1379 N94-19489
Surface science at the solid liquid interface
[AD-A271422] 05 p1678 N94-19839
Surface electrochemistry of metals
[AD-A272913] 05 p1691 N94-21245
Liquid oscillations in a spherical system with sliding edges boundary by two conical solid surfaces in zero-gravity
[LRT-WE-9-FB-5-1992] 06 p2318 N94-23197
Effects of thermal-solutal convection on temperature and solutal fields under various gravitational orientations
06 p2267 N94-24451
Surface-induced static undulations in multilayer films of liquid-crystalline polymers
[AD-A273517] 06 p2262 N94-25159
The hydrodynamics of a moving fluid-liquid contact line
[ETN-94-95352] 06 p2339 N94-25247
Bulletin of National Research Institute for Metals in Fiscal Year 1993, no. 14
[REPT-14] 07 p2722 N94-25544
Observation on metal surface in aqueous solution using an electrochemical Scanning Tunneling Microscope (STM) 07 p2724 N94-25554
Study on interfacial reaction analysis at interfacial joining 07 p2728 N94-25574
Morphology transitions during non-equilibrium growth processes
[ITN-94-85236] 07 p3065 N94-27243
On line quantification of crystal surfaces by stereo imaging
[NASA-CR-195277] 07 p3066 N94-27561

A solid-on-solid invasion percolation model for self-affine interfaces
[DE94-608102] 08 p3521 N94-30888
Interfacial behaviour: Wettability in SiC(sub p) metal matrix composites
[ISBN-0-315-87206-3] 09 p3621 N94-31835
Chemical structure and kinetics at liquid/solid interfaces
[AD-A277112] 09 p3636 N94-32304
Time-resolved analytical methods for liquid/solid interfaces
[DE94-008352] 09 p3637 N94-32826
Interface shape and convection during solidification and melting of succinonitrile
[NASA-TM-106487] 11 p4262 N94-35248
Determination of the dispersion constant in a constrained vapor bubble thermosyphon
[NASA-CR-196124] 12 p4442 N94-36992
Nonlinear optical spectroscopy for surface studies
[DE94-011623] 12 p4408 N94-37056

LIQUID-VAPOR EQUILIBRIUM
Explosive boiling at very low heat fluxes: A microgravity phenomenon
[NASA-TM-106325] 03 p1046 N94-15817
Effect of initial droplet-size distributions on fuel-vapor profiles in a shear-layer flow 06 p2160 N94-24283
Thermocapillary flow with evaporation and condensation and its effect on liquid retention in low-G fluid acquisition devices
[NASA-TP-3463] 07 p2797 N94-27639
Measurement of viscosity, density, and gas solubility of refrigerant blends in selected synthetic lubricants
[DE94-010426] 11 p4244 N94-35687

LIQUID-VAPOR INTERFACES
Studies of momentum and energy transfer across wavy gas-liquid interfaces
[AD-A266432] 02 p0635 N94-13699
Sloshing dynamics on rotating helium dewar tank
[NASA-CR-194403] 02 p0637 N94-13959
Space Station thermal storage/refrigeration system research and development
[NASA-CR-193841] 03 p0879 N94-15191
Mechanism of intermittent atomization
[AD-A266625] 03 p1021 N94-15770
Pressurization and expulsion of a flightweight liquid hydrogen tank
[NASA-TM-106427] 05 p1799 N94-20177
Experimental study of void formation during aluminum solidification in reduced gravity
[NASA-TM-106190] 05 p1692 N94-21604
The 2-D polymerized Langmuir-Blodgett films studied by STM
[AD-A273542] 06 p2261 N94-24930
Interface configuration experiment: Preliminary results
[NASA-TM-109684] 07 p2760 N94-25849
Calculating the surface properties for the liquid-vapour interface: Illustrating the thermodynamic stability of the spherical microstructures
[DE94-601992] 07 p3073 N94-26837
Report of three microgravity experiments by the drop shaft
[JTN-94-80579] 07 p2761 N94-27341
Thermocapillary flow with evaporation and condensation and its effect on liquid retention in low-G fluid acquisition devices
[NASA-TP-3463] 07 p2797 N94-27639
Liquid atomization in supersonic flows 08 p3276 N94-29839
Local two-phase flow simulations including interface tracking with mass transfer 08 p3283 N94-30954
Determination of the dispersion constant in a constrained vapor bubble thermosyphon
[NASA-CR-196124] 12 p4442 N94-36992
Nonlinear optical spectroscopy for surface studies
[DE94-011623] 12 p4408 N94-37056

LIQUIDS
NT BEVERAGES
NT CRYOGENIC FLUIDS
NT FERMI LIQUIDS
NT FERROFLUIDS
NT HYDRAULIC FLUIDS
NT LIQUEFIED GASES
NT LIQUEFIED NATURAL GAS
NT LIQUID AIR
NT LIQUID HELIUM
NT LIQUID HELIUM 2
NT LIQUID HYDROGEN
NT LIQUID LITHIUM
NT LIQUID METALS
NT LIQUID NITROGEN
NT LIQUID OXYGEN
NT LIQUID SODIUM
NT MERCURY (METAL)
NT MERCURY ISOTOPES
NT ORGANIC LIQUIDS
NT POTABLE WATER
NT ROTATING LIQUIDS
Marangoni Benard instabilities in liquid mixtures with Soret effect 01 p0119 N94-10215
Shielded open-circuited sample holders for dielectric and magnetic measurements of liquids and powders
[PB93-198851] 02 p0652 N94-14687
Contained liquids in microgravity, part 2 03 p0979 N94-16085
Partitioning of Nb, Mo, Ba, Ce, Pb, Th and U between immiscible carbonate and silicate liquids: Evaluating the effects of P2O5,F, and carbonate composition 03 p0953 N94-16283
A priori inequalities for an ideal-incompressible liquid in an electromagnetic field
[IFTR-9/1992] 03 p0998 N94-16652
Pulsed laser kinetic studies of liquids under high pressure
[DE93-017826] 03 p1041 N94-16998
An automated system for ultrasound measurements of liquids by the resonance (Eggers) method
[IFTR-17/1992] 03 p1178 N94-17087
Basic studies of the liquid state of matter: Electrical properties and laser interactions
[AD-A268311] 03 p1042 N94-17567
Structure, thermodynamics, and dynamical properties of supercooled liquids
[DE93-788387] 04 p1607 N94-18211
Performance of the Amorphous Materials Diffractometer GLAD at IPNS
[DE93-017746] 04 p1430 N94-18481
Femtosecond Raman-induced Kerr effect study of polar solvent dynamics: Amides
[DE93-017563] 05 p1678 N94-19924
Electron reactions in nonpolar liquids: Pressure effects
[DE93-040328] 05 p1970 N94-19931
Measuring liquid properties with smooth and textured-surface resonators
[DE93-019433] 05 p1749 N94-20054
Containerless measurements on liquids at high temperatures 06 p2238 N94-25125
Bulletin of the Institute for Chemical Reaction Science, Tohoku University, volume 2
[JTN-94-80602] 07 p2717 N94-27385
Development of liquid membrane separation processes 07 p2717 N94-27386
Orthobaric densities and molar volumes of liquids: Aliphatic and cyclic ketones
[ESDU-93010] 07 p2720 N94-28060
Viscosity of liquids: Halogenated ethanes
[ESDU-93012] 07 p2720 N94-28062
Orthobaric densities and molar volumes of liquids: Fused ring compounds
[ESDU-93029] 07 p2721 N94-28097
Vapour pressures and critical points of liquids: Fused ring compounds
[ESDU-93028] 07 p2721 N94-28142
Interaction of multiple spark-generated bubbles in a compressible liquid
[AD-A275037] 08 p3272 N94-29149
Empirical and semi-empirical relationships of liquid-vapor, solid-vapor, and solid-liquid surface energies
[AD-A276480] 09 p3631 N94-31248
Electronic balance and some gravimetric applications (the density of solids and liquids, pycnometry and mass)
[PB94-163052] 12 p4446 N94-36719
Microscopic theory of the dielectric response of highly dispersive biological media
[AD-A280516] 12 p4516 N94-37109

LIQUIDUS
Phase equilibria and volumetric properties for the system NaCl-CaCl2-H2O
[DE93-013590] 01 p0076 N94-11244
The ilmenite liquidus and depths of segregation for high-Ti picrite glasses 03 p0975 N94-16241
Transition metals in superheat melts 03 p0962 N94-16273
The rheology and composition of cryovolcanic flows on icy satellites 03 p1243 N94-16294
Liquidus equilibria of lunar analogs at high pressure 03 p1283 N94-16364
Origin of high-Ti lunar ultramafic glasses 05 p1686 N94-20853
Containerless measurements on liquids at high temperatures 06 p2238 N94-25125
Liquidus temperature and optical properties measurement by containerless techniques 06 p2247 N94-25126
Liquid and solid solubility of Ag in Bi2Sr2CaCu2O8
[DE94-002829] 07 p2735 N94-26273

LISP (PROGRAMMING LANGUAGE)
Common lisp framework
[AD-A265878] 02 p0742 N94-12933
An experimental comparison of CLOS and C(++) implementations of an object-oriented graphical simulation of walking robot kinematics
[AD-A267168] 03 p1165 N94-15855
OORA Automated Knowledge System (OAKS) code, appendix C
[AD-A270709] 04 p1531 N94-19573
A proposed research program in information processing
[NASA-CR-194271] 05 p2041 N94-20134
Emacs Lisp in Edwin scheme
[AD-A276721] 09 p3818 N94-32504
Translating an AI application from Lisp to Ada: A case study
[NASA-TM-103845] 09 p3820 N94-32906

LITERATURE
NT BIOGRAPHY
NT DOCUMENTATION
Third Annual Foreign Acquisitions Workshop: Improving Access to Foreign Gray Literature
[NASA-TM-109683] 06 p2593 N94-24759

LITHERGOLIC PROPELLANTS
U HYBRID PROPELLANTS

LITHIUM
NT LIQUID LITHIUM
NT LITHIUM ISOTOPES
Calculation of electron-lithium scattering using the coupled-channel optical method
[DE93-623049] 02 p0806 N94-13226
A quartz crystal microbalance study of lithium insertion and removal into evaporated films MO(y) (M = Mo, Fe, and V)
[DSIS-93-00649] 02 p0810 N94-14203
In situ Raman spectroscopy of lithium electrode surface in ambient temperature lithium secondary battery
[DE93-015238] 03 p1010 N94-16061
Lithium D-cell study
[NASA-CR-192705] 03 p1011 N94-16505
Thin composite solid electrolyte film for lithium batteries
[NASA-CASE-NPO-18694-1-CU] 03 p1014 N94-1 325
Characterization of the lithium/pan-based polymer electrolytes interface
[AD-A268401] 03 p0973 N94-17434
Shrinkage void formation and its effect on freeze and thaw processes of lithium and lithium-fluoride for space applications
[DE93-019303] 04 p1338 N94-19128
Transient studies of low temperature catalysts for methane conversion
[DE93-041232] 05 p1680 N94-20934
Heat transfer additives for absorption cooling system fluids
[PB93-202521] 05 p1714 N94-21426
Preliminary SP-100/Stirling heat exchanger designs
[NASA-TM-106444] 05 p1670 N94-21809
SP-100 heat transport technology development
[DE94-000769] 06 p2218 N94-23452
Lithium drifted silicon detector fabrication on gettered floating-zone silicon
[DE94-003890] 07 p3054 N94-26095
In situ spectroscopic applications to the study of rechargeable lithium batteries
[DE94-003478] 07 p2782 N94-26328
The reactivity of lithium toward non-aqueous solvents of relevance to energy storage applications as studied by surface analytical techniques
[DE94-003483] 07 p2856 N94-26464
High rate lithium/thionyl chloride bipolar battery development 07 p2864 N94-28133
Analytic cross sections for collisions of H, H2, He and Li atoms and ions with atoms and molecules
[DE94-707686] 08 p3485 N94-28788
Tris(trimethylsily)arsine and lithium bis(trimethylsily)arsenide
[AD-A275075] 08 p3189 N94-29140
Dendrite preventing separator for secondary lithium batteries
[NASA-CASE-NPO-18585-1-CU] 08 p3265 N94-29411
Anode for rechargeable ambient temperature lithium cells
[NASA-CASE-NPO-18580-1-CU] 08 p3265 N94-29505
Sodium sulfate corrosion of silicon carbide fiber-reinforced lithium aluminosilicate glass-ceramic matrix composites
[AD-A277224] 09 p3623 N94-32023
Status of developing a multifunctional aviation grease
[AD-A276755] 09 p3656 N94-32184
Performance of the Sony lithium-ion rechargeable battery
[AD-A277076] 09 p3693 N94-32303

Proceedings of the Ad Hoc Workshop on Ceramics for Li/FeS2 batteries
[DE94-007460] 09 p3694 N94-32607
Anionic states of LiFLi
[AD-A278830] 11 p4322 N94-35678
New anionic states of the lithium trimer
[AD-A278832] 11 p4323 N94-35797

LITHIUM ALLOYS
NT ALUMINUM-LITHIUM ALLOYS
Aluminium-lithium forgings: Properties and potential satellite applications 01 p0058 N94-10021
Mechanical and fatigue properties of fibre reinforced aluminium-lithium alloy and aluminium-lithium MMC based laminates 01 p0058 N94-10022
Investigations on aluminium-lithium alloys for damage tolerant application 01 p0059 N94-10023
Preparation and characterization of rapidly solidified Al-Li alloys
[ISBN-0-315-58948-5] 02 p0569 N94-13367
Phase separation and ordering process in Al-Li alloys studied by small-angle neutron scattering and neutron diffraction
[DE93-016750] 04 p1358 N94-17947
Segregation and oxidation studies of Al-Li and Al-Mg alloys
[ISBN-0-315-83993-7] 06 p2244 N94-24469
Issues for conversion coating of aluminum alloys with hydrotalcite
[DE94-003804] 07 p2732 N94-25819
An anodic dissolution-based mechanism for the rapid cracking, pre-exposure phenomenon demonstrated by Al-Li-Cu alloys
[DE94-004798] 07 p2742 N94-27788
NASA-UVA light aerospace alloy and structures technology program (LA2ST)
[NASA-CR-195275] 07 p2844 N94-27851
Calculations of nonspherically averaged charge densities for substitutionally disordered alloys
[DE94-008293] 09 p3646 N94-32754

LITHIUM CHLORIDES
Aluminum-phosphorus chemistry: Preparation and structural characterization of (Et2AlP(SiMe3)2)2, Et(Cl)2Al(dot)P(SiMe3)3, and i-Bu2(Cl)Al(dot)P(SiMe3)3
[AD-A265268] 01 p0078 N94-11683
Hydride-containing molten salts and their technology implications
[AD-A266458] 03 p1092 N94-16567
A Shuttle mechanism for molten-electrolyte lithium batteries
[DE94-002914] 07 p2781 N94-26144

LITHIUM COMPOUNDS
NT LITHIUM CHLORIDES
NT LITHIUM FLUORIDES
NT LITHIUM HYDRIDES
NT LITHIUM NIOBATES
NT LITHIUM OXIDES
Tritium diffusion and desorption in single crystal LiAlO2
[DE93-015140] 03 p1211 N94-16805
Issues for conversion coating of aluminum alloys with hydrotalcite
[DE94-003804] 07 p2732 N94-25819
Anionic states of LiFLi
[AD-A278830] 11 p4322 N94-35678

LITHIUM FLUORIDES
Modeling void growth and movement with phase change in thermal energy storage canisters
[NASA-TM-106288] 01 p0163 N94-12576
Heat storage module 03 p0946 N94-15172
An improved light source for laser ranging 03 p0913 N94-15567
Calculation of the LiF-CeF3-BeF2 and LiF-PuF3-BeF2 ternary phase diagrams
[DE93-017437] 04 p1360 N94-18501
Shrinkage void formation and its effect on freeze and thaw processes of lithium and lithium-fluoride for space applications
[DE93-019303] 04 p1338 N94-19128

LITHIUM HYDRIDES
Generation of neutronic thermal data in support of space nuclear propulsion
[DE93-013148] 02 p0549 N94-13034
Vacancy formation energy of Li(H, D) and Na(H, D) systems
[DE93-633452] 06 p2558 N94-22978
A future, intense source of negative hydrogen ions 08 p3494 N94-30485

LITHIUM ISOTOPES
Neutronics of a D-Li neutron source: An overview
[DE94-005372] 08 p3493 N94-30893

LITHIUM NIOBATES
Structural development in ceramic precursor sols and gels
[AD-A264354] 01 p0090 N94-11281
Implementation of manufacturing techniques for planar, single mode waveguides on lithium niobate
[DSIS-93-00101] 02 p0792 N94-13845
Liquid metal drop ejection
[NASA-CR-193718] 02 p0572 N94-14133
Development of the Mars Observer Laser Altimeter (MOLA) 03 p0921 N94-15617
Extracavity frequency doubling study of a pulsed photodissociation iodine laser
[AD-A267893] 03 p1042 N94-17394
IR materials producibility
[AD-A268849] 04 p1577 N94-18223
Investigation of a fiber optic frequency shifter and optical isolator
[AD-A269820] 04 p1579 N94-18738
High temperature sensor/microphone development for active noise control
[NASA-CR-195214] 07 p2812 N94-27214
Electro-optic materials by solid source MOCVD
[DE94-005120] 07 p2757 N94-27716
Manufacture of light-damage resistant, planar, single mode waveguide on lithium niobate
[DSIS-94-01503] 09 p3879 N94-31850
Fiber optic transceiver for interfacing digital superconducting electronics
[DE94-008284] 10 p4040 N94-33842
Characterization of lithium niobate electro-optic modulators at cryogenic temperatures
[DE94-010059] 11 p4333 N94-35697

LITHIUM OXIDES
Cathode materials for the molten carbonate fuel cell
[DE93-019515] 05 p1848 N94-21870
Overcharge and overdischarge protection of ambient temperature secondary lithium cells
[NASA-CASE-NPO-18343-1-CU] 06 p2310 N94-23823
Glass-ceramic Li-Al-Si-O composition and process for its production
[CA-PATENT-APPL-SN-2043757] 06 p2254 N94-24129
Reference electrodes for solid polymer electrolytes
[DE94-004583] 07 p2780 N94-25806
Fiber optic transceiver for interfacing digital superconducting electronics
[DE94-008284] 10 p4040 N94-33842
Kinetics of phase transformations in glass forming systems
[NASA-CR-196082] 11 p4245 N94-35977

LITHIUM SULFUR BATTERIES
The 1987 Goddard Space Flight Center Battery Workshop
[NASA-CP-3236] 03 p1012 N94-17062
The ANL electric vehicle battery R&D program for DOE-EHP
[DE93-017414] 04 p1394 N94-17750
Lithium batteries: Future batteries 05 p1752 N94-20630
Status of the development of rechargeable lithium cells 06 p2392 N94-23354
In situ spectroscopic applications to the study of rechargeable lithium batteries
[DE94-003478] 07 p2782 N94-26328

LITHIUM 4
U LITHIUM ISOTOPES

LITHIUM 6
U LITHIUM ISOTOPES

LITHOGRAPHY
NT PHOTOLITHOGRAPHY
X ray production (approximately)130 (Angstrom) from laser-produced plasmas for projection x ray lithography applications
[DE93-009256] 01 p0385 N94-10286
Physical optics modelling of Soft X ray Projection Lithography (SXPL) imaging experiments
[DE93-011556] 01 p0374 N94-10339
Wavelength considerations in soft x ray projection lithography
[DE93-014115] 01 p0381 N94-10651
Radiation hardness of Mo/Si multilayers designed for use in a soft x ray projection lithography system
[DE93-011879] 01 p0143 N94-11273
A novel photosensitive polyimide resist consisting of a soluble polyimide and a bis(perfluorophenyl azide) as a cross-linker
[AD-A265998] 01 p0093 N94-12353
Low voltage electron beam lithography
[AD-A265358] 01 p0145 N94-12405
Photogenerated base in polymer imaging. Synthesis and photopatterning of poly(2-cyano-2-(p-vinylphenyl) butanoic acid)
[AD-A265288] 01 p0095 N94-12585
Design and testing of planar magnetic micromotors fabricated by deep x ray lithography and electroplating
[DE93-012856] 02 p0618 N94-12821
Optical degradation issues for XUV projection lithography systems
[DE93-012658] 02 p0626 N94-14805
Laser lithography by photon scanning tunneling microscopy
[DE93-015962] 02 p0660 N94-14863
Aberration correction of unstable resonators
[NASA-CASE-NPO-18791-1-CU] 03 p1034 N94-15987
Subwavelength structured surfaces and their applications 03 p1194 N94-17337
Soft x ray emission from Alexandrite laser-matter-interaction
[AD-A267905] 03 p1042 N94-17378
Low voltage electron beam lithography
[AD-A267865] 03 p1215 N94-17389
Resist performance in soft x ray projection lithography
[DE93-016490] 03 p1036 N94-17647
Quantum Optoelectronics. Organization of the 1993 photonics science topical meetings. Technical digest series, volume 8
[AD-A269026] 04 p1578 N94-18488
Advanced Solid-State Lasers/Compact Blue-Green Lasers. 1993 technical digest series. Volume 2: Organization of the 1993 photonics science topical meetings
[AD-A269058] 04 p1438 N94-18492
RF vacuum microelectronics
[AD-A270003] 04 p1403 N94-18667
Soft X Ray Projection Lithography. Organization of the 1993 photonics science optical meetings
[AD-A269159] 04 p1579 N94-18693
Operational parameters of an opto-electronic neural network employing fixed planar holographic interconnects
[DE93-018795] 04 p1433 N94-19000
The 1982 to 1992 decade of research on the vacuum ultraviolet ring at National Synchrotron Light Source
[DE93-019469] 04 p1603 N94-19564
Nanofabrication by focused ion beam
[AD-A271290] 04 p1345 N94-19746
Uncertainty limited atomic position measurement using optical fields
[AD-A271013] 05 p1970 N94-19822
Characterization and possible repair of defects in soft x ray projection lithography masks
[DE93-019147] 05 p1750 N94-20231
The modification of polymer surfaces and the fabrication of submicron-scale functionalized structures by deep-UV and electron beam lithography
[AD-A265956] 05 p1700 N94-20328
Spectral characterization of lithographic sources
[DE93-019941] 05 p1997 N94-21848
Center for X-Ray Optics, 1992
[DE94-000726] 05 p1990 N94-21868
Proposed additions to the SHADOW ray-tracing code for general-asymmetric perfect-crystal optics
[DE94-001291] 06 p2560 N94-23188
Fabrication of sub-40-nm p-n junctions for 0.18 micron MOS device applications using a cluster-tool-compatible, nanosecond thermal doping technique
[DE94-001608] 06 p2309 N94-23520
Characteristics of products generated by selective sintering and stereolithography rapid prototyping processes 06 p2264 N94-24412
Scanning probe lithography. 2: Selective chemical vapor deposition of copper into scanning tunneling microscope-defined patterns
[AD-A273304] 06 p2547 N94-25144
High precision x ray lithographic masks
[AD-A273342] 06 p2346 N94-25154
Study on elucidation of damage generation process by electron beam lithography 07 p2729 N94-25581
Opportunities for High Aspect Ratio Micro-Electro-Magnetic-Mechanical Systems (HAR-MEMMS) at Lawrence Berkeley Laboratory
[DE94-003499] 07 p2827 N94-27722
Low voltage electron beam lithography
[AD-A275648] 08 p3262 N94-28650
Focused ion beam fabrication of microelectronic structures
[AD-A275384] 08 p3264 N94-29305
Microactuator production via high aspect ratio, high edge acuity metal fabrication technology 08 p3235 N94-29770
A combined electron beam/optical lithography process step for the fabrication of sub-half-micron-gate-length MMIC chips 08 p3240 N94-30445
Semiconductor microcavity lasers
[DE94-006143] 09 p3716 N94-31622
Development, characterization, and applications of high temperature superconductor nanobridge Josephson junctions
[DE94-008113] 09 p3903 N94-32409
Low voltage electron beam lithography
[AD-A278204] 10 p4038 N94-33375

Solid Freeform Fabrication Symposium Proceedings
[AD-A277718] 10 p4032 N94-33441
Planar rotational magnetic micromotors with integrated shaft encoder and magnetic rotor levitation
11 p4224 N94-35907
Advanced laser driver for soft x-ray projection lithography
[DE94-011643] 12 p4449 N94-37722

LITHOLOGY
Descriptions and preliminary interpretations of cores recovered from the Manson Impact Structure (Iowa)
01 p0281 N94-12032
Petrography and preliminary interpretations of the crystalline breccias from the Manson M-1 core
01 p0281 N94-12056
Oxygen isotopes as tracers of tektite source rocks: An example from the Ivory Coast tektites and Lake Bosumtwi Crater 01 p0430 N94-12146
Post-impact alteration of the Manson impact structure
01 p0282 N94-12188
Noble gas evidence of an aqueous reservoir near the surface of Mars more recently than 1.3 Ga
01 p0473 N94-12228
Assimilation in lunar basalts and volcanic glasses: Implications for a heterogenous mantle source region
01 p0478 N94-12250
Fluvial erosion on Mars: Implications for paleoclimatic change 03 p1241 N94-16210
Trace-element composition of Chicxulub crater melt rock, K/T tektites and Yucatan basement
03 p1242 N94-16245
A Monazite-bearing clast in Apollo 17 melt breccia
03 p1267 N94-16279
Apollo 17 materials viewed from 2 to 4 mm soil particles: Pre-serenitatis highlands components
03 p1267 N94-16280
The dregs of crystallization in Zagami
03 p1245 N94-16390
Bright soil units on Mars determined from ISM imaging spectrometer data 03 p1295 N94-16430
From minerals to rocks: Toward modeling lithologies with remote sensing 03 p1086 N94-16437
Mapping the mineralogy and lithology of Canyonlands, Utah with imaging spectrometer data and the multiple spectral feature mapping algorithm
03 p1066 N94-16670
First results from analysis of coordinated AVIRIS, TIMS, and ISM (French) data for the Ronda (Spain) and Beni Bousera (Morocco) peridotites 03 p1067 N94-16675
Twenty-Fourth Lunar and Planetary Science Conference. Part 3: N-Z
[NASA-CR-193149] 05 p2092 N94-20636
The Erevan howardite: Petrology of glassy clasts and mineral chemistry 05 p1684 N94-20640
Modelling the gravity and magnetic field anomalies of the Chicxulub crater 05 p1862 N94-20668
Opaque-rich lithology in the Divnoe achondrite: Petrology and origin 05 p2082 N94-20680
Chaunskij: The most highly metamorphosed, shock-modified and metal-rich mesosiderite
05 p2082 N94-20681
Spectral reflectance studies of the Humorum Basin region 05 p2101 N94-20682
Petrography of shock features in the 1953 Manson 2-A drill core 05 p1862 N94-20767
Distribution and geologic history of materials excavated by the lunar crater Bullialdus 05 p2128 N94-20832
Equilibrium and fractional crystallization of a primitive Shergottite composition 05 p2085 N94-20861
Highland crust at the Apollo 14 site: A review
06 p2614 N94-24364
The western highland province at the Apollo 14 site
06 p2615 N94-24369
Seafloor characterization/Galapagos propagating rift
[AD-A273586] 06 p2419 N94-25165
Analysis of deep seismic reflection and other data from the southern Washington Cascades
[DE94-005958] 09 p3771 N94-31525
Environmental process tomography in the United States
[DE94-006402] 10 p4081 N94-33718
The Twenty-Fifth Lunar and Planetary Science Conference. Part 1: A-G
[NASA-CR-195743] 11 p4355 N94-35395
Mineralogy of an unusual CM clast in the Kaidun meteorite 11 p4352 N94-35476

LITHOSPHERE
NT EARTH CORE
NT EARTH CRUST
NT EARTH MANTLE
NT EARTH SURFACE
A model for the subduction mechanics of flexible lithosphere and its viscous coupling to the mantle using power-law rheologies 01 p0277 N94-11585
Horizontal stresses induced by vertical processes in planetary lithospheres 01 p0281 N94-12042
Buoyant subduction on Venus: Implications for subduction around coronae 01 p0455 N94-12130
Transmantle flux tectonics 01 p0283 N94-12249
Regional tectonic analysis of Venus as part of the Pioneer Venus guest investigator project
[NASA-CR-194079] 02 p0842 N94-13561
LFASE report: Crustal study
[AD-A266893] 03 p1111 N94-14947
The formation and evolution of Alpha and Tellus tesserae on Venus 03 p1249 N94-16183
Ishtar deformed belts: Evidence for deformation from below? 03 p1256 N94-16218
Estimates of lithospheric thickness on Venus
03 p1267 N94-16277
Effective elastic thickness of the Venusian lithosphere with lateral viscosity variations in the mantle
03 p1293 N94-16421
Beta Regio rift system on Venus: Geologic interpretation of Magellan images 05 p2095 N94-20655
Venus magmatic and tectonic evolution
05 p2101 N94-20683
Rifting at Devana Chasma, Venus: Structure and estimation of the effective thickness of the elastic lithosphere 05 p2113 N94-20754
Geoid, topography, and convection-driven crustal deformation on Venus 05 p2116 N94-20769
A tectonic resurfacing model for Venus
05 p2118 N94-20781
Arcuate and circular structures in the Tharsis region: Evidence of coronae on Mars 05 p2134 N94-20863
Large floor-fractured craters and isostatic crater modification: Implications for lithospheric thickness on Venus 05 p2135 N94-20873
The national geomagnetic initiative
[LC-93-85739] 06 p2401 N94-23344
Patterns of deformation and volcanic flows associated with lithospheric loading by large volcanoes on Venus
09 p3776 N94-31106
State of stress, faulting, and eruption characteristics of large volcanoes on Mars 09 p3940 N94-31108
Origin and thermal evolution of Mars
09 p3940 N94-31109
The tectonic and volcanic evolution of Venus: Catastrophic or gradual? 09 p3940 N94-31111
Effects due to overlapping large impact basins on Mars 11 p4360 N94-35427
Rheology, tectonics, and the structure of the Venus lithosphere 11 p4367 N94-35479
Formation of fold and thrust belts on Venus due to horizontal shortening of a laterally heterogeneous lithosphere 11 p4367 N94-35480
Patterns of brittle deformation under extension on Venus 11 p4373 N94-36168

LITTORAL CURRENTS
U COASTAL CURRENTS

LITTORAL DRIFT
Coastal processes due to nearshore current around an upheaving island 01 p0199 N94-11942

LITTORAL TRANSPORT
Coastal processes due to nearshore current around an upheaving island 01 p0199 N94-11942

LIVER
A characterization of carboxylesterases in rat and guinea pig: Their heterogeneity and role in detoxication of organophosphorus compounds
[NDRE-PUBL-93-1001] 02 p0730 N94-14852
Space research on organs and tissues
04 p1503 N94-19214
In vitro system for studying metabolism of environmental chemicals in human cells
[AD-A273427] 06 p2421 N94-24688
Modulation by galactosamine-induced hepatitis of biological responses of the rat exposed to high altitude hypoxia 07 p2904 N94-27464
Cloning of rat RXR alpha cDNA and the expression of its mRNA in regenerating liver and primary cultured hepatocytes 07 p2905 N94-27479
Physiological investigations of the isolated rat's liver in hypothermia and hypoxia and their relevance in aircraft incidents above the sea 08 p3382 N94-28439

LIVERWORTS
U BRYOPHYTES

LMCR (REACTORS)
U LIQUID METAL COOLED REACTORS

LMFBR
U LIQUID METAL FAST BREEDER REACTORS

LNG
U LIQUEFIED NATURAL GAS

LOAD CARRYING CAPACITY
Influence of the loading rate on the endurance and deformability of cement matrix composites
[IFTR-1/1992] 03 p1060 N94-17052
Mechanics of cracking for composite material
09 p3624 N94-32501

LOAD DISTRIBUTION (FORCES)
Method of recertifying a loaded bearing member using a phase point
[NASA-CASE-LAR-14741-1] 01 p0185 N94-10671
Systematic study of effects of load misalignment in uniaxial low cycle fatigue testing at high temperatures
[NPL-DMM(A)-27] 03 p1057 N94-15015
Static analysis of beams on an elastic base as stated by generalized functions
[IFTR-27/1991] 03 p1060 N94-16923
The role of NASTRAN in the preliminary design cycle
04 p1450 N94-17835
Road march performance of special operations soldiers carrying various loads and load distributions
[AD-A269198] 04 p1512 N94-18882
Global dynamic stability of a shallow arch by poincare-like simple cell mapping
06 p2160 N94-24280
Reduction of structural loads using maneuver load control on the Advanced Fighter Technology Integration (AFTI)/F-111 mission adaptive wing
[NASA-TM-4526] 06 p2168 N94-24295
Coordinated control of multiple robot manipulators
08 p3306 N94-30289

LOAD FACTORS
U LOADS (FORCES)

LOAD TESTING MACHINES
High temperature tension test equipment of heat resistant composite materials
[NAL-TM-652] 07 p2710 N94-27255
SP/MSP tests for the evaluation of FGM
[NAL-SP-17] 07 p2710 N94-27279
SP/MSP tests for the evaluation of FGM
07 p2710 N94-27280
Research on the development of fracture characteristics evaluation system for ceramics and metal composite materials 07 p2710 N94-27281
Internally damped, self-arresting vertical drop-weight apparatus
[NASA-CASE-LAR-15003-1] 12 p4389 N94-36826
Characterization of mechanical properties degradation using small punch testing technique
[DE94-011202] 12 p4418 N94-37410

LOAD TESTS
Numerical simulation and experimental results of filament wound CFRP tubes tested under biaxial load
01 p0058 N94-10015
Analytical prediction and test verification of the multiaxial behaviour of high-strength steel for lightweight structures
01 p0058 N94-10016
A benchmark bending test of a thick specimen. Part 2: Surface displacement measurements
[ARL-RR-6-PT-2] 02 p0670 N94-12928
Systematic study of effects of load misalignment in uniaxial low cycle fatigue testing at high temperatures
[NPL-DMM(A)-27] 03 p1057 N94-15015
Measurement and analysis of critical CTOA for an aluminum alloy sheet
[NASA-TM-109024] 03 p0956 N94-15948
Mean strain effects on the strain life fatigue curve
[AD-A267211] 03 p0960 N94-16984
The IOSDL SeaSoar hydraulic unit
[IOS-300-1992] 03 p1114 N94-17516
Biaxial flexural testing of a carbon fiber reinforced epoxy composite
[AD-A271956] 05 p1674 N94-20577
Fatigue resistance under tension-compression of laminates IM6/5245C and AS4/3501-6
[IAR-CR-25] 07 p2708 N94-26711
Compatibility of refrigerants and lubricants with engineering plastics
[DE94-004959] 07 p2756 N94-27692
Creep rupture properties of a nickel-base heat-resistant alloy Hastelloy XR under varying temperature/stress condition
[DE94-701175] 07 p2743 N94-27807
A laboratory test on construction of ice domes and their load-carrying capacity 07 p2884 N94-27966
The estimation of pre-stress by deformation rate analysis and suggestion of a mechanism from the elast-plastical theory 07 p2871 N94-28156
Static fracture behavior of a ceramic matrix composite at elevated temperatures
[AD-A275363] 08 p3177 N94-29008
Root-sum-square structural strength verification approach
[NASA-TM-108453] 08 p3322 N94-30206
WISPER and WISPERX: Final definition of two standardised fatigue loading sequences for wind turbine blades
[AD-B175835] 08 p3324 N94-30872
Determining the bearing capacity of flexible airfield pavements using a heavy weight deflectometer
[ISBN-0-315-86210-6] 09 p3587 N94-31710
Structural testing of the technology integration box beam 09 p3628 N94-33125

Technology integration box beam failure study
09 p3628 N94-33126
Crack growth predictions using a crack closure model
10 p4071 N94-34584
Internally damped, self-arresting vertical drop-weight apparatus
[NASA-CASE-LAR-15003-1] 12 p4389 N94-36826
Methodologies for the thermomechanical characterization of continuous-fiber ceramic matrix composites: A review of test methods
[DE94-012111] 12 p4405 N94-37370
Characterization of mechanical properties degradation using small punch testing technique
[DE94-011202] 12 p4418 N94-37410

LOADING FORCES
U LOADS (FORCES)

LOADING OPERATIONS
Fatigue technology assessment and strategies for fatigue avoidance in marine structures. Appendices
[AD-A269053] 04 p1455 N94-18716
ASTRO-1 to explore invisible universe
[NASA-TM-109360] 04 p1336 N94-18956
Performance demonstration: UH-60Q external rescue hoist and cargo loadmeter
[AD-A277533] 10 p3989 N94-34080

LOADING RATE
An analysis of ways of determining the material constants for viscoelastic materials
[IFTR-28/91] 03 p0951 N94-17050
Influence of the loading rate on the endurance and deformability of cement matrix composites
[IFTR-1/1992] 03 p1060 N94-17052
Humidity effects on soluble core mechanical and thermal properties (polyvinyl alcohol/microballoon composite) type CG extendospheres, volume 2
[NASA-CR-193893] 06 p2229 N94-24224

LOADING WAVES
U ELASTIC WAVES
U LOADS (FORCES)

LOADS (FORCES)
NT AERODYNAMIC LOADS
NT AXIAL LOADS
NT BLAST LOADS
NT COMPRESSION LOADS
NT CONTACT LOADS
NT CRITICAL LOADING
NT CYCLIC LOADS
NT DYNAMIC LOADS
NT GUST LOADS
NT IMPACT LOADS
NT LANDING LOADS
NT RANDOM LOADS
NT ROLLING CONTACT LOADS
NT SHOCK LOADS
NT STATIC LOADS
NT TRANSIENT LOADS
NT TRANSVERSE LOADS
NT VARIABLE AMPLITUDE LOADING
NT VIBRATORY LOADS
NT WING LOADING
Perforated plates for thin-walled structures
01 p0063 N94-10056
Method of recertifying a loaded bearing member using a phase point
[NASA-CASE-LAR-14741-1] 01 p0185 N94-10671
Materials for adaptive structural acoustic control, volume 3
[AD-A264621] 01 p0358 N94-11262
A model for the subduction mechanics of flexible lithosphere and its viscous coupling to the mantle using power-law rheologies 01 p0277 N94-11585
Mechanical interaction between synthetic fiber and cement base matrix in FRC composites
[AD-A265310] 01 p0073 N94-11686
Structural design/margin assessment
[NASA-TP-3410] 02 p0669 N94-12831
A piloted simulation investigation of the normal load factor and longitudinal thrust required for air-to-air acquisition and tracking 02 p0522 N94-13301
Autofrettage: Stress distribution under load and retained stresses after depressurization. A modified plane-strain case
[AD-A266320] 02 p0671 N94-13579
An 8-node axisymmetric acoustic finite element for non-axisymmetric fluid-structure interaction analysis
[FFA-TN-1993-03] 02 p0673 N94-13689
Nonlinear wave forces on large ocean structures
[AD-A266820] 02 p0683 N94-14902
Helicopter structures: A review of loads, fatigue design techniques, and usage monitoring
[AD-A267115] 03 p0866 N94-15651
Investigation of the origin of hot spots in deformed crystals: Ammonium perchlorate studies
[AD-A267692] 03 p1214 N94-17270
Heat load analysis on the cable-in-conduit with central core conductor for the TF coil Rebut layer design
[DE93-013783] 04 p1395 N94-17872
The respectiveness of response in a bar under static and transient loads
[VTT-TIED-1377] 04 p1452 N94-17959
Road march performance of special operations soldiers carrying various loads and load distributions
[AD-A269198] 04 p1512 N94-18882
Plastic mechanism analysis of T-joints in RHS subject to combined bending and concentrated force
[PB93-195774] 04 p1456 N94-19061
Automatic locking orthotic knee device
[NASA-CASE-MFS-28633-1] 05 p1896 N94-20493
Loads produced by a suited subject performing tool tasks without the use of foot restraints
[NASA-TP-3424] 05 p1896 N94-20606
Possible flexural signatures around Olympus and Ascraeus Montes, Mars 05 p2142 N94-20911
Maximum team lifting capacity as a function of team size
[AD-A271642] 05 p1892 N94-21036
Results of the second Round Robin on opening-load measurement conducted by ASTM Task Group E24.04.04 on crack closure measurement and analysis
[NASA-TM-109032] 05 p1832 N94-21624
Strength capabilities and load requirements while performing torquing tasks in zero gravity
[NASA-TP-3433] 05 p1897 N94-21627
Analysis of thermal mechanical fatigue in titanium matrix composites 05 p1835 N94-22618
Split spline screw
[NASA-CASE-GSC-13434-1] 06 p2352 N94-23082
A study of the core module simulator floor capability
06 p2380 N94-24418
Buckling of circular cylindrical shells subjected to combined loads (axial compression, normal pressure, bending and transverse shear loading)
[PB93-215358] 06 p2378 N94-24745
Loading, electromyograph, and motion during exercise
06 p2427 N94-25359
Loading, electromyograph, and motion during exercise
06 p2427 N94-25380
Effect of loading mode on the fracture toughness of a reduced activation ferritic/martensitic stainless steel
[DE94-004290] 07 p2732 N94-25987
The identification of inflow fluid dynamics parameters that can be used to scale fatigue loading spectra of wind turbine structural components
[DE94-000231] 07 p2791 N94-26117
Modification of a model for fatigue life predictions based on level-crossing
[PB94-123395] 07 p2842 N94-27198
Influence of impeller shroud forces on turbopump rotor dynamics 07 p2796 N94-27378
Vibrations in engineering structures: A review of model and full-scale test of a cable-stayed bridge and a traffic sign gantry
[NLR-TP-92321-U] 07 p2843 N94-27553
Mechanically fastened composite laminates subjected to combined bearing-bypass and shear loading
07 p2712 N94-27914
Performance evaluation of a 22.5/30 kW 270 volts direct current generator system
[AD-A275106] 08 p3263 N94-28913
Growth condition of an ice layer in freezing soils under applied loads. Part 1: Experiment
[AD-A275215] 08 p3357 N94-29070
Rotary blood pump
[NASA-CASE-MSC-22424-1] 08 p3299 N94-29370
A compact roller-gear pitch-yaw joint module: Design and control issues 08 p3161 N94-29629
Closed form expressions for a consistent stress material nonlinear finite element 08 p3322 N94-30258
Patterns of deformation and volcanic flows associated with lithospheric loading by large volcanoes on Venus
09 p3776 N94-31106
Energy absorber for the CETA
09 p3604 N94-33303
Dexterous end effector flight demonstration
10 p4067 N94-34032
A user's manual for the program TRES4: Random vibration analysis of vertical-axis wind turbines in turbulent winds
[DE94-009012] 10 p4079 N94-34078
Performance demonstration: UH-60Q external rescue hoist and cargo loadmeter
[AD-A277533] 10 p3989 N94-34080
The crack severity index of monitored load spectra
10 p4071 N94-34585
High energy
[DE94-009477] 11 p4331 N94-36428
Replacement of silicone polymer A with silicone polymer B and the subsequent characterization of the new cellular silicone materials
[DE94-010105] 12 p4421 N94-36474
Predicting defect behaviour 12 p4455 N94-37331
A method for thermal analysis of spiral bevel gears
[NASA-TM-106612] 12 p4451 N94-37451
Dynamics of a split torque helicopter transmission
[NASA-TM-106410] 12 p4452 N94-37457
Fatigue case study and loading spectra for wind turbines
[DE94-010798] 12 p4457 N94-37622
Understanding and managing power system harmonics
[AD-A280627] 12 p4440 N94-37759

LOCAL AREA NETWORKS
Formal specification of the plain UCN layer in LOTOS
[MEMO-INF-92-83] 01 p0131 N94-10280
Using a private SMDS/ATM network to provide long-haul supercomputing visualization services
[DE93-010692] 01 p0325 N94-11109
Reliability analysis for FDDI dual homing networks
[AD-A266133] 01 p0337 N94-11475
Applying paperless technology to achieve excellence in manufacturing operations
[TABES PAPER 93-630] 03 p1052 N94-16147
Advanced optical fiber communication systems
[AD-A269120] 04 p1577 N94-18254
Inventory management plan for a research and development local area network
[DE93-018381] 04 p1617 N94-19026
A highly concurrent medium access control strategy for high speed multiwavelength networks using transceivers with limited tunability
[MEMO-INF-93-07] 04 p1390 N94-19230
A distributed reinforcement learning scheme for network routing
[AD-A270600] 05 p1938 N94-19845
Understanding Open Systems Interconnection (OSI)
[AD-A271877] 05 p1929 N94-20472
Using manufacturing message specification for monitor and control at Venus 05 p1932 N94-21333
Distributed intelligent control and status networking
05 p1932 N94-21335
The Test Analysis Retrieval System (TARS): Meeting the challenges of the network's test processes
05 p1933 N94-21337
Performance evaluation of video on ethernet
[DE93-040696] 05 p1936 N94-21749
Evaluation of DEC's GIGAswitch for distributed parallel computing
[DE94-001356] 05 p1936 N94-21853
Application development in a PC/LAN environment
05 p1923 N94-22067
File transfer performance in LAN interconnection through a satellite channel 05 p1746 N94-22209
Supercomputer networking for space science applications
[NASA-CR-194876] 06 p2465 N94-23085
Switch configuration for migration to optical fiber network 06 p2447 N94-23250
SPOT4 Operational Control Center (CMP)
06 p2197 N94-23856
The evolving trend in spacecraft health analysis
06 p2202 N94-23946
The experimental physics and industrial control system architecture: Past, present, and future
[DE94-002639] 06 p2457 N94-24626
Ground based mission planning systems
06 p2522 N94-25014
Code division multiple access local area network communications employing fiber optic signal processing techniques
[AD-A274897] 07 p3096 N94-26180
Modeling and simulation of a fiber distributed data interface local area network
[AD-A274838] 07 p3098 N94-26500
A tri-state optical switch for local area network communications 07 p2789 N94-27922
Evaluation of wireless Local Area Networks
[AD-A275133] 08 p3243 N94-29064
Remote observatory access via the advanced communications technology satellite
08 p3253 N94-29894
Validation experiments with an Ethernet model using the simulation tool 'PROMISE'
[AD-B174795] 08 p3429 N94-30912
Distributed Active Archive Center
10 p4157 N94-33826
High level modelling and design of asynchronous interface logic
[PB94-167822] 11 p4258 N94-35534
Network upgrades 12 p4541 N94-36851

LOCAL GROUP (ASTRONOMY)
NT MILKY WAY GALAXY
Angular momentum in the Local Group
[DE94-009322] 11 p4350 N94-35980

LOCAL SCIENTIFIC SURVEY MODULE
Using the SPICE system to help plan and interpret space science observations 06 p2517 N94-23950

LOCAL THERMODYNAMIC EQUILIBRIUM
The 8 to 11 keV x ray sources for imaging and absorption experiments
[DE93-015973] 02 p0803 N94-14865
Configuration interaction in LTE spectra of heavy elements
[DE93-017166] 04 p1584 N94-17990
Model atmosphere analysis of selected luminous B stars
[NASA-CR-195096] 06 p2599 N94-24051
The solar spectral irradiances from x ray to radio wavelengths
[NASA-CR-195203] 06 p2629 N94-25260
SHARC, a model for calculating atmospheric and infrared radiation under non-equilibrium conditions
[AD-A275207] 08 p3357 N94-28893
Abundance patterns in red-giant CH stars 08 p3539 N94-29820
SOLGAS refined: A computerized thermodynamic equilibrium calculation tool
[DE94-009021] 09 p3913 N94-32846
LOCALIZATION
U POSITION (LOCATION)
LOCATION
U POSITION (LOCATION)
LOCI
Mach reflection of spherical detonation waves
[DE93-016604] 07 p2797 N94-27705
Further investigation of curve veering phenomena 08 p3460 N94-30515
Design and initial testing of a facility to measure unsteady pressures on an oscillating cascade with supersonic leading edge locus 09 p3569 N94-31880
LOCKHEED AIRCRAFT
NT C-130 AIRCRAFT
NT C-141 AIRCRAFT
NT F-104 AIRCRAFT
NT P-3 AIRCRAFT
NT S-3 AIRCRAFT
NT SR-71 AIRCRAFT
NT U-2 AIRCRAFT
LOCKHEED U-2 AIRCRAFT
U U-2 AIRCRAFT
LOCKING
NT LASER MODE LOCKING
Connector systems for structures
[NASA-CASE-MSC-21998-1] 03 p1046 N94-15707
Automatic locking orthotic knee device
[NASA-CASE-MFS-28633-1] 05 p1896 N94-20493
Self locking set screw
[AD-D015969] 05 p1824 N94-21277
Prosthetic elbow joint
[NASA-CASE-MFS-28707-1] 10 p4100 N94-35115
Adaptable binary programs
[AD-A260243] 12 p4494 N94-37119
LOCKS (FASTENERS)
Activities Report of the Institute of Applied Physics
[ETN-93-93749] 05 p1966 N94-21798
Electronic locking system 05 p1796 N94-21801
Preloaded launch locking devices for SILEX 06 p2358 N94-24008
LOCOMOTION
NT ASTRONAUT LOCOMOTION
NT WALKING
Apparatus and method for measuring subject work rate on an exercise device
[NASA-CASE-MSC-21752-1] 05 p1895 N94-20194
Perception/action: An holistic approach 2
[AD-A271822] 05 p1891 N94-20627
Mechanical design of a planetary rover 06 p2369 N94-23403
Planetary rover locomotion mechanisms 06 p2369 N94-23404
Walking, jumping, and tumbling: More than one way to get around Mars 06 p2370 N94-23419
Physical modeling and dynamic simulation of planet vehicles: Application to the motion prediction 06 p2371 N94-23426
Computerized in vitro test for chemical toxicity based on tetrahymena swimming patterns 08 p3354 N94-30463
Biologically-inspired hexapod robot design and simulation
[AIAA PAPER 94-1178-CP] 08 p3439 N94-30530
ODYSSEUS autonomous walking robot: The leg/arm design
[AIAA PAPER 94-1180-CP] 08 p3439 N94-30531
LOCOMOTIVES
Electromechanical batteries and the electric locomotive
[DE93-013311] 01 p0142 N94-11009
Adaptation of model parameters of a rail model at measured rail compliances
[ILR-MITT-274(1992)] 05 p1831 N94-21153
Design and operation of a medium speed 12-cylinder coal-fueled diesel engine. Phase 2: Improvements
[DE94-009547] 11 p4275 N94-35815
LOGARITHMS
Quenched chiral logarithms
[DE93-010195] 01 p0346 N94-11663
Vanishing theorem on arithmetic surfaces
[PB93-215481] 05 p1961 N94-22263
Logarithm of probability measures and infinite divisibility of sub-stable random vectors
[PB94-118627] 06 p2486 N94-23758
A logarithmic barrier cutting plane method for convex programming
[REPT-93-43] 07 p2957 N94-25761
Unifying investigation of interior-point methods for convex programming
[PB94-126463] 07 p2967 N94-27031
An efficient off-line electronic cash system based on the representation problem
[CWI-CS-R9323] 07 p2776 N94-27551
Pairwise-comparison using the logarithmic least squares method and the generalized pseudoinverse
[REPT-93-84] 09 p3844 N94-31701
Logarithmic corrections of the two-body QED problem
[DE94-611157] 11 p4322 N94-35783
Graphing techniques for materials laboratory using Excel 11 p4232 N94-36414
LOGIC
Useful lambda notation
[PB93-191856] 04 p1524 N94-19066
Axiomatization, declarative semantics and operational semantics of passive and active updates in logic databases
[PB93-195956] 04 p1618 N94-19067
Correspondence theory for extended modal logics, version 3.0
[ML-93-16] 09 p3856 N94-31417
LOGIC CIRCUITS
Smart spatial light modulator research and development
[AD-A264928] 01 p0382 N94-11286
Programmable logic devices
[DE93-013117] 01 p0144 N94-11479
A formal language for the specification and verification of synchronous and asynchronous circuits
[NASA-CR-191509] 03 p1144 N94-15443
Digital laser range finder emulator
[AD-D015811] 03 p1040 N94-16540
Computer-aided design package for designers of digital optical computers
[AD-A267866] 03 p1154 N94-17390
Orpheus: A synthesis framework for regular architectures
[REPT-93-016] 03 p1156 N94-17504
New dynamic FET logic and serial memory circuits for VLSI GaAs technology 04 p1397 N94-18339
Automated ILA design for synchronous sequential circuits 04 p1397 N94-18340
Single phase dynamic CMOS PLA using charge sharing technique 04 p1397 N94-18341
An SEU immune logic family 04 p1398 N94-18342
Cellular logic array for computation of squares 04 p1398 N94-18343
Fault tolerant sequential circuits using sequence invariant state machines 04 p1398 N94-18344
Formal specification of a high speed CMOS correlator 04 p1401 N94-18371
Ultra low power CMOS technology 04 p1401 N94-18373
Canonical multi-valued input Reed-Muller trees and forms 04 p1401 N94-18375
Asynchronous sequential circuit design using pass transistor iterative logic arrays 04 p1402 N94-18376
Pulse mode VLSI asynchronous circuits 04 p1402 N94-18377
Improved self arbitrated VLSI asynchronous circuits 04 p1402 N94-18378
A special purpose silicon compiler for designing supercomputing VLSI systems 04 p1402 N94-18379
On timing faults in digital logic circuits
[AD-A268714] 04 p1402 N94-18400
Naval research reviews. Mixing enhancement for air-breathing propulsion. Non-axisymmetric jets increase mixing, volume 44 and volume 45
[AD-A268966] 04 p1521 N94-18543
An RS-170 to 700 frame per second CCD camera
[DE93-018367] 04 p1432 N94-18828
Motorola MC68040 high-speed design using Altera EPM5000 erasable programmable logic devices
[DE93-017635] 04 p1523 N94-19006
Superconducting flux flow devices, digital circuits and memories
[DE93-019072] 04 p1405 N94-19079
Evaluation of laser diode based optical switches for optical processors
[AD-A270949] 04 p1581 N94-19602
Reconfigurable fuzzy cell
[NASA-CASE-MSC-21613-1] 05 p1907 N94-20492
Design of CMOS logic gates for TID radiation 05 p1754 N94-21083
Complementary heterojunction FET technology for space application 05 p1755 N94-21094
Bridging faults in BiCMOS circuits 05 p1756 N94-21105
Fault detection in digital and analog circuits using an i(DD) temporal analysis technique 05 p1757 N94-21106
Faulty behavior of asynchronous storage elements 05 p1757 N94-21108
Detection of CMOS bridging faults using minimal stuck-at fault test sets 05 p1757 N94-21110
Practical issues in implementing roving spares in VLSI systolic arrays 05 p1758 N94-21114
Experiments on technology mapping using different cell libraries 05 p1758 N94-21118
Low-latency digital frequency synthesizer using the residue number system 05 p1759 N94-21121
Correctness properties for iterated hardware structures 05 p1759 N94-21124
Partition algebraic design of asynchronous sequential circuits 05 p1759 N94-21125
Defect-sensitivity analysis of an SEU immune CMOS logic family 05 p1765 N94-21711
Dimension scaling effects on the yield sensitivity of HEMT digital circuits 05 p1765 N94-21712
Detection of feed-through faults in CMOS storage elements 05 p1766 N94-21721
Bit-systolic arithmetic arrays using dynamic differential gallium arsenide circuits 05 p1767 N94-21724
A VLSI implementation of DCT using pass transistor technology 05 p1767 N94-21725
On fast carry select adders 05 p1767 N94-21728
A 1 GHz sample rate, 256-channel, 1-bit quantization, CMOS, digital correlator chip 05 p1768 N94-21732
Formal hardware verification in Maple 05 p1771 N94-22112
Impact of partitioning on parallel discrete event simulation of logic circuits 05 p1772 N94-22115
Logic oriented neural networks 05 p1782 N94-22182
A Hopfield neural net for discrete Fourier transform calculation 05 p1783 N94-22184
A new class of multi-function two-rail totally self-checking basic building blocks 05 p1788 N94-22215
Fuzzy and neural control
[NASA-TM-108753] 05 p1947 N94-22270
Formal verification of digital circuits described in VHDL
[ETN-94-95165] 06 p2306 N94-22833
Logic synthesis on programmable networks
[ETN-94-95174] 06 p2449 N94-23151
CADBIT 2: Computer-aided design for built-in test, volume 1
[AD-A273702] 06 p2463 N94-25455
CADBIT 2: Computer-aided design for built-in test, volume 2
[AD-A273703] 06 p2463 N94-25456
Use of parallel counters for triggering
[DE93-616656] 07 p2979 N94-25918
Processing, fabrication, and demonstration of HTS integrated microwave circuits, appendix A
[AD-A274600] 07 p2785 N94-26890
Symbolic model checking for sequential circuit verification
[AD-A274375] 07 p2786 N94-27061
DALIA: A language for the description and analysis of digital systems 07 p2954 N94-27192
Three dimensional transient analysis of microstrip circuits in multilayered anisotropic media
[AD-A274995] 08 p3263 N94-28995
Fault coverage measurement for digital microcircuits
[AD-A276226] 09 p3686 N94-31066
Formal verification of systolic multipliers with the Boyer-Moore theorem prover
[RR-897-M] 09 p3839 N94-31082
A neuron network for image classification: From algorithm to implantation
[TELECOM-93-E-005] 09 p3687 N94-31168
Study of continuous-time and mixed analog-digital operators
[TELECOM-93-E-010] 09 p3687 N94-31170
A hierarchical approach to test generation for CMOS VLSI circuits
[ISBN-9-09-005449-9] 09 p3689 N94-31535
Radiation tolerant, high speed, low power, gallium arsenide logic
[AD-A277293] 09 p3694 N94-32509
Multiple-valued programmable logic array minimization by solution space search
[AD-A278033] 09 p3821 N94-33090

A diagnostic expert system for digital circuits
09 p3699 N94-33340
Semiconductor single-electron digital devices and circuits
[AD-A278338] 10 p4147 N94-33969
Time delay measurement correlator and its application
10 p4042 N94-34350
Digital circuit test language and test pattern data base
10 p4042 N94-34364
High-speed digital project, HSD test capability
[DE94-010885] 11 p4260 N94-36197
High temperature superconducting digital circuits and subsystems
[DE94-001207] 12 p4436 N94-36557

LOGIC DESIGN
Models for reactivity
[AD-A266419] 03 p1149 N94-16554
Weakened negative introspection in autoepistemic reasoning
[PB93-187375] 04 p1520 N94-18118
A verification logic representation of indeterministic signal states 04 p1401 N94-18372
Ultra low power CMOS technology
04 p1401 N94-18373
Canonical multi-valued input Reed-Muller trees and forms 04 p1401 N94-18375
Asynchronous sequential circuit design using pass transistor iterative logic arrays 04 p1402 N94-18376
Pulse mode VLSI asynchronous circuits
04 p1402 N94-18377
Improved self arbitrated VLSI asynchronous circuits
04 p1402 N94-18378
A special purpose silicon compiler for designing supercomputing VLSI systems 04 p1402 N94-18379
VHDL simulation with access to transistor models
04 p1402 N94-18381
Naval research reviews. Mixing enhancement for air-breathing propulsion. Non-axisymmetric jets increase mixing, volume 44 and volume 45
[AD-A268966] 04 p1521 N94-18543
Power optimization in logic isomers
05 p1756 N94-21101
Test pattern generation for ILA sequential circuits
05 p1757 N94-21107
Partition algebraic design of asynchronous sequential circuits 05 p1759 N94-21125
High-speed Viterbi decoding with overlapping code sequences 05 p1760 N94-21130
Behavioral model simulation studies of an image compressor 05 p1760 N94-21133
HDL to verification logic translator
05 p1766 N94-21717
Detection of feed-through faults in CMOS storage elements 05 p1766 N94-21721
Formal hardware verification in Maple
05 p1771 N94-22112
Towards the formal verification of the requirements and design of a processor interface unit: HOL listings
[NASA-CR-191466] 05 p1937 N94-22414
A method for the general simultaneous full decomposition of sequential machines: Algorithms and implementation
[EUT-92-E-267] 06 p2445 N94-23170
Towards the formal specification of the requirements and design of a processor interface unit: HOL listings
[NASA-CR-191465] 06 p2466 N94-23252
Test methods and custom hardware for functional testing of a high speed GaAs DRAM
[AD-A274859] 07 p2781 N94-26175
Investigation into model-based fuzzy logic control
[AD-A274660] 07 p2985 N94-26336
Program derivation by proof transformation
[AD-A275260] 08 p3453 N94-29304
Yield and variability optimization of integrated circuits: Principles and practical solutions
08 p3266 N94-29805
Extension of the LUSTRE language and application to circuit design: The LUSTRE V4 language and the POLLUX system
[ETN-94-95918] 09 p3812 N94-31543
Radiation tolerant, high speed, low power, gallium arsenide logic
[AD-A277293] 09 p3694 N94-32509
Fuzzy logic approaches to multi-objective decision-making in aerospace applications
[NASA-TM-106599] 10 p4016 N94-33953
High level modelling and design of asynchronous interface logic
[PB94-167822] 11 p4258 N94-35534
The most abstract common refinement
[AD-A278870] 11 p4305 N94-36014

LOGIC NETWORKS
U LOGIC CIRCUITS

LOGIC PROGRAMMING
A correct and efficient interface for logical query languages with complex objects
[MEMO-INF-93-01] 01 p0320 N94-10167
Completing fault models for abductive diagnosis
[DE93-003832] 02 p0761 N94-12859
Efficient dynamic optimization of logic programs
[NASA-TM-109251] 02 p0761 N94-12889
Automatic translation of database integrity constraints into compensating production rules
[REPT-92-055] 03 p1234 N94-17502
Weakened negative introspection in autoepistemic reasoning
[PB93-187375] 04 p1520 N94-18118
A verification logic representation of indeterministic signal states 04 p1401 N94-18372
Ultra low power CMOS technology
04 p1401 N94-18373
Asynchronous rendezvous in the presence of backtracking
[PB93-197739] 04 p1524 N94-19062
Axiomatization, declarative semantics and operational semantics of passive and active updates in logic databases
[PB93-195956] 04 p1618 N94-19067
Integrity checking in deductive databases: An exposition
[PB93-191724] 04 p1619 N94-19709
Bottom-up abstract interpretation of logic programs
[PB93-191773] 05 p1928 N94-19995
Programming logic for F omega
[PB93-191781] 05 p1928 N94-19996
System at the cross-roads of functional and logic programming
[PB93-191823] 05 p1928 N94-20009
Parallel logic programming systems
[RR-891-I] 05 p1929 N94-20176
A declarative approach for first-order built-in's of PROLOG
[CWI-CS-R9246] 05 p1909 N94-21026
COCOLOG: A conditional observer and controller logic for finite machines
[INRIA-RR-1714] 05 p1910 N94-21063
Correctness properties for iterated hardware structures 05 p1759 N94-21124
Reasoning about update logic
[CWI-CS-R9312] 05 p1914 N94-21496
Changing preferences
[CWI-CS-R9310] 05 p1915 N94-21551
Termination and confluence of rule execution
[CWI-CS-R9309] 05 p1916 N94-21587
An information retrieval logical model applied to the formalism of conceptual graphs: The ELEN prototype and its experimentation on a corpus of software components
[ETN-94-95162] 06 p2588 N94-22879
Interpretation of evolutive environment by a multisensory perception machine
[LAAS-93111] 06 p2471 N94-22907
Asynchronous rendezvous in distributed logic programming
[PB93-220614] 06 p2448 N94-23096
Logic synthesis on programmable networks
[ETN-94-95174] 06 p2449 N94-23151
Applications of the Aurora parallel PROLOG system to computational molecular biology
[DE93-041166] 06 p2420 N94-23468
Transition system specifications in stalk format with bisimulation as a congruence
[PB94-110608] 06 p2453 N94-23707
Area-power-delay trade-off in logic synthesis
[ISBN-9-09-005332-8] 06 p2461 N94-25080
Deductive computer programming
[AD-A274966] 07 p2962 N94-26303
Process algebra of concurrent constraint programming
[PB94-126695] 07 p2966 N94-26919
Freeness analysis for logic programs-and correctness
[PB94-126703] 07 p2966 N94-26956
A characterization of stable models using a non-monotonic operator
[CWI-CS-R9315] 07 p2970 N94-27543
Modular termination proofs for logic and pure PROLOG programs
[CWI-CS-R9316] 07 p2970 N94-27544
A strategy for dynamic interpretation: A fragment and an implementation
[CWI-CS-R9317] 07 p2970 N94-27545
Partial support for the Second International Symposium on Artificial Intelligence and Mathematics
[AD-A275199] 08 p3434 N94-29026
Incorporating geometric constraints into rule-based systems using nonlinear optimization
[AD-A275093] 08 p3452 N94-29063
Neural network solutions to logic programs with geometric constraints
[AD-A275419] 08 p3435 N94-29198
Logic of transition systems
[CT-93-03] 08 p3424 N94-30371
Algorithmic problems concerning first-order definability of modal formulas on the class of all finite frames
[ML-93-07] 08 p3456 N94-30383
Remarks on the theory of semi-functors
[ML-93-08] 08 p3457 N94-30384
The Vanilla meta-interpreter for definite logic programs and ambivalent syntax
[CT-93-01] 08 p3424 N94-30386
Isomorphisms between predicate and state transformers
[CWI-CS-R9338] 08 p3459 N94-30430
Comparative semantics for linear arrays of communicating processes
[CWI-CS-R9336] 08 p3426 N94-30491
Unravelling nondeterminism: On having the ability to choose
[RUU-CS-93-30] 08 p3428 N94-30749
LORE and reason maintenance
[REPT-93-88] 09 p3812 N94-31522
Negation by default for framing in temporal logic programming
[PB94-148848] 10 p4107 N94-33978
Finding accurate frontiers: A knowledge-intensive approach to relational learning 10 p4098 N94-34044
Automated knowledge-base refinement
10 p4160 N94-34056
Projection in temporal logic programming
[PB94-148814] 10 p4108 N94-34123

LOGIC UNITS
U ARITHMETIC AND LOGIC UNITS

LOGICAL ELEMENTS
New automatic deduction techniques in first order finite and infinite polyvalent logic
[ETN-93-95003] 04 p1528 N94-19359

LOGISTICS
NT LUNAR LOGISTICS
NT SPACE LOGISTICS
Assessing the adequacy of the industrial base
[AD-A264954] 01 p0417 N94-11856
Sleep management user's guide for special operations personnel
[AD-A267746] 03 p1119 N94-14943
Defense Logistics Information System (DLIS) procedures manual. Products and services end-user manual
[AD-A267766] 03 p1232 N94-17007
CALS test network handbook
[AD-A267587] 03 p1160 N94-17209
A comparison of air force data systems
[AD-A269691] 04 p1616 N94-18575
Planning process software: A user guide for the DMCA
[AD-A271252] 05 p1902 N94-19911
The logistic model: The integration of business process redesign and information systems development based on logistic principles
[MEMO-INF-92-70] 05 p2045 N94-22276
The Columbus logistics support at the APMC: Requirements and implementation aspects
06 p2515 N94-23935
Timed coloured Petri nets and their application to logistics
[ETN-94-95310] 06 p2522 N94-25293
A comparative evaluation plan for the Maintenance, Inventory, and Logistics Planning (MILP) System Human-Computer Interface (HCI)
06 p2588 N94-25373
The 1993 Federal Aviation Administration Aviation System Capital Investment Plan
[AD-A279036] 08 p3136 N94-29445
The Nomad Explorer assembly assist vehicle: An architecture for rapid global extraterrestrial base infrastructure establishment 09 p3599 N94-31429
Knowledge-based commodity distribution planning
09 p3915 N94-32427
Space Station evolution study
[NASA-CR-193937] 09 p3611 N94-32898
Analysis of intermediate level maintenance following F404-GE-400 engine component life reductions
[AD-A277918] 09 p3585 N94-33283
NAVSPACECOM space surveillance sensor system digital signal processing receiver. Volume 3: Operating system functions
[AD-A278839] 11 p4212 N94-35799
NAVSPACECOM space surveillance sensor system digital signal processing receiver. Volume 4: Hardware interfaces
[AD-A278845] 11 p4212 N94-35801
The integrated model development environment
[AD-A278613] 11 p4308 N94-36250
A mean value analysis heuristic for analysis of aircraft sortie generation
[AD-A278578] 12 p4507 N94-36970

LOGISTICS MANAGEMENT
NT INVENTORY CONTROLS
NT INVENTORY MANAGEMENT
On-orbit refueling 01 p0038 N94-11565
Analysis of the Army's installation support modules with the private sector's open information systems
[AD-A265667] 01 p0421 N94-12579
Decision support for material planners
[ISBN-9-03-860201-4] 02 p0819 N94-14449
Facilities maintenance handbook
[NHB-8831.2] 03 p1224 N94-15934
Defense Logistics Information System (DLIS) procedures manual. Products and services end-user manual
[AD-A267766] 03 p1232 N94-17007
Defense Logistics Information System (DLIS). Procedures manual: Logistics On-Line Access (LOLA) procedures manual
[AD-A267685] 03 p1233 N94-17229
Multigrid approach to solving the long transportation problem on a regular grid in cost space
[AD-A272323] 05 p1909 N94-21038
A framework for SFC/DC system data analysis
06 p2523 N94-23234
Development of the Air Force contingency contracting course framework
[AD-A273921] 07 p3093 N94-25895
DOD Electronic Commerce (EC)/Electronic Data Interchange (EDI) in contracting report
[AD-A275298] 08 p3242 N94-28874
A study of theoretical models for managing technology change and a comparison to a radio frequency identification implementation
[AD-A276012] 09 p3672 N94-31385
Modular Simulator System (MSS) management guide
[AD-A277098] 09 p3588 N94-32014
The implementation of Electronic Data Interchange (EDI) with defense transportation operations
[AD-A280568] 12 p4493 N94-37040

LOH HELICOPTER
U OH-6 HELICOPTER

LONG DURATION EXPOSURE FACILITY
The magnitude of impact damage on LDEF materials
[NASA-CR-188258] 01 p0043 N94-10666
Space environmental effects on the integrity of chromic acid anodized coatings
[NASA-CR-191468] 01 p0055 N94-10947
Property changes induced by the space environment in composite materials on LDEF: Solar array materials passive LDEF experiment A0171 (SAMPLE)
[NASA-CR-192572] 01 p0073 N94-11484
Mineralogy of chondritic interplanetary dust particle impact residues from LDEF 01 p0080 N94-12045
Composition and modal frequencies of hypervelocity particles less than 1 millimeter in diameter in low-Earth orbit 01 p0429 N94-12063
Modelling hypervelocity impacts into aluminum structures based on LDEF data
01 p0190 N94-12178
Lessons learned from the Long Duration Exposure Facility
[AD-A266026] 01 p0044 N94-12394
Analysis of samples of reflector materials which are multicoated and metal samples with oxide coatings which have been exposed the space environment in LDEF testing
[NASA-CR-193647] 02 p0575 N94-12789
STS-32 mission highlights resource tape
[NASA-TM-109291] 02 p0531 N94-13631
Partial analysis of LDEF experiment A-0114
[NASA-CR-193826] 02 p0564 N94-14025
Surface characterization of LDEF materials
[NASA-CR-194519] 02 p0543 N94-14683
Long Duration Exposure Facility is coming home
[NASA-TM-109656] 03 p0884 N94-15227
STS-32 onboard 16mm photography quick release
[NASA-TM-109472] 03 p0880 N94-15376
STS-32 LDEF EVA training in WETF with Low and Dunbar
[NASA-TM-109473] 03 p1135 N94-15377
STS-32 LDEF approach in SES
[NASA-TM-109474] 03 p0880 N94-15379
Long Duration Exposure Facility retrieval animation
[NASA-TM-109426] 03 p0885 N94-15496
Long Duration Exposure Facility
[NASA-TM-109427] 03 p0885 N94-15497
Analysis of leading edge and trailing edge cover glass samples before and after treatment with advanced satellite contamination removal techniques
[AD-A267055] 03 p0885 N94-15666
Long Duration Exposure Facility experiment M0003 deintegration/findings and impacts
[AD-A267140] 03 p0885 N94-15749
Impact penetration experiments in teflon targets of variable thickness 03 p1063 N94-16253
Resolving LDEF's flux distribution: Orbital (debris?) and natural meteoroid populations 03 p1245 N94-16391
Third LDEF Post-Retrieval Symposium Abstracts
[NASA-CP-10120] 03 p1303 N94-16495
Performance of silvered Teflon thermal control blankets on spacecraft
[AD-A266284] 03 p0887 N94-16909
Long duration exposure facility experiment m0003 deintegration observation database
[AD-A267579] 03 p0951 N94-17207
LDEF update
[NASA-TM-109352] 04 p1334 N94-18921
The application of jet spray and ion beam contamination removal techniques to samples from the LDEF spacecraft
[AD-A270973] 04 p1354 N94-19755
Long Duration Exposure Facility (LDEF) contamination study
[AD-A272419] 05 p1658 N94-21147
Conversion of LDEF experiment M0003 sample observation database to MS-DOS formats
[AD-A272945] 05 p1681 N94-21226
Results of the post flight analyses on system materials for the LDEF-FRECOPA experiment
05 p1659 N94-21371
Measured space environmental effects to LDEF during retrieval 05 p1659 N94-21372
Space environmental effects on polymer matrix composites: The UTIAS/LDEF experiment
05 p1660 N94-21373
Some results of the oxidation investigation of copper and silver samples flown on LDEF
05 p1660 N94-21375
The implications of the LDEF results on Space Station Freedom power system materials
05 p1660 N94-21377
Gamma ray spectrometry of LDEF samples: Results of 1992 analyses
[DE94-001177] 05 p1684 N94-22046
Analysis of impactor residues in tray clamps from the Long Duration Exposure Facility. Part 2: Clamps from Bay B of the satellite
[NASA-TM-104784] 06 p2386 N94-24095
Analysis of selected materials flown on interior locations of the Long Duration Exposure Facility
[NASA-CR-4586] 08 p3175 N94-29458
Study of activation data of metal samples from LDEF-1 and Spacelab-2
[NASA-CR-193973] 08 p3205 N94-29736
LDEF Materials Results for Spacecraft Applications
[NASA-CP-3257] 09 p3591 N94-31012
The performance of thermal control coatings on LDEF and implications to future spacecraft
09 p3591 N94-31013
Performance of silvered Teflon (trademark) thermal control blankets on spacecraft 09 p3591 N94-31014
Space environment durability of beta cloth in LDEF thermal blankets 09 p3591 N94-31015
Space Station WP-2 application of LDEF MLI results
09 p3592 N94-31016
Anodized aluminum on LDEF
09 p3592 N94-31017
Follow-up on the effects of the space environment on UHCRE thermal blankets 09 p3592 N94-31018
Modeling of LDEF contamination environment
09 p3592 N94-31019
Spacecraft contamination issues from LDEF: Issues for design 09 p3592 N94-31020
Model of spacecraft atomic oxygen and solar exposure microenvironments 09 p3593 N94-31021
Atomic oxygen erosion considerations for spacecraft materials selection 09 p3593 N94-31022
Performance of selected polymeric materials on LDEF
09 p3593 N94-31023
Atomic oxygen interaction at defect sights in protective coatings on polymers flown on LDEF
09 p3593 N94-31024
Fluorescence observations of LDEF exposed materials as an indicator of induced material reactions
09 p3593 N94-31025
Laser-induced fluorescence of space-exposed polyurethane 09 p3593 N94-31026
On the linearity of fast atomic oxygen effects
09 p3594 N94-31027
Micrometeoroid/space debris effects on materials
09 p3595 N94-31032
Thermal-vacuum response of polymer matrix composites in space 09 p3595 N94-31033
The impact of LDEF results on the space application of metal matrix composites 09 p3595 N94-31034
Low-Earth orbit effects on organic composite materials flown on LDEF 09 p3595 N94-31036
Summary of materials and hardware performance on LDEF 09 p3595 N94-31037
LDEF materials special investigation group's data bases 09 p3596 N94-31038
Analysis of leading edge and trailing edge cover glass samples before and after treatment with advanced satellite contamination removal techniques
09 p3596 N94-31041
Effects of orbital exposure on RTV during the LDEF mission 09 p3597 N94-31043
Spacecraft materials: Comparison between flight results obtained on LDEF and MIR 09 p3597 N94-31045
Characterization of polymer decomposition products by laser desorption mass spectrometry
09 p3597 N94-31046
Design application and development of spacecraft in LEO utilizing LDEF results 09 p3597 N94-31047
An overview of the on-orbit contamination of the Long Duration Exposure Facility (LDEF)
09 p3598 N94-31049
What LDEF means for development and testing of materials 09 p3598 N94-31050
Solar radiation effects on glasses
[NASA-CR-195900] 10 p4029 N94-34232
Results from LDEF experiment A0114: The interaction of atomic oxygen with materials surfaces at orbital altitudes
[NASA-CR-196016] 11 p4235 N94-35388
Current activities and results of the Long Duration Exposure Facility Meteoroid and Debris Special Investigation Group 11 p4352 N94-35458
Morphology of meteoroid and space debris craters on LDEF metal targets 11 p4353 N94-36159
Evaluation of seals and lubricants used on the Long Duration Exposure Facility
[NASA-CR-4604] 12 p4399 N94-37614

LONG DURATION SPACE FLIGHT
Hormonal regulation of fluid and electrolyte metabolism in zero-g and bedrest 01 p0311 N94-12004
Hormonal regulation of fluid and electrolyte metabolism during periods of headward fluid shifts
01 p0311 N94-12005
Recycling in space
[NASA-TM-109307] 02 p0737 N94-13615
Magnetic resonance imaging after exposure to microgravity 02 p0594 N94-13771
An evaluation of noise and its effects on shuttle crewmembers during STS-50/USML-1
[NASA-TM-104775] 02 p0735 N94-13961
Physical countermeasures for long-term manned space flights
[ESA-SP-1160] 02 p0733 N94-14860
Supporting life in space
[NASA-TM-109593] 03 p1135 N94-15285
STS-26 long duration simulation: Crew entering SMS
[NASA-TM-109560] 03 p0876 N94-15474
Concepts and embodiment design of a reentry recumbent seating system for the NASA Space Shuttle
[NASA-CR-195504] 06 p2438 N94-24667
Project Minerva: A low-cost manned Mars mission based on indigenous propellant production
07 p2760 N94-25705
Simulation modeling for long duration spacecraft control systems 07 p2684 N94-26288
Psychophysiology in microgravity and the role of exercise 07 p2936 N94-28374
Gravity, the third dimension of life support in space
10 p4101 N94-33635

LONG PERIOD VARIABLES
U MIRA VARIABLES

LONG RANGE WEATHER FORECASTING
JPRS report: Science and technology. Central Eurasia: Earth Sciences
[JPRS-UES-93-004] 04 p1461 N94-19209
Thermospheric modeling accuracies using F10.7 and Ap
[AD-A277355] 09 p3773 N94-32337
US streamflow patterns associated with the extreme phases of the Southern Oscillation
10 p4088 N94-33359
Long range forecasts of the Northern Hemisphere anomalies with antecedent sea surface temperature patterns
[NASA-CR-189358] 11 p4292 N94-35380

LONG TERM EFFECTS
Property changes induced by the space environment in composite materials on LDEF: Solar array materials passive LDEF experiment A0171 (SAMPLE)
[NASA-CR-192572] 01 p0073 N94-11484
Lessons learned from the Long Duration Exposure Facility
[AD-A266026] 01 p0044 N94-12394
Surface characterization of LDEF materials
[NASA-CR-194519] 02 p0543 N94-14683
A fifteen years lifetime mechanism for an infrared Earth sensor 06 p2362 N94-24040
Static adhesion in preloaded contacts subjected to long-term vacuum exposure 06 p2363 N94-24043
Design and testing of a unique randomized gravity, continuous flow bioreactor 06 p2423 N94-25368

Preparation of creep data sheet: Material strength data sheet
07 p2723 N94-25548

LONG WAVE RADIATION
Stationary spectra of short-wave convective and magnetostatic fluctuations in a finite-pressure plasma and anomalous heat conductivity
[DE93-617852] 01 p0388 N94-10840
Studies of the net surface radiative flux from satellite radiances during FIFE
[NASA-CR-193150] 01 p0230 N94-10953
Simulation of clear-sky outgoing longwave radiation over the oceans using operational analysis
05 p1861 N94-22290
Development of a statistical method for estimating the downward longwave radiation at the surface from satellite observations 09 p3742 N94-31553

LONG WAVES (METEOROLOGY)
U PLANETARY WAVES

LONGITUDE
Venus gravity: New Magellan low altitude data
05 p2117 N94-20772
Differential global positioning system for the surface-towed ordnance locating system: Testing, results, and user's guide
[DE94-002980] 07 p2664 N94-26309

LONGITUDINAL CONTROL
Computation of a controlled store separation from a cavity 03 p0858 N94-16513
A combined Earth scanner and momentum wheel for attitude determination and control of small spacecraft
06 p2208 N94-24022
Feedback control laws for highly maneuverable aircraft
[NASA-CR-195195] 06 p2190 N94-25176
Techniques to improve maneuver stability characteristics of a nonlinear wide-body transport airplane in cruise flight
[NASA-TM-4521] 07 p2679 N94-27660

LONGITUDINAL STABILITY
On non-linear longitudinal stability of an aircraft in a dive in the presence of atmospheric disturbances
01 p0031 N94-11492
The dynamic stability of the helicopter
[LR-772] 04 p1321 N94-19615
Longitudinal beam dynamics for heavy ion fusion using WARPrz
[DE93-019154] 05 p1992 N94-19915
Determination of the stability and control derivatives of the NASA F/A-18 HARV using flight data
[NASA-CR-194838] 06 p2190 N94-24804
Effect of aeroelastic-propulsive interactions on flight dynamics of a hypersonic vehicle
06 p2164 N94-25113
Techniques to improve maneuver stability characteristics of a nonlinear wide-body transport airplane in cruise flight
[NASA-TM-4521] 07 p2679 N94-27660
An experimental and theoretical study of the aerodynamic characteristics of some generic missile concepts at Mach numbers from 2 to 6.8
[NASA-TM-109110] 08 p3130 N94-29473
X-29 flight control system: Lessons learned
[NASA-TM-4598] 10 p3984 N94-34384
Aerodynamic design of super maneuverable aircraft
10 p3992 N94-34617

LONGITUDINAL WAVES
NT PLANE WAVES
Turbulent boundary layer interacting with spanwise periodic longitudinal vortex arrays
01 p0165 N94-12626
Correction of longitudinal errors in accelerators for heavy-ion fusion
[DE93-018656] 04 p1575 N94-19106
The electromechanical properties of tetragonal BaTiO3 and PbTiO3 single crystals
[DE93-019008] 04 p1603 N94-19550
An electromagnetic finite difference time domain analog treatment of small signal acoustic interactions
[DE94-009978] 11 p4319 N94-35770
Fundamentals studies of radial wave thermoacoustic engines
[AD-A280534] 12 p4431 N94-37090

LONGSHORE CURRENTS
U COASTAL CURRENTS

LOOP ANTENNAS
Multiple Antenna Implementation System (MAntIS)
[DE93-012515] 01 p0131 N94-10270
Direct electron heating and current drive with fast waves in D3-D
[DE93-013028] 02 p0801 N94-14293
Arc detection and protection in high-power antenna systems
[DE93-013272] 04 p1382 N94-17695
Isolated and coupled superquadric loop antennas for mobile communications applications
06 p2289 N94-22834
Receiving antennas for electromagnetic pulses and transients
[ISBN-0-315-62312-8] 07 p2777 N94-27871
Three-dimensional effects for radio frequency antenna modeling
[DE94-006102] 08 p3255 N94-30105

LOOP TRANSFER FUNCTIONS
Application of programmable logic controller to pump regulation system for supplying water
10 p4067 N94-34344

LOOP TRANSFER RECOVERY
Asymptotic correctors: The LTR
[PB93-199701] 06 p2474 N94-24627
H infinity/LTR state feedback control
10 p4115 N94-34320

LOOPS
Analysis and effects of the number of nests of DO loops during vector supercomputing
[NAL-TR-1146] 02 p0748 N94-13453
The renormalization of the axial anomaly in dimensional regularization
[NIKHEF-H/92-18] 03 p1220 N94-17618
Material data representation of hysteresis loops for Hastelloy X using artificial neural networks
[NASA-TM-105990] 06 p2376 N94-23551
Method of implementing digital phase-locked loops
[NASA-CASE-NPO-18757-1-CU] 08 p3265 N94-29374
Butterfly and scaling law in YBa2Cu4O8
[DE94-006037] 08 p3519 N94-30338
Varying execution discipline to increase performance
[DE94-007844] 09 p3819 N94-32651
Performance evaluation of digital phase-locked loops for advanced deep space transponders
11 p4254 N94-35558

LORAN
NT LORAN C

LORAN C
Determination of Loran-C/GPS human factors issues
[AD-A266334] 02 p0514 N94-14563
MIMO recursive least squares control algorithm for the AN/FPN-44A Loran-C transmitter
[AD-A274820] 07 p2664 N94-26493
Realtime mitigation of GPS SA errors using Loran-C
07 p2642 N94-27291
Loran-C time management 08 p3144 N94-30644

LORENTZ CONTRACTION
On the Michelson-Morley experiment
[DE93-629908] 04 p1608 N94-18268

LORENTZ FORCE
Force and power efficiency of micro-g electromagnetic levitation coils 01 p0110 N94-10129
New mechanism of Ostwald ripening in Lorentz-force stabilized Cu-Pb dispersions 01 p0116 N94-10192
Electrode array electromagnetic velocimeter
[AD-D015950] 05 p1806 N94-19882
Modeling the minimum energy state of the Earth's magnetotail
[AD-A267984] 05 p1856 N94-20485
Magnetohydrodynamic boundary layer control system
[AD-D016120] 09 p3710 N94-32958

LORENTZ GAS
Theoretical and numerical studies in magnetic fusion
[DE94-000536] 05 p1993 N94-20937

LORENTZ TRANSFORMATIONS
On the Michelson-Morley experiment
[DE93-629908] 04 p1608 N94-18268
On the transverse size of a fast moving nucleon
[DE93-616891] 06 p2539 N94-25481
Principles of gauge theory of real hadrons
[DE93-613096] 07 p3013 N94-25835
Duality for multiparametric quantum GL(n) and for a Lorentz quantum group
[DE93-613048] 07 p3005 N94-25868
On the relativistic invariant representation of arbitrary bilinear combinations of Dirac spinors
[DE93-634343] 07 p3019 N94-26456
Possible explanation of the interaction cross-section growth at high energies
[DE94-606457] 08 p3494 N94-28612

LOSS OF COOLANT
GAM-HEAT: A computer code to compute heat transfer in complex enclosures
[DE93-014724] 03 p1023 N94-15980

LOSSES
Power losses of a type 2 superconducting slab of arbitrary thickness in the presence of alternating current conductors
[DE93-617892] 01 p0396 N94-10716
Recent study of beam stability in the PSR
[DE93-014473] 02 p0780 N94-13173
Regenerator optimization for Stirling cycle refrigeration
[DE93-018468] 04 p1380 N94-18818
Bounds for expected loss in Bayesian decision theory with imprecise prior probabilities
[PB93-197507] 04 p1558 N94-19327
Volatile loss from accreting icy protoplanets
05 p2084 N94-20793
Outgassing data for selecting spacecraft materials
[NASA-RP-1124-REV-3] 05 p1676 N94-21889
Momentum loss in proton-nucleus and nucleus-nucleus collisions
[NASA-TP-3405] 06 p2540 N94-24305
Broad geoacoustic assessment of some regional areas
[AD-A275504] 08 p3356 N94-28791
AC losses for the self field of an AC transport current with a DC transport current offset in high T(c) superconducting magnet coils for MagLev application
[DE94-005187] 08 p3268 N94-30907
Particle orbit analysis for LHD helical axis configurations
[DE94-718995] 11 p4336 N94-35773

LOSSLESS EQUIPMENT
Performance considerations for the application of the lossless browse and residual model
07 p2946 N94-28256

LOSSY MEDIA
Utilization of boundary element method for extraction of frequency dependent conductivity parameters of lossy intra-chip transmission lines
[ETN-93-94385] 02 p0771 N94-14807
Imaging targets embedded in a lossy half space with Synthetic Aperture Radar
[DE94-010807] 12 p4435 N94-37391

LOST WAX PROCESS
U INVESTMENT CASTING

LOUDNESS
A virtual acoustic orientation instrument
[AD-A268181] 03 p1134 N94-17510
Variability of measured sonic boom signatures. Volume 1: Technical report
[NASA-CR-191483-VOL-1] 06 p2526 N94-24172
Variability of measured sonic boom signatures. Volume 2: Data report
[NASA-CR-191483-VOL-2] 06 p2526 N94-24173
Experimental studies of loudness and annoyance response to sonic booms 07 p2651 N94-28195
Subjective response to sonic booms having different shapes, rise times, and durations
[NASA-TM-109090] 08 p3479 N94-29464
A laboratory study of subjective annoyance response to sonic booms and aircraft flyovers
[NASA-TM-109113] 10 p4132 N94-33610

LOUDSPEAKERS
On the formation process of Karman vortex street
01 p0016 N94-12621
Comparison of measured and predicted pure tone propagation levels from JAPE-1: An evaluation of the performance of ASOPRAT 06 p2527 N94-24212

LOUVERS
Icing of turbine intake louvers
[AD-A265714] 01 p0029 N94-12274
Solution of mixed convection heat transfer from isothermal in-line fins 06 p2321 N94-23644

LOVE WAVES
High resolution geological site characterization utilizing ground motion data
[AD-A268926] 04 p1481 N94-18485
Surface wave group velocity tomography of East Asia, part 1
[AD-A270100] 04 p1484 N94-18868
Extension of love wave transformation theory to laterally heterogeneous structures
[DE94-608098] 08 p3365 N94-30093

LOW ALLOY STEELS
U HIGH STRENGTH STEELS

LOW ALTITUDE
Low altitude plume impingement handbook
[NASA-CR-194193] 02 p0643 N94-14741
Radiocommunication problems of a position reporting and bidirectional messagery system using VHF/UHF with low-Earth orbit satellites 03 p0889 N94-17136
Delta launch vehicle: Accommodations for small satellites 03 p0878 N94-17139
Small imaging satellite for Earth observing system adjunct 03 p0891 N94-17151
Regulation of low Earth orbit satellites
03 p0892 N94-17159
LEOCOM-SPES: Low cost message communications
03 p0892 N94-17161
TAOS (S80): A (LEO-MSS) system for position reporting and telemanagement services 03 p0893 N94-17162
Feasibility study of a personal communications system IRIDIUM-like 03 p0893 N94-17165
Low-cost, dual-use platforms for environmental sensing, phase 1
[AD-A272951] 05 p1646 N94-21246
Regulated drag area parachute
[AD-D015992] 06 p2170 N94-25051

Methods for improving low-angle, low-altitude radar tracking accuracy
[AD-A274914] 07 p2768 N94-26347
Radar detection of low-altitude targets in a maritime environment. Volume 1: Final analysis
[AD-A278493] 10 p4037 N94-34376
Accurate estimation of object location in an image sequence using helicopter flight data
10 p3997 N94-35055
Minimum performance standards: Airborne low-range radar altimeters
[RTCA-DO-155] 11 p4198 N94-35344

LOW ASPECT RATIO
Off-design performance of crenulated blades in a linear compressor cascade
[AD-A273744] 06 p2340 N94-25534
Octahedral metallomesogens: Liquid crystallinity in low aspect ratio materials
[AD-A274830] 07 p3059 N94-26571
Program to develop a performance and heat load prediction system for multistage turbines
[NASA-CR-195223] 07 p2674 N94-26588
Design of a low aspect ratio transonic compressor stage using CFD techniques
[NASA-TM-106636] 10 p3998 N94-33971

LOW ASPECT RATIO WINGS
NT DELTA WINGS
An experimental investigation of the optimum slat setting on a combat aircraft model 04 p1308 N94-18431
Normal force of low aspect ratio cropped-delta wings at pre-stall angles of attack and subsonic speeds
[ESDU-93034] 07 p2648 N94-27955

LOW CARBON STEELS
Investigation of criteria for ductile fracture under fully-plastic conditions 02 p0672 N94-13593
Laser-shock damage of iron-based materials
[AD-A267196] 03 p1038 N94-15852
Crashworthiness analysis using advanced material models in DYNA3D
[DE94-002988] 06 p2229 N94-24632
The influence of TIG welding thermal cycles on HSLA-100 steel plate
[AD-A274248] 07 p2740 N94-27009

LOW CONCENTRATIONS
Study of the atmospheric chemistry of radon progeny in laboratory and real indoor atmospheres
[DE93-012236] 01 p0266 N94-11671
Reduction of Pu(6) with hydrogen peroxide: Effects of plutonium, peroxide, and iron concentrations and of reaction time
[DE93-013598] 02 p0564 N94-13487
Granulometry in environments with very small particle concentrations 08 p3259 N94-30511
Characterization of defects in Si and SiO2-Si using positrons
[DE94-009044] 10 p4147 N94-33877

LOW CONDUCTIVITY
Experimental study of multiple droplet evaporative cooling
[PB93-198463] 01 p0149 N94-10851
Properties of graphite fiber reinforced copper matrix composites for space power applications
[NASA-CR-191026] 08 p3178 N94-29208

LOW COST
Processing, properties, and wear resistance of aluminides
[DE93-012186] 01 p0083 N94-11141
Inexpensive capillary discharge x-ray laser driver
[AD-A265932] 01 p0176 N94-12382
Limitations to the quality of optical phase conjugation by stimulated Brillouin scattering
[AD-A266006] 01 p0383 N94-12389
A proposed ground segment design for small satellites 03 p0878 N94-17154
LEOCOM-SPES: Low cost message communications 03 p0892 N94-17161
The ORBCOMM system 03 p0893 N94-17163
S-80: A satellite for less than 50 MF 03 p0894 N94-17172
A mini satellite called Arsene: The way to make it at a minimum cost 03 p0895 N94-17179
TUBSAT: Low cost access to space technology 03 p0895 N94-17180
Laser materials processing applications at Lawrence Livermore National Laboratory
[DE93-017976] 04 p1437 N94-18093
A rugged, low-cost advanced data acquisition system for field test projects
[DE93-010041] 04 p1615 N94-18334
Optoelectronic packaging: A review
[DE93-040059] 04 p1515 N94-19535
High rate resistive plate chambers: An inexpensive, fast, large area detector of energetic charged particles for accelerator and non-accelerator applications
[DE93-018664] 04 p1572 N94-19545
Clementine: An inexpensive mission to the Moon and Geographos 05 p1652 N94-20765
A low cost alternative to high performance PCM bit synchronizers 05 p1813 N94-21347
Silicon microelectronic field-emissive devices for advanced display technology
[DE94-000397] 05 p1794 N94-22380
A low-cost vector processor boosting compute-intensive image processing operations 05 p1925 N94-22441
Wilbur: A low-cost CCD camera system for MDM Observatory 05 p1814 N94-22510
The Westinghouse Series 1000 Mobile Phone: Technology and applications 06 p2284 N94-22800
Low cost coherent demodulation for mobile satellite terminals 06 p2284 N94-22803
Low cost antennas for MSAT vehicular applications 06 p2289 N94-22830
Microstrip monopulse antenna for land mobile communications 06 p2289 N94-22833
L-band mobile terminal antennas for helicopters 06 p2289 N94-22835
An x ray diffraction investigation of alpha-Al2O2 addition to Yttria Stabilized Zirconia (YSZ) thermal barrier coatings subject to destabilizing vanadium pentoxide (V2O5) exposure
[AD-A273403] 06 p2261 N94-25072
Preceedings of the 12th International Congress: Corrosion Control for Low-Cost Reliability. Volume 2: Process Industries Plant Operations
[AD-A273662] 06 p2251 N94-25449
Low-cost photovoltaic inverters incorporating application-specific integrated circuits
[DE94-003270] 07 p2856 N94-26463
Low cost, radial flow, solid oxide fuel cell
[DE94-002982] 07 p2858 N94-26785
NPSNET: Integration of Distributed Interactive Simulation (DIS) protocol for communication architecture and information interchange
[AD-A275061] 08 p3530 N94-29139
The suitability of low-cost urban airshed modeling in the Chicago area
[DE94-005114] 08 p3349 N94-30023
Proceedings of the low cost materials of construction for biological processes workshop
[DE94-000218] 08 p3226 N94-30761
A low cost igniter utilizing an SCB and titanium sub-hydride potassium perchlorate pyrotechnic
[DE94-006467] 09 p3666 N94-31827
Design, manufacture, and test of a flight load recorder for small aircraft
[AD-A277752] 10 p3997 N94-33409
The servicing aid tool: A teleoperated robotics system for space applications 10 p4067 N94-34039
Technology Reinvestment Project's Focus Area: Low Cost Electronic Packaging
[PB94-161155] 11 p4259 N94-35748

LOW CURRENTS
Development of ultra-low noise, high sensitivity planar metal grating coupled 3 to 5 multiquantum well infrared detectors for focal plane array staring IR sensor systems
[AD-A265599] 01 p0404 N94-12375
Low-current traveling wave tube for use in the microwave power module
[NASA-TP-3344] 02 p0620 N94-13110
LHCD (low hybrid current drive) experiment on the HT-6B tokamak
[DE93-613720] 06 p2555 N94-25331
Effect of LHCD (low hybrid current drive) on tearing mode instability
[DE93-613700] 06 p2555 N94-25344
Experimental and theoretical studies of a high temperature cesium-barium tacitron, with application to low voltage-high current inversion
[DE94-008182] 11 p4228 N94-35349

LOW DENSITY FLOW
Simulation of low-density nozzle plumes in non-zero ambient pressures
[NASA-TM-106501] 09 p3615 N94-32742

LOW DENSITY GASES
U RAREFIED GASES

LOW DENSITY MATERIALS
An ultralight carbon-carbon composite with amorphous matrix 01 p0061 N94-10042
Fabrication of very-low-density, high-stiffness carbon fiber/aluminum hybridized composite with ultra-low density and high stiffness (M-11) 02 p0588 N94-13743
Removal of carbonaceous contaminants from silica aerogel 03 p0953 N94-16256
Shock compression of low-density foams
[DE93-040545] 05 p1707 N94-21546

LOW EARTH ORBITAL ENVIRONMENTS
U EARTH ORBITAL ENVIRONMENTS

LOW FREQUENCIES
NT VERY LOW FREQUENCIES
Stationary spectra in a magnetized current-carrying plasma
[DE93-617847] 01 p0386 N94-10397
Stationary spectra in a plasma with a shear (renormalized statistical approach with non-zero eigenfrequencies)
[DE93-617851] 01 p0386 N94-10523
Stationary spectra in a finite-pressure current-carrying plasma
[DE93-617848] 01 p0387 N94-10538
Stationary spectra in a quasi neutral current-carrying plasma
[DE93-617849] 01 p0387 N94-10539
Stationary spectra in a sheared plasma (linear limit)
[DE93-617850] 01 p0387 N94-10540
Low power digital recorder development
[AD-A265921] 01 p0170 N94-10704
Effects of energetic particle events on VLF/LF propagation parameters/1989
[AD-A265266] 01 p0275 N94-11013
The response of an electron in a biased double well to a strong laser: Delocalization and low frequency generation
[AD-A265169] 01 p0366 N94-11100
Energy transfer dynamics and impact sensitivity
[DE93-009551] 01 p0098 N94-11269
A 3D gyrokinetic particle-in-cell simulation of fusion plasma microturbulence on parallel computers
[DE93-012503] 02 p0794 N94-12846
1/f noise and oxide traps in MOSFETs
[DE93-007581] 02 p0619 N94-12942
The propagation characteristics and instability properties of low-frequency electromagnetic waves in the Io plasma torus 02 p0601 N94-13650
Low frequency acoustics of laminated composite axisymmetric structures
[DRA-TM(USGR)-93302] 04 p1344 N94-19391
Measurements of ocean surface and bottom backscattering strengths in the northwestern Atlantic Ocean
[AD-A270893] 04 p1500 N94-19786
High resolution infrared spectroscopy of cyclobutane: A study of vibrational mode coupling involving large amplitude, low frequency modes
[AD-A271987] 05 p1973 N94-20619
Modal structure of variations in the tropical climate system. Part 2: Origins of the low-frequency mode
[MPIM-96] 06 p2407 N94-23199
Multi-ion, multi-event test of ion cyclotron resonance heating
[NASA-CR-194859] 06 p2540 N94-23495
Nonlinear dynamics applied to atmospheric prediction
[AD-A273437] 06 p2404 N94-24674
Very low frequency and low frequency transmitting antenna parameter monitoring system
[AD-D015989] 06 p2302 N94-25049
Measurements and modeling of multitone, low-frequency acoustic data from the Arraial do Cabo range
[AD-A273406] 06 p2530 N94-25073
Improved magnetostrictive transducer drive elements achieved by reduction of crystalline defects and improved crystalline orientation
[AD-A273391] 06 p2313 N94-25276
Hydroacoustic wave-fields generated by different source types, a computational study
[PB94-123536] 07 p3010 N94-27037
Simulating high-frequency wind for long durations
[DE94-002739] 07 p2682 N94-27997
A study on adaptive active noise control 10 p4122 N94-34372
Simulation models for computational plasma physics: Concluding report
[DE94-009976] 11 p4335 N94-35647
A comparison of two examples of magnetic tracker systems 12 p4485 N94-37275

LOW FREQUENCY BANDS
NT VERY LOW FREQUENCIES
ALFIS: Astronomical Low Frequency Interferometry Satellites. A feasibility study
[LR-699] 02 p0542 N94-13988

LOW GRAVITY
U MICROGRAVITY

LOW GRAVITY MANUFACTURING
Solidification in immiscible systems: The influence of processing conditions on resulting microstructures 01 p0112 N94-10174
Ripening of immiscible liquid droplets in microgravity with constrained Marangoni drift 01 p0117 N94-10200
A study of the quasibinary Al-W-Mo system. Part 1: Preliminary investigations and preparation for microgravity experiments 01 p0119 N94-10211
A study of the quasibinary Al-Mo-W system. Part 2: A physico-mechanical investigation of the system fabricated under the gravitylessness conditions 01 p0119 N94-10212

Visualization of solidification front phenomena
[NASA-CR-193838] 03 p0976 N94-15006
The first flight of the QUESTS GAS payload G-521
04 p1325 N94-19170
Study on melted solution stirring under microgravity
07 p2730 N94-25585
Report of three microgravity experiments by the drop shaft
[JTN-94-80579] 07 p2761 N94-27341
Prometheus in space: Research Committee on Functional New Material
[JTN-94-80580] 07 p2761 N94-28002
Survey report of JSUP Space Environment Utilization Research Committee in fiscal year 1992: Protein Crystal Growth Session
[JTN-94-80584] 08 p3158 N94-28583
Fluid and transportation phenomena under microgravity 08 p3227 N94-28939
Combustion studies under microgravity
08 p3228 N94-28940
Glass studies under microgravity
08 p3228 N94-28941
Fabrication of electronic materials in space
08 p3228 N94-28942
Protein crystal growth in microgravity
08 p3228 N94-28943
Cell culture in space 08 p3228 N94-28944
Cosmic energy equipment 08 p3229 N94-28945
Survey report of JSUP Space Environment Utilization Research Committee in fiscal year 1992: Functional New Materials Session
[JTN-94-80582] 08 p3159 N94-30162
Survey report of JSUP Space Environment Utilization Research Committee in fiscal year 1992: Metallic Materials Session
[JTN-94-80583] 08 p3159 N94-30794
Design, characterization, and control of the NASA three degree of freedom reaction compensation platform
09 p3605 N94-33304

LOW LATITUDES
U TROPICAL REGIONS

LOW MASS
U MASS

LOW MOLECULAR WEIGHTS
Chain propagation/step propagation polymerization chemistry. The preparation of solvent resistant well phase-separated thermoplastic elastomers
[AD-A271128] 05 p1699 N94-20016
Polyimide processing additives
[NASA-CASE-LAR-13669-2] 06 p2252 N94-23079
Center for advanced electrical and structural polymers
[AD-A273415] 06 p2259 N94-24783
Solventless, curable fluid oligomeric systems for high performance microwave, acoustical and mechanical applications 08 p3223 N94-30478
Proposal to produce novel, transparent radiation hard low refractive index
[AD-A278476] 10 p4029 N94-34087

LOW NOISE
Flex-gear electrical power transmission
[NASA-CR-194422] 02 p0661 N94-13445
Position error determination for the speedometer and altimeter of the NAL QSTOL experimental aircraft ASKA
[NAL-TR-1144] 02 p0517 N94-13451
The (delta)f algorithm for beam dynamics
[DE93-015632] 03 p1187 N94-16660
High resolution SQUID magnetometry for non-destructive evaluation
[AD-A268884] 04 p1447 N94-18225
Low-noise oscillators for airborne radar applications, revision 1
[AD-A269372] 04 p1403 N94-18471
Monolithic low noise preamplifier for piezoelectric sensors
[AD-D015860] 04 p1563 N94-18734
A unified Monte Carlo interpretation of particle simulations and applications to nonneutral plasmas
[DE94-001231] 05 p1997 N94-21973
Cryogenic, low-noise high electron mobility transistor amplifiers for the Deep Space Network
06 p2291 N94-23262
Delta f Algorithm
[DE94-003120] 07 p2963 N94-26521
A gimbaled low noise momentum wheel
08 p3162 N94-29640
A high rate, low noise, x ray silicon strip detector system
[DE94-004557] 08 p3268 N94-30717
NASA HSR phase 1 low noise nozzle technology program overview 10 p3972 N94-33463
Processing, fabrication, and demonstration of HTS integrated microwave circuits
[AD-A277684] 10 p4040 N94-33893

LOW PASS FILTERS
Force reflection with compliance control
[NASA-CASE-NPO-18668-1-CU]
01 p0179 N94-10654
Spatially-varying IIR filter banks for image coding
[NASA-CR-193727] 02 p0619 N94-12897
The influence of lowpass filtering and the effects of fading on the group demodulation of QPSK signals
05 p1746 N94-22170
Probabilistic methods for image generation and encoding
[AD-A274294] 07 p2964 N94-26682
Variable-resolution imagery for flight simulation
[AD-A276199] 09 p3586 N94-31058
Third order LPF type compensator for flexible rotor suspension 11 p4217 N94-35863

LOW PRESSURE
NT HIGH ALTITUDE PRESSURE
Plating under reduced pressure
[DE93-011896] 01 p0084 N94-11668
Low pressure storage of natural gas on activated carbon
[DE93-014053] 02 p0660 N94-12851
NASA metrology and calibration, 1993
[NASA-TM-109280] 02 p0597 N94-14410
Discontinuous phase formation and selective attack of SiC materials exposed to low oxygen partial pressure environments
[DE93-040161] 06 p2231 N94-22933
Performance assessment of low pressure nuclear thermal propulsion 06 p2217 N94-23070
LPCVD of InN on GaAs(110) using HN3 and TMIn: Comparison with Si(100) results
[AD-A273555] 06 p2235 N94-24917
Mechanisms of anode power deposition in a low pressure free burning arc
[NASA-CR-194442] 06 p2553 N94-25190
Combustion synthesis method
07 p2721 N94-25561
Modulation by galactosamine-induced hepatitis of biological responses of the rat exposed to high altitude hypoxia 07 p2904 N94-27464
Studies on water electrolyte metabolism and endocrine responses at rest and during submaximal exercise at 6,000 m simulated altitude 08 p3388 N94-28496
Effects of training at simulated altitude of 6,000 m on endocrine responses at rest and during exercise at the same altitude 08 p3388 N94-28497
Large eddy simulation of subsonic mixing layers
08 p3276 N94-29851
Low pressure process for continuous fiber reinforced polyamic acid resin matrix composite laminates
[NASA-CASE-LAR-14954-1] 10 p4020 N94-35075
Theoretical aspect of low pressure discharges in simple gasses
[AD-A278762] 11 p4335 N94-35493
The optimization of interfaces in InAsSb/InGaAs strained-layer superlattices grown by metal-organic chemical vapor deposition
[DE94-010070] 11 p4340 N94-35698
Equations of state valid continuously from zero to extreme pressures with H2O and CO2 as examples
[DE94-011907] 11 p4238 N94-36230

LOW PRESSURE CHAMBERS
U VACUUM CHAMBERS

LOW REYNOLDS NUMBER
Least-squares finite element solutions for three-dimensional backward-facing step flow
[NASA-TM-106353] 02 p0770 N94-14407
Hoph bifurcation in viscous, low speed flows about an airfoil with structural coupling
[AD-A266542] 03 p0859 N94-16798
Two-equation models for low-Reynolds-number variants 04 p1415 N94-18587
Theoretical examination of the flow around a cylinder with a low dimensional Galerkin process
[MPIS-25/1992] 04 p1422 N94-19525
The use of transition region characteristics to improve the numerical simulation of heat transfer in bypass transitional flows
[NASA-TM-106445] 06 p2320 N94-23525
Evaluation of turbulence models in the PARC code for transonic diffuser flows
[NASA-TM-106391] 06 p2168 N94-24084
On streak spacing in wall-bounded turbulent flows
06 p2331 N94-24159
Detailed description of two calculation programs for incompressible, steady state boundary layer flows, applied to determine the aerodynamic characteristics of NACA12 and OA312 foils at low Reynolds numbers
[ISL-N-604/92] 06 p2171 N94-25461
A numerical determination of bifurcation points for low Reynolds number conical flows
[AD-A273984] 07 p2791 N94-25991
Aerodynamic drag of droplets in turbulent flow fields
[ISBN-0-315-75827-9] 09 p3571 N94-32491
An analysis of supersonic flows with low-Reynolds number compressible two-equation turbulence models using LU finite volume implicit numerical techniques
[NASA-CR-195302] 09 p3572 N94-32926
Backward-facing step measurements at low Reynolds number, Re(sub h)=5000
[NASA-TM-108807] 09 p3711 N94-33290

LOW SPEED
Strain concentration assessment of laminates subjected to low velocity impact
[AD-A264497] 01 p0073 N94-11446
Calibration of anemometers at low speed by means of towing carriage 01 p0164 N94-12619
Low-speed wind tunnel tests on four types of joined-wing aircraft models
[NAL-TR-1167] 02 p0501 N94-13340
Hoph bifurcation in viscous, low speed flows about an airfoil with structural coupling
[AD-A266542] 03 p0859 N94-16798
Experimental and computational investigation of the NASA low-speed centrifugal compressor flow field
[NASA-TM-4481] 03 p0869 N94-17386
Experimental and computational results from a large low-speed centrifugal impeller
[NASA-TM-106421] 05 p1636 N94-20136
The high Reynolds number flow through an axial-flow pump
[AD-A273844] 07 p2789 N94-25604
Laser Doppler velocimetry in a low speed multistage compressor
[AD-A274836] 07 p2818 N94-26498
Hopf bifurcation in viscous, low-speed flows about an airfoil with structural coupling 08 p3134 N94-30865
Control of low-speed turbulent separated flow over a backward-facing ramp
[NASA-TM-109740] 09 p3573 N94-33071

LOW SPEED STABILITY
HSCT high lift system aerodynamic requirements
10 p3980 N94-33522

LOW SPEED WIND TUNNELS
NT SUBSONIC WIND TUNNELS
A guide to the DRA 13 ft x 9 ft Low Speed Wind Tunnel Facility
[AD-A267739] 02 p0528 N94-14876
A software interface for the ARL wind tunnel data acquisition system
[AD-A267114] 03 p1146 N94-15650
NASA Lewis 9- by 15-foot low-speed wind tunnel user manual
[NASA-TM-106247] 03 p0872 N94-15819
Hot wire anemometry: A versatile instrumentation used for predevelopment studies and flight testing of the Do-328 aircraft 05 p1640 N94-22604
Installation of models in the 2 m x 3 m low speed wind tunnel
[LTR-LA-286] 07 p2681 N94-27594
Transient flow features of a supersonic jet in a low speed cross flow 07 p2800 N94-28005
Evaluation of the buoyancy drag on automobile models in low speed wind tunnels 07 p2658 N94-28352
Cylinder drag experiment: An upgraded laboratory
[AD-A277841] 10 p3982 N94-33835
Three-dimensional force data acquisition and boundary corrections for the Walter H. Beech Memorial 7 x 10 foot low speed wind tunnel
[AR93-2] 11 p4200 N94-36437

LOW TEMPERATURE
NT CRYOGENIC TEMPERATURE
Crystal growth from low temperature vapour phase
01 p0115 N94-10191
Experiments in ultracold collisions
[DE93-012110] 01 p0365 N94-11029
Phase equilibria and volumetric properties for the system NaCl-CaCl2-H2O
[DE93-013590] 01 p0076 N94-11244
Synthesis and magnetic properties of novel La*2-x*M*x*CuO*4 equals y* compositions (La equals La, Pr, Nd, Sm, Eu, Cd; M equals Ca, Sr, Ba; O (less than or equal) x 0.2; -0.5 (less than or equal) y (less than or equal) 0.5)
[DE93-011359] 01 p0403 N94-12383
Low temperature metal-organic chemical vapor deposition growth processes for high efficiency solar cells
[DE92-010562] 02 p0702 N94-13386
A microstructural approach to fatigue crack processes in poly crystalline BCC materials
[DE93-016666] 02 p0812 N94-14354
Spectroscopic investigations of nonambient systems with millimeter and submillimeter probes
[AD-A266537] 03 p0968 N94-16796
Amide and tetrazene complexes of transition and main group elements as precursors for the low temperature synthesis of elemental nitrides
[AD-A266246] 03 p0950 N94-16931

Transient studies of low temperature catalysts for methane conversion
[DE93-017710] 03 p0950 N94-16962
Molecular structure of low temperature form of triaminoguanidinium nitrate (TAGN)
[AD-A270409] 04 p1377 N94-18708
Ground movements associated with gas hydrate production
[DE93-019887] 04 p1486 N94-19018
Isolation mechanisms in III-V devices
[AD-A271197] 04 p1605 N94-19717
N,N'-bis(4,4,4-trinitro butyryl) hydrazine
[AD-D015897] 05 p1712 N94-20122
Transient studies of low temperature catalysts for methane conversion
[DE93-041232] 05 p1680 N94-20934
Cold starting an alcohol-fueled engine with ultrasonic fuel atomization
[PB93-206597] 05 p1826 N94-22093
A comparison of small and larger mesoscale latent heat and radiative fluxes: December 6 case study 05 p1879 N94-22335
Low temperature absorption spectra and ground state electronic structure of tetrakis(2,6-di-tert-butylphenoxide)uranium(IV)
[DE94-000774] 05 p2035 N94-22387
Spectroscopic studies of magnetic transitions in TbPO4
[DE94-001274] 05 p2035 N94-22565
Low temperature diffusion of hydrogenic species in oxide crystals: Radiation induced diffusion
[DE94-000374] 06 p2558 N94-22957
Thermally activated low temperature creep and primary water stress corrosion cracking of NiCrFe alloys
[DE94-001756] 06 p2241 N94-23219
On the electron mobility in slightly compensated heavily doped gallium arsenide at low temperatures
[DE93-634712] 07 p3057 N94-26387
Variable temperature cold stage for microscope observation 07 p2718 N94-27389
The addition of molecular oxygen to hydroperoxy-propyl radicals
[DE94-003662] 07 p2760 N94-27725
Low temperature behavior of virgin martensite
[PB94-132925] 08 p3204 N94-29142
A newly developed snow vehicle (SM100S) for Antarctica. Part 3: Low temperature toughness of the welded joints of the structural steel 08 p3364 N94-29983
Centrifugal atomization of lanthanide materials for cryogenic coolers
[DE94-006035] 08 p3219 N94-30337
Performance of silvered Teflon (trademark) thermal control blankets on spacecraft 09 p3591 N94-31014
Metal cluster-rare gas van der Waals complexes: Microscopic models of physisorption
[DE94-008134] 09 p3873 N94-32797
Low energy ion beam assisted growth of homoepitaxial silicon films at low temperature
[AD-A278092] 09 p3908 N94-33039
A low temperature scanning force microscope for biological samples
[DE94-011357] 11 p4297 N94-36269
Pairing and low temperature properties of 2D Fermi-systems with attraction between particles
[DE94-615510] 11 p4329 N94-36434

LOW TEMPERATURE ENVIRONMENTS
Icing of turbine intake louvers
[AD-A265714] 01 p0029 N94-12274
Search for lunar water ice in cometary impact craters
[AD-A270130] 04 p1627 N94-18877
Proceedings: International Symposium on Thermal Engineering and Science for Cold Regions
[AD-A270636] 04 p1487 N94-19529
The Support of Air Operations under Extreme Hot and Cold Weather Conditions
[AGARD-CP-540] 08 p3379 N94-28420
Medical support for British operations in the Antarctic 08 p3379 N94-28421
The concept of Royal Navy air operations under extreme environmental conditions 08 p3379 N94-28424
Toward a molecular scale understanding of frost heaving, phase 1
[AD-A275446] 08 p3356 N94-28882
Antarctic Record, vol. 36, no. 3
[REPT-108] 08 p3363 N94-29978
A newly developed snow vehicle (SM100S) for Antarctica. Part 1: Necessity and process of the development 08 p3314 N94-29981
A newly developed snow vehicle (SM100S) for Antarctica. Part 2: Design of the system 08 p3314 N94-29982
A newly developed snow vehicle (SM100S) for Antarctica. Part 4: Low temperature properties of crawler belt 08 p3314 N94-29984
A newly developed snow vehicle (SM100S) for Antarctica. Part 5: Result of general performance tests 08 p3314 N94-29985
Activities of the wintering party at Syowa Station by the 32nd Japanese Antarctic Research Expedition in 1991 08 p3364 N94-29986
Network analyzer calibration for cryogenic on-wafer measurements
[DE94-010089] 11 p4262 N94-36430

LOW TEMPERATURE PHYSICS
Realistic theories of heavy electron and other strongly correlated materials
[DE93-010350] 04 p1571 N94-19204
Finite element analysis of time-independent superconductivity 09 p3691 N94-31905
Quadrupolar effects in PrCu2Si2
[DE94-011509] 12 p4534 N94-37054

LOW TEMPERATURE PLASMAS
U COLD PLASMAS

LOW TEMPERATURE TESTS
Cryogenic probe station for use in automated microwave and noise figure measurements
[NASA-TM-106560] 08 p3286 N94-29000
Low temperature behavior of virgin martensite
[PB94-132925] 08 p3204 N94-29142
Evaluation of corrosion protecting properties of modern aircraft paint systems
[AD-B179388] 08 p3220 N94-30420
Improved construction materials for polar regions using microcellular thermoplastic foams 08 p3223 N94-30483

LOW THRUST
A laboratory model of a hydrogen/oxygen engine for combustion and nozzle studies
[NASA-TM-106281] 01 p0047 N94-11252
Analysis of reacting flowfields in low-thrust rocket engines and plumes 02 p0552 N94-14491
Design of a controllable pitch underwater thruster system
[AD-A271140] 05 p1821 N94-20021
Theory and computation of optimal low- and medium-thrust transfers
[NASA-CR-194812] 06 p2217 N94-23275
Design of a resistojet for Space Station Freedom
[NASA-CR-195506] 06 p2221 N94-24979

LOW THRUST PROPULSION
NT ELECTROMAGNETIC PROPULSION
NT ION PROPULSION
NT PLASMA PROPULSION
NT SOLAR ELECTRIC PROPULSION
NT SOLAR PROPULSION
Low thrust space propulsion
[NASA-TM-109286] 02 p0552 N94-13625
Molecular gas dynamics applied to low-thrust propulsion 06 p2214 N94-23053
Determination of pressure response times for gaseous flow in a tube
[AD-A275274] 08 p3272 N94-29435

LOW VELOCITY
U LOW SPEED

LOW VISIBILITY
Airport surface operations requirements analysis
[NASA-CR-191508] 06 p2172 N94-23288
Development and evaluation of a near infrared reflecting and low visibility paint scheme for RAAF P-3C Orion aircraft
[AD-A274881] 07 p2669 N94-26864
Extremely Low Visibility IFR Rotorcraft Approach (ELVIRA) operational concept development. Volume 1: Executive Summary
[AD-A278651] 08 p3142 N94-30189
Vision-based aircraft guidance
[NASA-CR-195937] 10 p4007 N94-34264

LOW VOLTAGE
Low voltage electron beam lithography
[AD-A265358] 01 p0145 N94-12405
Preparation and investigation of improved low voltage electron excitable phosphors
[AD-A266852] 03 p0963 N94-14948
Low voltage electron beam lithography
[AD-A267865] 03 p1215 N94-17389
Limiting factors for carbon based chemical double layer capacitors 06 p2394 N94-23365
Low voltage electron beam lithography
[AD-A275648] 08 p3262 N94-28650
Low voltage electron beam lithography
[AD-A278204] 10 p4038 N94-33375

LOW WEIGHT
The NASA sponsored HSCT propulsion studies 10 p3974 N94-33476

LOWER ATMOSPHERE
NT TROPOPAUSE
NT TROPOSPHERE
Atmospheric turbulence and diffusion research
[DE93-011842] 02 p0718 N94-14425
A ray trace model for propagation loss
[AD-A266314] 03 p0997 N94-16467
Refractive index structure in the lower atmosphere
[AD-A270935] 05 p1854 N94-19899
Empirical wind model for the middle and lower atmosphere. Part 2: Local time variations
[NASA-TM-104592] 05 p1870 N94-21862
Uniqueness of a solution of a steady state photochemical problem: Applications to Mars 11 p4370 N94-36151
First measurement of helium on Mars: Implications for the problem of radiogenic gases on the terrestrial planets 11 p4370 N94-36153

LOWER BODY NEGATIVE PRESSURE
Glycerol-induced hyperhydration 01 p0309 N94-11996
Spectral analysis of resting cardiovascular variables and responses to oscillatory LBNP before and after 6 degree head dowm bedrest 01 p0309 N94-11997
Effect of prolonged LBNP and saline ingestion on plasma volume and orthostatic responses during bed rest 01 p0310 N94-11998
Health monitoring of Japanese payload specialist: Autonomic nervous and cardiovascular responses under reduced gravity condition (L-0) 02 p0591 N94-13757
Countermeasure for reducing post-flight orthostatic intolerance: Lower Body Negative Pressure (LBNP) experiment E140 02 p0594 N94-13772
STS-32 crew training for lower body negative pressure unit and AFE
[NASA-TM-109475] 03 p1120 N94-15381
Responses to LBNP in men with varying profiles of strength and aerobic capacity: Implications for flight crews
[NASA-TP-3346] 06 p2426 N94-23530
Pulse waveform and transcranial Doppler analysis during lower body negative pressure
[AD-A274516] 07 p2911 N94-27088
Aerobic fitness and orthostatic tolerance: Evidence against an association 07 p2934 N94-28365
Response to graded Lower Body Negative Pressure (LBNP) after space flight 10 p4096 N94-33637

LOWER IONOSPHERE
NT D REGION

LOX (OXYGEN)
U LIQUID OXYGEN

LOX-HYDROGEN ENGINES
U HYDROGEN OXYGEN ENGINES

LQG CONTROL
U LINEAR QUADRATIC GAUSSIAN CONTROL

LQR
U LINEAR QUADRATIC REGULATOR

LRC CIRCUITS
U RLC CIRCUITS

LRV (VEHICLE)
U LUNAR ROVING VEHICLES

LSI
U LARGE SCALE INTEGRATION

LST
U HUBBLE SPACE TELESCOPE

LTE (ASTRONOMY)
U LOCAL THERMODYNAMIC EQUILIBRIUM

LUBRICANT TESTS
A vacuum four-ball tribometer to evaluate liquid lubricants for space applications
[NASA-TM-106264] 02 p0575 N94-12842
Dry film lubricant evaluation
[DE93-013114] 02 p0578 N94-13118
Surface analysis of bearings
[AD-A266800] 02 p0661 N94-13122
The use of screening tests in spacecraft lubricant evaluation
[AD-A272943] 05 p1705 N94-21225
An analytical ultra-high vacuum tribometer for solid lubricant studies 06 p2361 N94-24033
BLAST, a new lubricant screening tester for space oils and greases 06 p2362 N94-24042
An assessment of solid lubricant films for use in high temperature space applications 06 p2363 N94-24044
The development of dry-lubricated ceramic cages 06 p2363 N94-24045
Development of high temperature liquid lubricants for low-heat rejection: Heavy duty diesel engines
[NASA-CR-191197] 06 p2258 N94-24753
The use of screening tests in spacecraft lubricant evaluation 08 p3162 N94-29641

LUBRICANTS
NT GAS LUBRICANTS
NT HIGH TEMPERATURE LUBRICANTS
NT LUBRICATING OILS
NT SOLID LUBRICANTS
The properties of perfluoropolyethers used for space applications
[NASA-TM-106275] 01 p0088 N94-10864

Measurement of viscosity, density and gas solubility of refrigerant blends
[DE93-014772] 01 p0089 N94-11145
Accelerated screening methods for predicting lubricant performance in refrigerant compressors
[DE93-014773] 01 p0089 N94-11146
Ceramics technology project database
[DE93-012431] 01 p0091 N94-11672
Surface analysis of bearings
[AD-A266800] 02 p0661 N94-13122
Miscibility of lubricants with refrigerants, phase 1
[DE93-014766-PHASE-1] 02 p0596 N94-13407
Canadian Target Assembly (CTA) to Airborne Support Equipment (ASE) vibration test report
[IME-AMT-TR-001] 02 p0663 N94-14195
Compatibility of refrigerants and lubricants with motor materials
[DE93-014768] 02 p0583 N94-14801
Scholarly research program in fuel analysis and combustion research
[AD-A266789] 03 p0942 N94-14911
Heating of lubricant with an electric resistance heater
[VTT-TIED-1359] 03 p0974 N94-17547
Compatibility of refrigerants and lubricants with motor materials, volume 1
[DE93-040216] 04 p1350 N94-18895
Compatibility of refrigerants and lubricants with motor materials, volume 2
[DE93-040217] 04 p1350 N94-18896
Measurement of viscosity, density, and gas solubility of refrigerant blends in selected synthetic lubricants
[DE93-040221] 04 p1350 N94-18977
Accelerated screening methods for determining chemical and thermal stability of refrigerant-lubricant mixtures. Part 1: Method assessment
[DE93-040215] 04 p1351 N94-19136
Compatibility of refrigerants and lubricants with motor materials, volume 3
[DE93-040218] 04 p1352 N94-19191
Surface species in tribology
[AD-A270970] 04 p1446 N94-19754
Microscopic modeling of tribological and interfacial phenomena
[AD-A271864] 05 p1823 N94-20464
The use of screening tests in spacecraft lubricant evaluation
[AD-A272943] 05 p1705 N94-21225
Scanning tunneling microscopy investigations of metal dichalcogenide materials
[AD-A272910] 05 p2027 N94-21242
Utilization of metals to improve the lubrication of ceramic load-bearing devices
[PB93-202448] 05 p1825 N94-21424
Integrity testing of brush seal in a T-700 engine
05 p1654 N94-21792
Navy GTE seal development activity
05 p1655 N94-21794
Dynamics of face seals for high speed turbomachinery
05 p1655 N94-21796
New method for increasing machine service-life, phase 2
[PB93-200707] 06 p2354 N94-23533
New pin-on-disk equipment for vacuum tribometry
06 p2360 N94-24023
Measurement of viscosity, density, and gas solubility of refrigerant blends in selected synthetic lubricants
[DE94-003609] 07 p2713 N94-25934
Accelerated screening methods for determining chemical and thermal stability of refrigerant-lubricant mixtures. Part 2: Experimental comparison and verification of methods
[DE94-003664] 07 p2749 N94-26007
Using ferro-magnetic fluids to lubricate non-conformal isothermal contacts
[INPE-5520-TAE/021] 07 p2827 N94-27665
Compatibility of refrigerants and lubricants with engineering plastics
[DE94-004959] 07 p2756 N94-27692
Solubility, viscosity, and density of refrigerant/lubricant mixtures
[DE94-004237] 07 p2721 N94-28069
Calculation methods for steadily loaded central circumferential groove hydrodynamic journal bearings (guide to use of computer program A9304)
[ESDU-93004] 07 p2830 N94-28073
Calculation methods for steadily loaded axial groove hydrodynamic journal bearings (guide to use of computer program A9305)
[ESDU-93005] 07 p2830 N94-28074
Calculation methods for steadily loaded axial groove hydrodynamic journal bearings. Low viscosity process fluid lubrication (guide to use of computer program A9306)
[ESDU-93006] 07 p2830 N94-28075
The use of screening tests in spacecraft lubricant evaluation
08 p3162 N94-29641
Lubricant rheology at high shear rates
08 p3217 N94-29967
Materials compatibility and lubricants research on CFC-refrigerant substitutes
[DE94-004905] 08 p3220 N94-30692
Measurement of viscosity, density, and gas solubility of refrigerant blends in selected synthetic lubricants
[DE94-007723] 09 p3653 N94-31917
Compatibility of refrigerants and lubricants with elastomers
[DE94-008552] 09 p3658 N94-32518
Perfluoropolyalkylether decomposition on catalytic aluminas
[NASA-TM-106547] 09 p3617 N94-33021
A comparison of the performance of solid and liquid lubricants in oscillating spacecraft ball bearings
09 p3606 N94-33311
The preliminary evaluation of liquid lubricants for space applications by vacuum tribometry
09 p3606 N94-33313
Measurement of viscosity, density, and gas solubility of refrigerant blends in selected synthetic lubricants
[DE94-010426] 11 p4244 N94-35687
Solubility, viscosity and density of refrigerant/lubricant mixtures
[DE94-009996] 11 p4245 N94-35771
Research update: Materials Compatibility and Lubricant Research (MCLR) program
[DE94-010001] 11 p4247 N94-36387
Sealed tube comparisons of the compatibility of desiccants with refrigerants and lubricants
[DE94-010002] 11 p4251 N94-36388
Evaluation of the EHL film thickness and extreme pressure additives on gear surface fatigue life
[NASA-TM-106663] 12 p4451 N94-37319
Materials Compatibility and Lubricant Research on CFC-refrigerant substitutes
[DE94-012352] 12 p4425 N94-37373
Sealed tube comparisons of the compatibility of desiccants with refrigerants and lubricants
[DE94-012371] 12 p4425 N94-37421
Information on alternative refrigerants and lubricants: The ARTI refrigerant database
[DE94-009997] 12 p4426 N94-37490
Properties of perfluoropolyethers for space applications
[NASA-TM-106616] 12 p4426 N94-37520
Evaluation of seals and lubricants used on the Long Duration Exposure Facility
[NASA-CR-4604] 12 p4399 N94-37614
Perfluorodiethoxymethane on nickel and nickel oxide surfaces
[DE94-011200] 12 p4426 N94-37712

LUBRICATING OILS
Synthetic lubricants and high-performance functional fluids: Phosphazenes
[ARL-TR-45] 02 p0580 N94-14126
Contained liquids in microgravity, part 2
03 p0979 N94-16085
Vapor-delivered lubrication of steel-steel and steel-ceramic systems
[PB93-202364] 05 p1825 N94-21451
Tribological characterization of spatial wet lubricants under vacuum 06 p2264 N94-24010
In-vacuum performance of Fomblin Z25-lubricated, 52100 steel bearings with TiC-coated balls
06 p2358 N94-24011
BLAST, a new lubricant screening tester for space oils and greases 06 p2362 N94-24042
A colour image processing algorithm to identify copper-based particles in filter debris samples
[DREP-TM-93-19] 06 p2455 N94-24122
Status of developing a multifunctional aviation grease
[AD-A276755] 09 p3656 N94-32184
Lubrication with binary mixtures: Liquid-liquid emulsion in elastohydrodynamics and metal forming
09 p3658 N94-32490
The effect of alternative fuels on the stability and lubricity of crankcase lubricants
[DE94-010353] 11 p4245 N94-36108

LUBRICATION
NT BOUNDARY LUBRICATION
NT SELF LUBRICATION
NT SPACECRAFT LUBRICATION
Accelerated screening methods for predicting lubricant performance in refrigerant compressors
[DE93-014773] 01 p0089 N94-11146
Advanced model of gradual wear of viscoelastic surface film
[AD-A265130] 01 p0090 N94-11222
Tribological characteristics of sputtered Au/Cr films on alumina substrates at elevated temperatures
[NASA-TM-106078] 01 p0055 N94-11362
Properties of interfacial tribo-films
[AD-A265591] 01 p0182 N94-12374
Atomic-scale friction measurements using friction force microscopy. Part 1: General principles and new measurement techniques
[AD-A268391] 03 p1048 N94-17533
Interdisciplinary research on wear of materials
[AD-A268190] 04 p1443 N94-17730
Microscopic modeling of tribological and interfacial phenomena
[AD-A271864] 05 p1823 N94-20464
Utilization of metals to improve the lubrication of ceramic load-bearing devices
[PB93-202448] 05 p1825 N94-21424
Lubricated wear of steel-ceramic and ceramic-ceramic systems
[PB93-202356] 05 p1825 N94-21450
Vapor-delivered lubrication of steel-steel and steel-ceramic systems
[PB93-202364] 05 p1825 N94-21451
Navy GTE seal development activity
05 p1655 N94-21794
Dynamics of face seals for high speed turbomachinery
05 p1655 N94-21796
Lewis Research Center R and D Facilities
[NASA-TM-109400] 06 p2630 N94-23135
New method for increasing machine service-life, phase 2
[PB93-200707] 06 p2354 N94-23533
An application of small-gap equations in sealing devices 06 p2325 N94-23668
Development of a theory of the wear of ceramics
[DE94-002773] 06 p2254 N94-23783
Tribological characteristics of ball bearings lubricated with a sputtered molybdenum disulphide film in a vacuum under a high thrust load 06 p2355 N94-23992
The tribology of some MoS2-lubricated engineering ceramics 06 p2356 N94-23993
Thermal vacuum performance of cycloid and harmonic gearboxes with solid (MoS2) and liquid (Braycote 601) lubrication 06 p2358 N94-24009
Wear reduction in ceramic bearings by surface generated pyrolytic carbon continuously replenished by ethylene gas
[AD-A278264] 06 p2364 N94-24090
Investigation of the ultrafiltration technique using military greases
[AD-A273633] 06 p2261 N94-25029
Using ferro-magnetic fluids to lubricate non-conformal isothermal contacts
[INPE-5520-TAE/021] 07 p2827 N94-27665
Lubrication of space systems
[NASA-TM-106392] 08 p3214 N94-29399
An asymptotic analysis for compressible gas lubrication of rough surfaces 08 p3222 N94-30922
Lubrication with binary mixtures: Liquid-liquid emulsion in elastohydrodynamics and metal forming
09 p3658 N94-32490
Frictional behavior and adhesion of Ag and Au films applied to aluminum oxide by oxygen-ion assisted Screen Cage Ion Plating (SCIP)
[NASA-TM-106522] 09 p3647 N94-32931
Torque characteristics of solid lubricated precision bearings during oscillatory motion
[AD-A278133] 09 p3728 N94-33061
The effect of alternative fuels on the stability and lubricity of crankcase lubricants
[DE94-010353] 11 p4245 N94-36108
Evaluation of the EHL film thickness and extreme pressure additives on gear surface fatigue life
[NASA-TM-106663] 12 p4451 N94-37319

LUBRICATION SYSTEMS
AGBT advanced counter-rotating gearbox detailed design report
[NASA-CR-180883] 01 p0179 N94-10400
Lubrication of space systems
[NASA-TM-106392] 08 p3214 N94-29399
Design of a high-speed reliable ball bearing
09 p3606 N94-33314

LUCITE (TRADEMARK)
U POLYMETHYL METHACRYLATE

LUDER BANDS
U PLASTIC DEFORMATION
U YIELD POINT

LUGS
RSRM nozzle actuator bracket/lug fracture mechanics qualification test
[NASA-CR-193859] 03 p0927 N94-17080

LUMBERING AREAS
U FORESTS

LUMINAIRES
NT AIRCRAFT LIGHTS
NT ARC LAMPS
NT FLASH LAMPS
NT MERCURY LAMPS
NT QUARTZ LAMPS
NT RUNWAY LIGHTS

Parametric study of diffusion-enhancement networks for spatiotemporal grouping in real-time artificial vision
[AD-A265065] 01 p0331 N94-11652
An analysis of the maintenance performance measurement system for LAMPS MK 3 helicopter squadrons
[AD-A276421] 09 p3565 N94-31332
Evaluation for the development of taxiway lighting intensity standards
[AD-A276706] 09 p3588 N94-32120
SeaWiFS technical report series. Volume 16: The second SeaWiFS Intercalibration Round-Robin Experiment, SIRREX-2, June 1993
[NASA-TM-104566-VOL-16] 10 p4093 N94-34412

LUMINANCE
The effects of luminance boundaries on color perception
[AD-A268398] 03 p1133 N94-17397
Perception of lightness and brightness in complex patterns
[AD-A268435] 03 p1134 N94-17513
Validation of a second generation conspicuity meter
[IZF-1993-A-11] 06 p2542 N94-22895
Evaluation of visual acuity with Gen 3 night vision goggles
[NASA-TM-108792] 06 p2431 N94-23974
Night vision devices and characteristics 06 p2432 N94-23982
Luminance-brightness mapping: The missing decades
[ETN-94-95351] 06 p2428 N94-25298
Image quality and the display modulation transfer function: Experimental findings
[AD-A274061] 07 p2679 N94-25773
Fusion of range and luminance data from laser radar systems
[AD-A275608] 08 p3292 N94-28770

LUMINESCENCE
NT BIOLUMINESCENCE
NT CATHODOLUMINESCENCE
NT CHEMILUMINESCENCE
NT ELECTROLUMINESCENCE
NT FLUORESCENCE
NT LASER INDUCED FLUORESCENCE
NT LUNAR LUMINESCENCE
NT OPTICAL RESONANCE
NT PHOSPHORESCENCE
NT PHOTOLUMINESCENCE
NT RESONANCE FLUORESCENCE
NT SONOLUMINESCENCE
NT SPACECRAFT GLOW
NT THERMOLUMINESCENCE
NT X RAY FLUORESCENCE
Improved super luminescent light source specification
[AD-D015746] 01 p0176 N94-12329
Gordon Research Conference on Chronobiology, 1991
[AD-A266354] 02 p0728 N94-13698
A sum-rule of luminescence spectrum
[ITN-93-85223] 02 p0814 N94-14559
Optical luminescence spectroscopy as a probe of the surface mineralogy of Mars 05 p1813 N94-22437
Symbiosis in marine luminous bacteria
[AD-A273540] 06 p2422 N94-24791
Data analysis and interpretation of lunar dust exosphere 06 p2623 N94-25349
Development of intermetallic compounds for high performance luminescence elements 07 p2722 N94-25545
A miniaturized ASIC-based multichannel scaler instrument
[DE94-007222] 09 p3807 N94-32783
Light in Thermal Environments (LITE) Workshop
[NASA-CR-195851] 09 p3790 N94-32981
Growth, characterization, and device development in monocrystalline diamond films
[AD-A277863] 10 p4146 N94-33774
Visible and infrared (1.54 micrometers) LED based on Er-doped porous Si
[AD-A278528] 10 p4042 N94-34295
Flight testing of a luminescent surface pressure sensor
[NASA-TM-103970] 11 p4189 N94-35394
Optical studies of dynamical processes in disordered systems
[DE94-011945] 12 p4538 N94-37676

LUMINESCENT INTENSITY
U LUMINOUS INTENSITY

LUMINOSITY
NT STELLAR LUMINOSITY
Experimental efforts and results in finding new heavy scintillators
[DE93-010406] 01 p0371 N94-10156
Upgraded D(O) calorimeter electronics for short Tevatron bunch space and the effect of pile-up on the W mass measurement
[DE93-013566] 01 p0146 N94-12603
The evidence for clumpy accretion in the Herbig Ae star HR 5999
[NASA-CR-189314] 02 p0828 N94-12915
A search for scalar leptoquarks in D0
[DE93-012780] 02 p0779 N94-12954
Inclusive single muons at DO
[DE93-012779] 02 p0783 N94-13494
The origin of the far-infrared emission from galactic molecular clouds 02 p0848 N94-13654
X ray emission from Wolf-Rayet stars with recurrent dust formation
[NASA-CR-189321] 03 p1300 N94-15533
Search for top quark with D0 detector
[DE93-040170] 04 p1572 N94-19536
Energy and luminosity limits of hadron supercolliders
[DE93-019248] 05 p1980 N94-20300
The preservation of low emittance flat beams
[DE93-040964] 05 p1981 N94-21773
Silicon microelectronic field-emissive devices for advanced display technology
[DE94-000397] 05 p1794 N94-22380
Search for the top quark and other new particles at D0
[DE94-001220] 06 p2535 N94-24515
Secondary particle in background levels and effects on detectors at future hadron colliders
[DE94-003378] 07 p3011 N94-25598
Physical conditions in classical H2 regions in the Magellanic Clouds 08 p3543 N94-29722
A multiwavelength study of two prototypical supernova remnants 08 p3540 N94-29833
High redshift QSOs and the x ray background
[NASA-CR-195112] 08 p3540 N94-29957
Can a variable alpha induce limit cycle behavior and exponential luminosity decay in transient soft x ray sources? 09 p3929 N94-31129
Thermal continua of AGN accretion disks 09 p3931 N94-31137
Substorm aurorae and their connection to the inner magnetosphere
[AD-A277609] 10 p4086 N94-33850
Proceedings of the Workshop on TRISTAN Physics at High Luminosities
[DE94-737969] 12 p4523 N94-37727

LUMINOUS FLUX DENSITY
U LUMINOUS INTENSITY

LUMINOUS INTENSITY
NT ILLUMINANCE
NT LUMINANCE
Photocatalysis for the treatment of waste water: Applications involving the removal of metals
[DE93-011669] 02 p0561 N94-12841
Characterization of Spirulina biomass for CELSS diet potential
[NASA-CR-194123] 02 p0729 N94-14097
Optical switching devices
[AD-D015918] 05 p1984 N94-20059
Intensity and polarization of light scattered by size distributions of randomly oriented nonspherical particles 05 p1721 N94-20416
Absolute determination of local tropospheric OH concentrations 08 p3343 N94-28594
Strategies to sustain and enhance performance in stressful environments
[AD-A275223] 08 p3398 N94-29027
Optical flameout detector
[NASA-CASE-LAR-14997-1] 08 p3287 N94-29368
Radiation/remote sensing: Review of the principal definitions 09 p3757 N94-30996
Evaluation of intensity distribution profiles for US. Army rotorcraft position lighting adapted for image intensifier operations
[AD-A276459] 09 p3804 N94-32171
Bioluminescence bathyphotometer
[AD-D016102] 09 p3790 N94-32959
Multiple scattering of light in a comet atmosphere 10 p4163 N94-33388

LUMPED PARAMETER SYSTEMS
Improved approximations applied to the S(sub N) even-parity equation
[DE93-016467] 04 p1551 N94-19343

LUMPING
A weighted least-squares lump correction algorithm for transmission-corrected gamma ray nondestructive assay
[DE93-018474] 05 p1904 N94-20049

LUNAR ALBEDO
Mixing model analysis of telescopic lunar spectra 03 p1284 N94-16371

LUNAR ATMOSPHERE
Effects of levitated dust on astronomical observations from the lunar surface 03 p1239 N94-16433
Lunar horizon glow and the Clementine mission 11 p4366 N94-35478

LUNAR BASED EQUIPMENT
NT LUNAR CONSTRUCTION EQUIPMENT
NT LUNAR EXCAVATION EQUIPMENT
General overview of an integrated lunar oxygen production/brickmaking system 01 p0131 N94-12027
Galileo EM-2 contributions to the lunar control network 01 p0468 N94-12198
Interferometric astronomy on the Moon 06 p2601 N94-23378
Conceptual design and architecture of hexapod robotic vehicles for the (L)OVLA project 06 p2369 N94-23405
LOITA: Lunar Optical/Infrared Telescope Array
[NASA-CR-195532] 06 p2546 N94-24816
Mitigation of adverse environmental effects on lunar-based astronomical instruments 09 p3598 N94-31426

LUNAR BASES
Lunar campsite concept: Space transfer concepts and analysis for exploration missions
[NASA-CR-192602] 01 p0433 N94-10144
Radiation considerations for interplanetary missions 01 p0045 N94-11559
Cold press sintering of simulated lunar basalt 01 p0131 N94-12026
General overview of an integrated lunar oxygen production/brickmaking system 01 p0131 N94-12027
Thermodynamics of lunar ilmenite reduction 01 p0415 N94-12028
Mission to the Moon: An ESA study on future exploration 01 p0460 N94-12153
Exploration planning in the context of human exploration and development of the Moon 01 p0474 N94-12229
Conceptual studies report on lunar and planetary exploration
[NASDA-TK-SS0438] 01 p0481 N94-12323
Manned lunar exploration missions 01 p0482 N94-12326
Effects of radiobiological uncertainty on vehicle and habitat shield design for missions to the moon and Mars
[NASA-TP-3312] 02 p0846 N94-12875
Lunar base concepts
[NASA-TM-109607] 03 p1247 N94-15294
Building a lunar base
[NASA-TM-109674] 03 p0983 N94-15519
The first lunar outpost: The design reference mission and a new era in lunar science 03 p0874 N94-16362
Study of the National Science Foundation's South Pole Station as an analogous data base for the logistical support of a Moon laboratory
[NASA-TM-108429] 03 p1174 N94-17469
Lunar base Controlled Ecological Life Support System (LCELSS): Preliminary conceptual design study
[NASA-CR-188479] 04 p1511 N94-18484
Space transfer concepts and analyses for exploration missions
[NASA-CR-193876] 04 p1332 N94-18820
Space exploration initiative
[NASA-TM-109366] 04 p1323 N94-18981
Characterization of Minnesota lunar simulant for plant growth 05 p1897 N94-20665
Power beaming to space using a nuclear reactor-pumped laser
[DE94-001208] 06 p2348 N94-23185
Design of a lunar propellant processing facility. NASA/USRA advanced program
[NASA-CR-195502] 06 p2266 N94-24618
Space transfer vehicle concepts and requirements. Volume 4: Summary of special studies
[NASA-CR-193918] 06 p2201 N94-24970
Project Columbiad: Reestablishment of human presence on the Moon 07 p2689 N94-25687
First lunar outpost 07 p2943 N94-25694
The 1991-1992 project summaries 07 p2943 N94-25698
Lunar base habitat designs: Characterizing the environment, and selecting habitat designs for future trade-offs
[NASA-CR-195687] 07 p2943 N94-27934
The Second Annual International Space University Alumni Conference
[NASA-CP-3253] 09 p3598 N94-31425
Solar lunar power 09 p3599 N94-31427
The Nomad Explorer assembly assist vehicle: An architecture for rapid global extraterrestrial base infrastructure establishment 09 p3599 N94-31429
Design of a logistics model for building and supporting a lunar station
[ILR-MITT-282(1993)] 09 p3803 N94-31852

LUNAR CINEMATOGRAPHY
U LUNAR PHOTOGRAPHY

LUNAR COMMUNICATION
Conceptual communications system design in the 25.25-27.5 and 37.0-40.5 GHz frequency bands 06 p2306 N94-25379

LUNAR COMPOSITION
Multiple nitrogen components in lunar soil sample 12023 01 p0451 N94-12108
Solar wind-induced secondary ions and their relation to lunar surface composition 01 p0474 N94-12232
Measuring and distinguishing compositional and maturity properties of lunar soils by remote VIS-NIR spectroscopy 01 p0478 N94-12251
Deposition of impact-generated vapors in the lunar regolith 02 p0843 N94-14302
Why is the Moon dark? 03 p1256 N94-16219
Lunar scout missions: Galileo encounter results and application to scientific problems and exploration requirements 03 p1259 N94-16229
Earth-based and Galileo SSI multispectral observations of eastern mare serenitatis and the Apollo 17 landing site 03 p1261 N94-16244
On the composition of neuKREEP: QMD contamination at Apollo 11? 03 p1266 N94-16276
Composition and maturity of the 60013/14 core 03 p1275 N94-16327
Grain surface features of Apollo 17 orange and black glass 03 p1289 N94-16397
Gamma ray spectrometer for Lunar Scout 2 03 p1037 N94-16426
Core formation in the Moon: The mystery of the excess depletion of Mo, W and P 05 p2095 N94-20651
Fragments of ancient lunar crust: Ferroan noritic anorthosites from the descartes region of the Moon 05 p2096 N94-20660
Volatility in the lunar crust: Trace element analyses of lunar minerals by PIXE proton microprobe 05 p2097 N94-20661
Impact glasses from the ultrafine fraction of lunar soils 05 p2097 N94-20662
The Sm-(146,147)-Nd-(142,143) formation interval for the lunar mantle and implications for lunar evolution 05 p2097 N94-20663
MinMap: An imaging spectrometer for high resolution compositional mapping of the Moon 05 p1813 N94-20688
Chronology and genesis of high-Ti mare volcanism: Melting of cogenetic depleted and enriched reservoirs 05 p2118 N94-20777
Implantation of nitrogen: Effects of hydrogen and implantation energy 05 p1686 N94-20804
Mineralogy and cooling history of magnesian lunar granulite 67415 05 p2124 N94-20811
Ti-bearing oxide minerals in lunar meteorite Y793169 with the VLT affinity 05 p2084 N94-20812
Distribution and geologic history of materials excavated by the lunar crater Bulliaidus 05 p2128 N94-20832
Origin of high-Ti lunar ultramafic glasses 05 p1686 N94-20853
Petrology and geochemistry of VLT glasses from double drive tube 79001/2 05 p1687 N94-20870
Multispectral studies of selected crater- and basin-filling lunar Maria from Galileo Earth-Moon encounter 1 05 p2136 N94-20876
Basaltic Volcanism and Ancient Planetary Crusts [NASA-CR-193151] 06 p2614 N94-24363
Experimental study of lunar and SNC (Mars) magmas [NASA-CR-195274] 07 p3107 N94-27850
New prospects for analyzing lunar pyroclastic glass 11 p4355 N94-35397
Single agglutinates: A comparative study of compositions of agglutinitic glass, whole-grain, bulk soil, and FMR 11 p4355 N94-35401
Luna 24 regolith breccias: A possible source of the fine size material of the Luna 24 regolith 11 p4362 N94-35450
Alkali element constraints on Earth-Moon relations 11 p4354 N94-36169

LUNAR CONSTRUCTION EQUIPMENT
Cold press sintering of simulated lunar basalt 01 p0131 N94-12026
Lunar preform manufacturing 07 p2765 N94-25677

LUNAR CORE
Overturn of magma ocean ilmenite cumulate layer: Implications for lunar magmatic evolution and formation of a lunar core 03 p1261 N94-16242
Petrology and geochemistry of VLT glasses from double drive tube 79001/2 05 p1687 N94-20870

LUNAR CRATERS
Differential scaling: Implications for central structures in large lunar craters 01 p0461 N94-12158
Twenty-Fourth Lunar and Planetary Science Conference. Part 2: G-M [NASA-CR-193174] 03 p1247 N94-16173
Galileo imaging results from the second Earth-Moon flyby: Lunar Maria and related units 03 p1252 N94-16199
Remote sensing studies of the northeastern portion of the lunar nearside 03 p1258 N94-16225
Lunar impact basins: New data for the nearside northern high latitudes and eastern limb from the second Galileo flyby 03 p1258 N94-16228
Modes of formation of lunar light plains and the detection of cryptomaria deposits 03 p1259 N94-16231
The size of complex craters 03 p1262 N94-16249
The history of mare volcanism in the Orientale Basin: Mare deposit ages, compositions and morphologies 03 p1269 N94-16289
Galileo SSI lunar observations: Copernican craters and soils 03 p1288 N94-16395
Thermogeologic mapping of the Moon from lunar orbit 03 p1290 N94-16405
Working group for planetary system nomenclature [NASA-CR-194406] 04 p1626 N94-18841
Search for lunar water ice in cometary impact craters [AD-A270130] 04 p1627 N94-18877
Spectral reflectance studies of the Humorum Basin region 05 p2101 N94-20682
Compositional diversity of the lunar North Pole: Preliminary analyses of Galileo SSI data 05 p2101 N94-20686
Chronology of lunar granite 12033,576: Resetting of Rb-Sr and K-Ca isochrons 05 p2115 N94-20763
Distribution and geologic history of materials excavated by the lunar crater Bullialdus 05 p2128 N94-20832
Consortium study of lunar meteorites Yamato-793169 and Asuka-881757: Geochemical evidence of mutual similarity, and dissimilarity versus other mare basalts 05 p2085 N94-20857
Large floor-fractured craters and isostatic crater modification: Implications for lithospheric thickness on Venus 05 p2135 N94-20873
Degradation sequence of young lunar craters from orbital infrared survey 05 p2136 N94-20874
Multispectral studies of selected crater- and basin-filling lunar Maria from Galileo Earth-Moon encounter 1 05 p2136 N94-20876
The morphology of the lunar surface parts in the region of work of the mobile geological laboratory vehicle in Mare Imbrium 06 p2607 N94-23385
The Twenty-Fifth Lunar and Planetary Science Conference. Part 1: A-G [NASA-CR-195743] 11 p4355 N94-35395
Block distributions on the lunar surface: A comparison between measurements obtained from surface and orbital photography 11 p4359 N94-35419
Preliminary description of double drive tube 68002/68001 11 p4363 N94-35457

LUNAR CRUST
The granulite suite: Impact melts and metamorphic breccias of the early lunar crust 01 p0282 N94-12197
Assimilation in lunar basalts and volcanic glasses: Implications for a heterogenous mantle source region 01 p0478 N94-12250
Remote sensing studies of the northeastern portion of the lunar nearside 03 p1258 N94-16225
Mode of emplacement of lunar mare volcanic deposits: Graben formation due to near surface deformation accompanying dike emplacement at Rima Parry 5 03 p1258 N94-16227
The ilmenite liquidus and depths of segregation for high-Ti picrite glasses 03 p0975 N94-16241
Overturn of magma ocean ilmenite cumulate layer: Implications for lunar magmatic evolution and formation of a lunar core 03 p1261 N94-16242
Petrogenesis of Apollo 12 mare basalts. Part 2: An open system model to explain the pigeonite basalt compositions 05 p1684 N94-20645
Fragments of ancient lunar crust: Ferroan noritic anorthosites from the descartes region of the Moon 05 p2096 N94-20660
Volatility in the lunar crust: Trace element analyses of lunar minerals by PIXE proton microprobe 05 p2097 N94-20661
Compositional diversity of the lunar North Pole: Preliminary analyses of Galileo SSI data 05 p2101 N94-20686
Geology and deposits of the Serenitatis basin 05 p2119 N94-20786
The Mg-suite and the highland crust: An unsolved enigma 05 p2126 N94-20822
The Clementine Mission science return at the Moon and Geographos 05 p1652 N94-20850
Limits on differentiation of melt sheets from basin-scale lunar impacts 05 p2133 N94-20856
Basaltic Volcanism and Ancient Planetary Crusts [NASA-CR-193151] 06 p2614 N94-24363
Highland crust at the Apollo 14 site: A review 06 p2614 N94-24364
Whole rock major element chemistry of KREEP basalt clasts in lunar breccia 15205: Implications for the petrogenesis of volcanic KREEP basalts 06 p2614 N94-24365
Major element chemistry of Apollo 14 mare basalt clasts and highland plutonic clasts from lunar breccia 14321: Comparison with neutron activation results 06 p2614 N94-24366
The western highland province at the Apollo 14 site 06 p2615 N94-24369
Lunar mare volcanism: Mixing of distinct, mantle source regions with KREEP-like component 06 p2615 N94-24370
Heterogeneity in small aliquots of Apollo 15 olivine-normative basalt: Implications for breccia clast studies 06 p2616 N94-24373

LUNAR DUST
Solar wind-induced secondary ions and their relation to lunar surface composition 01 p0474 N94-12232
Lunar Curatorial Facility resource [NASA-TM-109531] 03 p0875 N94-15393
Effects of levitated dust on astronomical observations from the lunar surface 03 p1239 N94-16433
Data analysis and interpretation of lunar dust exosphere 06 p2623 N94-25349
Mitigation of adverse environmental effects on lunar-based astronomical instruments 09 p3598 N94-31426

LUNAR ECHOES
NT LUNAR RADAR ECHOES

LUNAR ECLIPSES
EUVE observations of the Moon 03 p1250 N94-16185

LUNAR EFFECTS
High Earth orbit design for lunar assisted small Explorer class missions 11 p4202 N94-35608

LUNAR ENVIRONMENT
NT LUNAR ATMOSPHERE
Laboratory simulations of lunar darkening processes 02 p0843 N94-14301
Space transfer concepts and analyses for exploration missions [NASA-CR-193876] 04 p1332 N94-18820
Design for producing fiberglass fabric in a lunar environment 07 p2765 N94-25676
Extraterrestrial surface propulsion systems 07 p2833 N94-25691
First lunar outpost 07 p2943 N94-25694
Lunar base habitat designs: Characterizing the environment, and selecting habitat designs for future trade-offs [NASA-CR-195687] 07 p2943 N94-27934
Operational environments for electrical power wiring on NASA space systems [NASA-TM-106655] 12 p4398 N94-36951

LUNAR EVOLUTION
Magnetic fields and nonuniform structures of the Moon 01 p0472 N94-12218
Overturn of magma ocean ilmenite cumulate layer: Implications for lunar magmatic evolution and formation of a lunar core 03 p1261 N94-16242
Tidal regime of intact planetoid capture model for the Earth-Moon system: Does it relate to the archean sedimentary rock record? 03 p1245 N94-16378
The Sm-(146,147)-Nd-(142,143) formation interval for the lunar mantle and implications for lunar evolution 05 p2097 N94-20663
Degradation sequence of young lunar craters from orbital infrared survey 05 p2136 N94-20874
Multispectral studies of selected crater- and basin-filling lunar Maria from Galileo Earth-Moon encounter 1 05 p2136 N94-20876

LUNAR EXCAVATION EQUIPMENT
Future energy source --- Mining Helium-3 on the moon [NASA-TM-109363] 04 p1628 N94-18959

LUNAR EXPLORATION
Lunar campsite concept: Space transfer concepts and analysis for exploration missions [NASA-CR-192602] 01 p0433 N94-10144
The Los Alamos neutron spectrometer for the Lunar Scout-1 mission 01 p0172 N94-12038
Mission to the Moon: An ESA study on future exploration 01 p0460 N94-12153
Remote sensing x ray fluorescence spectrometry for future lunar exploration missions 01 p0462 N94-12165
Exploration planning in the context of human exploration and development of the Moon 01 p0474 N94-12229
Terrestrial case studies of ilmenite exploration and lunar implications 01 p0478 N94-12247
Significance and scenarios of lunar and planetary exploration missions 01 p0482 N94-12324
Unmanned lunar exploration mission 01 p0482 N94-12325
Manned lunar exploration missions 01 p0482 N94-12326
The studies on lunar and planetary exploration and utilization: The study on lunar resources utilization [NASDA-CNT-930014] 02 p0842 N94-13655

Pre-phase a study report of lunar polar orbiter
[NASDA-TK-SS0440] 03 p0873 N94-15000
The 1966 highlights --- NASA research programs
[NASA-TM-109444] 03 p1302 N94-15343
Lunar scout missions: Galileo encounter results and application to scientific problems and exploration requirements 03 p1259 N94-16229
Clementine: Anticipated scientific datasets from the Moon and Geographos 03 p1288 N94-16392
Opportunity for early science return by the Artemis Program 03 p1291 N94-16408
The High Resolution Stereo Camera (HRSC) for the Lunar Scout 1 Mission 05 p1813 N94-20650
Clementine: An inexpensive mission to the Moon and Geographos 05 p1652 N94-20765
Powdered aluminum and oxygen rocket propellants: Subscale combustion experiments
[NASA-TM-106439] 05 p1713 N94-21760
The birth of NASA: The diary of T. Keith Glennan
[NASA-SP-4105] 06 p2630 N94-23333
Lunar science strategy: Exploring the Moon with humans and machines 06 p2605 N94-23376
Robotic exploration of Moon and Mars 06 p2606 N94-23379
The morphology of the lunar surface parts in the region of work of the mobile geological laboratory vehicle in Mare Imbrium 06 p2607 N94-23385
Unmanned lunar rovers: Utilization for exploration 06 p2607 N94-23387
Early lunar rover mission studies 06 p2607 N94-23388
Lunar exploration rover program developments
[DE93-040759] 06 p2613 N94-23469
The Extended Mission Rover (EMR) 07 p2689 N94-25674
Project Columbiad: Reestablishment of human presence on the Moon 07 p2689 N94-25687
Recent developments in the Robotic All Terrain Lunar Exploration Rover (RATLER) program
[DE93-040342] 07 p2821 N94-26110
The Robotic All-Terrain Lunar Exploration Rover (RATLER): Increased mobility through simplicity 07 p2685 N94-26291
Lunar Transportation Facilities and Operations Study, option 1
[NASA-CR-195700] 07 p3109 N94-27982
The Nomad Explorer assembly assist vehicle: An architecture for rapid global extraterrestrial base infrastructure establishment 09 p3599 N94-31429
Apollo 11 highlights
[NASA-TM-109763] 09 p3600 N94-31820
A multitasking behavioral control system for the Robotic All Terrain Lunar Exploration Rover (RATLER)
[DE94-007293] 09 p3835 N94-32787
NASA images 14
[NASA-TM-109823] 10 p4011 N94-33577
Lunar exploration rover program developments 10 p4066 N94-34023
Vehicle development of Lunar/Mars exploration 10 p4067 N94-34030
JPRS report. Central Eurasia: Aviation and cosmonautics, no. 2, February 1993
[JPRS-UAC-94-001] 10 p4011 N94-35117
Apollo 11 at twenty-five, version 1.0
[NASA-CR-193380] 11 p4376 N94-35363
Remote geochemical experiment package for Discovery class missions 11 p4350 N94-35420

LUNAR FAR SIDE
The history of mare volcanism in the Orientale Basin: Mare deposit ages, compositions and morphologies 03 p1269 N94-16289

LUNAR GEOLOGY
Twenty-fourth Lunar and Planetary Science Conference. Part 1: A-F
[NASA-CR-193095] 01 p0435 N94-12015
Measurements of cosmogenic nuclides in lunar rock 64455 01 p0437 N94-12033
Apollo 16 core 60013/14 as a product of path 1 and path 2 regolith evolution processes 01 p0440 N94-12050
Spectral and multispectral imaging studies of lunar mantled mare deposits 01 p0446 N94-12079
Multiple nitrogen components in lunar soil sample 12023 01 p0451 N94-12108
Viscous relaxation of the Moho under large lunar basins 01 p0452 N94-12113
Mission to the Moon: An ESA study on future exploration 01 p0460 N94-12153
Differential scaling: Implications for central structures in large lunar craters 01 p0461 N94-12158
Macroscopic electric charge separation during hypervelocity impacts: Potential implications for planetary paleomagnetism 01 p0431 N94-12181
The granulite suite: Impact melts and metamorphic breccias of the early lunar crust 01 p0282 N94-12197
Magnetic fields and nonuniform structures of the Moon 01 p0472 N94-12218
Solar wind-induced secondary ions and their relation to lunar surface composition 01 p0474 N94-12232
Assimilation in lunar basalts and volcanic glasses: Implications for a heterogenous mantle source region 01 p0478 N94-12250
Laboratory simulations of lunar darkening processes 02 p0843 N94-14301
Deposition of impact-generated vapors in the lunar regolith 02 p0843 N94-14302
The state of Fe in the lunar regolith and its relationship to the spectral reflectance properties of the moon 02 p0843 N94-14303
The SCR Ne-21 and Ar-38 in lunar rock 68815: The solar proton energy spectrum over the past 2 MYR 03 p1248 N94-16177
First oxygen from lunar basalt 03 p1249 N94-16182
Importance of expansion and contraction in the formation of tectonic features on the Moon 03 p1250 N94-16189
Remote sensing studies of the northeastern portion of the lunar nearside 03 p1258 N94-16225
Mode of emplacement of lunar mare volcanic deposits: Graben formation due to near surface deformation accompanying dike emplacement at Rima Parry 5 03 p1258 N94-16227
Lunar impact basins: New data for the nearside northern high latitudes and eastern limb from the second Galileo flyby 03 p1258 N94-16228
Modes of formation of lunar light plains and the detection of cryptomaria deposits 03 p1259 N94-16231
Galileo photometry of Apollo landing sites 03 p1259 N94-16234
An iridium-rich iron micrometeorite with silicate inclusions from the Moon 03 p1242 N94-16281
Nitrogen isotopic signatures in agglutinates from breccia 79035 03 p0954 N94-16314
Age determinations and Earth-based multispectral observations of lunar light plains 03 p1275 N94-16323
Composition of Apollo 17 core 76001 03 p1275 N94-16326
Composition and maturity of the 60013/14 core 03 p1275 N94-16327
Lunar phase function effects on spectral ratios used for resource assessment 03 p1278 N94-16342
Twenty-Fourth Lunar and Planetary Science Conference. Part 3: N-Z
[NASA-CR-193149] 05 p2092 N94-20636
Petrogenesis of Apollo 12 mare basalts. Part 1: Multiple melts and fractional crystallization to explain olivine and ilmenite basalt compositions 05 p1684 N94-20644
Petrogenesis of Apollo 12 mare basalts. Part 2: An open system model to explain the pigeonite basalt compositions 05 p1684 N94-20645
Core formation in the Moon: The mystery of the excess depletion of Mo, W and P 05 p2095 N94-20651
Fragments of ancient lunar crust: Ferroan noritic anorthosites from the descartes region of the Moon 05 p2096 N94-20660
Volatility in the lunar crust: Trace element analyses of lunar minerals by PIXE proton microprobe 05 p2097 N94-20661
Impact glasses from the ultrafine fraction of lunar soils 05 p2097 N94-20662
The Sm-(146,147)-Nd-(142,143) formation interval for the lunar mantle and implications for lunar evolution 05 p2097 N94-20663
Spectral reflectance studies of the Humorum Basin region 05 p2101 N94-20682
U-Pb isotopic ages and characteristics of ancient (greater than 4.0 Ga) lunar highland rocks 05 p2104 N94-20700
U-Pb isotopic systematics of ferroan anorthosite 60025 05 p1685 N94-20702
C-O volatiles in Apollo 15 and Apollo 17 picritic glasses 05 p1685 N94-20727
Basaltic magmatism on the Moon. A perspective from volcanic picritic glasses 05 p2114 N94-20758
Origin of the Apollo 15 very low Ti green glass. A perspective from the compositional diversity in the very low Ti glasses 05 p1685 N94-20759
Combined backscatter Moessbauer spectrometer/x ray fluorescence analyzer (BaMS/XRF) for extraterrestrial surfaces 05 p1686 N94-20761
Geochronology and petrogenesis of the western highlands alkali suite: Radiogenic isotopic evidence from Apollo 14 05 p2118 N94-20778
Magnesian anorthosites from the western highlands of the Moon: Isotope geochemistry and petrogenesis 05 p2118 N94-20779
Geology and deposits of the Serenitatis basin 05 p2119 N94-20786
Mineralogy and cooling history of magnesian lunar granulite 67415 05 p2124 N94-20811
Sparking young minds with Moon rocks and meteorites 05 p2039 N94-20819
Evaluation of lunar rocks and soils for resource utilization: Detailed image analysis of raw materials and beneficiated products 05 p2126 N94-20820
The Mg-suite and the highland crust: An unsolved enigma 05 p2126 N94-20822
Distribution and geologic history of materials excavated by the lunar crater Bullialdus 05 p2128 N94-20832
Limits on differentiation of melt sheets from basin-scale lunar impacts 05 p2133 N94-20856
Lunar science strategy: Exploring the Moon with humans and machines 06 p2605 N94-23376
The morphology of the lunar surface parts in the region of work of the mobile geological laboratory vehicle in Mare Imbrium 06 p2607 N94-23385
Catalog of Apollo 17 rocks. Volume 1: Stations 2 and 3 (South Massif)
[NASA-CR-194854] 06 p2613 N94-24058
Highland crust at the Apollo 14 site: A review 06 p2614 N94-24364
Major element chemistry of Apollo 14 mare basalt clasts and highland plutonic clasts from lunar breccia 14321: Comparison with neutron activation results 06 p2614 N94-24366
Auto-metasomatism of the western lunar highlands: Result of closed system fractionation and mobilization of a KREEPy trapped liquid 06 p2615 N94-24367
Polytopic vector analysis in igneous petrology: Application to lunar petrogenesis 06 p2615 N94-24368
The western highland province at the Apollo 14 site 06 p2615 N94-24369
The Lunar Scout Program: An international program to survey the Moon from orbit for geochemistry, mineralogy, imagery, geodesy, and gravity
[NASA-TM-104791] 09 p3943 N94-32923
The Twenty-Fifth Lunar and Planetary Science Conference. Part 1: A-G
[NASA-CR-195743] 11 p4355 N94-35395
High spatial resolution telescopic multispectral imaging and spectroscopy of the Moon. 1: The Serenitatis/Tranquillitatis border region 11 p4356 N94-35402
Lunar mineral feedstocks from rocks and soils: X-ray digital imaging in resource evaluation 11 p4358 N94-35415
The Twenty-Fifth Lunar and Planetary Science Conference. Part 3: P-Z
[NASA-CR-195745] 11 p4362 N94-35448
FeO and MgO in plagioclase of lunar anorthosites: Igneous or metamorphic? 11 p4351 N94-35449
The Twenty-Fifth Lunar and Planetary Science Conference. Part 2: H-O
[NASA-CR-195744] 11 p4367 N94-36136
New data supporting a Sm-146,147-Nd-142,143 formation interval for the lunar mantle 11 p4374 N94-36173

LUNAR GRAVITATION
Lunar Scout Two spacecraft gravity experiment 01 p0459 N94-12152
Magnetic fields and nonuniform structures of the Moon 01 p0472 N94-12218
Compositional diversity of the lunar North Pole: Preliminary analyses of Galileo SSI data 05 p2101 N94-20686
First lunar outpost 07 p2943 N94-25694
Lifetimes of lunar satellite orbits
[NASA-TP-3394] 07 p2690 N94-27771
Lunar LIGO and gravitational wave astronomy on the Moon 11 p4366 N94-35472
Preliminary solutions for the lunar gravity field from analysis of lunar orbiter tracking data 11 p4371 N94-36156

LUNAR IONOSPHERE
U LUNAR ATMOSPHERE

LUNAR LABORATORIES
The first lunar outpost: The design reference mission and a new era in lunar science 03 p0874 N94-16362
Study of the National Science Foundation's South Pole Station as an analogous data base for the logistical support of a Moon laboratory
[NASA-TM-108429] 03 p1174 N94-17469

LUNAR LANDING
Where no flag has gone before: Political and technical aspects of placing a flag on the Moon
[NASA-CR-188251] 02 p0827 N94-12800
Galileo photometry of Apollo landing sites 03 p1259 N94-16234
Lunar lander and return propulsion system trade study
[NASA-TP-3388] 03 p0925 N94-16496

Comparisons of selected laser beam power missions to conventionally powered missions
[NASA-TM-106110] 03 p1040 N94-16522
Apollo 11: 20th anniversary
[NASA-TM-109364] 04 p1323 N94-18979
Lunar Transportation Facilities and Operations Study, option 1
[NASA-CR-195700] 07 p3109 N94-27982
Lunar Transportation Facilities and Operations Study, option 2
[NASA-CR-195701] 07 p3109 N94-27983
Apollo 11 highlights
[NASA-TM-109763] 09 p3600 N94-31820
Load-limiting landing gear footpad energy absorption system 09 p3607 N94-33323
Apollo: A retrospective analysis
[NASA-TM-109853] 10 p4187 N94-34638

LUNAR LANDING MODULES
NT APOLLO LUNAR EXPERIMENT MODULE
Unmanned lunar exploration mission 01 p0482 N94-12325
Pre-phase a study report of lunar polar orbiter
[NASDA-TK-SS0440] 03 p0873 N94-15000
Lunar transportation system
[NASA-CR-195540] 06 p2365 N94-24805
Extended duration lunar lander
[NASA-CR-195527] 06 p2206 N94-24916
Low-cost unmanned lunar lander 07 p2697 N94-25699

LUNAR LANDING SITES
Auto-metasomatism of the western lunar highlands: Result of closed system fractionation and mobilization of a KREEPy trapped liquid 06 p2615 N94-24367
Block distributions on the lunar surface: A comparison between measurements obtained from surface and orbital photography 11 p4359 N94-35419

LUNAR LAUNCH
Lunar lander and return propulsion system trade study
[NASA-TP-3388] 03 p0925 N94-16496
Neighboring extremal guidance for systems with piecewise linear control using time as the reference variable
[AD-A267942] 03 p0874 N94-17010
Lunar Transportation Facilities and Operations Study, option 1
[NASA-CR-195700] 07 p3109 N94-27982
Lunar Transportation Facilities and Operations Study, option 2
[NASA-CR-195701] 07 p3109 N94-27983

LUNAR LIMB
Total solar eclipse of 3 November 1994
[NASA-RP-1318] 03 p1236 N94-15481

LUNAR LOGISTICS
Lunar campsite concept: Space transfer concepts and analysis for exploration missions
[NASA-CR-192602] 01 p0433 N94-10144
Design of a logistics model for building and supporting a lunar station
[ILR-MITT-282(1993)] 09 p3803 N94-31852

LUNAR LUMINESCENCE
Lunar horizon glow and the Clementine mission 11 p4366 N94-35478

LUNAR MAGNETIC FIELDS
Macroscopic electric charge separation during hypervelocity impacts: Potential implications for planetary paleomagnetism 01 p0431 N94-12181
Magnetic fields and nonuniform structures of the Moon 01 p0472 N94-12218

LUNAR MANTLE
Assimilation in lunar basalts and volcanic glasses: Implications for a heterogenous mantle source region 01 p0478 N94-12250
Mode of emplacement of lunar mare volcanic deposits: Graben formation due to near surface deformation accompanying dike emplacement at Rima Parry 5 03 p1258 N94-16227
The ilmenite liquidus and depths of segregation for high-Ti picrite glasses 03 p0975 N94-16241
Overturn of magma ocean ilmenite cumulate layer: Implications for lunar magmatic evolution and formation of a lunar core 03 p1261 N94-16242
The Sm-(146,147)-Nd-(142,143) formation interval for the lunar mantle and implications for lunar evolution 05 p2097 N94-20663
C-O volatiles in Apollo 15 and Apollo 17 picritic glasses 05 p1685 N94-20727
Lunar mare volcanism: Mixing of distinct, mantle source regions with KREEP-like component 06 p2615 N94-24370
New data supporting a Sm-146,147-Nd-142,143 formation interval for the lunar mantle 11 p4374 N94-36173

LUNAR MAPS
Galileo imaging results from the second Earth-Moon flyby: Lunar Maria and related units 03 p1252 N94-16199
Lunar impact basins: New data for the nearside northern high latitudes and eastern limb from the second Galileo flyby 03 p1258 N94-16228
Thermogeologic mapping of the Moon from lunar orbit 03 p1290 N94-16405
MinMap: An imaging spectrometer for high resolution compositional mapping of the Moon 05 p1813 N94-20688

LUNAR MARIA
Spectral and multispectral imaging studies of lunar mantled mare deposits 01 p0446 N94-12079
Graphite solubility and co-vesiculation in basalt-like melts at one-ATM 01 p0463 N94-12173
Using lunar sounder imagery to distinguish surface from subsurface reflectors in lunar highlands areas 01 p0464 N94-12179
Galileo imaging results from the second Earth-Moon flyby: Lunar Maria and related units 03 p1252 N94-16199
Confirmation of saturation equilibrium conditions in crater populations 03 p1103 N94-16222
Remote sensing studies of the northeastern portion of the lunar nearside 03 p1258 N94-16225
Mode of emplacement of lunar mare volcanic deposits: Graben formation due to near surface deformation accompanying dike emplacement at Rima Parry 5 03 p1258 N94-16227
Lunar impact basins: New data for the nearside northern high latitudes and eastern limb from the second Galileo flyby 03 p1258 N94-16228
Modes of formation of lunar light plains and the detection of cryptomaria deposits 03 p1259 N94-16231
Overturn of magma ocean ilmenite cumulate layer: Implications for lunar magmatic evolution and formation of a lunar core 03 p1261 N94-16242
Earth-based and Galileo SSI multispectral observations of eastern mare serenitatis and the Apollo 17 landing site 03 p1261 N94-16244
Petrologic models of 15388, a unique Apollo 15 mare basalt 03 p1264 N94-16258
Apollo 17 materials viewed from 2 to 4 mm soil particles: Pre-serenitatis highlands components 03 p1267 N94-16280
The history of mare volcanism in the Orientale Basin: Mare deposit ages, compositions and morphologies 03 p1269 N94-16289
Thermogeologic mapping of the Moon from lunar orbit 03 p1290 N94-16405
Petrogenesis of Apollo 12 mare basalts. Part 1: Multiple melts and fractional crystallization to explain olivine and ilmenite basalt compositions 05 p1684 N94-20644
Petrogenesis of Apollo 12 mare basalts. Part 2: An open system model to explain the pigeonite basalt compositions 05 p1684 N94-20645
Spectral reflectance studies of the Humorum Basin region 05 p2101 N94-20682
Compositional diversity of the lunar North Pole: Preliminary analyses of Galileo SSI data 05 p2101 N94-20686
C-O volatiles in Apollo 15 and Apollo 17 picritic glasses 05 p1685 N94-20727
Lunar basalt meteorite EET 87521: Petrology of the clast population 05 p2083 N94-20752
Basaltic magmatism on the Moon. A perspective from volcanic picritic glasses 05 p2114 N94-20758
Chronology of lunar granite 12033,576: Resetting of Rb-Sr and K-Ca isochrons 05 p2115 N94-20763
Chronology and genesis of high-Ti mare volcanism: Melting of cogenetic depleted and enriched reservoirs 05 p2118 N94-20777
Geology and deposits of the Serenitatis basin 05 p2119 N94-20786
Ti-bearing oxide minerals in lunar meteorite Y793169 with the VLT affinity 05 p2084 N94-20812
The U-Th-Pb, Sm-Nd, and Ar-Ar isotopic systematics of lunar meteorite Yamato-793169 05 p2084 N94-20834
Consortium study of lunar meteorites Yamato-793169 and Asuka-881757: Geochemical evidence of mutual similarity, and dissimilarity versus other mare basalts 05 p2085 N94-20857
Multispectral studies of selected crater- and basin-filling lunar Maria from Galileo Earth-Moon encounter 1 05 p2136 N94-20876
Consortium reports on lunar meteorites Yamato 793169 and Asuka 881757, a new type of mare basalt 05 p2086 N94-20893
Basaltic Volcanism and Ancient Planetary Crusts
[NASA-CR-193151] 06 p2614 N94-24363
Major element chemistry of Apollo 14 mare basalt clasts and highland plutonic clasts from lunar breccia 14321: Comparison with neutron activation results 06 p2614 N94-24366
Auto-metasomatism of the western lunar highlands: Result of closed system fractionation and mobilization of a KREEPy trapped liquid 06 p2615 N94-24367
Lunar mare volcanism: Mixing of distinct, mantle source regions with KREEP-like component 06 p2615 N94-24370
Reduction of lunar mare soil and pyroclastic glass 11 p4355 N94-35398
High spatial resolution telescopic multispectral imaging and spectroscopy of the Moon. 1: The Serenitatis/Tranquillitatis border region 11 p4356 N94-35402

LUNAR MINING
Terrestrial case studies of ilmenite exploration and lunar implications 01 p0478 N94-12247
Future energy source --- Mining Helium-3 on the moon
[NASA-TM-109363] 04 p1628 N94-18959
Design of a lunar propellant processing facility. NASA/USRA advanced program
[NASA-CR-195502] 06 p2266 N94-24618
Lunar surface operations. Volume 4: Lunar rover trailer
[NASA-CR-195554] 08 p3299 N94-29386

LUNAR MOBILE LABORATORIES
Pressurized Lunar Rover (PLR) 07 p2833 N94-25704

LUNAR MODULE
NT APOLLO LUNAR EXPERIMENT MODULE

LUNAR OBSERVATORIES
Interferometric astronomy on the Moon 06 p2601 N94-23378
LOLA: Lunar Optical Long-baseline Array. 1992-1993 space design
[NASA-CR-195533] 06 p2298 N94-24582
LOITA: Lunar Optical/Infrared Telescope Array
[NASA-CR-195532] 06 p2546 N94-24816

LUNAR OCCULTATION
NT SOLAR ECLIPSES

LUNAR ORBITER
The 1966 highlights --- NASA research programs
[NASA-TM-109444] 03 p1302 N94-15343
Preliminary solutions for the lunar gravity field from analysis of lunar orbiter tracking data 11 p4371 N94-36156

LUNAR ORBITS
A guidance and navigation system for two spacecraft rendezvous in translunar halo orbit
[AD-A267498] 03 p0898 N94-17368
Degradation sequence of young lunar craters from orbital infrared survey 05 p2136 N94-20874
The modal solution to the Moon's orbit using canonical Floquet perturbation theory
[AD-A273732] 07 p2690 N94-26001
Nasa Langley Research Center seventy-fifth anniversary publications, 1992
[NASA-TM-109691] 07 p3118 N94-27431
Lifetimes of lunar satellite orbits
[NASA-TP-3394] 07 p2690 N94-27771

LUNAR PERTURBATION
U LUNAR EFFECTS

LUNAR PHASES
Lunar phase function effects on spectral ratios used for resource assessment 03 p1278 N94-16342

LUNAR PHOTOGRAPHS
Lunar multispectral mosaics from Galileo's second Earth-Moon flyby 03 p1288 N94-16394
Compositional diversity of the lunar North Pole: Preliminary analyses of Galileo SSI data 05 p2101 N94-20686

LUNAR PHOTOGRAPHY
Lunar phase function effects on spectral ratios used for resource assessment 03 p1278 N94-16342
Preliminary results from Mariner 10: High resolution images of the Moon 05 p2107 N94-20719
Block distributions on the lunar surface: A comparison between measurements obtained from surface and orbital photography 11 p4359 N94-35419

LUNAR PROBES
Conceptual studies report on lunar and planetary exploration
[NASDA-TK-SS0438] 01 p0481 N94-12323
Unmanned lunar exploration mission 01 p0482 N94-12325
Pre-phase a study report of lunar polar orbiter
[NASDA-TK-SS0440] 03 p0873 N94-15000
The Clementine instrument complement 03 p1086 N94-16370

LUNAR PROGRAMS
NT APOLLO PROJECT
NT SURVEYOR PROJECT
The first lunar outpost: The design reference mission and a new era in lunar science 03 p0874 N94-16362
Opportunity for early science return by the Artemis Program 03 p1291 N94-16408
MinMap: An imaging spectrometer for high resolution compositional mapping of the Moon 05 p1813 N94-20688

Artemis common lunar lander. Phase 2: Study results for external review
[NASA-TM-109699] 07 p2692 N94-28205
The Lunar Scout Program: An international program to survey the Moon from orbit for geochemistry, mineralogy, imagery, geodesy, and gravity
[NASA-TM-104791] 09 p3943 N94-32923
JPRS report. Central Eurasia: Aviation and cosmonautics, no. 2, February 1993
[JPRS-UAC-94-001] 10 p4011 N94-35117

LUNAR RADAR ECHOES
Interpretation of lunar and planetary electromagnetic scattering using the full wave solutions
01 p0440 N94-12049

LUNAR RADIATION
CERN-derived analysis of lunar radiation backgrounds
05 p2080 N94-20880

LUNAR RANGEFINDING
Lunar ranging
[NASA-TM-109603] 03 p1236 N94-15311
Eighth International Workshop on Laser Ranging Instrumentation
[NASA-CP-3214] 03 p0911 N94-15552
Poisson filtering of laser ranging data
03 p0917 N94-15593
Lunar laser ranging data processing in a Unix/X windows environment 03 p0918 N94-15599
LLR: Activities in Wettzell 03 p0876 N94-15600
Performance of the upgraded Orroral laser ranging system 03 p0877 N94-15602
WLRS — Wettzell Laser Ranging System (WLRS)
03 p0877 N94-15606

LUNAR RESOURCES
Terrestrial case studies of ilmenite exploration and lunar implications 01 p0478 N94-12247
The studies on lunar and planetary exploration and utilization: The study on lunar resources utilization
[NASDA-CNT-930014] 02 p0842 N94-13655
Helium-3 inventory of lunar samples: A potential future energy resource for mankind? 03 p1295 N94-16428
Search for lunar water ice in cometary impact craters
[AD-A270130] 04 p1627 N94-18877
Future energy source — Mining Helium-3 on the moon
[NASA-TM-109363] 04 p1628 N94-18959
Production of O2 on the Moon: A lab-top demonstration of ilmenite reduction with hydrogen
05 p2126 N94-20821
Powdered aluminum and oxygen rocket propellants: Subscale combustion experiments
[NASA-TM-106439] 05 p1713 N94-21760
Design of a lunar propellant processing facility. NASA/USRA advanced program
[NASA-CR-195502] 06 p2266 N94-24618
Lunar mineral feedstocks from rocks and soils: X-ray digital imaging in resource evaluation
11 p4358 N94-35415

LUNAR ROCKS
NT KREEP
Production of electronic grade lunar silicon by disproportionation of silicon difluoride
01 p0435 N94-12017
Cold press sintering of simulated lunar basalt
01 p0131 N94-12026
General overview of an integrated lunar oxygen production/brickmaking system
01 p0131 N94-12027
Thermodynamics of lunar ilmenite reduction
01 p0415 N94-12028
Measurements of cosmogenic nuclides in lunar rock 64455 01 p0437 N94-12033
Vaporization by shock loading of albite, jadeite, and pyrex glass: Experimental study 01 p0097 N94-12039
Apollo 16 core 60013/14 as a product of path 1 and path 2 regolith evolution processes
01 p0440 N94-12050
Natural thermoluminescence profiles in lunar cores and implications for meteorites 01 p0443 N94-12060
Impact comminution of glasses: Implications for lunar regolith evolution 01 p0461 N94-12159
Macroscopic electric charge separation during hypervelocity impacts: Potential implications for planetary paleomagnetism 01 p0431 N94-12181
The granulite suite: Impact melts and metamorphic breccias of the early lunar crust
01 p0282 N94-12197
The Fe/Mn constraint on precursors of basaltic achondrites 01 p0432 N94-12208
Compositional heterogeneity within a dumbbell-shaped Apollo 15 green glass: Evidence for simultaneous eruption of different magmas 01 p0470 N94-12209
Magnetic fields and nonuniform structures of the Moon 01 p0472 N94-12218
The state of Fe in the lunar regolith and its relationship to the spectral reflectance properties of the moon
02 p0843 N94-14303
Lunar Curatorial Facility resource
[NASA-TM-109531] 03 p0875 N94-15393
Building a lunar base
[NASA-TM-109674] 03 p0983 N94-15519
The SCR Ne-21 and Ar-38 in lunar rock 68815: The solar proton energy spectrum over the past 2 MYR
03 p1248 N94-16177
First oxygen from lunar basalt
03 p1249 N94-16182
A test of the applicability of independent scattering to high albedo planetary regoliths
03 p1250 N94-16187
Why is the Moon dark? 03 p1256 N94-16219
Lunar impact basins: New data for the nearside northern high latitudes and eastern limb from the second Galileo flyby 03 p1258 N94-16228
Galileo photometry of Apollo landing sites
03 p1259 N94-16234
A Monazite-bearing clast in Apollo 17 melt breccia
03 p1267 N94-16279
Apollo 17 materials viewed from 2 to 4 mm soil particles: Pre-serenitatis highlands components
03 p1267 N94-16280
An iridium-rich iron micrometeorite with silicate inclusions from the Moon 03 p1242 N94-16281
Liquidus equilibria of lunar analogs at high pressure
03 p1283 N94-16364
Fragments of ancient lunar crust: Ferroan noritic anorthosites from the descartes region of the Moon
05 p2096 N94-20660
Volatility in the lunar crust: Trace element analyses of lunar minerals by PIXE proton microprobe
05 p2097 N94-20661
The Sm-(146,147)-Nd-(142,143) formation interval for the lunar mantle and implications for lunar evolution
05 p2097 N94-20663
Characterization of Minnesota lunar simulant for plant growth 05 p1897 N94-20665
Optical effects of space weathering on lunar soils and the role of the finest fraction 05 p2101 N94-20687
U-Pb isotopic ages and characteristics of ancient (greater than 4.0 Ga) lunar highland rocks
05 p2104 N94-20700
U-Pb isotopic systematics of ferroan anorthosite 60025 05 p1685 N94-20702
Euhedral metallic-Fe-Ni grains in extraterrestrial samples 05 p1697 N94-20724
Basaltic magmatism on the Moon. A perspective from volcanic picritic glasses 05 p2114 N94-20758
Geochronology and petrogenesis of the western highlands alkali suite: Radiogenic isotopic evidence from Apollo 14 05 p2118 N94-20778
Geology and deposits of the Serenitatis basin
05 p2119 N94-20786
Sparking young minds with Moon rocks and meteorites 05 p2039 N94-20819
A long-term change of the AR/KR/XE fractionation in the solar corpuscular radiation 05 p2136 N94-20875
Catalog of Apollo 17 rocks. Volume 1: Stations 2 and 3 (South Massif)
[NASA-CR-194854] 06 p2613 N94-24058
Highland crust at the Apollo 14 site: A review
06 p2614 N94-24364
Polytopic vector analysis in igneous petrology: Application to lunar petrogenesis
06 p2615 N94-24368
The western highland province at the Apollo 14 site
06 p2615 N94-24369
Heterogeneity in small aliquots of Apollo 15 olivine-normative basalt: Implications for breccia clast studies 06 p2616 N94-24373
A widely adaptable habitat construction system utilizing space resources 07 p2688 N94-27374
Lunar mineral feedstocks from rocks and soils: X-ray digital imaging in resource evaluation
11 p4358 N94-35415
Grain rims on ilmenite in the lunar regolith: Comparison to vapor deposits on regolith silicates
11 p4359 N94-35418
Solar proton produced neon in shergottite meteorites
11 p4351 N94-35428
FeO and MgO in plagioclase of lunar anorthosites: Igneous or metamorphic? 11 p4351 N94-35449
Luna 24 regolith breccias: A possible source of the fine size material of the Luna 24 regolith
11 p4362 N94-35450
Petrographic characterization of lunar soils: Application of x ray digital-imaging to quantitative and automated analysis 11 p4368 N94-36138

LUNAR ROVING VEHICLES
NT LUNOKHOD LUNAR ROVING VEHICLES
NT MANNED LUNAR SURFACE VEHICLES
Unmanned lunar exploration mission
01 p0482 N94-12325
Asynchronous transfer mode link performance over ground networks 02 p0610 N94-14385
Space transfer concepts and analyses for exploration missions, phase 4
[NASA-CR-193849] 03 p0882 N94-15831
Rover mounted ground penetrating radar as a tool for investigating the near-surface of Mars and beyong
03 p1007 N94-16197
The first lunar outpost: The design reference mission and a new era in lunar science
03 p0874 N94-16362
Power transmission by laser beam from lunar-synchronous satellite
[NASA-TM-4496] 05 p1669 N94-20102
Method for remotely powering a device such as a lunar rover
[NASA-CASE-LAR-14789-1] 05 p1824 N94-20587
Catalog of Apollo experiment operations
[NASA-RP-1317] 06 p2194 N94-23292
Missions, Technologies, and Design of Planetary Mobile Vehicles
[ISBN-2-85428-331-7] 06 p2605 N94-23373
Past US studies and developments for planetary rovers 06 p2369 N94-23375
Lunar science strategy: Exploring the Moon with humans and machines 06 p2605 N94-23376
Rover requirements for the planet surface segment of the space exploration initiative 06 p2369 N94-23377
Lunar rover navigation concepts
06 p2607 N94-23386
Unmanned lunar rovers: Utilization for exploration
06 p2607 N94-23387
Early lunar rover mission studies
06 p2607 N94-23388
The study of the mobile lunar explorer
06 p2607 N94-23389
Lunar exploration rover program developments
[DE93-040759] 06 p2613 N94-23469
Some useful innovations with TRASYS and SINDA-85
06 p2322 N94-23647
The Enabler: A concept for a lunar work vehicle
07 p2833 N94-25675
Planetary surface exploration MESUR/autonomous lunar rover 07 p2833 N94-25683
Recent developments in the Robotic All Terrain Lunar Exploration Rover (RATLER) program
[DE93-040342] 07 p2821 N94-26110
Early lunar rover mission studies
07 p2684 N94-26290
The Robotic All-Terrain Lunar Exploration Rover (RATLER): Increased mobility through simplicity
07 p2685 N94-26291
A multitasking behavioral control system for the Robotic All-Terrain Lunar Exploration Rover (RATLER)
07 p2685 N94-26292
Artemis common lunar lander. Phase 2: Study results for external review
[NASA-TM-109699] 07 p2692 N94-28205
Lunar surface operations. Volume 4: Lunar rover trailer
[NASA-CR-195554] 08 p3299 N94-29386
Lunar exploration rover program developments
10 p4066 N94-34023

LUNAR SATELLITES
NT IMP
NT LUNAR ORBITER
Conceptual studies report on lunar and planetary exploration
[NASDA-TK-SS0438] 01 p0481 N94-12323
Unmanned lunar exploration mission
01 p0482 N94-12325
Pre-phase a study report of lunar polar orbiter
[NASDA-TK-SS0440] 03 p0873 N94-15000
Copernicus: Lunar surface mapper
07 p3081 N94-25702
The Lunar Scout Program: An international program to survey the Moon from orbit for geochemistry, mineralogy, imagery, geodesy, and gravity
[NASA-TM-104791] 09 p3943 N94-32923

LUNAR SCATTERING
U DIFFUSE RADIATION
U LUNAR RADAR ECHOES

LUNAR SEISMOGRAPHS
Meteoroid environment near the Earth-Moon system
[NASA-CR-193670] 02 p0835 N94-13203

LUNAR SHADOW
Angular resolution studies of the CYGNUS array using the shadows of the Sun and Moon
[DE93-012723] 02 p0846 N94-12946
Total solar eclipse of 3 November 1994
[NASA-RP-1318] 03 p1236 N94-15481

LUNAR SHELTERS
Lunar campsite concept: Space transfer concepts and analysis for exploration missions
[NASA-CR-192602] 01 p0433 N94-10144
Lunar surface operations. Volume 1: Lunar surface emergency shelter
[NASA-CR-195551] 08 p3299 N94-29354

LUNAR SOIL
NT LUNAR DUST
Production of electronic grade lunar silicon by disproportionation of silicon difluoride
01 p0435 N94-12017
Effects of microscopic iron metal on the reflectance spectra of glass and minerals 01 p0436 N94-12024
Thermodynamics of lunar ilmenite reduction
01 p0415 N94-12028
Measurements of cosmogenic nuclides in lunar rock 64455 01 p0437 N94-12033
Vaporization by shock loading of albite, jadeite, and pyrex glass: Experimental study 01 p0097 N94-12039
Apollo 16 core 60013/14 as a product of path 1 and path 2 regolith evolution processes
01 p0440 N94-12050
Multiple nitrogen components in lunar soil sample 12023 01 p0451 N94-12108
A reexamination of amino acids in lunar soil
01 p0452 N94-12109
Impact comminution of glasses: Implications for lunar regolith evolution 01 p0461 N94-12159
Macroscopic electric charge separation during hypervelocity impacts: Potential implications for planetary paleomagnetism 01 p0431 N94-12181
Solar wind-induced secondary ions and their relation to lunar surface composition 01 p0474 N94-12232
Measuring and distinguishing compositional and maturity properties of lunar soils by remote VIS-NIR spectroscopy 01 p0478 N94-12251
Deposition of impact-generated vapors in the lunar regolith 02 p0843 N94-14302
The state of Fe in the lunar regolith and its relationship to the spectral reflectance properties of the moon
02 p0843 N94-14303
Lunar Curatorial Facility resource [NASA-TM-109531] 03 p0875 N94-15393
Building a lunar base [NASA-TM-109674] 03 p0983 N94-15519
First oxygen from lunar basalt
03 p1249 N94-16182
Galileo imaging results from the second Earth-Moon flyby: Lunar Maria and related units
03 p1252 N94-16199
Lunar impact basins: New data for the nearside northern high latitudes and eastern limb from the second Galileo flyby 03 p1258 N94-16228
Galileo photometry of Apollo landing sites
03 p1259 N94-16234
Apollo 17 materials viewed from 2 to 4 mm soil particles: Pre-serenitatis highlands components
03 p1267 N94-16280
An iridium-rich iron micrometeorite with silicate inclusions from the Moon 03 p1242 N94-16281
Composition of Apollo 17 core 76001
03 p1275 N94-16326
Composition and maturity of the 60013/14 core
03 p1275 N94-16327
Lunar phase function effects on spectral ratios used for resource assessment 03 p1278 N94-16342
Mixing model analysis of telescopic lunar spectra
03 p1284 N94-16371
Galileo SSI lunar observations: Copernican craters and soils 03 p1288 N94-16395
Grain surface features of Apollo 17 orange and black glass 03 p1289 N94-16397
JSC-1: A new lunar regolith simulant
03 p1289 N94-16398
Fragments of ancient lunar crust: Ferroan noritic anorthosites from the descartes region of the Moon
05 p2096 N94-20660
Impact glasses from the ultrafine fraction of lunar soils
05 p2097 N94-20662
The Sm-(146,147)-Nd-(142,143) formation interval for the lunar mantle and implications for lunar evolution
05 p2097 N94-20663
Characterization of Minnesota lunar simulant for plant growth 05 p1897 N94-20665
Compositional diversity of the lunar North Pole: Preliminary analyses of Galileo SSI data
05 p2101 N94-20686
Optical effects of space weathering on lunar soils and the role of the finest fraction 05 p2101 N94-20687
Implantation of nitrogen: Effects of hydrogen and implantation energy 05 p1686 N94-20804
Petrology and geochemistry of VLT glasses from double drive tube 79001/2 05 p1687 N94-20870
Degradation sequence of young lunar craters from orbital infrared survey 05 p2136 N94-20874
Highland crust at the Apollo 14 site: A review
06 p2614 N94-24364
Whole rock major element chemistry of KREEP basalt clasts in lunar breccia 15205: Implications for the petrogenesis of volcanic KREEP basalts
06 p2614 N94-24365
Major element chemistry of Apollo 14 mare basalt clasts and highland plutonic clasts from lunar breccia 14321: Comparison with neutron activation results
06 p2614 N94-24366
Polytopic vector analysis in igneous petrology: Application to lunar petrogenesis
06 p2615 N94-24368
Measuring track densities in lunar grains by image analysis 06 p2623 N94-25355
A widely adaptable habitat construction system utilizing space resources 07 p2688 N94-27374
Experimental study of lunar and SNC (Mars) magmas [NASA-CR-195274] 07 p3107 N94-27850
Computer image analysis of etched tracks from ionizing radiation [NASA-CR-196025] 11 p4319 N94-35264
New prospects for analyzing lunar pyroclastic glass
11 p4355 N94-35397
Reduction of lunar mare soil and pyroclastic glass
11 p4355 N94-35398
Single agglutinates: A comparative study of compositions of agglutinitic glass, whole-grain, bulk soil, and FMR 11 p4355 N94-35401
Measuring track densities in lunar grains using image analysis 11 p4357 N94-35409
Lunar mineral feedstocks from rocks and soils: X-ray digital imaging in resource evaluation
11 p4358 N94-35415
Preliminary description of double drive tube 68002/68001 11 p4363 N94-35457
Petrographic characterization of lunar soils: Application of x ray digital-imaging to quantitative and automated analysis 11 p4368 N94-36138
The nature of agglutinitic glass in the fine-size fraction of lunar soil 10084 11 p4369 N94-36148

LUNAR SPACECRAFT
NT APOLLO LUNAR EXPERIMENT MODULE
NT IMP
NT LUNAR LANDING MODULES
NT LUNAR ORBITER
NT LUNAR PROBES
NT LUNAR SATELLITES
Lunar campsite concept: Space transfer concepts and analysis for exploration missions [NASA-CR-192602] 01 p0433 N94-10144
The Los Alamos neutron spectrometer for the Lunar Scout-1 mission 01 p0172 N94-12038
Lunar Scout Two spacecraft gravity experiment
01 p0459 N94-12152
Space transfer concepts and analyses for exploration missions, phase 4 [NASA-CR-193849] 03 p0882 N94-15831
Lunar scout missions: Galileo encounter results and application to scientific problems and exploration requirements 03 p1259 N94-16229
Lunar lander and return propulsion system trade study [NASA-TP-3388] 03 p0925 N94-16496
Neighboring extremal guidance for systems with piecewise linear control using time as the reference variable [AD-A267942] 03 p0874 N94-17010
The High Resolution Stereo Camera (HRSC) for the Lunar Scout 1 Mission 05 p1813 N94-20650
Minimum accommodation for aerobrake assembly, phase 2 [NASA-TM-107608] 07 p2692 N94-27774
Artemis common lunar lander. Phase 2: Study results for external review [NASA-TM-109699] 07 p2692 N94-28205
Load-limiting landing gear footpad energy absorption system 09 p3607 N94-33323

LUNAR SURFACE
Spectral and multispectral imaging studies of lunar mantled mare deposits 01 p0446 N94-12079
Preliminary report of lunar observations by the Near-Infrared Mapping Spectrometer (NIMS) during the second Galileo Earth-Moon encounter
01 p0425 N94-12140
Using lunar sounder imagery to distinguish surface from subsurface reflectors in lunar highlands areas
01 p0464 N94-12179
Macroscopic electric charge separation during hypervelocity impacts: Potential implications for planetary paleomagnetism 01 p0431 N94-12181
Solar wind-induced secondary ions and their relation to lunar surface composition 01 p0474 N94-12232
Measuring and distinguishing compositional and maturity properties of lunar soils by remote VIS-NIR spectroscopy 01 p0478 N94-12251
The studies on lunar and planetary exploration and utilization: The study on lunar resources utilization [NASDA-CNT-930014] 02 p0842 N94-13655
Laboratory simulations of lunar darkening processes
02 p0843 N94-14301
The SCR Ne-21 and Ar-38 in lunar rock 68815: The solar proton energy spectrum over the past 2 MYR
03 p1248 N94-16177
Importance of expansion and contraction in the formation of tectonic features on the Moon
03 p1250 N94-16189
Confirmation of saturation equilibrium conditions in crater populations 03 p1103 N94-16222
Galileo photometry of Apollo landing sites
03 p1259 N94-16234
Earth-based and Galileo SSI multispectral observations of eastern mare serenitatis and the Apollo 17 landing site 03 p1261 N94-16244
Mixing model analysis of telescopic lunar spectra
03 p1284 N94-16371
Lunar multispectral mosaics from Galileo's second Earth-Moon flyby 03 p1288 N94-16394
Galileo SSI lunar observations: Copernican craters and soils 03 p1288 N94-16395
Remote visual detection of impacts on the lunar surface 03 p1290 N94-16404
Thermogeologic mapping of the Moon from lunar orbit
03 p1290 N94-16405
Opportunity for early science return by the Artemis Program 03 p1291 N94-16408
Gamma ray spectrometer for Lunar Scout 2
03 p1037 N94-16426
Effects of levitated dust on astronomical observations from the lunar surface 03 p1239 N94-16433
Search for lunar water ice in cometary impact craters [AD-A270130] 04 p1627 N94-18877
Impact glasses from the ultrafine fraction of lunar soils
05 p2097 N94-20662
Optical effects of space weathering on lunar soils and the role of the finest fraction 05 p2101 N94-20687
Preliminary results from Mariner 10: High resolution images of the Moon 05 p2107 N94-20719
Basaltic magmatism on the Moon. A perspective from volcanic picritic glasses 05 p2114 N94-20758
Chronology and genesis of high-Ti mare volcanism: Melting of cogenetic depleted and enriched reservoirs
05 p2118 N94-20777
Contributions of the Clementine mission to our understanding of the processes and history of the Moon
05 p2119 N94-20784
Earth-based measurement of lunar topography using delayed radar interferometry 05 p2119 N94-20787
Degradation sequence of young lunar craters from orbital infrared survey 05 p2136 N94-20874
CERN-derived analysis of lunar radiation backgrounds
05 p2080 N94-20880
Catalog of Apollo experiment operations [NASA-RP-1317] 06 p2194 N94-23292
Rover requirements for the planet surface segment of the space exploration initiative 06 p2369 N94-23377
The morphology of the lunar surface parts in the region of work of the mobile geological laboratory vehicle in Mare Imbrium 06 p2607 N94-23385
Design of a walking robot [NASA-CR-195200] 06 p2367 N94-25274
The Extended Mission Rover (EMR)
07 p2689 N94-25674
Design for producing fiberglass fabric in a lunar environment 07 p2765 N94-25676
Planetary surface exploration MESUR/autonomous lunar rover 07 p2833 N94-25683
Project Columbiad: Reestablishment of human presence on the Moon 07 p2689 N94-25687
Artemis common lunar lander. Phase 2: Study results for external review [NASA-TM-109699] 07 p2692 N94-28205
Lunar surface operations. Volume 4: Lunar rover trailer [NASA-CR-195554] 08 p3299 N94-29386
Backscatter Mossbauer Spectrometer (BaMS) for extraterrestrial applications 08 p3236 N94-29774
The Nomad Explorer assembly assist vehicle: An architecture for rapid global extraterrestrial base infrastructure establishment 09 p3599 N94-31429
High-resolution synthetic aperture radar observations of the Moon 09 p3676 N94-31952
Load-limiting landing gear footpad energy absorption system 09 p3607 N94-33323
Lunar Ultraviolet Telescope Experiment (LUTE), phase A [NASA-TM-4594] 10 p4162 N94-34920
Block distributions on the lunar surface: A comparison between measurements obtained from surface and orbital photography 11 p4359 N94-35419
Preliminary description of double drive tube 68002/68001 11 p4363 N94-35457
Lunar LIGO and gravitational wave astronomy on the Moon 11 p4366 N94-35472
Lunar horizon glow and the Clementine mission
11 p4366 N94-35478

LUNAR SURFACE VEHICLES
NT LUNAR MOBILE LABORATORIES
NT LUNAR ROVING VEHICLES
NT LUNOKHOD LUNAR ROVING VEHICLES
NT MANNED LUNAR SURFACE VEHICLES
Activities of the Center for Space Construction
[NASA-CR-193717] 04 p1335 N94-19371
Enabler operator station 07 p2943 N94-25679
Dust control for Enabler 07 p2943 N94-25680

LUNAR TEMPERATURE
Thermogeologic mapping of the Moon from lunar orbit 03 p1290 N94-16405

LUNAR TOPOGRAPHY
Viscous relaxation of the Moho under large lunar basins 01 p0452 N94-12113
Mode of emplacement of lunar mare volcanic deposits: Graben formation due to near surface deformation accompanying dike emplacement at Rima Parry 5 03 p1258 N94-16227
Lunar scout missions: Galileo encounter results and application to scientific problems and exploration requirements 03 p1259 N94-16229
Earth-based measurement of lunar topography using delayed radar interferometry 05 p2119 N94-20787
The morphology of the lunar surface parts in the region of work of the mobile geological laboratory vehicle in Mare Imbrium 06 p2607 N94-23385

LUNAR TRAJECTORIES
NT EARTH-MOON TRAJECTORIES
Lunar transportation system
[NASA-CR-195540] 06 p2365 N94-24805

LUNEBERG LENSES
U RADAR CORNER REFLECTORS

LUNGS
NT ALVEOLI
Evaluation of medical treatments to increase survival of ebullism in guinea pigs 01 p0302 N94-11548
Pulmonary function in microgravity: KC-135 experience 01 p0309 N94-11994
Flow limitation and flutter in membrane walled collapsible tubes: A model for expiratory wheezing
[ISBN-0-315-73875-8] 02 p0635 N94-13662
A characterization of carboxylesterases in rat and guinea pig: Their heterogeneity and role in detoxication of organophosphorus compounds
[NDRE-PUBL-93-1001] 02 p0730 N94-14852
Asbestos Surveillance Program 03 p1127 N94-16638
Spontaneous pneumothorax, cysts and bullae 06 p2425 N94-23326
Effects of combined breathing impediments on diver's respiratory performance
[AD-A277437] 09 p3805 N94-33084

LUNOKHOD LUNAR ROVING VEHICLES
Soviet developments of planet rovers in period of 1964 - 1990 06 p2369 N94-23374

LYAPUNOV FUNCTIONS
U LIAPUNOV FUNCTIONS

LYMAN ALPHA RADIATION
Model development for Ulysses and SOHO
[NASA-CR-193884] 06 p2627 N94-24484
Physical conditions in classical H2 regions in the Magellanic Clouds 08 p3543 N94-29722
Observation of Jovian auroral Ly-alpha line profile and emission variability with a sounding rocket and the IUE archives 08 p3550 N94-30798
A study of the neutral hydrogen distribution of the Milky Way through 21 cm emission and Lyman alpha absorption 09 p3938 N94-32309

LYMAN SPECTRA
The theory of QSO absorption line systems and their relationship to the galaxies
[NASA-CR-194596] 03 p1236 N94-15679

LYMPHOCYTES
Cellular responses to low-gravity: Pilot studies on suborbital rockets and orbiting spacecraft
[NASA-CR-194402] 02 p0729 N94-14494
A study of the effects of high power pulsed 2450 MHz microwaves, ELF modulated microwaves, and ELF fields on human lymphocytes and selected cell lines
[AD-A269070] 04 p1505 N94-18294

LYOPHILS
U COLLOIDS

LYRA CONSTELLATION
Analysis of the IUE spectra of the strongly interacting binary beta Lyrae
[NASA-CR-194118] 02 p0833 N94-14493

LYSINE
Quinoa: An emerging new crop with potential for CELSS
[NASA-TP-3422] 05 p1895 N94-20137

LYSOZYME
Convective flow effects on protein crystal growth
[NASA-CR-194560] 03 p1206 N94-15476
Temperature dependence of protein solubility-determination, application to crystallization, and growth kinetics studies 06 p2224 N94-24344
Convective flow effects on protein crystal growth
[NASA-CR-195785] 08 p3515 N94-30015

M

M REGION
A spectral atlas of the nu(sub 12) fundamental of (13)C(12)CH6 in the 12 micron region
[NASA-TM-104601] 10 p4138 N94-34945

M STARS
The 0.15 seconds near-infrared imaging of the central parsec of the galaxy
[MPE-PREPRINT-239] 04 p1621 N94-19415
Stellar coronae at the end of the main sequence: A Rosat survey of the late M dwarfs
[NASA-CR-194700] 04 p1628 N94-19794

M WINGS
U VARIABLE SWEEP WINGS

MAARS
U CRATERS

MACH NUMBER
Numerical calculation of scramjet inlet flow
[NAL-TR-1174T] 01 p0027 N94-10370
Exergy decrease in shock waves and boundary layers of space launch vehicles
[AD-A265272] 01 p0042 N94-10493
Kinetic approach to long wave length modes in rotating plasmas
[DE93-771286] 01 p0388 N94-10807
Progress in modeling hypersonic turbulent boundary layers 01 p0157 N94-12300
Improved aeroprediction code. Part 1: Summary of new methods and comparison with experiment
[AD-A266015] 02 p0500 N94-12989
A time-accurate numerical method for chemically reacting flows at all Mach numbers 02 p0500 N94-13198
Numerical simulations and experiments on physics of high Mach number shockwave: Turbulent flow interactions
[DE93-013424] 02 p0631 N94-13249
Topics on spatially high-order accurate methods and pre-conditioning for the Navier-Stokes equations with finite-rate chemistry 02 p0633 N94-13572
A solution algorithm for the prediction of compressible laminar and turbulent shear flows 02 p0634 N94-13635
A comparison of computational and experimental data for a subscale high speed propulsive nozzle at low mach numbers
[AD-A266543] 02 p0504 N94-13705
Flight-determined engine exhaust characteristics of an F404 engine in an F-18 airplane
[NASA-TM-4538] 03 p0869 N94-15141
Tollmien-Schlichting/vortex interactions in compressible boundary layer flows
[NASA-CR-191515] 03 p1017 N94-15183
Numerical investigations in three-dimensional internal flows
[NASA-CR-194594] 03 p1020 N94-15551
Wind tunnel investigation of three axisymmetric cowls of different lengths at Mach numbers from 0.60 to 0.92
[NASA-TM-4488] 03 p0856 N94-15681
Wind tunnel investigation with an operational turbojet engine
[TABES PAPER 93-662] 03 p0870 N94-16157
Aerothermoelastic analysis of a NASP demonstrator model
[NASA-TM-109007] 03 p0867 N94-17055
Higher-order accurate Osher schemes with application to compressible boundary layer stability
[NASA-TM-106355] 03 p1026 N94-17056
Boundary conditions and the simulation of low Mach number flows
[NASA-TM-106374] 03 p1029 N94-17448
Error propagation equations and tables for estimating the uncertainty in high-speed wind tunnel test results
[DE93-018685] 04 p1311 N94-18275
A comparative study of turbulence models in predicting hypersonic inlet flows 04 p1314 N94-18553
Acoustic intensity measurements in the presence of low Mach number flow
[AD-A269995] 04 p1562 N94-18664
Linear and nonlinear PSE for compressible boundary layers
[NASA-CR-191537] 05 p1797 N94-20033
Acoustic radiation damping of flat rectangular plates subjected to subsonic flows
[NASA-TM-109382] 05 p1967 N94-20211
Calibration of HYPULSE for hypervelocity air flows corresponding to flight Mach numbers 13.5, 15, and 17
[NASA-CR-191578] 06 p2192 N94-23564
Evaluation of turbulence models in the PARC code for transonic diffuser flows
[NASA-TM-106391] 06 p2168 N94-24084
Direct simulation of isothermal-wall supersonic channel flow 06 p2172 N94-24164
Effects of shock strength on shock turbulence interaction 06 p2332 N94-24165
An experimental investigation of a Mach 3.0 high-speed civil transport at supersonic speeds
[NASA-TP-3365] 06 p2169 N94-24311
The radiated noise from isotropic turbulence revisited
[AD-A276712] 06 p2333 N94-24356
Experimental cavity pressure measurements at subsonic and transonic speeds. Static-pressure results
[NASA-TP-3358] 06 p2169 N94-24464
Validation of the ROTAC code for the rotor noise prediction
[PB93-204311] 06 p2529 N94-24514
Relationship between transition and modes of instability in supersonic boundary layers
[NASA-CR-4562] 06 p2336 N94-24725
Development and implementation of a scramjet cycle analysis code with a finite-rate-chemistry combustion model for use on a personal computer
[AD-A273834] 07 p2673 N94-25617
Mix induced by single shock passage through a material interface
[DE93-019505] 07 p2792 N94-26427
Pressure distributions on a 0.02-scale Space Shuttle orbiter nose at Mach 21.5 in helium
[NASA-TM-4495] 07 p2646 N94-26592
Experimental and theoretical study of aerodynamic characteristics of some lifting bodies at angles of attack from -10 degrees to 53 degrees at Mach numbers from 2.30 to 4.62
[NASA-TM-4528] 07 p2646 N94-26693
The cryogenic tunnel Cologne at DLR
[DLR-MITT-93-10] 07 p2681 N94-27587
Normal force of low aspect ratio cropped-delta wings at pre-stall angles of attack and subsonic speeds
[ESDU-93034] 07 p2648 N94-27955
Transient flow features of a supersonic jet in a low speed cross flow 07 p2800 N94-28005
Wing lift increment at zero angle of attack due to deployment of single-slotted flaps at low speeds
[ESDU-93019] 07 p2649 N94-28140
Large amplitude Langmuir and ion-acoustic waves in a relativistic two-fluid plasma
[AD-B183694L] 08 p3506 N94-29547
Analysis of fluctuating static pressure measurements in a large high Reynolds number transonic cryogenic wind tunnel 08 p3158 N94-30788
Hypervelocity Tunnel 9 Mach 10/14 Calibration
[AD-A275960] 09 p3587 N94-31318
Hotwire measurements of the turbulent flow into a cascade of controlled-diffusion compressor blades
[AD-A277297] 09 p3706 N94-32042
A new method for calculating wing along aerodynamics to angle of attack 180 deg
[AD-A277965] 09 p3574 N94-33263
Sonic boom configuration minimization 10 p3973 N94-33473
Status of an inlet configuration trade study for the Douglas HSCT 10 p3977 N94-33506
Effect of pressure gradient on first mode of instability in high-speed boundary layers
[AD-280579] 10 p4048 N94-34130
Experimental studies of very-high Mach number hydrodynamics
[AD-A278761] 11 p4263 N94-35492
A shadowgraph study of Space Transportation System (STS): The Space Shuttle Launch Vehicle (SSLV)
[NASA-RP-1341] 12 p4382 N94-36741
Subsonic aerodynamic characteristic of semispan commercial transport model with wing-mounted advanced ducted propeller operating in reverse thrust --- conducted in the Langley 14 by 22 foot subsonic wind tunnel
[NASA-TP-3427] 12 p4384 N94-37505

MACH REFLECTION
Mach reflection of spherical detonation waves
[DE93-016604] 07 p2797 N94-27705

MACH-ZEHNDER INTERFEROMETERS
Balanced arrow Mach-Zehnder interferometer 05 p1789 N94-22221
A technique for multiplexing 3x3-coupler terminated interferometric fiber-optic sensors
[AD-A276739] 09 p3880 N94-32180

MACHINE LEARNING
A new HMM learning algorithm for continuous speech recognition
[NHK-SERIAL-413] 01 p0132 N94-10560
Toward intelligent flight control 01 p0033 N94-11503
Statistical and optimization methods to expedite neural network training for transient identification
[DE93-009985] 01 p0340 N94-11644

A pattern recognition system for locating small volvanoes in Magellan SAR images of Venus
01 p0455 N94-12126
Efficient dynamic optimization of logic programs
[NASA-TM-109251] 02 p0761 N94-12889
An analog clustering network from a biological model
[AD-A265637] 02 p0762 N94-12969
Obstacle detection by recognizing binary expansion patterns
[NASA-CR-194415] 02 p0514 N94-14495
Hidden Markov model approach to skill learning and its application to telerobotics
[AD-A266989] 03 p1164 N94-15502
Representation in incremental learning
[NASA-CR-194595] 03 p1221 N94-15719
Temporal segmentation of tasks from human hand motion
[AD-A266596] 03 p1166 N94-16725
Information technology division technical paper abstracts
[AD-A266227] 03 p1166 N94-16938
Integrating reactive and deliberative planning for agents
[AD-A267631] 03 p1166 N94-17201
Bias in planning and explanation-based learning
[AD-A269608] 04 p1610 N94-17746
Application of the network discriminant function to learning
[AD-A268793] 04 p1540 N94-18189
Dialog-Based Learning (DBL) for adaptive interface agents and programming-by-demonstrations systems
[AD-A269154] 04 p1540 N94-18261
Fast-training algorithm for hidden-layer forward-feed neural networks
[AD-A269253] 04 p1540 N94-18263
On masking effect
[AD-A269593] 04 p1541 N94-18462
Towards versatile and practical knowledge acquisition
[AD-A269596] 04 p1615 N94-18464
Geometrical pattern learning
[DE93-017641] 04 p1542 N94-19007
A refinement for nonmonotonic logic
[REPT-93-21] 04 p1542 N94-19092
Learning control of large-scale systems
[MATHS-REPT-A-186] 04 p1544 N94-19408
Explorations of the practical issues of learning prediction-control tasks using temporal difference learning methods
[AD-A270836] 04 p1544 N94-19599
VLSI implementation of neuromorphic learning networks
[AD-A270825] 04 p1407 N94-19665
Building brains for bodies
[AD-A270531] 05 p1939 N94-19875
Robot skill learning and the effects of basis function choice
[TR-437] 05 p1939 N94-20135
The Seventh International Symposium on Methodologies for Intelligent Systems (Poster Session)
[AD-A272125] 05 p1942 N94-20573
Design of a computer assisted tool for object oriented acquisition, modeling and simulation of knowledge structure
[ETN-93-94183] 05 p1910 N94-21152
High dimension action spaces in robot skill learning
[TR-458] 05 p1945 N94-21317
A neural M-ary tree method for data compression
05 p1780 N94-22166
Cascaded recursive artificial neural networks
05 p1780 N94-22167
Logic oriented neural networks
05 p1782 N94-22182
A framework of connectionist network toward speech waveform coding 05 p1746 N94-22211
Speaker-independent isolated-digit recognition using neural networks and hidden Markov model
05 p1747 N94-22213
Fuzzy and neural control
[NASA-TM-108753] 05 p1947 N94-22270
SkICAT: A cataloging and analysis tool for wide field imaging surveys 05 p2049 N94-22546
General asymmetric neural networks and structure design by genetic algorithms: A learning rule for temporal patterns
[DE94-001254] 05 p1947 N94-22563
Artificial neural networks: Application to the optical recognition of music partitions
[ETN-94-95166] 06 p2470 N94-22884
Increasing levels of assistance in refinement of knowledge-based retrieval systems
[NASA-CR-195144] 06 p2591 N94-24552
A methodology for software cost estimation using machine learning techniques
[AD-A273158] 06 p2459 N94-24775
High-level connectionist models
[AD-A273638] 06 p2468 N94-25030
A rough set approach to speech recognition
[ISBN-0-315-83894-9] 07 p2769 N94-26619
Using discovery-based learning to prove the behavior of an autonomous agent
[AD-A274131] 07 p2987 N94-27121
Translation and rotation invariant pattern recognition
[PB94-123676] 07 p2968 N94-27157
Artificial Intelligence Research Branch future plans
[NASA-TM-109733] 07 p2989 N94-28065
A neural network with modular hierarchical learning
[NASA-CASE-NPO-19077-1-CU] 08 p3435 N94-29492
On-line search for optimal controller parameters using interconnected learning automata
[MATHS-REPT-A-196] 08 p3436 N94-29526
Nonlinear PCA: Algorithms and applications
[PB94-137544] 08 p3419 N94-29680
Robotic hand-eye motor learning
08 p3436 N94-29835
Reinforcement learning for robots using neural networks 08 p3437 N94-29853
Unsupervised learning in analog networks
[ISBN-0-315-85959-8] 08 p3432 N94-30140
A lateral inhibition neural network that emulates a winner-takes-all algorithm
[RUU-CS-92-46] 08 p3438 N94-30334
An intelligent robotic aid system for human services
[AIAA PAPER 94-1232-CP] 08 p3447 N94-30580
Use of bad training data for better predictions
[DE94-006233] 08 p3427 N94-30705
ELF: Learning incomplete fuzzy rule sets for an autonomous robot
[REPT-93-043] 08 p3449 N94-30923
Some methodological issues about designing autonomous agents which learn their behaviors: The ELF experience
[REPT-93-068] 08 p3449 N94-30939
Report of the 'Mathematical Models for Neural Networks' course
[TELECOM-93-D-019] 09 p3828 N94-31100
Concepts and environment
[REPT-93-032] 09 p3829 N94-31186
Filtering and recognition of moving boats in radar images
[REPT-93-039] 09 p3671 N94-31190
A neural network methodology for engineering applications: The learning control of robotic systems
[RR-480] 09 p3830 N94-31500
Trajectory learning with a direct drive robotic manipulator 09 p3831 N94-31794
Neural network definitions of highly predictable protein secondary structure classes
[DE94-006234] 09 p3834 N94-32175
A differential theory of learning for efficient statistical pattern recognition
[AD-A277313] 09 p3800 N94-32277
Refining fuzzy logic controllers with machine learning
09 p3839 N94-32421
Analysis and synthesis of adaptive neural elements and assembles
[AD-A277423] 09 p3836 N94-32996
Investigation of drive-reinforcement learning and application of learning to flight control
[AD-A277442] 09 p3801 N94-33053
Research in VLSI system implementation of neuromorphic learning networks
[AD-A278247] 10 p4112 N94-33403
On stochastic approximation algorithms for classes of PAC learning problems
[DE94-007417] 10 p4113 N94-33690
An analysis of stopping criteria in artificial neural networks
[AD-A278491] 10 p4113 N94-33755
Learning procedures from interactive natural language instructions 10 p4110 N94-34047
Two frameworks for integrating knowledge in induction
10 p4160 N94-34050
Discovering operating modes in telemetry data from the Shuttle Reaction Control System
10 p4013 N94-34051
Self-calibrating models for dynamic monitoring and diagnosis 10 p4127 N94-34052
Filtering as a reasoning-control strategy: An experimental assessment 10 p4127 N94-34053
A machine-learning apprentice for the completion of repetitive forms 10 p4110 N94-34055
Automated knowledge-base refinement
10 p4160 N94-34056
Multiresolutional schemata for unsupervised learning of autonomous robots for 3D space operation
10 p4123 N94-35051
Automatic cataloguing and characterization of Earth science data using SE-trees 10 p4124 N94-35058
Developing interpretable models with optimized set reduction for identifying high risk software components
11 p4301 N94-35435
Combining left and right unlinking for matching a large number of learned rules
[AD-A278979] 11 p4311 N94-35527
Prodigy planning algorithm
[AD-A278900] 11 p4303 N94-35574
The breakdown of operators when interacting with the external world
[AD-A278936] 11 p4299 N94-35716
Fuzzy self-learning control for magnetic servo system
11 p4215 N94-35852
Subgrouped real time recurrent learning neural networks
[AD-A280618] 12 p4500 N94-37043
Adaptive learning of multi-sensor integration techniques with genetic algorithms
[DE94-012744] 12 p4500 N94-37083
Bootstrap planning: Theory and application
[DE94-006466] 12 p4501 N94-37425

MACHINE LIFE
U SERVICE LIFE

MACHINE RECOGNITION
U ARTIFICIAL INTELLIGENCE

MACHINE STORAGE
U COMPUTER STORAGE DEVICES
U CORE STORAGE

MACHINE TOOLS
NT BORING MACHINES
NT GRINDING MACHINES
NT MILLING MACHINES
Material removal processes: Engineering mechanics consideration
[DE93-010733] 01 p0126 N94-10293
Thermal error compensation feasibility study using artificial intelligence
[AD-A266084] 01 p0340 N94-12411
Measuring machines for digitalizing and measuring complex surfaces, models and matrices
[CRIF-MC-97] 04 p1444 N94-17963
Present evolution of tools management
[CRIF-MC-102] 04 p1444 N94-17964
The machine reception: A business of experts
[CRIF-MC-94] 04 p1611 N94-17980
A rational design change methodology based on experimental and analytical modal analysis
[DE93-018537] 04 p1521 N94-18271
Survey of ceramic machining in Japan
[DE93-018277] 04 p1372 N94-18946
The Milling assistant, case-based Reasoning, and machining strategy: A report on the development of automated numerical control programming systems at New Mexico State University
[DE93-041101] 05 p2029 N94-21690
Machines for moving in soil 06 p2369 N94-23411
JBK-75 stainless steel machinability study
[DE94-002268] 06 p2242 N94-23475
Composite material impregnation unit
[NASA-TM-107751] 06 p2254 N94-23486
Tool sharing, part 3
[PB94-111697] 06 p2467 N94-24524
Research experience for undergraduates in robotics and materials
[AD-A273659] 06 p2368 N94-25436
The National Center for Advanced Information Components Manufacturing: Program update
[DE94-002647] 07 p2960 N94-26118
Application of high-speed milling to the Finnish manufacturing industry
[PB94-135548] 08 p3230 N94-29187
Effect of non-metallic inclusions on the machinability of steel
[PB93-230233] 08 p3204 N94-29387
Generation of gear tooth surfaces by application of CNC machines
[NASA-CR-195306] 08 p3303 N94-30205
Precision and manufacturing at the Lawrence Livermore National Laboratory 08 p3240 N94-30449
Application of neural networks in multiple sensor fusion for on-line tool wear monitoring
10 p4119 N94-34347
Open architecture controllers for advanced manufacturing
[DE94-007572] 12 p4496 N94-37782

MACHINE TRANSLATION
Processing proper nouns in machine translation for English news
[NHK-SERIAL-414] 01 p0418 N94-10559
Machine translation technology: A potential key to the information age
[PB93-134336] 01 p0421 N94-12385
Using multiple adaptively-weighted strategies for the resolution of demonstratives
[AD-A266463] 03 p1150 N94-16585
Automatic generation of production rules for integrity maintenance
[REPT-92-054] 03 p1156 N94-17501

Automatic translation of database integrity constraints into compensating production rules
[REPT-92-055] 03 p1234 N94-17502
PATRAN 2.5/EAL interface guide
[NASA-TM-109053] 07 p2972 N94-27655
ARM: Abstract Rewriting Machine
[CWI-CS-R9330] 07 p2974 N94-27794
Automatic translation among spoken languages 09 p3685 N94-32437
Translation between representation languages 10 p4110 N94-34054
Good applications for crummy machine translation
[AD-A278689] 11 p4345 N94-35651
Machine Translation Project 12 p4541 N94-36846

MACHINE VISION
U COMPUTER VISION

MACHINE-INDEPENDENT PROGRAMS
SPPTOOLS: Programming tools for the IRAF SPP language 05 p1925 N94-22474
Development of the FITS tools package for multiple software environments 05 p1927 N94-22516
Dynamic data distributions in Vienna Fortran
[NASA-CR-191575] 06 p2448 N94-23092
The ergonomics of software porting: Automatically configuring software to the runtime environment or everything you wanted to know about your C compiler but didn't know who to ask
[CWI-CS-R9266] 07 p2961 N94-26221

MACHINERY
Transcript of workshop on machinery health monitoring
[IME-MET-TR-005] 02 p0733 N94-13847
Machinery dynamics activities in Canadian industries
[IME-MET-TR-006] 02 p0663 N94-14147
Applications of neural networks in fault detection of rotating machinery
[AD-A270755] 04 p1448 N94-19766
Vibrational power transmission analysis of machinery installations in ships with the objective of noise reduction
[ISVR-TR-216] 06 p2363 N94-24076
Variable speed controller 07 p2943 N94-25678
Identification of mechanical systems using probabilistic neural networks
[DE94-007555] 10 p4114 N94-34296

MACHINING
NT CHEMICAL MACHINING
NT ELECTROCHEMICAL MACHINING
NT MICROMACHINING
NT MILLING (MACHINING)
Material removal processes: Engineering mechanics consideration
[DE93-010733] 01 p0126 N94-10293
Thermal error compensation feasibility study using artificial intelligence
[AD-A266084] 01 p0340 N94-12411
Machining aspects of nickel-phosphorus coatings
[DE93-013037] 02 p0580 N94-14311
Computational diagnostics for detecting phase transitions during nanoindentation
[DE93-016536] 02 p0813 N94-14439
Machining and grinding: High rate deformation in practice
[DE93-010718] 02 p0664 N94-14457
Detection of subsurface defects in machined silicon nitride ceramics by optical scattering methods
[DE93-015554] 03 p0968 N94-16658
Predesign of diamond turned refractive/diffractive elements for IR objectives 03 p1198 N94-17359
Electrostatic micrometers: Recent developments and perspectives of uses in clock and watch making 04 p1425 N94-18014
Survey of ceramic machining in Japan
[DE93-018277] 04 p1372 N94-18946
Precision machining and polishing of scintillating crystals for large calorimeters and hodoscopes
[DE93-018663] 04 p1381 N94-19544
Evaluation of a scanning Hartmann device for single point turning applications
[DE93-019204] 05 p1821 N94-19891
High-power copper vapor lasers and their application to precision drilling and cutting
[DE93-019951] 05 p1819 N94-21844
JBK-75 stainless steel machinability study
[DE94-002268] 06 p2242 N94-23475
Effect of nitrocarburizing on shape of titanium alloy parts
[DE94-004040] 07 p2732 N94-25822
Opportunities for High Aspect Ratio Micro-Electro-Magnetic-Mechanical Systems (HAR-MEMMS) at Lawrence Berkeley Laboratory
[DE94-003499] 07 p2827 N94-27722
Effect of non-metallic inclusions on the machinability of steel
[PB93-230233] 08 p3204 N94-29387
The machining of fiber metal laminates. Part 1: An inventory of forming processes
[LR-710-PT-1] 08 p3184 N94-30343
Confessions of a robot lobotomist
[AIAA PAPER 94-1185-CP] 08 p3440 N94-30535
Material properties and fracture mechanics in relation to ceramic machining
[DE94-006623] 08 p3221 N94-30829
Cost-effective ceramic machining: Summary of three-body wear experiments
[DE94-007757] 09 p3650 N94-31354
Neutral ion sources in precision manufacturing 09 p3875 N94-32447
Leveraging metal matrix composites to reduce costs in space mechanisms 09 p3604 N94-33301
Application of neural networks in multiple sensor fusion for on-line tool wear monitoring 10 p4119 N94-34347

MACINTOSH PC
U MACINTOSH PERSONAL COMPUTERS

MACINTOSH PERSONAL COMPUTERS
Activity Catalog Tool (ACT) user manual, version 2.0
[NASA-CR-177634] 06 p2430 N94-23527
Performing speech recognition research with hypercard 06 p2306 N94-24194

MACROCLIMATE
U CLIMATE

MACROMOLECULES
Effects of a microgravity environment on the crystallization of biological macromolecules 01 p0117 N94-10198
Application of molecular modeling to biological processing
[AD-A272612] 05 p1974 N94-21185
Polymer morphologh 06 p2226 N94-24353
Ultrastructure processing of macromolecular materials
[AD-A273413] 06 p2258 N94-24782
Center for advanced electrical and structural polymers
[AD-A273415] 06 p2259 N94-24783
Ultrastructure processing of macromolecular materials
[AD-A274460] 07 p2754 N94-27086
Molecular structure of coal studied by solvent extraction 08 p3187 N94-28676
Crosslinking and surface reactions in macromolecules: Spectroscopic FT-IR studies 08 p3221 N94-30812
Multifunctional macromolecules
[AD-A277347] 09 p3656 N94-32246
Phase-sensitive flow cytometry: New technology for analyzing biochemical, functional, and structural features in fluorochrome-labeled cells and particles
[DE94-003960] 10 p4094 N94-33734

MACROSCOPIC EQUATIONS
Derivation of the macroscopic rate equations for the driven diffusive Ising model at pair level of approximation
[DE93-616839] 06 p2524 N94-25208
Volume averaged model for the mechanics of alloys solidification
[PB94-138617] 08 p3208 N94-30113

MACULAR VISION
U VISION

MAGELLAN PROJECT (NASA)
Russia's contribution to regional geologic mapping of Venus 01 p0454 N94-12122
Synthesis of global thematic mapping, Venus: Geologic correlations/questions for the Magellan gravity mission 01 p0467 N94-12194
Characteristics of arachnoids from Magellan data 01 p0469 N94-12204
STS-30 Magellan IUS/EVA training in WETF
[NASA-TM-109300] 02 p0737 N94-13601
Magellan: Principal Venus science findings 03 p0989 N94-15887
Guide to Magellan image interpretation
[NASA-CR-194340] 03 p1298 N94-17654
Magellan, Galileo, and Ulysses
[NASA-TM-109362] 04 p1628 N94-18958
Magellan vertical polarization radar observations 05 p1744 N94-20691
Magellan at Venus: Summary of science findings 05 p2110 N94-20734
Response of the topography and gravity field on Venus to mantle upwelling beneath a chemical boundary layer 05 p2117 N94-20775
Magellan Mission 05 p1652 N94-20829

MAGELLAN SPACECRAFT (NASA)
The origin of Venusian channels: Modelling of thermal erosion by lava 01 p0456 N94-12131
STS-30 Magellan deploy Sim in SMS and MOCR
[NASA-TM-109571] 03 p0875 N94-15301
STS-26 through STS-34, deploy activities
[NASA-TM-109566] 03 p1301 N94-15315
STS-30 onboard 16mm photography quick release
[NASA-TM-109579] 03 p0881 N94-15423
The depths of the largest impact craters on Venus 03 p1264 N94-16261
Tessera terrain on Venus: Global characterization from Magellan data 03 p1264 N94-16262
Magellan, Galileo, and Ulysses
[NASA-TM-109362] 04 p1628 N94-18958
Magellan vertical polarization radar observations 05 p1744 N94-20691
Venus gravity: New Magellan low altitude data 05 p2117 N94-20772
Magellan Mission 05 p1652 N94-20829
Magellan spacecraft and memory state tracking: Lessons learned, future thoughts 06 p2207 N94-23865
VMPLOT: A versatile analysis tool for mission operations 06 p2507 N94-23891
Using SFOC to fly the Magellan Venus mapping mission 06 p2516 N94-23941
Magellan to Venus
[NASA-CR-195779] 11 p4201 N94-35510
Field demonstration of X-band photonic antenna remoting in the Deep Space Network 11 p4252 N94-35545

MAGELLANIC CLOUDS
The first data from the MACHO experiment
[DE93-014423] 02 p0840 N94-14467
Dust in the Small Magellanic Cloud
[NASA-CR-193344] 04 p1624 N94-17764
Spectrophotometry of emission-line stars in the magellanic clouds
[NASA-CR-194082] 04 p1628 N94-19425
IRAS galaxies observed in the ROSAT survey: Starbursts or central activity 04 p1623 N94-19528
How to handle 6GBytes a night and not get swamped 05 p2058 N94-22444
Dust in the Small Magellanic Cloud
[NASA-CR-195764] 08 p3543 N94-29696
Physical conditions in classical H2 regions in the Magellanic Clouds 08 p3543 N94-29722
Study of stellar associations located in the region contained between the Magellanic Clouds
[ISBN-0-315-86692-6] 09 p3935 N94-31913

MAGIC TEES
An investigation of a novel microstrip magic-T
[ISBN-0-315-86218-1] 09 p3690 N94-31711

MAGMA
Th-230 - U-238 series disequilibrium of the Olkaria basalts Gregory Rift Valley, Kenya: Petrogenesis 01 p0281 N94-12074
Lava flows on Venus: Analysis of motion and cooling 01 p0457 N94-12137
Comparison of the distribution of large magmatic centers on Earth, Venus, and Mars 01 p0467 N94-12192
The Magellan volcanic and magmatic feature catalog 01 p0467 N94-12193
Compositional heterogeneity within a dumbbell-shaped Apollo 15 green glass: Evidence for simultaneous eruption of different magmas 01 p0470 N94-12209
Vulcanian explosive eruptions: A mechanism for localised pyroclast dispersal on Venus 01 p0477 N94-12243
Primitive SNC parent magmas and crystallization: Low PH2O experiments 01 p0433 N94-12264
Assimilation of solids during ascent of magmas from the Bartoy Field of the Baikal Region, Siberia 03 p1103 N94-16214
Bubble coalescence in magmas 03 p1103 N94-16237
Overturn of magma ocean ilmenite cumulate layer: Implications for lunar magmatic evolution and formation of a lunar core 03 p1261 N94-16242
Experimental constraints on CO2 and H2O in the Martian mantle and primary magmas 03 p1262 N94-16248
Petrologic models of 15388, a unique Apollo 15 mare basalt 03 p1264 N94-16258
Constraints on the differentiation of the Earth from the coupled Sm-146,147-Nd-142,143 systematics 03 p1103 N94-16271
Explosive volcanism and the compositions of the cores of differentiated asteroids 03 p1243 N94-16306
Venusian pancake domes: Insights from terrestrial voluminous silicic lavas and thermal modeling 03 p1286 N94-16381
Calderas produced by hydromagmatic eruptions through permafrost in northwest Alaska 05 p2089 N94-20385
Volatility in the lunar crust: Trace element analyses of lunar minerals by PIXE proton microprobe 05 p2097 N94-20661
Thermal and rheological controls on magma migration in dikes: Examples from the east rift zone of Kilauea volcano, Hawaii 05 p1862 N94-20673
Venus magmatic and tectonic evolution 05 p2101 N94-20683
Venus pancake dome formation: Morphologic effects of a cooling-induced variable viscosity during emplacement 05 p2110 N94-20732

Basaltic magmatism on the Moon. A perspective from volcanic picritic glasses 05 p2114 N94-20758
Origin of the Apollo 15 very low Ti green glass. A perspective from the compositional diversity in the very low Ti glasses 05 p1685 N94-20759
Orthopyroxenes as recorders of diogenite petrogenesis: Trace element systematics 05 p1686 N94-20760
FE-60 and the evolution of eucrites 05 p2083 N94-20768
Chronology and genesis of high-Ti mare volcanism: Melting of cogenetic depleted and enriched reservoirs 05 p2118 N94-20777
Geochronology and petrogenesis of the western highlands alkali suite: Radiogenic isotopic evidence from Apollo 14 05 p2118 N94-20778
Magnesian anorthosites from the western highlands of the Moon: Isotope geochemistry and petrogenesis 05 p2118 N94-20779
Differentiation of magma oceans and the thickness of the depleted layer on Venus 05 p2118 N94-20780
The parent magma of the Nakhla (SNC) meteorite: Reconciliation of composition estimates from magmatic inclusions and element partitioning 05 p2085 N94-20836
Elevation and igneous crater modification on Venus: Implications for magmatic volatile content 05 p2135 N94-20872
Lunar mare volcanism: Mixing of distinct, mantle source regions with KREEP-like component 06 p2615 N94-24370
The transition from diapirism to dike intrusion: Implications for planetary volcanism
[NASA-CR-195133] 06 p2403 N94-24580
Experimental study of lunar and SNC (Mars) magmas
[NASA-CR-195274] 07 p3107 N94-27850
The thermal consequences of giant impacts in the early solar system 08 p3543 N94-29698
Studies in Jurassic and Cretaceous North American apparent polar wander 08 p3362 N94-29940
The parent magma of xenoliths in shergottite EETA79001: Bulk and trace element composition inferred from magmatic inclusions 11 p4352 N94-35467
Role of magma-water interaction in very large explosive eruptions
[DE94-002698] 11 p4291 N94-36103
Vent processes during the 1912 eruption at Novarupta, Katmai National Park, Alaska
[DE94-010740] 12 p4468 N94-36451

MAGNESIUM
NT MAGNESIUM ISOTOPES
Inhibiting corrosion in Gr/Al and Gr/Mg metal matrix composites using nonequilibrium alloying techniques
[AD-A266547] 02 p0556 N94-13583
Mechanical properties of magnesium ammonium phosphate cements and their zeolite composites
[DE93-015155] 03 p0934 N94-16057
The Fe2(+)-Mg interdiffusion in orthopyroxene: Constraints from cation ordering and structural data and implications for cooling rates of meteorites 03 p1241 N94-16175
The resonance lines of MG2 as diagnostics of the upper solar chromosphere
[NASA-CR-195084] 06 p2627 N94-24300
Dissolution of secondary phases during extrusion
[PB94-124583] 07 p2732 N94-25908
The magnesium chelation step in chlorophyll biosynthesis
[DE94-008727] 09 p3794 N94-32890
Non-alloyed, refractory metal contact optimization with shallow implantations of Zn and Mg
[DE94-010392] 11 p4240 N94-36110
Cr, Mn, and Ca distributions for olivine in angritic systems: Constraints on the origins of Cr-rich and Ca-poor core olivine in angrite LEW87051 11 p4353 N94-36162
Using nonequilibrium alloying techniques for corrosion inhibition in Gr/Al and Gr/Mg metal matrix composites
[AD-A280529] 12 p4404 N94-37088

MAGNESIUM ALLOYS
Mechanical properties of magnesium/carbon composites developed by hot pressing under medium pressure 01 p0059 N94-10024
Aircraft carrier exposure tests of cast magnesium alloys
[AD-A268260] 03 p0962 N94-17418
The use of backscattered electron imaging mode to assess the effect of fine dispersions on development of superplastic microstructure in Al-Mg alloys
[AD-A272426] 05 p1691 N94-21258
New extensions in the development of deformation processed metal-metal matrix composites
[DE94-000692] 06 p2227 N94-23004
Quantitative analysis in the Al-Mg-Si system with small amounts of Mg and Si
[PB93-201499] 06 p2241 N94-23446
Segregation and oxidation studies of Al-Li and Al-Mg alloys
[ISBN-0-315-83993-7] 06 p2244 N94-24469
Formation of three types of quasi-crystals in Al-Pd-Mg system
[REPT-A-2667] 07 p3053 N94-26071
Hot deformation behaviour of Si(p)/Al composites and their matrices and an Al-Mg-Si alloy
[ISBN-0-315-84699-2] 07 p2711 N94-27314
The corrosion behavior of sputter-deposited magnesium-valve metal alloys 07 p2745 N94-28164
Failures to model the development of a cube texture during the high temperature compression of Al-Mg alloys
[DE94-005013] 08 p3201 N94-28544
Casting of weldable graphite/magnesium metal matrix composites with built-in metallic inserts 08 p3186 N94-30482
Shock tube ignition and combustion of aluminum/magnesium alloy particles in oxygen at high pressure 09 p3631 N94-31286

MAGNESIUM COMPOUNDS
NT CHLOROPHYLLS
NT DOLOMITE (MINERAL)
NT ENSTATITE
NT FORSTERITE
NT MAGNESIUM FLUORIDES
NT MAGNESIUM OXIDES
NT MAGNESIUM SULFATES
NT PERICLASE
NT TALC
Advanced civil engineering materials based on inorganic polymers
[AD-A270837] 04 p1374 N94-19600
The Mg-suite and the highland crust: An unsolved enigma 05 p2126 N94-20822

MAGNESIUM FLUORIDES
Novel Co:MgF2 lidar for aerosol profiler
[NASA-CR-191525] 02 p0654 N94-13091
SALI chemical analysis of provided samples
[NASA-CR-194138] 06 p2232 N94-23524
Ferroelectric fluoride memory FET development
[AD-A274341] 07 p2785 N94-27057

MAGNESIUM ISOTOPES
Isotopic and trace element characteristics of an unusual refractory inclusion from Essebi 01 p0471 N94-12212
Grosnaja ABCs: Magnesium isotope compositions 03 p1241 N94-16191
Petrography, mineralogy, and Mg isotope composition of VICTA: A vigarano CaAl4O7-bearing type A inclusion 03 p1103 N94-16203
Diffusion-controlled magnesium isotopic fractionation of a single crystal forsterite evaporated from the solid state 05 p1686 N94-20855
Mechanisms of formation and of de-excitation in the reaction Mg-24 + C-12 yields 9 alpha at 35MeV per nucleon
[ISBN-0-315-86746-9] 09 p3867 N94-31749
Laser cooling of 24Mg+ in the ASTRID storage ring
[DE94-010445] 12 p4523 N94-37619

MAGNESIUM OXIDES
NT PERICLASE
Properties of E-beam interactive oxide films for nanometer scale structures
[AD-A272848] 05 p1675 N94-21191
MOCVD growth and structure of PbTiO3 thin films
[DE93-040230] 05 p2033 N94-21994
Orientationally independent antiferromagnetic coupling in epitaxial Fe/Cr (211) and (100) superlattices
[DE94-001270] 05 p2035 N94-22564
Transparent polycrystalline body with high ultraviolet transmittance, process for making and applications thereof
[CA-PATENT-1325511] 07 p3066 N94-27276
FeO and MgO in plagioclase of lunar anorthosites: Igneous or metamorphic? 11 p4351 N94-35449
Substrate effects on the structure and optical properties of epitaxial PbTiO3 thin films prepared by metal-organic chemical vapor deposition
[DE94-010432] 12 p4535 N94-37192
Microstructure and chemistry of MgO- and CoO-doped nickel-titanate spinels
[DE94-012741] 12 p4537 N94-37382
The MBE growth and optical quality of BaTiO3 and SrTiO3 thin films on MgO
[DE94-011468] 12 p4538 N94-37570

MAGNESIUM SULFATES
Phase equilibria of the magnesium sulfate-water system to 4 kbars 03 p0953 N94-16247
Crustal structure and igneous processes in a chondritic Io 03 p1243 N94-16292

MAGNESYN (TRADEMARK)
U SERVOMOTORS

MAGNET COILS
High-field conductor testing at the FENIX facility
[DE93-012318] 01 p0387 N94-10737
Magnetic island suppression in torsatron configurations
[DE93-621681] 01 p0392 N94-11215
Electrodynamic forces of the cross-connected figure-eight null-flux coil suspension system
[DE93-015139] 03 p1048 N94-16969
Nonparaxial MHD stabilizers for an axisymmetric magnetic mirror
[DE93-017996] 04 p1587 N94-18505
Contribution to the study of the additional losses in coil elements used in static converters
[ECL-92-60] 04 p1406 N94-19297
Stability of an uncooled segment of a high-temperature superconductor
[DE94-000476] 05 p2032 N94-21932
Developments in materials for high-field magnets
[DE94-000761] 06 p2307 N94-22987
Study of a system for producing a pulsed magnetic field (B 2T) with a frequency of 50 Hz
[ISL-N-601/92] 06 p2314 N94-25460
Development of an industrial CO2 laser for mask marking
[DE93-632901] 07 p2816 N94-26184
AC losses for the self field of an AC transport current with a DC transport current offset in high T(c) superconducting magnet coils for MagLev application
[DE94-005187] 08 p3268 N94-30907
Structural design of the superconducting Poloidal Field coils for the Tokamak Physics Experiment
[DE94-007078] 09 p3887 N94-31406
Design and evaluation of coils for a 50 mm diameter induction coilgun launcher
[DE94-005244] 09 p3603 N94-32671
Coaxial slow source
[DE94-008191] 09 p3892 N94-32800
Models for interpreting interstrand resistance measurements in Rutherford cables
[DE94-010844] 11 p4259 N94-36194

MAGNETIC ABSORPTION
U ELECTROMAGNETIC ABSORPTION

MAGNETIC ANOMALIES
A study on the magnetospheric activity using the AE, ap, and Dst geomagnetic indices
[INPE-5470-TDI/501] 01 p0276 N94-11165
Polarity reversals and tilt of the Earth's magnetic dipole 01 p0283 N94-12219
Pseudo magnetic anomaly derived from satellite altimetry and its application to the tectonics in the North Fuji Basin 01 p0208 N94-12645
Aeromagnetic work in the Lincoln Sea: 1991 survey
[DSIS-93-00308] 02 p0715 N94-13830
Dynamical model for the distribution of geomagnetically trapped anomalous-component ions
[ATR-91(9558)-6] 02 p0784 N94-13936
Research in particle physics
[DE93-040875] 04 p1567 N94-18534
Fabrication and evaluation of superconducting and semiconducting materials
[AD-A271645] 05 p2018 N94-20558
Modelling the gravity and magnetic field anomalies of the Chicxulub crater 05 p1862 N94-20668
Characterization of the Marquez Dome buried impact crater using gravity and magnetic data 05 p1863 N94-20882
A scalar-vector model of quark-antiquark interaction under linear confinement
[DE93-616871] 06 p2536 N94-25317
Observations of the geomagnetic field by Polar Patrol Balloon (PPB) experiment in Antarctica 08 p3359 N94-29235
Steps toward understanding the solar dynamo
[AD-A277398] 09 p3953 N94-32343
Surface conforming flexible eddy current probe for scanning varying surface contours
[AD-D016173] 09 p3627 N94-33018

MAGNETIC BEARINGS
Development of passive superconducting bearings. Phase 3
[AD-A266050] 01 p0180 N94-10706
Improvement of azimuthal homogeneity in permanent-magnet bearing rotors
[DE93-009954] 01 p0144 N94-11607
Cryogenic fluid film bearing tester development study
[NASA-CR-192586] 02 p0660 N94-12791
Fuzzy control of magnetic bearings 04 p1399 N94-18357
Acceleration-augmented LQG control of an active magnetic bearing 05 p1757 N94-21112
A new eddy current model for magnetic bearing control system design 05 p1763 N94-21698
The low noise momentum wheel MW-X: EM design and predicted properties 06 p2360 N94-24024
Superconducting energy storage
[DE94-002248] 06 p2395 N94-24654
Current leads and magnetic bearings
[DE94-004607] 08 p3297 N94-28461

A gimbaled low noise momentum wheel
08 p3162 N94-29640
Adaptive automatic balancing of magnetic bearing systems 10 p4067 N94-34338
Advanced technology lunar telescope
11 p4350 N94-35473
Influence of backup bearings and support structure dynamics on the behavior of rotors with active supports
[NASA-CR-196119] 11 p4274 N94-35500
Flywheel energy storage using superconducting magnetic bearings
[DE94-009817] 11 p4282 N94-35829
Second International Symposium on Magnetic Suspension Technology, part 1
[NASA-CP-3247-PT-1] 11 p4212 N94-35836
Aerospace applications of magnetic bearings
11 p4213 N94-35837
Nonlinear control of magnetic bearings
11 p4213 N94-35838
High performance data acquisition, identification, and monitoring for active magnetic bearings
11 p4213 N94-35839
High temperature superconductors for magnetic suspension applications 11 p4214 N94-35843
Measurement and characterization of force dynamics in high T(sub c) superconductors
11 p4214 N94-35844
Materials for efficient high-flux magnetic bearing actuators 11 p4214 N94-35845
Design, construction, and testing of a five active axes magnetic bearing system 11 p4214 N94-35846
Experimental measurement and calculation of losses in planar radial magnetic bearings
11 p4214 N94-35847
Active magnetic bearing control loop modeling for a finite element rotordynamics code 11 p4216 N94-35857
Modelling and control of a rotor supported by magnetic bearings 11 p4216 N94-35858
Dynamic analysis of a magnetic bearing system with flux control 11 p4216 N94-35859
Third order LPF type compensator for flexible rotor suspension 11 p4217 N94-35863
Second International Symposium on Magnetic Suspension Technology, part 2
[NASA-CP-3247-PT-2] 11 p4223 N94-35902
Integration of magnetic bearings in the design of advanced gas turbine engines 11 p4223 N94-35903
Electromechanical simulation and test of rotating systems with magnetic bearing or piezoelectric actuator active vibration control 11 p4223 N94-35905
Planar rotational magnetic micromotors with integrated shaft encoder and magnetic rotor levitation
11 p4224 N94-35907
Concepts of flywheels for energy storage using autostable high-T(sub c) superconducting magnetic bearings 11 p4224 N94-35909
Manufacturing and testing of a magnetically suspended composite flywheel energy storage system
11 p4224 N94-35910
Rotor dynamic behaviour of a high-speed oil-free motor compressor with a rigid coupling supported on four radial magnetic bearings 11 p4224 N94-35911
Magnetically suspended stepping motors for clean room and vacuum environments 11 p4225 N94-35915
Large angle magnetic suspension test fixture
[NASA-CR-196138] 12 p4390 N94-37450

MAGNETIC CIRCUITS
Direct current transducer
[DE92-644548] 01 p0141 N94-10533
Advanced electric motor technology flux mapping
[NASA-CR-193824] 02 p0621 N94-13186

MAGNETIC CLOUDS
Fragmentation of magnetized filamentary interstellar clouds 05 p2008 N94-22687
Gravitational instability of magnetized filamentary clouds. 1: Helical magnetic fields
05 p2008 N94-22688

MAGNETIC COILS
NT FIELD COILS
NT MAGNET COILS
Processing and transport properties of high J(sub c) silver clad Bi-2223 tapes and coils
[DE93-010674] 01 p0398 N94-11073
Fabrication, properties, and microstructures of high (Tc) tapes and coils made from Ag-clad Bi-2223 superconductor
[DE93-017405] 04 p1602 N94-19122
Assessment of stellarators as reactors
[DE93-017775] 06 p2548 N94-22916
Performance analysis of the combined EDS maglev propulsion, levitation, and guidance system
[DE94-001346] 06 p2352 N94-22996
Proposal of Modular Heliotron: Advanced modular helical system compatible with closed helical divertor
[NIFS-261] 06 p2552 N94-24458
The use of harmonics in 3-D magnetic fields
[DE94-002274] 06 p2299 N94-24656
Formulae for the calculation of the magnetic field strength in a Helmholtz system with circular coils
[NPL-DES-130] 08 p3260 N94-30785

MAGNETIC COMPRESSION
MHD simulation of deuterium-fiber-initiated Z-pinches with two-fluid effects
[DE93-012682] 01 p0384 N94-10158
Compact lightweight CO2 laser for SDIO application
[AD-A273010] 05 p1817 N94-21284
Physics of transport phenomena in magnetic confinement plasmas 05 p2000 N94-22628
Use of magnetic compression to support turbine engine rotors 08 p3314 N94-30484

MAGNETIC CONTROL
Magnetic island suppression in torsatron configurations
[DE93-621681] 01 p0392 N94-11215
Optical metrology of magnetically trapped hydrogen
[AD-A272110] 05 p1680 N94-20584
Fusion Plasma Theory. Task 1: Magnetic confinement fusion plasma theory
[DE94-000778] 05 p1998 N94-22019
A scalar-vector model of quark-antiquark interaction under linear confinement
[DE93-616871] 06 p2538 N94-25317
High-speed repetitive pellet injector for plasma fueling of magnetic confinement fusion devices
[DE94-002792] 07 p3042 N94-26140
The effect of magnetic field configuration on particle pinch velocity in Compact Helical System (CHS)
[AD-B183299L] 08 p3505 N94-29398
Magnetically operated check valve
[NASA-CASE-MSC-22046-1] 11 p4274 N94-35661
Active magnetic bearing control loop modeling for a finite element rotordynamics code 11 p4216 N94-35857
Modelling and control of a rotor supported by magnetic bearings 11 p4216 N94-35858
Time-delay control of a magnetic levitated linear positioning system 11 p4217 N94-35862
Potential formation and transport in open field line systems
[DE94-718910] 11 p4337 N94-35983

MAGNETIC COOLING
Proceedings of the 7th International Cryocooler Conference, part 1
[AD-A268448] 03 p0985 N94-17482
Proceedings of the 7th International Cryocooler Conference, part 2
[AD-A268449] 03 p0985 N94-17484
Proceedings of the 7th International Cryocooler Conference, part 3
[AD-A268450] 03 p0985 N94-17485
The 7th International Cryocooler Conference
[AD-A268451] 04 p1379 N94-18147

MAGNETIC CORES
Expectations for the Martian core magnetic field
05 p2120 N94-20792

MAGNETIC DIFFUSION
Magnetic fields in spiral galaxies
05 p2010 N94-22697

MAGNETIC DIPOLES
Polarity reversals and tilt of the Earth's magnetic dipole 01 p0283 N94-12219
Neptune high-latitude emission: Dependence of angle on frequency
[NASA-CR-193280] 02 p0848 N94-13476
Toroidal solenoids in the electromagnetic field and Aharonov-Casher effect
[DE93-629861] 04 p1566 N94-18152
Convection algorithms for magnetospheric particles
[AD-A270103] 04 p1493 N94-18871
Examination of low level magnetic dipole intensities in the transition nuclei Sm-148, Sm-150, Sm-152 and Sm-154, with inelastic photon scattering at S-DALINAC
[ETN-93-95069] 05 p1971 N94-20030
Iterative electromagnetic Born inversion applied to earth conductivity imaging
[DE93-040668] 05 p1859 N94-21928
Stability of beam in the Fermilab Main Injector
[DE94-000619] 05 p1982 N94-21934
Variable-field permanent magnet dipole
[DE94-000800] 05 p1820 N94-22020
Evaluation of APC NbTi superconductor in a model dipole magnet
[DE94-003258] 07 p3060 N94-26795
Electromagnetic fields and interference
[PB94-126489] 07 p2771 N94-26877
Limitation on the magnetic dipole moment of the reactor neutrino
[DE94-611171] 11 p4320 N94-35566
Formation of iron metal and grain coagulation in the solar nebula 11 p4373 N94-36170
Beam energy absolute measurement using K-edge absorption spectrometers
[DE94-010019] 11 p4331 N94-36192

MAGNETIC DISKS
Static Computer Memory Integrity Testing (SCMIT): An experiment flown on STS-40 as part of GAS payload G-616 04 p1325 N94-19169
Picoindentation hardness measurements using atomic force microscopy
[AD-A270877] 04 p1604 N94-19579
Microtribology of magnetic media
[AD-A271209] 04 p1407 N94-19722
Atomic-scale friction measurements using friction force microscopy. Part 2: Application to magnetic media
[AD-A270759] 04 p1447 N94-19767
Tribological studies of silicon for magnetic recording applications (Invited)
[AD-A270878] 04 p1447 N94-19784
Atomic-scale friction measurements using friction force microscopy. Part 2: Application to magnetic media
[AD-A275202] 08 p3298 N94-29290
Evolution of dynamo-generated magnetic fields in accretion disks around compact and young stars
09 p3931 N94-31138
Nonthermal accretion disk models around neutron stars 09 p3931 N94-31139
A redundant disk array architecture for efficient small writes
[AD-A276645] 09 p3815 N94-31940
Eurocap program-ebre station
[AD-A277044] 09 p3772 N94-32007
Storage media pipelining: Making good use of fine-grained media 10 p4155 N94-33816

MAGNETIC DISPERSION
Magnetic field dissipation and contraction of molecular clouds
[REPT-337] 06 p2603 N94-24976

MAGNETIC DISTURBANCES
NT MAGNETIC STORMS
NT POLAR SUBSTORMS
Preliminary results of observations of solar flares with Nobeyama Radioheliograph 05 p2001 N94-22633
Utility of interplanetary scintillation maps in forecasting geomagnetic activity: A study based on single-station data from Cambridge, United Kingdom
[PB94-156775] 10 p4087 N94-34600
Space environment laboratory in review, 1993
[PB94-153004] 10 p4187 N94-34946
Solar-Terrestrial Predictions, 4: Proceedings of a workshop. Volume 1: Workshop overview papers; working group reports; User community reports; Regional Warning Center Reports
[PB94-173176] 12 p4471 N94-37780

MAGNETIC EFFECTS
The effect of a uniform magnetic field on the onset of steady Marangoni convection in a layer of conducting fluid 01 p0120 N94-10222
On thermodynamic properties of heavy fermion systems in magnetic field
[DE93-613819] 01 p0409 N94-10403
Analytical description of the torsatron Uragan-2M magnetic configuration with account of plasma pressure and external correcting magnetic field
[DE93-620983] 01 p0391 N94-11174
Are cosmic rays effective for ionization of the solar nebula? 01 p0472 N94-12220
Multiwavelength observations of unidentified high energy gamma ray sources
[NASA-CR-194536] 02 p0840 N94-14688
A study of relaxation transitions in the polymers under the influence of magnetic fields
[AD-A263878] 03 p0963 N94-15133
Magnetic effects in anomalous dispersion
[DE93-014291] 03 p1175 N94-15978
Magnetic effects in Venus/solar wind interaction
[NASA-CR-194666] 03 p1299 N94-17281
A general purpose ionospheric ray tracing procedure
[AD-A271058] 05 p1854 N94-19860
Study of possible energy upgrade for the ALS and modeling of the real lattice for the diagnosis of lattice problems
[DE93-040286] 05 p2016 N94-20323
Characterization of convection related defects in II-VI compound semiconductors
[NASA-CR-194704] 05 p2030 N94-21778
Effects of magnetic field perturbations in the ATF torsatron
[DE94-000474] 05 p1999 N94-22568
The structure and spin dynamics of lanthanide-bearing silicate glasses
[DE94-001320] 06 p2252 N94-22992
Steady induction effects in geomagnetism. Part 1C: Geomagnetic estimation of steady surficial core motions: Application to the definitive geomagnetic reference field models
[NASA-TP-3272-PT-1C] 06 p2403 N94-24465

An investigation of magnetic field effects on plume density and temperature profiles of an applied-field MPD thruster
[NASA-TM-106416] 07 p2700 N94-26090
Magnetostriction and magnetostrictive materials
[VTT-TIED-1434] 07 p3058 N94-26545
Direct evidence of the interplanetary magnetic field effect on the cosmic-ray shadow by the sun
[ICRR-296-93-8] 07 p3116 N94-27607
Cryogenic fracture behavior of 316LN in magnetic fields up to 14.6 T
[DE94-005215] 07 p2742 N94-27694
Potential hazards of magnetic resonance imagers to emergency medical service helicopter operations
[AD-A278873] 08 p3135 N94-29862
Electromagnetic effect on turbulent transport in liquid metals and electrolytes (bath)
[PB94-138450] 08 p3206 N94-29946
Localization in presence of magnetic field in 2-D disordered binary alloys
[DE94-608093] 08 p3208 N94-30108
Magnetic properties of a transverse spin-1 Ising model with longitudinal crystal field interactions
[DE94-608118] 08 p3517 N94-30165
Evolution of protoplanetary disks with dynamo magnetic fields 09 p3931 N94-31135
Magnetless magnetic fusion
[DE94-007114] 09 p3891 N94-32686
Anomalous transport equations in toroidal plasmas
[DE94-009206] 09 p3893 N94-32922
Magnetic field sources and their threat to magnetic media 10 p4151 N94-33794
Magnetic island effects, interactions in tokamaks
[DE94-009209] 10 p4145 N94-34221
Magnetic field effect on selective photoionization
[DE94-611079] 11 p4334 N94-36180

MAGNETIC ENERGY STORAGE

Technology assessments of advanced energy storage systems for electric and hybrid vehicles
[DE93-014395] 02 p0701 N94-12913
Engineering design of a high-temperature superconductor current lead
[DE93-015156] 03 p1013 N94-17226
Analysis of superconducting magnetic energy storage applications at a proposed wind farm site near Browning, Montana
[DE93-018793] 04 p1466 N94-18276
Superconducting energy storage
[DE94-002248] 06 p2395 N94-24654
Battery energy and superconducting magnetic energy storage for utility applications: A qualitative analysis
[DE94-005382] 08 p3336 N94-28489

MAGNETIC EQUATOR

The effects of magnetic storm phases on F-layer irregularities from auroral to equatorial latitudes
[AD-A275203] 08 p3356 N94-28891

MAGNETIC FIELD CONFIGURATIONS

NT MAGNETIC ISLANDS
Optimization of break-down conditions in tokamak TOTUS
[DE93-617863] 01 p0386 N94-10524
Calculation of Mercier stability criterium in stellarators
[DE93-621599] 01 p0389 N94-11091
Charged particle motion in torsatrons, part 1
[DE93-621639] 01 p0389 N94-11119
Particle transport analysis in torsatron configurations
[DE93-621640] 01 p0390 N94-11120
Analytical description of the torsatron Uragan-2M magnetic configuration with account of plasma pressure and external correcting magnetic field
[DE93-620983] 01 p0391 N94-11174
Simple kinetic model for plasma in stochastic helical field
[DE93-621643] 01 p0391 N94-11208
Magnetic island suppression in torsatron configurations
[DE93-621681] 01 p0392 N94-11215
Short pulse lasers for generation of fields exceeding 100 MG
[DE93-013346] 01 p0369 N94-11815
Nonlinear analysis of a magnicon output cavity
[AD-A265342] 01 p0145 N94-12424
Theory of field-reversed configurations
[DE93-015611] 02 p0794 N94-12862
Evolution of the interplanetary magnetic field
[DE93-012631] 02 p0836 N94-13262
Studies of non-inductive current drive in the CDX-U tokamak 02 p0799 N94-13680
Current distribution tomography for determination of internal current density distributions
[DE93-015463] 02 p0604 N94-13899
Stability and confinement properties of small-aspect-ratio tokamak
[INPE-5463-PRE/1771] 02 p0801 N94-14024
Method and apparatus for forming an agile plasma mirror effective as a microwave reflector
[AD-D015788] 03 p0998 N94-16535
The inverse problem to the evaluation of magnetic fields
[DE93-015239] 03 p1175 N94-17288
Profile stabilization of tilt mode in a field reversed configuration
[DE93-016770] 04 p1583 N94-17753
Filamentary magnetohydrodynamic plasmas
[DE93-015616] 04 p1583 N94-17945
Toroidal solenoids in the electromagnetic field and Aharonov-Casher effect
[DE93-629861] 04 p1566 N94-18152
Finite beta plasma equilibrium in toroidally linked mirrors
[DE93-040318] 04 p1590 N94-19193
Magnetic and crystallographic structures in UTX intermetallic compounds
[DE93-018291] 04 p1605 N94-19735
Magnetically controlled solar nebula
05 p2120 N94-20791
Temperature dependence of magnetic order in single-crystalline UPdSn
[DE93-040153] 05 p2033 N94-21991
Initial operation of a large-scale plasma source ion implantation experiment
[DE94-000805] 05 p2036 N94-22583
Numerical simulation of magnetic reconnection associated with emerging flux in the solar atmosphere
05 p2004 N94-22654
MHD relaxation in magnetic loops
05 p2004 N94-22658
Particle acceleration in a filamentary current sheet model 05 p2004 N94-22659
Dynamics of physical state during two current loops collision 05 p2005 N94-22663
Enhanced absorption of p-modes on sunspot and plage regions 05 p2006 N94-22671
Gamma ray burst as a result of the explosive instability in the magnetosphere of old neutron star
05 p2007 N94-22675
Asymptotic structure of magnetically driven MHD wind
05 p2008 N94-22682
MHD flows from compact objects: Effects on magnetic field configurations 05 p2008 N94-22684
Gravitational instability of magnetized filamentary clouds. 1: Helical magnetic fields
05 p2008 N94-22688
Gravitational instability of magnetized filamentary clouds. 2: Rotation 05 p2009 N94-22689
Magnetic superbubbles in the galactic disk and halo
05 p2009 N94-22694
Generation and maintenance of bisymmetric spiral magnetic fields in disk galaxies in differential rotation
05 p2010 N94-22695
The relaxed state and entropy production due to the electric resistivity and viscosity of plasma
05 p2010 N94-22696
Magnetic fields in spiral galaxies
05 p2010 N94-22697
Plasma initiation in a tokamak with conducting superstructure: First results from Alcator C-MOD
[DE94-001565] 06 p2552 N94-24504
Structure of the modulated magnetic phase of Mn3Sn
[DE94-002788] 07 p2733 N94-26092
The ZnO thin films with C-axis orientation prepared on the room temperature substrate by the ECR multipolar plasma sputtering method
[DE94-605039] 07 p2758 N94-27857
Atomic and magnetic structure of YBa2(Cu(1-x)Fe(x))3O(6+y) at 0.05 less than or equal to x less than or equal to 0.30, y is approximately equal to 1 and y is approximately equal to 0.5
[DE94-606852] 08 p3513 N94-29210
A 6MeV heavy ion beam probe for the Large Helical Device
[AD-B183695L] 08 p3505 N94-29397
The effect of magnetic field configuration on particle pinch velocity in Compact Helical System (CHS)
[AD-B183299L] 08 p3505 N94-29398
Magnetic field generation by circularly polarized laser light and inertial plasma confinement in a miniature magnetic bottle induced by circularly polarized laser light
[DE94-608353] 08 p3508 N94-30192
Dynamics of flux tubes in accretion disks
09 p3932 N94-31142
Radiation from an aperture into an anisotropic plasma half-space 09 p3885 N94-31205
Planetary magnetotails: Magnetic configuration and nonthermal plasma 09 p3942 N94-32326
Magnetless magnetic fusion
[DE94-007114] 09 p3891 N94-32686
Stability of bootstrap current driven magnetic islands in stellarators
[DE94-009207] 09 p3893 N94-32912
Summary of experimental progress and suggestions for future work
[DE94-008893] 10 p4145 N94-34012
Magnetic island effects, interactions in tokamaks
[DE94-009209] 10 p4145 N94-34221
LHD helical divertor
[DE94-727626] 11 p4336 N94-35752
Analysis of recent agile mirror data
[AD-A278758] 11 p4318 N94-36427

MAGNETIC FIELD INTENSITY

U MAGNETIC FLUX

MAGNETIC FIELD INVERSIONS

Polarity reversals and tilt of the Earth's magnetic dipole 01 p0283 N94-12219
Large-scale velocity fields and small-scale magnetic fields during the maximum of solar cycle 22
[AD-A278378] 10 p4165 N94-33743

MAGNETIC FIELD RECONNECTION

A study of the magnetic field annihilation process in the magnetosphere and some geotechnical applications
[DE93-013249] 01 p0273 N94-10305
A study of the magnetic field annihilation process in the magnetosphere and some geotechnical applications
[DE93-013248] 01 p0273 N94-10319
Simulation study of dynamo structure in reversed field pinch
[DE93-771406] 01 p0390 N94-11128
Macroscopic behaviour and discrete dynamo of RFP plasma in high theta discharge
[DE93-771408] 01 p0392 N94-11239
The interplanetary origins and the main-phase development of moderate geomagnetic storms (1978 - 1979)
[INPE-5445-TDI/491] 02 p0835 N94-13174
Resonant absorption of Alfven waves near a neutral point
[DE93-628761] 04 p1586 N94-18172
Driven reconnection and self-organization
05 p2000 N94-22625
Numerical simulation of magnetic reconnection associated with emerging flux in the solar atmosphere
05 p2004 N94-22654
Magnetic reconnection in emission nebulae in clusters of galaxies 05 p2010 N94-22700
Two populations and models of gamma ray bursts
[NASA-CR-194762] 06 p2629 N94-22947
Reduction of the anode fall in a coaxial plasma thruster with an applied magnetic nozzle
[DE94-000670] 06 p2218 N94-23283
Nonlinear growth of strongly unstable tearing modes
[DE94-003366] 07 p3042 N94-25958
Computer simulations on development of the fast reconnection mechanism 08 p3360 N94-29241
Nonthermal accretion disk models around neutron stars 09 p3931 N94-31139
A triggering mechanism of fast crash in sawtooth oscillation
[DE94-718974] 11 p4336 N94-35772
Studies of the dayside boundary layer processes based on ground observations in the Svalbard area
[AD-A280715] 11 p4292 N94-36265

MAGNETIC FIELDS

NT BIOMAGNETISM
NT FORCE-FREE MAGNETIC FIELDS
NT GEOMAGNETISM
NT INTERPLANETARY MAGNETIC FIELDS
NT INTERSTELLAR MAGNETIC FIELDS
NT LUNAR MAGNETIC FIELDS
NT MAGNETIC CLOUDS
NT MAGNETOSTATIC FIELDS
NT NONUNIFORM MAGNETIC FIELDS
NT PALEOMAGNETISM
NT PLANETARY MAGNETIC FIELDS
NT SOLAR MAGNETIC FIELD
NT STELLAR MAGNETIC FIELDS
The use of magnetic fields for damping unsteady Marangoni convection in GaAs floating zones under microgravity 01 p0100 N94-10073
Calculation of the effects of magnetic field damping in fluid flow: Comparison of magnetohydrodynamic models of different complexity 01 p0103 N94-10089
CdTe crystal growth in the Soviet facility zona 4
01 p0106 N94-10111
CdTe crystal growth by THM with a rotating magnetic field 01 p0107 N94-10116
New mechanism of Ostwald ripening in Lorentz-force stabilized Cu-Pb dispersions 01 p0116 N94-10192
Results of crystal growth experiments by FZM on Zona facilities in microgravity 01 p0116 N94-10193
THM-growth of III-V-semiconductors in the magnetic field 01 p0118 N94-10209
The effect of a uniform magnetic field on the onset of steady Marangoni convection in a layer of conducting fluid 01 p0120 N94-10222

Nonlinear second harmonic generation by light wave-plasma interaction in oscillating magnetic field
[DE93-613723] 01 p0386 N94-10387
Stationary spectra in a magnetized current-carrying plasma
[DE93-617847] 01 p0386 N94-10397
On thermodynamic properties of heavy fermion systems in magnetic field
[DE93-613819] 01 p0409 N94-10403
Stationary spectra in a finite-pressure current-carrying plasma
[DE93-617848] 01 p0387 N94-10538
Stationary spectra in a sheared plasma (linear limit)
[DE93-617850] 01 p0387 N94-10540
Quantum mechanical effects of topological origin
01 p0378 N94-10594
New squeezed landau states
01 p0379 N94-10601
Power losses of a type 2 superconducting slab of arbitrary thickness in the presence of alternating current conductors
[DE93-617892] 01 p0396 N94-10716
Reversed-field pinch studies in the Madison Symmetric Torus
[DE93-013464] 01 p0388 N94-10747
Stationary spectra of short-wave convective and magnetostatic fluctuations in a finite-pressure plasma and anomalous heat conductivity
[DE93-617852] 01 p0388 N94-10840
Calculation of Mercier stability criterium in stellarators
[DE93-621599] 01 p0389 N94-11091
Possibilities of magnetic diagnostics in stellarators
[DE93-621608] 01 p0389 N94-11092
Radiative properties of strongly magnetized plasmas
[DE93-014096] 01 p0389 N94-11118
Magnetic Earth Ionosphere Resonant Frequencies (MEIRF) project
[NASA-CR-193182] 01 p0276 N94-11355
Accretion disk viscosity and internal waves in disks
01 p0153 N94-11615
The magnetic field of rotating bodies
[DE93-619769] 01 p0427 N94-11812
Polarity reversals and tilt of the Earth's magnetic dipole 01 p0283 N94-12219
On the unique structure of the magnetic fields of Uranus and Neptune 01 p0472 N94-12221
Pilot trial of potentiating normal healing of stress fractures using pulsing electromagnetic fields
[AD-A264251] 01 p0311 N94-12364
A 3D gyrokinetic particle-in-cell simulation of fusion plasma microturbulence on parallel computers
[DE93-012503] 02 p0794 N94-12846
Investigation of dynamics of plasma fluxes generated by the quasi-stationary plasma accelerator P-50
[DE93-621665] 02 p0794 N94-12854
Plasma diffusion through multidipole magnetic fields
[INPE-5460-PRE/1768] 02 p0795 N94-12901
Kinetic simulations of ultra-intense laser plasma interactions and a novel method of generating odd harmonics
[DE93-014418] 02 p0797 N94-13207
Evolution of the interplanetary magnetic field
[DE93-012631] 02 p0836 N94-13262
Neptune high-latitude emission: Dependence of angle on frequency
[NASA-CR-193280] 02 p0848 N94-13476
The geometric phase in quantum physics
[DE93-011121] 02 p0817 N94-13479
ADP study of gamma-ray bursts
[NASA-CR-194311] 02 p0848 N94-13708
Casting of superconducting composite materials (M-4)
02 p0586 N94-13736
Energetic neutral atoms: Imaging the magnetospheric ring current
[NASA-CR-194339] 02 p0715 N94-13826
Mutual inductance between partially wound tori and a bifilar conductor
[ETN-93-94388] 02 p0624 N94-13998
Multi-bunch beam-break-up studies for a SWFEL/TBA
[DE93-016973] 02 p0658 N94-14414
Interactions among convection, magnetic fields and p-mode oscillations in the sun
[NASA-CR-194477] 02 p0845 N94-14479
Kinetic simulations of ultra-intense laser plasma interactions
[DE93-014419] 02 p0802 N94-14564
Theory of the negative magnetoresistance in magnetic metallic multilayers
[DE93-013912] 02 p0776 N94-14584
Investigations of transitions from order to chaos in dynamical systems
[DE93-014438] 02 p0818 N94-14738
Construction of the Courant-Snyder invariants for the non-linear equations of motion under presence of the linear coupling
[DE93-017565] 02 p0788 N94-14872
An adiabatic demagnetisation refrigerator with a mechanical pre-cooler for space applications
03 p0906 N94-15070
Benard convection of magnetic colloids under microgravity 03 p0943 N94-15159
Formation of the stable auroral arc that intensifies at substorm onset
[NASA-CR-193637] 03 p1098 N94-15433
The fractional quantum Hall effect and the rotation group
[DE93-010348] 03 p1207 N94-15972
Method and apparatus for forming an agile plasma mirror effective as a microwave reflector
[AD-D015788] 03 p0998 N94-16535
TransRapid TR-07 maglev-spectrum magnetic field effects on daily pineal indoleamine metabolic rhythms in rodents
[DE93-015143] 03 p1117 N94-16893
The inverse problem to the evaluation of magnetic fields
[DE93-015239] 03 p1175 N94-17288
High power steady state MPD thrusters
[AD-A267277] 03 p0928 N94-17308
Comparison of computer predictions and magnetic field measurements for an iron spectrometer magnet
[DE93-016164] 03 p1176 N94-17658
The phase mixing of shear Alfven waves
[DE93-624920] 04 p1581 N94-17688
Limits on m = 2, n = 1 error field induced locked mode instability in TPX with typical sources of poloidal field coil error field and a proto type correction coil, C-coil
[DE93-014408] 04 p1582 N94-17702
Corroboration of magnetic forces in US Maglev design
[DE93-014918] 04 p1443 N94-17785
Rapid geophysical surveyor
[DE93-016637] 04 p1461 N94-17851
Synthesis and study of high-T(sub c) superconducting electronic materials
[AD-A268851] 04 p1402 N94-18390
Comparison of ferrite materials for pulse applications
[DE93-017224] 04 p1574 N94-18497
Magnetic field measurements of a superconducting undulator for a Harmonic Generation FEL experiment at the NSLS
[DE93-017621] 04 p1438 N94-18504
Numerical modelling of fringing fields and their use for complex permittivity measurements at high frequencies
[AD-A270198] 04 p1388 N94-18782
Convection algorithms for magnetospheric particles
[AD-A270103] 04 p1493 N94-18871
Fabrication and characterization of high-T(sub c) tapes and coils made from Ag-clad Bi-2223 superconductors
[DE93-018615] 04 p1601 N94-18993
Three dimensional multipole decomposition of fields
[DE93-018530] 04 p1389 N94-19053
The Cluster magnetic field investigation: Scientific objectives and instrumentation 04 p1329 N94-19629
The Electron Drift Instrument for Cluster
04 p1329 N94-19630
Transient skin effect in a massive cylinder by eccentric location of exciting conduction bands
[ETN-93-95048] 04 p1391 N94-19646
Effect of exciton localization and delocalization on magnetic-field-dependent photoluminescence linewidths in semiconductors
[DE93-018860] 05 p1748 N94-19884
Space-charge dominated beam transport in magnetic quadrupoles with large aperture ratios
[DE93-040443] 05 p1992 N94-20004
Resistive gate magnetic field sensor
[AD-D015923] 05 p1749 N94-20199
Neoclassical kinetic theory near an X-point: Plateau regime
[DE93-019825] 05 p1951 N94-20224
Measurement and correction of magnetic fields in pulsed slotted-tube microwigglers
[DE93-040100] 05 p1815 N94-20272
The National High Magnetic Field Laboratory, a user facility in support of research in high magnetic fields
[DE93-040145] 05 p1714 N94-20278
Longitudinal instability of an induction linac with acceleration
[DE93-019249] 05 p1980 N94-20290
A study of the induction heating of organic composites
[AD-A272657] 05 p1675 N94-21187
Ionospheric photoelectrons measured at geosynchronous orbit
[AD-A272431] 05 p1857 N94-21202
The angular velocity spread of REB induced by magnetic field discontinuity
[IPPCZ-331] 05 p1996 N94-21573
Results from long conduction time plasma opening switch experiments at Sandia National Laboratories
[DE93-019063] 05 p1762 N94-21632
Relaxation of hysteresis loop in a single crystal of YBa2Cu4O8
[DE93-019519] 05 p2029 N94-21649
On the stability of shear-Alfven vortices
[DE93-040912] 05 p1996 N94-21752
Studies of electromagnetic ion cyclotron waves using AMPTE/CCE and Dynamics Explorer
[NASA-CR-194711] 05 p1982 N94-21878
Iterative electromagnetic Born inversion applied to earth conductivity imaging
[DE93-040668] 05 p1859 N94-21928
A moving finite element model of the tokamak scrapeoff layer
[DE94-000673] 05 p1997 N94-21965
Magnetic insulation of secondary electrons in plasma source ion implantation
[DE93-040106] 05 p1997 N94-21988
Variable-field permanent magnet dipole
[DE94-000800] 05 p1820 N94-22020
Effects of magnetic field perturbations in the ATF torsatron
[DE94-000474] 05 p1999 N94-22568
Test results of two high temperature superconducting sample coils
[DE94-000496] 05 p2035 N94-22570
The de Haas-van Alphen measurements in Ba(0.6)K(0.4)BiO3
[DE93-041169] 06 p2556 N94-22920
Simple estimate of stored energy and conductor insulation voltage-withstand requirements for advanced solenoid magnet designs
[DE93-041048] 06 p2307 N94-23019
Reduction of the anode fall in a coaxial plasma thruster with an applied magnetic nozzle
[DE94-000670] 06 p2218 N94-23283
Three-dimensional solidification and melting using magnetic field control 06 p2325 N94-23664
Application of multigrid methods to the solution of liquid crystal equations on a SIMD computer
06 p2484 N94-23686
Research for electric energy systems
[DE94-001839] 06 p2293 N94-23719
Review of a variational method applied to magnetoelastic buckling problems
[PB94-111184] 06 p2562 N94-23769
Exact transformation of the anisotropic Ginzburg-Landau model and its consequences
[DE94-002208] 06 p2562 N94-23795
Magnetic power piston fluid compressor
[NASA-CASE-GSC-13565-1] 06 p2354 N94-23831
Magnetic shielding of interplanetary spacecraft against solar flare radiation
[NASA-CR-195539] 06 p2204 N94-24334
The use of harmonics in 3-D magnetic fields
[DE94-002274] 06 p2299 N94-24656
Compact free electron lasers for medical applications
[AD-A273609] 06 p2350 N94-24934
The role of emitter states in magnetotunneling through double-barrier resonant-tunneling diodes at high magnetic fields
[REPT-A-2658] 06 p2564 N94-24959
On superconductivity of alpha-(BEDT-TTF)2KHg(SCN)4
[REPT-A-2660] 06 p2564 N94-24978
An active antenna for ELF magnetic fields
06 p2303 N94-25192
The nanostructure of multilayered films: A NMR study
[ETN-94-95347] 06 p2262 N94-25222
A relativistic theory on wave propagation in inhomogeneous magnetoplasmas
[ETN-94-95322] 06 p2554 N94-25285
The anomalous transport caused by particles transverse drift
[DE93-613685] 06 p2554 N94-25329
Study of a system for producing a pulsed magnetic field (B 2T) with a frequency of 50 Hz
[ISL-N-601/92] 06 p2314 N94-25460
Magnetic field-induced saddle point in GaAs/AlGaAs short period superlattices
[REPT-A-2656] 06 p2568 N94-25515
Diffusion in electronegative discharges with magnetic fields
[AD-A273826] 06 p2304 N94-25521
Shielded Coil Electrodynamic Propulsion (SCEP). A feasibility study
[AD-A273824] 06 p2314 N94-25539
Study on phase transformation due to deformation in ferromagnetic fields at cryogenic condition
07 p2724 N94-25556
An optimal constrained linear inverse method for magnetic source imaging
[DE94-004014] 07 p2957 N94-25663
Electromagnetic properties of a toroidal solenoid
[DE93-613032] 07 p2766 N94-25866

An investigation of magnetic field effects on plume density and temperature profiles of an applied-field MPD thruster
[NASA-TM-106416] 07 p2700 N94-26090
Detection of transient vector-fields in additive noise
[FFI-93/7028] 07 p2768 N94-26232
Ising critical behaviour in the one-dimensional frustrated quantum XY model
[DE93-634755] 07 p3057 N94-26390
The influence of energy losses with time in NbTi superconductors in pulsed magnetic fields
[DE93-634761] 07 p3058 N94-26512
A mechanism for resistive dissipation in Ag sheathed Bi2Sr2CaCu2O8 and Bi2Sr2Ca2Cu3O10
[DE94-003009] 07 p3060 N94-26771
Asymptotics for Kummer functions, Bose plasmas, and related special functions
[DE94-601853] 07 p3007 N94-26928
An optimal constrained linear inverse method for magnetic source imaging
[DE94-002264] 07 p2996 N94-26936
Detection of low-intensity magnetic fields with a magnetostrictive fiber optic sensor
[AD-A274120] 07 p3037 N94-27062
Technical report of ISSP. Ser. A, no. 2674: High-field cyclotron resonance and impurity transition in n- and p-3C-SiC at magnetic fields up to 175 T
[JTN-94-80560] 07 p3064 N94-27232
Technical report of ISSP. Ser. A, no. 2672: Magneto-optical effects of excitons in BiI3 crystals under pulsed high magnetic fields. 3: Excitons confined around a stacking disorder formed by a bending stress
[JTN-94-80558] 07 p3065 N94-27240
Technical report of ISSP. Ser. A, no. 2675: High-field cyclotron resonance and valence-band structure in semiconducting diamond
[JTN-94-80561] 07 p3065 N94-27245
Researches of the Electrotechnical Laboratory. No. 51: Study of formation and sustainment of reversed field pinch by slow control of magnetic field
[JTN-94-80548] 07 p3046 N94-27350
Study of the hyperfine magnetic field at Ta-181 site in the Heusler Co2ScSn, Co2ScGa, and Co2HfSn alloys
[DE94-603989] 07 p3067 N94-27623
Fiber optic Faraday flux transformer specification
[AD-D016058] 07 p3039 N94-27674
Cryogenic fracture behavior of 316LN in magnetic fields up to 14.6 T
[DE94-005215] 07 p2742 N94-27694
Mode analysis of gyrotron oscillation using a k-spectrometer
[DE94-701195] 07 p2813 N94-27703
Atomic processes in Inertial Electrostatic Confinement (IEC) devices
[DE94-005015] 07 p3047 N94-27715
Advanced development of particle beam probe diagnostic system
[DE94-002316] 07 p3047 N94-27720
Passive stabilization of MHD instabilities at high (beta)n in the HBT-EP tokamak
[DE94-003317] 07 p3047 N94-27735
Technical report of ISSP. Ser. A, no. 2687: Quantized persistent currents of a quantum dot in a strong magnetic field
[JTN-94-80573] 07 p3028 N94-27758
Experimental results of 40-kA Nb3Al conductor
[DE94-701207] 07 p2788 N94-27821
The three-dimensional hydrogen atom in crossed magnetic and electric fields
[DE94-606301] 07 p3029 N94-27847
Three-dimensional finite element modeling of a magnet array spinning above a conductor
[DE94-004573] 08 p3468 N94-28459
Effect of phonon dispersion on properties of exciton in magnetic field
[DE93-634756] 08 p3481 N94-28469
Estimation of geomagnetic conjugate points by using Pc5 pulsations 08 p3357 N94-29079
Transient internal probe
[AD-A275054] 08 p3505 N94-29134
Orbital applications of electrodynamic propulsion
[AD-A275413] 08 p3173 N94-29216
Observations of the geomagnetic field by Polar Patrol Balloon (PPB) experiment in Antarctica
08 p3359 N94-29235
Formation and self-healing of magnetic islands in finite-beta helias equilibria
[AD-B183271L] 08 p3505 N94-29483
Nonadiabatic effects in the quantum Hall regime
08 p3513 N94-29530
Fast gravity, gravity partials, normalized gravity, gravity gradient torque and magnetic field: Derivation, code and data
[NASA-CR-188243] 08 p3361 N94-29588
Three-axis fiber optic vector magnetometer
[AD-D016016] 08 p3288 N94-29699
Potential hazards of magnetic resonance imagers to emergency medical service helicopter operations
[AD-A278873] 08 p3135 N94-29862
Quasi-adiabatic motion of energetic particles in a dipole magnetic field
[DE94-607322] 08 p3362 N94-29935
Electromagnetic effect on turbulent transport in liquid metals and electrolytes (bath)
[PB94-138450] 08 p3206 N94-29946
Estimating the cost of large superconducting thin solenoid magnets
[DE94-006289] 08 p3468 N94-30026
Algorithm and program ORANGE for magnetic field simulation of magnetic system spectrometer STORS
[DE94-608013] 08 p3421 N94-30083
Localization in presence of magnetic field in 2-D disordered binary alloys
[DE94-608093] 08 p3208 N94-30108
Some results on the phase diagram of the antiferromagnetic Potts model in an external magnetic field
[DE94-608115] 08 p3468 N94-30110
Periodic electromagnetic vacuum in the two-dimensional Yang-Mills theory with the Chern-Simons mass
[DE94-608128] 08 p3525 N94-30170
Resistive ballooning mode in a gas-dynamic trap
[DE94-608328] 08 p3508 N94-30171
Magnetic field generation by circularly polarized laser light and inertial plasma confinement in a miniature magnetic bottle induced by circularly polarized laser light
[DE94-608353] 08 p3508 N94-30192
Electric power lines: Questions and answers on research into health effects
[DE94-005637] 08 p3353 N94-30757
Formulae for the calculation of the magnetic field strength in a Helmholtz system with circular coils
[NPL-DES-130] 08 p3260 N94-30785
Nonlinear optics response of semiconductor quantum wells under high magnetic fields
[DE94-003244] 08 p3520 N94-30835
Magnetotransport measurements in magnetic fields up to 50T in SmB6 and FeSi
[DE94-006227] 08 p3520 N94-30848
Calculating the J(c), B, T surface for commercial niobium tin conductors using a reduced state model
[DE94-006296] 08 p3520 N94-30850
Intra- versus interlayer pairing in the copper oxide superconductors: Response to a magnetic field
[DE94-005475] 08 p3521 N94-30898
Laboratory and space experiments as a key to the plasma universe
[TRITA-ALP-1993-01] 09 p3885 N94-31088
Evolution of protoplanetary disks with dynamo magnetic fields 09 p3931 N94-31135
Evolution of dynamo-generated magnetic fields in accretion disks around compact and young stars
09 p3931 N94-31138
Toroidal pinch experiments
[DE94-005876] 09 p3887 N94-31558
Fiberoptisk magnetfaltsensor (fiber optic magnetometer)
[PB94-148061] 09 p3878 N94-31584
Collective acceleration in solar flares
[DE94-006288] 09 p3953 N94-31632
Fermi surface instability at 0.4 K in a heavy-fermion YbBiPt: SDW?
[DE94-006224] 09 p3899 N94-31916
Transport phenomena in the Earth's plasma sheet
09 p3772 N94-31970
Stability of bootstrap current driven magnetic islands in stellarators
[DE94-009207] 09 p3893 N94-32912
Anomalous transport equations in toroidal plasmas
[DE94-009206] 09 p3893 N94-32922
Investigation of superconductivity and magnetism in d and f-electron materials
[DE94-008535] 09 p3907 N94-32933
Electron acceleration system
[AD-D016143] 09 p3893 N94-32977
An approximate Riemann solver for magnetohydrodynamics (that works in more than one dimension)
[AD-280296] 09 p3849 N94-33033
Magnetic field sources and their threat to magnetic media 10 p4151 N94-33794
CDAW-9 analysis of magnetospheric events on 3 May 1986: Event C
[AD-A277610] 10 p4086 N94-33851
Transport properties of interacting magnetic islands in tokamak plasmas
[DE94-009208] 10 p4145 N94-34140
Space environment laboratory in review, 1993
[PB94-153004] 10 p4187 N94-34946
The study of the local magnetic field in the oxide alpha-Bi2O3 by the mu SR-technique
[DE94-612636] 11 p4322 N94-35751
Particle orbit analysis for LHD helical axis configurations
[DE94-718995] 11 p4336 N94-35773
Magnetoresistance of films and strips with the diffuse surface scattering
[DE94-611100] 11 p4340 N94-35933
Zero modes of the two-dimensional Dirac operator on a noncompact Riemann surface in an external magnetic field
[DE94-616618] 11 p4343 N94-36071
Functional integration method for the one-dimensional localization, the higher correlators and mean current in mesoscopic ring in the arbitrary magnetic field
[DE94-616621] 11 p4325 N94-36073
Numerical method to study the stability of periodic solutions of particle motion in nonlinear magnetic fields
[DE94-610740] 11 p4325 N94-36088
Magnetic field effect on selective photoionization
[DE94-611079] 11 p4334 N94-36180
Magnetic properties of nanosize iron clusters
[DE94-011329] 11 p4318 N94-36204
Further studies of 60-Hz exposure effects on human function
[DE94-010192] 11 p4297 N94-36223
Magnetic metallic multilayers
[DE94-011913] 11 p4341 N94-36274
Simultaneous observations of the westward electrojet and the cross-tail current sheet during substorms
[AD-A278631] 11 p4292 N94-36383
Q-profile flattening due to nonlinear development of resistive kink mode and ensuing fast crash in sawtooth oscillations
[DE94-727625] 12 p4526 N94-36472
Pulsed field magnets at the United States National High Magnetic Field Laboratory
[DE94-002624] 12 p4436 N94-36514
Method of N-15 analysis by mass-spectroscopy on ion implanter MPB-200
[DE94-618203] 12 p4407 N94-36529
Design and analysis of high-field quasi-continuous magnets
[DE94-000762] 12 p4508 N94-36556
Relaxation of the density matrix for an arbitrary spin in random external fields
[DE94-618457] 12 p4509 N94-37078
Critical-state flux-density profiles in type-2 superconducting thin-film strips and disks
[DE94-011199] 12 p4535 N94-37166
A comparison of two examples of magnetic tracker systems 12 p4485 N94-37275
BMAP dipole magnetic field analysis and orbit tracking/calculations of energy deposition in GaAs WHEBY detectors
[DE94-012080] 12 p4522 N94-37303
Investigation of exposure to Extremely Low Frequency (ELF) magnetic and electric fields: Ongoing animals studies
[DE94-011239] 12 p4480 N94-37625
Symplectic tracking using point magnets and a reference orbit made of circular arcs and straight lines
[DE94-011919] 12 p4505 N94-37675
A freon-filled, holographic bubble chamber as a high energy photon burst spectrometer
[DE94-011645] 12 p4446 N94-37723

MAGNETIC FILMS

NRL review for 1993
[AD-A265666] 01 p0497 N94-12334
Epitaxial iron films
[AD-A268286] 03 p1217 N94-17579
Picoindentation hardness measurements using atomic force microscopy
[AD-A270877] 04 p1604 N94-19579
Magnetic Ultrathin Films: Multilayers and Surfaces, Interfaces, and Characterization, volume 313
[AD-A271402] 04 p1375 N94-19758
Magnetic circular dichroism in x ray absorption and core-level photoemission
[DE93-019381] 05 p1688 N94-19986
Giant magnetoresistance and microstructural characteristics of epitaxial Fe-Ag and Co-Ag granular thin films
[DE94-006287] 08 p3519 N94-30707
Resonant photoemission and magnetic x-ray circular dichroism in the M shell of ultrathin films of Fe
[DE94-007453] 10 p4029 N94-34120

MAGNETIC FLUX

Quantum mechanical effects of topological origin
01 p0378 N94-10594
On the possible unobservability of the Wu-Yang phase factor in curved space
[DE93-617645] 01 p0411 N94-10831
Advanced magnetic flux compression generator development issues: A comparison of coaxial and disk generators
[DE93-014025] 02 p0794 N94-12849

The study of structure-processing-property relations in copper oxide based high (Tc) superconductors
[DE93-015066] 02 p0804 N94-13003
Instability heating of the HDZP
[DE93-012641] 02 p0798 N94-13513
Review of the Procyon explosive pulsed power system
[DE93-016562] 02 p0802 N94-14532
Global auroral imaging: Dynamics of Explorer Miss ion
[NASA-CR-194284] 03 p1097 N94-15003
Effects of spin-orbit coupling on disordered mesoscopic systems
[ITN-93-85220] 03 p1180 N94-15288
Solar vector magnetic field research
[AD-A267367] 03 p1299 N94-17004
Microwave scattering from TAE modes
[DE93-018170] 04 p1583 N94-17809
Superconducting flux flow devices, digital circuits and memories
[DE93-019072] 04 p1405 N94-19079
Development, refinement, and testing of a short term solar flare prediction algorithm
[NASA-CR-194727] 05 p2147 N94-21832
The effect of correlated and point defects on the vortex lattice melting transition in single crystal YBa2Cu3O(7-delta)
[DE93-040277] 05 p2033 N94-21997
Research for electric energy systems
[DE94-001839] 06 p2293 N94-23719
Exact transformation of the anisotropic Ginzburg-Landau model and its consequences
[DE94-002208] 06 p2562 N94-23795
Magnetic field dissipation and contraction of molecular clouds
[REPT-337] 06 p2603 N94-24976
Mechanisms of anode power deposition in a low pressure free burning arc
[NASA-CR-194442] 06 p2553 N94-25190
Solar magnetic cycle
[NASA-CR-195202] 06 p2628 N94-25275
The Casimir energy of the rigid string with massive ends
[DE93-616851] 06 p2492 N94-25338
Diffusion in electronegative discharges with magnetic fields
[AD-A273826] 06 p2304 N94-25521
Flux flow, pinning, and resistive behavior in superconducting networks
[DE94-003400] 07 p3050 N94-25848
High resolution studies of sunspots and flux tubes
[NASA-CR-195216] 07 p3111 N94-27321
Technical report of ISSP. Ser. A, no. 2687: Quantized persistent currents of a quantum dot in a strong magnetic field
[JTN-94-80573] 07 p3028 N94-27758
Determination of the plasma column shape in the Tokamak Novillo cross section by magnetic probes
[DE94-604986] 07 p3048 N94-27844
The structure of solar magnetic fields and their associated electric currents 08 p3544 N94-29723
New evidence for flux cutting in type II superconductors
[ISBN-0-315-85830-3] 08 p3515 N94-30032
Periodic electromagnetic vacuum in the two-dimensional Yang-Mills theory with the Chern-Simons mass
[DE94-608128] 08 p3525 N94-30170
Magnetic flux reconstruction methods for shaped tokamaks
[DE94-005827] 08 p3510 N94-30882
Solar measurements from the Airglow-Solar Spectrometer Instrument (ASSI) on the San Marco 5 satellite
[NASA-CR-193815] 08 p3551 N94-30948
Dynamics of flux tubes in accretion disks
09 p3932 N94-31142
Theoretical principles for designing long stator/linear motors with iron
[ETN-94-95741] 09 p3688 N94-31374
Transport phenomena in the Earth's plasma sheet
09 p3772 N94-31970
Steps toward understanding the solar dynamo
[AD-A277398] 09 p3953 N94-32343
Substorm aurorae and their connection to the inner magnetosphere
[AD-A277609] 10 p4086 N94-33850
Studies on equatorial shock formation during plasmaspheric refilling
[NASA-CR-195864] 10 p4088 N94-34669
On the physics of waves in the solar atmosphere: Wave heating and wind acceleration
[NASA-CR-194119] 11 p4375 N94-36395
Critical-state flux-density profiles in type-2 superconducting thin-film strips and disks
[DE94-011199] 12 p4535 N94-37166

MAGNETIC INDUCTION
Simultaneous solution for core magnetic field and fluid flow beneath an electrically conducting mantle
[NASA-TM-4536] 02 p0716 N94-13960
Survey of subsurface geophysical exploration technologies adaptable to an airborne platform
[DE93-015080] 02 p0717 N94-14294
Calibration of a magnetic induction system for measurement of hypervelocities
[DE93-013949] 02 p0652 N94-14578
Footprint size of a helicopter-borne electromagnetic induction sounding system versus antenna altitude
[AD-A270468] 04 p1463 N94-19672
Projectile transverse motion and stability in electromagnetic induction launchers
[DE94-001557] 06 p2198 N94-23210
Excitation balances and transport in an inductively coupled plasma
[ETN-94-95330] 06 p2554 N94-25241
Time domain reflectometry for measuring bulk soil electrical conductivity and comparison with the Em38 instrument
[PB94-125432] 07 p2881 N94-27052
Analytical study of beam handling and emittance control
[AD-A274412] 07 p3033 N94-27078
A teleoperated system for remote site characterization
10 p4066 N94-34029
Advanced induction accelerator designs for ground based and space based FELs
[AD-A278885] 11 p4271 N94-35586

MAGNETIC INDUCTION PROBES
U MAGNETIC PROBES

MAGNETIC ISLANDS
Magnetic island suppression in torsatron configurations
[DE93-621681] 01 p0392 N94-11215
Analysis of stochastic particle behavior in a magnetic island due to electrostatic drift waves
[DE94-727553] 10 p4137 N94-33869
Magnetic island effects, interactions in tokamaks
[DE94-009209] 10 p4145 N94-34221

MAGNETIC LENSES
Spin characteristics of ion beams during the motion of electromagnetic elements
[DE93-617448] 01 p0364 N94-10848
The use of harmonics in 3-D magnetic fields
[DE94-002274] 06 p2299 N94-24656
A study on electrostatic quadrupole lenses and their application technologies
[REPT-948] 06 p2546 N94-24982
Focusing properties of a three-element quadrupole lens system and its stigmatic focusing behaviour
[DE93-616534] 07 p2766 N94-25915
Third-order beam optics of real solenoid magnetic lens
[DE94-608014] 08 p3500 N94-30084
ILSE combiner study
[DE94-011009] 11 p4331 N94-36202

MAGNETIC LEVITATION VEHICLES
Compendium of executive summaries from the maglev system concept definition
[PB93-154938/GAR] 02 p0661 N94-13285
Controls of maglev suspension systems
[DE93-015540] 03 p1011 N94-16443
Dynamics, stability, and control of maglev systems
[DE93-015163] 03 p1047 N94-16806
TransRapid TR-07 maglev-spectrum magnetic field effects on daily pineal indoleamine metabolic rhythms in rodents
[DE93-015143] 03 p1117 N94-16893
Electrodynamic forces of the cross-connected figure-eight null-flux coil suspension system
[DE93-015139] 03 p1048 N94-16969
The 13th International Conference on Magnetically Levitated Systems and Linear Drives MAGLEV 1993
[DE93-040381] 05 p1825 N94-21544
Vehicle/guideway interaction and ride comfort in maglev systems
[DE94-001319] 06 p2352 N94-22991
Performance analysis of the combined EDS maglev propulsion, levitation, and guidance system
[DE94-001346] 06 p2352 N94-22996
Review and status of Maglev in the United States
[DE94-006832] 09 p3722 N94-31319
Theoretical principles for designing long stator/linear motors with iron
[ETN-94-95741] 09 p3688 N94-31374
Applicable dimensioning and measure and technological examination of long stator-linear motors for magnetic high-speed railways
[ETN-94-95734] 09 p3689 N94-31575
On the unsteady-motion theory of magnetic forces for maglev
[DE94-007765] 09 p3727 N94-32778
Second International Symposium on Magnetic Suspension Technology, part 1
[NASA-CP-3247-PT-1] 11 p4212 N94-35836
System concept definition of the Grumman superconducting Electromagnetic Suspension (EMS) Maglev design 11 p4213 N94-35840
Transrapid (the first high-speed Maglev train system certified ready for application): Development status and prospects for deployment 11 p4213 N94-35841
Control of maglev vehicles with aerodynamic and guideway disturbances 11 p4213 N94-35842
Fault tolerant computer control for a Maglev transportation system 11 p4215 N94-35848
Superconducting Electromagnetic Suspension (EMS) system for Grumman Maglev concept
11 p4215 N94-35849
National Maglev initiative: California line electric utility power system requirements 11 p4215 N94-35850
Second International Symposium on Magnetic Suspension Technology, part 2
[NASA-CP-3247-PT-2] 11 p4223 N94-35902
Future ultra-speed tube-flight
11 p4225 N94-35918
Dynamic stability of maglev systems
[DE94-010451] 11 p4276 N94-36433
Study of Japanese electrodynamic-suspension maglev systems
[DE94-011486] 12 p4452 N94-37515

MAGNETIC MATERIALS
NT FERRIMAGNETIC MATERIALS
NT FERROFLUIDS
NT FERROMAGNETIC FILMS
NT FERROMAGNETIC MATERIALS
NT MAGNETITE
NT PERMALLOYS (TRADEMARK)
Thermal inertia and radar reflectivity of the Martian north polar ERG: Low-density aggregates
03 p1260 N94-16238
Magnetic Ultrathin Films: Multilayers and Surfaces, Interfaces, and Characterization, volume 313
[AD-A271402] 04 p1375 N94-19758
Influences of nitrogen absorption on the magnetic properties of YFe2, YFe3 and Y6Fe23
[REPT-A-2654] 06 p2564 N94-24958
Metallic multilayers: Experimental investigation of magnetic anisotropy and magnetic interlayer coupling
[ETN-94-95364] 06 p2250 N94-25242
First principle calculation for magneto-crystalline anisotropy
[DE93-634653] 07 p3052 N94-26012
Center for nonlinear phenomena and magnetic materials
[AD-A274176] 07 p3009 N94-27126
List of papers published by the members of Institute for Materials Research, Tohoku University 1992
[JTN-94-80608] 07 p3118 N94-27355
Report on the development of low magnetic permeability reference materials
[NPL-DES-119] 08 p3476 N94-30783
Piezoelectric materials research in Europe
[AD-A276207] 09 p3648 N94-31059
Correlations between micromagnetic, microstructural and microchemical properties in ultrathin epitaxial magnetic structures
[AD-A277200] 09 p3901 N94-32092
Surface conforming flexible eddy current probe for scanning varying surface contours
[AD-D016173] 09 p3627 N94-33018
Advanced induction accelerator designs for ground based and space based FELs
[AD-A278885] 11 p4271 N94-35586

MAGNETIC MEASUREMENT
Large array SQUID magnetometer for NDE
[AD-A264799] 01 p0304 N94-11449
Magnetic fields and nonuniform structures of the Moon 01 p0472 N94-12218
Survey of subsurface geophysical exploration technologies adaptable to an airborne platform
[DE93-015080] 02 p0717 N94-14294
Shielded open-circuited sample holders for dielectric and magnetic measurements of liquids and powders
[PB93-198851] 02 p0652 N94-14687
A high-precision direct current measuring device over a kiloampere range
[DE93-626409] 02 p0627 N94-14885
Comparison of computer predictions and magnetic field measurements for an iron spectrometer magnet
[DE93-016164] 03 p1176 N94-17658
High resolution SQUID magnetometry for non-destructive evaluation
[AD-A268884] 04 p1447 N94-18225
Magnetic field measurements of a superconducting undulator for a Harmonic Generation FEL experiment at the NSLS
[DE93-017621] 04 p1438 N94-18504

Resistive gate magnetic field sensor
[AD-D015923] 05 p1749 N94-20199
Measurement and correction of magnetic fields in pulsed slotted-tube microwigglers
[DE93-040100] 05 p1815 N94-20272
Narsarsuaq Geophysical Observatory: Magnetic results, 1985 - 1990
[DATA-REPT-93-1] 05 p1856 N94-20607
Thule Geophysical Observatory: Magnetic results 1985 - 1990
[DATA-REPT-92-4] 05 p1857 N94-20609
Magnetic properties and Moessbauer analyses of glass from the K-T boundary, Beloc, Haiti
05 p1685 N94-20753
Concept report: Experimental vector magnetograph (EXVM) operational configuration balloon flight assembly
[NASA-CR-194702] 05 p1638 N94-21776
Aeronautical satellite antenna steering using magnetic field sensors 06 p2289 N94-22836
Heavy ion irradiation of Bi-2223 silver-clad tapes for superconducting current density enhancement
[DE93-017416] 06 p2556 N94-22886
Magnetic properties and transmission electron microscopy investigations of Nd-Fe-B-Co-Al melt spun ribbons
[PB93-201531] 06 p2561 N94-23428
Research for electric energy systems
[DE94-001839] 06 p2293 N94-23719
Some theoretical problems of magnetic diagnostics in tokamaks and stellarators
[NIFS-262] 06 p2551 N94-24306
Measurement of magnetic fluctuation induced energy transport
[DE94-003846] 07 p3042 N94-26132
Detection of transient vector-fields in additive noise
[FFI-93/7028] 07 p2768 N94-26232
An optimal constrained linear inverse method for magnetic source imaging
[DE94-002264] 07 p2996 N94-26936
Determination of the plasma column shape in the Tokamak Novillo cross section by magnetic probes
[DE94-604986] 07 p3048 N94-27844
Observations of the geomagnetic field by Polar Patrol Balloon (PPB) experiment in Antarctica
08 p3359 N94-29235
Three-axis fiber optic vector magnetometer
[AD-D016016] 08 p3288 N94-29699
The structure of solar magnetic fields and their associated electric currents 08 p3544 N94-29723
Guidance notes for use with NPL low permeability reference materials
[NPL-DES-121] 08 p3476 N94-30780
Magnetic flux reconstruction methods for shaped tokamaks
[DE94-005827] 08 p3510 N94-30882
Element-specific magnetic hysteresis measurements, a new application of circularly polarized soft x-rays
[DE94-007122] 09 p3858 N94-31397
Fiberoptisk magnetfaltsensor (fiber optic magnetometer)
[PB94-148061] 09 p3878 N94-31584
Evaluation of the IHS transformation use on the integration of geophysical (aeromagnetometry) and remote sensing (TM-Landsat) data for the geological investigation in the Pojuca area (Serra dos Carajas, PA)
[INPE-5532-TDI/521] 10 p4077 N94-34223
Measurements of the SIS: Magnets and SIS control system 10 p4067 N94-34359
Flux creep: Its dependence on current denisty and relation to critical current densities from transport and magnetic measurements
[DE94-011701] 12 p4440 N94-37738

MAGNETIC MEMORIES

U MAGNETIC STORAGE

MAGNETIC METALS

U MAGNETIC MATERIALS
U METALS

MAGNETIC MIRRORS

NT TANDEM MIRRORS
Nonparaxial MHD stabilizers for an axisymmetric magnetic mirror
[DE93-017996] 04 p1587 N94-18505
Generalized energy principle for flute perturbations in axisymmetric mirror machines
[DE93-019399] 04 p1589 N94-19037
Finite beta plasma equilibrium in toroidally linked mirrors
[DE93-040318] 04 p1590 N94-19193
Toroidal plasma beta-FLR limit in a toroidally linked mirror system
[DE94-003119] 07 p3041 N94-25792
Experiments on the two-stage dense plasma heating on the GOL-3 device
[DE94-608356] 08 p3508 N94-30193
Hot-ion plasma in the quadrupole trap
[DE94-617216] 11 p4337 N94-36082
Bounce resonance heating and transport in a magnetic mirror
[DE94-727545] 12 p4531 N94-37466

MAGNETIC MOMENTS

Effect of a distribution of exchange parameters within a simple localized-itinerant model
[DE93-610314] 01 p0395 N94-10314
Canted magnetic moments at the Gd(0001) surface
[DE93-014327] 02 p0805 N94-13102
The geometric phase in quantum physics
[DE93-011121] 02 p0817 N94-13479
Quantum Monte Carlo by message passing
[DE93-012645] 02 p0760 N94-14177
Electric measurement of Lavet motors
04 p1408 N94-18022
Toroidal solenoids in the electromagnetic field and Aharonov-Casher effect
[DE93-629861] 04 p1566 N94-18152
Research in particle physics
[DE93-040875] 04 p1567 N94-18534
The anomalous magnetic moment of the muon
[DE93-018932] 04 p1572 N94-19320
Magnetic and crystallographic structures in UTX intermetallic compounds
[DE93-018291] 04 p1605 N94-19735
A relativistic constituent quark model
[DE93-041085] 05 p1946 N94-21689
A scalar-vector model of quark-antiquark interaction under linear confinement
[DE93-616871] 06 p2538 N94-25317
Volume dependence of vanadium magnetism
[DE94-601838] 07 p3050 N94-25843
Technical report of ISSP. Ser. A, no. 2678: Magnetic properties of carbon nanotubes
[JTN-94-80564] 07 p3064 N94-27174
Quasi-adiabatic motion of energetic particles in a dipole magnetic field
[DE94-607322] 08 p3362 N94-29935
Molecular/polymeric magnetism
[DE94-005888] 09 p3649 N94-31201
Element-specific magnetic hysteresis measurements, a new application of circularly polarized soft x-rays
[DE94-007122] 09 p3858 N94-31397
Hyperon polarization and magnetic moments
[DE94-006041] 09 p3864 N94-31507
Hyperon polarization, crystal channeling, and E781 at Fermilab
[DE94-008224] 09 p3877 N94-32802
Dependence of x ray absorption magnetic circular dichroism on layer periodicity in iron-platinum multilayers
[DE94-008786] 09 p3647 N94-32892
Limitation on the magnetic dipole moment of the reactor neutrino
[DE94-611171] 11 p4320 N94-35566
Magnetic metallic multilayers
[DE94-011913] 11 p4341 N94-36274

MAGNETIC MONOPOLES

Enhancement of the rate of radiative processes in the field of a magnetic monopole
[DE94-603717] 07 p3074 N94-27696

MAGNETIC PERMEABILITY

Remanent magnetism of HED meteorites: Implications for their evolution and ancient magnetic fields
01 p0431 N94-12172
Quantum Monte Carlo by message passing
[DE93-012645] 02 p0760 N94-14177
A high-precision direct current measuring device over a kiloampere range
[DE93-626409] 02 p0627 N94-14885
Comparative magnetic and thermoanalytical study of two enstatite chondrites: Adhi Kot and Atlanta
03 p1244 N94-16329
Structural phase transition and superconductivity in La(2-x)Ba(x)CuO4
[DE93-015812] 03 p1212 N94-16868
Synthesis and characterization of new low-dimensional metal complex conductors
[AD-A268251] 03 p0952 N94-17416
High resolution SQUID magnetometry for non-destructive evaluation
[AD-A268884] 04 p1447 N94-18225
Realistic theories of heavy electron and other strongly correlated materials
[DE93-010350] 04 p1571 N94-19204
Non-Fermi-liquid and multichannel Kondo phenomena in Y(1-x)U(x)Pd3 and related alloys
[DE93-040135] 05 p2015 N94-20275
Non-fermi liquid and spin-glass behavior of the Sc(1-x)U(x)Pd3 system
[DE93-040134] 05 p2016 N94-20335
Fabrication and evaluation of superconducting and semiconducting materials
[AD-A271645] 05 p2018 N94-20558
Alloying studies in U(1-x)Th(x)Pd2Al3 (0 (le) x (le) 1)
[DE94-000807] 05 p2036 N94-22584
Magnetic phases in UNiGe
[DE94-000793] 06 p2239 N94-22939
Crystal field in Nd2CuO4
[DE93-617054] 06 p2567 N94-25425
Technical report of ISSP. Ser. A, no. 2678: Magnetic properties of carbon nanotubes
[JTN-94-80564] 07 p3064 N94-27174
Technical report of ISSP. Ser. A, no. 2681: Orbital and spin susceptibilities of the plane copper sites in YBa2Cu3O(x) system
[JTN-94-80567] 07 p3064 N94-27177
Technical report of ISSP. Ser. A, no. 2669: Relations between oxygen deficiency and structures in the La-Sr-Cu-O system. 3: Oxygen contents and structure of (La, Sr)8Cu8O(16+delta) phase
[JTN-94-80555] 07 p3066 N94-27353
Scaling in heavy-fermion systems
[DE94-005002] 08 p3492 N94-30775
Guidance notes for use with NPL low permeability reference materials
[NPL-DES-121] 08 p3476 N94-30780
Report on the development of low magnetic permeability reference materials
[NPL-DES-119] 08 p3476 N94-30783
Synthesis, characterization, phase diagrams and superconducting, and normal state magnetic properties of La(2-x)Sr(x)CuO4 (0 is less than or equal to x which is less than or equal to 0.08) and electrochemically oxidized La(2-x)Sr(x)CuO(4 + delta) (0 is less than or equal to x which is less than or equal to 0.33, 0 is less than or equal to delta which is less than or equal to 0.12)
[DE94-005260] 09 p3895 N94-31067

MAGNETIC POLES

A method to determine asteroid poles
01 p0431 N94-12205
Polarity reversals and tilt of the Earth's magnetic dipole 01 p0283 N94-12219
Structural evidence for reorientation of Miranda about a paleo-pole 05 p2098 N94-20671
Compositional diversity of the lunar North Pole: Preliminary analyses of Galileo SSI data
05 p2101 N94-20686

MAGNETIC PROBES

Suggestion for extended Viking magnetic properties experiment on future Mars missions
03 p1285 N94-16375
Determination of the plasma column shape in the Tokamak Novillo cross section by magnetic probes
[DE94-604986] 07 p3048 N94-27844

MAGNETIC PROPERTIES

NT ANTIFERROMAGNETISM
NT BIOMAGNETISM
NT CURIE TEMPERATURE
NT DIAMAGNETISM
NT FERRIMAGNETISM
NT FERROMAGNETISM
NT GEOMAGNETISM
NT GYROFREQUENCY
NT GYROMAGNETISM
NT MAGNETIC EFFECTS
NT MAGNETIC FIELD RECONNECTION
NT MAGNETIC INDUCTION
NT MAGNETIC MOMENTS
NT MAGNETIC PERMEABILITY
NT MAGNETIC RELAXATION
NT MAGNETIC SUSPENSION
NT MAGNETORESISTIVITY
NT MAGNETOSTRICTION
NT PALEOMAGNETISM
NT PARAMAGNETISM
NT POLARIZATION CHARACTERISTICS
NT REMANENCE
NT SPIN-LATTICE RELAXATION
Effect of a distribution of exchange parameters within a simple localized-itinerant model
[DE93-610314] 01 p0395 N94-10314
Rietveld refinement of magnetic structures from pulsed-neutron-source powder-diffraction data
[DE93-012740] 01 p0363 N94-10743
Application of spin-sensitive electron spectroscopies to investigations of electronic and magnetic properties of solid surfaces and epitaxial systems
[DE93-015079] 01 p0076 N94-10854
Remanent magnetism of HED meteorites: Implications for their evolution and ancient magnetic fields
01 p0431 N94-12172
Synthesis and magnetic properties of novel La*2-x*M*x*CuO*4 equals y* compositions (La equals La, Pr, Nd, Sm, Eu, Cd; M equals Ca, Sr, Ba; O (less than or equal) x 0.2; -0.5 (less than or equal) y (less than or equal) 0.5)
[DE93-011359] 01 p0403 N94-12363
The 1990 Western Pacific Geophysics meeting
[NASA-CR-193456] 02 p0712 N94-13334

Spin polarized photoemission studies of interfacial and thin film magnetism
[DE93-014326] 02 p0580 N94-14142
Magnetic interactions and disorder - phase transitions in dilute spin-glasses and high temperature superconductors
[ITN-93-85217] 02 p0815 N94-14825
Magneto-optic superlattice thin films: Fabrication, structural and magnetic characterization 03 p0974 N94-14982
Fullerene superconductors
[AD-A266749] 03 p1010 N94-15954
Magnetic effects in anomalous dispersion
[DE93-014291] 03 p1175 N94-15978
Comparative magnetic and thermoanalytical study of two enstatite chondrites: Adhi Kot and Atlanta 03 p1244 N94-16329
Suggestion for extended Viking magnetic properties experiment on future Mars missions 03 p1285 N94-16375
Atomic-scale friction measurements using friction force microscopy. Part 1: General principles and new measurement techniques
[AD-A268391] 03 p1048 N94-17533
Epitaxial iron films
[AD-A268286] 03 p1217 N94-17579
Magnetic properties of single-crystalline UCu3Al2
[DE93-016607] 04 p1593 N94-17744
Spin-integrated and spin-dependent photoelectron diffraction
[DE93-016546] 04 p1565 N94-17850
Comparison of ferrite materials for pulse applications
[DE93-017224] 04 p1574 N94-18497
High pressure metallization of Mott Insulators: Magnetic, structural and electronic properties
[DE93-018295] 04 p1404 N94-18805
Superconductivity and magnetism in niobium doped YBa2Cu3O7 related high-(Tc) ceramics
[DE93-018086] 04 p1601 N94-19049
Some superhigh-frequency and magnetic properties of chemically precipitated films
[AD-A266195] 04 p1351 N94-19110
Magnetic Ultrathin Films: Multilayers and Surfaces, Interfaces, and Characterization, volume 313
[AD-A271402] 04 p1375 N94-19758
Optical metrology of magnetically trapped hydrogen
[AD-A272110] 05 p1680 N94-20584
Magnetic properties and Moessbauer analyses of glass from the K-T boundary, Beloc, Haiti 05 p1685 N94-20753
Magnetic record in chondrite meteorites 05 p2085 N94-20858
Magnetic force microscopy/current contrast imaging: A new technique for internal current probing of IC's
[DE93-040754] 05 p1761 N94-21532
Magnetic instability of Kondo insulators
[DE93-040064] 05 p1768 N94-21762
Magnetism in CeRu2Ge2 and CeRh2Ge2 and its pressure dependence
[DE93-040061] 05 p2032 N94-21987
Temperature dependence of magnetic order in single-crystalline UPdSn
[DE93-040153] 05 p2033 N94-21991
Orientationally independent antiferromagnetic coupling in epitaxial Fe/Cr (211) and (100) superlattices
[DE94-001270] 05 p2035 N94-22564
Spectroscopic studies of magnetic transitions in TbPO4
[DE94-001274] 05 p2035 N94-22565
Inelastic neutron scattering of (gamma)-iron, and the determination of the elastic constants by lattice dynamics
[DE94-000694] 05 p1978 N94-22573
The de Haas-van Alphen measurements in Ba(0.6)K(0.4)BiO3
[DE93-041169] 06 p2556 N94-22920
The structure and spin dynamics of lanthanide-bearing silicate glasses
[DE94-001320] 06 p2252 N94-22992
Muon spin relaxation studies of the interplay between magnetism and superconductivity in heavy fermion systems
[DE94-000700] 06 p2559 N94-23006
Magnetic properties and transmission electron microscopy investigations of Nd-Fe-B-Co-Al melt spun ribbons
[PB93-201531] 06 p2561 N94-23428
Instrument interface description for NOAA 2000 instruments with European morning spacecraft and/or NOAA-OPQ spacecraft
[NASA-TM-109406] 06 p2208 N94-23478
Influences of nitrogen absorption on the magnetic properties of YFe2, YFe3 and Y6Fe23
[REPT-A-2654] 06 p2564 N94-24958
Magnetic properties of NdCo3 and its gamma phase hydride NdCo3H(4.1)
[REPT-A-2655] 06 p2567 N94-25412
Study on characteristics and electronic structures of materials with strong electronic correlations by ferromagnetic fields 07 p2724 N94-25557
Magnetic properties of a quantum transverse spin-1 Blume-Emery-Griffiths model
[DE94-608114] 08 p3517 N94-30109
Magnetic properties of the three dimensional Ising model with interface single-ion anisotropy
[DE94-608116] 08 p3525 N94-30164
Magnetic properties of a transverse spin-1 Ising model with longitudinal crystal field interactions
[DE94-608118] 08 p3517 N94-30165
The bond diluted spin-1 Blume-Emery-Griffiths model in a transverse field
[DE94-608121] 08 p3525 N94-30167
Magnetic properties of a transverse spin-1 Ising model with random crystal field interactions
[DE94-608117] 08 p3517 N94-30181
MuSR measurement of the magnetic penetration depth and coherence length in the high-Tc superconductor YBa2Cu3O(6.95)
[ISBN-0-315-85385-9] 08 p3517 N94-30203
Piezoelectric materials research in Europe
[AD-A276207] 09 p3648 N94-31059
Molecular/polymeric magnetism
[DE94-005888] 09 p3649 N94-31201
On the unsteady-motion theory of magnetic forces for maglev
[DE94-007765] 09 p3727 N94-32778
Investigation of superconductivity and magnetism in d and f-electron materials
[DE94-008535] 09 p3907 N94-32933
Ocean magnetics
[PB94-149028] 10 p4092 N94-34142
Chondrule magnetic properties 11 p4352 N94-35471
Materials for efficient high-flux magnetic bearing actuators 11 p4214 N94-35845
Magnetic properties of nanosize iron clusters
[DE94-011329] 11 p4318 N94-36204

MAGNETIC PUMPING
Studies on the parametric decay of waves in fusion plasmas
[VTT-PUBS-110] 03 p1200 N94-15204
High frequency Raman current drive 03 p1201 N94-15208
On the decay of a dipole pump wave to half-harmonics 03 p1201 N94-15211
Review of tokamak experiments on direct electron heating and current drive with fast waves
[DE94-004185] 07 p3041 N94-25801
Performance analysis of reciprocating regenerative magnetic heat pumping
[DE94-009488] 11 p4264 N94-35683

MAGNETIC RECORDING
Magnetic and magneto-optical properties and domain structure of Co/Pd multilayers 03 p1227 N94-14991
Tribological studies of silicon for magnetic recording applications (Invited)
[AD-A270878] 04 p1447 N94-19784
An experimental compact Hi-Vision VCR using metal evaporated tape
[NHK-LABS-NOTE-423] 09 p3683 N94-33081
The Third NASA Goddard Conference on Mass Storage Systems and Technologies
[NASA-CP-3262] 10 p4151 N94-33791

MAGNETIC RELAXATION
NT SPIN-LATTICE RELAXATION
Filamentation, current profiles and transport in a tokamak
[DE93-016768] 04 p1584 N94-17948
Relaxation of polar orientational order in nonlinear optical polymers by second harmonic generation
[AD-A269059] 04 p1370 N94-18515
Relaxation of hysteresis loop in a single crystal of YBa2Cu4O8
[DE93-019519] 05 p2029 N94-21649
Muon spin relaxation studies of the interplay between magnetism and superconductivity in heavy fermion systems
[DE94-000700] 06 p2559 N94-23006
Dipolar relaxation in a second-order nonlinear optical interpenetrating polymer network
[AD-A273626] 06 p2258 N94-24732
On the (mu)SR activity at LNP JINR phasotron
[DE94-608385] 08 p3517 N94-30195
Nuclear magnetic relaxation studies of semiconductor nanocrystals and solids
[DE94-006301] 08 p3520 N94-30842
Low dispersion of the muon precession frequency in HTSC samples YBa2Cu3O(x) and EuBa2Cu3O(x)
[DE94-608388] 09 p3896 N94-31395
Experimental evidence for lattice effects in high temperature superconductors
[DE94-006250] 09 p3899 N94-31633

MAGNETIC RESONANCE
NT ELECTRON PARAMAGNETIC RESONANCE
NT FERROMAGNETIC RESONANCE
NT NUCLEAR MAGNETIC RESONANCE
Magnetic island suppression in torsatron configurations
[DE93-621681] 01 p0392 N94-11215
Magnetic resonance imaging after exposure to microgravity 02 p0594 N94-13771
The National High Magnetic Field Laboratory, a user facility in support of research in high magnetic fields
[DE93-040145] 05 p1714 N94-20278
Fabrication and evaluation of superconducting and semiconducting materials
[AD-A271645] 05 p2018 N94-20558
Magnetic resonance studies of 3d transition metal impurities in compound semiconductors
[PB93-232197] 06 p2243 N94-23714
Potential hazards of magnetic resonance imagers to emergency medical service helicopter operations
[AD-A278873] 08 p3135 N94-29862
Fast nonsupervised 3D registration of PET and MR images of the brain
[TELECOM-93-C-006] 09 p3798 N94-33069

MAGNETIC SHIELDING
Fabrication and evaluation of superconducting and semiconducting materials
[AD-A271645] 05 p2018 N94-20558
Magnetic shielding of interplanetary spacecraft against solar flare radiation
[NASA-CR-195539] 06 p2204 N94-24334
Applications of high transition temperature superconductors at the Savannah River Site
[DE94-012938] 12 p4536 N94-37311

MAGNETIC SIGNATURES
Solar vector magnetic field research
[AD-A267367] 03 p1299 N94-17004
Development, refinement, and testing of a short term solar flare prediction algorithm
[NASA-CR-194726] 05 p2147 N94-21815
Solar imaging vector magnetograph
[NASA-CR-194729] 05 p1810 N94-21876
Determination of coronal magnetic fields from vector magnetograms
[NASA-CR-194744] 05 p2147 N94-21877
Polarization analysis of a balloon-borne solar magnetograph
[NASA-CR-193908] 06 p2345 N94-24852
Kiruna geophysical data. Data summary 93/4-6, April-June 1993
[PB94-123700] 07 p2881 N94-27039
Kiruna geophysical data. Data summary 93/1-3, January-March, 1993
[PB94-123791] 07 p2881 N94-27043

MAGNETIC SPECTROSCOPY
NMR spectroscopy of experimentally shocked single crystal quartz: A reexamination of the NMR shock barometer 01 p0081 N94-12258
Implementation of a compact magnetic electron energy spectrometer for intense relativistic electron beams
[AD-A274451] 07 p3033 N94-27082
Simulation of experiments on deep inelastic scattering of muons on superconducting magnetic toroidal spectrometer STORS
[DE94-606267] 08 p3483 N94-28554
Experimental setups and methods to obtain new nuclear data at intermediate and high energies
[DE94-607850] 08 p3489 N94-30052
Spectroscopic and dynamical studies of highly energized small polyatomic molecules
[DE94-006509] 08 p3489 N94-30061
Algorithm and program ORANGE for magnetic field simulation of magnetic system spectrometer STORS
[DE94-608013] 08 p3421 N94-30083
Concept, construction and testing of a high resolution QCLAM electron spectrometer with large solid angle and high impulse acceptance for the electron accelerator S-DALINAC
[ETN-94-95755] 09 p3711 N94-31515
High Resolution Transmission Electron Microscopy (HRTEM) of nanophase ferric oxides 11 p4239 N94-35433
Beam energy absolute measurement using K-edge absorption spectrometers
[DE94-010019] 11 p4331 N94-36192

MAGNETIC STARS
ROSAT guest investigator program (AO-1). On a search for coronal x ray emissions from white dwarfs
[NASA-CR-193654] 02 p0835 N94-13171
Convective turbulence and transport in stars 08 p3546 N94-29913

MAGNETIC STORAGE
NT CORE STORAGE
NT MAGNETIC DISKS
Characterization facility for magneto-optic media and systems 03 p1226 N94-14983
Magnetic and magneto-optical properties and domain structure of Co/Pd multilayers 03 p1227 N94-14991
Atomic-scale friction measurements using friction force microscopy. Part 1: General principles and new measurement techniques
[AD-A268391] 03 p1048 N94-17533
The Third NASA Goddard Conference on Mass Storage Systems and Technologies
[NASA-CP-3262] 10 p4151 N94-33791
Magnetic field sources and their threat to magnetic media 10 p4151 N94-33794

MAGNETIC STORMS
NT POLAR SUBSTORMS
The interplanetary origins and the main-phase development of moderate geomagnetic storms (1978 - 1979)
[INPE-5445-TDI/491] 02 p0835 N94-13174
Formation of the stable auroral arc that intensifies at substorm onset
[NASA-CR-193637] 03 p1098 N94-15433
The Solar Flare Myth in solar-terrestrial physics
[DE93-016487] 03 p1299 N94-16895
A correlative comparison of geomagnetic storms and auroral substorms using geomagnetic indeces
[AD-A268081] 03 p1102 N94-17512
Penetrating radiation environment and effects study
[AD-A270126] 04 p1485 N94-18874
The effects of magnetic storm phases on f-layer irregularities from auroral to equatorial latitudes
[AD-A267388] 04 p1486 N94-19008
Dynamics Explorer 2: Continued FPI and NACS instrument data analysis and associated scientific activity at the University of Michigan
[NASA-CR-194689] 05 p1657 N94-20173
The effects of magnetic storm phases on F-layer irregularities from auroral to equatorial latitudes
[AD-A272685] 05 p1857 N94-21189
Data analysis and theoretical studies of the upper mesosphere and lower thermosphere
[NASA-CR-195108] 06 p2402 N94-24089
Dynamics explorer interdisciplinary scientist investigations
[NASA-CR-195226] 07 p2878 N94-26204
Region 5395 of March 1989 --- solar activity, geomagnetic disturbances, and terrestrial effects
[PB94-120714] 07 p3110 N94-26755
Compton Gamma Ray Observatory/BATSE observations of energetic electrons scattered by cyclotron resonance with waves from powerful VLF transmitters
[NASA-CR-189336] 07 p3115 N94-26790
The Sixteenth Symposium on Coordinated Observations of the Ionosphere and the Magnetosphere in the Polar Regions: Program and abstracts
[JTN-94-80601] 07 p2882 N94-27300
Configuration of the near-Earth plasma sheet
[NASA-CR-195271] 07 p2883 N94-27438
Proton aurora and substorm intensifications
[ATR-93(7248)-1] 07 p2887 N94-28218
The effects of magnetic storm phases on F-layer irregularities from auroral to equatorial latitudes
[AD-A275203] 08 p3356 N94-28891
Accurate modeling of F-region electron densities
[NASA-CR-195781] 08 p3364 N94-30014
Variations of electron fluxes, low-frequency radiations and plasma density during the geomagnetic storm on 9-12 March, 1979 according to data of the Interkosmos-19 satellites
[DE94-607323] 08 p3365 N94-30223
Self-consistent effects of magnetospheric hydromagnetic waves on ring current ions
[AD-A277406] 09 p3774 N94-32346
CDAW-9 analysis of magnetospheric events on 3 May 1986: Event C
[AD-A277610] 10 p4086 N94-33851
Utility of interplanetary scintillation maps in forecasting geomagnetic activity: A study based on single-station data from Cambridge, United Kingdom
[PB94-156775] 10 p4087 N94-34600
Collisonless dynamics of the magnetosphere
[AD-A278886] 11 p4290 N94-35708
Simultaneous observations of the westward electrojet and the cross-tail current sheet during substorms
[AD-A278631] 11 p4292 N94-36383
Analysis of plasma measurements for the Geotail mission
[NASA-CR-196274] 12 p4470 N94-37470
Random and periodic substorms and their origins in the solar wind
[DE94-011693] 12 p4549 N94-37668
Substorm statistics: Occurrences and amplitudes
[DE94-011694] 12 p4471 N94-37669

MAGNETIC SUBSTORMS
U MAGNETIC STORMS

MAGNETIC SURVEYS
Pseudo magnetic anomaly derived from satellite altimetry and its application to the tectonics in the North Fuji Basin 01 p0208 N94-12645
Application of transient airborne electromagnetic and ground resistivity methods to geological mapping in tropical terrains
[ISBN-0-315-57172-1] 02 p0685 N94-13542
Aeromagnetic work in the Lincoln Sea: 1991 survey
[DSIS-93-00308] 02 p0715 N94-13830
Rapid geophysical surveyor
[DE93-016637] 04 p1461 N94-17851
Analysis of deep seismic reflection and other data from the southern Washington Cascades
[DE94-005958] 09 p3771 N94-31525

MAGNETIC SUSCEPTIBILITY
U MAGNETIC PERMEABILITY

MAGNETIC SUSPENSION
Electromechanical batteries and the electric locomotive
[DE93-013311] 01 p0142 N94-11009
Improvement of azimuthal homogeneity in permanent-magnet bearing rotors
[DE93-009954] 01 p0144 N94-11607
Propulsion simulator for magnetically-suspended wind tunnel models
[NASA-CR-189560] 02 p0527 N94-13127
A superconducting large-angle magnetic suspension
[NASA-CR-189735] 02 p0596 N94-13141
Compendium of executive summaries from the maglev system concept definition
[PB93-154938/GAR] 02 p0661 N94-13285
Rolling moment control in the NAL 10 cm x 10 cm magnetic suspension and balance system
[NAL-TR-1164] 02 p0526 N94-13347
Controls of maglev suspension systems
[DE93-015540] 03 p1011 N94-16443
Dynamics, stability, and control of maglev systems
[DE93-015163] 03 p1047 N94-16806
Electrodynamic forces of the cross-connected figure-eight null-flux coil suspension system
[DE93-015139] 03 p1048 N94-16969
Corroboration of magnetic forces in US Maglev design
[DE93-014918] 04 p1443 N94-17785
Six degree of freedom fine motion positioning stage based on magnetic levitation
[DE93-017651] 04 p1446 N94-19547
The 13th International Conference on Magnetically Levitated Systems and Linear Drives MAGLEV 1993
[DE93-040381] 05 p1825 N94-21544
Vehicle/guideway interaction and ride comfort in maglev systems
[DE94-001319] 06 p2352 N94-22991
Performance analysis of the combined EDS maglev propulsion, levitation, and guidance system
[DE94-001346] 06 p2352 N94-22996
Preliminary eddy current modelling for the large angle magnetic suspension test fixture
[NASA-CR-194772] 06 p2192 N94-23539
Neural control of magnetic suspension systems 07 p2682 N94-27905
System identification of the Large-Angle Magnetic Suspension Test Facility (LAMSTF) 07 p2682 N94-27908
Neural network based time-optimal control of a magnetically levitated precision positioning system
[DE94-006573] 08 p3437 N94-30250
On the unsteady-motion theory of magnetic forces for maglev
[DE94-007765] 09 p3727 N94-32778
Vibration Isolation Technology (VIT) ATD project
[NASA-TM-106496] 09 p3567 N94-33064
Second International Symposium on Magnetic Suspension Technology, part 1
[NASA-CP-3247-PT-1] 11 p4212 N94-35836
Aerospace applications of magnetic bearings 11 p4213 N94-35837
System concept definition of the Grumman superconducting Electromagnetic Suspension (EMS) Maglev design 11 p4213 N94-35840
Transrapid (the first high-speed Maglev train system certified ready for application): Development status and prospects for deployment 11 p4213 N94-35841
High temperature superconductors for magnetic suspension applications 11 p4214 N94-35843
Measurement and characterization of force dynamics in high T(sub c) superconductors 11 p4214 N94-35844
Fault tolerant computer control for a Maglev transportation system 11 p4215 N94-35848
Superconducting Electromagnetic Suspension (EMS) system for Grumman Maglev concept 11 p4215 N94-35849
Fuzzy self-learning control for magnetic servo system 11 p4215 N94-35852
Implementation of a decoupled controller for a magnetic suspension system using electromagnets mounted in a planar array 11 p4216 N94-35853
Status of MSBS study at NAL 11 p4216 N94-35854
The simulation of a propulsive jet and force measurement using a magnetically suspended wind tunnel model 11 p4191 N94-35855
A dynamic method for magnetic torque measurement 11 p4216 N94-35856
Some further developments in the dynamic modelling and control of the large angle magnetic suspension test fixture 11 p4217 N94-35860
Neural network controller development for a magnetically suspended flywheel energy storage system 11 p4217 N94-35861
Time-delay control of a magnetic levitated linear positioning system 11 p4217 N94-35862
Third order LPF type compensator for flexible rotor suspension 11 p4217 N94-35863
Second International Symposium on Magnetic Suspension Technology, part 2
[NASA-CP-3247-PT-2] 11 p4223 N94-35902
Electromagnetically levitated vibration isolation system for the manufacturing process of silicon monocrystals 11 p4223 N94-35906
Planar rotational magnetic micromotors with integrated shaft encoder and magnetic rotor levitation 11 p4224 N94-35907
Manufacturing and testing of a magnetically suspended composite flywheel energy storage system 11 p4224 N94-35910
Nonlinear feedback model attitude control using CCD in magnetic suspension system 11 p4225 N94-35912
Robust tracking control of a magnetically suspended rigid body 11 p4225 N94-35913
Magnetically suspended stepping motors for clean room and vacuum environments 11 p4225 N94-35915
Six degree of freedom fine motion positioning stage based on magnetic levitation 11 p4225 N94-35916
Analysis of achievable disturbance attenuation in a precision magnetically-suspended motion control system 11 p4225 N94-35917
Future ultra-speed tube-flight 11 p4225 N94-35918
Maglev crude oil pipeline 11 p4226 N94-35919
Dynamic stability of maglev systems
[DE94-010451] 11 p4276 N94-36433
Optical position measurement for a large gap magnetic suspension system: Design and performance analysis
[NASA-TP-3438] 12 p4447 N94-36946
Melt-processing of Y-Ba-Cu-O superconductors for improved levitation
[DE94-011503] 12 p4537 N94-37377
Large angle magnetic suspension test fixture
[NASA-CR-196138] 12 p4390 N94-37450
Study of Japanese electrodynamic-suspension maglev systems
[DE94-011486] 12 p4452 N94-37515

MAGNETIC SWITCHING
Evolution of high-repetition-rate induction accelerators through advancements in switching
[DE93-012599] 02 p0654 N94-12963
Exciplex laser study: Discharge and magnetic switching systems
[PB93-199768] 06 p2349 N94-24629

MAGNETIC TAPE RECORDERS
U MAGNETIC RECORDING
U TAPE RECORDERS

MAGNETIC TAPES
NT COMPUTER COMPATIBLE TAPES
Contribution to the tribological study of magnetic-tape head contact
[ECL-92-57] 04 p1434 N94-19414
Microtribology of magnetic media
[AD-A271209] 04 p1407 N94-19722
Atomic-scale friction measurements using friction force microscopy. Part 2: Application to magnetic media
[AD-A270759] 04 p1447 N94-19767
The program for catalogization of magnetic tapes in EXCHARM experiment
[DE94-606271] 08 p3528 N94-28615
Atomic-scale friction measurements using friction force microscopy. Part 2: Application to magnetic media
[AD-A275202] 08 p3298 N94-29290
High performance quarter-inch cartridge tape systems 10 p4057 N94-33795
Architectural constructs of Ampex DST 10 p4153 N94-33805
Volume server: A scalable high speed and high capacity magnetic tape archive architecture with concurrent multi-host access 10 p4154 N94-33807

Performance measurements and operational characteristics of the Storage Tek ACS 4400 tape library with the Cray Y-MP EL 10 p4154 N94-33811
Using magnetic tape technology for data migration 10 p4154 N94-33812
A practical large scale/high speed data distribution system using 8 mm libraries 10 p4157 N94-33825
Marshall Space Flight Center head development program
[NASA-CR-193944] 10 p4056 N94-34073
An analysis of file system and installation of the file management system for NOS operating system
[DE94-611062] 11 p4346 N94-35833

MAGNETIC VARIATIONS
NT GEOMAGNETIC PULSATIONS
NT NOCTURNAL VARIATIONS
Chromospheric activity in agol binaries
[AD-A273546] 06 p2602 N94-24557
High latitude cusp signature observations for southward IMF B sub Z
[AD-A273801] 06 p2406 N94-25536
Comparative investigation of high-latitude ionospheric structure and effects near solar maximum
[AD-A273799] 07 p2877 N94-25877
Mesopause winds and OH intensities at Mid-Latitudes-Fabry-Perot interferometer observations of the OH emission at 8430 A from bear lake observatory
[AD-A275246] 08 p3361 N94-29430
Magnetohydrodynamics of the Earth's core. 1: Steady, rotating magnetoconvection. 2: Magnetic Rossby waves 09 p3770 N94-31104
A study of angular momentum loss in binaries using the free Lagrange method 09 p3931 N94-31134

MAGNETICALLY TRAPPED PARTICLES
NT INNER RADIATION BELT
NT PROTON BELTS
NT RADIATION BELTS
Investigations of YBaCuO materials with near-room-temperature resistivity transitions
[AD-A268016] 03 p1216 N94-17477
Ultracold atoms in traps and fountains
[ETN-94-95325] 06 p2537 N94-25239

MAGNETITE
Changes in Hawaiian palagonite FE mineralogy associated with thermal alteration: Implications for Mars 01 p0281 N94-12055
Iron and nickel isotopic mass fractionation in deep-sea spherules 01 p0282 N94-12199
Mineralogy and metallurgical properties of iron ore sinter based on magnetite fines
[DE94-763309] 12 p4414 N94-36525

MAGNETIZATION
Magnetization reversal by nucleation
[DE93-610313] 01 p0350 N94-10313
Theory of the negative magnetoresistance in magnetic metallic multilayers
[DE93-013912] 02 p0776 N94-14584
Magnetic and magneto-optical properties and domain structure of Co/Pd multilayers 03 p1227 N94-14991
Comparative magnetic and thermoanalytical study of two enstatite chondrites: Adhi Kot and Atlanta 03 p1244 N94-16329
Neutron and x ray scattering studies of (FeF2)(sub m)(CoF2)(sub n) multilayers
[DE93-015809] 03 p1184 N94-16838
Magnetic properties of single-crystalline UCu3Al2
[DE93-016607] 04 p1593 N94-17744
Ising model on tangled chain. Part 2: Magnetization and susceptibility
[DE93-628794] 04 p1607 N94-18174
Fermiology and De Haas-Van Alphen effect of beta-(ET)2IBr2
[DE93-019523] 05 p2011 N94-19807
Two-polarity magnetization in the Manson impact breccia 05 p1863 N94-20789
Observation of x ray absorption magnetic circular dichroism in well-characterized iron-cobalt-platinum multilayers
[DE94-000303] 05 p1694 N94-21944
Magnetic phases in UNiGe
[DE94-000793] 06 p2239 N94-22939
Spin fluctuations in an ordered Heisenberg ferromagnet with dipolar interactions
[PB93-204493] 06 p2524 N94-24533
Influences of nitrogen absorption on the magnetic properties of YFe2, YFe3 and Y6Fe23
[REPT-A-2654] 06 p2564 N94-24958
Metallic multilayers: Experimental investigation of magnetic anisotropy and magnetic interlayer coupling
[ETN-94-95364] 06 p2250 N94-25242
Modification in the kinetic solution for magnetized plasmas
[DE93-613687] 06 p2555 N94-25343
Critical currents in YBaCuO-ceramics
[DE93-617140] 06 p2263 N94-25404
Magnetic properties of NdCo3 and its gamma phase hydride NdCo3H(4.1)
[REPT-A-2655] 06 p2567 N94-25412
Power laws, flicker noise, and the barkhausen effect
[AD-A274702] 07 p3008 N94-26376
Technical report of ISSP. Ser. A, no. 2687: Quantized persistent currents of a quantum dot in a strong magnetic field
[JTN-94-80573] 07 p3028 N94-27758
Anisotropy in the electrical, magnetic and optical properties of Pb2Sr2RCu3O8
[ISBN-0-315-84930-4] 07 p3070 N94-27974
Observation of the phase shift of the wave function of the neutron under total reflection
[DE94-608244] 08 p3489 N94-30096
Magnetic properties of a quantum transverse spin-1 Blume-Emery-Griffiths model
[DE94-608114] 08 p3517 N94-30109
Magnetic properties of the three dimensional Ising model with interface single-ion anisotropy
[DE94-608116] 08 p3525 N94-30164
Magnetic properties of a transverse spin-1 Ising model with longitudinal crystal field interactions
[DE94-608118] 08 p3517 N94-30165
The bond diluted spin-1 Blume-Emery-Griffiths model in a transverse field
[DE94-608121] 08 p3525 N94-30167
Magnetic properties of a transverse spin-1 Ising model with random crystal field interactions
[DE94-608117] 08 p3517 N94-30181
Butterfly and scaling law in YBa2Cu4O8
[DE94-006037] 08 p3519 N94-30338
Molecular/polymeric magnetism
[DE94-005888] 09 p3649 N94-31201
Shape, size, and distribution of magnetic particles in Bjurbole chondrules 11 p4353 N94-36167
Magnetic metallic multilayers
[DE94-011913] 11 p4341 N94-36274
Consequences of competing hybridization for magnetic ordering in correlated-electron lattices
[DE94-011648] 12 p4534 N94-37057

MAGNETO-OPTICS
Experiments in ultracold collisions
[DE93-012110] 01 p0365 N94-11029
Research Studies on Advanced Optical Module/Head Designs for Optical Disk Recording Devices
[NASA-CR-194390] 03 p1226 N94-14981
Magneto-optic superlattice thin films: Fabrication, structural and magnetic characterization 03 p0974 N94-14982
Characterization facility for magneto-optic media and systems 03 p1226 N94-14983
Application of holographic optical elements to magneto-optic read/write heads 03 p1226 N94-14985
Measurement of birefringence for optical recording disk substrates 03 p1227 N94-14989
Magnetic and magneto-optical properties and domain structure of Co/Pd multilayers 03 p1227 N94-14991
A near-field scanning optical microscope for analysis of magneto-optic media 03 p1199 N94-14995
Determining the locations of the various CIRC recording format information blocks (user data blocks, C2 and C1 words and EFM frames) on a recorded compact disc 03 p1228 N94-14997
Magnetic Ultrathin Films: Multilayers and Surfaces, Interfaces, and Characterization, volume 313
[AD-A271402] 04 p1375 N94-19758
Transient internal probe
[AD-A275054] 08 p3505 N94-29134
Storage media pipelining: Making good use of fine-grained media 10 p4155 N94-33816

MAGNETOACOUSTIC WAVES
Simulation of enhanced tokamak performance on D3-D using fast wave current drive
[DE93-014009] 03 p1203 N94-16823

MAGNETOACTIVITY
NT MAGNETIC FIELD RECONNECTION
NT MAGNETORESISTIVITY

MAGNETOCARDIOGRAPHY
Detection geometry and reconstruction error in magnetic source imaging
[DE94-004012] 07 p2809 N94-25662

MAGNETOELASTIC WAVES
NT MAGNETOACOUSTIC WAVES

MAGNETOELASTICITY
U MAGNETOSTRICTION

MAGNETOGASDYNAMICS
U MAGNETOHYDRODYNAMICS

MAGNETOGRAMS
U MAGNETIC SIGNATURES

MAGNETOHYDRODYNAMIC ACCELERATION
U PLASMA ACCELERATION

MAGNETOHYDRODYNAMIC FLOW
Comparison of hydrodynamic and semi-kinetic treatments for plasma flow along closed field lines
[NASA-CR-193589] 01 p0387 N94-10641
Physics of tokamak scrape-off layer confinement
[DE93-011949] 01 p0390 N94-11125
Simulation study of dynamo structure in reversed field pinch
[DE93-771406] 01 p0390 N94-11128
The role of ionospheric plasma in the magnetosphere
[NASA-CR-194404] 02 p0716 N94-13967
Implicit multi-fluid simulation of interpenetrating plasmas
[DE93-013351] 02 p0801 N94-14342
Review of the Procyon explosive pulsed power system
[DE93-016562] 02 p0802 N94-14532
High power steady state MPD thrusters
[AD-A267277] 03 p0928 N94-17308
Plasma flow switch and foil implosion experiments on Pegasus 2
[DE93-016464] 03 p1013 N94-17318
Profile stabilization of tilt mode in a field reversed configuration
[DE93-016770] 04 p1583 N94-17753
Viscosity in the edge of tokamak plasmas
[DE93-018039] 04 p1588 N94-18988
Radiative divertor modeling studies
[DE93-018092] 04 p1590 N94-19290
On magnetodynamic effects initiated by a high-speed impact of a large cosmic body upon the Earth's surface 05 p2082 N94-20647
Driven reconnection and self-organization 05 p2000 N94-22625
Turbulization of free shear flows: 3D perturbations 05 p2000 N94-22626
Laboratory structure of the heliopause 05 p2003 N94-22648
Prompt high-energy particle acceleration during two current loops collision 05 p2005 N94-22661
Plasma structure in a plasma flow along a magnetic mirror field 05 p2005 N94-22664
Mean elemental composition and He-3 enrichments in solar energetic particles 05 p2006 N94-22670
MHD flows from compact objects: Effects on magnetic field configurations 05 p2008 N94-22684
Three-dimensional simulations of cosmic jets employing the smoothed particle hydrodynamics technique 05 p2008 N94-22685
Time variation of MHD accretion onto a black hole 05 p2009 N94-22692
Magnetic fields in spiral galaxies 05 p2010 N94-22697
Shock formation in magnetohydrodynamical accretion onto a black hole 05 p2010 N94-22699
Magnetohydrodynamic phenomena in star-forming processes and their environment 05 p2010 N94-22701
Three-dimensional solidification and melting using magnetic field control 06 p2325 N94-23664
Scientific study in solar and plasma physics relative to rocket and balloon projects
[NASA-CR-193885] 06 p2627 N94-24461
Liquid metal MHD research and development in Israel 07 p2854 N94-26055
Ways to improve MHD power plants and prospects of their application 07 p2854 N94-26056
Shear flow generation from the interaction of neoclassical and drift wave transport processes
[DE94-003135] 07 p2791 N94-26096
Quiet-time intensifications along the poleward auroral boundary near midnight
[ATR-93(7248)-2] 07 p2877 N94-26201
Scaling of sustained ZT-40 M reversed field pinches
[DE94-003318] 07 p3043 N94-26321
Researches of the Electrotechnical Laboratory. No. 53: Spectral emission from combustion gas containing scattering media
[JTN-94-80603] 07 p2717 N94-27246
Proceedings of the NIPR Symposium on Upper Atmosphere Physics, no. 6
[JTN-94-80593] 08 p3359 N94-29233
Computer simulations on development of the fast reconnection mechanism 08 p3360 N94-29241
The Seventh International Beer Sheva Seminar on MHD Flows and Turbulence
[DE94-607211] 08 p3506 N94-29831
Transport suppression by shear flow generation in multihelicity resistive-g turbulence
[DE94-007108] 09 p3886 N94-31366
Hydrodynamics of neutron star interiors and laboratory superfluids 09 p3936 N94-31949
Characteristics of ion flow in the quiet state of the inner plasma sheet
[AD-A277451] 09 p3894 N94-33106

Dynamical nature of inviscid power law for two-dimensional turbulences and self-consistent spectrum and transport of plasma filaments
[DE94-009425] 10 p4144 N94-33913
Studies on equatorial shock formation during plasmaspheric refilling
[NASA-CR-195864] 10 p4088 N94-34669
A triggering mechanism of fast crash in sawtooth oscillation
[DE94-718974] 11 p4336 N94-35772
Q-profile flattening due to nonlinear development of resistive kink mode and ensuing fast crash in sawtooth oscillations
[DE94-727625] 12 p4526 N94-36472
Momentum-energy transport from turbulence driven by parallel flow shear
[DE94-012765] 12 p4443 N94-37362

MAGNETOHYDRODYNAMIC GENERATORS

Advanced magnetic flux compression generator development issues: A comparison of coaxial and disk generators
[DE93-014025] 02 p0794 N94-12849
Heat and seed recovery technology project
[DE93-009203] 02 p0800 N94-13913
Application of a NEPTUNE propulsion concept to a manned Mars excursion
[AD-A268053] 03 p0929 N94-17587
Development of a multi-point two-color pyrometer for tube and wall temperature and emissivity measurement at the CFFF
[DE93-014716] 04 p1429 N94-18207
Study of multi-phase flow characteristics in an MHD power train
[DE93-018570] 04 p1586 N94-18272
MHD integrated topping cycle project
[DE93-040520] 04 p1588 N94-18978
MHD Integrated Topping Cycle Project
[DE93-040521] 04 p1589 N94-19055
The Lightcraft project: Flight technology for a hypersonic mass transit system 07 p2670 N94-25695
Liquid metal MHD research and development in Israel 07 p2854 N94-26055
Ways to improve MHD power plants and prospects of their application 07 p2854 N94-26056
MHD seed recovery/regeneration, phase 2
[DE94-006772] 09 p3886 N94-31273

MAGNETOHYDRODYNAMIC STABILITY

Kinetic approach to long wave length modes in rotating plasmas
[DE93-771286] 01 p0388 N94-10807
Magnetohydrodynamic computation of feedback stabilization of resistive-shell instabilities in the reversed field pinch
[DE93-013466] 01 p0388 N94-10852
Calculation of Mercier stability criterium in stellarators
[DE93-621599] 01 p0389 N94-11091
The angular structure of second harmonic emission from laser-produced plasmas irradiated at moderate intensity
[DE93-013102] 01 p0389 N94-11114
Gyrosheath near the tokamak edge
[DE93-012191] 01 p0390 N94-11142
Studies on the parametric decay of waves in fusion plasmas
[DE93-621659] 01 p0390 N94-11148
Elementary mechanism of electron beam dissipative instability development
[DE93-621653] 01 p0391 N94-11209
Experimental investigation of wake field excitation in plasma by a periodic succession of relativistic particle clots
[DE93-621655] 01 p0391 N94-11211
Negative viscosity and generation of dissipative solitons and zonal dissipative structures by drift waves
[DE93-621656] 01 p0392 N94-11212
Spreading of Bimodulated Ultra-relativistic Electron Beam (BUEB) in Atmospheric Plasma Channel (APCh)
[DE93-621658] 01 p0392 N94-11213
The role of plasma rotation on MHD instabilities in tokamaks
[DE93-013486] 01 p0393 N94-11512
Initial assessment of lower hybrid current drive in D3-D
[DE93-013310] 01 p0394 N94-12370
Two-dimensional simulations of foil implosion experiments on the Los Alamos capacitor bank
[DE93-012676] 02 p0794 N94-12814
Theory of field-reversed configurations
[DE93-015611] 02 p0794 N94-12862
Plasma diffusion through multidipole magnetic fields
[INPE-5460-PRE/1768] 02 p0795 N94-12901
Equilibrium reconstruction of the q-profile in tokamaks from motional Stark effect data
[DE93-015815] 02 p0796 N94-13046
Investigation of plasma instabilities in the Polar cusp
[NASA-CR-194283] 02 p0796 N94-13084
Recent study of beam stability in the PSR
[DE93-014473] 02 p0780 N94-13173
Parametric instabilities in large nonuniform laser plasmas
[DE93-013184] 02 p0797 N94-13393
Instability heating of the HDZP
[DE93-012641] 02 p0798 N94-13513
Nonlinear evolution of tearing modes in inhomogeneous plasmas
[PPL-133] 02 p0798 N94-13564
The propagation characteristics and instability properties of low-frequency electromagnetic waves in the Io plasma torus 02 p0601 N94-13650
Longitudinal beam dynamics for heavy ion fusion
[DE93-013850] 02 p0789 N94-13727
Small scale magnetic islands in collisionless plasmas
[PPL-131] 02 p0799 N94-13836
Semi-local kinetic analysis of the toroidal ion temperature gradient mode
[PPL-130] 02 p0800 N94-13851
Anomalous transport due to the ion acoustic instability in tokamaks
[PPL-129] 02 p0800 N94-13852
Numerical Studies of Collisionless Current Layers
[NASA-CR-194337] 02 p0800 N94-13854
On MHD mode equations in toroidal plasmas
[PPL-139] 02 p0800 N94-13877
Stability and confinement properties of small-aspect-ratio tokamak
[INPE-5463-PRE/1771] 02 p0801 N94-14024
Anomalous transport due to small scale electromagnetic and large scale electrostatic modes in tokamaks
[PPL-140] 02 p0801 N94-14206
Implicit multi-fluid simulation of interpenetrating plasmas
[DE93-013351] 02 p0801 N94-14342
The role of electric field shear stabilization of turbulence in the H-mode to VH-mode transition in D3-D
[DE93-015474] 02 p0802 N94-14583
Anomalous ion transport and feedback control
[DE93-018324] 02 p0803 N94-14874
Studies on the parametric decay of waves in fusion plasmas
[VTT-PUBS-110] 03 p1200 N94-15204
High beta and confinement studies of TFTR
[DE93-016204] 03 p1202 N94-16446
Direct drive foil implosion experiments on Pegasus 2
[DE93-012666] 03 p1202 N94-16776
Fundamental-mode RF design in e(+)e(-) storage ring factories
[DE93-015249] 03 p1183 N94-16809
Structure and damping of toroidal drift waves (and their implications for anomalous transport)
[DE93-014005] 03 p1203 N94-16822
Nonlinear gyrofluid models of shear Alfven instabilities in ignited and beam heated toroidal plasmas
[DE93-016235] 03 p1203 N94-16869
High power steady state MPD thrusters
[AD-A267277] 03 p0928 N94-17308
Plasma instabilities and transport in the MPD thruster
[AD-A268268] 03 p1204 N94-17575
Transformation of energy and momentum due to Landau damping in space
[DE93-624921] 04 p1581 N94-17689
Limits on m = 2, n = 1 error field induced locked mode instability in TPX with typical sources of poloidal field coil error field and a proto type correction coil, C-coil
[DE93-014408] 04 p1582 N94-17702
Self-regulated shear flow turbulence in confined plasmas
[DE93-015823] 04 p1583 N94-17743
Profile stabilization of tilt mode in a field reversed configuration
[DE93-016770] 04 p1583 N94-17753
Plasma properties research: Task 3
[DE93-017087] 04 p1583 N94-17854
Filamentary magnetohydrodynamic plasmas
[DE93-015616] 04 p1583 N94-17945
AEOLUS-IT MHD simulation code based on a toroidally incompressible plasma model
[DE93-788461] 04 p1586 N94-18157
Resonant absorption of Alfven waves near a neutral point
[DE93-628761] 04 p1586 N94-18172
Hydrodynamic instability modeling for ICF
[DE93-018634] 04 p1587 N94-18274
Nonparaxial MHD stabilizers for an axisymmetric magnetic mirror
[DE93-017996] 04 p1587 N94-18505
Generalized energy principle for flute perturbations in axisymmetric mirror machines
[DE93-019399] 04 p1589 N94-19037
On neutral plasma oscillations
[DE93-040319] 04 p1590 N94-19194
Finite Larmor radius flute mode theory with end loss
[DE93-040914] 05 p1991 N94-19872

Effect of limiter end loss in finite Larmor radius theory
[DE93-040913] 05 p1992 N94-19887
Beta-limiting instabilities in D3-D discharges with large bootstrap current
[DE93-015476] 05 p1993 N94-20326
Two-dimensional nonlinear Schrodinger equations and their properties
[AD-A272184] 05 p1952 N94-20923
Three-wave resonant interaction in a thin layer
[AD-A272331] 05 p1994 N94-21039
Shear flow generation by Reynolds stress and suppression of resistive g-modes
[DE93-040911] 05 p1995 N94-21514
On the stability of shear-Alfven vortices
[DE93-040912] 05 p1996 N94-21752
Continuum damping of ideal toroidal Alfven eigenmodes
[DE94-001233] 05 p1998 N94-22560
Kinetic resonance damping rate of the toroidal ion temperature gradient mode
[DE94-001234] 05 p1998 N94-22561
Fluid simulations of Delta T(sub e)-driven turbulence and transport in boundary plasmas
[DE94-001304] 05 p1999 N94-22566
Driven reconnection and self-organization 05 p2000 N94-22625
MHD instabilities of fusion oriented plasmas 05 p2000 N94-22627
Consequences of chaotic particle motion for the stability of space plasma current sheets 05 p2001 N94-22636
Tangential stress due to Kelvin-Helmholtz instability at the magnetospheric boundary 05 p2003 N94-22651
Non-linear thermal instability of optical thin molecular structures 05 p2006 N94-22667
On the nonlinear instability of thermal structures 05 p2006 N94-22668
Consequences of plasma-maser in plasma astrophysics 05 p2006 N94-22669
The onset and spectra of a magnetized Langmuir turbulence 05 p2006 N94-22673
Langmuir microstructures and pulsar radio emission 05 p2007 N94-22678
Helical kink instability of jets from young stellar objects 05 p2008 N94-22686
Fragmentation of magnetized filamentary interstellar clouds 05 p2008 N94-22687
Gravitational instability of magnetized filamentary clouds. 1: Helical magnetic fields 05 p2008 N94-22688
Gravitational instability of magnetized filamentary clouds. 2: Rotation 05 p2009 N94-22689
Spiral Alfven instability in accretion disks 05 p2010 N94-22696
Fluctuations and confinement in ATF
[DE94-000485] 06 p2549 N94-22998
Optimization of energy transfer in microwave electrothermal thrusters 06 p2216 N94-23065
Investigation of a subsonic-arc-attachment thruster using segmented anodes
[NASA-TM-106419] 06 p2219 N94-23531
Stabilization of the external kink and other MHD issues
[DE94-001541] 06 p2552 N94-24502
Plasma initiation in a tokamak with conducting superstructure: First results from Alcator C-MOD
[DE94-001565] 06 p2552 N94-24504
Effect of LHCD (low hybrid current drive) on tearing mode instability
[DE93-613700] 06 p2555 N94-25344
Toroidal plasma beta-FLR limit in a toroidally linked mirror system
[DE94-003119] 07 p3041 N94-25792
Nonlinear growth of strongly unstable tearing modes
[DE94-003366] 07 p3042 N94-25958
Investigation of plasma instabilities in the polar cusp
[NASA-CR-195212] 07 p2879 N94-26599
TFTR experimental data analysis collaboration
[DE94-004166] 07 p3047 N94-27690
Reduced Braginskii equations
[DE94-003510] 07 p3047 N94-27723
Numerical experiment on finite element method for matching data
[DE94-701208] 07 p3000 N94-27731
Passive stabilization of MHD instabilities at high (beta)n in the HBT-EP tokamak
[DE94-003317] 07 p3047 N94-27735
Nonlinear magnetohydrodynamics
[DE94-005654] 08 p3503 N94-28547
Active electron and ion beam experiments in space
[AD-A275570] 08 p3504 N94-28828
Towards experimental verification and device applications of current driven plasma instabilities in solid state systems
[AD-A275395] 08 p3504 N94-29055

Proceedings of the NIPR Symposium on Upper Atmosphere Physics, no. 6
[JTN-94-80593] 08 p3359 N94-29233
Computer simulations on development of the fast reconnection mechanism 08 p3360 N94-29241
Coupled magnetohydrodynamic oscillations in the magnetosphere-ionosphere system: Hall current effect 08 p3360 N94-29242
Scale-length dependence of the ratio between the magnetic and electric field perturbations in the ionospheric field-aligned current region 08 p3360 N94-29243
Formation and self-healing of magnetic islands in finite-beta helias equilibria
[AD-B183271L] 08 p3505 N94-29483
The structure of solar magnetic fields and their associated electric currents 08 p3544 N94-29723
Higher order collisionless ballooning mode in tokamaks
[PPL-143] 08 p3507 N94-30156
Eigenmode analysis of the destabilized ion acoustic mode in tokamaks
[PPL-142] 08 p3507 N94-30158
Resistive ballooning mode in a gas-dynamic trap
[DE94-608328] 08 p3508 N94-30171
Langmuir waves in the electron-positron plasma
[DE94-608330] 08 p3508 N94-30191
A review of the ablative stabilization of the Rayleigh-Taylor instability in regimes relevant to ICF
[DE94-005809] 08 p3509 N94-30597
Advanced steady-state operating scenarios
[DE94-004810] 08 p3509 N94-30768
On the nonlinear dynamics of ocean wave systems 08 p3378 N94-30790
Inertial confinement fusion
[DE94-005957] 08 p3510 N94-30875
Numerical method for the investigation of the magnetohydrodynamic stability of three dimensional plasma equilibria
[ETN-94-95752] 09 p3887 N94-31512
Toroidal pinch experiments
[DE94-005876] 09 p3887 N94-31558
High beta tokamak research
[DE94-006513] 09 p3888 N94-31664
Stability and instability criteria for magnetohydrodynamics
[PB94-148475] 09 p3889 N94-31772
Theoretical studies of magnetohydrodynamic equilibria and dynamics of a solar coronal loop 09 p3953 N94-31792
Instability heating of solid-fiber Z pinches
[DE94-007055] 09 p3889 N94-31809
Anomalous thermalization of fast ions in magnetized plasma
[DE94-007109] 09 p3891 N94-32631
Basic principles approach for studying nonlinear Alfven wave-alpha particle dynamics
[DE94-007112] 09 p3891 N94-32664
Cooperative program on D3-D (FY 1993)
[DE94-008343] 09 p3892 N94-32820
Stability of bootstrap current driven magnetic islands in stellarators
[DE94-009207] 09 p3893 N94-32912
Stabilization method of A.C. arc plasma
[DE94-757268] 09 p3893 N94-32916
The spatial development of the magnetospheric low-latitude boundary layer
[ISBN-0-315-77418-5] 09 p3776 N94-33111
Diffusion at the magnetopause: A theoretical perspective
[DE94-009356] 10 p4086 N94-33910
High beta and second stability region transport and stability analysis
[DE94-009654] 10 p4145 N94-33920
LLE review, volume 57
[DE94-009186] 10 p4145 N94-33990
Studies of ion acoustic decay
[DE94-009470] 10 p4138 N94-34168
Magnetic island effects, interactions in tokamaks
[DE94-009209] 10 p4145 N94-34221
A review of the ablative stabilization of the Rayleigh-Taylor instability in regimes relevant to inertial confinement region
[DE94-008300] 10 p4145 N94-35080
Collisionless dynamics of the magnetosphere
[AD-A278886] 11 p4290 N94-35708
A triggering mechanism of fast crash in sawtooth oscillation
[DE94-716974] 11 p4336 N94-35772
The kinetics of inhomogeneous plasma
[DE94-611459] 11 p4336 N94-35788
Analysis of current diffusive ballooning mode
[DE94-716992] 11 p4336 N94-35811
Neoclassical current and related MHD stability, gap modes, and radial electric field effects in heliotron and torsatron plasmas
[DE94-716987] 11 p4337 N94-35938
Improved models of beta-limit, anomalous transport and radial electric field with loss cone loss in heliotron/torsatron
[DE94-716976] 11 p4324 N94-35984
Initial studies of reflectometer for ITER
[DE94-012476] 12 p4528 N94-37167
Confinement improvement in H-mode-like plasmas in helical systems
[DE94-727619] 12 p4528 N94-37231
Anomalous cross field flux in CHS
[DE94-727547] 12 p4529 N94-37359
Isotope scaling and eta(i) mode with impurities in tokamak plasmas
[DE94-012763] 12 p4529 N94-37361
Recent DIII-D high power heating and current drive experiments
[DE94-012509] 12 p4530 N94-37436
Theory of anomalous transport in H-mode plasmas
[DE94-727546] 12 p4531 N94-37485
Langmuir waves in the electron-positron plasma
[DE94-618779] 12 p4531 N94-37728

MAGNETOHYDRODYNAMIC TURBULENCE
NT LANGMUIR TURBULENCE
NT PLASMA TURBULENCE
On energy transport equations for turbulent magnetized plasma
[PPL-135] 02 p0800 N94-13850
Broken symmetry in ideal magnetohydrodynamic turbulence
[NASA-TM-109017] 03 p1023 N94-15964
Compressible MHD turbulence in the interplanetary medium 05 p2003 N94-22650
Structure of accretion plasmas of x ray binary pulsars in MHD turbulence 05 p2007 N94-22679
Spiral Alfven instability in accretion disks 05 p2010 N94-22698
On the physics of waves in the solar atmosphere: Wave heating and wind acceleration
[NASA-CR-195197] 06 p2628 N94-25264
Acceleration in astrophysics
[DE94-004986] 08 p3552 N94-28580
The Seventh International Beer Sheva Seminar on MHD Flows and Turbulence
[DE94-607211] 08 p3506 N94-29831

MAGNETOHYDRODYNAMIC WAVES
NT ELECTROSTATIC WAVES
NT PLASMA WAVES
Efficiency of fast wave current drive for a weakly relativistic plasma
[DE93-012775] 01 p0385 N94-10159
Nonlinear MHD-waves in a dissipative plasma with hall currents
[DE93-617844] 01 p0386 N94-10395
Comment of parameter excitation of Alfven and Heliicon waves in a magnetoactive compensated semiconductor by microwave radiation
[DE93-623203] 02 p0806 N94-13228
Investigations of transitions from order to chaos in dynamical systems
[DE93-014438] 02 p0818 N94-14738
Linear and non-linear studies of Alfven waves in space. Stationary and dynamic processes in magnetospheric plasmas
[NASA-CR-193585] 03 p1239 N94-16647
Nonlinear gyrofluid models of shear Alfven instabilities in ignited and beam heated toroidal plasmas
[DE93-016235] 03 p1203 N94-16869
The phase mixing of shear Alfven waves
[DE93-624920] 04 p1581 N94-17688
Profile stabilization of tilt mode in a field reversed configuration
[DE93-016770] 04 p1583 N94-17753
Microwave scattering from TAE modes
[DE93-018170] 04 p1583 N94-17809
On the stability of shear-Alfven vortices
[DE93-040912] 05 p1996 N94-21752
Continuum damping of ideal toroidal Alfven eigenmodes
[DE94-001233] 05 p1998 N94-22560
MHD instabilities of fusion oriented plasmas 05 p2000 N94-22627
Theory of leaked auroral kilometric radiation 05 p2003 N94-22649
Compressible MHD turbulence in the interplanetary medium 05 p2003 N94-22650
Energy release at Alfvenic fronts in solar flares 05 p2003 N94-22652
Dynamo driven by weak plasma turbulence: The effect of differential rotation 05 p2005 N94-22665
The onset and spectra of a magnetized Langmuir turbulence 05 p2006 N94-22673
Langmuir microstructures and pulsar radio emission 05 p2007 N94-22678
Magnetic superbubbles in the galactic disk and halo 05 p2009 N94-22694
Spiral Alfven instability in accretion disks 05 p2010 N94-22698
Shock formation in magnetohydrodynamical accretion onto a black hole 05 p2010 N94-22699
On the physics of waves in the solar atmosphere: Wave heating and wind acceleration
[NASA-CR-195197] 06 p2628 N94-25264
Review of tokamak experiments on direct electron heating and current drive with fast waves
[DE94-004185] 07 p3041 N94-25801
TFTR experimental data analysis collaboration
[DE94-004166] 07 p3047 N94-27690
The calculation for energy balance of heating plasmas by Alfven waves
[DE94-604994] 07 p3049 N94-27855
Proceedings of the NIPR Symposium on Upper Atmosphere Physics, no. 6
[JTN-94-80593] 08 p3359 N94-29233
Coupled magnetohydrodynamic oscillations in the magnetosphere-ionosphere system: Hall current effect 08 p3360 N94-29242
Scale-length dependence of the ratio between the magnetic and electric field perturbations in the ionospheric field-aligned current region 08 p3360 N94-29243
ULF waves and magnetic field characteristics in the polar cusp observed at Godhavn 08 p3361 N94-29244
Study of generation mechanisms of magnetospheric VLF/ELF emissions based on the direction findings 08 p3361 N94-29245
Nonlinear wave packet evolution in a dispersive plasma: Application to rotational discontinuities 08 p3506 N94-29822
On determination of a momentum of Alfven wave packet
[DE94-608329] 08 p3255 N94-30172
Numerical simulation of interplanetary dynamics 09 p3933 N94-31566
Plasma confinement theory and transport simulation
[DE94-006065] 09 p3888 N94-31619
Self-consistent effects of magnetospheric hydromagnetic waves on ring current ions
[AD-A277406] 09 p3774 N94-32346
Basic principles approach for studying nonlinear Alfven wave-alpha particle dynamics
[DE94-007112] 09 p3891 N94-32664
On the ULF waves in the Earth's dayside magnetosphere 10 p4085 N94-33416
Magnetic field waves at Uranus
[NASA-CR-194807] 10 p4164 N94-34000
Theoretical studies of the solar atmosphere and interstellar pickup ions
[NASA-CR-195846] 10 p4166 N94-34716
On the physics of waves in the solar atmosphere: Wave heating and wind acceleration
[NASA-CR-194119] 11 p4375 N94-36395
Q-profile flattening due to nonlinear development of resistive kink mode and ensuing fast crash in sawtooth oscillations
[DE94-727625] 12 p4526 N94-36472

MAGNETOHYDRODYNAMICS
Calculation of the effects of magnetic field damping in fluid flow: Comparison of magnetohydrodynamic models of different complexity 01 p0103 N94-10089
Source to detector spectrum transformation and its inverse for the Pegasus Z-pinch
[DE93-012674] 01 p0384 N94-10157
MHD simulation of deuterium-fiber-initiated Z-pinches with two-fluid effects
[DE93-012682] 01 p0384 N94-10158
Reversed-field pinch studies in the Madison Symmetric Torus
[DE93-013464] 01 p0388 N94-10747
Magnetohydrodynamic computation of feedback stabilization of resistive-shell instabilities in the reversed field pinch
[DE93-013466] 01 p0388 N94-10852
Discrete vortex representation of magnetohydrodynamics
[DE93-012190] 01 p0393 N94-11669
On the unique structure of the magnetic fields of Uranus and Neptune 01 p0472 N94-12221
MHD shocks in coronal mass ejections
[NASA-CR-193418] 02 p0828 N94-12970
Magnetic fusion computing: A personal retrospective view
[DE93-014147] 02 p0797 N94-13217
Heat and seed recovery technology project
[DE93-009203] 02 p0800 N94-13913
Investigations of transitions from order to chaos in dynamical systems
[DE93-014438] 02 p0818 N94-14738
Magnetic effects in Venus/solar wind interaction
[NASA-CR-194666] 03 p1299 N94-17281
Profile stabilization of tilt mode in a field reversed configuration
[DE93-016770] 04 p1583 N94-17753

Filamentary magnetohydrodynamic plasmas
[DE93-015616] 04 p1583 N94-17945
Coupled MHD and transport analysis of improved confinement D3-D discharges
[DE93-016985] 04 p1585 N94-18057
AEOLUS-IT MHD simulation code based on a toroidally incompressible plasma model
[DE93-788461] 04 p1586 N94-18157
Study of multi-phase flow characteristics in an MHD power train
[DE93-018570] 04 p1586 N94-18272
Hydrodynamic instability modeling for ICF
[DE93-018634] 04 p1587 N94-18274
Nonparaxial MHD stabilizers for an axisymmetric magnetic mirror
[DE93-017996] 04 p1587 N94-18505
Contributions from geomagnetic inverse theory to the study of hydromagnetic conditions near the core-mantle boundary
[NASA-CR-194303] 04 p1484 N94-18853
MHD technology transfer, integration and review committee
[DE93-040519] 04 p1588 N94-18892
Viscosity in the edge of tokamak plasmas
[DE93-018039] 04 p1588 N94-18988
Generalized energy principle for flute perturbations in axisymmetric mirror machines
[DE93-019399] 04 p1589 N94-19037
Magnetically controlled solar nebula
05 p2120 N94-20791
On the stability of shear-Alfven vortices
[DE93-040912] 05 p1996 N94-21752
Physics of magnetospheric boundary layers
[NASA-CR-194725] 05 p1858 N94-21836
A spheromak ignition experiment reusing Mirror Fusion Test Facility (MFTF) equipment
[DE94-001856] 05 p2034 N94-22050
Compressible MHD turbulence in the interplanetary medium
05 p2003 N94-22650
MHD relaxation in magnetic loops
05 p2004 N94-22658
Formation of fast magnetosonic shock waves during two current loops collision in solar flare
05 p2005 N94-22662
Helical kink instability of jets from young stellar objects
05 p2008 N94-22686
Time variation of MHD accretion onto a black hole
05 p2009 N94-22692
Accretion of a hot plasma onto the central black hole: Fokker-Planck formulation
05 p2009 N94-22693
Magnetic superbubbles in the galactic disk and halo
05 p2009 N94-22694
Generation and maintenance of bisymmetric spiral magnetic fields in disk galaxies in differential rotation
05 p2010 N94-22695
Magnetohydrodynamic phenomena in star-forming processes and their environment
05 p2010 N94-22701
Plasma research in the Madison Symmetric Torus (MST)
[DE94-002318] 06 p2549 N94-22976
Lectures on magnetohydrodynamical drives
[PB93-224962] 06 p2308 N94-23104
The internal structure and dynamics of the railgun plasma armature between infinitely wide ablating rails
[DE94-001473] 06 p2198 N94-23208
Evolution of large-scale plasma structures in comets: Kinematics and physics
[NASA-CR-194777] 06 p2601 N94-23251
Scientific study in solar and plasma physics relative to rocket and balloon projects
[NASA-CR-193885] 06 p2627 N94-24461
Model development for Ulysses and SOHO
[NASA-CR-193884] 06 p2627 N94-24484
Stabilization of the external kink and other MHD issues
[DE94-001541] 06 p2552 N94-24502
Modelling of thermal argon plasmas
[ETN-94-95363] 06 p2554 N94-25300
LHCD (low hybrid current drive) experiment on the HT-6B tokamak
[DE93-613720] 06 p2555 N94-25331
Effect of LHCD (low hybrid current drive) on tearing mode instability
[DE93-613700] 06 p2555 N94-25344
The Lightcraft project: Flight technology for a hypersonic mass transit system
07 p2670 N94-25695
Nonlinear growth of strongly unstable tearing modes
[DE94-003366] 07 p3042 N94-25958
The First Energy Conference: Israel and the Former USSR
[ISBN-965-229-098-X] 07 p2853 N94-26050
Liquid metal MHD research and development in Israel
07 p2854 N94-26055
Nonlinear transverse propagation of photons in a ultrarelativistically hot and magnetized electron-positron plasma: Coupling of Langmuir and electromagnetic solitons
[DE94-603667] 07 p3046 N94-27630
TFTR experimental data analysis collaboration
[DE94-004166] 07 p3047 N94-27690
Numerical experiment on finite element method for matching data
[DE94-701208] 07 p3000 N94-27731
Analysis of density limit and efficiency in lower hybrid current drive
[DE94-604995] 07 p3049 N94-27856
Nonlinear magnetohydrodynamics
[DE94-005654] 08 p3503 N94-28547
Acceleration in astrophysics
[DE94-004986] 08 p3552 N94-28580
Formation and self-healing of magnetic islands in finite-beta helias equilibria
[AD-B183271L] 08 p3505 N94-29483
Liquid metal MHD and heat transfer in a tokamak blanket slotted coolant channel
[DE94-004622] 08 p3506 N94-29510
A relativistic solitary wave in electron positron plasma
[DE94-608107] 08 p3507 N94-30071
Advanced steady-state operating scenarios
[DE94-004810] 08 p3509 N94-30768
Magnetohydrodynamics of the Earth's core. 1: Steady, rotating magnetoconvection. 2: Magnetic Rossby waves
09 p3770 N94-31104
Evolution of dynamo-generated magnetic fields in accretion disks around compact and young stars
09 p3931 N94-31138
Numerical simulation of interplanetary dynamics
09 p3933 N94-31566
High beta tokamak research
[DE94-006513] 09 p3888 N94-31664
Stability and instability criteria for magnetohydrodynamics
[PB94-148475] 09 p3889 N94-31772
Pulsed expansion of plasma in a magnetic thruster
09 p3889 N94-31776
Theoretical studies of magnetohydrodynamic equilibria and dynamics of a solar coronal loop
09 p3953 N94-31792
Computer modeling of active experiments in space plasmas
09 p3890 N94-31927
Hydrodynamics of neutron star interiors and laboratory superfluids
09 p3936 N94-31949
Theoretical studies on ionospheric irregularities and ion diode performance
[AD-A277115] 09 p3772 N94-31984
Scenarios for multi-unit inertial fusion energy plants producing hydrogen fuel
[DE94-006614] 09 p3666 N94-32114
Self-consistent effects of magnetospheric hydromagnetic waves on ring current ions
[AD-A277406] 09 p3774 N94-32346
Magnetohydrodynamic boundary layer control system
[AD-D016120] 09 p3710 N94-32958
An approximate Riemann solver for magnetohydrodynamics (that works in more than one dimension)
[AD-280296] 09 p3849 N94-33033
The spatial development of the magnetospheric low-latitude boundary layer
[ISBN-0-315-77418-5] 09 p3776 N94-33111
High beta and second stability region transport and stability analysis
[DE94-009654] 10 p4145 N94-33920
Magnetic island effects, interactions in tokamaks
[DE94-009209] 10 p4145 N94-34221
Contributions of the low-latitude boundary layer to the finite width magnetotail convection model
[NASA-CR-196116] 11 p4289 N94-35392
A triggering mechanism of fast crash in sawtooth oscillation
[DE94-718974] 11 p4336 N94-35772
MHD and confinement characteristics in the high-beta regime on the CHS low-aspect-ratio heliotron/torsatron
[DE94-718981] 11 p4339 N94-36357
A study of physical mechanisms for filament eruption and coronal mass ejection via numerical simulation
[NASA-CR-196087] 12 p4549 N94-36469
Simulation of three-dimensional multi-phase flow characteristics in the deswirl section of the CDIF MHD power train
[DE94-012644] 12 p4443 N94-37176
Momentum-energy transport from turbulence driven by parallel flow shear
[DE94-012765] 12 p4443 N94-37362
Project JOVE --- microgravity experiments and applications
[NASA-CR-196292] 12 p4445 N94-37635
Magnetotail dynamics: MHD simulations of driven and spontaneous dynamic changes
[DE94-011702] 12 p4471 N94-37701

MAGNETOIONIC PLASMA

U PLASMAS (PHYSICS)

MAGNETOMETERS

NT VARIOMETERS

A phaseonium magnetometer: A new optical magnetometer based on index enhanced media
01 p0375 N94-10565
NASA Marshall Space Flight Center solar observatory report, January - June 1993
[NASA-TM-108417] 01 p0423 N94-10866
Large array SQUID magnetometer for NDE
[AD-A264799] 01 p0304 N94-11449
High resolution SQUID magnetometry for non-destructive evaluation
[AD-A268884] 04 p1447 N94-18225
Experience with custom processors in space flight applications
04 p1336 N94-18338
Aspects of the calibration and processing of the CRRES fluxgate magnetometer data
[AD-A270127] 04 p1432 N94-18875
STAFF (Spatio-Temporal Analysis of Field Fluctuations) experiment for the Cluster mission
04 p1328 N94-19625
The Cluster magnetic field investigation: Scientific objectives and instrumentation
04 p1329 N94-19629
Solar imaging vector magnetograph
[NASA-CR-194729] 05 p1810 N94-21876
Polarization analysis of a balloon-borne solar magnetograph
[NASA-CR-193908] 06 p2345 N94-24852
Detection geometry and reconstruction error in magnetic source imaging
[DE94-004012] 07 p2809 N94-25662
Determination of the geomagnetic external contribution by nonlinear optimization methods
[DE94-600882] 07 p2878 N94-26365
Fabrication issues in optimizing YBa(2)Cu(3)O(7-x) flux transformers for low I/f noise
[DE94-005209] 08 p3261 N94-28546
The computer-aided system for the high resolution SQUID-magnetometer
[DE94-606138] 08 p3286 N94-28553
NASA Marshall Space Flight Center Solar Observatory report, July - October 1993
[NASA-TM-108448] 08 p3160 N94-29470
Three-axis fiber optic vector magnetometer
[AD-D016016] 08 p3288 N94-29699
Fiberoptisk magnetfaltsensor (fiber optic magnetometer)
[PB94-148061] 09 p3878 N94-31584
A teleoperated system for remote site characterization
10 p4066 N94-34029
Operational support for Upper Atmosphere Research Satellite (UARS) attitude sensors
11 p4204 N94-35617
A new algorithm for attitude-independent magnetometer calibration
11 p4209 N94-35644
Magnetic properties of nanosize iron clusters
[DE94-011329] 11 p4318 N94-36204

MAGNETOMETRY

U MAGNETIC MEASUREMENT

MAGNETOPAUSE

A study of the magnetic field annihilation process in the magnetosphere and some geotechnical applications
[DE93-013249] 01 p0273 N94-10305
A study of the magnetic field annihilation process in the magnetosphere and some geotechnical applications
[DE93-013248] 01 p0273 N94-10319
Ion anisotropy driven waves in the Earth's magnetosheath and plasma depletion layer
[DE93-012751] 02 p0712 N94-12952
The interplanetary origins and the main-phase development of moderate geomagnetic storms (1978 - 1979)
[INPE-5445-TDI/491] 02 p0835 N94-13174
Terrestrial magnetospheric imaging: Numerical modeling of low energy neutral atoms
[DE93-014561] 02 p0717 N94-14328
Penetrating radiation environment and effects study
[AD-A270126] 04 p1485 N94-18874
Laboratory relations between the solar wind dynamic pressure and the magnetospheric structures of the Earth and comets
05 p2003 N94-22647
The spatial development of the magnetospheric low-latitude boundary layer
[ISBN-0-315-77418-5] 09 p3776 N94-33111
Diffusion at the magnetopause: A theoretical perspective
[DE94-009356] 10 p4086 N94-33910
Origins of energetic ions in the Earth's magnetosheath
[NASA-CR-189359] 12 p4471 N94-37703

MAGNETOPLASMADYNAMICS
Electric propulsion system technology
[NASA-CR-194099] 02 p0549 N94-13068
Low power pulsed MPD thruster system analysis and applications
[NASA-CR-191187] 02 p0550 N94-13415
High power steady state MPD thrusters
[AD-A267277] 03 p0928 N94-17308
Evaluation of externally heated pulsed MPD thruster cathodes
[NASA-CR-191090] 05 p1670 N94-21565
Reduction of the anode fall in a coaxial plasma thruster with an applied magnetic nozzle
[DE94-000670] 06 p2218 N94-23283
Numerical simulation of cylindrical, self-field MPD thrusters with multiple propellants
[NASA-CR-194458] 06 p2220 N94-24714
An investigation of magnetic field effects on plume density and temperature profiles of an applied-field MPD thruster
[NASA-TM-106416] 07 p2700 N94-26090
Flowing DPF design for propulsion experiments
[AD-A274973] 07 p2701 N94-26537
Performance of a quasi-steady, multi megawatt, coaxial plasma thruster
[NASA-CR-195311] 09 p3616 N94-32970

MAGNETOPLASMAS
U PLASMAS (PHYSICS)

MAGNETORESISTIVITY
Theory of the negative magnetoresistance in magnetic metallic multilayers
[DE93-013912] 02 p0776 N94-14584
The effect of correlated and point defects on the vortex lattice melting transition in single crystal YBa2Cu3O(7-delta)
[DE93-040277] 05 p2033 N94-21997
Magnetic phases in UNiGe
[DE94-000793] 06 p2239 N94-22939
Anomalous magnetoresistance behavior of superconducting Nd(2-x)Ce(x)CuO(4-y) single crystal
[DE94-000806] 06 p2558 N94-22941
Giant magnetoresistance and microstructural characteristics of epitaxial Fe-Ag and Co-Ag granular thin films
[DE94-006287] 08 p3519 N94-30707
Magnetotransport measurements in magnetic fields up to 50T in SmB6 and FeSi
[DE94-006227] 08 p3520 N94-30848
Effect of twin boundary density on the vortex melting transition in YBa2Cu3O(7-delta) single crystals
[DE94-007684] 09 p3904 N94-32601
Magnetoresistance of films and strips with the diffuse surface scattering
[DE94-611100] 11 p4340 N94-35933
Magnetic metallic multilayers
[DE94-011913] 11 p4341 N94-36274
Pressure dependence of the conductivity and magnetoconductance in oriented iodine-doped polyacetylene
[PB94-184488] 12 p4427 N94-37854

MAGNETOSHEATH
Ion anisotropy driven waves in the Earth's magnetosheath and plasma depletion layer
[DE93-012751] 02 p0712 N94-12952
Tangential stress due to Kelvin-Helmholtz instability at the magnetospheric boundary 05 p2003 N94-22651
Collisionless shock structures of Earth and other planets
[NASA-CR-195257] 07 p3104 N94-27407
The spatial development of the magnetospheric low-latitude boundary layer
[ISBN-0-315-77418-5] 09 p3776 N94-33111
Development of a preliminary solar wind transport magnetosheath forecast model
[AD-A278560] 10 p4165 N94-33785
Flank solar wind interaction
[NASA-CR-189327] 10 p4166 N94-35225
Origins of energetic ions in the Earth's magnetosheath
[NASA-CR-189359] 12 p4471 N94-37703

MAGNETOSONIC RESONANCE
Formation of fast magnetosonic shock waves during two current loops collision in solar flare
05 p2005 N94-22662
Mean elemental composition and He-3 enrichments in solar energetic particles 05 p2006 N94-22670

MAGNETOSPHERE-IONOSPHERE COUPLING
Modeling of the coupled magnetospheric and neutral wind dynamos
[NASA-CR-194728] 05 p1856 N94-20537
Implications of Viking dayside auroral measurements
[ISBN-0-315-83273-8] 05 p1861 N94-22575
Ionosphere-magnetosphere coupling
[NASA-CR-195222] 07 p2881 N94-27237
The Sixteenth Symposium on Coordinated Observations of the Ionosphere and the Magnetosphere in the Polar Regions: Program and abstracts
[JTN-94-80601] 07 p2882 N94-27300
Proceedings of the NIPR Symposium on Upper Atmosphere Physics, no. 6
[JTN-94-80593] 08 p3359 N94-29233
Signatures of dayside solar wind/magnetosphere/ionosphere coupling as revealed by the pace HF radars and associated experiments
08 p3359 N94-29236
A theory of current generator in the magnetosphere-ionosphere coupling
08 p3360 N94-29240
Coupled magnetohydrodynamic oscillations in the magnetosphere-ionosphere system: Hall current effect
08 p3360 N94-29242
Convection and electrodynamic signatures in the vicinity of a Sun-aligned arc: Results from the Polar Acceleration Regions and Convection Study (Polar ARCS)
09 p3954 N94-31102
Modeling of the magnetosphere-ionosphere-atmosphere system
[NASA-CR-195157] 11 p4288 N94-35244

MAGNETOSPHERIC INSTABILITY
Linear and non-linear studies of Alfven waves in space. Stationary and dynamic processes in magnetospheric plasmas
[NASA-CR-193585] 03 p1239 N94-16647
ULF waves in the low-latitude boundary layer and their relationship to magnetospheric pulsations: A multisatellite observation
[AD-A278906] 11 p4289 N94-35587
Analysis of plasma measurements for the Geotail mission
[NASA-CR-196274] 12 p4470 N94-37470
Substorm statistics: Occurrences and amplitudes
[DE94-011694] 12 p4471 N94-37669

MAGNETOSTATIC FIELDS
A study of relaxation transitions in the polymers under the influence of magnetic fields
[AD-A263878] 03 p0963 N94-15133
On radio frequency wave induced radial transport and wave helicity
[IPPCZ-326] 07 p2777 N94-27838

MAGNETOSTATICS
Stationary spectra of short-wave convective and magnetostatic fluctuations in a finite-pressure plasma and anomalous heat conductivity
[DE93-617852] 01 p0388 N94-10840
Magnetostatic waves-based integrated optic bragg cell modules with applications to RF signal processing
[AD-A269115] 04 p1577 N94-18295
Three dimensional multipole decomposition of fields
[DE93-018530] 04 p1389 N94-19053
The best of GYMNOS: A users guide
[DE93-041275] 05 p1992 N94-19991
Some challenging problems of the structured and dynamical solar atmosphere 06 p2624 N94-22838
Toward milli-Newton electro- and magneto-static microactuators 08 p3238 N94-29784

MAGNETOSTRICTION
On thermodynamic properties of heavy fermion systems in magnetic field
[DE93-613819] 01 p0409 N94-10403
Magnetostrictive actuators for human sensory feedback
[AD-A269266] 04 p1511 N94-17841
Review of a variational method applied to magnetoelastic buckling problems
[PB94-111184] 06 p2562 N94-23769
Improved magnetostrictive transducer drive elements achieved by reduction of crystalline defects and improved crystalline orientation
[AD-A273391] 06 p2313 N94-25276
Magnetostriction and magnetostrictive materials
[VTT-TIED-1434] 07 p3058 N94-26545
Ferrite phase shifters using stress insensitive materials
[AD-A274639] 07 p2708 N94-26895
Detection of low-intensity magnetic fields with a magnetostrictive fiber optic sensor
[AD-A274120] 07 p3037 N94-27062
Research on the improvement of shape-memory and magnetostrictive materials
[AD-A275397] 08 p3203 N94-29056
Fiberoptisk magnetfaltsensor (fiber optic magnetometer)
[PB94-148061] 09 p3878 N94-31584

MAGNETOTELLURIC PROFILING
U MAGNETIC SURVEYS

MAGNETOVARIOGRAPHS
U VARIOMETERS

MAGNETRON SPUTTERING
Ion assisted sputter deposition of Mo-Si multilayers
[DE93-013830] 02 p0583 N94-14693
Application of cylindrical distribution functions to anisotropic scattering from amorphous films
[DE93-015256] 03 p1183 N94-16811
Application of hard coatings to substrates at low temperatures
[NASA-CR-193867] 03 p0971 N94-17122
Anisotropic phase separation in amorphous Fe-Ge alloys
[DE93-015255] 03 p0961 N94-17251
Fundamental studies of defect generation in amorphous silicon alloys grown by remote plasma-enhanced chemical-vapor deposition
[DE93-017083] 05 p2029 N94-21615
Thin-film fabrication of Pb-doped BiSrCaCuO superconductor 05 p1781 N94-22176

MAGNETRONS
Anisotropic phase separation in amorphous Fe-Ge alloys
[DE93-015255] 03 p0961 N94-17251
Observation of x ray absorption magnetic circular dichroism in well-characterized iron-cobalt-platinum multilayers
[DE94-000303] 05 p1694 N94-21944
Transmission electron microscopy study of thick copper-304 stainless steel multilayers
[DE94-001045] 05 p1696 N94-22394
Novel two-stage selenization methods for fabrication of thin-film CIS cells and submodules
[DE94-000220] 06 p2390 N94-23296
Inverse free electron laser beat-wave accelerator research
[DE94-002597] 06 p2349 N94-23702
HPm-tubes: Literature survey comprising 1992
[PB94-123643] 07 p2785 N94-27038
Dependence of x ray absorption magnetic circular dichroism on layer periodicity in iron-platinum multilayers
[DE94-008786] 09 p3647 N94-32892
State of the art in high-power microwaves: An overview
[DE94-007075] 11 p4272 N94-35978

MAGNETS
NT ELECTROMAGNETS
NT FERRIMAGNETS
NT HIGH FIELD MAGNETS
NT PERMANENT MAGNETS
NT SUPERCONDUCTING MAGNETS
NT WIGGLER MAGNETS
Spin characteristics of ion beams during the motion of electromagnetic elements
[DE93-617448] 01 p0364 N94-10848
Operational characteristics of a 100-mA, 2-MeV radio-frequency quadrupole
[DE93-014474] 01 p0374 N94-12786
Calibration of a magnetic induction system for measurement of hypervelocities
[DE93-013949] 02 p0652 N94-14578
Automated directional solidification furnace
[NASA-TM-109662] 03 p1175 N94-15233
Comparison of computer predictions and magnetic field measurements for an iron spectrometer magnet
[DE93-016164] 03 p1176 N94-17658
A summary of studies of particle stability at RHIC
[DE93-040173] 05 p1970 N94-19868
Survey and alignment analysis for the ALS storage ring using computer spreadsheets
[DE93-019254] 05 p1917 N94-21917
Molecular/polymeric magnetism
[DE94-005888] 09 p3649 N94-31201
Magnetohydrodynamic boundary layer control system
[AD-D016120] 09 p3710 N94-32958
Measurements of the SIS: Magnets and SIS control system 10 p4067 N94-34359
Design and analysis of high-field quasi-continuous magnets
[DE94-000762] 12 p4508 N94-36556
BMAP dipole magnetic field analysis and orbit tracking/calculations of energy deposition in GaAs WHEBY detectors
[DE94-012080] 12 p4522 N94-37303

MAGNIFICATION
Optical displays: A tutorial on images and image formation
[AD-A266230] 03 p1192 N94-16926
Diffractive optical elements for generating arbitrary line foci 03 p1195 N94-17338

MAGNIFIERS
U MAGNIFICATION

MAGNITUDE
NT STELLAR MAGNITUDE

MAGNONS
The peculiarities of the spin glass state in Fe(x)Mn(1-x)TiO3
[DE93-617882] 01 p0395 N94-10525
Generalized spin systems and sigma-models
[DE93-613981] 01 p0410 N94-10802

A symmetrical form for equations of a nonlinear spiral magnetic
[DE93-621350] 01 p0344 N94-11033
Hydrodynamic asymptotics of Green functions in magnetics with spontaneously broken symmetry
[DE93-621349] 02 p0767 N94-13223
Theoretical high energy physics
[DE93-015884] 03 p1187 N94-16170
Lattice relaxation theory of localized excitations in quasi-one-dimensional systems
[DE93-624947] 03 p1215 N94-17437
Lectures of Fermi liquid theory
[DE93-016630] 04 p1592 N94-17714
Polaron tunneling in high-temperature superconductors
[DE93-016880] 04 p1593 N94-17754
Nonlinear dynamics and instabilities in ferromagnetic resonance experiments: Examinations of spheres from yttrium iron garnet in coincidence area of the first Suhl instabilities
[ETN-93-95072] 04 p1604 N94-19612
Spin fluctuations in an ordered Heisenberg ferromagnet with dipolar interactions
[PB93-204493] 06 p2524 N94-24533
Localized excitations in competing bond-order-wave, charge-density-wave and spin-density-wave systems. 2: Competing charge-density-wave and spin-density-wave
[DE93-617131] 06 p2538 N94-25388
Holes in a two-dimensional quantum antiferromagnet
[DE93-634753] 07 p3057 N94-26388
Fermi surface instability at 0.4 K in a heavy-fermion YbBiPt: SDW?
[DE94-006224] 09 p3899 N94-31916

MAIN SEQUENCE STARS
NT DWARF STARS
NT FLARE STARS
NT RED DWARF STARS
NT SUN
The abundances of the elements in sharp-lined early type stars
[NASA-CR-194055] 01 p0424 N94-12573
Stellar coronae at the end of the main sequence: A Rosat survey of the late M dwarfs
[NASA-CR-194700] 04 p1628 N94-19794
The circumstellar environments of intermediate mass main sequence stars
[NASA-CR-189311] 05 p2055 N94-21498
VVNRS: Variable phenomena in VV Cephei
[NASA-CR-194731] 05 p2056 N94-21835
ROSAT observations of the x ray binary HD 154791
[NASA-CR-195189] 06 p2600 N94-25198
Coronal heating via nanoflares
[DE94-000773] 07 p3110 N94-26696
Globular cluster photometry near the turnoff: Blue stragglers, relative ages, and the horizontal branch
08 p3538 N94-29732
Surface differential rotation in a sample of cool dwarf stars 08 p3545 N94-29827
The evolutionary status of PSR 1259-63
[DE94-007094] 09 p3938 N94-32503
Binary-binary collisions involving main-sequence stars, white dwarfs and neutron stars in globular clusters
[DE94-005086] 10 p4163 N94-33415

MAINTAINABILITY
More sense for less cents: Cost effective servicing of remote sensing satellites 01 p0348 N94-11572
RAMCAD (reliability, availability, and maintainability in computer-aided design)
[AD-A265143] 01 p0331 N94-11679
RAMCAD design methodology
[AD-A267010] 03 p1145 N94-15525
Conflict Resolution (CORE) for software quality factors
[AD-A267248] 03 p1151 N94-16941
Reliability and maintainability of modular robot systems: A roadmap for design
[AD-A268104] 03 p1168 N94-17517

MAINTENANCE
NT AIRCRAFT MAINTENANCE
NT FILE MAINTENANCE (COMPUTERS)
NT SPACE MAINTENANCE
NT SPACECRAFT MAINTENANCE
Applying reliability models to the maintenance of Space Shuttle software 01 p0330 N94-11434
Department of Energy fundamentals handbook: Engineering symbology, prints, and drawings
[DE93-012181] 01 p0129 N94-11456
Department of Energy fundamentals handbook: Engineering symbology, prints, and drawings
[DE93-012220] 01 p0129 N94-11670
Activities of Hawker Siddeley Canada Inc.
[CTN-93-60865] 02 p0849 N94-13505
Transcript of workshop on machinery health monitoring
[IME-MET-TR-005] 02 p0733 N94-13847
Optimal maintenance policies of a Markovian system
[ITN-93-85216] 02 p0774 N94-14502
Helicopter structures: A review of loads, fatigue design techniques, and usage monitoring
[AD-A267115] 03 p0866 N94-15651
Facilities maintenance handbook
[NHB-8831.2] 03 p1224 N94-15934
Effects of inspection error on optimal inspection policies and software fault detection models
[AD-A267511] 03 p1153 N94-17075
Application of thermal spray and ceramic coatings and reinforced epoxy for cavitation damage repair of hydroelectric turbines and pumps
[AD-A267624] 03 p0971 N94-17198
SUNRAYCE 1993: Working safely with lead-acid batteries and photovoltaic power systems
[DE93-016553] 04 p1464 N94-17712
Restoration of an 18th century English clock
04 p1427 N94-18026
Aircrew life support, AFSC 122X0(1T1X1)
[AD-A268998] 04 p1511 N94-18394
A case study in software maintenance
[AD-A269923] 04 p1521 N94-18659
Tehachapi solar thermal system
[DE93-018443] 04 p1468 N94-19014
Downsizing a database platform for increased performance and decreased costs
[DE93-018687] 04 p1618 N94-19099
Using electronic data interchange to report product quality
[AD-A271843] 05 p1828 N94-20468
Four-channel HF receiving antenna array simulator
[AD-A271876] 05 p1732 N94-20471
Engineering design, fabrication, installation, operation, and maintenance services in support of research on laser plasma physics
[AD-A272249] 05 p1994 N94-20943
N parallel queueing systems with server breakdown and repair
[CWI-BS-R9236] 05 p1944 N94-21232
Optimal repairman assignment in two maintenance models which are equivalent to routing models with early decisions
[CWI-BS-R9301] 05 p1930 N94-21234
Reducing the cognitive workload: Trouble managing power systems
[NASA-TM-106413] 05 p1714 N94-21564
Constraint-based scheduling 06 p2510 N94-23904
Reliability analysis of a repairable dependent parallel system
[ETN-94-95312] 06 p2373 N94-25295
Human factors in airway facilities maintenance: Development of a prototype outage assessment inventory
[DOT/FAA/AM-94/5] 07 p2941 N94-26136
Development of the gas turbine. Part 2: Manufacturing, commissioning, and operation 07 p2831 N94-28081
Towards an information model and mechanisms for design rationale capture and use
[AD-A275060] 08 p3530 N94-29138
A compact roller-gear pitch-yaw joint module: Design and control issues 08 p3161 N94-29629
Teleoperated systems for nuclear reactors: Inspection and maintenance
[AIAA PAPER 94-1176-CP] 08 p3439 N94-30528
The maintenance of operational flight program
[AD-A276363] 09 p3565 N94-31367
Common modeling system for digital simulation
09 p3823 N94-32429
Analysis of intermediate level maintenance following F404-GE-400 engine component life reductions
[AD-A277918] 09 p3585 N94-33283
Unique methods for on-orbit structural repair, maintenance, and assembly 10 p4102 N94-33663
Software architecture standard for simulation virtual machine, version 2.0
[NASA-CR-188291] 11 p4301 N94-35443
The development and application of composite complexity models and a relative complexity metric in a software maintenance environment
11 p4255 N94-35559
Implementation of a Computerized Maintenance Management System 11 p4343 N94-35970

MAINTENANCE TRAINING
Exercise countermeasures for bed-rest deconditioning
[NASA-TM-103987] 01 p0300 N94-11191
Forecasting the impact of virtual environment technology on maintenance training 01 p0314 N94-11570
Human factors in aviation maintenance: Phase 3, volume 1
[DOT/FAA/AM-93/15] 02 p0738 N94-14023
STS-31 crew training inflight maintenance and bailout exercises in CCT and WFTF
[NASA-TM-109483] 03 p0876 N94-15450
Knowledge organization in intelligent tutoring systems for diagnostic problem solving in complex dynamic domains
[AD-A273986] 07 p2984 N94-25899
Production of a computer based lesson teaching employees how to use an air data tester
[ISBN-0-315-84708-5] 07 p2969 N94-27316
Evaluation of a tool for producing and presenting interactive videodisc job aids
[AD-A278599] 12 p4432 N94-36473

MAJORITY CARRIERS
Electrochemical characterization of p(+)n and n(+)p diffused InP structures 01 p0049 N94-11385
Activation energy and capture cross section of majority carrier traps in Zn doped InP 01 p0049 N94-11386
The structural, chemical, and electrical properties of He-implantation-induced nanocavities in silicon
[DE94-002681] 07 p3052 N94-25971
A charge distribution analysis instrument for catalysis and material science applications
[DE94-008560] 10 p4146 N94-33407

MALAYA
U MALAYSIA

MALAYSIA
Atmospheric science research in Malaysia: Perspectives on international cooperation 07 p2874 N94-28285

MALES
Screening for prostate cancer
03 p1126 N94-16630
Effects of a high-energy food supplement on cold-induced thermogenesis
[AD-A269301] 04 p1504 N94-17823
Aeromedical disposition for coronary artery disease
06 p2423 N94-23316
Aeromedical implications of mitral valve prolapse
06 p2424 N94-23323
Spontaneous pneumothorax, cysts and bullae
06 p2425 N94-23326
Thermoregulatory effects of caffeine ingestion during rest and exercise in men
[NASA-TM-108783] 07 p2901 N94-26210
Effects of heat acclimation on heat-exercise tolerance in untrained and endurance-trained men wearing NBC protective clothing
[AD-A277522] 10 p4099 N94-33707

MALFUNCTIONS
Lock-up failure of a four-bar linkage deployment mechanism 08 p3163 N94-29646

MAMMALS
NT BABOONS
NT CATS
NT DOLPHINS
NT GUINEA PIGS
NT HUMAN BEINGS
NT MARINE MAMMALS
NT MICE
NT MONKEYS
NT PRIMATES
NT RABBITS
NT RATS
NT RODENTS
NT SHEEP
NT SWINE
The organization of the suprachiasmatic circadian pacemaker of the rat and its regulation by neurotransmitters and modulators
[AD-A266113] 01 p0301 N94-12417
An apparatus for measuring the biological oxidation of hydrogen gas under hyperbaric conditions
[AD-A266834] 03 p1119 N94-14916
Ontogenesis of mammals in microgravity
[NASA-TM-103978] 03 p1139 N94-17636
Physiologically based pharmacokinetic modelling of percutaneously absorbed dibromomethane utilizing multiple dermal sub-compartments
[AD-A271106] 05 p1889 N94-19981
Proposed law of nature linking impacts, plume volcanism, and Milankovitch cycles to terrestrial vertebrate mass extinctions via greenhouse-embryo death coupling
07 p2876 N94-28307
Multi-cellular, three-dimensional living mammalian tissue
[NASA-CASE-MSC-21560-2] 11 p4296 N94-35232

MAMMARY GLANDS
Bioeffects of radiofrequency radiation on cell growth and differentation. Volume 1: Engineering considerations
[AD-A267754] 03 p1118 N94-17232

MAN
U HUMAN BEINGS

MAN ENVIRONMENT INTERACTIONS
Chemistry and transport in a multi-dimensional model
[NASA-CR-194425] 02 p0716 N94-13969
Summary of conclusions and recommendations from a visibility science workshop
[DE93-012770] 02 p0710 N94-14523
Recent advances in radar remote sensing of forest
03 p0991 N94-15897

Statement on global climate change before the Subcommittee on Energy and Power, United States House of Representatives
[DE93-013163] 03 p1095 N94-16006
Global change research: Science and policy
[DE93-015675] 03 p1096 N94-16445
Global emissions and models of photochemically active compounds
[DE93-040490] 05 p1852 N94-21969
Fine resolution atmospheric sulfate model driven by operational meteorological data: Comparison with observations
[DE94-002994] 09 p3766 N94-32691
Asymetric change of daily temperature range: Proceedings
[DE94-010102] 11 p4293 N94-35703
Endangered and potentially endangered wildlife on John F. Kennedy Space Center and faunal integrity as a goal for maintaining biological diversity
[NASA-TM-109204] 11 p4288 N94-36422
Science priorities for the human dimensions of global change 12 p4464 N94-36987

MAN MACHINE SYSTEMS
NT HUMAN-COMPUTER INTERFACE
Virtual sound for virtual reality
[DE93-010519] 01 p0321 N94-10291
Aerospace medicine and biology: A continuing bibliography with indexes (supplement 375)
[NASA-SP-7011(375)] 01 p0303 N94-10398
Aerospace medicine and biology: A continuing bibliography with indexes (supplement 376)
[NASA-SP-7011(376)] 01 p0303 N94-10399
A new HMM learning algorithm for continuous speech recognition
[NHK-SERIAL-413] 01 p0132 N94-10560
Sixth Annual Workshop on Space Operations Applications and Research (SOAR 1992), volume 2
[NASA-CP-3187-VOL-2] 01 p0486 N94-11527
Noise levels and their effects on Shuttle crewmembers' performance: Operational concerns
01 p0314 N94-11538
Aerospace medicine and biology: A continuing bibliography with indexes (supplement 374)
[NASA-SP-7011(374)] 01 p0304 N94-11689
Flight crew interface aspects of forward-looking airborne windshear detection systems
[NASA-CR-191437] 02 p0516 N94-12829
Cognitive engineering in aerospace application: Pilot interaction with cockpit automation
[NASA-CR-177617] 02 p0510 N94-13247
Compatibility of information and mode of control: The case for natural control systems
02 p0523 N94-13307
Future developments of the NLR research flight simulator
[NLR-TP-92143-U] 02 p0528 N94-13498
Aerospace medicine and biology: A continuing bibliography with indexes (supplement 379)
[NASA-SP-7011(379)] 02 p0733 N94-14412
Manned vehicle systems research facility
[NASA-TM-109650] 03 p0875 N94-15318
Aerospace medicine and biology: A continuing bibliography with indexes (supplement 378)
[NASA-SP-7011(378)] 03 p1122 N94-16478
Aerospace medicine and biology: A continuing bibliography with indexes (supplement 380)
[NASA-SP-7011(380)] 03 p1122 N94-16479
OREMUS: Prototype of an orbit determination center dedicated to mini-satellite control
03 p0878 N94-17156
Acquisition and production of skilled behavior in dynamic decision-making tasks
[NASA-CR-194658] 03 p1133 N94-17296
Research on man-machine productivity in aviation at Human Engineering Institute of Hangzhou University
[AD-A269952] 04 p1512 N94-18673
Aerospace medicine and biology: A continuing bibliography with indexes (supplement 382)
[NASA-SP-7011(382)] 04 p1507 N94-18936
Aerospace medicine and biology: A continuing bibliography with indexes (supplement 381)
[NASA-SP-7011(381)] 04 p1507 N94-19069
Human-machine interfaces
[AD-A270730] 04 p1513 N94-19764
Research in image management and access
[NASA-CR-194797] 05 p1907 N94-20376
AIDA: A graphical interactive system, adapted to the user
[ETN-93-93792] 05 p1908 N94-21020
Aerospace medicine and biology: A continuing bibliography with indexes (supplement 383)
[NASA-SP-7011(383)] 05 p1892 N94-21288
Automating the control of robotic systems in unstructured environments
[DE93-040753] 05 p1946 N94-21929
Intervention strategies for the management of human error
[NASA-CR-4547] 05 p1642 N94-22373
Link monitor and control operator assistant: A prototype demonstrating semiautomated monitor and control
06 p2292 N94-23267
Lunar exploration rover program developments
[DE93-040759] 06 p2613 N94-23469
Activity Catalog Tool (ACT) user manual, version 2.0
[NASA-CR-177634] 06 p2430 N94-23527
Intelligent tutoring and aiding in satellite ground control 06 p2443 N94-23929
Programmable display pushbuttons on the Space Station's telerobot control panel
06 p2435 N94-24198
Simulation of the human-telerobot interface on the Space Station 06 p2436 N94-24202
Intelligent systems and advanced user interfaces for design, operation, and maintenance of command management systems
[NASA-CR-195172] 06 p2459 N94-24797
Human factors of mission planning systems: Theory and concepts 06 p2521 N94-25010
Mission planning and mission rehearsal systems: Displays and other interactive techniques
06 p2522 N94-25013
Sensor fusion display evaluation using information integration models in enhanced/synthetic vision applications 06 p2443 N94-25512
Quality metrics for sensor images
06 p2443 N94-25513
Institute for Information Technology
[NRC-37061] 07 p3118 N94-26709
Automated information management for designers: Functional requirements for computer based associates that support access and use of technical information in design
[AD-A274603] 07 p3099 N94-26891
Telepresence in the human exploration of Mars: Field studies in analog environments
07 p2685 N94-27360
Aerospace medicine and biology: A continuing bibliography with indexes (supplement 386)
[NASA-SP-7011(386)] 07 p2933 N94-28208
Aerospace medicine and biology: A continuing bibliography with indexes (supplement 387)
[NASA-SP-7011(387)] 07 p2933 N94-28213
Visit to CERMA: Centre d'Etudes et de Recherches de Medecine Aerospatiale, Centre for Studies and Research in Aviation and Space Medicine, Bretigny sur Orge, France, November 16-18, 1992
[PB94-132990] 07 p2937 N94-28392
Systematic safety consideration in product design
[PB94-132354] 08 p3229 N94-28410
Engineering of systems for application of scientific computing in industry 08 p3123 N94-28947
Stress and ergonomic design and evaluation of person-machine systems
[AD-A275156] 08 p3400 N94-29034
Future manned systems advanced avionics study
[NASA-CR-188277] 08 p3150 N94-29377
Cognitive approach to specifications on air traffic controllers' decision assistance systems
08 p3139 N94-29571
Elements of supervisory control for military robotic applications 08 p3309 N94-30303
Supervised autonomous control for Space Station Special Purpose Dextrous Manipulator (SPDM) robot
08 p3309 N94-30305
Aiding the operator in the manual control of a space manipulator
[PB94-125549] 08 p3402 N94-30390
A force-controllable macro-micro manipulator and its application to medical robots 08 p3314 N94-30441
Task automation in a successful industrial telerobot
[AIAA PAPER 94-1189-CP] 08 p3441 N94-30539
A real-time computer control and trajectory generation environment for Trussarm
[ISBN-0-315-87060-5] 09 p3832 N94-31833
Adaptive control of telerobotic systems worn by humans
[AD-A276608] 09 p3834 N94-32036
Aerospace medicine and biology: A continuing bibliography with indexes (supplement 389)
[NASA-SP-7011(389)] 09 p3797 N94-32347
Aerospace medicine and biology: A continuing bibliography with indexes (supplement 385)
[NASA-SP-7011(385)] 09 p3797 N94-32348
Technology transfer of operator-in-the-loop simulation
09 p3802 N94-32472
A rapid algorithm for realistic human reaching and its use in a virtual reality system 10 p4101 N94-33621
A human factors evaluation using tools for automated knowledge engineering 10 p4101 N94-33628
Quantitative 3-D imaging topogrammetry for telemedicine applications 10 p4096 N94-33645
On the design of flight-deck procedures
[NASA-CR-177642] 10 p3987 N94-33943
Seventh Annual Workshop on Space Operations Applications and Research (SOAR 1993), volume 1
[NASA-CP-3240-VOL-1] 10 p4179 N94-34019
Lunar exploration rover program developments
10 p4066 N94-34023
RoboLab and virtual environments
10 p4015 N94-34027
Controlling telerobots with video data and compensating for time-delayed video using Omniview
10 p4127 N94-34031
Intelligent vehicle control: Opportunities for terrestrial-space system integration
10 p4127 N94-34038
Robotic vehicle mobility and task performance: A flexible control modality for manned systems
10 p4067 N94-34040
Intelligent command and control systems for satellite ground operations
[NASA-CR-195852] 10 p4130 N94-34064
Bilateral control to coordinate operators with supporting systems by force sensed grips 10 p4067 N94-34335
Aerospace medicine and biology: A continuing bibliography with indexes (supplement 390)
[NASA-SP-7011(390)] 10 p4095 N94-34602
Expanding the pilot's envelope
10 p3994 N94-34627
Man-machine Integration Design and Analysis System (MIDAS) Task Loading Model (TLM) experimental and software detailed design report
[NASA-CR-177640] 10 p4100 N94-34706
Effects of checklist interface on non-verbal crew communications
[NASA-CR-177639] 10 p3987 N94-34915
Aerospace medicine and biology: A continuing bibliography with indexes (supplement 391)
[NASA-SP-7011(391)] 11 p4297 N94-35345
International Space Station alpha remote manipulator system workstation controls test report
[NASA-TM-104796] 11 p4274 N94-35481
MMI(exp 2) demonstrator systems: A multi-modal interface for man machine interaction with knowledge based systems. Deliverable D17 (TA 2) ESPRIT project 2474 MMI(exp 2)
[PB94-170537] 11 p4298 N94-35600
Virtual Interfaces: Research and Applications
[AGARD-CP-541] 12 p4482 N94-37261
Task-specific usability requirements for virtual information environments: Interface design and data representation for human operators of complex medical systems 12 p4483 N94-37262
On the feasibility of virtual environments in medicine
12 p4483 N94-37264
Interactive large screen: A multi-mode dialogue tool for future cockpits 12 p4484 N94-37266
The DRA Virtual Cockpit Research Program
12 p4484 N94-37269
Virtual reality evolution or revolution
12 p4484 N94-37270
A non-intrusive way to measure point-of-gaze
12 p4484 N94-37272
Operator gaze position control interfaces: Investigation of psychophysical and operational parameters
12 p4485 N94-37273
Visual accommodation to virtual image displays when knowledge of object distance conflicts with optical distance 12 p4485 N94-37278
Aerospace medicine and biology: A continuing bibliography with indexes (supplement 392)
[NASA-SP-7011(392)] 12 p4482 N94-37445

MAN TENDED FREE FLYERS
Mission activities planning for a Hermes mission by means of AI-technology 06 p2502 N94-23858

MAN-COMPUTER INTERFACE
U HUMAN-COMPUTER INTERFACE

MANAGEMENT
NT CONFIGURATION MANAGEMENT
NT CONTRACT MANAGEMENT
NT DATA MANAGEMENT
NT ENGINEERING MANAGEMENT
NT ENVIRONMENT MANAGEMENT
NT FINANCIAL MANAGEMENT
NT FOREST MANAGEMENT
NT INDUSTRIAL MANAGEMENT
NT INFORMATION MANAGEMENT
NT INVENTORY CONTROLS
NT INVENTORY MANAGEMENT
NT LAND MANAGEMENT
NT LOGISTICS MANAGEMENT
NT PERSONNEL MANAGEMENT
NT PROCUREMENT MANAGEMENT
NT PRODUCTION MANAGEMENT
NT PROJECT MANAGEMENT
NT RECORDS MANAGEMENT
NT REFORESTATION

NT RESEARCH MANAGEMENT
NT RESOURCES MANAGEMENT
NT SAFETY MANAGEMENT
NT SYSTEMS MANAGEMENT
NT TOTAL QUALITY MANAGEMENT
NT WATER MANAGEMENT
NT WEAPON SYSTEM MANAGEMENT
Discovery management workshop
[NASA-TM-108244] 02 p0531 N94-14080
Management: A bibliography for NASA managers
[NASA-SP-7500(27)] 06 p2586 N94-24708
Defense aerospace and the new world order
06 p2596 N94-25066

MANAGEMENT ANALYSIS
Development of a naming convention and data management system
[NASA-CR-193860] 05 p2042 N94-20268
Relevant costs or full costs? Explaining why managers use capacity cost allocations for short term decisions
[ISBN-9-06-215364-X] 06 p2587 N94-25279
An evaluation of aircraft maintenance performance factors in the objective wing
[AD-A276010] 09 p3565 N94-31362
Mapping analysis and planning system for the John F. Kennedy Space Center 09 p3757 N94-32463

MANAGEMENT INFORMATION SYSTEMS
Myths and realities: Defining re-engineering for a large organization 01 p0330 N94-11436
Design issues for high performance engineering information systems
[AD-A264839] 01 p0420 N94-11520
Data management strategy for the Tampa Bay National Estuary Program: Recommendations and implementation plan
[PB93-191633] 01 p0267 N94-11864
Analysis of the Army's installation support modules with the private sector's open information systems
[AD-A265667] 01 p0421 N94-12579
Making the connection between information modeling and implementation
[DE93-011588] 02 p0820 N94-12907
Building the repositories to serve --- Superconducting Super Collider information system
[DE93-014100] 02 p0821 N94-12983
Knowledge base technology for CT-DIMS: Report 1
[DE93-013118] 02 p0743 N94-13014
Program/project management resource lists
[NASA-TM-109268] 02 p0822 N94-13107
Department of Defense technical architecture framework for information management. Volume 2: Technical reference model and standards profile, version 2.0
[AD-A267194] 03 p1229 N94-15788
Department of Defense technical architecture framework for information management. Volume 3: Architecture concepts and design guidance, version 2.0
[AD-A267195] 03 p1230 N94-15789
Performance Information Management System (PIMS) communication
[AD-A267040] 03 p1231 N94-16458
Managing information as a corporate asset: Key strategies for information professionals to remain competitive
[DE93-015515] 03 p1232 N94-16875
Defense Logistics Information System (DLIS) procedures manual. Products and services end-user manual
[AD-A267766] 03 p1232 N94-17007
A proposed research program in strategic computing
[AD-A267516] 03 p1153 N94-17078
Defense Logistics Information System (DLIS). Procedures manual: Logistics On-Line Access (LOLA) procedures manual
[AD-A267685] 03 p1233 N94-17229
EDMS: Engineering data management system. User's reference
[PB93-187391] 04 p1614 N94-18119
Corporate Information Management (CIM) report on the simulation processes, version 2.0
[AD-A269119] 04 p1617 N94-18770
Denver TMA assessment
[NASA-CR-4554] 04 p1315 N94-18844
Results of a joint Navy/Air Force operational test to evaluate USAF Integrated Maintenance Information Systems (IMIS), Interactive Electronic Technical Manual (IETM) technology applied to the F/A-18 aircraft
[AD-A271322] 04 p1619 N94-19571
A comparison Air Force data systems --- Comments on IDA Paper P-2863
[AD-A270662] 04 p1619 N94-19780
Using electronic data interchange to report product quality
[AD-A271843] 05 p1828 N94-20468
A conceptual database design and performance analysis of the MILSATCOM requirements database
[AD-A272672] 05 p1658 N94-21217
Three original programmes for managers
05 p1923 N94-22083
A system for managing information at ATLAS
[DE94-001337] 06 p2590 N94-23190
Management: A bibliography for NASA managers
[NASA-SP-7500(27)] 06 p2586 N94-24708
Aviation system safety risk management tool analysis. Volume 2: Appendices
[AD-A273502] 06 p2173 N94-24864
COSMIC monthly progress report
[NASA-CR-195153] 06 p2460 N94-25023
Implementing a multiple criteria model base in co-op with a graphical user interface generator
[AD-A274901] 07 p3093 N94-26181
Information systems criteria for applying software reengineering: Guidelines for identifying information systems for software reengineering
[AD-A274699] 07 p3097 N94-26375
Data analysis and data fusion for intelligence analysis and decision support. Research plan 1993-2000
[PB94-123569] 07 p3005 N94-27173
University program management information system, FY 1993
[NASA-TM-109719] 07 p3100 N94-27413
The TMIS life-cycle process document, revision A
[NASA-TM-109698] 07 p2697 N94-27775
Software systems reengineering process model, version 1.0
[AD-A275711] 08 p3407 N94-28691
Environmental Compliance Assessment And Management System Program (ECAMP). US Air Force European Economic Community (EEC)
[AD-A275593] 08 p3346 N94-28727
An evaluation of techniques for ranking academic information systems journals
[AD-A275179] 08 p3529 N94-29066
Software engineering and software management in a distributed UNIX environment
[NLR-TP-92233-U] 08 p3422 N94-30314
Initial estimates of Integrated Maintenance Information System (IMIS) costs and benefits, volume 1
[AD-A276144] 09 p3565 N94-31830
Application of Artificial Intelligence to the DoD Corporate Information Management (CIM) program
[AD-A276656] 09 p3834 N94-32061
Lifting the fog of corporate information management
[AD-A276680] 09 p3918 N94-32090
Modular Simulator System (MSS). Executive report
[AD-A276966] 09 p3588 N94-32241
Managing performance of DB2 Ad Hoc Reports
[DE94-006669] 09 p3920 N94-32635
Developing a personal-computer-based records retention system using Paradox(tm)
[DE94-007984] 09 p3819 N94-32749
A parallel data management system for large-scale NASA datasets 10 p4157 N94-33828
COSMIC monthly progress report
[NASA-CR-195962] 11 p4302 N94-35514
Fire data management system, FDMS 2.0, technical documentation
[PB94-164019] 11 p4346 N94-35819

MANAGEMENT METHODS
NT PATTERN METHOD (FORECASTING)
Space Station Redesign Team: Final report to the Advisory Committee on the Redesign of the Space Station
[NASA-TM-109241] 01 p0042 N94-10663
Engineering performance metrics
[DE93-012084] 01 p0128 N94-11028
From red tape to results: Creating a government that works better and costs less 01 p0422 N94-11351
From red tape to results: Creating a government that works better and costs less. Executive summary
01 p0422 N94-11353
Maximizing reuse: Applying common sense and discipline 01 p0329 N94-11429
Insights into software development in Japan
01 p0330 N94-11435
Research and development of post-classical management tools for government program offices, volume 2
[DE93-010236] 01 p0417 N94-11600
International disaster research
01 p0307 N94-11805
Ninth Annual NASA/Contractors Conference on Quality and Productivity. World Class Excellence: The Journey Continues. Conference presentations
[NASA-CR-194514] 02 p0665 N94-13153
Measuring quality progress 02 p0666 N94-13154
Defining the performance gap: Conducting a self-assessment 02 p0666 N94-13155
What's the bottom line payback for TQM?
02 p0666 N94-13156
Partnership with the customer
02 p0666 N94-13157
Strategic planning as a focus for continuous improvement. A case study 02 p0666 N94-13158
The power of cross-functional teams in driving total quality 02 p0666 N94-13159
Kennedy Space Center's NASA/Contractor Team-Centered Total Quality Management Seminar: Results, methods, and lessons learned
02 p0667 N94-13162
Here's the beef: A case study in organizational transformation 02 p0667 N94-13163
NASA Johnson Space Center: Total quality partnership 02 p0668 N94-13165
The Eighth Annual NASA/Contractors Conference and 1991 National Symposium on Quality and Productivity: Extending the boundaries of total quality management
[NASA-TM-109276] 02 p0669 N94-14321
NASA directives master list and index
[NHB-1410.13L] 03 p1229 N94-15414
Facilities maintenance handbook
[NHB-8831.2] 03 p1224 N94-15934
NASA information resources management handbook
[NHB-2410.1E] 03 p1230 N94-15941
Creating and maintaining a visionary quality program
[DE93-015122] 03 p1050 N94-16055
Environmental management lessons to be learned from the upcoming CFC phase out or how to insure that we survive the next environmentally mandated process change
[TABES PAPER 93-570] 03 p1050 N94-16136
Development of a proposed international standard for certification of aircraft to High Intensity Radiated Fields (HIRF)
[NASA-TM-106357] 03 p0863 N94-16520
Software Engineering Guidebook
[NASA-CR-177625] 03 p1150 N94-16656
Applicability of computer spreadsheet simulation for solving resource allocation problems
[AD-A267436] 03 p1152 N94-17027
Module interconnection frameworks for a real-time spreadsheet
[AD-A267317] 03 p1153 N94-17220
Software Capability Evaluation (SCE) version 1.5 method description. Software capability evaluation project
[AD-A267895] 03 p1154 N94-17395
Present evolution of tools management
[CRIF-MC-102] 04 p1444 N94-17964
Quality, management, and the interplay of self-assessment, process assessments, and performance-based observations
[DE93-018787] 04 p1448 N94-19336
Performance management systems: A statistical analysis
[AD-A272989] 05 p2043 N94-21266
An evaluation of artificial neural network modeling for manpower analysis
[AD-A273001] 05 p1945 N94-21269
The NCC project: A quality management perspective
05 p1828 N94-21324
Let your fingers do the walking: The projects most invaluable tool 05 p1922 N94-21325
NCCDS configuration management process improvement 05 p1931 N94-21327
Issues in NASA program and project management. Special Report: 1993 conference
[NASA-SP-6101(07)] 05 p2039 N94-21497
Issues in NASA program and project management
[NASA-SP-6101(06)] 05 p2040 N94-21499
New mission requirements methodologies for services provided by the Office of Space Communications
06 p2519 N94-23961
Early manufacturing considerations in design
06 p2177 N94-24315
Extension of the critical path method
[PB94-118817] 06 p2488 N94-24527
Management: A bibliography for NASA managers
[NASA-SP-7500(27)] 06 p2586 N94-24708
Reuse-Driven Software Processes Guidebook, version 02.00.03
[AD-A273644] 06 p2461 N94-25148
Appendix B: Rapid development approaches for system engineering and design 06 p2272 N94-25195
Appendix C: Rapid development approaches for system engineering and design 06 p2272 N94-25196
Relevant costs or full costs? Explaining why managers use capacity cost allocations for short term decisions
[ISBN-9-06-215364-X] 06 p2587 N94-25279
Throughput time control and due date reliability in tool and die shops
[ISBN-9-03-860182-4] 06 p2587 N94-25283
Integrated risk management 06 p2588 N94-25361
Strategies for recruiting additional African Americans into the NASA JSC summer faculty fellows program
06 p2585 N94-25362
Module interconnection frameworks for a real-time spreadsheet
[AD-A273853] 07 p2956 N94-25588

The effectiveness of AMT investment in UK metal component manufacture
[IND-MANU-SCI-TECH-REPT-3] 07 p2762 N94-25775
An exploratory survey of methods used to develop measures of performance
[AD-A273945] 07 p2834 N94-25896
Business process redesign: Design the improved process
[AD-A274947] 07 p3093 N94-26299
Benefits estimation for simulation systems used for aircrew training in a multiship environment
[AD-A274313] 07 p2938 N94-26882
An investigation of integrated product development implementation issues: A case study of Bosma Machine and Tool Corp.
[AD-A273917] 07 p2942 N94-27320
Polyhedral characterization of the economic lot-sizing problem with start-up costs
[MEMO-COSOR-92-46] 07 p2969 N94-27396
Risk-based prioritization: A comparison of approaches
[DE94-003368] 08 p3526 N94-28474
The development and demonstration of the metric assessment tool
[AD-A275788] 08 p3230 N94-28742
A generalization of the software engineering maturity model 08 p3416 N94-29341
Application of information management methodologies for project quality improvement in a changing environment 08 p3416 N94-29342
Information engineering implementation and acceptance 08 p3530 N94-29533
Report on NATO PTTI 08 p3469 N94-30645
Why TQM fails (and what you can do about it)
[DE93-018945] 08 p3527 N94-30698
Software reuse case study: TRILLIUM
[AD-A276108] 09 p3811 N94-31465
Process mapping: A user-friendly tool for process improvement
[DE94-004357] 09 p3730 N94-31605
Budget allocation and monopolistic pricing in a multiproduct firm
[REPT-93-86] 09 p3924 N94-31617
Lifting the fog of corporate information management
[AD-A276680] 09 p3918 N94-32090
CIM in space: Corporate Information Management (CIM) implications for space-based information systems
[AD-A276882] 09 p3600 N94-32126
Case studies of software process improvement methods
[AD-A277289] 09 p3818 N94-32508
Agile total quality guidelines for enhancing teamwork and success
[DE93-019972] 09 p3915 N94-32678
Total Quality Management implementation guidelines
[DE94-007232] 09 p3915 N94-32723
The Virtual Mission Operations Center 10 p4150 N94-33615
Management issues in automated audit analysis
[DE94-007571] 10 p4112 N94-34297
CAirTOX: A compartment model for assessing the fate of and human exposure to toxic-chemical emissions to air
[DE94-010084] 11 p4284 N94-35700

MANAGEMENT PLANNING
NT PRODUCTION PLANNING
NT PROJECT PLANNING
An advisor module for tactical and strategic state-oriented planning systems with an application in manpower planning
[MEMO-COSOR-92-57] 01 p0416 N94-10868
US Coast Guard GPS Information Center (GPSIC) and its function within the Civil GPS Service (CGS) 01 p0024 N94-10966
Lunar-Ultraviolet Telescope Experiment (LUTE) integrated program plan
[NASA-CR-193267] 01 p0424 N94-11356
Software management guide
[DE93-012034] 01 p0330 N94-11452
Intergovernmental decisionmaking for environmental protection and public works
[PB93-176824] 01 p0266 N94-11584
Information resources management long-range plan, FY1994
[DE93-013898] 01 p0420 N94-11588
ESA Costing Software (ECOS) introduction
[ESA-F-28] 01 p0333 N94-12383
Defense: Health care
[AD-A265914] 01 p0421 N94-12445
Strategic planning as a focus for continuous improvement. A case study 02 p0666 N94-13158
Building a quality culture in the Office of Space Flight: Approach, lessons learned and implications for the future 02 p0667 N94-13164
Creating a strategic plan for configuration management using computer aided software engineering (CASE) tools
[DE93-013663] 02 p0746 N94-13394
Forest management for fixing and sequestering carbon
[DE93-013520] 02 p0707 N94-13486
Space and Earth sciences, computer systems, and scientific data analysis support, volume 1
[NASA-CR-189319] 02 p0741 N94-13788
Fourteenth National Industrial Energy Technology Conference: Proceedings
[DE93-016698] 02 p0710 N94-14516
Testing and management of flight instruments and their data
[NASA-CR-194332] 03 p0868 N94-15187
Facilities maintenance handbook
[NHB-8831.2] 03 p1224 N94-15934
NASA information resources management handbook
[NHB-2410.1E] 03 p1230 N94-15941
Design Quality Task Force survey comments
[AD-A266283] 03 p1225 N94-16473
Emergency preparedness and planning 03 p1124 N94-16613
Current information technology resource requirements of the federal government: Fiscal year 1994 04 p1612 N94-17756
Safeguarding our energy future
[DE93-016001] 04 p1466 N94-18109
The organizational preparation of existing relational databases for the integration of expert systems
[AD-A268823] 04 p1614 N94-18191
Environmental restoration and waste management five-year plan, fiscal years 1994-1998. Volume 3: Public concerns
[DOE/S-00097P-VOL-3] 04 p1475 N94-18835
Computing professionals: Changing needs for the 1990's
[B-030] 04 p1515 N94-19401
Strategic plan, 1991: A strategy for leadership in space through excellence in space science and applications
[NASA-TM-109256] 04 p1611 N94-19434
Planning process software: A user guide for the DMCA
[AD-A271252] 05 p1902 N94-19911
Government Open Systems Interconnection Profile (GOSIP) transition strategy
[AD-A273005] 05 p1740 N94-21308
Models of transient processes in centrally planned economy 05 p2051 N94-22071
Three original programmes for managers 05 p1923 N94-22083
Cost benefits of advanced software: A review of methodology used at Kennedy Space Center 06 p2464 N94-23240
New mission requirements methodologies for services provided by the Office of Space Communications 06 p2519 N94-23961
Software reuse in spacecraft planning and scheduling systems 06 p2520 N94-23966
Risk identification and reduction in integrated product teams 06 p2497 N94-24407
Management: A bibliography for NASA managers
[NASA-SP-7500(27)] 06 p2586 N94-24708
Design and application of electromechanical actuators for deep space missions
[NASA-CR-195134] 06 p2365 N94-24842
The future of manned spaceflight 06 p2195 N94-25067
Integrated risk management 06 p2588 N94-25361
Financial resource review model user's guide
[AD-A274979] 08 p3410 N94-29088
Software Management Environment (SME) concepts and architecture, revision 1
[NASA-CR-189293] 08 p3419 N94-29727
Triple Diagonal modeling: A mechanism to focus productivity improvement for business success
[DE94-004309] 08 p3527 N94-30041
Graphical simulation for aerospace manufacturing
[AIAA PAPER 94-1224-CP] 08 p3446 N94-30573
European business confronted with the 21st century: Men, the essential risk
[ESA-SP-1167] 09 p3914 N94-31181
Europe at the crossroads: The future of its satellite communications industry
[ESA-SP-1166] 09 p3670 N94-31182
An active computer supported medium for distributed planning in enterprises
[ETN-94-95738] 09 p3829 N94-31372
A study of theoretical models for managing technology change and a comparison to a radio frequency identification implementation
[AD-A276012] 09 p3672 N94-31385
NASCOM system development plan: System description, capabilities, and plans, FY 94-2
[NASA-TM-109744] 09 p3674 N94-31503
Modular Simulator System (MSS) management guide
[AD-A277098] 09 p3588 N94-32014
NASA strategic plan
[NASA-TM-109780] 09 p3915 N94-32222
Reuse strategy model: Planning aid for reuse-based projects
[AD-A277641] 10 p4106 N94-33891
National facilities study. Volume 5: Space research and development facilities task group
[NASA-TM-109859] 10 p4010 N94-34637
Johnson Space Center (JSC) research and technology
[NASA-TM-104788] 10 p4187 N94-34677
The Federal Aviation Administration plan for research, engineering and development 11 p4376 N94-35262
Apollo 11 at twenty-five, version 1.0
[NASA-CR-193380] 11 p4376 N94-35363
Earth Observing System/Advanced Microwave Sounding Unit-A (EOS/AMSU-A) software management plan
[NASA-CR-189362] 12 p4461 N94-36919
Earth Observing System (EOS)/Advanced Microwave Sounding Unit A (AMSU-A) configuration management plan
[NASA-CR-189371] 12 p4494 N94-37061
Toward a new National Weather Service: National Weather Service employee feedback 12 p4474 N94-37467

MANAGEMENT SYSTEMS
NT FLIGHT MANAGEMENT SYSTEMS
NT MANAGEMENT INFORMATION SYSTEMS
Financial management: NASA's financial reports are based on unreliable data
[AD-A265690] 01 p0418 N94-12443
Quality assurance for environmental chemistry: 1991, volume 2
[DE93-011792] 01 p0272 N94-12780
Measuring quality progress 02 p0666 N94-13154
Teamwork for Oversight of Processes and Systems (TOPS). Implementation guide for TOPS version 2.0, 10 August 1992 02 p0668 N94-13167
Quality assurance for environmental chemistry, 1991, volume 1
[DE93-011791] 02 p0709 N94-14020
Fault management for data systems
[NASA-TM-103953] 03 p1116 N94-15548
Equipment management user's handbook for property custodians
[NHB-4200.2A] 03 p1224 N94-15957
Equipment Management Manual
[NHB-4200.1D] 03 p1225 N94-16799
A comparison of queueing, cluster and distributed computing systems
[NASA-TM-109025] 03 p1160 N94-16878
Visual display principles for C3I system tasks
[AD-A267969] 03 p1005 N94-17498
Carbon Dioxide Information Analysis Center: FY 1992 activities
[DE93-013845] 04 p1471 N94-17774
User's manual of Tokamak Simulation Code
[DE93-788388] 04 p1586 N94-18212
Reference model for project support environments, version 1.0
[AD-A269110] 04 p1520 N94-18251
The J85 cost/benefit engine study
[AD-A269280] 04 p1320 N94-18333
Data management for support of the Oregon Transect Ecosystem Research (OTTER) project
[NASA-CR-4557] 05 p1905 N94-20149
Development of a naming convention and data management system
[NASA-CR-193860] 05 p2042 N94-20268
Performance management systems: A statistical analysis
[AD-A272989] 05 p2043 N94-21266
Problem reporting management system performance simulation 05 p1931 N94-21328
Information and decision structure in a Japanese type of management with respect to QCC and just-in-time systems 05 p2046 N94-22063
Structure and flow of data through an environmental data management system
[DE93-040487] 06 p2589 N94-22934
A system for managing information at ATLAS
[DE94-001337] 06 p2590 N94-23190
KSC management training system project 06 p2574 N94-23246
Space Station Freedom (SSF) Data Management System (DMS) performance model data base
[NASA-CR-188270] 06 p2590 N94-23289
GEWEX 06 p2385 N94-23614
An engineering code to analyze hypersonic thermal management systems 06 p2320 N94-23636
Columbus system support for telescience operations 06 p2505 N94-23877
Real-time automated failure identification in the Control Center Complex (CCC) 06 p2272 N94-23892

Performance of the engineering analysis and data system 2 common file system 06 p2576 N94-24413
Design and specification of a centralized manufacturing data management and scheduling system 06 p2577 N94-24416
Modular approach to project management [PB94-118833] 06 p2586 N94-24528
Intelligent systems and advanced user interfaces for design, operation, and maintenance of command management systems [NASA-CR-195172] 06 p2459 N94-24797
The use of design automation software by government-contracted architect/engineer firms: A status report [AD-A273181] 06 p2459 N94-24812
A comparative evaluation plan for the Maintenance, Inventory, and Logistics Planning (MILP) System Human-Computer Interface (HCI) 06 p2588 N94-25373
Automated information management for designers: Functional requirements for computer based associates that support access and use of technical information in design [AD-A274603] 07 p3099 N94-26891
On modeling and controlling intelligent systems [DE94-002446] 07 p2988 N94-27706
Environmental Compliance Assessment And Management System Program (ECAMP). US Air Force European Economic Community (EEC) [AD-A275593] 08 p3346 N94-28727
Object oriented design of the autonomous fixtaking management system 08 p3143 N94-29323
A common Ada run-time system for avionics software 08 p3150 N94-29331
DLR's ATM demonstration programme 08 p3140 N94-29575
ARC2000: Automatic radar control 08 p3141 N94-29583
Software Management Environment (SME) concepts and architecture, revision 1 [NASA-CR-189293] 08 p3419 N94-29727
Analysis of EDP performance [NASA-CR-195726] 08 p3420 N94-29945
Model borne data management system for wind tunnel testing, phase 2 [AD-A276296] 09 p3587 N94-31295
An analysis of the records management process to determine the impact of automation on productivity [AD-A275923] 09 p3916 N94-31344
The development and use of an evaluation mechanism for the assessment of software configuration management tools [AD-A275961] 09 p3810 N94-31383
A model and algorithms for a software evolution control system [AD-A276431] 09 p3811 N94-31449
Hierarchical storage management system evaluation 10 p4154 N94-33809
A parallel data management system for large-scale NASA datasets 10 p4157 N94-33828
Software Management Environment (SME): Components and algorithms [NASA-CR-189346] 10 p4109 N94-34996
An analysis of file system and installation of the file management system for NOS operating system [DE94-611062] 11 p4346 N94-35833
Implementation of a Computerized Maintenance Management System 11 p4343 N94-35970

MANDRELS
Equivalent performance in different helical resonator plasma polymerization coater platforms [DE94-001517] 07 p2753 N94-26933
Filament to mandrel gap analysis: Resulting gap from filament winding over a cone-cylinder transition mandrel (reference NMTP no. 93838) [DE94-004225] 08 p3175 N94-28528
Composite hot drape forming 08 p3240 N94-30448
Diamond turning in the production of x ray optics 09 p3604 N94-33298

MANEUVERABILITY
Physics of forebody flow control [NASA-CR-193626] 01 p0015 N94-11195
Comparing aircraft agility using mahalanobis distances [PB93-175446] 01 p0026 N94-11464
Adaptive reconfigurable flight controls for high angle of attack aircraft agility 01 p0032 N94-11502
A piloted simulation investigation of the normal load factor and longitudinal thrust required for air-to-air acquisition and tracking 02 p0522 N94-13301
In-flight simulation of high agility through active control: Taming complexity by design 02 p0523 N94-13306
Predicted structural response of the lightweight-interceptor technology demonstration vehicle [DE93-014676] 04 p1333 N94-17782
An investigation of fighter aircraft agility [NASA-CR-194608] 04 p1318 N94-19448
Thrust vectoring theory, laboratory and flight tests 06 p2155 N94-24251
Analysis and optimization of preliminary aircraft configurations in relationship to emerging agility metrics [NASA-CR-195228] 07 p2668 N94-26235
Exploring QDES as a tool for determining limits of achievable performance in aircraft design [AD-A275359] 08 p3146 N94-28998
Navy Omni-Directional Vehicle (ODV) development program 09 p3729 N94-32451
Technologies for Highly Manoeuvrable Aircraft [AD-280271] 10 p3990 N94-34605
Engine characteristics for agile aircraft 10 p3991 N94-34608
Thrust vector aided maneuvering of the YF-22 Advanced Tactical Fighter prototype 10 p3991 N94-34610
Aerodynamic design of super maneuverable aircraft 10 p3992 N94-34617
Application of current departure resistance criteria to the post-stall manoeuvering envelope 10 p3993 N94-34622
Study findings on the influence of maneuverability and agility on helicopter handling qualities 10 p3993 N94-34624
Operational agility: An overview of AGARD Working Group 19 10 p3993 N94-34625
Operational agility assessment with the AM-X aircraft 10 p3994 N94-34626
The influence of flying qualities on operational agility 10 p3994 N94-34628
An agility metric structure for operational agility 10 p3994 N94-34629
Application of centrifuge based dynamic flight simulation to enhanced maneuverability RDT/E 10 p3994 N94-34630
Optimal tactics for agile aircraft technology: A differential game methodology 10 p3994 N94-34631
Concepts and application of dynamic separation for agility and super-maneuverability of aircraft: An assessment 10 p3997 N94-34988

MANEUVERABLE REENTRY BODIES
NT HL-10 REENTRY VEHICLE
NT LIFTING REENTRY VEHICLES

MANEUVERABLE SPACECRAFT
NT AEROSPACE PLANES
NT APOLLO LUNAR EXPERIMENT MODULE
NT RENDEZVOUS SPACECRAFT
NT X-30 VEHICLE
The fragmentation of Kosmos 2163 [NASA-CR-191643] 03 p0887 N94-16503
Dynamic characterization of a lightweight, highly maneuverable spacecraft using modal and finite element analyses [DE93-018095] 04 p1335 N94-18942

MANEUVERS
NT AIRCRAFT MANEUVERS
NT EARTH ORBITAL RENDEZVOUS
NT EVASIVE ACTIONS
NT HOVERING
NT ORBITAL MANEUVERS
NT ORBITAL RENDEZVOUS
NT SIDESLIP
NT SPACECRAFT DOCKING
NT SPACECRAFT MANEUVERS
Hydrodynamics of maneuvering bodies: LDRD Final Report [DE94-009970] 11 p4265 N94-35769
Maneuvering and control of flexible space robots 11 p4218 N94-35867

MANGANESE
NT MANGANESE ISOTOPES
A detailed investigation of the benthic regime in the Clarion-Clipperton province of the Pacific and a forecast of consequences of manganese nodule mining 01 p0224 N94-12733
Synthesis, reactivity, and characterization of (-hexacarbocyclic) manganese dicarbonyl complexes with sulfur and phosphorus ligands [AD-A267592] 03 p0930 N94-17192
High performance heavy alloys by alloying and process control [AD-A271129] 05 p1689 N94-20019
Chemical zoning and diffusion of Ca, Al, Mn, and Cr in olivine of springwater pallasite 05 p2086 N94-20902
GGA study of the magnetic and cohesive properties of bcc, fcc and hcp Mn [REPT-A-2662] 06 p2564 N94-24960
An extraterrestrial event at the tertiary-quaternary boundary 07 p2890 N94-28309
Electron spin resonance measurements of Er(3+) and Mn(2+) in the high temperature superconductor compounds La(2-x)Sr(x)CuO(4-delta) [ETN-94-95746] 09 p3898 N94-31612
Mechanical behavior and phase stability of NiAl-based shape memory alloys [DE94-012336] 12 p4419 N94-37420
Superacid catalysis of light hydrocarbon conversion [DE94-011132] 12 p4411 N94-37431

MANGANESE ALLOYS
NT MANGANIN (TRADEMARK)
Structure and properties of an RS Al-Si-Ni-Mn-Zr alloy for high temperature applications 01 p0064 N94-10063
Containerless processing of equiatomic Mn50Bi50 in a drop tube 01 p0118 N94-10205
Bibliography on silicides [AD-A270516] 04 p1374 N94-19532
Microstructural development in low activation ferritic alloys irradiated to 200 dpa at 420 C [DE94-004269] 07 p2731 N94-25803
Structure of the modulated magnetic phase of Mn3Sn [DE94-002788] 07 p2733 N94-26092
NMR study of quasicrystal Al(70)Pd(20)T(M10) alloy (T(M):Cr, Mn, Fe, and Co) 07 p2745 N94-28162
Formation and high mechanical strength of Al-based alloys containing a nanoscale icosahedral phase as a main constituent 07 p2746 N94-28171
Mechanical properties and microstructure of thermomechanically processed, high manganese steel [ARL-TR-146] 07 p2747 N94-28212

MANGANESE COMPOUNDS
NT MANGANESE OXIDES
Synthesis, reactivity, and characterization of (-hexacarbocyclic) manganese dicarbonyl complexes with sulfur and phosphorus ligands [AD-A267592] 03 p0930 N94-17192
Fe/Mn in olivine of carbonaceous meteorites 05 p2084 N94-20788
Characterization of convection related defects in II-VI compound semiconductors [NASA-CR-194704] 05 p2030 N94-21778
Magnetic resonance studies of 3d transition metal impurities in compound semiconductors [PB93-232197] 06 p2243 N94-23714
Technical report of ISSP. Ser. A, no. 2673: Two successive spin glass transitions in non-diluted Heisenberg-like spin glass Ni(0.42)Mn(0.58) TiO3 [JTN-94-80559] 07 p2756 N94-27241
Optical properties of cadmium sulfide, zinc selenide, and zinc manganese selenide semiconductor films 08 p3500 N94-29759
Molecular/polymeric magnetism [DE94-005888] 09 p3649 N94-31201

MANGANESE IONS
Contribution of all excited states to ZFS of a (sup 6) S-state [DE93-617007] 06 p2568 N94-25483

MANGANESE ISOTOPES
Search for effects of a supernova explosion 30 to 40 thousand years ago in chondrites 01 p0428 N94-12022
The beta(+) decay and cosmic-ray half-life of Mn-54 [DE93-013913] 02 p0848 N94-13695
On possible Mn-53 heterogeneity in the early solar system 03 p1244 N94-16344

MANGANESE OXIDES
Cathode materials for the molten carbonate fuel cell [DE93-019515] 05 p1848 N94-21870

MANGANESE 53
U MANGANESE ISOTOPES

MANGANESE 54
U MANGANESE ISOTOPES

MANGANESE 56
U MANGANESE ISOTOPES

MANGANIN (TRADEMARK)
Deep ion implantation into manganin to modify its pressure and electrothermocharacteristics [DE93-630229] 04 p1359 N94-18218
Multiple shock initiation of LX-17 [DE94-001524] 06 p2265 N94-23807

MANIFOLDS (MATHEMATICS)
NT RIEMANN MANIFOLD
The structure of Hilbert flag varieties [MEMO-1095] 01 p0348 N94-10272
One dimensional representations in quantum optics 01 p0375 N94-10570
S(sup 1) x S(sup 2) as a bag membrane and its Einstein-Weyl geometry [DE93-613149] 01 p0410 N94-10635
Homoclinic intermittency [W-9302] 01 p0344 N94-10908
The Lip microbundle representation theorem [DE93-619671] 01 p0346 N94-11348
(1,1)-geodesic maps into Grassmann manifolds [DE93-624799] 04 p1545 N94-17684
Groups on transformations in Finslerian spaces [DE93-624765] 04 p1606 N94-17794

Some remarks on integrable Hamiltonian systems with two degrees of freedom
[DE93-624766] 04 p1546 N94-17815
A reduction of the globalization and U(1)-covering
[DE93-624769] 04 p1546 N94-17817
About structurally stable generating mechanism for invariant hyperbolic sets
[DE93-629858] 04 p1561 N94-18150
Path integrals on warped product manifolds
[DE93-629859] 04 p1561 N94-18151
On the numerical computation of invariant manifolds
[W-9306] 06 p2480 N94-23140
When an infinitely-renormalizable endomorphism of the interval can be smoothed
[PB93-238087] 06 p2481 N94-23548
Non-trivial examples of real isolated singularity at the origin
[PB94-110939] 06 p2487 N94-23787
Quasiconformal mappings, operators on Hilbert space, and local formulae for characteristic classes
[PB93-238079] 06 p2488 N94-24536
The renormalization group for flag manifolds
[DE93-616846] 06 p2491 N94-25213
Characterization of self-conjugate minimal surfaces in R(sup 3)
[DE94-601538] 07 p2993 N94-26409
Implementation of integral manifold control on a two degree of freedom flexible joint manipulator: Theory and experiments
[ISBN-0-315-83572-9] 07 p2823 N94-26658
Poisson-lie group of pseudodifferential symbols
[PB94-124393] 07 p2997 N94-26996
Illumination in diverse codimensions
[AD-A277602] 07 p2971 N94-27572
A survey of open problems in symplectic integration
[DE94-003966] 07 p3007 N94-27777
Symplectic topology of integrable Hamiltonian systems
[DE94-608120] 08 p3467 N94-30166
Elements for the recognition of three dimensional deformable shapes: Application to biomedical imagery
[TELECOM-93-E-006] 08 p3396 N94-30978
On the computation of simplical approximations of implicitly defined two-dimensional manifolds
[AD-A278132] 09 p3849 N94-33060
Generalized Fredholm determinants and Selberg zeta functions for axiom A dynamical systems
[PB94-167665] 11 p4314 N94-35758
Some theorems on a class of harmonic manifolds
[DE94-611102] 11 p4315 N94-35934
Quantum groups, non-commutative differential geometry and applications
[DE94-011358] 11 p4315 N94-36270
Localization of topological Pontryagin classes by propagation with finite speed
[PB94-180866] 12 p4506 N94-37852
Eigenfunction bounds for compact manifolds with integrable geodesic flow
[PB94-180874] 12 p4506 N94-37853

MANIPULATION
U MANIPULATORS

MANIPULATORS
NT REMOTE MANIPULATOR SYSTEM
Lightweight CFRP frame structures for a Rotex-derived manipulator system 01 p0056 N94-10005
Force reflection with compliance control
[NASA-CASE-NPO-18668-1-CU] 01 p0179 N94-10654
Telerobot control system
[NASA-CASE-NPO-18116-1-CU] 01 p0179 N94-10670
Momentum management in redundant manipulators for vibration suppression
[NASA-CR-194112] 01 p0180 N94-10821
Mechanical analysis of parallel manipulators with simulation, design, and control applications
[ISBN-0-315-72013-1] 01 p0181 N94-11156
Model reference adaptive control (MRAC) with applications to robotics 01 p0339 N94-11640
Derivation of three closed loop kinematic velocity models using normalized quaternion feedback for an autonomous redundant manipulator with application to inverse kinematics
[DE93-012823] 01 p0340 N94-12543
Roller-gear drives for robotic manipulators design, fabrication and test
[NASA-CR-194248] 02 p0660 N94-12802
Force reflecting hand controller for manipulator teleoperation
[NASA-CR-191345] 02 p0661 N94-13129
Control algorithm implementation for a redundant degree of freedom manipulator
[NASA-CR-191339] 02 p0762 N94-13131
Robot-task compliance: The energy criterion
[ITN-93-85196] 02 p0763 N94-13568
Generalized impedance control of a redundant manipulator 02 p0661 N94-13575
Decentralized control of uncertain systems via sensitivity models
[DE93-012963] 02 p0766 N94-14568
Modelling robotic systems with DADS 02 p0678 N94-14625
Parallel methods for dynamic simulation of multiple manipulator systems 02 p0680 N94-14637
Tactile sensing and control in humans and robotic/teleoperated systems
[AD-A267710] 03 p1163 N94-14937
Fuzzy control and fuzzy kinematic mapping for a redundant space robot
[AD-A266866] 03 p1163 N94-14950
Fuzzy inverse kinematic mapping: Rule generation, efficiency, and implementation
[AD-A266967] 03 p1163 N94-14954
Serpentine manipulator planning and control for NASA Space-Shuttle payload servicing
[AD-A266961] 03 p0879 N94-14969
Real-time implementation of neural network learning control of a flexible space manipulator
[AD-A266962] 03 p1045 N94-14970
Welding nozzle position manipulator
[NASA-CASE-MFS-29837-1] 03 p1047 N94-15882
Contextually dependent control strategies for manipulation
[TR-416] 03 p1165 N94-16580
A modular control architecture for real-time synchronous and asynchronous systems
[DE93-015439] 03 p1166 N94-16888
Development of a prototype kinestatic platform for application to space and ground servicing tasks. Phase 1: Concept Modeling
[NASA-CR-194036] 03 p0887 N94-16905
Three axis force override rate control of a PUMA 560 manipulator
[AD-A267313] 03 p1048 N94-16944
Joint stiffness estimation based on force sensor measurements in industrial manipulators
[REPT-92-053] 04 p1443 N94-17937
Efficient dynamic modeling of manipulators containing closed kinematic loops
[REPT-92-083] 04 p1444 N94-17940
Direct kinematics solution architectures for industrial robot manipulators: Bit-serial versus parallel 04 p1399 N94-18358
In-situ growth monitoring of molecular beam epitaxy processes
[AD-A269287] 04 p1598 N94-18616
Cooperative control of multiple space manipulators
[AD-A270291] 04 p1445 N94-18813
Adaptive path planning: Algorithm and analysis
[DE93-008348] 04 p1523 N94-18926
Application of change detection to dynamic contact sensing
[AD-A270523] 05 p1939 N94-20105
Teleoperation with virtual force feedback
[DE93-019406] 05 p1942 N94-20293
Development and testing of a reliability performance index for modular robotic systems
[AD-A271901] 05 p1942 N94-20488
Active damping of oscillations in a long compliant manipulator link
[DE93-018878] 05 p1826 N94-22038
A robust adaptive control design for flexible joint manipulators 05 p1790 N94-22230
Analytical representation of working articulation space of a plane manipulator in an encumbered environment 05 p1792 N94-22241
Control of multiple robot manipulators with optimal force distribution 05 p1794 N94-22255
Optimal control of the tip of a flexible arm 05 p1794 N94-22256
Dynamic analyses of flexible robotic manipulators
[ISBN-0-315-59251-6] 05 p1827 N94-22421
Robot link and contact surface dynamic interaction: An experimental study of contact instability
[ISBN-0-315-83439-0] 05 p1827 N94-22578
Normal forms of kinematic singularities of 3R robot manipulators
[MEMO-1124] 06 p2469 N94-22712
Graphical programming: A systems approach for telerobotic servicing of space assets
[DE93-019016] 06 p2472 N94-23201
NASA/ASEE Summer Faculty Fellowship Program
[NASA-CR-194678] 06 p2571 N94-23230
Control of a serpentine manipulator with collision avoidance 06 p2368 N94-23232
Micro-gravity compatible drive (MGCD) 06 p2355 N94-23988
Illumination requirements for operating a space remote manipulator 06 p2435 N94-24195
Robust stability of second-order systems
[NASA-CR-195175] 06 p2488 N94-24564
Genetic-based motion planning for articulated robotic manipulators
[RR-476] 06 p2368 N94-25322
Modelling the Shuttle Remote Manipulator System: Another flexible model 06 p2371 N94-25350
Robotics in a controlled, ecological life support system 06 p2444 N94-25371
A global approach to kinematic path planning to robots with holonomic and nonholonomic constraints 07 p2683 N94-26279
Inertial-space disturbance rejection for space-based manipulators 07 p2683 N94-26281
Performance measures from the explorer platform berthing experiment 07 p2683 N94-26283
Asymptotically stable neural networks for identification of nonlinear dynamic systems
[ISBN-0-315-84328-4] 07 p2985 N94-26629
Dynamics of a flexible extendible beam
[ISBN-0-315-84278-4] 07 p2838 N94-26639
Motion planning for serial manipulators with many degrees of freedom: Implementation of a sequential search strategy
[ISBN-0-315-83682-2] 07 p2822 N94-26642
Optimal architectural design of parallel and hybrid manipulators
[ISBN-0-315-84351-9] 07 p2822 N94-26657
Simulation dynamics of a multibody chain: Recursion based on chain modal coordinates
[ISBN-0-315-83555-9] 07 p2994 N94-26659
Interchangeable end effector tools utilized on the PFMA
[NASA-CR-193925] 07 p2823 N94-27149
Generalized finite element dynamic modelling and simulation for flexible robot manipulators
[ISBN-0-315-84623-2] 07 p2825 N94-27343
Dynamic control of kinematically redundant manipulators
[ISBN-0-315-84627-5] 07 p2825 N94-27344
Advanced control of a flexible spherical wrist
[ISBN-0-315-84424-8] 07 p2826 N94-27652
Local performance optimization for a class of redundant eight-degree-of-freedom manipulators
[NASA-TP-3417] 07 p2989 N94-27773
Comparison of dynamic analysis of a Schilling hydraulic manipulator with experimental results
[DE94-004597] 07 p2827 N94-27780
Design and construction of the Aerobot Robotic Manipulator (ARM)
[AD-A275362] 08 p3298 N94-28894
Experimental evaluation of fuzzy logic control of a flexible arm manipulator
[AD-A275375] 08 p3434 N94-29013
Feedback control of a three-link planar under-actuated manipulator using a surge velocity
[AD-A275159] 08 p3435 N94-29044
Kinematic functions for redundancy resolution using configuration control
[NASA-CASE-NPO-18608-1-CU] 08 p3436 N94-29504
Simplified and symmetrical five-bar linkage driver for manipulating a six-degree-of-freedom parallel minimanipulator with three inextensible limbs
[NASA-CASE-GSC-13485-2] 08 p3301 N94-29556
A compact roller-gear pitch-yaw joint module: Design and control issues 08 p3161 N94-29629
Six-degree-of-freedom parallel minimanipulator with three inextensible limbs
[NASA-CASE-GSC-13485-1] 08 p3288 N94-29726
Collision avoidance and control of multiple revolute manipulators 08 p3302 N94-29884
A study of the flexible space platform based deployable manipulator
[ISBN-0-315-85410-3] 08 p3303 N94-30135
Experimental sliding mode control of a flexible single link manipulator
[ISBN-0-315-85466-9] 08 p3304 N94-30238
Coordinated control of multiple robot manipulators 08 p3306 N94-30269
Force control techniques for robot manipulators and their military applications 08 p3307 N94-30291
An inverse kinematics algorithm for the DREP/Philips real-time radiographic manipulator system 08 p3307 N94-30292
Simulation of lightweight robots and their controllers 08 p3307 N94-30294
The response of flexible manipulators to a new computed torque control strategy: Simulation results 08 p3308 N94-30295
Symbolic generation of dynamics equations for manipulators mounted on moving bases 08 p3308 N94-30296
Supervised autonomous control for Space Station Special Purpose Dextrous Manipulator (SPDM) robot 08 p3309 N94-30305
A testbed for the development of ground-based control of space-based manipulators 08 p3309 N94-30306

Aiding the operator in the manual control of a space manipulator
[PB94-125549] 08 p3402 N94-30390
Development and validation of a linear recursive order-N algorithm for the simulation of flexible space manipulators dynamics
[AD-B173557] 08 p3311 N94-30391
A force-controllable macro-micro manipulator and its application to medical robots 08 p3314 N94-30441
Programmable Automated Welding System (PAWS): Control of welding through software and hardware 08 p3314 N94-30443
Space flight manipulator technologies and requirements for the NASA Flight Telerobotic Servicer (FTS)
[AIAA PAPER 94-1191-CP] 08 p3441 N94-30542
A highly redundant robot system for inspection
[AIAA PAPER 94-1194-CP] 08 p3442 N94-30545
Fuzzy logic based robotic controller
[AIAA PAPER 94-1202-CP] 08 p3443 N94-30553
Robotic NDE inspection of advanced solid rocket motor casings
[AIAA PAPER 94-1222-CP] 08 p3446 N94-30571
An intelligent robotic aid system for human services
[AIAA PAPER 94-1232-CP] 08 p3447 N94-30580
Kinematic analysis of platform-type robotic manipulators
[ISBN-0-315-78703-1] 08 p3311 N94-30793
Robust adaptive control of a mechanical manipulator 08 p3449 N94-30806
Kinematics and force analysis of a robot hand based on an artificial biological control scheme 08 p3313 N94-30957
A high-performance multi-arm environment: Theoretical aspects and practical implementation
[RR-479] 09 p3722 N94-31379
Kinematic synthesis and analysis of a novel class of six-DOF parallel minimanipulators 09 p3723 N94-31568
Remote robot manipulator coupled with remote-controlled guide vehicle for soil sampling in hazardous waste sites 09 p3723 N94-31569
Real-time control of the Trussarm variable-geometry-truss manipulator utilizing machine vision
[ISBN-0-315-87054-0] 09 p3830 N94-31735
Point-contact and point-impact dynamics for multibody chains
[ISBN-0-315-87056-7] 09 p3734 N94-31737
Development of a robotic simulator for studying interference and contact problems
[ISBN-0-315-86705-1] 09 p3588 N94-31747
Application of contact mechanics for the validation of robotized operations of grasping objects subjected to static and dynamic force fields
[ISBN-0-315-86831-7] 09 p3725 N94-31754
Strategy for tracking and grabbing a moving object with the aid of a decouplable manipulator with six degrees of freedom general architecture, guided by a vision system
[ISBN-0-315-86864-3] 09 p3831 N94-31757
Trajectory learning with a direct drive robotic manipulator 09 p3831 N94-31794
Development of a feedforward controller for a flexible manipulator
[ISBN-0-315-86515-6] 09 p3832 N94-31801
A real-time computer control and trajectory generation environment for Trussarm
[ISBN-0-315-87060-5] 09 p3832 N94-31833
Model identification of a reconfigurable robot manipulator
[ISBN-0-315-87109-1] 09 p3725 N94-31874
Automatic analysis of force distribution in multi-fingered articulated hands
[ISBN-0-315-87205-5] 09 p3725 N94-31878
High-speed path constrained manipulator operation using optimal-feedback combined controller 09 p3833 N94-31962
Control of a flexible-link robotic arm manipulating an unknown dynamic payload 09 p3725 N94-31973
Parallel methods for synthesizing whole-hand grasps from generalized prototypes
[AD-A276798] 09 p3726 N94-32166
An experimental testbed for a free-floating manipulator
[AD-A277350] 09 p3726 N94-32334
Trajectory planning for space manipulators
[AD-A277229] 09 p3611 N94-32369
Applying robotics to HAZMAT 09 p3729 N94-32452
Technology transfer of operator-in-the-loop simulation 09 p3802 N94-32472
Construction of a parallel processor for simulating manipulators and other mechanical systems
[NASA-CR-191327] 09 p3826 N94-32482
A new solution method for the inverse kinematic joint velocity calculations of redundant manipulators
[DE94-004427] 09 p3727 N94-32682
Development of an interchangeable end effector mechanism for the Ranger telerobotic vehicle 09 p3604 N94-33297
Experiments in autonomous navigation and control of multi-manipulator, free-flying space robots 10 p4013 N94-33383
The resolvability ellipsoid for sensor based manipulation
[AD-A277898] 10 p4055 N94-33549
Force override rate control for robotic manipulators 10 p4066 N94-33665
Graphical programming: A systems approach for telerobotic servicing of space assets 10 p4066 N94-33666
Controlling telerobots with video data and compensating for time-delayed video using Omniview 10 p4127 N94-34031
Robotic technologies of the Flight Telerobotic Servicer (FTS) including fault tolerance 10 p4067 N94-34034
Hardware interface for isolation of vibrations in flexible manipulators: Development and applications 10 p4067 N94-34036
The servicing aid tool: A teleoperated robotics system for space applications 10 p4067 N94-34039
Bilateral control to coordinate operators with supporting systems by force sensed grips 10 p4067 N94-34335
A test system of pose repeatability precision of multi-path robot 10 p4067 N94-34341
Kinematic modeling of a double octahedral Variable Geometry Truss (VGT) as an extensible gimbal
[NASA-TM-109127] 11 p4311 N94-35242
Technology demonstration of space intravehicular automation and robotics
[NASA-TM-109138] 12 p4501 N94-37589
Robust stability of second-order systems
[NASA-CR-196384] 12 p4501 N94-37590
A new technique for dynamic load distribution when two manipulators mutually lift a rigid object, part 2
[DE94-010126] 12 p4501 N94-37735

MANNED LUNAR SURFACE VEHICLES
The Extended Mission Rover (EMR) 07 p2689 N94-25674
Pressurized Lunar Rover (PLR) 07 p2833 N94-25704
Lunar surface operations. Volume 1: Lunar surface emergency shelter
[NASA-CR-195551] 08 p3299 N94-29354

MANNED MARS MISSIONS
In-space assembly-servicing requirements 01 p0348 N94-11569
Design, qualification and operation of nuclear rockets for safe Mars missions
[DE93-010792] 02 p0549 N94-12996
Mirror fusion propulsion system: A performance comparison with alternate propulsion systems for the manned Mars Mission
[NASA-TM-109248] 02 p0550 N94-13147
Optimizing interplanetary trajectories with deep space maneuvers
[NASA-CR-4546] 02 p0532 N94-14851
Application of a NEPTUNE propulsion concept to a manned Mars excursion
[AD-A268053] 03 p0929 N94-17587
Space exploration initiative
[NASA-TM-109366] 04 p1323 N94-18981
Mars exploration study workshop 2
[NASA-CP-3243] 05 p2146 N94-21883
Manned Mars mission on-orbit operations FTS capabilities assessment
[NASA-CR-189328] 06 p2430 N94-23080
Power generation technology options for a Mars mission
[NASA-TM-106451] 06 p2220 N94-24681
Preliminary design of a universal Martian lander
[NASA-CR-195529] 06 p2206 N94-25007
Manned mission to Mars with periodic refueling from electrically propelled tankers 07 p2689 N94-25670
Lowest cost, nearest term options for a manned Mars mission 07 p2689 N94-25682
Project APEX: Advanced manned exploration of the Martian moon Phobos 07 p3079 N94-25688
Project Minerva: A low-cost manned Mars mission based on indigenous propellant production 07 p2760 N94-25705
Pax: A permanent base for human habitation of Mars 07 p2943 N94-25706
Nuclear electric propulsion: A better, safer, cheaper transportation system for human exploration of Mars
[NASA-TM-106406] 08 p3171 N94-28833

MANNED ORBITAL LABORATORIES
NT SPACELAB
Docking mechanisms: An overview of different systems 06 p2357 N94-24004

MANNED ORBITAL SPACE STATIONS
U SPACE STATIONS

MANNED REENTRY
Concepts and embodiment design of a reentry recumbent seating system for the NASA Space Shuttle
[NASA-CR-195504] 06 p2438 N94-24667

MANNED SPACE FLIGHT
NT APOLLO FLIGHTS
NT APOLLO 11 FLIGHT
NT APOLLO 15 FLIGHT
NT APOLLO 16 FLIGHT
NT APOLLO 17 FLIGHT
NT MANNED REENTRY
NT MERCURY MA-6 FLIGHT
NT SPACE SHUTTLE MISSION 51-F
NT SPACE SHUTTLE MISSION 51-L
NT SPACE SHUTTLE MISSION 61-A
NT SPACE SHUTTLE MISSIONS
Lunar campsite concept: Space transfer concepts and analysis for exploration missions
[NASA-CR-192602] 01 p0433 N94-10144
PTTI-aided ephemeris calculation and rapid data link acquisition for manned space flight 01 p0042 N94-10974
Effects of CSF hormones and ionic composition on salt/water metabolism
[NASA-CR-193232] 01 p0300 N94-11045
Development of a nonazeotropic heat pump for crew hygiene water heating
[NASA-CR-194189] 02 p0737 N94-13674
Life support and habitability manual, volume 1
[ESA-PSS-03-406-ISSUE-1-VOL-1] 02 p0737 N94-13901
Life support and habitability manual, volume 2
[ESA-PSS-03-406-ISSUE-1-VOL-2] 02 p0738 N94-13902
An evaluation of noise and its effects on shuttle crewmembers during STS-50/USML-1
[NASA-TM-104775] 02 p0735 N94-13961
My experiences in manned space flight 02 p0698 N94-14276
The problem of traveling in outer space: The rocket motor
[NASA-TT-10002] 02 p0552 N94-14463
Physical countermeasures for long-term manned space flights
[ESA-SP-1160] 02 p0733 N94-14860
Cohen program management briefing
[NASA-TM-109536] 03 p1223 N94-15367
President Kennedy's speech at Rice University
[NASA-TM-109532] 03 p1302 N94-15394
History of the manned space flight program
[NASA-TM-109529] 03 p1303 N94-16069
Human Transportation System (HTS) study, volume 2
[NASA-TM-104779-VOL-2] 03 p0882 N94-17320
Human Transportation System (HTS) study: Executive summary
[NASA-TM-104780] 04 p1332 N94-18669
Human Transportation System (HTS) study, volume 1
[NASA-TM-104779] 04 p1332 N94-18670
Return to space
[NASA-TM-109356] 04 p1332 N94-18955
An antiproton driver for ICF propulsion 06 p2217 N94-23069
The birth of NASA: The diary of T. Keith Glennan
[NASA-SP-4105] 06 p2630 N94-23333
Space tourism: A flight of fantasy or the next major space product? Paper session 3: Products
[NASA-TM-109385] 06 p2194 N94-23710
Crew interface analysis: Selected articles on space human factors research, 1987 - 1991
[NASA-TM-104756] 06 p2433 N94-24185
Previous experience in manned space flight: A survey of human factors lessons learned 06 p2435 N94-24196
Suddenly, tomorrow came... A history of the Johnson Space Center
[NASA-SP-4307] 06 p2631 N94-24584
The future of manned spaceflight 06 p2195 N94-25067
Future of aerospace
[PB94-120185] 07 p2669 N94-26906
Research and Development Annual Report, 1992
[NASA-TM-104777] 07 p3119 N94-27993
Start of space tourism 08 p3164 N94-29714
Atmosphere quality standards in manned space vehicles
[ESA-PSS-03-401-ISSUE-1] 09 p3802 N94-31224
Legal regime of human activities in outer space law 09 p3599 N94-31431
Advanced transportation system study: Manned launch vehicle concepts for two way transportation system payloads to LEO
[NASA-CR-193951] 09 p3608 N94-33100
Load-limiting landing gear footpad energy absorption system 09 p3607 N94-33323
United States/Russia space cooperation documentary
[NASA-TM-109809] 10 p4014 N94-33561

Space educators' handbook
[NASA-TM-109779] 11 p4343 N94-35339
Budget estimates, fiscal year 1995. Volume 1: Agency summary, human space flight, and science, aeronautics and technology
[NASA-TM-109791] 11 p4347 N94-35899

MANNED SPACE FLIGHT NETWORK
Apollo 11: The Goddard connection
[NASA-TM-109815] 10 p4010 N94-33566

MANNED SPACECRAFT
NT AEROSPACE PLANES
NT APOLLO LUNAR EXPERIMENT MODULE
NT BURAN SPACE SHUTTLE
NT CHALLENGER (ORBITER)
NT COLUMBIA (ORBITER)
NT COLUMBUS SPACE STATION
NT DISCOVERY (ORBITER)
NT FRIENDSHIP 7
NT HERMES MANNED SPACEPLANE
NT MAN TENDED FREE FLYERS
NT MANNED ORBITAL LABORATORIES
NT MERCURY SPACECRAFT
NT MIR SPACE STATION
NT SOYUZ SPACECRAFT
NT SPACE SHUTTLE ORBITERS
NT SPACE SHUTTLES
NT SPACELAB
NT X-30 VEHICLE
Development of an advanced spacecraft tandem mass spectrometer
[NASA-CR-194195] 02 p0545 N94-13953
Human Transportation System (HTS) study, volume 2
[NASA-TM-104779-VOL-2] 03 p0882 N94-17320
Entry velocities at Mars and Earth for short transit times
[AD-A272591] 05 p1665 N94-21420
Suddenly, tomorrow came... A history of the Johnson Space Center
[NASA-SP-4307] 06 p2631 N94-24584
ESTEC wiring test programme materials related properties 08 p3165 N94-28698
Vulnerability of manned spacecraft to crew loss from orbital debris penetration
[NASA-TM-108452] 08 p3169 N94-30161
Advanced transportation system study: Manned launch vehicle concepts for two way transportation system payloads to LEO
[NASA-CR-193951] 09 p3608 N94-33100
Advanced transportation system study: Manned launch vehicle concepts for two way transportation system payloads to LEO. Work breakdown structure and work breakdown structure dictionary
[NASA-CR-193952] 10 p4012 N94-34911
Advanced transportation system study: Manned launch vehicle concepts for two way transportation system payloads to LEO. Program cost estimates document
[NASA-CR-193953] 10 p4013 N94-34912

MANPOWER
NT ENGINEERS
NT SCIENTISTS
An advisor module for tactical and strategic state-oriented planning systems with an application in manpower planning
[MEMO-COSOR-92-57] 01 p0416 N94-10868
An evaluation of artificial neural network modeling for manpower analysis
[AD-A273001] 05 p1945 N94-21269
Personnel shift assignment: Existence conditions and network models
[MEMO-1116] 06 p2585 N94-22704

MANTLE (EARTH STRUCTURE)
U EARTH MANTLE

MANUAL CONTROL
NT VISUAL CONTROL
Evaluation of two cockpit display concepts for civil tiltrotor instrument operations on steep approaches 02 p0517 N94-13323
Simulator study of uncoupled control functions. Use of manual pointing modes when aiming at ground targets and oncoming airborne target
[FFA-TN-1992-18] 02 p0528 N94-13588
Manual control in space research on perceptual-motor functions under zero gravity conditions (L-10) 02 p0593 N94-13767
Unistick vehicle controller
[NASA-TM-109618] 03 p1046 N94-15347
Visually guided touching and manual tracking
[TR-412] 03 p1166 N94-16581
Reducing video frame rate increases remote optimal focus time
[NASA-TM-104018] 06 p2431 N94-23970
Speech versus manual control of camera functions during a telerobotic task 06 p2436 N94-24199
Tactility as a function of grasp force: Effects of glove, orientation, pressure, load, and handle
[NASA-TP-3474] 08 p3402 N94-30210
Aiding the operator in the manual control of a space manipulator
[PB94-125549] 08 p3402 N94-30390
Manual tracking performance using a virtual hand controller: A comparison study 12 p4484 N94-37271

MANUALS
NT USER MANUALS (COMPUTER PROGRAMS)
The guide to Design For On-orbit Spacecraft Servicing (DFOSS) manual: Producing a consensus document 01 p0421 N94-11575
Environmental awareness
[DE93-014192] 02 p0707 N94-13218
Manual on the global data-processing system. Volume 1: (Annex 4 to the WMO regulations) global aspects (1992 edition)
[WMO-485-VOL-1] 02 p0721 N94-13686
Life support and habitability manual, volume 1
[ESA-PSS-03-406-ISSUE-1-VOL-1] 02 p0737 N94-13901
Life support and habitability manual, volume 2
[ESA-PSS-03-406-ISSUE-1-VOL-2] 02 p0738 N94-13902
National use of the groups 7wwW1W2 and 960ww for ground stations
[KNMI-PUBL-181] 02 p0722 N94-13926
Manual on the global data-processing system. Volume 2: Regional aspects (1992 edition)
[WMO-485-VOL-2] 02 p0722 N94-14071
Oak Ridge Environmental Information System (ORIES) site workstation information packet for OREIS 6.2
[DE93-010761] 02 p0825 N94-14458
A guide to the DRA 13 ft x 9 ft Low Speed Wind Tunnel Facility
[AD-A267739] 02 p0528 N94-14876
User's guide: Hot-mix recycling of asphalt concrete pavements
[AD-A266939] 03 p0983 N94-15177
Defense Logistics Information System (DLIS) procedures manual. Products and services end-user manual
[AD-A267766] 03 p1232 N94-17007
Results of a joint Navy/Air Force operational test to evaluate USAF Integrated Maintenance Information Systems (IMIS), Interactive Electronic Technical Manual (IETM) technology applied to the F/A-18 aircraft
[AD-A271322] 04 p1619 N94-19571
Publication of science data on CD-ROM: A guide and example
[NASA-CR-4560] 05 p1842 N94-21585
Everything you might want to know about the Internet but are afraid to ask!
[DE93-041118] 05 p2046 N94-22413
Tools reference manual for a Requirements Specification Language (RSL), version 2.0
[NASA-CR-191461] 06 p2445 N94-23125
Bibliographic Retrieval System (BARS), Sandia Shock Compression (SSC) database, Shock Physics Index (SPHINX) database, Volume 2: UNIX version user's guide
[DE94-001704] 06 p2589 N94-23128
Manual on measurement of methane and nitrous oxide emissions from agriculture
[DE93-616429] 06 p2399 N94-25167
Defense Technical Information Center cataloging guidelines
[AD-A275100] 08 p3529 N94-28911
Fundamentals of printing technology
[PB94-132602] 08 p3530 N94-29141
User's manual for the model interface and plugboard cabinets in the 14- by 22-foot subsonic tunnel
[NASA-TM-109062] 08 p3133 N94-30176
Laser safety manual for DREO
[AD-A276288] 09 p3714 N94-31255
CMS Distribution Subsystem user's guide
[DE94-005328] 09 p3816 N94-32146
Total Quality Management implementation guidelines
[DE94-007232] 09 p3915 N94-32723
Report of the workshops: Automated generation of electronic technical manuals
[AD-A278046] 10 p4150 N94-33401

MANUFACTURING
NT COMPUTER AIDED MANUFACTURING
NT LOW GRAVITY MANUFACTURING
NT SPACE MANUFACTURING
Lightweight CFRP frame structures for a Rotex-derived manipulator system 01 p0056 N94-10005
Cost effectiveness of structural applications of fibre reinforced thermoplastics 01 p0060 N94-10032
Spin-rolling, welding, and heat treatment of aluminium 2219 for Ariane 5 GAM high pressure vessel liners 01 p0062 N94-10045
PM technology and mechanical properties of metallic foams 01 p0064 N94-10059
Dry in-line thermoplastic matrix impregnation, phase 1
[AD-A265016] 01 p0067 N94-11221
Large array SQUID magnetometer for NDE
[AD-A264799] 01 p0304 N94-11449
The effect of processing on the microstructure and tensile properties of a (gamma)-TiAl based alloy
[DE93-013221] 01 p0084 N94-11488
Design issues for high performance engineering information systems
[AD-A264839] 01 p0420 N94-11520
Space Solar Power Program
[DE93-011750] 01 p0055 N94-11675
Statistical process control in the hybrid microelectronics manufacturing industry: A Navy view point
[AD-A265164] 01 p0145 N94-11884
Photovoltaics: Contract lists, fiscal year 1992
[DE93-000093] 02 p0701 N94-12902
Role of microstructure on fatigue durability of aluminum aircraft alloys
[AD-A265627] 02 p0568 N94-12993
Knowledge base technology for CT-DIMS: Report 1
[DE93-013118] 02 p0743 N94-13014
Rigid-flexible printed wiring boards
[DE93-013938] 02 p0620 N94-13094
Pollution prevention through total quality
[DE93-013814] 02 p0707 N94-13390
Rapid intelligent inspection process definition for dimensional measurement in advanced manufacturing
[DE93-011271] 02 p0748 N94-13480
Activities of Hawker Siddeley Canada Inc.
[CTN-93-60865] 02 p0849 N94-13505
Cesium iodide (CsI) crystal manufacture
[DE93-012146] 02 p0808 N94-13973
Continuous roll-to-roll a-Si photovoltaic manufacturing technology
[DE93-010006] 02 p0704 N94-14109
Knowledge based systems: From process control to policy analysis
[DE93-014582] 02 p0765 N94-14117
Welding technologies as applied to nuclear manufacturing
[DE93-010924] 02 p0664 N94-14565
Geometric tolerance assessment
[NPL-DITC-210/92] 03 p1049 N94-15013
Production Technology for Components from Nonmetallic Fiber Reinforced Materials
[ETN-93-94607] 03 p0931 N94-15254
Galileo probe spacecraft mission to Jupiter
[NASA-TM-109646] 03 p1247 N94-16070
Lithium D-cell study
[NASA-CR-192705] 03 p1011 N94-16505
Status of molten carbonate fuel cell technology development
[DE93-015666] 03 p1092 N94-16715
Manufacturing tolerance requirements for frequency selective surfaces
[AD-A266541] 03 p0999 N94-16797
Materials processing and manufacturing technologies for diamond substrate multichip modules (DSMCM)
[AD-A267316] 03 p0969 N94-16946
Integration ToolKit and Methods (ITKM) manufacturing methods and prototype toolkit. A combined modeling method using IDEFO, IDEF1x and XSpec
[AD-A266176] 03 p0984 N94-16981
Manufacturing the key to binary optics 03 p1194 N94-17332
Laser figuring for the generation of analog micro-optics and kineform surfaces 03 p1196 N94-17346
Applications of advanced diffractive optical elements 03 p1197 N94-17356
Factors which affect fatigue strength of fasteners
[DE93-017272] 04 p1453 N94-18084
Autonomous neural network controllers for adaptive material handling
[AD-A268908] 04 p1540 N94-18331
Performance of defect-tolerant set-associative cache memories 04 p1398 N94-18346
High-efficiency silicon concentrator cell commercialization
[DE93-018491] 04 p1467 N94-18409
Workshop on Innovation in Materials Processing and Manufacture: Exploratory Concepts for Energy Applications
[DE93-017674] 04 p1467 N94-18478
New applications for high average power beams
[DE93-018845] 04 p1439 N94-18522
Materials processing and manufacturing technologies for diamond substrates multichip modules
[AD-A268989] 04 p1599 N94-18764
Integrated circuits: Resistless processing simplifies production and cuts costs
[DE93-018069] 04 p1405 N94-18941
Conceptual design of a sodium sulfur cell for US electric van batteries
[DE93-018683] 04 p1405 N94-19035
MODIL cryocooler producibility demonstration project results
[DE93-017981] 04 p1335 N94-19275

Manufacturing technology
[DE93-019580] 04 p1381 N94-19480
Incology 908 database report: On process-structure-property relationship
[DE93-017616] 04 p1366 N94-19546
Shell designs
[AD-A270656] 04 p1460 N94-19606
Program descriptions
[NSF-92-123] 04 p1531 N94-19619
Amorphous silicon batch process cost analysis
[DE93-018203] 04 p1470 N94-19760
Materials processing and manufacturing technologies for Diamond Substrate MultiChip Modules (DSMCM)
[AD-A271011] 05 p2011 N94-19821
Solder technology in the manufacturing of electronic products
[DE93-018842] 05 p1699 N94-19960
Using electronic data interchange to report product quality
[AD-A271843] 05 p1828 N94-20468
Optimization of static traffic allocation policies
[CWI-BS-R9302] 05 p1930 N94-21161
Materials processing and manufacturing technologies for diamond substrate multichip modules
[AD-A271484] 05 p2027 N94-21319
Improvement of the stability of the process for synthesizing chemically prepared varistor powder
[DE94-000345] 05 p1763 N94-21654
Modeling of glass fabrication
05 p1711 N94-21800
Proceedings of the IMOG (Interagency Manufacturing Operations Group) Numerical Systems Group
[DE94-001009] 05 p1917 N94-21851
Progress in phases 2 and 3 of the Photovoltaic Manufacturing Technology Project (PVMaT)
[DE94-000206] 06 p2389 N94-22888
A novel process monitoring and control system based on a neural manufacturing concept
[DE94-001516] 06 p2471 N94-23011
Sensors for process control Focus Team report
[DE93-040897] 06 p2560 N94-23204
Amorphous silicon PVMaT, phase 2A
[DE93-018221] 06 p2390 N94-23295
SP-100 heat transport technology development
[DE94-000769] 06 p2218 N94-23452
Engineering for profitability
[PNR-90990] 06 p2595 N94-23580
The Electronics Quality/Reliability Center: Lessons learned from partnering with industry
[DE94-001501] 06 p2309 N94-23777
Integrated Airframe Design Technology
[AGARD-R-794] 06 p2177 N94-24313
Early manufacturing considerations in design
06 p2177 N94-24315
Applications of CFD codes and supercomputers to aircraft design activities 06 p2177 N94-24316
Frameworks for integrated airframe design
06 p2178 N94-24318
Design and specification of a centralized manufacturing data management and scheduling system
06 p2577 N94-24416
SEMATECH, a case study: Analysis of a government-industry partnership
[AD-A273166] 06 p2586 N94-24683
The Blue Emu
[NASA-CR-195535] 06 p2182 N94-24817
Production control and demand management in capacitated flow process industries
[ISBN-9-03-860211-1] 06 p2586 N94-25235
Study on utilization of super clean, high vacuum space
07 p2682 N94-25586
Lunar preform manufacturing
07 p2765 N94-25677
The effectiveness of AMT investment in UK metal component manufacture
[IND-MANU-SCI-TECH-REPT-3]
07 p2762 N94-25775
General Motors Corporation and Pacific Northwest Laboratory staff exchange: Inspection of case hardened steels and metal-matrix composites
[DE94-003470] 07 p2706 N94-25982
The National Center for Advanced Information Components Manufacturing: Program update
[DE94-002647] 07 p2960 N94-26118
Overview of the Photovoltaic Manufacturing Technology (PVMaT) project
[DE93-018234] 07 p2856 N94-26426
Adaptive path planning in changing environments
[DE94-003269] 07 p2985 N94-26462
Qualified manufacturing and interoperability for space applications 07 p2949 N94-26719
Fabrication technology
[DE94-003017] 07 p2763 N94-26778
Investigation of ACC/CCI tunnel diodes
[AD-A274549] 07 p2785 N94-26845
Material optimization and manufacturing development of reduced cost powder metal titanium alloy components for gas turbine engine application, phase 2
[AD-A274410] 07 p2709 N94-26978
Solar collector manufacturing activity, 1992
[DE94-003401] 07 p2859 N94-27048
A widely adaptable habitat construction system utilizing space resources 07 p2688 N94-27374
Multiple weight stepwise regression
[DE94-001602] 07 p3000 N94-27564
Continuous roll-to-roll a-Si photovoltaic manufacturing technology
[DE94-000260] 07 p2859 N94-27610
Development of the gas turbine. Part 2: Manufacturing, commissioning, and operation 07 p2831 N94-28081
Open communication in manufacturing automation
[PB94-132479] 07 p2976 N94-28377
Silicon-Film (tm) photovoltaic manufacturing technology
[DE94-000258] 08 p3336 N94-28501
NEMA wire and cable standards development programs 08 p3166 N94-28706
Electroset Technology: On the forefront of manufacturing
[AD-A275166] 08 p3263 N94-29045
Application of high-speed milling to the Finnish manufacturing industry
[PB94-135548] 08 p3230 N94-29187
Realizing the productivity potential of expeditious operations
[PB94-135555] 08 p3230 N94-29188
Technology transfer initiatives
[NASA-CR-195151] 08 p3537 N94-29410
Micromanufacturing: Recent developments in this country and abroad 08 p3235 N94-29769
Practical applications of plasma surface modification
[DE94-004892] 08 p3349 N94-29932
Logistics for the implementation of lead-free solders on electronic assemblies
[DE94-004800] 08 p3206 N94-29936
Non-aqueous cleaning solvent substitution
[DE94-005339] 08 p3219 N94-30245
The 1992 report on the next generation ultra clean technology for advanced microfabrication
[DE94-744171] 08 p3157 N94-30268
Technology 2003: The Fourth National Technology Transfer Conference and Exposition, volume 1
[NASA-CP-3249-VOL-1] 08 p3555 N94-30440
The use of interactive computer vision and robot hand controllers for enhancing manufacturing safety
08 p3314 N94-30442
Near-net-shape manufacturing: Spray-formed metal matrix composites and tooling 08 p3186 N94-30447
Precision and manufacturing at the Lawrence Livermore National Laboratory 08 p3240 N94-30449
Conference on Intelligent Robotics in Field, Factory, Service, and Space (CIRFFSS 1994), volume 1
[NASA-CP-3251] 08 p3439 N94-30526
Agile manufacturing: The factory of the future
[AIAA PAPER 94-1184-CP] 08 p3440 N94-30534
Confessions of a robot lobotomist
[AIAA PAPER 94-1185-CP] 08 p3440 N94-30535
PV Cz silicon manufacturing technology improvements
[DE94-000248] 08 p3339 N94-30603
Large-area triple-junction a-Si alloy production scale up
[DE94-000249] 08 p3339 N94-30604
Thin EFG octagons
[DE94-000257] 08 p3339 N94-30605
Automated solar cell assembly teamed process research
[DE94-000295] 09 p3759 N94-31279
The 18th annual electronics manufacturing seminar
[AD-A276038] 09 p3687 N94-31281
Fractional-factorial process development techniques
[DE94-005580] 09 p3690 N94-31593
The future of open architecture process control systems
[DE94-006163] 09 p3830 N94-31623
Laser applications in wood processing
[PB94-138567] 09 p3717 N94-31840
Advances in MOVPE compound semiconductor epitaxy manufacturing technology: From high throughput large area reactors to cluster tools
[DE94-006367] 09 p3901 N94-32104
Validation of the Environmentally Conscious Manufacturing Integrated Demonstration hardware
[DE94-003824] 09 p3765 N94-32144
Fiber optic chemical sensors
[AD-A277128] 09 p3881 N94-32380
From display and PWB to MCMs: Large panel manufacturing
[DE94-007855] 09 p3693 N94-32386
Empirical modeling for intelligent, real-time manufacture control 09 p3839 N94-32424
Neutral ion sources in precision manufacturing
09 p3875 N94-32447
Flexible manufacturing for photonics device assembly
09 p3669 N94-32449
LLNL casting technology
[DE94-008282] 09 p3669 N94-32839
Development of thermoplastic composite aircraft structures
[NASA-CR-189593] 09 p3626 N94-32860
Application of a design-build-team approach to low cost and weight composite fuselage structure
[NASA-CR-4418] 09 p3626 N94-32863
Second NASA Advanced Composites Technology Conference
[NASA-CP-3154] 09 p3627 N94-33121
Design, characterization, and control of the NASA three degree of freedom reaction compensation platform
09 p3605 N94-33304
Solid Freeform Fabrication Symposium Proceedings
[AD-A277718] 10 p4032 N94-33441
Detail design of a 10.4-m stretched-membrane dish
[DE94-009462] 10 p4079 N94-34167
Designing aluminum sealing glasses for manufacturability
[DE94-010081] 11 p4244 N94-35699
Intelligent processing of materials, technical activities, 1993 (NAS-NRC Assessment Panel, April 21-22 1994)
[PB94-164183] 11 p4251 N94-35737
CABPRO: An expert system for process planning multiwire cables
[DE94-010213] 11 p4312 N94-35810
Electromagnetically levitated vibration isolation system for the manufacturing process of silicon monocrystals
11 p4223 N94-35906
Report on the Workshop on Manufacturing Polymer Composites by Liquid Molding
[PB94-160066] 11 p4234 N94-36004
Design for manufacturability evaluation: Composite National Ignition Facility (NIF) pockel cell body
[DE94-010669] 11 p4338 N94-36284
Optimisation of composite aircraft structures by direct manufacturing approaches 11 p4194 N94-36327
Hardness variability in commercial and hardened technologies
[DE94-007270] 11 p4261 N94-36362
Using experimental design modules for process characterization in manufacturing/materials processes laboratories 11 p4230 N94-36405
Process capability determination of new and existing equipment 11 p4230 N94-36406
MODIL cryocooler producibility demonstration project results
[DE93-019213] 12 p4430 N94-36444
Amorphous silicon photovoltaic manufacturing technology, phase 2A
[DE94-006895] 12 p4461 N94-36476
Manufacture and properties of sigma fibre reinforced titanium 12 p4401 N94-36655
Opportunities for innovation: Biotechnology
[PB94-157831] 12 p4478 N94-36720
Advanced manufacturing technology for polymer composite structures in Japan 12 p4422 N94-36968
Scoping economics for the commercial manufacture of metallocene catalysts
[DE94-011526] 12 p4422 N94-37055
Using nonequilibrium alloying techniques for corrosion inhibition in Gr/Al and Gr/Mg metal matrix composites
[AD-A280529] 12 p4404 N94-37088
The control of cleanness in powder metallurgy materials for turbine disks 12 p4421 N94-37325
Maintaining constant standards during the forging process 12 p4421 N94-37326
Selected case studies in modeling and simulation applied to environmentally conscious design and manufacturing
[DE94-007556] 12 p4466 N94-37389
A graphic view of Geometric Dimensioning and Tolerancing
[DE94-011478] 12 p4435 N94-37736

MANY BODY PROBLEM

Satellite structure of the xenon valence shell by electron momentum spectroscopy
[DE93-609993] 01 p0360 N94-10327
Reduced gravity multibody dynamics testing
[NASA-CR-192589] 01 p0125 N94-11483
Highly anisotropic but nodeless gap from a valence-fluctuation pairing mechanism
[DE93-010738] 01 p0401 N94-11646
Many-body corrections in XAFS
[DE93-011002] 02 p0563 N94-13478
Many-body quantum mechanical studies of molecular clusters
[AD-A266624] 03 p1180 N94-15727
Dust grain resonant capture: A statistical study
03 p1245 N94-16384

Numerical studies of the photoluminescence spectrum of quantum Hall systems
[DE93-015822] 03 p1220 N94-16810
The physics of cellular automata and coherence and chaos in classical many-body dynamical systems
[DE93-018021] 04 p1561 N94-18177
A parallel hashed oct-tree N-body algorithm
[DE93-012654] 04 p1526 N94-19205
A microscopic theory of quantum optics and new photon-locked bistable states
[AD-A271250] 05 p1983 N94-19901
Method for simulating a vehicle shock test: Design and realization of the required implementation tools
[ECL-92-14] 06 p2352 N94-22885
Pions and neutrinos as probes of the nucleon and nuclear few-body system
[DE93-040127] 06 p2531 N94-22928
Calculations of Bose-Einstein correlations from Relativistic Quantum Molecular Dynamics
[DE94-000794] 06 p2569 N94-23453
Theoretical and computational studies in intermediate energy nuclear physics
[DE94-004177] 07 p3012 N94-25800
Stability of large scale interconnected dynamical systems
[DE94-601536] 07 p2993 N94-26408
How reliable is the HMSA integral equation for the pair structure of supercooled and amorphous mixtures?
[DE94-601543] 07 p3006 N94-26411
Study of the critical points at infinity arising from the failure of the Palais-smale condition for n-body type problems
[DE94-603656] 07 p3000 N94-27818
Equation of state of stellar plasmas
[DE94-004186] 08 p3542 N94-28526
The role of cloud collisions in N-body simulations of disk galaxies 08 p3545 N94-29755
The stability of perfect elliptic disks
08 p3545 N94-29834
Periodic orbits of n-body type problems: The fixed period case
[DE94-608096] 08 p3453 N94-30091
Exclusive many-particle diffusion in disordered media and correlation functions for random vertex models
[DE94-608134] 08 p3525 N94-30121
Micromechanics and effective properties of particulate composites and fluid suspensions
09 p3703 N94-31744
Numerical simulation of quantum many-body systems
[DE94-008451] 09 p3912 N94-32513
Near edge x ray spectroscopy theory
[DE94-008179] 09 p3905 N94-32799
On the theory of bounded many-particle systems with purely coulomb interactions
[DE94-617215] 11 p4325 N94-36081
Dust evolution from comets and asteroids: Their velocities at Earth orbit intersection
11 p4352 N94-36142

MANY ELECTRON EFFECTS
Semiempirical studies of atomic structure
[DE94-001568] 06 p2531 N94-22937
Numerical simulation of quantum many-body systems
[DE94-008451] 09 p3912 N94-32513

MANY PARTICLE THEORY
U MANY BODY PROBLEM

MAPPING
NT CADASTRAL MAPPING
NT COMPUTER AIDED MAPPING
NT ICE MAPPING
NT PHOTOMAPPING
NT PLANETARY MAPPING
NT SOIL MAPPING
NT THEMATIC MAPPING
NT THERMAL MAPPING
Mapping of the East Australian current with the ERS-1 SAR and shipborne studies 01 p0234 N94-11717
Techniques and applications of SAR interferometry for ERS-1: Topographic mapping, change detection, and slope measurement 01 p0236 N94-11734
The extraction of bottom characteristics and mapping in Kin Bay, Okinawa Main Island, Japan, using LANDSAT-5/TM and SPOT-1/HRV data
01 p0197 N94-11931
Mapping bathymetric slopes from bathymetry data
[AD-A265923] 01 p0290 N94-12350
Land cover monitoring with multi-temporal ERS-1 SAR observations in the Netherlands
01 p0246 N94-12473
Mapping a dynamic playa surface using multitemporal ERS-1 SAR data: First results 01 p0246 N94-12474
Preliminary studies on the application of ERS-1 data to topographic mapping 01 p0246 N94-12476
Combined analysis of ERS-1 SAR and visible/infrared remote sensing data for land cover/land use mapping in a tropical zone: A case study in Guinea
01 p0246 N94-12478
Example of SPOT/ERS-1 complementarity
01 p0247 N94-12479
Application of ERS-1 SAR data to snow mapping
01 p0247 N94-12483
Methodological considerations for use of ERS-1 imagery for the delineation of river networks in tropical forest areas 01 p0247 N94-12484
The TREES project: Pre-processing and generation of terrain data for inclusion in an ERS-1 SAR classification scheme 01 p0249 N94-12496
Mapping of sea bottom topography with ERS-1 C-band SAR 01 p0254 N94-12525
ERS-1 imaging radar over the Waddensea-North Netherlands 01 p0254 N94-12526
SAR imaging of geology and bathymetry: Kent coastal area - southern North Sea 01 p0254 N94-12527
Application of remote sensing for coastal management in the north coast of Java 01 p0218 N94-12701
Estimation of areal evapotranspiration using LANDSAT TM data: Kitami City, Hokkaido, Japan
01 p0219 N94-12703
Land use/land cover mapping of central water shed of Iran area based on satellite data interpretation
01 p0219 N94-12704
A method to minimize reference data in classifying satellite remote sensing data into land cover classes
01 p0219 N94-12705
Quantitative mapping of pore fraction variations in silicon nitride using an ultrasonic contact scan technique
[NASA-TP-3377] 02 p0665 N94-13056
Error analysis of real time and post processed or bit determination of GFO using GPS tracking
[NASA-CR-193646] 02 p0512 N94-13238
Perception for outdoor navigation
[AD-A266867] 03 p0863 N94-14919
Improved mapping system
[NASA-TM-109643] 03 p1082 N94-15428
Develop advanced nonlinear signal analysis topographical mapping system
[NASA-CR-194577] 03 p1082 N94-15646
The role of carbon and temperature in determining electrical conductivity of basins, crust and mantle
[DE93-015936] 03 p1101 N94-16840
CTD oxygen, tracer and nutrient data from RRS Charles Darwin Cruises 58/59 in the NE Atlantic as part of Vivaldi 1991
[IOS-296-1992] 04 p1496 N94-18065
SeaSoar CTD, fluorescence and scalar irradiance data from RRS Charles Darwin Cruises 58/59, NE Atlantic, Vivaldi 1991
[IOS-299-1992] 04 p1496 N94-18066
Resolution in radar mapping
[AD-A269730] 04 p1462 N94-18753
Topographic mapping using a monopulse SAR system
05 p1721 N94-20417
Performance evaluation of the JPL TOPSAR system: An across-track interferometric SAR system for topographic mapping 05 p1732 N94-20461
Ocean mapping using satellite radar altimetry
[ETN-93-93470] 05 p1841 N94-21017
Remote sensing for hydrology progress and prospects
[WMO-773] 05 p1841 N94-21069
Relational algebra and equational proofs
[PB94-110822] 06 p2486 N94-23724
Mapping closed tropical forest cover in West Africa using NOAA/AVHRR-LAC data 07 p2850 N94-27184
Fixed point type theorems and projection-interaction approximation
[DE94-603669] 07 p3000 N94-27632
Solution of the Heisenberg equation for the four-fermion contact interaction by the method of dynamical mappings
[DE94-606341] 07 p3075 N94-27858
Fractals and their applications to remote sensing and digital mapping
[ISBN-0-315-59469-1] 07 p2852 N94-27870
The uses and limitations of fractal geometry in digital terrain modelling 08 p3333 N94-29958
A monotonicity conjecture for real cubic maps
[DE94-003969] 08 p3335 N94-30610
NORSMAP 1989: Norwegian remote sensing spectroscopy for mapping and monitoring or algal blooms and pollution 09 p3744 N94-31856
Alternatives to hierarchical techniques in stereo correlation
[AD-A276570] 09 p3746 N94-31938
Optics and radar: Cohabitation, rivality or happy marriage. Towards new planning tools
09 p3748 N94-32529
The use of ERS images for mapping
09 p3749 N94-32531
The use of SPOT and ERS-1 images to map the eruption of Nevado Sabancaya (Province of Arequipa, South Peru) and evaluate associated risks 09 p3751 N94-32546
Evaluation of the potential of SAR data for mapping of landslide risks
[BRGM-93033] 09 p3753 N94-32552
Use of SPOT and ERS-1 to map tropical vegetation and mangrove dynamics in Guiana 09 p3753 N94-32555
Statistical analysis and mapping of cotton and food crop cultivation surfaces in the west of Burkina Faso: Contribution of combined SPOT P and XS data
09 p3757 N94-32575
Estimation of fractal dimensions from transect data
[DE94-009808] 11 p4281 N94-36018
Eurocap program: Ebre Station
[AD-A280418] 12 p4469 N94-37215

MAPS
NT ASTRONOMICAL MAPS
NT LUNAR MAPS
NT METEOROLOGICAL CHARTS
NT PHOTOMAPS
NT RADAR MAPS
NT RELIEF MAPS
Boundary of Fatou sets of hyperbolic rational maps or degree two
[DE93-613031] 01 p0348 N94-10412
Convergence theorems for a class of nonlinear maps in uniformly smooth Banach spaces
[DE92-641347] 01 p0343 N94-10531
Worldwide map of rainfall amount over the ocean derived from passive microwave radiometer
01 p0211 N94-12663
Pargo Chasma and its relationship to global tectonics
03 p1249 N94-16181
The Navy tessellated spheroid map projection system: A comprehensive definition
[AD-A269989] 04 p1462 N94-18677
Color palette considerations for digital map displays
[AD-A269991] 04 p1462 N94-18679
Detecting topographical regions in digital terrain maps
[AD-A272889] 05 p1841 N94-21453
Study of methods and structures for handling of digitized maps for geographical information systems
[PB93-204402] 06 p2590 N94-23741
The Mars mapper science and mission planning tool
06 p2503 N94-23867
Antarctic Meteorite Location and Mapping Project (AMLAMP): Antarctic meteorite location map series explanatory text and user's guide to AMLAMP data
[NASA-CR-194841] 06 p2603 N94-24964
A brief introduction to symplectic integrators and recent results
[DE94-006225] 09 p3845 N94-31763
Techniques and applications of SAR interferometry for ERS-1 09 p3756 N94-32568
MDFF HELP library, version 2: On-line documentation for the map data formatting facility
[AD-A277763] 09 p3922 N94-32987
Global color views of Mars 09 p3948 N94-33217
Digital mapping, charting, and geodesy analysis program technical review of Urban Vector Smart Map (UV(sub Map)) prototype 1
[AD-A277831] 10 p4076 N94-33832

MARAGING STEELS
Weldability of maraging steels
01 p0059 N94-10028

MARANGONI CONVECTION
Experimental study of axisymmetric thermocapillary flows 01 p0100 N94-10072
The use of magnetic fields for damping unsteady Marangoni convection in GaAs floating zones under microgravity 01 p0100 N94-10073
Instability of thermocapillary convection in floating zones 01 p0101 N94-10076
Thermocapillary instabilities in cylindrical liquid bridges: Mechanisms and transition boundaries
01 p0101 N94-10077
Transient three-dimensional numerical simulation of Marangoni flow in a liquid column under microgravity
01 p0101 N94-10079
Marangoni and buoyant convections in zone melting of GaAs with liquid encapsulation
01 p0101 N94-10081
Coupled thermovibrational and thermocapillary convection in liquid bridge (floating zone system)
01 p0101 N94-10082
Towards real time numerical stimulation of Marangoni convection: A help for telescience microgravity experiments 01 p0102 N94-10087
Surface-tension driven convection in finite-size containers 01 p0103 N94-10090
Marangoni instability induced convection in an evaporating liquid droplet 01 p0104 N94-10094
Thermocapillary migration of bubbles: A semi-analytical solution for large Marangoni numbers
01 p0104 N94-10095
High Prandtl number fluids in a multilayered system under 1-g or micro-g environment
01 p0104 N94-10096

Marangoni flows in open cavities with differentially heated end walls 01 p0104 N94-10097
Benard and Marangoni convection in multiple liquid layers 01 p0105 N94-10100
Coupled thermogravitational and thermocapillary convection in a two-layer fluid system 01 p0105 N94-10101
Thermocapillary slug flow in a capillary tube 01 p0105 N94-10104
Numerical simulation of Marangoni convection around gas bubbles in a liquid matrix 01 p0106 N94-10107
Microgravity experiments using TR-1A rocket 01 p0112 N94-10142
Thermocapillary convection instability in microgravity crystal growth 01 p0112 N94-10172
Marangoni motion during melting of a hypermonotectic alloy: Numerical simulations for the D2 experiment IHF04 01 p0113 N94-10177
Numerical calculation of the growth of InP by the travelling heater method in the first mission of the Space Flyer Unit 01 p0114 N94-10179
Ripening of immiscible liquid droplets in microgravity with constrained Marangoni drift 01 p0117 N94-10200
Marangoni-driven solitary waves 01 p0119 N94-10214
Marangoni Benard instabilities in liquid mixtures with Soret effect 01 p0119 N94-10215
Numerical investigations on Marangoni-Benard instability in multi layer systems 01 p0120 N94-10217
Instability of thermocapillary convection in multiple superposed immiscible liquid layers 01 p0120 N94-10218
Convective motion in a multi-layered system with a free surface 01 p0120 N94-10219
Vibrational-thermocapillary parallel flows and stability 01 p0120 N94-10220
Appearance of convective instabilities caused by liquid-liquid phase separation under small buoyancy forces 01 p0120 N94-10221
The effect of a uniform magnetic field on the onset of steady Marangoni convection in a layer of conducting fluid 01 p0120 N94-10222
The combined influence of anticonvective and thermocapillary mechanisms on the stability of systems with interface 01 p0121 N94-10223
Single bubble experiments in pool boiling: Results from TEXUS 26 01 p0124 N94-10243
Marangoni instability in a liquid layer with two free surfaces
[NASA-TM-106166] 01 p0152 N94-11376
Marangoni effect induced convection in material processing under microgravity (M-18) 02 p0589 N94-13750
Contributions to numerical solution of Navier-Stokes equations in two and three dimensional flows
[ETN-93-94395] 02 p0647 N94-14816
An investigation of low Marangoni number fluid flow in a cold corner
[AD-A271317] 04 p1422 N94-19569
Survey report of JSUP Space Environment Utilization Research Committee in fiscal year 1992: Metallic Materials Session
[JTN-94-80583] 08 p3159 N94-30794
Coupled Marangoni-Benard/Rayleigh-Benard instability with temperature dependent viscosity
[NASA-TM-106646] 12 p4444 N94-37507

MARIA

NT LUNAR MARIA
Assimilation of solids during ascent of magmas from the Bartoy Field of the Baikal Region, Siberia 03 p1103 N94-16214
The ilmenite liquidus and depths of segregation for high-Ti picrite glasses 03 p0975 N94-16241

MARINE BIOLOGY

Remote sensing of aquatic system
[INPE-5271-PRP/159] 02 p0684 N94-13426
Nonlinear relationships between particulate absorption and chlorophyll: Detritus or pigment packaging?
[AD-A266806] 02 p0731 N94-14899
Abstracts of manuscripts submitted in 1992 for publication
[AD-A267963] 03 p1113 N94-17383
Nutrients and light as factors controlling phytoplankton biomass on the Dutch continental shelf (North Sea), 1988-1990
[PB94-111143] 06 p2418 N94-24601
Coupling of pelagic and benthic communities over a seamount in the Eastern North Pacific
[AD-A274750] 07 p2899 N94-26149
Measuring variation in ecosystem sensitivity to stress
[AD-A274232] 07 p2868 N94-26817
Macrobenthic fauna in the dutch sector of the north sea in 1991
[PB94-126414] 07 p2868 N94-27200
Changes in phytoplankton population in the Chao Phraya estuary, Thailand, during the eutrophication mechanisms studies 07 p2875 N94-28287
SeaWiFS technical report series. Volume 17: Ocean color in the 21st century. A strategy for a 20-year time series
[NASA-TM-104566-VOL-17] 10 p4093 N94-34209
Proceedings: Integrated Research Planning Meeting for Gulf of Mexico Estuaries
[PB94-157799] 11 p4296 N94-35738

MARINE CHEMISTRY

Faulted structure of the bottom simulating reflector on the Blake Ridge, western North Atlantic
[AD-A271289] 04 p1500 N94-19745
An experimental study of plunging liquid jet induced air carryunder and dispersion
[AD-A274414] 07 p2794 N94-26979
The carbon cycle revisited 08 p3350 N94-30622
MarChem 93, the proceedings, the 1993 workshop on marine chemistry instrumentation
[AD-A279035] 12 p4475 N94-36446

MARINE ENVIRONMENTS

Near surface ocean processes: Acoustical observations, ambient sound, and Langmuir circulation 01 p0288 N94-11447
Biscayne bay: A bibliography of the marine environment
[PB93-184802] 01 p0266 N94-11451
Automatic classification system for zooplankton 01 p0203 N94-11969
Study on sea water purification using a substratum of marine organisms 01 p0217 N94-12696
DISTERM: A shipboard data system for satellite monitoring of ocean and atmosphere 01 p0226 N94-12749
Remote sensing of aquatic system
[INPE-5271-PRP/159] 02 p0684 N94-13426
STS-29 crew bailout in WETF
[NASA-TM-109548] 03 p1136 N94-15385
Chondritic ratios of Fe/Cr/Ir in Kerguelen Plateau (Hole 738C) K/T carbonate-rich sediments support asteroid-cometary impact at K/T time 03 p1244 N94-16357
AVIRIS calibration and application in coastal oceanic environments 03 p1069 N94-16685
Atmospheric correction of AVIRIS data in ocean waters 03 p1070 N94-16690
Development and evaluation of alternative radioanalytical methods, including mass spectrometry for marine materials
[DE93-625117] 04 p1345 N94-17691
Coastal Ocean Modeling Workshop
[AD-A268955] 04 p1497 N94-18393
Work plan for the Marine Aerosol Properties and the Thermal Imager Performance Trial (MAPTIP)
[AD-A270026] 04 p1483 N94-18712
Estimating the oceanic sound speed environmental for long-range acoustic propagation
[AD-A270231] 04 p1499 N94-18903
Microstructure and texture control of fatigue in hydrogen and marine environments
[AD-A271277] 04 p1344 N94-19744
Marine-modified LOWTRAN: The contribution of sun glint
[AD-A269547] 04 p1500 N94-19762
SIMA: An integrated environmental monitoring system 05 p1840 N94-20967
Estimating the rotation rate of mesoscale ocean rings from satellite altimetry
[AD-A272922] 05 p1883 N94-21222
Low-cost, dual-use platforms for environmental sensing, phase 1
[AD-A272951] 05 p1646 N94-21246
Diffraction analysis of transient acoustic waves: Half-plane in a layered medium
[PB94-110988] 06 p2526 N94-23726
Recent developments in the mathematical modelling and physical understanding of transport and dispersion in aquatic systems, with special reference to tidal waters
[PB94-111135] 06 p2418 N94-24600
Environmentally assisted cracking of high strength beta titanium alloys
[AD-A273598] 06 p2245 N94-24823
Study on fatigue crack propagation characteristics around welded joint interface in complexed conditions 07 p2730 N94-25584
Conversion of the CLUSE model for applications over open ocean
[AD-A273750] 07 p2893 N94-26013
The biostratigraphy and paleogeography of Maastrichtian inoceramids 07 p2889 N94-28303
Fundamental studies on the corrosion behavior of weldments in marine microbial environments
[AD-A275247] 08 p3203 N94-28900
Oceanic survey utilizing satellites 08 p3328 N94-29040
Tohoku district observed by artificial satellites 08 p3328 N94-29041
The effects of altimeter sampling characteristics: Some Geosat examples
[AD-A275225] 08 p3357 N94-29062
Research report on the potential of ocean development suitable for area characteristics
[JTN-94-80587] 08 p3377 N94-29595
High resolution properties of the marine atmospheric boundary layer
[DE94-006235] 09 p3774 N94-32736
SEASOAR and CTD observations during a COARE surveys cruise, W9211C, 22 January - 22 February, 1993
[AD-A277925] 09 p3791 N94-33244

MARINE MAMMALS

NT DOLPHINS
Sonic booms and marine mammals: Informational status and recommendations 07 p2651 N94-28198

MARINE METEOROLOGY

Development of a buoy system for monitoring marine weather and marine life abundance 01 p0217 N94-12694
Binary homogeneous nucleation: Temperature and relative humidity fluctuations and non-linearity
[DE93-007884] 02 p0709 N94-13911
An investigation of the Ground-Based High-Resolution Interferometer Sounder (GB-HIS) in a costal marine environment
[AD-A268052] 03 p1114 N94-17503
Ship-produced cloud line of 13 July 1991
[DE93-016879] 04 p1472 N94-17986
Rapid oceanic cyclogenesis studies
[AD-A269258] 04 p1490 N94-18265
The activities of equatorial anticyclones of the Western Pacific and the South China Sea and their effects on the tracks of typhoon movement
[AD-A269954] 04 p1492 N94-18675
Work plan for the Marine Aerosol Properties and the Thermal Imager Performance Trial (MAPTIP)
[AD-A270026] 04 p1483 N94-18712
The marine light-mixed layer experiment cruise and data report: R/V endeavor cruise EN-224, mooring deployment, 27 April-1 May 1991: Cruise EN-227, mooring recovery, 5-23 September 1991
[AD-A271175] 05 p1864 N94-20186
Scientific development of a massively parallel ocean climate model
[DE93-019446] 05 p1855 N94-20219
Four-dimensional remote sensing of the marine boundary layer with a digital beamforming radar wind profiler
[AD-A270627] 05 p1882 N94-20564
Low-cost, dual-use platforms for environmental sensing, phase 1
[AD-A272951] 05 p1646 N94-21246
NOVAM evaluation utilizing electro-optics and meteorological data from KEY-90
[AD-A271722] 05 p1868 N94-21356
Acoustic monitoring of global ocean variability
[AD-A271998] 05 p1883 N94-21366
A regional analysis of cloudy mean spherical albedo over the marine stratocumulus region and the tropical Atlantic Ocean
[NASA-CR-194771] 06 p2409 N94-24049
Naval Interactive Data Analysis System (NIDAS), software user's manual
[NASA-CR-195179] 07 p2956 N94-25606
Mesoscale frontal evolution of the ERICA IOP-5A Cyclone
[AD-A274906] 07 p2893 N94-26183
The numerical simulation of marine boundary layer clouds
[AD-A273669] 07 p2894 N94-26195
Propagation of cold air masses in East Asia and its associated planetary-scale function
[AD-A274304] 07 p2895 N94-26850
Studies of marine aerosols and their evolution in the eastern North Atlantic
[AD-A275011] 08 p3377 N94-29128
Hydrographic service Royal Australian Navy
[AD-A277134] 09 p3788 N94-32066
The influence of cumulus parameterization on model forecasts of rapid oceanic cyclogenesis
[AD-A277207] 09 p3784 N94-32094
Typhoon havens handbook for the western Pacific and Indian Oceans, change 3
[AD-A277030] 09 p3784 N94-32260
Evolution of diurnal surface winds and surface currents for Monterey Bay
[AD-A277649] 09 p3790 N94-33057
Comparison of numerical models for computing underwater light fields
[AD-A278256] 10 p4140 N94-33411
Detection and analysis of fog at night using GOES multispectral infrared imagery
[NOAA-TR-NESDIS-75] 10 p4143 N94-34913

Turbulent transfer in the marine planetary boundary layer
[AD-A280549] 12 p4476 N94-37038
The role of horizontal variability in air-sea interaction
[AD-A280561] 12 p4476 N94-37047
Experiment on rapidly intensifying cyclones over the Atlantic
[AD-A280365] 12 p4473 N94-37180

MARINE NAVIGATION
U SURFACE NAVIGATION

MARINE PROPULSION
Icing of turbine intake louvers
[AD-A265714] 01 p0029 N94-12274
Integration of interactive interfaces with intelligent tutoring systems: An implementation
[AD-A273869] 07 p2985 N94-25966
Experimental and computational studies on propeller noise due to inflow distortion 09 p3860 N94-31846

MARINE RESOURCES
Space research and remote sensing programmes in Bangladesh 01 p0035 N94-10679
Biscayne bay: A bibliography of the marine environment
[PB93-184802] 01 p0266 N94-11451
The requirement for global training programmes to meet the new remote sensing technology 01 p0196 N94-11929
Primary productivity in the Oyashio area in the spring and summer of 1990 01 p0211 N94-12658
Characterization of dissolved organic matter in the ocean by using the fluorescence excitation-emission matrix 01 p0211 N94-12659
Development of a buoy system for monitoring marine weather and marine life abundance 01 p0217 N94-12694
Acoustic estimation of plankton biomass 01 p0218 N94-12699
The 1970 highlights --- NASA programs and research
[NASA-TM-109628] 03 p1302 N94-15415
On United States-Japan Conference on Development and Utilization of Natural Resources: Report of the 14th Joint Meeting of U. S. and Japan Marine Mining Panel 08 p3188 N94-28683
Research report on the potential of ocean development suitable for area characteristics
[JTN-94-80587] 08 p3377 N94-29595
Reproduction in the Japanese anchovy (Engraulis japonica) as related to population fluctuation 08 p3235 N94-29708

MARINE TECHNOLOGY
Coastal scour problems and methods for prediction of maximum scour
[AD-A266658] 02 p0726 N94-14775
Abstracts of manuscripts submitted in 1992 for publication
[AD-A267963] 03 p1113 N94-17383
Fatigue technology assessment and strategies for fatigue avoidance in marine structures. Appendices
[AD-A269053] 04 p1455 N94-18716
SIMBAT theoretical manual
[AD-A271063] 05 p1882 N94-19979
Fire safety engineering research in Norway
[PB93-201630] 06 p2268 N94-23429
Fundamental studies on the corrosion behavior of weldments in marine microbial environments
[AD-A275247] 08 p3203 N94-28900
Research report on the potential of ocean development suitable for area characteristics
[JTN-94-80587] 08 p3377 N94-29595
Development of the breakwater with submerged mound for interchanging sea water 08 p3234 N94-29703
Photovoltaic power without batteries for continuous cathodic protection 08 p3341 N94-30465

MARINER PROGRAM
NT MARINER-MERCURY 1973

MARINER SPACE PROBES
NT MARINER 6 SPACE PROBE
NT MARINER 7 SPACE PROBE
NT MARINER 9 SPACE PROBE
NT MARINER 10 SPACE PROBE

MARINER SPACECRAFT
The 1971 highlights --- NASA programs and research
[NASA-TM-109629] 03 p1302 N94-15417
Mars Operational Environmental Satellite (MOES): A post-Mars Observer discovery mission 06 p2620 N94-24890
Wavelength calibration techniques and subtle surface and atmospheric absorption features in the Mariner 6, 7 IRS reflectance data 11 p4356 N94-35405

MARINER 6 SPACE PROBE
Wavelength calibration techniques and subtle surface and atmospheric absorption features in the Mariner 6, 7 IRS reflectance data 11 p4356 N94-35405

MARINER 7 SPACE PROBE
Wavelength calibration techniques and subtle surface and atmospheric absorption features in the Mariner 6, 7 IRS reflectance data 11 p4356 N94-35405

MARINER 9 SPACE PROBE
GMM-1: A 50 degree and order gravitational field model for Mars 05 p2117 N94-20774
Reanalysis of Mariner 9 UV Spectrometer Data for Ozone, Cloud, and Dust Abundances, and Their Interaction Over Climate Timescales
[NASA-CR-195244] 07 p3107 N94-27885
Probing the Martian atmosphere in the ultraviolet 07 p3108 N94-27890
How well was total ozone abundance inferred with Mariner 9? 07 p3108 N94-27891

MARINER 10 SPACE PROBE
Preliminary results from Mariner 10: High resolution images of the Moon 05 p2107 N94-20719

MARINER-MERCURY 1973
The 1973 highlights --- Pioneer and Mariner space probes and other advancements
[NASA-TM-109624] 03 p1302 N94-15410

MARITIME SATELLITES
NT ERS-1 (ESA SATELLITE)
Propagation research in Japan 03 p0996 N94-16043
Evolution of INMARSAT systems and applications: The land mobile experience 06 p2280 N94-22779
INMARSAT's personal communicator system 06 p2282 N94-22788
Low cost coherent demodulation for mobile satellite terminals 06 p2284 N94-22803
Improved frame synchronization schemes for INMARSAT-B/M SCPC and TDM channels 06 p2285 N94-22806
An analysis of cellular telephone and INMARSAT systems for providing radio data link computer communications for US Navy vessels
[AD-A278143] 09 p3684 N94-33160

MARKARIAN GALAXIES
Astrophysics with MILAGRO
[DE93-012722] 03 p1240 N94-17657
Finnish astronomy days, 1992-1993. Proceedings of the Finnish Astronomical Society
[PB94-136892] 08 p3538 N94-29170

MARKERS
Ion beam mixing of marker layers into amorphous aluminum oxide
[DE94-000901] 07 p2752 N94-26676

MARKET RESEARCH
Potential markets for advanced satellite communications
[NASA-CR-191145] 01 p0041 N94-10512
Business fleet refueling assessment
[PB93-189892] 01 p0098 N94-11017
Space Solar Power Program
[DE93-011750] 01 p0055 N94-11675
Photovoltaics: Program overview, fiscal year 1992
[DE93-000055] 02 p0701 N94-12914
The closing window of opportunity: Addressing the US space launch vehicle crisis
[TABES PAPER 93-640] 03 p0878 N94-16148
Status of molten carbonate fuel cell technology development
[DE93-015666] 03 p1092 N94-16715
Satellite communications systems and technology. Executive summary
[NASA-TM-109346] 03 p1006 N94-17661
Directory of Energy Information Administration Models 1993
[DE93-016987] 04 p1616 N94-18707
Wind energy: Program overview, FY 1992
[DE93-000056] 05 p1845 N94-19921
Development of satellite telecommunications during the period 1990 - 2005
[CRANFIELD-AERO-9301] 07 p2765 N94-25639
Powerful selling and sales strategy 07 p2662 N94-28245
Marketing tools for increasing proactivity in technical information centers
[AGARD-AR-326] 08 p3528 N94-30934
Europe at the crossroads: The future of its satellite communications industry
[ESA-SP-1166] 09 p3670 N94-31182
Photovoltaics: Program overview, fiscal year 1993
[DE94-000246] 09 p3758 N94-31235
Current Research Information in Europe: Conference proceedings
[PB94-127933] 09 p3917 N94-31768
Environmental issues related to biomass: An overview
[DE94-007226] 09 p3767 N94-32784
NASA Annual HSR Workshop: Boeing HSCT program summary 10 p3970 N94-33449
Update on Douglas' high-speed civil transport studies 10 p3970 N94-33450
Structural composite construction materials manufactured from municipal solid waste
[AD-A280635] 12 p4403 N94-36730

MARKETING
Powerful selling and sales strategy 07 p2662 N94-28245
Marketing tools for increasing proactivity in technical information centers
[AGARD-AR-326] 08 p3528 N94-30934
World jet airplane inventory at year-end 1993
[PB94-164993] 12 p4384 N94-36530
Opportunities for innovation: Biotechnology
[PB94-157831] 12 p4478 N94-36720

MARKING
NT ISOTOPIC LABELING
A tight lower bound for on-line monotonic list labeling
[TR-478] 04 p1531 N94-19508
Beginning the 21st century with advanced Automatic Parts Identification (API) 09 p3923 N94-32444

MARKOV CHAINS
Parametric analysis of atmospheric processes
[NASA-CR-192523] 01 p0347 N94-10757
Optimal maintenance policies of a Markovian system
[ITN-93-85216] 02 p0774 N94-14502
Nonparametric statistics: Weighted rankings analysis
[AD-A266607] 03 p1173 N94-16657
An approximation for computing reduction in bandwidth requirements using intelligent multiplexers
[AD-A267434] 03 p1001 N94-17026
Bayesian analysis of ARMA processes: Complete sampling based inference under full likelihoods
[AD-A269168] 04 p1557 N94-18694
Adaptive uniformization: Technical details
[PB94-149523] 04 p1558 N94-19265
Tandem queues with deterministic service times
[PB93-197465] 04 p1543 N94-19324
Adaptive uniformization
[MEMO-INF-92-88] 04 p1558 N94-19385
Finding optimal policies for Markov decision chains: A unifying framework for mean-variance-tradeoffs
[PB93-191930] 04 p1559 N94-19555
Production and test of pseudo random elements
[ETN-93-95070] 04 p1559 N94-19610
Some topics in regenerative steady-state simulation
[AD-A271145] 05 p1902 N94-19855
Determination of the optimal stochastic upper bound of a Markovian generator
[RR-906-I] 05 p1963 N94-20202
Specification and generation of Markov reward models
[MEMO-INF-92-60] 05 p1963 N94-21058
Linear programming for standard and nonstandard Markovian control problems. A survey
[PB93-191948] 05 p1963 N94-21066
A multi-level solution algorithm for steady-state Markov chains
[NASA-CR-191558] 05 p1914 N94-21462
Dependability and performability analysis
[NASA-CR-191565] 05 p1965 N94-21463
Algorithms for Markov decision chains with partial information
[PB93-220085] 05 p1918 N94-22098
Resolution of Markov models on distributed memory machines
[ETN-94-95182] 06 p2444 N94-22900
Modeling parallelism and synchronization
[ETN-94-95179] 06 p2465 N94-23134
Control algorithms for effective operation of variable-speed wind turbines
[DE94-002607] 06 p2394 N94-23704
General optimal stopping theorems for semi-Markov processes
[PB93-214989] 06 p2496 N94-24744
On finding optimal policies for Markov decision chains: A unifying framework for mean-variance-tradeoffs
[TW-92-13] 06 p2497 N94-25528
Single-server queues with spatially distributed arrivals
[PB94-126638] 07 p2986 N94-26916
The Communication Link and Error ANalysis (CLEAN) simulator
[NASA-CR-195243] 07 p2968 N94-27168
Markov chains for random urinalysis 3: Daily model and drug kinetics
[AD-A275540] 08 p3389 N94-28797
Dynamical entropy of generalized quantum Markov chains
[PB94-148483] 09 p3850 N94-31590
The Laplace functional and Palm measure of a quasi-Cox process which is driven by a Markov chain
[REPT-93-82] 09 p3851 N94-31699
Undiscounted Markov decision chains with partial information; an algorithm for computing a locally optimal periodic policy
[TW-93-10] 09 p3851 N94-32205
Adaptive control of nonlinear and stochastic systems
[AD-A278411] 09 p3839 N94-33325

MARKOV PROCESSES
NT MARKOV CHAINS
A new HMM learning algorithm for continuous speech recognition
[NHK-SERIAL-413] 01 p0132 N94-10560
Stochastic scheduling games with Markov decision arrival processes
[CWI-BS-R9231] 02 p0773 N94-14005
The effects of internal fluctuations on a class of nonequilibrium statistical field theories
[DE93-016620] 02 p0774 N94-14441
Optimal maintenance policies of a Markovian system
[ITN-93-85216] 02 p0774 N94-14502
Hidden Markov model approach to skill learning and its application to telerobotics
[AD-A266989] 03 p1164 N94-15502
A multilevel-multiresolution method for image processing. A Bayesian framework for reconstructing and representing shapes
[AD-A266772] 03 p1082 N94-15842
Nonparametric statistics: Weighted rankings analysis
[AD-A266607] 03 p1173 N94-16657
Using Markov chains to model the error behavior of data communications channels
[AD-A266468] 03 p0999 N94-16777
Longitudinal beam dynamics with RF noise
[DE93-018649] 04 p1574 N94-18994
Excursion theory of a finite set via resolvents
[REPT-93-19] 04 p1557 N94-19090
Excursions of stochastic processes, Cox-point processes, entrance behavior and resolvents
[PB93-197291] 04 p1558 N94-19323
Compensation approach for three or more dimensional random walks
[PB93-197499] 04 p1543 N94-19326
Sensitivity and uncertainty analysis of Markov reward models
[MEMO-INF-92-89] 04 p1559 N94-19386
Equivalence and reduction of hidden Markov models
[AD-A270762] 04 p1560 N94-19768
The effect of dissipative inhomogeneous medium on the statistics of the wave intensity 05 p1726 N94-20440
A semi-Markov model of a home network access protocol
[MEMO-INF-92-71] 05 p1909 N94-21045
Linear programming for standard and nonstandard Markovian control problems. A survey
[PB93-191948] 05 p1963 N94-21066
N parallel queueing systems with server breakdown and repair
[CWI-BS-R9236] 05 p1944 N94-21232
Throughput and blocking in circuit-switched interconnection networks 05 p1784 N94-22189
Speaker-independent isolated-digit recognition using neural networks and hidden Markov model
05 p1747 N94-22213
Product forms as a solution base for queueing systems
[MEMO-COSOR-92-37] 06 p2477 N94-25526
Application of Markov random field theory to image coding and motion estimation
[ISBN-0-315-83435-8] 07 p2964 N94-26632
Three dimensional object recognition using a complex autoregressive model
[AD-A274388] 07 p2995 N94-26829
Limit theorems for functionals of Markov processes and renormalizable stable fields
[AD-A274645] 07 p3004 N94-27106
White noise theory of robust nonlinear filtering with correlated state and observation noises
[PB94-126661] 07 p3004 N94-27211
Stability of dynamical systems in the presence of noise
[AD-A275383] 08 p3243 N94-29072
U-statistics of random-size samples and limit theorems for systems of Markovian particles with non-Poisson initial distributions
[AD-A275018] 08 p3464 N94-29129
Hierarchical structures and asymmetric stochastic processes on p-adics and adeles
[PB94-138203] 08 p3464 N94-29178
Subphonetic acoustic modeling for speaker-independent continuous speech recognition
[AD-A275217] 08 p3244 N94-29303
ASSIST internals reference manual
[NASA-TM-109102] 08 p3431 N94-29494
Representation, prediction and identification of cyclostationary processes: A state-space approach
[REPT-93-041] 09 p3850 N94-31191
High-performance speech recognition using consistency modeling
[AD-A276775] 09 p3679 N94-32185
Area-interaction point processes
[CWI-BS-R9318] 09 p3847 N94-32197
Robust multisource classification method using the Markov random field methods 09 p3750 N94-32537
Hierarchical modeling for reliability analysis using Markov models
[NASA-CR-188288] 09 p3731 N94-32862
A note on analytic recovery of transition probabilities in three dimensional diffuse tomography
[DE94-011378] 12 p4506 N94-37719
MARS
Significance and scenarios of lunar and planetary exploration missions 01 p0482 N94-12324
Mars exploration missions 01 p0482 N94-12327
Technical problems on lunar an planetary exploration mission 01 p0482 N94-12328
MARS (PLANET)
Evolution of steep Martian slopes
01 p0434 N94-11184
Giant impact-induced atmospheric blow-off
01 p0435 N94-12019
Marslink 01 p0438 N94-12034
Mars: The initial emplacement of ground ice in response to the thermal evolution of its early crust
01 p0462 N94-12168
Small volcanoes in Tempe Terra, Mars: Their detailed morphometry and inferred geologic significance
01 p0469 N94-12202
Shallow crustal discontinuities and graben and scarp formation in the Tharsis region of Mars
01 p0469 N94-12203
Classification of Martian deltas
01 p0470 N94-12207
A comparison of the visible and near infrared reflectance of hydrovolcanic palagonite tuffs and Martian weathered soils 01 p0477 N94-12245
Planetary astronomy of Mars. Mars data reduction
[NASA-CR-193515] 01 p0424 N94-12768
MARS Mission research center
[NASA-CR-194034] 02 p0841 N94-13088
Solar radiation on Mars: Stationary photovoltaic array
[NASA-TM-106321] 02 p0626 N94-14730
Mars laser altimeter based on a single photon ranging technique 03 p0921 N94-15619
Space transfer concepts and analyses for exploration missions, phase 4
[NASA-CR-193849] 03 p0882 N94-15831
A mineralized zone in Western Candor Chasma, Mars
03 p1248 N94-16179
Explosive mafic volcanism on Earth and Mars
03 p1253 N94-16204
A Moessbauer spectrometer for the mineralogical analysis of the Mars surface: First temperature dependent tests of the detector and drive system
03 p1259 N94-16233
Thermal inertia and radar reflectivity of the Martian north polar ERG: Low-density aggregates
03 p1260 N94-16238
Experimental constraints on CO2 and H2O in the Martian mantle and primary magmas 03 p1262 N94-16248
Geomorphic processes in the Argyre-Dorsa Argentea region of Mars 03 p1270 N94-16293
Was Martian mantle wet? A possible consequence of rapid core formation 03 p1277 N94-16335
Space transfer concepts and analyses for exploration missions
[NASA-CR-193876] 04 p1332 N94-18820
Spacework 17: O'Leary's Mars
[NASA-TM-109374] 04 p1629 N94-18966
Constraints on the rate of discharge and duration of the Mangala Valles flood 05 p2099 N94-20674
GMM-1: A 50 degree and order gravitational field model for Mars 05 p2117 N94-20774
Expectations for the Martian core magnetic field
05 p2120 N94-20792
Workshop on Early Mars: How Warm and How Wet?, part 1
[NASA-CR-193553] 05 p2142 N94-21659
Ancient Martian valley genesis and paleoclimatic inference: The present as a key to the past
05 p2142 N94-21661
Mars: Noachian hydrology by its statistics and topology 05 p2143 N94-21664
The hydrologic response of Mars to the onset of a colder climate and to the thermal evolution of its early crust
05 p2143 N94-21666
An attempt to comprehend Martian weathering conditions through the analysis of terrestrial palagonite samples 05 p2143 N94-21668
Briny lakes on early Mars? Terrestrial intracrater playas and Martian candidates 05 p2145 N94-21675
Early Mars was wet but not warm: Erosion, fluvial features, liquid water habitats, and life below freezing
05 p2145 N94-21677
Wet inside and out? Constraints on water in the Martian mantle and on outgassed water, based on melt inclusions in SNC meteorites 05 p2145 N94-21678
An improved gravity model for Mars: Goddard Mars Model-1 (GMM-1)
[NASA-TM-104584] 06 p2401 N94-23282
Robotic exploration of Moon and Mars
06 p2606 N94-23379
Science strategy for Mars exploration
06 p2606 N94-23380
Mars 96 small rover: Mission strategy
06 p2606 N94-23381
A reference Martian mission for a long range rover
06 p2606 N94-23382
Science objectives for short-range rovers on Mars
06 p2606 N94-23383
Prospects for using mobile vehicles in missions to Mars and other planets 06 p2607 N94-23384
The robotic Mars rover 06 p2608 N94-23390
Mission and system concepts for Mars robotic precursor missions 06 p2608 N94-23391
Mission and system design of a long range rover mission 06 p2608 N94-23392
Mars subsurface sounding with a ground penetrating radar 06 p2608 N94-23393
Balloon experiments at Mars 96 project
06 p2608 N94-23396
Rover: Autonomous concepts for Mars exploration
06 p2369 N94-23400
Mechanical design of a planetary rover
06 p2369 N94-23403
Dual rover concept for Mars exploration
06 p2370 N94-23415
Mars 96 rover: Technical vision and navigation
06 p2370 N94-23417
Marsohkod movement control
06 p2370 N94-23418
The influence of orography on the transport of atmospheric constituents 06 p2619 N94-24886
Retrieval of temperature profiles from Martian infrared spectra 06 p2620 N94-24893
Three-dimensional numerical simulation of near-surface flows over the Martian north polar cap
06 p2621 N94-24895
Project APEX: Advanced manned exploration of the Martian moon Phobos 07 p3079 N94-25688
Mars transportation system 07 p2833 N94-25689
Telepresence in the human exploration of Mars: Field studies in analog environments
07 p2685 N94-27360
Reanalysis of Mariner 9 UV Spectrometer Data for Ozone, Cloud, and Dust Abundances, and Their Interaction Over Climate Timescales
[NASA-CR-195244] 07 p3107 N94-27885
MUADEE: Mars Upper Atmosphere Dynamics, Energetics, and Evolution discovery mission. Executive summary volume
[NASA-CR-195732] 08 p3549 N94-28418
BAG: A code for predicting the performance of a gas bag impact attenuation system for the Pathfinder lander
[DE94-003688] 08 p3165 N94-28477
Origin and thermal evolution of Mars
09 p3940 N94-31109
Mars: Five views on what is known
[NASA-TM-109751] 09 p3942 N94-31805
Marsville: The cosmic village
[NASA-TM-109752] 09 p3913 N94-31806
Mars: Past, Present, and Future. Results from the MSATT Program, part 1
[NASA-CR-194279] 09 p3943 N94-33190
Depth-diameter ratios for Martian impact craters: Implications for target properties and episodes of degradation 09 p3943 N94-33191
Constraints on the Martian cratering rate imposed by the SNC meteorites and Vallis Marineris layered deposits 09 p3945 N94-33197
MARSNET: A European network of stations on the surface of Mars 09 p3945 N94-33199
Possible test of ancient dense Martian atmosphere
09 p3947 N94-33206
SNC meteorites and their implications for reservoirs of Martian volatiles 09 p3947 N94-33209
The Northern Plains MSATT Meeting, and a call for a field-oriented successor to MSATT
09 p3947 N94-33210
The effect of polar caps on obliquity
09 p3948 N94-33213
Might it be possible to predict the onset of major Martian dust storms? 09 p3948 N94-33215
The distribution of Martian ground ice at other epochs
09 p3948 N94-33218
Polar sediment accumulation: Role of surface winds at the two poles 09 p3951 N94-33233
The Martian sources of the SNC meteorites (two, not one), and what can and can't be learned from the SNC meteorites 09 p3951 N94-33234
Planetary protection issues and future Mars missions
[NASA-CP-10086] 10 p4164 N94-33533
Vehicle development of Lunar/Mars exploration
10 p4067 N94-34030

High degree gravitational sensitivity from Mars orbiters for the GMM-1 gravity model
[NASA-TM-104604] 10 p4088 N94-34992
An automatic planetary vehicle for exploring Mars
11 p4354 N94-35336
High resolution visible to short-wave near-infrared CCD spectra of Mars during 1990 11 p4356 N94-35403
Absolute calibration and atmospheric versus mineralogic origin of absorption features in 2.0 to 2.5 micron Mars spectra obtained during 1993 11 p4356 N94-35404
Wavelength calibration techniques and subtle surface and atmospheric absorption features in the Mariner 6, 7 IRS reflectance data 11 p4356 N94-35405
Fluvial processes in Ma'adim Vallis and the potential of Gusev crater as a high priority site
11 p4358 N94-35414
The mass of Mars, Phobos, and Deimos, from the analysis of the Mariner 9 and Viking Orbiter tracking data 11 p4364 N94-35461
The real-time display of interferometry data for Goldstone radar astronomy data acquisition
11 p4255 N94-35560
Progress in the development of the GMM-2 gravity field model for Mars 11 p4371 N94-36155

MARS ATMOSPHERE
Marslink 01 p0438 N94-12034
Behavior of vortices generated by an advancing ejecta curtain in theory, in the laboratory, and on Mars
01 p0169 N94-12044
An observational search for CO2 ice clouds on Mars
01 p0441 N94-12054
The effects of atmospheric pressure on infrared reflectance spectra of Martian analogs
01 p0445 N94-12071
Near-infrared spectra of the Martian surface: Reading between the lines 01 p0465 N94-12184
Dust in the Martian atmosphere: Polarimetric sensing
01 p0473 N94-12223
Noble gas evidence of an aqueous reservoir near the surface of Mars more recently than 1.3 Ga
01 p0473 N94-12228
Composition of the Martian aerosols through near-IR spectroscopy 01 p0475 N94-12235
Organic matter on the early surface of Mars: An assessment of the contribution by interplanetary dust
01 p0480 N94-12259
Optical properties of CO2 ice and CO2 snow in the ultraviolet, visible, and infrared
[NASA-CR-194110] 02 p0686 N94-14081
Mars laser altimeter based on a single photon ranging technique 03 p0921 N94-15619
Nitrates in SNCs: Implications for the nitrogen cycle on Mars 03 p1251 N94-16193
Sand transport on Mars: Preliminary results from models 03 p1252 N94-16198
Martian carbon dioxide: Clues from isotopes in SNC meteorites 03 p1270 N94-16295
Altitude profile of aerosols on Mars from measurements of its thermal radiation on limb 03 p1294 N94-16423
Dust-dynamic feedbacks in the Martian atmosphere: Surface dust lifting 03 p1296 N94-16434
Balloon exploration of the northern plains of Mars near and north of the Viking 2 landing site
05 p2092 N94-20401
Workshop on Early Mars: How Warm and How Wet?, part 1
[NASA-CR-193553] 05 p2142 N94-21659
A carbon dioxide/methane greenhouse atmosphere on early Mars 05 p2142 N94-21662
The early Martian environment: Clues from the cratered highlands and the Precambrian Earth
05 p2143 N94-21667
Requirements for the early atmosphere of Mars from nitrogen isotope ratios 05 p2144 N94-21669
A model for the evolution of CO2 on Mars
05 p2144 N94-21671
Mars atmosphere loss and isotopic fractionation by solar-wind-induced sputtering and photochemical escape
05 p2144 N94-21672
Possible solutions to the problem of channel formation on early Mars 05 p2144 N94-21673
Early Mars was wet but not warm: Erosion, fluvial features, liquid water habitats, and life below freezing
05 p2145 N94-21677
The young Sun and photochemistry of the primitive Martian atmosphere 05 p2145 N94-21679
Evolution of the Martian atmosphere
05 p2146 N94-21680
MSATT Workshop on Innovative Instrumentation for the In Situ Study of Atmosphere-Surface Interactions on Mars
[NASA-CR-194584] 05 p1811 N94-22430
Determination of Martian soil mineralogy and water content using the Thermal Analyzer for Planetary Soils (TAPS) 05 p1812 N94-22433
Temperature/pressure and water vapor sounding with microwave spectroscopy 05 p1812 N94-22436
Workshop on Atmospheric Transport on Mars
[NASA-CR-194855] 06 p2616 N94-24871
The NASA/GISS Mars general circulation model: Preliminary experiments 06 p2616 N94-24872
Optimal gains for a single polar orbiting satellite
06 p2208 N94-24873
A diagnostic model to estimate winds and small-scale drag from Mars Observer PMIRR data
06 p2617 N94-24874
Eddy mixing coefficient values derived from simulations with the NASA Ames Mars GCM
06 p2617 N94-24875
Mars dust-driven tides and their impact on the thermosphere 06 p2617 N94-24876
Cloud, dust, and ozone vertical profiles from solar occultation measurements: Implications for dynamics
06 p2617 N94-24877
Particle sizes and composition of Mars atmospheric dust based upon Viking and Mariner 9 observations
06 p2618 N94-24878
Aspects of the Martian global circulation
06 p2618 N94-24879
Impact of the CO2 and H2O clouds of the Martian polar hood on the polar energy balance
06 p2618 N94-24880
Multiannual simulations with the Mars climate model
06 p2618 N94-24881
Regarding tracer transport in Mars' winter atmosphere in the presence of nearly stationary, forced planetary waves 06 p2618 N94-24882
Analyzing Martian winds and tracer concentrations using Mars Observer data 06 p2619 N94-24883
The annual pressure cycle on Mars: Results from the LMD Martian atmospheric general circulation model
06 p2619 N94-24884
Northern hemisphere dust storms on Mars
06 p2619 N94-24885
Dynamics of the atmosphere of Mars: Review of some outstanding problems 06 p2620 N94-24888
Modeling and data assimilation for Mars Observer
06 p2620 N94-24889
Mars Operational Environmental Satellite (MOES): A post-Mars Observer discovery mission
06 p2620 N94-24890
A study of cloud motions on Mars. 2: Some examples of observations and analyses since 1969
06 p2620 N94-24891
Evidence for dust transport in Viking IR thermal mapper opacity data 06 p2620 N94-24892
Retrieval of temperature profiles from Martian infrared spectra 06 p2620 N94-24893
Dust transport in the Martian atmosphere
06 p2621 N94-24894
The role of atmospheric heat transport in the seasonal carbon dioxide cycle 06 p2621 N94-24896
Eddy mixing coefficient upper limit derived from the photochemical balance of O2 06 p2621 N94-24897
Diagnostic calculations of the circulation in the Martian atmosphere 06 p2622 N94-24898
Martian mesoscale circulations induced by variations in surface optical and thermal characteristics: A numerical study 06 p2622 N94-24899
Two-dimensional modeling of thermal inversion layers in the middle atmosphere of Mars
06 p2622 N94-24900
Three-dimensional numerical simulation of thermal tides in the Martian atmosphere 06 p2622 N94-24901
Vertical transport of water in the Martian boundary layer 06 p2622 N94-24902
The Mars Aerial Platform (MAP) mission
06 p2622 N94-24903
Mars Observer: Applications to atmospheric transport
06 p2623 N94-24904
Extraterrestrial surface propulsion systems
07 p2833 N94-25691
Reanalysis of Mariner 9 UV Spectrometer Data for Ozone, Cloud, and Dust Abundances, and Their Interaction Over Climate Timescales
[NASA-CR-195244] 07 p3107 N94-27885
Cooling the Martian atmosphere: The spectral overlap of the C02 15 micrometers band and dust
07 p3107 N94-27886
Martian atmospheric radiation budget
07 p3107 N94-27887
Mars ozone: Mariner 9 revisited
07 p3107 N94-27888
Why is the north polar cap on Mars different than the south polar cap? 07 p3107 N94-27889
Probing the Martian atmosphere in the ultraviolet
07 p3108 N94-27890
How well was total ozone abundance inferred with Mariner 9? 07 p3108 N94-27891
In situ Mars ozone detector 07 p3108 N94-27892
The Martian atmospheric planetary boundary layer stability, fluxes, spectra, and similarity
[NASA-CR-195711] 07 p3108 N94-27935
MUADEE: Mars Upper Atmosphere Dynamics, Energetics, and Evolution discovery mission. Executive summary volume
[NASA-CR-195732] 08 p3549 N94-28418
The 1992-1993 advanced design program. Part 1: The Mars methane engine project. Part 2: The Mars oxygen processor new furnace
[NASA-CR-195513] 08 p3299 N94-29409
The viability of photovoltaics on the Martian surface
[NASA-TM-106478] 08 p3338 N94-30196
Mars: Past, Present, and Future. Results from the MSATT Program, part 1
[NASA-CR-194279] 09 p3943 N94-33190
Stationary eddies in the Mars general circulation as simulated by the NASA-Ames GCM
09 p3944 N94-33192
Deposition rates of oxidized iron on Mars
09 p3945 N94-33198
Mars atmospheric dust properties: A synthesis of Mariner 9, Viking, and Phobos observations
09 p3945 N94-33200
Magmatic volatiles and the weathering of Mars
09 p3946 N94-33201
Aerosols scattering and near-infrared observations of the Martian surface 09 p3946 N94-33204
A model for the evolution of CO2 on Mars
09 p3946 N94-33205
Possible test of ancient dense Martian atmosphere
09 p3947 N94-33206
Groundbased monitoring of Martian atmospheric opacity 09 p3947 N94-33207
Mars atmospheric loss and isotopic fractionation by solar-wind-induced sputtering and photochemical escape
09 p3947 N94-33208
SNC meteorites and their implications for reservoirs of Martian volatiles 09 p3947 N94-33209
How well was total ozone abundance inferred with Mariner 9 09 p3947 N94-33212
Escape of Mars atmospheric carbon through time by photochemical means 09 p3948 N94-33214
Studies of atmospheric dust from Viking IR thermal mapper data 09 p3948 N94-33216
Eddy transport of water vapor in the Martian atmosphere 09 p3949 N94-33221
Numerical simulation of thermally induced near-surface flows over Martian terrain 09 p3949 N94-33223
The wavelength dependence of Martian atmospheric dust radiative properties 09 p3950 N94-33228
Carbonate formation on Mars: Latest experiments
09 p3950 N94-33231
Carbonates, surfates, phosphates, nitrates, and organic materials: Their association in a Martian meteorite
09 p3952 N94-33239
Simultaneous laboratory measurements of CO2 and H2O adsorption on palagonite: Implications for the Martian climate and volatile reservoir 09 p3952 N94-33240
Windblown sand on Mars: The effect of saltation threshold on drift potentials derived from Mars GCM
11 p4366 N94-35474
Simultaneous adsorption of CO2 and H2O under Mars-like conditions and application to the evolution of the Martian climate 11 p4366 N94-35475
Atmospheric effects on the mapping of Martian thermal inertia and thermally derived albedo
11 p4368 N94-36137
Mars atmospheric escape and isotopic fractionation: Synthesis of data and models 11 p4369 N94-36143
Uniqueness of a solution of a steady state photochemical problem: Applications to Mars 11 p4370 N94-36151
First measurement of helium on Mars: Implications for the problem of radiogenic gases on the terrestrial planets 11 p4370 N94-36153
Mars vertical axis wind machines. The design of a Darreus and a Giromill for use on Mars
[NASA-CR-196143] 12 p4462 N94-36807
Mars vertical axis wind machines: The design of a tornado vortex machine for use on Mars
[NASA-CR-196144] 12 p4462 N94-36823
An investigation of solar wind effects on the evolution of the Martian atmosphere
[NASA-CR-193424] 12 p4549 N94-37012

MARS CRATERS
Increased depth-diameter ratios in the Medusae Fossae Formation deposits of Mars 01 p0439 N94-12043
Behavior of vortices generated by an advancing ejecta curtain in theory, in the laboratory, and on Mars
01 p0169 N94-12044
Modern shelf ice, equatorial Aeolis Quadrangle, Mars
01 p0450 N94-12100
Fractal dimensions of rampart impact craters on Mars
01 p0460 N94-12154

Martian crater degradation by eolian processes: Analogy with the Rio Cuarto Crater Field, Argentina
03 p1251 N94-16196
The seismic response of an aquifer to the propagation of an impact generated shock wave: A possible trigger of the Martian outflow channels?
03 p1281 N94-16354
Morphologic and morphometric studies of impact craters in the northern plains of Mars 05 p2089 N94-20384
Evidence for an ice sheet/frozen lake in Utopia Planitia, Mars 05 p2089 N94-20388
Ice in the northern plains: Relic of a frozen ocean?
05 p2090 N94-20391
A model for the origin of Martian polygonal terrain
05 p2090 N94-20393
Determination of cosmic bodies size-velocity distribution by observation of current impacts on Mars
05 p2082 N94-20648
Arcuate and circular structures in the Tharsis region: Evidence of coronae on Mars 05 p2134 N94-20863
Early Mars: A regional assessment of denudation chronology 05 p2145 N94-21676
Depth-diameter ratios for Martian impact craters: Implications for target properties and episodes of degradation 09 p3943 N94-33191
Constraints on the Martian cratering rate imposed by the SNC meteorites and Vallis Marineris layered deposits 09 p3945 N94-33197
Regional sedimentological variations among dark crater floor features: Toward a model for modern eolian sand distribution on Mars 09 p3946 N94-33203
Possible test of ancient dense Martian atmosphere
09 p3947 N94-33206
Fluvial processes in Ma'adim Vallis and the potential of Gusev crater as a high priority site
11 p4358 N94-35414
Impact basins in Southern Daedalia, Mars: Evidence for clustered impactors? 11 p4360 N94-35426
Effects due to overlapping large impact basins on Mars 11 p4360 N94-35427
Noachian and Hesperian modification of the original Chryse impact basin topography
11 p4364 N94-35462

MARS ENVIRONMENT

NT MARS ATMOSPHERE
Dust in the Martian atmosphere: Polarimetric sensing
01 p0473 N94-12223
Mars look-alike
[NASA-TM-109667] 03 p1094 N94-15238
Sand transport on Mars: Preliminary results from models 03 p1252 N94-16198
International testing of a Mars rover prototype
03 p1273 N94-16312
Workshop on early Mars: How warm and how wet, part 2?
[NASA-CR-193503] 03 p1297 N94-17637
The fate of water deposited in the low-lying northern plains 05 p2089 N94-20387
K, U, and Th behavior in Martian environmental conditions 05 p2141 N94-20908
Workshop on Early Mars: How Warm and How Wet?, part 1
[NASA-CR-193553] 05 p2142 N94-21659
Mars: Noachian hydrology by its statistics and topology 05 p2143 N94-21664
The evolution of the early Martian climate and the initial emplacement of crustal H2O 05 p2143 N94-21665
The hydrologic response of Mars to the onset of a colder climate and to the thermal evolution of its early crust
05 p2143 N94-21666
The early Martian environment: Clues from the cratered highlands and the Precambrian Earth
05 p2143 N94-21667
Fluvial valleys in the heavily cratered terrains of Mars: Evidence for paleoclimatic change?
05 p2144 N94-21670
Possible solutions to the problem of channel formation on early Mars 05 p2144 N94-21673
Mars and the early Sun 05 p2146 N94-21683
Particle sizes and composition of Mars atmospheric dust based upon Viking and Mariner 9 observations
06 p2618 N94-24878
Multiannual simulations with the Mars climate model
06 p2618 N94-24881
Northern hemisphere dust storms on Mars
06 p2619 N94-24885
Mars Operational Environmental Satellite (MOES): A post-Mars Observer discovery mission
06 p2620 N94-24890
First lunar outpost 07 p2943 N94-25694
Why is the north polar cap on Mars different than the south polar cap? 07 p3107 N94-27889
The viability of photovoltaics on the Martian surface
[NASA-TM-106478] 08 p3338 N94-30196
Fiber optic chemical sensors on Mars
[DE94-005251] 09 p3941 N94-31145
The importance of environmental conditions in reflectance spectroscopy of laboratory analogs for Mars surface materials 09 p3944 N94-33195
The effect of polar caps on obliquity
09 p3948 N94-33213
Might it be possible to predict the onset of major Martian dust storms? 09 p3948 N94-33215
Controls on the CO2 seasonal cycle
09 p3950 N94-33227
Obliquity variation in a Mars climate evolution model
09 p3951 N94-33236
The influence of thermal inertia on Mars' seasonal pressure variation and the effect of the weather component 09 p3952 N94-33238
Planetary protection issues and future Mars missions
[NASA-CP-10086] 10 p4164 N94-33533
Exopaleontology and the search for a fossil record on Mars 11 p4360 N94-35425
Simultaneous adsorption of CO2 and H2O under Mars-like conditions and application to the evolution of the Martian climate 11 p4366 N94-35475
Operational environments for electrical power wiring on NASA space systems
[NASA-TM-106655] 12 p4398 N94-36951
Receiver design, performance analysis, and evaluation for space-borne laser altimeters and space-to-space laser ranging systems
[NASA-CR-194747] 12 p4397 N94-36988

MARS EXPLORATION

Mars exploration missions 01 p0482 N94-12327
Mars exploration study workshop 2
[NASA-CP-3243] 05 p2146 N94-21883
Science strategy for Mars exploration
06 p2606 N94-23380
Rover: Autonomous concepts for Mars exploration
06 p2369 N94-23400
Development/drilling test of auger boring machine on board Mars rover for Mars exploration
06 p2369 N94-23402
Dual rover concept for Mars exploration
06 p2370 N94-23415
Vehicle development of Lunar/Mars exploration
10 p4067 N94-34030

MARS GEOSCIENCE CLIMATOLOGY ORBITER

U MARS OBSERVER

MARS LANDING

Planetary protection implementation on future Mars lander missions
[NASA-CP-3216] 02 p0841 N94-13183
First US Mars landing
[NASA-TM-109669] 03 p0885 N94-15436
Mars exobiology landing sites for future exploration
03 p1278 N94-16339
Mars exploration study workshop 2
[NASA-CP-3243] 05 p2146 N94-21883
Descent and landing phase: Vision based robust spacecraft motion estimation and elevation modeling
06 p2608 N94-23394
Rover in the Mars 96 mission
06 p2609 N94-23397
Battery study for the Mars Environmental Survey (MESUR) Pathfinder 07 p2860 N94-28105
BAG: A code for predicting the performance of a gas bag impact attenuation system for the Pathfinder lander
[DE94-003688] 08 p3165 N94-28477
Autonomous hazard detection and avoidance
[NASA-CR-188331] 11 p4309 N94-36439

MARS OBSERVER

A simple model of clastic sediments on Mars
01 p0460 N94-12155
Development of the Mars Observer Laser Altimeter (MOLA) 03 p0921 N94-15617
Bench checkout equipment for spaceborne laser altimeter systems 03 p0921 N94-15618
The thumbprint terrain: What will Mars Observer tell us? 05 p2091 N94-20397
Distributed science operations for JPL planetary missions 06 p2500 N94-23850
The Mars mapper science and mission planning tool
06 p2503 N94-23867
An approach to the design of operations systems
06 p2506 N94-23884
Mars Observer screen display design for a multimission environment 06 p2197 N94-23888
Mars Observer data production, transfer, and archival: The data production assembly line
06 p2518 N94-23953
Modeling and data assimilation for Mars Observer
06 p2620 N94-24889
Mars Operational Environmental Satellite (MOES): A post-Mars Observer discovery mission
06 p2620 N94-24890
Mars Observer: Applications to atmospheric transport
06 p2623 N94-24904
Optical Chopper Assembly for the Mars Observer
08 p3162 N94-29639
The Mars Observer differential one-way range demonstration 11 p4210 N94-35543
The Mars Observer Ka-band link experiment
11 p4255 N94-35563

MARS PHOTOGRAPHS

Geologic history of central Chryse Planitia and the Viking 1 landing site, Mars 01 p0465 N94-12180
Rover imaging system for the Mars rover/sample return mission
[NASA-CR-193413] 02 p0649 N94-13464
Geomorphic evidence for an eolian contribution to the formation of the Martian northern plains
05 p2092 N94-20402
Regional sedimentological variations among dark crater floor features: Toward a model for modern eolian sand distribution on Mars 09 p3946 N94-33203
Subpixel resolution from multiple images
11 p4281 N94-35417

MARS PROBES

NT MARINER 6 SPACE PROBE
NT MARINER 7 SPACE PROBE
NT MARINER 9 SPACE PROBE
NT MARS OBSERVER
NT MARS 4 SPACECRAFT
NT VIKING LANDER SPACECRAFT
NT VIKING SPACECRAFT
A comparison of telescopic and Phobos-2 ISM spectra of Mars in the short-wave near-infrared (0.76-1.02 microns) 01 p0424 N94-12053
Conceptual studies report on lunar and planetary exploration
[NASDA-TK-SS0438] 01 p0481 N94-12323
Mars exploration missions 01 p0482 N94-12327
Exploring Mars
[NASA-TM-109306] 02 p0842 N94-13613
Mars Analog Site Study (MASS)
03 p1252 N94-16200
Mars 1994/1996: The French navigation tasks
06 p2195 N94-23924
Parachute Swivel Mechanism for planetary entry
08 p3162 N94-29643
Mars: Five views on what is known
[NASA-TM-109751] 09 p3942 N94-31805
Receiver design, performance analysis, and evaluation for space-borne laser altimeters and space-to-space laser ranging systems
[NASA-CR-194747] 12 p4397 N94-36988
Baseline antenna design for space exploration initiative
[NASA-CR-196298] 12 p4435 N94-37255

MARS ROVER SAMPLE RETURN MISSION

U MARS SAMPLE RETURN MISSIONS

MARS SAMPLE RETURN MISSIONS

Mars rover sample return mission
[NASA-TM-109521] 03 p0873 N94-15471
Science strategy for Mars exploration
06 p2606 N94-23380
Operations concepts for Mars missions with multiple mobile spacecraft 06 p2501 N94-23852

MARS SATELLITES

NT DEIMOS
NT PHOBOS

MARS SURFACE

Twenty-fourth Lunar and Planetary Science Conference. Part 1: A-F
[NASA-CR-193095] 01 p0435 N94-12015
Rates of fluvio-thermal erosion on Mars
01 p0435 N94-12018
Lineament analysis and tectonic interpretation for the Tharsis region 01 p0437 N94-12031
Increased depth-diameter ratios in the Medusae Fossae Formation deposits of Mars 01 p0439 N94-12043
Behavior of vortices generated by an advancing ejecta curtain in theory, in the laboratory, and on Mars
01 p0169 N94-12044
A comparison of telescopic and Phobos-2 ISM spectra of Mars in the short-wave near-infrared (0.76-1.02 microns) 01 p0424 N94-12053
Changes in Hawaiian palagonite FE mineralogy associated with thermal alteration: Implications for Mars
01 p0281 N94-12055
Thermal studies of Martian channels and valleys using Termoskan data 01 p0443 N94-12064
Spectral analysis of the gravity and topography of Mars 01 p0444 N94-12065
Reflectance spectra of sulfate-and carbonate-bearing Fe(3+)-doped montmorillonites as Mars soil analogs
01 p0445 N94-12070
The effects of atmospheric pressure on infrared reflectance spectra of Martian analogs
01 p0445 N94-12071
Using high spectral resolution spectrophotometry to study broad mineral absorption features on Mars
01 p0446 N94-12077
Modern shelf ice, equatorial Aeolis Quadrangle, Mars
01 p0450 N94-12100

Martian particle size based on thermal inertia corrected for elevation-dependent atmospheric properties
01 p0430 N94-12107
Chemical weathering on Mars: Rate of oxidation of iron dissolved in brines 01 p0455 N94-12128
An ancient inner lake in Maadim Vallis
01 p0456 N94-12133
Spatial variation in the seasonal south polar cap of Mars as observed by Mariner 7 01 p0456 N94-12134
Fault geometries and extension in the Valles Marineris, Mars 01 p0458 N94-12144
Basal scarp, paleoglacier, and fissure flows of Elysium Mons, Mars 01 p0459 N94-12148
Fractal dimensions of rampart impact craters on Mars
01 p0460 N94-12154
A simple model of clastic sediments on Mars
01 p0460 N94-12155
Mars: The initial emplacement of ground ice in response to the thermal evolution of its early crust
01 p0462 N94-12168
The role of the geothermal gradient in the emplacement and replenishment of ground ice on Mars
01 p0463 N94-12169
The thermodynamic case for a water-rich Mars
01 p0463 N94-12170
Geologic history of central Chryse Planitia and the Viking 1 landing site, Mars 01 p0465 N94-12180
Near-infrared spectra of the Martian surface: Reading between the lines 01 p0465 N94-12184
Comparison of the distribution of large magmatic centers on Earth, Venus, and Mars 01 p0467 N94-12192
Small volcanoes in Tempe Terra, Mars: Their detailed morphometry and inferred geologic significance
01 p0469 N94-12202
Shallow crustal discontinuities and graben and scarp formation in the Tharsis region of Mars
01 p0469 N94-12203
Classification of Martian deltas
01 p0470 N94-12207
Relation between ages and elevations of Martian channels 01 p0472 N94-12216
Noble gas evidence of an aqueous reservoir near the surface of Mars more recently than 1.3 Ga
01 p0473 N94-12228
Automatic definition of spectral units in the equatorial regions of Mars 01 p0432 N94-12234
Moessbauer spectrometer for mineralogical analysis of the Mars surface: Moessbauer source considerations
01 p0476 N94-12242
A comparison of the visible and near infrared reflectance of hydrovolcanic palagonite tuffs and Martian weathered soils 01 p0477 N94-12245
Organic matter on the early surface of Mars: An assessment of the contribution by interplanetary dust
01 p0480 N94-12259
Primitive SNC parent magmas and crystallization: Low PH2O experiments 01 p0433 N94-12264
Do large impact basins in the southern hemisphere of Mars control the distribution of polar structures and deposits? 01 p0481 N94-12266
Free-air and Bouguer gravity anomalies and the Martian crustal dichotomy 01 p0481 N94-12267
New Mars free-air and Bouguer gravity: Correlation with topography, geology and large impact basins
01 p0481 N94-12268
Interdisciplinary scientist participation in the Phobos mission
[NASA-CR-193715] 01 p0482 N94-12446
Planetary astronomy of Mars. Mars data reduction
[NASA-CR-193515] 01 p0424 N94-12768
The nature and origin of periodically spaced tectonic features on Mars
[NASA-CR-193821] 02 p0842 N94-13199
Martian sedimentary deposits
[NASA-CR-193266] 02 p0842 N94-13855
A widget based operations simulator for a planetary camera: A model for the high resolution stereo camera on Mars 94
[DLR-FB-92-30] 02 p0651 N94-14044
Optical properties of CO2 ice and CO2 snow in the ultraviolet, visible, and infrared
[NASA-CR-194110] 02 p0686 N94-14081
A mineralized zone in Western Candor Chasma, Mars
03 p1248 N94-16179
Nitrates in SNCs: Implications for the nitrogen cycle on Mars 03 p1251 N94-16193
Martian crater degradation by eolian processes: Analogy with the Rio Cuarto Crater Field, Argentina
03 p1251 N94-16196
Rover mounted ground penetrating radar as a tool for investigating the near-surface of Mars and beyong
03 p1007 N94-16197
Sand transport on Mars: Preliminary results from models 03 p1252 N94-16198
Explosive mafic volcanism on Earth and Mars
03 p1253 N94-16204
Fluvial erosion on Mars: Implications for paleoclimatic change 03 p1241 N94-16210
Modeling the reflectance of CO2 frost with new optical constants: Application to Martian south polar cap spectra 03 p1256 N94-16217
Confirmation of saturation equilibrium conditions in crater populations 03 p1103 N94-16222
A Moessbauer spectrometer for the mineralogical analysis of the Mars surface: First temperature dependent tests of the detector and drive system
03 p1259 N94-16233
Thermal inertia and radar reflectivity of the Martian north polar ERG: Low-density aggregates
03 p1260 N94-16238
Geomorphic processes in the Argyre-Dorsa Argentea region of Mars 03 p1270 N94-16293
Martian carbon dioxide: Clues from isotopes in SNC meteorites 03 p1270 N94-16295
Was Martian mantle wet? A possible consequence of rapid core formation 03 p1277 N94-16335
Hellas basin, Mars: Formation by oblique impact
03 p1280 N94-16350
The seismic response of an aquifer to the propagation of an impact generated shock wave: A possible trigger of the Martian outflow channels?
03 p1281 N94-16354
Sedimentation, volcanism, and ancestral lakes in the Valles Marineris: Clues from topography
03 p1283 N94-16369
Suggestion for extended Viking magnetic properties experiment on future Mars missions
03 p1285 N94-16375
The dregs of crystallization in Zagami
03 p1245 N94-16390
Global and regional/seasonal color mosaics of Mars
03 p1288 N94-16393
The effects of orbital and climatic variations on Martian surface heat flow 03 p1290 N94-16402
Equatorial ground ice on Mars: Steady-state stability
03 p1290 N94-16403
Deucalionis Regio, Mars: Evidence for a unique mineralogic endmember and a crusted surface
03 p1291 N94-16406
Analysis of pyroxene absorptions observed in Martian dark regions 03 p1292 N94-16411
Mars brine formation experiment
03 p1293 N94-16419
Terrestrial impact melts as analogues for the hematization of Martian surface materials
03 p1104 N94-16424
The influence of oceans on Martian volcanism
03 p1295 N94-16427
Bright soil units on Mars determined from ISM imaging spectrometer data 03 p1295 N94-16430
Variations in the Fe mineralogy of bright Martian soil
03 p1295 N94-16431
Dust-dynamic feedbacks in the Martian atmosphere: Surface dust lifting 03 p1296 N94-16434
Composition of weakly altered Martian crust
03 p1296 N94-16436
Working group for planetary system nomenclature
[NASA-CR-194406] 04 p1626 N94-18841
JPRS report: Science and technology. Central Eurasia: Space
[JPRS-USP-93-004] 04 p1323 N94-19146
Workshop on the Martian Northern Plains: Sedimentological, Periglacial, and Paleoclimatic Evolution
[NASA-CR-194831] 05 p2088 N94-20382
Hydrological consequences of ponded water on Mars
05 p2089 N94-20383
Morphologic and morphometric studies of impact craters in the northern plains of Mars 05 p2089 N94-20384
Evidence for an ice sheet/frozen lake in Utopia Planitia, Mars 05 p2089 N94-20388
A wet-geology and cold-climate Mars model: Punctuation of a slow dynamic approach to equilibrium
05 p2090 N94-20389
Possible occurrence and origin of massive ice in Utopia Planitia 05 p2090 N94-20390
Ice in the northern plains: Relic of a frozen ocean?
05 p2090 N94-20391
Observed climatic activity pertaining to the evolution of the northern plains 05 p2090 N94-20392
A model for the origin of Martian polygonal terrain
05 p2090 N94-20393
The distribution of ground ice on Mars
05 p2090 N94-20394
A marine sedimentary model for the evolution of the northern plains 05 p2091 N94-20395
The thumbprint terrain: What will Mars Observer tell us? 05 p2091 N94-20397
Stratigraphy of the Martian northern plains
05 p2091 N94-20398
Seismic-triggering history of the catastrophic outflows in the Chryse region of Mars 05 p2091 N94-20399
A formational model for the polygonal terrains of Mars: Taking a crack at the genesis of the Martian polygons
05 p2091 N94-20400
Balloon exploration of the northern plains of Mars near and north of the Viking 2 landing site
05 p2092 N94-20401
Geomorphic evidence for an eolian contribution to the formation of the Martian northern plains
05 p2092 N94-20402
Determination of cosmic bodies size-velocity distribution by observation of current impacts on Mars
05 p2082 N94-20648
Constraints on the rate of discharge and duration of the Mangala Valles flood 05 p2099 N94-20674
Wavelength dependence of limb-darkening of Mars from visible and near-IR telescopic spectral imaging
05 p2101 N94-20685
Eruption history of the Tharsis shield volcanoes, Mars
05 p2102 N94-20692
Geology of Biblis Patera, Ulysses Patera, and Jovis Tholus, Mars 05 p2103 N94-20693
Thermal conductivity measurements of particulate materials under Martian conditions
05 p1685 N94-20703
Geologic mapping of Harmakhis and Reull Valles region, Mars: Evidence for multiple resurfacing and drainage events 05 p1844 N94-20705
Derivation of the midinfrared (5.0-25.0 micron) optical constants of hydrous carbonate and sulfate
05 p2108 N94-20723
Detectability of crystalline ferric and ferrous minerals on Mars 05 p2110 N94-20730
Local topography of Mars and its relationship to surface weathering processes 05 p2111 N94-20737
Mars: New evidence for origin of some Valles Marineris layered deposits 05 p2112 N94-20748
The roughness of the Martian surface: A scale dependent model 05 p2115 N94-20762
Extensional history of Mars' Tharsis Region
05 p2125 N94-20814
Complex structure of the Thaumasia region of Mars
05 p2125 N94-20815
Large, ancient, compressional structures on Mars
05 p2125 N94-20816
Discharge rates in Ma'adim Vallis, Mars
05 p2128 N94-20830
The parent magma of the Nakhla (SNC) meteorite: Reconciliation of composition estimates from magmatic inclusions and element partitioning
05 p2085 N94-20836
Arcuate and circular structures in the Tharsis region: Evidence of coronae on Mars 05 p2134 N94-20863
A study of carbonates, sulfates, and phosphates using thermal emission spectroscopy
05 p1686 N94-20868
Spectral analysis of chemisorbed CO2 on Mars analog materials 05 p2140 N94-20900
Comparison of flank modification on Ascraeus and Arsia Montes volcanoes, Mars 05 p2140 N94-20903
K, U, and Th behavior in Martian environmental conditions 05 p2141 N94-20908
Wrinkle ridges, reverse faulting, and the depth penetration of lithospheric stress in lunae planum, Mars
05 p2141 N94-20910
Possible flexural signatures around Olympus and Ascraeus Montes, Mars 05 p2142 N94-20911
Workshop on Early Mars: How Warm and How Wet?, part 1
[NASA-CR-193553] 05 p2142 N94-21659
Evolution of the global water cycle on Mars: The geological evidence 05 p2142 N94-21660
Ancient Martian valley genesis and paleoclimatic inference: The present as a key to the past
05 p2142 N94-21661
A carbon dioxide/methane greenhouse atmosphere on early Mars 05 p2142 N94-21662
Oxidation of dissolved iron under warmer, wetter conditions on Mars: Transitions to present-day arid environments 05 p2143 N94-21663
Mars: Noachian hydrology by its statistics and topology 05 p2143 N94-21664
The evolution of the early Martian climate and the initial emplacement of crustal H2O 05 p2143 N94-21665
The hydrologic response of Mars to the onset of a colder climate and to the thermal evolution of its early crust
05 p2143 N94-21666
The early Martian environment: Clues from the cratered highlands and the Precambrian Earth
05 p2143 N94-21667
An attempt to comprehend Martian weathering conditions through the analysis of terrestrial palagonite samples 05 p2143 N94-21668
Fluvial valleys in the heavily cratered terrains of Mars: Evidence for paleoclimatic change?
05 p2144 N94-21670

Briny lakes on early Mars? Terrestrial intracrater playas and Martian candidates 05 p2145 N94-21675
Early Mars: A regional assessment of denudation chronology 05 p2145 N94-21676
Early Mars was wet but not warm: Erosion, fluvial features, liquid water habitats, and life below freezing 05 p2145 N94-21677
Wet inside and out? Constraints on water in the Martian mantle and on outgassed water, based on melt inclusions in SNC meteorites 05 p2145 N94-21678
Early Mars: The inextricable link between internal and external influences on valley network formation 05 p2146 N94-21681
The Martian valley networks: Origin by niveo-fluvial processes 05 p2146 N94-21682
Mars exploration study workshop 2 [NASA-CP-3243] 05 p2146 N94-21883
MSATT Workshop on Innovative Instrumentation for the In Situ Study of Atmosphere-Surface Interactions on Mars [NASA-CR-194584] 05 p1811 N94-22430
A Backscatter Moessbauer Spectrometer (BaMS) for use on Mars 05 p1811 N94-22431
Determination of Martian soil mineralogy and water content using the Thermal Analyzer for Planetary Soils (TAPS) 05 p1812 N94-22433
In situ identification of the Martian surface material and its interaction with the Martian atmosphere using DTA/GC 05 p1812 N94-22434
Mass spectrometer-pyrolysis experiment for atmospheric and soil sample analysis on the surface of Mars 05 p1812 N94-22435
Optical luminescence spectroscopy as a probe of the surface mineralogy of Mars 05 p1813 N94-22437
Missions, Technologies, and Design of Planetary Mobile Vehicles [ISBN-2-85428-331-7] 06 p2605 N94-23373
Rover requirements for the planet surface segment of the space exploration initiative 06 p2369 N94-23377
The robotic Mars rover 06 p2608 N94-23390
Mars subsurface sounding with a ground penetrating radar 06 p2608 N94-23393
Descent and landing phase: Vision based robust spacecraft motion estimation and elevation modeling 06 p2608 N94-23394
Mars 96 rover: Science, instrumentation, and control 06 p2369 N94-23395
Rover in the Mars 96 mission 06 p2609 N94-23397
Development/drilling test of auger boring machine on board Mars rover for Mars exploration 06 p2369 N94-23402
Planetary rover locomotion mechanisms 06 p2369 N94-23404
Machines for moving in soil 06 p2369 N94-23411
The Mars 96 balloon guiderope: An autonomous system in extreme environment conditions 06 p2369 N94-23412
Walking, jumping, and tumbling: More than one way to get around Mars 06 p2370 N94-23419
Perspective of creation of means for collecting information concerning transport situation 06 p2370 N94-23420
The Mars mapper science and mission planning tool 06 p2503 N94-23867
Impact of the CO2 and H2O clouds of the Martian polar hood on the polar energy balance 06 p2618 N94-24880
Temporal and spatial mapping of surface albedo and atmospheric dust opacity on Mars 06 p2619 N94-24887
Mars Operational Environmental Satellite (MOES): A post-Mars Observer discovery mission 06 p2620 N94-24890
Dust transport in the Martian atmosphere 06 p2621 N94-24894
Three-dimensional numerical simulation of near-surface flows over the Martian north polar cap 06 p2621 N94-24895
Martian mesoscale circulations induced by variations in surface optical and thermal characteristics: A numerical study 06 p2622 N94-24899
Three-dimensional numerical simulation of thermal tides in the Martian atmosphere 06 p2622 N94-24901
Vertical transport of water in the Martian boundary layer 06 p2622 N94-24902
The Mars Aerial Platform (MAP) mission 06 p2622 N94-24903
Tectonic Evolution of Mars [NASA-CR-194714] 06 p2623 N94-24996
The geophysical signal of the martian global dichotomy 06 p2623 N94-24997
Planetary surface exploration MESUR/autonomous lunar rover 07 p2833 N94-25683
Mars transportation system 07 p2833 N94-25689
Design and development of the second generation Mars Habitat 07 p2943 N94-25693
Project Ares 3 07 p2671 N94-25712
Why is the north polar cap on Mars different than the south polar cap? 07 p3107 N94-27889
In situ Mars ozone detector 07 p3108 N94-27892
Mars rover mechanisms designed for Rocky 4 08 p3161 N94-29630
Backscatter Mossbauer Spectrometer (BaMS) for extraterrestrial applications 08 p3236 N94-29774
A broad-band microseismometer for planetary operations 08 p3237 N94-29778
The viability of photovoltaics on the Martian surface [NASA-TM-106478] 08 p3338 N94-30196
State of stress, faulting, and eruption characteristics of large volcanoes on Mars 09 p3940 N94-31108
Origin and thermal evolution of Mars 09 p3940 N94-31109
Mars: Five views on what is known [NASA-TM-109751] 09 p3942 N94-31805
One: Microphysics of frost metamorphism: Applications to Triton and Mars. Two: A global analysis of the ozone deficit in the upper stratosphere and lower mesosphere. Three: The diabatic circulation in the stratosphere as diagnosed from Microwave Limb Sounder data 09 p3942 N94-31975
Mars: Past, Present, and Future. Results from the MSATT Program, part 1 [NASA-CR-194279] 09 p3943 N94-33190
Depth-diameter ratios for Martian impact craters: Implications for target properties and episodes of degradation 09 p3943 N94-33191
Thermal studies of Martian channels and valleys using Termoskan data: New results 09 p3944 N94-33194
The importance of environmental conditions in reflectance spectroscopy of laboratory analogs for Mars surface materials 09 p3944 N94-33195
Ferric sulfate montmorillonites as Mars soil analogs 09 p3944 N94-33196
Constraints on the Martian cratering rate imposed by the SNC meteorites and Vallis Marineris layered deposits 09 p3945 N94-33197
Deposition rates of oxidized iron on Mars 09 p3945 N94-33198
MARSNET: A European network of stations on the surface of Mars 09 p3945 N94-33199
Magmatic volatiles and the weathering of Mars 09 p3946 N94-33201
Thermal and hydraulic considerations regarding the fate of water discharged by the outflow channels to the Martian northern plains 09 p3946 N94-33202
Regional sedimentological variations among dark crater floor features: Toward a model for modern eolian sand distribution on Mars 09 p3946 N94-33203
Aerosols scattering and near-infrared observations of the Martian surface 09 p3946 N94-33204
Groundbased monitoring of Martian atmospheric opacity 09 p3947 N94-33207
SNC meteorites and their implications for reservoirs of Martian volatiles 09 p3947 N94-33209
The Northern Plains MSATT Meeting, and a call for a field-oriented successor to MSATT 09 p3947 N94-33210
Temporal and spatial mapping of atmospheric dust opacity and surface albedo on Mars 09 p3947 N94-33211
The effect of polar caps on obliquity 09 p3948 N94-33213
Might it be possible to predict the onset of major Martian dust storms? 09 p3948 N94-33215
Global color views of Mars 09 p3948 N94-33217
The distribution of Martian ground ice at other epochs 09 p3948 N94-33218
Mineralogical diversity (spectral reflectance and Moessbauer data) in compositionally similar impact melt rocks from Manicouagan Crater, Canada 09 p3948 N94-33219
Martian spectral units derived from ISM imaging spectrometer data 09 p3949 N94-33220
IRTM brightness temperature maps of the Martian south polar region during the polar night: The cold spots don't move 09 p3949 N94-33222
Numerical simulation of thermally induced near-surface flows over Martian terrain 09 p3949 N94-33223
Apron heights around stepped massifs in the Cydonia Mensae region: Do they record the local paleobathymetry of Oceanus Borealis? 09 p3949 N94-33224
The pH of Mars 09 p3950 N94-33225
The mineralogic evolution of the Martian surface through time: Implications from chemical reaction path modeling studies 09 p3950 N94-33226
Martian deltas: Morphology and distribution 09 p3950 N94-33230
Geologic controls of erosion and sedimentation on Mars 09 p3951 N94-33232
Polar sediment accumulation: Role of surface winds at the two poles 09 p3951 N94-33233
The Martian sources of the SNC meteorites (two, not one), and what can and can't be learned from the SNC meteorites 09 p3951 N94-33234
Temporal changes in the geographic distribution, elevation, and potential origin of the Martian outflow channels 09 p3951 N94-33235
Obliquity variation in a Mars climate evolution model 09 p3951 N94-33236
Dielectric properties of Mars' surface: Proposed measurement on a Mars lander 09 p3951 N94-33237
The influence of thermal inertia on Mars' seasonal pressure variation and the effect of the weather component 09 p3952 N94-33238
Carbonates, surfates, phosphates, nitrates, and organic materials: Their association in a Martian meteorite 09 p3952 N94-33239
Planetary protection issues and future Mars missions [NASA-CP-10086] 10 p4164 N94-33533
Design of the MESUR/pathfinder microrover 10 p4066 N94-34021
Mars aqueous chemistry experiment [NASA-CR-196024] 11 p4354 N94-35263
An automatic planetary vehicle for exploring Mars 11 p4354 N94-35336
Workshop on the Martian Northern Plains: Sedimentological, periglacial, and paleoclimatic evolution [NASA-CR-196134] 11 p4354 N94-35359
High resolution visible to short-wave near-infrared CCD spectra of Mars during 1990 11 p4356 N94-35403
Absolute calibration and atmospheric versus mineralogic origin of absorption features in 2.0 to 2.5 micron Mars spectra obtained during 1993 11 p4356 N94-35404
Wavelength calibration techniques and subtle surface and atmospheric absorption features in the Mariner 6, 7 IRS reflectance data 11 p4356 N94-35405
Fluvial processes in Ma'adim Vallis and the potential of Gusev crater as a high priority site 11 p4358 N94-35414
The fretted terrain of the Nilosyrtis Mensae region of Mars: Clues to the timing of dichotomy formation and the emplacement of the northern plains 11 p4360 N94-35424
Exopaleontology and the search for a fossil record on Mars 11 p4360 N94-35425
Effects due to overlapping large impact basins on Mars 11 p4360 N94-35427
Quantifying shapes of volcanoes on Venus 11 p4361 N94-35429
High Resolution Transmission Electron Microscopy (HRTEM) of nanophase ferric oxides 11 p4239 N94-35433
The topography of Mars: A re-evaluation of current data 11 p4364 N94-35460
Noachian and Hesperian modification of the original Chryse impact basin topography 11 p4364 N94-35462
The parent magma of xenoliths in shergottite EETA79001: Bulk and trace element composition inferred from magmatic inclusions 11 p4352 N94-35467
Windblown sand on Mars: The effect of saltation threshold on drift potentials derived from Mars GCM 11 p4366 N94-35474
Atmospheric effects on the mapping of Martian thermal inertia and thermally derived albedo 11 p4368 N94-36137
Mossbauer and spectral (visible and near-IR) data for Fe(3+)-substituted rutile 11 p4240 N94-36154

MARS SURFACE SAMPLES

Thermal imaging for a mobile robot 08 p3308 N94-30300

MARS VOLCANOES

Twenty-fourth Lunar and Planetary Science Conference. Part 1: A-F [NASA-CR-193095] 01 p0435 N94-12015
Lineament analysis and tectonic interpretation for the Tharsis region 01 p0437 N94-12031
Basal scarp, paleoglacier, and fissure flows of Elysium Mons, Mars 01 p0459 N94-12148
Small volcanoes in Tempe Terra, Mars: Their detailed morphometry and inferred geologic significance 01 p0469 N94-12202
Shallow crustal discontinuities and graben and scarp formation in the Tharsis region of Mars 01 p0469 N94-12203
Explosive mafic volcanism on Earth and Mars 03 p1253 N94-16204
Fractal geometry of some Martian lava flow margins: Alba Patera 03 p1270 N94-16298
Martian lavas: Three complementary remote sensing techniques to derive flow properties 03 p1283 N94-16366
The influence of oceans on Martian volcanism 03 p1295 N94-16427

Eruption history of the Tharsis shield volcanoes, Mars
05 p2102 N94-20692
Geology of Biblis Patera, Ulysses Patera, and Jovis Tholus, Mars 05 p2103 N94-20693
Chronology, eruption duration, and atmospheric contribution of Apollinaris Patera, Mars
05 p2108 N94-20720
Arcuate and circular structures in the Tharsis region: Evidence of coronae on Mars 05 p2134 N94-20863
Comparison of flank modification on Ascraeus and Arsia Montes volcanoes, Mars 05 p2140 N94-20903
Possible flexural signatures around Olympus and Ascraeus Montes, Mars 05 p2142 N94-20911
Tectonic History of the Terrestrial Planets
[NASA-CR-195696] 09 p3939 N94-31105
State of stress, faulting, and eruption characteristics of large volcanoes on Mars 09 p3940 N94-31108
Evidence for ultramafic lavas on Syrtis Major
09 p3950 N94-33229

MARS 4 SPACECRAFT
The 1982 highlights
[NASA-TM-109671] 03 p1303 N94-15508

MARSHES
U MARSHLANDS

MARSHLANDS
A preliminary study of the variability and magnitude of the flux of biogenic sulfur gases from a New Hampshire salt marsh 01 p0267 N94-12452
Sulfate reduction and other sedimentary biogeochemistry in a northern New England salt marsh
01 p0268 N94-12453
Emissions of sulfur gases from wetlands
01 p0269 N94-12458
Acetate concentrations and oxidation in salt marsh sediments 01 p0269 N94-12459
Sulfur transformations in the sediments of a New Hampshire salt marsh 01 p0270 N94-12463
Emissions of biogenic sulfur gases from northern bogs and fens 01 p0271 N94-12467
Elevated acetate concentrations in the rhizosphere of Spartina alterniflora and potential influences on sulfate reduction 01 p0271 N94-12468
The ecological and environmental impacts of manmade marshes
[AD-A269213] 04 p1475 N94-18885

MARTENSITE
Continuum modeling of materials that can undergo martensitic phase transitions
[AD-A268767] 04 p1360 N94-18386
Internal friction associated with dislocation relaxations in virgin martensite
[PB93-226280] 06 p2240 N94-23119
Microstructural development in low activation ferritic alloys irradiated to 200 dpa at 420 C
[DE94-004269] 07 p2731 N94-25803
Computer simulation of martensitic transformations
[DE94-005213] 08 p3201 N94-28479
Research on the improvement of shape-memory and magnetostrictive materials
[AD-A275397] 08 p3203 N94-29056
Low temperature behavior of virgin martensite
[PB94-132925] 08 p3204 N94-29142
Displacive transformation in ceramics
[AD-A278442] 10 p4026 N94-33539
Mechanical performance of austempered ductile iron
[AD-A280452] 12 p4420 N94-37758

MARTENSITIC STAINLESS STEELS
Weldability of maraging steels
01 p0059 N94-10028
Electrochemical properties of passive films on 440C stainless steel
[ISBN-0-315-64248-3] 07 p2757 N94-27801
Toughening mechanisms in ultrahigh-strength steels
[AD-A275439] 08 p3202 N94-28867
Characterization of the corrosion resistance of duplex stainless steels using local current density mapping techniques
[DE94-007980] 09 p3646 N94-32699
Characterization of nuclear transmutations in materials irradiated test facilities
[DE94-013309] 12 p4420 N94-37552

MARTENSITIC TRANSFORMATION
Transient phenomena following precipitation and re-solution anneals in a NiTi alloy
[AD-A267557] 03 p0961 N94-17106
Omega phase formation in shock-loaded zirconium
[DE93-018343] 04 p1595 N94-18162
Continuum modeling of materials that can undergo martensitic phase transitions
[AD-A268767] 04 p1360 N94-18386
The longitudinal free vibrations of a fixed-free two-phase elastic bar
[AD-A268768] 04 p1453 N94-18387
The temperature at the phase boundary during quasi-static motions of a two-phase thermoelastic bar
[AD-A268769] 04 p1596 N94-18388
Damping in ferrous shape memory alloys
[AD-A271009] 04 p1366 N94-19775
First principles calculations for analysis martensitic transformations
[DE94-000666] 05 p1695 N94-21964
Study on phase transformation due to deformation in ferromagnetic fields at cryogenic condition
07 p2724 N94-25556
Study on microscopic structural controls and electronic properties at material surfaces by ion beams
07 p2727 N94-25571
Stress-induced phase transformation in ZrO2 materials
[ISBN-0-315-83373-4] 07 p2752 N94-26661
Computer simulation of martensitic transformations
[DE94-005213] 08 p3201 N94-28479
Transformation plasticity in ductile solids
[DE94-010420] 11 p4240 N94-35953

MARTINGALES
Bisexual branching diffusions
[AD-A274698] 07 p3008 N94-26374

MARYLAND
Focused feasibility study final field sampling plan
[AD-A277445] 09 p3769 N94-33105

MASER MATERIALS
Collision and motional averaging effects in cryogenic atomic hydrogen masers
[AD-A278478] 10 p4057 N94-33746

MASER OUTPUTS
Collision and motional averaging effects in cryogenic atomic hydrogen masers
[AD-A278478] 10 p4057 N94-33746

MASER RESONATORS
U MASERS

MASERS
NT HYDROGEN MASERS
NT INTERSTELLAR MASERS
NT WATER MASERS
Fundamental theory of light for applications: Notes for five informal lectures
[DE93-016463] 03 p1192 N94-16953
Design of a tunable 4-MW free electron maser for heating fusion plasmas
[DE93-017172] 04 p1437 N94-18134
Proof of the feasibility of coherent and incoherent schemes for pumping a gamma ray laser
[AD-A269173] 04 p1440 N94-18880
Observation of pressure ridges in SAR images of sea ice: Scattering theory and comparison with observations
05 p1723 N94-20427
Infrared and SiO maser observations of OH/IR stars
[PB94-104890] 06 p2599 N94-24780
A dual-cavity ruby maser for the Ka-band link experiment 08 p3250 N94-29658
X-band ultralow-noise maser amplifier performance
08 p3251 N94-29672
Three-photon micromasers
[DE94-611106] 11 p4272 N94-35782

MASKING
A novel photosensitive polyimide resist consisting of a soluble polyimide and a bis(perfluorophenyl azide) as a cross-linker
[AD-A265998] 01 p0093 N94-12353
On masking effect
[AD-A269593] 04 p1541 N94-18462
X ray reflection masks: Manufacturing, characterization and first tests
[BONN-IR-92-31] 05 p1986 N94-21043
Joint Acoustic Propagation Experiment (JAPE)
06 p2527 N94-24208
JAPE 91: Influence of terrain masking of the acoustic propagation of helicopter noise
06 p2528 N94-24214
Auditory spectro-temporal pattern analysis
[AD-A273554] 06 p2427 N94-24865
Pattern analysis based models of masking by spatially separated sound sources
[AD-A277882] 10 p4095 N94-33779

MASKS
NT OXYGEN MASKS
RF vacuum microelectronics
[AD-A266066] 01 p0142 N94-10818
A prototype urine collection device for female aircrew
01 p0317 N94-11549
RF vacuum microelectronics
[AD-A270003] 04 p1403 N94-18667
Characterization and possible repair of defects in soft x ray projection lithography masks
[DE93-019147] 05 p1750 N94-20231
Development of an industrial CO2 laser for mask marking
[DE93-632901] 07 p2816 N94-26184
RF vacuum microelectronics
[AD-A275221] 08 p3263 N94-28915

MASONRY
NT BRICKS
Microstructure in mortar: A summary of a new project of research 05 p1708 N94-21896
Proceedings of the Fourth Euroseminar on Microscopy Applied to Building Materials
[PB94-119807] 07 p2839 N94-26754

MASS
NT CENTER OF MASS
NT CRITICAL MASS
NT ELECTRON MASS
NT GALACTIC MASS
NT PARTICLE MASS
NT PLANETARY MASS
NT STELLAR MASS
Quark and lepton masses
[DE93-012308] 01 p0370 N94-12787
Stability of reference masses 1: Evidence for posiible variations in the mass of reference kilograms arising from mercury contamination
[NPL-DMM(A)-86] 02 p0708 N94-13667
Neutrino mass
[DE93-018467] 04 p1567 N94-18269
Mass properties measurement system dynamics
06 p2368 N94-23235
Mass properties measurement system: Dynamics and statics measurements 06 p2368 N94-23236
Small low mass advanced PBR's for bi-modal operation
[DE94-003201] 07 p2699 N94-25798
Parametric analysis of the space power plants on the base of criterion of specific mass in generalized design variants
[DE93-634153] 07 p2701 N94-26166
A compact roller-gear pitch-yaw joint module: Design and control issues 08 p3161 N94-29629
A non-contacting vertical alignment system for mass properties measuring instruments
[DE94-004680] 08 p3289 N94-29927
Evolution of vaporizing pulsars
09 p3929 N94-31128
A test apparatus and facility to identify the rotordynamic coefficients of high-speed hydrostatic bearings
10 p4065 N94-34199
The mass of Mars, Phobos, and Deimos, from the analysis of the Mariner 9 and Viking Orbiter tracking data 11 p4364 N94-35461

MASS BALANCE
A carbon isotope mass balance for an anoxic marine sediment: Isotopic signatures of diagenesis
04 p1477 N94-19232
Space Station evolution study oxygen loop closure
[NASA-CR-193938] 07 p2941 N94-26788
Piggyback balance experiment: An illustration of Archimedes' principles and Newton's third law
[PB94-163060] 11 p4265 N94-35942

MASS DISTRIBUTION
Power-law confusion: You say incremental, I say differential 01 p0347 N94-12175
Mass and spatial distribution of carbonaceous component in Comet Halley 01 p0433 N94-12263
Accuracy and repeatability of the standard automated mass properties measurement system
[AD-A265897] 01 p0316 N94-12346
Incorporation of boundary layer heating predictive methodology into NSWCDD aeroprediction code
[AD-A267000] 03 p1020 N94-15632
Analysis and design of weight balancing system for laser velocimetry traverse
[AD-A271171] 05 p1816 N94-20546
Equilibrium models of mass distribution and collisional lifetimes of asteroids 05 p2086 N94-20877
Validation of a nonintrusive optical technique for the measurement of liquid mass distribution in a two-phase spray 06 p2548 N94-24420
Near surface analysis 06 p2407 N94-25364
Particulate and gaseous organic receptor modeling for the Southern California Air Quality Study
[PB94-156700] 11 p4285 N94-35735
Anthropogenic sulfate and organic aerosols, CCN, and cloud project concentration at a marine site
[DE94-004210] 11 p4286 N94-36025
Selected case studies in modeling and simulation applied to environmentally conscious design and manufacturing
[DE94-007556] 12 p4466 N94-37389

MASS FILTERS
U FLUID FILTERS

MASS FLOW
An overview of the capabilities of ARA for the measurement of nozzle discharge and thrust
[ARA-MEMO-378] 01 p0055 N94-12283
Sedimentation rates and particulate fluxes in the slope and deep sea areas off eastern Taiwan
01 p0220 N94-12709
Flow instability tests for a particle bed reactor nuclear thermal rocket fuel element
[AD-A268012] 03 p0929 N94-17474

Vane optimization for maximum efficiency using Design Of Experiments (DOX)
[AD-A270270] 04 p1320 N94-18907
Mathematical modeling of the free surface hydrodynamic and of transport in suspensions of non cohesive sediments: Aid to the interpretation of spatial images
[ETN-93-95011] 04 p1421 N94-19502
System and method for cancelling expansion waves in a wave rotor
[NASA-CASE-LEW-15218-1] 05 p1801 N94-20588
Speed of sound data and related models for mixtures of natural gas constituents
[PB93-200822] 05 p1968 N94-21447
A representation for the turbulent mass flux contribution to Reynolds-stress and two-equation closures for compressible turbulence
[NASA-CR-191569] 06 p2319 N94-23302
CFD assessment of orifice aspect ratio and mass flow ratio on jet mixing in rectangular ducts
[NASA-TM-106434] 06 p2187 N94-24082
Ethylene trace-gas techniques for high-speed flows
[NASA-TM-106491] 06 p2169 N94-24335
Propagation of cold air masses in East Asia and its associated planetary-scale function
[AD-A274304] 07 p2895 N94-26850
Disk irradiation and light curves of x ray novae 09 p3929 N94-31124

MASS FLOW RATE

Development of a high specific 1.5 to 5 kW thermal arcjet
[NASA-CR-193133] 01 p0047 N94-11354
High power steady state MPD thrusters
[AD-A267277] 03 p0928 N94-17308
Flow instability tests for a particle bed reactor nuclear thermal rocket fuel element
[AD-A268012] 03 p0929 N94-17474
Two stage turbine for rockets 06 p2215 N94-23059
Simplified, inverse, ejector design tool
[NASA-CR-194438] 06 p2166 N94-23511
Ethylene trace-gas techniques for high-speed flows
[NASA-TM-106491] 06 p2169 N94-24335
Carrying the mass flux terms exactly in the first and second moment equations of compressible turbulence
[AD-A276346] 06 p2335 N94-24712
Measurement of the volume mass by spontaneous Raman scattering. Study of turbulent fluctuations of mixing in a subsonic free jet. Measurements in supersonic wind tunnels
[ISL-R-102/92] 06 p2339 N94-25462
SP industry calorimeter for rate of heat release measurements up to 10MW
[PB94-124211] 07 p2811 N94-27044
Advanced diagnostics for reacting flows
[AD-A275057] 08 p3272 N94-29136
Disk irradiation and light curves of x ray novae 09 p3929 N94-31124
Control of hypersonic aerodynamic forces with surface blowing 09 p3567 N94-31216

MASS RATIOS

NT MIXING RATIOS
NT PAYLOAD MASS RATIO
NT PROPELLANT MASS RATIO
Dissociation rates of diatomic molecules
[AD-A266464] 03 p1182 N94-16586
Proof of stability of the hydrogen molecule
[PB93-221026] 05 p1977 N94-22271
Large amplitude Langmuir and ion-acoustic waves in a relativistic two-fluid plasma
[AD-B183694L] 08 p3506 N94-29547
A study of angular momentum loss in binaries using the free Lagrange method 09 p3931 N94-31134
Gravitational instabilities in protostellar disks 09 p3932 N94-31140
Double-lined pre-main-sequence binaries: A test of pre-main-sequence evolutionary theory 09 p3933 N94-31497
Applications of non-resonant RF forces for improvement of tokamak reactor performances. Part 1: Application of ponderomotive force
[DE94-718994] 11 p4336 N94-35813

MASS SPECTRA

Measurement of polycyclic aromatic hydrocarbon (PAHs) in interplanetary dust particles 01 p0431 N94-12167
Negative ion formation in small carbon clusters
[DE93-015436] 03 p1182 N94-16064
Crossed molecular beam studies of atmospheric chemical reaction dynamics
[DE93-019246] 04 p1478 N94-19303
Studies of clusters
[DE93-018961] 04 p1572 N94-19309
Evaluation of mass spectra for a verification database
[PML-1993-12] 04 p1619 N94-19453
Measurement of the B(+) and B(0) lifetimes
[DE93-019906] 05 p1969 N94-19814
Search for excited quarks in p(-p) collisions at the square root of s = 1.8 TeV
[DE93-019910] 05 p1975 N94-21840
Aspects of nonrenormalizable terms in a superstring standard-like models
[DE93-614530] 07 p3071 N94-25911
Quantizable configurations of the relativistic string
[DE93-634346] 07 p3072 N94-26036
Meson X(1814) as a candidate for a hybrid state
[DE93-634447] 07 p3017 N94-26045
Leptonic decay constants of heavy mesons in QCD
[DE93-634426] 07 p3022 N94-26767
A measurement of the W mass using electrons at CDF
[DE94-004656] 07 p3028 N94-27748
Decay constants of heavy mesons in the relativistic potential model with velocity dependent corrections
[DE94-606495] 07 p3030 N94-27860
Measurement of the W mass in the D0 detector
[DE94-006002] 08 p3490 N94-30103
Overlap of metal clusters and nuclear structure physics
[DE94-608387] 08 p3517 N94-30183
Imaging AMS
[DE94-006662] 09 p3632 N94-31349
Composition and properties of dust from Comet Halley 09 p3936 N94-31947
Performance of an ion trap inductively coupled plasma mass spectrometer
[DE94-007470] 09 p3713 N94-32811
Leptonic decay constants of heavy quarkonia in effective QCD sum rules
[DE94-611160] 11 p4322 N94-35784
Production of phi mesons in central Si + Au collisions at 14.6 A GeV/c
[DE94-011726] 12 p4516 N94-37152

MASS SPECTROMETERS

Ionization potentials of small carbon clusters
[AD-A264379] 01 p0067 N94-11260
Measurement of polycyclic aromatic hydrocarbon (PAHs) in interplanetary dust particles 01 p0431 N94-12167
Development of an advanced spacecraft tandem mass spectrometer
[NASA-CR-194195] 02 p0545 N94-13953
Precise flux control for lattice matched superlattice materials
[AD-A268254] 03 p1215 N94-17417
The minimum detection limits of RDX and TNT deposited on various surfaces as determined by ion mobility spectroscopy
[DE93-018521] 04 p1378 N94-19042
Novel mass spectrometric instrument for gaseous and particulate characterization and monitoring
[DE93-019992] 04 p1433 N94-19054
Crossed molecular beam studies of atmospheric chemical reaction dynamics
[DE93-019246] 04 p1478 N94-19303
The laser and its applications on environment and biotechnology research
[DE94-000376] 05 p1820 N94-21957
Atmospheric sampling glow discharge ionization and triple quadrupole tandem mass spectrometry for explosives vapor detection
[DE93-040593] 05 p1852 N94-22004
Prospects for future solar-wind missions 06 p2624 N94-22841
Interpretation of discrepancies in mass spectroscopy data obtained from different experimental configurations 06 p2237 N94-23245
Multi-ion, multi-event test of ion cyclotron resonance heating
[NASA-CR-194859] 06 p2540 N94-23495
Reactivity of ambident anions in the gas phase
[PB93-232189] 06 p2533 N94-23713
New high temperature plasmas and sample introduction systems for analytical atomic emission and mass spectrometry
[DE94-004564] 08 p3503 N94-28458
A study of solid propellants using a microprobe mass spectrometer system
[AD-A275325] 08 p3224 N94-28879
Adaption of the bubble detector for use as a LET spectrometer 08 p3291 N94-30216
Imaging AMS
[DE94-006662] 09 p3632 N94-31349
Performance of an ion trap inductively coupled plasma mass spectrometer
[DE94-007470] 09 p3713 N94-32811
Capillary column GC-MS/MS confirmation of phosphate esters with a hybrid tandem mass spectrometer
[AD-A278748] 11 p4238 N94-36091
Method of N-15 analysis by mass-spectroscopy on ion implanter MPB-200
[DE94-618203] 12 p4407 N94-36529
A fast spectroscopic diagnostic for the measurement of plasma impurity ion dynamics
[DE94-012985] 12 p4529 N94-37354

MASS SPECTROMETRY

U MASS SPECTROSCOPY

MASS SPECTROSCOPY

Progress in zirconium resonance ionization spectroscopy
[DE93-011881] 01 p0076 N94-11075
Tandem mass spectrometric analysis of phosphate esters
[AD-A265483] 01 p0078 N94-12009
Novel mass spectrometric instrument for gaseous and particulate characterization and monitoring
[DE93-014093] 01 p0272 N94-12783
EBIT Trapping Program
[DE93-014422] 02 p0788 N94-13208
Research in cosmic and gamma ray astrophysics: Cosmic physics portion
[NASA-CR-194127] 02 p0847 N94-13211
Low temperature metal-organic chemical vapor deposition growth processes for high efficiency solar cells
[DE92-010562] 02 p0702 N94-13386
Construction and test of a facility for photon-stimulated field description using excimer laser and time of flight
[ETN-93-94386] 02 p0657 N94-13996
UV and IR laser ablation for inductively coupled plasma mass spectrometry
[DE93-017124] 02 p0658 N94-14415
Osmium isotopes in Ivory Coast tektites: Confirmation of a meteoritic component and rhenium depletion 03 p1244 N94-16321
Space Shuttle solid rocket motor exposure monitoring 03 p0976 N94-16624
Elemental impurity analysis of mercuric iodide by ICP/MS
[DE93-015531] 03 p0949 N94-16876
Laser photoionization time-of-flight mass spectrometry of nitrated polycyclic aromatic hydrocarbons and nitrated heterocyclic compounds
[AD-A268126] 03 p0952 N94-17520
Growth of dielectric thin films by irradiation of condensed molecular precursors with synchrotron radiation
[DE93-016161] 03 p0974 N94-17676
Development and evaluation of alternative radioanalytical methods, including mass spectrometry for marine materials
[DE93-625117] 04 p1345 N94-17691
Detonation reaction steps frozen by free expansion and analyzed by mass spectrometry
[DE93-012734] 04 p1376 N94-17813
Matrix- and substrate-assisted laser desorption for fast DNA sequencing
[DE93-015332] 04 p1501 N94-18242
Flame structure studies of a lean 20-torr H2/N2O/Ar flame employing molecular beam mass spectrometry
[AD-A268889] 04 p1349 N94-18456
Novel mass spectrometric instrument for gaseous and particulate characterization and monitoring
[DE93-019992] 04 p1433 N94-19054
Research program activities of the ORNL Analytical Chemistry Division
[DE93-017938] 04 p1339 N94-19117
Evaluation of mass spectra for a verification database
[PML-1993-12] 04 p1619 N94-19453
Detailed structure study of an H2/N2O/Ar flame employing molecular beam mass spectrometry, laser spectroscopy, and modeling
[AD-A270720] 05 p1679 N94-20111
Hydrogen pickup and redistribution in alpha-annealed zircaloy-4
[DE93-018050] 05 p1689 N94-20182
Multielement analysis of interplanetary dust particles using TOF-SIMS 05 p2084 N94-20790
Analysis of semi-insulating bulk GaAs using glow discharge mass spectrometry
[AD-A273032] 05 p1682 N94-21435
On Plasma Edge Spectroscopy and Spectroscopic Studies of Impurity Densities and Impurity Transport
[IPF-92-2] 05 p1996 N94-21802
Plasma edge spectroscopy 05 p1996 N94-21803
Spectroscopic studies of impurity densities and impurity transport 05 p1997 N94-21804
Atmospheric sampling glow discharge ionization and triple quadrupole tandem mass spectrometry for explosives vapor detection
[DE93-040593] 05 p1852 N94-22004
Interpretation of discrepancies in mass spectroscopy data obtained from different experimental configurations 06 p2237 N94-23245
Condensed-phase thermal decomposition of TATB investigated by Atomic Force Microscopy (AFM) and Simultaneous Thermogravimetric Modulated Beam Mass Spectrometry (STMBMS)
[DE94-000396] 06 p2232 N94-23298

Fifty years of continuous improvement: What has DOE done for analytical chemistry?
[DE94-002539] 06 p2234 N94-24548
Isothiazolone volatility study of a water bottom from fuel treated with Kathon (tm) FP1.5 biocide
[AD-A273165] 06 p2266 N94-24728
Study on analyzing method establishment for metallic material development 07 p2729 N94-25578
Molecular beam mass spectrometry studies of the chemical vapor deposition of diamond
[DE94-003802] 07 p3049 N94-25601
Three methods to measure RH bond energies
[DE94-003795] 07 p3013 N94-25816
New FORTRAN computer programs to acquire and process isotopic mass spectrometric data: Operator's manual
[DE94-003174] 07 p2965 N94-26784
Antiproton studies in penning traps
[AD-A274250] 07 p3024 N94-27011
Determination of lead isotope ratios in seawater by purge and trap GC/MS after ethylation 07 p2870 N94-28152
New high temperature plasmas and sample introduction systems for analytical atomic emission and mass spectrometry
[DE94-004564] 08 p3503 N94-28458
Measurement of elemental speciation by liquid chromatography: Inductively coupled plasma mass spectrometry (LC-ICP-MS) with the Direct Injection Nebulizer (DIN)
[DE94-005261] 08 p3187 N94-28483
Matrix isolation studies of the interactions of BF3 with water and substituted diethyl ethers. Chemical ionization mass spectrometric determination of the proton affinity of (CF3CH2)2O
[NASA-TM-106422] 08 p3189 N94-28832
Reactions of metal ions and their clusters in the gas phase using laser ionization: Fourier transform mass spectrometry
[DE94-006208] 08 p3207 N94-30024
Novel mass spectrometric instrument for gaseous and particulate characterization and monitoring
[DE94-005896] 08 p3349 N94-30047
Characterization of polymer decomposition products by laser desorption mass spectrometry 09 p3597 N94-31046
Imaging AMS
[DE94-006662] 09 p3632 N94-31349
AMS beyond 2000
[DE94-006666] 09 p3632 N94-31352
Development of sample charge compensation for characterization of impurities in semiconductor materials
[AD-A277113] 09 p3899 N94-31983
Group 12 thiolates: Syntheses, characterization and decomposition pathways
[AD-A277055] 09 p3900 N94-32011
New zinc-bis(dialkylamides) potentially usable as site-selective dopants for p-type ZnSe
[AD-A276947] 09 p3902 N94-32218
Organic analyses of the Murchison meteorite 09 p3938 N94-32489
Performance of an ion trap inductively coupled plasma mass spectrometer
[DE94-007470] 09 p3713 N94-32811
A combined experimental and theoretical study of the neutral, cationic and anionic Si3N cluster molecule
[AD-A278834] 11 p4323 N94-35792
Capillary column GC-MS/MS confirmation of phosphate esters with a hybrid tandem mass spectrometer
[AD-A278748] 11 p4238 N94-36091
Metal-carbon nanostructures
[DE94-009177] 12 p4400 N94-36509
Physics Division annual review, 1 April 1992 - 31 March 1993
[DE94-002497] 12 p4512 N94-36513
United States Air Force Summer Research Program, 1993. Volume 16: Arnold Engineering Development Center, Frank J. Seiler Research Laboratory and Wilford Hall Medical Center
[AD-A278658] 12 p4550 N94-36978
Light stable isotope analysis of meteorites by ion microprobe
[NASA-CR-196096] 12 p4548 N94-37004
Probing flame chemistry with MBMS, theory, and modeling
[DE94-011224] 12 p4413 N94-37623

MASS TRANSFER
Heat and mass transfer mechanisms of the polymerization under terrestrial and microgravity conditions 01 p0103 N94-10092
Transport of heat and mass in near-critical fluids 01 p0122 N94-10230
Experimental study of multiple droplet evaporative cooling
[PB93-198463] 01 p0149 N94-10851
Research on chemical vapor deposition processes for advanced ceramic coatings
[NASA-CR-193613] 02 p0577 N94-13089
The corrosion behavior of 8001 Al under heat-transfer conditions in an aqueous loop system
[DE93-013450] 02 p0569 N94-13242
Destruction of waste energetic materials using base hydrolysis
[DE93-012738] 02 p0584 N94-13491
Studies of momentum and energy transfer across wavy gas-liquid interfaces
[AD-A266432] 02 p0635 N94-13699
Wind mass and energy deposition
[DE93-013345] 02 p0839 N94-14341
Density and temperature relaxation near the critical point of carbon dioxide under reduced gravity 03 p0944 N94-15164
Investigation of the influence of applied potential on erosion-corrosion of copper in alkaline chloride solutions
[AD-A266448] 03 p0958 N94-16562
Pulse-timing studies of x ray pulsars
[NASA-CR-193778] 04 p1621 N94-18611
Adsorption analysis of ammonia in an aqueous solution
[DE93-019512] 04 p1353 N94-19552
Supercritical thermodynamics of sulfur and nitrogen species
[DE93-041221] 04 p1610 N94-19670
Parameters affecting hydrogen chloride measurements
[AD-A271326] 05 p1851 N94-20025
Pressurization and expulsion of a flightweight liquid hydrogen tank
[NASA-TM-106427] 05 p1799 N94-20177
Heat transfer additives for absorption cooling system fluids
[PB93-202521] 05 p1714 N94-21426
A novel method for determination of transport parameters of H2 and O2 in PEMFCs
[DE94-001492] 06 p2389 N94-22962
Absorption technology for solar and waste heat utilization 07 p2854 N94-26053
An April 1991 outburst from 4U0115+63 observed by BATSE
[DE94-007093] 07 p3116 N94-27440
Volume averaged model for the mechanics of alloys solidification
[PB94-138617] 08 p3208 N94-30113
On the structure and atomic motions in liquid sodium
[DE94-608386] 08 p3490 N94-30182
Local two-phase flow simulations including interface tracking with mass transfer 08 p3283 N94-30954
Can a variable alpha induce limit cycle behavior and exponential luminosity decay in transient soft x ray sources? 09 p3929 N94-31129
The prediction of convective transfer on the thermal insulation of a solid-propellant rocket motor
[ONERA-NT-1993-15] 09 p3614 N94-31423
Cloud studies seen from a physical chemist's perspective
[DE94-006059] 09 p3771 N94-31527
Numerical simulations of monsoon rainfall with the NRL/NCSU regional nested grid model 09 p3782 N94-31791
Computational study of simultaneous heat and mass transfer in turbulent separated flows 09 p3704 N94-31843
A Lagrangian-Eulerian finite element method with adaptive gridding for advection-dispersion problems
[DE94-011372] 12 p4506 N94-37718

MASSIFS
Composition of Apollo 17 core 76001 03 p1275 N94-16326

MASSIVE STARS
A photometric study of massive x-ray binaries
[ITN-93-85207] 02 p0829 N94-13231
Charge-exchange reactions and weak interaction rates for Type 2 supernovae
[DE93-015104] 02 p0783 N94-13893
The astrophysical interpretation of isotope anomalies in graphite and SiC grains of chondrites 03 p1244 N94-16343
Detection of accreting gas toward HD 45677: A newly recognized, Herbig Be proto-planetary system
[NASA-CR-189312] 04 p1621 N94-19288
New production mechanisms for unstable nuclei in stars, supernovae, and the big bang
[DE93-018627] 05 p2081 N94-21618
The formation of massive stars: A 30 Mo case study
[ISBN-0-315-83944-9] 05 p2081 N94-22593
Physical conditions in classical H2 regions in the Magellanic Clouds 08 p3543 N94-29722
A multi wavelength observational study of the Cartwheel ring galaxy 08 p3539 N94-29821
Near infrared surveys of high mass star forming regions 09 p3925 N94-31898

MASSIVELY PARALLEL PROCESSORS
NT CONNECTION MACHINE
Massively parallel multifrontal methods for finite element analysis on MIMD computer systems
[DE93-009838] 01 p0335 N94-10257
A heterogeneous graphics procedure for visualization of massively parallel solutions
[DE93-009628] 01 p0336 N94-11270
Massively parallel hydrodynamics on unstructured grids
[DE93-007325] 01 p0153 N94-11601
The 3-D massively parallel impact simulations using PCTH
[DE93-011593] 02 p0670 N94-12908
A network evaluation and analysis tool
[DE93-012647] 02 p0758 N94-12917
An experimental regional scale climate simulation laboratory
[DE93-015935] 02 p0719 N94-13119
Implementation of ADI: Schemes on MIMD parallel computers
[NASA-CR-193720] 02 p0759 N94-13204
Advanced computers and simulation
[DE93-014354] 02 p0740 N94-13286
A data distributed parallel algorithm for ray-traced volume rendering
[NASA-CR-191520] 02 p0749 N94-13721
Efficient, massively parallel eigenvalue computation
[NASA-CR-194289] 02 p0760 N94-13921
VFGEN: A parallel volume fraction generator for hydrocodes
[DE93-011673] 02 p0752 N94-14019
Hybrid S(sub N)/Monte Carlo research and results
[DE93-012677] 02 p0773 N94-14178
An efficient parallel algorithm for matrix-vector multiplication
[DE93-015125] 02 p0754 N94-14399
An overview of parallel scientific visualization
[DE93-017105] 02 p0755 N94-14521
Particle simulations on massively parallel machines
[DE93-015644] 03 p1157 N94-14927
Overview of Enhanced Data Stream Array Processor (EDSAP)
[AD-A266986] 03 p1158 N94-15492
Requirements for supercomputing in energy research: The transition to massively parallel computing
[DE93-012376] 03 p1160 N94-16774
Efficient scheduling of real-time compute-intensive periodic graphs on large grain data flow multiprocessor
[AD-A267444] 03 p1141 N94-17030
Benchmarking massively parallel architectures
[DE93-016486] 03 p1162 N94-17646
PARX, kernel of a system for massively parallel computers: Control of communication between processes
[ETN-93-94353] 04 p1533 N94-17976
A fast adaptive convex hull algorithm on two-dimensional processor arrays with a reconfigurable BUS system 04 p1402 N94-18380
Three-dimensional shock wave physics simulations with MIMD PAGOSA on massively parallel computers
[DE93-011682] 04 p1455 N94-18829
A massively parallel adaptive finite element method with dynamic load balancing
[DE93-012844] 04 p1536 N94-19161
Experience in implementing a parallel file system
[DE93-012840] 04 p1536 N94-19188
MIMD massively parallel methods for engineering and science problems
[DE93-019409] 04 p1531 N94-19562
Scientific development of a massively parallel ocean climate model
[DE93-019446] 05 p1855 N94-20219
Fast data parallel polygon rendering
[DE93-040157] 05 p1929 N94-20279
Massively parallel computation of RCS with finite elements 05 p1726 N94-20437
Multi-CPU plasma fluid turbulence calculations on a CRAY Y-MP C90
[DE93-015425] 05 p1801 N94-20562
Multiple-fold clustered processor mesh array 05 p1757 N94-21113
A novel VLSI processor architecture for supercomputing arrays 05 p1758 N94-21115
Analysis of multigrid methods on massively parallel computers: Architectural implications 05 p1938 N94-21468
Visualization on massively parallel computers using CM/AVS
[DE93-040151] 05 p1936 N94-21746
The transition to massively parallel computing within a production environment at a DOE access center
[DE93-019155] 05 p1936 N94-21828
Scientific computing in the 1990ies: An astronomical perspective 05 p2057 N94-22440

Achieving high performance on the Intel Paragon
[DE94-003108] 07 p2979 N94-25953
Computational mechanics
[DE94-003015] 07 p2965 N94-26775
Efficient massively parallel simulation of dynamic channel assignment schemes for wireless cellular communications
[AD-A277558] 07 p2971 N94-27558
High performance computing in chemistry and massively parallel computers: A simple transition?
[DE94-004318] 07 p2982 N94-27600
Rome Laboratory software engineering technology program 08 p3414 N94-29330
Progress report for the PTUF Project-93 Q1 and Q2
[PB94-138591] 08 p3431 N94-29995
A heterogeneous computing environment for simulating astrophysical fluid flows 09 p3928 N94-31119
An efficient three-dimensional Poisson solver for SIMD high-performance-computing architectures
09 p3823 N94-31120
Three-dimensional radiative transfer calculations on an SIMD machine applied to accretion disks
09 p3932 N94-31141
Delft Ising computing engine
[PB94-148251] 09 p3806 N94-31587
Some calculations on supersymmetric graphs as communication networks
[REPT-93-72] 09 p3824 N94-31641
Massively parallel systems design for real-time embedded applications
[AD-A277256] 09 p3826 N94-32323
Spacecraft On-Board Information Extraction Computer (SOBIEC) 09 p3808 N94-32433
The Numerical Tokamak Project (NTP) simulation of turbulent transport in the core plasma: A grand challenge in plasma physics
[DE94-008279] 09 p3892 N94-32838
Overview of shock physics codes for armor analysis
[DE94-008948] 09 p3739 N94-32842
Parallel supercomputing: Advanced methods, algorithms, and software for large-scale linear and nonlinear problems
[DE94-008446] 09 p3836 N94-32992
Turbulence modeling of free shear layers for high performance aircraft
[NASA-CR-196137] 12 p4442 N94-36808
Parallelized direct execution simulation of message-passing parallel programs
[NASA-CR-194936] 12 p4497 N94-37411
A scalable high-performance I/O system
[DE94-011513] 12 p4498 N94-37519
Three-dimensional gyrokinetic particle-in-cell simulation of plasmas on a massively parallel computer: LDRD Core Competency Project
[DE94-013367] 12 p4532 N94-37732

MATCHED FILTERS
Further studies using matched filter theory and stochastic simulation for gust loads prediction
[NASA-TM-109010] 01 p0026 N94-11587
Signal processing in impulsive electromagnetic interference
[AD-A266425] 03 p0998 N94-16557
Expansions of cumulative distribution functions directly from characteristic functions
[AD-A267727] 03 p1173 N94-17372
Choice of filters for the detection of gravitational waves from coalescing binaries. 2: Detection in coloured noise
[DE93-616844] 06 p2604 N94-25211
A parallel algorithm for filtering gravitational waves from coalescing binaries
[DE93-616845] 06 p2604 N94-25212
Detection of transient vector-fields in additive noise
[FFI-93/7028] 07 p2768 N94-26232
Output statistics of the SALFAS FM normalizer Smoothing/Prediction function
[AD-A275758] 08 p3463 N94-28759
A computer program to obtain time-correlated gust loads for nonlinear aircraft using the matched-filter-based method
[NASA-TM-109768] 10 p4006 N94-33378

MATCHING
Screening of solar cells
[NASA-TM-106298] 02 p0620 N94-13134
Saving comparisons in the Crochemore-Perrin string matching algorithm
[CWI-CS-R9322] 07 p2971 N94-27550
The molecular matching problem
07 p3030 N94-27910
Variable-resolution stereo matching
08 p3308 N94-30298
On the unification free PROLOG programs
[CWI-CS-R9331] 08 p3427 N94-30733
Fast nonsupervised 3D registration of PET and MR images of the brain
[TELECOM-93-C-006] 09 p3798 N94-33069
Nearest-neighbour search in constant time: An alternative to neural networks for pattern matching applications 09 p3838 N94-33157

MATERIAL ABSORPTION
Hygroscopic absorption to falling films: The effects of the concentration level
[ITN-93-85198] 01 p0148 N94-10391

MATERIAL BALANCE
NT WATER BALANCE
Disintegrating ice front of Shirase Glacier, East Antarctica 01 p0210 N94-12654

MATERIAL REMOVAL (MACHINING)
U MACHINING

MATERIAL STRENGTH
U MECHANICAL PROPERTIES

MATERIALS
Development of the gas turbine. Part 1: Design philosophy and performance 07 p2831 N94-28080
Spacecraft materials: Comparison between flight results obtained on LDEF and MIR 09 p3597 N94-31045
Databases and demands for solar heating materials
[PB94-137494] 09 p3758 N94-31070

MATERIALS HANDLING
NT GROUND HANDLING
NT PROPELLANT TRANSFER
NT REMOTE HANDLING
Hydrogen peroxide safety issues
[DE93-013895] 02 p0565 N94-14346
Materials processing in space: Issues for the third decade
[TABES PAPER 93-260] 03 p0983 N94-16133
Biomass energy: State of the technology present obstacles and future potential
[DE93-016295] 03 p1092 N94-16766
Materials inventory management manual
[NHB-4100.1C] 03 p1225 N94-16830
Autonomous neural network controllers for adaptive material handling
[AD-A268908] 04 p1540 N94-18331
Workshop on Innovation in Materials Processing and Manufacture: Exploratory Concepts for Energy Applications
[DE93-017674] 04 p1467 N94-18478
Coordination of software-development activities among sites that are geographically separated
[DE93-019201] 04 p1524 N94-19076
Robotics in a controlled, ecological life support system
06 p2444 N94-25371
Automated in-situ inspection systems for underground storage tanks
[AD-A274644] 07 p2764 N94-27144

MATERIALS RECOVERY
NT WATER RECLAMATION
Investigations into the recovery of waste sulfuric acid with concentrated solar radiation
[DLR-FB-93-11] 03 p0952 N94-17594
Mechanically refuelable zinc/air electric vehicle cells
[DE93-016446] 04 p1394 N94-17770
Substrate recovery of Mo-Si multilayer coated optics
[DE93-019610] 05 p1698 N94-19810
Plasma-chemical conversion of hydrogen sulfide into hydrogen and sulfur
[DE93-041167] 05 p1682 N94-21789
MHD seed recovery/regeneration, phase 2
[DE94-006772] 09 p3886 N94-31273
Feasibility study for the recycling of nickel metal hydride electric vehicle batteries
[DE94-000268] 09 p3690 N94-31598
Investigation on optimization of carbon dioxide processing system and effective utilization technique of carbon
[DE94-757426] 10 p4082 N94-34224
Consolidation of zircaloy-4 end crops by induction melting
[DE94-010031] 11 p4240 N94-35650
AICD: Advanced Industrial Concepts Division Biological and Chemical Technologies Research Program
[DE94-006854] 11 p4283 N94-36051

MATERIALS SCIENCE
Recovery of materials impacted at high velocity
[DE93-014150] 02 p0576 N94-12885
Nonlinear analysis, scientific computation, and continuum mechanics applied to the science of materials
[AD-A266641] 02 p0817 N94-14680
Sounding Rocket Experiments in Fluid Science and Materials Sciences: TEXUS 25 to 27 and MASER 4, volume 3
[ESA-SP-1132-VOL-3] 03 p0943 N94-15157
QUESTS: A microgravity research facility for materials science experiments 03 p0978 N94-16082
Workshop on Innovation in Materials Processing and Manufacture: Exploratory Concepts for Energy Applications
[DE93-017674] 04 p1467 N94-18478
Contribution to the identification of nonlinear behavior laws in material mechanics
[ECL-92-36] 04 p1458 N94-19411
Materials Science and Engineering
[DE93-040497] 05 p1675 N94-21530
Chemistry and materials science
[DE94-001449] 05 p2152 N94-21858
Report on smart materials
[PB94-137528] 08 p3203 N94-29015
Journal of NIRE, vol. 2, no. 3
[JTN-94-80553] 08 p3553 N94-29512
Research laboratories annual report 1992
[DE94-608124] 08 p3555 N94-30168
Technology 2003: The Fourth National Technology Transfer Conference and Exposition, volume 1
[NASA-CP-3249-VOL-1] 08 p3555 N94-30440
Atomic oxygen erosion considerations for spacecraft materials selection 09 p3593 N94-31022
A cross-disciplinary report on the mathematical sciences applied to materials science, part 1
[AD-A276116] 09 p3843 N94-31529
Intelligent processing of materials, technical activities, 1993 (NAS-NRC Assessment Panel, April 21-22 1994)
[PB94-164183] 11 p4251 N94-35737
National Educators' Workshop: Update 1993. Standard Experiments in Engineering Materials Science and Technology
[NASA-CP-3259] 11 p4229 N94-36398
ASTM test methods for composite characterization and evaluation 11 p4229 N94-36399
Application of materials database (MAT.DB.) to materials education 11 p4230 N94-36402
Simulation of materials processing: Fantasy or reality?
11 p4230 N94-36404
Using experimental design modules for process characterization in manufacturing/materials processes laboratories 11 p4230 N94-36405
Process capability determination of new and existing equipment 11 p4230 N94-36406
Graphing techniques for materials laboratory using Excel 11 p4232 N94-36414
Collection, processing, and reporting of damage tolerant design data for non-aerospace structural materials
[NASA-CR-196046] 11 p4347 N94-36435
JPRS report: Science and technology. Central Eurasia: Materials science
[JPRS-UMS-93-008] 12 p4404 N94-37010
JPRS report: Science and technology. Central Eurasia: Engineering and equipment
[JPRS-UEQ-93-007] 12 p4431 N94-37523

MATERIALS TESTING REACTORS
U NUCLEAR RESEARCH AND TEST REACTORS

MATERIALS TESTS
Polyimide foam insulation systems: A major weight reduction and improvement in fire resistance of sidewall systems 01 p0017 N94-10769
A polyimide foam for advanced fire resistant aircraft applications 01 p0017 N94-10770
Development and testing of a superconducting link for an IR detector
[NASA-CR-193674] 01 p0170 N94-10948
Lessons learned from the Long Duration Exposure Facility
[AD-A266026] 01 p0044 N94-12394
Ohmic heating of composite candidate graphite-fiber/coating combinations
[NASA-TM-4491] 02 p0554 N94-12871
Flight service evaluation of composite components on the Bell helicopter model 206L
[NASA-CR-191499] 02 p0555 N94-13267
Effect of thermal processing practices on the properties of superplastic Al-Li alloys
[NASA-CR-4548] 02 p0574 N94-14850
Atomic research
[NASA-CR-193843] 02 p0788 N94-14905
Building a lunar base
[NASA-TM-109674] 03 p0983 N94-15519
Long Duration Exposure Facility experiment M0003 deintegration/findings and impacts
[AD-A267140] 03 p0885 N94-15749
Materials, processes, and environmental engineering network
[TABES PAPER 93-610] 03 p1051 N94-16142
Evaluation of materials proposed for the construction of the Plasma Electrode Pockels Cell (PEPC) on beamlet
[DE93-016952] 04 p1584 N94-17988
Limited Duration of Candidate Materials Exposure Experiment (LDCE): A Complex Autonomous Payload (CAP) using a Get Away Special (GAS) canister
04 p1326 N94-19176
Ceramic matrix composite parts design
06 p2256 N94-24237
On the deformation kinetics constitutive law of plastic deformation: The rate equation
06 p2161 N94-24289

Performance of selected polymeric materials on LDEF
09 p3593 N94-31023
Fluorescence observations of LDEF exposed materials as an indicator of induced material reactions
09 p3593 N94-31025
Laser-induced fluorescence of space-exposed polyurethane 09 p3593 N94-31026
What LDEF means for development and testing of materials 09 p3598 N94-31050
ASTM test methods for composite characterization and evaluation 11 p4229 N94-36399
Continuous unidirectional fiber reinforced composites: Fabrication and testing 11 p4229 N94-36400
Mechanical properties of crosslinked polymer coatings
11 p4231 N94-36410
Methodologies for thermal and mechanical testing of TMC materials 12 p4401 N94-36659
Experimental and finite-element simulation results for a plane-strain punch-test using isotropic and anisotropic materials
[DE94-011711] 12 p4457 N94-37670

MATHEMATICAL ANALYSIS
U APPLICATIONS OF MATHEMATICS

MATHEMATICAL LOGIC
NT ALGORITHMS
NT AXIOMS
NT BOOLEAN ALGEBRA
NT BOOLEAN FUNCTIONS
NT EQUIVALENCE
NT GENETIC ALGORITHMS
NT LATTICES (MATHEMATICS)
NT PARSING ALGORITHMS
NT PREDICATE CALCULUS
NT SET THEORY
NT SIMPLEX METHOD
NT THRESHOLD LOGIC
Finite state machine microarchitecture transformations described with relational algebra
[MEMO-INF-92-63] 01 p0319 N94-10278
Rare attributes in finite universe: Hypotheses testing specification and exact randomized upper confidence bounds
[DE93-012783] 02 p0775 N94-12955
Combinatorial semantics
[TR-444] 03 p1149 N94-16575
Notes on the use of Dempster-Shafer and fuzzy reasoning to fuse identity attribute data
[AD-A267426] 03 p1004 N94-17309
Using semantic information for processing negation and disjunction in logic programs
[DE93-017412] 04 p1614 N94-18099
Verification of VLSI designs 04 p1400 N94-18363
A refinement for nonmonotonic logic
[REPT-93-21] 04 p1542 N94-19092
Technical development of a theory of programs
[ETN-93-95058] 04 p1532 N94-19652
Are types needed for natural language?
[PB93-191831] 05 p1949 N94-19997
Set theory and nominalisation, part 1
[PB93-191807-PT-1] 05 p1962 N94-20007
Set theory and nominalisation, part 2
[PB93-191815-PT-2] 05 p1962 N94-20008
Back and forth bisimulations on prime event structures
[RR-888-I-IMAG-124-LIFIA] 05 p1929 N94-20124
Explanation closure, action closure, and the Sandewall test suite for reasoning about change
[TR-440] 05 p1907 N94-20522
Proving run-time properties of general programs w.r.t. constructive negation
[CWI-CS-R9245] 05 p1909 N94-21025
Beta(sub k)-complete problems and greediness
[TR-455] 05 p1913 N94-21318
Procedural dynamic semantics, verb-phrase ellipsis, and presupposition
[CWI-CS-R9311] 05 p1914 N94-21495
Reasoning about update logic
[CWI-CS-R9312] 05 p1914 N94-21496
Changing preferences
[CWI-CS-R9310] 05 p1915 N94-21551
Making some issues of implicit knowledge explicit
[PB93-220606] 06 p2478 N94-22984
Logic of capabilities
[PB94-110715] 06 p2473 N94-23747
Epistemic logic for defeasible reasoning using a meta-level architecture metaphor
[PB94-110723] 06 p2473 N94-23748
Typechecker for bijective pure type systems
[PB94-110814] 06 p2454 N94-23817
Real-time process logic
[PB94-101441] 06 p2446 N94-24540
PLANET: A hierarchical network simulator
[ISBN-9-09-005693-9] 06 p2313 N94-25083
New binary integration strategies and corresponding R90 calculations
[AD-A274786] 07 p2769 N94-26359
A formalization of objects using equational dynamic logic
[PB94-125218] 07 p2965 N94-26852
Combining logics
[PB94-125242] 07 p2965 N94-26908
A characterization of stable models using a non-monotonic operator
[CWI-CS-R9315] 07 p2970 N94-27543
Modal logic, transition systems and processes
[CWI-CS-R9321] 07 p2970 N94-27549
Parallel quantification
[LP-93-01] 08 p3422 N94-30318
Dynamic generalized quantifiers and monotonicity
[LP-93-02] 08 p3454 N94-30319
A smart child of Peano's
[ML-92-10] 08 p3455 N94-30325
Completeness of the Lambek calculus with respect to relativized relational semantics
[LP-93-03] 08 p3455 N94-30326
Identity: Quarrelling with an unproblematic notion
[LP-93-04] 08 p3455 N94-30327
A note on schema equivalence
[TR-92-30] 08 p3535 N94-30362
Logic of transition systems
[CT-93-03] 08 p3424 N94-30371
Bounded contraction and many-valued semantics
[ML-93-04] 08 p3456 N94-30380
Models of the untyped lambda-calculus in semi Cartesian closed categories
[ML-93-05] 08 p3456 N94-30381
Categorial generalization of algebraic recursion theory
[ML-93-06] 08 p3456 N94-30382
Algorithmic problems concerning first-order definability of modal formulas on the class of all finite frames
[ML-93-07] 08 p3456 N94-30383
Remarks on the theory of semi-functors
[ML-93-08] 08 p3457 N94-30384
Natural deduction for intuitionistic linear logic
[ML-93-09] 08 p3457 N94-30385
The conjoinability relation in Lambek calculus in linear logic
[ML-93-03] 08 p3457 N94-30397
Termination of term rewriting by semantic labelling
[RUU-CS-93-24] 08 p3459 N94-30424
Three metric domains of processes for bisimulation
[CWI-CS-R9335] 08 p3459 N94-30427
Perpetual reductions and strong normalization in orthogonal term rewriting systems
[CWI-CS-R9345] 08 p3426 N94-30437
Comparative semantics for linear arrays of communicating processes
[CWI-CS-R9336] 08 p3426 N94-30491
Design and analysis of dynamic leader election protocols in broadcast networks
[MEMO-INF-93-43] 08 p3260 N94-30520
A monotonicity conjecture for real cubic maps
[DE94-003969] 08 p3335 N94-30610
Unravelling nondeterminism: On having the ability to choose
[RUU-CS-93-30] 08 p3428 N94-30749
Termination of term rewriting by semantic labelling
[RUU-CS-92-38] 08 p3462 N94-30859
The structure of exponentials: Uncovering the dynamics of linear logic proofs
[ML-93-10] 08 p3430 N94-30973
Inventory of fragments and exact models in intuitionistic proportional logic
[ML-93-11] 08 p3463 N94-30974
Remarks on uniformly finitely precomplete positive equivalences
[ML-93-12] 08 p3463 N94-30975
OTTER 3.0 reference manual and guide
[DE94-007457] 09 p3829 N94-31315
What comes first in dynamic semantics: A compositional, non-representational account of natural language presupposition
[LP-93-15] 09 p3855 N94-31389
The meaning of duplicates in the relational database model
[CT-93-04] 09 p3916 N94-31392
Binary quantifiers and relational semantics
[LP-93-13] 09 p3855 N94-31404
On the independent axiomatizability of modal and intermediate logics
[ML-93-17] 09 p3856 N94-31407
Extensional realizability
[ML-93-18] 09 p3856 N94-31408
The decidability of dependency in intuitionistic propositional logic
[ML-93-20] 09 p3856 N94-31410
Sums and quantifiers
[LP-93-05] 09 p3856 N94-31411
Effective truth
[ML-93-15] 09 p3856 N94-31416
Information acquisition from multi-agent resources; abstract
[LP-93-08] 09 p3917 N94-31452
Completeness and decidability of the mixed style of inference with composition
[LP-93-09] 09 p3842 N94-31453
Tractable deduction in some fragments of auto-epistemic logic
[REPT-93-89] 09 p3844 N94-31673
An epistemic proof system for parallel processes
[TR-93-17] 09 p3826 N94-32291
Fuzzy logic application for modeling man-in-the-loop space shuttle proximity operations
[NASA-CR-188283] 09 p3835 N94-32359
From conditional oughts to qualitative decision theory
10 p4127 N94-34043
A critique of type systems for global overloading
[AD-A278800] 11 p4304 N94-35676
The most abstract common refinement
[AD-A278870] 11 p4305 N94-36014

MATHEMATICAL MODELS
NT ANALOG SIMULATION
NT BIOLOGICAL MODELS (MATHEMATICS)
NT DIGITAL SIMULATION
NT K-EPSILON TURBULENCE MODEL
NT PETRI NETS
NT THOMAS-FERMI MODEL
NT TURBULENCE MODELS
NT VENEZIANO MODEL
Constitutive laws for describing the service relevant creep behaviour of metallic materials
01 p0064 N94-10060
Effects of axial and centrifugal forces on the stability of liquid bridges 01 p0102 N94-10083
Liquid bridges and floating zones
01 p0102 N94-10085
Model of convective motion under low gravity
01 p0103 N94-10088
Space and temporal behavior and control of the residual convection in microgravity 01 p0104 N94-10099
Concept and design of ampoule for melt growth of gallium arsenide in first mission of space flyer unit
01 p0107 N94-10115
CdTe crystal growth by THM with a rotating magnetic field 01 p0107 N94-10116
Computational procedures for determining parameters in Ramberg-Osgood elastoplastic model based on modulus and damping versus strain
[DE93-013309] 01 p0185 N94-10306
Topex orbit determination using GPS tracking system
01 p0038 N94-10359
A lattice gas model for enzyme kinetics with alternate interactions
[DE93-613027] 01 p0395 N94-10411
A flexible modelling software for data acquisition
[DE93-612915] 01 p0322 N94-10484
A lattice gas model for enzyme kinetics with next-nearest neighbor interactions
[DE93-613026] 01 p0410 N94-10631
Arcjet space thrusters
[NASA-CR-193191] 01 p0046 N94-10700
System monitoring and diagnosis with qualitative models
[NASA-CR-193812] 01 p0323 N94-10711
Dimensional transition of the space-time at the minimum action near the planck scale
[DE93-754192] 01 p0410 N94-10718
Bringing theory to practice: The reality of interprocessor communication
[DE93-012346] 01 p0336 N94-10738
Applications of a model to predict flame spread over interior finish materials in a compartment
01 p0019 N94-10783
Practical hazard assessment: An approach to the fire safety 01 p0020 N94-10785
Developments needed to expand the role of fire modeling in material fire hazard assessment
01 p0020 N94-10787
Classical gravity coupled to Liouville theory
[DE93-613049] 01 p0275 N94-10798
The Langevin's approach to the statistical theory of bounded plasma
[DE93-617842] 01 p0388 N94-10839
Combustion-induced crack propagation process in a solid-propellant crack cavity 01 p0098 N94-10901
Evaluation of dual flow thrust vectored nozzles with exhaust stream impingement
[NASA-CR-193292] 01 p0150 N94-10912
Studies of the net surface radiative flux from satellite radiances during FIFE
[NASA-CR-193150] 01 p0230 N94-10953
Advances in time-scale algorithms
01 p0334 N94-10988
Synopsis of timing measurement techniques used in telecommunications 01 p0139 N94-10990

An analytic model for calculating pump-induced wavefront distortions in laser slabs
[DE93-011953] 01 p0174 N94-11126
The three-point function as a probe of models for large-scale structure
[NASA-CR-193249] 01 p0425 N94-11153
Comprehensive dynamic analysis of a bladed disk-turborotor-bearing system
[ISBN-0-315-73646-1] 01 p0180 N94-11155
Similarity of the leading contributions to the self-energy and the thermodynamics in two- and three-dimensional Fermi Liquids
[DE93-012673] 01 p0412 N94-11162
A version of superstring with four space-time dimensions
[DE93-608196] 01 p0412 N94-11163
The controlling parameters of the integrated flux of a stellar population 01 p0426 N94-11187
Blading models for TURBAN and CSPAN turbomachine design codes
[NASA-CR-191164] 01 p0015 N94-11203
A comparison between numerically modelled and experimentally measured loss mechanisms in wave rotors
[NASA-TM-106279] 01 p0029 N94-11255
Computational mechanics needs study
[NASA-CR-193712] 01 p0327 N94-11279
Submarine internal waves
[MRL-GD-0049] 01 p0098 N94-11303
Normal modes of the world's oceans: A numerical investigation using Proudman functions
[NASA-TM-104587] 01 p0288 N94-11358
Extended ecosystem signatures with application to Eos synergism requirements
[NASA-CR-193398] 01 p0266 N94-11374
Surface passivation of InP solar cells with InAlAs layers 01 p0049 N94-11389
The impact of vegetation on the atmospheric boundary layer and convective storms 01 p0277 N94-11480
A modeling investigation of thermal and strain induced recovery and nonlinear hardening in potential based viscoplasticity
[NASA-TM-106122] 01 p0188 N94-11482
On non-linear longitudinal stability of an aircraft in a dive in the presence of atmospheric disturbances 01 p0031 N94-11492
Modeling nonlinear aerodynamic loads for aircraft stability and control analysis 01 p0032 N94-11499
Accretion disk viscosity and internal waves in disks 01 p0153 N94-11615
Integral equation methods for mixed boundary problem of fracture mechanics 01 p0188 N94-11617
A C-band wind scatterometer model derived from the data obtained during the ERS-1 calibration/validation campaign 01 p0233 N94-11711
New tests of the equivalence principle using non-metric couplings of electromagnetism and gravitation 01 p0413 N94-11821
A simple model of melt fracture
[AD-A265311] 01 p0092 N94-11862
Effect of species structure and dielectric constant on C-band forest backscatter
[NASA-TM-109219] 01 p0245 N94-11885
The modelling of aerodynamic flows by solution of the Euler equations on mixed polyhedral grids
[ARA-84] 01 p0016 N94-11888
Evaluation of ECMWF latent heat flux in TOGA CD-ROM 01 p0195 N94-11921
Air-sea fluxes and universal constants in weak-turbulence theory of surface gravity waves 01 p0195 N94-11922
The extraction of bottom characteristics and mapping in Kin Bay, Okinawa Main Island, Japan, using LANDSAT-5/TM and SPOT-1/HRV data 01 p0197 N94-11931
The Pacific responses exhibited by an OGCM to various wind fields 01 p0202 N94-11964
Remote sensing for numerical modelling of radiative transfer processes in ocean environment 01 p0204 N94-11973
Rates of fluvio-thermal erosion on Mars 01 p0435 N94-12018
Ejecting basaltic achondrites from Vesta: Hydrodynamical impact models 01 p0429 N94-12036
Power-law confusion: You say incremental, I say differential 01 p0347 N94-12175
Deviations from the straight line: Bumps (and grinds) in the collisionally evolved size distribution of asteroids 01 p0431 N94-12201
Modelling of dispersal and deposition of impact glass spherules from the Cretaceous-Tertiary boundary deposit 01 p0432 N94-12238
Phase transitions and 2D spherical convection in a large icy satellite 01 p0433 N94-12265
A local dynamic model for large eddy simulation 01 p0155 N94-12285
Parameterization of subgrid-scale stress by the velocity gradient tensor 01 p0155 N94-12286
Experiments on near-wall structure of three-dimensional boundary layers 01 p0159 N94-12309
The evolution equation for the flame surface density in turbulent premixed combustion 01 p0081 N94-12316
Study and modeling of finite rate chemistry effects in turbulent non-premixed flames 01 p0081 N94-12317
Why does preferential diffusion strongly affect premixed turbulent combustion? 01 p0081 N94-12319
Analytical models for describing the mechanical behavior of fiber reinforced composites
[AD-A265906] 01 p0074 N94-12347
Project of an attitude control system (three axis) of a satellite using the LQG/LTR methodology
[INPE-5473-TDI/504] 01 p0044 N94-12356
Ultrasonic wave interaction with advanced complex materials for nondestructive evaluation applications
[AD-A265704] 01 p0074 N94-12401
Sampling and position effects in the Electronically Steered Thinned Array Radiometer (ESTAR)
[NASA-TM-108998] 01 p0245 N94-12432
Modeling void growth and movement with phase change in thermal energy storage canisters
[NASA-TM-106288] 01 p0163 N94-12576
Process modelling for materials preparation experiments
[NASA-CR-193556] 01 p0056 N94-12588
Proceedings of the PORSEC 1992 in Okinawa: Conference for Pacific Ocean Environments and Probing, volume 2
[JTN-93-80419] 01 p0207 N94-12635
A numerical study of deep convection at high latitudes 01 p0210 N94-12652
A basic consideration for remote sensing using microwave radars on a satellite 01 p0212 N94-12665
Variability of the mixed layer depth in the North Pacific Ocean as calculated by a 3-D semi-analytical mixed layer remote sensing model 01 p0221 N94-12718
SST assimilation: Eastern Mediterranean case study 01 p0221 N94-12719
Optimum selection of spectral channels in the problem of remote sensing of phytoplankton concentration in ocean water 01 p0223 N94-12726
The thermodynamics of the nonlinear shear flows 01 p0169 N94-12728
Turbulence generation in the Pacific undercurrent by shear 01 p0223 N94-12730
Verification of the atmosphere-ocean radiative transfer parametric models 01 p0225 N94-12738
Convective and dynamic instability in meridional trenches 01 p0225 N94-12739
Optical transfer operator of the atmosphere-ocean system 01 p0225 N94-12742
Trajectory curving in underwater propagation of light 01 p0226 N94-12748
Atmospheric correction for determination of average SST fields based on AVHRR data 01 p0227 N94-12750
Coupled numerical model for altimetric data assimilation and velocity field analysis 01 p0227 N94-12752
Complex (hydrodynamic, satellite) monitoring of dynamic structures in the western Pacific with the aim of forecasting the marine ecosystems behaviour 01 p0227 N94-12753
Mesoscale dynamic structures of the Subarctic Frontal Zone in the Pacific Ocean 01 p0227 N94-12754
Mixing of drifter ensemble by mesoscale currents 01 p0228 N94-12760
Non-image visible polarization remote sensing of the ocean 01 p0229 N94-12762
The 1991 version of the plume impingement computer program. Volume 1: Description
[NASA-CR-194192] 01 p0166 N94-12775
VIB2D: Quasi 3-D unsteady viscous flow method for blade flutter calculation
[CUED/A-TURBO/TR.129] 01 p0166 N94-12779
A computer model for liquid jet atomization in rocket thrust chambers
[NASA-CR-194194] 02 p0627 N94-12803
The 24 GHz measurements of 2.2 lambda conical horn antennas illuminating a conducting sheet
[NASA-TM-109002] 02 p0598 N94-12811
Venus gravity
[NASA-CR-194077] 02 p0841 N94-12823
Thermosolutal convection and macrosegregation in dendritic alloys
[NASA-CR-194039] 02 p0567 N94-12825
Artificial intelligence support for scientific model-building
[NASA-TM-109252] 02 p0761 N94-12890
An analytical investigation of transient effects on rewetting of heated thin flat plates
[NASA-TM-106120] 02 p0628 N94-12968
Tree reconstruction from partial orders
[DE93-009841] 02 p0743 N94-12991
Surrogates for numerical simulations; optimization of eddy-promoter heat exchangers
[NASA-CR-191510] 02 p0629 N94-13074
The three-dimensional flow past a rapidly rotating circular cylinder
[NASA-CR-191512] 02 p0630 N94-13075
A coherent flame model of premixed turbulent combustion in a counterflow geometry
[CUED/A-THERMO/TR.60] 02 p0562 N94-13085
Dynamics of adaptive structures: Design through simulations
[NASA-CR-193724] 02 p0540 N94-13112
Diagnostic studies of the HxOy-NxOy-O3 photochemical system using data from NASA GTE field expeditions
[NASA-CR-193672] 02 p0706 N94-13170
Lightning simulation and determination of expected striking points
[ITN-93-85202] 02 p0719 N94-13188
Radiative transfer in the dynamic atmospheres of Mira-type variables
[NASA-CR-193324] 02 p0829 N94-13287
A model for rotorcraft flying qualities studies 02 p0523 N94-13308
The development and potential of inverse simulation for the quantitative assessment of helicopter handling qualities 02 p0523 N94-13311
An analytic modeling and system identification study of rotor/fuselage dynamics at hover 02 p0524 N94-13312
Calculation of the required sensor accuracy to obtain a specified state estimation accuracy
[NAL-TR-1173] 02 p0649 N94-13343
Neptune high-latitude emission: Dependence of angle on frequency
[NASA-CR-193280] 02 p0848 N94-13476
Electron emission resulting from fast ion impact on thin metal foils: Implications of these data for development of track structure models
[DE93-013506] 02 p0782 N94-13485
Tidal interactions in the Earth Moon system
[COMMUNICATIONS-SER-B-160] 02 p0837 N94-13503
A knowledge-based model for the integration of remote sensing into a mineral exploration program
[ISBN-0-315-58982-5] 02 p0685 N94-13523
Analytical framework for modeling scale-related variabilities in remote sensing 02 p0685 N94-13592
A stochastic model for behavior analysis of fiber-reinforced quasi-brittle materials 02 p0672 N94-13594
Passage-averaged approximation of turbomachinery flows using vorticity-potential method
[ISBN-0-315-72716-0] 02 p0634 N94-13598
Minimal modeling of the bimodality of extratropical atmospheric planetary waves 02 p0713 N94-13622
Evaluation for rheological constitutive relations, using the indentation technique 02 p0775 N94-13627
Develop research plan for use of atlas data
[NASA-CR-194338] 02 p0714 N94-13709
Theoretical molecular studies of astrophysical interest
[NASA-CR-193300] 02 p0838 N94-13781
Event-driven simulation in SELMON: An overview of EDSE
[NASA-CR-194505] 02 p0749 N94-13784
Antenna pattern control using impedance surfaces
[NASA-CR-194517] 02 p0602 N94-13799
A review of robust detection
[DSIS-93-00400] 02 p0603 N94-13829
Modelling of the temperature distribution in a copper roll for the design of a system of cooled rolls adapted to vertical strip casting
[IMI-93RT-21200-1436-G] 02 p0557 N94-13866
Stochastic performance modeling and evaluation of obstacle detectability with imaging range sensors
[NASA-CR-194510] 02 p0605 N94-13946
Wind erosion in semiarid landscapes: Predictive models and remote sensing methods for the influence of vegetation
[NASA-CR-194029] 02 p0715 N94-13956
Sloshing dynamics on rotating helium dewar tank
[NASA-CR-194403] 02 p0637 N94-13959
Simultaneous solution for core magnetic field and fluid flow beneath an electrically conducting mantle
[NASA-TM-4536] 02 p0716 N94-13960
The role of ionospheric plasma in the magnetosphere
[NASA-CR-194404] 02 p0716 N94-13967
Computer program for thermal and transport properties of parahydrogen from 20 to 10,000 K
[NASA-TP-3378] 02 p0552 N94-14102

A performance prediction model for a fault-tolerant computer during recovery and restoration
[NASA-CR-194490] 02 p0741 N94-14136
Computational techniques and capabilities
02 p0506 N94-14162
Integration of remote sensing and mathematical modelling in disaster mitigation
02 p0692 N94-14239
Nonlinear wave predictions in ceramics
[DE93-016516] 02 p0582 N94-14436
Three-dimensional modeling of diesel engine intake flow, combustion and emissions-2
[NASA-CR-191189] 02 p0519 N94-14448
A conduction model for the vacuum arc remelting process
[NPL-DMM(A)-98] 02 p0639 N94-14464
The motion of a conical shaped liner driven by explosive load
[ITN-93-85215] 02 p0585 N94-14507
Atmospheric acoustic modeling
[DE93-016727] 02 p0718 N94-14518
Scattering calculations and confining interactions
[NASA-CR-194242] 02 p0786 N94-14549
Long duration measurements of fading on a low elevation angle, 11-GHz satellite path 02 p0613 N94-14661
A database for propagation models
02 p0614 N94-14665
Contribution towards a draft revision of recommendations 681: Propagation data required for the design of Earth-space land mobile telecommunications systems 02 p0614 N94-14666
Characterisation of the LMS propagation channel at L- and S-bands: Narrowband experimental data and channel modelling 02 p0615 N94-14669
ACTS propagation experiment discussion: Ka-band propagation measurements using the ACTS propagation terminal and the CSU-CHILL and Space Communications Technology Center Florida propagation program
02 p0616 N94-14678
Nonlinear analysis, scientific computation, and continuum mechanics applied to the science of materials
[AD-A266641] 02 p0817 N94-14680
A study of thin liquid sheet flows
[NASA-TM-106323] 02 p0642 N94-14732
Robust non convex optimization algorithms: Codes and numerical simulation of large scale
[ETN-93-94354] 02 p0756 N94-14813
Optical systems integrated modeling
02 p0547 N94-14837
Double inlet pulse tube cryocooler theory
[AD-A266832] 02 p0597 N94-14877
Toward a quasi-linear closure for compressible turbulence
[DE93-017185] 02 p0647 N94-14895
A mathematical model for the study of hemorrhagic shock and fluid resuscitation: The systemic and pulmonary vasculature
[AD-A266835] 03 p1119 N94-14917
Engineering Physics and Mathematics Division progress report, period ending 31 December 1992
[DE93-015118] 03 p1301 N94-14926
Static aeroelastic response of an aircraft with asymmetric wing planforms representative of combat damage
[AD-A266890] 03 p0865 N94-14951
Unsteady separated flows: Empirical model and control
[AD-A267282] 03 p0855 N94-14959
Modelling of creep data for plastics
[NPL-DMM(A)-92] 03 p1057 N94-15017
Inelastic deformation of metal matrix composites
[NASA-CR-191522] 03 p0930 N94-15106
Advanced methods for cascade testing
[AGARD-AG-328] 03 p1016 N94-15119
Predicted and real development in the aviation in the period 1961-1991 03 p0853 N94-15122
Rotary engine performance computer program (RCEMAP and RCEMAPPC): User's guide
[NASA-CR-191192] 03 p0869 N94-15192
On the use of the noncentral chi-square density function for the distribution of helicopter spectral estimates
[NASA-CR-191546] 03 p1176 N94-15487
Hidden Markov model approach to skill learning and its application to telerobotics
[AD-A266989] 03 p1164 N94-15502
Comparison of RADARC high-frequency radar performance prediction model and ROTHR Amchitka data
[AD-A267077] 03 p0967 N94-15540
Verification of a two-dimensional infiltration model for the resin transfer molding process
[NASA-CR-194597] 03 p0964 N94-15656
Mathematical model of frost heave and thaw settlement in pavements
[AD-A267037] 03 p0983 N94-15676
Nontidal gravity changes observed with a superconducting gravimeter 03 p1100 N94-15808
Report of the working group on theoretical tidal model
03 p1101 N94-15815
Fast simulation of steady-state availability in non-Markovian highly dependable systems
[AD-A266747] 03 p1174 N94-15823
Nuclear rocket plume studies
[AD-A267154] 03 p0925 N94-15837
A feasibility study of a microgravity enhancement system for Space Station Freedom
[NASA-CR-191550] 03 p0886 N94-15864
Effects of rotation on coolant passage heat transfer. Volume 2: Coolant passages with trips normal and skewed to the flow
[NASA-CR-4396-VOL-2] 03 p1023 N94-15991
A CCIR-based prediction model for Earth-Space propagation 03 p0997 N94-16050
Aerodynamic/dynamic/control interaction
[AD-A266187] 03 p0871 N94-16107
Cost-effective test methods for Shuttle payloads
[TABES PAPER 93-651] 03 p0883 N94-16151
Modeling and simulation: A key to future defense technology
[TABES PAPER 93-654] 03 p1054 N94-16153
Sand transport on Mars: Preliminary results from models 03 p1252 N94-16198
Explosive mafic volcanism on Earth and Mars
03 p1253 N94-16204
Morphology and models for the evolution of eastern Hecate Chasma, Venus 03 p1256 N94-16215
Ishtar deformed belts: Evidence for deformation from below? 03 p1256 N94-16218
Why is the Moon dark? 03 p1256 N94-16219
An experimental study of trace element partitioning between perovskite, hibonite and melt: Equilibrium values 03 p0954 N94-16313
Lava crusts and flow dynamics
03 p1103 N94-16316
On the relationship between tectonic plates and thermal mantle plume morphology 03 p1104 N94-16349
Aspects of modelling the tectonics of large volcanoes on the terrestrial planets 03 p1104 N94-16396
Controls of maglev suspension systems
[DE93-015540] 03 p1011 N94-16443
A mathematical model for the study of hemorrhagic shock and fluid resuscitation: Transcapillary exchange
[AD-A266427] 03 p1123 N94-16544
Numerical modeling of the temperature gradients and spectra of the plasma armature on Thunderbolt
[AD-A266414] 03 p0878 N94-16552
A mathematical model for the study of hemorrhagic shock and fluid resuscitation: Exchange of fluid and solutes between vascular, interstitial, and tissue cell compartments
[AD-A266426] 03 p1123 N94-16558
Spatial resolution and cloud optical thickness retrievals 03 p1066 N94-16671
Lossless compression of AVIRIS data: Comparison of methods and instrument constraints
03 p1075 N94-16713
Comparison of modeled backscatter with SAR data at P-band 03 p1076 N94-16735
SAR backscatter from coniferous forest gaps
03 p1076 N94-16736
Retrieval of pine forest biomass using JPL AIRSAR data 03 p1076 N94-16737
Sea bottom topography imaging with SAR
03 p1077 N94-16745
Development of a constitutive model for creep and life prediction of advanced silicon nitride ceramics
[DE93-015894] 03 p0968 N94-16813
Emissions of volatile organic compounds from stationary combustion sources: Numerical modeling capabilities
[DE93-014123] 03 p1096 N94-16825
Textile composite processing science
03 p0938 N94-16856
Development of braided fiber seals for engine applications 03 p0939 N94-16859
Quantification of processing artifacts in textile composites 03 p0939 N94-16860
Stochastic damage evolution in textile laminates
03 p0939 N94-16861
Integration ToolKit and Methods (ITKM) manufacturing methods and prototype toolkit. A combined modeling method using IDEFO, IDEF1x and XSpec
[AD-A266176] 03 p0984 N94-16981
Modeling, estimation and control of distributed parameter systems
[AD-A267325] 03 p1026 N94-17003
Ensemble forecasting techniques in medium-range forecasting
[AD-A267443] 03 p1107 N94-17029
Studies of changes in the energy stored in metals as a result of subjecting them to a surface type technological process
[IFTR-25/1991] 03 p0960 N94-17063
Proposal of a simple mathematical model for the action of a laser on a metal plate
[IFTR-36/1991] 03 p1041 N94-17065
Nonequilibrium radiation and chemistry models for aerocapture vehicle flowfields
[NASA-CR-194645] 03 p1027 N94-17095
Phased array antenna analysis using hybrid finite element methods
[AD-A267620] 03 p1002 N94-17196
Shielding from space radiations
[NASA-CR-194664] 03 p1301 N94-17255
Characterization of metallic multilayers using x ray diffraction analysis
[NIAR-93-13] 03 p0961 N94-17282
The roles of fluid motion and other transport phenomena in the morphology of materials
[NASA-CR-194665] 03 p1028 N94-17298
ONRASIA scientific information bulletin, volume 18, number 2
[AD-A267798] 03 p1304 N94-17305
Mathmatical modeling for diffractive optics
03 p1195 N94-17342
A Geographic Information System approach to modeling nutrient and sediment transport
[DE93-013747] 03 p1097 N94-17426
Energy deposition fluctuations induced by ions in microvolumes and nanovolumes: An analytic approach. 1: Theory
[AD-A267959] 03 p1173 N94-17495
Application of the finite-difference time-domain method to scattering and radiation problems involving wires and plates
[AD-A268396] 03 p1005 N94-17496
Compressible flow solvers using unstructured grids
[INRIA-RR-1732] 03 p1030 N94-17531
Structured finite volume modeling of US Navy aircraft engine test cells. Task 2: Turboprop engine. Volume 2: Code documentation and listings
[AD-A268386] 03 p0873 N94-17569
A basic principles description of liquid vapor phase transitions
[AD-A268331] 03 p1176 N94-17581
A two-layer quasi-geotrophic spherical model: Formulation and climatology
[DM-63] 03 p1110 N94-17593
On the Debye-Huckel's theory
[DE93-624789] 04 p1561 N94-17681
Further on the current algebra of WZNW models at and away from criticality
[DE93-624809] 04 p1545 N94-17686
Direct Monte Carlo simulation of the chemical equilibrium composition of detonation products
[DE93-014559] 04 p1376 N94-17751
Modeling and new equipment definition for the vibration isolation box equipment system
[NASA-CR-193185] 04 p1379 N94-17763
Dust in the Small Magellanic Cloud
[NASA-CR-193344] 04 p1624 N94-17764
CO2 laser with modulated losses: Theoretical models and experiments in the chaotic regime
[DE93-624901] 04 p1435 N94-17771
Air pollution effects field research facility. 3: UV-B exposure and monitoring system
[DE93-013098] 04 p1470 N94-17773
A one dimensional numerical model, with an application to the vertical distribution of dissolved oxygen in the ocean
[DE93-018481] 04 p1495 N94-17779
A radial transmission line material measurement apparatus
[DE93-018508] 04 p1394 N94-17780
A new multiphase equation of state for iron
[DE93-017629] 04 p1357 N94-17819
Considerations for the use of the modified line reversal technique for gas temperature measurement
[DE93-015752] 04 p1576 N94-17857
The value of windpower: An investigation using a qualified production cost model
[DE93-010043] 04 p1465 N94-17888
A preliminary model for crack-tip hydrogen transport
[NPL-DMM(A)-84] 04 p1451 N94-17899
On comparison and extensions of control methods for narrow-band disturbance rejection
[REPT-93-015] 04 p1540 N94-17922
Ratio of specimen thickness to detection area for reliable hydrogen permeation measurement
[NPL-DMM(A)-103] 04 p1451 N94-17929
TANGO: A notation for describing advanced transaction models
[REPT-93-014] 04 p1613 N94-17936

Linear parameter identification methods for ARMA models with periodic coefficients
[REPT-92-070] 04 p1556 N94-17938
Efficient dynamic modeling of manipulators containing closed kinematic loops
[REPT-92-083] 04 p1444 N94-17940
Kinetic growth of random-like and ballistic-like deposition models
[DE93-624946] 04 p1595 N94-17956
Format.m: A usage manual. Towards an efficient symbolic-numeric environment: Extending Mathematica's format rules
[MATHS-REPT-A-185] 04 p1547 N94-17969
Impact response of composite laminates: A guide to closed form solutions
[FFA-TN-1992-33] 04 p1339 N94-17971
A free boundary eigenvaue problem
[IPP-6/310] 04 p1584 N94-17981
Summary report for supercritical carbon dioxide extraction and carbonization of Resorcinol-Formaldehyde (RF) foams
[DE93-016924] 04 p1346 N94-17987
Limitations on the fidelity of 100 fs pulses produced by chirped pulse amplification
[DE93-017167] 04 p1396 N94-17991
Computational strategies for composite structures
[PB93-195097] 04 p1452 N94-18079
Cut and paste based modeling with boundary features
[PB93-187250] 04 p1520 N94-18117
Navigation in hypermedia applications: Modelling and semantics
[REPT-93-034] 04 p1520 N94-18136
The physics of cellular automata and coherence and chaos in classical many-body dynamical systems
[DE93-018021] 04 p1561 N94-18177
Non-linear flight dynamics 04 p1319 N94-18240
Mechanical modeling of the growth of salt structures
[DE93-015342] 04 p1596 N94-18243
A rational design change methodology based on experimental and analytical modal analysis
[DE93-018537] 04 p1521 N94-18271
Hydrodynamic instability modeling for ICF
[DE93-018634] 04 p1587 N94-18274
Bayesian model choice: Asymptotics and exact calculations
[AD-A269067] 04 p1557 N94-18516
Microwave (SSM/I) Estimates of the Precipitation Rate to Improve Numerical Atmospheric Model Forecasts
[NASA-CR-193566] 04 p1491 N94-18602
Diabatic forcing and initialization with assimilation of cloud and rain water in a forecast model: Methodology 04 p1491 N94-18603
Moist wind relationships 04 p1492 N94-18607
Initialization and assimilation of cloud and rainwater in a regional model 04 p1492 N94-18608
Full Boltzmann discrete spectral wave model, implementation and nondimensional tests
[AD-A269885] 04 p1498 N94-18685
Soft X Ray Projection Lithography. Organization of the 1993 photonics science optical meetings
[AD-A269159] 04 p1579 N94-18693
Bayesian analysis of ARMA processes: Complete sampling based inference under full likelihoods
[AD-A269168] 04 p1557 N94-18694
Directory of Energy Information Administration Models 1993
[DE93-016987] 04 p1616 N94-18707
Constant-thrust orbit-raising transfer charts
[AD-A269088] 04 p1334 N94-18718
Solar radiation in Saudi Arabia
[AD-A269970] 04 p1493 N94-18781
Numerical modelling of fringing fields and their use for complex permittivity measurements at high frequencies
[AD-A270198] 04 p1388 N94-18782
Knowledge sources for an intelligent MCM analyzer
[AD-A269224] 04 p1542 N94-18887
Flow volumes for interactive vector field visualization
[DE93-017102] 04 p1418 N94-18888
BACKSCATTER.FOR: A program to calculate the backscattering strength of an inhomogeneous seabed
[AD-A269235] 04 p1499 N94-18910
The intelligent processing of materials
[AD-A269250] 04 p1362 N94-18923
Dynamic characterization of a lightweight, highly maneuverable spacecraft using modal and finite element analyses
[DE93-018095] 04 p1335 N94-18942
Viscosity in the edge of tokamak plasmas
[DE93-018039] 04 p1588 N94-18988
A least-squares computational tool kit
[DE93-018400] 04 p1557 N94-19011
Modeling of the formation of microporosity in alloys
[DE93-017733] 04 p1364 N94-19044
Plastic mechanism analysis of T-joints in RHS subject to combined bending and concentrated force
[PB93-195774] 04 p1456 N94-19061
Deterministic growth-dispersal models and branching random walk
[REPT-93-14] 04 p1550 N94-19088
Similarity solutions for gravity-dominated spreading of a lens of organic contaminant
[REPT-93-24] 04 p1420 N94-19139
Inverse scattering of surface waves: A new look at surface consistency
[REPT-93-25] 04 p1486 N94-19140
Modelling software for structure metrics
[MEMO-INF-93-13] 04 p1526 N94-19200
Molecular dynamics modeling of the mechanical behavior of metallic multilayers
[DE93-017972] 04 p1365 N94-19263
A unified performability evaluation framework for computer and communication systems
[PB94-149549] 04 p1537 N94-19264
Adaptive uniformization: Technical details
[PB94-149523] 04 p1558 N94-19265
Design for cyclic loading endurance of composites
[NASA-TM-106407] 04 p1457 N94-19351
Modelization, numerical simulation and optimal control of NET tokamak plasma configuration evolution for the future generation of fusion reactors
[ETN-93-95019] 04 p1591 N94-19364
Tetravalent chromium (Cr(4+)) as laser-active ion for tunable solid-state lasers
[NASA-CR-194529] 04 p1441 N94-19369
Numerical analysis of pressure meter tests: Application of parameter identification of soils behavior
[ECL-92-52] 04 p1487 N94-19380
Contribution to the modelling and the identification of nonlinear mechanical systems
[ECL-92-32] 04 p1529 N94-19409
Contribution to the identification of nonlinear behavior laws in material mechanics
[ECL-92-36] 04 p1458 N94-19411
Numerical prediction of transition of the F-16 wing at supersonic speeds
[NASA-CR-194407] 04 p1312 N94-19433
Contribution to the study of a symmetric film flow (with or without tensio-active elements)
[ECL-93-13] 04 p1421 N94-19461
Computational Methods for Crashworthiness
[NASA-CP-3223] 04 p1458 N94-19465
Impact analysis of composite aircraft structures 04 p1458 N94-19468
Development and use of computational techniques in Army Aviation research and development programs for crash resistant helicopter technology 04 p1459 N94-19469
Explicit solution techniques for impact with contact constraints 04 p1459 N94-19470
Mathematical sciences, technology, and economic competitiveness
[LC-91-60253] 04 p1514 N94-19478
Structuration processes in protoplanetary accretion disks
[MPE-243] 04 p1628 N94-19519
Stability measurements of Rayleigh-Benard convection near the critical state using a spectral model
[MPIS-15/1992] 04 p1422 N94-19520
Methods for description and control of dynamical systems and their application
[MPIS-17/1992] 04 p1553 N94-19522
An iterative inverse scattering method for the removal of scattered surface waves
[REPT-93-18] 04 p1488 N94-19644
Modeling of driver behavior: Information perception, rule and control strategies in experiments and simulations
[ETN-93-95053] 04 p1510 N94-19649
Remote sensing of Earth terrain
[NASA-CR-194598] 04 p1464 N94-19681
Updated Contributions to the Twente Workshop on Hamiltonian Graph Theory
[MEMO-1076] 04 p1554 N94-19683
On Hamilton-connectedness of Cayley graphs 04 p1554 N94-19684
Toughness and the cycle structure of graphs 04 p1554 N94-19686
The Hopping Lemma 04 p1554 N94-19687
Cycles containing all vertices of maximum degree 04 p1554 N94-19688
Long paths and cycles in tough graphs 04 p1554 N94-19689
The complete closure of a graph 04 p1555 N94-19690
Twenty odd statements in Twente 04 p1555 N94-19691
Generalized closures of graphs 04 p1555 N94-19692
Two problems related to results of Chvatal-Erdoes 04 p1555 N94-19693
Concerning the circumference of certain families of graphs 04 p1555 N94-19694
Ore-type conditions for cycles through specified vertices 04 p1555 N94-19695
Hamilton cycles in path-tough graphs 04 p1555 N94-19696
Cubic graphs containing k vertex-disjoint subgraphs of given cyclomatic number 04 p1555 N94-19697
Reports of the 1992 Synoptic Symposium
[KNMI-TR-151] 04 p1494 N94-19698
HIRLAM 04 p1494 N94-19699
The WAQUA/CSM-16 model 04 p1494 N94-19700
The wave forecasting model NEDWAM 04 p1495 N94-19701
Amorphous silicon batch process cost analysis
[DE93-018203] 04 p1470 N94-19760
Equivalence and reduction of hidden Markov models
[AD-A270762] 04 p1560 N94-19768
A study of the amplification of laser and VLF waves using a simple pendulum model
[AD-A270857] 04 p1442 N94-19770
A Kirchhoff approach to seismic modeling and prestack depth migration
[AD-A271010] 05 p1854 N94-19820
SPICE macromodel for a 1-megawatt power MOSFET switch
[DE93-019415] 05 p1748 N94-19844
Performance potential of plasma thrusters: Arcjet and Hall thruster modeling
[AD-A271085] 05 p1667 N94-19847
Numerical modeling of fringing fields and their use for complex permittivity measurements at high frequencies
[AD-A270478] 05 p1966 N94-19917
Set theory and nominalisation, part 1
[PB93-191807-PT-1] 05 p1962 N94-20007
Set theory and nominalisation, part 2
[PB93-191815-PT-2] 05 p1962 N94-20008
Absorption heat pump for space applications
[NASA-CR-194693] 05 p1845 N94-20066
Cavitation modelling 05 p1668 N94-20079
Statistical object recognition
[AD-A270887] 05 p1962 N94-20113
Modeling of interactions between biosphere and atmosphere on the global scale
[NASA-CR-193423] 05 p1837 N94-20205
A breakdown model for the bipolar transistor to be used with circuit simulators
[DE93-019422] 05 p1750 N94-20218
Computational model of a magnetic modulator for copper lasers
[DE93-019603] 05 p1815 N94-20223
The CSIRO 9-level atmospheric general circulation model
[CSIRO-TP-26] 05 p1855 N94-20256
RCS Analysis of Plate Geometries, parts 1 and 2
[NASA-CR-194173] 05 p1717 N94-20269
High-frequency techniques for RCS prediction of plate geometries 05 p1717 N94-20270
A physical optics/equivalent currents model for the RCS of trihedral corner reflectors 05 p1717 N94-20271
Applying the INN model to the MaxClique
[DE93-040137] 05 p1906 N94-20276
Feature-based tolerancing for intelligent inspection process definition
[DE93-017984] 05 p1906 N94-20311
The life cycles of intense cyclonic and anticyclonic circulation systems observed over oceans
[NASA-CR-194760] 05 p1865 N94-20353
Process for the homoepitaxial growth of single-crystal silicon carbide films on silicon carbide wafers
[NASA-CASE-LEW-15223-1] 05 p2017 N94-20381
Seismic-triggering history of the catastrophic outflows in the Chryse region of Mars 05 p2091 N94-20399
A formational model for the polygonal terrains of Mars: Taking a crack at the genesis of the Martian polygons 05 p2091 N94-20400
Time-domain analysis of planar microstrip devices using a generalized Yee-algorithm based on unstructured grids 05 p1724 N94-20431
Retrieval of ice thickness from polarimetric SAR data 05 p1724 N94-20432
Synergism of active and passive microwave data for estimating bare surface soil moisture 05 p1727 N94-20444
Relationship of attenuation in a vegetation canopy to physical parameters of the canopy 05 p1729 N94-20450
Numerical modeling for an electric-field hyperthermia applicator 05 p1729 N94-20451
Application of the target decomposition theorem to a polarimetric random media model 05 p1730 N94-20453
Modeling the minimum energy state of the Earth's magnetotail
[AD-A267984] 05 p1856 N94-20485

Theoretical and experimental study of the winding of a thin plastic film: The role of aerodynamic effects
[ECL-93-04] 05 p1703 N94-20599

Hydrostatic/nonhydrostatic comparison with the MERCURE code on orographic flows
[ETN-93-94603] 05 p1866 N94-20600

A comparison of calculated and measured rheological properties of crystallising lavas in the field and in the laboratory 05 p1862 N94-20690

Magellan vertical polarization radar observations 05 p1744 N94-20691

Asteroid collisions: Target size effects and resultant velocity distributions 05 p2083 N94-20729

Venus pancake dome formation: Morphologic effects of a cooling-induced variable viscosity during emplacement 05 p2110 N94-20732

Core formation by giant impacts: Conditions for intact melt region formation 05 p1863 N94-20833

Numerical modeling of impact erosion of atmospheres: Preliminary results 05 p2131 N94-20847

Recondensation in the early solar system: Physical conditions and source material 05 p2085 N94-20849

Diffusion-controlled magnesium isotopic fractionation of a single crystal forsterite evaporated from the solid state 05 p1686 N94-20855

Convex set and linear mixing model 05 p1844 N94-20888

Tight comparison bounds for the string prefix-matching problem
[CWI-CS-R9250] 05 p1952 N94-21029

The correlated M/G/1 queue
[CWI-BS-R9303] 05 p1943 N94-21032

Routing of freeway traffic: A discrete-time state space model and routing problems
[CWI-BS-R9232] 05 p1944 N94-21033

Specification and generation of Markov reward models
[MEMO-INF-92-60] 05 p1963 N94-21058

Computation of signal delays in RC networks 05 p1744 N94-21102

Application of molecular modeling to biological processing
[AD-A272612] 05 p1974 N94-21185

Analysis of the effects of eurasian crustal and upper mantel structure on regional phases using broadband seismic data
[AD-A272446] 05 p1858 N94-21206

An evaluation of artificial neural network modeling for manpower analysis
[AD-A273001] 05 p1945 N94-21269

Forecasting technique of variations of the optical absorptivity of thermal control coatings under different simultaneous radiations 05 p1664 N94-21399

MINIFOLD: A kernel for a MANIFOLD-like coordination language
[CWI-CS-R9252] 05 p1915 N94-21534

Derivation of a model of the exciter of a brushless synchronous machine
[EUT-92-E-258] 05 p1761 N94-21538

Coupling of smooth particle hydrodynamics with PRONTO
[DE93-019080] 05 p1915 N94-21539

Defect motion as the origin of the 1/f conductance noise in solids
[EUT-92-E-259] 05 p2029 N94-21552

Survey of lift-fan aerodynamic technology
[NASA-CR-177615] 05 p1646 N94-21592

Local uniform grid refinement and brine transport in porous media with inhomogeneities
[CWI-NM-R9224] 05 p1803 N94-21609

Ultrafast gas switching experiments
[DE93-019071] 05 p1762 N94-21634

Some evidence on determinants of fuel economy as a function of driving cycle and test type
[DE93-019511] 05 p1825 N94-21637

Monitoring issues from a modeling perspective 05 p1868 N94-21640

Fluvial valleys in the heavily cratered terrains of Mars: Evidence for paleoclimatic change? 05 p2144 N94-21670

Mars atmosphere loss and isotopic fractionation by solar-wind-induced sputtering and photochemical escape 05 p2144 N94-21672

A methodology for quantifying uncertainty in models
[DE93-040154] 05 p1916 N94-21747

Stochastic simulation for imaging spatial uncertainty: Comparison and evaluation of available algorithms
[DE93-040058] 05 p1916 N94-21761

An analysis of pressure driven cross-flow through a long slot connecting two parallel channels
[DE93-040181] 05 p1804 N94-21765

Radio and optical emission: Spectral shapes and breaks in GRB
[NASA-CR-194763] 05 p2150 N94-21781

Modeling bristle lift-off in idealized brush seal configurations 05 p1655 N94-21797

Activities Report of the Institute of Applied Physics
[ETN-93-93749] 05 p1966 N94-21798

Edge plasma experiments on CASTOR tokamak
[IPPCZ-332] 05 p1997 N94-21816

Simulations of diffusion-reaction equations with implications to turbulent combustion modeling
[NASA-CR-191536] 05 p1804 N94-21861

Empirical wind model for the middle and lower atmosphere. Part 2: Local time variations
[NASA-TM-104592] 05 p1870 N94-21862

A quantitative model for interpreting nanometer scale hardness measurements of thin films
[DE93-040601] 05 p2034 N94-22005

Information Technology and Economic Modelling
[VTT-SYMP-135] 05 p2049 N94-22056

Mathematical modelling of economic systems 05 p2050 N94-22060

AJKA: An econometric macromodel for Finland 05 p2050 N94-22061

Macromodel of centrally planned economy 05 p2050 N94-22062

Models of transient processes in centrally planned economy 05 p2051 N94-22071

Multicriteria optimisation problem in the agricultural modelling 05 p1844 N94-22073

A model of negotiation in an extensive form game 05 p1965 N94-22075

APL-technology of computer simulation 05 p1923 N94-22077

Microdynamic model of reproduction: Taxation and currency issue as regulators of economy 05 p2053 N94-22084

Use of economic models in Finnish economic policy 05 p2053 N94-22085

Experiences of the bank of Finland's econometric simulation model 05 p2053 N94-22086

Full wave numerical model of arbitrarily-shaped proximity coupled microstrip antennas 05 p1745 N94-22137

Modeling of coaxial-fed microstrip patch antenna by finite difference time domain method 05 p1745 N94-22138

Formulation for numerical solution of radiation and transmission from arbitrary apertures 05 p1745 N94-22140

Effect of errors on the phase centre and pointing angle of phased array antennas 05 p1746 N94-22162

A simplified method for S-parameter calculations of metal septum waveguide filters 05 p1782 N94-22180

Transient acoustic wave modeling: Higher-order WKBJ asymptotics and symbolical manipulation (revised)
[PB93-215432] 05 p1969 N94-22262

The logistic model: The integration of business process redesign and information systems development based on logistic principles
[MEMO-INF-92-70] 05 p2045 N94-22276

A thermodynamic analysis of propagating subcritical cracks with cohesive zones 05 p1834 N94-22611

Brief summary of the evolution of high-temperature creep-fatigue life prediction models for crack initiation 05 p1834 N94-22613

On some approximately balanced combinatorial cooperative games
[MEMO-1113] 06 p2493 N94-22702

Personnel shift assignment: Existence conditions and network models
[MEMO-1116] 06 p2585 N94-22704

Nonlinear state space H(sub infinity) control theory
[MEMO-1119] 06 p2469 N94-22706

Nonlinear systems which have finite-dimensional H(sub infinity) suboptimal central controllers
[MEMO-1120] 06 p2469 N94-22707

Normal forms of kinematic singularities of 3R robot manipulators
[MEMO-1124] 06 p2469 N94-22712

Feedback linearization of parametrized nonlinear time-varying systems
[MEMO-1126] 06 p2470 N94-22714

Nonlocal models in continuum mechanics
[DE93-040146] 06 p2316 N94-22870

Identification for robust control using an H(sub infinity) norm
[EUT-92-E-261] 06 p2470 N94-22873

Method for simulating a vehicle shock test: Design and realization of the required implementation tools
[ECL-92-14] 06 p2352 N94-22885

Causal labeled transition systems: A new approach for describing the behavior of concurrent systems
[LAAS-93179] 06 p2447 N94-22911

Small rocket flowfield diagnostic chambers 06 p2210 N94-23030

A theoretical evaluation of aluminum gel propellant two-phase flow losses on vehicle performance 06 p2210 N94-23031

LOX droplet vaporization in a supercritical forced convective environment 06 p2211 N94-23034

Evaporation and combustion of LOX under supercritical and subcritical conditions 06 p2211 N94-23035

CFD modeling of microwave electrothermal thrusters 06 p2216 N94-23066

Nuclear propulsion control and health monitoring 06 p2217 N94-23071

Flames in dusty mixtures: Their structure and stability
[NASA-CR-191567] 06 p2317 N94-23089

Modelling of solid polymer and direct methanol fuel cells: Phenomenological equations and analytical solutions
[PB93-224897] 06 p2390 N94-23102

Atmospheric numerical modeling resource enhancement and model convective parameterization/scale interaction studies
[NASA-CR-194769] 06 p2400 N94-23124

Atmospheric flow in heterogeneous vegetated regions
[W-9303] 06 p2401 N94-23175

Mathematical modeling of MCFC cells/stacks and networks
[DE94-001914] 06 p2390 N94-23212

Experimental modification and identification of the DSS-13 antenna control system model 06 p2291 N94-23260

Viewing hybrid systems as products of control systems and automata
[NASA-CR-194792] 06 p2472 N94-23300

The ignition temperature of solid explosives exposed to a fire
[DE94-001047] 06 p2265 N94-23436

Mathematical addenda to Hopper's model of plane stokes flow driven by capillarity on a free surface
[PB93-237691] 06 p2480 N94-23438

Differential algebraic equations
[PB93-237618] 06 p2481 N94-23455

Bayesian decision theory with imprecise prior probabilities applied to replacement problems
[PB93-237634] 06 p2481 N94-23456

Mechanical and thermal buckling analysis of sandwich panels under different edge conditions
[NASA-TM-4535] 06 p2228 N94-23514

The computation of R(sub 0) for discrete-time epidemic models with dynamic heterogeneity
[CWI-AM-R9301] 06 p2420 N94-23521

Preliminary eddy current modelling for the large angle magnetic suspension test fixture
[NASA-CR-194772] 06 p2192 N94-23539

Material data representation of hysteresis loops for Hastelloy X using artificial neural networks
[NASA-TM-105990] 06 p2376 N94-23551

A linear model for corrugation and its limit of validity 06 p2269 N94-23584

Development of an analytical-numerical model to predict radiant emission or absorption
[NASA-CR-194860] 06 p2453 N94-23624

Thermal control system for SSF sensor/electronics
[SAND-92-0652C] 06 p2321 N94-23640

Study of transient behavior of finned coil heat exchangers 06 p2321 N94-23642

A direct approach to finding unknown boundary conditions in steady heat conduction 06 p2322 N94-23645

Some useful innovations with TRASYS and SINDA-85 06 p2322 N94-23647

Features of a SINDA/FLUINT model of a liquid oxygen supply line 06 p2322 N94-23649

Convection equation modeling: A non-iterative direct matrix solution algorithm for use with SINDA 06 p2323 N94-23651

An analytic study of a two-phase laminar airfoil in simulated heavy rain 06 p2171 N94-23661

An adaptive multigrid model for hurricane track prediction 06 p2416 N94-23687

Similarity in wave propagation under a global relaxation law
[PB94-111028] 06 p2524 N94-23730

Structured constraint satisfaction
[PB94-119039] 06 p2497 N94-23764

Two applications of a generic task model for solving boolean constraint satisfaction problems
[PB94-119047] 06 p2487 N94-23765

Investigations on detonation shock dynamics and related topics
[DE94-002570] 06 p2326 N94-23809

Dispersion of fire suppression agents discharged from high pressure vessels: Establishing initial/boundary conditions for the flow outside the vessel
[PB94-103660] 06 p2172 N94-23810

Boundary layer receptivity and control 06 p2327 N94-24141

The use of analytical models in human-computer interface design 06 p2434 N94-24190

Integrated approach in modelling, testing, and design of gradient-CVI derived CMC components 06 p2256 N94-24239

New features in Computational Fluid Dynamics (CFD) technology at the TASHAN Engineering Center at IAI
06 p2155 N94-24249
Development of a damage tolerance tool to analyze multiple-site damage in aircraft structure
06 p2157 N94-24261
Aerodynamic models for performance calculations of modern technology propellers 06 p2161 N94-24285
Integrated stress and strength analysis of airplane structures using the data processing tool ISSY
06 p2178 N94-24320
Trends of design methodology of airframe
06 p2179 N94-24327
Numerical modeling of physical vapor transport under microgravity conditions: Effect of thermal creep and stress 06 p2223 N94-24340
GEWEX Cloud Systems Study (GCSS)
06 p2411 N94-24377
Parameterization of sub-grid scale convection
06 p2413 N94-24386
Coupled land surface/hydrologic/atmospheric models
06 p2413 N94-24387
Session on validation of coupled models
06 p2414 N94-24399
A study of the core module simulator floor capability
06 p2380 N94-24418
A minimum cost tolerance allocation method for rocket engines and robust rocket engine design
06 p2222 N94-24419
Using neural networks to assist in OPAD data analysis
06 p2477 N94-24452
Evaluation of advanced materials through experimental mechanics and modelling 06 p2374 N94-24454
An Earth albedo model: A mathematical model for the radiant energy input to an orbiting spacecraft due to the diffuse reflectance of solar radiation from the Earth below
[NASA-TM-104596] 06 p2195 N94-24497
Improved gas core propulsion model
[DE94-000929] 06 p2220 N94-24511
Diagnosing process faults using neural network models
[DE94-002633] 06 p2473 N94-24518
The transition from diapirism to dike intrusion: Implications for planetary volcanism
[NASA-CR-195133] 06 p2403 N94-24580
Edge elements, their advantages and disadvantages
[PB94-111069] 06 p2298 N94-24593
Finite-element modelling of three-dimensional electromagnetic fields using edge and nodal elements
[PB94-111077] 06 p2298 N94-24597
Recent developments in the mathematical modelling and physical understanding of transport and dispersion in aquatic systems, with special reference to tidal waters
[PB94-111135] 06 p2418 N94-24600
Crashworthiness analysis using advanced material models in DYNA3D
[DE94-002988] 06 p2229 N94-24632
Non-brittleness of a DESIRE-model for an office assignment task
[PB94-119021] 06 p2489 N94-24643
A two-dimensional dispersion module for the TOUGH2 simulator
[DE94-002262] 06 p2335 N94-24655
An efficient data assimilation algorithm with a gaussian covariance structure
[AD-A273152] 06 p2418 N94-24671
Temporal model of an optically pumped co-doped solid state laser
[NASA-TM-109680] 06 p2350 N94-24851
Vertical transport of water in the Martian boundary layer 06 p2622 N94-24902
Exercise keevil: Noise levels of six military helicopters
[PB93-210722] 06 p2529 N94-25026
Parametric uncertainty modeling for application to robust control 06 p2163 N94-25103
A study of roll attractor and wing rock of delta wings at high angles of attack 06 p2164 N94-25111
The importance of properties in modeling
06 p2246 N94-25121
Thermophysical property sensitivity effects in steel solidification 06 p2246 N94-25122
A thermodynamic approach to obtain materials properties for engineering applications
06 p2248 N94-25131
An exploratory stochastic model for toxic effects on cells
[AD-A273438] 06 p2422 N94-25146
First results from the Fennoscandian GPS networks
06 p2405 N94-25204
Designs with a small number of runs for factorial experiments
[ISBN-9-03-860162-X] 06 p2462 N94-25237
Introduction to a behavioral approach for continuous time systems
[ETN-94-95301] 06 p2492 N94-25277
Modelling of premixed laminar flames
[ETN-94-95317] 06 p2236 N94-25284
Validating identified nonlinear models with chaotic dynamics
[RR-469] 06 p2523 N94-25314
Ring nuclei of strain for bonded dissimilar elastic half spaces with particular application to axisymmetric crack problems
[OUEL-1966/92] 06 p2379 N94-25325
On a new functional integral formalism for Hubbard model
[DE93-614017] 06 p2492 N94-25334
The Casimir energy of the rigid string with massive ends
[DE93-616851] 06 p2492 N94-25338
Deviation equations of Synge and Schild in spaces with affine connection and metric, and equations for gravitational waves detectors
[DE93-616852] 06 p2571 N94-25339
Loading, electromyograph, and motion during exercise
06 p2427 N94-25359
Influence of test configuration on the combustion characteristics of polymers as ignition sources
06 p2238 N94-25365
Modelling early failures in Space Station Freedom
06 p2374 N94-25372
Edge detection using a complex wavelet
[AD-A273699] 06 p2493 N94-25452
Fault detection in HVAC systems using fuzzy models
[OUEL-1977/93] 06 p2373 N94-25475
Quality metrics for sensor images
06 p2443 N94-25513
Shielded Coil Electrodynamic Propulsion (SCEP). A feasibility study
[AD-A273824] 06 p2314 N94-25539
The application of simulated annealing to stochastic systems
[AD-A273850] 07 p3001 N94-25607
A comparison of three approximate mathematical models for the gravity gradient stabilized satellite
[AD-A273832] 07 p2694 N94-25615
HDR reactor containment fire modeling with BRI2
[VTT-PUBS-113] 07 p3031 N94-25621
Binaural room simulation
[AD-A273823] 07 p3009 N94-25737
Hydrogen uptake into silicon from an ECR plasma
[DE94-003771] 07 p3050 N94-25815
Spatial symmetry, local integrability and tetrahedron equations in the Baxter-Bazhanov model
[DE93-634348] 07 p3002 N94-26038
Z(sub N)(sup n-1) broken model
[DE93-634357] 07 p3072 N94-26039
Geometric correction of SPOT images with use of digital elevation models
[ETN-94-95033] 07 p2847 N94-26107
The identification of inflow fluid dynamics parameters that can be used to scale fatigue loading spectra of wind turbine structural components
[DE94-000231] 07 p2791 N94-26117
SIMA: A model for forest succession based on the carbon and nitrogen cycles with application to silvicultural management of the forest ecosystem
[SILVA-CARELICA-22] 07 p2848 N94-26258
Simulation modeling for long duration spacecraft control systems 07 p2684 N94-26288
C-periodicity and the physical mass in the 3-state Potts model
[DE94-601551] 07 p3019 N94-26423
Subgraph approximations for large directed graphical models
[AD-A274813] 07 p3003 N94-26485
Simulation approaches for calculations in directed graphical models
[AD-A274825] 07 p3003 N94-26494
A concurrent, multigroup, discrete ordinates model of neutron transport
[DE94-004334] 07 p3020 N94-26577
Reconstruction of multiple cracks from experimental electrostatic boundary measurements
[AD-A277433] 07 p2994 N94-26601
Piloted simulation study of an ILS approach of a twin-pusher business/commuter turboprop aircraft configuration
[NASA-TM-4516] 07 p2646 N94-26602
Analysis of the influence of weather on infrared imagery
[FEL-92-A421] 07 p3036 N94-26649
Simulation dynamics of a multibody chain: Recursion based on chain modal coordinates
[ISBN-0-315-83555-9] 07 p2994 N94-26659
A constitutive model for layered wire mesh and aramid cloth fabric
[DE94-003275] 07 p2708 N94-26796
Calculations of material removal, removal rate, and Preston coefficient in continuous lapping/polishing machines
[DE94-002619] 07 p2763 N94-26804
Physical modelling and adaptive predictive control of diffusion/LPCVD reactors
[PB94-126398] 07 p2763 N94-26819
Modern photoacoustic spectroscopy problems. Theory and experiment (a review)
[IFTR-41/1993] 07 p2716 N94-26823
Three dimensional object recognition using a complex autoregressive model
[AD-A274388] 07 p2995 N94-26829
Calculation of the electromagnetic critical state response of high T(sub c) superconductor tape
[DE94-002894] 07 p3061 N94-26868
Recursive bundle event structures
[PB94-125275] 07 p3004 N94-26870
Annual conference on fire research, 1993: Book of abstracts
[PB94-121324] 07 p2717 N94-26907
Combining logics
[PB94-125242] 07 p2965 N94-26908
Some aspects of nonlinear discrete-time descriptor systems in economics
[PB94-126653] 07 p3101 N94-26918
A non-linear mathematical model or finite, periodic rail corrugations
[REPT-93-49] 07 p2996 N94-26967
Kinetics of 2-pentadecylaniline polymerizations in monolayers: Relationships between experimental data and a new theoretical model
[AD-A274419] 07 p2754 N94-27080
Research in improved assessment of software reliability
[AD-A274161] 07 p2968 N94-27140
Numerical Analysis Methods of Surface Cracks
[VTT-PUBS-119] 07 p2841 N94-27186
UAH mathematical model of the variable polarity plasma ARC welding system calculation
[NASA-CR-193926] 07 p2824 N94-27221
High resolution studies of sunspots and flux tubes
[NASA-CR-195216] 07 p3111 N94-27321
Compressibility effects on rotor forces in the leakage path between a shrouded pump impeller and its housing
07 p2796 N94-27379
Global barotropic response to a tropical forcing
[NASA-CR-195256] 07 p2896 N94-27408
A characterization of stable models using a non-monotonic operator
[CWI-CS-R9315] 07 p2970 N94-27543
Control of a hydrogen/oxygen steam generator
[DLR-FB-93-02] 07 p2826 N94-27589
Development of hypersonic engine seals: Flow effects of preload and engine pressures
[NASA-TM-106333] 07 p2826 N94-27599
An unavailability model for errors made during surveillance testing
[DE94-000816] 07 p2835 N94-27613
Lifetimes of lunar satellite orbits
[NASA-TP-3394] 07 p2690 N94-27771
Modeling of the coupled magnetospheric and neutral wind dynamos
[NASA-CR-195273] 07 p2883 N94-27852
Ion-driven permeation of deuterium in metals
[DE94-701104] 07 p2744 N94-27876
Reanalysis of Mariner 9 UV Spectrometer Data for Ozone, Cloud, and Dust Abundances, and Their Interaction Over Climate Timescales
[NASA-CR-195244] 07 p3107 N94-27885
A laboratory test on construction of ice domes and their load-carrying capacity 07 p2884 N94-27966
Numerical assessment of aerodynamic interactions on missiles with transverse jets control
07 p2659 N94-28031
Numerical simulation of a powered-lift landing
07 p2671 N94-28033
Gas Turbine Engine Transient Behaviour
[VKI-LS-1993-06] 07 p2828 N94-28043
Transient model applications. 2: Compressor stall modeling methods 07 p2829 N94-28049
Engine simulation technology
07 p2829 N94-28051
Landscape dynamics of northeastern forests
[NASA-CR-195272] 07 p2852 N94-28070
Nonequilibrium radiation and chemistry models for aerocapture vehicle flowfields
[NASA-CR-195706] 07 p2648 N94-28071
An initial investigation into methods of computing transonic aerodynamic sensitivity coefficients
[NASA-CR-195705] 07 p2648 N94-28072
A modelling of the noise from simple coaxial jets. Part 3: With hot primary flow
[ISVR-TR-230-PT-3] 07 p2807 N94-28173
Interaction of the sonic boom with atmospheric turbulence 07 p2650 N94-28191

The propagation of spark-produced N waves through turbulence 07 p2650 N94-28193
Performance considerations for the application of the lossless browse and residual model 07 p2946 N94-28256
Extraterrestrial accretion and glacial cycles 07 p2890 N94-28308
Intertemporal bargaining and dynamic consistency [PB94-133147] 07 p3095 N94-28386
Lisp interface to geometric modelling operations [PB94-133121] 07 p3001 N94-28398
Filament to mandrel gap analysis: Resulting gap from filament winding over a cone-cylinder transition mandrel (reference NMTP no. 93838) [DE94-004225] 08 p3175 N94-28528
Applied analysis/computational mathematics [DE94-005133] 08 p3451 N94-28571
Dissipative quantum dynamics and nonlinear sigma-model [DE94-606295] 08 p3523 N94-28617
A family of joint probability models for cost and schedule uncertainties [AD-A275513] 06 p3463 N94-28670
Controlling chaos in plasma filled diodes [AD-A275525] 08 p3504 N94-28686
On the linear stability of Verkley's modons 08 p3324 N94-28695
Similarity solutions and numerical modeling in buoyancy controlled turbulent diffusion flames [AD-A275820] 08 p3188 N94-28777
Modeling, analysis, and simulation of an optical time-division multiple-access network architecture [AD-A275847] 08 p3498 N94-28780
The lectures in complex systems, volume 5 [AD-A275458] 08 p3466 N94-28807
Approximation of solutions of the cubic NLSE by finite dimensional equations and non-squeezing properties [PB94-138294] 08 p3452 N94-29148
Model-oriented data analysis with applications to lake and soil water simulation [PB94-136942] 08 p3329 N94-29173
Computer simulations on development of the fast reconnection mechanism 08 p3360 N94-29241
Flowfield prediction of NO(x) and smoke production in aircraft engines 08 p3191 N94-29252
Numerical prediction of turbulent sooting diffusion flames 08 p3191 N94-29253
Numerical modelling of turbine combustion chambers 08 p3154 N94-29254
Modeling of the phase liquidates in combustion chambers 08 p3195 N94-29278
Scramjet CFD methods and analysis. Part 2: Scramjet CFD analysis. Numerical simulation of supersonic mixing and combustion applied to scramjet combustor 08 p3152 N94-29300
Attenuation of outdoor sound propagation levels by a snow cover [AD-A275387] 08 p3478 N94-29314
Damage meso-modeling of 3D evolutive composites [REPT-932-430-106] 08 p3179 N94-29442
On-line search for optimal controller parameters using interconnected learning automata [MATHS-REPT-A-196] 08 p3436 N94-29526
Development and verification of a model to predict impingement currents for ion thrusters [NASA-CR-195322] 08 p3173 N94-29546
Introduction to the design of ventilation systems 08 p3231 N94-29599
Ventilation models 08 p3232 N94-29603
Models for vibration-dissociation coupling in high-temperature gases 08 p3273 N94-29675
Spherical model for turbulence 08 p3274 N94-29730
Control of micromachined deformable mirrors 08 p3239 N94-29787
On fatigue crack closure: Analysis and measurement [ISBN-0-315-74873-7] 08 p3321 N94-29812
An analytical study of unsteady rotor/fuselage interaction in hover and forward flight 08 p3131 N94-29826
Radiation and scattering from cylindrically conformal printed antennas [NASA-CR-195546] 08 p3253 N94-29873
Acceptance sampling methods for sample results verification [DE94-002862] 08 p3465 N94-29925
Microgravity compatible drive system-rider. New technologies [PB94-138583] 08 p3229 N94-29996
Melt flow during alloy solidification: Dimensional analysis and model problems [PB94-138625] 08 p3206 N94-29997
Polynomial modeling of analog-to-digital converters [DE94-005579] 08 p3406 N94-30008
Triple Diagonal modeling: A mechanism to focus productivity improvement for business success [DE94-004309] 08 p3527 N94-30041
Boundary-induced phase transitions in equilibrium and non-equilibrium systems [DE94-608137] 08 p3199 N94-30111
Statistical description of hot and dense clustering matter [DE94-608155] 08 p3490 N94-30112
Volume averaged model for the mechanics of alloys solidification [PB94-138617] 08 p3208 N94-30113
Generalized augmented space theorem for correlated disorder and cluster coherent potential approximation [DE94-608110] 08 p3208 N94-30118
Modelling of multiparticle production by dynamical semigroup method [DE94-608132] 08 p3490 N94-30120
A framework for comparing conceptual modeling languages [TR-92-29] 08 p3535 N94-30361
Logic of transition systems [CT-93-03] 08 p3424 N94-30371
Bounded contraction and many-valued semantics [ML-93-04] 08 p3456 N94-30380
Models of the untyped lambda-calculus in semi Cartesian closed categories [ML-93-05] 08 p3456 N94-30381
The secrets of causality [RUU-CS-93-29] 08 p3426 N94-30490
Free-floating dual-arm robots for space assembly [AIAA PAPER 94-1195-CP] 08 p3442 N94-30546
The road plan model: Information model for planning road building activities [AIAA PAPER 94-1219-CP] 08 p3445 N94-30567
Simulation of composite material response under dynamic compressive loading [DE94-005272] 08 p3184 N94-30589
A review of the ablative stabilization of the Rayleigh-Taylor instability in regimes relevant to ICF [DE94-005809] 08 p3509 N94-30597
An evaluation of explicit pseudo-steady-state approximation schemes for stiff ODE systems from chemical kinetics [CWI-NM-R9312] 08 p3353 N94-30729
Engineering of systems for application of scientific computing in industry WP project management ISNaS 9209099 [PB94-126232] 08 p3428 N94-30739
Modeling data throughput on communication networks [DE94-005077] 08 p3260 N94-30772
Formulae for the calculation of the magnetic field strength in a Helmholtz system with circular coils [NPL-DES-130] 08 p3260 N94-30785
Using the log-normal distribution in analyzing aerosols: The mathematical reasoning underlying the various diameters used and the plotting procedure [DE94-006459] 08 p3461 N94-30817
Selecting model complexity in learning problems [DE94-000764] 08 p3461 N94-30821
Numerical simulation of a condenser in two-phase heat transport systems: A feasibility study [AD-B173650] 08 p3282 N94-30855
A solid-on-solid invasion percolation model for self-affine interfaces [DE94-608102] 08 p3521 N94-30888
Mathematical models of hysteresis [DE94-005681] 08 p3260 N94-30902
An investigation of the reacting vortex structures associated with pulse combustion 08 p3200 N94-30911
An asymptotic analysis for compressible gas lubrication of rough surfaces 08 p3222 N94-30922
Optimization techniques for a dial-a-ride transportation system in urban environment [REPT-93-051] 08 p3537 N94-30926
Identification of the damping ratio relationship of an autovehicle suspension [REPT-93-063] 08 p3313 N94-30937
Application of the extended Kalman filter to the estimation of the char mass in a fluidized bed combustor [REPT-93-065] 08 p3200 N94-30938
Numerical modeling and prediction of the thermomechanical behavior of fiber-reinforced composites 08 p3186 N94-30956
Numerical simulations of piano strings. Part 1: A physical model for a struck string using finite difference methods [TELECOM-93-C-003] 08 p3481 N94-30972
Elements for the recognition of three dimensional deformable shapes: Application to biomedical imagery [TELECOM-93-E-006] 08 p3396 N94-30978
Model updating of vibrating systems based on measured or calculated frequency response functions [CTH-E-93-03] 09 p3732 N94-31091
Report of the 'Mathematical Models for Neural Networks' course [TELECOM-93-D-019] 09 p3828 N94-31100
Tectonic History of the Terrestrial Planets [NASA-CR-195696] 09 p3939 N94-31105
Aspects of modelling the tectonics of large volcanoes on the terrestrial planets 09 p3940 N94-31107
Geoid-to-topography ratios on Venus: A global perspective 09 p3940 N94-31110
A tectonic resurfacing model for Venus 09 p3941 N94-31113
A Green's function approach to analysing the effects of random synaptic background activity in a model neural network [MATHS-REPT-A-202] 09 p3828 N94-31157
Representation, prediction and identification of cyclostationary processes: A state-space approach [REPT-93-041] 09 p3850 N94-31191
Interactive reconstruction of anatomical structures with free-form surfaces [TELECOM-93-E-002] 09 p3794 N94-31195
An investigation of the spin-coating process and a model for three-dimensional regular foams 09 p3649 N94-31206
A comparison of predictors for first-guess wind speed errors [AD-A276460] 09 p3781 N94-31239
Oscillations in piston-driven shear flow of a non-Newtonian fluid [AD-A276472] 09 p3701 N94-31245
ADCIRC: An advanced three-dimensional circulation model for shelves, coasts, and estuaries. User's manual for ADCIRC-2DDI [AD-A276150] 09 p3787 N94-31250
A study of theoretical models for managing technology change and a comparison to a radio frequency identification implementation [AD-A276012] 09 p3672 N94-31385
An algebraic view on Rosetta [CL-93-02] 09 p3841 N94-31391
Nonlinear model validation using correlation tests [RR-463] 09 p3842 N94-31394
A review of sensitivity analysis techniques [DE94-007192] 09 p3842 N94-31399
Identification of polynomial and rational NARMAX models [RR-483] 09 p3842 N94-31413
Modeling of fracture and damage in quasibrittle materials 09 p3734 N94-31479
On the mechanics of stress analysis of fiber-reinforced composites 09 p3619 N94-31481
Fully discrete arbitrary-order schemes for a model hyperbolic conservation law [CRANFIELD-AERO-9307] 09 p3843 N94-31539
A simplified Von Neumann method for linear stability analysis [CRANFIELD-AERO-9310] 09 p3843 N94-31540
Two models solving the increasing energy problem of the continuous Hopfield network model [REPT-93-87] 09 p3843 N94-31552
Development and implementation of a full-potential ASW method [ETN-94-95757] 09 p3858 N94-31560
Numerical simulation of interplanetary dynamics 09 p3933 N94-31566
Evidence for a correct SiO2 voltage acceleration model [DE94-006578] 09 p3690 N94-31594
Boundary-layer cumulus over land: Some observations and conceptual models [DE93-040820] 09 p3781 N94-31597
Plasma confinement theory and transport simulation [DE94-006065] 09 p3888 N94-31619
The influence of transmutation, void swelling, and flux/spectra uncertainties on the electrical properties of copper and copper alloys [DE94-006213] 09 p3641 N94-31626
Impurities and conductivity in a D-wave superconductor [DE94-006222] 09 p3898 N94-31628
On the validity of the BLP model [REPT-93-70] 09 p3917 N94-31640
Aeroacoustic sources in internal flows [ISBN-9-03-86-0282-0] 09 p3860 N94-31653
Aperture excitation of electrically large, lossy cavities [PB94-145711] 09 p3675 N94-31683
Numerical modelling of turbulence [ISBN-0-315-86439-7] 09 p3703 N94-31720
Micromechanics and effective properties of particulate composites and fluid suspensions 09 p3703 N94-31744
Stability and instability criteria for magnetohydrodynamics [PB94-148475] 09 p3889 N94-31772

Numerical simulations of monsoon rainfall with the NRL/NCSU regional nested grid model
09 p3782 N94-31791
A model of concurrent flow flame spread over a thin solid fuel 09 p3634 N94-31795
Attitude dynamics of spinning rockets in space with internal mass motion 09 p3601 N94-31802
Cometary molecules 09 p3935 N94-31869
Seasons and chaos in population dynamics
09 p3912 N94-31897
A paraperspective factorization method for shape and motion recovery
[AD-A276513] 09 p3712 N94-31929
Cumulus convection parameterization and numerical modelling of moist atmospheres
09 p3783 N94-31989
Computer modelling of cyclic deformation of high-temperature materials
[AD-A277056] 09 p3623 N94-32012
Minimization of computational requirements in the hybrid stress finite element method
[AD-A277120] 09 p3846 N94-32048
Wavevector-frequency analysis with applications to acoustics
[AD-A276618] 09 p3861 N94-32125
A polling system with a dormant server
[CWI-BS-R9313] 09 p3835 N94-32193
Area-interaction point processes
[CWI-BS-R9318] 09 p3847 N94-32197
Multiple inheritance via intersection types
[TR-93-18] 09 p3848 N94-32292
Finite element solution to the Helmholtz equation with high wave number. Part 1: The h-version of the FEM
[AD-A277396] 09 p3848 N94-32341
Mechanics of failure of high temperature metal matrix composites
[AD-A277397] 09 p3624 N94-32342
Fuzzy logic application for modeling man-in-the-loop space shuttle proximity operations
[NASA-CR-188283] 09 p3835 N94-32359
Chemical vapor deposition fluid flow simulation modelling tool
[NASA-CR-189648] 09 p3707 N94-32480
The p-q-r-medial axis algorithm requires only local operations
[CWI-BS-R9317] 09 p3849 N94-32507
Numerical simulation of quantum many-body systems
[DE94-008451] 09 p3912 N94-32513
Molecular Science Research Center
[DE94-007464] 09 p3871 N94-32605
Modeling of residual stress mitigation in austenitic stainless steel pipe girth weldment
[DE94-007184] 09 p3738 N94-32639
Basic principles approach for studying nonlinear Alfven wave-alpha particle dynamics
[DE94-007112] 09 p3891 N94-32664
Arithmetic averaging: A versatile technique for smoothing and trend removal
[DE94-005274] 09 p3852 N94-32673
Ethics and rationality in information-enriched decisions: A model for technical communication
[DE93-040251] 09 p3681 N94-32679
A new solution method for the inverse kinematic joint velocity calculations of redundant manipulators
[DE94-004427] 09 p3727 N94-32682
Aspects of modeling uncertainty and prediction
[DE94-007565] 09 p3852 N94-32744
A long-term simulation of surface fluxes and soil moisture
[DE94-006661] 09 p3774 N94-32772
New advances in the modeling of high-temperature superconductors
[DE94-007649] 09 p3905 N94-32815
The Numerical Tokamak Project (NTP) simulation of turbulent transport in the core plasma: A grand challenge in plasma physics
[DE94-008279] 09 p3892 N94-32838
Hierarchical modeling for reliability analysis using Markov models
[NASA-CR-188288] 09 p3731 N94-32862
Manual for automatic generation of finite element models of spiral bevel gears in mesh
[NASA-CR-191009] 09 p3728 N94-32900
A mathematical model for simulating noise suppression of lined ejectors
[NASA-TP-3425] 09 p3861 N94-32930
Modeling of aircraft unsteady aerodynamic characteristics. Part 1: Postulated models
[NASA-TM-109120] 09 p3586 N94-32951
Fluid Dynamics Lagrangian Simulation Model
[AD-A277438] 09 p3710 N94-33009
Effective computational strategy for predicting the response of complex systems
[AD-A277452] 09 p3740 N94-33011
Fast nonsupervised 3D registration of PET and MR images of the brain
[TELECOM-93-C-006] 09 p3798 N94-33069
Statistical characteristics of bistatic surface scatter and mean bistatic surface scattering strengths
[AD-A278155] 09 p3862 N94-33096
Real-time sensor data validation
[NASA-CR-195295] 09 p3616 N94-33099
Designer's unified cost model
09 p3627 N94-33122
A comparison of rough surface parabolic equation models
[AD-A278090] 09 p3791 N94-33185
An approximate model for vertical polarization and surface roughness using the parabolic equation
[AD-A278091] 09 p3684 N94-33186
A case-based approach to creative design
[AD-A278235] 10 p4104 N94-33377
Similarity in separated flow fields producing large-scale vortices 10 p3969 N94-33382
Environmental modeling with GIS: A strategy for dealing with spatial continuity 10 p4080 N94-33421
Stratospheric models and measurements: A critical comparison 10 p3971 N94-33457
Previous model comparisons
10 p3971 N94-33458
Stochastic models of attention and search
[AD-A278538] 10 p4097 N94-33674
Development of predictive reaction models of soot formation
[AD-A278366] 10 p4021 N94-33701
Meso-beta scale numerical simulation studies of terrain-induced jet streak mass and momentum perturbations
[NASA-CR-195863] 10 p4089 N94-33752
An RSM study of the effects of simulation work and metamodel specification on the statistical quality of metamodel estimates
[AD-A278551] 10 p4130 N94-33783
Infrared troubles of differential renormalization
[DE94-611119] 10 p4142 N94-33862
Modeling the transition region
10 p4046 N94-33890
Modeling the impact behavior of high strength ceramics
[AD-A277744] 10 p4028 N94-33894
Transition receptivity and control: Computations
[AD-A278339] 10 p4047 N94-33970
Self-calibrating models for dynamic monitoring and diagnosis 10 p4127 N94-34052
A toolbox and a record for scientific model development 10 p4110 N94-34062
The 2nd International Workshop on Discrete Time Domain Modelling of Electromagnetic Fields and Networks
[AD-A277551] 10 p4035 N94-34081
A multimaterial formalism
[DE94-009300] 10 p4048 N94-34097
Kinematic model of a beam riding air-to-air missile
[PB94-149085] 10 p3990 N94-34106
Experimental and analytical study on fluid whirl and fluid whip modes 10 p4054 N94-34191
Identification of mechanical systems using probabilistic neural networks
[DE94-007555] 10 p4114 N94-34296
Trim calculation of tandem rotor helicopter using simplified rotor system mathematical model
10 p4008 N94-34337
A dynamic model of the vacuum furnace for separating Pb from Sn-Pb alloy 10 p4026 N94-34346
Optimum design of wide frequency vibration absorbers
10 p4074 N94-34348
Analysis of woven and braided fabric reinforced composites
[NASA-CR-194930] 10 p4020 N94-34399
An assessment of fatigue crack growth prediction models for aerospace structures
10 p4071 N94-34586
Cost and schedule estimation study report
[NASA-CR-189344] 11 p4300 N94-35256
Introduction to Neural Networks: Neural Network Workshop for the Hanford Community
[DE94-006526] 11 p4311 N94-35348
Contributions of the low-latitude boundary layer to the finite width magnetotail convection model
[NASA-CR-196116] 11 p4289 N94-35392
Shoemaker-Levy 9 and the tidal disruption of comets
11 p4351 N94-35406
Developing interpretable models with optimized set reduction for identifying high risk software components
11 p4301 N94-35435
The temperature of nitrogen on Pluto
11 p4365 N94-35468
Influence of backup bearings and support structure dynamics on the behavior of rotors with active supports
[NASA-CR-196119] 11 p4274 N94-35500
Numerical modeling studies of wake vortex transport and evolution within the planetary boundary layer
[NASA-CR-196078] 11 p4192 N94-35522
Genetic algorithms
[PB94-171048] 11 p4303 N94-35602
Determination of extensional viscosity from capillary rheometer entrance pressure drop measurements using a numerical simulation of contraction flow
[PB94-171154] 11 p4263 N94-35603
Simulation models for computational plasma physics: Concluding report
[DE94-009976] 11 p4335 N94-35647
AFDM: An advanced fluid-dynamics model, volume 6
[DE94-009596] 11 p4264 N94-35669
Model documentation: Renewable Fuels Module of the National Energy Modeling System
[DE94-009962] 11 p4282 N94-35672
The breakdown of operators when interacting with the external world
[AD-A278936] 11 p4299 N94-35716
Three-photon micromasers
[DE94-611106] 11 p4272 N94-35782
Energy partitioning in high speed impact of analog solid rocket motors
[AD-A278771] 11 p4228 N94-35825
Integrated design of structures, controls, and materials
11 p4218 N94-35869
Effects of noise variance model on optimal feedback design and actuator placement
11 p4220 N94-35883
Comparison of PDF and moment closure methods in the modeling of turbulent reacting flows
[NASA-TM-106614] 11 p4265 N94-35948
A three dimensional multigrid Reynolds-averaged Navier-Stokes solver for unstructured meshes
[AD-A280998] 11 p4191 N94-35994
Analysis of mid-tropospheric carbon monoxide data using a three-dimensional global atmospheric chemistry numerical model
[DE94-004782] 11 p4286 N94-36026
A classical model for closed-loop diagrams of binary liquid mixtures
[DE94-011011] 11 p4237 N94-36033
A new association-model for binary VLE of alcohol/hydrocarbon and amine/hydrocarbon mixtures
[DE94-011012] 11 p4248 N94-36034
Theoretical and experimental study of air and hydrogen electrodes
[DE94-763308] 11 p4283 N94-36060
Classical time machine
[DE94-616616] 11 p4342 N94-36070
Functional integration method for the one-dimensional localization, the higher correlators and mean current in mesoscopic ring in the arbitrary magnetic field
[DE94-616621] 11 p4325 N94-36073
Distance dependent fractional statistics in a P, T-invariant model
[DE94-617360] 11 p4325 N94-36083
Progress in the development of the GMM-2 gravity field model for Mars 11 p4371 N94-36155
Three dimensional visualization of a coastal mesoscale model
[AD-A278576] 11 p4294 N94-36187
Kinetic theory of runaway air breakdown and the implications for lightning initiation
[DE94-001683] 11 p4295 N94-36240
An improved assessment approach for noise impacts from stationary point and traffic sources on humans and wildlife
[DE94-009728] 11 p4319 N94-36320
Analysis of high speed flow, thermal and structural interactions
[NASA-CR-196017] 11 p4268 N94-36420
Dynamic stability of maglev systems
[DE94-010451] 11 p4276 N94-36433
A mixture model for shock compression of porous multi-component reactive materials
[DE93-017638] 12 p4400 N94-36456
Modelling irradiation creep of zirconium alloys
[DE94-619055] 12 p4414 N94-36544
Elimination of numerical dispersion in finite-difference modeling and migration by flux-corrected transport
[DE94-004159] 12 p4510 N94-36551
Accelerated line-by-line calculations for the radiative transfer of trace gases related to climate studies
[DE94-004404] 12 p4464 N94-36552
Quantum and quasi-classical analyses of high order emission processes
[DE93-041348] 12 p4513 N94-36697
Modeling the Earth system in the Mission to Planet Earth era
[NASA-TM-109892] 12 p4461 N94-36827
A PDE-based methodology for modeling, parameter estimation and feedback control in structural and structural acoustic systems
[NASA-CR-194928] 12 p4500 N94-36924

JPRS report: Central Eurasia. Aviation and cosmonautics, No. 5, May 1993
[JPRS-UAC-94-004] 12 p4391 N94-37000
DDT modeling and shock compression experiments of porous or damaged energetic materials
[DE94-011419] 12 p4428 N94-37052
Propagation of radius-tailored laser pulses over extended distances in a uniform plasma
[AD-A280405] 12 p4528 N94-37182
Some effects of heat release in premixed flames
[DE94-011346] 12 p4409 N94-37199
Some considerations for modeling the creep behavior of composite materials
[DE94-012112] 12 p4404 N94-37205
Time-dependent simulations of filament propagation in photoconducting switches
[DE94-012146] 12 p4438 N94-37213
Spray combustion model improvement study, 1
[NASA-CR-196122] 12 p4410 N94-37250
Issues concerning the updating of finite-element models from experimental data
[NASA-TM-109116] 12 p4456 N94-37253
MARFE's in tokamak edge plasma: Pattern formation under nonlocal constraints
[DE94-012766] 12 p4529 N94-37309
Predicting defect behaviour 12 p4455 N94-37331
Selected case studies in modeling and simulation applied to environmentally conscious design and manufacturing
[DE94-007556] 12 p4466 N94-37389
Ionization balance and gain calculations for neon-like selenium x-ray laser plasmas
[DE94-012590] 12 p4530 N94-37437
Dynamics of a split torque helicopter transmission
[NASA-TM-106410] 12 p4452 N94-37457
Simple ocean carbon cycle models
[DE94-011745] 12 p4477 N94-37494
Theoretical studies of a molecular beam generator
[NASA-CR-196306] 12 p4522 N94-37508
Study of Japanese electrodynamic-suspension maglev systems
[DE94-011486] 12 p4452 N94-37515
A computational model for three-dimensional jointed media with a single joint set
[DE94-007582] 12 p4470 N94-37527
Operations and support cost modeling of conceptual space vehicles
[NASA-CR-196299] 12 p4397 N94-37580

MATHEMATICAL PROGRAMMING
NT DYNAMIC PROGRAMMING
NT LINEAR PROGRAMMING
NT NONLINEAR PROGRAMMING
NT QUADRATIC PROGRAMMING
A surrogate heuristic for set covering problems
[INPE-5462-PRE/1770] 01 p0325 N94-11178
The 8th Workshop on the Mathematical Foundations of Programming Semantics
[AD-A266436] 02 p0749 N94-13700
Mathematical optimization: A tool for aircraft design
[MBB-LME-251-S-PUB-0492] 02 p0751 N94-14006
Geometric tolerance assessment
[NPL-DITC-210/92] 03 p1049 N94-15013
MGD1M: A parallel multigrid code with a fast vectorized ILU-relaxation
[CWI-NM-R9222] 05 p1930 N94-21077
Parallelizing a highly vectorized multigrid code with zebra relaxation
[CWI-NM-R9225] 05 p1935 N94-21610
Simplicial variable dimension restart algorithm to find economic equilibria on the unit simplex using n(n+1) rays
[PB94-110541] 06 p2596 N94-24477
CORSS: Cylinder Optimization of Rings, Skin, and Stringers
[NASA-TP-3457] 06 p2490 N94-24727
Evolving recurrent perceptrons
[AD-A273241] 06 p2496 N94-24778
Determining neural network hidden layer size using evolutionary programming
[AD-A273242] 06 p2475 N94-25139
Data structures and amortized complexity in a functional setting
[ETN-94-95307] 06 p2476 N94-25290
A logarithmic barrier cutting plane method for convex programming
[REPT-93-43] 07 p2957 N94-25761
Research on primal-dual interior point algorithms for mathematical programming
[DE94-003962] 07 p2959 N94-25821
Formal methods for dependable real-time systems 07 p2953 N94-26740
The CODE-TOP (COncurrent system DEvelopment using Transformations Of Predicate-transition nets) method: Examples of using it for system architecture specification, software specification, and code generation 07 p2953 N94-26744
New mixed integer algorithm for classification and placement of measurements in process flow networks
[PB94-126752] 07 p2966 N94-26921
North American jumelage 'type systems'
[AD-A275342] 08 p3411 N94-29214
Program derivation by proof transformation
[AD-A275260] 08 p3453 N94-29304
A structural co-induction theorem
[CWI-CS-R9346] 08 p3461 N94-30753
A new methodology of system parameter estimation
[MATHS-REPT-A-208] 09 p3808 N94-31163
A parallel implementation of the column subtraction algorithm
[AD-A275922] 09 p3810 N94-31343
On the computation of simplical approximations of implicitly defined two-dimensional manifolds
[AD-A278132] 09 p3849 N94-33060
Mixed 0-1 programming by lift-and-project in a branch-and-cut framework
[AD-A278045] 09 p3822 N94-33183
An investigation of simulated annealing applied to structural optimization problems
[AD-A278461] 10 p4068 N94-33541

MATHEMATICS
Project TIMS (Teaching Integrated Math/Science)
[NASA-CR-194288] 01 p0416 N94-11599
Career Information in the Mathematical Sciences (CIMS)
[DE93-013780] 01 p0318 N94-11817
Workshop for coordinating South Carolina's pre-college systemic initiatives in science and mathematics
[DE93-012263] 02 p0818 N94-13216
Guide to programs, fiscal year 1993
[NSF-92-78] 04 p1633 N94-19620
Mathematics B for the study direction VWO: A reconnaissance
[REPT-92-80] 05 p1950 N94-20032
A cross-disciplinary report on the mathematical sciences applied to materials science, part 1
[AD-A276116] 09 p3843 N94-31529
OPTIONS for systemic change in mathematics, science, and technology education: Scientist/teacher partnerships
[DE94-007472] 09 p3914 N94-32910
Building on the foundation for an engineering career 11 p4343 N94-35973
Beginning a dialogue on the changing environment for the physical and mathematical sciences 12 p4509 N94-36948

MATRICES (MATHEMATICS)
NT ADJOINTS
NT CANONICAL FORMS
NT EIGENVALUES
NT EIGENVECTORS
NT HESSIAN MATRICES
NT STIFFNESS MATRIX
Vectorizing matrix operations arising from PDE discretization on 9-point stencils
[CWI-NM-R9221] 01 p0342 N94-10351
On renormalization group flow in matrix model
[DE93-613050] 01 p0409 N94-10413
Symbolic dynamics and description of complexity
[DE93-613030] 01 p0418 N94-10485
Operator substitution
[MEMO-COSOR-92-51] 01 p0343 N94-10867
Alleviating memory contention in matrix computations on large-scale shared-memory multiprocessors
[AD-A265009] 01 p0320 N94-11294
Discrete Kalman filtering equations of second-order form for control-structure interaction simulations
[NASA-CR-193723] 01 p0331 N94-11522
Direct solution of the mathematical adjoint equations for an interface current nodal formulation
[DE93-009961] 01 p0346 N94-11608
Tree reconstruction from partial orders
[DE93-009841] 02 p0743 N94-12991
A path-oriented matrix-based knowledge representation system
[NASA-CR-4539] 02 p0744 N94-13065
Codes from an N-dimensional torus simplicially or cellularly decomposed 02 p0747 N94-13438
Formally biorthogonal polynomials and a look-ahead Levinson algorithm for general Toeplitz systems
[NASA-CR-194297] 02 p0748 N94-13586
Stochastic realization of finite-valued processes and primes in the positive matrices
[CWI-BS-R9222] 02 p0773 N94-13677
Efficient, massively parallel eigenvalue computation
[NASA-CR-194289] 02 p0760 N94-13921
On the differential structure of matrix-valued rational inner functions
[CWI-BS-R9228] 02 p0770 N94-14003
An efficient parallel algorithm for matrix-vector multiplication
[DE93-015125] 02 p0754 N94-14399
The use of linked lists in the simulation of controller-structure interaction 02 p0679 N94-14630
Parallel O(log n) algorithms for open- and closed-chain rigid multibody systems based on a new mass matrix factorization technique 02 p0679 N94-14636
Splines, contours and SVD subroutines
[DE93-016088] 02 p0757 N94-14866
Automatic differentiation of limit functions
[DE93-016376] 03 p1168 N94-14928
Decomposition of large sparse symmetric systems for parallel computation. Part 2: Parallelization tool roadmap
[AD-A267072] 03 p1158 N94-15671
Decomposition of large sparse symmetric systems for parallel computation. Part 1: Theoretical foundations
[AD-A267144] 03 p1159 N94-15750
Generating local addresses and communication sets for data-parallel programs
[NASA-CR-194605] 03 p1159 N94-15796
Maximum likelihood techniques applied to quasi-elastic light scattering
[NASA-CR-193550] 03 p1192 N94-16718
Invariance of slip movements with respect to the control matrix
[IFTR-43/1991] 03 p1170 N94-17045
The renormalization of the axial anomaly in dimensional regularization
[NIKHEF-H/92-18] 03 p1220 N94-17618
Proposal for a numerical array library
[DE93-015017] 04 p1516 N94-17786
Differential geometry of CR-submanifolds of a normal almost para contact manifold
[DE93-624764] 04 p1545 N94-17793
A modified direct preconditioner for indefinite symmetric Toeplitz systems
[DE93-015234] 04 p1516 N94-17800
A zeta function approach to the semiclassical quantization of maps
[DE93-624774] 04 p1547 N94-17949
Deformed traces and covariant quantum algebras for quantum groups GL(sub qp)(2) and GL(sub qp)(1/1)
[DE93-629862] 04 p1561 N94-18153
Phase space representations and quantum probability theory
[DE93-629863] 04 p1556 N94-18154
Paragrassmann analysis and quantum groups
[DE93-628593] 04 p1561 N94-18168
On paragrassmann differential calculus
[DE93-628594] 04 p1548 N94-18169
A multigrid acceleration technique for computing steady solutions to the equations of compressible flow 04 p1412 N94-18559
A parallel and pipelined architecture for estimation of direction of arrival using a bilinear transformation method, volume 3
[AD-A270137] 04 p1389 N94-18897
New insights in GMRES-like methods with variable preconditioners
[REPT-93-10] 04 p1524 N94-19084
PUMMA: Parallel Universal Matrix Multiplication Algorithms on distributed memory concurrent computers
[DE93-019163] 04 p1538 N94-19299
The Fourier analysis technique and epsilon-pseudo-eigenvalues
[DE93-018805] 04 p1551 N94-19337
A comparison of iterative methods for a model coupled system of elliptic equations
[DE93-040482] 04 p1553 N94-19655
On the computation of versal family of matrices
[RR-892-M] 04 p1532 N94-19712
Geometric contact for curves and surfaces
[RR-893-M] 04 p1556 N94-19731
Segmented operations for sparse matrix computation on vector multiprocessors
[AD-A270601] 05 p1928 N94-19950
Determination of the optimal stochastic upper bound of a Markovian generator
[RR-906-I] 05 p1963 N94-20202
On the numerical stability of quasi-definite systems
[DE93-019404] 05 p1950 N94-20217
Parallel band reduction and tridiagonalization
[DE93-019566] 05 p1951 N94-20221
Numerical ranges and stability estimates
[TW-92-10] 05 p1953 N94-21060
Method for design rotation
[AD-A272440] 05 p1911 N94-21204
A new matrix formulation of classical electrodynamics. Part 3: Wave propagation through a multilayer dielectric medium with planar boundaries
[AD-A271610] 05 p1739 N94-21240
Using parallel banded linear system solvers in generalized eigenvalue problems
[NASA-CR-191540] 05 p1915 N94-21584
The quantum structure of matter grand challenge project: Large-scale 3-D solutions in relativistic quantum dynamics
[DE94-000328] 05 p1960 N94-21955

A sharp upper bound for departure from normality
| DE93-040457 | 05 p1960 N94-21966
Column reduced rational matrix functions with given null-pole data in the complex plane
| PB93-220531 | 05 p1960 N94-22099
Integration of parallel processing structures using a matrix approach 05 p1784 N94-22192
Registering and resampling images in STSDAS 05 p1927 N94-22550
Properties of the transfer matrices of deflecting magnet systems for free electron laser
| DE93-508257 | 06 p2347 N94-22922
Implementation and parallelization of fast matrix multiplication for a fast Legendre transform
| DE94-002184 | 06 p2478 N94-22975
On the Daubechies-based wavelet differentiation matrix
| NASA-CR-191583 | 06 p2479 N94-23090
Characterization of measures with a convex matrix-k-range
| PB93-220655 | 06 p2479 N94-23098
The p-ranks of Latin square graphs
| PB93-230498 | 06 p2479 N94-23107
Implementing abstract multigrid or multilevel methods 06 p2483 N94-23682
The Third Twente Workshop on Graphs and Combinatorial Optimization
| PB94-110947 | 06 p2486 N94-23722
Coordinate-free interpretations of the optimal costs for Lq problems subject to implicit systems
| PB94-118700 | 06 p2473 N94-23760
A matrix analysis of conjugate gradient algorithms
| DE94-002546 | 06 p2454 N94-23796
The HDTV digital audio matrix
| BBC-RD-1993/9 | 06 p2295 N94-24085
On the differentiation matrix for Daubechies-based wavelets on an interval
| AD-A276348 | 06 p2487 N94-24291
Stitching the Yukawa quilt
| PB93-204477 | 06 p2569 N94-24532
Conveying digital data in noisy, unstable, multipath environments
| AD-D015980 | 06 p2301 N94-25038
Designs with a small number of runs for factorial experiments
| ISBN-9-03-860162-X | 06 p2462 N94-25237
A reachability test for systems over polynomial rings using Groebner bases
| MEMO-COSOR-92-38 | 06 p2493 N94-25527
Piecewise least squares fitting technique using finite interval method with Hermite polynomials
| VTT-PUBS-135 | 07 p2990 N94-25733
Separable expansions of the NN t-matrix by way of exact half off the energy shell methods
| DE94-601615 | 07 p3015 N94-25890
Matrix near rings and pseudo distributivity
| DE94-601505 | 07 p2992 N94-26366
Parallel matrix transpose algorithms on distributed memory concurrent computers
| DE94-002424 | 07 p2964 N94-26764
Simple currents versus orbifolds with discrete torsion: A complete classification
| NIKHEF-H/93-13 | 07 p2995 N94-26812
Role of anticausal inverses in multirate filter-banks. Part 1: System theoretic fundamentals
| AD-A274279 | 07 p2997 N94-27015
Ma42: A new frontal code for solving sparse unsymmetric systems
| PB94-124302 | 07 p2998 N94-27115
The PRISM project: Infrastructure and algorithms for parallel eigensolvers
| DE94-005125 | 07 p2973 N94-27717
Hessenberg matrices in Krylov subspaces and the computation of the spectrum
| PB94-133170 | 07 p3001 N94-28389
Improved QCD sum rule estimates of the higher twist contributions to polarised and unpolarised nucleon structure functions
| PB94-138112 | 08 p3487 N94-29161
Integer cosine transform for image compression 08 p3247 N94-29619
The Stroemberg wavelet on the interval and the Franklin system
| TELECOM-93-C-002 | 08 p3462 N94-30971
Structural properties of inverse linear systems
| MATHS-REPT-A-200 | 09 p3840 N94-31156
Observations of the notion of minimality in the generalized state space
| MATHS-REPT-A-207 | 09 p3840 N94-31162
Arnoldi code for computing selected eigenvalues of sparse real unsymmetric matrices
| PB94-145182 | 09 p3813 N94-31682
Recursive analysis of matrix scattering functions
| AD-A277264 | 09 p3845 N94-32018
Multiparameter quantum groups and multiparameter R-matrices
| CWI-AM-R9307 | 09 p3846 N94-32106
Stability estimates for families of matrices of nonuniformly bounded order
| TW-93-14 | 09 p3847 N94-32207
N(exp n(n-1)/2)-state R-matrix related with U(sub q)(sl(n)) algebra at q(exp 2N) = 1
| DE94-608140 | 09 p3902 N94-32247
Perfect 0, +/- matrices
| AD-A277387 | 09 p3848 N94-32286
Balanced 0, + or - matrices. Part 1: Decomposition
| AD-A278170 | 10 p4128 N94-33384
Normal matrix in gravity field determination with satellite methods. Its stabilization, its information content and its use in error propagation
| PB94-149705 | 10 p4076 N94-34114
Systolic matrix inversion using a Monte Carlo method
| PB94-148798 | 10 p4130 N94-34257
Three-photon micromasers
| DE94-611106 | 11 p4272 N94-35782
Inverse problem for symmetric tridiagonal matrices. Calculation of discrete orthogonal polynomial system with arbitrary weight
| DE94-612434 | 11 p4315 N94-35789
Modelling and control of a rotor supported by magnetic bearings 11 p4216 N94-35858
Solving ill-conditioned matrix equations in control
| AD-A280502 | 12 p4503 N94-37146
Parallel tridiagnoalization through two-step band reduction
| DE94-011512 | 12 p4505 N94-37518
A new technique for dynamic load distribution when two manipulators mutually lift a rigid object, part 2
| DE94-010126 | 12 p4501 N94-37735

MATRIX ANALYSIS

U MATRICES (MATHEMATICS)

MATRIX MATERIALS

Fatigue-life behavior and matrix fatigue crack spacing in unnotched SCS-6/Timetal 21S metal matrix composites
| NASA-CR-191467 | 01 p0185 N94-10715
Interface considerations in Al2O3/NiAl composite
| NASA-CR-191167 | 01 p0066 N94-11202
An analysis of fiber-matrix interface failure stresses for a range of ply stress states
| NASA-TM-108999 | 01 p0067 N94-11276
Moessbauer spectrometer for mineralogical analysis of the Mars surface: Moessbauer source considerations 01 p0476 N94-12242
Proposed framework for thermomechanical life modeling of metal matrix composites
| NASA-TP-3320 | 01 p0074 N94-12449
Ceramic matrix composites by microwave assisted CVI
| DE93-012640 | 02 p0576 N94-12916
Graphite fiber textile preform/copper matrix composites
| NASA-CR-193797 | 02 p0558 N94-14050
Construction, testing, and representation of resin and fiber reinforced materials 03 p0931 N94-15255
Machine development 03 p0932 N94-15258
Carbon-carbon grid for ion engines
| NASA-CASE-NPO-19174-1-CU | 03 p0925 N94-15876
NEXTEL(trademark)/SiC composites using forced chemical vapor infiltration
| DE93-013532 | 03 p0934 N94-16008
Overview of chemical vapor infiltration
| DE93-015440 | 03 p0934 N94-16065
Wear resistant titanium material development
| AD-A266474 | 03 p0959 N94-16780
Influence of the loading rate on the endurance and deformability of cement matrix composites
| IFTR-1/1992 | 03 p1060 N94-17052
A comprehensive study of matrix fracture mechanisms in fiber-reinforced ceramic matrix composites
| AD-A268809 | 04 p1340 N94-18205
Process relationship as influenced by carbonization rate
| AD-A269680 | 04 p1341 N94-18572
Bibliography on ceramic matrix composites and reinforcing whiskers, platelets, and fibers, 1970-1990
| AD-A270139 | 04 p1371 N94-18750
Experiments and analysis of lateral piezoresistance gauges
| DE93-017874 | 04 p1433 N94-19111
Composite materials with improved properties in compression
| AD-A272837 | 05 p1675 N94-21176
Thermal stability relationships between PMR-15 resin and its composites
| NASA-TM-106265 | 05 p1675 N94-21488
Determination of fiber-matrix interface failure parameters from off-axis tests
| NASA-TM-109043 | 06 p2241 N94-23274
Time dependent behavior of a graphite/thermoplastic composite and the effects of stress and physical aging
| NASA-TM-109047 | 06 p2228 N94-23280
Test methods for composites: A status report. Volume 2: Compression test methods
| AD-A273522 | 06 p2230 N94-24779
Test methods for composites: A status report. Volume 1: Tension test methods
| AD-A273501 | 06 p2230 N94-24942
Test methods for composites: A status report. Volume 3: Shear test methods
| AD-A273561 | 06 p2230 N94-25163
Inner fiber observation for metal matrix composites under the stress load condition utilizing Synchrotron Orbital Radiation (SR) by X-ray CT 07 p2724 N94-25553
Lunar preform manufacturing 07 p2765 N94-25677
Characterization of fatigue damage in a metal matrix composite (SCS-6/Ti-15-3) at elevated temperature
| AD-A273797 | 07 p2706 N94-25876
Engineering limitations of ceramic composites for high performance and high temperature applications
| DE94-001676 | 07 p2754 N94-27021
Polyimide/inorganic composite-interpenetrating polymer network for stable second-order nonlinear optics
| AD-A274646 | 07 p2709 N94-27107
Thermoplastic or thermosetting composites in aircrafts
| PB94-123809 | 07 p2710 N94-27253
Innovative processing of composites for ultra-high temperature applications, book 2
| AD-A275598 | 08 p3177 N94-28730
3-D braided, continuous fiber ceramic composites produced by chemical vapor infiltration
| AD-A275192 | 08 p3178 N94-29024
Microwave assisted chemical vapor infiltration
| DE94-005005 | 08 p3185 N94-30771
Characterization of polymer decomposition products by laser desorption mass spectrometry 09 p3597 N94-31046
Ultrasonic tomography in fiber-reinforced composite materials 09 p3620 N94-31565
Dynamics of supermatrix semiconductor growth
| AD-A278380 | 10 p4147 N94-34085
Tough high performance composite matrix
| NASA-CASE-LAR-14239-2 | 11 p4232 N94-35372
Liquid crystalline thermosetting polyimides
| DE94-009939 | 11 p4244 N94-35768
Integrated design of structures, controls, and materials 11 p4218 N94-35869
Cement paste matrix composite materials center
| AD-A279017 | 11 p4233 N94-35952
Nanochannel glass matrix used in making mesoscopic structures
| AD-D016216 | 11 p4234 N94-36123
High temperature creep and oxidation resistant chromium silicide matrix alloy containing molybdenum
| NASA-CASE-LEW-15697-1 | 11 p4241 N94-36275
Properties of TMC processed by fibre coating and hiping 12 p4401 N94-36656
Oxidation behavior of titanium aluminide matrix materials 12 p4401 N94-36658
Modeling of outgassing and matrix decomposition in carbon-phenolic composites
| NASA-CR-196319 | 12 p4405 N94-37471

MATRIX METHODS

A lattice gas model for enzyme kinetics with alternate interactions
| DE93-613027 | 01 p0395 N94-10411
Spin characteristics of ion beams during the motion of electromagnetic elements
| DE93-617448 | 01 p0364 N94-10848
Development of time-dependent orthotropic constitutive law of a thermoplastic composite material 02 p0556 N94-13595
Finding stable orientations of assemblies with linear programming
| AD-A266990 | 03 p1143 N94-15212
Construction and calculation 03 p0931 N94-15256
Decomposition of large sparse symmetric systems for parallel computation. Part 1: Theoretical foundations
| AD-A267144 | 03 p1159 N94-15750
Eigenfunctions of the transfer matrix in the presence of linear coupling
| DE93-015020 | 03 p1151 N94-16892
Speckles statistics and decorrelation effects in complex ABCD optical systems
| AD-A267843 | 03 p1193 N94-17012
Improved omit set displacement recoveries in dynamic analysis 04 p1449 N94-17829
A noniterative improvement of Guyan reduction 04 p1449 N94-17833
A methodology to model physical contact between structural components in NASTRAN 04 p1450 N94-17836

The respectiveness of response in a bar under static and transient loads
[VTT-TIED-1377] 04 p1452 N94-17959
Fast-training algorithm for hidden-layer forward-feed neural networks
[AD-A269253] 04 p1540 N94-18263
Maximum likelihood modal parameter identification and realization of stochastic systems
06 p2157 N94-24265
Hydroacoustic wave-fields generated by different source types, a computational study
[PB94-123536] 07 p3010 N94-27037
Compound matrix method for multi-point boundary-value problems
[PB94-137791] 08 p3453 N94-29476
The 2nd International Workshop on Discrete Time Domain Modelling of Electromagnetic Fields and Networks
[AD-A277551] 10 p4035 N94-34081
Application of the compound-matrix method to wave propagation in range-independent fluid-solid media
[PB94-149077] 10 p4129 N94-34105
Infinite dimensional generalized time optimal control problem 10 p4115 N94-34321
Applying transfer matrix method to the estimation of the modal characteristics of the NASA Mini-Mass Truss
11 p4218 N94-35870
Numerical method to study the stability of periodic solutions of particle motion in nonlinear magnetic fields
[DE94-610740] 11 p4325 N94-36088

MATRIX STRESS CALCULATION
U MATRIX METHODS

MATRIX THEORY
The quantum mass shift of the soliton in Skyrme model
[ITN-93-85219] 03 p1180 N94-15283
On the computation of versal family of matrices
[RR-892-M] 04 p1532 N94-19712
Modifications to 8x8 dynamical theory: Polarizations redefined according to x ray diffraction convention
[DE94-001290] 06 p2560 N94-23187
Role of anticausal inverses in multirate filter-banks. Part 1: System theoretic fundamentals
[AD-A274279] 07 p2997 N94-27015
Causal fir matrices with anticausal fir inverses, and application in characterization of biorthonormal filter banks
[AD-A274509] 07 p2998 N94-27035
Structural properties of inverse linear systems
[MATHS-REPT-A-200] 09 p3840 N94-31156
Observations of the notion of minimality in the generalized state space
[MATHS-REPT-A-207] 09 p3840 N94-31162
Pairwise-comparison using the logarithmic least squares method and the generalized pseudoinverse
[REPT-93-84] 09 p3844 N94-31701
Simple Patch: A new heuristic for the product traveling salesman problem
[REPT-93-85] 09 p3845 N94-31702
Stability estimates for families of matrices of nonuniformly bounded order
[TW-93-14] 09 p3847 N94-32207
Perfect 0, +/- matrices
[AD-A277387] 09 p3848 N94-32286
An introduction to the conjugate gradient method that even an idiot can understand
[AD-A277565] 10 p4128 N94-33392

MATTER (PHYSICS)
NT DARK MATTER
NT DEGENERATE MATTER
A theoretical kinematical study of the gradient of any cosmic scalar field
[DE92-644731] 01 p0425 N94-11136
Fast pulsars, compact stars, and the strange matter hypothesis
[DE93-015039] 03 p1239 N94-16052
Basic studies of the liquid state of matter: Electrical properties and laser interactions
[AD-A268311] 03 p1042 N94-17567
Dibaryon-induced instability of neutron stars
[DE93-634453] 07 p3103 N94-26046
Rescattering and energy loss of fast partons in nuclear matter
[DE94-002918] 07 p3018 N94-26145
Equation of state of neutron star matter, limiting rotational periods of fast pulsars, and the properties of strange stars
[DE94-005214] 08 p3542 N94-28480
Theoretical studies in hadronic and nuclear physics
[DE94-003524] 08 p3492 N94-30838
The Mesozoic Era of relativistic heavy ion physics and beyond
[DE94-011341] 12 p4548 N94-37557

MATTER-ANTIMATTER PROPULSION
An antiproton driver for ICF propulsion
06 p2217 N94-23069

MATURING
U GROWTH

MAXIMA
Cycles containing all vertices of maximum degree
04 p1554 N94-19688
Concerning the circumference of certain families of graphs 04 p1555 N94-19694
On multiflow problems
[RR-889-M] 05 p1950 N94-20125
Joint essential maximal numerical range
[DE94-603674] 07 p3000 N94-27637
Stability estimates for families of matrices of nonuniformly bounded order
[TW-93-14] 09 p3847 N94-32207

MAXIMUM ENTROPY METHOD
Study of the surface circulation to the North of Bransfield Strait, Antarctica
[INPE-5472-TDI/503] 01 p0288 N94-11200
Maximum entropy spectral analysis of the geological time series of the oxygen isotope record from deep-sea cores
[INPE-5465-PRE/1773] 02 p0725 N94-13728
Quantum Monte Carlo by message passing
[DE93-012645] 02 p0760 N94-14177
Exact solution of the generalized time-dependent Jaynes-Cummings Hamiltonian
[DE93-624773] 04 p1546 N94-17811
Optimal resolution in maximum entropy image reconstruction from projections with multigrid acceleration 05 p1955 N94-21465
DECONV-TOOL: An IDL based deconvolution software package 05 p1927 N94-22542
First MEM task IRMEO in IRAF
05 p1928 N94-22551
Application of maximum entropy and irreducible cluster integrals to joint probability distributions for x ray structure determination
[PB93-224152] 06 p2559 N94-23109
Density estimation by maximum quantum entropy
[DE94-002626] 06 p2569 N94-24516
Quantum statistical inference for density estimation
[DE94-002625] 07 p3073 N94-26805
The maximum entropy approach applied to energy exchange, chemical reactions and ionisation in the direct simulation Monte Carlo method for rarefied hypersonic flows
[IC-AERO-93-01] 08 p3524 N94-29481
Procedures for basic inverse problems: Black body radiation problem and phonon density of states problem
[ISBN-0-315-85757-9] 08 p3525 N94-30244
Probability distributions with given marginals and given correlation that have maximal entropy
[REPT-93-81] 09 p3851 N94-31698
Determination of interface structure and bonding at atomic resolution in the stem
[DE94-011466] 12 p4517 N94-37238
The application of maximum entropy to Z-contrast imaging in a stem
[DE94-011470] 12 p4412 N94-37546

MAXIMUM LIKELIHOOD ESTIMATES
Segmented land use classification of multitemporal ERS-1 SAR data using a majority filter
01 p0245 N94-12472
Per-field filtering and classification of multitemporal ERS-1 SAR imagery 01 p0247 N94-12485
Cancellation of multipath for monopulse radars
[ITN-93-85191] 02 p0600 N94-13538
Maximum likelihood estimation for constrained or missing data models
[AD-A266563] 02 p0773 N94-13585
Enhanced decoding for the Galileo S-band mission
02 p0609 N94-14380
Supervised classification of remotely sensed images
[DLR-FB-92-07] 02 p0700 N94-14428
Robust estimators and tests in one-sample location problem with particular consideration on modified maximum likelihood process
[ETN-93-94391] 02 p0774 N94-14703
Generalized smooth models
[DE93-013045] 02 p0756 N94-14864
A new method for generating Bayes classifiers assuming mixtures of Gaussian densities
[FFI-91/4029] 03 p1172 N94-15298
Statistical analysis of trigonometric parallaxes
[NASA-CR-194558] 03 p1172 N94-15641
A multilevel-multiresolution method for image processing. A Bayesian framework for reconstructing and representing shapes
[AD-A266772] 03 p1082 N94-15842
Maximum likelihood techniques applied to quasi-elastic light scattering
[NASA-CR-193550] 03 p1192 N94-16718
EDF tests for normality in linear models after a Box-Cox transformation
[AD-A269068] 04 p1557 N94-18517
Spectral analysis on the canonical autoregressive decomposition
[AD-A270083] 04 p1549 N94-18798
Generalized regression trees: Function estimation via recursive partitioning and maximum likelihood
[AD-A271259] 04 p1560 N94-19726
Parameter estimation with cost function of second order in output-error-problem
[DLR-FB-92-38] 05 p1964 N94-21139
DECONV-TOOL: An IDL based deconvolution software package 05 p1927 N94-22542
Nonlinear smoothing for random fields
[PB94-149531] 06 p2493 N94-22728
Pseudo-coherent demodulation for mobile satellite systems 06 p2287 N94-22819
First order conditions for the maximum likelihood estimation of an exact ARMA model
[PB94-110533] 06 p2495 N94-23814
Maximum likelihood modal parameter identification and realization of stochastic systems
06 p2157 N94-24265
Density estimation by maximum quantum entropy
[DE94-002626] 06 p2569 N94-24516
Determination of the stability and control derivatives of the NASA F/A-18 HARV using flight data
[NASA-CR-194838] 06 p2190 N94-24804
A statistical analysis of recent Naval Experimental Diving Unit (NEDU) single-depth human exposures to 100 percent oxygen at pressure
[AD-A273488] 06 p2427 N94-24950
X-31 aerodynamic characteristics determined from flight data 06 p2164 N94-25109
Parameter estimation for ARMA models with infinite variance innovations
[AD-A274654] 07 p3003 N94-26355
Non-adaptive robust filters for speckle noise reduction
[INPE-5519-PRE/1794] 07 p2776 N94-27335
Digital combining-weight estimation for broadband sources using maximum-likelihood estimates
08 p3250 N94-29661
Hierarchical mixtures of experts and the EM algorithm
[AD-A276516] 09 p3814 N94-31932
An experimental study of pilot/vehicle dynamics using a tilt rotor flying machine
[AD-A277516] 09 p3805 N94-33349
Several modified goodness-of-fit tests for the cauchy distribution with unknown scale and location parameters
[AD-A278496] 10 p4130 N94-34301
Automatic cataloguing and characterization of Earth science data using SE-trees 10 p4124 N94-35058
Maximum-likelihood soft-decision decoding of block codes using the A* algorithm 11 p4254 N94-35555
Point and interval estimation of series system reliability using small data sets
[AD-A278647] 11 p4316 N94-35575
Radar tracking in multipath: Techniques for improved performance 12 p4395 N94-36631
Index and bulk parameters for frequency-direction spectra measured at CERC Field Research Facility, September 1990 to August 1991
[AD-A280423] 12 p4476 N94-37216
Index and bulk parameters for frequency-direction spectra measured at CERC Field Research Facility, September 1991 to August 1992
[AD-A280455] 12 p4477 N94-37229

MAXIMUM PRINCIPLE
Existence of a maximal solution for quasimonotone elliptic systems
[PB94-149689] 04 p1550 N94-19153
Some properties of generalized biregular functions with values in a Clifford algebra
[DE93-613024] 07 p2991 N94-25881
On some general properties of parabolic conservation equations
[DE94-006101] 08 p3461 N94-30758

MAXIMUM USABLE FREQUENCY
Northern Exposure 1992: An investigation of transauroral HF radio skywave propagation
[AD-A273363] 06 p2303 N94-25089
Analysis of ionospheric parameters in Europe and creation of the prediction algorithm
[AD-A276342] 09 p3771 N94-31326

MAXWELL EQUATION
A parallel implementation of particle tracking with space charge effects on an Intel iPSC/860
[DE93-012307] 01 p0335 N94-10340
Stationary spectra in a magnetized current-carrying plasma
[DE93-617847] 01 p0386 N94-10397
The heat transfer by radiation between two media
[DE93-617820] 01 p0149 N94-10838
Measurement of birefringence for optical recording disk substrates 03 p1227 N94-14989
Stress sensitivity of dielectric resonators
[AD-A266767] 03 p1009 N94-15825

An asymptotic expansion of an electromagnetic field in the velocity of a caustic in the form of simple waves
[IFTR-14/1991] 03 p1002 N94-17048
Mathmatical modeling for diffractive optics
03 p1195 N94-17342
Advances and applications of ABCI
[DE93-016971] 04 p1383 N94-18055
Current-potential characteristics of electrochemical systems
[DE93-040303] 04 p1352 N94-19192
Analysis of microstrip dipoles and slots transversely coupled to a microstrip line using the FDTD method
05 p1718 N94-20405
FD-TD modeling of 2-D dielectric waveguides for propagation and scattering of femtosecond optical solitons 05 p1719 N94-20406
Time-domain analysis of planar microstrip devices using a generalized Yee-algorithm based on unstructured grids
05 p1724 N94-20431
Modeling the minimum energy state of the Earth's magnetotail
[AD-A267984] 05 p1856 N94-20485
A new matrix formulation of classical electrodynamics. Part 3: Wave propagation through a multilayer dielectric medium with planar boundaries
[AD-A271610] 05 p1739 N94-21240
Characteristic based methods for the time-domain Maxwell equations
[AD-A272973] 05 p1802 N94-21263
Detailed analysis case studies of trapped plasmas at the Earth's magnetic equator
[AD-A272497] 05 p1858 N94-21432
Proposed additions to the SHADOW ray-tracing code for general-asymmetric perfect-crystal optics
[DE94-001291] 06 p2560 N94-23188
Compatibility relations and the finite-element formulation of electromagnetic field problems
[PB94-110996] 06 p2294 N94-23727
Study of a local absorbing boundary condition for the modeling of an infinite external domain in the time-domain finite-element package FEMAXT
[PB94-111002] 06 p2294 N94-23728
Analysis for the computational modeling of finite cladding and lossy coating effects in fibers
[PB94-111085] 06 p2544 N94-23732
Finite-element method for computing three-dimensional electromagnetic fields in inhomogeneous media (1993)
[PB94-111101] 06 p2298 N94-24637
Reduced Braginskii equations
[DE94-003510] 07 p3047 N94-27723
Fields and potentials in general uniaxial bianisotropic media I. Axial sources
[PB94-132875] 07 p2778 N94-28379
Plane wave propagation in an anisotropic chiral medium with isotropic permittivity and permeability
[PB94-133097] 07 p2778 N94-28384
Exact spherical wave solutions to Maxwell's equations with applications 08 p3252 N94-29733
Theory of fundamental interactions
[DE94-608126] 08 p3525 N94-30169
MOM3D method of moments code theory manual
[NASA-CR-189594] 09 p3682 N94-32897
On the boundary integral equation methods for an extended time-harmonic Maxwell type system
10 p4128 N94-33417
User's guide for ABCI version 8.8, azimuthal beam cavity interaction
[DE94-009638] 10 p4139 N94-33916

MAXWELL FLUIDS
Kinetic approach to long wave length modes in rotating plasmas
[DE93-771286] 01 p0388 N94-10807
Stability of viscoelastic flow: Physical and numerical considerations 01 p0031 N94-11493
Propagation of radius-tailored laser pulses over extended distances in a uniform plasma
[AD-A280405] 12 p4528 N94-37182

MAXWELL-BOLTZMANN DENSITY FUNCTION
Modelling ideal gas fluorides laser plasmas
[ETN-93-95073] 04 p1592 N94-19613
Atomic oxygen interaction at defect sights in protective coatings on polymers flown on LDEF
09 p3593 N94-31024
Fast electron generation and transport in a turbulent, magnetized plasma
[DE94-012986] 12 p4531 N94-37730

MAXWELLIAN DISTRIBUTION (DENSITY)
U MAXWELL-BOLTZMANN DENSITY FUNCTION

MCDONNELL AIRCRAFT
NT DC 10 AIRCRAFT
Numerical flow simulation for complete vehicle configurations
[AD-A273588] 06 p2170 N94-24849

MCDONNELL DOUGLAS AIRCRAFT
NT DC 8 AIRCRAFT
NT DC 10 AIRCRAFT
NT DOUGLAS AIRCRAFT
NT F-18 AIRCRAFT
NT MCDONNELL AIRCRAFT
NT MD 11 AIRCRAFT
Aircraft accident report: Inadvertent in-flight slat deployment, China Eastern Airlines Flight 583, McDonnell Douglas MD-11, B-2171, 950 nautical miles south of Shemya, Alaska, 6 April 1993
[PB93-910408] 06 p2172 N94-23579
Aircraft incident report: In-flight turbulence encounter and loss of portions of the elevators, China Airlines Flight CI-012, McDonnell Douglas MD-11-P, Taiwan Registration B-150 about 20 miles east of Japan, 7 December 1992
[PB94-910403] 09 p3576 N94-32936

MCMURDO SOUND
Telepresence in the human exploration of Mars: Field studies in analog environments
07 p2685 N94-27360

MD 11 AIRCRAFT
Aircraft incident report: In-flight turbulence encounter and loss of portions of the elevators, China Airlines Flight CI-012, McDonnell Douglas MD-11-P, Taiwan Registration B-150 about 20 miles east of Japan, 7 December 1992
[PB94-910403] 09 p3576 N94-32938

MDA
U MULTIPLE DOCKING ADAPTERS

MEADOWLANDS
U GRASSLANDS

MEAN
Bounds on inconsistent inferences for sequences of trials with varying probabilities
[AD-A267146] 03 p1172 N94-15733
Estimates of monthly mean soil moisture for 1979-1989
[NASA-TM-104571] 06 p2407 N94-23132

MEAN FREE PATH
Electron runaway in RF discharges
[DE93-771407] 01 p0363 N94-10661
Variance reduction unique to coupled electron/photon Monte Carlo transport
[DE93-014999] 02 p0782 N94-13409
Wave structure induced by fluid dynamic limits in the Broadwell model
[AD-A268512] 04 p1410 N94-18385

MEAN SQUARE VALUES
An investigation of the Ground-Based High-Resolution Interferometer Sounder (GB-HIS) in a costal marine environment
[AD-A268052] 03 p1114 N94-17503
An empirical evaluation of five circular error probable estimation techniques and a method for improving them
[AD-A266528] 04 p1556 N94-18397
Tracking with time-delayed data in multisensor systems
[AD-A271334] 04 p1391 N94-19582
Likelihood analysis of parity violation in the compound nucleus
[DE94-000671] 05 p1977 N94-22572
Development and validation of RNG methodology for compressible turbulence
[AD-A273469] 06 p2337 N94-24929
An optimal constrained linear inverse method for magnetic source imaging
[DE94-004014] 07 p2957 N94-25663
Short-range cloud amount forecasting with model output statistics
[AD-A274769] 07 p2895 N94-26798
An optimal constrained linear inverse method for magnetic source imaging
[DE94-002264] 07 p2996 N94-26936
The generalized multi delay adaptive filter: Structure and convergence analysis
[TELECOM-93-D-004] 09 p3808 N94-31094
H infinity control for nonlinear and linear systems
[AD-A280450] 12 p4494 N94-37226
X-ray diffraction studies of evaporated gold thin films deposited on aluminum nitride substates
[AD-A280454] 12 p4536 N94-37228

MEAN TIME BETWEEN FAILURES
U MTBF

MEANDERS
Meander properties of Venusian channels
03 p1275 N94-16324

MEASURE AND INTEGRATION
NT BINARY INTEGRATION
NT FUNCTIONAL INTEGRATION
NT INTEGRAL CALCULUS
NT J INTEGRAL
NT LEBESGUE THEOREM
NT NUMERICAL INTEGRATION
NT RUNGE-KUTTA METHOD
NT STIELTJES INTEGRAL
NT WEIGHTING FUNCTIONS
Finite difference schemes for long-time integration
[NASA-CR-191471] 01 p0343 N94-10642
An adaptive projection method for the incompressible Euler equations
[DE93-016428] 02 p0639 N94-14434
Volume integral equations applied to circular and square cylinders
[AD-A266635] 03 p1169 N94-15785
Numerical methods for molecular dynamics
[DE93-018321] 04 p1566 N94-18179
The explicit computation of integration algorithms and first integrals for ordinary differential equations with polynomials coefficients using trees
[NASA-CR-194787] 06 p2448 N94-23074
Characterization of measures with a convex range: A generalization of Lyapounov's theorem
[PB93-220523] 06 p2523 N94-23094
Characterization of measures with a convex matrix-k-range
[PB93-220655] 06 p2479 N94-23098
Response-coefficient method for heat-conduction transients with time-dependent inputs
06 p2326 N94-23671
On the continuity of limit capacity of central Cantor sets
[DE93-613022] 06 p2523 N94-25328
On invariant measures for some infinite-dimensional dynamical systems
[DE94-606342] 08 p3522 N94-28609
A note on cocycles in a semidirect product
[REPT-93-65] 09 p3851 N94-31661

MEASURE THEORY
U MEASURE AND INTEGRATION

MEASUREMENT
A measurement and evaluation process model applied to software engineering environments
[INPE-5345-PUD/048] 02 p0746 N94-13428
Lecture notes on engineering measurement for software engineers
[AD-A266959] 03 p1142 N94-14967
Mass properties measurement system: Dynamics and statics measurements 06 p2368 N94-23236
The development and demonstration of the metric assessment tool
[AD-A275788] 08 p3230 N94-28742

MEASURING
U MEASUREMENT

MEASURING INSTRUMENTS
NT ACCELEROMETERS
NT ADVANCED VERY HIGH RESOLUTION RADIOMETER
NT ALTIMETERS
NT AMMETERS
NT ANALYZERS
NT ANEMOMETERS
NT APPROACH INDICATORS
NT ATOMIC CLOCKS
NT ATTITUDE INDICATORS
NT AUTONOMOUS SPACECRAFT CLOCKS
NT BALLOON-BORNE INSTRUMENTS
NT BAROMETERS
NT BATHYMETERS
NT BATHYTHERMOGRAPHS
NT BOLOMETERS
NT CALORIMETERS
NT CERENKOV COUNTERS
NT CHRONOMETERS
NT CINETHEODOLITES
NT CLOCKS
NT CLOUD HEIGHT INDICATORS
NT COMPARATORS
NT COMPASSES
NT CONDUCTIVITY METERS
NT COUNTERS
NT DICKE RADIOMETERS
NT DIFFRACTOMETERS
NT DISTANCE MEASURING EQUIPMENT
NT DOSIMETERS
NT DYNAMOMETERS
NT EBERT SPECTROMETERS
NT ELECTROMETERS
NT ELECTRON COUNTERS
NT ELECTRON PROBES
NT ELECTROPHOTOMETERS
NT ELECTROSTATIC PROBES
NT ELLIPSOMETERS
NT ENGINE MONITORING INSTRUMENTS
NT ERGOMETERS
NT ETALONS
NT EXTENSOMETERS
NT FABRY-PEROT INTERFEROMETERS
NT FABRY-PEROT SPECTROMETERS
NT FLAME CALORIMETERS
NT FLIGHT LOAD RECORDERS
NT FLIGHT RECORDERS
NT FLIR DETECTORS

NT FLOWMETERS
NT GAMMA RAY SPECTROMETERS
NT GOLAY DETECTOR CELLS
NT GRAVIMETERS
NT GRAVITY GRADIOMETERS
NT HIGH DISPERSION SPECTROGRAPHS
NT HODOSCOPES
NT HOT-FILM ANEMOMETERS
NT HOT-WIRE ANEMOMETERS
NT HOT-WIRE FLOWMETERS
NT HYGROMETERS
NT HYPSOMETERS
NT IMAGING SPECTROMETERS
NT IMPEDANCE PROBES
NT INDICATING INSTRUMENTS
NT INFRARED DETECTORS
NT INFRARED INSTRUMENTS
NT INFRARED INTERFEROMETERS
NT INFRARED RADIOMETERS
NT INFRARED SCANNERS
NT INFRARED SPECTROMETERS
NT INFRARED SPECTROPHOTOMETERS
NT INTERFEROMETERS
NT ION PROBES
NT ION TRAPS (INSTRUMENTATION)
NT IONIZATION GAGES
NT IONOSONDES
NT LASER ALTIMETERS
NT LASER ANEMOMETERS
NT LASER DOPPLER VELOCIMETERS
NT LASER RANGE FINDERS
NT LASER SPECTROMETERS
NT LIGHT SCATTERING METERS
NT LUNAR SEISMOGRAPHS
NT MACH-ZEHNDER INTERFEROMETERS
NT MAGNETIC PROBES
NT MAGNETOMETERS
NT MASS SPECTROMETERS
NT METEOROLOGICAL INSTRUMENTS
NT MICHELSON INTERFEROMETERS
NT MICROBALANCES
NT MICROMETERS
NT MICROWAVE INTERFEROMETERS
NT MICROWAVE PROBES
NT MICROWAVE RADIOMETERS
NT MICROWAVE REFLECTOMETERS
NT MICROWAVE SENSORS
NT MICROWAVE SPECTROMETERS
NT MOISTURE METERS
NT MONOCHROMATORS
NT NEUTRON COUNTERS
NT NEUTRON SPECTROMETERS
NT OCULOMETERS
NT OPTICAL MEASURING INSTRUMENTS
NT OPTICAL PYROMETERS
NT OPTICAL RANGE FINDERS
NT OSCILLOGRAPHS
NT OXYGEN ANALYZERS
NT PARTICLE TELESCOPES
NT PENETROMETERS
NT PHOTOMETERS
NT PIEZOELECTRIC GAGES
NT PLAN POSITION INDICATORS
NT PLASMA PROBES
NT PNEUMATIC PROBES
NT POLARIMETERS
NT POSITION INDICATORS
NT PRESSURE GAGES
NT PRESSURE MODULATOR RADIOMETERS
NT PROFILOMETERS
NT PROPORTIONAL COUNTERS
NT PYRANOMETERS
NT PYROMETERS
NT QUANTUM COUNTERS
NT RADIATION COUNTERS
NT RADIATION DETECTORS
NT RADIATION MEASURING INSTRUMENTS
NT RADIATION PYROMETERS
NT RADIO ALTIMETERS
NT RADIO DIRECTION FINDERS
NT RADIO INTERFEROMETERS
NT RADIOGONIOMETERS
NT RADIOMETERS
NT RADIOSONDES
NT RAIN GAGES
NT RANGE FINDERS
NT RATIOMETERS
NT RAWINSONDES
NT REFLECTOMETERS
NT RESONANCE PROBES
NT RESPIROMETERS
NT RHEOMETERS
NT RIOMETERS
NT SATELLITE-BORNE INSTRUMENTS
NT SCATTEROMETERS
NT SCINTILLATION COUNTERS
NT SEISMOGRAPHS
NT SHOCK MEASURING INSTRUMENTS
NT SIGNAL ANALYZERS
NT SILICON RADIATION DETECTORS
NT SMOKE DETECTORS
NT SOLAR SPECTROMETERS
NT SONDES
NT SONIC ANEMOMETERS
NT SPACECRAFT POSITION INDICATORS
NT SPECTROHELIOGRAPHS
NT SPECTROMETERS
NT SPECTROPHOTOMETERS
NT SPECTRORADIOMETERS
NT SPEED INDICATORS
NT STRAIN GAGE BALANCES
NT STRAIN GAGES
NT TEMPERATURE MEASURING INSTRUMENTS
NT TEMPERATURE PROBES
NT THERMOMETERS
NT TILTMETERS
NT TIME MEASURING INSTRUMENTS
NT TIME OF FLIGHT SPECTROMETERS
NT TIMING DEVICES
NT TORQUEMETERS
NT TOTAL OZONE MAPPING SPECTROMETER
NT TRANSMISSOMETERS
NT TURBULENCE METERS
NT ULTRAVIOLET DETECTORS
NT ULTRAVIOLET SPECTROMETERS
NT VARIOMETERS
NT VIBRATION METERS
NT VISCOMETERS
NT VOLTMETERS
NT WEIGHT INDICATORS
NT WIND VANES
NT X RAY DETECTORS

Recommendations for future research in hypersonic instrumentation 01 p0004 N94-10433

Pressure and force measurements on models set in hypersonic flows: A review 01 p0005 N94-10435

Velocity measurements in hypersonic flows: A review 01 p0005 N94-10436

Thermal flux measurements in hypersonic flows: A review 01 p0005 N94-10438

Overview of the 1989 Wind Tunnel Calibration Workshop
[NASA-TP-3393] 01 p0034 N94-11869

Phobos/Harp post launch support
[NASA-CR-193676] 02 p0540 N94-13109

Perspective on the National Aero-Space Plane Program instrumentation development
[NASA-TM-4505] 02 p0516 N94-13256

Calculation of the required sensor accuracy to obtain a specified state estimation accuracy
[NAL-TR-1173] 02 p0649 N94-13343

DATAA: Data acquisition made easy
[DE93-014683] 02 p0823 N94-13406

The 3D pneumatic and 2D dynamic probes: Their development and subsequent use in a transonic fan
[RAE-TM-AERO/PROP-22] 02 p0653 N94-14827

A high-precision direct current measuring device over a kiloampere range
[DE93-626409] 02 p0627 N94-14885

Simultaneous measurement of temperature and strain using four connecting wires
[NASA-TM-104271] 03 p1032 N94-15754

Wind tunnel investigation with an operational turbojet engine
[TABES PAPER 93-662] 03 p0870 N94-16157

Passive tracking of a target using an array of sensors
[DE93-015870] 03 p0997 N94-16169

Cosmic dust and space debris measurements on board the small satellites HITEN and BREM-SAT 03 p0890 N94-17147

S 80/T: A micro satellite system combining high performances and limited resources 03 p0893 N94-17166

A radial transmission line material measurement apparatus
[DE93-018508] 04 p1394 N94-17780

Verification of VALISYS cad based CMM software at LLNL
[DE93-013854] 04 p1517 N94-17911

Measuring machines for digitalizing and measuring complex surfaces, models and matrices
[CRIF-MC-97] 04 p1444 N94-17963

Simulation of quartz resonators 04 p1426 N94-18021

Laser induced damage testing: Equipment and techniques
[DE93-017143] 04 p1437 N94-18060

C-band PARC manual
[FEL-92-B159] 04 p1383 N94-18070

Belgian Royal Observatory Communications, Series A, No. 104, Geophysics Series No. 175
[COMMUNICATIONS-SER-A-104] 04 p1482 N94-18622

Recent developments in fast response aerodynamic probe technology 04 p1431 N94-18645

Experiments and analysis of lateral piezoresistance gauges
[DE93-017874] 04 p1433 N94-19111

Pantex Plant Meteorological Monitoring Program
[DE93-018495] 04 p1493 N94-19127

Software quality in test and measurment equipment
[PB93-197846] 04 p1528 N94-19333

Six degree of freedom fine motion positioning stage based on magnetic levitation
[DE93-017651] 04 p1446 N94-19547

A comparison of polygraphic and actigraphic monitoring of sleep using a 5-channel programmable-sensitivity actigraph
[AD-A270731] 04 p1507 N94-19608

The Electron Drift Instrument for Cluster 04 p1329 N94-19630

The Cluster Ion Spectroscopy experiment 04 p1329 N94-19631

Charge collectors for the omega upgrade
[DE93-019684] 05 p1972 N94-20264

Enhanced software for the GT1022 automated gaging system
[DE94-001374] 05 p1918 N94-21977

Acoustic, fiber optic, and silicon microelectronic microsensors research and development activities at Sandia National Laboratories
[DE93-019075] 05 p1770 N94-22040

Writing instrument interfaces with xf/tktcl 05 p1925 N94-22480

Thermoelectric cooled, purge-and-trap device for enhancing the utility of fiber optic VOC sensors
[DE94-001772] 06 p2541 N94-22722

Unmanned lunar rovers: Utilization for exploration 06 p2607 N94-23387

Measuring electrically charged particle fluxes in space using a fiber optic loop sensor
[NASA-CR-191328] 06 p2544 N94-23829

New pin-on-disk equipment for vacuum tribometry 06 p2360 N94-24023

An analytical ultra-high vacuum tribometer for solid lubricant studies 06 p2361 N94-24033

Miniature convection cooled plug-type heat flux gauges
[NASA-TM-106483] 06 p2344 N94-24069

The CEBAF beam loss sensors
[CEBAF-PR-93-032] 06 p2540 N94-24662

Chemically sensitive interfacial force microscopy: Contact potential measurements of self-assembling monolayer films
[AD-A273135] 06 p2234 N94-24772

Bioregenerative life support systems for microgravity
[NASA-CR-195516] 06 p2422 N94-24810

Measurement of interfacial tension by use of pendant drop video techniques
[DE93-000168] 06 p2345 N94-24831

Conceptual design of an astronaut hand anthropometry device
[NASA-CR-195490] 06 p2439 N94-24956

Very low frequency and low frequency transmitting antenna parameter monitoring system
[AD-D015989] 06 p2302 N94-25049

Bundle Intensity and Beamgate Length recorder (BIBL)
[DIGEL-1993-7] 07 p3031 N94-25619

Primary standards laboratory report 1st half 1993
[DE94-003138] 07 p2762 N94-26027

Lepton masses in an SU(3)(sub L) x U(1)(sub N) gauge model
[DE93-634366] 07 p3016 N94-26040

Improved measurement accuracy in a Long Trace Profiler: Compensation for laser pointing instability
[DE94-003408] 07 p2816 N94-26130

Breakwire technique for hypervelocity measurement
[AD-A274779] 07 p2809 N94-26358

Calibrating/testing meters in hot water test bench VM7
[PB94-124294] 07 p2812 N94-27160

Trace organic chemical detection using an ultraviolet excitation molecular beam fluorometer
[DE94-002649] 07 p2704 N94-27708

Energy Dispersive X ray Diffraction (EDXD) apparatus for liquids at high temperature 07 p2721 N94-28159

Single specimen fracture toughness determination procedure using instrumented impact test
[PB94-132040] 08 p3316 N94-28402

Development and application of a thermistor current meter
[AD-A275816] 08 p3286 N94-28831

Improved in-flow acoustic sensor
[NASA-CASE-ARC-12001-1] 08 p3478 N94-29363

Stereo imaging based particle velocimeter
[NASA-CR-195800] 08 p3289 N94-29742
A non-contacting vertical alignment system for mass properties measuring instruments
[DE94-004680] 08 p3289 N94-29927
VHF impedance measurement: A review
[PB94-138682] 08 p3267 N94-30115
Theory of fundamental interactions
[DE94-608126] 08 p3525 N94-30169
User's manual for the model interface and plugboard cabinets in the 14- by 22-foot subsonic tunnel
[NASA-TM-109062] 08 p3133 N94-30176
Monitor for status epilepticus seizures
08 p3397 N94-30460
The performance of gloss meters on curving surfaces
[NPL-DMM(A)-111] 08 p3501 N94-30522
Guidance notes for use with NPL low permeability reference materials
[NPL-DES-121] 08 p3476 N94-30780
Report on the development of low magnetic permeability reference materials
[NPL-DES-119] 08 p3476 N94-30783
Guidance on eliminating interference from sensitive electrical circuits
[PB94-139300] 08 p3268 N94-30784
Fiber optic chemical sensors on Mars
[DE94-005251] 09 p3941 N94-31145
Implementation of instruments and facilities at the SGP CART site
[DE94-006839] 09 p3781 N94-31322
Microwave dielectric behavior of soils. Report 2: A unique coaxial measurement apparatus
[AD-A275982] 09 p3771 N94-31353
Continuous measurement of aircraft wing icing
09 p3576 N94-32454
Advanced high frequency partial discharge measuring system
[NASA-CR-195240] 09 p3697 N94-33044
Proceedings SPIE: Conference Digest, volume 2104
[AD-A278107] 09 p3884 N94-33187
Traineeship augmentation for aerosol optical properties study
[AD-A278466] 10 p4085 N94-33544
Performance demonstration: UH-60Q external rescue hoist and cargo loadmeter
[AD-A277533] 10 p3989 N94-34080
A new type of temperature and humidity detection-control system 10 p4057 N94-34365
Dual active surface, miniature, plug-type heat flux gauge
[NASA-CASE-LEW-15643-1] 10 p4056 N94-35078
Ionic contamination detection
[DE94-010212] 11 p4258 N94-35686
Six degree of freedom fine motion positioning stage based on magnetic levitation 11 p4225 N94-35916
Measurement of a surface heat flux and temperature
11 p4231 N94-36407
Summary of the extensions of the Standard Model working group
[DE94-002217] 12 p4512 N94-36527
Methods of calculation of higher power corrections in QCD
[DE94-618511] 12 p4521 N94-36748
United States Air Force Summer Research Program, 1993. Volume 16: Arnold Engineering Development Center, Frank J. Seiler Research Laboratory and Wilford Hall Medical Center
[AD-A278658] 12 p4550 N94-36978
A non-intrusive way to measure point-of-gaze
12 p4484 N94-37272

MECHANICAL DEVICES
Nonlinear analysis of mechanical systems under combined harmonic and stochastic excitation
[AD-A266217] 03 p1173 N94-16937
Electrorheological (ER) fluids: A research needs assessment
[AD-A267588] 03 p0951 N94-17210
Computer modeling and animation of mechanical systems
[NIAR-93-3] 03 p1153 N94-17299
Metal band drives in spacecraft mechanisms
06 p2355 N94-23987
Low melting temperature alloy deployment mechanism
06 p2356 N94-23997
An Earth observation telescope refocusing mechanism
[REPT-932-440-103] 08 p3332 N94-29417
Rotary actuator
[NASA-CASE-MFS-28581-1] 08 p3205 N94-29447
Metal band drives in spacecraft mechanisms
08 p3162 N94-29637
Proceedings of the Workshop on Microtechnologies and Applications to Space Systems
[NASA-CR-195688] 08 p3235 N94-29767
Identification of mechanical systems using probabilistic neural networks
[DE94-007555] 10 p4114 N94-34296
Preload release mechanism
[NASA-CASE-MSC-22327-1] 12 p4450 N94-36839

MECHANICAL DRAWINGS
U ENGINEERING DRAWINGS

MECHANICAL DRIVES
NT HELICOPTER PROPELLER DRIVE
NT TRANSMISSIONS (MACHINE ELEMENTS)
Roller-gear drives for robotic manipulators design, fabrication and test
[NASA-CR-194248] 02 p0660 N94-12802
Development of a high-speed mechanical drive system for oscillating an annular blade row in the bending mode
[NAL-TR-1170] 02 p0502 N94-13342
Experimental investigation of nozzle/plume aerodynamics at hypersonic speeds
[NASA-CR-194628] 05 p1636 N94-20014
Long range fast tool servo
[AD-A271614] 05 p1761 N94-21257
Lectures on magnetohydrodynamical drives
[PB93-224962] 06 p2308 N94-23104
The Fifth European Space Mechanisms and Tribology Symposium
[ESA-SP-334] 06 p2355 N94-23985
Micro-gravity compatible drive (MGCD)
06 p2355 N94-23988
Development steps on the basis of test with the LOCSTAR reflector deployment mechanism
06 p2356 N94-23998
Ultra-clean high-precision mechanisms for the SUMER EUV spectrometer on SOHO 06 p2356 N94-23999
Periscope mechanism for SWAN instrument
06 p2357 N94-24000
Thermal vacuum performance of cycloid and harmonic gearboxes with solid (MoS2) and liquid (Braycote 601) lubrication 06 p2358 N94-24009
Reliable redundant device for mechanisms
06 p2361 N94-24030
Viscous rotary damper 06 p2361 N94-24031
Recharge mechanism based on shape memory alloy
06 p2362 N94-24039
Electrical engineering and industrial electronics education days: Control of asynchronous generators
[PB94-135514] 08 p3266 N94-29523
Mars rover mechanisms designed for Rocky 4
08 p3161 N94-29630
SP-100 control drive assembly development
08 p3163 N94-29651
Microgravity compatible drive system-rider. New technologies
[PB94-138583] 08 p3229 N94-29996

MECHANICAL ENGINEERING
Material removal processes: Engineering mechanics consideration
[DE93-010733] 01 p0126 N94-10293
RAMCAD (reliability, availability, and maintainability in computer-aided design)
[AD-A265143] 01 p0331 N94-11679
Machinery dynamics activities in Canadian industries
[IME-MET-TR-006] 02 p0663 N94-14147
Krupp technical reports no. 2, English edition, October 1992
[ETN-93-94631] 03 p0984 N94-16000
Expert system for welding engineering
03 p0984 N94-16003
Remote diagnosis as used for mechanized parking systems 03 p0984 N94-16004
Research activities, Faculty of Civil Engineering, Delft University of Technology, 1990 - 1991
[PB93-195022] 04 p1380 N94-19254
Program descriptions
[NSF-92-123] 04 p1531 N94-19619
Production of NiAl and TiAl intermetallics by mechanical alloying
[VTT-JULK-760] 05 p1691 N94-20530
Computational and analytical methods in nonlinear fluid dynamics
[AD-A272722] 05 p1802 N94-21169
Stiffening of deployable space booms: Automated Protein Crystal Growth Facility
[NASA-CR-195547] 06 p2196 N94-24820
Design of gas bearing systems for precision applications
[ISBN-9-03-860112-3] 06 p2367 N94-25249
The 1991-1992 project summaries
07 p2943 N94-25698
Filament to mandrel gap analysis: Resulting gap from filament winding over a cone-cylinder transition mandrel (reference NMTP no. 93838)
[DE94-004225] 08 p3175 N94-28528
Implementation of a Computerized Maintenance Management System 11 p4343 N94-35970
Case based reasoning in engineering design
[AD-A278943] 11 p4305 N94-36006
Using experimental design modules for process characterization in manufacturing/materials processes laboratories 11 p4230 N94-36405
Integrated Engineering Information Technology, FY 1993 accomplishments
[DE94-011406] 12 p4545 N94-37563
Advanced Turbine Technology Applications Project (ATTAP)
[NASA-CR-195367] 12 p4452 N94-37763

MECHANICAL FINGERS
U END EFFECTORS

MECHANICAL HANDS
U END EFFECTORS

MECHANICAL IMPEDANCE
Computer code for scattering from impedance bodies of revolution. Part 3: Surface impedance with s and phi variation. Analytical and numerical results
[NASA-CR-193396] 02 p0599 N94-13264
Low melting temperature alloy deployment mechanism
06 p2356 N94-23997
Development steps on the basis of test with the LOCSTAR reflector deployment mechanism
06 p2356 N94-23998

MECHANICAL MEASUREMENT
NT DISPLACEMENT MEASUREMENT
NT DRAG MEASUREMENT
NT FLOW MEASUREMENT
NT FRICTION MEASUREMENT
NT PARTICLE IMAGE VELOCIMETRY
NT PRESSURE MEASUREMENT
NT STRESS MEASUREMENT
NT THRUST MEASUREMENT
NT VELOCITY MEASUREMENT
NT VIBRATION MEASUREMENT
NT WIND MEASUREMENT
NT WIND VELOCITY MEASUREMENT
A mechanical system damping measurement technique using a one-degree-of-freedom (1DOF) cylindrical gas bearing
[AD-A268402] 03 p1048 N94-17462
Omega phase formation in shock-loaded zirconium
[DE93-018343] 04 p1595 N94-18162
High accuracy die mechanical stress measurement with the ATC04 Assembly Test Chip
[DE93-019435] 05 p1830 N94-20477
An ultrasonic testing technique for monitoring the cure and mechanical properties of polymeric materials
[AD-A274536] 07 p2753 N94-26842
Shape from diameter: Negative results
[RUU-CS-93-16] 08 p3458 N94-30407
Shape from diameter: Positive results
[RUU-CS-93-17] 08 p3458 N94-30408
Fluid mechanical measurements within the bottom boundary layer over the Northern California continental shelf during stress
[AD-A277916] 09 p3791 N94-33243

MECHANICAL OSCILLATORS
NT GYROSCOPIC PENDULUMS
NT PENDULUMS

MECHANICAL PROPERTIES
NT ABRASION RESISTANCE
NT AEROELASTICITY
NT AEROSERVOELASTICITY
NT AEROTHERMOELASTICITY
NT ANELASTICITY
NT BRITTLENESS
NT BULK MODULUS
NT COMPRESSIBILITY
NT COMPRESSIVE STRENGTH
NT CREEP PROPERTIES
NT CREEP RUPTURE STRENGTH
NT CREEP STRENGTH
NT DIMENSIONAL STABILITY
NT DUCTILITY
NT EARTHQUAKE RESISTANCE
NT ELASTIC PROPERTIES
NT ELASTOPLASTICITY
NT ELECTROSTRICTION
NT FATIGUE LIFE
NT FIBER STRENGTH
NT FLEXIBILITY
NT FRACTURE STRENGTH
NT HARDNESS
NT HIGH STRENGTH
NT HYDROELASTICITY
NT IMPACT STRENGTH
NT KNOOP HARDNESS
NT LOAD CARRYING CAPACITY
NT MAGNETOSTRICTION
NT MICROHARDNESS
NT MODULUS OF ELASTICITY
NT NOTCH SENSITIVITY
NT NOTCH STRENGTH
NT PHOTOELASTICITY
NT PIEZOELECTRICITY
NT PLASTIC PROPERTIES
NT POISSON RATIO
NT PROPORTIONAL LIMIT
NT RESILIENCE

NT ROCKWELL HARDNESS
NT SHEAR PROPERTIES
NT SHEAR STRENGTH
NT SHELL STABILITY
NT STEADY STATE CREEP
NT STIFFNESS
NT STRESS CYCLES
NT STRESS RATIO
NT STRESS RELAXATION
NT STRUCTURAL STABILITY
NT SUPERPLASTICITY
NT TENSILE CREEP
NT TENSILE PROPERTIES
NT TENSILE STRENGTH
NT THERMAL RESISTANCE
NT THERMOELASTICITY
NT THERMOPLASTICITY
NT TOUGHNESS
NT VISCOELASTICITY
NT VISCOPLASTICITY
NT WEAR RESISTANCE
NT WELD STRENGTH
NT YIELD POINT
NT YIELD STRENGTH

The microstructure and mechanical properties of hot worked FeAl intermetallic alloys
01 p0058 N94-10020

Aluminium-lithium forgings: Properties and potential satellite applications 01 p0058 N94-10021

Weldability of maraging steels
01 p0059 N94-10028

Aluminum-beryllium alloys for aerospace applications
01 p0060 N94-10029

Ceramic matrix composites: High performance materials for space application 01 p0062 N94-10044

LAMINV: A computer code for creating laminates having prescribed properties 01 p0065 N94-10069

Physical properties of injection molded liquid crystal polymers and high temperature engineering polymers
[AD-A264912] 01 p0087 N94-10508

Computational simulation of hot composite structures
[NASA-TM-106200] 01 p0186 N94-10762

Primaset (tm): A safer material for aircraft interior applications 01 p0018 N94-10772

Fire resistance and mechanical properties for phenolic prepregs 01 p0020 N94-10786

Level 3 material characterization of NARC HRPF, HRHU, HRHF, and HRPU
[NASA-CR-192579] 01 p0065 N94-10812

Synthesis and properties of nanophase materials
[DE93-011757] 01 p0397 N94-10962

Fibre reinforced polymer matrix composites: Microstructure and mechanical properties
[DLR-FB-92-28] 01 p0066 N94-11085

Mechanical interaction between synthetic fiber and cement base matrix in FRC composites
[AD-A265310] 01 p0073 N94-11686

Experimental studies of the structure of grain boundaries
[DE93-013979] 01 p0402 N94-11700

Fracture behavior of ionomers and ionomeric blends
[AD-A265379] 01 p0094 N94-12407

Molecular properties of polymeric materials for space applications
[NASA-CR-194370] 01 p0094 N94-12450

Simulation studies for surfaces and materials strength
[NASA-CR-193305] 02 p0671 N94-13179

Measurements on two-dimensional arrays of mesoscopic Josephson junctions
[AD-A265129] 02 p0807 N94-13359

Measurement of strain in individual phases of composites before, during, and after mechanical loading
[DE93-014585] 02 p0558 N94-14119

Dynamic mechanical deformation of a SiC(sub p)/Al-Li (8090) composite
[DE93-014586] 02 p0558 N94-14121

Physical and structural properties of a sputtered zirconia-yttria layer used as a thermal resistance
[ONERA-NT-1992-10] 02 p0810 N94-14193

Nonlinear wave predictions in ceramics
[DE93-016516] 02 p0582 N94-14436

Machining and grinding: High rate deformation in practice
[DE93-010718] 02 p0664 N94-14457

The structure and mechanical properties of Ru-Cu and Ru-Ti nanolayer composites
[DE93-014453] 02 p0558 N94-14469

Microstructural influences on the mechanical properties of solder
[DE93-015044] 02 p0573 N94-14474

Structures and shear response of lipid monolayers
[DE93-015076] 02 p0730 N94-14802

Yield properties of tungsten and tungsten heavy alloys
[AD-A266833] 02 p0575 N94-14878

The effect of aging at 343 C on the mechanical properties and microstructure of type 308 stainless steel weldments
[DE93-015454] 03 p0957 N94-16103

Evaluation of the interfacial mechanical properties in fiber-reinforced ceramic composites
[DE93-015494] 03 p0935 N94-16461

Thermal stress effects in intermetallic matrix composites
[NASA-CR-191191] 03 p1054 N94-16518

Evolution of microstructure in face centered cubic metals during irradiation: A review
[DE93-015682] 03 p0958 N94-16662

The effect of oxygen, grain size, and strain rate on the mechanical behavior of forged P/M tantalum
[DE93-011251] 03 p0959 N94-16764

Processing of complex sintered reaction bonded silicon nitride parts by microwave heating
[DE93-015811] 03 p0969 N94-16877

Electrical conductivity of ion implanted ladder and semi-ladder polymers
[AD-A267432] 03 p0970 N94-16978

Mean strain effects on the strain life fatigue curve
[AD-A267211] 03 p0960 N94-16984

Dynamic testing and characterization of pre-fractured ceramic
[DE93-016457] 03 p0972 N94-17238

Micromechanics modeling and analysis of Haversian compact bone tissues as a fiber reinforced composite material
[AD-A268250] 03 p1129 N94-17456

Metals 2000
[DE93-016761] 04 p1355 N94-17752

Microstructural analysis of solid-state resistance welds
[DE93-017295] 04 p1443 N94-17761

Atlas of formability: ALLVAC 718
[AD-A268304] 04 p1357 N94-17804

Measurement and analysis of three 1.5-GPa shock-wave profiles in copper
[DE93-016559] 04 p1451 N94-17864

Mechanical properties of excimer laser modified titanium surfaces
[DE93-012663] 04 p1358 N94-17875

Impact modeling with smooth particle hydrodynamics
[DE93-016561] 04 p1451 N94-17906

Ceramic films and interfaces: Chemical and mechanical properties
[DE93-018416] 04 p1369 N94-18163

Study of mechanical behavior and internal structure of ferritic nanocrystalline material
[DE93-019264] 04 p1596 N94-18184

Mechanical properties of fiber-reinforced YBa2Cu3O(x) and Bi2Sr2CaCu2O(x) bars
[DE93-017689] 04 p1454 N94-18479

Carbon/carbon composites coated with SiC by chemical vapor deposition
[AD-A269934] 04 p1341 N94-18544

Pressureless densification of ceramic matrix composites
[AD-A269137] 04 p1371 N94-18691

Mechanical properties and impact damage resistance of composites fabricated by low cost, vacuum assisted, resin transfer molding
[AD-A270361] 04 p1342 N94-18702

Mechanical-property changes of structural composite materials after low-temperature proton irradiation: Implications for use in SSC magnet systems
[DE93-016735] 04 p1343 N94-18763

Intelligent materials systems and structures. Part 4: The influence of thermomechanical loading on the life of shape memory alloys
[PB93-195923] 04 p1363 N94-18952

High dose effects in neutron irradiated face-centered cubic metals
[DE93-017671] 04 p1364 N94-19043

Polymer technology publication. Series no. 14, 1993
[PB93-195964] 04 p1372 N94-19052

Molecular dynamics modeling of the mechanical behavior of metallic multilayers
[DE93-017972] 04 p1365 N94-19263

Low-aluminum-content iron-aluminum alloys
[DE93-017862] 04 p1365 N94-19274

Microstructure of the interfacial zone around aggregate particles in concrete
[PB93-195790] 04 p1380 N94-19322

Ni-Al2O3 solid state binding: Elaboration, state of thermal constraints, mechanical behavior
[ECL-92-31] 04 p1366 N94-19436

New aircraft materials and structures
[MBB-LME-202-S-PUB-502-A] 04 p1319 N94-19496

Incology 908 database report: On process-structure-property relationship
[DE93-017616] 04 p1366 N94-19546

Ceramic technology project data base
[DE93-019360] 04 p1374 N94-19561

Picoindentation hardness measurements using atomic force microscopy
[AD-A270877] 04 p1604 N94-19579

Advanced civil engineering materials based on inorganic polymers
[AD-A270837] 04 p1374 N94-19600

Simulation of dynamic material response with the PAGOSA code
[DE93-018285] 04 p1460 N94-19603

Structure and properties of polycarbonate alloys
[ETN-93-95071] 04 p1375 N94-19611

Commercialization effort in support of electroslag-casting technology
[DE93-017988] 04 p1366 N94-19733

Dynamic, multiaxial impact response of confined and unconfined ceramic rods
[DE93-040057] 05 p1829 N94-19824

Characterization studies of lower and non-TDI polyurethane encapsulants
[DE93-041129] 05 p1698 N94-19857

High performance heavy alloys by alloying and process control
[AD-A271129] 05 p1689 N94-20019

Fundamentals of mechanical behavior in structural intermetallics: A synthesis of atomistic and continuum modeling
[DE93-019166] 05 p1690 N94-20232

Properties and potential of high-temperature niobium beryllides
[DE93-019169] 05 p1690 N94-20233

Direct imaging of the surface microstructure of dielectric materials using an atomic force microscope
[AD-A272251] 05 p2018 N94-20575

Mechanical properties and reliability of semi-crystalline polymers
[AD-A271591] 05 p1704 N94-20946

Issues related to mechanical properties of neutron-irradiated ceramics
[DE93-040262] 05 p1707 N94-21560

Molecular dynamics modeling of the mechanical behavior of metallic multilayers
[DE93-019947] 05 p1694 N94-21921

Strengthening and toughening in refracto:y metal alloys
[DE93-019942] 05 p1695 N94-21986

Tensile strength of fiber reinforced plastics at 77K irradiated by various radiation sources
[DE93-040826] 05 p1709 N94-22008

The history of development of molybdenum alloys for structural applications
[DE94-000389] 06 p2239 N94-22958

Evaluation of A5Si3Z(x) intermetallics for use as high temperature structural materials
[DE93-041127] 06 p2227 N94-22977

Development of small punch testing technique and its application to evaluation of mechanical properties degradation
[DE94-001193] 06 p2375 N94-23184

Instrument interface description for NOAA 2000 instruments with European morning spacecraft and/or NOAA-OPQ spacecraft
[NASA-TM-109406] 06 p2208 N94-23478

Materials Science and Engineering
[DE94-003018] 06 p2228 N94-23493

The effects of texture and strain on the r-va lue of heavy gauge tantalum plate
[DE94-000690] 06 p2242 N94-23541

The mechanical properties of single crystal (alpha)-Si3N4
[DE94-002632] 06 p2563 N94-24517

A survey of metallurgical research on several actinides
[DE94-002643] 06 p2245 N94-24747

Environmentally assisted cracking of high strength beta titanium alloys
[AD-A273598] 06 p2245 N94-24823

An x ray diffraction investigation of alpha-Al2O2 addition to Yttria Stabilized Zirconia (YSZ) thermal barrier coatings subject to destabilizing vanadium pentoxide (V2O5) exposure
[AD-A273403] 06 p2261 N94-25072

The nanometer-scale mechanics of gold films
[AD-A273307] 06 p2565 N94-25086

Simulation studies for surfaces and materials strength
[NASA-CR-195185] 06 p2565 N94-25093

Surface compositional variations of Mo-47Re alloy as a function of temperature
[NASA-TP-3402] 06 p2245 N94-25117

Preparation and properties of translucent gamma-aluminium oxynitride
[ETN-94-95305] 06 p2263 N94-25281

Alternatives for reinforcement: Fiber composites
[VTT-TIED-1412] 06 p2230 N94-25386

Study on high temperature damage control and life improvement 07 p2729 N94-25580

Continuous fiber reinforced thermoplastic composites: Literature survey
[VTT-TIED-1422] 07 p2704 N94-25651
Structure and properties of intermetallic composites synthesized in situ using solid state displacement reactions
[DE94-004312] 07 p2705 N94-25805
Stress relaxation in dough moulding compounds
[PB94-124872] 07 p2748 N94-25894
An atom probe investigation of the influence of trace impurities on the mechanical behavior of NiAl
[DE94-002797] 07 p2734 N94-26272
Titanium 1992: Volume 3: Science and technology
[AD-A274800] 07 p2735 N94-26337
Titanium 1992: Science and technology, volume 2 rence (7th) in san diego, california on june 29-july 2, 1992. Volume 2
[AD-A274799] 07 p2736 N94-26362
Statistical mechanical properties of Z(N)(sup n-1) broken model
[DE93-634344] 07 p2993 N94-26457
Investigation of forced and isothermal chemical vapor infiltrated SiC/SiC ceramic matrix composites
[DE94-004544] 07 p2708 N94-26557
Mechanical properties of nanophase materials
[DE94-004625] 07 p2751 N94-26594
The influence of weld metal alloying additions to extend the heat input range for the submerged arc welding of high strength steels
[AD-A274284] 07 p2738 N94-26679
New rubber qualification for the igniter adapter
[NASA-CR-193936] 07 p2752 N94-26708
Proceedings of the Fourth Euroseminar on Microscopy Applied to Building Materials
[PB94-119807] 07 p2839 N94-26754
Mechanism of mechanical fatigue of silica glass
[DE94-003165] 07 p2753 N94-26783
An ultrasonic testing technique for monitoring the cure and mechanical properties of polymeric materials
[AD-A274536] 07 p2753 N94-26842
Thermoplastic or thermosetting composites in aircrafts
[PB94-123809] 07 p2710 N94-27253
Researches of the Electrotechnical Laboratory. No. 52: Studies of externally pressurized porous gas bearings
[JTN-94-80549] 07 p2825 N94-27351
Research into the microstructure and mechanical behavior of eutectic Bi-Sn and In-Sn
[DE94-004558] 07 p2741 N94-27619
Formation of glassy Pd-Ni-P alloys by mechanical alloying and their structure and thermal stability
07 p2746 N94-28168
High Quality Aluminium Castings Conference
[PB94-133592] 07 p2747 N94-28359
Studies in ice mechanics
[PB94-133055] 07 p2900 N94-28393
Joining silicon carbide to austenitic stainless steel through diffusion welding
[PB94-126331] 08 p3297 N94-28399
Viscous and elastic-plastic material model in the ABAQUS
[PB94-132347] 08 p3316 N94-28409
Analysis of data by long-time mechanical properties of 08KH18N10T steel irradiated by neutrons
[DE94-605337] 08 p3202 N94-28551
Robust 300 C wire insulation system
08 p3165 N94-28699
Electrical and mechanical testing of wire insulation for space applications 08 p3166 N94-28710
Innovative processing of composites for ultra-high temperature applications, book 1
[AD-A275597] 08 p3176 N94-28729
Probabilistic material strength degradation model for Inconel 718 components subjected to high temperature, mechanical fatigue, creep and thermal fatigue effects
[NASA-CR-195284] 08 p3318 N94-28840
On the dynamic mechanical behavior of 3-D integrated fabric reinforced composites
[AD-A275424] 08 p3177 N94-28865
Electronic structure and mechanical properties of grain boundaries
[AD-A275198] 08 p3512 N94-28890
Microstructure/property relationships for SCS6/Timetal 21-S composite
[AD-A275056] 08 p3178 N94-29135
Characterisation and processing of SiC/MAS-L glass ceramic matrix composite
[REPT-932-430-111] 08 p3179 N94-29412
Glass-ceramic matrix composites
[REPT-932-430-112] 08 p3179 N94-29413
The effect of various metallurgical parameters on the flow and fracture behavior of polycrystalline NiAl near the brittle-to-ductile transition
[NASA-TM-106534] 08 p3205 N94-29758
Estimation of Weibull modulus from dynamic and static fatigue experiments
[PB94-138641] 08 p3322 N94-30114
High elongation elastomers 08 p3223 N94-30477
Simulation of composite material response under dynamic compressive loading
[DE94-005272] 08 p3184 N94-30589
Effect of fiber coating on mechanical properties of Nicalon fibers and Nicalon-fiber/SiC matrix composites
[DE94-005477] 08 p3185 N94-30593
Studies on the optimization of deformation processed metal-metal matrix composites
[DE94-006033] 08 p3185 N94-30704
Influence of tungsten alloying additions on the mechanical properties and texture of tantalum
[DE94-004994] 08 p3210 N94-30774
Numerical modeling and prediction of the thermomechanical behavior of fiber-reinforced composites 08 p3186 N94-30956
Databases and demands for solar heating materials
[PB94-137494] 09 p3758 N94-31070
Performance predictions for composite materials
[AD-A276451] 09 p3618 N94-31261
Contributions to the validation of the CJS model for granular materials
[ECL-92-56] 09 p3733 N94-31376
On the constitutive response of transversely loaded fiber composites with compliant interphases
09 p3619 N94-31555
An experimental and analytical investigation of a threaded fastener
[VTT-JULK-786] 09 p3724 N94-31654
Powder metallurgical processing of fibre reinforced aluminium composites
[PB94-148285] 09 p3620 N94-31688
Passive vibration damping materials: Piezoelectric ceramic composites for vibration damping applications
[AD-A276550] 09 p3653 N94-31935
Mechanical properties of acrylate networks formed by visible laser-induced polymerization. 2. Control of the mechanical properties
[AD-A277111] 09 p3655 N94-31982
Recent advances and developments in refractory alloys
[DE94-007929] 09 p3644 N94-32374
Multiple size scale structures in silica/siloxane composites studied by small-angle scattering
[DE94-007300] 09 p3625 N94-32642
Inorganic polymer engineering materials
[DE94-008519] 09 p3659 N94-32655
Influence of volume fraction of component materials and interlayer bond strength on fracture toughness of multi-layer Al 6090-25 volume percent SiCp and Al 5182 laminates
[DE94-007141] 09 p3626 N94-32665
Structure, stability, and mechanical properties of intermetallic phases
[DE94-009178] 09 p3647 N94-32852
Acoustic window
[AD-D016171] 09 p3862 N94-33017
Interface engineering in oxide fiber/oxide matrix composites
[AD-A277672] 09 p3627 N94-33029
High Temperature Silicides and Refractory Alloys Symposium, volume 322
[AD-A278373] 10 p4024 N94-33741
Solar radiation effects on glasses
[NASA-CR-195900] 10 p4029 N94-34232
JPRS report: Science and technology. Central Eurasia: Materials science
[JPRS-UMS-93-007] 11 p4240 N94-35517
Thick film fabrication of aluminum nitride microcircuits
[DE94-010107] 11 p4259 N94-35706
Properties and bibliography of GaSe
[AD-A279064] 11 p4340 N94-35733
Continuous unidirectional fiber reinforced composites: Fabrication and testing 11 p4229 N94-36400
Laminated thermoplastic composite material from recycled high density polyethylene
11 p4230 N94-36403
Mechanical properties of crosslinked polymer coatings
11 p4231 N94-36410
Collection, processing, and reporting of damage tolerant design data for non-aerospace structural materials
[NASA-CR-196046] 11 p4347 N94-36435
Flame resistant fibrous structures development
[NASA-CR-185700] 12 p4421 N94-36641
Characterisation of Fibre Reinforced Titanium Matrix Composites
[AGARD-R-796] 12 p4400 N94-36649
Possibilities and pitfalls in aerospace applications of titanium matrix composites 12 p4400 N94-36650
Manufacture and properties of sigma fibre reinforced titanium 12 p4401 N94-36655
Fibre-matrix interface properties in Ti-matrix composites: Chemical compatibility and micromechanical behaviour
12 p4401 N94-36657
Methodologies for thermal and mechanical testing of TMC materials 12 p4401 N94-36659
Processing and mechanical properties of NiAl-based in-situ composites
[NASA-CR-195333] 12 p4416 N94-36954
Data compatibility for various Charpy-tests
[DE94-617534] 12 p4416 N94-37074
Chromium/molybdenum alloy plating. Part 1: The electrodeposition of low contraction chromium/molybdenum alloys using unipolar (on/off) pulse plating
[AD-A280236] 12 p4417 N94-37138
Defect initiation/growth and energy dissipation induced by deformation and fracture
[AD-A280411] 12 p4424 N94-37184
A fully coupled thermal, chemical, mechanical cookoff model
[DE94-011432] 12 p4428 N94-37201
Status review and accomplishments of the Materials Research Center at the University of Pittsburgh
[AD-A280422] 12 p4399 N94-37214
Mechanical behavior of MoSi2 and MoSi2 composites
[DE94-013116] 12 p4405 N94-37289
Atomic level characterization of defects in microalloyed NiAl: An atom probe investigation
[DE94-012732] 12 p4418 N94-37396
Characterization of mechanical properties degradation using small punch testing technique
[DE94-011202] 12 p4418 N94-37410
Development of durable high-temperature catalysts for natural gas combustion: Catalytic materials (CATMAT (trade name)) properties database
[PB94-171824] 12 p4412 N94-37462
Micromechanical modeling of advanced materials
[DE94-011249] 12 p4405 N94-37627
Double network elastomers and method of making same
[AD-D016323] 12 p4427 N94-37831

MECHANICAL RESONANCE
U RESONANT VIBRATION

MECHANICAL SHOCK
NT HYDRAULIC SHOCK
Development of test techniques to simulate high-frequency mechanical shock on weapon components
[KCP-613-4998] 02 p0675 N94-13907
Shear wave measurements in shock-induced, high-pressure phases
[DE93-016461] 03 p1062 N94-17664
A finite element scheme for shock capturing
[AD-A270182] 04 p1417 N94-18755
U.S. Tag for ISO/TC 43, acoustics, IEC/TC 29 electroacoustics, and ISO/TC 108/SC4 human exposure to mechanical vibration and shock: Minutes of the accredited standards committee on bioacoustics, S3
[AD-A273014] 05 p1897 N94-21309
US tag for ISO/TC 108 mechanical vibration and shock: Minutes of the accredited Standards Committee on Mechanical Vibration and Shock, S2
[AD-A273015] 06 p2376 N94-23789
Minutes: Accredited Standards Committee on Mechanical Vibration and Shock, S2. US TAG for ISO/TC 108 Mechanical Vibration and Shock
[AD-A275591] 08 p3316 N94-28726

MECHANICAL TWINNING
Slip, twinning and transformation in Laves phases
[DE93-018164] 03 p0960 N94-16972
Deformation twinning: Influence of strain rate
[DE94-002693] 07 p2738 N94-26621

MEDIA
NT ANISOTROPIC FLUIDS
NT ANISOTROPIC MEDIA
NT ELASTIC MEDIA
NT INTERGALACTIC MEDIA
NT INTERPLANETARY DUST
NT INTERPLANETARY MEDIUM
NT ZODIACAL DUST
Your GAS experiment and the media or why does that other can get all of the publicity?
04 p1327 N94-19182
Development of novel switchable protein surfaces
[AD-A275510] 08 p3384 N94-28667

MEDIAN (STATISTICS)
Robust estimators and tests in one-sample location problem with particular consideration on modified maximum likelihood process
[ETN-93-94391] 02 p0774 N94-14703

MEDICAL ELECTRONICS
Transcutaneous Analyte Measuring Methods (TAMM)
[AD-A271387] 04 p1408 N94-19756
Journal of rehabilitation research and development, volume 30, number 1, 1993
[AD-A272956] 05 p1893 N94-21613
The adaptive resonance theory network: (Clustering-) behaviour in relation with brainstem auditory evoked potential patterns
[EUT-92-E-264] 06 p2470 N94-22877

Monitoring activity with a wrist-worn actigraph: Effects of amplifier passband and threshold variations
[AD-A274705] 07 p2909 N94-26377
On the feasibility of virtual environments in medicine 12 p4483 N94-37264

MEDICAL EQUIPMENT
NT ARTIFICIAL HEART VALVES
NT BLOOD PUMPS
NT ENDOSCOPES
NT PROSTHETIC DEVICES
NT RESPIRATORS
NT SURGICAL INSTRUMENTS
NT X RAY APPARATUS
NT X RAY TUBES
Medical evaluations on the KC-135 1991 flight report summary
[NASA-TM-104755] 02 p0731 N94-12832
Cool suit
[NASA-TM-109639] 03 p1120 N94-15250
New insulin pump
[NASA-TM-109642] 03 p1120 N94-15253
Living well in space: Clinical care challenge
[NASA-TM-109539] 03 p1120 N94-15370
Medical imaging
[NASA-TM-109675] 03 p1229 N94-15520
Annual historical report, calendar year 1992
[AD-A267050] 03 p1121 N94-15663
Method and apparatus to characterize ultrasonically reflective contrast agents
[NASA-CASE-LAR-14969-1] 03 p1129 N94-17085
Automated data collection system for the TCM3 transcutaneous pO2/pCO2 monitoring system
[AD-A268400] 03 p1129 N94-17424
Legacy of the X Ray Laser Program
[DE93-019550] 04 p1442 N94-19554
Transcutaneous Analyte Measuring Methods (TAMM)
[AD-A271387] 04 p1408 N94-19756
Numerical modeling for an electric-field hyperthermia applicator 05 p1729 N94-20451
Compact free electron lasers for medical applications
[AD-A273609] 06 p2350 N94-24934
High impact strength poly(lactide) tough biodegradable materials
[ETN-94-95389] 07 p2747 N94-25748
Development of surgical CW Nd:YAG laser with optical fiber delivery system
[DE93-632902] 07 p2817 N94-26185
Biomedical polyurethane networks
[ETN-94-95391] 07 p2750 N94-26211
Technology 2003: The Fourth National Technology Transfer Conference and Exposition, volume 1
[NASA-CP-3249-VOL-1] 08 p3555 N94-30440
A force-controllable macro-micro manipulator and its application to medical robots 08 p3314 N94-30441
Composite redesign of obstetrical forceps 08 p3397 N94-30457
A fuzzy logic controller for hormone administration using an implantable pump 08 p3397 N94-30459
Hydrogenated amorphous silicon (a-Si:H) based gamma camera: Monte Carlo simulations
[DE94-007042] 09 p3795 N94-31323
Technical evaluation of the UH-60Q: Medical oxygen system
[AD-A276983] 09 p3579 N94-32242
Integration of the Molecular Sieve Oxygen Generating System (MSOGS) into the UH-60Q MEDEVAC Blackhawk
[AD-A277668] 10 p4099 N94-33589
On the feasibility of virtual environments in medicine 12 p4483 N94-37264

MEDICAL PERSONNEL
NT FLIGHT SURGEONS
NT PHYSICIANS
NT SURGEONS
US-USSR telemedicine consultation spacebridge to Armenia and Ufa 01 p0308 N94-11809
Illness/injury pattern complex 40 (Titan) 03 p1125 N94-16625
Tuberculosis: A case for increased screening 03 p1126 N94-16627
OSHA bloodborne pathogens standards exposure control plan 03 p1127 N94-16645
Aeromedical support for casualties in extremely hot climates 08 p3382 N94-28443
Technical evaluation of the UH-60Q: Aircraft in typical aeromedical evacuation missions
[AD-A276944] 09 p3586 N94-32217
Medical problems in high mountain environments. A handbook for medical officers
[AD-A278095] 09 p3798 N94-33268
Emergency medical services 10 p4096 N94-33644

MEDICAL SCIENCE
NT CARDIOLOGY
NT CLINICAL MEDICINE
NT ENDOCRINOLOGY
NT EPIDEMIOLOGY
NT HISTOLOGY
NT HUMAN PATHOLOGY
NT IMMUNOLOGY
NT NEUROLOGY
NT NUCLEAR MEDICINE
NT OPHTHALMOLOGY
NT PATHOLOGY
NT PSYCHIATRY
NT RADIOBIOLOGY
NT RADIOLOGY
NT SYMPTOMOLOGY
National Institute of Health Almanac, 1992
[PB93-183556] 01 p0303 N94-10828
Development of bioelastic materials for the prevention of adhesions: Polypenta- and polytetrapeptides
[AD-A264851] 01 p0088 N94-10863
The Department of Clinical Investigation, reports control symbol MED-300(R-1)
[AD-A264969] 01 p0304 N94-11649
Global considerations for implementation of telemedicine 01 p0305 N94-11792
A telemedicine health care delivery system 01 p0307 N94-11803
Clinical physiology of bed rest
[NASA-TM-104010] 02 p0727 N94-13447
Thyroid alterations in porcine after prolonged exposure to cold or heat
[AD-A266840] 02 p0733 N94-14879
New insulin pump
[NASA-TM-109642] 03 p1120 N94-15253
Annual historical report, calendar year 1992
[AD-A267050] 03 p1121 N94-15663
Localizing visual function in the brain
[AD-A267381] 03 p1133 N94-17020
Biomedical polyurethane networks
[ETN-94-95391] 07 p2750 N94-26211
Clinical investigation program
[AD-A275025] 08 p3391 N94-29116
Virtual reality in medical education and assessment 09 p3798 N94-32471
Bibliography of research reports and publications issued by the Human Engineering Division
[AD-A278787] 11 p4299 N94-35712
Activities of National Institute of Radiological Sciences
[DE94-727636] 11 p4296 N94-36101
Task-specific usability requirements for virtual information environments: Interface design and data representation for human operators of complex medical systems 12 p4483 N94-37262

MEDICAL SERVICES
International Telemedicine/Disaster Medicine Conference: Papers and Presentations
[NASA-NP-207] 01 p0304 N94-11787
Medical informatics and telemedicine: A vision 01 p0305 N94-11788
The Canadian experience: Using telemedicine for the support of medical care at remote sites 01 p0305 N94-11789
Telemedicine and international disaster response: Medical consultation to Armenia and Russia via a telemedicine spacebridge 01 p0305 N94-11790
Use of telescience for biomedical research during space flight 01 p0305 N94-11791
Global considerations for implementation of telemedicine 01 p0305 N94-11792
Tropical medicine: Telecommunications and technology transfer 01 p0305 N94-11793
Clinical aspects of telemedicine 01 p0306 N94-11795
Commercial applications of telemedicine 01 p0306 N94-11798
Space technology in remote health care 01 p0306 N94-11799
The use of communication technology in medicine 01 p0306 N94-11800
The National Disaster Medical System 01 p0307 N94-11801
A telemedicine health care delivery system 01 p0307 N94-11803
Communications infrastructure requirements for telemedicine/telehealth in the context of planning for and responding to natural disasters: Considering the need for shared regional networks 01 p0307 N94-11804
Use of satellite telecommunications for telemedicine 01 p0308 N94-11807
US-USSR telemedicine consultation spacebridge to Armenia and Ufa 01 p0308 N94-11809
The revitalization of health and education in Rural America Act of 1992 01 p0308 N94-11810
Defense: Health care
[AD-A265914] 01 p0421 N94-12445
In-flight demonstration of the Space Station Freedom Health Maintenance Facility fluid therapy system (E300/E05) 02 p0595 N94-13775
Living well in space: Clinical care challenge
[NASA-TM-109539] 03 p1120 N94-15370
Annual historical report, calendar year 1992
[AD-A267050] 03 p1121 N94-15663
Proceedings of the 1992 Annual Meeting NASA Occupational Health Program
[NASA-CR-193462] 03 p1123 N94-16609
Americans with Disabilities Act considerations for the practice of occupational medicine 03 p1124 N94-16611
Emergency preparedness and planning 03 p1124 N94-16613
Ongoing Recovery Basic Information Tool (ORBIT) 03 p1124 N94-16616
Illness/injury pattern complex 40 (Titan) 03 p1125 N94-16625
Identifying and responding to customer needs at the Kennedy Space Center 03 p1056 N94-16626
Tuberculosis: A case for increased screening 03 p1126 N94-16627
Summary of follow-up results from potential tuberculosis exposures 03 p1126 N94-16628
Screening for prostate cancer 03 p1126 N94-16630
Physical fitness and health education program at NASA Headquarters 03 p1126 N94-16631
Ames Fitness Program 03 p1126 N94-16632
Asbestos Surveillance Program 03 p1127 N94-16638
Hearing Conservation Medical Program 03 p1127 N94-16639
Lead Surveillance Program 03 p1127 N94-16640
Mercury Surveillance Program 03 p1127 N94-16641
Respiratory Protection Program medical clearance for respirator use 03 p1127 N94-16642
General Medical Surveillance Program 03 p1127 N94-16643
Bloodborne Pathogens Program 03 p1127 N94-16644
Annual research progress report, fiscal year 1992. Volume 2: Department of Clinical Investigation
[AD-A273584] 06 p2427 N94-24945
Practice patterns of US Army medical department psychiatrists and psychologists
[AD-A274787] 07 p2909 N94-26360
The role of hyperbaric oxygen as a prophylaxis for radiation enteritis
[AD-A274974] 07 p2901 N94-26517
Monograph of the aviation epidemiology data register for calendar year 1988
[AD-A274589] 07 p2911 N94-26985
The telemedicine spacebridge project: A joint US/Russian venture in long distance medicine via satellite
[NASA-TM-106523] 07 p2693 N94-27427
Clinical investigation program
[AD-A275025] 08 p3391 N94-29116
Potential hazards of magnetic resonance imagers to emergency medical service helicopter operations
[AD-A278873] 08 p3135 N94-29862
Technical evaluation of the UH-60Q: Aircraft in typical aeromedical evacuation missions
[AD-A276944] 09 p3586 N94-32217
Integration of the Molecular Sieve Oxygen Generating System (MSOGS) into the UH-60Q MEDEVAC Blackhawk
[AD-A277668] 10 p4099 N94-33589
Telemedicine, virtual reality, and surgery 10 p4096 N94-33641
Emergency medical services 10 p4096 N94-33644
Global Picture Archiving and Communication Systems (GPACS): An overview
[AD-A280617] 12 p4543 N94-37042
Night vision goggles in Emergency Medical Service (EMS) helicopters
[SCT-93RR-22] 12 p4487 N94-37742

MEDICINE
Science, technology, and the federal government: National goals for a new era 02 p0827 N94-14115

MEDITERRANEAN SEA
NT ADRIATIC SEA
Preliminary results of the comparison of ATSR measurements with in situ sea temperatures
[DE93-013399] 01 p0287 N94-10517
The activity of the ERS-1 Venice (Italy) group on scatterometry 01 p0233 N94-11713
SST assimilation: Eastern Mediterranean case study 01 p0221 N94-12719
Some aspects of the drought in North Africa and in the Mediterranean basin 09 p3778 N94-30989
The climate of the Mediterranean basin: Its sensitivity to global change 09 p3778 N94-30993
The ocean-atmosphere interactions in the Mediterranean Sea 09 p3779 N94-30995

The study of the Mediterranean outflow
[AD-A277742] 10 p4091 N94-33445
MEDIUM SCALE INTEGRATION
Investigation of advanced fault insertion and simulator methods
[NASA-CR-195241] 08 p3261 N94-28511
MEETINGS
U CONFERENCES
MEISSNER EFFECT
U DIAMAGNETISM
U SUPERCONDUCTIVITY
MELT SPINNING
Comparison of Al-Fe alloys produced by PFC and USGA techniques 01 p0058 N94-10019
Preparation and characterization of rapidly solidified Al-Li alloys
[ISBN-0-315-58948-5] 02 p0569 N94-13367
Melt spinning study
[NASA-CR-193823] 04 p1380 N94-19423
Melt-spin processing of high (Tc) oxide superconductors
[DE94-000696] 05 p2036 N94-22582
Ceramic silicon-boron-carbon fibers from organic silicon-boron-polymers
[NASA-CASE-ARC-11956-1-SB] 06 p2253 N94-23311
Microstructures and mechanical properties of Al3Ti-based alloys: Analysis in single phase and multiphase systems
[ONERA-NT-1993-6] 09 p3640 N94-31420
MELTING
NT ARC MELTING
NT FUSION (MELTING)
NT LEVITATION MELTING
NT VACUUM MELTING
Marangoni motion during melting of a hypermonotectic alloy: Numerical simulations for the D2 experiment IHF04 01 p0113 N94-10177
Preliminary results of Mn partitioning experiments on Murchison analogues 01 p0281 N94-12081
Simulation of possible regolith optical alteration effects on carbonaceous chondrite meteorites 01 p0430 N94-12163
Flash melting of chondrule precursors in excess of 1600 C. Series 1: Type 2 (B1) chondrule composition experiments 01 p0431 N94-12177
Primordial lightning: Evidence preserved in chondrites 01 p0432 N94-12230
Incomplete melting of the Au(100) surface
[DE93-623192] 02 p0569 N94-13227
High temperature behavior of glass (M-8) 02 p0587 N94-13740
Microwave hybrid heating of alumina filaments
[DE93-012642] 02 p0581 N94-14327
Statistical mechanical theory of liquid entropy
[DE93-016524] 02 p0817 N94-14593
Partial melting experiment of Y-Ba-Cu oxide 03 p0945 N94-15168
Remelting of Fe-C-Si-alloy in a ceramic mold skin 03 p0945 N94-15169
Mathematical model of frost heave and thaw settlement in pavements
[AD-A267037] 03 p0983 N94-15676
Partial melting of ordinary chondrites: Lost City (H) and St. Severin (LL) 03 p1243 N94-16286
On origin of the olivine inclusions from the Kainsaz CO carbonaceous chondrite 03 p1244 N94-16345
First results from analysis of coordinated AVIRIS, TIMS, and ISM (French) data for the Ronda (Spain) and Beni Bousera (Morocco) peridotites 03 p1067 N94-16675
Low-aluminum-content iron-aluminum alloys
[DE93-017862] 04 p1365 N94-19274
Proceedings: International Symposium on Thermal Engineering and Science for Cold Regions
[AD-A270636] 04 p1487 N94-19529
Orthopyroxenes as recorders of diogenite petrogenesis: Trace element systematics 05 p1686 N94-20760
Origin of high-Ti lunar ultramafic glasses 05 p1686 N94-20853
Ancient Martian valley genesis and paleoclimatic inference: The present as a key to the past 05 p2142 N94-21661
The Martian valley networks: Origin by niveo-fluvial processes 05 p2146 N94-21682
Modeling of glass fabrication 05 p1711 N94-21800
The incongruent melting and melt textured solidification process of Bi2Sr2CaCu3O8
[DE93-041123] 05 p2032 N94-21936
The effect of correlated and point defects on the vortex lattice melting transition in single crystal YBa2Cu3O(7-delta)
[DE93-040277] 05 p2033 N94-21997
Shock temperature measurements of iron to 350 GPa
[DE94-001058] 05 p1695 N94-22024
First-principles pressure-temperature phase diagrams in metals
[DE94-001056] 05 p1696 N94-22398
Processing of YBCO superconductors for improved levitation force
[DE94-001326] 06 p2559 N94-22994
Generalized melting criterion for beam-induced amorphization
[DE94-001333] 06 p2560 N94-23189
Three-dimensional solidification and melting using magnetic field control 06 p2325 N94-23664
A dynamic melting model for the origin of Apollo 15 olivine-normative and quartz-normative mare basalts 06 p2615 N94-24371
Detection of velocity in high temperature liquid metals 06 p2247 N94-25127
Liquid and solid solubility of Ag in Bi2Sr2CaCu2O8
[DE94-002829] 07 p2735 N94-26273
Iron: What is melt?
[DE94-003373] 07 p2735 N94-26322
Morphology transitions during non-equilibrium growth processes
[ITN-94-85236] 07 p3065 N94-27243
Laser-material interactions: A study of laser energy coupling with solids
[DE94-005212] 08 p3292 N94-28478
Dislocation theory of melting for iron, revisited
[DE94-002715] 08 p3355 N94-28538
Melt flow during alloy solidification: Dimensional analysis and model problems
[PB94-138625] 08 p3206 N94-29997
A toy model of sea ice growth 08 p3351 N94-30626
Effect of twin boundary density on the vortex melting transition in YBa2Cu3O(7-delta) single crystals
[DE94-007684] 09 p3904 N94-32601
Snowmelt forecasting. Further cold regions development of operational hydrological forecasting, volume 2
[AD-A278123] 09 p3757 N94-33269
Mantle melting and crustal recycling in subduction zones 10 p4084 N94-33368
Interface shape and convection during solidification and melting of succinonitrile
[NASA-TM-106487] 11 p4262 N94-35248
Consolidation of zircaloy-4 end crops by induction melting
[DE94-010031] 11 p4240 N94-35650
Partial melting of the St. Severin (LL) and Lost City (H) ordinary chondrites: One step backwards and two steps forward 11 p4353 N94-36146
Production of ferroan andesites by the experimental partial melting of an LL chondrite 11 p4353 N94-36160
Partition coefficients for Al, Ca, Ti, Cr, and Ni in olivine obtained by melting experiment on an LL6 chondrite 11 p4353 N94-36163
Alternate melting and refining routes 12 p4421 N94-37323
Process enhancements of superalloy material 12 p4421 N94-37324
MELTING POINTS
Micromechanisms of monotonic and cyclic subcritical crack growth in advanced high melting point low-ductility intermetallics
[AD-A267764] 03 p0961 N94-17223
Studies on gel electrolyte based on nitrile-butadiene copolymers
[AD-A269450] 04 p1370 N94-18282
High performance heavy alloys by alloying and process control
[AD-A271129] 05 p1689 N94-20019
The incongruent melting and melt textured solidification process of Bi2Sr2CaCu3O8
[DE93-041123] 05 p2032 N94-21936
Shock temperature measurements of iron to 350 GPa
[DE94-001058] 05 p1695 N94-22024
Low melting temperature alloy deployment mechanism 06 p2356 N94-23997
High strain rate superplasticity in metals and composites
[DE94-001521] 06 p2229 N94-24547
Synthesis of soluble halogenated polyphenylenes: Mechanism for the coupling halogenated lithiobenzenes
[AD-A273547] 06 p2257 N94-24558
Metal-catalyzed alkynylation of brominated polyphenylenes: Thermoset precursors of high density monolithic glassy carbon
[AD-A273232] 06 p2259 N94-24789
Iron: What is melt?
[DE94-003373] 07 p2735 N94-26322
Microspheres for laser velocimetry in high temperature wind tunnel 07 p2682 N94-27903
Thermal conductivity of liquid carboxylic acids
[ESDU-93017] 07 p2721 N94-28138
Directional solidification studies in Ni-Al alloys
[DE94-005562] 08 p3201 N94-28527
Dislocation theory of melting for iron, revisited
[DE94-002715] 08 p3355 N94-28538
On the temperature distribution near a cold surface
[AD-A275162] 08 p3332 N94-29288
The ferroelectric behavior of odd-numbered nylons
[AD-A278126] 09 p3663 N94-33058
MELTS (CRYSTAL GROWTH)
NT CONTAINERLESS MELTS
NT IMPACT MELTS
NT MELT SPINNING
Effect of rotation on microgravity floating-zone crystal growth 01 p0101 N94-10080
Coupled thermovibrational and thermocapillary convection in liquid bridge (floating zone system) 01 p0101 N94-10082
On shape of single crystals grown by FZM in microgravity 01 p0102 N94-10084
Liquid bridges and floating zones 01 p0102 N94-10085
Space and temporal behavior and control of the residual convection in microgravity 01 p0104 N94-10099
CdTe crystal growth in the Soviet facility zona 4 01 p0106 N94-10111
Concept and design of ampoule for melt growth of gallium arsenide in first mission of space flyer unit 01 p0107 N94-10115
CdTe crystal growth by THM with a rotating magnetic field 01 p0107 N94-10116
Proceedings of the 8th European Symposium on Materials and Fluid Sciences in Microgravity, volume 2
[ESA-SP-333-VOL-2] 01 p0112 N94-10171
On the role of Soret effect in concentration distribution in crystals growing from the melt 01 p0112 N94-10173
Solidification from supercooled melt under microgravity 01 p0113 N94-10176
Numerical calculation of the growth of InP by the travelling heater method in the first mission of the Space Flyer Unit 01 p0114 N94-10179
Scientific specifications for an automated facility for growing large semiconducting crystals from the melt in space 01 p0114 N94-10180
TEXUS 28 experiment: Convections and crystal growth of Ge:Ga. Analysis of temperature measurements 01 p0114 N94-10184
Results of crystal growth experiments by FZM on Zona facilities in microgravity 01 p0116 N94-10193
Non-equilibrium solidification in undercooled Ni-B alloys 01 p0086 N94-10196
Conductive-radiative model for predicting the shape of HgI2 crystal grown in the LTVG furnace 01 p0117 N94-10201
THM-growth of III-V-semiconductors in the magnetic field 01 p0118 N94-10209
Crystal growth in the Zone Melting Facility (ZMF) 01 p0119 N94-10213
The stability of hibonite and other aluminous phases in silicate melts: Implications for the origin of hibonite-bearing inclusions 01 p0080 N94-12052
The solubility of gold in silicate melts: First results 01 p0087 N94-12086
Graphite solubility and co-vesiculation in basalt-like melts at one-ATM 01 p0463 N94-12173
Flash melting of chondrule precursors in excess of 1600 C. Series 1: Type 2 (B1) chondrule composition experiments 01 p0431 N94-12177
Process modelling for materials preparation experiments
[NASA-CR-193556] 01 p0056 N94-12588
Growth experiment of narrow band-gap semiconductor PbSnTe single crystals in space (M-1) 02 p0586 N94-13733
Growth of Si spherical crystals and the surface oxidation (M-9) 02 p0587 N94-13741
Crystal growth of compound semiconductors in a low-gravity environment (InGaAs crystals) (M-22) 02 p0590 N94-13754
Containerless processing of undercooled melts
[NASA-CR-194350] 02 p0572 N94-14123
Siderophile elements in the upper mantle of the Earth: New clues from metal-silicate partition coefficients 03 p1103 N94-16250
Os isotopes in SNC meteorites and their implications to the early evolution of Mars and Earth 03 p1242 N94-16272
Transition metals in superheat melts 03 p0962 N94-16273
Angrite LEW87051: Are the olivines pheno's or xeno's? A continuing story 03 p1103 N94-16285
Explosive volcanism and the compositions of the cores of differentiated asteroids 03 p1243 N94-16306
Evaporation kinetics of Mg2SiO4 crystals and melts from molecular dynamics simulations 03 p1219 N94-16331
Was Martian mantle wet? A possible consequence of rapid core formation 03 p1277 N94-16335

Hydride-containing molten salts and their technology implications
[AD-A266458] 03 p1092 N94-16567
Convection effects on radial segregation and crystal melt interface in vertical Bridgman growth
[NASA-CR-191541] 03 p1029 N94-17387
Polymer technology publication. Series no. 14, 1993
[PB93-195964] 04 p1372 N94-19052
Frequency dependent electrical properties of minerals and partial melts
[DE93-019918] 05 p2012 N94-19861
Evaporation of a sodium tellurite melt in the jamic low gravity drop shaft 05 p1713 N94-20605
The incongruent melting and melt textured solidification process of Bi2Sr2CaCu3O8
[DE93-041123] 05 p2032 N94-21936
Theoretical considerations for Reaction-Formed Silicon Carbide (RFSC) formation by molten silicon infiltration into slurry-derived preforms
[NASA-TM-106414] 06 p2222 N94-23500
Three-dimensional solidification and melting using magnetic field control 06 p2325 N94-23664
Study on melted solution stirring under microgravity 07 p2730 N94-25585
Nonlinear dynamics and pattern selection at the crystal-melt interface
[DE94-003112] 07 p3060 N94-26780
Channel model for AC electric arc
[PB94-124591] 07 p2786 N94-27327
Float zone crystal growth using laser radiation
[DLR-FB-93-10] 07 p3066 N94-27590
Characterization of semi-insulating gallium arsenide
[AD-A273781] 07 p3068 N94-27704
A novel approach to the fabrication of SiC structures of arbitrary shape
[AD-A275475] 08 p3214 N94-29073
Process modelling for materials preparation experiments
[NASA-CR-195782] 08 p3175 N94-30242
Investigation of the phase equilibria and phase transformations associated with the Bi2Sr2CaCu2O(y) superconductor
[DE94-004889] 08 p3519 N94-30691
On the possible role of elemental carbon in the formation of reduced chondrules 11 p4351 N94-35421
Synthetic and natural Nakhla pyroxenes: Parent melt composition and REE partition coefficients 11 p4353 N94-36161

MEMBRANE ANALOGY
U MEMBRANE STRUCTURES
U STRUCTURAL ANALYSIS

MEMBRANE STRUCTURES
NT SKIN (STRUCTURAL MEMBER)
Evaluation for membrane components of water recycling system
[NAL-TM-646] 02 p0737 N94-13388
Cellular and molecular level responses after radiofrequency radiation exposure, alone or in combination with x rays or chemicals
[AD-A268189] 04 p1501 N94-17729
Benchmarking the QUAD4/TRIA3 element 04 p1450 N94-17837
Electrochemical synthesis of ultrathin film composite membranes
[AD-A272721] 05 p1681 N94-21168
High power density proton exchange membrane fuel cells 06 p2393 N94-23359
Advances in direct oxidation methanol fuel cells 06 p2393 N94-23361

MEMBRANE THEORY
U STRUCTURAL ANALYSIS

MEMBRANES
NT CELL MEMBRANES (BIOLOGY)
NT ION EXCHANGE MEMBRANE ELECTROLYTES
NT MEMBRANE STRUCTURES
NT SKIN (STRUCTURAL MEMBER)
Aluminum and membrane channels
[AD-A265241] 01 p0300 N94-11020
A theory of membrane absorbers
[ISVR-TR-217] 01 p0076 N94-11216
Probability of alamethicin conductance states varies with nonlamellar tendancy of bilayer phospholipids
[AD-A264957] 01 p0301 N94-11648
Predicting the vibrations of a spinning inflated membrane
[DE93-010690] 02 p0676 N94-14456
Upgrading of raw natural gas using high-performance polymer membranes
[DE93-014041] 02 p0586 N94-14586
Primary and secondary electrical space power based on advanced PEM systems
[DE93-012643] 02 p0553 N94-14689
Structures and shear response of lipid monolayers
[DE93-015076] 02 p0730 N94-14802
Gas separations using ceramic membranes
[DE93-000278] 03 p0947 N94-15861
Modification of fluoropolymer surfaces with electronically conductive polymers
[AD-A266294] 03 p0967 N94-16475
Morphology of polymerized membranes on an amorphous substrate at molecular resolution by AFM
[AD-A268760] 04 p1370 N94-18403
Intracellular physiology of the rat suprachiasmatic nucleus: Electrical properties, neurotransmission and effects of neuromodulators
[AD-A268829] 04 p1505 N94-18538
Molten carbonate fuel cell networks: Principles, analysis, and performance
[DE93-000281] 04 p1468 N94-18925
Lateral distribution of lipids in membranes at high pressure
[AD-A271183] 05 p1700 N94-20299
High temperature size selective membranes
[DE93-019865] 05 p1709 N94-21982
Cellular and tissue injury during nonfreezing cold injury and frostbite
[AD-A270883] 06 p2423 N94-22732
A novel method for determination of transport parameters of H2 and O2 in PEMFCs
[DE94-001492] 06 p2389 N94-22962
Primary and secondary electrical space power based on advanced PEM systems 06 p2392 N94-23357
PEM regenerative fuel cells 06 p2392 N94-23358
A high performance H2-Cl2 fuel cell for space power applications 06 p2394 N94-23366
Selective hydrogen separation by palladium-based composite membranes
[PB93-201671] 06 p2254 N94-23431
Gauging of Chern-Simons p-Barnes
[DE94-601553] 07 p2993 N94-26425
Bulletin of the Institute for Chemical Reaction Science, Tohoku University, volume 2
[JTN-94-80602] 07 p2717 N94-27385
Development of liquid membrane separation processes 07 p2717 N94-27386
Effects of high-intensity electric field stimulation on the electromechanical performance of cardiac muscle: Influence of fiber orientation 07 p2904 N94-27467
On the mechanism of reentrant arrhythmias following DC defibrillation: Influence of fiber orientation to the effects of low-energy electric field stimulation on the effective refractory period of cardiac muscle 07 p2904 N94-27468
Development of a 2f optical performance measurement system
[DE94-003489] 07 p3039 N94-27721
Polyaniline membranes for gas and liquid separation
[AD-A275851] 08 p3408 N94-28790
Effects of pressure on membrane-associated receptors and effector elements
[AD-A275813] 08 p3384 N94-28829
Inorganic polymer-derived ceramic membranes
[DE94-000082] 08 p3216 N94-29830
Adhesion of phospholipid monolayers to planar supports deposited with the Langmuir-Blodgett technique
[PB94-148699] 10 p4029 N94-34102
Detail design of a 10.4-m stretched-membrane dish
[DE94-009462] 10 p4079 N94-34167
Combined SO(x)/NO(x) control via SOXAL (tm) process: An electrodialytic regenerative wet scrubbing process
[DE94-009053] 11 p4284 N94-35346
A low temperature scanning force microscope for biological samples
[DE94-011357] 11 p4297 N94-36269
Effects of freezing and cold acclimation on the plasma membrane of isolated protoplasts
[DE94-012487] 12 p4479 N94-37248

MEMORY
The 12th Annual Carmel Conference, distinctiveness and Memory: Cognitive Psychophysiological and Physiological Considerations
[AD-A267181] 03 p1131 N94-15148
Theoretical and experimental research into biological mechanisms underlying learning and memory
[AD-A267441] 03 p1133 N94-17022
Synaptic plasticity and memory formation
[AD-A267988] 03 p1133 N94-17453
Cortical substrate of haptic representation
[AD-A269583] 04 p1508 N94-18304
The identification of the computational significance of key neurobiological characteristics found in a number of telencephalic brain regions
[AD-A269374] 04 p1505 N94-18407
Comparing performance on implicit memory tests
[AD-A269900] 04 p1508 N94-18657
Visual perception of features and objects
[AD-A269879] 04 p1508 N94-18682
First results with utile distinction memory for reinforcement learning
[TR-446] 04 p1610 N94-19485
Research, Development, Training, and Evaluation (RDTE) support delivery order 1: Computational cognitive models
[AD-A271837] 05 p1894 N94-20610
Air traffic controller working memory: Considerations in air traffic control tactical operations
[AD-A273722] 07 p2664 N94-26197
The central executive component of working memory
[AD-A274295] 07 p2938 N94-26683
Effects of methamphetamine and fatigue on long- and short-term memory
[AD-A276452] 09 p3799 N94-32187
Reading: Interaction with memory
[AD-A277547] 09 p3801 N94-32956
Analysis and synthesis of adaptive neural elements and assembles
[AD-A277423] 09 p3836 N94-32996
Reminding-based learning
[AD-A277424] 09 p3801 N94-32997

MEMORY (COMPUTERS)
Radiation hardened nonvolatile memory for space and strategic applications
[DE93-000746] 01 p0319 N94-10146
A proof-of-concept implementation of persistence in a hierarchical storage system
[DE93-009959] 01 p0319 N94-10318
Simulation of a parallel computer
[NAL-TR-1154] 01 p0335 N94-10368
Low latency messages on distributed memory multiprocessors
[NASA-CR-191479] 01 p0323 N94-10643
Flexible language constructs for large parallel programs
[NASA-CR-191478] 01 p0326 N94-11196
Alleviating memory contention in matrix computations on large-scale shared-memory multiprocessors
[AD-A265009] 01 p0320 N94-11294
Data processing units for eight magnetospheric particle and field sensors
[AD-A264403] 01 p0276 N94-11463
Gallium arsenide dynamic random access memory support circuitry
[AD-A265176] 01 p0320 N94-11875
Beyond core: Making parallel computer I/O practical
[DE93-012347] 02 p0758 N94-12878
The KSR1: Experimentation and modeling of poststore
[DE93-012539] 02 p0759 N94-13470
Hashing and rehashing in emulated shared memory
[CWI-CS-R9240] 02 p0740 N94-13525
The National Storage Laboratory: A collaborative research project
[DE93-015099] 02 p0760 N94-14475
Execution methods, and parallel virtual machines for distributed implementation of the LCS parallel programming language
[LAAS-93032] 02 p0761 N94-14716
Relaxing consistency in recoverable distributed shared memory
[AD-A266931] 03 p1140 N94-15174
The design of self-checking reduced instruction set computers
[AD-A267012] 03 p1140 N94-15763
Generating local addresses and communication sets for data-parallel programs
[NASA-CR-194605] 03 p1159 N94-15796
The alignment-distribution graph
[NASA-CR-194609] 03 p1148 N94-15956
Unipolar terminal-attractor based neural associative memory with adaptive threshold
[NASA-CASE-NPO-18790-1-CU] 03 p1165 N94-15958
A decision criteria to select an associative-memory organization that minimizes the execution time of a mix of associative-search operations
[AD-A266438] 03 p1149 N94-16560
A trace-based comparison of shared memory multiprocessor architectures
[TR-432] 03 p1159 N94-16577
Shared-memory multiprocessor trends and the implications for parallel program performance
[TR-420] 03 p1159 N94-16578
SONOS technology for commercial and military nonvolatile memory applications
[DE93-015647] 03 p1011 N94-16661
Fault-tolerant architectures for multiprocessor and VLSI-based systems
[AD-A267370] 03 p1140 N94-17005
Superconducting/semiconducting hybrids and advance memory concepts for superconducting electronics
[AD-A268679] 04 p1397 N94-18312
An SEU immune logic family 04 p1398 N94-18342
Performance of defect-tolerant set-associative cache memories 04 p1398 N94-18346
An improved distributed arithmetic architecture 04 p1398 N94-18349

Low power signal processing research at Stanford
04 p1393 N94-18351
Technology, design, simulation, and evaluation for SEP-hardened circuits 04 p1399 N94-18352
Formal verification of an MMU and MMU cache
04 p1400 N94-18366
A programming paradigm for distributed-memory computers
[DE93-018336] 04 p1524 N94-19024
Performance and scalability aspects of directory-based cache coherence in shared-memory multiprocessors
[DE93-016442] 04 p1536 N94-19115
Static Computer Memory Integrity Testing (SCMIT): An experiment flown on STS-40 as part of GAS payload G-616 04 p1325 N94-19169
Radiation hardened microprocessor for small payloads
04 p1327 N94-19184
Wide-address spaces: Exploring the design space
[MEMO-INF-92-77] 04 p1537 N94-19219
Toward a high performance distributed memory climate model
[DE93-019156] 04 p1494 N94-19298
PUMMA: Parallel Universal Matrix Multiplication Algorithms on distributed memory concurrent computers
[DE93-019163] 04 p1538 N94-19299
Data-Machine Independence (DMI)
[DE93-018008] 04 p1539 N94-19734
A novel method for characterizing the electrical Priorities of lead Zirconate Titanate (PZT) ferroelectric films and memory devices
[AD-A270463] 05 p2013 N94-19966
A methodology for formal hardware verification, with application to microprocessors
[AD-A270550] 05 p1898 N94-20085
Mint tutorial and user manual
[TR-452] 05 p1905 N94-20143
Memory contention in scalable cache-coherent multiprocessors
[TR-448] 05 p1929 N94-20144
Single-event upset testing of the performance semiconductor 1750A CMOS/SOS chip set
[AD-A271158] 05 p2015 N94-20184
DISCERN: A distributed neural network model of script processing and memory 05 p1941 N94-20255
Optoelectronic associative memory
[NASA-CASE-NPO-18278-1-CU]
05 p1985 N94-20303
M-dimensional computer memory with M-1 dimensional hyperplane access
[AD-D015960] 05 p1898 N94-20357
Measuring the effects of thread placement on the Kendall Square KSR1
[DE93-040655] 05 p1908 N94-20932
Avoiding and tolerating latency in large-scale next-generation shared-memory multiprocessors
05 p1753 N94-21081
Test results for SEU and SEL immune memory circuits
05 p1754 N94-21087
An ASIC memory buffer controller for a high speed disk system 05 p1754 N94-21089
A CAM-based LZ data compression IC
05 p1759 N94-21129
The effects of block size on the performance of coherent caches in shared-memory multiprocessors
[AD-A272838] 05 p1899 N94-21177
Fast mutual exclusion, even with contention
[AD-A272947] 05 p1912 N94-21227
Software coherence in multiprocessor memory systems
[NASA-CR-194696] 05 p1931 N94-21272
High dimension action spaces in robot skill learning
[TR-458] 05 p1945 N94-21317
A simple modern correctness condition for a space-based high-performance multiprocessor
05 p1766 N94-21718
Detection of feed-through faults in CMOS storage elements 05 p1766 N94-21721
A novel cache mechanism 05 p1767 N94-21730
A set-associative, fault-tolerant cache design
05 p1768 N94-21731
The quantum structure of matter grand challenge project: Large-scale 3-D solutions in relativistic quantum dynamics
[DE94-000328] 05 p1960 N94-21955
The design of linear algebra libraries for high performance computers
[DE93-040458] 05 p1960 N94-21967
Efficient communication primitives on mesh architectures with hardware routing
[DE93-018791] 05 p1936 N94-22032
Reverse automatic differentiation of modular FORTRAN programs
[DE94-000336] 05 p1918 N94-22088
Crystal ball gazing 05 p1925 N94-22477
Dynamic data distributions in Vienna Fortran
[NASA-CR-191575] 06 p2448 N94-23092
Distributed Operating Systems and Mach. Proceedings of the Spring 1992 Graduate Seminar on Distributed Systems
[PB93-224905] 06 p2449 N94-23103
Fault tolerant onboard packet switch architecture for communication satellites: Shared memory per beam approach
[NASA-TM-106397] 06 p2201 N94-23567
Vectorization and parallelization of the finite strip method for dynamic Mindlin plate problems
06 p2483 N94-23679
Design and implementation issues of end-to-end protocols in high-speed networks
[PB94-110905] 06 p2467 N94-23752
Algorithm on addition chains with restricted memory
[PB94-118692] 06 p2454 N94-23759
Non-volatile, solid state bistable electrical switch
[NASA-CASE-NPO-17621-1-CU]
06 p2309 N94-23820
A quick uplink, expandable executable for the NSSC-1 of the Hubble Space Telescope
06 p2305 N94-23859
Magellan spacecraft and memory state tracking: Lessons learned, future thoughts
06 p2207 N94-23865
The design of a standard message passing interface for distributed memory concurrent computers
[DE94-002536] 06 p2446 N94-24538
Crosstie random access memory element having associated read/write circuitry
[AD-D016027] 06 p2446 N94-24724
MOS analog memory with injection capacitors
[AD-D015990] 06 p2312 N94-25050
Fast parallel algorithms for short-range molecular dynamics
[DE93-018519] 07 p3016 N94-26033
Virtual data
[DE94-002718] 07 p2986 N94-26807
Memory subsystem performance of programs using copying garbage collection
[AD-A274258] 07 p3099 N94-27014
Memory subsystem performance of programs with intensive heap allocation
[AD-A274122] 07 p2967 N94-27063
Binary snapshots
[CWI-CS-R9319] 07 p2955 N94-27547
Parallel computing for probabilistic response analysis of high temperature composites
[NASA-CR-194467] 07 p2843 N94-27656
Review and analysis of dense linear system solver package for distributed memory machines
07 p2978 N94-27916
Performance analysis of memory hierachies in high performance systems
[DE94-005549] 08 p3404 N94-28517
A common Ada run-time system for avionics software
08 p3150 N94-29331
Multi-speed multi-phase resolver converter
[NASA-CASE-MFS-28855-1] 08 p3264 N94-29372
A comparison of distributed memory and virtual shared memory parallel programming models
[DE94-005473] 09 p3825 N94-31663
Compiler techniques for managing data motion
[AD-A276514] 09 p3918 N94-31930
Interpreter composition issues in the formal verification of a processor-memory module
[NASA-CR-4594] 09 p3820 N94-32775
Toroidal computer memory for serial and parallel processors
[AD-D016144] 09 p3807 N94-32978
A petabyte size electronic library using the N-Gram memory engine 10 p4153 N94-33802
An analog memory integrated circuit for waveform acquisition up to 900 MHz
[DE94-009020] 10 p4041 N94-33928
A format for storing and managing multiple level of detail terrain for simulated environments
[AD-A278497] 10 p4159 N94-34377
Communication and memory requirements as the basis for mapping task and data parallel programs
[AD-A278954] 11 p4310 N94-35806
A critical examination of charge funneling and its impact on single-event upset in Si devices
[DE94-007868] 11 p4261 N94-36373
Software use control
[DE94-008429] 12 p4489 N94-36480
Cost-effective computations with boundary interface operators in elliptic problems
[DE94-621506] 12 p4503 N94-37098
Adaptable binary programs
[AD-A280243] 12 p4494 N94-37119
SACS: A cache simulator incorporating timing analysis with buffer and memory management
[AD-A280472] 12 p4494 N94-37230

MENISCI
Evaporation from a meniscus within a capillary tube in microgravity
[NASA-CR-194593] 03 p0976 N94-15654
Finite element modeling of evaporation and condensation during sol-gel film and fiber formation
[DE93-017655] 04 p1345 N94-17820
Sol-gel metal oxide and metal oxide/polymer multilayers applied by meniscus coating
[DE94-005813] 09 p3649 N94-31199
Transient body force effects on the dryout and rewet of a heated capillary structure
[AD-A278677] 11 p4264 N94-35690
Determination of the dispersion constant in a constrained vapor bubble thermosyphon
[NASA-CR-196124] 12 p4442 N94-36992

MENTAL HEALTH
Incongruity, incongruity resolution, and mental states: The measure and modification of situational awareness and control
[NASA-CR-194568] 05 p1893 N94-20168
Practice patterns of US Army medical department psychiatrists and psychologists
[AD-A274787] 07 p2909 N94-26360
Human dimensions research team, operation restore hope
[AD-A274340] 07 p2939 N94-27056
La Chalupa-30: Lessons learned from a 30-day subsea mission analogue 10 p4096 N94-33654

MENTAL PERFORMANCE
Psychophysiological measures of cognitive workload in laboratory and flight 01 p0317 N94-11529
Analyzing human errors in flight mission operations
01 p0314 N94-11534
Work/rest schedules and performance of S-3 aviators during fleet exercise
[AD-A265807] 02 p0734 N94-12975
Work/rest schedules and performance of F/A-18 aviators during Fleet Exercise 1992
[AD-A265826] 02 p0735 N94-12982
Selection of behavioral tasks and development of software for evaluation of rhesus monkey behavior during spaceflight
[NASA-CR-194176] 02 p0728 N94-13865
The influence of ATC message length and timing on pilot communication
[NASA-CR-177621] 02 p0512 N94-14744
Complex information coordination performance: Differential changes in working memory contributions following training
[AD-A267007] 03 p1132 N94-15762
Scuba-diving, anxiety and task performance
03 p1132 N94-15938
Cognitive engineering models in space systems
[NASA-CR-193473] 03 p1140 N94-16716
The behavioral toxicology of high-peak, low average power, pulsed microwave irradiation
[AD-A268392] 03 p1134 N94-17535
A method for cognitive task analysis
[IZF-1992-B5] 04 p1508 N94-17967
Cognitive limitations in coordination in hierarchical information processing structures
[AD-A268825] 04 p1616 N94-18535
Comparing performance on implicit memory tests
[AD-A269900] 04 p1508 N94-18657
Research on man-machine productivity in aviation at Human Engineering Institute of Hangzhou University
[AD-A269952] 04 p1512 N94-18673
Cognitive ability and whole-body rotation
[IZF-1993-B-4] 04 p1510 N94-19440
Development of the UTC-PAB normative database
[AD-A271319] 05 p1893 N94-20023
Incongruity, incongruity resolution, and mental states: The measure and modification of situational awareness and control
[NASA-CR-194568] 05 p1893 N94-20168
Cognition and the brain: A continuation of the university research initiative at New York University
[AD-A271872] 05 p1894 N94-20467
Compatibility evaluation and research on the Computerized Adaptive Screening Test (CAST): User and programmer's guide
[AD-A273112] 05 p1894 N94-21510
Mental images 06 p2429 N94-23980
Investigation of time and intensity effects in operator workload and performance
[CTN-94-60927] 06 p2433 N94-24171
Automated system function allocation and display format: Task information processing requirements
06 p2434 N94-24189
EEG and chaos: Description of underlying dynamics and its relation to dissociative states
[NASA-CR-195171] 06 p2428 N94-24799
Human factors of mission planning systems: Theory and concepts 06 p2521 N94-25010

Study on knowledge extraction and systematization for material design 07 p2727 N94-25568
Extending the rule space model to a semantically-rich domain: Diagnostic assessment in architecture
[AD-A273789] 07 p2948 N94-25864
A diagnostic classification model for document processing skills
[AD-A273790] 07 p3096 N94-25925
The use of EEG as a workload assessment tool in flight test
[AD-A274568] 07 p2910 N94-26847
Task demand, workload, and performance
[PB94-123627] 07 p2942 N94-27155
Brain wave correlates of attentional states: Event related potentials and quantitative EEG analysis during performance of cognitive and perceptual tasks
07 p2940 N94-27901
Symptoms of hypoxia at simulated altitude of 25,000 feet 07 p2933 N94-27945
Toward a model of expert knowledge structure and their role in cognitive task performance
[AD-A275641] 08 p3529 N94-28645
Designing for performance: A cognitive systems engineering approach to modifying an AWACS human computer interface
[AD-A275187] 08 p3399 N94-28861
Temporal and qualitative decomposition of plausible reasoning
[AD-A275073] 08 p3398 N94-29154
Spectral analysis of heart rate and psychological state: A review of its validity as a workload index
[AD-B179387] 08 p3399 N94-30969
Assessing design activity in complex CMOS circuit design
[AD-A277620] 10 p4040 N94-33854
Immersive virtual environments as trainer: System design from a cognitive stance
12 p4484 N94-37267

MENTAL STRESS
U STRESS (PSYCHOLOGY)

MERCAPTAN
U THIOLS

MERCAPTO COMPOUNDS
U THIOLS

MERCURY (METAL)
NT MERCURY ISOTOPES
Stability of reference masses 1: Evidence for posiible variations in the mass of reference kilograms arising from mercury contamination
[NPL-DMM(A)-86] 02 p0708 N94-13667
Mercury Surveillance Program
03 p1127 N94-16641
Sodium-mercury excimer laser, phase 1
[AD-A267728] 03 p1042 N94-17230
Measurement of volatile metal species at elevated temperatures
[PB94-132321] 08 p3186 N94-28407
Processable, chemical routes to binary metal sulfides
[AD-A277006] 09 p3642 N94-32004
Modeling atmospheric concentrations and deposition of Hg
[DE94-012633] 12 p4467 N94-37440

MERCURY (PLANET)
A mission to Mercury and a mission to the moons of Mars
[NASA-CR-195530] 06 p2195 N94-24619
Forced libration of Mercury and geodetic determination of a possible fluid core 09 p3774 N94-32493
The real-time display of interferometry data for Goldstone radar astronomy data acquisition
11 p4255 N94-35560

MERCURY CADMIUM TELLURIDES
Process modelling for materials preparation experiments
[NASA-CR-193556] 01 p0056 N94-12588
Advanced high performance CdHgTe multiplexed arrays 03 p0903 N94-15051
A 12.5 micron infrared detector for Earth observation
03 p0903 N94-15052
Proceedings of the 6th International Conference on Narrow Gap Semiconductors
[AD-A268097] 03 p1015 N94-17570
IR materials producibility
[AD-A268849] 04 p1577 N94-18223
Theory of energy-assisted epitaxy; theory of ordered semiconductor alloys: In(1-x)Tl(x)Sb as a long-wave infrared material
[AD-A271007] 05 p2012 N94-19835
The quantum efficiency of HgCdTe photodiodes in relation to the direction of illumination and to their geometry 05 p1735 N94-20512
IR materials producibility
[AD-A273031] 05 p1987 N94-21321
Effects of thermal-solutal convection on temperature and solutal fields under various gravitational orientations
06 p2267 N94-24451
Modeling the total dose radiation effects of Hg(1-x)Cd(x)Te photodiodes using numerical device simulators
[AD-A275235] 08 p3263 N94-29028
Dual-use applications of infrared sensitive materials
[AD-A275140] 08 p3499 N94-29694
Indium-vacancy complexes in mercury cadmium telluride
[AD-A276177] 09 p3894 N94-31055
IR materials producibility
[AD-A277028] 09 p3879 N94-32006
Comprehensive investigation of HgCdTe metalorganic chemical vapor deposition
[NASA-CR-195933] 10 p4030 N94-34278
Use of rotation to suppress thermosolutal convection in directionally solidified binary alloys
[NASA-CR-196372] 12 p4415 N94-36811

MERCURY COMPOUNDS
NT MERCURY CADMIUM TELLURIDES
NT MERCURY TELLURIDES
Conductive-radiative model for predicting the shape of HgI2 crystal grown in the LTVG furnace
01 p0117 N94-10201
Optical properties and surface morphology studies of palladium contacts on mercuric iodide single crystals
[DE93-012510] 03 p1207 N94-15973
Elemental impurity analysis of mercuric iodide by ICP/MS
[DE93-015531] 03 p0949 N94-16876
X ray analysis of alpha mercuric iodide crystal structure and processing effects
[DE93-017620] 05 p2027 N94-21296
New concepts for HgI2 scintillator gamma ray spectroscopy
[NASA-CR-194819] 06 p2233 N94-24113
Measurement of volatile metal species at elevated temperatures
[PB94-132321] 08 p3186 N94-28407
Measurement of elemental speciation by liquid chromatography: Inductively coupled plasma mass spectrometry (LC-ICP-MS) with the Direct Injection Nebulizer (DIN)
[DE94-005261] 08 p3187 N94-28483
High T(sub c) superconductor tunnel junctions for photon detectors
[DE94-007686] 09 p3904 N94-32602

MERCURY FLIGHTS
NT MERCURY MA-6 FLIGHT

MERCURY ISOTOPES
Radiations from hot nuclei 07 p3030 N94-27915

MERCURY LAMPS
Process to fabricate thick coplanar microwave electrode structures
[AD-D015913] 05 p1748 N94-19892

MERCURY MA-6 FLIGHT
Astronauts number 3 --- Friendship 7
[NASA-TM-109430] 03 p0874 N94-15501
Astronauts number 3, part 2
[NASA-TM-109822] 10 p4011 N94-33576

MERCURY PROJECT
Astronauts number 1 --- mercury project
[NASA-TM-109428] 03 p1131 N94-15499

MERCURY SPACECRAFT
NT FRIENDSHIP 7
Astronauts number 2
[NASA-TM-109429] 03 p0873 N94-15500

MERCURY SURFACE
Mercury: Mid-infrared (7.3 - 13.5 microns) spectroscopic observations showing features characteristic of plagioclase 11 p4370 N94-36150

MERCURY TELLURIDES
NT MERCURY CADMIUM TELLURIDES
Characterization of convection related defects in II-VI compound semiconductors
[NASA-CR-194704] 05 p2030 N94-21778
Vibrational properties of homopolar and heteropolar surfaces and interfaces of the CdTe/HgTe system
[DE94-608105] 08 p3516 N94-30069

MERGING ROUTINES
Paradigms for very fast parallel algorithms
[ITN-93-85212] 02 p0755 N94-14556
Tests of a simple data merging algorithm for the GONG project 05 p1927 N94-22549

MERIDIONAL FLOW
Numerical simulations of thermal convection in rapidly rotating spherical fluid shells 01 p0153 N94-11635
Empirical wind model for the middle and lower atmosphere. Part 2: Local time variations
[NASA-TM-104592] 05 p1870 N94-21862
Observed and Navy operational global model climatologies of synoptic disturbances over the tropical western Pacific during winter 1991-1992
[AD-A273400] 06 p2416 N94-25071
Interpreting the implied meridional oceanic energy transport in AMIP
[DE94-001538] 07 p2898 N94-26072

MEROMORPHIC FUNCTIONS
NT ELLIPTIC FUNCTIONS
NT RATIONAL FUNCTIONS
On a class of two-dimensional nearest neighboring random walks
[CWI-BS-R9220] 01 p0347 N94-10353
Controlled invariance of nonlinear systems: Nonexact forms speak louder than exact forms
[PB93-237790] 06 p2475 N94-24755

MERRITT ISLAND (FL)
A study of the Merritt Island, Florida sea breeze flow regimes and their effect on surface heat and moisture fluxes
[NASA-CR-4537] 01 p0286 N94-12580
An in-depth analysis and modelling of the Shuttle to MILA S-band telemetry link 05 p1657 N94-21340
Development and implementation of a scrub habitat compensation plan for Kennedy Space Center
[NASA-TM-109202] 08 p3347 N94-29099

MESAS
Geologic mapping of Harmakhis and Reull Valles region, Mars: Evidence for multiple resurfacing and drainage events 05 p1844 N94-20705

MESFETS
U FIELD EFFECT TRANSISTORS

MESH (MATHEMATICS)
U COMPUTATIONAL GRIDS

MESH GENERATION (MATHEMATICS)
U GRID GENERATION (MATHEMATICS)

MESOMETEOROLOGY
Sensitivity testing of a single-Doppler temperature retrieval and forecast system
[AD-A267278] 03 p1105 N94-14958
Mesoscale frontogenesis: An analysis of two cold front case studies
[AD-A267950] 03 p1107 N94-17054
Opposing mesoscale flows in a broken midlatitude squall line
[AD-A268011] 03 p1109 N94-17492
Clouds: Their prediction and simulation
[AD-A271161] 05 p1864 N94-19900
Incorporation and comparative evaluation of a non-convective cloud parameterization scheme in the Naval Research Laboratory west coast mesoscale weather prediction model
[AD-A272417] 05 p1867 N94-21146
Mesoscale simulations of the November 25-26 and December 5-6 cirrus cases using the RAMS model
05 p1878 N94-22331
A comparison of small and larger mesoscale latent heat and radiative fluxes: December 6 case study
05 p1879 N94-22335
United States Weather Research Program (USWRP)
06 p2411 N94-24375
Validation of mesoscale models
06 p2413 N94-24391
Session on validation of coupled models
06 p2414 N94-24399
Development and testing of the Coupled Ocean/Atmosphere Mesoscale Prediction System (COAMPS)
[AD-A273925] 07 p2892 N94-25793
Mesoscale meteorological measurements characterizing complex flows
[DE94-002359] 07 p2895 N94-26761
Evaluation of the National Meteorological Center mesoscale model for prediction of severe convection over Central Arizona 08 p3371 N94-29744
An observational and numerical study of sea/land-breeze circulations in an area of complex coastal heating 08 p3372 N94-29813
Coordination of mesoscale meteorological research between ASL and European group
[AD-A276730] 09 p3784 N94-32162
Use of cloud observations and mesoscale meteorology models to evaluate and improve cloud parameterizations
[DE94-003610] 09 p3785 N94-32717
Development and testing of improved techniques for modeling the hydrologic cycle in a mesoscale weather prediction system
[AD-A277416] 09 p3786 N94-32921
Atmospheric and dispersion modeling in areas of highly complex terrain employing a four-dimensional data assimilation technique
[DE94-004041] 11 p4285 N94-35823

MESON RESONANCE
Further study of the X(1910) meson
[DE93-621443] 02 p0782 N94-13362
On the hadron formation time in pion-nucleus interaction
[DE93-616879] 06 p2539 N94-25476
Issues in light hadron spectroscopy
[PB94-138229] 08 p3486 N94-29112
Hybrid mesons (Q(anti Q)g) in N(anti N) annihilation
[DE94-001491] 11 p4327 N94-36239

MESON-MESON INTERACTIONS
Theoretical high energy physics
[DE93-015884] 03 p1187 N94-16170
Low energy theorems from the effective Lagrangian with vector mesons
[DE94-611173] 11 p4322 N94-35785
MESON-NUCLEON INTERACTIONS
Strangeness production with protons and pions
[DE93-010879] 01 p0359 N94-10304
Crossing-odd spin effects in the dipole model of hadron scattering
[DE93-617692] 01 p0362 N94-10551
Dynamics of pion-nucleus systems
[DE93-014449] 02 p0785 N94-14468
The quantum mass shift of the soliton in Skyrme model
[ITN-93-85219] 03 p1180 N94-15283
Past, present and future ((pi),(eta)) experiments
[DE93-016631] 03 p1182 N94-16115
Unitary (pi)(pi)N model of N* excitations in (pi)N and (gamma)N reactions
[DE93-017422] 04 p1568 N94-18826
Eta-nucleon interaction and nuclear production of eta mesons
[DE93-018469] 04 p1571 N94-19259
Pions and neutrinos as probes of the nucleon and nuclear few-body system
[DE93-040127] 06 p2531 N94-22928
Momentum and coordinate space three-nucleon potentials
[DE93-040868] 06 p2531 N94-22951
Theoretical and computational studies in intermediate energy nuclear physics
[DE94-004177] 07 p3012 N94-25800
A dependence of exclusive vector meson production in muon-nucleus scattering
[DE94-003363] 07 p3016 N94-25957
Proceedings of the workshop on (pi), K, (eta)-nucleon interactions
[DE94-701314] 07 p3027 N94-27733
Deep inelastic lepton scattering on nuclei: operator product expansion and meson-nucleon theory
[DE94-606442] 08 p3484 N94-28610
Possible explanation of the interaction cross-section growth at high energies
[DE94-606457] 08 p3494 N94-28612
Pion-nucleon interaction in nuclear matter above the Delta resonance energy
[DE94-727455] 10 p4137 N94-33994
Studies in intermediate energy nuclear physics
[DE94-007602] 10 p4140 N94-34381
Search for the H dibaryon by Xi(-) capture on the deuteron
[DE94-011733] 12 p4520 N94-37672
MESONS
NT ETA-MESONS
NT HYPERONS
NT KAONS
NT MESON RESONANCE
NT MUONS
NT OMEGA-MESONS
NT PIONS
NT RHO-MESONS
NT VECTOR MESONS
Proceedings of the third workshop on light quark meson spectroscopy
[DE93-754138] 01 p0363 N94-10696
Strange meson spectroscopy in K(omega) and K(phi) at 11 GeV/c and Cherenkov ring imaging at SLD
[DE93-013593] 01 p0363 N94-10748
Aspects of symmetry violation
[DE93-011003] 02 p0779 N94-12997
Further study of the X(1910) meson
[DE93-621443] 02 p0782 N94-13362
The off shell (rho)-(omega) mixing in the QCD sum rules
[DE93-014845] 02 p0786 N94-14527
Early baryon and meson spectroscopy culminating in the discovery of the Omega minus SU(3) and quarks
[DE93-014321] 02 p0787 N94-14580
Tests of non-local interferences in kaon physics at asymmetric phi-factories
[DE93-013905] 02 p0787 N94-14857
Closed orbit distortion and the beam-beam interaction
[DE93-015284] 03 p1190 N94-15854
Status of (alpha)(sub s) measurements
[DE93-015179] 03 p1181 N94-16059
Mesons at finite temperature in the NJL model with gluon condensate
[DE93-626697] 03 p1185 N94-17310
Production of D-mesons in pp-collisions and quark-gluon string model
[DE93-626721] 03 p1185 N94-17312
Gauge unification of fundamental forces: The story of success
[DE93-624813] 04 p1383 N94-17952
Beauty without charm in B-meson decays
[PREPRINT-732] 04 p1565 N94-17972
Unitary (pi)(pi)N model of N* excitations in (pi)N and (gamma)N reactions
[DE93-017422] 04 p1568 N94-18826
Investigation of physical structures and interactions at high energy
[DE93-014444] 04 p1574 N94-18927
Measurement of the B(+) and B(0) lifetimes
[DE93-019906] 05 p1969 N94-19814
The cross section for the production of b(bar-b) pairs in p(bar p) collisions at the square root of s equals 1.8 TeV
[DE93-019900] 05 p1972 N94-20225
Recent results on top, bottom and exotic physics at the Tevatron
[DE94-000578] 05 p1975 N94-21786
Measurement of the B meson and b quark cross-section in (-p)p collisions at the square root of s = 1.8 TeV using the exclusive decays B(+) and B(exp 0) yields J/psiK*(exp 0)
[DE93-019907] 05 p1975 N94-21806
Low mass muon pair production in 450 GeV p-Be collisions
[PB94-110699] 06 p2533 N94-23746
Strong interactions studies with medium energy probes
[DE94-001446] 06 p2540 N94-23791
Relativistic hadrons in an external field
[ETN-94-95387] 06 p2538 N94-25259
A quark structure of hadrons and nuclei
[DE93-616872] 06 p2539 N94-25474
Weak interactions in a bilocal chiral theory
[DE93-616887] 06 p2539 N94-25477
On the transverse size of a fast moving nucleon
[DE93-616891] 06 p2539 N94-25481
Quark-antiquark bound states
[DE93-613054] 07 p3013 N94-25826
Weak interactions in a bilocal chiral theory
[DE93-613097] 07 p3013 N94-25836
Algorithms of the vertex coordinate reconstruction for straight tracks of short-lived particles
[DE93-616661] 07 p3015 N94-25919
Heavy quark production and spectroscopy
[DE94-003619] 07 p3015 N94-25935
Meson X(1814) as a candidate for a hybrid state
[DE93-634447] 07 p3017 N94-26045
Mesons and diquarks in a NJL-model at finite temperature and chemical potential
[DE93-634375] 07 p3020 N94-26505
Signatures for hybrids
[DE94-004244] 07 p3020 N94-26574
Measuring the time dependence of B(sub s)(sup 0) meson - anti B(sub s)(sup 0) meson oscillations
[ISBN-0-315-84367-5] 07 p3021 N94-26665
Light-quark, heavy-quark systems: An update
[DE94-002298] 07 p3021 N94-26759
Leptonic decay constants of heavy mesons in QCD
[DE93-634426] 07 p3022 N94-26767
Low-energy hadronic interactions beyond the current algebra approach
[DE94-602600] 07 p3022 N94-26900
Meson spectroscopy and particle astrophysics
[DE94-001799] 07 p3115 N94-27003
Measurements of the B(sup 0)(bar B)(sup 0)CP asymmetry
[DE94-003379] 07 p3063 N94-27047
Charmonium physics at a tau-charm factory
[PB94-124344] 07 p3024 N94-27199
Observation of excited charmed mesons
[ISBN-0-315-57014-8] 07 p3026 N94-27400
Weak hadronic decays of heavy flavor mesons
[ISBN-0-315-55542-4] 07 p3026 N94-27402
Indiana University high energy physics, task A
[DE94-000961] 07 p3033 N94-27614
Decay constants of heavy mesons in the relativistic potential model with velocity dependent corrections
[DE94-606495] 07 p3030 N94-27860
B production and B(0)(bar B)(0) mixing at DO
[DE94-004664] 08 p3484 N94-28574
Glueball and meson dispersion and diffusion relations in compact U(1)(2+1) gauge theory
[ISBN-0-315-85577-0] 08 p3490 N94-30234
Heavy flavor production at fixed target photo- and hadroproduction
[DE94-004651] 08 p3491 N94-30719
Theoretical studies in hadronic and nuclear physics
[DE94-003524] 08 p3492 N94-30838
Study of B(0) - bar-B(0) mixing in D0
[DE94-006000] 09 p3897 N94-31506
F0-975, A0-980 as eye-witnesses of confinement
[PB94-147105] 09 p3868 N94-31923
Semileptonic decays of mesons in the SO(4) model
[DE94-008108] 09 p3873 N94-32708
Studies in intermediate energy nuclear physics
[DE94-007602] 10 p4140 N94-34381
The silent phase transition in mesonic bags and lattice theory
[DE94-616852] 11 p4321 N94-35583
Hybrid mesons (Q(anti Q)g) in N(anti N) annihilation
[DE94-001491] 11 p4327 N94-36239
Decay of the D(sub s)-meson
[DE94-611209] 11 p4329 N94-36308
B-lifetime measurements at the tevatron
[DE94-003617] 12 p4513 N94-36528
B quark production cross sections and the b- (bar b) correlated production cross section at CDF
[DE94-000620] 12 p4514 N94-36700
Sum rules for 1/m corrections to the form factors of semileptonic B decays
[DE94-618548] 12 p4514 N94-37065
Mass identified particle production and Bose Einstein correlations at 1800 GeV
[DE94-013418] 12 p4515 N94-37067
A study of jet handedness in hadronic Z0 decays
[DE94-013358] 12 p4515 N94-37087
Five-lepton decay modes of muon and tau mesons
[DE94-621636] 12 p4516 N94-37099
Production of phi mesons in central Si+Au collisions at 14.6 A GeV/c
[DE94-011726] 12 p4516 N94-37152
Physics with primary beams of the KEK-PS
[DE94-748635] 12 p4522 N94-37234
Prospects for measuring B(s) mixing at CDF
[DE94-013147] 12 p4518 N94-37298
MESOPAUSE
Mesopause winds and OH intensities at Mid-Latitudes-Fabry-Perot interferometer observations of the OH emission at 8430 A from bear lake observatory
[AD-A275246] 08 p3361 N94-29430
Study of gravity wave in the upper atmosphere by way of OH* (9-4) and O2(b 1 Sigma(+,g), 0-1) bands nightglow observations
[INPE-5539-TDI/527] 10 p4087 N94-34227
MESOSCALE PHENOMENA
NT JET STREAMS (METEOROLOGY)
On the importance of mesoscale potential vorticity anomalies and topographic forcing during cyclone redevelopment across the Appalachians: A GALE case study 01 p0284 N94-10822
Study of the surface circulation to the North of Bransfield Strait, Antarctica
[INPE-5472-TDI/503] 01 p0288 N94-11200
A four-dimensional, mesoscale, non-gaussian multispectral smoke model. Phase 1: Feasibility study
[AD-A264805] 01 p0152 N94-11519
Activities relating to understanding the initiation, organization and structure of moist convection in the Southeast environment
[NASA-CR-193829] 01 p0285 N94-11598
Ocean circulation revealed by altimeter data 01 p0245 N94-11786
Ocean-ice interaction study of waves and mesoscale features 01 p0197 N94-11935
Comparison of ERS-1 SAR images of the Western Mediterranean to in situ oceanographic data: PRIM-1 Cruise (May 1992) 01 p0255 N94-12529
On a nonstationary dynamics of the north-west Pacific Ocean 01 p0222 N94-12724
Mesoscale dynamic structures of the Subarctic Frontal Zone in the Pacific Ocean 01 p0227 N94-12754
Circulation model experiments of the Gulf Stream using satellite-derived fields
[AD-A266067] 02 p0725 N94-12990
Effects of surface thermal forcing on stratified flow past an isolated obstacle 02 p0633 N94-13553
Numerical simulation and parameterization of orographic gravity waves 02 p0713 N94-13647
Regional climatology sensitivity studies
[DE93-010712] 02 p0722 N94-14057
Sensitivity testing of a single-Doppler temperature retrieval and forecast system
[AD-A267278] 03 p1105 N94-14958
Mesoscale modeling of the atmosphere
[AD-A263236] 03 p1098 N94-15132
Short term weather forecasting in real time in a base weather station setting
[AD-A266872] 03 p1105 N94-15142
Mesoscale lightning
[NASA-TM-109655] 03 p1105 N94-15226
Mesoscale frontogenesis: An analysis of two cold front case studies
[AD-A267950] 03 p1107 N94-17054
Opposing mesoscale flows in a broken midlatitude squall line
[AD-A268011] 03 p1109 N94-17492
Propagation characteristics of mesoscale convective systems
[AD-A268130] 03 p1109 N94-17522
Forecasting the ducting of electromagnetic waves on the mesoscale
[AD-A268101] 03 p1109 N94-17571

Surface energy balance modeling at mesoscale: The contribution of the future Earth observing system
[BCRS-91-04] 03 p1085 N94-17616
The vertical distribution of heating in the tropical atmosphere
[AD-A270452] 04 p1490 N94-18514
Diabatic forcing and initialization with assimilation of cloud and rain water in a forecast model: Methodology 04 p1491 N94-18603
Moist wind relationships 04 p1492 N94-18607
Initialization and assimilation of cloud and rainwater in a regional model 04 p1492 N94-18608
Preparation of data assimilation and model evaluation experiment data sets
[AD-A269996] 04 p1498 N94-18665
JPRS report: Science and technology. Central Eurasia: Earth Sciences
[JPRS-UES-93-004] 04 p1461 N94-19209
Clouds: Their prediction and simulation
[AD-A271161] 05 p1864 N94-19900
Incorporation and comparative evaluation of a non-convective cloud parameterization scheme in the Naval Research Laboratory west coast mesoscale weather prediction model
[AD-A272417] 05 p1867 N94-21146
Estimating the rotation rate of mesoscale ocean rings from satellite altimetry
[AD-A272922] 05 p1883 N94-21222
Development and tests of a cloud physics parameterization for real-time aviation and public numerical weather forecasting
[PB93-202711] 05 p1868 N94-21427
Cloud fields derived from satellite and surface data during FIRE cirrus phase 2 05 p1872 N94-22302
Analysis of the GOES 6.7 micrometer channel observations during FIRE 2 05 p1875 N94-22316
Three dimensional modeling of cirrus during the 1991 FIRE IFO 2: Detailed process study 05 p1877 N94-22327
Cirrus cloud development in a mobile upper tropospheric trough: The November 26th FIRE cirrus case study 05 p1878 N94-22329
A comparison of small and larger mesoscale latent heat and radiative fluxes: December 6 case study 05 p1879 N94-22335
Development of advanced cloud parameterizations to examine air quality, cloud properties, and cloud-radiation feedback in mesoscale models
[DE93-041164] 05 p1853 N94-22384
Scientific investigations of atmospheric processes
[NASA-CR-194805] 06 p2401 N94-23271
Methodology for the assessment of surface resistance and soil water storage variability at mesoscale based on remote sensing measurements. A case study with HAPEX-EFEDA data. UNESCO-International Hydrological Program 4
[PB94-111721] 06 p2386 N94-23734
Report of the proceedings of the Colloquium and Workshop on Multiscale Coupled Modeling
[NASA-CP-3217] 06 p2410 N94-24374
United States Weather Research Program (USWRP) 06 p2411 N94-24375
Scientific goals of the Cooperative Multiscale Experiment (CME) 06 p2411 N94-24381
Grand challenge scientific questions in coupled modeling 06 p2412 N94-24382
Examples of data assimilation in mesoscale models 06 p2412 N94-24384
Measurement and modeling of moist processes 06 p2413 N94-24385
Parameterization of sub-grid scale convection 06 p2413 N94-24386
Coupled land surface/hydrologic/atmospheric models 06 p2413 N94-24387
Incorporation of the planetary boundary layer in atmospheric models 06 p2413 N94-24388
The role of radiation in mesoscale flows: Physics, parameterizations, codes 06 p2413 N94-24389
Chemistry on the mesoscale: Modeling and measurement issues 06 p2413 N94-24390
Validation of mesoscale models 06 p2413 N94-24391
Techniques and resources for storm-scale numerical weather prediction 06 p2414 N94-24392
Session on cumulus parameterization 06 p2414 N94-24394
Joint sessions on modeling of boundary layer and radiative transfer processes 06 p2414 N94-24396
Session on modeling of radiative transfer processes 06 p2414 N94-24397
Session on validation of coupled models 06 p2414 N94-24399
Session on techniques and resources for storm-scale numerical weather prediction 06 p2415 N94-24400
Vertical motion in the SYNOP central array
[AD-A273593] 06 p2418 N94-24795
Three-dimensional numerical simulation of near-surface flows over the Martian north polar cap 06 p2621 N94-24895
Martian mesoscale circulations induced by variations in surface optical and thermal characteristics: A numerical study 06 p2622 N94-24899
Development and testing of the Coupled Ocean/Atmosphere Mesoscale Prediction System (COAMPS)
[AD-A273925] 07 p2892 N94-25793
A modeling study of the mesocyclone
[AD-A274889] 07 p2893 N94-26168
Mesoscale frontal evolution of the ERICA IOP-5A Cyclone
[AD-A274906] 07 p2893 N94-26183
A preliminary analysis of the US west climatology
[DE94-003028] 07 p2894 N94-26313
Investigation of mesoscale convective cloud clusters in South China
[AD-A274303] 07 p2895 N94-26678
Mesoscale meteorological measurements characterizing complex flows
[DE94-002359] 07 p2895 N94-26761
Objective analysis of a coastal ocean eddy using satellite AVHRR and in situ hydrographic data
[AD-A275715] 08 p3376 N94-28642
Prototype terminal aerodrome forecasts using a mesoscale model
[AD-A275308] 08 p3369 N94-29194
Evaluation of the National Meteorological Center mesoscale model for prediction of severe convection over Central Arizona 08 p3371 N94-29744
Four-dimensional data assimilation using the adjoint method 08 p3455 N94-30353
Coordination of mesoscale meteorological research between ASL and European group
[AD-A276730] 09 p3784 N94-32162
Proceedings of the Ninth Annual Pacific Climate (PACLIM) Workshop
[DE94-003024] 09 p3766 N94-32693
Use of cloud observations and mesoscale meteorology models to evaluate and improve cloud parameterizations
[DE94-003610] 09 p3785 N94-32717
Development and testing of improved techniques for modeling the hydrologic cycle in a mesoscale weather prediction system
[AD-A277416] 09 p3786 N94-32921
Evolution of upwelling fronts off the coast of Portugal
[NASA-CR-195692] 09 p3790 N94-33045
Meso-beta scale numerical simulation studies of terrain-induced jet streak mass and momentum perturbations
[NASA-CR-195863] 10 p4089 N94-33752
Effects of mesoscale convective organization and vertical wind shear on the cumulus-environment interaction 10 p4090 N94-34910
Mesoscale roughness of Venus 11 p4361 N94-35430
Atmospheric and dispersion modeling in areas of highly complex terrain employing a four-dimensional data assimilation technique
[DE94-004041] 11 p4285 N94-35823
Three dimensional visualization of a coastal mesoscale model
[AD-A278576] 11 p4294 N94-36187
Variability of the California Current System off Point Sur, California from April 1988 to December 1990
[AD-A278579] 12 p4476 N94-36985
On the development of boundary layer secondary circulations resulting from horizontally varying surface heat flux
[DE94-011234] 12 p4472 N94-37048
Long-range mesoscale modeling of pollutant transport for the European Tracer EXperiment (ETEX)
[DE94-010820] 12 p4465 N94-37093
Factors influencing the parameterization of anvil clouds within GCMs
[DE94-010794] 12 p4475 N94-37621

MESOSPHERE
NT MESOPAUSE
Polar mesospheric waves and structure
[AD-A265360] 01 p0279 N94-12561
Internal instability of nonparallel flow on an equatorial beta-plane
[AD-A268927] 04 p1490 N94-18486
Measurement of mesospheric turbulence in the framework of the metal campaign and development of a sensor for static pressure free measurements of neutral and electron density
[BONN-IR-92-45] 05 p1857 N94-21149
An analysis of Solar Mesospheric Explorer temperatures for the upper stratosphere and mesosphere
[NASA-CR-194861] 06 p2626 N94-23626
Data analysis and theoretical studies of the upper mesosphere and lower thermosphere
[NASA-CR-195108] 06 p2402 N94-24089
Mesospheric and lower thermospheric winds, temperatures densities, and volume emission rates
[NASA-CR-195147] 06 p2403 N94-24486
Photochemical processes and the atmospheric airglow emissions of OH and Na in the mesospheric region
[INPE-5380-PUD/050] 07 p2882 N94-27334
Odin aeronomy science: A phase-A report by the Aeronomy Science Working Group for the Odin satellite
[AP-31] 09 p3770 N94-31222
One: Microphysics of frost metamorphism: Applications to Triton and Mars. Two: A global analysis of the ozone deficit in the upper stratosphere and lower mesosphere. Three: The diabatic circulation in the stratosphere as diagnosed from Microwave Limb Sounder data 09 p3942 N94-31975
Radar scattering from the summer polar mesosphere: Theory and observations 09 p3772 N94-32077

MESOZOIC ERA
NT CRETACEOUS PERIOD
Earth's partial pressure of CO2 over the past 100-500 Ma; evidence from Ce anomalies in mostly shallow seas (less than 200 m) as recorded in carbonate sediments, 2 03 p1104 N94-16360

MESSAGE PROCESSING
Low latency messages on distributed memory multiprocessors
[NASA-CR-191479] 01 p0323 N94-10643
Design and analysis of an optical interface message processor
[AD-A266079] 01 p0381 N94-10697
The Zipcode message-passing system
[DE93-011958] 01 p0336 N94-11027
A formally verified algorithm for interactive consistency under a hybrid fault model
[NASA-CR-4527] 01 p0326 N94-11188
Effective software reuse in an embedded realtime system
[AD-A264993] 01 p0326 N94-11220
Portable programming on parallel/networked computers using the Application Portable Parallel Library (APPL)
[NASA-TM-106238] 01 p0327 N94-11232
The PVM systems: An in-depth analysis and documenting study. Concise edition
[DE93-011959] 01 p0336 N94-11248
Fail-safe PVM: A portable package for distributed programming with transparent recovery
[AD-A266594] 02 p0749 N94-13779
The influence of ATC message length and timing on pilot communication
[NASA-CR-177621] 02 p0512 N94-14744
VDM specification of the MD4 message digest algorithm
[NPL-DITC-204/92] 03 p1142 N94-14944
RAISE specification of the MD4 message digest algorithm
[NPL-DITC-206/92] 03 p1142 N94-15010
Understanding partitions and the no partition assumption
[AD-A266296] 03 p1000 N94-16911
Ground wave emergency network final operational capability: Environmental assessment for central Wyoming relay node, site number RN 8C928WY
[AD-A267842] 03 p1001 N94-17011
Intel NX to PVM 3.2 message passing conversion library
[NASA-TM-109038] 03 p1152 N94-17060
Causality-preserving timestamps in distributed programs
[AD-A267534] 03 p1153 N94-17118
Radiocommunication problems of a position reporting and bidirectional messagery system using VHF/UHF with low-Earth orbit satellites 03 p0889 N94-17136
LEOCOM-SPES: Low cost message communications 03 p0892 N94-17161
STARSYS: A view after WARC-92 — satellite position and messaging system 03 p0893 N94-17168
Embedded Computer Performance Measurement (ECPM). Advanced avionics subsystems and technology multiprocessor ECPM software documentation
[AD-A269921] 04 p1320 N94-18658
Efficient transparent optimistic rollback recovery for distributed application programs
[AD-A268981] 04 p1522 N94-18696
Corporate Information Management (CIM) report on the simulation processes, version 2.0
[AD-A269119] 04 p1617 N94-18770
Experience in implementing a parallel file system
[DE93-012840] 04 p1536 N94-19188
Message passing in PUMA
[DE93-012841] 04 p1537 N94-19206
Abstracting inter-object communications using composition filters
[MEMO-INF-92-78] 04 p1526 N94-19220
Automated processing of military messages according to ADatP-3
[FEL-92-A044] 04 p1393 N94-19798

ATC/pilot voice communications: A survey of the literature
[DOT/FAA/AM-93/20] 05 p1738 N94-21201
Using manufacturing message specification for monitor and control at Venus 05 p1932 N94-21333
Developing a space network interface simulator: The NTS approach 05 p1933 N94-21343
A self-defining hierarchical data system 05 p2046 N94-22448
The Keck Task Library (KTL) 05 p2048 N94-22504
EUTELTRACS: The European experience on mobile satellite services 06 p2281 N94-22781
Users manual for the Chameleon parallel programming tools
[DE94-001934] 06 p2465 N94-22973
Arc consistency problem: An exercise in parallel programming with shared objects
[PB94-110590] 06 p2466 N94-23706
The design of a standard message passing interface for distributed memory concurrent computers
[DE94-002536] 06 p2446 N94-24538
Special signature schemes
[ETN-94-95296] 06 p2446 N94-25081
Interface technical specification of the V.25 bis emulator
[AD-A273754] 07 p2948 N94-25720
Programming in Fortran M
[DE94-002756] 07 p2963 N94-26407
An efficient communication scheme for solving the S(sub n) equations on message-passing multiprocessors
[DE94-000378] 07 p2769 N94-26482
Example of the EXPANSE signalling protocol
[PB94-125283] 07 p2771 N94-26872
Communication on the Paragon
[DE94-003103] 07 p2983 N94-27713
An all pairs shortest paths distributed algorithm using 2n(exp 2) messages
[RUU-CS-93-19] 08 p3432 N94-30411
Analysis of the effect of routing strategies for parallel implementations of a selected avionics application
[AD-A276069] 09 p3581 N94-31458
MICA, a facility to achieve portability for message-passing and dynamic memory management in FORTRAN
[DE94-006692] 09 p3807 N94-32147
On the design of Chant: A talking threads package
[AD-280503] 10 p4109 N94-34952
The rel/REL: A family of reliable multicast protocols for distributed real-time systems
[PB94-167830] 11 p4310 N94-35535
A compile time model for composing parallel programs
[AD-A278896] 11 p4310 N94-35597

MESSAGES

The influence of ATC message length and timing on pilot communication
[NASA-CR-177621] 02 p0512 N94-14744
Toward a verifiable approach to the design of concurrent computations
[DE93-012908] 02 p0756 N94-14844
Multiphase complete exchange: A theoretical analysis
[NASA-CR-191531] 03 p1145 N94-15489
A parallel adaptive mesh refinement algorithm
[NASA-CR-191530] 03 p1168 N94-15724
Securing electronic mail: The risks and future of electronic mail
[DE93-017187] 04 p1383 N94-17994
Message passing in PUMA
[DE93-012841] 04 p1537 N94-19206
Ground wave emergency network. Final operational capability. Environmental assessment for south central Montana relay node, site no. RN8C925MT
[AD-A267795] 05 p1716 N94-19964
The data acquisition system for the Anglo-Australian Observatory 2-degree field project 05 p2048 N94-22529
A packet-based concept for spacecraft command planning 06 p2504 N94-23873
The design of a standard message passing interface for distributed memory concurrent computers
[DE94-002536] 06 p2446 N94-24538
A doubly logarithmic communication algorithm for the Completely Connected Optical Communication Parallel Computer
[DE93-019408] 07 p2980 N94-26473
Security aspects of computer supported collaborative work
[AD-A275636] 08 p3528 N94-28640
PEM public key certificate cache server
[DE94-006404] 09 p3675 N94-31784
On the design of Chant: A talking threads package
[AD-280503] 10 p4109 N94-34952

METABOLIC DISEASES

Modulation by galactosamine-induced hepatitis of biological responses of the rat exposed to high altitude hypoxia 07 p2904 N94-27464
Protective action of an amiloride derivative (amiloride, 5-(N, N-dimethyl) hydrochloride) against in isolated ischemia/reperfusion newborn rabbit hearts 07 p2904 N94-27466

METABOLIC WASTES

NT HUMAN WASTES
NT URINE

METABOLISM

NT ADRENAL METABOLISM
NT CALCIUM METABOLISM
NT CARBOHYDRATE METABOLISM
NT ELECTROLYTE METABOLISM
NT ENZYME ACTIVITY
NT FERMENTATION
NT HORMONE METABOLISMS
NT HYDROGEN METABOLISM
NT LIPID METABOLISM
NT MINERAL METABOLISM
NT OXYGEN METABOLISM
NT PROTEIN METABOLISM

Effect of intermittent cold exposure on the fiber-type composition of selected skeletal muscles in rats
[AD-A265309] 01 p0301 N94-11861
Clinical physiology of bed rest
[NASA-TM-104010] 02 p0727 N94-13447
Endocrine and metabolic changes in payload specialist (L-1) 02 p0591 N94-13758
Metabolic rate measurements comparing supine with upright upper-body exercises
[NASA-CR-4549] 02 p0729 N94-14028
Cellular responses to low-gravity: Pilot studies on suborbital rockets and orbiting spacecraft
[NASA-CR-194402] 02 p0729 N94-14494
TransRapid TR-07 maglev-spectrum magnetic field effects on daily pineal indoleamine metabolic rhythms in rodents
[DE93-015143] 03 p1117 N94-16893
Metabolic changes and hemodynamic dysfunction following hypothermic shock
[AD-A269780] 04 p1506 N94-18598
Microgravity research in plant biological systems: Realizing the potential of molecular biology 04 p1503 N94-19216
A study of the effect of hydrocarbon structure on the induction of male rat nephropathy and metabolic structure
[AD-A270969] 04 p1504 N94-19789
In vitro system for studying metabolism of environmental chemicals in human cells
[AD-A273427] 06 p2421 N94-24688
Prediction of survival times on land in a cold climate 08 p3379 N94-28423
Physiological investigations of the isolated rat's liver in hypothermia and hypoxia and their relevance in aircraft incidents above the sea 08 p3382 N94-28439
The organization of the suprachiasmatic circadian pacemaker of the rat and its regulation by neurotransmitters and modulators
[AD-A277324] 09 p3793 N94-32622
Numerical model of the thermal behavior of an extremity in a cold environment including counter-current heat exchange between the blood vessels
[AD-A278099] 09 p3798 N94-33040
Effect of microgravity on plant growth
[NASA-CR-196004] 11 p4296 N94-35257
Chemical and structural characterization of nitroaromatic adducts with hemoglobins
[AD-A280533] 12 p4480 N94-37089

METABOLITES

Cumulative effect of repeated brief cerebral ischemia
[AD-A267155] 03 p1121 N94-15736
Nuclear Medicine Program
[DE93-013896] 04 p1504 N94-17699
Biological determinants of photobioreactor design
[DE94-011665] 12 p4468 N94-37740

METAGALAXY

U UNIVERSE

METAL AIR BATTERIES

Mechanically refuelable zinc/air electric vehicle cells
[DE93-016446] 04 p1394 N94-17770
Advanced batteries for electric vehicle applications: Nontechnical summary
[DE93-019007] 05 p1748 N94-19885
High energy density aluminum-oxygen cell 06 p2393 N94-23363
Promising future energy storage systems: Nanomaterial based systems, Zn-air, and electromechanical batteries
[DE94-007443] 09 p3692 N94-32136
Overview of Sandia's electric vehicle battery program
[DE94-008944] 09 p3696 N94-32806

METAL BONDING

NT METAL-METAL BONDING

High temperature stability, interface bonding, and mechanical behavior in (beta)-NiAl and Ni3Al matrix composites with reinforcements modified by ion beam enhanced deposition
[DE93-013977] 01 p0398 N94-11115
Electronic and total energy properties of ternary and quaternary semiconductor compounds, alloys and superlattices
[NASA-CR-192905] 01 p0405 N94-12570
The thermal dissociation of NH2CHO(ND2CHO) on Si(100)-2x1
[AD-A266903] 03 p0942 N94-14956
Metal/ceramic interfaces: Relationships between structure and chemistry
[AD-A268792] 04 p1369 N94-18188
High performance YBCO films
[AD-A269090] 04 p1599 N94-18719
Joining and Adhesion of Advanced Inorganic Materials Symposium
[AD-A269748] 04 p1342 N94-18720
Binding of copper to nanocavity surfaces in silicon
[DE93-019073] 04 p1364 N94-19080
Cratering evaluations and results
[DE93-040347] 05 p1691 N94-20478
Transferable tight-binding parameters: An application to Ni and Ni-Al alloys
[DE94-001044] 05 p1695 N94-22023
Interface science of controlled metal/metal and metal/ceramic interfaces prepared using ultrahigh vacuum diffusion bonding
[DE94-001066] 05 p1696 N94-22025
Strength, ultrasonic and metallurgical evaluation of diffusion bonds
[DE94-000665] 05 p1697 N94-22571
Gas-pressure forming of superplastic ceramic sheet
[DE94-001520] 06 p2252 N94-22930
Ge-Au eutectic bonding of Ge (100) single crystals
[DE94-002281] 06 p2564 N94-24657
Joining of fibre reinforced metal matrix composite materials
[PB94-132453] 07 p2712 N94-28376
Joining silicon carbide to austenitic stainless steel through diffusion welding
[PB94-126331] 08 p3297 N94-28399
Joining of alumina by vacuum brazing
[VTT-TIED-1495] 09 p3724 N94-31656
Soft x ray photoelectron spectroscopy study of the interaction of Cr with MoS2(0001)
[AD-A276916] 09 p3635 N94-32233
Liquid-assisted diffusion bonding of NiAl
[DE94-006687] 09 p3645 N94-32522
A review of weldment failure modes and weldability testing methods
[AD-A278096] 09 p3729 N94-33251
Mapping of residual strains of a ceramic-to-metal joint using x ray diffraction
[DE94-007421] 10 p4069 N94-33691

METAL CLUSTERS

Structure of s - p bonded metal clusters with 8, 20 and 40 valence electrons
[DE93-613643] 01 p0361 N94-10503
Size dependence of chemical reactivity of gaseous metal clusters: A new mechanistic probe
[AD-A264690] 01 p0077 N94-11264
Structure stability and spectroscopy of metal clusters
[DE93-016142] 02 p0567 N94-12836
Synthesis and properties of novel cluster phases
[DE93-017056] 02 p0577 N94-13072
Thermochemistry of transition metal clusters
[DE93-016201] 02 p0571 N94-13977
Neutral copper cluster sputtering yields: Ne(+), Ar(+) and Xe(+) bombardment
[DE93-019010] 05 p1690 N94-20288
Simulation studies for surfaces and materials strength
[NASA-CR-195185] 06 p2565 N94-25093
Peculiarities and application perspectives of metal-ion implants in glasses
[DE94-004671] 07 p3035 N94-26248
Realtime structural electrochemistry of platinum clusters using dispersive XAFS
[DE94-005093] 08 p3208 N94-30101
Generalized augmented space theorem for correlated disorder and cluster coherent potential approximation
[DE94-608110] 08 p3208 N94-30118
Overlap of metal clusters and nuclear structure physics
[DE94-608387] 08 p3517 N94-30183
Theoretical studies of zirconium and carbon clusters with molecular dynamics simulations
[DE94-005276] 09 p3862 N94-31146
Metal clusters: Dynamics and structure
[AD-A276842] 09 p3643 N94-32091
Metal cluster-rare gas van der Waals complexes: Microscopic models of physisorption
[DE94-008134] 09 p3873 N94-32797

Theoretical study of novel bonding in molecules: Metastable molecular fuels
[AD-A277807] 10 p4031 N94-33895
Nonlinear optical composites of metal cluster laden polymers
[AD-D016217] 11 p4234 N94-36124
Metal cluster alloys and oxides: Elucidating structural and electronic effects in governing the reactivity and catalytic role of matter in finite dimensions
[DE94-010224] 11 p4328 N94-36298
Supersonic bare metal cluster beams
[DE94-010790] 12 p4532 N94-36454
Metal-carbon nanostructures
[DE94-009177] 12 p4400 N94-36509
Low-energy electron collisions with metal clusters: Electron capture and cluster fragmentation
[DE94-003623] 12 p4512 N94-36516
Photodissociation and spectroscopy of gas phase bimetallic clusters
[DE94-012607] 12 p4419 N94-37438

METAL COATINGS
NT ALUMINUM COATINGS
NT GOLD COATINGS
NT NICKEL COATINGS
NT ZINC COATINGS
Analysis of samples of reflector materials which are multicoated and metal samples with oxide coatings which have been exposed the space environment in LDEF testing
[NASA-CR-193647] 02 p0575 N94-12789
Ohmic heating of composite candidate graphite-fiber/coating combinations
[NASA-TM-4491] 02 p0554 N94-12871
Absorption and damage thresholds of low defect density hafnia deposited with activated oxygen
[DE93-013853] 02 p0655 N94-13243
Laser CO2 beam transmission through hollow metallic waveguide coated by a thin internal dielectric layer
[ITN-93-85201] 02 p0656 N94-13571
Metastability of yttrium-oxides
[DE93-016548] 02 p0813 N94-14440
JPRS report: Science and technology. Central Eurasia: Materials science
[JPRS-UMS-93-006] 02 p0558 N94-14573
JPRS report: Science and technology. Central Eurasia: Materials science
[JPRS-UMS-93-004] 02 p0559 N94-14574
Materials and structures 02 p0546 N94-14835
Restoring Miss Liberty --- inorganic coatings
[NASA-TM-109605] 03 p0963 N94-15313
Optical properties and surface morphology studies of palladium contacts on mercuric iodide single crystals
[DE93-012510] 03 p1207 N94-15973
Transparent conductive coatings in the far ultraviolet
[NASA-CR-194632] 03 p1191 N94-16024
The role of carbon and temperature in determining electrical conductivity of basins, crust and mantle
[DE93-015936] 03 p1101 N94-16840
Robotic weld overlay coatings for erosion control
[DE93-016938] 03 p0970 N94-16959
Application of hard coatings to substrates at low temperatures
[NASA-CR-193867] 03 p0971 N94-17122
Thermal analysis of coatings and substrate materials during a disruption in fusion reactors
[DE93-017688] 04 p1588 N94-18971
Silver lined ceramic vessel
[AD-D015917] 05 p1700 N94-20057
Field emitter array RF amplifier development project, phase 1, option 1
[AD-A272567] 05 p1740 N94-21361
Structural characterization and thermal cycling behaviour of EB-PVD thermal barrier coating systems
[ISBN-0-315-83365-3] 06 p2257 N94-24468
Robotic weld overlay coatings for erosion control
[DE94-002665] 06 p2258 N94-24749
Electrochemical behavior of ion-plated TiN and Cu-Cr coatings
[AD-A273411] 06 p2235 N94-24784
Laser ablation and deposition of metals
[ETN-94-95311] 06 p2351 N94-25294
Plasma sprayed thermal barrier coatings: Production, characterization and testing
[ISBN-9-03-860082-8] 06 p2555 N94-25439
Proceedings of the 12th International Congress: Corrosion Control for Low-Cost Reliability. Volume 1: Coatings
[AD-A273661] 06 p2251 N94-25448
Proceedings of the 12th International Congress: Corrosion Control for Low-Cost Reliability. Volume 3B: Corrosion: Specific issues
[AD-A273664] 06 p2251 N94-25451
Hydrogen trapping with Pd coated alloy films 07 p2723 N94-25551
Issues for conversion coating of aluminum alloys with hydrotalcite
[DE94-003804] 07 p2732 N94-25819
Comparison of technology for high-power laser mirrors and synchrotron radiation mirrors
[DE94-002913] 07 p3035 N94-26276
Vapor deposition of copper on stainless steel 304L
[DE94-001945] 07 p2740 N94-27006
Electrodeposition of bismuth alloys by the controlled potential method
[DE94-605318] 08 p3212 N94-28550
Anodization of copper in chloride media
[AD-A275565] 08 p3202 N94-28793
Thick thermal barrier coatings for diesel components
[NASA-CR-187111] 08 p3537 N94-29350
Metafusion: A breakthrough in metallurgy 08 p3211 N94-30446
Atomic oxygen damage characterization by photothermal scanning 09 p3598 N94-31051
Robotic weld overlay coatings for erosion control
[DE94-008004] 09 p3658 N94-32408
Robotic weld overlay coatings for erosion control
[DE94-009703] 10 p4060 N94-33902
Proceedings of the 57th National Congress of Japan Thermal Spraying Society
[DE94-731734] 10 p4029 N94-34133
Efficient chemistry for selective modification and metallization of substrates
[AD-D016162] 10 p4023 N94-34287
Oxidation performance of platinum-clad Mo-47Re alloy
[NASA-TM-4559] 10 p4025 N94-34398
A novel method for depositing precious metal films on difficult surfaces
[NASA-TM-106607] 11 p4243 N94-35260
Field emitter array RF amplifier development project. Cathode technology development. Phase 1
[AD-A280515] 12 p4437 N94-37108
Chromium/molybdenum alloy plating. Part 1: The electrodeposition of low contraction chromium/molybdenum alloys using unipolar (on/off) pulse plating
[AD-A280236] 12 p4417 N94-37138
Development of intermetallic coatings for fusion power applications
[DE94-012647] 12 p4419 N94-37442

METAL COMBUSTION
Shear flow control of gas jets in liquids
[AD-A264673] 01 p0152 N94-11448
Distributed combustion in solid propellants
[AD-A265727] 01 p0099 N94-12564
Metal slurry droplet and spray combustion
[AD-A269648] 04 p1349 N94-18736
Influence of test configuration on the combustion characteristics of polymers as ignition sources 06 p2238 N94-25365
Shock tube ignition and combustion of aluminum/magnesium alloy particles in oxygen at high pressure 09 p3631 N94-31286
Control experiments in liquid metal combustion
[AD-A276918] 09 p3635 N94-32234

METAL CORROSION
U CORROSION

METAL CRYSTALS
Deformation mechanisms in tungsten single crystals in ballistic impact experiments
[AD-A265701] 01 p0405 N94-12563
Atomic structure of the 310 twin in niobium: Theoretical predictions and comparison with experimental observation
[DE93-013421] 02 p0806 N94-13136
Growth experiment of organic metal crystal in low gravity (M-21) 02 p0590 N94-13753
High temperature materials technology research for advanced thermionic systems
[DE93-018302] 03 p0960 N94-16964
Photorefractive tungsten bronze crystals for optical computing
[AD-A268859] 04 p1596 N94-18320
The effect of crystallographic orientation on the performance of single crystal tungsten subscale penetrators
[AD-A268988] 04 p1597 N94-18468
Pit initiation on passivated metal surfaces: Crystallographic orientation and environmental effects
[ISBN-0-315-85433-2] 08 p3208 N94-30138
High temperature materials technology research for advanced thermionic systems
[DE94-008341] 09 p3646 N94-32825

METAL CUTTING
JBK-75 stainless steel machinability study
[DE94-002268] 06 p2242 N94-23475
Effect of non-metallic inclusions on the machinability of steel
[PB93-230233] 08 p3204 N94-29387

METAL DRAWING
Plane strain finite element analysis of sheet forming operations including bending effects 08 p3322 N94-30354

METAL FATIGUE
Fatigue in single crystal nickel superalloys
[AD-A266116] 01 p0085 N94-12418
Isothermal fatigue mechanisms in Ti-based metal matrix composites
[NASA-CR-191181] 01 p0074 N94-12594
Role of microstructure on fatigue durability of aluminum aircraft alloys
[AD-A265627] 02 p0568 N94-12993
Role of microstructure on fatigue durability of aluminum aircraft alloys
[AD-A266350] 02 p0571 N94-13697
Fatigue design curves for 6061-T6 aluminum
[DE93-011849] 02 p0571 N94-14021
Laser-shock damage of iron-based materials
[AD-A267196] 03 p1038 N94-15852
Ion implantation effects on surface-mechanical properties of metals and polymers
[DE93-014661] 03 p0958 N94-16453
Fatigue life program using strain-life methods
[AD-A267310] 03 p1060 N94-16943
Mean strain effects on the strain life fatigue curve
[AD-A267211] 03 p0960 N94-16984
Factors which affect fatigue strength of fasteners
[DE93-017272] 04 p1453 N94-18084
Development of the microstructure based stochastic life prediction models
[AD-A269880] 04 p1454 N94-18683
Fatigue resistant Ti3Al composites
[AD-A270305] 04 p1341 N94-18692
Development of the microstructure based stochastic life prediction model
[AD-A269742] 04 p1361 N94-18742
Intelligent materials systems and structures. Part 4: The influence of thermomechanical loading on the life of shape memory alloys
[PB93-195923] 04 p1363 N94-18952
Results of the second Round Robin on opening-load measurement conducted by ASTM Task Group E24.04.04 on crack closure measurement and analysis
[NASA-TM-109032] 05 p1832 N94-21624
A high temperature fatigue life prediction computer code based on the total strain version of StrainRange Partitioning (SRP) 05 p1835 N94-22620
Fatigue life and crack growth prediction methodology
[NASA-TM-109044] 06 p2228 N94-23279
Mean stress models for low cycle fatigue of a nickel-base superalloy 06 p2159 N94-24276
Elevated temperature crack propagation
[NASA-TM-106490] 06 p2377 N94-24715
Variable amplitude fatigue, modelling and testing
[PB93-204469] 06 p2378 N94-24742
The mechanical property data base from an Air Force/Industry Cooperative Test Program on advanced aluminum alloys (7064 and CW67)
[AD-A273741] 06 p2251 N94-25531
Interactions between corrosion fatigue and stress corrosion crack on steel for light water reactors 07 p2722 N94-25547
Study on variation of damage generation mechanism by fatigue on TiAl compounds due to different slip systems 07 p2729 N94-25579
Study on evaluation of crack generation and crack growth behaviors under static loading at high temperature and under combined loading 07 p2730 N94-25583
Study on fatigue crack propagation characteristics around welded joint interface in complexed conditions 07 p2730 N94-25584
An experimental study on the effects of compressive stress on the fatigue crack growth of low-alloy steel
[DE94-004447] 07 p2737 N94-26582
Status and prospects for aluminium-lithium alloys in aircraft structures
[NLR-TP-92193-U] 07 p2743 N94-27797
An experimental investigation of fatigue damage in aluminum 2024-T3 alloys 07 p2747 N94-27900
The transition from stress corrosion cracking to corrosion fatigue in AA-7075 and AA-8090
[ISBN-0-315-59526-4] 07 p2744 N94-27950
Fatigue propagation behaviour of short cracks (1-2 mm) in steels
[ESDU-93033] 07 p2845 N94-28145
An analysis of isothermal, bithermal, and thermomechanical fatigue data of Haynes 188 and B1900+Hf by energy considerations
[NASA-TM-106359] 08 p3317 N94-28619
Role of microstructure on the fatigue durability of aluminum aircraft alloys
[AD-A275814] 08 p3202 N94-28830
Cyclic axial-torsional deformation behavior of a cobalt-base superalloy
[NASA-TM-106372] 08 p3203 N94-28921

Cold expansion and interference for extending the fatigue life of multi-layer metal joints
[AD-A274982] 08 p3318 N94-29091
The effect of mechanical paint stripping on the fatigue and fracture of thin aluminum airplane skin
08 p3205 N94-29900
Fatigue of carbon and low-alloy steels in LWR environments
[DE94-005116] 08 p3207 N94-30021
An investigation of fatigue crack propagation under mode 1 and mixed mode 1/2 loadings
08 p3323 N94-30814
Fractographic and microstructural analysis of fatigue crack growth in Ti-6Al-4V fan disc forgings
[AD-B174765] 08 p3153 N94-30914
Multiple-site damage in aircraft fuselage structures
[LR-729] 09 p3578 N94-31675
Thermal-mechanical fatigue crack growth in aircraft engine materials
[ISBN-0-315-86543-1] 09 p3734 N94-31707
Acoustic emission from crack growth in 7050 aluminum and 7075 aluminum as a function of temperature and heat treatment
[DREP-CRS-93-15] 09 p3642 N94-31871
Creep-fatigue criteria and inelastic behavior of modified 9Cr-1Mo steel at elevated temperatures
[DE94-007915] 09 p3642 N94-31918
Fracture micromechanics of continuous fiber and textile reinforced metal and ceramic matrix composites
[AD-A277434] 09 p3627 N94-33008
Risk analysis of the C-141 WS405 inner-to-outer wing joint 10 p3996 N94-34592
The role of fatigue analysis for design of military aircraft 10 p3996 N94-34594
An overview of the F-16 service life approach
10 p3996 N94-34599
Fatigue and residual strength behaviour of ARALL3 panels with bonded-on doublers
[AD-B181062] 11 p4279 N94-36226
Ability of the total strain version of strainrange partitioning to characterize thermomechanical fatigue behavior
[NASA-TM-4556] 12 p4455 N94-37102
Physical and mechanical metallurgy of NiAl
[NASA-TP-3398] 12 p4419 N94-37503

METAL FIBERS

Elastic-plastic finite element analyses of an unidirectional, 9 vol percent tungsten fiber reinforced copper matrix composite
[NASA-TM-106304] 02 p0559 N94-14719
Integrated fundamental research on current collection
[AD-A266987] 03 p1008 N94-15494
Aerosol filtration with steel fiber filters
[DE93-016990] 04 p1380 N94-18710
Composite fiber structures for catalysts and electrodes
06 p2393 N94-23364
Surface and interfacial properties of polymer blends. A literature survey
[PB93-230191] 06 p2254 N94-23561
Impact tests on fibre metal laminates under a tensile load
[PB94-126570] 07 p2710 N94-27201
Continuous unidirectional fiber reinforced composites: Fabrication and testing 11 p4229 N94-36400

METAL FILMS

Tribological characteristics of sputtered Au/Cr films on alumina substrates at elevated temperatures
[NASA-TM-106078] 01 p0055 N94-11362
In situ XANES studies of the passive film on Fe and Fe-26Cr
[DE93-010869] 01 p0084 N94-11459
The laser ablation of gold films at the electrode surface of a quartz crystal microbalance
[AD-A265535] 01 p0175 N94-12012
The x ray dichroism experiments using circular polarization
[DE93-013195] 02 p0568 N94-13036
Microstructural mechanisms that enhance electromigration resistance in Al-Cu thin films
[DE93-013770] 02 p0812 N94-14345
Ion mixing of thin ZrO2 films on sapphire
[DE93-015214] 03 p1206 N94-14925
Laboratory for x ray optics
[AD-A267149] 03 p1189 N94-15735
Cellulose triacetate, thin film dielectric capacitor
[NASA-CASE-NPO-18935-1-CU]
03 p1010 N94-15952
Aberration correction of unstable resonators
[NASA-CASE-NPO-18791-1-CU]
03 p1034 N94-15987
Weibull analysis applied to the pull adhesion test and fracture of a metal-ceramic interface
[DE93-012913] 03 p1059 N94-15997
Design and fabrication of a reflection far ultraviolet polarizer and retarder
[NASA-CR-194630] 03 p1191 N94-16023
Transparent conductive coatings in the far ultraviolet
[NASA-CR-194632] 03 p1191 N94-16024
UHV-stem studies on nucleation and growth of thin metal silicide films on silicon
[DE93-017604] 03 p1212 N94-16961
Characterization of metallic multilayers using x ray diffraction analysis
[NIAR-93-13] 03 p0961 N94-17282
Epitaxial iron films
[AD-A268286] 03 p1217 N94-17579
Superhardness effect in Au/Ni multilayers
[DE93-016444] 04 p1357 N94-17860
Infrared detection with high-(Tc bolometers and response of Nb tunnel junctions to picosecond voltage pulses
[DE93-016963] 04 p1595 N94-17989
Metal Film Surface Plasmon Resonance (MFSPR) fibre couplers
[AD-A268871] 04 p1579 N94-18635
The Coulomb anomaly in strongly disordered films
[AD-A271095] 05 p2012 N94-19849
Microscopic origins of metastable effects in a-Si:H and deep defect characterization in a-Si,Ge:H alloys
[DE93-018205] 05 p1688 N94-19985
Magnetic circular dichroism in x ray absorption and core-level photoemission
[DE93-019381] 05 p1688 N94-19986
Study of mechanisms for long wavelength Schottky-barrier infrared detectors
[AD-A270538] 05 p1971 N94-20083
The metallic bond for monolayer transition metal layers on transition metal surfaces
[DE93-019060] 05 p1691 N94-20313
Growth, characterization and device development in monocrystalline diamond films
[AD-A272715] 05 p2026 N94-21190
Shock temperature measurements of iron to 350 GPa
[DE94-001058] 05 p1695 N94-22024
Selective hydrogen separation by palladium-based composite membranes
[PB93-201671] 06 p2254 N94-23431
Soft x ray optics by pulsed laser deposition
[NASA-CR-195139] 06 p2546 N94-24967
The nanometer-scale mechanics of gold films
[AD-A273307] 06 p2565 N94-25086
Laser ablation and deposition of metals
[ETN-94-95311] 06 p2351 N94-25294
Study on alloy films for hydrogen separation
07 p2726 N94-25565
Study on substance diffusion in thin films with controlled structures 07 p2727 N94-25570
The formation of conducting gold films by thermal decomposition and direct patterning using electron beam lithography of the gold cluster Au55P(C6H5)312C16
[AD-A273720] 07 p2749 N94-26074
Chemical vapor deposition and characterization of tungsten boron alloy films
[DE94-002648] 07 p2738 N94-26610
Geometric structures of thin film: Pt on Pd(110) and NiO on Ni(100)
[DE94-005564] 08 p3211 N94-28530
Sweep rate and concentration effects on metastable structures formed in the underpotential deposition of silver on Pt(111)
[AD-A275369] 08 p3189 N94-29010
Vacuum vapor deposition
[NASA-CASE-MFS-28652-1] 08 p3215 N94-29446
Microstructure and mechanical properties of nitrided molybdenum silicide coatings
[DE94-006249] 08 p3217 N94-30025
Effects of hydrogen on the resistivity of thin Au and Cu films 08 p3218 N94-30225
Giant magnetoresistance and microstructural characteristics of epitaxial Fe-Ag and Co-Ag granular thin films
[DE94-006287] 08 p3519 N94-30707
Preliminary results from the CONCAP-2-01 and EIOM-3 experiments on STS-46 09 p3596 N94-31042
Process parameter-growth environment-film property relationships for reactive sputter deposited metal (V, Nb, Zr, Y, Au) oxide, nitride, and oxynitride films
[AD-A276382] 09 p3640 N94-31258
Reliability of multilayer copper/polyimide
[AD-A276228] 09 p3650 N94-31284
Computerized Ultrasonic Testing System (CUTS) for in-process thickness determination
09 p3862 N94-32456
Anisotropic phase separation through the metal-insulator transition in amorphous Mo-Ge and Fe-Ge alloys
[DE94-007259] 09 p3646 N94-32795
Atomic force microscopy
[AD-A277589] 10 p4026 N94-33429
A novel method for depositing precious metal films on difficult surfaces
[NASA-TM-106607] 11 p4243 N94-35260
Effect of niobium interlayer on high-temperature sliding friction and wear of silver films on alumina
[DE94-010462] 11 p4275 N94-36232
Irradiation effects in Fe-30 percent Ni alloy during Ar ion implantation
[DE94-619057] 12 p4415 N94-36564
X-ray diffraction studies of evaporated gold thin films deposited on aluminum nitride substates
[AD-A280454] 12 p4536 N94-37228
Scanning x-ray diffraction: A technique with high compositional resolution for studying phase formation in co-deposited thin films
[DE94-011496] 12 p4420 N94-37516

METAL FINISHING

NT SHOT PEENING
Dry stripping as a surface treatment method
[VTT-TIED-1348] 03 p0985 N94-17544

METAL FLUORIDES

NT ALUMINUM FLUORIDES
NT BERYLLIUM FLUORIDES
NT CALCIUM FLUORIDES
NT COBALT FLUORIDES
NT LANTHANUM FLUORIDES
NT LITHIUM FLUORIDES
NT MAGNESIUM FLUORIDES
NT PLUTONIUM FLUORIDES
NT SODIUM FLUORIDES
NT TUNGSTEN FLUORIDES
NT URANIUM FLUORIDES
Neutron and x ray scattering studies of (FeF2)(sub m)(CoF2)(sub n) multilayers
[DE93-015809] 03 p1184 N94-16838
Optical properties of chromium and neodymium in zirconium - barium - lanthanum - aluminum fluoride glass
[AD-A271609] 05 p1987 N94-21236

METAL FOAMS

PM technology and mechanical properties of metallic foams 01 p0064 N94-10059
Indentability of conventional and negative Poisson's ratio foams 09 p3629 N94-33131

METAL FOILS

Two-dimensional simulations of foil implosion experiments on the Los Alamos capacitor bank
[DE93-012676] 02 p0794 N94-12814
Stripping efficiencies for 277 MeV/amu gold beam on copper foils
[DE93-014306] 02 p0569 N94-13221
Electron emission resulting from fast ion impact on thin metal foils: Implications of these data for development of track structure models
[DE93-013506] 02 p0782 N94-13485
Thermal conductance of pressed metallic contacts augmented with Indium foil or Apiezon-N (tm) grease at liquid helium temperatures
[NASA-TM-108779] 02 p0776 N94-14027
Direct drive foil implosion experiments on Pegasus 2
[DE93-012666] 03 p1202 N94-16776
Plasma flow switch and foil implosion experiments on Pegasus 2
[DE93-016464] 03 p1013 N94-17318
Foil bearing research at Penn State
06 p2215 N94-23058
Phase transformations in Cu-Zr multilayers
[DE94-000393] 06 p2241 N94-23297
Reference electrodes for solid polymer electrolytes
[DE94-004583] 07 p2780 N94-25806

METAL FORGING

U FORGING

METAL FORMING

U FORMING TECHNIQUES
U METAL WORKING

METAL FUELS

Shear flow control of gas jets in liquids
[AD-A264673] 01 p0152 N94-11448
Aluminum powder/water reaction ignited by electrical pulsed power
[AD-A269223] 04 p1376 N94-17840
An apparatus for measurement of ignition and burning characteristics of metallic particles
[AD-A274815] 07 p2716 N94-26487
Nonswelling behavior of HT9 alloy irradiated to high exposure
[DE94-003502] 07 p2736 N94-26522

METAL GRINDING

JBK-75 stainless steel machinability study
[DE94-002268] 06 p2242 N94-23475

METAL HALIDES

NT ALKALI HALIDES
NT ALUMINUM CHLORIDES
NT ALUMINUM FLUORIDES
NT BARIUM FLUORIDES
NT BERYLLIUM FLUORIDES
NT CALCIUM FLUORIDES
NT CESIUM IODIDES
NT COBALT FLUORIDES
NT COPPER CHLORIDES

NT IRON CHLORIDES
NT LANTHANUM CHLORIDES
NT LANTHANUM FLUORIDES
NT LITHIUM CHLORIDES
NT LITHIUM FLUORIDES
NT MAGNESIUM FLUORIDES
NT METAL FLUORIDES
NT PLUTONIUM FLUORIDES
NT SILVER BROMIDES
NT SODIUM CHLORIDES
NT SODIUM FLUORIDES
NT SODIUM IODIDES
NT TITANIUM CHLORIDES
NT TUNGSTEN FLUORIDES
NT URANIUM FLUORIDES
NT ZINC CHLORIDES
Chemical Vapor Deposition of Refractory Metals and Ceramics 2. Materials Research Society Symposium proceedings
[AD-A265072] 01 p0092 N94-11866
Structure of ionic fluids in equilibrium with a microporous ionic matrix
[DE94-600563] 07 p2715 N94-26391

METAL HARDENING
U HARDENING (MATERIALS)

METAL HYDRIDES
NT LITHIUM HYDRIDES
NT SODIUM HYDRIDES
X ray and gamma ray spectroscopy of solids under pressure
[DE93-014847] 01 p0076 N94-10653
Materials compatibility of hydride storage materials with austenitic stainless steels
[DE93-013688] 02 p0703 N94-13691
Catalytic arene hydrogenation using early transition metal hydride compounds
[DE93-015500] 02 p0573 N94-14402
Small satellite nickel-hydrogen and nickel-metal hydride power applications 03 p0895 N94-17175
Structural stability of 1100 C heated Pd/k during absorption cycling in protium
[DE93-016270] 04 p1346 N94-18048
Current status of environmental, health, and safety issues of nickel metal-hydride batteries for electric vehicles
[DE93-017079] 05 p1748 N94-19902
High-power gas switch with hydride electrodes
[AD-D015956] 05 p1751 N94-20354
Ovonic nickel metal hydride batteries for space applications 06 p2391 N94-23352
Alloys for hydrogen storage in nickel/hydrogen and nickel/metal hydride batteries 06 p2391 N94-23353
Impedance measurements on a spiral-wound nickel/metal hydride cell cycled in a simulated Leo orbit 06 p2392 N94-23355
Hydride thermodynamic machines
[VTT-JULK-768] 06 p2571 N94-25416
Metal hydride storage
[VTT-JULK-769] 06 p2396 N94-25417
Lighter alkali hydride and deuteride 1: Electronic properties of pure solids
[DE93-616188] 07 p3051 N94-25914
Development of nickel-metal hydride cell: An update 07 p2864 N94-28130
Ni-MH storage test and cycle life test 07 p2864 N94-28131
Determination of thermal properties of commercial Ni-MH cells 07 p2864 N94-28132
Feasibility study for the recycling of nickel metal hydride electric vehicle batteries
[DE94-000268] 09 p3690 N94-31598
Metal hydrides in hydrogen energy systems
[VTT-TIED-1407] 09 p3759 N94-31655
Metal hydride heat pump engineering demonstration and evaluation model
[NASA-CR-188286] 09 p3669 N94-32857
Development of nickel and metal hydride secondary battery
[DE94-757270] 09 p3697 N94-32917
Theoretical and experimental study of air and hydrogen electrodes
[DE94-763308] 11 p4283 N94-36060

METAL INSULATOR SEMICONDUCTORS
U MIS (SEMICONDUCTORS)

METAL IONS
NT FERRIC IONS
NT MANGANESE IONS
Photodetachment studies on few-electron atomic negative ions
[DE93-008474] 01 p0358 N94-10154
X ray absorption spectroscopy of electrochemically generated species
[AD-A264749] 01 p0077 N94-11265
Thermochemistry of transition metal clusters
[DE93-016201] 02 p0571 N94-13977
Tetravalent chromium (Cr(4+)) as laser-active ion for tunable solid-state lasers
[NASA-CR-194527] 02 p0659 N94-14576
Reactor studies of metal ions associated with chromatographic silica
[AD-A266675] 02 p0573 N94-14779
Ion mixing of thin ZrO2 films on sapphire
[DE93-015214] 03 p1206 N94-14925
Optical and infrared spectra of thermally annealed Pb implanted SiO2 glasses
[DE93-015304] 03 p0965 N94-15828
Application of in situ scanning x ray fluorescence to study the concentration of metal ions in simulated pits
[DE93-014054] 03 p0956 N94-15921
Investigation of the effects of polyelectrolyte coatings on colloid transport in porous media
[DE93-018300] 03 p0970 N94-16973
Single crystal diamond thin films
[AD-A266457] 03 p1214 N94-17216
Modified aequorin shows increased bioluminescence activity
[AD-A268774] 04 p1347 N94-18185
Novel electrochemical materials prepared by sol-gel chemistry
[AD-A269060] 04 p1578 N94-18405
Kinetic studies of electrochemical generation of Ag(II) ion and catalytic oxidation of selected organics
[DE93-016601] 04 p1352 N94-19240
Tetravalent chromium (Cr(4+)) as laser-active ion for tunable solid-state lasers
[NASA-CR-194529] 04 p1441 N94-19369
Formation of colloidal Ag precipitates in fused silica by MeV ion implantation
[DE93-040268] 05 p2012 N94-19869
A process for preparing an assembly of an article and a soluble polyimide which resists dimensional change, delamination, and debonding when exposed to changes in temperature
[NASA-CASE-LAR-14763-1] 05 p1702 N94-20373
Shattering the myth of the resonantly photo-pumped neon-like titanium laser
[DE93-019624] 05 p1819 N94-21873
High oxygen pressure synthesis of new copper oxide superconductors
[DE93-040278] 05 p2033 N94-21998
Miniaturized disk-bend testing, nano-indentation, and the microstructure of ion-irradiated titanium aluminides
[DE93-040600] 05 p1697 N94-22559
Excited state dynamics of thulium ions in yttrium aluminum garnets
[NASA-CR-195159] 06 p2564 N94-25024
Excitation mechanisms for XUV and x ray lasers
[DE93-617006] 06 p2351 N94-25482
Peculiarities and application perspectives of metal-ion implants in glasses
[DE94-004671] 07 p3035 N94-26246
Structure of ionic fluids in equilibrium with a microporous ionic matrix
[DE94-600563] 07 p2715 N94-26391
Microstructures of Si surface layers implanted with Cu
[DE94-004690] 07 p3058 N94-26565
Modulation wavelength dependence of ion mixing in metallic superlattices
[DE94-004608] 07 p3059 N94-26591
Secondary electron emission from copper surface due to neodymium and gadolinium ion bombardment
[DE94-701115] 07 p3027 N94-27718
Hypersensitive transition spectrum of f-element and coordination structure
[DE94-604133] 07 p3070 N94-27843
Property enchancement of polyimide films by way of the incorporation of lanthanide metal ions 07 p2758 N94-27926
Study of iron exchanged zeolites by Moessbauer effect and electron spin resonance spectroscopy
[DE94-605138] 08 p3514 N94-29691
Reactions of metal ions and their clusters in the gas phase using laser ionization: Fourier transform mass spectrometry
[DE94-006208] 08 p3207 N94-30024
Nanosize metal alloy particle formation in Ag and Cu sequentially implanted silica
[DE94-005592] 08 p3207 N94-30042
Rotator phases in narrow-gap semiconductors
[DE94-005472] 08 p3521 N94-30897
Enhancement of oxidation resistance of silicon carbide by high-dose and multi-energy aluminum implantation
[DE94-006560] 09 p3640 N94-31314
Performance of the Sony lithium-ion rechargeable battery
[AD-A277076] 09 p3693 N94-32303
Metal-ion spin-on glasses: Novel materials for active waveguides
[DE94-007738] 09 p3882 N94-32649
Performance of an ion trap inductively coupled plasma mass spectrometer
[DE94-007470] 09 p3713 N94-32811
Ultrahigh-current-density metal-ion implantation and diamondlike-hydrocarbon films for tribological applications
[DE94-008958] 09 p3906 N94-32843
Metal ion complexation by ionizable crown ethers
[DE94-008301] 09 p3661 N94-32847
Optical properties of lanthanide-doped RbTiOAsO4 and transition metal-doped KTiOPO4
[DE94-008433] 09 p3907 N94-32963
Rare Earth Doped Semiconductors and Materials Research Society Symposium Proceedings, Volume 301
[AD-A277517] 09 p3908 N94-33055
Effects of isotope selection on solution convergence in HZE transport
[NASA-TP-3445] 10 p4167 N94-33686
Generalized syntheses of periodic surfactant and inorganic composite materials
[AD-A278001] 10 p4019 N94-34160
New calculations of Fe spectra in high-temperature plasmas
[DE94-009919] 11 p4339 N94-36386
Direct catalytic decomposition of nitric oxide
[DE94-005025] 12 p4407 N94-36475
Determination of copper in tap water using solid-phase spectrophotometry
[NASA-TM-106480] 12 p4408 N94-36537
Consequences of competing hybridization for magnetic ordering in correlated-electron lattices
[DE94-011648] 12 p4534 N94-37057
Photodissociation and spectroscopy of gas phase bimetallic clusters
[DE94-012607] 12 p4419 N94-37438

METAL JOINTS
NT SOLDERED JOINTS
NT SPOT WELDS
NT WELDED JOINTS
Physical interpretation and development of ultrasonic nondestructive evaluation techniques applied to the quantitative characterization of textile composite materials
[NASA-CR-194549] 03 p0931 N94-15190
Wetting behavior of alternative solder alloys
[DE93-016730] 04 p1359 N94-18127
Cold expansion and interference for extending the fatigue life of multi-layer metal joints
[AD-A274982] 08 p3318 N94-29091
Automation of the NDT diagnostic using neural nets. Application: Inspection of Airbus longitudinal joints during maintenance
[REPT-932-600-104] 08 p3315 N94-29474
Feasibility study of cold expansion processes modelling
[DSIS-94-01186] 09 p3735 N94-31849

METAL MATRIX COMPOSITES
NT ALUMINUM GRAPHITE COMPOSITES
NT EUTECTIC COMPOSITES
Hybrid materials for use at elevated temperatures 01 p0057 N94-10013
Mechanical and fatigue properties of fibre reinforced aluminium-lithium alloy and aluminium-lithium MMC based laminates 01 p0058 N94-10022
Mechanical properties of magnesium/carbon composites developed by hot pressing under medium pressure 01 p0059 N94-10024
Design evaluation of GLARE laminate lay-ups 01 p0063 N94-10051
Joints between dissimilar metallic and ceramic materials 01 p0063 N94-10052
Introducing SMaSE: An aide memoire on structural materials and space engineering 01 p0063 N94-10053
Constitutive laws for describing the service relevant creep behaviour of metallic materials 01 p0064 N94-10060
Liquid phase sintering of tungsten composites under microgravity. Effect of matrix composition 01 p0118 N94-10207
A study of the quasibinary Al-W-Mo system. Part 1: Preliminary investigations and preparation for microgravity experiments 01 p0119 N94-10211
A study of the quasibinary Al-Mo-W system. Part 2: A physico-mechanical investigation of the system fabricated under the gravitylessness conditions 01 p0119 N94-10212
Interface reactions of (Ni3Al) ribbons/Al-MMC in ground preparation as preliminary test for microgravity experiments 01 p0123 N94-10237
Fatigue-life behavior and matrix fatigue crack spacing in unnotched SCS-6/Timetal 21S metal matrix composites
[NASA-CR-191467] 01 p0185 N94-10715
Computational simulation of hot composite structures
[NASA-TM-106200] 01 p0186 N94-10762

Tribological characteristics of hot-pressed self-lubricating composites
[NAL-TR-1160] 01 p0066 N94-10858
Micromechanisms of fatigue crack growth and fracture toughness in metal matrix composites
[AD-A265153] 01 p0187 N94-11096
Corrosion behavior of metal matrix composites
[AD-A265352] 01 p0085 N94-12404
Proposed framework for thermomechanical life modeling of metal matrix composites
[NASA-TP-3320] 01 p0074 N94-12449
Isothermal fatigue mechanisms in Ti-based metal matrix composites
[NASA-CR-191181] 01 p0074 N94-12594
Ohmic heating of composite candidate graphite-fiber/coating combinations
[NASA-TM-4491] 02 p0554 N94-12871
NDE of titanium alloy MMC rings for gas turbine engines
[NASA-TM-106188] 02 p0555 N94-13138
An advanced test technique to quantify thermomechanical fatigue damage accumulation in composite materials
[NASA-CR-191147] 02 p0555 N94-13139
Inelastic deformation mechanisms in SCS-6/Ti 15-3 MMC lamina under compression
[NASA-CR-191170] 02 p0555 N94-13378
Inhibiting corrosion in Gr/Al and Gr/Mg metal matrix composites using nonequilibrium alloying techniques
[AD-A266547] 02 p0556 N94-13583
Evaluation for rheological constitutive relations, using the indentation technique 02 p0775 N94-13627
Modified carbon for improved corrosion resistance
[AD-D015741] 02 p0556 N94-13663
UK interlaboratory tensile tests on Al alloy/SiC particulate metal matrix composites
[NPL-DMM(A)-77] 02 p0570 N94-13666
Preparation of particle-dispersion alloys (M-6)
02 p0587 N94-13738
Fabrication of very-low-density, high-stiffness carbon fiber/aluminum hybridized composite with ultra-low density and high stiffness (M-11) 02 p0588 N94-13743
Fatigue and residual strength characteristics of fiber metal laminates subjected to incidental damage
[LR-708] 02 p0674 N94-13803
Modelling of the temperature distribution in a copper roll for the design of a system of cooled rolls adapted to vertical strip casting
[IMI-93RT-21200-1436-G] 02 p0557 N94-13866
Hierarchical nonlinear behavior of hot composite structures
[NASA-TM-106229] 02 p0676 N94-14041
Optimal synthesis of hot composite laminates with interphase layers
[NASA-TM-106326] 02 p0557 N94-14042
Elastic-plastic finite element analyses of an unidirectional, 9 vol percent tungsten fiber reinforced copper matrix composite
[NASA-TM-106304] 02 p0559 N94-14719
Thermomechanical and isothermal fatigue behavior of a (90)sub 8 titanium matrix composite
[NASA-CR-191196] 02 p0560 N94-14822
Thermoelastic response of metal matrix composites with large-diameter fibers subjected to thermal gradients
[NASA-TM-106344] 02 p0560 N94-14823
Fracture toughness tests for particulate MMC UK COSI (IACFA) task group. Meeting report, October 1992
[NPL-DMM(A)-81] 03 p1057 N94-15021
Inelastic deformation of metal matrix composites
[NASA-CR-191522] 03 p0930 N94-15106
Liquid phase sintering of tungsten composites under microgravity. Effect of matrix composition
03 p0945 N94-15171
Anisotropic damage mechanics modeling in metal matrix composites
[AD-A266328] 03 p0934 N94-16440
The processing and mechanical properties of high temperature/high performance composites. Book 1: Coonstituent properties of composites
[AD-A266394] 03 p0935 N94-16483
The processing and mechanical properties of high temperature/high performance composites. Book 3: Coonstituent properties and macroscopic performance
[AD-A266396] 03 p0935 N94-16485
Thermal stress effects in intermetallic matrix composites
[NASA-CR-191191] 03 p1054 N94-16518
The processing and mechanical properties of high temperature/high performance composites. Book 4: Coonstitutive laws and design
[AD-A266397] 03 p0935 N94-16528
The processing and mechanical properties of high temperature/high performance composites. Book 5: Processing and miscellaneous properties
[AD-A266398] 03 p0935 N94-16529
Continuous fabrication of SiC fiber tows by chemical vapor deposition
[AD-A266460] 03 p0936 N94-16569
Techniques for preparation of ingot metallurgical discontinuous composites
[AD-D015748] 03 p0940 N94-16933
Interfacial shear behavior and its influence on fiber damage in sapphire-reinforced gamma titanium aluminide composites
[AD-A267943] 03 p1060 N94-17043
Ceramic fiber coatings development and demonstration
[AD-A267286] 03 p0972 N94-17242
Elastic-plastic finite-difference analysis of unidirectional composites subjected to thermomechanical cyclic loading
[AD-A267666] 03 p1061 N94-17269
Aspects of high temperature damage in fiber reinforced titanium metal matrix composites
[AD-A267907] 03 p0941 N94-17379
Metals 2000
[DE93-016761] 04 p1355 N94-17752
Strength optimization of C/Al metal matrix composites produced from prepregs
[DLR-FB-92-39] 04 p1340 N94-18122
NSWCWODET participation in Space Shuttle mission STS-46
[AD-A268875] 04 p1332 N94-18321
Fatigue resistant Ti3Al composites
[AD-A270305] 04 p1341 N94-18692
Wettability and reaction kinetics in metal matrix composites
[AD-A270377] 04 p1342 N94-18704
Bibliography on ceramic matrix composites and reinforcing whiskers, platelets, and fibers, 1970-1990
[AD-A270139] 04 p1371 N94-18750
The applications of modified metals in the construction industry
[VTT-TIED-1329] 04 p1365 N94-19374
Residual strength predictions for fibre metal laminates: The R-curves approach
[LR-717] 04 p1344 N94-19666
Damage accumulation in advanced metal matrix composites under thermal cycling/creep loadings
[AD-A271207] 04 p1344 N94-19720
Micromechanics of interfaces in metal matrix composites
[AD-A271012] 04 p1345 N94-19776
The Seventh International Conference on Composite Structures, volume 25, numbers 1-4
[AD-A269961] 05 p1672 N94-20031
Metal-glass composite field-emitting arrays
[AD-D015942] 05 p1673 N94-20064
Strengthening of NiAl matrix composites
[AD-A271491] 05 p1674 N94-20550
Strength and toughness improvement of silicide intermetallics by nanophase and microphase reinforcements
[AD-A272914] 05 p1692 N94-21320
Analysis of thermal mechanical fatigue in titanium matrix composites 05 p1835 N94-22618
New extensions in the development of deformation processed metal-metal matrix composites
[DE94-000692] 06 p2227 N94-23004
Materials Science and Engineering
[DE94-003018] 06 p2228 N94-23493
Engine materials characterization and damage monitoring by using x ray technologies
[NASA-TP-3328] 06 p2372 N94-24074
High strain rate superplasticity in metals and composites
[DE94-001521] 06 p2229 N94-24547
Crashworthiness analysis using advanced material models in DYNA3D
[DE94-002988] 06 p2229 N94-24632
Matrix fatigue cracking mechanisms of alpha(2) TMC for hypersonic applications
[NASA-TM-106506] 06 p2230 N94-25186
Bulletin of National Research Institute for Metals in Fiscal Year 1993, no. 14
[REPT-14] 07 p2722 N94-25544
Inner fiber observation for metal matrix composites under the stress load condition utilizing Synchrotron Orbital Radiation (SR) by X-ray CT 07 p2724 N94-25553
Investigation of compressive behavior for metal matrix composites with a circular hole
[AD-A273835] 07 p2705 N94-25739
Structure and properties of intermetallic composites synthesized in situ using solid state displacement reactions
[DE94-004312] 07 p2705 N94-25805
Characterization of fatigue damage in a metal matrix composite (SCS-6/Ti-15-3) at elevated temperature
[AD-A273797] 07 p2706 N94-25876
Numerical simulations of interfacial debonding in ductile-phase reinforced intermetallic matrix composites
[DE94-003639] 07 p2706 N94-25938
An investigation of cavitation in a mechanically alloyed 15 volume percent SiCp/IN9021 aluminum composite
[DE94-003371] 07 p2748 N94-25959
General Motors Corporation and Pacific Northwest Laboratory staff exchange: Inspection of case hardened steels and metal-matrix composites
[DE94-003470] 07 p2706 N94-25982
Investigation of tension-compression fatigue behavior of a cross-ply metal matrix composite at room and elevated temperatures
[AD-A273731] 07 p2706 N94-25999
Effects of post-fabrication processing on the tensile properties of centrifugally cast SiC particulate reinforced aluminum composites
[AD-A274865] 07 p2707 N94-26190
Titanium 1992: Volume 3: Science and technology
[AD-A274800] 07 p2735 N94-26337
Bimaterial interfaces and their role in the mechanical performance of the in-situ composites
[AD-A274688] 07 p2707 N94-26447
Processing and mechanical properties of laminated metal composites of Al 6090-25 volume percent SiC(sub p) and Al 5182
[DE94-001070] 07 p2708 N94-26930
Development of fibre-metal laminates, ARALL and GLARE, new fatigue resistant materials
[PB94-126471] 07 p2669 N94-26969
Interface phenomena in metal-ceramic composites
[AD-A274167] 07 p2709 N94-27125
Impact tests on fibre metal laminates under a tensile load
[PB94-126570] 07 p2710 N94-27201
High intensity x ray instrumentation for residual strain measurements in composites and textured materials
[ISBN-0-315-85169-4] 07 p2842 N94-27278
SP/MSP tests for the evaluation of FGM
[NAL-SP-17] 07 p2710 N94-27279
SP/MSP tests for the evaluation of FGM
07 p2710 N94-27280
Research on the development of fracture characteristics evaluation system for ceramics and metal composite materials 07 p2710 N94-27281
Hot deformation behaviour of Si(p)/Al composites and their matrices and an Al-Mg-Si alloy
[ISBN-0-315-84699-2] 07 p2711 N94-27314
Finite element analysis of damped vibrations of laminated composite plates
[ISBN-0-315-84928-2] 07 p2843 N94-27585
A hydrostatic stress-dependent anisotropic model of viscoplasticity
[NASA-TM-106525] 07 p2711 N94-27640
Implementation of thermal residual stresses in the analysis of fiber bridged matrix crack growth in titanium matrix composites
[NASA-TM-109082] 07 p2711 N94-27658
The deformation of copper-tungsten composites
[ISBN-0-315-84939-8] 07 p2712 N94-27688
Low strain behaviour of a particulate reinforced aluminum alloy
[ISBN-0-315-84906-1] 07 p2744 N94-27961
Joining of fibre reinforced metal matrix composite materials
[PB94-132453] 07 p2712 N94-28376
Technology base enhancement program. Metal matrix composites
[AD-A275531] 08 p3176 N94-28688
Innovative processing of composites for ultra-high temperature applications, book 1
[AD-A275597] 08 p3176 N94-28729
Innovative processing of composites for ultra-high temperature applications, book 2
[AD-A275598] 08 p3177 N94-28730
An anisotropic extension of Bodner's model of viscoplasticity: Model development
[NASA-CR-195289] 08 p3318 N94-28821
Prediction of stress-strain response of SCS-6/Timetal-21S subjected to a hypersonic flight profile
[NASA-TM-109026] 08 p3177 N94-28823
Electrical conductivity measurements on a SiCp/Al alloy metal matrix composite
[PB94-138310] 08 p3263 N94-29120
Microstructure/property relationships for SCS6/Timetal 21-S composite
[AD-A275056] 08 p3178 N94-29135
An analysis of the microstructure and reinforcement distribution of an extruded particle-reinforced Al 6061-10 volume percent Al2O3 metal matrix composite
[AD-A275050] 08 p3178 N94-29166
Properties of graphite fiber reinforced copper matrix composites for space power applications
[NASA-CR-191026] 08 p3178 N94-29208

Thermodynamic analysis of chemical compatibility of several compounds with Fe-Cr-Al alloys
[NASA-CR-191166] 08 p3181 N94-29684
Multiple Concentric Cylinder Model (MCCM) user's guide
[NASA-CR-195299] 08 p3183 N94-30125
The machining of fiber metal laminates. Part 1: An inventory of forming processes
[LR-710-PT-1] 08 p3184 N94-30343
Particulate metal matrix composites: Draft procedure for tensile tests at ambient temperature
[PB94-149721] 08 p3184 N94-30419
Near-net-shape manufacturing: Spray-formed metal matrix composites and tooling 08 p3186 N94-30447
Casting of weldable graphite/magnesium metal matrix composites with built-in metallic inserts
08 p3186 N94-30482
Studies on the optimization of deformation processed metal-metal matrix composites
[DE94-006033] 08 p3185 N94-30704
A class of inclusion problems for the strengthening of brittle and ductile composites 08 p3186 N94-30959
The impact of LDEF results on the space application of metal matrix composites 09 p3595 N94-31034
Inelastic deformation of metal matrix composites
09 p3618 N94-31285
Development and characterization of intermediary layers allowing the bond between a metal alloy and a plasma sprayed ceramic
[ECL-91-39] 09 p3619 N94-31377
Powder metallurgical processing of fibre reinforced aluminium composites
[PB94-148285] 09 p3620 N94-31688
Characterization and growth mechanisms of the MgAl2O4 phase in Al2O3-reinforced Al-Mg composites
[ISBN-0-315-86531-8] 09 p3620 N94-31706
Interfacial behaviour: Wettability in SiC(sub p) metal matrix composites
[ISBN-0-315-87206-3] 09 p3621 N94-31835
Mechanics of failure of high temperature metal matrix composites
[AD-A277397] 09 p3624 N94-32342
Influence of volume fraction of component materials and interlayer bond strength on fracture toughness of multi-layer Al 6090-25 volume percent SiCp and Al 5182 laminates
[DE94-007141] 09 p3626 N94-32665
METCAN demonstration manual, version 1.0
[NASA-TM-105607] 09 p3626 N94-32858
Fracture micromechanics of continuous fiber and textile reinforced metal and ceramic matrix composites
[AD-A277434] 09 p3627 N94-33008
Briefing and review meeting implementation of the military handbook 17 for polymer matrix and metal matrix composites
[AD-A277446] 09 p3663 N94-33010
On the mechanics of microballoon-reinforced metal matrix composites
[AD-A277928] 09 p3630 N94-33178
Leveraging metal matrix composites to reduce costs in space mechanisms 09 p3604 N94-33301
Laser processing of discontinuously reinforced aluminum composites
[AD-A277903] 10 p4018 N94-33593
A fully associative, non-linear kinematic, unified viscoplastic model for titanium based matrices
[NASA-TM-106609] 10 p4069 N94-33958
The effect of thermomechanical processing on mechanical properties of a cast 6061 aluminum metal matrix composite
[AD-A277995] 10 p4019 N94-34220
Implementation of the military handbook 17 for polymer matrix composites and metal matrix composites
[AD-A278795] 11 p4244 N94-35757
Isothermal damage and fatigue behavior of SCS-6/Timetal 21S (0/90)s composite at 650 C
[NASA-CR-195345] 11 p4234 N94-35995
Advanced composites in Japan
11 p4234 N94-36045
Fatigue and residual strength behaviour of ARALL3 panels with bonded-on doublers
[AD-B181062] 11 p4279 N94-36226
A coupled/uncoupled deformation and fatigue damage algorithm utilizing the finite element method
[NASA-TM-106526] 12 p4455 N94-36561
Characterisation of Fibre Reinforced Titanium Matrix Composites
[AGARD-R-796] 12 p4400 N94-36649
Possibilities and pitfalls in aerospace applications of titanium matrix composites 12 p4400 N94-36650
Applications of Titanium Matrix Composite to large airframe structure 12 p4400 N94-36651
SCS-6 (tm) fiber reinforced titanium
12 p4400 N94-36652
Processing of titanium matrix composites
12 p4401 N94-36653
Composites based on titanium with external and internal reinforcement 12 p4401 N94-36654
Manufacture and properties of sigma fibre reinforced titanium 12 p4401 N94-36655
Properties of TMC processed by fibre coating and hiping 12 p4401 N94-36656
Oxidation behavior of titanium aluminide matrix materials 12 p4401 N94-36658
Methodologies for thermal and mechanical testing of TMC materials 12 p4401 N94-36659
Ultrasonic nondestructive characterization methods for the development and life prediction of titanium matrix composites 12 p4401 N94-36660
Metal matrix composites: Analysis of simple specimens and model components under creep and fatigue loading
12 p4402 N94-36661
Residual strength and life prediction techniques for Ti MMC 12 p4402 N94-36662
Process/composite concurrent tailoring of SiC/Ti composites 12 p4402 N94-36663
Micromechanical modeling of damage growth in titanium based metal-matrix composites
12 p4402 N94-36664
Crack growth under cycle loading in fibre reinforced titanium metal matrix composites
12 p4402 N94-36665
Prediction of thermal and mechanical stress-strain responses of TMC's subjected to complex TMF histories
12 p4402 N94-36666
Pre-standardisation work on fatigue and fracture testing of titanium matrix composites 12 p4402 N94-36667
ASTM and VAMAS activities in titanium matrix composites test methods development
12 p4403 N94-36668
Development of mechanical testing methods for titanium matrix composites (traction-ogligo-cyclic fatigue)
12 p4403 N94-36669
Modelling and testing fibre reinforced titanium for design purposes 12 p4403 N94-36670
NiAl-base composite containing high volume fraction of AlN for advanced engines
[NASA-CASE-LEW-15818-1] 12 p4403 N94-36752
Feasibility of (IMC)(sub d)-reinforced metal matrix composites
[AD-A280626] 12 p4404 N94-37044
Using nonequilibrium alloying techniques for corrosion inhibition in Gr/Al and Gr/Mg metal matrix composites
[AD-A280529] 12 p4404 N94-37088
Status review and accomplishments of the Materials Research Center at the University of Pittsburgh
[AD-A280422] 12 p4399 N94-37214
A methodology to predict damage initiation, damage growth and residual strength in titanium matrix composites
[NASA-TM-109135] 12 p4405 N94-37320
Physical and mechanical metallurgy of NiAl
[NASA-TP-3398] 12 p4419 N94-37503

METAL NITRIDES
NT ALUMINUM NITRIDES
NT GALLIUM NITRIDES
NT TITANIUM NITRIDES
Amide and tetrazene complexes of transition and main group elements as precursors for the low temperature synthesis of elemental nitrides
[AD-A266246] 03 p0950 N94-16931
Study on microscopic structural controls and electronic properties at material surfaces by ion beams
07 p2727 N94-25571
Mechanistic studies of opto-electronic materials and syntheses using multiple laser and surface diagnostics
[AD-A274528] 07 p3036 N94-26834
Synthesis and neutron diffraction study of Na3WN3 and Na3MoN3
[AD-A275158] 08 p3203 N94-29043
Digital control programmer for temperature control
[DE94-615584] 11 p4309 N94-36382

METAL ORGANIC CHEMICAL VAPOR DEPOSITION
U METALORGANIC CHEMICAL VAPOR DEPOSITION

METAL OXIDE SEMICONDUCTORS
NT CMOS
NT SOS (SEMICONDUCTORS)
1/f noise and oxide traps in MOSFETs
[DE93-007581] 02 p0619 N94-12942
Molecular simulator: A basic tool for submicron MOS processes development
[LAAS-92484] 02 p0814 N94-14697
Design and optimization of high voltage lateral DMOS devices using RESURF technology
[LAAS-92511] 02 p0626 N94-14711
DLTS and dynamic transconductance analysis of deep-submicron fully-depleted SOI MOSFET's
[AD-A267291] 03 p1214 N94-17243
Development of analog watch with minute repeater
04 p1429 N94-18043
ARPA/CSTO rapid VLSI implementation
[AD-A269170] 04 p1403 N94-18695
Design of power electronics for TVC EMA systems
[NASA-CR-193839] 04 p1407 N94-19642
Modeling failure and reliability in new-generation devices
[AD-A271150] 05 p1748 N94-19910
Simple method to estimate MOS oxide-trap, interface-trap, and border-trap densities
[DE93-041138] 05 p2032 N94-21939
Fabrication of sub-40-nm p-n junctions for 0.18 micron MOS device applications using a cluster-tool-compatible, nanosecond thermal doping technique
[DE94-001608] 06 p2309 N94-23520
Object imaging accomplished with an integrated circuit robotic tactile sensor incorporating a piezoelectric polyvinylidene fluoride thin film
[AD-A274038] 07 p2780 N94-25845
Demonstration of monolithic co-fabrication of Y1Ba2Cu3O7-Sigma and CMOS devices on the same sapphire substrate
[AD-A274757] 07 p3059 N94-26566
The analysis of thermal and 1/F noise in MOS devices, circuits and systems
[ISBN-0-315-57811-4] 07 p2787 N94-27642
A study of DC-DC converters with MCT's for arcjet power supplies
[NASA-CR-191204] 07 p2703 N94-27662
Nonvolatile programmable neural network synaptic array
[NASA-CASE-NPO-18578-1-CU]
08 p3265 N94-29426
Charge collection spectroscopy applied to MOS RAM's 08 p3201 N94-30220
Process parameter-growth environment-film property relationships for reactive sputter deposited metal (V, Nb, Zr, Y, Au) oxide, nitride, and oxynitride films
[AD-A276382] 09 p3640 N94-31258
An extended approach to oxidations and nitridations of Si and Ge(x)Si(1-x) materials
[AD-A276056] 09 p3631 N94-31282
Hydrogen incorporation and radiation induced dynamics in metal-oxide-silicon structures: A study using nuclear reaction analysis
[ETN-94-95742] 09 p3898 N94-31610
Analysis and synthesis of MOS translinear circuits
[ISBN-9-09-005495-2] 09 p3690 N94-31616
Temperature dependence of single-event burnout in n-channel power MOSFET's
[AD-A277921] 09 p3698 N94-33177
Estimating low-dose rate irradiation response of MOSFETs
[DE94-007292] 11 p4342 N94-36367

METAL OXIDES
NT ALUMINUM OXIDES
NT ANATASE
NT BARIUM OXIDES
NT BISMUTH OXIDES
NT BSCCO SUPERCONDUCTORS
NT CALCIUM OXIDES
NT CERIUM OXIDES
NT CHROMIUM OXIDES
NT COBALT OXIDES
NT COPPER OXIDES
NT GALLIUM OXIDES
NT HAFNIUM OXIDES
NT HEMATITE
NT ILMENITE
NT IRON OXIDES
NT LANTHANUM OXIDES
NT LEAD OXIDES
NT LITHIUM OXIDES
NT MAGNESIUM OXIDES
NT MAGNETITE
NT MANGANESE OXIDES
NT MIXED OXIDES
NT MOLYBDENUM OXIDES
NT NICKEL OXIDES
NT NIOBIUM OXIDES
NT PERICLASE
NT PLATINUM OXIDES
NT POTASSIUM OXIDES
NT RUTILE
NT SAPPHIRE
NT SCANDIUM OXIDES
NT SILVER OXIDES
NT STRONTIUM OXIDES
NT TANTALUM OXIDES
NT TIN OXIDES
NT TITANIUM OXIDES
NT TUNGSTEN OXIDES
NT URANIUM OXIDES
NT VANADIUM OXIDES
NT YBCO SUPERCONDUCTORS
NT YTTRIA-STABILIZED ZIRCONIA
NT YTTRIUM OXIDES
NT ZINC OXIDES
NT ZIRCONIUM OXIDES

Kinetics of photodeposition of superconducting films
[DE93-015511] 02 p0812 N94-14348
Ion mixing of thin ZrO2 films on sapphire
[DE93-015214] 03 p1206 N94-14925
Molten salt electrodeposition of high temperature superconductors
[AD-A266620] 03 p1009 N94-15726
The friction and wear of ceramic/ceramic and ceramic/metal combinations in sliding contact
[NASA-TM-106348] 03 p0930 N94-15769
Catalytic hydrocarbon reactions over supported metals
[DE93-018168] 04 p1345 N94-17808
Surface phases and their influence on metal-oxide interfaces
[DE93-019931] 04 p1601 N94-19020
Electrocatalysts for oxygen electrodes
[DE93-040446] 04 p1354 N94-19653
Development of durable high-temperature catalysts for natural gas combustion
[PB93-226447] 06 p2232 N94-23477
Pulsed Ion Beam Surface Analysis (PIBSA) as a means of in-situ real-time analysis of thin films during growth
[DE94-001276] 06 p2562 N94-23805
Surface compositional variations of Mo-47Re alloy as a function of temperature
[NASA-TP-3402] 06 p2245 N94-25117
Investigation of the solid-solid surface adsorption of Eu2O3 on amorphous Al2O3
[DE93-613824] 06 p2566 N94-25332
Reference electrodes for solid polymer electrolytes
[DE94-004583] 07 p2780 N94-25806
Studies of thin-film growth, adsorption, and oxidation by in situ, real-time, and ex situ ion beam analysis
[DE94-002907] 07 p3055 N94-26275
Ion implantation and dynamic recovery of tin-doped indium oxide films
[DE94-001126] 07 p3062 N94-26932
Epitaxial heterojunctions of oxide semiconductors and metals on high temperature superconductors
[NASA-CASE-NPO-18483-1-CU] 08 p3513 N94-29501
Bench-scale synthesis of nanoscale materials 08 p3240 N94-30473
Influence of surface defects and local structure on oxygenate reaction pathways over metal oxide surfaces
[DE94-005680] 08 p3522 N94-30901
Sol-gel metal oxide and metal oxide/polymer multilayers applied by meniscus coating
[DE94-005813] 09 p3649 N94-31199
Experimental investigations and molecular dynamics simulations of radiation induced surface damage
[AD-A277323] 09 p3871 N94-32621
Development of a catalyst for conversion of syngas-derived materials to isobutylene
[DE94-009698] 10 p4021 N94-33901
Activities of the Tandem Accelerator Center, University of Tsukuba
[DE94-748687] 12 p4522 N94-37237

METAL PARTICLES
NT METAL POWDER
NT POWDERED ALUMINUM
Processing, properties, and wear resistance of aluminides
[DE93-012186] 01 p0083 N94-11141
Effects of microscopic iron metal on the reflectance spectra of glass and minerals 01 p0436 N94-12024
The spectral effects of subsolidus reduction of olivine and pyroxene 01 p0081 N94-12110
Iron and nickel isotopic mass fractionation in deep-sea spherules 01 p0282 N94-12199
The unusual metallic particles in Krymka LL3.0 chondrite 01 p0433 N94-12253
Distributed combustion in solid propellants
[AD-A265727] 01 p0099 N94-12564
The effect of crystal tilt on high resolution micrographs of small metal particles
[DE93-013915] 02 p0574 N94-14795
Metal slurry droplet and spray combustion
[AD-A269648] 04 p1349 N94-18736
Atomic-scale friction measurements using friction force microscopy. Part 2: Application to magnetic media
[AD-A270759] 04 p1447 N94-19767
Preliminary AEM study of the microstructure and composition of metal particles in ordinary chondrites 05 p2086 N94-20894
An apparatus for measurement of ignition and burning characteristics of metallic particles
[AD-A274815] 07 p2716 N94-26487
Template synthesized nanoscopic gold particles: Optical spectra and the effects of particle size and shape
[AD-A275378] 08 p3197 N94-29312
Study on the formation of ultrafine particles of Sm-Co intermetallic compounds using RF thermal plasma 08 p3211 N94-29516
Nanosize metal alloy particle formation in Ag and Cu sequentially implanted silica
[DE94-005592] 08 p3207 N94-30042
Oxidation resistant copper
[AD-D016099] 09 p3696 N94-32721
Validation and implementation of optical diagnostics for particle sizing in rocket motors
[AD-A278581] 12 p4428 N94-36972

METAL PLATES
Advances in low carbon, high strength ferrous alloys
[AD-A265264] 01 p0085 N94-12532
Experimental technique to simulate orbital-debris impact on space shields at impact velocities over 10 km/s
[DE93-011619] 02 p0539 N94-12909
Development of test techniques to simulate high-frequency mechanical shock on weapon components
[KCP-613-4998] 02 p0675 N94-13907
High counting rate resistive-plate chamber
[DE93-014928] 02 p0651 N94-14452
Heavy section steel irradiation experiment
[DE93-015517] 02 p0573 N94-14537
Microwave interaction with plasmas
[AD-A267048] 03 p1201 N94-15661
Analysis of electromagnetic scattering from irregularly shaped, thin, metallic flat plates
[NASA-TP-3361] 03 p0998 N94-16655
Proposal of a simple mathematical model for the action of a laser on a metal plate
[IFTR-36/1991] 03 p1041 N94-17065
Metallurgical evaluation of SRAM 2/SRAM A program mer base plates
[DE93-018689] 04 p1364 N94-19100
The fire resistance of profiled thin steel sheet structures
[VTT-TIED-1320] 04 p1380 N94-19373
Thermal information regarding the cooldown and operation of liquid argon calorimeters
[DE93-019391] 05 p1807 N94-19987
Numerical simulations of hypervelocity impact experiments involving single Whipple bumper shields
[AD-A272123] 05 p1831 N94-20572
A simplified method for S-parameter calculations of metal septum waveguide filters 05 p1782 N94-22180
Performance of the X-/Ka/KABLE-band dichroic plate in the DSS-13 beam waveguide antenna 06 p2291 N94-23261
The effects of texture and strain on the r-va lue of heavy gauge tantalum plate
[DE94-000690] 06 p2242 N94-23541
Unsegmented electromagnetic calorimeter prototype. Energy and coordinate resolution
[DE93-634185] 07 p2810 N94-26396
Evaluation of crack arrest fracture toughness of parent plate, weld metal and heat affected zone of BIS 812 EMA ship plate steel
[AD-A274871] 07 p2839 N94-26859
The influence of TIG welding thermal cycles on HSLA-100 steel plate
[AD-A274248] 07 p2740 N94-27009
Aluminum alloy 8090-T8771 thick plate material characterization
[AD-A274146] 07 p2987 N94-27077
Electrical conductivity measurements on a SiCp/Al alloy metal matrix composite
[PB94-138310] 08 p3263 N94-29120
Effect of vibratory stress relief during welding of thick stainless steel plate
[DE94-006557] 09 p3733 N94-31312
Transient body force effects on the dryout and rewet of a heated capillary structure
[AD-A278677] 11 p4264 N94-35690
Residual stresses in a multi-pass weld in an austenitic stainless steel plate before and after thermal stress relief
[DE94-013278] 12 p4420 N94-37548

METAL POWDER
NT POWDERED ALUMINUM
The effect of processing on the microstructure and tensile properties of a (gamma)-TiAl based alloy
[DE93-013221] 01 p0084 N94-11488
Study on the mechanism of liquid phase sintering (M-12) 02 p0588 N94-13744
Reverse micelle synthesis of nanoscale metal containing catalysts
[DE93-012869] 02 p0572 N94-14184
Solid lubricants for space structures, phase 2
[AD-A266653] 03 p0968 N94-16767
Characterization of nanoscale oxide and oxyhydroxide powders using EXAFS spectroscopy
[DE93-015683] 03 p0940 N94-17235
Aluminum powder/water reaction ignited by electrical pulsed power
[AD-A269223] 04 p1376 N94-17840
Field emission cathode and vacuum microelectronic microwave amplifier development
[AD-A269526] 04 p1403 N94-18639
Metastable bcc phase formation in the Nb-Cr system
[DE93-018376] 05 p2012 N94-19926
Shock response of porous Al-2 + Fe2O3 powder mixtures
[DE93-018851] 05 p1688 N94-19944
Transmission electron microscopy study of thick copper-304 stainless steel multilayers
[DE94-001045] 05 p1696 N94-22394
Material optimization and manufacturing development of reduced cost powder metal titanium alloy components for gas turbine engine application, phase 2
[AD-A274410] 07 p2709 N94-26978
Mechanical alloying processing with application to structural materials: ASSERT supplement
[AD-A275400] 08 p3204 N94-29205
Studies of high temperature ternary phases in mixed-metal-rich early transition metal sulfide and phosphide systems
[DE94-006034] 08 p3209 N94-30336
Centrifugal atomization of lanthanide materials for cryogenic coolers
[DE94-006035] 08 p3219 N94-30337
The new Metals and Alloys Indexes, search manual: A phase diagram research tool
[DE94-005371] 09 p3643 N94-32098
On the formation of muon- and zeta-phases in Ag-Al system by mechanical alloying
[DE94-007125] 09 p3645 N94-32636
Development of nickel and metal hydride secondary battery
[DE94-757270] 09 p3697 N94-32917
NiAl-base composite containing high volume fraction of AlN for advanced engines
[NASA-CASE-LEW-15818-1] 12 p4403 N94-36752
Substantiating powder metal life methodologies for engines 12 p4455 N94-37330

METAL PROPELLANTS
Shear flow control of gas jets in liquids
[AD-A264673] 01 p0152 N94-11448
Combustion-induced crack/debond propagation in solid propellants 02 p0584 N94-13560
Aluminum powder/water reaction ignited by electrical pulsed power
[AD-A269223] 04 p1376 N94-17840
Powdered aluminum and oxygen rocket propellants: Subscale combustion experiments
[NASA-TM-106439] 05 p1713 N94-21760
Experimental investigation of ignition of boron/titanium composite particles 06 p2159 N94-24275
Ignition and combustion characteristics of metallized propellants, phase 2
[NASA-CR-195107] 06 p2266 N94-24700
Shock tube ignition and combustion of aluminum/magnesium alloy particles in oxygen at high pressure 09 p3631 N94-31286
Validation and implementation of optical diagnostics for particle sizing in rocket motors
[AD-A278581] 12 p4428 N94-36972

METAL SHEETS
Hybrid materials for use at elevated temperatures 01 p0057 N94-10013
Failure prediction of thin beryllium sheets used in spacecraft structures
[NASA-CR-194164] 01 p0187 N94-11190
Measurement and analysis of critical CTOA for an aluminum alloy sheet
[NASA-TM-109024] 03 p0956 N94-15948
Laser weld repair of tantalum sheet
[DE93-016417] 03 p1041 N94-16871
The fire resistance of profiled thin steel sheet structures
[VTT-TIED-1320] 04 p1380 N94-19373
Formulation and identification of the anisotropic laws for thin sheets drawing
[ECL-92-55] 04 p1365 N94-19400
Weld cladding of hard surfaces
[PB93-201598] 06 p2353 N94-23448
On experimental studies of yield surfaces of metals: A more general approach
[IFTR-42/1993] 07 p2739 N94-26824
Production of an amorphous Fe(75)Si(10)B(15) sheet by a metallic mold casting method and its properties 07 p2746 N94-28170
Electrical conductivity measurements on a SiCp/Al alloy metal matrix composite
[PB94-138310] 08 p3263 N94-29120
Delamination growth in composites under cyclic loads 08 p3183 N94-30256
Plane strain finite element analysis of sheet forming operations including bending effects 08 p3322 N94-30354
Photovoltaic power without batteries for continuous cathodic protection 08 p3341 N94-30465

Design of a variable-conductance vacuum insulation
[DE94-000270] 08 p3268 N94-30819
Composite repairs of cracked metallic airframe structures
[AD-A277680] 10 p3969 N94-33590
Transformation plasticity in ductile solids
[DE94-010420] 11 p4240 N94-35953

METAL SHELLS
Foil bearing research at Penn State
06 p2215 N94-23058

METAL SPINNING
Spinforming characteristics of a net shape forming process 01 p0056 N94-10004
Spin-rolling, welding, and heat treatment of aluminium 2219 for Ariane 5 GAM high pressure vessel liners
01 p0062 N94-10045

METAL SPRAYING
Performance aspects of de Laval spray-forming nozzles
[DE93-013671] 01 p0163 N94-12604
Proceedings of the 57th National Congress of Japan Thermal Spraying Society
[DE94-731734] 10 p4029 N94-34133
Method for producing closed cell spherical porosity in spray formed metals
[AD-D016126] 10 p4025 N94-34152

METAL SURFACES
Hydrogen partitioning and transport in titanium aluminides
[NASA-CR-194117] 01 p0076 N94-10713
Application of spin-sensitive electron spectroscopies to investigations of electronic and magnetic properties of solid surfaces and epitaxial systems
[DE93-015079] 01 p0076 N94-10854
Real-space formation and dissipation dynamics of hexagonal reconstruction on Au(100) in aqueous media as explored by potentiodynamic scanning tunneling microscopy
[AD-A266138] 01 p0368 N94-11658
Nonlinear optical spectroscopy of Ag(111) in electrolyte and in vacuum
[AD-A265622] 01 p0079 N94-12534
Incomplete melting of the Au(100) surface
[DE93-623192] 02 p0569 N94-13227
About the influence of inert gas ion implantation on metal corrosion stability
[DE93-620574] 02 p0569 N94-13360
Surfaces and interfaces of ceramics and metals
[DE93-014959] 02 p0578 N94-13408
Excimer laser surface processing of titanium
[DE93-012633] 02 p0570 N94-13512
Materials compatibility of hydride storage materials with austenitic stainless steels
[DE93-013688] 02 p0703 N94-13691
Determination of the surface cleanliness of metals by FT-IR spectroscopy
[DE93-013252] 02 p0565 N94-14525
Quantum state resolved desorption of CO from solid surfaces
[DE93-016876] 02 p0814 N94-14597
The friction and wear of ceramic/ceramic and ceramic/metal combinations in sliding contact
[NASA-TM-106348] 03 p0930 N94-15769
Passive oxide films on well-defined nickel surfaces: An examination of film growth on Ni(100) with ex situ scanning tunneling microscopy
[DE93-014056] 03 p1207 N94-15923
A Moessbauer spectrometer for the mineralogical analysis of the Mars surface: First temperature dependent tests of the detector and drive system
03 p1259 N94-16233
Hydride-containing molten salts and their technology implications
[AD-A266458] 03 p1092 N94-16567
Vectorial electron transfer in spatially ordered arrays
[DE93-018150] 03 p1185 N94-16971
Mechanical properties of excimer laser modified titanium surfaces
[DE93-012663] 04 p1358 N94-17875
Process for applying high application-temperature coating to heat-sensitive aluminum alloys
[AD-D015823] 04 p1368 N94-17905
Surface phases and their influence on metal-oxide interfaces
[DE93-019931] 04 p1601 N94-19020
Binding of copper to nanocavity surfaces in silicon
[DE93-019073] 04 p1364 N94-19080
Surface species in tribology
[AD-A270970] 04 p1446 N94-19754
Segregation of Si to the surface of Fe-29Ni-17Co alloy
[DE93-040053] 05 p1687 N94-19864
The metallic bond for monolayer transition metal layers on transition metal surfaces
[DE93-019060] 05 p1691 N94-20313
In-situ electrochemical surface science
[AD-A265942] 05 p1680 N94-20330
Surface electrochemistry of metals
[AD-A272913] 05 p1691 N94-21245
Vapor-delivered lubrication of steel-steel and steel-ceramic systems
[PB93-202364] 05 p1825 N94-21451
Laser Raman and x ray scattering studies of corrosion films on metals
[DE93-040243] 05 p1692 N94-21558
Inelastic electron scattering from surfaces
[DE94-001738] 05 p1977 N94-22049
Inelastic electron scattering from surfaces
[DE94-001368] 06 p2531 N94-22733
Chromate-free talc chemical conversion coatings for aluminum alloys
[DE94-001567] 06 p2238 N94-22932
Density functional studies: First principles and semi-emperical calculations of clusters and surfaces
[DE94-002836] 06 p2561 N94-23214
Thermal phase behavior of metal surfaces: X-ray scattering studies of Pt(001)
[DE94-002991] 06 p2245 N94-24612
Free energy profiles for Li(+) and I(-) ions approaching Pt(100) surface: A molecular dynamics study
[AD-A273455] 06 p2536 N94-24675
Use of scanning tunneling microscope in corrosion studies
[VTT-TIED-1416] 06 p2250 N94-25346
Proceedings of the 12th International Congress: Corrosion Control for Low-Cost Reliability. Volume 5A: Corrosion: General issues
[AD-A273666] 06 p2250 N94-25406
Proceedings of the 12th International Congress: Corrosion Control for Low-Cost Reliability. Volume 1: Coatings
[AD-A273661] 06 p2251 N94-25448
Observation on metal surface in aqueous solution using an electrochemical Scanning Tunneling Microscope (STM) 07 p2724 N94-25554
Study on interfacial reaction analysis at interfacial joining 07 p2728 N94-25574
Atomic-scale chemistry of metal surfaces
[REPT-A-2657] 07 p3012 N94-25636
Binding of copper and nickel to cavities in silicon formed by helium ion implantation
[DE94-003769] 07 p3050 N94-25814
A mimic model of Pt-Rh catalyst prepared by electrochemical deposition of Rh on Pt (100) surface
[REPT-A-2664] 07 p2715 N94-26476
An investigation of the effect of surface impurities on the adsorption kinetics of hydrogen chemisorbed onto iron
[NASA-CR-195213] 07 p2716 N94-26643
Stability of reference masses 2: The effect of environment and cleaning methods on the surfaces of stainless steel and allied materials
[NPL-DMM(A)-95] 07 p2738 N94-26653
On experimental studies of yield surfaces of metals: A more general approach
[IFTR-42/1993] 07 p2739 N94-26824
Secondary electron emission from copper surface due to neodymium and gadolinium ion bombardment
[DE94-701115] 07 p3027 N94-27718
Image potential of a tunnelling electron moving near two different metals
[DE94-603657] 07 p3069 N94-27819
Sweep rate and concentration effects on metastable structures formed in the underpotential deposition of silver on Pt(111)
[AD-A275369] 08 p3189 N94-29010
X ray standing wave studies of underpotentially deposited metal monolayers
[AD-A275409] 08 p3513 N94-29215
Pit initiation on passivated metal surfaces: Crystallographic orientation and environmental effects
[ISBN-0-315-85433-2] 08 p3208 N94-30138
XPS analysis of 440C steel surfaces lubricated with perfluoropolyethers under sliding conditions in high vacuum
[NASA-TM-106548] 08 p3218 N94-30177
Effects of hydrogen on the resistivity of thin Au and Cu films 08 p3218 N94-30225
Computer simulation of the interaction of fast hydrogen atoms with a molybdenum containing sorbed hydrogen
[DE94-608419] 08 p3209 N94-30253
An investigation of the corrosion properties of aluminum-tantalum alloys using electrochemical impedance spectroscopy and local electrochemical impedance spectroscopy 08 p3209 N94-30521
Interaction of water with metal surfaces
[AD-A276260] 09 p3632 N94-31293
Fiber optic sensors for the detection of surface acoustic waves on metals
[ISBN-0-315-87055-9] 09 p3878 N94-31736
A new-type of long-range restructuring of ordered metal surfaces induced by lateral adsorbate interactions: Iodide on AU(110) electrodes
[AD-A276633] 09 p3643 N94-32060
Vibrational spectroscopy at metal-solution interfaces: Some perspectives and prospects for electrochemical surface science
[AD-A276781] 09 p3644 N94-32169
Molten metal analysis by laser produced plasmas
[DE94-007014] 09 p3646 N94-32782
Metal cluster-rare gas van der Waals complexes: Microscopic models of physisorption
[DE94-008134] 09 p3873 N94-32797
Method and apparatus for inhibiting the disbonding of a paint from metal surfaces
[AD-D016106] 09 p3663 N94-32960
Atomic force microscopy
[AD-A277589] 10 p4026 N94-33429
The underpotential deposition of copper on Pt(311): Site selective deposition and anion effects
[AD-A278022] 10 p4023 N94-33436
Continuing research on friction and wear of materials
[AD-A277690] 10 p4059 N94-33437
Unique methods for on-orbit structural repair, maintenance, and assembly 10 p4102 N94-33663
Slow collisions of multicharged ions with metal surfaces
[DE94-009449] 10 p4136 N94-33684
Stainless steel surface treatment
[AD-D016135] 10 p4024 N94-33758
Bistatic clutter RCS simulation using scale model surfaces with two scale roughness
[AD-A277604] 10 p4035 N94-33847
Ion beam surface treatment: A new capability for rapid melt and resolidification of surfaces
[DE94-008955] 10 p4025 N94-34014
Processing and properties of high temperature metal/fiber-reinforced-thermoplastic laminates
[AD-A278791] 11 p4232 N94-35654
Morphology of meteoroid and space debris craters on LDEF metal targets 11 p4353 N94-36159
Formation and stability of Fe-rich precipitates in dilute Zr(Fe) single-crystal alloys
[DE94-619027] 11 p4242 N94-36288
First results from the Los Alamos plasma source ion implantation experiment
[DE94-003931] 12 p4414 N94-36461
Atomic and electronic structure of metals and alloys: Rare earths, ultrathin films and surface alloys
[DE94-011581] 12 p4516 N94-37113
Modelling of surfaces. Part 1: Monatomic metallic surfaces using equivalent crystal theory
[NASA-TM-106680] 12 p4419 N94-37459
Perfluorodiethoxymethane on nickel and nickel oxide surfaces
[DE94-011200] 12 p4426 N94-37712
Morphological aspects of surface reactions
[DE94-011208] 12 p4413 N94-37713

METAL VAPOR LASERS
Recent results from material processing studies on new generation lasers
[DE93-013841] 02 p0653 N94-12898
Absorption and damage thresholds of low defect density hafnia deposited with activated oxygen
[DE93-013853] 02 p0655 N94-13243
Laser beam control and diagnostic systems for the copper-pumped dye laser system at Lawrence Livermore National Laboratory
[DE93-016529] 02 p0658 N94-14437
The copper-pumped dye laser system at Lawrence Livermore National Laboratory
[DE93-014429] 04 p1435 N94-17723
Safety approaches for high power modular laser operation
[DE93-017213] 04 p1435 N94-17759
Laser materials processing applications at Lawrence Livermore National Laboratory
[DE93-017976] 04 p1437 N94-18093
Cutting and drilling studies using high power visible lasers
[DE93-019149] 04 p1441 N94-19294
Computational model of a magnetic modulator for copper lasers
[DE93-019603] 05 p1815 N94-20223
High-power copper vapor lasers and their application to precision drilling and cutting
[DE93-019951] 05 p1819 N94-21844
An externally heated copper vapour laser
[DE94-619484] 12 p4447 N94-36565
New hollow-cathode electrode for high-power copper lasers
[DE94-011637] 12 p4448 N94-37244

METAL VAPORS
NT SODIUM VAPOR

Design of CCD camera system for use inside electron beam furnace
[DE93-009525] 01 p0170 N94-11267
Gas-evaporation in low-gravity field (cogelation mechanism of metal vapors) (M-14)
02 p0588 N94-13746
Bench-scale screening tests for a boiling sodium-potassium alloy solar receiver
[DE93-018512] 04 p1469 N94-19040
Impact of copper vapour contamination on argon arcs
05 p1994 N94-21053
Artificial plasma experiments. Chemical release observations associated with the CRRES program
[NASA-CR-194871] 06 p2550 N94-23565
The reaction mechanism of W-CVD in Si
[ETN-94-95329] 06 p2261 N94-25084
Hook spectroscopy as an atomic number density diagnostic applied to laser-ablated copper plasmas
[DE94-002645] 07 p3042 N94-26081
Studies of interfaces and vapors with Optical Second Harmonic Generation
[DE94-006295] 08 p3476 N94-30841
Using laser absorption spectroscopy to monitor composition and physical properties of metal vapors
[DE94-001530] 09 p3716 N94-31599
Ultrahigh-current-density metal-ion implantation and diamondlike-hydrocarbon films for tribological applications
[DE94-008958] 09 p3906 N94-32843

METAL WHISKER REINFORCEMENT
U WHISKER COMPOSITES

METAL WORKING
NT CLADDING
NT EXPLOSIVE FORMING
NT FORGING
NT HYDROFORMING
NT METAL DRAWING
NT METAL SPINNING
Atlas of formability: Ultimet
[AD-A268352] 04 p1355 N94-17767
Atlas of formability: HAYNES 556
[AD-A268354] 04 p1356 N94-17768
Atlas of formability: HAYNES 188
[AD-A268355] 04 p1356 N94-17769
Atlas of formability: NICKELVAC K-500
[AD-A268351] 04 p1356 N94-17772
Atlas of formability: Haynes 230
[AD-A268325] 04 p1356 N94-17788
Atlas of formability: INCONEL 718
[AD-A268350] 04 p1356 N94-17789
Atlas of formability: Hastelloy C-22
[AD-A268324] 04 p1356 N94-17796
Atlas of formability: Permalloy - 80 flow stress curves
[AD-A268263] 04 p1356 N94-17801
Atlas of formability: Nickelvac C-276
[AD-A268264] 04 p1357 N94-17802
Atlas of formability: Ti-6Al-4V ELI
[AD-A268300] 04 p1357 N94-17803
Atlas of formability: ALLVAC 718
[AD-A268304] 04 p1357 N94-17804
Atlas of formability: Waspaloy
[AD-A268323] 04 p1593 N94-17805
Formulation and identification of the anisotropic laws for thin sheets drawing
[ECL-92-55] 04 p1365 N94-19400
Titanium 1992: Volume 3: Science and technology
[AD-A274800] 07 p2735 N94-26337
Titanium 1992: Science and Technology, volume 1
[AD-A274798-VOL-1] 07 p2739 N94-26799
Plane strain finite element analysis of sheet forming operations including bending effects
08 p3322 N94-30354
Application of ALE techniques to metal forming simulations
[DE94-005358] 08 p3211 N94-30892
Lubrication with binary mixtures: Liquid-liquid emulsion in elastohydrodynamics and metal forming
09 p3658 N94-32490

METAL-GAS SYSTEMS
Atomic structures and compositions of internal interfaces
[DE93-014840] 01 p0363 N94-10750
First-principles studies of phase stability and the structural and dynamical properties of hydrogen-metal systems
[DE93-016129] 02 p0570 N94-13374
Effect of oxygen concentration and ordering on vanadium-oxygen alloy vibrational spectra
[DE93-627003] 04 p1355 N94-17692
Report of the 1991 Workshop on Particle-Material Interactions for Fusion Research
[DE93-788393] 04 p1573 N94-18156
Evaluation of a diffusion/trapping model for hydrogen ingress in high-strength alloys
[AD-A271328] 05 p1689 N94-20027
Diffusion of hydrogen in iron oxides
[DE93-632430] 06 p2239 N94-22966
Exploratory Technology Research Program for Electrochemical Energy Storage
[DE94-003479] 07 p2781 N94-26047
The 10th International Conference on Internal Friction and Ultrasonic Attenuation in Solids (ICIFUAS)
[AD-A276849] 09 p3902 N94-32209
Metal-carbon nanostructures
[DE94-009177] 12 p4400 N94-36509

METAL-METAL BONDING
A high voltage dielectrically isolated smart power technology based on silicon direct bonding
[LAAS-92492] 02 p0626 N94-14698
Beryllium processing technology review for applications in plasma-facing components
[DE93-018396] 04 p1363 N94-19028
Organometallic chemistry of bimetallic compounds
[DE94-002313] 06 p2238 N94-22897
Strength, acoustic evaluation and metallurgy of diffusion bonds
[DE94-001804] 06 p2243 N94-23717
Method of bonding molybdenum to steel
[AD-D016079] 07 p2747 N94-28187
Small cylindrical adhesive bonds
[PB94-148210] 09 p3651 N94-31585
Metal clusters: Dynamics and structure
[AD-A276842] 09 p3643 N94-32091

METAL-SEMICONDUCTOR-METAL SEMICONDUCTORS
U MSM (SEMICONDUCTORS)

METAL-WATER REACTIONS
Proceedings of the 12th International Congress: Corrosion Control for Low-Cost Reliability. Volume 5B: Corrosion: General issues
[AD-A273667] 06 p2250 N94-25407
Fundamental study on monitoring technology on local surface damages 07 p2724 N94-25555
Interfaces of high-protection performance polyaryls-coated zinc phosphated steels
[DE94-011732] 12 p4417 N94-37153

METALLIC GLASSES
Detection of low-intensity magnetic fields with a magnetostrictive fiber optic sensor
[AD-A274120] 07 p3037 N94-27062
Production of amorphous metal layers using ion implantation and investigation of the related modification of some surface properties
[DE94-617509] 12 p4414 N94-36541

METALLIC PLASMAS
Hook spectroscopy as an atomic number density diagnostic applied to laser-ablated copper plasmas
[DE94-002645] 07 p3042 N94-26081

METALLIC STARS
The controlling parameters of the integrated flux of a stellar population 01 p0426 N94-11187

METALLICITY
On inhomogeneous halo collapse and the globular cluster metallicity gradient
[DE93-013090] 02 p0834 N94-13011
Globular cluster photometry near the turnoff: Blue stragglers, relative ages, and the horizontal branch
08 p3538 N94-29732
Study of the stellar populations of the Fornax dwarf spheroidal galaxy
[ISBN-0-315-85526-6] 08 p3541 N94-30231
Line-strength gradients and kinematic profiles in elliptical galaxies 09 p3934 N94-31788
The role of galaxy type and environment in determining the properties of globular cluster systems
[ISBN-0-315-76447-3] 09 p3939 N94-33112

METALLIZING
Method for producing a hybridization of detector array and integrated circuit for readout
[NASA-CASE-NPO-18062-1-CU]
01 p0141 N94-10656
Effects of solar cell environment on contact integrity
01 p0049 N94-11387
Chemical Vapor Deposition of Refractory Metals and Ceramics 2. Materials Research Society Symposium proceedings
[AD-A265072] 01 p0092 N94-11866
Electrochemical planarization for microelectronic circuits
[DE93-017214] 02 p0627 N94-14870
Ablation, surface activation, and electroless metallization of insulating materials by pulsed excimer laser irradiation
[DE93-015808] 03 p1040 N94-16664
Robotic weld overlay coatings for erosion control
[DE93-016938] 03 p0970 N94-16959
Low dielectric constant insulators and gold metallization for GHz multi-chip modules, part 2
[AD-A268590] 03 p1176 N94-17605
Development of large-area monolithically integrated silicon-film photovoltaic modules
[DE93-010037] 04 p1464 N94-17731
RF vacuum microelectronics
[AD-A270003] 04 p1403 N94-18667
High pressure metallization of Mott Insulators: Magnetic, structural and electronic properties
[DE93-018295] 04 p1404 N94-18805
Pressure induced metallization of the Mott Insulator 6(sub 2)
[DE93-018296] 04 p1600 N94-18969
Metallization and charge-transfer gap closure of transition-metal iodides under pressure
[DE93-040301] 04 p1353 N94-19538
Adhesive electroless metallization of fluoropolymeric substrates
[AD-A271858] 05 p1703 N94-20526
Diagnostics and methods for real-time laser microchemistry
[AD-A270871] 05 p1680 N94-20566
Direct imaging of the surface microstructure of dielectric materials using an atomic force microscope
[AD-A272251] 05 p2018 N94-20575
Low-gravity electrodeposition and growth of polymer thin films with large third-order optical nonlinearities by electrochemical processes for devices: Thiophene-based polymers 06 p2225 N94-24346
Robotic weld overlay coatings for erosion control
[DE94-002665] 06 p2258 N94-24749
Experimental determination of the CU-IN-PB ternary phase diagram
[DE94-003765] 07 p2735 N94-26349
X ray standing wave studies of underpotentially deposited metal monolayers
[AD-A275409] 08 p3513 N94-29215
Vacuum vapor deposition
[NASA-CASE-MFS-28652-1] 08 p3215 N94-29446
The organometallic chemical vapor deposition of transition metal carbides: The use of homoleptic alkyls
[DE94-005577] 08 p3206 N94-30007
Research on high reliability refractory ohmic contacts for GaAs FETs and MODFETs
[AD-A276848] 09 p3697 N94-33034
Efficient chemistry for selective modification and metallization of substrates
[AD-D016162] 10 p4023 N94-34287
A novel method for depositing precious metal films on difficult surfaces
[NASA-TM-106607] 11 p4243 N94-35260
Au/Zn contacts to Rho-InP: Electrical and metallurgical characteristics and the relationship between them
[NASA-TM-106590] 11 p4281 N94-35271

METALLOGRAPHY
Metallographic cooling rates of L-group ordinary chondrites 01 p0429 N94-12061
Estimation of strain in 1-kW primary containment vessels by microstructural examination
[DE93-013053] 02 p0573 N94-14316
Cation ordering in orthopyroxenes and cooling rates of meteorites: Low temperature cooling rates of Estherville, Bondoc and Shaw 03 p1241 N94-16176
Effects of processing and prolonged high temperature exposure on the microstructure of Nb-1Zr-C sheet
[NASA-TM-106370] 03 p0959 N94-16883
Microstructural analysis of solid-state resistance welds
[DE93-017295] 04 p1443 N94-17761
Dynamical behavior of octahedrite from the Henbury meteorite
[DE93-018834] 04 p1627 N94-19339
Investigation of cracking and erratic behavior of the uranium-titanium alloy
[DE93-018591] 05 p1688 N94-19957
Influence of sintering atmospheres on the aluminum sintering characteristics
[DE93-632412] 06 p2239 N94-22965
Determination of the compatibility between structural alloys and molten metals at high temperatures
[DE94-000954] 06 p2241 N94-23434
Large-scale production of Si(0.8)Ge(0.2) thermoelectric alloys by mechanical alloying
[DE94-000695] 06 p2243 N94-23753
Robotic weld overlay coatings for erosion control
[DE94-002665] 06 p2258 N94-24749
Upset welding process for 21-6-9 spherical vessels
[DE93-018194] 07 p2832 N94-28229
Development of evaluated data bank of physical properties of perspective nuclear engineering steels and alloys
[DE94-607999] 08 p3207 N94-30078
Nature of dissolution of binary tantalum-titanium alloys by molten plutonium
[DE94-005090] 08 p3210 N94-30776
Method of test for cleanness assessment of metal alloys: The preparation of button specimens by electron beam melting and the characterisation of recovered inclusions
[NPL-DMM(A)-130] 08 p3210 N94-30796
Nd-YAG laser welding of the fiber optic connector to the header shell on the 2SL actuator
[DE94-006104] 09 p3723 N94-31621

METALLOIDS
NT AMORPHOUS SILICON
NT ANTIMONY
NT ARSENIC
NT BORON
NT BORON ISOTOPES
NT GERMANIUM
NT GERMANIUM ISOTOPES
NT POLONIUM ISOTOPES
NT SILICON
NT SILICON ISOTOPES
NT TELLURIUM
Electronic and atomic structure of semiconductors and of high-temperature superconductors
[AD-A266805] 03 p1205 N94-14913
List of papers published by the members of Institute for Materials Research, Tohoku University 1992
[JTN-94-80606] 07 p3118 N94-27355
METALLORGANIC COMPOUNDS
U ORGANOMETALLIC COMPOUNDS
METALLURGY
Fabrication of advanced design (grooved) cermet anodes
[DE93-014590] 03 p1012 N94-16765
The use of backscattered electron imaging mode to assess the effect of fine dispersions on development of superplastic microstructure in Al-Mg alloys
[AD-A272426] 05 p1691 N94-21258
Irradiation damage behavior of low alloy steel wrought and weld materials
[DE94-000519] 06 p2239 N94-22999
New extensions in the development of deformation processed metal-metal matrix composites
[DE93-000692] 06 p2227 N94-23004
COMPETENCE 2000: Study on training requirements of the Norwegian metallurgical industry
[PB94-124609] 07 p2741 N94-27328
Metafusion: A breakthrough in metallurgy 08 p3211 N94-30446
A dynamic model of the vacuum furnace for separating Pb from Sn-Pb alloy 10 p4026 N94-34346
METALORGANIC CHEMICAL VAPOR DEPOSITION
High temperature annealing of minority carrier traps in irradiated MOCVD n(+)p InP solar cell junctions 01 p0048 N94-11382
Investigation of ZnSe-coated silicon substrates for GaAs solar cells 01 p0052 N94-11405
Heteroepitaxial InP, and ultrathin, directly glassed, GaAs 3-5 solar cells 01 p0052 N94-11406
Remote plasma enhanced chemical vapor deposition of GaP with in situ generation of phosphine precursors 01 p0399 N94-11440
Organometallic chemical vapor deposition and characterization of ZnGeP2/GaP multiple heterostructures on GaP substrates 01 p0400 N94-11442
Organometallic chemical vapor deposition and characterization of ZnGe(1-x)Si(x)P2-Ge alloys on GaP substrates 01 p0400 N94-11443
Low temperature metal-organic chemical vapor deposition growth processes for high efficiency solar cells
[DE92-010562] 02 p0702 N94-13386
Fabrication of AlGaAs/GaAs-light-emitting devices by selective MOCVD using dialkylmetalchloride 02 p0627 N94-13433
Characterization of InTlSb grown by low pressure metalorganic chemical vapor deposition on GaAs substrate
[AD-A266878] 03 p1206 N94-14922
Ion doped quantum well lasers
[AD-A267198] 03 p1038 N94-15853
The growth of InAs(1-x)Sb(x)/InAs strained-layer superlattices by metal-organic chemical vapor deposition
[DE93-015028] 03 p1208 N94-16012
Rare earth doped III-V semiconductors for optoelectronics
[AD-A268279] 03 p1216 N94-17577
Growth of structures for integrated optoelectronic devices
[AD-A269014] 04 p1598 N94-18527
Single source precursors for the OMCVD of 3/5 compound semiconductors
[AD-A271147] 04 p1606 N94-19739
MOCVD-grown InGaAsP heterostructure diode lasers
[AD-A270848] 04 p1606 N94-19769
Development of high-efficiency CdTe solar cells
[DE93-018206] 05 p1845 N94-19925
Common Themes and Mechanisms of Epitaxial Growth, volume 312 --- Materials Research Society symposium proceedings
[AD-A270513] 05 p2013 N94-19967
Alumoxanes: Rationalization of black box materials
[AD-A272805] 05 p1704 N94-21170
The n-p(p(+))-n Al(yGa)(1-y) As-GaAs-In(x)Ga(1-x) as quantum well laser with p(+)-n(+)GaAs-InGaAs tunnel contact on n GaAs
[AD-A271292] 05 p2030 N94-21805
MOCVD growth and structure of PbTiO3 thin films
[DE93-040230] 05 p2033 N94-21994
Ordering and phase separation in MOCVD InGaP alloys and unicompositional quantum wells
[DE94-004693] 07 p3056 N94-26352
Mechanistic studies of opto-electronic materials and syntheses using multiple laser and surface diagnostics
[AD-A274528] 07 p3036 N94-26834
Nitride semiconductors for ultraviolet detection
[AD-A274246] 07 p3060 N94-26840
High-efficiency, thin-film solar cells
[DE94-000250] 07 p2860 N94-27625
Electro-optic materials by solid source MOCVD
[DE94-005120] 07 p2757 N94-27716
MOCVD growth of GaN, AlN and AlGaN for UV photodetector applications
[AD-A275078] 08 p3512 N94-28871
InTlSb for long-wavelength infrared photodetectors and arrays
[AD-A275079] 08 p3512 N94-28872
GaAs/GaN strained layer superlattice materials for high temperature transistors, phase 1
[AD-A276115] 09 p3897 N94-31528
Novel growth technologies for in situ formation of semiconductor quantum wire structures
[AD-A277188] 09 p3902 N94-32255
Comprehensive investigation of HgCdTe metalorganic chemical vapor deposition
[NASA-CR-195933] 10 p4030 N94-34278
The optimization of interfaces in InAsSb/InGaAs strained-layer superlattices grown by metal-organic chemical vapor deposition
[DE94-010070] 11 p4340 N94-35698
Development of novel II-VI solar cells
[PB94-159415] 11 p4282 N94-35739
High temperature heterojunction bipolar transistors
[AD-A278605] 11 p4261 N94-36360
InTlSb for long-wavelength infrared photodetectors and arrays
[AD-A280207] 12 p4524 N94-37149
Substrate effects on the structure and optical properties of epitaxial PbTiO3 thin films prepared by metal-organic chemical vapor deposition
[DE94-010432] 12 p4535 N94-37192
Investigation of polycrystalline thin-film CuInSe2 solar cells based on ZnSe windows
[DE94-006936] 12 p4462 N94-37381
METALS
NT ACTINIDE SERIES
NT ALKALI METALS
NT ALKALINE EARTH METALS
NT ALUMINUM
NT ALUMINUM ISOTOPES
NT ALUMINUM 26
NT ALUMINUM 27
NT AMERICIUM
NT BARIUM
NT BERYLLIUM
NT BERYLLIUM ISOTOPES
NT BERYLLIUM 10
NT BISMUTH
NT CADMIUM
NT CALCIUM
NT CALCIUM ISOTOPES
NT CALIFORNIUM
NT CALIFORNIUM ISOTOPES
NT CERIUM
NT CESIUM
NT CESIUM ISOTOPES
NT CESIUM VAPOR
NT CESIUM 137
NT CHROMIUM
NT COBALT
NT COBALT ISOTOPES
NT COBALT 60
NT COPPER
NT CURIUM
NT DYSPROSIUM
NT ERBIUM
NT EUROPIUM
NT FERROUS METALS
NT GADOLINIUM
NT GALLIUM
NT GALLIUM ISOTOPES
NT GOLD
NT GOLD ISOTOPES
NT HAFNIUM ISOTOPES
NT HOLMIUM
NT INDIUM
NT INDIUM ISOTOPES
NT IRIDIUM
NT IRON
NT IRON ISOTOPES
NT IRON 57
NT LANTHANUM
NT LANTHANUM ISOTOPES
NT LEAD (METAL)
NT LEAD ISOTOPES
NT LIQUID LITHIUM
NT LIQUID METALS
NT LIQUID SODIUM
NT LITHIUM
NT LITHIUM ISOTOPES
NT MAGNESIUM
NT MAGNESIUM ISOTOPES
NT MANGANESE
NT MANGANESE ISOTOPES
NT MERCURY (METAL)
NT MERCURY ISOTOPES
NT METAL VAPORS
NT MOLYBDENUM
NT NEODYMIUM
NT NEODYMIUM ISOTOPES
NT NEPTUNIUM
NT NICKEL
NT NICKEL ISOTOPES
NT NIOBIUM
NT NOBLE METALS
NT OSMIUM
NT OSMIUM ISOTOPES
NT PALLADIUM
NT PLATINUM
NT PLUTONIUM
NT PLUTONIUM 238
NT POTASSIUM
NT POTASSIUM ISOTOPES
NT POTASSIUM 40
NT PRASEODYMIUM
NT RADIUM ISOTOPES
NT RARE EARTH ELEMENTS
NT REFRACTORY METALS
NT RHENIUM
NT RHENIUM ISOTOPES
NT RHODIUM
NT RUBIDIUM
NT RUTHENIUM
NT SAMARIUM
NT SAMARIUM ISOTOPES
NT SCANDIUM
NT SILVER
NT SODIUM
NT SODIUM ISOTOPES
NT SODIUM VAPOR
NT STRONTIUM
NT STRONTIUM ISOTOPES
NT TANTALUM
NT TERBIUM
NT THALLIUM
NT THORIUM
NT THORIUM ISOTOPES
NT THULIUM
NT THULIUM ISOTOPES
NT TIN
NT TITANIUM
NT TRANSITION METALS
NT TRANSURANIUM ELEMENTS
NT TUNGSTEN
NT URANIUM
NT URANIUM ISOTOPES
NT URANIUM 238
NT VANADIUM
NT YTTERBIUM
NT YTTRIUM
NT ZINC
NT ZIRCONIUM
NT ZIRCONIUM ISOTOPES
Structure of s - p bonded metal clusters with 8, 20 and 40 valence electrons
[DE93-613643] 01 p0361 N94-10503
Monte Carlo simulations of phase transformations in Fe-Cr alloys
[DE93-013847] 01 p0081 N94-10522
A method of influence regions in the theory of vacancy swelling of metals
[DE93-620579] 01 p0083 N94-11363
Structure stability and spectroscopy of metal clusters
[DE93-016142] 02 p0567 N94-12836
A benchmark bending test of a thick specimen. Part 2: Surface displacement measurements
[ARL-RR-6-PT-2] 02 p0670 N94-12928
Metal-semiconductor, composite radiation detectors
[DE93-013313] 02 p0619 N94-12994
Boundary stability under nonequilibrium conditions
[DE93-016259] 02 p0809 N94-13980
Machining and grinding: High rate deformation in practice
[DE93-010718] 02 p0664 N94-14457

The effect of crystal tilt on high resolution micrographs of small metal particles
[DE93-013915] 02 p0574 N94-14795

Vacancy condensation as the precursor to passivity breakdown
[DE93-012925] 03 p0956 N94-15998

Evolution of microstructure in face centered cubic metals during irradiation: A review
[DE93-015682] 03 p0958 N94-16662

Studies of changes in the energy stored in metals as a result of subjecting them to a surface type technological process
[IFTR-25/1991] 03 p0960 N94-17063

Metals 2000
[DE93-016761] 04 p1355 N94-17752

Lightweight materials for transportation: Program plan
[DE93-017381] 04 p1340 N94-18087

A review of the stages of work hardening
[DE93-016456] 04 p1359 N94-18114

Modified aequorin shows increased bioluminescence activity
[AD-A268774] 04 p1347 N94-18185

A comparison of wet and dry scrubbing systems for control of metals and dioxin/furan emissions from incinerators
[DE93-017446] 04 p1474 N94-18502

Self-organized criticality and the Barkhausen effect in amorphous and polycrystalline metals
[AD-A269817] 04 p1361 N94-18735

Diamond brazed to a metal
[AD-D015877] 04 p1371 N94-18746

High dose effects in neutron irradiated face-centered cubic metals
[DE93-017671] 04 p1364 N94-19043

An ab initio Monte Carlo study of low energy positron and electron implantation in elemental metals and multilayers
[DE93-019847] 04 p1603 N94-19541

General introduction to microstructural evolution under cascade damage conditions
[DE93-017443] 05 p2012 N94-19923

Lewis Cliff 87057: A new metal-rich E3 chondrite with similarities to Mt. Egerton, Shallowater and Happy Canyon 05 p2086 N94-20901

Utilization of metals to improve the lubrication of ceramic load-bearing devices
[PB93-202448] 05 p1825 N94-21424

Electron emission from nanometer-size metallic clusters: Electronic states and structural stability of supported Au clusters
[DE93-040184] 05 p1975 N94-21766

Theoretical studies of structural phase transitions in actinide metals
[DE94-000796] 05 p1696 N94-22388

Development of an analytical-numerical model to predict radiant emission or absorption
[NASA-CR-194860] 06 p2453 N94-23624

Variable amplitude fatigue, modelling and testing
[PB93-204469] 06 p2378 N94-24742

A thermodynamic approach to obtain materials properties for engineering applications 06 p2248 N94-25131

Three-dimensional, inelastic response of single-edge notch bend specimens subjected to impact loading
[AD-A273302] 06 p2378 N94-25143

Knowledge base systems for chemical compounds designing support 07 p2723 N94-25550

Study on analyzing method establishment for metallic material development 07 p2729 N94-25578

Study on elucidation of damage generation process by electron beam lithography 07 p2729 N94-25581

The effectiveness of AMT investment in UK metal component manufacture
[IND-MANU-SCI-TECH-REPT-3] 07 p2762 N94-25775

Debye-Waller factors of the light actinide metals
[DE94-000685] 07 p2733 N94-26069

Power laws, flicker noise, and the barkhausen effect
[AD-A274702] 07 p3008 N94-26376

Template synthesis of metal microtubule ensembles utilizing chemical, electrochemical, and vacuum deposition techniques
[AD-A274676] 07 p2715 N94-26444

A new materials data compilation can help in actinide phase-diagram research
[DE94-000797] 07 p3058 N94-26514

Mechanical properties of nanophase materials
[DE94-004625] 07 p2751 N94-26594

Technical report of ISSP. Ser. A, no. 2679: Novel electronic states of partially deuterated (DMe-DCNQI)2Cu
[JTN-94-80565] 07 p3064 N94-27175

Resonant holographic measurements of laser ablation plume expansion in vacuum and argon gas backgrounds
[DE94-001407] 07 p2813 N94-27615

Image potential of a tunnelling electron moving near two different metals
[DE94-603657] 07 p3069 N94-27819

Speciation in Water and Soil: A literature review
[PB94-132388] 08 p3341 N94-28412

Dislocation theory of melting for iron, revisited
[DE94-002715] 08 p3355 N94-28538

Study of activation data of metal samples from LDEF-1 and Spacelab-2
[NASA-CR-193973] 08 p3205 N94-29736

Microactuator production via high aspect ratio, high edge acuity metal fabrication technology 08 p3235 N94-29770

Mechanisms and effects of heat generation at the tips of dynamic cracks and notches in metals 08 p3321 N94-29808

Novel mass spectrometric instrument for gaseous and particulate characterization and monitoring
[DE94-005896] 08 p3349 N94-30047

A new material for removing heavy metals from water 08 p3354 N94-30471

A comparison of the evolution of cold and hot deformation microstructures and textures in fcc metals
[DE94-005103] 08 p3210 N94-30777

Metal induced embrittlement
[DE94-007450] 09 p3640 N94-31325

Control and monitoring of heavy metal emissions
[VTT-TIED-1508] 09 p3765 N94-31657

New molecular-based routes to binary main group metal sulfides
[AD-A277005] 09 p3900 N94-32003

The new Metals and Alloys Indexes, search manual: A phase diagram research tool
[DE94-005371] 09 p3643 N94-32098

Experimental measurement of dynamic failure and fragmentation properties of metals
[DE94-007377] 09 p3737 N94-32135

Characterization of nanoparticles and nanophase materials
[DE94-008348] 09 p3907 N94-32990

Ceramic and metal composite circuit-board-level technology for application specific electronic modules (ASEM)
[AD-A277961] 09 p3630 N94-33180

A model of the atmospheric metal deposition by cosmic dust particles
[AD-A278561] 10 p4163 N94-33786

Calculation of phase stability in Zr-Nb-Ru using LMTO and the cluster variation method
[AD-A278556] 10 p4137 N94-33896

Method for producing closed cell spherical porosity in spray formed metals
[AD-D016126] 10 p4025 N94-34152

Intelligent processing of materials, technical activities, 1993 (NAS-NRC Assessment Panel, April 21-22 1994)
[PB94-164183] 11 p4251 N94-35737

Modeling the atmospheric input of nutrients, heavy metals, and pesticides to the Great Lakes
[DE94-005481] 11 p4286 N94-36007

The relationship between hydroxyl groups on oxide surfaces and the properties of supported metals
[DE94-010786] 11 p4241 N94-36233

Ion modulated electroactivity in thin film metallopolymers
[AD-A278618] 11 p4246 N94-36253

Data compatibility for various Charpy-tests
[DE94-617534] 12 p4416 N94-37074

Atomic and electronic structure of metals and alloys: Rare earths, ultrathin films and surface alloys
[DE94-011581] 12 p4516 N94-37113

Defect initiation/growth and energy dissipation induced by deformation and fracture
[AD-A280411] 12 p4424 N94-37184

Theory of metal insulator transition in strongly correlated electron systems
[DE94-013135] 12 p4438 N94-37295

Positron implantation in solids
[DE94-013029] 12 p4537 N94-37499

METAMORPHIC ROCKS

NT QUARTZITE

The role of carbon and temperature in determining electrical conductivity of basins, crust and mantle
[DE93-015936] 03 p1101 N94-16840

METAMORPHISM (GEOLOGY)

Shock transformations in quartzite 01 p0097 N94-12040

Mineralogy of chondritic interplanetary dust particle impact residues from LDEF 01 p0080 N94-12045

Petrography and preliminary interpretations of the crystalline breccias from the Manson M-1 core 01 p0281 N94-12056

Metallographic cooling rates of L-group ordinary chondrites 01 p0429 N94-12061

Chondrite thermal histories from Low-CA pyroxene microstructures: Autometamorphism versus prograde metamorphism revisited 01 p0429 N94-12105

Anomalous REE patterns in unequilibrated enstatite chondrites: Evidence and implications 01 p0431 N94-12191

The granulite suite: Impact melts and metamorphic breccias of the early lunar crust 01 p0282 N94-12197

Trace element distributions in primitive achondrites 01 p0431 N94-12200

Isotopic and trace element characteristics of an unusual refractory inclusion from Essebi 01 p0471 N94-12212

The Karakul depression in Pamirs: The first impact structure in Central Asia 03 p1241 N94-16212

Pyroxene equilibration temperatures in metamorphosed ordinary chondrites 03 p1242 N94-16224

Comparison of reflectance spectra of C asteroids and unique C chondrites Y86720, Y82162, and B7904 03 p1242 N94-16246

The group A3 chondrules of Krymka: Further evidence for major evaporative loss during the formation of chondrules 03 p1242 N94-16257

Different radiation and metamorphic history of the Kainsaz CO 3.2 chondrules 03 p1243 N94-16296

Heterogeneous plagioclase compositions in the Maralinga CK4 chondrite 03 p1243 N94-16308

A hydrogen isotope study of CO3 type carbonaceous chondrites; comparison with type 3 ordinary chondrites 03 p1246 N94-16425

Fragments of ancient lunar crust: Ferroan noritic anorthosites from the descartes region of the Moon 05 p2096 N94-20660

Orthopyroxenes as recorders of diogenite petrogenesis: Major and minor element systematics 05 p1684 N94-20670

Lamellar olivine in the Divnoe achondrite: Evidence for high-pressure exsolution? 05 p1685 N94-20679

Chaunskij: The most highly metamorphosed, shock-modified and metal-rich mesosiderite 05 p2082 N94-20681

Post-igneous redistribution of components in eucrites 05 p1685 N94-20684

Micrometeorite dynamic pyrometamorphism: Nonstoichiometric clinoenstatite (CLEN) 05 p2083 N94-20715

Euhedral metallic-Fe-Ni grains in extraterrestrial samples 05 p1697 N94-20724

Post-metamorphic brecciation in type 3 ordinary chondrites 05 p2083 N94-20749

Petrography of shock features in the 1953 Manson 2-A drill core 05 p1862 N94-20767

FE-60 and the evolution of eucrites 05 p2083 N94-20768

Fine resolution chronology based on initial Sr-87/Sr-86
[CONTRIB-5230(794)] 05 p1686 N94-20794

Original size of the Vredefort structure, South Africa 05 p1863 N94-20825

Shock attenuation at the Slate Islands revisited 05 p1863 N94-20887

Chemical composition of new Acapulcoites and Lodranites 05 p2086 N94-20905

A geochemical study of acapulcoite and lodranite meteorites 06 p2605 N94-25358

Geochemical and fluid dynamic investigations into the nature of chemical variability in the Earth's mantle 08 p3367 N94-30917

FeO and MgO in plagioclase of lunar anorthosites: Igneous or metamorphic? 11 p4351 N94-35449

More shock recovery experiments on mesosiderite analogs 11 p4351 N94-35455

Shocked materials from the Dutch Peak diamictite, Utah 11 p4352 N94-36140

Calorimetric thermobarometry of experimentally shocked quartz 11 p4240 N94-36174

METASTABILITY

U METASTABLE STATE

METASTABLE ATOMS

Measurement of metastable population distribution in gadolinium atomic beam by laser resonance photoionization method
[DE94-701194] 07 p3029 N94-27820

First observation of laser-induced resonant annihilation in metastable antiprotonic helium atoms
[DE94-748668] 12 p4519 N94-37417

METASTABLE STATE

Photodetachment studies on few-electron atomic negative ions
[DE93-008474] 01 p0358 N94-10154

Application of spin-sensitive electron spectroscopies to investigations of electronic and magnetic properties of solid surfaces and epitaxial systems
[DE93-015079] 01 p0076 N94-10854

Non-barrier tunneling in presence of dissipations
[DE93-621381] 01 p0412 N94-11086

Polymeric nitrogen
[DE93-012600] 01 p0089 N94-11151

Metastable enhancement of C(+) and O(+) capture reactions
[DE93-015075] 02 p0807 N94-13373
Metastability of yttrium-oxides
[DE93-016548] 02 p0813 N94-14440
Astronomy and astrophysics 03 p1239 N94-15970
Metastable phases in mechanically alloyed aluminum germanium powders
[DE93-008727] 03 p0958 N94-16463
The processing and mechanical properties of high temperature/high performance composites. Book 5: Processing and miscellaneous properties
[AD-A266398] 03 p0935 N94-16529
Pulsed laser deposition of metastable Ca(1-x)Sr(x)CuO2 thin films
[DE93-015804] 03 p1040 N94-16663
Kinetics of silica-phase transitions
[DE93-016231] 03 p1217 N94-17659
The microstructural mechanism of electromigration failure in narrow interconnects of Al alloys
[DE93-018598] 04 p1365 N94-19282
A microscopic theory of quantum optics and new photon-locked bistable states
[AD-A271250] 05 p1983 N94-19901
Metastable bcc phase formation in the Nb-Cr system
[DE93-018376] 05 p2012 N94-19926
Microscopic origins of metastable effects in a-Si:H and deep defect characterization in a-Si,Ge:H alloys
[DE93-018205] 05 p1688 N94-19985
Phonons and metastability in compressed nitrogen
[DE93-019913] 05 p2016 N94-20318
Theoretical investigations of metastability and energy storage in molecular systems
[AD-A271849] 05 p1973 N94-20612
The stability of oxyamphiboles: Existence of Ferric-bearing minerals under the reducing conditions on the surface of Venus 05 p2122 N94-20800
Reliable interface design for combining asynchronous and synchronous circuits 05 p1758 N94-21119
Electronically metastable molecules of high symmetry
[AD-A272015] 05 p1974 N94-21461
Polymeric nitrogen
[DE93-040544] 05 p1706 N94-21512
Generalized melting criterion for beam-induced amorphization
[DE94-001333] 06 p2560 N94-23189
Electrochemical behavior of ion-plated TiN and Cu-Cr coatings
[AD-A273411] 06 p2235 N94-24784
Excitation mechanisms for XUV and x ray lasers
[DE93-617006] 06 p2351 N94-25482
Collaborative research on ion implantation of ceramics
[DE93-019177] 07 p2749 N94-26080
Recombination and metastability in amorphous silicon and silicon germanium alloys
[DE94-000237] 07 p2736 N94-26481
Dynamics of metastable states in supersonic beams
[ITN-94-85232] 07 p3028 N94-27760
Measurement of metastable population distribution in gadolinium atomic beam by laser resonance photoionization method
[DE94-701194] 07 p3029 N94-27820
Directional solidification studies in Ni-Al alloys
[DE94-005562] 08 p3201 N94-28527
Laboratory studies of chemical and photochemical processes relevant to stratospheric ozone
[NASA-CR-189351] 08 p3347 N94-29549
Production and detection of metastable atomic oxygen
[ISBN-0-315-87364-7] 09 p3868 N94-31915
NN-interaction in (1)S0-state: Virtual level or dibaryon resonance?
[DE94-606492] 09 p3869 N94-32097
Amorphous/crystalline structure and phase transformations in metastable semiconducting Ge(1-x)Sn(x)
[DE94-006659] 09 p3901 N94-32115
Stability and precipitation kinetics in Si(1-y)C(y)/Si and Si(1-x-y)Ge(x)C(y)/Si heterostructures prepared by solid phase epitaxy
[DE94-006589] 09 p3902 N94-32296
Structural studies of photoinduced intramolecular electron transfer in cyclopentadienylnickelnitrosyl
[DE94-008467] 09 p3874 N94-32876
Theoretical study of novel bonding in molecules: Metastable molecular fuels
[AD-A277807] 10 p4031 N94-33895
On the origin of porphyritic chondrules
[DE94-010464] 11 p4351 N94-36418

METATHESIS
Strained ring energetic binders
[AD-A269056] 04 p1377 N94-18491
Rotational isomers of Mo(VI) alkylidene complexes and Cis/trans polymer structure: Investigations in ring-opening metathesis polymerization
[AD-A272647] 05 p1704 N94-21184
Photochemical approaches to conversion of light to electricity or fuel
[DE94-001650] 05 p1849 N94-22048

METAZOA
U ANIMALS

METEOR BURSTS
U METEOROID SHOWERS

METEOR CRATERS
U CRATERS

METEOR TRAILS
Meteor burst communications improvement study
[AD-A270866] 04 p1393 N94-19793
Meteor Burst Communications (MBC) throughput improvement tests
[AD-A273941] 07 p2767 N94-25990
Performance statistics bulletin. High latitude meteor scatter propagation October, November, December 1990, January 1991
[AD-A276693] 09 p3676 N94-31998
Performance statistics bulletin. High latitude meteor scatter propagation, February, March, April, May 1992
[AD-A276667] 09 p3677 N94-32083
Performance statistics bulletin. High latitude meteor scatter propagation February, March, April, May 1991
[AD-A276723] 09 p3678 N94-32158
Performance statistics bulletin. High latitude meteor scatter propagation October, November, December 1991, January 1992
[AD-A276724] 09 p3678 N94-32159
Performance statistics bulletin. High latitude meteor scatter propagation, November and December 1989, and January 1990
[AD-A276688] 09 p3680 N94-32297
Performance statistics bulletin. High latitude meteor scatter propagation
[AD-A276694] 09 p3680 N94-32298
Performance statistics bulletin. High latitude meteor scatter propagation
[AD-A276695] 09 p3680 N94-32299
Performance statistics bulletin. High latitude meteor scatter propagation
[AD-A276696] 09 p3680 N94-32300
Performance statistics bulletin. High latitude meteor scatter propagation, June, July, August, September 1992
[AD-A277508] 09 p3685 N94-33347
Antarctic meteor scatter test, December 1992
[AD-A277894] 10 p4033 N94-33547

METEORITE COLLISIONS
Explicit 3D continuum fracture modeling with smooth particle hydrodynamics 01 p0429 N94-12062
Collisions of small Spacewatch asteroids with the Earth 01 p0430 N94-12157
Macroscopic electric charge separation during hypervelocity impacts: Potential implications for planetary paleomagnetism 01 p0431 N94-12181
Modelling of dispersal and deposition of impact glass spherules from the Cretaceous-Tertiary boundary deposit 01 p0432 N94-12238
Osmium isotopes in Ivory Coast tektites: Confirmation of a meteoritic component and rhenium depletion 03 p1244 N94-16321
Geochemical evidences for two chondritic-like cometary or asteroidal impacts before and at the K/T boundary 03 p1244 N94-16359
Possible sources of H2 to H2O enrichment at evaporation of parent chondritic material 03 p1244 N94-16377
CO2 production by impact in carbonates? An ATEM and stable isotope (C,O) study 03 p0954 N94-16383
Remote visual detection of impacts on the lunar surface 03 p1290 N94-16404
Search for lunar water ice in cometary impact craters
[AD-A270130] 04 p1627 N94-18877
Impact glasses from the ultrafine fraction of lunar soils 05 p2097 N94-20662
Global blackout following the K/T Chicxulub impact: Results of impact and atmospheric modeling 05 p1854 N94-20698
Impact disturbance of the Venus atmosphere 05 p2106 N94-20709
Euhedral metallic-Fe-Ni grains in extraterrestrial samples 05 p1697 N94-20724
Chicxulub impact basin: Gravity characteristics and implications for basin morphology and deep structure 05 p1862 N94-20757
Chronology of lunar granite 12033,576: Resetting of Rb-Sr and K-Ca isochrons 05 p2115 N94-20763
Multivariate statistical analysis: Principles and applications to coorbital streams of meteorite falls 05 p1964 N94-20881
LREE variability in CM matrices: Another look at meteorite compaction ages 05 p2086 N94-20884
Geometrical analysis of the microcraters found on LDEF samples 05 p1666 N94-20890
Impacts, extinctions, volcanism, glaciations, and tectonics: Matches and mismatches 07 p2888 N94-28298
Science observed: The mass-extinction debates 07 p2888 N94-28300
Consequences of impacts of small asteroids and comets with Earth 07 p2889 N94-28301
An extraterrestrial event at the tertiary-quaternary boundary 07 p2890 N94-28309
JPRS report: Science and technology. Central Eurasia: Space
[JPRS-USP-94-001] 11 p4201 N94-35518
Shocked materials from the Dutch Peak diamictite, Utah 11 p4352 N94-36140
Hematite formed from pyroxene on Mars by meteoritic impact 11 p4372 N94-36165

METEORITE COMPRESSION TESTS
U COMPRESSION TESTS
U MECHANICAL PROPERTIES
U METEORITES

METEORITE CRATERS
Morphology of large impact craters and basins on Venus: Implications for ring formation 01 p0436 N94-12023
Descriptions and preliminary interpretations of cores recovered from the Manson Impact Structure (Iowa) 01 p0281 N94-12032
Increased depth-diameter ratios in the Medusae Fossae Formation deposits of Mars 01 p0439 N94-12043
Behavior of vortices generated by an advancing ejecta curtain in theory, in the laboratory, and on Mars 01 p0169 N94-12044
Strontium and oxygen isotope study of M-1, M-3 and M-4 drill core samples from the Manson impact structure, Iowa: Comparison with Haitian K-T impact glasses 01 p0281 N94-12080
Si-29 NMR spectroscopy of naturally-shocked quartz from Meteor Crater, Arizona: Correlation to Kieffer's classification scheme 01 p0080 N94-12087
Age of Popigai impact event using the Ar-40 - Ar-39 method 01 p0282 N94-12093
Shock induced reaction in Chicxulub target materials (CaSO4 and SiO2) and their relation to extinctions 01 p0282 N94-12149
Collisions of small Spacewatch asteroids with the Earth 01 p0430 N94-12157
Microtektite-like glass spherules in Late Devonian (367 MA) shales 01 p0461 N94-12160
KT boundary impact glasses from the Gulf of Mexico region 01 p0282 N94-12161
Post-impact alteration of the Manson impact structure 01 p0282 N94-12188
Model of optical scatter from microimpacts on the Hubble Telescope 01 p0384 N94-12189
Laboratory studies on the velocity of fragments from impact disruptions 01 p0189 N94-12359
Twenty-Fourth Lunar and Planetary Science Conference. Part 2: G-M
[NASA-CR-193174] 03 p1247 N94-16173
Martian crater degradation by eolian processes: Analogy with the Rio Cuarto Crater Field, Argentina 03 p1251 N94-16196
Collisional and dynamical history of Gaspra 03 p1241 N94-16202
The Acraman impact structure: Estimation of the diameter by the ejecta layer thickness 03 p1103 N94-16211
The Karakul depression in Pamirs: The first impact structure in Central Asia 03 p1241 N94-16212
Confirmation of saturation equilibrium conditions in crater populations 03 p1103 N94-16222
Corvid meteoroids and a Giordano Bruno ray are genetically related 03 p1242 N94-16223
Lunar impact basins: New data for the nearside northern high latitudes and eastern limb from the second Galileo flyby 03 p1258 N94-16228
Trace-element composition of Chicxulub crater melt rock, K/T tektites and Yucatan basement 03 p1242 N94-16245
The depths of the largest impact craters on Venus 03 p1264 N94-16261
Density of impact craters on tessera, Venus 03 p1264 N94-16263
A first-order model for impact crater degradation on Venus 03 p1265 N94-16268
A discontinuous melt sheet in the Manson impact structure 03 p1103 N94-16269
Al-26 production profile and model comparisons in Canyon Diablo 03 p1245 N94-16409
Siderophile element fractionation in meteor crater impact glasses and metallic spherules 03 p1246 N94-16414
Ejecta patterns of Meteor Crater, Arizona derived from the linear un-mixing of TIMS data and laboratory thermal emission spectra 03 p1065 N94-16607

Twenty-Fourth Lunar and Planetary Science Conference. Part 3: N-Z
[NASA-CR-193149] 05 p2092 N94-20636
Largest impact features on Venus: Non-preserved or non-recognizable? 05 p2096 N94-20657
Modelling the gravity and magnetic field anomalies of the Chicxulub crater 05 p1862 N94-20668
Structural evidence for reorientation of Miranda about a paleo-pole 05 p2098 N94-20671
U-Pb provenance ages of shocked zircons from the K-T boundary, Raton Basin, Colorado 05 p1685 N94-20701
The Manson impact crater: Estimation of the energy of formation, possible size of the impacting asteroid or comet, and ejecta volume and mass 05 p2083 N94-20721
Preliminary estimation of tagamite cooling conditions (Puchezh-Katunki Astrobleme, Russia) 05 p2083 N94-20735
Searching for ancient Venus 05 p2111 N94-20743
Chicxulub impact basin: Gravity characteristics and implications for basin morphology and deep structure 05 p1862 N94-20757
Research program on the Manson impact structure, Iowa 05 p1862 N94-20766
A tectonic resurfacing model for Venus 05 p2118 N94-20781
The missing impact craters on Venus 05 p2119 N94-20782
Delimitation of terrestrial impact craters by way of pseudotachylytic rock distribution 05 p1863 N94-20783
Two-polarity magnetization in the Manson impact breccia 05 p1863 N94-20789
The age of the Pretoria Saltpan impact crater, South Africa 05 p1863 N94-20798
Parabolic features and the erosion rate on Venus 05 p2122 N94-20801
Triton's cratering record and its time of capture 05 p2122 N94-20802
Multivariate statistical analysis: Principles and applications to coorbital streams of meteorite falls 05 p1964 N94-20881
Shock attenuation at the Slate Islands revisited 05 p1863 N94-20887
Geometrical analysis of the microcraters found on LDEF samples 05 p1666 N94-20890
Age and thermochronology of K-feldspars from the Manson Impact Structure 05 p1863 N94-20899
Some implications of large impact craters and basins on Venus for terrestrial ringed craters and planetary evolution 07 p2890 N94-28306
Keeping that youthful look --- impact cratering of Venus 09 p3941 N94-31112
Biospheric effects of a large extraterrestrial impact: Case study of the Cretaceous/Tertiary boundary crater
[NASA-CR-195827] 09 p3942 N94-32740
Constraints on the Martian cratering rate imposed by the SNC meteorites and Vallis Marineris layered deposits 09 p3945 N94-33197
Possible test of ancient dense Martian atmosphere 09 p3947 N94-33206
Mineralogical diversity (spectral reflectance and Moessbauer data) in compositionally similar impact melt rocks from Manicouagan Crater, Canada 09 p3948 N94-33219
Impact basins in Southern Daedalia, Mars: Evidence for clustered impactors? 11 p4360 N94-35426
Effects due to overlapping large impact basins on Mars 11 p4360 N94-35427
Distribution of siderophile and other trace elements in melt rock at the Chicxulub impact structure 11 p4352 N94-35456
Current activities and results of the Long Duration Exposure Facility Meteoroid and Debris Special Investigation Group 11 p4352 N94-35458
Morphology of meteoroid and space debris craters on LDEF metal targets 11 p4353 N94-36159

METEORITES

NT ACHONDRITES
NT ALLENDE METEORITE
NT AUSTRALITES
NT BONDOC METEORITE
NT BRUDERHEIM METEORITE
NT CARBONACEOUS CHONDRITES
NT CARBONACEOUS METEORITES
NT CHASSIGNITES
NT CHONDRITES
NT COLD BOKKEVELD METEORITE
NT IRON METEORITES
NT KAPOETA ACHONDRITE
NT MICROMETEORITES
NT MURCHISON METEORITE
NT MURRAY METEORITE
NT NAKHLITES
NT ORGUEIL METEORITE
NT SHERGOTTITES
NT STONY METEORITES
NT STONY-IRON METEORITES
NT TEKTITES
NT UREILITES
Meteorites from recent amor-type orbits 01 p0429 N94-12059
Natural thermoluminescence profiles in lunar cores and implications for meteorites 01 p0443 N94-12060
Arroyo el Mimbral, Mexico, K/T unit: Origin as debris flow/turbidite, not a tsunami deposit 01 p0281 N94-12084
Chondrule formation by clumpy accretion onto the solar nebula 01 p0448 N94-12089
Twenty-Fourth Lunar and Planetary Science Conference. Part 2: G-M
[NASA-CR-193174] 03 p1247 N94-16173
Cation ordering in orthopyroxenes and cooling rates of meteorites: Low temperature cooling rates of Estherville, Bondoc and Shaw 03 p1241 N94-16176
Petrography, mineralogy, and Mg isotope composition of VICTA: A vigarano CaAl4O7-bearing type A inclusion 03 p1103 N94-16203
The group A3 chondrules of Krymka: Further evidence for major evaporative loss during the formation of chondrules 03 p1242 N94-16257
I-Xe structure of ILAFEGH 009 and shallowater: Evidence for early formation and rapid cooling of impact-derived enstatite meteorites 03 p1243 N94-16305
Isotopic signatures and distribution of nitrogen and trapped and radiogenic xenon in the Acapulco and FRO90011 meteorites 03 p1243 N94-16317
Effects of bulk composition on production rates of cosmogenic nuclides in meteorites 03 p1245 N94-16385
Classificational parameters for acapulcoites and lodranites: The cases of FRO 90011, EET 84302 and ALH A81187/84190 03 p1245 N94-16389
The dregs of crystallization in Zagami 03 p1245 N94-16390
The Nakhla parent melt: REE partition coefficients and clues to major element composition 03 p1245 N94-16399
More on the cooling history of angrite LEW 86010 03 p1245 N94-16400
Limited subsolidus diffusion in type B1 CAI: Evidence from Ti distribution in spinel 03 p0954 N94-16401
Remote visual detection of impacts on the lunar surface 03 p1290 N94-16404
Identification of new meteorite, Mihonoseki (L), from broken fragments in Japan 03 p1246 N94-16415
The thickness of eucritic crust in the HED parent body 03 p1104 N94-16416
Twenty-Fourth Lunar and Planetary Science Conference. Part 3: N-Z
[NASA-CR-193149] 05 p2092 N94-20636
Determination of cosmic bodies size-velocity distribution by observation of current impacts on Mars 05 p2082 N94-20648
Euhedral metallic-Fe-Ni grains in extraterrestrial samples 05 p1697 N94-20724
Lunar basalt meteorite EET 87521: Petrology of the clast population 05 p2083 N94-20752
Molecular equilibria and condensation sequences in carbon rich gases 05 p2083 N94-20756
Fine resolution chronology based on initial Sr-87/Sr-86
[CONTRIB-5230(794)] 05 p1686 N94-20794
Ti-bearing oxide minerals in lunar meteorite Y793169 with the VLT affinity 05 p2084 N94-20812
Sparking young minds with Moon rocks and meteorites 05 p2039 N94-20819
The parent magma of the Nakhla (SNC) meteorite: Reconciliation of composition estimates from magmatic inclusions and element partitioning 05 p2085 N94-20836
On modelling nuclear reactions in meteorites 05 p2085 N94-20844
Aluminum-26 activities in meteorites 05 p1686 N94-20851
LREE variability in CM matrices: Another look at meteorite compaction ages 05 p2086 N94-20884
Consortium reports on lunar meteorites Yamato 793169 and Asuka 881757, a new type of mare basalt 05 p2086 N94-20893
Wet inside and out? Constraints on water in the Martian mantle and on outgassed water, based on melt inclusions in SNC meteorites 05 p2145 N94-21678
Antarctic Meteorite Location and Mapping Project (AMLAMP): Antarctic meteorite location map series explanatory text and user's guide to AMLAMP data
[NASA-CR-194841] 06 p2603 N94-24964
Constraints on the Martian cratering rate imposed by the SNC meteorites and Vallis Marineris layered deposits 09 p3945 N94-33197
Carbonates, surfates, phosphates, nitrates, and organic materials: Their association in a Martian meteorite 09 p3952 N94-33239
What initiated planetesimal formation? 11 p4351 N94-35422
Inhomogeneous distribution of materials in lodranites-acapulcoites and IAB irons and their common formation processes 11 p4364 N94-35463
Pigeonholing planetary meteorites: The lessons of misclassification of EET87521 and ALH84001 11 p4353 N94-36157
Synthetic and natural Nakhla pyroxenes: Parent melt composition and REE partition coefficients 11 p4353 N94-36161
On the origin of porphyritic chondrules
[DE94-010464] 11 p4351 N94-36418

METEORITIC COMPOSITION

Twenty-fourth Lunar and Planetary Science Conference. Part 1: A-F
[NASA-CR-193095] 01 p0435 N94-12015
Moessbauer spectroscopy of the SNC meteorite Zagami 01 p0428 N94-12016
Dispersion of the ratios of cosmogenic isotopes of noble gases in chondrites of different cosmic-ray exposure ages 01 p0428 N94-12020
Peculiarities of distributions of the cosmic-ray exposure ages of H chondrite falls and finds 01 p0428 N94-12021
Search for effects of a supernova explosion 30 to 40 thousand years ago in chondrites 01 p0428 N94-12022
Calorimetric thermometry of meteoritic troilite: A feasibility study 01 p0428 N94-12025
Interstellar graphite in Murchison: Continued search for isotopically distinct components 01 p0097 N94-12029
Fourier domain target transformation analysis in the thermal infrared 01 p0258 N94-12030
Carbon in weathered ordinary chondrites from Roosevelt County 01 p0428 N94-12035
Nitrogen and noble gases in a glass sample from LEW88516 01 p0080 N94-12051
The stability of hibonite and other aluminous phases in silicate melts: Implications for the origin of hibonite-bearing inclusions 01 p0080 N94-12052
The great 8 MA event and the structure of the H-chondrite parent body 01 p0429 N94-12058
Natural thermoluminescence profiles in lunar cores and implications for meteorites 01 p0443 N94-12060
Composition and modal frequencies of hypervelocity particles less than 1 millimeter in diameter in low-Earth orbit 01 p0429 N94-12063
The asteroid-meteorite connection: Forging a new link to Vesta as the parent body of basaltic achondrite (HED) meteorites 01 p0429 N94-12068
Alkali-granitoids as fragments within the ordinary chondrite Adzhi-Bogdo: Evidence for highly fractionated, alkali-granitic liquids on asteroids 01 p0429 N94-12069
Preliminary results of Mn partitioning experiments on Murchison analogues 01 p0281 N94-12081
Noble gases in LEW88516 shergottite: Evidence for exposure age pairing with ALH77005 01 p0080 N94-12082
Ar-39 - Ar-40 ages of acapulcoites and lodranites: Evidence for early parent body heating 01 p0281 N94-12083
Midplane temperatures in the solar nebula 01 p0448 N94-12088
Chondrule formation by clumpy accretion onto the solar nebula 01 p0448 N94-12089
Minor and trace element composition and age of Yukon probable-microtektites 01 p0429 N94-12094
Trace-element abundances in several new ureilites 01 p0080 N94-12096
Mineralogy versus bulk composition of the carbonaceous chondrite clast Kaidun 2 01 p0429 N94-12101
Carbonaceous chondrite clasts in the Kapoeta howardite 01 p0282 N94-12104
SXRF determination of trace elements in chondrule rims in the unequilibrated CO3 chondrite, ALH A77307 01 p0429 N94-12106
Determining the relative extent of alteration in CM chondrites 01 p0430 N94-12114
The EET87513 clast N: A CM2 fragment in an HED polymict breccia 01 p0453 N94-12117
Volatiles in fourteen interplanetary dust particles: A comparison with CI and CM chondrites 01 p0430 N94-12132
Distribution of vanadium and melting of opaque assemblages in Efremovka CAI's 01 p0282 N94-12141
Metal-rich meteorites from the aubrite parent body 01 p0430 N94-12142

Oxygen isotopes as tracers of tektite source rocks: An example from the Ivory Coast tektites and Lake Bosumtwi Crater 01 p0430 N94-12146
LEW88516 and SNC meteorites 01 p0430 N94-12150
The Th and U abundances in chondritic meteorites 01 p0430 N94-12151
Microtektite-like glass spherules in Late Devonian (367 MA) shales 01 p0461 N94-12160
KT boundary impact glasses from the Gulf of Mexico region 01 p0282 N94-12161
Simulation of possible regolith optical alteration effects on carbonaceous chondrite meteorites 01 p0430 N94-12163
Spectral mixing models of S-Type asteroids 01 p0431 N94-12164
Olivine-rich asteroids, pallasitic olivine and olivine-metal mixtures: Comparisons of reflectance spectra 01 p0431 N94-12171
Remanent magnetism of HED meteorites: Implications for their evolution and ancient magnetic fields 01 p0431 N94-12172
The experimental production of matrix lumps within chondrules: Evidence of post-formational processes 01 p0431 N94-12176
Flash melting of chondrule precursors in excess of 1600 C. Series 1: Type 2 (B1) chondrule composition experiments 01 p0431 N94-12177
Trace element distributions in primitive achondrites 01 p0431 N94-12200
Cathodoluminescence properties of components in enstatite chondrites 01 p0432 N94-12206
The Fe/Mn constraint on precursors of basaltic achondrites 01 p0432 N94-12208
Soret diffusion: A possible cause of compositional heterogeneity within tektites 01 p0432 N94-12211
Isotopic and trace element characteristics of an unusual refractory inclusion from Essebi 01 p0471 N94-12212
On high-temperature formation of iron-rich olivine in the early solar system 01 p0432 N94-12225
Recondensation of chondritic material in the early solar system: Results of thermodynamic simulation 01 p0432 N94-12226
Primordial lightning: Evidence preserved in chondrites 01 p0432 N94-12230
Micro-zoning in minerals of a Landes silicate inclusion 01 p0432 N94-12231
A new carbon-rich phase (COPS) in Antarctic micrometeorites 01 p0432 N94-12233
The Xe-Q in Iodranites and a hint for Xe-L. FRO90011 another Iodranite? 01 p0432 N94-12239
Projectile-target mixing in melted ejecta formed during a hypervelocity impact cratering event 01 p0432 N94-12241
The unusual metallic particles in Krymka LL3.0 chondrite 01 p0433 N94-12253
On possibility of diamond formations in radiation process 01 p0433 N94-12254
The carbon isotopic composition of Novo Urei diamonds 01 p0433 N94-12255
The fractionation of noble gases in diamonds of CV3 Efremovka chondrite 01 p0081 N94-12256
Cronstedtite and iron sulfide mineralogy of CM-type carbonaceous chondrites from cryogenic Moessbauer spectra 01 p0433 N94-12257
Primitive SNC parent magmas and crystallization: Low PH2O experiments 01 p0433 N94-12264
Twenty-Fourth Lunar and Planetary Science Conference. Part 2: G-M [NASA-CR-193174] 03 p1247 N94-16173
The Fe2(+)-Mg interdiffusion in orthopyroxene: Constraints from cation ordering and structural data and implications for cooling rates of meteorites 03 p1241 N94-16175
Cation ordering in orthopyroxenes and cooling rates of meteorites: Low temperature cooling rates of Estherville, Bondoc and Shaw 03 p1241 N94-16176
Extraction and isotopic analysis of medium molecular weight hydrocarbons from Murchison using supercritical carbon dioxide 03 p1241 N94-16184
Cretaceous-tertiary boundary spherules and Cenozoic microtektites: Similarities and differences 03 p1241 N94-16186
Stalking the LREE-enriched component in ureilites 03 p1241 N94-16190
Grosnaja ABCs: Magnesium isotope compositions 03 p1241 N94-16191
Euromet Ureilite Consortium: A preliminary report on carbon and nitrogen geochemistry 03 p1241 N94-16192
Nitrates in SNCs: Implications for the nitrogen cycle on Mars 03 p1251 N94-16193
Martian crater degradation by eolian processes: Analogy with the Rio Cuarto Crater Field, Argentina 03 p1251 N94-16196
Petrography, mineralogy, and Mg isotope composition of VICTA: A vigarano CaAl4O7-bearing type A inclusion 03 p1103 N94-16203
Petrologic constraints on the surface processes on asteroid 4 Vesta and on excavation depths of diogenite fragments 03 p1241 N94-16208
Systematic chemical variations in large 3AB iron meteorites: Clues to core crystallization 03 p1241 N94-16213
Nd-142/Nd-144 in bulk planetary reservoirs, the problem of incomplete mixing of interstellar components and significance of very high precision Nd-145/Nd-144 measurements 03 p1256 N94-16220
Comparison of reflectance spectra of C asteroids and unique C chondrites Y86720, Y82162, and B7904 03 p1242 N94-16246
Gas-grain energy transfer in solar nebula shock waves: Implications for the origin of chondrules 03 p1262 N94-16251
The group A3 chondrules of Krymka: Further evidence for major evaporative loss during the formation of chondrules 03 p1242 N94-16257
Potassium isotope cosmochemistry, volatile depletion and the origin of the Earth 03 p0953 N94-16259
First investigation of noble gases in the Dengli H3,8 chondrite 03 p0953 N94-16264
Shock-thermal history of Kapoeta howardite matter on data of thermoluminescence analysis of individual mineral grains 03 p0953 N94-16267
Os isotopes in SNC meteorites and their implications to the early evolution of Mars and Earth 03 p1242 N94-16272
Complex zoning behavior in pyroxene in FeO-rich chondrules in the Semarkona ordinary chondrite 03 p1243 N94-16284
Partial melting of ordinary chondrites: Lost City (H) and St. Severin (LL) 03 p1243 N94-16286
Experimental partitioning of Zr, Ti, and Nb between silicate liquid and a complex noble metal alloy and the partitioning of Ti between perovskite and platinum metal 03 p0962 N94-16287
Experimental segregation of iron-nickel metal, iron-sulfide, and olivine in a thermal gradient: Preliminary results 03 p1243 N94-16288
The Al Rais meteorite: A CR chondrite or close relative? 03 p1243 N94-16290
Chemical and isotopic compositions in acid residues from various meteorites 03 p1243 N94-16291
Martian carbon dioxide: Clues from isotopes in SNC meteorites 03 p1270 N94-16295
Different radiation and metamorphic history of the Kainsaz CO 3.2 chondrules 03 p1243 N94-16296
Complex radiation-thermal history of Kaidun meteorite on data of track study of silicate minerals 03 p1243 N94-16297
I-Xe structure of ILAFEGH 009 and shallowater: Evidence for early formation and rapid cooling of impact-derived enstatite meteorites 03 p1243 N94-16305
Heterogeneous plagioclase compositions in the Maralinga CK4 chondrite 03 p1243 N94-16308
An experimental study of trace element partitioning between perovskite, hibonite and melt: Equilibrium values 03 p0954 N94-16313
Isotopic signatures and distribution of nitrogen and trapped and radiogenic xenon in the Acapulco and FRO90011 meteorites 03 p1243 N94-16317
Osmium isotopes in Ivory Coast tektites: Confirmation of a meteoritic component and rhenium depletion 03 p1244 N94-16321
Terrestrial bitumen analogue of orgueil organic material demonstrates high sensitivity to usual HF-HCl treatment 03 p0930 N94-16325
Chromite-rich mafic silicate chondrules in ordinary chondrites: Formation by impact melting 03 p1244 N94-16330
The astrophysical interpretation of isotope anomalies in graphite and SiC grains of chondrites 03 p1244 N94-16343
On possible Mn-53 heterogeneity in the early solar system 03 p1244 N94-16344
On origin of the olivine inclusions from the Kainsaz CO carbonaceous chondrite 03 p1244 N94-16345
A search for noble-gas evidence for presolar oxide grains 03 p0954 N94-16353
INAA of CAIs from the Maralinga CK4 chondrite: Effects of parent body thermal metamorphism 03 p1244 N94-16355
Chondritic ratios of Fe/Cr/Ir in Kerguelen Plateau (Hole 738C) K/T carbonate-rich sediments support asteroid-cometary impact at K/T time 03 p1244 N94-16357
Noble gases in twenty Yamato H-chondrites: Comparison with Allan Hills chondrites and modern falls 03 p1244 N94-16361
Experimentally reproduced relict enstatite in porphyritic chondrules of enstatite chondrite composition 03 p1244 N94-16363
Possible sources of H2 to H2O enrichment at evaporation of parent chondritic material 03 p1244 N94-16377
Effects of bulk composition on production rates of cosmogenic nuclides in meteorites 03 p1245 N94-16385
Classificational parameters for acapulcoites and lodranites: The cases of FRO 90011, EET 84302 and ALH A81187/84190 03 p1245 N94-16389
The dregs of crystallization in Zagami 03 p1245 N94-16390
The Nakhla parent melt: REE partition coefficients and clues to major element composition 03 p1245 N94-16399
More on the cooling history of angrite LEW 86010 03 p1245 N94-16400
Limited subsolidus diffusion in type B1 CAI: Evidence from Ti distribution in spinel 03 p0954 N94-16401
Remote visual detection of impacts on the lunar surface 03 p1290 N94-16404
Al-26 production profile and model comparisons in Canyon Diablo 03 p1245 N94-16409
Exsolved kirschsteinite in angrite LEW86010 olivine 03 p1245 N94-16410
Refractory precursor components in an Allende ferromagnesian chondrule 03 p1245 N94-16412
Igneous fractionation and subsolidus equilibration of diogenite meteorites 03 p1245 N94-16413
Siderophile element fractionation in meteor crater impact glasses and metallic spherules 03 p1246 N94-16414
Identification of new meteorite, Mihonoseki (L), from broken fragments in Japan 03 p1246 N94-16415
The thickness of eucritic crust in the HED parent body 03 p1104 N94-16416
Zaoyang chondrite cooling history from pyroxene Fe(2+)-Mg intracrystalline ordering and exolutions 03 p1246 N94-16417
A hydrogen isotope study of CO3 type carbonaceous chondrites; comparison with type 3 ordinary chondrites 03 p1246 N94-16425
Solar noble gases revealed by closed system stepped etching of a metal separate from Fayetteville 03 p0954 N94-16432
Nitrogen and light noble gases in Parsa enstatite chondrite 03 p1246 N94-16435
Dynamical behavior of octahedrite from the Henbury meteorite [DE93-018834] 04 p1627 N94-19339
Twenty-Fourth Lunar and Planetary Science Conference. Part 3: N-Z [NASA-CR-193149] 05 p2092 N94-20636
REE and other trace lithophiles in MAC88177, LEW88280 and LEW88763 05 p2082 N94-20639
The Erevan howardite: Petrology of glassy clasts and mineral chemistry 05 p1684 N94-20640
Carbonaceous xenoliths from the Erevan howardite 05 p1684 N94-20642
Igneous rock from Severnyi Kolchim (H3) chondrite: Nebular origin 05 p2082 N94-20643
Core formation in the Moon: The mystery of the excess depletion of Mo, W and P 05 p2095 N94-20651
Exposure ages of carbonaceous chondrites, 1 05 p2082 N94-20658
Identification of an interstellar oxide grain from the Murchison meteorite by ion imaging 05 p2082 N94-20659
Fragments of ancient lunar crust: Ferroan noritic anorthosites from the descartes region of the Moon 05 p2096 N94-20660
Volatility in the lunar crust: Trace element analyses of lunar minerals by PIXE proton microprobe 05 p2097 N94-20661
Impact glasses from the ultrafine fraction of lunar soils 05 p2097 N94-20662
The Sm-(146,147)-Nd-(142,143) formation interval for the lunar mantle and implications for lunar evolution 05 p2097 N94-20663
Tambo Quemado: Extraordinary concentrations of REE and refractory trace elements caused by artificial heating 05 p1684 N94-20667
Modelling the gravity and magnetic field anomalies of the Chicxulub crater 05 p1862 N94-20668
Self diffusion of alkaline-Earth in Ca-Mg-aluminosilicate melts: Experimental improvements on the determination of the self-diffusion coefficients 05 p1684 N94-20669
Orthopyroxenes as recorders of diogenite petrogenesis: Major and minor element systematics 05 p1684 N94-20670
Abundance and composition of solar KR in the H3-H6 chondrite ACFER111 05 p1684 N94-20676

C/O atomic ratios in micrometer-size crushed grains from Antarctic micrometeorites and two carbonaceous meteorites 05 p2082 N94-20678
Lamellar olivine in the Divnoe achondrite: Evidence for high-pressure exsolution? 05 p1685 N94-20679
Opaque-rich lithology in the Divnoe achondrite: Petrology and origin 05 p2082 N94-20680
Chaunskij: The most highly metamorphosed, shock-modified and metal-rich mesosiderite 05 p2082 N94-20681
Post-igneous redistribution of components in eucrites 05 p1685 N94-20684
Elevated initial Sr-87/Sr-86 in ordinary chondrite metal 05 p1685 N94-20695
Elemental depletions in Antarctic micrometeorites and Arctic cosmic spherules: Comparison and relationships 05 p2082 N94-20704
Oxygen isotopic relationships between the LEW85332 carbonaceous chondrite and CR chondrites 05 p2083 N94-20708
SCR neon and argon in Kapoeta feldspar: Evidence for an active ancient Sun 05 p2106 N94-20712
Cosmogenic-radionuclide profiles in Knyahinya: New measurements and models 05 p2106 N94-20713
Euhedral metallic-Fe-Ni grains in extraterrestrial samples 05 p1697 N94-20724
Further analyses of Rio Cuarto impact glass 05 p1685 N94-20745
Post-metamorphic brecciation in type 3 ordinary chondrites 05 p2083 N94-20749
Cathodoluminescence observations of in situ aqueous destruction of chondrules in the Murchison CM chondrite 05 p2083 N94-20750
Lunar basalt meteorite EET 87521: Petrology of the clast population 05 p2083 N94-20752
Orthopyroxenes as recorders of diogenite petrogenesis: Trace element systematics 05 p1686 N94-20760
The chondrite Mihonoseki: New observed fall 05 p2083 N94-20764
FE-60 and the evolution of eucrites 05 p2083 N94-20768
Size distributions and aerodynamic equivalence of metal chondrules and silicate chondrules in Acfer 059 05 p2084 N94-20773
Fe/Mn in olivine of carbonaceous meteorites 05 p2084 N94-20788
The Sm-Nd systematics of silicate inclusions in iron meteorites: Results from Caddo (IAB) [CONTRIB-5241(804)] 05 p2084 N94-20795
Hydrothermal alteration experiments of olivine with varying Fe contents: An attempt to simulate aqueous alteration of the carbonaceous chondrites 05 p1686 N94-20810
Ti-bearing oxide minerals in lunar meteorite Y793169 with the VLT affinity 05 p2084 N94-20812
The U-Th-Pb, Sm-Nd, and Ar-Ar isotopic systematics of lunar meteorite Yamato-793169 05 p2084 N94-20834
The parent magma of the Nakhla (SNC) meteorite: Reconciliation of composition estimates from magmatic inclusions and element partitioning 05 p2085 N94-20836
Rare Earth elements in individual minerals in Shergottites 05 p1686 N94-20852
Rhenium-osmium isotope systematics of ordinary chondrites and iron meteorites 05 p2085 N94-20854
Consortium study of lunar meteorites Yamato-793169 and Asuka-881757: Geochemical evidence of mutual similarity, and dissimilarity versus other mare basalts 05 p2085 N94-20857
Equilibrium and fractional crystallization of a primitive Shergottite composition 05 p2085 N94-20861
The formation of FeO-rich pyroxene and enstatite in unequilibrated enstatite chondrites: A petrologic-trace element (SIMS) study 05 p2086 N94-20866
Weathering features and secondary minerals in Antarctic Shergottites ALHA77005 and LEW88516 05 p2086 N94-20869
LREE variability in CM matrices: Another look at meteorite compaction ages 05 p2086 N94-20884
The carbon components in SNC meteorites of feldspathic harzburgite composition 05 p2086 N94-20885
Further carbon isotope measurements of LEW 88516 05 p2086 N94-20886
Regolith breccia consisting of H and LL chondrite mixture 05 p2080 N94-20892
Consortium reports on lunar meteorites Yamato 793169 and Asuka 881757, a new type of mare basalt 05 p2086 N94-20893
Preliminary AEM study of the microstructure and composition of metal particles in ordinary chondrites 05 p2086 N94-20894
Trace element compositions of spinel-rich refractory inclusions from the Murchison meteorite 05 p2086 N94-20897
Inter- and intra-crystalline oxygen isotope distribution of fassaites in Allende CAI 05 p2086 N94-20898
Lewis Cliff 87057: A new metal-rich E3 chondrite with similarities to Mt. Egerton, Shallowater and Happy Canyon 05 p2086 N94-20901
Chemical zoning and diffusion of Ca, Al, Mn, and Cr in olivine of springwater pallasite 05 p2086 N94-20902
Chemical composition of new Acapulcoites and Lodranites 05 p2086 N94-20905
Diffuse reflectance spectra of orthopyroxene, olivine, and plagioclase as a function of composition and structure 05 p2087 N94-20906
Mineralogy of dark clasts in primitive versus differentiated meteorites 05 p2087 N94-20907
Wet inside and out? Constraints on water in the Martian mantle and on outgassed water, based on melt inclusions in SNC meteorites 05 p2145 N94-21678
Correlated petrographic, electron microprobe, and ion microprobe studies of selected primitive and processed phase assemblages in meteorites [NASA-CR-194827] 06 p2601 N94-23499
A geochemical study of acapulcoite and lodranite meteorites 06 p2605 N94-25358
Experimental study of lunar and SNC (Mars) magmas [NASA-CR-195274] 07 p3107 N94-27850
Extraterrestrial accretion and glacial cycles 07 p2890 N94-28308
An extraterrestrial event at the tertiary-quaternary boundary 07 p2890 N94-28309
The origin of neon-E: Neon-E in single interstellar silicon carbide and graphite grains 09 p3933 N94-31556
Organic analyses of the Murchison meteorite 09 p3938 N94-32489
SNC meteorites and their implications for reservoirs of Martian volatiles 09 p3947 N94-33209
The Twenty-Fifth Lunar and Planetary Science Conference. Part 1: A-G [NASA-CR-195743] 11 p4355 N94-35395
Calorimetric thermometry of meteoritic troilite: Preliminary thermometer relationships 11 p4355 N94-35399
Alteration and formation of rims on the CM parent body 11 p4357 N94-35411
On the possible role of elemental carbon in the formation of reduced chondrules 11 p4351 N94-35421
The occurrence of blue luminescing enstatite in E3 and E4 chondrites 11 p4351 N94-35423
Antarctic weathering of the CK chondrites EET90004, 90007, and 90022: Nickel and sulfur mobility 11 p4351 N94-35451
More shock recovery experiments on mesosiderite analogs 11 p4351 N94-35455
Distribution of siderophile and other trace elements in melt rock at the Chicxulub impact structure 11 p4352 N94-35456
The parent magma of xenoliths in shergottite EETA79001: Bulk and trace element composition inferred from magmatic inclusions 11 p4352 N94-35467
Chondrule magnetic properties 11 p4352 N94-35471
Mineralogy of an unusual CM clast in the Kaidun meteorite 11 p4352 N94-35476
The Twenty-Fifth Lunar and Planetary Science Conference. Part 2: H-O [NASA-CR-195744] 11 p4367 N94-36136
Textural constraints on the formation of alteration phases in CM chondrites 11 p4353 N94-36145
Partial melting of the St. Severin (LL) and Lost City (H) ordinary chondrites: One step backwards and two steps forward 11 p4353 N94-36146
Preliminary results of sulfide melt/silicate wetting experiments in a partially melted ordinary chondrite 11 p4353 N94-36147
Pigeonholing planetary meteorites: The lessons of misclassification of EET87521 and ALH84001 11 p4353 N94-36157
On the origin of enstatite chondrite chondrules based on their petrography and comparison with experimentally produced chondrules 11 p4353 N94-36158
Production of ferroan andesites by the experimental partial melting of an LL chondrite 11 p4353 N94-36160
Synthetic and natural Nakhla pyroxenes: Parent melt composition and REE partition coefficients 11 p4353 N94-36161
Cr, Mn, and Ca distributions for olivine in angritic systems: Constraints on the origins of Cr-rich and Ca-poor core olivine in angrite LEW87051 11 p4353 N94-36162
Partition coefficients for Al, Ca, Ti, Cr, and Ni in olivine obtained by melting experiment on an LL6 chondrite 11 p4353 N94-36163
Ferromagnetic resonance spectra of H2-reduced minerals and glasses 11 p4240 N94-36164
Shape, size, and distribution of magnetic particles in Bjurbole chondrules 11 p4353 N94-36167
Pre-bombardment crystallization ages of basaltic clasts from Antarctic howardites EET87503 and EET87513 11 p4354 N94-36172
On the origin of porphyritic chondrules [DE94-010464] 11 p4351 N94-36418
Light stable isotope analysis of meteorites by ion microprobe [NASA-CR-196096] 12 p4548 N94-37004

METEORITIC DAMAGE

Post-impact alteration of the Manson impact structure 01 p0282 N94-12188
Laboratory studies on the velocity of fragments from impact disruptions 01 p0189 N94-12359
Collisional and dynamical history of Gaspra 03 p1241 N94-16202
The depths of the largest impact craters on Venus 03 p1264 N94-16261
On magnetodynamic effects initiated by a high-speed impact of a large cosmic body upon the Earth's surface 05 p2082 N94-20647
Determination of cosmic bodies size-velocity distribution by observation of current impacts on Mars 05 p2082 N94-20648
Dynamics of large scale impacts on Venus and Earth 05 p2098 N94-20666
The missing impact craters on Venus 05 p2119 N94-20782
A fresh look at crater scaling laws for normal and oblique hypervelocity impacts 05 p1666 N94-20864
Large floor-fractured craters and isostatic crater modification: Implications for lithospheric thickness on Venus 05 p2135 N94-20873
Multivariate statistical analysis: Principles and applications to coorbital streams of meteorite falls 05 p1964 N94-20881
Geometrical analysis of the microcraters found on LDEF samples 05 p1666 N94-20890
Meteoroids and debris impact risk assessment on Columbus and Hermes using a realistic geometrical analysis tool 05 p1662 N94-21388
Combination of on ground experiments and analysis software for the evaluation of material degradation in space (SILEX project) 05 p1662 N94-21389
An attempt to comprehend Martian weathering conditions through the analysis of terrestrial palagonite samples 05 p2143 N94-21668
Consequences of impacts of small asteroids and comets with Earth 07 p2889 N94-28301
Were all extinction events caused by impacts? 07 p2891 N94-28311
Morphology correlation of craters formed by hypervelocity impacts 09 p3594 N94-31031
Biospheric effects of a large extraterrestrial impact: Case study of the Cretaceous/Tertiary boundary crater [NASA-CR-195827] 09 p3942 N94-32740
Impact basins in Southern Daedalia, Mars: Evidence for clustered impactors? 11 p4360 N94-35426
Effects due to overlapping large impact basins on Mars 11 p4360 N94-35427
Distribution of siderophile and other trace elements in melt rock at the Chicxulub impact structure 11 p4352 N94-35456
Current activities and results of the Long Duration Exposure Facility Meteoroid and Debris Special Investigation Group 11 p4352 N94-35458
Shocked materials from the Dutch Peak diamictite, Utah 11 p4352 N94-36140

METEORITIC DIAMONDS

On possibility of diamond formations in radiation process 01 p0433 N94-12254
The carbon isotopic composition of Novo Urei diamonds 01 p0433 N94-12255
The fractionation of noble gases in diamonds of CV3 Efremovka chondrite 01 p0081 N94-12256
Micrometeorite pre-solar diamonds from Greenland cryoconite? 05 p2086 N94-20895
A general theory of impacts and mass extinctions, and the consequences of large-body impact on the Earth 07 p2891 N94-28310

METEORITIC DUST

U MICROMETEOROIDS

METEORITIC IONIZATION

U ATMOSPHERIC IONIZATION
U METEOR TRAILS

METEORITIC MICROSTRUCTURES

Metallographic cooling rates of L-group ordinary chondrites 01 p0429 N94-12061
Microtektite-like glass spherules in Late Devonian (367 MA) shales 01 p0461 N94-12160
Experimentally reproduced relict enstatite in porphyritic chondrules of enstatite chondrite composition 03 p1244 N94-16363
Coagulation of grains in static and collapsing protostellar clouds 05 p2085 N94-20865

The formation of FeO-rich pyroxene and enstatite in unequilibrated enstatite chondrites: A petrologic-trace element (SIMS) study 05 p2086 N94-20866
Preliminary AEM study of the microstructure and composition of metal particles in ordinary chondrites 05 p2086 N94-20894
Micrometeorite pre-solar diamonds from Greenland cryoconite? 05 p2086 N94-20895
Diffuse reflectance spectra of orthopyroxene, olivine, and plagioclase as a function of composition and structure 05 p2087 N94-20906
More shock recovery experiments on mesosiderite analogs 11 p4351 N94-35455
Textural constraints on the formation of alteration phases in CM chondrites 11 p4353 N94-36145

METEOROID CONCENTRATION
A CM chondrite cluster and CM streams 01 p0432 N94-12215
Meteoroid environment near the Earth-Moon system [NASA-CR-193670] 02 p0835 N94-13203
Extraterrestrial accretion and glacial cycles 07 p2890 N94-28308

METEOROID CRATERS
U METEORITE CRATERS

METEOROID DUST CLOUDS
NT ZODIACAL DUST

METEOROID PROTECTION
Comparison of analytic Whipple bumper shield ballistic limits with CTH simulations [DE93-015126] 02 p0539 N94-13006
BALLIST: A computer program to empirically predict the bumper thickness required to prevent perforation of the Space Station by orbital debris [NASA-CR-193825] 02 p0543 N94-14120
Meteoroids and debris impact risk assessment on Columbus and Hermes using a realistic geometrical analysis tool 05 p1662 N94-21388

METEOROID SHOWERS
Meteorites from recent amor-type orbits 01 p0429 N94-12059
Meteoroid environment near the Earth-Moon system [NASA-CR-193670] 02 p0835 N94-13203
Corvid meteoroids and a Giordano Bruno ray are genetically related 03 p1242 N94-16223
Meteor burst communications improvement study [AD-A270866] 04 p1393 N94-19793
High Frequency (HF) and meteor burst communications in a polar environment [AD-A271604] 05 p1737 N94-20949
Low noise measurements in an RF environment [AD-A273813] 07 p2767 N94-25960
Meteor Burst Communications (MBC) throughput improvement tests [AD-A273941] 07 p2767 N94-25990
Performance statistics bulletin: High altitude meteor scatter propagation, August, September, October 1989 [AD-A274455] 07 p2773 N94-27085
Performance statistics bulletin. High latitude meteor scatter propagation October, November, December 1990, January 1991 [AD-A276693] 09 p3676 N94-31998
Performance statistics bulletin. High latitude meteor scatter propagation February, March, April, May 1991 [AD-A276723] 09 p3678 N94-32158
Performance statistics bulletin. High latitude meteor scatter propagation October, November, December 1991, January 1992 [AD-A276724] 09 p3678 N94-32159
Performance statistics bulletin. High latitude meteor scatter propagation [AD-A276694] 09 p3680 N94-32298
Performance statistics bulletin. High latitude meteor scatter propagation [AD-A276695] 09 p3680 N94-32299
Performance statistics bulletin. High latitude meteor scatter propagation [AD-A276696] 09 p3680 N94-32300
Performance statistics bulletin. High latitude meteor scatter propagation, June, July, August, September 1992 [AD-A277508] 09 p3685 N94-33347

METEOROIDS
NT BOLIDES
NT MICROMETEOROIDS
NT RADIO METEORS
NT ZODIACAL DUST
The magnitude of impact damage on LDEF materials [NASA-CR-188258] 01 p0043 N94-10666
Meteorites from recent amor-type orbits 01 p0429 N94-12059
A CM chondrite cluster and CM streams 01 p0432 N94-12215
Meteor forward scatter studies [DSIS-93-00382] 02 p0602 N94-13801
Corvid meteoroids and a Giordano Bruno ray are genetically related 03 p1242 N94-16223
Resolving LDEF's flux distribution: Orbital (debris?) and natural meteoroid populations 03 p1245 N94-16391
Remote visual detection of impacts on the lunar surface 03 p1290 N94-16404
Effects of hydrodynamics and thermal radiation in the atmosphere after comet impacts 05 p1862 N94-20649
Meteoroids and debris impact risk assessment on Columbus and Hermes using a realistic geometrical analysis tool 05 p1662 N94-21388
Performance statistics bulletin. High latitude meteor scatter propagation October, November, December 1990, January 1991 [AD-A276693] 09 p3676 N94-31998
Performance statistics bulletin. High latitude meteor scatter propagation February, March, April, May 1991 [AD-A276723] 09 p3678 N94-32158
Performance statistics bulletin. High latitude meteor scatter propagation October, November, December 1991, January 1992 [AD-A276724] 09 p3678 N94-32159
Performance statistics bulletin. High latitude meteor scatter propagation [AD-A276694] 09 p3680 N94-32298
Performance statistics bulletin. High latitude meteor scatter propagation [AD-A276695] 09 p3680 N94-32299
Performance statistics bulletin. High latitude meteor scatter propagation [AD-A276696] 09 p3680 N94-32300
Performance statistics bulletin. High latitude meteor scatter propagation, June, July, August, September 1992 [AD-A277508] 09 p3685 N94-33347
Eureka! Aerogel capture of meteoroids in space 11 p4351 N94-35412
Current activities and results of the Long Duration Exposure Facility Meteoroid and Debris Special Investigation Group 11 p4352 N94-35458
Natural orbital environment definition guidelines for use in aerospace vehicle development [NASA-TM-4527] 11 p4291 N94-36175

METEOROLOGICAL BALLOONS
Attitude determination of stratospheric balloons using Kalman filters [INPE-5498-TDI/513] 02 p0649 N94-13366

METEOROLOGICAL CHARTS
Use of ERS-1 scatterometer winds in Canadian forecast centres 01 p0250 N94-12504
An analysis of cloud-cover reporting in the 1977 surface observation database [AD-A271102] 05 p1864 N94-19852
Analyzing Martian winds and tracer concentrations using Mars Observer data 06 p2619 N94-24883
Investigation of mesoscale convective cloud clusters in South China [AD-A274303] 07 p2895 N94-26678
The polygon-ellipse method of data compression of weather maps [AD-A278958] 11 p4293 N94-35719

METEOROLOGICAL INSTRUMENTS
NT BAROMETERS
NT CLOUD HEIGHT INDICATORS
NT IONOSONDES
NT RADIOSONDES
NT RAIN GAGES
NT RAWINSONDES
NT WIND VANES
The subduction experiment. Cruise report, R/V Oceanus, cruise number 250 legs 1 and 2. Subduction 2 mooring deployment and recovery cruise, 25 January-26 February 1992 [AD-A264922] 01 p0289 N94-11853
A comparison of ceiling and visibility observation for NWS manned observation sites and ASOS sites [AD-A268356] 03 p1108 N94-17459
A rugged, low-cost advanced data acquisition system for field test projects [DE93-010041] 04 p1615 N94-18334
Micro-sensors for in-situ meteorological measurements 08 p3236 N94-29777
Comparison of Savannah River Site's meteorological databases [DE94-001751] 08 p3373 N94-29817
Implementation of instruments and facilities at the SGP CART site [DE94-006839] 09 p3781 N94-31322
Low power, constant-flow air pump systems [DE94-007463] 09 p3727 N94-32758

METEOROLOGICAL PARAMETERS
Database blending for the climatology of cloud statistics program [AD-A265034] 01 p0283 N94-10336
Parametric analysis of atmospheric processes [NASA-CR-192523] 01 p0347 N94-10757
The Air Force Interactive Meteorological System: A research tool for satellite meteorology [AD-A265957] 01 p0284 N94-11113
TOVS soundings: Impact on the synoptic analysis over the south and southeast regions of Brazil from March 18 to March 19, 1991 [INPE-5497-TDI/512] 01 p0230 N94-11179
Global monitoring of atmospheric properties by the EOS MODIS [NASA-TM-109237] 01 p0231 N94-11485
Development of a graphical user interface and graphics display for the WIND system [DE93-011780] 01 p0285 N94-11614
Characteristic scales and vortex features of mesoscale vortices observed by the satellites during the winter 01 p0199 N94-11943
Scatterometer observations: Review 01 p0201 N94-11956
An atmospheric boundary layer stability estimator for urban areas [AD-A265189] 01 p0279 N94-12422
A study of the Merritt Island, Florida sea breeze flow regimes and their effect on surface heat and moisture fluxes [NASA-CR-4537] 01 p0286 N94-12580
An integrated approach to total end-to-end quality control of ocean data in the real-time environment 01 p0211 N94-12662
Worldwide map of rainfall amount over the ocean derived from passive microwave radiometer 01 p0211 N94-12663
Bibliography of urban climate in tropical/subtropical areas, 1981-1991 [WCASP-25] 02 p0718 N94-12918
The role of clouds and oceans in global greenhouse warming [DE93-016206] 02 p0706 N94-13079
Study on TRMM data utilization for meteorology [NASDA-CNT-930007] 02 p0721 N94-13643
National use of the groups 7wwW1W2 and 960ww for ground stations [KNMI-PUBL-181] 02 p0722 N94-13926
The MADONA experiments (Meteorology and Diffusion Over Non-uniform Areas): High-resolution in-plume concentration fluctuations measurements using lidar remote sensing technique [AD-A267711] 03 p1105 N94-14938
IAI topic: El Nino. Southern oscillation and interannual climate variability [INPE-5410-PRE/1757] 03 p1111 N94-15186
Determination of sunshine duration from radiation intensity pyranometric measurements of global and sky radiation [BER-181] 03 p1105 N94-15302
TAFVER 2 users manual [AD-A266850] 03 p1106 N94-15757
Environmental characterization for target acquisition. Report 1: Site descriptions and measurements [AD-A267192] 03 p1106 N94-15851
A comparison of cloud attenuation models using measured cloud data 03 p0996 N94-16044
Spatial and frequency diversity in lidar systems [AD-A266192] 03 p1039 N94-16124
Earth imaging results from Galileo's second encounter 03 p1252 N94-16201
The multivariate optimum interpolation analysis of meteorological data at the Fleet Numerical Oceanography Center [AD-A266459] 03 p1106 N94-16568
Investigation of cloud properties and atmospheric stability with MODIS [NASA-CR-193475] 03 p1107 N94-16717
Mesoscale frontogenesis: An analysis of two cold front case studies [AD-A267950] 03 p1107 N94-17054
Phillips Laboratory global spectral numerical weather prediction model [AD-A267293] 03 p1107 N94-17244
Windshear database for forward-looking systems certification [NASA-TM-109012] 03 p1108 N94-17283
Arctic cyclones and Marginal Ice Zone (MIZ) variability [AD-A268610] 03 p1108 N94-17465
Atmospheric propagation analysis program [AD-A268231] 03 p1006 N94-17565
Forecasting the ducting of electromagnetic waves on the mesoscale [AD-A268101] 03 p1109 N94-17571
An empirical study of tropical cloud clusters using special sensor microwave imager data [AD-A268072] 03 p1110 N94-17595
The Central American cold surge: An observational analysis of the deep southward penetration of North American cold fronts [AD-A268592] 03 p1110 N94-17607

Cloudiest year study: An analysis of the 3DNEPH and RTNEPH databases
[AD-A269403] 04 p1490 N94-18281
Eastern Europe: A climatological study
[AD-A269200] 04 p1493 N94-18883
Protocol for computation of surface boundary layer parameters used to determine soil moisture flux from meteorological data collected at LLNL, 1992-1993
[DE93-018906] 04 p1463 N94-19003
Pantex Plant Meteorological Monitoring Program
[DE93-018495] 04 p1493 N94-19127
Report of the Experts Meeting on Reference Climatological Stations (RCS) and National Climate Data Catalogues (NCC)
[WMO-TD-535] 04 p1494 N94-19312
Interactive Production Line (IPL)
04 p1495 N94-19704
The marine light-mixed layer experiment cruise and data report: R/V endeavor cruise EN-224, mooring deployment, 27 April-1 May 1991: Cruise EN-227, mooring recovery, 5-23 September 1991
[AD-A271175] 05 p1864 N94-20186
Simulated retrieval of land surface parameters using multichannel satellite microwave radiometry
05 p1727 N94-20443
Weather tutor 1: Stability basics
[AD-A270758] 05 p1866 N94-20565
Mathematical model and analysis of the Tactical Unmanned Ground Vehicle (TUGV) using computer simulation
[AD-A272258] 05 p1824 N94-20576
A parametric representation of a thunderstorm cell
[AD-A271983] 05 p1866 N94-20579
Remote sensing for hydrology progress and prospects
[WMO-773] 05 p1841 N94-21069
NOVAM evaluation utilizing electro-optics and meteorological data from KEY-90
[AD-A271722] 05 p1868 N94-21356
Low-power millimeter-wave radar observations of the atmosphere
[NASA-CR-194738] 05 p1858 N94-21811
Design document and database specifications for the Naval Interactive Data Analysis System (NIDAS), version 1.0
[NASA-CR-194817] 05 p2045 N94-21865
The FIRE Cirrus Science Results 1993
[NASA-CP-3238] 05 p1871 N94-22292
Atmospheric parameterization schemes for satellite cloud property retrieval during FIRE IFO 2
05 p1874 N94-22312
Cirrus cloud development in a mobile upper tropospheric trough: The November 26th FIRE cirrus case study
05 p1878 N94-22329
Studies in remotely sensed geophysical parameter retrieval and analysis
[NASA-CR-193914] 05 p1842 N94-22374
Atmospheric numerical modeling resource enhancement and model convective parameterization/scale interaction studies
[NASA-CR-194769] 06 p2400 N94-23124
An adaptive multigrid model for hurricane track prediction
06 p2416 N94-23687
Joint Acoustic Propagation Experiment (JAPE)
06 p2527 N94-24208
Some results gained from JAPE: An overview
06 p2527 N94-24209
Intercomparison of remote and balloon-borne sensors operated at JAPE-91
06 p2527 N94-24210
Comparison of measured and predicted pure tone propagation levels from JAPE-1: An evaluation of the performance of ASOPRAT
06 p2527 N94-24212
GEWEX Cloud Systems Study (GCSS)
06 p2411 N94-24377
Grand challenge scientific questions in coupled modeling
06 p2412 N94-24382
Session on cumulus parameterization
06 p2414 N94-24394
Modeling and data assimilation for Mars Observer
06 p2620 N94-24889
The evaluation of ASOS for the Kennedy Space Center's Shuttle Landing Facility
[NASA-CR-195685] 06 p2416 N94-25271
A preliminary analysis of the US west climatology
[DE94-003028] 07 p2894 N94-26313
Radar detection of low-altitude targets in a maritime environment. Volume 2: Meteorological and radar data
[AD-A274658] 07 p2768 N94-26335
Analysis and interpretation of the meteorology of the 1988 coastal transition zone experiment
[AD-A274710] 07 p2894 N94-26431
Overall analysis of meteorological information in the Daeduk nuclear complex
[DE93-632594] 07 p2894 N94-26469
Analysis of the influence of weather on infrared imagery
[FEL-92-A421] 07 p3036 N94-26649
Mesoscale meteorological measurements characterizing complex flows
[DE94-002359] 07 p2895 N94-26761
Surface roughness lengths
[AD-A274550] 07 p2895 N94-26846
Kiruna geophysical data. Data summary 93/4-6, April-June 1993
[PB94-123700] 07 p2881 N94-27039
Kiruna geophysical data. Data summary 93/1-3, January-March, 1993
[PB94-123791] 07 p2881 N94-27043
Meteorological data at the Nagaoka Institute of Snow and Ice Studies
[REPT-158] 07 p2896 N94-27169
The validation of ATSR measurements with in situ sea temperatures
[DE94-003195] 07 p2852 N94-27875
Report of the National Research Institute for Earth Science and Disaster Prevention, No. 51
[JTN-94-80509] 07 p2886 N94-27985
Development of a method for predicting snowfall intensity and compacted snow on roads
07 p2853 N94-27990
Conception of snow information network system in Yamagata Prefecture
07 p2853 N94-27991
Research activities on the meteorology over the Asia-Pacific region
07 p2853 N94-28271
A global forecast model comparison study - year 1
[AD-A275674] 08 p3369 N94-28663
Lead detection and mapping with reference to relationships between scale, sensor characteristics, surface conditions and atmospheric properties
[AD-A275321] 08 p3377 N94-28877
Oceanic survey utilizing satellites
08 p3328 N94-29040
Antarctic Record, volume 36, no. 1
[REPT-106-VOL-36-NO-1] 08 p3357 N94-29078
Micro-sensors for in-situ meteorological measurements
08 p3236 N94-29777
The incorporation and initialization of cloud water/ice in an operational forecast model
08 p3373 N94-29814
Atmospheric Propagation Effects Through Natural and Man-Made Obscurants for Visible to MM-Wave Radiation
[AD-A276919] 08 p3256 N94-30495
Propagation modeling of moist air and suspended water/ice particles at frequencies below 1000 GHz
08 p3256 N94-30497
Tropospheric corrections to GPS measurements using locally measured meteorological parameters compared with general tropospheric corrections
08 p3144 N94-30655
A comparison of predictors for first-guess wind speed errors
[AD-A276460] 09 p3781 N94-31239
Station climatic summaries: China, the former USSR, and Mongolia
[AD-A276548] 09 p3784 N94-32057
Recommendations for meteorological data collection during physiological field studies
[AD-A276834] 09 p3901 N94-32153
Recurvature dynamics of a typhoon
[AD-A276792] 09 p3784 N94-32164
Fine resolution atmospheric sulfate model driven by operational meteorological data: Comparison with observations
[DE94-002994] 09 p3766 N94-32691
Proceedings of the Ninth Annual Pacific Climate (PACLIM) Workshop
[DE94-003024] 09 p3766 N94-32693
Use of cloud observations and mesoscale meteorology models to evaluate and improve cloud parameterizations
[DE94-003610] 09 p3785 N94-32717
Mexico City ozone concentrations as a function of readily-available meteorological parameters
[DE94-007576] 09 p3768 N94-32814
Statistical and numerical study of the relation between weather and sonic boom characteristics
10 p3976 N94-33498
Development of a radiative cloud parameterization scheme of stratocumulus and stratus clouds which includes the impact of CCN on cloud albedo
[DE94-005476] 10 p4081 N94-33714
Sensitivity of cloud forcing to the cloud cover parameterization in a GCM
[DE94-000678] 10 p4089 N94-33728
University of North Dakota citation FIRE Cirrus 2 mission summary and data report
[NASA-CR-195842] 10 p4090 N94-34135
Radar detection of low-altitude targets in a maritime environment. Volume 1: Final analysis
[AD-A278493] 10 p4037 N94-34376
The analysis of rapidly developing fog at the Kennedy Space Center
[NASA-CR-195888] 10 p4090 N94-34939
Implementation of a low-cost, commercial orbit determination system
11 p4205 N94-35621
Three dimensional visualization of a coastal mesoscale model
[AD-A278576] 11 p4294 N94-36187
Environmental measurements in the Beaufort Sea, Spring 1993
[AD-A278718] 11 p4296 N94-36293
Chilbolton Advanced Meteorological Radar: A tool for multi-disciplinary atmospheric research
[PB94-167467] 12 p4432 N94-36567
Terminal Doppler Weather Radar (TDWR) build 5 Test and Evaluation Master Plan (TEMP)
[AD-A280426] 12 p4434 N94-37218

METEOROLOGICAL PROBES

U SONDES

METEOROLOGICAL RADAR

Impact of shutting down en route primary radars within CONUS interior
[DOT-VNTSC-FAA-93-1] 01 p0023 N94-11626
Rainfall-runoff estimation using digital radar
[AD-A265390] 01 p0286 N94-12408
Preliminary meteorological results for 1992 West Coast Scotland Experiment
[DE93-014677] 02 p0720 N94-13404
Remote identification of rain and hail with a polarization diversity radar
[ISBN-0-315-55623-4] 02 p0720 N94-13516
TRMM precipitation radar algorithm
02 p0690 N94-14224
Estimate of sampling errors of TRMM rainfall observation by using radar-AMeDAS composite data
02 p0690 N94-14225
Multiparameter airborne rain radar development for TRMM validation and TRMM-follow-on study
02 p0690 N94-14226
Future TRMM follow-on mission
02 p0691 N94-14228
Sensitivity testing of a single-Doppler temperature retrieval and forecast system
[AD-A267278] 03 p1105 N94-14958
The Next Generation Weather Radar (NEXRAD)/Air Route Surveillance Radar (ARSR) operational comparison
[REPT-93W0000145] 03 p0987 N94-15439
Designing clutter rejection filters with complex coefficients for airborne pulsed Doppler weather radar
[NASA-CR-4550] 03 p0862 N94-15444
TRMM radar
03 p0990 N94-15894
Windshear detection radar signal processing studies
[NASA-CR-194615] 03 p0994 N94-16022
Radar diagnostic parameters as indicators of severe weather in central Florida
[PB93-183507] 03 p1106 N94-16465
Remote sensing of precipitation and electrification with a dual-polarization, coherent, wideband radar system
[AD-A267479] 03 p1004 N94-17364
Automatic suppression of anomalous propagation clutter for noncoherent weather radars
[KNMI-WR-92-06] 03 p1004 N94-17407
A technique for measuring winds in the lower atmosphere using incoherent Doppler lidar
[DE93-017163] 04 p1488 N94-17758
Boundary layer heat budgets from wind profiler/RASS data: A feasibility study
[DE93-013187] 04 p1489 N94-18052
SPNDL: A concept for a small satellite Doppler lidar wind sounder
04 p1327 N94-19181
Investigations of a coherent vector radar technique for the observation of the atmosphere near 10 GHz
[KFK-5068] 04 p1494 N94-19616
Description and availability of airborne Doppler radar data
05 p1722 N94-20419
Next Generation Weather Radar (NEXRAD) Principal User Processor (PUP) Operational Test and Evaluation (OT/E)
[AD-A273075] 05 p1868 N94-21519
Microphysical properties of the November 26 cirrus cloud retrieved by Doppler radar/IR radiometer technique
05 p1873 N94-22304
Lidar and radar derived cirrus microphysical properties for the 26 November 1991 case study
05 p1873 N94-22305
Progress in interpreting CO2 lidar signatures to obtain cirrus microphysical and optical properties
05 p1874 N94-22308
Observations of multi-layered clouds using K-band radar
05 p1874 N94-22311
Urban/rural application of weather radar for flow forecasting. Proceedings of the Informal CEc -Workshop
[PB93-220135] 06 p2407 N94-23129
Implementation and evaluation of the new wind algorithm in NASA's 50 MHz doppler radar wind profiler
[NASA-CR-194880] 06 p2408 N94-23576

Estimation of the rain signal in the presence of large surface clutter
[NASA-CR-195105] 06 p2409 N94-24087
Further studies to extend and test the area-time-integral technique applied to satellite data
[NASA-CR-195132] 06 p2415 N94-24705
ASR-9 microburst detection algorithm
[AD-A273591] 06 p2415 N94-24850
Machine intelligent gust front algorithm
[AD-A273695] 07 p2680 N94-26196
Radar detection of low-altitude targets in a maritime environment. Volume 2: Meteorological and radar data
[AD-A274658] 07 p2768 N94-26335
Cloud liquid water content measurement tests using dual-wavelength radar
[PB94-125960] 07 p2896 N94-26959
Encoding approaches for data link transmission of weather graphics
[AD-A274497] 07 p2772 N94-26963
Numerical simulations of a mountain thunderstorm. A comparison with Doppler radar observations
[AD-A275296] 08 p3369 N94-28873
A study of precipitation in the coastal area of Antarctica as observed at Syowa Station using a vertical pointing radar 08 p3363 N94-29979
Evaluation of dual polarization attenuation of millimeter frequencies through a meteorological radar 08 p3256 N94-30496
Radar measurements 09 p3685 N94-31002
Field studies of raindrop oscillations with applications to radar meteorology 09 p3782 N94-31743
Radar rainfall measurements from space 09 p3782 N94-31889
Gyrotrons and free electron lasers for atmospheric sensing
[AD-A277281] 09 p3718 N94-32406
An integrated cloud observation and modeling investigation in support of the ARM program
[DE94-003160] 09 p3785 N94-32716
Terminal Doppler Weather Radar (TDWR) Low Level Wind Shear Alert System 3 (LLWAS 3) integration studies at Orlando International Airport
[AD-A278957] 11 p4294 N94-35807
Doppler weather radar studies of precipitation systems
[AD-A279417] 11 p4295 N94-36262
Chilbolton Advanced Meteorological Radar: A tool for multi-disciplinary atmospheric research
[PB94-167467] 12 p4432 N94-36567
Terminal Doppler Weather Radar (TDWR) build 5 Test and Evaluation Master Plan (TEMP)
[AD-A280426] 12 p4434 N94-37218
NASA ER-2 Doppler radar reflectivity calibration for the CAMEX project
[NASA-TM-104611] 12 p4475 N94-37790

METEOROLOGICAL ROCKETS
U SOUNDING ROCKETS

METEOROLOGICAL SATELLITES
NT DMSP SATELLITES
NT METEOSAT SATELLITE
NT NIMBUS 6 SATELLITE
NT NIMBUS 7 SATELLITE
NT NOAA SATELLITES
NT NOAA 9 SATELLITE
NT NOAA 10 SATELLITE
NT SAN MARCO SATELLITES
NT TIROS N SERIES SATELLITES
NT TIROS SATELLITES
Database blending for the climatology of cloud statistics program
[AD-A265034] 01 p0263 N94-10336
Meteorological Satellite Center
[MSC-TN-26] 01 p0190 N94-11079
Simulation of images of water vapor channel and infrared split channel 01 p0190 N94-11081
Statistical study on the regional and seasonal distribution of fog in the far east region by using GMS imagery 01 p0190 N94-11082
Overview of training seminar for the use of Japanese Earth Resources Satellite-1 (JERS-1) data 01 p0190 N94-11083
The 1980 highlights
[NASA-TM-109672] 03 p1303 N94-15509
Optical measurements of NASA/USAF CRRES high altitude rocket borne chemical release experiments in conjunction with the USAF airborne ionospheric observatory aircraft
[AD-A266404] 03 p1101 N94-16551
The multivariate optimum interpolation analysis of meteorological data at the Fleet Numerical Oceanography Center
[AD-A266459] 03 p1106 N94-16568
Nowcasting methods for satellite imagery
[AD-A267294] 03 p1108 N94-17267
Some potential errors in satellite wind estimates using the geostrophic approximation and the thermal wind
[AD-A269784] 04 p1491 N94-18599
SERCAA cloud analysis integration: Design concepts and interaction with cloud forecast models
[AD-A269104] 04 p1492 N94-18637
The future of remote sensing from space: Civilian satellite systems and applications
[OTA-ISC-558] 05 p1837 N94-20209
Comparison of radiation and cloud parameters derived from satellite and aircraft measurements during FIRE 2 cirrus IFO 05 p1872 N94-22299
Managing an archive of weather satellite images 05 p2048 N94-22525
The AGRHYMET data communications project 06 p2280 N94-22776
An AVHRR cloud classification database typed by experts
[AD-A273560] 06 p2416 N94-25162
A preliminary method for atmospheric soundings in real time using satellite and ground-based remotely sensed data
[AD-A274381] 07 p2880 N94-26828
TacSats for NATO
[AD-A277710] 08 p3169 N94-30350
The use of meteorological satellite data for studying tropical atmospheric phenomena 09 p3779 N94-31000
Satellite direct readout: Opportunities for science education
[AD-A276257] 09 p3609 N94-31292
Use of Air Force cloud cover data to evaluate and improve cloud forecasts and parameterizations in mesocale meteorological models
[AD-A277384] 09 p3784 N94-32054
Typhoon monitoring using passive satellite observations
[AD-A277859] 10 p4089 N94-33769
Looking at Earth from space: Direct readout from environmental satellites
[NASA-EP-300] 10 p4078 N94-34268

METEOROLOGICAL SERVICES
Development of a graphical user interface and graphics display for the WIND system
[DE93-011780] 01 p0285 N94-11614
Weather forecasting support for AASE-2
[NASA-CR-194342] 02 p0721 N94-13675
TAFVER 2 users manual
[AD-A266850] 03 p1106 N94-15757
A comparison of ceiling and visibility observation for NWS manned observation sites and ASOS sites
[AD-A268356] 03 p1108 N94-17459
Integrated Terminal Weather System (ITWS)
[AD-A269884] 04 p1492 N94-18684
Organized track system: Air ways above the ocean 04 p1495 N94-19702
Calamity weather: Environmental calamities and meteorology 04 p1495 N94-19703
Report of the Second CLICOM Experts Meeting
[WCDMP-19] 04 p1495 N94-19705
Next Generation Weather Radar (NEXRAD) Principal User Processor (PUP) Operational Test and Evaluation (OT/E)
[AD-A273075] 05 p1868 N94-21519
Meteorological analysis of the November 25 FIRE cirrus-2 case: A well-defined ridge-crest cirrus system over Oklahoma 05 p1877 N94-22328
AFGWC Dial-In Subsystem (AFDIS) software users manual, version 2.2
[AD-A275844] 08 p3371 N94-29747
Impact of weather on flight operations at a major airport
[PB94-127990] 10 p4090 N94-34408
The influence of data link-provided graphical weather on pilot decision-making
[AD-A278871] 11 p4293 N94-35596
Data requirements for ceiling and visibility products development
[AD-A278959] 11 p4293 N94-35720
Toward a new National Weather Service: Weather for those who fly 12 p4472 N94-36947
Toward a new National Weather Service: National Weather Service employee feedback 12 p4474 N94-37467

METEOROLOGICAL SOLENOIDS
Characteristic scales and vortex features of mesoscale vortices observed by the satellites during the winter 01 p0199 N94-11943

METEOROLOGICAL STATIONS
U WEATHER STATIONS

METEOROLOGY
NT AGROMETEOROLOGY
NT ALPINE METEOROLOGY
NT AVIATION METEOROLOGY
NT HYDROMETEOROLOGY
NT LONG RANGE WEATHER FORECASTING
NT MARINE METEOROLOGY
NT MESOMETEOROLOGY
NT MICROBURSTS (METEOROLOGY)
NT MICROMETEOROLOGY
NT NOWCASTING
NT NUMERICAL WEATHER FORECASTING
NT PLANETARY METEOROLOGY
NT POLAR METEOROLOGY
NT RADIO METEOROLOGY
NT STATISTICAL WEATHER FORECASTING
NT SYNOPTIC METEOROLOGY
NT TROPICAL METEOROLOGY
NT WEATHER FORECASTING
Preliminary results of the comparison of ATSR measurements with in situ sea temperatures
[DE93-013399] 01 p0287 N94-10517
Environmental Sciences Division
[DE93-013865] 01 p0264 N94-10650
The Air Force Interactive Meteorological System: A research tool for satellite meteorology
[AD-A265957] 01 p0284 N94-11113
An overview of intertropical convergence and intertropical discontinuity
[DE93-619229] 01 p0277 N94-11603
Development of a graphical user interface and graphics display for the WIND system
[DE93-011780] 01 p0285 N94-11614
Effects of satellite spectral resolution and atmospheric water vapor on retrieval of near-ground temperatures
[AD-A264920] 01 p0245 N94-11851
The subduction experiment. Cruise report, R/V Oceanus, cruise number 250 legs 1 and 2. Subduction 2 mooring deployment and recovery cruise, 25 January-26 February 1992
[AD-A264922] 01 p0289 N94-11853
Optimization and eigenvalue computation with application to meteorology and oceanography
[DE93-015310] 02 p0744 N94-13024
Preliminary meteorological results for 1992 West Coast Scotland Experiment
[DE93-014677] 02 p0720 N94-13404
Evaluation of infrared sensors for autonomous landing guidance
[AD-A266450] 02 p0513 N94-13703
Activities report of the Netherlands Remote Sensing Board
[ETN-93-93880] 02 p0686 N94-14073
CCl working group on climate data and its rapporteurs
[WCDMP-21] 02 p0723 N94-14118
The MADONA experiments (Meteorology and Diffusion Over Non-uniform Areas): High-resolution in-plume concentration fluctuations measurements using lidar remote sensing technique
[AD-A267711] 03 p1105 N94-14938
Mesoscale modeling of the atmosphere
[AD-A263236] 03 p1098 N94-15132
Ensemble forecasting techniques in medium-range forecasting
[AD-A267443] 03 p1107 N94-17029
Phillips Laboratory global spectral numerical weather prediction model
[AD-A267293] 03 p1107 N94-17244
Geography and meteorological studies in the Far East
[DE93-013563] 04 p1461 N94-17893
Cloud CCN feedback
[DE93-016878] 04 p1472 N94-17985
Overview of physical oceanographic measurements taken during the Mount Mitchell cruise to ROPME sea area
[DE93-018460] 04 p1497 N94-18494
An investigation of warm-cloud microphysics using a multi-component cloud model: Interactive effects of the aerosol spectrum
[AD-A270273] 04 p1493 N94-18812
Eastern Europe: A climatological study
[AD-A269200] 04 p1493 N94-18883
Pantex Plant Meteorological Monitoring Program
[DE93-018495] 04 p1493 N94-19127
A survey of current approaches to modelling of hydrological time-series with respect to climate variability and change
[WMO/TD-534] 04 p1463 N94-19435
Shape of wind gusts at a 130m tower at Wilhelmshaven (Germany)
[BER-BAND-B3] 04 p1494 N94-19503
Reports of the 1992 Synoptic Symposium
[KNMI-TR-151] 04 p1494 N94-19698
HIRLAM 04 p1494 N94-19699
The WAQUA/CSM-16 model 04 p1494 N94-19700
The wave forecasting model NEDWAM 04 p1495 N94-19701
Calamity weather: Environmental calamities and meteorology 04 p1495 N94-19703
Interactive Production Line (IPL) 04 p1495 N94-19704
Worldwide frequency of temperatures at selected altitudes
[AD-A271111] 05 p1864 N94-19908

Hydrostatic/nonhydrostatic comparison with the MERCURE code on orographic flows
[ETN-93-94603] 05 p1866 N94-20600
Measurement of mesospheric turbulence in the framework of the metal campaign and development of a sensor for static pressure free measurements of neutral and electron density
[BONN-IR-92-45] 05 p1857 N94-21149
Analysis of a sandstorm weather process-translation
[AD-A272959] 05 p1867 N94-21250
The early Martian environment: Clues from the cratered highlands and the Precambrian Earth 05 p2143 N94-21667
Role of surface characteristics in urban meteorology and air quality
[DE93-040929] 05 p1851 N94-21740
Meteorological analysis of the December 4-6 FIRE cirrus-2 case 05 p1875 N94-22314
Meteorological analysis of the November 25 FIRE cirrus-2 case: A well-defined ridge-crest cirrus system over Oklahoma 05 p1877 N94-22328
Locally modified Bott-scheme for highly convective flows
[MPIM-99] 06 p2400 N94-23157
Visualization of results from meteorological simulations on CRAY
[PB93-201358] 06 p2451 N94-23443
Atmospheric moisture fields derived by satellite observations over the tropical Pacific Ocean
[NASA-CR-194852] 06 p2408 N94-23542
Implementation and evaluation of the new wind algorithm in NASA's 50 MHz doppler radar wind profiler
[NASA-CR-194880] 06 p2408 N94-23576
Uncertainties in climate data sets
[NASA-CR-194848] 06 p2408 N94-23577
Convective organization in the Pacific ITCZ: Merging OLR, TOVS, and SSM/I information
[NASA-CR-194850] 06 p2408 N94-23619
Methodology for the assessment of surface resistance and soil water storage variability at mesoscale based on remote sensing measurements. A case study with HAPEX-EFEDA data. UNESCO-International Hydrological Program 4
[PB94-111721] 06 p2386 N94-23734
MAMS data for the Convection and Moisture Experiment (CAMEX)
[NASA-TM-108435] 06 p2409 N94-24080
Report of the proceedings of the Colloquium and Workshop on Multiscale Coupled Modeling
[NASA-CP-3217] 06 p2410 N94-24374
GEWEX Water Vapor Project (GVaP) 06 p2411 N94-24378
Developing prediction regions for a time series model for hurricane forecasting
[AD-A273777] 07 p2892 N94-25861
The effect of elevation data representation on nocturnal drainage wind simulations
[DE94-003624] 07 p2892 N94-25936
Active layer dynamics and arctic hydrology and meteorology
[DE94-001724] 07 p2892 N94-25951
Testbed model and data assimilation for ARM
[DE94-000432] 07 p2893 N94-26082
A preliminary analysis of the US west climatology
[DE94-003028] 07 p2894 N94-26313
Overall analysis of meteorological information in the Daeduk nuclear complex
[DE93-632594] 07 p2894 N94-26469
Recent ASCOT experiments in multi-layered flows
[DE94-002360] 07 p2880 N94-26762
Surface roughness lengths
[AD-A274550] 07 p2895 N94-26846
Atmospheric science research in Malaysia: Perspectives on international cooperation 07 p2874 N94-28285
The active titration method for measuring local hydroxyl radical concentration 08 p3345 N94-28602
Catalog of Air Force weather technical publications 1992-1993
[AD-A275635] 08 p3368 N94-28638
Papers in meteorology and geophysics, vol. 44, no.1
[JTN-94-80585] 08 p3324 N94-28693
Activities report of the International Meteorological Institute
[ETN-94-95524] 08 p3370 N94-29423
Comparison of Savannah River Site's meteorological databases
[DE94-001751] 08 p3373 N94-29817
The suitability of low-cost urban airshed modeling in the Chicago area
[DE94-005114] 08 p3349 N94-30023
Multiple weather regimes and baroclinically forced spherical resonance
[DM-65] 08 p3376 N94-30966
Implementation of instruments and facilities at the SGP CART site
[DE94-006839] 09 p3781 N94-31322
Regional sources of error growth in the National Meteorological Center's medium-range forecast model 09 p3781 N94-31554
Use of Air Force cloud cover data to evaluate and improve cloud forecasts and parameterizations in mesocale meteorological models
[AD-A277384] 09 p3784 N94-32054
Recommendations for meteorological data collection during physiological field studies
[AD-A276834] 09 p3901 N94-32153
Proceedings of the Ninth Annual Pacific Climate (PACLIM) Workshop
[DE94-003024] 09 p3766 N94-32693
Development and testing of improved techniques for modeling the hydrologic cycle in a mesoscale weather prediction system
[AD-A277416] 09 p3786 N94-32921
Performance of a new wind updating system for a prognostic meteorological model in the environs of Mexico City
[DE94-006243] 09 p3786 N94-32937
Operations summary for the convection and moisture experiment (CAMEX)
[NASA-TM-108445] 09 p3786 N94-33004
Atmospheric Sciences Program summaries of research in FY 1993
[DE94-003486] 10 p4086 N94-33731
Observations and modelling of winds and waves during the surface wave dynamics experiment. Report 2: Intensive observation period IOP-3
[AD-A278368] 10 p4093 N94-34375
Computer animation of clouds
[DE94-008289] 11 p4292 N94-35350

METEORS
U METEOROIDS

METEOSAT SATELLITE
Instrument interface description for NOAA 2000 instruments with European morning spacecraft and/or NOAA-OPQ spacecraft
[NASA-TM-109406] 06 p2208 N94-23478
Command/telemetry bus general specification for the NOAA-OPQ polar orbiting environmental satellites and EUMETSAT polar satellite systems
[NASA-TM-109407] 06 p2208 N94-23479

METERS
U MEASURING INSTRUMENTS

METHACRYLATE RESINS
U ACRYLIC RESINS

METHAMPHETAMINE
Effects of methamphetamine on vigilance and tracking during extended wakefulness
[AD-A274896] 07 p2909 N94-26179
Effects of methamphetamine and fatigue on long- and short-term memory
[AD-A276452] 09 p3799 N94-32187

METHANATION
Novel catalysts for methane activation
[DE93-040630] 04 p1349 N94-18532
The carbon isotope biogeochemistry of (epsilon)CO2 production in a methanogenic marine sediment 04 p1477 N94-19233
The carbon isotope biogeochemistry of methane production in anoxic sediments. 1: Field observations 04 p1477 N94-19234
Factors that control the stable carbon isotopic composition of methane produced in an anoxic marine sediment 04 p1477 N94-19235
New methane chemistry synthesis of materials for reversible uptake and useful functionalization of methane
[PB94-112786] 06 p2233 N94-23801
CO2 methanation catalysts prepared from amorphous Ni-valve metal alloys containing platinum group elements 07 p2745 N94-28166
Methane production and consumption in grassland and boreal ecosystems
[NASA-CR-196085] 11 p4284 N94-35486
Conversion of acetic acid to methane by thermophiles
[DE94-012478] 12 p4479 N94-37434

METHANE
Influence of neutral particles concentration on flame propagation in methane-air mixtures at zero and normal gravity conditions 01 p0121 N94-10224
Conversion of acetic acid to methane by thermophiles
[DE93-014433] 01 p0300 N94-10652
Solid-state structures of guanidinium methane, ethane, and trifluoromethanesulfonate
[AD-A265293] 01 p0402 N94-11654
Conversion of light hydrocarbon gases to metal carbides for production of liquid fuels and chemicals
[DE93-014962] 02 p0583 N94-13002
IMG: Interferometric monitor for greenhouse gases 02 p0689 N94-14217
Biomimetic methane oxidation
[DE93-013196] 02 p0705 N94-14510
Development of vanadium-phosphate catalysts for methanol production by selective oxidation of methane
[DE93-016850] 03 p0949 N94-16897
The photochemistry of poly(methylphenylphosphazene)
[AD-A267320] 03 p0970 N94-16948
Transient studies of low temperature catalysts for methane conversion
[DE93-017710] 03 p0950 N94-16962
Biofilm structure and diversity
[AD-A267254] 03 p1118 N94-16989
Methyl chloride via oxyhydrochlorination of methane
[DE93-017548] 03 p0952 N94-17218
Strategy for the reduction of total integrated fluid logistics to the Space Station Freedom
[NASA-TM-107744] 03 p1138 N94-17452
Titanium carbon-hydrogen layers on decorative surfaces 04 p1375 N94-18010
Fundamental studies of the mechanism of catalytic reactions with catalysts effective in the gasification of carbon solids and the oxidative coupling of methane
[DE93-015262] 04 p1347 N94-18193
Novel catalysts for methane activation
[DE93-040630] 04 p1349 N94-18532
Growth, characterization and device development in monocrystalline diamond films
[AD-A270074] 04 p1599 N94-18797
CDIAC catalog of numeric data and computer model packages
[DE93-017675] 04 p1475 N94-18832
Land-use related sources of CO2, CH4 and N2O: Current global emissions and projections for the period 1990-2100
[PB93-194819] 04 p1475 N94-18949
The CAESAR project: Experimental and modeling investigations of methane reforming in a catalytically enhanced solar absorption receiver on a parabolic dish
[DE93-040203] 04 p1469 N94-19109
Selective methane oxidation over promoted oxide catalysts
[DE93-040002] 04 p1351 N94-19132
Selective methane oxidation over promoted oxide catalysts
[DE93-040001] 04 p1351 N94-19150
Carbon Isotope Biogeochemistry of Methane from Anoxic Sediments
[NASA-CR-194620] 04 p1477 N94-19231
Analysis of satellite-derived ozone and water vapor measurements
[NASA-CR-193810] 04 p1486 N94-19237
Faulted structure of the bottom simulating reflector on the Blake Ridge, western North Atlantic
[AD-A271289] 04 p1500 N94-19745
Transient studies of low temperature catalysts for methane conversion
[DE93-041232] 05 p1680 N94-20934
Molten carbonate fuel cell networks: Principles, analysis, and performance
[DE93-019872] 05 p1846 N94-21527
A carbon dioxide/methane greenhouse atmosphere on early Mars 05 p2142 N94-21662
Survey on chemical engineering technologies for the global environmental protection
[DE94-714887] 05 p1852 N94-22044
Investigations on trends in global environment adaptive industrial technologies
[DE94-714888] 05 p1853 N94-22258
Radiative forcing calculations for SF6 and CH4 using a correlated k-distribution transmission model
[DE94-001855] 06 p2397 N94-23700
Fundamental and experimental studies on the catalytic combustion of methane
[PB94-112661] 06 p2233 N94-23736
New methane chemistry synthesis of materials for reversible uptake and useful functionalization of methane
[PB94-112786] 06 p2233 N94-23801
Fundamental study of NO(x) control in catalytic combustion
[PB94-112323] 06 p2398 N94-23818
Rice cultivation and methane emission: Documentation of distributed geographic data sets
[NASA-TM-104595] 06 p2381 N94-24800
Design of novel catalysts for the partial oxidation of methane to methanol
[PB94-114212] 06 p2235 N94-24920
Carbon and hydrogen isotope composition and C-14 concentration in methane from sources and from the atmosphere: Implications for a global methane budget
[NASA-CR-195166] 06 p2399 N94-25092
Manual on measurement of methane and nitrous oxide emissions from agriculture
[DE93-616429] 06 p2399 N94-25167
Methane emissions from natural wetlands
[DE93-040796] 07 p2865 N94-25790

Implications of policies and prevent climate change for future food security
[DE93-018872] 07 p2866 N94-25948
A conceptual framework for the evaluation of cost-effectiveness of projects to reduce GHG emissions and sequester carbon
[DE93-040448] 07 p2867 N94-26419
Laser probes of natural gas ignition chemistry
[PB94-128345] 07 p2717 N94-27226
Basic research on natural gas combustion phenomena
[PB94-129046] 07 p2717 N94-27256
The electrocatalytic oxidation of ethylene and methane, and reduction of oxygen on gas-diffusion electrodes made of amorphous nickel-valve metal-platinum group metal alloys 07 p2722 N94-28165
Methane challenge of high performance molecular sieve oxygen concentrator
[AD-A275155] 08 p3337 N94-29033
Prediction of prompt NO(x) in hydrocarbon air flames 08 p3190 N94-29250
The 1992-1993 advanced design program. Part 1: The Mars methane engine project. Part 2: The Mars oxygen processor new furnace
[NASA-CR-195513] 08 p3299 N94-29409
Preparation and structure of amorphous hydrogenated carbon film deposited with RF plasma CVD 08 p3223 N94-29518
Numerical prediction of mixing process in a methane-fueled engine 08 p3304 N94-30230
The development and evaluation of a tunable diode laser trace gas sensor for the measurement of N2O and CH4 fluxes using micrometeorological techniques
[ISBN-0-315-78975-1] 08 p3296 N94-30801
Transient studies of low temperature catalysts for methane conversion
[DE94-005767] 08 p3200 N94-30877
An investigation of the reacting vortex structures associated with pulse combustion 08 p3200 N94-30911
Feasibility study to evaluate plasma quench process for natural gas conversion applications
[DE94-000086] 09 p3758 N94-31234
Development of vanadium-phosphate catalysts for methanol production by selective oxidation of methane
[DE94-006759] 09 p3759 N94-31272
Volatiles combustion in fluidized beds
[DE94-008382] 09 p3636 N94-32414
Methyl chloride by way of oxyhydrochlorination of methane
[DE94-009129] 09 p3637 N94-32767
Direct aromatization of methane
[DE94-008719] 09 p3638 N94-32888
A correlated k-distribution model of the heating rates for atmospheric mixtures of H2O, CO2, O3, CH4, and N2O in the 0-2500 cm(exp -1) wave number region at altitudes between 0 and 60 km
[DE94-005136] 09 p3775 N94-32895
The potential impact of externalities considerations on the market for biomass power technologies
[DE94-000247] 10 p4078 N94-33726
Methane production and consumption in grassland and boreal ecosystems
[NASA-CR-196085] 11 p4284 N94-35486
Novel catalysts for methane activation
[DE94-009705] 11 p4237 N94-35778
Gasoline from natural gas by sulfur processing
[DE94-011130] 11 p4248 N94-36035
Advanced hydrogen/method utilization technology demonstration
[DE94-000214] 11 p4248 N94-36191
Methyl chloride via oxyhydrochlorination of methane
[DE94-010691] 12 p4406 N94-36450
Rich methane/air flames: Burning velocities, extinction limits, and flammability limit
[DE94-004340] 12 p4407 N94-36462
UK methane emissions inventory: A scoping study on the use of ambient measurements to reduce uncertainties
[PB94-167855] 12 p4463 N94-36533
Accelerated line-by-line calculations for the radiative transfer of trace gases related to climate studies
[DE94-004404] 12 p4464 N94-36552
California residential indoor air quality study. Volume 1: Methodology and descriptive statistics
[PB94-166048] 12 p4464 N94-36994
Influences of flame-vortex interactions on formation of oxides of nitrogen in curved methane-air diffusion flamelets
[DE94-005105] 12 p4409 N94-37221
Finite-rate chemistry and transient effects in Direct Numerical Simulations of turbulent non-premixed flames
[DE94-005250] 12 p4410 N94-37222
Conversion of acetic acid to methane by thermophiles
[DE94-012478] 12 p4479 N94-37434
Tropospheric radiative forcing of CH4
[DE94-011628] 12 p4468 N94-37631

METHANOL
U METHYL ALCOHOL

METHIONINE
The relationship of metallothionein induction to the heat shock response
[AD-A266634] 03 p1122 N94-15741
Stress and brain protein synthesis
[PB94-170750] 11 p4296 N94-35601

METHOD OF CHARACTERISTICS
Method of characteristics design of a supersonic wind tunnel nozzle with square cross-section, supplement 3
[NASA-CR-194359] 02 p0527 N94-12824
Shock-free supersonic elliptic nozzles and method of forming same
[NASA-CASE-LAR-14054-1] 03 p0925 N94-15947
General order characteristic methods for solving neutron transport problems
[DE93-015824] 03 p1170 N94-16167
The (delta)f algorithm for beam dynamics
[DE93-015632] 03 p1187 N94-16660
Characteristic based methods for the time-domain Maxwell equations
[AD-A272973] 05 p1802 N94-21263
Supersonic minimum length nozzle design for dense gases 06 p2171 N94-23656
Transonic expanding flow through axially symmetric orifices 08 p3128 N94-28985
Cylinder drag experiment: An upgraded laboratory
[AD-A277841] 10 p3982 N94-33835
Solid state acoustics information time region separating methods for gear diagnosis of failures 10 p4068 N94-34351

METHOD OF MOMENTS
Design of a continuous resistively loaded monopole antenna
[AD-A265852] 01 p0138 N94-12281
Antenna pattern control using impedance surfaces
[NASA-CR-194517] 02 p0602 N94-13799
Resonant frequencies of irregularly shaped microstrip antennas using method of moments
[NASA-TP-3386] 03 p0989 N94-15767
Analysis of electromagnetic scattering from irregularly shaped, thin, metallic flat plates
[NASA-TP-3361] 03 p0998 N94-16655
Application of the finite-difference time-domain method to scattering and radiation problems involving wires and plates
[AD-A268396] 03 p1005 N94-17496
Numerical modeling of fringing fields and their use for complex permittivity measurements at high frequencies
[AD-A270478] 05 p1966 N94-19917
An extended UTD analysis for the scattering and diffraction from cubic polynomial strips
[NASA-CR-194581] 05 p1716 N94-20139
Polarimetric thermal emission from rough surfaces 05 p1727 N94-20441
Comparison of higher order moment spectrum estimation techniques
[AD-A272967] 05 p1967 N94-21260
A modified moment invariants technique for classification of noisy objects 05 p1780 N94-22165
Modelling short bent, graded index dielectric slab waveguides
[PB93-215283] 05 p1742 N94-22349
Isolated and coupled superquadric loop antennas for mobile communications applications 06 p2289 N94-22834
Rigorous analysis of thick microstrip antennas and wire antennas embedded in a substrate
[EUT-92-E-263] 06 p2290 N94-22876
Numeric solution of the electric field integral equation using Galerkin's method for axially symmetric cases
[ESA-TT-1264] 07 p2768 N94-26315
Computer program for numerical evaluation of the performance of an overmoded TM01 circular to TE10 rectangular waveguide mode converter
[AD-A274548] 07 p2771 N94-26844
A jet calculus approach including coherence effects and the associated problem of moment inversion
[ISBN-0-315-51715-8] 07 p3025 N94-27266
Hybrid techniques for complex aerospace electromagnetics problems 07 p2779 N94-27894
Integral equation analysis of composite bodies of revolution and arbitrary surfaces with application to cavity-backed antennas 08 p3253 N94-29883
Electromagnetic scattering through loaded aperture panels with nonzero contact impedance
[ONERA-NT-1993-2] 09 p3673 N94-31418
MOM3D method of moments code theory manual
[NASA-CR-189594] 09 p3682 N94-32897
The use of L-moments to fit the generalized lambda distribution to sample data
[AD-A278549] 10 p4130 N94-33678
Comparison of PDF and moment closure methods in the modeling of turbulent reacting flows
[NASA-TM-106614] 11 p4265 N94-35948

METHODS
U PROCEDURES

METHOXY SYSTEMS
Preparation, characterization, and thermal behaviour study of lanthanides (3) and yttrium (3) 4-methoxy benzylidene pyruvate in solid state
[DE94-604079] 07 p3068 N94-27697

METHYL ALCOHOL
Methanol pan fires in an enclosed space: Effect of pressure and oxygen concentration
[AD-A266108] 01 p0079 N94-12415
Solvent dynamical effects in electron transfer: Molecular dynamics simulations of reactions in methanol
[AD-A266061] 01 p0369 N94-12420
Biofuels for transportation: The road from research to the marketplace
[DE93-000091] 02 p0585 N94-14454
Biomimetic methane oxidation
[DE93-013196] 02 p0705 N94-14510
Contained liquids in microgravity, part 2 03 p0979 N94-16085
Development of vanadium-phosphate catalysts for methanol production by selective oxidation of methane
[DE93-016850] 03 p0949 N94-16897
Fuel processing requirements and techniques for fuel cell propulsion power
[DE93-019516] 05 p1750 N94-20257
Cold starting an alcohol-fueled engine with ultrasonic fuel atomization
[PB93-206597] 05 p1826 N94-22093
Modelling of solid polymer and direct methanol fuel cells: Phenomenological equations and analytical solutions
[PB93-224897] 06 p2390 N94-23102
The electrolyte challenge for a direct methanol-air polymer electrolyte fuel cell operating at temperatures up to 200 C 06 p2393 N94-23360
Advances in direct oxidation methanol fuel cells 06 p2393 N94-23361
New methane chemistry synthesis of materials for reversible uptake and useful functionalization of methane
[PB94-112786] 06 p2233 N94-23801
Design of novel catalysts for the partial oxidation of methane to methanol
[PB94-114212] 06 p2235 N94-24920
Feasibility study on introduction of transportation-use petroleum substitution energy
[DE94-725205] 07 p2759 N94-26905
Feasibility study on introduction of a large methanol engine power generation plant
[DE94-732338] 08 p3224 N94-28629
Methanol-mediated continuous extraction of phenolic compounds from coal liquid 08 p3188 N94-28679
Technical analysis of alternative fueled vehicles
[DE94-744238] 08 p3304 N94-30269
Fuel cycle evaluations of biomass-ethanol and reformulated gasoline
[DE94-000227] 08 p3226 N94-30818
Investigation of the technology development status of alternate fuel vehicles
[DE94-744237] 08 p3312 N94-30831
Assessment of costs and benefits of flexible and alternative fuel use in the US transportation sector
[DE94-006100] 08 p3226 N94-30885
Development of vanadium-phosphate catalysts for methanol production by selective oxidation of methane
[DE94-006759] 09 p3759 N94-31272
Novel approaches to the production of higher alcohols from synthesis gas
[DE94-006770] 09 p3666 N94-32132
High octane ethers from synthesis gas-derived alcohols
[DE94-006774] 09 p3667 N94-32133
Development of a catalyst for conversion of syngas-derived materials to isobutylene
[DE94-009698] 10 p4021 N94-33901
Methanol electrooxidation on well-characterized Pt-Ru alloys
[DE94-009640] 10 p4022 N94-33918
Hynol: An economic process for methanol production from biomass and natural gas with reduced CO2 emission
[DE94-008872] 10 p4079 N94-34139
Methanol fuel additive demonstration
[PB94-156668] 11 p4247 N94-35941
The effect of alternative fuels on the stability and lubricity of crankcase lubricants
[DE94-010353] 11 p4245 N94-36108
Research and development of Proton-Exchange Membrane (PEM) fuel cell system for transportation applications: Initial conceptual design report
[DE94-010576] 11 p4283 N94-36243
Heterogeneous catalytic process for alcohol fuels from syngas
[DE94-010263] 11 p4248 N94-36299

Rich flammability limits in CH3OH/CO/diluent mixtures
[DE94-004341] 12 p4407 N94-36482

METHYL CHLORIDE

Methyl chloride via oxyhydrochlorination of methane
[DE93-017548] 03 p0952 N94-17218

Methyl chloride by way of oxyhydrochlorination of methane
[DE94-009129] 09 p3637 N94-32767

Methyl chloride via oxyhydrochlorination of methane
[DE94-010691] 12 p4406 N94-36450

METHYL COMPOUNDS

NT ACETONITRILE
NT METHYL POLYSILOXANES

Vibrational overtone activation of methylcyclopropene
[AD-A265588] 01 p0079 N94-12373

Experimental and kinetic modeling of acid/base and redox reactions over oxide catalysts
[DE93-016203] 02 p0563 N94-13375

High-valent oxo, methoxorhenium complexes: Models for intermediates and transition states in proton-coupled multi-electron transfer reactions
[AD-A266492] 03 p1211 N94-16782

High octane ethers from synthesis gas-derived alcohols
[DE93-016861] 03 p0975 N94-16898

The photophysics of poly(methylphenylphosphazene)
[AD-A267321] 03 p0970 N94-16949

Photodissociation studies of polyatomic free radicals
[AD-A270084] 04 p1350 N94-18799

Polymerization of enantiomerically pure 2,3-dicarboalkoxy norbornadienes and 5,6-disubstituted norbornenes by well-characterized molybdenum ROMP catalysts
[AD-A272649] 05 p1704 N94-21186

Surface science and modeling studies of endothermic fuels catalysis
[AD-A272850] 05 p1712 N94-21192

The 13C-NMR spectra of poly (4-((2-(acryloyloxy) ethyl) ethyl amino)- 4-nitroazobenzene-co-methyl methacrylate)
[AD-A273016] 05 p1705 N94-21238

Feasibility study: Monodisperse polymer particles containing laser-excitable dyes
06 p2225 N94-24350

Potent solvents for C60 and their utility for the rapid acquisition of 13CNMR data for fullerenes
[AD-A273349] 06 p2235 N94-24925

The electrochemistry of the solvated electron: A study of its properties and of its applications
[ETN-94-95313] 06 p2236 N94-25296

Effects of plastic media blasting on aircraft skin
[AD-A274817] 07 p2668 N94-26488

Basic research on natural gas combustion phenomena
[PB94-129046] 07 p2717 N94-27256

Novel oxidizing reagents derived from elemental fluorine
[ITN-94-85231] 07 p2719 N94-27687

New monomers for high performance polymers
07 p2758 N94-27904

Tris(trimethylsily)arsine and lithium bis(trimethylsily)arsenide
[AD-A275075] 08 p3189 N94-29140

X ray crystal structures of ((Me3SiCH2)2InCl)2 and ((Me3SiCH2)InCl2)
[AD-A275074] 08 p3513 N94-29155

Combustion and heat transfer in a high speed diesel engine operating with rape seed oil methyl ester fuel
[PB94-137536] 08 p3301 N94-29679

Group transfer and electron transfer reactions of organometallic complexes: Summary of research accomplished in 1993
[DE94-004963] 08 p3200 N94-30770

High-temperature study of O+H2CO yields OH+HCO
[DE94-006837] 09 p3864 N94-31321

Solvent diffusion coefficient concentration dependence in polymer solutions
[AD-A277023] 09 p3655 N94-32005

Microstructure of copolymers containing disperse red 1 and methyl methacrylate
[AD-A277140] 09 p3660 N94-32722

Conversion of polymers of methyl- and vinylsilane to Si-C ceramics
[NASA-TM-106554] 09 p3662 N94-32945

Infrared spectroscopy of organic free radicals related to combustion processes
[DE94-012481] 12 p4409 N94-37168

Thermal cis-trans isomerization rates of azobenzenes bound in the side chain of some copolymers and blends
[AD-A280451] 12 p4424 N94-37227

Thermodynamic and kinetic aspects of surface acidity
[DE94-012351] 12 p4411 N94-37372

METHYL CYANIDE

U ACETONITRILE

METHYL POLYSILOXANES

Sol-gel derived silica/siloxane composite materials: The effect of loading level and catalyst activity on silica domain formation
[DE94-002734] 07 p2712 N94-27710

Crosslinking and surface reactions in macromolecules: Spectroscopic FT-IR studies 08 p3221 N94-30812

METHYLATION

Studies in bioorganic chemistry
[AD-A265532] 01 p0055 N94-12011

Group transfer and electron transfer reactions of organometallic complexes: Summary of research accomplished in 1993
[DE94-004963] 08 p3200 N94-30770

METHYLENE

Vibrational overtone activation of methylcyclopropene
[AD-A265588] 01 p0079 N94-12373

Diosmacycloalkanes as models for the formation of hydrocarbons from surface methylenes
[DE94-011211] 12 p4413 N94-37754

METRIC CONVERSION

U METRICATION

METRIC SPACE

NT HILBERT SPACE

S(sup 1) x S(sup 2) as a bag membrane and its Einstein-Weyl geometry
[DE93-613149] 01 p0410 N94-10635

New tests of the equivalence principle using non-metric couplings of electromagnetism and gravitation
01 p0413 N94-11821

On the foundations of final semantics: Non-standard sets, metric spaces, partial orders
[CWI-CS-R9241] 02 p0768 N94-13526

Differential geometry of CR-submanifolds of a normal almost para contact manifold
[DE93-624764] 04 p1545 N94-17793

Geometrical pattern learning
[DE93-017641] 04 p1542 N94-19007

Excursion theory of a finite set via resolvents
[REPT-93-19] 04 p1557 N94-19090

Half-integral flows in a planar graph with four holes
[RR-894-M] 05 p1951 N94-20302

Modular interval spaces
[PB93-220663] 05 p1961 N94-22266

Median stabilization degree of a median algebra
[PB93-220010] 06 p2479 N94-23093

Medians and steiner trees
[PB94-110616] 06 p2486 N94-23708

On the continuity of limit capacity of central Cantor sets
[DE93-613022] 06 p2523 N94-25328

Three metric domains of processes for bisimulation
[CWI-CS-R9335] 08 p3459 N94-30427

Topological models for higher order control flow
[CWI-CS-R9340] 08 p3425 N94-30432

Comparative semantics for linear arrays of communicating processes
[CWI-CS-R9336] 08 p3426 N94-30491

A structural co-induction theorem
[CWI-CS-R9346] 08 p3461 N94-30753

Line transects, covariance functions and set approximation
[CWI-BS-R9311] 09 p3846 N94-32084

The p-q-r-medial axis algorithm requires only local operations
[CWI-BS-R9317] 09 p3849 N94-32507

Successive minima on arithmetic varieties
[PB94-167699] 11 p4314 N94-35759

Entropy of graphs, semigroups and groups
[PB94-167749] 11 p4314 N94-35763

Note on certain rigid subshifts
[PB94-179058] 12 p4506 N94-37833

METRIC SYSTEM

U INTERNATIONAL SYSTEM OF UNITS

METRICATION

The MERMAID project 01 p0329 N94-11426

SI (Metric) handbook
[NASA-TM-109197] 08 p3231 N94-29376

METROLOGY

Needs for super-smooth surfaces
[DE93-012482] 01 p0382 N94-11242

Activities report of the National Electrotechnical Institute Galileo Ferraris
[ETN-93-94224] 02 p0627 N94-14812

Investigation of Zerodur material processing
[NASA-CR-193842] 02 p0793 N94-14903

An optically modulated scatterer for microwave antenna metrology
[NPL-DES-126] 03 p0986 N94-15020

Improved optical radiation detectors and their calibration: 200 nm - 30 microns 03 p0906 N94-15075

Soft X Ray Projection Lithography. Organization of the 1993 photonics science optical meetings
[AD-A269159] 04 p1579 N94-18693

Evaluation of a scanning Hartmann device for single point turning applications
[DE93-019204] 05 p1821 N94-19891

Optical metrology of magnetically trapped hydrogen
[AD-A272110] 05 p1680 N94-20584

An exploratory survey of methods used to develop measures of performance
[AD-A273945] 07 p2834 N94-25896

SI (Metric) handbook
[NASA-TM-109197] 08 p3231 N94-29376

A normative frame of reference for the metrology function
[REPT-932-430-102] 08 p3231 N94-29477

Solid state laser systems for space application
[NASA-CR-195777] 08 p3294 N94-29914

European PTTI report 08 p3468 N94-30642

Russian national time scale long-term stability
08 p3475 N94-30679

Application of the modified voltage-dividing potentiometer to overlay metrology in a CMOS/bulk process
[DE94-007937] 09 p3695 N94-32700

The development and application of composite complexity models and a relative complexity metric in a software maintenance environment
11 p4255 N94-35559

Piggyback balance experiment: An illustration of Archimedes' principles and Newton's third law
[PB94-163060] 11 p4265 N94-35942

METROPOLITAN AREAS

U CITIES

MEXICO

The Mexico City 1991 lidar measurements campaign
[DE93-019960] 04 p1478 N94-19272

Field guide to Cretaceous-tertiary boundary sections in northeastern Mexico
[NASA-CR-195719] 08 p3354 N94-28416

Performance of a new wind updating system for a prognostic meteorological model in the environs of Mexico City
[DE94-006243] 09 p3786 N94-32937

MGCO

U MARS OBSERVER

MICA

NT BIOTITE

The processing and mechanical properties of high temperature/high performance composites. Book 1: Coonstituent properties of composites
[AD-A266394] 03 p0935 N94-16483

The direct synthesis of organic and organometallic-containing MICA-type aluminosilicates
[DE93-019001] 04 p1373 N94-19321

Application of an alkylammonium method for characterization of phyllosilicates in CI chondrites
11 p4351 N94-35432

Thermodynamics of minerals stable near the Earth's surface
[DE94-012479] 12 p4539 N94-37094

MICE

Compaction-like blastomere aggregation caused by 1-oleoyl-2-acetylglycerol in mouse embryos: An electron microscopic observation 07 p2905 N94-27487

MICHELSON INTERFEROMETERS

Study of Einstein-Podolsky-Rosen state for space-time variables in a two photon interference experiment
01 p0370 N94-10582

Localized and distributed fiber-optic strain sensors embedded in composite materials
[UTIAS-346] 01 p0073 N94-12013

IMG: Interferometric monitor for greenhouse gases
02 p0689 N94-14217

Suppression of backscatter and stray reflection induced phase noise in Michelson interferometers
[AD-D015809] 04 p1382 N94-17902

On the Michelson-Morley experiment
[DE93-629908] 04 p1608 N94-18268

Developmental testing of a prototype all-reflection Michelson interferometer
[AD-A269064] 04 p1430 N94-18406

Fiber optic Michelson sensor and arrays with passive elimination of polarization fading and source feedback isolation
[AD-D015944] 05 p1984 N94-20065

Thermal dilation fiber optical flow sensor
[AD-D015926] 05 p1797 N94-20094

Validation of the design of a high resolution all-reflection Michelson interferometer for atmospheric spectroscopy
[AD-A272505] 05 p1987 N94-21410

Mirror velocity sampling errors in a Michelson interferometer
[AD-A273105] 05 p1809 N94-21508

Michelson Interferometer (MINT)
05 p1813 N94-21646

Fiber optic detection of laser generated ultrasound for materials characterization
[ISBN-0-315-83541-9] 06 p2541 N94-22891

Fiber optic detection of ultrasound and its application to cure monitoring
[ISBN-0-315-83424-2] 06 p2544 N94-24466
On the importance of the Michelson-Morley experiment
[DE94-606298] 08 p3523 N94-28620
Three high duty cycle, space-qualified mechanisms 08 p3162 N94-29642
Solid state laser systems for space application
[NASA-CR-195777] 08 p3294 N94-29914
Microwave Michelson interferometer system report of first use on a railgun, Green Farm, San Diego, CA
[DE94-005294] 08 p3289 N94-30059
Fiber optic sensors for the detection of surface acoustic waves on metals
[ISBN-0-315-87055-9] 09 p3878 N94-31736
Coastal boundary layer and refractivity measurements using the ground-based high resolution interferometer sounder (GB-HIS)
[AD-A277980] 09 p3683 N94-33159
Development of long-life, low-noise linear bearings for atmospheric interferometry 09 p3606 N94-33312
Spectrally-selective fiber transmission filter system
[AD-D016133] 10 p4141 N94-33698
Gaseous effluent monitoring and identification using an imaging Fourier transform spectrometer
[DE94-012627] 12 p4467 N94-37428

MICROANALYSIS
Microanalysis of directionally solidified cobalt oxide-zirconia eutectic
[DE93-013207] 01 p0088 N94-10527
Procedures for analysis of debris relative to Space Shuttle systems
[NASA-TM-109190] 02 p0534 N94-12900
High spatial resolution x ray microanalysis: Comparison of experiment and incoherent scattering calculations
[DE93-011685] 02 p0648 N94-13044
Microstructural evolution of NARloy-Z at elevated temperatures
[NASA-TM-108419] 02 p0571 N94-13715
Application of Z-contrast imaging to obtain column-by-column spectroscopic analysis of materials
[DE93-015333] 03 p0947 N94-16014
The role of carbon and temperature in determining electrical conductivity of basins, crust and mantle
[DE93-015936] 03 p1101 N94-16840
Insights into semiconducting materials and growth phenomena through Z-contrast STEM
[DE93-015964] 03 p1212 N94-16841
Electron spectroscopy analysis
[NASA-CR-193591] 03 p0951 N94-17039
Detection of single molecules in microspheres
[DE93-017776] 04 p1567 N94-18493
Atomic resolution electron energy loss spectroscopy in the scanning transmission electron microscope
[DE93-015334] 04 p1352 N94-19239
Near atomic resolution microanalysis of interfaces by analytical electron microscopy
[DE93-019437] 05 p1687 N94-19904
Microanalysis of iron oxidation state in iron oxides using X Ray Absorption Near Edge Structure (XANES) 05 p1686 N94-20808
Study of the homogeneity of InP wafers
[AD-A273658] 07 p3055 N94-26194
Determination of lead isotope ratios in seawater by purge and trap GC/MS after ethylation 07 p2870 N94-28152
A study of solid propellants using a microprobe mass spectrometer system
[AD-A275325] 08 p3224 N94-28879
Electron microscopy: Metal alloy x ray microanalysis
[REPT-932-600-101] 08 p3205 N94-29525
Atomic-scale structure and chemistry of interfaces by Z-contrast imaging and electron energy loss spectroscopy in the STEM
[DE94-006563] 08 p3516 N94-30064
Correlations between micromagnetic, microstructural and microchemical properties in ultrathin epitaxial magnetic structures
[AD-A277200] 09 p3901 N94-32092
Deuterium absorption and material phase characteristics of SAES St198 Zr-Fe alloy
[DE94-008275] 09 p3646 N94-32781
New prospects for analyzing lunar pyroclastic glass 11 p4355 N94-35397
Single agglutinates: A comparative study of compositions of agglutinitic glass, whole-grain, bulk soil, and FMR 11 p4355 N94-35401
The anatomy of a cluster IDP. Part 1: Carbon abundance, bulk chemistry, and mineralogy of fragments from L2008#5 11 p4352 N94-35466
Continuum fluorescence of Cu in NbTi/Cu composite wires
[DE94-006940] 11 p4241 N94-36242
Density and composition analysis using focused MeV ion microbeam techniques
[DE94-012241] 12 p4517 N94-37210
Elemental mapping of segregation in stainless steels with an imaging filter
[DE94-012659] 12 p4417 N94-37304
AEM and AES of radiation-induced segregation in proton-irradiated stainless steels
[DE94-012734] 12 p4418 N94-37398
ALCHEMI formulated for delocalization and anti-site defects
[DE94-012740] 12 p4537 N94-37400
Scanning x-ray diffraction: A technique with high compositional resolution for studying phase formation in co-deposited thin films
[DE94-011496] 12 p4420 N94-37516

MICROBALANCES
The laser ablation of gold films at the electrode surface of a quartz crystal microbalance
[AD-A265535] 01 p0175 N94-12012
A novel test method for fuel thermal stability
[AD-A265853] 01 p0099 N94-12275
A quartz crystal microbalance study of lithium insertion and removal into evaporated films MO(y) (M = Mo, Fe, and V)
[DSIS-93-00649] 02 p0810 N94-14203
Atomic oxygen fluence detector for Bremsat: Scientific and technical description 05 p1663 N94-21396
Application of an electrochemical quartz crystal microbalance to the study of electrocatalytic films
[DE93-041124] 05 p2029 N94-21691
Pre-flight testing of Thermoelectric Quartz Crystal Microbalances (TQCM) for midcourse space experiment (MSX) spacecraft
[AD-A277054] 09 p3610 N94-32010

MICROBALLOONS
Properties and processing characteristics of low density carbon cloth phenolic composites 06 p2231 N94-24450
On the mechanics of microballoon-reinforced metal matrix composites
[AD-A277928] 09 p3630 N94-33178

MICROBE
U MICROORGANISMS

MICROBEAMS
He(+) and H(+) microbeam damage, swelling and annealing in diamonds
[DE94-601912] 07 p3063 N94-26987
Density and composition analysis using focused MeV ion microbeam techniques
[DE94-012241] 12 p4517 N94-37210

MICROBIOLOGY
NT BACTERIOLOGY
Chaos and microbial systems
[DE93-016814] 02 p0730 N94-14596
Microbiological analysis of debris from Space Transportation System (STS)-55 Spacelab D-2
[NASA-CR-193883] 06 p2421 N94-24310
Microbial biofilm formation and its consequences for the CELSS program
[NASA-CR-195146] 06 p2438 N94-24706
Proceedings of the 12th International Congress: Corrosion Control for Low-Cost Reliability. Volume 5B: Corrosion: General issues
[AD-A273667] 06 p2250 N94-25407
Proceedings of the 12th International Congress: Corrosion Control for Low-Cost Reliability. Volume 6: Electric Power Industry
[AD-A273668] 06 p2250 N94-25408
Microbiology research at some research institutes in the former Soviet Union: A survey of scientific publications
[PB94-123320] 07 p2902 N94-27171
Physiology and molecular-genetics of thermus and bacillus
[PB94-135571] 08 p3385 N94-29190

MICROBURSTS (METEOROLOGY)
Optimal lateral escape maneuvers for microburst encounters during final approach
[LR-691] 02 p0511 N94-13534
Windshear database for forward-looking systems certification
[NASA-TM-109012] 03 p1108 N94-17283
The relationship of an integral wind shear hazard to aircraft performance limitations
[NASA-TM-109080] 07 p2677 N94-26593
A data fusion algorithm for multi-sensor microburst hazard assessment 07 p2641 N94-27287
Investigation of air transportation technology at Princeton University, 1992-1993 07 p2643 N94-27294
Optimal nonlinear estimation for aircraft flight control in wind shear 07 p2643 N94-27296
Terminal Doppler Weather Radar (TDWR) Low Level Wind Shear Alert System 3 (LLWAS 3) integration studies at Orlando International Airport
[AD-A278957] 11 p4294 N94-35807

MICROCALORIMETERS
U CALORIMETERS

MICROCHANNEL PLATES
Absolute detection efficiency of a micro-channel plate detector to x rays in the 1-100 KeV energy range
[DE93-012592] 02 p0789 N94-14460
Microchannel plate imaging detectors for the ultraviolet 03 p0901 N94-15037
Microchannel plate detectors for space astronomy 03 p0901 N94-15038
The MIC photon counting detector 03 p0901 N94-15039
The STIS MAMA status: Current detector performance 03 p0905 N94-15069
The Rutherford Appleton Laboratory photon counting detector 03 p0910 N94-15096
Testing and management of flight instruments and their data
[NASA-CR-194332] 03 p0868 N94-15187
Performance optimization of detector electronics for millimeter laser ranging 03 p0913 N94-15569
Performance comparison of high speed microchannel plate photomultiplier tubes 03 p0922 N94-15624
Multi-frame x ray imaging with a large area 40ps camera
[DE93-017179] 03 p1035 N94-16960
Detecting small debris using a ground-based photon counting detector
[DE93-012623] 03 p0898 N94-17669
Neutron detectors for fusion reaction-rate measurements
[DE94-010407] 11 p4330 N94-36114
Design and construction of a imaging instrument for studying ion emission from pure ion emitters
[DE94-010702] 11 p4328 N94-36302

MICROCHANNELS
Liquid Cooled Heat Sink with through Vias (LCHS)
[AD-A266008] 01 p0073 N94-12344
Microchannel cooled heatsinks for high average power laser diode arrays
[DE93-016533] 02 p0658 N94-14442
High- and low-temperature bonding techniques for microstructures
[DE93-017173] 04 p1595 N94-17992
Active neutral particle diagnostics for high temperature plasma
[DE93-788457] 04 p1586 N94-18214
Thermal stresses in the microchannel heatsink cooled by liquid nitrogen
[DE93-018660] 04 p1418 N94-18995
High power, electron-beam induced switching in diamond
[DE93-040535] 05 p1768 N94-21770
Design of microchannels for cryostabilization of high temperature superconducting magnets
[DE94-001324] 06 p2559 N94-22993

MICROCIRCUITS
U MICROELECTRONICS

MICROCLIMATOLOGY
USAF physiological studies of personal microclimate cooling: A review
[AD-A267203] 03 p1022 N94-15858
Cold-start minidiesel engine development
[AD-A271064] 05 p1823 N94-20567
An overview of the ASCOT program
[DE94-004356] 07 p2869 N94-27601
The use of liquid and air microclimate conditioning systems to alleviate heat stress in helicopter NBC operations 08 p3384 N94-28453
Study of the energy partition in complex terrains (deforested and forested areas)
[INPE-5522-TDI/519] 10 p4083 N94-34225
Surface-layer response over shrub-steppe canopy during springtime
[DE94-011235] 12 p4468 N94-37624

MICROCOMPUTERS
NT IBM PERSONAL COMPUTERS
NT MACINTOSH PERSONAL COMPUTERS
NT PERSONAL COMPUTERS
Controller of serial multiplex communication channel
[DE92-641157] 01 p0336 N94-10544
Upgrading NASA/DOSE laser ranging system control computers 03 p0918 N94-15595
The Hough transform algorithm for sea ice lead analysis: An evaluation
[AD-A274535] 07 p2899 N94-26853
Microcomputer-based protective functions in industrial production systems: Assessment method
[PB94-137817] 08 p3411 N94-29159
Design and Monte Carlo analysis of an unmanned aerial vehicle
[AD-A277648] 09 p3580 N94-33056
An intelligent on-line failure-diagnosis card with extensive usage 10 p4068 N94-34334

Application of microcomputer governed speed rise and loadcontrol appliance in the 200MW steam turbine
10 p4118 N94-34342
A microcomputer measuring-controlling system for the performance test of fogging nozzles
10 p4032 N94-34362
A new type of temperature and humidity detection-control system 10 p4057 N94-34365
Digital control programmer for temperature control
[DE94-615584] 11 p4309 N94-36382

MICROCRACKS

Micromechanisms of fatigue crack growth and fracture toughness in metal matrix composites
[AD-A265153] 01 p0187 N94-11096
Fatigue in single crystal nickel superalloys
[AD-A266116] 01 p0085 N94-12418
Modeling the impact behavior of AD85 ceramic under multi-axial loading
[AD-A265877] 02 p0576 N94-12932
Automated crack identification for cement paste
[AD-A265753] 02 p0665 N94-13042
A stochastic model for behavior analysis of fiber-reinforced quasi-brittle materials
02 p0672 N94-13594
Micromechanical damage theories for brittle solids with interacting microcracks
[AD-A266348] 02 p0673 N94-13778
Thermo-mechanical analysis of oxidation protected carbon-carbon composites
[AD-A268191] 03 p0941 N94-17597
Helium-induced weld degradation of HT-9 steel
[DE93-015981] 04 p1358 N94-17915
Initiation and growth of microcracks in high strength steel butt welds
[AD-A268751] 04 p1454 N94-18466
Process relationship as influenced by carbonization rate
[AD-A269680] 04 p1341 N94-18572
A numerical analysis of crack growth in brittle microcracking composites
[DE93-011562] 04 p1343 N94-18914
A numerical analysis of crack propagation in microcracking ceramic and ceramic composites
[DE94-001192] 06 p2253 N94-23183
Micromechanical failure modes in brittle matrix composites 06 p2255 N94-24232
Characterization of fatigue damage in a metal matrix composite (SCS-6/Ti-15-3) at elevated temperature
[AD-A273797] 07 p2706 N94-25876
The fracture behavior of a CVD crystalline Si3N4/amorphous Si3N4 composite
[DE94-002646] 07 p2750 N94-26124
Brittle composites modeling: Comparisons with MoSi2/ZrO2
[DE94-004978] 08 p3182 N94-29933
Micromechanics of the dynamic response of ceramics and ceramic composites 08 p3217 N94-29975
Modeling the impact behavior of high strength ceramics
[AD-A277744] 10 p4028 N94-33894
Acoustical-optical fracture analysis
[PB94-170602] 11 p4279 N94-36216
Defect initiation/growth and energy dissipation induced by deformation and fracture
[AD-A280411] 12 p4424 N94-37184
A simple evaluation of thermally-induced streses in the vicinity of the stitch in a through-thickness reinforced cross-ply laminate
[NASA-CR-196317] 12 p4406 N94-37653
Effects of ply thickness on thermal cycle induced damage and thermal strain 12 p4459 N94-37806

MICROCRYSTALS

HRTEM in protein crystallography
[DE93-610322] 01 p0395 N94-10406
Boundary stability under nonequilibrium conditions
[DE93-016259] 02 p0809 N94-13980
A discontinuous melt sheet in the Manson impact structure 03 p1103 N94-16269
Fundamental studies of defect generation in amorphous silicon alloys grown by remote plasma-enhanced chemical-vapor deposition
[DE93-017083] 05 p2029 N94-21615
Prometheus in space: Research Committee on Functional New Material
[JTN-94-80580] 07 p2761 N94-28002
Oriented Si and Ge nanocrystals formed in Al2O3 by ion implantation and annealing
[DE94-005593] 09 p3901 N94-32172
Materials processing apparatus development for fluoride glass
[NASA-CR-193963] 10 p4030 N94-34388

MICROELECTRONICS

NT LARGE SCALE INTEGRATION
NT MEDIUM SCALE INTEGRATION
NT VERY LARGE SCALE INTEGRATION
RF vacuum microelectronics
[AD-A266066] 01 p0142 N94-10818
Applications of spectroscopic ellipsometry to microelectronics
[AD-A265148] 01 p0143 N94-11159
Resist materials design: Base-catalyzed chemical amplification
[AD-A265286] 01 p0145 N94-11819
Statistical process control in the hybrid microelectronics manufacturing industry: A Navy view point
[AD-A265164] 01 p0145 N94-11884
Polymers for microelectronics
[AD-A266036] 01 p0094 N94-12396
Multicomponent and multilayered thin films for advanced microtechnologies: Techniques, fundamentals, and devices
[AD-A265685] 01 p0405 N94-12442
Solderability of surface mount devices
[AD-A265751] 02 p0620 N94-13040
Mongoose ASIC microcontroller programming guide
[NASA-RP-1319] 02 p0623 N94-13871
An ultra-compact processor module based on the R3000
[DE93-012549] 02 p0625 N94-14427
Microwave interconnection
[DE93-016580] 02 p0625 N94-14533
Electrochemical planarization for microelectronic circuits
[DE93-017214] 02 p0627 N94-14870
Reliability characterization of digital microcircuits: Investigation of an in-process oxide reliability screening method
[AD-A267053] 03 p1008 N94-15665
The specific heat of titanium disilicide
[AD-A267543] 03 p0960 N94-17100
Reliability analysis of Surface Mount Technology (SMT)
[AD-A267598] 03 p1055 N94-17194
RF vacuum microelectronics
[AD-A268399] 03 p1014 N94-17423
Field-emitter arrays for RF vacuum microelectronics
[AD-A268397] 03 p1015 N94-17526
Smart Power: New power integrated circuit technologies and their applications
[VTT-TIED-1356] 03 p1015 N94-17546
Field emitter arrays for RF vacuum microelectronics
[AD-A268595] 03 p1015 N94-17608
Aerogels for microelectronic applications: Fast, inexpensive, and light as air
[DE93-017170] 04 p1395 N94-17882
Silicon micro-actuator 04 p1408 N94-18017
RF vacuum microelectronics
[AD-A269454] 04 p1396 N94-18284
Update on parts SEE susceptibility from heavy ions
[AD-A268735] 04 p1596 N94-18316
Field emission cathode and vacuum microelectronic microwave amplifier development
[AD-A269526] 04 p1403 N94-18639
RF vacuum microelectronics
[AD-A270003] 04 p1403 N94-18667
Engineering research, development and technology thrust area report, FY92
[DE93-016334] 04 p1632 N94-18856
Integrated circuits: Resistless processing simplifies production and cuts costs
[DE93-018069] 04 p1405 N94-18941
Optoelectronic packaging: A review
[DE93-040059] 04 p1515 N94-19535
Simulation of the behavior of micro-electronic capacitive pressure sensors
[LAAS-93190] 04 p1434 N94-19659
Solder technology in the manufacturing of electronic products
[DE93-018842] 05 p1699 N94-19960
Automated HMC assembly
[DE93-040641] 05 p1749 N94-20005
The aerogel mesh contamination collector
[AD-A270537] 05 p1651 N94-20011
Single-event upset testing of the performance semiconductor 1750A CMOS/SOS chip set
[AD-A271158] 05 p2015 N94-20184
Method for anisotropic etching in the manufacture of semiconductor devices
[NASA-CASE-MSC-21631-1] 05 p1993 N94-20491
X ray reflection masks: Manufacturing, characterization and first tests
[BONN-IR-92-31] 05 p1986 N94-21043
Comparison of single event upset rates for microelectronic memory devices during interplanetary solar particle events 05 p1754 N94-21085
Single event phenomena: Testing and prediction
05 p1763 N94-21696
Self assembly: An approach to terascale integration
[DE93-040104] 05 p1769 N94-21846
Microtechnology: The key to the technical challenges of the 21st century
[DE94-000403] 05 p1769 N94-21959
Fluorescent microthermographic imaging
[DE93-040332] 05 p1810 N94-22000
Acoustic, fiber optic, and silicon microelectronic microsensors research and development activities at Sandia National Laboratories
[DE93-019075] 05 p1770 N94-22040
Silicon microelectronic field-emissive devices for advanced display technology
[DE94-000397] 05 p1794 N94-22380
Multidisciplinary specification and design of microelectronics in products
[EUT-93-E-269] 06 p2308 N94-23136
Generic microelectronic smart sensor platform for detection of toxic, hazardous, and flammable gases
[DE93-017626] 06 p2343 N94-23200
CRRES microelectronics package flight data analysis
[NASA-TP-3423] 06 p2540 N94-23273
Solid state research
[AD-A274063] 07 p3049 N94-25645
Advanced qualification techniques
[DE94-003709] 07 p2780 N94-25812
A general purpose I(sub DDQ) measurement circuit
[DE94-002733] 07 p2781 N94-25977
The National Center for Advanced Information Components Manufacturing: Program update
[DE94-002647] 07 p2960 N94-26118
Experimental determination of the CU-IN-PB ternary phase diagram
[DE94-003765] 07 p2735 N94-26349
The 12-channel flash-ADC FASTBUS module
[DE93-634229] 07 p2783 N94-26380
Signal amplifier-shapers for multiwire detectors
[DE93-634171] 07 p2783 N94-26438
Diagnostics and microelectronics
[DE94-003016] 07 p2784 N94-26777
Generalized emulation microcircuit program
[AD-A274749] 07 p2785 N94-26797
Center for space microelectronics technology
[NASA-CR-195282] 07 p2786 N94-27574
Micro-electron deflector
[AD-D016055] 07 p2787 N94-27672
Opportunities for High Aspect Ratio Micro-Electro-Magnetic-Mechanical Systems (HAR-MEMMS) at Lawrence Berkeley Laboratory
[DE94-003499] 07 p2827 N94-27722
RF vacuum microelectronics
[AD-A275221] 08 p3263 N94-28915
Focused ion beam fabrication of microelectronic structures
[AD-A275384] 08 p3264 N94-29305
The influence of temperature on microelectronic device failure mechanisms, phase 2
[AD-A275029] 08 p3265 N94-29511
Proceedings of the Workshop on Microtechnologies and Applications to Space Systems
[NASA-CR-195688] 08 p3235 N94-29767
Micromanufacturing: Recent developments in this country and abroad 08 p3235 N94-29769
Overview of microoptics: Past, present, and future
08 p3235 N94-29771
Micro guidance and control technology overview
08 p3144 N94-29772
Micro guidance and control synthesis: New components, architectures, and capabilities 08 p3144 N94-29792
The bases for the development of high-temperature integrated SQUID-systems
[DE94-607901] 08 p3267 N94-30073
The bases for the development of high-temperature integrated SQUID-systems
[DE94-608462] 08 p3517 N94-30082
Proceedings of the 1991 Single Event Upset Symposium
[DSIS-92-00652] 08 p3495 N94-30211
Advanced development of the Spectrum Sciences Model 5005-TF, single event test fixture
08 p3291 N94-30218
Direct measurement of the reactivity of NH and OH on a silicon nitride surface
[DE94-005286] 08 p3199 N94-30260
Optoelectronic packaging activities at Sandia National Laboratories
[DE94-005287] 08 p3501 N94-30261
A combined electron beam/optical lithography process step for the fabrication of sub-half-micron-gate-length MMIC chips 08 p3240 N94-30445
Fault coverage measurement for digital microcircuits
[AD-A276226] 09 p3686 N94-31066
RF vacuum microelectronics
[AD-A276512] 09 p3691 N94-31928
Sandia technology engineering and science accomplishments
[DE94-008312] 09 p3668 N94-32412

Aerospace sponsored research
[ATR-93(8498)-1] 09 p3966 N94-32949
Silicon-Based Optoelectronic Materials Symposium and Materials Research Society Proceedings, volume 298
[AD-A277518] 09 p3662 N94-32952
The impact of ASIC devices on the SEU vulnerability of space-borne computers
[AD-A278134] 09 p3808 N94-33252
Microelectronic photomultiplier device with integrated circuitry
[AD-D016176] 10 p4039 N94-33723
A PC-based measurement and test system for digital controller 10 p4110 N94-34363
Thick film fabrication of aluminum nitride microcircuits
[DE94-010107] 11 p4259 N94-35706
Space-based crystal growth and thermocapillary flow 11 p4342 N94-35971
Rapid and accurate timing simulation of radiation-hardened digital microelectronics using VHDL
[AD-A278644] 11 p4261 N94-36361
Hardness variability in commercial and hardened technologies
[DE94-007270] 11 p4261 N94-36362
Measurement of a surface heat flux and temperature 11 p4231 N94-36407
Single event mirroring and sense amplifier designs for enhanced SE tolerance of DRAMs
[DE94-010397] 12 p4438 N94-37190
Development of low dielectric constant alumina-based ceramics for microelectronic substrates
[DE94-011360] 12 p4439 N94-37302

MICROFIBERS
Microinjection of the Yersinia YopE cytotoxin in mammalian cells induces actin microfilament disruption
[FOA-B-40418-4.4] 06 p2421 N94-24290

MICROGRAPHY
U PHOTOMICROGRAPHY

MICROGRAVITY
Project ARGO: Gas phase formation in simulated microgravity
[NASA-TM-104762] 01 p0125 N94-11235
Reduced gravity multibody dynamics testing
[NASA-CR-192589] 01 p0125 N94-11483
SWIRL as a means of liquid management in low gravity
[NASA-CR-4545] 01 p0412 N94-11523
Five biomedical experiments flown in an Earth orbiting laboratory: Lessons learned from developing these experiments on the first international microgravity mission from concept to landing 01 p0302 N94-11556
Microgravity vibration isolation technology: Development to demonstration
[NASA-TM-106320] 01 p0001 N94-11703
An application of reduced gravity model to mesoscale eddies 01 p0199 N94-11945
Echocardiography in the flight program 01 p0309 N94-11993
Space truss zero gravity dynamics
[AD-A266130] 01 p0044 N94-12541
The Third Workshop on Two Phase Fluid Experiment in the Space Environment
[NASDA-CON-930002] 01 p0161 N94-12547
Research on two phase flow in microgravity 01 p0162 N94-12554
Modeling void growth and movement with phase change in thermal energy storage canisters
[NASA-TM-106288] 01 p0163 N94-12576
Monoclonal antibodies directed against surface molecules of multicell spheroids
[NASA-CR-193560] 02 p0727 N94-12795
Medical evaluations on the KC-135 1991 flight report summary
[NASA-TM-104755] 02 p0731 N94-12832
Reduce fluid experiment system flight data from IML-1
[NASA-CR-193835] 02 p0804 N94-12873
Advanced protein crystal growth programmatic sensitivity study
[NASA-CR-193827] 02 p0804 N94-12934
Calcitonin control of calcium metabolism during weightlessness
[NASA-CR-193622] 02 p0731 N94-12960
Capillary surfaces in a wedge: Differing contact angles
[DE93-013903] 02 p0631 N94-13244
Temperature dependence of diffusivities, preliminary definition phase
[NASA-CR-192613] 02 p0648 N94-13326
Crystal growth of ZnSe and related ternary compound semiconductors by physical vapor transport
[NASA-CR-193834] 02 p0807 N94-13444
Thermal gravitational modelling and scaling of two-phase heat transport systems: Similarity considerations and useful equations predictions versus experimental results
[NLR-TP-91477-U] 02 p0632 N94-13533
STS-30 Magellan IUS/EVA training in WETF
[NASA-TM-109300] 02 p0737 N94-13601
Spacelab J experiment descriptions
[NASA-TM-4517] 02 p0586 N94-13732
Growth experiment of narrow band-gap semiconductor PbSnTe single crystals in space (M-1) 02 p0586 N94-13733
Growth of PbSnTe single crystal by traveling-zone method in low gravity (M-2) 02 p0586 N94-13734
Growth of semiconductor compound single crystal InSb by floating zone method (M-3) 02 p0586 N94-13735
Casting of superconducting composite materials (M-4) 02 p0586 N94-13736
Formation of deoxidization products in iron ingot by the addition of Al, Si, and/or Mn (M-5) 02 p0587 N94-13737
Preparation of particle-dispersion alloys (M-6) 02 p0587 N94-13738
Diffusion in liquid state and solidification of binary system (M-7) 02 p0587 N94-13739
High temperature behavior of glass (M-8) 02 p0587 N94-13740
Growth of Si spherical crystals and the surface oxidation (M-9) 02 p0587 N94-13741
Study on solidification of immisible alloys (M-10) 02 p0588 N94-13742
Fabrication of very-low-density, high-stiffness carbon fiber/aluminum hybridized composite with ultra-low density and high stiffness (M-11) 02 p0588 N94-13743
Study on the mechanism of liquid phase sintering (M-12) 02 p0588 N94-13744
Fabrication of Si-As-Te ternary amorphous semiconductor in the microgravity environment (M-13) 02 p0588 N94-13745
Gas-evaporation in low-gravity field (cogelation mechanism of metal vapors) (M-14) 02 p0588 N94-13746
Drop dynamics in space and interference with acoustic field (M-15) 02 p0588 N94-13747
Study of bubble behavior in weightlessness (effects of thermal gradient and acoustic stationary wave) (M-16) 02 p0589 N94-13748
Preparation of optical materials used in non-visible region (M-17) 02 p0589 N94-13749
Marangoni effect induced convection in material processing under microgravity (M-18) 02 p0589 N94-13750
Solidification of eutectic system alloys in space (M-19) 02 p0589 N94-13751
Growth of samarskite crystal under microgravity conditions (M-20) 02 p0590 N94-13752
Growth experiment of organic metal crystal in low gravity (M-21) 02 p0590 N94-13753
Crystal growth of compound semiconductors in a low-gravity environment (InGaAs crystals) (M-22) 02 p0590 N94-13754
Microgravity acceleration measurement environment characterization 02 p0590 N94-13755
Protein crystal growth 02 p0591 N94-13756
Health monitoring of Japanese payload specialist: Autonomic nervous and cardiovascular responses under reduced gravity condition (L-0) 02 p0591 N94-13757
Neurophysiological study on visuo-vestibular control of posture and movement in fish during adaptation to weightlessness 02 p0591 N94-13759
Separation of biogenic materials by electrophoresis under zero gravity (L-3) 02 p0592 N94-13760
Comparative measurement of visual stability in Earth and cosmic space (L-4) 02 p0592 N94-13761
Crystal growth of enzymes in low gravity (L-5) 02 p0592 N94-13762
Studies on the effects of microgravity on the ultrastructure and functions of cultured mammalian cells (L-6) 02 p0592 N94-13763
Gravity, chromosomes, and organized development in aseptically cultured plant cells 02 p0592 N94-13764
Effect of low gravity on calcium metabolism and bone formation (L-7) 02 p0593 N94-13765
Manual control in space research on perceptual-motor functions under zero gravity conditions (L-10) 02 p0593 N94-13767
Study on the biological effect of cosmic radiation and the development of radiation protection technology (L-11) 02 p0593 N94-13768
Amphibian fertilization and development in microgravity 02 p0594 N94-13770
Magnetic resonance imaging after exposure to microgravity 02 p0594 N94-13771
Countermeasure for reducing post-flight orthostatic intolerance: Lower Body Negative Pressure (LBNP) experiment E140 02 p0594 N94-13772
Bone culture research 02 p0595 N94-13773
Autogenic feedback training experiment: A preventative method for space motion sickness 02 p0595 N94-13774
In-flight demonstration of the Space Station Freedom Health Maintenance Facility fluid therapy system (E300/E05) 02 p0595 N94-13775
Renal function alterations during skeletal muscle disuse in simulated microgravity
[NASA-CR-194258] 02 p0733 N94-13824
The influence of a microgravity environment on the dendritic morphology during directional solidification of hypoeutectic Al-Si alloys
[NASA-CR-194139] 02 p0571 N94-13891
Sloshing dynamics on rotating helium dewar tank
[NASA-CR-194403] 02 p0637 N94-13959
Cellular responses to low-gravity: Pilot studies on suborbital rockets and orbiting spacecraft
[NASA-CR-194402] 02 p0729 N94-14494
Sounding Rocket Experiments in Fluid Science and Materials Sciences: TEXUS 25 to 27 and MASER 4, volume 3
[ESA-SP-1132-VOL-3] 03 p0943 N94-15157
Measurements of Interfacial Tension: MITE 03 p0943 N94-15158
Orientation of DNA during free-solution electrophoresis 03 p0944 N94-15162
Density and temperature relaxation near the critical point of carbon dioxide under reduced gravity 03 p0944 N94-15164
Temperature propagation in near-critical fluids prior to and during separation 03 p0944 N94-15165
Pressures of supercritical salt solutions 03 p0945 N94-15166
Unidirectional solidification of liquid-crystal material 03 p0945 N94-15167
Partial melting experiment of Y-Ba-Cu oxide 03 p0945 N94-15168
Liquid phase sintering of tungsten composites under microgravity. Effect of matrix composition 03 p0945 N94-15171
Heat storage module 03 p0946 N94-15172
Movement in microgravity
[NASA-TM-109526] 03 p0881 N94-15389
Evaporation from a meniscus within a capillary tube in microgravity
[NASA-CR-194593] 03 p0976 N94-15654
Mechanisms of combustion limits in premixed gas flames at microgravity
[NASA-CR-194557] 03 p0946 N94-15713
Explosive boiling at very low heat fluxes: A microgravity phenomenon
[NASA-TM-106325] 03 p1046 N94-15817
A feasibility study of a microgravity enhancement system for Space Station Freedom
[NASA-CR-191550] 03 p0886 N94-15864
Cultured normal mammalian tissue and process
[NASA-CASE-MSC-21984-1] 03 p1117 N94-15969
Proceedings of the Second Workshop on Microgravity Experimentation
[DSS-NR15-43-1990] 03 p0977 N94-16071
Scientific use of Space Station Freedom 03 p0977 N94-16072
The Japanese Space Station utilization plan 03 p0977 N94-16074
Canadian microgravity experiments flown in 1989-1990 03 p0977 N94-16075
New findings and instrumentation from the NASA Lewis Microgravity Facility 03 p0977 N94-16076
Laser-liquid interactions under reduced gravity conditions 03 p0977 N94-16077
The vibro-acoustic mapping of low gravity trajectories on a Learjet aircraft 03 p0978 N94-16078
MAXUS: The new sounding rocket program for long duration microgravity flight 03 p0978 N94-16079
Optical systems for the visualization of fluid and solid transparent media under microgravity conditions 03 p0978 N94-16081
QUESTS: A microgravity research facility for materials science experiments 03 p0978 N94-16082
Payloads for the processing of high temperature materials 03 p0979 N94-16083
The Canadian Space Station user development program. Where do we go from here? 03 p0898 N94-16084
Contained liquids in microgravity, part 2 03 p0979 N94-16085
Study of fractal aggregates 03 p0979 N94-16086
Investigation of two-phase flow and boiling heat transfer during quenching of a tube under microgravity 03 p0979 N94-16087
Use of microgravity in the synthesis of ceramics using sol gel techniques 03 p0979 N94-16088
Gas bubble generation and transport in microgravity 03 p0980 N94-16089
Infra Link: A data transmission system for microgravity research 03 p0980 N94-16091
Characteristics of aimed arm movements in humans under low gravity 03 p0980 N94-16093
Statistical techniques for study design of microgravity life sciences experiments 03 p0980 N94-16094
Transcranial Doppler ultrasound studies of cerebral blood-flow in microgravity 03 p0981 N94-16095

Human ocular torsion during parabolic flight: An investigation using electromagnetic scleral search coil
03 p0981 N94-16096
Heart rate response to parabolic flight manoeuvres
03 p0981 N94-16098
Finite element analytical techniques for ceramic production in microgravity: A hypoelastic model
03 p0981 N94-16099
Precise measurement and utilization of acceleration data
03 p0923 N94-16100
The design and analysis of a modular microgravity test platform for use aboard the NASA KC-135 aircraft
03 p0899 N94-16101
Solution behaviour in microgravity: Considerations for protein crystal growth
03 p0982 N94-16102
Materials processing in space: Issues for the third decade
[TABES PAPER 93-260] 03 p0983 N94-16133
Growth of single crystals of mercuric iodide on the ground and in space
[DE93-015523] 03 p1209 N94-16442
Looking at science on board Eureca
[ESA-BR-80] 03 p0874 N94-16584
Studies of premixed laminar and turbulent flames at microgravity
[NASA-CR-194656] 03 p0951 N94-17125
The 1990-1991 NASA space biology accomplishments
[NASA-TM-4501] 03 p1118 N94-17257
Ground testing for the no-vent fill of cryogenic tanks: Results of tests for a 71 cubic foot tank
[NASA-TM-106293] 03 p1030 N94-17486
Ontogenesis of mammals in microgravity
[NASA-TM-103978] 03 p1139 N94-17636
Spacelab 3
[NASA-TM-108750] 04 p1323 N94-18849
Characterization of fluid physics effects on cardiovascular response to microgravity (G-572)
04 p1323 N94-19163
MUZO flight experience with the programmable multizone furnace
04 p1324 N94-19167
Space Applications Industrial Laser System (SAILS)
04 p1325 N94-19173
Space Life Sciences Research: The Importance of Long-Term Space Experiments
[NASA-TM-4502] 04 p1502 N94-19210
Space research on organs and tissues
04 p1503 N94-19214
A scientific role for Space Station Freedom: Research at the cellular level
04 p1503 N94-19215
Microgravity research in plant biological systems: Realizing the potential of molecular biology
04 p1503 N94-19216
Life: Origin and evolution on Earth--How can we escape?
04 p1503 N94-19217
Stability limits and dynamics of nonaxisymmetric liquid bridges
[NASA-CR-194706] 05 p1797 N94-20037
Growth of zinc selenide single crystals by physical vapor transport in microgravity
[NASA-CR-194679] 05 p2017 N94-20346
Evaporation of a sodium tellurite melt in the jamic low gravity drop shaft
05 p1713 N94-20605
Loads produced by a suited subject performing tool tasks without the use of foot restraints
[NASA-TP-3424] 05 p1896 N94-20606
Experimental study of void formation during aluminum solidification in reduced gravity
[NASA-TM-106190] 05 p1692 N94-21604
Strength capabilities and load requirements while performing torquing tasks in zero gravity
[NASA-TP-3433] 05 p1897 N94-21627
Rewetting of monogroove heat pipe in Space Station radiators
[NASA-CR-194781] 05 p1804 N94-21820
Lewis Research Center R and D Facilities
[NASA-TM-109400] 06 p2630 N94-23135
Microgravity sciences application visiting scientist program
[NASA-CR-194804] 06 p2267 N94-23287
High power density proton exchange membrane fuel cells
06 p2393 N94-23359
Responses to LBNP in men with varying profiles of strength and aerobic capacity: Implications for flight crews
[NASA-TP-3346] 06 p2426 N94-23530
The study of dopant segregation behavior during the growth of GaAs in microgravity
[NASA-CR-193905] 06 p2267 N94-23549
Studies of two phase flow
[NASA-CR-195099] 06 p2267 N94-23594
Micro-gravity compatible drive (MGCD)
06 p2355 N94-23988
The development of the HERA Test Facility (HTF)
06 p2197 N94-24020
Roles, uses, and benefits of general aviation aircraft in aerospace engineering education
[NASA-TM-106463] 06 p2153 N94-24100
Autogenic-feedback training: A potential treatment for post-flight orthostatic intolerance in aerospace crews
[NASA-TM-108785] 06 p2426 N94-24102
Conceptual design of a device to measure hand swelling in a micro-gravity environment
[NASA-CR-195509] 06 p2437 N94-24330
NASA project 1: Full-body dynamometer
[NASA-CR-195507] 06 p2438 N94-24331
Microgravity Studies of Organic and Polymeric Materials
[NASA-CP-3250] 06 p2223 N94-24338
Numerical modeling of physical vapor transport under microgravity conditions: Effect of thermal creep and stress
06 p2223 N94-24340
Low-gravity electrodeposition and growth of polymer thin films with large third-order optical nonlinearities by electrochemical processes for devices: Thiophene-based polymers
06 p2225 N94-24346
Processing of semicrystalline polymers
06 p2226 N94-24351
Polymer morphologh
06 p2226 N94-24353
Measuring the dynamics of structural changes in biological macromolecules from light scattering data
06 p2422 N94-24426
Torque equilibrium attitudes for the Space Station
06 p2208 N94-24449
Effects of thermal-solutal convection on temperature and solutal fields under various gravitational orientations
06 p2267 N94-24451
JOVE NASA-FIT program: Microgravity and aeronomy projects
[NASA-CR-195121] 06 p2631 N94-24493
Japanese aerospace science and technology 1992. A bibliography with indexes
[NASA-SP-7104] 06 p2631 N94-24585
Concepts and embodiment design of a reentry recumbent seating system for the NASA Space Shuttle
[NASA-CR-195504] 06 p2438 N94-24667
Artificial gravity in space flight
[AD-A273420] 06 p2427 N94-24928
The role of visual context in manual target localization
06 p2429 N94-25351
Loading, electromyograph, and motion during exercise
06 p2427 N94-25359
Development of a model to assess orthostatic responses
06 p2427 N94-25376
Study on melted solution stirring under microgravity
07 p2730 N94-25585
Autonomous support for microorganism research in space
07 p2903 N94-25672
Bioregenerative system components for microgravity
07 p2903 N94-25673
First lunar outpost
07 p2943 N94-25694
Microgravity ignition experiment
07 p2761 N94-25707
Risks and issues in fire safety on the Space Station
[NASA-TM-106430] 07 p2692 N94-27436
Annals of the Research Inst. of Environmental Medicine, Nagoya Univ., volume 44
[REPT-44-VOL-44] 07 p2911 N94-27442
Changes in circadian variations of urine excretion in tail-suspended rats
07 p2911 N94-27443
Endocrinological evaluations of muscle and bone atrophy in tail-suspended rats
07 p2903 N94-27444
Changes in fluid and electrolyte metabolism during water immersion at high or thermoneutral temperature
07 p2912 N94-27445
Study on posture control and adaption mechanism under weightlessness: Results of second rehearsal for space experiment using carp
07 p2912 N94-27446
The mechanism of caloric nystagmus under microgravity. 1: Changes of endolymphatic pressure in the semicircular canal of pigeon by caloric stimulation
07 p2914 N94-27457
Comparative measurement of visual stability in cosmic space: Onboard experiment and pre-flight activities
07 p2916 N94-27463
Thermocapillary flow with evaporation and condensation and its effect on liquid retention in low-G fluid acquisition devices
[NASA-TP-3463] 07 p2797 N94-27639
Construction and test of experiment hardware for a space experiment on Spacelab mission IML-2
[DLR-FB-93-23] 07 p2903 N94-27743
Gravity dependence or pressure drop and heat transfer in straight two-phase heat transport system condenser ducts
[NLR-TP-92167-U] 07 p2798 N94-27853
An analysis of the loads applied to a heavy Space Station rack during translation and rotation tasks
[NASA-TM-104790] 07 p2697 N94-28183
Workshop on Countering Space Adaptation with Exercise: Current Issues
[NASA-CP-3252] 07 p2934 N94-28361
Exercise detraining: Applicability to microgravity
07 p2934 N94-28364
Weightlessness and the human skeleton: A new perspective
07 p2935 N94-28368
The use of biomechanics in the study of movement in microgravity
07 p2936 N94-28373
Psychophysiology in microgravity and the role of exercise
07 p2936 N94-28374
Microgravity science and applications. Program tasks and bibliography for FY 1993
[NASA-TM-4569] 08 p3227 N94-28415
Japanese Journal of Aerospace and Environmental Medicine, vol. 30, no. 3
[JTN-94-80606] 08 p3387 N94-28495
Some issues on Japan's space food development and relating preliminary experimental study
08 p3388 N94-28498
Japanese Journal of Aerospace and Environmental Medicine, volume 30, no. 1
[JTN-94-80598] 08 p3389 N94-28850
Image technology and information analysis of bone change with gravitational exposure
08 p3389 N94-28851
Overview of space environment utilization science
[JTN-94-80581] 08 p3227 N94-28938
Fluid and transportation phenomena under microgravity
08 p3227 N94-28939
Combustion studies under microgravity
08 p3228 N94-28940
Glass studies under microgravity
08 p3228 N94-28941
Fabrication of electronic materials in space
08 p3228 N94-28942
Protein crystal growth in microgravity
08 p3228 N94-28943
Cell culture in space
08 p3228 N94-28944
Cosmic energy equipment
08 p3229 N94-28945
The MERSS 5th Symposium on Space Medicine: Medical and Physiological Experiment Utilizing Parabolic Flight
[JTN-94-80588] 08 p3392 N94-29709
Microgravity by parabolic flight with MU-300 aircraft
08 p3392 N94-29710
Space movement of Trichinella spiralis under microgravity
08 p3387 N94-29711
Posture control of goldfishes under microgravity
08 p3387 N94-29712
Behavior and visual control of cyprinodonts under microgravity
08 p3387 N94-29713
A discussion of eye-head coordinative movement under microgravity during parabolic flight
08 p3393 N94-29715
Analysis of various biological activity parameters during parabolic flight
08 p3393 N94-29716
Hemodynamic measurement during parabolic flight
08 p3393 N94-29717
Motion sickness in parabolic flight: Possibility of electrogastrography as an objective index
08 p3393 N94-29718
Summary report of mission acceleration measurements for Spacehab-01, STS-57 launched 21 June 1993
[NASA-TM-106514] 08 p3168 N94-29757
Japanese Journal of Aerospace and Environmental Medicine, vol. 30, no. 2
[JTN-94-80599] 08 p3394 N94-29863
Effect of water immersion on muscle sympathetic nerve response during static muscle contraction
08 p3394 N94-29865
Shortening velocity and calcium sensitivity of single fibers from hindlimb suspended muscle in rats
08 p3387 N94-29866
Microgravity compatible drive system-rider. New technologies
[PB94-138583] 08 p3229 N94-29996
Laser beam welding of AISI 316 stainless steel in microgravity environment: Experiments aboard a KC-135 flight
[ISBN-0-315-86095-2] 08 p3229 N94-30145
Directional solidification characteristics of hyper-eutectic Al-Cu alloys under varying gravity conditions
[ISBN-0-315-86108-8] 08 p3209 N94-30146
Survey report of JSUP Space Environment Utilization Research Committee in fiscal year 1992: Functional New Materials Session
[JTN-94-80582] 08 p3159 N94-30162
Microgravity fluid science research in Europe
[AD-B179178] 08 p3229 N94-30409
Control system design for A and R supported microgravity experiments: An experiment payload control development
[AD-B179107] 08 p3229 N94-30421

Microencapsulation of anti-tumor, antibiotic and thrombolytic drugs in microgravity
08 p3397 N94-30453
Survey report of JSUP Space Environment Utilization Research Committee in fiscal year 1992: Metallic Materials Session
[JTN-94-80583] 08 p3159 N94-30794
Space acceleration measurement system
[NASA-TM-109754] 09 p3913 N94-31807
Steady thermal convection in multiple liquid layers
09 p3705 N94-31844
Solid surface
[NASA-TM-109746] 09 p3634 N94-31883
Defying gravity
[NASA-TM-109747] 09 p3667 N94-31884
An experimental study of void formation during aluminum solidification in reduced gravity
09 p3667 N94-31944
Boundary element analysis of three-dimensional nonlinear hydrodynamics in a reduced gravity environment 09 p3668 N94-32715
Vibration Isolation Technology (VIT) ATD project
[NASA-TM-106496] 09 p3567 N94-33064
Design, characterization, and control of the NASA three degree of freedom reaction compensation platform
09 p3605 N94-33304
The second giant leap
[NASA-TM-109827] 10 p4149 N94-33581
Investigation of moving belt radiator technology issues
[NASA-CR-195340] 10 p4032 N94-33950
Gas-grain simulation facility: Aerosol and particle research in microgravity
[NASA-CP-10135] 10 p4161 N94-34212
Partial gravity simulation using a pneumatic actuator with closed loop mechanical amplification
[NASA-TM-104798] 10 p4012 N94-34395
Cargo systems manual: Heat Pipe Performance (HPP) STS-66
[NASA-TM-109784] 10 p4131 N94-34720
US experiment flown on the Soviet biosatellite Cosmos 1667
[NASA-TM-108803] 10 p4102 N94-34951
Analysis of phase distribution phenomena in microgravity environments
[NASA-CR-196038] 11 p4249 N94-35237
Effect of microgravity on plant growth
[NASA-CR-196004] 11 p4296 N94-35257
The control of satellites with microgravity constraints: The COMET Control System 11 p4207 N94-35632
Microgravity isolation system design: A modern control synthesis framework 11 p4215 N94-35851
Space-based crystal growth and thermocapillary flow
11 p4342 N94-35971
Design and development of experimental facilities for short duration, low-gravity combustion and fire experiments
[NASA-CR-196107] 12 p4389 N94-36967
Methodologies to determine forces on bones and muscles of body segments during exercise, employing compact sensors suitable for use in crowded space vehicles
[NASA-CR-196272] 12 p4487 N94-37458
Project JOVE --- microgravity experiments and applications
[NASA-CR-196292] 12 p4445 N94-37635

MICROGRAVITY APPLICATIONS
Protein, glass, aerosol research, containerless processing and diagnostics technology for microgravity application 01 p0106 N94-10112
Design of a CVD reactor for the deposition of diamond in a microgravity environment 01 p0109 N94-10127
Force and power efficiency of micro-g electromagnetic levitation coils 01 p0110 N94-10129
Determination of the viscous acoustic field for liquid drop positioning/forcing in an acoustic levitation chamber in microgravity 01 p0110 N94-10131
The surface plasmon spectroscopy as diagnostic technique in microgravity experiments
01 p0110 N94-10133
Microgravity experiments using TR-1A rocket
01 p0112 N94-10142
Thermocapillary convection instability in microgravity crystal growth 01 p0112 N94-10172
Solidification in immiscible systems: The influence of processing conditions on resulting microstructures
01 p0112 N94-10174
Scientific specifications for an automated facility for growing large semiconducting crystals from the melt in space 01 p0114 N94-10180
Crystal growth from low temperature vapour phase
01 p0115 N94-10191
Reduce fluid experiment system flight data from IML-1
[NASA-CR-193835] 02 p0804 N94-12873
Scientific use of Space Station Freedom
03 p0977 N94-16072
The ESA telescience program
03 p0977 N94-16073
The Japanese Space Station utilization plan
03 p0977 N94-16074
New findings and instrumentation from the NASA Lewis Microgravity Facility 03 p0977 N94-16076
Laser-liquid interactions under reduced gravity conditions 03 p0977 N94-16077
The vibro-acoustic mapping of low gravity trajectories on a Learjet aircraft 03 p0978 N94-16078
MAXUS: The new sounding rocket program for long duration microgravity flight 03 p0978 N94-16079
Development of the Laser-based R/D Test-bed System (LTS) 03 p0978 N94-16080
Optical systems for the visualization of fluid and solid transparent media under microgravity conditions
03 p0978 N94-16081
QUESTS: A microgravity research facility for materials science experiments 03 p0978 N94-16082
Payloads for the processing of high temperature materials 03 p0979 N94-16083
Materials processing in space: Issues for the third decade
[TABES PAPER 93-260] 03 p0983 N94-16133
The first flight of the QUESTS GAS payload G-521
04 p1325 N94-19170
Cooling apparatus and couplings therefor
[NASA-CASE-ARC-11921-1] 05 p1800 N94-20371
Microgravity science and applications. Program tasks and bibliography for FY 1993
[NASA-TM-4569] 08 p3227 N94-28415
Plasma heating for containerless and microgravity materials processing
[NASA-CASE-NPO-18819-1-CU]
08 p3229 N94-29371
Summary report of mission acceleration measurements for Spacehab-01, STS-57 launched 21 June 1993
[NASA-TM-106514] 08 p3168 N94-29757
Survey report of JSUP Space Environment Utilization Research Committee in fiscal year 1992: Functional New Materials Session
[JTN-94-80582] 08 p3159 N94-30162
Vibration Isolation Technology (VIT) ATD project
[NASA-TM-106496] 09 p3567 N94-33064
Design, characterization, and control of the NASA three degree of freedom reaction compensation platform
09 p3605 N94-33304
Gas-grain simulation facility: Aerosol and particle research in microgravity
[NASA-CP-10135] 10 p4161 N94-34212
Materials processing apparatus development for fluoride glass
[NASA-CR-193963] 10 p4030 N94-34388
Space-based crystal growth and thermocapillary flow
11 p4342 N94-35971
Project JOVE --- microgravity experiments and applications
[NASA-CR-196292] 12 p4445 N94-37635

MICROHARDNESS
DBTT measurement by use of Small Punch (SP) test
[DE93-753188] 01 p0183 N94-11168
Fracture behavior of vanadium/vanadium silicide in-situ composites
[DE93-013422] 02 p0556 N94-13389
Laser-shock damage of iron-based materials
[AD-A267196] 03 p1038 N94-15852
Ion implantation effects on surface-mechanical properties of metals and polymers
[DE93-014661] 03 p0958 N94-16453
Investigation of the origin of hot spots in deformed crystals: Ammonium perchlorate studies
[AD-A267692] 03 p1214 N94-17270
Mechanical properties and crystal growth studies of semiconductor alloys
[AD-A268144] 03 p1216 N94-17454
Superhardness effect in Au/Ni multilayers
[DE93-016444] 04 p1357 N94-17860
Developing and understanding the high temperature behavior of niobium aluminides and niobium aluminide composites
[AD-A268874] 04 p1341 N94-18636
Metastable bcc phase formation in the Nb-Cr system
[DE93-018376] 05 p2012 N94-19926
Contribution to the interface micromechanical study and to the damage fundamental phenomena in glass fiber epoxy resin model composites
[ISAL-93-0027] 06 p2227 N94-23133
Robotic weld overlay coatings for erosion control
[DE94-002665] 06 p2258 N94-24749
The fracture behavior of a CVD crystalline Si3N4/amorphous Si3N4 composite
[DE94-002646] 07 p2750 N94-26124
The influence of TIG welding thermal cycles on HSLA-100 steel plate
[AD-A274248] 07 p2740 N94-27009
Characterization of structure and mechanical properties of MoSi2-SiC nanolayer composites
[DE94-004982] 08 p3175 N94-28579
Robotic weld overlay coatings for erosion control
[DE94-008004] 09 p3658 N94-32408
Robotic weld overlay coatings for erosion control
[DE94-009703] 10 p4060 N94-33902
First results from the Los Alamos plasma source ion implantation experiment
[DE94-003931] 12 p4414 N94-36461

MICROINDENTATION
U MICROHARDNESS

MICROINSTRUMENTATION
High- and low-temperature bonding techniques for microstructures
[DE93-017173] 04 p1595 N94-17992
Diagnostics and microelectronics
[DE94-003016] 07 p2784 N94-26777
Opportunities for High Aspect Ratio Micro-Electro-Magnetic-Mechanical Systems (HAR-MEMMS) at Lawrence Berkeley Laboratory
[DE94-003499] 07 p2827 N94-27722
Micro-sensors for in-situ meteorological measurements 08 p3236 N94-29777
Smart focal-plane technology for micro-instruments and micro-rovers 08 p3237 N94-29780
Microfabricated silicon biosensors for microphysiometry 08 p3238 N94-29783
Electrostatically suspended and sensed micro-mechanical rate gyroscope
11 p4224 N94-35908

MICROMACHINING
Fabrication process for cantilever beam micromechanical switches
[AD-A269716] 04 p1404 N94-18749
Cutting and drilling studies using high power visible lasers
[DE93-019149] 04 p1441 N94-19294
Micromachined actuator and sensor capabilities at the Microelectronics Development Laboratory
[DE93-019417] 05 p1769 N94-21918
Diagnostics and microelectronics
[DE94-003016] 07 p2784 N94-26777
Proceedings of the Workshop on Microtechnologies and Applications to Space Systems
[NASA-CR-195688] 08 p3235 N94-29767
Micromanufacturing: Recent developments in this country and abroad 08 p3235 N94-29769
Microactuator production via high aspect ratio, high edge acuity metal fabrication technology
08 p3235 N94-29770
Micro guidance and control technology overview
08 p3144 N94-29772
A broad-band microseismometer for planetary operations 08 p3237 N94-29778
Macro, mini, micro and nano (M(sup 3)N) technologies for the future 08 p3238 N94-29786
Emerging technologies in microguidance and control
08 p3144 N94-29788
The application of micromachined sensors to manned space systems 08 p3171 N94-29791
RF vacuum microelectronics
[AD-A276512] 09 p3691 N94-31928

MICROMECHANICS
Sensor abstractions to support many-robot systems
[AD-A265907] 01 p0180 N94-10803
Micromechanisms of fatigue crack growth and fracture toughness in metal matrix composites
[AD-A265153] 01 p0187 N94-11096
An analysis of fiber-matrix interface failure stresses for a range of ply stress states
[NASA-TM-108999] 01 p0067 N94-11276
Mechanical interaction between synthetic fiber and cement base matrix in FRC composites
[AD-A265310] 01 p0073 N94-11686
Analytical models for describing the mechanical behavior of fiber reinforced composites
[AD-A265906] 01 p0074 N94-12347
Properties of interfacial tribo-films
[AD-A265591] 01 p0182 N94-12374
Micromechanical strength effects in shock compression of solids
[DE93-014425] 02 p0670 N94-12887
A stochastic model for behavior analysis of fiber-reinforced quasi-brittle materials
02 p0672 N94-13594
Micromechanical damage theories for brittle solids with interacting microcracks
[AD-A266348] 02 p0673 N94-13778
Hierarchical nonlinear behavior of hot composite structures
[NASA-TM-106229] 02 p0676 N94-14041
Probabilistic micromechanics for high-temperature composites
[NASA-CR-191150] 02 p0676 N94-14408

Elastic-plastic finite element analyses of an unidirectional, 9 vol percent tungsten fiber reinforced copper matrix composite
[NASA-TM-106304] 02 p0559 N94-14719
Thermoelastic response of metal matrix composites with large-diameter fibers subjected to thermal gradients
[NASA-TM-106344] 02 p0560 N94-14823
Inelastic deformation of metal matrix composites
[NASA-CR-191522] 03 p0930 N94-15106
Environmental effects on elevated temperature subcritical crack growth of SiC/SiC composites
[DE93-015688] 03 p0934 N94-16158
Micromechanisms of monotonic and cyclic subcritical crack growth in advanced high melting point low-ductility intermetallics
[AD-A267764] 03 p0961 N94-17223
Micromechanics modeling and analysis of Haversian compact bone tissues as a fiber reinforced composite material
[AD-A268250] 03 p1129 N94-17456
Thermo-mechanical analysis of oxidation protected carbon-carbon composites
[AD-A268191] 03 p0941 N94-17597
Fabrication process for cantilever beam micromechanical switches
[AD-A269716] 04 p1404 N94-18749
The intelligent processing of materials
[AD-A269250] 04 p1362 N94-18923
Computational mechanics of composite materials
[PB93-195782] 04 p1343 N94-19281
Subcritical crack growth in continuous-fiber reinforced ceramic composites
[DE93-018784] 04 p1343 N94-19335
Micromechanics of interfaces in metal matrix composites
[AD-A271012] 04 p1345 N94-19776
Biotechnology and composite materials
[AD-A264278] 05 p1673 N94-20327
Direct imaging of the surface microstructure of dielectric materials using an atomic force microscope
[AD-A272251] 05 p2018 N94-20575
Thermal stress analysis of composites in the space environment 05 p1661 N94-21379
Determination of fiber-matrix interface failure parameters from off-axis tests
[NASA-TM-109043] 06 p2241 N94-23274
Micromechanical failure modes in brittle matrix composites 06 p2255 N94-24232
Micromechanical characterization of ceramic-matrix composites using the instrumented microindentation technique 06 p2256 N94-24233
Role of interfaces on the cyclic fatigue behaviour of ceramic matrix composites 06 p2256 N94-24234
Microstructure and micromechanical behaviour of CMCs 06 p2256 N94-24236
Micromechanical simulation of damage progression in carbon phenolic composites 06 p2231 N94-24446
Environmentally assisted cracking of high strength beta titanium alloys
[AD-A273598] 06 p2245 N94-24823
A nonlinear three-dimensional micromechanics model for fiber-reinforced laminated composites
[AD-A273772] 07 p2705 N94-25857
Computer modelling of cyclic deformation of high-temperature materials
[AD-A274504] 07 p2840 N94-27034
Deformation, constitutive behavior, and damage of advanced structural materials under multiaxial loading
[AD-A274165] 07 p2709 N94-27142
Prediction of stress-strain response of SCS-6/Timetal-21S subjected to a hypersonic flight profile
[NASA-TM-109026] 08 p3177 N94-28823
Proceedings of the Workshop on Microtechnologies and Applications to Space Systems
[NASA-CR-195688] 08 p3235 N94-29767
Microactuator production via high aspect ratio, high edge acuity metal fabrication technology 08 p3235 N94-29770
Toward milli-Newton electro- and magneto-static microactuators 08 p3238 N94-29784
Macro, mini, micro and nano (M(sup 3)N) technologies for the future 08 p3238 N94-29786
Integrated microgyroscope 08 p3239 N94-29789
Micro-opto-mechanical devices and systems using epitaxial lift off 08 p3239 N94-29793
Micromechanics of the dynamic response of ceramics and ceramic composites 08 p3217 N94-29975
Multiple Concentric Cylinder Model (MCCM) user's guide
[NASA-CR-195299] 08 p3183 N94-30125
Micromechanical analysis of thermo-inelastic multiphase short-fiber composites
[NASA-CR-195290] 08 p3183 N94-30178
Simulation of composite material response under dynamic compressive loading
[DE94-005272] 08 p3184 N94-30589
Numerical modeling and prediction of the thermomechanical behavior of fiber-reinforced composites 08 p3186 N94-30956
A class of inclusion problems for the strengthening of brittle and ductile composites 08 p3186 N94-30959
Micromechanical analysis of the interface and basic damage modes in glass fiber/epoxy resin model composites
[ONERA-NT-1993-4] 09 p3618 N94-31225
Unidirectional composites compressive behaviour: Test methods and micromechanical approach
[ONERA-NT-1993-10] 09 p3618 N94-31232
Inelastic deformation of metal matrix composites 09 p3618 N94-31285
On the constitutive response of transversely loaded fiber composites with compliant interphases 09 p3619 N94-31555
Micromechanics and effective properties of particulate composites and fluid suspensions 09 p3703 N94-31744
Toughening mechanisms in fiber-reinforced ceramic-matrix composites 09 p3622 N94-31943
Fracture mechanics and micromechanisms in fiber-reinforced composites 09 p3622 N94-31986
Finite element analysis of damage in fibrous composites using a micromechanical model
[AD-A277226] 09 p3623 N94-32024
Mechanics of the single fiber pullout problem with several interface conditions 09 p3623 N94-32078
New micro- and macroscopic models of contact and friction
[AD-A277240] 09 p3726 N94-32320
Development of an advanced continuum theory for composite laminates, volume 1
[AD-A277275] 09 p3625 N94-32591
Development of an advanced continuum theory for composite laminates, volume 2
[AD-A277276] 09 p3625 N94-32592
Fracture micromechanics of continuous fiber and textile reinforced metal and ceramic matrix composites
[AD-A277434] 09 p3627 N94-33008
Nonlocal theory for fracturing of quasibrittle materials
[AD-A278283] 09 p3740 N94-33143
Micromechanical characterization of nonlinear behavior of advanced polymer matrix composites
[NASA-TM-109129] 10 p4025 N94-34397
Analysis of woven and braided fabric reinforced composites
[NASA-CR-194930] 10 p4020 N94-34399
Planar rotational magnetic micromotors with integrated shaft encoder and magnetic rotor levitation 11 p4224 N94-35907
Fibre-matrix interface properties in Ti-matrix composites: Chemical compatibility and micromechanical behaviour 12 p4401 N94-36657
Metal matrix composites: Analysis of simple specimens and model components under creep and fatigue loading 12 p4402 N94-36661
Micromechanical modeling of damage growth in titanium based metal-matrix composites 12 p4402 N94-36664
Modelling and testing fibre reinforced titanium for design purposes 12 p4403 N94-36670
A fully coupled thermal, chemical, mechanical cookoff model
[DE94-011432] 12 p4428 N94-37201
A methodology to predict damage initiation, damage growth and residual strength in titanium matrix composites
[NASA-TM-109135] 12 p4405 N94-37320
Micromechanical modeling of advanced materials
[DE94-011249] 12 p4405 N94-37627
Strength characteristics and crack growth behavior of a composite with well aligned fibers 12 p4459 N94-37804
Statistical scaling relationships and size effects in the strength and creep rupture of fibrous composites 12 p4460 N94-37809

MICROMETEORITES
K/T spherules from Haiti and Wyoming: Origin, diagenesis, and similarity to some microtektites 01 p0281 N94-12085
A new carbon-rich phase (COPS) in Antarctic micrometeorites 01 p0432 N94-12233
Removal of carbonaceous contaminants from silica aerogel 03 p0953 N94-16256
An iridium-rich iron micrometeorite with silicate inclusions from the Moon 03 p1242 N94-16281
Size distribution of interplanetary iron and stony particles related with deep-sea spherules 03 p1245 N94-16388
C/O atomic ratios in micrometer-size crushed grains from Antarctic micrometeorites and two carbonaceous meteorites 05 p2082 N94-20678
Elemental depletions in Antarctic micrometeorites and Arctic cosmic spherules: Comparison and relationships 05 p2082 N94-20704
Micrometeorite dynamic pyrometamorphism: Nonstoichiometric clinoenstatite (CLEN) 05 p2083 N94-20715
Micrometeorite dynamic pyrometamorphism: Observation of a thermal gradient in iron-nickel sulfide 05 p2083 N94-20716
Micrometeorite pre-solar diamonds from Greenland cryoconite? 05 p2086 N94-20895
Mechanical failure probability of glasses in Earth orbit
[NASA-CR-195912] 10 p4031 N94-34947

MICROMETEOROIDS
NT ZODIACAL DUST
Dimensional scaling for impact cratering and perforation
[NASA-CR-188259] 01 p0042 N94-10665
Composition and modal frequencies of hypervelocity particles less than 1 millimeter in diameter in low-Earth orbit 01 p0429 N94-12063
Modelling hypervelocity impacts into aluminum structures based on LDEF data 01 p0190 N94-12178
Model of optical scatter from microimpacts on the Hubble Telescope 01 p0384 N94-12189
Interactions between spacecraft and their environments
[NASA-TM-106115] 02 p0541 N94-13917
Secondary impact hazard assessment
[NASA-CR-188261] 02 p0543 N94-14483
Long Duration Exposure Facility experiment M0003 deintegration/findings and impacts
[AD-A267140] 03 p0885 N94-15749
Impact penetration experiments in teflon targets of variable thickness 03 p1063 N94-16253
Densities of 5-15 micron interplanetary dust particles 03 p1244 N94-16367
The effect of an on-orbit near encounter on the number flux density of micron sized particles 03 p0899 N94-16374
Dust grain resonant capture: A statistical study 03 p1245 N94-16384
Resolving LDEF's flux distribution: Orbital (debris?) and natural meteoroid populations 03 p1245 N94-16391
Determination of parameters for hypervelocity dust grains encountered in near-Earth space 05 p2084 N94-20817
Intact capture of hypervelocity particles on Shuttle 05 p2085 N94-20837
A fresh look at crater scaling laws for normal and oblique hypervelocity impacts 05 p1666 N94-20864
Geometrical analysis of the microcraters found on LDEF samples 05 p1666 N94-20890
On dust emissions from the jovian system 05 p2141 N94-20909
Orbital debris and micrometeoroids: LDEF and Mir data 05 p1659 N94-21368
Combination of on ground experiments and analysis software for the evaluation of material degradation in space (SILEX project) 05 p1662 N94-21389
Hypervelocity impact induced arcing and Kapton pyrolization in a plasma environment
[NASA-TM-106528] 08 p3167 N94-28814
Space Station WP-2 application of LDEF MLI results 09 p3592 N94-31016
Morphology correlation of craters formed by hypervelocity impacts 09 p3594 N94-31031
Micrometeoroid/space debris effects on materials 09 p3595 N94-31032
Purity and cleanness of aerogel as a cosmic dust capture medium 11 p4247 N94-35469
Morphology of meteoroid and space debris craters on LDEF metal targets 11 p4353 N94-36159

MICROMETEOROLOGY
NT MICROBURSTS (METEOROLOGY)
The footprint area influencing a high-volume air sampler
[DE93-013947] 02 p0706 N94-13095
Atmospheric turbulence and diffusion research
[DE93-011842] 02 p0718 N94-14425
On the temperature distribution near a cold surface
[AD-A275162] 08 p3332 N94-29288
Study of the energy partition in complex terrains (deforested and forested areas)
[INPE-5522-TDI/519] 10 p4083 N94-34225

MICROMETEORS
U MICROMETEOROIDS

MICROMETERS
Proceedings of the 4th European Congress on Chronometry
[ETN-93-94633] 04 p1424 N94-18006

Development of ultrasonic motor and application to silent alarm analog quartz watch 04 p1425 N94-18016

MICROMINIATURIZATION

Toward milli-Newton electro- and magneto-static microactuators 08 p3238 N94-29784

Macro, mini, micro and nano (M(sup 3)N) technologies for the future 08 p3238 N94-29786

Emerging technologies in microguidance and control 08 p3144 N94-29788

Micro guidance and control synthesis: New components, architectures, and capabilities 08 p3144 N94-29792

The universal applications of microtubes and microtube composites 08 p3186 N94-30452

MICROMINIATURIZED ELECTRONIC DEVICES

Microfabricated silicon biosensors for microphysiometry 08 p3238 N94-29783

Macro, mini, micro and nano (M(sup 3)N) technologies for the future 08 p3238 N94-29786

Control of micromachined deformable mirrors 08 p3239 N94-29787

Emerging technologies in microguidance and control 08 p3144 N94-29788

The application of micromachined sensors to manned space systems 08 p3171 N94-29791

Micro guidance and control synthesis: New components, architectures, and capabilities 08 p3144 N94-29792

Single event upset and latchup measurements at Brookhaven National Laboratory 08 p3495 N94-30212

Electrostatically suspended and sensed micro-mechanical rate gyroscope 11 p4224 N94-35908

MICROMOTORS

Design and testing of planar magnetic micromotors fabricated by deep x ray lithography and electroplating [DE93-012856] 02 p0618 N94-12821

Electrostatic micrometers: Recent developments and perspectives of uses in clock and watch making 04 p1425 N94-18014

Piezo-electric motor: Perspectives and miniaturization 04 p1408 N94-18015

Silicon micro-actuator 04 p1408 N94-18017

Simulation of a quartz-clockwork 04 p1426 N94-18019

Electric measurement of Lavet motors 04 p1408 N94-18022

New current reduction system for watches with integrated current regulation motors 04 p1428 N94-18034

Some variation in the movement base of the ETA 251 series 04 p1428 N94-18035

Lavet type stepping motors and associated controls 05 p1752 N94-20632

Microactuator production via high aspect ratio, high edge acuity metal fabrication technology 08 p3235 N94-29770

Planar rotational magnetic micromotors with integrated shaft encoder and magnetic rotor levitation 11 p4224 N94-35907

MICROORGANISMS

NT ARCHAEBACTERIA
NT BACILLUS
NT BACTERIA
NT CLOSTRIDIUM BOTULINUM
NT ESCHERICHIA
NT HUMAN IMMUNODEFICIENCY VIRUS
NT PARAMECIA
NT PROTOZOA
NT PSEUDOMONAS
NT SALMONELLA
NT VIRUSES

Spacelab J air filter debris analysis [NASA-CR-192569] 01 p0301 N94-11201

The role of certain infauna and vascular plants in the mediation of redox reactions in marine sediments 01 p0268 N94-12454

Biodiesel/aquatic species project report, FY 1992 [DE93-010024] 02 p0709 N94-14087

Regulation of attached bacterial growth by adsorbed proteins [AD-A267756] 03 p1118 N94-17275

Improving the biodegradative capacity of subsurface bacteria [DE93-013171] 04 p1501 N94-18051

Microbial degradation of poly-b-esters: A mechanistic study, cellulose acetate biodegradability [AD-A271368] 04 p1374 N94-19586

Microbial biofilm formation and its consequences for the CELSS program [NASA-CR-195146] 06 p2438 N94-24706

Symbiosis in marine luminous bacteria [AD-A273540] 06 p2422 N94-24791

Autonomous support for microorganism research in space 07 p2903 N94-25672

Journal of NIRE, volume 2, number 4 [JTN-94-80554] 07 p2869 N94-28147

Collaboration of chemical oxidation and biological treatment for removal of refractory organic substances 07 p2870 N94-28149

Treatment of refractory organic substances with combined use of chemical oxidation and biological treatment. Part 2: Biodegradability of ozonation products of chlorophenol 07 p2870 N94-28151

Researches on bioconversion of coal into liquid product 08 p3187 N94-28677

Fundamental studies on the corrosion behavior of weldments in marine microbial environments [AD-A275247] 08 p3203 N94-28900

Stable RNA sequences as a tool for DNA probes and phylogenetic studies [PB94-135423] 08 p3385 N94-29156

Growth of hydrocarbon-rich microalga Botryococcus braunii in secondarily treated sewage and its consumption of nitrate ion and phosphate ion 08 p3387 N94-29519

Microfabricated silicon biosensors for microphysiometry 08 p3238 N94-29783

Biodiesel from aquatic species [DE94-000275] 08 p3225 N94-30038

Exopaleontology and the search for a fossil record on Mars 11 p4360 N94-35425

Studying of ion implantation effect on the biology in China [DE94-620692] 12 p4479 N94-37535

Biological determinants of photobioreactor design [DE94-011665] 12 p4468 N94-37740

MICROPARTICLES

Detection of single molecules in microspheres [DE93-017776] 04 p1567 N94-18493

Feasibility study: Monodisperse polymer particles containing laser-excitable dyes [NASA-CR-194280] 04 p1373 N94-19402

Microspheres for laser velocimetry in high temperature wind tunnel 07 p2682 N94-27903

The impact of electrically charged microspheres with planar surfaces under vacuum conditions 08 p3320 N94-29765

Microencapsulation of anti-tumor, antibiotic and thrombolytic drugs in microgravity 08 p3397 N94-30453

Space hypervelocity microparticle impact damage in polymer matrix composites [ISBN-0-315-87057-5] 09 p3652 N94-31692

Stabilized alumina/ethanol colloidal dispersion for seeding high temperature air flows [NASA-TM-106591] 09 p3713 N94-32983

Counting particles emitted by stratospheric aircraft and measuring size of particles emitted by stratospheric aircraft [NASA-CR-195908] 09 p3769 N94-33170

JPRS report: Science and technology. Central Eurasia: Physics and mathematics [JPRS-UPM-93-003] 10 p4132 N94-35118

Digital control programmer for temperature control [DE94-615584] 11 p4309 N94-36382

MICROPHONES

Free-field sensitivity calibration of laboratory standard microphones by the reciprocity technique: Measurements for the 1991 EEC intercomparison [NPL-RSA(EXT)-0043] 03 p1176 N94-15019

Acoustic intensity measurements in the presence of low Mach number flow [AD-A269995] 04 p1562 N94-18664

Head related transfer function pseudo-stereophony [NASA-CASE-ARC-11919-1-NP] 06 p2525 N94-23312

Comparison of measured and predicted pure tone propagation levels from JAPE-1: An evaluation of the performance of ASOPRAT 06 p2527 N94-24212

High temperature sensor/microphone development for active noise control [NASA-CR-195214] 07 p2812 N94-27214

Improved in-flow acoustic sensor [NASA-CASE-ARC-12001-1] 08 p3478 N94-29363

A silicon condenser microphone: Modelling and electronic circuitry [ISBN-9-09-005279-8] 09 p3688 N94-31517

A silicon condenser microphone: Materials and technology [ISBN-9-09-005899-0] 09 p3688 N94-31518

MICROPHOTOGRAPHS

The effect of an on-orbit near encounter on the number flux density of micron sized particles 03 p0899 N94-16374

MICROPHOTOMETERS

U PHOTOMETERS

MICROPLASMAS

Rapid analysis of mixed waste samples via the optical emission from laser initiated microplasmas [DE93-014563] 04 p1582 N94-17727

MICROPOROSITY

Amorphous sol-gel insulating films [DE93-012859] 02 p0576 N94-12866

Quantitative mapping of pore fraction variations in silicon nitride using an ultrasonic contact scan technique [NASA-TP-3377] 02 p0665 N94-13056

Gas separations using ceramic membranes [DE93-000278] 03 p0947 N94-15861

Modeling of the formation of microporosity in alloys [DE93-017733] 04 p1364 N94-19044

High temperature size selective membranes [DE93-019865] 05 p1709 N94-21982

Template synthesis of electronically conductive polymers [AD-A273673] 06 p2263 N94-25409

Structure of ionic fluids in equilibrium with a microporous ionic matrix [DE94-600563] 07 p2715 N94-26391

Template synthesis of metal microtubule ensembles utilizing chemical, electrochemical, and vacuum deposition techniques [AD-A274676] 07 p2715 N94-26444

Microporous structure with layered interstitial surface treatment, and method and apparatus for preparation thereof [NASA-CASE-MSC-21487-3] 11 p4235 N94-35229

Atomic oxygen reactor having at least one sidearm conduit [NASA-CASE-MSC-21487-4] 11 p4250 N94-35445

Mechanical performance of austempered ductile iron [AD-A280452] 12 p4420 N94-37758

MICROPROCESSORS

User's manual for the DAD-1 data acquisition daughter board for the SuperCard-2 [DE93-012153] 01 p0325 N94-11139

Data processing units for eight magnetospheric particle and field sensors [AD-A264403] 01 p0276 N94-11463

The KSR1: Experimentation and modeling of poststore [DE93-012539] 02 p0759 N94-13470

Mongoose ASIC microcontroller programming guide [NASA-RP-1319] 02 p0623 N94-13871

Test report for single event effects of the 80386DX microprocessor [NASA-CR-194509] 02 p0741 N94-13943

Adaptive Signal Processing Testbed: VME-based DSP board market survey [DSIS-93-00274] 02 p0605 N94-14015

An ultra-compact processor module based on the R3000 [DE93-012549] 02 p0625 N94-14427

VLSI for high-speed digital signal processing [AD-A267709] 03 p1007 N94-14936

A microprocessor controller for a towing tank drive and flow visualisation system [AD-A267087] 03 p0872 N94-15543

Embedded computer systems: Status of C-17 software [AD-A267307] 03 p1160 N94-16993

Some variation in the movement base of the ETA 251 series 04 p1428 N94-18035

Experience with custom processors in space flight applications 04 p1336 N94-18338

Simplified microprocessor design for VLSI control applications 04 p1400 N94-18359

Verification of VLSI designs 04 p1400 N94-18363

VLSI for high-speed digital signal processing [AD-A270406] 04 p1404 N94-18706

Motorola MC68040 high-speed design using Altera EPM5000 erasable programmable logic devices [DE93-017635] 04 p1523 N94-19006

VPU(tm) demonstration mission vicinity processor unit(tm) overview 04 p1325 N94-19171

Radiation hardened microprocessor for small payloads 04 p1327 N94-19184

On-line test methods of microprocessor based systems [ETN-93-95008] 04 p1530 N94-19498

A methodology for formal hardware verification, with application to microprocessors [AD-A270550] 05 p1898 N94-20085

Mongoose: Creation of a Rad-Hard MIPS R3000 05 p1754 N94-21090

Network command processing system overview 05 p1935 N94-21351

A 20 MHz CMOS reorder buffer for a superscalar microprocessor 05 p1764 N94-21700

A mechanized process algebra for verification of device synchronization protocols 05 p1766 N94-21716

Instruction set commutivity 05 p1766 N94-21719

IRAF and STSDAS under the new ALPHA architecture 05 p2049 N94-22553

Installation of an artificial neural network on distributed memory microprocessors [ETN-94-95175] 06 p2471 N94-23152

Contribution to the evaluation of efficiency of a microprocessor functional test
[ETN-94-95176] 06 p2445 N94-23153
Towards the formal specification of the requirements and design of a processor interface unit: HOL listings
[NASA-CR-191465] 06 p2466 N94-23252
Design and implementation issues of end-to-end protocols in high-speed networks
[PB94-110905] 06 p2467 N94-23752
Towards the formal verification of the requirements and design of a processor interface unit
[NASA-CR-4522] 06 p2467 N94-24075
Towards the formal specification of the requirements and design of a processor interface unit
[NASA-CR-4521] 06 p2467 N94-24463
Crosstie random access memory element having associated read/write circuitry
[AD-D016027] 06 p2446 N94-24724
The transputer
[AD-A273688] 06 p2446 N94-25438
Low-cost photovoltaic inverters incorporating application-specific integrated circuits
[DE94-003270] 07 p2856 N94-26463
Development of a MIL-STD-1750 microprocessor system for space applications 07 p2949 N94-26715
High performance flight computer developed for deep space applications 07 p2949 N94-26718
Fault tolerant real-time processing system for space use 07 p2949 N94-26720
NASA's spacecraft data system 07 p2950 N94-26723
Arithmetic performances of onboard computers 07 p2952 N94-26738
Microprocessor chip incorporating optical signal coupling transceiver
[AD-D016077] 07 p2788 N94-28186
Data fusion and correlation techniques testbed development audio processing study
[SKD-1600-73-014] 08 p3241 N94-28532
NSC 800, 8-bit CMOS microprocessor
[NASA-CR-195736] 08 p3405 N94-28845
Microcomputer-based protective functions in industrial production systems: Assessment method
[PB94-137817] 08 p3411 N94-29159
On ground system integration and testing: A modern approach 08 p3150 N94-29334
Communications technology for unattended sensors
[DE94-005685] 08 p3254 N94-30043
Maestro: An open system architecture for multi-robot control 08 p3306 N94-30288
Interpreter composition issues in the formal verification of a processor-memory module
[NASA-CR-4594] 09 p3820 N94-32775
The time domain crossbar (TDX): A high speed, high density, FPGA design
[DE94-007862] 10 p4034 N94-33840
Overview of the MSTI 2 processor-in-the-loop simulator 11 p4207 N94-35631

MICROSCALES
U MICROBALANCES

MICROSCOPES
NT ACOUSTIC MICROSCOPES
NT ELECTRON MICROSCOPES
NT ION MICROSCOPES
NT OPTICAL MICROSCOPES
Interferometric and optical tests of water window imaging x ray microscopes
[NASA-CR-193866] 01 p0375 N94-10506
A Fourier transform microscope for x ray and/or gamma ray imaging
[AD-D015742] 02 p0791 N94-13664
Optical displays: A tutorial on images and image formation
[AD-A266230] 03 p1192 N94-16926
Center-of-Excellence: Microlaser microscope
[DE93-040688] 04 p1442 N94-19658
Atomic-scale friction measurements using friction force microscopy. Part 2: Application to magnetic media
[AD-A270759] 04 p1447 N94-19767
X ray imaging and x ray source development at Lawrence Livermore National Laboratory
[DE94-007077] 09 p3719 N94-32629
Simplified ultra-high resolution optic for soft x ray imaging
[AD-A278424] 09 p3885 N94-33331

MICROSCOPY
NT ATOMIC FORCE MICROSCOPY
NT ELECTRON MICROSCOPY
NT LASER MICROSCOPY
NT PHOTOACOUSTIC MICROSCOPY
NT SCANNING ELECTRON MICROSCOPY
NT SCANNING TUNNELING MICROSCOPY
NT TRANSMISSION ELECTRON MICROSCOPY
NT ULTRAVIOLET MICROSCOPY
Ballistic electron transport studies using BEEM
[AD-A266029] 01 p0369 N94-12395
Crystallographic and metallurgical characterization of radiation detector grade cadmium telluride materials
[DE93-014335] 02 p0806 N94-13150
Imaging microscopy with x ray lasers at Lawrence Livermore National Laboratory
[DE93-013419] 02 p0655 N94-13258
Image reconstruction for x ray holographic microscopy
[DE93-013094] 02 p0653 N94-14772
Atomic-scale friction measurements using friction force microscopy. Part 1: General principles and new measurement techniques
[AD-A268391] 03 p1048 N94-17533
Tunneling microscopy of semiconductors
[AD-A270232] 04 p1600 N94-18904
Atomic-scale friction measurements using friction force microscopy. Part 1: General principles and new measurement techniques
[AD-A270749] 04 p1446 N94-19678
Atomic-scale friction and microfriction of graphite and diamond using friction force microscopy
[AD-A270952] 04 p1605 N94-19679
Atomic-scale friction measurements using friction force microscopy. Part 2: Application to magnetic media
[AD-A270759] 04 p1447 N94-19767
Acoustic microscopy and nonlinear effects in pressurized superfluid helium
[AD-A270598] 05 p1967 N94-19949
Atom probe field ion microscopy characterizations of VVER steels
[DE93-017864] 05 p1689 N94-20180
Ultrafast scanning microscopy
[DE93-040121] 05 p1985 N94-20320
Magnetic force microscopy/current contrast imaging: A new technique for internal current probing of IC's
[DE93-040754] 05 p1761 N94-21532
Material optimization for hard x ray Fresnel zone plates
[DE93-019569] 05 p1990 N94-21837
Center for X-Ray Optics, 1992
[DE94-000726] 05 p1990 N94-21868
Orientation imaging microscopy: New possibilities for microstructural investigations using automated BKD analysis
[DE94-000777] 06 p2557 N94-22938
Chemically sensitive interfacial force microscopy: Contact potential measurements of self-assembling monolayer films
[AD-A273135] 06 p2234 N94-24772
The nanometer-scale mechanics of gold films
[AD-A273307] 06 p2565 N94-25086
Detecting actin fibers in cell images using minimal spanning trees
[AD-A273914] 07 p2984 N94-25591
Regrowth zones in laser annealed radiation damaged diamond
[DE94-600821] 07 p3056 N94-26364
Proceedings of the Fourth Euroseminar on Microscopy Applied to Building Materials
[PB94-119807] 07 p2839 N94-26754
High definition Raman microscopic imaging
[DE94-003158] 07 p2716 N94-26781
The x ray holographic microscopy using the atomic-force microscope
[DE94-004003] 07 p2814 N94-27779
Atomic oxygen damage characterization by photothermal scanning 09 p3598 N94-31051
New and emerging techniques for imaging surfaces
[AD-A276497] 09 p3878 N94-31262
Differential phase acoustic microscope for micro-NDE
[NASA-CR-189617] 09 p3731 N94-32481
IMIS: An intelligence microscope imaging system 10 p4127 N94-33646
Fluorescence detection of single molecules using pulsed near-field optical excitation and time correlated photon counting
[DE94-007553] 11 p4320 N94-35376
Density and composition analysis using focused MeV ion microbeam techniques
[DE94-012241] 12 p4517 N94-37210
Submicrometer fiber-optic chemical sensors: Measuring pH inside single cells
[DE94-004160] 12 p4525 N94-37532

MICROSEISMS
Macroseismic study of the Dour (Belgium) earthquakes of 22 March 1987 and of Gulpen (Belgium) 17 October 1988 04 p1482 N94-18625
Long transect seafloor seismic array: A component of SAMSON (Sources of Ambient Micro Seismic Ocean ic Noise)
[AD-A277009] 09 p3789 N94-32401

MICROSTRIP ANTENNAS
Analysis of microstrip patch antennas with nonzero surface resistance
[NASA-TP-3362] 02 p0604 N94-13916
Proceedings of the 1992 Antenna Applications Symposium, volume 2
[AD-A266916] 03 p0986 N94-14998
Resonant frequencies of irregularly shaped microstrip antennas using method of moments
[NASA-TP-3386] 03 p0989 N94-15767
Dual polarization microstrip array antenna
[CA-PATENT-1-307-842] 03 p0994 N94-15986
Proceedings of the 1992 Antenna Applications Symposium, volume 1
[AD-A268167] 03 p1005 N94-17431
Two microstrip arrays for interferometric SAR applications 05 p1722 N94-20421
Bandwidth enhancement of dielectric resonator antennas 05 p1734 N94-20507
A 10 GHz Y-Ba-Cu-O/GaAs hybrid oscillator proximity coupled to a circular microstrip patch antenna 05 p1736 N94-20517
Full wave numerical model of arbitrarily-shaped proximity coupled microstrip antennas 05 p1745 N94-22137
Modeling of coaxial-fed microstrip patch antenna by finite difference time domain method 05 p1745 N94-22138
Applications of planar near-field measurements to electromagnetic radiation and interference problems 05 p1747 N94-22252
An active K/Ka-band antenna array for the NASA ACTS mobile terminal 06 p2289 N94-22832
Microstrip monopulse antenna for land mobile communications 06 p2289 N94-22833
Rigorous analysis of thick microstrip antennas and wire antennas embedded in a substrate
[EUT-92-E-263] 06 p2290 N94-22876
A constrained optimization technique for arbitrary antenna arrays and various performance indices
[ISBN-0-315-59455-1] 06 p2297 N94-24179
Printed circuit elements with applications to antennas, scattering, and circuits
[AD-A275512] 08 p3262 N94-28669
Three dimensional transient analysis of microstrip circuits in multilayered anisotropic media
[AD-A274995] 08 p3263 N94-28995
Theoretical and experimental study of a cylindrical microstrip antenna
[REPT-932-440-109] 08 p3245 N94-29456
A 32 GHz microstrip array antenna for microspacecraft application 08 p3251 N94-29668
Radiation and scattering from cylindrically conformal printed antennas
[NASA-CR-195546] 08 p3253 N94-29873
Radial microstrip slotline feed network for circular mobile communications array
[NASA-TM-106540] 08 p3267 N94-30198
The development of active integrated antennas and a design methodology
[ISBN-0-315-86119-3] 09 p3675 N94-31708
Proceedings of the 1993 Antenna Applications Symposium, volume 1
[AD-A277202] 09 p3676 N94-32049
Proceedings of the 1993 Antenna Applications Symposium, volume 2
[AD-A277203] 09 p3677 N94-32050
Microwave sensor for ice detection 09 p3583 N94-32457
COVICS: A covert video communications system
[DE94-007568] 09 p3682 N94-32745
Reconfigurable Array of Radiating Elements (RARE) controlled by light
[NASA-CR-195828] 09 p3884 N94-33073
The 20 GHz circularly polarized, high temperature superconducting microstrip antenna array
[NASA-CR-195097] 09 p3683 N94-33083

MICROSTRIP DEVICES
NT MICROSTRIP ANTENNAS
NT MICROSTRIP TRANSMISSION LINES
Development of microstrip gas chamber and application to imaging gamma-ray detector
[DE93-754294] 01 p0034 N94-11041
The imaging microstrip proportional counter: Features of a practical design 03 p0900 N94-15030
Monte Carlo simulation of the microstrip gas counter
[NIKHEF-H/93-07] 03 p1035 N94-17619
Time-domain analysis of planar microstrip devices using a generalized Yee-algorithm based on unstructured grids 05 p1724 N94-20431
TlCaBaCuO high Tc superconducting microstrip ring resonators designed for 12 GHz 05 p1735 N94-20516
Temperature dependence of the radiation induced change of depletion voltage in silicon PIN detectors
[DE94-002705] 07 p3052 N94-25972
Gamma Large Area Silicon Telescope (GLAST): Applying silicon strip detector technology to the detection of gamma rays in space
[DE94-003451] 07 p3116 N94-27740

An investigation of a novel microstrip magic-T
[ISBN-0-315-86218-1] 09 p3690 N94-31711
Experimental characterisation of gas microstrip detectors. Part 2: Counting rate characteristics
[PB94-167095] 11 p4269 N94-36061
Submillimeter quasioptical Josephson junction oscillator with integrated tuning elements
[AD-A280380] 12 p4534 N94-37036

MICROSTRIP TRANSMISSION LINES
Analysis and characterizations of planar transmission structures and components for superconducting and monolithic integrated circuits
[NASA-CR-193675] 02 p0619 N94-13026
Analysis of microstrip dipoles and slots transversely coupled to a microstrip line using the FDTD method 05 p1718 N94-20405
Linearly tapered slot antenna circular array for mobile communications
[NASA-TM-106441] 05 p1769 N94-21808
Three dimensional transient analysis of microstrip circuits in multilayered anisotropic media
[AD-A274995] 08 p3263 N94-28995
Simulation of non-uniform transmission lines for weakly dispersive structures
[ISBN-0-315-86525-3] 09 p3690 N94-31726
Theoretical and experimental study of microstrip-to-slot line uniplanar transition
[NASA-TM-106566] 09 p3696 N94-32905
Reconfigurable Array of Radiating Elements (RARE) controlled by light
[NASA-CR-195828] 09 p3884 N94-33073
Switched-beam radiometer front-end network analysis
[NASA-CR-194922] 11 p4252 N94-35247
Microwave detection of a superconducting infrared sensor
[AD-D016297] 12 p4440 N94-37769

MICROSTRUCTURE
NT METEORITIC MICROSTRUCTURES
NT WIDMANSTATTEN STRUCTURE
The microstructure and mechanical properties of hot worked FeAl intermetallic alloys 01 p0058 N94-10020
Structure and properties of an RS Al-Si-Ni-Mn-Zr alloy for high temperature applications 01 p0064 N94-10063
Solidification in immiscible systems: The influence of processing conditions on resulting microstructures 01 p0112 N94-10174
TEM study of a space processed Al-Al2O3 metallic composite 01 p0075 N94-10186
Pulsatile instability in rapid directional solidification: Strongly-nonlinear analysis 01 p0115 N94-10188
Solidification of undercooled Ni-32.5 wt percent Sn eutectic alloy 01 p0086 N94-10194
Undercooled W-Re and Mo-Re drops in an ultra high vacuum drop tube 01 p0086 N94-10195
Microanalysis of directionally solidified cobalt oxide-zirconia eutectic
[DE93-013207] 01 p0088 N94-10527
Preparation of carbon monoliths having tailored pore structure from porous polymer precursors
[DE93-011576] 01 p0089 N94-10958
Synthesis and properties of nanophase materials
[DE93-011757] 01 p0397 N94-10962
Microstructure and associated properties of YB2Cu3O(x) superconductors prepared by melt processing techniques
[DE93-010675] 01 p0398 N94-11004
Damping measurements for ultra-high carbon steel/brass laminates
[DE93-011886] 01 p0082 N94-11076
Fibre reinforced polymer matrix composites: Microstructure and mechanical properties
[DLR-FB-92-28] 01 p0066 N94-11085
Damping mechanisms in chemically vapor deposited SiC fibers
[NASA-TM-106334] 01 p0066 N94-11135
Structural development in ceramic precursor sols and gels
[AD-A264354] 01 p0090 N94-11281
High-temperature corrosion of ceramic-ceramic composites in a waste incinerator environment
[DE93-012430] 01 p0072 N94-11368
Organometallic chemical vapor deposition and characterization of ZnGe(1-x)Si(x)P2-Ge alloys on GaP substrates 01 p0400 N94-11443
The effect of processing on the microstructure and tensile properties of a (gamma)-TiAl based alloy
[DE93-013221] 01 p0084 N94-11488
Mechanical interaction between synthetic fiber and cement base matrix in FRC composites
[AD-A265310] 01 p0073 N94-11686
Processing and properties of coated HPZ fiber reinforced glass-ceramic matrix composites
[AD-A265177] 01 p0092 N94-11876
Chondrite thermal histories from Low-CA pyroxene microstructures: Autometamorphism versus prograde metamorphism revisited 01 p0429 N94-12105
Fracture behavior of ionomers and ionomeric blends
[AD-A265379] 01 p0094 N94-12407
Microstructure-based fatigue life prediction methods for naval steel structures
[AD-A265429] 01 p0085 N94-12426
Multicomponent and multilayered thin films for advanced microtechnologies: Techniques, fundamentals, and devices
[AD-A265685] 01 p0405 N94-12442
Deformation mechanisms in tungsten single crystals in ballistic impact experiments
[AD-A265701] 01 p0405 N94-12563
Amorphous sol-gel insulating films
[DE93-012859] 02 p0576 N94-12866
Deposition of crystalline boron thick layers from gas phase
[DE93-620499] 02 p0576 N94-12867
Recovery of materials impacted at high velocity
[DE93-014150] 02 p0576 N94-12885
Role of microstructure on fatigue durability of aluminum aircraft alloys
[AD-A265627] 02 p0568 N94-12993
Gas atomized Er3Ni powder for cryocooler applications
[DE93-011564] 02 p0568 N94-13000
Effect of microstructure on passive film formation and breakdown on Al alloys
[AD-A265339] 02 p0569 N94-13050
Transport properties of disordered porous media from the microstructure
[DE93-016065] 02 p0806 N94-13152
Fracture behavior of vanadium/vanadium silicide in-situ composites
[DE93-013422] 02 p0556 N94-13389
Tensile properties of LE-7 engine material with welded joint
[NAL-TR-1188] 02 p0570 N94-13460
Excimer laser surface processing of titanium
[DE93-012633] 02 p0570 N94-13512
Processing and mechanical properties of silicon carbide platelet reinforced alumina composites 02 p0556 N94-13557
Role of microstructure on fatigue durability of aluminum aircraft alloys
[AD-A266350] 02 p0571 N94-13697
Microstructural evolution of NARloy-Z at elevated temperatures
[NASA-TM-108419] 02 p0571 N94-13715
The microstructural response of near gamma-TiAl+W to heat treatment
[DSIS-93-00237] 02 p0571 N94-13840
The influence of a microgravity environment on the dendritic morphology during directional solidification of hypoeutectic Al-Si alloys
[NASA-CR-194139] 02 p0571 N94-13891
High-resolution Z-contrast imaging and hole concentration mapping of YBCO thin films
[DE93-015803] 02 p0808 N94-13930
Radiation hardening and radiation-induced chromium depletion effects on intergranular stress corrosion cracking of austenitic stainless steels
[DE93-011602] 02 p0572 N94-14058
Physical and structural properties of a sputtered zirconia-yttria layer used as a thermal resistance
[ONERA-NT-1992-10] 02 p0810 N94-14193
Theory of the electronic and structural properties of solid state oxides
[DE93-016051] 02 p0811 N94-14296
Estimation of strain in 1-kW primary containment vessels by microstructural examination
[DE93-013053] 02 p0573 N94-14316
Microstructural mechanisms that enhance electromigration resistance in Al-Cu thin films
[DE93-013770] 02 p0812 N94-14345
A microstructural approach to fatigue crack processes in poly crystalline BCC materials
[DE93-016666] 02 p0812 N94-14354
Pore-size-distribution of cationic polyacrylamide hydrogels
[DE93-015218] 02 p0581 N94-14400
Room temperature degradation of YBa2Cu3O(7-x) superconductors in varying relative humidity environments
[NASA-TP-3368] 02 p0813 N94-14409
Theoretical studies of breakdown in random media
[DE93-018107] 02 p0558 N94-14418
Computational diagnostics for detecting phase transitions during nanoindentation
[DE93-016536] 02 p0813 N94-14439
Microstructural influences on the mechanical properties of solder
[DE93-015044] 02 p0573 N94-14474
Processing and testing of high toughness silicon nitride ceramics
[NASA-CR-191190] 02 p0582 N94-14543
Current titles — National Center for Electron Microscopy
[DE93-015859] 02 p0851 N94-14587
Solution chemistry optimization of sol-gel processed PZT thin films
[DE93-013776] 02 p0814 N94-14695
Molecular simulator: A basic tool for submicron MOS processes development
[LAAS-92484] 02 p0814 N94-14697
An investigation of the role of second phase particles in the design of ultra high strength steels of improved toughness
[AD-A266774] 02 p0573 N94-14786
Office of Naval Research/DARPA publications: Composite materials with improved properties in compression
[AD-A265509] 02 p0560 N94-14794
Microstructural origins and modeling of intergranular crack initiation in an Al-Li-Cu-Mg-(Zr) alloy
[ISAL-91-0012] 02 p0574 N94-14814
Influence of heat treatment on microstructure of Ti-35wt Al prepared by elemental powder metallurgy
[GKSS/92/E/27] 02 p0574 N94-14821
Phases and phase transitions of polymeric liquid crystals: A high resolution x ray diffraction and light scattering study
[ITN-93-85218] 02 p0816 N94-14826
Characterization of the cyclic plasticity of polycrystalline aluminum in the 90-300K domain: Use of the ultrasonic wave coupling technique - low frequency restraint
[ISAL-92-0083] 03 p0954 N94-14930
Dynamic behavior of fiber and particle reinforced composites
[AD-A266905] 03 p0930 N94-15143
Partial melting experiment of Y-Ba-Cu oxide 03 p0945 N94-15168
Self-diffusion coefficients of sol-gel intermediates
[AD-A266957] 03 p0963 N94-15179
Structural investigation of electrochemically etched silicon
[DE93-015300] 03 p1207 N94-15827
Laser-shock damage of iron-based materials
[AD-A267196] 03 p1038 N94-15852
Ternary alloying effects in polycrystalline (beta)-NiAl
[DE93-012675] 03 p0955 N94-15885
Passive oxide films on well-defined nickel surfaces: An examination of film growth on Ni(100) with ex situ scanning tunneling microscopy
[DE93-014056] 03 p1207 N94-15923
Dynamical Ising model simulations of nucleation and growth in copper-cobalt alloys
[DE93-015336] 03 p0957 N94-16015
Rheology and microstructure of concentrated zirconia-alumina suspensions for gelcasting composites
[DE93-015339] 03 p0966 N94-16016
The influence of microstructure on the mechanical behavior of silicon nitride ceramics
[DE93-015363] 03 p0966 N94-16018
The effect of long-term aging on the impact properties of modified 9Cr-1Mo steel
[DE93-015453] 03 p0957 N94-16068
The influence of thermal aging on the microstructure and fatigue properties of modified 9Cr-1Mo steel
[DE93-015489] 03 p0957 N94-16106
Cation ordering in orthopyroxenes and cooling rates of meteorites: Low temperature cooling rates of Estherville, Bondoc and Shaw 03 p1241 N94-16176
Classificational parameters for acapulcoites and lodranites: The cases of FRO 90011, EET 84302 and ALH A81187/84190 03 p1245 N94-16389
Ion implantation effects on surface-mechanical properties of metals and polymers
[DE93-014661] 03 p0958 N94-16453
Thermal stress effects in intermetallic matrix composites
[NASA-CR-191191] 03 p1054 N94-16518
Evolution of microstructure in face centered cubic metals during irradiation: A review
[DE93-015682] 03 p0958 N94-16662
Ultrafast processes in tunneling microstructure devices
[AD-A266570] 03 p1210 N94-16720
Microstructure of Zr3Al after 2 MeV proton bombardment
[DE93-015331] 03 p1211 N94-16814
The Ceramic Technology Project: Ten years of progress
[DE93-015991] 03 p0968 N94-16843
Effects of processing and prolonged high temperature exposure on the microstructure of Nb-1Zr-C sheet
[NASA-TM-106370] 03 p0959 N94-16883
Slip, twinning and transformation in Laves phases
[DE93-018164] 03 p0960 N94-16972

Transformation toughening of composite ceramics
[AD-A267304] 03 p0971 N94-16980
Investigation of the origin of hot spots in deformed crystals: Ammonium perchlorate studies
[AD-A267692] 03 p1214 N94-17270
Micromechanics modeling and analysis of Haversian compact bone tissues as a fiber reinforced composite material
[AD-A268250] 03 p1129 N94-17456
Modeling microstructural evolution and the mechanical response of superplastic materials
[DE93-014417] 04 p1355 N94-17711
Microstructural analysis of solid-state resistance welds
[DE93-017295] 04 p1443 N94-17761
Atlas of formability: Ultimet
[AD-A268352] 04 p1355 N94-17767
Atlas of formability: HAYNES 556
[AD-A268354] 04 p1356 N94-17768
Atlas of formability: HAYNES 188
[AD-A268355] 04 p1356 N94-17769
Atlas of formability: NICKELVAC K-500
[AD-A268351] 04 p1356 N94-17772
Atlas of formability: Nickelvac C-276
[AD-A268264] 04 p1357 N94-17802
Plastic anisotropy in MoSi2 single crystals
[DE93-012650] 04 p1594 N94-17874
Mechanical properties of excimer laser modified titanium surfaces
[DE93-012663] 04 p1358 N94-17875
High- and low-temperature bonding techniques for microstructures
[DE93-017173] 04 p1595 N94-17992
Microstructurally based thermomechanical fatigue lifetime model of solder joints for electronic applications
[DE93-016508] 04 p1452 N94-17995
Embrittlement of surface mount solder joints by hot solder-dipped, gold-plated leads
[DE93-017659] 04 p1358 N94-18003
Omega phase formation in shock-loaded zirconium
[DE93-018343] 04 p1595 N94-18162
Advanced in macrostatistical hydrodynamics
[DE93-018479] 04 p1410 N94-18270
Several fundamental issues in the mechanics of inelastic behavior
[AD-A269455] 04 p1453 N94-18285
Nanostructured materials: Mind over matter
[DE93-017690] 04 p1597 N94-18480
Fabrication and microstructural development of Ag-clad TlBa2Ca2Cu3O(x) tapes
[DE93-017407] 04 p1597 N94-18500
Research on stable, high-efficiency amorphous silicon multijunction modules
[DE93-010046] 04 p1467 N94-18518
Developing and understanding the high temperature behavior of niobium aluminides and niobium aluminide composites
[AD-A268874] 04 p1341 N94-18636
Development of the microstructure based stochastic life prediction models
[AD-A269880] 04 p1454 N94-18683
Development of the microstructure based stochastic life prediction models
[AD-A270453] 04 p1455 N94-18714
Development of the microstructure based stochastic life prediction model
[AD-A269742] 04 p1361 N94-18742
Fundamental concepts relating local atomic arrangements, deformation, and fracture of intermetallic alloys
[AD-A268745] 04 p1361 N94-18788
High pressure metallization of Mott Insulators: Magnetic, structural and electronic properties
[DE93-018295] 04 p1404 N94-18805
Morphology, deformation, and defect structures of TiCr2 in Ti-Cr alloys
[DE93-018332] 04 p1361 N94-18807
Effects of shock loading on a solid-solution strengthened superalloy
[DE93-018345] 04 p1362 N94-18809
Development of ductile Fe3Al-based aluminides
[DE93-017865] 04 p1362 N94-18938
Tensile properties of as-cast iron-aluminide alloys
[DE93-017852] 04 p1363 N94-18975
Modeling of single-crystal laser-weld microstructures
[DE93-017853] 04 p1445 N94-18976
Fabrication and characterization of high-T(sub c) tapes and coils made from Ag-clad Bi-2223 superconductors
[DE93-018615] 04 p1601 N94-18993
High dose effects in neutron irradiated face-centered cubic metals
[DE93-017671] 04 p1364 N94-19043
X ray studies of microstructures in semiconductor and superconducting materials
[DE93-040690] 04 p1601 N94-19056
Metallurgical evaluation of SRAM 2/SRAM A program mer base plates
[DE93-018689] 04 p1364 N94-19100
Fabrication, properties, and microstructures of high (Tc) tapes and coils made from Ag-clad Bi-2223 superconductor
[DE93-017405] 04 p1602 N94-19122
The microstructural mechanism of electromigration failure in narrow interconnects of Al alloys
[DE93-018598] 04 p1365 N94-19282
Analytical and experimental evaluation of joining silicon nitride to metal and silicon carbide to metal for advanced heat engine applications
[DE93-018128] 04 p1446 N94-19291
Cutting and drilling studies using high power visible lasers
[DE93-019149] 04 p1441 N94-19294
Microstructure of the interfacial zone around aggregate particles in concrete
[PB93-195790] 04 p1380 N94-19322
Dynamical behavior of octahedrite from the Henbury meteorite
[DE93-018834] 04 p1627 N94-19339
Role of pressure in the study of fullerenes
[DE93-018839] 04 p1602 N94-19340
Melt spinning study
[NASA-CR-193823] 04 p1380 N94-19423
Microstructure and texture control of fatigue in hydrogen and marine environments
[AD-A271277] 04 p1344 N94-19744
Damping in ferrous shape memory alloys
[AD-A271009] 04 p1366 N94-19775
General introduction to microstructural evolution under cascade damage conditions
[DE93-017443] 05 p2012 N94-19923
Particles on surfaces of laser ablated Y1Ba2Cu3O(7-delta) films
[DE93-040269] 05 p2013 N94-19929
Investigation of cracking and erratic behavior of the uranium-titanium alloy
[DE93-018591] 05 p1688 N94-19957
Microstructural stability of wrought, laser and electron beam glazed NARloy-Z alloy at elevated temperatures
[NASA-TM-108431] 05 p1689 N94-20100
Atom probe field ion microscopy characterizations of VVER steels
[DE93-017864] 05 p1689 N94-20180
Sol-spray preparation, particulate characteristics, and sintering of alumina powders
[DE93-018577] 05 p1690 N94-20183
Microscopic evaluation of low-temperature embrittlement in type 308 stainless steel welds
[DE93-040266] 05 p1690 N94-20282
Transport in microstructures in the microwave and millimeter-wave regime
[AD-A271875] 05 p2017 N94-20470
The effects of processing and constituent materials on compressive strength of thick composite laminates
[AD-A271912] 05 p1673 N94-20490
Direct imaging of the surface microstructure of dielectric materials using an atomic force microscope
[AD-A272251] 05 p2018 N94-20575
Microstructure evolution in the presence of constraints and implications on the properties of Mg-Li and Nb-Al constraints
[AD-A272088] 05 p1674 N94-20623
Regolith breccia consisting of H and LL chondrite mixture 05 p2080 N94-20892
Microstructural modeling and toughening of Si3N4 ceramics for high temperature engine applications
[AD-A272897] 05 p1704 N94-21197
The use of backscattered electron imaging mode to assess the effect of fine dispersions on development of superplastic microstructure in Al-Mg alloys
[AD-A272426] 05 p1691 N94-21258
Applicability and performance benefits of XD (Tradename) titanium aluminides to expendable gas turbine engines
[AD-A272998] 05 p1648 N94-21268
Investigation of the effect of various oxide and fluoride additives on the microstructure, electronic properties, and phase shifting ability of Ba(1-x)Sr(x)TiO3
[AD-A271756] 05 p2027 N94-21303
Deformation of an alumina-zirconia-silicon carbide-whisker reinforced composite
[DE93-040244] 05 p1676 N94-21559
High resolution, three dimensional soft x ray imaging
[DE93-018667] 05 p1989 N94-21630
Surface and subsurface defect detection in Si3N4 components by laser scattering
[DE93-040829] 05 p1832 N94-21772
Ductile-brittle transition behavior of tungsten under shock loading conditions
[DE93-019945] 05 p1693 N94-21843
Symposium on Microscopy and Image Analysis of Building Materials
[VTT-SYMP-136] 05 p1707 N94-21890
Preparation of concrete specimens for microstructural image analysis studies 05 p1707 N94-21891
A quantitative S.E.M. image analysis of cement paste microstructure 05 p1708 N94-21894
Determination of pore structure of concrete from thin sections by image analysis 05 p1708 N94-21895
Microstructure in mortar: A summary of a new project of research 05 p1708 N94-21896
The effect of microstructural evolution on superplasticity in Ni3Si(V, Mo)
[DE93-041320] 05 p1694 N94-21943
Dynamic properties of ceramic materials
[DE94-000654] 05 p1708 N94-21963
Microtextural characterization of annealed and deformed copper
[DE93-040144] 05 p1695 N94-21990
Benefits of thread rolling process to the stress corrosion cracking and fatigue resistance of high strength fasteners
[DE93-040438] 05 p1833 N94-22001
Microstructural evolution of neutron-irradiated Fe-Cr-Ni ternary alloys at high helium generation rates
[DE93-018786] 05 p1696 N94-22037
Quantitative analysis of scanning tunneling microscopy images for surface structure determination: Sulfur on Re(0001)
[DE93-019235] 05 p2034 N94-22041
Miniaturized disk-bend testing, nano-indentation, and the microstructure of ion-irradiated titanium aluminides
[DE93-040600] 05 p1697 N94-22559
Strength, ultrasonic and metallurgical evaluation of diffusion bonds
[DE94-000665] 05 p1697 N94-22571
Relationship of microstructure and mechanical properties for V-Cr-Ti alloys
[DE94-001431] 06 p2238 N94-22718
Carbon aerogels: An update on structure, properties, and applications
[DE94-001528] 06 p2252 N94-22931
Orientation imaging microscopy: New possibilities for microstructural investigations using automated BKD analysis
[DE94-000777] 06 p2557 N94-22938
The history of development of molybdenum alloys for structural applications
[DE94-000389] 06 p2239 N94-22958
Damage under monotonic or cyclic loads of new AlSiFe alloys prepared by the Osprey (tm) process
[ISAL-93-0008] 06 p2239 N94-22972
Atomic-scale structure of grain boundaries: Correlations to grain boundary properties
[DE94-001289] 06 p2558 N94-22990
Texture gradient effects in tantalum
[DE94-000689] 06 p2240 N94-23021
Internal friction associated with dislocation relaxations in virgin martensite
[PB93-226280] 06 p2240 N94-23119
Magnetic properties and transmission electron microscopy investigations of Nd-Fe-B-Co-Al melt spun ribbons
[PB93-201531] 06 p2561 N94-23428
Theory of extrusion: Advances and challenges
[PB93-201572] 06 p2241 N94-23447
Characterization of the microstructure of Nb-1wt.%Zr-0.1wt.%C tubes as affected by thermomechanical processing
[NASA-TM-106381] 06 p2242 N94-23550
Strength, acoustic evaluation and metallurgy of diffusion bonds
[DE94-001804] 06 p2243 N94-23717
Combustion synthesis and engineering of nanoparticles for electronic, structural and superconductor applications
[DE94-001865] 06 p2254 N94-23720
Large-scale production of Si(0.8)Ge(0.2) thermoelectric alloys by mechanical alloying
[DE94-000695] 06 p2243 N94-23753
Metal-mullite reactions
[DE94-002038] 06 p2244 N94-23811
Catalog of Apollo 17 rocks. Volume 1: Stations 2 and 3 (South Massif)
[NASA-CR-194854] 06 p2613 N94-24058
Microstructure and micromechanical behaviour of CMCs 06 p2256 N94-24236
Ordered organic thin films self-assembled from the vapor phase 06 p2223 N94-24339
Defects in electro-optically active polymer solids 06 p2223 N94-24342
Microstructural analysis of the 2195 aluminum-lithium alloy welds 06 p2251 N94-24448
Integral equations for the microstructures of supercritical fluids
[DE94-002460] 06 p2535 N94-24589

Ultrastructure processing of macromolecular materials
[AD-A273413] 06 p2258 N94-24782
Thermophysical property sensitivity effects in steel solidification 06 p2246 N94-25122
Microstructure of styrene methyl methacrylate copolymers grafted onto polybutadiene seeds
[ETN-94-95360] 06 p2262 N94-25225
Evaluation of multiaxial fracture models for technical ceramics
[ISBN-9-03-860192-1] 06 p2263 N94-25299
Frost effects on the microstructure of high strength concrete, and methods for their analysis
[VTT-PUBS-126] 06 p2379 N94-25529
Study on microscopic structural controls and electronic properties at material surfaces by ion beams
07 p2727 N94-25571
Study on production of materials with one direction solidification texture 07 p2727 N94-25572
Study on solidification of non-homogeneous melting/solidification materials 07 p2728 N94-25573
Study on interfacial reaction analysis at interfacial joining 07 p2728 N94-25574
Study on elucidation of damage generation process by electron beam lithography 07 p2729 N94-25581
Computer modelling of cyclic deformation of high-temperature materials
[AD-A273852] 07 p2704 N94-25608
Langmuir-Blodgett film of amylose-esters and chiral azo-dyes (structure and second order nonlinear optical behaviour)
[ETN-94-95390] 07 p2747 N94-25749
Microstructural development in low activation ferritic alloys irradiated to 200 dpa at 420 C
[DE94-004269] 07 p2731 N94-25803
Radiation hardening effects on localized deformation and stress corrosion cracking of stainless steels
[DE94-004308] 07 p2731 N94-25804
Structure and properties of intermetallic composites synthesized in situ using solid state displacement reactions
[DE94-004312] 07 p2705 N94-25805
Grain boundary degradation of YBCO superconductors sintered in CO2-containing atmospheres
[DE94-003206] 07 p3053 N94-26029
Modeling defect production in high energy collision cascades
[DE94-003810] 07 p3017 N94-26049
Collaborative research on ion implantation of ceramics
[DE93-019177] 07 p2749 N94-26080
Influence of grain structure and solute composition on the work hardening behavior of aluminium at cryogenic temperatures
[DE94-003415] 07 p2733 N94-26087
The fracture behavior of a CVD crystalline Si3N4/amorphous Si3N4 composite
[DE94-002646] 07 p2750 N94-26124
Zr-rich corner of the Zr-Sn-O diagram
[DE93-633764] 07 p2734 N94-26161
The study of single-pass GMA welds with different cover gas compositions on HSLA-100 steel
[AD-A274857] 07 p2822 N94-26174
Stress relaxation in sputtered W films and W/GeSi/Si heterostructures
[DE94-004007] 07 p3055 N94-26239
The effect of processing on the microstructure of Ag-sheathed Bi-2223 wires
[DE94-004627] 07 p3055 N94-26243
An atom probe investigation of the influence of trace impurities on the mechanical behavior of NiAl
[DE94-002797] 07 p2734 N94-26272
The microstructural response of granular soil under uniaxial strain
[AD-A274808] 07 p2763 N94-26341
Ordering and phase separation in MOCVD InGaP alloys and unicompositional quantum wells
[DE94-004693] 07 p3056 N94-26352
Template synthesis of metal microtubule ensembles utilizing chemical, electrochemical, and vacuum deposition techniques
[AD-A274676] 07 p2715 N94-26444
A study on the development of high-T(c) superconducting wire
[DE93-632438] 07 p2783 N94-26546
Microstructural development in irradiated vanadium alloys
[DE94-004307] 07 p2737 N94-26556
Microstructures of Si surface layers implanted with Cu
[DE94-004690] 07 p3058 N94-26565
Structure and properties of composites synthesized in situ using solid state displacement reactions
[DE94-004589] 07 p2737 N94-26585
Mechanical properties of nanophase materials
[DE94-004625] 07 p2751 N94-26594
The processing of powder metallurgically produced near gamma-titanium aluminide
[ISBN-0-315-84018-8] 07 p2738 N94-26633
The influence of weld metal alloying additions to extend the heat input range for the submerged arc welding of high strength steels
[AD-A274284] 07 p2738 N94-26679
Proceedings of the Fourth Euroseminar on Microscopy Applied to Building Materials
[PB94-119807] 07 p2839 N94-26754
Diagnostics and microelectronics
[DE94-003016] 07 p2784 N94-26777
Titanium 1992: Science and Technology, volume 1
[AD-A274798-VOL-1] 07 p2739 N94-26799
Ferroelectric thin film microstructure development and related property enhancement
[DE94-002741] 07 p3061 N94-26856
Controlled heterogeneous nucleation of melt-textured YBa2Cu3O(6+x) by addition of Al2O3 particles
[AD-A274605] 07 p3062 N94-26892
Fabrication and characterization of nano-crystalline diamond films
[DE94-002202] 07 p3062 N94-26934
Interface phenomena in metal-ceramic composites
[AD-A274167] 07 p2709 N94-27125
Accordion-like polymers for nonlinear applications
[AD-D016031] 07 p2755 N94-27148
Squeeze casting: A literature review
[PB94-124575] 07 p2741 N94-27326
Utility fog: A universal physical substance
07 p2687 N94-27367
Research into the microstructure and mechanical behavior of eutectic Bi-Sn and In-Sn
[DE94-004558] 07 p2741 N94-27619
Effect of precipitate structure on hot deformation of Al-Mg-Mn alloys
[DE94-004596] 07 p2741 N94-27622
Electron microscopy studies of undoped and phosphorus doped Si:H and Si,C:H films
[DE94-004738] 07 p3069 N94-27757
An anodic dissolution-based mechanism for the rapid cracking, pre-exposure phenomenon demonstrated by Al-Li-Cu alloys
[DE94-004798] 07 p2742 N94-27788
Hydrothermal growth and characterization of oxides in zirconium alloys
[DE94-602981] 07 p2743 N94-27829
Fragmentation of Ge(1-x) Sn(x) Se2 glasses
[DE94-603009] 07 p2758 N94-27837
An experimental investigation of fatigue damage in aluminum 2024-T3 alloys 07 p2747 N94-27900
Application of the Positron Annihilation Technique to the study of vapor absorption process in polyethylene (LDPE) and in imide polymer (6FDA-TMPD PI)
[DE94-602737] 07 p2720 N94-27998
Mechanical properties and microstructure of thermomechanically processed, high manganese steel
[ARL-TR-146] 07 p2747 N94-28212
Studies in ice mechanics
[PB94-133055] 07 p2900 N94-28393
Computer simulation of martensitic transformations
[DE94-005213] 08 p3201 N94-28479
Directional solidification studies in Ni-Al alloys
[DE94-005562] 08 p3201 N94-28527
On the prediction of HAZ grain size using Monte Carlo simulation
[DE94-005465] 08 p3511 N94-28535
Failures to model the development of a cube texture during the high temperature compression of Al-Mg alloys
[DE94-005013] 08 p3201 N94-28544
Characterization of structure and mechanical properties of MoSi2-SiC nanolayer composites
[DE94-004982] 08 p3175 N94-28579
Role of microstructure on the fatigue durability of aluminum aircraft alloys
[AD-A275814] 08 p3202 N94-28830
Toughening mechanisms in ultrahigh-strength steels
[AD-A275439] 08 p3202 N94-28867
Research on the improvement of shape-memory and magnetostrictive materials
[AD-A275397] 08 p3203 N94-29056
Effect of microstructure on the strength and fracture energy of bimaterial interfaces
[AD-A274987] 08 p3178 N94-29126
Microstructure/property relationships for SCS6/Timetal 21-S composite
[AD-A275056] 08 p3178 N94-29135
Low temperature behavior of virgin martensite
[PB94-132925] 08 p3204 N94-29142
An analysis of the microstructure and reinforcement distribution of an extruded particle-reinforced Al 6061-10 volume percent Al2O3 metal matrix composite
[AD-A275050] 08 p3178 N94-29166
Mechanical alloying processing with application to structural materials: ASSERT supplement
[AD-A275400] 08 p3204 N94-29205
Characterisation and processing of SiC/MAS-L glass ceramic matrix composite
[REPT-932-430-111] 08 p3179 N94-29412
Assessment of the fibre volume distribution around optical fibres
[FFA-TN-1993-12] 08 p3179 N94-29425
Microstructure and mechanical properties of nitrided molybdenum silicide coatings
[DE94-006249] 08 p3217 N94-30025
Development of evaluated data bank of physical properties of perspective nuclear engineering steels and alloys
[DE94-607999] 08 p3207 N94-30076
Plasma enhanced chemical vapor deposition of ZrO2 thin films
[DE94-008031] 08 p3218 N94-30104
On the structure and atomic motions in liquid sodium
[DE94-608386] 08 p3490 N94-30182
Dislocation loops in spinel crystals irradiated successively with deep and shallow ion implants
[DE94-005083] 08 p3517 N94-30201
Studies on the optimization of deformation processed metal-metal matrix composites
[DE94-006033] 08 p3185 N94-30704
Giant magnetoresistance and microstructural characteristics of epitaxial Fe-Ag and Co-Ag granular thin films
[DE94-006287] 08 p3519 N94-30707
Microstructural development and mechanical behavior of eutectic bismuth-tin and eutectic indium-tin in response to high temperature deformation
[DE94-005202] 08 p3210 N94-30710
A comparison of the evolution of cold and hot deformation microstructures and textures in fcc metals
[DE94-005103] 08 p3210 N94-30777
Fractographic and microstructural analysis of fatigue crack growth in Ti-6Al-4V fan disc forgings
[AD-B174765] 08 p3153 N94-30914
Microstructures and mechanical properties of Al3Ti-based alloys: Analysis in single phase and multiphase systems
[ONERA-NT-1993-6] 09 p3640 N94-31420
Structure and dynamics of microemulsions in bulk, at interfaces, and in confined geometries
[DE94-006043] 09 p3633 N94-31526
Aging effects on the microstructure, surface characteristics and wettability of Cu pretinned with Sn-Pb solders
[DE94-007033] 09 p3641 N94-31638
Effect of irradiation damage and helium on the swelling and structure of vanadium-base alloys
[DE94-006540] 09 p3641 N94-31666
High-temperature deformation and fracture toughness of duplex ceramic microstructures
09 p3653 N94-31945
Sodium sulfate corrosion of silicon carbide fiber-reinforced lithium aluminosilicate glass-ceramic matrix composites
[AD-A277224] 09 p3623 N94-32023
Work hardening behavior in aluminum alloy 2090
[DE94-007036] 09 p3643 N94-32064
Correlations between micromagnetic, microstructural and microchemical properties in ultrathin epitaxial magnetic structures
[AD-A277200] 09 p3901 N94-32092
Robotic weld overlay coatings for erosion control
[DE94-008004] 09 p3658 N94-32408
Mechanical properties of vacuum-sintered yttria ceramics
[DE94-008138] 09 p3659 N94-32617
Microstructure of copolymers containing disperse red 1 and methyl methacrylate
[AD-A277140] 09 p3660 N94-32722
Microanalytical study of defect formation in thin bismuth strontium calcium copper oxide films
[DE94-008217] 09 p3661 N94-32751
Isothermal sintering, microstructure, and superconducting properties of Y1Ba2Cu3O(7-x) compound
[DE94-008132] 09 p3905 N94-32779
NMR characterization of shocked quartz
[DE94-007733] 09 p3774 N94-32816
Light scattering studies of a model electrorheological fluid
[DE94-007860] 09 p3883 N94-32818
Phase behavior, structure, and properties of model block polymers
[AD-A277530] 09 p3662 N94-32954
Characterization of nanoparticles and nanophase materials
[DE94-008348] 09 p3907 N94-32990
Interface engineering in oxide fiber/oxide matrix composites
[AD-A277672] 09 p3627 N94-33029
Fine and microstructure observations at Fieberlin g Guyot R/V new horizon cruise report
[AD-A277917] 09 p3791 N94-33109

Cruise report: Oceanus 250 leg 4 high resolution profiler survey for the North Atlantic Tracer Release Experiment, 25 March - 24 April, 1992
[AD-A277935] 09 p3791 N94-33245
The path for long range conduction in high J(sub c) TiBa2Ca2Cu3O(8+x) spray-pyrolyzed deposits
[DE94-007211] 09 p3909 N94-33271
Microstructures and epitaxy in oxide superconductor thin films and devices
[AD-A278427] 09 p3910 N94-33332
Microstructurally based model of fatigue initiation and growth
[AD-A278198] 10 p4023 N94-33373
Microforces in electromigration
[AD-A276229] 10 p4132 N94-33397
Atomic force microscopy
[AD-A277589] 10 p4026 N94-33429
The effects of in-situ processing methods on the microstructure and fracture toughness of V-V3Si composites
[DE94-009093] 10 p4019 N94-33681
Solidification microstructures in single-crystal stainless steel melt pools
[DE94-009839] 10 p4024 N94-33880
Robotic weld overlay coatings for erosion control
[DE94-009703] 10 p4060 N94-33902
Fabrication, phase transformation studies, and characterization of SiC-AlN-Al2OC ceramics
[DE94-009649] 10 p4028 N94-33919
Dynamics of supermatrix semiconductor growth
[AD-A278380] 10 p4147 N94-34085
The microstructure and morphology of carbon black: A study using small angle neutron scattering and contrast variation
[DE94-009315] 10 p4022 N94-34098
Structures and properties of materials recovered from high shock pressures
[DE94-010057] 11 p4232 N94-35696
Integrated design of structures, controls, and materials
11 p4218 N94-35869
Cement paste matrix composite materials center
[AD-A279017] 11 p4233 N94-35952
Investigation of moisture-induced embrittlement of iron aluminides
[DE94-010881] 11 p4241 N94-36196
Microstructural development in solution derived PZT thin films
[DE94-008744] 11 p4246 N94-36209
Studies of the effect of microstructure on the dynamic behavior of granular and particulate media
[AD-A279012] 12 p4455 N94-36520
Characterization and processing of sintered products from nano-crystalline powders generated by the RTDS method
[DE94-004765] 12 p4415 N94-36553
Properties of TMC processed by fibre coating and hiping 12 p4401 N94-36656
Small-angle x ray scattering studies of microvoids in amorphous-silicon-based semiconductors
[DE94-006931] 12 p4533 N94-36745
Low temperature materials --- indium gallium arsenides
[AD-A278703] 12 p4533 N94-36755
Feasibility of (IMC)(sub d)-reinforced metal matrix composites
[AD-A280626] 12 p4404 N94-37044
Chromium/molybdenum alloy plating. Part 1: The electrodeposition of low contraction chromium/molybdenum alloys using unipolar (on/off) pulse plating
[AD-A280236] 12 p4417 N94-37138
Interaction effects of cracks, flaws and damage in ceramic
[AD-A280368] 12 p4423 N94-37181
Microstructure and chemistry of MgO- and CoO-doped nickel-titanate spinels
[DE94-012741] 12 p4537 N94-37382
Atomic level characterization of defects in microalloyed NiAl: An atom probe investigation
[DE94-012732] 12 p4418 N94-37396
The effect of reactive elements on the segregation behavior and microstructure of alpha-Al2O3 scales on beta-NiAl
[DE94-012739] 12 p4418 N94-37399
Micromechanical modeling of advanced materials
[DE94-011249] 12 p4405 N94-37627
Strength characteristics and crack growth behavior of a composite with well aligned fibers
12 p4459 N94-37804
Scaling effects of defects in fiber-reinforced composites 12 p4459 N94-37807

MICROWAVE ABSORPTION
H2S data reduction
[NASA-CR-193389] 02 p0617 N94-14743
Basic studies in plasma wave interactions
[AD-A280465] 12 p4527 N94-37139

MICROWAVE AMPLIFIERS
NT CYCLOTRON RESONANCE DEVICES
Wide band 140 GHz TWTA 01 p0132 N94-10514
Nonlinear analysis of a magnicon output cavity
[AD-A265342] 01 p0145 N94-12424
Microwave generation for magnetic fusion energy applications
[DE93-013864] 02 p0654 N94-13058
Field-emitter arrays for RF vacuum microelectronics
[AD-A268397] 03 p1015 N94-17526
Plasma klystron amplifier
[AD-D015819] 04 p1395 N94-17903
Field emission cathode and vacuum microelectronic microwave amplifier development
[AD-A269526] 04 p1403 N94-18639
Cryogenic, low-noise high electron mobility transistor amplifiers for the Deep Space Network
06 p2291 N94-23262
Towards experimental verification and device applications of current driven plasma instabilities in solid state systems
[AD-A275395] 08 p3504 N94-29055
X-band ultralow-noise maser amplifier performance
08 p3251 N94-29672
Design of a high power x-band magnicon amplifier
[AD-A277001] 09 p3692 N94-32199
Field emitter array RF amplifier development project phase one, cathode technology development
[AD-A280334] 12 p4437 N94-37033
Field emitter array RF amplifier development project. Phase 1, option 1
[AD-A280377] 12 p4437 N94-37035
Microwave generation for magnetic fusion energy applications
[DE94-012107] 12 p4448 N94-37368
Study on the measurement uncertainty of noise properties of a millimeter wave amplifier
[PB94-170917] 12 p4510 N94-37632

MICROWAVE ANTENNAS
NT HORN ANTENNAS
NT RECTENNAS
Enhanced decoding for the Galileo S-band mission
02 p0609 N94-14380
An optically modulated scatterer for microwave antenna metrology
[NPL-DES-126] 03 p0986 N94-15020
Experimental evaluation of an adaptive focusing algorithm for a microwave planar phased-array hyperthermia system at UCSF
[AD-A267004] 03 p1121 N94-15634
Method and apparatus for forming an agile plasma mirror effective as a microwave reflector
[AD-D015788] 03 p0998 N94-16535
The TOPSAR interferometric radar topographic mapping instrument 03 p1078 N94-16749
True time delay optically controlled dual band transmitter
[AD-A267663] 03 p1003 N94-17228
Design and fabrication of a Multichannel Adaptive Optical Processor (MADOP)
[AD-A270004] 04 p1579 N94-18668
Space applications of superconducting microwave electronics at NASA Lewis Research Center
05 p1671 N94-20513
AlGaAs laser diode FM spectrum: Phased array antenna application 05 p1746 N94-22196
Numerical method for computing the electric field produced by a microwave beam in a stratified medium
05 p1746 N94-22197
K- and Ka-band mobile-vehicular satellite-tracking reflector antenna system for the NASA ACTS mobile terminal 06 p2289 N94-22831
An active K/Ka-band antenna array for the NASA ACTS mobile terminal 06 p2289 N94-22832
A digital combining-weight estimation algorithm for broadband sources with the array feed compensation system 08 p3250 N94-29660
Digital combining-weight estimation for broadband sources using maximum-likelihood estimates
08 p3250 N94-29661
A 32 GHz microstrip array antenna for microspacecraft application 08 p3251 N94-29668
The development of active integrated antennas and a design methodology
[ISBN-0-315-86119-3] 09 p3675 N94-31708
SATCOM feasibility study for search and rescue aircraft
[DSIS-94-01083] 09 p3575 N94-31902
Reconfigurable Array of Radiating Elements (RARE) controlled by light
[NASA-CR-195828] 09 p3884 N94-33073
The 20 GHz circularly polarized, high temperature superconducting microstrip antenna array
[NASA-CR-195097] 09 p3683 N94-33083
Two-axis antenna positioning mechanism
09 p3605 N94-33308
Field demonstration of X-band photonic antenna remoting in the Deep Space Network
11 p4252 N94-35545
Submillimeter quasioptical Josephson junction oscillator with integrated tuning elements
[AD-A280380] 12 p4534 N94-37036

MICROWAVE ATTENUATION
A basic consideration for remote sensing using microwave radars on a satellite
01 p0212 N94-12665
Dispersion effects on millimeter wavelength attenuation efficiencies for a variety of fibers
[AD-A268992] 04 p1386 N94-18454
Attenuation of epsilon(sub eff) of coplanar waveguide transmission lines on silicon substrates
05 p1733 N94-20504
Evaluation of dual polarization attenuation of millimeter frequencies through a meteorological radar
08 p3256 N94-30496
Chilbolton Advanced Meteorological Radar: A tool for multi-disciplinary atmospheric research
[PB94-167467] 12 p4432 N94-36567

MICROWAVE CIRCUITS
Three-cavity circuit studies of the Maryland gyroklystron
[DE93-010173] 01 p0145 N94-11645
Limited bandwidth microwave filter
[AD-D015744] 01 p0145 N94-12322
Low cost high efficiency GaAs monolithic RF module for SARSAT distress beacons
[NASA-CR-194235] 01 p0146 N94-12773
Processing, fabrication and demonstration of HTS integrated microwave circuits
[AD-A265789] 02 p0619 N94-12892
A millimeter-wave tunneladder TWT
[NASA-CR-182183] 02 p0620 N94-13106
Electrical noise in microwave field effect and bipolar transistors
[LAAS-93042] 02 p0616 N94-14717
High efficiency low cost monolithic module for SARSAT distress beacons
[NASA-CR-194234] 04 p1315 N94-18852
Automated HMC assembly
[DE93-040641] 05 p1749 N94-20005
Interinjection-locked quasioptical power combiners and phased arrays
[AD-A271178] 05 p2015 N94-20214
Quartz/fused silica chip carriers
[NASA-CR-194154] 05 p2016 N94-20340
Recent activities in printed Antennas at LeRC
05 p1722 N94-20422
Solid State Technology Branch of NASA Lewis Research Center: Fifth Annual Digest
[NASA-TM-106303] 05 p1732 N94-20497
An x-band peeled HEMT amplifier
05 p1732 N94-20498
Coplanar waveguide radial line stub
05 p1733 N94-20503
Space applications of superconducting microwave electronics at NASA Lewis Research Center
05 p1671 N94-20513
Ten GHz YBa2Cu3O(7-delta) superconducting ring resonators on NdGaO3 substrates
05 p1735 N94-20515
Non-destructive semiconductor wafer probing system using laser pulses to generate and detect millimeter-wave signals
[CA-PATENT-APPL-SN-2,020,733]
05 p1760 N94-21178
Hybrid finite element/waveguide mode analysis of passive RF devices
[AD-A273074] 05 p1740 N94-21518
High temperature superconducting planar circuit structure for high frequency applications
[AD-A273083] 05 p2028 N94-21521
Characterization and modelling of extremely high frequency enclosures 05 p1782 N94-22177
Non-linear analysis of the electrical properties of the active circuits of high-frequency oscillators
05 p1785 N94-22195
MHMIC: Technology for the integration of microwave sub-assemblies 05 p1785 N94-22199
Microwave analog frequency dividers: Design, modeling and realization
[LAAS-93139] 06 p2307 N94-22909
Spatial frequency multiplier with active linearly tapered slot antenna array
[NASA-TM-106494] 06 p2310 N94-24308
Modeling electromagnetic effects in MMICs for T/R modules
[AD-A273808] 07 p2766 N94-25736
Processing, fabrication, and demonstration of HTS integrated microwave circuits, appendix A
[AD-A274600] 07 p2785 N94-26890

An efficient and accurate Green's function analysis of packaged microwave integrated circuits
[ISBN-0-315-84425-6] 07 p2787 N94-27653
Frequency-domain analysis of nonlinear microwave circuits
[PB94-132024] 08 p3261 N94-28400
Three dimensional transient analysis of microstrip circuits in multilayered anisotropic media
[AD-A274995] 08 p3263 N94-28995
Towards experimental verification and device applications of current driven plasma instabilities in solid state systems
[AD-A275395] 08 p3504 N94-29055
A combined electron beam/optical lithography process step for the fabrication of sub-half-micron-gate-length MMIC chips 08 p3240 N94-30445
Precision frequency synthesizing sources with excellent time/frequency performances 08 p3473 N94-30671
Microwave dielectric behavior of soils. Report 3: Measurement and modeling
[AD-A276060] 09 p3771 N94-31457
High-performance GaAs/AlGaAs optical phase modulators for microwave/photonic integrated circuits
[DE94-006361] 09 p3688 N94-31483
High performance YBCO films
[AD-A276493] 09 p3897 N94-31531
Simulation of non-uniform transmission lines for weakly dispersive structures
[ISBN-0-315-86525-3] 09 p3690 N94-31726
Design of a high power x-band magnicon amplifier
[AD-A277001] 09 p3692 N94-32199
High-performance GaAs/AlGaAs optical phase modulators for microwave photonic integrated circuits
[DE94-007376] 09 p3696 N94-32809
YBCO Josephson Junction arrays
[AD-A277426] 09 p3908 N94-33005
Advanced silicon technology for microwave circuits
[AD-A278039] 09 p3698 N94-33091
Processing, fabrication, and demonstration of HTS integrated microwave circuits
[AD-A277684] 10 p4040 N94-33893
The 2nd International Workshop on Discrete Time Domain Modelling of Electromagnetic Fields and Networks
[AD-A277551] 10 p4035 N94-34081
A 32-GHz solid-state power amplifier for deep space communications 11 p4255 N94-35562
Radially combined 30 W, 14-16 GHz amplifier
[DE94-010078] 12 p4432 N94-36471
A novel transition between rectangular waveguide and layered ridge dielectric waveguide
[NASA-TM-106661] 12 p4433 N94-36955
Microwave detection of a superconducting infrared sensor
[AD-D016297] 12 p4440 N94-37769

MICROWAVE COUPLING
Aperture coupling of circular cylindrical dielectric resonator antenna
[ISBN-0-315-60632-0] 05 p1743 N94-22409
Microwave excitation of pulsed high pressure gas discharge lasers
[DLR-FB-93-12] 06 p2351 N94-25304
Microwave coupling into a slotted cavity
[PB94-123742] 07 p2772 N94-27041
An investigation of a novel microstrip magic-T
[ISBN-0-315-86218-1] 09 p3690 N94-31711

MICROWAVE EMISSION
Estimations of temperature and humidity of the canopy in Amazon Forest using microwave data from SMMR sensor of Nimbus-7 satellite
[INPE-5444-TDI/490] 02 p0720 N94-13614
Comparative study of x ray and microwave emissions during solar flares
[NASA-CR-194532] 02 p0845 N94-14577
Radiation from solar flares 05 p2001 N94-22634
High sensitivity and resolution decimetric spectroscope: Preliminary analysis of solar bursts
[INPE-5537-TDI/525] 09 p3954 N94-33080
Studies of impulsive solar bursts observed with high spectral resolution in the range of 18 to 23 GHz
[INPE-5538-TDI/526] 10 p4165 N94-34219
State of the art in high-power microwaves: An overview
[DE94-007075] 11 p4272 N94-35978

MICROWAVE EQUIPMENT
NT BACKWARD WAVE TUBES
NT CYCLOTRON RESONANCE DEVICES
NT HORN ANTENNAS
NT KLYSTRONS
NT MAGNETRONS
NT MICROWAVE AMPLIFIERS
NT MICROWAVE ANTENNAS
NT MICROWAVE FILTERS
NT MICROWAVE INTERFEROMETERS
NT MICROWAVE OSCILLATORS
NT MICROWAVE PROBES
NT MICROWAVE RADIOMETERS
NT MICROWAVE TUBES
NT RECTENNAS
NT THYRATRONS
NT TRAVELING WAVE TUBES
Microwave multiplexer with channels of varying fractional bandwidths
[AD-D015754] 01 p0140 N94-10389
Microwave interconnection
[DE93-016580] 02 p0625 N94-14533
Synthesis of ceramic oxide powders in a microwave plasma device
[DE93-012741] 03 p0965 N94-15920
A modified two-fluid model of conductivity for superconducting surface resistance calculation
[AD-A267549] 03 p1013 N94-17104
Engineering research, development and technology thrust area report, FY92
[DE93-016334] 04 p1632 N94-18856
Automated HMC assembly
[DE93-040641] 05 p1749 N94-20005
Interinjection-locked quasioptical power combiners and phased arrays
[AD-A271178] 05 p2015 N94-20214
Three point lead screw positioning apparatus for a cavity tuning plate
[NASA-CASE-LEW-15216-1] 05 p1822 N94-20375
TlCaBaCuO high Tc superconducting microstrip ring resonators designed for 12 GHz
05 p1735 N94-20516
Microwave and pulsed power
[DE94-003019] 07 p2782 N94-26312
Four phase microwave pulse generator for pulsed EPR spectrometer 07 p2718 N94-27388
Photoconductive switching for high power microwave generation
[PB94-137460] 08 p3244 N94-29177
Hydrogen maser clocks in space for solid-Earth research and time-transfer applications: Experiment overview and evaluation of Russian miniature sapphire loaded cavity
08 p3474 N94-30676
Simulation of non-uniform transmission lines for weakly dispersive structures
[ISBN-0-315-86525-3] 09 p3690 N94-31726
Performance evaluation and operating characteristics of a waveguide microwave applicator for space propulsion applications 09 p3614 N94-31908
Division of Microwave Technology
[PB94-148079] 09 p3676 N94-31925
Estimation and analysis of climate-scale rainfall over the Tropical Pacific 09 p3783 N94-32030
Proceedings SPIE: Conference Digest, volume 2104
[AD-A278107] 09 p3884 N94-33187
Influence of an externally modulated photonic link on a microwave communications system
11 p4252 N94-35544
DSS-13 S-/X-band microwave feed system
11 p4253 N94-35550
Earth Observing System/Advanced Microwave Sounding Unit-A (EOS/AMSU-A) software management plan
[NASA-CR-189362] 12 p4461 N94-36919

MICROWAVE FILTERS
Limited bandwidth microwave filter
[AD-D015744] 01 p0145 N94-12322
Manual design technique for broadband passive thin-film attenuators using the Smith chart
05 p1782 N94-22178
X-/Ka-band dichroic plate design and grating lobe study 08 p3247 N94-29616

MICROWAVE FREQUENCIES
NT C BAND
NT EXTREMELY HIGH FREQUENCIES
NT P BAND
NT SUPERHIGH FREQUENCIES
Hard x ray/microwave spectroscopy of solar flares
[NASA-CR-194399] 02 p0844 N94-13958
Recent scientific advances in the use of radar in scientific hydrology 03 p0991 N94-15895
Application of Cloude's target decomposition theorem to polarimetric imaging radar data
05 p1724 N94-20429
C-band radar backscatter of sea ice in the Weddell Sea, Antarctica during the austral winter of 1992
05 p1725 N94-20435
A physics-based heterojunction bipolar transistor model for integrated circuit simulation
[AD-A274081] 07 p2781 N94-25995
Over-the-horizon propagation measurements at six radar-frequency bands at the Atlantic Ocean Coast
[AD-A274151] 07 p2773 N94-27136
Effective conductivity of wire mesh reflectors for space deployable antenna systems
[NASA-CR-191605] 07 p2788 N94-27770
Cryogenic probe station for use in automated microwave and noise figure measurements
[NASA-TM-106560] 08 p3286 N94-29000
RF and microwave dielectric measurements upon layered materials using reflectometric coaxial sensor
[NPL-DES-125] 08 p3476 N94-30781
Development of a frequency-domain electromagnetic scattering measurement system
[AD-A276738] 09 p3678 N94-32179
Processing and characterization of functionally gradient ceramic materials
[AD-A277154] 09 p3657 N94-32367
Dielectric measurements of selected ceramics at microwave frequencies 11 p4232 N94-36412
A high power microwave frequency modulated KrF laser
[DE94-009303] 12 p4447 N94-36510
Study on the measurement uncertainty of noise properties of a millimeter wave amplifier
[PB94-170917] 12 p4510 N94-37632

MICROWAVE HOLOGRAPHY
Automated inspection of turbine blades: Challenges and opportunities
[AIAA PAPER 94-1226-CP] 08 p3446 N94-30575

MICROWAVE IMAGERY
Summer Arctic ice concentrations and characteristics from SAR and SSM/I data 01 p0241 N94-11762
Ocean wave detection by SAR
01 p0197 N94-11932
On the determination of the SAR ocean surface scattering patch size 01 p0197 N94-11933
Measurements of ocean cross-section with a side-looking airborne radar 01 p0201 N94-11954
SSMI wind speed variability over the Pacific Ocean
01 p0207 N94-12637
Microwave radiometry of ice cover in polar regions
01 p0210 N94-12655
Fine scale measurements of microwave backscatter from the ocean surface
[AD-A264516] 03 p1111 N94-15134
A summary of microwave remote sensing investigations planned for BOREAS 03 p0993 N94-15914
An analysis of simulated and actual DMSP SSM/T-2 brightness temperatures
[AD-A268103] 03 p1109 N94-17573
An empirical study of tropical cloud clusters using special sensor microwave imager data
[AD-A268072] 03 p1110 N94-17595
Packaging, deployment, and panel design concepts for a truss-stiffened 7-panel precision deployable reflector with feed boom
[NASA-TM-109000] 04 p1333 N94-17765
Microwave (SSM/I) Estimates of the Precipitation Rate to Improve Numerical Atmospheric Model Forecasts
[NASA-CR-193566] 04 p1491 N94-18602
Physical retrieval of precipitation water contents from Special Sensor Microwave/Imager (SSM/I) data. Part 1: A cloud ensemble/radiative parameterization for sensor response (report version) 04 p1491 N94-18604
Physical retrieval of precipitation water contents from Special Sensor Microwave/Imager (SSM/I) data. Part 2: Retrieval method and applications (report version)
04 p1491 N94-18605
Atlas of SSM/I satellite ice concentration interpolated to operational ice model domains of the Arctic for 1992
[AD-A270306] 04 p1499 N94-18727
Millimeter wave imaging technology
[AD-A271257] 05 p1715 N94-19912
Comparison of remote sensing measurements with a two-scale polarimetric emission and scattering model for sea surfaces 05 p1721 N94-20415
On evaluating the accuracy of SAR sea-ice classification using multifrequency polarimetric AIRSAR data
05 p1724 N94-20428
Millimeter-wave imaging of composite materials
[DE93-041160] 05 p1677 N94-21940
Investigation of passive atmospheric sounding using millimeter and submillimeter wavelength channels
[NASA-CR-194858] 06 p2404 N94-24843
Passive millimeter-wave imaging
06 p2306 N94-25494
Advanced radiometric and interferometric milimeter-wave scene simulations
06 p2306 N94-25498
A model-based approach for detection of objects in low resolution passive-millimeter wave images
06 p2442 N94-25507
Polarimetric investigation of edge scattering by mono- and bistatic microwave imaging
[ESA-TT-1284] 07 p2768 N94-26317
Leadex environmental phenomena and effects observed by DMSP, NOAA, and ERS-1 satellites
[AD-A274596] 07 p2868 N94-26888
Model for the simulation of atmospheric effects on targets to background passive signatures
08 p3258 N94-30507

Polarimetric backscatter measurements of natural surfaces at millimeter wavelengths
08 p3259 N94-30509
Estimation and analysis of climate-scale rainfall over the Tropical Pacific
09 p3783 N94-32030
Production of long-term global water vapor and liquid water data set using ultra-fast methods to assimilate multi-satellite and radiosonde observations
[NASA-CR-196044] 11 p4292 N94-35355
A model-based approach for detection of runways and other objects in image sequences acquired using an on-board camera
[NASA-CR-196424] 12 p4446 N94-36812

MICROWAVE INTERFEROMETERS
Microwave Michelson interferometer system report of first use on a railgun, Green Farm, San Diego, CA
[DE94-005294] 08 p3289 N94-30059

MICROWAVE LANDING SYSTEMS
Flight evaluations of approach/landing navigation sensor systems: Summary of 1990 flight experiments
[NAL-TR-1175] 02 p0513 N94-13344
MLS signal-in-space category 3 landing hazard analysis
05 p1644 N94-22134
Application of scattering by arrays of cylinders to MLS signal propagation error estimation
05 p1644 N94-22135
Testing of DME/P equipment performance for complex MLS procedures
05 p1644 N94-22136
MLS pointing angle error sources and effects
05 p1644 N94-22154
Developing software to RTCA DO-178A
05 p1645 N94-22155
A flight test system design for the microwave landing system
05 p1645 N94-22156
Automatic, real-time fault monitor verifying network in a microwave landing system
[CA-PATENT-1325261] 07 p2665 N94-27275
Ground independent landing system
08 p3137 N94-29564
Flight simulator evaluation of advanced MLS procedures
[AD-B174270] 08 p3143 N94-30915
An analysis of operational suitability for test and evaluation of highly reliable systems
[AD-A278573] 11 p4192 N94-36184
A model-based approach for detection of runways and other objects in image sequences acquired using an on-board camera
[NASA-CR-196424] 12 p4446 N94-36812

MICROWAVE OSCILLATORS
NT MAGNETRONS
Dielectric resonator
[US-PATENT-4,580,116] 01 p0141 N94-10668
Measurements of the operation of the SINUS-6/BWO system
[AD-A266423] 03 p1011 N94-16556
Optically-switched submillimeter-wave oscillator and radiator
[NASA-CASE-NPO-18547-1-CU]
03 p1014 N94-17324
Optically controlled active impedance element and filters employing the same
[AD-D015863] 04 p1396 N94-18062
The gyrotron backward-wave-oscillator experiment --- final progress report
[AD-A268982] 04 p1403 N94-18452
Interinjection-locked quasioptical power combiners and phased arrays
[AD-A271178] 05 p2015 N94-20214
A 10 GHz Y-Ba-Cu-O/GaAs hybrid oscillator proximity coupled to a circular microstrip patch antenna
05 p1736 N94-20517
Improvement of the performance of IMPATT oscillators through appropriate modification of resonant-cap activity
05 p1782 N94-22179
Non-linear analysis of the electrical properties of the active circuits of high-frequency oscillators
05 p1785 N94-22195
Electrical analysis of wideband and distributed windows using time-dependent field codes
[DE94-002987] 07 p2768 N94-26310
HPm-tubes: Literature survey comprising 1992
[PB94-123643] 07 p2785 N94-27038
Computer simulations of radiation generation from relativistic electron beams
[AD-A274139] 07 p3024 N94-27133
Synchronization of microwave oscillators by direct optical injection
[ISBN-0-315-85546-0] 08 p3500 N94-30233
Repetitively pulsed backward-wave oscillator investigations
[AD-A278281] 09 p3698 N94-33142
Optically switched submillimeter-wave oscillator
[AD-A278014] 09 p3698 N94-33249
A 1- to 10-GHz downconverter for high-resolution microwave survey
11 p4253 N94-35551
Submillimeter quasioptical Josephson junction oscillator with integrated tuning elements
[AD-A280380] 12 p4534 N94-37036

MICROWAVE POWER BEAMING
Construction and testing of a space ready rectenna
[NASA-CR-193310] 01 p0137 N94-11357
Low-current traveling wave tube for use in the microwave power module
[NASA-TP-3344] 02 p0620 N94-13110
WISPER: Wirless Space Power Experiment
[NASA-CR-195538] 06 p2396 N94-24701
A transportronic solution to the problem of interorbital transportation
[NASA-CR-191152] 08 p3164 N94-29355

MICROWAVE PROBES
An optically modulated scatterer for microwave antenna metrology
[NPL-DES-126] 03 p0986 N94-15020
Network analyzer calibration for cryogenic on-wafer measurements
[DE94-010089] 11 p4262 N94-36430

MICROWAVE RADIATION
U MICROWAVES

MICROWAVE RADIOMETERS
Investigation of passive atmospheric sounding using millimeter and submillimeter wavelength channels
[NASA-CR-193627] 01 p0274 N94-10726
Physical processes of microwave backscattering from laboratory wind-wave surfaces 01 p0200 N94-11952
Dependence of oceanic microwave emission on wind direction 01 p0201 N94-11957
On the variability of wind speeds in the North Western Pacific observed by altimeter/GEOSAT and SSM/I/DMSP 01 p0201 N94-11960
Sampling and position effects in the Electronically Steered Thinned Array Radiometer (ESTAR)
[NASA-TM-108998] 01 p0245 N94-12432
Validation of the ATSR/M microwave radiometer data
01 p0252 N94-12511
SSMI wind speed variability over the Pacific Ocean
01 p0207 N94-12637
Microwave radiometry of ice cover in polar regions
01 p0210 N94-12655
Worldwide map of rainfall amount over the ocean derived from passive microwave radiometer
01 p0211 N94-12663
Estimations of temperature and humidity of the canopy in Amazon Forest using microwave data from SMMR sensor of Nimbus-7 satellite
[INPE-5444-TDI/490] 02 p0720 N94-13614
Phase aligner for the Electronically Scanned Thinned Array Radiometer (ESTAR) instrument
[NASA-TM-4518] 02 p0623 N94-13878
Future TRMM follow-on mission
02 p0691 N94-14228
Radiometric observations of atmospheric attenuation at 20.6 and 31.65 GHz: The Wave Propagation Laboratory data base 02 p0613 N94-14660
Comparison of OLYMPUS beacon and radiometric attenuation measurements at Blacksburg, Virginia
03 p0996 N94-16046
Earth observation from small satellites
03 p0891 N94-17150
Validation and analysis of microwave-derived rainfall over the tropics
[AD-A267785] 03 p1108 N94-17303
Arctic and Antarctic sea ice, 1978-1987: Satellite passive-microwave observations and analysis
[NASA-SP-511] 03 p1114 N94-17439
A conceptual design study for a two-dimensional, electronically scanned thinned array radiometer
[NASA-TM-109051] 03 p1085 N94-17665
Physical retrieval of precipitation water contents from Special Sensor Microwave/Imager (SSM/I) data. Part 1: A cloud ensemble/radiative parameterization for sensor response (report version) 04 p1491 N94-18604
Atmospheric infrared sounder
[NASA-CR-194814] 05 p1856 N94-20362
Simulated retrieval of land surface parameters using multichannel satellite microwave radiometry
05 p1727 N94-20443
Polarimetric thermal emission from periodic water surfaces 05 p1728 N94-20445
Spatial and temporal variations of satellite microwave measurements of latent heat release in tropic cyclones due to environmental forcing obtained from a numerical model
[AD-A267947] 05 p1865 N94-20482
A field evaluation of remote sensor measurements of wind, temperature, and moisture for ARM integrated sounding system research
[DE94-000565] 06 p2381 N94-23001
Application of ERS-1 active microwave instrumentation data to remote sensing of snow
[PB93-224756] 06 p2382 N94-23224
Feasibility of detecting aircraft wake vortices using passive microwave radiometers
[NASA-CR-191553] 06 p2343 N94-23498
Investigation of passive atmospheric sounding using millimeter and submillimeter wavelength channels
[NASA-CR-194858] 06 p2404 N94-24843
Cloud liquid water content measurement tests using dual-wavelength radar
[PB94-125960] 07 p2896 N94-26959
Conceptual radiometer design studies for Earth observations from low Earth orbit
[NASA-CR-4588] 08 p3329 N94-29098
On the relation between SMMR 37-GHz polarization difference and the rainfall over Africa and Australia
[NASA-TM-104598] 08 p3370 N94-29408
Model for the simulation of atmospheric effects on targets to background passive signatures
08 p3258 N94-30507
Remote sensor observations during WISP91: The use of microwave radiometers, RASS, and lidar ceilometers for detection of aircraft icing conditions
[PB94-142106] 08 p3136 N94-30890
An integrated cloud observation and modeling investigation in support of the ARM program
[DE94-003160] 09 p3785 N94-32716
Water vapor from sunradiometry in comparison with microwave and balloon-sonde measurements at the Southern Great Plains ARM Site
[DE94-007479] 09 p3786 N94-32759
The multiple scattering contributions in the strong fluctuation theory to the microwave brightness temperature
[AD-A277721] 10 p4075 N94-33442
Two-channel microwave radiometer for observations of total column precipitable water vapor and cloud liquid water path
[DE94-007480] 12 p4471 N94-36479

MICROWAVE REFLECTOMETERS
The MRIS feasibility study
[NASA-TM-107763] 02 p0597 N94-12804
Scattering of reflectometer signals from rippled surfaces
[PPL-138] 02 p0602 N94-13802
Microwave reflectometer ionization sensor
[NASA-CR-191464] 03 p0922 N94-17083
Microwave reflectometry for fusion plasma diagnostics
[DE94-620118] 12 p4527 N94-36566

MICROWAVE RESONANCE
Applications of in-situ ellipsometry to microwave electron cyclotron resonance plasma processes
[AD-A265197] 01 p0373 N94-11880
Measurement electronics of industrial microwave resonator sensors
[TKK-S-RAD-S194] 02 p0625 N94-14096
Improvement of the performance of IMPATT oscillators through appropriate modification of resonant-cap activity
05 p1782 N94-22179
Investigation and application of microwave electron cyclotron resonance plasma physical vapour deposition
[DE93-613909] 06 p2555 N94-25333
Plasma surface cleaning using microwave plasmas
[DE94-002754] 07 p2713 N94-26014

MICROWAVE SCATTERING
ERS-1 studies at the Department of Oceanography from Space, IFREMER/Brest (France)
01 p0233 N94-11712
The activity of the ERS-1 Venice (Italy) group on scatterometry 01 p0233 N94-11713
A preliminary C-band scatterometer model function for the ERS-1 AMI instrument 01 p0233 N94-11715
On the determination of the SAR ocean surface scattering patch size 01 p0197 N94-11933
Experiment and results of the Italian activity in the field of ocean microwave backscattering
01 p0200 N94-11953
Scatterometer observations: Review
01 p0201 N94-11956
The microwave backscattering from wind waves
01 p0201 N94-11959
A basic consideration for remote sensing using microwave radars on a satellite
01 p0212 N94-12665
Scattering of reflectometer signals from rippled surfaces
[PPL-138] 02 p0602 N94-13802
Fine scale measurements of microwave backscatter from the ocean surface
[AD-A264516] 03 p1111 N94-15134
Microwave scattering from TAE modes
[DE93-018170] 04 p1583 N94-17809
The split-step algorithm for microwave propagation modeling above a conducting surface
[FEL-92-A430] 04 p1390 N94-19447
Theoretical and experimental research on coherent microwave backscatter from the ocean
[AD-A271276] 04 p1500 N94-19743

Radar backscatter measurements from simulated sea ice during CRRELEX 1990
[AD-A271034] 05 p1715 N94-19823
Comparison of remote sensing measurements with a two-scale polarimetric emission and scattering model for sea surfaces 05 p1721 N94-20415
Use of microwave polarimetry to enhance SAR images of the ocean surface
[AD-A271911] 05 p1882 N94-20489
Presenting the Rain-Sea Interaction Facility
[NASA-RP-1322] 05 p1884 N94-21628
Application of scattering by arrays of cylinders to MLS signal propagation error estimation 05 p1644 N94-22135
A simplified method for S-parameter calculations of metal septum waveguide filters 05 p1782 N94-22180
Overview of the ATF stellarator program
[DE94-000371] 06 p2550 N94-23462
Use of microwave polarimetry to enhance SAR images of the ocean surface
[AD-A273568] 06 p2419 N94-24944
A hybrid electromagnetic-statistical approach for characterizing MMW scattering by terrain 08 p3259 N94-30510

MICROWAVE SENSORS
Measurement electronics of industrial microwave resonator sensors
[TKK-S-RAD-S194] 02 p0625 N94-14096
ERS-1 system
[ESA-SP-1146] 02 p0699 N94-14353
Relating multifrequency radar backscattering to forest biomass: Modeling and AIRSAR measurement 03 p1077 N94-16741
Physical retrieval of precipitation water contents from Special Sensor Microwave/Imager (SSM/I) data. Part 1: A cloud ensemble/radiative parameterization for sensor response (report version) 04 p1491 N94-18604
Synergism of active and passive microwave data for estimating bare surface soil moisture 05 p1727 N94-20444
Mission planning for an Earth observation low Earth orbiter: ERS-1 06 p2503 N94-23868
Conceptual radiometer design studies for Earth observations from low Earth orbit
[NASA-CR-4588] 08 p3329 N94-29098
Radar rainfall measurements from space 09 p3782 N94-31889
Microwave sensor for ice detection 09 p3583 N94-32457
Application of ERS-1 SAR data for hydrological studies 09 p3754 N94-32558
Synergy of thermal infrared and microwave remote sensing for evaporation estimation 09 p3754 N94-32559

MICROWAVE SIGNATURES
Arctic sea ice microwave signature and geophysical processes study 01 p0240 N94-11754
Microwave properties and systems overview 03 p0924 N94-15222
The split-step algorithm for microwave propagation modeling above a conducting surface
[FEL-92-A430] 04 p1390 N94-19447
A comparison between several computer codes for calculations on microwave propagation
[FEL-92-A435] 04 p1390 N94-19449
Model for the simulation of atmospheric effects on targets to background passive signatures 08 p3258 N94-30507

MICROWAVE SOUNDING
Submillimeter wave observation experiment of Earth atmosphere with SIS mixer 01 p0130 N94-11837
DMSP F11 SSM/T-2 calibration and validation
[AD-A265817] 02 p0719 N94-12978
Water-vapour, total water and rainrate from passive microwave satellite data over ocean
[DLR-FB-92-37] 02 p0723 N94-14189
Earth Observing System (EOS) Advanced Microwave Sounding Unit-A (AMSU-A) schedule plan
[NASA-CR-194856] 11 p4281 N94-35734
Application of differential inversion to DMSP microwave sounder data
[AD-A278575] 11 p4294 N94-36186
Earth Observing System/Advanced Microwave Sounding Unit-A (EOS/AMSU-A) software management plan
[NASA-CR-189362] 12 p4461 N94-36919
Earth Observing System (EOS)/Advanced Microwave Sounding Unit A (AMSU-A) configuration management plan
[NASA-CR-189371] 12 p4494 N94-37061

MICROWAVE SPECTRA
Validation of directional wave spectra from the ERS-1 during the ESA CAL/VAL campaign 01 p0232 N94-11707
The Grand Banks ERS-1 SAR wave spectra validation experiment 01 p0232 N94-11708
Submillimeter, millimeter, and microwave spectral line catalogue, revision 3
[NASA-CR-194501] 02 p0602 N94-13813
On the relationship between spectral domain approach and method of lines 05 p1794 N94-22254
Laboratory detection of C5S by pulsed-discharge-nozzle Fourier-transform microwave spectroscopy
[JTN-94-80519] 06 p2235 N94-24984
Evaluation of wireless Local Area Networks
[AD-A275133] 08 p3243 N94-29064
Cometary molecules 09 p3935 N94-31869

MICROWAVE SPECTROMETERS
Temperature/pressure and water vapor sounding with microwave spectroscopy 05 p1812 N94-22436

MICROWAVE SWITCHING
Ferrite phase shifters using stress insensitive materials
[AD-A274639] 07 p2708 N94-26895
Photoconductive switching for high power microwave generation
[PB94-137460] 08 p3244 N94-29177

MICROWAVE TRANSMISSION
Construction and testing of a space ready rectenna
[NASA-CR-193310] 01 p0137 N94-11357
One-dimensional calculation of high-power microwave pulse compression by the earth's ionosphere
[DE93-009517] 01 p0137 N94-11466
True time delay optically controlled dual band transmitter
[AD-A267663] 03 p1003 N94-17228
The split-step algorithm for microwave propagation modeling above a conducting surface
[FEL-92-A430] 04 p1390 N94-19447
A comparison between several computer codes for calculations on microwave propagation
[FEL-92-A435] 04 p1390 N94-19449
Microwave coupling into a slotted cavity
[PB94-123742] 07 p2772 N94-27041
Preliminary analysis of Asynchronous Transfer Mode (ATM) over microwave channels
[AD-A275214] 08 p3243 N94-29069
Propagation modeling of moist air and suspended water/ice particles at frequencies below 1000 GHz 08 p3256 N94-30497
The influence of the evaporation duct on the angle of arrival and amplitude of the backscattered signal from targets low above the sea 08 p3256 N94-30498
Theoretical, experimental, and computational evaluation of disk-loaded circular wave guides
[NASA-TM-106640] 10 p4041 N94-33944

MICROWAVE TUBES
NT BACKWARD WAVE TUBES
NT CYCLOTRON RESONANCE DEVICES
NT KLYSTRONS
NT MAGNETRONS
NT TRAVELING WAVE TUBES
Electrical analysis of wideband and distributed windows using time-dependent field codes
[DE94-002987] 07 p2768 N94-26310
HPm-tubes: Literature survey comprising 1992
[PB94-123643] 07 p2785 N94-27038
High-power microwave-tube transmitters
[DE94-005340] 09 p3686 N94-31150
Dielectric loaded broadband gyro-TWT system
[AD-A277889] 10 p4040 N94-33861
State of the art in high-power microwaves: An overview
[DE94-007075] 11 p4272 N94-35978
Evaluation of some slow-wave vane structures for aminiature traveling-wave tube at 30 GHz
[NASA-TM-106654] 12 p4437 N94-36819

MICROWAVES
NT MICROWAVE EMISSION
NT MILLIMETER WAVES
Single-electron tunneling
[DE93-013337] 01 p0396 N94-10648
The possibility of using carbon-graphite materials for microwave plasma diagnostics in large fusion devices
[DE93-621609] 01 p0066 N94-11143
Characteristics of ICR-produced peripheral plasma in the Uragan-3M torsatron
[DE93-621666] 01 p0392 N94-11214
The excitation of cyanogen and ionized carbon in interstellar and extragalactic gas clouds 01 p0426 N94-11582
Search for structures in the cosmic microwave background radiation
[INPE-5491-TDI/508] 01 p0484 N94-12357
Ceramic matrix composites by microwave assisted CVI
[DE93-012640] 02 p0576 N94-12916
Search for extraterrestrial intelligence/high resolution microwave survey team member
[NASA-CR-194177] 02 p0739 N94-13086
Comment of parameter excitation of Alfven and Helicon waves in a magnetoactive compensated semiconductor by microwave radiation
[DE93-623203] 02 p0806 N94-13228
Problems and opportunities in microwave joining of ceramics
[DE93-014998] 02 p0579 N94-13888
Microwave hybrid heating of alumina filaments
[DE93-012642] 02 p0581 N94-14327
Microwave sintering of large alumina bodies
[DE93-012752] 02 p0581 N94-14340
Microwave interconnection
[DE93-016580] 02 p0625 N94-14533
Velocity matched millimeterwave electro-optic modulator
[AD-A267264] 03 p1188 N94-14957
Microwave interaction with plasmas
[AD-A267048] 03 p1201 N94-15661
The pressure broadening of HDO by O2, N2, H2, and He between 100 K and 600 K
[AD-A267118] 03 p0946 N94-15684
Crystallization of grain boundary phases in silicon nitride with low additive contents by microwave annealing
[DE93-015801] 03 p1209 N94-16164
Efficient computational methods to study new and innovative signal detection techniques in SETI
[NASA-CR-193602] 03 p0998 N94-16649
Processing of complex sintered reaction bonded silicon nitride parts by microwave heating
[DE93-015811] 03 p0969 N94-16877
Large signal characterization and modeling of heterojunction bipolar transistors
[AD-A266184] 03 p1012 N94-16935
The behavioral toxicology of high-peak, low average power, pulsed microwave irradiation
[AD-A268392] 03 p1134 N94-17535
Design of a tunable 4-MW free electron maser for heating fusion plasmas
[DE93-017172] 04 p1437 N94-18134
A study of the effects of high power pulsed 2450 MHz microwaves, ELF modulated microwaves, and ELF fields on human lymphocytes and selected cell lines
[AD-A269070] 04 p1505 N94-18294
High-power microwave breakdown of dielectric interfaces
[AD-A268844] 04 p1397 N94-18318
The gyrotron backward-wave-oscillator experiment --- final progress report
[AD-A268982] 04 p1403 N94-18452
General geometry PIC for MIMD computers
[AD-A269085] 04 p1534 N94-18767
Electron cyclotron resonance heating in the microwave tokamak experiment
[DE93-018083] 04 p1590 N94-19289
Optical frequency division using an optical parametric oscillator
[AD-A270847] 04 p1581 N94-19578
Quasi-optical transponder using FET's and patch antennas
[AD-A271339] 04 p1407 N94-19584
Transport in microstructures in the microwave and millimeter-wave regime
[AD-A271875] 05 p2017 N94-20470
Spatial and temporal variations of satellite microwave measurements of latent heat release in tropic cyclones due to environmental forcing obtained from a numerical model
[AD-A267947] 05 p1865 N94-20482
Use of microwave polarimetry to enhance SAR images of the ocean surface
[AD-A271911] 05 p1882 N94-20489
Rotational spectrum of a dark state in 2-fluoroethanol using microwave/radiofrequency-infrared multiple resonance
[AD-A272101] 05 p1817 N94-20583
Particle behavior in an ECR plasma etch tool
[DE93-040343] 05 p1996 N94-21769
Plasma-chemical conversion of hydrogen sulfide into hydrogen and sulfur
[DE93-041167] 05 p1682 N94-21789
An assessment of the cost of microwave sintering ceramic tiles for armor applications
[DE94-000978] 05 p1693 N94-21850
Optimization of energy transfer in microwave electrothermal thrusters 06 p2216 N94-23065
CFD modeling of microwave electrothermal thrusters 06 p2216 N94-23066
Proceedings of the 1993 Bi-Isotropics Workshop on Novel Microwave Materials
[PB93-224772] 06 p2290 N94-23225
Synthesis of passive microwave and radar altimeter data for estimating accumulation rates of polar snow
[NASA-CR-194864] 06 p2382 N94-23573
Multigrid and cyclic reduction applied to the Helmholtz equation 06 p2304 N94-23676

Microwave techniques for physical property measurements 06 p2238 N94-25134
Microwave excitation of pulsed high pressure gas discharge lasers
[DLR-FB-93-12] 06 p2351 N94-25304
Theoretical aspects of the agile mirror
[AD-A274890] 07 p2767 N94-26177
Microwave and pulsed power
[DE94-003019] 07 p2782 N94-26312
Experimental and theoretical investigation of RF absorption and reflection from preformed plasmas
[AD-A274189] 07 p3046 N94-27098
A direct current rectification scheme for microwave space power conversion using traveling wave electron acceleration 07 p2687 N94-27371
Electromagnetic modeling of bi-isotropic media
[PB94-132909] 07 p2778 N94-28382
Analysis of microwave induced interference in pn-diodes
[PB94-136983] 08 p3243 N94-28906
Deployable reflector structure
[NASA-CASE-LAR-14513-1-SB] 08 p3245 N94-29360
Energetic events in the early universe 08 p3547 N94-30012
Microwave vision for robots
[AIAA PAPER 94-0687-CP] 08 p3443 N94-30550
Remote pumping of solid state lasers with nuclear driven fluorescers
[DE94-004846] 08 p3296 N94-30614
Microwave dielectric behavior of soils. Report 1: Summary of related research and applications
[AD-A275980] 09 p3771 N94-31351
Microwave dielectric behavior of soils. Report 2: A unique coaxial measurement apparatus
[AD-A275982] 09 p3771 N94-31353
Two-gigawatt burst-mode operation of the Intense Microwave Prototype (IMP) Free-Electron Laser (FEL) for the Microwave Tokamak Experiment (MTX)
[DE94-006613] 09 p3715 N94-31580
Structure estimation of phase objects from the diffraction near field: Microwave and model calculations
[ETN-94-95737] 09 p3674 N94-31608
High peak power microwaves: A health hazard
[AD-A277168] 09 p3681 N94-32576
Water vapor from sunradiometry in comparison with microwave and balloon-sonde measurements at the Southern Great Plains ARM Site
[DE94-007479] 09 p3786 N94-32759
Experimental observations of thermal spikes in microwave processing of ceramic oxide fibers
[DE94-009348] 10 p4027 N94-33683
Influence of an externally modulated photonic link on a microwave communications system 11 p4252 N94-35544
A 1- to 10-GHz downconverter for high-resolution microwave survey 11 p4253 N94-35551
State of the art in high-power microwaves: An overview
[DE94-007075] 11 p4272 N94-35978
On the effects of transforming the vibrational spectra of molecular systems under microwave radiation
[DE94-617057] 11 p4329 N94-36310
Astronomy in the region between 1 mm and 0.1 mm wavelength
[NASA-CR-196020] 11 p4349 N94-36419
Analysis of recent agile mirror data
[AD-A278758] 11 p4318 N94-36427
Network analyzer calibration for cryogenic on-wafer measurements
[DE94-010089] 11 p4262 N94-36430
A high power microwave frequency modulated KrF laser
[DE94-009303] 12 p4447 N94-36510
New plasma source of hydrides for epitaxial growth
[DE94-006918] 12 p4533 N94-36744
Behavioral performance in monkeys exposed to TEMPO high-peak-power microwave pulses at 3 GHz
[AD-A280551] 12 p4478 N94-37045
Turning soot into diamonds with microwaves
[DE94-013426] 12 p4422 N94-37068
Suppression of beam-break-up in a standing wave free electron laser two-beam accelerator
[DE94-011348] 12 p4521 N94-37200

MICROWEIGHING
U WEIGHT MEASUREMENT

MID-OCEAN RIDGES
Assimilation of solids during ascent of magmas from the Bartoy Field of the Baikal Region, Siberia 03 p1103 N94-16214
Faulted structure of the bottom simulating reflector on the Blake Ridge, western North Atlantic
[AD-A271289] 04 p1500 N94-19745
Light in Thermal Environments (LITE) Workshop
[NASA-CR-195851] 09 p3790 N94-32981

MID-OCEANIC RIDGES
U MID-OCEAN RIDGES

MIDAIR COLLISIONS
NT BIRD-AIRCRAFT COLLISIONS
National Transportation Safety Board annual review of aircraft accident data, US general aviation, calendar year 1989
[PB93-160687] 03 p0863 N94-16464
Aircraft accident report: Midair collision, Mitsubishi MU-2B-60, N74FB, and PIPER PA-32-301, N82419, Greenwood Municipal Airport, Greenwood, Indiana, 11 September 1992
[PB93-910406] 04 p1315 N94-19352
A fresh look at crater scaling laws for normal and oblique hypervelocity impacts 05 p1666 N94-20864
Effectiveness of protection clothing for cold weather conditions after ejection over sea: A case report 08 p3381 N94-28435
Annual review of aircraft accident data: US general aviation calendar year 1991
[PB94-127982] 10 p3988 N94-34991

MIDALTITUDE
MAGSS-14: Medium Altitude Global Mobile Satellite System with enhanced regional coverage 03 p0893 N94-17164

MIDCOURSE GUIDANCE
Evaluation of GPS position and attitude determination for automated rendezvous and docking missions
[NASA-CR-4614] 12 p4397 N94-37506

MIDDLE ATMOSPHERE
NT MESOPAUSE
NT MESOSPHERE
NT OZONOSPHERE
NT STRATOSPHERE
Electrodynamics of the middle atmosphere: Superpressure balloon program
[NASA-CR-193671] 02 p0712 N94-13293
A rocket-borne lidar for studies of the middle atmosphere
[FFI/RAPPORT-92/7034] 02 p0715 N94-13949
Chemistry and transport in a multi-dimensional model
[NASA-CR-194425] 02 p0716 N94-13969
Second flight of the Spacelab grille spectrometer during the Atlas-1 mission
[AERONAUTICA-ACTA-A-367-1992] 03 p0923 N94-17592
Analysis of satellite-derived ozone and water vapor measurements
[NASA-CR-193810] 04 p1486 N94-19237
Interactions of free modes, tides, and gravity waves in the middle atmosphere
[REPT-84] 05 p1855 N94-20155
Empirical wind model for the middle and lower atmosphere. Part 2: Local time variations
[NASA-TM-104592] 05 p1870 N94-21862
Two-dimensional modeling of thermal inversion layers in the middle atmosphere of Mars 06 p2622 N94-24900
Theory and observations of horizontal and vertical structure of gravity wave perturbations in the middle atmosphere 08 p3366 N94-30802
Uniqueness of a solution of a steady state photochemical problem: Applications to Mars 11 p4370 N94-36151

MIDLATITUDES
U TEMPERATE REGIONS

MIE SCATTERING
NT RAYLEIGH SCATTERING
Model of optical scatter from microimpacts on the Hubble Telescope 01 p0384 N94-12189
Light scattering from a spherical particle on a conducting plane. Part 1: Normal incidence
[AD-A265920] 01 p0383 N94-12341
Bridging the gap between the Rayleigh and Thomson limits for various convex bodies
[DSIS-93-00613] 02 p0607 N94-14204
A test of the applicability of independent scattering to high albedo planetary regoliths 03 p1250 N94-16187
Remote sensing of Earth terrain
[NASA-CR-194598] 04 p1464 N94-19681
Multiple scattering effects on the Linear Depolarization Ratio (LDR) measured during CaPE by a Ka-band air-borne radar 05 p1728 N94-20446
On the theory of morphology-dependent resonances: Shape resonances, width formulas, and graphical representations
[AD-A272279] 05 p2037 N94-20945
Particle sizes and composition of Mars atmospheric dust based upon Viking and Mariner 9 observations 06 p2618 N94-24878
Template synthesized nanoscopic gold particles: Optical spectra and the effects of particle size and shape
[AD-A275378] 08 p3197 N94-29312
Optical modeling of visibility and visibility instrumentation using stratified Mie theory 08 p3348 N94-29750

MIE THEORY
U MIE SCATTERING

MIGRATION
Warm streamers extended from Warm Core Rings (WCRs) and their role on fish migration and fishing ground formation 01 p0198 N94-11938

MILANKOVITCH THEORY
U CLIMATOLOGY

MILITARY AIR FACILITIES
The use of the Air Force Academy high wind alert system in forecasting moderate intensity wind events for military bases in the Colorado Springs area
[AD-A267648] 03 p1107 N94-17245

MILITARY AIRCRAFT
Thermal stability of sealants for military aircraft: Modification of polysulfide prepolymers with ether and thioether monomers
[AD-A264079] 01 p0089 N94-11107
Naval aviation: The Navy is taking actions to improve the combat capabilities of its tactical aircraft. Report to Congressional Requesters
[AD-A268002] 03 p0868 N94-17472
Naval aviation: Consider all alternatives before proceeding with the F/A-18E/F
[AD-A269302] 04 p1305 N94-18279
JPRS report: Central Eurasia. Aviation and cosmonautics, no. 12, December 1992
[JPRS-UAC-93-006] 04 p1632 N94-19148
JPRS report: Central Eurasia: Aviation and cosmonautics, no. 11, November 1992
[JPRS-UAC-93-005] 04 p1632 N94-19208
Audit report. Navy's aircraft structural life surveillance program data recorders
[AD-A270391] 05 p1645 N94-20040
A cost model for USAF acquisition of commercial aircraft for service in the special air mission fleet
[AD-A274012] 07 p3093 N94-25796
Unmanned Air Vehicle/Remotely Piloted Vehicle analysis for lethal UAV/RPV
[AD-A276052] 09 p3578 N94-31442
Aircraft weight prediction capability. Volume 1: Weight study and results
[AD-A277206] 09 p3579 N94-32062
A comparison of military and commercial aircraft development
[AD-A276830] 09 p3575 N94-32168
Anthropometric accommodation in USAF cockpits 10 p4101 N94-33630
Aircraft battle damage repair for the 1990's and beyond
[AD-A278635] 12 p4386 N94-36465

MILITARY AVIATION
Naval aviation: The Navy is taking actions to improve the combat capabilities of its tactical aircraft. Report to Congressional Requesters
[AD-A268002] 03 p0868 N94-17472

MILITARY HELICOPTERS
NT AH-1G HELICOPTER
NT AH-64 HELICOPTER
NT H-53 HELICOPTER
NT H-60 HELICOPTER
NT OH-6 HELICOPTER
NT SH-3 HELICOPTER
NT UH-1 HELICOPTER
NT UH-60A HELICOPTER
ADS-33C related handling qualities research performed using the NRC Bell 205 airborne simulator 02 p0521 N94-13295
MIL-H-8501B: Application to shipboard terminal operations 02 p0521 N94-13296
Some lessons learned in three years with ADS-33C --- rotorcraft handling qualities specification 02 p0521 N94-13299
Investigation of the effects of bandwidth and time delay on helicopter roll-axis handling qualities 02 p0522 N94-13300
Improvements in hover display dynamics for a combat helicopter 02 p0523 N94-13310
Design and pilot evaluation of the RAH-66 Comanche Core AFCS 02 p0525 N94-13321
Design and pilot evaluation of the RAH-66 Comanche selectable control modes 02 p0525 N94-13322
An analysis of helicopter attrition using a low level combat simulation
[DSIS-93-00262] 02 p0515 N94-13839
HELSCAM V2.0: Development and application guide
[DSIS-93-00137] 02 p0515 N94-13867
Army Cockpit Delethalization Program (CDP)
[AD-A268990] 04 p1512 N94-18765
Research and design activities and the economic balance of MBB
[ETN-93-94909] 04 p1310 N94-19383
Night operations 06 p2431 N94-23977
Evaluation of the UH-1N instrument panel
[AD-A273145] 06 p2186 N94-24774

Exercise keevil: Noise levels of six military helicopters
[PB93-210722] 06 p2529 N94-25026
An analysis of the maintenance performance measurement system for LAMPS MK 3 helicopter squadrons
[AD-A276421] 09 p3565 N94-31332
Army scout/reconnaissance helicopters versus unmanned aerial vehicles
[AD-A276902] 09 p3579 N94-32232
Estimating the impact of crashworthiness standards on mortality and morbidity events in the US Army rotary-wing aircraft mishaps
[AD-A277121] 09 p3575 N94-32363
Study findings on the influence of maneuverability and agility on helicopter handling qualities
10 p3993 N94-34624
Planning German Army helicopter maintenance and mission assignment
[AD-A280483] 12 p4381 N94-37352

MILITARY OPERATIONS
NT COMBAT
NT ELECTRONIC WARFARE
Assessing the adequacy of the industrial base
[AD-A264954] 01 p0417 N94-11856
Improved Many-On-Many ROUTE software description
[DE93-013961] 01 p0334 N94-12608
Sleep management user's guide for special operations personnel
[AD-A267746] 03 p1119 N94-14943
Space countersurveillance: A requisite for theater defense planning
[AD-A266871] 03 p0884 N94-15147
Technical evaluation report on the AGARD-PEP Specialists Meeting on Combat Aircraft Noise
[NLR-TP-91445-U] 03 p1177 N94-15506
Annual historical report, calendar year 1992
[AD-A267050] 03 p1121 N94-15663
Technical urban search and rescue, System To Locate Survivors (STOLS) units: Operator's manual
[AD-A266317] 03 p0862 N94-16438
Design Quality Task Force survey comments
[AD-A266283] 03 p1225 N94-16473
Not ready for the first space war. What about the second?
[AD-A266557] 03 p1174 N94-16665
Nonlinear methods for communications
[AD-A267376] 03 p1001 N94-17019
Military space programs in the press: An analysis for change
[AD-A267799] 03 p0874 N94-17306
Coastal Ocean Modeling Workshop
[AD-A268955] 04 p1497 N94-18393
A comparison of air force data systems
[AD-A269691] 04 p1616 N94-18575
Road march performance of special operations soldiers carrying various loads and load distributions
[AD-A269198] 04 p1512 N94-18882
Coordination of software-development activities among sites that are geographically separated
[DE93-019201] 04 p1524 N94-19076
Planning process software: A user guide for the DMCA
[AD-A271252] 05 p1902 N94-19911
HERMES, a report generator for research on information processing in command posts: The effect of missing information
[IZF-1992-A-28] 05 p2042 N94-20310
In-flight measurement of aircrew breathing in Navy aircraft
[AD-A271811] 05 p1896 N94-21154
Night operations 06 p2431 N94-23977
Safety guidelines for the operation of the DREO 10 m EMP simulator DREMPS
[DREO-TN-93-5] 06 p2193 N94-24117
Operation Friction: Development and introduction of personal cooling for CH124 Sea King aircrew
[DCIEM-93-06] 06 p2433 N94-24119
Overall system concepts in mission planning
06 p2521 N94-25009
Human factors of mission planning systems: Applications and implementation
06 p2522 N94-25011
Ground based mission planning systems
06 p2522 N94-25014
In flight mission planning in the Copilote Electronique
06 p2522 N94-25015
Mission rehearsal in the SOF-ATS program
06 p2522 N94-25016
Development of the Air Force contingency contracting course framework
[AD-A273921] 07 p3093 N94-25895
Report of the defense science board task force on aircraft assessment
[AD-A274531] 07 p2669 N94-26835
Human dimensions research team, operation restore hope
[AD-A274340] 07 p2939 N94-27056
The Support of Air Operations under Extreme Hot and Cold Weather Conditions
[AGARD-CP-540] 08 p3379 N94-28420
The concept of Royal Navy air operations under extreme environmental conditions 08 p3379 N94-28424
The Environmental Symptoms Questionnaire: Assessing reactions to environmental extremes in military operations 08 p3383 N94-28447
The management issues of implementing telecommuting: A case study
[AD-A275267] 08 p3527 N94-28905
Clinical investigation program
[AD-A275025] 08 p3391 N94-29116
TacSats for NATO
[AD-A277710] 08 p3169 N94-30350
Report on NATO PTTI 08 p3469 N94-30645
Coordination of mesoscale meteorological research between ASL and European group
[AD-A276730] 09 p3784 N94-32162
DOD space based requirements: Increasing DOD access to space
[AD-A276874] 09 p3601 N94-32211
Medical problems in high mountain environments. A handbook for medical officers
[AD-A278095] 09 p3798 N94-33268
Proceedings of the Symposium/Workshop on Applications of Expert Systems in DND
[DSIS-93-00343] 09 p3853 N94-33335
Management of uncertainty in knowledge-based systems: A military perspective
09 p3854 N94-33341
Ground vehicle control at NIST: From teleoperation to autonomy 10 p4127 N94-34037
Future tanker considerations and requirements
11 p4197 N94-36342
Hose-drogue versus boom receptacle air refueling
11 p4197 N94-36345

MILITARY PSYCHIATRY
U MILITARY PSYCHOLOGY

MILITARY PSYCHOLOGY
The 27th International Applied Military Psychology Symposium: A Focus on Decision Making Research
[AD-A265278] 01 p0313 N94-11701
Practice patterns of US Army medical department psychiatrists and psychologists
[AD-A274787] 07 p2909 N94-26360
Human dimensions research team, operation restore hope
[AD-A274340] 07 p2939 N94-27056

MILITARY SPACECRAFT
NT DMSP SATELLITES
NT RECONNAISSANCE SPACECRAFT
Fuzzification of ASAT's rule based aimpoint selection
[AD-A266068] 01 p0043 N94-11223
Military satellite communications: Opportunity to save billions of dollars. Report to the Chairman, Legislation, and National Security Subcommittee, Committee on Government Operations, House of Representatives
[AD-A267627] 03 p1002 N94-17199
TacSats for NATO
[AD-A277710] 08 p3169 N94-30350
CIM in space: Corporate Information Management (CIM) implications for space-based information systems
[AD-A276882] 09 p3600 N94-32126

MILITARY TECHNOLOGY
Assured Mission Support Space Architecture (AMSSA) study 01 p0348 N94-11573
Solderability of surface mount devices
[AD-A265751] 02 p0620 N94-13040
Knowledge-based oceanographic image compression
[AD-A265752] 02 p0821 N94-13041
Symposium on the Future of Aeronautics in the Netherlands
[ETN-93-93780] 03 p0853 N94-15120
Expectations for the future of military aviation
03 p0854 N94-15128
Annual historical report, calendar year 1992
[AD-A267050] 03 p1121 N94-15663
Multiobjective functions optimization for task allocation mapping to multicomputer nodes
[AD-A267071] 03 p1146 N94-15670
TABES 1993: 9th Annual Technical and Business Exhibition and Symposium 03 p1050 N94-16129
Modeling and simulation: A key to future defense technology
[TABES PAPER 93-654] 03 p1054 N94-16153
SONOS technology for commercial and military nonvolatile memory applications
[DE93-015647] 03 p1011 N94-16661
Not ready for the first space war. What about the second?
[AD-A266557] 03 p1174 N94-16665
Diffractive optics in adverse environments
03 p1197 N94-17352
Radar transmitter procedures
[AD-A268274] 03 p1005 N94-17523
Military applications of high-accuracy frequency standards and clocks
[AD-A269303] 04 p1430 N94-18299
An investigation of methods for updating ionospheric scintillation models using topside in-situ plasma density measurements
[AD-A269872] 04 p1483 N94-18655
Utilization of Shuttle small payload accommodations in the DOD Space Test Program 04 p1326 N94-19180
Millimeter wave imaging technology
[AD-A271257] 05 p1715 N94-19912
Tactical laser weapons and other directed-energy weapons
[AD-A267961] 05 p1816 N94-20484
Documents on the history of aeronautical and space research in Germany, 1900 - 1970
[DLR-MITT-92-08] 05 p2152 N94-20543
Chemistry and materials science
[DE94-001449] 05 p2152 N94-21858
Microtechnology: The key to the technical challenges of the 21st century
[DE94-000403] 05 p1769 N94-21959
Operation Friction: Development and introduction of personal cooling for CH124 Sea King aircrew
[DCIEM-93-06] 06 p2433 N94-24119
UAV current technology and future trends
06 p2154 N94-24245
Design project: LONGBOW supersonic interceptor
[NASA-CR-195510] 06 p2180 N94-24581
Advanced avionics architecture and technology review. Executive summary and volume 1: Avionics tech nology. Volume 2: Avionics systems engineering
[AD-A273630] 06 p2186 N94-24733
Information systems strategy in air transport
[AD-A273125] 06 p2173 N94-24781
Overall system concepts in mission planning
06 p2521 N94-25009
Research interests and broad agency announcement 94-1 of the Air Force Office of Scientific Research
[AD-A273410] 06 p2632 N94-2..075
Object interaction in a parallel object-oriented discrete-event simulation
[AD-A274084] 07 p2959 N94-25942
Optoelectronic technology consortium
[AD-A274595] 07 p3036 N94-26857
Air Force standards for nickel hydrogen battery
07 p2862 N94-28116
AF Ni-Cd cell qualification program
07 p2863 N94-28122
Visit to CERMA: Centre d'Etudes et de Recherches de Medecine Aerospatiale, Centre for Studies and Research in Aviation and Space Medicine, Bretigny sur Orge, France, November 16-18, 1992
[PB94-132990] 07 p2937 N94-28392
The management issues of implementing telecommuting: A case study
[AD-A275267] 08 p3527 N94-28905
Spectral and polarimetric analysis of hyperspectral data collected by an acousto-optic tunable filter system
[AD-A275076] 08 p3329 N94-29095
NPSNET: Integration of Distributed Interactive Simulation (DIS) protocol for communication architecture and information interchange
[AD-A275061] 08 p3530 N94-29139
Software testing practices and their evolution for the 1990's 08 p3415 N94-29335
A disciplined approach to software test and evaluation
08 p3416 N94-29339
Proceedings of the 3rd Conference on Military Robotic Applications
[DRES-SP-149] 08 p3304 N94-30275
Autonomous intelligent military robots: Army ants, killer bees, and cybernetic soldiers 08 p3304 N94-30276
Robotics and the battlefield of the future
08 p3304 N94-30277
DREV activities related to military vehicles robotization
08 p3305 N94-30278
Autonomous Robotic Refueling System (ARRS) for rapid aircraft turnaround 08 p3305 N94-30279
Force control techniques for robot manipulators and their military applications 08 p3307 N94-30291
Elements of supervisory control for military robotic applications 08 p3309 N94-30303
Aspects of the operator interface for military robotic applications in unstructured environments
08 p3309 N94-30304
Cubanes: Super explosives and potential pharmaceutical intermediates 08 p3227 N94-30454
Automated detection of ship tracks in multispectral satellite data
[AD-A276697] 09 p3746 N94-32119

Common modeling system for digital simulation
09 p3823 N94-32429
Interagency Advanced Power Group: Steering Group meeting minutes
[DE94-007951] 09 p3761 N94-32701
An investigation of methods for improving models of ionospheric plasma-density irregularities and radio-frequency scintillation
[AD-A278568] 10 p4033 N94-33703
Controlled atmospheric breakdown: Applications and research opportunities
[AD-A278584] 12 p4464 N94-36973
United States Air Force Summer Research Program, 1993. Volume 13: Phillips Laboratory
[AD-A278657] 12 p4550 N94-36977
United States Air Force Summer Research Program, 1993. Volume 16: Arnold Engineering Development Center, Frank J. Seiler Research Laboratory and Wilford Hall Medical Center
[AD-A278658] 12 p4550 N94-36978
United States Air Force Summer Research Program, 1993. Volume 3: Phillips Laboratory
[AD-A278694] 12 p4550 N94-36979
United States Air Force Summer Research Program, 1993. Volume 4: Rome Laboratory
[AD-A278695] 12 p4551 N94-36980
United States Air Force Summer Research Program, 1993. Volume 8: Phillips Laboratory
[AD-A278698] 12 p4551 N94-36983
United States Air Force Summer Research Program, 1993. Volume 9: Rome Laboratory
[AD-A278699] 12 p4551 N94-36984

MILK

Hydrogen peroxide electrodes based on electrical connection of redox centers of various peroxidases to electrodes through a three-dimensional electron relaying polymer network
[AD-A276543] 09 p3691 N94-32056

MILKY WAY GALAXY

The 0.15 seconds near-infrared imaging of the central parsec of the galaxy
[MPE-PREPRINT-239] 04 p1621 N94-19415
Spatial distribution of near infrared line radiation in galactic nuclei measured with Fabry-Perot spectrometer FAST
[MPE-239] 05 p2081 N94-21138
Extracting galactic structure parameters from multivariated density estimation
05 p1964 N94-22458
A study of the neutral hydrogen distribution of the Milky Way through 21 cm emission and Lyman alpha absorption 09 p3938 N94-32309
And then there was Voyager
[NASA-CR-195928] 10 p4164 N94-33587

MILLIMETER WAVES

Investigation of passive atmospheric sounding using millimeter and submillimeter wavelength channels
[NASA-CR-193627] 01 p0274 N94-10726
A millimeter-wave tunneladder TWT
[NASA-CR-182183] 02 p0620 N94-13106
Long-pulse operation of a gyrotron with beam/RF separation
[DE93-015007] 02 p0649 N94-13410
Millimeter and infrared studies of young stellar objects in dark cloud L1641 02 p0838 N94-13648
Submillimeter, millimeter, and microwave spectral line catalogue, revision 3
[NASA-CR-194501] 02 p0602 N94-13813
Velocity matched millimeterwave electro-optic modulator
[AD-A267264] 03 p1188 N94-14957
Applications of SLR 03 p0911 N94-15556
New methods of generation of ultrashort laser pulses for ranging 03 p0913 N94-15565
Millimeter accuracy satellites for two color ranging
03 p0916 N94-15583
Improvement of SLR accuracy, a possible new step
03 p0917 N94-15588
Dispersion effects on millimeter wavelength attenuation efficiencies for a variety of fibers
[AD-A268992] 04 p1385 N94-18454
Millimeter wave reflectivity measurement system
[AD-A270008] 04 p1387 N94-18601
Optical properties of redispersed iron fibers measured at 94 GHz
[AD-A269739] 04 p1342 N94-18756
Environmental characterization for target acquisition. Report 3: New concepts for evaluating low-grazing angle radar measurements
[AD-A269956] 04 p1388 N94-18777
Quasi-optical transponder using FET's and patch antennas
[AD-A271339] 04 p1407 N94-19584
Experimental and theoretical investigation of broadband high-power windows for millimeter waves
[KFK-5157] 04 p1391 N94-19617
Millimeter wave imaging technology
[AD-A271257] 05 p1715 N94-19912
Interinjection-locked quasioptical power combiners and phased arrays
[AD-A271178] 05 p2015 N94-20214
Transport in microstructures in the microwave and millimeter-wave regime
[AD-A271875] 05 p2017 N94-20470
An 85 GHz quasioptical gyroklystron experiment
[AD-A272020] 05 p1752 N94-20931
Low-power millimeter-wave radar observations of the atmosphere
[NASA-CR-194738] 05 p1858 N94-21811
Millimeter-wave imaging of composite materials
[DE93-041160] 05 p1677 N94-21940
Adaptive data rate control TDMA systems as a rain attenuation compensation technique
06 p2287 N94-22821
Advanced mobile satellite communications using COMETS satellite in MM-wave and Ka-band
06 p2288 N94-22829
Planar varactor frequency multiplier devices with blocking barrier
[NASA-CASE-NPO-18428-1-CU]
06 p2310 N94-23821
Investigation of passive atmospheric sounding using millimeter and submillimeter wavelength channels
[NASA-CR-194858] 06 p2404 N94-24843
Passive millimeter-wave imaging
06 p2306 N94-25494
Advanced radiometric and interferometric milimeter-wave scene simulations
06 p2306 N94-25498
Simulation of a passive millimeter wave sensor
06 p2346 N94-25499
A model-based approach for detection of objects in low resolution passive-millimeter wave images
06 p2442 N94-25507
Electrical analysis of wideband and distributed windows using time-dependent field codes
[DE94-002987] 07 p2768 N94-26310
Laboratory plasma studies
[AD-A274655] 07 p3043 N94-26356
Focal plane antenna array for millimeter waves
[AD-D016034] 07 p2774 N94-27202
Characterization of a diffraction grating as a simulant of a selective frequency antenna for radiometric applications
[AD-A275793] 08 p3241 N94-28745
A combined electron beam/optical lithography process step for the fabrication of sub-half-micron-gate-length MMIC chips 08 p3240 N94-30445
Evaluation of dual polarization attenuation of millimeter frequencies through a meteorological radar
08 p3256 N94-30496
Propagation modeling of moist air and suspended water/ice particles at frequencies below 1000 GHz
08 p3256 N94-30497
Model for the simulation of atmospheric effects on targets to background passive signatures
08 p3258 N94-30507
Polarimetric backscatter measurements of natural surfaces at millimeter wavelengths
08 p3259 N94-30509
A hybrid electromagnetic-statistical approach for characterizing MMW scattering by terrain
08 p3259 N94-30510
Millimeter wave, high-resolution, holographic surveillance system
[DE94-004289] 09 p3712 N94-31831
Optical processing of MMW for agile beamsteering and beamforming
[AD-A277161] 09 p3880 N94-32068
Fusion applications of high power millimeter wave sources
[DE94-007374] 09 p3718 N94-32202
YBCO Josephson Junction arrays
[AD-A277426] 09 p3908 N94-33005
Synthetic vision technology demonstration. Volume 1: Executive summary
[AD-280564] 09 p3582 N94-33076
Synthetic vision technology demonstration. Volume 2: Sensor tower testing
[DOT/FAA/RD-93/40-VOL-2] 09 p3582 N94-33077
Synthetic vision technology demonstration. Volume 3: Flight tests
[AD-A281051] 09 p3582 N94-33078
Synthetic vision technology demonstration. Volume 4: Appendices
[AD-A281052] 09 p3583 N94-33079
Proceedings SPIE: Conference Digest, volume 2104
[AD-A278107] 09 p3884 N94-33187
High temperature superconducting Josephson junction array systems, phase 1
[AD-A277937] 09 p3908 N94-33246
Theoretical, experimental, and computational evaluation of a tunnel ladder slow-wave structure
[NASA-TM-106642] 10 p4041 N94-33945
The 2nd International Workshop on Discrete Time Domain Modelling of Electromagnetic Fields and Networks
[AD-A277551] 10 p4035 N94-34081
Detection of the 267 GHz J = 1-0 rotational transition of PH3 in Saturn with a new Fourier transform spectrometer
[NASA-CR-194364] 10 p4162 N94-34718
A 32-GHz solid-state power amplifier for deep space communications 11 p4255 N94-35562
State of the art in high-power microwaves: An overview
[DE94-007075] 11 p4272 N94-35978
Intensity of waves diffracted from symmetrical profile lamellar gratings
[DE94-611101] 12 p4433 N94-36753
A novel transition between rectangular waveguide and layered ridge dielectric waveguide
[NASA-TM-106661] 12 p4433 N94-36955
Microwave generation for magnetic fusion energy applications
[DE94-012107] 12 p4448 N94-37368
Study on the measurement uncertainty of noise properties of a millimeter wave amplifier
[PB94-170917] 12 p4510 N94-37632

MILLING

Titanium alloys milling assistance by high pressure lubricoolant jet
[DE93-013302] 01 p0082 N94-11008
Selective formation of porous silicon
[NASA-CASE-NPO-18735-1-CU]
03 p0966 N94-15960
NiAl-base composite containing high volume fraction of AlN for advanced engines
[NASA-CASE-LEW-15818-1] 12 p4403 N94-36752

MILLING (MACHINING)

Focused-ion-beam material removal rates
[AD-A270852] 05 p1713 N94-19834
Application of high-speed milling to the Finnish manufacturing industry
[PB94-135548] 08 p3230 N94-29187

MILLING MACHINES

Focused-ion-beam material removal rates
[AD-A270852] 05 p1713 N94-19834
Accuracy analysis of multi-axis machines
[ETN-94-95341] 07 p3002 N94-26000

MILNE METHOD

Miln equation for the calculation of the phases and amplitudes of wave functions for continuum spectrum of Coulomb two-center problem
[DE94-606292] 08 p3522 N94-28616

MIMD (COMPUTERS)

Massively parallel multifrontal methods for finite element analysis on MIMD computer systems
[DE93-009838] 01 p0335 N94-10257
Layering techniques for development of parallel systems: An algebraic approach
[MEMO-INF-92-62] 01 p0335 N94-10277
A parallel implementation of particle tracking with space charge effects on an Intel iPSC/860
[DE93-012307] 01 p0335 N94-10340
Flexible language constructs for large parallel programs
[NASA-CR-191478] 01 p0326 N94-11196
Portable programming on parallel/networked computers using the Application Portable Parallel Library (APPL)
[NASA-TM-106238] 01 p0327 N94-11232
A heterogeneous graphics procedure for visualization of massively parallel solutions
[DE93-009628] 01 p0336 N94-11270
Parallel molecular dynamics with the embedded atom method
[DE93-010683] 01 p0367 N94-11455
Parallelizing Timed Petri Net simulations
[NASA-CR-194278] 02 p0758 N94-12938
Parallel implementation of an algorithm for Delaunay triangulation
[NASA-TM-103951] 02 p0740 N94-12973
Implementation of ADI: Schemes on MIMD parallel computers
[NASA-CR-193720] 02 p0759 N94-13204
An overview of parallel scientific visualization
[DE93-017105] 02 p0755 N94-14521
On the solution of a class of graph problems by parallel algorithms
[LAAS-92514] 02 p0756 N94-14712
Identification of continuous-time dynamical systems: Neural network based algorithms and parallel implementation
[DE93-014427] 02 p0766 N94-14737
A trace-based comparison of shared memory multiprocessor architectures
[TR-432] 03 p1159 N94-16577

Distributed memory parallel computers and computational fluid dynamics 04 p1413 N94-18568
General geometry PIC for MIMD computers
[AD-A269085] 04 p1534 N94-18767
Optimal eigenvalue computation on distributed-memory MIMD multiprocessors
[DE93-018337] 04 p1535 N94-18808
Three-dimensional shock wave physics simulations with MIMD PAGOSA on massively parallel computers
[DE93-011682] 04 p1455 N94-18829
A massively parallel adaptive finite element method with dynamic load balancing
[DE93-012844] 04 p1536 N94-19161
MIMD massively parallel methods for engineering and science problems
[DE93-019409] 04 p1531 N94-19562
Building brains for bodies
[AD-A270531] 05 p1939 N94-19875
Parallel band reduction and tridiagonalization
[DE93-019566] 05 p1951 N94-20221
The design of linear algebra libraries for high performance computers
[DE93-040458] 05 p1960 N94-21967
Parallelizing a maximum entropy image deconvolution algorithm 05 p1787 N94-22208
The design of a standard message passing interface for distributed memory concurrent computers
[DE94-002536] 06 p2446 N94-24538
A Multitransputer Parallel Processing System (MTPPS)
[DE94-604652] 07 p2981 N94-26903
MIMD parallel approaches to object labeling
[ISBN-0-315-60198-1] 07 p2982 N94-27644
Building brains for bodies
[AIAA PAPER 94-1208-CP] 08 p3444 N94-30559
Studies of an optical multi-processor interconnect
[AD-A277093] 09 p3881 N94-32392
Iwmeter: A real-time and interactive parallel software monitor for iWarp
[AD-A277587] 10 p4104 N94-33427
Parallel programming methodologies for non-uniform structured problems in materials science
[AD-A277868] 10 p4111 N94-33777
Overset grid applications on distributed memory MIMD computers
[NASA-CR-196081] 11 p4268 N94-36397
Porting industrial codes and developing sparse linear solvers on parallel computers
[PB94-170503] 12 p4497 N94-36547

MIMO (CONTROL SYSTEMS)
Utilizing quantitative feedback theory design technique for flight control system 01 p0032 N94-11501
Transmission zeros of spacecraft attitude control system
[NAL-TR-1166] 02 p0540 N94-13339
Control system design for flexible structures using data models 02 p0527 N94-14646
Design of a state-space controller for an advanced gas turbine engine
[AD-A270859] 05 p1647 N94-20042
Telerobotic control of a mobile coordinated robotic server, executive summary
[NASA-CR-194685] 05 p1821 N94-20044
A homotopy algorithm for digital optimal projection control GASD-HADOC
[NASA-CR-193881] 06 p2456 N94-24470
MIMO system identification for H(infinity) robust control: A frequency domain approach with minimum error bounds
[ETN-94-95354] 06 p2476 N94-25262
Flight controller design using mixed H2/H infinity optimization with a singular H infinity constraint
[AD-A273831] 06 p2191 N94-25525
Design of a subsonic envelope flight control system for the Vista F-16 using quantitative feedback theory
[AD-A274057] 07 p2676 N94-25771
Evaluation of moderate angle of attack roll of a dual engine, thrust vectoring aircraft using quantitative feedback theory
[AD-A274118] 07 p2667 N94-25905
MIMO recursive least squares control algorithm for the AN/FPN-44A Loran-C transmitter
[AD-A274820] 07 p2664 N94-26493
Identification and H(infinity)/(mu)-synthesis control of the Sandia truss
[DE94-002735] 07 p2839 N94-26810
Integrated active and passive control design methodology for the LaRC CSI evolutionary model
[NASA-CR-4580] 08 p3164 N94-28417
Antiwindup analysis and design approaches for MIMO systems
[NASA-CR-195304] 09 p3584 N94-32075
Control strategies for systems with limited actuators
[NASA-CR-195307] 09 p3727 N94-32741
Microgravity isolation system design: A modern control synthesis framework 11 p4215 N94-35851
Adaptive model reduction for continuous systems via recursive rational interpolation 11 p4219 N94-35876
Mixed H2/H-infinity optimization with multiple H infinity constraints
[AD-A280572] 12 p4388 N94-36733
Eigensystem realization algorithm user's guide forVAX/VMS computers: Version 931216
[NASA-TM-109066] 12 p4493 N94-36818
H infinity control for nonlinear and linear systems
[AD-A280450] 12 p4494 N94-37226

MINE DETECTORS
Constructing a reference event list for ARCESS
[AD-A269288] 04 p1481 N94-18297
Numerical computation and measurement of radar cross section for impulse radar
[PB94-149200] 10 p4036 N94-34096

MINERAL DEPOSITS
Twenty-fourth Lunar and Planetary Science Conference. Part 1: A-F
[NASA-CR-193095] 01 p0435 N94-12015
Increased depth-diameter ratios in the Medusae Fossae Formation deposits of Mars 01 p0439 N94-12043
Petrography and preliminary interpretations of the crystalline breccias from the Manson M-1 core 01 p0281 N94-12056
A mineralized zone in Western Candor Chasma, Mars 03 p1248 N94-16179
Explosive mafic volcanism on Earth and Mars 03 p1253 N94-16204
A Moessbauer spectrometer for the mineralogical analysis of the Mars surface: First temperature dependent tests of the detector and drive system 03 p1259 N94-16233
A Monazite-bearing clast in Apollo 17 melt breccia 03 p1267 N94-16279
The influence of oceans on Martian volcanism 03 p1295 N94-16427
AVIRIS study of Death Valley evaporite deposits using least-squares band-fitting methods 03 p1067 N94-16676
Ground-truthing AVIRIS mineral mapping at Cuprite, Nevada 03 p1069 N94-16682
Expert system-based mineral mapping using AVIRIS 03 p1073 N94-16704
Mechanical modeling of the growth of salt structures
[DE93-015342] 04 p1596 N94-18243
Dating native gold by noble gas analyses 05 p1684 N94-20652
C/O atomic ratios in micrometer-size crushed grains from Antarctic micrometeorites and two carbonaceous meteorites 05 p2082 N94-20678
Mineralogy and cooling history of magnesian lunar granulite 67415 05 p2124 N94-20811
A new Antarctic meteorite with chromite, orthopyroxene and metal with reference to a formation model of S asteroids 05 p2084 N94-20813
Evaluation of lunar rocks and soils for resource utilization: Detailed image analysis of raw materials and beneficiated products 05 p2126 N94-20820
On United States-Japan Conference on Development and Utilization of Natural Resources: Report of the 14th Joint Meeting of U. S. and Japan Marine Mining Panel 08 p3188 N94-28683
Thermal emission measurements (5-25 microns) of Hawaiian palagonitic soils with implications for Mars 09 p3944 N94-33193
Deposition rates of oxidized iron on Mars 09 p3945 N94-33198
Aerosols scattering and near-infrared observations of the Martian surface 09 p3946 N94-33204
Grain rims on ilmenite in the lunar regolith: Comparison to vapor deposits on regolith silicates 11 p4359 N94-35418
Petrographic characterization of lunar soils: Application of x ray digital-imaging to quantitative and automated analysis 11 p4368 N94-36138

MINERAL EXPLORATION
Terrestrial case studies of ilmenite exploration and lunar implications 01 p0478 N94-12247
A knowledge-based model for the integration of remote sensing into a mineral exploration program
[ISBN-0-315-58982-5] 02 p0685 N94-13523

MINERAL METABOLISM
Space research on organs and tissues 04 p1503 N94-19214
Endocrinological evaluations of muscle and bone atrophy in tail-suspended rats 07 p2903 N94-27444

MINERAL OILS
Measurement of viscosity, density, and gas solubility of refrigerant blends in selected synthetic lubricants
[DE94-003609] 07 p2713 N94-25934
Calculation methods for steadily loaded axial groove hydrodynamic journal bearings (guide to use of computer program A9305)
[ESDU-93005] 07 p2830 N94-28074

MINERALOGY
Twenty-fourth Lunar and Planetary Science Conference. Part 1: A-F
[NASA-CR-193095] 01 p0435 N94-12015
Moessbauer spectroscopy of the SNC meteorite Zagami 01 p0428 N94-12016
Carbon in weathered ordinary chondrites from Roosevelt County 01 p0428 N94-12035
Mineralogy of chondritic interplanetary dust particle impact residues from LDEF 01 p0080 N94-12045
Nitrogen and noble gases in a glass sample from LEW88516 01 p0080 N94-12051
Changes in Hawaiian palagonite FE mineralogy associated with thermal alteration: Implications for Mars 01 p0281 N94-12055
Alkali-granitoids as fragments within the ordinary chondrite Adzhi-Bogdo: Evidence for highly fractionated, alkali-granitic liquids on asteroids 01 p0429 N94-12069
Spectral and multispectral imaging studies of lunar mantled mare deposits 01 p0446 N94-12079
Impact mineralogy and chemistry of the cretaceous-tertiary boundary at DSDP site 576 01 p0282 N94-12091
Mineralogy versus bulk composition of the carbonaceous chondrite clast Kaidun 2 01 p0429 N94-12101
Carbonaceous chondrite clasts in the Kapoeta howardite 01 p0282 N94-12104
The EET87513 clast N: A CM2 fragment in an HED polymict breccia 01 p0453 N94-12117
Venus mountain-top mineralogy: Misconceptions about pyrite as the high radar-reflecting phase 01 p0455 N94-12129
LEW88516 and SNC meteorites 01 p0430 N94-12150
First results of the seven-color asteroid survey 01 p0430 N94-12162
Simulation of possible regolith optical alteration effects on carbonaceous chondrite meteorites 01 p0430 N94-12163
Crystal-chemistry and partitioning of REE in whitlockite 01 p0408 N94-12174
Post-impact alteration of the Manson impact structure 01 p0282 N94-12188
The correlation of alkalis and aluminum during high-temperature volatilization of albite and nepheline 01 p0081 N94-12214
Micro-zoning in minerals of a Landes silicate inclusion 01 p0432 N94-12231
The Xe-Q in Iodranites and a hint for Xe-L. FRO90011 another Iodranite? 01 p0432 N94-12239
Moessbauer spectrometer for mineralogical analysis of the Mars surface: Moessbauer source considerations 01 p0476 N94-12242
Measuring and distinguishing compositional and maturity properties of lunar soils by remote VIS-NIR spectroscopy 01 p0478 N94-12251
Cronstedtite and iron sulfide mineralogy of CM-type carbonaceous chondrites from cryogenic Moessbauer spectra 01 p0433 N94-12257
Spectral analysis for automated exploration and sample acquisition
[NASA-CR-194095] 02 p0545 N94-13189
A mineralized zone in Western Candor Chasma, Mars 03 p1248 N94-16179
Grosnaja ABCs: Magnesium isotope compositions 03 p1241 N94-16191
Euromet Ureilite Consortium: A preliminary report on carbon and nitrogen geochemistry 03 p1241 N94-16192
Rover mounted ground penetrating radar as a tool for investigating the near-surface of Mars and beyong 03 p1007 N94-16197
Petrography, mineralogy, and Mg isotope composition of VICTA: A vigarano CaAl4O7-bearing type A inclusion 03 p1103 N94-16203
Explosive mafic volcanism on Earth and Mars 03 p1253 N94-16204
Pyroxene equilibration temperatures in metamorphosed ordinary chondrites 03 p1242 N94-16224
Lunar impact basins: New data for the nearside northern high latitudes and eastern limb from the second Galileo flyby 03 p1258 N94-16228
Lunar scout missions: Galileo encounter results and application to scientific problems and exploration requirements 03 p1259 N94-16229
A Moessbauer spectrometer for the mineralogical analysis of the Mars surface: First temperature dependent tests of the detector and drive system 03 p1259 N94-16233
The group A3 chondrules of Krymka: Further evidence for major evaporative loss during the formation of chondrules 03 p1242 N94-16257

Shock-thermal history of Kapoeta howardite matter on data of thermoluminescence analysis of individual mineral grains 03 p0953 N94-16267
Searching for neuKREEP: An EMP study of Apollo 11 Group A basalts 03 p1266 N94-16275
A Monazite-bearing clast in Apollo 17 melt breccia 03 p1267 N94-16279
Carbon abundances, major element chemistry, and mineralogy of hydrated interplanetary dust particles 03 p1243 N94-16309
An initial perspective of S-asteroid subtypes within asteroid families 03 p1243 N94-16310
Isotopic signatures and distribution of nitrogen and trapped and radiogenic xenon in the Acapulco and FRO90011 meteorites 03 p1243 N94-16317
Chromite-rich mafic silicate chondrules in ordinary chondrites: Formation by impact melting 03 p1244 N94-16330
On possible Mn-53 heterogeneity in the early solar system 03 p1244 N94-16344
The Nakhla parent melt: REE partition coefficients and clues to major element composition 03 p1245 N94-16399
More on the cooling history of angrite LEW 86010 03 p1245 N94-16400
Deucalionis Regio, Mars: Evidence for a unique mineralogic endmember and a crusted surface 03 p1291 N94-16406
Exsolved kirschsteinite in angrite LEW86010 olivine 03 p1245 N94-16410
Analysis of pyroxene absorptions observed in Martian dark regions 03 p1292 N94-16411
Igneous fractionation and subsolidus equilibration of diogenite meteorites 03 p1245 N94-16413
Siderophile element fractionation in meteor crater impact glasses and metallic spherules 03 p1246 N94-16414
Identification of new meteorite, Mihonoseki (L), from broken fragments in Japan 03 p1246 N94-16415
The thickness of eucritic crust in the HED parent body 03 p1104 N94-16416
Optical effects of regolith processes on S asteroids as simulated by laser impulse alteration of ordinary chondrite 03 p1246 N94-16422
Bright soil units on Mars determined from ISM imaging spectrometer data 03 p1295 N94-16430
Variations in the Fe mineralogy of bright Martian soil 03 p1295 N94-16431
Composition of weakly altered Martian crust 03 p1296 N94-16436
Mapping the mineralogy and lithology of Canyonlands, Utah with imaging spectrometer data and the multiple spectral feature mapping algorithm 03 p1066 N94-16670
First results from analysis of coordinated AVIRIS, TIMS, and ISM (French) data for the Ronda (Spain) and Beni Bousera (Morocco) peridotites 03 p1067 N94-16675
Integrating remote sensing techniques at Cuprite, Nevada: AVIRIS, Thematic Mapper, and field spectroscopy 03 p1072 N94-16701
Expert system-based mineral mapping using AVIRIS 03 p1073 N94-16704
The Koshak section: Evidence for element fractionation and an oxidation event at the K/T boundary 05 p1862 N94-20641
Petrogenesis of Apollo 12 mare basalts. Part 1: Multiple melts and fractional crystallization to explain olivine and ilmenite basalt compositions 05 p1684 N94-20644
Volatility in the lunar crust: Trace element analyses of lunar minerals by PIXE proton microprobe 05 p2097 N94-20661
Opaque-rich lithology in the Divnoe achondrite: Petrology and origin 05 p2082 N94-20680
Chaunskij: The most highly metamorphosed, shock-modified and metal-rich mesosiderite 05 p2082 N94-20681
Post-igneous redistribution of components in eucrites 05 p1685 N94-20684
Micrometeorite dynamic pyrometamorphism: Observation of a thermal gradient in iron-nickel sulfide 05 p2083 N94-20716
Derivation of the midinfrared (5.0-25.0 micron) optical constants of hydrous carbonate and sulfate 05 p2108 N94-20723
Detectability of crystalline ferric and ferrous minerals on Mars 05 p2110 N94-20730
Combined backscatter Moessbauer spectrometer/x ray fluorescence analyzer (BaMS/XRF) for extraterrestrial surfaces 05 p1686 N94-20761
The chondrite Mihonoseki: New observed fall 05 p2083 N94-20764
The stability of oxyamphiboles: Existence of Ferric-bearing minerals under the reducing conditions on the surface of Venus 05 p2122 N94-20800
Mineralogy and cooling history of magnesian lunar granulite 67415 05 p2124 N94-20811
Ti-bearing oxide minerals in lunar meteorite Y793169 with the VLT affinity 05 p2084 N94-20812
A new Antarctic meteorite with chromite, orthopyroxene and metal with reference to a formation model of S asteroids 05 p2084 N94-20813
Evaluation of lunar rocks and soils for resource utilization: Detailed image analysis of raw materials and beneficiated products 05 p2126 N94-20820
Cometary interplanetary dust particles? An update on carbon in anhydrous IDPS 05 p2084 N94-20828
Reverse polarity magnetized melt rocks from the Chicxulub impact structure, Yucatan Peninsula, Mexico 05 p1863 N94-20843
Origin of high-Ti lunar ultramafic glasses 05 p1686 N94-20853
Multiplicity of chondrule heating events and the coarsening of chondrule textures 05 p2085 N94-20860
A study of carbonates, sulfates, and phosphates using thermal emission spectroscopy 05 p1686 N94-20868
Weathering features and secondary minerals in Antarctic Shergottites ALHA77005 and LEW88516 05 p2086 N94-20869
Lewis Cliff 87057: A new metal-rich E3 chondrite with similarities to Mt. Egerton, Shallowater and Happy Canyon 05 p2086 N94-20901
Mineralogy of dark clasts in primitive versus differentiated meteorites 05 p2087 N94-20907
A Backscatter Moessbauer Spectrometer (BaMS) for use on Mars 05 p1811 N94-22431
Determination of Martian soil mineralogy and water content using the Thermal Analyzer for Planetary Soils (TAPS) 05 p1812 N94-22433
In situ identification of the Martian surface material and its interaction with the Martian atmosphere using DTA/GC 05 p1812 N94-22434
Optical luminescence spectroscopy as a probe of the surface mineralogy of Mars 05 p1813 N94-22437
Highland crust at the Apollo 14 site: A review 06 p2614 N94-24364
Whole rock major element chemistry of KREEP basalt clasts in lunar breccia 15205: Implications for the petrogenesis of volcanic KREEP basalts 06 p2614 N94-24365
Lunar mare volcanism: Mixing of distinct, mantle source regions with KREEP-like component 06 p2615 N94-24370
A geochemical study of acapulcoite and lodranite meteorites 06 p2605 N94-25358
Experimental study of lunar and SNC (Mars) magmas [NASA-CR-195274] 07 p3107 N94-27850
Possibilities of GER data for soil surface characteristics in the Almaden area 09 p3744 N94-31859
Magmatic volatiles and the weathering of Mars 09 p3946 N94-33201
Mineralogical diversity (spectral reflectance and Moessbauer data) in compositionally similar impact melt rocks from Manicouagan Crater, Canada 09 p3948 N94-33219
The mineralogic evolution of the Martian surface through time: Implications from chemical reaction path modeling studies 09 p3950 N94-33226
Evidence for ultramafic lavas on Syrtis Major 09 p3950 N94-33229
Absolute calibration and atmospheric versus mineralogic origin of absorption features in 2.0 to 2.5 micron Mars spectra obtained during 1993 11 p4356 N94-35404
Wavelength calibration techniques and subtle surface and atmospheric absorption features in the Mariner 6, 7 IRS reflectance data 11 p4356 N94-35405
A mineralogical instrument for planetary applications 11 p4357 N94-35408
Grain rims on ilmenite in the lunar regolith: Comparison to vapor deposits on regolith silicates 11 p4359 N94-35418
On the possible role of elemental carbon in the formation of reduced chondrules 11 p4351 N94-35421
Exopaleontology and the search for a fossil record on Mars 11 p4360 N94-35425
High Resolution Transmission Electron Microscopy (HRTEM) of nanophase ferric oxides 11 p4239 N94-35433
Antarctic weathering of the CK chondrites EET90004, 90007, and 90022: Nickel and sulfur mobility 11 p4351 N94-35451
Thermal emission measurements (5-25 microns) of Hawaiian palagonitic soils with implications for Mars 11 p4292 N94-35452
Transmission measurements (4000-400 cm(exp -1), 2.5-25 microns) of crystalline ferric oxides and ferric oxyhydroxides: Implications for Mars 11 p4292 N94-35454
Distribution of siderophile and other trace elements in melt rock at the Chicxulub impact structure 11 p4352 N94-35456
Innovative instrumentation for mineralogical and elemental analyses of solid extraterrestrial surfaces: The Backscatter Moessbauer Spectrometer/X Ray Fluorescence analyzer (BaMS/XRF) 11 p4239 N94-35459
Inhomogeneous distribution of materials in lodranites-acapulcoites and IAB irons and their common formation processes 11 p4364 N94-35463
The anatomy of a cluster IDP. Part 1: Carbon abundance, bulk chemistry, and mineralogy of fragments from L2008#5 11 p4352 N94-35466
A quick look method of detecting water of hydration in small solar system bodies 11 p4352 N94-35470
Mineralogy of an unusual CM clast in the Kaidun meteorite 11 p4352 N94-35476
Mineralogy of artificially heated carbonaceous chondrites 11 p4352 N94-35477
The Twenty-Fifth Lunar and Planetary Science Conference. Part 2: H-O [NASA-CR-195744] 11 p4367 N94-36136
Electron energy-loss spectroscopy of carbon in interplanetary dust particles 11 p4353 N94-36149
Synthetic and natural Nakhla pyroxenes: Parent melt composition and REE partition coefficients 11 p4353 N94-36161
Cr, Mn, and Ca distributions for olivine in angritic systems: Constraints on the origins of Cr-rich and Ca-poor core olivine in angrite LEW87051 11 p4353 N94-36162
Moessbauer mineralogy of calcined Murchison meteorite 11 p4353 N94-36166
Mineralogy and metallurgical properties of iron ore sinter based on magnetite fines [DE94-763309] 12 p4414 N94-36525
Light stable isotope analysis of meteorites by ion microprobe [NASA-CR-196096] 12 p4548 N94-37004
Thermodynamics of minerals stable near the Earth's surface [DE94-012479] 12 p4539 N94-37094

MINERALS

NT ALEXANDRITE
NT AMPHIBOLES
NT ANATASE
NT ARAGONITE
NT ASBESTOS
NT BIOTITE
NT CALCITE
NT CHROMITES
NT DOLOMITE (MINERAL)
NT ENSTATITE
NT FAYALITE
NT FELDSPARS
NT FORSTERITE
NT GADOLINIUM-GALLIUM GARNET
NT GARNETS
NT GRAPHITE
NT GYPSUM
NT HEMATITE
NT ILMENITE
NT IRON ORES
NT KAMACITE
NT KREEP
NT MAGNETITE
NT MICA
NT MONTMORILLONITE
NT NEPHELINE
NT OLIVINE
NT PEROVSKITES
NT PYRITES
NT PYROLYTIC GRAPHITE
NT PYROXENES
NT QUARTZ
NT SCHREIBERSITE
NT SIDERITES
NT SPINEL
NT STISHOVITE
NT TALC
NT TROILITE
NT WURTZITE
NT YTTRIUM-ALUMINUM GARNET
NT YTTRIUM-IRON GARNET
NT ZINCBLENDE

Distribution of mineral aerosols over the North Pacific 01 p0204 N94-11976
Effects of microscopic iron metal on the reflectance spectra of glass and minerals 01 p0436 N94-12024
Fourier domain target transformation analysis in the thermal infrared 01 p0258 N94-12030
Petrography and preliminary interpretations of the crystalline breccias from the Manson M-1 core 01 p0281 N94-12056
Using high spectral resolution spectrophotometry to study broad mineral absorption features on Mars 01 p0446 N94-12077

Near-infrared spectra of the Martian surface: Reading between the lines 01 p0465 N94-12184
Trace element distributions in primitive achondrites 01 p0431 N94-12200
Primitive SNC parent magmas and crystallization: Low PH2O experiments 01 p0433 N94-12264
The Fe2(+)-Mg interdiffusion in orthopyroxene: Constraints from cation ordering and structural data and implications for cooling rates of meteorites 03 p1241 N94-16175
Stalking the LREE-enriched component in ureilites 03 p1241 N94-16190
Euromet Ureilite Consortium: A preliminary report on carbon and nitrogen geochemistry 03 p1241 N94-16192
Lunar impact basins: New data for the nearside northern high latitudes and eastern limb from the second Galileo flyby 03 p1258 N94-16228
A Moessbauer spectrometer for the mineralogical analysis of the Mars surface: First temperature dependent tests of the detector and drive system 03 p1259 N94-16233
Complex radiation-thermal history of Kaidun meteorite on data of track study of silicate minerals 03 p1243 N94-16297
Refractory precursor components in an Allende ferromagnesian chondrule 03 p1245 N94-16412
From minerals to rocks: Toward modeling lithologies with remote sensing 03 p1086 N94-16437
Preliminary analysis of thermal-infrared multispectral scanner data of the Iron Hill, Colorado carbonatite-alkalic rock complex 03 p1065 N94-16605
Ejecta patterns of Meteor Crater, Arizona derived from the linear un-mixing of TIMS data and laboratory thermal emission spectra 03 p1065 N94-16607
Mapping the mineralogy and lithology of Canyonlands, Utah with imaging spectrometer data and the multiple spectral feature mapping algorithm 03 p1066 N94-16670
AVIRIS as a tool for carbonatite exploration: Comparison of SPAM and Mbandmap data analysis methods 03 p1073 N94-16703
In situ observation of radiation induced amorphization of crystals with apatite structure [DE93-018450] 04 p1599 N94-18816
Frequency dependent electrical properties of minerals and partial-melts [DE93-019918] 05 p2012 N94-19861
Evaporation in equilibrium, in vacuum, and in hydrogen gas 05 p1684 N94-20638
Fragments of ancient lunar crust: Ferroan noritic anorthosites from the descartes region of the Moon 05 p2096 N94-20660
Volatility in the lunar crust: Trace element analyses of lunar minerals by PIXE proton microprobe 05 p2097 N94-20661
Characterization of Minnesota lunar simulant for plant growth 05 p1897 N94-20665
Abundance and composition of solar KR in the H3-H6 chondrite ACFER111 05 p1684 N94-20676
Post-igneous redistribution of components in eucrites 05 p1685 N94-20684
U-Pb provenance ages of shocked zircons from the K-T boundary, Raton Basin, Colorado 05 p1685 N94-20701
Detectability of crystalline ferric and ferrous minerals on Mars 05 p2110 N94-20730
Research program on the Manson impact structure, Iowa 05 p1862 N94-20766
FE-60 and the evolution of eucrites 05 p2083 N94-20768
Magnesian anorthosites from the western highlands of the Moon: Isotope geochemistry and petrogenesis 05 p2118 N94-20779
Microanalysis of iron oxidation state in iron oxides using X Ray Absorption Near Edge Structure (XANES) 05 p1686 N94-20808
Regolith breccia consisting of H and LL chondrite mixture 05 p2080 N94-20892
Lewis Cliff 87057: A new metal-rich E3 chondrite with similarities to Mt. Egerton, Shallowater and Happy Canyon 05 p2086 N94-20901
An attempt to comprehend Martian weathering conditions through the analysis of terrestrial palagonite samples 05 p2143 N94-21668
Effect of powder characteristics on gas-pressure sintering of Si3N4 with rare earth additives [DE94-000330] 05 p1694 N94-21945
Integrated hydrometallurgical jarosite treatment [PB93-217990] 06 p2232 N94-22983
Demonstration of the feasibility of an integrated x ray laboratory for planetary exploration [NASA-CR-177631] 06 p2598 N94-24832
Some properties of graphs with local Ore conditions [PB94-126612] 07 p2996 N94-26962
Image processing for hyperspectral data 08 p3326 N94-28930
JERS-1 data and information system for resources exploration 08 p3327 N94-28932
Inorganic polymer engineering materials [DE94-008519] 09 p3659 N94-32655
The mineralogic evolution of the Martian surface through time: Implications from chemical reaction path modeling studies 09 p3950 N94-33226
National Geoscience Data Repository System [DE94-000120] 11 p4344 N94-35347
Lunar mineral feedstocks from rocks and soils: X-ray digital imaging in resource evaluation 11 p4358 N94-35415
Exopaleontology and the search for a fossil record on Mars 11 p4360 N94-35425
Application of an alkylammonium method for characterization of phyllosilicates in CI chondrites 11 p4351 N94-35432
High Resolution Transmission Electron Microscopy (HRTEM) of nanophase ferric oxides 11 p4239 N94-35433
Inhomogeneous distribution of materials in lodranites-acapulcoites and IAB irons and their common formation processes 11 p4364 N94-35463
Mossbauer and spectral (visible and near-IR) data for Fe(3+)-substituted rutile 11 p4240 N94-36154
Ferromagnetic resonance spectra of H2-reduced minerals and glasses 11 p4240 N94-36164
Thermodynamics of minerals stable near the Earth's surface [DE94-012479] 12 p4539 N94-37094

MINES (EXCAVATIONS)
Joint research activities with CCMRI (China) 08 p3240 N94-29521
Emissions of greenhouse gases from the use of transportation fuels and electricity [DE94-006166] 09 p3765 N94-31625

MINES (ORDNANCE)
Earth Penetration Radar Imaging System (EPRIS) [DE93-019890] 04 p1391 N94-19542

MINIATURE ELECTRONIC EQUIPMENT
Miniature color display, phase 4 [AD-A272920] 05 p1760 N94-21221
Micromachined electron tunneling infrared sensors 08 p3238 N94-29785
Integrated microgyroscope 08 p3239 N94-29789

MINIATURIZATION
NT MICROMINIATURIZATION
Design and development of a miniature column-based interface (MCBI) stress gage [AD-A266054] 01 p0170 N94-10873
Performance evaluation of the honeywell GG1308 miniature ring laser gyroscope [AD-A266694] 02 p0653 N94-14782
Piezo-electric motor: Perspectives and miniaturization 04 p1408 N94-18015
Self assembly: An approach to terascale integration [DE93-040104] 05 p1769 N94-21846
Microtechnology: The key to the technical challenges of the 21st century [DE94-000403] 05 p1769 N94-21959
Laser light scattering instrument advanced technology development [NASA-CR-194803] 06 p2349 N94-23286
Pigs in cyberspace 07 p2689 N94-27376
Miniaturization in x ray and gamma ray spectroscopy 08 p3236 N94-29773
A sub-cm micromachined electron microscope 08 p3236 N94-29775
Micromachined electron tunneling infrared sensors 08 p3238 N94-29785
Miniature wide field-of-view star trackers for spacecraft attitude sensing and navigation 08 p3144 N94-29794
A miniaturized ASIC-based multichannel scaler instrument [DE94-007222] 09 p3807 N94-32783
The ALEXIS mission recovery [DE94-007549] 09 p3611 N94-32813
Evaluation of some slow-wave vane structures for aminiature traveling-wave tube at 30 GHz [NASA-TM-106654] 12 p4437 N94-36819

MINICOMPUTERS
Upgrading NASA/DOSE laser ranging system control computers 03 p0918 N94-15595
Fifty years of continuous improvement: What has DOE done for analytical chemistry? [DE94-002539] 06 p2234 N94-24548

MINIMA
Modifications of the Griesmer bound 08 p3247 N94-29618
On the minimum of independent geometrically distributed random variables [AD-A279629] 09 p3821 N94-33075
Successive minima on arithmetic varieties [PB94-167699] 11 p4314 N94-35759

MINIMAL SURFACES
Characterization of self-conjugate minimal surfaces in R(sup 3) [DE94-601538] 07 p2993 N94-26409
Some remarks on the symmetry of self-conjugate minimal surfaces in R3 [DE94-603670] 07 p3007 N94-27633
The Klein-Fock equation, minimal surfaces and gravitational fields [DE94-606340] 08 p3356 N94-28803
The problems of the minimal surface and minimal lineal measure in three dimensions [DE94-013002] 12 p4479 N94-37355

MINIMAX TECHNIQUE
Finding stable orientations of assemblies with linear programming [AD-A266990] 03 p1143 N94-15212
Tool sharing: An application of max-algebra, part 2 [MEMO-1122] 06 p2478 N94-22710
Tool sharing: An application of max-algebra, part 1 [MEMO-1108] 06 p2478 N94-22726
The least energy critical set [DE93-616820] 06 p2493 N94-25434
Phase portraits of quadratic systems with finite multiplicity three and one critical point of infinity [REPT-93-41] 07 p2991 N94-26215
The transient period of a cyclic process: An horizon theorem [MEMO-1149] 08 p3427 N94-30585
H-infinity estimation 10 p4114 N94-34313
Asymetric change of daily temperature range: Proceedings [DE94-010102] 11 p4293 N94-35703

MINIMIZATION
U OPTIMIZATION

MINIMUM DRAG
Identification of integrated airframe: Propulsion effects on an F-15 aircraft for application to drag minimization [NASA-TM-4532] 06 p2188 N94-24106
Examples of flight path optimisation using a multivariate gradient-search method [ESDU-93021] 07 p2670 N94-28092

MINIMUM ENTROPY METHOD
The relaxed state and entropy production due to the electric resistivity and viscosity of plasma 05 p2010 N94-22696

MINING
NT LUNAR MINING
NT STRIP MINING
Asteroid exploration and utilization 07 p3080 N94-25697
On United States-Japan Conference on Development and Utilization of Natural Resources: Report of the 14th Joint Meeting of U. S. and Japan Marine Mining Panel 08 p3188 N94-28683
An electromagnetic noncontacting sensor for thickness measurement in a dispersive medium [AIAA PAPER 94-1200-CP] 08 p3443 N94-30551
Opportunities for innovation: Biotechnology [PB94-157831] 12 p4478 N94-36720

MINKOWSKI SPACE
On local frame fields and fermion dynamics in space with nontrivial topologies [DE93-617657] 01 p0349 N94-10548
Non-Euclidean space for local hidden variables [DE93-621341] 01 p0344 N94-11032
Green-Schwarz superstrings in the generalized harmonical Newmann-Penrose formalism [DE93-621422] 01 p0412 N94-11088
Impulsive moving mirror model in a Schroedinger picture with impulse effect in a Banach space [DE93-629864] 04 p1561 N94-18155
Impulsive moving mirror model and the stability of linear homogeneous differential equations with impulse effect in a Banach space [DE93-629906] 04 p1549 N94-18200
Dimensional crossover from non-renormalizability to renormalizability [DE93-613052] 07 p3006 N94-26193
Classical solutions of Yang-Mills-Chern-Simons theory in 2+1 dimensions: A quasi-linear superposition [DE93-634335] 07 p3006 N94-26270
The extensions of space-time. Physics in the 8-dimensional homogeneous space D is equal to SU(2,2)/K [DE93-634336] 07 p3072 N94-26551

MINNESOTA
Satellite inventory of Minnesota forest resources [NASA-CR-193565] 01 p0231 N94-11521

MINOR PLANETS
U ASTEROIDS

MINORITIES
Flight Dynamics Directorate (FDD) Historically Black Colleges and Universities (HBCU's) database managment system: A user's guide
[AD-A264947] 01 p0419 N94-11288
A summer program in mathematics and computer science for academically oriented student
[AD-A263467] 01 p0415 N94-11517
Pattern of federal procurement from minority and women-owned small business
[PB93-189355] 01 p0417 N94-11844
Strategies for recruiting additional African Americans into the NASA JSC summer faculty fellows program
06 p2585 N94-25362
The Seventh Annual National Conference of Black Physics Students
[NASA-CR-195735] 08 p3526 N94-28746

MINORITY CARRIERS
High temperature annealing of minority carrier traps in irradiated MOCVD n(+)p InP solar cell junctions
01 p0048 N94-11382
Measurement of the minority carrier diffusion length and edge surface-recombination velocity in InP
01 p0049 N94-11388
Surface passivation of InP solar cells with InAlAs layers 01 p0049 N94-11389
Investigation of ZnSe-coated silicon substrates for GaAs solar cells 01 p0052 N94-11405
Intrinsic and interfacial recombination in OMVPE- and MBE-prepared GaAs/Al(x)Ga(1-x)As heterostructures
[DE93-009844] 02 p0809 N94-14083
Multicrystalline silicon solar cells: Gettering optimization and characterization
[DE93-015001] 02 p0705 N94-14861
Development of large-area monolithically integrated silicon-film photovoltaic modules
[DE93-010037] 04 p1464 N94-17731
Defect behavior of polycrystalline solar cell silicon
[DE93-018490] 04 p1468 N94-19016
Polycrystalline thin film materials and devices
[DE93-018213] 06 p2389 N94-22862
Passivation of III-V compound semiconductor based devices
[AD-A276178] 09 p3894 N94-31056
Experimental and theoretical studies of hydrogenated amorphous semiconductor alloys and superlattices
[AD-A276159] 09 p3686 N94-31079

MINUTEMAN ICBM
Uncertainties in the characterization of the thermal environment of a solid rocket propellant fire
[DE94-002023] 07 p2760 N94-27719

MINUTEMAN MISSILES
U MINUTEMAN ICBM

MIR SPACE STATION
A stereoscopic vision system with applications to automated docking and tracking
[AD-A270754] 04 p1333 N94-19765
Orbital docking system centerline color television camera system test
[NASA-TM-104783] 06 p2205 N94-24625
Concepts and embodiment design of a reentry recumbent seating system for the NASA Space Shuttle
[NASA-CR-195504] 06 p2438 N94-24667
Spacecraft materials: Comparison between flight results obtained on LDEF and MIR 09 p3597 N94-31045
Technical assessment of Mir-1 life support hardware for the international space station
[NASA-TM-108441] 09 p3803 N94-31380

MIRA VARIABLES
Infrared and SiO maser observations of OH/IR stars
[PB94-104890] 06 p2599 N94-24780

MIRANDA
Voyager encounters Uranus
[NASA-TM-109619] 03 p1247 N94-15348
Spacework 16 --- Simulated Space Shuttle Program
[NASA-TM-109436] 03 p1221 N94-15420
Structural evidence for reorientation of Miranda about a paleo-pole 05 p2098 N94-20671
Triton's cratering record and its time of capture
05 p2122 N94-20802

MIRROR FUSION
Applying design principles to fusion reactor configurations for propulsion in space
[NASA-TM-108247] 01 p0047 N94-11053
Mirror fusion propulsion system: A performance comparison with alternate propulsion systems for the manned Mars Mission
[NASA-TM-109248] 02 p0550 N94-13147

MIRRORS
NT ETALONS
NT FRESNEL REFLECTORS
NT MAGNETIC MIRRORS
NT PARABOLOID MIRRORS
NT TANDEM MIRRORS
Zerodur polishing process for high surface quality and high efficiency
[DE93-012596] 01 p0087 N94-10271
Spin characteristics of ion beams during the motion of electromagnetic elements
[DE93-617448] 01 p0364 N94-10848
Damage thresholds of fluoride multilayers at 355 nm
[DE93-009523] 01 p0090 N94-11230
Needs for super-smooth surfaces
[DE93-012482] 01 p0382 N94-11242
Model of optical scatter from microimpacts on the Hubble Telescope 01 p0384 N94-12189
Light scattering from a spherical particle on a conducting plane. Part 1: Normal incidence
[AD-A265920] 01 p0383 N94-12341
Comparison of multiresolution techniques for digital signal processing
[AD-A265364] 01 p0138 N94-12406
Project proposal for partial computational physics support for Survivability of Coatings program
[DE93-013788] 02 p0576 N94-12939
Reflective coatings for solar applications
[DE93-010026] 02 p0702 N94-13381
Design and performance of an automated video-based laser beam alignment system
[DE93-012571] 02 p0656 N94-13481
Laser-damage susceptibility of nodular defects in dielectric mirror coatings: AFM measurements and electric-field modeling
[DE93-014655] 02 p0580 N94-14124
Determination of the surface cleanliness of metals by FT-IR spectroscopy
[DE93-013252] 02 p0565 N94-14525
Fabrication 02 p0546 N94-14834
Rotary encoding device
[NASA-CASE-GSC-13556-1] 03 p1148 N94-15943
Method and apparatus for forming an agile plasma mirror effective as a microwave reflector
[AD-D015788] 03 p0998 N94-16535
Profile stabilization of tilt mode in a field reversed configuration
[DE93-016770] 04 p1583 N94-17753
Impulsive moving mirror model and the stability of Schroedinger equation with impulse effect in a Banach space
[DE93-629866] 04 p1548 N94-18196
Impulsive moving mirror model and impulsive differential equations in Banach space
[DE93-629867] 04 p1549 N94-18197
Impulsive moving mirror model and the stability of linear homogeneous differential equations with impulse effect in a Banach space
[DE93-629906] 04 p1549 N94-18200
Developmental testing of a prototype all-reflection Michelson interferometer
[AD-A269064] 04 p1430 N94-18406
Testing and evaluation of large-area heliostats for solar thermal applications
[DE93-018509] 04 p1467 N94-18520
Development of robust multilayer optics for use in high-peak power radiation environments
[DE93-018557] 04 p1580 N94-18931
Tetravalent chromium (Cr(4+)) as laser-active ion for tunable solid-state lasers
[NASA-CR-194529] 04 p1441 N94-19369
Synchrotron/crystal sample preparation
[NASA-CR-193837] 04 p1603 N94-19513
Evaluation of a scanning Hartmann device for single point turning applications
[DE93-019204] 05 p1821 N94-19891
Circular polarizing mirrors for high power lasers
[AD-A267820] 05 p1815 N94-19965
Characterization and possible repair of defects in soft x ray projection lithography masks
[DE93-019147] 05 p1750 N94-20231
Wide-angle imaging system with fiberoptic components providing angle-dependent virtual material stops
[NASA-CASE-NPO-18146-1-CU] 05 p1986 N94-20345
X ray reflection masks: Manufacturing, characterization and first tests
[BONN-IR-92-31] 05 p1986 N94-21043
Mirror velocity sampling errors in a Michelson interferometer
[AD-A273105] 05 p1809 N94-21508
Generation of harmonic radiation using the multi-cavity free-electron laser
[DE94-001261] 05 p1820 N94-21975
X ray characterization of a three-element condenser system for soft x ray projection lithography
[DE93-019916] 05 p1990 N94-21985
HST PSF simulation using Tiny Tim
05 p1926 N94-22498
Theoretical investigation of variable periodicity (graded) multilayers for hard x ray applications
[NASA-CR-193913] 06 p2543 N94-23502
SALI chemical analysis of provided samples
[NASA-CR-194138] 06 p2232 N94-23524
Flight solar calibrations using the Mirror Attenuator Mosaic (MAM): Low scattering mirror
06 p2384 N94-23602
Investigate zero-stress replicated optics
[NASA-CR-193889] 06 p2545 N94-24665
Elastic backscattering lidar for a MSTI satellite
[DE94-002701] 07 p2816 N94-26126
Theoretical aspects of the agile mirror
[AD-A274890] 07 p2767 N94-26177
Mounting of SSM's
[VTT-TIED-1442] 07 p2695 N94-26250
Comparison of technology for high-power laser mirrors and synchrotron radiation mirrors
[DE94-002913] 07 p3035 N94-26276
Phase conjugated lasers applied to commercial x ray lithography
[DE94-001529] 07 p2819 N94-27018
Reflectometer employing an integrating sphere and lens-mirror concentrator
[AD-D016061] 07 p3039 N94-27676
The PROTEL contamination code
[RXR-93071] 07 p3040 N94-28202
Design and testing of the LITE Variable Field Stop mechanism 08 p3161 N94-29633
Determining noise temperatures in beam waveguide systems 08 p3249 N94-29657
Control of micromachined deformable mirrors
08 p3239 N94-29787
Nonlinear absorption in high reflector multilayers
[DE94-005818] 08 p3295 N94-30598
Characterization of defect geometries in multilayer optical coatings
[DE94-005820] 08 p3501 N94-30599
Degradation of optical components in space
09 p3594 N94-31029
Automatic resonator alignment and power stabilization of high power C02 lasers
[ISBN-0-315-77217-4] 09 p3714 N94-31472
Fast acting optical deflection
[AD-A276630] 09 p3879 N94-32037
Electromagnetic wave reflection from irregular plasma layers
[AD-A276727] 09 p3678 N94-32161
Neutral ion sources in precision manufacturing
09 p3875 N94-32447
X ray imaging and x ray source development at Lawrence Livermore National Laboratory
[DE94-007077] 09 p3719 N94-32629
Multi-line passive fiber optic slipring
[AD-D016092] 09 p3883 N94-32738
Operational experience and evaluation of a dual-element stretched-membrane heliostat
[DE94-008827] 09 p3763 N94-32965
Diamond turning in the production of x ray optics
09 p3604 N94-33298
Performance of adaptive optics at Lick Observatory
[DE94-009382] 10 p4142 N94-33911
Design and implementation of a beam-waveguide mirror control system for vernier pointing of the DSS-13 antenna 11 p4253 N94-35548
Issues in the design and optimization of adaptive optics and laser guide stars for the Keck Telescopes
[DE94-009384] 11 p4349 N94-35565
Analysis of recent agile mirror data
[AD-A278758] 11 p4318 N94-36427
Adaptive optics for laser beamforming in the atmosphere 12 p4393 N94-36621

MIS (SEMICONDUCTORS)
Squeezed states of electrons and transitions of the density of states 01 p0370 N94-10593
Atomic layer epitaxy of boron nitride
[AD-A266260] 03 p1212 N94-16932
Passivation of III-V compound semiconductor based devices
[AD-A276178] 09 p3894 N94-31056

MISALIGNMENT
Systematic study of effects of load misalignment in uniaxial low cycle fatigue testing at high temperatures
[NPL-DMM(A)-27] 03 p1057 N94-15015
Stability of beam in the Fermilab Main Injector
[DE94-000619] 05 p1982 N94-21934
Performance impacts for actuator misalignments and failures in large-aperture adaptive-optic telescopes
[AD-A273838] 07 p3034 N94-25742
Enhanced simulation software for rocket turbopump, turbulent, annular liquid seals
[NASA-CR-195239] 07 p2825 N94-27383

MISCIBILITY
U SOLUBILITY

MISFETS
U FIELD EFFECT TRANSISTORS

MISORIENTATION
U MISALIGNMENT

MISS DISTANCE
Hypervelocity orbital intercept guidance using certainty control
[AD-A267297] 03 p1174 N94-17219
An empirical evaluation of five circular error probable estimation techniques and a method for improving them
[AD-A266528] 04 p1556 N94-18397
Comparison of c.t.s. based prediction of store trajectory with flight test data 06 p2158 N94-24268
MISSILE ANTENNAS
Missile antenna pattern coordinate system and data formats
[AD-A269153] 04 p1385 N94-18260
MISSILE BODIES
Numerical assessment of aerodynamic interactions on missiles with transverse jets control 07 p2659 N94-28031
MISSILE CASES
U MISSILE BODIES
MISSILE COMPONENTS
NT MISSILE ANTENNAS
NT MISSILE BODIES
Transparent polycrystalline body with high ultraviolet transmittance, process for making and applications thereof
[CA-PATENT-1325511] 07 p3066 N94-27276
MISSILE CONFIGURATIONS
Missile datcom user's manual
[AD-A267447] 03 p1152 N94-17032
Holographic testing of composite propfans for a cruise missile wind tunnel model
[NASA-TM-105271] 06 p2187 N94-23545
State-of-the-art engineering aeroprediction methods with emphasis on new semiempirical techniques for predicting nonlinear aerodynamics on complete missile configurations
[AD-A273680] 06 p2171 N94-25411
A numerical study of high-speed missile configurations using a block-structured parallel algorithm
[AD-A273776] 07 p2979 N94-25860
Numerical assessment of aerodynamic interactions on missiles with transverse jets control 07 p2659 N94-28031
User's guide for an interactive personal computer interface for the aeroprediction code
[NSWCDD/TR-94/107] 11 p4305 N94-35958
The analysis of a generic air-to-air missile simulation model
[NASA-TM-109057] 11 p4309 N94-36438
An aerodynamic and static-stability analysis of the Hypersonic Applied Research Technology (HART) missile
[AD-A280631] 12 p4382 N94-36729
MISSILE CONSTRUCTION
U MISSILE STRUCTURES
MISSILE CONTROL
Test/analysis correlation and model updating of the STARS 1 and 2 missile systems
[DE93-013774] 02 p0748 N94-13578
Wind tunnel investigation with an operational turbojet engine
[TABES PAPER 93-662] 03 p0870 N94-16157
Military applications of high-accuracy frequency standards and clocks
[AD-A269303] 04 p1430 N94-18299
A mixed map/variable structure observer for target tracking 06 p2157 N94-24263
Recent developments in the simulation of steady and transient transverse jet interactions for missile, rotorcraft, and propulsive applications 07 p2804 N94-28030
Numerical assessment of aerodynamic interactions on missiles with transverse jets control 07 p2659 N94-28031
Fast adaptive control and its application to missile guidance 10 p4008 N94-34332
MISSILE DEFENSE
Plume radiation 03 p0924 N94-15223
Corporate Information Management (CIM) report on the simulation processes, version 2.0
[AD-A269119] 04 p1617 N94-18770
Standard atmospheres for engagement modeling
[AD-A272447] 05 p1858 N94-21207
High-velocity interceptors for boost-phase intercepts
[DE94-001077] 05 p1965 N94-22403
Elastic backscattering lidar for a MSTI satellite
[DE94-002701] 07 p2816 N94-26126
Laser beam steering with semiconductor waveguide
[AD-A275775] 08 p3292 N94-28765
Optical processing of MMW for agile beamsteering and beamforming
[AD-A277161] 09 p3880 N94-32068
MISSILE DESIGN
Test/analysis correlation and model updating of the STARS 1 and 2 missile systems
[DE93-013774] 02 p0748 N94-13578
Missile datcom user's manual
[AD-A267447] 03 p1152 N94-17032
An experimental and theoretical study of the aerodynamic characteristics of some generic missile concepts at Mach numbers from 2 to 6.8
[NASA-TM-109110] 08 p3130 N94-29473
MISSILE DETECTION
NT RADAR DETECTION
Estimation with multisensor/multiscan detection fusion
[AD-A265673] 01 p0138 N94-12338
Rocket Motor Plume Technology
[AGARD-LS-188] 03 p0923 N94-15217
Plume primary smoke 03 p0923 N94-15218
Microwave properties and systems overview 03 p0924 N94-15222
Super-resolution of multi-pixel and sub-pixel images for the SDI
[AD-A268537] 04 p1462 N94-18631
A feasibility study of a parallax-based passive missile approach warning system
[ISBN-0-315-60640-1] 05 p1743 N94-22410
Radar detection of low-altitude targets in a maritime environment. Volume 2: Meteorological and radar data
[AD-A274658] 07 p2768 N94-26335
Missile launch detection electric field perturbation experiment
[DE94-004224] 08 p3466 N94-30586
UVPI imaging from the LACE satellite: The Low Cost Launch Vehicle (LCLV) rocket plume
[AD-A278785] 12 p4398 N94-36445
MISSILE ENGINE CASES
U ROCKET ENGINE CASES
MISSILE GUIDANCE
U MISSILE CONTROL
MISSILE LAUNCHERS
Test/analysis correlation and model updating of the STARS 1 and 2 missile systems
[DE93-013774] 02 p0748 N94-13578
MISSILE RANGES
Joint Acoustic Propagation Experiment (JAPE-91) Workshop
[NASA-CP-3231] 06 p2526 N94-24207
MISSILE SIGNATURES
Propulsion 03 p0924 N94-15219
Microwave properties and systems overview 03 p0924 N94-15222
Boost-phase discrimination research
[NASA-TM-109347] 05 p1666 N94-19818
MISSILE STABILIZATION
U MISSILE CONTROL
U STABILIZATION
MISSILE STRUCTURES
Metals 2000
[DE93-016761] 04 p1355 N94-17752
MISSILE SYSTEMS
Test/analysis correlation and model updating of the STARS 1 and 2 missile systems
[DE93-013774] 02 p0748 N94-13578
Propulsion 03 p0924 N94-15219
Dependable software technology exchange
[AD-A267103] 03 p1146 N94-15638
The analysis of a generic air-to-air missile simulation model
[NASA-TM-109057] 11 p4309 N94-36438
MISSILE TESTS
Comparison of c.t.s. based prediction of store trajectory with flight test data 06 p2158 N94-24268
MISSILE TRACKING
Ultraviolet plume instrument description and plume data reduction methodology
[AD-A266141] 01 p0054 N94-11643
UVPI imaging from the LACE satellite: The Nihka rocket plume
[AD-A268456] 04 p1334 N94-18149
Super-resolution of multi-pixel and sub-pixel images for the SDI
[AD-A268537] 04 p1462 N94-18631
UVPI imaging from the LACE satellite: The Strypi rocket plume
[AD-A270967] 04 p1335 N94-19787
NPAC distributed-parallel system feasibility study
[AD-A270972] 04 p1539 N94-19790
UVPI imaging from the LACE satellite: The Starbird rocket plume
[AD-A271981] 05 p1658 N94-20617
Optimal control design advantages utilizing two-degree-of-freedom controllers
[AD-A273839] 07 p2984 N94-25743
Elastic backscattering lidar for a MSTI satellite
[DE94-002701] 07 p2816 N94-26126
Overview of the Miniature Sensor Technology Integration (MSTI) spacecraft attitude control system 11 p4206 N94-35627
Overview of the MSTI 2 on-orbit alignment 11 p4206 N94-35629
UVPI imaging from the LACE satellite: The Low Cost Launch Vehicle (LCLV) rocket plume
[AD-A278785] 12 p4398 N94-36445
MISSILE TRAJECTORIES
Hypervelocity orbital intercept guidance using certainty control
[AD-A267297] 03 p1174 N94-17219
Missile antenna pattern coordinate system and data formats
[AD-A269153] 04 p1385 N94-18260
Comparison of c.t.s. based prediction of store trajectory with flight test data 06 p2158 N94-24268
Kinematic model of a beam riding air-to-air missile
[PB94-149085] 10 p3990 N94-34106
MISSILE VIBRATION
Aeroelastic vibrations of lifting surfaces
[ECL-91-01] 09 p3585 N94-31677
MISSILES
NT AIR TO AIR MISSILES
NT ANTIMISSILE MISSILES
NT BALLISTIC MISSILES
NT CRUISE MISSILES
NT FLEET BALLISTIC MISSILES
NT INTERCONTINENTAL BALLISTIC MISSILES
NT MINUTEMAN ICBM
NT RADAR HOMING MISSILES
NT SIDEWINDER MISSILES
Test/analysis correlation and model updating of the STARS 1 and 2 missile systems
[DE93-013774] 02 p0748 N94-13578
Electromagnetic wave test 02 p0508 N94-14173
The effect of the nose shape and wing location toward the wing vortex breakdown
[AD-A267724] 03 p0855 N94-14942
Wind tunnel investigation with an operational turbojet engine
[TABES PAPER 93-662] 03 p0870 N94-16157
Missile datcom user's manual
[AD-A267447] 03 p1152 N94-17032
Missile antenna pattern coordinate system and data formats
[AD-A269153] 04 p1385 N94-18260
Two-dimensional boundary surfaces for axi-symmetric external transonic flows
[AD-A269678] 04 p1312 N94-18571
Dynamic response analysis of composite structural members during missile launch
[AD-A270023] 04 p1332 N94-18760
Aerospace: Facts and figures, 1992-1993
[AD-A272571] 05 p1635 N94-21419
An overview on the main available ceramic composites and their processing routes 06 p2255 N94-24229
A numerical study of high-speed missile configurations using a block-structured parallel algorithm
[AD-A273776] 07 p2979 N94-25860
Numerical assessment of aerodynamic interactions on missiles with transverse jets control 07 p2659 N94-28031
Experimental investigation of three-dimensional vortex-airfoil interaction in a supersonic stream
[AD-A275107] 08 p3122 N94-28899
Exposure assessment of JAVELIN missile combustion products
[AD-A278128] 09 p3616 N94-33059
Compact diffusers for small transonic compressors 10 p4002 N94-34449
Numerical simulation of shock interaction with above-ground structures
[AD-A278713] 11 p4279 N94-35949
An aerodynamic and static-stability analysis of the Hypersonic Applied Research Technology (HART) missile
[AD-A280631] 12 p4382 N94-36729
MISSION ADAPTIVE WINGS
Mission adaptive wing
[NASA-TM-109448] 03 p0865 N94-15321
Reduction of structural loads using maneuver load control on the Advanced Fighter Technology Integration (AFTI)/F-111 mission adaptive wing
[NASA-TM-4526] 06 p2168 N94-24295
MISSION PLANNING
Results of mission preparation support to microgravity experiments on board of Eureca 1 01 p0111 N94-10138
Mission support for crystal growth experiments in Russian unmanned carriers 01 p0111 N94-10139
Numerical calculation of the growth of InP by the travelling heater method in the first mission of the Space Flyer Unit 01 p0114 N94-10179
Aerodynamic and aerothermal challenges for the design of the Hermes spaceplane 01 p0003 N94-10423
An analysis of the modes and states for generic avionics
[NASA-CR-188253] 01 p0027 N94-10664
Parametric analysis of atmospheric processes
[NASA-CR-192523] 01 p0347 N94-10757

Lunar-Ultraviolet Telescope Experiment (LUTE) integrated program plan
[NASA-CR-193267] 01 p0424 N94-11356
Five biomedical experiments flown in an Earth orbiting laboratory: Lessons learned from developing these experiments on the first international microgravity mission from concept to landing 01 p0302 N94-11556
Operational radiological support for the US manned space program 01 p0318 N94-11561
On-orbit refueling 01 p0038 N94-11565
The rational behavior model: A multi-paradigm, tri-level software architecture for the control of autonomous vehicles
[AD-A265175] 01 p0332 N94-11874
The requirement for global training programmes to meet the new remote sensing technology 01 p0196 N94-11929
Conceptual studies report on lunar and planetary exploration
[NASDA-TK-SS0438] 01 p0481 N94-12323
Significance and scenarios of lunar and planetary exploration missions 01 p0482 N94-12324
Unmanned lunar exploration mission 01 p0482 N94-12325
Manned lunar exploration missions 01 p0482 N94-12326
Mars exploration missions 01 p0482 N94-12327
The Third Workshop on Two Phase Fluid Experiment in the Space Environment
[NASDA-CON-930002] 01 p0161 N94-12547
Summary of studies on JEM utilization experiment projects 01 p0161 N94-12548
METEOSAT second generation programme SEVIRI: An enhanced visible and IR radiometer for meteorology 01 p0212 N94-12667
MARS Mission research center
[NASA-CR-194034] 02 p0841 N94-13088
Present status of JEM utilization projects 02 p0530 N94-13273
Earth Observation Center Annual Report on Research and Development, Fiscal Year 1992
[EOC-92-01-0007] 02 p0687 N94-14091
Earth observation experiment data analysis 02 p0687 N94-14093
ADEOS project 02 p0687 N94-14094
Asia-Pacific ISY conference, volume 1
[NASDA-CM-199-1] 02 p0532 N94-14098
European space for exclusively peaceful purposes
[ESA-BR-86] 02 p0851 N94-14137
TRMM system overview and status in the United States 02 p0690 N94-14221
TRMM Project in Japan: Overview and status 02 p0690 N94-14222
Future TRMM follow-on mission 02 p0691 N94-14228
Space transportation systems within ESA programmes: Current status and perspectives 02 p0537 N94-14275
Mission scenario of HOPE 02 p0537 N94-14279
Primary and secondary electrical space power based on advanced PEM systems
[DE93-012643] 02 p0553 N94-14689
Pre-phase a study report of lunar polar orbiter
[NASDA-TK-SS0440] 03 p0873 N94-15000
HSTS: Integrating planning and scheduling
[AD-A266991] 03 p1222 N94-15213
Dare to dream --- The Space Station Freedom development
[NASA-TM-109512] 03 p0885 N94-15458
STS-26 crew participation in meetings
[NASA-TM-109519] 03 p0873 N94-15469
Mars rover sample return mission
[NASA-TM-109521] 03 p0873 N94-15471
Commitment to challenge
[NASA-TM-109523] 03 p0876 N94-15473
Long Duration Exposure Facility
[NASA-TM-109427] 03 p0885 N94-15497
SATCOP mission planning software package 03 p0912 N94-15562
AIRSAR South American deployment: Operation plan, version 3.0 03 p0994 N94-15919
Scientific use of Space Station Freedom 03 p0977 N94-16072
Approaching the new reality
[TABES PAPER 93-230] 03 p1050 N94-16131
A mission concept of Phobos/Deimos exploration 03 p1287 N94-16387
Chairmanship of the Neptune/Pluto outer planets science working group
[NASA-CR-194625] 03 p1297 N94-16832
AMIGAU: A prototype tool aimed at mission analysis for satellites and satellite constellations 03 p0888 N94-17133
Small missions for space science 03 p0874 N94-17142
Strategy for a small satellite program and a proposal for a first mission 03 p0874 N94-17143
Small satellite missions to long-period comets 03 p0874 N94-17144
Big results with small space systems: What small systems are doing today 03 p0896 N94-17187
Human Transportation System (HTS) study, volume 2
[NASA-TM-104779-VOL-2] 03 p0882 N94-17320
Human Transportation System (HTS) study: Executive summary
[NASA-TM-104780] 04 p1332 N94-18669
Human Transportation System (HTS) study, volume 1
[NASA-TM-104779] 04 p1332 N94-18670
The Navy tessellated spheroid map projection system: A comprehensive definition
[AD-A269989] 04 p1462 N94-18677
Spacelab 3
[NASA-TM-108750] 04 p1323 N94-18849
Cluster ground segment and mission operations 04 p1330 N94-19636
The Cluster Joint Science Operations Centre 04 p1331 N94-19639
The EXOSAT operational experience
[ESA-STM-248] 05 p1657 N94-20235
Clementine: An inexpensive mission to the Moon and Geographos 05 p1652 N94-20765
Mars exploration study workshop 2
[NASA-CP-3243] 05 p2146 N94-21883
SPIKE: Application for ASTRO-D mission planning 05 p1926 N94-22486
Solar physics within ESA's planning 06 p2624 N94-22844
Lunar science strategy: Exploring the Moon with humans and machines 06 p2605 N94-23376
Mars 96 small rover: Mission strategy 06 p2606 N94-23381
A reference Martian mission for a long range rover 06 p2606 N94-23382
Early lunar rover mission studies 06 p2607 N94-23388
The robotic Mars rover 06 p2608 N94-23390
Mission and system concepts for Mars robotic precursor missions 06 p2608 N94-23391
Mission and system design of a long range rover mission 06 p2608 N94-23392
Balloon experiments at Mars 96 project 06 p2608 N94-23396
Evolving directions in NASA's planetary rover requirements and technology 06 p2370 N94-23414
Walking, jumping, and tumbling: More than one way to get around Mars 06 p2370 N94-23419
Strategies in transition 06 p2498 N94-23833
Mission operations update for the restructured Earth Observing System (EOS) mission 06 p2499 N94-23839
Mission planning for Shuttle Imaging Radar-C (SIR-C) with a real-time interactive planning software 06 p2305 N94-23842
ATOS-1: Designing the infrastructure for an advanced spacecraft operations system 06 p2197 N94-23849
Operations concepts for Mars missions with multiple mobile spacecraft 06 p2501 N94-23852
NASDA satellite mission operation system and operations 06 p2501 N94-23854
Mission activities planning for a Hermes mission by means of AI-technology 06 p2502 N94-23858
A review of mission planning systems 06 p2503 N94-23866
The Mars mapper science and mission planning tool 06 p2503 N94-23867
Mission planning for an Earth observation low Earth orbiter: ERS-1 06 p2503 N94-23868
Integrating payload design, planning, and control in the Dutch Utilisation Centre 06 p2207 N94-23869
Voyager uplink planning in the interstellar mission era 06 p2305 N94-23870
Science planning and sequencing for Cassini 06 p2504 N94-23871
Techniques and software for optimum and efficient mission science sequence development 06 p2504 N94-23872
A packet-based concept for spacecraft command planning 06 p2504 N94-23873
Connecting science and operations: The operations coordinator 06 p2504 N94-23874
The instant sequencing task: Toward constraint-checking a complex spacecraft command sequence interactively 06 p2504 N94-23875
AGENDA: A task organizer and scheduler 06 p2504 N94-23876
Generic mission planning concepts for space astronomy missions 06 p2505 N94-23878
A MOS for all seasons 06 p2505 N94-23879
An operations concept methodology to achieve low-cost mission operations 06 p2505 N94-23880
Mission engineering 06 p2505 N94-23881
Manned Space-laboratories Control Center (MSCC) operations concept 06 p2505 N94-23882
Making adaptable systems work for mission operations: A case study 06 p2506 N94-23883
An approach to the design of operations systems 06 p2506 N94-23884
Management of information for mission operations using automated keyword referencing 06 p2506 N94-23886
The FOT tool kit concept 06 p2507 N94-23889
GSMS and space views: Advanced spacecraft monitoring tools 06 p2507 N94-23890
Influence of a new generation of operations support systems on current spacecraft operations philosophy: The users feedback 06 p2507 N94-23894
The Advanced Technology Operations System: ATOS 06 p2508 N94-23897
Mission and science activity scheduling language 06 p2515 N94-23938
Toward lowering the cost of mission operations 06 p2519 N94-23960
New mission requirements methodologies for services provided by the Office of Space Communications 06 p2519 N94-23961
An intelligent planning and scheduling system for the HST servicing missions 06 p2520 N94-23964
Software reuse in spacecraft planning and scheduling systems 06 p2520 N94-23966
Planning: Management of predictability and uncertainty and keeping abreast of developments 06 p2520 N94-23967
Estimating the Deep Space Network modification costs to prepare for future space missions by using major cost drivers 06 p2520 N94-23968
The Far Ultraviolet (FUV) auroral imager for the Inner Magnetospheric Imager (IMI) mission: Options 06 p2209 N94-24453
A mission to Mercury and a mission to the moons of Mars
[NASA-CR-195530] 06 p2195 N94-24619
Power generation technology options for a Mars mission
[NASA-TM-106451] 06 p2220 N94-24681
WISPER: Wirless Space Power Experiment
[NASA-CR-195538] 06 p2396 N94-24701
Near Earth asteroid rendezvous
[NASA-CR-195518] 06 p2195 N94-24808
Ultraviolet, visible, and gravity astrophysics: A plan for the 1990's
[NASA-NP-152] 06 p2603 N94-24973
PERCIVAL mission to Mars
[NASA-CR-195541] 06 p2195 N94-24995
New Advances in Mission Planning and Rehearsal Systems
[AGARD-LS-192] 06 p2521 N94-25008
Overall system concepts in mission planning 06 p2521 N94-25009
Human factors of mission planning systems: Theory and concepts 06 p2521 N94-25010
Human factors of mission planning systems: Applications and implementation 06 p2522 N94-25011
Computing techniques in mission planning 06 p2522 N94-25012
Mission planning and mission rehearsal systems: Displays and other interactive techniques 06 p2522 N94-25013
Ground based mission planning systems 06 p2522 N94-25014
In flight mission planning in the Copilote Electronique 06 p2522 N94-25015
Effect of power system technology and mission requirements on high altitude long endurance aircraft
[NASA-CR-194455] 06 p2189 N94-25200
ROSAT mission planning using artificial intelligence methods
[DLR-FB-93-14] 06 p2476 N94-25345
A comparative evaluation plan for the Maintenance, Inventory, and Logistics Planning (MILP) System Human-Computer Interface (HCI) 06 p2588 N94-25373
The Extended Mission Rover (EMR) 07 p2689 N94-25674
Lowest cost, nearest term options for a manned Mars mission 07 p2689 N94-25682
Comet nucleus and asteroid sample return missions 07 p2689 N94-25692
First lunar outpost 07 p2943 N94-25694
Project Minerva: A low-cost manned Mars mission based on indigenous propellant production 07 p2760 N94-25705
Pax: A permanent base for human habitation of Mars 07 p2943 N94-25706
Access to space study
[NASA-TM-109693] 07 p2685 N94-27151
Interdisciplinary technology 07 p2686 N94-27363

Space science: Causes and impacts of cutbacks to NASA's outer solar system exploration missions. Report to the Chairman, Subcommittee on Investigations and Oversight, Committee on Science, Space, and Technology, House of Representatives
[GAO/NSIAD-94-24] 07 p3106 N94-27418
MUADEE: Mars Upper Atmosphere Dynamics, Energetics, and Evolution discovery mission. Executive summary volume
[NASA-CR-195732] 08 p3549 N94-28418
Proceedings of the 3rd International Symposium: JERS-1 and Remote Sensing in the Future
[JTN-94-80597] 08 p3329 N94-29217
A capacity planning model for Canadian military airlift requests
[ISBN-0-315-86079-0] 08 p3136 N94-30144
Development status of the Communications and Broadcasting Engineering Test Satellite (COMETS)
[JTN-94-80545] 08 p3169 N94-30811
NASA strategic plan
[NASA-TM-109780] 09 p3915 N94-32222
Forced libration of Mercury and geodetic determination of a possible fluid core 09 p3774 N94-32493
The Lunar Scout Program: An international program to survey the Moon from orbit for geochemistry, mineralogy, imagery, geodesy, and gravity
[NASA-TM-104791] 09 p3943 N94-32923
MARSNET: A European network of stations on the surface of Mars 09 p3945 N94-33199
Scheduling fighter missions using an expert system with an operations research module 09 p3853 N94-33337
The PLAID graphics analysis impact on the space program 10 p4110 N94-33632
Constraint-based integration of planning and scheduling for space-based observatory management 10 p4150 N94-34046
SeaWiFS technical report series. Volume 17: Ocean color in the 21st century. A strategy for a 20-year time series
[NASA-TM-104566-VOL-17] 10 p4093 N94-34209
Advanced timeline systems
[NASA-CR-193958] 10 p4131 N94-34281
Johnson Space Center (JSC) research and technology
[NASA-TM-104788] 10 p4187 N94-34677
Cargo systems manual: Heat Pipe Performance (HPP) STS-66
[NASA-TM-109784] 10 p4131 N94-34720
Apollo 11 at twenty-five, version 1.0
[NASA-CR-193380] 11 p4376 N94-35363
Materials processing in space tasks. WBS task 5.4: Generic tasks
[NASA-CR-193979] 11 p4249 N94-35485
Automated maneuver planning using a fuzzy logic algorithm 11 p4203 N94-35610
Spacecraft attitude determination accuracy from mission experience 11 p4204 N94-35618
Application of star identification using pattern matching to space ground systems at GSFC 11 p4209 N94-35640
Planning German Army helicopter maintenance and mission assignment
[AD-A280483] 12 p4381 N94-37352

MISSISSIPPI
Remote sensing and the Mississippi high accuracy reference network 09 p3758 N94-32466

MISSISSIPPI RIVER (US)
Modeling present and future river runoff using global atmospheric models
[AD-A265274] 01 p0285 N94-11685

MITOCHONDRIA
Effect of intermittent cold exposure on the fiber-type composition of selected skeletal muscles in rats
[AD-A265309] 01 p0301 N94-11861

MIXED CRYSTALS
Symmetry lowering in crystalline solid solutions: A study of cinnamamide-thienylacrylamide by x ray and neutron diffraction and solid-state photochemistry
[DE93-010871] 01 p0394 N94-10301
The Lindemann criterion of melting for pure and mixed ionic crystals
[ITN-93-85210] 02 p0814 N94-14554

MIXED FLOW
U MULTIPHASE FLOW

MIXED OXIDES
NT BSCCO SUPERCONDUCTORS
NT YBCO SUPERCONDUCTORS
Grain boundaries in complex oxides
[DE93-013986] 01 p0398 N94-11012
Fabrication and microstructural development of Ag-clad TlBa2Ca2Cu3O(x) tapes
[DE93-017407] 04 p1597 N94-18500
Synthesis and characterization of novel ternary and quaternary reduced molybdenum oxides
[DE94-005563] 08 p3510 N94-28529
Nonaqueous slip casting of YBa2Cu3O(7-x) superconductive ceramics
[NASA-CR-4575] 08 p3512 N94-29101

MIXERS
A comparison of free-space and fiber mixer performances
[AD-A273558] 06 p2547 N94-25161
Frequency-domain analysis of nonlinear microwave circuits
[PB94-132024] 08 p3261 N94-28400

MIXING
NT DISSOLVING
NT HOMOGENIZING
NT LAMINAR MIXING
NT PREMIXING
NT SIGNAL MIXING
NT SUSPENDING (MIXING)
NT TURBULENT MIXING
Projectile-target mixing in melted ejecta formed during a hypervelocity impact cratering event 01 p0432 N94-12241
Hot electron mixers, the potential competition 03 p0903 N94-15055
Analysis of supersonic flows using k-epsilon model and the RPLUS code: Progress towards high speed combustor analysis 04 p1411 N94-18551
Convex set and linear mixing model 05 p1844 N94-20888
Ethylene trace-gas techniques for high-speed flows
[NASA-TM-106491] 06 p2169 N94-24335
Modulation wavelength dependence of ion mixing in metallic superlattices
[DE94-004608] 07 p3059 N94-26591
Methods of testing parameterizations: Vertical ocean mixing 08 p3352 N94-30633
Competition between crystallization and mixing/demixing in polymer mixture
[ETN-94-95753] 09 p3651 N94-31513

MIXING CIRCUITS
Theoretical SIS mixer research
[AD-A266323] 02 p0807 N94-13580
Broadband IF matching for quasioptical mixers
[MPE-PREPRINT-240] 04 p1390 N94-19416
Quasi-optical transponder using FET's and patch antennas
[AD-A271339] 04 p1407 N94-19584
Quantum noise studies with superconducting tunnel junction mixers
[AD-A270897] 05 p2012 N94-19897
Development of a 4-bit parallel analog-to-digital converter and a four-quadrant double-balanced mixer using heterojunction bipolar transistor technology
[AD-A274074] 07 p2947 N94-25648
A compact 150 GHz SIS receiver cooled by 4 K GM refrigerator
[REPT-36] 07 p2776 N94-27340
Spectral-domain optical processing techniques
[AD-A278371] 10 p4141 N94-33739

MIXING DEPTH
U MIXING HEIGHT

MIXING LAYERS (FLUIDS)
The kinematics of buoyancy induced mixing 01 p0123 N94-10239
Seasonal variation of the surface mixed layer in the subtropical re-circulation area of the North Pacific during OMLET 01 p0195 N94-11924
Mixed layer heat budget of Kuroshio-Tango triangle using satellite and ship observations 01 p0196 N94-11925
A normal stress subgrid-scale eddy viscosity model in large eddy simulation 01 p0155 N94-12288
LIF measurements of scalar mixing in turbulent shear layers 01 p0159 N94-12312
Plane mixing layer vortical structure kinematics 01 p0159 N94-12313
Numerical simulation of the non-Newtonian mixing layer 01 p0159 N94-12314
A multiple-scale turbulence model for incompressible flow
[NASA-TM-106113] 02 p0631 N94-13385
Modeling and simulation of transport and combustion phenomena in a supersonic mixing layer
[ONERA-NT-1992-11] 02 p0565 N94-14194
Linear instability of curved free shear layers
[NASA-TM-106290] 02 p0642 N94-14729
A study of the fine scale motions of incompressible time-developing mixing layers 02 p0644 N94-14751
Behavior of streamwise rib vortices in a three-dimensional mixing layer 02 p0644 N94-14754
Direct simulation of polymer drag reduction in free shear flows and vortex dipoles 02 p0644 N94-14755
Investigation of the dilatational dissipation in compressible homogeneous shear flow 02 p0645 N94-14758
Large eddy simulation and direct numerical simulation of high speed turbulent reacting flows
[NASA-CR-193131] 03 p1018 N94-15427
Parametric resonant triad interactions in a free shear layer
[NASA-TM-106365] 03 p1021 N94-15751
Three dimensional hydrodynamic calculations with adaptive mesh refinement of the evolution of Rayleigh Taylor and Richtmyer Meshkov instabilities in converging geometry: Multi-mode perturbations
[DE93-017155] 03 p1025 N94-16903
Transmission of light through a turbulent mixing layer
[AD-A267266] 03 p1193 N94-17264
Studies on high pressure and unsteady flame phenomena: Revision
[AD-A269138] 04 p1348 N94-18257
The application of front tracking to the simulation of shock refractions and shock accelerated interface mixing
[DE93-018342] 04 p1419 N94-19025
The effects of initial conditions on the 3-D topology of temporally evolving wakes (ARI on 3-D bluff body wakes)
[AD-A271008] 04 p1423 N94-19774
Turbulence modeling for high speed compressible flows
[NASA-CR-194547] 05 p1799 N94-20210
Mixing of a chemically buoyant layer at the top of a thermally convecting fluid: Implications for mantle dynamics with application to Venus 05 p2099 N94-20675
Green Sheet project: Dye sheet evolution
[AD-A272019] 05 p1883 N94-21443
Direct simulation of shock-induced mixing layer
[DE93-040498] 05 p1803 N94-21531
Image analysis applications to mixing phenomena and turbulent dispersions
[ECL-92-29] 06 p2317 N94-22971
Small rocket flowfield diagnostic chambers 06 p2210 N94-23030
A random distribution reacting mixing layer model
[NASA-CR-194445] 06 p2187 N94-23552
Numerical simulation of non-Newtonian free shear flows 06 p2331 N94-24160
Vortical structure in a forced plane mixing layer 06 p2331 N94-24162
Measurement of the volume mass by spontaneous Raman scattering. Study of turbulent fluctuations of mixing in a subsonic free jet. Measurements in supersonic wind tunnels
[ISL-R-102/92] 06 p2339 N94-25462
Transverse vorticity measurements in the University of Houston two stream shear layer facility
[AD-A273910] 07 p2797 N94-27562
Scalar mixing in the subsonic jet in crossflow 07 p2800 N94-28008
A random distribution reacting mixing layer model
[NASA-TM-106517] 08 p3150 N94-28923
Evolution of the large-scale vortices in turbulent mixing-layers 08 p3273 N94-29686
Large eddy simulation of subsonic mixing layers 08 p3276 N94-29851
The enhancement of compressible turbulent mixing via streamwise vorticity 08 p3280 N94-30487
Transition to turbulence in confined compressible mixing layers 08 p3283 N94-30958
Reacting compressible mixing layers: Structure and stability
[AD-A278319] 10 p4047 N94-33965
Controlling combustion and maximizing heat release in a reacting compressible free shear layer
[AD-A278328] 10 p3982 N94-33966
Numerical simulation of two-dimensional spatially-developing mixing layers
[AD-A281683] 10 p4049 N94-34686
The stabilizing effect of compressibility in turbulent shear flow
[NASA-CR-194932] 12 p4444 N94-37605
Towards enhancing and delaying disturbances in free shear flows
[NASA-CR-194945] 12 p4445 N94-37606

MIXING LENGTH FLOW THEORY
Why convective heat transport in the solar nebula was inefficient 01 p0458 N94-12143
Mixing in a stratified shear flow: Energetics and sampling 01 p0159 N94-12311
On memory effects in turbulence
[DLR-FB-93-03] 04 p1409 N94-18124
Turbulence modeling for non-equilibrium flows 06 p2328 N94-24144
Development and implementation of a scramjet cycle analysis code with a finite-rate-chemistry combustion model for use on a personal computer
[AD-A273834] 07 p2673 N94-25617
Performance of renormalization group algebraic turbulence model on boundary layer transition simulation
[NASA-CR-194466] 07 p2644 N94-26131
Numerical simulation of turbulent free jet by TFKE model 07 p2871 N94-28157

Modification of the MML turbulence model for adverse pressure gradient flows
[NASA-TM-106544] 09 p3709 N94-32947

MIXING RATIOS
Eddy mixing coefficient upper limit derived from the photochemical balance of O2 06 p2621 N94-24897
Evaluation of a concentration probe for application in a supersonic flow field
[AD-A273915] 07 p2643 N94-25592
Analysis of mid-tropospheric carbon monoxide data using a three-dimensional global atmospheric chemistry numerical model
[DE94-004782] 11 p4286 N94-36026
First measurement of helium on Mars: Implications for the problem of radiogenic gases on the terrestrial planets 11 p4370 N94-36153
The E2/M1 mixing ratio in the excitation of the Delta from polarized photo-reactions
[DE94-004235] 12 p4510 N94-36442

MIXTURES
NT ADMIXTURES
NT AEROSOLS
NT AIR
NT AQUEOUS SOLUTIONS
NT BINARY FLUIDS
NT BINARY MIXTURES
NT COLLOIDAL PROPELLANTS
NT COLLOIDS
NT COMPRESSED AIR
NT DETONABLE GAS MIXTURES
NT DISPERSIONS
NT EMULSIONS
NT EUTECTIC ALLOYS
NT EUTECTICS
NT FOG
NT GAS MIXTURES
NT HIGH TEMPERATURE AIR
NT LIQUID AIR
NT LIQUID-GAS MIXTURES
NT NUCLEAR EMULSIONS
NT PHOTOGRAPHIC EMULSIONS
NT POLYMER BLENDS
NT SIALON
NT SLURRIES
NT SMOKE
NT SOLID SOLUTIONS
NT SOLID SUSPENSIONS
NT SOLUTIONS
Marangoni Benard instabilities in liquid mixtures with Soret effect 01 p0119 N94-10215
Measurement of viscosity, density and gas solubility of refrigerant blends
[DE93-014772] 01 p0089 N94-11145
Chemical equilibrium in high pressure molecular fluid mixtures
[DE93-040160] 05 p1796 N94-19829
One- and multi-component theories of mixtures
[DE93-040543] 05 p1966 N94-21511
Ultrastructure processing of macromolecular materials
[AD-A273413] 06 p2258 N94-24782
Analysis and computer tools for separation processes involving nonideal mixtures
[DE94-004162] 07 p2960 N94-25986
Studies in physico-chemical hydrodynamics of extended systems
[DE94-006752] 09 p3706 N94-32149
Thermal cis-trans isomerization rates of azobenzenes bound in the side chain of some copolymers and blends
[AD-A280451] 12 p4424 N94-37227

MMS
U MULTIMISSION MODULAR SPACECRAFT

MNEMONICS
Comparing performance on implicit memory tests
[AD-A269900] 04 p1508 N94-18657

MOBILE COMMUNICATION SYSTEMS
NT LAND MOBILE SATELLITE SERVICE
Trellis coding with Continuous Phase Modulation (CPM) for satellite-based land-mobile communications
[NASA-CR-191325] 02 p0604 N94-13909
Opening remarks: Current and future activities 02 p0612 N94-14655
Propagation issues for emerging mobile and portable communications: A systems perspective 02 p0614 N94-14667
Propagation considerations in the American Mobile Satellite system design 02 p0614 N94-14668
Tree attenuation at 20 GHz: Foliage effects 02 p0615 N94-14672
Propagation-related AMT design aspects and supporting experiments 03 p0995 N94-16042
Propagation research in Japan 03 p0996 N94-16043
The ORBCOMM system 03 p0893 N94-17163
MAGSS-14: Medium Altitude Global Mobile Satellite System with enhanced regional coverage 03 p0893 N94-17164
The ELLIPSO (tm) system: Elliptical low orbits for mobile communications 03 p0893 N94-17167
Mobile antenna development at JPL 05 p1731 N94-20457
Mobile terminal antennas for helicopters 05 p1731 N94-20458
Linearly tapered slot antenna circular array for mobile communications
[NASA-TM-106441] 05 p1769 N94-21808
A consideration of the integration of terrestrial and satellite mobile systems 05 p1746 N94-22172
ARQ on fading channels 05 p1747 N94-22242
Proceedings of the Third International Mobile Satellite Conference (IMSC 1993)
[NASA-CR-194516] 06 p2273 N94-22735
Worldwide survey of direct-to-listener digital audio delivery systems development since WARC-1992 06 p2273 N94-22736
ESA personal communications and digital audio broadcasting systems based on non-geostationary satellites 06 p2273 N94-22737
Utilizing a TDRS satellite for direct broadcast satellite-radio propagation experiments and demonstrations 06 p2274 N94-22740
Aeronautical audio broadcasting via satellite 06 p2274 N94-22741
The MSAT spacecraft of Telesat Mobile Inc. 06 p2207 N94-22742
Adaptive digital beamforming for a CDMA mobile communications payload 06 p2274 N94-22743
Electrical performance of wire mesh for spacecraft deployable reflector antennas 06 p2275 N94-22744
Adaptive array antenna for satellite cellular and direct broadcast communications 06 p2275 N94-22745
SAW based systems for mobile communications satellites 06 p2275 N94-22746
US domestic and international regulatory issues 06 p2275 N94-22748
International organizations to enable world-wide mobile satellite services 06 p2275 N94-22749
Use of negotiated rulemaking in developing technical rules for low-Earth orbit mobile satellite systems 06 p2276 N94-22750
The provision of spectrum for feeder links of non-geostationary mobile satellites 06 p2276 N94-22751
The possibilities for mobile and fixed services in the 20/30 GHz frequency bands 06 p2276 N94-22752
Use of the 30/20 GHz band by multipurpose satellite systems 06 p2276 N94-22753
Power attenuation characteristics as switch-over criterion in personal satellite mobile communications 06 p2277 N94-22756
Integration of mobile satellite and cellular systems 06 p2277 N94-22757
Interworking evolution of mobile satellite and terrestrial networks 06 p2277 N94-22758
Interworking and integration of the Inmarsat Standard-M with Pan-European GSM system 06 p2277 N94-22759
Architectures and protocols for an integrated satellite-terrestrial mobile system 06 p2277 N94-22760
Handover procedures in integrated satellite and terrestrial mobile systems 06 p2277 N94-22761
MSAT and cellular hybrid networking 06 p2278 N94-22762
Trends in mobile satellite communication 06 p2278 N94-22763
Optimizing space constellations for mobile satellite systems 06 p2278 N94-22764
A system architecture for an advanced Canadian wideband mobile satellite system 06 p2278 N94-22766
Applicability of different onboard routing and processing techniques to mobile satellite systems 06 p2278 N94-22767
A European mobile satellite system concept exploiting CDMA and OBP 06 p2279 N94-22768
Study of LEO-SAT microwave link for broad-band mobile satellite communication system 06 p2279 N94-22769
The FAA satellite communications program 06 p2279 N94-22772
Canadian aeronautical mobile data trials 06 p2279 N94-22773
ACTS mobile SATCOM experiments 06 p2280 N94-22774
Cockpit weather graphics using mobile satellite communications 06 p2280 N94-22775
Using satellite communications for a mobile computer network 06 p2280 N94-22777
Design and implementation considerations of a MSAT packet data network 06 p2280 N94-22778
ACTS advanced system concepts and experimentation 06 p2280 N94-22780
The Iridium (tm) system: Personal communications anytime, anyplace 06 p2281 N94-22785
The Globalstar mobile satellite system for worldwide personal communications 06 p2282 N94-22786
Odyssey personal communications satellite system 06 p2282 N94-22787
INMARSAT's personal communicator system 06 p2282 N94-22788
The European Mobile System (EMS) 06 p2282 N94-22789
Electromagnetic field strength prediction in an urban environment: A useful tool for the planning of LMSS 06 p2283 N94-22795
Systems implications of L-band fade data statistics for LEO mobile systems 06 p2284 N94-22799
The Westinghouse Series 1000 Mobile Phone: Technology and applications 06 p2284 N94-22800
First satellite mobile communication trials using BLQS-CDMA 06 p2284 N94-22801
Channel and terminal description of the ACTS mobile terminal 06 p2284 N94-22802
Low cost coherent demodulation for mobile satellite terminals 06 p2284 N94-22803
Asynchronous timing and Doppler recovery in DSP based DPSK modems for fixed and mobile satellite applications 06 p2285 N94-22805
Estimation of frequency offset in mobile satellite modems 06 p2285 N94-22807
A pattern jitter free AFC scheme for mobile satellite systems 06 p2285 N94-22809
A CDMA synchronisation scheme 06 p2285 N94-22810
A high quality voice coder with integrated echo canceller and voice activity detector for mobile satellite applications 06 p2286 N94-22812
Performance of the unique-word-reverse-modulation type demodulator for mobile satellite communications 06 p2286 N94-22813
Diversity reception for advanced multi-satellite networks: A CDMA approach 06 p2286 N94-22816
System services and architecture of the TMI satellite mobile data system 06 p2286 N94-22817
A comparison between coherent and noncoherent mobile systems in large Doppler shift, delay spread, and C/I environment 06 p2287 N94-22818
Pseudo-coherent demodulation for mobile satellite systems 06 p2287 N94-22819
Transmission over EHF mobile satellite channels 06 p2287 N94-22820
Adaptive data rate control TDMA systems as a rain attenuation compensation technique 06 p2287 N94-22821
SATCOM simulator speeds MSS deployment and lowers costs 06 p2287 N94-22822
Development of a multilayer interference simulation program for MSS systems 06 p2287 N94-22823
Handover aspects for a Low Earth Orbit (LEO) CDMA Land Mobile Satellite (LMS) system 06 p2288 N94-22824
Study on networking issues of medium earth orbit satellite communications systems 06 p2288 N94-22825
The design and networking of dynamic satellite constellations for global mobile communication systems 06 p2288 N94-22826
Low earth orbit satellite/terrestrial mobile service compatibility 06 p2288 N94-22827
A practical system for regional mobile satellite services 06 p2288 N94-22828
Advanced mobile satellite communications using COMETS satellite in MM-wave and Ka-band 06 p2288 N94-22829
Low cost antennas for MSAT vehicular applications 06 p2289 N94-22830
K- and Ka-band mobile-vehicular satellite-tracking reflector antenna system for the NASA ACTS mobile terminal 06 p2289 N94-22831
An active K/Ka-band antenna array for the NASA ACTS mobile terminal 06 p2289 N94-22832
Microstrip monopulse antenna for land mobile communications 06 p2289 N94-22833
Isolated and coupled superquadric loop antennas for mobile communications applications 06 p2289 N94-22834
L-band mobile terminal antennas for helicopters 06 p2289 N94-22835
Satellite communications systems and technology. Volume 1: Analytical chapters
[NASA-TM-109398] 06 p2293 N94-23627
Low Earth orbit communications satellite 07 p2698 N94-25701
Evaluation of wireless Local Area Networks
[AD-A275133] 08 p3243 N94-29064
Radial microstrip slotline feed network for circular mobile communications array
[NASA-TM-106540] 08 p3267 N94-30198

Fast autodidactic adaptive equalization algorithms
[TELECOM-93-E-018] 09 p3670 N94-31174
Communications networks in stressed environments
[AD-A275967] 09 p3672 N94-31384
Channel and terminal description of the ACTS mobile terminal 09 p3599 N94-31428
Multisatellite constellation configuration selection for multiregional highly elliptical orbit constellations 09 p3600 N94-31437
A multichannel architecture for Naval Task Force Communication
[AD-A276230] 09 p3673 N94-31446
Call sign intelligibility improvement using a spatial auditory display 10 p4038 N94-33617
Large granularity cache coherence for intermittent connectivity
[AD-A278897] 11 p4345 N94-35571
Application of a Monte Carlo accuracy assessment tool to TDRS and GPS 11 p4207 N94-35635

MOBILITY
NT CARRIER MOBILITY
NT ELECTRON MOBILITY
NT HOLE MOBILITY
NT IONIC MOBILITY
In situ observation of radiation induced amorphization of crystals with apatite structure
[DE93-018450] 04 p1599 N94-18816
Conceptual design and architecture of hexapod robotic vehicles for the (L)OVLA project 06 p2369 N94-23405
Mobility analysis, simulation, and scale model testing for the design of wheeled planetary rovers 06 p2370 N94-23425
Preliminary results on time-varying feedback stabilization of a nonholonomic car-like mobile robot
[INRIA-RR-1512] 06 p2475 N94-24963
The Robotic All-Terrain Lunar Exploration Rover (RATLER): Increased mobility through simplicity 07 p2685 N94-26291
Effect of temperature and recoil-energy spectra on irradiation-induced amorphization in Ca2La8(SiO4)6O2
[DE94-004371] 07 p3067 N94-27602
RHEED studies of the nucleation, growth, and mobility of Ag atoms on the Si(111)7 x 7 surface
[DE94-005551] 08 p3521 N94-30899
Studying transient mobility and energy loss using scanning tunneling microscopy
[AD-A276292] 09 p3877 N94-31256

MOCVD (VAPOR DEPOSITION)
U METALORGANIC CHEMICAL VAPOR DEPOSITION

MODAL RESPONSE
Nonlinear response of a clamped-clamped beam with internal resonance under sinusoidel excitation 01 p0186 N94-10897
Dynamic tests on the NASA Langley CSI evolutionary model 01 p0045 N94-11320
System identification for Space Station Freedom using observer/Kalman filter Markov parameters
[NASA-CR-191521] 02 p0539 N94-12976
A component modes projection and assembly model reduction methodology for articulated, multi-flexible body structures 02 p0677 N94-14622
A simplistic look at limit stresses from random loading
[NASA-TM-108427] 03 p1058 N94-15710
Improved omit set displacement recoveries in dynamic analysis 04 p1449 N94-17829
Dynamic characterization of a lightweight, highly maneuverable spacecraft using modal and finite element analyses
[DE93-018095] 04 p1335 N94-18942
Modal combination in response spectrum modal dynamic analysis
[DE94-000339] 05 p1833 N94-21956
Modal test of the Brazilian satellite launcher (VLS) configuration burn-out of the first stage 06 p2156 N94-24257
Maximum likelihood modal parameter identification and realization of stochastic systems 06 p2157 N94-24265
Mode analysis of gyrotron oscillation using a k-spectrometer
[DE94-701195] 07 p2813 N94-27703
Stiffness-generated rigid-body mode shapes for Lanczos eigensolution with SUPORT DOF by way of a MSC/NASTRAN DMAP alter
[NASA-TM-106537] 08 p3319 N94-29406
Transient analysis mode participation for modal survey target mode selection using MSC/NASTRAN DMAP
[NASA-TM-106536] 08 p3319 N94-29469
Modelling soft impacts for vibrational excitation of civil engineering structures
[PB94-137619] 08 p3320 N94-29681
Pulse response based minimum time control of flexible structures 08 p3436 N94-29720
Modal analysis of solar panels using boundary integral equations
[NLT-TP-92218-U] 08 p3338 N94-30328
Second-order structural identification via state space-based system realizations 08 p3323 N94-30815
Decentralized control of flexible, multibody systems 10 p4058 N94-33366

MODE COUPLING
U COUPLED MODES

MODE OF VIBRATION
U VIBRATION MODE

MODE SHAPES
U MODAL RESPONSE

MODEL REFERENCE ADAPTIVE CONTROL
Model reference adaptive control (MRAC) with applications to robotics 01 p0339 N94-11640
Control algorithm implementation for a redundant degree of freedom manipulator
[NASA-CR-191339] 02 p0762 N94-13131
Direct model reference adaptive control of robotic arms 07 p2683 N94-26282
Investigation into model-based fuzzy logic control
[AD-A274660] 07 p2985 N94-26336
Using generic tool kits to build intelligent systems
[AIAA PAPER 94-1214-CP] 08 p3445 N94-30565
High-speed path constrained manipulator operation using optimal-feedback combined controller 09 p3833 N94-31962
An accelerated gradient method for adaptive control using only input and output measurements 10 p4115 N94-34319

MODELS
NT AIRCRAFT MODELS
NT ANALOG SIMULATION
NT ASTRONOMICAL MODELS
NT ATMOSPHERIC GENERAL CIRCULATION MODELS
NT ATMOSPHERIC MODELS
NT BIOLOGICAL MODELS (MATHEMATICS)
NT BREADBOARD MODELS
NT DIGITAL SIMULATION
NT DYNAMIC MODELS
NT ELECTROWEAK MODEL
NT ENVIRONMENT MODELS
NT HYDROLOGY MODELS
NT K-EPSILON TURBULENCE MODEL
NT LIGHTHILL GAS MODEL
NT MATHEMATICAL MODELS
NT NUCLEAR MODELS
NT OCEAN MODELS
NT PETRI NETS
NT QUARK MODELS
NT QUARK PARTON MODEL
NT SCALE MODELS
NT SEMISPAN MODELS
NT SPACECRAFT MODELS
NT STANDARD MODEL (PARTICLE PHYSICS)
NT STELLAR MODELS
NT THOMAS-FERMI MODEL
NT THREE DIMENSIONAL MODELS
NT TURBULENCE MODELS
NT TWO DIMENSIONAL MODELS
NT VECTOR DOMINANCE MODEL
NT VENEZIANO MODEL
NT WIND TUNNEL MODELS
Neural network model selection using asymptotic jackknife estimator and cross-validation method
[AD-A264960] 01 p0339 N94-11289
An experimental study of tether reel system: A laboratory model
[NAL-TR-1176T] 02 p0539 N94-12943
Infrared remote activity transceiver universal model
[AD-A266965] 03 p1188 N94-15144
Geophysical models of Western Aphrodite-Niobe region: Venus 03 p1286 N94-16382
Multi-resolution processing for fractal analysis of airborne remotely sensed data 03 p1065 N94-16604
The dynamics of hydroponic crops for simulation studies of the CELSS initial reference configurations
[NASA-CR-194654] 03 p1118 N94-17279
Rockets: Physical science teacher's guide with activities
[NASA-EP-291] 05 p1669 N94-20226
Current status: Animal models of nausea 05 p1889 N94-21915
An experimental investigation of the effect of upper surface blowing on dynamic stall
[NASA-CR-194863] 06 p2165 N94-22894
Flexible framework for contingent information systems modelling
[PB93-220549] 06 p2589 N94-23095
Designers' models of the human-computer interface 06 p2433 N94-24188
Systems engineering: A formal approach. Part 3: Modeling methods
[PB94-101409] 06 p2456 N94-24513
An object model for multimedia programming
[CWI-CS-R9327] 07 p2971 N94-27552
One from many: Selecting an appropriate human performance model
[DCIEM-93-25] 07 p2942 N94-27683
Molecular structure of coal studied by solvent extraction 08 p3187 N94-28676
Reference model for project support environments, version 2.0
[AD-A275191] 08 p3410 N94-29068
On a formal approach to the methodology of information planning
[MEMO-INF-93-42] 09 p3917 N94-31415
A compile time model for composing parallel programs
[AD-A278896] 11 p4310 N94-35597

MODEMS
Two way time transfer results at NRL and USNO 01 p0353 N94-10983
Performances of a date dissemination code on telephone lines using commercial modems 01 p0139 N94-10984
Asynchronous timing and Doppler recovery in DSP based DPSK modems for fixed and mobile satellite applications 06 p2285 N94-22805
Estimation of frequency offset in mobile satellite modems 06 p2285 N94-22807
A comparison between coherent and noncoherent mobile systems in large Doppler shift, delay spread, and C/I environment 06 p2287 N94-22818
Two-way satellite time transfer: Overview and recent developments 08 p3469 N94-30646

MODERATION (ENERGY ABSORPTION)
NT THERMALIZATION (ENERGY ABSORPTION)

MODERATORS
Generation of neutronic thermal data in support of space nuclear propulsion
[DE93-013148] 02 p0549 N94-13034
Temperature and Doppler coefficients of various space nuclear reactors
[DE94-001388] 05 p1671 N94-21979
Characteristics and control response of the TOPAZ 2 reactor system real-time dynamic simulator
[DE94-003788] 07 p2699 N94-25600
Space-R thermionic space nuclear power system: Design and technology demonstration
[DE94-001890] 07 p2699 N94-25929

MODES
NT BALLOONING MODES
NT COUPLED MODES
NT FAILURE MODES
NT LASER MODES
NT MODES (STANDING WAVES)
NT PROPAGATION MODES
NT PUSHBROOM SENSOR MODES
NT VIBRATION MODE
NT WHISPERING GALLERY MODES

MODES (STANDING WAVES)
Experiments on the aerodynamic generation of noise in centrifugal turbomachinery 08 p3480 N94-30804

MODFETS
Characteristics of 0.8- and 0.2-microns gate length In(x)Ga(1-x) As/In(0.52)Al(0.48)As/InP (0.53 less than or equal to x less than or equal to 0.70) modulation-doped field-effect transistors at cryogenic temperatures 05 p1733 N94-20499

MODULARITY
A modular design for connectionist parsing 05 p1941 N94-20252
MAYGEN: A symbolic debugger generation system
[AD-A272512] 05 p1913 N94-21413
Modular interval spaces
[PB93-220663] 05 p1961 N94-22266
Laser light scattering instrument advanced technology development
[NASA-CR-194803] 06 p2349 N94-23286
Modular approach to project management
[PB94-118833] 06 p2586 N94-24528
A type-theoretic approach to higher-order modules with sharing
[AD-A273566] 06 p2458 N94-24693
Modular Simulator System (MSS). Engineering design guide
[AD-A276967] 09 p3589 N94-32394
Use of formal calculation to automatically obtain adjoint programs
[PB94-170701] 11 p4308 N94-36259

MODULATED CONTINUOUS RADIATION
Microwave reflectometer ionization sensor
[NASA-CR-191464] 03 p0922 N94-17083

MODULATION
NT AMPLITUDE MODULATION
NT BINARY PHASE SHIFT KEYING
NT DELTA MODULATION

NT DIFFERENTIAL PULSE CODE MODULATION
NT FM/PM (MODULATION)
NT FREQUENCY MODULATION
NT FREQUENCY SHIFT KEYING
NT LIGHT MODULATION
NT PHASE MODULATION
NT PHASE SHIFT KEYING
NT PULSE CODE MODULATION
NT PULSE DURATION MODULATION
NT PULSE MODULATION
NT PULSE POSITION MODULATION
NT QUADRATURE AMPLITUDE MODULATION
NT QUADRATURE PHASE SHIFT KEYING
NT VELOCITY MODULATION

Controlling chaotic behavior in CO2 and other lasers
[AD-A264811] 01 p0174 N94-10870

To the theory of irregular auto modulation in electron beam-backward electromagnetic wave dynamic system
[DE93-620982] 01 p0133 N94-11030

Telemetering and telecommunications research
[NASA-CR-193235] 01 p0042 N94-11297

Experimental and theoretical investigations of Cs-Ba vapor tacitron inverter for power conditioning in space power systems
[DE93-012971] 01 p0048 N94-11372

Modulational stability of periodic solutions of the Kuramoto-Sivaskinsky equation
[NASA-CR-191502] 02 p0628 N94-12888

Controlling chaotic behavior in CO2 and other lasers
[AD-A266431] 03 p1040 N94-16546

Diffuse scattering and image contrast of tweed in superconducting oxides: A simulation and interpretation
[DE93-016131] 03 p1212 N94-16844

Nonlinear methods for communications
[AD-A267376] 03 p1001 N94-17019

Field-emitter arrays for RF vacuum microelectronics
[AD-A268397] 03 p1015 N94-17526

Plasma klystron amplifier
[AD-D015819] 04 p1395 N94-17903

Advanced optical fiber communication systems
[AD-A269120] 04 p1577 N94-18254

Extrathalamic modulation of cortical function
[AD-A270869] 04 p1507 N94-19783

Computational model of a magnetic modulator for copper lasers
[DE93-019603] 05 p1815 N94-20223

Stability analysis of unsteady ablation fronts
[DE93-019689] 05 p1819 N94-21839

Direct digital RF synthesis and modulation for MSAT mobile applications 06 p2285 N94-22804

An introduction to digital modulation and OFDM techniques
[BBC-RD-1993/10] 06 p2295 N94-24086

Automatic modulation recognition based on spatial pattern classification using artificial neural networks
[CTN-94-60897] 06 p2296 N94-24115

Modulation and synchronization technique for MF-TDMA system
[NASA-CR-194448] 06 p2304 N94-25266

Modulation Simulation Program: Programmer's manual, version 1.00
[DREO-16] 07 p2973 N94-27761

Modulation Simulation Program: Operator's manual, version 1.00
[DREO-16] 07 p2975 N94-27951

Tropospheric HO2 determination by FAGE 08 p3345 N94-28606

Modulation and coding for the Gaussian channel, possibly affected by fluctuations
[TELECOM-93-E-009] 09 p3840 N94-31169

A simple model for determining photoelectron-generated radiation scaling laws
[DE94-006130] 09 p3761 N94-32660

Long distance transmission of 15 Gb/s digital using subcarrier multiplexing and external modulation
[DE94-008298] 09 p3682 N94-32756

Automatic modulation recognition 09 p3686 N94-33153

Activities of the optoelectronics laboratory
[PB94-171196] 11 p4334 N94-36190

Attention and signal detection. A study of attention divided between visual and auditory signals
[PB94-170594] 11 p4298 N94-36215

Picosecond laser induced electric field modulation of carotenoid absorption bands
[DE94-009692] 12 p4512 N94-36524

MODULATION DOPED FETS
U MODFETS

MODULATION DOPING

Synthesis and properties of mismatched heterojunction/substrate interfaces
[AD-A272904] 05 p1760 N94-21229

MODULATION TRANSFER FUNCTION

Fundamental studies of radar scattering from water surfaces: The Lake Washington experiment
[NASA-CR-194030] 01 p0139 N94-12778

Image quality and the display modulation transfer function: Experimental findings
[AD-A274061] 07 p2679 N94-25773

Optical and image transmission through desert atmospheres
[AD-A276022] 09 p3742 N94-31496

MODULATORS
NT BRAGG CELLS
NT MODEMS

Variable rate transfer of optical information
[AD-D015758] 01 p0418 N94-10374

Controlling chaotic behavior in CO2 and other lasers
[AD-A264811] 01 p0174 N94-10870

Smart spatial light modulator research and development
[AD-A264928] 01 p0382 N94-11286

GaAs sigma-delta modulator modeling for Analog to Digital Converters (ADC's)
[AD-A263419] 01 p0144 N94-11516

Radiation effects on optoelectronic analog link for particle detectors
[DE93-015794] 02 p0793 N94-14529

Optical residue processing module
[AD-A267721] 03 p1188 N94-14940

Velocity matched millimeterwave electro-optic modulator
[AD-A267264] 03 p1188 N94-14957

Controlling chaotic behavior in CO2 and other lasers
[AD-A266431] 03 p1040 N94-16546

Four Frequency-Shift Keying (4-FSK) spread spectrum modulator and demodulator
[AD-A267433] 03 p1000 N94-16979

High-speed nonlinear switching mechanisms and devices for multi-gigabit data processing
[AD-A267753] 03 p1014 N94-17375

Optimal pulse modulator design criteria for plasma source ion implanters
[DE93-016465] 03 p1205 N94-17645

Spatial light modulators and applications: Summaries of papers presented at the Spatial Light Modulators and Applications Topical Meeting
[AD-A269452] 04 p1577 N94-18283

High efficiency low cost monolithic module for SARSAT distress beacons
[NASA-CR-194234] 04 p1315 N94-18852

Spice modeling of a FET-switched induction accelerator cell
[DE93-018662] 04 p1575 N94-18996

Computational model of a magnetic modulator for copper lasers
[DE93-019603] 05 p1815 N94-20223

Diagnostics and microelectronics
[DE94-003016] 07 p2784 N94-26777

Spatial light modulators with arbitrary quantum wells profiles
[AD-A275023] 08 p3499 N94-29114

Design and analysis of a low-loss linear analog phase modulator for deep space spacecraft X-band transponder applications 08 p3248 N94-29625

Optical Chopper Assembly for the Mars Observer 08 p3162 N94-29639

High-performance GaAs/AlGaAs optical phase modulators for microwave/photonic integrated circuits
[DE94-006361] 09 p3688 N94-31483

Fiber optic continuous true time-delay modulator
[AD-D016098] 09 p3883 N94-32720

High-performance GaAs/AlGaAs optical phase modulators for microwave photonic integrated circuits
[DE94-007376] 09 p3696 N94-32809

Phase-only 128x128 spatial light modulator based on LASLM technology
[AD-A277901] 10 p4141 N94-33591

Fiber optic transceiver for interfacing digital superconducting electronics
[DE94-008284] 10 p4040 N94-33842

Characterization of lithium niobate electro-optic modulators at cryogenic temperatures
[DE94-010059] 11 p4333 N94-35697

Design of a composite filter realizable on practical spatial light modulators
[NASA-CR-196297] 12 p4525 N94-37579

MODULATORS-DEMODULATORS
U MODEMS

MODULES
NT AIRLOCK MODULES
NT APOLLO LUNAR EXPERIMENT MODULE
NT COMMAND MODULES
NT ELECTRONIC MODULES
NT LANDING MODULES
NT LOCAL SCIENTIFIC SURVEY MODULE
NT LUNAR LANDING MODULES
NT SIM
NT SPACECRAFT DOCKING MODULES
NT SPACECRAFT MODULES

A tool for generation of expert system shells
[INPE-5493-TDI/510] 01 p0325 N94-11181

On-line upgrade of program modules using AdaPT
[NASA-CR-194331] 02 p0754 N94-14472

SAR sensor electronics: T/R modules 03 p0993 N94-15911

Research on stable, high-efficiency amorphous silicon multijunction modules
[DE93-010046] 04 p1467 N94-18518

Knowledge sources for an intelligent MCM analyzer
[AD-A269224] 04 p1542 N94-18887

Research on stable, high-efficiency amorphous silicon multijunction modules
[DE93-018220] 05 p1850 N94-22257

Module interconnection frameworks for a real-time spreadsheet
[AD-A273853] 07 p2956 N94-25588

Design and development of the second generation Mars Habitat 07 p2943 N94-25693

A modular approach to evaluation cryptographic protocols using Petri nets
[ISBN-0-315-85354-9] 07 p2972 N94-27595

A modular approach for automated sample preparation and chemical analysis 08 p3354 N94-30464

Modular Simulator System (MSS). System/segment specification for the generic modular simulator system-flight station module, volume 2
[AD-A276969] 09 p3588 N94-32313

Research on stable, high-efficiency amorphous silicon multijunction modules
[DE94-000298] 09 p3695 N94-32680

Laser drilling of vertical vias in silicon
[DE94-009250] 11 p4270 N94-35351

The development and application of composite complexity models and a relative complexity metric in a software maintenance environment 11 p4255 N94-35559

Amorphous silicon photovoltaic manufacturing technology, phase 2A
[DE94-006895] 12 p4461 N94-36476

MODULUS OF ELASTICITY

High temperature stability, interface bonding, and mechanical behavior in (beta)-NiAl and Ni3Al matrix composites with reinforcements modified by ion beam enhanced deposition
[DE93-013977] 01 p0398 N94-11115

An advanced test technique to quantify thermomechanical fatigue damage accumulation in composite materials
[NASA-CR-191147] 02 p0555 N94-13139

Micromechanical damage theories for brittle solids with interacting microcracks
[AD-A266348] 02 p0673 N94-13778

Optical and physical properties of the LiSrAlF6:Cr laser crystal
[DE93-014657] 02 p0808 N94-13881

Shock compression and quasielastic release in tantalum
[DE93-014566] 02 p0811 N94-14329

Experimental study of nonassociated flow and instability of frictional materials
[AD-A266421] 03 p1024 N94-16555

The determination of the Young moduli of a material after exposure to laser light and delineation of the zone of laser alterations
[IFTR-37/1991] 03 p1061 N94-17058

New test method to determine modulus of elasticity of rocket grain material
[AD-A269758] 04 p1377 N94-18758

Elastic properties of amorphous thin films studied by Rayleigh waves
[DE93-018375] 04 p1372 N94-19202

Molecular dynamics modeling of the mechanical behavior of metallic multilayers
[DE93-017972] 04 p1365 N94-19263

Metastable bcc phase formation in the Nb-Cr system
[DE93-018376] 05 p2012 N94-19926

Adaptation of model parameters of a rail model at measured rail compliances
[ILR-MITT-274(1992)] 05 p1831 N94-21153

Results of the second Round Robin on opening-load measurement conducted by ASTM Task Group E24.04.04 on crack closure measurement and analysis
[NASA-TM-109032] 05 p1832 N94-21624

Molecular dynamics modeling of the mechanical behavior of metallic multilayers
[DE93-019947] 05 p1694 N94-21921

Miniaturized disk-bend testing, nano-indentation, and the microstructure of ion-irradiated titanium aluminides
[DE93-040600] 05 p1697 N94-22559

FR/GE/UK/US International Test Operations Procedure (ITOP) 1-1-050 development of laboratory vibration test schedules
[AD-A273887] 07 p2836 N94-25732

Users manual for CATNIP: A Computer Analysis Tool for Normal Impact Penetration
[DE94-003671] 07 p2962 N94-26371

Effects of physical aging on long-term behavior of composites 07 p2712 N94-27897
Alumina ceramic: A cost effective replacement for titanium in deep submergence pressure housings
[AD-A275640] 08 p3212 N94-28641
Thermal expansion and elastic anisotropy in single crystal Al2O3 and SiC reinforcements
[NASA-TM-106516] 08 p3214 N94-29105
Experimental determination of orthotropic elastic constants
[FFA-TN-1991-35] 08 p3215 N94-29424
Creep and physical aging of PVC: Dependence on stress and temperature
[NPL-DMM(A)-115] 08 p3217 N94-29886
Resonant ultrasound spectroscopy for elastic constant measurements
[DE94-005016] 08 p3480 N94-30098
A class of inclusion problems for the strengthening of brittle and ductile composites 08 p3186 N94-30959
Evaluation of nondestructive inspection techniques for quality control of alumina-ceramic housing components
[AD-A276220] 09 p3730 N94-31065
Considering ties elasticities in high frequency rail dynamics
[ILR-MITT-281(1993)] 09 p3733 N94-31375
Elastic modulus measurements of LDEF glasses and glass-ceramics using a speckle technique
[NASA-CR-195911] 09 p3653 N94-31851
Ceramic Technology Project database
[DE94-008494] 09 p3659 N94-32632

MOHR CIRCLES
U FRACTURE MECHANICS

MOIRE EFFECTS
Steep geometric grating for use in moire interferometry
[AD-A268759] 04 p1453 N94-18328
Plane stress stable crack growth and J-integral/HRR field
[AD-A275761] 08 p3317 N94-28761

MOIRE FRINGES
A Fourier transform microscope for x ray and/or gamma ray imaging
[AD-D015742] 02 p0791 N94-13664
Steep geometric grating for use in moire interferometry
[AD-A268759] 04 p1453 N94-18328

MOIRE INTERFEROMETRY
Optical systems for the visualization of fluid and solid transparent media under microgravity conditions
03 p0978 N94-16081
J-integral and HRR field associated with stable crack growth in thin aluminum SEN specimen
[AD-A267879] 03 p0960 N94-17041
Steep geometric grating for use in moire interferometry
[AD-A268759] 04 p1453 N94-18328
A comparative evaluation of in-plane shear test methods for laminated graphite-epoxy composites
[NASA-CR-193808] 04 p1456 N94-19095
Plane stress stable crack growth and J-integral/HRR field
[AD-A275761] 08 p3317 N94-28761
Fracture process zone of brittle composites
08 p3182 N94-29876
Four beam interferometer manual: Operating instructions for the INEL diffraction Moire interferometer
[DE94-010772] 12 p4453 N94-36452

MOISTURE
NT ATMOSPHERIC MOISTURE
NT SOIL MOISTURE
Moisture meter evaluation
[DE93-016581] 02 p0652 N94-14534
Durability predictions for adhesively bonded joints in humid environments
[AD-A271177] 05 p1830 N94-20001
Humidity effects on soluble core mechanical and thermal properties (polyvinyl alcohol/microballoon composite) type CG extendospheres, volume 2
[NASA-CR-193893] 06 p2229 N94-24224
Package integrity measurement technology and quality assurance
[AD-A273881] 07 p2834 N94-25727
Adsorption of water to the metal/polymer interface studied by neutron and x ray reflectivity
[DE94-005578] 09 p3651 N94-31649
Evaluating plastic assembly processes for high reliability applications using HAST and Assembly Test Chips
[DE94-010750] 12 p4439 N94-37363

MOISTURE CONTENT
NT ATMOSPHERIC MOISTURE
Photochemical modelling of Venus clouds using Pioneer Venus data
[NASA-CR-194108] 01 p0434 N94-10823
Microtektite-like glass spherules in Late Devonian (367 MA) shales 01 p0461 N94-12160
Analytic expression for epithermal neutron spectra amplitudes as a function of water content
01 p0473 N94-12227
Cloud liquid water content over the Pacific Ocean tropical zone derived from ship microwave radiometric measurement 01 p0225 N94-12743
Measuring surface fluxes in CAPE
[NASA-CR-193664] 02 p0711 N94-12788
Moisture meter evaluation
[DE93-016581] 02 p0652 N94-14534
An assessment of acid fog
[DE93-009347] 03 p1095 N94-15940
A detailed model for simulation of catchment scale subsurface hydrologic processes
[PAPER-92WR02333] 03 p1084 N94-16032
Water in Earth's mantle: Hydrogen analysis of mantle olivine, pyroxenes and garnet using the SIMS
03 p1104 N94-16336
Bright soil units on Mars determined from ISM imaging spectrometer data 03 p1295 N94-16430
A snow wetness retrieval algorithm for SAR
03 p1075 N94-16732
Microwave (SSM/I) Estimates of the Precipitation Rate to Improve Numerical Atmospheric Model Forecasts
[NASA-CR-193566] 04 p1491 N94-18602
Physical retrieval of precipitation water contents from Special Sensor Microwave/Imager (SSM/I) data. Part 1: A cloud ensemble/radiative parameterization for sensor response (report version) 04 p1491 N94-18604
Physical retrieval of precipitation water contents from Special Sensor Microwave/Imager (SSM/I) data. Part 2: Retrieval method and applications (report version)
04 p1491 N94-18605
Forecast model applications of retrieved three dimensional liquid water fields 04 p1492 N94-18606
Relationship of attenuation in a vegetation canopy to physical parameters of the canopy
05 p1729 N94-20450
Comparison of cloud microphysical parameters derived from surface and satellite measurements during FIRE phase 2 05 p1873 N94-22306
Normalized vertical ice mass flux profiles from vertically pointing 8-mm-wavelength Doppler radar
05 p1879 N94-22334
An overview of a model rotor icing test in the NASA Lewis Icing Research Tunnel
[NASA-TM-106471] 06 p2166 N94-23299
Spatial and temporal variability of soil temperature, moisture and surface soil properties
[NASA-CR-194109] 06 p2401 N94-23337
Methodology for the assessment of surface resistance and soil water storage variability at mesoscale based on remote sensing measurements. A case study with HAPEX-EFEDA data. UNESCO-International Hydrological Program 4
[PB94-111721] 06 p2386 N94-23734
Groundtruth collection for the JPL-SAR and ERS-1 campaign in Flevoland and Veluwe, Netherlands, 1991
[BCRS-92-26] 06 p2386 N94-23755
Water cycle research associated with the CaPE hydrometeorology project (CHymP
06 p2416 N94-24414
Drying deformable media: Kinetics, shrinkage and stresses
[ETN-94-95314] 06 p2236 N94-25302
Package integrity measurement technology and quality assurance
[AD-A273881] 07 p2834 N94-25727
Mechanism of mechanical fatigue of silica glass
[DE94-003165] 07 p2753 N94-26783
Cloud liquid water content measurement tests using dual-wavelength radar
[PB94-125960] 07 p2896 N94-26959
Time domain reflectometry for measuring bulk soil electrical conductivity and comparison with the Em38 instrument
[PB94-125432] 07 p2881 N94-27052
Global patterns of cloud optical thickness variation with temperature and the implications for climate change
08 p3374 N94-29972
Recurvature dynamics of a typhoon
[AD-A276792] 09 p3784 N94-32164
Effects of interphases on the mechanical, thermal and hygromechanical response of fiber-reinforced composites 09 p3624 N94-32496
Development and testing of improved techniques for modeling the hydrologic cycle in a mesoscale weather prediction system
[AD-A277416] 09 p3786 N94-32921
The importance of environmental conditions in reflectance spectroscopy of laboratory analogs for Mars surface materials 09 p3944 N94-33195
Production of long-term global water vapor and liquid water data set using ultra-fast methods to assimilate multi-satellite and radiosonde observations
[NASA-CR-195981] 11 p4293 N94-35499

MOISTURE DETECTORS
U MOISTURE METERS

MOISTURE METERS
NT HYGROMETERS
Moisture meter evaluation
[DE93-016581] 02 p0652 N94-14534

MOISTURE RESISTANCE
Polyimides containing pendent siloxane groups
[NASA-CASE-LAR-14638-1] 08 p3215 N94-29555

MOL (ORBITAL LABORATORIES)
U MANNED ORBITAL LABORATORIES

MOLABS
U LUNAR MOBILE LABORATORIES

MOLDING MATERIALS
Universal adjustable mould for antenna reflectors
01 p0059 N94-10027
Fabrication of advanced design (grooved) cermet anodes
[DE93-014590] 03 p1012 N94-16765
Machinable oxide ceramic
[AD-D015927] 05 p1699 N94-20017
Improved ceramic slip casting technique --- application to aircraft model fabrication
[NASA-CASE-LAR-14471-1] 05 p1702 N94-20377
Technique to predict the curing behaviour of unsaturated polyester materials
[PB94-124856] 07 p2748 N94-25892
Modelling the inhibition cure behaviour of unsaturated polyester moulding materials
[PB94-124864] 07 p2748 N94-25893
Stress relaxation in dough moulding compounds
[PB94-124872] 07 p2748 N94-25894

MOLDS
Universal adjustable mould for antenna reflectors
01 p0059 N94-10027
Remelting of Fe-C-Si-alloy in a ceramic mold skin
03 p0945 N94-15169
Production of an amorphous Fe(75)Si(10)B(15) sheet by a metallic mold casting method and its properties
07 p2746 N94-28170
Advanced manufacturing technology for polymer composite structures in Japan 12 p4422 N94-36968

MOLECULAR ABSORPTION
The effect of turbulence and molecular relaxation on sonic boom signatures 10 p3976 N94-33497
Integration of the Molecular Sieve Oxygen Generating System (MSOGS) into the UH-60Q MEDEVAC Blackhawk
[AD-A277668] 10 p4099 N94-33589

MOLECULAR BEAM EPITAXY
Crack suppression in GaInSb buffer layers initially under tensile stress
[DE93-012839] 01 p0396 N94-10745
Rapid thermal processing for strained-layer semiconductor devices
[DE93-013754] 01 p0396 N94-10809
Memory effects in the organometallic chemical beam epitaxy of compound semiconductors
[NASA-CR-193106] 01 p0399 N94-11439
Ballistic electron transport studies using BEEM
[AD-A266029] 01 p0369 N94-12395
Intrinsic and interfacial recombination in OMVPE- and MBE-prepared GaAs/Al(x)Ga(1-x)As heterostructures
[DE93-009844] 02 p0809 N94-14083
Evolving surface cusps during strained-layer epitaxy
[DE93-015430] 02 p0813 N94-14478
Magneto-optic superlattice thin films: Fabrication, structural and magnetic characterization
03 p0974 N94-14982
High temperature superconductivity
[AD-A267006] 03 p1008 N94-15635
Laboratory for x ray optics
[AD-A267149] 03 p1189 N94-15735
A high flux radical beam diamond growth
[AD-A266754] 03 p1207 N94-15955
JSEP fellowship
[AD-A266568] 03 p1211 N94-16800
Growth and doping of Al(x)Ga(1-x)N films by electron cyclotron resonance assisted molecular beam epitaxy
[AD-A267305] 03 p1212 N94-16992
Nitride semiconductors for ultraviolet detection
[AD-A267877] 03 p1012 N94-17040
Photo-assisted epitaxial growth for III-V semiconductors
[AD-A267889] 03 p1213 N94-17042
Curved grating fabrication techniques for concentric-circle grating, surface-emitting semiconductor lasers 03 p1045 N94-17349
Interface properties of wide bandgap semiconductor structures
[AD-A268269] 03 p1215 N94-17377
Precise flux control for lattice matched superlattice materials
[AD-A268254] 03 p1215 N94-17417

Low temperature deposition and characterization of n- and p-type silicon carbide thin films and associated ohmic and Schottky contacts
[AD-A267966] 03 p0973 N94-17490
Epitaxial iron films
[AD-A268286] 03 p1217 N94-17579
Mechanical properties of interfaces and superlattices
[AD-A268591] 03 p1217 N94-17606
Kinetic aspects of lattice mismatch in molecular beam epitaxial growth on planar and patterned substrates
[AD-A270424] 04 p1597 N94-18506
In-situ growth monitoring of molecular beam epitaxy processes
[AD-A269287] 04 p1598 N94-18616
Isolation mechanisms in III-V devices
[AD-A271197] 04 p1605 N94-19717
Investigation of quantum effects in heterostructures
[AD-A270938] 05 p2011 N94-19817
Theory of energy-assisted epitaxy; theory of ordered semiconductor alloys: In(1-x)Tl(x)Sb as a long-wave infrared material
[AD-A271007] 05 p2012 N94-19835
Common Themes and Mechanisms of Epitaxial Growth, volume 312 --- Materials Research Society symposium proceedings
[AD-A270513] 05 p2013 N94-19967
Monocrystalline germanium film on sapphire
[AD-D015925] 05 p2017 N94-20348
Center for the integration of optical computing
[AD-A271874] 05 p1899 N94-20469
Surface treatment of InP and contribution to the optimization of the InP(p)/InP(p) regrown interfaces grown by GSMBE
[ECL-92-48] 05 p2018 N94-20598
Ga delta-doping layers in silicon
[PB93-224632] 06 p2561 N94-23222
Method of forming silicon structures with selectable optical characteristics
[NASA-CASE-NPO-18625-1-CU] 06 p2563 N94-23972
On the origin of 1/f noise in epitaxial GaAs
[ISBN-9-09-006067-7] 06 p2566 N94-25297
Ultra-high aggregate bandwidth two-dimensional multiple-wavelength diode laser arrays
[AD-A274018] 07 p2815 N94-25756
Investigation of a normal incidence high-performance p-type strained layer In(0.3)Ga(0.7)As / In(0.52)Al(0.48) as quantum well infrared photodetector
[AD-A274854] 07 p3055 N94-26188
MBE grown 3 to 5 strain relaxed buffer layers and superlattices characterized by atomic force microscopy
[DE94-002931] 07 p3056 N94-26308
Nitride semiconductors for ultraviolet detection
[AD-A274246] 07 p3060 N94-26840
Pseudomorphic semiconducting heterostructures from combinations of AlN, GaN and selected SiC polytypes: Theoretical advancement and its coordination with experimental studies of nucleation, growth, characterization and device development
[AD-A274247] 07 p3061 N94-26841
Low temperature deposition and characterization of N- and p-type silicon carbide thin films and associated ohmic and Schottky contacts
[AD-A274345] 07 p2754 N94-26974
Visible light emitting materials and injection devices
[AD-A274418] 07 p2786 N94-27079
Observation of stimulated emission from an MBE grown GaN film on sapphire
[DE94-003638] 07 p3068 N94-27724
Exploratory research for a high temperature superconducting integrated circuit
[AD-A275798] 08 p3262 N94-28767
Spatial light modulators with arbitrary quantum wells profiles
[AD-A275023] 08 p3499 N94-29114
Research on the atomic layer-by-layer growth of high-temperature superconductor thin films at the Institute of Scientific and Industrial Research, Japan
[DE94-003739] 08 p3519 N94-30611
Growth and characterization of III-V semiconductors with rare earth impurities for optoelectronic devices
[AD-A276021] 09 p3896 N94-31455
Semiconductor microcavity lasers
[DE94-006143] 09 p3716 N94-31622
High speed, strained layer, multiquantum well, GaInAsP and GaAs lasers and heterostructures
[AD-A277287] 09 p3719 N94-32608
Compositions and chemical bonding in ceramics by quantitative electron energy-loss spectrometry
[DE94-007208] 09 p3659 N94-32640
Research in the optical sciences
[AD-A278271] 09 p3884 N94-33140
Development of ultra-low noise, high performance 3 to 5 Quantum Well Infrared Photodetectors (QWIPs) for focal plane array staring image sensor systems
[AD-A278861] 11 p4642 N94-36385
Low temperature materials --- indium gallium arsenides
[AD-A278703] 12 p4533 N94-36755
The MBE growth and optical quality of BaTiO3 and SrTiO3 thin films on MgO
[DE94-011468] 12 p4538 N94-37570

MOLECULAR BEAMS

In situ secondary ion mass spectrometry analysis
[DE93-012185] 01 p0076 N94-11140
Development of a molecular beam technique to study early solar system silicon reactions 01 p0432 N94-12224
Lawrence Berkeley Laboratory Chemical Sciences Division
[DE93-015260] 02 p0851 N94-14401
Molecular beam studies of reaction dynamics
[DE93-015035] 03 p1181 N94-15995
Metal/ceramic interfaces: Relationships between structure and chemistry
[AD-A268792] 04 p1369 N94-18188
Flame structure studies of a lean 20-torr H2/N2O/Ar flame employing molecular beam mass spectrometry
[AD-A268889] 04 p1349 N94-18456
The Fourteenth Symposium on Molecular Beams
[AD-A268721] 04 p1568 N94-18787
Crossed molecular beam studies of atmospheric chemical reaction dynamics
[DE93-019246] 04 p1478 N94-19303
Transport in microstructures in the microwave and millimeter-wave regime
[AD-A271875] 05 p2017 N94-20470
Theoretical studies of a molecular beam generator
[NASA-CR-194779] 06 p2540 N94-23485
Molecular beam mass spectrometry studies of the chemical vapor deposition of diamond
[DE94-003802] 07 p3049 N94-25601
Investigation of a normal incidence high-performance p-type strained layer In(0.3)Ga(0.7)As / In(0.52)Al(0.48) as quantum well infrared photodetector
[AD-A274854] 07 p3055 N94-26188
Trace organic chemical detection using an ultraviolet excitation molecular beam fluorometer
[DE94-002649] 07 p2704 N94-27708
Dynamics of metastable states in supersonic beams
[ITN-94-85232] 07 p3028 N94-27760
Surface structure and stereochemical properties of self-assembled monolayer materials
[DE94-004960] 08 p3484 N94-28578
RHEED studies of the nucleation, growth, and mobility of Ag atoms on the Si(111)7 x 7 surface
[DE94-005551] 08 p3521 N94-30899
Metal cluster-rare gas van der Waals complexes: Microscopic models of physisorption
[DE94-008134] 09 p3873 N94-32797
Ultrafast chemical dynamics of reactions in beams
[AD-A278939] 11 p4323 N94-35805
Molecular beam surface analysis
[DE94-010773] 12 p4406 N94-36453
Theoretical studies of a molecular beam generator
[NASA-CR-196306] 12 p4522 N94-37508

MOLECULAR BIOLOGY

Solitons and 1/f noise in molecular chains
[DE93-622898] 02 p0778 N94-12879
Gordon Research Conference on Chronobiology, 1991
[AD-A266354] 02 p0728 N94-13698
The role of chemical inhibition of gap junctional intercellular communication in toxicology
[AD-A269251] 04 p1502 N94-18924
Microgravity research in plant biological systems: Realizing the potential of molecular biology 04 p1503 N94-19216
High resolution electron crystallography of protein molecules
[DE93-040114] 05 p1884 N94-19826
A complex systems approach to computational molecular biology
[DE93-040062] 05 p1884 N94-19866
Application of molecular modeling to biological processing
[AD-A272612] 05 p1974 N94-21185
Applications of the Aurora parallel PROLOG system to computational molecular biology
[DE93-041166] 06 p2420 N94-23468
Molecular biological studies on the human radioresistance and drug resistance
[DE93-632682] 07 p2910 N94-26549
NCVS, volume 5
[AD-A274975] 07 p2902 N94-27165
Space radiation health research, 1991-1992
[NASA-TM-109721] 07 p2932 N94-27556
Neutrons in biology
[DE94-701085] 07 p2903 N94-27862
Biodiesel from aquatic species
[DE94-000275] 08 p3225 N94-30038
Lattice gas simulations of replicating domains
[DE94-005008] 08 p3200 N94-30748
Neural network definitions of highly predictable protein secondary structure classes
[DE94-006234] 09 p3834 N94-32175
Future directions of nonlinear dynamics in physical and biological systems. (Physica D nonlinear, volume 68, number 1)
[AD-A278085] 09 p3794 N94-33250
Enzymology and molecular biology of cell wall biosynthesis
[DE94-008585] 10 p4094 N94-34008
High resolution electron diffraction analysis of structural changes associated with the photocycle of bacteriorhodopsin
[DE94-011800] 12 p4479 N94-37156

MOLECULAR BONDS

U CHEMICAL BONDS

MOLECULAR CHAINS

Structural and electronic properties of atomic chains
[DE93-617758] 01 p0366 N94-11349
Theoretical treatment of the bulk and surface properties of fluids containing long, flexible molecules
[DE93-015560] 02 p0575 N94-12861
Solitons and 1/f noise in molecular chains
[DE93-622898] 02 p0778 N94-12879
Computer simulations for the adsorption of polymers onto surfaces
[DE93-016667] 02 p0577 N94-13070
Chain propagation/step propagation polymerization chemistry. The preparation of solvent resistant well phase-separated thermoplastic elastomers
[AD-A271128] 05 p1699 N94-20016
Light scattering studies of an electrorheological fluid
[DE93-019419] 05 p1700 N94-20315
Spatial organization of polymer chains in a crystallizable diblock polyethylene and polystyrene
[AD-A271862] 05 p1702 N94-20463
Atomic-scale chemistry of metal surfaces
[REPT-A-2657] 07 p3012 N94-25636
Localization properties of one-dimensional electrified chains
[DE94-603672] 07 p3067 N94-27635

MOLECULAR CLOUDS

Cosmological gamma-ray burst model
[NASA-CR-193368] 01 p0484 N94-10507
The excitation of cyanogen and ionized carbon in interstellar and extragalactic gas clouds 01 p0426 N94-11582
Initiating solar system formation through stellar shock waves 01 p0448 N94-12090
UV extinction properties of carina nebular dust
[NASA-CR-189308] 02 p0835 N94-13233
Analysis of interstellar cloud structure based on IRAS images
[NASA-CR-194341] 02 p0836 N94-13332
Search for x ray emitting young stars outside of massive molecular clouds
[NASA-CR-193609] 02 p0830 N94-13462
The origin of the far-infrared emission from galactic molecular clouds 02 p0848 N94-13654
Analysis of the IUE spectra of the strongly interacting binary beta Lyrae
[NASA-CR-194118] 02 p0833 N94-14493
Boundary conditions for the paleoenvironment: Chemical and physical processes in the pre-solar nebula
[NASA-CR-194418] 03 p1298 N94-15421
ROSAT-IUE observations of symbiotic stars. The x ray morphology of high latitude associations
[NASA-CR-194616] 03 p1236 N94-16492
Collisional dynamics of perturbed particle disks in the solar system
[NASA-CR-193584] 03 p1239 N94-16648
The molecular environment of S106 IR
[MPE-PREPRINT-241] 04 p1622 N94-19417
Coagulation of grains in static and collapsing protostellar clouds 05 p2085 N94-20865
Factor analysis as a tool for spectral line component separation 21cm emission in the direction of L1780 05 p1965 N94-22536
Fragmentation of magnetized filamentary interstellar clouds 05 p2008 N94-22687
Gravitational instability of magnetized filamentary clouds. 1: Helical magnetic fields 05 p2008 N94-22688
Gravitational instability of magnetized filamentary clouds. 2: Rotation 05 p2009 N94-22689
Magnetic field dissipation and contraction of molecular clouds
[REPT-337] 06 p2603 N94-24976
CO-to-H2 conversion factor in dwarf irregular galaxies
[REPT-333] 06 p2603 N94-24985
High spatial resolution observations of CO in CRL 618
[REPT-334] 06 p2604 N94-24986
The Nobeyama millimeter array survey for protoplanetary disks around protostar candidates and T Tauri stars in Taurus
[REPT-336] 06 p2604 N94-24987

Investigations of the dynamical evolution of protoplanetary nebulae
[NASA-CR-195278] 07 p3105 N94-27428
Modulating terrestrial impacts from Oort cloud comets by the adiabatically changing galactic tides
07 p2890 N94-28305
The role of cloud collisions in N-body simulations of disk galaxies 08 p3545 N94-29755
Circumstellar material around young stars in Orion
09 p3930 N94-31133
Theory of protostellar accretion disks
09 p3931 N94-31136
Evolution of dynamo-generated magnetic fields in accretion disks around compact and young stars
09 p3931 N94-31138
CO observations in external galaxies and gas mass determination 09 p3925 N94-31790
A study of physical conditions, radiative transfer and shocks in the interstellar medium
09 p3937 N94-31963

MOLECULAR CLUSTERS
Many-body quantum mechanical studies of molecular clusters
[AD-A266624] 03 p1180 N94-15727
Vibrational and electronic properties of clusters and ultrathin films
[DE93-012291] 04 p1367 N94-17678
Embedded microclusters in zeolites and cluster beam sputtering: Simulation on parallel computers
[DE94-000741] 05 p1701 N94-20352
Molecular Science Research Center
[DE94-007464] 09 p3871 N94-32605
Metal cluster alloys and oxides: Elucidating structural and electronic effects in governing the reactivity and catalytic role of matter in finite dimensions
[DE94-010224] 11 p4328 N94-36298
Status review and accomplishments of the Materials Research Center at the University of Pittsburgh
[AD-A280422] 12 p4399 N94-37214
Quantum confinement in GaP nanoclusters
[DE94-013119] 12 p4536 N94-37290
Photodissociation and spectroscopy of gas phase bimetallic clusters
[DE94-012607] 12 p4419 N94-37438

MOLECULAR COLLISIONS
Collision-induced squeezing in a harmonic oscillator
01 p0379 N94-10597
Theoretical molecular studies of astrophysical interest
[NASA-CR-193300] 02 p0838 N94-13781
Lawrence Berkeley Laboratory Chemical Sciences Division
[DE93-015260] 02 p0851 N94-14401
Single-collision studies of energy transfer and chemical reaction
[DE93-017603] 03 p1182 N94-16121
Atomic processes in hydrogen and deuterium negative ion discharges
[DE93-013432] 03 p1183 N94-16817
Femtosecond Fourier-transform spectroscopy of low-frequency intermolecular motions in weakly interacting liquids
[DE93-017312] 04 p1566 N94-18085
The quantum dynamics of electronically nonadiabatic chemical reactions
[NASA-CR-194309] 04 p1568 N94-18837
Calculation of molecular excitation rates
[NASA-CR-193782] 04 p1571 N94-19236
Collisions of molecules with clusters: A quasiclassical study
[DE93-018614] 05 p1971 N94-20050
Non-adiabatic effects in low-energy electron-molecule scattering
[DE93-040485] 05 p1976 N94-21968
Vibrational energy transfer within the B 3Pi (O(+) sub u) state of 79BR2 upon collision with N2, O2, NO, and SF6
[AD-A273905] 07 p3011 N94-25589
International bulletin on atomic and molecular data for fusion. No. 42-45, Mar. 1991 - Dec. 1992
[DE94-601817] 07 p3045 N94-26946
International bulletin on atomic and molecular data for fusion. No. 46
[DE94-601818] 07 p3023 N94-26947
Theoretical studies of zirconium and carbon clusters with molecular dynamics simulations
[DE94-005276] 09 p3862 N94-31146
Spectroscopic study of the molecular collisions (hydrogen-nitrogen and hydrogen-oxygen) at energies of several MeV
[ISBN-0-315-86794-9] 09 p3867 N94-31753
Analysis of forward and inverse problems in chemical dynamics and spectroscopy
[DE94-007607] 09 p3635 N94-32140
Time-resolved IR spectroscopy, energy transfer, and state-to-state collision dynamics of atmospheric species
[AD-A277372] 09 p3773 N94-32338
Energy transfer properties and mechanisms
[DE94-007403] 09 p3636 N94-32594
Charge-changing collision cross sections of low-energy carbon ions with carbon containing molecules
[DE94-727628] 10 p4137 N94-33935
Comment on observation of the striking departure from velocity proportionality in low-energy electronic stopping
[DE94-009821] 10 p4138 N94-34242
A two-dimensional model for collisional energy transfer in bimolecular ion-molecule dynamics
[AD-A278913] 11 p4321 N94-35589
State-to-state dynamics of molecular energy transfer
[DE94-009651] 11 p4324 N94-35816

MOLECULAR DIFFUSION
Why does preferential diffusion strongly affect premixed turbulent combustion? 01 p0081 N94-12319
Mapping closures for turbulent combustion
[AD-A265671] 01 p0079 N94-12378
Reaction and diffusion in turbulent combustion
[DE93-017085] 03 p0943 N94-15146
The influence of an electric field on the kinetics of nucleation
[IFTR-2/91] 03 p1213 N94-17046
Defects in GaAs bulk crystals and multi-layers caused by In diffusion
[DE93-016968] 04 p1595 N94-18054
A database of selected transport coefficients for combustion studies
[DE93-041278] 05 p1678 N94-19889
Model for liquid boron oxide droplet gasification in H/O/C/F combustion environments
[AD-A272911] 05 p1682 N94-21243
Combustion in turbulent jets and buoyant flames
[PB93-202372] 05 p1682 N94-21452
Modeling of outgassing and matrix decomposition in carbon-phenolic composites
[NASA-CR-194741] 05 p1676 N94-21743
A two-dimensional dispersion module for the TOUGH2 simulator
[DE94-002262] 06 p2335 N94-24655
Molecular aspects of transport in thin films of controlled architecture
[DE94-004552] 08 p3211 N94-28457
Effects of diffusion and inertia on chaotic mixing: A computational and experimental study
08 p3488 N94-29903
Lattice gas simulations of replicating domains
[DE94-005008] 08 p3200 N94-30748
Flooded cell permeation testing of elastomers
[AD-A277698] 10 p4026 N94-33438

MOLECULAR DISSOCIATION
U DISSOCIATION

MOLECULAR DYNAMICS
Computer-aided molecular design of fire resistant aircraft materials 01 p0019 N94-10779
A new decomposition strategy for parallel bonded molecular dynamics
[DE93-009839] 01 p0366 N94-11284
Parallel molecular dynamics with the embedded atom method
[DE93-010683] 01 p0367 N94-11455
A molecular dynamics simulation code ISIS
[DE93-753187] 01 p0368 N94-11592
Solvent dynamical effects in electron transfer: Molecular dynamics simulations of reactions in methanol
[AD-A266061] 01 p0369 N94-12420
Molecular dynamics simulation of electronically excited polyatomic molecules
[DE93-623045] 02 p0781 N94-13225
Computational diagnostics for detecting phase transitions during nanoindentation
[DE93-016536] 02 p0813 N94-14439
Particle simulations on massively parallel machines
[DE93-015644] 03 p1157 N94-14927
Evaporation kinetics of Mg2SiO4 crystals and melts from molecular dynamics simulations
03 p1219 N94-16331
A molecular dynamics simulator for optimal control of molecular motion
[AD-A266572] 03 p1183 N94-16722
Crystalline beam ground state
[DE93-014331] 03 p1211 N94-16827
Continuum solvent models for computational chemistry
[DE93-016329] 03 p0953 N94-17660
Numerical methods for molecular dynamics
[DE93-018321] 04 p1566 N94-18179
Computer simulation of macromolecular crystals and their defects
[DE93-015213] 04 p1596 N94-18192
Molecular dynamics modeling of the mechanical behavior of metallic multilayers
[DE93-017972] 04 p1365 N94-19263
Embedded microclusters in zeolites and cluster beam sputtering: Simulation on parallel computers
[DE94-000741] 05 p1701 N94-20352
Integral equation calculation of solvent activation free energies for electron and proton transfer reactions
[AD-A272665] 05 p1681 N94-21216
Molecular dynamics modeling of the mechanical behavior of metallic multilayers
[DE93-019947] 05 p1694 N94-21921
Transferable tight-binding parameters: An application to Ni and Ni-Al alloys
[DE94-001044] 05 p1695 N94-22023
Microscopic and macroscopic dynamics
[DE93-019576] 05 p1937 N94-22042
Computer simulation of molecular response at a shock front
[DE94-001050] 05 p1977 N94-22396
Smoothed-particle hydrodynamics and nonequilibrium molecular dynamics
[DE94-001059] 05 p1977 N94-22400
Fracture simulations via massively parallel molecular dynamics
[DE93-040159] 06 p2374 N94-22871
Calculations of Bose-Einstein correlations from Relativistic Quantum Molecular Dynamics
[DE94-000794] 06 p2569 N94-23453
Momentum loss in proton-nucleus and nucleus-nucleus collisions
[NASA-TP-3405] 06 p2540 N94-24305
The torsion space nucleic acids molecular mechanics program DUPLEX: Surveying conformation space by potential energy minimization
[DE94-002441] 06 p2563 N94-24567
Integral equations for the microstructures of supercritical fluids
[DE94-002460] 06 p2535 N94-24569
Free energy profiles for Li(+) and I(-) ions approaching Pt(100) surface: A molecular dynamics study
[AD-A273455] 06 p2536 N94-24675
Structures of Cl(-)(H2O)(n) and F(-)(H2O)(n) (n equal to 2,3...15) clusters: Molecular dynamics computer simulations
[AD-A273474] 06 p2537 N94-24940
Fast parallel algorithms for short-range molecular dynamics
[DE93-018519] 07 p3016 N94-26033
Modeling defect production in high energy collision cascades
[DE94-003810] 07 p3017 N94-26049
How reliable is the HMSA integral equation for the pair structure of supercooled and amorphous mixtures?
[DE94-601543] 07 p3006 N94-26411
Nanoscale plasticity in silica glass
[DE94-004212] 07 p2751 N94-26554
A semiclassical reactive flux method for the calculation of condensed phase activated rate constants
[AD-A274850] 07 p3020 N94-26562
Modeling Group 4 elements with new transferable tight-binding models
[DE94-000770] 07 p3059 N94-26695
International journal of quantum chemistry. Quantum Chemistry Symposium Number 27: Proceedings of the International Symposium on Atomic, Molecular, and Condensed Matter Theory and Computational Methods
[AD-A274352] 07 p3023 N94-26926
First principles calculations for the cleaved and annealed Ge(111) surfaces
[DE93-617048] 07 p3066 N94-27347
Computer simulation of aqueous Na-Cl electrolytes
[DE94-002622] 07 p3030 N94-28001
Experimental and theoretical studies of molecular solids
[AD-A275511] 08 p3485 N94-28668
Computer simulation of molecular interactions in supercritical solvents
[AD-A274977] 08 p3486 N94-29087
Nanodislocation structures generated in shocked crystals 08 p3514 N94-29915
Exclusive many-particle diffusion in disordered media and correlation functions for random vertex models
[DE94-608134] 08 p3525 N94-30121
Theoretical studies of solid-fluid phase equilibria
[DE94-006406] 08 p3226 N94-30708
Molecular dynamics simulations of dense plasmas
[DE94-005082] 08 p3509 N94-30752
Theoretical studies of zirconium and carbon clusters with molecular dynamics simulations
[DE94-005276] 09 p3862 N94-31146
Molecular dynamics computer simulations of charged metal electrode-aqueous electrolyte interfaces
[AD-A276401] 09 p3863 N94-31237
The threshold energy for defect production in SiC: A molecular dynamic study
[DE94-007123] 09 p3896 N94-31499
Modern integral equation techniques for quantum reactive scattering theory
[DE94-007039] 09 p3857 N94-31639
Atomic and molecular data needs for fusion
[DE94-006555] 09 p3870 N94-32177

Chemical structure and kinetics at liquid/solid interfaces
[AD-A277112] 09 p3636 N94-32304
Point defect production, geometry, and stability in silicon: A molecular dynamics simulation study
[DE94-008292] 09 p3903 N94-32411
Wave packet studies of the vibrational predissociation of three and four-atom van der Waals complexes
[DE94-007623] 09 p3871 N94-32598
Chemisorbed-molecule potential-energy surfaces and electronically-stimulated processes
[DE94-007932] 09 p3719 N94-32603
Experimental investigations and molecular dynamics simulations of radiation induced surface damage
[AD-A277323] 09 p3871 N94-32621
Molecular interactions in dilute supercritical mixtures: Molecular dynamics investigation
[DE94-007610] 09 p3872 N94-32644
Future directions of nonlinear dynamics in physical and biological systems. (Physica D nonlinear, volume 68, number 1)
[AD-A278085] 09 p3794 N94-33250
High resolution molecular spectroscopy of atmospheric species
[AD-A278382] 09 p3776 N94-33351
Simulation of rotary-drum and repose tests for frictional spheres and rigid sphere clusters
[DE94-008094] 10 p4044 N94-33841
Object-oriented particle simulation on parallel computers
[DE94-009353] 10 p4111 N94-33908
Vacuum ultraviolet studies of molecular dynamics
[AD-A278940] 11 p4321 N94-35657
Ultrafast chemical dynamics of reactions in beams
[AD-A278939] 11 p4323 N94-35805
State-to-state dynamics of molecular energy transfer
[DE94-009651] 11 p4324 N94-35816
Multicomponent glass surfaces: Structure and adsorption
[DE94-010516] 11 p4246 N94-36283
United States Air Force Summer Research Program, 1993. Volume 5A: Wright Laboratory
[AD-A278696] 12 p4551 N94-36981

MOLECULAR ELECTRONICS
Charge storage and switching phenomena with molecular assemblies of metal complexes
[AD-A266673] 02 p0787 N94-14778
Photosynthetic reaction centers as active molecular electronic components, phase 1
[AD-A271388] 04 p1503 N94-19757
Ab initio potential energy surface for the H + OCS reaction
[AD-A270577] 05 p1698 N94-19947
Molecular surface electrostatic potentials in the analysis of non-hydrogen-bonding noncovalent interactions
[AD-A274612] 07 p3022 N94-26894
Electrical microengineering of redox enzymes
[AD-A279015] 11 p4236 N94-35745

MOLECULAR ENERGY LEVELS
NT INTERMOLECULAR FORCES
NT ROTATIONAL STATES
NT VIBRATIONAL STATES
Dynamics of charge-transfer excited states relevant to photochemical energy conversion
[DE93-013981] 01 p0263 N94-11116
The A((2)pi(sub u))-X((2)pi(sub g)) system of Br2(+) studied by velocity modulation spectroscopy
[USIP-93-04] 04 p1569 N94-18847
Dynamics of metastable states in supersonic beams
[ITN-94-85232] 07 p3028 N94-27760
Predissociation in N2(C'4, 1 Sigma u +) and other N2 states and its importance in the atmospheres of Titan and Triton
[NASA-CR-195727] 08 p3549 N94-28816
Intramolecular energy transfer reactions in polymetallic complexes
[DE94-010114] 11 p4326 N94-36126

MOLECULAR EXCITATION
Dynamics of dissociation versus ionization in strong laser fields
[DE93-009261] 01 p0173 N94-10287
Review of SHARC 2.0 O3 kinetics and spectroscopy
[AD-A265481] 01 p0274 N94-10496
Phasing operator for two oscillators in classical field
01 p0370 N94-10579
The excitation of cyanogen and ionized carbon in interstellar and extragalactic gas clouds
01 p0426 N94-11582
Thermal-infrared emission spectroscopy of natural surfaces: Application to coated surfaces
01 p0081 N94-12156
Kinetic studies following state-selective laser excitation
[DE93-012970] 02 p0654 N94-13013
Molecular dynamics simulation of electronically excited polyatomic molecules
[DE93-623045] 02 p0781 N94-13225
Theoretical molecular studies of astrophysical interest
[NASA-CR-193300] 02 p0838 N94-13781
Photochemical dynamics of surface oriented molecules
[DE93-016289] 02 p0784 N94-13983
Structure and stability of microvoids in A-Si:H
[DE93-016625] 02 p0813 N94-14413
Theoretical prediction of the UV adsorption and fluorescence spectra of tyrosine and phenylalanine
[AD-A266970] 03 p0943 N94-15111
Molecular processes in comets
[NASA-CR-194148] 03 p1239 N94-15188
Synthesis and chemistry of novel cyclic fluorocarbons
[AD-A267148] 03 p0929 N94-15734
The photophysics of poly(methylphenylphosphazene)
[AD-A267321] 03 p0970 N94-16949
Interface properties of wide bandgap semiconductor structures
[AD-A268269] 03 p1215 N94-17377
In-situ electron and optical spectroscopies of translational and vibrational activated bond breaking and formation on semiconductors
[AD-A268192] 03 p1015 N94-17560
Experimental and theoretical investigation of surface chemistry induced by direct and indirect electronic excitation
[AD-A268846] 04 p1348 N94-18221
Vibrational dynamics in photoinduced electron transfer
[DE93-040874] 04 p1567 N94-18533
Nonlinear optical properties of molecules
[AD-A270199] 04 p1567 N94-18783
Calculation of molecular excitation rates
[NASA-CR-193782] 04 p1571 N94-19236
Unimolecular photodissociation dynamics of ketene (CH2CO): The singlet/triplet branching ratio and experimental observation of the vibrational level thresholds of the transition-state
[DE93-019252] 04 p1352 N94-19304
Contribution of all excited states to ZFS of a (sup 6) S-state
[DE93-617007] 06 p2568 N94-25483
The importance of vibrationally excited nitrogen in silicon nitride deposition systems
[AD-A274874] 07 p2750 N94-26167
Dynamics of metastable states in supersonic beams
[ITN-94-85232] 07 p3028 N94-27760
Spectroscopic and dynamical studies of highly energized small polyatomic molecules
[DE94-006509] 08 p3489 N94-30061
Cometary molecules 09 p3935 N94-31869
Electronic and nuclear factors in intramolecular charge and excitation transfer processes
[DE94-006598] 09 p3870 N94-32178
Energy transfer properties and mechanisms
[DE94-007403] 09 p3636 N94-32594
Fluorescence detection of single molecules using pulsed near-field optical excitation and time correlated photon counting
[DE94-007553] 11 p4320 N94-35376
Anionic states of LiFLi
[AD-A278830] 11 p4322 N94-35678
Periodicity and peculiarity in 120 first and second row diatomic molecules
[AD-A278836] 11 p4323 N94-35793
Intramolecular energy transfer reactions in polymetallic complexes
[DE94-010114] 11 p4326 N94-36126
Molecular nitrogen fluorescence lidar for remote sensing of the auroral ionosphere
[AD-A280716] 11 p4291 N94-36263

MOLECULAR FLOW
NT TRANSITION FLOW
Molecular gas dynamics applied to low-thrust propulsion 06 p2214 N94-23053
Comprehensive investigation of HgCdTe metalorganic chemical vapor deposition
[NASA-CR-195933] 10 p4030 N94-34278

MOLECULAR GASES
NT DIATOMIC GASES
Dynamics of dissociation versus ionization in strong laser fields
[DE93-009261] 01 p0173 N94-10287
Quantum dynamics of helium clusters
[AD-A266060] 01 p0411 N94-10874
Resonant x ray Raman scattering from atoms and molecules
[DE93-015158] 02 p0784 N94-13896
Charge storage and switching phenomena with molecular assemblies of metal complexes
[AD-A266673] 02 p0787 N94-14778
Study of multi-dimensional radiative energy transfer in molecular gases
[NASA-CR-194613] 03 p1181 N94-15752
BACKSCAT lidar simulation version 3.0: Technical documentation and users guide
[AD-A267296] 03 p1003 N94-17268
Molecular and polymeric ceramic precursors
[DE93-040364] 04 p1372 N94-18891
Molecular abundances in the envelopes around evolved stars
[PB94-104916] 06 p2602 N94-23812
An investigation of the effect of surface impurities on the adsorption kinetics of hydrogen chemisorbed onto iron
[NASA-CR-195213] 07 p2716 N94-26643
The kinematics of molecular gas and dust in the nearby galaxies Centaurus A and M82
08 p3544 N94-29738
CO observations in external galaxies and gas mass determination 09 p3925 N94-31790
The manifestations of energetic activity in the galactic center 09 p3937 N94-32028
Molecular nitrogen fluorescence lidar for remote sensing of the auroral ionosphere
[AD-A280716] 11 p4291 N94-36263

MOLECULAR INTERACTIONS
NT MOLECULAR COLLISIONS
Engineering solid-state materials. Strategies for modeling and packing control of molecular assemblies into 3-D networks
[AD-A265291] 01 p0404 N94-12438
Molecular solvent-dynamical effects on activated electron-transfer kinetics: How important is solvent friction?
[AD-A265886] 02 p0779 N94-12894
Theory, modeling, and simulation
[DE93-015607] 02 p0755 N94-14571
Modeling study to evaluate the ionic mechanism of soot formation in flames
[AD-A266242] 03 p0950 N94-16930
Supercritical thermodynamics of sulfur and nitrogen species
[DE93-017727] 03 p1220 N94-16997
Interface properties of wide bandgap semiconductor structures
[AD-A268269] 03 p1215 N94-17377
Cathode sheath charge transfer effects
[AD-A268393] 03 p1186 N94-17536
Femtosecond Fourier-transform spectroscopy of low-frequency intermolecular motions in weakly interacting liquids
[DE93-017312] 04 p1566 N94-18085
The Fourteenth Symposium on Molecular Beams
[AD-A268721] 04 p1568 N94-18787
Supercritical thermodynamics of sulfur and nitrogen species
[DE93-041221] 04 p1610 N94-19670
Embedded microclusters in zeolites and cluster beam sputtering: Simulation on parallel computers
[DE94-000741] 05 p1701 N94-20352
Integral equations for the microstructures of supercritical fluids
[DE94-002460] 06 p2535 N94-24569
Study on computerized experiment of amorphous transformation process by solid phase reaction
07 p2726 N94-25564
International bulletin on atomic and molecular data for fusion. No. 46
[DE94-601818] 07 p3023 N94-26947
Spectroscopy and dynamics of molecular and ionic impurities embedded in solid hydrogen
[AD-A274149] 07 p3064 N94-27095
Low energy ion-molecule reactions and chemiionization kinetics
[DE94-005414] 08 p3481 N94-28491
Monte Carlo simulation or normal shock wave. Part 2: VHS model and VSS model 08 p3123 N94-28948
Computer simulation of molecular interactions in supercritical solvents
[AD-A274977] 08 p3486 N94-29087
Theoretical studies of solid-fluid phase equilibria
[DE94-006406] 08 p3226 N94-30708
Molecular interactions at metal/polyimide interfaces: A correlation with adhesion and bond durability
[AD-A276301] 09 p3650 N94-31297
High-temperature study of O+H2CO yields OH+HCO
[DE94-006837] 09 p3864 N94-31321
The 14th Annual West Coast Theoretical Chemistry/Statistical Mechanics Conference
[AD-A276942] 09 p3656 N94-32239
Molecular interactions in dilute supercritical mixtures: Molecular dynamics investigation
[DE94-007610] 09 p3872 N94-32644
Radiation and photochemistry section
[DE94-008880] 09 p3873 N94-32757
Implementation of a vibrationally linked chemical reaction model for DSMC
[NASA-TM-109109] 09 p3710 N94-33020

High resolution molecular spectroscopy of atmospheric species
[AD-A278382] 09 p3776 N94-33351
Microscopic theory of the dielectric response of highly dispersive biological media
[AD-A280516] 12 p4516 N94-37109
Effects of molecular transport on turbulence-chemistry interactions in a hydrogen-argon-air jet diffusion flame
[DE94-005107] 12 p4413 N94-37711

MOLECULAR IONS
NT HYDRONIUM IONS
Merged beam studies of laser stimulated radiative recombination
[AD-A267186] 03 p1037 N94-15145
The Fourteenth Symposium on Molecular Beams
[AD-A268721] 04 p1568 N94-18787
The A((2)pi(sub u))-X((2)pi(sub g)) system of Br2(+) studied by velocity modulation spectroscopy
[USIP-93-04] 04 p1569 N94-18847
Collisional processes involving atmospheric gases
[AD-A270729] 05 p1854 N94-19954
Examination of the response capacity of a silicon pixel detector for ions and molecules in the energy area 100 to 300 keV
[MPE-241] 06 p2346 N94-25415
Experimental and theoretical studies of molecular solids
[AD-A275511] 08 p3485 N94-28668
A two-dimensional model for collisional energy transfer in bimolecular ion-molecule dynamics
[AD-A278913] 11 p4321 N94-35589
Dissociative recombination of stored and phase-spaced cooled molecular ions in CRYRING
[DE94-002459] 11 p4327 N94-36267

MOLECULAR ORBITALS
Charge storage and switching phenomena with molecular assemblies of metal complexes
[AD-A266673] 02 p0787 N94-14778
Theoretical prediction of the UV adsorption and fluorescence spectra of tyrosine and phenylalanine
[AD-A266970] 03 p0943 N94-15111
Thermochemistry of silicate speciation in aqueous sodium silicate solutions: Ionization and polymerization of small silicate ion
[AD-A266825] 03 p0964 N94-15683
Ab initio study of vibrational frequency shift upon the 1:1 acetone-iodine complex formation
08 p3188 N94-28681
Anionic states of LiFLi
[AD-A278830] 11 p4322 N94-35678
Periodicity and peculiarity in 120 first and second row diatomic molecules
[AD-A278836] 11 p4323 N94-35793

MOLECULAR OSCILLATIONS
A molecular dynamics simulator for optimal control of molecular motion
[AD-A266572] 03 p1183 N94-16722
Proton transfer dynamics and cluster ion fragmentation in phenol/ammonia clusters
[AD-A269133] 04 p1348 N94-18256

MOLECULAR OSCILLATORS
Design, synthesis and characterization of novel nonlinear optical polymers
[AD-A267035] 03 p0964 N94-15675
A molecular dynamics simulator for optimal control of molecular motion
[AD-A266572] 03 p1183 N94-16722

MOLECULAR PHYSICS
Polar solvation and electron transfer
[DE93-013328] 01 p0365 N94-11010
Parallel molecular dynamics with the embedded atom method
[DE93-010683] 01 p0367 N94-11455
Chaos, entropy, and reversibility: A simple example
01 p0031 N94-11495
A molecular dynamics simulation code ISIS
[DE93-753187] 01 p0368 N94-11592
Experimental and theoretical study of inhomogeneous electron transfer in betaine: Comparisons of measured and predicted spectral dynamics
[AD-A265703] 02 p0780 N94-13051
Phase transition in polymer blends and structure of ionomers and copolymers
[DE93-016256] 02 p0579 N94-13978
Computational diagnostics for detecting phase transitions during nanoindentation
[DE93-016536] 02 p0813 N94-14439
Particle simulations on massively parallel machines
[DE93-015644] 03 p1157 N94-14927
Molecular dynamics modeling of the mechanical behavior of metallic multilayers
[DE93-017972] 04 p1365 N94-19263
One- and multi-component theories of mixtures
[DE93-040543] 05 p1966 N94-21511
Dynamics of metastable states in supersonic beams
[ITN-94-85232] 07 p3028 N94-27760

MOLECULAR RELAXATION
Femtosecond dynamics, photoexcitation, and ESR spectra of MX chain solids
[AD-A264689] 01 p0399 N94-11263
Vibrational relaxation in hypersonic flow fields
[NASA-TP-3367] 02 p0776 N94-14733
Computational techniques for high-speed flows with viscous and chemical effects 04 p1412 N94-18560
Hydrolysis reaction and positronium decay in silica gels
[AD-A270028] 04 p1371 N94-18713
Shock induced condensation in fluids of high molar specific heat: Shock structure and relaxation
[MPIS-106/1993] 05 p1798 N94-20145
A study of vibrational relaxation of electronically-excited molecules
[DE93-613553] 07 p3013 N94-25827
Spectroscopic and vibrational energy transfer studies in molecular bromine
[AD-A273795] 07 p3014 N94-25875
Progress in modeling atmospheric propagation of sonic booms 07 p2650 N94-28189
Vibrational energy transfer of diatomic gases in hypersonic expanding flows 09 p3570 N94-31958
Implementation of a vibrationally linked chemical reaction model for DSMC
[NASA-TM-109109] 09 p3710 N94-33020
The effect of turbulence and molecular relaxation on sonic boom signatures 10 p3976 N94-33497

MOLECULAR ROTATION
The excitation of cyanogen and ionized carbon in interstellar and extragalactic gas clouds
01 p0426 N94-11582
The influence of an electric field on the kinetics of nucleation
[IFTR-2/91] 03 p1213 N94-17046
High resolution infrared spectroscopy of cyclobutane: A study of vibrational mode coupling involving large amplitude, low frequency modes
[AD-A271987] 05 p1973 N94-20619
Collective and quasiparticle excitations in light Pb isotopes
[ETN-94-96014] 09 p3865 N94-31548
Recovery of frozen flow losses in arcjets
[AD-A278739] 11 p4228 N94-36089

MOLECULAR SIEVES
U ABSORBENTS

MOLECULAR SPECTRA
NT ELECTRONIC SPECTRA
NT RAMAN SPECTRA
NT ROTATIONAL SPECTRA
NT VIBRATIONAL SPECTRA
Spectroscopy Division
[DE94-604074] 07 p2717 N94-26988
Ab initio study of vibrational frequency shift upon the 1:1 acetone-iodine complex formation
08 p3188 N94-28681
Summary of some data processing routines in the molecular physics group of Stockholm University
[USIP-93-05] 09 p3808 N94-31087
Detection of the 267 GHz J = 1-0 rotational transition of PH3 in Saturn with a new Fourier transform spectrometer
[NASA-CR-194364] 10 p4162 N94-34718

MOLECULAR SPECTROSCOPY
NT RAMAN SPECTROSCOPY
Kinetic studies following state-selective laser excitation
[DE93-012970] 02 p0654 N94-13013
The infrared solar spectrum
[COMMUNICATIONS-SER-B-159]
02 p0844 N94-13502
Plasma edge spectroscopy 05 p1996 N94-21803
Laboratory detection of C5S by pulsed-discharge-nozzle Fourier-transform microwave spectroscopy
[JTN-94-80519] 06 p2235 N94-24984
CO-to-H2 conversion factor in dwarf irregular galaxies
[REPT-333] 06 p2603 N94-24985
High spatial resolution observations of CO in CRL 618
[REPT-334] 06 p2604 N94-24986
The Nobeyama millimeter array survey for protoplanetary disks around protostar candidates and T Tauri stars in Taurus
[REPT-336] 06 p2604 N94-24987
Molecular surface electrostatic potentials in the analysis of non-hydrogen-bonding noncovalent interactions
[AD-A274612] 07 p3022 N94-26894
Summary of some data processing routines in the molecular physics group of Stockholm University
[USIP-93-05] 09 p3808 N94-31087
Laser and Fourier transform spectroscopy of novel propellant molecules
[AD-A277506] 09 p3667 N94-33013
High resolution molecular spectroscopy of atmospheric species
[AD-A278382] 09 p3776 N94-33351
A spectral atlas of the nu(sub 12) fundamental of (13)C(12)CH6 in the 12 micron region
[NASA-TM-104601] 10 p4138 N94-34945

MOLECULAR STRUCTURE
Chemical pattern formation under microgravity
01 p0121 N94-10227
Electron momentum spectroscopy of atoms, molecules and solids
[DE93-610148] 01 p0360 N94-10332
Recent advances in electron momentum spectroscopy
[DE93-610149] 01 p0361 N94-10333
Site dependence of the apparent shape of a molecule in STM images: Benzene on Pt(111)
[AD-A263488] 01 p0365 N94-11093
Femtosecond dynamics, photoexcitation, and ESR spectra of MX chain solids
[AD-A264689] 01 p0399 N94-11263
Adsorption and dissociation of disilane on Si(001) studied by STM
[AD-A265269] 01 p0402 N94-11684
The global potential energy surfaces of the lowest two 1A' states of the ozone molecule: Theoretical determination and analysis 01 p0267 N94-12269
Fracture behavior of ionomers and ionomeric blends
[AD-A265379] 01 p0094 N94-12407
Engineering solid-state materials. Strategies for modeling and packing control of molecular assemblies into 3-D networks
[AD-A265291] 01 p0404 N94-12438
Resonant x ray Raman scattering from atoms and molecules
[DE93-015158] 02 p0784 N94-13896
Workshop on Formation of Supermolecular Structures in Composite Fluid: Phase Rule and Dynamics
[DE93-782887] 02 p0581 N94-14421
Theory, modeling, and simulation
[DE93-015607] 02 p0755 N94-14571
CarbBank: A structural and bibliographic database for complex carbohydrates
[DE93-015582] 02 p0827 N94-14803
Thermochemistry of silicate speciation in aqueous sodium silicate solutions: Ionization and polymerization of small silicate ion
[AD-A266825] 03 p0964 N94-15683
Many-body quantum mechanical studies of molecular clusters
[AD-A266624] 03 p1180 N94-15727
Study of protein-H2O interactions by multidimensional NMR spectroscopy
[AD-A266955] 03 p0946 N94-15760
Chemical and displacement atomic pair correlations in crystalline solid solutions recovered by anomalous x ray scattering in Fe-Ni alloys
[DE93-015906] 03 p1209 N94-16171
Structural effects in electron transfer reactions: Comparative interfacial electrochemical kinetics for cis- versus trans-dioxorhenium (V) (bi)pyridine oxidation
[AD-A266307] 03 p1182 N94-16466
Structural studies of sol-gel glasses
[AD-A266277] 03 p0967 N94-16472
The photochemistry of poly(methylphenylphosphazene)
[AD-A267320] 03 p0970 N94-16948
Responsive copolymers for enhanced petroleum recovery
[DE93-018030] 03 p0971 N94-16999
Synthesis, characterization, and polymerization of new ferrocene-fluorene complexes. A novel high-molecular weight conjugated polymer with pendant ferrocene groups
[AD-A267717] 03 p0972 N94-17273
Theoretical crystallography with the Advanced Visualization System
[DE93-015692] 03 p1215 N94-17319
X ray absorption spectroscopic studies of the active sites of nickel- and copper-containing metalloproteins
[DE93-017142] 04 p1347 N94-18059
Numerical methods for molecular dynamics
[DE93-018321] 04 p1566 N94-18179
Metal/ceramic interfaces: Relationships between structure and chemistry
[AD-A268792] 04 p1369 N94-18188
Morphology of polymerized membranes on an amorphous substrate at molecular resolution by AFM
[AD-A268760] 04 p1370 N94-18403
Mesoepitaxy: A universal route to oriented materials
[AD-A270437] 04 p1598 N94-18511
Molecular structure of low temperature form of triaminoguanidinium nitrate (TAGN)
[AD-A270409] 04 p1377 N94-18708
A numerical study of hybrid optimization methods for the molecular conformation problems
[DE93-017898] 04 p1569 N94-18985

Structure-property relationships in radical-cation (electron-donor molecule) and anion-based (including fullerides) organic superconductors and their use in the design of new materials
[DE93-018617] 04 p1601 N94-19022
Polymer films with enhanced dielectric properties
[AD-A271148] 04 p1375 N94-19740
Cooperative formation of inorganic-organic interfaces in the synthesis of silicate mesostructures
[AD-A271196] 04 p1375 N94-19742
Characterization studies of lower and non-TDI polyurethane encapsulants
[DE93-041129] 05 p1698 N94-19857
Femtosecond Raman-induced Kerr effect study of polar solvent dynamics: Amides
[DE93-017563] 05 p1678 N94-19924
Light scattering studies of an electrorheological fluid
[DE93-019419] 05 p1700 N94-20315
High energy ionization in liquids: The free ion yield
[DE93-040329] 05 p1973 N94-20324
In-situ electrochemical surface science
[AD-A265942] 05 p1680 N94-20330
Molecular and atomic arrays in nano- and mesoporous materials synthesis
[AD-A271500] 05 p2017 N94-20544
Rotational isomers of Mo(VI) alkylidene complexes and Cis/trans polymer structure: Investigations in ring-opening metathesis polymerization
[AD-A272647] 05 p1704 N94-21184
Polymerization of enantiomerically pure 2,3-dicarboalkoxy norbornadienes and 5,6-disubstituted norbornenes by well-characterized molybdenum ROMP catalysts
[AD-A272649] 05 p1704 N94-21186
Surface electrochemistry of metals
[AD-A272913] 05 p1691 N94-21245
Optically induced birefringence in copolymers and blends containing azobenzene groups
[AD-A273085] 05 p1706 N94-21523
Column chromatographic separation of Y(3+) from Sr(2+) by polymeric ionizable crown ether resins
[DE94-000935] 05 p1683 N94-22021
Theoretical research program to study chemical reactions in AOTV bow shock tubes
[NASA-CR-194710] 05 p1804 N94-22027
Non-linear thermal instability of optical thin molecular structures 05 p2006 N94-22667
Measuring the dynamics of structural changes in biological macromolecules from light scattering data 06 p2422 N94-24426
Interactions between organized, surface-confined monolayers and vapor-phase probe molecules. 7: Comparison of self-assemblying organomercaptan monolayers deposited on gold from liquid and vapor phases
[AD-A273196] 06 p2535 N94-24555
Center for advanced electrical and structural polymers
[AD-A273415] 06 p2259 N94-24783
Synthesis of molecular wires by a novel divergent/convergent approach
[AD-A273332] 06 p2537 N94-25087
On the mechanism of action of 3',5'-cyclic adenosine monophosphate: A study of four- and five-coordinated phosphorus compounds, modelling the activated state of cAMP
[ISBN-9-03-860222-7] 06 p2226 N94-25238
Contribution of all excited states to ZFS of a (sup 6) S-state
[DE93-617007] 06 p2568 N94-25483
Morphological analysis of ionomers
[DE94-003660] 07 p2749 N94-26005
Radiation-Induced Structural Changes, 2
[DE93-520314] 07 p3054 N94-26109
Transition metals in highly correlated discotic phases: Designing metallomesogens with selected intermolecular organizations
[AD-A274695] 07 p2736 N94-26452
An x ray absorption fine structure study of ordering in polythiophene thin films
[AD-A274235] 07 p2753 N94-26822
Controlled heterogeneous nucleation of melt-textured YBa2Cu3O(6+x) by addition of Al2O3 particles
[AD-A274605] 07 p3062 N94-26892
NCVS, volume 5
[AD-A274975] 07 p2902 N94-27165
Molecular dynamics simulation and crystal-field theory: Predicting the optical spectra and structure of rare-earth doped inorganic glasses
[ISBN-0-315-84679-8] 07 p3025 N94-27310
The molecular matching problem 07 p3030 N94-27910
Thermal conductivity of liquid carboxylic acids
[ESDU-93017] 07 p2721 N94-28138
Journal of NIRE, Vol. 2, No. 2
[JTN-94-80552] 08 p3187 N94-28675
Molecular structure of coal studied by solvent extraction 08 p3187 N94-28676
Structural changes during carbonization and oxidation of coal 08 p3187 N94-28678
Ab initio study of vibrational frequency shift upon the 1:1 acetone-iodine complex formation 08 p3188 N94-28681
Structure of ordinary ice I(sub h). Part 1: Ideal structure of ice
[AD-A275149] 08 p3486 N94-29021
Synthesis and molecular structures of R(Me3CCH2)2In-E(SiMe3) (R = Me3CCH2, E = P or As; R = Me, E = P)
[AD-A275020] 08 p3486 N94-29131
Polymer technology publication series no. 16
[PB94-135522] 08 p3214 N94-29157
Organic materials that respond to molecules
[AD-A275392] 08 p3174 N94-29307
Insensitive energetic materials: The importance of physical properties and molecular structure
[AD-A275393] 08 p3225 N94-29308
Theoretical investigation of gas-surface interactions
[NASA-CR-195755] 08 p3272 N94-29378
Summary of some data processing routines in the molecular physics group of Stockholm University
[USIP-93-05] 09 p3808 N94-31087
Theoretical studies of zirconium and carbon clusters with molecular dynamics simulations
[DE94-005276] 09 p3862 N94-31146
Analytical applications of scanning tunneling microscopy
[AD-A276066] 09 p3711 N94-31283
Infrared and near infrared transient absorption spectroscopy of molecular free radicals
[DE94-005446] 09 p3632 N94-31305
Collective and quasiparticle excitations in light Pb isotopes
[ETN-94-96014] 09 p3865 N94-31548
Double rotation NMR studies of zeolites and aluminophosphate molecular sieves
[DE94-007032] 09 p3866 N94-31637
Chemical interactions between protein molecules and polymer membrane materials
[DE94-006987] 09 p3651 N94-31672
Recent developments in polymeric charge transfer complexes
[AD-A277108] 09 p3654 N94-31979
New molecular-based routes to binary main group metal sulfides
[AD-A277005] 09 p3900 N94-32003
Neural network definitions of highly predictable protein secondary structure classes
[DE94-006234] 09 p3834 N94-32175
Towards a detailed understanding of the structural variability in lignins: A new approach
[DE94-007449] 09 p3793 N94-32267
Chemical structure and kinetics at liquid/solid interfaces
[AD-A277112] 09 p3636 N94-32304
Molecular Science Research Center
[DE94-007464] 09 p3871 N94-32605
Nonlinear optical polymers derived from organic/inorganic composites
[AD-A277408] 09 p3659 N94-32610
Ionization probes of molecular structure and chemistry
[DE94-007605] 09 p3872 N94-32643
Calculation of phase stability in Zr-Nb-Ru using LMTO and the cluster variation method
[AD-A278556] 10 p4137 N94-33896
Theoretical aspect of low pressure discharges in simple gasses
[AD-A278762] 11 p4335 N94-35493
Structural investigations of 1-ethyl-3-methylimidazolium hydrogen dichloride: Neutron diffraction studies of an ambient-temperature molten salt
[DE94-009680] 11 p4237 N94-35777
United States Air Force Summer Research Program, 1993. Volume 5A: Wright Laboratory
[AD-A278696] 12 p4551 N94-36981
Comparison of the crystal structure and molecular models of N,N-diisobutyl-2- (octylphenylphosphinyl) acetamide (CMPO)
[DE94-013434] 12 p4534 N94-37069
High resolution electron diffraction analysis of structural changes associated with the photocycle of bacteriorhodopsin
[DE94-011800] 12 p4479 N94-37156
Organometallic NLO polymers. 4: Organometallic main-chain, side-chain, and guest-host polymers: A study of their orientation and relaxation using second harmonic generation
[AD-A280347] 12 p4423 N94-37179
Copper-containing ceramic precursor synthesis: Solid-state transformations and materials technology
[NASA-TM-106556] 12 p4399 N94-37315
First-principles determination of the polarizabilities of carbon tubules as a function of length
[DE94-013015] 12 p4537 N94-37356
Tert-butylalumoxanes: Synthetic analogs for methylalumoxane (MAO) and new catalytic routes to polyolefins and polyketones
[AD-A280532] 12 p4399 N94-37650

MOLECULAR THEORY

Theory, modeling, and simulation
[DE93-015607] 02 p0755 N94-14571
A molecular dynamics simulator for optimal control of molecular motion
[AD-A266572] 03 p1183 N94-16722
Calculation of molecular excitation rates
[NASA-CR-193782] 04 p1571 N94-19236

MOLECULAR TRAJECTORIES

Collisions of molecules with clusters: A quasiclassical study
[DE93-018614] 05 p1971 N94-20050

MOLECULAR WEIGHT

NT LOW MOLECULAR WEIGHTS

Synthesis, characterization, and modification of poly(organophosphazenes), that bear both 2,2,2-trifluoroethoxy and phenoxy groups
[AD-A264913] 01 p0092 N94-11847
Radiation-induced modifications of allylamino-substituted polyphosphazenes
[AD-A264914] 01 p0092 N94-11848
Glucose electrodes based on cross-linked (Os(bpy)2Cl)(sup +/2+) complexed poly(1-vinylimidazole) films
[AD-A265404] 01 p0094 N94-12425
Characterization of 1:1 random copolymers obtained from 6-, 7-, 11-, and 12-carbon amino acids
[AD-A265827] 02 p0577 N94-12985
Hemoglobin
[AD-A266455] 03 p1123 N94-16566
Photodegradation of MDI based polyurethane/urea elastomers
[AD-A267308] 03 p0971 N94-16994
Synthesis and structural characterization of new light molecular weight inorganic oxidizers and relative derivatives, volume 1
[AD-A271437] 05 p2012 N94-19842
Polybenzoxazole via aromatic nucleophilic displacement
[NASA-CASE-LAR-14606-1-CU] 05 p1672 N94-20540
Phenylethynl-terminated poly(arylene ethers)
[NASA-CASE-LAR-14797-1] 06 p2253 N94-23307
Measuring the dynamics of structural changes in biological macromolecules from light scattering data 06 p2422 N94-24426
Chemical polymerization and Langmuir-Blodgett techniques. 2: The polymerization of monolayers of 3-substituted pyrroles
[AD-A274478] 07 p2755 N94-27163
Method and apparatus for inhibiting the disbonding of a paint from metal surfaces
[AD-D016106] 09 p3663 N94-32960
Addition polyimides with enhanced processability
[NASA-CASE-LEW-15043-1] 11 p4242 N94-35234
Probing flame chemistry with MBMS, theory, and modeling
[DE94-011224] 12 p4413 N94-37623

MOLECULES

NT DIATOMIC MOLECULES
NT MACROMOLECULES
NT POLYATOMIC MOLECULES
NT TRIATOMIC MOLECULES
Pulsed plasma processing for control of diesel engine emissions
[DE93-011884] 01 p0181 N94-11247
A new decomposition strategy for parallel bonded molecular dynamics
[DE93-009839] 01 p0366 N94-11284
FEFF5: An ab initio multiple scattering XAFS code
[DE93-011000] 01 p0367 N94-11470
Ultrafast photoinduced electron transfer reactions in supramolecular arrays: Studies of electronic coupling and solvation
[DE93-012910] 02 p0782 N94-13484
Selective excitation, relaxation, and energy channeling in molecular systems
[DE93-018819] 02 p0785 N94-14420
Dissociation rates of diatomic molecules
[AD-A266464] 03 p1182 N94-16586
Optical properties of water released in low Earth orbit
[AD-A266197] 03 p1192 N94-16936
Experimental and theoretical investigation of surface chemistry induced by direct and indirect electronic excitation
[AD-A268846] 04 p1348 N94-18221
Detection of single molecules in microspheres
[DE93-017776] 04 p1567 N94-18493

Electronically metastable molecules of high symmetry
[AD-A272015] 05 p1974 N94-21461
Measuring the dynamics of structural changes in biological macromolecules from light scattering data
06 p2422 N94-24426
Interactions between organized, surface-confined monolayers and vapor-phase probe molecules. 7: Comparison of self-assemblying organomercaptan monolayers deposited on gold from liquid and vapor phases
[AD-A273196] 06 p2535 N94-24555
Synthesis and characterization of two-dimensional molecular recognition interfaces
[AD-A273177] 06 p2536 N94-24729
Atomic-scale chemistry of metal surfaces
[REPT-A-2657] 07 p3012 N94-25636
On the classification scheme for resonant states of muonic molecules
[DE93-613645] 07 p3014 N94-25853
Transition metal activation and functionalization of carbon-hydrogen bonds
[DE94-003650] 07 p2715 N94-26369
Influence of surface defects and local structure on oxygenate reaction pathways over metal oxide surfaces
[DE94-005680] 08 p3522 N94-30901
Modification of semiconductor surface properties with chemically bound molecular films
[AD-A276162] 09 p3895 N94-31081
Physical chemistry of molecules and grains in space
[AD-A276037] 09 p3932 N94-31280
Positron-molecule interactions
[AD-A276542] 09 p3869 N94-32082
A genetic algorithm based method for docking flexible molecules
[DE94-007525] 09 p3793 N94-32269
Theoretical study of novel bonding in molecules: Metastable molecular fuels
[AD-A277807] 10 p4031 N94-33895
A combined experimental and theoretical study of the neutral, cationic and anionic Si3N cluster molecule
[AD-A278834] 11 p4323 N94-35792
The 1st International Symposium on Organic Photochromism: Molecules and Systems
[PB94-179488] 12 p4399 N94-37531

MOLIERE FORMULA
U COSMIC RAY SHOWERS
U SPATIAL DISTRIBUTION

MOLLUSKS
An experimental study of siphonal jets in a turbulent boundary layer crossflow 07 p2802 N94-28015

MOLNIYA SATELLITES
Orbital applications of electrodynamic propulsion
[AD-A275413] 08 p3173 N94-29216

MOLTEN SALT ELECTROLYTES
Carbonate fuel cell endurance: Hardware corrosion and electrolyte management status
[DE93-013800] 02 p0701 N94-13093
Molten carbonate fuel cell networks: Principles, analysis, and performance
[DE93-019872] 05 p1846 N94-21527
Molten salt techniques for reproducible excess heat
[AD-A274935] 07 p2714 N94-26296
Fundamental stack and system issues in molten carbonate fuel cell development
[DE94-005960] 08 p3338 N94-30048
Room temperature molten salts for advanced energy conversion and storage
[AD-A277777] 09 p3763 N94-33015

MOLTEN SALTS
Ultrasound absorption in molten salts
03 p0944 N94-15161
Molten salt electrodeposition of high temperature superconductors
[AD-A266620] 03 p1009 N94-15726
Hydride-containing molten salts and their technology implications
[AD-A266458] 03 p1092 N94-16567
Molten salt reactor for potentiostatic electroplating
[AD-D016020] 06 p2258 N94-24720
X ray diffraction analysis of electrodeposited beta-tantalum
[AD-A273254] 06 p2249 N94-25142
Structure of ionic fluids in equilibrium with a microporous ionic matrix
[DE94-600563] 07 p2715 N94-26391
Isothermal corrosion testing of steels in molten nitrate salts
[DE94-004695] 07 p2742 N94-27755
Room temperature molten salts for advanced energy conversion and storage
[AD-A277777] 09 p3763 N94-33015
Structural investigations of 1-ethyl-3-methylimidazolium hydrogen dichloride: Neutron diffraction studies of an ambient-temperature molten salt
[DE94-009680] 11 p4237 N94-35777
Neutron diffraction study of aluminum chloride imidazolium chloride molten salts
[DE94-009679] 11 p4239 N94-36349
The logic behind thick, liquid-walled, fusion concepts
[DE94-012678] 12 p4528 N94-37307

MOLYBDATES
New mechanism for toughening ceramic materials
[AD-A278479] 10 p4027 N94-33747

MOLYBDENUM
Radiation hardness of Mo/Si multilayers designed for use in a soft x ray projection lithography system
[DE93-011879] 01 p0143 N94-11273
Optical degradation issues for XUV projection lithography systems
[DE93-012658] 02 p0626 N94-14805
Plastic anisotropy in MoSi2 single crystals
[DE93-012650] 04 p1594 N94-17874
Substrate recovery of Mo-Si multilayer coated optics
[DE93-019610] 05 p1698 N94-19810
Core formation in the Moon: The mystery of the excess depletion of Mo, W and P 05 p2095 N94-20651
Rotational isomers of Mo(VI) alkylidene complexes and Cis/trans polymer structure: Investigations in ring-opening metathesis polymerization
[AD-A272647] 05 p1704 N94-21184
Polymerization of enantiomerically pure 2,3-dicarboalkoxy norbornadienes and 5,6-disubstituted norbornenes by well-characterized molybdenum ROMP catalysts
[AD-A272649] 05 p1704 N94-21186
Interface science of controlled metal/metal and metal/ceramic interfaces prepared using ultrahigh vacuum diffusion bonding
[DE94-001066] 05 p1696 N94-22025
Soft x ray optics by pulsed laser deposition
[NASA-CR-195139] 06 p2546 N94-24967
Surface compositional variations of Mo-47Re alloy as a function of temperature
[NASA-TP-3402] 06 p2245 N94-25117
Study on development of chemical measurement method utilizing plasmas 07 p2728 N94-25576
Method of bonding molybdenum to steel
[AD-D016079] 07 p2747 N94-28187
A photoemission electron microscope investigation of chemical vapor deposition diamond films and diamond nucleation 08 p3215 N94-29745
Brittle composites modeling: Comparisons with MoSi2/ZrO2
[DE94-004978] 08 p3182 N94-29933
Microstructure and mechanical properties of nitrided molybdenum silicide coatings
[DE94-006249] 08 p3217 N94-30025
Computer simulation of the interaction of fast hydrogen atoms with a molybdenum containing sorbed hydrogen
[DE94-608419] 08 p3209 N94-30253
Creep behavior of MoSi2-SiC composites
[DE94-004980] 08 p3185 N94-30693
Studies of supported molybdenum and tungsten
[DE94-006207] 08 p3210 N94-30839
Electronic structure and stability of simple and complex phases in transition metals
[DE94-009090] 10 p4024 N94-33679
Design of a high activity and selectivity alcohol catalyst
[DE94-003633] 11 p4237 N94-36023
An investigation of molybdenum and molybdenum oxide catalyzed hydrocarbon formation reactions
[DE94-013700] 12 p4409 N94-37132

MOLYBDENUM ALLOYS
A history of tungsten- and molybdenum-base alloys
[DE93-010283] 01 p0082 N94-11108
Tensile and stress-rupture behavior of hafnium carbide dispersed molybdenum and tungsten base alloy wires
[NASA-TM-106350] 03 p0962 N94-17652
Atlas of formability: Ultimet
[AD-A268352] 04 p1355 N94-17767
Bibliography on silicides
[AD-A270516] 04 p1374 N94-19532
The effect of microstructural evolution on superplasticity in Ni3Si(V, Mo)
[DE93-041320] 05 p1694 N94-21943
Alloying effects on mechanical and metallurgical properties of NiAl
[DE93-040814] 05 p1694 N94-21948
Strengthening and toughening in refractory metal alloys
[DE93-019942] 05 p1695 N94-21986
The history of development of molybdenum alloys for structural applications
[DE94-000389] 06 p2239 N94-22958
Evaluation of A5Si3Z(x) intermetallics for use as high temperature structural materials
[DE93-041127] 06 p2227 N94-22977
Study on alloy films for hydrogen separation
07 p2726 N94-25565
Innovative processing of composites for ultra-high temperature applications, book 2
[AD-A275598] 08 p3177 N94-28730
Creep-fatigue criteria and inelastic behavior of modified 9Cr-1Mo steel at elevated temperatures
[DE94-007915] 09 p3642 N94-31918
High Temperature Silicides and Refractory Alloys Symposium, volume 322
[AD-A278373] 10 p4024 N94-33741
High temperature creep and oxidation resistant chromium silicide matrix alloy containing molybdenum
[NASA-CASE-LEW-15697-1] 11 p4241 N94-36275
Chromium/molybdenum alloy plating. Part 1: The electrodeposition of low contraction chromium/molybdenum alloys using unipolar (on/off) pulse plating
[AD-A280236] 12 p4417 N94-37138

MOLYBDENUM COMPOUNDS
NT MOLYBDATES
NT MOLYBDENUM DISULFIDES
NT MOLYBDENUM OXIDES
Strength and toughness improvement of silicide intermetallics by nanophase and microphase reinforcements
[AD-A272914] 05 p1692 N94-21320
Design of a resistojet for Space Station Freedom
[NASA-CR-195506] 06 p2221 N94-24979
Characterization of structure and mechanical properties of MoSi2-SiC nanolayer composites
[DE94-004982] 08 p3175 N94-28579
Fabrication and testing of plasma-spray formed MoSi2 and MoSi2 composite tubes
[DE94-004995] 08 p3175 N94-28581
Novel approaches to the production of higher alcohols from synthesis gas
[DE94-006770] 09 p3666 N94-32132
The effect of ductile phase (Nb) reinforcement morphology on the mechanical behavior of an intermetallic matrix (MoSi2) 09 p3615 N94-32500
Mechanical behavior of MoSi2 and MoSi2 composites
[DE94-013116] 12 p4405 N94-37289

MOLYBDENUM DISULFIDES
Dry film lubricant evaluation
[DE93-013114] 02 p0578 N94-13118
Applications of surface science to solid lubricants
[SMC-TR-93-24] 02 p0579 N94-13903
Scanning tunneling microscopy investigations of metal dichalcogenide materials
[AD-A272910] 05 p2027 N94-21242
LB-Deposited, side-chain substituted polyaniline, polypyrrole and the corresponding monomers, studied by STM
[AD-A274405] 07 p2754 N94-26977
Soft x ray photoelectron spectroscopy study of the interaction of Cr with MoS2(0001)
[AD-A276916] 09 p3635 N94-32233
Torque characteristics of solid lubricated precision bearings during oscillatory motion
[AD-A278133] 09 p3728 N94-33061

MOLYBDENUM OXIDES
A quartz crystal microbalance study of lithium insertion and removal into evaporated films MO(y) (M = Mo, Fe, and V)
[DSIS-93-00649] 02 p0810 N94-14203
Siderophile elements in the upper mantle of the Earth: New clues from metal-silicate partition coefficients
03 p1103 N94-16250
Synthesis and characterization of novel ternary and quaternary reduced molybdenum oxides
[DE94-005563] 08 p3510 N94-28529
An investigation of molybdenum and molybdenum oxide catalyzed hydrocarbon formation reactions
[DE94-013700] 12 p4409 N94-37132

MOLYBDENUM SULFIDES
NT MOLYBDENUM DISULFIDES
Low temperature pathways to Chevrel phases via reduced molybdenum sulfide cluster complexes
[DE93-013282] 01 p0405 N94-12599
Tribological characteristics of ball bearings lubricated with a sputtered molybdenum disulphide film in a vacuum under a high thrust load 06 p2355 N94-23992
The tribology of some MoS2-lubricated engineering ceramics 06 p2356 N94-23993
Development of long-life, low-noise linear bearings for atmospheric interferometry 09 p3606 N94-33312

MOMENT DISTRIBUTION
Techniques for estimating Space Station aerodynamic characteristics
[NASA-CR-193394] 02 p0541 N94-13955
Error propagation equations and tables for estimating the uncertainty in high-speed wind tunnel test results
[DE93-018685] 04 p1311 N94-18275

MOMENTS
NT BENDING MOMENTS
NT DIPOLE MOMENTS
NT DISTRIBUTION MOMENTS

NT MAGNETIC MOMENTS
NT MEAN
NT MOMENTS OF INERTIA
NT ORTHOGONALITY
NT PITCHING MOMENTS
NT ROLLING MOMENTS
NT STABILITY DERIVATIVES
NT STANDARD DEVIATION
NT TORQUE
NT YAWING MOMENTS

MOMENTS OF INERTIA

Porosity and the ecology of icy satellites
01 p0431 N94-12186

Accuracy and repeatability of the standard automated mass properties measurement system
[AD-A265897] 01 p0316 N94-12346

Friction drive position transducer
[AD-D015851] 04 p1424 N94-17717

Torque equilibrium attitudes for the Space Station
06 p2208 N94-24449

Numerical analysis of the motion of a rigid body with an attached spring-mass-damper
[AD-A273825] 06 p2379 N94-25520

Normal forms for perturbations of the euler top
[PB94-125390] 07 p3009 N94-26968

Theory of fundamental interactions
[DE94-608126] 08 p3525 N94-30169

Forced libration of Mercury and geodetic determination of a possible fluid core 09 p3774 N94-32493

MOMENTUM

NT ANGULAR MOMENTUM

On a Lagrange-Hamilton formalism describing position and momentum uncertainties 01 p0349 N94-10583

Momentum and heat frictions between fast ions and thermal plasma species
[DE93-771240] 01 p0390 N94-11149

Momentum induced by laser-tissue interaction
[DE93-010737] 01 p0301 N94-11667

Surface eddy fluxes from the GEOSAT satellite altimeter 01 p0208 N94-12643

On transport of energy, momentum, orbital angular momentum and self-angular momentum of electromagnetic wave in dispersal media
[DE93-624179] 02 p0617 N94-14883

Determination of momentum flux using a bivane and cup anemometer
[AD-A265414] 03 p1105 N94-15137

Longitudinal beam dynamics for heavy ion fusion using WARPrz
[DE93-019154] 05 p1992 N94-19915

Meso-Beta scale numerical simulation studies of terrain-induced jet streak mass/momentum perturbations
[NASA-CR-194627] 05 p1864 N94-20138

Neutron and PIMC determination of the longitudinal momentum distribution of HCP, BCC and normal liquid He-4
[DE93-019009] 05 p1972 N94-20187

Momentum and coordinate space three-nucleon potentials
[DE93-040868] 06 p2531 N94-22951

Momentum loss in proton-nucleus and nucleus-nucleus collisions
[NASA-TP-3405] 06 p2540 N94-24305

On the hadron formation time in pion-nucleus interaction
[DE93-616879] 06 p2539 N94-25476

On the estimation of matrix elements for optical transitions in semiconductors
[DE93-613550] 07 p3051 N94-25851

How to build analogues of the Bessel-Clifford expansions for the sum of the repulsive Coulomb potential and central potential decreasing more rapidly than the centrifugal one?
[DE93-634308] 07 p3007 N94-26472

Study of the process (pi)(sup -)A(yields)(pi)(sup -)(eta)'(eta)A at the moment 36 GeV/c
[DE93-634530] 07 p3024 N94-27250

Predictions of momentum and scalar fields in a jet in cross-flow using first and second order turbulence closures 07 p2803 N94-28025

Melt flow during alloy solidification: Dimensional analysis and model problems
[PB94-138625] 08 p3206 N94-29997

On determination of a momentum of Alfven wave packet
[DE94-608329] 08 p3255 N94-30172

Deexcitation processes in nuclear reactions: The study of hot hadronic matter
[DE94-003396] 08 p3492 N94-30836

Gas dynamics for accretion disk simulations
09 p3932 N94-31144

MOMENTUM ENERGY

U KINETIC ENERGY

MOMENTUM THEORY

Dynamics of adaptive structures: Design through simulations
[NASA-CR-193724] 02 p0540 N94-13112

Pinching solutions of slender cylindrical jets
[NASA-CR-191482] 02 p0630 N94-13114

Momentum loss in proton-nucleus and nucleus-nucleus collisions
[NASA-TP-3405] 06 p2540 N94-24305

Unified approach for incompressible flows
06 p2342 N94-25356

Computation of non-isentropic internal flows with variable density
[AD-A274848] 07 p2794 N94-26801

Excited Landau levels, orbital angular momentum and axial anomaly
[DE94-606407] 07 p3068 N94-27679

Measuring attitude with a gradiometer
11 p4206 N94-35630

MOMENTUM TRANSFER

Crossing-odd spin effects in the dipole model of hadron scattering
[DE93-617692] 01 p0362 N94-10551

Momentum management in redundant manipulators for vibration suppression
[NASA-CR-194112] 01 p0180 N94-10821

Accretion disk viscosity and internal waves in disks
01 p0153 N94-11615

Air-sea fluxes and universal constants in weak-turbulence theory of surface gravity waves
01 p0195 N94-11922

Mixed layer heat budget of Kuroshio-Tango triangle using satellite and ship observations 01 p0196 N94-11925

High freestream turbulence effects on the transport of heat and momentum 02 p0633 N94-13559

Studies of momentum and energy transfer across wavy gas-liquid interfaces
[AD-A266432] 02 p0635 N94-13699

The role of electric field shear stabilization of turbulence in the H-mode to VH-mode transition in D3-D
[DE93-015474] 02 p0802 N94-14583

On transport of energy, momentum, orbital angular momentum and self-angular momentum of electromagnetic wave in dispersal media
[DE93-624179] 02 p0617 N94-14883

A global traveling wave on Venus
[NASA-CR-194356] 03 p1246 N94-15182

Gas-grain energy transfer in solar nebula shock waves: Implications for the origin of chondrules
03 p1262 N94-16251

The pp elastic scattering experiment at RHIC and polarization studies in the Coulomb Nuclear Interference region
[DE93-015391] 03 p1187 N94-16829

Production of D-mesons in pp-collisions and quark-gluon string model
[DE93-626721] 03 p1185 N94-17312

Transformation of energy and momentum due to Landau damping in space
[DE93-624921] 04 p1581 N94-17689

Neutron and PIMC determination of the longitudinal momentum distribution of HCP, BCC and normal liquid He-4
[DE93-019009] 05 p1972 N94-20187

Physical chemistry of energetic nitrogen compounds
[AD-A271819] 05 p1712 N94-20625

Studies of the deuteron at high energy and momentum transfer
[DE93-041162] 05 p1976 N94-21941

Momentum loss in proton-nucleus and nucleus-nucleus collisions
[NASA-TP-3405] 06 p2540 N94-24305

Proton spin: The role of quark-gluon and hadron degrees of freedom
[DE93-616867] 06 p2538 N94-25341

The amplitude of the elastic hadron-hadron scattering in the coulombic range of transfer momenta
[DE93-613183] 07 p3014 N94-25869

Two dimensional self-consistent fluid simulation of RF inductive sources
[DE94-003635] 07 p2767 N94-25937

A study of LPM suppression of bremsstrahlung at 25 GeV
[DE94-003457] 07 p3018 N94-26133

Topics in longshore currents
[AD-A274788] 07 p2899 N94-26361

Relativistic collision rate calculations for electron-air interactions
[DE94-004204] 07 p3020 N94-26527

The challenges of exclusive processes in QCD
[DE94-003429] 07 p3024 N94-27050

Experimental measurement of local displacement and chemical pair correlations in crystalline solid solutions
[DE94-001124] 07 p3065 N94-27251

Volume averaged model for the mechanics of alloys solidification
[PB94-138617] 08 p3208 N94-30113

On determination of a momentum of Alfven wave packet
[DE94-608329] 08 p3255 N94-30172

On the structure and atomic motions in liquid sodium
[DE94-608386] 08 p3490 N94-30182

The dynamical settling of warped disks and angular momentum transport in galaxies
09 p3928 N94-31121

Theory of protostellar accretion disks
09 p3931 N94-31136

A fully two-dimensional, non-oscillatory advection scheme for momentum and scalar transport equations
[DM-66] 09 p3700 N94-31221

State-to-state dynamics of molecular energy transfer
[DE94-009651] 11 p4324 N94-35816

MONATOMIC GASES

Measurements of scattering processes in negative ion-atom collisions
[DE93-013863] 02 p0779 N94-12940

Calculation of hypersonic shock structure using flux-split algorithms
[NASA-CR-194296] 02 p0504 N94-13607

To extend the thirteen-moment theory and its application to problems in rarefied hypersonic flow
[AD-A267384] 03 p0859 N94-17021

The stellar and gaseous content of massive low surface brightness disk galaxies 09 p3933 N94-31495

On the various forms of the energy equation for a dilute, monatomic mixture of nonreacting gases
[NASA-CR-4612] 11 p4190 N94-35864

MONAURAL SIGNALS

Head related transfer function pseudo-stereophony
[NASA-CASE-ARC-11919-1-NP]
06 p2525 N94-23312

Monaural and binaural processing of complex waveforms
[AD-A274209] 07 p3010 N94-27067

Modelling the late part of room impulse responses using adaptive filtering: On the recreation of reality
[CTH-E-93-01] 09 p3859 N94-31076

MONGOLIA

National space programmes and application of the remote sensing data in Mongolia
01 p0036 N94-10686

Station climatic summaries: China, the former USSR, and Mongolia
[AD-A276548] 09 p3784 N94-32057

MONITORS

Measurement of display transfer characteristics using test pictures
[BBC-RD-1992/13] 01 p0133 N94-11023

A high-precision direct current measuring device over a kiloampere range
[DE93-626409] 02 p0627 N94-14885

Automated data collection system for the TCM3 transcutaneous pO2/pCO2 monitoring system
[AD-A268400] 03 p1129 N94-17424

Measuring emittance using beam position monitors
[DE93-014470] 04 p1434 N94-17709

Solid-state, resistive hydrogen sensors for safety monitoring
[DE93-017769] 04 p1424 N94-17778

VPU(tm) demonstration mission vicinity processor unit(tm) overview 04 p1325 N94-19171

An embedded fibre optic for damage growth monitoring in Kevlar composites
[ISBN-0-315-83501-X] 05 p1677 N94-22589

Generic microelectronic smart sensor platform for detection of toxic, hazardous, and flammable gases
[DE93-017626] 06 p2343 N94-23200

Particle size measurement for the control of industrial crystallizers
[PB94-119104] 06 p2562 N94-23766

Mars Observer screen display design for a multimission environment 06 p2197 N94-23888

A comparison of sleep scored from electroencephalography to sleep scored by wrist actigraphy
[AD-A273739] 07 p2910 N94-26748

Automatic, real-time fault monitor verifying network in a microwave landing system
[CA-PATENT-1325261] 07 p2665 N94-27275

Monitor for status epilepticus seizures
08 p3397 N94-30460

A transmission-loss monitor using current transformers
[DE94-003974] 08 p3267 N94-30716

Pre-flight testing of Thermoelectric Quartz Crystal Microbalances (TQCM) for midcourse space experiment (MSX) spacecraft
[AD-A277054] 09 p3610 N94-32010

Continuous measurement of aging response in aluminum alloys by eddy current methods
[AD-A277233] 09 p3644 N94-32371

Iwmeter: A real-time and interactive parallel software monitor for iWarp
[AD-A277587] 10 p4104 N94-33427
Development of large area, tiled, liquid crystal display
[AD-A277564] 10 p4039 N94-33588
Application of neural networks in multiple sensor fusion for on-line tool wear monitoring
10 p4119 N94-34347
A real-time 2-D composite damage monitoring system employing neural network 10 p4074 N94-34355
Adjustable control station with movable monitors and cameras for viewing systems in robotics and teleoperations
[NASA-CASE-NPO-17837-1-CU]
11 p4332 N94-35384
Intelligent processing of materials, technical activities, 1993 (NAS-NRC Assessment Panel, April 21-22 1994)
[PB94-164183] 11 p4251 N94-35737

MONKEYS
Computer software and hardware to determine contrast sensitivity using three methods: Tracking, limits, and constant stimuli
[AD-A265168] 01 p0324 N94-11099
Locus coeruleus, vigilance, and stress: Brain mechanisms of adaptive behavioral responsiveness
[AD-A265657] 01 p0302 N94-12441
Selection of behavioral tasks and development of software for evaluation of rhesus monkey behavior during spaceflight
[NASA-CR-194176] 02 p0728 N94-13865
Somatosensory responsiveness in behaving monkeys and human subjects
[AD-A268924] 04 p1501 N94-18231
Extrathalamic modulation of cortical function
[AD-A270869] 04 p1507 N94-19783
Susceptibility of the squirrel monkey to different motion conditions 05 p1885 N94-21899
Recovery of the vomiting reflex following area postrema ablation in squirrel monkeys 05 p1886 N94-21904
Motion sickness elicited by passive rotation in squirrel monkeys 05 p1887 N94-21905
Conditioned taste aversion and motion sickness in cats and squirrel monkeys 05 p1888 N94-21914

MONOCHROMATIC RADIATION
A comparison of calculated and observed monochromatic type Ia supernova light curves
[MPA-709] 03 p1237 N94-17629
The coherent backscattering opposition effect
05 p1991 N94-20646

MONOCHROMATIZATION
Conical geometry for sagittal focusing as applied to x rays from synchrotrons
[DE93-017238] 04 p1593 N94-17760

MONOCHROMATORS
Monochromator SP-017. The results of the first experiments
[DE93-617463] 01 p0372 N94-10849
Magnetic circular dichroism in x ray absorption and core-level photoemission
[DE93-019381] 05 p1688 N94-19986
Modifications to 8x8 dynamical theory: Polarizations redefined according to x ray diffraction convention
[DE94-001290] 06 p2560 N94-23187
Proposed additions to the SHADOW ray-tracing code for general-asymmetric perfect-crystal optics
[DE94-001291] 06 p2560 N94-23188
Design of a high-precision double crystal tunable monochromator
[DE94-003004] 07 p2811 N94-26787

MONOCRYSTALS
U SINGLE CRYSTALS

MONOCULAR VISION
Motion and structure from planar motion in noisy monocular image sequences 08 p3308 N94-30299

MONOIDS
On semisimple cocommutative bialgebras
[CWI-AM-R9210] 05 p1954 N94-21158

MONOLITHIC CIRCUITS
U INTEGRATED CIRCUITS

MONOMERS
Photoinitiated radical polymerization of liquid monomers in microgravity 01 p0124 N94-10246
New aromatic activated dihalides and bisphenol monomers for the preparation of novel poly(arylene ethers)
[NASA-CR-193190] 01 p0055 N94-10513
Thermal stability of sealants for military aircraft: Modification of polysulfide prepolymers with ether and thioether monomers
[AD-A264079] 01 p0089 N94-11107
The 13C and 15N solid-state NMR of copolymers of nylon 6 and 7: Observation of a stable pseudohexagonal phase
[AD-A265799] 01 p0094 N94-12381
Synthesis and polymerization of oligomeric multiple aromatic ether-containing phthalonitriles
[AD-D015729] 01 p0094 N94-12399
Unexpectedly rapid hydrosilation polymerization of the diallyl derivative of bisphenol A and 2,6-diallylphenol
[AD-A265832] 02 p0577 N94-12986
Poling of thin polymer films in electro optic applications
[AD-A266562] 02 p0579 N94-13584
Phases and phase transitions of polymeric liquid crystals: A high resolution x ray diffraction and light scattering study
[ITN-93-85218] 02 p0816 N94-14826
Compounds containing meta-biphenylenedioxy moieties and polymers therefrom
[NASA-CASE-LAR-14517-1] 03 p0965 N94-15879
Swelling equilibria for temperature-sensitive ampholytic hydrogels
[DE93-015264] 03 p0966 N94-15996
Photochemically induced transformations of transition complexes
[AD-A271112] 05 p2014 N94-19982
Lateral distribution of lipids in membranes at high pressure
[AD-A271183] 05 p1700 N94-20299
Column chromatographic separation of Y(3+) from Sr(2+) by polymeric ionizable crown ether resins
[DE94-000935] 05 p1683 N94-22021
The use of expanding monomers in carbon fibre composites
[ISBN-0-315-83550-8] 06 p2226 N94-22890
Di(hydroxyphenyl)- 1,2,4-triazole monomers
[NASA-CASE-LAR-14440-2] 06 p2252 N94-23075
Di(hydroxyphenyl)- benzimidazole monomers
[NASA-CASE-LAR-14643-2] 06 p2253 N94-23305
Phenylethynyl-terminated poly(arylene ethers)
[NASA-CASE-LAR-14797-1] 06 p2253 N94-23307
Method of determining shear stress employing a monomer-polymer laminate structure
[NASA-CASE-LAR-14654-2] 06 p2375 N94-23308
Reaction of isocyanates with carboxylic acids and its application to polymer synthesis
[PB94-118858] 06 p2254 N94-23763
STM studies of LB deposited alkyl substituted polyaniline and its corresponding monomer
[AD-A273553] 06 p2257 N94-24562
High temperature adhesive
[AD-D016019] 06 p2258 N94-24737
Synthesis of polyphenylenes via Bergman cyclization of enediyne monomers
[AD-A273298] 06 p2260 N94-24924
Curing phthalonitriles with acid
[AD-D015996] 06 p2261 N94-25054
Synthesis of molecular wires by a novel divergent/convergent approach
[AD-A273332] 06 p2537 N94-25087
LB-Deposited, side-chain substituted polyaniline, polypyrrole and the corresponding monomers, studied by STM
[AD-A274405] 07 p2754 N94-26977
Langmuir-Blodgett and STM investigations of conducting polymer thin films
[AD-A274512] 07 p2755 N94-27087
New monomers for high performance polymers
07 p2758 N94-27904
Isomeric poly(benzophenone)s: Synthesis of highly crystalline poly (4, 4 foot-benzophenone) and amorphous poly (2, 5-benzophenone), a soluble poly (p-phenylene) derivative
[AD-A277261] 09 p3655 N94-32017
Recovery of carboxylic acids at pH greater than pKa
[DE94-007030] 09 p3636 N94-32376
Novel polydiacetylenes as materials for second and third order nonlinear optics
[AD-A277512] 09 p3664 N94-33082
Polymers of BIS (Ethynylstyryl) benzene and related monomers
[AD-D016194] 10 p4030 N94-34407
Polymer from DIIMIDO-DI-PHTHALONITRILE
[AD-D016189] 10 p4030 N94-34682
Tough, processable semi-interpenetrating polymer networks from monomer reactants
[NASA-CASE-LAR-14838-1] 11 p4242 N94-35233
Addition polyimides with enhanced processability
[NASA-CASE-LEW-15043-1] 11 p4242 N94-35234
Thermal cis-trans isomerization rates of azobenzenes bound in the side chain of some copolymers and blends
[AD-A280451] 12 p4424 N94-37227
Basic solutions to carbon/carbon oxidation: Science and technology
[AD-A280447] 12 p4404 N94-37232
Synthesis of phthalonitrile resins containing ether and imide linkages with aromatic diamine curing agent
[AD-D016309] 12 p4427 N94-37778

MONOMOLECULAR FILMS
NT LANGMUIR-BLODGETT FILMS
Nanofabrication by focused ion beam
[AD-A271290] 04 p1345 N94-19746
Chemically sensitive interfaces on SAW devices
[DE94-001832] 06 p2526 N94-23718
Synthesis and characterization of two-dimensional molecular recognition interfaces
[AD-A273177] 06 p2536 N94-24729
Liquid crystalline side-chain polysiloxanes with 4-amino-4'-stilbene-carboxylic ester mesogens
[AD-A274510] 07 p2754 N94-27036
Surface structure and stereochemical properties of self-assembled monolayer materials
[DE94-004960] 08 p3484 N94-28578
Adhesion of phospholipid monolayers to planar supports deposited with the Langmuir-Blodgett technique
[PB94-148699] 10 p4029 N94-34102
SAW chemical sensor arrays using new thin-film materials
[DE94-011940] 12 p4411 N94-37365
Magnetic and structural instabilities of ferromagnetic and antiferromagnetic Fe/Cu(100)
[DE94-011504] 12 p4509 N94-37517

MONOPLANES
NT B-50 AIRCRAFT
NT B-52 AIRCRAFT
NT B-70 AIRCRAFT
NT BOEING 720 AIRCRAFT
NT BOEING 737 AIRCRAFT
NT BOEING 757 AIRCRAFT
NT BOEING 767 AIRCRAFT
NT C-130 AIRCRAFT
NT C-131 AIRCRAFT
NT C-135 AIRCRAFT
NT C-141 AIRCRAFT
NT DC 8 AIRCRAFT
NT F-5 AIRCRAFT
NT F-104 AIRCRAFT
NT F-106 AIRCRAFT
NT MYSTERE 20 AIRCRAFT
NT P-3 AIRCRAFT
NT S-2 AIRCRAFT
NT S-3 AIRCRAFT
NT T-38 AIRCRAFT
NT T-39 AIRCRAFT
NT U-2 AIRCRAFT
NT X-14 AIRCRAFT
NT X-31 AIRCRAFT
NT XV-5 AIRCRAFT

MONOPOLE ANTENNAS
NT WHIP ANTENNAS
Design of a matching network for dipole antennas
[AD-A265115] 01 p0136 N94-11158
Design of a continuous resistively loaded monopole antenna
[AD-A265852] 01 p0138 N94-12281
Design of broadband wire antennas for frequency hopping applications
[AD-A267405] 03 p1001 N94-17025
The analysis of low-profile, broadband, monopole, vehicle antennas and matching network synthesis
[AD-A268340] 03 p1006 N94-17582
A broadband V-antenna for pulsed field measurements: Experimental results 05 p1745 N94-22139
Receiving antennas for electromagnetic pulses and transients
[ISBN-0-315-62312-8] 07 p2777 N94-27871
Time domain spectroscopy for studying a monopole antenna immersed in a plasma
[ISBN-0-315-86526-1] 09 p3888 N94-31727

MONOPOLES
NT MAGNETIC MONOPOLES
Design of a continuous resistively loaded monopole antenna
[AD-A265852] 01 p0138 N94-12281
Moduli space of monopoles and some invariants of 3-manifolds
[PB94-167756] 11 p4314 N94-35764

MONOPROPELLANTS
Monopropellant aqueous hydroxyl ammonium nitrate/fuel
[AD-D015922] 05 p1712 N94-20061
Chemistry of the burning surface
[AD-A272725] 05 p1681 N94-21181
Weld joint concepts for on-orbit repair of Space Station Freedom fluid system tube assemblies
06 p2371 N94-24427
Liquid monopropellants
[AD-D016074] 07 p2760 N94-28226

MONOPULSE ANTENNAS
Topographic mapping using a monopulse SAR system
05 p1721 N94-20417
Microstrip monopulse antenna for land mobile communications 06 p2289 N94-22833
Beam-waveguide antenna servo design issues for tracking low earth-orbiting satellites
06 p2292 N94-23268

MONOPULSE RADAR
Cancellation of multipath for monopulse radars
[ITN-93-85191] 02 p0600 N94-13538
Enhanced down-range profiles of complex targets using wideband radar echo returns
[AD-A266508] 03 p0999 N94-16788
Radome depolarization effects on monopulse receiver tracking performance
[AD-A267446] 03 p1001 N94-17031
Topographic mapping using a monopulse SAR system
05 p1721 N94-20417
Method and apparatus of generating sum or difference signals corresponding to an apparent beam in a monopulse radar system
[AD-D015998] 06 p2302 N94-25056
Method and apparatus for determining target elevation angle, altitude and range, and the like in a monopulse radar system with reduced multipath errors
[AD-D016005] 06 p2302 N94-25058
Methods for improving low-angle, low-altitude radar tracking accuracy
[AD-A274914] 07 p2768 N94-26347
Radar cross sections of ground clutter at 95 GHz for summer and fall conditions 08 p3259 N94-30512
Estimation with multisensor/multiscan detection fusion
[AD-A278753] 11 p4256 N94-36092
MONOSACCHARIDES
NT GLUCOSE
MONOTECTIC ALLOYS
Marangoni motion during melting of a hypermonotectic alloy: Numerical simulations for the D2 experiment IHF04 01 p0113 N94-10177
Study on solidification of immisible alloys (M-10)
02 p0588 N94-13742
Immiscible phase incorporation during directional solidification of hypermonotectics
[NASA-CR-194412] 02 p0565 N94-14480
Separation behaviour of monotectic alloys
03 p0945 N94-15170
MONOTONE FUNCTIONS
Monotone approximate query processing
[AD-A267153] 03 p1169 N94-15779
Existence of a maximal solution for quasimonotone elliptic systems
[PB94-149689] 04 p1550 N94-19153
Using geometric techniques to improve dynamic programming algorithms for the economic lot-sizing problem and extensions
[PB93-197556] 04 p1528 N94-19330
Isotonic estimation and rates of convergence in Wicksell's problem
[REPT-93-39] 07 p3002 N94-26213
MONSOONS
Climate variability in a coupled GCM. Part 2: The Indian Ocean and monsoon
[MPIM-104] 06 p2401 N94-23159
Investigation of mesoscale convective cloud clusters in South China
[AD-A274303] 07 p2895 N94-26678
Propagation of cold air masses in East Asia and its associated planetary-scale function
[AD-A274304] 07 p2895 N94-26850
Simulation of the Indian and East-Asian summer monsoon in the ECMWF model: Sensitivity to horizontal resolution
[DE94-004276] 07 p2897 N94-27571
Study of dynamic characteristics of a monsoon circulation tube
[AD-A275238] 08 p3370 N94-29394
Numerical simulations of monsoon rainfall with the NRL/NCSU regional nested grid model
09 p3782 N94-31791
Forecasters handbook for the Philippine Islands and surrounding waters
[AD-A277993] 09 p3787 N94-33089
MONTE CARLO METHOD
Deformation mechanisms of continuous fibre-reinforced thermoplastic composites during manufacturing: A probabilistic approach 01 p0060 N94-10030
Heat analysis of thermoplastic components during the initial stages of manufacturing: A probabilistic approach
01 p0060 N94-10031
Techniques, processes, and measures for software safety and reliability
[DE93-012379] 01 p0322 N94-10347
Three-dimensional hypersonic rarefied flow calculations using direct simulation Monte Carlo method
01 p0007 N94-10449
Monte Carlo simulations of a two-dimensional hard dimer system
[DE93-613535] 01 p0361 N94-10502
Cosmological gamma-ray burst model
[NASA-CR-193368] 01 p0484 N94-10507
Acceleration of positrons in supernova shocks
[NASA-CR-193713] 01 p0425 N94-10511
Monte Carlo simulations of phase transformations in Fe-Cr alloys
[DE93-013847] 01 p0081 N94-10522
Monte Carlo algorithms in simulation of 2beta-decay and penetration of electrons through matter
[DE93-617741] 01 p0364 N94-10837
ACARA user's manual
[NASA-TM-106277] 01 p0183 N94-11167
Bi-directional reflectance by oceanic waters studied via Monte-Carlo simulations 01 p0203 N94-11971
The evaluation of radiative process in the atmosphere-ground system by Monte Carlo method
01 p0205 N94-11980
Venus resurfacing rates: Constraints provided by 3-D Monte Carlo simulations 01 p0453 N94-12119
PDF approach for turbulent scalar field: Some recent developments 01 p0160 N94-12315
Propagation of light pulses through a three-layer medium (cloud, pure air, and ocean water)
01 p0222 N94-12725
A new method to assess Monte Carlo convergence
[DE93-012667] 02 p0772 N94-12919
Parallelizing Timed Petri Net simulations
[NASA-CR-194278] 02 p0758 N94-12938
HIJET with AGS physics and N(sup *)'s
[DE93-014022] 02 p0780 N94-13097
GRO: Black hole models for gamma ray bursts
[NASA-CR-193244] 02 p0829 N94-13178
Beta/gamma test problems for ITS
[DE93-013522] 02 p0781 N94-13349
Variance reduction unique to coupled electron/photon Monte Carlo transport
[DE93-014999] 02 p0782 N94-13409
Maximum likelihood estimation for constrained or missing data models
[AD-A266563] 02 p0773 N94-13585
Determining the solar-flare photospheric scale height from SMM gamma-ray measurements
[NASA-CR-194084] 02 p0844 N94-13671
ADP study of gamma-ray bursts
[NASA-CR-194311] 02 p0848 N94-13708
Distributed processor Monte Carlo: MCNP results on a 16-node IBM cluster
[DE93-012639] 02 p0752 N94-14176
Quantum Monte Carlo by message passing
[DE93-012645] 02 p0760 N94-14177
Hybrid S(sub N)/Monte Carlo research and results
[DE93-012677] 02 p0773 N94-14178
Monte Carlo simulation of the OCP freezing transition
[DE93-013039] 02 p0811 N94-14313
Deconvolution for positive signals
[DE93-013044] 02 p0773 N94-14314
Development and application of the automated Monte Carlo biasing procedure in SAS4
[DE93-015205] 02 p0774 N94-14334
Results from a water-Cerenkov array
[DE93-012715] 02 p0849 N94-14461
Measuring parity violation using the neutron capture reaction
[DE93-016629] 02 p0786 N94-14514
Robust estimators and tests in one-sample location problem with particular consideration on modified maximum likelihood process
[ETN-93-94391] 02 p0774 N94-14703
Statics and kinetics of phase transformations in bcc Fe-Cr
[DE93-013839] 02 p0574 N94-14793
The LAHET code system: Introduction, development, and benchmarking
[DE93-012657] 02 p0787 N94-14804
Particle simulations on massively parallel machines
[DE93-015644] 03 p1157 N94-14927
DSMC simulations of Mach 20 nitrogen flows about a 70 degree blunted cone and its wake
[NASA-TM-107762] 03 p1018 N94-15291
Particle kinetic simulation of high altitude hypervelocity flight
[NASA-CR-194599] 03 p0856 N94-15678
Study of multi-dimensional radiative energy transfer in molecular gases
[NASA-CR-194613] 03 p1181 N94-15752
Particle simulation of hypersonic flow
[AD-A267185] 03 p0857 N94-15787
Investigation of radiative interaction in laminar flows using Monte Carlo simulation
[NASA-CR-194604] 03 p1021 N94-15795
General Monte Carlo reliability simulation code including common mode failures and HARP fault/error-handling
[NASA-CR-187587] 03 p1150 N94-16594
Abundance recovery error analysis using simulated AVIRIS data 03 p1074 N94-16708
Diffuse scattering and image contrast of tweed in superconducting oxides: A simulation and interpretation
[DE93-016131] 03 p1212 N94-16844
Simulation reduction using the Taguchi method
[NASA-CR-4542] 03 p1055 N94-17082
Planning under uncertainty solving large-scale stochastic linear programs
[DE93-013920] 04 p1516 N94-17701
Direct Monte Carlo simulation of the chemical equilibrium composition of detonation products
[DE93-014559] 04 p1376 N94-17751
Heavy ion nuclear physics research
[DE93-018862] 04 p1565 N94-17776
Investigation of the relative abundance of heavy versus light nuclei in primary cosmic rays using underground muon bundles
[DE93-017601] 04 p1630 N94-17818
Criticality benchmark comparisons leading to cross-section upgrades
[DE93-017184] 04 p1556 N94-18073
Recent studies of short-range order in alloys: The Cowley theory revisited
[DE93-016416] 04 p1358 N94-18111
Diffusion in ordered alloys
[AD-A268232] 04 p1359 N94-18322
Simulation of emittance dilution in electron storage ring from Compton backscattering
[DE93-017611] 04 p1386 N94-18503
Bayesian model choice: Asymptotics and exact calculations
[AD-A269067] 04 p1557 N94-18516
Bayesian analysis of ARMA processes: Complete sampling based inference under full likelihoods
[AD-A269168] 04 p1557 N94-18694
Polarimetric statistics of electromagnetic waves scattered by distributed targets
[PB93-195907] 04 p1389 N94-18951
The PAPAGENO Partonic Monte-Carlo Program
[DE93-018524] 04 p1571 N94-19247
Single sided tomography of extremely large dense objects
[DE93-017993] 04 p1580 N94-19268
Sensitivity and uncertainty analysis of Markov reward models
[MEMO-INF-92-89] 04 p1559 N94-19386
An ab initio Monte Carlo study of low energy positron and electron implantation in elemental metals and multilayers
[DE93-019847] 04 p1603 N94-19541
Uncertainty versus interindividual variability
[DE93-018105] 04 p1559 N94-19549
Chemical equilibrium in high pressure molecular fluid mixtures
[DE93-040160] 05 p1796 N94-19829
Neutron and PIMC determination of the longitudinal momentum distribution of HCP, BCC and normal liquid He-4
[DE93-019009] 05 p1972 N94-20187
The GEM Silicon Tracking System
[DE93-040133] 05 p2016 N94-20322
A theoretical and numerical study of polarimetric scattering and emission from random rough surfaces with anisotropic directional spectrum
05 p1730 N94-20454
One- and multi-component theories of mixtures
[DE93-040543] 05 p1966 N94-21511
Interpolative modeling of GaAs FET S-parameter data bases for use in Monte Carlo simulations
05 p1767 N94-21723
High power, electron-beam induced switching in diamond
[DE93-040535] 05 p1768 N94-21770
A simulation model for probabilistic analysis of Space Shuttle abort modes
[NASA-TM-108432] 05 p1656 N94-21859
Toward a QCD analysis of jet rates in deep-inelastic Muon-Proton scattering
[DE94-000618] 05 p1976 N94-21962
A unified Monte Carlo interpretation of particle simulations and applications to nonneutral plasmas
[DE94-001231] 05 p1997 N94-21973
Monte Carlo calculation of multi-electron effects on synchrotron radiation
[DE94-001259] 05 p1982 N94-21974
A High Resolution Liquid Xenon Imaging Telescope for 0.3-10 MeV Gamma Ray Astrophysics: Construction and Initial Balloon Flights
[NASA-CR-194709] 05 p2056 N94-22281
The polarization sensitivity of the liquid xenon imaging telescope 05 p2056 N94-22282
Simulating the Euclidean time Schroedinger equations using an INTEL iPSC/860 hypercube: Application to the t-J model of high-T(sub c) superconductivity
[DE94-000489] 05 p2035 N94-22385
Algorithmic advances in stochastic programming
[DE94-001160] 05 p1921 N94-22406
A Monte Carlo study of the Sudbury Neutrino Observatory small test detector experiment
[ISBN-0-315-59056-4] 05 p1977 N94-22416

Likelihood analysis of parity violation in the compound nucleus
[DE94-000671] 05 p1977 N94-22572
Analysis of a proposed Compton backscatter imaging technique
[DE93-040537] 06 p2371 N94-22935
Coherence lost? Not-so-fast escapes from the in-phase attractor of a set of globally coupled nonlinear oscillators
[DE94-000799] 06 p2557 N94-22940
Molecular gas dynamics applied to low-thrust propulsion 06 p2214 N94-23053
Monte Carlo climate change forecasts with a global coupled ocean-atmosphere model
[MPIM-97] 06 p2407 N94-23156
Accuracy control in Monte Carlo radiative calculations 06 p2321 N94-23639
Thermal analysis of combinatorial solid geometry models using SINDA 06 p2323 N94-23650
Integral equations for the microstructures of supercritical fluids
[DE94-002460] 06 p2535 N94-24569
Bounds and simulation results of 32-ary and 64-ary quadrature amplitude modulation for broadband-ISDN via satellite
[NASA-TM-106484] 06 p2202 N94-25095
Effect of high frequency field on the transport properties of superlattice
[DE93-617047] 06 p2568 N94-25447
On the hadron formation time in pion-nucleus interaction
[DE93-616879] 06 p2539 N94-25476
Penetrating nature of very collimated high-energy shower-clusters of hadrons and gamma rays 07 p3113 N94-25631
NNN-Ising model simulation of nanodomain textures in relaxor-type lead scandium tantalate
[DE94-601884] 07 p2748 N94-25844
On radiation defects in strip detectors
[DE93-616646] 07 p3015 N94-25916
Monte Carlo event generators for hadron-hadron collisions
[DE94-003212] 07 p3015 N94-25955
Crossover between BCS and performed-Boson theories with increasing interactions
[DE93-019018] 07 p3017 N94-26078
Laser manipulation of metastable neon atoms
[ETN-94-95344] 07 p2817 N94-26225
Modelling of ionisation reactions and of the resulting electric fields in one-dimensional hypersonic shock waves with the direct simulation Monte Carlo method
[IC-AERO-92-01] 07 p2644 N94-26248
Ising critical behaviour in the one-dimensional frustrated quantum XY model
[DE93-634755] 07 p3057 N94-26390
C-periodicity and the physical mass in the 3-state Potts model
[DE94-601551] 07 p3019 N94-26423
Subgraph approximations for large directed graphical models
[AD-A274813] 07 p3003 N94-26485
Simulation approaches for calculations in directed graphical models
[AD-A274825] 07 p3003 N94-26494
Stochastic solution to quantum dynamics
[NASA-TP-3408] 07 p3114 N94-26550
Measuring the time dependence of B(sub s)(sup 0) meson - anti B(sub s)(sup 0) meson oscillations
[ISBN-0-315-84367-5] 07 p3021 N94-26665
Direct simulation Monte-Carlo of near continuum hypersonic flow with chemical reactions
[DLR-FB-93-01] 07 p2797 N94-27588
Monte Carlo calculations of low background detector response
[DE94-004593] 07 p3116 N94-27621
Numerical and experimental analyses of the radiant heat flux produced by quartz heating systems
[NASA-TP-3387] 07 p3011 N94-27659
BATSE burst location accuracy and constraints on the fraction of repeating GRB sources
[DE94-004981] 07 p3116 N94-27714
Modeling the DMSP and CRRES dosimeters using the path length distribution method
[RXR-93051] 07 p2698 N94-28200
The PROTEL contamination code
[RXR-93071] 07 p3040 N94-28202
A measurement of the LMP effect
[DE94-005225] 08 p3482 N94-28493
On the prediction of HAZ grain size using Monte Carlo simulation
[DE94-005465] 08 p3511 N94-28535
Energy losses of fast charged particles in thin silicon detectors
[DE94-606065] 08 p3483 N94-28552
Solution of charged particle transport equation by Monte-Carlo method in the BRANDZ code system
[DE94-606270] 08 p3484 N94-28614
A family of joint probability models for cost and schedule uncertainties
[AD-A275513] 08 p3463 N94-28670
SOCRATES simulation of the emission at wavelength 6300 A generated by the interaction between the atmosphere and the Space Shuttle exhaust
[AD-A275567] 08 p3164 N94-28827
Proceedings of the 10th NAL Symposium on Aircraft Computational Aerodynamics
[NAL-SP-19] 08 p3123 N94-28946
Monte Carlo simulation or normal shock wave. Part 2: VHS model and VSS model 08 p3123 N94-28948
Variable soft sphere molecular model in the Monte Carlo simulation of air species 08 p3123 N94-28949
The appearance of the Sun and Moon seen through clouds
[AD-A275338] 08 p3551 N94-29212
Focused ion beam fabrication of microelectronic structures
[AD-A275384] 08 p3264 N94-29305
The maximum entropy approach applied to energy exchange, chemical reactions and ionisation in the direct simulation Monte Carlo method for rarefied hypersonic flows
[IC-AERO-93-01] 08 p3524 N94-29481
Efficiencies of the ICRF minority heating in the CHS and LHD plasmas
[AD-B183300L] 08 p3506 N94-29499
Performance of MCNP4A on seven computing platforms
[DE93-040101] 08 p3419 N94-29816
Particle kinetic simulation of high altitude hypervelocity flight
[NASA-CR-194535] 08 p3131 N94-29893
Measurement of the W mass in the D0 detector
[DE94-006002] 08 p3490 N94-30103
Estimation of Weibull modulus from dynamic and static fatigue experiments
[PB94-138641] 08 p3322 N94-30114
Ten new checks to assess the statistical quality of Monte Carlo solutions in MCNP
[DE94-006137] 08 p3465 N94-30366
Systematic error estimation in multisensor fusion systems
[AD-B179298] 08 p3428 N94-30764
Hydrogenated amorphous silicon (a-Si:H) based gamma camera: Monte Carlo simulations
[DE94-007042] 09 p3795 N94-31323
Using Monte Carlo techniques and parallel processing for debris hazard analysis of rocket systems
[DE94-007250] 09 p3609 N94-31382
Mixture model simulating reactive turbulent flows: Testing of Eulerian-Lagrangian probabilistic models
[ONERA-NT-1993-13] 09 p3702 N94-31477
Diagonal band probability distributions
[REPT-93-80] 09 p3851 N94-31697
Cometary molecules 09 p3935 N94-31869
ITS version 3.0: Powerful, user-friendly software for radiation modelling
[DE94-006607] 09 p3678 N94-32113
A comparison between two Monte Carlo codes on determination of transient chemical yields
[DE94-007224] 09 p3636 N94-32251
An algorithm for probabilistic, totally-ordered temporal projection
[AD-A277341] 09 p3817 N94-32257
Planetary magnetotails: Magnetic configuration and nonthermal plasma 09 p3942 N94-32326
Parallel Monte Carlo reactor neutronics
[DE94-007642] 09 p3826 N94-32357
Parallel particle simulations of low-density fluid flows
[DE94-007858] 09 p3707 N94-32373
Numerical simulation of quantum many-body systems
[DE94-008451] 09 p3912 N94-32513
Characterization of atomic and molecular impurity sources and transport at the tokamak edge
[DE94-007212] 09 p3891 N94-32619
Complete model description of an electron beam using ACCEPT Monte Carlo simulation code
[DE94-007063] 09 p3872 N94-32628
Implementation and display of Computer Aided Design (CAD) models in Monte Carlo radiation transport and shielding applications
[DE94-007221] 09 p3819 N94-32641
Simulation of low-density nozzle plumes in non-zero ambient pressures
[NASA-TM-106501] 09 p3615 N94-32742
Studies of jet production with the D0 detector
[DE94-008271] 09 p3873 N94-32780
Analytic properties of the OCP and ionic mixtures in the strongly coupled fluid state
[DE94-008216] 09 p3637 N94-32801
Implementation of a vibrationally linked chemical reaction model for DSMC
[NASA-TM-109109] 09 p3710 N94-33020
Design and Monte Carlo analysis of an unmanned aerial vehicle
[AD-A277648] 09 p3580 N94-33056
Simulation of CO2 release at 800 km altitude
[AD-A276692] 09 p3776 N94-33272
Comparison of numerical models for computing underwater light fields
[AD-A278256] 10 p4140 N94-33411
Systolic matrix inversion using a Monte Carlo method
[PB94-148798] 10 p4130 N94-34257
Several modified goodness-of-fit tests for the cauchy distribution with unknown scale and location parameters
[AD-A278496] 10 p4130 N94-34301
Monolith catalysts for closed-cycle carbon dioxide lasers
[NASA-CR-196093] 11 p4271 N94-35489
Point and interval estimation of series system reliability using small data sets
[AD-A278647] 11 p4316 N94-35575
Stopping rules for a class of sampling-based stochastic programming algorithms
[AD-A278654] 11 p4303 N94-35577
Beam tests of a prototype level-1 calorimeter trigger for LHC experiments
[PB94-170495] 11 p4269 N94-35599
Application of a Monte Carlo accuracy assessment tool to TDRS and GPS 11 p4207 N94-35635
Computer simulations of benzene in faujasite-type zeolites
[DE94-007533] 11 p4242 N94-36369
Can we break intractability using randomization or the average case setting?
[AD-A278598] 11 p4316 N94-36425
MCNP: Multigroup/adjoint capabilities
[DE94-010682] 12 p4506 N94-36449
Time-step stability for self-consistent Monte Carlo device simulation
[DE94-012145] 12 p4528 N94-37207
Statistical characterization of rare events 12 p4454 N94-37327
Positron implantation in solids
[DE94-013029] 12 p4537 N94-37499
Probability techniques for reliability analysis of composite materials
[NASA-CR-195294] 12 p4406 N94-37633

MONTEREY BAY (CA)
Evolution of diurnal surface winds and surface currents for Monterey Bay
[AD-A277649] 09 p3790 N94-33057
Characterization of tidal currents in Monterey Bay from remote and in-situ measurements
[AD-A277844] 10 p4092 N94-33767
A comparison of modeled and observed ocean mixed layer behavior in a sea breeze influenced coastal region
[AD-A277911] 10 p4092 N94-33922

MONTMORILLONITE
Reflectance spectra of sulfate-and carbonate-bearing Fe(3+)-doped montmorillonites as Mars soil analogs 01 p0445 N94-12070
Ferric sulfate montmorillonites as Mars soil analogs 09 p3944 N94-33196
Mars atmospheric dust properties: A synthesis of Mariner 9, Viking, and Phobos observations 09 p3945 N94-33200
Thermal emission measurements (5-25 microns) of palagonite/Fe-substituted montmorillonite intimate mixtures: Applications to Mars 11 p4292 N94-35453

MOODS
Determinants of subjective fatigue for C-141 crews during Operation Desert Storm 11 p4196 N94-36338

MOON
Lunar Scout Two spacecraft gravity experiment 01 p0459 N94-12152
Mission to the Moon: An ESA study on future exploration 01 p0460 N94-12153
Exploration planning in the context of human exploration and development of the Moon 01 p0474 N94-12229
Significance and scenarios of lunar and planetary exploration missions 01 p0482 N94-12324
Technical problems on lunar an planetary exploration mission 01 p0482 N94-12328
Tidal interactions in the Earth Moon system
[COMMUNICATIONS-SER-B-160] 02 p0837 N94-13503
The studies on lunar and planetary exploration and utilization: The study on lunar resources utilization
[NASDA-CNT-930014] 02 p0842 N94-13655
Extrapolation of space weathering processes to other small solar system bodies 02 p0843 N94-14300
EUVE observations of the Moon 03 p1250 N94-16185
The Clementine Mission science return at the Moon and Geographos 05 p1652 N94-20650
The Extended Mission Rover (EMR) 07 p2689 N94-25674

The modal solution to the Moon's orbit using canonical Floquet perturbation theory
[AD-A273732] 07 p2690 N94-26001
The appearance of the Sun and Moon seen through clouds
[AD-A275338] 08 p3551 N94-29212
Apollo 11 highlights
[NASA-TM-109763] 09 p3600 N94-31820
Apollo 11: The Goddard connection
[NASA-TM-109815] 10 p4010 N94-33566
High spatial resolution telescopic multispectral imaging and spectroscopy of the Moon. 1: The Serenitatis/Tranquillitatis border region
11 p4356 N94-35402

MOONS
U NATURAL SATELLITES

MOORING
Real-time tomography mooring
[AD-A264923] 01 p0289 N94-11854
The marine light-mixed layer experiment cruise and data report: R/V endeavor cruise EN-224, mooring deployment, 27 April-1 May 1991: Cruise EN-227, mooring recovery, 5-23 September 1991
[AD-A271175] 05 p1864 N94-20186
Vertical motion in the SYNOP central array
[AD-A273593] 06 p2418 N94-24795

MOORINGS
U MOORING

MORAINES
U GLACIAL DRIFT

MORALE
Stress and ergonomic design and evaluation of person-machine systems
[AD-A275156] 08 p3400 N94-29034

MORL
U MANNED ORBITAL LABORATORIES

MORNING
Space-time structure of the morning aurora inferred from coincident DMSP-F6, -F8, and Sondrestrom incoherent scatter radar observations
[AD-A275442] 08 p3356 N94-28869

MORPHOLOGY
NT GEOMORPHOLOGY
NT ISOMORPHISM
NT POLYMORPHISM
Ground results of the Mephisto program: Benefits and space experiments orientation 01 p0086 N94-10197
Physical studies of planetary and satellite surfaces
[NASA-CR-193545] 01 p0434 N94-10817
Characterization of the Si/SiO2 interfere morphology from quantum oscillations in Fowler-Nordheim tunneling currents
[AD-A265149] 01 p0143 N94-11160
Characterization of gas-aerosol interaction kinetics using morphology dependent stimulated Raman scattering
[DE93-012324] 01 p0077 N94-11359
The morphologies of distant radio galaxies
01 p0426 N94-11597
Yana ring structure, North-Eastern Siberia: A possible counterpart of coronae on Venus
01 p0282 N94-12121
Differential scaling: Implications for central structures in large lunar craters 01 p0461 N94-12158
Small volcanoes in Tempe Terra, Mars: Their detailed morphometry and inferred geologic significance
01 p0469 N94-12202
Gravity as a probe for understanding pattern specification
[NASA-CR-194142] 02 p0713 N94-13418
Formation of deoxidization products in iron ingot by the addition of Al, Si, and/or Mn (M-5)
02 p0587 N94-13737
Ion assisted sputter deposition of Mo-Si multilayers
[DE93-013830] 02 p0583 N94-14693
Effects of aging time on V205 sol-gel coatings
[AD-A266824] 03 p0965 N94-15843
Micro- and meso-scale simulations of magnetospheric processes related to the aurora and substorm morphology
[NASA-CR-193437] 03 p1102 N94-17527
Morphology of polymerized membranes on an amorphous substrate at molecular resolution by AFM
[AD-A268760] 04 p1370 N94-18403
Morphology, deformation, and defect structures of TiCr2 in Ti-Cr alloys
[DE93-018332] 04 p1361 N94-18807
A scientific role for Space Station Freedom: Research at the cellular level 04 p1503 N94-19215
Development of a technique to determine the morphology and dynamics of agglomerates in chemically reacting flows
[AD-A271160] 05 p1678 N94-20000
Morphologic and morphometric studies of impact craters in the northern plains of Mars 05 p2089 N94-20384
Response of the topography and gravity field on Venus to mantle upwelling beneath a chemical boundary layer
05 p2117 N94-20775
Contributions of the Clementine mission to our understanding of the processes and history of the Moon
05 p2119 N94-20784
A classification scheme for the morphology of lava flow fields 05 p1863 N94-20879
Structure and morphology of Pd overlayers on epitaxial SnO2 films studies with the atomic force microscope
[AD-A271827] 05 p2028 N94-21458
Growth and morphology of crystals: Theory and observations
[PB93-221166] 05 p2035 N94-22273
Electric field-mediated processing of polymer blend solutions 06 p2223 N94-24341
Polymer morphologh 06 p2226 N94-24353
Hydraulics and morphology of mountain rivers: A literature survey. Communications on hydraulic and geotechnical engineering
[PB94-110772] 06 p2388 N94-24636
Morphology of highly textured polyethylene/polyethylene- propylene semicrystalline diblock copolymers
[AD-A273683] 06 p2263 N94-25413
Characterization of physically vapor deposited AF2400 thin films
[DE94-004019] 07 p2749 N94-25985
Morphological analysis of ionomers
[DE94-003660] 07 p2749 N94-26005
Oxygen reduction at a YSZ interface with cathode materials La(1-x)(Ca or Sr)(x)MnO3(1-x)CaMnO3
[DE94-002954] 07 p3054 N94-26147
MBE grown 3 to 5 strain relaxed buffer layers and superlattices characterized by atomic force microscopy
[DE94-002931] 07 p3056 N94-26308
High definition Raman microscopic imaging
[DE94-003158] 07 p2716 N94-26781
The morphological processing of binary images
[AD-A274310] 07 p2996 N94-26972
Morphology transitions during non-equilibrium growth processes
[ITN-94-85236] 07 p3065 N94-27243
Hydrothermal growth and characterization of oxides in zirconium alloys
[DE94-602981] 07 p2743 N94-27829
Elements for the recognition of three dimensional deformable shapes: Application to biomedical imagery
[TELECOM-93-E-006] 08 p3396 N94-30978
Morphological directional coding of images
[ISBN-0-315-86336-6] 09 p3814 N94-31715
The p-q-r-medial axis algorithm requires only local operations
[CWI-BS-R9317] 09 p3849 N94-32507
Martian deltas: Morphology and distribution
09 p3950 N94-33230
The microstructure and morphology of carbon black: A study using small angle neutron scattering and contrast variation
[DE94-009315] 10 p4022 N94-34098
Morphological aspects of surface reactions
[DE94-010184] 11 p4236 N94-35685
Computational methods for material failure processes
[AD-A278716] 11 p4278 N94-36292
Morphological aspects of surface reactions
[DE94-011208] 12 p4413 N94-37713

MORPHOTROPISM
U ISOMORPHISM

MORTALITY
Evaluation of medical treatments to increase survival of ebullism in guinea pigs 01 p0302 N94-11548
Longitudinal study of astronaut health: Mortality in the years 1959-1991 01 p0312 N94-11560
Health effects of global warming: Problems in assessment
[DE93-040323] 05 p1850 N94-19930
Estimating the impact of crashworthiness standards on mortality and morbidity events in the US Army rotary-wing aircraft mishaps
[AD-A277121] 09 p3575 N94-32363

MOS (JAPANESE SPACECRAFT)
U JAPANESE SPACECRAFT

MOS (SEMICONDUCTORS)
U METAL OXIDE SEMICONDUCTORS

MOSAICS
Radarmap of Germany: First mosaic and classification
01 p0246 N94-12477
Global Magellan-image map of Venus at full resolution
03 p1274 N94-16319
Global and regional/seasonal color mosaics of Mars
03 p1288 N94-16393
Lunar multispectral mosaics from Galileo's second Earth-Moon flyby 03 p1288 N94-16394
Cathodoluminescence observations of in situ aqueous destruction of chondrules in the Murchison CM chondrite
05 p2083 N94-20750
Flight solar calibrations using the Mirror Attenuator Mosaic (MAM): Low scattering mirror
06 p2384 N94-23602
Automating geographically referenced digital mosaics from aerial videography with area-based feature matching 08 p3333 N94-29540
Global color views of Mars 09 p3948 N94-33217
First Galileo image of asteroid 243 Ida
11 p4351 N94-35416

MOSFET
U FIELD EFFECT TRANSISTORS

MOSS (SPACE STATIONS)
U SPACE STATIONS

MOSSBAUER EFFECT
A new matrix for the ageless 21.6-keV Eu-151 nuclear gamma ray Moessbauer source
[DE93-009795] 01 p0075 N94-10338
The peculiarities of the spin glass state in Fe(x)Mn(1-x)TiO3
[DE93-617882] 01 p0395 N94-10525
X ray and gamma ray spectroscopy of solids under pressure
[DE93-014847] 01 p0076 N94-10653
Moessbauer spectroscopy of the SNC meteorite Zagami 01 p0428 N94-12016
Moessbauer spectrometer for mineralogical analysis of the Mars surface: Moessbauer source considerations
01 p0476 N94-12242
Cronstedtite and iron sulfide mineralogy of CM-type carbonaceous chondrites from cryogenic Moessbauer spectra 01 p0433 N94-12257
A Moessbauer spectrometer for the mineralogical analysis of the Mars surface: First temperature dependent tests of the detector and drive system
03 p1259 N94-16233
Suppression of charge scattering in Moessbauer experiments using synchrotron radiation
[DE93-015406] 03 p1212 N94-16887
Pressure induced metallization of the Mott Insulator 6(sub 2)
[DE93-018296] 04 p1600 N94-18969
Gamma scattering in condensed matter with high intensity Moessbauer radiation
[DE93-019461] 04 p1601 N94-19031
Fabrication and evaluation of superconducting and semiconducting materials
[AD-A271645] 05 p2018 N94-20558
Magnetic properties and Moessbauer analyses of glass from the K-T boundary, Beloc, Haiti
05 p1685 N94-20753
Combined backscatter Moessbauer spectrometer/x ray fluorescence analyzer (BaMS/XRF) for extraterrestrial surfaces 05 p1686 N94-20761
Investigation of the solid-solid surface adsorption of Eu2O3 on amorphous Al2O3
[DE93-613824] 06 p2566 N94-25332
The Latin American conference on the applications of the Moessbaer effect
[DE93-615942] 07 p3051 N94-25912
Atomic and magnetic structure of YBa2(Cu(1-x)Fe(x))3O(6+y) at 0.05 less than or equal to x less than or equal to 0.30, y is approximately equal to 1 and y is approximately equal to 0.5
[DE94-606852] 08 p3513 N94-29210
Study of iron exchanged zeolites by Moessbauer effect and electron spin resonance spectroscopy
[DE94-605138] 08 p3514 N94-29691
Backscatter Mossbauer Spectrometer (BaMS) for extraterrestrial applications 08 p3236 N94-29774

MOSSES
U BRYOPHYTES

MOTILITY
U LOCOMOTION

MOTION EQUATIONS
U EQUATIONS OF MOTION

MOTION PERCEPTION
Visual psychophysics of egomotion
[AD-A265253] 01 p0304 N94-11681
Bayesian estimation of motion fields from image sequences
[ISBN-0-315-57212-4] 02 p0772 N94-13540
Comparative measurement of visual stability in Earth and cosmic space (L-4) 02 p0592 N94-13761
Neural basis of motion perception
[AD-A267267] 03 p1133 N94-17265
Overview of research in progress at the Center of Excellence
[NASA-CR-194329] 04 p1618 N94-19256
Pilot studies on object motion perception during linear self-motion after long duration centrifugation of human subjects
[IZF-1993-B-3] 04 p1510 N94-19439
Applications of motion estimation in image processing
[FEL-92-B356] 04 p1580 N94-19455

A non-homogeneous, spatio-temporal, wavelet multiresolution analysis and its application to the analysis of motion
[AD-A270621] 04 p1538 N94-19534
The local measurement and global interpretation of 3D motion field generated by several moving objects from range image sequences 05 p1777 N94-22146
Segmenting the optical flow due to the motion of several rigid objects 05 p1777 N94-22147
Mobile robot perception in unknown and unstructured dynamic voxel environments
[ISBN-0-315-83951-1] 05 p1947 N94-22591
Perception in flight: Shape and motion perception, space perception, spatial orientation, and visual vestibular interaction 06 p2429 N94-23979
Extracting heading and temporal range from optic flow: Human performance issues 06 p2442 N94-25510
Application of Markov random field theory to image coding and motion estimation
[ISBN-0-315-83435-8] 07 p2964 N94-26632
Motion analysis from a sequence of range images
[ISBN-0-315-84684-4] 07 p2969 N94-27311
Estimation of image motion in scenes containing multiple moving objects
[ISBN-0-315-85208-9] 07 p2969 N94-27346
Frequency analysis of body sway induced by optokinetic stimulation 07 p2914 N94-27455
Effects of imaginary target on induced eye movements by linear acceleration 07 p2914 N94-27456
Motion and structure from planar motion in noisy monocular image sequences 08 p3308 N94-30299
Obstacle detection for an autonomous vehicle 08 p3309 N94-30302
Aspects of vision and planning in a dynamic, uncertain environment 08 p3448 N94-30803
Sensory sensitivities and discriminations and their roles in aviation
[AD-A277312] 09 p3800 N94-32276
Visual motion perception and visual information processing
[AD-A278530] 10 p4096 N94-33595
Visual motion perception and visual information processing
[AD-A278370] 10 p4097 N94-33738
The cognitive, perceptual, and neural bases of skilled performance
[AD-A277608] 10 p4097 N94-33849
Neural models of motion perception
[AD-A278362] 10 p4097 N94-33857
Evaluation of lens distortion errors using an underwater camera system for video-based motion analysis
[NASA-TM-104795] 10 p4099 N94-33957
Visual-vestibular interaction
[NASA-CR-196097] 11 p4297 N94-35379
Relation of motion sickness susceptibility to vestibular and behavioral measures of orientation
[NASA-CR-196121] 12 p4480 N94-37005
The use of a tactile interface to convey position and motion perceptions 12 p4486 N94-37281

MOTION PICTURES
Animation techniques in BRL-CAD
[AD-A275232] 08 p3417 N94-29392

MOTION SICKNESS
Motion and spatial disorientation systems: Special research capabilities
[AD-A265155] 01 p0303 N94-11097
Promethazine and its use as a treatment for space motion sickness 01 p0312 N94-11550
Update on the incidence and treatment of space motion sickness 01 p0312 N94-11551
Cardiovascular dynamics during space sickness and deconditioning 01 p0311 N94-12007
Health monitoring of Japanese payload specialist: Autonomic nervous and cardiovascular responses under reduced gravity condition (L-0) 02 p0591 N94-13757
Neurophysiological study on visuo-vestibular control of posture and movement in fish during adaptation to weightlessness 02 p0591 N94-13759
Comparative measurement of visual stability in Earth and cosmic space (L-4) 02 p0592 N94-13761
Autogenic feedback training experiment: A preventative method for space motion sickness 02 p0595 N94-13774
Psychophysiological investigations of the biomedical problems of manned spaceflight
[NASA-CR-194107] 02 p0732 N94-13782
Autogenic-Feedback Training (AFT) as a preventive method for space motion sickness: Background and experimental design
[NASA-TM-108780] 03 p1120 N94-15537
Reliability of autonomic responses and malaise across multiple motion sickness stimulation tests
[NASA-TM-108787] 03 p1121 N94-15711
Flight simulator-induced sickness and visual displays evaluation
[AD-A267019] 03 p1122 N94-15845
Evaluation of putative neurochemical intermediaries in space/motion sickness
[NASA-CR-193607] 03 p1118 N94-17090
The brain electrical activity in different G situations
[AERONAUTICA-ACTA-A-372-1993] 04 p1507 N94-19523
Self-Motion Perception and Motion Sickness
[NASA-CR-194276] 05 p1885 N94-21897
Changes in plasma vasopressin during motion sickness in cats 05 p1885 N94-21898
Susceptibility of the squirrel monkey to different motion conditions 05 p1885 N94-21899
Relationship of area postrema to three putative measures of motion sickness 05 p1885 N94-21900
Reassessment of area postrema's role in motion sickness and conditioned taste aversion 05 p1886 N94-21901
Gamma-aminobutyric acid (GABA) and neuropeptides in neural areas mediating motion-induced emesis 05 p1886 N94-21902
Motion sickness elicited by passive rotation in squirrel monkeys 05 p1887 N94-21905
Area postrema ablations in cats: Evidence for separate neural routes for motion- and xylazine-induced CTA and emesis 05 p1887 N94-21906
Immunocytochemical localization of glutamic acid decarboxylase (GAD) and substance P in neural areas mediating motion-induced emesis: Effects of vagal stimulation on GAD immunoreactivity 05 p1887 N94-21909
The effects of area postrema lesions and selective vagotomy on motion-induced conditioned taste aversion 05 p1888 N94-21910
Experimental studies of gastric dysfunction in motion sickness: The effect of gastric and vestibular stimulation on the vagal and splanchnic gastric efferents 05 p1888 N94-21911
Role of the area postrema in three putative measures of motion sickness in the rat 05 p1888 N94-21912
Investigating motion sickness using the conditioned taste aversion paradigm 05 p1888 N94-21913
Conditioned taste aversion and motion sickness in cats and squirrel monkeys 05 p1888 N94-21914
Increasing accuracy in the assessment of motion sickness: A construct methodology
[NASA-TM-108797] 06 p2420 N94-23088
Perception in flight: Shape and motion perception, space perception, spatial orientation, and visual vestibular interaction 06 p2429 N94-23979
Transfer of perceptual adaptation to space sickness: What enhances an individual's ability to adapt?
[NASA-CR-188256] 06 p2427 N94-24227
The electrogastrogram during parabolic flight 07 p2913 N94-27452
Effect of seasickness on aircrew student survivor ability after ditching in cold water 08 p3379 N94-28425
Japanese Journal of Aerospace and Environmental Medicine, volume 30, no. 1
[JTN-94-80598] 08 p3389 N94-28850
Disturbance of equilibrium on JAL flight crew 08 p3390 N94-28856
Space and vertigo: In relation to space motion sickness 08 p3390 N94-28857
The MERSS 5th Symposium on Space Medicine: Medical and Physiological Experiment Utilizing Parabolic Flight
[JTN-94-80588] 08 p3392 N94-29709
Motion sickness in parabolic flight: Possibility of electrogastrography as an objective index 08 p3393 N94-29718
Autogenic-feedback training as a treatment for airsickness in high-performance military aircraft: Two case studies
[NASA-TM-108810] 09 p3801 N94-33068
Relation of motion sickness susceptibility to vestibular and behavioral measures of orientation
[NASA-CR-196121] 12 p4480 N94-37005
Profile analysis of after-effects experienced during exposure to several virtual reality environments 12 p4482 N94-37263

MOTION SICKNESS DRUGS
Susceptibility of the squirrel monkey to different motion conditions 05 p1885 N94-21899

MOTION SIMULATION
Mechanical analysis of parallel manipulators with simulation, design, and control applications
[ISBN-0-315-72013-1] 01 p0181 N94-11156
Vertical motion simulator familiarization guide
[NASA-TM-103923] 02 p0527 N94-13008
Computational Control Workstation: Users' perspectives 02 p0681 N94-14648
Temporal segmentation of tasks from human hand motion
[AD-A266596] 03 p1166 N94-16725
Strategy for motion of a moving body of quasi-polygonal form within a polygonal space 05 p1792 N94-22240
Reach performance while wearing the Space Shuttle launch and entry suit during exposure to launch accelerations 06 p2436 N94-24204
Motion planning for serial manipulators with many degrees of freedom: Implementation of a sequential search strategy
[ISBN-0-315-83682-2] 07 p2822 N94-26642
Application of centrifuge based dynamic flight simulation to enhanced maneuverability RDT/E 10 p3994 N94-34630

MOTION SIMULATORS
Future developments of the NLR research flight simulator
[NLR-TP-92143-U] 02 p0528 N94-13498
Future directions in flight simulation: A user perspective 06 p2162 N94-25101
The effect of platform motion on human energy expenditure during walking. An exploratory experiment
[AD-A273760] 07 p2940 N94-25724
ANOPP/VMS HSCT ground contour system 10 p3975 N94-33492

MOTION STABILITY
NT AERODYNAMIC STABILITY
NT AIRCRAFT STABILITY
NT ATTITUDE STABILITY
NT BOUNDARY LAYER STABILITY
NT DIRECTIONAL STABILITY
NT FLAME STABILITY
NT FLOW STABILITY
NT GYROSCOPIC STABILITY
NT HOVERING STABILITY
NT LATERAL STABILITY
NT LONGITUDINAL STABILITY
NT LOW SPEED STABILITY
NT MAGNETOHYDRODYNAMIC STABILITY
NT ROTARY STABILITY
NT SPACECRAFT STABILITY
Projectile transverse motion and stability in electromagnetic induction launchers
[DE94-001557] 06 p2198 N94-23210
A comparison of three approximate mathematical models for the gravity gradient stabilized satellite
[AD-A273832] 07 p2694 N94-25615
Recent trend of domestic and international regulations on intact stability of ships for safety 07 p2764 N94-27977
Some remarks about pseudo-Hamiltonian
[DE94-003273] 08 p3487 N94-29700
Analysis of achievable disturbance attenuation in a precision magnetically-suspended motion control system 11 p4225 N94-35917

MOTOR SYSTEMS (BIOLOGY)
U EFFERENT NERVOUS SYSTEMS

MOTOR VEHICLES
NT AUTOMOBILES
NT CRAWLER TRACTORS
NT ELECTRIC AUTOMOBILES
NT ELECTRIC MOTOR VEHICLES
NT TRACKED VEHICLES
NT TRUCKS
Coprocessing of fossil fuels and biomass for CO2 emission reduction in the transportation sector
[PB93-194165] 01 p0267 N94-11845
Effects of RVP, T(50), and oxygenates on hot-start and driveability performance at high and low altitude
[AD-A266382] 03 p0869 N94-16516
The causes of contact noise
[REPT-92-100] 05 p1822 N94-20157
Dead reckoning navigation
[VTT-TIED-1402] 07 p2664 N94-25808
Unscreened low tension cables scrape abrasion testing
[PB94-123767] 07 p2823 N94-26849
Optimising BMW four-cylinder two-valve engines
[PB94-125101] 07 p2824 N94-27254
TCM exemptions to promote alternative-fuel vehicles: The good, the bad, and the ugly
[DE94-005924] 08 p3311 N94-30703

MOTORS
NT ASYNCHRONOUS MOTORS
NT ELECTRIC MOTORS
NT INDUCTION MOTORS
NT MICROMOTORS
NT SERVOMOTORS
NT STEPPING MOTORS
NT SYNCHRONOUS MOTORS
NT TORQUE MOTORS

MOUNTAINS
NT ADIRONDACK MOUNTAINS (NY)
NT ALPS MOUNTAINS (EUROPE)
NT ANDES MOUNTAINS (SOUTH AMERICA)
NT APPALACHIAN MOUNTAINS (NORTH AMERICA)
NT CASCADE RANGE (CA-OR-WA)
NT ROCKY MOUNTAINS (NORTH AMERICA)

The Lathrop Wells Volcanic Center: Status of field and geochronology studies
[DE93-008917] 01 p0273 N94-10285
The evaluation of radiative process in the atmosphere-ground system by Monte Carlo method 01 p0205 N94-11980
Monitoring of snowcover in high mountain terrain with ERS-1 SAR 01 p0247 N94-12482
Net radiation mapping of mountainous terrain using Landsat-5 thematic mapper imagery and digital terrain data
[ISBN-0-315-57755-X] 02 p0685 N94-13475
Ishtar deformed belts: Evidence for deformation from below? 03 p1256 N94-16218
The Mexico City 1991 lidar measurements campaign
[DE93-019960] 04 p1478 N94-19272
Hydraulics and morphology of mountain rivers: A literature survey. Communications on hydraulic and geotechnical engineering
[PB94-110772] 06 p2388 N94-24636
GPS survey of the western Tien Shan
[NASA-CR-195174] 06 p2175 N94-24826
Glacial landforms and late Cenozoic history of the western Soer-Rondane mountains 08 p3357 N94-29080
Recommendations for meteorological data collection during physiological field studies
[AD-A276834] 09 p3901 N94-32153
Medical problems in high mountain environments. A handbook for medical officers
[AD-A278095] 09 p3798 N94-33268
Paleoclimate validation of a numerical climate model
[DE94-009287] 12 p4463 N94-36470

MOUNTING
Mounting of SSM's
[VTT-TIED-1442] 07 p2695 N94-26250
RF vacuum microelectronics
[AD-A275221] 08 p3263 N94-28915
An analytical study of the vibration of beams fitted with neutralizers. Part 2: Assessment of the effects of mounting configurations
[ISVR-TR-225-PT-2] 09 p3740 N94-32982

MOUNTS
U SUPPORTS

MOVING TARGET INDICATORS
Moving target indicator using higher order statistics
[AD-D015890] 03 p1000 N94-16917
Low-noise oscillators for airborne radar applications, revision 1
[AD-A269372] 04 p1403 N94-18471
Enhanced adaptive statistical filter providing improved performance for target motion analysis noise discrimination statement of government interest
[AD-D016039] 07 p2786 N94-27109
Some neural computing approaches to target tracking 09 p3837 N94-33151
MTI compatible coherent sidelobe canceller
[AD-D016300] 12 p4435 N94-37771

MPP (COMPUTERS)
U MASSIVELY PARALLEL PROCESSORS

MRAC (SYSTEMS)
U MODEL REFERENCE ADAPTIVE CONTROL

MSAT
Mobile antenna development at JPL 05 p1731 N94-20457
Comparison of theoretical and simulated performance results for sloppy-slotted Aloha signaling 05 p1746 N94-22204
The MSAT spacecraft of Telesat Mobile Inc. 06 p2207 N94-22742
MSAT and cellular hybrid networking 06 p2278 N94-22762
Design and implementation considerations of a MSAT packet data network 06 p2280 N94-22778
The Westinghouse Series 1000 Mobile Phone: Technology and applications 06 p2284 N94-22800
Direct digital RF synthesis and modulation for MSAT mobile applications 06 p2285 N94-22804
A practical system for regional mobile satellite services 06 p2288 N94-22828
Low cost antennas for MSAT vehicular applications 06 p2289 N94-22830
SATCOM feasibility study for search and rescue aircraft
[DSIS-94-01083] 09 p3575 N94-31902
MSAT boom joint testing and load absorber design 09 p3606 N94-33315
Special test equipment and fixturing for MSAT reflector assembly alignment 09 p3606 N94-33316

MSM (SEMICONDUCTORS)
Effects of solar cell environment on contact integrity 01 p0049 N94-11387
Fiber optic transceiver for interfacing digital superconducting electronics
[DE94-008284] 10 p4040 N94-33842
Low temperature materials --- indium gallium arsenides
[AD-A278703] 12 p4533 N94-36755

MTBF
Algorithms for treating redundancy in repairable and non-repairable systems
[DE94-005289] 08 p3315 N94-29020

MTF
U MODULATION TRANSFER FUNCTION

MTFF (SPACE STATION)
U MAN TENDED FREE FLYERS

MTI RADAR
U MOVING TARGET INDICATORS

MUBIS (SCANNERS)
U MULTIPLE BEAM INTERVAL SCANNERS

MULLITES
Interface chemistry in ceramic matrix composites
[AD-A266629] 03 p0973 N94-17466
Metal-mullite reactions
[DE94-002038] 06 p2244 N94-23811
Enhancement of oxidation resistance of silicon carbide by high-dose and multi-energy aluminum implantation
[DE94-006560] 09 p3640 N94-31314
Interface engineering in oxide fiber/oxide matrix composites
[AD-A277672] 09 p3627 N94-33029

MULTIBEAM ANTENNAS
Proceedings of the 1992 Antenna Applications Symposium, volume 2
[AD-A266916] 03 p0986 N94-14998
Proceedings of the 1992 Antenna Applications Symposium, volume 1
[AD-A268167] 03 p1005 N94-17431
Proceedings of the 1993 Antenna Applications Symposium, volume 1
[AD-A277202] 09 p3676 N94-32049
Proceedings of the 1993 Antenna Applications Symposium, volume 2
[AD-A277203] 09 p3677 N94-32050

MULTICHANNEL COMMUNICATION
An efficient medium access control strategy for high speed WDM multiaccess networks
[MEMO-INF-92-74] 01 p0131 N94-10165
Call sign intelligibility improvement using a spatial auditory display
[NASA-TM-104014] 03 p1177 N94-15549
On-board packet switch architectures for communication satellites
[NASA-TM-106328] 03 p0883 N94-17488
Multichannel error correction code decoder
[NASA-TM-106331] 04 p1333 N94-19313
State-space models for multichannel detection
[AD-A270608] 05 p1715 N94-19816
Simulated retrieval of land surface parameters using multichannel satellite microwave radiometry 05 p1727 N94-20443
Four-channel HF receiving antenna array simulator
[AD-A271876] 05 p1732 N94-20471
Recording system using multiplexed inputs to a multichannel recorder
[AD-D015971] 05 p1808 N94-21278
Electrical performance of wire mesh for spacecraft deployable reflector antennas 06 p2275 N94-22744
Fault tolerant onboard packet switch architecture for communication satellites: Shared memory per beam approach
[NASA-TM-106397] 06 p2201 N94-23567
Advanced technology for a satellite multichannel demultiplexer/demodulator
[NASA-CR-194435] 06 p2202 N94-23631
Interference analysis of multichannel transmission lines: A system's analysis
[PB94-126505] 07 p2772 N94-26909
Design and test of a regenerative satellite transmultiplexer
[ISBN-0-315-85280-1] 07 p2786 N94-27303
A multichannel architecture for Naval Task Force Communication
[AD-A276230] 09 p3673 N94-31446
Passive, multi-channel fiber optic rotary joint assembly
[AD-D016116] 09 p3882 N94-32626
Long distance transmission of 15 Gb/s digital using subcarrier multiplexing and external modulation
[DE94-008298] 09 p3682 N94-32756
Method providing optimum optical trains alignment in a passive multi-channel fiber optic rotary joint
[AD-D016125] 10 p4143 N94-34151

MULTICHANNEL PLATES
U MICROCHANNEL PLATES

MULTICHARGED IONS
U IONS

MULTIGRID METHODS
Hypersonic flow computations around re-entry vehicles 01 p0009 N94-10461
Looking for O(N) Navier-Stokes solutions on non-structured meshes
[NASA-CR-191472] 01 p0345 N94-11277
Viscous analysis of three-dimensional rotor flows using a multigrid method
[NASA-TM-106266] 01 p0152 N94-11481
Grid optimization and multigrid techniques for fluid flow and transport problems 01 p0154 N94-11824
Application of incremental unknowns to the Burgers equation 01 p0156 N94-12293
Towards a cell-vertex Navier-Stokes algorithm for three-dimensional structured/unstructured meshes
[ARA-MEMO-366] 01 p0161 N94-12437
Analysis of the Harrier forebody/inlet design using computational techniques
[NASA-CR-193616] 02 p0503 N94-13463
Development of a general purpose multigrid accelerated Navier-Stokes solver 02 p0641 N94-14613
Development of an explicit multiblock/multigrid flow solver for viscous flows in complex geometries
[NASA-TM-106356] 02 p0642 N94-14728
A parallel adaptive mesh refinement algorithm
[NASA-CR-191530] 03 p1168 N94-15724
A multilevel-multiresolution method for image processing. A Bayesian framework for reconstructing and representing shapes
[AD-A266772] 03 p1082 N94-15842
An upwind multigrid method for solving viscous flows on unstructured triangular meshes
[NASA-TM-109343] 03 p1027 N94-17061
Multigrid time-accurate integration of Navier-Stokes equations
[NASA-TM-106373] 03 p1028 N94-17258
Multigrid direct numerical simulation of the whole process of flow transition in 3-D boundary layers
[NASA-TM-106369] 03 p1030 N94-17557
Thin-layer and full Navier-Stokes calculations for turbulent supersonic flow over a cone at an angle of attack
[NASA-CR-189103] 03 p0861 N94-17558
Numerical calculations of high lift flows using structured and unstructured methods 04 p1307 N94-18428
A multigrid acceleration technique for computing steady solutions to the equations of compressible flow 04 p1412 N94-18559
Computational techniques for high-speed flows with viscous and chemical effects 04 p1412 N94-18560
Multigrid methods for flow transition in three-dimensional boundary layers with surface roughness
[NASA-CR-4540] 04 p1417 N94-18843
3D composite grids using Bezier curves and surfaces in component adaptive methods
[AD-A269188] 04 p1549 N94-18863
Multigrid for a groundwater flow problem
[PB94-149655] 04 p1420 N94-19144
Multigrid approach to solving the long transportation problem on a regular grid in cost space
[AD-A272323] 05 p1909 N94-21038
MGD1M: A parallel multigrid code with a fast vectorized ILU-relaxation
[CWI-NM-R9222] 05 p1930 N94-21077
A multi-level solution algorithm for steady-state Markov chains
[NASA-CR-191558] 05 p1914 N94-21482
The Sixth Copper Mountain Conference on Multigrid Methods, part 2
[NASA-CP-3224-PT-2] 05 p1955 N94-21464
Optimal resolution in maximum entropy image reconstruction from projections with multigrid acceleration 05 p1955 N94-21465
Multilevel methods for transport equations in diffusive regimes 05 p1955 N94-21467
Analysis of multigrid methods on massively parallel computers: Architectural implications 05 p1938 N94-21468
Time-accurate Navier-Stokes calculations with multigrid acceleration 05 p1956 N94-21469
Looking for O(N) Navier-Stokes solutions on non-structured meshes 05 p1806 N94-21471
The block adaptive multigrid method applied to the solution of the Euler equations 05 p1641 N94-21472
Multigrid schemes for viscous hypersonic flows 05 p1641 N94-21473
Layout optimization with algebraic multigrid methods 05 p1957 N94-21474
A multigrid method for steady Euler equations on unstructured adaptive grids 05 p1957 N94-21476
An automatic multigrid method for the solution of sparse linear systems 05 p1957 N94-21478
A multigrid algorithm for the cell-centered finite difference scheme 05 p1957 N94-21479
A semi-Lagrangian approach to the shallow water equation 05 p1806 N94-21480
Multigrid solution of the Navier-Stokes equations on highly stretched grids with defect correction 05 p1806 N94-21481

The multigrid preconditioned conjugate gradient method 05 p1958 N94-21482
Mapping robust parallel multigrid algorithms to scalable memory architectures 05 p1922 N94-21483
Unstructured multigrid through agglomeration 05 p1958 N94-21484
Multigrid properties of upwind-biased data reconstructions 05 p1806 N94-21485
On the prediction of multigrid efficiency through local mode analysis 05 p1959 N94-21486
Numerical study of a multigrid method with four smoothing methods for the incompressible Navier-Stokes equations in general coordinates 05 p1806 N94-21487
Parallelizing a highly vectorized multigrid code with zebra relaxation
[CWI-NM-R9225] 05 p1935 N94-21610
Numerical multigrid software (MGD5M): A parallel multigrid code with a twisted ILLU-relaxation
[CWI-NM-R9226] 05 p1916 N94-21611
The 3-D unstructured mesh generation using local transformations 05 p1919 N94-22356
A multigrid multiblock solver for compressible turbulent flow
[MEMO-1125] 06 p2315 N94-22713
Local grid refinement method for the euler equations
[PB93-223329] 06 p2317 N94-22985
The Sixth Copper Mountain Conference on Multigrid Methods, part 1
[NASA-CP-3224-PT-1] 06 p2482 N94-23673
A multigrid solver for the semiconductor equations 06 p2482 N94-23674
FAS multigrid calculations of three dimensional flow using non-staggered grids 06 p2341 N94-23675
Multigrid and cyclic reduction applied to the Helmholtz equation 06 p2304 N94-23676
Uniform convergence of multigrid V-cycle iterations for indefinite and nonsymmetric problems 06 p2482 N94-23677
A multilevel cost-space approach to solving the balanced long transportation problem 06 p2483 N94-23678
Domain decomposition methods for nonconforming finite element spaces of Lagrange-type 06 p2483 N94-23680
Implementing abstract multigrid or multilevel methods 06 p2483 N94-23682
Numerical solution of flame sheet problems with and without multigrid methods 06 p2237 N94-23683
A mixed method Poisson solver for three-dimensional self-gravitating astrophysical fluid dynamical systems 06 p2484 N94-23684
Multigrid methods for differential equations with highly oscillatory coefficients 06 p2484 N94-23685
Application of multigrid methods to the solution of liquid crystal equations on a SIMD computer 06 p2484 N94-23686
An adaptive multigrid model for hurricane track prediction 06 p2416 N94-23687
Relaxation schemes for Chebyshev spectral multigrid methods 06 p2484 N94-23688
Multigrid methods for a semilinear PDE in the theory of pseudoplastic fluids 06 p2341 N94-23689
A comparison of locally adaptive multigrid methods: LDC, FAC and FIC 06 p2485 N94-23692
Compressible turbulent flow simulation with a multigrid multiblock method 06 p2342 N94-23694
A nonconforming multigrid method using conforming subspaces 06 p2485 N94-23695
Multigrid method for integral equations and automatic programs 06 p2464 N94-23696
Toward large eddy simulation of turbulent flow over an airfoil 06 p2172 N94-24150
An integrated runtime and compile-time approach for parallelizing structured and block structured applications
[NASA-CR-191554] 06 p2458 N94-24740
Lubrication in cold rolling: Numerical simulation using multigrid techniques
[ISBN-9-09-005313-1] 06 p2262 N94-25230
On the robustness of a multiple semi-coarsened grid method
[REPT-93-51] 07 p2992 N94-26252
Grid-independent convergence based on preconditioning techniques
[PB94-125358] 07 p2997 N94-27000
Agglomeration multigrid for the three-dimensional Euler equations
[AD-A277557] 07 p2999 N94-27557
TVD flux-difference split methods for high-speed thermochemical nonequilibrium flows with strong shocks
[UTIAS-350] 07 p2799 N94-27880
A parallel multigrid algorithm for solving the Navier-Stokes equations on a transputer system
[PREPRINT-699] 07 p2807 N94-28099
ENGRID: A graphical interactive code for the computation of structured grids for blocked flow domains 08 p3124 N94-28956
An elliptic-hyperbolic grid generation method and application to compressor flows 08 p3128 N94-28981
RNS optimization procedure for three-dimensional composite velocity multi-block applications 08 p3273 N94-29534
Computational methods for the shape shading problem
[ISBN-0-315-85430-8] 08 p3421 N94-30136
Canonical-variables multigrid method for steady-state Euler equations
[AD-A279020] 08 p3454 N94-30208
Prediction of transonic potential flow with slipstreams around configurations
[FFA-TN-1992-15] 09 p3568 N94-31220
Development and application of a multimesh auto-adaptive finite element method for the calculation of an electric arc plasma
[ECL-89-03] 09 p3886 N94-31378
Solution of the incompressible Navier-Stokes equations in general coordinates by Krylov subspace and multigrid methods
[REPT-93-64] 09 p3703 N94-31660
Numerical simulation of combined external/internal transonic flow on the forebody/inlet of the AV-8B Harrier 2 09 p3569 N94-31759
Multigrid diagonal implicit solutions for compressible turbulent flows and their evaluation 09 p3705 N94-31941
A three-dimensional multigrid technique for unsteady incompressible viscous flows 10 p4042 N94-33364
TIGGERC: Turbomachinery interactive grid generator for 2-D grid applications and users guide
[NASA-TM-106586] 10 p3998 N94-33974
A three dimensional multigrid Reynolds-averaged Navier-Stokes solver for unstructured meshes
[AD-A260998] 11 p4191 N94-35994
A multilevel adaptive projection method for unsteady incompressible flow
[DE93-016418] 11 p4267 N94-36315
Overset grid applications on distributed memory MIMD computers
[NASA-CR-196081] 11 p4268 N94-36397
A method for flow simulation about complex geometries using both structured and unstructured grids
[NASA-TM-106633] 12 p4383 N94-37283
Prediction of film cooling on gas turbine airfoils
[NASA-TM-106653] 12 p4387 N94-37448
Unstructured grid methods for the simulation of 3D transient flows
[NASA-CR-196139] 12 p4444 N94-37525

MULTILAYER INSULATION
CFM technologies for space transportation: Multipurpose hydrogen testbed system definition and tank procurement
[NASA-CR-194355] 02 p0539 N94-12827
Approximate Green's function methods for HZE transport in multilayered materials
[NASA-TM-4519] 03 p1300 N94-17084
SRB thermal curtain design support
[NASA-CR-193858] 03 p0928 N94-17124
Outgassing rate of Reemay Spunbonded Polyester and DuPont Double Aluminized Mylar
[DE93-040015] 05 p1699 N94-19973
Space environment durability of beta cloth in LDEF thermal blankets 09 p3591 N94-31015
Space Station WP-2 application of LDEF MLI results 09 p3592 N94-31016

MULTILAYER STRUCTURES
U LAMINATES

MULTILOOP SYSTEMS
U CASCADE CONTROL

MULTIMEDIA
Development of a hypermedia knowledge base of aircraft fire safety regulations 01 p0021 N94-10793
Design issues for high performance engineering information systems
[AD-A264839] 01 p0420 N94-11520
The use of communication technology in medicine 01 p0306 N94-11800
Programming the multimodal interface
[DE93-013084] 02 p0748 N94-13576
Hypertext Compiling Tools (HCT): Developing model based applications with standard hypertext systems
[REPT-92-049] 02 p0750 N94-13822
Bandwidth characteristics of multimedia data traffic on a local area network
[NASA-TM-104026] 03 p0883 N94-15648
Processor capacity reserves for multimedia operating systems
[AD-A266639] 03 p1158 N94-15745
A computer-based training system combining virtual reality and multimedia
[DE93-013768] 03 p1132 N94-16819
Information technology resources assessment
[DE93-015276] 04 p1613 N94-17894
Pegasus project description
[MEMO-INF-92-75] 04 p1536 N94-19159
Pegasus: Operating system support for distributed multimedia systems
[MEMO-INF-92-76] 04 p1536 N94-19160
A concept for implementing hypermedia technology in computer aided workplaces in medicine
[ETN-93-95057] 05 p1889 N94-20022
Telecommunications services for multimedia data exchange support
[AD-A271704] 05 p1740 N94-21352
CMIFed: A presentation environment for porta ble hypermedia documents
[CWI-CS-R9305] 05 p2044 N94-21494
Structured multimedia authoring
[CWI-CS-R9304] 05 p2044 N94-21535
The Amsterdam hypermedia model: Extending hypertext to support real multimedia
[CWI-CS-R9306] 05 p2045 N94-21536
Publication of science data on CD-ROM: A guide and example
[NASA-CR-4560] 05 p1842 N94-21585
Transparent data service with multiple wireless access 06 p2276 N94-22754
Internetworking satellite and local exchange networks for personal communications applications 06 p2276 N94-22755
NASDA's Advanced On-Line System (ADOLIS) 06 p2509 N94-23903
Service description of communication systems supporting multi-media multi-user applications
[PB94-110855] 06 p2299 N94-24650
Performance measurements of the multimedia testbed on Mach 3.0: Experience writing real-time device drivers, servers, and applications
[AD-A273600] 06 p2460 N94-24932
Considerations regarding the deployment of hypermedia at JSC 06 p2595 N94-25366
A multimedia adult literacy program: Combining NASA technology, instructional design theory, and authentic literacy concepts 06 p2585 N94-25384
Development of satellite telecommunications during the period 1990 - 2005
[CRANFIELD-AERO-9301] 07 p2765 N94-25639
Multimedia in Views
[CWI-CS-R9263] 07 p2961 N94-26218
Hypermedia support for engineering design systems: Application to fatigue analysis
[VTT-TIED-1432] 07 p2837 N94-26255
An object model for multimedia programming
[CWI-CS-R9327] 07 p2971 N94-27552
Application of digital video to hypermedia training systems
[AD-A274989] 08 p3409 N94-28910
HYPER-NPSNET: Embedded multimedia in a 3D virtual world
[AD-A275063] 08 p3410 N94-29152
End-to-end delay reduction in narrow bandwidth real-time multimedia tele-education applications
[AD-B179614] 08 p3260 N94-30518
Developing the Multimedia User Interface Component (MUSIC) for the Icarus Presentation System (IPS)
[AD-A276341] 09 p3810 N94-31335
The vision machines
[NASA-TM-109757] 09 p3806 N94-31816
Problems in survivable multi-media networks
[AD-A277370] 09 p3825 N94-32052
An information system organized as stratified hypermedia
[TR-93-12] 09 p3918 N94-32289
Literacity: A multimedia adult literacy package combining NASA technology, recursive ID theory, and authentic instruction theory 09 p3924 N94-32462
Voice and video transmission using XTP and FDDI 09 p3685 N94-32468
Long distance transmission of 15 Gb/s digital using subcarrier multiplexing and external modulation
[DE94-008298] 09 p3682 N94-32756
Multimedia as a desktop and classroom tool
[DE94-009118] 09 p3807 N94-32766
MADE: A Multiple Application Development Environment
[CWI-CS-R9360] 09 p3822 N94-33097
ATM technology and beyond 10 p4156 N94-33820
Space educators' handbook
[NASA-TM-109779] 11 p4343 N94-35339
Exploring hypermedia information services for disseminating software engineering information
[AD-A278765] 11 p4302 N94-35495
The impact of scaling on a multimedia connection architecture
[AD-A278700] 11 p4300 N94-35652

CAirTOX: A compartment model for assessing the fate of and human exposure to toxic-chemical emissions to air
[DE94-010084] 11 p4284 N94-35700
Evaluation of a tool for producing and presenting interactive videodisc job aids
[AD-A278599] 12 p4432 N94-36473
Multimedia 12 p4541 N94-36847
Low cost software-based rendering and stereoscopic interfaces for teleoperation and virtual reality 12 p4486 N94-37279
The Canadian network for the advancement of research, industry and education (CANARIE) 12 p4543 N94-37336
Portable color multimedia training systems based on monochrome laptop computers (CBT-in-a-briefcase), with spinoff implications for video uplink and downlink in spaceflight operations
[NASA-TM-108460] 12 p4496 N94-37556
Interactive Collaborative Environments (ICE): Platform independent X application sharing and multi-media over wide area networks
[DE94-008868] 12 p4502 N94-37784

MULTIMISSION MODULAR SPACECRAFT
NASA experiences in the Goddard MMS
[NASA-TM-109290] 02 p0819 N94-13629
Earth observation from small satellites 03 p0891 N94-17150
Performance measures from the explorer platform berthing experiment 07 p2683 N94-26283

MULTIMODE RESONATORS
Stability curves for a thermoacoustic prime mover
[AD-A272607] 05 p1968 N94-21422

MULTIPATH TRANSMISSION
Cancellation of multipath for monopulse radars
[ITN-93-85191] 02 p0600 N94-13538
MUSIC and maximum likelihood using a refined propagation model: Performance comparison for radar low-angle tracking
[DREO-RN-1122] 02 p0603 N94-13832
Portable multipath measurement system
[DSIS-93-00177] 02 p0603 N94-13843
Results of multiband (L, S, Ku band) propagation measurements and model for high elevation angle land mobile satellite channel 02 p0615 N94-14670
Coverage aspects of a single frequency network designed for digital audio broadcasting
[BBC-RD-1993/3] 02 p0616 N94-14742
Diffraction of microwaves at rectangular facades of buildings with and without ground reflections (Fresnel-Kirchhoff-Approximation)
[DLR-FB-92-35] 03 p0987 N94-15155
Johnson-Gierhart program predictions of excess propagation loss for super-high frequency air-to-ground paths. Volume 2: Appendices
[AD-A267021] 03 p0987 N94-15527
Broadband conventional beamforming incorporating adaptive equalization
[AD-A267090] 03 p0987 N94-15544
Alternative optical architectures for multichannel adaptive optical processing
[AD-A267052] 03 p1189 N94-15664
Development and analysis of ARMA parameter estimation schemes in the presence of noise
[AD-A267184] 03 p0989 N94-15786
Satellite sound broadcast propagation measurements 03 p0996 N94-16047
An overview of the text propagation effects for land-mobile-satellite systems: Experimental and modeling results 03 p0996 N94-16048
A study of land mobile satellite service multipath effects using SATLAB software 03 p0997 N94-16051
ATCRBS reply environment at Memphis International Airport
[AD-A266322] 03 p0864 N94-16439
Design and fabrication of a Multichannel Adaptive Optical Processor (MADOP)
[AD-A270004] 04 p1579 N94-18668
Generalized multichannel signal detection
[AD-A271385] 04 p1391 N94-19587
Robust, high-speed network design for large-scale multiprocessing
[AD-A271003] 05 p1716 N94-19977
Optical signal processing
[AD-A271036] 05 p1983 N94-20013
Adaptive digital beamforming for a CDMA mobile communications payload 06 p2274 N94-22743
ROCSAT-1 telecommunication experiments 06 p2279 N94-22770
Land mobile satellite propagation measurements in Japan using ETS-V satellite 06 p2282 N94-22790
K-band mobile propagation measurements using ACTS 06 p2283 N94-22792
Measurement of multipath delay profile in land mobile satellite channels 06 p2283 N94-22793
A study of satellite motion-induced multipath phenomena 06 p2283 N94-22794
Diversity reception for advanced multi-satellite networks: A CDMA approach 06 p2286 N94-22816
Transmission over EHF mobile satellite channels 06 p2287 N94-22820
Global acoustic mapping of ocean temperatures (GAMOT)
[AD-A273387] 06 p2418 N94-24719
Conveying digital data in noisy, unstable, multipath environments
[AD-D015980] 06 p2301 N94-25038
Measurements and modeling of multitone, low-frequency acoustic data from the Arraial do Cabo range
[AD-A273406] 06 p2530 N94-25073
Northern Exposure 1992: An investigation of transauroral HF radio skywave propagation
[AD-A273363] 06 p2303 N94-25089
Analyzing adaptive beamformer performance in a stable multipath environment
[AD-A274029] 07 p2766 N94-25766
Methods for improving low-angle, low-altitude radar tracking accuracy
[AD-A274914] 07 p2768 N94-26347
Laser phase induced intensity noise in fiber-optic signal processing and sensing systems
[ITN-94-85234] 07 p2819 N94-27179
Ground station siting considerations for DGPS 07 p2642 N94-27293
Radar returns from a low-flying target over a rough sea surface under multipath and clutter conditions 08 p3253 N94-29882
Direct-sequence spread-spectrum performance in a multipath fading environment
[AD-A276080] 09 p3673 N94-31464
The effects of a multipath channel and interference on coherent M-PSK digital communication systems
[AD-A278158] 09 p3684 N94-33254
Impact of Multipath on MFSK. A complement to FOA report C 30671-3.5
[PB94-149226] 10 p4036 N94-34107
Radar tracking in multipath: Techniques for improved performance 12 p4395 N94-36631
Array element gain and phase estimation in the presence of interference
[AD-A280381] 12 p4434 N94-37162

MULTIPHASE FLOW
NT TWO PHASE FLOW
Nonlinear aspects of transonic aeroelasticity 01 p0002 N94-10357
Nonlinear aspects of transonic aeroelasticity
[UTIAS-345] 01 p0015 N94-11857
A multiphase model for shock-induced flow in low density foam
[DE93-013767] 02 p0632 N94-13397
Implicit multi-fluid simulation of interpenetrating plasmas
[DE93-013351] 02 p0801 N94-14342
Fundamental studies of rocket combustion chemistry and combustion instability
[AD-A266248] 03 p0925 N94-16482
Study of multi-phase flow characteristics in an MHD power train
[DE93-018570] 04 p1586 N94-18272
Transport phenomena and interfacial kinetics in multiphase combustion systems
[AD-A270202] 04 p1349 N94-18785
Technology to prevent greenhouse effect gases
[DE94-707421] 05 p1850 N94-19976
High-resolution numerical methods for compressible multi-phase flow in hierarchical porous media
[DE94-000740] 05 p1799 N94-20351
Eleventh Symposium on Energy Engineering Sciences: Proceedings
[DE93-019930] 07 p2763 N94-26429
High-resolution numerical methods for compressible multi-phase flow in hierarchical porous media
[DE94-008261] 09 p3707 N94-32410
A multimaterial formalism
[DE94-009300] 10 p4048 N94-34097
Verification and benchmark testing of the NUFT computer code
[DE94-005650] 10 p4048 N94-34138
Aerodynamic design and investigation of a mixed flow compressor stage 10 p4002 N94-34450
Design and aerodynamic performance evaluation of a high-work mixed flow turbine stage 10 p4003 N94-34459
Multiphase flow with interphase exchanges (MFIX) documentation theory guide
[DE94-000087] 12 p4441 N94-36550
Simulation of three-dimensional multi-phase flow characteristics in the deswirl section of the CDIF MHD power train
[DE94-012644] 12 p4443 N94-37176

MULTIPHOTON ABSORPTION
Nonperturbative methods in the problem of multiphoton excitation of atom by squeezed light 01 p0376 N94-10575
New infrared photon absorption processes
[DE93-017017] 02 p0780 N94-13071
A search for strong-field direct two electron ionization using coincidence spectroscopy
[DE93-013435] 02 p0781 N94-13241
Multiphoton ionization studies of WF6 and UF6
[DE93-016232] 03 p1181 N94-15863
Characterization of UV emissions resulting from electronic energy transfer in atmospheric molecules
[AD-A266244] 03 p1101 N94-16469
Sensitive detection of gas-phase nitro-containing energetic materials employing 226-nm radiation
[AD-A267633] 03 p0951 N94-17203
Laser photoionization time-of-flight mass spectrometry of nitrated polycyclic aromatic hydrocarbons and nitrated heterocyclic compounds
[AD-A268126] 03 p0952 N94-17520
Removing CFC's from the atmosphere with lasers: A second look
[DE93-017516] 04 p1473 N94-18101
Harmonic generation at high intensities
[DE93-018632] 04 p1572 N94-19283
Direct detection of atomic ions from molecular photofragmentation during nonresonant multiphoton ionization of sputtered species
[DE93-040886] 05 p1976 N94-21951

MULTIPLE ACCESS
NT ALOHA SYSTEM
NT CODE DIVISION MULTIPLE ACCESS
NT DEMAND ASSIGNMENT MULTIPLE ACCESS
NT FREQUENCY DIVISION MULTIPLE ACCESS
NT TIME DIVISION MULTIPLE ACCESS
An efficient medium access control strategy for high speed WDM multiaccess networks
[MEMO-INF-92-74] 01 p0131 N94-10165
Optimal routing of IP packets to multi-homed servers
[DE93-010949] 01 p0133 N94-10709
Signal processing in impulsive electromagnetic interference
[AD-A266425] 03 p0998 N94-16557
Communication in the presence of unknown interference
[AD-A271146] 04 p1392 N94-19738
Analysis of the TDRS multiple access system for possible use as an attitude control system sensor 05 p1666 N94-21338
A one-shot access scheme for a multicast switch 05 p1773 N94-22120
Transparent data service with multiple wireless access 06 p2276 N94-22754
A protocol for satellite access via use of spot-beams 06 p2286 N94-22811
DS-SSMA capacity for a mobile satellite system 06 p2286 N94-22814
Multi-access laser communications terminal
[NASA-CR-191251] 06 p2295 N94-23830
Validation experiments with an Ethernet model using the simulation tool 'PROMISE'
[AD-B174795] 08 p3429 N94-30912
Information-seeking in hypertext: Multiple access methods in a full-text hypertext database 08 p3536 N94-30918
Hubless satellite communications networks 09 p3600 N94-31433
Applied harmonic analysis
[AD-A278384] 09 p3685 N94-33353

MULTIPLE BEAM INTERVAL SCANNERS
An initial study of using the 34-m antenna for lunar mission support 02 p0611 N94-14396

MULTIPLE DOCKING ADAPTERS
Docking mechanisms: An overview of different systems 06 p2357 N94-24004

MULTIPLE FREQUENCY RADAR
U MULTISPECTRAL RADAR

MULTIPLE INPUT MULTIPLE OUTPUT
U MIMO (CONTROL SYSTEMS)

MULTIPLE INSTRUCTION MULTIPLE DATA STREAM
U MIMD (COMPUTERS)

MULTIPLE TARGET TRACKING
Multiple target track-while-scan in the airborne EO environment 12 p4394 N94-36629
Multitarget track initiation using a modified Hough transform 12 p4395 N94-36630

MULTIPLETS
U FINE STRUCTURE

MULTIPLEX TRANSMISSION
U MULTIPLEXING

MULTIPLEXERS
U MULTIPLEXING

MULTIPLEXING
NT CODE DIVISION MULTIPLEXING
NT FREQUENCY DIVISION MULTIPLEXING
NT TIME DIVISION MULTIPLEXING
NT WAVELENGTH DIVISION MULTIPLEXING
Multiplexed and distributed optical fibre sensors
01 p0064 N94-10065
A fiber optic network system with low crosstalk using code-division multiplexing
[AD-D015763] 01 p0374 N94-10376
Microwave multiplexer with channels of varying fractional bandwidths
[AD-D015754] 01 p0140 N94-10389
Controller of serial multiplex communication channel
[DE92-641157] 01 p0336 N94-10544
SONET synchronization: What's happening
01 p0355 N94-10992
Analysis of the eastern range multiplexed fiber optic IRIG B120 distribution system 01 p0139 N94-10996
Holographic multiplexing for 3D optical memory
[AD-A266099] 01 p0171 N94-11420
Superconducting SQUID amplifiers for IR detectors and other applications, phase 2
[AD-A265447] 01 p0145 N94-12333
HYMOSS signal processing for pushbroom spectral imaging
[NASA-CR-191341] 02 p0620 N94-13125
Advanced high performance CdHgTe multiplexed arrays 03 p0903 N94-15051
A linear monolithic 4-6 on silicon IR detector array
03 p0910 N94-15098
An approximation for computing reduction in bandwidth requirements using intelligent multiplexers
[AD-A267434] 03 p1001 N94-17026
Review of rigorous coupled-wave analysis and of homogeneous effective medium approximations for high spatial-frequency surface-relief gratings
03 p1194 N94-17335
3-D optical memory disk
[AD-A267908] 03 p1141 N94-17380
VHF air/ground communications for air traffic control: A decision tree approach to system innovations, volume 2
[AD-A268632] 04 p1386 N94-18495
Specifying and proving communication closedness in protocols
[PB94-149515] 04 p1390 N94-19267
Tandem queues with deterministic service times
[PB93-197465] 04 p1543 N94-19324
Recording system using multiplexed inputs to a multichannel recorder
[AD-D015971] 05 p1808 N94-21278
Wide passband wavelength multi/demultiplexer at 1.3/1.55 micrometers based on etched Fresnel mirror, appendix 8 05 p1989 N94-21602
Quadrature biorthogonal modulation
05 p1747 N94-22232
InGaAsP/InP based 1.3/1.55 micron vertical cavity surface emitting lasers for wavelength division multiplexed high speed distributed computing, phase 1
[AD-A271081] 06 p2348 N94-23123
Design and implementation issues of end-to-end protocols in high-speed networks
[PB94-110905] 06 p2467 N94-23752
Digital data, composite video multiplexer and demultiplexer boards for an IBM PC/AT compatible computer 06 p2447 N94-25377
Modeling of the ground-to-SSFMB link networking features using SPW 06 p2306 N94-25381
The AFIT multielectrode array for neural recording and simulation: Design, testing, and encapsulation
[AD-A274086] 07 p2909 N94-25943
A VHDL register transfer level model of the linear token passing multiplex data bus protocol for the high speed data bus
[AD-A273734] 07 p2980 N94-26009
Comparative analysis of different configurations of PLC-based safety systems from reliability point of view
07 p2836 N94-27925
A multiplexed two-way solid communications link for teleoperated robots 08 p3310 N94-30310
A technique for multiplexing 3x3-coupler terminated interferometric fiber-optic sensors
[AD-A276739] 09 p3880 N94-32180
ATM technology and beyond
10 p4156 N94-33820
Computer assisted multiplex sequencing
[DE94-008549] 10 p4107 N94-34007

MULTIPLICATION
An efficient parallel algorithm for matrix-vector multiplication
[DE93-015125] 02 p0754 N94-14399
Implementation and parallelization of fast matrix multiplication for a fast Legendre transform
[DE94-002184] 06 p2478 N94-22975
The PRISM project: Infrastructure and algorithms for parallel eigensolvers
[DE94-005125] 07 p2973 N94-27717
A new tool for signal processing
[AD-A278385] 09 p3685 N94-33354

MULTIPLIER PHOTOTUBES
U PHOTOMULTIPLIER TUBES

MULTIPLIERS
Method and apparatus for spur-reduced digital sinusoid synthesis
[NASA-CASE-NPO-18789-1-CU]
03 p1154 N94-17326
Complementary heterojunction FET technology for space application 05 p1755 N94-21094
Synthesis algorithm of VLSI multipliers for ASIC
05 p1758 N94-21116
Evaluation of floating-point sum or difference of products in carry-save domain 05 p1764 N94-21705
Radar target discrimination systems using artificial neural network topology
[AD-D015984] 06 p2301 N94-25041
Formal verification of systolic multipliers with the Boyer-Moore theorem prover
[RR-897-M] 09 p3839 N94-31082

MULTIPOLAR FIELDS
On the unique structure of the magnetic fields of Uranus and Neptune 01 p0472 N94-12221
X-SAR: The X-band synthetic aperture radar on board the Space Shuttle 03 p0990 N94-15891
Multipolar-like form of nonabelian gauge theories
[DE93-626690] 03 p1171 N94-17314

MULTIPOLES
Model for the pomeron
[DE93-617693] 01 p0362 N94-10552
Three dimensional multipole decomposition of fields
[DE93-018530] 04 p1389 N94-19053
A summary of studies of particle stability at RHIC
[DE93-040173] 05 p1970 N94-19868
Fast fourier transforms for nonequispaced data
[AD-A272687] 05 p1954 N94-21164
General-relativistic celestial mechanics. 4: Theory of satellite motion
[PB94-147782] 09 p3601 N94-31769
Selected applications of planar permanent magnet multipoles in FEL insertion device design
[DE94-009014] 09 p3721 N94-32845
RHIC chromatic correction system
[DE94-008532] 09 p3883 N94-32994

MULTIPROCESSING (COMPUTERS)
Efficient partitioning and assignment on programs for multiprocessor execution
[NASA-CR-193458] 01 p0324 N94-10942
The Zipcode message-passing system
[DE93-011958] 01 p0336 N94-11027
Node assignment in heterogeneous computing
[NASA-CR-4534] 01 p0142 N94-11131
Portable programming on parallel/networked computers using the Application Portable Parallel Library (APPL)
[NASA-TM-106238] 01 p0327 N94-11232
Alleviating memory contention in matrix computations on large-scale shared-memory multiprocessors
[AD-A265009] 01 p0320 N94-11294
Scalable concurrent programming project
[AD-A266097] 01 p0328 N94-11295
Scalable spin locks for multiprogrammed systems
[AD-A265007] 01 p0337 N94-11650
High speed packet switching
[NASA-CR-191334] 02 p0759 N94-13177
Simulator for heterogeneous dataflow architectures
[NASA-CR-191545] 02 p0622 N94-13797
A performance prediction model for a fault-tolerant computer during recovery and restoration
[NASA-CR-194490] 02 p0741 N94-14136
Distributed processor Monte Carlo: MCNP results on a 16-node IBM cluster
[DE93-012639] 02 p0752 N94-14176
Nonrecursive formulations of multibody dynamics and concurrent multiprocessing 02 p0679 N94-14632
On the solution of a class of graph problems by parallel algorithms
[LAAS-92514] 02 p0756 N94-14712
Relaxing consistency in recoverable distributed shared memory
[AD-A266931] 03 p1140 N94-15174
Multiobjective functions optimization for task allocation mapping to multicomputer nodes
[AD-A267071] 03 p1146 N94-15670
A trace-based comparison of shared memory multiprocessor architectures
[TR-432] 03 p1159 N94-16577
Shared-memory multiprocessor trends and the implications for parallel program performance
[TR-420] 03 p1159 N94-16578
Efficient compilation of array statements for private memory multicomputers
[AD-A266595] 03 p1160 N94-16724
Applications and development of communication models for the touchstone GAMMA and DELTA prototypes
[NASA-CR-193617] 03 p0999 N94-16867
Fault-tolerant architectures for multiprocessor and VLSI-based systems
[AD-A267370] 03 p1140 N94-17005
SPROC: A multiple-processor DSP IC
04 p1398 N94-18347
High-performance multiprocessor architecture for a 3-D lattice gas model 04 p1400 N94-18362
Parallelization of the Air Force Space Command (AFSPACECOM) satellite motion models
[AD-A269327] 04 p1334 N94-18470
A programming paradigm for distributed-memory computers
[DE93-018336] 04 p1524 N94-19024
The p4 Linda: A portable implementation of Linda
[DE93-017752] 04 p1535 N94-19046
Performance and scalability aspects of directory-based cache coherence in shared-memory multiprocessors
[DE93-016442] 04 p1536 N94-19115
Pegasus project description
[MEMO-INF-92-75] 04 p1536 N94-19159
Pegasus: Operating system support for distributed multimedia systems
[MEMO-INF-92-76] 04 p1536 N94-19160
Wide-address spaces: Exploring the design space
[MEMO-INF-92-77] 04 p1537 N94-19219
A multi-level data-flow architecture for signal and data processing applications
[DE93-041272] 04 p1539 N94-19588
Segmented operations for sparse matrix computation on vector multiprocessors
[AD-A270601] 05 p1928 N94-19950
Robust, high-speed network design for large-scale multiprocessing
[AD-A271003] 05 p1716 N94-19977
Multilist scheduling: A new parallel programming model
[AD-A270549] 05 p1929 N94-20084
Memory contention in scalable cache-coherent multiprocessors
[TR-448] 05 p1929 N94-20144
Parallel logic programming systems
[RR-891-I] 05 p1929 N94-20176
Time warp operating system version 2.7 internals manual
[NASA-CR-194798] 05 p1899 N94-20549
Measuring the effects of thread placement on the Kendall Square KSR1
[DE93-040655] 05 p1908 N94-20932
Analysis and evaluation of configuring of graphical systems on multiprocessor architectures
[ETN-93-93618] 05 p1930 N94-21018
Avoiding and tolerating latency in large-scale next-generation shared-memory multiprocessors
05 p1753 N94-21081
The effects of block size on the performance of coherent caches in shared-memory multiprocessors
[AD-A272838] 05 p1899 N94-21177
Scheduling for locality in shared-memory multiprocessors
[AD-A272948] 05 p1930 N94-21228
Software coherence in multiprocessor memory systems
[NASA-CR-194696] 05 p1931 N94-21272
Using parallel banded linear system solvers in generalized eigenvalue problems
[NASA-CR-191540] 05 p1915 N94-21584
A simple modern correctness condition for a space-based high-performance multiprocessor
05 p1766 N94-21718
Low energy CMOS for space applications
05 p1768 N94-21735
Using stream interleaving to eliminate the need for interlocks in deeply pipelined processors
05 p1781 N94-22175
Integration of parallel processing structures using a matrix approach 05 p1784 N94-22192
Fault tolerance for real-time multiprocessor operating systems 05 p1788 N94-22216
Distributed input/output processing in data-driven multiprocessors
[DE94-000323] 05 p1937 N94-22378
The ADAM environment and transputers
05 p1926 N94-22494
A new programming metaphor for image processing procedures 05 p1927 N94-22531
A dataflow analysis tool for parallel processing of algorithms
[NASA-TM-109054] 06 p2448 N94-23086
Distributed Operating Systems and Mach. Proceedings of the Spring 1992 Graduate Seminar on Distributed Systems
[PB93-224905] 06 p2449 N94-23103

Installation of an artificial neural network on distributed memory microprocessors
[ETN-94-95175] 06 p2471 N94-23152
A parallel PROLOG system for distributed memory multiprocessor
[ETN-94-95173] 06 p2465 N94-23167
Towards real-time stereovision systems for planetary missions 06 p2370 N94-23422
Linear time algorithm to schedule trees with communication delays optimally on two machines
[PB93-237782] 06 p2451 N94-23441
Preemptive scheduling in a two-stage multiprocessor flow shop is Np-hard
[PB94-111648] 06 p2467 N94-23756
Three, four, five, six or the complexity of scheduling with communication delays
[PB94-111630] 06 p2467 N94-23767
Mission planning for Shuttle Imaging Radar-C (SIR-C) with a real-time interactive planning software 06 p2305 N94-23842
The design of the EMPS multiprocessor executive for distributed computing
[ETN-94-95336] 06 p2468 N94-25062
Multiprocessor scheduling with communication delays
[ETN-94-95346] 06 p2468 N94-25221
An efficient communication scheme for solving the S(sub n) equations on message-passing multiprocessors
[DE94-000378] 07 p2769 N94-26482
Design and implementation of a multiprocessor for DSP and communications systems algorithm evaluation
[ISBN-0-315-84128-1] 07 p2980 N94-26674
On-board computer for control subsystem of satellite 07 p2949 N94-26716
Real time avionics constraints: Silicon solutions 07 p2949 N94-26717
Test of onboard real time applications (LICE (tm)) 07 p2952 N94-26737
Specification performance optimization and executive generation for onboard multiprocessor real time application with SynDEx 07 p2954 N94-26745
Partitioning structural VHDL circuits for parallel execution on hypercubes
[AD-A274390] 07 p2785 N94-26830
Hard real-time reliable multicast in the DEDOS system
[PB94-126745] 07 p2966 N94-26920
Automatic mapping of task and data parallel programs for efficient execution on multicomputers
[AD-A274125] 07 p2982 N94-27117
Design of a parallel discrete event simulation coprocessor
[AD-A274135] 07 p2982 N94-27123
Garbage collection in a multiprocessor Smalltalk system
[ISBN-0-315-51159-1] 07 p2982 N94-27332
Unified distributed simulation
[ISBN-0-315-59019-X] 07 p2983 N94-27685
An enhanced global spectral model
[PL-TR-92-2011] 07 p2898 N94-28223
Design and packaging of fault tolerant optoelectronic multiprocessor computing system
[AD-A275896] 08 p3405 N94-28798
Model-oriented analysis of a communications protocol
[PB94-138146] 08 p3244 N94-29109
NPSNET: Integration of Distributed Interactive Simulation (DIS) protocol for communication architecture and information interchange
[AD-A275061] 08 p3530 N94-29139
Design of a thinwire real-time multiprocessor operating system 08 p3415 N94-29333
High throughput network for multiprocessor interconnections
[VTT-PUBS-147] 08 p3245 N94-29468
Hypra/TR: A tuple oriented recovery method for a continuously available distributed DBMS on a shared nothing multi-computer
[PB94-141264] 08 p3533 N94-29921
Computational balance in real-time cyclic spectral analysis
[DE94-005091] 08 p3432 N94-30100
A locally synchronous globally asynchronous Vertex-8 processing element for image reconstruction on a mesh
[ISBN-0-315-86005-7] 08 p3432 N94-30143
Common spaceborne multicomputer operating system and development environment
[NASA-TM-109092] 08 p3422 N94-30197
Maestro: An open system architecture for multi-robot control 08 p3306 N94-30288
Improving the execution speed of robot control computations: An allocation scheme for heterogeneous multiprocessors 08 p3310 N94-30308
Scheduling techniques for multiple processor systems in real-time environments
[AD-A276149] 09 p3824 N94-31249
List ranking and list scan on the CRAY C-90
[AD-A276411] 09 p3824 N94-31259
DOME: Dynamic optimization on multiprocessor engines, a statistical approach 09 p3807 N94-31972
VME rollback hardware for time warp multiprocessor systems
[NASA-CR-191796] 09 p3826 N94-32483
Development of a low-latency scalar communication routine on message-passing architectures
[DE94-007061] 09 p3827 N94-32683
Investigation of modularly configured attached processors with intelligent memories
[AD-A278418] 09 p3839 N94-33330
Iwmeter: A real-time and interactive parallel software monitor for iWarp
[AD-A277587] 10 p4104 N94-33427
Program composition
[AD-A278377] 10 p4105 N94-33742
Software fault tolerance: Dynamic combination of dependability and efficiency
[PB94-148830] 10 p4106 N94-33977
Analyzing PICL trace data with MEDEA
[DE94-009173] 10 p4111 N94-33987
Constraints and system primitives in achieving multilevel security in real time distributed system environment
[AD-A278407] 10 p4107 N94-34086
The design and realization of a real-time multitasking control system by using AMX multitasking executive 10 p4118 N94-34343
Modeling heterogeneous processor scheduling for real time systems 10 p4124 N94-35053
Parallel algorithms for LU decomposition on a shared memory multiprocessor
[PB94-167798] 11 p4314 N94-35531
Porting industrial codes and developing sparse linear solvers on parallel computers
[PB94-170503] 12 p4497 N94-36547

MULTIPROGRAMMING
Scalable concurrent programming project
[AD-A266097] 01 p0328 N94-11295
Scalable spin locks for multiprogrammed systems
[AD-A265007] 01 p0337 N94-11650
The p4 Linda: A portable implementation of Linda
[DE93-017752] 04 p1535 N94-19046
Scheduling for locality in shared-memory multiprocessors
[AD-A272948] 05 p1930 N94-21228
Exercises in multiprogramming
[PB94-101458] 06 p2454 N94-23768
Ada multiple-programming for hard real time applications in space systems 07 p2951 N94-26730

MULTIPROPELLANTS
U ROCKET PROPELLANTS

MULTIRADAR TRACKING
U RADAR NETWORKS

MULTISENSOR APPLICATIONS
NT MULTISENSOR FUSION
Estimation with multisensor/multiscan detection fusion
[AD-A265673] 01 p0138 N94-12338
Non-scanned LADAR imaging and applications
[DE93-013772] 02 p0655 N94-13261
Reasoning with uncertain and incomplete information in aerospace applications
[NLR-TP-91366-U] 02 p0763 N94-13529
Computer vision and sensor fusion for detecting buried objects
[DE93-012605] 02 p0700 N94-14566
Comparison of JPL-AIRSAR and DLR E-SAR images from the MAC Europe 1991 campaign over testsite Oberpfaffenhofen: Frequency and polarization dependent backscatter variations from agricultural fields 03 p1075 N94-16733
Image accuracy and representational enhancement through low-level, multi-sensor integration techniques
[DE93-014888] 03 p1167 N94-17287
Operator performance in pattern matching as a function of reference material structure
[AD-A269889] 04 p1509 N94-18686
Tracking with time-delayed data in multisensor systems
[AD-A271334] 04 p1391 N94-19582
Integrated display of multi-sensor geophysical and electromagnetic flight data 05 p1721 N94-20418
Multisensor pinhole yawsonde
[AD-A271715] 05 p1808 N94-20930
Multi-sensoral approach to night flight: Perceptive and Cognitive limitations 06 p2432 N94-23981
Radar E-O image fusion 06 p2306 N94-25503
Development of a multi-sensor in situ fiber optic fluorometer
[DE94-003399] 07 p3035 N94-26100
An analysis of multiple sensor system payloads for unmanned aerial vehicles
[AD-A274905] 07 p2667 N94-26182
A data fusion algorithm for multi-sensor microburst hazard assessment 07 p2641 N94-27287
Multi-sensor data fusion in a distributed environment: Architectural solutions
[NLR-TP-92243-U] 07 p2989 N94-27800
ACCS Surveillance Exploratory Prototype (ASEP) 08 p3138 N94-29566
Multi-sensor data fusion and the use of artificial intelligence
[PB94-126216] 08 p3448 N94-30741
Systematic error estimation in multisensor fusion systems
[AD-B179298] 08 p3428 N94-30764
Automatic extraction of cartographic objects by fusion of data extracted from satellite images
[TELECOM-93-E-001] 09 p3742 N94-31165
Chamber optics for testing passive remote sensing vapor detectors
[AD-A275909] 09 p3878 N94-31340
Multiparameter bifurcations and applications
[AD-A278365] 10 p4133 N94-33858
Application of neural networks in multiple sensor fusion for on-line tool wear monitoring 10 p4119 N94-34347
JPRS report: Science and technology. Central Eurasia
[JPRS-UST-94-007] 11 p4249 N94-35227
Adaptive multisensor fusion for the perception and interpretation of outdoor robot scenes
[PB94-170719] 12 p4499 N94-36535
Studies and simulations on sensor fusion and cueing for fighter application 12 p4395 N94-36632
Sensor data fusion for air to air situation awareness beyond visual range 12 p4395 N94-36633
Contact level fusion of radar and IRST contacts on almost electromagnetically silent platform 12 p4395 N94-36634
Adaptive learning of multi-sensor integration techniques with genetic algorithms
[DE94-012744] 12 p4500 N94-37083

MULTISENSOR FUSION
Systematic error estimation in multisensor fusion systems
[AD-B179298] 08 p3428 N94-30764
Adaptive multisensor fusion for the perception and interpretation of outdoor robot scenes
[PB94-170719] 12 p4499 N94-36535

MULTISPECTRAL BAND CAMERAS
Development of a portable multispectral thermal infrared camera
[NASA-CR-191340] 02 p0648 N94-13176

MULTISPECTRAL BAND SCANNERS
NT THEMATIC MAPPERS (LANDSAT)
Thermal-infrared emission spectroscopy of natural surfaces: Application to coated surfaces 01 p0081 N94-12156
Medical imaging
[NASA-TM-109675] 03 p1229 N94-15520
Summaries of the Third Annual JPL Airborne Geoscience Workshop. Volume 2: TIMS Workshop
[NASA-CR-194541] 03 p1063 N94-16595
TIMS performance evaluation summary 03 p1063 N94-16596
A quantitative analysis of TIMS data obtained on the Learjet 23 at various altitudes 03 p1063 N94-16597
Analysis of TIMS performance subjected to simulated wind blast 03 p1063 N94-16598
Sensitivity of blackbody reference panels to wind blast 03 p1063 N94-16599
Comparison of preliminary results from Airborne Aster Simulator (AAS) with TIMS data 03 p1064 N94-16600
Application of split window technique to TIMS data 03 p1064 N94-16601
Atmospheric corrections for TIMS estimated emittance 03 p1064 N94-16602
An algorithm for the estimation of bounds on the emissivity and temperatures from thermal multispectral airborne remotely sensed data 03 p1064 N94-16603
Preliminary analysis of thermal-infrared multispectral scanner data of the Iron Hill, Colorado carbonatite-alkalic rock complex 03 p1065 N94-16605
Summaries of the Third Annual JPL Airborne Geoscience Workshop. Volume 1: AVIRIS Workshop
[NASA-CR-194540] 03 p1066 N94-16666
Method for selection of wavelength bands for multispectral classification
[PB93-204378] 06 p2388 N94-24741
Mapping coastal habitats using an imaging spectrometer
[ISBN-0-315-84362-4] 07 p2848 N94-26664
Analysis of GER imaging spectrometry data for the identification of soil and vegetation parameters in land degradation studies 09 p3744 N94-31857
Possibilities of GER data for soil surface characteristics in the Almaden area 09 p3744 N94-31859
The effects of vegetation on the ability to map soils using GERIS data 09 p3744 N94-31860

Extraction of forests stand age parameters from airborne imaging spectroscopy data 09 p3745 N94-31867
Remote sensing for hurricane Andrew impact assessment 09 p3758 N94-32464
Space Shuttle orbit determination using empirical force modeling of attitude maneuvers for the German MOMS-02/D2 mission 11 p4207 N94-35634

MULTISPECTRAL PHOTOGRAPHY
NT INFRARED PHOTOGRAPHY
Age determinations and Earth-based multispectral observations of lunar light plains 03 p1275 N94-16323
Lunar multispectral mosaics from Galileo's second Earth-Moon flyby 03 p1288 N94-16394
Information extraction for multispectral images using radiation interaction models
[BCRS-90-22] 05 p1841 N94-21015
MAMS data for the Convection and Moisture Experiment (CAMEX)
[NASA-TM-108435] 06 p2409 N94-24080
Morphodynamics of inter-tidal areas: The Wadden Sea
[NLR-TP-92356-U] 07 p2851 N94-27555
SPECTRUM analysis of multispectral imagery in conjunction with wavelet/KLT data compression
[DE94-003961] 07 p2851 N94-27727
Multispectral and textural classifications of a SPOT HRV-1 image, region of Sherbrooke, Quebec, Canada
[ISBN-0-315-84978-9] 07 p2851 N94-27863
Assessment of region-based methods for automated SAR/optical registration, attribute extraction, and classification 09 p3750 N94-32536
Earth observational research using multistage EOS-like data
[NASA-CR-195833] 09 p3757 N94-33019
High spatial resolution telescopic multispectral imaging and spectroscopy of the Moon. 1: The Serenitatis/Tranquillitatis border region 11 p4356 N94-35402

MULTISPECTRAL RADAR
Use of microwave polarimetry to enhance SAR images of the ocean surface
[AD-A271911] 05 p1882 N94-20489

MULTISPECTRAL RESOURCE SAMPLER
Earth observational research using multistage EOS-like data
[NASA-CR-194626] 03 p1084 N94-16831

MULTISTAGE COMPRESSORS
U TURBOCOMPRESSORS

MULTISTAGE ROCKET VEHICLES
NT ARIANE LAUNCH VEHICLE
NT ATLAS LAUNCH VEHICLES
NT ELDO LAUNCH VEHICLE
NT PEGASUS AIR-LAUNCHED BOOSTER
NT SATURN 5 LAUNCH VEHICLES
NT SCOUT LAUNCH VEHICLE
NT TITAN LAUNCH VEHICLES
NT TITAN 4 LAUNCH VEHICLE
ARIANE 5 light derivatives 03 p0878 N94-17140
NEXT launch system 03 p0878 N94-17141
Modal test of the Brazilian satellite launcher (VLS) configuration burn-out of the first stage 06 p2156 N94-24257
Aerodynamic characteristics of the National Launch System (NLS) 1 1/2 stage launch vehicle
[NASA-TP-3488] 12 p4384 N94-37577

MULTISTATIC RADAR
Interpretation of lunar and planetary electromagnetic scattering using the full wave solutions 01 p0440 N94-12049
The accuracy of monostatic and bistatic radar imaging by range-Doppler-processing with and without motion compensation
[DLR-FB-93-07] 04 p1384 N94-18071
Statistical description of the bistatic radar cross section distributions for a right circular cylinder
[AD-A270001] 04 p1387 N94-18666
Calibration network intended for phase-array antennas at 3 GHz
[PB93-204352] 06 p2297 N94-24530
RL/ERCT automated swept-angle bistatic measurement system
[AD-A275763] 08 p3241 N94-28763
Synchronization in multistatic radar
[PB94-136975] 08 p3242 N94-28885
Synchronization, positioning, and communication in multistatic radar systems for air defence
[PB94-137478] 08 p3243 N94-28908
Simulator for multistatic radar
[PB94-135506] 08 p3245 N94-29311
Bistatic clutter RCS simulation using scale model surfaces with two scale roughness
[AD-A277604] 10 p4035 N94-33847

MULTITASKING (COMPUTERS)
U MULTIPROGRAMMING

MULTITEMPORAL ANALYSIS
U TEMPORAL RESOLUTION

MULTIVARIABLE CONTROL
Rotorcraft flying qualities improvement using advanced control 02 p0522 N94-13303
Robust synthesis of discrete-time multivariable control systems with induced delays 02 p0662 N94-13642
Self-tuning control techniques for multivariable systems
[INPE-5449-TDI/495] 02 p0765 N94-14084
Active control of a multivariable system by way of polynomial neural networks: Computer simulation evaluations and laboratory experimental results
[AD-A270033] 04 p1541 N94-18790
Reduced-order modelling and control of a class of systems for which balanced truncation is Hankel-norm optimal
[OUEL-1922/92] 06 p2472 N94-23163
A reliable algorithm for optimal control synthesis
[NASA-CR-194809] 06 p2472 N94-23332
Parametric uncertainty reduction in robust multivariable control
[AD-A273412] 06 p2460 N94-24927
On-line evaluation of multiloop digital controller performance 06 p2163 N94-25105
Kernels of anti-causal operators and the multivariable generalized predictive control problem
[MATHS-REPT-A-191] 06 p2476 N94-25428
Grey-box modelling and identification topics
[PB94-126380] 07 p2986 N94-27029
A direct digital design for a multichannel structural test system using the characteristic locus method
[MATHS-REPT-A-206] 09 p3828 N94-31161
Robust tracking control of a magnetically suspended rigid body 11 p4225 N94-35913

MULTIVARIATE STATISTICAL ANALYSIS
NT BIVARIATE ANALYSIS
NT COVARIANCE
NT ORTHOGONALITY
NT REGRESSION ANALYSIS
A multi-variance analysis in the time domain 01 p0146 N94-10999
Applications of multivariate analysis
[AD-A265250] 01 p0347 N94-11882
Development of pattern recognition techniques for the evaluation of toxicant impacts to multispecies systems
[AD-A267197] 03 p1095 N94-15790
The multivariate optimum interpolation analysis of meteorological data at the Fleet Numerical Oceanography Center
[AD-A266459] 03 p1106 N94-16568
Nonparametric statistics: Weighted rankings analysis
[AD-A266607] 03 p1173 N94-16657
Computing science and statistics. Volume 24: Graphics and visualization
[AD-A266571] 03 p1150 N94-16721
Multivariate wavelet representations and approximations
[AD-A269350] 04 p1546 N94-17825
Active control of a multivariable system by way of polynomial neural networks: Computer simulation evaluations and laboratory experimental results
[AD-A270033] 04 p1541 N94-18790
A multivariate anthropometric method for crew station design
[AD-A270652] 04 p1513 N94-19531
Fast scalar algorithms for multivariate partial correlations and their empirical counterparts
[RR-903-M] 05 p1905 N94-20201
Multivariate statistical analysis: Principles and applications to coorbital streams of meteorite falls 05 p1964 N94-20881
Method for design rotation
[AD-A272440] 05 p1911 N94-21204
Extracting galactic structure parameters from multivariated density estimation 05 p1964 N94-22458
SIMBAD quality-control 05 p2048 N94-22502
Factor analysis as a tool for spectral line component separation 21cm emission in the direction of L1780 05 p1965 N94-22536
Parametric uncertainty reduction in robust multivariable control
[AD-A273412] 06 p2460 N94-24927
Topics in probability and dynamics
[AD-A273543] 06 p2496 N94-24931
Radial base functions: L(sup p)-approximation orders with scattered centers
[AD-A274682] 07 p3003 N94-26445
A multivariate anthropometric method for crew station design: Abridged
[AD-A274588] 07 p2941 N94-26984
Radial basis function approximation: From gridded centers to scattered centers
[AD-A274184] 07 p2998 N94-27103
Multivariate spectral analysis to extract materials from multispectral data
[AD-A274142] 07 p2709 N94-27135
Examples of flight path optimisation using a multivariate gradient-search method
[ESDU-93021] 07 p2670 N94-28092
Noise and drift analysis of non-equally spaced timing data 08 p3472 N94-30667
A radial basis function approach to financial time series analysis
[AD-A276408] 09 p3924 N94-31361
Multivariate spline approximation
[AD-A276034] 09 p3842 N94-31441
Probability distributions with given marginals and given correlation that have maximal entropy
[REPT-93-81] 09 p3851 N94-31698
Gauss elimination by segments and multivariate polynomial interpolation
[AD-A278646] 11 p4315 N94-36012
Chemical recognition software
[DE94-012918] 12 p4495 N94-37496

MULTIVIBRATORS
NT FLIP-FLOPS

MUON SPIN ROTATION
Muon spin relaxation studies of heavy fermion superconductors
[DE93-014576] 02 p0815 N94-14773
Interplay of magnetic and superconducting heavy fermion ground states
[DE94-000680] 06 p2240 N94-23003
Muon spin relaxation studies of the interplay between magnetism and superconductivity in heavy fermion systems
[DE94-000700] 06 p2559 N94-23006
On the (mu)SR activity at LNP JINR phasotron
[DE94-608385] 08 p3517 N94-30195
MuSR measurement of the magnetic penetration depth and coherence length in the high-Tc superconductor YBa2Cu3O(6.95)
[ISBN-0-315-85385-9] 08 p3517 N94-30203
Low dispersion of the muon precession frequency in HTSC samples YBa2Cu3O(x) and EuBa2Cu3O(x)
[DE94-608388] 09 p3896 N94-31395
The study of the local magnetic field in the oxide alpha-Bi2O3 by the mu SR-technique
[DE94-612636] 11 p4322 N94-35751

MUONIUM
Five-lepton decay modes of muon and tau mesons
[DE94-621636] 12 p4516 N94-37099

MUONS
Conceptual design report for the SDC barrel and intermediate muon detectors based on a jet-type drift chamber
[DE93-753173] 01 p0367 N94-11510
Experiments with energetic (mu)d and (mu)t emitted from solid hydrogen
[DE93-010252] 01 p0373 N94-12542
Detection of hot muonic hydrogen atoms emitted in vacuum using x-rays
[DE93-010253] 02 p0778 N94-12860
Double semi-leptonic charm decay in HELIOS-I 450 GeV/c p-Be data
[DE93-013493] 02 p0781 N94-13348
Study of electroweak interactions
[DE93-015067] 02 p0782 N94-13412
Inclusive single muons at DO
[DE93-012779] 02 p0783 N94-13494
Effects of additional isoscalar vector bosons in e(sup +)e)(sup -)(yields)ff-bar processes at the TRISTAN and LEP energies
[DE93-621451] 02 p0783 N94-13506
The (mu)(+) yields e(+)gamma
[DE93-012750] 02 p0785 N94-14181
Rare muon processes
[DE93-012646] 02 p0785 N94-14366
Characteristics of a high energy muon(+)muon(-) collider based on electro-production of muons
[DE93-017154] 02 p0790 N94-14893
Electroweak physics from D0
[DE93-015041] 03 p1181 N94-16053
PHENIX Conceptual Design Report
[DE93-015759] 03 p1182 N94-16161
The 3D-Flow processor for a programmable level-1 trigger (feasibility study)
[DE93-016045] 03 p1159 N94-16172
Calorimeter based detectors for high energy hadron colliders
[DE93-017055] 03 p1188 N94-16900
Electroweak results from D0
[DE93-014926] 03 p1185 N94-16968
Investigation of the relative abundance of heavy versus light nuclei in primary cosmic rays using underground muon bundles
[DE93-017601] 04 p1630 N94-17818
Investigation of physical structures and interactions at high energy
[DE93-014444] 04 p1574 N94-18927
SSC detector muon sub-system beam tests
[DE93-018415] 04 p1569 N94-19013

The anomalous magnetic moment of the muon
[DE93-018932] 04 p1572 N94-19320
Energy loss measurement of cosmic ray muons
[KFK-5158] 04 p1631 N94-19504
Measurement of the energy of horizontal cosmic ray muons
[KFK-5163] 04 p1631 N94-19505
Measurements of cosmic ray muons with multi-wire proportional chambers with a prototype setup for KASCADE
[KFK-5173] 04 p1631 N94-19506
High rate resistive plate chambers: An inexpensive, fast, large area detector of energetic charged particles for accelerator and non-accelerator applications
[DE93-018664] 04 p1572 N94-19545
Measurement of the B(+) and B(0) lifetimes
[DE93-019906] 05 p1969 N94-19814
B production at D0
[DE93-019250] 05 p1972 N94-20291
Evaluation of the chemical composition of cosmic radiation in energy area of 10(exp 15) eV
[ETN-93-93682] 05 p2150 N94-21056
Toward a QCD analysis of jet rates in deep-inelastic Muon-Proton scattering
[DE94-000618] 05 p1976 N94-21962
A measurement of the forward-backward asymmetry and sin(sup 2)(theta)(sub W) from the process Z(sup 0) (yields) (mu)(sup +)(mu)(sup (minus)) at (radical)s = 1.8 TeV
[DE94-001908] 06 p2532 N94-23018
Low mass muon pair production in 450 GeV p-Be collisions
[PB94-110699] 06 p2533 N94-23746
New evaluation of hadronic contributions to the anomalous magnetic moment of charged leptons
[DE93-634394] 06 p2536 N94-24844
A research of possibility for negative muon production by a low energy electron beam accompanying ion beam
[NIFS-266] 06 p2536 N94-24868
The L3 visualization system and its use in the Z(zero) line shape analysis
[ETN-94-95382] 06 p2537 N94-25231
On the classification scheme for resonant states of muonic molecules
[DE93-613645] 07 p3014 N94-25853
Theoretical and experimental studies of elementary physics
[DE94-002310] 07 p3008 N94-25988
Heavy charged leptons in an SU(3)(sub L) x U(1)(sub N) model
[DE93-634367] 07 p3016 N94-26041
Harvard University High Energy Physics
[DE94-002406] 07 p3032 N94-26119
Separation and reconstruction of electron neutrino interaction in the IHEP-JINR neutrino detector and BARS detector
[DE93-634182] 07 p3019 N94-26393
Measurements of the p (mu)d-molecule formation rate at different hydrogen temperature
[DE93-634636] 07 p3020 N94-26511
Indiana University high energy physics, task A
[DE94-000961] 07 p3033 N94-27614
Monte Carlo calculations of low background detector response
[DE94-004593] 07 p3116 N94-27621
Jet production in muon scattering at Fermilab E665
[DE94-004663] 07 p3028 N94-27752
Muon transfer rates in collisions of hydrogen isotope mesic atoms on bare nuclei: Multichannel adiabatic approach
[DE94-606752] 07 p3030 N94-27861
Simulation of experiments on deep inelastic scattering of muons on superconducting magnetic toroidal spectrometer STORS
[DE94-606267] 08 p3483 N94-28554
B production and B(0)(bar B)(0) mixing at DO
[DE94-004664] 08 p3484 N94-28574
Project of the experiment to test the hypothesis on existence of white and black p(mu)-atoms
[DE94-606751] 08 p3485 N94-28625
A study of the ultrahigh-energy cosmic ray mass composition with the MACRO and EAS-TOP experiments 08 p3552 N94-29687
On the (mu)SR activity at LNP JINR phasotron
[DE94-608385] 08 p3517 N94-30195
Search for the top quark in the electron-electron and electron-muon channels at D0
[DE94-006174] 08 p3492 N94-30779
Inclusive single muon production in D0
[DE94-006175] 08 p3493 N94-30887
Low dispersion of the muon precession frequency in HTSC samples YBa2Cu3O(x) and EuBa2Cu3O(x)
[DE94-608388] 09 p3896 N94-31395
Proceedings of the International Workshop on Low Energy Muon Science: LEMS 1993
[DE94-006495] 09 p3874 N94-32804
Ionization EM calorimetry with accordion electrodes and liquid krypton or argon
[DE94-009082] 09 p3713 N94-32821
Deuteron-induced fusion in various environments
[DE94-009305] 10 p4140 N94-34077
Isoscalar vector bosons at LEP 2
[DE94-611253] 11 p4323 N94-35787
J/psi absorption effects in the coherent production on nuclei
[DE94-616870] 11 p4326 N94-36129
Critical issues in muon colliders: A summary
[DE94-011382] 11 p4331 N94-36271
Older muons are wiser: Using time information in (mu)LCR spectroscopy
[DE93-018556] 12 p4511 N94-36457
Measurement and processing of gammas accompanying muon pairs in the reaction pi(-)C yields mu(+)mu(-) + gamma + X at 38 GeV
[DE94-617044] 12 p4512 N94-36523
Radiative and rare mu and pi decays
[DE94-618549] 12 p4515 N94-37066
Five-lepton decay modes of muon and tau mesons
[DE94-621636] 12 p4516 N94-37099
The 24/36/48 Cathode Strip Chamber layout for SSC GEM detector muon subsystem
[DE94-012676] 12 p4439 N94-37306

MURCHISON METEORITE
Interstellar graphite in Murchison: Continued search for isotopically distinct components
01 p0097 N94-12029
Determining the relative extent of alteration in CM chondrites 01 p0430 N94-12114
A new carbon-rich phase (COPS) in Antarctic micrometeorites 01 p0432 N94-12233
Extraction and isotopic analysis of medium molecular weight hydrocarbons from Murchison using supercritical carbon dioxide 03 p1241 N94-16184
Do SiC grains in Orgueil differ from those in Murchison? 03 p1242 N94-16260
Identification of an interstellar oxide grain from the Murchison meteorite by ion imaging
05 p2082 N94-20659
Petrography and origin of refractory inclusions from the Murray and Murchison C2 chondrites
05 p2084 N94-20770
Trace element compositions of spinel-rich refractory inclusions from the Murchison meteorite
05 p2086 N94-20897
Organic analyses of the Murchison meteorite
09 p3938 N94-32489
Moessbauer mineralogy of calcined Murchison meteorite 11 p4353 N94-36166

MURRAY METEORITE
Petrography and origin of refractory inclusions from the Murray and Murchison C2 chondrites
05 p2084 N94-20770

MUSCLE RELAXANTS
Computer automation and artificial intelligence
[DE94-611058] 11 p4312 N94-35831

MUSCLES
NT MYOCARDIUM
NT TENDONS
Magnetic resonance imaging after exposure to microgravity 02 p0594 N94-13771
Currents induced in the human body for exposure to ultrawideband electromagnetic pulses
[AD-A268570] 03 p1130 N94-17621
Control of shoulder muscles during goal directed movements
[PB93-195139] 04 p1504 N94-18080
Space research on organs and tissues
04 p1503 N94-19214
Cosmos 2229
[NASA-CR-194734] 05 p1895 N94-20338
Cellular and tissue injury during nonfreezing cold injury and frostbite
[AD-A270883] 06 p2423 N94-22732
Left ventricular hypertrophy and athlete's heart
06 p2424 N94-23321
Skeletal muscle metabolism in hypokinetic rats
[NASA-CR-195082] 06 p2420 N94-24124
Microinjection of the Yersinia YopE cytotoxin in mammalian cells induces actin microfilament disruption
[FOA-B-40418-4.4] 06 p2421 N94-24290
Loading, electromyograph, and motion during exercise
06 p2427 N94-25359
Loading, electromyograph, and motion during exercise
06 p2427 N94-25380
Effects of perfusion of amiodarone on electrophysiological properties in single rabbit ventricular myocytes 07 p2906 N94-27503
Impaired associated movement in Parkinson's disease: An evaluation of Bell's phenomenon
07 p2928 N94-27520
Contribution of muscle spindle afferent activity to transient pause in EMG during voluntary tonic contraction 07 p2928 N94-27522
Sympathetic nerve activity during dynamic leg exercise
07 p2929 N94-27527
Analysis on one minute wave in body fluid volume and muscle pumping referred to body parts generating the one minute wave during human active standing
07 p2929 N94-27528
The measurements of muscle blood flow by laser Doppler flowmetry with needle type probe
07 p2908 N94-27530
Muscle sympathetic nerve activity in patients with hyper-and hypothyroidism: A microneurographic study
07 p2930 N94-27531
Enhancement of skin sympathetic nerve activity in amyotrophic lateral sclerosis 07 p2930 N94-27532
Treatment of orthostatic hypotension by nasal administration of vasopressin 07 p2930 N94-27533
Muscle sympathetic nerve activity in humans
07 p2932 N94-27538
Muscular activity and its relationship to biomechanics and human performance 07 p2934 N94-28362
Eccentric exercise testing and training
07 p2934 N94-28363
Electrical stimulation in exercise training
07 p2935 N94-28371
Leg muscle volume during 30-day 6-degree head-down bed rest with isotonic and isokinetic exercise training
[NASA-TM-4580] 08 p3385 N94-29401
Japanese Journal of Aerospace and Environmental Medicine, vol. 30, no. 2
[JTN-94-80599] 08 p3394 N94-29863
Effect of water immersion on muscle sympathetic nerve response during static muscle contraction
08 p3394 N94-29865
Shortening velocity and calcium sensitivity of single fibers from hindlimb suspended muscle in rats
08 p3387 N94-29866
Muscle disuse through tail-suspension: Etiology and therapeutics 09 p3796 N94-31746
Typology of skeletal muscle in humans undergoing intense physical training or prolonged akinesia
[PB94-170644] 11 p4297 N94-36217
Methodologies to determine forces on bones and muscles of body segments during exercise, employing compact sensors suitable for use in crowded space vehicles
[NASA-CR-196272] 12 p4487 N94-37458

MUSCULAR FUNCTION
Effect of intermittent cold exposure on the fiber-type composition of selected skeletal muscles in rats
[AD-A265309] 01 p0301 N94-11861
Evaluation of physiological and psychological impairment of human performance in cold stressed subjects
[AD-A268637] 04 p1506 N94-18632
Cosmos 2229
[NASA-CR-194734] 05 p1895 N94-20338
Impaired associated movement in Parkinson's disease: An evaluation of Bell's phenomenon
07 p2928 N94-27520
Contribution of muscle spindle afferent activity to transient pause in EMG during voluntary tonic contraction 07 p2928 N94-27522
Japanese Journal of Aerospace and Environmental Medicine, vol. 30, no. 2
[JTN-94-80599] 08 p3394 N94-29863
Shortening velocity and calcium sensitivity of single fibers from hindlimb suspended muscle in rats
08 p3387 N94-29866

MUSCULAR STRENGTH
Exercise countermeasures for bed-rest deconditioning
[NASA-TM-103987] 01 p0300 N94-11191
Maximum team lifting capacity as a function of team size
[AD-A271642] 05 p1892 N94-21036
Strength capabilities and load requirements while performing torquing tasks in zero gravity
[NASA-TP-3433] 05 p1897 N94-21627
Responses to LBNP in men with varying profiles of strength and aerobic capacity: Implications for flight crews
[NASA-TP-3346] 06 p2426 N94-23530
NASA project 1: Full-body dynamometer
[NASA-CR-195507] 06 p2438 N94-24331
The value of electrical stimulation as an exercise training modality 07 p2936 N94-28372
Typology of skeletal muscle in humans undergoing intense physical training or prolonged akinesia
[PB94-170644] 11 p4297 N94-36217

MUSCULAR TONUS
NT HYPOTONIA
Contribution of muscle spindle afferent activity to transient pause in EMG during voluntary tonic contraction 07 p2928 N94-27522

MUSCULOSKELETAL SYSTEM
NT BONE MARROW
NT BONES
NT COLLAGENS
NT CONNECTIVE TISSUE
NT CRANIUM
NT ELBOW (ANATOMY)
NT FEMUR
NT JOINTS (ANATOMY)
NT KNEE (ANATOMY)
NT MUSCLES
NT SPINE
NT TENDONS
NT WRIST
Risk of decompression sickness in the presence of circulating microbubbles 01 p0312 N94-11546
Body/cushion contact stress analysis during sitting [ITN-93-85204] 02 p0736 N94-13229
Effect of low gravity on calcium metabolism and bone formation (L-7) 02 p0593 N94-13765
Renal function alterations during skeletal muscle disuse in simulated microgravity [NASA-CR-194258] 02 p0733 N94-13824
In vivo animal models of body composition in aging [DE93-012527] 04 p1501 N94-17889
Skeletal muscle metabolism in hypokinetic rats [NASA-CR-195082] 06 p2420 N94-24124
Muscular activity and its relationship to biomechanics and human performance 07 p2934 N94-28362
Exercise detraining: Applicability to microgravity 07 p2934 N94-28364
Shortening velocity and calcium sensitivity of single fibers from hindlimb suspended muscle in rats 08 p3387 N94-29866
Isolating strain parameters correlated to skeletal adaptation 09 p3797 N94-31960
Typology of skeletal muscle in humans undergoing intense physical training or prolonged akinesia [PB94-170644] 11 p4297 N94-36217
MUSEUMS
Pathfinder: Shuttle exhibit [NASA-TM-109357] 04 p1333 N94-19071
Indianapolis CIP review [NASA-TM-109821] 10 p4149 N94-33575
MUSIC
Study of computer system as a musical instrument 02 p0747 N94-13439
Sights and sounds of space [NASA-TM-109610] 03 p1302 N94-15424
Analysis, representation and processing of the instrumental gesture: Application to keyboard instruments [ETN-93-94402] 04 p1519 N94-17977
Numerical simulations of piano strings. Part 1: A physical model for a struck string using finite difference methods [TELECOM-93-C-003] 08 p3481 N94-30972
Noise reduction techniques for the restoration of musical recordings [TELECOM-93-E-019] 08 p3291 N94-30979
MUTAGENS
Studying of ion implantation effect on the biology in China [DE94-620692] 12 p4479 N94-37535
MUTATIONS
Proceedings of the Symposium on Radiation Research in Life Science [DE93-754137] 01 p0300 N94-10888
Evolution of catalytic RNA in the laboratory [NASA-CR-194124] 02 p0727 N94-13210
Isolation of thermostable enzyme mutants by cloning and selection in thermophilic bacteria [AD-A266378] 03 p1117 N94-16514
Studies on the application of radiation for genetic transformation in higher plants [DE93-632656] 07 p2901 N94-26470
Molecular biological studies on the human radioresistance and drug resistance [DE93-632682] 07 p2910 N94-26549
Vacuum-UV-effects on E. coli plasmid pUC19: Inactivation, strand break induction and mutation induction [DLR-FB-93-26] 07 p2903 N94-27754
Estimates of cellular mutagenesis from cosmic rays [NASA-TP-3453] 12 p4481 N94-37282
Studying of ion implantation effect on the biology in China [DE94-620692] 12 p4479 N94-37535
MYLAR (TRADEMARK)
Thermal testing of aluminized Mylar [NASA-TM-108414] 01 p0089 N94-11175
Outgassing rate of Reemay Spunbonded Polyester and DuPont Double Aluminized Mylar [DE93-040015] 05 p1699 N94-19973
MYOCARDIUM
Protective action of platelet-activating factor antagonist, TCV-309, against ischemia reperfusion injury in isolated rabbit hearts 07 p2904 N94-27465
Protective action of an amiloride derivative (amiloride, 5-(N, N-dimethyl) hydrochloride) against in isolated ischemia/reperfusion newborn rabbit hearts 07 p2904 N94-27466
Effects of high-intensity electric field stimulation on the electromechanical performance of cardiac muscle: Influence of fiber orientation 07 p2904 N94-27467
On the mechanism of reentrant arrhythmias following DC defibrillation: Influence of fiber orientation to the effects of low-energy electric field stimulation on the effective refractory period of cardiac muscle 07 p2904 N94-27468
Positive chronotropic effect of mechanical stretch on the sinoatrial node: Roles of neurotransmitters and stretch activated channels 07 p2904 N94-27469
Effects of perfusion of amiodarone on electrophysiological properties in single rabbit ventricular myocytes 07 p2906 N94-27503
Fast and slow onsets of Na channel blocking actions due to lidocaine and disopyramide using concentration-clamp method 07 p2907 N94-27504
Electrophysiological effects of MS-551, a new Class 3 antiarrhythmic agent, on isolated rabbit ventricular muscles 07 p2907 N94-27505
Comparative investigation of new Class 3 antiarrhythmic drugs, E-4031 and MS-551, on electrophysiological properties in isolated rabbit ventricular myocytes 07 p2907 N94-27506
Effects of Class 1 antiarrhythmic drugs on the intraventricular conduction: Influence of fiber orientation 07 p2907 N94-27507
Effects of Class 3 antiarrhythmic agents, E-4031 and MS-551 on ventricular repolarization in isolated rabbit hearts 07 p2907 N94-27508
Electrical coupling between the sino-atrial node and atrial muscle: Cell to cell interaction through an external circuit and its simulation by computer modeling 07 p2907 N94-27509
A study on tissue excitation of cardiac muscle under electrical field stimulation 07 p2907 N94-27510
Block of cardiac sodium channels by Ro 22-9194 (R), a new antiarrhythmic agent: Effects on the maximum upstroke velocity (Vmax) of single guinea pig ventricular myocytes 07 p2907 N94-27511
Electrophysiological effects of an antiarrhythmic drug, moricizine on isolated guinea pig ventricular muscles 07 p2907 N94-27512
Postnatal changes in the autonomic modulation of L-type Ca(exp 2+) currents of rabbit ventricular cells 07 p2931 N94-27535
Mechanism for regulation of myocardial contractility by autonomic drugs: Pathophysiological relevance in congestive heart failure 07 p2931 N94-27536
MYOELECTRICITY
Application of dexterous space robotics technology to myoelectric prostheses 09 p3729 N94-32450
MYOGLOBIN
Quasi-elastic neutron scattering studies of protein dynamics [DE93-015074] 02 p0782 N94-13414
MYOPIA
Accommodation during instrument viewing can be influenced by knowledge of object distance [AD-A278987] 11 p4298 N94-35528
Is increased accommodation a necessary condition for instrument myopia? [AD-A278962] 11 p4298 N94-35659
MYSTERE 20 AIRCRAFT
Evaluation of Night Vision Goggles (NVG) for maritime search and rescue (HH-3/HH-60) comparison report [AD-A266493] 03 p1138 N94-16793

N

N-BODY PROBLEM
U MANY BODY PROBLEM
N-P JUNCTIONS
U P-N JUNCTIONS
N-TYPE SEMICONDUCTORS
Effects of growth conditions and substrate orientation on the properties of InSb [DE93-013766] 02 p0812 N94-14344
Diamond p-n junction cold cathode [AD-A266926] 03 p1206 N94-15107
Selective electrochemical wafer thinning for silicon characterization [DE93-015083] 04 p1592 N94-17742
Silicon concentrator solar cell research [DE93-018489] 04 p1468 N94-19015
Visible light emitting materials and injection devices [AD-A274418] 07 p2786 N94-27079
N-156 AIRCRAFT
U F-5 AIRCRAFT
NACELLES
Application of composite materials for production nacelle structures 01 p0056 N94-10006
The application of advanced materials to aircraft nacelle structures 01 p0057 N94-10011
Flow analysis for the nacelle of an advanced ducted propeller at high angle-of-attack and at cruise with boundary layer control [NASA-TM-106371] 03 p0858 N94-16571
Supersonic flow visualization of a nacelle in close proximity to a simulated wing [NASA-CR-194675] 03 p0860 N94-17260
Wind tunnel investigation of an STOL aircraft model: An effect of engine nacelle shape [NAL-TM-653] 07 p2647 N94-27235
Propeller off-axis loads due to thrust axis incidence and nacelle magnus force 07 p2652 N94-28319
A new approach to turboprop forward nacelle design 07 p2655 N94-28336
NAKHLITES
Nitrates in SNCs: Implications for the nitrogen cycle on Mars 03 p1251 N94-16193
Os isotopes in SNC meteorites and their implications to the early evolution of Mars and Earth 03 p1242 N94-16272
Martian carbon dioxide: Clues from isotopes in SNC meteorites 03 p1270 N94-16295
An attempt to comprehend Martian weathering conditions through the analysis of terrestrial palagonite samples 05 p2143 N94-21668
Cosmogenic C-14 in Antarctic and non-Antarctic meteorites and lunar samples [NASA-CR-195795] 08 p3546 N94-29905
SNC meteorites and their implications for reservoirs of Martian volatiles 09 p3947 N94-33209
The Martian sources of the SNC meteorites (two, not one), and what can and can't be learned from the SNC meteorites 09 p3951 N94-33234
Pigeonholing planetary meteorites: The lessons of misclassification of EET87521 and ALH84001 11 p4353 N94-36157
NAMING
NT NORMS
Model designation of military aerospace vehicles [AD-A267852] 03 p0898 N94-17388
Named Venusian craters 05 p2109 N94-20725
NAP-OF-THE-EARTH NAVIGATION
Visual cueing considerations in Nap-of-the-Earth helicopter flight head-slaved helmet-mounted displays 02 p0524 N94-13315
Multiple-camera/motion stereoscopy for range estimation in helicopter flight 06 p2441 N94-25505
Accurate estimation of object location in an image sequence using helicopter flight data 10 p3997 N94-35055
Advanced information processing system: The Army Fault-Tolerant Architecture detailed design overview [NASA-CR-194924] 12 p4497 N94-36962
NAPHTHALENE
The thermodynamic properties to 700 K of naphthalene and 2,7-dimethylnaphthalene [DE93-000160] 05 p2037 N94-20473
Computer simulation of molecular interactions in supercritical solvents [AD-A274977] 08 p3486 N94-29087
Minipilot solar system: Design/operation of system and results of non-solar testing at MRI [PB94-152238] 10 p4079 N94-34165
NAPPES
U FOLDS (GEOLOGY)
NARROWBAND
Continued development of an ultra-narrow bandpass filter for solar research [NASA-CR-194169] 01 p0381 N94-10735
Non-linear dynamics of automodulation processes in coupled distributed autovibration systems with delay [DE93-620976] 01 p0143 N94-11365
Filters for the International Solar Terrestrial Physics (ISTP) mission far ultraviolet imager [NASA-CR-194633] 03 p1190 N94-15868
Use of AVIRIS data to the definition of optimised specifications for land applications with future spaceborne imaging spectrometers 03 p1071 N94-16694
On comparison and extensions of control methods for narrow-band disturbance rejection [REPT-93-015] 04 p1540 N94-17922
Evaluation of a single stage of the LADS filter [AD-A271101] 05 p1814 N94-19851
RADCAL: A narrow-band model for radiation calculations in a combustion environment [PB93-200889] 05 p1682 N94-21448
Conductors with small Fermi energies and small gap energies [DE93-040887] 06 p2561 N94-23432

Investigation of Raman beam cleanup and phase conjugation
[AD-A273157] 06 p2545 N94-24672
COVICS: A covert video communications system
[DE94-007568] 09 p3682 N94-32745
Detection of possible burst transmissions in a dense signal environment
[PB94-149259] 10 p4036 N94-34109

NASA COMMUNICATION NETWORK
U NASCOM NETWORK

NASA PROGRAMS
NT APOLLO PROJECT
NT GALILEO PROJECT
NT MAGELLAN PROJECT (NASA)
NT MARINER-MERCURY 1973
NT MERCURY PROJECT
NT NASA SPACE PROGRAMS
NT NATIONAL AEROSPACE PLANE PROGRAM
NT NATIONAL LAUNCH VEHICLE PROGRAM
NT PIONEER PROJECT
NT PROJECT SETI
NT SCOUT PROJECT
NT SUPERSONIC CRUISE AIRCRAFT RESEARCH
NT SURVEYOR PROJECT
NT TILT ROTOR RESEARCH AIRCRAFT PROGRAM
NT VIKING MARS PROGRAM
NT VOYAGER PROJECT
The NASA Lewis Research Center SBIR program: An assessment
[NASA-TM-106205] 01 p0485 N94-10356
NASA Marshall Space Flight Center solar observatory report, January - June 1993
[NASA-TM-108417] 01 p0423 N94-10866
National Aero-Space Plane: A need for program direction and funding decisions
[GAO/NSIAD-93-207] 01 p0416 N94-10910
NASA procurement: Proposed changes to the Jet Propulsion Laboratory contract. Report to Congressional Requesters
[GAO/NSIAD-93-178] 01 p0416 N94-10941
Advanced statistical methods for improved data analysis of NASA astrophysics missions
[NASA-CR-193514] 01 p0425 N94-10943
The 1987 RIACS annual report
[NASA-CR-193220] 01 p0324 N94-11046
The role of metrics and measurements in a software intensive total quality management environment
01 p0329 N94-11428
Development and application of an acceptance testing model 01 p0330 N94-11432
Financial management: NASA's financial reports are based on unreliable data
[AD-A265690] 01 p0418 N94-12443
National atmospheric sciences program, fiscal years 1987-1990
[NSF-92-16] 02 p0711 N94-12794
Technology Applications Team: Applications of aerospace technology
[NASA-CR-194362] 02 p0828 N94-13104
Program/project management resource lists
[NASA-TM-109268] 02 p0822 N94-13107
Ninth Annual NASA/Contractors Conference on Quality and Productivity. World Class Excellence: The Journey Continues. Keynote presentations
[NASA-CR-194513] 02 p0665 N94-13148
Ninth Annual NASA/Contractors Conference on Quality and Productivity. World Class Excellence: The Journey Continues. Conference presentations
[NASA-CR-194514] 02 p0665 N94-13153
Strategic planning as a focus for continuous improvement. A case study 02 p0666 N94-13158
Building a quality culture in the Office of Space Flight: Approach, lessons learned and implications for the future 02 p0667 N94-13164
NASA Johnson Space Center: Total quality partnership 02 p0668 N94-13165
Shared visions: Partnership of Rockwell International and NASA Cost Effectiveness Enhancements (CEE) for the space shuttle system integration program
02 p0668 N94-13166
NASA/contractor partnership on the second TDRSS ground terminal program: Breaking barriers
02 p0668 N94-13168
Government/contractor partnerships for continuous improvement. A Goddard Space Flight Center example
02 p0669 N94-13169
User observations on information sharing (corporate knowledge and lessons learned)
[NASA-TM-104781] 02 p0819 N94-13400
NASA aerospace database subject scope: An overview
[NASA-SP-7107] 02 p0823 N94-13401
Goddard Space Flight Center robotics demo
[NASA-TM-109302] 02 p0662 N94-13604
Highlights, 1981
[NASA-TM-109305] 02 p0850 N94-13612
NASA experiences in the Goddard MMS
[NASA-TM-109290] 02 p0819 N94-13629
The Eighth Annual NASA/Contractors Conference and 1991 National Symposium on Quality and Productivity: Extending the boundaries of total quality management
[NASA-TM-109276] 02 p0669 N94-14321
NASA Space Engineering Research Center for VLSI systems design
[NASA-CR-194035] 02 p0625 N94-14325
SHARP
[NASA-TM-109659] 03 p1221 N94-15230
University Joint Venture: JOVE
[NASA-TM-109660] 03 p1229 N94-15231
Space classroom
[NASA-TM-109661] 03 p1221 N94-15232
Return to flight 1
[NASA-TM-109663] 03 p1223 N94-15234
Teacher in space
[NASA-TM-109666] 03 p1131 N94-15237
The 1969 highlights
[NASA-TM-109630] 03 p1301 N94-15241
The 1972 highlights
[NASA-TM-109631] 03 p1301 N94-15242
The 1965 highlights --- NASA programs
[NASA-TM-109632] 03 p1301 N94-15243
The 1967 highlights
[NASA-TM-109633] 03 p1301 N94-15244
From space to Earth
[NASA-TM-109638] 03 p1235 N94-15249
GAS highlights, 1988 --- Get Away Specials
[NASA-TM-109600] 03 p0873 N94-15308
Space Shuttle highlights
[NASA-TM-109606] 03 p0880 N94-15314
Return to flight 3, the journey continues
[NASA-TM-109651] 03 p1223 N94-15319
IG nuts and bolts
[NASA-TM-109652] 03 p1049 N94-15320
NACA-NASA: 75 years of flight
[NASA-TM-109449] 03 p1302 N94-15322
NASA images 6
[NASA-TM-109437] 03 p0862 N94-15336
NASA images 7
[NASA-TM-109438] 03 p1235 N94-15337
NASA images 16
[NASA-TM-109440] 03 p1235 N94-15339
Back to propellers
[NASA-TM-109445] 03 p0869 N94-15344
Better airplane wings
[NASA-TM-109446] 03 p0933 N94-15345
Cohen program management briefing
[NASA-TM-109536] 03 p1223 N94-15367
CORE/TRC
[NASA-TM-109434] 03 p1221 N94-15418
Improved mapping system
[NASA-TM-109643] 03 p1082 N94-15428
Challenger Center: Orientation
[NASA-TM-109433] 03 p1221 N94-15505
Coast encounters: A space age adventure in science literacy
[NASA-TM-109334] 03 p1229 N94-15523
NASA Space Engineering Research Center for VLSI System Design
[NASA-CR-194587] 03 p1008 N94-15547
NASA trend analysis procedures
[NASA-RP-1290] 03 p1223 N94-15782
NAS technical summaries: Numerical aerodynamic simulation program, March 1991 - February 1992
[NASA-TM-109335] 03 p0854 N94-15798
NASA/DOD Aerospace Knowledge Diffusion Research Project. Paper 33: Technical communications practices and the use of information technologies as reported by Dutch and US aerospace engineers
[NASA-TM-109337] 03 p1230 N94-15839
The strategic environmental research and development program: A new paradigm for space, the environment, and national security
[AD-A266222] 03 p1174 N94-16109
Proceedings of the 1992 Annual Meeting NASA Occupational Health Program
[NASA-CR-193462] 03 p1123 N94-16609
The Goddard Space Flight Center ergonomics program 03 p1125 N94-16621
Industrial Hygiene Laboratory accreditation: The JSC experience 03 p1125 N94-16623
Summary of follow-up results from potential tuberculosis exposures 03 p1126 N94-16628
Physical fitness and health education program at NASA Headquarters 03 p1126 N94-16631
Ames Fitness Program 03 p1126 N94-16632
Johnson Space Center health related fitness program
03 p1126 N94-16633
Kennedy Space Center exercise program
03 p1126 N94-16634
The Langley Fitness Center 03 p1126 N94-16635
Physical Exercise Program 03 p1127 N94-16636
Arsenic surveillance program
03 p1127 N94-16637
Asbestos Surveillance Program
03 p1127 N94-16638
Hearing Conservation Medical Program
03 p1127 N94-16639
Lead Surveillance Program 03 p1127 N94-16640
Mercury Surveillance Program
03 p1127 N94-16641
Respiratory Protection Program medical clearance for respirator use 03 p1127 N94-16642
General Medical Surveillance Program
03 p1127 N94-16643
Bloodborne Pathogens Program
03 p1127 N94-16644
Mission management aircraft operations manual
[NHB-7900.3] 03 p1225 N94-16729
Aircraft operations management manual
[NHB-7900.3(V1)] 03 p1225 N94-16730
Equipment Management Manual
[NHB-4200.1D] 03 p1225 N94-16799
OSSA Information Systems Program
[NASA-TM-108774] 04 p1612 N94-17737
The 1994 NASA authorization, volume 2
[GPO-71-510] 04 p1620 N94-18842
National Boy Scout Jamboree
[NASA-TM-109367] 04 p1610 N94-18982
California Student Get Away Special Payload GAS-450
04 p1324 N94-19164
The GAMCIT gamma ray burst detector
04 p1324 N94-19168
The first flight of the QUESTS GAS payload G-521
04 p1325 N94-19170
Marshall Space Flight Center 1989 annual chronology of events
[NASA-TM-109381] 04 p1633 N94-19486
NASA's Education Program
[NASA-EP-297] 05 p2038 N94-20129
NASA property: Improving management of government equipment provided to contractors. Report to the Chairman, Subcommittee on Investigations and Oversight, Committee on Science, Space, and Technology, House of Representatives
[GAO/NSIAD-93-191] 05 p2039 N94-20206
NASA procurement: Planning for pilot test of new procurement procedures is adequate. Report to the Chairman, Committee on Governmental Affairs, US Senate
[GAO/NSIAD-94-67] 05 p2039 N94-20236
The manager's guide to NASA graphics standards
[NHB-1430.2] 05 p2042 N94-20308
NASA patent abstracts bibliography: A continuing bibliography. Section 1: Abstracts (supplement 44)
[NASA-SP-7039(44)-SECT-1] 05 p2043 N94-21254
Network command processing system overview
05 p1935 N94-21351
Issues in NASA program and project management. Special Report: 1993 conference
[NASA-SP-6101(07)] 05 p2039 N94-21497
Issues in NASA program and project management
[NASA-SP-6101(06)] 05 p2040 N94-21499
NASA procurement report, FY 1992
[NASA-TM-109390] 05 p2040 N94-21623
NASA procurement report, FY 1993
[NASA-TM-109393] 05 p2040 N94-21625
Summary data on all NASA procurement actions
[NASA-TM-109392] 05 p2040 N94-21638
NASA SERC digital correlator projects
05 p1765 N94-21708
Index to 1992 NASA Tech Briefs, volume 16, numbers 1-12
[NASA-TM-109377] 05 p2053 N94-21736
Index to 1991 NASA Tech Briefs, volume 15, numbers 1-12
[NASA-TM-109376] 05 p2053 N94-21737
Cumulative index to NASA Tech Briefs, 1986-1990, volumes 10-14
[NASA-TM-109378] 05 p2054 N94-21738
An overview of the radiation component of the NASA TOGA-COARE experiment 05 p1881 N94-22344
Johnson Space Center CFD grid generation requirements 05 p1919 N94-22355
NASA's astrophysics archives at the National Space Science Data Center 05 p2049 N94-22541
NASA patent abstracts bibliography: A continuing bibliography. Section 2: Indexes (supplement 44)
[NASA-SP-7039(44)-SECT-2] 06 p2590 N94-23712
NASA printing, duplicating, and copying management handbook
[NASA-NHB-1490.5] 06 p2590 N94-23971
NASA high performance computing and communications program
[NASA-TM-4554] 06 p2591 N94-24337
A compilation of technology spinoffs from the US Space Shuttle Program 06 p2578 N94-24424
Access to space studies 06 p2199 N94-24434

Suddenly, tomorrow came... A history of the Johnson Space Center
[NASA-SP-4307] 06 p2631 N94-24584
NASA/DOD Aerospace Knowledge Diffusion Research Project. Report number 20: The use of selected information products and services by US aerospace engineers and scientists: Results of two surveys
[AD-A276068] 06 p2592 N94-24649
Management: A bibliography for NASA managers
[NASA-SP-7500(27)] 06 p2586 N94-24708
NASA tech brief evaluations
[NASA-CR-195150] 06 p2597 N94-24829
NASA STI program database: Journal coverage (1990-1992)
[NASA-TM-109720] 06 p2593 N94-25168
National Aeronautics and Space Administration (NASA)/American Society for Engineering Education (ASEE) Summer Faculty Fellowship Program, 1993, volume 1
[NASA-CR-198271-VOL-1] 06 p2632 N94-25348
Strategies for recruiting additional African Americans into the NASA JSC summer faculty fellows program 06 p2585 N94-25362
An assessment of testing requirement impacts on nuclear thermal propulsion ground test facility design
[DE94-002933] 07 p2702 N94-26560
Aerospace safety advisory panel
[NASA-TM-109692] 07 p3118 N94-27381
Nasa Langley Research Center seventy-fifth anniversary publications, 1992
[NASA-TM-109691] 07 p3118 N94-27431
Small business innovation research program solicitation
[NASA-TM-109695] 07 p3094 N94-27661
NASA SBIR abstracts of 1992, phase 1 projects
[NASA-TM-109694] 07 p3094 N94-27772
The 1993 NASA-ODU American Society for Engineering Education (ASEE) Summer Faculty Fellowship Program
[NASA-CR-191544] 07 p3085 N94-27893
Research and Development Annual Report, 1992
[NASA-TM-104777] 07 p3119 N94-27993
NASA: Major challenges for management. Testimony before the Legislation and National Security Subcommittee, Committee on Government Operations, House of Representatives
[GAO/T-NSIAD-94-18] 07 p3095 N94-28176
NASA space and Earth science data on CD-ROM
[NASA-TM-109709] 08 p3528 N94-28414
BAG: A code for predicting the performance of a gas bag impact attenuation system for the Pathfinder lander
[DE94-003688] 08 p3165 N94-28477
NASA Parts Program Office responsibilities 08 p3165 N94-28702
NASA Parts Project Office: Basic goals 08 p3166 N94-28703
Research and technology, 1992
[NASA-TM-103996] 08 p3555 N94-29891
A survey of NASA and military standards on fault tolerance and reliability applied to robotics
[AIAA PAPER 94-1211-CP] 08 p3445 N94-30562
Terrestrial applications of NASA space telerobotics technologies
[AIAA PAPER 94-1235-CP] 08 p3448 N94-30582
Global change research and NASA's Earth Observing System
[PB94-126992] 09 p3741 N94-31068
NASCOM system development plan: System description, capabilities, and plans, FY 94-2
[NASA-TM-109744] 09 p3674 N94-31503
Marsville: The cosmic village
[NASA-TM-109752] 09 p3913 N94-31806
Aerospace test facilities at NASA LERC Plumbrook
[NASA-TM-109755] 09 p3602 N94-31814
Welcome to the Ohio Aerospace Institute
[NASA-TM-109756] 09 p3913 N94-31815
The sky is your classroom
[NASA-TM-109759] 09 p3914 N94-31887
Index to NASA news releases and speeches, 1993
[NASA-TM-109722] 09 p3917 N94-31888
NASA strategic plan
[NASA-TM-109780] 09 p3915 N94-32222
Management of government quality assurance functions for NASA contracts
[NHB-5300.4(2B-2)] 09 p3731 N94-32387
NASA/DOD Aerospace Knowledge Diffusion Research Project. Paper 10: The NASA/DOD Aerospace Knowledge Diffusion Research Project
[NASA-TM-109769] 09 p3921 N94-32831
Research and Technology Objectives and Plans Summary (RTOPS)
[NASA-TM-105441] 09 p3966 N94-32885
Opinion polls and the US civil space program
[NASA-TM-109700] 09 p3914 N94-33066
Space history, space policy, and executive leadership
[NASA-TM-109787] 09 p3924 N94-33067
NASA HSR phase 1 low noise nozzle technology program overview 10 p3972 N94-33463
LeRC in-house experimental research 10 p3975 N94-33484
The making of the time capsule
[NASA-TM-109807] 10 p4011 N94-33560
NASA report to education, volume 6
[NASA-TM-109818] 10 p4167 N94-33573
Indianapolis CIP review
[NASA-TM-109821] 10 p4149 N94-33575
Space electronics video: Research for today and tomorrow
[NASA-TM-109829] 10 p4039 N94-33583
Automating the training development process for mission flight operations 10 p4098 N94-33625
Emergency medical services 10 p4096 N94-33644
Activities of the NASA centers
[NASA-TM-109836] 10 p4068 N94-33721
Way station to space: The history of Stennis Space Center
[NASA-TM-109819] 10 p4011 N94-33771
Nomination of Daniel S. Goldin to be administrator of the National Aeronautics and Space Administration
[S-HRG-102-744] 10 p4150 N94-33947
NASA historical data book. Volume 4: NASA resources 1969-1978
[NASA-SP-4012-VOL-4] 10 p4179 N94-33949
SeaWiFS technical report series. Volume 16: The second SeaWiFS Intercalibration Round-Robin Experiment, SIRREX-2, June 1993
[NASA-TM-104566-VOL-16] 10 p4093 N94-34412
NASA/DOD Aerospace Knowledge Diffusion Research Project. Paper 42: An analysis of the transfer of Scientific and Technical Information (STI) in the US aerospace industry
[NASA-TM-109863] 10 p4159 N94-34730
Director's discretionary fund
[NASA-TM-103997] 11 p4376 N94-35370
NASA patent abstracts bibliography: A continuing bibliography. Section 1: Abstracts (supplement 45)
[NASA-SP-7039(45)-SECT-1] 11 p4344 N94-35382
Aerospace Safety Advisory Panel
[NASA-TM-109840] 11 p4201 N94-35390
Statement by Bill D. Colvin, Inspector General
[NASA-TM-109793] 11 p4348 N94-35446
Trace-shortened Reed-Solomon codes 11 p4254 N94-35554
Challenging the Future - Journey to Excellence. Aeropropulsion strategic plan for the 1990's
[NASA-TM-109250] 11 p4228 N94-35591
TDRSS Onboard Navigation System (TONS) flight qualification experiment 11 p4206 N94-35625
NASA patent abstracts bibliography: A continuing bibliography. Section 2: Indexes (supplement 45)
[NASA-SP-7039(45)-SECT-2] 11 p4346 N94-35835
Budget estimates, fiscal year 1995. Volume 1: Agency summary, human space flight, and science, aeronautics and technology
[NASA-TM-109791] 11 p4347 N94-35899
Budget estimates, fiscal year 1995. Volume 2: Mission support and Inspector General
[NASA-TM-109792] 11 p4348 N94-35900
A biased historical perspective of women in the engineering field at Dryden from 1946 to November 1992 11 p4251 N94-35967
Research and technology, 1993
[NASA-TM-108816] 11 p4380 N94-36117
National Educators' Workshop: Update 1993. Standard Experiments in Engineering Materials Science and Technology
[NASA-CP-3259] 11 p4229 N94-36398
Profile of NASA software engineering: Lessons learned from building the baseline 12 p4492 N94-36500
Impact of Ada in the Flight Dynamics Division: Excitement and frustration 12 p4492 N94-36501
Software engineering technology transfer: Understanding the process 12 p4492 N94-36502
NASA STI Program Coordinating Council Eleventh Meeting: NASA STI Modernization Plan
[NASA-TM-109415] 12 p4540 N94-36841
NASA STI modernization plan 12 p4540 N94-36842
The Engineering Review Board 12 p4540 N94-36843
RECON Replacement Project 12 p4541 N94-36844
Electronic SCAN (Selected Current Aerospace Notices) 12 p4541 N94-36845
Machine Translation Project 12 p4541 N94-36846
Multimedia 12 p4541 N94-36847
Electronic document interchange 12 p4541 N94-36848
Electronic document interchange 12 p4541 N94-36849
NASA Access Mechanism (NAM) 12 p4541 N94-36850
Network upgrades 12 p4541 N94-36851
Standards in the architectural effort 12 p4541 N94-36852
NASA STI Program Coordinating Council Twelfth Meeting: Standards
[NASA-TM-109925] 12 p4541 N94-36853
STI Architectural Framework Working Group 12 p4542 N94-36854
Design and development of experimental facilities for short duration, low-gravity combustion and fire experiments
[NASA-CR-196107] 12 p4389 N94-36967
Engineering directorate technical facilities catalog
[NASA-TM-109895] 12 p4390 N94-37443
NASA reload program
[NASA-CR-193972] 12 p4429 N94-37446
NASA commercial technology. Agenda for change
[NASA-TM-109898] 12 p4546 N94-37765

NASA SPACE PROGRAMS

NT APOLLO PROJECT
NT GALILEO PROJECT
NT MAGELLAN PROJECT (NASA)
NT MARINER-MERCURY 1973
NT MERCURY PROJECT
NT NATIONAL LAUNCH VEHICLE PROGRAM
NT PIONEER PROJECT
NT PROJECT SETI
NT SCOUT PROJECT
NT SURVEYOR PROJECT
NT VIKING MARS PROGRAM
NT VOYAGER PROJECT
Transportation systems analyses: Volume 1: Executive Summary
[NASA-CR-192583] 01 p0041 N94-10826
Transportation systems analyses. Volume 2: Technical/programmatics
[NASA-CR-192582] 01 p0041 N94-10827
Access to Japanese aerospace-related scientific and technical information: The NASA Aerospace Database
[NASA-TM-109413] 02 p0822 N94-13105
Highlights, 1981
[NASA-TM-109305] 02 p0850 N94-13612
Research and technology highlights, 1992
[NASA-TM-4452] 02 p0850 N94-13962
The 1969 highlights
[NASA-TM-109630] 03 p1301 N94-15241
The 1972 highlights
[NASA-TM-109631] 03 p1301 N94-15242
The 1965 highlights --- NASA programs
[NASA-TM-109632] 03 p1301 N94-15243
The 1967 highlights
[NASA-TM-109633] 03 p1301 N94-15244
Stock footage of Goddard Space Flight Center and Headquarters
[NASA-TM-109589] 03 p0875 N94-15273
Space Station: The link to America's future
[NASA-TM-109653] 03 p0884 N94-15274
Lunar base concepts
[NASA-TM-109607] 03 p1247 N94-15294
NASA: The 25th year
[NASA-TM-109457] 03 p1302 N94-15352
NASA's Hubble Space Telescope: The challenge and complexity of operations
[NASA-TM-109577] 03 p1236 N94-15422
Mars rover sample return mission
[NASA-TM-109521] 03 p0873 N94-15471
Commitment to challenge
[NASA-TM-109523] 03 p0876 N94-15473
History of the manned space flight program
[NASA-TM-109529] 03 p1303 N94-16069
TABES 1993: 9th Annual Technical and Business Exhibition and Symposium 03 p1050 N94-16129
Approaching the new reality
[TABES PAPER 93-230] 03 p1050 N94-16131
Commercial space opportunities advanced concepts and technology overview
[TABES PAPER 93-240] 03 p1050 N94-16132
Human Transportation System (HTS) study: Executive summary
[NASA-TM-104780] 04 p1332 N94-18669
Human Transportation System (HTS) study, volume 1
[NASA-TM-104779] 04 p1332 N94-18670
The future of remote sensing from space: Civilian satellite systems and applications
[OTA-ISC-558] 05 p1837 N94-20209
Solar physics within NASA's planning 06 p2625 N94-22845
The birth of NASA: The diary of T. Keith Glennan
[NASA-SP-4105] 06 p2630 N94-23333
Past US studies and developments for planetary rovers 06 p2369 N94-23375
Strategies in transition 06 p2498 N94-23833
Future trends in NASA space operations 06 p2498 N94-23836

Ultraviolet, visible, and gravity astrophysics: A plan for the 1990's
[NASA-NP-152] 06 p2603 N94-24973
The future of manned spaceflight 06 p2195 N94-25067
New Ways Of Doing Business (NWODB) cost quantification analysis
[NASA-CR-195186] 06 p2586 N94-25197
JSC almanac
[NASA-TM-109702] 07 p3119 N94-28204
Status of frequency and time support for NASA systems 08 p3468 N94-30640
NASA's space platform technology program and planning 09 p3597 N94-31044
MSFC orbital spacecraft development emphases for this decade 09 p3598 N94-31048
Chronology of KSC and KSC related events for 1993
[NASA-TM-109196] 09 p3966 N94-33072
Stennis Space Center 1992
[NASA-TM-109796] 10 p4011 N94-33558
United States/Russia space cooperation documentary
[NASA-TM-109809] 10 p4014 N94-33561
Technology for small spacecraft
[NASA-CR-196041] 10 p4015 N94-34411
NASA Space Geodesy Program: GSFC data analysis, 1993. VLBI geodetic results 1979 - 1992
[NASA-TM-104605] 11 p4281 N94-35261
Space educators' handbook
[NASA-TM-109779] 11 p4343 N94-35339
Space and the American imagination
[NASA-CR-196131] 11 p4376 N94-35356
Planetary Rover Program
[NASA-CR-196108] 11 p4201 N94-35511
The history of space expioration
[NASA-TM-109888] 11 p4201 N94-36440

NASA STRUCTURAL ANALYSIS PROGRAM
U NASTRAN

NASCOM NETWORK
NASCOM system development plan: System description, capabilities, and plans, FY 94-2
[NASA-TM-109744] 09 p3674 N94-31503

NASTRAN
NASTRAN modeling of flight test components for UH-60A airloads program test configuration
[NASA-CR-193614] 01 p0186 N94-10937
Design optimization studies using COSMIC NASTRAN 04 p1450 N94-17834
The role of NASTRAN in the preliminary design cycle 04 p1450 N94-17835
Benchmarking the QUAD4/TRIA3 element 04 p1450 N94-17837
Stiffness-generated rigid-body mode shapes for Lanczos eigensolution with SUPORT DOF by way of a MSC/NASTRAN DMAP alter
[NASA-TM-106537] 08 p3319 N94-29406
Transient analysis mode participation for modal survey target mode selection using MSC/NASTRAN DMAP
[NASA-TM-106536] 08 p3319 N94-29469
QUAD4 seminar
[AD-A277366] 09 p3818 N94-32330

NATIONAL AEROSPACE PLANE PROGRAM
CFD analysis of hypersonic, chemically reacting flow fields 01 p0002 N94-10422
National Aero-Space Plane: A need for program direction and funding decisions
[GAO/NSIAD-93-207] 01 p0416 N94-10910
An environmental study of the National Aerospace Plane
[AD-A266071] 01 p0025 N94-10945
Perspective on the National Aero-Space Plane Program instrumentation development
[NASA-TM-4505] 02 p0516 N94-13256
Trajectory optimization for the national aerospace plane
[NASA-CR-194146] 02 p0516 N94-14104
National Aero-Space Plane
[NASA-TM-109450] 03 p0865 N94-15323
National Aero-Space Plane resource reel
[NASA-TM-109451] 03 p0865 N94-15324
Fluid flow and heat convection studies for actively cooled airframes
[NASA-CR-194624] 03 p1024 N94-16491
Trajectory optimization for the National Aerospace Plane
[NASA-CR-194618] 03 p0867 N94-16498
A conceptual design of an unmanned test vehicle using an airbreathing propulsion system
[NASA-CR-195550] 06 p2189 N94-25085
A numerical study of mixing and combustion in hypervelocity flows through a scramjet combustor model 07 p2808 N94-27911
Hypervelocity Tunnel 9 Mach 10/14 Calibration
[AD-A275960] 09 p3587 N94-31318
High temperature NASP engine seal development
[NASA-TM-109750] 09 p3725 N94-31804
Futurepath 3
[NASA-TM-109762] 09 p3735 N94-31819
The National Aerospace Plane (NASP): Development issues for the follow-on vehicle
[AD-A278417] 09 p3581 N94-33329
John C. Stennis Space Center overview
[NASA-TM-109816] 10 p4011 N94-33567
High Heat Flux Facility
[NASA-TM-109834] 10 p4009 N94-33570
National aerospace plane
[NASA-TM-109843] 10 p4019 N94-33750
Turbulence compressibility corrections
[NASA-TM-108827] 10 p4047 N94-33999

NATIONAL AIRSPACE SYSTEM
National Airspace System operational concept
[DOT/FAA/SE-93/1] 01 p0023 N94-10933
FAA air traffic activity
[AD-A266043] 01 p0022 N94-12397
Determination of Loran-C/GPS human factors issues
[AD-A266334] 02 p0514 N94-14563
The FAA Technical Center Human Factors Laboratory information guide
[AD-A269343] 04 p1513 N94-18992
Conflict-free trajectory planning for air traffic control automation
[NASA-TM-108790] 06 p2174 N94-25272
Rotorcraft low altitude IFR benefit/cost analysis: Conclusions and recommendations
[AD-A274241] 07 p2665 N94-26826
Optical communications for transport aircraft 07 p2643 N94-27298
The 1993 Federal Aviation Administration plan for research, engineering and development
[AD-A279037] 07 p2643 N94-27960
1.8 gigahertz (GHz) digital Low Density Radio Communications Link (LDRCL) Operational Test and Evaluation (OT&E) integration and OT&E operational final test report
[AD-A275800] 08 p3241 N94-28771
The 1993 Federal Aviation Administration Aviation System Capital Investment Plan
[AD-A279036] 08 p3136 N94-29445
Loran-C time management 08 p3144 N94-30644
Civil tiltrotor market penetration: Effects on Northeast corridor airport delay
[AD-A277534] 09 p3576 N94-32955
The Federal Aviation Administration plan for research, engineering and development 11 p4376 N94-35262
AWOS Data Acquisition System (ADAS) Operational Test and Evaluation (OT/E) integration and OT/E operational test report
[AD-A280492] 12 p4473 N94-37143

NATIONAL AVIATION SYSTEM
FAA aviation forecasts, fiscal years 1994-2005
[AD-A277808] 09 p3566 N94-33016

NATIONAL LAUNCH VEHICLE PROGRAM
The National Launch System Advanced Development Program: A brief overview 01 p0040 N94-11576
Aerodynamic flight control to increase payload capability of future launch vehicles
[NASA-CR-193850] 03 p0870 N94-15532
Flame trench analysis of NLS vehicles 06 p2199 N94-23249
Aerodynamic characteristics of the National Launch System (NLS) 1 1/2 stage launch vehicle
[NASA-TP-3488] 12 p4384 N94-37577

NATIONAL PARKS
NT YELLOWSTONE NATIONAL PARK (ID-MT-WY)
Multisensor remote sensing data and GIS techniques for monitoring preservation areas: A case study
[INPE-5317-PRE/1714] 02 p0688 N94-14131
Linear mixing model applied to AVHRR LAC data 05 p1838 N94-20958
Dose-response relationships derived from data collected at Grand Canyon, Haleakala and Hawaii Volcanoes National Parks
[PB94-151941] 10 p4134 N94-34380
Vent processes during the 1912 eruption at Novarupta, Katmai National Park, Alaska
[DE94-010740] 12 p4468 N94-36451

NATIONS
NT ALASKA
NT ARGENTINA
NT ARIZONA
NT ARKANSAS
NT ARMENIA
NT AUSTRALIA
NT AZERBAIJAN
NT BANGLADESH
NT BELARUS
NT BELGIUM
NT BRAZIL
NT CALIFORNIA
NT CANADA
NT CHINA
NT CONNECTICUT
NT DENMARK
NT FINLAND
NT FRANCE
NT FRENCH GUIANA
NT GERMANY
NT HAWAII
NT ICELAND
NT IDAHO
NT INDIA
NT INDIANA
NT INDONESIA
NT IOWA
NT IRAN
NT ISRAEL
NT ITALY
NT JAPAN
NT KAZAKHSTAN
NT KENYA
NT MALAYSIA
NT MARYLAND
NT MEXICO
NT MINNESOTA
NT MISSISSIPPI
NT MONGOLIA
NT NETHERLANDS
NT NEWFOUNDLAND
NT NIGER
NT NORWAY
NT ONTARIO
NT PHILIPPINES
NT PORTUGAL
NT REPUBLIC OF SOUTH AFRICA
NT RUSSIAN FEDERATION
NT SAUDI ARABIA
NT SINGAPORE
NT SOMALIA
NT SOUTH CAROLINA
NT SOUTH KOREA
NT SUDAN
NT SWEDEN
NT TAIWAN
NT THAILAND
NT TIBET
NT TUNISIA
NT U.S.S.R.
NT UNITED KINGDOM
NT UNITED STATES
NT VIETNAM
NT WASHINGTON
NT YUKON TERRITORY

NATURAL FREQUENCIES
U RESONANT FREQUENCIES

NATURAL GAS
Vehicular fleet operation on natural gas and propane: An overview
[PB93-194603] 01 p0098 N94-10844
Business fleet refueling assessment
[PB93-189892] 01 p0098 N94-11017
Low pressure storage of natural gas on activated carbon
[DE93-014053] 02 p0660 N94-12851
Overview: Gas hydrate geology and geography
[DE93-014043] 02 p0688 N94-14151
Upgrading of raw natural gas using high-performance polymer membranes
[DE93-014041] 02 p0566 N94-14586
Biomass energy: State of the technology present obstacles and future potential
[DE93-016295] 03 p1092 N94-16766
Methyl chloride via oxyhydrochlorination of methane
[DE93-017548] 03 p0952 N94-17218
Report to Congress: Comprehensive Program Plan for Advanced Turbine Systems
[DE93-016718] 04 p1467 N94-18475
EIA publications directory, 1992
[DE93-016833] 04 p1617 N94-18983
Speed of sound data and related models for mixtures of natural gas constituents
[PB93-200822] 05 p1968 N94-21447
Vapor-delivered lubrication of steel-steel and steel-ceramic systems
[PB93-202364] 05 p1825 N94-21451
Combustion in turbulent jets and buoyant flames
[PB93-202372] 05 p1682 N94-21452
Current situation in developing petroleum substituting energy (the United Kingdom)
[DE94-714897] 05 p1713 N94-22091
Development of durable high-temperature catalysts for natural gas combustion
[PB93-226447] 06 p2232 N94-23477
Evaluation of reducing gas turbine emissions through hydrogen-enhanced steam-injected combustion
[PB94-109873] 06 p2187 N94-23709
Fundamental and experimental studies on the catalytic combustion of methane
[PB94-112661] 06 p2233 N94-23736

Fundamental study of NO(x) control in catalytic combustion
[PB94-112323] 06 p2398 N94-23818
Near-surface seismic imaging
[PB94-119096] 06 p2404 N94-24647
Modelling of premixed laminar flames
[ETN-94-95317] 06 p2236 N94-25284
Natural gas applications for hybrid vehicles.
[PB94-117108] 07 p2759 N94-26753
Feasibility study on introduction of transportation-use petroleum substitution energy
[DE94-725205] 07 p2759 N94-26905
Sequential multi-point injection of a natural gas engine. Topical report, November 1991 - April 1992
[PB94-126794] 07 p2824 N94-27224
Laser probes of natural gas ignition chemistry
[PB94-128345] 07 p2717 N94-27226
Basic research on natural gas combustion phenomena
[PB94-129046] 07 p2717 N94-27256
Combined Cycles for Power Plants
[VKI-LS-1993-08] 07 p2830 N94-28077
Introduction to combined cycles
07 p2789 N94-28078
Numerical prediction of mixing process in a methane-fueled engine 08 p3304 N94-30230
Technical analysis of alternative fueled vehicles
[DE94-744238] 08 p3304 N94-30269
Configuration and performance of the indirect-fired fuel cell bottomed turbine cycle
[DE94-005961] 08 p3338 N94-30313
Investigation of the technology development status of alternate fuel vehicles
[DE94-744237] 08 p3312 N94-30831
Compressed natural gas fueled vehicles: The Houston experience
[DE94-005804] 08 p3312 N94-30878
Assessment of costs and benefits of flexible and alternative fuel use in the US transportation sector
[DE94-006100] 08 p3226 N94-30885
Feasibility study to evaluate plasma quench process for natural gas conversion applications
[DE94-000086] 09 p3758 N94-31234
Economic feasibility analysis of distributed electric power generation based upon the natural gas fired fuel cell
[DE94-005795] 09 p3759 N94-31487
Gas hydrate detection and mapping on the US east coast
[DE94-005959] 09 p3742 N94-31504
Analysis of deep seismic reflection and other data from the southern Washington Cascades
[DE94-005958] 09 p3771 N94-31525
Emissions of greenhouse gases from the use of transportation fuels and electricity
[DE94-006166] 09 p3765 N94-31625
EIA directory of electronic products, fourth quarter 1993
[DE94-007368] 10 p4151 N94-33596
Hynol: An economic process for methanol production from biomass and natural gas with reduced CO2 emission
[DE94-008872] 10 p4079 N94-34139
Infrared multiphoton ignition and combustion enhancement of natural gas.
[PB94-165438] 11 p4236 N94-35755
Analysis of the injection process in direct injected natural gas engines
[PB94-156494] 11 p4275 N94-35931
Gasoline from natural gas by sulfur processing
[DE94-011130] 11 p4248 N94-36035
A comparison between direct spark ignition and prechamber ignition in an internal combustion engine
[DE94-008218] 11 p4275 N94-36206
Effects of natural gas composition on ignition delay under diesel conditions
[DE94-006405] 11 p4276 N94-36378
Alternative fuel information: Facts about CNG and LPG conversion
[DE94-006888] 12 p4429 N94-37402
Technical evaluation and assessment of CNG/LPG bi-fuel and flex-fuel vehicle viability
[DE94-006925] 12 p4451 N94-37408

NATURAL GAS EXPLORATION
Analysis of deep seismic reflection and other data from the Southern Washington Cascades
[DE94-004075] 12 p4470 N94-37489

NATURAL LANGUAGE (COMPUTERS)
A real-time spoken-language system for interactive problem solving
[AD-A266046] 01 p0324 N94-11104
Transactions of the 10th Army Conference on Applied Mathematics and Computing
[AD-A265098] 01 p0318 N94-11678
Machine translation technology: A potential key to the information age
[PB93-134336] 01 p0421 N94-12385
Proceedings of the Seventh International Symposium on Methodologies for Intelligent Systems (poster session)
[DE93-013470] 01 p0340 N94-12428
Using multiple adaptively-weighted strategies for the resolution of demonstratives
[AD-A266463] 03 p1150 N94-16585
Information technology division technical paper abstracts
[AD-A266227] 03 p1166 N94-16938
Employing knowledge resources in a new text planner architecture
[AD-A269669] 04 p1516 N94-17732
EXPECT: Intelligent support for knowledge base refinement
[AD-A269602] 04 p1612 N94-17745
Intelligent help facilities: Generating natural language descriptions with examples
[AD-A269555] 04 p1521 N94-18290
Automatic documentation generation: The interaction of text and examples
[AD-A269670] 04 p1616 N94-18570
Generating object descriptions: Intergrating examples with text
[AD-A269992] 04 p1522 N94-18680
Computer-assisted instruction and natural language systems
[MEMO-INF-92-86] 04 p1527 N94-19225
Are types needed for natural language?
[PB93-191831] 05 p1949 N94-19997
Nominalization, prediction and type containment
[PB93-191799] 05 p1898 N94-20082
Connectionism and Natural Language Processing
[MEMO-INF-92-64] 05 p1940 N94-20242
A single layer higher order neural net and its application to grammar recognition 05 p1941 N94-20251
A modular design for connectionist parsing
05 p1941 N94-20252
Syntactic neural networks for natural language processing 05 p1941 N94-20254
DISCERN: A distributed neural network model of script processing and memory 05 p1941 N94-20255
The Seventh International Symposium on Methodologies for Intelligent Systems (Poster Session)
[AD-A272125] 05 p1942 N94-20573
A strategy for dynamic interpretation: A fragment and an implementation
[CWI-CS-R9317] 07 p2970 N94-27545
Engineering specification editing tools
[AD-A275116] 08 p3419 N94-29746
What comes first in dynamic semantics: A compositional, non-representational account of natural language presupposition
[LP-93-15] 09 p3855 N94-31389
Methods for parallelizing search paths in phrasing
[AD-A276876] 09 p3817 N94-32212
High-speed data search 09 p3923 N94-32441
Finding all periods and initial palindromes of a string in parallel
[AD-B175069] 09 p3827 N94-33002
MMI(exp 2) demonstrator systems: A multi-modal interface for man machine interaction with knowledge based systems. Deliverable D17 (TA 2) ESPRIT project 2474 MMI(exp 2)
[PB94-170537] 11 p4298 N94-35600

NATURAL LANGUAGE PROCESSING
Automatic word categorization: An information-theoretic approach
[CS-9209] 01 p0419 N94-10903
Automatic documentation generation: The interaction of text and examples
[AD-A269670] 04 p1616 N94-18570
Feasibility study in linguistically motivated object-oriented conceptual design of information systems
[PB93-197754] 04 p1618 N94-19331
Non-well-foundedness and type freeness can unify the interpretation of functional application
[PB93-191849] 04 p1560 N94-19710
A real-time spoken-language system for interactive problem-solving, combining linguistic and statistical technology for improved spoken language understanding
[AD-A270901] 04 p1392 N94-19749
Are types needed for natural language?
[PB93-191831] 05 p1949 N94-19997
A computational theory of lexical relatedness
[TR-421] 05 p1904 N94-20067
Causal reconstruction
[AD-A271692] 05 p1908 N94-20929
Recognizing hesitation phenomena in continuous, spontaneous speech 05 p1746 N94-22210
Intelligent text retrieval in the NASA astrophysics data system 05 p2048 N94-22499
An architecturally-based theory of human sentence comprehension
[AD-A275380] 08 p3398 N94-29313
Generalized left-corner parsing
[TR-92-21] 08 p3432 N94-30356
Interrogatives and adverbs of quantification
[LP-92-14] 08 p3456 N94-30372
Updates in dynamic semantics
[LP-93-06] 09 p3856 N94-31450
Weaks vs. strong readings of donkey sentences and monotonicity inference in a dynamic setting
[LP-93-10] 09 p3856 N94-31468
Finding all periods and initial palindromes of a string in parallel
[AD-B175069] 09 p3827 N94-33002
Dialog structure and plan recognition in spontaneous spoken dialog
[AD-A277566] 10 p4032 N94-33393
Learning procedures from interactive natural language instructions 10 p4110 N94-34047
An error-resistant linguistic protocol for air traffic control
[NASA-CR-196098] 12 p4385 N94-37013

NATURAL LASERS
U LASERS

NATURAL SATELLITES
NT CALLISTO
NT CHARON
NT DEIMOS
NT EUROPA
NT GANYMEDE
NT ICY SATELLITES
NT IO
NT JUPITER SATELLITES
NT MIRANDA
NT MOON
NT NEPTUNE SATELLITES
NT PHOBOS
NT SATURN SATELLITES
NT TITAN
NT TITANIA
NT TRITON
Physical studies of planetary and satellite surfaces
[NASA-CR-193545] 01 p0434 N94-10817
Orbital simulations of satellite escape/capture and the origin of satellites such as Triton
01 p0429 N94-12057
Rover mounted ground penetrating radar as a tool for investigating the near-surface of Mars and beyong
03 p1007 N94-16197

NAUSEA
Reliability of autonomic responses and malaise across multiple motion sickness stimulation tests
[NASA-TM-108787] 03 p1121 N94-15711
Changes in plasma vasopressin during motion sickness in cats 05 p1885 N94-21898
Current status: Animal models of nausea
05 p1889 N94-21915
Profile analysis of after-effects experienced during exposure to several virtual reality environments
12 p4482 N94-37263
Some side-effects of immersion virtual reality
12 p4482 N94-37277

NAUTICAL CHARTS
The Navy tessellated spheroid map projection system: A comprehensive definition
[AD-A269989] 04 p1462 N94-18677
MDFF HELP library, version 2: On-line documentation for the map data formatting facility
[AD-A277763] 09 p3922 N94-32987

NAVIER-STOKES EQUATION
Numerical calculation of scramjet inlet flow
[NAL-TR-1174T] 01 p0027 N94-10370
Experimental, analytical, and computational methods applied to hypersonic compression ramp flows
01 p0006 N94-10444
A CFD-based aerodynamic design procedure for hypersonic wind-tunnel nozzles
01 p0009 N94-10458
Hypersonic multi block flow simulations around space vehicles including non-equilibrium chemistry
01 p0009 N94-10460
Aerodynamic characteristics analysis of Garabedian-Korn 75-06-12 airfoil
[PAPER-2D-2] 01 p0010 N94-10468
Aerodynamic characteristics analysis of Garabedian-Korn 75-06-12 airfoil
[PAPER-2D-3] 01 p0010 N94-10469
Aerodynamic characteristics analysis of Garabedian-Korn 75-06-12 airfoil: Computation using q-omega 2 equation turbulence model
[PAPER-2D-4] 01 p0010 N94-10470
Aerodynamic characteristics analysis of Garabedian-Korn 75-06-12 airfoils: Computation using Baldwin-Lomax turbulence model
[PAPER-2D-5] 01 p0011 N94-10471
Aerodynamic characteristics analysis of Garabedian-Korn 75-06-12 aircraft
[PAPER-2D-7] 01 p0011 N94-10472

Aerodynamic characteristics analysis of Garabedian-Korn 75-06-12 airfoil
[PAPER-2D-9] 01 p0011 N94-10474
Flow analysis around ONERA model M5 configuration
[PAPER-3D-1] 01 p0011 N94-10477
Flow analysis around ONERA model M5 configuration
[PAPER-3D-2] 01 p0012 N94-10478
Flow analysis around ONERA model M5 configuration
[PAPER-3D-4] 01 p0012 N94-10480
Flow analysis around ONERA model M5 configuration
[PAPER-3D-5] 01 p0012 N94-10481
Navier-Stokes flowfield computation of wing/rotor interaction for a tilt rotor aircraft in hover
[NASA-CR-4532] 01 p0013 N94-10758
A comparative study of full Navier-Stokes and Reduced Navier-Stokes analyses for separating flows within a diffusing inlet S-duct
[NASA-TM-106250] 01 p0039 N94-10764
Development of an unstructured solution adaptive method for the quasi-three-dimensional Euler and Navier-Stokes equations
[NASA-CR-191161] 01 p0028 N94-10816
A dynamically adaptive mesh method for internal flows 01 p0149 N94-10896
Combustion chamber analysis code
[NASA-CR-192585] 01 p0046 N94-10934
New developments in the method of space-time conservation element and solution element: Applications to the Euler and Navier-Stokes equations
[NASA-TM-106226] 01 p0150 N94-10939
Theoretical investigation of 3-D shock wave turbulent boundary layer interactions
[AD-A265275] 01 p0150 N94-11014
Examination of wall functions for a parabolized Navier-Stokes code for supersonic flow
[DE93-011590] 01 p0014 N94-11111
High order accurate solutions of viscous problems
[NASA-TM-106267] 01 p0151 N94-11253
Looking for O(N) Navier-Stokes solutions on non-structured meshes
[NASA-CR-191472] 01 p0345 N94-11277
Computation of hypersonic nosetip heat transfer rates for an M829-like projectile
[AD-A263226] 01 p0016 N94-11870
A local dynamic model for large eddy simulation 01 p0155 N94-12285
Application of incremental unknowns to the Burgers equation 01 p0156 N94-12293
Direct numerical simulation of turbulent flow over a backward-facing step 01 p0156 N94-12296
Towards a cell-vertex Navier-Stokes algorithm for three-dimensional structured/unstructured meshes
[ARA-MEMO-366] 01 p0161 N94-12437
Proceedings of the 9th and 10th NAL Workshop on Investigation and Control of Boundary-Layer Transition
[NAL-SP-18] 01 p0163 N94-12611
Turbulence modeling of free shear layers for high-performance aircraft
[NASA-CR-193659] 02 p0520 N94-12799
Numerical simulation of hypersonic flow for the design of the H-2 orbiting plane (HOPE), part 3
[NAL-TR-1168-PT-3] 02 p0499 N94-12948
Integration of viscous effects into inviscid computational methods
[NASA-CR-193677] 02 p0629 N94-13007
Two-dimensional Navier-Stokes heat transfer analysis for rough turbine blades
[NASA-TM-106008] 02 p0629 N94-13027
Averaging techniques for steady and unsteady calculations of a transonic fan stage
[NASA-TM-106231] 02 p0499 N94-13108
Analysis of the Harrier forebody/inlet design using computational techniques
[NASA-CR-193616] 02 p0503 N94-13463
Topics on spatially high-order accurate methods and pre-conditioning for the Navier-Stokes equations with finite-rate chemistry 02 p0633 N94-13572
Passage-averaged approximation of turbomachinery flows using vorticity-potential method
[ISBN-0-315-72716-0] 02 p0634 N94-13598
A computational study of the base region flow field for the M865 projectile
[ARL-TR-109] 02 p0504 N94-13795
CNSFV code development, virtual zone Navier-Stokes computations of oscillating control surfaces and computational support of the laminar flow supersonic wind tunnel
[NASA-CR-194259] 02 p0504 N94-14030
Multigrid solution of internal flows using unstructured solution adaptive meshes
[NASA-CR-194233] 02 p0638 N94-14356
Analysis of reacting flowfields in low-thrust rocket engines and plumes 02 p0552 N94-14491
A vertex-based finite-volume algorithm for the Navier-Stokes equations 02 p0639 N94-14599
The structure of laminar flow in a three-dimensional driven cavity 02 p0640 N94-14601
An implicit finite volume nodal point scheme for the solution of two-dimensional compressible Navier-Stokes equations 02 p0640 N94-14603
Navier-Stokes simulation of transonic vortex flow over a delta wing 02 p0640 N94-14606
Computation of nonequilibrium flows using PNS equations 02 p0641 N94-14610
Hypersonic viscous flow computations 02 p0510 N94-14612
Development of a general purpose multigrid accelerated Navier-Stokes solver 02 p0641 N94-14613
Analysis, approximation, and computation of a coupled solid/fluid temperature control problem
[NASA-TM-106351] 02 p0771 N94-14731
Low altitude plume impingement handbook
[NASA-CR-194193] 02 p0643 N94-14741
DNS and modeling of the interaction between turbulent premixed flames and walls 02 p0646 N94-14763
Contributions to numerical solution of Navier-Stokes equations in two and three dimensional flows
[ETN-93-94395] 02 p0647 N94-14816
Analytical description of the breakup of liquid jets in air
[NASA-CR-191503] 02 p0647 N94-14849
Toward a quasi-linear closure for compressible turbulence
[DE93-017185] 02 p0647 N94-14895
Rocket motor plume flowfields: Phenomenology and simulation 03 p0924 N94-15221
Proteus two-dimensional Navier-Stokes computer code, version 2.0. Volume 2: User's guide
[NASA-TM-106338-VOL-2] 03 p1019 N94-15475
Proteus two-dimensional Navier-Stokes computer code, version 2.0. Volume 1: Analysis description
[NASA-TM-106336-VOL-1] 03 p1019 N94-15485
Proteus three-dimensional Navier-Stokes computer code, version 1.0. Volume 2: User's guide
[NASA-TM-106340-VOL-2] 03 p1020 N94-15488
On the stability analysis of approximate factorization methods for 3D Euler and Navier-Stokes equations
[NASA-TM-106314] 03 p1169 N94-15818
Proteus three-dimensional Navier-Stokes computer code, version 1.0. Volume 3: Programmer's reference
[NASA-TM-106341] 03 p1022 N94-15865
Proteus two-dimensional Navier-Stokes computer code, version 2.0. Volume 3: Programmer's reference
[NASA-TM-106339] 03 p1022 N94-15867
Computation of a controlled store separation from a cavity 03 p0858 N94-16513
Proteus three-dimensional Navier-Stokes computer code, version 1.0. Volume 1: Analysis description
[NASA-TM-106337] 03 p1024 N94-16527
Flow analysis for the nacelle of an advanced ducted propeller at high angle-of-attack and at cruise with boundary layer control
[NASA-TM-106371] 03 p0858 N94-16571
Hoph bifurcation in viscous, low speed flows about an airfoil with structural coupling
[AD-A266542] 03 p0859 N94-16798
Adaptive Navier-Stokes calculations for vortical flow
[AD-A266236] 03 p1026 N94-16966
An upwind multigrid method for solving viscous flows on unstructured triangular meshes
[NASA-TM-109343] 03 p1027 N94-17061
Computational aerodynamics with icing effects
[AD-A267509] 03 p0860 N94-17074
On solving the compressible Navier-Stokes equations for unsteady flows at very low Mach numbers
[NASA-TM-106380] 03 p1027 N94-17128
Multigrid time-accurate integration of Navier-Stokes equations
[NASA-TM-106373] 03 p1028 N94-17258
Convection effects on radial segregation and crystal melt interface in vertical Bridgman growth
[NASA-CR-191541] 03 p1029 N94-17387
Boundary conditions and the simulation of low Mach number flows
[NASA-TM-106374] 03 p1029 N94-17448
Thin-layer and full Navier-Stokes calculations for turbulent supersonic flow over a cone at an angle of attack
[NASA-CR-189103] 03 p0861 N94-17558
Granular fluctuations in plasma turbulence and their role in transport
[DE93-013465] 03 p1187 N94-17674
Finite element modeling of evaporation and condensation during sol-gel film and fiber formation
[DE93-017655] 04 p1345 N94-17820
Investigation of a matrix-model for the artificial dissipation in a cell vertex finite volume scheme for solving the Navier-Stokes equations
[DLR-FB-92-33] 04 p1409 N94-18076
Parabolized Navier-Stokes computation of surface heat transfer characteristics for supersonic and hypersonic KE projectiles
[AD-A268858] 04 p1410 N94-18391
Navier-Stokes computations of turbulent flow around high-lift configurations 04 p1306 N94-18420
Efficient simulation of incompressible viscous flow over multi-element airfoils 04 p1306 N94-18421
Navier-Stokes calculations on multi-element airfoils using a chimera-based solver 04 p1306 N94-18422
Numerical solution of the Navier-Stokes equations for high-lift configurations on structured composite grids 04 p1306 N94-18423
Prediction of the high-lift performance of multi-element aerofoils using an unstructured Navier-Stokes solver 04 p1307 N94-18427
Numerical calculations of high lift flows using structured and unstructured methods 04 p1307 N94-18428
Navier-Stokes simulation of flow field around a blown-flap high-lift system 04 p1307 N94-18429
An algebraic turbulence model for turbomachinery 04 p1411 N94-18554
Variational approaches to CFD: Applications to potential Euler and Navier-Stokes equations 04 p1413 N94-18565
Introduction to spectral methods: Application to the Stokes problem 04 p1413 N94-18566
An introduction to the modelling of turbulence 04 p1414 N94-18579
Turbulence modeling for compressible flows and implementation in Navier-Stokes solvers 04 p1416 N94-18597
Theoretical study and modelling of homogeneous turbulence under rotation for implantation in a code for solving Navier-Stokes equations
[ECL-93-05] 04 p1420 N94-19381
On the numerical analysis of nonlinear Galerkin methods: Spectral approximation and finite elements
[ETN-93-94900] 04 p1552 N94-19407
Numerical prediction of transition of the F-16 wing at supersonic speeds
[NASA-CR-194407] 04 p1312 N94-19433
Numerical investigation of the incompressible flow around a wing with a fixed spoiler
[ISL-R-109/91] 04 p1313 N94-19524
Navier-Stokes, dynamics and aeroelastic computations for vortical flows, buffet and flutter applications
[NASA-CR-194520] 04 p1313 N94-19621
Linear and nonlinear PSE for compressible boundary layers
[NASA-CR-191537] 05 p1797 N94-20033
A comparison of two incompressible Navier-Stokes algorithms for unsteady internal flow
[NASA-TM-108794] 05 p1798 N94-20104
Head-on collision of drops: A numerical investigation
[NASA-TM-106394] 05 p1798 N94-20167
Some practical turbulence modeling options for Reynolds-averaged full Navier-Stokes calculations of three-dimensional flows
[NASA-TM-106399] 05 p1637 N94-20534
Prediction and control of vortex-dominated and vortex-wake flows
[NASA-CR-194722] 05 p1637 N94-21054
Computational and analytical methods in nonlinear fluid dynamics
[AD-A272722] 05 p1802 N94-21169
An efficient numerical method for three-dimensional hypersonic flow
[AD-A272506] 05 p1637 N94-21411
Time-accurate Navier-Stokes calculations with multigrid acceleration 05 p1956 N94-21469
Looking for O(N) Navier-Stokes solutions on non-structured meshes 05 p1806 N94-21471
Multigrid solution of the Navier-Stokes equations on highly stretched grids with defect correction 05 p1806 N94-21481
On the prediction of multigrid efficiency through local mode analysis 05 p1959 N94-21486
Numerical study of a multigrid method with four smoothing methods for the incompressible Navier-Stokes equations in general coordinates 05 p1806 N94-21487
A study of the compressible flow through a diffusing S-duct
[NASA-TM-106411] 05 p1638 N94-21591
Mixed finite element and finite volume methods
[ISBN-0-315-63035-3] 05 p1805 N94-22417
A multigrid multiblock solver for compressible turbulent flow
[MEMO-1125] 06 p2315 N94-22713
CFD analyses of combustor and nozzle flowfields 06 p2210 N94-23033
Heat transfer in rocket combustion chambers 06 p2214 N94-23051
Computational fluid dynamic modelling of cavitation 06 p2215 N94-23060

Reliability enhancement of Navier-Stokes codes through convergence enhancement 06 p2216 N94-23064
CFD modeling of microwave electrothermal thrusters 06 p2216 N94-23066
Two-dimensional Navier-Stokes computations of subsonic and supersonic flows through turbine cascades [PB93-226223] 06 p2317 N94-23114
POISs3: A 3D poisson smoother of structured grids [PB93-226231] 06 p2318 N94-23115
Computational study of GA(W)-1: Airfoil near stall [PB93-226249] 06 p2165 N94-23116
Tracking sharp interface of two fluids by the CIP (Cubic-Interpolated Propagation) scheme [DE93-508322] 06 p2319 N94-23460
Unsteady jet flow computation towards noise prediction [NASA-CR-194449] 06 p2153 N94-23553
An implicit numerical scheme for the simulation of internal viscous flows on unstructured grids [NASA-TM-106437] 06 p2481 N94-23554
Numerical analysis of a vortex controlled diffuser 06 p2324 N94-23659
An application of small-gap equations in sealing devices 06 p2325 N94-23668
A comparative study of computational solutions to flow over a backward-facing step 06 p2326 N94-23670
Multi-grid domain decomposition approach for solution of Navier-Stokes equations in primitive variable form 06 p2341 N94-23693
Efficient interpolation of velocity and flux components defined on 2- and 3-dimensional non-cartesian grids [PB94-118619] 06 p2486 N94-23757
Drag reduction at a plane wall 06 p2327 N94-24140
On the large eddy simulation of turbulent flows in complex geometry 06 p2329 N94-24148
Transition to turbulence in an elliptic vortex 06 p2331 N94-24161
On the dynamics of approximating schemes for dissipative nonlinear equations 06 p2332 N94-24168
Discrete sensitivity derivatives of the Navier-Stokes equations with a parallel Krylov solver [NASA-TM-106481] 06 p2265 N94-24301
Implementation of the Baldwin-Barth turbulence model into the ZETA code and its diagnosis [NASA-CR-194795] 06 p2335 N94-24640
Solution of the discretized incompressible Navier-Stokes equations with iterative methods [PB94-118635] 06 p2335 N94-24641
Carrying the mass flux terms exactly in the first and second moment equations of compressible turbulence [AD-A276346] 06 p2335 N94-24712
Numerical solutions of the complete Navier-Stokes equations [NASA-CR-194780] 06 p2337 N94-24858
Computational fluid mechanics [NASA-CR-194765] 06 p2337 N94-24859
Triangular spectral elements for incompressible fluid flow [AD-A276838] 06 p2490 N94-24914
Turbulence models and Reynolds analogy for two-dimensional supersonic compression ramp flow [NASA-TM-106474] 06 p2337 N94-25119
Development and application of new algorithms for the simulation of viscous compressible flows with moving bodies in three dimensions [AD-A273514] 06 p2338 N94-25157
A continuing search for a near-perfect numerical flux scheme. Part 1: AUSM+ [NASA-TM-106524] 06 p2338 N94-25180
Two-dimensional CFD modeling of wave rotor flow dynamics [NASA-TM-106261] 06 p2189 N94-25185
A numerical investigation of the artificial compressibility method for the solution of the Navier-Stokes equations [CRANFIELD-AERO-9213] 06 p2340 N94-25486
Riemann solvers for solving the incompressible Navier-Stokes equations using the artificial compressibility method [CRANFIELD-AERO-9208] 07 p2790 N94-25778
A numerical determination of bifurcation points for low Reynolds number conical flows [AD-A273984] 07 p2791 N94-25991
Comments regarding two upwind methods for solving two-dimensional external flows using unstructured grids [NASA-TM-109078] 07 p2644 N94-26154
Computational prediction of isolated performance of an axisymmetric nozzle at Mach number 0.90 [NASA-TM-4506] 07 p2646 N94-26547
The dynamics of interacting nonlinearities governing long wavelength driftwave turbulence [DE94-001785] 07 p2793 N94-26558
Numerical studies on the dynamics of bubble, turbulent, free shear flows: Effect of the inter-phase coupling on the global flow evolution [AD-A274521] 07 p2794 N94-26832
Numerical simulation of receptivity and transition in a boundary layer on a flat plate with a suction hole [NASA-CR-195708] 07 p2798 N94-27782
New constitutive equation for the volume viscosity in fluids [NASA-TM-109104] 07 p2798 N94-27867
Navier-Stokes simulation of two and three dimensional jets in crossflow, effects of grid, and boundary conditions 07 p2804 N94-28026
Theoretical and experimental investigation of a delta wing with turbulent leading-edge jets 07 p2659 N94-28029
Recent developments in the simulation of steady and transient transverse jet interactions for missile, rotorcraft, and propulsive applications 07 p2804 N94-28030
Numerical assessment of aerodynamic interactions on missiles with transverse jets control 07 p2659 N94-28031
Navier-Stokes analysis of a swirling jet in crossflow 07 p2806 N94-28038
A parallel multigrid algorithm for solving the Navier-Stokes equations on a transputer system [PREPRINT-699] 07 p2807 N94-28099
Euler and Navier-Stokes wing/fuselage computations of the De Havilland Dash 8 aircraft 07 p2654 N94-28329
A study of blunt trailing edge airfoils using the Navier Stokes code: ARC2D 07 p2656 N94-28340
Thin-layer Navier-Stokes computations for multi-element airfoils 07 p2656 N94-28341
Solution-adaptive simulation of transonic cascade flows 07 p2657 N94-28344
Multigrid solutions of the 2D Euler/Navier-Stokes equations on unstructured meshes 07 p2658 N94-28349
Large eddy simulations using lattice Boltzmann algorithms [DE94-005666] 08 p3270 N94-28549
Numerical simulation of unsteady aerodynamic heating induced by shock reflections 08 p3123 N94-28952
ENGRID: A graphical interactive code for the computation of structured grids for blocked flow domains 08 p3124 N94-28956
A design of third-generation airfoils for helicopter rotor blades using Navier-Stokes 08 p3124 N94-28957
Unsteady aerodynamic computations around NACA0012 at high angles of attack 08 p3126 N94-28969
Study of modeling of turbulence of renormalization group analysis 08 p3126 N94-28970
The upsilon-q method and the psi-q method for incompressible flows 08 p3126 N94-28971
Theoretical study of the incompressible Navier-Stokes equations by the least-squares method [NASA-TM-106535] 08 p3272 N94-29096
A free-wake Euler and Navier-Stokes CFD method and its application to helicopter rotors including dynamic stall [AD-A275416] 08 p3129 N94-29197
Investigation of advanced counterrotation blade configuration concepts for high speed turboprop systems. Task 2: Unsteady ducted propfan analysis computer program users manual [NASA-CR-187105] 08 p3152 N94-29438
A new flux-conserving numerical scheme for the steady, incompressible Navier-Stokes equations [NASA-TM-106520] 08 p3273 N94-29471
RNS optimization procedure for three-dimensional composite velocity multi-block applications 08 p3273 N94-29534
Finite element method for numerical simulation of turbulent flows. The N3S code 08 p3233 N94-29612
Spherical model for turbulence 08 p3274 N94-29730
Numerical study of the trailing vortex of a wing with wing-tip blowing [NASA-CR-195803] 08 p3130 N94-29760
Direct and large-eddy simulations of turbulent flow in a square duct 08 p3275 N94-29809
The h-p adaptive methods for incompressible viscous flow problems 08 p3275 N94-29836
Numerical solution of 3-D Navier-Stokes equations in vorticity-velocity form for incompressible flows 08 p3276 N94-29843
Algorithm and code development for unsteady three-dimensional Navier-Stokes equations [NASA-CR-195774] 08 p3277 N94-29942
High-resolution algorithms for the Navier-Stokes equations for generalized discretizations 08 p3278 N94-29965
Aircraft aerodynamics with deflected jets in ground effect 08 p3132 N94-29973
Three dimensional compressible turbulent flow computations for a diffusing S-duct with/without vortex generators 08 p3281 N94-30519
Euler results of the ISNaS compressible multi-block flow solver [AD-B179299] 08 p3281 N94-30756
Information system for flow simulation based on the Navier-Stokes equations vectorization [AD-B179293] 08 p3281 N94-30763
CFD-based drag prediction: State-of-the-art, theory, prospects [AD-B179297] 09 p3567 N94-31180
A priori tests of large eddy simulation of the compressible plane mixing layer [MEMO-1152] 09 p3699 N94-31185
A solution adaptive structured-unstructured grid procedure for unsteady flows 09 p3700 N94-31217
On the structure and stability of slender viscous vortices 09 p3700 N94-31218
Solution of the incompressible Navier-Stokes equations in general coordinates by Krylov subspace and multigrid methods [REPT-93-64] 09 p3703 N94-31660
Cell-vertex discretisation of the driven cavity flow without artificial diffusion [W-9317] 09 p3703 N94-31689
Simulations of the creation and motion of vortex rings [W-9319] 09 p3703 N94-31691
Finite volume discretization of the k-epsilon turbulence model in general coordinates [REPT-93-90] 09 p3703 N94-31703
Finite element numerical simulation of turbulent flows [ISBN-0-315-86416-8] 09 p3703 N94-31717
Numerical modelling of turbulence [ISBN-0-315-86439-7] 09 p3703 N94-31720
Finite element vorticity-based methods for the solution of the incompressible and compressible Navier-Stokes equations [ISBN-0-315-87265-9] 09 p3703 N94-31730
Multigrid diagonal implicit solutions for compressible turbulent flows and their evaluation 09 p3705 N94-31941
Chemical vapor deposition fluid flow simulation modeling tool [NASA-CR-189648] 09 p3707 N94-32480
Additive turbulent decomposition of the incompressible and compressible Navier-Stokes equations [AD-A277321] 09 p3708 N94-32511
Advanced CFD methodology for fast transients encountered in nonlinear combustion instability problems. Volume 2: User's guide [NASA-CR-191352] 09 p3637 N94-32694
Advanced CFD methodology for fast transients encountered in nonlinear combustion instability problems. Volume 1: Theory and validation [NASA-CR-191351] 09 p3637 N94-32696
Study of dynamic stall phenomenon and its control using vorticity, stream function and circulation form of the unsteady Navier-Stokes equations 09 p3572 N94-32714
Modification of the MML turbulence model for adverse pressure gradient flows [NASA-TM-106544] 09 p3709 N94-32947
Use of Navier-Stokes methods for the calculation of high-speed nozzle flow fields [NASA-TM-106551] 09 p3573 N94-32984
A study of weak solutions and their regularizations by numerical methods [AD-A277453] 09 p3850 N94-33175
A three-dimensional multigrid technique for unsteady incompressible viscous flows 10 p4042 N94-33364
Code validation for the simulation of supersonic viscous flow about the F-16XL 10 p3981 N94-33528
Spatio-temporal complexity and large-scale structures in problems of continuum mechanic [AD-A278473] 10 p4044 N94-33702
Special Course on Progress in Transition Modelling [AGARD-R-793] 10 p4045 N94-33884
A free-wake Euler and Navier-Stokes CFD method and its application to helicopter rotors including dynamic stall [AD-A278000] 10 p3983 N94-34159
Semi-span model testing in the national transonic facility [NASA-CR-195952] 10 p4048 N94-34300
Combined LAURA-UPS solution procedure for chemically-reacting flows [NASA-TM-107964] 10 p4049 N94-34721
Characterization of dynamic stall phenomenon using two-dimensional unsteady Navier-Stokes equations 10 p3986 N94-34974
Computation of unsteady flows over airfoils 10 p3986 N94-34977
Departure solutions of the unsteady thin-layer and full Navier-Stokes equations solved using streamline curvature based iteration techniques 10 p4052 N94-34980

On the nonlinear stability of viscous modes within the Rayleigh problem on an infinite flat plate
[NASA-CR-194909] 11 p4263 N94-35497
Boundary conditions for jet flow computations
[NASA-TM-106648] 11 p4266 N94-35976
A three dimensional multigrid Reynolds-averaged Navier-Stokes solver for unstructured meshes
[AD-A280998] 11 p4191 N94-35994
An efficient, intelligent solution for viscous flows inside solid rocket motors
[AD-A278629] 11 p4228 N94-36255
An equal-order approximate projection FEM
[DE94-010101] 11 p4268 N94-36374
Numerical investigation of multi-element airfoils
[NASA-CR-194592] 11 p4191 N94-36394
Preconditioned implicit solvers for the Navier-Stokes equations on distributed-memory machines
[NASA-TM-106449] 12 p4502 N94-36647
An aerodynamic and static-stability analysis of the Hypersonic Applied Research Technology (HART) missile
[AD-A280631] 12 p4382 N94-36729
An arbitrary grid CFD algorithm for configuration aerodynamics analysis. Volume 1: Theory and validations
[NASA-CR-195918] 12 p4493 N94-36914
An arbitrary grid CFD algorithm for configuration aerodynamics analysis. Volume 2: FEMNAS user guide
[NASA-CR-196135] 12 p4493 N94-36922
Navier-Stokes and potential theory solutions for ahelicopter fuselage and comparison with experiment
[NASA-TM-4586] 12 p4383 N94-36966
A fundamental study of hypersonic unstarts
[AD-A280506] 12 p4443 N94-37128
Flow visualization for Lagrangian particle methods
[DE94-010757] 12 p4443 N94-37195
Prediction of film cooling on gas turbine airfoils
[NASA-TM-106653] 12 p4387 N94-37448
Development of advanced Navier-Stokes solver
[NASA-CR-195094] 12 p4504 N94-37449

NAVIGATION
NT AIR NAVIGATION
NT ALL-WEATHER AIR NAVIGATION
NT DEAD RECKONING
NT DIGITAL NAVIGATION
NT DOPPLER NAVIGATION
NT INERTIAL NAVIGATION
NT INTERPLANETARY NAVIGATION
NT LORAN C
NT NAP-OF-THE-EARTH NAVIGATION
NT RADAR NAVIGATION
NT RADIO NAVIGATION
NT SPACE NAVIGATION
NT SURFACE NAVIGATION
Helicopter approach capability using the differential Global Positioning System
[NASA-CR-177618] 01 p0024 N94-12355
Experiments in mobile robot navigation and range imaging
[DE93-013280] 01 p0341 N94-12598
Wide-area Differential Global Positioning System (WDGPS)/Wide-area Integrity Broadcast (WIB) alternatives analysis
[DOT/FAA/SE-93/3] 03 p0864 N94-16906
Military applications of high-accuracy frequency standards and clocks
[AD-A269303] 04 p1430 N94-18299
HERACLITUS, phase 1. Harbour Entrance of Rotterdam Radar based Current Related Information for Traffic Guidance of Ships: Feasibility of deriving current profile data from sea surface observations in the Rotterdam (Netherlands) port entrance
[BCRS-93-04] 06 p2417 N94-24107
NASA LaRC Workshop on Guidance, Navigation, Controls, and Dynamics for Atmospheric Flight, 1993
[NASA-CP-10127] 06 p2162 N94-25096
Sensor-based navigation of a mobile robot using automatically constructed fuzzy rules
[DE94-001137] 07 p2986 N94-26948
Fault detection and isolation 07 p2642 N94-27289
Micro guidance and control synthesis: New components, architectures, and capabilities 08 p3144 N94-29792
ARK: Autonomous mobile robot in an industrial environment
[AIAA PAPER 94-1177-CP] 08 p3439 N94-30529
Meeting the challenges of installing a mobile robotic system
[AIAA PAPER 94-1187-CP] 08 p3440 N94-30537
Hydrographic service Royal Australian Navy
[AD-A277134] 09 p3788 N94-32066
An investigation of methods for improving models of ionospheric plasma-density irregularities and radio-frequency scintillation
[AD-A278568] 10 p4033 N94-33703
A study of navigation in virtual space
10 p3988 N94-34026
Evaluation of flame-sprayed polymer coatings for civil works navigation structures
[AD-A280507] 12 p4422 N94-37104
Progress in navigation filter estimate fusion and its application to spacecraft rendezvous
[NASA-TM-104794] 12 p4392 N94-37386

NAVIGATION AIDS
NT ATTITUDE INDICATORS
NT BEACONS
NT COMPASSES
NT NAVIGATION INSTRUMENTS
NT RADAR BEACONS
NT RADIO BEACONS
NT RADIO DIRECTION FINDERS
NT TERCOM
National Airspace System operational concept
[DOT/FAA/SE-93/1] 01 p0023 N94-10933
Toward intelligent flight control
01 p0033 N94-11503
Definition of spacecraft standard interfaces by the NASA Space Assembly and Servicing Working Group (SASWG) 01 p0348 N94-11574
Flight evaluations of approach/landing navigation sensor systems: Summary of 1990 flight experiments
[NAL-TR-1175] 02 p0513 N94-13344
Some frequency and damping measurements of laminated beryllium beams
[DE93-015909] 02 p0676 N94-14530
Comparison of a distributed Kalman filter versus a centralized Kalman filter with fault detection considerations
[AD-A270713] 05 p1903 N94-19969
Lunar rover navigation concepts
06 p2607 N94-23386
Expansion-based passive ranging
06 p2176 N94-25504
A simulation of GPS and differential GPS sensors
07 p2666 N94-27918
Software engineering methods in the Hermes on-board software 08 p3414 N94-29326
Ground independent landing system
08 p3137 N94-29564
GPS/GNSS for ATM 08 p3138 N94-29565
Hydrographic service Royal Australian Navy
[AD-A277134] 09 p3788 N94-32066
A study of navigation in virtual space
10 p3988 N94-34026
Coupled ice-ocean model supporting winter navigation in the Baltic Sea. Part 1: Ice dynamics and water levels
[PB94-148780] 10 p4092 N94-34121

NAVIGATION INSTRUMENTS
NT ATTITUDE INDICATORS
NT COMPASSES
NT RADIO DIRECTION FINDERS
Flight evaluations of approach/landing navigation sensor systems: Summary of 1990 flight experiments
[NAL-TR-1175] 02 p0513 N94-13344
Performance evaluation tests of the GPS/DGPS navigation system installed in the NAL Dornier 228: Preliminary ground test results
[NAL-TM-649] 02 p0513 N94-13346
Perception for outdoor navigation
[AD-A266867] 03 p0863 N94-14919
Automatic AVHRR image navigation software
[NASA-CR-194602] 05 p1643 N94-20148
A software architecture for a small autonomous underwater vehicle navigation system
[AD-A272322] 05 p1643 N94-21037
An overview of a generic multi-sensor integrated navigation system design
[CTN-94-60916] 06 p2174 N94-24120
Application of aircraft navigation sensors to enhanced vision systems 06 p2176 N94-25495
Dead reckoning navigation
[VTT-TIED-1402] 07 p2664 N94-25808
A simulation of GPS and differential GPS sensors
07 p2666 N94-27918
An electromagnetic noncontacting sensor for thickness measurement in a dispersive medium
[AIAA PAPER 94-1200-CP] 08 p3443 N94-30551
Evaluation of flame-sprayed polymer coatings for civil works navigation structures
[AD-A280507] 12 p4422 N94-37104

NAVIGATION SATELLITES
NT NAVSTAR SATELLITES
The time keeping system for GPS block IIR
01 p0024 N94-10964
Not ready for the first space war. What about the second?
[AD-A266557] 03 p1174 N94-16665
A GPS coverage model 07 p2642 N94-27292
GPS/GNSS for ATM 08 p3138 N94-29565
TacSats for NATO
[AD-A277710] 08 p3169 N94-30350
The 25th Annual Precise Time and Time Interval (PTTI) Applications and Planning Meeting
[AD-A280955] 08 p3488 N94-30639

NAVSTAR SATELLITES
Cesium and rubidium frequency standards status and performance on the GPS program
08 p3145 N94-30663
A review of the status and capabilities of Navstar GPS
[AD-B174629] 08 p3143 N94-30854

NAVY
Statistical process control in the hybrid microelectronics manufacturing industry: A Navy view point
[AD-A265164] 01 p0145 N94-11884
Structured finite volume modeling of US Navy aircraft engine test cells task 2: Turboprop engine, volume 1
[AD-A267833] 03 p0872 N94-17405
Structured finite volume modeling of US Navy aircraft engine test cells. Task 1: Turboshaft engine, volume 1
[AD-A268176] 03 p0873 N94-17432
Naval aviation: The Navy is taking actions to improve the combat capabilities of its tactical aircraft. Report to Congressional Requesters
[AD-A268002] 03 p0868 N94-17472
Structured finite volume modeling of US Navy aircraft engine test cells. Task 1: Turboshaft engine-code documentation and listings, volume 2
[AD-A268177] 03 p0873 N94-17508
Coastal Ocean Modeling Workshop
[AD-A268955] 04 p1497 N94-18393
The Navy tessellated spheroid map projection system: A comprehensive definition
[AD-A269989] 04 p1462 N94-18677
Compilation of 1992 annual reports of the navy ELF communications system ecological monitoring program, volume 2
[AD-A269726] 04 p1388 N94-18751
Audit report. Navy's aircraft structural life surveillance program data recorders
[AD-A270391] 05 p1645 N94-20040
Design project: LONGBOW supersonic interceptor
[NASA-CR-195510] 06 p2180 N94-24581
ELF communications system ecological monitoring program
[AD-A273456] 06 p2299 N94-24676
Observed and Navy operational global model climatologies of synoptic disturbances over the tropical western Pacific during winter 1991-1992
[AD-A273400] 06 p2416 N94-25071
Report of the defense science board task force on aircraft assessment
[AD-A274531] 07 p2669 N94-26835
The NOGAPS ten year AMIP integration
[AD-A274332] 07 p2900 N94-26887
Communications subsystem for the Petite Amateur Navy Satellite (PANSAT)
[AD-A275532] 08 p3242 N94-28812
Procedures for computing site seismicity
[AD-A277666] 09 p3775 N94-33028

NC-130 AIRCRAFT
U C-130 AIRCRAFT

NEAR FIELDS
A near-field scanning optical microscope for analysis of magneto-optic media 03 p1199 N94-14995
Phased array antenna analysis using hybrid finite element methods
[AD-A267620] 03 p1002 N94-17196
How to deduce the far field of an antenna from planar near-field measurements
[NPL-DES-123] 03 p1006 N94-17545
Probe compensation in cylindrical near-field scanning: A novel simulation methodology
05 p1718 N94-20404
Massively parallel computation of RCS with finite elements 05 p1726 N94-20437
Applications of planar near-field measurements to electromagnetic radiation and interference problems
05 p1747 N94-22252
Mixing and unmixedness in plasma jets 1: Near-field analysis 06 p2323 N94-23655
Toward modeling wingtip vortices
06 p2171 N94-24142
Unstructured adaptive mesh computations of rotorcraft high-speed impulsive noise
[NASA-CR-195090] 06 p2529 N94-24307
Nonlinear hysteresis in an endochronic solid
[AD-A274594] 07 p2880 N94-26855
Experiments into the scaling parameters required for exhaust gas ingestion testing of vertical landing aircraft
07 p2671 N94-28017
Measurement basis of near fields in spherical coordinates in the 100 MHz to 6 GHz band
[REPT-932-430-107] 08 p3255 N94-30153
Formulation of time-domain planar near-field measurements without probe correction
[AD-A276380] 09 p3672 N94-31371

Structure estimation of phase objects from the diffraction near field: Microwave and model calculations
[ETN-94-95737] 09 p3674 N94-31608
Use of the sampling theorem to speed up near-field physical optics scattering calculations
11 p4253 N94-35549
EM-ANIMATE: A computer program for displaying and animating electromagnetic near-field and surface-current solutions: Video supplement to NASA Technical Memorandum 4539
[NASA-TM-4539-VIDEO-SUPPL] 12 p4492 N94-36518

NEAR INFRARED RADIATION
Formulating infrared coatings for defence applications
[MRL-RR-1-93] 01 p0090 N94-11302
A comparison of telescopic and Phobos-2 ISM spectra of Mars in the short-wave near-infrared (0.76-1.02 microns) 01 p0424 N94-12053
Compositional and textural information from the dual inversion of visible, near and thermal infrared remotely sensed data 01 p0258 N94-12097
A comparison of the visible and near infrared reflectance of hydrovolcanic palagonite tuffs and Martian weathered soils 01 p0477 N94-12245
Planetary astronomy of Mars. Mars data reduction
[NASA-CR-193515] 01 p0424 N94-12768
A near-infrared faint galaxy survey: Evolution and the cosmological geometry from K band photometry
02 p0830 N94-13591
Millimeter and infrared studies of young stellar objects in dark cloud L1641 02 p0838 N94-13648
The 1 to 5 micron imaging of deeply embedded young stellar objects 02 p0831 N94-13657
New K type asteroids 03 p1241 N94-16195
The 0.15 seconds near-infrared imaging of the central parsec of the galaxy
[MPE-PREPRINT-239] 04 p1621 N94-19415
Wavelength dependence of limb-darkening of Mars from visible and near-IR telescopic spectral imaging
05 p2101 N94-20685
Spatial distribution of near infrared line radiation in galactic nuclei measured with Fabry-Perot spectrometer FAST
[MPE-239] 05 p2081 N94-21138
Deep near-infrared survey of the Southern Sky (DENIS) 05 p2062 N94-22467
Optimization of techniques to reconstruct images disturbed by atmospheric turbulence in the near infra-red
[PB93-199784] 06 p2298 N94-24630
Multivariate calibration applied to near-infrared spectroscopy for the quantitative analysis of dilute aqueous solutions
[DE94-003231] 07 p2716 N94-26794
Development and evaluation of a near infrared reflecting and low visibility paint scheme for RAAF P-3C Orion aircraft
[AD-A274881] 07 p2669 N94-26864
Planetary Instrument Definition and Development Program (PIDDP). Instrument for future planetary flight missions: A visible-infrared imaging spectrometer for planetary missions
[NASA-CR-195254] 07 p3106 N94-27409
Evaluation of near-infrared spectrophotometric method for individual tolerance to +Gz acceleration
07 p2933 N94-27944
Measurement of atmospheric OH by titration of near-IR fluorescent dyes 08 p3344 N94-28599
Near-IR diode laser absorption for measurement of tropospheric HO2 08 p3345 N94-28607
HO2 detection by near infrared absorption using tunable diode lasers 08 p3346 N94-28608
Imaging spectrometry of the Earth and other solar system bodies 08 p3237 N94-29779
Evolution of miniature detectors and focal plane arrays for infrared sensors 08 p3237 N94-29781
Infrared properties of obscuring dust tori in active galactic nuclei 08 p3545 N94-29832
Correlation studies of Pioneer Venus imagery obtained from PV experiments with near IR imagery obtained from ground-based observations during Venus inferior conjunction
[NASA-CR-195772] 08 p3550 N94-29892
A near-infrared survey of the star forming region NGC 2264 08 p3540 N94-29971
Infrared and near infrared transient absorption spectroscopy of molecular free radicals
[DE94-005446] 09 p3632 N94-31305
Near infrared surveys of high mass star forming regions 09 p3925 N94-31898
Aerosols scattering and near-infrared observations of the Martian surface 09 p3946 N94-33204
Instrumentation on the RAIDS experiment 2: Extreme ultraviolet spectrometer, photometer, and near IR spectrometer
[AD-A278543] 10 p4085 N94-33676
High spatial resolution telescopic multispectral imaging and spectroscopy of the Moon. 1: The Serenitatis/Tranquillitatis border region
11 p4356 N94-35402
Absolute calibration and atmospheric versus mineralogic origin of absorption features in 2.0 to 2.5 micron Mars spectra obtained during 1993 11 p4356 N94-35404
Theoretical studies of ultrashort phenomena
[AD-A278938] 11 p4332 N94-35664
Dynamic structural effects and ultrafast biomolecular kinetics in photoinduced charge transfer reactions
[DE94-010421] 11 p4329 N94-36390
Intensity of waves diffracted from symmetrical profile lamellar gratings
[DE94-611101] 12 p4433 N94-36753
Holmium quasi-two level laser
[AD-D016302] 12 p4449 N94-37772

NEAR ULTRAVIOLET RADIATION
Near-ultraviolet laser photoemission: Scanning microscopy, buried interfaces and image-potential states
08 p3294 N94-29531

NEAR WAKES
The effects of initial conditions on the 3-D topology of temporally evolving wakes (ARI on 3-D bluff body wakes)
[AD-A271008] 04 p1423 N94-19774
Near wake measurements on a rotor model with Mie-vanes in the Delft open jet tunnel
[PB93-215382] 05 p1638 N94-22260
Flow past a circular cylinder with a permeable wake splitter plate
[AD-A273765] 07 p2790 N94-25872
The effects of three-dimensional imposed 3-d disturbances on bluff-body near wake flows
[AD-A274845] 07 p2791 N94-26187
Nominally 2-dimensional flow about a normal flat plate
[AD-A274472] 07 p2794 N94-27026
Research on bluff body vortex wakes
[AD-A273780] 07 p2796 N94-27319
An experimental study of wing tip vortex in the near wake of a rectangular wing
[AD-A275389] 08 p3129 N94-29306
Flow past a circular cylinder with a permeable wake splitter plate 08 p3275 N94-29764

NEARSHORE WATER
NT COASTAL WATER
Wind products for use in coastal wave and surge models
[AD-A269753] 04 p1497 N94-18414

NEBULAE
NT CRAB NEBULA
NT H I REGIONS
NT H II REGIONS
NT HERBIG-HARO OBJECTS
NT ORION NEBULA
NT PLANETARY NEBULAE
Midplane temperatures in the solar nebula
01 p0448 N94-12088
Initiating solar system formation through stellar shock waves 01 p0448 N94-12090
Boundary conditions for the paleoenvironment: Chemical and physical processes in the pre-solar nebula
[NASA-CR-194418] 03 p1298 N94-15421
Formation of the low-mass solar nebula
05 p2109 N94-20728
Diffusive redistribution of water vapor in the solar nebula revisited 05 p2113 N94-20751
Magnetically controlled solar nebula
05 p2120 N94-20791
Magnetic reconnection in emission nebulae in clusters of galaxies 05 p2010 N94-22700
X ray enhancement of SN 1987A due to interaction with its ring-like nebula
[NIFS-265] 06 p2602 N94-24867
Investigations of the dynamical evolution of protoplanetary nebulae
[NASA-CR-195278] 07 p3105 N94-27428
Convective solar nebula 09 p3930 N94-31130
Formation of iron metal and grain coagulation in the solar nebula 11 p4373 N94-36170

NECK (ANATOMY)
Mass properties test procedure for manikin headforms and helmet systems
[AD-A265654] 01 p0315 N94-10296
An assessment of the potential for neck injury due to padding of aircraft interior walls for head impact protection
[DOT/FAA/AM-93/14] 02 p0738 N94-13972

NEEDLE BEARINGS
Development of long-life, low-noise linear bearings for atmospheric interferometry 09 p3606 N94-33312

NEEL TEMPERATURE
The low-temperature specific heat of CeCu2Ge2 at 0 and 9.5 kbar
[DE93-014914] 04 p1360 N94-18398

NEGATIVE ELECTRON AFFINITY
Diamond p-n junction cold cathode
[AD-A266926] 03 p1206 N94-15107
Characterization of diamond film nucleation and growth surface
[AD-A269400] 04 p1597 N94-18459
Growth, characterization and device development in monocrystalline diamond films
[AD-A272715] 05 p2026 N94-21190
Electron beam analysis for cyclotron harmonic and free-electron laser devices
[AD-A275070] 08 p3293 N94-29179

NEGATIVE FEEDBACK
The Lever oscillator for use in high resistance resonator applications
[DE93-017652] 04 p1404 N94-18827
Temperature and Doppler coefficients of various space nuclear reactors
[DE94-001388] 05 p1671 N94-21979
High speed electronic analog computers using low-gain amplifiers
[AD-D015974] 06 p2446 N94-25034
Robust stabilization of marginally stable positive-real systems
[NASA-TM-109136] 12 p4500 N94-37058

NEGATIVE IONS
NT ANIONS
Photodetachment studies on few-electron atomic negative ions
[DE93-008474] 01 p0358 N94-10154
Measurements of scattering processes in negative ion-atom collisions
[DE93-013863] 02 p0779 N94-12940
Swelling equilibria for temperature-sensitive ampholytic hydrogels
[DE93-015264] 03 p0966 N94-15996
Negative ion formation in small carbon clusters
[DE93-015436] 03 p1182 N94-16064
Atomic processes in hydrogen and deuterium negative ion discharges
[DE93-013432] 03 p1183 N94-16817
Atomic beam studies relevant to the space environment
[AD-A268628] 03 p1186 N94-17436
Oligomer and mixed-metal compounds, potential multielectron transfer catalysts
[DE93-019592] 04 p1350 N94-19017
Optimization and control of a small angle ion source using an adaptive neural network controller
[DE93-040063] 05 p1946 N94-21845
Semiempirical studies of atomic structure
[DE94-001588] 06 p2531 N94-22937
Diffusion in electronegative discharges with magnetic fields
[AD-A273826] 06 p2304 N94-25521
High gas-efficiency hydrogen negative ion sources
[PB93-232163] 07 p3025 N94-27348
A future, intense source of negative hydrogen ions
08 p3494 N94-30485
Symposium on Inorganic and Organometallic Polymers
[AD-A277860] 10 p4027 N94-33772
Proceedings of the Workshop on Negative Ion Formation and Beam Handling
[DE94-748683] 12 p4518 N94-37360
Production of high current H(-) beams in a cesium seeded volume negative ion source equipped with PG filter
[DE94-718962] 12 p4522 N94-37463

NEGATIVE RESISTANCE CIRCUITS
Interinjection-locked quasioptical power combiners and phased arrays
[AD-A271178] 05 p2015 N94-20214

NEGATIVE RESISTANCE DEVICES
Interinjection-locked quasioptical power combiners and phased arrays
[AD-A271178] 05 p2015 N94-20214

NEODYMIUM
Optical properties of chromium and neodymium in zirconium - barium - lanthanum - aluminum fluoride glass
[AD-A271609] 05 p1987 N94-21236
Hypersensitive transition spectrum of f-element and coordination structure
[DE94-604133] 07 p3070 N94-27843
Solubility of Nd in brine
[DE94-005099] 08 p3187 N94-28567
Ion-beam-driven amorphization of Ca2La8(Si4)6O2 single crystals
[DE94-006219] 09 p3895 N94-31307
Sensitivity and signal to noise ratio improvement of a one micron ladar system incorporating a neodymium doped optical fiber preamplifier. Laser radar testbed
[AD-A280235] 12 p4447 N94-37137

NEODYMIUM ALLOYS
Magnetic properties and transmission electron microscopy investigations of Nd-Fe-B-Co-Al melt spun ribbons
[PB93-201531] 06 p2561 N94-23428

NEODYMIUM COMPOUNDS
Crystal structure and short-range oxygen defects in La- and Nd-modified ZrO2
[DE93-040229] 05 p2033 N94-21993
Anomalous magnetoresistance behavior of superconducting Nd(2-x)Ce(x)CuO(4-y) single crystal
[DE94-000806] 06 p2156 N94-22941
Magnetic properties of NdCo3 and its gamma phase hydride NdCo3H(4.1)
[REPT-A-2655] 06 p2567 N94-25412
NEODYMIUM ISOTOPES
Radiogenic age and isotopic studies
[DE93-610548] 01 p0274 N94-10407
Nd-142/Nd-144 in bulk planetary reservoirs, the problem of incomplete mixing of interstellar components and significance of very high precision Nd-145/Nd-144 measurements 03 p1256 N94-16220
Constraints on the differentiation of the Earth from the coupled Sm-146,147-Nd-142,143 systematics 03 p1103 N94-16271
The Sm-(146,147)-Nd-(142,143) formation interval for the lunar mantle and implications for lunar evolution 05 p2097 N94-20663
The Sm-Nd systematics of silicate inclusions in iron meteorites: Results from Caddo (IAB)
[CONTRIB-5241(804)] 05 p2084 N94-20795
New data supporting a Sm-146,147-Nd-142,143 formation interval for the lunar mantle 11 p4374 N94-36173
NEODYMIUM LASERS
Thermal-optical switching of a silicon based interference filter
[AD-A265152] 01 p0174 N94-11095
An analytic model for calculating pump-induced wavefront distortions in laser slabs
[DE93-011953] 01 p0174 N94-11126
Short pulse lasers for generation of fields exceeding 100 MG
[DE93-013346] 01 p0369 N94-11815
Numerical simulations of Nd:YAG laser amplifiers
[FFI/RAPPORT-92/7028] 02 p0657 N94-13970
The interaction of intense femtosecond laser pulses with solid targets
[DE93-014415] 02 p0658 N94-14114
Nd:YLF laser for airborne/spaceborne laser ranging 03 p0913 N94-15563
An improved light source for laser ranging 03 p0913 N94-15567
Two color satellite laser ranging upgrades at Goddard's 1.2m telescope facility 03 p0915 N94-15581
Measuring atmospheric dispersion with WLRS in multiple wavelength mode 03 p0916 N94-15582
Upgrading of the Borowiec laser station 03 p0877 N94-15604
Results of the MTLRS-1 upgrade 03 p0877 N94-15610
The new MTLRS transmitting system 03 p0877 N94-15612
Effects of turbulence on the geodynamic laser ranging system 03 p0921 N94-15616
Development of the Mars Observer Laser Altimeter (MOLA) 03 p0921 N94-15617
The third generation SLR station Potsdam no. 7836 03 p0877 N94-15623
Laser weld repair of tantalum sheet
[DE93-016417] 03 p1041 N94-16871
Design, development and characterization studies of a large aperture high power Nd: Glass rod amplifier stage
[DE93-624944] 03 p1042 N94-17630
Analysis of neon soft x ray spectra from short-pulse laser-produced plasmas
[DE93-014420] 04 p1582 N94-17708
Pulsed power supply for Nova Upgrade
[DE93-019626] 04 p1441 N94-19307
Development of a lidar for integration with the Naval Postgraduate School Infrared Search and Target Designation (NPS-IRSTD) system
[AD-A271847] 05 p1817 N94-20611
Simulations of spectral broadening by cross-phase modulation (XPM) with chaotic light pulses
[DE93-019623] 05 p1819 N94-21872
Effect of bandwidth on beam smoothing and frequency conversion at the third harmonic of the Nova laser
[DE93-019917] 05 p1819 N94-21920
Progress toward ultra-stable lasers for use in space
[NASA-TM-109678] 06 p2349 N94-24488
Numerical simulation and analysis of experimental results on stimulated Raman scattering in laser-plasma Hohlraum targets
[DE93-613719] 06 p2554 N94-25330
Elastic backscattering lidar for a MSTI satellite
[DE94-002701] 07 p2816 N94-26126
Development of surgical CW Nd:YAG laser with optical fiber delivery system
[DE93-632902] 07 p2817 N94-26185
Development of high average power industrial Nd:YAG laser with peak power of 10 kW class
[DE93-633201] 07 p2818 N94-26520
Beam-quality measurements for materials processing lasers and the proposed ISO standard
[DE94-002738] 07 p2819 N94-26811
High-power CW diode-laser-array-pumped solid-state lasers and efficient nonlinear optical frequency conversion
[AD-A276126] 09 p3714 N94-31278
High average power pulsed phase conjugate laser with birefringence correction
[DE94-006049] 09 p3719 N94-32659
Greater than 100 watt average power at 0.53 micron with 25 ns, 2.5 kHz repetition rate pulses from a single power oscillator
[DE94-011641] 12 p4447 N94-37114
High average power pulsed phase conjugate laser with birefringence correction
[DE94-012062] 12 p4447 N94-37160
Advanced laser driver for soft x-ray projection lithography
[DE94-011643] 12 p4449 N94-37722
NEON
NT NEON ISOTOPES
High-order harmonic generation with short-pulse lasers
[DE93-016532] 02 p0659 N94-14594
Observation of nonsequential ionization of helium and its impact on intensity monitoring
[DE93-017174] 03 p0949 N94-16904
Analysis of neon soft x ray spectra from short-pulse laser-produced plasmas
[DE93-014420] 04 p1582 N94-17708
Helium in interplanetary dust particles 05 p2082 N94-20653
Intramultiplet mixing for Ne(**)(3p) + He at superthermal energies
[ETN-94-95327] 06 p2538 N94-25240
Laser manipulation of metastable neon atoms
[ETN-94-95344] 07 p2817 N94-26225
Computer simulation of molecular interactions in supercritical solvents
[AD-A274977] 08 p3486 N94-29087
Optical field ionization of atoms and ions using ultrashort laser pulses
[DE94-006643] 08 p3488 N94-29845
Wave packet studies of the vibrational predissociation of three and four-atom van der Waals complexes
[DE94-007623] 09 p3871 N94-32598
Collision and motional averaging effects in cryogenic atomic hydrogen masers
[AD-A278478] 10 p4057 N94-33746
Solar proton produced neon in shergottite meteorites 11 p4351 N94-35428
NEON ISOTOPES
Dispersion of the ratios of cosmogenic isotopes of noble gases in chondrites of different cosmic-ray exposure ages 01 p0428 N94-12020
Peculiarities of distributions of the cosmic-ray exposure ages of H chondrite falls and finds 01 p0428 N94-12021
Noble gases in LEW88516 shergottite: Evidence for exposure age pairing with ALH77005 01 p0080 N94-12082
The SCR Ne-21 and Ar-38 in lunar rock 68815: The solar proton energy spectrum over the past 2 MYR 03 p1248 N94-16177
Effects of bulk composition on production rates of cosmogenic nuclides in meteorites 03 p1245 N94-16385
Solar noble gases revealed by closed system stepped etching of a metal separate from Fayetteville 03 p0954 N94-16432
SCR neon and argon in Kapoeta feldspar: Evidence for an active ancient Sun 05 p2106 N94-20712
The Cherenkov hadronic like-jets
[DE93-634525] 07 p3016 N94-26010
The origin of neon-E: Neon-E in single interstellar silicon carbide and graphite grains 09 p3933 N94-31556
NEON 19
U NEON ISOTOPES
NEOPLASMS
NT CANCER
Molecular biological studies on the human radioresistance and drug resistance
[DE93-632682] 07 p2910 N94-26549
NEOPRENES
U CHLOROPRENE RESINS
NEPHANALYSIS
Cloudiest year study: An analysis of the 3DNEPH and RTNEPH databases
[AD-A269403] 04 p1490 N94-18281
SERCAA cloud analysis integration: Design concepts and interaction with cloud forecast models
[AD-A269104] 04 p1492 N94-18637
An analysis of cloud-cover reporting in the 1977 surface observation database
[AD-A271102] 05 p1864 N94-19852
Short-range cloud amount forecasting with model output statistics
[AD-A274769] 07 p2895 N94-26798
NEPHELINE
The correlation of alkalis and aluminum during high-temperature volatilization of albite and nepheline 01 p0081 N94-12214
NEPTUNE (PLANET)
Detection of dust impacts by the Voyager planetary radio astronomy experiment
[NASA-CR-193281] 01 p0423 N94-11305
Models of Neptune's smooth recurrent radio emission
[NASA-CR-193283] 01 p0484 N94-11312
Orbital simulations of satellite escape/capture and the origin of satellites such as Triton 01 p0429 N94-12057
On the unique structure of the magnetic fields of Uranus and Neptune 01 p0472 N94-12221
Precession of Uranus and Neptune and their magnetic field 01 p0473 N94-12222
Neptune high-latitude emission: Dependence of angle on frequency
[NASA-CR-193280] 02 p0848 N94-13476
Neptune encounter highlights
[NASA-TM-109421] 03 p1246 N94-15240
NASA report to education, volume 7
[NASA-TM-109435] 03 p1247 N94-15419
Voyager 2: Neptune encounter
[NASA-TM-109423] 03 p1247 N94-15491
Tidal interaction: A possible explanation for geysers and other fluid phenomena in the Neptune-Triton system 03 p1272 N94-16311
Mapping the stability region of the 3:2 Neptune-Pluto resonance 03 p1280 N94-16351
Detailed analysis of low energy plasma data under the Voyager Uranus data analysis program
[NASA-CR-193668] 04 p1628 N94-17842
Working group for planetary system nomenclature
[NASA-CR-194406] 04 p1626 N94-18841
Voyager's last encounter
[NASA-TM-109361] 04 p1628 N94-18957
The Jet Propulsion Laboratory space exploration: Past, present and future 06 p2153 N94-24242
Analysis of energetic proton and electron data in Neptune's magnetosphere
[NASA-CR-195707] 07 p3107 N94-27784
Radio science ground data system for the Voyager-Neptune encounter, part 1 08 p3248 N94-29623
Plasma and radio waves from Neptune: Source mechanisms and propagation
[NASA-CR-195877] 09 p3943 N94-33103
Voyager last picture show
[NASA-CR-195796] 11 p4367 N94-35506
Plasma and radio waves from Neptune: Source mechamisms and propagation
[NASA-CR-196284] 12 p4550 N94-37251
NEPTUNE ATMOSPHERE
Voyager's last encounter
[NASA-TM-109361] 04 p1628 N94-18957
NEPTUNE SATELLITES
NT TRITON
Voyager's last encounter
[NASA-TM-109361] 04 p1628 N94-18957
NEPTUNIUM
Crystallographic phase transitions in actinide metals as a function of pressure
[DE93-040138] 05 p2011 N94-19827
A survey of metallurgical research on several actinides
[DE94-002643] 06 p2245 N94-24747
NEPTUNIUM COMPOUNDS
Theoretical studies of the structures and electronic properties of U(NH2)(sub 3) and Np(NH2)(sub 3)
[DE94-000768] 05 p2031 N94-21857
NERVA (ENGINE)
U NUCLEAR ENGINE FOR ROCKET VEHICLES
NERVES
NT GANGLIA
NT OCULOMOTOR NERVES
Cortical adaptive filtering in bioacoustic signal classification
[AD-A266229] 03 p1177 N94-16939
Coupled neural-dendritic processes: Cooperative stochastic effects and the analysis of spike trains
[AD-A270041] 04 p1506 N94-18793
The role of axon-Schwann cell interactions in nervous system ionic homeostasis
[AD-A270936] 05 p1890 N94-20045
Theoretical and numerical examinations of nonlinear parameter dependent advanced differential difference equations
[ETN-93-93681] 05 p1952 N94-21042

Immunocytochemical localization of glutamic acid decarboxylase (GAD) and substance P in neural areas mediating motion-induced emesis: Effects of vagal stimulation on GAD immunoreactivity
05 p1887 N94-21909
Disturbed neuronal migration in the cerebral cortex of mice by low-dose gamma radiation
07 p2904 N94-27470
Abnormal development of serotonin nerve fibers in the cerebral cortex of young rats with methylazoxymethanol induced microcephaly 07 p2905 N94-27485
Inductive differentiation of nerve cells in mouse embryonic ectoderm at early primitive streak stage by retinoic acid 07 p2905 N94-27488
Cellular analysis of the startle reflex
[AD-A278243] 10 p4094 N94-33380

NERVOUS SYSTEM
NT AFFERENT NERVOUS SYSTEMS
NT AUTONOMIC NERVOUS SYSTEM
NT BRAIN
NT CENTRAL NERVOUS SYSTEM
NT CEREBELLUM
NT CEREBRAL CORTEX
NT CEREBRUM
NT EFFERENT NERVOUS SYSTEMS
NT GANGLIA
NT HIPPOCAMPUS
NT HYPOTHALAMUS
NT NERVES
NT OCULOMOTOR NERVES
NT PINEAL GLAND
NT SYMPATHETIC NERVOUS SYSTEM
NT THALAMUS
An analog clustering network from a biological model
[AD-A265637] 02 p0762 N94-12969
Development of the OMPAT neuropsychological/psychomotor performance evaluation and OMPAT data and timing support programs
[AD-A266954] 03 p1122 N94-15759
Neural mechanisms of attention
[AD-A266315] 03 p1132 N94-16456
The role of axon-Schwann cell interactions in nervous system ionic homeostasis
[AD-A270936] 05 p1890 N94-20045
The effects of area postrema lesions and selective vagotomy on motion-induced conditioned taste aversion
05 p1888 N94-21910
Electrophysiology of the rat nucleus accumbens: Local circuitry, neuromodulation and synaptic plasticity
[PB93-232254] 06 p2420 N94-23454
Photonic technology for implementation of generalizable neural networks: A synthetic approach
[AD-A273497] 06 p2474 N94-24622
Influence of mechanical stimulation on inflammatory edema 07 p2906 N94-27497
The effect of naloxone on sleeping time in adjuvant arthritic rats 07 p2906 N94-27498
Effects of capsaicin on freshly dissociated rat dorsal root ganglion cells 07 p2906 N94-27499
Size distribution of retrogradely labeled dorsal root ganglion cells: Test of normality
07 p2906 N94-27500
Interaction between endogenous opioid and Cholecystokinin (CCK) in modulating respiratory responses induced by thin-fiber muscular afferents
07 p2906 N94-27502
Electrical coupling between the sino-atrial node and atrial muscle: Cell to cell interaction through an external circuit and its simulation by computer modeling
07 p2907 N94-27509
Correlation between electrical activity and the size of single sinoatrial node cells 07 p2907 N94-27513
The ionic mechanism underlying the negative chronotropic effect of acetylcholine: Experimental study in rabbit single sinoatrial node cells
07 p2908 N94-27514
The ionic mechanism underlying the negative chronotropic effect of acetylcholine: Experiments using small sinoatrial node tissue preparations isolated from rabbit hearts 07 p2908 N94-27515
The ionic mechanism underlying the negative chronotropic effect of acetylcholine: Postganglionic vagal stimulation in isolated rabbit hearts
07 p2908 N94-27516
Hyperalgesia to cold in patients with Subacute Myelo-Optico-Neuropathy (SMON)
07 p2928 N94-27521
Effect of food intake on skin vasomotor responses to head-up tilt in humans 08 p3390 N94-28854
Research in VLSI system implementation of neuromorphic learning networks
[AD-A278247] 10 p4112 N94-33403

NETHERLANDS
Symposium on the Future of Aeronautics in the Netherlands
[ETN-93-93780] 03 p0853 N94-15120
Aviation and the KLM: Past and future
03 p0853 N94-15126
Developments in the Higher Technical Aerospace Education 03 p0854 N94-15130
Reports of the 1992 Synoptic Symposium
[KNMI-TR-151] 04 p1494 N94-19698
The WAQUA/CSM-16 model
04 p1494 N94-19700
Soil temperatures
[KNMI-WR-92-05] 05 p1865 N94-20309
Exploratory report nickel and nickel compounds
[PB93-223998] 06 p2242 N94-23496
Exploratory report antimony and antimony compounds
[PB93-224004] 06 p2397 N94-23497
Analysis of vulnerability to the impacts of sea level rise: A case study for The Netherlands
[PB94-111150] 06 p2399 N94-24573
Soil pollution at former industrial sites, the heritage of 150 years of industrial development in Noord-Brabant, The Netherlands
[ISBN-9-09-005758-7] 06 p2400 N94-25223
Remote sensing and GIS for the management and investigation of the Wadden Sea
[BCRS-92-20] 07 p2847 N94-26228

NETS
NT NEURAL NETS
NT PETRI NETS
Studies of Shuttle orbiter arrestment system
[NASA-TP-3370] 06 p2177 N94-24304
Conditional dependence in probabilistic networks
[RUU-CS-92-34] 08 p3464 N94-29450
Pearl's belief propagation: The proofs
[RUU-CS-92-47] 08 p3456 N94-30378

NETWORK ANALYSIS
NT CRITICAL PATH METHOD
Networks of real-time processes
[DE93-013049] 01 p0338 N94-12597
A network evaluation and analysis tool
[DE93-012647] 02 p0758 N94-12917
Proceedings of the 11th Space Surveillance Workshop, volume 1
[AD-A265120] 02 p0531 N94-13358
Stochastic scheduling in in-forest networks
[INRIA-RR-1719] 03 p1164 N94-15695
Congestion control of high-speed networks
[AD-A267013] 03 p0989 N94-15748
State space partitioning methods for solving a class of stochastic network problems
[AD-A267494] 03 p1173 N94-17585
APLAC: An object-oriented analog circuit simulator and design tool. 6.1 reference manual
[PB93-187193] 04 p1396 N94-18091
Exact cost flow problems in acyclic networks
[REPT-93-030] 04 p1520 N94-18138
Specification and analysis of a high speed transport protocol
[AD-A268941] 04 p1386 N94-18449
Naval research reviews. Mixing enhancement for air-breathing propulsion. Non-axisymmetric jets increase mixing, volume 44 and volume 45
[AD-A268966] 04 p1521 N94-18543
Improved HF data network simulator, volume 1
[AD-A270953] 04 p1393 N94-19752
Improved HF data network simulator, software user's manual, volume 2
[AD-A270954] 04 p1393 N94-19753
SPICE macromodel for a 1-megawatt power MOSFET switch
[DE93-019415] 05 p1748 N94-19844
High resolution signal processing
[AD-A271181] 05 p1717 N94-20215
An evaluation of artificial neural network modeling for manpower analysis
[AD-A273001] 05 p1945 N94-21269
Sorting network for the partial selection problem
05 p1773 N94-22121
A neural network approach to the maximum flow problem 05 p1783 N94-22183
Throughput and blocking in circuit-switched interconnection networks 05 p1784 N94-22189
Neural networks for optimum routing in packet-switched communications networks 05 p1746 N94-22205
Handover procedures in integrated satellite and terrestrial mobile systems 06 p2277 N94-22761
MSAT and cellular hybrid networking
06 p2278 N94-22762
Trends in mobile satellite communication
06 p2278 N94-22763
A system architecture for an advanced Canadian wideband mobile satellite system
06 p2278 N94-22766
Transient analysis of circuits including frequency-dependent components using transgyrator and convolution
[PB93-225001] 06 p2308 N94-23130
Mathematical modeling of MCFC cells/stacks and networks
[DE94-001914] 06 p2390 N94-23212
Extension of the critical path method
[PB94-118817] 06 p2488 N94-24527
Modular approach to project management
[PB94-118833] 06 p2586 N94-24528
Irreducible core of a minimum cost spanning tree game
[PB94-110962] 06 p2489 N94-24653
New directions in network flows
[AD-A273467] 06 p2468 N94-24939
Development of a 4-bit parallel analog-to-digital converter and a four-quadrant double-balanced mixer using heterojunction bipolar transistor technology
[AD-A274074] 07 p2947 N94-25648
New mixed integer algorithm for classification and placement of measurements in process flow networks
[PB94-126752] 07 p2966 N94-26921
Integrated model development for liquid fueled rocket propulsion systems
[NASA-CR-195253] 07 p2702 N94-27166
Modeling, analysis, and simulation of an optical time-division multiple-access network architecture
[AD-A275847] 08 p3498 N94-28780
Digitally programmable composite operational amplifier applications
[AD-A275081] 08 p3262 N94-28842
High throughput network for multiprocessor interconnections
[VTT-PUBS-147] 08 p3245 N94-29468
Customer creation and combination in queueing networks
[MEMO-INF-93-35] 08 p3438 N94-30375
An intrinsic Hamiltonian formulation of the dynamics of LC-circuits
[MEMO-1154] 08 p3462 N94-30964
A Green's function approach to analysing the effects of random synaptic background activity in a model neural network
[MATHS-REPT-A-202] 09 p3828 N94-31157
Some calculations on supersymmetric graphs as communication networks
[REPT-93-72] 09 p3824 N94-31641
Analysis and design of a formal neural network for filtering a dynamic signal
[ISBN-0-315-86932-1] 09 p3832 N94-31873
Multicast communication with guaranteed quality of service
[AD-A277650] 09 p3682 N94-33025
Assessing the vulnerability of multi-commodity networks with failing components
[AD-A278434] 09 p3684 N94-33334
Worst case circuit analysis application guidelines
[AD-A278216] 10 p4038 N94-33376
Data communication network at the ASRM facility
[NASA-CR-195901] 10 p4033 N94-33535
Assessment of the current European research and developments in non-invasive integrated circuit analysis
[DE94-004042] 10 p4039 N94-33735
Topological properties of typical interconnection networks: Fault tolerance, communication delay and connection cost
[PB94-148822] 10 p4111 N94-33976
The 2nd International Workshop on Discrete Time Domain Modelling of Electromagnetic Fields and Networks
[AD-A277551] 10 p4035 N94-34081
Switched-beam radiometer front-end network analysis
[NASA-CR-194922] 11 p4252 N94-35247
An analysis of file system and installation of the file management system for NOS operating system
[DE94-611062] 11 p4346 N94-35833

NETWORK CONTROL
Galileo EM-2 contributions to the lunar control network 01 p0468 N94-12198
Communications and control for electric power systems
[NASA-CR-194503] 02 p0622 N94-13811
Real-time implementation of neural network learning control of a flexible space manipulator
[AD-A266962] 03 p1045 N94-14970
Panacea: An active sensor controller for the ALVINN autonomous driving system
[AD-A266964] 03 p0864 N94-14972
The distributed database dynamic reconfiguration project
[AD-A267116] 03 p1229 N94-15652
The IMS software integration platform
[AD-A266285] 03 p1151 N94-16910
Models and building blocks for secure open systems
[FEL-92-B365] 04 p1619 N94-19457
Protocol service decomposition for high-performance networking
[AD-A270613] 04 p1538 N94-19533

Congestion/flow control and routing in data networks: A control-theoretic approach
[AD-A271121] 04 p1392 N94-19737
Physics Detector Simulation Facility. Phase 2: System software description
[DE93-019745] 05 p1928 N94-19812
Networks Technology Conference
[NASA-CP-3241] 05 p1931 N94-21323
The NCC project: A quality management perspective 05 p1828 N94-21324
Let your fingers do the walking: The projects most invaluable tool 05 p1922 N94-21325
Software metrics: The key to quality software on the NCC project 05 p1922 N94-21326
Enhanced networks operations using the X Window System 05 p1932 N94-21329
The automated ground network system 05 p1932 N94-21330
Mission Operations Support Area (MOSA) for ground network support 05 p1932 N94-21331
Space network scheduling benchmark: A proof-of-concept process for technology transfer 05 p1932 N94-21332
Distributed intelligent control and status networking 05 p1932 N94-21335
Developing a space network interface simulator: The NTS approach 05 p1933 N94-21343
A packet switched communications system for GRO 05 p1744 N94-21345
A laboratory system for the investigation of rain fade compensation techniques for Ka-band satellites
[NASA-CR-191200] 05 p1762 N94-21566
Interworking evolution of mobile satellite and terrestrial networks 06 p2277 N94-22758
Interworking and integration of the Inmarsat Standard-M with Pan-European GSM system 06 p2277 N94-22759
Architectures and protocols for an integrated satellite-terrestrial mobile system 06 p2277 N94-22760
Handover procedures in integrated satellite and terrestrial mobile systems 06 p2277 N94-22761
Optimizing space constellations for mobile satellite systems 06 p2278 N94-22764
ACTS mobile SATCOM experiments 06 p2280 N94-22774
The ORBCOMM data communications system 06 p2281 N94-22782
System services and architecture of the TMI satellite mobile data system 06 p2286 N94-22817
Study on networking issues of medium earth orbit satellite communications systems 06 p2288 N94-22825
Specifications of ETS, the Enhanced Transport Service
[RR-907-I] 06 p2589 N94-23150
Source spacing in B-ISDN
[PB93-201747] 06 p2293 N94-23508
NASDA satellite mission operation system and operations 06 p2501 N94-23854
NASDA knowledge-based network planning system 06 p2508 N94-23898
Deep Space Network (DSN), Network Operations Control Center (NOCC) computer-human interfaces 06 p2447 N94-23917
EOS ground data systems: A description and interface overview 06 p2517 N94-23948
Video transmission on ATM networks
[NASA-CR-195124] 08 p3244 N94-29106
High throughput network for multiprocessor interconnections
[VTT-PUBS-147] 08 p3245 N94-29468
Remote observatory access via the advanced communications technology satellite 08 p3253 N94-29894
Performance evaluation of intelligent network services
[PB94-149564] 08 p3438 N94-30373
Self-stabilizing I-exclusion algorithms
[RUU-CS-93-01] 08 p3424 N94-30379
An all pairs shortest paths distributed algorithm using 2n(exp 2) messages
[RUU-CS-93-19] 08 p3432 N94-30411
Communications networks in stressed environments
[AD-A275967] 09 p3672 N94-31384
The use of service limits for efficient operation of multi-station single-medium communication systems
[CWI-BS-R9312] 09 p3677 N94-32085
Undiscounted Markov decision chains with partial information; an algorithm for computing a locally optimal periodic policy
[TW-93-10] 09 p3851 N94-32205
Discrete-event-dynamic-system-based approaches for scheduling transmissions in multihop packet radio networks
[AD-A276566] 09 p3679 N94-32230
Voice and video transmission using XTP and FDDI 09 p3685 N94-32468
Use and administration of UNIX (tm) systems 09 p3821 N94-33051
Group-oriented coordination models for distributed client-server computing 10 p4126 N94-35068
Large granularity cache coherence for intermittent connectivity
[AD-A278897] 11 p4345 N94-35571
A comparison of queueing, cluster and distributed computing systems
[NASA-TM-109025-REV-1] 12 p4497 N94-36932

NETWORK SYNTHESIS

Models for asynchronous circuit behaviour with OR causality
[PB94-148897] 10 p4112 N94-34126
High level modelling and design of asynchronous interface logic
[PB94-167822] 11 p4258 N94-35534

NETWORKS

Design of a matching network for dipole antennas
[AD-A265115] 01 p0136 N94-11158
Galileo EM-2 contributions to the lunar control network 01 p0468 N94-12198
Tests of a simple data merging algorithm for the GONG project 05 p1927 N94-22549
Bayesian belief networks and conditional independencies
[RUU-CS-92-36] 08 p3465 N94-30376

NEUMANN PROBLEM

A simplified Von Neumann method for linear stability analysis
[CRANFIELD-AERO-9310] 09 p3843 N94-31540
Finite volume discretization of the k-epsilon turbulence model in general coordinates
[REPT-93-90] 09 p3703 N94-31703

NEURAL NETS

The applicability of neural nets for decision support
[MEMO-COSOR-92-49] 01 p0338 N94-10169
Nonlinear stability and control study of highly maneuverable high performance aircraft
[NASA-CR-193480] 01 p0025 N94-10344
Unsupervised splitting rules for neural tree classifiers
[AD-A264961] 01 p0338 N94-10487
Functional approximation using artificial neural networks in structural mechanics
[NASA-TM-105820] 01 p0188 N94-11254
Three-dimensional object recognition using an unsupervised BCM network: The usefulness of distinguishing features
[AD-A264576] 01 p0304 N94-11261
Neural network model selection using asymptotic jackknife estimator and cross-validation method
[AD-A264960] 01 p0339 N94-11289
Fault location in structures using neural networks 01 p0070 N94-11335
Spatial light rebroadcaster architecture study
[AD-A266102] 01 p0382 N94-11421
Adaptive reconfigurable flight controls for high angle of attack aircraft agility 01 p0032 N94-11502
Toward intelligent flight control 01 p0033 N94-11503
Bounding the Vapnik-Chervonenkis dimension of concept classes parameterized by real numbers
[DE93-011600] 01 p0331 N94-11611
Model reference adaptive control (MRAC) with applications to robotics 01 p0339 N94-11640
Statistical and optimization methods to expedite neural network training for transient identification
[DE93-009985] 01 p0340 N94-11644
Parametric study of diffusion-enhancement networks for spatiotemporal grouping in real-time artificial vision
[AD-A265065] 01 p0331 N94-11652
A hybrid neural network and feature extraction technique for target recognition
[AD-D015732] 01 p0333 N94-12386
Signal feature analysis using neural networks and psychoacoustics
[AD-A266048] 01 p0340 N94-12398
Thermal error compensation feasibility study using artificial intelligence
[AD-A266084] 01 p0340 N94-12411
Proceedings of the Seventh International Symposium on Methodologies for Intelligent Systems (poster session)
[DE93-013470] 01 p0340 N94-12428
An analog clustering network from a biological model
[AD-A265637] 02 p0762 N94-12969
Adaptive Transfer Function Networks
[DE93-014344] 02 p0745 N94-13151
A review and analysis of neural networks for classification of remotely sensed multispectral imagery
[NASA-CR-194291] 02 p0763 N94-13603
ANNS: An X Window based version of the AFIT neural network simulator
[AD-A266540] 02 p0764 N94-13704
Satellite imagery and exogenous data integration by neural network in automation land-cover classification
[INPE-5480-PRE/1778] 02 p0686 N94-13729
Nonlinear aspects of data integration for land-cover classification in a neural network environment
[INPE-5479-PRE/1778] 02 p0686 N94-13789
Tomographic methods in flow diagnostics
[NASA-TM-106330] 02 p0650 N94-13876
Communications and control for electric power systems: Power flow classification for static security assessment
[NASA-CR-194512] 02 p0624 N94-13948
Feature discovery on segmented objects in SAR imagery using self-organizing neural networks
[DE93-010685] 02 p0686 N94-14056
Identification and interpretation of patterns in rocket engine data
[NASA-CR-194534] 02 p0552 N94-14309
Obstacle detection by recognizing binary expansion patterns
[NASA-CR-194415] 02 p0514 N94-14495
Computer vision and sensor fusion for detecting buried objects
[DE93-012605] 02 p0700 N94-14566
A neural-network approach to robotic control 02 p0679 N94-14634
Retrieval properties of neural networks with infinitely many marked patterns
[PREPRINT-729] 02 p0766 N94-14718
Speaker independent recognition of isolated words using vector quantization and neural networks
[ETN-93-94390] 02 p0616 N94-14724
Identification of continuous-time dynamical systems: Neural network based algorithms and parallel implementation
[DE93-014427] 02 p0766 N94-14737
Mathematic methods and algorithms for real-time applications
[AD-A266776] 02 p0771 N94-14789
Determining neural network connectivity using evolutionary programming
[AD-A266853] 02 p0766 N94-14882
Unsteady separated flows: Empirical model and control
[AD-A267282] 03 p0855 N94-14959
Real-time implementation of neural network learning control of a flexible space manipulator
[AD-A266962] 03 p1045 N94-14970
Panacea: An active sensor controller for the ALVINN autonomous driving system
[AD-A266964] 03 p0864 N94-14972
Multiobjective functions optimization for task allocation mapping to multicomputer nodes
[AD-A267071] 03 p1146 N94-15670
The bootstrapped algorithm: Fast algorithm for blind signal separation
[AD-A266671] 03 p1147 N94-15772
Unipolar terminal-attractor based neural associative memory with adaptive threshold
[NASA-CASE-NPO-18790-1-CU] 03 p1165 N94-15958
Neural-network-directed alignment of optical systems using the laser-beam spatial filter as an example
[NASA-TP-3372] 03 p1034 N94-15961
Real-time adaptive neural network data processing
[TABES PAPER 93-660] 03 p1054 N94-16155
Neural mechanisms of attention
[AD-A266315] 03 p1132 N94-16456
AVIRIS data and neural networks applied to an urban ecosystem 03 p1073 N94-16705
Information technology division technical paper abstracts
[AD-A266227] 03 p1166 N94-16938
ONRASIA scientific information bulletin, volume 18, number 2
[AD-A267798] 03 p1304 N94-17305
An object-oriented environment for computer vision and pattern recognition
[DE93-017098] 04 p1517 N94-17867
Neural networks to classify speaker independent isolated words recorded in radio car environments
[REPT-93-013] 04 p1383 N94-17935
Application of the network discriminant function to learning
[AD-A268793] 04 p1540 N94-18189
Proceedings of the 3rd Workshop on Balloon-Borne Experiments with Superconducting Magnet Spectrometers
[DE93-788362] 04 p1630 N94-18219
Optical associative processors and directed graphs
[AD-A268881] 04 p1615 N94-18224
Preliminary structural design: Defining the design space
[AD-A268898] 04 p1317 N94-18227
Fast-training algorithm for hidden-layer forward-feed neural networks
[AD-A269253] 04 p1540 N94-18263

Cortical substrate of haptic representation
[AD-A269583] 04 p1508 N94-18304
Autonomous neural network controllers for adaptive material handling
[AD-A268908] 04 p1540 N94-18331
Optical computing. Organization of the 1993 Photonics Science Topical Meetings. Technical digest series, volume 7
[AD-A269025] 04 p1578 N94-18332
Low power signal processing research at Stanford
04 p1393 N94-18351
Pulse-firing winner-take-all networks
04 p1399 N94-18353
Training product unit neural networks with genetic algorithms 04 p1399 N94-18354
VLSI synthesis of digital application specific neural networks 04 p1399 N94-18355
Measurement selection for parametric IC fault diagnosis 04 p1399 N94-18356
The identification of the computational significance of key neurobiological characteristics found in a number of telencephalic brain regions
[AD-A269374] 04 p1505 N94-18407
Joint services electronics program
[AD-A269383] 04 p1403 N94-18638
Interaction of intense lasers and relativistic electron beams with solids, gases and plasmas
[AD-A269655] 04 p1439 N94-18737
Neutral networks: An NRL perspective
[AD-A269122] 04 p1541 N94-18773
Active control of a multivariable system by way of polynomial neural networks: Computer simulation evaluations and laboratory experimental results
[AD-A270033] 04 p1541 N94-18790
Coupled neural-dendritic processes: Cooperative stochastic effects and the analysis of spike trains
[AD-A270041] 04 p1506 N94-18793
Operational parameters of an opto-electronic neural network employing fixed planar holographic interconnects
[DE93-018795] 04 p1433 N94-19000
An innovative neural manufacturing concept
[DE93-017212] 04 p1527 N94-19238
Use of shape memory alloys in the robust control of smart structures
[AD-A270827] 04 p1366 N94-19594
Explorations of the practical issues of learning prediction-control tasks using temporal difference learning methods
[AD-A270836] 04 p1544 N94-19599
VLSI implementation of neuromorphic learning networks
[AD-A270825] 04 p1407 N94-19665
Transcutaneous Analyte Measuring Methods (TAMM)
[AD-A271387] 04 p1408 N94-19756
Applications of neural networks in fault detection of rotating machinery
[AD-A270755] 04 p1448 N94-19766
Metrics for specifying and/or testing neural networks statement of government interest
[AD-D015946] 05 p1938 N94-19843
A complex systems approach to computational molecular biology
[DE93-040062] 05 p1884 N94-19866
Building brains for bodies
[AD-A270531] 05 p1939 N94-19875
Center for neural engineering
[AD-A271164] 05 p1890 N94-20185
Proceedings of the Twentieth Annual Technologyfest
05 p1645 N94-20188
Self-organization via active exploration in robotic applications. Phase 2: Hybrid hardware prototype
[NASA-CR-194723] 05 p1939 N94-20212
Connectionism and Natural Language Processing
[MEMO-INF-92-64] 05 p1940 N94-20242
Representation of spoken words in a self-organizing neural net 05 p1940 N94-20243
Modeling the human mental lexicon with self-organizing feature maps 05 p1743 N94-20244
Speech synthesis with artificial neural networks
05 p1743 N94-20245
Generalization performance of backpropagation learning on a syllabification task 05 p1940 N94-20246
Hopfield models as neural-network acceptors
05 p1941 N94-20250
A single layer higher order neural net and its application to grammar recognition 05 p1941 N94-20251
Syntactic neural networks for natural language processing 05 p1941 N94-20254
DISCERN: A distributed neural network model of script processing and memory 05 p1941 N94-20255
Applying the INN model to the MaxClique
[DE93-040137] 05 p1906 N94-20276
Electronic neural network for solving traveling salesman and similar global optimization problems
[NASA-CASE-NPO-17807-2-CU] 05 p1942 N94-20360
Neural network for processing both spatial and temporal data with time based back-propagation
[NASA-CASE-MSC-21874-1] 05 p1942 N94-20366
Retrieval of ice thickness from polarimetric SAR data
05 p1724 N94-20432
Application of neural network to remote sensing of soil moisture using theoretical polarimetric backscattering coefficients 05 p1730 N94-20455
Center for the integration of optical computing
[AD-A271874] 05 p1899 N94-20469
The Seventh International Symposium on Methodologies for Intelligent Systems (Poster Session)
[AD-A272125] 05 p1942 N94-20573
Simulating a user's preferences: Towards automated artificial evolution for computer generated images
[AD-A272058] 05 p1942 N94-20621
Algorithm/architecture study for artificial neural nets
[AD-A271820] 05 p1943 N94-20626
An application of the Cerebellar Model Articulation Controller for a switched reluctance rotor position estimator
[AD-A271769] 05 p1943 N94-20926
Neural network studies
[AD-A271593] 05 p1943 N94-20947
Robust neural classifier circuits using asynchronous design 05 p1757 N94-21111
An evaluation of artificial neural network modeling for manpower analysis
[AD-A273001] 05 p1945 N94-21269
Application of a back-propagation neural network to isolated-word speech recognition
[AD-A272495] 05 p1945 N94-21430
A mean field neural network for hierarchical module placement 05 p1766 N94-21720
A comparative robustness evaluation of feedforward neurofilters
[NASA-TM-106440] 05 p1650 N94-21742
Simulated behaviour of large scale SCI rings and tori
[DE93-040149] 05 p1935 N94-21745
Optimization and control of a small angle ion source using an adaptive neural network controller
[DE93-040063] 05 p1946 N94-21845
Estimation of AR signal patterns using competitive neural networks 05 p1744 N94-22102
Signal classification and noise filtering using artificial neural networks 05 p1744 N94-22103
Noise filtering using multilayer feedforward neural network 05 p1770 N94-22104
A neural network for multiresolution image detection
05 p1779 N94-22163
Improvement in invariant pattern recognition with neural networks and Fourier-Mellin filters
05 p1780 N94-22164
A neural M-ary tree method for data compression
05 p1780 N94-22166
Cascaded recursive artificial neural networks
05 p1780 N94-22167
On the discovery of approximate arithmetic relations by backpropagation networks 05 p1782 N94-22181
Logic oriented neural networks
05 p1782 N94-22182
A neural network approach to the maximum flow problem 05 p1783 N94-22183
A Hopfield neural net for discrete Fourier transform calculation 05 p1783 N94-22184
Interference reduction using neural networks
05 p1783 N94-22186
A pyramid neural network architecture for stereo fusion 05 p1785 N94-22201
Neural networks for optimum routing in packet-switched communications networks 05 p1746 N94-22205
Acceleration of backpropagation learning using a parallel DSP machine 05 p1786 N94-22206
A framework of connectionist network toward speech waveform coding 05 p1746 N94-22211
Speaker-independent isolated-digit recognition using neural networks and hidden Markov model
05 p1747 N94-22213
Fuzzy and neural control
[NASA-TM-108753] 05 p1947 N94-22270
A neural network prototyping package within IRAF
05 p1949 N94-22451
STARBASE: Database software for the automated plate scanner 05 p1927 N94-22512
General asymmetric neural networks and structure design by genetic algorithms: A learning rule for temporal patterns
[DE94-001254] 05 p1947 N94-22563
The adaptive resonance theory network: (Clustering-) behaviour in relation with brainstem auditory evoked potential patterns
[EUT-92-E-264] 06 p2470 N94-22877
Artificial neural networks: Application to the optical recognition of music partitions
[ETN-94-95166] 06 p2470 N94-22884
Customizable VLSI artificial neural network chips based on a novel technology
[DE94-001418] 06 p2307 N94-23008
A novel process monitoring and control system based on a neural manufacturing concept
[DE94-001516] 06 p2471 N94-23011
Installation of an artificial neural network on distributed memory microprocessors
[ETN-94-95175] 06 p2471 N94-23152
Neural network research in Finland. Symposium
[PB93-224822] 06 p2472 N94-23463
Material data representation of hysteresis loops for Hastelloy X using artificial neural networks
[NASA-TM-105990] 06 p2376 N94-23551
Adaptive nonlinear polynomial neural networks for control of boundary layer/structural interaction
[NASA-CR-189645] 06 p2525 N94-23698
Automatic modulation recognition based on spatial pattern classification using artificial neural networks
[CTN-94-60897] 06 p2296 N94-24115
Acoustic target detection and classification using neural networks 06 p2529 N94-24221
Preliminary analysis of the JAPE ground vehicle test data with an artificial neural network classifier
06 p2529 N94-24222
Neural network-based control using Lyapunov functions 06 p2477 N94-24433
Using neural networks to assist in OPAD data analysis
06 p2477 N94-24452
Optimal Space Station solar array gimbal angle determination via radial basis function neural networks
[NASA-TM-106482] 06 p2195 N94-24482
Diagnosing process faults using neural network models
[DE94-002633] 06 p2473 N94-24518
Systematic construction of trigonometric neural networks
[PB93-200228] 06 p2474 N94-24544
Photonic technology for implementation of generalizable neural networks: A synthetic approach
[AD-A273497] 06 p2474 N94-24622
Hyperspectral imagery classification using a backpropagation neural network
[AD-A273615] 06 p2545 N94-24730
A methodology for software cost estimation using machine learning techniques
[AD-A273158] 06 p2459 N94-24775
Evolving recurrent perceptrons
[AD-A273241] 06 p2496 N94-24778
Evolving neural network connectivity
[AD-A273134] 06 p2490 N94-24921
High-level connectionist models
[AD-A273638] 06 p2468 N94-25030
Radar target discrimination systems using artificial neural network topology
[AD-D015984] 06 p2301 N94-25041
Determining neural network hidden layer size using evolutionary programming
[AD-A273242] 06 p2475 N94-25139
The determination of the branching ratios of the Z(zero) boson into heavy quarks using neural networks
[ETN-94-95381] 06 p2538 N94-25246
On-line control of dynamic systems using feedforward neural networks
[RR-457] 06 p2476 N94-25307
Development of programmable artificial neural networks 06 p2477 N94-25370
Color image segmentation
[AD-A274027] 07 p2984 N94-25759
A feasibility study on bird classification with neural network
[AD-A273753] 07 p2659 N94-25780
Neural networks for dynamic flight control
[AD-A274089] 07 p2676 N94-25785
Predicting nonlinear time series
[AD-A274051] 07 p2990 N94-25834
The AFIT multielectrode array for neural recording and simulation: Design, testing, and encapsulation
[AD-A274086] 07 p2909 N94-25943
Adaptive optimization and control using neural networks
[DE94-003941] 07 p2985 N94-25983
Zernike moments and rotation invariant object recognition. A neural network oriented case study
[AD-A273749] 07 p2767 N94-26011
Asymptotically stable neural networks for identification of nonlinear dynamic systems
[ISBN-0-315-84328-4] 07 p2985 N94-26629
Parallel computational geometry on analog Hopfield networks
[ISBN-0-315-84093-5] 07 p2980 N94-26635
Smart structures, an overview
[AD-A274147] 07 p2987 N94-27093

Translation and rotation invariant pattern recognition
[PB94-123676] 07 p2968 N94-27157
Motion analysis from a sequence of range images
[ISBN-0-315-84684-4] 07 p2969 N94-27311
Center for space microelectronics technology
[NASA-CR-195282] 07 p2786 N94-27574
On modeling and controlling intelligent systems
[DE94-002446] 07 p2988 N94-27706
Neural control of magnetic suspension systems
07 p2682 N94-27905
An overview on development of neural network technology 07 p2990 N94-27913
A space-based classification system for RF transients
[DE94-003933] 08 p3240 N94-28522
Track filtering by robust neural network
[DE94-606067] 08 p3434 N94-28613
Modeling, analysis, and simulation of an optical time-division multiple-access network architecture
[AD-A275847] 08 p3498 N94-28780
Non-intrusive gaze tracking using artificial neural networks
[AD-A275186] 08 p3397 N94-28860
Intelligent automated process planning and code generation for computer-controlled inspection
[AD-A275346] 08 p3409 N94-28920
Initial wave-type identification with neural networks and its contribution to automated processing in IMS version 3.0
[AD-A275058] 08 p3359 N94-29137
Neural network solutions to logic programs with geometric constraints
[AD-A275419] 08 p3435 N94-29198
Nonvolatile programmable neural network synaptic array
[NASA-CASE-NPO-18578-1-CU]
08 p3265 N94-29426
Automation of the NDT diagnostic using neural nets. Application: Inspection of Airbus longitudinal joints during maintenance
[REPT-932-600-104] 08 p3315 N94-29474
A neural network with modular hierarchical learning
[NASA-CASE-NPO-19077-1-CU]
08 p3435 N94-29492
Nonlinear PCA: Algorithms and applications
[PB94-137544] 08 p3419 N94-29680
Stereo imaging based particle velocimeter
[NASA-CR-195800] 08 p3289 N94-29742
Neural network with dynamically adaptable neurons
[NASA-CASE-NPO-17803-1-CU]
08 p3436 N94-29756
Activities of Ishikawajima-Harima Heavy Industries Co. Ltd.
[PB94-137981] 08 p3555 N94-29798
Robotic hand-eye motor learning
08 p3436 N94-29835
Neural network application to Particle Impact Noise Detection 08 p3437 N94-29840
Reinforcement learning for robots using neural networks 08 p3437 N94-29853
Genetic algorithms at UC Davis/LLNL
[DE94-006625] 08 p3421 N94-30117
Unsupervised learning in analog networks
[ISBN-0-315-85959-8] 08 p3432 N94-30140
A novel approach to noise-filtering based on a gain-scheduling neural network architecture
[NASA-TM-106563] 08 p3155 N94-30204
Taxonomy of gamma ray burster data using a self-organizing neural network
[DE94-006480] 08 p3553 N94-30248
Neural network based time-optimal control of a magnetically levitated precision positioning system
[DE94-006573] 08 p3437 N94-30250
A lateral inhibition neural network that emulates a winner-takes-all algorithm
[RUU-CS-92-46] 08 p3438 N94-30334
A multiscale approach to image segmentation using Kohonen networks
[RUU-CS-93-06] 08 p3438 N94-30349
Microwave vision for robots
[AIAA PAPER 94-0887-CP] 08 p3443 N94-30550
A neural network-based technique for structural identification of SISO systems
[REPT-93-076] 08 p3449 N94-30941
Machinery monitoring and diagnostics using pseudo Wigner-Ville distribution and backpropagation neural network
[AD-A276219] 09 p3828 N94-31064
Report of the 'Mathematical Models for Neural Networks' course
[TELECOM-93-D-019] 09 p3828 N94-31100
A Green's function approach to analysing the effects of random synaptic background activity in a model neural network
[MATHS-REPT-A-202] 09 p3828 N94-31157
A neuron network for image classification: From algorithm to implantation
[TELECOM-93-E-005] 09 p3687 N94-31168
Filtering and recognition of moving boats in radar images
[REPT-93-039] 09 p3671 N94-31190
ART: Adaptive Resonance Theory
[TELECOM-93-D-020] 09 p3829 N94-31193
Smart environmental monitor based on neural networks and multi-spectral pattern recognition
[AD-A276445] 09 p3829 N94-31301
A neural network methodology for engineering applications: The learning control of robotic systems
[RR-480] 09 p3830 N94-31500
Two models solving the increasing energy problem of the continuous Hopfield network model
[REPT-93-87] 09 p3843 N94-31552
A neural network model for the visual perception of the depth of a scene from stereoscopy and shading
[ISBN-0-315-86753-1] 09 p3831 N94-31750
The vision machines
[NASA-TM-109757] 09 p3806 N94-31816
Universal approximation in p-mean by neural networks
[W-9320] 09 p3832 N94-31821
Analysis and design of a formal neural network for filtering a dynamic signal
[ISBN-0-315-86932-1] 09 p3832 N94-31873
Hierarchical mixtures of experts and the EM algorithm
[AD-A276516] 09 p3814 N94-31932
Neural networks for model-based recognition
[AD-A277375] 09 p3834 N94-32053
Exploring phase space concepts in the forecasting of time series with artificial neural networks
[DE94-005810] 09 p3834 N94-32127
On the relationship between generalization error, hypothesis complexity, and sample complexity for radial basis functions
[AD-A276802] 09 p3851 N94-32142
Neural network definitions of highly predictable protein secondary structure classes
[DE94-006234] 09 p3834 N94-32175
Undergraduate robotics projects in support of research on neural networks
[AD-A277331] 09 p3835 N94-32281
Neural models of spatial orientation in novel environments
[AD-A277383] 09 p3835 N94-32340
Fuzzy-neural control of an aircraft tracking camera platform 09 p3839 N94-32423
Empirical modeling for intelligent, real-time manufacture control 09 p3839 N94-32424
Neural network wavelet technology: A frontier of automation 09 p3839 N94-32425
Analysis and synthesis of adaptive neural elements and assembles
[AD-A277423] 09 p3836 N94-32996
Proceedings of the NIPS 1993 Postconference Workshop on Pulling It All Together: Methods for Combining Neural Networks
[AD-A277507] 09 p3836 N94-33014
Correlation filter synthesis using neural networks
[AD-A278124] 09 p3836 N94-33043
CRAD Signal and Information Processing Working Group Workshop on Neural networks, volume 1
[DREA-TC-93-305-VOL-1] 09 p3836 N94-33149
The application of a radial basis function neural network for radar tracking over the sea 09 p3686 N94-33150
Some neural computing approaches to target tracking
09 p3837 N94-33151
Neural networks applied to the phonemic segmentation of speech 09 p3686 N94-33152
Automatic modulation recognition
09 p3686 N94-33153
Multi-sensor data fusion for target acquisition
09 p3837 N94-33154
Periodic and chaotic signal generation in a recursive artificial neural network 09 p3686 N94-33155
Modular neural network architectures
09 p3838 N94-33156
Nearest-neighbour search in constant time: An alternative to neural networks for pattern matching applications 09 p3838 N94-33157
Numerical optimization techniques in neural network training 09 p3838 N94-33158
A neural network application to search and rescue satellite aided tracking (SARSAT)
09 p3613 N94-33345
Assembly of a neural analog computer, phase 2
[AD-A278192] 10 p4103 N94-33402
A Fortran based learning system using multilayer back-propagation neural network techniques
[AD-A278463] 10 p4112 N94-33542
On stochastic approximation algorithms for classes of PAC learning problems
[DE94-007417] 10 p4113 N94-33690
A self-organizing neural network architecture for auditory and speech perception with applications to acoustic and other temporal prediction problems
[AD-A277526] 10 p4095 N94-33708
Using neural networks as an event trigger in elementary particle physics experiments
[DE94-006316] 10 p4136 N94-33716
An analysis of stopping criteria in artificial neural networks
[AD-A278491] 10 p4113 N94-33755
Pattern analysis based models of masking by spatially separated sound sources
[AD-A277882] 10 p4095 N94-33779
The cognitive, perceptual, and neural bases of skilled performance
[AD-A277608] 10 p4097 N94-33849
Neural models of motion perception
[AD-A278362] 10 p4097 N94-33857
Seismic event interpretation using fuzzy logic and neural networks
[DE94-009469] 10 p4087 N94-33931
A neural/expert based client server architecture for MITE ITS
[AD-A278330] 10 p4113 N94-33968
Fuzzy logic, neural networks, and soft computing
10 p4127 N94-34048
Theoretical and experimental studies of auditory processing
[AD-A278505] 10 p4134 N94-34293
Identification of mechanical systems using probabilistic neural networks
[DE94-007555] 10 p4114 N94-34296
The study of optimal control with neural networks
10 p4115 N94-34316
A continuously tuned adaptive robust controller
10 p4115 N94-34317
Process control using neural networks
10 p4116 N94-34324
Application of neural networks in multiple sensor fusion for on-line tool wear monitoring
10 p4119 N94-34347
A real-time 2-D composite damage monitoring system employing neural network 10 p4074 N94-34355
A combined approach to buffet response analyses and fatigue life prediction 10 p4072 N94-34587
The 1994 Goddard Conference on Space Applications of Artificial Intelligence
[NASA-CP-3268] 10 p4122 N94-35043
Application of artificial neural networks in hydrological modeling: A case study of runoff simulation of a Himalayan glacier basin 10 p4125 N94-35061
An intelligent control system for failure detection and controller reconfiguration 10 p4126 N94-35066
Introduction to Neural Networks: Neural Network Workshop for the Hanford Community
[DE94-006526] 11 p4311 N94-35348
Genetic algorithms
[PB94-171048] 11 p4303 N94-35602
High-resolution subsurface imaging and neural network recognition
[DE94-009546] 11 p4290 N94-35666
Computer automation and artificial intelligence
[DE94-611058] 11 p4312 N94-35831
Neural network controller development for a magnetically suspended flywheel energy storage system
11 p4217 N94-35861
A comparison of artificial neural networks and statistical analyses
[DE94-010846] 11 p4312 N94-36195
Multidisciplinary studies of integrated neural network systems
[AD-A278774] 11 p4312 N94-36309
High energy
[DE94-009477] 11 p4331 N94-36428
Hardware implementation of a desktop supercomputer for high performance image processing
[AD-A280550] 12 p4489 N94-36731
Neural network for positioning Space Station solar arrays
[NASA-TM-106656] 12 p4431 N94-36943
Subgrouped real time recurrent learning neural networks
[AD-A280618] 12 p4500 N94-37043
Simple and efficient method of secondary vertex searching
[DE94-618542] 12 p4514 N94-37064
Feature and model selection in feedforward neural networks
[AD-A280709] 12 p4501 N94-37526
Open architecture controllers for advanced manufacturing
[DE94-007572] 12 p4496 N94-37782
Neurocontrol of a broadband (ATM) Clos' switching network
[PB94-179389] 12 p4441 N94-37851

NEUROBLASTS
Analysis of the Electrically Evoked Response (EER) of the cat . 07 p2908 N94-27519
NEUROLOGY
Transcranial Doppler ultrasound and the etiology of neurologic decompression sickness during altitude decompression 01 p0312 N94-11544
Development of the OMPAT neuropsychological/psychomotor performance evaluation and OMPAT data and timing support programs
[AD-A266954] 03 p1122 N94-15759
Localizing visual function in the brain
[AD-A267381] 03 p1133 N94-17020
Cortical substrate of haptic representation
[AD-A269583] 04 p1508 N94-18304
Strategies for enhancing catecholamine-mediated neurotransmission
[NASA-CR-193807] 04 p1506 N94-18862
Interdisciplinary training in life science (FY 1991 ASSERT)
[AD-A269220] 04 p1512 N94-18886
Incongruity, incongruity resolution, and mental states: The measure and modification of situational awareness and control
[NASA-CR-194568] 05 p1893 N94-20168
Relationship of area postrema to three putative measures of motion sickness 05 p1885 N94-21900
The effects of area postrema lesions and selective vagotomy on motion-induced conditioned taste aversion 05 p1888 N94-21910
Current status: Animal models of nausea 05 p1889 N94-21915
Muscular activity and its relationship to biomechanics and human performance 07 p2934 N94-28362
Monitor for status epilepticus seizures 08 p3397 N94-30460
Visual neural development and chromatic aberration
[AD-A277402] 09 p3800 N94-32345
Stress and brain protein synthesis
[PB94-170750] 11 p4296 N94-35601
Multidisciplinary studies of integrated neural network systems
[AD-A278774] 11 p4312 N94-36309
Cardiac pressure changes with venous gas embolism and decompression
[AD-A280412] 12 p4481 N94-37224
NEUROMUSCULAR TRANSMISSION
Synaptic plasticity and memory formation
[AD-A267988] 03 p1133 N94-17453
Positive chronotropic effect of mechanical stretch on the sinoatrial node: Roles of neurotransmitters and stretch activated channels 07 p2904 N94-27469
Interaction between endogenous opioid and Cholecystokinin (CCK) in modulating respiratory responses induced by thin-fiber muscular afferents 07 p2906 N94-27502
The value of electrical stimulation as an exercise training modality 07 p2936 N94-28372
The use of biomechanics in the study of movement in microgravity 07 p2936 N94-28373
NEURON TRANSMISSION
U BIOELECTRICITY
NEURONS
NT AXONS
NT NEUROBLASTS
Three-dimensional object recognition using an unsupervised BCM network: The usefulness of distinguishing features
[AD-A264576] 01 p0304 N94-11261
Role of spatially distributed ion channels in single neuron computation
[AD-A265972] 01 p0079 N94-12351
Locus coeruleus, vigilance, and stress: Brain mechanisms of adaptive behavioral responsiveness
[AD-A265657] 01 p0302 N94-12441
An analog clustering network from a biological model
[AD-A265637] 02 p0762 N94-12969
Neurotoxicity of hemoglobin in cortical cell culture
[AD-A266506] 03 p1128 N94-16786
Theoretical and experimental research into biological mechanisms underlying learning and memory
[AD-A267441] 03 p1133 N94-17022
Somatosensory responsiveness in behaving monkeys and human subjects
[AD-A268924] 04 p1501 N94-18231
Cortical substrate of haptic representation
[AD-A269583] 04 p1508 N94-18304
Intracellular physiology of the rat suprachiasmatic nucleus: Electrical properties, neurotransmission and effects of neuromodulators
[AD-A268829] 04 p1505 N94-18538
Operational parameters of an opto-electronic neural network employing fixed planar holographic interconnects
[DE93-018795] 04 p1433 N94-19000
The role of axon-Schwann cell interactions in nervous system ionic homeostasis
[AD-A270936] 05 p1890 N94-20045
Toward a neurobiological theory of visual attention
[AD-A270724] 05 p1890 N94-20112
Customizable VLSI artificial neural network chips based on a novel technology
[DE94-001418] 06 p2307 N94-23008
Cortical mechanisms of attention, discrimination, and motor response to somesthetic stimuli
[AD-A274163] 07 p2940 N94-27141
Distribution of GABA immunoreactive neurons in the brain of rolling mouse Nagoya and gamma-irradiated mouse 07 p2904 N94-27471
Effects of gamma ray radiation on the developing mouse cerebellum: Apoptotic cell death and induction of tissue transglutaminase 07 p2904 N94-27472
Development of Purkinje cells in vitro 07 p2905 N94-27483
Developmental expression of protein kinase C type 1 isozyme in suncus and rat cerebella 07 p2905 N94-27484
Synaptogenesis, selective stabilization, and free association
[AD-A275250] 08 p3392 N94-29431
A lateral inhibition neural network that emulates a winner-takes-all algorithm
[RUU-CS-92-46] 08 p3438 N94-30334
Towards simplicity: Noise and cooperation in the perfect integrator
[AD-A276256] 09 p3799 N94-31291
Two models solving the increasing energy problem of the continuous Hopfield network model
[REPT-93-87] 09 p3843 N94-31552
Empirical modeling for intelligent, real-time manufacture control 09 p3839 N94-32424
The organization of the suprachiasmatic circadian pacemaker of the rat and its regulation by neurotransmitters and modulators
[AD-A277324] 09 p3793 N94-32622
Models of the neuronal mechanisms of target localization of the barn owl
[AD-A277332] 09 p3797 N94-32623
Analysis and synthesis of adaptive neural elements and assembles
[AD-A277423] 09 p3836 N94-32996
Neostriatal neuronal activity and behavior
[AD-A278429] 09 p3802 N94-33333
Assembly of a neural analog computer, phase 2
[AD-A278192] 10 p4103 N94-33402
Research in VLSI system implementation of neuromorphic learning networks
[AD-A278247] 10 p4112 N94-33403
NEUROPHYSIOLOGY
Monitoring cognitive function and need with the automated neuropsychological assessment metrics in Decompression Sickness (DCS) research 01 p0314 N94-11533
Nonlinear resonance: Noise-assisted information processing in physical and neurophysiological systems
[AD-A265161] 01 p0313 N94-11890
NRL review for 1993
[AD-A265666] 01 p0497 N94-12334
The organization of the suprachiasmatic circadian pacemaker of the rat and its regulation by neurotransmitters and modulators
[AD-A266113] 01 p0301 N94-12417
Neurophysiological study on visuo-vestibular control of posture and movement in fish during adaptation to weightlessness 02 p0591 N94-13759
Feature discovery on segmented objects in SAR imagery using self-organizing neural networks
[DE93-010685] 02 p0686 N94-14056
The 12th Annual Carmel Conference, distinctiveness and Memory: Cognitive Psychophysiological and Physiological Considerations
[AD-A267181] 03 p1131 N94-15148
Cumulative effect of repeated brief cerebral ischemia
[AD-A267155] 03 p1121 N94-15736
Unipolar terminal-attractor based neural associative memory with adaptive threshold
[NASA-CASE-NPO-18790-1-CU] 03 p1165 N94-15958
Neurotoxicity of hemoglobin in cortical cell culture
[AD-A266506] 03 p1128 N94-16786
Cortical adaptive filtering in bioacoustic signal classification
[AD-A266229] 03 p1177 N94-16939
Localizing visual function in the brain
[AD-A267381] 03 p1133 N94-17020
Evaluation of putative neurochemical intermediaries in space/motion sickness
[NASA-CR-193607] 03 p1118 N94-17090
Neural basis of motion perception
[AD-A267267] 03 p1133 N94-17265
Localization of figure background segregation mechanisms in primate visual cortex
[PB93-187961] 04 p1508 N94-18121
Somatosensory responsiveness in behaving monkeys and human subjects
[AD-A268924] 04 p1501 N94-18231
Cortical substrate of haptic representation
[AD-A269583] 04 p1508 N94-18304
Intracellular physiology of the rat suprachiasmatic nucleus: Electrical properties, neurotransmission and effects of neuromodulators
[AD-A268829] 04 p1505 N94-18538
Strategies for enhancing catecholamine-mediated neurotransmission
[NASA-CR-193807] 04 p1506 N94-18862
The role of axon-Schwann cell interactions in nervous system ionic homeostasis
[AD-A270936] 05 p1890 N94-20045
Toward a neurobiological theory of visual attention
[AD-A270724] 05 p1890 N94-20112
Gamma-aminobutyric acid (GABA) and neuropeptides in neural areas mediating motion-induced emesis 05 p1886 N94-21902
Electrophysiology of the rat nucleus accumbens: Local circuitry, neuromodulation and synaptic plasticity
[PB93-232254] 06 p2420 N94-23454
Top down influences on bottom-up processing
[AD-A274220] 07 p2939 N94-27072
Cortical mechanisms of attention, discrimination, and motor response to somesthetic stimuli
[AD-A274163] 07 p2940 N94-27141
Visit to CERMA: Centre d'Etudes et de Recherches de Medecine Aerospatiale, Centre for Studies and Research in Aviation and Space Medicine, Bretigny sur Orge, France, November 16-18, 1992
[PB94-132990] 07 p2937 N94-28392
Models of the neuronal mechanisms of target localization of the barn owl
[AD-A277332] 09 p3797 N94-32623
Analysis and synthesis of adaptive neural elements and assembles
[AD-A277423] 09 p3836 N94-32996
Neostriatal neuronal activity and behavior
[AD-A278429] 09 p3802 N94-33333
US experiment flown on the Soviet biosatellite Cosmos 1667
[NASA-TM-108803] 10 p4102 N94-34951
Proceedings of SPIE: The International Society for Optical Engineering, Computational Vision Based on Neurobiology, volume 2054
[AD-A278731] 12 p4523 N94-36468
Cerebral neurochemical mechanisms in stress and anxiety
[AD-A280473] 12 p4482 N94-37233
Investigation of exposure to Extremely Low Frequency (ELF) magnetic and electric fields: Ongoing animals studies
[DE94-011239] 12 p4480 N94-37625
NEUROSCIENCE
U NEUROLOGY
NEUROSPORA
A circadian rhythm of conidiation in Neurospora crassa (L-12) 02 p0593 N94-13769
NEUROTRANSMITTERS
The organization of the suprachiasmatic circadian pacemaker of the rat and its regulation by neurotransmitters and modulators
[AD-A266113] 01 p0301 N94-12417
Synaptic plasticity and memory formation
[AD-A267988] 03 p1133 N94-17453
Intracellular physiology of the rat suprachiasmatic nucleus: Electrical properties, neurotransmission and effects of neuromodulators
[AD-A268829] 04 p1505 N94-18538
Strategies for enhancing catecholamine-mediated neurotransmission
[NASA-CR-193807] 04 p1506 N94-18862
The role of axon-Schwann cell interactions in nervous system ionic homeostasis
[AD-A270936] 05 p1890 N94-20045
Gamma-aminobutyric acid (GABA) and neuropeptides in neural areas mediating motion-induced emesis 05 p1886 N94-21902
Immunocytochemical localization of glutamic acid decarboxylase (GAD) and substance P in neural areas mediating motion-induced emesis: Effects of vagal stimulation on GAD immunoreactivity 05 p1887 N94-21909
Electrophysiology of the rat nucleus accumbens: Local circuitry, neuromodulation and synaptic plasticity
[PB93-232254] 06 p2420 N94-23454
Annals of the Research Inst. of Environmental Medicine, Nagoya Univ., volume 44
[REPT-44-VOL-44] 07 p2911 N94-27442

Distribution of GABA immunoreactive neurons in the brain of rolling mouse Nagoya and gamma-irradiated mouse
07 p2904 N94-27471
The ionic mechanism underlying the negative chronotropic effect of acetylcholine: Experimental study in rabbit single sinoatrial node cells
07 p2908 N94-27514
The ionic mechanism underlying the negative chronotropic effect of acetylcholine: Experiments using small sinoatrial node tissue preparations isolated from rabbit hearts
07 p2908 N94-27515
The ionic mechanism underlying the negative chronotropic effect of acetylcholine: Postganglionic vagal stimulation in isolated rabbit hearts
07 p2908 N94-27516
Postnatal changes in the autonomic modulation of L-type Ca(exp 2+) currents of rabbit ventricular cells
07 p2931 N94-27535
Desensitization to acethylcholine in pacemaker cells of the sinoatrial node
07 p2908 N94-27537
The role of beta-adrenoceptor stimulation in the progression of chronic heart failure
07 p2932 N94-27541
The organization of the suprachiasmatic circadian pacemaker of the rat and its regulation by neurotransmitters and modulators
[AD-A277324] 09 p3793 N94-32622
Cerebral neurochemical mechanisms in stress and anxiety
[AD-A280473] 12 p4482 N94-37233

NEUTRAL ATMOSPHERES
Modeling of the coupled magnetospheric and neutral wind dynamos
[NASA-CR-194728] 05 p1856 N94-20537
Upper atmosphere neutral and plasma density modeling
[AD-A274768] 07 p2879 N94-26569
Modeling of the coupled magnetospheric and neutral wind dynamos
[NASA-CR-195273] 07 p2883 N94-27852
The Pluto fast flyby mission: Completing the reconnaissance of the solar system
08 p3235 N94-29768

NEUTRAL ATOMS
Imaging of magnetospheric dynamics using low energy neutral atom detection
[DE93-012656] 01 p0275 N94-10742
Low energy neutral atom imaging techniques
[DE93-012744] 02 p0779 N94-12950
Advances in low energy neutral atom imaging techniques
[DE93-012745] 02 p0782 N94-13492
Energetic neutral atoms: Imaging the magnetospheric ring current
[NASA-CR-194339] 02 p0715 N94-13826
Terrestrial magnetospheric imaging: Numerical modeling of low energy neutral atoms
[DE93-014561] 02 p0717 N94-14328
Kinetics of photodeposition of superconducting films
[DE93-015511] 02 p0812 N94-14348
Uncertainty limited atomic position measurement using optical fields
[AD-A271013] 05 p1970 N94-19822
Cooling and trapping of neutral atoms
[AD-A276957] 09 p3870 N94-32360

NEUTRAL BEAMS
NT MOLECULAR BEAMS
NT NEUTRON BEAMS
A PC-PCL-based control system for the high-voltage pulsed-power operation of the Intense Diagnostic Neutral Beam (IDNB) Experiment
[DE93-014144] 02 p0797 N94-13100
High beta and confinement studies of TFTR
[DE93-016204] 03 p1202 N94-16446
Active neutral particle diagnostics for high temperature plasma
[DE93-788457] 04 p1586 N94-18214
Fast ion behavior during neutral beam injection in ATF
[DE93-040267] 05 p1992 N94-20058
IPP Prague Contributions to the IAEA Technical Committee Meeting on Research Using Small Tokamaks
[IPPCZ-329] 06 p2551 N94-24293
Investigation of the heat handling capabilities of DIII-D neutral beamline internal components
[DE94-001107] 06 p2553 N94-24756
Heavy neutral beam probe for edge plasma analysis in tokamaks
[DE94-003391] 07 p3041 N94-25846
New conditioning procedure derived from operating experience with the Common Long-Pulse Ion Source
[DE94-002891] 07 p3045 N94-26865
High gas-efficiency hydrogen negative ion sources
[PB93-232163] 07 p3025 N94-27348
Shine through measurements with hydrogen beam in JT-60
[DE94-701113] 07 p3047 N94-27899
Laser blow-off lithium beam probing with high temporal resolution for edge plasma diagnostics
[DE94-701176] 07 p2820 N94-27701
Experimental survey of the L-H transition conditions in the D3-D tokamak
[DE94-007428] 09 p3891 N94-32595
Heating experiments using neutral beams with variable injection angle and ICRF waves in CHS
[DE94-718982] 11 p4337 N94-35936
Feasibility study for a novel pulsed neutral beam diagnostics for tokamaks
[DE94-617129] 11 p4339 N94-36417

NEUTRAL BUOYANCY SIMULATION
Propellant management in surface tension tanks
01 p0106 N94-10110
Structural assembly demonstration experiment, phase 1
[NASA-CR-193967] 11 p4212 N94-35484

NEUTRAL CURRENTS
Future high precision experiments and new physics beyond Standard Model
[DE93-011004] 01 p0373 N94-11618
The electric field of a current-carrying conductor
[DE93-626637] 02 p0617 N94-14892
Neutral-current detection in the Sudbury Neutrino Observatory
[DE93-014481] 03 p1185 N94-16951
Weak neutral currents and collapse initiated supernova
[DE93-018652] 04 p1627 N94-19284
Flavor changing neutral currents in SU(3) x U(1) models
[DE94-602576] 07 p3022 N94-26899
First observation of neutral current proton electron scattering at the square root of s = 300 GeV
[DE94-701107] 07 p3030 N94-27877

NEUTRAL GASES
The distance to the high velocity clouds of neutral hydrogen
[NASA-CR-194343] 02 p0838 N94-13716
Physics of gas breakdown for ion beam transport in gas
[DE93-015646] 02 p0801 N94-14349
Radiative divertor modeling studies
[DE93-018092] 04 p1590 N94-19290
Design aspects and parametric characterisation of a neutral rare gas laser
[AD-A271100] 05 p1814 N94-19850
Electronically metastable molecules of high symmetry
[AD-A272015] 05 p1974 N94-21461
The manifestations of energetic activity in the galactic center
09 p3937 N94-32028
A role of neutral hydrogen in CHS plasmas with reheat and collapse and comparison with JIPPT-IIU tokamak plasmas
[DE94-718985] 12 p4530 N94-37384

NEUTRAL PARTICLES
NT COLD NEUTRONS
NT FAST NEUTRONS
NT NEUTRONS
NT SOLAR NEUTRONS
NT THERMAL NEUTRONS
Influence of neutral particles concentration on flame propagation in methane-air mixtures at zero and normal gravity conditions
01 p0121 N94-10224
Neutral strange particle production at the AGS
[DE93-014044] 02 p0780 N94-13098
Measurement of H zero excited states produced by foil stripping of 800-MeV H(-) ions
[DE93-014391] 02 p0788 N94-13103
Advances in low energy neutral atom imaging techniques
[DE93-012745] 02 p0782 N94-13492
Hybrid S(sub N)/Monte Carlo research and results
[DE93-012677] 02 p0773 N94-14178
Terrestrial magnetospheric imaging: Numerical modeling of low energy neutral atoms
[DE93-014561] 02 p0717 N94-14328
Linear characteristic spatial quadrature for discrete ordinates neutral particle transport on arbitrary triangles
[AD-A267485] 03 p1185 N94-17365
Active neutral particle diagnostics for high temperature plasma
[DE93-788457] 04 p1586 N94-18214
Exponential characteristic spatial quadrature for discrete ordinates neutral particle transport in two-dimensional cartesian coordinates
[AD-A270458] 04 p1554 N94-19671
Secondary particle in background levels and effects on detectors at future hadron colliders
[DE94-003378] 07 p3011 N94-25598
Two dimensional self-consistent fluid simulation of RF inductive sources
[DE94-003635] 07 p2767 N94-25937
Monoenergetic neutral particle transport in semi-infinite media
[AD-A277155] 09 p3870 N94-32368
A combined experimental and theoretical study of the neutral, cationic and anionic Si3N cluster molecule
[AD-A278834] 11 p4323 N94-35792
About existence of a baryon with the 3.52 GeV/c2 mass
[DE94-621641] 12 p4519 N94-37414

NEUTRALIZERS
An analytical study of the vibration of beams fitted with neutralizers. Part 2: Assessment of the effects of mounting configurations
[ISVR-TR-225-PT-2] 09 p3740 N94-32982
An analytical study of the vibration of beams fitted with neutralizers. Part 1: Assessment of the effects of neutralizer design parameters
[ISVR-TR-224-PT-1] 10 p4070 N94-34304

NEUTRINO BEAMS
High energy physics at Tufts University
[DE93-018299] 04 p1575 N94-19023
Accelerator-based neutrino oscillation searches
[DE94-000818] 06 p2626 N94-23515

NEUTRINOS
NT SOLAR NEUTRINOS
The effect of a scalar boson coupled to neutrinos on the behavior of the tritium beta decay spectrum near the end point
[DE93-012655] 01 p0361 N94-10349
On parity conservation and the question of the missing, right-handed neutrino
[DE93-613092] 01 p0361 N94-10414
Planck scale effects on the Majoron
[DE93-613120] 01 p0410 N94-10545
Tau physics
[DE93-010956] 01 p0367 N94-11469
Charged scalar particles and (tau) leptonic decay
[DE93-622969] 02 p0779 N94-12882
A program of correlated observations using the EGRET instrument on GRO and the IMB neutrino detector
[NASA-CR-194367] 02 p0783 N94-13856
Are there atmospheric neutrino oscillations?
[DE93-015550] 02 p0783 N94-13890
Angular correlations in neutron beta decay
[DE93-014349] 02 p0785 N94-14466
On the 17-keV neutrino
[DE93-012638] 03 p1181 N94-15974
Possible dust contamination of the early solar system
03 p1244 N94-16352
Contained (nu) events observed in Soudan 2
[DE93-015548] 03 p1300 N94-17233
Neutrino masses in superstring derived standard-like models
[DE93-624802] 04 p1565 N94-17951
Neutrino mass
[DE93-018467] 04 p1567 N94-18269
Inverse neutrinoless double (beta)-decay at the NLC?
[DE93-017397] 04 p1568 N94-18825
Investigation of physical structures and interactions at high energy
[DE93-014444] 04 p1574 N94-18927
Weak neutral currents and collapse initiated supernova
[DE93-018652] 04 p1627 N94-19284
CERN-derived analysis of lunar radiation backgrounds
05 p2080 N94-20880
A Monte Carlo study of the Sudbury Neutrino Observatory small test detector experiment
[ISBN-0-315-59056-4] 05 p1977 N94-22416
Neutrino emission processes in dense high-temperature plasmas
05 p2001 N94-22638
Pions and neutrinos as probes of the nucleon and nuclear few-body system
[DE93-040127] 06 p2531 N94-22928
Accelerator-based neutrino oscillation searches
[DE94-000818] 06 p2626 N94-23515
Kamiokande results on solar neutrinos and a supernova search
[ICRR-REPT-294-93-6] 06 p2627 N94-24961
A research program in experimental and theoretical high energy physics
[DE94-002156] 07 p3031 N94-25931
Theoretical and experimental studies of elementary physics
[DE94-002310] 07 p3008 N94-25988
Separation and reconstruction of electron neutrino interaction in the IHEP-JINR neutrino detector and BARS detector
[DE93-634182] 07 p3019 N94-26393
Physical characteristics of polymethylmethacrylate scintillator SOFG-120
[DE93-634184] 07 p2810 N94-26395
About possible types of neutrino oscillations
[DE93-634449] 07 p3020 N94-26508

Constraints on singlet right-handed neutrinos coming from the Z(0)-width
[DE93-634393] 07 p3022 N94-26766
An analysis of monojet data in p(bar-p) collisions at square root of s equal to 1.8 TEV
[DE94-001822] 07 p3026 N94-27565
Cosmological constraints on very heavy stable neutrinos
[DE94-601669] 07 p3117 N94-28066
Emission of supersymmetric neutron pair by charged lepton in magnetic field
[DE93-634365] 08 p3481 N94-28468
Properties of W + jet events in proton-antiproton collisions at 1.8 TeV
[DE94-004002] 08 p3482 N94-28524
Proceedings of the workshop on quark and lepton mass matrices
[DE94-707692] 08 p3485 N94-28624
A Tevatron collider beauty factory
[DE94-004879] 08 p3488 N94-29930
On possibility to create the scintillation trigger for liquid-argon neutrino detector
[DE94-607844] 08 p3489 N94-30050
Search for heavy neutrinos at the IHEP-JINR neutrino detector
[DE94-608175] 08 p3489 N94-30095
Research in elementary particle physics
[DE94-001657] 08 p3491 N94-30762
Probing lepton number violation via Majorana neutrinos at hadron supercolliders
[PB94-147055] 09 p3868 N94-31922
Convection in Type 2 supernovae
[DE94-009373] 09 p3938 N94-32914
A search for radiative neutrino decay from supernovae
[NASA-CR-196011] 11 p4376 N94-35515
Limitation on the magnetic dipole moment of the reactor neutrino
[DE94-611171] 11 p4320 N94-35566
Radiatively induced electron and electron-neutrino masses
[DE94-616775] 11 p4321 N94-35582
Nonadiabatic neutrino oscillations revisited
[DE94-616649] 11 p4321 N94-35593
Some consequences in weak processes of three generations mixing in the leptonic sector
[DE94-616650] 11 p4321 N94-35594
Collective plasma corrections to the solar opacity
[PB94-170511] 11 p4375 N94-36210
Five-lepton decay modes of muon and tau mesons
[DE94-621636] 12 p4516 N94-37099
Neutrino-nucleon scattering
[DE94-011720] 12 p4520 N94-37671

NEUTRON ABSORBERS
Generation of neutronic thermal data in support of space nuclear propulsion
[DE93-013148] 02 p0549 N94-13034
Experiment of neutron multiplication in beryllium
[DE94-604605] 07 p2742 N94-27730
Irradiation-assisted stress corrosion cracking of materials from commercial BWRs: Role of grain-boundary microchemistry
[DE94-006542] 09 p3643 N94-32109

NEUTRON ACTIVATION ANALYSIS
Fine-powder Al2O3 and SiO2 for preparation of multielement standards for rare-earth elements analysis
[DE93-625118] 02 p0567 N94-14884
INAA of CAIs from the Maralinga CK4 chondrite: Effects of parent body thermal metamorphism
03 p1244 N94-16355
Development and evaluation of alternative radioanalytical methods, including mass spectrometry for marine materials
[DE93-625117] 04 p1345 N94-17691
Study on neutron activation analysis
[DE93-632191] 07 p3017 N94-26116

NEUTRON BEAMS
Possibility of a crossed-beam experiment involving slow-neutron capture by unstable nuclei rapid-process-tron
[DE93-754288] 01 p0363 N94-10720
Measurement of the Fe-56(n,p)Mn-56, Al-27(n,p)Mg-27 and Al-27(n,alpha)Na-24 cross sections at 16.0, 17.0 and 18.3 MeV
[NPL-RSA(EXT)-38] 02 p0783 N94-13883
Multiplicity spectrometry on neutron filtered beams
[DE93-617529] 02 p0790 N94-14843
On radiation defects in strip detectors
[DE93-616646] 07 p3015 N94-25916
Neutron reflection interferometry
[DE94-601876] 07 p2714 N94-26170
Neutron-neutron scattering: Possibility of in-beam experiment
[DE94-606459] 07 p3027 N94-27682
The use of pulsed neutron diffraction to measure strain in composites
[DE94-007536] 10 p4019 N94-33693
Physics with primary beams of the KEK-PS
[DE94-748635] 12 p4522 N94-37234

NEUTRON COUNTERS
NT NEUTRON SPECTROMETERS
Preliminary results from bubble detector measurements aboard Biocosmos-2044 03 p0981 N94-16097
Neutral-current detection in the Sudbury Neutrino Observatory
[DE93-014481] 03 p1185 N94-16951
Heavy ion nuclear physics research
[DE93-018862] 04 p1565 N94-17776
LAHET calculations for accelerator neutron production
[DE93-016518] 04 p1570 N94-19120
Thermal neutron multiplicity measurements using the pyrochemical multiplicity counter at Lawrence Livermore National Laboratory
[DE93-018538] 04 p1571 N94-19278
Experimental characterization of the AFIT Neutron Facility
[AD-A273822] 06 p2539 N94-25519
Surface physics with cold and thermal neutron reflectometry
[DE94-001447] 07 p2733 N94-26070
Performance of a 14-MeV neutron generator as an in situ calibration source for TFTR
[DE94-004993] 07 p3048 N94-27825
Preliminary detector design ST862-prototype neutron detector
[DE94-004714] 08 p3491 N94-30695
Neutron measurements at the commercial aircraft altitudes
[ISBN-0-315-86201-7] 09 p3955 N94-31709
Resistivity measurements on the neutron irradiated detector grade silicon materials
[DE94-009083] 09 p3906 N94-32822
Neutron detectors for fusion reaction-rate measurements
[DE94-010407] 11 p4330 N94-36114
Stopping power of charged particles from 10 eV/amu to 10 GeV/amu
[DE94-719024] 12 p4518 N94-37387

NEUTRON CROSS SECTIONS
Criticality benchmark comparisons leading to cross-section upgrades
[DE93-017184] 04 p1556 N94-18073
Computer codes for checking, plotting and processing of neutron cross-section covariance data and their application
[DE93-018459] 04 p1570 N94-19129

NEUTRON DECAY
Angular correlations in neutron beta decay
[DE93-014349] 02 p0785 N94-14466
Radiations from hot nuclei 07 p3030 N94-27915

NEUTRON DETECTORS
U NEUTRON COUNTERS

NEUTRON DIFFRACTION
Symmetry lowering in crystalline solid solutions: A study of cinnamamide-thienylacrylamide by x ray and neutron diffraction and solid-state photochemistry
[DE93-010871] 01 p0394 N94-10301
Rietveld refinement of magnetic structures from pulsed-neutron-source powder-diffraction data
[DE93-012740] 01 p0363 N94-10743
Measurement of residual strain in composites by means of time-of-flight neutron diffraction
[DE93-012939] 02 p0555 N94-13248
Quasi-elastic neutron scattering studies of protein dynamics
[DE93-015074] 02 p0782 N94-13414
Measurement of strain in individual phases of composites before, during, and after mechanical loading
[DE93-014585] 02 p0558 N94-14119
Workshop on Formation of Supermolecular Structures in Composite Fluid: Phase Rule and Dynamics
[DE93-782887] 02 p0581 N94-14421
Roles of oxygen defects in copper-oxide superconductors
[DE93-014875] 03 p1208 N94-15982
Thermal stress effects in intermetallic matrix composites
[NASA-CR-191191] 03 p1054 N94-16518
Phase separation and ordering process in Al-Li alloys studied by small-angle neutron scattering and neutron diffraction
[DE93-016750] 04 p1358 N94-17947
Performance of the Amorphous Materials Diffractometer GLAD at IPNS
[DE93-017746] 04 p1430 N94-18481
Neutron and PIMC determination of the longitudinal momentum distribution of HCP, BCC and normal liquid He-4
[DE93-019009] 05 p1972 N94-20187
Neutron-scattering studies of Yb-bearing silicate glasses
[DE93-019768] 05 p1700 N94-20265
Non-Fermi-liquid and multichannel Kondo phenomena in Y(1-x)U(x)Pd3 and related alloys
[DE93-040135] 05 p2015 N94-20275
The structure and spin dynamics of lanthanide-bearing silicate glasses
[DE94-001320] 06 p2252 N94-22992
Dual-purpose RTOF diffractometer facility at the ET-RR-1 reactor
[VTT-TIED-1425] 06 p2566 N94-25347
Debye-Waller factors of the light actinide metals
[DE94-000685] 07 p2733 N94-26069
Neutrons in biology
[DE94-701085] 07 p2903 N94-27862
Hysteresis phenomena at spin-flop transition induced by the pulsed magnetic field
[DE94-606851] 08 p3511 N94-28626
Synthesis and neutron diffraction study of Na3WN3 and Na3MoN3
[AD-A275158] 08 p3203 N94-29043
Adsorption of water to the metal/polymer interface studied by neutron and x ray reflectivity
[DE94-005578] 09 p3651 N94-31649
Structural ordering in liquid K-Te alloys
[DE94-008477] 09 p3645 N94-32514
Extended-range order in glasses
[DE94-008135] 09 p3661 N94-32798
The use of pulsed neutron diffraction to measure strain in composites
[DE94-007536] 10 p4019 N94-33693
Structural investigations of 1-ethyl-3-methylimidazolium hydrogen dichloride: Neutron diffraction studies of an ambient-temperature molten salt
[DE94-009680] 11 p4237 N94-35777
Neutron diffraction study of aluminum chloride imidazolium chloride molten salts
[DE94-009679] 11 p4239 N94-36349
Structural ground-state of La2CuO4 in the LTO phase: Evidence of local disorder
[DE94-013126] 12 p4536 N94-37291

NEUTRON DISTRIBUTION
Thermal neutron multiplicity measurements using the pyrochemical multiplicity counter at Lawrence Livermore National Laboratory
[DE93-018538] 04 p1571 N94-19278
Experiment of neutron multiplication in beryllium
[DE94-604605] 07 p2742 N94-27730
Two-dimensional over-all neutronics analysis of the ITER device
[DE94-718963] 12 p4530 N94-37464

NEUTRON EMISSION
The LAHET code system: Introduction, development, and benchmarking
[DE93-012657] 02 p0787 N94-14804
Radiations from hot nuclei 07 p3030 N94-27915
Control heavy ion collisions in the systems Ar-40 + Ca-40 and Si-28 + Si-28, and the nature of particle emission in fusion-evaporation reactions
[ETN-94-95749] 09 p3866 N94-31614
Search for neutrons from deuterated palladium subject to high electrical currents
[DE94-009342] 10 p4139 N94-33907
Hot-ion plasma in the quadrupole trap
[DE94-617216] 11 p4337 N94-36082
D-D fusion experiments using fast z-pinches
[DE94-010090] 12 p4526 N94-36448

NEUTRON FLUX
U FLUX (RATE)

NEUTRON FLUX DENSITY
Neutron-neutron scattering: Possibility of in-beam experiment
[DE94-606459] 07 p3027 N94-27682

NEUTRON IRRADIATION
Szilard-Chalmers effect in solid HIO4.2H2O by neutron irradiation
[DE93-617173] 01 p0397 N94-10830
Facility for stress corrosion cracking test of irradiated material in high temperature water
[DE93-753189] 01 p0084 N94-11593
AlGaAs diode laser blue shift resulting from fast neutron irradiation
[AD-A266642] 02 p0659 N94-14681
Investigations of low-temperature neutron embrittlement of ferritic steels
[DE93-015460] 02 p0573 N94-14700
The effect of irradiation on the mechanical properties of 6061-T651 aluminum
[DE93-015825] 03 p0958 N94-16168
Charpy impact toughness of martensitic steels irradiated in FFTF: Effect of heat treatment
[DE93-015960] 04 p1450 N94-17848
Effects of irradiation temperature on embrittlement of nuclear pressure vessel steels
[DE93-015428] 04 p1359 N94-18245
Evaluation of fiber optic performance in the ACRR
[DE93-018515] 04 p1580 N94-18970

High dose effects in neutron irradiated face-centered cubic metals
[DE93-017671] 04 p1364 N94-19043
AGB stars as a source of short-lived radioactive nuclei in the solar nebula 05 p2133 N94-20859
Tensile and shear fracture behavior of fiber reinforced plastics at 77K irradiated by various radiation sources
[DE93-040280] 05 p1706 N94-21542
Issues related to mechanical properties of neutron-irradiated ceramics
[DE93-040262] 05 p1707 N94-21560
Microstructural evolution of neutron-irradiated Fe-Cr-Ni ternary alloys at high helium generation rates
[DE93-018786] 05 p1696 N94-22037
Effects of neutron irradiation and hydrogen on ductile-brittle transition temperatures of V-Cr-Ti alloys
[DE94-001466] 06 p2240 N94-23009
Development of small punch testing technique and its application to evaluation of mechanical properties degradation
[DE94-001193] 06 p2375 N94-23184
Effect of neutron irradiation on tensile properties of V-Cr-Ti alloys
[DE94-001433] 06 p2240 N94-23194
Radiation hardening effects on localized deformation and stress corrosion cracking of stainless steels
[DE94-004308] 07 p2731 N94-25804
Temperature dependence of static RAM volatility
[DE93-040345] 07 p2948 N94-26111
Microstructural development in irradiated vanadium alloys
[DE94-004307] 07 p2737 N94-26556
Geological Dating by Ar-40 - Ar-39 method
[DE94-601975] 07 p2880 N94-26874
Relationship between swelling and irradiation creep in cold-worked PCA stainless steel irradiated to approximately 178 dpa at approximately 400 C
[DE94-004368] 08 p3201 N94-28456
Radiation effects in beryllium used for plasma protection
[DE94-004599] 08 p3201 N94-28460
Irradiation-induced structure and property changes in tokamak plasma-facing, carbon-carbon composites
[DE94-006046] 08 p3508 N94-30365
Effect of irradiation damage and helium on the swelling and structure of vanadium-base alloys
[DE94-006540] 09 p3641 N94-31666
Defect cascades produced by neutron irradiation in YBa2Cu3O(7-delta) superconductors
[DE94-007700] 09 p3903 N94-32372
Resistivity measurements on the neutron irradiated detector grade silicon materials
[DE94-009083] 09 p3906 N94-32822
Development of high temperature property database for Alloy 800H
[DE94-727589] 10 p4024 N94-33870
Determination of the Fermi level position for neutron irradiated high resistivity silicon detectors and materials using the Transient Charge Technique (TChT)
[DE94-009107] 11 p4260 N94-36221
Study of point defect mobilities in zirconium during electron irradiation in a HVEM
[DE94-619028] 11 p4242 N94-36289
Modelling irradiation creep of zirconium alloys
[DE94-619055] 12 p4414 N94-36544
Irradiation assisted stress corrosion cracking of HTH Alloy X-750 and Alloy 625
[DE94-012667] 12 p4416 N94-37080
Characterization of mechanical properties degradation using small punch testing technique
[DE94-011202] 12 p4418 N94-37410
Characterization of nuclear transmutations in materials irradiated test facilities
[DE94-013309] 12 p4420 N94-37552

NEUTRON PHYSICS

An overview of the current status of resonance theory in reactor physics applications
[DE94-010465] 12 p4521 N94-37194

NEUTRON RADIOGRAPHY

Practical neutron training course: Course notes
[PB94-145158] 09 p3867 N94-31681

NEUTRON SCATTERING

Rietveld refinement of magnetic structures from pulsed-neutron-source powder-diffraction data
[DE93-012740] 01 p0363 N94-10743
The searchlight problem for neutrons in a semi-infinite medium
[DE93-010796] 01 p0365 N94-10952
Energy transfer dynamics and impact sensitivity
[DE93-009551] 01 p0098 N94-11269
X-ray and neutron scattering studies of magnetic critical fluctuations in holmium
[DE93-010873] 01 p0400 N94-11467
Generation of neutronic thermal data in support of space nuclear propulsion
[DE93-013148] 02 p0549 N94-13034
Quasi-elastic neutron scattering studies of protein dynamics
[DE93-015074] 02 p0782 N94-13414
The use of polarised neutron reflection for unique density profile determination in thin films
[PB93-187136] 02 p0579 N94-13783
Workshop on Formation of Supermolecular Structures in Composite Fluid: Phase Rule and Dynamics
[DE93-782887] 02 p0581 N94-14421
Small-angle scattering, contrast variation and the study of complex composite materials: A study of the structure of carbon black
[DE93-012707] 02 p0559 N94-14690
Multiple process simulations for correction factor calculations in experiments with neutrons. LUSMK program
[DE93-623957] 03 p1179 N94-14932
Structural investigation of electrochemically etched silicon
[DE93-015300] 03 p1207 N94-15827
Neutron and x ray scattering studies of (FeF2)(sub m)(CoF2)(sub n) multilayers
[DE93-015809] 03 p1184 N94-16838
Polaron tunneling in high-temperature superconductors
[DE93-016880] 04 p1593 N94-17754
Phase transitions and neutron scattering
[DE93-016748] 04 p1594 N94-17866
Phase separation and ordering process in Al-Li alloys studied by small-angle neutron scattering and neutron diffraction
[DE93-016750] 04 p1358 N94-17947
The use of chopper spectrometers for cold-to-epithermal neutron scattering at IPNS
[DE93-017798] 04 p1598 N94-18531
T violating neutron spin rotation asymmetry
[DE93-018470] 04 p1570 N94-19126
Neutron and PIMC determination of the longitudinal momentum distribution of HCP, BCC and normal liquid He-4
[DE93-019009] 05 p1972 N94-20187
Non-Fermi-liquid and multichannel Kondo phenomena in Y(1-x)U(x)Pd3 and related alloys
[DE93-040135] 05 p2015 N94-20275
Spectroscopic studies of magnetic transitions in TbPO4
[DE94-001274] 05 p2035 N94-22565
Inelastic neutron scattering of (gamma)-iron, and the determination of the elastic constants by lattice dynamics
[DE94-000694] 05 p1978 N94-22573
Spin-hole doping in the Kondo insulator Ce3Bi4Pt3 studied by neutron scattering
[DE93-040107] 06 p2557 N94-22925
The structure and spin dynamics of lanthanide-bearing silicate glasses
[DE94-001320] 06 p2252 N94-22992
Microscopic dynamics in dense helium-neon mixtures: Neutron scattering, kinetic theory and computer simulations
[ISBN-9-07-386105-5] 06 p2537 N94-25228
Lattice dynamics of Ba(1-x)K(x)BiO3 as studied by neutron scattering and computer simulation
[DE93-617053] 06 p2567 N94-25424
Crystal field in Nd2CuO4
[DE93-617054] 06 p2567 N94-25425
The Haldane energy gap of a doped linear-chain Heisenberg antiferromagnet
[DE93-617130] 06 p2567 N94-25426
Morphological analysis of ionomers
[DE94-003660] 07 p2749 N94-26005
Neutron reflection interferometry
[DE94-601876] 07 p2714 N94-26170
Neutrons in biology
[DE94-701085] 07 p2903 N94-27862
Hysteresis phenomena at spin-flop transition induced by the pulsed magnetic field
[DE94-606851] 08 p3511 N94-28626
Double-crystal analyser system for the PRISMA spectrometer: Test of a prototype
[PB94-138245] 08 p3286 N94-29113
Incommensurate magnetic order in UNi2Al3
[DE94-005449] 08 p3209 N94-30246
Structure and dynamics of microemulsions in bulk, at interfaces, and in confined geometries
[DE94-006043] 09 p3633 N94-31526
Practical neutron training course: Course notes
[PB94-145158] 09 p3867 N94-31681
Multiple size scale structures in silica/siloxane composites studied by small-angle scattering
[DE94-007300] 09 p3625 N94-32642
Strongly anisotropic s-wave versus d-wave gap in cuprate superconductors: Evidence and theory
[DE94-007579] 09 p3904 N94-32746
Investigation of superconductivity and magnetism in d and f-electron materials
[DE94-008535] 09 p3907 N94-32933
Porosity in plasma sprayed alumina coatings
[DE94-008874] 10 p4028 N94-34011
The microstructure and morphology of carbon black: A study using small angle neutron scattering and contrast variation
[DE94-009315] 10 p4022 N94-34098
Relativistic three-particle dynamical equations. 2: Application to the trinucleon system
[DE94-616653] 11 p4320 N94-35580
The dynamics of hydrogen atoms dissolved in Zr Cr2 alloy
[DE94-618756] 12 p4520 N94-37652

NEUTRON SOURCES

Intense neutron sources for fusion materials studies
[DE93-009782] 01 p0391 N94-11171
Design for low beam loss in accelerators for intense neutron source applications
[DE93-014557] 02 p0789 N94-13327
Beam halo in high-intensity beams
[DE93-014565] 02 p0789 N94-13328
INGDB-90. The International Neutron Nuclear Data Base for geophysics applications
[DE93-624095] 02 p0827 N94-14880
Heavy ion nuclear physics research
[DE93-018862] 04 p1565 N94-17776
The use of chopper spectrometers for cold-to-epithermal neutron scattering at IPNS
[DE93-017798] 04 p1598 N94-18531
Generalized energy principle for flute perturbations in axisymmetric mirror machines
[DE93-019399] 04 p1589 N94-19037
LAHET calculations for accelerator neutron production
[DE93-016518] 04 p1570 N94-19120
Neutron and PIMC determination of the longitudinal momentum distribution of HCP, BCC and normal liquid He-4
[DE93-019009] 05 p1972 N94-20187
Toroidal plasma beta-FLR limit in a toroidally linked mirror system
[DE94-003119] 07 p3041 N94-25792
Surface physics with cold and thermal neutron reflectometry
[DE94-001447] 07 p2733 N94-26070
Atomic processes in Inertial Electrostatic Confinement (IEC) devices
[DE94-005015] 07 p3047 N94-27715
Performance of a 14-MeV neutron generator as an in situ calibration source for TFTR
[DE94-004993] 07 p3048 N94-27825
Double-crystal analyser system for the PRISMA spectrometer: Test of a prototype
[PB94-138245] 08 p3286 N94-29113
Neutronics of a D-Li neutron source: An overview
[DE94-005372] 08 p3493 N94-30893
Analysis of beam-on-target interaction in a neutron-source test facility
[DE94-005392] 09 p3863 N94-31151
H(-) injection simulation for a 5 MW spallation neutron source
[DE94-009003] 10 p4140 N94-33983
Time-of-flight diffraction at pulsed neutron sources: An introduction to the symposium
[DE94-010442] 11 p4327 N94-36225
D-D fusion experiments using fast z-pinches
[DE94-010090] 12 p4526 N94-36448
Inertial Electrostatic Confinement (IEC) devices
[DE94-013114] 12 p4529 N94-37316

NEUTRON SPECTRA

Analytic expression for epithermal neutron spectra amplitudes as a function of water content
01 p0473 N94-12227
Preliminary results from bubble detector measurements aboard Biocosmos-2044 03 p0981 N94-16097
LAHET calculations for accelerator neutron production
[DE93-016518] 04 p1570 N94-19120
Crystal field in Nd2CuO4
[DE93-617054] 06 p2567 N94-25425
Experimental characterization of the AFIT Neutron Facility
[AD-A273822] 06 p2539 N94-25519
A search for energetic ion directivity in large solar flares
[NASA-CR-196036] 11 p4374 N94-35993
User's manual for SNL-SAND-2 code
[DE94-011744] 12 p4496 N94-37673

NEUTRON SPECTROMETERS

The Los Alamos neutron spectrometer for the Lunar Scout-1 mission 01 p0172 N94-12038
Multiplicity spectrometry on neutron filtered beams
[DE93-617529] 02 p0790 N94-14843
Phase transitions and neutron scattering
[DE93-016748] 04 p1594 N94-17866

The use of chopper spectrometers for cold-to-epithermal neutron scattering at IPNS
[DE93-017798] 04 p1598 N94-18531
Double-crystal analyser system for the PRISMA spectrometer: Test of a prototype
[PB94-138245] 08 p3286 N94-29113
Experimental setups and methods to obtain new nuclear data at intermediate and high energies
[DE94-607850] 08 p3489 N94-30052

NEUTRON STARS
NT PULSARS
A photometric study of massive x-ray binaries
[ITN-93-85207] 02 p0829 N94-13231
Astronomy and astrophysics 03 p1239 N94-15970
Relativistic mean-field calculations of lambda and sigma hypernuclei
[DE93-015269] 03 p1181 N94-16013
Fast pulsars, compact stars, and the strange matter hypothesis
[DE93-015039] 03 p1239 N94-16052
Evolution of r-process elements in the hot supernova bubble
[DE93-017169] 04 p1624 N94-17897
Dark matter: Neutron star halo and the nature of gamma-bursts 05 p2002 N94-22643
Relativistically expanding pair plasmas as bursting sources of cosmic gamma rays 05 p2003 N94-22646
Gamma ray burst as a result of the explosive instability in the magnetosphere of old neutron star 05 p2007 N94-22675
Neutron star mergers and gamma-ray bursts
[NASA-CR-195176] 06 p2629 N94-25091
Dibaryon-induced instability of neutron stars
[DE93-634453] 07 p3103 N94-26046
TEV emission from close binaries
[DE93-634330] 07 p3104 N94-26268
Magnetic field induced contributions of supersymmetric particles to energy losses of neutron star
[DE93-634331] 07 p3104 N94-26269
Gamma ray bursts from the accretion of solid bodies onto high-velocity Galactic neutron stars
[DE94-005006] 07 p3117 N94-27827
Equation of state of neutron star matter, limiting rotational periods of fast pulsars, and the properties of strange stars
[DE94-005214] 08 p3542 N94-28480
On observing neutron star oscillations 08 p3538 N94-29795
Near-critical spherically symmetric accretion by neutron stars 08 p3546 N94-29991
Nonthermal accretion disk models around neutron stars 09 p3931 N94-31139
Reactive flows in compact objects 09 p3934 N94-31567
Structure and stability of spherical accretion flows onto compact objects 09 p3935 N94-31946
Hydrodynamics of neutron star interiors and laboratory superfluids 09 p3936 N94-31949
Binary-binary collisions involving main-sequence stars, white dwarfs and neutron stars in globular clusters
[DE94-005086] 10 p4163 N94-33415
Absolute limit on rotation of gravitationally bound stars
[DE94-011367] 12 p4548 N94-37049

NEUTRON TRANSMUTATION
U NUCLEAR REACTIONS

NEUTRONS
NT COLD NEUTRONS
NT FAST NEUTRONS
NT SOLAR NEUTRONS
NT THERMAL NEUTRONS
A spectral nodal method for the solution of the Sn equations in x, y geometry for highly absorbing deep penetration problems
[DE93-613520] 01 p0349 N94-10636
The searchlight problem for neutrons in a semi-infinite medium
[DE93-010796] 01 p0365 N94-10952
Development of deterministic transport methods for low energy neutrons for shielding in space
[NASA-CR-194172] 01 p0366 N94-11199
On the neutron EDM search in the Laue diffraction by the crystal without a centre of symmetry
[DE93-622971] 02 p0804 N94-12828
Workshop on Formation of Supermolecular Structures in Composite Fluid: Phase Rule and Dynamics
[DE93-782887] 02 p0581 N94-14421
Measuring parity violation using the neutron capture reaction
[DE93-016629] 02 p0786 N94-14514
The status of cold fusion
[DE93-012731] 02 p0802 N94-14567
Multiplicity spectrometry on neutron filtered beams
[DE93-617529] 02 p0790 N94-14843
INGDB-90. The International Neutron Nuclear Data Base for geophysics applications
[DE93-624095] 02 p0827 N94-14880
Multiple process simulations for correction factor calculations in experiments with neutrons. LUSMK program
[DE93-623957] 03 p1179 N94-14932
General order characteristic methods for solving neutron transport problems
[DE93-015824] 03 p1170 N94-16167
A calibration of the production rate ratio P-21/P-26 by low energy secondry neutrons: Identification of Ne spallation components at the 10(exp 6) atoms/g level in terrestrial samples 03 p1187 N94-16194
ARIES tokamak reactor study
[DE93-017059] 03 p1203 N94-16901
Energy-loss cross sections for inclusive charge-exchange reactions at intermediate energies
[NASA-TM-4522] 03 p1188 N94-17018
Heavy ion nuclear physics research
[DE93-018862] 04 p1565 N94-17776
Characteristics and pulsed radiation response of non-ideal quartz shock stress gauges
[DE93-017628] 04 p1424 N94-17999
Neutron-induced collision cascade mixing in Nb/V superlattices
[DE93-018575] 04 p1600 N94-18933
LAHET calculations for accelerator neutron production
[DE93-016518] 04 p1570 N94-19120
T violating neutron spin rotation asymmetry
[DE93-018470] 04 p1570 N94-19126
Neutron and PIMC determination of the longitudinal momentum distribution of HCP, BCC and normal liquid He-4
[DE93-019009] 05 p1972 N94-20187
SLAC measurement of the neutron spin structure function
[DE93-040998] 05 p1975 N94-21788
Spin dynamics and implications for superconductivity: Some problems with the d-wave scenario
[DE94-001183] 05 p2032 N94-21972
Polarized structure functions of the nucleon in the resonance region
[CEBAF-PR-94-001] 06 p2540 N94-24663
Experimental characterization of the AFIT Neutron Facility
[AD-A273822] 06 p2539 N94-25519
Data on parity violation in the compound nucleus and its interpretation
[DE94-003965] 07 p3013 N94-25820
Index to BROND-2, CENDL-2, ENDF/B-6, JEF-2, JENDL-3
[DE93-634500] 07 p3016 N94-26034
Fusion Energy Advisory Committee: Advice and recommendations to the US Department of Energy in response to the charge letter of September 1, 1992
[DE93-019842] 07 p3043 N94-26428
A concurrent, multigroup, discrete ordinates model of neutron transport
[DE94-004334] 07 p3020 N94-26577
Pre-orbital criticality safety for the NEPSTP mission
[DE94-002600] 07 p3005 N94-26802
Monte Carlo calculations of low background detector response
[DE94-004593] 07 p3116 N94-27621
Neutron-neutron scattering: Possibility of in-beam experiment
[DE94-606459] 07 p3027 N94-27682
Atomic processes in Inertial Electrostatic Confinement (IEC) devices
[DE94-005015] 07 p3047 N94-27715
Experiment of neutron multiplication in beryllium
[DE94-604605] 07 p2742 N94-27730
Neutrons in biology
[DE94-701085] 07 p2903 N94-27862
Radiations from hot nuclei 07 p3030 N94-27915
Results on structure functions from fixed-target experiments
[DE94-005233] 08 p3482 N94-28541
Determination of the neutron spin-structure function
[DE94-005234] 08 p3483 N94-28542
The effects of relativistic neutrons on nonthermal models of active galactic nuclei 08 p3547 N94-29993
Experimental setups and methods to obtain new nuclear data at intermediate and high energies
[DE94-607850] 08 p3489 N94-30052
Observation of the phase shift of the wave function of the neutron under total reflection
[DE94-608244] 08 p3489 N94-30096
Intercomparison of theoretical calculations of important activation cross sections for fusion reactor technology
[DE94-002642] 08 p3497 N94-30825
Neutron measurements at the commercial aircraft altitudes
[ISBN-0-315-86201-7] 09 p3955 N94-31709
NN-interaction in (1)S0-state: Virtual level or dibaryon resonance?
[DE94-606492] 09 p3869 N94-32097
Parallel Monte Carlo reactor neutronics
[DE94-007642] 09 p3826 N94-32357
Adjacent-cell Preconditioners for solving optically thick neutron transport problems
[DE94-007219] 09 p3872 N94-32666
Irradiation-induced phase transformations in zirconium alloys
[DE94-008484] 09 p3648 N94-32993
Spin-structure function of the neutron He-3: SLAC results
[DE94-008927] 09 p3875 N94-33189
A new point-centered diffusion differencing for unstructured meshes
[DE94-006399] 10 p4128 N94-33717
Search for neutrons from deuterated palladium subject to high electrical currents
[DE94-009342] 10 p4139 N94-33907
CALTRANS: A parallel, deterministic, 3D neutronics code
[DE94-010667] 11 p4326 N94-36127
Study of point defect mobilities in zirconium during electron irradiation in a HVEM
[DE94-619028] 11 p4242 N94-36289
MCNP: Multigroup/adjoint capabilities
[DE94-010682] 12 p4506 N94-36449
Forward scattering of neutrons from polymeric and magnetic multilayers
[DE93-041158] 12 p4513 N94-36696
An overview of the current status of resonance theory in reactor physics applications
[DE94-010465] 12 p4521 N94-37194
Physics with primary beams of the KEK-PS
[DE94-748635] 12 p4522 N94-37234
Data simulation for the Associated Particle Imaging system
[DE94-012664] 12 p4518 N94-37305
The logic behind thick, liquid-walled, fusion concepts
[DE94-012678] 12 p4528 N94-37307
Neutron transport methods on scalable shared memory multiprocessors
[DE94-012324] 12 p4498 N94-37419

NEWS
Index to NASA news releases and speeches, 1993
[NASA-TM-109722] 09 p3917 N94-31888

NEWS MEDIA
COBE video news
[NASA-TM-109598] 03 p0987 N94-15292
Emerging computer technologies and the news media of the future 07 p2688 N94-27372

NEWTON METHODS
NT NEWTON-RAPHSON METHOD
Newton iterative methods for large scale nonlinear systems
[DE93-015357] 02 p0767 N94-13025
Calculation of the required sensor accuracy to obtain a specified state estimation accuracy
[NAL-TR-1173] 02 p0649 N94-13343
On a convergence of iterative Newton's scheme
[DE93-626604] 02 p0772 N94-14886
Comparing quasi-Newton methods for solving sparse interface problems
[CWI-NM-R9303] 05 p1959 N94-21576
First MEM task IRMEO in IRAF 05 p1928 N94-22551
Error due to the stopping of the Newton iteration in implicit linear multistep methods
[PB94-101425] 06 p2487 N94-23786
Generalized Gaussian quadrature rules for systems of arbitrary functions
[AD-A273610] 06 p2491 N94-24947
Correlation between the gravity field and the bathymetry in the North Atlantic Ocean
[ETN-94-95036] 07 p2899 N94-26108
Numerical solution of the two-dimensional time-dependent incompressible Euler equations
[NASA-CR-195775] 08 p3277 N94-29859
Lattice geometrodynamics 09 p3857 N94-31825
On the error committed by stopping the Newton iteration in Runge-Kutta methods and linear multistep methods
[TW-93-13] 09 p3847 N94-32206

NEWTON SECOND LAW
Piggyback balance experiment: An illustration of Archimedes' principles and Newton's third law
[PB94-163060] 11 p4265 N94-35942

NEWTON THEORY
Essential shift: Scientific revolution in the 20th century
[AD-A270810] 04 p1610 N94-19663

NEWTON-RAPHSON METHOD
Evaluation of the Shuttle remote manipulator
[NASA-CR-194351] 02 p0662 N94-13800
Calculation of a 3-D pose of a known object in a single perspective view
[VTT-PUBS-122] 07 p2957 N94-25642

Computation of iodine species concentrations in water
10 p4102 N94-33660
Hierarchically parallelized constrained nonlinear solvers with automated substructuring
[NASA-CR-194474] 12 p4456 N94-37554

NEWTONIAN FLUIDS
Canonically covariant formulation of Landau's Newtonian superfluid dynamics
[PB93-221034] 05 p1805 N94-22272
An application of small-gap equations in sealing devices 06 p2325 N94-23668
Calculation methods for steadily loaded central circumferential groove hydrodynamic journal bearings (guide to use of computer program A9304)
[ESDU-93004] 07 p2830 N94-28073
Calculation methods for steadily loaded axial groove hydrodynamic journal bearings. Low viscosity process fluid lubrication (guide to use of computer program A9306)
[ESDU-93006] 07 p2830 N94-28075
Piggyback balance experiment: An illustration of Archimedes' principles and Newton's third law
[PB94-163060] 11 p4265 N94-35942

NICHROME (TRADEMARK)
Wear reduction in ceramic bearings by surface generated pyrolytic carbon continuously replenished by ethylene gas
[AD-A278264] 06 p2364 N94-24090

NICKEL
NT NICKEL ISOTOPES
Plating under reduced pressure
[DE93-011896] 01 p0084 N94-11668
Quantum state resolved desorption of CO from solid surfaces
[DE93-016876] 02 p0814 N94-14597
Optimization study of x ray laser coherence in Ni-like Ta
[DE93-016419] 02 p0660 N94-14888
Passive oxide films on well-defined nickel surfaces: An examination of film growth on Ni(100) with ex situ scanning tunneling microscopy
[DE93-014056] 03 p1207 N94-15923
Thin Ni silicide formation by low temperature-induced metal atom reaction with ion implanted amorphous silicon
[DE93-015449] 03 p1209 N94-16066
Characterization of Ni on Si wafers: Comparison of surface analysis techniques
[DE93-016501] 03 p0953 N94-17649
X ray absorption spectroscopic studies of the active sites of nickel- and copper-containing metalloproteins
[DE93-017142] 04 p1347 N94-18059
Environmentally assisted cracking of nickel anode substrates in Li/SOCl2 cells: An engineering approach
[DE93-015130] 04 p1405 N94-18928
Molecular dynamics modeling of the mechanical behavior of metallic multilayers
[DE93-017972] 04 p1365 N94-19263
Ni-Al2O3 solid state binding: Elaboration, state of thermal constraints, mechanical behavior
[ECL-92-31] 04 p1366 N94-19436
Collisions of molecules with clusters: A quasiclassical study
[DE93-018614] 05 p1971 N94-20050
Lightweight battery electrode and method of making it
[AD-D015895] 05 p1749 N94-20120
Stable Ni isotopes and Be-10 and Al-26 in metallic spheroids from Meteor Crater, Arizona
05 p1863 N94-20889
Preliminary AEM study of the microstructure and composition of metal particles in ordinary chondrites
05 p2086 N94-20894
Shattering the myth of the resonantly photo-pumped neon-like titanium laser
[DE93-019624] 05 p1819 N94-21873
The effect of microstructural evolution on superplasticity in Ni3Si(V, Mo)
[DE93-041320] 05 p1694 N94-21943
Transferable tight-binding parameters: An application to Ni and Ni-Al alloys
[DE94-001044] 05 p1695 N94-22023
High surface area, low weight composite nickel fiber electrodes 06 p2391 N94-23351
Exploratory report nickel and nickel compounds
[PB93-223998] 06 p2242 N94-23496
Strength, acoustic evaluation and metallurgy of diffusion bonds
[DE94-001804] 06 p2243 N94-23717
Binding of copper and nickel to cavities in silicon formed by helium ion implantation
[DE94-003769] 07 p3050 N94-25814
Molten salt techniques for reproducible excess heat
[AD-A274935] 07 p2714 N94-26296
Suppression of thermal grain growth in nickel by prior electron irradiation
[DE94-004602] 07 p2737 N94-26587
Detection of low-intensity magnetic fields with a magnetostrictive fiber optic sensor
[AD-A274120] 07 p3037 N94-27062
Development of nickel-metal hydride cell: An update
07 p2864 N94-28130
Ni-MH storage test and cycle life test
07 p2864 N94-28131
Determination of thermal properties of commercial Ni-MH cells 07 p2864 N94-28132
Geometric structures of thin film: Pt on Pd(110) and NiO on Ni(100)
[DE94-005564] 08 p3211 N94-28530
Pit initiation on passivated metal surfaces: Crystallographic orientation and environmental effects
[ISBN-0-315-85433-2] 08 p3208 N94-30138
Interface controlled amorphization of crystalline Ni/Ti multilayers
[DE94-008685] 09 p3906 N94-32884
Antarctic weathering of the CK chondrites EET90004, 90007, and 90022: Nickel and sulfur mobility
11 p4351 N94-35451
Computation of dendrites using a phase field model
[PB94-160744] 11 p4236 N94-35736
Partition coefficients for Al, Ca, Ti, Cr, and Ni in olivine obtained by melting experiment on an LL6 chondrite
11 p4353 N94-36163
Sodium/nickel-chloride battery development
[DE94-011481] 12 p4437 N94-37053
XAFS-like structure of resonant Raman scattering
[DE94-618410] 12 p4517 N94-37171
Perfluorodiethoxymethane on nickel and nickel oxide surfaces
[DE94-011200] 12 p4426 N94-37712

NICKEL ALLOYS
NT ASTROLOY (TRADEMARK)
NT HASTELLOY (TRADEMARK)
NT INCONEL (TRADEMARK)
NT KAMACITE
NT NICHROME (TRADEMARK)
NT NITINOL ALLOYS
NT WASPALOY
Structure and properties of an RS Al-Si-Ni-Mn-Zr alloy for high temperature applications
01 p0064 N94-10063
Solidification and metastable phase formation of highly undercooled Fe-Cr-Ni alloy melts
01 p0087 N94-10204
Interface reactions of (Ni3Al) ribbons/Al-MMC in ground preparation as preliminary test for microgravity experiments 01 p0123 N94-10237
Production of reactive sintered nickel aluminide
[DE93-014434] 01 p0083 N94-11127
Fatigue in single crystal nickel superalloys
[AD-A266116] 01 p0085 N94-12418
NiAl alloys for structural uses
[NASA-CR-194113] 01 p0085 N94-12447
JPRS report: Science and technology. Central Eurasia: Materials science
[JPRS-UMS-93-004] 02 p0559 N94-14574
The friction and wear of ceramic/ceramic and ceramic/metal combinations in sliding contact
[NASA-TM-106348] 03 p0930 N94-15769
Ternary alloying effects in polycrystalline (beta)-NiAl
[DE93-012675] 03 p0955 N94-15885
A sulfur segregation study of PWA 1480, NiCrAl, and NiAl alloys
[NASA-TM-106289] 03 p0956 N94-15992
A reexamination of grain boundary fracture in Ni3Al: Environmental and alloying effects
[DE93-015431] 03 p1208 N94-16063
Robotic weld overlay coatings for erosion control
[DE93-016938] 03 p0970 N94-16959
Transient phenomena following precipitation and re-solution anneals in a NiTi alloy
[AD-A267557] 03 p0961 N94-17106
Characterization of metallic multilayers using x ray diffraction analysis
[NIAR-93-13] 03 p0961 N94-17282
Atlas of formability: Ultimet
[AD-A268352] 04 p1355 N94-17767
Atlas of formability: HAYNES 556
[AD-A268354] 04 p1356 N94-17768
Atlas of formability: HAYNES 188
[AD-A268355] 04 p1356 N94-17769
Atlas of formability: NICKELVAC K-500
[AD-A268351] 04 p1356 N94-17772
Atlas of formability: Haynes 230
[AD-A268325] 04 p1356 N94-17788
Atlas of formability: Nickelvac C-276
[AD-A268264] 04 p1357 N94-17802
Atlas of formability: ALLVAC 718
[AD-A268304] 04 p1357 N94-17804
Summary of work on coatings and claddings for fossil energy applications
[DE93-017005] 04 p1367 N94-17881
Evaluation of the nickel release by horological products 04 p1367 N94-18009
Diffusion in ordered alloys
[AD-A268232] 04 p1359 N94-18322
Effects of shock loading on a solid-solution strengthened superalloy
[DE93-018345] 04 p1362 N94-18809
Environmental degradation of Alloy 600 and welded filler metal EN82 in an elevated temperature aqueous environment
[DE93-018049] 04 p1363 N94-18940
Intelligent materials systems and structures. Part 4: The influence of thermomechanical loading on the life of shape memory alloys
[PB93-195923] 04 p1363 N94-18952
Bibliography on silicides
[AD-A270516] 04 p1374 N94-19532
Incology 908 database report: On process-structure-property relationship
[DE93-017616] 04 p1366 N94-19546
Segregation of Si to the surface of Fe-29Ni-17Co alloy
[DE93-040053] 05 p1687 N94-19864
Current status of environmental, health, and safety issues of nickel metal-hydride batteries for electric vehicles
[DE93-017079] 05 p1748 N94-19902
Production of NiAl and TiAl intermetallics by mechanical alloying
[VTT-JULK-760] 05 p1691 N94-20530
Magnetic instability of Kondo insulators
[DE93-040064] 05 p1768 N94-21762
Molecular dynamics modeling of the mechanical behavior of metallic multilayers
[DE93-019947] 05 p1694 N94-21921
Ni3Al aluminide alloys
[DE94-000493] 05 p1694 N94-21933
Alloying effects on mechanical and metallurgical properties of NiAl
[DE93-040814] 05 p1694 N94-21948
First principles calculations for analysis martensitic transformations
[DE94-000666] 05 p1695 N94-21964
Shape memory metals
[DE94-001373] 05 p1695 N94-21976
Transferable tight-binding parameters: An application to Ni and Ni-Al alloys
[DE94-001044] 05 p1695 N94-22023
Microstructural evolution of neutron-irradiated Fe-Cr-Ni ternary alloys at high helium generation rates
[DE93-018786] 05 p1696 N94-22037
Magnetic phases in UNiGe
[DE94-000793] 06 p2239 N94-22939
Generic microelectronic smart sensor platform for detection of toxic, hazardous, and flammable gases
[DE93-017626] 06 p2343 N94-23200
Material data representation of hysteresis loops for Hastelloy X using artificial neural networks
[NASA-TM-105990] 06 p2376 N94-23551
Multilayer relaxation and surface structure of ordered alloys
[NASA-TM-106433] 06 p2243 N94-23578
Mean stress models for low cycle fatigue of a nickel-base superalloy 06 p2159 N94-24276
Structural characterization and thermal cycling behaviour of EB-PVD thermal barrier coating systems
[ISBN-0-315-83365-3] 06 p2257 N94-24468
Investigate zero-stress replicated optics
[NASA-CR-193889] 06 p2545 N94-24665
Robotic weld overlay coatings for erosion control
[DE94-002665] 06 p2258 N94-24749
Hydrogen trapping with Pd coated alloy films
07 p2723 N94-25551
Study on alloy films for hydrogen separation
07 p2726 N94-25565
Study on film generation phenomena by particle deposition 07 p2728 N94-25575
The role of grain boundary chemistry and structure in the environmentally-assisted intergranular cracking of nickel-base alloys
[DE94-003159] 07 p2732 N94-25954
Influence of helium generation rate and temperature history on mechanical properties of model Fe-Cr-Ni alloys irradiated in FFTF at relatively low displacement rates
[DE94-004264] 07 p2737 N94-26575
Deformation twinning: Influence of strain rate
[DE94-002693] 07 p2738 N94-26621
Stability of reference masses 2: The effect of environment and cleaning methods on the surfaces of stainless steel and allied materials
[NPL-DMM(A)-95] 07 p2738 N94-26653
Experimental measurement of local displacement and chemical pair correlations in crystalline solid solutions
[DE94-001124] 07 p3065 N94-27251
Current status of research and development on nickel and iron aluminides
[DE94-004247] 07 p2741 N94-27616

A transmission electron microscope study of Ni4W precipitates in a Ni-37 wt. percent W alloy
[ISBN-0-315-59932-4] 07 p2743 N94-27803
Effect of different ions on the anodic behaviour of alloy 800 in chloride solutions at high temperature
[DE94-602982] 07 p2743 N94-27832
Differential scanning calorimetric study of solid state amorphization and crystallization in Zr/Co and Zr/Ni multilayers 07 p2745 N94-28161
The electrocatalytic oxidation of ethylene and methane, and reduction of oxygen on gas-diffusion electrodes made of amorphous nickel-valve metal-platinum group metal alloys 07 p2722 N94-28165
CO2 methanation catalysts prepared from amorphous Ni-valve metal alloys containing platinum group elements 07 p2745 N94-28166
Mechanical behavior of amorphous alloys at elevated temperatures 07 p2746 N94-28167
Formation of glassy Pd-Ni-P alloys by mechanical alloying and their structure and thermal stability 07 p2746 N94-28168
Directional solidification studies in Ni-Al alloys
[DE94-005562] 08 p3201 N94-28527
Fusion welding with self-generated filler metal
[NASA-CASE-LEW-15671-1] 08 p3301 N94-29557
The effect of various metallurgical parameters on the flow and fracture behavior of polycrystalline NiAl near the brittle-to-ductile transition
[NASA-TM-106534] 08 p3205 N94-29758
Incommensurate magnetic order in UNi2Al3
[DE94-005449] 08 p3209 N94-30246
Transmissibility of nickel-titanium shape memory alloy springs
[AD-A276055] 09 p3640 N94-31456
Thermal-mechanical fatigue crack growth in aircraft engine materials
[ISBN-0-315-86543-1] 09 p3734 N94-31707
Fatigue in single crystal nickel superalloys
[AD-A276662] 09 p3643 N94-32047
Liquid-assisted diffusion bonding of NiAl
[DE94-008687] 09 p3645 N94-32522
Boron and hydrogen in Ni3Al. Part 2: Mechanical testing of bicrystals
[DE94-007441] 09 p3904 N94-32606
Structure, stability, and mechanical properties of intermetallic phases
[DE94-009178] 09 p3647 N94-32852
Effect of boron and hydrogen on the electronic structure of Ni3Al
[DE94-009092] 10 p4024 N94-33680
Weldability of Ni-Cr-W superalloy manufactured on industrial scale
[DE94-727593] 10 p4059 N94-33873
Characterization and processing of sintered products from nano-crystalline powders generated by the RTDS method
[DE94-004765] 12 p4415 N94-36553
Irradiation effects in Fe-30 percent Ni alloy during Ar ion implantation
[DE94-619057] 12 p4415 N94-36564
NiAl-base composite containing high volume fraction of AlN for advanced engines
[NASA-CASE-LEW-15818-1] 12 p4403 N94-36752
Processing and mechanical properties of NiAl-based in-situ composites
[NASA-CR-195333] 12 p4416 N94-36954
Process enhancements of superalloy material 12 p4421 N94-37324
Maintaining constant standards during the forging process 12 p4421 N94-37326
Defects and their effects on the integrity of nickel based aeroengine discs 12 p4421 N94-37328
Substantiating powder metal life methodologies for engines 12 p4455 N94-37330
Examination of weldability of Ni-Cr-W superalloys
[DE94-719014] 12 p4418 N94-37385
Atomic level characterization of defects in microalloyed NiAl: An atom probe investigation
[DE94-012732] 12 p4418 N94-37396
The effect of reactive elements on the segregation behavior and microstructure of alpha-Al2O3 scales on beta-NiAl
[DE94-012739] 12 p4418 N94-37399
Mechanical behavior and phase stability of NiAl-based shape memory alloys
[DE94-012336] 12 p4419 N94-37420
Physical and mechanical metallurgy of NiAl
[NASA-TP-3398] 12 p4419 N94-37503

NICKEL CADMIUM BATTERIES

The 1987 Goddard Space Flight Center Battery Workshop
[NASA-CP-3236] 03 p1012 N94-17062
A power system for a microsatellite 03 p0895 N94-17176
Advanced batteries for electric vehicle applications: Nontechnical summary
[DE93-019007] 05 p1748 N94-19885
Aerospace applications of batteries 06 p2390 N94-23346
Review of super Ni/Cd cell designs and performance 06 p2391 N94-23348
Thermodynamics of nickel-cadmium and nickel-hydrogen batteries 06 p2391 N94-23349
Characteristics and development report for the T1576 power supply and the MC3935 battery
[DE94-003675] 07 p2783 N94-26372
Handbook for handling and storage of nickel-cadmium batteries: Lessons learned
[NASA-RP-1326] 07 p2702 N94-26613
The 1993 NASA Aerospace Battery Workshop
[NASA-CP-3254] 07 p2860 N94-28100
Summary of NASA Aerospace Flight Battery Systems Program activities 07 p2860 N94-28101
Advanced energy storage for space applications: A follow-up 07 p2860 N94-28103
Experimental evaluation of battery cells for space-based radar application 07 p2860 N94-28104
Screen test for cadmium and nickel plates 07 p2860 N94-28106
Analysis for nickel (3 and 4) in positive plates from nickel-cadmium cells 07 p2861 N94-28107
Calculation of the thermoneutral potential of NiCd and NiH2 cells 07 p2861 N94-28111
Orbital management and design considerations for NiCd satellite power systems 07 p2862 N94-28118
TOPEX/Poseidon battery performance during the first year of operation 07 p2862 N94-28119
Nickel cadmium battery operations on-orbit: Trials, tribulations, and success on the Upper Atmosphere Research Satellite 07 p2862 N94-28120
Performance test results of ETS-6 Ni-Cd cells 07 p2863 N94-28121
AF Ni-Cd cell qualification program 07 p2863 N94-28122
Discriminating performance parameters for 50 amp-hour and 60 amp-hour nickel-cadmium plates and battery cells 07 p2863 N94-28123
Some observations on battery charge control 07 p2863 N94-28125
Construction of temperature compensated constant voltage (VT) curves for super Ni-Cd (tm) cells 07 p2863 N94-28126
The 1988 Goddard Space Flight Center Battery Workshop
[NASA-CP-3237] 09 p3758 N94-31233

NICKEL COATINGS

JPRS report: Science and technology. Central Eurasia: Materials science
[JPRS-UMS-93-005] 02 p0559 N94-14575
Insoluble coatings for Stirling engine heat pipe condenser surfaces
[NASA-CR-191188] 02 p0554 N94-14771
Superhardness effect in Au/Ni multilayers
[DE93-016444] 04 p1357 N94-17860
Lightweight battery electrode and method of making it
[AD-D015895] 05 p1749 N94-20120
Adhesion of electrolessly deposited Ni(P) on alumina ceramic
[ETN-94-95358] 08 p3212 N94-28539

NICKEL COMPOUNDS

NT NICKEL OXIDES
NT SCHREIBERSITE
Ovonic nickel metal hydride batteries for space applications 06 p2391 N94-23352
Alloys for hydrogen storage in nickel/hydrogen and nickel/metal hydride batteries 06 p2391 N94-23353
Exploratory report nickel and nickel compounds
[PB93-223998] 06 p2242 N94-23496
Successive structural phase transitions in stoichiometric La2NiO4 observed by x ray diffraction
[REPT-A-2665] 07 p3051 N94-25921
Technical report of ISSP. Ser. A, no. 2673: Two successive spin glass transitions in non-diluted Heisenberg-like spin glass Ni(0.42)Mn(0.58) TiO3
[JTN-94-80559] 07 p2756 N94-27241
Interstitially stabilized phases in the zirconium-nickel system
[DE94-005561] 08 p3201 N94-28525
Development of nickel and metal hydride secondary battery
[DE94-757270] 09 p3697 N94-32917

NICKEL HYDROGEN BATTERIES

Space Station Freedom advanced photovoltaics and battery technology development planning 01 p0052 N94-11401
NASA handbook for nickel-hydrogen batteries
[NASA-RP-1314] 02 p0550 N94-13265
The 1987 Goddard Space Flight Center Battery Workshop
[NASA-CP-3236] 03 p1012 N94-17062
Small satellite nickel-hydrogen and nickel-metal hydride power applications 03 p0895 N94-17175
System performance predictions for Space Station Freedom's electric power system
[NASA-TM-106396] 05 p1667 N94-20062
Thermodynamics of nickel-cadmium and nickel-hydrogen batteries 06 p2391 N94-23349
High specific energy, high capacity nickel-hydrogen cell design 06 p2391 N94-23350
High surface area, low weight composite nickel fiber electrodes 06 p2391 N94-23351
Alloys for hydrogen storage in nickel/hydrogen and nickel/metal hydride batteries 06 p2391 N94-23353
Impedance measurements on a spiral-wound nickel/metal hydride cell cycled in a simulated Leo orbit 06 p2392 N94-23355
NASA Lewis advanced IPV nickel-hydrogen technology 06 p2392 N94-23356
The 1993 NASA Aerospace Battery Workshop
[NASA-CP-3254] 07 p2860 N94-28100
Summary of NASA Aerospace Flight Battery Systems Program activities 07 p2860 N94-28101
Advanced energy storage for space applications: A follow-up 07 p2860 N94-28103
Experimental evaluation of battery cells for space-based radar application 07 p2860 N94-28104
Space Station Freedom NiH2 cell testing program 07 p2861 N94-28108
Ni-H2 cell characterization for INTELSAT programs 07 p2861 N94-28109
SAFT nickel hydrogen cell cycling status 07 p2861 N94-28110
Calculation of the thermoneutral potential of NiCd and NiH2 cells 07 p2861 N94-28111
Performance model of a recirculating stack nickel hydrogen cell 07 p2861 N94-28112
Thermal modeling of NiH2 batteries 07 p2862 N94-28113
Nickel-hydrogen cell reversal characteristics 07 p2862 N94-28114
Cycle life versus depth of discharge update on modeling studies --- Nickel-Hydrogen Batteries 07 p2862 N94-28115
Air Force standards for nickel hydrogen battery 07 p2862 N94-28116
Charge efficiency of Ni/H2 cells during transfer orbit of Telstar 4 satellites 07 p2862 N94-28117
Discriminating performance parameters for 50 amp-hour and 60 amp-hour nickel-cadmium plates and battery cells 07 p2863 N94-28123
A pressure based charge control system for the DSPSE NiH2 CPV battery 07 p2863 N94-28127
Advanced nickel-hydrogen spacecraft battery development 07 p2863 N94-28129
The 1988 Goddard Space Flight Center Battery Workshop
[NASA-CP-3237] 09 p3758 N94-31233
Development of nickel and metal hydride secondary battery
[DE94-757270] 09 p3697 N94-32917

NICKEL IRON BATTERIES

Advanced batteries for electric vehicle applications: Nontechnical summary
[DE93-019007] 05 p1748 N94-19885

NICKEL ISOTOPES

Iron and nickel isotopic mass fractionation in deep-sea spherules 01 p0282 N94-12199
FE-60 and the evolution of eucrites 05 p2083 N94-20768
Stable Ni isotopes and Be-10 and Al-26 in metallic spheroids from Meteor Crater, Arizona 05 p1863 N94-20889

NICKEL OXIDES

Passive oxide films on well-defined nickel surfaces: An examination of film growth on Ni(100) with ex situ scanning tunneling microscopy
[DE93-014056] 03 p1207 N94-15923
Siderophile elements in the upper mantle of the Earth: New clues from metal-silicate partition coefficients 03 p1103 N94-16250
Applications of x ray absorption fine structure to the in situ study of the effect of cobalt in nickel hydrous oxide electrodes for fuel cells and rechargeable batteries 06 p2391 N94-23347
Atomic-scale chemistry of metal surfaces
[REPT-A-2657] 07 p3012 N94-25636
Interstitially stabilized phases in the zirconium-nickel system
[DE94-005561] 08 p3201 N94-28525
Geometric structures of thin film: Pt on Pd(110) and NiO on Ni(100)
[DE94-005564] 08 p3211 N94-28530
Transient studies of low temperature catalysts for methane conversion
[DE94-005767] 08 p3200 N94-30877

Perfluorodiethoxymethane on nickel and nickel oxide surfaces
[DE94-011200] 12 p4426 N94-37712

NICKEL PLATE
Screen test for cadmium and nickel plates
07 p2860 N94-28106
Analysis for nickel (3 and 4) in positive plates from nickel-cadmium cells 07 p2861 N94-28107

NICKEL STEELS
Stress corrosion cracking of 316 SS and Incoloy-800 in high temperature aqueous containing sulfate and chloride
[DE93-623325] 03 p0952 N94-17302
Irradiation damage behavior of low alloy steel wrought and weld materials
[DE94-000519] 06 p2239 N94-22999

NICKEL ZINC BATTERIES
Exploratory Technology Research Program for Electrochemical Energy Storage
[DE94-003479] 07 p2781 N94-26047

NIGER
Monitoring landsurface characteristics in Niger using complementary SPOT and ERS-1 SAR data
09 p3754 N94-32560

NIGHT
Sleep management user's guide for special operations personnel
[AD-A267746] 03 p1119 N94-14943
A nighttime structure model of atmospheric optical turbulence, c2(n), derived from thermosonde and high resolution rawinsonde measurements
[AD-A273803] 06 p2406 N94-25537
Detection and analysis of fog at night using GOES multispectral infrared imagery
[NOAA-TR-NESDIS-75] 10 p4143 N94-34913
Laser designation pods optimized concept for day/night operations 12 p4393 N94-36620

NIGHT AIRGLOW
U NIGHTGLOW

NIGHT E LAYER
U E REGION
U NIGHT SKY

NIGHT F LAYER
U F REGION
U NIGHT SKY

NIGHT FLIGHTS (AIRCRAFT)
Visual Problems in Night Operations
[AGARD-LS-187] 06 p2431 N94-23976
Civil use of night vision devices: Evaluation pilot's guide, part 1
[SCT-91RR-43] 12 p4487 N94-37741
Night vision goggles in Emergency Medical Service (EMS) helicopters
[SCT-93RR-22] 12 p4487 N94-37742
Assessment of night vision goggle workload: Flight test engineer's guide
[SCT-91RR-45] 12 p4487 N94-37743

NIGHT SKY
Tip-tilt compensation: Resolution limits for ground-based telescopes using laser guide star adaptive optics
[DE93-016426] 03 p1237 N94-16872

NIGHT VISION
Perceptual response to visual noise and display media
[NASA-CR-193406] 01 p0313 N94-11511
Comparative night vision goggle visual acuity measurements performed in the A-10 aircraft in an operational setting
[AD-A266721] 03 p1137 N94-15820
Evaluation of Night Vision Goggles (NVG) for maritime search and rescue (HH-3/HH-60) comparison report
[AD-A266493] 03 p1138 N94-16793
SYDONI: An intensified system for night observation
03 p0891 N94-17153
Human integration evaluation of three helmet systems
[AD-A271320] 04 p1513 N94-19570
Electro-optics display research, test, and evaluation laboratory program
[AD-A270947] 04 p1408 N94-19751
Night vision goggle model F4949 preflight adjustment/assessment procedures
[AD-A271079] 05 p1895 N94-19935
Evaluation of visual acuity with Gen 3 night vision goggles
[NASA-TM-108792] 06 p2431 N94-23974
Visual Problems in Night Operations
[AGARD-LS-187] 06 p2431 N94-23976
Night operations 06 p2431 N94-23977
Physical aspects of the visual stimulus
06 p2431 N94-23978
Perception in flight: Shape and motion perception, space perception, spatial orientation, and visual vestibular interaction 06 p2429 N94-23979
Mental images 06 p2429 N94-23980
Multi-sensoral approach to night flight: Perceptive and Cognitive limitations 06 p2432 N94-23981
Night vision devices and characteristics
06 p2432 N94-23982
Cockpit/NVG visual integration issues
06 p2432 N94-23983
Night vision goggle illusions and visual training
06 p2432 N94-23984
An investigation of stereopsis with AN/AVS-6 night vision goggles at varying levels of illuminance and contrast
[AD-A275332] 08 p3400 N94-28918
Night vision camcorder system
[AD-A277004] 09 p3712 N94-32002
Assessment of interior modifications in C-130 and C-141 aircraft for night vision goggle operations
[AD-A276843] 09 p3582 N94-32223
Methods for measuring characteristics of night vision goggles
[AD-A277046] 09 p3804 N94-32302
An evaluation framework for designing a night vision, computer-based trainer
[AD-A278005] 09 p3590 N94-33139
Forward-looking infrared: Capabilities for search and rescue
[AD-A277895] 10 p4141 N94-33548
Vision-based aircraft guidance
[NASA-CR-195937] 10 p4007 N94-34264
Accommodation during instrument viewing can be influenced by knowledge of object distance
[AD-A278987] 11 p4298 N94-35528
Is increased accommodation a necessary condition for instrument myopia?
[AD-A278962] 11 p4298 N94-35659
Visual accommodation to virtual image displays when knowledge of object distance conflicts with optical distance 12 p4485 N94-37278
Civil use of night vision devices: Evaluation pilot's guide, part 1
[SCT-91RR-43] 12 p4487 N94-37741
Night vision goggles in Emergency Medical Service (EMS) helicopters
[SCT-93RR-22] 12 p4487 N94-37742
Assessment of night vision goggle workload: Flight test engineer's guide
[SCT-91RR-45] 12 p4487 N94-37743

NIGHTGLOW
Upper atmosphere neutral and plasma density modeling
[AD-A274768] 07 p2879 N94-26569
A model of the atmospheric metal deposition by cosmic dust particles
[AD-A278561] 10 p4163 N94-33786
Study of gravity wave in the upper atmosphere by way of OH* (9-4) and O2(b 1 Sigma(+,g), 0-1) bands nightglow observations
[INPE-5539-TDI/527] 10 p4087 N94-34227

NIMBUS SATELLITES
NT NIMBUS 6 SATELLITE
NT NIMBUS 7 SATELLITE

NIMBUS 6 SATELLITE
The fragmentation of the Nimbus 6 rocket body
[NASA-CR-191645] 03 p0926 N94-16504

NIMBUS 7 SATELLITE
Coastal zone color scanner: Nimbus 7
[NASA-TM-109590] 03 p1111 N94-15281
Arctic and Antarctic sea ice, 1978-1987: Satellite passive-microwave observations and analysis
[NASA-SP-511] 03 p1114 N94-17439
Nimbus-7 Earth radiation budget calibration history. Part 2: The Earth flux channels
[NASA-RP-1335-PT-2] 07 p2814 N94-27981

NIMPHE (ENGINE)
U HYDRAZINE ENGINES

NIOBATES
NT LITHIUM NIOBATES
Electrooptic crystal growth and properties
[AD-A276023] 09 p3896 N94-31439
On the nature of striae in strontium barium niobate
[DE94-006486] 09 p3901 N94-32176
Displacive transformation in ceramics
[AD-A278442] 10 p4026 N94-33539

NIOBIUM
Experimental approach to non-contact calorimetry in space 01 p0112 N94-10143
Space Storable Rocket Technology program (SSRT). Option 1 program
[NASA-CR-191171] 01 p0046 N94-10938
Atomic structure of the 310 twin in niobium: Theoretical predictions and comparison with experimental observation
[DE93-013421] 02 p0806 N94-13136
Submillimeterwave SIS mixer developments
03 p0903 N94-15054
Nb-based SJTJ for nuclear detection: Preliminary results with alpha radiation 03 p0905 N94-15068
Preparation and properties of Nb/Al SIS and SIN junctions for millimeter and submillimeter radioastronomical receivers 03 p0907 N94-15078
Superconductivity and magnetism in niobium doped YBa2Cu3O7 related high-(Tc) ceramics
[DE93-018086] 04 p1601 N94-19049
Total hemispherical emittance of Niobium-1 percent zirconium fuel cladding for the SP-100 space reactor
[AD-A270456] 04 p1576 N94-19589
Welding of niobium to stainless
[DE94-003365] 06 p2365 N94-24614
Experimental results of 40-kA Nb3Al conductor
[DE94-701207] 07 p2788 N94-27821
Inorganic materials for anomalous-dispersion phase-matched second harmonic generation: Rubidium titanyl arsenate isomorphs, Rb(Ti(1-2x)Ln(x)Nb(x))OAsO4
[DE94-006141] 09 p3899 N94-31847
Characterization of interface structure in multilayers using specular x ray reflectance
[DE94-007698] 09 p3657 N94-32358
Effect of niobium interlayer on high-temperature sliding friction and wear of silver films on alumina
[DE94-010462] 11 p4275 N94-36232

NIOBIUM ALLOYS
Processing and protection of high temperature structural materials
[AD-A267292] 03 p0954 N94-14961
Effects of processing and prolonged high temperature exposure on the microstructure of Nb-1Zr-C sheet
[NASA-TM-106370] 03 p0959 N94-16883
Developing and understanding the high temperature behavior of niobium aluminides and niobium aluminide composites
[AD-A268874] 04 p1341 N94-18636
Bibliography on silicides
[AD-A270516] 04 p1374 N94-19532
Metastable bcc phase formation in the Nb-Cr system
[DE93-018376] 05 p2012 N94-19926
Effects of processing history on the creep strength of Nb-1Zr
[DE93-015905] 05 p1689 N94-20093
Properties and potential of high-temperature niobium beryllides
[DE93-019169] 05 p1690 N94-20233
Strengthening and toughening in refractory metal alloys
[DE93-019942] 05 p1695 N94-21986
New extensions in the development of deformation processed metal-metal matrix composites
[DE94-000692] 06 p2227 N94-23004
Characterization of the microstructure of Nb-1wt.%Zr-0.1wt.%C tubes as affected by thermomechanical processing
[NASA-TM-106381] 06 p2242 N94-23550
Effect of hydrogen exposure on a Cu-8 Cr-4 Nb alloy
[NASA-TM-106429] 06 p2243 N94-23556
Fracture behavior of 20% Nb particulate reinforced alumina composite
[DE94-002830] 07 p2706 N94-26019
The influence of energy losses with time in NbTi superconductors in pulsed magnetic fields
[DE93-634761] 07 p3058 N94-26512
A tri-junction diffusion couple analysis of the Nb-Cr-Ti system at 950 C
[DE94-002637] 07 p2737 N94-26607
Evaluation of APC NbTi superconductor in a model dipole magnet
[DE94-003258] 07 p3060 N94-26795
The effect of Ti conduit on the critical current in (Nb, Ti)3Sn cable-in-conduit conductors
[DE94-701204] 07 p2788 N94-27817
The corrosion behavior of sputter-deposited magnesium-valve metal alloys 07 p2745 N94-28164
CO2 methanation catalysts prepared from amorphous Ni-valve metal alloys containing platinum group elements
07 p2745 N94-28166
Effects of thermomechanical processing on tensile and long-time creep behavior of Nb-1 percent Zr-0.1 percent C sheet
[NASA-TM-106319] 08 p3202 N94-28822
Calculating the J(c), B, T surface for commercial niobium tin conductors using a reduced state model
[DE94-006296] 08 p3520 N94-30850
High Temperature Silicides and Refractory Alloys Symposium, volume 322
[AD-A278373] 10 p4024 N94-33741
Multifilamentary superconducting cable and a method of manufacturing it
[AD-D016146] 10 p4040 N94-33837
Continuum fluorescence of Cu in NbTi/Cu composite wires
[DE94-008940] 11 p4241 N94-36242
Precipitation in Zr-2.5 Nb enhanced by proton irradiation
[DE94-619056] 12 p4415 N94-36563

NIOBIUM CARBIDES
Effects of processing and prolonged high temperature exposure on the microstructure of Nb-1Zr-C sheet
[NASA-TM-106370] 03 p0959 N94-16883
Performance of carbon-based hot frit substrates
[DE94-000509] 05 p1676 N94-21754
The influence of weld metal alloying additions to extend the heat input range for the submerged arc welding of high strength steels
[AD-A274284] 07 p2738 N94-26679
NIOBIUM COMPOUNDS
NT LITHIUM NIOBATES
NT NIOBATES
NT NIOBIUM CARBIDES
NT NIOBIUM OXIDES
High frequency behavior of long and small junctions
[AD-A265670] 01 p0403 N94-12336
Study on measurement and evaluation methods for superconductive characteristics
07 p2725 N94-25560
NIOBIUM OXIDES
Synthesis and thermal evolution of structure in alkoxide-derived niobium pentoxide gels
[NASA-TM-106259] 01 p0090 N94-11257
Fiber optic transceiver for interfacing digital superconducting electronics
[DE94-008284] 10 p4040 N94-33842
NITINOL ALLOYS
Experimental and analytical analysis of the response of a smart beam to rate feedback
[AD-A266544] 02 p0557 N94-13706
NITRAMINE PROPELLANTS
Time-temperature shift factors for gun propellants
[AD-A264979] 01 p0097 N94-10489
Spectral studies of solid propellant combustion 4: Absorption and burn rate results for M43, XM39, and M10 propellants
[AD-A267119] 03 p0946 N94-15685
Laser ignition of solid propellants: 1. Ignition delays
[AD-A268454] 03 p0976 N94-17538
Detailed structure study of an H2/N2O/Ar flame employing molecular beam mass spectrometry, laser spectroscopy, and modeling
[AD-A270720] 05 p1679 N94-20111
Chemistry of the burning surface
[AD-A272725] 05 p1681 N94-21181
Insensitive energetic materials: The importance of physical properties and molecular structure
[AD-A275393] 08 p3225 N94-29308
Condensed-phase processes during solid propellant combustion. 3: Preliminary depth-profiling studies on XM39, JA2, M9, M30, and HMX2
[AD-A276595] 09 p3635 N94-32124
NITRATE ESTERS
Laser ignition of solid propellants: 1. Ignition delays
[AD-A268454] 03 p0976 N94-17538
High melting amino aromatic nitrate esters
[AD-D015929] 05 p1711 N94-19801
Condensed-phase processes during solid propellant combustion. 3: Preliminary depth-profiling studies on XM39, JA2, M9, M30, and HMX2
[AD-A276595] 09 p3635 N94-32124
NITRATES
NT AMMONIUM NITRATES
NT CELLULOSE NITRATE
NT NITROGLYCERIN
NT PETN
NT POTASSIUM NITRATES
The phytoplankton bloom in the Kinu-ura Bay, Japan in the rainy season 01 p0211 N94-12660
Variation of the photosynthetic products in the regional upwelling area around the Izu Islands, Japan
01 p0211 N94-12661
Characterization of Spirulina biomass for CELSS diet potential
[NASA-CR-194123] 02 p0729 N94-14097
Nitrates in SNCs: Implications for the nitrogen cycle on Mars 03 p1251 N94-16193
Atmospheric ionization by solar particles detected by nitrate measurement in antarctic snow
[AD-A267583] 03 p1299 N94-17208
Chemical tracer studies at IOSDL. 3: The measurement of silicate, nitrate and phosphate in seawater
[IOS-302-1992] 03 p1114 N94-17489
Solar proton events from a 180 year depth profile of nitrate concentrations from the central Greenland ice sheet
[AD-A272868] 05 p2147 N94-21196
Bulletin of the Institute for Chemical Reaction Science, Tohoku University, volume 2
[JTN-94-80602] 07 p2717 N94-27385
Reactivity of nitrate radical (NO3) toward organic compounds 07 p2704 N94-27387
Growth of hydrocarbon-rich microalga Botryococcus braunii in secondarily treated sewage and its consumption of nitrate ion and phosphate ion
08 p3387 N94-29519
Dry deposition of PAN to grassland vegetation
[DE94-005111] 09 p3768 N94-32894
Carbonates, surfates, phosphates, nitrates, and organic materials: Their association in a Martian meteorite
09 p3952 N94-33239
NITRATION
Study of chemical reactions under the influence of ultrasound
[DE93-016458] 02 p0778 N94-14867
NITRIC ACID
Reduction of Pu(6) with hydrogen peroxide: Effects of plutonium, peroxide, and iron concentrations and of reaction time
[DE93-013598] 02 p0564 N94-13487
Study of chemical reactions under the influence of ultrasound
[DE93-016458] 02 p0778 N94-14867
An assessment of acid fog
[DE93-009347] 03 p1095 N94-15940
NITRIC OXIDE
In situ detection of tropospheric OH, HO2, NO2, and NO by laser-induced fluorescence in detection chambers at reduced pressures
[NASA-CR-193189] 01 p0274 N94-10701
Direct catalytic decomposition of nitric oxide
[DE93-016689] 03 p0949 N94-16896
Factors determining the release of nitric oxide --- Calcium/cadmium transport by renal cortical collectin duct cells
[AD-A266232] 03 p1118 N94-17224
UV absorption technique for monitoring mobile source NO emissions
[AD-A273858] 07 p2713 N94-25964
Ozone production at a rural site in Georgia during the summer 1992 SOS campaign
[DE94-003989] 08 p3342 N94-28523
Simulation of pollutant formation in turbulent combustors using an extended coherent flame model
08 p3190 N94-29251
Flowfield prediction of NO(x) and smoke production in aircraft engines 08 p3191 N94-29252
Fuel property effects on engine combustion processes
[DE94-005529] 09 p3631 N94-31153
NO decomposition in non-reducing atmospheres
[DE94-011157] 11 p4237 N94-36036
Direct catalytic decomposition of nitric oxide
[DE94-005025] 12 p4407 N94-36475
NITRIDES
NT ALUMINUM NITRIDES
NT BORON NITRIDES
NT GALLIUM NITRIDES
NT METAL NITRIDES
NT OXYNITRIDES
NT SILICON NITRIDES
NT TITANIUM NITRIDES
SONOS technology for commercial and military nonvolatile memory applications
[DE93-015647] 03 p1011 N94-16661
Atomic layer epitaxy of boron nitride
[AD-A266260] 03 p1212 N94-16932
Nitride semiconductors for ultraviolet detection
[AD-A267877] 03 p1012 N94-17040
Interface chemistry in ceramic matrix composites
[AD-A268629] 03 p0973 N94-17466
Nitridation of GaAs(100) by laser-induced decomposition of HN3
[AD-A269147] 04 p1438 N94-18258
LPCVD of InN on GaAs(110) using HN3 and TMIn: Comparison with Si(100) results
[AD-A273555] 06 p2235 N94-24917
Influences of nitrogen absorption on the magnetic properties of YFe2, YFe3 and Y6Fe23
[REPT-A-2654] 06 p2564 N94-24958
Process parameter-growth environment-film property relationships for reactive sputter deposited metal (V, Nb, Zr, Y, Au) oxide, nitride, and oxynitride films
[AD-A276382] 09 p3640 N94-31258
Cost-effective ceramic machining: Summary of three-body wear experiments
[DE94-007757] 09 p3650 N94-31354
High temperature heterojunction bipolar transistors
[AD-A278605] 11 p4261 N94-36360
NiAl-base composite containing high volume fraction of AlN for advanced engines
[NASA-CASE-LEW-15818-1] 12 p4403 N94-36752
NITRIDING
Nitridation of GaAs(100) by laser-induced decomposition of HN3
[AD-A269147] 04 p1438 N94-18258
Evaluation of radiation effects in re-oxidized nitrided oxide devices by hot carrier stressing at 77 K
05 p1754 N94-21084
Selection of polymer binders and fabrication of SiC fiber-reinforced reaction-bonded silicon nitride matrix composites
[NASA-CR-194874] 06 p2255 N94-24223
Combustion synthesis method
07 p2721 N94-25561
Study on microscopic structural controls and electronic properties at material surfaces by ion beams
07 p2727 N94-25571
Effect of nitrocarburizing on shape of titanium alloy parts
[DE94-004040] 07 p2732 N94-25822
Microstructure and mechanical properties of nitrided molybdenum silicide coatings
[DE94-006249] 08 p3217 N94-30025
Charge trapping and breakdown in N2O oxides
[DE94-003775] 08 p3266 N94-30040
NITRILES
NT ACETONITRILE
NT ACRYLONITRILES
NT POLYACRYLONITRILE
Coupled growth of cells and bubbles in directional solidification of succinonitrile-acetone alloys
01 p0118 N94-10206
Curing phthalonitrile resins with acid and amine
[AD-D016021] 06 p2258 N94-24721
Curing phthalonitriles with acid
[AD-D015996] 06 p2261 N94-25054
Interface shape and convection during solidification and melting of succinonitrile
[NASA-TM-106487] 11 p4262 N94-35248
Synthesis of phthalonitrile resins containing ether and imide linkages with aromatic diamine curing agent
[AD-D016309] 12 p4427 N94-37778
NITRO COMPOUNDS
NT NITROBENZENES
NT NITROGLYCERIN
NT NITROGUANIDINE
NT NITROMETHANE
NT TRINITRO COMPOUNDS
NT TRINITROTOLUENE
Synthesis and characterization of 1,4-dinitroglycoluril (DINGU)
[DE93-014111] 02 p0584 N94-13099
Study of chemical reactions under the influence of ultrasound
[DE93-016458] 02 p0778 N94-14867
Sensitive detection of gas-phase nitro-containing energetic materials employing 226-nm radiation
[AD-A267633] 03 p0951 N94-17203
Computational studies of energetic organic molecules
[AD-A274726] 07 p3018 N94-26172
Superior energetic materials that contain carbocations and anions. Energetic materials restricted in composition to C, H, N, and O atoms
[AD-A275449] 08 p3225 N94-29310
The thermochemistry and reaction mechanisms in the decomposition of energetic materials
[DE94-011420] 11 p4248 N94-36376
NITROBENZENES
NT TRINITROTOLUENE
Evaluation of pre-extraction analytical holding times for nitroaromatic and nitramine explosives in water
[AD-A271547] 05 p1712 N94-20927
Chemical and structural characterization of nitroaromatic adducts with hemoglobins
[AD-A280533] 12 p4480 N94-37089
NITROCELLULOSE
U CELLULOSE NITRATE
NITROGEN
NT LIQUID NITROGEN
NT NITROGEN ISOTOPES
NT NITROGEN 15
NT SOLID NITROGEN
Polymeric nitrogen
[DE93-012600] 01 p0089 N94-11151
Nitrogen and noble gases in a glass sample from LEW88516 01 p0080 N94-12051
Multiple nitrogen components in lunar soil sample 12023 01 p0451 N94-12108
Carbon and nitrogen in Type 2 supernova diamonds
01 p0431 N94-12166
Characterization of 1:1 random copolymers obtained from 6-, 7-, 11-, and 12-carbon amino acids
[AD-A265827] 02 p0577 N94-12985
Modeling of the partitioning of reactive odd nitrogen in the lower stratosphere using aircraft measurements of NOy, NO, and other trace species
[NASA-CR-194305] 02 p0714 N94-13707
Euromet Ureilite Consortium: A preliminary report on carbon and nitrogen geochemistry
03 p1241 N94-16192
Nitrates in SNCs: Implications for the nitrogen cycle on Mars 03 p1251 N94-16193
A Pluto thermal model 03 p1256 N94-16216

Nitrogen and light noble gases in Parsa enstatite chondrite 03 p1246 N94-16435
Static characteristics of a conduction and radiation dominated electric arc in nitrogen
[DE93-627106] 03 p1204 N94-17311
Laser ignition of solid propellants: 1. Ignition delays
[AD-A268454] 03 p0976 N94-17538
Dense energetic compounds of C, H, N, and O atoms. 3: 5-(4-nitro-(1,2,5) oxadiazolyl)-5H-(1,2,3) triazolo (4,5-c)(1,2,5) oxadiazole
[AD-A268715] 04 p1338 N94-18314
Determination of nitrogen to carbon abundance ratios from transition layer emission lines
[NASA-CR-191921] 04 p1622 N94-19421
Chemical equilibrium in high pressure molecular fluid mixtures
[DE93-040160] 05 p1796 N94-19829
Phonons and metastability in compressed nitrogen
[DE93-019913] 05 p2016 N94-20318
Implantation of nitrogen: Effects of hydrogen and implantation energy 05 p1686 N94-20804
Are the C delta light nitrogen and noble gases located in the same carrier? 05 p2085 N94-20846
Polymeric nitrogen
[DE93-040544] 05 p1706 N94-21512
Reburning rich-lean kinetics
[PB93-220887] 06 p2232 N94-23100
Combustion synthesis method 07 p2721 N94-25561
The importance of vibrationally excited nitrogen in silicon nitride deposition systems
[AD-A274874] 07 p2750 N94-26167
Peroxy radical measurements with NCAR's chemical amplifier 08 p3345 N94-28603
Predissociation in N2(C'4, 1 Sigma u +) and other N2 states and its importance in the atmospheres of Titan and Triton
[NASA-CR-195727] 08 p3549 N94-28816
Microstructure and mechanical properties of nitrided molybdenum silicide coatings
[DE94-006249] 08 p3217 N94-30025
Spectroscopic study of the molecular collisions (hydrogen-nitrogen and hydrogen-oxygen) at energies of several MeV
[ISBN-0-315-86794-9] 09 p3867 N94-31753
Vibrational energy transfer of diatomic gases in hypersonic expanding flows 09 p3570 N94-31958
Simulation of low-density nozzle plumes in non-zero ambient pressures
[NASA-TM-106501] 09 p3615 N94-32742
Global changes in biogeochemical cycles in response to human activities
[NASA-CR-191896] 10 p4083 N94-34685
Vacuum ultraviolet studies of molecular dynamics
[AD-A278940] 11 p4321 N94-35657
Tritiated ammonia formation
[DE94-011170] 11 p4237 N94-36056
Molecular nitrogen fluorescence lidar for remote sensing of the auroral ionosphere
[AD-A280716] 11 p4291 N94-36263
Direct catalytic decomposition of nitric oxide
[DE94-005025] 12 p4407 N94-36475
Theoretical studies of a molecular beam generator
[NASA-CR-196306] 12 p4522 N94-37508
Optical spectroscopy of a nitrogen-hydrogen complex in ZnSe
[DE94-011622] 12 p4413 N94-37630

NITROGEN ATOMS

Enhanced thermal capacity aerogels summary report, FY 1993
[DE94-008888] 09 p3639 N94-33260

NITROGEN COMPOUNDS

NT ALUMINUM NITRIDES
NT AMIDES
NT AMINO RADICAL
NT AMMONIA
NT AMMONIUM NITRATES
NT ATROPINE
NT AZIDES (INORGANIC)
NT AZIDES (ORGANIC)
NT AZO COMPOUNDS
NT BETAINES
NT BISMALEIMIDE
NT BORON NITRIDES
NT CAFFEINE
NT CELLULOSE NITRATE
NT CYANO COMPOUNDS
NT DIISOCYANATES
NT GALLIUM NITRIDES
NT HMX
NT HYDROCYANIC ACID
NT IMIDES
NT IMINES
NT ISOCYANATES
NT KAPTON (TRADEMARK)
NT METAL NITRIDES
NT NITRATE ESTERS
NT NITRATES
NT NITRIC ACID
NT NITRIC OXIDE
NT NITRIDES
NT NITRO COMPOUNDS
NT NITROBENZENES
NT NITROGEN DIOXIDE
NT NITROGEN OXIDES
NT NITROGEN POLYMERS
NT NITROGEN TETROXIDE
NT NITROGLYCERIN
NT NITROGUANIDINE
NT NITROMETHANE
NT NITROUS OXIDES
NT OXYNITRIDES
NT PETN
NT POLYIMIDES
NT POTASSIUM NITRATES
NT RDX
NT SILICON NITRIDES
NT THIOUREAS
NT TITANIUM NITRIDES
NT TRINITRO COMPOUNDS
NT TRINITROTOLUENE
NT TRYPTOPHAN
NT UREAS
NT XANTHINES

Importance of sprays for long range transport of harmful substances in the troposphere
[MITT-81] 02 p0711 N94-14723
Supercritical thermodynamics of sulfur and nitrogen species
[DE93-017727] 03 p1220 N94-16997
Molecular and polymeric ceramic precursors
[DE93-040364] 04 p1372 N94-18891
Supercritical thermodynamics of sulfur and nitrogen species
[DE93-041221] 04 p1610 N94-19670
Physical chemistry of energetic nitrogen compounds
[AD-A271819] 05 p1712 N94-20625
Phase diagram of La2NiO(4 + delta) (0 less than or equal to delta less than or equal to 0.18). 1: Phases at room temperature and phase transition above delta equal to 0.15
[REPT-A-2661] 07 p3053 N94-26089
Reactions and spectroscopy of excited nitrenes
[AD-A278475] 10 p4136 N94-33745

NITROGEN DIOXIDE

In situ detection of tropospheric OH, HO2, NO2, and NO by laser-induced fluorescence in detection chambers at reduced pressures
[NASA-CR-193189] 01 p0274 N94-10701
The mobile lidar system ARGOS for spatial resolution remote measuring of gaseous air pollutants
[GKSS/92/E/26] 02 p0617 N94-14820
The radical amplifier 08 p3345 N94-28604
California residential indoor air quality study. Volume 1: Methodology and descriptive statistics
[PB94-166048] 12 p4464 N94-36994

NITROGEN FIXATION

U NITROGENATION

NITROGEN HYDRIDES

NT AMINO RADICAL

NITROGEN IONS

Electron spectroscopic studies of the neutralization of slow multicharged ions during interactions with a metal surface
[DE93-041046] 06 p2532 N94-22956
Radiative properties of molecular nitrogen ions produced by helium Penning ionization and argon effects
[NASA-CR-195126] 06 p2534 N94-24487
Study on microscopic structural controls and electronic properties at material surfaces by ion beams 07 p2727 N94-25571
Energy parameters of the incident auroral electrons derived by the intensity ratio of auroral emissions 07 p2779 N94-27964

NITROGEN ISOTOPES

NT NITROGEN 15

Interstellar graphite in Murchison: Continued search for isotopically distinct components 01 p0097 N94-12029
Euromet Ureilite Consortium: A preliminary report on carbon and nitrogen geochemistry 03 p1241 N94-16192
Nitrogen isotopic signatures in agglutinates from breccia 79035 03 p0954 N94-16314
A carbon and nitrogen isotope study of carbonaceous vein material in ureilite meteorites 05 p2083 N94-20726
Requirements for the early atmosphere of Mars from nitrogen isotope ratios 05 p2144 N94-21669

NITROGEN LASERS

Bibliography of short wavelength chemical laser research
[AD-A267619] 03 p1041 N94-17195

NITROGEN OXIDES

NT NITRIC OXIDE
NT NITROGEN DIOXIDE
NT NITROGEN TETROXIDE
NT NITROUS OXIDES

User's manual for the plume visibility model PLUVUE 2 (revised)
[PB93-188233] 01 p0265 N94-11016
Application of jet-shear-layer mixing and effervescent atomization to the development of a low-NO(x) combustor
[NASA-TM-105888] 01 p0028 N94-11234
An examination of utility emissions contributions to elevated ozone concentrations in the Chicago area
[DE93-012852] 02 p0708 N94-13495
IMG: Interferometric monitor for greenhouse gases 02 p0689 N94-14217
Summary of conclusions and recommendations from a visibility science workshop
[DE93-012770] 02 p0710 N94-14523
Application of non-thermal plasmas to pollution control
[DE93-016432] 03 p1096 N94-16449
SONOS technology for commercial and military nonvolatile memory applications
[DE93-015647] 03 p1011 N94-16661
Atomic beam studies relevant to the space environment
[AD-A268628] 03 p1186 N94-17436
Title 1 implementation: Status report on nonattainment areas
[DE93-017677] 04 p1471 N94-17777
Land-use related sources of CO2, CH4 and N2O: Current global emissions and projections for the period 1990-2100
[PB93-194819] 04 p1475 N94-18949
Detailed structure study of an H2/N2O/Ar flame employing molecular beam mass spectrometry, laser spectroscopy, and modeling
[AD-A270720] 05 p1679 N94-20111
Advanced Turbine Systems (ATS). Phase 1: System scoping and feasibility studies
[DE93-041130] 05 p1826 N94-21938
Investigations on trends in global environment adaptive industrial technologies
[DE94-714888] 05 p1853 N94-22258
Experimental evaluation of oxygen-enriched air and emulsified fuels in a six-cylinder diesel engine
[DE94-000907] 05 p1811 N94-22391
Economics of electron beam and electrical discharge processing for post-combustion NO(x) control in internal combustion engines
[DE93-019574] 06 p2351 N94-22865
Fundamental limitations of non-thermal plasma processing for internal combustion engine NO(x) control
[DE93-019622] 06 p2351 N94-22866
Reburning rich-lean kinetics
[PB93-220887] 06 p2232 N94-23100
Flue gas cleaning by pulse corona streamer
[EUT-93-E-272] 06 p2268 N94-23174
Evaluation of reducing gas turbine emissions through hydrogen-enhanced steam-injected combustion
[PB94-109873] 06 p2187 N94-23709
Fundamental study of NO(x) control in catalytic combustion
[PB94-112323] 06 p2398 N94-23818
Alternative control techniques document: NOx emissions from stationary reciprocating internal combustion engines
[PB94-104494] 06 p2398 N94-24476
Development of SO(x) and NO(x) solid electrolyte sensors 07 p2725 N94-25562
Technical Report of National Research Institute of Fisheries Engineering: Fishing Boat and Instrument, No. 12
[JTN-94-80595] 07 p2764 N94-27976
The emission characteristics of a high speed diesel engine 07 p2764 N94-27980
Emissions of nitrogen oxides (NO(x) and N2O) in pressurized fluidized bed combustion
[PB94-133071] 07 p2876 N94-28395
Catalytic fabric filtration for simultaneous NO(x) and particulate control
[DE94-001660] 08 p3341 N94-28463
The radical amplifier 08 p3345 N94-28604
Fuels and Combustion Technology for Advanced Aircraft Engines
[AD-A275879] 08 p3189 N94-29246
On the effect of emissions from aircraft engines on the state of the atmosphere 08 p3189 N94-29247
Prediction of prompt NO(x) in hydrocarbon air flames 08 p3190 N94-29250

Ultra low NO(x) ultra lean gas turbine primary zones with liquid fuels 08 p3154 N94-29267
Reduction of NO(x) by fuel-staging in gas turbine engines: A commitment to the future 08 p3194 N94-29272
Chambers of turboreactors with variable geometry: A response to the matrix of pollution in cycles at high temperature, high pressure 08 p3194 N94-29273
The influence of air distribution on homogeneity and pollutant formation in the primary zone of a tubular combustor 08 p3194 N94-29274
Effects of hydrogen addition on pollutant emissions in a gas turbine combustor 08 p3195 N94-29275
Charge trapping and breakdown in N2O oxides [DE94-003775] 08 p3266 N94-30040
Identification of research relating to the critical loads concept and its potential application to the regulation of acidic deposition [DE94-008234] 09 p3767 N94-32752
Dry deposition of PAN to grassland vegetation [DE94-005111] 09 p3768 N94-32894
A correlated k-distribution model of the heating rates for atmospheric mixtures of H2O, CO2, O3, CH4, and N2O in the 0-2500 cm(exp -1) wave number region at altitudes between 0 and 60 km [DE94-005136] 09 p3775 N94-32895
Low emissions combustor technology for high-speed civil transport engines 10 p3974 N94-33481
HSR combustion analytical research 10 p3974 N94-33483
Application of pulsed plasma NO(x) reduction to diesel engine exhaust [DE94-007454] 10 p4080 N94-33692
Combustor technology for future small gas turbine aircraft 10 p4002 N94-34452
Combined SO(x)/NO(x) control via SOXAL (tm) process: An electrodialytic regenerative wet scrubbing process [DE94-009053] 11 p4284 N94-35346
State-to-state dynamics of molecular energy transfer [DE94-009651] 11 p4324 N94-35816
Modeling the atmospheric input of nutrients, heavy metals, and pesticides to the Great Lakes [DE94-005481] 11 p4286 N94-36007
Air quality implications associated with the selection of power plants in the Pacific Northwest [DE94-004783] 11 p4287 N94-36027
Treatment of toxic gases SO2 and NO(x) by electron beam irradiation [DE94-615424] 11 p4330 N94-36028
Dipole forbidden vibrational modes for NO and CO on Cu observed in the far IR [DE94-003199] 12 p4408 N94-36559
SIHTI: Energy and environmental technology [DE94-763290] 12 p4464 N94-37007
Influences of flame-vortex interactions on formation of oxides of nitrogen in curved methane-air diffusion flamelets [DE94-005105] 12 p4409 N94-37221
Stratospheric emissions effects database development [NASA-CR-4592] 12 p4467 N94-37607

NITROGEN PLASMA
Initial operation of a large-scale plasma source ion implantation experiment [DE94-000805] 05 p2036 N94-22583
Investigation of intense XUV emission of nitrogen-puff Z-pinch with small energy input [PH-23] 08 p3505 N94-29075
Multichannel x ray spectral measurement of hot plasma evolution in nitrogen-puff Z-pinch [PH-24] 08 p3505 N94-29076
The growth of silicon nitride crystalline films using microwave plasma enhanced chemical vapor deposition [AD-A278862] 11 p4340 N94-35828
First results from the Los Alamos plasma source ion implantation experiment [DE94-003931] 12 p4414 N94-36461

NITROGEN POLYMERS
Ballistic performance of polycarbonate/polyester and polycarbonate/styrene- acrylonitrile microlayer sheets [AD-A275462] 08 p3177 N94-28735
Basic solutions to carbon/carbon oxidation: Science and technology [AD-A280447] 12 p4404 N94-37232

NITROGEN TETROXIDE
Freon recovery from nitrogen tetroxide and freon solutions [PL-TR-92-3051] 07 p2721 N94-28215

NITROGEN 15
The 13C and 15N solid-state NMR of copolymers of nylon 6 and 7: Observation of a stable pseudohexagonal phase [AD-A265799] 01 p0094 N94-12381
NMR studies of enriched species at interfaces [AD-A264703] 04 p1367 N94-17878
Manual on measurement of methane and nitrous oxide emissions from agriculture [DE93-616429] 06 p2399 N94-25167
Method of N-15 analysis by mass-spectroscopy on ion implanter MPB-200 [DE94-618203] 12 p4407 N94-36529

NITROGENATION
Gordon Research Conference on Chronobiology, 1991 [AD-A266354] 02 p0728 N94-13698

NITROGLYCERIN
Closed-chamber analysis of M5 propellant lot RAD-64597 [AD-A266321] 02 p0585 N94-14145
Processing solid propellants for recycling [DE94-011433] 12 p4428 N94-37202

NITROGUANIDINE
Condensed-phase processes during solid propellant combustion. 3: Preliminary depth-profiling studies on XM39, JA2, M9, M30, and HMX2 [AD-A276595] 09 p3635 N94-32124

NITROMETHANE
Computer simulation of molecular response at a shock front [DE94-001050] 05 p1977 N94-22396

NITROUS OXIDES
Analysis of satellite-derived ozone and water vapor measurements [NASA-CR-193810] 04 p1486 N94-19237
Manual on measurement of methane and nitrous oxide emissions from agriculture [DE93-616429] 06 p2399 N94-25167
Implications of policies and prevent climate change for future food security [DE93-018872] 07 p2866 N94-25948
Ozone production at a rural site in Georgia during the summer 1992 SOS campaign [DE94-003989] 08 p3342 N94-28523
An improved method of measuring tropospheric NO2, NO3, HO2, and RO2 by Matrix Isolation and Electronic Spin Resonance (MIESR) 08 p3345 N94-28605
Charge trapping and breakdown in N2O oxides [DE94-003775] 08 p3266 N94-30040
A toy model for estimating N2O emissions from natural soils 08 p3351 N94-30627
The development and evaluation of a tunable diode laser trace gas sensor for the measurement of N2O and CH4 fluxes using micrometeorological techniques [ISBN-0-315-78975-1] 08 p3296 N94-30801
A correlated k-distribution model of the heating rates for atmospheric mixtures of H2O, CO2, O3, CH4, and N2O in the 0-2500 cm(exp -1) wave number region at altitudes between 0 and 60 km [DE94-005136] 09 p3775 N94-32895
Vacuum ultraviolet studies of molecular dynamics [AD-A278940] 11 p4321 N94-35657
Influences of flame-vortex interactions on formation of oxides of nitrogen in curved methane-air diffusion flamelets [DE94-005105] 12 p4409 N94-37221
Tropospheric radiative forcing of CH4 [DE94-011628] 12 p4468 N94-37631

NMR
U NUCLEAR MAGNETIC RESONANCE

NOAA F SATELLITE
U NOAA 9 SATELLITE

NOAA G SATELLITE
U NOAA 10 SATELLITE

NOAA SATELLITES
NT NOAA 9 SATELLITE
NT NOAA 10 SATELLITE
Radiometer offsets and count conversion coefficients for the Earth Radiation Budget Experiment (ERBE) spacecraft for the years 1987, 1988, and 1989 [NASA-CR-191489] 01 p0286 N94-12772
An algorithm for the remote sensing of fog using satellite-data and additional information [DLR-FB-92-23] 02 p0688 N94-14135
Scientific studies in association with the Shuttle Solar Backscatter Ultraviolet (SSBUV) project [NASA-CR-193404] 04 p1630 N94-19437
Instrument interface description for NOAA 2000 instruments with European morning spacecraft and/or NOAA-OPQ spacecraft [NASA-TM-109406] 06 p2208 N94-23478
Command/telemetry bus general specification for the NOAA-OPQ polar orbiting environmental satellites and EUMETSAT polar satellite systems [NASA-TM-109407] 06 p2208 N94-23479
Evaluating NOAA satellite products for global climate monitoring 06 p2384 N94-23604
Leadex environmental phenomena and effects observed by DMSP, NOAA, and ERS-1 satellites [AD-A274596] 07 p2868 N94-26888
Development of a statistical method for estimating the downward longwave radiation at the surface from satellite observations 09 p3742 N94-31553
Variability of the California Current System off Point Sur, California from April 1988 to December 1990 [AD-A278579] 12 p4476 N94-36985
NOAA polar satellite calibration: A system description [NOAA-TR-NESDIS-77] 12 p4396 N94-37009

NOAA 9 SATELLITE
Radiometer offsets and count conversion coefficients for the Earth Radiation Budget Experiment (ERBE) spacecraft for the years 1987, 1988, and 1989 [NASA-CR-191489] 01 p0286 N94-12772

NOAA 10 SATELLITE
Radiometer offsets and count conversion coefficients for the Earth Radiation Budget Experiment (ERBE) spacecraft for the years 1987, 1988, and 1989 [NASA-CR-191489] 01 p0286 N94-12772

NOBLE GASES
U RARE GASES

NOBLE METALS
NT GOLD
NT GOLD ISOTOPES
NT RUTHENIUM
NT SILVER
Field evaluation of six protective coatings applied to T-56 turbine blades after 2500 hours of engine use [ARL-TR-27] 01 p0090 N94-11311
Examination of the surface second harmonic response at infrared wavelengths [AD-A265206] 01 p0403 N94-12371
Spin polarized photoemission studies of interfacial and thin film magnetism [DE93-014326] 02 p0580 N94-14142
Experimental partitioning of Zr, Ti, and Nb between silicate liquid and a complex noble metal alloy and the partitioning of Ti between perovskite and platinum metal 03 p0962 N94-16287

NOCTILUCENCE
U LUMINESCENCE

NOCTURNAL VARIATIONS
Formation of the stable auroral arc that intensifies at substorm onset [NASA-CR-193637] 03 p1098 N94-15433

NODULES
A detailed investigation of the benthic regime in the Clarion-Clipperton province of the Pacific and a forecast of consequences of manganese nodule mining 01 p0224 N94-12733
Sarcoidosis and the aviator 06 p2425 N94-23325

NOE NAVIGATION
U NAP-OF-THE-EARTH NAVIGATION

NOISE
A window least squares algorithm for statistical noise smoothing of 2D-ACAR data [DE93-613828] 01 p0395 N94-10537
In-flight estimation of gyro noise on the Upper Atmosphere Research Satellite (UARS) and Extreme Ultraviolet Explorer (EUVE) missions 11 p4204 N94-35616

NOISE (SOUND)
NT AERODYNAMIC NOISE
NT AIRCRAFT NOISE
NT BLADE SLAP NOISE
NT ENGINE NOISE
NT JET AIRCRAFT NOISE
NT PROPELLER NOISE
NT SONIC BOOMS
NT THERMAL NOISE
Active control of periodic noise with time-varying frequency [REPT-93-012] 04 p1562 N94-17934
Parallel and vector adaptations of the underwater finite element parabolic equation model [AD-A269990] 04 p1563 N94-18678
Analysis of data from Columbia Point Arena Ocean-Bottom Seismic Station (OBSS) [AD-A271263] 04 p1500 N94-19727
A register of underwater acoustic test facilities in the US, Canada, and the United Kingdom [AD-A270884] 04 p1500 N94-19785
Noise measurements on two types of airplanes used for spraying in agriculture [LR-706] 04 p1319 N94-19796
The causes of contact noise [REPT-92-100] 05 p1822 N94-20157
Bulletin of Precision and Intelligence Laboratory, No. 68 [JTN-94-80609] 07 p3010 N94-27282
Minutes. Accredited Standards Committee on Noise, S12. US tag for ISO/TC 43/SC1 noise and ISO/TC 94/SC12 hearing protection [AD-A275622] 08 p3477 N94-28636
Evaluation of monitoring audiometry in the United States Air Force Hearing Conservation Program [AD-A275309] 08 p3391 N94-29211
Neural network application to Particle Impact Noise Detection 08 p3437 N94-29840

Parameter identification of the rotordynamic coefficients of high-Reynolds-number hydrostatic bearings
08 p3311 N94-30792
An investigation of acoustic noise requirements for the Space Station centrifuge facility
[NASA-TM-108811] 09 p3805 N94-32936
Improvements in spiral-bevel gears to reduce noise and increase strength
[NASA-TM-106613] 10 p4059 N94-33609
Comparison of transmission error predictions with noise measurements for several spur and helical gears
[NASA-TM-106647] 10 p4060 N94-33954
Influence of gear design parameters on gearbox radiated noise
[NASA-TM-106511] 10 p4060 N94-33972
Proceedings of the 6th International Congress on Noise as a Public Health Problem, volume 2
[AD-A278217] 10 p4134 N94-34290
Theoretical and experimental studies of auditory processing
[AD-A278505] 10 p4134 N94-34293
Measurements of correlation coefficients of vibration on a car body shell
[ISVR-TR-220] 10 p4070 N94-34307
Ground and space flight experiments of the effects of light, sound and/or temperature on animals
[NASA-CR-196102] 12 p4478 N94-36986

NOISE ATTENUATION
U NOISE REDUCTION

NOISE ELIMINATION
U NOISE REDUCTION

NOISE GENERATORS
Control of jet noise
[NASA-CR-193612] 01 p0358 N94-11176
Acoustic intensity measurements in the presence of low Mach number flow
[AD-A269995] 04 p1562 N94-18664
Fluid dynamic noise in a centrifugal pump
[AD-A275264] 08 p3477 N94-28904
Experiments on the aerodynamic generation of noise in centrifugal turbomachinery 08 p3480 N94-30804
Study on the measurement uncertainty of noise properties of a millimeter wave amplifier
[PB94-170917] 12 p4510 N94-37632

NOISE HAZARDS
U HAZARDS
U NOISE (SOUND)

NOISE INTENSITY
Spacecraft signal sources portable test system
01 p0139 N94-11000
Noise levels and their effects on Shuttle crewmembers' performance: Operational concerns
01 p0314 N94-11538
Preliminary analysis of the FLIP array data from the NOBS experiment
[AD-A265911] 01 p0289 N94-12349
1/f noise and oxide traps in MOSFETs
[DE93-007581] 02 p0619 N94-12942
An evaluation of noise and its effects on shuttle crewmembers during STS-50/USML-1
[NASA-TM-104775] 02 p0735 N94-13961
Underwater hearing: A review
[ISVR-TR-212] 02 p0777 N94-14130
Cruise noise measurements of a scale model advanced ducted propulsor
[NASA-TM-105808] 03 p1176 N94-15115
Technical evaluation report on the AGARD-PEP Specialists Meeting on Combat Aircraft Noise
[NLR-TP-91445-U] 03 p1177 N94-15506
Radar backscattering from snow facies of the Greenland ice sheet: Results from the AIRSAR 1991 campaign
05 p1725 N94-20434
The relative noise levels of parallel axis gear sets with various contact ratios and gear tooth forms
[AD-A276299] 05 p1826 N94-21756
Spatial frequency multiplier with active linearly tapered slot antenna array
[NASA-TM-106494] 06 p2310 N94-24308
Exercise keevil: Noise levels of six military helicopters
[PB93-210722] 06 p2529 N94-25026
VHF-UHF noise surveys at Gulkana, Elmensdorf AFB, Galena AFB, Kotzebue and Cape Lisburne, Alaska and NRL, Pomonkey, Maryland
[PL-TR-93-2136] 07 p2777 N94-28211
Subjective response to sonic booms having different shapes, rise times, and durations
[NASA-TM-109090] 08 p3479 N94-29464
Investigation of sonic boom for the Space Shuttle: High cross-range orbiter
[NASA-TM-108238] 09 p3860 N94-31336
Investigation of sonic boom for the Space Shuttle: Low cross-range orbiter
[NASA-TM-108237] 09 p3860 N94-31337
Experimental and computational studies on propeller noise due to inflow distortion 09 p3860 N94-31846
Aero acoustic analysis and community noise. HSCT climb to cruise noise assessment
10 p3975 N94-33491
A laboratory study of subjective annoyance response to sonic booms and aircraft flyovers
[NASA-TM-109113] 10 p4132 N94-33610
Comparison of transmission error predictions with noise measurements for several spur and helical gears
[NASA-TM-106647] 10 p4060 N94-33954
Influence of gear design parameters on gearbox radiated noise
[NASA-TM-106511] 10 p4060 N94-33972
Dose-response relationships derived from data collected at Grand Canyon, Haleakala and Hawaii Volcanoes National Parks
[PB94-151941] 10 p4134 N94-34380
A low temperature scanning force microscope for biological samples
[DE94-011357] 11 p4297 N94-36269
An improved assessment approach for noise impacts from stationary point and traffic sources on humans and wildlife
[DE94-009728] 11 p4319 N94-36320
Three flights into thunderstorms with the revised Rocket Electric Field Sounding (REFS) payload
[AD-A280424] 12 p4473 N94-37217

NOISE MEASUREMENT
An experimental assessment of the use of ground-level microphones to measure the fly-over noise of jet-engined aircraft
[NPL-RSA(EXT)-0039] 02 p0777 N94-13885
An evaluation of noise and its effects on shuttle crewmembers during STS-50/USML-1
[NASA-TM-104775] 02 p0735 N94-13961
Cruise noise measurements of a scale model advanced ducted propulsor
[NASA-TM-105808] 03 p1176 N94-15115
Cryogenic measurements of aerojet GaAs n-JFETs
[NASA-TM-103972] 03 p1009 N94-15765
Noise measurement flight test of five light helicopters
[AD-A268566] 03 p1179 N94-17599
Gear sound levels with various tooth contact ratios and forms
[NASA-TM-106432] 04 p1446 N94-19318
Noise measurements on two types of airplanes used for spraying in agriculture
[LR-706] 04 p1319 N94-19796
Interinjection-locked quasioptical power combiners and phased arrays
[AD-A271178] 05 p2015 N94-20214
Detector noise statistics in the non-linear regime
05 p1748 N94-22526
Validation of the ROTAC code for the rotor noise prediction
[PB93-204311] 06 p2529 N94-24514
Fan noise research at NASA
[NASA-TM-106512] 06 p2530 N94-25172
On the origin of 1/f noise in epitaxial GaAs
[ISBN-9-09-006067-7] 06 p2566 N94-25297
The ISL rotor bench
[ISL-R-108/92] 06 p2185 N94-25301
On the application of Allan variance method for Ring Laser Gyro performance characterization
[DE94-003880] 07 p2810 N94-26525
Report of National Institute for Resources and Environment. No. 8: Research on blasting sound related to it's measurement, propagation prediction, control and evaluation
[JTN-94-80605] 08 p3479 N94-29597
A high rate, low noise, x ray silicon strip detector system
[DE94-004557] 08 p3268 N94-30717
Long transect seafloor seismic array: A component of SAMSON (Sources of Ambient Micro Seismic Ocean ic Noise)
[AD-A277009] 09 p3789 N94-32401
HSCT design for reduced sonic boom
10 p3973 N94-33471
P and W propulsion systems studies results/status
10 p3974 N94-33480
Community noise technology needs: Boeing's perspective 10 p3975 N94-33490
High performance jet-engine flight test data base for HSR . 10 p3976 N94-33493
Relaxation and turbulence effects on sonic boom signatures 10 p3976 N94-33496
Overview of NASA human response to sonic boom program 10 p3976 N94-33499
Sonic boom acceptability studies
10 p3977 N94-33500
Georgia Tech sonic boom simulator
10 p3977 N94-33501
Sonic boom (human response and atmospheric effects) outdoor-to-indoor response to minimized sonic booms
10 p3977 N94-33502
Comparison of transmission error predictions with noise measurements for several spur and helical gears
[NASA-TM-106647] 10 p4060 N94-33954
Solid state acoustics information time region separating methods for gear diagnosis of failures
10 p4068 N94-34351
Activity report 1990-1992 and proceedings, volume 1
[DE94-610480] 11 p4290 N94-35830
Study on the measurement uncertainty of noise properties of a millimeter wave amplifier
[PB94-170917] 12 p4510 N94-37632

NOISE POLLUTION
Strategic planning for aircraft noise route impact analysis: A three dimensional approach
[NASA-CR-191484] 03 p1178 N94-17278
Transport policy options for reducing noise at airports; Hamburg airport taken as an example
[DLR-FB-92-40] 04 p1322 N94-18123
Aircraft noise effects on cultural resources: Recommendation and rationale for further research
[PB93-205326] 05 p1968 N94-22053
Aircraft noise effects on cultural resources: Annotated bibliography
[PB93-205334] 05 p1969 N94-22054
Silence amenity engineering: Past and present
07 p3011 N94-27283
Cooling towers for combined cycles: New developments to meet environmental requirements
07 p2832 N94-28088
The single European market: Economical advance, ecological problem? 07 p2661 N94-28235
Common property resources and low-level flying in Labrador: Flight, fight or fancy?
[ISBN-0-315-87318-3] 09 p3924 N94-31732
First Annual High-Speed Research Workshop, part 1
[NASA-CP-10087-PT-1] 10 p3970 N94-33447
Headquarters summary reports
10 p3970 N94-33452
Community noise sources and noise control issues
10 p3972 N94-33467
A NASA Lewis comparative propulsion system assessment for the High-Speed Civil Transport
10 p3974 N94-33477
Aeroacoustics analysis and community noise overview
10 p3975 N94-33488
Flying on the ground
[NASA-TM-109825] 10 p4132 N94-33579
Proceedings of the 6th International Congress on Noise as a Public Health Problem, volume 2
[AD-A278217] 10 p4134 N94-34290
A review of an updated synthesis of noise/annoyance relationships
[NASA-CR-194950] 10 p4134 N94-34303
Dose-response relationships derived from data collected at Grand Canyon, Haleakala and Hawaii Volcanoes National Parks
[PB94-151941] 10 p4134 N94-34380
An improved assessment approach for noise impacts from stationary point and traffic sources on humans and wildlife
[DE94-009728] 11 p4319 N94-36320

NOISE PREDICTION
Activities Report of the Institute of Applied Physics
[ETN-93-93749] 05 p1966 N94-21798
Traffic noise in a roundabout way
05 p1966 N94-21799
A modelling of the noise from simple co-axial jets. Part 2: In a simulated flightstream
[ISVR-TR-226] 06 p2525 N94-22959
Unsteady jet flow computation towards noise prediction
[NASA-CR-194449] 06 p2153 N94-23553
Silence amenity engineering: Past and present
07 p3011 N94-27283
A modelling of the noise from simple coaxial jets. Part 3: With hot primary flow
[ISVR-TR-230-PT-3] 07 p2807 N94-28173
Report of National Institute for Resources and Environment. No. 8: Research on blasting sound related to it's measurement, propagation prediction, control and evaluation
[JTN-94-80605] 08 p3479 N94-29597
Scattering of a random acoustic field by an infinite cylinder: Application to the modelization of the acoustic environment of the 'Ariane 5' launcher scale-model using experimental data
[ONERA-NT-1993-11] 09 p3860 N94-31226
HSCT noise reduction technology development at GE Aircraft Engines 10 p3972 N94-33466
Coupled 2-dimensional cascade theory for noise and unsteady aerodynamics of blade row interaction in turbofans. Volume 1: Theory development and parametric studies
[NASA-CR-4506-VOL-1] 10 p3998 N94-34146

Flow structure generated by perpendicular blade vortex interaction and implications for helicopter noise predictions
[NASA-CR-195824] 10 p3984 N94-34207

NOISE PREDICTION (AIRCRAFT)

Strategic planning for aircraft noise route impact analysis: A three dimensional approach
[NASA-CR-191484] 03 p1178 N94-17278

Validation of the ROTAC code for the rotor noise prediction
[PB93-204311] 06 p2529 N94-24514

INM, Integrated Noise Model. Version 4.11: User's guide, supplement
[AD-A273885] 07 p3009 N94-25731

Assessing the effects of Tuned Vibration Absorbers (TVAs) on interior cabin noise levels: A correlation between analytical acoustic predictions and flight test measurements 07 p2652 N94-28318

Experimental validation of finite element and boundary element methods for predicting structural vibration and radiated noise
[NASA-CR-4561] 08 p3301 N94-29552

Sonic boom prediction and minimization using computational fluid dynamics 10 p3973 N94-33472

Sonic boom predictions using a modified Euler code 10 p3973 N94-33474

Aeroacoustics analysis and community noise overview 10 p3975 N94-33488

Community noise technology needs: Boeing's perspective 10 p3975 N94-33490

Aero acoustic analysis and community noise. HSCT climb to cruise noise assessment 10 p3975 N94-33491

ANOPP/VMS HSCT ground contour system 10 p3975 N94-33492

High performance jet-engine flight test data base for HSR 10 p3976 N94-33493

Status and plans for the ANOPP/HSR prediction system 10 p3976 N94-33494

Overview of NASA HSR high-lift program 10 p3979 N94-33518

Status of LaRC HSCT high-lift research 10 p3979 N94-33519

Engine exhaust characteristics evaluation in support of aircraft acoustic testing 11 p4319 N94-35963

NOISE PROPAGATION

Sound exposure level prediction for impulse sound sources above variable terrain
[AD-A267535] 03 p1178 N94-17119

JAPE 91: Influence of terrain masking of the acoustic propagation of helicopter noise 06 p2528 N94-24214

Attenuation of outdoor sound propagation levels by a snow cover
[AD-A275387] 08 p3478 N94-29314

Report of National Institute for Resources and Environment. No. 8: Research on blasting sound related to it's measurement, propagation prediction, control and evaluation
[JTN-94-80605] 08 p3479 N94-29597

Reciprocity-based experimental determination of dynamic forces and moments: A feasibility study
[NASA-CR-194905] 09 p3862 N94-33023

ANOPP/VMS HSCT ground contour system 10 p3975 N94-33492

Computation of helicopter rotor acoustics in forward flight
[NASA-CR-196132] 11 p4319 N94-36031

An improved assessment approach for noise impacts from stationary point and traffic sources on humans and wildlife
[DE94-009728] 11 p4319 N94-36320

NOISE REDUCTION

Control of jet noise
[NASA-CR-193612] 01 p0058 N94-11176

A theory of membrane absorbers
[ISVR-TR-217] 01 p0076 N94-11216

Using lunar sounder imagery to distinguish surface from subsurface reflectors in lunar highlands areas 01 p0464 N94-12179

An analog clustering network from a biological model
[AD-A265637] 02 p0762 N94-12969

Active control of acoustic pressure fields using smart material technologies
[NASA-CR-191480] 02 p0768 N94-13354

Piston engine intake and exhaust system design
[ISVR-TR-222] 02 p0663 N94-13874

Study on the possibilities to apply spectrumindex
[VTT-PUBS-109] 02 p0777 N94-14034

Noise levels from a model turbofan engine with simulated noise control measures applied
[NASA-TM-106318] 02 p0518 N94-14036

Study of speckle reduction when using a CO2 waveguide laser close to its threshold state
[DSIS-93-00250] 02 p0657 N94-14067

Mixing noise reduction for rectangular supersonic jets by nozzle shaping and induced screech mixing
[NASA-TM-106364] 02 p0508 N94-14208

Active control of fan-generated plane wave noise
[NASA-TM-109008] 02 p0777 N94-14481

Removing noise from discontinuous data
[ITN-93-85211] 02 p0826 N94-14555

The 1968 highlights --- NASA programs and research
[NASA-TM-109627] 03 p1302 N94-15413

The 1971 highlights --- NASA programs and research
[NASA-TM-109629] 03 p1302 N94-15417

Technical evaluation report on the AGARD-PEP Specialists Meeting on Combat Aircraft Noise
[NLR-TP-91445-U] 03 p1177 N94-15506

Hydraulic pump with integral electric motor
[AD-D015782] 03 p1011 N94-16549

Suppression of backscatter and stray reflection induced phase noise in Michelson interferometers
[AD-D015809] 04 p1382 N94-17902

Transport policy options for reducing noise at airports; Hamburg airport taken as an example
[DLR-FB-92-40] 04 p1322 N94-18123

Inverse scattering of surface waves: A new look at surface consistency
[REPT-93-25] 04 p1486 N94-19140

Gear sound levels with various tooth contact ratios and forms
[NASA-TM-106432] 04 p1446 N94-19318

Applications of motion estimation in image processing
[FEL-92-B356] 04 p1580 N94-19455

Supersonic jets from bevelled rectangular nozzles
[NASA-TM-106403] 04 p1313 N94-19484

Oceanic in situ Fraunhofer-line characteristics: Fraunhofer-line underwater experiment (FLUX)
[AD-A270659] 05 p1881 N94-19952

VLSI mixed signal processing system 05 p1744 N94-21100

Survey of lift-fan aerodynamic technology
[NASA-CR-177615] 05 p1646 N94-21592

Active control of wake/blade-row interaction noise through the use of blade surface actuators
[NASA-CR-4556] 05 p1968 N94-21608

Journal of rehabilitation research and development, volume 30, number 1, 1993
[AD-A272956] 05 p1893 N94-21613

The relative noise levels of parallel axis gear sets with various contact ratios and gear tooth forms
[AD-A276299] 05 p1826 N94-21756

Signal classification and noise filtering using artificial neural networks 05 p1744 N94-22103

Noise filtering using multilayer feedforward neural network 05 p1770 N94-22104

Sub-band adaptive noise cancelling 05 p1774 N94-22125

Applications of a two-dimensional nonlinear filters to image restoration 05 p1789 N94-22225

Estimation of frequency offset in mobile satellite modems 06 p2285 N94-22807

Low noise electric motor 06 p2315 N94-23989

Vibrational power transmission analysis of machinery installations in ships with the objective of noise reduction
[ISVR-TR-216] 06 p2363 N94-24076

Fan noise research at NASA
[NASA-TM-106512] 06 p2530 N94-25172

Adaptive noise cancellation using recurrent radial basis function networks
[RR-472] 06 p2313 N94-25319

Evaluation of an Acoustic Charge Transport (ACT) device for adaptive interference suppression in spread spectrum communications systems
[AD-A274073] 07 p2765 N94-25647

High temperature sensor/microphone development for active noise control
[NASA-CR-195214] 07 p2812 N94-27214

Optimising BMW four-cylinder two-valve engines
[PB94-125101] 07 p2824 N94-27254

Silence amenity engineering: Past and present 07 p3011 N94-27283

Non-adaptive robust filters for speckle noise reduction
[INPE-5519-PRE/1794] 07 p2776 N94-27335

On the use of feedback to control sound radiation from a plate excited by a turbulent boundary layer
[ISVR-TR-227] 07 p2807 N94-28175

Assessing the effects of Tuned Vibration Absorbers (TVAs) on interior cabin noise levels: A correlation between analytical acoustic predictions and flight test measurements 07 p2652 N94-28318

Removal of coherent Extremely Low Frequency (ELF) background noise by adaptive noise cancellation
[AD-A275016] 08 p3243 N94-28898

Fluid dynamic noise in a centrifugal pump
[AD-A275264] 08 p3477 N94-28904

Boundary layer control device for duct silencers
[NASA-CASE-ARC-12030-1] 08 p3478 N94-29362

A novel approach to noise-filtering based on a gain-scheduling neural network architecture
[NASA-TM-106563] 08 p3155 N94-30204

Noise reduction techniques for the restoration of musical recordings
[TELECOM-93-E-019] 08 p3291 N94-30979

An adaptive Kalman filter excisor for suppressing narrowband interference
[AD-A276286] 09 p3671 N94-31253

Mitigation of adverse environmental effects on lunar-based astronomical instruments 09 p3598 N94-31426

A silicon condenser microphone: Modelling and electronic circuitry
[ISBN-9-09-005279-8] 09 p3688 N94-31517

A silicon condenser microphone: Materials and technology
[ISBN-9-09-005899-0] 09 p3688 N94-31518

Restoration of interferometric, polarimetric, radiometric, and textural information in SAR images 09 p3750 N94-32535

A mathematical model for simulating noise suppression of lined ejectors
[NASA-TP-3425] 09 p3861 N94-32930

An investigation of acoustic noise requirements for the Space Station centrifuge facility
[NASA-TM-108811] 09 p3805 N94-32936

Noise cancellation for CELP voice encoders in an F/A-18 noise environment
[AD-A277652] 09 p3683 N94-33026

First Annual HSR Program Workshop: Headquarters perspective 10 p3970 N94-33448

General Electric/Pratt and Whitney summary report 10 p3970 N94-33451

Headquarters summary reports 10 p3970 N94-33452

Airframe systems studies review 10 p3970 N94-33453

Douglas Aircraft HSCT status and future research needs 10 p3970 N94-33454

Overview of Langley systems studies 10 p3971 N94-33456

First Annual High-Speed Research Workshop, part 2
[NASA-CP-10087-PT-2] 10 p3972 N94-33462

NASA HSR phase 1 low noise nozzle technology program overview 10 p3972 N94-33463

High speed jet noise research at NASA Lewis 10 p3972 N94-33464

HSCT nozzle source noise programs at Pratt and Whitney 10 p3972 N94-33465

HSCT noise reduction technology development at GE Aircraft Engines 10 p3972 N94-33466

Community noise sources and noise control issues 10 p3972 N94-33467

NASA/LaRC jet plume research 10 p3972 N94-33468

HSCT design for reduced sonic boom 10 p3973 N94-33471

Sonic boom configuration minimization 10 p3973 N94-33473

P and W propulsion systems studies results/status 10 p3974 N94-33480

Community noise technology needs: Boeing's perspective 10 p3975 N94-33490

Aero acoustic analysis and community noise. HSCT climb to cruise noise assessment 10 p3975 N94-33491

HSCT integrated propulsion control issues 10 p3978 N94-33510

Enabling propulsion materials for high-speed civil transport engines 10 p3978 N94-33511

Nozzle material requirements and the status of intermetallic matrix composites 10 p3979 N94-33513

Overview of NASA HSR high-lift program 10 p3979 N94-33518

Status of LaRC HSCT high-lift research 10 p3979 N94-33519

HSCT high lift system aerodynamic requirements 10 p3980 N94-33522

HSCT high-lift technology requirements 10 p3980 N94-33523

Improvements in spiral-bevel gears to reduce noise and increase strength
[NASA-TM-106613] 10 p4059 N94-33609

Energy absorption apparatus
[AD-D016163] 10 p4133 N94-33699

A study on adaptive active noise control 10 p4122 N94-34372

Error reduction in images with the use of additional information
[AD-A278636] 11 p4334 N94-36257

A low temperature scanning force microscope for biological samples
[DE94-011357] 11 p4297 N94-36269

Forward sweep, low noise rotor blade
[NASA-CASE-LAR-14569-1] 12 p4386 N94-36767
A PDE-based methodology for modeling, parameter estimation and feedback control in structural and structural acoustic systems
[NASA-CR-194928] 12 p4500 N94-36924
Noise reduction for speech enhancement using non-linear wavelet processing
[AD-A280469] 12 p4434 N94-37141

NOISE SPECTRA
Preliminary analysis of the FLIP array data from the NOBS experiment
[AD-A265911] 01 p0289 N94-12349
1/f noise and oxide traps in MOSFETs
[DE93-007581] 02 p0619 N94-12942
Maximum likelihood techniques applied to quasi-elastic light scattering
[NASA-CR-193550] 03 p1192 N94-16718
Study of the utilization of thin oxides in indium phosphides for the realisation of electron components
[ECL-92-38] 05 p2018 N94-20593
Defect motion as the origin of the 1/f conductance noise in solids
[EUT-92-E-259] 05 p2029 N94-21552
Laser linewidth measurement in the presence of RIN and using the recirculating self heterodyne method
[EUT-92-E-262] 06 p2347 N94-22874
A modelling of the noise from simple co-axial jets. Part 2: In a simulated flightstream
[ISVR-TR-226] 06 p2525 N94-22959
Ground characterization for JAPE
06 p2527 N94-24213
Some subjects in digital audio, noise shaping, sample rate conversion, dynamic range compression and testing
[ISBN-9-09-005162-7] 06 p2530 N94-25220
Study of the blade/vortex interaction: Acoustics, aerodynamics and models
[ISL-R-104/92] 06 p2340 N94-25463
An analysis of FM jamming and noise quality measures
[AD-A274349] 07 p2772 N94-26924
Laser phase induced intensity noise in fiber-optic signal processing and sensing systems
[ITN-94-85234] 07 p2819 N94-27179
Geometrical resonances in the nyquist noise spectrum for ballistic conductors
[DE94-603668] 07 p3027 N94-27631
Parameter identification of the rotordynamic coefficients of high-Reynolds-number hydrostatic bearings
08 p3311 N94-30792
Blast overpressure studies with animals and man
[AD-A280240] 12 p4480 N94-37118

NOISE SUPPRESSORS
U NOISE REDUCTION

NOISE TEMPERATURE
Insertion loss and noise-temperature contribution of high-temperature superconducting bandpass filters centered at 2.3 and 8.45 GHz 02 p0608 N94-14376
Quantum noise studies with superconducting tunnel junction mixers
[AD-A270897] 05 p2012 N94-19897
Cryogenic, low-noise high electron mobility transistor amplifiers for the Deep Space Network
06 p2291 N94-23262
Determining noise temperatures in beam waveguide systems 08 p3249 N94-29657
A dual-cavity ruby maser for the Ka-band link experiment 08 p3250 N94-29658
X-band ultralow-noise maser amplifier performance
08 p3251 N94-29672
The electrical conductivities of candidate beam-waveguide antenna shroud materials
11 p4252 N94-35546
Spacecraft-spacecraft radio-metric tracking: Signal acquisition requirements and application to Mars approach navigation 11 p4254 N94-35557
Study on the measurement uncertainty of noise properties of a millimeter wave amplifier
[PB94-170917] 12 p4510 N94-37632

NOISE TOLERANCE
An evaluation of noise and its effects on shuttle crewmembers during STS-50/USML-1
[NASA-TM-104775] 02 p0735 N94-13961
Proceedings of the 6th International Congress on Noise as a Public Health Problem, volume 1
[AD-A278259] 10 p4133 N94-33961
Proceedings of the Sixth International Congress on Noise as a Public Health Problem, volume 3
[AD-A278218] 11 p4319 N94-36176

NOMENCLATURES
Effect of switched-bias bakes on the postirradiation electrical response of MOS devices
[DE93-009629] 01 p0143 N94-11271
Working group for planetary system nomenclature
[NASA-CR-194406] 04 p1626 N94-18841

NOMINAL VALUES
U APPROXIMATION

NOMOGRAMS
U NOMOGRAPHS

NOMOGRAPHS
Experimental determination of the CU-IN-PB ternary phase diagram
[DE94-003765] 07 p2735 N94-26349

NON-INTRUSIVE MEASUREMENT
U NONINTRUSIVE MEASUREMENT

NONADIABATIC CONDITIONS
The geometric phase in quantum physics
[DE93-011121] 02 p0817 N94-13479
Adiabatic and non adiabatic effects in Free Electron Laser (FEL) non linear interactions
[ITN-93-85224] 02 p0659 N94-14547
Supersymmetry of gauge equations and geometric nonadiabatic phases
[DE93-626671] 03 p1219 N94-14935
Polaron tunneling in high-temperature superconductors
[DE93-016880] 04 p1593 N94-17754
The quantum dynamics of electronically nonadiabatic chemical reactions
[NASA-CR-194309] 04 p1568 N94-18837
Nonlinear ion-mixing-mode particle transport in the dissipative trapped electron regime
[DE94-000989] 06 p2533 N94-23435
Nonadiabatic effects in the quantum Hall regime
08 p3513 N94-29530
Theory for electron-transfer reactions in a three-component system: The degenerate regime
[DE94-005919] 08 p3493 N94-30903
Nonadiabatic neutrino oscillations revisited
[DE94-616649] 11 p4321 N94-35593

NONADIABATIC PROCESSES
U HEAT TRANSFER

NONADIABATIC THEORY
Consequences of chaotic particle motion for the stability of space plasma current sheets
05 p2001 N94-22636

NONCONDENSABLE GASES
Fin-efficiency calculation for condensation in the presence of noncondensable gases
[DE93-017684] 04 p1409 N94-18004
The FY1992 survey on commercialization of Stirling engine utilization equipment
[DE94-707416] 05 p1849 N94-22029
Thermodynamic models for bounding pressurant mass requirements of cryogenic tanks
[NASA-TM-106476] 06 p2346 N94-25202
A computer program for condensing heat exchanger performance in the presence of noncondensable gases
[NASA-CR-177643] 10 p4048 N94-34259

NONCONDUCTORS
U ELECTRICAL INSULATION

NONDESTRUCTIVE TESTS
NT NEUTRON RADIOGRAPHY
Special problems of 3-D ultrasonic QNDI techniques and applications to composites aerospace structures
01 p0061 N94-10036
Design of inspection and acceptance test methodology for TIG welded aluminum-alloy bracket for camera housings for IRS-1A space craft and executing it
01 p0061 N94-10037
Quantifying disbond area 01 p0061 N94-10038
New x ray scanning topographic approaches to nondestructive evaluation of composites
01 p0061 N94-10039
Material characterization and modeling with shear ography
[NASA-CR-192576] 01 p0185 N94-10342
Report of the IAEA Consultants' Meeting on Real-Time Nondestructive Monitoring of Wear and Corrosion Using the Thin Layer Activation Technique
[DE93-617422] 01 p0183 N94-10847
Response of composite laminates to dynamic surface loads 01 p0066 N94-10902
A Recommended Methodology for Quantifying NDE/NDI Based on Aircraft Engine Experience
[AGARD-LS-190] 01 p0028 N94-11022
Fibre reinforced polymer matrix composites: Microstructure and mechanical properties
[DLR-FB-92-28] 01 p0066 N94-11085
Ultrasonic inspection, material noise and surface roughness
[DE93-011560] 01 p0183 N94-11110
A survey of techniques for corrosion monitoring
[DE93-012131] 01 p0083 N94-11250
Large array SQUID magnetometer for NDE
[AD-A264799] 01 p0304 N94-11449
Potential techniques for non-destructive evaluation of cable materials
[DE93-008350] 01 p0183 N94-11586
Ultrasonic wave interaction with advanced complex materials for nondestructive evaluation applications
[AD-A265704] 01 p0074 N94-12401
Development of nondestructive evaluation methods and prediction of effects of flaws on the fracture behavior of structural ceramics
[DE93-012942] 02 p0577 N94-13032
Quantitative mapping of pore fraction variations in silicon nitride using an ultrasonic contact scan technique
[NASA-TP-3377] 02 p0665 N94-13056
NDE of titanium alloy MMC rings for gas turbine engines
[NASA-TM-106188] 02 p0555 N94-13138
Structural investigation of a damaged GRP/foam sandwich composite using x ray computed tomography
02 p0669 N94-13857
The development of inspection and repair methods for the C-17 aft cargo door
[LR-704] 02 p0499 N94-13904
High frame rate thermal imager for hypersonic wind tunnel applications
[ONERA-NT-1992-12] 02 p0850 N94-14009
Enhanced NDE systems
[NASA-CR-192603] 02 p0669 N94-14101
JPRS report: Science and technology. Central Eurasia: Materials science
[JPRS-UMS-93-006] 02 p0558 N94-14573
Study of deferred acoustic emission in carbon epoxy composites
[ISAL-91-0078] 02 p0560 N94-14815
Physical interpretation and development of ultrasonic nondestructive evaluation techniques applied to the quantitative characterization of textile composite materials
[NASA-CR-194549] 03 p0931 N94-15190
Component testing and quality assurance
03 p0932 N94-15259
The Marshall Automated Weld System (MAWS)
[TABES PAPER 93-602] 03 p1049 N94-16138
Detection of subsurface defects in machined silicon nitride ceramics by optical scattering methods
[DE93-015554] 03 p0968 N94-16658
Ultrasonic wave propagation model for nondestructive evaluation of solid rocker motor propellant
[AD-A267653] 03 p0976 N94-17248
Synthesis and evaluation of polymeric materials
[AD-A267809] 03 p0973 N94-17408
X ray computed tomography for failure analysis investigations
[AD-A268086] 03 p1055 N94-17515
X ray computed tomography for casting demonstration
[AD-A268084] 03 p1056 N94-17596
The application of nondestructive techniques to the testing of a wind turbine blade
[DE93-016731] 04 p1447 N94-18128
High resolution SQUID magnetometry for non-destructive evaluation
[AD-A268884] 04 p1447 N94-18225
Nondestructive inspection of graphite-epoxy laminates for heat damage using DRIFT and LPF spectroscopies
[DE93-017228] 04 p1343 N94-18761
Metallurgical evaluation of SRAM 2/SRAM A program mer base plates
[DE93-018689] 04 p1364 N94-19100
Ultrasonic technique for inspection of GPHS capsule girth weld integrity
[DE93-040072] 04 p1448 N94-19189
Three dimensional ultrasonic imaging: An aging aircraft nondestructive inspection tool
[DE93-018088] 04 p1448 N94-19252
Materials characterization of propellants using ultrasonics
[NASA-CR-193877] 04 p1378 N94-19494
New aircraft materials and structures
[MBB-LME-202-S-PUB-502-A] 04 p1319 N94-19496
Thermal wave image processing for characterization of subsurface of flaws in materials
[DE93-019024] 04 p1344 N94-19551
Quantitative evaluation of material composition of composites using x ray energy-dispersive NDE technique
[DE93-041157] 05 p1672 N94-19688
Microscopic origins of metastable effects in a-Si:H and deep defect characterization in a-Si,Ge:H alloys
[DE93-018205] 05 p1688 N94-19985
Three-dimensional dynamic thermal imaging of structural flaws by dual-band infrared computed tomography
[DE93-019575] 05 p1906 N94-20316
Development of improved processing and evaluation methods for high reliability structural ceramics for advanced heat engine applications, phase 1
[DE93-040528] 05 p1702 N94-20481
Spectroscopic ellipsometry studies of HF treated Si(100) surfaces 05 p1734 N94-20508
Ellipsometric study of Si(0.5)Ge(0.5)/Si strained-layer superlattices 05 p1734 N94-20509

The 1992 USAF structural integrity program conference
[AD-A272876] 05 p1635 N94-21194
Damage states around fastener holes in thick graphite/epoxy composite laminates
[AD-A272613] 05 p1675 N94-21504
Surface and subsurface defect detection in Si3N4 components by laser scattering
[DE93-040829] 05 p1832 N94-21772
Millimeter-wave imaging of composite materials
[DE93-041160] 05 p1677 N94-21940
Three dimensional ultrasonic imaging
[DE93-040549] 05 p1968 N94-22003
Strength, ultrasonic and metallurgical evaluation of diffusion bonds
[DE94-000665] 05 p1697 N94-22571
An embedded fibre optic for damage growth monitoring in Kevlar composites
[ISBN-0-315-83501-X] 05 p1677 N94-22589
Theoretical studies of wave propagation in multilayered piezoelectric media
[DE93-040273] 06 p2371 N94-22872
Strength, acoustic evaluation and metallurgy of diffusion bonds
[DE94-001804] 06 p2243 N94-23717
An evaluation of Compton scatter imaging using COMSCAN
[DREP-TM-93-38] 06 p2372 N94-24136
Ultrasonic nondestructive evaluation as a tool for the development of aerospace structural ceramic composites 06 p2257 N94-24240
Nondestructive evaluations
[DE94-003020] 06 p2373 N94-24613
Investigation of the effects of manufacturing variations and materials on fatigue crack detection methods in gear teeth
[NASA-CR-195093] 06 p2373 N94-24769
Demonstration of polyscann ultrasonic butt-fusion inspection system for polyethylene pipes
[AD-A273279] 06 p2373 N94-24814
Development of a nondestructive vibration technique for bond assessment of Space Shuttle tiles
[NASA-CR-195163] 06 p2201 N94-24919
Nuclear magnetic resonance imaging with short gradient pulses
[AD-D016006] 06 p2537 N94-25047
General Motors Corporation and Pacific Northwest Laboratory staff exchange: Inspection of case hardened steels and metal-matrix composites
[DE94-003470] 07 p2706 N94-25982
Non-contact ultrasonic inspection
[VTT-TIED-1454] 07 p2835 N94-26257
Design and life-time of polymer matrix composite structures: Summary
[VTT-TIED-1415] 07 p2707 N94-26260
Development of non-destructive testing technology for the crack of steam generator tubes
[DE93-632953] 07 p2835 N94-26399
Reconstruction of multiple cracks from experimental electrostatic boundary measurements
[AD-A277433] 07 p2994 N94-26601
A comparison of Probability Of Detection (POD) data determined using different statistical methods
[LTR-ST-1947] 07 p2835 N94-26644
Optical surface contouring for non-destructive inspection of turbomachinery
[NASA-CR-195245] 07 p2835 N94-26691
Calculation of the electromagnetic critical state response of high T(sub c) superconductor tape
[DE94-002894] 07 p3061 N94-26868
Space Shuttle main engine turbopump bearing assessment program
[NASA-TM-108447] 07 p2833 N94-26265
Portable electronically based method for the nondestructive remote sensing of crevice corrosion
[AD-A275403] 08 p3318 N94-29057
Automation of the NDT diagnostic using neural nets. Application: Inspection of Airbus longitudinal joints during maintenance
[REPT-932-600-104] 08 p3315 N94-29474
Bolt and nut evaluator
[NASA-CASE-GSC-13468-1] 08 p3288 N94-29538
Method and apparatus for indicating disbonds in joint regions
[NASA-CASE-LAR-14626-1] 08 p3315 N94-29548
Improved ground-penetrating radar, bridge decks
[DE94-004863] 08 p3254 N94-29929
Vacuum chamber and adaptors for shearography and holography
[NASA-CR-192467] 08 p3157 N94-29956
Physical interpretation and development of ultrasonic nondestructive evaluation techniques applied to the quantitative characterization of textile composite materials
[NASA-CR-195766] 08 p3183 N94-30016
Development of evaluated data bank of physical properties of perspective nuclear engineering steels and alloys
[DE94-607999] 08 p3207 N94-30076
Resonant ultrasound spectroscopy for elastic constant measurements
[DE94-005016] 08 p3480 N94-30098
Radar jet engine health monitoring project
[ASSGI-301] 08 p3153 N94-30130
Robotic NDE inspection of advanced solid rocket motor casings
[AIAA PAPER 94-1222-CP] 08 p3446 N94-30571
Automation for nondestructive inspection of aircraft
[AIAA PAPER 94-1223-CP] 08 p3446 N94-30572
Evaluation of nondestructive inspection techniques for quality control of alumina-ceramic housing components
[AD-A276220] 09 p3730 N94-31065
Naval Surface Warfare Center Dahlgren Division Technical Digest: Advanced materials technology
[AD-A276448] 09 p3668 N94-31364
Determining the bearing capacity of flexible airfield pavements using a heavy weight deflectometer
[ISBN-0-315-86210-6] 09 p3587 N94-31710
Ultrasonic characterization of damage in a simulated CF-18 composite structure
[DREP-LN-93-26] 09 p3730 N94-31872
Location of impact damage sites in composite aircraft structures, task 3.4.1
[DSIS-94-01590] 09 p3621 N94-31892
Benchmarking of the state-of-the-art in nondestructive testing/evaluation for applicability in the Composite Armored Vehicle (CAV) Advanced Technology Demonstrator (ATD) program, phase 1
[AD-A276660] 09 p3730 N94-32088
Shearographic inspection of a DeHavilland DHC-7
[AD-A276716] 09 p3566 N94-32157
A versatile nondestructive evaluation imaging workstation 09 p3732 N94-32458
Differential phase acoustic microscope for micro-NDE
[NASA-CR-189617] 09 p3731 N94-32481
Dual-band infrared imaging to detect corrosion damage within airframes and concrete structures
[DE94-006047] 09 p3580 N94-32658
PSIDD: A Post-Scan Interactive Data Display system for ultrasonic scans
[NASA-TM-4545] 09 p3732 N94-33038
On-orbit NDE: A novel approach to tube weld inspection 10 p4066 N94-33664
NDE activities and technology transfer at Sandia National Laboratories
[DE94-007294] 10 p4067 N94-33688
The use of pulsed neutron diffraction to measure strain in composites
[DE94-007536] 10 p4019 N94-33693
Assessment of the current European research and developments in non-invasive integrated circuit analysis
[DE94-004042] 10 p4039 N94-33735
Solid state acoustics information time region separating methods for gear diagnosis of failures 10 p4068 N94-34351
Characterisation of Fibre Reinforced Titanium Matrix Composites
[AGARD-R-796] 12 p4400 N94-36649
Ultrasonic nondestructive characterization methods for the development and life prediction of titanium matrix composites 12 p4401 N94-36660
Detection of delaminations in composite beams using piezoelectric sensors
[NASA-TM-106611] 12 p4403 N94-36956
Density and composition analysis using focused MeV ion microbeam techniques
[DE94-012241] 12 p4517 N94-37210
Process enhancements of superalloy material 12 p4421 N94-37324
Development of nondestructive evaluation methods and prediction of effects of flaws on the fracture behavior of structural ceramics
[DE94-012466] 12 p4425 N94-37423

NONEQUILIBRIUM CONDITIONS
The High Precision Thermostat HPT-HYDRA 01 p0109 N94-10124
Non-equilibrium solidification in undercooled Ni-B alloys 01 p0086 N94-10196
Boundary stability under nonequilibrium conditions
[DE93-016259] 02 p0809 N94-13980
Characterization of flow fields in hypersonic ground test facilities 02 p0505 N94-14157
Nonequilibrium radiation and chemistry models for aerocapture vehicle flowfields
[NASA-CR-195706] 07 p2648 N94-28071
Models for vibration-dissociation coupling in high-temperature gases 08 p3273 N94-29675
Using nonequilibrium alloying techniques for corrosion inhibition in Gr/Al and Gr/Mg metal matrix composites
[AD-A280529] 12 p4404 N94-37088

NONEQUILIBRIUM DRAG
U FRICTION DRAG

NONEQUILIBRIUM FLOW
Studies on scramjet nozzles. Part 1: Performance of two dimensional nozzles
[NAL-TR-1149] 01 p0027 N94-10367
Calculations of viscous nonequilibrium flows in nozzles 01 p0008 N94-10455
Nonequilibrium hypersonic flow in a wind-tunnel nozzle 01 p0008 N94-10456
Hypersonic, nonequilibrium flow over a cylindrically blunted 6 deg wedge
[NASA-TM-108994] 01 p0162 N94-12571
Computation of nonequilibrium flows using PNS equations 02 p0641 N94-14610
Particle kinetic simulation of high altitude hypervelocity flight
[NASA-CR-194599] 03 p0856 N94-15678
Studies on nonequilibrium phenomena in supersonic chemically reacting flows
[NASA-CR-194662] 03 p1027 N94-17215
Establishing the basis for validated predictions of highly non-equilibrium flows (with 9 attachments)
[AD-A272918] 05 p1802 N94-21220
Upwind MacCormack Euler solver with non-equilibrium chemistry 06 p2326 N94-23672
Radiative properties of molecular nitrogen ions produced by helium Penning ionization and argon effects
[NASA-CR-195126] 06 p2534 N94-24487
Chemical and vibrational nonequilibrium viscous flows: Modelling, internal and external flow applications
[ESA-TT-1274] 07 p2791 N94-26316
Approximate Riemann solvers: Improvement of the HLLEM scheme and its generalization for chemically reacting flows
[NAL-TR-1189] 07 p2795 N94-27205
TVD flux-difference split methods for high-speed thermochemical nonequilibrium flows with strong shocks
[UTIAS-350] 07 p2799 N94-27880
Numerical analysis of two dimensional/axisymmetric non-equilibrium hypersonic flow 08 p3125 N94-28963
On approximate Riemann solvers: Improvement of HLLEM scheme and its generalization for chemically reacting flows 08 p3126 N94-28973
Models for vibration-dissociation coupling in high-temperature gases 08 p3273 N94-29675
Response of wall turbulence to high frequency streamwise and spanwise oscillations 09 p3700 N94-31211
Development and application of computational aerothermodynamics flowfield computer codes
[NASA-CR-196136] 11 p4189 N94-35498
NEQPAK, the AEDC thermochemical nonequilibrium package: Theory and use
[AD-A279005] 11 p4266 N94-35951
A flux splitting scheme with high-resolution and robustness for discontinuities
[NASA-TM-106452] 12 p4441 N94-36646
Experimental investigation of nozzle/plume aerodynamics at hypersonic speeds
[NASA-CR-195829] 12 p4382 N94-36687
Hypersonic, nonequilibrium flow over the FIRE 2 forebody at 1634 sec
[NASA-TM-109141] 12 p4444 N94-37455
Theoretical studies of a molecular beam generator
[NASA-CR-196306] 12 p4522 N94-37508

NONEQUILIBRIUM IONIZATION
Nonequilibria in thermal emission from supernova remnants
[NIFS-264] 06 p2602 N94-24866
Modelling of ionisation reactions and of the resulting electric fields in one-dimensional hypersonic shock waves with the direct simulation Monte Carlo method
[IC-AERO-92-01] 07 p2644 N94-26248

NONEQUILIBRIUM PLASMAS
Synthesis of ceramic oxide powders in a microwave plasma device
[DE93-012741] 03 p0965 N94-15920
Modelling of thermal argon plasmas
[ETN-94-95363] 06 p2554 N94-25300

NONEQUILIBRIUM RADIATION
Nonequilibrium radiation and chemistry models for aerocapture vehicle flowfields
[NASA-CR-194645] 03 p1027 N94-17095
Nonequilibrium radiation and chemistry models for aerocapture vehicle flowfields
[NASA-CR-195706] 07 p2648 N94-28071

NONEQUILIBRIUM THERMODYNAMICS
Canonical operator formulation of nonequilibrium thermodynamics
[DE93-613028] 01 p0409 N94-10388
Nonequilibrium hypersonic flow in a wind-tunnel nozzle 01 p0008 N94-10456

Hypersonic multi block flow simulations around space vehicles including non-equilibrium chemistry
01 p0009 N94-10460
Thermal and chemical non equilibrium hypersonic flow computations 01 p0010 N94-10465
Arcjet space thrusters
[NASA-CR-193191] 01 p0046 N94-10700
Topics on spatially high-order accurate methods and pre-conditioning for the Navier-Stokes equations with finite-rate chemistry 02 p0633 N94-13572
Numerical simulation of viscous flows in chemical nonequilibrium
[MBB-LME-211-S-PUB-506] 04 p1421 N94-19497
Essential shift: Scientific revolution in the 20th century
[AD-A270810] 04 p1610 N94-19663

NONEUCLIDIAN GEOMETRY
U DIFFERENTIAL GEOMETRY

NONFLAMMABLE MATERIALS
Proceedings of the International Conference for the Promotion of Advanced Fire Resistant Aircraft Interior Materials
[DOT/FAA/CT-93/3] 01 p0017 N94-10766
Fire-resistant hydrolytically stable poly(arylene phosphine oxide) material systems
01 p0019 N94-10780
A non-halogenated, flame retarded polycarbonate
01 p0019 N94-10781
Flammability parameters of materials: Ignition, combustion, and flame spread 01 p0020 N94-10788
Future material development trends for commercial airplane interiors 01 p0021 N94-10792
Future needs in the development of materials for aircraft interiors and equipment 01 p0021 N94-10794
Proceedings of the International Conference for the Promotion of Advanced Fire Resistant Aircraft Interior Materials
[AD-A266057] 01 p0022 N94-12384
Fire-resistant barriers for composite materials
[AD-D016014] 06 p2230 N94-24735
Impact of improved materials and cabin water spray on commuter aircraft postcrash fire survivability
[AD-A274421] 07 p2660 N94-27081

NONGRAY GAS
Study of multi-dimensional radiative energy transfer in molecular gases
[NASA-CR-194613] 03 p1181 N94-15752

NONHOLONOMIC EQUATIONS
Dynamics and design of nonholonomic robotic mechanical systems
[ISBN-0-315-72009-3] 02 p0662 N94-13597
Trajectory planning for space manipulators
[AD-A277229] 09 p3611 N94-32369

NONHOMOGENEITY
U INHOMOGENEITY

NONINTRUSIVE MEASUREMENT
Local measurement of temperatures and concentrations: A review for hypersonic flows
01 p0004 N94-10434
Hypersonic flow-field measurements: Nonintrusive
02 p0507 N94-14167
Nonintrusive fast response oxygen monitoring system for high temperature flows
[NASA-CR-4553] 03 p1036 N94-17655
Studies on high pressure and unsteady flame phenomena: Revision
[AD-A269138] 04 p1348 N94-18257
Earth Penetration Radar Imaging System (EPRIS)
[DE93-019890] 04 p1391 N94-19542
Measurement of thermal-hydraulic parameters in two-phase flow using flow visualization image analysis
[DE93-006255] 05 p1805 N94-22269
An experimental study of characteristic combustion-driven flows for CFD validation
06 p2212 N94-23040
Design of a surface deformation measuring instrument for the Surface Tension Driven Convection Experiment (STDCE-2)
[NASA-CR-194758] 06 p2343 N94-23285
Doppler global velocimetry: Development of a flight research instrumentation system for application to non-intrusive measurements of the flow field
[NASA-CR-191490] 06 p2344 N94-24360
Temperature measurement using infrared imaging systems during turbine engine altitude testing
[NASA-TM-105871] 06 p2193 N94-25184
Non-invasive optical detection of glucose in cell culture nutrient medium 06 p2422 N94-25357
Non-intrusive gaze tracking using artificial neural networks
[AD-A275186] 08 p3397 N94-28860
An actively cooled floating element skin friction balance for direct measurement in high enthalpy supersonic flows 08 p3289 N94-29824
Non-invasive temperature measurements using electron paramagnetic resonance spectroscopy
08 p3198 N94-29881
Photopyroelectric spectroscopy as a non-intrusive technique for the determination of the optical absorption spectra of multiple quantum well samples
[ISBN-0-315-87164-4] 09 p3833 N94-31875
Design of a two dimensional planer pressurized air labyrinth seal test rig
[AD-A277232] 09 p3726 N94-32370
Scalar imaging velocimetry studies of turbulent flow structure and dynamics
[AD-A278395] 09 p3710 N94-33164
The 3rd International Symposium on Special Topics in Chemical Propulsion: Non-Intrusive Combustion Diagnostics
[AD-A277443] 10 p4016 N94-34079
Measurement of a surface heat flux and temperature
11 p4231 N94-36407
A non-intrusive way to measure point-of-gaze
12 p4484 N94-37272

NONISOTHERMAL PROCESSES
Chemical vapour deposition of tungsten for the application in integrated circuits
[ISBN-9-09-005151-1] 09 p3641 N94-31519

NONISOTROPIC PLATES
U ANISOTROPIC PLATES

NONISOTROPY
U ANISOTROPY

NONLINEAR EQUATIONS
NT CUBIC EQUATIONS
NT DUFFING DIFFERENTIAL EQUATION
NT NONLINEAR EVOLUTION EQUATIONS
NT QUADRATIC EQUATIONS
NT QUARTIC EQUATIONS
Non-linear liquid bridge dynamics
01 p0100 N94-10074
General renormalized statistical approach with finite cross-field correlations
[DE93-617846] 01 p0386 N94-10396
A symmetrical form for equations of a nonlinear spiral magnetic
[DE93-621350] 01 p0344 N94-11033
Dynamics and control of coherent structures in the turbulent wall layer: An overview
01 p0031 N94-11494
Nonlinear and dynamic analysis of flight
01 p0032 N94-11496
Spline approximation for system of n-th order nonlinear ordinary differential equations
[DE93-608188] 01 p0346 N94-11507
Open boundary conditions for incompletely parabolic systems
[FFI/RAPPORT-92/7029] 02 p0770 N94-13971
Multiplicative noise: Applications in cosmology and field theory
[DE93-016624] 02 p0840 N94-14536
Large spatial, temporal, and algorithmic adaptivity for implicit nonlinear finite element analysis
[DE93-016438] 02 p0771 N94-14589
Construction of the Courant-Snyder invariants for the non-linear equations of motion under presence of the linear coupling
[DE93-017565] 02 p0788 N94-14872
On a convergence of iterative Newton's scheme
[DE93-626604] 02 p0772 N94-14886
Adaptive wavelet collocation methods for initial value boundary problems of nonlinear PDE's
[NASA-CR-191507] 03 p1169 N94-15833
Nonlinear problems in fluid dynamics and inverse scattering
[AD-A266234] 03 p1026 N94-16927
Applications of the phi-transform
[AD-A266247] 03 p1170 N94-16940
Numerically solving a transient heat conduction problem with convection and radiation
[AD-A268521] 03 p1220 N94-17540
SAND contact in DYNA3D
[DE93-016451] 04 p1340 N94-18113
On higher dimensional Ermakov systems: Canonical reductions
[MATHS-REPT-A-182] 04 p1548 N94-18140
ASYS: a computer algebra package for analysis of nonlinear algebraic equations systems
[DE93-629819] 04 p1548 N94-18175
On the numerical analysis of nonlinear Galerkin methods: Spectral approximation and finite elements
[ETN-93-94900] 04 p1552 N94-19407
Dynamical systems and nonlinear partial differential equations
[AD-A271514] 05 p1951 N94-20545
Two-dimensional nonlinear Schrodinger equations and their properties
[AD-A272184] 05 p1952 N94-20923
Universality in blow-up for non linear heat equations
[PB93-215465] 05 p2038 N94-22095
Non-linear analysis of the electrical properties of the active circuits of high-frequency oscillators
05 p1785 N94-22195
On the nonlinear instability of thermal structures
05 p2006 N94-22668
Nonlinear smoothing for random fields
[PB94-149531] 06 p2493 N94-22728
The characterization of reaction-convection-diffusion processes by travelling waves
[PB94-150315] 06 p2273 N94-22729
Incomplete corrections in nonlinear problems
[PB93-225746] 06 p2479 N94-23106
On the estimation of the correlation dimension and its application to radar reflector discrimination
[NASA-CR-4564] 06 p2309 N94-23304
Periodic nonlinear Schroedinger equation and invariant measures
[PB93-238012] 06 p2487 N94-23775
Error due to the stopping of the Newton iteration in implicit linear multistep methods
[PB94-101425] 06 p2487 N94-23786
On the dynamics of some grid adaption schemes
[NASA-CR-195092] 06 p2454 N94-24110
On the dynamics of approximating schemes for dissipative nonlinear equations
06 p2332 N94-24168
Global dynamic stability of a shallow arch by poincare-like simple cell mapping
06 p2160 N94-24280
Stable non-Gaussian diffusive profiles
[PB93-238053] 06 p2489 N94-24610
Stability analysis of anisotropic conical shells
[PB94-119054] 06 p2377 N94-24645
Nonlinear equations of motion for a panel subject to external loads
[AD-A273142] 06 p2170 N94-24773
Approximation to nonlinear equations using nonlinear rational models
[RR-448] 06 p2492 N94-25306
Selfsimilar solutions of a nonlinear transport equation
[REPT-93-42] 07 p2865 N94-25760
Predicting nonlinear time series
[AD-A274051] 07 p2990 N94-25834
Continuation and multi-grid for bifurcation problems
[AD-A274965] 07 p2992 N94-26302
A parametric sensitivity study for single-stage-to-orbit hypersonic vehicles using trajectory optimization
[NASA-CR-195703] 07 p2697 N94-27789
Nonlinear solvers 07 p2829 N94-28053
Numerical analysis and computation of nonlinear partial differential equations from applied mathematics
[AD-A275582] 08 p3451 N94-28723
Approximation of solutions of the cubic NLSE by finite dimensional equations and non-squeezing properties
[PB94-138294] 08 p3452 N94-29148
A non-linear simulation for an autonomous unmanned air vehicle
[AD-A275062] 08 p3146 N94-29200
Nonlinear wave packet evolution in a dispersive plasma: Application to rotational discontinuities
08 p3506 N94-29822
Approximation methods for nonlinear operator equations of the m-accretive type
[DE94-608099] 08 p3467 N94-30065
Fuzzy logic based robotic controller
[AIAA PAPER 94-1202-CP] 08 p3443 N94-30553
On wavelet representations of differential equations
[RR-482] 09 p3842 N94-31412
The finite element method with asymptotic self-similar solutions 09 p3736 N94-31904
Design and Monte Carlo analysis of an unmanned aerial vehicle
[AD-A277648] 09 p3580 N94-33056
Whiskered tori for integrable pde's: Chaotic behavior in near integrable pde's
[AD-A278390] 10 p4128 N94-33430
Self-similar regimes of subsonic Langmuir wave collapse
[DE94-611466] 11 p4335 N94-35750
Variations in the modal characteristics of a telescopically deploying beam 11 p4218 N94-35872
Multiquadric collocation methods in the numerical solution of Volterra integral equations with weakly singular kernels
[DE94-013000] 12 p4505 N94-37497
Hierarchically parallelized constrained nonlinear solvers with automated substructuring
[NASA-CR-194474] 12 p4456 N94-37554
Tensor-GMRES method for large sparse systems of nonlinear equations
[NASA-CR-196379] 12 p4505 N94-37655

NONLINEAR EVOLUTION EQUATIONS
Cauchy problem for periodic KDV-type equations
[PB93-238020] 06 p2487 N94-23776

NONLINEAR FEEDBACK
Nonlinear disturbance decoupling and linearization: A partial interpretation of integral feedback
[PB93-197515] 04 p1543 N94-19328

Adaptive nonlinear polynomial neural networks for control of boundary layer/structural interaction
[NASA-CR-189645] 06 p2525 N94-23698
Stabilization of flexible systems under a certain class of nonlinear feedback controls 10 p4114 N94-34314
Nonlinear feedback model attitude control using CCD in magnetic suspension system 11 p4225 N94-35912

NONLINEAR FILTERS
Nonlinear resonance: Noise-assisted information processing in physical and neurophysiological systems
[AD-A265161] 01 p0313 N94-11890
Development and analysis of ARMA parameter estimation schemes in the presence of noise
[AD-A267184] 03 p0989 N94-15786
High order nonlinear estimation with signal processing applications
[AD-A268407] 03 p1005 N94-17463
A comparative robustness evaluation of feedforward neurofilters
[NASA-TM-106440] 05 p1650 N94-21742
Applications of a two-dimensional nonlinear filters to image restoration 05 p1789 N94-22225
Evolving recurrent perceptrons
[AD-A273241] 06 p2496 N94-24778
White noise theory of robust nonlinear filtering with correlated state and observation noises
[PB94-126661] 07 p3004 N94-27211
A novel approach to noise-filtering based on a gain-scheduling neural network architecture
[NASA-TM-106563] 08 p3155 N94-30204
Linearly separable stack-like architecture for the design of weighted order statistic filters with application in image processing
[ISBN-0-315-87284-5] 09 p3675 N94-31731

NONLINEAR OPTICS
Nonlinear Dynamics in Optical Systems. Postdeadline papers presented at the Optical Society of America Conference
[AD-A264958] 01 p0375 N94-10486
Nonclassical states of the second optical harmonic in the presence of self-action 01 p0375 N94-10567
Disturbance, the uncertainty principle and quantum optics 01 p0375 N94-10569
Photon number amplification/duplication through parametric conversion 01 p0376 N94-10572
Non classical effects in planar waveguides 01 p0376 N94-10574
Squeezing in phase-conjugated resonance fluorescence 01 p0376 N94-10576
Second and third order nonlinear optical properties of crystalline inorganic/organic complexes
[DE93-011883] 01 p0173 N94-10755
Lattice-matched heteroepitaxy of wide gap ternary compound semiconductors 01 p0400 N94-11441
The laser second threshold: Its exact analytical dependence on detuning and relaxation rates
[DE93-619706] 01 p0175 N94-11633
A relaxation study of poled nonlinear optical polymers by infrared reflection-absorption spectroscopy
[AD-A265797] 01 p0093 N94-12380
Limitations to the quality of optical phase conjugation by stimulated Brillouin scattering
[AD-A266006] 01 p0383 N94-12389
Engineering solid-state materials. Strategies for modeling and packing control of molecular assemblies into 3-D networks
[AD-A265291] 01 p0404 N94-12438
Nonlinear optical spectroscopy of Ag(111) in electrolyte and in vacuum
[AD-A265622] 01 p0079 N94-12534
Preparation of stable photopatternable polymeric materials for non-linear optics
[AD-A265359] 01 p0095 N94-12577
Nonlinear laser spectroscopy studies of semiconductor heterostructures
[AD-A265728] 02 p0805 N94-13037
Beam halo formation from space-charge dominated beams in uniform focusing channels
[DE93-014458] 02 p0789 N94-13209
Poling of thin polymer films in electro optic applications
[AD-A266562] 02 p0579 N94-13584
Optimum wavelengths for two color ranging 03 p0915 N94-15580
Design, synthesis and characterization of novel nonlinear optical polymers
[AD-A267035] 03 p0964 N94-15675
Organic polymeric electro-optic materials: Synthesis, processing, and device applications
[AD-A267133] 03 p0964 N94-15688
High-performance nonlinear optical material developed in Japan
[AD-A266194] 03 p1191 N94-16126
Rational design, construction, and processing of high-performance nonlinear optical materials
[AD-A266185] 03 p1191 N94-16454
New organic materials for nonlinear optics applications
[AD-A266451] 03 p1192 N94-16563
Main chain chromophoric polymers with second order nonlinear optical properties
[AD-D015893] 03 p0969 N94-16920
Theoretical studies of nonlinear optical properties of conjugated polymers
[AD-A267390] 03 p1193 N94-17024
Two-dimensional acousto-optical interaction theory and experimental analysis
[AD-A267761] 03 p1193 N94-17254
High-speed nonlinear switching mechanisms and devices for multi-gigabit data processing
[AD-A267753] 03 p1014 N94-17375
Spectral inverse scattering theory for dielectric media: Application to optical devices
[AD-A268635] 03 p1199 N94-17427
Optical studies of glasses embedded with inorganic ions and organic dyes
[AD-A268146] 03 p1199 N94-17455
Polaron tunneling in high-temperature superconductors
[DE93-016880] 04 p1593 N94-17754
Metal-nanocluster composites made by ion implantation: A novel third-order nonlinear material
[DE93-015908] 04 p1339 N94-17846
Development of short pulse soft x ray lasers
[DE93-017150] 04 p1437 N94-18131
IR materials producibility
[AD-A268849] 04 p1577 N94-18223
Tunable synchronously pumped intracavity two-stage optical frequency upconversion
[AD-A269105] 04 p1438 N94-18250
Integrated photonics research volume 10. Conference edition
[AD-A269298] 04 p1577 N94-18298
Applications of nonlinear optic effects in new specialty fibers
[AD-A268890] 04 p1578 N94-18457
Theory of electromagnetic waves propagating in nonlinear anisotropic optical materials
[AD-A269305] 04 p1386 N94-18469
Quantum Optoelectronics. Organization of the 1993 photonics science topical meetings. Technical digest series, volume 8
[AD-A269026] 04 p1578 N94-18488
Advanced Solid-State Lasers/Compact Blue-Green Lasers. 1993 technical digest series. Volume 2: Organization of the 1993 photonics science topical meetings
[AD-A269058] 04 p1438 N94-18492
Relaxation of polar orientational order in nonlinear optical polymers by second harmonic generation
[AD-A269059] 04 p1370 N94-18515
Photonics in Switching: Organization of the 1993 photonics science topical meetings. Technical digest
[AD-A269024] 04 p1578 N94-18528
Phase conjugation and beam combination using stimulated brillouin scattering
[AD-A269899] 04 p1439 N94-18656
Nonlinear optical properties of molecules
[AD-A270199] 04 p1567 N94-18783
Molecular nonlinear optical susceptibilities in condensed phases
[AD-A270200] 04 p1568 N94-18784
Consortium for materials development in space
[NASA-CR-194411] 04 p1379 N94-18840
Final report on subcontract B076260 --- borate synthesis
[DE93-019501] 04 p1604 N94-19565
Electro-optic beam steering using non-linear organic materials
[AD-A270809] 04 p1374 N94-19577
Ionized-cluster beam/partially ionized beam deposition of electro-optical and nonlinear optical organic materials and device development
[AD-A270832] 04 p1604 N94-19596
Optical switch evaluation support
[AD-A270948] 04 p1581 N94-19601
Complex and stereoregular nonlinear optical materials
[AD-A271067] 05 p1983 N94-19846
Multidimensional solitons in fiber arrays
[DE93-019923] 05 p1983 N94-19862
Photoluminescence spectroscopy of zinc germanium diphosphide (ZnGeP2)
[AD-A270705] 05 p1678 N94-19953
Optical switching devices
[AD-D015918] 05 p1984 N94-20059
FD-TD modeling of 2-D dielectric waveguides for propagation and scattering of femtosecond optical solitons 05 p1719 N94-20406
Investigation of heterojunctions and multiple quantum well structures using crystalline organic semiconductors
[AD-A272113] 05 p2018 N94-20569
Statistical fluctuations in lasers
[DE94-000710] 05 p1817 N94-20939
Recent developments in aromatic azo polymers research
[AD-A272966] 05 p1705 N94-21259
Azo polymers for optical storage 3: Effect of film thickness on net phase retardation and writing speed
[AD-A272994] 05 p1705 N94-21267
Photonics and nonlinear optics with molecular materials and polymers
[AD-A271747] 05 p1988 N94-21457
Techniques for the flux growth of optical materials: Growth of beta-barium borate
[AD-A272717] 05 p2028 N94-21505
Optical processing in photorefractive media 05 p1789 N94-22222
A fully automated stage for optical waveguide measurements
[AD-A273042] 06 p2542 N94-22915
Microgravity sciences application visiting scientist program
[NASA-CR-194804] 06 p2267 N94-23287
Spatiotemporal behavior and nonlinear dynamics in a phase conjugate resonator
[NASA-CR-4567] 06 p2543 N94-23529
Inertial confinement fusion
[DE94-002602] 06 p2551 N94-23703
Prediction of nonlinear optical properties of organic materials. General theoretical considerations 06 p2224 N94-24343
Low-gravity electrodeposition and growth of polymer thin films with large third-order optical nonlinearities by electrochemical processes for devices: Thiophene-based polymers 06 p2225 N94-24346
Polydiacetylene thin films for nonlinear optical applications 06 p2225 N94-24347
Crystal growth of organics for nonlinear optical applications 06 p2225 N94-24348
Nonlinear optical thin films 06 p2225 N94-24349
Optimization of microscopic and macroscopic second order optical nonlinearities 06 p2226 N94-24354
Dipolar relaxation in a second-order nonlinear optical interpenetrating polymer network
[AD-A273626] 06 p2258 N94-24732
Ultrastructure processing of macromolecular materials
[AD-A273413] 06 p2258 N94-24782
Center for advanced electrical and structural polymers
[AD-A273415] 06 p2259 N94-24783
Extension of On-Surface Radiation Condition (OSRC) theory to full-vector electromagnetic wave scattering by three-dimensional conducting, dielectric, and coated targets
[AD-A274023] 07 p2766 N94-25757
Studies of non-linear optical effects for agile beam steering
[AD-A273998] 07 p3034 N94-25902
Microtubules for nonlinear optical limiting
[AD-A273940] 07 p3035 N94-25941
Three-wave nonlinear interactions in KTiOPO4 (KTP) and KTP isomorphs
[AD-A274079] 07 p3052 N94-25993
Instantaneous amplitude and frequency dynamics of coherent wave mixing in semiconductor quantum wells
[DE94-003262] 07 p3054 N94-26128
Peculiarities and application perspectives of metal-ion implants in glasses
[DE94-004671] 07 p3035 N94-26246
An x ray absorption fine structure study of ordering in polythiophene thin films
[AD-A274235] 07 p2753 N94-26822
Research and development within nonlinear optics for protection of optical sensors against laser irradiation on of optical sensors against laser irradiation. Quarterannual report 1 (april 1993))
[PB94-124245] 07 p3037 N94-27046
Polyimide/inorganic composite-interpenetrating polymer network for stable second-order nonlinear optics
[AD-A274646] 07 p2709 N94-27107
Accordion-like polymers for nonlinear applications
[AD-D016031] 07 p2755 N94-27148
Predoctoral training grant in the area of physical sciences
[DE94-004406] 07 p3039 N94-27603
Optical pattern recognition system utilizing resonator array
[AD-D016071] 07 p3040 N94-28224
High-power CW diode-laser-array-pumped solid-state lasers and efficient nonlinear optical frequency
[AD-A275394] 08 p3293 N94-29309
Study of nonlinear optical polymers and their applications in optical waveguides 08 p3216 N94-29807

Nonlinear absorption in high reflector multilayers
[DE94-005818] 08 p3295 N94-30598
Nonlinear optics response of semiconductor quantum wells under high magnetic fields
[DE94-003244] 08 p3520 N94-30835
New material for high average power infrared generation: QPM-DB GaAs
[AD-A276389] 09 p3714 N94-31358
Compatibility studies of some azo polymer blends
[AD-A277141] 09 p3657 N94-32365
Mathematical nonlinear optics
[AD-A277320] 09 p3882 N94-32510
New developments in second-order nonlinear optical polymeric materials
[AD-A277409] 09 p3658 N94-32578
Stable second-order nonlinear optical materials based on interpenetrating polymer networks
[AD-A277410] 09 p3658 N94-32579
Nonlinear optical polymers derived from organic/inorganic composites
[AD-A277408] 09 p3659 N94-32610
Nonlinear optical properties of rigid-rod polymers
[NASA-CR-191349] 09 p3882 N94-32702
Low loss second-order nonlinear optical polymers based on all organic sol-gel materials
[AD-A277482] 09 p3663 N94-32985
A relaxation study of poled nonlinear optical polymers by infrared reflection-absorption spectroscopy
[AD-A277513] 09 p3663 N94-33054
Novel polydiacetylenes as materials for second and third order nonlinear optics
[AD-A277512] 09 p3664 N94-33082
Research in the optical sciences
[AD-A278271] 09 p3884 N94-33140
Studies of optical beam phase conjugation and electromagnetic scattering process
[AD-A278389] 09 p3884 N94-33145
Advanced material processing for integrated-optic frequency doubling systems
[AD-A278394] 09 p3698 N94-33163
Future directions of nonlinear dynamics in physical and biological systems. (Physica D nonlinear, volume 68, number 1)
[AD-A278085] 09 p3794 N94-33250
Optical properties of doped sol-gel silica glasses
[AD-A278094] 09 p3884 N94-33267
Second-order nonlinear optical polymers: From fundamentals to applications
[AD-A277514] 09 p3664 N94-33348
Organosilicon polymeric nonlinear optical materials for optical switching and modulation
[AD-A278245] 10 p4140 N94-33381
Spectral-domain optical processing techniques
[AD-A278371] 10 p4141 N94-33739
Defect structure of semiconducting and insulating epitaxial oxides
[DE94-009650] 10 p4146 N94-33845
Nonlinear frequency conversion optical filter
[AD-D016127] 10 p4036 N94-34283
Concurrent stabilization and imaging of a novel polymer for second harmonic generation via in situ photopolymerization
[AD-A278912] 11 p4243 N94-35588
Theoretical studies of ultrashort phenomena
[AD-A278938] 11 p4332 N94-35664
Properties and bibliography of GaSe
[AD-A279064] 11 p4340 N94-35733
Nonlinear optical composites of metal cluster laden polymers
[AD-D016217] 11 p4234 N94-36124
Application of GaSe and AgGaSe2 crystal growth to non-linear optics
[PB94-170552] 11 p4341 N94-36212
Nonlinear optical spectroscopy for surface studies
[DE94-011623] 12 p4408 N94-37056
Poly(p-phenylene) derivatives new high performance nonlinear optical polymers
[AD-A280248] 12 p4422 N94-37121
Organic NLO polymers. 2: Main-chain and guest-host Chi(2)NLO polymers: NLO-phore structure versus poling
[AD-A280230] 12 p4423 N94-37133
Organic nonlinear optical (NLO) polymers. 4: Thermally stable NLO polymers
[AD-A280196] 12 p4423 N94-37148
Organic NLO polymers. 5: Homopolymerization of indole based NLO-phore: A heterocycle Chi(2)NLO main-chain polymer
[AD-A280229] 12 p4423 N94-37151
Abstracts of 2nd International Conference on Lasers and their Applications
[DE94-617409] 12 p4448 N94-37169
Organometallic NLO polymers. 4: Organometallic main-chain, side-chain, and guest-host polymers: A study of their orientation and relaxation using second harmonic generation
[AD-A280347] 12 p4423 N94-37179
Laser probing of interfaces
[DE94-011300] 12 p4449 N94-37628

NONLINEAR PROGRAMMING

Boundary formulations for nonlinear design sensitivity analysis 02 p0672 N94-13669
A sequential quadratic programming algorithm using an incomplete solution of the subproblem
[DE93-017439] 03 p1149 N94-16120
Design optimization studies using COSMIC NASTRAN 04 p1450 N94-17834
A structural design decomposition method utilizing substructuring
[NASA-TM-107750] 06 p2376 N94-23368
PLANET: A hierarchical network simulator
[ISBN-9-09-005693-9] 06 p2313 N94-25083
Unifying investigation of interior-point methods for convex programming
[PB94-126463] 07 p2967 N94-27031
Center for Parallel Optimization
[AD-A274988] 08 p3431 N94-29127
Investigation on application of genetic algorithms to optimal reactive power dispatch of power systems
[MATHS-REPT-A-197] 08 p3266 N94-29527
Optimal reactive power dispatch of power systems using nonlinear programming
[MATHS-REPT-A-209] 09 p3808 N94-31164
Parallel structured optimization algorithms for inverse problems
[AD-A276053] 09 p3811 N94-31443
A Gauss-Seidel type solver for special convex programs, with application to frictional contact mechanics
[REPT-93-77] 09 p3813 N94-31694
OPT++: An object-oriented class library for nonlinear optimization
[DE94-008890] 09 p3818 N94-32584
Application of sequential quadratic programming to large-scale structural design problems
[AD-A278574] 11 p4307 N94-36185

NONLINEAR SYSTEMS

Chemical pattern formation under microgravity 01 p0121 N94-10227
Balancing of the normalized right coprime factorization of a nonlinear system
[MEMO-1096] 01 p0341 N94-10273
On output linearization of observable dynamics
[MEMO-1105] 01 p0341 N94-10276
Nonlinear Dynamics in Optical Systems. Postdeadline papers presented at the Optical Society of America Conference
[AD-A264958] 01 p0375 N94-10486
On the Sobolev systems with ellipsoid cavities
[DE92-641290] 01 p0148 N94-10530
Convergence theorems for a class of nonlinear maps in uniformly smooth Banach spaces
[DE92-641347] 01 p0343 N94-10531
Classical gravity coupled to Liouville theory
[DE93-613049] 01 p0275 N94-10798
Detecting non-linearities in stationary time series
[W-9223] 01 p0344 N94-10906
Creation and annihilation of solitons in nonlinear integrable systems
[DE93-621379] 01 p0365 N94-11078
Optimisation methods for solving separable nonlinear least squares problems
[ISVR-TR-219] 01 p0345 N94-11217
Trajectory pattern inverse dynamics and control of nonlinear dynamics systems with application to flexible structures 01 p0181 N94-11219
Stability in Aerospace Systems
[AGARD-R-789] 01 p0031 N94-11489
Chaotic time series analysis 01 p0031 N94-11490
On non-linear longitudinal stability of an aircraft in a dive in the presence of atmospheric disturbances 01 p0031 N94-11492
Modeling nonlinear aerodynamic loads for aircraft stability and control analysis 01 p0032 N94-11499
Transactions of the 10th Army Conference on Applied Mathematics and Computing
[AD-A265098] 01 p0318 N94-11678
Nonlinear stability calculations of pipe flow 01 p0163 N94-12612
Nonlinear instability of a laminar flow in a rectangular duct and generation of the turbulent secondary flow 01 p0164 N94-12622
The thermodynamics of the nonlinear shear flows 01 p0169 N94-12728
Modulational stability of periodic solutions of the Kuramoto-Sivaskinsky equation
[NASA-CR-191502] 02 p0628 N94-12888
Newton iterative methods for large scale nonlinear systems
[DE93-015357] 02 p0767 N94-13025
Relegation for decentralized control
[AD-A265720] 02 p0819 N94-13059
Stability of subharmonics and escape phenomena in the twin-well potential duffing system 02 p0775 N94-13235
Nonlinear vibrations of thick composite plates: Higher-order shear deformation plate theory 02 p0556 N94-13558
Nonlinear aspects of data integration for land-cover classification in a neural network environment
[INPE-5479-PRE/1778] 02 p0686 N94-13789
Multi-dimensional high order essentially non-oscillatory finite difference methods in generalized coordinates
[NASA-CR-194031] 02 p0770 N94-14429
Nonlinear wave predictions in ceramics
[DE93-016516] 02 p0582 N94-14436
Chaos and microbial systems
[DE93-016814] 02 p0730 N94-14596
Identification of continuous-time dynamical systems: Neural network based algorithms and parallel implementation
[DE93-014427] 02 p0766 N94-14737
A new treatment of periodic systems with applications to helicopter rotor blade dynamics
[AD-A266770] 02 p0510 N94-14784
Iteration scheme for the multiparameter nonlinear boundary value problem with the additional conditions and its application to some field models
[DE93-626638] 03 p1168 N94-14933
Controlling chaotic behavior in CO2 and other lasers
[AD-A266431] 03 p1040 N94-16548
Operator overloading as an enabling technology for automatic differentiation
[DE93-012899] 03 p1170 N94-16778
Nonlinear problems in fluid dynamics and inverse scattering
[AD-A266234] 03 p1026 N94-16927
Nonlinear analysis of mechanical systems under combined harmonic and stochastic excitation
[AD-A266217] 03 p1173 N94-16937
Stochastic chaos: An analog of quantum chaos
[DE93-016619] 03 p1220 N94-16956
Nonlinear methods for communications
[AD-A267376] 03 p1001 N94-17019
Discrete sliding mode control for nonlinear sampled data systems
[AD-A267500] 03 p1167 N94-17369
Extracavity frequency doubling study of a pulsed photodissociation iodine laser
[AD-A267893] 03 p1042 N94-17394
Robust control of uncertain nonlinear systems
[AD-A268056] 03 p1167 N94-17506
Nonlinear random response prediction using MSC/NASTRAN
[NASA-TM-109029] 03 p1179 N94-17650
Modelling chaotic vibrations using NASTRAN 04 p1449 N94-17830
Generalization of optimal control theory: Linear and nonlinear structures
[PB93-188621] 04 p1540 N94-18125
On higher dimensional Ermakov systems: Canonical reductions
[MATHS-REPT-A-182] 04 p1548 N94-18140
Non Linear Dynamics and Chaos
[AGARD-LS-191] 04 p1607 N94-18236
Stability analysis through bifurcation theory, 1 04 p1608 N94-18238
Non-linear flight dynamics 04 p1319 N94-18240
An ab initio study of the weakly bonded CO-Cl2 complex
[AD-A269000] 04 p1349 N94-18395
Fundamental research in nonlinear random vibration for aerospace applications
[AD-A268929] 04 p1454 N94-18487
Competitive dynamics and self-organization in photorefractive systems
[AD-A269663] 04 p1430 N94-18569
Phase-space description of plasma waves: Linear and nonlinear theory
[IRF-SR-211] 04 p1587 N94-18860
Control of nonlinear systems
[AD-A270141] 04 p1542 N94-18898
Statistical learning theory and algorithms
[AD-A270209] 04 p1523 N94-18901
The intelligent processing of materials
[AD-A269250] 04 p1362 N94-18923
Analysis and design of robust decentralized controllers for nonlinear systems
[DE93-019224] 04 p1543 N94-19302
Nonlinear disturbance decoupling and linearization: A partial interpretation of integral feedback
[PB93-197515] 04 p1543 N94-19328
Time dependent identification of nonlinear structures
[ECL-92-64] 04 p1457 N94-19403
Contribution to the modelling and the identification of nonlinear mechanical systems
[ECL-92-32] 04 p1529 N94-19409

Contribution to the identification of nonlinear behavior laws in material mechanics
[ECL-92-36] 04 p1458 N94-19411
Acoustic microscopy and nonlinear effects in pressurized superfluid helium
[AD-A270598] 05 p1967 N94-19949
Computational and analytical methods in nonlinear fluid dynamics
[AD-A272722] 05 p1802 N94-21169
The block adaptive multigrid method applied to the solution of the Euler equations 05 p1641 N94-21472
High temperature superconducting planar circuit structure for high frequency applications
[AD-A273083] 05 p2028 N94-21521
Improvements to a method for the geometrically nonlinear analysis of compressively loaded stiffened composite panels
[NASA-CR-194715] 05 p1832 N94-21814
The spectral world coordinate systems in IRAF/NOAO 05 p2049 N94-22539
Response statistics of shell structures with geometrical and material nonlinearities, volume 1
[ISBN-0-315-84006-4] 05 p1833 N94-22590
Decoupling problems around a trajectory: From linearity to nonlinearity
[MEMO-1115] 06 p2469 N94-22703
Balancing for unstable nonlinear systems
[MEMO-1118] 06 p2469 N94-22705
Nonlinear state space H(sub infinity) control theory
[MEMO-1119] 06 p2469 N94-22706
Nonlinear systems which have finite-dimensional H(sub infinity) suboptimal central controllers
[MEMO-1120] 06 p2469 N94-22707
On dynamic input-output linearization of discrete-time nonlinear systems
[MEMO-1123] 06 p2447 N94-22711
Feedback linearization of parametrized nonlinear time-varying systems
[MEMO-1126] 06 p2470 N94-22714
Probabilistic analysis of mechanical systems
[DE93-041145] 06 p2371 N94-22918
Chaos and simple determinism in reversed field pinch plasmas: Nonlinear analysis of numerical simulation and experimental data
[DE94-001575] 06 p2550 N94-23211
Viewing hybrid systems as products of control systems and automata
[NASA-CR-194792] 06 p2472 N94-23300
On the estimation of the correlation dimension and its application to radar reflector discrimination
[NASA-CR-4564] 06 p2309 N94-23304
Nonlinear analysis using a modal based reduction technique 06 p2161 N94-24288
Neural network-based control using Lyapunov functions 06 p2477 N94-24433
Discrete applied mathematics
[AD-A273552] 06 p2488 N94-24561
Robust stability of second-order systems
[NASA-CR-195175] 06 p2488 N94-24564
Hamiltonian approach to fairly low and long gravity waves
[PB94-111119] 06 p2404 N94-24598
Control of nonlinear systems represented in quasilinear form
[NASA-CR-194840] 06 p2475 N94-24760
Nonlinear dynamical control of lasers
[AD-A273359] 06 p2350 N94-24938
System for producing synchronized signals
[AD-D016003] 06 p2302 N94-25057
Modeling transonic aerodynamic response using nonlinear systems theory for use with modern control theory 06 p2164 N94-25112
Center for Analysis of Heterogeneous and Nonlinear Media
[AD-A273515] 06 p2230 N94-25158
Practical evaluation of robust control for a class of nonlinear mechanical dynamic systems
[ISBN-9-03-860092-5] 06 p2475 N94-25224
Approximation to nonlinear equations using nonlinear rational models
[RR-448] 06 p2492 N94-25306
The phase response of nonlinear systems
[RR-458] 06 p2476 N94-25308
On the inversion of the n-dimensional Laplace transform
[RR-461] 06 p2492 N94-25310
Unwrapping the phase response functions for nonlinear systems
[RR-465] 06 p2462 N94-25311
Validating identified nonlinear models with chaotic dynamics
[RR-469] 06 p2523 N94-25314
Frequency response functions for nonlinear rational models
[RR-471] 06 p2492 N94-25318
Relationship between the structure and performance of identified nonlinear polynomial models
[RR-474] 06 p2492 N94-25320
Characterization of nonlinear effects in optically pumped vertical cavity surface emitting lasers
[AD-A273840] 07 p2815 N94-25744
Evaluation of moderate angle of attack roll of a dual engine, thrust vectoring aircraft using quantitative feedback theory
[AD-A274118] 07 p2667 N94-25905
Determination of the geomagnetic external contribution by nonlinear optimization methods
[DE94-600882] 07 p2878 N94-26365
On the phi(sub 0)-stability of perturbed nonlinear differential systems
[DE93-634304] 07 p2993 N94-26441
Asymptotically stable neural networks for identification of nonlinear dynamic systems
[ISBN-0-315-84328-4] 07 p2985 N94-26629
Computation of stress intensity factors by the mode enrichment technique with applications to geometrically nonlinear problems
[PB94-126513] 07 p2840 N94-26910
Some aspects of nonlinear discrete-time descriptor systems in economics
[PB94-126653] 07 p3101 N94-26918
Parallel mathematical software
[DE94-001587] 07 p2967 N94-27020
Development of K(1-x)Na(x)TiOPO4 crystals for nonlinear applications
[AD-A274336] 07 p3063 N94-27055
Control oriented system identification
[AD-A274162] 07 p2987 N94-27124
Center for nonlinear phenomena and magnetic materials
[AD-A274176] 07 p3009 N94-27126
Operator theoretic methods in the control of distributed and nonlinear systems
[AD-A274160] 07 p2988 N94-27139
The onset of chaos in a periodically forced nonlinear oscillator
[ISBN-0-315-84564-3] 07 p2842 N94-27272
The deterministic power-spectral-density method
[AD-B175894] 07 p2678 N94-27395
Control system for tracking nonlinear systems
[AD-D016057] 07 p2787 N94-27673
Super finite elements for nonlinear static and dynamic analysis of stiffened plate structures
[ISBN-0-315-63903-2] 07 p2844 N94-27808
Neural control of magnetic suspension systems 07 p2682 N94-27905
The deterministic power-spectral-density-method for nonlinear systems
[AD-B179687] 07 p3001 N94-28353
Frequency-domain analysis of nonlinear microwave circuits
[PB94-132024] 08 p3261 N94-28400
Nonlinear magnetohydrodynamics
[DE94-005654] 08 p3503 N94-28547
Annual summary of basic research thermoacoustic heat transport, 1993
[AD-A275751] 08 p3230 N94-28644
The solving of the relativistic two-body problem with a nonlinear dependence upon a spectrum parameter
[DE94-606343] 08 p3451 N94-28783
General theory and algorithms for the non-casual inversion, slewing and control of space-based articulated structures
[AD-A275118] 08 p3167 N94-29002
Incorporating geometric constraints into rule-based systems using nonlinear optimization
[AD-A275093] 08 p3452 N94-29063
Evolution of the large-scale vortices in turbulent mixing-layers 08 p3273 N94-29686
Large-scale computations in analysis of structures
[DE94-004022] 08 p3321 N94-29951
Stochastic stability and nonlinear control in mechanical systems 08 p3303 N94-29966
On the nonlinear dynamics of ocean wave systems 08 p3378 N94-30790
An experimental study of nonlinear wave coupling and energy transfer characterizing the transition of a planar jet shear layer 08 p3282 N94-30953
A radial basis function approach to financial time series analysis
[AD-A276408] 09 p3924 N94-31361
Nonlinear model validation using correlation tests
[RR-463] 09 p3842 N94-31394
On wavelet representations of differential equations
[RR-482] 09 p3842 N94-31412
Adaptive nonlinear control of spacecraft 09 p3609 N94-31564
Chaotic attitude motion of satellites in the central gravitational field
[ISBN-0-315-78768-6] 09 p3610 N94-31723
Asymptotic behavior of dynamic systems 09 p3911 N94-31894
Structural stability and bifurcations 09 p3911 N94-31895
Deterministic chaos 09 p3912 N94-31896
Modeling and control of nonlinear systems
[AD-A277377] 09 p3834 N94-32095
Basic principles approach for studying nonlinear Alfven wave-alpha particle dynamics
[DE94-007112] 09 p3891 N94-32664
Advanced CFD methodology for fast transients encountered in nonlinear combustion instability problems. Volume 1: Theory and validation
[NASA-CR-191351] 09 p3637 N94-32696
State-space self-tuner for on-line adaptive control
[NASA-CR-195836] 09 p3835 N94-32943
RHIC chromatic correction system
[DE94-008532] 09 p3883 N94-32994
Investigation of drive-reinforcement learning and application of learning to flight control
[AD-A277442] 09 p3801 N94-33053
On the computation of simplical approximations of implicitly defined two-dimensional manifolds
[AD-A278132] 09 p3849 N94-33060
Future directions of nonlinear dynamics in physical and biological systems. (Physica D nonlinear, volume 68, number 1)
[AD-A278085] 09 p3794 N94-33250
Adaptive control of nonlinear and stochastic systems
[AD-A278411] 09 p3839 N94-33325
A computer program to obtain time-correlated gust loads for nonlinear aircraft using the matched-filter-based method
[NASA-TM-109768] 10 p4006 N94-33378
Robust control of nonlinear flexible multibody systems using quaternion feedback and dissipative compensation
[NASA-TM-109099] 10 p4014 N94-34103
Investigation and simulation of nonlinear processors for spread spectrum receivers, volume 1
[AD-A278025] 10 p4037 N94-34288
Investigation and simulation of nonlinear processors for spread spectrum receivers. Volume 2: Users manual
[AD-A278026] 10 p4037 N94-34289
Resonance capture in unbalanced dual-spin spacecraft
[AD-A278501] 10 p4015 N94-34292
Identification of 2nd and 3rd Volterra kernel of nonlinear systems 10 p4114 N94-34312
Robust stabilization of nonlinear systems with a class of unmatched uncertainties 10 p4115 N94-34322
The tracking control of nonlinear uncertain systems 10 p4008 N94-34331
Techniques for aerodynamic characterization and performance evaluation at high angle of attack 10 p3991 N94-34614
A genetic technique for planning a control sequence to navigate the state space with a quasi-minimum-cost output trajectory for a non-linear multi-dimnensional system 10 p4123 N94-35052
Dynamic analysis of a magnetic bearing system with flux control 11 p4216 N94-35859
Maneuvering and control of flexible space robots 11 p4218 N94-35867
Improved models of beta-limit, anomalous transport and radial electric field with loss cone loss in heliotron/torsatron
[DE94-718976] 11 p4324 N94-35984
Combining nonlinear multiresolution system and vector quantization for still image compression
[DE94-009422] 11 p4305 N94-36017
Nonlinearity with disorder: Spatio-temporal complex behavior arising from length scales competition
[DE94-000675] 12 p4502 N94-36685
Parameter estimation in a structural acoustic system with fully nonlinear coupling conditions
[NASA-CR-194926] 12 p4503 N94-36991
Theoretical investigations of chaotic dynamics
[AD-A280325] 12 p4507 N94-37028
H infinity control for nonlinear and linear systems
[AD-A280450] 12 p4494 N94-37226
The canonical symmetry for integral systems
[DE94-618486] 12 p4504 N94-37375

NONLINEARITY

Effects of axial and centrifugal forces on the stability of liquid bridges 01 p0102 N94-10083
Nonlinear second harmonic generation by light wave-plasma interaction in oscillating magnetic field
[DE93-613723] 01 p0386 N94-10387
Nonlinear MHD-waves in a dissipative plasma with hall currents
[DE93-617844] 01 p0386 N94-10395
Singularity spectrum of self-organized criticality
[DE93-613820] 01 p0348 N94-10404
On the Sobolev systems with ellipsoid cavities
[DE92-641290] 01 p0148 N94-10530

On the stability of stationary regimes in a distributed autovibration system with external feedback
[DE93-620979] 01 p0141 N94-10543
An exactly solvable model of an oscillator with nonlinear coupling and zeros of Bessel functions
01 p0349 N94-10573
Non-stationary and non-linear dispersive medium as external field which generates the squeezed states
01 p0380 N94-10605
The nonlinear evolution of modes on unstable stratified shear layers
[NASA-CR-191492] 01 p0149 N94-10810
A self-consistent model of non-linear parameterization of turbulent diffusion in atmospheric boundary layer
[DE93-011950] 01 p0275 N94-11052
Time-resolved optical studies of charge relaxation and charge transfer at electrode interfaces
[DE93-013985] 01 p0398 N94-11117
Simulation study of dynamo structure in reversed field pinch
[DE93-771406] 01 p0390 N94-11128
Negative viscosity and generation of dissipative solitons and zonal dissipative structures by drift waves
[DE93-621656] 01 p0392 N94-11212
Non-linear dynamics of automodulation processes in coupled distributed autovibration systems with delay
[DE93-620976] 01 p0143 N94-11365
Effects of wave nonlinearity on ERS-1 radar altimeter returns: A preliminary investigation
01 p0235 N94-11722
Nonlinear aspects of transonic aeroelasticity
[UTIAS-345] 01 p0015 N94-11857
Nonlinear resonance: Noise-assisted information processing in physical and neurophysiological systems
[AD-A265161] 01 p0313 N94-11890
Cardiovascular dynamics during space sickness and deconditioning 01 p0311 N94-12007
Estimation with multisensor/multiscan detection fusion
[AD-A265673] 01 p0138 N94-12338
A relaxation study of poled nonlinear optical polymers by infrared reflection-absorption spectroscopy
[AD-A265797] 01 p0093 N94-12380
Nonlinear optical spectroscopy of Ag(111) in electrolyte and in vacuum
[AD-A265622] 01 p0079 N94-12534
Three-dimensional finite element analysis of explosive safety facilities: A technology assessment
[AD-A265700] 01 p0035 N94-12562
Preparation of stable photopatternable polymeric materials for non-linear optics
[AD-A265359] 01 p0095 N94-12577
Nonlinear effects in ferrite tuned cavities
[DE93-014136] 01 p0374 N94-12785
A general contact detection algorithm for finite element analysis
[DE93-012846] 02 p0742 N94-12956
Linear and nonlinear spectroscopic probing of solute interactions with chemically modified silica surface
[DE93-014648] 02 p0562 N94-13001
Beam halo formation from space-charge dominated beams in uniform focusing channels
[DE93-014458] 02 p0789 N94-13209
Brillouin scattering from fluctuations produced by stimulated Raman scattering
[DE93-016531] 02 p0792 N94-14438
Kinetic simulations of ultra-intense laser plasma interactions
[DE93-014419] 02 p0802 N94-14564
Stress stiffening and approximate equations in flexible multibody dynamics 02 p0677 N94-14620
Nonrecursive formulations of multibody dynamics and concurrent multiprocessing 02 p0679 N94-14632
Nonlinear analysis, scientific computation, and continuum mechanics applied to the science of materials
[AD-A266641] 02 p0817 N94-14680
High-performance nonlinear optical material developed in Japan
[AD-A266194] 03 p1191 N94-16126
Nonlinear gyrofluid models of shear Alfven instabilities in ignited and beam heated toroidal plasmas
[DE93-016235] 03 p1203 N94-16869
Processing of resonance parameter covariance files
[DE93-015506] 03 p1231 N94-16874
Acoustic waves in complicated geometries and their interactions with liquid-propellant droplet combustion
[AD-A267260] 03 p1178 N94-16991
Nonlinear methods for communications
[AD-A267376] 03 p1001 N94-17019
Theoretical studies of nonlinear optical properties of conjugated polymers
[AD-A267390] 03 p1193 N94-17024
A search for evidence of nonlinear elasticity in the earth
[DE93-015279] 03 p1102 N94-17252
High order nonlinear estimation with signal processing applications
[AD-A268407] 03 p1005 N94-17463
The 1992 annual report on scientific programs: A broad research program on the sciences of complexity
[DE93-018151] 04 p1561 N94-18178
Nonlinear Thomson scattering of intense laser pulse from beams and plasmas
[AD-A269556] 04 p1438 N94-18460
Fundamental research in nonlinear random vibration for aerospace applications
[AD-A268929] 04 p1454 N94-18487
Multidimensional wave decompositions for the Euler equations 04 p1413 N94-18562
Effects of harmonics on EMI/RFI filters operating under nonlinear loading conditions
[AD-A269559] 04 p1388 N94-18769
Active control of a multivariable system by way of polynomial neural networks: Computer simulation evaluations and laboratory experimental results
[AD-A270033] 04 p1541 N94-18790
Application of differential sensitivity theory to continuum mechanics
[DE93-012732] 04 p1609 N94-19187
Singularities and symmetries of nonlinear ordinary and partial differential equations
[DE93-040083] 04 p1550 N94-19190
Analysis and design of robust decentralized controllers for nonlinear systems
[DE93-019224] 04 p1543 N94-19302
Time dependent identification of nonlinear structures
[ECL-92-64] 04 p1457 N94-19403
A comparison of iterative methods for a model coupled system of elliptic equations
[DE93-040482] 04 p1553 N94-19655
Theoretical studies of turbulence and anomalous transport in toroidal confinement devices
[DE93-040684] 04 p1592 N94-19656
Nonlinear acoustics: Periodic waveguide, finite-amplitude propagation in a medium having a distribution of relaxation processes, and production of an isolated negative pulse in water
[AD-A270530] 05 p1967 N94-19894
Study of transverse coupled bunch instabilities by using non-linear Taylor maps for the Advanced Light Source (ALS)
[DE93-040287] 05 p1979 N94-19989
Design of a controllable pitch underwater thruster system
[AD-A271140] 05 p1821 N94-20021
Emittance measurement and modeling of the ALS 50 MeV LINAC to booster line
[DE93-040116] 05 p1979 N94-20273
The coherent backscattering opposition effect
05 p1991 N94-20646
RADCAL: A narrow-band model for radiation calculations in a combustion environment
[PB93-200889] 05 p1682 N94-21448
A unified Monte Carlo interpretation of particle simulations and applications to nonneutral plasmas
[DE94-001231] 05 p1997 N94-21973
Theoretical and simulated performance for a novel frequency estimation technique
06 p2285 N94-22808
Chaos in plasma simulation and experiment
[DE94-001574] 06 p2549 N94-22963
Computation of flows in a turn-around duct and a turbine cascade using advanced turbulence models
06 p2216 N94-23062
Fully coupled nonlinear thermomechanical analysis including general contact in PALM2D
[DE94-001661] 06 p2568 N94-23216
Nonlinear ion-mixing-mode particle transport in the dissipative trapped electron regime
[DE94-000989] 06 p2533 N94-23435
Tracking sharp interface of two fluids by the CIP (Cubic-Interpolated Propagation) scheme
[DE93-508322] 06 p2319 N94-23460
Implementing abstract multigrid or multilevel methods
06 p2483 N94-23682
Energy and maximum norm estimates for nonlinear conservation laws
[NASA-CR-195091] 06 p2569 N94-24109
Prediction of nonlinear optical properties of organic materials. General theoretical considerations
06 p2224 N94-24343
Optimization of microscopic and macroscopic second order optical nonlinearities 06 p2226 N94-24354
Diagnosing process faults using neural network models
[DE94-002633] 06 p2473 N94-24518
Computer modeling of nonlinearities
06 p2458 N94-24661
Nonlinear dynamics applied to atmospheric prediction
[AD-A273437] 06 p2404 N94-24674
Robust, nonlinear, high angle-of-attack control design for a supermaneuverable vehicle
06 p2164 N94-25108
Nonlinear aerodynamic modeling using multivariate orthogonal functions 06 p2164 N94-25110
Infinitely divisible processes and their nonlinear functionals; a study of their structural, statistical and sample path properties and their prediction problems
[AD-A273468] 06 p2496 N94-25147
A comparison of three approximate mathematical models for the gravity gradient stabilized satellite
[AD-A273832] 07 p2694 N94-25615
Microtubules for nonlinear optical limiting
[AD-A273940] 07 p3035 N94-25941
Three-wave nonlinear interactions in KTiOPO4 (KTP) and KTP isomorphs
[AD-A274079] 07 p3052 N94-25993
Nonlinear ocean waves
[AD-A274651] 07 p2899 N94-26354
Determination of the geomagnetic external contribution by nonlinear optimization methods
[DE94-600882] 07 p2878 N94-26385
Nonlinear dynamics and pattern selection at the crystal-melt interface
[DE94-003112] 07 p3060 N94-26780
Nonlinear hysteresis in an endochronic solid
[AD-A274594] 07 p2880 N94-26855
Center for nonlinear phenomena and magnetic materials
[AD-A274176] 07 p3009 N94-27126
Optimal nonlinear estimation for aircraft flight control in wind shear 07 p2643 N94-27296
Transmittance fluctuations and non-linearity in random chains in the presence of applied electric fields
[DE94-603665] 07 p2787 N94-27628
Optical parametric oscillator modeling with diffraction, depletion, and double refraction
[DE94-001504] 07 p3040 N94-27999
Dissipative quantum dynamics and nonlinear sigma-model
[DE94-606295] 08 p3523 N94-28617
Computational methods in continuum mechanics
[AD-A275560] 08 p3451 N94-28792
A non-linear simulation for an autonomous unmanned air vehicle
[AD-A275062] 08 p3146 N94-29200
Screening of flexible cables by nonlinear resistance measurements
[AD-A275193] 08 p3264 N94-29289
An investigation of distributed coupling in a nonlinear semiconductor waveguide 08 p3246 N94-29529
Large amplitude Langmuir and ion-acoustic waves in a relativistic two-fluid plasma
[AD-B183694L] 08 p3506 N94-29547
Nonlinear wave packet evolution in a dispersive plasma: Application to rotational discontinuities
08 p3506 N94-29822
Robotic hand-eye motor learning
08 p3436 N94-29835
A guidance and navigation system for two spacecraft rendezvous in translunar halo orbit
08 p3142 N94-29837
Large-scale computations in analysis of structures
[DE94-004022] 08 p3321 N94-29951
Closed form expressions for a consistent stress material nonlinear finite element 08 p3322 N94-30258
Nonlinear multibody formulation for rotorcraft analysis
08 p3149 N94-30787
Nonlinear calculations of the time evolution of black hole accretion disks 09 p3929 N94-31127
Taming chaotic circuits 09 p3910 N94-31289
Towards simplicity: Noise and cooperation in the perfect integrator
[AD-A276256] 09 p3799 N94-31291
Nonlinearity as an origin of nonuniqueness in solution of Hartree's equation
[DE94-006538] 09 p3841 N94-31311
On the relationship between generalization error, hypothesis complexity, and sample complexity for radial basis functions
[AD-A276802] 09 p3851 N94-32142
Advanced CFD methodology for fast transients encountered in nonlinear combustion instability problems. Volume 2: User's guide
[NASA-CR-191352] 09 p3637 N94-32694
Parallel supercomputing: Advanced methods, algorithms, and software for large-scale linear and nonlinear problems
[DE94-008446] 09 p3836 N94-32992
A relaxation study of poled nonlinear optical polymers by infrared reflection-absorption spectroscopy
[AD-A277513] 09 p3663 N94-33054
Novel polydiacetylenes as materials for second and third order nonlinear optics
[AD-A277512] 09 p3664 N94-33082

Growth and nonlinearity
[DE94-007366] 10 p4021 N94-33689
Asymptotic approaches to transition modelling
10 p4045 N94-33887
A fully associative, non-linear kinematic, unified viscoplastic model for titanium based matrices
[NASA-TM-106609] 10 p4069 N94-33958
Investigation and simulation of nonlinear processors for spread spectrum receivers, volume 1
[AD-A278025] 10 p4037 N94-34288
Non-linear numerical analysis of the losipescu specimen for composite materials
[NASA-CR-195934] 10 p4020 N94-34306
Parallel processing for nonlinear dynamics simulations of structures including rotating bladed-disk assemblies
[NASA-CR-194567] 10 p4112 N94-34683
Non-local sub-characteristic zones of influence in unsteady interactive boundary-layers
10 p4053 N94-34982
Linear and nonlinear pattern selection in Rayleigh-Benard stability problems
[NASA-TM-104007] 11 p4263 N94-35371
Nonlinear control of magnetic bearings
11 p4213 N94-35838
A case study in nonlinear dynamics and control of articulated spacecraft: The Space Station Freedom with a mobile remote manipulator system
11 p4220 N94-35879
Numerical method to study the stability of periodic solutions of particle motion in nonlinear magnetic fields
[DE94-610740] 11 p4325 N94-36088
Application of GaSe and AgGaSe2 crystal growth to non-linear optics
[PB94-170552] 11 p4341 N94-36212
Local instabilities and the transition to chaos of non-linear waves
[PB94-170578] 11 p4341 N94-36213
Non-linear interaction of gravity waves with average jet flows, instabilities, and turbulence
[PB94-170586] 11 p4291 N94-36214
Recovering depth from focus using iterative image estimation techniques
[DE94-010994] 12 p4524 N94-37165
Understanding and managing power system harmonics
[AD-A280627] 12 p4440 N94-37759

NONNEWTONIAN FLOW
Numerical simulation of the non-Newtonian mixing layer 01 p0159 N94-12314

NONNEWTONIAN FLUIDS
A comparison of calculated and measured rheological properties of crystallising lavas in the field and in the laboratory 05 p1862 N94-20690
Multigrid methods for a semilinear PDE in the theory of pseudoplastic fluids 06 p2341 N94-23689

NONOSCILLATORY ACTION
A fully two-dimensional, non-oscillatory advection scheme for momentum and scalar transport equations
[DM-66] 09 p3700 N94-31221

NONPARAMETRIC STATISTICS
Nonparametric statistics: Weighted rankings analysis
[AD-A266607] 03 p1173 N94-16657
Computing science and statistics. Volume 24: Graphics and visualization
[AD-A266571] 03 p1150 N94-16721
Introduction to bayesian nonparametric theory
[PB94-125002] 07 p3004 N94-26939
Stochastic models in reliability theory
[AD-A277529] 09 p3731 N94-32953

NONPOINT SOURCES
A Geographic Information System approach to modeling nutrient and sediment transport
[DE93-013747] 03 p1097 N94-17426

NONREFLECTION
U ENERGY ABSORPTION

NONRELATIVISTIC ELECTRONS
U ELECTRONS

NONRELATIVISTIC MECHANICS
Observables, measurements and phase operators from a Bohmian perspective 01 p0378 N94-10589
Non-gauge phase transformations in quantum transition amplitudes 01 p0378 N94-10596
Effects of spin-orbit coupling on disordered mesoscopic systems
[ITN-93-85220] 03 p1180 N94-15288

NONRESONANCE
Particle-In-Cell (PIC) code simulation results and comparison with theory scaling laws for photoelectron-generated radiation
[DE94-006132] 09 p3695 N94-32662

NONRIGIDITY
U FLEXIBILITY

NONTHERMAL EMISSION
U NONTHERMAL RADIATION

NONTHERMAL RADIATION
NT CYCLOTRON RADIATION
NT ION CYCLOTRON RADIATION
NT SYNCHROTRON RADIATION
Nonthermal planetary radio emissions: Theories and observations 05 p2001 N94-22635
Voyager planetary radio astronomy studies
[NASA-CR-194776] 06 p2614 N94-24328

NONUNIFORM FLOW
Internal instability of nonparallel flow on an equatorial beta-plane
[AD-A268927] 04 p1490 N94-18486
Rotordynamic effects driven by fluid forces from a geometrically imperfect labyrinth
[AD-A276424] 09 p3722 N94-31333
Additional capabilities of the unified waves model
[AD-A276114] 09 p3702 N94-31467
Inlet distortion in engines on VSTOL aircraft
[NASA-CR-195841] 09 p3584 N94-33035

NONUNIFORM MAGNETIC FIELDS
Using ferro-magnetic fluids to lubricate non-conformal isothermal contacts
[INPE-5520-TAE/021] 07 p2827 N94-27665

NONUNIFORM PLASMAS
Parametric instabilities in large nonuniform laser plasmas
[DE93-013184] 02 p0797 N94-13393

NONUNIFORMITY
DILUTE: A code for studying beam evolution under RF noise
[DE93-011605] 01 p0133 N94-10960
Locally non-uniform finite-difference time domain with application to stealth, crosstalk, and narrow apertures
[DE93-013958] 02 p0601 N94-13696
Machining and grinding: High rate deformation in practice
[DE93-010718] 02 p0664 N94-14457
The MADONA experiments (Meteorology and Diffusion Over Non-uniform Areas): High-resolution in-plume concentration fluctuations measurements using lidar remote sensing technique
[AD-A267711] 03 p1105 N94-14938
Some problems in the rheological characterisation of composite rocket propellants
[AD-A268806] 04 p1376 N94-18203
Radial basis function approximation: From gridded centers to scattered centers
[AD-A274184] 07 p2998 N94-27103
Experimental and computational studies on propeller noise due to inflow distortion 09 p3860 N94-31846
Effect of surface forces on the rheology of particle-liquid systems and the consolidation of ceramic powders
[AD-A277092] 09 p3657 N94-32391
Parallel programming methodologies for non-uniform structured problems in materials science
[AD-A277868] 10 p4111 N94-33777

NONVISCOUS FLOW
U INVISCID FLOW

NOREPINEPHRINE
Neuropeptide-Y (NPY) increases total blood flow in the tail, and reduces cutaneous microvascular blood flow in the tail and foot of the rat
[AD-A266839] 03 p1115 N94-14918
The role of beta-adrenoceptor stimulation in the progression of chronic heart failure
07 p2932 N94-27541
Cerebral neurochemical mechanisms in stress and anxiety
[AD-A280473] 12 p4482 N94-37233

NORMAL DENSITY FUNCTIONS
Positive phase space distributions and uncertainty relations 01 p0379 N94-10598
A new method to assess Monte Carlo convergence
[DE93-012667] 02 p0772 N94-12919
High order nonlinear estimation with signal processing applications
[AD-A268407] 03 p1005 N94-17463
An empirical evaluation of five circular error probable estimation techniques and a method for improving them
[AD-A266528] 04 p1556 N94-18397
The roughness of the Martian surface: A scale dependent model 05 p2115 N94-20762
The missing impact craters on Venus
05 p2119 N94-20782
Measure fields for function approximation
[AD-A272660] 05 p1964 N94-21215
Setting test limits under prescribed consumer loss
[MEMO-1107] 06 p2478 N94-22725
Subset selection for the best of two populations: Tables of the expected subset size
[PB93-237857] 06 p2494 N94-23546
A random distribution reacting mixing layer model
[NASA-CR-194445] 06 p2187 N94-23552
Solving the ranking and selection indifference-zone formulation for normal distributions using computer software
[AD-A273821] 06 p2496 N94-25518
Simulating high-frequency wind for long durations
[DE94-002739] 07 p2682 N94-27997

NORMAL DISTRIBUTIONS
U NORMAL DENSITY FUNCTIONS

NORMAL FORCE DISTRIBUTION
U FORCE DISTRIBUTION

NORMAL SHOCK WAVES
An experimental investigation of shock wave/vortex interaction 02 p0634 N94-13574
Laser Doppler velocimetry measurements across a normal shock in transonic flow
[AD-A267240] 03 p0855 N94-14973
Stability of hypersonic flow of a detonable gas mixture in the stagnation region of a blunt body and a forward facing step 06 p2154 N94-24248
Modelling of ionisation reactions and of the resulting electric fields in one-dimensional hypersonic shock waves with the direct simulation Monte Carlo method
[IC-AERO-92-01] 07 p2644 N94-26248
A supersonic tunnel for laser and flow-seeding techniques
[NASA-TM-106588] 11 p4265 N94-35945

NORMALITY
Balancing of the normalized right coprime factorization of a nonlinear system
[MEMO-1096] 01 p0341 N94-10273
EDF tests for normality in linear models after a Box-Cox transformation
[AD-A269068] 04 p1557 N94-18517
On estimation and testing in Poisson regression models with over-dispersion
[MEMO-1083] 05 p1963 N94-21076
A sharp upper bound for departure from normality
[DE93-040457] 05 p1960 N94-21966
Size distribution of retrogradely labeled dorsal root ganglion cells: Test of normality
07 p2906 N94-27500

NORMALIZING
Comparing curried and uncurried rewriting
[CWI-CS-R9350] 08 p3425 N94-30415
Perpetual reductions and strong normalization in orthogonal term rewriting systems
[CWI-CS-R9345] 08 p3426 N94-30437

NORMALIZING (STATISTICS)
ERS-1 scatterometer data characteristics and wind retrieval skill 01 p0233 N94-11709
EDF tests for normality in linear models after a Box-Cox transformation
[AD-A269068] 04 p1557 N94-18517
Set theory and nominalisation, part 2
[PB93-191815-PT-2] 05 p1962 N94-20008
The detection performance of a long-term spectral integrator using normalized and quantized data
[DREP-TM-93-11] 06 p2455 N94-24130
Output statistics of the SALFAS FM normalizer Smoothing/Prediction function
[AD-A275758] 08 p3463 N94-28759
Perpetual reductions in orthogonal combinatory reduction systems
[CWI-CS-R9349] 08 p3459 N94-30413
Higher order recursive program schemes are Turing incomplete
[CWI-CS-R9348] 08 p3425 N94-30414
Comparing curried and uncurried rewriting
[CWI-CS-R9350] 08 p3425 N94-30415
Airborne SAR as a complement to SPOT HRV in land-cover classification: The use of normalization and principal components analysis 09 p3750 N94-32539

NORMS
A posteriori error estimation for hierarchic models of elliptic boundary value problems on thin domains
[AD-A267714] 03 p1168 N94-14939
Identification for robust control using an H(sub infinity) norm
[EUT-92-E-261] 06 p2470 N94-22873
Triangular norms and conorms: A general tool for generating fuzzy mathematical morphologies
[TELECOM-93-D-001] 09 p3839 N94-31092

NORTH AMERICA
Implementation of a system to provide mobile satellite services in North America 06 p2281 N94-22784
Propagation of cold air masses in East Asia and its associated planetary-scale function
[AD-A274304] 07 p2895 N94-26850

NORTH AMERICAN AIRCRAFT
NT B-1 AIRCRAFT
NT B-70 AIRCRAFT
NT T-39 AIRCRAFT
NT X-15 AIRCRAFT

NORTH ATLANTIC TREATY ORGANIZATION (NATO)
AGARD highlights 92/2, September 1992
[AGARD-HIGHLIGHTS-92/2] 01 p0497 N94-11820

Activities report to NATO
[ETN-94-95047] 06 p2318 N94-23227
Cardiovascular and pulmonary disease in NATO aircrew: An overview 06 p2423 N94-23314
Report on NATO PTTI 08 p3469 N94-30645
AGARD highlights 94/1, April 1994
[AGARD-HIGHLIGHTS-94/1] 09 p3956 N94-31196
AGARD membership, 1994
[AGARD-MEMB-94] 09 p3914 N94-31197
NATO contributions to European environmental security
[AD-A275918] 09 p3763 N94-31275
AGARD highlights 93/2
[AGARD-HIGHLIGHTS-93/2] 11 p4376 N94-35444

NORTH SEA
Calibration of ERS-1 altimetry over the North Sea 01 p0234 N94-11716
Nutrients and light as factors controlling phytoplankton biomass on the Dutch continental shelf (North Sea), 1988-1990
[PB94-111143] 06 p2418 N94-24601
Macrobenthic fauna in the dutch sector of the north sea in 1991
[PB94-126414] 07 p2868 N94-27200

NORTH VIETNAM
U VIETNAM

NORTHERN HEMISPHERE
NT ARCTIC REGIONS
Southern and Northern Hemisphere total ozone as seen by TOMS
[NASA-TM-109591] 03 p1098 N94-15282
Northern hemisphere tropospheric mid-latitude circulation after violent volcanic eruptions
[MPIM-107] 06 p2403 N94-24491
Northern hemisphere dust storms on Mars 06 p2619 N94-24885
An AVHRR cloud classification database typed by experts
[AD-A273560] 06 p2416 N94-25162
Long range forecasts of the Northern Hemisphere anomalies with antecedent sea surface temperature patterns
[NASA-CR-189358] 11 p4292 N94-35380

NORTHERN SKY
Search for continuous and single day emission from ultra-high-energy sources
[DE93-012724] 02 p0846 N94-12947
Sloan Digital Sky Survey
[DE94-004662] 07 p3103 N94-27750
Sloan Digital Sky Survey
[DE94-011749] 12 p4547 N94-37667

NORTHROP AIRCRAFT
NT F-5 AIRCRAFT
NT F-18 AIRCRAFT
NT T-38 AIRCRAFT

NORWAY
Coastal ocean studies with ERS-1 SAR during NORCSEX 1991 01 p0234 N94-11720
Fire safety engineering research in Norway
[PB93-201630] 06 p2268 N94-23429
Norwegian ionospheric satellite experiment: High latitude, low Earth orbit plasma measurements
[FFI-93/7025] 07 p2876 N94-25807
The Norwegian seismic array (NORSAR), phase 3
[AD-A275440] 08 p3356 N94-28868

NOSE CAPS
U NOSE CONES

NOSE CONES
NT ROCKET NOSE CONES
The effect of the nose shape and wing location toward the wing vortex breakdown
[AD-A267724] 03 p0855 N94-14942
Compilation of reinforced carbon-carbon transatlantic abort landing arc jet test results
[NASA-TM-104778] 05 p1676 N94-21834
Tip effects on the vortex wake of an axisymmetric body at angle of attack 09 p3570 N94-31907
Calibration and validation studies in the LENS facility
[AD-A278403] 09 p3591 N94-33167

NOSE FINS
Supersonic aerodynamic characteristics of a circular body Earth-to-Orbit vehicle
[NASA-TM-4533] 06 p2170 N94-24716

NOSE TIPS
Computation of hypersonic nosetip heat transfer rates for an M829-like projectile
[AD-A263226] 01 p0016 N94-11870
An aerodynamic and static-stability analysis of the Hypersonic Applied Research Technology (HART) missile
[AD-A280631] 12 p4382 N94-36729

NOSE WHEELS
Computational methods for frictional contact with applications to the Space Shuttle orbiter nose-gear tire 09 p3608 N94-32295

NOSES (FOREBODIES)
NT NOSE CONES
NT ROCKET NOSE CONES
A theoretical investigation of unsteady separation phenomena related to dynamic stall
[AD-A271865] 05 p1636 N94-20465
Controlled oscillation of forebody vortices by nozzle jet blowing
[ISBN-0-315-84134-6] 07 p2678 N94-27648
Pneumatic management of blunted-forebody flow asymmetry for high-angle-of-attack directional control 07 p2679 N94-28028
An experimental investigation of the effect of leading edge extensions on directional stability and the effectiveness of forebody nose strakes 08 p3155 N94-29728

NOTATION
U CODING

NOTCH SENSITIVITY
The processing and mechanical properties of high temperature/high performance composites. Book 2: Coonstituent properties and macroscopic performance
[AD-A266395] 03 p0935 N94-16484
The processing and mechanical properties of high temperature/high performance composites. Book 4: Coonstitutive laws and design
[AD-A266397] 03 p0935 N94-16528
Investigation of compressive behavior for metal matrix composites with a circular hole
[AD-A273835] 07 p2705 N94-25739
Tension fracture of laminates for transport fuselage. Part 1: Material screening 09 p3629 N94-33130

NOTCH STRENGTH
The effect of electric discharge machined notches on the fracture toughness of several structural alloys
[AD-A268605] 03 p0962 N94-17464
Three-dimensional, inelastic response of single-edge notch bend specimens subjected to impact loading
[AD-A273302] 06 p2378 N94-25143
Structure and properties of intermetallic composites synthesized in situ using solid state displacement reactions
[DE94-004312] 07 p2705 N94-25805

NOTCH TESTS
NT CHARPY IMPACT TEST
Micromechanical characterization of ceramic-matrix composites using the instrumented microindentation technique 06 p2256 N94-24233
Structure and properties of intermetallic composites synthesized in situ using solid state displacement reactions
[DE94-004312] 07 p2705 N94-25805
Non-linear numerical analysis of the losipescu specimen for composite materials
[NASA-CR-195934] 10 p4020 N94-34306

NOTCHED METALS
U NOTCH TESTS

NOTCHES
A computer program to calculate growth rates for cracks at notches in regions of residual stress
[RAE-TM-MAT/STR-1207] 02 p0683 N94-14818
The effect of electric discharge machined notches on the fracture toughness of several structural alloys
[AD-A268605] 03 p0962 N94-17464
Off-design performance of crenulated blades in a linear compressor cascade
[AD-A273744] 06 p2340 N94-25534
Effects of crenulations on three dimensional losses in a linear compressor cascade
[AD-A273778] 07 p2790 N94-25862
Mechanisms and effects of heat generation at the tips of dynamic cracks and notches in metals 08 p3321 N94-29808
Growth of artificially and naturally initiating notch root cracks under FALSTAFF spectrum loading 10 p4072 N94-34589

NOVA LASER SYSTEM
Evaluation of materials proposed for the construction of the Plasma Electrode Pockels Cell (PEPC) on beamlet
[DE93-016952] 04 p1584 N94-17988
Effect of bandwidth on beam smoothing and frequency conversion at the third harmonic of the Nova laser
[DE93-019917] 05 p1819 N94-21920
Precision operation of the Nova laser for fusion experiments
[DE94-007073] 10 p4057 N94-33405
ICF program
[DE94-006281] 10 p4145 N94-35079
X ray radiographic imaging of hydrodynamic phenomena in radiation driven materials: Shock propagation, material compression and shear flow
[DE94-009515] 11 p4266 N94-35982

NOVAE
The spectroscopic evolution of novae in the bulge of M31 and a search for their possible origin in the M31 globular cluster system 02 p0831 N94-13668
Properties of x ray emission from x ray novae 05 p2007 N94-22676
Disk instability and the spectral evolution of the 1992 outburst of the intermediate polar GK Persei 09 p3928 N94-31123
Disk irradiation and light curves of x ray novae 09 p3929 N94-31124
Observational constraints on black hole accretion disks 09 p3929 N94-31126
Can a variable alpha induce limit cycle behavior and exponential luminosity decay in transient soft x ray sources? 09 p3929 N94-31129
The physics of black hole x ray novae 09 p3932 N94-31143

NOWCASTING
Nowcasting methods for satellite imagery
[AD-A267294] 03 p1108 N94-17267
Design document and database specifications for the Naval Interactive Data Analysis System (NIDAS), version 1.0
[NASA-CR-194817] 05 p2045 N94-21865
An efficient data assimilation algorithm with a gaussian covariance structure
[AD-A273152] 06 p2418 N94-24671
Data requirements for ceiling and visibility products development
[AD-A278959] 11 p4293 N94-35720
Atmospheric and dispersion modeling in areas of highly complex terrain employing a four-dimensional data assimilation technique
[DE94-004041] 11 p4285 N94-35823
Use of wind profiler data in short-range forcasting
[AD-A279482] 11 p4295 N94-36228

NOXIOUS MATERIALS
U CONTAMINANTS

NOZZLE COEFFICIENT
U NOZZLE FLOW

NOZZLE DESIGN
Gas-liquid jets under reduced gravity conditions 01 p0103 N94-10091
A CFD-based aerodynamic design procedure for hypersonic wind-tunnel nozzles 01 p0009 N94-10458
Control of jet noise
[NASA-CR-193612] 01 p0358 N94-11176
Method of characteristics design of a supersonic wind tunnel nozzle with square cross-section, supplement 3
[NASA-CR-194359] 02 p0527 N94-12824
Propulsion integration 02 p0508 N94-14174
Qualification test of the Ross Double Planetary Mixer
[NASA-CR-192600] 02 p0652 N94-14497
Heat transfer and aerodynamics of a 3D design nozzle guide vane tested in the Pyestock isentropic light piston facility
[RAE-TM-AERO/PROP-19] 03 p0856 N94-15696
Welding nozzle position manipulator
[NASA-CASE-MFS-29837-1] 03 p1047 N94-15882
Shock-free supersonic elliptic nozzles and method of forming same
[NASA-CASE-LAR-14054-1] 03 p0925 N94-15947
Flight 20 (STS-45) polysulfide gas path investigation
[NASA-CR-193861] 03 p0928 N94-17213
Experimental investigation of nozzle/plume aerodynamics at hypersonic speeds
[NASA-CR-194628] 05 p1636 N94-20014
A tutorial on the aero/thermodynamical design of liquid-propellant rocket engine nozzles 05 p1668 N94-20074
Shape optimization governed by the Euler equations using an adjoint method
[NASA-CR-191555] 05 p1950 N94-20092
Development of phased twin flip-flop jets
[NASA-TM-106404] 05 p1637 N94-20563
Dual-bell altitude compensating nozzles 06 p2215 N94-23057
Development of a code for wall contour design in the transonic region of axisymmetric and square nozzles
[NASA-CR-194857] 06 p2167 N94-23625
Supersonic minimum length nozzle design for dense gases 06 p2171 N94-23656
Final postflight hardware evaluation report RSRM-28 (STS-53)
[NASA-CR-193902] 06 p2200 N94-24112
Controlled oscillation of forebody vortices by nozzle jet blowing
[ISBN-0-315-84134-6] 07 p2678 N94-27648
The interaction region associated with twin jets and a normal crossflow 07 p2800 N94-28009
Fuel injector design for high temperature aircraft engine 08 p3154 N94-29263

Shear flow control of cold and heated rectangular jets by mechanical tabs. Volume 1: Results and discussion
[NASA-CR-182296-VOL-1] 09 p3708 N94-32867
Shear flow control of cold and heated rectangular jets by mechanical tabs. Volume 2: Tabulated data
[NASA-CR-182296-VOL-2] 09 p3709 N94-32869
Enhancement of mixing in a rectangular jet by mechanical tabs
[NASA-CR-185207] 09 p3709 N94-32872
HSCT noise reduction technology development at GE Aircraft Engines 10 p3972 N94-33466
Community noise sources and noise control issues 10 p3972 N94-33467
NASA/LaRC jet plume research 10 p3972 N94-33468
Results of GEAE HSCT propulsion system studies 10 p3974 N94-33479
P and W propulsion systems studies results/status 10 p3974 N94-33480
NASA reload program
[NASA-CR-193972] 12 p4429 N94-37446

NOZZLE EFFICIENCY
Internal performance of a nonaxisymmetric nozzle with a rotating upper flap and a center-pivoted lower flap
[NASA-TP-3385] 05 p1637 N94-21569
Postflight hardware evaluation RSRM-29 (STS-54). Appendix C: Nozzle PFORs
[NASA-CR-193894] 06 p2219 N94-24064

NOZZLE FLOW
Numerical simulation of the flow through a scramjet engine 01 p0003 N94-10425
Calculations of viscous nonequilibrium flows in nozzles 01 p0008 N94-10455
Static internal performance of a single expansion ramp nozzle with multiaxis thrust vectoring capability
[NASA-TM-4450] 01 p0012 N94-10675
Control of jet noise
[NASA-CR-193612] 01 p0358 N94-11176
An overview of the capabilities of ARA for the measurement of nozzle discharge and thrust
[ARA-MEMO-378] 01 p0055 N94-12283
An experimental investigation of the redistribution of gas stream total temperature in a high turning angle transonic planar cascade
[ISBN-0-315-60791-2] 02 p0502 N94-13369
Chemical reactions in scramjet engines: Reduced kinetic models for ignition, combustion and nozzle flow
[NAL-TR-1184] 02 p0563 N94-13458
Investigation of the feasibility of optical diagnostic measurements at the exit of the SSME
[NASA-CR-193832] 02 p0553 N94-14682
Numerical investigations in three-dimensional internal flows
[NASA-CR-194594] 03 p1020 N94-15551
Design of round-to-square transition section; analysis and computer code
[AD-A267173] 03 p0872 N94-15847
Effects of internal yaw-vectoring devices on the static performance of a pitch-vectoring nonaxisymmetric convergent-divergent nozzle
[NASA-TP-3369] 03 p0858 N94-16572
Flight 20 (STS-45) polysulfide gas path investigation
[NASA-CR-193861] 03 p0928 N94-17213
Two-dimensional, high flow, precisely controlled monodisperse drop source
[AD-A267660] 03 p1028 N94-17250
Experimental studies on a gas dynamic laser with narrow throat and high area-ratio grid nozzles
[AD-A267818] 03 p1042 N94-17400
Adaptations to micropep and rocket to allow performance evaluation of multiple grain and/or airbreathing motors
[AD-A268798] 04 p1337 N94-18202
Workshop on Computational Turbulence Modeling
[NASA-TM-109266] 04 p1410 N94-18545
High order non-oscillatory schemes for the compressible Euler equations 04 p1412 N94-18558
Molecular gas dynamics applied to low-thrust propulsion 06 p2214 N94-23053
Dual-bell altitude compensating nozzles 06 p2215 N94-23057
Two stage turbine for rockets 06 p2215 N94-23059
Theoretical studies of a molecular beam generator
[NASA-CR-194779] 06 p2540 N94-23485
Effect of delta tabs on mixing and axis switching in jets from asymmetric nozzles
[NASA-TM-106450] 06 p2167 N94-23592
Ignition and combustion characteristics of metallized propellants, phase 2
[NASA-CR-195107] 06 p2266 N94-24700
Chemical and vibrational nonequilibrium viscous flows: Modelling, internal and external flow applications
[ESA-TT-1274] 07 p2791 N94-26316
Numerical investigation of thrust vectoring by injection of secondary air into nozzle flows 07 p2801 N94-28013
Experiments on interaction force of jets in hypervelocity cross-flow in a shock tunnel 07 p2659 N94-28022
A study of jet effect and ground effect interference on a STOL fighter 07 p2671 N94-28034
Calculation of propulsive nozzle flowfields in multidiffusing chemically reacting environments
[NASA-TM-106532] 08 p3271 N94-28835
Fuel injector design for high temperature aircraft engine 08 p3154 N94-29263
Scramjet CFD methods and analysis. Part 1: Scramjet CFD methods. Numerical simulation of the flow in scramjet duct 08 p3152 N94-29296
Particle kinetic simulation of high altitude hypervelocity flight
[NASA-CR-194535] 08 p3131 N94-29893
Eigenvalue analysis of the convergence behaviour of an Euler method
[PB94-1255722-U] 08 p3281 N94-30743
Evaluation of flip-flop jet nozzles for use as practical excitation devices
[NASA-TM-106377] 08 p3135 N94-30949
The small-scale topology of a 2:1 aspect-ratio elliptic jet 09 p3699 N94-31184
Boundary layer study on nozzle wall at hypersonic velocities 09 p3569 N94-31882
Simulation of low-density nozzle plumes in non-zero ambient pressures
[NASA-TM-106501] 09 p3615 N94-32742
Shear flow control of cold and heated rectangular jets by mechanical tabs. Volume 1: Results and discussion
[NASA-CR-182296-VOL-1] 09 p3708 N94-32867
Shear flow control of cold and heated rectangular jets by mechanical tabs. Volume 2: Tabulated data
[NASA-CR-182296-VOL-2] 09 p3709 N94-32869
Enhancement of mixing in a rectangular jet by mechanical tabs
[NASA-CR-185207] 09 p3709 N94-32872
Use of Navier-Stokes methods for the calculation of high-speed nozzle flow fields
[NASA-TM-106551] 09 p3573 N94-32984
Experimental studies of shock-wave/wall-jet interaction in hypersonic flow
[NASA-CR-195844] 10 p4048 N94-34171
Computational study of generic hypersonic vehicle flow fields
[NASA-CR-195938] 10 p3984 N94-34277
Nozzle guide vane flow in radial inflow turbines 10 p4004 N94-34460
The prediction of nozzle performance and heat transfer in hydrogen/oxygen rocket engines with transpiration cooling, film cooling, and high area ratios
[NASA-TM-106617] 10 p4017 N94-34924
Fundamental studies in blow-down and cryogenic cooling
[AD-A278967] 11 p4250 N94-35524
Tipjet 80-inch model rotor hover test: Test no. 1198
[AD-A279680] 11 p4191 N94-36261
An experimental investigation of active control of thrust vectoring nozzle flow fields
[AD-A278702] 11 p4229 N94-36291
Experimental investigation of nozzle/plume aerodynamics at hypersonic speeds
[NASA-CR-195829] 12 p4382 N94-36687
Computational investigation of an improved cowl concept for hypersonic propulsive nozzles
[AD-A280596] 12 p4441 N94-36724
Theoretical studies of a molecular beam generator
[NASA-CR-196306] 12 p4522 N94-37508

NOZZLE GEOMETRY
Studies on scramjet nozzles. Part 1: Performance of two dimensional nozzles
[NAL-TR-1149] 01 p0027 N94-10367
Mixing noise reduction for rectangular supersonic jets by nozzle shaping and induced screech mixing
[NASA-TM-106364] 02 p0508 N94-14208
Shock-free supersonic elliptic nozzles and method of forming same
[NASA-CASE-LAR-14054-1] 03 p0925 N94-15947
Experimental studies on a gas dynamic laser with narrow throat and high area-ratio grid nozzles
[AD-A267818] 03 p1042 N94-17400
Study of multi-phase flow characteristics in an MHD power train
[DE93-018570] 04 p1586 N94-18272
Supersonic jets from bevelled rectangular nozzles
[NASA-TM-106403] 04 p1313 N94-19484
A tutorial on the aero/thermodynamical design of liquid-propellant rocket engine nozzles 05 p1668 N94-20074
Internal performance of a nonaxisymmetric nozzle with a rotating upper flap and a center-pivoted lower flap
[NASA-TP-3385] 05 p1637 N94-21569
Dual-bell altitude compensating nozzles 06 p2215 N94-23057
Effect of delta tabs on mixing and axis switching in jets from asymmetric nozzles
[NASA-TM-106450] 06 p2167 N94-23592
Computational prediction of isolated performance of an axisymmetric nozzle at Mach number 0.90
[NASA-TM-4506] 07 p2646 N94-26547
Control experiments in liquid metal combustion
[AD-A276918] 09 p3635 N94-32234
Static performance investigation of a skewed-throat multiaxis thrust-vectoring nozzle concept
[NASA-TP-3411] 10 p3983 N94-34172
Probabilistic assessment of space nuclear propulsion system nozzle
[NASA-TM-106539] 12 p4457 N94-37704

NOZZLE INSERTS
SRB thermal curtain design support
[NASA-CR-193857] 03 p0927 N94-17123
Shear flow control of cold and heated rectangular jets by mechanical tabs. Volume 1: Results and discussion
[NASA-CR-182296-VOL-1] 09 p3708 N94-32867
Shear flow control of cold and heated rectangular jets by mechanical tabs. Volume 2: Tabulated data
[NASA-CR-182296-VOL-2] 09 p3709 N94-32869
Mixing and noise benefit versus thrust penalty in supersonic jets using impingement tones
[NASA-TM-106583] 12 p4382 N94-36686

NOZZLE THRUST COEFFICIENTS
A tutorial on the aero/thermodynamical design of liquid-propellant rocket engine nozzles 05 p1668 N94-20074
Internal performance of a nonaxisymmetric nozzle with a rotating upper flap and a center-pivoted lower flap
[NASA-TP-3385] 05 p1637 N94-21569

NOZZLE WALLS
Numerical investigations in three-dimensional internal flows
[NASA-CR-194594] 03 p1020 N94-15551
Analysis of film cooling in rocket nozzles
[NASA-CR-194674] 04 p1338 N94-19438
Development of a code for wall contour design in the transonic region of axisymmetric and square nozzles
[NASA-CR-194857] 06 p2167 N94-23625
Boundary layer study on nozzle wall at hypersonic velocities 09 p3569 N94-31882

NOZZLES
Welding nozzle position manipulator
[NASA-CASE-MFS-29837-1] 03 p1047 N94-15882
Postflight hardware evaluation RSRM-29 (STS-54). Case, seals, and joints PFORs, appendix B
[NASA-CR-193899] 06 p2367 N94-25020
Gas-turbine engine steady-state behavior 07 p2828 N94-28044
A microcomputer measuring-controlling system for the performance test of fogging nozzles 10 p4032 N94-34362

NUCLEAR ASTROPHYSICS
Nuclear astrophysics
[DE93-010569] 01 p0425 N94-10292
Planck scale effects on the Majoron
[DE93-613120] 01 p0410 N94-10545
Experimental and theoretical high energy physics program
[DE93-013336] 01 p0373 N94-12600
Research in theoretical nuclear physics
[DE93-015096] 02 p0839 N94-14330
Fast pulsars, compact stars, and the strange matter hypothesis
[DE93-015039] 03 p1239 N94-16052
Properties of nuclei in astrophysical environments: Binding energies, weak-interaction rates
[MPA-706] 03 p1240 N94-17628
New production mechanisms for unstable nuclei in stars, supernovae, and the big bang
[DE93-018627] 05 p2081 N94-21618
Reactive flows in compact objects 09 p3934 N94-31567

NUCLEAR AUXILIARY POWER UNITS
NT SPACE POWER REACTORS

NUCLEAR BINDING ENERGY
Recent advances in electron momentum spectroscopy
[DE93-610149] 01 p0361 N94-10333
Three-nucleon problem with phase equivalent potentials
[DE93-617731] 01 p0363 N94-10722
Quantum dynamics of helium clusters
[AD-A266060] 01 p0411 N94-10874
Interatomic interactions in BCC and FCC lattices of transition metals
[DE93-621541] 01 p0398 N94-11090
A generalized Bethe-Weizsaecker mass formula for strange hadronic matter
[DE93-011010] 01 p0368 N94-11620
Simulation studies for surfaces and materials strength
[NASA-CR-193305] 02 p0671 N94-13179

Thermochemistry of transition metal clusters
[DE93-016201] 02 p0571 N94-13977
Spin polarized photoemission studies of interfacial and thin film magnetism
[DE93-014326] 02 p0580 N94-14142
Electronic spectroscopy of the gas-phase OH-Kr van der Waals complex
[AD-A266891] 03 p0942 N94-14946
Simulation studies for surfaces and materials strength
[NASA-CR-193387] 03 p1056 N94-15004
Photoemission study of diamond (100) surface
[DE93-015251] 03 p1208 N94-16062
Effect of oxygen concentration and ordering on vanadium-oxygen alloy vibrational spectra
[DE93-627003] 04 p1355 N94-17692
Binding of copper to nanocavity surfaces in silicon
[DE93-019073] 04 p1364 N94-19080
Theoretical research program to study chemical reactions in AOTV bow shock tubes
[NASA-CR-194710] 05 p1804 N94-22027
Binding of copper and nickel to cavities in silicon formed by helium ion implantation
[DE94-003769] 07 p3050 N94-25814
Three methods to measure RH bond energies
[DE94-003795] 07 p3013 N94-25816
The structural, chemical, and electrical properties of He-implantation-induced nanocavities in silicon
[DE94-002681] 07 p3052 N94-25971
The bond diluted spin-1 Blume-Emery-Griffiths model in a transverse field
[DE94-608121] 08 p3525 N94-30167
Indium-vacancy complexes in mercury cadmium telluride
[AD-A276177] 09 p3894 N94-31055
Nonthermal accretion disk models around neutron stars 09 p3931 N94-31139
IR materials producibility
[AD-A277028] 09 p3879 N94-32006
Gettering of metal impurities by cavities in silicon
[DE94-005248] 09 p3645 N94-32672
Relativistic three-particle dynamical equations. 2: Application to the trinucleon system
[DE94-616653] 11 p4320 N94-35580

NUCLEAR BULGE (GALAXIES)
U GALACTIC BULGE

NUCLEAR CAPTURE
NT ELECTRON CAPTURE

NUCLEAR CHEMISTRY
Fifty years of continuous improvement: What has DOE done for analytical chemistry?
[DE94-002539] 06 p2234 N94-24548
Radiochemistry Division annual progress report : 1991
[DE94-600652] 07 p2715 N94-26392
TRIUMF scientific activities
[CTN-94-61062] 07 p3117 N94-26656

NUCLEAR DEFORMATION
Overlap of metal clusters and nuclear structure physics
[DE94-608387] 08 p3517 N94-30183

NUCLEAR ELECTRIC POWER GENERATION
NT NUCLEAR POWER PLANTS
NT NUCLEAR POWER REACTORS
NT SPACE POWER REACTORS
NT THERMONUCLEAR POWER GENERATION
Directory of Energy Information Administration Models 1993
[DE93-016987] 04 p1616 N94-18707
Technology to prevent greenhouse effect gases
[DE94-707420] 05 p1851 N94-20116
Current situation of development of petroleum substituting energies (USA)
[DE94-707492] 05 p1848 N94-22013
Mars transportation system 07 p2833 N94-25689
The First Energy Conference: Israel and the Former USSR
[ISBN-965-229-098-X] 07 p2853 N94-26050
Present situation of the development of petroleum substitution energy (France)
[DE94-725201] 07 p2760 N94-26914
International bulletin on atomic and molecular data for fusion. No. 42-45, Mar. 1991 - Dec. 1992
[DE94-601817] 07 p3045 N94-26946
International bulletin on atomic and molecular data for fusion. No. 46
[DE94-601818] 07 p3023 N94-26947
Research laboratories annual report 1992
[DE94-608124] 08 p3555 N94-30168
Aerospace test facilities at NASA LERC Plumbrook
[NASA-TM-109755] 09 p3602 N94-31814
EIA directory of electronic products, fourth quarter 1993
[DE94-007368] 10 p4151 N94-33596
International Energy: Subject Thesaurus, revision 1
[DE94-002590] 10 p4151 N94-33730
Safeguards Information Management Systems (SIMS)
[DE94-008936] 10 p4158 N94-34013
Multi-unit Inertial Fusion Energy (IFE) plants producing hydrogen fuel
[DE94-007241] 10 p4079 N94-34088
Logarithmic corrections of the two-body QED problem
[DE94-611157] 11 p4322 N94-35783

NUCLEAR ELECTRIC PROPULSION
Space exploration initiative fuels, materials and related nuclear propulsion technologies panel
[NASA-TM-105706] 03 p0923 N94-15118
Application of a NEPTUNE propulsion concept to a manned Mars excursion
[AD-A268053] 03 p0929 N94-17587
Critical technologies for reactors used in nuclear electric propulsion
[DE93-017685] 04 p1337 N94-17908
Potassium-Rankine power conversion subsystem modeling for nuclear electric propulsion
[NASA-CR-191134] 04 p1468 N94-18821
Power conditioning system modelling for nuclear electric propulsion
[NASA-CR-191136] 05 p1846 N94-21179
NEP Early Flight program: System performance and development considerations
[NASA-TM-106415] 05 p1654 N94-21570
Brayton power conversion system parametric design modelling for nuclear electric propulsion
[NASA-CR-191135] 05 p1671 N94-21874
Advanced nuclear thermal propulsion concepts 06 p2217 N94-23068
Utilization of recently developed codes for high power Brayton and Rankine cycle power systems 06 p2222 N94-23641
Heat pipe cooled heat rejection subsystem modelling for nuclear electric propulsion
[NASA-CR-191132] 06 p2219 N94-24061
Characteristics and control response of the TOPAZ 2 reactor system real-time dynamic simulator
[DE94-003788] 07 p2699 N94-25600
Risk perspectives for Topaz 2 flight mission
[DE94-003229] 07 p2700 N94-25956
Nuclear electric propulsion for future NASA space science missions
[DE93-019086] 07 p2700 N94-25969
Nuclear electric propulsion: A better, safer, cheaper transportation system for human exploration of Mars
[NASA-TM-106406] 08 p3171 N94-28833
Utilizing a Russian space nuclear reactor for a United States space mission: Flight qualification issues
[DE94-004674] 09 p3613 N94-31265
Integrated safety program for the Nuclear Electric Propulsion Space Test Program
[DE94-004670] 09 p3615 N94-32669
Utilizing a Russian space nuclear reactor for a US space mission: Systems integration issues
[DE94-005585] 10 p4017 N94-34137
Scoping calculations of power sources for nuclear electric propulsion
[NASA-CR-191133] 10 p4017 N94-34211

NUCLEAR EMULSIONS
Meso-optical Fourier transform microscope with double focusing
[DE94-607851] 08 p3290 N94-30148
Sigma minus-nucleus interactions in emulsion at 350 GeV
[DE94-616886] 11 p4326 N94-36130

NUCLEAR ENERGY
Directory of IAEA databases
[DE93-622837] 01 p0420 N94-11818
JPRS report: Science and technology. Central Eurasia: Engineering and equipment
[JPRS-UEQ-93-006] 02 p0776 N94-14431
Cosmic energy equipment 08 p3229 N94-28945
JPRS report: Science and technology. Central Eurasia
[JPRS-UST-94-004] 11 p4249 N94-35341
JPRS report: Science and technology. Central Eurasia
[JPRS-UST-94-005] 11 p4249 N94-35342

NUCLEAR ENGINE FOR ROCKET VEHICLES
Nuclear propulsion systems engineering
[DE93-010791] 02 p0548 N94-12870
Entry velocities at Mars and Earth for short transit times
[AD-A272591] 05 p1665 N94-21420

NUCLEAR EXPLOSION EFFECT
Controlled atmospheric breakdown: Applications and research opportunities
[AD-A278584] 12 p4464 N94-36973

NUCLEAR EXPLOSIONS
NT THERMONUCLEAR EXPLOSIONS
Sensitivities of calculated residual stress to separation distances of two simultaneous events
[DE92-019571] 01 p0098 N94-10751
Atmospheric acoustic modeling
[DE93-016727] 02 p0718 N94-14518
Ground wave emergency network environmental assessment for northwestern Colorado relay node site number RN 8C924CO
[AD-A267654] 03 p1003 N94-17249
Ground wave emergency network final operational capability. Environmental assessment for southern Arkansas relay node site no. RN 8C912AR
[AD-A268001] 03 p1004 N94-17376
Environmental assessment for northwestern Indiana relay node site no. RN 8C902IN
[AD-A267849] 03 p1004 N94-17406
Proceedings of the 15th Annual Seismic Research Symposium
[AD-A271458] 05 p1855 N94-20090
On magnetodynamic effects initiated by a high-speed impact of a large cosmic body upon the Earth's surface 05 p2082 N94-20647
Parametric and nonparametric discriminants for regional earthquakes and explosions
[AD-A273807] 06 p2406 N94-25538
Research in pulsed power plasma physics
[AD-A274323] 07 p3045 N94-27074
Investigations on local seismic phases and modeling of seismic signals
[AD-A277891] 10 p4085 N94-33537
Processed seismic motion records from earthquakes, 1982-1993: Recorded at Scotty's Castle, California
[DE94-001371] 10 p4086 N94-33729
A comparison of artificial neural networks and statistical analyses
[DE94-010846] 11 p4312 N94-36195
Controlled atmospheric breakdown: Applications and research opportunities
[AD-A278584] 12 p4464 N94-36973

NUCLEAR FISSION
A modular gas-cooled cermet reactor system for planetary base power
[DE93-013672] 02 p0550 N94-13351
The LAHET code system: Introduction, development, and benchmarking
[DE93-012657] 02 p0787 N94-14804
Engineering Physics and Mathematics Division progress report, period ending 31 December 1992
[DE93-015118] 03 p1301 N94-14926

NUCLEAR FUEL ELEMENTS
Space nuclear thermal propulsion nuclear element tests at Sandia National Laboratories
[DE93-002301] 01 p0045 N94-10282
A critical assembly designed to measure neutronic benchmarks in support of the Space Nuclear Thermal Propulsion program
[DE92-040974] 01 p0371 N94-10529
TFE verification program
[DE93-009609] 01 p0373 N94-11694
Flow instability tests for a particle bed reactor nuclear thermal rocket fuel element
[AD-A268012] 03 p0929 N94-17474
An F2D analysis of the Flow Instability Test (FIT) experiment
[DE94-001420] 06 p2217 N94-23193
Space-R thermionic space nuclear power system design and technology demonstration
[DE94-002017] 07 p2700 N94-25930
TFE verification program
[DE94-009870] 12 p4398 N94-37514

NUCLEAR FUELS
NT SPENT FUELS
Review of nuclear thermal propulsion carbide reactor fuel corrosion and exhibit
[DE93-016605] 02 p0585 N94-14535
Space reactor fuel element testing in upgraded TREAT
[DE93-012524] 02 p0554 N94-14806
Space exploration initiative fuels, materials and related nuclear propulsion technologies panel
[NASA-TM-105706] 03 p0923 N94-15118
Space Nuclear Facility test capability at the Baikal-1 and IGR sites Semipalatinsk-21, Kazakhstan
[DE93-011662] 03 p0926 N94-16773
EIA publications directory, 1992
[DE93-016833] 04 p1617 N94-18983
Total hemispherical emittance of Niobium-1 percent zirconium fuel cladding for the SP-100 space reactor
[AD-A270456] 04 p1576 N94-19589
Pellet ablation in the large helical device
[NIFS-260] 06 p2551 N94-24358
Grain by grain study of the mechanisms of crack propagation during iodine SCC of Zry-4
[DE93-633765] 07 p2734 N94-26162
Nonswelling behavior of HT9 alloy irradiated to high exposure
[DE94-003502] 07 p2736 N94-26522
Application of railgun principle to high-velocity hydrogen pellet injection for magnetic fusion reactor fueling
[DE94-004411] 07 p3044 N94-26579

List of papers published by the members of Institute for Materials Research, Tohoku University 1992
[JTN-94-80608] 07 p3118 N94-27355
Fuel ion rotation measurement and its implications on H-mode theories
[DE94-004860] 07 p3048 N94-27791
The development of CVR coatings for PBR fuels
[DE94-004233] 09 p3875 N94-31480

NUCLEAR FUSION
NT CONTROLLED FUSION
Heavy ion fusion at sub-barrier energies: Progress and questions
[DE93-011764] 01 p0372 N94-11124
Experiments with energetic (mu)d and (mu)t emitted from solid hydrogen
[DE93-010252] 01 p0373 N94-12542
Microwave generation for magnetic fusion energy applications
[DE93-013864] 02 p0654 N94-13058
Nuclear fusion of protons with ions of boron
[DE93-014284] 02 p0781 N94-13219
Long-pulse operation of a gyrotron with beam/RF separation
[DE93-015007] 02 p0649 N94-13410
The status of cold fusion
[DE93-012731] 02 p0802 N94-14567
Nuclear fusion of protons with ions of boron
[DE93-015399] 03 p1202 N94-16019
Chemical and isotopic compositions in acid residues from various meteorites 03 p1243 N94-16291
The astrophysical interpretation of isotope anomalies in graphite and SiC grains of chondrites 03 p1244 N94-16343
Magnetic Fusion Energy Technology Fellowship: Report on survey of institutional coordinators
[DE93-014646] 04 p1583 N94-17739
Plasma properties research: Task 3
[DE93-017087] 04 p1583 N94-17854
Evolution of r-process elements in the hot supernova bubble
[DE93-017169] 04 p1624 N94-17897
Electron stripping cross sections for light impurity ions in colliding with atomic hydrogens relevant to fusion research
[DE93-788476] 04 p1566 N94-18158
Institute of Geophysics and Planetary Physics, 1992
[DE93-019209] 04 p1627 N94-19077
Transverse beam combiner for ILSE
[DE93-019239] 04 p1591 N94-19559
Longitudinal beam dynamics for heavy ion fusion using WARPrz
[DE93-019154] 05 p1992 N94-19915
Space-charge dominated beam transport in magnetic quadrupoles with large aperture ratios
[DE93-040443] 05 p1992 N94-20004
AGB stars as a source of short-lived radioactive nuclei in the solar nebula 05 p2133 N94-20859
Theoretical and numerical studies in magnetic fusion
[DE94-000536] 05 p1993 N94-20937
New production mechanisms for unstable nuclei in stars, supernovae, and the big bang
[DE93-018627] 05 p2081 N94-21618
Fourth International Toki Conference on Plasma Physics and Controlled Nuclear Fusion
[ESA-SP-351] 05 p2000 N94-22624
Fusion Energy Advisory Committee: Advice and recommendations to the US Department of Energy in response to the charge letter of September 1, 1992
[DE93-019842] 07 p3043 N94-26428
Researches of the Electrotechnical Laboratory. No. 51: Study of formation and sustainment of reversed field pinch by slow control of magnetic field
[JTN-94-80548] 07 p3046 N94-27350
Broadband EUV survey spectrometer for short-timescale experiments
[DE94-005459] 08 p3498 N94-28534
Project of the experiment to test the hypothesis on existence of white and black p(mu)-atoms
[DE94-606751] 08 p3485 N94-28625
Transient internal probe
[AD-A275054] 08 p3505 N94-29134
Comparison of 14 MeV isomer production of Hf-178m1 and Hf-179m2 using Feshbach-Kerman-Koonin and exciton preequilibrium models
[DE94-002640] 08 p3488 N94-30039
Overview of the US stellarator reactor study
[DE94-006042] 08 p3508 N94-30339
Plasma confinement theory and transport simulation
[DE94-006065] 09 p3888 N94-31619
Mechanisms of formation and of de-excitation in the reaction Mg-24 + C-12 yields 9 alpha at 35MeV per nucleon
[ISBN-0-315-86746-9] 09 p3867 N94-31749
Atomic and molecular data needs for fusion
[DE94-006555] 09 p3870 N94-32177
Fusion applications of high power millimeter wave sources
[DE94-007374] 09 p3718 N94-32202
Magnetless magnetic fusion
[DE94-007114] 09 p3891 N94-32686
Convection in Type 2 supernovae
[DE94-009373] 09 p3938 N94-32914
Deuteron-induced fusion in various environments
[DE94-009305] 10 p4140 N94-34077
Applications of non-resonant RF forces for improvement of tokamak reactor performances. Part 1: Application of ponderomotive force
[DE94-718994] 11 p4336 N94-35813
Neutron detectors for fusion reaction-rate measurements
[DE94-010407] 11 p4330 N94-36114
Stellar alchemy: The origin of the chemical elements
[DE94-011903] 11 p4350 N94-36229
Primordial nucleosynthesis in conformal Weyl gravity
[DE94-003002] 11 p4327 N94-36241
Towards nuclear fusion reactors
[DE94-748680] 12 p4528 N94-37235
Three-dimensional gyrokinetic particle-in-cell simulation of plasmas on a massively parallel computer: LDRD Core Competency Project
[DE94-013367] 12 p4532 N94-37732

NUCLEAR HEAT
Development of lightweight radiators for lunar based power systems
[NASA-TM-106604] 09 p3726 N94-32272

NUCLEAR INTERACTIONS
NT ELECTRON CAPTURE
NT SPIN-ORBIT INTERACTIONS
NT WEAK INTERACTIONS (FIELD THEORY)
Measurements of transverse energy and forward energy in high-energy nuclear collisions
[DE93-012755] 02 p0788 N94-12817
HIJET with AGS physics and N(sup *)'s
[DE93-014022] 02 p0780 N94-13097
Scattering calculations and confining interactions
[NASA-CR-194242] 02 p0786 N94-14549
Calculations of cosmic-ray helium transport in shielding materials
[NASA-TP-3354] 03 p1301 N94-17666
Heavy-ion collisions and the nuclear equation of state
[DE93-019263] 04 p1566 N94-18104
Momentum loss in proton-nucleus and nucleus-nucleus collisions
[NASA-TP-3405] 06 p2540 N94-24305
Behavior of the intermittency exponents and a quark-gluon plasma formation in the heavy ion collisions
[DE93-616869] 06 p2541 N94-25342
Energy concentration in high energy hadron-gamma families 07 p3113 N94-25632
A search for the production of direct leptons in nucleon-nucleus and nucleus-nucleus collisions
[DE94-004640] 07 p3018 N94-26244
Stopping powers and cross sections due to two-photon processes in relativistic nucleus-nucleus collisions
[NASA-CR-4574] 07 p3033 N94-27646
Experimental setup for study of hadron and hard photon production in nucleus-nucleus collisions
[DE94-607849] 08 p3489 N94-30051
Experimental setups and methods to obtain new nuclear data at intermediate and high energies
[DE94-607850] 08 p3489 N94-30052
Theory of ultra dense matter and the dynamics of high energy interactions involving nuclei
[DE94-004178] 08 p3491 N94-30686
Transverse energy production with Si and Au beams at AGS energy: Towards hot and dense hadronic matter
[DE94-007178] 09 p3938 N94-32638
Solar proton produced neon in shergottite meteorites 11 p4351 N94-35428
SCATTER program of cross section calculation of the hadron and lepton interactions with nuclei
[DE94-617006] 11 p4326 N94-36134
High baryon density from relativistic heavy ion collisions
[DE94-003894] 12 p4511 N94-36460
An overview of the current status of resonance theory in reactor physics applications
[DE94-010465] 12 p4521 N94-37194
Strangeness and the quark-gluon plasma: An experimenter's perspective
[DE94-011377] 12 p4519 N94-37558

NUCLEAR LIGHTBULB ENGINES
In-reactor testing of the closed cycle gas core reactor: The Nuclear Light Bulb concept
[DE93-004053] 01 p0370 N94-10149

NUCLEAR MAGNETIC RESONANCE
Si-29 NMR spectroscopy of naturally-shocked quartz from Meteor Crater, Arizona: Correlation to Kieffer's classification scheme 01 p0080 N94-12087
NMR spectroscopy of experimentally shocked single crystal quartz: A reexamination of the NMR shock barometer 01 p0081 N94-12258
The 13C and 15N solid-state NMR of copolymers of nylon 6 and 7: Observation of a stable pseudohexagonal phase
[AD-A265799] 01 p0094 N94-12381
NMR characterization of polymers formed in diazotizing mixtures of luminol and 3-amino-L-tyrosine
[AD-A266093] 01 p0094 N94-12536
Development of nondestructive evaluation methods and prediction of effects of flaws on the fracture behavior of structural ceramics
[DE93-012942] 02 p0577 N94-13032
Transport properties of disordered porous media from the microstructure
[DE93-016065] 02 p0806 N94-13152
Office of Naval Research/DARPA publications: Composite materials with improved properties in compression
[AD-A265509] 02 p0560 N94-14794
Multinuclear NMR study of aluminosilicate sol-gel synthesis reasons for the homogeneous gelation using the prehydrolysis method
[AD-A266877] 03 p0962 N94-14921
NMR and theoretical investigation of cation binding with sol-gel silicates
[AD-A266999] 03 p0963 N94-15631
Study of protein-H2O interactions by multidimensional NMR spectroscopy
[AD-A266955] 03 p0946 N94-15760
Detection and dosimetry of chemical contaminants in polymeric materials
[AD-A266605] 03 p0968 N94-16727
Suppression of charge scattering in Moessbauer experiments using synchrotron radiation
[DE93-015406] 03 p1212 N94-16887
NMR studies of enriched species at interfaces
[AD-A264703] 04 p1367 N94-17878
Advanced in macrostatistical hydrodynamics
[DE93-018479] 04 p1410 N94-18270
Synthesis and structural characterization of new light molecular weight inorganic oxidizers and relative derivatives, volume 1
[AD-A271437] 05 p2012 N94-19842
Examination of low level magnetic dipole intensities in the transition nuclei Sm-148, Sm-150, Sm-152 and Sm-154, with inelastic photon scattering at S-DALINAC
[ETN-93-95069] 05 p1971 N94-20030
Characterization of amorphous material in shocked quartz by NMR spectroscopy
[DE93-019069] 05 p1679 N94-20307
The 13C-NMR spectra of poly (4-((2-(acryloyloxy) ethyl) ethyl amino)- 4-nitroazobenzene-co-methyl methacrylate)
[AD-A273016] 05 p1705 N94-21238
Dynamics of adsorbed, swollen block copolymers
[AD-A272013] 05 p1706 N94-21460
Local structure in oxygen-doped La2CuO(4+delta)
[DE93-040248] 05 p2030 N94-21768
Spin dynamics and implications for superconductivity: Some problems with the d-wave scenario
[DE94-001183] 05 p2032 N94-21972
NMR studies of oxygen-doped La2CuO(4+delta)
[DE93-040756] 05 p2034 N94-22007
Magnetic resonance studies of 3d transition metal impurities in compound semiconductors
[PB93-232197] 06 p2243 N94-23714
Synthesis and in-vivo detection of boronated compounds for use in BNCT
[DE94-001899] 06 p2233 N94-23780
Nuclear magnetic resonance imaging with short gradient pulses
[AD-D016006] 06 p2537 N94-25047
The nanostructure of multilayered films: A NMR study
[ETN-94-95347] 06 p2262 N94-25222
Microstructure of styrene methyl methacrylate copolymers grafted onto polybutadiene seeds
[ETN-94-95360] 06 p2262 N94-25225
On the mechanism of action of 3',5'-cyclic adenosine monophosphate: A study of four- and five-coordinated phosphorus compounds, modelling the activated state of cAMP
[ISBN-9-03-860222-7] 06 p2226 N94-25238
Microscopic study of local structure and charge distribution in metallic La2CuO(4+delta)
[DE94-003801] 07 p3050 N94-25817
Morphological analysis of ionomers
[DE94-003660] 07 p2749 N94-26005
Use of oxygen-17 isotope in the characterization of zeolites and related structures by nuclear magnetic resonance spectroscopy
[VTT-TIED-1448] 07 p2714 N94-26251
Technical report of ISSP. Ser. A, no. 2681: Orbital and spin susceptibilities of the plane copper sites in YBa2Cu3O(x) system
[JTN-94-80567] 07 p3064 N94-27177

Technical report of ISSP. Ser. A, no. 2683: Itinerant character of 5f electrons in UNi2Ga
[JTN-94-80569] 07 p3025 N94-27337
NMR study of quasicrystal Al(70)Pd(20)T(M10) alloy (T(M):Cr, Mn, Fe, and Co) 07 p2745 N94-28162
Fundamental studies of hydrogen interaction with supported meta and bimetallic catalysts
[DE94-004887] 08 p3202 N94-28562
Structural changes during carbonization and oxidation of coal 08 p3187 N94-28678
Nuclear magnetic relaxation studies of semiconductor nanocrystals and solids
[DE94-006301] 08 p3520 N94-30842
New molecular-based routes to binary main group metal sulfides
[AD-A277005] 09 p3900 N94-32003
NMR studies of organic thin films
[AD-A276953] 09 p3656 N94-32221
Advances and applications of dynamic-angle spinning nuclear magnetic resonance
[DE94-007031] 09 p3870 N94-32250
Dynamics of block poly(styrene-co-vinylpyridine) (SVP) in solution and on silica
[AD-A277139] 09 p3657 N94-32364
Strongly anisotropic s-wave versus d-wave gap in cuprate superconductors: Evidence and theory
[DE94-007579] 09 p3904 N94-32746
NMR characterization of shocked quartz
[DE94-007733] 09 p3774 N94-32816
A quest for a new superconducting state
[DE94-008439] 09 p3908 N94-32991
Cross-condensation reactions in an organically modified silica sol-gel
[DE94-010086] 11 p4244 N94-35701
NMR imaging of components and materials for DOE application
[DE94-010664] 11 p4238 N94-36084
Diamond deposition and defect chemistry studied via solid state NMR
[AD-A280609] 12 p4533 N94-36727
Sodium-23 NMR and complex impedance studies of gel electrolytes based on poly(acrylonitrile)
[AD-A280330] 12 p4408 N94-37031
Activities of the Tandem Accelerator Center, University of Tsukuba
[DE94-748687] 12 p4522 N94-37237
Thermal-oxidative pretreatment and evaluation of poly (hexafluoropropene oxide) fluids
[NASA-TM-106659] 12 p4424 N94-37300
The effects of proton-beam quality on the production of gamma rays for nuclear resonance absorption in nitrogen
[DE94-011609] 12 p4523 N94-37629

NUCLEAR MEDICINE
NT RADIOBIOLOGY
Nuclear Medicine Program
[DE93-013896] 04 p1504 N94-17699
TRIUMF scientific activities
[CTN-94-61062] 07 p3117 N94-26656

NUCLEAR MODELS
Coulomb effects in low-energy nuclear fragmentation
[NASA-TP-3352] 01 p0485 N94-12434
Engineering Physics and Mathematics Division progress report, period ending 31 December 1992
[DE93-015118] 03 p1301 N94-14926
Investigation of the relative abundance of heavy versus light nuclei in primary cosmic rays using underground muon bundles
[DE93-017601] 04 p1630 N94-17818
Momentum loss in proton-nucleus and nucleus-nucleus collisions
[NASA-TP-3405] 06 p2540 N94-24305
Hadron jets and nucleon clusters in the relativistic nuclear collisions
[DE93-613434] 07 p3031 N94-25850
Nucleon-nucleon scattering lengths in QCD sum rules
[DE93-520239] 07 p3015 N94-25922
Nucleon and nuclei at finite temperature, as a phenomenological test of the entropy bound
[DE94-608094] 08 p3489 N94-30097
Influence of long-range correlations on the spectral functions and response of 48Ca and 90Zr
[ETN-94-96017] 09 p3865 N94-31537

NUCLEAR PARTICLES
NT ALPHA PARTICLES
NT ANTINEUTRINOS
NT ANTINUCLEONS
NT ANTIPARTICLES
NT ANTIPROTONS
NT BETA PARTICLES
NT BOSONS
NT ETA-MESONS
NT HYPERONS
NT KAONS
NT MESON RESONANCE
NT MESONS
NT MUONS
NT NUCLEONS
NT PHOTOELECTRONS
NT PHOTONS
NT PIONS
NT POSITRONS
NT RHO-MESONS
NT VECTOR MESONS
NT XI HYPERONS

NUCLEAR PHYSICS
NT NUCLEAR ASTROPHYSICS
NT REACTOR PHYSICS
Report of the Workshop on Light Particle-Induced Reactions
[DE93-752300] 01 p0360 N94-10317
The legacy of uncertainty 01 p0376 N94-10577
Report of the third Seminar on Nuclear Physics at the Energy Region of the JAERI Tandem-Booster Accelerator
[DE93-754330] 01 p0372 N94-11043
Directory of IAEA databases
[DE93-622837] 01 p0420 N94-11818
Advanced computers and simulation
[DE93-014354] 02 p0740 N94-13286
Research in theoretical nuclear physics
[DE93-015096] 02 p0839 N94-14330
Some tools of the trade we've developed for our cross-section calculations
[DE93-013835] 02 p0786 N94-14569
Engineering Physics and Mathematics Division progress report, period ending 31 December 1992
[DE93-015118] 03 p1301 N94-14926
Heavy ion nuclear physics research
[DE93-018862] 04 p1565 N94-17776
Activities report of the Rutherford Appleton Laboratory
[ETN-93-94555] 04 p1631 N94-17968
Institute for Nuclear Theory
[DE93-017369] 04 p1568 N94-18824
F-spin concept and g-bosons in the interceding boson model
[ETN-93-93607] 05 p1973 N94-21136
Summary of the Hadronic Weak Interaction session
[DE94-000592] 05 p1975 N94-21775
Likelihood analysis of parity violation in the compound nucleus
[DE94-000671] 05 p1977 N94-22572
Accelerator-based neutrino oscillation searches
[DE94-000818] 06 p2626 N94-23515
Polarized structure functions of the nucleon in the resonance region
[CEBAF-PR-94-001] 06 p2540 N94-24663
Theoretical and computational studies in intermediate energy nuclear physics
[DE94-004177] 07 p3012 N94-25800
Pion-nucleus interactions and the STAR experiment at RHIC
[DE94-000658] 07 p3021 N94-26586
TRIUMF scientific activities
[CTN-94-61062] 07 p3117 N94-26656
Nuclear Theory Group, University of Washington recent and planned research
[DE94-002729] 07 p3022 N94-26809
Quantum chromodynamics and nuclear physics at extreme energy density
[DE94-004418] 07 p3026 N94-27604
Electroweak and other interactions in medium-energy nuclear physics
[DE94-004161] 07 p3027 N94-27689
Future directions in particle and nuclear physics at multi-GeV hadron beam facilities
[DE94-002946] 07 p3027 N94-27711
Proceedings of the workshop on (pi), K, (eta)-nucleon interactions
[DE94-701314] 07 p3027 N94-27733
Research laboratories annual report 1992
[DE94-608124] 08 p3555 N94-30168
Overlap of metal clusters and nuclear structure physics
[DE94-608387] 08 p3517 N94-30183
Theoretical studies in hadronic and nuclear physics
[DE94-003524] 08 p3492 N94-30838
Nuclear physics and astrophysics
[DE94-007168] 09 p3939 N94-33147
The PS 200 catching trap: A new tool for ultra-low energy antiproton physics
[DE94-009309] 10 p4137 N94-34089
Studies in intermediate energy nuclear physics
[DE94-007602] 10 p4140 N94-34381
Summary: Hadron dynamics sessions
[DE94-003011] 11 p4328 N94-36303
Physics Division annual review, 1 April 1992 - 31 March 1993
[DE94-002497] 12 p4512 N94-36513

NUCLEAR POTENTIAL
Quasi-relativistic effects in barrier-penetration processes
[DE93-617730] 01 p0410 N94-10721
Development and implementation of a full-potential ASW method
[ETN-94-95757] 09 p3858 N94-31560
P-matrix approach and three-nucleon problem
[DE94-616887] 11 p4326 N94-36131

NUCLEAR POWER GENERATION
U NUCLEAR ELECTRIC POWER GENERATION

NUCLEAR POWER PLANTS
Techniques, processes, and measures for software safety and reliability
[DE93-012379] 01 p0322 N94-10347
Renewable energy sources 1991, part 3
[DE93-605594] 01 p0263 N94-11505
Statistical and optimization methods to expedite neural network training for transient identification
[DE93-009985] 01 p0340 N94-11644
Department of Energy fundamentals handbook: Engineering symbology, prints, and drawings
[DE93-012220] 01 p0129 N94-11670
A data base for aging of structural materials
[DE93-009714] 02 p0824 N94-13915
Computational problems with the binomial failure rate model and incomplete common cause failure reliability data
[DE93-014346] 02 p0669 N94-14143
Current situation of development of petroleum substituting energies (USA)
[DE94-707492] 05 p1848 N94-22013
Fire simulation based on convection calculation
[VTT-TIED-1411] 07 p2762 N94-26259
Development of an automated fracture assessment system for nuclear structures (appendix 1/1)
07 p2841 N94-27187
Issues arising with the application of optical fiber transmission in class 1E systems in nuclear power plants
[DE94-004743] 08 p3500 N94-29928
Risk measures in living probabilistic safety assessment
[VTT-PUBS-146] 08 p3465 N94-30154
Diode-pumped solid-state-laser drivers and the competitiveness of inertial fusion energy
[DE94-006654] 08 p3296 N94-30830
HFE safety reviews of advanced nuclear power plant control rooms 10 p4100 N94-33613
Guidelines for design and development of computer/microprocessor based systems in research and power reactors
[DE94-616271] 11 p4300 N94-35570
Activity report 1990-1992 and proceedings, volume 1
[DE94-610480] 11 p4290 N94-35830

NUCLEAR POWER REACTORS
NT SPACE POWER REACTORS
Power generation technology options for a Mars mission
[NASA-TM-106451] 06 p2220 N94-24681
Small low mass advanced PBR's for bi-modal operation
[DE94-003201] 07 p2699 N94-25798

NUCLEAR PROPULSION
NT NUCLEAR ELECTRIC PROPULSION
Space nuclear thermal propulsion nuclear element tests at Sandia National Laboratories
[DE93-002301] 01 p0045 N94-10282
Space nuclear technology
[DE93-010184] 01 p0045 N94-10299
A critical assembly designed to measure neutronic benchmarks in support of the Space Nuclear Thermal Propulsion program
[DE92-040974] 01 p0371 N94-10529
Applying design principles to fusion reactor configurations for propulsion in space
[NASA-TM-108247] 01 p0047 N94-11053
Nuclear propulsion systems engineering
[DE93-010791] 02 p0548 N94-12870
MCNP benchmark analyses of critical experiments for the Space Nuclear Thermal Propulsion program
[DE93-014046] 02 p0548 N94-12981
Design, qualification and operation of nuclear rockets for safe Mars missions
[DE93-010792] 02 p0549 N94-12996
Generation of neutronic thermal data in support of space nuclear propulsion
[DE93-013148] 02 p0549 N94-13034
Gas core nuclear thermal rocket engine research and development in the former USSR
[DE93-012165] 02 p0552 N94-14013
Computer program for thermal and transport properties of parahydrogen from 20 to 10,000 K
[NASA-TP-3378] 02 p0552 N94-14102

Nuclear thermal propulsion engine based on particle bed reactor using light water steam as a propellant
[DE93-014336] 02 p0552 N94-14111
Review of nuclear thermal propulsion carbide reactor fuel corrosion and exhibit
[DE93-016605] 02 p0585 N94-14535
Space reactor fuel element testing in upgraded TREAT
[DE93-012524] 02 p0554 N94-14806
Space exploration initiative fuels, materials and related nuclear propulsion technologies panel
[NASA-TM-105706] 03 p0923 N94-15118
Space Nuclear Facility test capability at the Baikal-1 and IGR sites Semipalatinsk-21, Kazakhstan
[DE93-011662] 03 p0926 N94-16773
Development and analysis of startup strategies for particle bed nuclear rocket engine
[AD-A267949] 03 p0927 N94-17053
Mission needs and system commonality for space nuclear power and propulsion
[DE93-016557] 04 p1337 N94-17863
KINETIC: A system code for analyzing Nuclear thermal propulsion rocket engine transients
[DE93-016825] 04 p1337 N94-17884
Performance assessment of low pressure nuclear thermal propulsion
[NASA-TM-108433] 05 p1671 N94-21860
F2D users manual: A two-dimensional compressible gas flow code
[DE94-000653] 05 p1805 N94-22386
NASA Propulsion Engineering Research Center, volume 2
[NASA-CR-194719-VOL-2] 06 p2209 N94-23028
Advanced nuclear thermal propulsion concepts
06 p2217 N94-23068
Performance assessment of low pressure nuclear thermal propulsion 06 p2217 N94-23070
Nuclear propulsion control and health monitoring
06 p2217 N94-23071
Improved gas core propulsion model
[DE94-000929] 06 p2220 N94-24511
A review of carbide fuel corrosion for nuclear thermal propulsion applications
[DE94-003938] 07 p2699 N94-25613
Mars transportation system 07 p2833 N94-25689
Small low mass advanced PBR's for bi-modal operation
[DE94-003201] 07 p2699 N94-25798
An assessment of testing requirement impacts on nuclear thermal propulsion ground test facility design
[DE94-002933] 07 p2702 N94-26560
Small low mass advanced PBR's for propulsion
[DE94-005142] 08 p3497 N94-30588
Summary of particle bed reactor designs for the Space Nuclear Thermal Propulsion Program
[DE94-007434] 09 p3615 N94-32266
One fantastic ride
[NASA-TM-109828] 10 p4016 N94-33582
Probabilistic assessment of space nuclear propulsion system nozzle
[NASA-TM-106539] 12 p4457 N94-37704

NUCLEAR PUMPED LASERS
DOE reactor-pumped laser program
[DE94-006372] 09 p3715 N94-31485

NUCLEAR PUMPING
Reactor-pumped laser experimental results
[DE94-005247] 08 p3292 N94-28482
Reactor-pumped laser facility at DOE's Nevada Test Site
[DE94-006371] 08 p3295 N94-30265
Remote pumping of solid state lasers with nuclear driven fluorescers
[DE94-004846] 08 p3296 N94-30614

NUCLEAR QUADRUPOLE RESONANCE
Phase separation and superconductivity in La2CuO(4 + delta): Effects of oxygen diffusion
[DE93-016610] 04 p1594 N94-17907
Microscopic study of local structure and charge distribution in metallic La2CuO(4 + delta)
[DE94-003801] 07 p3050 N94-25817
Technical report of ISSP. Ser. A, no. 2683: Itinerant character of 5f electrons in UNi2Ga
[JTN-94-80569] 07 p3025 N94-27337

NUCLEAR RADIATION
NT BETA PARTICLES
NT FAST NEUTRONS
NT GAMMA RAY BURSTS
NT GAMMA RAYS
NT NEUTRON BEAMS
NT SPALLATION
NT THERMAL NEUTRONS
AFRRI reports, first quarter 1993
[AD-A266380] 03 p1123 N94-16515
Infrared properties of obscuring dust lon in active galactic nuclei 08 p3545 N94-29832
Atomic physics and radiation processes in plasmas
[DE94-727617] 11 p4337 N94-35939

NUCLEAR RADIATION SPECTROSCOPY
Proceedings of the third workshop on light quark meson spectroscopy
[DE93-754138] 01 p0363 N94-10696
Proceedings of the Fourth Conference on Hyperfine Interaction Spectroscopic Investigations
[DE94-614944] 10 p4147 N94-33866

NUCLEAR REACTIONS
NT ALPHA DECAY
NT CONTROLLED FUSION
NT ELECTRON CAPTURE
NT NEUTRON EMISSION
NT NEUTRON SCATTERING
NT NUCLEAR FISSION
NT NUCLEAR FUSION
NT NUCLEAR INTERACTIONS
NT NUCLEAR SCATTERING
NT PHOTONUCLEAR REACTIONS
NT PROTON SCATTERING
NT PROTON-PROTON REACTIONS
NT RADIOACTIVE DECAY
NT RESONANCE SCATTERING
NT SPALLATION
NT SPIN-ORBIT INTERACTIONS
NT THERMONUCLEAR REACTIONS
NT TRANSMUTATION
NT WEAK INTERACTIONS (FIELD THEORY)
Report of the Workshop on Light Particle-Induced Reactions
[DE93-752300] 01 p0360 N94-10317
The multiplicity spectra of the (169)Tm(n, gamma) reaction
[DE93-617733] 01 p0364 N94-10835
Monochromator SP-017. The results of the first experiments
[DE93-617463] 01 p0372 N94-10849
Double-lambda compound nucleus and the formation of double hypernuclei
[DE93-754289] 01 p0365 N94-11040
Report of the third Seminar on Nuclear Physics at the Energy Region of the JAERI Tandem-Booster Accelerator
[DE93-754330] 01 p0372 N94-11043
Coulomb effects in low-energy nuclear fragmentation
[NASA-TP-3352] 01 p0485 N94-12434
Final state interactions and inclusive nuclear collisions
[NASA-TP-3353] 01 p0373 N94-12435
Semiempirical fragmentation models on galactic cosmic ray transport calculations with hydrogen target
[NASA-TP-3350] 02 p0847 N94-13263
The theory of relativistic heavy ion collisions
[DE93-015934] 02 p0784 N94-13952
Angular correlations in neutron beta decay
[DE93-014349] 02 p0785 N94-14466
Measuring parity violation using the neutron capture reaction
[DE93-016629] 02 p0786 N94-14514
Some tools of the trade we've developed for our cross-section calculations
[DE93-013835] 02 p0786 N94-14569
Multiplicity spectrometry on neutron filtered beams
[DE93-617529] 02 p0790 N94-14843
INGDB-90. The International Neutron Nuclear Data Base for geophysics applications
[DE93-624095] 02 p0827 N94-14880
Multiple process simulations for correction factor calculations in experiments with neutrons. LUSMK program
[DE93-623957] 03 p1179 N94-14932
Al-26-Mg-26 ages of iron meteorites
03 p1242 N94-16240
Possible dust contamination of the early solar system
03 p1244 N94-16352
Evolution of r-process elements in the hot supernova bubble
[DE93-017169] 04 p1624 N94-17897
T violating neutron spin rotation asymmetry
[DE93-018470] 04 p1570 N94-19126
On modelling nuclear reactions in meteorites
05 p2085 N94-20844
Advanced far infrared detectors
[DE93-040289] 05 p1988 N94-21528
Semiconductor isotope engineering
[DE93-040119] 05 p2030 N94-21744
Ferroelectric thin films 3
[AD-A273394] 06 p2565 N94-25027
Data on parity violation in the compound nucleus and its interpretation
[DE94-003965] 07 p3013 N94-25820
Hadron jets and nucleon clusters in the relativistic nuclear collisions
[DE93-613434] 07 p3031 N94-25850
Index to BROND-2, CENDL-2, ENDF/B-6, JEF-2, JENDL-3
[DE93-634500] 07 p3016 N94-26034
Radiochemistry Division annual progress report : 1991
[DE94-600652] 07 p2715 N94-26392
Measurements of the p (mu)d-molecule formation rate at different hydrogen temperature
[DE93-634636] 07 p3020 N94-26511
Comparison of 14 MeV isomer production of Hf-178m1 and Hf-179m2 using Feshbach-Kerman-Koonin and exciton preequilibrium models
[DE94-002640] 08 p3488 N94-30039
Intercomparison of theoretical calculations of important activation cross sections for fusion reactor technology
[DE94-002642] 08 p3497 N94-30825
Deexcitation processes in nuclear reactions: The study of hot hadronic matter
[DE94-003396] 08 p3492 N94-30836
Neutronics of a D-Li neutron source: An overview
[DE94-005372] 08 p3493 N94-30893
Reactive flows in compact objects
09 p3934 N94-31567
Hydrogen incorporation and radiation induced dynamics in metal-oxide-silicon structures: A study using nuclear reaction analysis
[ETN-94-95742] 09 p3898 N94-31610
Effects of isotope selection on solution convergence in HZE transport
[NASA-TP-3445] 10 p4167 N94-33686
A three-body calculation of the O-16(d,p)O-17 reaction using a two-term separable potential for the s-wave nucleon-core interaction
[DE94-616652] 11 p4320 N94-35579
Relativistic three-particle dynamical equations. 2: Theoretical development
[DE94-616654] 11 p4320 N94-35581
Activities of the Tandem Accelerator Center, University of Tsukuba
[DE94-748687] 12 p4522 N94-37237

NUCLEAR REACTOR CONTROL
GRISET certification package
[DE93-011783] 01 p0327 N94-11246
System performance modeling and analysis of a fault-tolerant, real time parallel processor
[AD-A268070] 03 p1162 N94-17551
SP-100 control drive assembly development
08 p3163 N94-29651
Development of a VME and CAMAC based data acquisition and transfer system for JT-60 control
[DE94-727590] 10 p4158 N94-33871

NUCLEAR REACTORS
NT ADVANCED TEST REACTORS
NT FAST NUCLEAR REACTORS
NT FUSION REACTORS
NT GAS COOLED REACTORS
NT HEAVY WATER REACTORS
NT HELIOTRONS
NT HIGH FLUX ISOTOPE REACTORS
NT HIGH TEMPERATURE GAS COOLED REACTORS
NT JOINT EUROPEAN TORUS
NT LIGHT WATER REACTORS
NT LIQUID METAL COOLED REACTORS
NT LIQUID METAL FAST BREEDER REACTORS
NT NUCLEAR POWER REACTORS
NT NUCLEAR RESEARCH AND TEST REACTORS
NT PEBBLE BED REACTORS
NT PRESSURIZED WATER REACTORS
NT SPACE POWER REACTORS
NT SPHEROMAKS
NT STELLARATORS
NT THERMAL REACTORS
NT TOKAMAK DEVICES
NT WATER COOLED REACTORS
NT WATER MODERATED REACTORS
GRISET certification package
[DE93-011783] 01 p0327 N94-11246
Research results
[DE93-753403] 01 p0372 N94-11595
The corrosion behavior of 8001 Al under heat-transfer conditions in an aqueous loop system
[DE93-013450] 02 p0569 N94-13242
A modular gas-cooled cermet reactor system for planetary base power
[DE93-013672] 02 p0550 N94-13351
Fatigue design curves for 6061-T6 aluminum
[DE93-011849] 02 p0571 N94-14021
Estimation of strain in 1-kW primary containment vessels by microstructural examination
[DE93-013053] 02 p0573 N94-14316
Welding technologies as applied to nuclear manufacturing
[DE93-010924] 02 p0664 N94-14565
GAM-HEAT: A computer code to compute heat transfer in complex enclosures
[DE93-014724] 03 p1023 N94-15980

System performance modeling and analysis of a fault-tolerant, real time parallel processor
[AD-A268070] 03 p1162 N94-17551
Fluid-structure-interaction analyses of reactor vessel using improved hybrid Lagrangian Eulerian code ALICE-II
[DE93-015536] 04 p1409 N94-18248
Power transmission by laser beam from lunar-synchronous satellite
[NASA-TM-4496] 05 p1669 N94-20102
Method for remotely powering a device such as a lunar rover
[NASA-CASE-LAR-14789-1] 05 p1824 N94-20587
A review of carbide fuel corrosion for nuclear thermal propulsion applications
[DE94-003938] 07 p2699 N94-25613
HDR reactor containment fire modeling with BRI2
[VTT-PUBS-113] 07 p3031 N94-25621
Overall analysis of meteorological information in the Daeduk nuclear complex
[DE93-632594] 07 p2894 N94-26469
Mesoscale meteorological measurements characterizing complex flows
[DE94-002359] 07 p2895 N94-26761
Neutron-neutron scattering: Possibility of in-beam experiment
[DE94-606459] 07 p3027 N94-27682
Single specimen fracture toughness determination procedure using instrumented impact test
[PB94-132040] 08 p3316 N94-28402
Teleoperated systems for nuclear reactors: Inspection and maintenance
[AIAA PAPER 94-1176-CP] 08 p3439 N94-30528
Small low mass advanced PBR's for propulsion
[DE94-005142] 08 p3497 N94-30588
Modeling of residual stress mitigation in austenitic stainless steel pipe girth weldment
[DE94-007184] 09 p3738 N94-32639
Integrated safety program for the Nuclear Electric Propulsion Space Test Program
[DE94-004670] 09 p3615 N94-32669
Reactor pressure vessel structural integrity research in the US Nuclear Regulatory Commission HSST and HSSI Programs
[DE94-006550] 09 p3739 N94-32771
ONED90: 1-dimensional diffusion code
[DE94-611063] 11 p4305 N94-35834
Thermodynamic behaviour of tellurium at high temperatures
[DE94-612823] 11 p4240 N94-35960
Activities of the Chemical Technology Division
[DE94-013050] 12 p4410 N94-37357

NUCLEAR RESEARCH
Directory of IAEA databases
[DE93-622837] 01 p0420 N94-11818
Magnetic Fusion Energy Technology Fellowship: Report on survey of institutional coordinators
[DE93-014646] 04 p1583 N94-17739
Testing new technology for the heavy ion experiment at CERN
[DE94-004747] 12 p4521 N94-37220

NUCLEAR RESEARCH AND TEST REACTORS
NT ADVANCED TEST REACTORS
In-reactor testing of the closed cycle gas core reactor: The Nuclear Light Bulb concept
[DE93-004053] 01 p0370 N94-10149
Space nuclear technology
[DE93-010184] 01 p0045 N94-10299
A critical assembly designed to measure neutronic benchmarks in support of the Space Nuclear Thermal Propulsion program
[DE92-040974] 01 p0371 N94-10529
Development of plastic capsule for research reactor irradiation
[DE93-753186] 01 p0372 N94-11591

NUCLEAR ROCKET ENGINES
NT NUCLEAR LIGHTBULB ENGINES
Space nuclear technology
[DE93-010184] 01 p0045 N94-10299
Applying design principles to fusion reactor configurations for propulsion in space
[NASA-TM-108247] 01 p0047 N94-11053
Gas core nuclear thermal rocket engine research and development in the former USSR
[DE93-012165] 02 p0552 N94-14013
Space reactor fuel element testing in upgraded TREAT
[DE93-012524] 02 p0554 N94-14806
Nuclear rocket plume studies
[AD-A267154] 03 p0925 N94-15837
Space Nuclear Facility test capability at the Baikal-1 and IGR sites Semipalatinsk-21, Kazakhstan
[DE93-011662] 03 p0926 N94-16773
Development and analysis of startup strategies for particle bed nuclear rocket engine
[AD-A267949] 03 p0927 N94-17053
Flow instability tests for a particle bed reactor nuclear thermal rocket fuel element
[AD-A268012] 03 p0929 N94-17474
SPACE-R Thermionic Space Nuclear Power System: Design and Technology Demonstration Program
[DE93-013969] 05 p1670 N94-21824
Nuclear propulsion control and health monitoring
06 p2217 N94-23071
Project WISH: The Emerald City
07 p2703 N94-25690
Conceptual design: TFE verification program
[DE94-012469] 12 p4398 N94-37433

NUCLEAR SCATTERING
NT NEUTRON SCATTERING
NT RESONANCE SCATTERING
Medium energy hadron-nucleus scattering in the 1/N expansion formalism
[DE93-622957] 02 p0778 N94-12848
Suppression of charge scattering in Moessbauer experiments using synchrotron radiation
[DE93-015406] 03 p1212 N94-16887
A dependence of exclusive vector meson production in muon-nucleus scattering
[DE94-003363] 07 p3016 N94-25957
Jet production in muon scattering at Fermilab E665
[DE94-004663] 07 p3028 N94-27752
The 14th Annual West Coast Theoretical Chemistry/Statistical Mechanics Conference
[AD-A276942] 09 p3656 N94-32239
H(-) injection simulation for a 5 MW spallation neutron source
[DE94-009003] 10 p4140 N94-33983
Alternating series fit to the total cross sections
[DE94-616888] 11 p4326 N94-36132

NUCLEAR SHIELDING
U RADIATION SHIELDING

NUCLEAR SPIN
High spin properties of nuclei
[DE93-008788] 01 p0358 N94-10254
The multiplicity spectra of the (169)Tm(n, gamma) reaction
[DE93-617733] 01 p0364 N94-10835
F-spin concept and g-bosons in the interceding boson model
[ETN-93-93607] 05 p1973 N94-21136

NUCLEAR STRUCTURE
High spin properties of nuclei
[DE93-008788] 01 p0358 N94-10254
Nuclear structure models: Applications and development
[DE93-u12934] 01 p0368 N94-11813
Research in theoretical nuclear physics
[DE93-015096] 02 p0839 N94-14330
Dynamics of pion-nucleus systems
[DE93-014449] 02 p0785 N94-14468
Institute for Nuclear Theory
[DE93-017369] 04 p1568 N94-18824
Symmetry-dictated trucation: Solutions of the spherical shell model for heavy nuclei
[DE94-000482] 05 p1976 N94-21961
Nucleon-nucleon scattering lengths in QCD sum rules
[DE93-520239] 07 p3015 N94-25922
Nuclear Theory Group, University of Washington recent and planned research
[DE94-002729] 07 p3022 N94-26809
Overlap of metal clusters and nuclear structure physics
[DE94-608387] 08 p3517 N94-30183

NUCLEAR TEST REACTORS
U NUCLEAR RESEARCH AND TEST REACTORS

NUCLEAR TRANSFORMATIONS
NT TRANSMUTATION

NUCLEAR WARHEADS
Propellants and explosives in ballistic missiles
[UCRL-LR-113578] 07 p2760 N94-28222

NUCLEAR WASTES
U RADIOACTIVE WASTES

NUCLEAR WEAPONS
NT FUSION WEAPONS
Inertial Confinement Fusion
[DE93-013303] 02 p0795 N94-13017
A model for fuel fire duration and application to the B-1B bomber
[DE93-013000] 02 p0512 N94-14292
Computer/information security design approaches for Complex 21/Reconfiguration facilities
[DE93-018547] 04 p1535 N94-18930
A qualified radiation hardened nonvolatile memory for space and tactical weapons applications
[DE94-001211] 06 p2559 N94-23186
Nondestructive evaluations
[DE94-003020] 06 p2373 N94-24613
The relative performance of FeS2 and CoS in long-life thermal-battery applications
[DE94-006145] 09 p3695 N94-32663
Vulnerability assessment of a space based weapon platform electronic system exposed to a thermonuclear weapon detonation
[DE94-007229] 09 p3611 N94-32667
Software use control
[DE94-008429] 12 p4489 N94-36480

NUCLEATE BOILING
NT LEIDENFROST PHENOMENON
Gravity and electric field effects on pool boiling heat transfer 01 p0121 N94-10226

NUCLEATION
NT CLOUD SEEDING
STARDUST: A simulation experiment of cosmic dust analogues production in microgravity conditions
01 p0113 N94-10175
Coupled growth of cells and bubbles in directional solidification of succinonitrile-acetone alloys
01 p0118 N94-10206
Study of vapor bubble growth in a supersaturated liquid 01 p0122 N94-10232
Magnetization reversal by nucleation
[DE93-610313] 01 p0350 N94-10313
Structural development in ceramic precursor sols and gels
[AD-A264354] 01 p0090 N94-11281
Joint pain and Doppler-detectable bubbles in altitude (Hypobaric) decompression 01 p0312 N94-11542
A mechanism for the reduction in risk of decompression sickness in microgravity environment
01 p0312 N94-11545
An ellipsometry investigation of nucleation and growth of electron cyclotron resonance plasma deposited silicon films
[AD-A265037] 01 p0401 N94-11651
Carbon and nitrogen in Type 2 supernova diamonds
01 p0431 N94-12166
Development of a molecular beam technique to study early solar system silicon reactions
01 p0432 N94-12224
A parameterization of cloud droplet nucleation
[DE93-007998] 02 p0718 N94-12903
Binary homogeneous nucleation: Temperature and relative humidity fluctuations and non-linearity
[DE93-007884] 02 p0709 N94-13911
Optimization of the processing parameters of high temperature superconducting glass-ceramics: Center Director's discretionary fund final report
[NASA-TM-108421] 02 p0808 N94-13938
Containerless processing of undercooled melts
[NASA-CR-194350] 02 p0572 N94-14123
Multiplicative noise: Applications in cosmology and field theory
[DE93-016624] 02 p0840 N94-14536
Characterization of diamond film growth in a combustion flame
[AD-A266659] 02 p0816 N94-14839
Diamond epitaxy and diamondlike coatings
[AD-A266657] 03 p1206 N94-15747
Dynamical Ising model simulations of nucleation and growth in copper-cobalt alloys
[DE93-015336] 03 p0957 N94-16015
The role of interfacial chemistry in surface nucleation and growth of calcium oxalate
[DE93-015689] 03 p1209 N94-16159
Creep ductility of iron at very low strain rates: The effects of sulfur
[DE93-015490] 03 p0959 N94-16890
UHV-stem studies on nucleation and growth of thin metal silicide films on silicon
[DE93-017604] 03 p1212 N94-16961
The influence of an electric field on the kinetics of nucleation
[IFTR-2/91] 03 p1213 N94-17046
Pseudomorphic semiconducting heterostructures from combinations of AlN, GaN and selected SiC polytypes: Theoretical advancement and its coordination with experimental studies of nucleation, growth, characterization and device deployment
[AD-A267561] 03 p1213 N94-17108
Atomic layer epitaxy group IV materials: Surface processes, thin films, devices and their characterization
[AD-A267527] 03 p1213 N94-17116
Diamond growth on carbide surfaces using a selective etching technique
[AD-A267989] 03 p0973 N94-17413
Growth, characterization and device development in monocrystalline diamond films
[AD-A268206] 03 p1216 N94-17553
Characterization of diamond film nucleation and growth surface
[AD-A269400] 04 p1597 N94-18459
Growth, characterization and device development in monocrystalline diamond films
[AD-A270074] 04 p1599 N94-18797

A numerical analysis of crack growth in brittle microcracking composites
[DE93-011562] 04 p1343 N94-18914
Surface phases and their influence on metal-oxide interfaces
[DE93-019931] 04 p1601 N94-19020
Melt spinning study
[NASA-CR-193823] 04 p1380 N94-19423
Shock induced condensation in fluids of high molar specific heat: Shock structure and relaxation
[MPIS-106/1993] 05 p1798 N94-20145
Kinetics of phase transformations in glass forming systems
[NASA-CR-194270] 05 p1701 N94-20347
Growth, characterization and device development in monocrystalline diamond films
[AD-A273097] 05 p2028 N94-21506
Development of advanced cloud parameterizations to examine air quality, cloud properties, and cloud-radiation feedback in mesoscale models
[DE93-041164] 05 p1853 N94-22384
Microgravity sciences application visiting scientist program
[NASA-CR-194804] 06 p2267 N94-23287
Characterization of 3-D particle distributions and effects on recrystallization studied by computer simulation
[PB93-201408] 06 p2562 N94-23535
Temperature dependence of protein solubility-determination, application to crystallization, and growth kinetics studies 06 p2224 N94-24344
Polymer morphologh 06 p2226 N94-24353
The chemistry of particulate formation in fluorocarbon plasmas
[DE94-001500] 06 p2552 N94-24546
Containerless measurements on liquids at high temperatures 06 p2238 N94-25125
Particle nucleation and growth in butadiene emulsion polymerization
[ETN-94-95300] 06 p2262 N94-25236
The in situ observation of epitaxial diamond thin film nucleation and growth using emission electron microscopy
[AD-A273698] 06 p2263 N94-25489
Dissolution of secondary phases during extrusion
[PB94-124583] 07 p2732 N94-25908
Study of precipitation and recrystallization in Al alloy 2519 by backscattered electron imaging methods
[AD-A274919] 07 p2736 N94-26533
Pseudomorphic semiconducting heterostructures from combinations of AlN, GaN and selected SiC polytypes: Theoretical advancement and its coordination with experimental studies of nucleation, growth, characterization and device development
[AD-A274247] 07 p3061 N94-26841
Controlled heterogeneous nucleation of melt-textured YBa2Cu3O(6+x) by addition of Al2O3 particles
[AD-A274605] 07 p3062 N94-26892
Development of K(1-x)Na(x)TiOPO4 crystals for nonlinear applications
[AD-A274336] 07 p3063 N94-27055
A photoemission electron microscope investigation of chemical vapor deposition diamond films and diamond nucleation 08 p3215 N94-29745
Study of nucleation and growth in Al-Zn alloys using TEM
[DE94-006312] 08 p3211 N94-30852
RHEED studies of the nucleation, growth, and mobility of Ag atoms on the Si(111)7 x 7 surface
[DE94-005551] 08 p3521 N94-30899
Solidification structure synthesis in undercooled liquids
[AD-A276166] 09 p3910 N94-31054
Characterization and growth mechanisms of the MgAl2O4 phase in Al2O3-reinforced Al-Mg composites
[ISBN-0-315-86531-8] 09 p3620 N94-31706
A parameterization of cloud droplet nucleation
[DE94-007469] 09 p3785 N94-32268
Nucleation and growth of cubic boron nitride films produced by ion-assisted pulsed laser deposition
[DE94-007295] 09 p3861 N94-32796
Interface controlled amorphization of crystalline Ni/Ti multilayers
[DE94-008685] 09 p3906 N94-32884
Displacive transformation in ceramics
[AD-A278442] 10 p4026 N94-33539
Transformation plasticity in ductile solids
[DE94-010420] 11 p4240 N94-35953
Kinetics of phase transformations in glass forming systems
[NASA-CR-196082] 11 p4245 N94-35977
Local instabilities and the transition to chaos of non-linear waves
[PB94-170578] 11 p4341 N94-36213
In situ studies of zeolite syntheses using powder diffraction methods: Crystallization of instant zeolite A powder and CoAPO-5
[DE94-006570] 11 p4341 N94-36358
Literature review and preliminary studies of fretting and fretting fatigue including special applications to aircraft joints
[AD-A280310] 12 p4456 N94-37125
Numerical analysis of an impinging jet reactor for the CVD and gas-phase nucleation of titania
[NASA-TM-106619] 12 p4431 N94-37254

NUCLEI
A quark structure of hadrons and nuclei
[DE93-616872] 06 p2539 N94-25474
On the hadron formation time in pion-nucleus interaction
[DE93-616879] 06 p2539 N94-25476

NUCLEI (CYTOLOGY)
Stress-induced enhancement of the startle reflex
[AD-A278414] 09 p3802 N94-33327

NUCLEI (NUCLEAR PHYSICS)
NT ALPHA PARTICLES
NT DEUTERONS
NT EVEN-EVEN NUCLEI
NT HEAVY NUCLEI
NT HYPERNUCLEI
NT ODD-EVEN NUCLEI
NT ODD-ODD NUCLEI
Report of the third Seminar on Nuclear Physics at the Energy Region of the JAERI Tandem-Booster Accelerator
[DE93-754330] 01 p0372 N94-11043
Research in cosmic and gamma ray astrophysics: Cosmic physics portion
[NASA-CR-194127] 02 p0847 N94-13211
Properties of nuclei in astrophysical environments: Binding energies, weak-interaction rates
[MPA-706] 03 p1240 N94-17628
Eta-nucleon interaction and nuclear production of eta mesons
[DE93-018469] 04 p1571 N94-19259
Examination of low level magnetic dipole intensities in the transition nuclei Sm-148, Sm-150, Sm-152 and Sm-154, with inelastic photon scattering at S-DALINAC
[ETN-93-95069] 05 p1971 N94-20030
Low p(sub T) phenomena observed in high energy nuclear collisions
[DE94-000825] 05 p1982 N94-21849
Likelihood analysis of parity violation in the compound nucleus
[DE94-000671] 05 p1977 N94-22572
Momentum loss in proton-nucleus and nucleus-nucleus collisions
[NASA-TP-3405] 06 p2540 N94-24305
Correlations in inelastic collisions of relativistic nuclei with emulsion at (4.1 - 4.5) A GeV/c
[DE93-634526] 07 p3030 N94-27994
Nucleon and nuclei at finite temperature, as a phenomenological test of the entropy bound
[DE94-608094] 08 p3489 N94-30097

NUCLEIC ACIDS
NT DEOXYRIBONUCLEIC ACID
NT RIBONUCLEIC ACIDS
Release of iron from hemoglobin
[AD-A266503] 03 p1128 N94-16784
The torsion space nucleic acids molecular mechanics program DUPLEX: Surveying conformation space by potential energy minimization
[DE94-002441] 06 p2563 N94-24567

NUCLEON-NUCLEON INTERACTIONS
Workshop on NN Bremsstrahlung and Polarization Observables
[DE93-010181] 01 p0361 N94-10334
P-matrix description of the two-particle interaction
[DE93-617690] 01 p0361 N94-10549
Studies of P-matrix formalism on the basis of the potential description of two-particle interaction
[DE93-617691] 01 p0362 N94-10550
The determination of nucleon-nucleon scattering phases by the phase functions method
[DE93-617729] 01 p0362 N94-10557
Three-nucleon problem with phase equivalent potentials
[DE93-617731] 01 p0363 N94-10722
HIJET with AGS physics and N(sup *)'s
[DE93-014022] 02 p0780 N94-13097
Resonances in the Sigma NN system
[DE93-014353] 02 p0785 N94-14144
The off shell (rho)-(omega) mixing in the QCD sum rules
[DE93-014845] 02 p0786 N94-14527
Relativistic proton-nucleus scattering and one-boson-exchange models 02 p0786 N94-14550
Theoretical antideuteron-nucleus absorptive cross sections 02 p0786 N94-14551
Isospin flip as a relativistic effect: NN interactions
[CEBAF-PR-89-023] 02 p0786 N94-14552
The LAHET code system: Introduction, development, and benchmarking
[DE93-012657] 02 p0787 N94-14804
Energy-loss cross sections for inclusive charge-exchange reactions at intermediate energies
[NASA-TM-4522] 03 p1188 N94-17018
Momentum and coordinate space three-nucleon potentials
[DE93-040868] 06 p2531 N94-22951
On the transverse size of a fast moving nucleon
[DE93-616891] 06 p2539 N94-25481
Separable expansions of the NN t-matrix by way of exact half off the energy shell methods
[DE94-601615] 07 p3015 N94-25890
Nucleon-nucleon scattering lengths in QCD sum rules
[DE93-520239] 07 p3015 N94-25922
The Nijmegen hyperon-nucleon potentials
[DE94-007557] 09 p3869 N94-32139
Medium energy measurements of N-N parameters
[DE94-006067] 09 p3869 N94-32173
Medium energy measurements of N-N parameters
[DE94-008340] 10 p4137 N94-33923
Complex Kohn variational principle for two-nucleon bound-state and scattering with the tensor potential
[DE94-616651] 11 p4321 N94-35595
The nucleon-nucleon potential in the chromodielectric soliton model
[DE94-004646] 11 p4329 N94-36305
Hadron production in S+nucleus collisions at 200 GeV/nucleon
[DE94-011344] 12 p4520 N94-37715

NUCLEON-NUCLEON SCATTERING
Crossing-odd spin effects in the dipole model of hadron scattering
[DE93-617692] 01 p0362 N94-10551
The determination of nucleon-nucleon scattering phases by the phase functions method
[DE93-617729] 01 p0362 N94-10557
No-lost theorem for parity violating nucleon-nucleon scattering experiments
[DE93-012737] 02 p0779 N94-12949
Theoretical antideuteron-nucleus absorptive cross sections 02 p0786 N94-14551
Isospin flip as a relativistic effect: NN interactions
[CEBAF-PR-89-023] 02 p0786 N94-14552
Energy-loss cross sections for inclusive charge-exchange reactions at intermediate energies
[NASA-TM-4522] 03 p1188 N94-17018
Theoretical and computational studies in intermediate energy nuclear physics
[DE94-004177] 07 p3012 N94-25800
Nucleon-nucleon scattering lengths in QCD sum rules
[DE93-520239] 07 p3015 N94-25922
Complex Kohn variational principle for two-nucleon bound-state and scattering with the tensor potential
[DE94-616651] 11 p4321 N94-35595
The spin observables of electron-nucleon scattering from the formalism of nucleon-nucleon scattering
[DE94-011368] 12 p4520 N94-37717

NUCLEONS
Crossing-odd spin effects in the dipole model of hadron scattering
[DE93-617692] 01 p0362 N94-10551
A generalized Bethe-Weizsaecker mass formula for strange hadronic matter
[DE93-011010] 01 p0368 N94-11620
Measuring strangeness in the nucleon
[DE93-014861] 02 p0785 N94-14471
Isospin flip as a relativistic effect: NN interactions
[CEBAF-PR-89-023] 02 p0786 N94-14552
On the statistical theory of the even-even nucleons levels' density
[DE93-623990] 02 p0788 N94-14875
Unitary (pi)(pi)N model of N* excitations in (pi)N and (gamma)N reactions
[DE93-017422] 04 p1568 N94-18826
Eta-nucleon interaction and nuclear production of eta mesons
[DE93-018469] 04 p1571 N94-19259
A relativistic constituent quark model
[DE93-041085] 05 p1946 N94-21689
SLAC measurement of the neutron spin structure function
[DE93-040998] 05 p1975 N94-21788
Pions and neutrinos as probes of the nucleon and nuclear few-body system
[DE93-040127] 06 p2531 N94-22928
Momentum and coordinate space three-nucleon potentials
[DE93-040868] 06 p2531 N94-22951
Polarized structure functions of the nucleon in the resonance region
[CEBAF-PR-94-001] 06 p2540 N94-24663
On the transverse size of a fast moving nucleon
[DE93-616891] 06 p2539 N94-25481
Theoretical and computational studies in intermediate energy nuclear physics
[DE94-004177] 07 p3012 N94-25800

Hadron jets and nucleon clusters in the relativistic nuclear collisions
[DE93-613434] 07 p3031 N94-25850
Nucleon-nucleon scattering lengths in QCD sum rules
[DE93-520239] 07 p3015 N94-25922
Theoretical and experimental studies of elementary physics
[DE94-002310] 07 p3008 N94-25988
The STAR experiment at the Relativistic Heavy Ion Collider
[DE94-003409] 07 p3017 N94-26083
Rescattering and energy loss of fast partons in nuclear matter
[DE94-002918] 07 p3018 N94-26145
Proceedings of the workshop on (pi), K, (eta)-nucleon interactions
[DE94-701314] 07 p3027 N94-27733
Study of invisible nucleon decay, N approaches nu nu nu bar, and a forbidden nuclear transition in the Kamiokande detector
[ICRR-299-93-11] 07 p3028 N94-27759
Improved QCD sum rule estimates of the higher twist contributions to polarised and unpolarised nucleon structure functions
[PB94-138112] 08 p3487 N94-29161
Nucleon and nuclei at finite temperature, as a phenomenological test of the entropy bound
[DE94-608094] 08 p3489 N94-30097
Theoretical studies in hadronic and nuclear physics
[DE94-003524] 08 p3492 N94-30838
The form factors of the nucleons
[DE94-007096] 09 p3872 N94-32630
Transverse energy production with Si and Au beams at AGS energy: Towards hot and dense hadronic matter
[DE94-007178] 09 p3938 N94-32638
Polarized lepton-nucleon scattering
[DE94-009027] 09 p3875 N94-33278
Pion-nucleon interaction in nuclear matter above the Delta resonance energy
[DE94-727455] 10 p4137 N94-33994
Studies in intermediate energy nuclear physics
[DE94-007602] 10 p4140 N94-34381
J/psi absorption effects in the coherent production on nuclei
[DE94-616870] 11 p4326 N94-36129
Hybrid mesons (Q(anti Q)g) in N(anti N) annihilation
[DE94-001491] 11 p4327 N94-36239
The form factors of the nucleons
[DE94-013357] 12 p4515 N94-37086
Neutrino-nucleon scattering
[DE94-011720] 12 p4520 N94-37671
The spin observables of electron-nucleon scattering from the formalism of nucleon-nucleon scattering
[DE94-011368] 12 p4520 N94-37717

NUCLEOPHILES
Synthesis, characterization, and modification of poly(organophosphazenes), that bear both 2,2,2-trifluoroethoxy and phenoxy groups
[AD-A264913] 01 p0092 N94-11847
Amide and tetrazene complexes of transition and main group elements as precursors for the low temperature synthesis of elemental nitrides
[AD-A266246] 03 p0950 N94-16931
Phenylethynyl endcapping reagents and reactive diluents
[NASA-CASE-LAR-14796-1] 10 p4023 N94-35077

NUCLEOSYNTHESIS
U NUCLEAR FUSION

NUCLEOTIDES
NT ADENOSINE TRIPHOSPHATE
NT CYCLIC AMP

NUCLIDES
NT ALUMINUM ISOTOPES
NT ALUMINUM 26
NT ALUMINUM 27
NT AMERICIUM
NT ARGON ISOTOPES
NT BERYLLIUM ISOTOPES
NT BERYLLIUM 10
NT BORON ISOTOPES
NT BROMINE ISOTOPES
NT CALCIUM ISOTOPES
NT CALIFORNIUM
NT CALIFORNIUM ISOTOPES
NT CARBON ISOTOPES
NT CARBON 12
NT CARBON 13
NT CARBON 14
NT CESIUM ISOTOPES
NT CESIUM VAPOR
NT CESIUM 137
NT COBALT ISOTOPES
NT COBALT 60
NT CURIUM
NT DEUTERIUM
NT GALLIUM ISOTOPES
NT GERMANIUM ISOTOPES
NT GOLD ISOTOPES
NT HAFNIUM ISOTOPES
NT HELIUM ISOTOPES
NT HYDROGEN ISOTOPES
NT INDIUM ISOTOPES
NT IODINE ISOTOPES
NT IRON ISOTOPES
NT IRON 57
NT ISOTOPES
NT LANTHANUM ISOTOPES
NT LEAD ISOTOPES
NT LITHIUM ISOTOPES
NT MANGANESE ISOTOPES
NT MERCURY ISOTOPES
NT NEODYMIUM ISOTOPES
NT NEON ISOTOPES
NT NEPTUNIUM
NT NICKEL ISOTOPES
NT NITROGEN ISOTOPES
NT NITROGEN 15
NT OXYGEN ISOTOPES
NT OXYGEN 18
NT PHOSPHORUS ISOTOPES
NT PLUTONIUM
NT PLUTONIUM 238
NT POLONIUM ISOTOPES
NT POTASSIUM ISOTOPES
NT POTASSIUM 40
NT RADIOACTIVE ISOTOPES
NT RADIUM ISOTOPES
NT RADON ISOTOPES
NT RHENIUM ISOTOPES
NT SODIUM ISOTOPES
NT STRONTIUM ISOTOPES
NT TELLURIUM
NT THORIUM ISOTOPES
NT THULIUM ISOTOPES
NT TRANSURANIUM ELEMENTS
NT TRITIUM
NT URANIUM ISOTOPES
NT URANIUM 238
NT XENON ISOTOPES
NT XENON 129
NT ZIRCONIUM ISOTOPES
Measurements of cosmogenic nuclides in lunar rock 64455 01 p0437 N94-12033
Effects of bulk composition on production rates of cosmogenic nuclides in meteorites 03 p1245 N94-16385
Cosmogenic-radionuclide profiles in Knyahinya: New measurements and models 05 p2106 N94-20713
Production rates of terrestrial in-situ-produced cosmogenic nuclides
[DE94-005156] 08 p3543 N94-28545
SYNTH: A spectrum synthesizer
[DE94-004719] 11 p4331 N94-36317
An overview of the current status of resonance theory in reactor physics applications
[DE94-010465] 12 p4521 N94-37194

NULL HYPOTHESIS
Rare attributes in finite universe: Hypotheses testing specification and exact randomized upper confidence bounds
[DE93-012783] 02 p0775 N94-12955
State-space models for multichannel detection
[AD-A270608] 05 p1715 N94-19816
Wieand's theorem
[PB94-126711] 07 p3004 N94-27223

NUMBER THEORY
NT ARITHMETIC
NT CONGRUENCES
NT DIOPHANTINE EQUATION
NT EXPONENTS
NT FLOATING POINT ARITHMETIC
NT INDUCTION (MATHEMATICS)
NT INTEGERS
NT MULTIPLICATION
Mathematics and string theory
[DE93-017903] 02 p0817 N94-14417
Semi-stability and heights of cycles
[PB93-215507] 05 p1961 N94-22377
A rational elliptic surface related to the question of expressing squares as sum of consecutive squares
[W-9305] 06 p2479 N94-23139
Fast methods for computation with algebraic numbers
[ISBN-0-315-57888-2] 07 p2998 N94-27269

NUMERICAL ANALYSIS
NT APPROXIMATION
NT BORN APPROXIMATION
NT BORN-OPPENHEIMER APPROXIMATION
NT BOUNDARY INTEGRAL METHOD
NT CHEBYSHEV APPROXIMATION
NT COMPUTATIONAL CHEMISTRY
NT COMPUTATIONAL FLUID DYNAMICS
NT CONJUGATE GRADIENT METHOD
NT DIFFERENCE EQUATIONS
NT ERROR ANALYSIS
NT ESSENTIALLY NON-OSCILLATORY SCHEMES
NT FINITE DIFFERENCE THEORY
NT FINITE ELEMENT METHOD
NT FINITE VOLUME METHOD
NT FLUX VECTOR SPLITTING
NT HARTREE APPROXIMATION
NT INTERPOLATION
NT ITERATION
NT ITERATIVE SOLUTION
NT LEAST SQUARES METHOD
NT MEAN SQUARE VALUES
NT MILNE METHOD
NT MONTE CARLO METHOD
NT MULTIGRID METHODS
NT NEWTON METHODS
NT NEWTON-RAPHSON METHOD
NT NOMOGRAPHS
NT NUMERICAL INTEGRATION
NT PADE APPROXIMATION
NT PARTICLE IN CELL TECHNIQUE
NT PREDICTOR-CORRECTOR METHODS
NT RAYLEIGH-RITZ METHOD
NT RELAXATION METHOD (MATHEMATICS)
NT RUNGE-KUTTA METHOD
NT SOMMERFELD APPROXIMATION
NT TRUNCATION ERRORS
NT TVD SCHEMES
NT UPWIND SCHEMES (MATHEMATICS)
Aerosol sampling models survey
[AD-A265903] 01 p0075 N94-10337
Summary of research in progress at ICASE
[NASA-CR-191481] 01 p0318 N94-11198
Normal modes of the world's oceans: A numerical investigation using Proudman functions
[NASA-TM-104587] 01 p0288 N94-11358
Numerical simulations of thermal convection in rapidly rotating spherical fluid shells 01 p0153 N94-11635
Research in computing and applied mathematics
[AD-A266137] 01 p0331 N94-11657
Measurement of wave parameters by HF ocean radar 01 p0192 N94-11903
Time evolution of cross-stream exchange associated with the variations in the Kuroshio 01 p0197 N94-11936
An application of reduced gravity model to mesoscale eddies 01 p0199 N94-11945
Remote sensing for numerical modelling of radiative transfer processes in ocean environment 01 p0204 N94-11973
A development on estimation method of undersea light 01 p0204 N94-11974
Atmospheric correction plans for SeaWiFS 01 p0204 N94-11975
Implications of aerosol retrieval and atmospheric correction in remote sensing 01 p0205 N94-11978
The upwelling radiation at the top of the atmosphere in coastal region 01 p0205 N94-11981
Incident shortwave and longwave radiations over the western North Pacific and the Sea of Okhotsk derived from GMS-WEFAX images 01 p0205 N94-11982
Studies of dynamical processes affecting the distribution of stratospheric ozone
[NASA-CR-193477] 01 p0279 N94-12560
Observations of eddy fields in the Northwest Pacific by GEOSAT altimetry 01 p0207 N94-12639
Theory and oceanographic applications of satellite altimeter measurements 01 p0208 N94-12641
A numerical study of deep convection at high latitudes 01 p0210 N94-12652
Microwave radiometry of ice cover in polar regions 01 p0210 N94-12655
Study on diffusion phenomena of river effluents issued into sea around Japan with satellite remote sensing data 01 p0212 N94-12664
Delineation of mesoscale features of ocean on satellite IR image 01 p0214 N94-12675
The warm eddy detection from NOAA/AVHRR thermal images using the Hough transformation 01 p0220 N94-12713
Variability of the mixed layer depth in the North Pacific Ocean as calculated by a 3-D semi-analytical mixed layer remote sensing model 01 p0221 N94-12718
Coupled numerical model for altimetric data assimilation and velocity field analysis 01 p0227 N94-12752
MHD shocks in coronal mass ejections
[NASA-CR-193418] 02 p0828 N94-12970
Combustor technology for future small gas turbine aircraft
[NASA-TM-106312] 02 p0517 N94-13142
Magnetic fusion computing: A personal retrospective view
[DE93-014147] 02 p0797 N94-13217

A probabilistic method for the buckling assessment of stiffened composite shells
[NASA-TM-106286] 02 p0671 N94-13379
Numerical simulation and parameterization of orographic gravity waves 02 p0713 N94-13647
Mathematical algorithms for multidimensional inverse scattering problems in inhomogeneous medium
[AD-A266440] 02 p0749 N94-13702
A comparison of computational and experimental data for a subscale high speed propulsive nozzle at low mach numbers
[AD-A266543] 02 p0504 N94-13705
High order hybrid numerical simulations of two dimensional detonation waves
[NASA-CR-191506] 02 p0769 N94-13792
The numerical simulation of the collapse process of axially compressed cylindrical shells with measured imperfections
[LR-705] 02 p0674 N94-13905
Numerical simulations of Nd:YAG laser amplifiers
[FFI/RAPPORT-92/7028] 02 p0657 N94-13970
Engineering Physics and Mathematics Division progress report, period ending 31 December 1992
[DE93-015118] 03 p1301 N94-14926
Prediction of stable tearing of 2024-T3 aluminum alloy using the crack-tip opening angle approach
[NASA-TM-109023] 03 p0955 N94-15708
C++ as a language for object-oriented numerics
[DE93-015027] 03 p1148 N94-15985
Analysis of electromagnetic scattering from irregularly shaped, thin, metallic flat plates
[NASA-TP-3361] 03 p0998 N94-16655
Numerical studies of the photoluminescence spectrum of quantum Hall systems
[DE93-015822] 03 p1220 N94-16810
Applications of the phi-transform
[AD-A266247] 03 p1170 N94-16940
Elastic waves in discretely continuous mechanical systems
[IFTR-21/1992] 03 p1061 N94-17091
Phillips Laboratory global spectral numerical weather prediction model
[AD-A267293] 03 p1107 N94-17244
Mathematical Sciences Division 1992 programs
[AD-A268586] 03 p1140 N94-17623
The calculation methods of a cracked plastic composite laminate: A literature survey
[VTT-TIED-1362] 04 p1339 N94-17958
Format.m: A usage manual. Towards an efficient symbolic-numeric environment: Extending Mathematica's format rules
[MATHS-REPT-A-185] 04 p1547 N94-17969
Numerical methods for one-dimensional hyperbolic conservation laws
[PB93-194801] 04 p1547 N94-18078
Numerical methods for molecular dynamics
[DE93-018321] 04 p1566 N94-18179
Numerical and symbolic signal representation and processing
[AD-A270271] 04 p1389 N94-18811
A numerical study of hybrid optimization methods for the molecular conformation problems
[DE93-017898] 04 p1569 N94-18985
Using geometric techniques to improve dynamic programming algorithms for the economic lot-sizing problem and extensions
[PB93-197556] 04 p1528 N94-19330
Numerical analysis of proximal methods: Decomposition and parallelization
[ETN-93-95017] 04 p1552 N94-19362
Numerical experiments on the Ginzburg-Landau equations
[DE93-019504] 04 p1604 N94-19567
Numerical solution of differential-algebraic equations with ill-conditioned constraints
[AD-A270934] 05 p1949 N94-19898
Multi-disciplinary coupling effects for integrated design of propulsion systems
[NASA-TM-106349] 05 p1830 N94-20170
High-resolution numerical methods for compressible multi-phase flow in hierarchical porous media
[DE94-000740] 05 p1799 N94-20351
Numerical methods for singularly perturbed differential equations with applications
[AD-A272112] 05 p1952 N94-20568
Numerical simulation of lava flows: Applications to the terrestrial planets 05 p1863 N94-20904
Theoretical and numerical studies in magnetic fusion
[DE94-000536] 05 p1993 N94-20937
Numerical ranges and stability estimates
[TW-92-10] 05 p1953 N94-21060
Mathcad computer applications predicting antenna parameters from antenna physical dimensions and ground characteristics
[AD-A272987] 05 p1740 N94-21264
Users manual for the NASA Lewis three-dimensional ice accretion code (LEWICE 3D)
[NASA-TM-105974] 05 p1642 N94-21590
Numerical method for computing the electric field produced by a microwave beam in a stratified medium
05 p1746 N94-22197
Performance of a simple circular polarization selective surface 05 p1746 N94-22198
A numerical analysis of crack propagation in microcracking ceramic and ceramic composites
[DE94-001192] 06 p2253 N94-23183
Chaos and simple determinism in reversed field pinch plasmas: Nonlinear analysis of numerical simulation and experimental data
[DE94-001575] 06 p2550 N94-23211
Study of transient behavior of finned coil heat exchangers 06 p2321 N94-23642
Solution of mixed convection heat transfer from isothermal in-line fins 06 p2321 N94-23644
Unsteady three-dimensional thermal field prediction in turbine blades using nonlinear BEM
06 p2325 N94-23665
Temporal model of an optically pumped co-doped solid state laser
[NASA-TM-109680] 06 p2350 N94-24851
Research in progress and other activities of the Institute for Computer Applications in Science and Engineering
[AD-A276215] 06 p2444 N94-25090
Space Station flexible dynamics under plume impingement 06 p2208 N94-25383
Numerical analysis of the motion of a rigid body with an attached spring-mass-damper
[AD-A273825] 06 p2379 N94-25520
Studies in nonlinear numerical analysis
[AD-A273911] 07 p2959 N94-25968
Analysis and computer tools for separation processes involving nonideal mixtures
[DE94-004162] 07 p2960 N94-25986
A transient symmetrical method for the measurement of temperature dependent thermal diffusivity
[VTT-TIED-1452] 07 p3008 N94-26256
Continuation and multi-grid for bifurcation problems
[AD-A274965] 07 p2992 N94-26302
A robust upwind discretization method for advection, diffusion and source terms
[CWI-NM-R9308] 07 p2868 N94-26774
Computer program for numerical evaluation of the performance of an overmoded TM01 circular to TE10 rectangular waveguide mode converter
[AD-A274548] 07 p2771 N94-26844
Improved numerical methods for quantum field theory (Outstanding Junior Investigator Award)
[DE94-001793] 07 p3073 N94-27002
Numerical and experimental analyses of the radiant heat flux produced by quartz heating systems
[NASA-TP-3387] 07 p3011 N94-27659
The calculation for energy balance of heating plasmas by Alfven waves
[DE94-604994] 07 p3049 N94-27855
A laboratory test on construction of ice domes and their load-carrying capacity 07 p2884 N94-27966
Numerical simulation of turbulent free jet by TFKE model 07 p2871 N94-28157
Frequency-domain analysis of nonlinear microwave circuits
[PB94-132024] 08 p3261 N94-28400
Applied analysis/computational mathematics
[DE94-005133] 08 p3451 N94-28571
On the linear stability of Verkley's modons
08 p3324 N94-28695
Numerical analysis and computation of nonlinear partial differential equations from applied mathematics
[AD-A275582] 08 p3451 N94-28723
Computational methods in continuum mechanics
[AD-A275560] 08 p3451 N94-28792
A numerical solver for initial and boundary value problems in differential-algebraic systems
[AD-A275447] 08 p3452 N94-28883
Numerical analysis of airfoil for helicopter blade at high angle of attack using Navier-Stokes code
08 p3124 N94-28958
Modeling the total dose radiation effects of Hg(1-x)Cd(x)Te photodiodes using numerical device simulators
[AD-A275235] 08 p3263 N94-29028
Scale-length dependence of the ratio between the magnetic and electric field perturbations in the ionospheric field-aligned current region 08 p3360 N94-29243
An improvement of the slender body theory for oscillating ships with finite forward speed 08 p3234 N94-29705
Investigations of dispersion characteristics of microwave/optical guided wave structures by using transmission line matrix method
[ISBN-0-315-85856-7] 08 p3254 N94-30034
Numerical detection and continuation of codimension-two homoclinic bifurcations
[CWI-AM-R9308] 09 p3847 N94-32191
Advanced CFD methodology for fast transients encountered in nonlinear combustion instability problems. Volume 2: User's guide
[NASA-CR-191352] 09 p3637 N94-32694
Parallel programming methodologies for non-uniform structured problems in materials science
[AD-A277868] 10 p4111 N94-33777
Squeeze film dampers with oil hole feed
10 p4065 N94-34195
Pseudospectral collocation methods for fourth order differential equations
[AD-A281653] 10 p4129 N94-34260
Analysis of wavelet technology for NASA applications
[NASA-CR-195929] 10 p3985 N94-34704
Aspects of robust computational modeling for plain and reinforced concrete
[PB94-169240] 11 p4251 N94-35820
Numerical methods for multibody systems
11 p4222 N94-35897
Numerical analysis of an impinging jet reactor for the CVD and gas-phase nucleation of titania
[NASA-TM-106619] 12 p4431 N94-37254
Two-dimensional over-all neutronics analysis of the ITER device
[DE94-718963] 12 p4530 N94-37464
Langmuir waves in the electron-positron plasma
[DE94-618779] 12 p4531 N94-37728

NUMERICAL CONTROL

Position and force control of a vehicle with two or more steerable drive wheels
[DE93-012512] 01 p0177 N94-10269
AD100/ADSIM, ACSL, and MATLAB output comparisons using frequency-response analysis
[DE93-009640] 01 p0047 N94-11122
Airborne optical tracking control system design study
[DE93-009515] 01 p0382 N94-11662
An experimental study of tether reel system: A laboratory model
[NAL-TR-1176T] 02 p0539 N94-12943
Data fusion for adaptive control in manufacturing: Impact on engineering information models
[DE93-011555] 02 p0743 N94-12999
Inertial confinement fusion program
[DE93-013372] 02 p0796 N94-13047
A PC-PCL-based control system for the high-voltage pulsed-power operation of the Intense Diagnostic Neutral Beam (IDNB) Experiment
[DE93-014144] 02 p0797 N94-13100
DATAA: Data acquisition made easy
[DE93-014683] 02 p0823 N94-13406
Knowledge based systems: From process control to policy analysis
[DE93-014582] 02 p0765 N94-14117
Eye-gaze and intent: Application in 3D interface control
[DE93-015210] 02 p0738 N94-14335
Laser beam control and diagnostic systems for the copper-pumped dye laser system at Lawrence Livermore National Laboratory
[DE93-016529] 02 p0658 N94-14437
A fast frame rate 512 x 512 CCD digital camera system
[DE93-013048] 02 p0653 N94-14792
Performance seeking control: Program overview and future directions
[NASA-TM-4531] 02 p0519 N94-14855
A microprocessor controller for a towing tank drive and flow visualisation system
[AD-A267087] 03 p0872 N94-15543
A computer-controlled x-y offset guiding stage for the MLRS 03 p0918 N94-15598
A modular control architecture for real-time synchronous and asynchronous systems
[DE93-015439] 03 p1166 N94-16888
Automated strain gauge plethysmograph
[AD-A267323] 03 p1035 N94-17002
A measurement station for study of Earth moving tools and ground cutting processes
[IFTR-10/1991] 03 p0985 N94-17068
A state-of-the-art plasma polymerization coater for ICF targets
[DE93-016452] 03 p1204 N94-17237
Experience with custom processors in space flight applications 04 p1336 N94-18338
Simplified microprocessor design for VLSI control applications 04 p1400 N94-18359
Optimizing wind turbine control system parameters
[DE93-018861] 04 p1469 N94-19036
Analysis and design of robust decentralized controllers for nonlinear systems
[DE93-019224] 04 p1543 N94-19302

The Milling assistant, case-based Reasoning, and machining strategy: A report on the development of automated numerical control programming systems at New Mexico State University
[DE93-041101] 05 p2029 N94-21690
Performance evaluation of video on ethernet
[DE93-040696] 05 p1936 N94-21749
Proceedings of the IMOG (Interagency Manufacturing Operations Group) Numerical Systems Group
[DE94-001009] 05 p1917 N94-21851
Model-based reasoning for power system management using KATE and the SSM/PMAD
[NASA-CR-193942] 05 p1671 N94-21882
Enhanced software for the GT1022 automated gaging system
[DE94-001374] 05 p1918 N94-21977
Use of open systems for control, analysis, and data acquisition of the DIII-D tokamak
[DE94-001101] 05 p1998 N94-22089
Wilbur: A low-cost CCD camera system for MDM Observatory 05 p1814 N94-22510
K- and Ka-band mobile-vehicular satellite-tracking reflector antenna system for the NASA ACTS mobile terminal 06 p2289 N94-22831
Link monitor and control operator assistant: A prototype demonstrating semiautomated monitor and control 06 p2292 N94-23267
A reliable algorithm for optimal control synthesis
[NASA-CR-194809] 06 p2472 N94-23332
Imaging System (INEL) T805 prototype
[DE94-002807] 06 p2382 N94-23492
Calibration block for digital beam forming antenna
[PB93-204550] 06 p2294 N94-23773
Characteristics of products generated by selective sintering and stereolithography rapid prototyping processes 06 p2264 N94-24412
Octave: A MARSYAS post-processor for computer-aideed control system design 06 p2465 N94-24422
The experimental physics and industrial control system architecture: Past, present, and future
[DE94-002639] 06 p2457 N94-24626
Bioregenerative life support systems for microgravity
[NASA-CR-195516] 06 p2422 N94-24810
NASA/Army rotorcraft transmission research, a review of recent significant accomplishments
[NASA-TM-106508] 06 p2367 N94-25181
Research experience for undergraduates in robotics and materials
[AD-A273659] 06 p2368 N94-25436
Graphical programming at Sandia National Laboratories
[DE94-003803] 07 p2958 N94-25818
A large high vacuum, high pumping speed space simulation chamber for electric propulsion
[NASA-TM-106453] 07 p2690 N94-26142
New Thomson scattering laser control for D3-D
[DE94-002890] 07 p3043 N94-26274
Automated system for gas detectors providing with binary mixtures
[DE93-634192] 07 p2715 N94-26406
Low-cost photovoltaic inverters incorporating application-specific integrated circuits
[DE94-003270] 07 p2856 N94-26463
Distributed Nd:YAG laser welding and process control in inert glove boxes
[DE94-002629] 07 p2818 N94-26605
Virtual data
[DE94-002718] 07 p2986 N94-26807
Object-oriented software construction at ALS
[DE94-003418] 07 p2967 N94-27049
The universal robot 07 p2686 N94-27361
Inverted pendulum control apparatus using transputers
[DE94-701224] 07 p2973 N94-27732
Experimental apparatus for optimization of flap position for a three-element airfoil model 07 p2682 N94-27912
Digital tracking and control of retinal images
[AD-A275469] 08 p3389 N94-28810
Intelligent automated process planning and code generation for computer-controlled inspection
[AD-A275346] 08 p3409 N94-28920
Reactive system software concept with automation using the LDS language 08 p3414 N94-29327
Communications technology for unattended sensors
[DE94-005685] 08 p3254 N94-30043
Application of fuzzy logic to the control of wind tunnel settling chamber temperature
[NASA-TM-109105] 08 p3157 N94-30200
Generation of gear tooth surfaces by application of CNC machines
[NASA-CR-195306] 08 p3303 N94-30205
Maestro: An open system architecture for multi-robot control 08 p3306 N94-30288
An inverse kinematics algorithm for the DREP/Philips real-time radiographic manipulator system 08 p3307 N94-30292
Simulation of lightweight robots and their controllers 08 p3307 N94-30294
Elements of supervisory control for military robotic applications 08 p3309 N94-30303
Supervised autonomous control for Space Station Special Purpose Dextrous Manipulator (SPDM) robot 08 p3309 N94-30305
A testbed for the development of ground-based control of space-based manipulators 08 p3309 N94-30306
Achieving robot autonomy 08 p3310 N94-30307
Improving the execution speed of robot control computations: An allocation scheme for heterogeneous multiprocessors 08 p3310 N94-30308
Programmable Automated Welding System (PAWS): Control of welding through software and hardware 08 p3314 N94-30443
Confessions of a robot lobotomist
[AIAA PAPER 94-1185-CP] 08 p3440 N94-30535
Controlling multiple security robots in a warehouse environment
[AIAA PAPER 94-1300-CP] 08 p3441 N94-30540
Object-based task-level control: A hierarchical control architecture for remote operation of space robots
[AIAA PAPER 94-1209-CP] 08 p3444 N94-30560
ControlShell: A real-time software framework
[AD-A276481] 09 p3811 N94-31475
The future of open architecture process control systems
[DE94-006163] 09 p3830 N94-31623
Digital state-feedback H(infinity) control of Pritchard-Salamon systems: A Popov function approach
[REPT-93-69] 09 p3830 N94-31647
Quench detection and instrumentation for the Tokamak Physics Experiment magnets
[DE94-006656] 09 p3888 N94-31667
Real-time control and application to robotics: Hardware and software architectures
[ISBN-0-315-87192-X] 09 p3833 N94-31876
Evolving software reengineering technology for the emerging innovative-competitive era 09 p3823 N94-32439
The expanded role of software in a control system
[DE94-007524] 10 p4113 N94-33838
Development of a VME and CAMAC based data acquisition and transfer system for JT-60 control
[DE94-727590] 10 p4158 N94-33871
Integrated control and management of advanced aircraft electrical power system 10 p4042 N94-34333
Bilateral control to coordinate operators with supporting systems by force sensed grips 10 p4067 N94-34335
Improvement of control system reliability with analytical redundancy technique 10 p4118 N94-34340
The design and realization of a real-time multitasking control system by using AMX multitasking executive 10 p4118 N94-34343
Computational methods for HSCT-inlet controls/CFD interdisciplinary research
[NASA-TM-106618] 11 p4198 N94-35352
Microprocessor control of multiple peak power tracking DC/DC converters for use with solar cell arrays
[NASA-CASE-GSC-13450-2] 11 p4282 N94-35540
Guidelines for design and development of computer/microprocessor based systems in research and power reactors
[DE94-616271] 11 p4300 N94-35570
Computer automation and artificial intelligence
[DE94-611058] 11 p4312 N94-35831
High performance data acquisition, identification, and monitoring for active magnetic bearings 11 p4213 N94-35839
Fault tolerant computer control for a Maglev transportation system 11 p4215 N94-35848
NIPER Lab WARDEN: Description and LabVIEW executable code of a general-purpose laboratory-automation program
[DE94-000125] 12 p4492 N94-36698
Creation of a virtual world to study human spetial perception during sustained acceleration 12 p4484 N94-37268
Operator gaze position control interfaces: Investigation of psychophysical and operational parameters 12 p4485 N94-37273
Advanced information processing system: Hosting of advanced guidance, navigation and control algorithms on AIPS using ASTER
[NASA-CR-194960] 12 p4499 N94-37583
Open architecture controllers for advanced manufacturing
[DE94-007572] 12 p4496 N94-37782
What is an open architecture robot controller?
[DE94-007854] 12 p4501 N94-37783

NUMERICAL DATA BASES

SeaWiFS technical report series. Volume 20: The SeaWiFS bio-optical archive and storage system (SeaBASS), part 1
[NASA-TM-104566-VOL-20-PT-1] 12 p4475 N94-36958

NUMERICAL FLOW VISUALIZATION

Study on diffusion phenomena of river effluents issued into sea around Japan with satellite remote sensing data 01 p0212 N94-12664
Aspects of applying a relaxation method to computing sea surface velocities from sea surface temperature images 01 p0214 N94-12679
High speed transition prediction
[NASA-CR-194125] 02 p0502 N94-13422
Rotor stator CGI
[NASA-TM-109313] 02 p0518 N94-13608
Numerical simulation of steady three-dimensional flows in axial turbomachinery bladerows 02 p0634 N94-13630
Analysis of reacting flowfields in low-thrust rocket engines and plumes 02 p0552 N94-14491
Simulation of hypersonic, reacting flow around reentry bodies: Comparisons of numerical and experimental results
[MBB-LME-211-S-PUB-507] 02 p0509 N94-14710
The 1989 computational fluid dynamics highlights
[NASA-TM-109635] 03 p1018 N94-15246
Large eddy simulation and direct numerical simulation of high speed turbulent reacting flows
[NASA-CR-193131] 03 p1018 N94-15427
The 1988 computational fluid dynamics highlights
[NASA-TM-109645] 03 p1019 N94-15431
NAS technical summaries: Numerical aerodynamic simulation program, March 1991 - February 1992
[NASA-TM-109335] 03 p0854 N94-15798
Infrared thermography 04 p1432 N94-18652
3D composite grids using Bezier curves and surfaces in component adaptive methods
[AD-A269188] 04 p1549 N94-18863
Content based-grid node selection for vector field visualization
[REPT-93-35] 04 p1525 N94-19155
Numerical simulation of turbulent free jet by TFKE model 07 p2871 N94-28157
Analytic rendering of curvilinear volume data
[DE94-004934] 08 p3407 N94-28506
Characterization of dynamic stall phenomenon using two-dimensional unsteady Navier-Stokes equations 10 p3986 N94-34974
Vortex tubes in turbulent flows: Identification, representation, reconstruction
[AD-A280504] 11 p4267 N94-35992

NUMERICAL INTEGRATION

NT RUNGE-KUTTA METHOD

On the depletion in the outer asteroid belt and the structure of the 4 to 3 mean motion resonance 01 p0426 N94-11596
Comparison of level-1 and level-2 buckling and postbuckling solutions
[NASA-CR-194611] 03 p1057 N94-15154
Volume integral equations applied to circular and square cylinders
[AD-A266635] 03 p1169 N94-15785
Fast algorithms for polynomial interpolation, integration and differentiation
[AD-A267505] 03 p1154 N94-17370
Numerical integration of structural elements in NIKE3D and DYNA3D
[DE93-016325] 04 p1452 N94-18049
Calculation of turbulent boundary layer wall pressure spectra
[AD-A269549] 04 p1416 N94-18642
Implementation of a nonisothermal unified inelastic-strain theory into ADINA6.0 for a titanium alloy: User guide
[AD-A269927] 04 p1360 N94-18660
On the numeric integration of dynamic attitude equations
[NASA-CR-194788] 06 p2448 N94-23073
Comparison of time integration methods for the evolution of galaxies
[PB94-111671] 06 p2602 N94-24522
Geoid determination: With help of the alternative scattering method
[ETN-94-95375] 07 p2847 N94-25746
Analysis and control of hourglass instabilities in underintegrated linear and nonlinear elasticity
[NASA-CR-195293] 07 p2846 N94-28266
Finite-part integrals and the Euler-Maclaurin expansion
[DE94-006539] 09 p3844 N94-31665
Description and use of LSODE, the Livermore Solver for Ordinary Differential Equations
[NASA-RP-1327] 11 p4313 N94-35259

NUMERICAL STABILITY
A reliable stability test for exponential polynomials
[MEMO-COSOR-92-48] 01 p0341 N94-10168
Numerical simulations of thermal convection in rapidly rotating spherical fluid shells 01 p0153 N94-11635
Summation by parts, projections, and stability
[NASA-CR-194290] 01 p0346 N94-12776
Modulational stability of periodic solutions of the Kuramoto-Sivaskinsky equation
[NASA-CR-191502] 02 p0628 N94-12888
Stability of subharmonics and escape phenomena in the twin-well potential duffing system
02 p0775 N94-13235
Linear stability of stationary solutions of the Vlasov-Poisson system in three dimensions
[DE93-013873] 03 p1174 N94-16820
A modified direct preconditioner for indefinite symmetric Toeplitz systems
[DE93-015234] 04 p1516 N94-17800
Robustness and efficiency of generalized predictive control algorithms with guaranteed stability
[MATHS-REPT-A-190] 04 p1530 N94-19412
On the numerical stability of quasi-definite systems
[DE93-019404] 05 p1950 N94-20217
Stability behavior of systems obtained by index-reduction
[PB93-237709] 06 p2481 N94-23439
Infinite divisible and stable distributions modulo 1
[PB94-110640] 06 p2495 N94-23815
Dynamic localization and second-order subgrid-scale models in large eddy simulations of channel flow
06 p2329 N94-24149
Octave: A MARSYAS post-processor for computer-aideed control system design
06 p2465 N94-24422
Exploiting structure: Introduction and motivation
[NASA-CR-195136] 06 p2490 N94-24847
Parameter estimation for ARMA models with infinite variance innovations
[AD-A274654] 07 p3003 N94-26355
Analysis and control of hourglass instabilities in underintegrated linear and nonlinear elasticity
[NASA-CR-195293] 07 p2846 N94-28266
Concurrent simulation and constraint stabilization for flexible multibody systems 08 p3154 N94-29532
Aspects of the modeling and numerical simulation of leading-edge vortex flow
[AD-B179108] 08 p3133 N94-30492
Numerical precision and roundoff considerations concerning computer code migration
[DE94-005421] 08 p3427 N94-30590
A simplified Von Neumann method for linear stability analysis
[CRANFIELD-AERO-9310] 09 p3843 N94-31540
A stability estimate based on numerical ranges with application to a spectral discretization of a convection-diffusion equation
[TW-93-12] 09 p3847 N94-32200
Stability estimates for families of matrices of nonuniformly bounded order
[TW-93-14] 09 p3847 N94-32207
Eta percent-superconvergence in the interior of locally refined meshes of quadrilaterals: Superconvergence of the gradient in finite element solutions of Laplace's and Poisson's equations
[AD-A277242] 09 p3848 N94-32331
Finite element solution to the Helmholtz equation with high wave number. Part 1: The h-version of the FEM
[AD-A277396] 09 p3848 N94-32341
Preconditioned time-difference methods for advection-diffusion-reaction equations
[DE94-006472] 09 p3638 N94-32840
Time-step stability for self-consistent Monte Carlo device simulation
[DE94-012145] 12 p4528 N94-37207

NUMERICAL WEATHER FORECASTING
Simulation of images of water vapor channel and infrared split channel 01 p0190 N94-11081
Validation of ERS-1 wind and wave data by use of operational forecast models 01 p0233 N94-11710
A preliminary C-band scatterometer model function for the ERS-1 AMI instrument 01 p0233 N94-11715
The nocturnal wind maximum: An interactive forecast method
[KNMI-TR-142] 02 p0722 N94-13985
Precipitation verification LAM
[KNMI-TR-143] 02 p0722 N94-13991
Adaptation of humidity-cloud cover relations in the LAM
[KNMI-TR-144] 02 p0722 N94-13992
A verification of the Euroguidance: A guidance forecast for transportation and tourism
[KNMI-TR-145] 02 p0722 N94-13993
Sensitivity testing of a single-Doppler temperature retrieval and forecast system
[AD-A267278] 03 p1105 N94-14958
TAFVER 2 users manual
[AD-A266850] 03 p1106 N94-15757
Ensemble forecasting techniques in medium-range forecasting
[AD-A267443] 03 p1107 N94-17029
Phillips Laboratory global spectral numerical weather prediction model
[AD-A267293] 03 p1107 N94-17244
Microwave (SSM/I) Estimates of the Precipitation Rate to Improve Numerical Atmospheric Model Forecasts
[NASA-CR-193566] 04 p1491 N94-18602
Diabatic forcing and initialization with assimilation of cloud and rain water in a forecast model: Methodology
04 p1491 N94-18603
Physical retrieval of precipitation water contents from Special Sensor Microwave/Imager (SSM/I) data. Part 2: Retrieval method and applications (report version)
04 p1491 N94-18605
Forecast model applications of retrieved three dimensional liquid water fields 04 p1492 N94-18606
Moist wind relationships 04 p1492 N94-18607
Initialization and assimilation of cloud and rainwater in a regional model 04 p1492 N94-18608
SERCAA cloud analysis integration: Design concepts and interaction with cloud forecast models
[AD-A269104] 04 p1492 N94-18637
On the use of semi-Lagrangian methods for accurate predictions of gravity waves
[DM-61] 04 p1562 N94-18859
Toward a high performance distributed memory climate model
[DE93-019156] 04 p1494 N94-19298
Reports of the 1992 Synoptic Symposium
[KNMI-TR-151] 04 p1494 N94-19698
HIRLAM 04 p1494 N94-19699
The WAQUA/CSM-16 model
04 p1494 N94-19700
The wave forecasting model NEDWAM
04 p1495 N94-19701
Meso-Beta scale numerical simulation studies of terrain-induced jet streak mass/momentum perturbations
[NASA-CR-194627] 05 p1864 N94-20138
The CSIRO 9-level atmospheric general circulation model
[CSIRO-TP-26] 05 p1855 N94-20256
Development and tests of a cloud physics parameterization for real-time aviation and public numerical weather forecasting
[PB93-202711] 05 p1868 N94-21427
A synoptic-scale overview of the TOGA COARE intensive observing period November 1992 to February 1993 based on analyses from US operational global data assimilation systems
[NASA-TM-104593] 05 p1868 N94-21605
Use of satellite data for validation of operational forecast models and operational analyses
05 p1861 N94-22291
Monte Carlo climate change forecasts with a global coupled ocean-atmosphere model
[MPIM-97] 06 p2407 N94-23156
Hurricane risk assessment: Rollback or ride out
06 p2416 N94-23248
Visualization of results from meteorological simulations on CRAY
[PB93-201358] 06 p2451 N94-23443
Modelling TOVS radiances of synoptic systems
[NASA-CR-194847] 06 p2408 N94-23620
Implementation of a state of the art automated system for the production of cloud/water vapor motion winds from geostationary satellites
[NASA-CR-195087] 06 p2410 N94-24125
GEWEX Cloud Systems Study (GCSS)
06 p2411 N94-24377
Validation of mesoscale models
06 p2413 N94-24391
Techniques and resources for storm-scale numerical weather prediction 06 p2414 N94-24392
Session on cumulus parameterization
06 p2414 N94-24394
Session on techniques and resources for storm-scale numerical weather prediction 06 p2415 N94-24400
Development and testing of the Coupled Ocean/Atmosphere Mesoscale Prediction System (COAMPS)
[AD-A273925] 07 p2892 N94-25793
Testbed model and data assimilation for ARM
[DE94-000432] 07 p2893 N94-26082
Simulation of the Indian and East-Asian summer monsoon in the ECMWF model: Sensitivity to horizontal resolution
[DE94-004276] 07 p2897 N94-27571
A global forecast model comparison study - year 1
[AD-A275674] 08 p3369 N94-28663
Error growth in poor ECMWF forecasts over the contiguous United States
[AD-A275297] 08 p3369 N94-29183
Prototype terminal aerodrome forecasts using a mesoscale model
[AD-A275308] 08 p3369 N94-29194
Evaluation of the National Meteorological Center mesoscale model for prediction of severe convection over Central Arizona 08 p3371 N94-29744
Physical processes associated with variability in successive operational model forecasts of cyclogenesis
[ISBN-0-315-74753-6] 08 p3371 N94-29751
An observational and numerical study of sea/land-breeze circulations in an area of complex coastal heating 08 p3372 N94-29813
The incorporation and initialization of cloud water/ice in an operational forecast model
08 p3373 N94-29814
A comparison of predictors for first-guess wind speed errors
[AD-A276460] 09 p3781 N94-31239
Regional sources of error growth in the National Meteorological Center's medium-range forecast model
09 p3781 N94-31554
Numerical simulations of monsoon rainfall with the NRL/NCSU regional nested grid model
09 p3782 N94-31791
Recurvature dynamics of a typhoon
[AD-A276792] 09 p3784 N94-32164
Tropical cyclone forecasters reference guide. 5: Numerical track forecast guidance
[AD-A277318] 09 p3785 N94-32278
Coupled ice-ocean model supporting winter navigation in the Baltic Sea. Part 1: Ice dynamics and water levels
[PB94-148780] 10 p4092 N94-34121
Long range forecasts of the Northern Hemisphere anomalies with antecedent sea surface temperature patterns
[NASA-CR-189358] 11 p4292 N94-35380

NUSSELT NUMBER
On temperature distribution in non-participating medium with radiation boundary condition
[DE93-619375] 01 p0153 N94-11604
A parametric study of heat transfer within a planar thermosyphon
[DE93-019546] 05 p1799 N94-20258
Validated heat-transfer and pressure-drop prediction methods based on the discrete-element method. Phase 2: Two-dimensional rib roughness
[DE94-002379] 07 p2794 N94-26763
Forced convection heat transfer in straight tubes. Part 2: Laminar and transitional flow
[ESDU-93018-PT-2] 07 p2807 N94-28139
Local heat transfer in an enclosed corotating disk with axial throughflow 08 p3276 N94-29849

NUTATION
State-of-the-art satellite laser range modeling for geodetic and oceanographic applications
03 p0916 N94-15586
Ulysses log 1992 06 p2502 N94-23863
Numerical simulation of Ulysses nutation
06 p2207 N94-24017
Wobble-nutation modes of the Earth
[ISBN-0-315-84246-6] 07 p3102 N94-26669
Attitude dynamics of spinning rockets in space with internal mass motion 09 p3601 N94-31802
Resonance capture in unbalanced dual-spin spacecraft
[AD-A278501] 10 p4015 N94-34292

NUTATION DAMPERS
Reactive thrust cruise for a geosynchronous satellite with minimum fuel consumption
06 p2158 N94-24271
Numerical analysis of the motion of a rigid body with an attached spring-mass-damper
[AD-A273825] 06 p2379 N94-25520
Attitude dynamics of spinning rockets in space with internal mass motion 09 p3601 N94-31802

NUTATIONAL OSCILLATION
U NUTATION

NUTRIENTS
Microbial biofilm formation and its consequences for the CELSS program
[NASA-CR-195146] 06 p2438 N94-24706

NUTRITION
International food research project
[NASA-TM-109540] 03 p1135 N94-15371
Visit to CERMA: Centre d'Etudes et de Recherches de Medecine Aerospatiale, Centre for Studies and Research in Aviation and Space Medicine, Bretigny sur Orge, France, November 16-18, 1992
[PB94-132990] 07 p2937 N94-28392
Nutrition and hydration status of aircrew members consuming an improved survival ration during a simulated survival scenario 08 p3380 N94-28429
Food security in the context of global environmental change
[DE94-007481] 09 p3768 N94-32812

NUTRITIONAL REQUIREMENTS
NT CALORIC REQUIREMENTS
Characterization of Spirulina biomass for CELSS diet potential
[NASA-CR-194123] 02 p0729 N94-14097
Nutrition and hydration status of aircrew members consuming an improved survival ration during a simulated survival scenario 08 p3380 N94-28429
NUTS (FASTENERS)
Tilt mechanism
[AD-D015780] 03 p1047 N94-16548
Bolt and nut evaluator
[NASA-CASE-GSC-13468-1] 08 p3288 N94-29538
An experimental and analytical investigation of a threaded fastener
[VTT-JULK-786] 09 p3724 N94-31654
NYLON (TRADEMARK)
Wetting effects on nylon spheres engulfment in ice 01 p0115 N94-10189
The 13C and 15N solid-state NMR of copolymers of nylon 6 and 7: Observation of a stable pseudohexagonal phase
[AD-A265799] 01 p0094 N94-12381
Soluble precursor route to polyanilines
[AD-A268015] 03 p0973 N94-17494
Analysis of selected materials flown on interior locations of the Long Duration Exposure Facility
[NASA-CR-4586] 08 p3175 N94-29458
The ferroelectric behavior of odd-numbered nylons
[AD-A278126] 09 p3663 N94-33058
Electric field-induced changes in odd-numbered nylons
[AD-A278003] 09 p3664 N94-33138
NYLON RESINS
U POLYAMIDE RESINS
NYQUIST DIAGRAM
Parameter estimation of linear systems from frequency response measurements (computer program)
[ESDU-93016] 07 p2976 N94-28137
NYQUIST FREQUENCIES
Investigation of spectral analysis techniques for randomly sampled velocimetry data 07 p3009 N94-27924
NYSTAGMUS
NT VESTIBULAR NYSTAGMUS
Vertical gaze direction during parabolic flight 07 p2913 N94-27453
The mechanism of caloric nystagmus under microgravity. 1: Changes of endolymphatic pressure in the semicircular canal of pigeon by caloric stimulation 07 p2914 N94-27457
Disturbance of equilibrium on JAL flight crew 08 p3390 N94-28856

O

O RING SEALS
Durability of a carbon segmented circumferential seal for a liquid oxygen turbopump
[NAL-TR-1155] 01 p0178 N94-10369
Check valve with poppet dashpot/frictional damping mechanism
[NASA-CASE-MSC-21950-1] 01 p0179 N94-10658
Flight 20 (STS-45) polysulfide gas path investigation
[NASA-CR-193861] 03 p0928 N94-17213
Effect of temperature and O-ring gland finish on sealing ability of Viton V747-75
[NASA-TP-3391] 04 p1368 N94-18075
Viscoelastic analysis of seals for extended service life 06 p2371 N94-24408
Postflight hardware evaluation RSRM-29 (STS-54). Case, seals, and joints PFORs, appendix B
[NASA-CR-193899] 06 p2367 N94-25020
Outgas and vacuum seal characteristics of irradiated polyimide O-ring
[DE94-701200] 07 p2757 N94-27812
OAO
The 1968 highlights --- NASA programs and research
[NASA-TM-109627] 03 p1302 N94-15413
OBJECT PROGRAMS
A distributed, visual object system using aggregation objects with a local namespace
[IME-MET-TR-007] 02 p0764 N94-13860
Reviews of computing technology: Object-oriented technology
[DE93-014740] 02 p0754 N94-14470
Structural modeling: An application framework and development process for flight simulators
[AD-A271348] 05 p1650 N94-19880
Mint tutorial and user manual
[TR-452] 05 p1905 N94-20143
Maestro: An open system architecture for multi-robot control 08 p3306 N94-30288
The Vanilla meta-interpreter for definite logic programs and ambivalent syntax
[CT-93-01] 08 p3424 N94-30386
Symbolic debugging of globally optimized code: Data value problems and their solutions
[AD-A278898] 11 p4302 N94-35572
OBJECT-ORIENTED PROGRAMMING
An object-oriented model for extensible concurrent systems: The composition-filters approach
[MEMO-INF-92-87] 01 p0320 N94-10166
Database computing in HEP
[DE93-011765] 01 p0419 N94-11105
Object oriented implementation of adaptive mesh refinement algorithms
[DE93-011885] 01 p0325 N94-11112
Development of generic field classes for finite element and finite difference problems
[DE93-011678] 01 p0345 N94-11225
Impacts of object-oriented technologies: Seven years of SEL studies 01 p0329 N94-11425
The MERMAID project 01 p0329 N94-11426
Reuse: A knowledge-based approach 01 p0329 N94-11430
Large project experiences with object-oriented methods and reuse 01 p0329 N94-11431
The relational-to-object-oriented cross-model accessing capability in a multi-model and multi-lingual database system
[AD-A264911] 01 p0420 N94-11846
Object-oriented productivity metrics 02 p0667 N94-13161
Programming languages made in Italy
[REPT-93-002] 02 p0750 N94-13805
A distributed, visual object system using aggregation objects with a local namespace
[IME-MET-TR-007] 02 p0764 N94-13860
The OOA technique in information systems
[REPT-72-92] 02 p0823 N94-13863
Efficient, massively parallel eigenvalue computation
[NASA-CR-194289] 02 p0760 N94-13921
Discrete event simulation using object-oriented programming: Application to manufacturing
[ERB-1037] 02 p0753 N94-14200
Reviews of computing technology: Object-oriented technology
[DE93-014740] 02 p0754 N94-14470
Development of a computer supported instrumentation for economic planning and evaluation of production facilities for fiber reinforced composites elements 03 p0932 N94-15260
The distributed database dynamic reconfiguration project
[AD-A267116] 03 p1229 N94-15652
An experimental comparison of CLOS and C(++) implementations of an object-oriented graphical simulation of walking robot kinematics
[AD-A267168] 03 p1165 N94-15855
Integration ToolKit and Methods (ITKM) manufacturing methods and prototype toolkit. A combined modeling method using IDEFO, IDEF1x and XSpec
[AD-A266176] 03 p0984 N94-16981
An object-oriented program specification for a mobile robot motion control language
[AD-A267213] 03 p1166 N94-16986
Design and implementation of an interface editor for the Amadeus multi-relational database front-end system
[AD-A267403] 03 p1233 N94-17114
An object-oriented dynamic software process model
[AD-A267726] 03 p1154 N94-17371
Research in presistent simulation: Development of the persistent ModSim object-oriented programming language
[AD-A268568] 03 p1157 N94-17620
Proposal for a numerical array library
[DE93-015017] 04 p1516 N94-17786
An object-oriented environment for computer vision and pattern recognition
[DE93-017098] 04 p1517 N94-17867
A structured approach for modeling, analyzing and simulating real-time control systems
[REPT-93-044] 04 p1539 N94-17916
An environment for requirement reuse
[REPT-92-082] 04 p1613 N94-17939
Object-oriented extension of a relational DBMS
[ETN-93-94403] 04 p1519 N94-17978
The development of a course sequence in real-time systems design
[AD-A269459] 04 p1522 N94-18726
NASA Electronic Library System (NELS) optimization
[NASA-CR-193688] 04 p1617 N94-18839
Software engineering for effective utilization of parallel processing computing system
[AD-A269191] 04 p1535 N94-18865
Asynchronous rendezvous in the presence of backtracking
[PB93-197739] 04 p1524 N94-19062
Abstracting inter-object communications using composition filters
[MEMO-INF-92-78] 04 p1526 N94-19220
DataTypeLog: A deductive object oriented query language
[MEMO-INF-92-79] 04 p1526 N94-19221
The TM typing rules
[MEMO-INF-92-80] 04 p1526 N94-19222
The TM manual version 1.3 working document
[MEMO-INF-93-06] 04 p1527 N94-19229
Feasibility study in linguistically motivated object-oriented conceptual design of information systems
[PB93-197754] 04 p1618 N94-19331
Advanced software development workstation: Object-oriented methodologies and applications for flight planning and mission operations
[NASA-CR-193706] 04 p1513 N94-19349
Managing persistent objects: From the programming language to the system
[ETN-93-95021] 04 p1529 N94-19368
Contribution to applications systems design MOSAIC method in the Aristote project
[ETN-93-95022] 04 p1529 N94-19370
OORA Automated Knowledge System (OAKS) code, appendix C
[AD-A270709] 04 p1531 N94-19573
Computer security. Evolutions 1987 to 1992: Trends and perspectives
[RR-905-I] 04 p1532 N94-19713
On the automation of object-oriented requirements analysis
[AD-A270673] 04 p1532 N94-19782
A parallelizing compiler based on partial evaluation
[AD-A270838] 05 p1898 N94-19832
PREVAIL-DM: A framework-based environment for formal hardware verification
[RR-899] 05 p1905 N94-20164
Object-oriented DFD models to present the functional and behavioral views
[DE93-040206] 05 p1906 N94-20280
Design of a computer assisted tool for object oriented acquisition, modeling and simulation of knowledge structure
[ETN-93-94183] 05 p1910 N94-21152
The Mercury user's manual
[TR-465] 05 p1913 N94-21316
The three-dimensional Event-Driven Graphics Environment (3D-EDGE) 05 p1922 N94-21342
Reducing the cognitive workload: Trouble managing power systems
[NASA-TM-106413] 05 p1714 N94-21564
Termination and confluence of rule execution
[CWI-CS-R9309] 05 p1916 N94-21587
An evaluation of integration of the trace assertion method with the box structure method for coding in C++
[DE93-040480] 05 p1918 N94-21924
Database computing in HEP
[NASA-CR-194791] 05 p1921 N94-22375
An object-oriented data reduction system in Fortran 05 p2046 N94-22447
A structured data transfer protocol 05 p2047 N94-22450
C++, objected-oriented programming, and astronomical data models 05 p2063 N94-22473
Programmability in AIPS++ 05 p1926 N94-22482
An object-oriented approach for supporting both X and terminal interfaces 05 p1926 N94-22491
StarView: The object oriented design of the ST DADS user interface 05 p2049 N94-22548
A general model for dynamic and complex information management: The ELEN prototype object manager for software engineering
[ETN-94-95163] 06 p2588 N94-22880
Asynchronous rendezvous in distributed logic programming
[PB93-220614] 06 p2448 N94-23096
APLAC: An object-oriented analog circuit simulator and design tool. 6.1 system simulations manual
[PB93-224871] 06 p2450 N94-23226
An object-oriented approach for parallel self adaptive mesh refinement on block structured grids 06 p2469 N94-23697
Object-oriented technologies in a multi-mission data system 06 p2506 N94-23885
Using Mach threads to control DSN operational sequences 06 p2477 N94-23916
SIMSAT: An object oriented architecture for real-time satellite simulation 06 p2197 N94-23940
Telemetry ground system development via the component approach 06 p2203 N94-23949
A simulation and evaluation of NATO Standardization Agreement (STANAG) 4214
[AD-A273195] 06 p2297 N94-24554
Declarative Object Manipulation Environment (DOME): Alpha version
[AD-A273233] 06 p2460 N94-24935

Proposed Object Oriented Programming (OOP) enhancements to the Very High Speed Integrated Circuits (VHSIC) Hardware Description Language (VHDL)
[AD-A274004] 07 p2957 N94-25661
Performance measurement of three commercial object-oriented database management systems
[AD-A274028] 07 p3096 N94-25765
Domain analysis and modeling of a model-based software executive
[AD-A274087] 07 p2958 N94-25783
Object-oriented design and implementation of a parallel Ada simulation system
[AD-A274119] 07 p2979 N94-25906
Object interaction in a parallel object-oriented discrete-event simulation
[AD-A274084] 07 p2959 N94-25942
Using database technology to support domain-oriented application composition systems
[AD-A274091] 07 p3096 N94-26024
Coordinated scheduling for dynamic real-time systems
[NASA-CR-195231] 07 p3093 N94-26206
MATRA Marconi Space: The Silex on-board processor and on-board software 07 p2950 N94-26726
Implementing hard real-time systems: A case study 07 p2951 N94-26731
Developing with Ada using HOOD design methodology 07 p2953 N94-26741
The CODE-TOP (COncurrent system DEvelopment using Transformations Of Predicate-transition nets) method: Examples of using it for system architecture specification, software specification, and code generation 07 p2953 N94-26744
A formalization of objects using equational dynamic logic
[PB94-125218] 07 p2965 N94-26852
Example of the EXPANSE signalling protocol
[PB94-125283] 07 p2771 N94-26872
Object-oriented software construction at ALS
[DE94-003418] 07 p2967 N94-27049
An object-oriented database interface for Ada
[AD-A274391] 07 p2968 N94-27075
Active database architectures and the design of sentinel for constraint management
[AD-A274205] 07 p3099 N94-27101
Parallel computers for advanced information processing 07 p2955 N94-27193
Schema integration in object-oriented databases
[CWI-CS-R9320] 07 p2970 N94-27548
An object model for multimedia programming
[CWI-CS-R9327] 07 p2971 N94-27552
Comparison of Object-Oriented Analysis and Design Methods: A Collection of Papers
[MEMO-INF-92-69] 07 p2975 N94-27936
A formal approach to the comparison of object-oriented analysis and design methodologies 07 p2975 N94-27937
Object-oriented development methods 07 p2975 N94-27938
CASE tools for the support of object-oriented analysis and design methods 07 p2975 N94-27939
Object-based design of embedded software
[PB94-132073] 08 p3407 N94-28403
Object-oriented CAD tool implementations for the construction industry
[PB94-132370] 08 p3407 N94-28411
A concurrent, object-based implementation for the tactical level of the rational behavior model
[AD-A275024] 08 p3410 N94-29115
The covering property of the object-oriented data model: Design and implementation issues
[AD-A275048] 08 p3530 N94-29165
Basic research in computer science
[AD-A275184] 08 p3405 N94-29181
Aerospace Software Engineering for Advanced Systems Architectures
[AD-A277101] 08 p3412 N94-29315
Object versus functional oriented design 08 p3413 N94-29321
Hierarchical Object Oriented Design (HOOD): Possibilities, limitations, and challenges 08 p3413 N94-29322
Object oriented design of the autonomous fixtaking management system 08 p3143 N94-29323
A distributed object-based environment in Ada 08 p3417 N94-29347
Constrained objects
[AD-A275273] 08 p3418 N94-29434
The effects of inheritance on the properties of physical storage models in object-oriented databases 08 p3531 N94-29537
Object-oriented database support for scientific data management: A system for experimentation 08 p3531 N94-29677
Maestro: An open system architecture for multi-robot control 08 p3306 N94-30288
DTL: A deductive and typed object-oriented language
[MEMO-INF-93-41] 08 p3425 N94-30417
Mapping objects to files: A UNIX file system interface to an object management system
[RUU-CS-93-08] 08 p3428 N94-30746
A generic model for data acquisition: Connectionist methods of information processing
[TELECOM-93-E-003] 09 p3730 N94-31166
Design patterns mixing genericity and inheritance in the development of reusable components
[REPT-93-021] 09 p3808 N94-31178
A finite state machine model for object oriented systems
[REPT-93-040] 09 p3809 N94-31212
Real time simulation model for designing converter regulation
[ETN-94-95735] 09 p3689 N94-31576
Report on implementing part relationships using VML metaclasses
[PB94-147485] 09 p3813 N94-31686
EVORM: A conceptual modelling technique for evolving application domains
[TR-93-16] 09 p3918 N94-32290
Multiple inheritance via intersection types
[TR-93-18] 09 p3848 N94-32292
CONFIG: Integrated engineering of systems and their operation 09 p3823 N94-32432
OPT++: An object-oriented class library for nonlinear optimization
[DE94-008890] 09 p3818 N94-32584
A framework for developing and managing reusable avionics software
[AD-A276846] 09 p3582 N94-32909
A++ and P++ array classes for architecture independent finite difference computations
[DE94-009321] 10 p4106 N94-33906
Object-oriented particle simulation on parallel computers
[DE94-009353] 10 p4111 N94-33908
Ada developers' supplement to the recommended approach
[NASA-CR-189345] 10 p4109 N94-34921
C++ Planning and Resource Reasoning (PARR) shell 10 p4124 N94-35054
Measuring and assessing maintainability at the end of high level design 11 p4301 N94-35438
Impacts of object-oriented technologies: Seven years of SEL studies 11 p4301 N94-35439
An object-oriented implementation of a graphical-programming system
[DE94-009298] 11 p4304 N94-35808
Object-oriented simulation pictures (OOSPic) for design and testing
[AD-A278798] 11 p4305 N94-36013
Integrating end-to-end threads of control into object-oriented analysis and design 12 p4491 N94-36496
Fusing modeling techniques to support domain analysis for reuse opportunities identification 12 p4491 N94-36497
Impact of Ada in the Flight Dynamics Division: Excitement and frustration 12 p4492 N94-36501
Design, implementaion and evaluation of a declarative object-oriented programming language
[PB94-169208] 12 p4492 N94-36546
ZLIB++: Object-oriented numerical library for differential algebra
[DE94-010839] 12 p4495 N94-37453

OBLATE SPHEROIDS
Intensity and polarization of light scattered by size distributions of randomly oriented nonspherical particles 05 p1721 N94-20416
Orbital applications of electrodynamic propulsion
[AD-A275413] 08 p3173 N94-29216
The Earth Satellite Program (ESP), version 2.0
[AD-A278860] 11 p4201 N94-35827

OBLIQUE SHOCK WAVES
Numerical calculation of scramjet inlet flow
[NAL-TR-1174T] 01 p0027 N94-10370
Flow development in a circular pipe in the UTIAS/RPI M = 8.3 gun tunnel 01 p0006 N94-10442
Development of a Delaunay-based adaption scheme with applications to complex three-dimensional rotational flows 01 p0149 N94-10824
Evaluation of dual flow thrust vectored nozzles with exhaust stream impingement
[NASA-CR-193292] 01 p0150 N94-10912
An experimental investigation of shock wave/vortex interaction 02 p0634 N94-13574
On the interaction between the shock wave attached to a wedge and freestream disturbances
[NASA-CR-191528] 03 p1019 N94-15478
An investigation of oblique shock/boundary layer interaction control
[AD-A268106] 03 p0861 N94-17574
Experimental investigation of three-dimensional vortex-airfoil interaction in a supersonic stream
[AD-A275107] 08 p3122 N94-28899
Experimental studies of transpiration cooling with shock interaction in hypersonic flow, part B
[NASA-CR-195958] 10 p3985 N94-34965
Investigation of Burnett equations for two-dimensional hypersonic flow
[AD-A278942] 11 p4190 N94-35717
A supersonic tunnel for laser and flow-seeding techniques
[NASA-TM-106588] 11 p4265 N94-35945

OBLIQUE WINGS
The 1980 highlights
[NASA-TM-109672] 03 p1303 N94-15509
High-speed research program systems analysis activities at Ames Research Center 10 p3971 N94-33455

OBLIQUENESS
The connection between Venus' free obliquity and its CMB oblateness 05 p2139 N94-20896
The effect of polar caps on obliquity 09 p3948 N94-33213

OBSERVABILITY (SYSTEMS)
On output linearization of observable dynamics
[MEMO-1105] 01 p0341 N94-10276

OBSERVATION
NT EARTH OBSERVATIONS (FROM SPACE)
NT SATELLITE OBSERVATION
NT SKY SURVEYS (ASTRONOMY)
NT SPACE OBSERVATIONS (FROM EARTH)
NT VISUAL OBSERVATION
Aircraft weight prediction capability. Volume 1: Weight study and results
[AD-A277206] 09 p3579 N94-32062

OBSERVATION AIRCRAFT
NT F-5 AIRCRAFT
NT OH-6 HELICOPTER
NT U-2 AIRCRAFT

OBSERVATORIES
NT ASTRONOMICAL OBSERVATORIES
NT ASTRONOMICAL SATELLITES
NT GAMMA RAY OBSERVATORY
NT GEOPHYSICAL OBSERVATORIES
NT GINGA SATELLITE
NT HEAO
NT HEAO 1
NT HEAO 2
NT HUBBLE SPACE TELESCOPE
NT INFRARED ASTRONOMY SATELLITE
NT INFRARED SPACE OBSERVATORY (ISO)
NT IUE
NT KUIPER AIRBORNE OBSERVATORY
NT LUNAR OBSERVATORIES
NT OAO
NT OGO
NT OSO
NT ROSAT MISSION
NT SAS
NT SOFIA (AIRBORNE OBSERVATORY)
NT SOLAR OBSERVATORIES
NT SPACE INFRARED TELESCOPE FACILITY
NT SPARTAN SATELLITES
NT X RAY ASTROPHYSICS FACILITY
Search for ultra-high-energy radiation from gamma-ray bursts
[DE93-012721] 02 p0847 N94-12964
Unmasking the Sun
[NASA-TM-109595] 03 p1298 N94-15287
Lunar ranging
[NASA-TM-109603] 03 p1236 N94-15311
A computer-controlled x-y offset guiding stage for the MLRS 03 p0918 N94-15598
Neutral-current detection in the Sudbury Neutrino Observatory
[DE93-014481] 03 p1185 N94-16951
Site comparison for optical visibility statistics in southern California 08 p3247 N94-29617
ARM: A climate process observatory
[DE94-007473] 12 p4463 N94-36477

OBSTACLE AVOIDANCE
Measures for simulator evaluation of a helicopter obstacle avoidance system 01 p0035 N94-11535
Obstacle detection by recognizing binary expansion patterns
[NASA-CR-194415] 02 p0514 N94-14495
Perception for outdoor navigation
[AD-A266867] 03 p0863 N94-14919
Environmental use of a Laser Range Finder and the Advanced Visualization System
[DE93-016163] 03 p1043 N94-17677
Object recognition through image understanding for an autonomous mobile robot
[AD-A273206] 06 p2475 N94-24862
Collision avoidance and control of multiple revolute manipulators 08 p3302 N94-29884

Extended occupancy grid method for modelling unknown dynamic environments 08 p3144 N94-30281
Navigation of military and space unmanned ground vehicles in unstructured terrains 08 p3144 N94-30282
An optimal obstacle avoidance path planning algorithm for the Excalibur robot 08 p3306 N94-30287
Sonar sensing and obstable detection 08 p3309 N94-30301
Obstacle detection for an autonomous vehicle 08 p3309 N94-30302
Motion control of mobile robots 08 p3310 N94-30309
A probabilistic approach to motion planning for car-like robots
[RUU-CS-93-18] 08 p3438 N94-30410
A robotic wheelchair
[AIAA PAPER 94-1229-CP] 08 p3447 N94-30578
Piecewise linear paths among convex obstacles
[RUU-CS-93-20] 08 p3460 N94-30721
Iterative removal of boundary minima of harmonic potential function for mobile robot navigation
[REPT-93-059] 08 p3449 N94-30962
Safe navigation and active vision for autonomous vehicles: A purposive and direct solution 09 p3832 N94-31842
Tripping over obstacles: Biomechanical analyses of how young and old try to avoid it 09 p3803 N94-31954
Intelligent vehicle control: Opportunities for terrestrial-space system integration 10 p4127 N94-34038
A genetic technique for planning a control sequence to navigate the state space with a quasi-minimum-cost output trajectory for a non-linear multi-dimnensional system 10 p4123 N94-35052
Accurate estimation of object location in an image sequence using helicopter flight data 10 p3997 N94-35055

OBSTRUCTING
U BLOCKING

OCCLUSION
Optimal hemicube sampling
[DE93-010499] 01 p0334 N94-12591
Incompressible viscous flow in tubes with occlusions
[ISBN-0-315-75467-2] 09 p3704 N94-31778

OCCULTATION
NT RADIO OCCULTATION
NT SOLAR ECLIPSES
NT STELLAR OCCULTATION

OCCUPATION
A summer program in mathematics and computer science for academically oriented student
[AD-A263467] 01 p0415 N94-11517
Career Information in the Mathematical Sciences (CIMS)
[DE93-013780] 01 p0318 N94-11817
Carpal tunnel syndrome and other cumulative trauma disorders of the arm and hand and occupation in US Navy enlisted personnel
[AD-A267747] 03 p1129 N94-17374
Interdisciplinary training in life science (FY 1991 ASSERT)
[AD-A269220] 04 p1512 N94-18886
NASA/DOD Aerospace Knowledge Diffusion Research Project. Paper 40: Technical communications in aerospace education: A study of AIAA student members
[NASA-TM-109868] 11 p4344 N94-35254
Mentoring for 2000 and beyond 11 p4343 N94-35964

OCCUPATIONAL DISEASES
Proceedings of the 1992 Annual Meeting NASA Occupational Health Program
[NASA-CR-193462] 03 p1123 N94-16609
New health and safety initiatives at the Department of Energy (DOE) 03 p1124 N94-16610
Americans with Disabilities Act considerations for the practice of occupational medicine 03 p1124 N94-16611
Programs and resources for control of job stress in the Federal workplace 03 p1124 N94-16617
Tuberculosis: A case for increased screening 03 p1126 N94-16627
Summary of follow-up results from potential tuberculosis exposures 03 p1126 N94-16628
Legionella: An overview 03 p1126 N94-16629
Asbestos Surveillance Program 03 p1127 N94-16638
Lead Surveillance Program 03 p1127 N94-16640
Mercury Surveillance Program 03 p1127 N94-16641
General Medical Surveillance Program 03 p1127 N94-16643
OSHA bloodborne pathogens standards exposure control plan 03 p1127 N94-16645
Carpal tunnel syndrome and other cumulative trauma disorders of the arm and hand and occupation in US Navy enlisted personnel
[AD-A267747] 03 p1129 N94-17374
Review of short-term, high-level exposure to metals: Antimony, barium, and cadmium
[AD-A268896] 04 p1505 N94-18392
Minimization of carpal tunnel syndrome
[AD-A276409] 09 p3795 N94-31363

OCEAN BOTTOM
Low power digital recorder development
[AD-A265921] 01 p0170 N94-10704
Acoustics of bubbly sediments
[AD-A263726] 01 p0288 N94-11299
A model for the subduction mechanics of flexible lithosphere and its viscous coupling to the mantle using power-law rheologies 01 p0277 N94-11585
Acoustic characteristics of side scan sonar and sub-bottom profiler for 10,000 m class ROV 01 p0172 N94-11916
The extraction of bottom characteristics and mapping in Kin Bay, Okinawa Main Island, Japan, using LANDSAT-5/TM and SPOT-1/HRV data 01 p0197 N94-11931
On resolution of underwater stereo photogrammetry 01 p0172 N94-11966
Impact mineralogy and chemistry of the cretaceous-tertiary boundary at DSDP site 576 01 p0282 N94-12091
Iron and nickel isotopic mass fractionation in deep-sea spherules 01 p0282 N94-12199
Preliminary analysis of the FLIP array data from the NOBS experiment
[AD-A265911] 01 p0289 N94-12349
Mapping bathymetric slopes from bathymetry data
[AD-A265923] 01 p0290 N94-12350
Mapping of sea bottom topography with ERS-1 C-band SAR 01 p0254 N94-12525
Integrated marine survey system 01 p0217 N94-12693
A detailed investigation of the benthic regime in the Clarion-Clipperton province of the Pacific and a forecast of consequences of manganese nodule mining 01 p0224 N94-12733
Bottom currents and possibilities for near bottom layer environmental investigations in the Pacific by means of self contained bottom stations 01 p0224 N94-12734
Autonomous self contained bottom pop-up stations for study of the benthic layer and seismicity of the ocean's bottom 01 p0224 N94-12735
Convective and dynamic instability in meridional trenches 01 p0225 N94-12739
Model of Kuroshio region circulation 01 p0229 N94-12765
LFASE report: Crustal study
[AD-A266893] 03 p1111 N94-14947
Composite refraction-reflection stack sections: Tracing faults in the Atlantic coastal plain sediments
[DE93-013581] 03 p1112 N94-16009
Mapping of sea bottom topography 03 p1077 N94-16744
Sea bottom topography imaging with SAR 03 p1077 N94-16745
The Megascience Forum
[DE93-014445] 03 p1303 N94-16804
Real time system for practical acoustic monitoring of global ocean temperature
[AD-A267868] 03 p1113 N94-17391
Fabrication of a NAVMAP, a deep-sea mapping system
[AD-A268630] 03 p1085 N94-17467
Report detailing modifications to the 1/8 degree global bathymetry
[AD-A268178] 03 p1114 N94-17509
Constraints on crustal structure from long period pressure and displacement measurements on the deep seafloor
[AD-A269931] 04 p1498 N94-18663
BACKSCATTER.FOR: A program to calculate the backscattering strength of an inhomogeneous seabed
[AD-A269235] 04 p1499 N94-18910
The interpretation of crustal dynamics data in terms of plate motions and regional deformation near plate boundaries
[NASA-CR-194302] 04 p1487 N94-19432
Analysis of data from Columbia Point Arena Ocean-Bottom Seismic Station (OBSS)
[AD-A271263] 04 p1500 N94-19727
Faulted structure of the bottom simulating reflector on the Blake Ridge, western North Atlantic
[AD-A271289] 04 p1500 N94-19745
Seismic studies of the geologic structure and physical properties of the seabed
[AD-A270895] 04 p1500 N94-19747
Measurements of ocean surface and bottom backscattering strengths in the northwestern Atlantic Ocean
[AD-A270893] 04 p1500 N94-19786
A laboratory model of a cooled continental shelf
[AD-A270862] 04 p1500 N94-19792
On the sources of North Atlantic deep water
[AD-A270854] 05 p1881 N94-19895
Seafloor characterization/Galapagos propagating rift
[AD-A272001] 05 p1882 N94-20581
First discovery of the organic materials in deep-sea iron cosmic spherule 05 p1685 N94-20677
Iridium in sediments containing large abundances of Australasian microtektites from DSDP hole 758B in the Eastern Indian Ocean and from DSDP hole 769A in the Sulu Sea 05 p2083 N94-20741
Green Sheet project: Dye sheet evolution
[AD-A272019] 05 p1883 N94-21443
Reactive trace metals as indicators of subduction and ventilation processes in the ocean
[AD-A273585] 06 p2419 N94-25164
Seafloor characterization/Galapagos propagating rift
[AD-A273586] 06 p2419 N94-25165
Analysis of modal evolution caused by a weakly range-dependent seabed in shallow water and its application to inversion for geoacoustic properties
[AD-A273656] 06 p2419 N94-25435
Coupling of pelagic and benthic communities over a seamount in the Eastern North Pacific
[AD-A274750] 07 p2899 N94-26149
Topics in longshore currents
[AD-A274788] 07 p2899 N94-26361
Macrobenthic fauna in the dutch sector of the north sea in 1991
[PB94-126414] 07 p2868 N94-27200
An extraterrestrial event at the tertiary-quaternary boundary 07 p2890 N94-28309
Updated deep-tow acoustics/geophysics system compressional velocity database
[AD-A275477] 08 p3355 N94-28685
Seafloor characterization using texture
[AD-A275399] 08 p3377 N94-29204
Considerations in the modelling of seafloor acoustic backscatter
[AD-A275404] 08 p3478 N94-29206
Multi-scale studies of seafloor topography
[AD-A277006] 09 p3789 N94-32400
Long transect seafloor seismic array: A component of SAMSON (Sources of Ambient Micro Seismic Ocean ic Noise)
[AD-A277009] 09 p3789 N94-32401
Light in Thermal Environments (LITE) Workshop
[NASA-CR-195851] 09 p3790 N94-32981
Quantitative modeling of bottom morphology and subbottom properties
[AD-A278142] 09 p3790 N94-33062
Bottom boundary layer stress measurements with BASS tripods: Data report STRESS 1988-1989
[AD-A277864] 10 p4092 N94-33775
A geoacoustic model for fine-grained, unconsolidated calcareous sediments (ARSRP natural laboratory)
[AD-A277830] 10 p4092 N94-33831
Variability of the California Current System off Point Sur, California from April 1988 to December 1990
[AD-A278579] 12 p4476 N94-36985

OCEAN COLOR SCANNER
Application of the airborne ocean color imager for commercial fishing
[NASA-TM-103986] 01 p0231 N94-11378
SeaWiFS technical report series. Volume 12, SeaWiFS technical report series cumulative index: Volumes 1-11
[NASA-TM-104566-VOL-12] 03 p1111 N94-15529
SeaWiFS technical report series. Volume 16: The second SeaWiFS Intercalibration Round-Robin Experiment, SIRREX-2, June 1993
[NASA-TM-104566-VOL-16] 10 p4093 N94-34412

OCEAN CURRENTS
NT COASTAL CURRENTS
NT EL NINO
NT GULF STREAM
Topex/Poseidon: A United States/France mission. Oceanography from space: The oceans and climate
[NASA-TM-108253] 01 p0043 N94-10699
Study of the surface circulation to the North of Bransfield Strait, Antarctica
[INPE-5472-TDI/503] 01 p0288 N94-11200
Near surface ocean processes: Acoustical observations, ambient sound, and Langmuir circulation 01 p0288 N94-11447
Mapping of the East Australian current with the ERS-1 SAR and shipborne studies 01 p0234 N94-11717
Preliminary analysis of circulations over the Indian Ocean and adjoining regions using ERS-1 surface winds in the NCMRWF data assimilation system 01 p0234 N94-11719

Ocean circulation revealed by ice floe tracking
01 p0240 N94-11759
ERS-1 radar altimetry over the North Atlantic
01 p0242 N94-11772
An investigation using empirical orthogonal functions and objective analysis to analyse the vertical temperature structure of a gulf stream meander
[AD-A265116] 01 p0289 N94-11868
Proceedings of the PORSEC 1992 in Okinawa: Conference for Pacific Ocean Environments and Probing, volume 1
[JTN-93-80418] 01 p0191 N94-11894
HF ocean radar system at Okinawa Radio Observatory 01 p0139 N94-11902
Exchange of bay water with ocean current monitored by the NOAA satellite 01 p0193 N94-11908
Current structures in the western equatorial Pacific during JAPACS cruises 01 p0193 N94-11911
Ocean-ice interaction study of waves and mesoscale features 01 p0197 N94-11935
The coherent structure in the oceanic turbulence around Japan Islands Chain forced by an air, sea, and solid Earth interaction 01 p0198 N94-11940
An application of reduced gravity model to mesoscale eddies 01 p0199 N94-11945
A study of pollution courses of spilled oil floatation in the outer ocean 01 p0205 N94-11983
Circulation of North Pacific Intermediate Water
01 p0206 N94-11985
Roles of the NEC and MC in the formation and evolution of the Equatorial Pacific Warm Pool
01 p0206 N94-11990
Proceedings of the PORSEC 1992 in Okinawa: Conference for Pacific Ocean Environments and Probing, volume 2
[JTN-93-80419] 01 p0207 N94-12635
Surface eddy fluxes from the GEOSAT satellite altimeter 01 p0208 N94-12643
Measurement of eddy structure and movement in the north-east Pacific with the GEOSAT altimeter
01 p0209 N94-12647
Observation of warm current at the boundary from north equatorial current to Kuroshio by NOAA/AVHRR
01 p0214 N94-12676
The WOCE/TOGA Surface Velocity Programme (SVP)
01 p0216 N94-12691
The acoustic arrangement for measuring vertical structure of sea current 01 p0223 N94-12729
Turbulence generation in the Pacific undercurrent by shear 01 p0223 N94-12730
A detailed investigation of the benthic regime in the Clarion-Clipperton province of the Pacific and a forecast of consequences of manganese nodule mining
01 p0224 N94-12733
Bottom currents and possibilities for near bottom layer environmental investigations in the Pacific by means of self contained bottom stations 01 p0224 N94-12734
Autonomous self contained bottom pop-up stations for study of the benthic layer and seismicity of the ocean's bottom 01 p0224 N94-12735
Complex (hydrodynamic, satellite) monitoring of dynamic structures in the western Pacific with the aim of forecasting the marine ecosystems behaviour
01 p0227 N94-12753
Study of the admixture diffusion in the sea using remote techniques 01 p0228 N94-12759
Mixing of drifter ensemble by mesoscale currents
01 p0228 N94-12760
Experimental and theoretical investigation of undular bore formation upstream the bank
01 p0229 N94-12764
Circulation model experiments of the Gulf Stream using satellite-derived fields
[AD-A266067] 02 p0725 N94-12990
An experimental regional scale climate simulation laboratory
[DE93-015935] 02 p0719 N94-13119
Ocean uptake of carbon dioxide
[DE93-012967] 02 p0707 N94-13384
Tidal interactions in the Earth Moon system
[COMMUNICATIONS-SER-B-160]
02 p0837 N94-13503
Radar imaging of sub-mesoscale ocean phenomena
[AD-A266339] 02 p0725 N94-13581
On the space-time ocean current variability and its effects on the length-of-day
[ISBN-0-315-59510-8] 02 p0726 N94-14205
On the sea truth data of the Kuroshio meander and cold eddy movement 02 p0696 N94-14266
Tracking of change of a warm-core ring structure
02 p0696 N94-14267
Outline of ISY Kuroshio observation experiment
02 p0697 N94-14268
Warm streamers extended from Warm Core Rings (WCR's) and their role on fish migration and fishing ground formation 02 p0697 N94-14270
IAI topic: El Nino. Southern oscillation and interannual climate variability
[INPE-5410-PRE/1757] 03 p1111 N94-15186
Optical properties of the Red Sea
[AD-A266466] 03 p1113 N94-16588
SAR observations in the Gulf of Mexico
03 p1077 N94-16742
Real time system for practical acoustic monitoring of global ocean temperature
[AD-A267868] 03 p1113 N94-17391
Meridional circulation in the tropical north atlantic
[AD-A268222] 03 p1114 N94-17555
Wind products for use in coastal wave and surge models
[AD-A269753] 04 p1497 N94-18414
ADCIRC: An advanced three-dimensional circulation model for shelves, coasts, and estuaries. Report 3: Development of a tidal constituent database for the western North Atlantic and Gulf of Mexico
[AD-A268685] 04 p1497 N94-18455
Acoustic travel time perturbations due to an internal tide and internal wave field in the Barents Sea
[AD-A270879] 04 p1499 N94-19580
Shipboard ADCP observations during RRS Charles Darwin Cruise 62
[IOS-298-1992] 05 p1882 N94-20531
Offshore decision support system: ERS-1 pilot project WAVEWATCH
[BCRS-92-09] 05 p1865 N94-20532
Ocean mapping using satellite radar altimetry
[ETN-93-93470] 05 p1841 N94-21017
Estimating the rotation rate of mesoscale ocean rings from satellite altimetry
[AD-A272922] 05 p1883 N94-21222
Comparison of satellite-derived velocity fields in the coastal transition zone
[AD-A272565] 05 p1883 N94-21360
Acoustic monitoring of global ocean variability
[AD-A271998] 05 p1883 N94-21366
Green Sheet project: Dye sheet evolution
[AD-A272019] 05 p1883 N94-21443
Influence of geoid model uncertainty on the determination of ocean circulation with satellite altimetry
[PB93-219301] 05 p1842 N94-22097
HERACLITUS, phase 1. Harbour Entrance of Rotterdam Radar based Current Related Information for Traffic Guidance of Ships: Feasibility of deriving current profile data from sea surface observations in the Rotterdam (Netherlands) port entrance
[BCRS-93-04] 06 p2417 N94-24107
An efficient data assimilation algorithm with a gaussian covariance structure
[AD-A273152] 06 p2418 N94-24671
Vertical motion in the SYNOP central array
[AD-A273593] 06 p2418 N94-24795
A study on structure of benthic boundary layer in coastal waters
[REPT-4] 07 p2898 N94-25635
Hydrographic and Acoustic Doppler Current Profiler (ADCP) data from the ONR eastern boundary current accelerated research initiative, 9-16 June 1992
[AD-A274115] 07 p2898 N94-26076
Meeting of the Eighth Session of the Scientific Advisory Committee of the World Climate Impact Assessment and Response Strategies Programme
[DE93-633954] 07 p2866 N94-26163
An XCP user's guide and reference manual
[AD-A274519] 07 p2900 N94-27090
An oceanographical observation in the Western Pacific and international cooperations 07 p2872 N94-28272
Global atmospheric and ocean modeling on the connection machine
[DE94-003930] 08 p3342 N94-28521
The velocity field in the Northeast Atlantic from satellite-tracked drifting buoys
[AD-A275704] 08 p3376 N94-28690
Papers in meteorology and geophysics, vol. 44, no.1
[JTN-94-80585] 08 p3324 N94-28693
The Japan Sea proper water and water circulation in the Japan Sea 08 p3324 N94-28694
Development and application of a thermistor current meter
[AD-A275816] 08 p3286 N94-28831
A model analysis of potential vorticity on isopycnal surfaces for the global ocean
[AD-A275047] 08 p3377 N94-29164
SAR-related stress variability in the Marine Atmospheric Boundary Layer (MABL)
[AD-A275275] 08 p3377 N94-29436
Modeling deep equatorial circulation
08 p3378 N94-29815
Atmosphere, ocean, and land: Critical gaps in Earth system models 08 p3350 N94-30617
Cryosphere and climate 08 p3352 N94-30632
Methods of testing parameterizations: Vertical ocean mixing 08 p3352 N94-30633
Altimeter data processing from sea surface topography to horizontal eddy momentum fluxes
[PB94-147550] 08 p3378 N94-30714
General ocean circulation 09 p3777 N94-30984
Low frequency variability observed in the tropical Atlantic Ocean 09 p3778 N94-30991
The effect of westerly wind bursts on a tropical ocean general circulation model
[AD-A276423] 09 p3788 N94-31448
Observations of turbulence, internal waves and background flows: An inquiry into the relationships between scales of motion 09 p3705 N94-31988
Three dimensional vorticity field in the California current system
[AD-A276951] 09 p3788 N94-32220
Estimating subpycnocline density fluctuations in the California current region from upper ocean observations
[AD-A277278] 09 p3789 N94-32325
Deep water studies of CTD data
[AD-A277741] 09 p3791 N94-33176
Cruise report: Oceanus 250 leg 4 high resolution profiler survey for the North Atlantic Tracer Release Experiment, 25 March - 24 April, 1992
[AD-A277935] 09 p3791 N94-33245
The study of the Mediterranean outflow
[AD-A277742] 10 p4091 N94-33445
CO2 impulse response curves for GWP calculations
[DE94-004277] 10 p4081 N94-33736
Bottom boundary layer stress measurements with BASS tripods: Data report STRESS 1988-1989
[AD-A277864] 10 p4092 N94-33775
Operational Baltic Sea circulation model. Part 1: Baratropic version
[PB94-149101] 10 p4093 N94-34143
Modernization of the graphics post-processors of the Hamburg German Climate Computer Center Carbon Cycle Codes
[DE94-011604] 11 p4288 N94-36273
Cooling of the West Spitzbergen Current: Wintertime observations west of Svalbard
[AD-A280648] 12 p4475 N94-36762
Simple ocean carbon cycle models
[DE94-011745] 12 p4477 N94-37494

OCEAN DATA ACQUISITIONS SYSTEMS

One-year mooring of an ADCP in the central region of the Kuroshio west of Okinawa 01 p0194 N94-11913
Acoustic Doppler current profiling of the Kuroshio over the East China Sea shelf slope
01 p0194 N94-11914
Measurement of the surface layer current averaged vertically using Multipaths Inverted Echosounder
01 p0194 N94-11915
Acoustic characteristics of side scan sonar and sub-bottom profiler for 10,000 m class ROV
01 p0172 N94-11916
The development of phytoplankton sensing system with optical fiber 01 p0203 N94-11967
Ocean measuring experiments using optical fiber distributed temperature sensor 01 p0172 N94-11968
ERS-1 and Almaz SAR ocean wave imaging over the Gulf Stream and the Grand Banks
01 p0251 N94-12505
Proceedings of the PORSEC 1992 in Okinawa: Conference for Pacific Ocean Environments and Probing, volume 2
[JTN-93-80419] 01 p0207 N94-12635
A surface water monitoring system: A device for the sea-truth observations 01 p0210 N94-12657
ADCP evidence for upper layer circulation in northeast of the South China Sea 01 p0215 N94-12686
Development of a shuttle AUV for oceanographic measurement 01 p0217 N94-12692
Integrated marine survey system
01 p0217 N94-12693
Development of a buoy system for monitoring marine weather and marine life abundance
01 p0217 N94-12694
Laser photoheterodyne interferometers for oceanographic investigations 01 p0177 N94-12732
Autonomous self contained bottom pop-up stations for study of the benthic layer and seismicity of the ocean's bottom 01 p0224 N94-12735
DISTERM: A shipboard data system for satellite monitoring of ocean and atmosphere
01 p0226 N94-12749
The structure of hydrophysical measuring systems of vertical sounding and self-contained stations
01 p0227 N94-12751
Buoy experiments to obtain the sea-truth data for OCTS/NSCAT, part 1
[NASDA-CNT-930005-PT-1] 02 p0725 N94-13653
Phase aligner for the Electronically Scanned Thinned Array Radiometer (ESTAR) instrument
[NASA-TM-4518] 02 p0623 N94-13878
ERS-1 system
[ESA-SP-1146] 02 p0699 N94-14353

The IOSDL SeaSoar hydraulic unit
[IOS-300-1992] 03 p1114 N94-17516
CTD and XBT data collected on ERS-1 validation cruise RRS Charles Darwin Cruise 62A, Iceland-Faeroes region
[IOS-294-1992] 04 p1461 N94-18063
CTD oxygen, tracer and nutrient data from RRS Charles Darwin Cruises 58/59 in the NE Atlantic as part of Vivaldi 1991
[IOS-296-1992] 04 p1496 N94-18065
SeaSoar CTD, fluorescence and scalar irradiance data from RRS Charles Darwin Cruises 58/59, NE Atlantic, Vivaldi 1991
[IOS-299-1992] 04 p1496 N94-18066
Modifications of airborne oceanographic lidar for the long range P-3 missions
[NASA-CR-194682] 04 p1499 N94-18819
Method for extracting tidal and inertial motion from ARGOS ice buoys applied to the Barents Sea during CEAREX
[PB93-190213] 04 p1499 N94-19063
Shipboard ADCP observations during RRS Charles Darwin Cruise 62
[IOS-298-1992] 05 p1882 N94-20531
SeaWiFS technical report series. Volume 9: The simulated SeaWiFS data set, version 1
[NASA-TM-104566-VOL-9] 06 p2417 N94-23291
An oceanographical observation in the Western Pacific and international cooperations 07 p2872 N94-28272
Global Acoustic Mapping of Ocean Temperatures (GAMOT)
[AD-A275777] 08 p3376 N94-28740
Profiling ALACE instruments
[AD-A277246] 09 p3789 N94-32321
Long transect seafloor seismic array: A component of SAMSON (Sources of Ambient Micro Seismic Ocean ic Noise)
[AD-A277009] 09 p3789 N94-32401
SEASOAR and CTD observations during a COARE surveys cruise, W9211C, 22 January - 22 February, 1993
[AD-A277925] 09 p3791 N94-33244
Tracking system options for future altimeter satellite missions 11 p4205 N94-35622

OCEAN DATA PLATFORMS
U OCEAN DATA ACQUISITIONS SYSTEMS

OCEAN DATA STATIONS
U OCEAN DATA ACQUISITIONS SYSTEMS

OCEAN DYNAMICS
Normal modes of the world's oceans: A numerical investigation using Proudman functions
[NASA-TM-104587] 01 p0288 N94-11358
Use of ERS-1 data at Saclant Undersea Research Centre 01 p0233 N94-11714
Mapping of the East Australian current with the ERS-1 SAR and shipborne studies 01 p0234 N94-11717
SAR imaging of dynamical features in the English Channel 01 p0234 N94-11721
SAR ocean imaging in the Gulf of Alaska 01 p0235 N94-11723
Comparisons of ERS-1 altimeter height data and the Fine Resolution Antarctic Model (FRAM) 01 p0235 N94-11725
Air-sea-ice interactions in the Weddell Sea 01 p0239 N94-11753
Space and time variability of the Gulf Stream using ERS-1 ALT-OPR02 data 01 p0242 N94-11769
Circulation of North Pacific Intermediate Water 01 p0206 N94-11985
Shear, strain and thermohaline vertical fine structure in the upper ocean
[AD-A265961] 01 p0289 N94-12348
ERS-1 and Almaz SAR ocean wave imaging over the Gulf Stream and the Grand Banks 01 p0251 N94-12505
A new model for Synthetic Aperture Radar (SAR) images from ocean scatter 01 p0251 N94-12508
On the extraction of ocean wave spectra from ERS-1 SAR wave mode image spectra 01 p0251 N94-12509
Coastal morphodynamics and energetic characteristics of swell studied with ERS-1 SAR 01 p0254 N94-12524
ERS-1 imaging radar over the Waddensea-North Netherlands 01 p0254 N94-12526
Comparison of GEOSAT sea surface height and model-simulated surface dynamic height 01 p0208 N94-12644
Wind-wave and foam dynamics from optical and radar airborne observations 01 p0226 N94-12745
Circulation model experiments of the Gulf Stream using satellite-derived fields
[AD-A266067] 02 p0725 N94-12990
An experimental regional scale climate simulation laboratory
[DE93-015935] 02 p0719 N94-13119
Integration of space and in-situ observations to study atmosphere, ocean and land processes
[NASA-CR-194495] 02 p0683 N94-14500
Nonlinear wave forces on large ocean structures
[AD-A266820] 02 p0683 N94-14902
On the application and evaluation of the relocatable diecast ocean circulation model in coastal and semi-enclosed seas
[AD-A266626] 03 p1112 N94-15771
Observations and modelling of winds and waves during the Surface Wave Dynamics Experiment. Report 1: Intensive observation period IOP-1, 20-31 October 1990
[AD-A266384] 03 p1113 N94-16517
Earth system dynamics: The interrelation of atmospheric, ocean and solid earth dynamics
[NASA-CR-193487] 03 p1081 N94-17444
Statistics and physical oceanography
[AD-A268565] 03 p1115 N94-17598
Two microstrip arrays for interferometric SAR applications 05 p1722 N94-20421
Optical climatology of the Northeast Pacific Ocean
[AD-A271671] 05 p1866 N94-20559
Ocean wave height transformation model using surface roller theory
[AD-A272610] 05 p1883 N94-21423
GEWEX Continental-scale International Project (GCIP) 06 p2411 N94-24376
Statistical methods in physical oceanography
[AD-A273612] 06 p2419 N94-24948
Meeting of the Eighth Session of the Scientific Advisory Committee of the World Climate Impact Assessment and Response Strategies Programme
[DE93-633954] 07 p2866 N94-26163
Topics in longshore currents
[AD-A274788] 07 p2899 N94-26361
A model analysis of potential vorticity on isopycnal surfaces for the global ocean
[AD-A275047] 08 p3377 N94-29164
The dynamics of tropical intraseasonal variability 08 p3371 N94-29741
Modeling deep equatorial circulation 08 p3378 N94-29815
Modeling the Earth System, volume 3
[NASA-CR-194256] 08 p3350 N94-30616
Towards coupled physical-biogeochemical models of the ocean carbon cycle 08 p3350 N94-30618
Dynamic constraints on CO2 uptake by an iron-fertilized Antarctic 08 p3350 N94-30619
The role of sea ice dynamics in global climate change 08 p3350 N94-30620
On the nonlinear dynamics of ocean wave systems 08 p3378 N94-30790
General ocean circulation 09 p3777 N94-30984
Low frequence variability of the ocean atmosphere coupled system 09 p3777 N94-30986
The effect of westerly wind bursts on a tropical ocean general circulation model
[AD-A276423] 09 p3788 N94-31448
Validation support of the ERIM ocean model
[AD-A277364] 09 p3788 N94-32284
ENSO forced variations of the sea surface temperature and adjusted sea level along the west coast of the United States
[AD-A277306] 09 p3789 N94-32327
The study of the Mediterranean outflow
[AD-A277742] 10 p4091 N94-33445
Operational Baltic Sea circulation model. Part 1: Baratropic version
[PB94-149101] 10 p4093 N94-34143

OCEAN FLOOR SPREADING
U SEA FLOOR SPREADING

OCEAN MODELS
Validation of ERS-1 wind and wave data by use of operational forecast models 01 p0233 N94-11710
Use of ERS-1 data at Saclant Undersea Research Centre 01 p0233 N94-11714
Evaluation of two January - June 1992 ERS-1 AMI wind vector data sets 01 p0235 N94-11724
Comparisons of ERS-1 altimeter height data and the Fine Resolution Antarctic Model (FRAM) 01 p0235 N94-11725
Air-sea-ice interactions in the Weddell Sea 01 p0239 N94-11753
Remote sensing and the air-sea boundary layers 01 p0191 N94-11896
Evaluation of ECMWF latent heat flux in TOGA CD-ROM 01 p0195 N94-11921
Circulation of North Pacific Intermediate Water 01 p0206 N94-11985
A new model for Synthetic Aperture Radar (SAR) images from ocean scatter 01 p0251 N94-12508
Proceedings of the PORSEC 1992 in Okinawa: Conference for Pacific Ocean Environments and Probing, volume 2
[JTN-93-80419] 01 p0207 N94-12635
Comparison of GEOSAT sea surface height and model-simulated surface dynamic height 01 p0208 N94-12644
Measurement of eddy structure and movement in the north-east Pacific with the GEOSAT altimeter 01 p0209 N94-12647
Preliminary results from a satellite altimetric data assimilation using a Kalman filter and smoother 01 p0209 N94-12648
Fluctuations of the Kuroshio extension detected by the GEOSAT altimetry data 01 p0209 N94-12649
Mean flow and variability in the Kuroshio extension from GEOSAT altimetry data 01 p0209 N94-12650
A numerical study of deep convection at high latitudes 01 p0210 N94-12652
Verification of the atmosphere-ocean radiative transfer parametric models 01 p0225 N94-12738
Convective and dynamic instability in meridional trenches 01 p0225 N94-12739
Atmospheric correction for determination of average SST fields based on AVHRR data 01 p0227 N94-12750
Coupled numerical model for altimetric data assimilation and velocity field analysis 01 p0227 N94-12752
Complex (hydrodynamic, satellite) monitoring of dynamic structures in the western Pacific with the aim of forecasting the marine ecosystems behaviour 01 p0227 N94-12753
Mesoscale dynamic structures of the Subarctic Frontal Zone in the Pacific Ocean 01 p0227 N94-12754
Generation of internal waves near the shelf boundary 01 p0229 N94-12763
Experimental and theoretical investigation of undular bore formation upstream the bank 01 p0229 N94-12764
Model of Kuroshio region circulation 01 p0229 N94-12765
Problem of climate change predictability and satellite radiation budget observations 01 p0229 N94-12766
Circulation model experiments of the Gulf Stream using satellite-derived fields
[AD-A266067] 02 p0725 N94-12990
Radar imaging of sub-mesoscale ocean phenomena
[AD-A266339] 02 p0725 N94-13581
Exploring the southern ocean response to climate change
[NASA-CR-194601] 03 p1112 N94-15680
On the application and evaluation of the relocatable diecast ocean circulation model in coastal and semi-enclosed seas
[AD-A266626] 03 p1112 N94-15771
Observations and modelling of winds and waves during the Surface Wave Dynamics Experiment. Report 1: Intensive observation period IOP-1, 20-31 October 1990
[AD-A266384] 03 p1113 N94-16517
The use of General Circulation Models in detecting climate change induced by greenhouse gases
[DE93-014369] 03 p1096 N94-16802
Real time system for practical acoustic monitoring of global ocean temperature
[AD-A267868] 03 p1113 N94-17391
Report detailing modifications to the 1/8 degree global bathymetry
[AD-A268178] 03 p1114 N94-17509
Statistics and physical oceanography
[AD-A268565] 03 p1115 N94-17598
The performance of drag relations in the WAQUA storm surge model
[KNMI-TR-149] 04 p1496 N94-17923
Coastal Ocean Modeling Workshop
[AD-A268955] 04 p1497 N94-18393
ADCIRC: An advanced three-dimensional circulation model for shelves, coasts, and estuaries. Report 3: Development of a tidal constituent database for the western North Atlantic and Gulf of Mexico
[AD-A268685] 04 p1497 N94-18455
Preparation of data assimilation and model evaluation experiment data sets
[AD-A269996] 04 p1498 N94-18665
Work plan for the Marine Aerosol Properties and the Thermal Imager Performance Trial (MAPTIP)
[AD-A270026] 04 p1483 N94-18712
DYNLET1 model formulation and user's guide
[AD-A269843] 04 p1498 N94-18723
Connection machine software conversion of a Navy oceans model
[AD-A269876] 04 p1535 N94-18772
Estimating the oceanic sound speed environmental for long-range acoustic propagation
[AD-A270231] 04 p1499 N94-18903
Modeling of current features in Gulf Stream SAR imagery
[AD-A270734] 04 p1499 N94-19609
A laboratory model of a cooled continental shelf
[AD-A270862] 04 p1500 N94-19792

SIMBAT theoretical manual
[AD-A271063] 05 p1882 N94-19979
The CSIRO 9-level atmospheric general circulation model
[CSIRO-TP-26] 05 p1855 N94-20256
Processing of climatological data for model initialization
[AD-A271878] 05 p1865 N94-20487
Seafloor characterization/Galapagos propagating rift
[AD-A272001] 05 p1882 N94-20581
Estimating the rotation rate of mesoscale ocean rings from satellite altimetry
[AD-A272922] 05 p1883 N94-21222
Ocean wave height transformation model using surface roller theory
[AD-A272610] 05 p1883 N94-21423
Green Sheet project: Dye sheet evolution
[AD-A272019] 05 p1883 N94-21443
VIERS-1, phase 3
[BCRS-92-24] 06 p2381 N94-23145
Monte Carlo climate change forecasts with a global coupled ocean-atmosphere model
[MPIM-97] 06 p2407 N94-23156
Climate variability in a coupled GCM. Part 2: The Indian Ocean and monsoon
[MPIM-104] 06 p2401 N94-23159
Modal structure of variations in the tropical climate system. Part 2: Origins of the low-frequency mode
[MPIM-96] 06 p2407 N94-23199
Global ocean modeling on the Connection Machine
[DE94-000888] 06 p2417 N94-23517
HERACLITUS, phase 1. Harbour Entrance of Rotterdam Radar based Current Related Information for Traffic Guidance of Ships: Feasibility of deriving current profile data from sea surface observations in the Rotterdam (Netherlands) port entrance
[BCRS-93-04] 06 p2417 N94-24107
Techniques and resources for storm-scale numerical weather prediction 06 p2414 N94-24392
An efficient data assimilation algorithm with a gaussian covariance structure
[AD-A273152] 06 p2418 N94-24671
Global acoustic mapping of ocean temperatures (GAMOT)
[AD-A273387] 06 p2418 N94-24719
Vertical motion in the SYNOP central array
[AD-A273593] 06 p2418 N94-24795
Statistical methods in physical oceanography
[AD-A273612] 06 p2419 N94-24948
Seafloor characterization/Galapagos propagating rift
[AD-A273586] 06 p2419 N94-25165
Simulation of the carbon cycle in the oceans
[DE94-000780] 07 p2898 N94-25791
Development and testing of the Coupled Ocean/Atmosphere Mesoscale Prediction System (COAMPS)
[AD-A273925] 07 p2892 N94-25793
Conversion of the CLUSE model for applications over open ocean
[AD-A273750] 07 p2893 N94-26013
Topics in longshore currents
[AD-A274788] 07 p2899 N94-26361
Bathymetric data set extraction program. Users guide
[AD-A274761] 07 p2899 N94-26567
Global atmospheric and ocean modeling on the connection machine
[DE94-003930] 08 p3342 N94-28521
Global Acoustic Mapping of Ocean Temperatures (GAMOT)
[AD-A275777] 08 p3376 N94-28740
A model analysis of potential vorticity on isopycnal surfaces for the global ocean
[AD-A275047] 08 p3377 N94-29164
The dynamics of tropical intraseasonal variability 08 p3371 N94-29741
On the annual cycle of the tropical Pacific atmosphere and ocean 08 p3371 N94-29763
Modeling deep equatorial circulation 08 p3378 N94-29815
Splines and ocean wave modelling
[PB94-139409] 08 p3378 N94-30002
Modeling the Earth System, volume 3
[NASA-CR-194256] 08 p3350 N94-30616
Atmosphere, ocean, and land: Critical gaps in Earth system models 08 p3350 N94-30617
Towards coupled physical-biogeochemical models of the ocean carbon cycle 08 p3350 N94-30618
Dynamic constraints on CO2 uptake by an iron-fertilized Antarctic 08 p3350 N94-30619
The role of sea ice dynamics in global climate change 08 p3350 N94-30620
Four simple ocean carbon models 08 p3351 N94-30625
Methods of testing parameterizations: Vertical ocean mixing 08 p3352 N94-30633
Comprehensive system models: Strategies for evaluation 08 p3353 N94-30638
Subtropical Climates and Their Evolution: From Space-Based Observation to Modelling
[ISBN-2-85-428333-3] 09 p3776 N94-30981
General ocean circulation 09 p3777 N94-30984
Climatologic flux in tropical ocean 09 p3777 N94-30985
The effect of westerly wind bursts on a tropical ocean general circulation model
[AD-A276423] 09 p3788 N94-31448
The influence of cumulus parameterization on model forecasts of rapid oceanic cyclogenesis
[AD-A277207] 09 p3784 N94-32094
Validation support of the ERIM ocean model
[AD-A277364] 09 p3788 N94-32284
Ocean variability and its influence on the detectability of greenhouse warming signals
[DE94-008670] 09 p3790 N94-32881
Quantitative modeling of bottom morphology and subbottom properties
[AD-A278142] 09 p3790 N94-33062
Comparison of numerical models for computing underwater light fields
[AD-A278256] 10 p4140 N94-33411
The study of the Mediterranean outflow
[AD-A277742] 10 p4091 N94-33445
A predictive parametric model for volume scattering strength in the deep ocean with an application to nighttime near-surface scattering in the North Sargasso Sea below 16 kHz
[AD-A277902] 10 p4091 N94-33592
A comparison of modeled and observed ocean mixed layer behavior in a sea breeze influenced coastal region
[AD-A277911] 10 p4092 N94-33922
Coupled ice-ocean model supporting winter navigation in the Baltic Sea. Part 1: Ice dynamics and water levels
[PB94-148780] 10 p4092 N94-34121
Operational Baltic Sea circulation model. Part 1: Baratropic version
[PB94-149101] 10 p4093 N94-34143
Modernization of the graphics post-processors of the Hamburg German Climate Computer Center Carbon Cycle Codes
[DE94-011604] 11 p4288 N94-36273
Atmospheric gas
[DE94-007439] 12 p4465 N94-37187

OCEAN SURFACE

Preliminary results on backscattering strength from a wind generated bubbly ocean surface
[AD-A265006] 01 p0287 N94-10490
Topex/Poseidon: A United States/France mission. Oceanography from space: The oceans and climate
[NASA-TM-108253] 01 p0043 N94-10699
Study of the surface circulation to the North of Bransfield Strait, Antarctica
[INPE-5472-TDI/503] 01 p0288 N94-11200
Near surface ocean processes: Acoustical observations, ambient sound, and Langmuir circulation 01 p0288 N94-11447
A C-band wind scatterometer model derived from the data obtained during the ERS-1 calibration/validation campaign 01 p0233 N94-11711
Calibration of ERS-1 altimetry over the North Sea 01 p0234 N94-11716
Preliminary analysis of circulations over the Indian Ocean and adjoining regions using ERS-1 surface winds in the NCMRWF data assimilation system 01 p0234 N94-11719
First results for the simultaneous estimation of the geoid and the sea surface topography by ERS-1 altimeter data 01 p0241 N94-11765
Separation of geoid and sea surface topography in shallow water regions: A first ERS-1 radar altimeter data evaluation 01 p0242 N94-11766
A stochastic-deterministic approach as an alternative to classical cross-over techniques in small ocean basins 01 p0242 N94-11767
ERS-1 radar altimetry over the North Atlantic 01 p0242 N94-11772
Preliminary geophysical investigation with ERS-1 35-day altimeter data 01 p0243 N94-11775
Quick-look monitoring of the sea surface with ERS-1 fast delivery altimeter data 01 p0243 N94-11777
Spatial scales of wave height 01 p0244 N94-11782
Proceedings of the PORSEC 1992 in Okinawa: Conference for Pacific Ocean Environments and Probing, volume 1
[JTN-93-80418] 01 p0191 N94-11894
Remote sensing and the air-sea boundary layers 01 p0191 N94-11896
Effects of wind-roughened sea surface on ocean color remote sensing: Noise derived from reflected light and whitecaps 01 p0191 N94-11898
An algorithm for the detection of mucilage (green slime) in the Adriatic Sea 01 p0191 N94-11900
Remote sensing of the suspended matter distribution with high concentration in China Sea 01 p0192 N94-11901
Statistical study of HF ocean radar echo 01 p0139 N94-11905
Exchange of bay water with ocean current monitored by the NOAA satellite 01 p0193 N94-11908
Variability of wind stress, and sensible and latent heat flux in the North Atlantic during SEASAT 01 p0194 N94-11918
Evaporation and thermal/hydrologic balance in the Pacific 01 p0195 N94-11919
A new expression for the production rate of sea water droplets on the sea surface 01 p0195 N94-11920
Evaluation of ECMWF latent heat flux in TOGA CD-ROM 01 p0195 N94-11921
Air-sea fluxes and universal constants in weak-turbulence theory of surface gravity waves 01 p0195 N94-11922
Sea surface heat flux in the beginning of the Kuroshio 01 p0195 N94-11923
Seasonal variation of the surface mixed layer in the subtropical re-circulation area of the North Pacific during OMLET 01 p0195 N94-11924
Mixed layer heat budget of Kuroshio-Tango triangle using satellite and ship observations 01 p0196 N94-11925
Estimation of solar radiation at the sea surface with geostationary meteorological satellite data 01 p0196 N94-11926
Ocean wave detection by SAR 01 p0197 N94-11932
On the determination of the SAR ocean surface scattering patch size 01 p0197 N94-11933
The optical/computer hybrid processing of extracting ocean wave directional spectrum by airborne photograph 01 p0197 N94-11934
Ocean-ice interaction study of waves and mesoscale features 01 p0197 N94-11935
Time evolution of cross-stream exchange associated with the variations in the Kuroshio 01 p0197 N94-11936
Warm streamers extended from Warm Core Rings (WCRs) and their role on fish migration and fishing ground formation 01 p0198 N94-11938
The Kyucho events in Sukumo Bay induced by Kuroshio front disturbances 01 p0198 N94-11939
The coherent structure in the oceanic turbulence around Japan Islands Chain forced by an air, sea, and solid Earth interaction 01 p0198 N94-11940
Westward propagation of sea surface anomalies in the western North Pacific as seen by the altimeter and radiometer 01 p0198 N94-11941
An application of reduced gravity model to mesoscale eddies 01 p0199 N94-11945
The use of CZCS for primary production estimate in the Pacific 01 p0199 N94-11946
CZCS derived chlorophyll distribution in Antarctic water during austral summer 01 p0199 N94-11947
Seasonal changes of phytoplankton distributions in the Northwest Pacific detected by Coastal Zone Color Scanner 01 p0200 N94-11948
Satellite-derived oceanic features 01 p0200 N94-11949
Particle dynamics in the western subarctic Pacific: Implications from CZCS imagery 01 p0200 N94-11950
High-reflectance water mass in Off-Sanriku area observed by CZCS 01 p0200 N94-11951
Physical processes of microwave backscattering from laboratory wind-wave surfaces 01 p0200 N94-11952
Experiment and results of the Italian activity in the field of ocean microwave backscattering 01 p0200 N94-11953
Measurements of ocean cross-section with a side-looking airborne radar 01 p0201 N94-11954
Dependence of oceanic microwave emission on wind direction 01 p0201 N94-11957
Surface roughness variations across the Iceland-Faroes frontal region observed by the GEOSAT altimeter and NOAA AVHRR 01 p0201 N94-11958
On the variability of wind speeds in the North Western Pacific observed by altimeter/GEOSAT and SSM/I/DMSP 01 p0201 N94-11960
Observation of wind and waves by GEOSAT altimeter 01 p0202 N94-11961
Availability of wind field over the North Pacific derived from data on ships-of-opportunity and analysis of long-term variabilities 01 p0202 N94-11962
Wind field estimate by using one hour GMS data 01 p0202 N94-11963
The Pacific responses exhibited by an OGCM to various wind fields 01 p0202 N94-11964
Development of shipboard ocean lidar 01 p0140 N94-11965

Bi-directional reflectance by oceanic waters studied via Monte-Carlo simulations 01 p0203 N94-11971
Optical characteristics in Tokyo Bay 01 p0204 N94-11972
Remote sensing for numerical modelling of radiative transfer processes in ocean environment 01 p0204 N94-11973
Observations of the fractal properties of the Japan sea surface temperature patterns 01 p0205 N94-11984
Sea surface temperature anomalies in the Arabian Sea 01 p0206 N94-11988
Preliminary analysis of the FLIP array data from the NOBS experiment [AD-A265911] 01 p0289 N94-12349
A statistical analysis of sea state surface ERS-1 SAR-wave mode imagettes 01 p0251 N94-12507
Ship traffic monitoring using the ERS-1 SAR 01 p0253 N94-12521
Topography of the Western Mediterranean from the ERS-1 altimeter 01 p0255 N94-12531
Proceedings of the PORSEC 1992 in Okinawa: Conference for Pacific Ocean Environments and Probing, volume 2 [JTN-93-80419] 01 p0207 N94-12635
Analysis of GEOSAT wind data 01 p0207 N94-12636
SSMI wind speed variability over the Pacific Ocean 01 p0207 N94-12637
Observation of wave crests by satellite remote sensed data 01 p0207 N94-12638
Observations of eddy fields in the Northwest Pacific by GEOSAT altimetry 01 p0207 N94-12639
Variability of sea level and sea surface temperature anomalies in the equatorial Pacific 01 p0208 N94-12640
Theory and oceanographic applications of satellite altimeter measurements 01 p0208 N94-12641
Analysis of collinear passes of satellite altimeter data 01 p0208 N94-12642
Surface eddy fluxes from the GEOSAT satellite altimeter 01 p0208 N94-12643
Comparison of GEOSAT sea surface height and model-simulated surface dynamic height 01 p0208 N94-12644
Principal oscillation pattern analysis of sea level variations in the tropical Pacific measured by the GEOSAT altimeter 01 p0209 N94-12646
Measurement of eddy structure and movement in the north-east Pacific with the GEOSAT altimeter 01 p0209 N94-12647
Preliminary results from a satellite altimetric data assimilation using a Kalman filter and smoother 01 p0209 N94-12648
Fluctuations of the Kuroshio extension detected by the GEOSAT altimetry data 01 p0209 N94-12649
Mean flow and variability in the Kuroshio extension from GEOSAT altimetry data 01 p0209 N94-12650
Pacific rim sea ice as observed with the NIMBUS-7 SMMR 01 p0210 N94-12651
The seasonal change of phytoplankton size distribution using optical fiber sensor 01 p0210 N94-12656
A surface water monitoring system: A device for the sea-truth observations 01 p0210 N94-12657
The phytoplankton bloom in the Kinu-ura Bay, Japan in the rainy season 01 p0211 N94-12660
Evaluating the spread of red soil with LANDSAT TM data in coral reefs of Okinawa main island, southwestern Japan 01 p0212 N94-12668
Measurement of the sea surface emissivity 01 p0213 N94-12672
Evaluation of the method of geostrophic flow using NOAA-AVHRR data 01 p0213 N94-12673
Satellite observations of the northeast monsoon coastal current 01 p0214 N94-12678
Aspects of applying a relaxation method to computing sea surface velocities from sea surface temperature images 01 p0214 N94-12679
Sea surface temperature difference between NOAA/AVHRR and in-situ observation 01 p0215 N94-12680
Statistical features of mesoscale eddies at the Kuroshio front 01 p0215 N94-12682
Intrusion of Kuroshio warm water into Sagami Bay 01 p0215 N94-12683
A study of front dynamics off northeastern Taiwan based on the NOAA-AVHRR satellite remote sensing data 01 p0215 N94-12684
Satellite thermal variations of Kuroshio in relation to storm floods 01 p0215 N94-12685
Frontal zones in Pacific Ocean: Satellite and ship data analysis 01 p0216 N94-12687
Swordfish (Xiphias gladius) catch distributions relative to environmental features observed from satellites off Coquimbo, Chile (30 deg S) 01 p0216 N94-12688
Observation of cold coastal water with high turbidity around the southwestern tip of Korean Peninsula 01 p0216 N94-12689
On the error characteristics of the sea surface temperature observed by satellite 01 p0216 N94-12690
Seasonal variability of surface ocean color in the Omura Bay using multitemporal LANDSAT-5 TM data 01 p0218 N94-12698
Study on air-sea interactions in the OMLET (Ocean Mixed Layer Experiment) area using satellite remote sensing 01 p0220 N94-12710
The warm eddy detection from NOAA/AVHRR thermal images using the Hough transformation 01 p0220 N94-12713
Applicability of satellite infrared data for the monitoring of coastal environments 01 p0220 N94-12714
Satellite and moored buoy observations of polar frontal system over the Yamato Rise in the Japan Sea 01 p0221 N94-12715
The relationship between skin and bulk sea surface temperatures 01 p0221 N94-12716
Variability of the Kuroshio observed from satellite thermal imagery 01 p0221 N94-12717
Variability of the mixed layer depth in the North Pacific Ocean as calculated by a 3-D semi-analytical mixed layer remote sensing model 01 p0221 N94-12718
SST assimilation: Eastern Mediterranean case study 01 p0221 N94-12719
Mapping of high density area of benthic diatom in Ariake Sea 01 p0222 N94-12720
Advective surface velocity in the north west Pacific derived from NOAA AVHRR images 01 p0222 N94-12721
Polarisation of backscattering radiation at remote sensing of ocean with impulse laser beam 01 p0177 N94-12722
The method of investigation of the horizontal structure of the thermal fronts 01 p0222 N94-12723
On a nonstationary dynamics of the north-west Pacific Ocean 01 p0222 N94-12724
Optimum selection of spectral channels in the problem of remote sensing of phytoplankton concentration in ocean water 01 p0223 N94-12726
Field research of wind wave spectrum variability 01 p0223 N94-12727
Influence of the Kuroshio warm-core rings on hydrographic and fishery conditions off southern Kuril Islands 01 p0224 N94-12737
Spatial variability of the ocean underwater dynamic noise from satellite radar sensing data 01 p0225 N94-12740
Observations of film slicks and internal waves with Ka-band scatterometer 01 p0225 N94-12741
Optical transfer operator of the atmosphere-ocean system 01 p0225 N94-12742
Variability of spectral reflectance in coastal waters near the river plumes 01 p0226 N94-12744
Wind-wave and foam dynamics from optical and radar airborne observations 01 p0226 N94-12745
Observations of surface signatures in the north-west Pacific Ocean with the spaceborne SAR 01 p0226 N94-12746
Radar observation of internal waves field in the north-west Pacific 01 p0226 N94-12747
Atmospheric correction for determination of average SST fields based on AVHRR data 01 p0227 N94-12750
Coupled numerical model for altimetric data assimilation and velocity field analysis 01 p0227 N94-12752
Complex (hydrodynamic, satellite) monitoring of dynamic structures in the western Pacific with the aim of forecasting the marine ecosystems behaviour 01 p0227 N94-12753
Mesoscale dynamic structures of the Subarctic Frontal Zone in the Pacific Ocean 01 p0227 N94-12754
A possibility to define the location of epipelagic fish concentrations with assistance of satellite sensing 01 p0228 N94-12757
High biological production of the tidal mixing zones on Japan Sea shelf 01 p0228 N94-12758
Study of the admixture diffusion in the sea using remote techniques 01 p0228 N94-12759
The algorithm of primary production determination 01 p0228 N94-12761
Non-image visible polarization remote sensing of the ocean 01 p0229 N94-12762
Generation of internal waves near the shelf boundary 01 p0229 N94-12763
Experimental and theoretical investigation of undular bore formation upstream the bank 01 p0229 N94-12764
Model of Kuroshio region circulation 01 p0229 N94-12765
DMSP F11 SSM/T-2 calibration and validation [AD-A265817] 02 p0719 N94-12978
Error analysis of real time and post processed or bit determination of GFO using GPS tracking [NASA-CR-193646] 02 p0512 N94-13238
Radar imaging of sub-mesoscale ocean phenomena [AD-A266339] 02 p0725 N94-13581
Artificial oil pollution detection and wave observation in the sea adjacent to Japan by ERS-1 SAR 02 p0688 N94-14212
Image processing and analysis of airborne POLDER data 02 p0689 N94-14219
Outline of ISY sea surface temperature data sets 02 p0696 N94-14261
Integration of SST data sets using MOS-1 satellite data: For validation and monitoring 02 p0696 N94-14262
Geophysical validation of ATSR sea surface temperatures 02 p0696 N94-14263
Accuracy validation test of estimated sea surface temperature by satellite data 02 p0696 N94-14264
Sea surface effect on the sea surface temperature estimation by satellite data 02 p0696 N94-14265
On the sea truth data of the Kuroshio meander and cold eddy movement 02 p0696 N94-14266
Tracking of change of a warm-core ring structure 02 p0696 N94-14267
Outline of ISY Kuroshio observation experiment 02 p0697 N94-14268
Warm streamers extended from Warm Core Rings (WCR's) and their role on fish migration and fishing ground formation 02 p0697 N94-14270
Fine scale measurements of microwave backscatter from the ocean surface [AD-A264516] 03 p1111 N94-15134
Arctic internal waves (CEAREX) [AD-A265822] 03 p1111 N94-15139
Testing the waters from space --- Thermal mapping [NASA-TM-109623] 03 p1082 N94-15409
Exploring the southern ocean response to climate change [NASA-CR-194601] 03 p1112 N94-15680
Observations and modelling of winds and waves during the Surface Wave Dynamics Experiment. Report 1: Intensive observation period IOP-1, 20-31 October 1990 [AD-A266384] 03 p1113 N94-16517
Field observations of infragravity, sea and swell directional spectra [AD-A266439] 03 p1113 N94-16561
Investigation of AIRSAR signatures of the Gulf Stream 03 p1077 N94-16743
Preliminary estimates of frequency-direction spectra derived from the SAMSON pressure gage array, November 1990 to May 1991 [AD-A267960] 03 p1114 N94-17497
Rapid oceanic cyclogenesis studies [AD-A269258] 04 p1490 N94-18265
Wind products for use in coastal wave and surge models [AD-A269753] 04 p1497 N94-18414
Full Boltzmann discrete spectral wave model, implementation and nondimensional tests [AD-A269885] 04 p1498 N94-18685
Development of ISY data set, part 2 [NASDA-CNT-930006-PT-2] 04 p1463 N94-19384
The split-step algorithm for microwave propagation modeling above a conducting surface [FEL-92-A430] 04 p1390 N94-19447
Acoustic travel time perturbations due to an internal tide and internal wave field in the Barents Sea [AD-A270879] 04 p1499 N94-19580
Modeling of current features in Gulf Stream SAR imagery [AD-A270734] 04 p1499 N94-19609
Remote sensing of Earth terrain [NASA-CR-194598] 04 p1464 N94-19681
Theoretical and experimental research on coherent microwave backscatter from the ocean [AD-A271276] 04 p1500 N94-19743
Measurements of ocean surface and bottom backscattering strengths in the northwestern Atlantic Ocean [AD-A270893] 04 p1500 N94-19786
SIMBAT theoretical manual [AD-A271063] 05 p1882 N94-19979
ERS-1 and Seasat scatterometer measurements of ocean winds: Model functions and the directional distribution of short waves 05 p1720 N94-20412
Ku-band ocean radar backscatter observations during SWADE 05 p1720 N94-20413
Analysis of Ku-band cross section at low incidence angles 05 p1720 N94-20414
Comparison of remote sensing measurements with a two-scale polarimetric emission and scattering model for sea surfaces 05 p1721 N94-20415
Two microstrip arrays for interferometric SAR applications 05 p1722 N94-20421
Near grazing scattering from non-Gaussian ocean surfaces 05 p1726 N94-20438

Rough surface scattering from moving ocean surfaces as an indicator of scattering mechanisms
05 p1726 N94-20439
Polarimetric thermal emission from rough surfaces
05 p1727 N94-20441
Polarimetric thermal emission from periodic water surfaces 05 p1728 N94-20445
A theoretical and numerical study of polarimetric scattering and emission from random rough surfaces with anisotropic directional spectrum
05 p1730 N94-20454
Use of microwave polarimetry to enhance SAR images of the ocean surface
[AD-A271911] 05 p1882 N94-20489
Optical climatology of the Northeast Pacific Ocean
[AD-A271671] 05 p1866 N94-20559
Four-dimensional remote sensing of the marine boundary layer with a digital beamforming radar wind profiler
[AD-A270627] 05 p1882 N94-20564
Neural network studies
[AD-A271593] 05 p1943 N94-20947
Models of refraction in the marine atmosphere surface layer
[AD-A271724] 05 p1858 N94-21357
Airborne surface backscattering strength measurements in the western Atlantic Ocean
[AD-A271737] 05 p1883 N94-21358
Presenting the Rain-Sea Interaction Facility
[NASA-RP-1322] 05 p1884 N94-21628
Marine boundary layer model evaluation by using a height gain measurement technique in the interference region 05 p1777 N94-22145
Modes of ocean variability in the tropical Pacific as derived from Geosat altimetry
[MPIM-103] 06 p2382 N94-23158
Global ocean modeling on the Connection Machine
[DE94-000888] 06 p2417 N94-23517
The effect of sub-surface volume scattering on the accuracy of ice-sheet altimeter retracking algorithms
[NASA-CR-194825] 06 p2386 N94-24060
Factors affecting the identification of phytoplankton groups by means of remote sensing
[NASA-TM-108799] 06 p2387 N94-24403
Free-surface/vorticity interaction
[AD-A273263] 06 p2335 N94-24686
Use of microwave polarimetry to enhance SAR images of the ocean surface
[AD-A273568] 06 p2419 N94-24944
Interpreting the implied meridional oceanic energy transport in AMIP
[DE94-001538] 07 p2898 N94-26072
A comparative evaluation of SAR and SLAR
[DE94-002922] 07 p2848 N94-26277
Nonlinear ocean waves
[AD-A274651] 07 p2899 N94-26354
The NOGAPS ten year AMIP integration
[AD-A274332] 07 p2900 N94-26887
Acoustic bubble sizing, using active and passive techniques to compare ambient and entrained populations
[ISVR-TR-229] 07 p2807 N94-28172
Sea ice and oceans applications of SAR
08 p3327 N94-28934
Tohoku district observed by artificial satellites
08 p3328 N94-29041
A model analysis of potential vorticity on isopycnal surfaces for the global ocean
[AD-A275047] 08 p3377 N94-29164
SAR-related stress variability in the Marine Atmospheric Boundary Layer (MABL)
[AD-A275275] 08 p3377 N94-29436
Radar returns from a low-flying target over a rough sea surface under multipath and clutter conditions
08 p3253 N94-29882
Splines and ocean wave modelling
[PB94-139409] 08 p3378 N94-30002
The influence of the evaporation duct on the angle of arrival and amplitude of the backscattered signal from targets low above the sea 08 p3256 N94-30498
Altimeter data processing from sea surface topography to horizontal eddy momentum fluxes
[PB94-147550] 08 p3378 N94-30714
The validation of ocean surface heat fluxes in AMIP
[DE94-001539] 08 p3378 N94-30823
The effects of altimeter sampling characteristics: Some Geosat examples
[AD-A276899] 09 p3747 N94-32214
Validation support of the ERIM ocean model
[AD-A277364] 09 p3788 N94-32284
Almaz marine applications 09 p3751 N94-32544
A comparison of rough surface parabolic equation models
[AD-A278090] 09 p3791 N94-33185
An approximate model for vertical polarization and surface roughness using the parabolic equation
[AD-A278091] 09 p3684 N94-33186
Ocean surface roughness from infrared measurements: A failure of shape from reflection
[AD-A278008] 10 p4091 N94-33435
Ocean magnetics
[PB94-149028] 10 p4092 N94-34142
The modelling of the ocean surface image in optical remote sensing 10 p4078 N94-34369
Tracking system options for future altimeter satellite missions 11 p4205 N94-35622
Evaluation of synthetic aperture radar for oil-spill response
[AD-A278796] 11 p4284 N94-35674
Wedge scattering by the method of iteration
[DE94-010404] 11 p4256 N94-36112
Index and bulk parameters for frequency-direction spectra measured at CERC Field Research Facility, September 1992 to August 1993
[AD-A280233] 12 p4476 N94-37135
Experiment on rapidly intensifying cyclones over the Atlantic
[AD-A280365] 12 p4473 N94-37180
Airborne ROWS data report for the high resolution experiment, June 1993
[NASA-TM-104609] 12 p4477 N94-37397

OCEAN TEMPERATURE
NT SEA SURFACE TEMPERATURE
Preliminary results of the comparison of ATSR measurements with in situ sea temperatures
[DE93-013399] 01 p0287 N94-10517
Proceedings of the PORSEC 1992 in Okinawa: Conference for Pacific Ocean Environments and Probing, volume 1
[JTN-93-80418] 01 p0191 N94-11894
Ocean measuring experiments using optical fiber distributed temperature sensor 01 p0172 N94-11968
Remote sensing of subsurface water temperature profile and backscattering coefficient in the China Sea by Ocean Lidar (OLIDAR) 01 p0203 N94-11970
On an upwelling front, propagation of upwelling and vertical velocity in the eastern Arabian Sea during monsoon, 1987 01 p0206 N94-11987
Roles of the NEC and MC in the formation and evolution of the Equatorial Pacific Warm Pool
01 p0206 N94-11990
Shear, strain and thermohaline vertical fine structure in the upper ocean
[AD-A265961] 01 p0289 N94-12348
Proceedings of the PORSEC 1992 in Okinawa: Conference for Pacific Ocean Environments and Probing, volume 2
[JTN-93-80419] 01 p0207 N94-12635
A possibility to define the location of epipelagic fish concentrations with assistance of satellite sensing
01 p0228 N94-12757
Generation of internal waves near the shelf boundary
01 p0229 N94-12763
Real time system for practical acoustic monitoring of global ocean temperature
[AD-A267868] 03 p1113 N94-17391
CTD and XBT data collected on ERS-1 validation cruise RRS Charles Darwin Cruise 62A, Iceland-Faeroes region
[IOS-294-1992] 04 p1461 N94-18063
SeaSoar and CTD sections across the Iceland-Faeroes Front and Faeroe Shetland Channel, August 1990
[IOS-295-1992] 04 p1496 N94-18064
An atlas of bathy-thermograph temperature cross-sections for Coral and Tasman Sea transects from 1960 to 1987
[AD-A268775] 04 p1497 N94-18329
On the sources of North Atlantic deep water
[AD-A270854] 05 p1881 N94-19895
Estimating the rotation rate of mesoscale ocean rings from satellite altimetry
[AD-A272922] 05 p1883 N94-21222
Global acoustic mapping of ocean temperatures (GAMOT)
[AD-A273387] 06 p2418 N94-24719
An XCP user's guide and reference manual
[AD-A274519] 07 p2900 N94-27090
The validation of ATSR measurements with in situ sea temperatures
[DE94-003195] 07 p2852 N94-27875
Global Acoustic Mapping of Ocean Temperatures (GAMOT)
[AD-A275777] 08 p3376 N94-28740
Profiling ALACE instruments
[AD-A277246] 09 p3789 N94-32321
Observations and modelling of winds and waves during the surface wave dynamics experiment. Report 2: Intensive observation period IOP-3
[AD-A278368] 10 p4093 N94-34375
Cooling of the West Spitzbergen Current: Wintertime observations west of Svalbard
[AD-A280648] 12 p4475 N94-36762

OCEANOGRAPHIC PARAMETERS
NT OCEAN TEMPERATURE
NT SEA SURFACE TEMPERATURE
Remote sensing and the air-sea boundary layers
01 p0191 N94-11896
Satellite observations of red tide events: Plans for EESI 01 p0191 N94-11899
An algorithm for the detection of mucilage (green slime) in the Adriatic Sea 01 p0191 N94-11900
Remote sensing of the suspended matter distribution with high concentration in China Sea
01 p0192 N94-11901
Measurement of wave parameters by HF ocean radar
01 p0192 N94-11903
Kuroshio observations by the HF ocean radar
01 p0192 N94-11904
Groundwave HF ocean surface radar
01 p0139 N94-11906
Air-sea interaction: Fluxes, a review
01 p0201 N94-11955
Impact of ERS-1 wind/wave/ice data on operational ocean forecasting 01 p0250 N94-12500
A surface water monitoring system: A device for the sea-truth observations 01 p0210 N94-12657
An integrated approach to total end-to-end quality control of ocean data in the real-time environment
01 p0211 N94-12662
Preliminary estimates of frequency-direction spectra derived from the SAMSON pressure gage array, November 1990 to May 1991
[AD-A267960] 03 p1114 N94-17497
Development and evaluation of alternative radioanalytical methods, including mass spectrometry for marine materials
[DE93-625117] 04 p1345 N94-17691
SeaSoar and CTD sections across the Iceland-Faeroes Front and Faeroe Shetland Channel, August 1990
[IOS-295-1992] 04 p1496 N94-18064
CTD oxygen, tracer and nutrient data from RRS Charles Darwin Cruises 58/59 in the NE Atlantic as part of Vivaldi 1991
[IOS-296-1992] 04 p1496 N94-18065
The marine light-mixed layer experiment cruise and data report: R/V endeavor cruise EN-224, mooring deployment, 27 April-1 May 1991: Cruise EN-227, mooring recovery, 5-23 September 1991
[AD-A271175] 05 p1864 N94-20186
Proceedings of the 15th Earth Observation Symposium
[JTN-94-80607] 08 p3328 N94-29036
Oceanic survey utilizing satellites
08 p3328 N94-29040
The effects of altimeter sampling characteristics: Some Geosat examples
[AD-A275225] 08 p3357 N94-29062
Tidal atlas software development
[AD-A275251] 08 p3377 N94-29432
Application of radon transformation for improved analysis of sparsely sampled data: A feasibility study
[PB94-147535] 09 p3741 N94-31075
Hydrographic service Royal Australian Navy
[AD-A277134] 09 p3788 N94-32066
The effects of altimeter sampling characteristics: Some Geosat examples
[AD-A276899] 09 p3747 N94-32214
Ocean variability and its influence on the detectability of greenhouse warming signals
[DE94-008670] 09 p3790 N94-32881
Forecasters handbook for the Philippine Islands and surrounding waters
[AD-A277993] 09 p3787 N94-33089
SEASOAR and CTD observations during a COARE surveys cruise, W9211C, 22 January - 22 February, 1993
[AD-A277925] 09 p3791 N94-33244
Storm evolution of directional seas in shallow water
[AD-A278541] 10 p4089 N94-33404
Environmental measurements in the Beaufort Sea, Spring 1993
[AD-A278718] 11 p4296 N94-36293
SeaWiFS technical report series. Volume 20: The SeaWiFS bio-optical archive and storage system (SeaBASS), part 1
[NASA-TM-104566-VOL-20-PT-1]
12 p4475 N94-36958
Variability of the California Current System off Point Sur, California from April 1988 to December 1990
[AD-A278579] 12 p4476 N94-36985
Atmospheric gas
[DE94-007439] 12 p4465 N94-37187

OCEANOGRAPHY
Preliminary results of the comparison of ATSR measurements with in situ sea temperatures
[DE93-013399] 01 p0287 N94-10517

Topex/Poseidon: A United States/France mission. Oceanography from space: The oceans and climate
[NASA-TM-108253] 01 p0043 N94-10699
Study of the surface circulation to the North of Bransfield Strait, Antarctica
[INPE-5472-TDI/503] 01 p0288 N94-11200
Validation of directional wave spectra from the ERS-1 during the ESA CAL/VAL campaign
01 p0232 N94-11707
ERS-1 studies at the Department of Oceanography from Space, IFREMER/Brest (France)
01 p0233 N94-11712
Use of ERS-1 data at Saclant Undersea Research Centre 01 p0233 N94-11714
Arctic sea ice microwave signature and geophysical processes study 01 p0240 N94-11754
Spatial scales of wave height
01 p0244 N94-11782
The subduction experiment. Cruise report, R/V Oceanus, cruise number 250 legs 1 and 2. Subduction 2 mooring deployment and recovery cruise, 25 January-26 February 1992
[AD-A264922] 01 p0289 N94-11853
Real-time tomography mooring
[AD-A264923] 01 p0289 N94-11854
The requirement for global training programmes to meet the new remote sensing technology
01 p0196 N94-11929
Remote sensing for numerical modelling of radiative transfer processes in ocean environment
01 p0204 N94-11973
Use of SAR-wave, altimeter, and wind-scatterometer data in an operational swell forecasting system
01 p0250 N94-12503
Real time processing wave spectra from satellite SAR
01 p0251 N94-12506
DISTERM: A shipboard data system for satellite monitoring of ocean and atmosphere
01 p0226 N94-12749
Ocean acoustic processing: A model-based approach
[DE93-011902] 02 p0725 N94-12876
Optimization and eigenvalue computation with application to meteorology and oceanography
[DE93-015310] 02 p0744 N94-13024
Knowledge-based oceanographic image compression
[AD-A265752] 02 p0821 N94-13041
An experimental regional scale climate simulation laboratory
[DE93-015935] 02 p0719 N94-13119
Activities report of the Netherlands Remote Sensing Board
[ETN-93-93880] 02 p0686 N94-14073
Volume 14: The first SeaWiFS intercalibration round-robin experiment, SIRREX-1, July 1992
[NASA-TM-104566-VOL-14] 02 p0725 N94-14090
Short walk to everywhere --- Space, Earth, Ocean Center
[NASA-TM-109541] 03 p1221 N94-15372
State-of-the-art satellite laser range modeling for geodetic and oceanographic applications
03 p0916 N94-15586
On the application and evaluation of the relocatable diecast ocean circulation model in coastal and semi-enclosed seas
[AD-A266626] 03 p1112 N94-15771
Proceedings of the Third Spaceborne Imaging Radar Symposium
[NASA-CR-194104] 03 p0989 N94-15886
The multivariate optimum interpolation analysis of meteorological data at the Fleet Numerical Oceanography Center
[AD-A266459] 03 p1106 N94-16568
SAR observations in the Gulf of Mexico
03 p1077 N94-16742
The Megascience Forum
[DE93-014445] 03 p1303 N94-16804
Adequation of mini satellites to oceanic altimetry missions 03 p0891 N94-17152
Abstracts of manuscripts submitted in 1992 for publication
[AD-A267963] 03 p1113 N94-17383
Arctic cyclones and Marginal Ice Zone (MIZ) variability
[AD-A268610] 03 p1108 N94-17465
Fabrication of a NAVMAP, a deep-sea mapping system
[AD-A268630] 03 p1085 N94-17467
Report detailing modifications to the 1/8 degree global bathymetry
[AD-A268178] 03 p1114 N94-17509
List of the scientific and personal papers of Sir George Deacon, FRS
[IOS-301-1992] 03 p1114 N94-17518
Statistics and physical oceanography
[AD-A268565] 03 p1115 N94-17598
Development and evaluation of alternative radioanalytical methods, including mass spectrometry for marine materials
[DE93-625117] 04 p1345 N94-17691
A one dimensional numerical model, with an application to the vertical distribution of dissolved oxygen in the ocean
[DE93-018481] 04 p1495 N94-17779
Technologies for assessing the geologic and geomorphic history of coasts
[AD-A268780] 04 p1496 N94-18215
Synoptic ocean prediction experiment. EN216 CTD section data report
[AD-A268903] 04 p1497 N94-18230
An atlas of bathy-thermograph temperature cross-sections for Coral and Tasman Sea transects from 1960 to 1987
[AD-A268775] 04 p1497 N94-18329
Overview of physical oceanographic measurements taken during the Mount Mitchell cruise to ROPME sea area
[DE93-018460] 04 p1497 N94-18494
Preparation of data assimilation and model evaluation experiment data sets
[AD-A269996] 04 p1498 N94-18665
Atlas of SSM/I satellite ice concentration interpoiated to operational ice model domains of the Arctic for 1992
[AD-A270306] 04 p1499 N94-18727
Estimating the oceanic sound speed environmental for long-range acoustic propagation
[AD-A270231] 04 p1499 N94-18903
Distribution of turbidity in Australian tropical waters
[AD-A271059] 05 p1881 N94-19905
The marine light-mixed layer experiment cruise and data report: R/V endeavor cruise EN-224, mooring deployment, 27 April-1 May 1991: Cruise EN-227, mooring recovery, 5-23 September 1991
[AD-A271175] 05 p1864 N94-20186
Progress In Electromagnetics Research Symposium (PIERS)
[NASA-CR-194629] 05 p1718 N94-20403
Ocean mapping using satellite radar altimetry
[ETN-93-93470] 05 p1841 N94-21017
Acoustic monitoring of global ocean variability
[AD-A271998] 05 p1883 N94-21366
Low-cost Unmanned Air Vehicle (UAV) for oceanographic research
[AD-A273103] 05 p1646 N94-21507
A synoptic-scale overview of the TOGA COARE intensive observing period November 1992 to February 1993 based on analyses from US operational global data assimilation systems
[NASA-TM-104593] 05 p1868 N94-21605
Influence of geoid model uncertainty on the determination of ocean circulation with satellite altimetry
[PB93-219301] 05 p1842 N94-22097
Global acoustic mapping of ocean temperatures (GAMOT)
[AD-A273387] 06 p2418 N94-24719
Vertical motion in the SYNOP central array
[AD-A273593] 06 p2418 N94-24795
Statistical methods in physical oceanography
[AD-A273612] 06 p2419 N94-24948
Active control of oscillatory lift forces on a circular cylinder
[AD-A273243] 06 p2338 N94-25140
Naval Interactive Data Analysis System (NIDAS), software user's manual
[NASA-CR-195179] 07 p2956 N94-25606
Hydrographic and Acoustic Doppler Current Profiler (ADCP) data from the ONR eastern boundary current accelerated research initiative, 9-16 June 1992
[AD-A274115] 07 p2898 N94-26076
Coupling of pelagic and benthic communities over a seamount in the Eastern North Pacific
[AD-A274750] 07 p2899 N94-26149
Meeting of the Eighth Session of the Scientific Advisory Committee of the World Climate Impact Assessment and Response Strategies Programme
[DE93-633954] 07 p2866 N94-26163
A comparative evaluation of SAR and SLAR
[DE94-002922] 07 p2848 N94-26277
Bibliography of technical reports, 1992
[AD-A274849] 07 p3098 N94-26561
Effects of p-chlorophenol on sulfate reduction in marine sediments 07 p2870 N94-28150
Extraterrestrial accretion and glacial cycles
07 p2890 N94-28308
Global change research: Summaries of research in FY 1993
[DE94-003150] 08 p3341 N94-28473
Papers in meteorology and geophysics, vol. 44, no.1
[JTN-94-80585] 08 p3324 N94-28693
A model analysis of potential vorticity on isopycnal surfaces for the global ocean
[AD-A275047] 08 p3377 N94-29164
Modeling the Earth System, volume 3
[NASA-CR-194256] 08 p3350 N94-30616
Towards coupled physical-biogeochemical models of the ocean carbon cycle 08 p3350 N94-30618
Ocean acoustic propagation measurements and wave propagation in random media
[AD-A276165] 09 p3787 N94-31053
Evaluating success levels of mega-projects
09 p3599 N94-31432
The effects of altimeter sampling characteristics: Some Geosat examples
[AD-A276899] 09 p3747 N94-32214
Almaz marine applications 09 p3751 N94-32544
Forecasters handbook for the Philippine Islands and surrounding waters
[AD-A277993] 09 p3787 N94-33089
Fluid mechanical measurements within the bottom boundary layer over the Northern California continental shelf during stress
[AD-A277916] 09 p3791 N94-33243
Ultraviolet Absorption Spectrometry (UVAS) and Liquid Atomic Emission Spectrometry (LAES) for oceanographic analysis systems
[AD-A278263] 10 p4091 N94-33413
SeaWiFS technical report series. Volume 17: Ocean color in the 21st century. A strategy for a 20-year time series
[NASA-TM-104566-VOL-17] 10 p4093 N94-34209
Oceanography in the next decade: Building new partnerships
[NASA-CR-195926] 10 p4093 N94-34265
SeaWiFS technical report series. Volume 16: The second SeaWiFS Intercalibration Round-Robin Experiment, SIRREX-2, June 1993
[NASA-TM-104566-VOL-16] 10 p4093 N94-34412
Mission to Planet Earth. The living ocean: Observing ocean color from space
[NASA-PAM-554] 11 p4295 N94-35343
Tracking system options for future altimeter satellite missions 11 p4205 N94-35622
Evaluation of synthetic aperture radar for oil-spill response
[AD-A278796] 11 p4284 N94-35674
Variability of the California Current System off Point Sur, California from April 1988 to December 1990
[AD-A278579] 12 p4476 N94-36985
The role of horizontal variability in air-sea interaction
[AD-A280561] 12 p4476 N94-37047

OCEANS

NT ANTARCTIC OCEAN
NT ARCTIC OCEAN
NT ATLANTIC OCEAN
NT INDIAN OCEAN
NT PACIFIC OCEAN
Sandia ocean modeling system programmer's guide and user's manual
[DE93-007427] 01 p0287 N94-10153
Normal modes of the world's oceans: A numerical investigation using Proudman functions
[NASA-TM-104587] 01 p0288 N94-11358
Real-time tomography mooring
[AD-A264923] 01 p0289 N94-11854
The thermodynamic case for a water-rich Mars
01 p0463 N94-12170
Study on diffusion phenomena of river effluents issued into sea around Japan with satellite remote sensing data
01 p0212 N94-12664
Trajectory curving in underwater propagation of light
01 p0226 N94-12748
DISTERM: A shipboard data system for satellite monitoring of ocean and atmosphere
01 p0226 N94-12749
The role of clouds and oceans in global greenhouse warming
[DE93-016206] 02 p0706 N94-13079
Error analysis of real time and post processed or bit determination of GFO using GPS tracking
[NASA-CR-193646] 02 p0512 N94-13238
Ocean uptake of carbon dioxide
[DE93-012967] 02 p0707 N94-13384
Coastal zone color scanner: Nimbus 7
[NASA-TM-109590] 03 p1111 N94-15281
What we can learn about ocean tides from tide gauge and gravity loading measurements?
03 p1100 N94-15811
A study of the observed tidal residue vectors B versus oceanic tidal load vectors L 03 p1100 N94-15813
The influence of oceans on Martian volcanism
03 p1295 N94-16427
AVIRIS calibration and application in coastal oceanic environments 03 p1069 N94-16685
Fabrication of a NAVMAP, a deep-sea mapping system
[AD-A268630] 03 p1085 N94-17467
Statistics and physical oceanography
[AD-A268565] 03 p1115 N94-17598

A one dimensional numerical model, with an application to the vertical distribution of dissolved oxygen in the ocean
[DE93-018481] 04 p1495 N94-17779
Comments on computational underwater acoustics
[DE93-013789] 04 p1562 N94-17873
Synoptic ocean prediction experiment. EN216 CTD section data report
[AD-A268903] 04 p1497 N94-18230
Technology to prevent greenhouse effect gases
[DE94-707421] 05 p1850 N94-19976
A survey of the impact on acoustic propagation of warm core ocean eddys
[AD-A272188] 05 p1883 N94-20925
Estimating the rotation rate of mesoscale ocean rings from satellite altimetry
[AD-A272922] 05 p1883 N94-21222
Simulation of clear-sky outgoing longwave radiation over the oceans using operational analysis 05 p1861 N94-22290
Simulation of the carbon cycle in the oceans
[DE94-000780] 07 p2898 N94-25791
The biostratigraphy and paleogeography of Maastrichtian inoceramids 07 p2889 N94-28303
Quadruplet expansion of the acoustic pressure field in a wedge shaped ocean
[AD-A275121] 08 p3477 N94-29003
Atmosphere, ocean, and land: Critical gaps in Earth system models 08 p3350 N94-30617
The carbon cycle revisited 08 p3350 N94-30622
Ocean-atmospheric linkages 08 p3350 N94-30623
Four simple ocean carbon models 08 p3351 N94-30625
Ocean acoustic propagation measurements and wave propagation in random media
[AD-A276165] 09 p3787 N94-31053
Observations of turbulence, internal waves and background flows: An inquiry into the relationships between scales of motion 09 p3705 N94-31988
Characterization of tidal currents in Monterey Bay from remote and in-situ measurements
[AD-A277844] 10 p4092 N94-33767
A comparison of modeled and observed ocean mixed layer behavior in a sea breeze influenced coastal region
[AD-A277911] 10 p4092 N94-33922
Ocean magnetics
[PB94-149028] 10 p4092 N94-34142
SeaWiFS technical report series. Volume 17: Ocean color in the 21st century. A strategy for a 20-year time series
[NASA-TM-104566-VOL-17] 10 p4093 N94-34209
The life cycles of intense cyclonic and anticyclonic circulation systems observed over oceans
[NASA-CR-196271] 12 p4473 N94-37294

OCTAHEDRAL RESEARCH SATELLITES
U ENVIRONMENTAL RESEARCH SATELLITES

OCTAHEDRITE
U ANATASE

OCTANE
Comparative ignition of hexane and octane isomers in a shock tube
[DE93-016535] 02 p0566 N94-14869

OCTANE NUMBER
CRC customer versus rater octane number requirement program (1990)
[AD-A273997] 07 p2758 N94-25901

OCTAVES
Artificial neural networks: Application to the optical recognition of music partitions
[ETN-94-95166] 06 p2470 N94-22884

OCULOMETERS
Techniques used for the analysis of oculometer eye-scanning data obtained from an air traffic control display
[NASA-CR-191559] 05 p1643 N94-21629
Interactive large screen: A multi-mode dialogue tool for future cockpits 12 p4484 N94-37266
Gaze orientation under G(z)-load. Methodological aspects: Preliminary results 12 p4485 N94-37274

OCULOMOTOR NERVES
Japanese Journal of Aerospace and Environmental Medicine, volume 30, no. 1
[JTN-94-80598] 08 p3369 N94-28850
Basic understanding of vertigo 08 p3390 N94-28855
Equilibrium dysfunction in the clinical field 08 p3390 N94-28858

ODAS
U OCEAN DATA ACQUISITIONS SYSTEMS

ODD-EVEN NUCLEI
High spin properties of nuclei
[DE93-008788] 01 p0358 N94-10254

ODD-ODD NUCLEI
Nuclear structure models: Applications and development
[DE93-012934] 01 p0368 N94-11813

ODORS
Study on improvement of flammability, odor and offgassing tests for materials
[NASDA-CNT-930009] 02 p0563 N94-13471
Flammability, odor, offgassing, thermal vacuum stability, and compatibility with aerospace fluids of wire insulations 08 p3166 N94-28709

OFF-ON CONTROL
Increasing mission reliability using open-loop control
[AD-A271208] 04 p1545 N94-19721

OFFGASSING
Study on improvement of flammability, odor and offgassing tests for materials
[NASDA-CNT-930009] 02 p0563 N94-13471
Space Shuttle solid rocket motor exposure monitoring 03 p0976 N94-16624
Flammability, odor, offgassing, thermal vacuum stability, and compatibility with aerospace fluids of wire insulations 08 p3166 N94-28709

OFFICE AUTOMATION
Concepts and techniques for an active database approach to office procedure support
[PB94-110749] 06 p2590 N94-23816
A machine-learning apprentice for the completion of repetitive forms 10 p4110 N94-34055
Network upgrades 12 p4541 N94-36851

OFFSHORE ENERGY SOURCES
Computer-aided design system for objects location and reservoir with dispersed resource evolution investigation 05 p1923 N94-22064

OFFSHORE PLATFORMS
Nonlinear wave forces on large ocean structures
[AD-A266820] 02 p0683 N94-14902
Fire safety engineering research in Norway
[PB93-201630] 06 p2268 N94-23429

OFT
U SPACE TRANSPORTATION SYSTEM FLIGHTS

OFT 3
U SPACE TRANSPORTATION SYSTEM 3 FLIGHT

OFT 4
U SPACE TRANSPORTATION SYSTEM 4 FLIGHT

OGEE WINGS
U VARIABLE SWEEP WINGS

OGIVES
Pneumatic management of blunted-forebody flow asymmetry for high-angle-of-attack directional control 07 p2679 N94-28028

OGO
The 1966 highlights --- NASA research programs
[NASA-TM-109444] 03 p1302 N94-15343
The 1968 highlights --- NASA programs and research
[NASA-TM-109627] 03 p1302 N94-15413

OH-6 HELICOPTER
Advanced rotorcraft flight simulation: Model development, validation and parallel implementation 01 p0025 N94-11056

OHMIC DISSIPATION
Non-barrier tunneling in presence of dissipations
[DE93-621381] 01 p0412 N94-11086
Elementary mechanism of electron beam dissipative instability development
[DE93-621653] 01 p0391 N94-11209
Spreading of Bimodulated Ultra-relativistic Electron Beam (BUEB) in Atmospheric Plasma Channel (APCh)
[DE93-621658] 01 p0392 N94-11213
Ohmic heating of composite candidate graphite-fiber/coating combinations
[NASA-TM-4491] 02 p0554 N94-12871
Modeling of the coupled magnetospheric and neutral wind dynamos
[NASA-CR-194728] 05 p1856 N94-20537
Complementary heterojunction FET technology for space application 05 p1755 N94-21094
A spheromak ignition experiment reusing Mirror Fusion Test Facility (MFTF) equipment
[DE94-001856] 05 p2034 N94-22050
Time-resolved analytical methods for liquid/solid interfaces
[DE94-008352] 09 p3637 N94-32826
Energy absorption apparatus
[AD-D016163] 10 p4133 N94-33699
Self-similar regimes of subsonic Langmuir wave collapse
[DE94-611466] 11 p4335 N94-35750
Scaling laws for TEXT plasma profiles
[DE94-010832] 11 p4338 N94-36200

OHMS LAW
Nonlinear gyrofluid models of shear Alfven instabilities in ignited and beam heated toroidal plasmas
[DE93-016235] 03 p1203 N94-16869

OHZORA SATELLITE
U EXOS-C SATELLITE

OIL ADDITIVES
Surface species in tribology
[AD-A270970] 04 p1446 N94-19754
The effect of alternative fuels on the stability and lubricity of crankcase lubricants
[DE94-010353] 11 p4245 N94-36108

OIL EXPLORATION
Gulf of Mexico sales 147 and 150: Central and western planning areas. Draft environmental impact statement. Volume 1: Sections 1 through 4.C
[PB93-190304] 01 p0265 N94-11018
Gulf of Mexico sales 147 and 150: Central and western planning areas. Draft environmental impact statement. Volume 2: Sections 4.D through 9
[PB93-190312] 01 p0265 N94-11019
Near-surface seismic imaging
[PB94-119096] 06 p2404 N94-24647
Application of remote sensing techniques in petroleum exploration: The Indonesian experience 08 p3331 N94-29225
ACE: A distributed system to manage large data archives 10 p4156 N94-33818

OIL FIELDS
Information capability of NOAA-AVHRR data for monitoring oceanographic and atmospheric pollution 01 p0214 N94-12677

OIL POLLUTION
A study of pollution courses of spilled oil floatation in the outer ocean 01 p0205 N94-11983
Artificial oil pollution detection and wave observation in the sea adjacent to Japan by ERS-1 SAR 02 p0688 N94-14212
Oil spreading in surface waters with an ice cover
[PB93-190767] 04 p1476 N94-19064

OIL RECOVERY
BOAST 2 for the IBM 3090 and RISC 6000
[DE93-000138] 02 p0638 N94-14351
Responsive copolymers for enhanced petroleum recovery
[DE93-018030] 03 p0971 N94-16999
High-resolution numerical methods for compressible multi-phase flow in hierarchical porous media
[DE94-000740] 05 p1799 N94-20351
Measurement of interfacial tension by use of pendant drop video techniques
[DE93-000168] 06 p2345 N94-24831

OIL SLICKS
Gulf of Mexico sales 147 and 150: Central and western planning areas. Draft environmental impact statement. Volume 1: Sections 1 through 4.C
[PB93-190304] 01 p0265 N94-11018
Gulf of Mexico sales 147 and 150: Central and western planning areas. Draft environmental impact statement. Volume 2: Sections 4.D through 9
[PB93-190312] 01 p0265 N94-11019
Methodologies for estimating air emissions from three non-traditional source categories: Oil spills, petroleum vessel loading and unloading, and cooling towers
[PB93-181592] 01 p0266 N94-11471
A study of pollution courses of spilled oil floatation in the outer ocean 01 p0205 N94-11983
Artificial oil pollution detection and wave observation in the sea adjacent to Japan by ERS-1 SAR 01 p0253 N94-12520
Ship traffic monitoring using the ERS-1 SAR 01 p0253 N94-12521
Oil spill detection using satellite-based SAR: Experience from a field experiment 01 p0253 N94-12522
Observations of film slicks and internal waves with Ka-band scatterometer 01 p0225 N94-12741
Artificial oil pollution detection and wave observation in the sea adjacent to Japan by ERS-1 SAR 02 p0688 N94-14212
Overview of physical oceanographic measurements taken during the Mount Mitchell cruise to ROPME sea area
[DE93-018460] 04 p1497 N94-18494
Oil spreading in surface waters with an ice cover
[PB93-190767] 04 p1476 N94-19064
A comparative evaluation of SAR and SLAR
[DE94-002922] 07 p2848 N94-26277
Ship traffic monitoring and oil spill detection using the ERS-1 SAR 09 p3751 N94-32542
Evaluation of synthetic aperture radar for oil-spill response
[AD-A278796] 11 p4284 N94-35674

OILS
NT CRUDE OIL
NT LUBRICATING OILS
NT MINERAL OILS
NT SHALE OIL
Compatibility of refrigerants and lubricants with motor materials, volume 1
[DE93-040216] 04 p1350 N94-18895
Biofuels: Project summaries
[DE93-010003] 05 p1712 N94-19984
EHD enhancement of pool and in-tube boiling of alternate refrigerants
[DE94-000787] 05 p1798 N94-20101

New technique for oil backstreaming contamination measurements 05 p1652 N94-20511
Navy GTE seal development activity 05 p1655 N94-21794
New methane chemistry synthesis of materials for reversible uptake and useful functionalization of methane
[PB94-112786] 06 p2233 N94-23801
Skin friction measurement in complex flows using thin oil film techniques
[NASA-CR-194872] 06 p2327 N94-24098
Accelerated screening methods for determining chemical and thermal stability of refrigerant-lubricant mixtures. Part 2: Experimental comparison and verification of methods
[DE94-003664] 07 p2749 N94-26007
Oil production from buckwheat stillage by thermochemical liquefaction 07 p2871 N94-28154
Biodiesel from aquatic species
[DE94-000275] 08 p3225 N94-30038
Squeeze film dampers with oil hole feed 10 p4065 N94-34195
Environmental risk management
[DE94-620987] 12 p4467 N94-37492

OKAZAKI-LEVY-RUDENKO COMET
Infrared observations of cometary dust by COBE 08 p3541 N94-29994

OLEFINS
U ALKENES

OLEIC ACID
Contained liquids in microgravity, part 2 03 p0979 N94-16085

OLIGOMERS
Synthesis and polymerization of oligomeric multiple aromatic ether-containing phthalonitriles
[AD-D015729] 01 p0094 N94-12399
Unexpectedly rapid hydrosilation polymerization of the diallyl derivative of bisphenol A and 2,6-diallylphenol
[AD-A265832] 02 p0577 N94-12986
Charge storage and switching phenomena with molecular assemblies of metal complexes
[AD-A266673] 02 p0787 N94-14778
New organic materials for nonlinear optics applications
[AD-A266451] 03 p1192 N94-16563
Photodegradation of MDI based polyurethane/urea elastomers
[AD-A267308] 03 p0971 N94-16994
Nonlinear optical properties of molecules
[AD-A270199] 04 p1567 N94-18783
Oligomer and mixed-metal compounds, potential multielectron transfer catalysts
[DE93-019592] 04 p1350 N94-19017
Cooperative formation of inorganic-organic interfaces in the synthesis of silicate mesostructures
[AD-A271196] 04 p1375 N94-19742
Electrochemical and electronic properties of neural and oxidized soluble orthogonally-fused thiophene oligomers
[AD-A273283] 06 p2260 N94-24815
Metal-catalyzed alkynylation of (Bromophenyl)Oligophenylenes: A rapid route to thermoset precursors of high density monolithic glass-like carbon
[AD-A273219] 06 p2260 N94-24863
Synthesis of molecular wires by a novel divergent/convergent approach
[AD-A273332] 06 p2537 N94-25087
Synthesis and characterization of novel ternary and quaternary reduced molybdenum oxides
[DE94-005563] 08 p3510 N94-28529
Solventless, curable fluid oligomeric systems for high performance microwave, acoustical and mechanical applications 08 p3223 N94-30478
Conjugated polymer fluorescence: Interplay of correlations and alternation
[DE94-005587] 09 p3660 N94-32729
Phenylethynyl endcapping reagents and reactive diluents
[NASA-CASE-LAR-14796-1] 10 p4023 N94-35077
Liquid crystalline thermosetting polyimides
[DE94-009939] 11 p4244 N94-35768
Substituted silyl-terminated compounds and polymers thereof
[AD-D016310] 12 p4427 N94-37779

OLIVINE
NT FORSTERITE
Changes in Hawaiian palagonite FE mineralogy associated with thermal alteration: Implications for Mars 01 p0281 N94-12055
Olivine-rich asteroids, pallasitic olivine and olivine-metal mixtures: Comparisons of reflectance spectra 01 p0431 N94-12171
On high-temperature formation of iron-rich olivine in the early solar system 01 p0432 N94-12225
Micro-zoning in minerals of a Landes silicate inclusion 01 p0432 N94-12231
The Fe2(+)-Mg interdiffusion in orthopyroxene: Constraints from cation ordering and structural data and implications for cooling rates of meteorites 03 p1241 N94-16175
Stalking the LREE-enriched component in ureilites 03 p1241 N94-16190
Angrite LEW87051: Are the olivines pheno's or xeno's? A continuing story 03 p1103 N94-16285
Experimental segregation of iron-nickel metal, iron-sulfide, and olivine in a thermal gradient: Preliminary results 03 p1243 N94-16288
Water in Earth's mantle: Hydrogen analysis of mantle olivine, pyroxenes and garnet using the SIMS 03 p1104 N94-16336
On origin of the olivine inclusions from the Kainsaz CO carbonaceous chondrite 03 p1244 N94-16345
Liquidus equilibria of lunar analogs at high pressure 03 p1283 N94-16364
Mixing model analysis of telescopic lunar spectra 03 p1284 N94-16371
Possible sources of H2 to H2O enrichment at evaporation of parent chondritic material 03 p1244 N94-16377
More on the cooling history of angrite LEW 86010 03 p1245 N94-16400
The thickness of eucritic crust in the HED parent body 03 p1104 N94-16416
Petrogenesis of Apollo 12 mare basalts. Part 1: Multiple melts and fractional crystallization to explain olivine and ilmenite basalt compositions 05 p1684 N94-20644
Petrogenesis of Apollo 12 mare basalts. Part 2: An open system model to explain the pigeonite basalt compositions 05 p1684 N94-20645
Lamellar olivine in the Divnoe achondrite: Evidence for high-pressure exsolution? 05 p1685 N94-20679
Determining the composition of olivine on asteroidal surfaces 05 p1686 N94-20805
The x ray microprobe determination of chromium oxidation state in olivine from lunar basalt and kimberlitic diamonds 05 p1686 N94-20807
Hydrothermal alteration experiments of olivine with varying Fe contents: An attempt to simulate aqueous alteration of the carbonaceous chondrites 05 p1686 N94-20810
Measurements of the dielectric properties of simulated comet material as part of the KOSI 10 experiment 05 p2085 N94-20841
Chemical zoning and diffusion of Ca, Al, Mn, and Cr in olivine of springwater pallasite 05 p2086 N94-20902
Diffuse reflectance spectra of orthopyroxene, olivine, and plagioclase as a function of composition and structure 05 p2087 N94-20906
A dynamic melting model for the origin of Apollo 15 olivine-normative and quartz-normative mare basalts 06 p2615 N94-24371
Electrical conductivity of perovskite-magnesiowuestite as a function of pressure and temperature
[DE94-002714] 07 p2880 N94-26806
Reduction of lunar mare soil and pyroclastic glass 11 p4355 N94-35398
Alteration and formation of rims on the CM parent body 11 p4357 N94-35411
Partial melting of the St. Severin (LL) and Lost City (H) ordinary chondrites: One step backwards and two steps forward 11 p4353 N94-36146
Cr, Mn, and Ca distributions for olivine in angritic systems: Constraints on the origins of Cr-rich and Ca-poor core olivine in angrite LEW87051 11 p4353 N94-36162
Partition coefficients for Al, Ca, Ti, Cr, and Ni in olivine obtained by melting experiment on an LL6 chondrite 11 p4353 N94-36163

OMCVD (VAPOR DEPOSITION)
U METALORGANIC CHEMICAL VAPOR DEPOSITION

OMEGA-MESONS
Omega omega and rho+ rho- production in two photon interactions at ARGUS
[ISBN-0-315-63748-X] 07 p3026 N94-27399

OMNIDIRECTIONAL ANTENNAS
NT MONOPOLE ANTENNAS
NT WHIP ANTENNAS
Mobile antenna development at JPL 05 p1731 N94-20457
Mobile terminal antennas for helicopters 05 p1731 N94-20458
L-band mobile terminal antennas for helicopters 06 p2289 N94-22835

ON-LINE PROGRAMMING
High precision on-line standard arithmetic operators: Design and implementation
[ETN-93-95006] 04 p1552 N94-19487
Practical issues in implementing roving spares in VLSI systolic arrays 05 p1758 N94-21114

ON-LINE SYSTEMS
TOLS (Telescience On-Line Simulator): An essential instrument for micro-gravity interactive experiment 01 p0039 N94-10134
Estimation of critical values and vibration characteristics on supersonic delta wings. Part 1: On-line time series analysis of stationary random response
[NAL-TR-1153] 01 p0002 N94-10363
The First Text Retrieval Conference (TREC-1)
[PB93-191641] 01 p0419 N94-10829
A survey of techniques for corrosion monitoring
[DE93-012131] 01 p0083 N94-11250
Transition of building energy consumption using multi-input, single-output dynamic model
[VTT-PUBS-116] 02 p0597 N94-14055
On-line upgrade of program modules using AdaPT
[NASA-CR-194331] 02 p0754 N94-14472
Portable acoustic wave sensor systems for real-time monitoring of volatile organic compounds
[DE93-013753] 02 p0582 N94-14511
Complexity analysis of real-time reinforcement learning applied to finding shortest paths in deterministic domains
[AD-A266636] 03 p1131 N94-15742
RELMA: On-line quality control in the rubber mixing room using laser analysis 03 p0984 N94-16005
NASA Electronic Library System (NELS): The system impact of security
[NASA-CR-194614] 03 p1231 N94-16499
Development of dynamic, contex-driven help systems
[AD-A267409] 03 p1152 N94-16974
Critically evaluated/distributed database of IRAS LRS spectra
[NASA-CR-193611] 03 p1232 N94-17038
Defense RDT&E online system (DROLS) handbook
[AD-A267546] 03 p1232 N94-17101
Defense Logistics Information System (DLIS). Procedures manual: Logistics On-Line Access (LOLA) procedures manual
[AD-A267685] 03 p1233 N94-17229
Processes involved in the integration of pictures and discourse
[AD-A268150] 03 p1134 N94-17468
FEDIX on-line information service: Design, develop, test, and implement an on-line research and education information service
[DE93-018818] 04 p1614 N94-18181
Intelligent help facilities: Generating natural language descriptions with examples
[AD-A269555] 04 p1521 N94-18290
Handbook for users
[AD-A268726] 04 p1615 N94-18323
On-line monitoring of incinerator emissions
[DE93-017406] 04 p1474 N94-18499
Automatic documentation generation: The interaction of text and examples
[AD-A269670] 04 p1616 N94-18570
Software distribution using xnetlib
[DE93-018278] 04 p1523 N94-18989
On-line test methods of microprocessor based systems
[ETN-93-95008] 04 p1530 N94-19498
Recommendations resulting from the SPDS Community-Wide Workshop
[NASA-CR-194684] 05 p2042 N94-20363
Research in image management and access
[NASA-CR-194797] 05 p1907 N94-20376
Practical issues in implementing roving spares in VLSI systolic arrays 05 p1758 N94-21114
Data management for interdisciplinary field experiments: OTTER project support
[NASA-CR-4559] 05 p1842 N94-22345
ASpect: A new spectrum and line analysis package for IRAF 05 p1926 N94-22485
The NSO FTS database program and archive (FTSDBM) 05 p1926 N94-22506
The EXOSAT database and archive 05 p2048 N94-22521
Recommendations for a service framework to access astronomical archives 05 p2049 N94-22537
Translative interface for data sharing and integrating: A paradigm for distributed data systems
[DE93-018790] 06 p2588 N94-22863
A novel process monitoring and control system based on a neural manufacturing concept
[DE94-001516] 06 p2471 N94-23011
SPDB (science processing database): Quick reference guide 06 p2383 N94-23597
Particle size measurement for the control of industrial crystallizers
[PB94-119104] 06 p2562 N94-23766
Columbus system support for telescience operations 06 p2505 N94-23877
NASDA's Advanced On-Line System (ADOLIS) 06 p2509 N94-23903

Intelligent tutoring and aiding in satellite ground control 06 p2443 N94-23929
On-line evaluation of multiloop digital controller performance 06 p2163 N94-25105
On-line control of dynamic systems using feedforward neural networks
[RR-457] 06 p2476 N94-25307
Proceedings of the 12th International Congress: Corrosion Control for Low-Cost Reliability. Volume 6: Electric Power Industry
[AD-A273668] 06 p2250 N94-25408
CADBIT 2: Computer-aided design for built-in test, volume 1
[AD-A273702] 06 p2463 N94-25455
CADBIT 2: Computer-aided design for built-in test, volume 2
[AD-A273703] 06 p2463 N94-25456
Factors influencing perceived usability and utility of LIBERTAS at Cranfield: Implications for system modification and user education
[CRANFIELD-AERO-9212] 06 p2594 N94-25485
Module interconnection frameworks for a real-time spreadsheet
[AD-A273853] 07 p2956 N94-25588
The use of on-line ion chromatography for high temperature and high pressure reaction studies
[DE94-002525] 07 p2713 N94-26075
Federal Information Exchange (FEDIX) user's guide: Fall 1993, Version 5.0/Release 1.0
[DE94-003826] 07 p3097 N94-26350
The 12-channel flash-ADC FASTBUS module
[DE93-634229] 07 p2783 N94-26380
Design of an online help facility for ExSpect
[PB94-126687] 07 p2966 N94-26955
Electronic document distribution: Design of the anonymous FTP Langley Technical Report Server
[NASA-TM-4567] 07 p2971 N94-27573
Defense Technical Information Center cataloging guidelines
[AD-A275100] 08 p3529 N94-28911
Decision Making Aids (DMA) in on-line ATC systems 08 p3139 N94-29570
AFGWC Dial-In Subsystem (AFDIS) software users manual, version 2.2
[AD-A275844] 08 p3371 N94-29747
Pausing behavior of end-users in online searching 08 p3533 N94-29960
Hierarchical mixtures of experts and the EM algorithm
[AD-A276516] 09 p3814 N94-31932
A redundant disk array architecture for efficient small writes
[AD-A276645] 09 p3815 N94-31940
Moving BASISplus and TECHLIBplus from VAX/VMS to UNIX
[DE94-004696] 09 p3826 N94-32248
A hypertext system that learns from user feedback 09 p3923 N94-32428
Relationships between access and use in information systems: Remote access to and browsing of online catalogs 09 p3919 N94-32488
State-space self-tuner for on-line adaptive control
[NASA-CR-195836] 09 p3835 N94-32943
MDFF HELP library, version 2: On-line documentation for the map data formatting facility
[AD-A277763] 09 p3922 N94-32987
Ultraviolet Absorption Spectrometry (UVAS) and Liquid Atomic Emission Spectrometry (LAES) for oceanographic analysis systems
[AD-A278263] 10 p4091 N94-33413
Diagnosing anomalies of spacecraft for space maintenance and servicing 10 p4015 N94-33667
Vista goes online: Decision-analytic systems for real-time decision-making in mission control 10 p4125 N94-35063
Defense RDT and E online system (DROLS) retrieval reference guide
[AD-A278972] 11 p4344 N94-35525
Adaptive model reduction for continuous systems via recursive rational interpolation 11 p4219 N94-35876
Netlib services and resources
[DE94-010307] 11 p4347 N94-36300
NASA Access Mechanism: Lessons learned document
[NASA-TM-109924] 12 p4540 N94-36750
Electronic SCAN (Selected Current Aerospace Notices) 12 p4541 N94-36845
Network upgrades 12 p4541 N94-36851
Data compatibility for various Charpy-tests
[DE94-617534] 12 p4416 N94-37074
Wide aperture scintillation hodoscope with FEU-143 photomultipliers
[DE94-618211] 12 p4515 N94-37075

ONBOARD COMPUTERS
U AIRBORNE/SPACEBORNE COMPUTERS

ONBOARD DATA PROCESSING
Data processing units for eight magnetospheric particle and field sensors
[AD-A264403] 01 p0276 N94-11463
DISTERM: A shipboard data system for satellite monitoring of ocean and atmosphere 01 p0226 N94-12749
ALFIS: Astronomical Low Frequency Interferometry Satellites. A feasibility study
[LR-699] 02 p0542 N94-13988
NASA Lewis Meshed VSAT Workshop meeting summary
[NASA-TM-106332] 03 p0883 N94-17487
VPU(tm) demonstration mission vicinity processor unit(tm) overview 04 p1325 N94-19171
Multichannel error correction code decoder
[NASA-TM-106331] 04 p1333 N94-19313
On-board closed-loop congestion control for satellite based packet switching networks
[NASA-TM-106446] 05 p1656 N94-21581
CREIR: A multiaccess protocol for on-board processing satellite systems 05 p1780 N94-22168
Timing recovery in the channel processor of a digital group demodulator 05 p1780 N94-22169
Experiences in airborne computing at NRC for geophysical exploration applications 05 p1783 N94-22185
SAW based systems for mobile communications satellites 06 p2275 N94-22746
Applicability of different onboard routing and processing techniques to mobile satellite systems 06 p2278 N94-22767
A European mobile satellite system concept exploiting CDMA and OBP 06 p2279 N94-22768
Cockpit weather graphics using mobile satellite communications 06 p2280 N94-22775
Towards real-time stereovision systems for planetary missions 06 p2370 N94-23422
Fault tolerant onboard packet switch architecture for communication satellites: Shared memory per beam approach
[NASA-TM-106397] 06 p2201 N94-23567
Advanced technology for a satellite multichannel demultiplexer/demodulator
[NASA-CR-194435] 06 p2202 N94-23631
UAV current technology and future trends 06 p2154 N94-24245
Decentralized autonomous attitude determination using an inertially stabilized payload 06 p2157 N94-24264
Modulation and synchronization technique for MF-TDMA system
[NASA-CR-194448] 06 p2304 N94-25266
Real-Time Embedded Processing for Space Applications
[ISBN-2-85428-335-X] 07 p2948 N94-26713
Computing in space: Issues and answers 07 p2948 N94-26714
Real time avionics constraints: Silicon solutions 07 p2949 N94-26717
MATRA Marconi Space: The Silex on-board processor and on-board software 07 p2950 N94-26726
On-board software for the JET-X telescope on the Spectrum-X mission 07 p2951 N94-26727
Implementing hard real-time systems: A case study 07 p2951 N94-26731
Early real-time performance measurements on the Columbus processor system 07 p2952 N94-26736
Test of onboard real time applications (LICE (tm)) 07 p2952 N94-26737
Verification and validation of the on-board software real time requirements 07 p2953 N94-26739
Ada reusable software for satellite on-board data handling 07 p2953 N94-26743
Specification performance optimization and executive generation for onboard multiprocessor real time application with SynDEx 07 p2954 N94-26745
Asynchronous and packetized systems engineering tools 07 p2954 N94-26746
Advanced End-to-end Simulation for On-board Processing (AESOP) 07 p2945 N94-28255
Software engineering methods in the Hermes on-board software 08 p3414 N94-29326
GPS/GNSS for ATM 08 p3138 N94-29565
Unmanned vehicle mobility: Limits of autonomous navigation 08 p3310 N94-30311
Error analysis of real-time and post-processed orbit determination for the Geosat Follow-On altimetric satellite using GPS tracking 09 p3576 N94-31845
Aerospace sponsored research
[ATR-93(8498)-1] 09 p3966 N94-32949
Data processing algorithms for on-board satellite event analysis
[AD-A278406] 09 p3838 N94-33168
Microrover research at JPL 10 p4066 N94-34020
Experience with Ada on the F-18 High Alpha Research Vehicle flight test program 11 p4310 N94-35968
Space Generic Open Avionics Architecture (SGOAA) standard specification
[NASA-CR-188290] 12 p4387 N94-36933

ONBOARD EQUIPMENT
NT AIRBORNE EQUIPMENT
NT AIRBORNE LASERS
NT AIRBORNE/SPACEBORNE COMPUTERS
NT AIRCRAFT EQUIPMENT
NT EJECTION SEATS
NT SPACECRAFT ELECTRONIC EQUIPMENT
NT SPACECRAFT EQUIPMENT
NT TERCOM
Integrated marine survey system 01 p0217 N94-12693
DISTERM: A shipboard data system for satellite monitoring of ocean and atmosphere 01 p0226 N94-12749
STS-29 crew IMAX camera training
[NASA-TM-109546] 03 p1031 N94-15380
Regulated emergency oxygen system
[AD-A266228] 03 p1138 N94-16983
The STRV On Board Data Handling (OBDH) system: An introduction 03 p0895 N94-17178
MINISAT programme 03 p0896 N94-17182
The space technology research vehicle: Development status 03 p0896 N94-17183
TITUS: A micro-satellite for technology demonstration 03 p0896 N94-17186
Key trends of the small satellite market 03 p0897 N94-17191
TDRSS Onboard Navigation System (TONS) flight qualification experiment 11 p4206 N94-35625

ONE DIMENSIONAL FLOW
A comparison between numerically modelled and experimentally measured loss mechanisms in wave rotors
[NASA-TM-106279] 01 p0029 N94-11255
Formulation of a next-generation interior ballistic code
[AD-A271539] 05 p1801 N94-20915
Dynamic response of a compressor research facility
[AD-A273836] 07 p2679 N94-25740
Integrated model development for liquid fueled rocket propulsion systems
[NASA-CR-195253] 07 p2702 N94-27166
Eigenvalue analysis of the convergence behaviour of an Euler method
[PB94-1255722-U] 08 p3281 N94-30743

ONISOTROPY
U ANISOTROPY

ONTARIO
The basement fracture pattern of southern Ontario: A tectonic interpretation based on Landsat TM imagery, airphotos and field data
[ISBN-0-315-87086-9] 09 p3772 N94-31834

ONTOGENESIS
U ONTOGENY

ONTOGENY
Ontogenesis of mammals in microgravity
[NASA-TM-103978] 03 p1139 N94-17636

OORT CLOUD
Studies of extra-solar Oort Clouds and the Kuiper Disk
[NASA-CR-195242] 07 p3103 N94-26789
Modulating terrestrial impacts from Oort cloud comets by the adiabatically changing galactic tides 07 p2890 N94-28305

OPACITY
H2S data reduction
[NASA-CR-193389] 02 p0617 N94-14743
FEEST: A method for tabulating equation of state and opacity tables
[DE93-017965] 04 p1347 N94-18092
Opacity measurements in shock-generated argon plasmas
[DE94-001057] 05 p1998 N94-22399
Physical properties of dense astrophysical plasmas 05 p2001 N94-22637
Groundbased monitoring of Martian atmospheric opacity 09 p3947 N94-33207
Collective plasma corrections to the solar opacity
[PB94-170511] 11 p4375 N94-36210

OPEN CIRCUIT VOLTAGE
Potential transients, transmission and electrochemical corrosion detection
[DE93-014055] 03 p0956 N94-15922
Techniques for reducing error in the calorimetric measurement of low wattage items
[DE93-018472] 05 p1807 N94-20114

OPEN CLUSTERS
UV extinction properties of carina nebular dust
[NASA-CR-189308] 02 p0835 N94-13233
Photometry and spectroscopy in the open cluster Alpha Persei, 2
[NASA-CR-193397] 02 p0833 N94-14358
A near-infrared survey of the star forming region NGC 2264 08 p3540 N94-29971

OPENINGS
NT APERTURES
NT SLITS
NT SYNTHETIC APERTURES

OPERATING COSTS
Space transportation alternatives for large space programs: The International Space University Summer Session, 1992
[NASA-TM-106271] 01 p0040 N94-10811
Transportation systems analyses. Volume 2: Technical/programmatics
[NASA-CR-192582] 01 p0041 N94-10827
Pulsed plasma processing for control of diesel engine emissions
[DE93-011884] 01 p0181 N94-11247
Life-cycle cost analysis of conventional and fuel cell/battery powered urban passenger vehicles
[DE93-010770] 01 p0182 N94-11438
Forecasting the impact of virtual environment technology on maintenance training 01 p0314 N94-11570
Robot-task compliance: The energy criterion
[ITN-93-85196] 02 p0763 N94-13568
Optimal maintenance policies of a Markovian system
[ITN-93-85216] 02 p0774 N94-14502
Optimizing wind turbine control system parameters
[DE93-018861] 04 p1469 N94-19036
Downsizing a database platform for increased performance and decreased costs
[DE93-018687] 04 p1618 N94-19099
Spaceplane flight simulation: Project definition
[PB93-211399] 05 p1651 N94-22094
Future trends in NASA space operations 06 p2498 N94-23836
Design of an airborne launch vehicle for an air launched space booster
[NASA-CR-195534] 06 p2198 N94-24860
The Bunny: A simulated commercial air transportation study
[NASA-CR-195537] 06 p2183 N94-25001
Development of advanced high temperature in-cylinder components and tribological systems for low heat rejection diesel engines, phase 1
[NASA-CR-187158] 07 p2827 N94-27984
Development of the gas turbine. Part 2: Manufacturing, commissioning, and operation 07 p2831 N94-28081
Aircraft age impacts on maintenance requirements
[AD-A275701] 08 p3121 N94-28666
Aircraft age impact on individual operating and support cost elements
[AD-A275739] 08 p3121 N94-28732
The 1993 Federal Aviation Administration Aviation System Capital Investment Plan
[AD-A279036] 08 p3136 N94-29445
Ventilation cost and air cleaning 08 p3232 N94-29605
Specifications of auxiliary power units for conformity with helicopter turboshaft engines 10 p4001 N94-34441
Future ultra-speed tube-flight 11 p4225 N94-35918

OPERATING SYSTEMS (COMPUTERS)
NT DISK OPERATING SYSTEM (DOS)
NT UNIX (OPERATING SYSTEM)
Transportable Applications Environment (TAE) Tenth Users' Conference
[NASA-CP-3225] 01 p0333 N94-12448
Integrated trusted systems development environment
[AD-A267029] 03 p1146 N94-15674
Fast interrupt priority management in operating system kernels
[AD-A266638] 03 p1140 N94-15744
Processor capacity reserves for multimedia operating systems
[AD-A266639] 03 p1158 N94-15745
Disconnected operation in a distributed file system
[AD-A266461] 03 p1231 N94-16570
An internetwork authentication architecture
[AD-A268579] 03 p1162 N94-17622
PARX: Architecture of an operating system for parallel machines
[ETN-93-94401] 04 p1533 N94-18068
Embedded Computer Performance Measurement (ECPM). Advanced avionics subsystems and technology multiprocessor ECPM software documentation
[AD-A269921] 04 p1320 N94-18658
Control of nonlinear systems
[AD-A270141] 04 p1542 N94-18898
Pegasus project description
[MEMO-INF-92-75] 04 p1536 N94-19159
Pegasus: Operating system support for distributed multimedia systems
[MEMO-INF-92-76] 04 p1536 N94-19160
Experience in implementing a parallel file system
[DE93-012840] 04 p1536 N94-19188
ACOS: A performance based approach to build a parallel complex object server
[MEMO-INF-93-11] 04 p1537 N94-19198
Message passing in PUMA
[DE93-012841] 04 p1537 N94-19206
Wide-address spaces: Exploring the design space
[MEMO-INF-92-77] 04 p1537 N94-19219
Service without servers
[AD-A270612] 04 p1515 N94-19591
A response to Cheriton and Skeen's criticism of casual and totally ordered communication
[AD-A271486] 05 p1912 N94-21300
Use of open systems for control, analysis, and data acquisition of the DIII-D tokamak
[DE94-001101] 05 p1998 N94-22089
Fault tolerance for real-time multiprocessor operating systems 05 p1788 N94-22216
ACOS: The performance based approach to build a parallel complex object server
[PB93-223816] 06 p2465 N94-22986
Distributed Operating Systems and Mach. Proceedings of the Spring 1992 Graduate Seminar on Distributed Systems
[PB93-224905] 06 p2449 N94-23103
Performance measurements of the multimedia testbed on Mach 3.0: Experience writing real-time device drivers, servers, and applications
[AD-A273600] 06 p2460 N94-24932
Analyzing the properties of user interface software
[AD-A273601] 06 p2460 N94-24933
The design of the EMPS multiprocessor executive for distributed computing
[ETN-94-95336] 06 p2468 N94-25062
Domain analysis and modeling of a model-based software executive
[AD-A274087] 07 p2958 N94-25783
Achieving high performance on the Intel Paragon
[DE94-003108] 07 p2979 N94-25953
Ada multiple-programming for hard real time applications in space systems 07 p2951 N94-26730
Implementing hard real-time systems: A case study 07 p2951 N94-26731
Object-based design of embedded software
[PB94-132073] 08 p3407 N94-28403
Reference model for project support environments, version 2.0
[AD-A275191] 08 p3410 N94-29068
Design of a thinwire real-time multiprocessor operating system 08 p3415 N94-29333
Adaptive operating systems concepts
[ETN-94-95754] 09 p3830 N94-31514
Moving BASISplus and TECHLIBplus from VAX/VMS to UNIX
[DE94-004696] 09 p3826 N94-32248
Predictable and adaptable complex real-time systems
[AD-A277827] 10 p4105 N94-33830
NAVSPACECOM space surveillance sensor system digital signal processing receiver. Volume 3: Operating system functions
[AD-A278839] 11 p4212 N94-35799
An analysis of file system and installation of the file management system for NOS operating system
[DE94-611062] 11 p4346 N94-35833

OPERATING TEMPERATURE
Thin film preparation and interfacial reaction study of solid oxide fuel cell materials 01 p0263 N94-11313
Cryogenic measurements of aerojet GaAs n-JFETs
[NASA-TM-103972] 03 p1009 N94-15765
Development of a cryogenic heat pipe
[DE93-018448] 04 p1417 N94-18831
Silicon device performance measurements to support temperature range enhancement
[NASA-CR-195265] 07 p2844 N94-27824
Development of advanced high temperature in-cylinder components and tribological systems for low heat rejection diesel engines, phase 1
[NASA-CR-187158] 07 p2827 N94-27984
The influence of temperature on microelectronic device failure mechanisms, phase 2
[AD-A275029] 08 p3265 N94-29511
Performance of silvered Teflon (trademark) thermal control blankets on spacecraft 09 p3591 N94-31014
The optimization of interfaces in InAsSb/InGaAs strained-layer superlattices grown by metal-organic chemical vapor deposition
[DE94-010070] 11 p4340 N94-35698

OPERATIONAL AMPLIFIERS
Stray insensitive switched capacitor composite operational amplifiers
[AD-A267412] 03 p1012 N94-16976
An 18 bit 50 kHz ADC for low earth orbit 05 p1764 N94-21702
Fifty years of continuous improvement: What has DOE done for analytical chemistry?
[DE94-002539] 06 p2234 N94-24548
High speed electronic analog computers using low-gain amplifiers
[AD-D015974] 06 p2446 N94-25034
Digitally programmable composite operational amplifier applications
[AD-A275081] 08 p3262 N94-28842
A magnetically coupled quench detector for superconducting magnets
[DE94-006040] 08 p3268 N94-30904
VLSI implementation of stray insensitive switched capacitor composite operational amplifiers
[AD-A276461] 09 p3687 N94-31240
Active antenna
[NASA-CASE-GSC-13309-1] 11 p4251 N94-35231
A gallium arsenide MESFET operational amplifier for use in composite operational amplifiers
[AD-A277843] 11 p4258 N94-35539
BJT model in APLAC
[PB94-171022] 11 p4259 N94-35822

OPERATIONAL HAZARDS
Safety guidelines for the operation of the DREO 10 m EMP simulator DREMPS
[DREO-TN-93-5] 06 p2193 N94-24117
Rotorwash analysis handbook. Volume 1: Development and analysis
[SCT-93RR-17-VOL-1] 12 p4381 N94-36466
Rotorwash analysis handbook. Volume 2: Appendixes
[SCT-93RR-17-VOL-2] 12 p4382 N94-36467

OPERATIONAL PROBLEMS
Criteria for assessing problem solving and decision making in complex environments 01 p0314 N94-11532
The airline quality report 1993
[NIAR-93-11] 03 p0863 N94-17262
Planning process software: A user guide for the DMCA
[AD-A271252] 05 p1902 N94-19911
Operability engineering in the Deep Space Network 06 p2514 N94-23930
An examination of the operational error database for air route traffic control centers
[AD-A275986] 06 p2175 N94-24472
Safety concerns for first entry operations of orbiting spacecraft 10 p4102 N94-33662

OPERATIONS RESEARCH
An advisor module for tactical and strategic state-oriented planning systems with an application in manpower planning
[MEMO-COSOR-92-57] 01 p0416 N94-10868
Gate assignment using linear programming
[LR-698] 02 p0775 N94-13987
Logarithmic asymptotics for steady-state tail probabilities in a single-server queue
[AD-A266746] 03 p1165 N94-15775
Fast simulation of steady-state availability in non-Markovian highly dependable systems
[AD-A266747] 03 p1174 N94-15823
Research and development: Engine of innovation at Krupp 03 p0984 N94-16001
Kennedy Space Center exercise program 03 p1126 N94-16634
An object-oriented dynamic software process model
[AD-A267726] 03 p1154 N94-17371
Mathematical Sciences Division 1992 programs
[AD-A268586] 03 p1140 N94-17623
Contribution to the analysis of tableaus based decision methods
[ETN-93-94355] 04 p1560 N94-18067
Polling systems: Moment stability of station times and central limit theorems
[PB93-191955] 04 p1560 N94-18990
Controlling multisupplier operations by intelligent EDI 05 p1744 N94-22076
Tool sharing: An application of max-algebra, part 2
[MEMO-1122] 06 p2478 N94-22710
A multilevel cost-space approach to solving the balanced long transportation problem 06 p2483 N94-23678
Design and specification of a generic task model for solving boolean constraint satisfaction problems
[PB94-118841] 06 p2486 N94-23762
Verification and validation of models
[PB94-110566] 06 p2456 N94-24507
Tool sharing, part 3
[PB94-111697] 06 p2467 N94-24524
Throughput time control and due date reliability in tool and die shops
[ISBN-9-03-860182-4] 06 p2587 N94-25283
The effectiveness of AMT investment in UK metal component manufacture
[IND-MANU-SCI-TECH-REPT-3] 07 p2762 N94-25775
The general pickup and delivery problem
[MEMO-COSOR-92-44] 07 p2992 N94-26226
Polyhedral characterization of the economic lot-sizing problem with start-up costs
[MEMO-COSOR-92-46] 07 p2969 N94-27396
The molecular matching problem 07 p3030 N94-27910

Realizing the productivity potential of expeditious operations
[PB94-135555] 08 p3230 N94-29188
A capacity planning model for Canadian military airlift requests
[ISBN-0-315-86079-0] 08 p3136 N94-30144
Mathematical research in materials science opportunities and perspectives, part 2
[AD-A276298] 09 p3852 N94-31296
A cross-disciplinary report on the mathematical sciences applied to materials science, part 1
[AD-A276116] 09 p3843 N94-31529
Seventh Annual Workshop on Space Operations Applications and Research (SOAR 1993), volume 2
[AD-A278178] 10 p4167 N94-33612
National facilities study. Volume 3: Mission and requirements model report
[NASA-TM-109857] 10 p4009 N94-34635
National facilities study. Volume 4: Space operations facilities task group
[NASA-TM-109858] 10 p4010 N94-34636
National facilities study. Volume 5: Space research and development facilities task group
[NASA-TM-109859] 10 p4010 N94-34637

OPERATOR PERFORMANCE
Analyzing human errors in flight mission operations 01 p0314 N94-11534
Vigilance problems in orbiter processing 01 p0314 N94-11536
Measuring human performance on NASA's microgravity aircraft 01 p0317 N94-11537
Visual Earth observation performance in the space environment. Human performance measurement 4: Flight experiments 01 p0314 N94-11539
SATORI: Situation Assessment Through the Re-creation of Incidents
[DOT/FAA/AM-93/12] 01 p0038 N94-12567
Cognitive engineering models in space systems
[NASA-CR-193473] 03 p1140 N94-16716
Preliminary validation of the task analysis/workload methodology
[AD-A267514] 03 p1138 N94-17077
Operator performance in pattern matching as a function of reference material structure
[AD-A269889] 04 p1509 N94-18686
Pushing technology to satisfy world applications
[DE94-001365] 06 p2353 N94-23191
Operability engineering in the Deep Space Network 06 p2514 N94-23930
Investigation of time and intensity effects in operator workload and performance
[CTN-94-60927] 06 p2433 N94-24171
Task demand, workload, and performance
[PB94-123627] 07 p2942 N94-27155
Designing for performance: A cognitive systems engineering approach to modifying an AWACS human computer interface
[AD-A275187] 08 p3399 N94-28861
Aiding the operator in the manual control of a space manipulator
[PB94-125549] 08 p3402 N94-30390
Sampling behaviour in a four instrument monitoring task: Effects of signal bandwidth and number of events per signal
[AD-B179613] 08 p3402 N94-30422
Use of a pitch adjustable foot restraint system: Operator strength capability and load requirements
[NASA-TP-3477] 09 p3805 N94-33050
Man-machine Integration Design and Analysis System (MIDAS) Task Loading Model (TLM) experimental and software detailed design report
[NASA-CR-177640] 10 p4100 N94-34706

OPERATORS (MATHEMATICS)
NT LINEAR OPERATORS
Deformations and recursion operators for evolution equations
[MEMO-1104] 01 p0341 N94-10163
The super vectorfield package for REDUCE. Version 1.0
[MEMO-1099] 01 p0321 N94-10265
Balancing of the normalized right coprime factorization of a nonlinear system
[MEMO-1096] 01 p0341 N94-10273
The ring structure of chiral operators for minimal models coupled to 2D gravity
[DE93-613119] 01 p0409 N94-10500
On local frame fields and fermion dynamics in space with nontrivial topologies
[DE93-617657] 01 p0349 N94-10548
Observables, measurements and phase operators from a Bohmian perspective 01 p0378 N94-10589
Nonunitary and unitary approach to Eigenvalue problem of Boson operators and squeezed coherent states 01 p0350 N94-10595
Wave and pseudo-diffusion equations from squeezed states 01 p0347 N94-10607
Operator substitution
[MEMO-COSOR-92-51] 01 p0343 N94-10867
The Nehari problem for the Pritchard-Salamon class of infinite-dimensional linear systems: A direct approach
[CS-9216] 01 p0344 N94-10905
Optical transfer operator of the atmosphere-ocean system 01 p0225 N94-12742
On some results by Fuhrmann on Hankel operators
[CWI-BS-R9224] 02 p0764 N94-13999
On relations between Schmidt pairs arising in robust control
[CWI-BS-R9225] 02 p0764 N94-14000
On the Schmidt pairs of multivariable Hankel operators and robust control
[CWI-BS-R9226] 02 p0765 N94-14001
Steepest descent approximations for accretive operator equations
[DE93-628586] 03 p1171 N94-17667
Functional analysis of subelliptic operators on lie groups
[PB93-194793] 04 p1547 N94-18077
L(sub p)-regularity of subelliptic operators on Lie groups
[PB93-194785] 04 p1549 N94-18948
Numerical analysis of proximal methods: Decomposition and parallelization
[ETN-93-95017] 04 p1552 N94-19362
High precision on-line standard arithmetic operators: Design and implementation
[ETN-93-95006] 04 p1552 N94-19487
Computation of large numbers and VLSI: Application to GCD, to stretched GCD and at euclidian distance
[ETN-93-95009] 04 p1552 N94-19499
Explicit results on gl(lambda) and sl(lambda)
[MEMO-1075] 05 p1953 N94-21072
On the closure properties of #P in the context of PF of #P
[TR-445] 05 p1955 N94-21456
Note on the use of spherical vectorfields in Clifford analysis
[PB93-237667] 06 p2480 N94-23437
A comparison of locally adaptive multigrid methods: LDC, FAC and FIC 06 p2485 N94-23692
Tensoral for post-processing users and simulation authors 06 p2333 N94-24169
Some maximality results for effect-valued measures
[PB94-111176] 06 p2569 N94-24575
Signatures of selfadjoint pencils
[PB94-111127] 06 p2457 N94-24599
Downward extrapolation of multi-component seismic data
[ISBN-9-09-005213-5] 06 p2405 N94-25229
Introduction to a behavioral approach for continuous time systems
[ETN-94-95301] 06 p2492 N94-25277
Parallel matrix transpose algorithms on distributed memory concurrent computers
[DE94-002424] 07 p2964 N94-26764
Q - difference intertwining operators for a Lorentz quantum algebra
[DE94-602559] 07 p2997 N94-27023
A characterization of stable models using a non-monotonic operator
[CWI-CS-R9315] 07 p2970 N94-27543
Joint essential maximal numerical range
[DE94-603674] 07 p3000 N94-27637
Calculation of eigenvalues of Schroedinger operators for arbitrary coupling
[DE94-606302] 08 p3522 N94-28582
A note on the Poisson brackets associated with Lax operators
[MATHS-REPT-A-195] 08 p3464 N94-29482
Approximation methods for nonlinear operator equations of the m-accretive type
[DE94-608099] 08 p3467 N94-30065
Graded Froelicher-Nijenhuis brackets and the theory of recursion operators for super differential equations
[MEMO-1147] 08 p3460 N94-30736
A cell-cycle model revisited
[CWI-AM-R9305] 09 p3851 N94-32229
Conference on operator, wavelet and control theory
[AD-A277429] 09 p3838 N94-33174
Dynamic subtrees: A new data structure for manipulating trees
[DE94-009168] 10 p4128 N94-33985

OPERATORS (PERSONNEL)
NT AIRCRAFT PILOTS
NT PILOTS (PERSONNEL)
NT TEST PILOTS
Department of Energy fundamentals handbook: Engineering symbology, prints, and drawings
[DE93-012181] 01 p0129 N94-11456
Department of Energy fundamentals handbook: Engineering symbology, prints, and drawings
[DE93-012220] 01 p0129 N94-11670
Operational training for the mission operations at the Brazilian National Institute for Space Research (INPE) 06 p2429 N94-23933
Modular Simulator System (MSS). System/segment specification for the generic modular simulator system-instructor/operator station module, volume 12
[AD-A276979] 09 p3589 N94-32318

OPHIUCHI CLOUDS
Pre-main sequence stars in the Chamaeleon cloud and pre-main sequence stars in the Rho Ophiuchi cloud core
[NASA-CR-194713] 05 p2080 N94-20337

OPHTHALMOLOGY
Vision impairment and corrective considerations of civil airmen
[DOT/FAA/AM-93/21] 06 p2426 N94-23623
Digital tracking and control of retinal images
[AD-A275469] 08 p3389 N94-28810
The Portable Dynamic Fundus Instrument: Uses in telemedicine and research 10 p4096 N94-33647

OPTICAL ABSORPTION
U ELECTROMAGNETIC ABSORPTION
U LIGHT TRANSMISSION

OPTICAL ACTIVITY
Kinetic aspects of lattice mismatch in molecular beam epitaxial growth on planar and patterned substrates
[AD-A270424] 04 p1597 N94-18506

OPTICAL AMPLIFIERS
U LIGHT AMPLIFIERS

OPTICAL BISTABILITY
Characteristics of semiconductor lasers with optical feedback
[ISBN-0-315-55435-5] 02 p0656 N94-13522
System for solving Boolean equations using optical lookup tables
[AD-D015962] 05 p1951 N94-20358

OPTICAL COMMUNICATION
Design and analysis of an optical interface message processor
[AD-A266079] 01 p0381 N94-10697
Experimental comparison of time synchronization techniques by means of light signals and clock transport on the rotating earth 01 p0351 N94-10970
Development of an on-board aircraft optical fiber data bus system
[NAL-TR-1163] 02 p0514 N94-13338
An overview of the Galileo Optical Experiment (GOPEX) 02 p0610 N94-14386
Galileo Optical Experiment (GOPEX) optical train: Design and validation at the Table Mountain Facility 02 p0610 N94-14390
GOPEX laser transmission and monitoring systems 02 p0611 N94-14391
GOPEX at the Starfire Optical Range 02 p0611 N94-14392
Congestion control of high-speed networks
[AD-A267013] 03 p0989 N94-15748
A formal protocol test procedure for the Survivable Adaptable Fiber Optic Embedded Network (SAFENET)
[AD-A267410] 03 p1192 N94-16975
Performance of coded coherent FSK lightwave system with noncoherent detection
[AD-A267442] 03 p1193 N94-17028
Non-blocking crossbar permutation engine with constant routing latency
[NASA-CASE-NPO-18864-1-CU] 03 p1161 N94-17328
A scalable wrap-around shuffle exchange network with deflection routing
[NASA-CASE-NPO-18983-1-CU] 03 p1161 N94-17330
Laser beam steering device 03 p1045 N94-17357
Activities of the Research Laboratory of Electronics
[AD-A266730] 03 p1304 N94-17651
Intentionally Short Range Communications (ISRC)
[AD-A268788] 04 p1384 N94-18216
Advanced optical fiber communication systems
[AD-A269120] 04 p1577 N94-18254
Integrated photonics research volume 10. Conference edition
[AD-A269298] 04 p1577 N94-18298
Competitive dynamics and self-organization in photorefractive systems
[AD-A269663] 04 p1430 N94-18569
Integrated Photonics Research: Post-deadline papers
[AD-A269232] 04 p1609 N94-18908
A highly concurrent medium access control strategy for high speed multiwavelength networks using transceivers with limited tunability
[MEMO-INF-93-07] 04 p1390 N94-19230
Optical frequency division using an optical parametric oscillator
[AD-A270847] 04 p1581 N94-19578
Experimental examinations of semiconductor laser amplifiers for optical communication technology
[ETN-93-95050] 04 p1442 N94-19647

Oceanic in situ Fraunhofer-line characteristics: Fraunhofer-line underwater experiment (FLUX)
[AD-A270659] 05 p1881 N94-19952
Optical signal processing
[AD-A271036] 05 p1983 N94-20013
Design considerations for a fiber optic communications network for power systems
[DE93-018404] 05 p1984 N94-20179
Silicon retina for optical tracking systems 05 p1755 N94-21098
QPPM receiver for free-space laser communications
[NASA-TM-106424] 05 p1741 N94-21567
Laser linewidth measurement in the presence of RIN and using the recirculating self heterodyne method
[EUT-92-E-262] 06 p2347 N94-22874
InGaAsP/InP based 1.3/1.55 micron vertical cavity surface emitting lasers for wavelength division multiplexed high speed distributed computing, phase 1
[AD-A271081] 06 p2348 N94-23123
Wide band fiber-optic communications 06 p2304 N94-23231
Optical subnet concepts for the deep space network 06 p2292 N94-23269
A lower bound for routing on a completely connected optical communication parallel computer
[DE93-040752] 06 p2466 N94-23491
Analysis for the computational modeling of finite cladding and lossy coating effects in fibers
[PB94-111085] 06 p2544 N94-23732
Measuring electrically charged particle fluxes in space using a fiber optic loop sensor
[NASA-CR-191328] 06 p2544 N94-23829
Multi-access laser communications terminal
[NASA-CR-191251] 06 p2295 N94-23830
Preloaded launch locking devices for SILEX 06 p2358 N94-24008
Integration and test of high-speed transmitter electronics for free-space laser communications
[NASA-TM-106295] 06 p2295 N94-24101
Optimization of microscopic and macroscopic second order optical nonlinearities 06 p2226 N94-24354
Japanese aerospace science and technology 1992. A bibliography with indexes
[NASA-SP-7104] 06 p2631 N94-24585
Crosstalk analysis of synchronous and asynchronous optical chip interconnects with direct detection
[AD-A273261] 06 p2311 N94-24685
Design of a shared coherent cache for a multiple channel architecture
[AD-A274026] 07 p3034 N94-25758
System design analysis of a lightweight laser satellite terminal
[AD-A274033] 07 p2690 N94-25769
Study of the homogeneity of InP wafers
[AD-A273658] 07 p3055 N94-26194
Laser-based communication link
[FFI-93/7023] 07 p2817 N94-26203
A doubly logarithmic communication algorithm for the Completely Connected Optical Communication Parallel Computer
[DE93-019408] 07 p2980 N94-26473
Accordion-like polymers for nonlinear applications
[AD-D016031] 07 p2755 N94-27148
Investigation of air transportation technology at Princeton University, 1992-1993 07 p2643 N94-27294
Optical communications for transport aircraft 07 p2643 N94-27298
Microprocessor chip incorporating optical signal coupling transceiver
[AD-D016077] 07 p2788 N94-28186
Lasercom system architecture with reduced complexity
[NASA-CASE-NPO-19069-1-CU] 08 p3293 N94-29493
Site comparison for optical visibility statistics in southern California 08 p3247 N94-29617
The Rb 780-nanometer Faraday anomalous dispersion optical filter: Theory and experiment 08 p3250 N94-29659
Overview of microoptics: Past, present, and future 08 p3235 N94-29771
Photonics at Sandia National Laboratories: From research to applications
[DE94-006463] 08 p3501 N94-30828
Standard testing procedures for optical fiber and unshielded twisted pair at Sandia National Laboratories
[DE94-005315] 08 p3501 N94-30910
Advanced optical fiber communication systems
[AD-A276416] 09 p3878 N94-31330
Pulse-splitting and AM-FM conversion in a nonlinear dispersive medium
[AD-A277041] 09 p3861 N94-32262
Control and reliability of optical networks in multiprocessors
[AD-A277385] 09 p3881 N94-32285
Passive, multi-channel fiber optic rotary joint assembly
[AD-D016116] 09 p3882 N94-32626
Multi-line passive fiber optic slipring
[AD-D016092] 09 p3883 N94-32738
Long distance transmission of 15 Gb/s digital using subcarrier multiplexing and external modulation
[DE94-008298] 09 p3682 N94-32756
Pointing and tracking space mechanism for laser communication 09 p3606 N94-33310
Photonic fast packet switching using optically processed control
[AD-A278195] 10 p4038 N94-33386
Spectral-domain optical processing techniques
[AD-A278371] 10 p4141 N94-33739
Silica Fresnel lens for laser communications
[AD-A278329] 10 p4058 N94-33967
Method providing optimum optical trains alignment in a passive multi-channel fiber optic rotary joint
[AD-D016125] 10 p4143 N94-34151
The Canadian network for the advancement of research, industry and education (CANARIE) 12 p4543 N94-37336

OPTICAL COMPUTERS

Design and analysis of an optical interface message processor
[AD-A266079] 01 p0381 N94-10697
Spatial light rebroadcaster architecture study
[AD-A266102] 01 p0382 N94-11421
Optical residue processing module
[AD-A267721] 03 p1188 N94-14940
Database system studies in fine grain optoelectronic computing
[AD-A267026] 03 p1145 N94-15627
Alternative optical architectures for multichannel adaptive optical processing
[AD-A267052] 03 p1189 N94-15664
Wideband acousto-optic correlator for an ESM receiver upgrade
[TABES PAPER 93-661] 03 p1054 N94-16156
Optical computing
[AD-A267881] 03 p1141 N94-17015
Low cost paths to binary optics 03 p1197 N94-17353
Computer-aided design package for designers of digital optical computers
[AD-A267866] 03 p1154 N94-17390
Coherent transient systems evaluation
[AD-A268808] 04 p1576 N94-18204
Optical associative processors and directed graphs
[AD-A268881] 04 p1615 N94-18224
Optical computing. Organization of the 1993 Photonics Science Topical Meetings. Technical digest series, volume 7
[AD-A269025] 04 p1578 N94-18332
Advanced Solid-State Lasers/Compact Blue-Green Lasers. 1993 technical digest series. Volume 2: Organization of the 1993 photonics science topical meetings
[AD-A269058] 04 p1438 N94-18492
Design and fabrication of a Multichannel Adaptive Optical Processor (MADOP)
[AD-A270004] 04 p1579 N94-18668
Center for the integration of optical computing
[AD-A271874] 05 p1899 N94-20469
Addition of decimal numbers in optical computing architecture by Walsh coded digits 05 p1773 N94-22122
Optical wavelet transform processor
[AD-A273625] 06 p2546 N94-24731
Photorefractive adaptive antenna array processor
[AD-A275762] 08 p3241 N94-28762
A/GATECH DOSP fabrication --- optical programmable logic array
[AD-A275848] 08 p3430 N94-28781
Overview of microoptics: Past, present, and future 08 p3235 N94-29771
Control and reliability of optical networks in multiprocessors
[AD-A277385] 09 p3881 N94-32285
Spectral-domain optical processing techniques
[AD-A278371] 10 p4141 N94-33739
Hardware implementation of time lenses and ultrafast optical temporal processors, phase 1
[AD-A278352] 10 p4143 N94-34006
Fault tolerance in opto-electronic computing
[AD-A280219] 12 p4453 N94-37150

OPTICAL CONTROL

Executive summary 02 p0545 N94-14831
Wavefront sensing, control, and pointing 02 p0546 N94-14833
True time delay optically controlled dual band transmitter
[AD-A267663] 03 p1003 N94-17228
Design considerations for a fiber optic communications network for power systems
[DE93-018404] 05 p1984 N94-20179
A theory for optical wavelength control in short pulse free electron laser oscillators
[AD-A271706] 05 p1817 N94-21353
Reconfigurable Array of Radiating Elements (RARE) controlled by light
[NASA-CR-195828] 09 p3884 N94-33073
Photonic fast packet switching using optically processed control
[AD-A278195] 10 p4038 N94-33386

OPTICAL CORRECTION PROCEDURE

Optical transfer operator of the atmosphere-ocean system 01 p0225 N94-12742
Emittance and beam size distortion due to linear coupling
[DE93-015402] 03 p1184 N94-16886
Space Shuttle Mission STS-61: Hubble Space Telescope servicing mission-01
[NASA-TM-109344] 05 p1653 N94-20192
Holographic optical elements correcting the off-axis aberrations of a parabolic mirror
[ISBN-0-315-57581-6] 05 p1990 N94-22411
HST image restoration: A comparison of pre- and post-servicing mission results 05 p1925 N94-22478
A study on electrostatic quadrupole lenses and their application technologies
[REPT-948] 06 p2546 N94-24982
High average power pulsed phase conjugate laser with birefringence correction
[DE94-006049] 09 p3719 N94-32659
Phase-only correction of scintillated laser beams: Downrange experimental results
[AD-A277778] 09 p3722 N94-33282

OPTICAL CORRELATORS

Application of normalized gray-scale correlation
[DE93-013765] 01 p0141 N94-10521
Alternative optical architectures for multichannel adaptive optical processing
[AD-A267052] 03 p1189 N94-15664
Spatial filters for optical correlation
[AD-A267199] 03 p1189 N94-15791
Coherent transient systems evaluation
[AD-A268808] 04 p1576 N94-18204
Evaluation of a liquid crystal spatial light modulator capable of amplitude- and phase-modulating modes
[AD-A269252] 04 p1577 N94-18262
Optimal design of binary phase-only filters using genetic algorithms
[AD-A268737] 04 p1396 N94-18278
Development of phase-only filters for sensor imagery
[AD-A276722] 09 p3880 N94-32151
Correlation filter synthesis using neural networks
[AD-A278124] 09 p3836 N94-33043
A novel optoelectronic system for distortion-invariant ATR
[AD-A277985] 09 p3884 N94-33087
Design of a composite filter realizable on practical spatial light modulators
[NASA-CR-196297] 12 p4525 N94-37579

OPTICAL COUNTERMEASURES

Millimeter wave reflectivity measurement system
[AD-A270008] 04 p1387 N94-18601
Atmospheric Propagation Effects Through Natural and Man-Made Obscurants for Visible to MM-Wave Radiation
[AD-A276919] 08 p3256 N94-30495
Experimental evaluation of camouflage effectiveness in the thermal infrared 08 p3257 N94-30502
NATO SOCMET trials 08 p3258 N94-30503
Global approach towards the evaluation of thermal infrared countermeasures 08 p3258 N94-30504
The effects of man-made smokes and battlefield-induced smokes on the propagation of electromagnetic radiation 08 p3258 N94-30505
Time-gated imaging through defense-scattering materials using stimulated Raman amplification
[AD-D016305] 12 p4440 N94-37775

OPTICAL COUPLING

Optical coupling elements for coherent optical multiport receivers
[ETN-93-94398] 03 p1188 N94-15447
Optical computing. Organization of the 1993 Photonics Science Topical Meetings. Technical digest series, volume 7
[AD-A269025] 04 p1578 N94-18332
Phase conjugation and beam combination using stimulated brillouin scattering
[AD-A269899] 04 p1439 N94-18656
Effects of stimulated Raman scattering on light beam properties during high-power laser beam long-path propagation
[AD-A273109] 05 p1818 N94-21509
Integrated optical coupling element on silicon substrate, appendix 2 05 p1988 N94-21596
An optical ASK and FSK phase diversity transmission system
[EUT-92-E-268] 06 p2542 N94-23171

A study of multiple guide optical couplers
[ISBN-0-315-84633-X] 07 p3038 N94-27441
An investigation of distributed coupling in a nonlinear semiconductor waveguide 08 p3246 N94-29529
Study of the dynamics of a nonlinear coupled-cavity laser system
[ISBN-0-315-86717-5] 09 p3716 N94-31748
Optimization of Y junctions in integrated optics
[ISBN-0-315-86782-5] 09 p3879 N94-31751
Method providing optimum optical trains alignment in a passive multi-channel fiber optic rotary joint
[AD-D016125] 10 p4143 N94-34151
High power diode laser Master Oscillator-Power Amplifier (MOPA)
[NASA-CR-196095] 11 p4271 N94-35488

OPTICAL DATA PROCESSING
NT SCENE ANALYSIS
Variable rate transfer of optical information
[AD-D015758] 01 p0418 N94-10374
Design and analysis of an optical interface message processor
[AD-A266079] 01 p0381 N94-10697
The optical/computer hybrid processing of extracting ocean wave directional spectrum by airborne photograph 01 p0197 N94-11934
Development of an on-board aircraft optical fiber data bus system
[NAL-TR-1163] 02 p0514 N94-13338
High speed all-optical networks
[NASA-CR-194384] 02 p0791 N94-13682
Optical residue processing module
[AD-A267721] 03 p1188 N94-14940
Research Studies on Advanced Optical Module/Head Designs for Optical Disk Recording Devices
[NASA-CR-194390] 03 p1226 N94-14981
Spatial filters for optical correlation
[AD-A267199] 03 p1189 N94-15791
Optical computing
[AD-A267881] 03 p1141 N94-17015
A scalable wrap-around shuffle exchange network with deflection routing
[NASA-CASE-NPO-18983-1-CU] 03 p1161 N94-17330
Asymmetric three-beam binary optic grating 03 p1195 N94-17340
Low cost paths to binary optics 03 p1197 N94-17353
Color separation gratings 03 p1198 N94-17362
The photonical, pure grid method
[NLR-TP-91478-U] 03 p1062 N94-17600
Examination of metrics and assumptions used in correlation filter design
[DE93-017636] 04 p1576 N94-18000
Evaluation of a liquid crystal spatial light modulator capable of amplitude- and phase-modulating modes
[AD-A269252] 04 p1577 N94-18262
Optimal design of binary phase-only filters using genetic algorithms
[AD-A268737] 04 p1396 N94-18278
Integrated photonics research volume 10. Conference edition
[AD-A269298] 04 p1577 N94-18298
Photorefractive tungsten bronze crystals for optical computing
[AD-A268859] 04 p1596 N94-18320
Optical computing. Organization of the 1993 Photonics Science Topical Meetings. Technical digest series, volume 7
[AD-A269025] 04 p1578 N94-18332
Quantum Optoelectronics. Organization of the 1993 photonics science topical meetings. Technical digest series, volume 8
[AD-A269026] 04 p1578 N94-18488
Photonics in Switching: Organization of the 1993 photonics science topical meetings. Technical digest
[AD-A269024] 04 p1578 N94-18528
Design and fabrication of a Multichannel Adaptive Optical Processor (MADOP)
[AD-A270004] 04 p1579 N94-18668
Integrated Photonics Research: Post-deadline papers
[AD-A269232] 04 p1609 N94-18908
Ultrafast Electronics and Optoelectronics: Summaries of papers. Technical digest conference edition
[AD-A269233] 04 p1405 N94-18909
Evaluation of laser diode based optical switches for optical processors
[AD-A270949] 04 p1581 N94-19602
Optical signal processing
[AD-A271036] 05 p1983 N94-20013
Optical encoding of imaging data
[AD-D015915] 05 p1984 N94-20056
Center for the integration of optical computing
[AD-A271874] 05 p1899 N94-20469
Addition of decimal numbers in optical computing architecture by Walsh coded digits 05 p1773 N94-22122
Optical processing in photorefractive media 05 p1789 N94-22222
Encoders for space applications 06 p2363 N94-24046
Optical pattern recognition system utilizing resonator array
[AD-D016071] 07 p3040 N94-28224
Modeling, analysis, and simulation of an optical time-division multiple-access network architecture
[AD-A275847] 08 p3498 N94-28780
Photonic devices and systems for optical signal processing
[AD-A275818] 08 p3498 N94-28804
Gordon research conference on optical signal processing and holography
[AD-A275092] 08 p3499 N94-28848
Overview of microoptics: Past, present, and future 08 p3235 N94-29771
Correlation filter synthesis using neural networks
[AD-A278124] 09 p3836 N94-33043
Design of free space interconnected signal processor
[AD-A278129] 09 p3683 N94-33093

OPTICAL DATA STORAGE MATERIALS
MeV ion-beam analysis of optical data storage films 03 p1226 N94-14984
Application of holographic optical elements to magneto-optic read/write heads 03 p1226 N94-14985
Dynamic testbed laboratory and micro-optics 03 p1199 N94-14986
Magnetic and magneto-optical properties and domain structure of Co/Pd multilayers 03 p1227 N94-14991
Effects of a shading band in the data path of an optical drive 03 p1199 N94-14993
Optical processing in photorefractive media 05 p1789 N94-22222
Azo polymers for reversible optical storage. 4. Cooperative motion of rigid groups in semicrystalline polymers
[AD-A277107] 09 p3654 N94-31978
Reversible optical storage in azo polymers
[AD-A277109] 09 p3654 N94-31980
The Third NASA Goddard Conference on Mass Storage Systems and Technologies
[NASA-CP-3262] 10 p4151 N94-33791
A new tape product for optical data storage 10 p4152 N94-33796
Certification of ICI 1012 optical data storage tape 10 p4152 N94-33797

OPTICAL DENSITY
Temperature depencence of the far infrared optical constants of polyethylene
[PB94-124336] 08 p3213 N94-28795

OPTICAL DEPTH
U OPTICAL THICKNESS

OPTICAL DISKS
Characterization facility for magneto-optic media and systems 03 p1226 N94-14983
Compact disk error measurements 03 p1227 N94-14988
Measurement of birefringence for optical recording disk substrates 03 p1227 N94-14989
Ring lens focusing and push-pull tracking scheme for optical disk systems 03 p1227 N94-14990
Determining the locations of the various CIRC recording format information blocks (user data blocks, C2 and C1 words and EFM frames) on a recorded compact disc 03 p1228 N94-14997
3-D optical memory disk
[AD-A267908] 03 p1141 N94-17380
Photorefractive tungsten bronze crystals for optical computing
[AD-A268859] 04 p1596 N94-18320
An ASIC memory buffer controller for a high speed disk system 05 p1754 N94-21089
Earth observation archive activities at DRA Farnborough 06 p2519 N94-23958
Spacecraft optical disk recorder memory buffer control 07 p2815 N94-27907
Virtual file system for PSDS 10 p4153 N94-33806
Using magnetic tape technology for data migration 10 p4154 N94-33812
Mass storage at NSA 10 p4155 N94-33817

OPTICAL EMISSION
U LIGHT EMISSION

OPTICAL EMISSION SPECTROSCOPY
NT LASER SPECTROSCOPY
Optical fiber spectroscopy: A study of the luminescent properties of the europium ion for thermal sensors
[NASA-CR-194576] 03 p1189 N94-15647
Growth and doping of Al(x)Ga(1-x)N films by electron cyclotron resonance assisted molecular beam epitaxy
[AD-A267305] 03 p1212 N94-16992
Imaging and blackbody emission spectra of hot particulates generated during laser ablation
[DE93-015818] 04 p1439 N94-18724
Spectroscopic studies of magnetic transitions in TbPO4
[DE94-001274] 05 p2035 N94-22565
Fifty years of continuous improvement: What has DOE done for analytical chemistry?
[DE94-002539] 06 p2234 N94-24548
Total light loss optic spectroscopy: Progress towards a fiber optic Raman organic vapor sensor
[DE94-002545] 06 p2234 N94-24549
Researches of the Electrotechnical Laboratory. No. 53: Spectral emission from combustion gas containing scattering media
[JTN-94-80603] 07 p2717 N94-27246

OPTICAL EQUIPMENT
NT CAMERAS
NT CINETHEODOLITES
NT COLLIMATORS
NT DIFFRACTOMETERS
NT EBERT SPECTROMETERS
NT ELECTROPHOTOMETERS
NT ELLIPSOMETERS
NT ENDOSCOPES
NT ETALONS
NT EYEPIECES
NT FAINT OBJECT CAMERA
NT FRAMING CAMERAS
NT HIGH DISPERSION SPECTROGRAPHS
NT HIGH SPEED CAMERAS
NT INFRARED SPECTROMETERS
NT INFRARED SPECTROPHOTOMETERS
NT LASER DOPPLER VELOCIMETERS
NT LASER RANGE FINDERS
NT LIGHT SCATTERING METERS
NT MICROWAVE REFLECTOMETERS
NT MULTISPECTRAL BAND CAMERAS
NT MULTISPECTRAL BAND SCANNERS
NT OCULOMETERS
NT OPTICAL GYROSCOPES
NT OPTICAL MEASURING INSTRUMENTS
NT OPTICAL MICROSCOPES
NT OPTICAL PYROMETERS
NT OPTICAL RANGE FINDERS
NT OPTICAL SCANNERS
NT PANORAMIC CAMERAS
NT PERISCOPES
NT PHOTOMETERS
NT PINHOLE CAMERAS
NT POLARIMETERS
NT PRISMS
NT REFLECTOMETERS
NT SPECTROHELIOGRAPHS
NT SPECTROPHOTOMETERS
NT STREAK CAMERAS
NT STROBOSCOPES
NT TELEVISION CAMERAS
NT THEMATIC MAPPERS (LANDSAT)
NT TOTAL OZONE MAPPING SPECTROMETER
NT TRANSMISSOMETERS
NT ULTRAVIOLET SPECTROMETERS
NT WIDE ANGLE LENSES
Development tests for a high stability optical bench 01 p0062 N94-10047
Technique to prepare high-reflectance optical fiber bragg gratings with single exposure in-line on fiber draw tower
[AD-D015757] 01 p0374 N94-10373
Wavelength considerations in soft x ray projection lithography
[DE93-014115] 01 p0381 N94-10651
Optoelectronic technology consortium
[AD-A265691] 01 p0383 N94-12444
Fabrication of AlGaAs/GaAs-light-emitting devices by selective MOCVD using dialkylmetalchloride 02 p0627 N94-13433
Optical degradation issues for XUV projection lithography systems
[DE93-012658] 02 p0626 N94-14805
Optical testing 02 p0547 N94-14836
Optical systems integrated modeling 02 p0547 N94-14837
Advanced optical instruments technology 02 p0547 N94-14838
A novel solid-state optical temporal analyzer with picosecond resolution and picowatt sensitivity
[AD-A266804] 03 p0986 N94-14912
Design of pulse stretching cell for a sodium guide star optical system
[DE93-016436] 03 p1236 N94-14929
Velocity matched millimeterwave electro-optic modulator
[AD-A267264] 03 p1188 N94-14957
Visualization of solidification front phenomena
[NASA-CR-193838] 03 p0976 N94-15006
Polished substrate surface and cleaning study for coated optic quality
[DE93-014116] 03 p1190 N94-15975

Optical ionospheric instrumentation and research
[AD-A266403] 03 p1192 N94-16550
Conference on Binary Optics: An Opportunity for Technical Exchange
[NASA-CP-3227] 03 p1194 N94-17331
Manufacturing the key to binary optics
03 p1194 N94-17332
Binary optics: Trends and limitations
03 p1194 N94-17333
Diffractive optics: Design, fabrication, and applications
03 p1194 N94-17334
Scalar limitations of diffractive optical elements
03 p1194 N94-17336
Diffractive optical elements for generating arbitrary line foci 03 p1195 N94-17338
Asymmetric three-beam binary optic grating
03 p1195 N94-17340
Scattering from binary optics
03 p1195 N94-17341
Mathmatical modeling for diffractive optics
03 p1195 N94-17342
Binary optics at Hughes Danbury Optical Systems
03 p1195 N94-17344
Diffractive optics fabricated by direct write methods with an electron beam 03 p1196 N94-17347
Applications of advanced diffractive optical elements
03 p1197 N94-17356
SURPHEX (tm): New dry photopolymers for replication of surface relief diffractive optics
03 p1198 N94-17358
Predesign of diamond turned refractive/diffractive elements for IR objectives 03 p1198 N94-17359
Optical system storage design with diffractive optical elements 03 p1198 N94-17360
Spectral inverse scattering theory for dielectric media: Application to optical devices
[AD-A268635] 03 p1199 N94-17427
Test methods for acceptance testing of telescopes
[AD-A268316] 03 p1237 N94-17568
Comparison of computer predictions and magnetic field measurements for an iron spectrometer magnet
[DE93-016164] 03 p1176 N94-17658
Experiments in sideband suppression on the Los Alamos National Laboratory Free-Electron Laser
[DE93-014466] 04 p1435 N94-17724
Considerations for the use of the modified line reversal technique for gas temperature measurement
[DE93-015752] 04 p1576 N94-17857
Designs for optical components related to the Los Alamos free-electron laser
[DE93-016617] 04 p1436 N94-17865
Calibration of a high frequency monostatic acoustic echosounder
[AD-A268901] 04 p1481 N94-18229
Evaluation of a liquid crystal spatial light modulator capable of amplitude- and phase-modulating modes
[AD-A269252] 04 p1577 N94-18262
Photorefractive receiver study
[AD-A269352] 04 p1577 N94-18302
Optical design for photonics. Organization of the 1993 Photonics Science Topical Meetings. Technical digest series, volume 9
[AD-A269027] 04 p1578 N94-18396
Quantum Optoelectronics. Organization of the 1993 photonics science topical meetings. Technical digest series, volume 8
[AD-A269026] 04 p1578 N94-18488
Advanced Solid-State Lasers/Compact Blue-Green Lasers. 1993 technical digest series. Volume 2: Organization of the 1993 photonics science topical meetings
[AD-A269058] 04 p1438 N94-18492
Liquid sound speeds at pressure from the optical analyzer technique
[DE93-018362] 04 p1563 N94-19151
Optical frequency division using an optical parametric oscillator
[AD-A270847] 04 p1581 N94-19578
The aerogel mesh contamination collector
[AD-A270537] 05 p1651 N94-20011
Feedback controlled optics with wavefront compensation
[NASA-CASE-NPO-18194-1-CU]
05 p1985 N94-20305
Optical metrology of magnetically trapped hydrogen
[AD-A272110] 05 p1680 N94-20584
Dual-beam multiple wavelength light transmittance measurement for particle sizing in rocket motor plumes
[AD-A272491] 05 p1670 N94-21206
QPPM receiver for free-space laser communications
[NASA-TM-106424] 05 p1741 N94-21567
The Keck keyword layer 05 p1925 N94-22460
The optohydraulic servovalve: A novel device for the precise optical control of hydraulic pressure
[ISBN-0-315-83580-X] 05 p1827 N94-22577
Measuring electrically charged particle fluxes in space using a fiber optic loop sensor
[NASA-CR-191328] 06 p2544 N94-23829
Mesospheric and lower thermospheric winds, temperatures densities, and volume emission rates
[NASA-CR-195147] 06 p2403 N94-24486
Germanium x ray phase plates for the production of circularly polarized x rays
[DE94-002908] 06 p2545 N94-24550
Heterodyne array for measurement of target velocity
[AD-D016025] 06 p2545 N94-24722
A study on electrostatic quadrupole lenses and their application technologies
[REPT-948] 06 p2546 N94-24982
Solutions of the 2-D Helmoholtz equation for optical waveguides
[DE93-616840] 06 p2547 N94-25209
The National Center for Advanced Information Components Manufacturing: Program update
[DE94-002647] 07 p2960 N94-26118
Optoelectronic Technology Consortium
[AD-A274909] 07 p2782 N94-26344
Optoelectronic technology consortium
[AD-A274595] 07 p3036 N94-26857
Helmet head tracking mounting device
[AD-D016048] 07 p2942 N94-27114
Binary optical elements: Studies in design, manufacture and performance
[ISBN-0-315-60643-6] 07 p3039 N94-27643
Aberrated point-spread functions and beam quality for optical systems with annular pupils
[AD-A275311] 08 p3499 N94-28875
Lasercom system architecture with reduced complexity
[NASA-CASE-NPO-19069-1-CU]
08 p3293 N94-29493
Design and testing of the LITE Variable Field Stop mechanism 08 p3161 N94-29633
Optical Chopper Assembly for the Mars Observer
08 p3162 N94-29639
Overview of microoptics: Past, present, and future
08 p3235 N94-29771
Hybrid optics for space applications
[ESA-CP-1158] 08 p3501 N94-30418
Precision and manufacturing at the Lawrence Livermore National Laboratory 08 p3240 N94-30449
Degradation of optical components in space
09 p3594 N94-31029
Mitigation of adverse environmental effects on lunar-based astronomical instruments
09 p3598 N94-31426
Neutral ion sources in precision manufacturing
09 p3875 N94-32447
Proceedings SPIE: Conference Digest, volume 2104
[AD-A278107] 09 p3884 N94-33187
Traineeship augmentation for aerosol optical properties study
[AD-A278466] 10 p4085 N94-33544
Multifunctional gel-silica optics
[AD-A278531] 10 p4141 N94-33670
Hardware implementation of time lenses and ultrafast optical temporal processors, phase 1
[AD-A278352] 10 p4143 N94-34006
Nonlinear frequency conversion optical filter
[AD-D016127] 10 p4036 N94-34283
Method and apparatus for removing unwanted reflections from an interferometer
[NASA-CASE-NPO-18478-1-CU]
11 p4333 N94-35749
A new, optical-lever based atomic force microscope
[AD-A280524] 12 p4524 N94-37110

OPTICAL FIBERS

NT SCINTILLATING FIBERS
Multiplexed and distributed optical fibre sensors
01 p0064 N94-10065
Fibre optic strain and temperature measurement in composite materials: A review of the OSTIC programme
01 p0065 N94-10066
The sensitivity of an optical fiber holographic interferometer 01 p0107 N94-10117
Method and apparatus for polarization-maintaining fiber optical amplification with orthogonal polarization output
[AD-D015756] 01 p0374 N94-10372
Technique to prepare high-reflectance optical fiber bragg gratings with single exposure in-line on fiber draw tower
[AD-D015757] 01 p0374 N94-10373
Fabrication and analysis of a special optical connector containing a 1/4-inch-long optical fiber for DOI tests
[DE93-013115] 01 p0381 N94-10647
Journal of Research of the National Institute of Standards and Technology, volume 98, number 2, March - April 1993
[PB93-196228] 01 p0485 N94-10850
Factors affecting the embedding of optical fibre sensors in advanced composite structures
01 p0070 N94-11336
Ocean measuring experiments using optical fiber distributed temperature sensor 01 p0172 N94-11968
Localized and distributed fiber-optic strain sensors embedded in composite materials
[UTIAS-346] 01 p0073 N94-12013
Development of an on-board aircraft optical fiber data bus system
[NAL-TR-1163] 02 p0514 N94-13338
Optical fiber sensors for materials and structures characterization
[NASA-CR-194090] 02 p0791 N94-13353
Measurements of optical properties of waveshifting optical fiber for liquid scintillator hadron calorimetry
[DE93-012606] 02 p0791 N94-13482
Liquid and gas evanescent wave spectroscopy via tunable lasers and silver halide fibers
[ITN-93-65226] 02 p0565 N94-14465
Radiation effects on optoelectronic analog link for particle detectors
[DE93-015794] 02 p0793 N94-14529
Optical fibre Fabry-Perot interferometers for calorimetric heat transfer gauges
[RAE-TM-AERO/PROP-20] 02 p0653 N94-14701
Optical residue processing module
[AD-A267721] 03 p1188 N94-14940
Prospects for high pressure imaging gas scintillation drift chambers 03 p0901 N94-15040
Optical coupling elements for coherent optical multiport receivers
[ETN-93-94398] 03 p1188 N94-15447
Optical fiber spectroscopy: A study of the luminescent properties of the europium ion for thermal sensors
[NASA-CR-194576] 03 p1189 N94-15647
The three-dimensional ray trajectories of the WKB optical fiber modes
[AD-A267167] 03 p1189 N94-15739
Pulse propagation in inhomogeneous optical waveguides
[DE93-013378] 03 p1191 N94-16007
Fundamental theory of light for applications: Notes for five informal lectures
[DE93-016463] 03 p1192 N94-16953
Investigation of the optical, electronic, and structural properties of fiber optic glasses
[AD-A267645] 03 p0971 N94-17204
The stability and dynamics of elastic structures and fluid flows
[AD-A267990] 03 p1029 N94-17414
Laser induced damage testing: Equipment and techniques
[DE93-017143] 04 p1437 N94-18060
Advanced optical fiber communication systems
[AD-A269120] 04 p1577 N94-18254
Applications of nonlinear optic effects in new specialty fibers
[AD-A268890] 04 p1578 N94-18457
Metal Film Surface Plasmon Resonance (MFSPR) fibre couplers
[AD-A268871] 04 p1579 N94-18635
Apparatus and method for varying a Bragg wavelength of a Bragg grating formed in an optical fiber
[AD-D015876] 04 p1579 N94-18743
Evaluation of fiber optic performance in the ACRR
[DE93-018515] 04 p1580 N94-18970
Penetrometer compatible, fiber-optic sensor for continuous monitoring of chlorinated hydrocarbons: Field test results
[DE93-017974] 04 p1352 N94-19266
Delamination in composite materials as observed using an optical fiber strain gage
[AD-A270803] 04 p1344 N94-19662
Multidimensional solitons in fiber arrays
[DE93-019923] 05 p1983 N94-19862
Fiber optic Michelson sensor and arrays with passive elimination of polarization fading and source feedback isolation
[AD-D015944] 05 p1984 N94-20065
Plasma chemical vapor deposition of halide glasses
[AD-D015933] 05 p1701 N94-20331
Wide-angle imaging system with fiberoptic components providing angle-dependent virtual material stops
[NASA-CASE-NPO-18146-1-CU]
05 p1986 N94-20345
Disengagable adapter for an optical fiber connector
[AD-D015959] 05 p1822 N94-20356
Optical fibers and Fluorosensors having improved power efficiency and methods of producing same
[NASA-CASE-LAR-14525-1-CU]
05 p1986 N94-20378
Delivery of very high bandwidth with ATM switches and SONET
[DE93-019432] 05 p1899 N94-20476
Optical fiber sensor having an active core
[NASA-CASE-LAR-14607-1-SB]
05 p1986 N94-20586

Integrated optical coupling element on silicon substrate, appendix 2
05 p1988 N94-21596
Fibre pigtailed silicon based low cost passive optical components, appendix 5
05 p1989 N94-21599
A new innovative instrument for space plasma instrumentation
[NASA-CR-194736] 05 p1666 N94-21780
Simulations of spectral broadening by cross-phase modulation (XPM) with chaotic light pulses
[DE93-019623] 05 p1819 N94-21872
OTDR strain gauge for smart skins
[DE93-041043] 05 p1810 N94-21953
The data acquisition system for the Anglo-Australian Observatory 2-degree field project
05 p2048 N94-22529
Demodulation of a fiber Fabry-Perot strain rosette using white light interferometry
[ISBN-0-315-83427-7] 05 p1990 N94-22579
Phase demodulation of interferometric fiber-optic sensors
[ISBN-0-315-83425-0] 05 p1991 N94-22581
An embedded fibre optic for damage growth monitoring in Kevlar composites
[ISBN-0-315-83501-X] 05 p1677 N94-22589
SFOLDA: A semiconductor LDA for measurements in complex flows
06 p2316 N94-22856
Fiber optic detection of laser generated ultrasound for materials characterization
[ISBN-0-315-83541-9] 06 p2541 N94-22891
NASA/ASEE Summer Faculty Fellowship Program
[NASA-CR-194678] 06 p2571 N94-23230
Output optics for laser velocimeters
[NASA-CASE-ARC-11889-1-SB]
06 p2543 N94-23309
Fiber optic temperature sensor using a Y2O2S:Eu thermographic phosphor
[DE94-000331] 06 p2543 N94-23461
Analysis for the computational modeling of finite cladding and lossy coating effects in fibers
[PB94-111085] 06 p2544 N94-23732
Measuring electrically charged particle fluxes in space using a fiber optic loop sensor
[NASA-CR-191328] 06 p2544 N94-23829
Fiber optic detection of ultrasound and its application to cure monitoring
[ISBN-0-315-83424-2] 06 p2544 N94-24466
Fiber optical angular sensor: Literature study and experimental results
[PB93-204345] 06 p2545 N94-24529
Total light loss optic spectroscopy: Progress towards a fiber optic Raman organic vapor sensor
[DE94-002545] 06 p2234 N94-24549
White-light, pressure, and temperature interferopolarimetric sensor featuring optical fibers
[PB93-199792] 06 p2545 N94-24631
Layered parallel interface for an active antenna array
[AD-D016002] 06 p2301 N94-25045
Influence of embedded optical fibers on compressive strength of advanced composites
[AD-A273775] 07 p2705 N94-25859
Development of surgical CW Nd:YAG laser with optical fiber delivery system
[DE93-632902] 07 p2817 N94-26185
Inert strength of pristine silica glass fibers
[DE94-004685] 07 p2750 N94-26247
Multichip module high speed testing
[AD-A274873] 07 p2782 N94-26343
Calorimeter with WLS fibers and parallel to beam scintillators
[DE93-634188] 07 p2810 N94-26378
Cad of GeO2-SiO2 double-layer core dispersion-shifted single-mode fibre
[DE93-634325] 07 p3035 N94-26383
All-optical gain switching of erbium-doped fibre amplifiers
[ISBN-0-315-84120-6] 07 p2784 N94-26704
Method of measuring liquid level
[AD-D016049] 07 p3038 N94-27153
Evanescent field infrared spectroscopy using chalcogenide glass fiber
[ITN-94-85233] 07 p3038 N94-27178
Ir-fibers in a laser threat warning system and robot shot warning system
[PB94-124476] 07 p3038 N94-27209
Intelligent material systems and structures. Part 6: Measurements of adhesion between optical fibres and composite materials
[PB94-123577] 07 p2756 N94-27215
Kinoform/lens system for injecting a high power laser beam into an optical fiber
[DE94-003226] 07 p2819 N94-27262
Fiber optic Faraday flux transformer specification
[AD-D016058] 07 p3039 N94-27674
Fiber optic true time-delay array antenna feed system
[AD-D016063] 07 p2777 N94-27734
Optical flameout detector
[NASA-CASE-LAR-14997-1] 08 p3287 N94-29368
Assessment of the fibre volume distribution around optical fibres
[FFA-TN-1993-12] 08 p3179 N94-29425
Intelligent material systems and structures. Part 7: Debonding and pull-out of two optical fibers from two epoxies
[PB94-137767] 08 p3180 N94-29475
A sub-cm micromachined electron microscope
08 p3236 N94-29775
Issues arising with the application of optical fiber transmission in class 1E systems in nuclear power plants
[DE94-004743] 08 p3500 N94-29928
Optical studies of dynamical processes in disordered systems
[DE94-006751] 08 p3501 N94-30252
Standard testing procedures for optical fiber and unshielded twisted pair at Sandia National Laboratories
[DE94-005315] 08 p3501 N94-30910
An axial approach to detection in capillary electrophoresis
[DE94-005556] 09 p3631 N94-31154
Advanced optical fiber communication systems
[AD-A276416] 09 p3878 N94-31330
Nd-YAG laser welding of the fiber optic connector to the header shell on the 2SL actuator
[DE94-006104] 09 p3723 N94-31621
Post-calibration correction for rotating-analyzer ellipsometer with optical fiber bundle detection system
[AD-A277329] 09 p3881 N94-32280
Studies of an optical multi-processor interconnect
[AD-A277093] 09 p3881 N94-32392
Flexible manufacturing for photonics device assembly
09 p3669 N94-32449
Passive, multi-channel fiber optic rotary joint assembly
[AD-D016116] 09 p3882 N94-32626
Torque-balanced extendable fiber optic cable
[AD-D016097] 09 p3882 N94-32719
Fiber optic continuous true time-delay modulator
[AD-D016098] 09 p3883 N94-32720
Multi-line passive fiber optic slipring
[AD-D016092] 09 p3883 N94-32738
Strain sensing using optical fibers
[NASA-CR-195807] 09 p3740 N94-32940
Fiber optic microcable produced with radiation cured composite
[AD-D016155] 10 p4142 N94-33761
Fiber-optical testing system having a detection circuit
[AD-D016159] 10 p4142 N94-33764
Proposal to produce novel, transparent radiation hard low refractive index
[AD-A278476] 10 p4029 N94-34087
A distributed optical fiber strain sensor for monitoring structural deformations
10 p4057 N94-34361
Plasma arc welding weld imaging
[NASA-CASE-MFS-28797-1] 11 p4273 N94-35367
Coatings for SiO2 optical fibers
[AD-D016197] 11 p4334 N94-36363
Sensitivity and signal to noise ratio improvement of a one micron ladar system incorporating a neodymium doped optical fiber preamplifier. Laser radar testbed
[AD-A280235] 12 p4447 N94-37137
Final report on spectral broadening by cross-phase modulation in linearly birefringent optical fibers
[DE94-010406] 12 p4524 N94-37191
Guiding hard x rays with glass polycapillary fiber
[DE94-004949] 12 p4525 N94-37258
Method of forming waveguides with ion exchange of halogen ions
[AD-D016304] 12 p4526 N94-37774

OPTICAL FILTERS
NT BIREFRINGENT FILTERS
NT INFRARED FILTERS
NT ULTRAVIOLET FILTERS
Continued development of an ultra-narrow bandpass filter for solar research
[NASA-CR-194169] 01 p0381 N94-10735
Thermal-optical switching of a silicon based interference filter
[AD-A265152] 01 p0174 N94-11095
Design of CCD camera system for use inside electron beam furnace
[DE93-009525] 01 p0170 N94-11267
Presort processor — optical filtering
[AD-A263872] 01 p0382 N94-11300
Comparison of multiresolution techniques for digital signal processing
[AD-A265364] 01 p0138 N94-12406
Advanced optical instruments technology
02 p0547 N94-14838
Display system employing acousto-optic tunable filter
[NASA-CASE-NPO-18736-1-CU]
03 p1190 N94-15933
Experiments in sideband suppression on the Los Alamos National Laboratory Free-Electron Laser
[DE93-014466] 04 p1435 N94-17724
Optimal design of binary phase-only filters using genetic algorithms
[AD-A268737] 04 p1396 N94-18278
Integrated Photonics Research: Post-deadline papers
[AD-A269232] 04 p1609 N94-18908
Design refinement of multilayer optical thin film devices with two optimization techniques
[DE93-634228] 06 p2542 N94-22979
Germanium x ray phase plates for the production of circularly polarized x rays
[DE94-002908] 06 p2545 N94-24550
Investigation of Raman beam cleanup and phase conjugation
[AD-A273157] 06 p2545 N94-24672
Calorimeter with WLS fibers and parallel to beam scintillators
[DE93-634188] 07 p2810 N94-26378
Long Duration Exposure Facility space optics handbook
[AD-A274831] 07 p3035 N94-26572
The Rb 780-nanometer Faraday anomalous dispersion optical filter: Theory and experiment
08 p3250 N94-29659
Degradation of optical components in space
09 p3594 N94-31029
Development of phase-only filters for sensor imagery
[AD-A276722] 09 p3880 N94-32151
Correlation filter synthesis using neural networks
[AD-A278124] 09 p3836 N94-33043
Analysis and design of a high speed, wide range stepwise tunable optical filter/amplifier
[PB94-149572] 09 p3698 N94-33169
Spectrally-selective fiber transmission filter system
[AD-D016133] 10 p4141 N94-33698
Nonlinear frequency conversion optical filter
[AD-D016127] 10 p4036 N94-34283
Design of a composite filter realizable on practical spatial light modulators
[NASA-CR-196297] 12 p4525 N94-37579

OPTICAL FLOW (IMAGE ANALYSIS)
Compatibility of information and mode of control: The case for natural control systems
02 p0523 N94-13307
Segmenting the optical flow due to the motion of several rigid objects
05 p1777 N94-22147
Extracting heading and temporal range from optic flow: Human performance issues
06 p2442 N94-25510
Optical information in landing scenes
06 p2442 N94-25511
Safe navigation and active vision for autonomous vehicles: A purposive and direct solution
09 p3832 N94-31842
Neural models of spatial orientation in novel environments
[AD-A277383] 09 p3835 N94-32340

OPTICAL GENERATORS
U LASER CAVITIES

OPTICAL GYROSCOPES
NASA's first in-space optical gyroscope: A technology experiment on the X ray Timing Explorer spacecraft
[NASA-TM-109242] 01 p0170 N94-10667

OPTICAL HETERODYNING
Impact of shorter wavelengths on optical quality for laws
[NASA-CR-193433] 02 p0792 N94-14473
Optical coupling elements for coherent optical multiport receivers
[ETN-93-94398] 03 p1188 N94-15447
Photorefractive receiver study
[AD-A269352] 04 p1577 N94-18302
Impact of shorter wavelengths on optical quality for laws
[NASA-CR-193873] 04 p1579 N94-18858
Coherent lidar design and performance verification
[NASA-CR-193813] 05 p1816 N94-20341
Laser linewidth measurement in the presence of RIN and using the recirculating self heterodyne method
[EUT-92-E-262] 06 p2347 N94-22874
Airborne astronomy with a 150 micrometer - 500 micrometer heterodyne spectrometer
[NASA-CR-195940] 10 p4162 N94-34705

OPTICAL IMAGES
U IMAGES

OPTICAL MASER MODULATION
U LIGHT MODULATION

OPTICAL MASERS
U LASERS

OPTICAL MATERIALS
Second and third order nonlinear optical properties of crystalline inorganic/organic complexes
[DE93-011883] 01 p0173 N94-10755

Arcjet exploratory tests of ARC optical window design for the AFE vehicle
[NASA-CR-192655] 01 p0034 N94-10930
Enhanced Damage-Resistant Optics for Spaceflight Laser Systems: Workshop findings and recommendations
[NASA-TM-109243] 01 p0381 N94-11054
Damage thresholds of fluoride multilayers at 355 nm
[DE93-009523] 01 p0090 N94-11230
Vacuum stability requirements of polymeric material for spacecraft application
[NASA-TM-109216] 01 p0091 N94-11350
New challenges in optical materials development
[DE93-011889] 01 p0383 N94-11676
Effect of microstructure on passive film formation and breakdown on Al alloys
[AD-A265339] 02 p0569 N94-13050
Optical fiber sensors for materials and structures characterization
[NASA-CR-194090] 02 p0791 N94-13353
Reflective coatings for solar applications
[DE93-010026] 02 p0702 N94-13381
Barium fluoride research and development at Lawrence Livermore National Laboratory
[DE93-014682] 02 p0807 N94-13405
Preparation of optical materials used in non-visible region (M-17) 02 p0589 N94-13749
Workshop Proceedings: Optical Systems Technology for Space Astrophysics in the 21st Century, volume 3
[NASA-CR-194102] 02 p0545 N94-14830
Executive summary 02 p0545 N94-14831
Materials and structures 02 p0546 N94-14835
Advanced optical instruments technology 02 p0547 N94-14838
Investigation of Zerodur material processing
[NASA-CR-193842] 02 p0793 N94-14903
Design, synthesis and characterization of novel nonlinear optical polymers
[AD-A267035] 03 p0964 N94-15675
Organic polymeric electro-optic materials: Synthesis, processing, and device applications
[AD-A267133] 03 p0964 N94-15688
High-performance nonlinear optical material developed in Japan
[AD-A266194] 03 p1191 N94-16126
Rational design, construction, and processing of high-performance nonlinear optical materials
[AD-A266185] 03 p1191 N94-16454
Main chain chromophoric polymers with second order nonlinear optical properties
[AD-D015893] 03 p0969 N94-16920
Static and dynamic investigations of brittle elasto-optical material
[IFTR-3/1992] 03 p1061 N94-17086
IR materials producibility
[AD-A268849] 04 p1577 N94-18223
Spatial light modulators and applications: Summaries of papers presented at the Spatial Light Modulators and Applications Topical Meeting
[AD-A269452] 04 p1577 N94-18283
Novel electrochemical materials prepared by sol-gel chemistry
[AD-A269060] 04 p1578 N94-18405
Theory of electromagnetic waves propagating in nonlinear anisotropic optical materials
[AD-A269305] 04 p1386 N94-18469
Relaxation of polar orientational order in nonlinear optical polymers by second harmonic generation
[AD-A269059] 04 p1370 N94-18515
Consortium for materials development in space
[NASA-CR-194411] 04 p1379 N94-18840
Radiation induced darkening of the optical elements in the Startracker camera
[DE93-018907] 04 p1433 N94-19004
Surface modification of sapphire for IR window application
[DE93-019168] 04 p1602 N94-19075
Ionized-cluster beam/partially ionized beam deposition of electro-optical and nonlinear optical organic materials and device development
[AD-A270832] 04 p1604 N94-19596
Optical switch evaluation support
[AD-A270948] 04 p1581 N94-19601
Complex and stereoregular nonlinear optical materials
[AD-A271067] 05 p1983 N94-19846
Optical switching devices
[AD-D015918] 05 p1984 N94-20059
X ray, extreme and far ultraviolet optical thin films for space applications
[NASA-CR-194635] 05 p1984 N94-20128
Optics survivability support, volume 1
[DE93-019616] 05 p1985 N94-20262
Optics survivability support, volume 2
[DE93-040310] 05 p1985 N94-20283
Optical metrology of magnetically trapped hydrogen
[AD-A272110] 05 p1680 N94-20584
The 13C-NMR spectra of poly (4-((2-(acryloyloxy) ethyl) ethyl amino)- 4-nitroazobenzene-co-methyl methacrylate)
[AD-A273016] 05 p1705 N94-21238
IR materials producibility
[AD-A273031] 05 p1987 N94-21321
Combination of on ground experiments and analysis software for the evaluation of material degradation in space (SILEX project) 05 p1662 N94-21389
Techniques for the flux growth of optical materials: Growth of beta-barium borate
[AD-A272717] 05 p2028 N94-21505
Polyimide-based electrooptic materials
[DE93-019416] 05 p1706 N94-21526
A fully automated stage for optical waveguide measurements
[AD-A273042] 06 p2542 N94-22915
Crystal growth of organics for nonlinear optical applications 06 p2225 N94-24348
Nonlinear optical thin films 06 p2225 N94-24349
Optimization of microscopic and macroscopic second order optical nonlinearities 06 p2226 N94-24354
Dipolar relaxation in a second-order nonlinear optical interpenetrating polymer network
[AD-A273626] 06 p2258 N94-24732
Ultrastructure processing of macromolecular materials
[AD-A273413] 06 p2258 N94-24782
Three-wave nonlinear interactions in KTiOPO4 (KTP) and KTP isomorphs
[AD-A274079] 07 p3052 N94-25993
Long Duration Exposure Facility space optics handbook
[AD-A274831] 07 p3035 N94-26572
An x ray absorption fine structure study of ordering in polythiophene thin films
[AD-A274235] 07 p2753 N94-26822
Mechanistic studies of opto-electronic materials and syntheses using multiple laser and surface diagnostics
[AD-A274528] 07 p3036 N94-26834
Polyimide/inorganic composite-interpenetrating polymer network for stable second-order nonlinear optics
[AD-A274646] 07 p2709 N94-27107
Dual-use applications of infrared sensitive materials
[AD-A275140] 08 p3499 N94-29694
An outdoor exposure testing program for optical materials used in solar thermal electric technologies
[DE94-000265] 08 p3500 N94-29799
Study of nonlinear optical polymers and their applications in optical waveguides 08 p3216 N94-29807
Nonlinear absorption in high reflector multilayers
[DE94-005818] 08 p3295 N94-30598
Characterization of defect geometries in multilayer optical coatings
[DE94-005820] 08 p3501 N94-30599
Remote pumping of solid state lasers with nuclear driven fluorescers
[DE94-004846] 08 p3296 N94-30614
Transient radiation-induced absorption in the materials for a GSGG laser
[DE94-005316] 09 p3714 N94-31148
New material for high average power infrared generation: QPM-DB GaAs
[AD-A276389] 09 p3714 N94-31358
Large-area conditioning of optics for high-power laser systems
[DE94-007028] 09 p3716 N94-31636
Advanced infrared photodetectors: Materials review
[AD-A277058] 09 p3879 N94-32013
The sol-gel-xerogel transition
[AD-A276647] 09 p3616 N94-32038
Multifunctional macromolecules
[AD-A277347] 09 p3656 N94-32246
Sol-gel coatings for high power laser optics: Past, present, and future
[DE94-007240] 09 p3718 N94-32252
New developments in second-order nonlinear optical polymeric materials
[AD-A277409] 09 p3658 N94-32578
Stable second-order nonlinear optical materials based on interpenetrating polymer networks
[AD-A277410] 09 p3658 N94-32579
Nonlinear optical polymers derived from organic/inorganic composites
[AD-A277408] 09 p3659 N94-32610
A historical perspective on fifteen years of laser damage thresholds at LLNL
[DE94-007930] 09 p3719 N94-32613
Nonlinear optical properties of rigid-rod polymers
[NASA-CR-191349] 09 p3882 N94-32702
Pump-probe method for investigating laser ablation and optical damage threshold mechanisms in optical materials
[DE94-008291] 09 p3720 N94-32753
Silicon-Based Optoelectronic Materials Symposium and Materials Research Society Proceedings, volume 298
[AD-A277518] 09 p3662 N94-32952
Low loss second-order nonlinear optical polymers based on all organic sol-gel materials
[AD-A277482] 09 p3663 N94-32985
Novel polydiacetylenes as materials for second and third order nonlinear optics
[AD-A277512] 09 p3664 N94-33082
Research in the optical sciences
[AD-A278271] 09 p3884 N94-33140
Development of materials for spectral hole burning applications
[AD-A278408] 09 p3909 N94-33324
Organosilicon polymeric nonlinear optical materials for optical switching and modulation
[AD-A278245] 10 p4140 N94-33381
Multifunctional gel-silica optics
[AD-A278531] 10 p4141 N94-33670
Detail design of a 10.4-m stretched-membrane dish
[DE94-009462] 10 p4079 N94-34167
Concurrent stabilization and imaging of a novel polymer for second harmonic generation via in situ photopolymerization
[AD-A278912] 11 p4243 N94-35588
Properties and bibliography of GaSe
[AD-A279064] 11 p4340 N94-35733
Determining the refractive index of a lambda/4 thin film on a thick substrate from a transmittance measurement
[DE93-019584] 12 p4523 N94-36693
Organic NLO polymers. 2: Main-chain and guest-host Chi(2)NLO polymers: NLO-phore structure versus poling
[AD-A280230] 12 p4423 N94-37133
Organic nonlinear optical (NLO) polymers. 4: Thermally stable NLO polymers
[AD-A280196] 12 p4423 N94-37148
Organic NLO polymers. 5: Homopolymerization of indole based NLO-phore: A heterocycle Chi(2)NLO main-chain polymer
[AD-A280229] 12 p4423 N94-37151
Substrate effects on the structure and optical properties of epitaxial PbTiO3 thin films prepared by metal-organic chemical vapor deposition
[DE94-010432] 12 p4535 N94-37192
Investigation of polycrystalline thin-film CuInSe2 solar cells based on ZnSe windows
[DE94-006936] 12 p4462 N94-37381
An amorphous fluoropolymer: Next generation optical coating candidate
[DE94-012386] 12 p4425 N94-37422

OPTICAL MEASUREMENT

NT ASTRONOMICAL PHOTOMETRY
NT ASTRONOMICAL POLARIMETRY
NT COLORIMETRY
NT INFRARED PHOTOMETRY
NT OPTOMETRY
NT PHOTOMETRY
NT POLARIMETRY
NT SPECTROPHOTOMETRY
NT STELLAR SPECTROPHOTOMETRY
NT ULTRAVIOLET PHOTOMETRY

Holographic interferometry for microgravity applications 01 p0108 N94-10123
Pressure and force measurements on models set in hypersonic flows: A review 01 p0005 N94-10435
Flow visualization and spectroscopy in hypersonic flows: New trends 01 p0005 N94-10437
A preliminary study on ice shape tracing with a laser light sheet
[NASA-TM-105964] 01 p0174 N94-11132
The evolution of whole field optical diagnostics for external transonic testing
[ARA-MEMO-379] 01 p0383 N94-11887
Adaptive control of interface by temperature and interface profile feedback in transparent multi-zone crystal growth furnace
[NASA-CR-194140] 02 p0762 N94-13253
Tomographic methods in flow diagnostics
[NASA-TM-106330] 02 p0650 N94-13876
Investigation of the feasibility of optical diagnostic measurements at the exit of the SSME
[NASA-CR-193832] 02 p0553 N94-14682
Executive summary 02 p0545 N94-14831
Measurement of birefringence for optical recording disk substrates 03 p1227 N94-14989
Sensor modelling for the Cyclops focal plane detector array based technology demonstrator
[AD-A267172] 03 p1190 N94-15846
Optical measurements of NASA/USAF CRRES high altitude rocket borne chemical release experiments in conjunction with the USAF airborne ionospheric observatory aircraft
[AD-A266404] 03 p1101 N94-16551
A 27 channels, 1 MHz fibre-optic measuring system
[AD-A266943] 03 p1003 N94-17307
High power steady state MPD thrusters
[AD-A267277] 03 p0928 N94-17308
Gear train behavior analyzer using laser beam scanning for watch movement 04 p1427 N94-18028

Space debris detection
[AD-A269254] 04 p1334 N94-18264
Survey of collision avoidance and ranging sensors for mobile robots, revision 1
[AD-A269846] 04 p1541 N94-18474
Pressure sensitive paint technique 04 p1431 N94-18647
Optical switch evaluation support
[AD-A270948] 04 p1581 N94-19601
Wavefront sensors for optical diagnostics in fluid mechanics: Application to heated flow, turbulence, and droplet evaporation
[DE93-040060] 05 p1797 N94-19974
Optical climatology of the Northeast Pacific Ocean
[AD-A271671] 05 p1866 N94-20559
Long Duration Exposure Facility (LDEF) contamination study
[AD-A272419] 05 p1658 N94-21147
Precision prism coupling setup applied to measure planar silica films on silicon, appendix 9 05 p1989 N94-21603
OTDR strain gauge for smart skins
[DE93-041043] 05 p1810 N94-21953
A fully automated stage for optical waveguide measurements
[AD-A273042] 06 p2542 N94-22915
Acoustic and optical investigations of superfluid He-3
[PB93-224889] 06 p2523 N94-23101
Capillary electrokinetic separations with optical detection
[DE94-001639] 06 p2233 N94-23716
Validation of a nonintrusive optical technique for the measurement of liquid mass distribution in a two-phase spray 06 p2548 N94-24420
Mesospheric and lower thermospheric winds, temperatures densities, and volume emission rates
[NASA-CR-195147] 06 p2403 N94-24486
Method and apparatus for the non-invasive measurement of pressure inside pipes using a fiber optic interferometer sensor
[AD-D016013] 06 p2344 N94-24734
A comparison of free-space and fiber mixer performances
[AD-A273558] 06 p2547 N94-25161
Non-invasive optical detection of glucose in cell culture nutrient medium 06 p2422 N94-25357
Surface physics with cold and thermal neutron reflectometry
[DE94-001447] 07 p2733 N94-26070
Research and development within nonlinear optics for protection of optical sensors against laser irradiation on of optical sensors against laser irradiation. Quarterannual report 1 (april 1993))
[PB94-124245] 07 p3037 N94-27046
Time domain reflectometry for measuring bulk soil electrical conductivity and comparison with the Em38 instrument
[PB94-125432] 07 p2881 N94-27052
Experimental verification of tomographic reconstruction of turbulent air flow structure using optical wavefront measurements
[AD-A274392] 07 p2795 N94-27129
Development of a 2f optical performance measurement system
[DE94-003489] 07 p3039 N94-27721
Detection of water on road surface by the polarized light 07 p2886 N94-27989
Optical flameout detector
[NASA-CASE-LAR-14997-1] 08 p3287 N94-29368
An experimental and comprehensive method to measure emission characteristics 08 p3257 N94-30501
Fiber optic chemical sensors on Mars
[DE94-005251] 09 p3941 N94-31145
Noninvasive spectral analysis and beam mapping of focused ultrasound, part 2
[AD-A276629] 09 p3861 N94-32059
Methods for measuring characteristics of night vision goggles
[AD-A277046] 09 p3804 N94-32302
Photothermal laser deflection, an innovative technique to measure particles in exhausts
[AD-A277151] 09 p3718 N94-32366
Calibration and validation studies in the LENS facility
[AD-A278403] 09 p3591 N94-33167
Real-time adaptive control of mixing in a plane shear layer
[AD-A278379] 10 p4113 N94-33744
Method of determining the concentration of a chemical of interest in a solution
[AD-D016165] 10 p4021 N94-33765
Sputter process investigation: Material and environment interaction processes investigation
[NASA-CR-193946] 10 p4026 N94-34076
A distributed optical fiber strain sensor for monitoring structural deformations 10 p4057 N94-34361
A survey of reflectometry techniques with applications to TFTR
[DE94-010202] 11 p4338 N94-36093
A multi-tiered wavefront sensor using binary optics
[DE94-010393] 11 p4267 N94-36111
Microwave reflectometry for fusion plasma diagnostics
[DE94-620118] 12 p4527 N94-36566
Initial studies of reflectometer for ITER
[DE94-012476] 12 p4528 N94-37167

OPTICAL MEASURING INSTRUMENTS

NT CINETHEODOLITES
NT DIFFRACTOMETERS
NT EBERT SPECTROMETERS
NT ELECTROPHOTOMETERS
NT ELLIPSOMETERS
NT ETALONS
NT HIGH DISPERSION SPECTROGRAPHS
NT INFRARED SPECTROMETERS
NT INFRARED SPECTROPHOTOMETERS
NT LASER RANGE FINDERS
NT LIGHT SCATTERING METERS
NT MICROWAVE REFLECTOMETERS
NT OCULOMETERS
NT OPTICAL PYROMETERS
NT OPTICAL RANGE FINDERS
NT PHOTOMETERS
NT POLARIMETERS
NT REFLECTOMETERS
NT SPECTROPHOTOMETERS
NT TOTAL OZONE MAPPING SPECTROMETER
NT TRANSMISSOMETERS
NT ULTRAVIOLET SPECTROMETERS

Local measurement of temperatures and concentrations: A review for hypersonic flows 01 p0004 N94-10434
Possibility of a crossed-beam experiment involving slow-neutron capture by unstable nuclei rapid-process-tron
[DE93-754288] 01 p0363 N94-10720
Optical fibre techniques for structural monitoring in composites 01 p0069 N94-11324
Strain measurement of carbon/epoxy composite with fibre optics white light quasi distributed polarimetric sensor 01 p0069 N94-11328
The development of phytoplankton sensing system with optical fiber 01 p0203 N94-11967
The seasonal change of phytoplankton size distribution using optical fiber sensor 01 p0210 N94-12656
Recent flight-test results of optical airdata techniques
[NASA-TM-4504] 02 p0517 N94-13791
Tomographic methods in flow diagnostics
[NASA-TM-106330] 02 p0650 N94-13876
Earth Observation Center Annual Report on Research and Development, Fiscal Year 1992
[EOC-92-01-0007] 02 p0687 N94-14091
Calibration and in-house validation results of JERS-1 data 02 p0687 N94-14092
Earth observation experiment data analysis 02 p0687 N94-14093
ADEOS project 02 p0687 N94-14094
Spectroscopic method and data reduction algorithm for laser long-path absorption measurements using RIS 02 p0689 N94-14218
Image processing and analysis of airborne POLDER data 02 p0689 N94-14219
Intra-blade quantitative transonic flow measurements at the DRA Pyestock Isentropic Light Piston Facility using PIV (Particle Image Velocimetry)
[RAE-TM-AERO/PROP-21] 02 p0509 N94-14706
Workshop Proceedings: Optical Systems Technology for Space Astrophysics in the 21st Century, volume 3
[NASA-CR-194102] 02 p0545 N94-14830
Executive summary 02 p0545 N94-14831
Optical testing 02 p0547 N94-14836
Neural-network-directed alignment of optical systems using the laser-beam spatial filter as an example
[NASA-TP-3372] 03 p1034 N94-15961
Revisiting the BCS, a measurement system for characterizing the optics of solar collectors
[DE93-015030] 03 p1091 N94-15993
Earth observation from small satellites 03 p0891 N94-17150
Portable, solid state, fiber optic coupled Doppler interferometer system for detonation and shock diagnostics
[DE93-013917] 04 p1423 N94-17700
Survey of collision avoidance and ranging sensors for mobile robots, revision 1
[AD-A269846] 04 p1541 N94-18474
Crossed molecular beam studies of atmospheric chemical reaction dynamics
[DE93-019246] 04 p1478 N94-19303
Pointing control design for autonomous space vehicle applications
[DE93-019943] 05 p1657 N94-19863
Wavefront sensors for optical diagnostics in fluid mechanics: Application to heated flow, turbulence, and droplet evaporation
[DE93-040060] 05 p1797 N94-19974
Thermal dilation fiber optical flow sensor
[AD-D015926] 05 p1797 N94-20094
Photonic electromagnetic field sensor apparatus
[AD-D015938] 05 p1717 N94-20333
Photonic electromagnetic field sensor apparatus
[AD-D015939] 05 p1718 N94-20334
Mathematical model and analysis of the Tactical Unmanned Ground Vehicle (TUGV) using computer simulation
[AD-A272258] 05 p1824 N94-20576
Army aircraft fire-detection systems operation and reliability
[AD-A271327] 05 p1641 N94-20912
Description and assessment of a new Optical Pressure Measurement System (OPMS) demonstrated in the high speed wind tunnel in Goettingen (Germany)
[DLR-FB-92-24] 05 p1651 N94-21280
CMU very fast range-imaging system
[AD-A272057] 05 p1761 N94-21282
Models of refraction in the marine atmosphere surface layer
[AD-A271724] 05 p1858 N94-21357
Integrated optical coupling element on silicon substrate, appendix 2 05 p1988 N94-21596
Design of a surface deformation measuring instrument for the Surface Tension Driven Convection Experiment (STDCE-2)
[NASA-CR-194758] 06 p2343 N94-23285
Fiber optical angular sensor: Literature study and experimental results
[PB93-204345] 06 p2545 N94-24529
LOLA: Lunar Optical Long-baseline Array. 1992-1993 space design
[NASA-CR-195533] 06 p2298 N94-24582
Method and apparatus for the non-invasive measurement of pressure inside pipes using a fiber optic interferometer sensor
[AD-D016013] 06 p2344 N94-24734
System for cancelling phase noise in an interferometric fiber optic sensor arrangement
[AD-D015994] 06 p2345 N94-25053
Non-invasive optical detection of glucose in cell culture nutrient medium 06 p2422 N94-25357
Numerical simulation of tomographic reconstruction for the study of turbulence using optical wavefront sensor measurements
[AD-A273851] 07 p2789 N94-25587
Development of a multi-sensor in situ fiber optic fluorometer
[DE94-003399] 07 p3035 N94-26100
Optical surface contouring for non-destructive inspection of turbomachinery
[NASA-CR-195245] 07 p2835 N94-26691
Research and development within nonlinear optics for protection of optical sensors against laser irradiation on of optical sensors against laser irradiation. Quarterannual report 1 (april 1993))
[PB94-124245] 07 p3037 N94-27046
Method of measuring liquid level
[AD-D016049] 07 p3038 N94-27153
Reflectometer employing an integrating sphere and lens-mirror concentrator
[AD-D016061] 07 p3039 N94-27676
Energy Dispersive X ray Diffraction (EDXD) apparatus for liquids at high temperature 07 p2721 N94-28159
A novel spectroscopic measurement method of RF plasma for temperature and electron density diagnoses 08 p3188 N94-28682
Three-axis fiber optic vector magnetometer
[AD-D016016] 08 p3288 N94-29699
Overview of microoptics: Past, present, and future 08 p3235 N94-29771
A commercialized, continuous flow fiber optic sensor for trichloroethylene and haloforms 08 p3502 N94-30462
Space equipment for Earth observations 09 p3613 N94-30997
Correlation filter synthesis using neural networks
[AD-A278124] 09 p3836 N94-33043
Design, development, and testing of a lightweight optical sensor cover system 09 p3604 N94-33302
Fiber optic probes for laser light scattering: Ground based evaluation for micgrogravity flight experimentation. Integrated coherent imaging fiber optic systems for laser light scattering and other applications
[NASA-CR-194377] 10 p4144 N94-34914
Is increased accommodation a necessary condition for instrument myopia?
[AD-A278962] 11 p4298 N94-35659
A multi-tiered wavefront sensor using binary optics
[DE94-010393] 11 p4267 N94-36111

Optical position measurement for a large gap magnetic suspension system: Design and performance analysis
[NASA-TP-3438] 12 p4447 N94-36946

OPTICAL MEMORY (DATA STORAGE)

Holographic multiplexing for 3D optical memory
[AD-A266099] 01 p0171 N94-11420
Database system studies in fine grain optoelectronic computing
[AD-A267026] 03 p1145 N94-15627
Optical system storage design with diffractive optical elements 03 p1198 N94-17360
3-D optical memory disk
[AD-A267908] 03 p1141 N94-17380
Coherent transient systems evaluation
[AD-A268808] 04 p1576 N94-18204
Photo-induced and electrooptic properties of (Pb,La)(Zr,Ti)O3 films
[DE93-017496] 04 p1371 N94-18519
Optoelectronic associative memory
[NASA-CASE-NPO-18278-1-CU] 05 p1985 N94-20303
Efficiency of reversible optical storage in azo polymers
[AD-A272923] 05 p1705 N94-21223
Azo polymers for optical storage 3: Effect of film thickness on net phase retardation and writing speed
[AD-A272994] 05 p1705 N94-21267
A novel process monitoring and control system based on a neural manufacturing concept
[DE94-001516] 06 p2471 N94-23011
Photo-induced and electrooptic properties of (Pb,La)(Zr,Ti)O3 films for optical memories
[DE93-019820] 06 p2542 N94-23202
Earth observation archive activities at DRA Farnborough 06 p2519 N94-23958
High-speed, high-density, coherent time-domain optical memory
[AD-A274249] 07 p3037 N94-27010
Spacecraft optical disk recorder memory buffer control 07 p2815 N94-27907
Photonic devices and systems for optical signal processing
[AD-A275818] 08 p3498 N94-28804
Gordon research conference on optical signal processing and holography
[AD-A275092] 08 p3499 N94-28848
Azo polymers for reversible optical storage. 4. Cooperative motion of rigid groups in semicrystalline polymers
[AD-A277107] 09 p3654 N94-31978
Reversible optical storage in azo polymers
[AD-A277109] 09 p3654 N94-31980
High frequency active auroral research program (HAARP) imager
[AD-A277469] 09 p3775 N94-32999

OPTICAL METHODS

U OPTICS

OPTICAL MICROSCOPES

Two dimensional measurement and evaluation of point images at microscope objectives
[ETN-93-94397] 02 p0793 N94-14856
A near-field scanning optical microscope for analysis of magneto-optic media 03 p1199 N94-14995
Optical air pore analysis 05 p1708 N94-21892
Bulletin of the Institute for Chemical Reaction Science, Tohoku University, volume 2
[JTN-94-80602] 07 p2717 N94-27385
Variable temperature cold stage for microscope observation 07 p2718 N94-27389
Meso-optical Fourier transform microscope with double focusing
[DE94-607851] 08 p3290 N94-30148
The conoscopic microscope
[TELECOM-93-E-017] 09 p3877 N94-31173
Novel failure analysis techniques using photon probing with a scanning optical microscope
[DE94-006594] 09 p3692 N94-32112
Combined atomic force and scanning reflection interference contrast microscopy
[AD-A280341] 12 p4514 N94-37034
A new, optical-lever based atomic force microscope
[AD-A280524] 12 p4524 N94-37110

OPTICAL MODULATION

U LIGHT MODULATION

OPTICAL PATHS

Study of Einstein-Podolsky-Rosen state for space-time variables in a two photon interference experiment 01 p0370 N94-10582
A method of detecting and locating electrical current imbalances
[NASA-CASE-LEW-15407-1] 03 p1009 N94-15706
Fabrication and phase tuning of an optical waveguide device
[AD-D015815] 03 p1191 N94-16489
Photonic electromagnetic field sensor apparatus
[AD-D015938] 05 p1717 N94-20333
Photonic electromagnetic field sensor apparatus
[AD-D015939] 05 p1718 N94-20334
Mode transition matrix measuring system
[AD-D015973] 05 p1987 N94-21279
Laser phase induced intensity noise in fiber-optic signal processing and sensing systems
[ITN-94-85234] 07 p2819 N94-27179
Spectral and temporal correlations of multifrequency waves in the turbulent atmosphere
[ITN-94-85229] 07 p2774 N94-27233
A technique for multiplexing 3x3-coupler terminated interferometric fiber-optic sensors
[AD-A276739] 09 p3880 N94-32180
Phase-only correction of scintillated laser beams: Downrange experimental results
[AD-A277778] 09 p3722 N94-33282
A study of the impact of cirrus clouds on high altitude, long horizontal path laser transmission
[AD-A278563] 10 p4090 N94-33859
Method providing optimum optical trains alignment in a passive multi-channel fiber optic rotary joint
[AD-D016125] 10 p4143 N94-34151
Fabrication and phase tuning of an optical waveguide device
[AD-D016215] 11 p4334 N94-36122

OPTICAL POLARIZATION

The continuum emission of active galactic nuclei
[ITN-93-85208] 02 p0847 N94-13232
Application of holographic optical elements to magneto-optic read/write heads 03 p1226 N94-14985
Optically induced rotation diffusion in polymer liquid crystals: Phenomenological theory and experimental verification
[ETN-93-95068] 05 p2014 N94-20026
An integrated-optic polarization splitter on silicon substrate, appendix 4 05 p1989 N94-21598
Optical spin polarization and state-sensitive detection of a cesium atomic beam
[ATR-92(8436)-1] 06 p2534 N94-24077
The effects of optical feedback on polarization of vertical cavity surface emitting lasers
[AD-A273728] 06 p2351 N94-25445
Spin effects in hard interactions (interest in accelerated polarized beam)
[DE93-634398] 07 p3031 N94-26044
Detection of water on road surface by the polarized light 07 p2886 N94-27989
Dust in the Small Magellanic Cloud
[NASA-CR-195764] 08 p3543 N94-29696
Multiple scattering of polarized radiation in planetary atmospheres
[ETN-94-96018] 09 p3674 N94-31551

OPTICAL PROPERTIES

NT ABSORPTANCE
NT ABSORPTIVITY
NT BIDIRECTIONAL REFLECTANCE
NT BIREFRINGENCE
NT BRIGHTNESS
NT BRIGHTNESS DISTRIBUTION
NT COLOR
NT DICHROISM
NT LUMINOSITY
NT OPACITY
NT OPTICAL BISTABILITY
NT OPTICAL REFLECTION
NT PHOSPHORESCENCE
NT PHOTOCONDUCTIVITY
NT RADIANCE
NT REFLECTANCE
NT REFRACTIVITY
NT SPECTRAL REFLECTANCE
NT STELLAR LUMINOSITY
NT TRANSMISSIVITY
NT TRANSMITTANCE
NT TRANSPARENCE
NT TURBIDITY
NT WATER COLOR

Invariance of the mobility edge in anodic titanium oxides
[DE92-642136] 01 p0394 N94-10281
Solid state ionics 3. Materials Research Society Symposium Proceedings, volume 293
[AD-A265675] 01 p0395 N94-10416
Interferometric and optical tests of water window imaging x ray microscopes
[NASA-CR-193866] 01 p0375 N94-10506
Fabrication and analysis of a special optical connector containing a 1/4-inch-long optical fiber for DOI tests
[DE93-013115] 01 p0381 N94-10647
Space environmental effects on the integrity of chromic acid anodized coatings
[NASA-CR-191468] 01 p0055 N94-10947
Investigation of optically generated electronic defects and protonic transport in hydrogen-bonded molecular solids: Isomorphs of potassium dihydrogen phosphate
[DE93-012498] 01 p0399 N94-11243
Implementation and use of a computational ray-tracing program for the design and analysis of complex optical systems
[AD-A265075] 01 p0382 N94-11653
Applications of in-situ ellipsometry to microwave electron cyclotron resonance plasma processes
[AD-A265197] 01 p0373 N94-11880
Optical characteristics in Tokyo Bay 01 p0204 N94-11972
Progress toward atomic layer epitaxy of diamond: Diamond films grown one layer at a time
[AD-A265530] 01 p0403 N94-12010
Effects of microscopic iron metal on the reflectance spectra of glass and minerals 01 p0436 N94-12024
Simulation of possible regolith optical alteration effects on carbonaceous chondrite meteorites 01 p0430 N94-12163
Measurements of optical properties of waveshifting optical fiber for liquid scintillator hadron calorimetry
[DE93-012606] 02 p0791 N94-13482
Optical and physical properties of the LiSrAlF6:Cr laser crystal
[DE93-014657] 02 p0808 N94-13881
Optimization of transparent and reflecting electrodes for amorphous silicon solar cells
[DE93-010009] 02 p0704 N94-14110
Laser and spectroscopic properties of Yb-doped apatite crystals
[DE93-014656] 02 p0810 N94-14125
Theory of the electronic and structural properties of solid state oxides
[DE93-016051] 02 p0811 N94-14296
Workshop on the Space Environment: The Effects on the Optical Properties of Airless Bodies
[NASA-CR-194417] 02 p0842 N94-14298
Impact of shorter wavelengths on optical quality for laws
[NASA-CR-193433] 02 p0792 N94-14473
Relativistic proton-nucleus scattering and one-boson-exchange models 02 p0786 N94-14550
Theoretical antideuteron-nucleus absorptive cross sections 02 p0786 N94-14551
Plume primary smoke 03 p0923 N94-15218
Design, synthesis and characterization of novel nonlinear optical polymers
[AD-A267035] 03 p0964 N94-15675
Why is the Moon dark? 03 p1256 N94-16219
Optical effects of regolith processes on S asteroids as simulated by laser impulse alteration of ordinary chondrite 03 p1246 N94-16422
Variations in the Fe mineralogy of bright Martian soil 03 p1295 N94-16431
Optical properties of the Red Sea
[AD-A266466] 03 p1113 N94-16588
Elastooptical brittle materials in experimental studies of the state of stress and deformation
[IFTR-22/1991] 03 p1059 N94-16651
Detection of subsurface defects in machined silicon nitride ceramics by optical scattering methods
[DE93-015554] 03 p0968 N94-16658
Main chain chromophoric polymers with second order nonlinear optical properties
[AD-D015893] 03 p0969 N94-16920
Optical properties of water released in low Earth orbit
[AD-A266197] 03 p1192 N94-16936
Speckles statistics and decorrelation effects in complex ABCD optical systems
[AD-A267843] 03 p1193 N94-17012
Theoretical studies of nonlinear optical properties of conjugated polymers
[AD-A267390] 03 p1193 N94-17024
Transmission of light through a turbulent mixing layer
[AD-A267266] 03 p1193 N94-17264
Laser ignition of solid propellants: 1. Ignition delays
[AD-A268454] 03 p0976 N94-17538
A new method of designing multilayer optical thin film coatings
[DE93-624683] 03 p0974 N94-17611
Dust in the Small Magellanic Cloud
[NASA-CR-193344] 04 p1624 N94-17764
Metal-nanocluster composites made by ion implantation: A novel third-order nonlinear material
[DE93-015908] 04 p1339 N94-17846
Considerations for the use of the modified line reversal technique for gas temperature measurement
[DE93-015752] 04 p1576 N94-17857
Photorefractive tungsten bronze crystals for optical computing
[AD-A268859] 04 p1596 N94-18320
Kinetic aspects of lattice mismatch in molecular beam epitaxial growth on planar and patterned substrates
[AD-A270424] 04 p1597 N94-18506

Research on stable, high-efficiency amorphous silicon multijunction modules
[DE93-010046] 04 p1467 N94-18518
An ultraviolet faraday rotator glass
[AD-D015879] 04 p1371 N94-18529
Optical and transport properties of metallic and semiconductor nanostructures
[AD-A270009] 04 p1598 N94-18609
In-situ growth monitoring of molecular beam epitaxy processes
[AD-A269287] 04 p1598 N94-18616
Integration of ferroelectric/semiconductor thin films for SLM and photorefractive applications
[AD-A268645] 04 p1598 N94-18633
Optical properties of oxide coatings prepared by ion-assisted deposition
[AD-A270024] 04 p1599 N94-18711
Optical properties of redispersed iron fibers measured at 94 GHz
[AD-A269739] 04 p1342 N94-18756
Nonlinear optical properties of molecules
[AD-A270199] 04 p1567 N94-18783
Development of robust multilayer optics for use in high-peak power radiation environments
[DE93-018557] 04 p1580 N94-18931
Evaluation of fiber optic performance in the ACRR
[DE93-018515] 04 p1580 N94-18970
Surface modification of sapphire for IR window application
[DE93-019168] 04 p1602 N94-19075
Feasibility study: Monodisperse polymer particles containing laser-excitable dyes
[NASA-CR-194280] 04 p1373 N94-19402
Refinement of unit cell parameters by least-squares: Comments on an old technique and the development of a new computer program
[AD-A270610] 04 p1531 N94-19590
Ionized-cluster beam/partially ionized beam deposition of electro-optical and nonlinear optical organic materials and device development
[AD-A270832] 04 p1604 N94-19596
The deposition of electro-optic films on semiconductors
[AD-A270823] 04 p1605 N94-19664
Complex and stereoregular nonlinear optical materials
[AD-A271067] 05 p1983 N94-19846
Innovative acoustic technique for studying new materials and new developments in solid state physics
[AD-A270540] 05 p2013 N94-19933
Study of electromagnetic wave scattering from characterized rough surfaces
[AD-A270931] 05 p1716 N94-19934
Research on defects and transport in amorphous-silicon-based semiconductors
[DE93-017117] 05 p2013 N94-19939
Photoluminescence spectroscopy of zinc germanium diphosphide (ZnGeP2)
[AD-A270705] 05 p1678 N94-19953
The marine light-mixed layer experiment cruise and data report: R/V endeavor cruise EN-224, mooring deployment, 27 April-1 May 1991: Cruise EN-227, mooring recovery, 5-23 September 1991
[AD-A271175] 05 p1864 N94-20186
Optical and transport properties of metallic and semiconductor nanostructures
[AD-A271716] 05 p2018 N94-20554
Optical climatology of the Northeast Pacific Ocean
[AD-A271671] 05 p1866 N94-20559
Investigation of heterojunctions and multiple quantum well structures using crystalline organic semiconductors
[AD-A272113] 05 p2018 N94-20569
Optical effects of space weathering on lunar soils and the role of the finest fraction 05 p2101 N94-20687
MinMap: An imaging spectrometer for high resolution compositional mapping of the Moon
05 p1813 N94-20688
Visible-infrared properties of controlled laboratory soils
05 p1685 N94-20689
Sunphotometer network for monitoring aerosol properties in the Brazilian Amazon
05 p1839 N94-20961
Obtaining surface optical properties from space-based lidar systems
[AD-A272831] 05 p1987 N94-21172
Optical properties of chromium and neodymium in zirconium - barium - lanthanum - aluminum fluoride glass
[AD-A271609] 05 p1987 N94-21236
Solid-state dynamics and quantum transport in novel semiconductor nanostructures
[AD-A272955] 05 p2027 N94-21248
Long-range laser imaging
[AD-A273020] 05 p1817 N94-21253
Fundamental studies of defect generation in amorphous silicon alloys grown by remote plasma-enhanced chemical-vapor deposition
[DE93-017083] 05 p2029 N94-21615
Optical properties of cirrus derived from airborne measurements during FIRE IFO 2
05 p1872 N94-22297
Progress in interpreting CO2 lidar signatures to obtain cirrus microphysical and optical properties
05 p1874 N94-22308
A numerical technique for the calculation of cloud optical extinction from lidar 05 p1874 N94-22309
Investigation of the effects of the macrophysical and microphysical properties of cirrus clouds on the retrieval of optical properties: Results for FIRE 2
05 p1880 N94-22339
A new automatic design method to develop multilayer thin film devices for high power laser applications
[DE93-632490] 06 p2347 N94-22967
Interferometry in rarefied gas flows
[ISL-CO-207/92] 06 p2318 N94-23160
Transparent conducting thin films for spacecraft applications
[NASA-TM-106466] 06 p2218 N94-23370
Spectroscopic IR ellipsometry of 100 and 001 oriented YBa2Cu3O(7-delta) films
[PB93-201481] 06 p2561 N94-23445
The possible effects of the natural and induced space environment on the optical and thermal properties of EOS surfaces 06 p2207 N94-23596
Method of forming silicon structures with selectable optical characteristics
[NASA-CASE-NPO-18625-1-CU]
06 p2563 N94-23972
Night vision devices and characteristics
06 p2432 N94-23982
Cockpit/NVG visual integration issues
06 p2432 N94-23983
Prediction of nonlinear optical properties of organic materials. General theoretical considerations
06 p2224 N94-24343
Center for advanced electrical and structural polymers
[AD-A273415] 06 p2259 N94-24783
Retrieval of temperature profiles from Martian infrared spectra 06 p2620 N94-24893
A study on electrostatic quadrupole lenses and their application technologies
[REPT-948] 06 p2546 N94-24982
Liquidus temperature and optical properties measurement by containerless techniques
06 p2247 N94-25126
Optical properties and emissivities of liquid metals and alloys 06 p2248 N94-25129
Preparation and properties of translucent gamma-aluminium oxynitride
[ETN-94-95305] 06 p2263 N94-25281
Results from the VISA project
[AD-A273752] 06 p2406 N94-25540
Langmuir-Blodgett film of amylose-esters and chiral azo-dyes (structure and second order nonlinear optical behaviour)
[ETN-94-95390] 07 p2747 N94-25749
Studies of non-linear optical effects for agile beam steering
[AD-A273998] 07 p3034 N94-25902
Lighter alkali hydride and deuteride 1: Electronic properties of pure solids
[DE93-616188] 07 p3051 N94-25914
Optical conductivity and resistivity in the two-band Emery model
[DE94-601943] 07 p3051 N94-25945
Physical characteristics of polymethylmethacrylate scintillator SOFG-120
[DE93-634184] 07 p2810 N94-26395
Research and development within nonlinear optics for protection of optical sensors against laser irradiation on of optical sensors against laser irradiation. Quarterannual report 1 (april 1993))
[PB94-124245] 07 p3037 N94-27046
Accordion-like polymers for nonlinear applications
[AD-D016031] 07 p2755 N94-27148
Ir-fibers in a laser threat warning system and robot shot warning system
[PB94-124476] 07 p3038 N94-27209
Molecular dynamics simulation and crystal-field theory: Predicting the optical spectra and structure of rare-earth doped inorganic glasses
[ISBN-0-315-84679-8] 07 p3025 N94-27310
Technical report of ISSP. Ser. A, no. 2685: ASE-free terawatt KrF/Ti : sapphire hybrid laser system
[JTN-94-80571] 07 p2820 N94-27339
High damage threshold anti-reflectors by physical vapor deposited amorphous fluoropolymer
[DE94-004865] 08 p3212 N94-28560
Experimental and theoretical studies of molecular solids
[AD-A275511] 08 p3485 N94-28668
WINDOW 4.0: Documentation of calculation procedures
[DE94-004935] 08 p3410 N94-29019
Template synthesized nanoscopic gold particles: Optical spectra and the effects of particle size and shape
[AD-A275378] 08 p3197 N94-29312
Optical properties of cadmium sulfide, zinc selenide, and zinc manganese selenide semiconductor films
08 p3500 N94-29759
Nanosize metal alloy particle formation in Ag and Cu sequentially implanted silica
[DE94-005592] 08 p3207 N94-30042
Optical studies of dynamical processes in disordered systems
[DE94-006751] 08 p3501 N94-30252
Hybrid optics for space applications
[ESA-CP-1158] 08 p3501 N94-30418
Nonlinear optics response of semiconductor quantum wells under high magnetic fields
[DE94-003244] 08 p3520 N94-30835
Matter-radiation interactions in the atmosphere
09 p3776 N94-30998
Space environment durability of beta cloth in LDEF thermal blankets 09 p3591 N94-31015
Treatment of cloud radiative effects in general circulation models
[DE94-001864] 09 p3764 N94-31600
Inorganic materials for anomalous-dispersion phase-matched second harmonic generation: Rubidium titanyl arsenate isomorphs, Rb(Ti(1-2x)Ln(x)Nb(x))OAsO4
[DE94-006141] 09 p3899 N94-31847
Sensitivity analysis of the AVHRR infrared cirrus model
[AD-A276690] 09 p3784 N94-32117
Compatibility studies of some azo polymer blends
[AD-A277141] 09 p3657 N94-32365
Nonlinear optical properties of rigid-rod polymers
[NASA-CR-191349] 09 p3882 N94-32702
Short-pulse, high-intensity lasers at Los Alamos
[DE94-007545] 09 p3720 N94-32760
Optical properties of lanthanide-doped RbTiOAsO4 and transition metal-doped KTiOPO4
[DE94-008433] 09 p3907 N94-32963
Optical properties of doped sol-gel silica glasses
[AD-A278094] 09 p3884 N94-33267
Comparison of numerical models for computing underwater light fields
[AD-A278256] 10 p4140 N94-33411
Traineeship augmentation for aerosol optical properties study
[AD-A278466] 10 p4085 N94-33544
A study of the impact of cirrus clouds on high altitude, long horizontal path laser transmission
[AD-A278563] 10 p4090 N94-33859
Silica Fresnel lens for laser communications
[AD-A278329] 10 p4058 N94-33967
Dynamics of supermatrix semiconductor growth
[AD-A278380] 10 p4147 N94-34085
Solar radiation effects on glasses
[NASA-CR-195900] 10 p4029 N94-34232
The effects of cloud inhomogeneities upon radiative fluxes, and the supply of a cloud truth validation dataset
[NASA-CR-196080] 11 p4293 N94-35391
Properties and bibliography of GaSe
[AD-A279064] 11 p4340 N94-35733
Activities of the optoelectronics laboratory
[PB94-171196] 11 p4334 N94-36190
Selected translated abstracts of Russian-language climate-change publications. 2: Clouds
[DE94-011465] 11 p4295 N94-36244
Azobenzene-containing polymers: Some optoelectronic properties
[AD-A280448] 12 p4424 N94-37185
Substrate effects on the structure and optical properties of epitaxial PbTiO3 thin films prepared by metal-organic chemical vapor deposition
[DE94-010432] 12 p4535 N94-37192
The MBE growth and optical quality of BaTiO3 and SrTiO3 thin films on MgO
[DE94-011468] 12 p4538 N94-37570
Optical studies of dynamical processes in disordered systems
[DE94-011945] 12 p4538 N94-37676

OPTICAL PUMPING

NT LASER PUMPING

A phaseonium magnetometer: A new optical magnetometer based on index enhanced media
01 p0375 N94-10565
High power z pinches as x ray laser photopumps
[DE93-012842] 01 p0173 N94-10746
New challenges in optical materials development
[DE93-011889] 01 p0383 N94-11676
The Livermore x ray laser program
[DE93-014118] 02 p0658 N94-14152
Theoretical studies relating to the interaction of radiation with matter
[AD-A267134] 03 p1180 N94-15689

Problems related to stimulated electromagnetic emissions, strong turbulence and ionospheric modification
[IRF-SR-212] 04 p1480 N94-17720
Pulsed power supply for Nova Upgrade
[DE93-019626] 04 p1441 N94-19307
Photopumped x ray laser research on Saturn
[DE93-019430] 05 p1816 N94-20298
Generation of intense ultrashort x ray pulses
[DE93-019607] 05 p1817 N94-21299
Optical spin polarization and state-sensitive detection of a cesium atomic beam
[ATR-92(8436)-1] 06 p2534 N94-24077
Experimental and theoretical features of strong suppression and shifting phenomena in odd-photon resonant excitations and stimulated emissions
[DE94-000341] 06 p2535 N94-24510
Computer modeling of nonlinearities 06 p2458 N94-24661
Temporal model of an optically pumped co-doped solid state laser
[NASA-TM-109680] 06 p2350 N94-24851
Characterization of nonlinear effects in optically pumped vertical cavity surface emitting lasers
[AD-A273840] 07 p2815 N94-25744
Broad band tunable dye laser development
[DE93-632978] 07 p2816 N94-26157
Multiple exposure CCD detector for high-speed laser pump, x ray probe Laue scattering
[DE94-004618] 07 p2820 N94-27781
Optical parametric oscillator modeling with diffraction, depletion, and double refraction
[DE94-001504] 07 p3040 N94-27999
Visible vertical cavity surface emitting lasers
[AD-A275334] 08 p3293 N94-28919
High conversion efficiency pumped-cavity second harmonic generation of a diode laser
[DE94-006805] 09 p3717 N94-32134
Repetitively pulsed Cr:LiSAF laser for lidar applcations
[DE94-007546] 09 p3720 N94-32761
A reliable low-maintenance flashlamp-pumped Ti:sapphire laser operating at 120 PPS
[DE94-009030] 09 p3721 N94-32848
Fluorescence detection of single molecules using pulsed near-field optical excitation and time correlated photon counting
[DE94-007553] 11 p4320 N94-35376
Chirped-pulse amplification with flashlamp-pumped Ti:Sapphire amplifiers
[DE94-010055] 11 p4272 N94-35695
System for end-pumping a solid state laser using a large aperture laser diode bar
[AD-D016213] 11 p4273 N94-36370
Advanced laser driver for soft x-ray projection lithography
[DE94-011643] 12 p4449 N94-37722

OPTICAL PYROMETERS

Fiber optic temperature sensor using a Y2O2S:Eu thermographic phosphor
[DE94-000331] 06 p2543 N94-23461
Multiwavelength pyrometer for gray and non-gray surfaces in the presence of interfering radiation
[NASA-CASE-LEW-15250-1] 11 p4269 N94-35383

OPTICAL RADAR

NT DIFFERENTIAL ABSORPTION LIDAR
Characterization of a scannerless LADAR system
[DE93-011582] 01 p0174 N94-10959
Measures for simulator evaluation of a helicopter obstacle avoidance system 01 p0035 N94-11535
Development of shipboard ocean lidar 01 p0140 N94-11965
Remote sensing of subsurface water temperature profile and backscattering coefficient in the China Sea by Ocean Lidar (OLIDAR) 01 p0203 N94-11970
Polarisation of backscattering radiation at remote sensing of ocean with impulse laser beam 01 p0177 N94-12722
Remote sensing of light scattering coefficient of sea water vertical distribution by the means of airborne lidar 01 p0224 N94-12736
Novel Co:MgF2 lidar for aerosol profiler
[NASA-CR-191525] 02 p0654 N94-13091
Non-scanned LADAR imaging and applications
[DE93-013772] 02 p0655 N94-13261
Coherent Doppler lidar signal covariance including wind shear and wind turbulence
[NASA-CR-194492] 02 p0721 N94-13723
A rocket-borne lidar for studies of the middle atmosphere
[FFI/RAPPORT-92/7034] 02 p0715 N94-13949
Signal and reference wavelengths for the elimination of SO2 cross sensitivity in remote measurements of tropospheric ozone with lidar
[GKSS/92/E/24] 02 p0617 N94-14819
The mobile lidar system ARGOS for spatial resolution remote measuring of gaseous air pollutants
[GKSS/92/E/26] 02 p0617 N94-14820
The MADONA experiments (Meteorology and Diffusion Over Non-uniform Areas): High-resolution in-plume concentration fluctuations measurements using lidar remote sensing technique
[AD-A267711] 03 p1105 N94-14938
IR detectors and subsystems for space applications 03 p0909 N94-15091
Prelaunch optical characterization of the Laser Geodynamic Satellite (LAGEOS 2)
[NASA-TP-3400] 03 p0884 N94-15193
Heterodyne efficiency for a coherent laser radar with diffuse or aerosol targets
[NASA-CR-194563] 03 p1038 N94-15477
System architecture of optically controlled phased array radar
[AD-A267056] 03 p0988 N94-15667
Spatial filters for optical correlation
[AD-A267199] 03 p1189 N94-15791
Spatial and frequency diversity in lidar systems
[AD-A266192] 03 p1039 N94-16124
Clementine: Anticipated scientific datasets from the Moon and Geographos 03 p1288 N94-16392
BACKSCAT lidar simulation version 3.0: Technical documentation and users guide
[AD-A267296] 03 p1003 N94-17268
Laser beam steering device 03 p1045 N94-17357
A technique for measuring winds in the lower atmosphere using incoherent Doppler lidar
[DE93-017163] 04 p1488 N94-17758
Data fusion through simulated annealing of registered range and reflectance images
[DE93-015910] 04 p1612 N94-17858
Laser imaging radar system
[AD-A270436] 04 p1387 N94-18510
Modifications of airborne oceanographic lidar for the long range P-3 missions
[NASA-CR-194682] 04 p1499 N94-18819
Impact of shorter wavelengths on optical quality for laws
[NASA-CR-193873] 04 p1579 N94-18858
SPNDL: A concept for a small satellite Doppler lidar wind sounder 04 p1327 N94-19181
The Mexico City 1991 lidar measurements campaign
[DE93-019960] 04 p1478 N94-19272
Optics survivability support, volume 1
[DE93-019616] 05 p1985 N94-20262
Coherent lidar design and performance verification
[NASA-CR-193813] 05 p1816 N94-20341
Integrated display of multi-sensor geophysical and electromagnetic flight data 05 p1721 N94-20418
Conically scanned holographic lidar telescope
[NASA-CASE-GSC-13462-1] 05 p1986 N94-20591
Development of a lidar for integration with the Naval Postgraduate School Infrared Search and Target Designation (NPS-IRSTD) system
[AD-A271847] 05 p1817 N94-20611
Examinations of a thallium atomic vapor filter for a Raman temperature lidar
[GKSS-92/E/13] 05 p1857 N94-21044
Obtaining surface optical properties from space-based lidar systems
[AD-A272831] 05 p1987 N94-21172
NOVAM evaluation utilizing electro-optics and meteorological data from KEY-90
[AD-A271722] 05 p1868 N94-21356
Green Sheet project: Dye sheet evolution
[AD-A272019] 05 p1883 N94-21443
The use of lidar for the evaluation of traffic-related urban pollution
[DE94-000704] 05 p1852 N94-22017
Cirrus properties deduced from CO2 lidar observations of zenith-enhanced backscatter from oriented crystals 05 p1871 N94-22295
Bi-directional reflectance and other radiation parameters of cirrus from ER-2 observations 05 p1871 N94-22296
Remote sensing of multilevel clouds during FIRE IFO 2 05 p1844 N94-22303
Lidar and radar derived cirrus microphysical properties for the 26 November 1991 case study 05 p1873 N94-22305
Progress in interpreting CO2 lidar signatures to obtain cirrus microphysical and optical properties 05 p1874 N94-22308
A numerical technique for the calculation of cloud optical extinction from lidar 05 p1874 N94-22309
Observations of multi-layered clouds using K-band radar 05 p1874 N94-22311
Comparison of cloud boundaries measured with 8.6 mm radar and 10.6 micrometer lidar 05 p1875 N94-22317
CO2 lidar observations of Mount Pinatubo debris: FIRE 2 and longer-term measurements 05 p1876 N94-22323
Micro pulse laser radar
[NASA-CASE-GSC-13493-1] 06 p2294 N94-23627
Tropospheric Ozone Lidar Intercomparison Experiment, TROLIX 1991
[MPIM-102] 06 p2402 N94-24108
Nonlinear dynamical control of lasers
[AD-A273359] 06 p2350 N94-24938
A comparison of free-space and fiber mixer performances
[AD-A273558] 06 p2547 N94-25161
Improvement of system properties of a pulsed laser Doppler anemometer with respect to an optical amplifier
[DLR-FB-93-19] 06 p2547 N94-25305
Results from the VISA project
[AD-A273752] 06 p2406 N94-25540
Wind measurements with an incoherent lidar
[AD-A273756] 07 p2891 N94-25722
Design analysis of a combined optical/LADAR deep-space surveillance satellite
[AD-A274040] 07 p2694 N94-25832
An overview of the TNO contribution to VAST 92
[AD-A273751] 07 p2893 N94-26016
Elastic backscattering lidar for a MSTI satellite
[DE94-002701] 07 p2816 N94-26126
The development of Cr, Tm, Ho:YAG lasers for airborne lidar
[AD-A274895] 07 p2816 N94-26178
Compilation of corrections for postprocessing of laser bathymetry data
[PB94-123668] 07 p2900 N94-27156
Sum frequency generation using an optical parametric oscillator
[DE94-001827] 07 p3040 N94-28000
Innovative direct detection range-Doppler laser radar
[AD-A275619] 08 p3292 N94-28635
Laser beam steering with semiconductor waveguide
[AD-A275775] 08 p3292 N94-28765
Fusion of range and luminance data from laser radar systems
[AD-A275608] 08 p3292 N94-28770
Design and testing of the LITE Variable Field Stop mechanism 08 p3161 N94-29633
Automated inspection of turbine blades: Challenges and opportunities
[AIAA PAPER 94-1226-CP] 08 p3446 N94-30575
Cloud and aerosol characterization for the ARM central facility: Multiple remote sensor techniques development
[DE94-003523] 08 p3365 N94-30608
Remote sensor observations during WISP91: The use of microwave radiometers, RASS, and lidar ceilometers for detection of aircraft icing conditions
[PB94-142106] 08 p3136 N94-30890
The development and testing of a backscatter absorption gas imaging (BAGI) system designed to image at a range of 300 m
[DE94-006192] 09 p3675 N94-31761
Wind-speed measurements with a scanning elastic-backscatter lidar
[DE94-004974] 09 p3785 N94-32726
High resolution properties of the marine atmospheric boundary layer
[DE94-006235] 09 p3774 N94-32736
Water vapor from sunradiometry in comparison with microwave and balloon-sonde measurements at the Southern Great Plains ARM Site
[DE94-007479] 09 p3786 N94-32759
Repetitively pulsed Cr:LiSAF laser for lidar applcations
[DE94-007546] 09 p3720 N94-32761
Comparison of coherent to incoherent detection at 2.09 micrometers using a solid state LADAR system
[AD-A277159] 09 p3721 N94-33102
Radio wave refractivity deduced from lidar measurements
[AD-D016147] 10 p4034 N94-33780
A study of the impact of cirrus clouds on high altitude, long horizontal path laser transmission
[AD-A278563] 10 p4090 N94-33859
FOA 33
[PB94-149184] 10 p4143 N94-34094
Laser/lidar analysis and testing
[NASA-CR-193954] 10 p4058 N94-34136
Nonlinear frequency conversion optical filter
[AD-D016127] 10 p4036 N94-34283
A precise passive narrow-beam filter infrared radiometer and its use with LIDAR in the ARM program
[DE94-004167] 11 p4269 N94-36085
Molecular nitrogen fluorescence lidar for remote sensing of the auroral ionosphere
[AD-A280716] 11 p4291 N94-36263
Implementation of Raman lidar for profiling of atmospheric water vapor and aerosols at the SGP CART site
[DE94-011754] 11 p4295 N94-36285

Receiver design, performance analysis, and evaluation for space-borne laser altimeters and space-to-space laser ranging systems
[NASA-CR-194747] 12 p4397 N94-36988
Sensitivity and signal to noise ratio improvement of a one micron ladar system incorporating a neodymium doped optical fiber preamplifier. Laser radar testbed
[AD-A280235] 12 p4447 N94-37137

OPTICAL RANGE FINDERS
NT LASER RANGE FINDERS
The conceptual design of a short-range distance sensor 05 p1774 N94-22129
A feasibility study of a parallax-based passive missile approach warning system
[ISBN-0-315-60640-1] 05 p1743 N94-22410

OPTICAL REFLECTION
An expert system shell for inferring vegetation characteristics: Prototype help system (Task 1)
[NASA-CR-193411] 01 p0231 N94-11236
Effects of wind-roughened sea surface on ocean color remote sensing: Noise derived from reflected light and whitecaps 01 p0191 N94-11898
The upwelling radiation at the top of the atmosphere in coastal region 01 p0205 N94-11981
Determination of the surface cleanliness of metals by FT-IR spectroscopy
[DE93-013252] 02 p0565 N94-14525
Engineering design of sub-micron topographies for simultaneously adherent and reflective metal-polymer interfaces
[NASA-CR-194573] 03 p0964 N94-15700
Fullerene superconductors
[AD-A266749] 03 p1010 N94-15954
Optical properties and surface morphology studies of palladium contacts on mercuric iodide single crystals
[DE93-012510] 03 p1207 N94-15973
Photodetector array having high pixel density
[AD-D015859] 04 p1432 N94-18731
OTDR strain gauge for smart skins
[DE93-041043] 05 p1810 N94-21953
Chromaticity analysis of LANDSAT multispectral scanner and thematic mapper imagery of Chilko Lake, British Columbia, using a theoretical optical water quality model
[ISBN-0-315-63832-X] 05 p1843 N94-22422
The performance of gloss meters on curving surfaces
[NPL-DMM(A)-111] 08 p3501 N94-30522
Estimation of visible and near-infrared reflectivity for Peyto Glacier Basin using satellite data
[ISBN-0-315-87039-7] 09 p3743 N94-31733
Sputter process investigation: Material and environment interaction processes investigation
[NASA-CR-193946] 10 p4028 N94-34076

OPTICAL RELAY SYSTEMS
Designs for optical components related to the Los Alamos free-electron laser
[DE93-016617] 04 p1436 N94-17865

OPTICAL RESONANCE
Feasibility study: Monodisperse polymer particles containing laser-excitable dyes
[NASA-CR-194280] 04 p1373 N94-19402
The resonance lines of MG2 as diagnostics of the upper solar chromosphere
[NASA-CR-195084] 06 p2627 N94-24300
Measurement of metastable population distribution in gadolinium atomic beam by laser resonance photoionization method
[DE94-701194] 07 p3029 N94-27820
Near resonant absorption by atoms in intense fluctuating laser fields
[DE94-005873] 09 p3714 N94-31200

OPTICAL RESONATORS
Horizontal-cavity surface-emitting lasers, superluminescent LEDs, and amplifiers, and parabolic gain unstable resonator semiconductor lasers 02 p0656 N94-13573
Theoretical investigation of scattering by homogeneous or coated dielectric spheres illuminated with a steady state or pulsed laser beam 02 p0657 N94-13624
Pulsed hydrogen fluoride overtone chemical laser studies
[AD-A267597] 03 p1041 N94-17193
Novel N x N integrated channel waveguide optical crossbars for large scale high speed non-blocking data switching
[AD-A272065] 05 p1986 N94-20922
Optical pattern recognition system utilizing resonator array
[AD-D016071] 07 p3040 N94-28224
Automatic resonator alignment and power stabilization of high power C02 lasers
[ISBN-0-315-77217-4] 09 p3714 N94-31472
Multifrequency, rapidly sequenced or simultaneous tunable laser
[AD-D016169] 09 p3721 N94-32968

OPTICAL SCANNERS
NT MULTISPECTRAL BAND SCANNERS
NT THEMATIC MAPPERS (LANDSAT)
A near-field scanning optical microscope for analysis of magneto-optic media 03 p1199 N94-14995
High rate resistive plate chambers: An inexpensive, fast, large area detector of energetic charged particles for accelerator and non-accelerator applications
[DE93-018664] 04 p1572 N94-19545
Evaluation of a scanning Hartmann device for single point turning applications
[DE93-019204] 05 p1821 N94-19891
Conically scanned holographic lidar telescope
[NASA-CASE-GSC-13462-1] 05 p1986 N94-20591
Surface acquisition through virtual milling 05 p1920 N94-22372
Microstructural analysis of the 2195 aluminum-lithium alloy welds 06 p2251 N94-24448
Channel to energy calibration results for the BATSE large area detectors 07 p3115 N94-26690
Characterization and calibration of the Agema 880+ imaging radiometer
[AD-A274417] 07 p3036 N94-26981
Synchronized laser scanning three dimensional acquisition system
[ISBN-0-315-86848-1] 09 p3879 N94-31756
Novel failure analysis techniques using photon probing with a scanning optical microscope
[DE94-006594] 09 p3692 N94-32112
A scanning defect mapping system for semiconductor characterization 09 p3885 N94-32446
Formation and stability of Fe-rich precipitates in dilute Zr(Fe) single-crystal alloys
[DE94-619027] 11 p4242 N94-36288

OPTICAL SENSORS
U OPTICAL MEASURING INSTRUMENTS

OPTICAL SIGNALS
U OPTICAL COMMUNICATION

OPTICAL SPECTRUM
U LIGHT (VISIBLE RADIATION)
U SPECTRA

OPTICAL SWITCHING
Design and analysis of an optical interface message processor
[AD-A266079] 01 p0381 N94-10697
Thermal-optical switching of a silicon based interference filter
[AD-A265152] 01 p0174 N94-11095
A thermal ionization model for the sustaining phase of lock-on in GaAs
[DE93-011558] 01 p0144 N94-11624
Preliminary surface-emitting laser logic device evaluation
[AD-A266111] 01 p0383 N94-12416
Infrared remote activity transceiver universal model
[AD-A266965] 03 p1188 N94-15144
Optical coupling elements for coherent optical multiport receivers
[ETN-93-94398] 03 p1188 N94-15447
Optically-switched submillimeter-wave oscillator and radiator
[NASA-CASE-NPO-18547-1-CU] 03 p1014 N94-17324
A scalable wrap-around shuffle exchange network with deflection routing
[NASA-CASE-NPO-18983-1-CU] 03 p1161 N94-17330
High-speed nonlinear switching mechanisms and devices for multi-gigabit data processing
[AD-A267753] 03 p1014 N94-17375
Evaluation of materials proposed for the construction of the Plasma Electrode Pockels Cell (PEPC) on beamlet
[DE93-016952] 04 p1584 N94-17988
Integrated photonics research volume 10. Conference edition
[AD-A269298] 04 p1577 N94-18298
Quantum Optoelectronics. Organization of the 1993 photonics science topical meetings. Technical digest series, volume 8
[AD-A269026] 04 p1578 N94-18488
Photonics in Switching: Organization of the 1993 photonics science topical meetings. Technical digest
[AD-A269024] 04 p1578 N94-18528
Ultrafast Electronics and Optoelectronics: Summaries of papers. Technical digest conference edition
[AD-A269233] 04 p1405 N94-18909
Improved optical pseudospark switch
[AD-D015821] 04 p1580 N94-18947
Optical switch evaluation support
[AD-A270948] 04 p1581 N94-19601
Evaluation of laser diode based optical switches for optical processors
[AD-A270949] 04 p1581 N94-19602
Stochastic differential equations and numerical simulation for pedestrians
[DE93-040851] 05 p1949 N94-20006
Optical signal processing
[AD-A271036] 05 p1983 N94-20013
Optical switching devices
[AD-D015918] 05 p1984 N94-20059
Optically controlled current filamentation in GaAs photoconductive semiconductor switches
[DE93-019427] 05 p2016 N94-20296
FD-TD modeling of 2-D dielectric waveguides for propagation and scattering of femtosecond optical solitons 05 p1719 N94-20406
Center for the integration of optical computing
[AD-A271874] 05 p1899 N94-20469
Novel N x N integrated channel waveguide optical crossbars for large scale high speed non-blocking data switching
[AD-A272065] 05 p1986 N94-20922
Non-destructive semiconductor wafer probing system using laser pulses to generate and detect millimeter-wave signals
[CA-PATENT-APPL-SN-2,020,733] 05 p1760 N94-21178
Mode transition matrix measuring system
[AD-D015973] 05 p1987 N94-21279
The effects of optical feedback on polarization of vertical cavity surface emitting lasers
[AD-A273728] 06 p2351 N94-25445
Low threshold all-optical crossbar switch on GaAs-GaAlAs channel waveguide arrays
[AD-A274971] 07 p2783 N94-26536
All-optical gain switching of erbium-doped fibre amplifiers
[ISBN-0-315-84120-6] 07 p2784 N94-26704
Advanced optical A/D converter
[AD-A275663] 08 p3498 N94-28656
Photonic devices and systems for optical signal processing
[AD-A275818] 08 p3498 N94-28804
Photoconductive switching for high power microwave generation
[PB94-137460] 08 p3244 N94-29177
Advanced optical fiber communication systems
[AD-A276416] 09 p3878 N94-31330
Reconfigurable optical switches with monolithic electrical-to-optical interfaces
[DE94-007745] 09 p3881 N94-32385
Mathematical nonlinear optics
[AD-A277320] 09 p3882 N94-32510
Fiber optic continuous true time-delay modulator
[AD-D016098] 09 p3883 N94-32720
Design of free space interconnected signal processor
[AD-A278129] 09 p3683 N94-33093
Research in the optical sciences
[AD-A278271] 09 p3884 N94-33140
Optically switched submillimeter-wave oscillator
[AD-A278014] 09 p3698 N94-33249
Organosilicon polymeric nonlinear optical materials for optical switching and modulation
[AD-A278245] 10 p4140 N94-33381
Photonic fast packet switching using optically processed control
[AD-A278195] 10 p4038 N94-33386
Theoretical studies of ultrashort phenomena
[AD-A278938] 11 p4332 N94-35664
Molecular systems for ultrafast optical switching: Controlling electron transfer reactions with femtosecond laser pulses
[DE94-009695] 11 p4332 N94-35671
Time-dependent simulations of filament propagation in photoconducting switches
[DE94-012146] 12 p4438 N94-37213

OPTICAL THICKNESS
Implications of aerosol retrieval and atmospheric correction in remote sensing 01 p0205 N94-11978
The effects of anthropogenic aerosols on optical thickness and particle size of clouds. Part 1: Retrieval algorithm 02 p0691 N94-14230
Earth radiation budget, cloud, and aerosol parameters derived from AVHRR and TOVS measurements 02 p0691 N94-14233
Solar radiation on Mars: Stationary photovoltaic array
[NASA-TM-106321] 02 p0626 N94-14730
Altitude profile of aerosols on Mars from measurements of its thermal radiation on limb 03 p1294 N94-16423
Spatial resolution and cloud optical thickness retrievals 03 p1066 N94-16671
Application of fractal methods to estimate the aerosol-optical depth for atmospheric correction of high resolution satellite data
[DLR-FB-93-04] 04 p1480 N94-18088
Bi-directional reflectance and other radiation parameters of cirrus from ER-2 observations 05 p1871 N94-22296

Optical properties of cirrus derived from airborne measurements during FIRE IFO 2
05 p1872 N94-22297
Development of methods for inferring cloud thickness and cloud-base height from satellite radiance data
05 p1872 N94-22301
A numerical technique for the calculation of cloud optical extinction from lidar 05 p1874 N94-22309
Ground-based passive remote sensing during FIRE IFO 2 05 p1844 N94-22319
Cloud-free aerosol optical depth determination over oceans from satellite radiometry
[DE94-001897] 06 p2386 N94-23779
Participation in TOMS missions
[NASA-CR-195110] 06 p2398 N94-24078
Mars dust-driven tides and their impact on the thermosphere 06 p2617 N94-24876
The appearance of the Sun and Moon seen through clouds
[AD-A275338] 08 p3551 N94-29212
Global patterns of cloud optical thickness variation with temperature and the implications for climate change
08 p3374 N94-29972
Optical depth effects in cluster cooling flows
08 p3541 N94-30800
Matter-radiation interactions in the atmosphere
09 p3776 N94-30998
Time-dependent behavior of Mount Pinatubo aerosol
[DE94-001877] 09 p3764 N94-31601
Evaluation of sulfate aerosol optical depths over the North Atlantic and comparison with satellite observations
[DE94-005457] 09 p3746 N94-32100
Sensitivity analysis of the AVHRR infrared cirrus model
[AD-A276690] 09 p3784 N94-32117
Adjacent-cell Preconditioners for solving optically thick neutron transport problems
[DE94-007219] 09 p3872 N94-32666
The wavelength dependence of Martian atmospheric dust radiative properties 09 p3950 N94-33228
Multiple scattering of light in a comet atmosphere
10 p4163 N94-33388
Comparison of the impact of volcanic eruptions and aircraft emissions on the aerosol mass loading and sulfur budget in the stratosphere 10 p3971 N94-33460
Sputter process investigation: Material and environment interaction processes investigation
[NASA-CR-193946] 10 p4028 N94-34076
Aerosol optical depth derived from solar radiometry observations at northern mid-latitude sites
[DE94-007476] 11 p4287 N94-36053

OPTICAL TRACKING

The 24th Annual Precise Time and Time Interval (PTTI) Applications and Planning Meeting
[NASA-CP-3218] 01 p0350 N94-10963
Airborne optical tracking control system design study
[DE93-009515] 01 p0382 N94-11662
DMSP F11 SSM/T-2 calibration and validation
[AD-A265817] 02 p0719 N94-12978
Three dimensional tracking of four point planar patterns using corners
[ISBN-0-315-52149-X] 02 p0791 N94-13490
Electromagnetic wave test 02 p0508 N94-14173
RACCOON: A Real-Time Autonomous Car Chaser Operating Optimally at Night
[AD-A266963] 03 p0863 N94-14971
Laser tracking for vertical control
03 p0911 N94-15553
Historical MOBLAS system characterization
03 p0915 N94-15579
Two color satellite laser ranging upgrades at Goddard's 1.2m telescope facility 03 p0915 N94-15581
Millimeter accuracy satellites for two color ranging
03 p0916 N94-15583
Two wavelength satellite laser ranging using SPAD
03 p0916 N94-15584
State-of-the-art satellite laser range modeling for geodetic and oceanographic applications
03 p0916 N94-15586
On the accuracy of ERS-1 orbit predictions
03 p0874 N94-15589
HP upgrade operational streamlining
03 p0918 N94-15596
A computer-controlled x-y offset guiding stage for the MLRS 03 p0918 N94-15598
Ground based laser ranging for satellite location
03 p0919 N94-15607
Station report on the Goddard Space Flight Center (GSFC) 1.2 meter telescope facility
03 p0922 N94-15625
Visual tracking
[AD-A271686] 05 p1943 N94-20920
Silicon retina for optical tracking systems
05 p1755 N94-21098
Image quality and the display modulation transfer function: Experimental findings
[AD-A274061] 07 p2679 N94-25773
Capture and location of blobs in digital images
[ISBN-0-315-84382-9] 07 p3036 N94-26666
Helmet head tracking mounting device
[AD-D016048] 07 p2942 N94-27114
The 25th Annual Precise Time and Time Interval (PTTI) Applications and Planning Meeting
[AD-A280955] 08 p3468 N94-30639
Digit-Eyes: Vision-based human hand tracking
[NASA-CR-195913] 09 p3803 N94-31447
Strategy for tracking and grabbing a moving object with the aid of a decouplable manipulator with six degrees of freedom general architecture, guided by a vision system
[ISBN-0-315-86864-3] 09 p3831 N94-31757
Optical processing of MMW for agile beamsteering and beamforming
[AD-A277161] 09 p3880 N94-32068
Correlation filter synthesis using neural networks
[AD-A278124] 09 p3836 N94-33043
A novel optoelectronic system for distortion-invariant ATR
[AD-A277965] 09 p3884 N94-33087
Task and environment-sensitive tracking
[AD-A278846] 11 p4312 N94-35802
Pointing and Tracking Systems
[AGARD-CP-539] 12 p4392 N94-36616
Pointing and tracking concept for a high energy laser weapon application 12 p4393 N94-36619
Global Positioning System Synchronized Active Light Autonomous Docking System
[NASA-CASE-MFS-28853-1] 12 p4395 N94-36825
Optical position measurement for a large gap magnetic suspension system: Design and performance analysis
[NASA-TP-3438] 12 p4447 N94-36946
United States Air Force Summer Research Program, 1993. Volume 13: Phillips Laboratory
[AD-A278657] 12 p4550 N94-36977
A more exact analysis of Sandia Laser Tracker data
[DE94-011411] 12 p4447 N94-37051

OPTICAL TRANSFER FUNCTION

Optical transfer operator of the atmosphere-ocean system 01 p0225 N94-12742
Performance impacts for actuator misalignments and failures in large-aperture adaptive-optic telescopes
[AD-A273838] 07 p3034 N94-25742
Calculation of turbulence degraded point spread function of an imaging system 08 p3260 N94-30514
The conoscopic microscope
[TELECOM-93-E-017] 09 p3877 N94-31173
A diffraction-based model of anisoplanatism effects in adaptive optic systems
[AD-A280491] 12 p4524 N94-37142

OPTICAL TRANSITION

Evaluation of hemoglobin-oxygen equilibrium binding by rapid-scanning spectrophotometry and singular-value decomposition
[AD-A266453] 03 p1123 N94-16564
On the estimation of matrix elements for optical transitions in semiconductors
[DE93-613550] 07 p3051 N94-25851

OPTICAL WAVEGUIDES

NT OPTICAL FIBERS
Semiconductor ring lasers
[DE93-012386] 01 p0174 N94-11005
Implementation of manufacturing techniques for planar, single mode waveguides on lithium niobate
[DSIS-93-00101] 02 p0792 N94-13845
Integrated optics technology transfer
[DSIS-93-00179] 02 p0792 N94-13868
Liquid and gas evanescent wave spectroscopy via tunable lasers and silver halide fibers
[ITN-93-85226] 02 p0565 N94-14465
Manufacturing and examination of integrated optical waveguide components in silicon
[ETN-93-94393] 02 p0793 N94-14704
Pulse propagation in inhomogeneous optical waveguides
[DE93-013378] 03 p1191 N94-16007
OETC optical backplane bus testbed. IBM tasks: Receiver OEIC and link simulation tools and analysis
[AD-A266198] 03 p1191 N94-16128
Fabrication and phase tuning of an optical waveguide device
[AD-D015815] 03 p1191 N94-16489
Performance of coded coherent FSK lightwave system with noncoherent detection
[AD-A267442] 03 p1193 N94-17028
Spectral inverse scattering theory for dielectric media: Application to optical devices
[AD-A268635] 03 p1199 N94-17427
Magnetostatic waves-based integrated optic bragg cell modules with applications to RF signal processing
[AD-A269115] 04 p1577 N94-18295
High-power microwave breakdown of dielectric interfaces
[AD-A268844] 04 p1397 N94-18318
Optical design for photonics. Organization of the 1993 Photonics Science Topical Meetings. Technical digest series, volume 9
[AD-A269027] 04 p1578 N94-18396
Photonics in Switching: Organization of the 1993 photonics science topical meetings. Technical digest
[AD-A269024] 04 p1578 N94-18528
A tunable compact high power far-infrared grating free-electron laser
[AD-A269875] 04 p1440 N94-18771
Integrated Photonics Research: Post-deadline papers
[AD-A269232] 04 p1609 N94-18908
Novel N x N integrated channel waveguide optical crossbars for large scale high speed non-blocking data switching
[AD-A272065] 05 p1986 N94-20922
Optical amplification and threshold behavior on InGaAs/InGaAsP multiquantum well structures
[ETN-93-94181] 05 p2026 N94-21151
Optical integrated structures and circuits on silicon
[VTT-PUBS-106] 05 p1988 N94-21594
A novel semiconductor process for optoelectronic applications on silicon substrate
05 p1988 N94-21595
Bidirectional method for optical channel waveguide attenuation measurement by detectors integrated on the wafer, appendix 3 05 p1988 N94-21597
An integrated-optic polarization splitter on silicon substrate, appendix 4 05 p1989 N94-21598
Fibre pigtailed silicon based low cost passive optical components, appendix 5 05 p1989 N94-21599
Birefringence control and dispersion characteristics of silicon oxynitride optical waveguides, appendix 6
05 p1989 N94-21600
Refractive index behaviour of phosphorus-doped planar silica waveguides, appendix 7 05 p1989 N94-21601
Time-laplace-transform-domain analysis of wave propagation in planar waveguides
[PB93-215226] 05 p1960 N94-22096
Architectures of the free space optical interconnects
05 p1789 N94-22220
Balanced arrow Mach-Zehnder interferometer
05 p1789 N94-22221
Modelling short bent, graded index dielectric slab waveguides
[PB93-215283] 05 p1742 N94-22349
A fully automated stage for optical waveguide measurements
[AD-A273042] 06 p2542 N94-22915
Conformal method of fabricating and optical waveguide on a semiconductor substrate
[AD-D015988] 06 p2546 N94-25043
Solutions of the 2-D Helmoholtz equation for optical waveguides
[DE93-616840] 06 p2547 N94-25209
Microtubules for nonlinear optical limiting
[AD-A273940] 07 p3035 N94-25941
Optoelectronic Technology Consortium
[AD-A274909] 07 p2782 N94-26344
Low threshold all-optical crossbar switch on GaAs-GaAlAs channel waveguide arrays
[AD-A274971] 07 p2783 N94-26536
Optoelectronic technology consortium
[AD-A274595] 07 p3036 N94-26857
Optical characterization and guided wave loss measurements for end-capped 6F-polybenzoxazole
[AD-A274586] 07 p3036 N94-26982
Focal plane antenna array for millimeter waves
[AD-D016034] 07 p2774 N94-27202
A study of multiple guide optical couplers
[ISBN-0-315-84633-X] 07 p3038 N94-27441
Electro-optic materials by solid source MOCVD
[DE94-005120] 07 p2757 N94-27716
Laser beam steering with semiconductor waveguide
[AD-A275775] 08 p3292 N94-28765
A new guided wave lens structure and its application
[AD-A275541] 08 p3499 N94-28813
An investigation of distributed coupling in a nonlinear semiconductor waveguide 08 p3246 N94-29529
Study of nonlinear optical polymers and their applications in optical waveguides 08 p3216 N94-29807
III-V compound semiconductor strip-loaded waveguide devices for PICs: Design for minimum crosstalk and high density
[DE94-006588] 09 p3897 N94-31502
Optimization of Y junctions in integrated optics
[ISBN-0-315-86782-5] 09 p3879 N94-31751
Low loss second-order nonlinear optical polymers based on all organic sol-gel materials
[AD-A277482] 09 p3663 N94-32985
Advanced material processing for integrated-optic frequency doubling systems
[AD-A278394] 09 p3698 N94-33163

Fabrication and phase tuning of an optical waveguide device
[AD-D016215] 11 p4334 N94-36122
Method of forming waveguides with ion exchange of halogen ions
[AD-D016304] 12 p4526 N94-37774

OPTICS
VUV thin films, chapter 7
[NASA-CR-194634] 03 p0967 N94-16494
Conference on Binary Optics: An Opportunity for Technical Exchange
[NASA-CP-3227] 03 p1194 N94-17331
Manufacturing the key to binary optics 03 p1194 N94-17332
Binary optics: Trends and limitations 03 p1194 N94-17333
Diffractive optics: Design, fabrication, and applications 03 p1194 N94-17334
Scattering from binary optics 03 p1195 N94-17341
Quantum optoelectronics technical digest, 1993. Voolume 8: Postconference edition
[AD-A268209] 04 p1576 N94-17887

OPTIMAL CONTROL
NT H-INFINITY CONTROL
NT LINEAR QUADRATIC GAUSSIAN CONTROL
NT LINEAR QUADRATIC REGULATOR
NT TIME OPTIMAL CONTROL
Nonlinear stability and control study of highly maneuverable high performance aircraft
[NASA-CR-193480] 01 p0025 N94-10344
Sample-data and discrete-time H2 optimal control
[MEMO-COSOR-92-53] 01 p0339 N94-10869
Application of controller partitioning optimization procedure to integrated flight/propulsion control design for a STOVL aircraft
[NASA-TM-106265] 01 p0030 N94-11251
Active control of acoustic pressure fields using smart material technologies
[NASA-CR-191480] 02 p0768 N94-13354
Optimal lateral escape maneuvers for microburst encounters during final approach
[LR-691] 02 p0511 N94-13534
On some results by Fuhrmann on Hankel operators
[CWI-BS-R9224] 02 p0764 N94-13999
On relations between Schmidt pairs arising in robust control
[CWI-BS-R9225] 02 p0764 N94-14000
On the Schmidt pairs of multivariable Hankel operators and robust control
[CWI-BS-R9226] 02 p0765 N94-14001
Development of an hp-version finite element method for computational optimal control
[NASA-CR-194149] 02 p0766 N94-14444
Decentralized control of uncertain systems via sensitivity models
[DE93-012963] 02 p0766 N94-14568
Analysis, approximation, and computation of a coupled solid/fluid temperature control problem
[NASA-TM-106351] 02 p0771 N94-14731
Functional differential equations with piecewise continuous argument
[AD-A266660] 02 p0772 N94-14840
Performance seeking control: Program overview and future directions
[NASA-TM-4531] 02 p0519 N94-14855
A molecular dynamics simulator for optimal control of molecular motion
[AD-A266572] 03 p1183 N94-16722
Neighboring extremal guidance for systems with piecewise linear control using time as the reference variable
[AD-A267942] 03 p0874 N94-17010
A comparative study of analog and digital control laws for the UMCSL truss
[AD-A267980] 03 p0871 N94-17412
Robust control of uncertain nonlinear systems
[AD-A268056] 03 p1167 N94-17506
Generalization of optimal control theory: Linear and nonlinear structures
[PB93-188621] 04 p1540 N94-18125
Parallel optimization algorithms and their implementation in VLSI design 04 p1401 N94-18374
Optimizing wind turbine control system parameters
[DE93-018861] 04 p1469 N94-19036
The optimal projection equations for finite-dimensional fixed-order H2-optimal control of infinite-dimensional discrete-time systems
[REPT-93-11] 04 p1542 N94-19085
The fixed, finite-order L(sup 2)-optimal control of infinite-dimensional time-varying discrete-time systems
[REPT-93-23] 04 p1542 N94-19138
Digital control of Pritchard-Salamon systems
[REPT-93-33] 04 p1543 N94-19286
Analysis and design of robust decentralized controllers for nonlinear systems
[DE93-019224] 04 p1543 N94-19302
Phasing strategies of the Hermes type space shuttle: Its optimization considering the thrust failures
[LAAS-93242] 04 p1544 N94-19361
Modeling of driver behavior: Information perception, rule and control strategies in experiments and simulations
[ETN-93-95053] 04 p1510 N94-19649
Acceleration-augmented LQG control of an active magnetic bearing 05 p1757 N94-21112
On the estimation algorithm used in adaptive performance optimization of turbofan engines
[NASA-TM-4551] 05 p1649 N94-21879
Control of multiple robot manipulators with optimal force distribution 05 p1794 N94-22255
Optimal control of the tip of a flexible arm 05 p1794 N94-22256
A mixed H2/H(infinity) function for a discrete time system
[MEMO-COSOR-92-36] 06 p2480 N94-23144
A reliable algorithm for optimal control synthesis
[NASA-CR-194809] 06 p2472 N94-23332
Coordinate-free interpretations of the optimal costs for Lq problems subject to implicit systems
[PB94-118700] 06 p2473 N94-23760
Identification of integrated airframe: Propulsion effects on an F-15 aircraft for application to drag minimization
[NASA-TM-4532] 06 p2188 N94-24106
Optimal feedback control of turbulent channel flow 06 p2327 N94-24139
Approximate optimal guidance for the advanced launch system
[NASA-CR-4568] 06 p2198 N94-24752
Control of nonlinear systems represented in quasilinear form
[NASA-CR-194840] 06 p2475 N94-24760
Optimal RTLS abort trajectories for an HL-20 personnel launch vehicle 06 p2165 N94-25114
Genetic algorithms in control systems engineering
[RR-470] 06 p2463 N94-25315
Flight controller design using mixed H2/H infinity optimization with a singular H infinity constraint
[AD-A273831] 06 p2191 N94-25525
Optimal control design advantages utilizing two-degree-of-freedom controllers
[AD-A273839] 07 p2984 N94-25743
Studies in nonlinear numerical analysis
[AD-A273911] 07 p2959 N94-25968
One machine scheduling with delayed precedence constraints
[PB93-237626] 07 p3094 N94-26314
Development of a performance evaluation tool (MMSOFE) for detection of failures with Multiple Model Adaptive Estimation (MMAE)
[AD-A274218] 07 p2665 N94-27071
Impulsive control and stabilization
[ISBN-0-315-84563-5] 07 p2988 N94-27271
Advanced control of a flexible spherical wrist
[ISBN-0-315-84424-8] 07 p2826 N94-27652
Pulse control method and its characteristics
[DE94-701187] 07 p2989 N94-27809
On identified predictive control 07 p2990 N94-27896
Topics in the design, analysis and implementation of feedback control systems
[ISBN-0-315-84934-7] 07 p2989 N94-27975
On the use of feedback to control sound radiation from a plate excited by a turbulent boundary layer
[ISVR-TR-227] 07 p2807 N94-28175
Application of digital control theory to adaptive grid generation 08 p3127 N94-28980
On-line search for optimal controller parameters using interconnected learning automata
[MATHS-REPT-A-196] 08 p3436 N94-29526
Reinforcement learning for robots using neural networks 08 p3437 N94-29853
Second order necessary conditions in optimal control
[ISBN-0-315-85443-X] 08 p3437 N94-30255
An optimal obstacle avoidance path planning algorithm for the Excalibur robot 08 p3306 N94-30287
Coordinated control of multiple robot manipulators 08 p3306 N94-30289
Calculus of variations applied to 2D multi-point airfoil design
[PB94-125457] 08 p3133 N94-30401
A stochastic control approach to flight path monitoring
[AD-B174630] 08 p3143 N94-30853
Integrated structure/control design of nonrigid robot arms for high-speed manipulation 08 p3312 N94-30866
Optimal low-thrust, Earth-Moon trajectories 08 p3159 N94-30961
Feasibility and stability results for constrained stable generalized predictive control
[MATHS-REPT-A-203] 09 p3828 N94-31158
Optimal reactive power dispatch of power systems using nonlinear programming
[MATHS-REPT-A-209] 09 p3808 N94-31164
Vibration control and design of composite cantilevers taking into account structural uncertainties and damage 09 p3733 N94-31213
Motion and force control of coordinated robots
[ISBN-0-315-86323-4] 09 p3724 N94-31714
Control of a random walk with noisy delayed information
[CWI-BS-R9316] 09 p3846 N94-32108
Undiscounted Markov decision chains with partial information; an algorithm for computing a locally optimal periodic policy
[TW-93-10] 09 p3851 N94-32205
Investigation of drive-reinforcement learning and application of learning to flight control
[AD-A277442] 09 p3801 N94-33053
The study of optimal control with neural networks 10 p4115 N94-34316
Aircraft optimal variable structure control system 10 p4007 N94-34328
Modelling and optimal control of Pb-Sn continuous crystallization process 10 p4118 N94-34345
A genetic technique for planning a control sequence to navigate the state space with a quasi-minimum-cost output trajectory for a non-linear multi-dimnensional system 10 p4123 N94-35052
JPRS report: Science and technology. Central Eurasia
[JPRS-UST-94-007] 11 p4249 N94-35227
Theory and computation of optimal low- and medium-thrust transfers
[NASA-CR-196077] 11 p4202 N94-35487
Control of flexible structures with distributed sensing and processing 11 p4218 N94-35871
Optimal disturbance rejecting control of hyperbolic systems 11 p4220 N94-35882
Magnetically suspended stepping motors for clean room and vacuum environments 11 p4225 N94-35915
Improvement of endurance performance by periodic optimal control of variable camber 11 p4194 N94-36329
Mixed H2/H-infinity optimization with multiple H infinity constraints
[AD-A280572] 12 p4388 N94-36733
H2 optimal control with H-infinity, mu, and L1 constraints
[AD-A280593] 12 p4500 N94-36736
Optimal control theory determination of feasible return-to-launch-site aborts for the HL-20 Personnel Launch System vehicle
[NASA-TP-3449] 12 p4396 N94-37260
Finite element approximation of an optimal control problem for the von Karman equations
[NASA-CR-194955] 12 p4505 N94-37540

OPTIMIZATION
NT DYNAMIC PROGRAMMING
NT GENETIC ALGORITHMS
NT H-INFINITY CONTROL
NT LINEAR PROGRAMMING
NT LINEAR QUADRATIC GAUSSIAN CONTROL
NT LINEAR QUADRATIC REGULATOR
NT MATHEMATICAL PROGRAMMING
NT NONLINEAR PROGRAMMING
NT OPERATIONS RESEARCH
NT OPTIMAL CONTROL
NT QUADRATIC PROGRAMMING
NT SIMPLEX METHOD
NT TIME OPTIMAL CONTROL
NT TRAJECTORY OPTIMIZATION
Perforated plates for thin-walled structures 01 p0063 N94-10056
LAMINV: A computer code for creating laminates having prescribed properties 01 p0065 N94-10069
Marginal allocations in the core of minimal chain-games
[MEMO-1103] 01 p0348 N94-10162
Applications of cut polyhedra
[CWI-BS-R9221] 01 p0347 N94-10354
Optimization algorithms for integer networks with side constraints for application in routing and scheduling
[AD-A265254] 01 p0322 N94-10492
The d-edge shortest-path problem for a Monge graph
[DE93-009828] 01 p0343 N94-10708
Progress in multidisciplinary design optimization at NASA Langley
[NASA-TM-107754] 01 p0318 N94-10814
Multilevel computer-aided optimum design of structural systems using multiple basis vectors 01 p0187 N94-11055
Optimisation methods for solving separable nonlinear least squares problems
[ISVR-TR-219] 01 p0345 N94-11217
Grid optimization and multigrid techniques for fluid flow and transport problems 01 p0154 N94-11824

A new heuristic for set covering problems
[INPE-5471-TDI/502] 01 p0333 N94-12358
Efficient dynamic optimization of logic programs
[NASA-TM-109251] 02 p0761 N94-12889
Tree reconstruction from partial orders
[DE93-009841] 02 p0743 N94-12991
Surrogates for numerical simulations; optimization of eddy-promoter heat exchangers
[NASA-CR-191510] 02 p0629 N94-13074
Multidisciplinary design techniques applied to conceptual aerospace vehicle design
[NASA-CR-194409] 02 p0515 N94-13618
An expert system for integrated structural analysis and design optimization for aerospace structures
[NASA-CR-194225] 02 p0673 N94-13673
Fast parallel string prefix-matching
[AD-A267758] 02 p0760 N94-13924
Mathematical optimization: A tool for aircraft design
[MBB-LME-251-S-PUB-0492] 02 p0751 N94-14006
VFGEN: A parallel volume fraction generator for hydrocodes
[DE93-011673] 02 p0752 N94-14019
Optimal synthesis of hot composite laminates with interphase layers
[NASA-TM-106326] 02 p0557 N94-14042
Development of an hp-version finite element method for computational optimal control
[NASA-CR-194149] 02 p0766 N94-14444
Paradigms for very fast parallel algorithms
[ITN-93-85212] 02 p0755 N94-14556
Computational issues in optimal tuning and placement of passive dampers 02 p0681 N94-14647
Development of x ray CCDs 03 p0900 N94-15033
Optimisation of FIR photoconductors for atmospheric spectroscopy 03 p0902 N94-15048
Preliminary analysis and design optimization of the short spacer truss of Space Station Freedom
[NASA-TM-4470] 03 p1058 N94-15709
Stochastic scheduling in a multiclass G/G/1 queue
[INRIA-RR-1746] 03 p1162 N94-17537
Optimisation and specification of Auger electron spectrometers for signal-to-noise ratio performance
[NPL-DMM(A)-101] 03 p1006 N94-17549
State space partitioning methods for solving a class of stochastic network problems
[AD-A267494] 03 p1173 N94-17585
Applications of an algebraic Monge property
[DE93-016869] 04 p1546 N94-17885
Heuristics from nature for hard combinatorial optimization problems
[REPT-93-025] 04 p1547 N94-17961
The optimal numerical algorithm for processing of phase coded time signals for radio-clocks 04 p1426 N94-18018
New current reduction system for watches with integrated current regulation motors 04 p1428 N94-18034
A study of the automatic generating system. 3: Improvement of the total system performance 04 p1429 N94-18040
Preliminary structural design: Defining the design space
[AD-A268898] 04 p1317 N94-18227
Learning database abstractions for query reformulation
[AD-A269531] 04 p1616 N94-18641
A numerical study of hybrid optimization methods for the molecular conformation problems
[DE93-017898] 04 p1569 N94-18985
Numerical analysis of proximal methods: Decomposition and parallelization
[ETN-93-95017] 04 p1552 N94-19362
Optimal safety system design using fault tree analysis
[MATHS-REPT-A-187] 04 p1529 N94-19382
On network representation of the solutions in combinatorial optimization
[RR-910-I] 04 p1552 N94-19392
Reanalysis of structure models
[ECL-93-07] 04 p1458 N94-19460
The complexity of the optimal spanning hypertree problem
[TR-471] 04 p1561 N94-19481
Finding optimal policies for Markov decision chains: A unifying framework for mean-variance-tradeoffs
[PB93-191930] 04 p1559 N94-19555
Shell designs
[AD-A270656] 04 p1460 N94-19606
A comparison of data-parallel algorithms for connected components
[AD-A270551] 05 p1902 N94-19918
On multiflow problems
[RR-889-M] 05 p1950 N94-20125
A design optimization procedure for epicyclic gears
[MATHS-REPT-A-188] 05 p1822 N94-20146
Determination of the optimal stochastic upper bound of a Markovian generator
[RR-906-I] 05 p1963 N94-20202
Applying the INN model to the MaxClique
[DE93-040137] 05 p1906 N94-20276
An investigation into the integration of meter-level range and millimeter-level phase data using a multimode stimulation for optimal filter estimation software package
[AD-A267955] 05 p1751 N94-20483
Design structuring and allocation optimization (Destination) prototype level 1 user's manual
[AD-A272115] 05 p1929 N94-20571
Optimization of a satellite localization and message sending system
[ETN-93-94448] 05 p1737 N94-20592
Routing of freeway traffic: A discrete-time state space model and routing problems
[CWI-BS-R9232] 05 p1944 N94-21033
On the core-structure of minimum cost spanning tree games
[MEMO-1085] 05 p1953 N94-21047
On the optimality of FCFS for networks of multi-server queues
[CWI-BS-R9235] 05 p1944 N94-21160
Optimization of static traffic allocation policies
[CWI-BS-R9302] 05 p1930 N94-21161
Optimization of fixed time polling schemes
[CWI-BS-R9237] 05 p1945 N94-21233
Optimal repairman assignment in two maintenance models which are equivalent to routing models with early decisions
[CWI-BS-R9301] 05 p1930 N94-21234
Selectivity: Reductions, nondeterminism, and function classes
[TR-469] 05 p1912 N94-21273
A mean field neural network for hierarchical module placement 05 p1766 N94-21720
Multicriteria optimisation problem in the agricultural modelling 05 p1844 N94-22073
The combinatorial algorithms for large scale discrete optimization problems 05 p1923 N94-22079
Improvements on the design of optimum SAW filters with the Remez Exchange Algorithm 05 p1773 N94-22123
Neural networks for optimum routing in packet-switched communications networks 05 p1746 N94-22205
Some best rate 1/p and rate (p-1)/p systematic quasi-cyclic codes over GF(3) and GF(4) 05 p1792 N94-22243
The Westinghouse Series 1000 Mobile Phone: Technology and applications 06 p2284 N94-22800
A mixed H2/H(infinity) function for a discrete time system
[MEMO-COSOR-92-36] 06 p2480 N94-23144
A structural design decomposition method utilizing substructuring
[NASA-TM-107750] 06 p2376 N94-23368
Object oriented simulation implementation in support of robust system design
[DE93-011687] 06 p2452 N94-23488
An engineering code to analyze hypersonic thermal management systems 06 p2320 N94-23636
Low noise electric motor 06 p2315 N94-23989
A constrained optimization technique for arbitrary antenna arrays and various performance indices
[ISBN-0-315-59455-1] 06 p2297 N94-24179
Application of concurrent engineering principles to aircraft structural design 06 p2178 N94-24321
Current and future design methods for large transport aircraft 06 p2179 N94-24324
Trends of design methodology of airframe 06 p2179 N94-24327
Next generation initiation techniques 06 p2412 N94-24383
Discrete applied mathematics
[AD-A273552] 06 p2488 N94-24561
A programming environment for distributed complex computing. An overview of the Framework for Interdisciplinary Design Optimization (FIDO) project. NASA Langley TOPS exhibit H120b
[NASA-TM-109058] 06 p2457 N94-24603
Tokamak Physics Experiment (TPX) cost and performance trade studies using supercode
[DE94-002720] 06 p2553 N94-24628
The Third Twente Workshop on Graphs and Combinatorial Optimization: Abstracts and late extended abstracts
[PB94-110954] 06 p2489 N94-24652
Runtime support and compilation methods for user-specified data distributions
[AD-A276326] 06 p2458 N94-24679
Sensitivity analysis of list scheduling heuristics
[PB93-237766] 06 p2468 N94-24764
Merits and limitations of optimality criteria method for structural optimization
[NASA-TP-3373] 06 p2378 N94-24845
RIACS/USRA
[NASA-CR-195117] 06 p2631 N94-25003
Computing techniques in mission planning 06 p2522 N94-25012
On the characterization and optimization of high-speed silicon bipolar transistors
[ETN-94-95367] 06 p2313 N94-25253
MIMO system identification for H(infinity) robust control: A frequency domain approach with minimum error bounds
[ETN-94-95354] 06 p2476 N94-25262
New algorithm for minimizing (chi)(sup 2) functionals with constraints
[DE93-616800] 06 p2463 N94-25432
Adaptive optimization and control using neural networks
[DE94-003941] 07 p2985 N94-25983
Determination of the geomagnetic external contribution by nonlinear optimization methods
[DE94-600882] 07 p2878 N94-26365
A technique for integrating engine cycle and aircraft configuration optimization
[NASA-CR-191602] 07 p2668 N94-26606
Thermal/structural tailoring of engine blades (T/STAEBL). User's manual
[NASA-CR-194463] 07 p2839 N94-26692
Specification performance optimization and executive generation for onboard multiprocessor real time application with SynDEx 07 p2954 N94-26745
Nested Krylov methods based on GCR
[PB94-125317] 07 p2995 N94-26818
Query optimization strategies for browsing sessions
[CWI-CS-R9268] 07 p3100 N94-27394
A sensitivity equation approach to shape optimization in fluid flows
[AD-A278423] 07 p2999 N94-27415
Fast parallel permutation algorithms
[CWI-CS-R9303] 07 p2982 N94-27579
Thermal/Structural Tailoring of Engine Blades (T/STAEBL): User's manual
[NASA-CR-194461] 07 p2843 N94-27776
Reliability-based structural optimization: A proposed analytical-experimental study
[NASA-TM-109055] 07 p2844 N94-27830
An optimization program based on the method of feasible directions: Theory and users guide
[NASA-TM-4552] 07 p2845 N94-27865
The molecular matching problem 07 p3030 N94-27910
Examples of flight path optimisation using a multivariate gradient-search method
[ESDU-93021] 07 p2670 N94-28092
Aerodynamic design using parallel processors
[AD-A275470] 08 p3122 N94-28674
Thermal/structural tailoring of engine blades (T/SEAEBL). Theoretical manual
[NASA-CR-194462] 08 p3317 N94-28815
Incorporating geometric constraints into rule-based systems using nonlinear optimization
[AD-A275093] 08 p3452 N94-29063
Investigation on application of genetic algorithms to optimal reactive power dispatch of power systems
[MATHS-REPT-A-197] 08 p3266 N94-29527
Yield and variability optimization of integrated circuits: Principles and practical solutions 08 p3266 N94-29805
Complicated problem solution techniques in optimal parameter searching
[DE94-608007] 08 p3421 N94-30077
A note on the complexity of local search problems
[CT-93-02] 08 p3456 N94-30370
Hybrid optics for space applications
[ESA-CP-1158] 08 p3501 N94-30418
Optimization techniques for a dial-a-ride transportation system in urban environment
[REPT-93-051] 08 p3537 N94-30926
On the use of genetic algorithms to solve the time-table problem
[REPT-90-060-REV] 09 p3829 N94-31176
The ant system: An autocatalytic optimizing process
[REPT-91-016-REV] 09 p3824 N94-31177
Techniques for increasing the robustness of iterative algorithms for multi-resources location problems
[REPT-93-037] 09 p3809 N94-31188
A worst-case analysis of an approximate algorithm for finding the minimum hamiltonian cycle on paths
[REPT-93-042] 09 p3809 N94-31192
Two models solving the increasing energy problem of the continuous Hopfield network model
[REPT-93-87] 09 p3843 N94-31552
Optimization of the forming parameters of PEEK/carbon fiber composite
[ISBN-0-315-86410-9] 09 p3620 N94-31716
Multidisciplinary optimization of high-speed civil transport configurations using variable-complexity modeling 09 p3578 N94-31881

Principal component analysis with missing data and its application to object modeling
[AD-A276644] 09 p3845 N94-31939
Minimization of computational requirements in the hybrid stress finite element method
[AD-A277120] 09 p3846 N94-32048
Experiences with EDO: An Evolutionary Database Optimizer
[TR-93-23] 09 p3918 N94-32105
Mesh optimization
[AD-A277644] 09 p3820 N94-32972
Local design optimization for composite transport fuselage crown panels 09 p3629 N94-33132
Numerical optimization techniques in neural network training 09 p3838 N94-33158
Mixed 0-1 programming by lift-and-project in a branch-and-cut framework
[AD-A278045] 09 p3822 N94-33183
Multilevel decomposition approach to integrated aerodynamic/dynamic/structural optimization of helicopter rotor blades
[NASA-TM-109084] 10 p3989 N94-33900
On optimal placement of spacers in bundled conductors 11 p4258 N94-35354
The development and application of composite complexity models and a relative complexity metric in a software maintenance environment
11 p4255 N94-35559
Symbolic debugging of globally optimized code: Data value problems and their solutions
[AD-A278898] 11 p4302 N94-35572
Reformulating query plans for multidatabase systems
[AD-A278688] 11 p4345 N94-35663
Optimization of turn position of tokamak inductor
[DE94-612627] 11 p4336 N94-35791
Optimisation of composite aircraft structures by direct manufacturing approaches 11 p4194 N94-36327
New method for minimizing regular functions with constraints on parameter region
[DE94-618340] 12 p4515 N94-37076
Optimization for minimum sensitivity to uncertain parameters
[NASA-TM-109139] 12 p4386 N94-37256

OPTIMUM CONTROL
U OPTIMAL CONTROL

OPTOELECTRONIC DEVICES
NT PHOTODIODES
NT PHOTOTRANSISTORS
Multiplexed and distributed optical fibre sensors
01 p0064 N94-10065
Ultrastable reference frequency distribution utilizing a fiber optic link 01 p0355 N94-10994
Lattice-matched heteroepitaxy of wide gap ternary compound semiconductors 01 p0400 N94-11441
Activities of Institute for Microstructural Sciences
[NRC-32815] 02 p0810 N94-14198
Activities of Institute for Microstructural Sciences
[CNR-32815] 02 p0810 N94-14199
Radiation effects on optoelectronic analog link for particle detectors
[DE93-015794] 02 p0793 N94-14529
Optical coupling elements for coherent optical multiport receivers
[ETN-93-94398] 03 p1188 N94-15447
System architecture of optically controlled phased array radar
[AD-A267056] 03 p0988 N94-15667
Organic polymeric electro-optic materials: Synthesis, processing, and device applications
[AD-A267133] 03 p0964 N94-15688
Almaz 03 p0898 N94-15889
Sputtered ferroelectric thin films of KTN for electro-optic devices
[AD-A266573] 03 p0968 N94-16723
JSEP fellowship
[AD-A266568] 03 p1211 N94-16800
Laser figuring for the generation of analog micro-optics and kineform surfaces 03 p1196 N94-17346
Diffractive optics fabricated by direct write methods with an electron beam 03 p1196 N94-17347
Micro-optics technology and sensor systems applications 03 p1197 N94-17350
Fabrication of micro-optical devices
03 p1197 N94-17351
Diffractive optics in adverse environments
03 p1197 N94-17352
Thermal Weapon Sight (TWS) AN/PAS-13 diffractive optics designed for producibility
03 p1197 N94-17354
Measurements of microlens performance
03 p1197 N94-17355
Laser beam steering device 03 p1045 N94-17357
Theory of dispersive microlenses
03 p1198 N94-17361
Color separation gratings 03 p1196 N94-17362
OSA proceedings on Ultrafast Electronics and Optoelectronics, volume 14
[AD-A267972] 03 p1014 N94-17410
Mechanical properties and crystal growth studies of semiconductor alloys
[AD-A268144] 03 p1216 N94-17454
Optically controlled active impedance element and filters employing the same
[AD-D015863] 04 p1396 N94-18062
Growth of structures for integrated optoelectronic devices
[AD-A269014] 04 p1598 N94-18527
Joint services electronics program
[AD-A269383] 04 p1403 N94-18638
Photodetector array having high pixel density
[AD-D015859] 04 p1432 N94-18731
Attitude sensor package 04 p1325 N94-19172
Electro-optic beam steering using non-linear organic materials
[AD-A270809] 04 p1374 N94-19577
Experimental examinations of semiconductor laser amplifiers for optical communication technology
[ETN-93-95050] 04 p1442 N94-19647
Feasibility study for a measuring system velocity projectile
[FEL-91-A368] 04 p1434 N94-19797
Optoelectronic associative memory
[NASA-CASE-NPO-18278-1-CU]
05 p1985 N94-20303
System for solving Boolean equations using optical lookup tables
[AD-D015962] 05 p1951 N94-20358
Investigation of heterojunctions and multiple quantum well structures using crystalline organic semiconductors
[AD-A272113] 05 p2018 N94-20569
Surface treatment of InP and contribution to the optimization of the InP(p)/InP(p) regrown interfaces grown by GSMBE
[ECL-92-48] 05 p2018 N94-20598
Non-destructive semiconductor wafer probing system using laser pulses to generate and detect millimeter-wave signals
[CA-PATENT-APPL-SN-2,020,733]
05 p1760 N94-21178
Optical integrated structures and circuits on silicon
[VTT-PUBS-106] 05 p1988 N94-21594
A novel semiconductor process for optoelectronic applications on silicon substrate
05 p1988 N94-21595
Bidirectional method for optical channel waveguide attenuation measurement by detectors integrated on the wafer, appendix 3 05 p1988 N94-21597
The conceptual design of a short-range distance sensor 05 p1774 N94-22129
Charge integrating optical position sensor
05 p1778 N94-22152
Visual Problems in Night Operations
[AGARD-LS-187] 06 p2431 N94-23976
Ferroelectric thin films 3
[AD-A273394] 06 p2565 N94-25027
Bridge type optoelectronic sample and hold circuit
[AD-D015986] 06 p2312 N94-25042
Radar E-O image fusion 06 p2306 N94-25503
Solid state research
[AD-A274063] 07 p3049 N94-25645
Optoelectronic technology consortium
[AD-A274595] 07 p3036 N94-26857
Research and development within nonlinear optics for protection of optical sensors against laser irradiation on of optical sensors against laser irradiation. Quarterannual report 1 (april 1993))
[PB94-124245] 07 p3037 N94-27046
Innovative optoelectronic materials and structures using OMVPE
[AD-A275811] 08 p3511 N94-28773
Optoelectronic integrated circuits fabricated using atomic layer epitaxy
[AD-A275454] 08 p3262 N94-28805
Gordon research conference on optical signal processing and holography
[AD-A275092] 08 p3499 N94-28848
Carrier collection and scattering in quantum well and superlattice devices
[AD-A275443] 08 p3512 N94-28880
An investigation of distributed coupling in a nonlinear semiconductor waveguide 08 p3246 N94-29529
Overview of microoptics: Past, present, and future
08 p3235 N94-29771
Micro guidance and control technology overview
08 p3144 N94-29772
Micro-opto-mechanical devices and systems using epitaxial lift off 08 p3239 N94-29793
Synchronization of microwave oscillators by direct optical injection
[ISBN-0-315-85546-0] 08 p3500 N94-30233
Optoelectronic packaging activities at Sandia National Laboratories
[DE94-005287] 08 p3501 N94-30261
Growth and characterization of III-V semiconductors with rare earth impurities for optoelectronic devices
[AD-A276021] 09 p3896 N94-31455
High-performance GaAs/AlGaAs optical phase modulators for microwave/photonic integrated circuits
[DE94-006361] 09 p3688 N94-31483
III-V compound semiconductor strip-loaded waveguide devices for PICs: Design for minimum crosstalk and high density
[DE94-006588] 09 p3897 N94-31502
Epitaxial liftoff technology onto processed silicon foundry wafers
[AD-A277116] 09 p3900 N94-31985
Novel optoelectronic devices based on combining GaAs and InP on Si
[AD-A277018] 09 p3693 N94-32301
WOCSDICE 1993 --- 17th European Workshop on Compound Semiconductor Devices and Integrated Circuits
[AD-A276766] 09 p3693 N94-32307
Flexible manufacturing for photonics device assembly
09 p3669 N94-32449
Automated fiber pigtailing technology
[DE94-007072] 09 p3695 N94-32688
Sandia's photonic program and its changing national role
[DE94-008616] 09 p3883 N94-32878
Silicon-Based Optoelectronic Materials Symposium and Materials Research Society Proceedings, volume 298
[AD-A277518] 09 p3662 N94-32952
Large-diameter InGaAs/AlGaAs vertical-cavity surface-emitting lasers with low threshold current density fabricated using a simple chemical etch process
[AD-A277733] 09 p3721 N94-33003
A novel optoelectronic system for distortion-invariant ATR
[AD-A277985] 09 p3884 N94-33087
Advanced material processing for integrated-optic frequency doubling systems
[AD-A278394] 09 p3698 N94-33163
Phase-only 128x128 spatial light modulator based on LASLM technology
[AD-A277901] 10 p4141 N94-33591
Dynamics of supermatrix semiconductor growth
[AD-A278380] 10 p4147 N94-34085
FOA 33
[PB94-149184] 10 p4143 N94-34094
Design of a composite filter realizable on practical spatial light modulators
[NASA-CR-196297] 12 p4525 N94-37579

OPTOELECTRONIC SWITCHING
U OPTICAL SWITCHING

OPTOMETRY
Enhancing sight
[NASA-TM-109637] 03 p1221 N94-15248
Image remapping strategies applied as protheses for the visually impaired 06 p2444 N94-25363

OR-GATES
U GATES (CIRCUITS)

ORATORY
U PUBLIC SPEAKING

ORBIT CALCULATION
Topex orbit determination using GPS tracking system
01 p0038 N94-10359
Precision GPS ephemerides and baselines
[NASA-CR-194171] 01 p0023 N94-11177
Removal of orbital error and the local geoid effects from ERS-1 altimeter data 01 p0242 N94-11770
ERS-1 precise orbits and altimetry analysis
01 p0242 N94-11771
Operational ERS-1 orbit determination at D-PAF
01 p0243 N94-11774
The Earth's gravity model for the ERS-1 commissioning phase 01 p0243 N94-11778
ERS-1 precise orbit determination
01 p0244 N94-11779
Lunar Scout Two spacecraft gravity experiment
01 p0459 N94-12152
Investigation for improving Global Positioning System (GPS) orbits using a discrete sequential estimator and stochastic models of selected physical processes
[NASA-CR-194167] 02 p0512 N94-13082
Error analysis of real time and post processed or bit determination of GFO using GPS tracking
[NASA-CR-193646] 02 p0512 N94-13238
Improved treatment of global positioning system force parameters in precise orbit determination applications
02 p0514 N94-14371
Failure modes of reduced-order orbit determination filters and their remedies 02 p0532 N94-14373
Laser ranging network performance and routine orbit determination at D-PAF 03 p0911 N94-15554

State-of-the-art satellite laser range modeling for geodetic and oceanographic applications
03 p0916 N94-15586
Closed orbit distortion and the beam-beam interaction
[DE93-015284] 03 p1190 N94-15854
Implementing a 50x50 gravity field model in an orbit determination system
[AD-A267548] 03 p0888 N94-17103
BRIDGE: A small scientific satellite for geodesy
03 p0890 N94-17146
Adequation of mini satellites to oceanic altimetry missions 03 p0891 N94-17152
OREMUS: Prototype of an orbit determination center dedicated to mini-satellite control
03 p0878 N94-17156
SeaTrack: Ground station orbit prediction and planning software for sea-viewing satellites
[NASA-RP-1331] 04 p1532 N94-19761
A new procedure for orbit determination based on three lines of sight: Angles only
[AD-A272937] 05 p1652 N94-21224
A review of GPS-based tracking techniques for TDRS orbit determination 06 p2196 N94-23257
New approaches for tracking earth orbiters using modified GPS ground receivers
06 p2196 N94-23258
Improved thermal force modeling for GPS satellites
06 p2207 N94-23259
Real-time on-board orbit determination with DORIS
06 p2196 N94-23919
TOPEX/Poseidon precision orbit determination production and expert system 06 p2196 N94-23920
Kalman filtering applied to real-time monitoring of apogee maneuvers 06 p2196 N94-23923
Navigation of space VLBI missions: Radioastron and VSOP 06 p2513 N94-23926
The geo-control system for station keeping and colocation of geostationary satellites
06 p2464 N94-23927
Comparison of time integration methods for the evolution of galaxies
[PB94-111671] 06 p2602 N94-24522
Hill equations for satellite orbit determination
[ETN-94-95374] 07 p2690 N94-25787
Enhanced orbit determination filter sensitivity analysis: Error budget development 08 p3159 N94-29655
Enhanced orbit determination filter: Inclusion of ground system errors as filter parameters
08 p3159 N94-29656
TOPEX/POSEIDON operational orbit determination results using global positioning satellites
08 p3160 N94-29666
Application of extended Lagrange series to the precise determination of Global Positioning Satellite orbits
[ISBN-0-315-85724-2] 08 p3159 N94-30237
Time transfer using geostationary satellites: Implementation of a Kalman filter
08 p3471 N94-30657
Air Force Space Command satellite orbit predictor using parallel virtual machines
[AD-A276316] 09 p3601 N94-31298
Multisatellite constellation configuration selection for multiregional highly elliptical orbit constellations
09 p3600 N94-31437
Possible improvements of satellite ephemeris programs used in geodesy
[PB94-148681] 09 p3743 N94-31592
Testing for preferred-frame effects in gravity with artificial Earth satellites
[PB94-148459] 09 p3610 N94-31771
Semianalytic Satellite Theory (SST): Mathematical algorithms
[AD-A276836] 09 p3610 N94-32208
Normal matrix in gravity field determination with satellite methods. Its stabilization, its information content and its use in error propagation
[PB94-149705] 10 p4076 N94-34114
The mass of Mars, Phobos, and Deimos, from the analysis of the Mariner 9 and Viking Orbiter tracking data 11 p4364 N94-35461
Flight Mechanics/Estimation Theory Symposium, 1994
[NASA-CP-3265] 11 p4202 N94-35605
Compatibility of TOPEX/Poseidon trajectory propagation with JPL and GSFC/FDF operational software
11 p4204 N94-35619
Improved solution accuracy for TDRSS-based TOPEX/Poseidon orbit determination
11 p4205 N94-35620
Implementation of a low-cost, commercial orbit determination system 11 p4205 N94-35621
Improved solution accuracy for Landsat-4 (TDRSS-user) orbit determination 11 p4205 N94-35623
Space Shuttle orbit determination using empirical force modeling of attitude maneuvers for the German MOMS-02/D2 mission 11 p4207 N94-35634
Application of a Monte Carlo accuracy assessment tool to TDRS and GPS 11 p4207 N94-35635
Evaluation of semiempirical atmospheric density models for orbit determination applications
11 p4208 N94-35636
Filter parameter tuning analysis for operational orbit determination support 11 p4208 N94-35637

ORBIT DECAY
On the delivery of planetesimals to a protoplanet in the solar nebula 03 p1245 N94-16379

ORBIT EQUATIONS
U ORBITAL MECHANICS

ORBIT INSERTION
Inertial Upper Stage
[NASA-TM-109654] 03 p0885 N94-15278
Tidal regime of intact planetoid capture model for the Earth-Moon system: Does it relate to the archean sedimentary rock record? 03 p1245 N94-16378
Small launchers (current and future projects in the world) 03 p0878 N94-17137
NEXT launch system 03 p0878 N94-17141
TITUS: A micro-satellite for technology demonstration
03 p0896 N94-17186
MERCATOR: Methods and Realization for Control of the Attitude and the Orbit of spacecraft
06 p2202 N94-23925
HISPASAT launch and early operations phases: Computation and monitoring of geostationary satellite positioning 06 p2514 N94-23928

ORBIT PERTURBATION
NT SATELLITE PERTURBATION
A simultaneous estimation of the mass of Mars and its natural satellites, Phobos and Deimos, from the orbital perturbations on the Mariner 9, Viking 1, and Viking 2 orbiters 03 p1279 N94-16347
On the delivery of planetesimals to a protoplanet in the solar nebula 03 p1245 N94-16379
Dust grain resonant capture: A statistical study
03 p1245 N94-16384
Improved thermal force modeling for GPS satellites
06 p2207 N94-23259
Hill equations for satellite orbit determination
[ETN-94-95374] 07 p2690 N94-25787

ORBIT TRANSFER VEHICLES
Workshop on Solar Electric Propulsion
01 p0054 N94-11416
Low power pulsed MPD thruster system analysis and applications
[NASA-CR-191187] 02 p0550 N94-13415
Guidance law development for aeroassisted transfer vehicles using matched asymptotic expansions
[NASA-CR-194523] 02 p0508 N94-14538
Minimum accommodation for aerobrake assembly. Phase 2: Structural concepts for a lunar transfer vehicle aerobrake which can be assembled on orbit
[NASA-TM-107610] 03 p0885 N94-15446
Space transfer concepts and analyses for exploration missions, phase 4
[NASA-CR-193849] 03 p0882 N94-15831
Comparisons of selected laser beam power missions to conventionally powered missions
[NASA-TM-106110] 03 p1040 N94-16522
Evaluation of externally heated pulsed MPD thruster cathodes
[NASA-CR-191090] 05 p1670 N94-21565
Theoretical research program to study chemical reactions in AOTV bow shock tubes
[NASA-CR-194710] 05 p1804 N94-22027
Power beaming to space using a nuclear reactor-pumped laser
[DE94-001208] 06 p2348 N94-23185
Lunar transportation system
[NASA-CR-195540] 06 p2365 N94-24805
Space transfer vehicle concepts and requirements. Volume 4: Summary of special studies
[NASA-CR-193918] 06 p2201 N94-24970
Orbit transfer rocket engine technology program enhanced heat transfer combustor technology
[AD-A277123] 07 p2700 N94-26156
Test results of the RS-44 integrated component evaluator liquid oxygen/hydrogen rocket engine
[AD-A277085] 07 p2701 N94-26231
Orbit transfer rocket engine technology program
[AD-A277021] 07 p2702 N94-26542
Orbital transfer vehicle engine technology high velocity ratio diffusing crossover
[AD-A277180] 07 p2703 N94-27212
Orbital transfer rocket engine technology 7.5K-LB thrust rocket engine preliminary design
[AD-A276954] 07 p2703 N94-27213
A transportronic solution to the problem of interorbital transportation
[NASA-CR-191152] 08 p3164 N94-29355
Computational radiative heat transfer in homogeneous and nonhomogeneous nonscattering media
09 p3702 N94-31563
The 7.5K lbf thrust engine preliminary design for Orbit Transfer Vehicle
[AD-A277519] 09 p3614 N94-31618
Attitude dynamics of spinning rockets in space with internal mass motion 09 p3601 N94-31802

ORBITAL ASSEMBLY
In-space operations for lunar and Mars space transfer vehicles 01 p0348 N94-11568
On-orbit servicing for USAF space missions: A phased development approach 01 p0348 N94-11571
Definition of spacecraft standard interfaces by the NASA Space Assembly and Servicing Working Group (SASWG) 01 p0348 N94-11574
The Second Workshop on Deployment and Assembly Experiment of Large Space Structure on Orbit
[NASDA-CON-930003] 02 p0529 N94-13268
Structural design of hexa-link truss deployable antenna 02 p0529 N94-13269
Thermal distortion measurement of TETRUS type thermal test model of large deployable antenna for mobile communications satellite 02 p0529 N94-13270
Development of modular cable mesh deployable antenna 02 p0530 N94-13274
Research on inflatable structure for space use
02 p0530 N94-13275
Helical truss beam development for large space structure 02 p0530 N94-13276
Application of intelligently adaptable structure and robot to large space structure 02 p0530 N94-13277
Trial manufacture model and in-space verification method of deployable antenna 02 p0530 N94-13278
Development and application of one dimensional deployable truss 02 p0531 N94-13281
The study on large space structure assembly technology: The study on deployable truss structure, part 1
[NASDA-TMR-930002] 02 p0541 N94-13658
The study on large space structure assembly technology: The study on deployable truss structure, part 2 and 3
[NASDA-TMR-930003-PT-2-3] 02 p0541 N94-13659
Large space structures and systems in the space station era: A bibliography with indexes (supplement 05)
[NASA-SP-7085(05)] 02 p0543 N94-14411
Minimum accommodation for aerobrake assembly. Phase 2: Structural concepts for a lunar transfer vehicle aerobrake which can be assembled on orbit
[NASA-TM-107610] 03 p0885 N94-15446
Ground integrated ET-derived space platforms for onorbit applications
[TABES PAPER 93-652] 03 p0899 N94-16152
End-effector: Joint conjugates for robotic assembly of large truss structures in space: Extended concepts
[NASA-CR-193576] 03 p1048 N94-17088
Space Station/Orbiter berthing dynamics during an assembly flight
[NASA-TM-109049] 03 p1062 N94-17451
Designing Space Station
[NASA-TM-109353] 04 p1334 N94-18922
Shuttle-C, the future is now
[NASA-TM-109355] 04 p1332 N94-18954
Space Applications Industrial Laser System (SAILS)
04 p1325 N94-19173
An expert system executive for automated assembly of large space truss structures
[NASA-TM-4487] 05 p1939 N94-20089
Manned Mars mission on-orbit operations FTS capabilities assessment
[NASA-CR-189328] 06 p2430 N94-23080
Space Habitat, assembly and repair facility
07 p2691 N94-25696
Selected topics in robotics for space exploration
[NASA-CP-10131] 07 p2682 N94-26278
Performance measures from the explorer platform berthing experiment 07 p2683 N94-26283
Berthing of Space Station Freedom using the shuttle remote manipulator system 07 p2684 N94-26284
An analysis of the loads applied to a heavy Space Station rack during translation and rotation tasks
[NASA-TM-104790] 07 p2697 N94-28183
Free-floating dual-arm robots for space assembly
[AIAA PAPER 94-1195-CP] 08 p3442 N94-30546
The SCRAM tool-kit 10 p4066 N94-33668
Structural assembly demonstration experiment, phase 1
[NASA-CR-193967] 11 p4212 N94-35484

ORBITAL BREAKUP
U SPACECRAFT BREAKUP

ORBITAL ELEMENTS
The long-term dynamical behavior of short-period comets 01 p0427 N94-11629
On the accuracy of ERS-1 orbit predictions
03 p0874 N94-15589
Formation of on-site normal points
03 p0917 N94-15592
The effects of orbital and climatic variations on Martian surface heat flow 03 p1290 N94-16402

SeaTrack: Ground station orbit prediction and planning software for sea-viewing satellites
[NASA-RP-1331] 04 p1532 N94-19761
SeaWiFS technical report series. Volume 11: Analysis of selected orbit propagation models for the SeaWiFS mission
[NASA-TM-104566-VOL-11] 06 p2417 N94-23338
A virtual environment for satellite modeling and orbital analysis in a distributed interactive simulation
[AD-A274114] 07 p2694 N94-25904
An April 1991 outburst from 4U0115+63 observed by BATSE
[DE94-007093] 07 p3116 N94-27440
Time transfer using geostationary satellites: Implementation of a Kalman filter
08 p3471 N94-30657
Dust evolution from comets and asteroids: Their velocities at Earth orbit intersection
11 p4352 N94-36142

ORBITAL FLIGHT TEST 3 (SHUTTLE)
U SPACE TRANSPORTATION SYSTEM 3 FLIGHT

ORBITAL FLIGHT TEST 4 (SHUTTLE)
U SPACE TRANSPORTATION SYSTEM 4 FLIGHT

ORBITAL FLIGHT TESTS (SHUTTLE)
U SPACE TRANSPORTATION SYSTEM FLIGHTS

ORBITAL LAUNCHING
STS-26 through STS-34, deploy activities
[NASA-TM-109566] 03 p1301 N94-15315

ORBITAL LIFETIME
Lifetimes of lunar satellite orbits
[NASA-TP-3394] 07 p2690 N94-27771

ORBITAL MANEUVERING VEHICLES
Computational analysis of Variable Thrust Engine (VTE) performance
[NASA-CR-193852] 03 p0928 N94-17442
Shuttle-C, the future is now
[NASA-TM-109355] 04 p1332 N94-18954

ORBITAL MANEUVERS
Guidance law development for aeroassisted transfer vehicles using matched asymptotic expansions
[NASA-CR-194523] 02 p0508 N94-14538
Effects of thrust vector control on the performance of the aerobang orbital plane change maneuver
[AD-A272532] 05 p1646 N94-21418
MERCATOR: Methods and Realization for Control of the Attitude and the Orbit of spacecraft
06 p2202 N94-23925
The geo-control system for station keeping and colocation of geostationary satellites
06 p2464 N94-23927
HISPASAT launch and early operations phases: Computation and monitoring of geostationary satellite positioning 06 p2514 N94-23928
Orbital applications of electrodynamic propulsion
[AD-A275413] 08 p3173 N94-29216
The influence of the deorbit-burn manoeuvre on the footprint of a re-entry capsule
[LR-727] 09 p3609 N94-31705
Ulysses: A solar odyssey
[NASA-TM-109820] 10 p4010 N94-33574
Theory and computation of optimal low- and medium-thrust transfers
[NASA-CR-196077] 11 p4202 N94-35487
Automated maneuver planning using a fuzzy logic algorithm 11 p4203 N94-35610

ORBITAL MECHANICS
Orbital simulations of satellite escape/capture and the origin of satellites such as Triton
01 p0429 N94-12057
Space flight: The application of orbital mechanics
[NASA-TM-109424] 03 p0874 N94-15493
Tidal regime of intact planetoid capture model for the Earth-Moon system: Does it relate to the archean sedimentary rock record? 03 p1245 N94-16378
The Cluster orbit and mission scenario
04 p1330 N94-19637
Inclined orbits and interference to stationary service and to stationary service by satellite
05 p1653 N94-22188
Improved thermal force modeling for GPS satellites
06 p2207 N94-23259
CNES organization for station positioning of geostationary satellites 06 p2501 N94-23857
Steady motions of rigid body satellites in a central gravitational field
[AD-A273742] 06 p2206 N94-25532
A virtual environment for satellite modeling and orbital analysis in a distributed interactive simulation
[AD-A274114] 07 p2694 N94-25904
Symplectic topology of integrable Hamiltonian systems
[DE94-608120] 08 p3467 N94-30166
Testing for preferred-frame effects in gravity with artificial Earth satellites
[PB94-148459] 09 p3610 N94-31771
Spatio-temporal complexity and large-scale structures in problems of continuum mechanic
[AD-A278473] 10 p4044 N94-33702
Compression of a radar track of a near Earth satellite into an Earth centered inertial state vector using least squares differential correction
[AD-A278498] 10 p4037 N94-34302
Configurational evolution dynamics and stability during in-situ development of large orbiting spacecraft
[AD-A280482] 12 p4397 N94-37351

ORBITAL MOTION
U ORBITS

ORBITAL POSITION ESTIMATION
Pre-operation analysis of ERS-1 tracking and operation, part 2-F
[NASDA-CNT-930002-PT-2-F] 01 p0230 N94-11130
Regional orbit precision in the Mediterranean area
01 p0039 N94-12530
Orbit determination error analysis based on the requirements of ADEOS mission
[NASDA-CNT-930008] 02 p0532 N94-13644
On the accuracy of ERS-1 orbit predictions
03 p0874 N94-15589
Laser ranging data analysis
[NASA-CR-193547] 03 p1041 N94-16719
Using the USCCS for sub microsecond spacecraft clock calibration 05 p1813 N94-21346
A review of GPS-based tracking techniques for TDRS orbit determination 06 p2196 N94-23257
New approaches for tracking earth orbiters using modified GPS ground receivers
06 p2196 N94-23258
Real-time on-board orbit determination with DORIS
06 p2196 N94-23919
TOPEX/Poseidon precision orbit determination production and expert system 06 p2196 N94-23920
Satellite autonomous navigation and orbit determination using magnetometers 06 p2156 N94-24258
TOPEX/POSEIDON operational orbit determination results using global positioning satellites
08 p3160 N94-29666
Time transfer using geostationary satellites: Implementation of a Kalman filter
08 p3471 N94-30657
Air Force Space Command satellite orbit predictor using parallel virtual machines
[AD-A276316] 09 p3601 N94-31298
Possible improvements of satellite ephemeris programs used in geodesy
[PB94-148681] 09 p3743 N94-31592
Error analysis of real-time and post-processed orbit determination for the Geosat Follow-On altimetric satellite using GPS tracking 09 p3576 N94-31845
Thermospheric modeling accuracies using F10.7 and Ap
[AD-A277355] 09 p3773 N94-32337
Aerospace sponsored research
[ATR-93(8498)-1] 09 p3966 N94-32949
Filter parameter tuning analysis for operational orbit determination support 11 p4208 N94-35637

ORBITAL RENDEZVOUS
NT EARTH ORBITAL RENDEZVOUS
STS-32 mission highlights resource tape
[NASA-TM-109291] 02 p0531 N94-13631
Phasing strategies of the Hermes type space shuttle: Its optimization considering the thrust failures
[LAAS-93242] 04 p1544 N94-19361
Telerobotic rendezvous and docking vision system architecture
[NASA-CR-191329] 06 p2204 N94-23828
Autonomous rendezvous and docking for Space Station Freedom 07 p2684 N94-26286
Nasa Langley Research Center seventy-fifth anniversary publications, 1992
[NASA-TM-109691] 07 p3118 N94-27431
Orbital applications of electrodynamic propulsion
[AD-A275413] 08 p3173 N94-29216
Evaluation of GPS position and attitude determination for automated rendezvous and docking missions
[NASA-CR-4614] 12 p4397 N94-37506

ORBITAL RESONANCES (CELESTIAL MECHANICS)
The IR properties of ringed galaxies and the IRAS database
[NASA-CR-194286] 01 p0426 N94-11590
On the depletion in the outer asteroid belt and the structure of the 4 to 3 mean motion resonance
01 p0426 N94-11596
Mapping the stability region of the 3:2 Neptune-Pluto resonance 03 p1280 N94-16351
On the delivery of planetesimals to a protoplanet in the solar nebula 03 p1245 N94-16379
Dust grain resonant capture: A statistical study
03 p1245 N94-16384
The design and networking of dynamic satellite constellations for global mobile communication systems
06 p2288 N94-22826
Binary-single star scattering: An investigation of a realistic chaotic scattering system
08 p3543 N94-29719

ORBITAL SERVICING
On-orbit refueling 01 p0038 N94-11565
On-orbit refueling 01 p0038 N94-11566
Preliminary analysis of the benefits derived to US Air Force spacecraft from on-orbit refueling
01 p0038 N94-11567
In-space operations for lunar and Mars space transfer vehicles 01 p0348 N94-11568
In-space assembly-servicing requirements
01 p0348 N94-11569
Definition of spacecraft standard interfaces by the NASA Space Assembly and Servicing Working Group (SASWG) 01 p0348 N94-11574
Supervised autonomous control, shared control, and teleoperation for space servicing
01 p0183 N94-11577
STS-37 CETA evaluation with Ross
[NASA-TM-109495] 03 p1135 N94-15330
Superfluid Helium On-Orbit Transfer (SHOOT) flight demonstration 04 p1327 N94-19185
Spline screw payload fastening system
[NASA-CASE-GSC-13454-1] 05 p1821 N94-20126
Graphical programming: A systems approach for telerobotic servicing of space assets
[DE93-019016] 06 p2472 N94-23201
Ground operation of robotics on Space Station Freedom 06 p2371 N94-23841
An intelligent planning and scheduling system for the HST servicing missions 06 p2520 N94-23964
Illumination requirements for operating a space remote manipulator 06 p2435 N94-24195
Manned mission to Mars with periodic refueling from electrically propelled tankers 07 p2689 N94-25670
System for the installation and replacement of components in hostile environments
[NASA-CASE-LEW-14906-1-SB]
08 p3300 N94-29427
Development and testing of the Automated Fluid Interface System 08 p3161 N94-29636
Technology transfer and evaluation for Space Station telerobotics
[AIAA PAPER 94-1190-CP] 08 p3441 N94-30541
Space flight manipulator technologies and requirements for the NASA Flight Telerobotic Servicer (FTS)
[AIAA PAPER 94-1191-CP] 08 p3441 N94-30542
A Space Station robot walker and its shared control software
[AIAA PAPER 94-1192-CP] 08 p3442 N94-30543
Technology for robotic surface inspection in space
[AIAA PAPER 94-1193-CP] 08 p3442 N94-30544
On-orbit spacecraft servicing: An element in the evolution of space robotics applications
[AIAA PAPER 94-1236-CP] 08 p3448 N94-30583
Experiments in autonomous navigation and control of multi-manipulator, free-flying space robots
10 p4013 N94-33383
Task network models in the prediction of workload imposed by extravehicular activities during the Hubble Space Telescope servicing mission
10 p4101 N94-33627
Graphical programming: A systems approach for telerobotic servicing of space assets
10 p4066 N94-33666
Diagnosing anomalies of spacecraft for space maintenance and servicing 10 p4015 N94-33667
Robotic technologies of the Flight Telerobotic Servicer (FTS) including fault tolerance 10 p4067 N94-34034
EVA-SCRAM operations 10 p4102 N94-34035

ORBITAL SIMULATORS
U SPACE SIMULATORS

ORBITAL SPACE TESTS
Third LDEF Post-Retrieval Symposium Abstracts
[NASA-CP-10120] 03 p1303 N94-16495

ORBITAL TRANSFER
U TRANSFER ORBITS

ORBITAL VELOCITY
Optical properties of water released in low Earth orbit
[AD-A266197] 03 p1192 N94-16936
Variety in planetary systems 05 p2086 N94-20871
Entry velocities at Mars and Earth for short transit times
[AD-A272591] 05 p1665 N94-21420
Dust evolution from comets and asteroids: Their velocities at Earth orbit intersection
11 p4352 N94-36142

ORBITAL WORKERS
A simulation system for Space Station extravehicular activity 06 p2434 N94-24192
An analysis of the loads applied to a heavy Space Station rack during translation and rotation tasks
[NASA-TM-104790] 07 p2697 N94-28183

Use of a pitch adjustable foot restraint system: Operator strength capability and load requirements
[NASA-TP-3477] 09 p3805 N94-33050

ORBITALS
NT ELECTRON ORBITALS
NT MOLECULAR ORBITALS

ORBITING ASTRONOMICAL OBSERVATORY
U OAO

ORBITING GEOPHYSICAL OBSERVATORY
U OGO

ORBITING SOLAR OBSERVATORY
U OSO

ORBITS
NT CIRCULAR ORBITS
NT EARTH ORBITS
NT ECCENTRIC ORBITS
NT ELLIPTICAL ORBITS
NT EQUATORIAL ORBITS
NT GEOSYNCHRONOUS ORBITS
NT INTERPLANETARY TRANSFER ORBITS
NT LUNAR ORBITS
NT PARKING ORBITS
NT PLANETARY ORBITS
NT POLAR ORBITS
NT SATELLITE ORBITS
NT SOLAR ORBITS
NT SPACECRAFT ORBITS
NT STELLAR ORBITS
NT TRANSFER ORBITS

The long-term dynamical behavior of short-period comets 01 p0427 N94-11629

Correlations in the actions of periodic orbits derived from quantum chaos
[DE93-616866] 06 p2571 N94-25340

Orbit spaces over commutative rings and projectives as semi-isomorphisms
[DE93-616822] 06 p2493 N94-25473

Towards a theory of growing surfaces: Mapping two-dimensional Laplacian growth onto Hamiltonian dynamics and statistics
[DE94-002636] 07 p2991 N94-26079

A semiclassical study of quantum maps 08 p3524 N94-29987

Periodic orbits of n-body type problems: The fixed period case
[DE94-608096] 08 p3453 N94-30091

Numerical detection and continuation of codimension-two homoclinic bifurcations
[CWI-AM-R9308] 09 p3847 N94-32191

New proof and extension of Sarkovskii's theorem
[AD-A278347] 10 p4129 N94-34004

ORDER-DISORDER TRANSFORMATIONS

X-ray and neutron scattering studies of magnetic critical fluctuations in holmium
[DE93-010873] 01 p0400 N94-11467

Effect of pressure on order and stability in alloys: The case of Al-Ge
[DE93-013842] 02 p0567 N94-12899

Transport properties of disordered porous media from the microstructure
[DE93-016065] 02 p0806 N94-13152

Electron-microscopy study of antiphase boundaries in Cu3Pd and Fe3Al alloys near the order-disorder transition
[ONERA-NT-1993-1] 03 p1206 N94-15295

Structural studies of sol-gel glasses
[AD-A266277] 03 p0967 N94-16472

Thermal disorder in adsorbed Cl on Si(100)
[AD-A266295] 03 p1210 N94-16476

Microstructure of Zr3Al after 2 MeV proton bombardment
[DE93-015331] 03 p1211 N94-16814

Kinetics of silica-phase transitions
[DE93-016231] 03 p1217 N94-17659

Effect of oxygen concentration and ordering on vanadium-oxygen alloy vibrational spectra
[DE93-627003] 04 p1355 N94-17692

Surface phases and their influence on metal-oxide interfaces
[DE93-019931] 04 p1601 N94-19020

A free energy simulation method based study of interfacial segregation
[DE93-019462] 04 p1364 N94-19032

The Coulomb anomaly in strongly disordered films
[AD-A271095] 05 p2012 N94-19849

Effect of exciton localization and delocalization on magnetic-field-dependent photoluminescence linewidths in semiconductors
[DE93-018860] 05 p1748 N94-19884

Disorder effects on small-polaron formation and hopping
[DE94-001205] 06 p2534 N94-23804

Two micron stimulated emission of activated insulating crystals
[REPT-94-002] 06 p2565 N94-25025

Fermi-liquid to non-Fermi-liquid transition in a dynamical generalization of the CPA in a disordered Hubbard model
[DE94-601875] 07 p2714 N94-26169

The origins of ordering in CuPt
[DE94-003864] 07 p2736 N94-26351

Ordering and phase separation in MOCVD InGaP alloys and unicompositional quantum wells
[DE94-004693] 07 p3056 N94-26352

Regrowth zones in laser annealed radiation damaged diamond
[DE94-600821] 07 p3056 N94-26364

Structure of ionic fluids in equilibrium with a microporous ionic matrix
[DE94-600563] 07 p2715 N94-26391

Transition metals in highly correlated discotic phases: Designing metallomesogens with selected intermolecular organizations
[AD-A274695] 07 p2736 N94-26452

Length-scale dependent ensemble-averaged conductance of a 1D disordered conductor: Conductance minimum
[DE94-602732] 07 p3062 N94-26902

First principles pseudopotential calculations on aluminum and aluminum alloys
[DE94-004890] 08 p3206 N94-29931

Structural analysis of amorphous phosphates using high performance liquid chromatography
[DE94-004791] 08 p3199 N94-30723

Experimental and theoretical studies of hydrogenated amorphous semiconductor alloys and superlattices
[AD-A276159] 09 p3686 N94-31079

Reversible optical storage in azo polymers
[AD-A277109] 09 p3654 N94-31980

Calculations of nonspherically averaged charge densities for substitutionally disordered alloys
[DE94-008293] 09 p3646 N94-32754

X ray absorption study of pulsed laser deposited boron nitride films
[DE94-008295] 09 p3662 N94-32855

Interface controlled amorphization of crystalline Ni/Ti multilayers
[DE94-008685] 09 p3906 N94-32884

Phase behavior, structure, and properties of model block polymers
[AD-A277530] 09 p3662 N94-32954

A theoretical study of ordering phenomena in K-In and K-Sb molten alloys
[DE94-611103] 11 p4240 N94-35935

Investigation of moisture-induced embrittlement of iron aluminides
[DE94-010881] 11 p4241 N94-36196

Modelling of the structure and physical properties of simple disordered systems
[DE94-617087] 11 p4329 N94-36311

ORDNANCE

Earth Penetration Radar Imaging System (EPRIS)
[DE93-019890] 04 p1391 N94-19542

Differential global positioning system for the surface-towed ordnance locating system: Testing, results, and user's guide
[DE94-002980] 07 p2664 N94-26309

Advanced release technologies program 09 p3607 N94-33322

Development and demonstration of a telerobotic excavation system 10 p4066 N94-34028

ORES
U MINERALS

ORGANELLES
NT CHLOROPLASTS
NT MITOCHONDRIA
NT NUCLEI (CYTOLOGY)

Probability of alamethicin conductance states varies with nonlamellar tendency of bilayer phospholipids
[AD-A264957] 01 p0301 N94-11648

ORGANIC ALUMINUM COMPOUNDS

Ignition delays, heats of combustion, and reaction rates of aluminum alkyl derivatives used as ignition and combustion enhancers for supersonic combustion
[NASA-CR-189581] 09 p3638 N94-32868

ORGANIC CHEMISTRY

Studies in bioorganic chemistry
[AD-A265532] 01 p0055 N94-12011

Royal Society of Chemistry, Heterocyclic Chemistry Group, Lakeland Heterocyclic Symposium
[AD-A270374] 04 p1338 N94-18703

Research program activities of the ORNL Analytical Chemistry Division
[DE93-017938] 04 p1339 N94-19117

The intramolecular cyclization of bis-2,5-dimethylene-2,5-dihydrofurans and bis-2,5-dimethylene-2,5-dihydrothiophenes: An approach to macrocycles
[DE94-007060] 09 p3657 N94-32377

Organic analyses of the Murchison meteorite 09 p3938 N94-32489

Anatomy of a cluster IDP, Part 2: Noble gas abundances, trace element geochemistry, isotopic abundances, and trace organic chemistry of several fragments from L2008#5 11 p4352 N94-35465

ORGANIC COMPOUNDS
NT ACETIC ACID
NT ACETYLENE
NT ACRYLIC ACID
NT ADENOSINE TRIPHOSPHATE
NT ALANINE
NT ALBUMINS
NT ALDOLASE
NT ALIPHATIC HYDROCARBONS
NT ALKANES
NT ALKENES
NT ALKYNES
NT AMINO ACIDS
NT ANTHRACENE
NT ATROPINE
NT AZOLES
NT AZULENE
NT BENZENE
NT BENZOIC ACID
NT BETAINES
NT BUTADIENE
NT BUTANES
NT BUTENES
NT CAFFEINE
NT CALMODULIN
NT CARBOHYDRATES
NT CARBOXYHEMOGLOBIN
NT CARBOXYLIC ACIDS
NT CAROTENE
NT CELLULOSE
NT CHLOROFLUOROMETHANE
NT CHOLESTEROL
NT CHOLINE
NT CITRIC ACID
NT CUBANE
NT CYCLIC AMP
NT CYCLIC COMPOUNDS
NT CYCLIC HYDROCARBONS
NT CYCLOBUTANE
NT CYCLOHEXANE
NT CYCLOPROPANE
NT CYSTEINE
NT DEOXYRIBONUCLEIC ACID
NT DEXTRANS
NT DICARBOXYLIC ACIDS
NT DIENES
NT DIETHYL ETHER
NT DIMETHYL COMPOUNDS
NT DIPHENYL COMPOUNDS
NT DOPA
NT ELASTIN
NT ENZYMES
NT ETHANE
NT ETHYLENE
NT ETHYLENEDIAMINETETRAACETIC ACIDS
NT FATTY ACIDS
NT FLUORINE ORGANIC COMPOUNDS
NT FLUOROCARBONS
NT FLUOROHYDROCARBONS
NT FLUOROPOLYMERS
NT FURANS
NT GLOBULINS
NT GLUCOSE
NT GLUCOSIDES
NT GLUTAMIC ACID
NT GLYCINE
NT GLYCOGENS
NT HEMOGLOBIN
NT HEPTANES
NT HETEROCYCLIC COMPOUNDS
NT HEXADIENE
NT HMX
NT HYDROCARBONS
NT INDENE
NT INDOLES
NT LIPIDS
NT LIQUEFIED NATURAL GAS
NT LYSINE
NT LYSOZYME
NT METHANE
NT METHIONINE
NT METHYLENE
NT MYOGLOBIN
NT NAPHTHALENE
NT NATURAL GAS
NT NUCLEIC ACIDS
NT OLEIC ACID
NT ORGANIC BORON COMPOUNDS
NT ORGANIC LIQUIDS
NT ORGANIC PEROXIDES
NT ORGANIC PHOSPHORUS COMPOUNDS
NT ORGANIC SILICON COMPOUNDS

NT ORGANIC SULFUR COMPOUNDS
NT OXALIC ACID
NT OXAZOLE
NT OXIDASE
NT PARAFFINS
NT PENTANES
NT PEPTIDES
NT PHENYLALANINE
NT PHOSPHAZENE
NT PHTHALOCYANIN
NT POLYBUTADIENE
NT POLYNUCLEAR ORGANIC COMPOUNDS
NT POLYPEPTIDES
NT POLYSACCHARIDES
NT POLYTETRAFLUOROETHYLENE
NT POLYVINYL FLUORIDE
NT PROMETHAZINE
NT PROPANE
NT PROPARGYL GROUPS
NT PROPIONIC ACID
NT PROPYLENE
NT PROSTAGLANDINS
NT PROTEASE
NT PROTEINS
NT PYRENES
NT PYRIDINES
NT PYRROLES
NT QUINONES
NT RDX
NT RETINENE
NT RHODAMINE
NT RIBONUCLEIC ACIDS
NT SEROTONIN
NT STARCHES
NT STEROIDS
NT STILBENE
NT SUCROSE
NT SUGARS
NT TEFLON (TRADEMARK)
NT TETRAHYDROFURAN
NT THYROXINE
NT TOCOPHEROL
NT TOLUENE
NT TRYPSIN
NT TRYPTOPHAN
NT TYROSINE
NT VINYLIDENE
NT XANTHINES

Second and third order nonlinear optical properties of crystalline inorganic/organic complexes
[DE93-011883] 01 p0173 N94-10755

Comprehensive analysis of airborne contaminants from recent Spacelab missions 01 p0318 N94-11553

Synthesis, characterization, and modification of poly(organophosphazenes), that bear both 2,2,2-trifluoroethoxy and phenoxy groups
[AD-A264913] 01 p0092 N94-11847

Tandem mass spectrometric analysis of phosphate esters
[AD-A265483] 01 p0078 N94-12009

A reexamination of amino acids in lunar soil 01 p0452 N94-12109

Oxidation state of the Earth's upper mantle during the last 3800 million years: Implications for the origin of life 01 p0283 N94-12210

Integrated, flexible, and rapid geophysical surveying
[DE93-009989] 02 p0712 N94-12906

Biomass production chamber air analysis of wheat study (BWT931)
[NASA-TM-109192] 02 p0737 N94-13712

Development of an advanced spacecraft tandem mass spectrometer
[NASA-CR-194195] 02 p0545 N94-13953

Portable acoustic wave sensor systems for real-time monitoring of volatile organic compounds
[DE93-013753] 02 p0582 N94-14511

Emissions of volatile organic compounds from stationary combustion sources: Numerical modeling capabilities
[DE93-014123] 03 p1096 N94-16825

Optical studies of glasses embedded with inorganic ions and organic dyes
[AD-A268146] 03 p1199 N94-17455

Title 1 implementation: Status report on nonattainment areas
[DE93-017677] 04 p1471 N94-17777

Indoor environment program
[DE93-018601] 04 p1513 N94-18935

Organic carbonyl compounds in Albuquerque, New Mexico, air: A preliminary study of the effects of oxygenated fuel use
[DE93-017748] 04 p1476 N94-19045

Kinetic studies of electrochemical generation of Ag(II) ion and catalytic oxidation of selected organics
[DE93-016601] 04 p1352 N94-19240

Surface electrochemistry of metals
[AD-A272913] 05 p1691 N94-21245

Laser driven hydrodynamic instability experiments
[DE93-040550] 05 p1818 N94-21547

Surface acoustic wave sensing of VOC's in harsh chemical environments
[DE93-040721] 05 p1968 N94-21751

Ordered organic thin films self-assembled from the vapor phase 06 p2223 N94-24339

On superconductivity of alpha-(BEDT-TTF)2KHg(SCN)4
[REPT-A-2660] 06 p2564 N94-24978

Computational studies of energetic organic molecules
[AD-A274726] 07 p3018 N94-26172

A materials compatibility study in FM-1, a liquid component of a paste extrudable explosive
[DE94-001166] 07 p2759 N94-26198

Numerical analysis of the photo-dissociation/radical oxidation of formaldehyde by ultraviolet light in a photolytic reactor
[AD-A274539] 07 p2868 N94-26843

Development of a sparging technique for volatile emissions from potato (Solanum tuberosum)
[NASA-TM-109199] 07 p2903 N94-27412

Trace organic chemical detection using an ultraviolet excitation molecular beam fluorometer
[DE94-002649] 07 p2704 N94-27708

Collaboration of chemical oxidation and biological treatment for removal of refractory organic substances 07 p2870 N94-28149

Treatment of refractory organic substances with combined use of chemical oxidation and biological treatment. Part 2: Biodegradability of ozonation products of chlorophenol 07 p2870 N94-28151

Surface structure and stereochemical properties of self-assembled monolayer materials
[DE94-004960] 08 p3484 N94-28578

Advanced fuel properties: A computer program for estimating property values
[AD-A275248] 08 p3224 N94-28901

Novel mass spectrometric instrument for gaseous and particulate characterization and monitoring
[DE94-005896] 08 p3349 N94-30047

Remote infrared vapor detection of volatile organic compounds
[AD-A276982] 09 p3746 N94-31999

The sol-gel-xerogel transition
[AD-A276647] 09 p3616 N94-32038

Techniques for the evaluation of outgassing from polymeric wafer pods
[DE94-008427] 10 p4028 N94-33926

Morphological aspects of surface reactions
[DE94-010184] 11 p4236 N94-35685

Particulate and gaseous organic receptor modeling for the Southern California Air Quality Study
[PB94-156700] 11 p4285 N94-35735

Vapor-fortified QA/QC samples for the analysis of volatile organic compounds
[AD-A278712] 11 p4229 N94-35776

Dual cure low-VOC coating process
[DE94-009346] 11 p4245 N94-35809

Real-time SAW measurements of NVR in cleanroom and in microenvironment
[DE94-011937] 12 p4389 N94-37159

SAW chemical sensor arrays using new thin-film materials
[DE94-011940] 12 p4411 N94-37365

The 1st International Symposium on Organic Photochromism: Molecules and Systems
[PB94-179488] 12 p4399 N94-37531

ORGANIC FLUORINE COMPOUNDS
U FLUORINE ORGANIC COMPOUNDS

ORGANIC LASERS
NT DYE LASERS

ORGANIC LIQUIDS

Similarity solutions for gravity-dominated spreading of a lens of organic contaminant
[REPT-93-24] 04 p1420 N94-19139

Electrochemically mediated polymerization of 2-pentadecylaniline confined to a planar liquid-liquid interface
[AD-A273541] 06 p2259 N94-24792

Flooded cell permeation testing of elastomers
[AD-A277698] 10 p4026 N94-33438

ORGANIC MATERIALS
NT PEAT

Organic matter on the early surface of Mars: An assessment of the contribution by interplanetary dust 01 p0480 N94-12259

Mass and spatial distribution of carbonaceous component in Comet Halley 01 p0433 N94-12263

The effects of organic adsorbates on the underpotential deposition of silver on Pt(111) electrodes
[AD-A265623] 01 p0404 N94-12376

Primary productivity in the Oyashio area in the spring and summer of 1990 01 p0211 N94-12658

Characterization of dissolved organic matter in the ocean by using the fluorescence excitation-emission matrix 01 p0211 N94-12659

Variation of the photosynthetic products in the regional upwelling area around the Izu Islands, Japan 01 p0211 N94-12661

Non-image visible polarization remote sensing of the ocean 01 p0229 N94-12762

Organic polymeric electro-optic materials: Synthesis, processing, and device applications
[AD-A267133] 03 p0964 N94-15688

Terrestrial bitumen analogue of orgueil organic material demonstrates high sensitivity to usual HF-HCl treatment 03 p0930 N94-16325

Bioorganic models for protein ion channels
[AD-A266365] 03 p1117 N94-16441

New organic materials for nonlinear optics applications
[AD-A266451] 03 p1192 N94-16563

Process relationship as influenced by carbonization rate
[AD-A269680] 04 p1341 N94-18572

Ionized-cluster beam/partially ionized beam deposition of electro-optical and nonlinear optical organic materials and device development
[AD-A270832] 04 p1604 N94-19596

First discovery of the organic materials in deep-sea iron cosmic spherule 05 p1685 N94-20677

A study of the induction heating of organic composites
[AD-A272657] 05 p1675 N94-21187

Algorithm-development activities
[NASA-CR-193225] 06 p2420 N94-23538

Microgravity Studies of Organic and Polymeric Materials
[NASA-CP-3250] 06 p2223 N94-24338

Prediction of nonlinear optical properties of organic materials. General theoretical considerations 06 p2224 N94-24343

Crystal growth of organics for nonlinear optical applications 06 p2225 N94-24348

Test methods for composites: A status report. Volume 1: Tension test methods
[AD-A273501] 06 p2230 N94-24942

Test methods for composites: A status report. Volume 3: Shear test methods
[AD-A273561] 06 p2230 N94-25163

Research and development within nonlinear optics for protection of optical sensors against laser irradiation on of optical sensors against laser irradiation. Quarterannual report 1 (april 1993))
[PB94-124245] 07 p3037 N94-27046

Organic materials that respond to molecules
[AD-A275392] 08 p3174 N94-29307

Low-Earth orbit effects on organic composite materials flown on LDEF 09 p3595 N94-31036

A compatibility study of FEFO with various containment materials
[DE94-005753] 09 p3649 N94-31198

NMR studies of organic thin films
[AD-A276953] 09 p3656 N94-32221

Development and application of photosensitive device systems to studies of biological and organic materials
[DE94-008503] 09 p3793 N94-32516

Ultrastructure processing of advanced materials
[AD-A278285] 10 p4018 N94-33962

Residual Gas Analysis (RGA) and shear strength characteristics of a silver-filled epoxy and polyimide under long-term, high-temperature storage conditions
[DE94-010106] 11 p4244 N94-35705

ORGANIC NITRATES
NT CELLULOSE NITRATE
NT NITROGLYCERIN
NT PETN

ORGANIC PEROXIDES

Formation of gas-phase peroxides in a rural atmosphere: An interpretation of the recent SOS/SERON field results
[DE94-002995] 09 p3766 N94-32692

ORGANIC PHOSPHORUS COMPOUNDS
NT PHOSPHAZENE

A characterization of carboxylesterases in rat and guinea pig: Their heterogeneity and role in detoxication of organophosphorus compounds
[NDRE-PUBL-93-1001] 02 p0730 N94-14852

Study on extraction behavior of TRPO with different composition
[DE94-620287] 12 p4412 N94-37534

ORGANIC SEMICONDUCTORS

Studies of interactions between conducting polymer and organic vapors: Applications to chemical sensing
[DE93-015694] 04 p1369 N94-18233

Investigation of heterojunctions and multiple quantum well structures using crystalline organic semiconductors
[AD-A272113] 05 p2018 N94-20569

ORGANIC SILICON COMPOUNDS
Sol-gel derived silica/siloxane composite materials: The effect of loading level and catalyst activity on silica domain formation
[DE94-002734] 07 p2712 N94-27710
Cross-condensation reactions in an organically modified silica sol-gel
[DE94-010086] 11 p4244 N94-35701
Spinnability of silica sols: The role of alkoxy group exchange
[DE94-010087] 11 p4244 N94-35702
ORGANIC SOLIDS
Laser fluorescent monitoring of dissolved organic matter in natural water 01 p0177 N94-12755
Ecological application of Surface Enhanced Raman Spectroscopy 01 p0227 N94-12756
ORGANIC SULFUR COMPOUNDS
Supercritical thermodynamics of sulfur and nitrogen species
[DE93-017727] 03 p1220 N94-16997
Nuclear magnetic relaxation studies of semiconductor nanocrystals and solids
[DE94-006301] 08 p3520 N94-30842
ORGANIC SUPERCONDUCTORS
The de Haas-van Alphen studies and Fermi surface properties of organic superconductors (ET)2X
[DE93-015157] 02 p0623 N94-13925
Structure-property relationships in radical-cation (electron-donor molecule) and anion-based (including fullerides) organic superconductors and their use in the design of new materials
[DE93-018617] 04 p1601 N94-19022
Fermiology and De Haas-Van Alphen effect of beta-(ET)2IBr2
[DE93-019523] 05 p2011 N94-19807
Microreflectance infrared study of electron-molecular vibrational coupling and lattice softness in BEDT-TTF salts
[DE94-008490] 09 p3907 N94-32989
ORGANIC WASTES (FUEL CONVERSION)
Statement on global climate change before the Subcommittee on Energy and Power, United States House of Representatives
[DE93-013163] 03 p1095 N94-16006
ORGANISMS
Compatibility tests for biological specimens to on-board experiments in the Space Shuttle flight
[NASDA-CNT-930003] 01 p0301 N94-12278
Study on sea water purification using a substratum of marine organisms 01 p0217 N94-12696
Application of remote sensing for coastal management in the north coast of Java 01 p0218 N94-12701
The algorithm of primary production determination 01 p0228 N94-12761
Non-image visible polarization remote sensing of the ocean 01 p0229 N94-12762
Space research with intact organisms: The role of Space Station Freedom 04 p1502 N94-19213
Coupling of pelagic and benthic communities over a seamount in the Eastern North Pacific
[AD-A274750] 07 p2899 N94-26149
Macrobenthic fauna in the dutch sector of the north sea in 1991
[PB94-126414] 07 p2868 N94-27200
Light utilization and photoinhibition of photosynthesis in marine phytoplankton
[DE94-005505] 09 p3794 N94-32896
Bioluminescence bathyphotometer
[AD-D016102] 09 p3790 N94-32959
ORGANIZATIONS
NT EUROPEAN SPACE AGENCY
NT NORTH ATLANTIC TREATY ORGANIZATION (NATO)
NT WORLD METEOROLOGICAL ORGANIZATION
Engineering performance metrics
[DE93-012084] 01 p0128 N94-11028
Insights into software development in Japan 01 p0330 N94-11435
Myths and realities: Defining re-engineering for a large organization 01 p0330 N94-11436
Research and development of post-classical management tools for government program offices, volume 2
[DE93-010236] 01 p0417 N94-11600
Electric and hybrid vehicle site operators program: Thinking of the future
[DE93-011231] 01 p0144 N94-11609
AGARD highlights 92/2, September 1992
[AGARD-HIGHLIGHTS-92/2] 01 p0497 N94-11820
Here's the beef: A case study in organizational transformation 02 p0667 N94-13163
Fifty years of the Netherlands Association of Aeronautical Engineers 03 p0853 N94-15121
PET team
[NASA-TM-109599] 03 p1223 N94-15293
Managing information as a corporate asset: Key strategies for information professionals to remain competitive
[DE93-015515] 03 p1232 N94-16875
Research grant handbook
[NHB-5800.1C] 03 p1225 N94-16907
Plasma Science Committee (PLSC) and the Panel on Opportunities in Plasma Science and Technology (OPST)
[DE93-018142] 03 p1204 N94-16995
Establishing a software measurement process
[AD-A267896] 03 p1154 N94-17396
Trends in Information Management at Department of Energy Headquarters
[DE93-017197] 04 p1615 N94-18496
Quality, management, and the interplay of self-assessment, process assessments, and performance-based observations
[DE93-018787] 04 p1448 N94-19336
A FET-switched induction accelerator cell
[DE93-019604] 05 p1769 N94-21838
International organizations to enable world-wide mobile satellite services 06 p2275 N94-22749
Towards a new radiation protection organization
[FOA-C-40304-4.3] 06 p2437 N94-24292
SEMATECH, a case study: Analysis of a government-industry partnership
[AD-A273166] 06 p2586 N94-24683
Federal Information Exchange (FEDIX) user's guide: Fall 1993, Version 5.0/Release 1.0
[DE94-003826] 07 p3097 N94-26350
International energy: Research organizations, 1988-1992
[DE93-017267] 07 p3098 N94-26398
Pigs in cyberspace 07 p2689 N94-27376
Measuring the impact of investments in information technologies on business performance
[REPT-93-056] 08 p3536 N94-30929
Piezoelectric materials research in Europe
[AD-A276207] 09 p3648 N94-31059
A redundant disk array architecture for efficient small writes
[AD-A276645] 09 p3815 N94-31940
Untying the gordian data knot. A paper on Information Engineering (IE) and Corporate Information Management (CIM)
[AD-A276862] 09 p3918 N94-32210
ORDIT: A new methodology to assist in the process of eliciting and modelling organisational requirements
[PB94-167814] 11 p4345 N94-35533
Introduction to USRA
[NASA-CR-195980] 11 p4376 N94-35590
ORGANOMETALLIC COMPOUNDS
NT CARBOXYHEMOGLOBIN
NT CHLOROPHYLLS
NT FERROCENES
NT HEMOGLOBIN
NT ORGANIC ALUMINUM COMPOUNDS
Aluminum-phosphorus chemistry: Preparation and structural characterization of (Et2AlP(SiMe3)2)2, Et(Cl)2Al(dot)P(SiMe3)3, and i-Bu2(Cl)Al(dot)P(SiMe3)3
[AD-A265268] 01 p0078 N94-11683
Anchoring strategies for bimetallic species in zeolites
[DE93-015622] 02 p0567 N94-12834
Growth experiment of organic metal crystal in low gravity (M-21) 02 p0590 N94-13753
Effects of growth conditions and substrate orientation on the properties of InSb
[DE93-013766] 02 p0812 N94-14344
Amide and tetrazene complexes of transition and main group elements as precursors for the low temperature synthesis of elemental nitrides
[AD-A266246] 03 p0950 N94-16931
X ray absorption spectroscopic studies of the active sites of nickel- and copper-containing metalloproteins
[DE93-017142] 04 p1347 N94-18059
Molecular and polymeric ceramic precursors
[DE93-040364] 04 p1372 N94-18891
The direct synthesis of organic and organometallic-containing MICA-type aluminosilicates
[DE93-019001] 04 p1373 N94-19321
Photochemically induced transformations of transition complexes
[AD-A271112] 05 p2014 N94-19982
Catalytic hydrogenation of carbon monoxide
[DE94-000881] 05 p1678 N94-20103
Sulfur-bonded thiophenes in organometallic rhenium complexes and adsorption of isocyanides on gold
[DE93-041126] 05 p1694 N94-21937
Low temperature absorption spectra and ground state electronic structure of tetrakis(2,6-di-tert-butylphenoxide)uranium(IV)
[DE94-000774] 05 p2035 N94-22387
Organometallic chemistry of bimetallic compounds
[DE94-002313] 06 p2238 N94-22897
Synthesis and in-vivo detection of boronated compounds for use in BNCT
[DE94-001899] 06 p2233 N94-23780
Scanning probe lithography. 2: Selective chemical vapor deposition of copper into scanning tunneling microscope-defined patterns
[AD-A273304] 06 p2547 N94-25144
Processing of LaCrO3 for solid oxide fuel cell applications
[DE94-002981] 07 p2857 N94-26747
Electro-optic materials by solid source MOCVD
[DE94-005120] 07 p2757 N94-27716
Alkylene-bridged polygerm- and polygermsilsesqui-oxanes: New hybrid organic-inorganic materials
[DE94-005096] 08 p3174 N94-28557
Gas phase thermochemistry of organogermanium compounds
[DE94-004885] 08 p3187 N94-28561
Innovative optoelectronic materials and structures using OMVPE
[AD-A275811] 08 p3511 N94-28773
Polymer technology publication series no. 16
[PB94-135522] 08 p3214 N94-29157
The organometallic chemical vapor deposition of transition metal carbides: The use of homoleptic alkyls
[DE94-005577] 08 p3206 N94-30007
Plasma enhanced chemical vapor deposition of ZrO2 thin films
[DE94-006031] 08 p3218 N94-30104
Group transfer and electron transfer reactions of organometallic complexes: Summary of research accomplished in 1993
[DE94-004963] 08 p3200 N94-30770
Molecular/polymeric magnetism
[DE94-005888] 09 p3649 N94-31201
Silicone grease as a precursor to a pseudo crown-ether ligand: Crystal structure of (K(+)K(Me2SiO)7(+))(HIn(CH2CMe3)3(-))4
[AD-A276343] 09 p3895 N94-31327
Tetraalkyldiarsines as potential precursors for electronic materials: Synthesis and characterization of various iso-propyl arsenic compounds
[AD-A277003] 09 p3900 N94-32001
Advances in MOVPE compound semiconductor epitaxy manufacturing technology: From high throughput large area reactors to cluster tools
[DE94-006367] 09 p3901 N94-32104
New zinc-bis(dialkylamides) potentially usable as site-selective dopants for p-type ZnSe
[AD-A276947] 09 p3902 N94-32218
Tert-butylalumoxanes: Synthetic analogs for methylalumoxane (MAO) and new catalytic routes to polyolefins and polyketones
[AD-A280511] 12 p4399 N94-37106
Tert-butylalumoxanes: Synthetic analogs for methylalumoxane (MAO) and new catalytic routes to polyolefins and polyketones
[AD-A280532] 12 p4399 N94-37650
ORGANOMETALLIC POLYMERS
A process for preparing an assembly of an article and a soluble polyimide which resists dimensional change, delamination, and debonding when exposed to changes in temperature
[NASA-CASE-LAR-14763-1] 05 p1702 N94-20373
Symposium on Inorganic and Organometallic Polymers
[AD-A277860] 10 p4027 N94-33772
Organometallic NLO polymers. 4: Organometallic main-chain, side-chain, and guest-host polymers: A study of their orientation and relaxation using second harmonic generation
[AD-A280347] 12 p4423 N94-37179
ORGANOMETALLIC VAPOR DEPOSITION
U METALORGANIC CHEMICAL VAPOR DEPOSITION
ORGANS
NCVS, volume 5
[AD-A274975] 07 p2902 N94-27165
ORGUEIL METEORITE
Do SiC grains in Orgueil differ from those in Murchison? 03 p1242 N94-16260
Terrestrial bitumen analogue of orgueil organic material demonstrates high sensitivity to usual HF-HCl treatment 03 p0930 N94-16325
Recondensation in the early solar system: Physical conditions and source material 05 p2085 N94-20849
ORIENTATION
Challenger Center: Orientation
[NASA-TM-109433] 03 p1221 N94-15505
Effects of pressure on the orientational ordering and phase transitions in solid C(60) and C(70)
[DE93-018858] 04 p1603 N94-19347

ORIFICE FLOW
Dispersion of fire suppression agents discharged from high pressure vessels: Establishing initial/boundary conditions for the flow outside the vessel
[PB94-103660] 06 p2172 N94-23810
Transonic expanding flow through axially symmetric orifices 08 p3128 N94-28985
ORIFICES
Shock-induced turbulent flow in baffle systems
[DE94-001532] 06 p2319 N94-23470
Optimization of orifice geometry for cross-flow mixing in a cylindrical duct
[NASA-TM-106436] 06 p2481 N94-23593
CFD assessment of orifice aspect ratio and mass flow ratio on jet mixing in rectangular ducts
[NASA-TM-106434] 06 p2187 N94-24082
ORIGINS
Using solar flare track densities to determine the origin of interplanetary dust particles 01 p0429 N94-12078
ORION AIRCRAFT
U P-3 AIRCRAFT
ORION CONSTELLATION
Theory of protostellar accretion disks
09 p3931 N94-31136
ORION NEBULA
Circumstellar material around young stars in Orion
09 p3930 N94-31133
ORNITHOPTER AIRCRAFT
U RESEARCH AIRCRAFT
OROGRAPHY
Numerical simulation and parameterization of orographic gravity waves 02 p0713 N94-13647
Orographic microbursts in a severe winter windstorm
[AD-A267651] 03 p1108 N94-17247
Effect of spatial resolution on the simulation of regional precipitation in China in a global climate model
[DE93-013433] 04 p1489 N94-18053
Hydrostatic/nonhydrostatic comparison with the MERCURE code on orographic flows
[ETN-93-94603] 05 p1866 N94-20600
GPS survey of the western Tien Shan
[NASA-CR-195174] 06 p2175 N94-24826
The influence of orography on the transport of atmospheric constituents 06 p2619 N94-24886
Investigation of mesoscale convective cloud clusters in South China
[AD-A274303] 07 p2895 N94-26678
An observational study of the extratropical anticyclones in the South American continent
[INPE-5387-TDI/476] 07 p2896 N94-27356
ORR-SOMMERFELD EQUATIONS
Stability of spatially developing boundary layers
02 p0640 N94-14605
On the stability of a time dependent boundary layer
[NASA-CR-191542] 03 p1030 N94-17450
ORRERIES
U ASTRONOMICAL MODELS
ORTHOGONAL FUNCTIONS
NT WALSH FUNCTION
An investigation using empirical orthogonal functions and objective analysis to analyse the vertical temperature structure of a gulf stream meander
[AD-A265116] 01 p0289 N94-11868
Simulation reduction using the Taguchi method
[NASA-CR-4542] 03 p1055 N94-17082
Canonical multi-valued input Reed-Muller trees and forms 04 p1401 N94-18375
Orthogonal pairs and zeros of Sobolev-type orthogonal polynomials
[REPT-92-46] 05 p1953 N94-21059
Orthogonalization method for determination of boundary layer receptivity coefficients
[ISBN-0-315-83426-9] 05 p1805 N94-22580
Polynomials orthogonal with respect to an inner product involving differences
[PB94-110731] 06 p2489 N94-24572
Responses of a finite baffled plate subject to turbulent and mean flow excitations
[NASA-CR-191570] 06 p2334 N94-24605
Nonlinear aerodynamic modeling using multivariate orthogonal functions 06 p2164 N94-25110
Two-dimensional pattern analysis and classification using a complex orthogonal estimation algorithm
[RR-475] 06 p2463 N94-25321
Statistical analysis of a satellite imagery time series: Implications for the study of coastal and estuarine circulation 08 p3335 N94-30919
The Stroemberg wavelet on the interval and the Franklin system
[TELECOM-93-C-002] 08 p3462 N94-30971
Estimating subpycnocline density fluctuations in the California current region from upper ocean observations
[AD-A277278] 09 p3789 N94-32325
ORTHOGONAL MULTIPLEXING THEORY
An introduction to digital modulation and OFDM techniques
[BBC-RD-1993/10] 06 p2295 N94-24086
ORTHOGONALITY
On a difference equation for generalizations of Charlier polynomials
[REPT-92-101] 02 p0770 N94-14150
A hydrogen atom in the curved space: Orthogonality of radial wave functions with respect to the critical momentum
[DE93-626623] 02 p0788 N94-14891
Parallel inverse iteration with reorthogonalization
[DE93-012867] 04 p1533 N94-17693
On polynomials orthogonal with respect to an inner product involving differences (the general case)
[REPT-93-32] 04 p1551 N94-19285
Orthogonal pairs and zeros of Sobolev-type orthogonal polynomials
[REPT-92-46] 05 p1953 N94-21059
Nested Krylov methods and preserving the orthogonality 06 p2483 N94-23681
Geometric correction of SPOT images with use of digital elevation models
[ETN-94-95033] 07 p2847 N94-26107
Event structures and orthogonal term graph rewriting
[CWI-CS-R9347] 08 p3459 N94-30412
Perpetual reductions in orthogonal combinatory reduction systems
[CWI-CS-R9349] 08 p3459 N94-30413
Perpetual reductions and strong normalization in orthogonal term rewriting systems
[CWI-CS-R9345] 08 p3426 N94-30437
A new orthogonal decomposition method for turbulent flows 08 p3281 N94-30494
Subspace estimation without eigenvectors for adaptive beamforming
[AD-A276287] 09 p3671 N94-31254
Combinatory reduction systems: Introduction and survey
[CWI-CS-R9362] 09 p3849 N94-32349
Gauss elimination by segments and multivariate polynomial interpolation
[AD-A278646] 11 p4315 N94-36012
ORTHOGRAPHY
Generalization performance of backpropagation learning on a syllabification task 05 p1940 N94-20246
ORTHONORMAL FUNCTIONS
Mathematic methods and algorithms for real-time applications
[AD-A266776] 02 p0771 N94-14789
Deviation equations of Synge and Schild in spaces with affine connection and metric, and equations for gravitational waves detectors
[DE93-616852] 06 p2571 N94-25339
The Stroemberg wavelet on the interval and the Franklin system
[TELECOM-93-C-002] 08 p3462 N94-30971
On interpolating random fields using a finite number of observations
[CWI-BS-R9314] 09 p3847 N94-32194
On constructing multi-variate orthonormal polynomials associated with spectral distribution functions
[CWI-BS-R9310] 09 p3851 N94-32225
ORTHOSTATIC TOLERANCE
Exercise countermeasures for bed-rest deconditioning
[NASA-TM-103987] 01 p0300 N94-11191
Proceedings of the First Joint NASA Cardiopulmonary Workshop
[NASA-CP-10068] 01 p0308 N94-11991
Carotid-cardiac baroreflex: Relation with orthostatic hypotension following simulated microgravity and implications for development of countermeasures
01 p0308 N94-11992
Echocardiography in the flight program
01 p0309 N94-11993
Effect of prolonged LBNP and saline ingestion on plasma volume and orthostatic responses during bed rest
01 p0310 N94-11998
Fitness, autonomic regulation and orthostatic tolerance 01 p0310 N94-11999
Hormonal regulation of fluid and electrolyte metabolism in zero-g and bedrest 01 p0311 N94-12004
Autogenic-feedback training: A countermeasure for orthostatic intolerance 01 p0311 N94-12006
Autogenic-feedback training: A potential treatment for post-flight orthostatic intolerance in aerospace crews
[NASA-TM-108785] 06 p2426 N94-24102
Development of a model to assess orthostatic responses 06 p2427 N94-25376
Evaluation of bioimpedance for the measurement of physiologic variables as related to hemodynamic studies in space flight 06 p2427 N94-25378
Intermittent gravity: How much, how often, how long?
[NASA-TM-108800] 07 p2944 N94-26098
Analysis on one minute wave in body fluid volume and muscle pumping referred to body parts generating the one minute wave during human active standing
07 p2929 N94-27528
Treatment of orthostatic hypotension by nasal administration of vasopressin 07 p2930 N94-27533
Workshop on Countering Space Adaptation with Exercise: Current Issues
[NASA-CP-3252] 07 p2934 N94-28361
Aerobic fitness and orthostatic tolerance: Evidence against an association 07 p2934 N94-28365
Does training-induced orthostatic hypotension result from reduced carotid baroreflex responsiveness?
07 p2935 N94-28366
Response to graded Lower Body Negative Pressure (LBNP) after space flight 10 p4096 N94-33637
ORTHOTROPIC CYLINDERS
Imperfection sensitivity of the Brazier effect for orthotropic cylindrical shells
[LR-687] 01 p0186 N94-10879
Series solution for a cylindrical composite shell subject to axisymmetric loadings
[ISBN-0-315-60559-6] 07 p2844 N94-27810
ORTHOTROPIC PLATES
Measuring methods for CFRP laminates' bending and torsion rigidities characteristics
02 p0529 N94-13272
Nonlinear equations of motion for a panel subject to external loads
[AD-A273142] 06 p2170 N94-24773
Flat rectangular orthotropic plates under uniformly distributed normal pressure. Elastic stresses and deflections for various forms of edge restraint
[ESDU-93011] 07 p2845 N94-28061
ORTHOTROPIC SHELLS
On the orthotropicity assumption and discontinuity conditions of conical shells
[LR-703] 02 p0673 N94-13787
Forced harmonic vibration of the generally orthotropic cylindrical shell with inner and outer fluid loading
[AD-A266985] 03 p1057 N94-15150
ORTHOTROPISM
Experimental determination of orthotropic elastic constants
[FFA-TN-1991-35] 08 p3215 N94-29424
Approximate estimation of the effects of asymmetry on the testing of tensile specimens
[NPL-DMM(A)-117] 08 p3322 N94-30523
Mechanics of cracking for composite material
09 p3624 N94-32501
OSCILLATING CYLINDERS
Vortex-induced forces on oscillating bluff cylinders
[AD-A265056] 01 p0154 N94-11865
Forces on an oscillating cylinder and related fluid flow phenomena
[ISBN-9-09-005589-4] 06 p2338 N94-25243
OSCILLATING FLOW
On the combustion of a laminar spray
[NASA-TM-106210] 01 p0028 N94-11238
High order accurate solutions of viscous problems
[NASA-TM-106267] 01 p0151 N94-11253
A simple model of melt fracture
[AD-A265311] 01 p0092 N94-11862
Establishing baseline data for an experimental appratus that measures heat transfer under conditions of oscillating pressure and flow
[NASA-CR-193772] 01 p0413 N94-12343
Study of possible mechanisms of instability due to heat transfer
[INPE-5448-TDI/494] 02 p0628 N94-12966
Stability of oscillatory two phase Couette flow
[NASA-CR-191501] 02 p0636 N94-13817
ENO schemes on unstructured meshes
04 p1412 N94-18561
Heat exchanger with oscillating flow
[NASA-CASE-LAR-14033-2] 05 p1800 N94-20495
Development of phased twin flip-flop jets
[NASA-TM-106404] 05 p1637 N94-20563
Response of wall turbulence to high frequency streamwise and spanwise oscillations
09 p3700 N94-31211
Design and initial testing of a facility to measure unsteady pressures on an oscillating cascade with supersonic leading edge locus 09 p3569 N94-31880
Oscillating-flow loss test results in rectangular heat exchanger passages
[NASA-CR-185297] 09 p3615 N94-32792
Flutter analysis of a supersonic cascade in time domain using an ADI Euler solver
[NASA-TM-105625] 09 p3739 N94-32883
The velocity field created by a shallow bump in a boundary layer
[AD-A281064] 11 p4266 N94-35975
A flux splitting scheme with high-resolution and robustness for discontinuities
[NASA-TM-106452] 12 p4441 N94-36646

OSCILLATION DAMPERS
Tuned mass damper for integrally bladed turbine rotor
[NASA-CASE-MFS-28697-1] 08 p3298 N94-29353
OSCILLATIONS
NT AIRFOIL OSCILLATIONS
NT ELECTRON OSCILLATIONS
NT H WAVES
NT HARMONIC OSCILLATION
NT MOLECULAR OSCILLATIONS
NT NONOSCILLATORY ACTION
NT PLASMA OSCILLATIONS
NT PRESSURE OSCILLATIONS
NT SELF OSCILLATION
NT SOLAR OSCILLATIONS
NT SOUTHERN OSCILLATION
NT STABLE OSCILLATIONS
NT STELLAR OSCILLATIONS
NT TRANSIENT OSCILLATIONS
NT TRANSVERSE OSCILLATION
NT UNDAMPED OSCILLATIONS
NT WING OSCILLATIONS
Aharonov-Bohm effect in Luttinger liquid
[DE93-613818] 01 p0408 N94-10148
Pulsatile instability in rapid directional solidification: Strongly-nonlinear analysis 01 p0115 N94-10188
A group-theoretic approach to the study of small oscillations of a dynamical system with a known symmetry
[DE93-612971] 01 p0409 N94-10402
Characterization of the Si/SiO2 interfere morphology from quantum oscillations in Fowler-Nordheim tunneling currents
[AD-A265149] 01 p0143 N94-11160
Sine and random vibration program evaluation on vibration control systems
[DE93-011974] 01 p0188 N94-11460
Decay interaction of bulk and surface Langmuir waves
[DE93-617843] 01 p0393 N94-11477
On the coupling of electromagnetic radiation into cavities
[DE93-011406] 01 p0137 N94-11621
Are there atmospheric neutrino oscillations?
[DE93-015550] 02 p0783 N94-13890
Predicting the vibrations of a spinning inflated membrane
[DE93-010690] 02 p0676 N94-14456
Breakdown of adiabatic invariance
[AD-A267246] 03 p1219 N94-14977
Effect of wind tunnel acoustic modes on linear oscillating cascade aerodynamics
[NASA-TM-106367] 03 p0869 N94-15866
Ventilated oscillatory boundary layers
[AD-A266226] 03 p1023 N94-16110
Search for chaos in free shear flows
[AD-A266245] 03 p1023 N94-16470
The (delta)f algorithm for beam dynamics
[DE93-015632] 03 p1187 N94-16660
Decoherence and recoherence of beam in phase space
[DE93-014885] 04 p1573 N94-17784
FY 1991 AASERT: Spatio-temporal making in human vision and its application to image coding
[AD-A268795] 04 p1505 N94-18190
Neutrino mass
[DE93-018467] 04 p1567 N94-18269
Close-coupled oscillating canard effects on post-stall lift enhancement
[AD-A268938] 04 p1321 N94-18541
Suppression of relaxation oscillations in flashpumped, two-micron tunable solid state lasers
[AD-D015928] 05 p1814 N94-19800
A synoptic-scale overview of the TOGA COARE intensive observing period November 1992 to February 1993 based on analyses from US operational global data assimilation systems
[NASA-TM-104593] 05 p1868 N94-21605
Active damping of oscillations in a long compliant manipulator link
[DE93-018878] 05 p1826 N94-22038
The current status of observational constraints on cosmic strings
[DE94-001505] 06 p2601 N94-23010
Accelerator-based neutrino oscillation searches
[DE94-000818] 06 p2626 N94-23515
Lateral high frequency oscillations and stability of a wheel rolling on a flexible track
06 p2269 N94-23585
Surface observations of stick-slip oscillations in tightly conformal wheel/rail contacts 06 p2270 N94-23588
Multigrid methods for differential equations with highly oscillatory coefficients 06 p2484 N94-23685
Nonlinear dynamics applied to atmospheric prediction
[AD-A273437] 06 p2404 N94-24674
About possible types of neutrino oscillations
[DE93-634449] 07 p3020 N94-26508
Measuring the time dependence of B(sub s)(sup 0) meson - anti B(sub s)(sup 0) meson oscillations
[ISBN-0-315-84367-5] 07 p3021 N94-26665
Polar optical oscillation modes in GaAs-based double heterostructures: Long wavelength limit
[DE94-601874] 07 p3062 N94-26897
Pressure-gain combustion
[DE94-002975] 07 p2719 N94-27712
The status of the solar neutrino problem
[DE94-003934] 07 p3111 N94-27742
An improvement of the slender body theory for oscillating ships with finite forward speed 08 p3234 N94-29705
Observational constraints on black hole accretion disks 09 p3929 N94-31126
Oscillations in piston-driven shear flow of a non-Newtonian fluid
[AD-A276472] 09 p3701 N94-31245
Considering ties elasticities in high frequency rail dynamics
[ILR-MITT-281(1993)] 09 p3733 N94-31375
Torque characteristics of solid lubricated precision bearings during oscillatory motion
[AD-A278133] 09 p3728 N94-33061
The analysis of wake-induced unsteady aerodynamics related to higher harmonic control
[AD-A277914] 09 p3573 N94-33108
Solar neutrino oscillations
[DE94-007265] 10 p4165 N94-33687
Real-time RMS active damping augmentation: Heavy and very light payload evaluations
[NASA-TM-109134] 10 p4015 N94-34386
Techniques for aerodynamic characterization and performance evaluation at high angle of attack
10 p3991 N94-34614
Nonadiabatic neutrino oscillations revisited
[DE94-616649] 11 p4321 N94-35593
Some consequences in weak processes of three generations mixing in the leptonic sector
[DE94-616650] 11 p4321 N94-35594
A triggering mechanism of fast crash in sawtooth oscillation
[DE94-718974] 11 p4336 N94-35772
A procedure for oscillatory parameter identification
[DE94-008047] 11 p4259 N94-36054
Numerical method to study the stability of periodic solutions of particle motion in nonlinear magnetic fields
[DE94-610740] 11 p4325 N94-36088
Q-profile flattening due to nonlinear development of resistive kink mode and ensuing fast crash in sawtooth oscillations
[DE94-727625] 12 p4526 N94-36472
Suppression of beam-break-up in a standing wave free electron laser two-beam accelerator
[DE94-011348] 12 p4521 N94-37200
OSCILLATOR STRENGTHS
The International Colloquium on Atomic Spectra and Oscillator Strengths for Astrophysical and Laboratory Plasmas
[NASA-TM-109255] 02 p0849 N94-13376
Optical and infrared spectra of thermally annealed Pb implanted SiO2 glasses
[DE93-015304] 03 p0965 N94-15828
Spectral characterization of lithographic sources
[DE93-019941] 05 p1997 N94-21848
International bulletin on atomic and molecular data for fusion. No. 46
[DE94-601818] 07 p3023 N94-26947
OSCILLATORS
NT CRYSTAL OSCILLATORS
NT GYROSCOPIC PENDULUMS
NT HARMONIC OSCILLATORS
NT MAGNETRONS
NT MICROWAVE OSCILLATORS
NT MOLECULAR OSCILLATORS
NT PENDULUMS
NT RELAXATION OSCILLATORS
NT VACUUM TUBE OSCILLATORS
NT VOLTAGE CONTROLLED OSCILLATORS
Numerical simulation of sidebands in free electron laser oscillators
[DE93-612675] 01 p0173 N94-10483
Nonlinear Dynamics in Optical Systems. Postdeadline papers presented at the Optical Society of America Conference
[AD-A264958] 01 p0375 N94-10486
Review of SHARC 2.0 O3 kinetics and spectroscopy
[AD-A265481] 01 p0274 N94-10496
Quantum noise and squeezing in optical parametric oscillator with arbitrary output coupling
01 p0375 N94-10568
An exactly solvable model of an oscillator with nonlinear coupling and zeros of Bessel functions
01 p0349 N94-10573
Dissipation in a squeezed-state environment
01 p0370 N94-10584
Disciplined rubidium oscillator with GPS selective availability 01 p0353 N94-10977
A multi-variance analysis in the time domain
01 p0146 N94-10999
A new method of time difference measurement: The time difference method by dual phase coincidence points detection 01 p0357 N94-11002
Confidence of the three-point estimator of frequency drift 01 p0357 N94-11003
Predicted performance of a dc beam driven FEM oscillator designed for fusion applications at 200-250 GHz
[DE93-013414] 02 p0655 N94-13145
Development of UHF spark-switched L-C Oscillators
[DE93-015019] 02 p0823 N94-13892
Investigation of an aeroelastic oscillator: Analysis of one-degree-of-freedom galloping with combined translational and torsional effects
[LR-707] 02 p0527 N94-13906
Melatonin, the pineal gland, and circadian rhythms
[AD-A268200] 03 p1129 N94-17478
X-ray laser oscillator-amplifier experiments
[DE93-017165] 04 p1436 N94-17868
On a possible algebra morphism of U(sub q)(osp1/2) onto the deformed oscillator algebra W(sub q)(N)
[DE93-629857] 04 p1548 N94-18176
High-power microwave breakdown of dielectric interfaces
[AD-A268844] 04 p1397 N94-18318
Designs for a 10.6 micrometer electromagnetic wiggler Free-Electron Laser (FEL)
[AD-A269695] 04 p1439 N94-18576
The Lever oscillator for use in high resistance resonator applications
[DE93-017652] 04 p1404 N94-18827
Contribution to the modelling and the identification of nonlinear mechanical systems
[ECL-92-32] 04 p1529 N94-19409
Optical frequency division using an optical parametric oscillator
[AD-A270847] 04 p1581 N94-19578
A theory for optical wavelength control in short pulse free electron laser oscillators
[AD-A271706] 05 p1817 N94-21353
Coherence lost? Not-so-fast escapes from the in-phase attractor of a set of globally coupled nonlinear oscillators
[DE94-000799] 06 p2557 N94-22940
Modulation characteristics of a high-power semiconductor Master Oscillator Power Amplifier (MOPA)
[NASA-TM-104577] 06 p2308 N94-23281
Controlling regular and chaotic dynamics in the Duffing-Ueda oscillator
[RR-477] 06 p2523 N94-25323
Deviation equations of Synge and Schild in spaces with affine connection and metric, and equations for gravitational waves detectors
[DE93-616852] 06 p2571 N94-25339
Wigner quantum oscillators
[DE94-601508] 07 p3073 N94-26758
HPm-tubes: Literature survey comprising 1992
[PB94-123643] 07 p2785 N94-27038
The onset of chaos in a periodically forced nonlinear oscillator
[ISBN-0-315-84564-3] 07 p2842 N94-27272
Optical parametric oscillator modeling with diffraction, depletion, and double refraction
[DE94-001504] 07 p3040 N94-27999
Sum frequency generation using an optical parametric oscillator
[DE94-001827] 07 p3040 N94-28000
Fiber laser amplifiers and oscillators
[AD-A274231] 07 p2820 N94-28068
Research on elementary particle physics. Task P: Studies in theory and phenomenology of elementary physics
[DE94-004955] 08 p3483 N94-28566
Time and frequency technology at NIST
08 p3468 N94-30641
Accuracy metrics for judging time scale algorithms
08 p3471 N94-30656
Noise and drift analysis of non-equally spaced timing data 08 p3472 N94-30667
Frequency standards from industry over the next 25 years 08 p3475 N94-30683
Laser/lidar analysis and testing
[NASA-CR-193954] 10 p4058 N94-34136
High power diode laser Master Oscillator-Power Amplifier (MOPA)
[NASA-CR-196095] 11 p4271 N94-35488
900-mW average power and tunability from a diode-pumped 2.94 micron Er:YAG oscillator
[DE94-009511] 11 p4271 N94-35679
Coherent states versus de Broglie-wavelets
[DE94-611075] 11 p4343 N94-36381

The 250 watt average power electro-quality Q-switched diode pumped power oscillator
[DE94-011644] 12 p4449 N94-37737
OSCILLOGRAMS
U OSCILLOGRAPHS
OSCILLOGRAPHS
A 10 GHz bandwidth, single transient, digitized oscilloscope with 20 GHz capability
[DE94-005400] 09 p3713 N94-32728
OSCILLOSCOPES
A 10 GHz bandwidth, single transient, digitized oscilloscope with 20 GHz capability
[DE94-005400] 09 p3713 N94-32728
OSCULATIONS
U DOUBLE CUSPS
OSMIUM
NT OSMIUM ISOTOPES
Glucose electrodes based on cross-linked (Os(bpy)2Cl)(sup +/2+) complexed poly(1-vinylimidazole) films
[AD-A265404] 01 p0094 N94-12425
OSMIUM ISOTOPES
Rhenium-osmium isotope systematics of Group 2A and Group 4A iron meteorites 01 p0431 N94-12182
Re-Os dating of 3AB iron meteorites 01 p0432 N94-12237
Os isotopes in SNC meteorites and their implications to the early evolution of Mars and Earth 03 p1242 N94-16272
Osmium isotopes in Ivory Coast tektites: Confirmation of a meteoritic component and rhenium depletion 03 p1244 N94-16321
Rhenium-osmium isotope systematics of ordinary chondrites and iron meteorites 05 p2085 N94-20854
OSMOSIS
NT REVERSE OSMOSIS
Physiological water model development 01 p0316 N94-12367
OSMOTIC PRESSURE
U OSMOSIS
OSO
The 1971 highlights --- NASA programs and research
[NASA-TM-109629] 03 p1302 N94-15417
OSPREY AIRCRAFT
U V-22 AIRCRAFT
OSTEOPOROSIS
Irreversibility of advanced osteoporosis: Limited role for pharmacologic intervention 07 p2935 N94-28369
Exercise and osteoporosis: Methodological and practical considerations 07 p2935 N94-28370
OSTWALD COARSENING
U OSTWALD RIPENING
OSTWALD RIPENING
New mechanism of Ostwald ripening in Lorentz-force stabilized Cu-Pb dispersions 01 p0116 N94-10192
Ripening of immiscible liquid droplets in microgravity with constrained Marangoni drift 01 p0117 N94-10200
Ostwald ripening of solid cobalt particles in liquid copper 01 p0087 N94-10202
Experimental studies on the effect of coherency strains on coarsening kinetics: Current status and future outlook
[DE94-008480] 09 p3647 N94-32964
OTF
U OPTICAL TRANSFER FUNCTION
OTOLITH ORGANS
Study on posture control and adaption mechanism under weightlessness: Differences in weight and shape of utricular otolith of carp 07 p2912 N94-27448
OTV
U ORBIT TRANSFER VEHICLES
OUTCROPS
Arroyo el Mimbral, Mexico, K/T unit: Origin as debris flow/turbidite, not a tsunami deposit 01 p0281 N94-12084
Field guide to Cretaceous-tertiary boundary sections in northeastern Mexico
[NASA-CR-195719] 08 p3354 N94-28416
OUTER PLANET MISSIONS
U GRAND TOURS
OUTER SPACE TREATY
Contributions to CD Space Committee 1992
[PB94-124401] 07 p3101 N94-27218
OUTGASSING
Vacuum stability requirements of polymeric material for spacecraft application
[NASA-TM-109216] 01 p0091 N94-11350
Oxidation state of the Earth's upper mantle during the last 3800 million years: Implications for the origin of life 01 p0283 N94-12210
BAKEOUT: A computer program for predicting diffusive outgassing from stainless steel
[DE93-012613] 02 p0573 N94-14364
Solar absorptance of optical surfaces contaminated with spacecraft material outgassing products
[AD-A267202] 03 p0886 N94-15857
Evolutionary implications of a steady-state water abundance on Venus 03 p1254 N94-16206
CO2 production by impact in carbonates? An ATEM and stable isotope (C,O) study 03 p0954 N94-16383
Outgassing rate of Reemay Spunbonded Polyester and DuPont Double Aluminized Mylar
[DE93-040015] 05 p1699 N94-19973
Space environmental effects on polymer matrix composites: The UTIAS/LDEF experiment 05 p1660 N94-21373
Materials evaluation at ESA/ESTEC 05 p1662 N94-21386
Wet inside and out? Constraints on water in the Martian mantle and on outgassed water, based on melt inclusions in SNC meteorites 05 p2145 N94-21678
Modeling of outgassing and matrix decomposition in carbon-phenolic composites
[NASA-CR-194741] 05 p1676 N94-21743
Outgassing data for selecting spacecraft materials
[NASA-RP-1124-REV-3] 05 p1676 N94-21889
Outgas and vacuum seal characteristics of irradiated polyimide O-ring
[DE94-701200] 07 p2757 N94-27812
ESTEC wiring test programme materials related properties 08 p3165 N94-28698
Thermal-vacuum response of polymer matrix composites in space 09 p3595 N94-31033
Origin and thermal evolution of Mars 09 p3940 N94-31109
Operation of D3-D with all-graphite walls
[DE94-004858] 09 p3886 N94-31304
The structural changes of water ice I during warmup 11 p4239 N94-36144
Development of high sensitivity techniques for characterizing outgassing of polymeric construction materials for microenvironments
[DE94-012068] 12 p4424 N94-37204
Modeling of outgassing and matrix decomposition in carbon-phenolic composites
[NASA-CR-196319] 12 p4405 N94-37471
OUTLET FLOW
Non-isoenergetic inviscid slot flow 07 p2655 N94-28333
OUTLETS
NT VENTS
OUTLETS (GEOLOGY)
U ESTUARIES
OUTPUT
NT CARDIAC OUTPUT
NT LASER OUTPUTS
NT MASER OUTPUTS
NT STROKE VOLUME
Implementation and experimentation with a motion planning system
[ITN-93-85213] 02 p0755 N94-14505
On dynamic input-output linearization of discrete-time nonlinear systems
[MEMO-1123] 06 p2447 N94-22711
OVER-THE-HORIZON RADAR
HF-OTH radar performance results
[AD-A266106] 01 p0138 N94-11655
Comparison of RADARC high-frequency radar performance prediction model and ROTHR Amchitka data
[AD-A267077] 03 p0987 N94-15540
RADARC HF ionospheric prediction program for OTH radar
[AD-A269557] 04 p1385 N94-18291
New algorithm of ground track processing in high-frequency skywave over-the-horizon-B radar
[AD-A267821] 05 p1717 N94-20207
Over-the-horizon propagation measurements at six radar-frequency bands at the Atlantic Ocean Coast
[AD-A274151] 07 p2773 N94-27136
Channel probe measurements for the American Sector Clutter Experiment, January 1994
[DE94-013086] 12 p4469 N94-37314
OVERCAST
U CLOUD COVER
OVERPRESSURE
Air blast measurements at 20 and 40 km distance from detonating 10 and 20 ton high explosive charges
[PB93-195949] 04 p1419 N94-19068
Variability of measured sonic boom signatures. Volume 1: Technical report
[NASA-CR-191483-VOL-1] 06 p2526 N94-24172
Variability of measured sonic boom signatures. Volume 2: Data report
[NASA-CR-191483-VOL-2] 06 p2526 N94-24173
Shock wave interaction with L-shaped structures
[AD-A273774] 07 p2790 N94-25858
Blast overpressure studies with animals and man
[AD-A275038] 08 p3391 N94-29150
Investigation of sonic boom for the Space Shuttle: High cross-range orbiter
[NASA-TM-108238] 09 p3860 N94-31336
Investigation of sonic boom for the Space Shuttle: Low cross-range orbiter
[NASA-TM-108237] 09 p3860 N94-31337
Blast overpressure studies with animals and man
[AD-A280240] 12 p4480 N94-37118
OVERTONES
U HARMONICS
OVERVOLTAGE
Induced voltages at air gaps due to electromagnetic field caused by direct and indirect lightning strokes
[ITN-93-85203] 02 p0599 N94-13237
Ultrafast gas switching experiments
[DE93-019071] 05 p1762 N94-21634
The zinc electrode: Reactions and mechanisms
[DE94-007977] 09 p3691 N94-31919
OXALATES
The role of interfacial chemistry in surface nucleation and growth of calcium oxalate
[DE93-015689] 03 p1209 N94-16159
OXALIC ACID
Improvement of the stability of the process for synthesizing chemically prepared varistor powder
[DE94-000345] 05 p1763 N94-21654
OXAZOLE
Characterization of thermally stable dye-doped polyimide based electrooptic materials
[DE94-005309] 09 p3882 N94-32674
OXIDASE
Bienzyme sensors based on electrically wired peroxidase
[AD-A271364] 04 p1374 N94-19585
Electrical communication between glucose oxidase and electrodes based on poly(vinylimidazole) complex of Os(bpy)2Cl2
[AD-A276585] 09 p3635 N94-32231
OXIDATION
NT ELECTROCHEMICAL OXIDATION
NT RUSTING
Atomic structures and compositions of internal interfaces
[DE93-014840] 01 p0363 N94-10750
Assessment of damage in ceramics and ceramic matrix composites using ultrasonic techniques
[NASA-TM-106121] 01 p0067 N94-11237
Catalytic oxidation of organics in vapor streams at remediation sites
[PB93-182962] 01 p0266 N94-11472
Potential techniques for non-destructive evaluation of cable materials
[DE93-008350] 01 p0183 N94-11586
Chemical weathering on Mars: Rate of oxidation of iron dissolved in brines 01 p0455 N94-12128
Oxidation state of the Earth's upper mantle during the last 3800 million years: Implications for the origin of life 01 p0283 N94-12210
Absorption and damage thresholds of low defect density hafnia deposited with activated oxygen
[DE93-013853] 02 p0655 N94-13243
Reduction of Pu(6) with hydrogen peroxide: Effects of plutonium, peroxide, and iron concentrations and of reaction time
[DE93-013598] 02 p0564 N94-13487
Growth of Si spherical crystals and the surface oxidation (M-9) 02 p0587 N94-13741
Homogeneous-hetergeneous combustion: Thermal and chemical coupling
[DE93-016050] 02 p0565 N94-14403
Biomimetic methane oxidation
[DE93-013196] 02 p0705 N94-14510
Molecular simulator: A basic tool for submicron MOS processes development
[LAAS-92484] 02 p0814 N94-14697
Study of chemical reactions under the influence of ultrasound
[DE93-016458] 02 p0778 N94-14867
An apparatus for measuring the biological oxidation of hydrogen gas under hyperbaric conditions
[AD-A266834] 03 p1119 N94-14916
Processing and protection of high temperature structural materials
[AD-A267292] 03 p0954 N94-14961
Effects of alloying and temperature on the high-temperature oxidation of Cr-Cr2Nb
[DE93-015800] 03 p0957 N94-16163
Powder diffraction studies using anomalous dispersion
[DE93-012531] 03 p1210 N94-16775
Development of vanadium-phosphate catalysts for methanol production by selective oxidation of methane
[DE93-016850] 03 p0949 N94-16897
Transient studies of low temperature catalysts for methane conversion
[DE93-017710] 03 p0950 N94-16962
Mechanistic models of soot formation
[AD-A267806] 03 p0950 N94-17008

Synthesis, characterization, and polymerization of new ferrocene-fluorene complexes. A novel high-molecular weight conjugated polymer with pendant ferrocene groups
[AD-A267717] 03 p0972 N94-17273
Thermo-mechanical analysis of oxidation protected carbon-carbon composites
[AD-A268191] 03 p0941 N94-17597
Catalytic hydrocarbon reactions over supported metals
[DE93-018168] 04 p1345 N94-17808
Fundamental studies of the mechanism of catalytic reactions with catalysts effective in the gasification of carbon solids and the oxidative coupling of methane
[DE93-015262] 04 p1347 N94-18193
Environmental effects on intermetallic compounds: A guide to the literature
[AD-A269587] 04 p1359 N94-18306
Analysis of deposit precursors in jet fuels using Fourier transform infrared spectroscopy
[AD-A269035] 04 p1377 N94-18489
Surface phases and their influence on metal-oxide interfaces
[DE93-019931] 04 p1601 N94-19020
Selective methane oxidation over promoted oxide catalysts
[DE93-040002] 04 p1351 N94-19132
Selective methane oxidation over promoted oxide catalysts
[DE93-040001] 04 p1351 N94-19150
Factors that control the stable carbon isotopic composition of methane produced in an anoxic marine sediment 04 p1477 N94-19235
Oxidation-reduction induced roughening of platinum (111) surface
[DE93-017408] 05 p1687 N94-19922
Fuel processing requirements and techniques for fuel cell propulsion power
[DE93-019516] 05 p1750 N94-20257
Spectroscopic ellipsometric characterization of Si/Si(1-x)Ge(x) strained-layer superlattices 05 p1734 N94-20510
The Koshak section: Evidence for element fractionation and an oxidation event at the K/T boundary 05 p1862 N94-20641
The formation of FeO-rich pyroxene and enstatite in unequilibrated enstatite chondrites: A petrologic-trace element (SIMS) study 05 p2086 N94-20866
Transient studies of low temperature catalysts for methane conversion
[DE93-041232] 05 p1680 N94-20934
Chemical reaction fouling model for single-phase heat transfer
[DE93-019556] 05 p1802 N94-20942
Space environmental effects on polymer matrix composites: The UTIAS/LDEF experiment 05 p1660 N94-21373
Some results of the oxidation investigation of copper and silver samples flown on LDEF 05 p1660 N94-21375
Review of corrosion behavior of ceramic heat exchanger materals: Corrosion characteristics of silicon carbide and silicon nitride
[DE93-041307] 05 p1706 N94-21516
Oxidation of dissolved iron under warmer, wetter conditions on Mars: Transitions to present-day arid environments 05 p2143 N94-21663
Application of an electrochemical quartz crystal microbalance to the study of electrocatalytic films
[DE93-041124] 05 p2029 N94-21691
Fundamental studies of stress distributions and stress relaxation in oxide scales on high temperature alloys
[DE94-001444] 05 p1693 N94-21854
High oxygen pressure synthesis of new copper oxide superconductors
[DE93-040278] 05 p2033 N94-21998
Surface modification of Ti3Al for improved oxidation resistance
[DE93-018297] 05 p1696 N94-22034
Investigations on trends in global environment adaptive industrial technologies
[DE94-714888] 05 p1853 N94-22258
Discontinuous phase formation and selective attack of SiC materials exposed to low oxygen partial pressure environments
[DE93-040161] 06 p2231 N94-22933
Influence of sintering atmospheres on the aluminum sintering characteristics
[DE93-632412] 06 p2239 N94-22965
Modelling of solid polymer and direct methanol fuel cells: Phenomenological equations and analytical solutions
[PB93-224897] 06 p2390 N94-23102
Advances in direct oxidation methanol fuel cells 06 p2393 N94-23361
The possible effects of the natural and induced space environment on the optical and thermal properties of EOS surfaces 06 p2207 N94-23596
Fundamental and experimental studies on the catalytic combustion of methane
[PB94-112661] 06 p2233 N94-23736
On the stability of the process of formation of combustion generated particles by coagulation and simultaneous shrinkage due to particle oxidation 06 p2159 N94-24274
Segregation and oxidation studies of Al-Li and Al-Mg alloys
[ISBN-0-315-83993-7] 06 p2244 N94-24469
Design of novel catalysts for the partial oxidation of methane to methanol
[PB94-114212] 06 p2235 N94-24920
Studies of thin-film growth, adsorption, and oxidation by in situ, real-time, and ex situ ion beam analysis
[DE94-002907] 07 p3055 N94-26275
Stability of reference masses 2: The effect of environment and cleaning methods on the surfaces of stainless steel and allied materials
[NPL-DMM(A)-95] 07 p2738 N94-26653
Numerical analysis of the photo-dissociation/radical oxidation of formaldehyde by ultraviolet light in a photolytic reactor
[AD-A274539] 07 p2868 N94-26843
Engineering limitations of ceramic composites for high performance and high temperature applications
[DE94-001676] 07 p2754 N94-27021
Thermogravimetric study of oxidation of a PdCr alloy used for high-temperature sensors
[NASA-TM-106473] 07 p2741 N94-27426
Novel oxidizing reagents derived from elemental fluorine
[ITN-94-85231] 07 p2719 N94-27687
High temperature grain growth and oxidation of Fe-29Ni-17Co (Kovar (tm)) alloy leads
[DE94-004691] 07 p3069 N94-27753
Kinetic parameters from thermogravimetric analysis 07 p2721 N94-27909
Collaboration of chemical oxidation and biological treatment for removal of refractory organic substances 07 p2870 N94-28149
Treatment of refractory organic substances with combined use of chemical oxidation and biological treatment. Part 2: Biodegradability of ozonation products of chlorophenol 07 p2870 N94-28151
Structural changes during carbonization and oxidation of coal 08 p3187 N94-28678
Polymer technology publication series no. 16
[PB94-135522] 08 p3214 N94-29157
Simulation of pollutant formation in turbulent combustors using an extended coherent flame model 08 p3190 N94-29251
Charge trapping and breakdown in N2O oxides
[DE94-003775] 08 p3266 N94-30040
Studies of supported molybdenum and tungsten
[DE94-006207] 08 p3210 N94-30839
Transient studies of low temperature catalysts for methane conversion
[DE94-005767] 08 p3200 N94-30877
Space environmental effects on polymer composites: Research needs and opportunities 09 p3595 N94-31035
Fuel property effects on engine combustion processes
[DE94-005529] 09 p3631 N94-31153
Development of vanadium-phosphate catalysts for methanol production by selective oxidation of methane
[DE94-006759] 09 p3759 N94-31272
An extended approach to oxidations and nitridations of Si and Ge(x)Si(1-x) materials
[AD-A276056] 09 p3631 N94-31282
Effects of oxidation and creep damage mechanisms on creep behavior in HIPed silicon nitrides
[DE94-006559] 09 p3618 N94-31313
Si/SiO2 interface studies by immersion ellipsometry
[AD-A277277] 09 p3881 N94-32324
Carbon cycle modeling calculations for the IPCC
[DE94-004332] 09 p3765 N94-32354
Catalytic methods using molecular oxygen for treatment of PMMS and ECLSS waste streams, volume 2
[NASA-CR-190299] 09 p3804 N94-32697
Oxidation resistant copper
[AD-D016099] 09 p3696 N94-32721
Electron cyclotron resonance plasma oxidation studies of InP
[AD-A277431] 09 p3893 N94-33007
Nanoscale structural changes upon electrooxidation of Au(111) as probed by potentiodynamic scanning tunneling microscopy
[AD-A276780] 09 p3909 N94-33275
Thermal cyclic oxidation behavior of the developed compositionally gradient graphite material of SiC and C in air environment
[DE94-727591] 10 p4027 N94-33872
Oxidation performance of platinum-clad Mo-47Re alloy
[NASA-TM-4559] 10 p4025 N94-34398
Microporous structure with layered interstitial surface treatment, and method and apparatus for preparation thereof
[NASA-CASE-MSC-21487-3] 11 p4235 N94-35229
Innovative instrumentation for mineralogical and elemental analyses of solid extraterrestrial surfaces: The Backscatter Moessbauer Spectrometer/X Ray Fluorescence analyzer (BaMS/XRF) 11 p4239 N94-35459
Methane production and consumption in grassland and boreal ecosystems
[NASA-CR-196085] 11 p4284 N94-35486
Evaluation of Oxygen Interactions with Materials 3: Mission and induced environments
[NASA-TM-109349] 11 p4236 N94-35680
Hematite formed from pyroxene on Mars by meteoritic impact 11 p4372 N94-36165
Investigation of moisture-induced embrittlement of iron aluminides
[DE94-010881] 11 p4241 N94-36196
Simulation of materials processing: Fantasy or reality? 11 p4230 N94-36404
Sintering of dioxide pellets in an oxidizing atmosphere (CO2)
[DE94-613046] 12 p4414 N94-36517
Oxidation behavior of titanium aluminide matrix materials 12 p4401 N94-36658
Basic solutions to carbon/carbon oxidation: Science and technology
[AD-A280447] 12 p4404 N94-37232
The effect of reactive elements on the segregation behavior and microstructure of alpha-Al2O3 scales on beta-NiAl
[DE94-012739] 12 p4418 N94-37399
Bibliography of work on the photocatalytic removal of hazardous compounds from water and air
[DE94-006906] 12 p4467 N94-37405

OXIDATION RESISTANCE

Protective coatings for high-temperature polymer matrix composites
[NASA-TM-106276] 01 p0074 N94-12431
Electrophoretic and electrolytic deposition of ceramic particles on porous substrates
[AD-A265141] 02 p0575 N94-12812
A sulfur segregation study of PWA 1480, NiCrAl, and NiAl alloys
[NASA-TM-106289] 03 p0956 N94-15992
Overview of chemical vapor infiltration
[DE93-015440] 03 p0934 N94-16065
Effects of alloying and temperature on the high-temperature oxidation of Cr-Cr2Nb
[DE93-015800] 03 p0957 N94-16163
Development and commercialization status of Fe3Al-based intermetallic alloys
[DE93-015802] 03 p0957 N94-16165
Environmental effects on iron aluminides
[DE93-015820] 03 p0958 N94-16166
Thermo-mechanical analysis of oxidation protected carbon-carbon composites
[AD-A268191] 03 p0941 N94-17597
Environmental effects on intermetallic compounds: A guide to the literature
[AD-A269587] 04 p1359 N94-18306
Carbon/carbon composites coated with SiC by chemical vapor deposition
[AD-A269934] 04 p1341 N94-18544
Polyimides containing amide and perfluoroisopropylidene connecting groups
[NASA-CASE-LAR-14608-1] 05 p1702 N94-20374
Oxidation resistant protective coating system for gas turbine components and process for penetration thereof
[CA-PATENT-1,294,155] 05 p1704 N94-21143
Alloying effects on mechanical and metallurgical properties of NiAl
[DE93-040814] 05 p1694 N94-21948
Surface modification of Ti3Al for improved oxidation resistance
[DE93-018297] 05 p1696 N94-22034
Evaluation of A5Si3Z(x) intermetallics for use as high temperature structural materials
[DE93-041127] 06 p2227 N94-22977
Advanced materials for radiation-cooled rockets 06 p2214 N94-23052
New method for increasing machine service-life, phase 2
[PB93-200707] 06 p2354 N94-23533
High temperature, oxidation resistant noble metal-Al alloy thermocouple
[NASA-CASE-LEW-15515-1] 06 p2343 N94-23826
Selection of the Space Station Freedom (SSF) Flat Collector Circuit (FCC) insulation material 08 p3165 N94-28701
Evaluation of oxide-coated iridium-rhenium chambers
[NASA-TM-106442] 08 p3172 N94-29097
Polyimides containing pendent siloxane groups
[NASA-CASE-LAR-14638-1] 08 p3215 N94-29555

Development of radiation resistant electrical cable insulations 08 p3223 N94-30480
Four advances in carbon-carbon materials technology 08 p3186 N94-30481
Enhancement of oxidation resistance of silicon carbide by high-dose and multi-energy aluminum implantation [DE94-006560] 09 p3640 N94-31314
Improved oxidation resistance of 3-D carbon/carbon composites [AD-A277349] 09 p3625 N94-32624
Oxidation resistant copper [AD-D016099] 09 p3696 N94-32721
Analysis of the Shuttle Orbiter reinforced carbon-carbon oxidation protection system [NASA-TM-104792] 11 p4262 N94-35245
Atomic oxygen protective coating with resistance to undercutting at defect sites [NASA-CASE-LEW-15306-1] 11 p4243 N94-35502
High temperature creep and oxidation resistant chromium silicide matrix alloy containing molybdenum [NASA-CASE-LEW-15697-1] 11 p4241 N94-36275
The effect of reactive elements on the segregation behavior and microstructure of alpha-Al2O3 scales on beta-NiAl [DE94-012739] 12 p4418 N94-37399
Physical and mechanical metallurgy of NiAl [NASA-TP-3398] 12 p4419 N94-37503

OXIDATION-REDUCTION REACTIONS
Technical Update: Johnson Space Center system using a solid electrolytic cell in a remote location to measure oxygen fugacities in CO/CO2 controlled-atmosphere furnaces [NASA-TM-104774] 01 p0423 N94-11183
X ray absorption spectroscopy of electrochemically generated species [AD-A264749] 01 p0077 N94-11265
Publications/Patents/Presentations/Honors/Student eport [AD-A265136] 01 p0078 N94-11873
The Fe/Mn constraint on precursors of basaltic achondrites 01 p0432 N94-12208
Glucose electrodes based on cross-linked (Os(bpy)2Cl)(sup +/2+) complexed poly(1-vinylimidazole) films [AD-A265404] 01 p0094 N94-12425
Sulfate reduction and other sedimentary biogeochemistry in a northern New England salt marsh 01 p0268 N94-12453
The role of certain infauna and vascular plants in the mediation of redox reactions in marine sediments 01 p0268 N94-12454
Acetate concentrations and oxidation in salt marsh sediments 01 p0269 N94-12459
The effects of acid deposition on sulfate reduction and methane production in peatlands 01 p0270 N94-12465
Elevated acetate concentrations in the rhizosphere of Spartina alterniflora and potential influences on sulfate reduction 01 p0271 N94-12468
Photocatalysis for the treatment of waste water: Applications involving the removal of metals [DE93-011669] 02 p0561 N94-12841
Experimental and kinetic modeling of acid/base and redox reactions over oxide catalysts [DE93-016203] 02 p0563 N94-13375
Charge storage and switching phenomena with molecular assemblies of metal complexes [AD-A266673] 02 p0787 N94-14778
In situ Raman spectroscopy of lithium electrode surface in ambient temperature lithium secondary battery [DE93-015238] 03 p1010 N94-16061
Earth's partial pressure of CO2 over the past 120 Ma; evidence from Ce anomalies in the deep (greater than 600 m) Pacific Ocean, 1 03 p1104 N94-16358
High-valent oxo, methoxorhenium complexes: Models for intermediates and transition states in proton-coupled multi-electron transfer reactions [AD-A266492] 03 p1211 N94-16782
Release of iron from hemoglobin [AD-A266503] 03 p1128 N94-16784
A simple chemical procedure for extending the conductive state of polypyrrole to more negative potentials [AD-A266235] 03 p0969 N94-16928
Solvational barriers to interfacial electron transfer: Minimization by way of valence delocalization [AD-A267371] 03 p0950 N94-17006
Oxygen reduction at a stabilized zirconia interface with Y(1-x)Ca(x)MnO3 or La(1-x)Sr(x)MnO3 cathode materials [DE93-015681] 04 p1593 N94-17747
Applications of scanning tunneling microscopy to electrochemistry [AD-A269129] 04 p1348 N94-18255
Kinetic studies of electrochemical generation of Ag(II) ion and catalytic oxidation of selected organics [DE93-016601] 04 p1352 N94-19240
Bienzyme sensors based on electrically wired peroxidase [AD-A271364] 04 p1374 N94-19585
Oxidation-reduction induced roughening of platinum (111) surface [DE93-017408] 05 p1687 N94-19922
Production of O2 on the Moon: A lab-top demonstration of ilmenite reduction with hydrogen 05 p2126 N94-20821
Development of an electrochemical hydrogen separator [DE93-019877] 05 p1683 N94-21984
Electrochemically mediated polymerization of 2-pentadecylaniline confined to a planar liquid-liquid interface [AD-A273541] 06 p2259 N94-24792
The coordination and atom transfer chemistry of titanium porphyrin complexes [DE94-003091] 07 p2704 N94-26779
Quenching of the excited state of hydrated Europium(3) ions by electron transfer [DE94-005553] 08 p3482 N94-28518
Realtime structural electrochemistry of platinum clusters using dispersive XAFS [DE94-005093] 08 p3208 N94-30101
Hydrogen peroxide electrodes based on electrical connection of redox centers of various peroxidases to electrodes through a three-dimensional electron relaying polymer network [AD-A276543] 09 p3691 N94-32056
The kinetics of heterogeneous electron transfer reactions in polar solvents [AD-A278459] 10 p4136 N94-33540
Electrical microengineering of redox enzymes [AD-A279015] 11 p4236 N94-35745
Some perspectives on solution-phase electron-transfer processes [AD-A278616] 11 p4238 N94-36252
Ion modulated electroactivity in thin film metallopolymers [AD-A278618] 11 p4246 N94-36253

OXIDE FILMS
Damage threshold study of ion beam sputtered coatings for a visible high-repetition laser at LLNL [DE93-013430] 01 p0095 N94-12602
Analysis of samples of reflector materials which are multicoated and metal samples with oxide coatings which have been exposed the space environment in LDEF testing [NASA-CR-193647] 02 p0575 N94-12789
Metastability of yttrium-oxides [DE93-016548] 02 p0813 N94-14440
Ion mixing of thin ZrO2 films on sapphire [DE93-015214] 03 p1206 N94-14925
Passive oxide films on well-defined nickel surfaces: An examination of film growth on Ni(100) with ex situ scanning tunneling microscopy [DE93-014056] 03 p1207 N94-15923
Vacancy condensation as the precursor to passivity breakdown [DE93-012925] 03 p0956 N94-15998
Surface phases and their influence on metal-oxide interfaces [DE93-019931] 04 p1601 N94-19020
Optical switch evaluation support [AD-A270948] 04 p1581 N94-19601
Nanofabrication by focused ion beam [AD-A271290] 04 p1345 N94-19746
Direct imaging of the surface microstructure of dielectric materials using an atomic force microscope [AD-A272251] 05 p2018 N94-20575
Study of the utilization of thin oxides in indium phosphides for the realisation of electron components [ECL-92-38] 05 p2018 N94-20593
Properties of E-beam interactive oxide films for nanometer scale structures [AD-A272848] 05 p1675 N94-21191
A quantitative model for interpreting nanometer scale hardness measurements of thin films [DE93-040601] 05 p2034 N94-22005
Stability of reference masses 2: The effect of environment and cleaning methods on the surfaces of stainless steel and allied materials [NPL-DMM(A)-95] 07 p2738 N94-26653
Ion implantation and dynamic recovery of tin-doped indium oxide films [DE94-001126] 07 p3062 N94-26932
The ZnO thin films with C-axis orientation prepared on the room temperature substrate by the ECR multipolar plasma sputtering method [DE94-605039] 07 p2758 N94-27857
Pull-test adhesion measurements of diamondlike carbon films on silicon carbide, silicon nitride, aluminum oxide, and zirconium oxide [DE94-005469] 08 p3211 N94-28536
Low Earth orbit durability evaluation of protected silicone for advanced refractive photovoltaic concentrator arrays [NASA-TM-106543] 08 p3172 N94-28999
Pitting corrosion of titanium [AD-A274980] 08 p3203 N94-29089
Distribution functions of electrons within aluminium oxide thin films [DE94-608418] 08 p3490 N94-30184
Ionic conduction mechanisms in CaF2 and CaF2-Al2O3 nanocomposite films on Al2O3 substrates [DE94-004792] 08 p3520 N94-30773
Process parameter-growth environment-film property relationships for reactive sputter deposited metal (V, Nb, Zr, Y, Au) oxide, nitride, and oxynitride films [AD-A276382] 09 p3640 N94-31258
Chemical vapor deposition of metal nitrides, phosphides, and arsenides [DE94-008096] 09 p3654 N94-31976
Sol-gel coatings for high power laser optics: Past, present, and future [DE94-007240] 09 p3718 N94-32252
Si/SiO2 interface studies by immersion ellipsometry [AD-A277277] 09 p3881 N94-32324
Energetics, bonding mechanism, and electronic structure of ceramic/ceramic and metal/ceramic interfaces [DE94-008551] 09 p3659 N94-32656
Microanalytical study of defect formation in thin bismuth strontium calcium copper oxide films [DE94-008217] 09 p3661 N94-32751
Evaluation of the Hughes conversion coating touch-up pen [AD-A278398] 09 p3664 N94-33166
Nanoscale structural changes upon electrooxidation of Au(111) as probed by potentiodynamic scanning tunneling microscopy [AD-A276780] 09 p3909 N94-33275
Microstructures and epitaxy in oxide superconductor thin films and devices [AD-A278427] 09 p3910 N94-33332
The relationship between hydroxyl groups on oxide surfaces and the properties of supported metals [DE94-010786] 11 p4241 N94-36233
Superconducting transistors [PB94-170743] 11 p4260 N94-36260
Wear-resisting oxide films for 900 C [DE94-010093] 11 p4246 N94-36306
Substrate effects on the structure and optical properties of epitaxial PbTiO3 thin films prepared by metal-organic chemical vapor deposition [DE94-010432] 12 p4535 N94-37192
Time-of-flight pulsed ion beam surface analysis as a means of in situ, real-time characterization of the growth of ferro-electric and conductive oxide heterostructures [DE94-012628] 12 p4517 N94-37249
Low temperature atmospheric pressure chemical vapor deposition of group 14 oxide films [DE94-013115] 12 p4425 N94-37317

OXIDES
NT ALUMINUM OXIDES
NT ANATASE
NT ANHYDRIDES
NT BARIUM OXIDES
NT BISMUTH OXIDES
NT BORON OXIDES
NT BSCCO SUPERCONDUCTORS
NT CALCIUM OXIDES
NT CARBON DIOXIDE
NT CARBON MONOXIDE
NT CERIUM OXIDES
NT CHLORINE OXIDES
NT CHROMIUM OXIDES
NT COBALT OXIDES
NT COPPER OXIDES
NT DIOXIDES
NT ENSTATITE
NT GALLIUM OXIDES
NT GERMANIUM OXIDES
NT HAFNIUM OXIDES
NT HEAVY WATER
NT HEMATITE
NT HYDROGEN PEROXIDE
NT ILMENITE
NT IRON OXIDES
NT LANTHANUM OXIDES
NT LEAD OXIDES
NT LITHIUM OXIDES
NT MAGNESIUM OXIDES
NT MAGNETITE
NT MANGANESE OXIDES
NT METAL OXIDES
NT MIXED OXIDES
NT MOLYBDENUM OXIDES
NT NICKEL OXIDES
NT NIOBIUM OXIDES
NT NITRIC OXIDE

NT NITROGEN DIOXIDE
NT NITROGEN OXIDES
NT NITROGEN TETROXIDE
NT NITROUS OXIDES
NT ORGANIC PEROXIDES
NT PERICLASE
NT PEROXIDES
NT PLATINUM OXIDES
NT POTASSIUM OXIDES
NT PYROXENES
NT QUARTZ
NT RUTILE
NT SAPPHIRE
NT SCANDIUM OXIDES
NT SELENIUM OXIDES
NT SILICON DIOXIDE
NT SILICON OXIDES
NT SILVER OXIDES
NT STISHOVITE
NT STRONTIUM OXIDES
NT SULFUR DIOXIDES
NT SULFUR OXIDES
NT TANTALUM OXIDES
NT TIN OXIDES
NT TITANIUM OXIDES
NT TUNGSTEN OXIDES
NT URANIUM OXIDES
NT VANADIUM OXIDES
NT YBCO SUPERCONDUCTORS
NT YTTRIA-STABILIZED ZIRCONIA
NT YTTRIUM OXIDES
NT ZINC OXIDES
NT ZIRCONIUM OXIDES

Multicomponent and multilayered thin films for advanced microtechnologies: Techniques, fundamentals, and devices
[AD-A265685] 01 p0405 N94-12442

Experimental and kinetic modeling of acid/base and redox reactions over oxide catalysts
[DE93-016203] 02 p0563 N94-13375

Synthesis of organic ligands for f-element separations
[DE93-012915] 02 p0554 N94-14290

A search for noble-gas evidence for presolar oxide grains 03 p0954 N94-16353

Thin composite solid electrolyte film for lithium batteries
[NASA-CASE-NPO-18694-1-CU] 03 p1014 N94-17325

Office of Naval Research Publications/Patents /Presentations/Honors report, 1 October 1992 - 30 September 1993
[AD-A270037] 04 p1632 N94-18791

Selective methane oxidation over promoted oxide catalysts
[DE93-040002] 04 p1351 N94-19132

Selective methane oxidation over promoted oxide catalysts
[DE93-040001] 04 p1351 N94-19150

Identification of an interstellar oxide grain from the Murchison meteorite by ion imaging 05 p2082 N94-20659

Further analyses of Rio Cuarto impact glass 05 p1685 N94-20745

Evaluation of radiation effects in re-oxidized nitrided oxide devices by hot carrier stressing at 77 K 05 p1754 N94-21084

Investigation of the effect of various oxide and fluoride additives on the microstructure, electronic properties, and phase shifting ability of Ba(1-x)Sr(x)TiO3
[AD-A271756] 05 p2027 N94-21303

Fundamental studies of stress distributions and stress relaxation in oxide scales on high temperature alloys
[DE94-001444] 05 p1693 N94-21854

Simple method to estimate MOS oxide-trap, interface-trap, and border-trap densities
[DE93-041138] 05 p2032 N94-21939

Melt-spin processing of high (Tc) oxide superconductors
[DE94-000696] 05 p2036 N94-22582

Low temperature diffusion of hydrogenic species in oxide crystals: Radiation induced diffusion
[DE94-000374] 06 p2558 N94-22957

The structure and spin dynamics of lanthanide-bearing silicate glasses
[DE94-001320] 06 p2252 N94-22992

PEM regenerative fuel cells 06 p2392 N94-23358

Contaminant effects in solid oxide fuel cells
[DE94-002963] 06 p2395 N94-23785

Study on measurement and evaluation methods for superconductive characteristics 07 p2725 N94-25560

Successive structural phase transitions in stoichiometric La2NiO4 observed by x ray diffraction
[REPT-A-2665] 07 p3051 N94-25921

Phase diagram of La2NiO(4 + delta) (0 less than or equal to delta less than or equal to 0.18). 1: Phases at room temperature and phase transition above delta equal to 0.15
[REPT-A-2661] 07 p3053 N94-26089

In situ spectroscopic applications to the study of rechargeable lithium batteries
[DE94-003478] 07 p2782 N94-26328

Sealant research for solid oxide fuel cells
[DE94-000015] 07 p2857 N94-26584

Processing of LaCrO3 for solid oxide fuel cell applications
[DE94-002981] 07 p2857 N94-26747

Fibrous emissive burners selective and broad band
[PB94-128329] 07 p2859 N94-27225

The radical amplifier 08 p3345 N94-28604

Effects of oxide charge and surface recombination velocity on the excess base current of BJT's
[DE94-003711] 08 p3263 N94-29025

Dislocation loops in spinel crystals irradiated successively with deep and shallow ion implants
[DE94-005083] 08 p3517 N94-30201

Remote pumping of solid state lasers with nuclear driven fluorescers
[DE94-004846] 08 p3296 N94-30614

Process parameter-growth environment-film property relationships for reactive sputter deposited metal (V, Nb, Zr, Y, Au) oxide, nitride, and oxynitride films
[AD-A276382] 09 p3640 N94-31258

Ionizing radiation effects on silicon test structures
[DE94-006060] 09 p3865 N94-31607

Photopolymerization of cyclohexene oxide: A visible light initiating system and mechanistic investigations
[AD-A277110] 09 p3654 N94-31981

Heterogeneous catalytic process for alcohol fuels from syngas
[DE94-008729] 09 p3667 N94-32583

Theoretical study of reactions at the electrode-electrolyte interface
[DE94-009658] 10 p4138 N94-34100

The relationship between hydroxyl groups on oxide surfaces and the properties of supported metals
[DE94-010786] 11 p4241 N94-36233

Heterogeneous catalytic process for alcohol fuels from syngas
[DE94-010263] 11 p4248 N94-36299

Processing, packaging, and characterization of electroceramic materials for phased array antennas
[AD-A280251] 12 p4432 N94-36743

Thermodynamics of minerals stable near the Earth's surface
[DE94-012479] 12 p4539 N94-37094

Time-of-flight pulsed ion beam surface analysis as a means of in situ, real-time characterization of the growth of ferro-electric and conductive oxide heterostructures
[DE94-012628] 12 p4517 N94-37249

Thermal-oxidative pretreatment and evaluation of poly (hexafluoropropene oxide) fluids
[NASA-TM-106659] 12 p4424 N94-37300

Study on extraction behavior of TRPO with different composition
[DE94-620287] 12 p4412 N94-37534

OXIDIZERS
NT LIQUID OXYGEN
NT ROCKET OXIDIZERS
NT TAGN

Synthesis and structural characterization of new light molecular weight inorganic oxidizers and relative derivatives, volume 1
[AD-A271437] 05 p2012 N94-19842

Cryogenic propellant rocket engine problems 05 p1668 N94-20076

Dynamics of face seals for high speed turbomachinery 05 p1655 N94-21796

Multiple flames in counterflow spray combustion 06 p2161 N94-24284

Advanced launch system. Advanced development oxidizer turbopump program
[NASA-CR-193920] 06 p2367 N94-25174

Novel oxidizing reagents derived from elemental fluorine
[ITN-94-85231] 07 p2719 N94-27687

Control experiments in liquid metal combustion
[AD-A276918] 09 p3635 N94-32234

Formation of gas-phase peroxides in a rural atmosphere: An interpretation of the recent SOS/SERON field results
[DE94-002995] 09 p3766 N94-32692

Laser-saturated fluorescence measurements in laminar sooting diffusion flames
[NASA-CR-191025] 12 p4508 N94-36643

OXIMETRY

Pulse waveform and transcranial Doppler analysis during lower body negative pressure
[AD-A274516] 07 p2911 N94-27088

OXOSILANES
U POLYSILANES

OXYALKYLATION
U ALKYLATION

OXYGEN
NT LIQUID OXYGEN
NT OXYGEN ISOTOPES
NT OXYGEN 17
NT OXYGEN 18

Hypobaric decompression prebreathe requirements and breathing environment 01 p0317 N94-11541

Methanol pan fires in an enclosed space: Effect of pressure and oxygen concentration
[AD-A266108] 01 p0079 N94-12415

Preliminary results on the hydrological measurements in the Aegean Sea off Crete: Cruise, Georgia, 1989
[PREPRINT-736] 02 p0725 N94-13500

Roles of oxygen defects in copper-oxide superconductors
[DE93-014875] 03 p1208 N94-15982

First oxygen from lunar basalt 03 p1249 N94-16182

The effect of oxygen, grain size, and strain rate on the mechanical behavior of forged P/M tantalum
[DE93-011251] 03 p0959 N94-16764

Regulated emergency oxygen system
[AD-A266228] 03 p1138 N94-16983

Automated data collection system for the TCM3 transcutaneous pO2/pCO2 monitoring system
[AD-A268400] 03 p1129 N94-17424

Oxygen diffusion in YBa2Cu3O(6 + delta) ceramics on heating
[DE93-629161] 03 p0974 N94-17633

Influence of the granular surface on the oxygen uptake in YBa2Cu3O(6 + delta) ceramics
[DE93-629162] 03 p0974 N94-17634

Effect of oxygen concentration and ordering on vanadium-oxygen alloy vibrational spectra
[DE93-627003] 04 p1355 N94-17692

Selective electrochemical wafer thinning for silicon characterization
[DE93-015083] 04 p1592 N94-17742

Oxygen reduction at a stabilized zirconia interface with Y(1-x)Ca(x)MnO3 or La(1-x)Sr(x)MnO3 cathode materials
[DE93-015681] 04 p1593 N94-17747

A one dimensional numerical model, with an application to the vertical distribution of dissolved oxygen in the ocean
[DE93-018481] 04 p1495 N94-17779

Phase separation and superconductivity in La2CuO(4 + delta): Effects of oxygen diffusion
[DE93-016610] 04 p1594 N94-17907

Dense energetic compounds of C, H, N, and O atoms. 3: 5-(4-nitro-(1,2,5) oxadiazolyl)-5H-(1,2,3) triazolo (4,5-c)(1,2,5) oxadiazole
[AD-A268715] 04 p1338 N94-18314

Temperature, kinetic energy, and rotational temperature dependences for the reactions of Ar(+)(2)P3/2 with O2 and CO
[AD-A268974] 04 p1567 N94-18526

Electrocatalysts for oxygen electrodes
[DE93-040446] 04 p1354 N94-19653

Chemical equilibrium in high pressure molecular fluid mixtures
[DE93-040160] 05 p1796 N94-19829

Encounters of H and D atoms with O2 in water: Relative diffusion and reaction rates
[DE93-018587] 05 p1970 N94-19956

High-temperature, high-pressure oxygen metering valve
[NASA-CASE-MSC-21823-1] 05 p1824 N94-20589

C/O atomic ratios in micrometer-size crushed grains from Antarctic micrometeorites and two carbonaceous meteorites 05 p2082 N94-20678

C-O volatiles in Apollo 15 and Apollo 17 picritic glasses 05 p1685 N94-20727

Durability of thermal control and environmental protective materials for the SSRMS in simulated LEO environment 05 p1663 N94-21392

Fast oxygen atom studies related to low Earth orbit activities 05 p1663 N94-21395

Atomic oxygen fluence detector for Bremsat: Scientific and technical description 05 p1663 N94-21396

Powdered aluminum and oxygen rocket propellants: Subscale combustion experiments
[NASA-TM-106439] 05 p1713 N94-21760

Local structure in oxygen-doped La2CuO(4 + delta)
[DE93-040248] 05 p2030 N94-21768

High oxygen pressure synthesis of new copper oxide superconductors
[DE93-040278] 05 p2033 N94-21998

A novel method for determination of transport parameters of H2 and O2 in PEMFCs
[DE94-001492] 06 p2389 N94-22962

Eddy mixing coefficient upper limit derived from the photochemical balance of O2 06 p2621 N94-24897

Design of novel catalysts for the partial oxidation of methane to methanol
[PB94-114212] 06 p2235 N94-24920
A statistical analysis of recent Naval Experimental Diving Unit (NEDU) single-depth human exposures to 100 percent oxygen at pressure
[AD-A273488] 06 p2427 N94-24950
The effects of zinc borate addition on the flammability characteristics of polyester, vinyl ester, and epoxy glass reinforced plastics
[AD-A273164] 06 p2262 N94-25136
Isotopically labeled CO2 from stratosphere: A tracer of carbon biogeochemistry
[DE94-002777] 07 p2877 N94-26015
The role of hyperbaric oxygen as a prophylaxis for radiation enteritis
[AD-A274974] 07 p2901 N94-26517
Electronic structure of a single oxygen vacancy in rutile TiO2
[DE94-002717] 07 p3062 N94-26901
Numerical simulation of the reignition of detonation by reflected shocks
[AD-A274755] 07 p2795 N94-27252
Technical report of ISSP. Ser. A, no. 2669: Relations between oxygen deficiency and structures in the La-Sr-Cu-O system. 3: Oxygen contents and structure of (La, Sr)8Cu8O(16 + delta) phase
[JTN-94-80555] 07 p3066 N94-27353
The addition of molecular oxygen to hydroperoxy-propyl radicals
[DE94-003662] 07 p2760 N94-27725
Peroxy radical measurements with NCAR's chemical amplifier 08 p3345 N94-28603
Japanese Journal of Aerospace and Environmental Medicine, volume 30, no. 1
[JTN-94-80596] 08 p3389 N94-28850
Arterial oxygen saturation during + Gz acceleration by short-radius centrifuge 08 p3389 N94-28852
Methane challenge of high performance molecular sieve oxygen concentrator
[AD-A275155] 08 p3337 N94-29033
High resistivity buffer layers by oxygen doping
[AD-A274986] 08 p3513 N94-29125
Fullerenes as precursors for diamond film growth without hydrogen or oxygen additions
[DE94-004582] 08 p3519 N94-30718
Spectroscopic study of the molecular collisions (hydrogen-nitrogen and hydrogen-oxygen) at energies of several MeV
[ISBN-0-315-86794-9] 09 p3867 N94-31753
Technical evaluation of the UH-60Q: Medical oxygen system
[AD-A276983] 09 p3579 N94-32242
Rate coefficient for the reaction H + O2 yields OH + O: Results from 2000 to 5300 K
[DE94-008105] 09 p3871 N94-32615
A model for predicting central nervous system toxicity from hyperbaric oxygen exposure in man: Effects of immersion, exercise, and old and new data
[AD-A278348] 10 p4095 N94-34005
Study of gravity wave in the upper atmosphere by way of OH* (9-4) and O2(b 1 Sigma(+,g), 0-1) bands nightglow observations
[INPE-5539-TDI/527] 10 p4087 N94-34227
High temperature sorbents for oxygen
[NASA-CASE-NPO-18409-1-CU] 11 p4235 N94-35255
Bus application of oxygen-enrichment technology and diesel-electric hybrid systems
[DE94-009835] 11 p4285 N94-35765
The reaction of hydroperoxy-propyl radicals with molecular oxygen
[DE94-006392] 11 p4239 N94-36319
Atmospheric gas
[DE94-007439] 12 p4465 N94-37187
Comparison of oxygen and silicon induced reactions at 14.6 A(GeV/C)
[DE94-011923] 12 p4518 N94-37364

OXYGEN ANALYZERS
CTD oxygen, tracer and nutrient data from RRS Charles Darwin Cruises 58/59 in the NE Atlantic as part of Vivaldi 1991
[IOS-296-1992] 04 p1496 N94-18065

OXYGEN ATOMS
Atomic structures and compositions of internal interfaces
[DE93-014840] 01 p0363 N94-10750
Novel oxygen atom source for material degradation studies
[NASA-CR-191323] 02 p0562 N94-13115
Atomic hydrogen and nitrogen distributions from atmosphere explorer measurements
[NASA-CR-194336] 02 p0714 N94-13825
Atomic research
[NASA-CR-193843] 02 p0788 N94-14905
Analysis of leading edge and trailing edge cover glass samples before and after treatment with advanced satellite contamination removal techniques
[AD-A267055] 03 p0885 N94-15666
Long Duration Exposure Facility experiment M0003 deintegration/findings and impacts
[AD-A267140] 03 p0885 N94-15749
Analytical and experimental investigation of the feasibility of accelerated lifetime testing of materials exposed to an atomic oxygen beam
[NASA-CR-193851] 03 p0946 N94-15766
Local environment about O atoms in Pr-Y-Ba-Cu-O films studied by O K-edge XAFS
[DE93-016218] 03 p1209 N94-16447
Atomic beam studies relevant to the space environment
[AD-A268628] 03 p1186 N94-17436
Effect of oxygen concentration and ordering on vanadium-oxygen alloy vibrational spectra
[DE93-627003] 04 p1355 N94-17692
NSWCWODET participation in Space Shuttle mission STS-46
[AD-A268875] 04 p1332 N94-18321
Method for anisotropic etching in the manufacture of semiconductor devices
[NASA-CASE-MSC-21631-1] 05 p1993 N94-20491
Combination of on ground experiments and analysis software for the evaluation of material degradation in space (SILEX project) 05 p1662 N94-21389
German space experiments on Spacelab D-2 and Eureca-1 to investigate atomic oxygen interaction with materials 05 p1662 N94-21390
The International Telecommunications Satellite (INTELSAT) Solar Array Coupon (ISAC) atomic oxgyen flight experiment: Techniques, results and summary 05 p1662 N94-21391
Atomic oxygen interaction with spacecraft materials: Relationship between orbital and ground-based testing for materials certification 05 p1663 N94-21393
Evaluation of plasma-deposited protective coatings for spacecraft applications 05 p1663 N94-21394
Method and apparatus for producing a thermal atomic oxygen beam
[NASA-CASE-LEW-15614-1] 06 p2534 N94-23825
Low Earth orbit durability evaluation of protected silicone for advanced refractive photovoltaic concentrator arrays
[NASA-TM-106543] 08 p3172 N94-28999
Space Station WP-2 application of LDEF MLI results 09 p3592 N94-31016
Follow-up on the effects of the space environment on UHCRE thermal blankets 09 p3592 N94-31018
Model of spacecraft atomic oxygen and solar exposure microenvironments 09 p3593 N94-31021
Atomic oxygen erosion considerations for spacecraft materials selection 09 p3593 N94-31022
Performance of selected polymeric materials on LDEF 09 p3593 N94-31023
Atomic oxygen interaction at defect sights in protective coatings on polymers flown on LDEF 09 p3593 N94-31024
Fluorescence observations of LDEF exposed materials as an indicator of induced material reactions 09 p3593 N94-31025
On the linearity of fast atomic oxygen effects 09 p3594 N94-31027
Low-Earth orbit effects on organic composite materials flown on LDEF 09 p3595 N94-31036
Ground-based simulation of LEO environment: Investigations of a select LDEF material: FEP Teflon (trademark) 09 p3596 N94-31039
An overview of the Evaluation of Oxygen Interaction with Materials-third phase (EOIM-3) experiment: Space Shuttle Mission 46 09 p3596 N94-31040
Analysis of leading edge and trailing edge cover glass samples before and after treatment with advanced satellite contamination removal techniques 09 p3596 N94-31041
Spacecraft materials: Comparison between flight results obtained on LDEF and MIR 09 p3597 N94-31045
Atomic oxygen damage characterization by photothermal scanning 09 p3598 N94-31051
Production and detection of metastable atomic oxygen
[ISBN-0-315-87364-7] 09 p3868 N94-31915
Enhanced thermal capacity aerogels summary report, FY 1993
[DE94-008888] 09 p3639 N94-33260
A comparison of atomic oxygen erosion yields of carbon and selected polymers exposed in ground based facilities and in low Earth orbit
[NASA-TM-106622] 11 p4243 N94-35243
Results from LDEF experiment A0114: The interaction of atomic oxygen with materials surfaces at orbital altitudes
[NASA-CR-196016] 11 p4235 N94-35388
Atomic oxygen reactor having at least one sidearm conduit
[NASA-CASE-MSC-21487-4] 11 p4250 N94-35445
Atomic oxygen protective coating with resistance to undercutting at defect sites
[NASA-CASE-LEW-15306-1] 11 p4243 N94-35502
Evaluation of Oxygen Interactions with Materials 3: Mission and induced environments
[NASA-TM-109349] 11 p4236 N94-35680

OXYGEN BREATHING
Hypobaric decompression prebreathe requirements and breathing environment 01 p0317 N94-11541
Decompression sickness risk versus time and altitude
[AD-A275261] 08 p3391 N94-29071
Exercise with prebreathe appears to increase protection from decompression sickness: Preliminary findings 10 p4096 N94-33639
The effectiveness of ground level post-flight 100 percent oxygen breathing as therapy for pain-only altitude Decompression Sickness (DCS) 10 p4096 N94-33643

OXYGEN COMPOUNDS
The multicomponent lineshape of the anharmonic A(1)(TO) phonon in PbTiO3
[DE93-018995] 05 p1970 N94-19971

OXYGEN CONSUMPTION
The OSU heat release rate test using the oxygen consumption principle 01 p0020 N94-10784
Variability of prediction of maximal oxygen concumption on the cycle ergometer using standard equations
[NASA-TP-3412] 02 p0729 N94-14032
Increased vascular resistance with hemoglobin-based oxygen carriers
[AD-A266454] 03 p1123 N94-16565
Metabolic monitoring of hypobaric subjects
[AD-A268221] 03 p1130 N94-17554
Intermittent gravity: How much, how often, how long?
[NASA-TM-108800] 07 p2944 N94-26098
Dual-cycle ergometry as an exercise modality during prebreathe with 100 percent oxygen 10 p4096 N94-33638

OXYGEN DEFICIENCY
U HYPOXIA

OXYGEN DETECTORS
U OXYGEN ANALYZERS

OXYGEN FLUORIDES
Research for electric energy systems
[DE94-001839] 06 p2293 N94-23719

OXYGEN IONS
Analytical and experimental investigation of the feasibility of accelerated lifetime testing of materials exposed to an atomic oxygen beam
[NASA-CR-193851] 03 p0946 N94-15766
Atomic beam studies relevant to the space environment
[AD-A268628] 03 p1186 N94-17436
Low-energy continuum-electron emission at 0 degrees from O(q+) + He collisions
[DE93-018777] 04 p1570 N94-19108
Local structure in oxygen-doped La2CuO(4 + delta)
[DE93-040248] 05 p2030 N94-21768
Multi-ion, multi-event test of ion cyclotron resonance heating
[NASA-CR-194859] 06 p2540 N94-23495
Ion implantation and dynamic recovery of tin-doped indium oxide films
[DE94-001126] 07 p3062 N94-26932
Energy parameters of the incident auroral electrons derived by the intensity ratio of auroral emissions 07 p2779 N94-27964
Low energy ion-molecule reactions and chemiionization kinetics
[DE94-005414] 08 p3481 N94-28491
Follow-up on the effects of the space environment on UHCRE thermal blankets 09 p3592 N94-31018
Frictional behavior and adhesion of Ag and Au films applied to aluminum oxide by oxygen-ion assisted Screen Cage Ion Plating (SCIP)
[NASA-TM-106522] 09 p3647 N94-32931

OXYGEN ISOTOPES
NT OXYGEN 17
NT OXYGEN 18
Interstellar graphite in Murchison: Continued search for isotopically distinct components 01 p0097 N94-12029
The EET87513 clast N: A CM2 fragment in an HED polymict breccia 01 p0453 N94-12117
Oxygen isotopes as tracers of tektite source rocks: An example from the Ivory Coast tektites and Lake Bosumtwi Crater 01 p0430 N94-12146
Trace element distributions in primitive achondrites 01 p0431 N94-12200
Maximum entropy spectral analysis of the geological time series of the oxygen isotope record from deep-sea cores
[INPE-5465-PRE/1773] 02 p0725 N94-13728

CO2 production by impact in carbonates? An ATEM and stable isotope (C,O) study 03 p0954 N94-16383
Oxygen isotopic relationships between the LEW85332 carbonaceous chondrite and CR chondrites 05 p2083 N94-20708
Inter- and intra-crystalline oxygen isotope distribution of fassaites in Allende CAI 05 p2086 N94-20898
A three-body calculation of the O-16(d,p)O-17 reaction using a two-term separable potential for the s-wave nucleon-core interaction
[DE94-616652] 11 p4320 N94-35579

OXYGEN MASKS
Creation of prototype aircrew protection equipment based on face anthropometry
[AD-A273865] 07 p2940 N94-25611
Portable ventilatory resuscitation systems
[AD-A274984] 08 p3401 N94-29093

OXYGEN METABOLISM
Exercise countermeasures for bed-rest deconditioning
[NASA-TM-103987] 01 p0300 N94-11191

OXYGEN PLASMA
Plasma surface cleaning using microwave plasmas
[DE94-002754] 07 p2713 N94-26014
Atomic oxygen treatment for non-contact removal of organic protective coatings from painting surfaces
[NASA-TM-106650] 12 p4421 N94-36952

OXYGEN PRODUCTION
General overview of an integrated lunar oxygen production/brickmaking system 01 p0131 N94-12027
Thermodynamics of lunar ilmenite reduction 01 p0415 N94-12028
Characterization of Spirulina biomass for CELSS diet potential
[NASA-CR-194123] 02 p0729 N94-14097
First oxygen from lunar basalt 03 p1249 N94-16182
Strategy for the reduction of total integrated fluid logistics to the Space Station Freedom
[NASA-TM-107744] 03 p1138 N94-17452
Production of O2 on the Moon: A lab-top demonstration of ilmenite reduction with hydrogen 05 p2126 N94-20821
Recent advances in SPE (tm) water electrolyzer 06 p2393 N94-23362
Nutrients and light as factors controlling phytoplankton biomass on the Dutch continental shelf (North Sea), 1988-1990
[PB94-111143] 06 p2418 N94-24601
Extraterrestrial surface propulsion systems 07 p2833 N94-25691
Space Station evolution study oxygen loop closure
[NASA-CR-193938] 07 p2941 N94-26788
The 1992-1993 advanced design program. Part 1: The Mars methane engine project. Part 2: The Mars oxygen processor new furnace
[NASA-CR-195513] 08 p3299 N94-29409

OXYGEN SPECTRA
Effect of oxygen concentration and ordering on vanadium-oxygen alloy vibrational spectra
[DE93-627003] 04 p1355 N94-17692
JOVE NASA-FIT program: Microgravity and aeronomy projects
[NASA-CR-195121] 06 p2631 N94-24493

OXYGEN SUPPLY EQUIPMENT
NT OXYGEN MASKS
General overview of an integrated lunar oxygen production/brickmaking system 01 p0131 N94-12027
Liquid hydrogen and liquid oxygen feedline passive recirculation analysis
[TABES PAPER 93-620] 03 p1031 N94-16145
Regulated emergency oxygen system
[AD-A266228] 03 p1138 N94-16983
Laboratory test and evaluation report of the essex model 60C-0037-2 molecular sieve oxygen generating system
[AD-A269967] 04 p1445 N94-18778
In-flight measurement of aircrew breathing in Navy aircraft
[AD-A271811] 05 p1896 N94-21154
Technical evaluation of the UH-60Q: Medical oxygen system
[AD-A276983] 09 p3579 N94-32242
Integration of the Molecular Sieve Oxygen Generating System (MSOGS) into the UH-60Q MEDEVAC Blackhawk
[AD-A277668] 10 p4099 N94-33589

OXYGEN SYSTEMS
U OXYGEN SUPPLY EQUIPMENT

OXYGEN TENSION
Effect of barbiturates and hyperoxia on lipid peroxidation in hypoxic neurons
[AD-A278467] 10 p4094 N94-33545

OXYGEN TOXICITY
U HYPEROXIA

OXYGEN 17
Development of a molecular beam technique to study early solar system silicon reactions 01 p0432 N94-12224
Design of a formaldehyde photodissociation process for carbon and oxygen isotope separation
[DE93-016435] 03 p1039 N94-16450
Use of oxygen-17 isotope in the characterization of zeolites and related structures by nuclear magnetic resonance spectroscopy
[VTT-TIED-1448] 07 p2714 N94-26251

OXYGEN 18
Strontium and oxygen isotope study of M-1, M-3 and M-4 drill core samples from the Manson impact structure, Iowa: Comparison with Haitian K-T impact glasses 01 p0281 N94-12080
Development of a molecular beam technique to study early solar system silicon reactions 01 p0432 N94-12224
Design of a formaldehyde photodissociation process for carbon and oxygen isotope separation
[DE93-016435] 03 p1039 N94-16450

OXYGENATION
Organic carbonyl compounds in Albuquerque, New Mexico, air: A preliminary study of the effects of oxygenated fuel use
[DE93-017748] 04 p1476 N94-19045
Fatigue crack growth rate studies of medium sulfur low alloy steels tested in high temperature water
[DE93-040437] 06 p2238 N94-22861
Fatigue of carbon and low-alloy steels in LWR environments
[DE94-005116] 08 p3207 N94-30021
Potential benefits of oxygen-enriched intake air in a vehicle powered by a spark-ignition engine
[DE94-013452] 12 p4451 N94-37070

OXYNITRIDES
Birefringence control and dispersion characteristics of silicon oxynitride optical waveguides, appendix 6 05 p1989 N94-21600
The synthesis and structural characterization of Na3WO3N
[AD-A275243] 08 p3204 N94-29395
Process parameter-growth environment-film property relationships for reactive sputter deposited metal (V, Nb, Zr, Y, Au) oxide, nitride, and oxynitride films
[AD-A276382] 09 p3640 N94-31258
Joining of silicon nitrides using oxynitride glasses
[DE94-008517] 09 p3658 N94-32517

OZONE
Review of SHARC 2.0 O3 kinetics and spectroscopy
[AD-A265481] 01 p0274 N94-10496
The global potential energy surfaces of the lowest two 1A' states of the ozone molecule: Theoretical determination and analysis 01 p0267 N94-12269
Studies of dynamical processes affecting the distribution of stratospheric ozone
[NASA-CR-193477] 01 p0279 N94-12560
An examination of utility emissions contributions to elevated ozone concentrations in the Chicago area
[DE93-012852] 02 p0708 N94-13495
Arctic ozone expedition
[NASA-TM-109301] 02 p0708 N94-13602
Develop research plan for use of atlas data
[NASA-CR-194338] 02 p0714 N94-13709
Chemistry and transport in a multi-dimensional model
[NASA-CR-194425] 02 p0716 N94-13969
Effects of typhoon on TOMS data 02 p0693 N94-14243
The role of the dynamics for the deviation of the total ozone from the long-term mean at the edge of the polar vortex 02 p0694 N94-14250
The European Arctic ozone experiment: An investigation of Northern Hemisphere ozone depletion 02 p0694 N94-14251
Space-based activities: SAM 2 and SAGE 2 02 p0694 N94-14252
New evidences supported the Wei hypothesis about the formation of the Antarctic ozone hole 02 p0694 N94-14253
Signal and reference wavelengths for the elimination of SO2 cross sensitivity in remote measurements of tropospheric ozone with lidar
[GKSS/92/E/24] 02 p0817 N94-14819
The mobile lidar system ARGOS for spatial resolution remote measuring of gaseous air pollutants
[GKSS/92/E/26] 02 p0817 N94-14820
Southern and Northern Hemisphere total ozone as seen by TOMS
[NASA-TM-109591] 03 p1098 N94-15282
Atlas of TOMS ozone, 1978-1988
[NASA-TM-109456] 03 p1094 N94-15329
Emerging technologies for the changing global market
[TABES PAPER 93-612] 03 p0930 N94-16144
Geochemistry and cosmochemistry of fullerenes 3: Reaction of C60 and C70 with ozone 03 p0953 N94-16243
The feasibility of tropospheric and total ozone determination using a Fabry-Perot interferometer as a satellite-based nadir-viewing atmospheric sensor
[NASA-TM-109342] 03 p1102 N94-17214
Air pollution effects field research facility. 3: UV-B exposure and monitoring system
[DE93-013098] 04 p1470 N94-17773
Title 1 implementation: Status report on nonattainment areas
[DE93-017677] 04 p1471 N94-17777
Screening analysis for chlorine-free alternative refrigerants to replace R-22 in air conditioning applications
[DE93-015920] 04 p1367 N94-17847
Analysis of meteorological conditions during AGASP-4: 30 March - 23 April 1992
[PB93-190205] 04 p1489 N94-18126
Upper atmospheric effects of the HF Active Auroral Research Program Ionospheric Research Instrument (HAARP IRI)
[AD-A268948] 04 p1481 N94-18451
October 1979-1989 Southern Hemisphere total ozone as seen by TOMS
[NASA-TM-109375] 04 p1476 N94-18967
Spatiotemporal variability of non-urban ozone concentrations over the eastern United States and its potential replication by satellite data
[PB93-191328] 04 p1476 N94-19065
Analysis of satellite-derived ozone and water vapor measurements
[NASA-CR-193810] 04 p1486 N94-19237
Crossed molecular beam studies of atmospheric chemical reaction dynamics
[DE93-019246] 04 p1478 N94-19303
Intrusion of stratospheric ozone in the troposphere through tropopause folding and cold air droplets
[REPT-87] 05 p1851 N94-20154
Tropospheric chemistry of natural hydrocarbons, aldehydes, and peroxy radicals: Their connections to sulfuric acid production and climate effects
[DE93-019525] 05 p1855 N94-20220
Stratospheric Aerosol and Gas Experiment (SAGE 3) 05 p1869 N94-21644
The young Sun and photochemistry of the primitive Martian atmosphere 05 p2145 N94-21679
Studies in remotely sensed geophysical parameter retrieval and analysis
[NASA-CR-193914] 05 p1842 N94-22374
Infrared FEL photochemistry: Multiple-photon dissociation of freon gas
[DE94-000817] 05 p1820 N94-22585
Overview of global greenhouse effects
[DE93-041165] 06 p2396 N94-22887
High precision double four bar linkage mechanism for interferometric linear scanning 06 p2359 N94-24013
Participation in TOMS missions
[NASA-CR-195110] 06 p2398 N94-24078
Tropospheric Ozone Lidar Intercomparison Experiment, TROLIX 1991
[MPIM-102] 06 p2402 N94-24108
Nimbus-7 Total Ozone Mapping Spectrometer (TOMS) data products user's guide
[NASA-RP-1323] 06 p2410 N94-24355
Design of a vehicle based system to prevent ozone loss
[NASA-CR-195498] 06 p2180 N94-24479
Ozone depletion, paradigms, and politics
[DE94-001600] 06 p2398 N94-24506
Cloud, dust, and ozone vertical profiles from solar occultation measurements: Implications for dynamics 06 p2617 N94-24877
Reanalysis of Mariner 9 UV Spectrometer Data for Ozone, Cloud, and Dust Abundances, and Their Interaction Over Climate Timescales
[NASA-CR-195244] 07 p3107 N94-27885
Martian atmospheric radiation budget 07 p3107 N94-27887
Mars ozone: Mariner 9 revisited 07 p3107 N94-27888
Why is the north polar cap on Mars different than the south polar cap? 07 p3107 N94-27889
Probing the Martian atmosphere in the ultraviolet 07 p3108 N94-27890
How well was total ozone abundance inferred with Mariner 9? 07 p3108 N94-27891
In situ Mars ozone detector 07 p3108 N94-27892
Ozone control of biological activity during Earth's history, including the KT catastrophe 07 p2876 N94-28312
Ozone production at a rural site in Georgia during the summer 1992 SOS campaign
[DE94-003989] 08 p3342 N94-28523
Harvard ER-2 OH laser-induced fluorescence instrument 08 p3343 N94-28592

Peroxy radical measurements with NCAR's chemical amplifier 08 p3345 N94-28603
Surface energy changes produced by ultraviolet-ozone irradiation of poly(methylmethacrylate), polycarbone and polytetrafluoroethylene
[NASA-TM-106460] 08 p3213 N94-28922
System requirements review for the High-Resolution Ozone Imager (HIROIG)
[AD-A275151] 08 p3347 N94-29023
Activities of the wintering party at Showa Station by the 31st Japanese Antarctic Research Expedition in 1990 08 p3358 N94-29083
GOME: Global Ozone Monitoring Experiment
[ESA-SP-1151] 08 p3347 N94-29452
Laboratory studies of chemical and photochemical processes relevant to stratospheric ozone
[NASA-CR-189351] 08 p3347 N94-29549
The suitability of low-cost urban airshed modeling in the Chicago area
[DE94-005114] 08 p3349 N94-30023
Regenerating using aqueous cleaners with ozone and electrolysis 08 p3240 N94-30468
Radiative flux calculations at UV and visible wavelengths
[DE94-004278] 08 p3350 N94-30613
Tropospheric radiative forcing of O3 for the 1994 IPCC report
[DE94-005698] 08 p3367 N94-30876
One: Microphysics of frost metamorphism: Applications to Triton and Mars. Two: A global analysis of the ozone deficit in the upper stratosphere and lower mesosphere. Three: The diabatic circulation in the stratosphere as diagnosed from Microwave Limb Sounder data 09 p3942 N94-31975
Formation of gas-phase peroxides in a rural atmosphere: An interpretation of the recent SOS/SERON field results
[DE94-002995] 09 p3766 N94-32692
Mexico City ozone concentrations as a function of readily-available meteorological parameters
[DE94-007576] 09 p3768 N94-32814
Quantified estimates of total GWPs for greenhouse gases taking into account tropospheric chemistry
[DE94-007846] 09 p3768 N94-32817
A correlated k-distribution model of the heating rates for atmospheric mixtures of H2O, CO2, O3, CH4, and N2O in the 0-2500 cm(exp -1) wave number region at altitudes between 0 and 60 km
[DE94-005136] 09 p3775 N94-32895
How well was total ozone abundance inferred with Mariner 9 09 p3947 N94-33212
Atmospheric Sciences Program summaries of research in FY 1993
[DE94-003486] 10 p4086 N94-33731
A statistical inference approach for the retrieval of the atmospheric ozone profile from simulated satellite measurements of solar backscattered ultraviolet radiation 10 p4083 N94-35060
JPRS report: Science and technology. Central Eurasia: Space
[JPRS-USP-94-001] 11 p4201 N94-35518
Vacuum ultraviolet studies of molecular dynamics
[AD-A278940] 11 p4321 N94-35657
Tropospheric radiative forcing of CH4
[DE94-011628] 12 p4468 N94-37631

OZONE DEPLETION
Mid-latitude ionospheric response to active experiments
[NASA-CR-193549] 01 p0280 N94-12583
Theoretical support for the Airborne Antarctic Ozone Experiment
[NASA-CR-193669] 02 p0713 N94-13465
Airborne Arctic stratospheric expedition: Ozone
[NASA-TM-109312] 02 p0515 N94-13606
Modeling of the partitioning of reactive odd nitrogen in the lower stratosphere using aircraft measurements of NOy, NO, and other trace species
[NASA-CR-194305] 02 p0714 N94-13707
The role of the dynamics for the deviation of the total ozone from the long-term mean at the edge of the polar vortex 02 p0694 N94-14250
The European Arctic ozone experiment: An investigation of Northern Hemisphere ozone depletion 02 p0694 N94-14251
Space-based activities: SAM 2 and SAGE 2 02 p0694 N94-14252
New evidences supported the Wei hypothesis about the formation of the Antarctic ozone hole 02 p0694 N94-14253
Long-range global warming impact of gaseous diffusion plant operation
[DE93-011686] 02 p0710 N94-14459
Atlas of TOMS ozone, 1978-1988
[NASA-TM-109456] 03 p1094 N94-15329
Arctic ozone
[NASA-TM-109614] 03 p1095 N94-15365
Prioritization methodology for chemical replacement
[NASA-TP-3421] 03 p0976 N94-15723
Environmental management lessons to be learned from the upcoming CFC phase out or how to insure that we survive the next environmentally mandated process change
[TABES PAPER 93-570] 03 p1050 N94-16136
NASA Operational Environment Team (NOET): NASA's key to environmental technology
[TABES PAPER 93-611] 03 p1052 N94-16143
Emerging technologies for the changing global market
[TABES PAPER 93-612] 03 p0930 N94-16144
Removing CFC's from the atmosphere with lasers: A second look
[DE93-017516] 04 p1473 N94-18101
Upper atmospheric effects of the HF Active Auroral Research Program Ionospheric Research Instrument (HAARP IRI)
[AD-A268948] 04 p1481 N94-18451
Ozone hole
[NASA-TM-109368] 04 p1476 N94-18960
US Department of Energy phaseout of CFC-refrigerants
[DE94-001668] 06 p2397 N94-23016
Ozone depletion, paradigms, and politics
[DE94-001600] 06 p2398 N94-24506
A three-dimensional chemical transport model study of the 1991 Antarctic ozone hole using objectively analysed data
[ISBN-0-315-84250-4] 07 p2867 N94-26670
Mission to Planet Earth: A program to understand global environmental change
[NASA-PAM-556] 07 p2869 N94-27958
System requirements review for the High-Resolution Ozone Imager (HIROIG)
[AD-A275151] 08 p3347 N94-29023
The ozone and the physico-chemical processes in tropical regions 09 p3770 N94-31010
Odin aeronomy science: A phase-A report by the Aeronomy Science Working Group for the Odin satellite
[AP-31] 09 p3770 N94-31222
Ionization probes of molecular structure and chemistry
[DE94-007605] 09 p3872 N94-32643
Possible effect of the chlorine oxide dimer on transient ozone loss in rocket plumes
[AD-A278135] 09 p3616 N94-33094
Headquarters summary reports 10 p3970 N94-33452
A NASA Lewis comparative propulsion system assessment for the High-Speed Civil Transport 10 p3974 N94-33477
Low emissions combustor technology for high-speed civil transport engines 10 p3974 N94-33481
HSR combustion analytical research 10 p3974 N94-33483
Ozone hole airborne Arctic stratospheric expedition (pre-flight)
[NASA-TM-109800] 10 p4080 N94-33551

OZONE HOLES
U OZONE DEPLETION

OZONE LAYER
U OZONOSPHERE

OZONOMETRY
Activities of the wintering party at Showa Station by the 31st Japanese Antarctic Research Expedition in 1990 08 p3358 N94-29083
Ozone hole airborne Arctic stratospheric expedition (pre-flight)
[NASA-TM-109800] 10 p4080 N94-33551

OZONOSPHERE
Atmospheric and spectroscopic research in the far infrared
[NASA-CR-193551] 01 p0280 N94-12582
Atlas of TOMS ozone, 1978-1988
[NASA-TM-109456] 03 p1094 N94-15329
NASA Operational Environment Team (NOET): NASA's key to environmental technology
[TABES PAPER 93-611] 03 p1052 N94-16143
Air pollution effects field research facility. 3: UV-B exposure and monitoring system
[DE93-013098] 04 p1470 N94-17773
Removing CFC's from the atmosphere with lasers: A second look
[DE93-017516] 04 p1473 N94-18101
Upper atmospheric effects of the HF Active Auroral Research Program Ionospheric Research Instrument (HAARP IRI)
[AD-A268948] 04 p1481 N94-18451
Ozone depletion, paradigms, and politics
[DE94-001600] 06 p2398 N94-24506
Initial ultraviolet-B intensity data at Lawrence Livermore National Laboratory
[DE94-004279] 07 p2869 N94-27267
System requirements review for the High-Resolution Ozone Imager (HIROIG)
[AD-A275151] 08 p3347 N94-29023
Radiative flux calculations at UV and visible wavelengths
[DE94-004278] 08 p3350 N94-30613
HSR combustion analytical research 10 p3974 N94-33483

P

P BAND
Application of Cloude's target decomposition theorem to polarimetric imaging radar data 05 p1724 N94-20429

P WAVES
NORSAR basic seismological research
[AD-A266193] 03 p1101 N94-16125
A comparison of single-station backazimuth estimates with regional event locations in the Central Appalachians
[AD-A269697] 04 p1483 N94-18690
Analysis of the effects of eurasian crustal and upper mantel structure on regional phases using broadband seismic data
[AD-A272446] 05 p1858 N94-21206
Downward extrapolation of multi-component seismic data
[ISBN-9-09-005213-5] 06 p2405 N94-25229
Decomposition of multi-component measurements into P and S waves
[ISBN-9-09-005197-X] 06 p2405 N94-25251
Elastic scattering by a spherical inclusion
[AD-A274713] 07 p2878 N94-26433
Dynamic and kinematic P wave tracing for a three-dimensional elastic inhomogeneous media by the asymptotic ray theory and application
[ITN-94-85239] 07 p2775 N94-27244
Initial wave-type identification with neural networks and its contribution to automated processing in IMS version 3.0
[AD-A275058] 08 p3359 N94-29137
Body-wave radiation patterns and AVO in transversely isotropic media
[DE94-009214] 10 p4036 N94-34162
Detection of the electrocardiogram P-wave using wavelet analysis
[DE94-010791] 12 p4481 N94-37197

P-I-N DIODES
U DIODES
U P-I-N JUNCTIONS

P-I-N JUNCTIONS
Radiation effects in Ga(0.47)In(0.53)As solar cells 01 p0052 N94-11404
Measurement and modeling of the stability of hydrogenated amorphous silicon solar cells and films after intense illumination 01 p0263 N94-11638
Design of broadband wire antennas for frequency hopping applications
[AD-A267405] 03 p1001 N94-17025
Electric-field dependence of electroreflectance and photocurrent spectra at visible wavelengths in MOVPE-grown InAlGaP multiple strained quantum-well structures
[DE94-004692] 07 p2780 N94-25664
Recombination and metastability in amorphous silicon and silicon germanium alloys
[DE94-000237] 07 p2736 N94-26481
Hydrogenated amorphous silicon (a-Si:H) based gamma camera: Monte Carlo simulations
[DE94-007042] 09 p3795 N94-31323
Development of novel II-VI solar cells
[PB94-159415] 11 p4282 N94-35739

P-N JUNCTIONS
Electrochemical characterization of p(+)n and n(+)p diffused InP structures 01 p0049 N94-11385
New experimental techniques for solar cells 01 p0052 N94-11403
Changes in electrical device characteristics during the formation of dislocations in situ in the TEM
[DE93-013910] 02 p0808 N94-13694
The XMM pn-CCD detector system: First results 03 p0900 N94-15034
Gallium arsenide-based ternary compounds and multi-band-gap solar cell research
[DE93-010049] 04 p1467 N94-18483
Defect behavior of polycrystalline solar cell silicon
[DE93-018490] 04 p1468 N94-19016
MOCVD-grown InGaAsP heterostructure diode lasers
[AD-A270848] 04 p1606 N94-19769
Some experiences of solving 1-D semiconductor device equations on a matrix coprocessor by a domain decomposition method
[CWI-NM-R9304] 05 p1935 N94-21492
Method for fabricating self-aligned gate diffused junction field effect transistor
[AD-D015975] 06 p2312 N94-25035

Analysis of microwave induced interference in pn-diodes
[PB94-136983] 08 p3243 N94-28906
The influence of an in-situ electric field on H(+) and He(+) implantation induced defects insil icon
[DE94-006553] 08 p3518 N94-30249

P-TYPE SEMICONDUCTORS
Organometallic chemical vapor deposition and characterization of ZnGe(1-x)Si(x)P2-Ge alloys on GaP substrates 01 p0400 N94-11443
Effects of growth conditions and substrate orientation on the properties of InSb
[DE93-013766] 02 p0812 N94-14344
Selective electrochemical wafer thinning for silicon characterization
[DE93-015083] 04 p1592 N94-17742
Atomic layer epitaxy of group 4 materials: Surface processes, thin films, devices and their characterization
[AD-A274325] 07 p3061 N94-26885
Visible light emitting materials and injection devices
[AD-A274418] 07 p2786 N94-27079
Non-alloyed, refractory metal contact optimization with shallow implantations of Zn and Mg
[DE94-010392] 11 p4240 N94-36110

P-3 AIRCRAFT
Development and evaluation of a near infrared reflecting and low visibility paint scheme for RAAF P-3C Orion aircraft
[AD-A274881] 07 p2669 N94-26864

PACIFIC ISLANDS
NT JAPAN
NT PHILIPPINES
Schools of the Pacific rainfall climate experiment 05 p1881 N94-20699

PACIFIC OCEAN
Central Equatorial Pacific Experiment (CEPEX)
[DE93-011656] 01 p0190 N94-11674
Proceedings of the PORSEC 1992 in Okinawa: Conference for Pacific Ocean Environments and Probing, volume 1
[JTN-93-80418] 01 p0191 N94-11894
Acoustic Doppler current profiling of the Kuroshio over the East China Sea shelf slope 01 p0194 N94-11914
Seasonal variation of the surface mixed layer in the subtropical re-circulation area of the North Pacific during OMLET 01 p0195 N94-11924
The Kyucho events in Sukumo Bay induced by Kuroshio front disturbances 01 p0198 N94-11939
Westward propagation of sea surface anomalies in the western North Pacific as seen by the altimeter and radiometer 01 p0198 N94-11941
Coastal processes due to nearshore current around an upheaving island 01 p0199 N94-11942
Availability of wind field over the North Pacific derived from data on ships-of-opportunity and analysis of long-term variabilities 01 p0202 N94-11962
Circulation of North Pacific Intermediate Water 01 p0206 N94-11985
Roles of the NEC and MC in the formation and evolution of the Equatorial Pacific Warm Pool 01 p0206 N94-11990
SSMI wind speed variability over the Pacific Ocean 01 p0207 N94-12637
Observations of eddy fields in the Northwest Pacific by GEOSAT altimetry 01 p0207 N94-12639
Variability of sea level and sea surface temperature anomalies in the equatorial Pacific 01 p0208 N94-12640
Pseudo magnetic anomaly derived from satellite altimetry and its application to the tectonics in the North Fuji Basin 01 p0208 N94-12645
Principal oscillation pattern analysis of sea level variations in the tropical Pacific measured by the GEOSAT altimeter 01 p0209 N94-12646
Measurement of eddy structure and movement in the north-east Pacific with the GEOSAT altimeter 01 p0209 N94-12647
Preliminary results from a satellite altimetric data assimilation using a Kalman filter and smoother 01 p0209 N94-12648
Mean flow and variability in the Kuroshio extension from GEOSAT altimetry data 01 p0209 N94-12650
Pacific rim sea ice as observed with the NIMBUS-7 SMMR 01 p0210 N94-12651
Variation of the photosynthetic products in the regional upwelling area around the Izu Islands, Japan 01 p0211 N94-12661
Sea surface temperature images of Geostationary Meteorological Satellite (GMS) and sea truth data from ferry boats 01 p0213 N94-12671
Intrusion of Kuroshio warm water into Sagami Bay 01 p0215 N94-12683
On a nonstationary dynamics of the north-west Pacific Ocean 01 p0222 N94-12724
Linkage of anthropogenic aerosol to clouds and climate
[DE93-016434] 02 p0719 N94-13080
IAI topic: El Nino. Southern oscillation and interannual climate variability
[INPE-5410-PRE/1757] 03 p1111 N94-15186
Spectral analysis of synoptic time scale disturbances over the tropical eastern Pacific during summer 1989, 1990 and 1991
[AD-A268821] 04 p1490 N94-18206
Optical climatology of the Northeast Pacific Ocean
[AD-A271671] 05 p1866 N94-20559
Observed and Navy operational global model climatologies of synoptic disturbances over the tropical western Pacific during winter 1991-1992
[AD-A273400] 06 p2416 N94-25071
Propagation of cold air masses in East Asia and its associated planetary-scale function
[AD-A274304] 07 p2895 N94-26850
Tropical cyclone report, 1992
[AD-A274464] 07 p2896 N94-27025
Global Acoustic Mapping of Ocean Temperatures (GAMOT)
[AD-A275777] 08 p3376 N94-28740
On the annual cycle of the tropical Pacific atmosphere and ocean 08 p3371 N94-29763
On interannual variability and climate change in the North Pacific 08 p3374 N94-29963
Satellite estimation of the global distribution and interannual variability of photosynthetically active radiation 08 p3334 N94-29970
Investigation of carbon dioxide in the central South Pacific Ocean (WOCE Sections P-16C and P-17C) during the TUNES/2 expedition of the R/V Thomas Washington, July-August, 1991
[DE94-006638] 09 p3763 N94-31347
The effect of westerly wind bursts on a tropical ocean general circulation model
[AD-A276423] 09 p3788 N94-31448
Air-sea interaction patterns in the equatorial Pacific
[AD-A277305] 09 p3788 N94-32072
Typhoon havens handbook for the western Pacific and Indian Oceans, change 3
[AD-A277030] 09 p3784 N94-32260
ENSO forced variations of the sea surface temperature and adjusted sea level along the west coast of the United States
[AD-A277306] 09 p3789 N94-32327
Fine and microstructure observations at Fieberlin g Guyot R/V new horizon cruise report
[AD-A277917] 09 p3791 N94-33109
SEASOAR and CTD observations during a COARE surveys cruise, W9211C, 22 January - 22 February, 1993
[AD-A277925] 09 p3791 N94-33244

PACKAGES
NT APOLLO LUNAR SURFACE EXPERIMENTS PACKAGE
NT INSTRUMENT PACKAGES

PACKAGING
NT ELECTRONIC PACKAGING
Environmental Protection Agency's life cycle methodology: Guidelines for use in development of packaging
[PB93-194199] 01 p0265 N94-10841
Package integrity measurement technology and quality assurance
[AD-A273881] 07 p2834 N94-25727
Codes on the unit sphere
[PB94-136991] 08 p3453 N94-29174
Processing, packaging, and characterization of electroceramic materials for phased array antennas
[AD-A280251] 12 p4432 N94-36743

PACKET SWITCHING
Technical support for digital systems technology development. Task order 1: ISP contention analysis and control
[NASA-CR-190758] 02 p0537 N94-12809
Destination-directed, packet-switched architecture for a geostationary communications satellite network
[NASA-TP-3379] 02 p0538 N94-13111
High speed packet switching
[NASA-CR-191334] 02 p0759 N94-13177
Overview of Enhanced Data Stream Array Processor (EDSAP)
[AD-A266986] 03 p1158 N94-15492
On-board B-ISDN fast packet switching architectures. Phase 1: Study
[NASA-CR-191143] 03 p0883 N94-17111
Non-blocking crossbar permutation engine with constant routing latency
[NASA-CASE-NPO-18864-1-CU] 03 p1161 N94-17328
A scalable wrap-around shuffle exchange network with deflection routing
[NASA-CASE-NPO-18983-1-CU] 03 p1161 N94-17330
Isochronets: A high-speed network switching architecture
[AD-A267811] 03 p1161 N94-17409
NASA Lewis Meshed VSAT Workshop meeting summary
[NASA-TM-106332] 03 p0883 N94-17487
On-board packet switch architectures for communication satellites
[NASA-TM-106328] 03 p0883 N94-17488
A distributed reinforcement learning scheme for network routing
[AD-A270600] 05 p1938 N94-19845
Reduction of network cost and wiring in Ranade's butterfly routing
[CWI-CS-R9243] 05 p1930 N94-21023
A packet switched communications system for GRO 05 p1744 N94-21345
Tandem queues with deterministic service times
[CWI-BS-R9238] 05 p1946 N94-21577
On-board closed-loop congestion control for satellite based packet switching networks
[NASA-TM-106446] 05 p1656 N94-21581
IAS telecommunication infrastructure and value added network services provided by IASNET 05 p1744 N94-22069
A shared buffer memory switch with maximum queue and minimum allocation 05 p1773 N94-22119
A one-shot access scheme for a multicast switch 05 p1773 N94-22120
Sorting network for the partial selection problem 05 p1773 N94-22121
Throughput, blocking, and interference in packet radio networks 05 p1746 N94-22190
Buffer allocation in an ATM switch with output buffer and speed constraints 05 p1746 N94-22203
Design and implementation considerations of a MSAT packet data network 06 p2280 N94-22778
Fault tolerant onboard packet switch architecture for communication satellites: Shared memory per beam approach
[NASA-TM-106397] 06 p2201 N94-23567
Fast simulation of packet loss rates in a shared buffer communications switch
[NASA-CR-191556] 06 p2457 N94-24638
Asynchronous and packetized systems engineering tools 07 p2954 N94-26746
Analysis of a multiaccess/switching technique for multibeam satellites in a prioritized ISDN environment
[ISBN-0-315-84632-1] 07 p2776 N94-27345
Communications networks in stressed environments
[AD-A275967] 09 p3672 N94-31384
Discrete-event-dynamic-system-based approaches for scheduling transmissions in multihop packet radio networks
[AD-A276566] 09 p3679 N94-32230
Principles of ultradependability in chaotic routing
[AD-A277422] 09 p3827 N94-32995
Multicast communication with guaranteed quality of service
[AD-A277650] 09 p3682 N94-33025
Photonic fast packet switching using optically processed control
[AD-A278195] 10 p4038 N94-33386
ATM technology and beyond 10 p4156 N94-33820
Neurocontrol of a broadband (ATM) Clos' switching network
[PB94-179389] 12 p4441 N94-37851

PACKET TRANSMISSION
NT ALOHA SYSTEM
Characteristics of the amateur radio means of the Arsene satellite
[CNES-NT-131] 02 p0605 N94-13950
Bandwidth characteristics of multimedia data traffic on a local area network
[NASA-TM-104026] 03 p0883 N94-15648
Non-blocking crossbar permutation engine with constant routing latency
[NASA-CASE-NPO-18864-1-CU] 03 p1161 N94-17328
Application guide for universal source encoding for space
[NASA-TP-3441] 05 p1741 N94-21783
A packet based, data driven telemetry system for autonomous experimental sub-orbital spacecraft
[DE94-000399] 05 p1657 N94-21980
CREIR: A multiaccess protocol for on-board processing satellite systems 05 p1780 N94-22168
Design and implementation considerations of a MSAT packet data network 06 p2280 N94-22778
The EURECA telecommanding chain: Experience with packet telecommand and telemetry systems 06 p2305 N94-23909
Modeling of the ground-to-SSFMB link networking features using SPW 06 p2306 N94-25381

Packet radio data link applications in the NASA Langley Research Center Transport Systems Research Vehicle
[NASA-TM-109071] 07 p2665 N94-27423
Video transmission on ATM networks
[NASA-CR-195124] 08 p3244 N94-29106
Discrete-event-dynamic-system-based approaches for scheduling transmissions in multihop packet radio networks
[AD-A276566] 09 p3679 N94-32230

PACKETS (COMMUNICATION)

Technical support for digital systems technology development. Task order 1: ISP contention analysis and control
[NASA-CR-190758] 02 p0537 N94-12809
Mathematic methods and algorithms for real-time applications
[AD-A266776] 02 p0771 N94-14789
An approximation for computing reduction in bandwidth requirements using intelligent multiplexers
[AD-A267434] 03 p1001 N94-17026
Non-blocking crossbar permutation engine with constant routing latency
[NASA-CASE-NPO-18864-1-CU] 03 p1161 N94-17328
A packet switched communications system for GRO 05 p1744 N94-21345
On-board closed-loop congestion control for satellite based packet switching networks
[NASA-TM-106446] 05 p1656 N94-21581
A one-shot access scheme for a multicast switch 05 p1773 N94-22120
Sorting network for the partial selection problem 05 p1773 N94-22121
Buffer allocation in an ATM switch with output buffer and speed constraints 05 p1746 N94-22203
Design and implementation considerations of a MSAT packet data network 06 p2280 N94-22778
A packet-based concept for spacecraft command planning 06 p2504 N94-23873
AMFESYS: Modelling and diagnosis functions for operations support 06 p2506 N94-23887
The European Space Agency standard for space packet utilisation 06 p2203 N94-23954
Fast simulation of packet loss rates in a shared buffer communications switch
[NASA-CR-191556] 06 p2457 N94-24638
Gigabits to the Desktop: Installing tomorrow's networks today
[DE94-007701] 09 p3827 N94-32646
Principles of ultradependability in chaotic routing
[AD-A277422] 09 p3827 N94-32995
Photonic fast packet switching using optically processed control
[AD-A278195] 10 p4038 N94-33386

PACKING DENSITY

Dynamic high-pressure shock compaction of diamond powders
[AD-A266004] 01 p0093 N94-12354
Equipment for investigation of cryogenic compaction of nanosize silicon nitride powders
[DE93-018740] 04 p1340 N94-18180
Molecular dynamics modeling of the mechanical behavior of metallic multilayers
[DE93-017972] 04 p1365 N94-19263
The 2-D polymerized Langmuir-Blodgett films studied by STM
[AD-A273542] 06 p2261 N94-24930

PADE APPROXIMATION

A hybrid Pade-Galerkin technique for differential equations
[NASA-CR-191494] 02 p0767 N94-13289
Rational trigonometric approximations using Fourier series partial sums
[NASA-CR-191535] 05 p1959 N94-21568
The accuracy-through-order and the equivalence properties in the algebraic approximant
[DE93-040188] 05 p1960 N94-21946
Unsteady jet flow computation towards noise prediction
[NASA-CR-194449] 06 p2153 N94-23553
Two-point PADE approximants for Stieltjes series 06 p2490 N94-24768

PAH

U POLYCYCLIC AROMATIC HYDROCARBONS

PAIN

Project ARGO: Gas phase formation in simulated microgravity
[NASA-TM-104762] 01 p0125 N94-11235
Joint pain and Doppler-detectable bubbles in altitude (Hypobaric) decompression 01 p0312 N94-11542

PAIN SENSITIVITY

Excitation of cutaneous polymodal receptor induced by sympathetic stimulation in adjuvant-induced arthritis rats 07 p2906 N94-27495
Influence of mechanical stimulation on inflammatory edema 07 p2906 N94-27497
The effect of naloxone on sleeping time in adjuvant arthritic rats 07 p2906 N94-27498
Changes in pain sensation induced by repetitive application of noxious heat pulses to the human skin 07 p2924 N94-27501
Hyperalgesia to cold in patients with Subacute Myelo-Optico-Neuropathy (SMON) 07 p2928 N94-27521
The polymodal receptor 07 p2908 N94-27539

PAINTS

Environmentally Safe and Effective Processes for Paint Removal
[AGARD-R-791] 01 p0126 N94-10613
Paint removal activities in the US Navy 01 p0126 N94-10614
Paint removal activities in Canada 01 p0126 N94-10615
Procedures without danger to the environment and efficiency (PSDEE) for the removal of paint. Point on the French activities concerning the removal of paint 01 p0126 N94-10616
Paint removal activities in Germany 01 p0126 N94-10617
The development of alternative paint removal techniques in the RAF 01 p0126 N94-10618
Operational aspects of F.16 plastic media blasting, as carried out by Fokker Aircraft Services 01 p0126 N94-10619
Use of robots for aircraft dry stripping via plastic media blasting 01 p0127 N94-10620
German Air Forces experiences with plastic media blasting and future requirements 01 p0127 N94-10621
Plastic media blasting activities at Hill Air Force Base 01 p0127 N94-10622
Large Aircraft Robotic Paint Stripping (LARPS) system and the high pressure water process 01 p0127 N94-10623
Automated Laser Paint Stripping (ALPS) update 01 p0127 N94-10624
Aquastrip (tm): An innovative paint removal technology 01 p0127 N94-10625
Paint removal and surface cleaning using ice particles 01 p0128 N94-10626
Paint removal using wheat starch blast media 01 p0128 N94-10627
IATA taskforce: Paintstripping 01 p0128 N94-10628
Selectively strippable paint schemes 01 p0128 N94-10629
Experimental measurement of the plasma conductivity of Z93 and Z93P thermal control paint
[NASA-TM-106284] 01 p0043 N94-10756
Understanding cracking failures of coatings: A fracture mechanics approach 01 p0187 N94-11218
Formulating infrared coatings for defence applications
[MRL-RR-1-93] 01 p0090 N94-11302
Study of novel conductive paints for solar cell electromagnetic fields
[DE93-015088] 02 p0581 N94-14337
XPS analysis of Al/EPDM bondlines from IUS SRM-1 polar bosses
[AD-A266851] 03 p1056 N94-14945
Automated image analysis method for the detection of cracks on wood surface
[VTT-JULK-755] 03 p1056 N94-17542
Dry stripping as a surface treatment method
[VTT-TIED-1348] 03 p0985 N94-17544
Pressure sensitive paint technique 04 p1431 N94-18647
An improved patch for radiative coolers
[NASA-CASE-GSC-13503-1] 05 p1822 N94-20127
Thermal control coatings 05 p1664 N94-21400
Evaluation of electroconductivity of two surface paints for spacecraft
[AD-A273063] 05 p1706 N94-21437
Development and evaluation of a near infrared reflecting and low visibility paint scheme for RAAF P-3C Orion aircraft
[AD-A274881] 07 p2669 N94-26864
Rules and definition of the range of paints applied on aeronautical structrural composites
[REPT-932-600-106] 08 p3215 N94-29459
Effects of make-up on the heat transfer from the head in hyperthermic conditions 08 p3394 N94-29864
The effect of mechanical paint stripping on the fatigue and fracture of thin aluminum airplane skin 08 p3205 N94-29900
Evaluation of corrosion protecting properties of modern aircraft paint systems
[AD-B179388] 08 p3220 N94-30420
Development of a unique polyurethane primer/topcoat 08 p3223 N94-30476
Evaluation of corrosion protective organic coatings for steel structures in fresh water
[PB94-138484] 09 p3649 N94-31072
Oxide pigments in water: The colloid-chemical point of view
[PB94-148616] 09 p3633 N94-31591
Conductive paints
[DE94-008508] 09 p3661 N94-32788
Method and apparatus for inhibiting the disbonding of a paint from metal surfaces
[AD-D016106] 09 p3663 N94-32960
The electrical conductivities of candidate beam-waveguide antenna shroud materials 11 p4252 N94-35548
Dual cure low-VOC coating process
[DE94-009346] 11 p4245 N94-35809
Atomic oxygen treatment for non-contact removal of organic protective coatings from painting surfaces
[NASA-TM-106650] 12 p4421 N94-36952
Evaluation of flame-sprayed polymer coatings for civil works navigation structures
[AD-A280507] 12 p4422 N94-37104
Diode array alternative to paint removal solid-state cw laser
[DE94-011482] 12 p4448 N94-37203

PAIR PRODUCTION

Coherence influence on the intensity of Bose-Einstein correlations and visible size of a source
[DE93-617697] 01 p0349 N94-10556
Top quark search in D(O) from the lepton + jets mode
[DE93-014027] 01 p0370 N94-12781
Top quark polarization and T-odd spin correlations as tools for testing (non) Standard Model predictions
[DE93-622956] 02 p0778 N94-12847
A search for scalar leptoquarks in D0
[DE93-012780] 02 p0779 N94-12954
Characteristics of a high energy muon(+)muon(-) collider based on electro-production of muons
[DE93-017154] 02 p0790 N94-14893
Crystal optics of high energy gamma-beams
[DE93-630228] 04 p1577 N94-18217
Low mass muon pair production in 450 GeV p-Be collisions
[PB94-110699] 06 p2533 N94-23746
Photon-photon collisions at the next linear collider: Theory
[DE93-041025] 06 p2534 N94-23803
CP test in the W pair production by way of photon fusion at NLC
[DE94-601608] 07 p3014 N94-25889
Magnetic field induced contributions of supersymmetric particles to energy losses of neutron star
[DE93-634331] 07 p3104 N94-26269
Chance to use W-decay lepton channels for width determination
[DE93-634438] 07 p3020 N94-26507
Search for the top quark in the single lepton + jets channel at D0
[DE94-004660] 07 p3028 N94-27749
Emission of supersymmetric neutron pair by charged lepton in magnetic field
[DE93-634365] 08 p3481 N94-28468
Time-dependent behavior of active galactic nuclei with pair production 09 p3929 N94-31125
A constraint on the pair-density ratio (Z+) in an electron-positron pair wind 09 p3930 N94-31132
Perturbative and nonperturbative EM lepton pair production in relativistic heavy-ion collisions
[DE94-006315] 09 p3867 N94-31779
Probing lepton number violation via Majorana neutrinos at hadron supercolliders
[PB94-147055] 09 p3868 N94-31922
A quark model of bar Lambda production in bar Rho interactions
[DE94-008071] 11 p4324 N94-35824
Processes of the reciprocal transformation vector charged particles pairs and electron-positron pairs
[DE94-616787] 11 p4325 N94-36077
Angular dependence of parton-parton scattering extracted from hadron pair production in pp collisions at radicals equal to 11.5 GeV
[DE94-611174] 12 p4511 N94-36504
Measurement and processing of gammas accompanying muon pairs in the reaction pi(-)C yields mu(+)mu(-) + gamma + X at 38 GeV
[DE94-617044] 12 p4512 N94-36523
Five-lepton decay modes of muon and tau mesons
[DE94-621636] 12 p4516 N94-37099
A freon-filled, holographic bubble chamber as a high energy photon burst spectrometer
[DE94-011645] 12 p4446 N94-37723

PAKISTAN SPACE PROGRAM

Pakistan Space and Upper Atmosphere Research Commission 01 p0037 N94-10693

PALEOBIOLOGY

The end-Permian mass extinction: A complex, multicausal extinction 07 p2888 N94-28299

Mass extinctions: Persistent problems and new directions 07 p2889 N94-28302
Ozone control of biological activity during Earth's history, including the KT catastrophe 07 p2876 N94-28312

PALEOCLIMATOLOGY
Earth's partial pressure of CO2 over the past 100-500 Ma; evidence from Ce anomalies in mostly shallow seas (less than 200 m) as recorded in carbonate sediments, 2 03 p1104 N94-16360
Workshop on Early Mars: How Warm and How Wet?, part 1
[NASA-CR-193553] 05 p2142 N94-21659
Ancient Martian valley genesis and paleoclimatic inference: The present as a key to the past 05 p2142 N94-21661
Early Mars was wet but not warm: Erosion, fluvial features, liquid water habitats, and life below freezing 05 p2145 N94-21677
The Martian valley networks: Origin by niveo-fluvial processes 05 p2146 N94-21682
Sensitivity of climate models: Comparison of simulated and observed patterns for past climates
[DE93-019934] 07 p2865 N94-25789
Impact of biomass burning on the atmosphere
[DE94-004333] 08 p3349 N94-29954
Modeling Earth system changes of the past 08 p3353 N94-30635
The Earth's climate: Past, present, and future 09 p3777 N94-30982
Biospheric effects of a large extraterrestrial impact: Case study of the Cretaceous/Tertiary boundary crater
[NASA-CR-195827] 09 p3942 N94-32740
Carbonate formation on Mars: Latest experiments 09 p3950 N94-33231
Exopaleontology and the search for a fossil record on Mars 11 p4360 N94-35425
Mars atmospheric escape and isotopic fractionation: Synthesis of data and models 11 p4369 N94-36143

PALEOMAGNETISM
Macroscopic electric charge separation during hypervelocity impacts: Potential implications for planetary paleomagnetism 01 p0431 N94-12181
Magnetic fields and nonuniform structures of the Moon 01 p0472 N94-12218
Frequency dependent electrical properties of minerals and partial-melts
[DE93-019918] 05 p2012 N94-19861
Two-polarity magnetization in the Manson impact breccia 05 p1863 N94-20789
An extraterrestrial event at the tertiary-quaternary boundary 07 p2890 N94-28309
Motion and development of the Pacific Plate from the Middle Jurassic to the Late Cretaceous 08 p3362 N94-29939

PALEONTOLOGY
Fluvial erosion on Mars: Implications for paleoclimatic change 03 p1241 N94-16210
Technologies for assessing the geologic and geomorphic history of coasts
[AD-A268780] 04 p1496 N94-18215
Structural evidence for reorientation of Miranda about a paleo-pole 05 p2098 N94-20671
The biostratigraphy and paleogeography of Maastrichtian inoceramids 07 p2889 N94-28303
An evaluation of criteria that may be used to identify species surviving a mass extinction 07 p2889 N94-28304
Ozone control of biological activity during Earth's history, including the KT catastrophe 07 p2876 N94-28312
Exopaleontology and the search for a fossil record on Mars 11 p4360 N94-35425

PALEOZOIC ERA
Earth's partial pressure of CO2 over the past 100-500 Ma; evidence from Ce anomalies in mostly shallow seas (less than 200 m) as recorded in carbonate sediments, 2 03 p1104 N94-16360
The end-Permian mass extinction: A complex, multicausal extinction 07 p2888 N94-28299

PALLADIUM
Optical properties and surface morphology studies of palladium contacts on mercuric iodide single crystals
[DE93-012510] 03 p1207 N94-15973
Study of mechanical behavior and internal structure of ferritic nanocrystalline material
[DE93-019264] 04 p1596 N94-18184
The metallic bond for monolayer transition metal layers on transition metal surfaces
[DE93-019060] 05 p1691 N94-20313
Structure and morphology of Pd overlayers on epitaxial SnO2 films studies with the atomic force microscope
[AD-A271827] 05 p2028 N94-21458
Selective hydrogen separation by palladium-based composite membranes
[PB93-201671] 06 p2254 N94-23431
Fundamental and experimental studies on the catalytic combustion of methane
[PB94-112661] 06 p2233 N94-23736
Metal-catalyzed alkynylation of brominated polyphenylenes: Thermoset precursors of high density monolithic glassy carbon
[AD-A273232] 06 p2259 N94-24789
Hydrogen trapping with Pd coated alloy films 07 p2723 N94-25551
Geometric structures of thin film: Pt on Pd(110) and NiO on Ni(100)
[DE94-005564] 08 p3211 N94-28530
Chemisorbed-molecule potential-energy surfaces and electronically-stimulated processes
[DE94-007932] 09 p3719 N94-32603
Search for neutrons from deuterated palladium subject to high electrical currents
[DE94-009342] 10 p4139 N94-33907

PALLADIUM ALLOYS
A survey and analysis of experimental hydrogen sensors
[NASA-TM-106300] 02 p0648 N94-13135
Realistic theories of heavy electron and other strongly correlated materials
[DE93-010350] 04 p1571 N94-19204
Non-Fermi-liquid and multichannel Kondo phenomena in Y(1-x)U(x)Pd3 and related alloys
[DE93-040135] 05 p2015 N94-20275
Non-fermi liquid and spin-glass behavior of the Sc(1-x)U(x)Pd3 system
[DE93-040134] 05 p2016 N94-20335
Magnetic instability of Kondo insulators
[DE93-040064] 05 p1768 N94-21762
First principles calculations for analysis martensitic transformations
[DE94-000666] 05 p1695 N94-21964
Temperature dependence of magnetic order in single-crystalline UPdSn
[DE93-040153] 05 p2033 N94-21991
Interplay of magnetic and superconducting heavy fermion ground states
[DE94-000680] 06 p2240 N94-23003
Generic microelectronic smart sensor platform for detection of toxic, hazardous, and flammable gases
[DE93-017626] 06 p2343 N94-23200
Formation of three types of quasi-crystals in Al-Pd-Mg system
[REPT-A-2667] 07 p3053 N94-26071
Toward insulating quasicrystalline alloy in Al-Pd-Re icosahedral phase
[REPT-A-2666] 07 p2736 N94-26477
Thermogravimetric study of oxidation of a PdCr alloy used for high-temperature sensors
[NASA-TM-106473] 07 p2741 N94-27426
NMR study of quasicrystal Al(70)Pd(20)T(M10) alloy (T(M):Cr, Mn, Fe, and Co) 07 p2745 N94-28162
Formation of glassy Pd-Ni-P alloys by mechanical alloying and their structure and thermal stability 07 p2746 N94-28168

PALLADIUM COMPOUNDS
Muon spin relaxation studies of heavy fermion superconductors
[DE93-014576] 02 p0815 N94-14773
Structural stability of 1100 C heated Pd/k during absorption cycling in protium
[DE93-016270] 04 p1346 N94-18048

PAN (POLYACRYLONITRILE)
U POLYACRYLONITRILE

PANCREAS
Nuclear Medicine Program
[DE93-013896] 04 p1504 N94-17699

PANEL METHOD (FLUID DYNAMICS)
VSAERO analysis of a Piper Cub aircraft 02 p0516 N94-14616
Panel codes for aerodynamic analysis at NAL 02 p0510 N94-14617
Flow analysis for the nacelle of an advanced ducted propeller at high angle-of-attack and at cruise with boundary layer control
[NASA-TM-106371] 03 p0858 N94-16571
Computational aerodynamics with icing effects
[AD-A267509] 03 p0860 N94-17074
A computational and experimental investigation of incompressible oscillatory airfoil flow and flutter problems
[AD-A268748] 04 p1311 N94-18402
ADAS implementation of a panel method for the prediction of aerodynamic loads
[LR-723] 04 p1313 N94-19667
Users manual for the NASA Lewis three-dimensional ice accretion code (LEWICE 3D)
[NASA-TM-105974] 05 p1642 N94-21590
A numerical study of airplanes flying in proximity
[AD-A273373] 06 p2173 N94-24718
Computational investigation of the compressible dynamic stall characteristics of the Sikorsky SSC-A09 airfoil
[AD-A274867] 07 p2644 N94-26191
Calculation of unsteady incompressible inviscid flow about wings and bodies using CANAERO-T panel model 07 p2655 N94-28334
Aircraft aerodynamics with deflected jets in ground effect 08 p3132 N94-29973
Computation of wind tunnel wall effects for complex models using a low-order panel method
[NASA-TM-104019] 08 p3132 N94-30151
Aerodynamic analysis of slipstream/wing/nacelle interference for preliminary design of aircraft configurations
[AD-B173651] 08 p3135 N94-30916
Computation of unsteady flows over airfoils 10 p3986 N94-34977
Navier-Stokes and potential theory solutions for ahelicopter fuselage and comparison with experiment
[NASA-TM-4566] 12 p4383 N94-36966

PANELS
NT CURVED PANELS
NT RECTANGULAR PANELS
NT WING PANELS
Stress relaxation forming of Ariane 5 front skirt outer skin panels 01 p0062 N94-10046
The feasibility of producing aluminum-lithium structures for cryogenic tankage applications by laser beam welding
[NASA-CR-191527] 02 p0595 N94-14026
Packaging, deployment, and panel design concepts for a truss-stiffened 7-panel precision deployable reflector with feed boom
[NASA-TM-109000] 04 p1333 N94-17765
Out of plane gradients in laminated composites
[NASA-CR-194875] 06 p2228 N94-23566
Adaptive nonlinear polynomial neural networks for control of boundary layer/structural interaction
[NASA-CR-189645] 06 p2525 N94-23698
The Columbus solar array mechanisms 06 p2356 N94-23994
Post buckling behaviour of stiffened composite panels loaded in cyclic compression and shear 06 p2157 N94-24260
Nonlinear equations of motion for a panel subject to external loads
[AD-A273142] 06 p2170 N94-24773
Evaluation of the UH-1N instrument panel
[AD-A273145] 06 p2186 N94-24774
Experimental and numerical vibration analyses of a stiffened panel
[VTT-PUBS-129] 07 p2836 N94-25650
Formulae for the buckling of simply-supported corrugated panels of orthotropic material under shear load
[PB94-126547] 07 p2840 N94-26911
Design and test of postbuckled stiffened curved plates: A literature survey
[PB94-126521] 07 p2840 N94-26961
Development of Alternating Current Potential Drop (ACPD) procedures for crack detection in aluminum aircraft panels
[AD-A275755] 08 p3315 N94-28646
Composite panel failure analysis and improvement plan
[AD-A275655] 08 p3176 N94-28653
Test and analysis of a stitched RFI graphite-epoxy panel with a fuel access door
[NASA-TM-108992] 08 p3178 N94-29100
Deployable reflector structure
[NASA-CASE-LAR-14513-1-SB] 08 p3245 N94-29360
Free vibration of thermally loaded panels including initial imperfections and post-buckling effects
[NASA-TM-109097] 08 p3479 N94-29461
Preliminary evaluation of hybrid titanium composite laminates
[NASA-TM-109095] 08 p3180 N94-29472
Dual-Band Infrared (DBIR) imaging inspections of Boeing 737 and KC-135 aircraft panels
[DE94-005700] 08 p3122 N94-29842
Three-dimensional free vibration analysis of thick arbitrarily laminated, rectangular, cylindrical and spherical composite panels 08 p3184 N94-30257
AGARD membership, 1994
[AGARD-MEMB-94] 09 p3914 N94-31197
Damage tolerance aspects of a full composite airplane fuselage: Requirements, modelling, predictions, experiments
[LR-728] 09 p3578 N94-31674
From display and PWB to MCMs: Large panel manufacturing
[DE94-007855] 09 p3693 N94-32386
Local design optimization for composite transport fuselage crown panels 09 p3629 N94-33132

Composite fuselage crown panel manufacturing technology 09 p3629 N94-33133
Frequency domain analysis of the random loading of cracked panels
[NASA-CR-196021] 11 p4279 N94-35974
Fatigue and residual strength behaviour of ARALL3 panels with bonded-on doublers
[AD-B181062] 11 p4279 N94-36226

PANORAMIC CAMERAS
Rover imaging system for the Mars rover/sample return mission
[NASA-CR-193413] 02 p0649 N94-13464

PAPER (MATERIAL)
The chemical detector paper as a potential alarm
[FFI-93/6007] 07 p2712 N94-25745
Structural composite construction materials manufactured from municipal solid waste
[AD-A280635] 12 p4403 N94-36730

PAPERS
STELAR: An experiment in the electronic distribution of astronomical literature 05 p2049 N94-22544
Index of NPL acoustics publications 1981-1990
[NPL-RSA(EXT)-0044] 08 p3480 N94-30786

PARA HYDROGEN
Theoretical phase diagrams for solid H(sub 2)
[DE94-001049] 05 p1684 N94-22395

PARABOLIC ANTENNAS
Environmental projects. Volume 15: Environmental assessment: Proposed 1-megawatt radar transmitter at the Mars site
[NASA-CR-194098] 02 p0598 N94-13090
Structural design of hexa-link truss deployable antenna 02 p0529 N94-13269
Thermal distortion measurement of TETRUS type thermal test model of large deployable antenna for mobile communications satellite 02 p0529 N94-13270

PARABOLIC DIFFERENTIAL EQUATIONS
Summation by parts, projections, and stability
[NASA-CR-194290] 01 p0346 N94-12776
Open boundary conditions for incompletely parabolic systems
[FFI/RAPPORT-92/7029] 02 p0770 N94-13971
The method of Laplace Transform MultiQuadrics (LTMQ) for the solution of the groundwater flow equation
[DE93-010408] 02 p0637 N94-14053
Computation of nonequilibrium flows using PNS equations 02 p0641 N94-14610
Higher-order accurate Osher schemes with application to compressible boundary layer stability
[NASA-TM-106355] 03 p1026 N94-17056
Linear and nonlinear PSE for compressible boundary layers
[NASA-CR-191537] 05 p1797 N94-20033
Adaptive grids for quasilinear parabolic systems in one space dimension
[ETN-93-93611] 05 p1954 N94-21137
Interface reflection of spherical acoustic waves in the first- and second-order rational parabolic approximations and their artifacts
[PB93-215424] 05 p1969 N94-22261
The characterization of reaction-convection-diffusion processes by travelling waves
[PB94-150315] 06 p2273 N94-22729
A nonlinear degenerating parabolic problem from the theory of type 2 superconductors
[PB94-150299] 06 p2555 N94-22730
Balanced truncation is Hankel-norm optimal when used to approximate a finite-difference model of a parabolic PDE
[OUEL-1921/92] 06 p2492 N94-25324
Applications of the homogenization method to flow and transport in porous media
[BER-9110] 06 p2340 N94-25467
Arbitrary-order numerical schemes for model parabolic equations
[CRANFIELD-AERO-9210] 07 p3005 N94-25781
Computation of numerical solution of parabolic PDEs by monotone iterative methods
[ISBN-0-315-84553-8] 07 p2999 N94-27404
On the zeros of solutions of forced parabolic differential equations of neutral type
[DE93-613019] 07 p3001 N94-28228
Unstructured space-time finite element method of heat conduction 08 p3279 N94-30224
On some general properties of parabolic conservation equations
[DE94-006101] 08 p3461 N94-30758
Texture generation on irregular regions
[AD-A275999] 09 p3841 N94-31359
THERM3D: A boundary element computer program for transient heat conduction problems
[DE94-008112] 09 p3708 N94-32709
A comparison of rough surface parabolic equation models
[AD-A278090] 09 p3791 N94-33185
Parabolized stability equations 10 p4046 N94-33888

PARABOLIC FLIGHT
The formation and breakage of liquid bridges under microgravity 01 p0100 N94-10071
Microgravity Applications Furnace Facility (MAFF) for parabolic flights 01 p0109 N94-10128
The vibro-acoustic mapping of low gravity trajectories on a Learjet aircraft 03 p0978 N94-16078
Heart rate response to parabolic flight manoeuvres 03 p0981 N94-16098
The electrogastrogram during parabolic flight 07 p2913 N94-27452
Vertical gaze direction during parabolic flight 07 p2913 N94-27453
Heart rate change in normal and labyrinthectomized hamsters during parabolic flight 07 p2914 N94-27454
The MERSS 5th Symposium on Space Medicine: Medical and Physiological Experiment Utilizing Parabolic Flight
[JTN-94-80588] 08 p3392 N94-29709
Microgravity by parabolic flight with MU-300 aircraft 08 p3392 N94-29710
A discussion of eye-head coordinative movement under microgravity during parabolic flight 08 p3393 N94-29715
Determination of acceleration field parameters with linear accelerometers
[PB94-125606] 08 p3290 N94-30742

PARABOLIC REFLECTORS
NT PARABOLOID MIRRORS
High-flux testing of heat pipes for point-focus solar collector systems
[DE93-011581] 02 p0628 N94-12884
Environmental projects. Volume 15: Environmental assessment: Proposed 1-megawatt radar transmitter at the Mars site
[NASA-CR-194098] 02 p0598 N94-13090
Development of UHF spark-switched L-C Oscillators
[DE93-015019] 02 p0623 N94-13892
Packaging, deployment, and panel design concepts for a truss-stiffened 7-panel precision deployable reflector with feed boom
[NASA-TM-109000] 04 p1333 N94-17765
The CAESAR project: Experimental and modeling investigations of methane reforming in a catalytically enhanced solar absorption receiver on a parabolic dish
[DE93-040203] 04 p1469 N94-19109
Development steps on the basis of test with the LOCSTAR reflector deployment mechanism 06 p2356 N94-23998
Numerical and experimental analyses of the radiant heat flux produced by quartz heating systems
[NASA-TP-3387] 07 p3011 N94-27659
Development of a 2f optical performance measurement system
[DE94-003489] 07 p3039 N94-27721
Performance of the Southern California Edison Company Stirling dish
[DE94-004676] 08 p3337 N94-29018
Predicting antenna parameters from antenna physical dimensions
[AD-A276442] 09 p3672 N94-31300
Radar rainfall measurements from space 09 p3782 N94-31889
Detail design of a 10.4-m stretched-membrane dish
[DE94-009462] 10 p4079 N94-34167
A new, optical-lever based atomic force microscope
[AD-A280524] 12 p4524 N94-37110

PARABOLIC VELOCITY
U ESCAPE VELOCITY

PARABOLOID MIRRORS
Long range fast tool servo
[AD-A271614] 05 p1761 N94-21257
Holographic optical elements correcting the off-axis aberrations of a parabolic mirror
[ISBN-0-315-57581-6] 05 p1990 N94-22411

PARACHUTE DESCENT
1990 ASCAN ground egress/parasail
[NASA-TM-109528] 03 p1136 N94-15391
Galileo probe ready to go
[NASA-TM-109648] 03 p1247 N94-15432
Parachute Swivel Mechanism for planetary entry 08 p3162 N94-29643

PARACHUTES
NT PARAFOILS
NT RECOVERY PARACHUTES
Parachute having improved vent line stacking
[NASA-CASE-MFS-28508-1] 01 p0014 N94-11021
Parachute system design, analysis, and simulation tool
[DE93-013755] 02 p0501 N94-13260
Galileo probe ready to go
[NASA-TM-109648] 03 p1247 N94-15432
Adamson, Jim — ASCAN training programs
[NASA-TM-109507] 03 p1137 N94-15454
Radially constructed cruciform parachute
[CA-PATENT-1323021] 06 p2168 N94-24182
Parachute Swivel Mechanism for planetary entry 08 p3162 N94-29643
A novel CFD/structural analysis of a cross parachute
[DE94-005271] 09 p3568 N94-31578

PARACHUTING
U PARACHUTE DESCENT

PARADOXES
Study of Einstein-Podolsky-Rosen state for space-time variables in a two photon interference experiment 01 p0370 N94-10582
Observables, measurements and phase operators from a Bohmian perspective 01 p0378 N94-10589
Believing in the basis of the evidence
[TR-438] 05 p2039 N94-20364
On non-informativeness in a classical Bayesian inference problem
[MEMO-COSOR-92-35] 06 p2494 N94-23143

PARAFFINS
The addition of molecular oxygen to hydroperoxy-propyl radicals
[DE94-003662] 07 p2760 N94-27725

PARAFOILS
The development and flight test of a deployable precision landing system for spacecraft recovery
[NASA-TM-4525] 02 p0537 N94-14853
The development and flight test of a deployable precision landing system for spacecraft recovery
[NASA-TM-4525] 02 p0537 N94-14853
Wind tunnel testing and research
[NASA-CR-188273] 08 p3156 N94-29052
Wind tunnel testing and research
[NASA-CR-188273] 08 p3156 N94-29052

PARALLAX
NT STELLAR PARALLAX
In search of Nemesis 07 p2888 N94-28297
Gaze orientation under G(z)-load. Methodological aspects: Preliminary results 12 p4485 N94-37274

PARALLEL COMPUTERS
NT CONNECTION MACHINE
NT MASSIVELY PARALLEL PROCESSORS
NT MIMD (COMPUTERS)
NT SIMD (COMPUTERS)
Simulation of a parallel computer
[NAL-TR-1154] 01 p0335 N94-10368
Low latency messages on distributed memory multiprocessors
[NASA-CR-191479] 01 p0323 N94-10643
The PVM systems: An in-depth analysis and documenting study. Concise edition
[DE93-011959] 01 p0336 N94-11248
A heterogeneous graphics procedure for visualization of massively parallel solutions
[DE93-009628] 01 p0336 N94-11270
Optimal cube-connected cube multiprocessors
[NASA-CR-191463] 01 p0337 N94-11308
Turbulence modeling of free shear layers for high-performance aircraft
[NASA-CR-193659] 02 p0520 N94-12799
Beyond core: Making parallel computer I/O practical
[DE93-012347] 02 p0758 N94-12878
Surrogates for numerical simulations; optimization of eddy-promoter heat exchangers
[NASA-CR-191510] 02 p0629 N94-13074
Adaptive Transfer Function Networks
[DE93-014344] 02 p0745 N94-13151
Parametric binary dissection
[NASA-CR-191496] 02 p0762 N94-13184
The NAS parallel benchmarks
[NASA-TM-103863] 02 p0740 N94-13200
USRA/RIACS
[NASA-CR-194334] 02 p0750 N94-13932
A design methodology for portable software on parallel computers
[NASA-CR-194181] 02 p0752 N94-14139
Development of parallel processing at NAL: A retrospect 02 p0641 N94-14614
A task adaptive parallel graphics renderer
[DE93-017123] 03 p1149 N94-16119
Computation of the Fluid and Optical Fields About the Stratospheric Observatory for Infrared Astronomy (SOFIA) and the Coupling of Fluids, Dynamics, and Control Laws on Parallel Computers
[NASA-CR-193168] 03 p0858 N94-16510
Requirements for supercomputing in energy research: The transition to massively parallel computing
[DE93-012376] 03 p1160 N94-16774
Asynchronous design for parallel processing architectures
[AD-A266523] 03 p1160 N94-16791
Testing string superprimitivity in parallel
[AD-A267814] 03 p1155 N94-17399

Optical computing. Organization of the 1993 Photonics Science Topical Meetings. Technical digest series, volume 7
[AD-A269025] 04 p1578 N94-18332
Case studies of software development tools for parallel architectures
[AD-A269193] 04 p1535 N94-18866
Early experiences with the IBM SP-1
[DE93-018398] 04 p1535 N94-19010
MIMD massively parallel methods for engineering and science problems
[DE93-019409] 04 p1531 N94-19562
Embedded microclusters in zeolites and cluster beam sputtering: Simulation on parallel computers
[DE94-000741] 05 p1701 N94-20352
Measuring the effects of thread placement on the Kendall Square KSR1
[DE93-040655] 05 p1908 N94-20932
MGD1M: A parallel multigrid code with a fast vectorized ILU-relaxation
[CWI-NM-R9222] 05 p1930 N94-21077
Comparing quasi-Newton methods for solving sparse interface problems
[CWI-NM-R9303] 05 p1959 N94-21576
Parallelizing a highly vectorized multigrid code with zebra relaxation
[CWI-NM-R9225] 05 p1935 N94-21610
Numerical multigrid software (MGD5M): A parallel multigrid code with a twisted ILLU-relaxation
[CWI-NM-R9226] 05 p1916 N94-21611
Simulated behaviour of large scale SCI rings and tori
[DE93-040149] 05 p1935 N94-21745
Visualization on massively parallel computers using CM/AVS
[DE93-040151] 05 p1936 N94-21746
Physics Detector Simulation Facility (PDSF) architecture/utilization
[DE93-019744] 05 p1936 N94-21919
Scientific computing in the 1990ies: An astronomical perspective 05 p2057 N94-22440
Users manual for the Chameleon parallel programming tools
[DE94-001934] 06 p2465 N94-22973
Modeling parallelism and synchronization
[ETN-94-95179] 06 p2465 N94-23134
Linear time algorithm to schedule trees with communication delays optimally on two machines
[PB93-237782] 06 p2451 N94-23441
Applications of the Aurora parallel PROLOG system to computational molecular biology
[DE93-041166] 06 p2420 N94-23468
The instant sequencing task: Toward constraint-checking a complex spacecraft command sequence interactively 06 p2504 N94-23875
Discrete sensitivity derivatives of the Navier-Stokes equations with a parallel Krylov solver
[NASA-TM-106481] 06 p2265 N94-24301
High-performance computing and communications
[DE94-002215] 06 p2457 N94-24566
Transputer benchmarks and performance comparisons with other computing machines
[RR-467] 06 p2446 N94-25312
Abstraction in, specification and proof of software for a 1D heat-transfer problem
[REPT-93-45] 07 p2790 N94-25763
Using a transfer function to describe the load-balancing problem
[DE94-004218] 07 p2979 N94-25802
A doubly logarithmic communication algorithm for the Completely Connected Optical Communication Parallel Computer
[DE93-019408] 07 p2980 N94-26473
Computational mechanics
[DE94-003015] 07 p2965 N94-26775
Parallel computers for advanced information processing 07 p2955 N94-27193
The High Performance Storage System
[DE94-004350] 08 p3404 N94-28505
Rome Laboratory software engineering technology program 08 p3414 N94-29330
Dependability analysis of parallel systems using a simulation-based approach
[NASA-CR-195762] 08 p3431 N94-29846
PCCM2: A GCM adapted for scalable parallel computers
[DE94-005113] 08 p3350 N94-30116
Early experiences with the IBM SP1 and the high-performance switch
[DE94-006261] 08 p3429 N94-30840
Implanting algorithms on parallel machines
[TELECOM-93-D-017] 09 p3823 N94-31099
Analysis of the effect of routing strategies for parallel implementations of a selected avionics application
[AD-A276069] 09 p3581 N94-31458
Computational chemistry on parallel computers
[DE94-008106] 09 p3636 N94-32616
Toroidal computer memory for serial and parallel processors
[AD-D016144] 09 p3807 N94-32978
Principles of ultradependability in chaotic routing
[AD-A277422] 09 p3827 N94-32995
Investigation of modularly configured attached processors with intelligent memories
[AD-A278418] 09 p3839 N94-33330
Parallel programming methodologies for non-uniform structured problems in materials science
[AD-A277868] 10 p4111 N94-33777
A parallel data management system for large-scale NASA datasets 10 p4157 N94-33828
Advanced information processing system: The Army Fault-Tolerant Architecture detailed design overview
[NASA-CR-194924] 12 p4497 N94-36962
Parallelized direct execution simulation of message-passing parallel programs
[NASA-CR-194936] 12 p4497 N94-37411
Three-dimensional gyrokinetic particle-in-cell simulation of plasmas on a massively parallel computer: LDRD Core Competency Project
[DE94-013367] 12 p4532 N94-37732

PARALLEL FLOW

NT PIPE FLOW
NT THREE DIMENSIONAL FLOW
Vibrational-thermocapillary parallel flows and stability 01 p0120 N94-10220
Receptivity in parallel flows: An adjoint approach 01 p0157 N94-12301
Heat load analysis on the cable-in-conduit with central core conductor for the TF coil Rebut layer design
[DE93-013783] 04 p1395 N94-17872
Refraction of high frequency noise in an arbitrary jet flow
[NASA-TM-106465] 06 p2525 N94-23464
On wave interactions of rotational and irrotational flows 09 p3700 N94-31219
Neoclassical current and related MHD stability, gap modes, and radial electric field effects in heliotron and torsatron plasmas
[DE94-718987] 11 p4337 N94-35938
The alternative faces of turbulent flow
[TM-5-94] 12 p4442 N94-36934
Momentum-energy transport from turbulence driven by parallel flow shear
[DE94-012765] 12 p4443 N94-37362

PARALLEL PLATES

Stability of liquid bridges between parallel plates 01 p0101 N94-10078
Stability of oscillatory two phase Couette flow
[NASA-CR-191501] 02 p0636 N94-13817
High counting rate resistive-plate chamber
[DE93-014928] 02 p0651 N94-14452
Investigation of radiative interaction in laminar flows using Monte Carlo simulation
[NASA-CR-194604] 03 p1021 N94-15795
On the stability of a time dependent boundary layer
[NASA-CR-191542] 03 p1030 N94-17450
Anomalous dielectric properties of carbon-black filled elastomers
[AD-A269378] 04 p1370 N94-18280
Method for controlling protein crystallization
[NASA-CASE-MFS-28688-1] 05 p2017 N94-20528
A study of non-ideal focus properties of 30 deg parallel plate energy analyzers
[NIFS-263] 06 p2311 N94-24457

PARALLEL PROCESSING (COMPUTERS)

Massively parallel multifrontal methods for finite element analysis on MIMD computer systems
[DE93-009838] 01 p0335 N94-10257
Layering techniques for development of parallel systems: An algebraic approach
[MEMO-INF-92-62] 01 p0335 N94-10277
A parallel implementation of particle tracking with space charge effects on an Intel iPSC/860
[DE93-012307] 01 p0335 N94-10340
CFD analysis of hypersonic, chemically reacting flow fields 01 p0002 N94-10422
Application of parallel processing to a surface patch/wire junction EFIE code
[AD-A264965] 01 p0336 N94-10488
Optimization algorithms for integer networks with side constraints for application in routing and scheduling
[AD-A265254] 01 p0322 N94-10492
Bringing theory to practice: The reality of interprocessor communication
[DE93-012346] 01 p0336 N94-10738
Efficient partitioning and assignment on programs for multiprocessor execution
[NASA-CR-193458] 01 p0324 N94-10942
The Zipcode message-passing system
[DE93-011958] 01 p0336 N94-11027
Basic experiment on an ultrasonic method of localization
[DE93-754295] 01 p0358 N94-11042
Advanced rotorcraft flight simulation: Model development, validation and parallel implementation 01 p0025 N94-11056
Summary of research in progress at ICASE
[NASA-CR-191481] 01 p0318 N94-11198
A distributed version of the NASA Engine Performance Program
[NASA-TM-106208] 01 p0327 N94-11231
Portable programming on parallel/networked computers using the Application Portable Parallel Library (APPL)
[NASA-TM-106238] 01 p0327 N94-11232
The PVM systems: An in-depth analysis and documenting study. Concise edition
[DE93-011959] 01 p0336 N94-11248
A heterogeneous graphics procedure for visualization of massively parallel solutions
[DE93-009628] 01 p0336 N94-11270
Heterogeneous SuperConcurrent Parallelism (HeSCP)
[AD-A265004] 01 p0336 N94-11293
Optimal cube-connected cube multiprocessors
[NASA-CR-191463] 01 p0337 N94-11308
Parallel molecular dynamics with the embedded atom method
[DE93-010683] 01 p0367 N94-11455
Massively parallel hydrodynamics on unstructured grids
[DE93-007325] 01 p0153 N94-11601
High-performance distributed systems architecture
[AD-A265297] 01 p0337 N94-11829
Problem specific environments for parallel systems
[AD-A266129] 01 p0337 N94-12540
Networks of real-time processes
[DE93-013049] 01 p0338 N94-12597
The DOE Program in High-Performance Computing and Communications (HPCC)
[DE93-013813] 01 p0334 N94-12606
Beyond core: Making parallel computer I/O practical
[DE93-012347] 02 p0758 N94-12878
The 3-D massively parallel impact simulations using PCTH
[DE93-011593] 02 p0670 N94-12908
A network evaluation and analysis tool
[DE93-012647] 02 p0758 N94-12917
Parallelizing Timed Petri Net simulations
[NASA-CR-194278] 02 p0758 N94-12938
Parallel implementation of an algorithm for Delaunay triangulation
[NASA-TM-103951] 02 p0740 N94-12973
An experimental regional scale climate simulation laboratory
[DE93-015935] 02 p0719 N94-13119
Parametric binary dissection
[NASA-CR-191496] 02 p0762 N94-13184
Implementation of ADI: Schemes on MIMD parallel computers
[NASA-CR-193720] 02 p0759 N94-13204
Advanced computers and simulation
[DE93-014354] 02 p0740 N94-13286
A data distributed parallel algorithm for ray-traced volume rendering
[NASA-CR-191520] 02 p0749 N94-13721
Tomographic methods in flow diagnostics
[NASA-TM-106330] 02 p0650 N94-13876
Efficient, massively parallel eigenvalue computation
[NASA-CR-194289] 02 p0760 N94-13921
USRA/RIACS
[NASA-CR-194334] 02 p0750 N94-13932
Three, four, five, six or the complexity of scheduling with communication delays
[CWI-BS-R9229] 02 p0751 N94-14004
VFGEN: A parallel volume fraction generator for hydrocodes
[DE93-011673] 02 p0752 N94-14019
Quantum Monte Carlo by message passing
[DE93-012645] 02 p0760 N94-14177
Hybrid S(sub N)/Monte Carlo research and results
[DE93-012677] 02 p0773 N94-14178
An efficient parallel algorithm for matrix-vector multiplication
[DE93-015125] 02 p0754 N94-14399
An overview of parallel scientific visualization
[DE93-017105] 02 p0755 N94-14521
Paradigms for very fast parallel algorithms
[ITN-93-85212] 02 p0755 N94-14556
Development of parallel processing at NAL: A retrospect 02 p0641 N94-14614
Parallel O(log n) algorithms for open- and closed-chain rigid multibody systems based on a new mass matrix factorization technique 02 p0679 N94-14636
On the solution of a class of graph problems by parallel algorithms
[LAAS-92514] 02 p0756 N94-14712
Identification of continuous-time dynamical systems: Neural network based algorithms and parallel implementation
[DE93-014427] 02 p0766 N94-14737

The development of a scalable parallel 3-D CFD algorithm for turbomachinery
[NASA-CR-193604] 02 p0664 N94-14848
Engineering Physics and Mathematics Division progress report, period ending 31 December 1992
[DE93-015118] 03 p1301 N94-14926
Particle simulations on massively parallel machines
[DE93-015644] 03 p1157 N94-14927
The alignment-distribution graph
[NASA-CR-194292] 03 p1168 N94-15112
Mobile and replicated alignment of arrays in data-parallel programs
[NASA-CR-194294] 03 p1158 N94-15113
The application of compiler-assisted multiple instruction retry to VLIW architectures
[AD-A266930] 03 p1158 N94-15173
Parallel spatial direct numerical simulations on the Intel iPSC/860 hypercube
[NASA-CR-191513] 03 p1144 N94-15483
Multiphase complete exchange: A theoretical analysis
[NASA-CR-191531] 03 p1145 N94-15489
Overview of Enhanced Data Stream Array Processor (EDSAP)
[AD-A266986] 03 p1158 N94-15492
Massively parallel, adaptive, color image processing for autonomous road following
[AD-A266988] 03 p0864 N94-15498
Decomposition of large sparse symmetric systems for parallel computation. Part 2: Parallelization tool roadmap
[AD-A267072] 03 p1158 N94-15671
A parallel adaptive mesh refinement algorithm
[NASA-CR-191530] 03 p1168 N94-15724
Decomposition of large sparse symmetric systems for parallel computation. Part 1: Theoretical foundations
[AD-A267144] 03 p1159 N94-15750
Particle simulation of hypersonic flow
[AD-A267185] 03 p0857 N94-15787
Generating local addresses and communication sets for data-parallel programs
[NASA-CR-194605] 03 p1159 N94-15796
Parallel processing and scientific applications
[AD-A267179] 03 p1159 N94-15849
Distributed computing feasibility in a non-dedicated homogeneous distributed system
[NASA-CR-191532] 03 p1149 N94-15989
Information Technology Resources Assessment
[DE93-013899] 03 p1230 N94-16010
A task adaptive parallel graphics renderer
[DE93-017123] 03 p1149 N94-16119
The 3D-Flow processor for a programmable level-1 trigger (feasibility study)
[DE93-016045] 03 p1159 N94-16172
A decision criteria to select an associative-memory organization that minimizes the execution time of a mix of associative-search operations
[AD-A266438] 03 p1149 N94-16560
Requirements for supercomputing in energy research: The transition to massively parallel computing
[DE93-012376] 03 p1160 N94-16774
Asynchronous design for parallel processing architectures
[AD-A266523] 03 p1160 N94-16791
Information technology division technical paper abstracts
[AD-A266227] 03 p1166 N94-16938
Optical computing
[AD-A267881] 03 p1141 N94-17015
Efficient scheduling of real-time compute-intensive periodic graphs on large grain data flow multiprocessor
[AD-A267444] 03 p1141 N94-17030
Networked workstations and parallel processing utilizing functional languages
[AD-A267464] 03 p1160 N94-17034
Intel NX to PVM 3.2 message passing conversion library
[NASA-TM-109038] 03 p1152 N94-17060
Visual parallel programming with determinacy: A language specification, an analysis technique, and a programming tool
[AD-A267560] 03 p1153 N94-17107
Development of iterative techniques for the solution of unsteady compressible viscous flows
[NASA-CR-194657] 03 p1027 N94-17129
ONRASIA scientific information bulletin, volume 18, number 2
[AD-A267798] 03 p1304 N94-17305
Estimating task execution delay in a real-time system via static source code analysis
[AD-A267496] 03 p1161 N94-17367
Accurate analysis of array references
[AD-A268069] 03 p1162 N94-17550
System performance modeling and analysis of a fault-tolerant, real time parallel processor
[AD-A268070] 03 p1162 N94-17551
Benchmarking massively parallel architectures
[DE93-016486] 03 p1162 N94-17646
Parallel inverse iteration with reorthogonalization
[DE93-012867] 04 p1533 N94-17693
An efficient implementation of error-valued semantics on imperative machines
[DE93-014658] 04 p1516 N94-17740
PARX, kernel of a system for massively parallel computers: Control of communication between processes
[ETN-93-94353] 04 p1533 N94-17976
PARX: Architecture of an operating system for parallel machines
[ETN-93-94401] 04 p1533 N94-18068
High performance Fortran: An overview
[DE93-017181] 04 p1519 N94-18072
An evolving infrastructure for scientific computing and the integration of new graphics technology
[DE93-017164] 04 p1520 N94-18133
Parallel optimization algorithms and their implementation in VLSI design 04 p1401 N94-18374
A fast adaptive convex hull algorithm on two-dimensional processor arrays with a reconfigurable BUS system 04 p1402 N94-18380
Parallelization of the Air Force Space Command (AFSPACECOM) satellite motion models
[AD-A269327] 04 p1334 N94-18470
The evolution of the PVM concurrent computing system
[DE93-017764] 04 p1534 N94-18482
Development of parallel architectures for sensor array processing. Volume 2: A parallel architecture for broad-band direction-of-arrival estimation
[AD-A270427] 04 p1534 N94-18508
Distributed memory parallel computers and computational fluid dynamics 04 p1413 N94-18568
Parallel and vector adaptations of the underwater finite element parabolic equation model
[AD-A269990] 04 p1563 N94-18678
Connection machine software conversion of a Navy oceans model
[AD-A269876] 04 p1535 N94-18772
Neutral networks: An NRL perspective
[AD-A269122] 04 p1541 N94-18773
Software engineering for effective utilization of parallel processing computing system
[AD-A269191] 04 p1535 N94-18865
Case studies of software development tools for parallel architectures
[AD-A269193] 04 p1535 N94-18866
A parallel and pipelined architecture for estimation of direction of arrival using a bilinear transformation method, volume 3
[AD-A270137] 04 p1389 N94-18897
Early experiences with the IBM SP-1
[DE93-018398] 04 p1535 N94-19010
Implementation of the turn function method in KIVA-F90
[DE93-018394] 04 p1419 N94-19027
The p4 Linda: A portable implementation of Linda
[DE93-017752] 04 p1535 N94-19046
Performance and scalability aspects of directory-based cache coherence in shared-memory multiprocessors
[DE93-016442] 04 p1536 N94-19115
A massively parallel adaptive finite element method with dynamic load balancing
[DE93-012844] 04 p1536 N94-19161
A multi-thread approach to coalescing small transfers generated by portable tool sets
[DE93-012128] 04 p1525 N94-19186
Experience in implementing a parallel file system
[DE93-012840] 04 p1536 N94-19188
ACOS: A performance based approach to build a parallel complex object server
[MEMO-INF-93-11] 04 p1537 N94-19198
A parallel hashed oct-tree N-body algorithm
[DE93-012654] 04 p1526 N94-19205
Message passing in PUMA
[DE93-012841] 04 p1537 N94-19206
Action systems and action refinement in the development of parallel systems: An algebraic approach
[MEMO-INF-93-14] 04 p1538 N94-19296
PUMMA: Parallel Universal Matrix Multiplication Algorithms on distributed memory concurrent computers
[DE93-019163] 04 p1538 N94-19299
Process allocation on distributed memory parallel architectures
[ETN-93-95004] 04 p1538 N94-19514
MIMD massively parallel methods for engineering and science problems
[DE93-019409] 04 p1531 N94-19562
CVL: A C vector library manual. Version 2
[AD-A270614] 04 p1531 N94-19592
Simulation of dynamic material response with the PAGOSA code
[DE93-018285] 04 p1460 N94-19603
Systolic design with asynchronous controls for digital-signal processing
[AD-A270976] 04 p1392 N94-19680
Implementation of parallel algorithms
[AD-A271035] 04 p1539 N94-19682
NPAC distributed-parallel system feasibility study
[AD-A270972] 04 p1539 N94-19790
A parallelizing compiler based on partial evaluation
[AD-A270838] 05 p1898 N94-19832
Exploiting the parallelism exposed by partial evaluation
[AD-A270678] 05 p1928 N94-19877
A comparison of data-parallel algorithms for connected components
[AD-A270551] 05 p1902 N94-19918
Implementation of a portable nested data-parallel language
[AD-A270524] 05 p1902 N94-19932
Two-dimensional particle-in-cell simulation on transputer arrays
[DE93-017977] 05 p1972 N94-20181
High resolution signal processing
[AD-A271181] 05 p1717 N94-20215
Scientific development of a massively parallel ocean climate model
[DE93-019446] 05 p1855 N94-20219
Parallel band reduction and tridiagonalization
[DE93-019566] 05 p1951 N94-20221
Fast data parallel polygon rendering
[DE93-040157] 05 p1929 N94-20279
Embedded microclusters in zeolites and cluster beam sputtering: Simulation on parallel computers
[DE94-000741] 05 p1701 N94-20352
Massively parallel computation of RCS with finite elements 05 p1726 N94-20437
Time warp operating system version 2.7 internals manual
[NASA-CR-194798] 05 p1899 N94-20549
Design structuring and allocation optimization (Destination) prototype level 1 user's manual
[AD-A272115] 05 p1929 N94-20571
Algorithm/architecture study for artificial neural nets
[AD-A271820] 05 p1943 N94-20626
Analysis and evaluation of configuring of graphical systems on multiprocessor architectures
[ETN-93-93618] 05 p1930 N94-21018
A novel VLSI processor architecture for supercomputing arrays 05 p1758 N94-21115
Scheduling for locality in shared-memory multiprocessors
[AD-A272948] 05 p1930 N94-21228
Optimal repairman assignment in two maintenance models which are equivalent to routing models with early decisions
[CWI-BS-R9301] 05 p1930 N94-21234
The Mercury user's manual
[TR-465] 05 p1913 N94-21316
Analysis of multigrid methods on massively parallel computers: Architectural implications 05 p1938 N94-21468
Mapping robust parallel multigrid algorithms to scalable memory architectures 05 p1922 N94-21483
MINIFOLD: A kernel for a MANIFOLD-like coordination language
[CWI-CS-R9252] 05 p1915 N94-21534
A data distributed, parallel algorithm for ray-traced volume rendering
[DE93-040150] 05 p1935 N94-21622
Simulated behaviour of large scale SCI rings and tori
[DE93-040149] 05 p1935 N94-21745
Visualization on massively parallel computers using CM/AVS
[DE93-040151] 05 p1936 N94-21746
The transition to massively parallel computing within a production environment at a DOE access center
[DE93-019155] 05 p1936 N94-21828
Evaluation of DEC's GIGAswitch for distributed parallel computing
[DE94-001356] 05 p1936 N94-21853
Physics Detector Simulation Facility (PDSF) architecture/utilization
[DE93-019744] 05 p1936 N94-21919
The design of linear algebra libraries for high performance computers
[DE93-040458] 05 p1960 N94-21967
Impact of partitioning on parallel discrete event simulation of logic circuits 05 p1772 N94-22115
VLSI design of a bit serial parallel processing 4 extender chip for M-path convolutional decoding 05 p1775 N94-22132
VLSI design of a parallel video output interface 05 p1778 N94-22153
The Schur Berlekamp-Massey algorithm is parallelizable 05 p1784 N94-22191
Integration of parallel processing structures using a matrix approach 05 p1784 N94-22192

Acceleration of backpropagation learning using a parallel DSP machine 05 p1786 N94-22206
Image convolution using the Myrias SPS-2 parallel computer 05 p1786 N94-22207
Parallelizing a maximum entropy image deconvolution algorithm 05 p1787 N94-22208
Distributed input/output processing in data-driven multiprocessors
[DE94-000323] 05 p1937 N94-22378
Simulating the Euclidean time Schroedinger equations using an INTEL iPSC/860 hypercube: Application to the t-J model of high-T(sub c) superconductivity
[DE94-000489] 05 p2035 N94-22385
Scientific computing in the 1990ies: An astronomical perspective 05 p2057 N94-22440
Seeing the forest for the trees: Networked workstations as a parallel processing computer 05 p1938 N94-22454
Contribution to geometric and dynamic modeling of parallel robots
[LAAS-93089] 06 p2470 N94-22904
Users manual for the Chameleon parallel programming tools
[DE94-001934] 06 p2465 N94-22973
Implementation and parallelization of fast matrix multiplication for a fast Legendre transform
[DE94-002184] 06 p2478 N94-22975
ACOS: The performance based approach to build a parallel complex object server
[PB93-223816] 06 p2465 N94-22986
Asynchronous rendezvous in distributed logic programming
[PB93-220614] 06 p2448 N94-23096
Incomplete corrections in nonlinear problems
[PB93-225746] 06 p2479 N94-23106
Programming in Fortran M
[DE94-000541] 06 p2450 N94-23207
Automated parallelization of timed Petri-net simulations
[NASA-CR-191574] 06 p2451 N94-23341
Linear time algorithm to schedule trees with communication delays optimally on two machines
[PB93-237782] 06 p2451 N94-23441
A lower bound for routing on a completely connected optical communication parallel computer
[DE93-040752] 06 p2466 N94-23491
Extending substructure based iterative solvers to multiple load and repeated analyses
[NASA-CR-194822] 06 p2466 N94-23504
Experience with parametric binary dissection
[NASA-CR-191552] 06 p2473 N94-23558
Real-time dynamics and control strategies for space operations of flexible structures
[NASA-CR-194794] 06 p2203 N94-23618
Vectorization and parallelization of the finite strip method for dynamic Mindlin plate problems 06 p2483 N94-23679
An object-oriented approach for parallel self adaptive mesh refinement on block structured grids 06 p2469 N94-23697
Multi-set extended relational algebra: A formal approach to a practical issue
[PB94-110830] 06 p2486 N94-23725
Advanced design concepts for open distributed systems development
[PB94-110897] 06 p2454 N94-23751
Preemptive scheduling in a two-stage multiprocessor flow shop is Np-hard
[PB94-111648] 06 p2467 N94-23756
Three, four, five, six or the complexity of scheduling with communication delays
[PB94-111630] 06 p2467 N94-23767
High performance, low cost, self-contained, multipurpose PC based ground systems 06 p2516 N94-23943
Decentralized autonomous attitude determination using an inertially stabilized payload 06 p2157 N94-24264
The design of a standard message passing interface for distributed memory concurrent computers
[DE94-002536] 06 p2446 N94-24538
High-performance computing and communications
[DE94-002215] 06 p2457 N94-24566
A programming environment for distributed complex computing. An overview of the Framework for Interdisciplinary Design Optimization (FIDO) project. NASA Langley TOPS exhibit H120b
[NASA-TM-109058] 06 p2457 N94-24603
Runtime support and compilation methods for user-specified data distributions
[AD-A276326] 06 p2458 N94-24679
Optimizing parallelization
[AD-A273565] 06 p2467 N94-24692
Sensitivity analysis of list scheduling heuristics
[PB93-237766] 06 p2468 N94-24764
RIACS/USRA
[NASA-CR-195117] 06 p2631 N94-25003
A parallel algorithm for filtering gravitational waves from coalescing binaries
[DE93-616845] 06 p2604 N94-25212
Multiprocessor scheduling with communication delays
[ETN-94-95346] 06 p2468 N94-25221
Designing parallel programs of parameterized granularity
[ETN-94-95302] 06 p2468 N94-25278
A design method for parallel programs
[ETN-94-95331] 06 p2469 N94-25282
Parallel processing methods for space based power systems 06 p2222 N94-25352
The transputer
[AD-A273688] 06 p2446 N94-25438
Expert system rule-base evaluation using real-time parallel processing
[AD-A273701] 06 p2469 N94-25454
System software and tools for high performance computing environments: A report on the findings of the Pasadena Workshop
[DE94-003918] 07 p2956 N94-25602
Using a transfer function to describe the load-balancing problem
[DE94-004218] 07 p2979 N94-25802
A numerical study of high-speed missile configurations using a block-structured parallel algorithm
[AD-A273776] 07 p2979 N94-25860
Object-oriented design and implementation of a parallel Ada simulation system
[AD-A274119] 07 p2979 N94-25906
Use of parallel counters for triggering
[DE93-616656] 07 p2979 N94-25918
Out of core, out of mind: Practical parallel I/O
[DE94-003107] 07 p2979 N94-25952
Achieving high performance on the Intel Paragon
[DE94-003108] 07 p2979 N94-25953
Real-time tracking with a 3D-flow processor array
[DE94-003981] 07 p2980 N94-25984
Fast parallel algorithms for short-range molecular dynamics
[DE93-018519] 07 p3016 N94-26033
Run-time recognition of task parallelism within the P++ parallel array class library
[DE94-002707] 07 p2980 N94-26120
The Chaco user's guide
[DE94-003669] 07 p2962 N94-26370
Parallel grid generation algorithm for distributed memory computers
[NASA-TP-3429] 07 p2963 N94-26466
The High Performance Storage System
[DE94-004351] 07 p2948 N94-26578
Parallel computational geometry on analog Hopfield networks
[ISBN-0-315-84093-5] 07 p2980 N94-26635
Parallel matrix transpose algorithms on distributed memory concurrent computers
[DE94-002424] 07 p2964 N94-26764
Computational mechanics
[DE94-003015] 07 p2965 N94-26775
A Multitransputer Parallel Processing System (MTPPS)
[DE94-604652] 07 p2981 N94-26903
An optoelectronic graphics display processor
[AD-A274401] 07 p3037 N94-26990
Parallel mathematical software
[DE94-001587] 07 p2967 N94-27020
Interactive control of a parallel simulation from a remote graphics workstation
[AD-A274217] 07 p2981 N94-27070
Implementation and performance of a domain decomposition algorithm in Sisal
[DE94-002012] 07 p2981 N94-27092
Static task allocation for parallel processing systems during software development
[AD-A274204] 07 p2981 N94-27100
Automatic mapping of task and data parallel programs for efficient execution on multicomputers
[AD-A274125] 07 p2982 N94-27117
A parallel computational fluid dynamics unstructured grid generator
[AD-A274129] 07 p2795 N94-27119
Design of a parallel discrete event simulation coprocessor
[AD-A274135] 07 p2982 N94-27123
Virtual memory management and virtual bus overloading on multiple channel architectures
[AD-A274127] 07 p2954 N94-27152
Parallel string matching algorithms
[AD-A274502] 07 p3100 N94-27164
Proceedings of the Third Workshop Computersystems: Research Forum on Design, Realization and Use of Computersystems
[ISBN-90-6144-995-2] 07 p2954 N94-27191
Parallel computers for advanced information processing 07 p2955 N94-27193
Parallel discrete event simulation 07 p2955 N94-27194
Sculpting in cyberspace: Parallel processing the development of new software 07 p2686 N94-27365
Shared virtual memory and generalized speedup
[AD-A277573] 07 p2969 N94-27416
Parallel implicit unstructured grid Euler solvers
[AD-A277581] 07 p2999 N94-27434
Efficient massively parallel simulation of dynamic channel assignment schemes for wireless cellular communications
[AD-A277558] 07 p2971 N94-27558
Iterative methods for the WLS state estimation on RISC, vector, and parallel computers
[DE94-004260] 07 p3000 N94-27569
Center for space microelectronics technology
[NASA-CR-195282] 07 p2786 N94-27574
High performance computing in chemistry and massively parallel computers: A simple transition?
[DE94-004318] 07 p2982 N94-27600
MIMD parallel approaches to object labeling
[ISBN-0-315-60198-1] 07 p2982 N94-27644
A fast Fourier transform radix-2 complex butterfly with built-in self-test
[ISBN-0-315-84139-7] 07 p2982 N94-27649
Parallel computing for probabilistic response analysis of high temperature composites
[NASA-CR-194467] 07 p2843 N94-27656
Communication on the Paragon
[DE94-003103] 07 p2983 N94-27713
The PRISM project: Infrastructure and algorithms for parallel eigensolvers
[DE94-005125] 07 p2973 N94-27717
Review and analysis of dense linear system solver package for distributed memory machines 07 p2978 N94-27916
The High Performance Storage System
[DE94-004350] 08 p3404 N94-28505
Performance analysis of memory hierachies in high performance systems
[DE94-005549] 08 p3404 N94-28517
Design of parallel systems for signal processing
[AD-A275490] 08 p3430 N94-28659
Aerodynamic design using parallel processors
[AD-A275470] 08 p3122 N94-28674
Parallelization techniques for highly parallel vector computer 08 p3129 N94-28990
Parallel Fortran programming for NWT 08 p3129 N94-28991
Performance evaluation of the NWT with parallel Fortran 08 p3129 N94-28992
A method of user interface for NWT 08 p3129 N94-28993
A porting methodology for parallel database systems
[AD-A275256] 08 p3529 N94-29053
Center for Parallel Optimization
[AD-A274988] 08 p3431 N94-29127
Rome Laboratory software engineering technology program 08 p3414 N94-29330
Distributed applications and failure tolerance programs using a reconfigurable parallel architecture 08 p3417 N94-29345
ECSU home-institution support program (1993)
[AD-A275244] 08 p3431 N94-29396
Stereo imaging based particle velocimeter
[NASA-CR-195800] 08 p3289 N94-29742
Checkpoint-based forward recovery using lookahead execution and rollback validation in parallel and distributed systems
[NASA-CR-195760] 08 p3431 N94-29869
First principles pseudopotential calculations on aluminum and aluminum alloys
[DE94-004890] 08 p3206 N94-29931
Progress report for the PTUF Project-93 Q1 and Q2
[PB94-138591] 08 p3431 N94-29995
Computational fluid and combustion dynamics
[DE94-006596] 08 p3279 N94-30003
Computational balance in real-time cyclic spectral analysis
[DE94-005091] 08 p3432 N94-30100
PCCM2: A GCM adapted for scalable parallel computers
[DE94-005113] 08 p3350 N94-30116
A locally synchronous globally asynchronous Vertex-8 processing element for image reconstruction on a mesh
[ISBN-0-315-86005-7] 08 p3432 N94-30143
Common spaceborne multicomputer operating system and development environment
[NASA-TM-109092] 08 p3422 N94-30197
Large-scale 3-D solutions of the time-dependent Dirac equation
[DE94-005591] 08 p3454 N94-30317
Manray: A replicated workers program in MANIFOLD
[CWI-CS-R9337] 08 p3433 N94-30429
Parallel iteration across the steps of high order Runge-Kutta methods for nonstiff initial value problems
[CWI-NM-R9313] 08 p3433 N94-30730

Parallel language constructs for paradigm integration and deterministic computations
[DE94-005119] 08 p3428 N94-30754
Early experiences with the IBM SP1 and the high-performance switch
[DE94-006261] 08 p3429 N94-30840
Computing at the leading edge: Research in the energy sciences
[DE94-006121] 08 p3563 N94-30844
Implanting algorithms on parallel machines
[TELECOM-93-D-017] 09 p3823 N94-31099
A heterogeneous computing environment for simulating astrophysical fluid flows 09 p3928 N94-31119
A probabilistic view of Datalog parallelization
[TELECOM-93-D-021] 09 p3824 N94-31183
Design and analysis of scalable parallel algorithms
[AD-A276255] 09 p3809 N94-31251
List ranking and list scan on the CRAY C-90
[AD-A276411] 09 p3824 N94-31259
Proof of concept for the rewrite rule machine: Interensemble studies
[AD-A276506] 09 p3809 N94-31263
Air Force Space Command satellite orbit predictor using parallel virtual machines
[AD-A276316] 09 p3601 N94-31298
A parallel implementation of the column subtraction algorithm
[AD-A275922] 09 p3810 N94-31343
Using Monte Carlo techniques and parallel processing for debris hazard analysis of rocket systems
[DE94-007250] 09 p3609 N94-31382
Parallel structured optimization algorithms for inverse problems
[AD-A276053] 09 p3811 N94-31443
Analysis of the effect of routing strategies for parallel implementations of a selected avionics application
[AD-A276069] 09 p3581 N94-31458
Some calculations on supersymmetric graphs as communication networks
[REPT-93-72] 09 p3824 N94-31641
A comparison of distributed memory and virtual shared memory parallel programming models
[DE94-005473] 09 p3825 N94-31663
Generalized steady-state method for solving 2-D diffusion systems
[REPT-93-83] 09 p3825 N94-31700
Methods of implementing the Viterbi algorithm on a massively parallel computer of the SIMD (single instruction multiple data) type
[ISBN-0-315-86783-3] 09 p3814 N94-31752
Algorithms and parallel architectures for laser acoustic imaging
[ISBN-0-315-86456-4] 09 p3716 N94-31797
Large-scale shape optimization: Numerical methods, parallel algorithms, and applications to aerodynamic design 09 p3815 N94-31966
The named-state register file
[AD-A276796] 09 p3825 N94-32165
MULTIGRAPH: An architecture for model-based programming. Model-based program synthesis for parallel computing. PREMOS: Programming environment for model-based program synthesis, version 01.00.00
[AD-A276949] 09 p3817 N94-32219
Parallel and distributed computing combinatorial algorithms
[AD-A277333] 09 p3826 N94-32243
Parallel processing for differencing and histogramming
[AD-A277060] 09 p3826 N94-32274
An epistemic proof system for parallel processes
[TR-93-17] 09 p3826 N94-32291
Parallel Monte Carlo reactor neutronics
[DE94-007642] 09 p3826 N94-32357
Parallel particle simulations of low-density fluid flows
[DE94-007858] 09 p3707 N94-32373
Studies of an optical multi-processor interconnect
[AD-A277093] 09 p3881 N94-32392
A high-speed linear algebra library with automatic parallelism 09 p3828 N94-32440
Construction of a parallel processor for simulating manipulators and other mechanical systems
[NASA-CR-191327] 09 p3826 N94-32482
Computational chemistry on parallel computers
[DE94-008105] 09 p3636 N94-32616
Development of a low-latency scalar communication routine on message-passing architectures
[DE94-007061] 09 p3827 N94-32683
Overview of shock physics codes for armor analysis
[DE94-008948] 09 p3739 N94-32842
Toroidal computer memory for serial and parallel processors
[AD-D016144] 09 p3807 N94-32978
Principles of ultradependability in chaotic routing
[AD-A277422] 09 p3827 N94-32995
Investigation of modularly configured attached processors with intelligent memories
[AD-A278418] 09 p3839 N94-33330
A self-organizing neural network architecture for auditory and speech perception with applications to acoustic and other temporal prediction problems
[AD-A277526] 10 p4095 N94-33708
Wavelet transforms in parallel image processing
[AD-A278372] 10 p4111 N94-33740
Effective parallel algorithm animation
[AD-A278552] 10 p4105 N94-33784
A parallel data management system for large-scale NASA datasets 10 p4157 N94-33828
Object-oriented particle simulation on parallel computers
[DE94-009353] 10 p4111 N94-33908
Analyzing PICL trace data with MEDEA
[DE94-009173] 10 p4111 N94-33987
Scientific data storage solutions: Meeting the high-performance challenge
[DE94-009312] 10 p4158 N94-34090
Implementation of a fully-balanced periodic tridiagonal solver on a parallel distributed memory architecture
[AD-A281651] 10 p4108 N94-34205
High-performance parallel analysis of coupled problems for aircraft propulsion
[NASA-CR-195883] 10 p3998 N94-34216
Fast adaptive control and its application to missile guidance 10 p4008 N94-34332
Parallel processing for nonlinear dynamics simulations of structures including rotating bladed-disk assemblies
[NASA-CR-194567] 10 p4112 N94-34683
Analysis of optimistic window-based synchronization
[AD-280468] 10 p4102 N94-34918
Interactive archives of scientific data 10 p4122 N94-35044
Runtime support for data parallel tasks
[AD-A280899] 11 p4300 N94-35240
Parallel algorithms for LU decomposition on a shared memory multiprocessor
[PB94-167798] 11 p4314 N94-35531
Task allocation for parallel real-time execution
[AD-A278789] 11 p4310 N94-35653
Communication and memory requirements as the basis for mapping task and data parallel programs
[AD-A278954] 11 p4310 N94-35806
Computer automation and artificial intelligence
[DE94-611058] 11 p4312 N94-35831
Computationally efficient multibody simulations 11 p4222 N94-35896
The most abstract common refinement
[AD-A278870] 11 p4305 N94-36014
CALTRANS: A parallel, deterministic, 3D neutronics code
[DE94-010667] 11 p4326 N94-36127
The EASE Visualization Community Club
[PB94-170529] 11 p4308 N94-36211
Computational methods for material failure processes
[AD-A278716] 11 p4278 N94-36292
Overset grid applications on distributed memory MIMD computers
[NASA-CR-196081] 11 p4268 N94-36397
A transient FETI methodology for large-scale parallel implicit computations in structural mechanics, part 2
[NASA-CR-194823] 12 p4497 N94-36503
Porting industrial codes and developing sparse linear solvers on parallel computers
[PB94-170503] 12 p4497 N94-36547
Preconditioned implicit solvers for the Navier-Stokes equations on distributed-memory machines
[NASA-TM-106449] 12 p4502 N94-36647
Turbulence modeling of free shear layers for high performance aircraft
[NASA-CR-196137] 12 p4442 N94-36808
Research in parallel computing
[NASA-CR-196267] 12 p4442 N94-36960
The impact of HPF data layout on the design of efficient and maintainable parallel linear algebra libraries
[DE94-012382] 12 p4504 N94-37246
Parallelized direct execution simulation of message-passing parallel programs
[NASA-CR-194936] 12 p4497 N94-37411
Neutron transport methods on scalable shared memory multiprocessors
[DE94-012324] 12 p4498 N94-37419
Experience with automatic, dynamic load balancing and adaptive finite element computation
[DE94-001422] 12 p4498 N94-37487
Distributed VIRtual System (DIVIRS) project
[NASA-CR-196262] 12 p4495 N94-37509
Parallel tridiagnoalization through two-step band reduction
[DE94-011512] 12 p4505 N94-37518
A scalable parallel algorithm for multiple objective linear programs
[NASA-CR-194920] 12 p4495 N94-37539
Hierarchically parallelized constrained nonlinear solvers with automated substructuring
[NASA-CR-194474] 12 p4456 N94-37554
Parallel Spectral Transform Shallow Water Model: A runtime-tunable parallel benchmark code
[DE94-011460] 12 p4498 N94-37568
Improved load distribution in parallel sparse Cholesky factorization
[NASA-CR-196380] 12 p4499 N94-37654
Three-dimensional gyrokinetic particle-in-cell simulation of plasmas on a massively parallel computer: LDRD Core Competency Project
[DE94-013367] 12 p4532 N94-37732
Techniques for real-time parallel processing: Sensor processing case studies
[AD-A280633] 12 p4499 N94-37760

PARALLEL PROGRAMMING

Advanced rotorcraft flight simulation: Model development, validation and parallel implementation 01 p0025 N94-11056
Flexible language constructs for large parallel programs
[NASA-CR-191478] 01 p0326 N94-11196
Scalable spin locks for multiprogrammed systems
[AD-A265007] 01 p0337 N94-11650
Transactions of the 10th Army Conference on Applied Mathematics and Computing
[AD-A265098] 01 p0318 N94-11678
An introduction to chordal graphs and clique trees
[DE93-012508] 01 p0332 N94-11695
Problem specific environments for parallel systems
[AD-A266129] 01 p0337 N94-12540
Calculating intersections of surfaces in screen space
[NASA-CR-191498] 02 p0745 N94-13185
Hashing and rehashing in emulated shared memory
[CWI-CS-R9240] 02 p0740 N94-13525
Fast parallel string prefix-matching
[AD-A267758] 02 p0760 N94-13924
A design methodology for portable software on parallel computers
[NASA-CR-194181] 02 p0752 N94-14139
Paradigms for very fast parallel algorithms
[ITN-93-85212] 02 p0755 N94-14556
Execution methods, and parallel virtual machines for distributed implementation of the LCS parallel programming language
[LAAS-93032] 02 p0761 N94-14716
Reactive system verification case study: Fault-tolerant transputer communication
[NASA-TM-108784] 03 p1145 N94-15538
Decomposition of large sparse symmetric systems for parallel computation. Part 1: Theoretical foundations
[AD-A267144] 03 p1159 N94-15750
The alignment-distribution graph
[NASA-CR-194609] 03 p1148 N94-15956
Shared-memory multiprocessor trends and the implications for parallel program performance
[TR-420] 03 p1159 N94-16578
Networked workstations and parallel processing utilizing functional languages
[AD-A267464] 03 p1160 N94-17034
Visual parallel programming with determinacy: A language specification, an analysis technique, and a programming tool
[AD-A267560] 03 p1153 N94-17107
Testing string superprimitivity in parallel
[AD-A267814] 03 p1155 N94-17399
Construction of d-dimensional hyperoctrees on a hypercube multiprocessor
[INRIA-RR-1752] 03 p1162 N94-17539
PARX: Architecture of an operating system for parallel machines
[ETN-93-94401] 04 p1533 N94-18068
High performance Fortran: An overview
[DE93-017181] 04 p1519 N94-18072
The evolution of the PVM concurrent computing system
[DE93-017764] 04 p1534 N94-18482
Software engineering for effective utilization of parallel processing computing system
[AD-A269191] 04 p1535 N94-18865
Asynchronous rendezvous in the presence of backtracking
[PB93-197739] 04 p1524 N94-19062
Performance and scalability aspects of directory-based cache coherence in shared-memory multiprocessors
[DE93-016442] 04 p1536 N94-19115
An annotated bibliography on parallel parsing: Updated version
[MEMO-INF-92-84] 04 p1537 N94-19223
Heap construction in the parallel comparison tree model
[TR-409] 04 p1538 N94-19512
Multilist scheduling: A new parallel programming model
[AD-A270549] 05 p1929 N94-20084
Mint tutorial and user manual
[TR-452] 05 p1905 N94-20143

Parallel logic programming systems
[RR-891-I] 05 p1929 N94-20176
Scheduling for locality in shared-memory multiprocessors
[AD-A272948] 05 p1930 N94-21228
Behavioural semantics of parallel functional programming languages
[MEMO-INF-92-66] 05 p1913 N94-21313
Butcher-Kuntzmann methods for nonstiff problems on parallel computers
[CWI-NM-R9305] 05 p1935 N94-21493
MINIFOLD: A kernel for a MANIFOLD-like coordination language
[CWI-CS-R9252] 05 p1915 N94-21534
Using parallel banded linear system solvers in generalized eigenvalue problems
[NASA-CR-191540] 05 p1915 N94-21584
A simple modern correctness condition for a space-based high-performance multiprocessor 05 p1766 N94-21718
Image convolution using the Myrias SPS-2 parallel computer 05 p1786 N94-22207
Parallelizing a maximum entropy image deconvolution algorithm 05 p1787 N94-22208
Parallel functional programming in SISAL: Fictions, facts, and future
[DE93-040486] 05 p1937 N94-22558
Users manual for the Chameleon parallel programming tools
[DE94-001934] 06 p2465 N94-22973
Installation of an artificial neural network on distributed memory microprocessors
[ETN-94-95175] 06 p2471 N94-23152
Applications of the Aurora parallel PROLOG system to computational molecular biology
[DE93-041166] 06 p2420 N94-23468
The Automated Instrumentation and Monitoring System (AIMS) reference manual
[NASA-TM-108795] 06 p2452 N94-23510
Arc consistency problem: An exercise in parallel programming with shared objects
[PB94-110590] 06 p2466 N94-23706
Object distribution in orca using compile-time and run-time techniques
[PB94-110574] 06 p2453 N94-23745
NASA high performance computing and communications program
[NASA-TM-4554] 06 p2591 N94-24337
The Adam language: Ada extended with support for multiway activities
[NASA-CR-4565] 06 p2456 N94-24480
An integrated runtime and compile-time approach for parallelizing structured and block structured applications
[NASA-CR-191554] 06 p2458 N94-24740
Design and implementation of a distributed version of the NASA Engine Performance Program
[NASA-CR-194475] 06 p2462 N94-25179
Designing parallel programs of parameterized granularity
[ETN-94-95302] 06 p2468 N94-25278
A design method for parallel programs
[ETN-94-95331] 06 p2469 N94-25282
Parallel processing methods for space based power systems 06 p2222 N94-25352
Abstraction in, specification and proof of software for a 1D heat-transfer problem
[REPT-93-45] 07 p2790 N94-25763
Parallel Assessment Window System (PAWS) enhancements
[AD-A274094] 07 p2979 N94-25786
Object interaction in a parallel object-oriented discrete-event simulation
[AD-A274084] 07 p2959 N94-25942
Out of core, out of mind: Practical parallel I/O
[DE94-003107] 07 p2979 N94-25952
Preconditioning in parallel Runge-Kutta methods for stiff initial value problems
[CWI-NM-R9310] 07 p2991 N94-26217
Programming in Fortran M
[DE94-002756] 07 p2963 N94-26407
Computational strategies for three-dimensional flow simulations on distributed computer systems
[NASA-CR-195249] 07 p2793 N94-26595
Efficient implementation of high-level parallel symbolic languages 07 p2955 N94-27196
Parallel algorithm for dominant points correspondences in robot binocular stereo vision 07 p2686 N94-27364
Semantics of MANIFOLD: Specification in ASF+SDF and extension
[CWI-CS-R9269] 07 p2971 N94-27575
Fast parallel permutation algorithms
[CWI-CS-R9303] 07 p2982 N94-27579
Global atmospheric and ocean modeling on the connection machine
[DE94-003930] 08 p3342 N94-28521
Reasoning about programs by exploiting the environment
[AD-A275852] 08 p3408 N94-28794
Investigation into formalization of domain-oriented parallel software development
[AD-A275177] 08 p3430 N94-29050
Progress report for the PTUF Project-93 Q1 and Q2
[PB94-138591] 08 p3431 N94-29995
Three metric domains of processes for bisimulation
[CWI-CS-R9335] 08 p3459 N94-30427
MANIFOLD version 1.0 programming: Programs and problems
[CWI-CS-R9334] 08 p3425 N94-30428
Manray: A replicated workers program in MANIFOLD
[CWI-CS-R9337] 08 p3433 N94-30429
Isomorphisms between predicate and state transformers
[CWI-CS-R9338] 08 p3459 N94-30430
Relating state transformation semantics and predicate transformer semantics for parallel programs
[CWI-CS-R9339] 08 p3433 N94-30431
Topological models for higher order control flow
[CWI-CS-R9340] 08 p3425 N94-30432
Comparative semantics for linear arrays of communicating processes
[CWI-CS-R9336] 08 p3426 N94-30491
On the relation between Unity properties and sequences of states
[RUU-CS-93-07] 08 p3433 N94-30720
Parallel iteration across the steps of high order Runge-Kutta methods for nonstiff initial value problems
[CWI-NM-R9313] 08 p3433 N94-30730
Parallel language constructs for paradigm integration and deterministic computations
[DE94-005119] 08 p3428 N94-30754
Implanting algorithms on parallel machines
[TELECOM-93-D-017] 09 p3823 N94-31099
The ant system: An autocatalytic optimizing process
[REPT-91-016-REV] 09 p3824 N94-31177
A probabilistic view of Datalog parallelization
[TELECOM-93-D-021] 09 p3824 N94-31183
A comparison of distributed memory and virtual shared memory parallel programming models
[DE94-005473] 09 p3825 N94-31663
The named-state register file
[AD-A276796] 09 p3825 N94-32165
Transformational derivation of (parallel) programs using skeletons
[TR-93-20] 09 p3825 N94-32196
Methods for parallelizing search paths in phrasing
[AD-A276876] 09 p3817 N94-32212
Computational chemistry on parallel computers
[DE94-008106] 09 p3636 N94-32616
A software architecture for multidisciplinary applications: Integrating task and data parallelism
[AD-A279750] 09 p3820 N94-32928
Finding all periods and initial palindromes of a string in parallel
[AD-B175069] 09 p3827 N94-33002
Program composition
[AD-A278377] 10 p4105 N94-33742
Parallel programming methodologies for non-uniform structured problems in materials science
[AD-A277868] 10 p4111 N94-33777
Implementation of a fully-balanced periodic tridiagonal solver on a parallel distributed memory architecture
[AD-A281651] 10 p4108 N94-34205
An overview of the Opus language and runtime system
[AD-A281616] 10 p4108 N94-34206
Extending HPF for advanced data parallel applications
[AD-A281652] 10 p4109 N94-34387
Parallel algorithms for LU decomposition on a shared memory multiprocessor
[PB94-167798] 11 p4314 N94-35531
A compile time model for composing parallel programs
[AD-A278896] 11 p4310 N94-35597
Communication and memory requirements as the basis for mapping task and data parallel programs
[AD-A278954] 11 p4310 N94-35806
The CMU task parallel program suite
[AD-A278951] 11 p4311 N94-36015
Porting industrial codes and developing sparse linear solvers on parallel computers
[PB94-170503] 12 p4497 N94-36547
A compilation system that integrates high performance FORTRAN and FORTRAN M
[DE94-013308] 12 p4496 N94-37551

PARALLEL STRIP LINES
U MICROSTRIP TRANSMISSION LINES

PARAMAGNETIC AMPLIFIERS
U MASERS

PARAMAGNETIC RESONANCE
NT ELECTRON PARAMAGNETIC RESONANCE

PARAMAGNETISM
Orbital glass in HTSC
[DE93-613988] 01 p0395 N94-10415
Volume dependence of vanadium magnetism
[DE94-601838] 07 p3050 N94-25843
Molecular/polymeric magnetism
[DE94-005888] 09 p3649 N94-31201

PARAMECIA
Space movement of Trichinella spiralis under microgravity 08 p3387 N94-29711

PARAMETER IDENTIFICATION
Microwave radiometry of ice cover in polar regions 01 p0210 N94-12655
Trajectory curving in underwater propagation of light 01 p0226 N94-12748
Mixing of drifter ensemble by mesoscale currents 01 p0228 N94-12760
Improvement of method for experimental determination of flutter speed by parameter identification
[NASA-CR-193555] 01 p0033 N94-12769
Bounds on time delay estimation given unknown signal spectral parameters
[ITN-93-85194] 02 p0601 N94-13566
Parameter identification of a model of the process of software development
[REPT-93-008] 02 p0750 N94-13807
Exploitation of cyclostationarity for signal-parameter estimation and system identification
[AD-A267137] 03 p0988 N94-15690
Development and analysis of ARMA parameter estimation schemes in the presence of noise
[AD-A267184] 03 p0989 N94-15786
Operator overloading as an enabling technology for automatic differentiation
[DE93-012899] 03 p1170 N94-16778
Small satellite constellation system: Optimization criteria 03 p0888 N94-17132
Linear parameter identification methods for ARMA models with periodic coefficients
[REPT-92-070] 04 p1556 N94-17938
Comparative examinations of several field oriented position control structures for asynchronous servomotors with a multitransputer system
[ETN-93-95051] 04 p1406 N94-19390
Contribution to the identification of nonlinear behavior laws in material mechanics
[ECL-92-36] 04 p1458 N94-19411
Methods for description and control of dynamical systems and their application
[MPIS-17/1992] 04 p1553 N94-19522
A learning autopilot for automatically controlled robust regulation
[ETN-93-95075] 04 p1321 N94-19711
Algorithms and architectures for high speed signal processing
[AD-A271000] 04 p1392 N94-19736
Literature review of the errors-in-variables approach to the problem of system identification
[AD-A271098] 05 p1949 N94-19907
Parameter estimation with cost function of second order in output-error-problem
[DLR-FB-92-38] 05 p1964 N94-21139
A project on parameter identification in reaction kinetics
[CWI-NM-R9301] 05 p1682 N94-21574
Identification for robust control using an H(sub infinity) norm
[EUT-92-E-261] 06 p2470 N94-22873
Failure-proof estimation under conditions of lack of information 06 p2158 N94-24267
A comparison of approximate interval estimators for the Bernoulli parameter
[AD-A276322] 06 p2458 N94-24680
Determination of the stability and control derivatives of the NASA F/A-18 HARV using flight data
[NASA-CR-194838] 06 p2190 N94-24804
Advanced ballistic range technology
[NASA-CR-195198] 06 p2165 N94-25169
Frequency response functions for nonlinear rational models
[RR-471] 06 p2492 N94-25318
Grey-box modelling and identification topics
[PB94-126380] 07 p2986 N94-27029
Multiple model adaptive control of a large flexible space structure with purposeful dither for enhanced identifiability
[AD-A274132] 07 p2987 N94-27122
Multiple weight stepwise regression
[DE94-001602] 07 p3000 N94-27564
A parametric sensitivity study for single-stage-to-orbit hypersonic vehicles using trajectory optimization
[NASA-CR-195703] 07 p2697 N94-27789
A variable selection heuristic for solid rocket motor design 08 p3173 N94-29544

Parameter identification of the rotordynamic coefficients of high-Reynolds-number hydrostatic bearings
08 p3311 N94-30792
A new methodology of system parameter estimation
[MATHS-REPT-A-208] 09 p3808 N94-31163
Identification of polynomial and rational NARMAX models
[RR-483] 09 p3842 N94-31413
A contribution to the representation and identification of semi-flexible robots
[ISBN-0-315-86450-8] 09 p3724 N94-31721
Model identification of a reconfigurable robot manipulator
[ISBN-0-315-87109-1] 09 p3725 N94-31874
On-line physical parameter identification and adaptive control of a launch vehicle 09 p3602 N94-31891
Approximation theory and computational methods for the identification and control of distributed parameter systems
[AD-A277335] 09 p3848 N94-32244
Parameter identification of a rotor supported in a pressurized bearing lubricated with water
10 p4065 N94-34197
NTT crosscorrelation recursive least squares procedure for on-line identification of process parameters
10 p4116 N94-34325
Fast adaptive control and its application to missile guidance 10 p4008 N94-34332
Adaptive autopilot
[AD-D016193] 10 p4007 N94-34406
High performance data acquisition, identification, and monitoring for active magnetic bearings
11 p4213 N94-35839
NASA Workshop on Distributed Parameter Modeling and Control of Flexible Aerospace Systems
[NASA-CP-3242] 11 p4217 N94-35865
Parameter estimation of the vibrational model for the SCOLE experimental facility 11 p4219 N94-35878
A procedure for oscillatory parameter identification
[DE94-008047] 11 p4259 N94-36054
A PDE-based methodology for modeling, parameter estimation and feedback control in structural and structural acoustic systems
[NASA-CR-194928] 12 p4500 N94-36924
Parameter estimation in a structural acoustic system with fully nonlinear coupling conditions
[NASA-CR-194926] 12 p4503 N94-36991

PARAMETERIZATION
NT PARAMETER IDENTIFICATION
A self-consistent model of non-linear parameterization of turbulent diffusion in atmospheric boundary layer
[DE93-011950] 01 p0275 N94-11052
Supervised autonomous control, shared control, and teleoperation for space servicing
01 p0183 N94-11577
Parameterization of subgrid-scale stress by the velocity gradient tensor 01 p0155 N94-12286
A parameterization of cloud droplet nucleation
[DE93-007998] 02 p0718 N94-12903
Extremal polygon containment problems and other issues in parametric searching
[ITN-93-85214] 02 p0771 N94-14506
Scattering calculations and confining interactions
[NASA-CR-194242] 02 p0786 N94-14549
On l(1): Optimal decentralized performance
02 p0681 N94-14643
Search for subgrid scale parameterization by projection pursuit regression 02 p0643 N94-14749
Adaptation of model parameters of a rail model at measured rail compliances
[ILR-MITT-274(1992)] 05 p1831 N94-21153
Atmospheric parameterization schemes for satellite cloud property retrieval during FIRE IFO 2
05 p1874 N94-22312
Development of advanced cloud parameterizations to examine air quality, cloud properties, and cloud-radiation feedback in mesoscale models
[DE93-041164] 05 p1853 N94-22384
Atmospheric numerical modeling resource enhancement and model convective parameterization/scale interaction studies
[NASA-CR-194769] 06 p2400 N94-23124
On testing two major cumulus parameterization schemes using the CSU regional atmospheric modeling system
[DE94-000703] 06 p2407 N94-23284
Parameterization of sub-grid scale convection
06 p2413 N94-24386
Session on cumulus parameterization
06 p2414 N94-24394
Joint sessions on modeling of boundary layer and radiative transfer processes 06 p2414 N94-24396
Super Beltrami differentials and N equal to 4 superconformal anomalies
[DE93-613047] 06 p2491 N94-25166
MIMO system identification for H(infinity) robust control: A frequency domain approach with minimum error bounds
[ETN-94-95354] 06 p2476 N94-25262
Designing parallel programs of parameterized granularity
[ETN-94-95302] 06 p2468 N94-25278
Parameter estimation of linear systems from frequency response measurements (computer program)
[ESDU-93016] 07 p2976 N94-28137
An observational and numerical study of sea/land-breeze circulations in an area of complex coastal heating 08 p3372 N94-29813
The incorporation and initialization of cloud water/ice in an operational forecast model
08 p3373 N94-29814
Use of satellite data to improve parameterization of spatial and temporal variations of gaseous dry deposition in regional-scale models
[DE94-005110] 08 p3334 N94-30022
Methods of testing parameterizations: Vertical ocean mixing 08 p3352 N94-30633
Use of Air Force cloud cover data to evaluate and improve cloud forecasts and parameterizations in mesocale meteorological models
[AD-A277384] 09 p3784 N94-32054
The influence of cumulus parameterization on model forecasts of rapid oceanic cyclogenesis
[AD-A277207] 09 p3784 N94-32094
A parameterization of cloud droplet nucleation
[DE94-007469] 09 p3785 N94-32268
Development of a radiative cloud parameterization scheme of stratocumulus and stratus clouds which includes the impact of CCN on cloud albedo
[DE94-005476] 10 p4081 N94-33714
Sensitivity of cloud forcing to the cloud cover parameterization in a GCM
[DE94-000678] 10 p4089 N94-33728
The Atmospheric Radiation Measurement Program and interfaces with external data sources
[DE94-003699] 11 p4286 N94-36024
Two-channel microwave radiometer for observations of total column precipitable water vapor and cloud liquid water path
[DE94-007480] 12 p4471 N94-36479
Assessing efficiency of software production for NASA-SEL data 12 p4490 N94-36490
Representing the influence of subgrid topography on hydrology
[DE94-004595] 12 p4474 N94-37379
Evaluation of parameterizations for pollutant transport and dispersion in an urban street canyon using a three-dimensional dynamic flow model
[DE94-012641] 12 p4467 N94-37429
A stratiform cloud parameterization for general circulation models
[DE94-011442] 12 p4474 N94-37566
Factors influencing the parameterization of anvil clouds within GCMs
[DE94-010794] 12 p4475 N94-37621

PARAMETERS
U INDEPENDENT VARIABLES

PARAMETRIC AMPLIFIERS
Quantum noise and squeezing in optical parametric oscillator with arbitrary output coupling
01 p0375 N94-10568
Photon number amplification/duplication through parametric conversion 01 p0376 N94-10572
Optical frequency division using an optical parametric oscillator
[AD-A270847] 04 p1581 N94-19578
Optical parametric oscillator modeling with diffraction, depletion, and double refraction
[DE94-001504] 07 p3040 N94-27999
Sum frequency generation using an optical parametric oscillator
[DE94-001827] 07 p3040 N94-28000
A noncritically phase matched femtosecond optical parametric oscillator near 3 microns
[DE94-008050] 09 p3720 N94-32704

PARAMETRIC OSCILLATORS
U PARAMETRIC AMPLIFIERS

PARASITES
Assisting wine growers
[NASA-TM-109812] 10 p4094 N94-33564

PARASITIC ANTENNAS
U PARASITIC ELEMENTS (ANTENNAS)

PARASITIC DISEASES
Satellite, environmental, and medical information applied to epidemiological monitoring 01 p0307 N94-11802
Combating malaria
[NASA-TM-109609] 03 p1081 N94-15297

PARASITIC ELEMENTS (ANTENNAS)
Bandwidth enhancement of dielectric resonator antennas 05 p1734 N94-20507

PARASITIC REFLECTORS
U PARASITIC ELEMENTS (ANTENNAS)

PARITY
Discrete space-time symmetries
[DE93-010199] 01 p0341 N94-10259
On parity conservation and the question of the missing, right-handed neutrino
[DE93-613092] 01 p0361 N94-10414
Nuclear structure models: Applications and development
[DE93-012934] 01 p0368 N94-11813
No-lost theorem for parity violating nucleon-nucleon scattering experiments
[DE93-012737] 02 p0779 N94-12949
On the theory of the decaying developed turbulence with spontaneous parity violation
[DE93-623190] 02 p0632 N94-13511
Coherent excitation of autoionizing resonances by electron impact
[DE93-018169] 02 p0785 N94-14419
Measuring parity violation using the neutron capture reaction
[DE93-016629] 02 p0786 N94-14514
On the difference caused by CP violation in the energy spectra of pions in K(sup (+-))(yields)(pi)(+-)(pi)(+-)(pi)-+ decays
[DE93-624828] 04 p1564 N94-17687
Improved approximations applied to the S(sub N) even-parity equation
[DE93-016467] 04 p1551 N94-19343
Links between N-modular redundancy and the theory of error-correcting codes 05 p1765 N94-21713
Likelihood analysis of parity violation in the compound nucleus
[DE94-000671] 05 p1977 N94-22572
Data on parity violation in the compound nucleus and its interpretation
[DE94-003965] 07 p3013 N94-25820
Dynamic breaking of U(N) and appearance of Chern-Simons term in 4-fermion theories
[DE93-634342] 07 p3019 N94-26455
The Hamiltonian structures of the super KP hierarchy associated with an even parity superlax operator
[DE94-601506] 07 p2994 N94-26459
Space-time symmetries: P and CP violation
[DE94-005012] 08 p3526 N94-30750
About G-parity violation in tau yields nu pi eta decay
[DE94-611146] 10 p4136 N94-33863

PARKING ORBITS
Prediction of three sigma maximum dispersed density for aerospace applications 06 p2207 N94-23654
Lifetimes of lunar satellite orbits
[NASA-TP-3394] 07 p2690 N94-27771
Optimal low-thrust, Earth-Moon trajectories
08 p3159 N94-30961
A geometric model of a V-slit Sun sensor correcting for spacecraft wobble 11 p4206 N94-35628

PARKINSON DISEASE
Impaired associated movement in Parkinson's disease: An evaluation of Bell's phenomenon
07 p2928 N94-27520
Effect of L-dopa on hemodynamic functions in humans 07 p2929 N94-27526

PARKS
NT NATIONAL PARKS
NT YELLOWSTONE NATIONAL PARK (ID-MT-WY)

PARSING ALGORITHMS
Layering techniques for development of parallel systems: An algebraic approach
[MEMO-INF-92-62] 01 p0335 N94-10277
An annotated bibliography on parallel parsing: Updated version
[MEMO-INF-92-84] 04 p1537 N94-19223
Attribute evaluation during generalized parsing
[MEMO-INF-92-85] 04 p1526 N94-19224
Non-well-foundedness and type freeness can unify the interpretation of functional application
[PB93-191849] 04 p1560 N94-19710
Neural data oriented parsing
05 p1940 N94-20248
A modular design for connectionist parsing
05 p1941 N94-20252
Parsing schemata: A framework for parallel and sequential parsing
[PB94-125267] 07 p2981 N94-26998
Engineering specification editing tools
[AD-A275116] 08 p3419 N94-29746
Maintaining presentation invariants in the Views system
[CWI-CS-R9262] 08 p3423 N94-30324
Increasing the applicability of LR parsing
[TR-93-06] 08 p3423 N94-30332
Generalized left-corner parsing
[TR-92-21] 08 p3432 N94-30356
Parsing in ISBES
[TR-92-32] 08 p3432 N94-30363

Methods for parallelizing search paths in phrasing
[AD-A276876] 09 p3817 N94-32212
Informal introduction to the extended affix grammar formalism and its compiler
[TR-93-19] 09 p3817 N94-32287

PARTIAL DIFFERENTIAL EQUATIONS
NT BIHARMONIC EQUATIONS
NT BURGER EQUATION
NT CAUCHY-RIEMANN EQUATIONS
NT ELLIPTIC DIFFERENTIAL EQUATIONS
NT FOKKER-PLANCK EQUATION
NT GAUSS EQUATION
NT HELMHOLTZ VORTICITY EQUATION
NT LIOUVILLE EQUATIONS
NT PARABOLIC DIFFERENTIAL EQUATIONS
NT POISSON EQUATION
NT VLASOV EQUATIONS
Vectorizing matrix operations arising from PDE discretization on 9-point stencils
[CWI-NM-R9221] 01 p0342 N94-10351
The INTEGRATOR package for REDUCE, version 1.0
[MEMO-1100] 01 p0322 N94-10418
Wave and pseudo-diffusion equations from squeezed states 01 p0347 N94-10607
DILUTE: A code for studying beam evolution under RF noise
[DE93-011605] 01 p0133 N94-10960
Quality factors and local adaption (with applications in Eulerian hydrodynamics)
[DE93-010502] 01 p0151 N94-11272
Control of large space structures with varying configuration
[AD-A265764] 01 p0044 N94-12387
Newton iterative methods for large scale nonlinear systems
[DE93-015357] 02 p0767 N94-13025
Simplification-driven automated partial evaluation
[DE93-012890] 02 p0768 N94-13391
Integrable system describing surfaces of non-constant curvature
[PREPRINT-734] 02 p0768 N94-13499
Adaptive wavelet collocation methods for initial value boundary problems of nonlinear PDE's
[NASA-CR-191507] 03 p1169 N94-15833
C++ as a language for object-oriented numerics
[DE93-015027] 03 p1148 N94-15985
Operator overloading as an enabling technology for automatic differentiation
[DE93-012899] 03 p1170 N94-16778
Applications of the phi-transform
[AD-A266247] 03 p1170 N94-16940
Numerical methods for one-dimensional hyperbolic conservation laws
[PB93-194801] 04 p1547 N94-18078
Introduction to spectral methods: Application to the Stokes problem 04 p1413 N94-18566
3D composite grids using Bezier curves and surfaces in component adaptive methods
[AD-A269188] 04 p1549 N94-18863
Application of differential sensitivity theory to continuum mechanics
[DE93-012732] 04 p1609 N94-19187
Singularities and symmetries of nonlinear ordinary and partial differential equations
[DE93-040083] 04 p1550 N94-19190
Group-invariant solutions of hydrodynamics and radiation hydrodynamics
[DE93-018373] 04 p1423 N94-19604
Stochastic differential equations and numerical simulation for pedestrians
[DE93-040651] 05 p1949 N94-20006
Linear and nonlinear PSE for compressible boundary layers
[NASA-CR-191537] 05 p1797 N94-20033
Dynamical systems and nonlinear partial differential equations
[AD-A271514] 05 p1951 N94-20545
Symmetries and conservation laws of the system: u(x)=vw(x), v(y)=uw(y), uv+w(xx)+w(yy)=0
[MEMO-1084] 05 p1953 N94-21046
MGD1M: A parallel multigrid code with a fast vectorized ILU-relaxation
[CWI-NM-R9222] 05 p1930 N94-21077
Interactive simulation package for coupled bending and torsional vibrations in flexible robot arms
[MEMO-1089] 05 p1944 N94-21140
A multi-level solution algorithm for steady-state Markov chains
[NASA-CR-191558] 05 p1914 N94-21462
MGGHAT: Elliptic PDE software with adaptive refinement, multigrid and high order finite elements 05 p1956 N94-21470
An automatic multigrid method for the solution of sparse linear systems 05 p1957 N94-21478
A semi-Lagrangian approach to the shallow water equation 05 p1806 N94-21480
A note on singularities caused by the hydrodynamic dispersion tensor
[CWI-NM-R9302] 05 p1803 N94-21575
Parallelizing a highly vectorized multigrid code with zebra relaxation
[CWI-NM-R9225] 05 p1935 N94-21610
Numerical multigrid software (MGD5M): A parallel multigrid code with a twisted ILLU-relaxation
[CWI-NM-R9226] 05 p1916 N94-21611
Universality in blow-up for non linear heat equations
[PB93-215465] 05 p2038 N94-22095
A working algorithm to isolate integrable surfaces in E cubed
[SSCL-PREPRINT-761] 06 p2452 N94-23518
A dual reciprocal boundary element formulation for viscous flows 06 p2325 N94-23666
A theorem regarding roots of the zero-order Bessel function of the first kind 06 p2325 N94-23667
Implementing abstract multigrid or multilevel methods 06 p2483 N94-23682
Multigrid methods for a semilinear PDE in the theory of pseudoplastic fluids 06 p2341 N94-23689
Wavelet multiresolution analyses adapted for the fast solution of boundary value ordinary differential equations 06 p2485 N94-23691
An object-oriented approach for parallel self adaptive mesh refinement on block structured grids 06 p2469 N94-23697
On the dynamics of approximating schemes for dissipative nonlinear equations 06 p2332 N94-24168
Global dynamic stability of a shallow arch by poincare-like simple cell mapping 06 p2160 N94-24280
Modelling the Shuttle Remote Manipulator System: Another flexible model 06 p2371 N94-25350
Development of programmable artificial neural networks 06 p2477 N94-25370
Continuation and multi-grid for bifurcation problems
[AD-A274965] 07 p2992 N94-26302
VLUGR2: A vectorized local uniform grid refinement code for PDE's in 2D
[CWI-NM-R9306] 07 p2965 N94-26772
Local uniform grid refinement and systems of coupled partial differential equations
[CWI-NM-R9307] 07 p2995 N94-26773
Fields and potentials in general uniaxial bianisotropic media I. Axial sources
[PB94-132875] 07 p2778 N94-28379
Applied analysis/computational mathematics
[DE94-005133] 08 p3451 N94-28571
Numerical analysis and computation of nonlinear partial differential equations from applied mathematics
[AD-A275582] 08 p3451 N94-28723
On approximate Riemann solvers: Improvement of HLLEM scheme and its generalization for chemically reacting flows 08 p3126 N94-28973
A design methodology for synthesizing low-order robust controllers for flexible structures 08 p3302 N94-29870
Large-scale shape optimization: Numerical methods, parallel algorithms, and applications to aerodynamic design 09 p3815 N94-31966
Control and stabilization of distributed parameter systems; theoretical and computational aspects
[AD-A277239] 09 p3738 N94-32275
Coherent processes in atom in strong radiation fields
[AD-A278388] 09 p3874 N94-33144
Whiskered tori for integrable pde's: Chaotic behavior in near integrable pde's
[AD-A278390] 10 p4128 N94-33430
Analysis of wavelet technology for NASA applications
[NASA-CR-195929] 10 p3985 N94-34704
Variations in the modal characteristics of a telescopically deploying beam 11 p4218 N94-35872
Computational Mathematics Laboratory for multiscale analysis
[AD-A278597] 11 p4315 N94-36424
A Galerkin method for linear PDE systems in circular geometries with structural acoustic applications
[NASA-CR-194925] 12 p4503 N94-36923

PARTIAL PRESSURE
NT OXYGEN TENSION
A mechanism for the reduction in risk of decompression sickness in microgravity environment 01 p0312 N94-11545
Binary homogeneous nucleation: Temperature and relative humidity fluctuations and non-linearity
[DE93-007884] 02 p0709 N94-13911
Earth's partial pressure of CO2 over the past 120 Ma; evidence from Ce anomalies in the deep (greater than 600 m) Pacific Ocean, 1 03 p1104 N94-16358
Earth's partial pressure of CO2 over the past 100-500 Ma; evidence from Ce anomalies in mostly shallow seas (less than 200 m) as recorded in carbonate sediments, 2 03 p1104 N94-16360
Control of catalytic hydrotreating selectivity with ammonia
[DE93-041223] 04 p1354 N94-19660
High oxygen pressure synthesis of new copper oxide superconductors
[DE93-040278] 05 p2033 N94-21998
Discontinuous phase formation and selective attack of SiC materials exposed to low oxygen partial pressure environments
[DE93-040161] 06 p2231 N94-22933
Simultaneous laboratory measurements of CO2 and H2O adsorption on palagonite: Implications for the Martian climate and volatile reservoir 09 p3952 N94-33240

PARTICLE ACCELERATION
Acceleration of positrons in supernova shocks
[NASA-CR-193713] 01 p0425 N94-10511
Wake-field and space charge effects on high brightness beams calculations and measured results for the laser driven photoelectrons at BNL-ATF
[DE93-015787] 02 p0659 N94-14572
Enhanced acceleration in a self-modulated-laser wakefield accelerator
[AD-A268452] 04 p1586 N94-18148
Parametric instabilities in picosecond time scales
[DE94-000384] 05 p1966 N94-21958
Particle acceleration in a filamentary current sheet model 05 p2004 N94-22659
Prompt high-energy particle acceleration during two current loops collision 05 p2005 N94-22661
Plasma structure in a plasma flow along a magnetic mirror field 05 p2005 N94-22664
Mean elemental composition and He-3 enrichments in solar energetic particles 05 p2006 N94-22670
Acceleration of solar-flare particles as viewed from their chemical composition 05 p2006 N94-22672
Particle acceleration on the Alfven surface of a plasma ejecting axisymmetric rotator 05 p2008 N94-22681
Spin effects in hard interactions (interest in accelerated polarized beam)
[DE93-634398] 07 p3031 N94-26044
Ionosphere-magnetosphere coupling
[NASA-CR-195222] 07 p2881 N94-27237
Acceleration of electrons and ions by strong lower-hybrid turbulence in solar flares
[NASA-TM-109723] 07 p3111 N94-27953
Acceleration in astrophysics
[DE94-004986] 08 p3552 N94-28580
A single-fluid, self-consistent formulation of particle transport and fluid dynamics 08 p3280 N94-30352
Collective acceleration in solar flares
[DE94-006288] 09 p3953 N94-31632
Cosmic rays: Physics and astrophysics. A research briefing
[NASA-CR-196118] 12 p4550 N94-36921
High Altitude Plasma Instrument (HAPI) data analysis
[NASA-CR-189360] 12 p4469 N94-36949

PARTICLE ACCELERATOR TARGETS
Fast trigger algorithm for B-events selection
[DE93-621452] 01 p0365 N94-11089
Experiments to measure the gluon helicity distribution in protons
[DE93-011756] 01 p0368 N94-11613
Charged-particle evaluation methodology at Lawrence Livermore National Laboratory
[DE93-013429] 02 p0781 N94-13251
Application of synchrotron radiation in chemical dynamics
[DE93-015040] 02 p0563 N94-13411
Longitudinal beam dynamics for heavy ion fusion
[DE93-013850] 02 p0789 N94-13727
Characteristics of a high energy muon(+)muon(-) collider based on electro-production of muons
[DE93-017154] 02 p0790 N94-14893
E789 and P865: High-rate fixed-target studies of charm and beauty
[DE93-017223] 02 p0788 N94-14898
Past, present and future ((pi),(eta)) experiments
[DE93-016631] 03 p1182 N94-16115
3D and r,z particle simulations of heavy ion fusion beams
[DE93-013417] 03 p1205 N94-17670
Compound-lens injector for a 19-MeV, 700-kA electron beam
[DE93-013752] 04 p1573 N94-17698
Overview of WARP: A particle code for heavy ion fusion
[DE93-018637] 04 p1588 N94-19034
High energy physics program. Task A: Experiment and theory. Task B: Numerical simulation
[DE93-018140] 04 p1575 N94-19050
Induction accelerator development for heavy ion fusion
[DE93-019228] 04 p1591 N94-19479

Development and characterization of a time-, position- and energy-resolved x ray diagnostic for PBFA 2 target experiments
[DE93-019429] 05 p1808 N94-20297
A high-intensity He-jet production source for radioactive beams
[DE93-040247] 05 p1981 N94-21767
SLAC measurement of the neutron spin structure function
[DE93-040998] 05 p1975 N94-21788
Studies of the deuteron at high energy and momentum transfer
[DE93-041162] 05 p1976 N94-21941
An antiproton driver for ICF propulsion
06 p2217 N94-23069
JLC-1
[DE93-520380] 07 p3031 N94-26113
Study of the process (pi)(sup -)A(yields)(pi)(sup -)(eta)'(eta)A at the moment 36 GeV/c
[DE93-634530] 07 p3024 N94-27250
Heavy flavor production at fixed target photo- and hadroproduction
[DE94-004651] 08 p3491 N94-30719
Transverse energy production with Si and Au beams at AGS energy: Towards hot and dense hadronic matter
[DE94-007178] 09 p3938 N94-32638
Spin-structure function of the neutron He-3: SLAC results
[DE94-008927] 09 p3875 N94-33189
Coherent multiple-foil x-ray transition radiation
[DE93-040831] 12 p4525 N94-37486
Experimental particle physics at the University of Pittsburgh
[DE94-011636] 12 p4521 N94-37721

PARTICLE ACCELERATORS
NT BETATRONS
NT CYCLIC ACCELERATORS
NT CYCLOTRONS
NT ELECTRON ACCELERATORS
NT ION ACCELERATORS
NT LINEAR ACCELERATORS
NT STORAGE RINGS (PARTICLE ACCELERATORS)
NT SUPERCONDUCTING SUPER COLLIDER
NT SYNCHROCYCLOTRONS
NT SYNCHROPHASOTRONS
NT SYNCHROTRONS
NT VAN DE GRAAFF ACCELERATORS
Proceedings of the Second KEK Topical Conference on e(sup +)e(sup -) collision physics
[DE93-754139] 01 p0364 N94-10889
Stripping efficiencies for 277 MeV/amu gold beam on copper foils
[DE93-014306] 02 p0569 N94-13221
Study of electroweak interactions
[DE93-015067] 02 p0782 N94-13412
Characteristics of a high energy muon(+)muon(-) collider based on electro-production of muons
[DE93-017154] 02 p0790 N94-14893
Calorimeter based detectors for high energy hadron colliders
[DE93-017055] 03 p1188 N94-16900
Search for the top quark from (e(mu)) and (e,e) events in the D0 detector in p(bar-p) collisions at the square root of s = 1.8 TeV
[DE93-016350] 03 p1186 N94-17662
The design of the MAD Design Program
[DE93-013343] 04 p1539 N94-17696
Enhanced acceleration in a self-modulated-laser wakefield accelerator
[AD-A268452] 04 p1586 N94-18148
Halo formation in mismatched, space-charge-dominated beams
[DE93-018581] 04 p1574 N94-18934
High energy physics at Tufts University
[DE93-018299] 04 p1575 N94-19023
Top search at the TEVATRON
[DE93-019392] 05 p1978 N94-19988
Heavy ion fusion injector experiments
[DE93-019188] 05 p1993 N94-20234
High current injector for heavy ion fusion
[DE93-019241] 05 p1979 N94-20289
B production at D0
[DE93-019250] 05 p1972 N94-20291
Engineering design, fabrication, installation, operation, and maintenance services in support of research on laser plasma physics
[AD-A272249] 05 p1994 N94-20943
Parton-parton elastic scattering and rapidity gaps at Tevatron energies
[DE93-041024] 05 p1974 N94-21515
Multibunch beam break-up in detuned structures
[DE93-041056] 05 p1981 N94-21686
Simulation and compensation of multibunch energy variation in NLC
[DE93-041057] 05 p1981 N94-21687
Search for excited quarks in p(-p) collisions at the square root of s = 1.8 TeV
[DE93-019910] 05 p1975 N94-21840
The lepton charge asymmetry in the decay of W bosons produced in p(bar p) collisions at (radical)s = 1.8 TeV
[DE93-019903] 05 p1976 N94-21847
Report of the Joint Seminar on Solid State Physics, Atomic and Molecular Physics, and Materials Science in the Energy Region of Tandem Accelerators
[DE93-508268] 06 p2548 N94-22924
Search for the top quark and other new particles at D0
[DE94-001220] 06 p2535 N94-24515
Electro-weak, QCD and top physics at the Tevatron
[DE94-002304] 06 p2535 N94-24611
Welding of niobium to stainless
[DE94-003365] 06 p2365 N94-24614
The L3 visualization system and its use in the Z(zero) line shape analysis
[ETN-94-95382] 06 p2537 N94-25231
Object-oriented software construction at ALS
[DE94-003418] 07 p2967 N94-27049
Space Experiments with Particle Accelerators (SEPAC)
[NASA-CR-193935] 07 p2761 N94-27664
Performance of a 14-MeV neutron generator as an in situ calibration source for TFTR
[DE94-004993] 07 p3048 N94-27825
A Tevatron collider beauty factory
[DE94-004879] 08 p3488 N94-29930
AMS beyond 2000
[DE94-006666] 09 p3632 N94-31352
The D0 upgrade
[DE94-006953] 09 p3867 N94-31671
Probing lepton number violation via Majorana neutrinos at hadron supercolliders
[PB94-147055] 09 p3868 N94-31922
Jet physics and QCD tests at the Tevatron collider
[DE94-008987] 09 p3871 N94-32587
The future of high-energy physics in the US: Statement for the 1994 HEPAP Subpanel
[DE94-008994] 09 p3876 N94-32588
A search for rapidity gaps in jet events and a study of color coherence in multijet events at D0
[DE94-006849] 09 p3872 N94-32627
Minimax: Multiparticle physics at the Tevatron collider
[DE94-007095] 09 p3873 N94-32689
Simulation of the beam halo from the beam-beam interaction in LEP
[DE94-009097] 10 p4139 N94-33682
Measurement of the ratio R = (sigma x B(p(bar p) yields W(sup (+-)) yields e(sup(+-))(nu)))/(sigma x B(p(bar p) yields Z(sup 0) yields e(sup +e(sup -)) in p(bar p) collisions at the square root of s = 1,800 GeV
[DE94-006846] 10 p4138 N94-35073
Beam tests of a prototype level-1 calorimeter trigger for LHC experiments
[PB94-170495] 11 p4269 N94-35599
Criticai issues in muon colliders: A summary
[DE94-011382] 11 p4331 N94-36271
High Energy Physics Division of research activities
[DE93-019681] 12 p4521 N94-36694
Propagation of radius-tailored laser pulses over extended distances in a uniform plasma
[AD-A280405] 12 p4528 N94-37182
Activities of the Tandem Accelerator Center, University of Tsukuba
[DE94-748687] 12 p4522 N94-37237
Particle physics
[DE94-012944] 12 p4518 N94-37312
Experimental particle physics at the University of Pittsburgh
[DE94-011636] 12 p4521 N94-37721

PARTICLE BEAMS
NT ATOMIC BEAMS
NT ELECTRON BEAMS
NT ION BEAMS
NT MOLECULAR BEAMS
NT NEUTRAL BEAMS
NT NEUTRINO BEAMS
NT NEUTRON BEAMS
NT PION BEAMS
NT PROTON BEAMS
NT RELATIVISTIC ELECTRON BEAMS
Kinetic effects in stochastic topologically nontrivial field
[DE93-621642] 01 p0391 N94-11207
Spectrum analysis in beam diagnostics
[DE93-013401] 01 p0373 N94-12601
Stripping efficiencies for 277 MeV/amu gold beam on copper foils
[DE93-014306] 02 p0569 N94-13221
Intra-blade quantitative transonic flow measurements at the DRA Pyestock Isentropic Light Piston Facility using PIV (Particle Image Velocimetry)
[RAE-TM-AERO/PROP-21] 02 p0509 N94-14706
Channel of the system for pulse charged particle beam diagnostics
[DE93-623867] 03 p1179 N94-14931
Confinement and stability of a Crystal Beam
[DE93-015400] 03 p1181 N94-16020
The (delta)f algorithm for beam dynamics
[DE93-015632] 03 p1187 N94-16660
Evolution of hadron beams under intrabeam scattering
[DE93-014330] 03 p1184 N94-16826
A review of some dynamics models in six-dimensional phase space and their suitable conditions of motion equation
[DE93-623741] 03 p1175 N94-17317
The Intense Slow Positron Source concept: A theoretical perspective on a proposed INEL Facility
[DE93-013675] 04 p1564 N94-17738
Advanced methods for the computation of particle beam transport and the computation of electromagnetic fields and beam-cavity interactions
[DE93-018160] 04 p1573 N94-17807
The Fourteenth Symposium on Molecular Beams
[AD-A268721] 04 p1568 N94-18787
SSC detector muon sub-system beam tests
[DE93-018415] 04 p1569 N94-19013
Simulation of the ALS longitudinal multibunch feedback system
[DE93-019227] 04 p1575 N94-19152
Transverse beam combiner for ILSE
[DE93-019239] 04 p1591 N94-19559
Space-charge dominated beam transport in magnetic quadrupoles with large aperture ratios
[DE93-040443] 05 p1992 N94-20004
Heavy ion fusion injector experiments
[DE93-019188] 05 p1993 N94-20234
Tactical laser weapons and other directed-energy weapons
[AD-A267961] 05 p1816 N94-20484
Plasma lens experiments at the Final Focus Test Beam
[DE93-041081] 05 p1981 N94-21688
SLD results from the study of polarized Z(sup 0) produced at the SLC
[DE93-041020] 05 p1982 N94-21952
Bundle Intensity and Beamgate Length recorder (BIBL)
[DIGEL-1993-7] 07 p3031 N94-25619
Advanced development of particle beam probe diagnostic system
[DE94-002316] 07 p3047 N94-27720
Third-order beam optics of real solenoid magnetic lens
[DE94-608014] 08 p3500 N94-30084
BNL possibilities
[DE94-007179] 09 p3864 N94-31398
Simulation of the beam halo from the beam-beam interaction in LEP
[DE94-009097] 10 p4139 N94-33682
Symplectic tracking using point magnets and a reference orbit made of circular arcs and straight lines
[DE94-011919] 12 p4505 N94-37675

PARTICLE COLLISIONS
Strangeness production with protons and pions
[DE93-010879] 01 p0359 N94-10304
Possibility of a crossed-beam experiment involving slow-neutron capture by unstable nuclei rapid-process-tron
[DE93-754288] 01 p0363 N94-10720
Strange meson spectroscopy in K(omega) and K(phi) at 11 GeV/c and Cherenkov ring imaging at SLD
[DE93-013593] 01 p0363 N94-10748
The intra-atomic motion of bound electrons as a possible source of a systematic error in electron beam polarization measurements by means of a Moeller polarimeter
[DE93-620984] 01 p0364 N94-10875
Proceedings of the Second KEK Topical Conference on e(sup +)e(sup -) collision physics
[DE93-754139] 01 p0364 N94-10889
Experiments in ultracold collisions
[DE93-012110] 01 p0365 N94-11029
Electronic excitation of ground state atoms by collision with heavy gas particles
[NASA-CR-193364] 01 p0366 N94-11360
Experiments to measure the gluon helicity distribution in protons
[DE93-011756] 01 p0368 N94-11613
Top quark search in D(O) from the lepton + jets mode
[DE93-014027] 01 p0370 N94-12781
Measurements of transverse energy and forward energy in high-energy nuclear collisions
[DE93-012755] 02 p0788 N94-12817
Low energy neutral atom imaging techniques
[DE93-012744] 02 p0779 N94-12950
Kinetic studies following state-selective laser excitation
[DE93-012970] 02 p0654 N94-13013

EBIT Trapping Program
[DE93-014422] 02 p0788 N94-13208
Nuclear fusion of protons with ions of boron
[DE93-014284] 02 p0781 N94-13219
Metastable enhancement of C(+) and O(+) capture reactions
[DE93-015075] 02 p0807 N94-13373
Study of electroweak interactions
[DE93-015067] 02 p0782 N94-13412
Electron emission resulting from fast ion impact on thin metal foils: Implications of these data for development of track structure models
[DE93-013506] 02 p0782 N94-13485
Inclusive single muons at DO
[DE93-012779] 02 p0783 N94-13494
High energy hadron-hadron collisions
[DE93-015584] 02 p0784 N94-13927
Top quark search: Results and prospects at Fermilab
[DE93-013016] 02 p0786 N94-14524
Scattering calculations and confining interactions
[NASA-CR-194242] 02 p0786 N94-14549
Theoretical antideuteron-nucleus absorptive cross sections 02 p0786 N94-14551
The pressure broadening of HDO by O2, N2, H2, and He between 100 K and 600 K
[AD-A267118] 03 p0946 N94-15684
Theoretical studies relating to the interaction of radiation with matter
[AD-A267134] 03 p1180 N94-15689
The cooling of confined ions driven by laser beams
[DE93-016612] 03 p1039 N94-16114
Fundamental-mode RF design in e(+)e(-) storage ring factories
[DE93-015249] 03 p1183 N94-16809
Energy-loss cross sections for inclusive charge-exchange reactions at intermediate energies
[NASA-TM-4522] 03 p1188 N94-17018
Production of D-mesons in pp-collisions and quark-gluon string model
[DE93-626721] 03 p1185 N94-17312
Search for the top quark from (e(mu)) and (e,e) events in the D0 detector in p(bar-p) collisions at the square root of s = 1.8 TeV
[DE93-016350] 03 p1186 N94-17662
Correlated charge-changing ion-atom collisions
[DE93-018717] 04 p1564 N94-17775
High-performance multiprocessor architecture for a 3-D lattice gas model 04 p1400 N94-18362
Research in particle physics
[DE93-040875] 04 p1567 N94-18534
A bit serial first level calorimeter trigger for an LHC detector
[USIP-92-08] 04 p1574 N94-18845
Neutron-induced collision cascade mixing in Nb/V superlattices
[DE93-018575] 04 p1600 N94-18933
Search for resonant electron transfer and double excitation in Kr(sup 34+) + H2 collisions
[DE93-018776] 04 p1569 N94-18999
High energy physics at Tufts University
[DE93-018299] 04 p1575 N94-19023
Electron impact polarization and correlation properties of the inert gases
[DE93-018358] 04 p1570 N94-19125
Experimental study of interactions of highly charged ions with atoms at keV energies
[DE93-040222] 04 p1571 N94-19257
Simulating supersymmetry with ISAJET 7.0/ISASUSY 1.0
[DE93-018266] 05 p1969 N94-19804
A search for new gauge bosons in (bar p)p collisions at square root of s equals 1.8 TeV in the dielectron decay mode
[DE93-019901] 05 p1969 N94-19813
Measurements of atomic interactions and frequency stability with a cryogenic hydrogen maser
[AD-A271132] 05 p1814 N94-19853
Collisional processes involving atmospheric gases
[AD-A270729] 05 p1854 N94-19954
A study of events with the highest total transverse energy in CDF
[DE93-019904] 05 p1978 N94-19972
Top search at the TEVATRON
[DE93-019392] 05 p1978 N94-19988
New relativistic S-matrix results for scattering -- beyond the usual anomalous factors/beyond impulse approximation
[DE93-019148] 05 p1971 N94-20096
Jet shapes in hadron and electron colliders
[DE93-019386] 05 p1979 N94-20216
The cross section for the production of b(bar-b) pairs in p(bar p) collisions at the square root of s equals 1.8 TeV
[DE93-019900] 05 p1972 N94-20225
Detection of traveling ionospheric disturbances induced by atmospheric gravity waves using the global positioning system 05 p1723 N94-20425
Theoretical and numerical studies in magnetic fusion
[DE94-000536] 05 p1993 N94-20937
Parton-parton elastic scattering and rapidity gaps at Tevatron energies
[DE93-041024] 05 p1974 N94-21515
Single and double ionization of helium by high-energy photon impact
[DE94-000381] 05 p1975 N94-21785
Measurement of the B meson and b quark cross-section in (-p)p collisions at the square root of s = 1.8 TeV using the exclusive decays B(+) and B(exp 0) yields J/psiK*(exp 0)
[DE93-019907] 05 p1975 N94-21806
Search for excited quarks in p(-p) collisions at the square root of s = 1.8 TeV
[DE93-019910] 05 p1975 N94-21840
The lepton charge asymmetry in the decay of W bosons produced in p(bar p) collisions at (radical)s = 1.8 TeV
[DE93-019903] 05 p1976 N94-21847
Low p(sub T) phenomena observed in high energy nuclear collisions
[DE94-000825] 05 p1982 N94-21849
Recent Fermilab results on hadroproduction of heavy flavors
[DE94-000595] 05 p1976 N94-21867
Low p(sub T) photon production in proton-nucleus collisions at 18 GeV/c
[DE94-001380] 06 p2532 N94-23007
A measurement of the forward-backward asymmetry and sin(sup 2)(theta)(sub W) from the process Z(sup 0) (yields) (mu)(sup +)(mu)(sup (minus)) at (radical)s = 1.8 TeV
[DE94-001908] 06 p2532 N94-23018
Calculations of Bose-Einstein correlations from Relativistic Quantum Molecular Dynamics
[DE94-000794] 06 p2569 N94-23453
Low mass muon pair production in 450 GeV p-Be collisions
[PB94-110699] 06 p2533 N94-23746
Photon-photon collisions at the next linear collider: Theory
[DE93-041025] 06 p2534 N94-23803
Search for the top quark and other new particles at D0
[DE94-001220] 06 p2535 N94-24515
Electro-weak, QCD and top physics at the Tevatron
[DE94-002304] 06 p2535 N94-24611
Analysis of SOFCAL calibration data
[NASA-CR-193910] 06 p2345 N94-25000
Production of (phi) mesons in central Si + Au collisions at 14.6 AGeV/c
[DE94-003196] 07 p3012 N94-25795
Convergent close-coupling calculation of electron-sodium scattering
[DE94-601815] 07 p3014 N94-25842
Hadron jets and nucleon clusters in the relativistic nuclear collisions
[DE93-613434] 07 p3031 N94-25850
The amplitude of the elastic hadron-hadron scattering in the coulombic range of transfer momenta
[DE93-613183] 07 p3014 N94-25869
Spectroscopic and vibrational energy transfer studies in molecular bromine
[AD-A273795] 07 p3014 N94-25875
Monte Carlo event generators for hadron-hadron collisions
[DE94-003212] 07 p3015 N94-25955
The Cherenkov hadronic like-jets
[DE93-634525] 07 p3016 N94-26010
Modeling defect production in high energy collision cascades
[DE94-003810] 07 p3017 N94-26049
The STAR experiment at the Relativistic Heavy Ion Collider
[DE94-003409] 07 p3017 N94-26083
Harvard University High Energy Physics
[DE94-002406] 07 p3032 N94-26119
Predictive modeling of particle-laden, turbulent flows
[DE94-003298] 07 p2792 N94-26319
Nuclear Theory Group, University of Washington recent and planned research
[DE94-002729] 07 p3022 N94-26809
D0 results on searches for the top quark
[DE94-003361] 07 p3023 N94-26938
Calculation of electron-potassium scattering
[DE94-601812] 07 p3023 N94-26942
Antiproton studies in penning traps
[AD-A274250] 07 p3024 N94-27011
An analysis of monojet data in p(bar-p) collisions at square root of s equal to 1.8 TEV
[DE94-001822] 07 p3026 N94-27565
Quantum chromodynamics and nuclear physics at extreme energy density
[DE94-004418] 07 p3026 N94-27604
Double excitation of He and H(-) by fast proton and anti-proton impact
[DE94-004581] 07 p3026 N94-27620
Stopping powers and cross sections due to two-photon processes in relativistic nucleus-nucleus collisions
[NASA-CR-4574] 07 p3033 N94-27646
Studies of heavy-ion reactions and transuranic nuclei
[DE94-004642] 07 p3029 N94-27783
Properties of W + jet events in proton-antiproton collisions at 1.8 TeV
[DE94-004002] 08 p3482 N94-28524
Properties of events containing a photon and several jets seen in p(bar p) collisions at (radical)s = 1.8 TeV
[DE94-005596] 08 p3482 N94-28531
Search for excited quarks in p(bar p) collisions at the square root of s = 1.8 TeV
[DE94-004658] 08 p3484 N94-28573
B production and B(0)(bar B)(0) mixing at DO
[DE94-004664] 08 p3484 N94-28574
A Tevatron collider beauty factory
[DE94-004879] 08 p3488 N94-29930
Inclusive jet and direct photon production at the D0 experiment
[DE94-006001] 08 p3488 N94-30049
Direct anti-b b production in anti-pp collisions at the square root of s = 1.8 TeV
[DE94-006167] 08 p3491 N94-30069
A search for rapidity gap events in p(bar p) collisions at D(0)
[DE94-004654] 08 p3491 N94-30722
Deexcitation processes in nuclear reactions: The study of hot hadronic matter
[DE94-003396] 08 p3492 N94-30836
Atomic physics with highly charged ions
[DE94-003397] 08 p3492 N94-30837
The measurement of the hadronic energy flow and jet production with the ZEUS calorimeter in deep inelastic scattering events at HERA
[ETN-94-96021] 09 p3865 N94-31534
Perturbative and nonperturbative EM lepton pair production in relativistic heavy-ion collisions
[DE94-006315] 09 p3867 N94-31779
Collisional and chaotic transport of energetic particles in toroidal plasma
[DE94-006504] 09 p3889 N94-31787
Monoenergetic neutral particle transport in semi-infinite media
[AD-A277155] 09 p3870 N94-32368
Jet physics and QCD tests at the Tevatron collider
[DE94-008987] 09 p3871 N94-32587
Transverse energy production with Si and Au beams at AGS energy: Towards hot and dense hadronic matter
[DE94-007178] 09 p3938 N94-32638
Electron: Cluster interactions
[DE94-009089] 09 p3874 N94-32807
The e(+)e(-) collisions at the SLC: The left-right asymmetry
[DE94-009031] 10 p4139 N94-33876
Charge-changing collision cross sections of low-energy carbon ions with carbon containing molecules
[DE94-727628] 10 p4137 N94-33935
Measurement of the ratio R = (sigma x B(p(bar p) yields W(sup (+-)) yields e(sup(+-))(nu)))/(sigma x B(p(bar p) yields Z(sup 0) yields e(sup +e(sup -)) in p(bar p) collisions at the square root of s = 1,800 GeV
[DE94-006846] 10 p4138 N94-35073
Theoretical aspect of low pressure discharges in simple gasses
[AD-A278762] 11 p4335 N94-35493
Proceedings of 2nd Working Meeting on Physics at VLEPP, volume 2
[DE94-616167] 11 p4326 N94-36182
B quark production cross sections and the b- (bar b) correlated production cross section at CDF
[DE94-000620] 12 p4514 N94-36700
Hard diffraction and deep inelastic scattering
[DE94-013353] 12 p4515 N94-37084
Precise determination of the weak mixing angle from a measurement of ALR in e(+)e(-) yields Z0
[DE94-013355] 12 p4515 N94-37085
Direct photoionization of excited helium
[DE94-618732] 12 p4516 N94-37097
A rejection method for selection of scattered states
[DE94-012232] 12 p4517 N94-37209
Stopping power of charged particles from 10 eV/amu to 10 GeV/amu
[DE94-719024] 12 p4518 N94-37387
The angular and energy distributions of ejected electrons in electron-impact ionization of helium
[DE94-618748] 12 p4519 N94-37528
Hadron production in S+nucleus collisions at 200 GeV/nucleon
[DE94-011344] 12 p4520 N94-37715

PARTICLE COUNTERS
U RADIATION COUNTERS

PARTICLE DECAY
NT NEUTRON DECAY
U RADIOACTIVE DECAY
Charged scalar particles and (tau) leptonic decay
[DE93-622969] 02 p0779 N94-12882
Double semi-leptonic charm decay in HELIOS-I 450 GeV/c p-Be data
[DE93-013493] 02 p0781 N94-13348
On the difference caused by CP violation in the energy spectra of pions in K(sup (+-))(yields)(pi)(+-)(pi)(+-)(pi)-+ decays
[DE93-624828] 04 p1564 N94-17687
Beauty without charm in B-meson decays
[PREPRINT-732] 04 p1565 N94-17972
A search for new gauge bosons in (bar p)p collisions at square root of s equals 1.8 TeV in the dielectron decay mode
[DE93-019901] 05 p1969 N94-19813
Measurement of the B meson and b quark cross-section in (-p)p collisions at the square root of s = 1.8 TeV using the exclusive decays B(+) and B(exp 0) yields J/psiK*(exp 0)
[DE93-019907] 05 p1975 N94-21806
The lepton-charge asymmetry in the decay of W bosons produced in p(bar p) collisions at (radical)s = 1.8 TeV
[DE93-019903] 05 p1976 N94-21847
Chance to use W-decay lepton channels for width determination
[DE93-634438] 07 p3020 N94-26507
Leptonic decay constants of heavy mesons in QCD
[DE93-634426] 07 p3022 N94-26767
Weak hadronic decays of heavy flavor mesons
[ISBN-0-315-55542-4] 07 p3026 N94-27402
Study of invisible nucleon decay, N approaches nu nu nu bar, and a forbidden nuclear transition in the Kamiokande detector
[ICRR-299-93-11] 07 p3028 N94-27759
Decay constants of heavy mesons in the relativistic potential model with velocity dependent corrections
[DE94-606495] 07 p3030 N94-27860
Energy distribution of the leptons in top decay to charged Higgs
[DE94-005231] 08 p3482 N94-28494
Weak decays of charged K-mesons and charm particles
[PB94-138062] 08 p3486 N94-29143
B lifetimes at CDF
[DE94-006850] 09 p3866 N94-31669
Medium energy measurements of N-N parameters
[DE94-006067] 09 p3869 N94-32173
Semileptonic decays of mesons in the SO(4) model
[DE94-008108] 09 p3873 N94-32708
Medium energy measurements of N-N parameters
[DE94-008340] 10 p4137 N94-33923
Measurement of the ratio R = (sigma x B(p(bar p) yields W(sup (+-)) yields e(sup(+-))(nu)))/(sigma x B(p(bar p) yields Z(sup 0) yields e(sup +e(sup -)) in p(bar p) collisions at the square root of s = 1,800 GeV
[DE94-006846] 10 p4138 N94-35073
A search for radiative neutrino decay from supernovae
[NASA-CR-196011] 11 p4376 N94-35515
Low energy theorems from the effective Lagrangian with vector mesons
[DE94-611173] 11 p4322 N94-35785
Pseudogoldstone boson decay induced by light and search for the solar axion radiation
[DE94-616907] 11 p4326 N94-36133
Decay of the D(sub s)-meson
[DE94-611209] 11 p4329 N94-36308
Top quark search at CDF
[DE94-003643] 12 p4511 N94-36459
A search for first generation scalar leptoquarks at radical s equal to 1.8 TeV with the D0 detector
[DE94-008846] 12 p4511 N94-36506
B-lifetime measurements at the tevatron
[DE94-003617] 12 p4513 N94-36528
High Energy Physics Division of research activities
[DE93-019681] 12 p4521 N94-36694
Sum rules for 1/m corrections to the form factors of semileptonic B decays
[DE94-618548] 12 p4514 N94-37065
Radiative and rare mu and pi decays
[DE94-618549] 12 p4515 N94-37066
New method for minimizing regular functions with constraints on parameter region
[DE94-618340] 12 p4515 N94-37076
A study of jet handedness in hadronic Z0 decays
[DE94-013358] 12 p4515 N94-37087
Five-lepton decay modes of muon and tau mesons
[DE94-621636] 12 p4516 N94-37099
Physics with primary beams of the KEK-PS
[DE94-748635] 12 p4522 N94-37234
Prospects for measuring B(s) mixing at CDF
[DE94-013147] 12 p4518 N94-37298
CDF results on electroweak physics
[DE94-011750] 12 p4520 N94-37674
Experimental particle physics at the University of Pittsburgh
[DE94-011636] 12 p4521 N94-37721

PARTICLE DENSITY (CONCENTRATION)
NT CARRIER DENSITY (SOLID STATE)
NT ELECTRON DENSITY (CONCENTRATION)
NT ELECTRON DENSITY PROFILES
NT ELECTRON DISTRIBUTION
NT ION DENSITY (CONCENTRATION)
NT IONOSPHERIC ELECTRON DENSITY
NT IONOSPHERIC ION DENSITY
NT PLASMA DENSITY
NT PROTON DENSITY (CONCENTRATION)
Nonlinear space charge effect of bunched beam in linac
[DE93-612176] 01 p0371 N94-10409
Effects of depositon rate on Bi2Sr2CaCu2O(8+x) and Bi2Sr(1.6)La(0.4)CuO(6+x) epitaxial thin film growth by pulsed-laser ablation
[DE93-015797] 02 p0812 N94-14362
A field-based technique for the longitudinal profiling of ultrarelativistic electron or positron bunches down to lengths of less than or equal to 10 microns
[DE93-040954] 05 p1978 N94-19873
Searching for high baryon density at the AGS with ARC
[DE93-041155] 05 p1975 N94-21693
The influence of flow type, particle type and gravity on orthokinetic coagulation
[ETN-94-95333] 06 p2267 N94-25060
Finite density effects in gauge theories
[ISBN-0-315-50637-7] 07 p3074 N94-27403
A study of the ultrahigh-energy cosmic ray mass composition with the MACRO and EAS-TOP experiments 08 p3552 N94-29687
High baryon density from relativistic heavy ion collisions
[DE94-003894] 12 p4511 N94-36460

PARTICLE DETECTORS
U RADIATION COUNTERS

PARTICLE DIFFUSION
NT ELECTRON DIFFUSION
NT IONIC DIFFUSION
Diffusion in liquid state and solidification of binary system (M-7) 02 p0587 N94-13739
Turbulent particle dispersion in confined swirling flows
[DLR-FB-92-32] 02 p0637 N94-14045
The (delta)f algorithm for beam dynamics
[DE93-015632] 03 p1187 N94-16660
Radial diffusion of toroidally trapped particles induced by lower hybrid and fast waves
[IPPCZ-327] 05 p1996 N94-21593
Recent developments in the mathematical modelling and physical understanding of transport and dispersion in aquatic systems, with special reference to tidal waters
[PB94-111135] 06 p2418 N94-24600
Bisexual branching diffusions
[AD-A274698] 07 p3008 N94-26374
Boundary-induced phase transitions in equilibrium and non-equilibrium systems
[DE94-608137] 08 p3199 N94-30111
Exclusive many-particle diffusion in disordered media and correlation functions for random vertex models
[DE94-608134] 08 p3525 N94-30121
Glueball and meson dispersion and diffusion relations in compact U(1)(2+1) gauge theory
[ISBN-0-315-85577-0] 08 p3490 N94-30234
Notes on the Langevin model for turbulent diffusion of marked particles
[DE94-007847] 09 p3708 N94-32652
Particle diffusion from the beam-beam interaction in synchrotron colliders
[DE94-007111] 09 p3876 N94-32685
A new point-centered diffusion differencing for unstructured meshes
[DE94-006399] 10 p4128 N94-33717
Analysis of stochastic particle behavior in a magnetic island due to electrostatic drift waves
[DE94-727553] 10 p4137 N94-33869
Diffusion at the magnetopause: A theoretical perspective
[DE94-009356] 10 p4086 N94-33910
Dynamic aperture and transverse proton diffusion in HERA
[DE94-010309] 11 p4331 N94-36224
Neutron transport methods on scalable shared memory multiprocessors
[DE94-012324] 12 p4498 N94-37419

PARTICLE EMISSION
NT ELECTRON EMISSION
NT FIELD EMISSION
NT ION EMISSION
NT NEUTRON EMISSION
NT PHOTOELECTRIC EMISSION
NT SECONDARY EMISSION
NT THERMIONIC EMISSION
NASCAP programmer's reference manual
[NASA-CR-191044] 01 p0278 N94-11702
The Intense Slow Positron Source concept: A theoretical perspective on a proposed INEL Facility
[DE93-013675] 04 p1564 N94-17738
Electrostatic charging and secondary effects in materials submitted to radiation in space 05 p1661 N94-21383
Superconducting cosmic strings near the electroweak scale and cosmic-ray propagation
[MPI-PHE/93-05] 06 p2629 N94-25459
Counting particles emitted by stratospheric aircraft and measuring size of particles emitted by stratospheric aircraft
[NASA-CR-195908] 09 p3769 N94-33170
Space environment laboratory in review, 1993
[PB94-153004] 10 p4187 N94-34946

PARTICLE ENERGY
NT ELECTRON ENERGY
NT ELECTRON STATES
NT PROTON ENERGY
Convection algorithms for magnetospheric particles
[AD-A270103] 04 p1493 N94-18871
Advanced fusion diagnostics
[DE93-040085] 04 p1589 N94-19133
An ab initio Monte Carlo study of low energy positron and electron implantation in elemental metals and multilayers
[DE93-019847] 04 p1603 N94-19541
Edge plasma experiments on CASTOR tokamak
[IPPCZ-332] 05 p1997 N94-21816
Examination of the response capacity of a silicon pixel detector for ions and molecules in the energy area 100 to 300 keV
[MPE-241] 06 p2346 N94-25415
Exploration of GaAs structures for solid-state detectors
[DE93-634191] 07 p3056 N94-26379
Influence of long-range correlations on the spectral functions and response of 48Ca and 90Zr
[ETN-94-96017] 09 p3865 N94-31537
JPRS report: Science and technology. Central Eurasia: Space
[JPRS-USP-94-001] 11 p4201 N94-35518
Fundamentals studies of radial wave thermoacoustic engines
[AD-A280534] 12 p4431 N94-37090
Positron implantation in solids
[DE94-013029] 12 p4537 N94-37499

PARTICLE FLUX
U FLUX (RATE)

PARTICLE FLUX DENSITY
NT ELECTRON FLUX DENSITY
NT NEUTRON FLUX DENSITY
NT PROTON FLUX DENSITY
The effect of an on-orbit near encounter on the number flux density of micron sized particles 03 p0899 N94-16374
Filamentation, current profiles and transport in a tokamak
[DE93-016768] 04 p1584 N94-17948
Measuring electrically charged particle fluxes in space using a fiber optic loop sensor
[NASA-CR-191328] 06 p2544 N94-23829
Surface fluxes of trace gases derived from convective-layer profiles 09 p3704 N94-31774

PARTICLE IMAGE DISPLACEMENT VELOCIMETRY
U PARTICLE IMAGE VELOCIMETRY

PARTICLE IMAGE VELOCIMETRY
The evolution of whole field optical diagnostics for external transonic testing
[ARA-MEMO-379] 01 p0383 N94-11887
Unsteady flow past a NACA 0012 airfoil pitching at constant rates
[AD-A265159] 01 p0016 N94-11889
Evaporation from a meniscus within a capillary tube in microgravity
[NASA-CR-194593] 03 p0976 N94-15654
Fluid dynamic mechanisms and interactions within separated flows
[AD-A271037] 05 p1797 N94-19978
Particle image velocimetry
[DE93-040657] 05 p1804 N94-21748
Droplet turbulence interactions under subcritical and supercritical conditions 06 p2211 N94-23036
Evolution of the large-scale vortices in turbulent mixing-layers 08 p3273 N94-29686
Development and application of particle image velocimetry in high-speed separated flow: Two-dimensional base cavities 08 p3282 N94-30791
Stabilized alumina/ethanol colloidal dispersion for seeding high temperature air flows
[NASA-TM-106591] 09 p3713 N94-32983
A qualitative and quantitative laser-based computer-aided flow visualization method
[NASA-CR-195300] 10 p3984 N94-34391

Unsteady flow past an airfoil pitched at constant rate
10 p3986 N94-34969
Data reduction procedures for laser velocimeter measurements in turbomachinery rotors
[NASA-CR-195343] 10 p4057 N94-35224

PARTICLE IN CELL TECHNIQUE

Emittance growth in displaced, space-charge-dominated beams with energy spread
[DE93-016514] 03 p1188 N94-17672
General geometry PIC for MIMD computers
[AD-A269085] 04 p1534 N94-18767
A particle method for history-dependent materials
[DE93-018696] 04 p1456 N94-19060
Pulsed expansion of plasma in a magnetic thruster
09 p3889 N94-31776

PARTICLE INTENSITY

Application of higher-order multipoint statistics to the ideal spray
[DE94-005104] 11 p4268 N94-36318

PARTICLE INTERACTIONS

NT ELECTRON CAPTURE
NT ELECTROWEAK INTERACTIONS (FIELD THEORY)
NT ELEMENTARY PARTICLE INTERACTIONS
NT HIGH ENERGY INTERACTIONS
NT ION ATOM INTERACTIONS
NT MESON-MESON INTERACTIONS
NT MESON-NUCLEON INTERACTIONS
NT MOLECULAR COLLISIONS
NT MOLECULAR INTERACTIONS
NT NUCLEAR INTERACTIONS
NT NUCLEON-NUCLEON INTERACTIONS
NT PLASMA-PARTICLE INTERACTIONS
NT SPIN-ORBIT INTERACTIONS
NT STRONG INTERACTIONS (FIELD THEORY)
NT WAVE-PARTICLE INTERACTIONS
NT WEAK ENERGY INTERACTIONS
NT WEAK INTERACTIONS (FIELD THEORY)

Indication on the existence of the bound state in the p anti p-system
[DE92-641575] 01 p0361 N94-10532
Studies of P-matrix formalism on the basis of the potential description of two-particle interaction
[DE93-617691] 01 p0362 N94-10550
Gas-Grain Simulation Facility (GGSF). Volume 2: Conceptual design definition
[NASA-CR-177613] 01 p0423 N94-11229
Studies of electrostatic waves and VLF-wave particle interaction in the ionosphere
[AD-A266013] 01 p0278 N94-12392
Predicted performance of a dc beam driven FEM oscillator designed for fusion applications at 200-250 GHz
[DE93-013414] 02 p0655 N94-13145
Beam halo formation from space-charge dominated beams in uniform focusing channels
[DE93-014458] 02 p0789 N94-13209
Measuring strangeness in the nucleon
[DE93-014861] 02 p0785 N94-14471
Analytical and experimental investigation of the feasibility of accelerated lifetime testing of materials exposed to an atomic oxygen beam
[NASA-CR-193851] 03 p0946 N94-15766
The three-loop QCD beta-function and anomalous dimensions
[NIKHEF-H/92-17] 03 p1186 N94-17617
Variable time-step integration for intense field effects
[DE93-013296] 04 p1382 N94-17909
Report of the 1991 Workshop on Particle-Material Interactions for Fusion Research
[DE93-788393] 04 p1573 N94-18156
Technology, design, simulation, and evaluation for SEP-hardened circuits 04 p1399 N94-18352
Charmonium physics from (bar p)p interactions
[DE93-017809] 04 p1569 N94-18973
Task A: Yale Accelerator Users Group (YAUG)
[DE93-018417] 04 p1570 N94-19029
Simulating supersymmetry with ISAJET 7.0/ISASUSY 1.0
[DE93-018266] 05 p1969 N94-19804
A study of events with the highest total transverse energy in CDF
[DE93-019904] 05 p1978 N94-19972
Recent Fermilab results on hadroproduction of heavy flavors
[DE94-000595] 05 p1976 N94-21867
Electron spectroscopic studies of the neutralization of slow multicharged ions during interactions with a metal surface
[DE93-041046] 06 p2532 N94-22956
Computer modeling of nonlinearities
06 p2458 N94-24661
Thermophysical properties of simple liquid metals: A brief review of theory 06 p2248 N94-25130
On the connection of classical mechanics, physical kinetics and quantum theory
[DE93-616823] 06 p2570 N94-25207
Fermionic field theory and gauge interactions on random lattices
[DE94-601565] 07 p3051 N94-25885
CP test in the W pair production by way of photon fusion at NLC
[DE94-601608] 07 p3014 N94-25889
Principles of gauge theory of real hadrons
[DE93-616857] 07 p3015 N94-25920
Energy distribution of the leptons in top decay to charged Higgs
[DE94-005231] 08 p3482 N94-28494
Theory of fundamental interactions
[DE94-608126] 08 p3525 N94-30169
Atomic physics with highly charged ions
[DE94-003397] 08 p3492 N94-30837
Analysis of the high energy behavior of the forward scattering parameters - sigma(tot), rho and B
[DE94-006537] 09 p3864 N94-31310
The measurement of the hadronic energy flow and jet production with the ZEUS calorimeter in deep inelastic scattering events at HERA
[ETN-94-96021] 09 p3865 N94-31534
Proceedings of the Fourth Conference on Hyperfine Interaction Spectroscopic Investigations
[DE94-614944] 10 p4147 N94-33866
GRACE manual
[DE94-727456] 10 p4105 N94-33867
The kinetics of inhomogeneous plasma
[DE94-611459] 11 p4336 N94-35788
On the theory of bounded many-particle systems with purely coulomb interactions
[DE94-617215] 11 p4325 N94-36081
P-matrix approach and three-nucleon problem
[DE94-616887] 11 p4326 N94-36131
Alternating series fit to the total cross sections
[DE94-616888] 11 p4326 N94-36132
Proceedings of the Twenty-First All-Union Conference on Physics of Charged Particles Interaction with Crystals
[DE94-615768] 11 p4341 N94-36181
P-matrix description of charged particles interaction
[DE94-616853] 11 p4329 N94-36391
Measurement and processing of gammas accompanying muon pairs in the reaction pi(-)C yields mu(+)mu(-) + gamma + X at 38 GeV
[DE94-617044] 12 p4512 N94-36523
Blois 5: Experimental summary
[DE94-001219] 12 p4513 N94-36558
High Energy Physics Division of research activities
[DE93-019681] 12 p4521 N94-36694

PARTICLE MASS

NT ELECTRON MASS

Top and Higgs masses in a composite boson model
[DE93-010874] 01 p0359 N94-10302
Report of the Workshop on Light Particle-Induced Reactions
[DE93-752300] 01 p0360 N94-10317
Comparing the Z(sup 0) mass and inclusive widths to the standard electroweak theory
[PREPRINT-731] 02 p0787 N94-14721
Densities of 5-15 micron interplanetary dust particles
03 p1244 N94-16367
Cabibbo mixing in superstring derived standard-like models
[DE93-624814] 04 p1607 N94-17953
Low mass muon pair production in 450 GeV p-Be collisions
[PB94-110699] 06 p2533 N94-23746
Stitching the Yukawa quilt
[PB93-204477] 06 p2569 N94-24532
C-periodicity and the physical mass in the 3-state Potts model
[DE94-601551] 07 p3019 N94-26423
Spectroscopy and strong decays of baryons
[ISBN-0-315-49073-X] 07 p3024 N94-27258
Finding the missing pieces of the standard model
[ISBN-0-315-57174-8] 07 p3024 N94-27259
On the model of the relativistic particle with curvature and torsion
[DE94-606330] 07 p3029 N94-27848
Cosmological constraints on very heavy stable neutrinos
[DE94-601669] 07 p3117 N94-28066
Operator analysis for quark and lepton masses in SO(10)
[DE94-005201] 08 p3491 N94-30709
Attitude dynamics of spinning rockets in space with internal mass motion 09 p3601 N94-31802
Solar neutrino oscillations
[DE94-007265] 10 p4165 N94-33687
Goldstone pion and other mesons using a scalar confining interaction
[DE94-010016] 11 p4321 N94-35649
Universal SU(2/1) and the Higgs and fermion masses
[DE94-009182] 11 p4323 N94-35814
Top dilepton search at CDF
[DE94-002302] 11 p4327 N94-36266
Top quark search at CDF
[DE94-003643] 12 p4511 N94-36459
About existence of a baryon with the 3.52 GeV/c2 mass
[DE94-621641] 12 p4519 N94-37414

PARTICLE MOTION

Exact and quasi-classical density matrix and Wigner functions for a particle in the box and half space
01 p0350 N94-10600
New squeezed landau states
01 p0379 N94-10601
Charged particle motion in torsatrons, part 1
[DE93-621639] 01 p0389 N94-11119
Particle transport analysis in torsatron configurations
[DE93-621640] 01 p0390 N94-11120
Development of deterministic transport methods for low energy neutrons for shielding in space
[NASA-CR-194172] 01 p0386 N94-11199
Helium transport scaling law studies
[DE93-013487] 01 p0393 N94-11513
Short pulse lasers for generation of fields exceeding 100 MG
[DE93-013346] 01 p0369 N94-11815
Spectrum analysis in beam diagnostics
[DE93-013401] 01 p0373 N94-12601
Stochastic dynamics: Crossover from 1/f(sup 3) to flicker noise
[DE93-622862] 02 p0772 N94-12896
Kinetic simulations of ultra-intense laser plasma interactions and a novel method of generating odd harmonics
[DE93-014418] 02 p0797 N94-13207
Numerical studies of spray combustion in liquid-fueled engines 02 p0564 N94-13685
Stormtime transport of ring current and radiation belt ions
[NASA-CR-194416] 02 p0714 N94-13793
Granular fluctuations in plasma turbulence and their role in transport
[DE93-013465] 03 p1187 N94-17674
High-performance multiprocessor architecture for a 3-D lattice gas model 04 p1400 N94-18362
Effects of transverse coupling on transverse beam size, simulation and measurements
[DE93-017804] 04 p1574 N94-18972
Visualization of turbulent flow with particles
[PB94-149671] 04 p1423 N94-19645
Aperture determination of RHIC92 from randomly generated initial coordinates
[DE93-040174] 05 p1978 N94-19945
Stochastic resonance in a periodic potential system under a constant force
[DE93-616817] 07 p3008 N94-25831
The effect of magnetic field configuration on particle pinch velocity in Compact Helical System (CHS)
[AD-B183299L] 08 p3505 N94-29398
X ray pulse considerations and electron flow in high voltage diodes
[AD-A277301] 09 p3868 N94-32044
Analysis of stochastic particle behavior in a magnetic island due to electrostatic drift waves
[DE94-727553] 10 p4137 N94-33869
Magnetoresistance of films and strips with the diffuse surface scattering
[DE94-611100] 11 p4340 N94-35933
Numerical method to study the stability of periodic solutions of particle motion in nonlinear magnetic fields
[DE94-610740] 11 p4325 N94-36088
Application of higher-order multipoint statistics to the ideal spray
[DE94-005104] 11 p4268 N94-36318

PARTICLE PRECIPITATION

NT ELECTRON PRECIPITATION
NT PROTON PRECIPITATION

Processing, properties, and wear resistance of aluminides
[DE93-012186] 01 p0083 N94-11141
Global zones of particle precipitation as observed EXOS-C
[AD-A268758] 04 p1481 N94-18467
Importance of aggregation and small ice crystals in cirrus clouds, based on observations and an ice particle growth model 05 p1879 N94-22336
Quiet-time intensifications along the poleward auroral boundary near midnight
[ATR-93(7248)-2] 07 p2877 N94-26201

PARTICLE PRODUCTION

NT KAON PRODUCTION
NT PAIR PRODUCTION
NT PHOTOPRODUCTION

Production of strange clusters in relativistic heavy ion collisions
[DE93-010876] 01 p0359 N94-10303
Strangeness production with protons and pions
[DE93-010879] 01 p0359 N94-10304
Fast trigger algorithm for B-events selection
[DE93-621452] 01 p0365 N94-11089
Relativistic heavy-ion collisions
[DE93-014844] 01 p0366 N94-11147
Tau physics
[DE93-010956] 01 p0367 N94-11469
Experiments to measure the gluon helicity distribution in protons
[DE93-011756] 01 p0368 N94-11613
Detection of hot muonic hydrogen atoms emitted in vacuum using x-rays
[DE93-010253] 02 p0778 N94-12860
HIJET with AGS physics and N(sup *)'s
[DE93-014022] 02 p0780 N94-13097
Neutral strange particle production at the AGS
[DE93-014044] 02 p0780 N94-13098
Further study of the X(1910) meson
[DE93-621443] 02 p0782 N94-13362
Study of electroweak interactions
[DE93-015067] 02 p0782 N94-13412
Inclusive single muons at DO
[DE93-012779] 02 p0783 N94-13494
Effects of additional isoscalar vector bosons in e(sup +)e)(sup -)(yields)ff-bar processes at the TRISTAN and LEP energies
[DE93-621451] 02 p0783 N94-13506
Top quark search: Results and prospects at Fermilab
[DE93-013016] 02 p0786 N94-14524
E789 and P865: High-rate fixed-target studies of charm and beauty
[DE93-017223] 02 p0788 N94-14898
Electroweak physics from D0
[DE93-015041] 03 p1181 N94-16053
Status of (alpha)(sub s) measurements
[DE93-015179] 03 p1181 N94-16059
Past, present and future ((pi),(eta)) experiments
[DE93-016631] 03 p1182 N94-16115
A calibration of the production rate ratio P-21/P-26 by low energy secondry neutrons: Identification of Ne spallation components at the 10(exp 6) atoms/g level in terrestrial samples 03 p1187 N94-16194
Electroweak results from D0
[DE93-014926] 03 p1185 N94-16968
Energy-loss cross sections for inclusive charge-exchange reactions at intermediate energies
[NASA-TM-4522] 03 p1188 N94-17018
Production of D-mesons in pp-collisions and quark-gluon string model
[DE93-626721] 03 p1185 N94-17312
Search for the top quark from (e(mu)) and (e,e) events in the D0 detector in p(bar-p) collisions at the square root of s = 1.8 TeV
[DE93-016350] 03 p1186 N94-17662
Beauty without charm in B-meson decays
[PREPRINT-732] 04 p1565 N94-17972
Experimental consequences of supersymmetry
[DE93-018270] 04 p1569 N94-18945
Task A: Yale Accelerator Users Group (YAUG)
[DE93-018417] 04 p1570 N94-19029
Extraction of Z(prime) coupling data from Z(prime) (yields) jj at the LHC and SSC
[DE93-018576] 04 p1570 N94-19096
Eta-nucleon interaction and nuclear production of eta mesons
[DE93-018469] 04 p1571 N94-19259
Simulating supersymmetry with ISAJET 7.0/ISASUSY 1.0
[DE93-018266] 05 p1969 N94-19804
A search for new gauge bosons in (bar p)p collisions at square root of s equals 1.8 TeV in the dielectron decay mode
[DE93-019901] 05 p1969 N94-19813
The two-jet differential cross-section at CDF
[DE93-019905] 05 p1978 N94-19983
The cross section for the production of b(bar-b) pairs in p(bar p) collisions at the square root of s equals 1.8 TeV
[DE93-019900] 05 p1972 N94-20225
B production at D0
[DE93-019250] 05 p1972 N94-20291
Search for excited quarks in p(-p) collisions at the square root of s = 1.8 TeV
[DE93-019910] 05 p1975 N94-21840
The lepton charge asymmetry in the decay of W bosons produced in p(bar p) collisions at (radical)s = 1.8 TeV
[DE93-019903] 05 p1976 N94-21847
Recent Fermilab results on hadroproduction of heavy flavors
[DE94-000595] 05 p1976 N94-21867
SLD results from the study of polarized Z(sup 0) produced at the SLC
[DE93-041020] 05 p1982 N94-21952
Toward a QCD analysis of jet rates in deep-inelastic Muon-Proton scattering
[DE94-000618] 05 p1976 N94-21962
Production, collection and utilization of very long-lived heavy charged leptons
[DE93-040867] 05 p1977 N94-22009
Time evolution of the quark-gluon plasma
[DE94-000804] 05 p1998 N94-22389
B-quark production at hadron colliders
[DE94-001459] 06 p2534 N94-23806
A research of possibility for negative muon production by a low energy electron beam accompanying ion beam
[NIFS-266] 06 p2536 N94-24868
Bottom quark production at the Z resonance
[ISBN-9-09-006217-3] 06 p2538 N94-25255
Behavior of the intermittency exponents and a quark-gluon plasma formation in the heavy ion collisions
[DE93-616869] 06 p2541 N94-25342
On the hadron formation time in pion-nucleus interaction
[DE93-616879] 06 p2539 N94-25476
Production of (phi) mesons in central Si + Au collisions at 14.6 AGeV/c
[DE94-003196] 07 p3012 N94-25795
Heavy quark production and spectroscopy
[DE94-003619] 07 p3015 N94-25935
Monte Carlo event generators for hadron-hadron collisions
[DE94-003212] 07 p3015 N94-25955
A dependence of exclusive vector meson production in muon-nucleus scattering
[DE94-003363] 07 p3016 N94-25957
The STAR experiment at the Relativistic Heavy Ion Collider
[DE94-003409] 07 p3017 N94-26083
Rescattering and energy loss of fast partons in nuclear matter
[DE94-002918] 07 p3018 N94-26145
A search for the production of direct leptons in nucleon-nucleus and nucleus-nucleus collisions
[DE94-004640] 07 p3018 N94-26244
Photon and hadron production of heavy flavors
[DE94-004655] 07 p3018 N94-26245
Strange Dibaryons
[DE94-003005] 07 p3022 N94-26769
D0 results on searches for the top quark
[DE94-003361] 07 p3023 N94-26938
Measurements of the B(sup 0)(bar B)(sup 0)CP asymmetry
[DE94-003379] 07 p3063 N94-27047
Study of the process (pi)(sup -)A(yields)(pi)(sup -)(eta)'(eta)A at the moment 36 GeV/c
[DE93-634530] 07 p3024 N94-27250
A jet calculus approach including coherence effects and the associated problem of moment inversion
[ISBN-0-315-51715-8] 07 p3025 N94-27266
Jet production in muon scattering at Fermilab E665
[DE94-004663] 07 p3028 N94-27752
Correlations in inelastic collisions of relativistic nuclei with emulsion at (4.1 - 4.5) A GeV/c
[DE93-634526] 07 p3030 N94-27994
Report of the subgroup on the top quark
[DE94-004624] 08 p3481 N94-28462
Properties of W + jet events in proton-antiproton collisions at 1.8 TeV
[DE94-004002] 08 p3482 N94-28524
Properties of events containing a photon and several jets seen in p(bar p) collisions at (radical)s = 1.8 TeV
[DE94-005596] 08 p3482 N94-28531
B production and B(0)(bar B)(0) mixing at DO
[DE94-004664] 08 p3484 N94-28574
Experimental setup for study of hadron and hard photon production in nucleus-nucleus collisions
[DE94-607849] 08 p3489 N94-30051
Experimental setups and methods to obtain new nuclear data at intermediate and high energies
[DE94-607850] 08 p3489 N94-30052
Search for heavy neutrinos at the IHEP-JINR neutrino detector
[DE94-608175] 08 p3489 N94-30095
Modelling of multiparticle production by dynamical semigroup method
[DE94-608132] 08 p3490 N94-30120
Direct anti-b b production in anti-pp collisions at the square root of s = 1.8 TeV
[DE94-006167] 08 p3491 N94-30369
Heavy flavor production at fixed target photo- and hadroproduction
[DE94-004651] 08 p3491 N94-30719
Search for the top quark in the electron-electron and electron-muon channels at D0
[DE94-006174] 08 p3492 N94-30779
Charmonium and bottomonium in (-p)p interactions
[DE94-006173] 08 p3493 N94-30886
Inclusive single muon production in D0
[DE94-006175] 08 p3493 N94-30887
State of hadron collider physics
[DE93-005279] 09 p3863 N94-31147
Elimination of two atomic electrons by a single high energy photon
[DE94-006834] 09 p3864 N94-31320
Study of B(0) - bar-B(0) mixing in D0
[DE94-006000] 09 p3897 N94-31506
Elementary particle physics
[DE94-006071] 09 p3866 N94-31620
Study of associated gauge boson production at D0: W gamma production
[DE94-006951] 09 p3866 N94-31670
Perturbative and nonperturbative EM lepton pair production in relativistic heavy-ion collisions
[DE94-006315] 09 p3867 N94-31779
Baryogenesis from a primordial lepton asymmetry
[PB94-145166] 09 p3868 N94-31921
Medium energy measurements of N-N parameters
[DE94-006067] 09 p3869 N94-32173
Antiproton production in heavy ion collisions
[DE94-007552] 09 p3870 N94-32271
Jet physics and QCD tests at the Tevatron collider
[DE94-008987] 09 p3871 N94-32587
A search for rapidity gaps in jet events and a study of color coherence in multijet events at D0
[DE94-006849] 09 p3872 N94-32627
Proceedings of the Workshop on B Physics at Hadron Accelerators
[DE94-007961] 09 p3877 N94-32748
Studies of jet production with the D0 detector
[DE94-008271] 09 p3873 N94-32780
Hyperon polarization, crystal channeling, and E781 at Fermilab
[DE94-008224] 09 p3877 N94-32802
The e(+)e(-) collisions at the SLC: The left-right asymmetry
[DE94-009031] 10 p4139 N94-33876
Measurement of the ratio R = (sigma x B(p(bar p) yields W(sup (+-)) yields e(sup(+-))(nu)))/(sigma x B(p(bar p) yields Z(sup 0) yields e(sup +e(sup -)) in p(bar p) collisions at the square root of s = 1,800 GeV
[DE94-006846] 10 p4138 N94-35073
Proceedings of 2nd Working meeting: Physics at VLEPP, volume 1
[DE94-616200] 11 p4320 N94-35569
Low energy theorems from the effective Lagrangian with vector mesons
[DE94-611173] 11 p4322 N94-35785
Isoscalar vector bosons at LEP 2
[DE94-611253] 11 p4323 N94-35787
Support of hadroproduction of bottom using the 800 GeV/c primary photon beam at the Fermilab tevatron
[DE94-009411] 11 p4324 N94-36016
CDF electroweak studies and the search for the top quark
[DE94-010333] 11 p4326 N94-36107
Proceedings of 2nd Working Meeting on Physics at VLEPP, volume 2
[DE94-616167] 11 p4326 N94-36182
Precise measurement of the left-right cross section asymmetry in Z boson production by electron-positron collisions
[DE94-010751] 11 p4326 N94-36198
Hybrid mesons (Q(anti Q)g) in N(anti N) annihilation
[DE94-001491] 11 p4327 N94-36239
Top dilepton search at CDF
[DE94-002302] 11 p4327 N94-36266
High baryon density from relativistic heavy ion collisions
[DE94-003894] 12 p4511 N94-36460
High Energy Physics Division of research activities
[DE93-019681] 12 p4521 N94-36694
Electroweak physics at the Tevatron collider
[DE93-040927] 12 p4513 N94-36695
B quark production cross sections and the b- (bar b) correlated production cross section at CDF
[DE94-000620] 12 p4514 N94-36700
Mass identified particle production and Bose Einstein correlations at 1800 GeV
[DE94-013418] 12 p4515 N94-37067
The mathematical simulation of physical processes in ECR multicharged ions sources
[DE94-618343] 12 p4515 N94-37077
Hard diffraction and deep inelastic scattering
[DE94-013353] 12 p4515 N94-37084
Precise determination of the weak mixing angle from a measurement of ALR in e(+)e(-) yields Z0
[DE94-013355] 12 p4515 N94-37085
Production of phi mesons in central Si+Au collisions at 14.6 A GeV/c
[DE94-011726] 12 p4516 N94-37152

Kaon correlation systematics in E859
[DE94-011927] 12 p4516 N94-37158
Comparison of oxygen and silicon induced reactions at 14.6 A(GeV/C)
[DE94-011923] 12 p4518 N94-37364
About existence of a baryon with the 3.52 GeV/c2 mass
[DE94-621641] 12 p4519 N94-37414
Strangeness and the quark-gluon plasma: An experimenter's perspective
[DE94-011377] 12 p4519 N94-37558
CDF results on electroweak physics
[DE94-011750] 12 p4520 N94-37674
Hadron production in S+nucleus collisions at 200 GeV/nucleon
[DE94-011344] 12 p4520 N94-37715
Pre-equilibrium parton dynamics: Proceedings
[DE94-011347] 12 p4520 N94-37716

PARTICLE SIZE DISTRIBUTION
Ostwald ripening of solid cobalt particles in liquid copper 01 p0087 N94-10202
Granular instability in fluidized beds: A small-over-large instability 01 p0122 N94-10235
Martian particle size based on thermal inertia corrected for elevation-dependent atmospheric properties 01 p0430 N94-12107
Organic matter on the early surface of Mars: An assessment of the contribution by interplanetary dust 01 p0480 N94-12259
Dynamic high-pressure shock compaction of diamond powders
[AD-A266004] 01 p0093 N94-12354
Size distribution of interplanetary iron and stony particles related with deep-sea spherules 03 p1245 N94-16388
From minerals to rocks: Toward modeling lithologies with remote sensing 03 p1086 N94-16437
Sol-spray preparation, particulate characteristics, and sintering of alumina powders
[DE93-018577] 05 p1690 N94-20183
Zinc and titanium smoke: Chemical composition and physical characteristics
[FOA-C-40277-4.9] 05 p1680 N94-20552
Thermal conductivity measurements of particulate materials under Martian conditions 05 p1685 N94-20703
Coagulation of grains in static and collapsing protostellar clouds 05 p2085 N94-20865
Holographic measurements of ice crystals in cirrus clouds during International Cirrus Experiment ICE
[GKSS-92/E/14] 05 p1866 N94-21052
A documentation of icing relevant cloud physical parameters on horizontal soundings of stratiform clouds (continuation)
[DLR-MITT-92-10] 05 p1871 N94-22280
Spectral variation of scattering and absorption by cirrus 05 p1876 N94-22321
Importance of aggregation and small ice crystals in cirrus clouds, based on observations and an ice particle growth model 05 p1879 N94-22336
Development of a droplet breakup model considering aerodynamic and droplet collision effects 06 p2213 N94-23045
Characterization of 3-D particle distributions and effects on recrystallization studied by computer simulation
[PB93-201408] 06 p2562 N94-23535
Gas-grain simulation experiment module conceptual design and gas-grain simulation facility breadboard development
[NASA-CR-177632] 06 p2598 N94-23536
Particle size measurement for the control of industrial crystallizers
[PB94-119104] 06 p2562 N94-23766
On the stability of the process of formation of combustion generated particles by coagulation and simultaneous shrinkage due to particle oxidation 06 p2159 N94-24274
Effect of initial droplet-size distributions on fuel-vapor profiles in a shear-layer flow 06 p2160 N94-24283
Low-gravity electrodeposition and growth of polymer thin films with large third-order optical nonlinearities by electrochemical processes for devices: Thiophene-based polymers 06 p2225 N94-24346
LRAT: Lightning Radiative Transfer 06 p2416 N94-24443
The influence of flow type, particle type and gravity on orthokinetic coagulation
[ETN-94-95333] 06 p2267 N94-25060
Mechanisms of droplet formation
[ISBN-9-06-275765-0] 06 p2338 N94-25227
Using the log-normal distribution in analyzing aerosols: The mathematical reasoning underlying the various diameters used and the plotting procedure
[DE94-006459] 08 p3461 N94-30817
Combustor and nozzle effects on particulate behavior in solid rocket motors
[AD-A277304] 09 p3614 N94-32071
Drop size distributions and related properties of fog for five locations measured from aircraft
[NASA-CR-4585] 09 p3787 N94-33065
Counting particles emitted by stratospheric aircraft and measuring size of particles emitted by stratospheric aircraft
[NASA-CR-195908] 09 p3769 N94-33170
The wavelength dependence of Martian atmospheric dust radiative properties 09 p3950 N94-33228
Shape, size, and distribution of magnetic particles in Bjurbole chondrules 11 p4353 N94-36167

PARTICLE SPIN
NT ELECTRON SPIN
NT ISOTOPIC SPIN
NT NUCLEAR SPIN
Aharonov-Bohm effect in Luttinger liquid
[DE93-613818] 01 p0408 N94-10148
Top quark polarization and T-odd spin correlations as tools for testing (non) Standard Model predictions
[DE93-622956] 02 p0778 N94-12847
Electromagnetic deflection of spinning particles
[DE93-622866] 02 p0778 N94-12858
Aspects of symmetry violation
[DE93-011003] 02 p0779 N94-12997
Calculation of electron-lithium scattering using the coupled-channel optical method
[DE93-623049] 02 p0806 N94-13226
Magnetic interactions and disorder - phase transitions in dilute spin-glasses and high temperature superconductors
[ITN-93-85217] 02 p0815 N94-14825
Quark-loop effects in high energy spin-flip processes
[DE93-626692] 03 p1188 N94-17313
Measuring the sea quark polarization
[DE93-015792] 04 p1566 N94-18234
Research activity on particle spin systems and related problems
[AD-A269456] 04 p1562 N94-18286
A conceptual design for the STAR endcap electromagnetic calorimeter
[DE93-040801] 05 p1807 N94-19990
Polarized structure functions of the nucleon in the resonance region
[CEBAF-PR-94-001] 06 p2540 N94-24663
Proton spin: The role of quark-gluon and hadron degrees of freedom
[DE93-616867] 06 p2538 N94-25341
A quark structure of hadrons and nuclei
[DE93-616872] 06 p2539 N94-25474
On the relativistic invariant representation of arbitrary bilinear combinations of Dirac spinors
[DE93-634343] 07 p3019 N94-26456
Correlated mean field Ansatz for the Kondo necklace
[DE94-603671] 07 p3067 N94-27634
On the model of the relativistic particle with curvature and torsion
[DE94-606330] 07 p3029 N94-27848
Axial anomaly in e(+)e(-) yields gamma gamma and anyon superconductivity
[DE94-606406] 07 p3070 N94-27859
Determination of the neutron spin-structure function
[DE94-005234] 08 p3483 N94-28542
On relativity principle violation in local measurements of spin precession of moving particles
[DE94-608067] 08 p3489 N94-30085
Magnetic properties of a quantum transverse spin-1 Blume-Emery-Griffiths model
[DE94-608114] 08 p3517 N94-30109
RHIC spin physics
[DE94-005452] 09 p3876 N94-32099
Marshall Space Flight Center head development program
[NASA-CR-193944] 10 p4056 N94-34073
Periodicity and peculiarity in 120 first and second row diatomic molecules
[AD-A278836] 11 p4323 N94-35793
Spin dynamics in storage rings and linear accelerators
[DE94-010320] 11 p4330 N94-36106
The E2/M1 mixing ratio in the excitation of the Delta from polarized photo-reactions
[DE94-004235] 12 p4510 N94-36442
Relaxation of the density matrix for an arbitrary spin in random external fields
[DE94-618457] 12 p4509 N94-37078
Polarization phenomena in quantum chromodynamics
[DE94-010663] 12 p4539 N94-37543
Neutrino-nucleon scattering
[DE94-011720] 12 p4520 N94-37671
The spin observables of electron-nucleon scattering from the formalism of nucleon-nucleon scattering
[DE94-011368] 12 p4520 N94-37717

PARTICLE TELESCOPES
CRRES high energy proton flux map
[AD-A274803] 07 p2878 N94-26338
The PROTEL contamination code
[RXR-93071] 07 p3040 N94-28202

PARTICLE THEORY
Top and Higgs masses in a composite boson model
[DE93-010874] 01 p0359 N94-10302
The legacy of uncertainty 01 p0376 N94-10577
S(sup 1) x S(sup 2) as a bag membrane and its Einstein-Weyl geometry
[DE93-613149] 01 p0410 N94-10635
All possible electroweak models from Z orbifold
[DE93-617656] 01 p0411 N94-10880
Elementary particle physics and high energy phenomena
[DE93-013971] 01 p0370 N94-12609
Electric charge quantization
[DE93-622901] 02 p0778 N94-12845
Radiative corrections in the strongly interacting limit of the standard electroweak model
[DE93-013906] 02 p0780 N94-13018
Comparing the Z(sup 0) mass and inclusive widths to the standard electroweak theory
[PREPRINT-731] 02 p0787 N94-14721
On the nature of mirror particles
[DE93-626670] 03 p1179 N94-14934
On the 17-keV neutrino
[DE93-012638] 03 p1181 N94-15974
Particle physics and cosmology, Task C
[DE93-016865] 03 p1239 N94-16118
Multipolar-like form of nonabelian gauge theories
[DE93-626690] 03 p1171 N94-17314
Research in particle physics
[DE93-040875] 04 p1567 N94-18534
High energy physics program. Task A: Experiment and theory. Task B: Numerical simulation
[DE93-018140] 04 p1575 N94-19050
Electrokinetic transport of heterogeneous particles in suspensions
[NASA-CR-194478] 04 p1353 N94-19367
Aperture determination of RHIC92 from randomly generated initial coordinates
[DE93-040174] 05 p1978 N94-19945
High energy physics program at Texas A/M University
[DE93-041089] 05 p1980 N94-20933
Recent results on top, bottom and exotic physics at the Tevatron
[DE94-000578] 05 p1975 N94-21786
Towards a theory of quark and lepton masses
[DE94-001726] 06 p2533 N94-23218
Applications of supersymmetric quantum mechanics
[ETN-94-95385] 06 p2570 N94-25257
Correlations in the actions of periodic orbits derived from quantum chaos
[DE93-616866] 06 p2571 N94-25340
Heavy flavour physics at LEP
[NIKHEF-H/92-19] 06 p2539 N94-25465
Cosmoparticle physics of family symmetry breaking
[DE94-601623] 07 p3013 N94-25837
Measurement of tau lepton branching fractions
[DE94-003423] 07 p3018 N94-26325
Construction of a new electroweak sphaleron
[NIKHEF-H/93-09] 07 p3020 N94-26540
On the model of the relativistic particle with curvature and torsion
[DE94-606330] 07 p3029 N94-27848
Twistor-like type 2 superstring and bosonic string
[DE94-606339] 08 p3523 N94-28802
Statistical description of hot and dense clustering matter
[DE94-608155] 08 p3490 N94-30112
Modelling of multiparticle production by dynamical semigroup method
[DE94-608132] 08 p3490 N94-30120
Problems in particle theory
[DE94-003665] 08 p3491 N94-30685
Semileptonic decays of mesons in the SO(4) model
[DE94-008108] 09 p3873 N94-32708
Summary: Hadron dynamics sessions
[DE94-003011] 11 p4328 N94-36303
Decay of the D(sub s)-meson
[DE94-611209] 11 p4329 N94-36308
The E2/M1 mixing ratio in the excitation of the Delta from polarized photo-reactions
[DE94-004235] 12 p4510 N94-36442
High baryon density from relativistic heavy ion collisions
[DE94-003894] 12 p4511 N94-36460
Radiative and rare mu and pi decays
[DE94-618549] 12 p4515 N94-37066
Particle physics
[DE94-012944] 12 p4518 N94-37312

PARTICLE TRACKS
Conceptual design report for the SDC barrel and intermediate muon detectors based on a jet-type drift chamber
[DE93-753173] 01 p0367 N94-11510
Theory of elementary particles and accelerator theory. Task C: Experimental high energy physics
[DE93-013139] 01 p0368 N94-11696
EGS (underscore) windows 2: An enhanced graphical interface to EGS
[DE93-010447] 02 p0746 N94-13382
Distributed processor Monte Carlo: MCNP results on a 16-node IBM cluster
[DE93-012639] 02 p0752 N94-14176
Measurements of cosmic ray muons with multi-wire proportional chambers with a prototype setup for KASCADE
[KFK-5173] 04 p1631 N94-19506
A summary of studies of particle stability at RHIC
[DE93-040173] 05 p1970 N94-19868
High energy ionization in liquids: The free ion yield
[DE93-040329] 05 p1973 N94-20324
LREE variability in CM matrices: Another look at meteorite compaction ages 05 p2086 N94-20884
Fast vertex search (in plane)
[DE93-616655] 07 p2959 N94-25917
Algorithms of the vertex coordinate reconstruction for straight tracks of short-lived particles
[DE93-616661] 07 p3015 N94-25919
Track filtering by robust neural network
[DE94-606067] 08 p3434 N94-28613
Meso-optical Fourier transform microscope with double focusing
[DE94-607851] 08 p3290 N94-30148
Proceedings of the Workshop on B Physics at Hadron Accelerators
[DE94-007961] 09 p3877 N94-32748
Using neural networks as an event trigger in elementary particle physics experiments
[DE94-006316] 10 p4136 N94-33716
Computer image analysis of etched tracks from ionizing radiation
[NASA-CR-196025] 11 p4319 N94-35264
Measuring track densities in lunar grains using image analysis 11 p4357 N94-35409
Eureka! Aerogel capture of meteoroids in space 11 p4351 N94-35412
Simple and efficient method of secondary vertex searching
[DE94-618542] 12 p4514 N94-37064

PARTICLE TRAJECTORIES
NT ELECTRON TRAJECTORIES
Spin characteristics of ion beams during the motion of electromagnetic elements
[DE93-617448] 01 p0364 N94-10848
Quantized conic sections; quantum gravity
[DE93-010950] 01 p0411 N94-10956
Non-barrier tunneling in presence of dissipations
[DE93-621381] 01 p0412 N94-11086
Probability of particle trapping/detrapping in torsatrons
[DE93-621641] 01 p0390 N94-11121
A four-dimensional, mesoscale, non-gaussian multispectral smoke model. Phase 1: Feasibility study
[AD-A264805] 01 p0152 N94-11519
Coulomb effects in low-energy nuclear fragmentation
[NASA-TP-3352] 01 p0485 N94-12434
Low energy neutral atom imaging techniques
[DE93-012744] 02 p0779 N94-12950
Molecular processes in comets
[NASA-CR-194148] 03 p1239 N94-15188
Experimental research in high energy physics
[DE93-011912] 04 p1574 N94-18916
Electrokinetic transport of heterogeneous particles in suspensions
[NASA-CR-194478] 04 p1353 N94-19367
Modeling of particle dispersion in a stationary isotropic homogeneous turbulence by large scale numerical simulation
[ETN-93-94604] 05 p1601 N94-20601
Surface path lines in plane Stokes flow driven by capillarity
[DE93-041277] 05 p1603 N94-21651
Monte Carlo calculation of multi-electron effects on synchrotron radiation
[DE94-001259] 05 p1982 N94-21974
Particle acceleration in a filamentary current sheet model 05 p2004 N94-22659
Current loop coalescence studied by 3-D electromagnetic particle code 05 p2005 N94-22660
Structure functions of sea quarks, Kogut-Susskind pole and dynamics of pp- and pp-bar-interactions at high energies
[DE93-613184] 07 p3031 N94-25870
IRMA: A program for three-dimensional color display of data
[AD-A273811] 07 p2959 N94-25879
Ice accretion on aircraft wings 07 p2657 N94-28345
A 6MeV heavy ion beam probe for the Large Helical Device
[AD-B183695L] 08 p3505 N94-29397
Some remarks about pseudo-Hamiltonian
[DE94-003273] 08 p3487 N94-29700
The impact of electrically charged microspheres with planar surfaces under vacuum conditions 08 p3320 N94-29765
Monoenergetic neutral particle transport in semi-infinite media
[AD-A277155] 09 p3870 N94-32368
An improved analytic solution for analysis of particle trajectories in fibrous, two-dimensional filters
[DE94-008969] 10 p4047 N94-34016
Q-deformations of the Veneziano model
[DE94-616769] 11 p4315 N94-36076
Simple and efficient method of secondary vertex searching
[DE94-618542] 12 p4514 N94-37064
Symplectic tracking using point magnets and a reference orbit made of circular arcs and straight lines
[DE94-011919] 12 p4505 N94-37675

PARTICLES
NT AEROSOLS
NT ALPHA PARTICLES
NT ANTINEUTRINOS
NT ANTINUCLEONS
NT ANTIPARTICLES
NT ANTIPROTONS
NT ARGON PLASMA
NT BARYONS
NT BETA PARTICLES
NT BOSONS
NT BOUNDARY LAYER PLASMAS
NT CHARGED PARTICLES
NT COLD NEUTRONS
NT COLD PLASMAS
NT COLLISIONAL PLASMAS
NT COLLISIONLESS PLASMAS
NT CONDUCTION ELECTRONS
NT COSMIC DUST
NT COSMIC PLASMA
NT CYLINDRICAL PLASMAS
NT DENSE PLASMAS
NT DEUTERONS
NT DROPS (LIQUIDS)
NT DUST
NT ELECTRON BEAMS
NT ELECTRON PLASMA
NT ELECTRON PRECIPITATION
NT ELECTRON RADIATION
NT ELECTRON-POSITRON PAIRS
NT ELECTRON-POSITRON PLASMAS
NT ELECTRONS
NT ELEMENTARY PARTICLES
NT ENERGETIC PARTICLES
NT ETA-MESONS
NT EVEN-EVEN NUCLEI
NT FAST NEUTRONS
NT FERMIONS
NT FINES
NT FOG
NT FREE ELECTRONS
NT GLUONS
NT GRAVITONS
NT HADRONS
NT HEAVY NUCLEI
NT HELIUM PLASMA
NT HIGGS BOSONS
NT HIGH ENERGY ELECTRONS
NT HIGH TEMPERATURE PLASMAS
NT HOT ELECTRONS
NT HYDROGEN PLASMA
NT HYPERNUCLEI
NT HYPERONS
NT INNER RADIATION BELT
NT INTERPLANETARY DUST
NT IONIZED GASES
NT KAONS
NT LASER PLASMAS
NT LEPTONS
NT LORENTZ GAS
NT LUNAR DUST
NT MAGNETIC CLOUDS
NT MAGNETIC MONOPOLES
NT MAGNETICALLY TRAPPED PARTICLES
NT MESON RESONANCE
NT MESONS
NT METAL PARTICLES
NT METAL POWDER
NT METALLIC PLASMAS
NT MICROPARTICLES
NT MICROPLASMAS
NT MUONS
NT NEUTRAL PARTICLES
NT NEUTRINOS
NT NEUTRONS
NT NITROGEN PLASMA
NT NONEQUILIBRIUM PLASMAS
NT NONUNIFORM PLASMAS
NT NUCLEI (NUCLEAR PHYSICS)
NT NUCLEONS
NT ODD-EVEN NUCLEI
NT ODD-ODD NUCLEI
NT OMEGA-MESONS
NT OXYGEN PLASMA
NT PARTICULATES
NT PARTONS
NT PHOTOELECTRONS
NT PHOTONS
NT PI-ELECTRONS
NT PIONS
NT PLASMA CLOUDS
NT PLASMA FOCUS
NT PLASMA JETS
NT PLASMA LAYERS
NT PLASMA SHEATHS
NT PLASMA SLABS
NT PLASMAS (PHYSICS)
NT POLARONS
NT POLLEN
NT POSITRONS
NT POWDER (PARTICLES)
NT POWDERED ALUMINUM
NT PRIMARY COSMIC RAYS
NT PROTON BELTS
NT PROTONS
NT QUARKS
NT RADIATION BELTS
NT RADIO JETS (ASTRONOMY)
NT RAINDROPS
NT RAREFIED PLASMAS
NT RELATIVISTIC ELECTRON BEAMS
NT RELATIVISTIC PARTICLES
NT RELATIVISTIC PLASMAS
NT RHO-MESONS
NT ROTATING PLASMAS
NT SOLAR CORPUSCULAR RADIATION
NT SOLAR COSMIC RAYS
NT SOLAR ELECTRONS
NT SOLAR NEUTRINOS
NT SOLAR NEUTRONS
NT SOLAR PROTONS
NT SOLAR WIND
NT SOOT
NT SPACE PLASMAS
NT STELLAR WINDS
NT STRONGLY COUPLED PLASMAS
NT TACHYONS
NT TERRESTRIAL DUST BELT
NT THERMAL NEUTRONS
NT THERMAL PLASMAS
NT TOROIDAL PLASMAS
NT TRAPPED PARTICLES
NT VECTOR MESONS
NT XI HYPERONS
NT ZODIACAL DUST
Light scattering from a spherical particle on a conducting plane. Part 1: Normal incidence
[AD-A265920] 01 p0383 N94-12341
Bridging the gap between the Rayleigh and Thomson limits for various convex bodies
[DSIS-93-00613] 02 p0607 N94-14204
An assessment of acid fog
[DE93-009347] 03 p1095 N94-15940
Particle Engulfment and Pushing by Solidifying Interfaces (PEPSI)
[NASA-CR-193856] 03 p0960 N94-17079
Study on neutron activation analysis
[DE93-632191] 07 p3017 N94-26116
Single scattering of light by ensembles of particles with various shapes
[ETN-94-96016] 09 p3878 N94-31550
Simulation of rotary-drum and repose tests for frictional spheres and rigid sphere clusters
[DE94-008094] 10 p4044 N94-33841

PARTICULATE FILTERS
U FLUID FILTERS

PARTICULATE REINFORCED COMPOSITES
Fracture toughness tests for particulate MMC UK COSI (IACFA) task group. Meeting report, October 1992
[NPL-DMM(A)-81] 03 p1057 N94-15021
Fracture behavior of 20% Nb particulate reinforced alumina composite
[DE94-002830] 07 p2706 N94-26019
Effects of post-fabrication processing on the tensile properties of centrifugally cast SiC particulate reinforced aluminum composites
[AD-A274865] 07 p2707 N94-26190

Processing of novel nanoparticle dispersion strengthened ceramics for improved mechanical performance
[AD-A275965] 09 p3649 N94-31276
NiAl-base composite containing high volume fraction of AlN for advanced engines
[NASA-CASE-LEW-15818-1] 12 p4403 N94-36752

PARTICULATE SAMPLING
Suggestion for extended Viking magnetic properties experiment on future Mars missions
03 p1285 N94-16375
Novel mass spectrometric instrument for gaseous and particulate characterization and monitoring
[DE93-019992] 04 p1433 N94-19054
Bioregenerative life support systems for microgravity
[NASA-CR-195516] 06 p2422 N94-24810
Remote robot manipulator coupled with remote-controlled guide vehicle for soil sampling in hazardous waste sites 09 p3723 N94-31569
Counting particles emitted by stratospheric aircraft and measuring size of particles emitted by stratospheric aircraft
[NASA-CR-195908] 09 p3769 N94-33170

PARTICULATES
NT SOOT
Advanced diagnostics for in situ measurement of particle formation and deposition in thermally stressed jet fuels
[DE93-009798] 01 p0098 N94-11366
Novel mass spectrometric instrument for gaseous and particulate characterization and monitoring
[DE93-014093] 01 p0272 N94-12783
Discussion of stress tensor nonuniqueness with application to nonuniform, particulate systems
[DE93-014352] 02 p0816 N94-13206
Nonlinear relationships between particulate absorption and chlorophyll: Detritus or pigment packaging?
[AD-A266806] 02 p0731 N94-14899
Analysis of leading edge and trailing edge cover glass samples before and after treatment with advanced satellite contamination removal techniques
[AD-A267055] 03 p0885 N94-15666
Near-surface temperature gradients and their effects on thermal-infrared emission spectra of particulate planetary surfaces 03 p1260 N94-16236
Title 1 implementation: Status report on nonattainment areas
[DE93-017677] 04 p1471 N94-17777
Imaging and blackbody emission spectra of hot particulates generated during laser ablation
[DE93-015818] 04 p1439 N94-18724
Development of a technique to determine the morphology and dynamics of agglomerates in chemically reacting flows
[AD-A271160] 05 p1678 N94-20000
Sol-spray preparation, particulate characteristics, and sintering of alumina powders
[DE93-018577] 05 p1690 N94-20183
Spiral fluid separator
[NASA-CASE-MFS-28658-1] 05 p1800 N94-20361
The coherent backscattering opposition effect
05 p1991 N94-20646
Thermal conductivity measurements of particulate materials under Martian conditions
05 p1685 N94-20703
Composite fiber structures for catalysts and electrodes
06 p2393 N94-23364
On the determination of local instantaneous averages in particulate flow measurements
06 p2325 N94-23663
Particle size measurement for the control of industrial crystallizers
[PB94-119104] 06 p2562 N94-23766
On the stability of the process of formation of combustion generated particles by coagulation and simultaneous shrinkage due to particle oxidation
06 p2159 N94-24274
The chemistry of particulate formation in fluorocarbon plasmas
[DE94-001500] 06 p2552 N94-24546
Study on neutron activation analysis
[DE93-632191] 07 p3017 N94-26116
Catalytic fabric filtration for simultaneous NO(x) and particulate control
[DE94-001660] 08 p3341 N94-28463
Novel mass spectrometric instrument for gaseous and particulate characterization and monitoring
[DE94-005896] 08 p3349 N94-30047
Centrifugal atomization of lanthanide materials for cryogenic coolers
[DE94-006035] 08 p3219 N94-30337
Particulate metal matrix composites: Draft procedure for tensile tests at ambient temperature
[PB94-149721] 08 p3184 N94-30419
Electrostatic reduction of particulates for laser resistant hafnia coatings
[DE94-005824] 09 p3651 N94-31557
Micromechanics and effective properties of particulate composites and fluid suspensions
09 p3703 N94-31744
Combustor and nozzle effects on particulate behavior in solid rocket motors
[AD-A277304] 09 p3614 N94-32071
Photothermal laser deflection, an innovative technique to measure particles in exhausts
[AD-A277151] 09 p3718 N94-32366
Air quality assessment and control
[DE94-000046] 10 p4081 N94-33725
Current activities and results of the Long Duration Exposure Facility Meteoroid and Debris Special Investigation Group 11 p4352 N94-35458
Particulate and gaseous organic receptor modeling for the Southern California Air Quality Study
[PB94-156700] 11 p4285 N94-35735
Studies of the effect of microstructure on the dynamic behavior of granular and particulate media
[AD-A279012] 12 p4455 N94-36520

PARTITIONS (MATHEMATICS)
A lattice gas model for enzyme kinetics with alternate interactions
[DE93-613027] 01 p0395 N94-10411
Parametric binary dissection
[NASA-CR-191496] 02 p0762 N94-13184
Understanding partitions and the no partition assumption
[AD-A266296] 03 p1000 N94-16911
A domain-partition method for the advection-diffusion equation
[INRIA-RR-1740] 03 p1030 N94-17534
An efficient implementation of error-valued semantics on imperative machines
[DE93-014658] 04 p1516 N94-17740
Software engineering for effective utilization of parallel processing computing system
[AD-A269191] 04 p1535 N94-18865
Decomposition invariance of generalized steady-state of a 1-D diffusion system
[REPT-93-26] 04 p1550 N94-19141
Algorithms for Markov decision chains with partial information
[PB93-220085] 05 p1918 N94-22098
Impact of partitioning on parallel discrete event simulation of logic circuits 05 p1772 N94-22115
Characterization of measures with a convex matrix-k-range
[PB93-220655] 06 p2479 N94-23098
A knowledge based system for scientific data visualization
[NASA-CR-194879] 06 p2452 N94-23507
Experience with parametric binary dissection
[NASA-CR-191552] 06 p2473 N94-23558
The Chaco user's guide
[DE94-003669] 07 p2962 N94-26370
Statistical mechanical properties of Z(N)(sup n-1) broken model
[DE93-634344] 07 p2993 N94-26457
Computer code for controller partitioning with IFPC application: A user's manual
[NASA-CR-195291] 07 p2678 N94-27414
Codes on the unit sphere
[PB94-136991] 08 p3453 N94-29174
Rectilinear decompositions with low stabbing number
[RUU-CS-93-25] 08 p3459 N94-30425
Dynamic microsets for RAMs
[RUU-CS-93-22] 08 p3406 N94-30727
Perfect binary space partitions
[RUU-CS-93-23] 08 p3460 N94-30728
SU(2) WZNW model at higher genera from gauge field functional integral
[PB94-148467] 09 p3857 N94-31589
Identity for propagator in four-fermion theory
[DE94-611104] 11 p4342 N94-35781
Partition coefficients for Al, Ca, Ti, Cr, and Ni in olivine obtained by melting experiment on an LL6 chondrite
11 p4353 N94-36163
Ability of the total strain version of strainrange partitioning to characterize thermomechanical fatigue behavior
[NASA-TM-4556] 12 p4455 N94-37102

PARTITIONS (STRUCTURES)
Continuum representations of cellular solids
[DE94-001706] 06 p2375 N94-23217

PARTONS
Quark and gluon jets at CDF
[DE93-014919] 02 p0783 N94-13884
Measuring the sea quark polarization
[DE93-015792] 04 p1566 N94-18234
Investigation of physical structures and interactions at high energy
[DE93-014444] 04 p1574 N94-18927
The PAPAGENO Partonic Monte-Carlo Program
[DE93-018524] 04 p1571 N94-19247
Direct photon results from CDF
[DE93-019908] 05 p1980 N94-20317
Parton-parton elastic scattering and rapidity gaps at Tevatron energies
[DE93-041024] 05 p1974 N94-21515
The lepton charge asymmetry in the decay of W bosons produced in p(bar p) collisions at (radical)s = 1.8 TeV
[DE93-019903] 05 p1976 N94-21847
Proton spin: The role of quark-gluon and hadron degrees of freedom
[DE93-616867] 06 p2538 N94-25341
The STAR experiment at the Relativistic Heavy Ion Collider
[DE94-003409] 07 p3017 N94-26083
Rescattering and energy loss of fast partons in nuclear matter
[DE94-002918] 07 p3018 N94-26145
A jet calculus approach including coherence effects and the associated problem of moment inversion
[ISBN-0-315-51715-8] 07 p3025 N94-27266
High energy parton-parton elastic scattering in QCD
[DE94-003432] 07 p3028 N94-27736
The small-x behaviour of parton distribution functions
[DE94-606414] 08 p3485 N94-28758
Inclusive jet and direct photon production at the D0 experiment
[DE94-006001] 08 p3488 N94-30049
String-parton model description of relativistic heavy-ion collisions
[DE94-009164] 09 p3874 N94-32850
QCD parametrizations of the parton distribution of deep inelastic scattering
[DE94-616660] 11 p4325 N94-36074
Angular dependence of parton-parton scattering extracted from hadron pair production in pp collisions at radicals equal to 11.5 GeV
[DE94-611174] 12 p4511 N94-36504
The Mesozoic Era of relativistic heavy ion physics and beyond
[DE94-011341] 12 p4548 N94-37557
Pre-equilibrium parton dynamics: Proceedings
[DE94-011347] 12 p4520 N94-37716

PASCAL (PROGRAMMING LANGUAGE)
The solving of equations by the method of boundary elements 01 p0326 N94-11182
A comprehensive software engineering educational experience
[AD-A270583] 05 p1905 N94-20109
Algorithms for speech coding systems based on linear prediction
[EUT-92-E-260] 06 p2447 N94-22731

PASSAGEWAYS
NT STRAITS

PASSENGER AIRCRAFT
NT A-310 AIRCRAFT
NT BOEING 720 AIRCRAFT
NT BOEING 727 AIRCRAFT
NT BOEING 737 AIRCRAFT
NT BOEING 747 AIRCRAFT
NT BOEING 757 AIRCRAFT
NT BOEING 767 AIRCRAFT
NT COMMUTER AIRCRAFT
NT DC 8 AIRCRAFT
NT DC 10 AIRCRAFT
NT EUROPEAN AIRBUS
NT H-53 HELICOPTER
NT MD 11 AIRCRAFT
NT MYSTERE 20 AIRCRAFT
NT T-39 AIRCRAFT
Radiometry in commercial aircraft
[GSF-41/91] 05 p1892 N94-21141
JB-300: An advanced medium size transport for 2005
[NASA-CR-195499] 06 p2179 N94-24401
NASA/USRA University Advanced Design Program, 1992-1993. The Diamondback: A simulated commercial air transportation study
[NASA-CR-195523] 06 p2180 N94-24462
The airplane: A simulated commercial air transportation study
[NASA-CR-195525] 06 p2182 N94-24837
The AC-120: The advanced commercial transport
[NASA-CR-195491] 06 p2182 N94-24966
Weasel works SA-150: Design study of a 100 to 150 passenger transport aircraft
[NASA-CR-195489] 06 p2183 N94-24975
The Bunny: A simulated commercial air transportation study
[NASA-CR-195537] 06 p2183 N94-25001
The Gold Rush: A simulated commercial air transportation study
[NASA-CR-195528] 06 p2184 N94-25002
The RTL-46: A simulated commercial air transportation study
[NASA-CR-195524] 06 p2184 N94-25017
High-order technology: Applying technical excellence to new airplane development 06 p2185 N94-25069

Design of the advanced regional aircraft, the DART-75
07 p2671 N94-25708
The design of a long-range megatransport aircraft
07 p2671 N94-25718
A symbol of reliability: Ju 52 07 p2663 N94-28250
Fracture and fatigue strength evaluation of multiple site damaged aircraft fuselages - curved panel testing and analysis
[PB94-152808] 09 p3579 N94-32015
A comparison of military and commercial aircraft development
[AD-A276830] 09 p3575 N94-32168
NASA Annual HSR Workshop: Boeing HSCT program summary 10 p3970 N94-33449
Update on Douglas' high-speed civil transport studies
10 p3970 N94-33450
Douglas Aircraft HSCT status and future research needs 10 p3970 N94-33454
The effects of cold exposure on wet aircraft passengers: A review
[AD-280253] 10 p4100 N94-34389
A review of computer evacuation models and their data needs
[AD-280707] 11 p4191 N94-35236

PASSENGERS
Federal Aviation Administration aviation forecasts
[AD-A265611] 01 p0002 N94-12578
Evaluation of head injury criteria
[NIAR-93-2] 05 p1890 N94-20190
Passenger terminal simulation model
[ISBN-0-315-61113-8] 05 p1652 N94-22423
Aircraft evacuation testing: Research and technology issues
[PB94-107620] 06 p2173 N94-24750
Powerful selling and sales strategy
07 p2662 N94-28245
Lufthansa long range services: More simplicity
07 p2663 N94-28246
Crash impact survival in light planes
[NASA-TM-109799] 10 p3987 N94-33749
The effects of cold exposure on wet aircraft passengers: A review
[AD-280253] 10 p4100 N94-34389
Future ultra-speed tube-flight
11 p4225 N94-35918

PASSIVATION
U PASSIVITY

PASSIVE ELEMENTS
U PARASITIC ELEMENTS (ANTENNAS)

PASSIVE SATELLITES
NT BEACON SATELLITES
NT LAGEOS (SATELLITE)
Ice surface temperature retrieval from AVHRR, ATSR, and passive microwave satellite data: Algorithm development and application
[NASA-CR-195276] 07 p2851 N94-27849
Typhoon monitoring using passive satellite observations
[AD-A277859] 10 p4089 N94-33769

PASSIVITY
Surface passivation of InP solar cells with InAlAs layers 01 p0049 N94-11389
In situ XANES studies of the passive film on Fe and Fe-26Cr
[DE93-010869] 01 p0084 N94-11459
Corrosion and passivation of high temperature superconductors
[AD-A265402] 01 p0405 N94-12586
Effect of microstructure on passive film formation and breakdown on Al alloys
[AD-A265339] 02 p0569 N94-13050
Vacancy condensation as the precursor to passivity breakdown
[DE93-012925] 03 p0956 N94-15998
In situ studies of passive film chemistry using x ray absorption spectroscopy
[DE93-014023] 03 p0947 N94-16011
ALE project
[AD-A271080] 05 p2014 N94-19980
The use of x ray techniques in the in situ study of corrosion
[DE93-019845] 05 p1690 N94-20301
Ultraviolet photosulfidation of III-V compound semiconductors for electronic passivation
[DE94-001417] 06 p2555 N94-22717
Chromate-free talc chemical conversion coatings for aluminum alloys
[DE94-001567] 06 p2238 N94-22932
Electrochemical sulfur passivation of visible (approximately 670nm) AlGaInP lasers
[DE94-002293] 06 p2350 N94-24659
Electrochemical properties of passive films on 440C stainless steel
[ISBN-0-315-64248-3] 07 p2757 N94-27801
Pit initiation on passivated metal surfaces: Crystallographic orientation and environmental effects
[ISBN-0-315-85433-2] 08 p3208 N94-30138
An investigation of the corrosion properties of aluminum-tantalum alloys using electrochemical impedance spectroscopy and local electrochemical impedance spectroscopy 08 p3209 N94-30521
Passivation of III-V compound semiconductor based devices
[AD-A276178] 09 p3894 N94-31056
Modification of semiconductor surface properties with chemically bound molecular films
[AD-A276162] 09 p3895 N94-31081
Determination of BPSG thin-film properties using IR reflection spectroscopy of product wafers
[DE94-006591] 09 p3634 N94-32110

PASTES
Automated crack identification for cement paste
[AD-A265753] 02 p0665 N94-13042
A materials compatibility study in FM-1, a liquid component of a paste extrudable explosive
[DE94-001166] 07 p2759 N94-26198
Cement paste matrix composite materials center
[AD-A279017] 11 p4233 N94-35952

PATENT APPLICATIONS
Supersonic bare metal cluster beams
[DE94-010790] 12 p4532 N94-36454

PATENT POLICY
NASA patent abstracts bibliography: A continuing bibliography. Section 1: Abstracts (supplement 44)
[NASA-SP-7039(44)-SECT-1] 05 p2043 N94-21254
NASA patent abstracts bibliography: A continuing bibliography. Section 2: Indexes (supplement 44)
[NASA-SP-7039(44)-SECT-2] 06 p2590 N94-23712
NASA patent abstracts bibliography: A continuing bibliography. Section 1: Abstracts (supplement 45)
[NASA-SP-7039(45)-SECT-1] 11 p4344 N94-35382
NASA patent abstracts bibliography: A continuing bibliography. Section 2: Indexes (supplement 45)
[NASA-SP-7039(45)-SECT-2] 11 p4346 N94-35835

PATENTS
Numerical and symbolic signal representation and processing
[AD-A270271] 04 p1389 N94-18811
The official gazette of the United States Patent and Trademark Office, vol. 1145, no. 4
[PB93-202240] 05 p2044 N94-21449

PATH PLANNING
U TRAJECTORY PLANNING

PATHOGENESIS
Asthma in aircrew 06 p2425 N94-23327

PATHOGENS
Bloodborne Pathogens Program
03 p1127 N94-16644
OSHA bloodborne pathogens standards exposure control plan 03 p1127 N94-16645
Bakteriella toxiner-morgondagens hot (bacterial toxins-the threat of tomorrow)
[PB94-124229] 07 p2902 N94-27045
Continuous monitoring of bacterial attachment
10 p4094 N94-33658

PATHOLOGY
NT HUMAN PATHOLOGY
Bakteriella toxiner-morgondagens hot (bacterial toxins-the threat of tomorrow)
[PB94-124229] 07 p2902 N94-27045
High peak power microwaves: A health hazard
[AD-A277168] 09 p3681 N94-32576
Activities of National Institute of Radiological Sciences
[DE94-727636] 11 p4296 N94-36101

PATHS
Neural networks for optimum routing in packet-switched communications networks 05 p1746 N94-22205

PATIENTS
Aeromedical support for casualties in extremely hot climates 08 p3382 N94-28443

PATROLS
Using satellite communications for a mobile computer network 06 p2280 N94-22777

PATTERN DISTRIBUTION
U DISTRIBUTION (PROPERTY)

PATTERN METHOD (FORECASTING)
Predicting lightning events in the KSC area: A feasibility study using single station data
[AD-A271440] 05 p1864 N94-20088

PATTERN RECOGNITION
NT CHARACTER RECOGNITION
Object recognition in industrial environment by means of tactile sensor
[ITN-93-85200] 01 p0178 N94-10393
Model-based recognition of 3-D objects by geometric hashing technique
[DE93-612916] 01 p0322 N94-10410
Unsupervised splitting rules for neural tree classifiers
[AD-A264961] 01 p0338 N94-10487
Automaticity of processing location versus identity information in brief visual displays
[AD-A265013] 01 p0418 N94-10491
Application of normalized gray-scale correlation
[DE93-013765] 01 p0141 N94-10521
Introduction to Bayesian image analysis
[DE93-012628] 01 p0347 N94-11006
A high-speed object recognition chip based on biologically-realistic hybrid temporal processing element
[AD-A265490] 01 p0339 N94-11049
Three-dimensional object recognition using an unsupervised BCM network: The usefulness of distinguishing features
[AD-A264576] 01 p0304 N94-11261
A summary of image segmentation techniques
[NASA-TM-104022] 01 p0327 N94-11274
Remote sensing of the suspended matter distribution with high concentration in China Sea
01 p0192 N94-11901
A pattern recognition system for locating small volvanoes in Magellan SAR images of Venus
01 p0455 N94-12126
VISART: Artificial vision for industrial use. A comprehensive system
[INPE-5379-TDI/474] 02 p0665 N94-12941
Feature extraction and classification algorithms for high dimensional data
[NASA-CR-194298] 02 p0743 N94-13023
View generated database
[NASA-CR-191397] 02 p0822 N94-13116
Design of partially supervised classifiers for multispectral image data
[NASA-CR-194299] 02 p0823 N94-13192
Close range 3-D position sensing using stereo vision and point-of-correspondance through mathematical morphology
[ISBN-0-315-61012-3] 02 p0763 N94-13515
A review and analysis of neural networks for classification of remotely sensed multispectral imagery
[NASA-CR-194291] 02 p0763 N94-13603
Fast parallel string prefix-matching
[AD-A267758] 02 p0760 N94-13924
Determination of position and orientation of rigid bodies from image segments
[FFI-92-4005] 02 p0752 N94-14039
Feature discovery on segmented objects in SAR imagery using self-organizing neural networks
[DE93-010685] 02 p0686 N94-14056
Identification and interpretation of patterns in rocket engine data
[NASA-CR-194534] 02 p0552 N94-14309
Obstacle detection by recognizing binary expansion patterns
[NASA-CR-194415] 02 p0514 N94-14495
Computer vision and sensor fusion for detecting buried objects
[DE93-012605] 02 p0700 N94-14566
Retrieval properties of neural networks with infinitely many marked patterns
[PREPRINT-729] 02 p0766 N94-14718
Speaker independent recognition of isolated words using vector quantization and neural networks
[ETN-93-94390] 02 p0616 N94-14724
Segmenting textured 3D surfaces using the space/frequency representation
[AD-A266960] 03 p1163 N94-14968
A new method for generating Bayes classifiers assuming mixtures of Gaussian densities
[FFI-91/4029] 03 p1172 N94-15298
Cooperativity and 3-D representation
[AD-A267180] 03 p1131 N94-15694
The bootstrapped algorithm: Fast algorithm for blind signal separation
[AD-A266671] 03 p1147 N94-15772
Efficient algorithmic techniques for combinatorial problems
[AD-A267151] 03 p1172 N94-15777
Development of pattern recognition techniques for the evaluation of toxicant impacts to multispecies systems
[AD-A267197] 03 p1095 N94-15790
Spatial filters for optical correlation
[AD-A267199] 03 p1189 N94-15791
Exploiting world structure to efficiently search for objects
[TR-434] 03 p1231 N94-16576
Discovering sequence similarity by the algorithmic significance method
[DE93-015556] 03 p1150 N94-16659
Image accuracy and representational enhancement through low-level, multi-sensor integration techniques
[DE93-014888] 03 p1167 N94-17287
A high-speed object recognition chip based on a biologically-realistic hybrid temporal processing
[AD-A268270] 03 p1134 N94-17576

An object-oriented environment for computer vision and pattern recognition
[DE93-017098] 04 p1517 N94-17867
Examination of metrics and assumptions used in correlation filter design
[DE93-017636] 04 p1576 N94-18000
Application of the network discriminant function to learning
[AD-A268793] 04 p1540 N94-18189
Optical associative processors and directed graphs
[AD-A268881] 04 p1615 N94-18224
Evaluation of a liquid crystal spatial light modulator capable of amplitude- and phase-modulating modes
[AD-A269252] 04 p1577 N94-18262
Optimal design of binary phase-only filters using genetic algorithms
[AD-A268737] 04 p1396 N94-18278
Constructing a reference event list for ARCESS
[AD-A269288] 04 p1481 N94-18297
Psychophysical analyses of perceptual representations
[AD-A268711] 04 p1508 N94-18313
Visual perception of features and objects
[AD-A269879] 04 p1508 N94-18682
Operator performance in pattern matching as a function of reference material structure
[AD-A269889] 04 p1509 N94-18686
Neutral networks: An NRL perspective
[AD-A269122] 04 p1541 N94-18773
Geometrical pattern learning
[DE93-017641] 04 p1542 N94-19007
Serial pattern complexity: Irregularity and hierarchy
[PB93-191914] 04 p1509 N94-19348
A non-homogeneous, spatio-temporal, wavelet multiresolution analysis and its application to the analysis of motion
[AD-A270621] 04 p1538 N94-19534
Transcutaneous Analyte Measuring Methods (TAMM)
[AD-A271387] 04 p1408 N94-19756
A stereoscopic vision system with applications to automated docking and tracking
[AD-A270754] 04 p1333 N94-19765
Applications of neural networks in fault detection of rotating machinery
[AD-A270755] 04 p1448 N94-19766
Equivalence and reduction of hidden Markov models
[AD-A270762] 04 p1560 N94-19768
Recognizing 3-D objects using 2-D images
[AD-A271005] 05 p1983 N94-19819
Representation and recognition with algebraic invariants and geometric constraint models
[AD-A271395] 05 p1949 N94-19838
Robust and efficient 3D recognition by alignment
[AD-A270839] 05 p1904 N94-20041
Statistical object recognition
[AD-A270887] 05 p1962 N94-20113
New algorithm of ground track processing in high-frequency skywave over-the-horizon-B radar
[AD-A267821] 05 p1717 N94-20207
Generalization performance of backpropagation learning on a syllabification task 05 p1940 N94-20246
Multivariate statistical analysis: Principles and applications to coorbital streams of meteorite falls 05 p1964 N94-20881
Recognition by prototypes
[AD-A271687] 05 p1943 N94-20921
Efficient comparison based string matching
[CWI-CS-R9249] 05 p1909 N94-21028
Tight comparison bounds for the string prefix-matching problem
[CWI-CS-R9250] 05 p1952 N94-21029
Data and model-driven selection using parallel-line groups
[AD-A271702] 05 p1913 N94-21365
Mathematical theory of thermodynamics of computation
[CWI-CS-R9251] 05 p2038 N94-21533
Determining the 3-D structure and motion of objects using a scanning laser range sensor
[NASA-CR-194745] 05 p1818 N94-21817
Improvement in invariant pattern recognition with neural networks and Fourier-Mellin filters 05 p1780 N94-22164
A modified moment invariants technique for classification of noisy objects 05 p1780 N94-22165
Interference reduction using neural networks 05 p1783 N94-22186
An insensitive algorithm for template matching with correlation 05 p1793 N94-22249
STAR-1 SAR road extraction using texture analysis and mathematical morphology
[ISBN-0-315-83255-X] 05 p1843 N94-22429
A neural network prototyping package within IRAF 05 p1949 N94-22451
The adaptive resonance theory network: (Clustering-) behaviour in relation with brainstem auditory evoked potential patterns
[EUT-92-E-264] 06 p2470 N94-22877
Artificial neural networks: Application to the optical recognition of music partitions
[ETN-94-95166] 06 p2470 N94-22884
Image pattern recognition supporting interactive analysis and graphical visualization
[NASA-CR-194878] 06 p2451 N94-23369
Sensing and modelling concepts for autonomous and remote mobile robot control 06 p2370 N94-23421
Neural network research in Finland. Symposium
[PB93-224822] 06 p2472 N94-23463
Imaging System (INEL) T805 prototype
[DE94-002807] 06 p2382 N94-23492
Joint Acoustic Propagation Experiment (JAPE) 06 p2527 N94-24208
Heterodyne array for measurement of target velocity
[AD-D016025] 06 p2545 N94-24722
Method for selection of wavelength bands for multispectral classification
[PB93-204378] 06 p2388 N94-24741
Object recognition through image understanding for an autonomous mobile robot
[AD-A273206] 06 p2475 N94-24862
Image remapping strategies applied as protheses for the visually impaired 06 p2444 N94-25363
An evaluation of three-dimensional sensors for the extravehicular activity helper/retreiver 06 p2444 N94-25369
Extracting projective information from single views of 3D point sets
[OUEL-1973/93] 06 p2464 N94-25471
Parametric and nonparametric discriminants for regional earthquakes and explosions
[AD-A273807] 06 p2406 N94-25538
Calculation of a 3-D pose of a known object in a single perspective view
[VTT-PUBS-122] 07 p2957 N94-25642
Solid estimation feature based correlation method for measuring control points required for correcting satellite images
[VTT-JULK-772] 07 p2848 N94-26253
Colour object recognition
[ISBN-0-315-83684-9] 07 p2994 N94-26614
A rough set approach to speech recognition
[ISBN-0-315-83894-9] 07 p2769 N94-26619
Three dimensional object recognition using a complex autoregressive model
[AD-A274388] 07 p2995 N94-26829
Interacting cortical filters for object recognition
[PB94-125374] 07 p2938 N94-26873
Orientation competition in cortical filters
[PB94-125366] 07 p2939 N94-27001
High-speed, high-density, coherent time-domain optical memory
[AD-A274249] 07 p3037 N94-27010
Combining shape and color information for 3D object recognition
[AD-A274123] 07 p2967 N94-27064
Translation and rotation invariant pattern recognition
[PB94-123676] 07 p2968 N94-27157
Parallel string matching algorithms
[AD-A274502] 07 p3100 N94-27164
Parallel algorithm for dominant points correspondences in robot binocular stereo vision 07 p2686 N94-27364
Saving comparisons in the Crochemore-Perrin string matching algorithm
[CWI-CS-R9322] 07 p2971 N94-27550
Thunderstorm Hypothesis Reasoner
[NASA-CR-195714] 07 p2897 N94-27884
Optical pattern recognition system utilizing resonator array
[AD-D016071] 07 p3040 N94-28224
A new method for recognizing quadric surfaces from range data and its application to telerobotics and automation, final phase
[NASA-CR-195733] 08 p3408 N94-28825
Animators and error reporters for generated programming environments
[CWI-CS-R9253] 08 p3418 N94-29503
A locally synchronous globally asynchronous Vertex-8 processing element for image reconstruction on a mesh
[ISBN-0-315-86005-7] 08 p3432 N94-30143
Shape from diameter: Negative results
[RUU-CS-93-16] 08 p3458 N94-30407
Shape from diameter: Positive results
[RUU-CS-93-17] 08 p3458 N94-30408
The use of interactive computer vision and robot hand controllers for enhancing manufacturing safety 08 p3314 N94-30442
Unsupervised texture image segmentation by improved neural network ART2
[AIAA PAPER 94-1199-CP] 08 p3442 N94-30549
Use of bad training data for better predictions
[DE94-006233] 08 p3427 N94-30705
Placing registration marks
[RUU-CS-93-21] 08 p3427 N94-30725
Elements for the recognition of three dimensional deformable shapes: Application to biomedical imagery
[TELECOM-93-E-006] 08 p3396 N94-30978
Tracking roads in an aerial image by Kalman filtering
[TELECOM-93-D-007] 09 p3711 N94-31096
Automatic extraction of cartographic objects by fusion of data extracted from satellite images
[TELECOM-93-E-001] 09 p3742 N94-31165
Filtering and recognition of moving boats in radar images
[REPT-93-039] 09 p3671 N94-31190
Feature discovery in gray level imagery for one-class object recognition
[DE94-005268] 09 p3671 N94-31267
Smart environmental monitor based on neural networks and multi-spectral pattern recognition
[AD-A276445] 09 p3829 N94-31301
Digit-Eyes: Vision-based human hand tracking
[NASA-CR-195913] 09 p3803 N94-31447
Polyhedric object recognition by indexing in a model base
[ETN-94-95913] 09 p3812 N94-31542
CAD-based off-line planning for an active-vision system
[ISBN-0-315-86317-X] 09 p3813 N94-31713
Morphological directional coding of images
[ISBN-0-315-86336-6] 09 p3814 N94-31715
Neural networks for model-based recognition
[AD-A277375] 09 p3834 N94-32053
High performance hardware and software for pattern recognition and image processing
[AD-A276405] 09 p3816 N94-32130
Development of phase-only filters for sensor imagery
[AD-A276722] 09 p3880 N94-32151
Algebraic functions for recognition
[AD-A276803] 09 p3846 N94-32167
A differential theory of learning for efficient statistical pattern recognition
[AD-A277313] 09 p3800 N94-32277
Wavelet transform of fixed pattern noise in focal plane arrays
[AD-A276963] 09 p3712 N94-32393
SAR image feature extraction system: A pre-operational application of ERS-1 SAR 09 p3751 N94-32543
Mechanisms of temporal pattern discrimination by human observers
[AD-A277407] 09 p3801 N94-32577
Correlation filter synthesis using neural networks
[AD-A278124] 09 p3836 N94-33043
A novel optoelectronic system for distortion-invariant ATR
[AD-A277985] 09 p3884 N94-33087
CRAD Signal and Information Processing Working Group Workshop on Neural networks, volume 1
[DREA-TC-93-305-VOL-1] 09 p3836 N94-33149
Neural networks applied to the phonemic segmentation of speech 09 p3686 N94-33152
Automatic modulation recognition 09 p3686 N94-33153
Nearest-neighbour search in constant time: An alternative to neural networks for pattern matching applications 09 p3838 N94-33157
Projective and object space geometry for monocular building extraction
[AD-A277586] 10 p4075 N94-33426
A Fortran based learning system using multilayer back-propagation neural network techniques
[AD-A278463] 10 p4112 N94-33542
Using neural networks as an event trigger in elementary particle physics experiments
[DE94-006316] 10 p4136 N94-33716
Dyadic wavelet features for isolated word speaker dependent speech recognition
[AD-A278492] 10 p4034 N94-33756
Neural models of motion perception
[AD-A278362] 10 p4097 N94-33857
Dimensional measurement to subpixel value 10 p4110 N94-34353
Application of star identification using pattern matching to space ground systems at GSFC 11 p4209 N94-35640
Clustering techniques in speaker recognition
[AD-A278676] 11 p4255 N94-35689
Estimation of fractal dimensions from transect data
[DE94-009808] 11 p4281 N94-36018
A model-based approach for detection of runways and other objects in image sequences acquired using an on-board camera
[NASA-CR-196424] 12 p4446 N94-36812
Subgrouped real time recurrent learning neural networks
[AD-A280618] 12 p4500 N94-37043

Simple and efficient method of secondary vertex searching
[DE94-618542] 12 p4514 N94-37064
Detection of the electrocardiogram P-wave using wavelet analysis
[DE94-010791] 12 p4481 N94-37197
Design of a composite filter realizable on practical spatial light modulators
[NASA-CR-196297] 12 p4525 N94-37579

PATTERN REGISTRATION
Automatic focus and registration of synthetic aperture radar images 08 p3246 N94-29536
Pre- and intra-radiotherapy multimodal image registration: Principles and first experiments 08 p3395 N94-30030
Fast nonsupervised 3D registration of PET and MR images of the brain
[TELECOM-93-C-006] 09 p3798 N94-33069
Subpixel resolution from multiple images 11 p4281 N94-35417

PATTERNS
Spatial patterns in semiconductor lasers
[DE93-040056] 05 p1814 N94-19865

PAVEMENTS
Mathematical model of frost heave and thaw settlement in pavements
[AD-A267037] 03 p0983 N94-15676
Performance of prefabricated geocomposite subdrainage system in an airport runway
[DOT/FAA/RD-93/23] 06 p2192 N94-23303
Airport pavement test machine design and cost study
[DOT/FAA/CT-93/51] 06 p2192 N94-24072
Granular bases for heavily loaded pavements
[AD-A275171] 08 p3156 N94-29047
Asphaltic concrete performance under heavy fighter aircraft loading
[AD-A275046] 08 p3157 N94-29151
Determining the bearing capacity of flexible airfield pavements using a heavy weight deflectometer
[ISBN-0-315-86210-6] 09 p3587 N94-31710

PAYLOAD CONTROL
Superfluid Helium On-Orbit Transfer (SHOOT) flight demonstration 04 p1327 N94-19185
The Cluster Joint Science Operations Centre 04 p1331 N94-19639
SAMPEX payload operation control center implementation 06 p2197 N94-23843
Integrating payload design, planning, and control in the Dutch Utilisation Centre 06 p2207 N94-23869
Customizing graphical user interface technology for spacecraft control centers 06 p2510 N94-23905
Spatial interpretation of NASA's Marshall Space Flight Center Payload Operations Control Center using virtual reality technology 06 p2198 N94-24432
Control system design for A and R supported microgravity experiments: An experiment payload control development
[AD-B179107] 08 p3229 N94-30421
Virtual reality as a human factors design analysis tool: Macro-ergonomic application validation and assessment of the Space Station Freedom payload control area 10 p4100 N94-33620

PAYLOAD DELIVERY (STS)
Inertial Upper Stage
[NASA-TM-109654] 03 p0885 N94-15278

PAYLOAD DEPLOYMENT & RETRIEVAL SYSTEM
NT REMOTE MANIPULATOR SYSTEM
Cognitive engineering models in space systems
[NASA-CR-193473] 03 p1140 N94-16716

PAYLOAD INTEGRATION
The advanced fluid physics module: How to achieve scientific goals for Spacelab D2 01 p0039 N94-10136
Serpentine manipulator planning and control for NASA Space-Shuttle payload servicing
[AD-A266961] 03 p0879 N94-14969
The first flight of the QUESTS GAS payload G-521 04 p1325 N94-19170
Kennedy Space Center processing of Shuttle small payloads 04 p1326 N94-19177
Payload holddown and release mechanism 09 p3607 N94-33321

PAYLOAD INTEGRATION PLAN
Development concept for Dutch user support
[PB94-125523] 09 p3598 N94-31208

PAYLOAD RETRIEVAL (STS)
STS-32 onboard 16mm photography quick release
[NASA-TM-109472] 03 p0880 N94-15376
STS-32 LDEF EVA training in WETF with Low and Dunbar
[NASA-TM-109473] 03 p1135 N94-15377
STS-32 LDEF approach in SES
[NASA-TM-109474] 03 p0880 N94-15379

PAYLOAD STATIONS
STS-30 onboard 16mm photography quick release
[NASA-TM-109579] 03 p0881 N94-15423

PAYLOAD TRANSFER
A transportronic solution to the problem of interorbital transportation
[NASA-CR-191152] 08 p3164 N94-29355

PAYLOADS
NT ASTRO MISSIONS (STS)
NT ATMOSPHERIC GENERAL CIRCULATION EXPERIMENT
NT EARTH RADIATION BUDGET EXPERIMENT
NT GET AWAY SPECIALS (STS)
NT PLASMA INTERACTION EXPERIMENT
NT SEPAC (PAYLOAD)
NT SHUTTLE IMAGING RADAR
NT SPACE SHUTTLE PAYLOADS
NT SPACE STATION PAYLOADS
NT SPACELAB
NT SPACELAB PAYLOADS
NT X RAY ASTROPHYSICS FACILITY
Description of the liquid structure facility architecture and experimental demonstration of the diagnostic capabilities 01 p0039 N94-10118
Temperature dependence of diffusivities, preliminary definition phase
[NASA-CR-192613] 02 p0648 N94-13326
STS-53 Space Shuttle mission report
[NASA-CR-193101] 02 p0535 N94-13934
Payload/GSE/data system interface: Users guide for the VPF (Vertical Processing Facility)
[NASA-CR-194385] 02 p0532 N94-14148
ECS: Eighth year in orbit
[ESA-BR-82] 02 p0543 N94-14352
STS-35 EVA payload training in WETF
[NASA-TM-109492] 02 p0739 N94-14790
Non-lethal Unmanned Aerial Vehicles (UAVs)
[AD-A267139] 03 p0866 N94-15692
MAXUS: The new sounding rocket program for long duration microgravity flight 03 p0978 N94-16079
QUESTS: A microgravity research facility for materials science experiments 03 p0978 N94-16082
Choosing ESRO's first scientific satellites
[ESA-HSR-3] 03 p0887 N94-16523
ARIANE 5 light derivatives 03 p0878 N94-17140
Cooperative control of multiple space manipulators
[AD-A270291] 04 p1445 N94-18813
The star identification, pointing and tracking system of UVSTAR, an attached payload instrument system for the Shuttle Hitchhiker-M platform 04 p1326 N94-19179
Cluster: Mission, Payload, and Supporting Activities
[ESA-SP-1159] 04 p1328 N94-19622
Database of proposed payloads and instruments for SEI missions 05 p1811 N94-22432
Geostationary payload concepts for personal satellite communications 06 p2278 N94-22765
Results of a laboratory experiment that tests rotating unbalanced-mass devices for scanning gimbaled payloads and free-flying spacecraft
[NASA-TP-3458] 06 p2269 N94-23574
A review of mission planning systems 06 p2503 N94-23866
Recharge mechanism based on shape memory alloy 06 p2362 N94-24039
Satellite situation report, volume 33, number 4
[NASA-TM-109677] 06 p2205 N94-24824
Effect of power system technology and mission requirements on high altitude long endurance aircraft
[NASA-CR-194455] 06 p2189 N94-25200
Project Columbiad: Reestablishment of human presence on the Moon 07 p2689 N94-25687
STS-57 Space Shuttle mission report
[NASA-CR-195739] 07 p2693 N94-28220
STS-56 Space Shuttle mission report
[NASA-CR-195740] 07 p2693 N94-28221
BAG: A code for predicting the performance of a gas bag impact attenuation system for the Pathfinder lander
[DE94-003688] 08 p3165 N94-28477
Suspension system for gimbal supported scanning payloads
[NASA-CASE-MFS-28817-1] 08 p3287 N94-29358
GOME: Global Ozone Monitoring Experiment
[ESA-SP-1151] 08 p3347 N94-29452
Imaging spectrometry of the Earth and other solar system bodies 08 p3237 N94-29779
Root-sum-square structural strength verification approach
[NASA-TM-108453] 08 p3322 N94-30206
Theoretical basis for state vector comparison, relative position display, and relative position/rendezvous prediction
[AD-A277216] 09 p3608 N94-32020
DOD space based requirements: Increasing DOD access to space
[AD-A276874] 09 p3601 N94-32211
Pip pin reliability and design 09 p3605 N94-33305
Payload holddown and release mechanism 09 p3607 N94-33321
Rotating unbalanced mass proof-of-concept
[NASA-TM-109814] 10 p4141 N94-33720
Hardware interface for isolation of vibrations in flexible manipulators: Development and applications 10 p4067 N94-34036
On-board emergent scheduling of autonomous spacecraft payload operations 10 p4123 N94-35047
Maneuvering and control of flexible space robots 11 p4218 N94-35867

PBRE (REACTORS)
U PEBBLE BED REACTORS

PCB
U POLYCHLORINATED BIPHENYLS

PCM (MATERIALS)
U PHASE CHANGE MATERIALS

PCM (MODULATION)
U PULSE CODE MODULATION

PDM (MODULATION)
U PULSE DURATION MODULATION

PEAKS (LANDFORMS)
Morphologic classes of impact basins on Venus 05 p2137 N94-20883

PEARSON DISTRIBUTIONS
The distribution of a sum of binomial random variables
[AD-A266969] 03 p1172 N94-15002
Synchronisation of cold induced vasodilation at various locations of one hand
[IZF-1992-B3] 04 p1504 N94-17966

PEAT
Application of static and dynamic enclosures in determining DMS and OCS fluxes in Sphagnum peatlands 01 p0269 N94-12460
Effects of inorganic sulfur addition on fluxes of volatile sulfur compounds in Sphagnum peatlands 01 p0270 N94-12461
Environmental factors controlling fluxes of dimethyl sulfide in a New Hampshire fen 01 p0270 N94-12462
Methane production and consumption in grassland and boreal ecosystems
[NASA-CR-196085] 11 p4284 N94-35486

PEBBLE BED REACTORS
Nuclear thermal propulsion engine based on particle bed reactor using light water steam as a propellant
[DE93-014336] 02 p0552 N94-14111
Small low mass advanced PBR's for bi-modal operation
[DE94-003201] 07 p2699 N94-25798
Summary of particle bed reactor designs for the Space Nuclear Thermal Propulsion Program
[DE94-007434] 09 p3615 N94-32266

PECULIAR GALAXIES
Guaranteed time observations support for Faint Object Spectrograph (FOS) on HST
[NASA-CR-196305] 12 p4547 N94-37037

PECULIAR STARS
NT SHELL STARS
NT SYMBIOTIC STARS
What is normal among the A-type stars?
[ISBN-0-315-83947-3] 05 p2081 N94-22592

PEDOLOGY
U SOIL SCIENCE

PEEK
Advanced zinc phosphate conversion and pre-ceramic polymetallosiloxane coatings for corrosion protection of steel and aluminum, and characteristics of polyphenyletheretherketone-based materials
[DE93-008717] 01 p0088 N94-10891
Crystallinity and dielectric properties of PEEK, a thermoplastic poly(ether ether ketone)
[AD-A266027] 01 p0091 N94-11487
Development of time-dependent orthotropic constitutive law of a thermoplastic composite material 02 p0556 N94-13595
Progress in the modeling of the shock response and mitigation of thick composite shells
[AD-A267009] 03 p1057 N94-15524
Creep damage of carbon fiber reinforced PEEK
[ISBN-0-315-58962-0] 05 p1677 N94-22420
A study of graphite peek composite with central elliptical holes under tension
[AD-A273779] 07 p2705 N94-25863
Optimization of the forming parameters of PEEK/carbon fiber composite
[ISBN-0-315-86410-9] 09 p3620 N94-31716
Low velocity impact damage in carbon fiber/PEEK composite laminates
[ISBN-0-315-86546-6] 09 p3622 N94-31909
Interfaces of high-protection performance polyaryls-coated zinc phosphated steels
[DE94-011732] 12 p4417 N94-37153

PEELING
The effect of plasma treatment on interfacial bond characteristics of Kevlar/epoxy laminates as measured by T-peel tests
[AD-A266920] 03 p0930 N94-14999

PEENING
NT SHOT PEENING
PEGASUS AIR-LAUNCHED BOOSTER
In-flight evaluation of aerodynamic predictions of an air-launched space booster 01 p0003 N94-10427
Special investigation report: Commercial space launch incident, launch procedure anomaly orbital sciences corporation PEGASUS/SCD-1, 80 nautical miles east of Cape Canaveral, Florida, February 9, 1993
[PB93-917003] 01 p0040 N94-11893
NASA report to education, volume 7
[NASA-TM-109435] 03 p1247 N94-15419
Preliminary analysis for a Mach 8 crossflow transition experiment on the Pegasus (R) space booster
[NASA-TM-104272] 12 p4381 N94-36648
PELLETS
Dielectric breakdown and its influence on ignition
[AD-A264925] 01 p0078 N94-11855
Pellet ablation in the large helical device
[NIFS-260] 06 p2551 N94-24358
High-speed repetitive pellet injector for plasma fueling of magnetic confinement fusion devices
[DE94-002792] 07 p3042 N94-26140
Sintering of dioxide pellets in an oxidizing atmosphere (CO2)
[DE94-613046] 12 p4414 N94-36517
PENALTY FUNCTION
Quantum statistical inference for density estimation
[DE94-002625] 07 p3073 N94-26805
The numerical calculation of laminar and turbulent flows using penalty function finite volume methods
[ISBN-0-315-61377-7] 07 p2799 N94-27947
PENCIL BEAMS
Analysis of a proposed Compton backscatter imaging technique
[DE93-040537] 06 p2371 N94-22935
PENDULOUS GYROSCOPES
U GYROSCOPIC PENDULUMS
PENDULUMS
NT GYROSCOPIC PENDULUMS
Results of tidal gravity observations with a conical pendulum 03 p1100 N94-15810
Design of non-sled setup to measure head injury criteria
[NIAR-92-20] 03 p0872 N94-17263
A study of the amplification of laser and VLF waves using a simple pendulum model
[AD-A270857] 04 p1442 N94-19770
Integrated accelerometer assembly
[CA-PATENT-1322107] 06 p2344 N94-24184
Modeling and control of nonlinear systems
[AD-A277377] 09 p3834 N94-32095
An automated digital data collection and analysis system for the Charpy Impact Tester 11 p4232 N94-36415
PENETRANTS
Detection and dosimetry of chemical contaminants in polymeric materials
[AD-A266605] 03 p0968 N94-16727
PENETRATION
A spectral nodal method for the solution of the Sn equations in x, y geometry for highly absorbing deep penetration problems
[DE93-613520] 01 p0349 N94-10636
Monte Carlo algorithms in simulation of 2beta-decay and penetration of electrons through matter
[DE93-617741] 01 p0364 N94-10837
Deformation mechanisms in tungsten single crystals in ballistic impact experiments
[AD-A265701] 01 p0405 N94-12563
Prediction of alumina penetration
[DE93-014017] 01 p0095 N94-12610
Measurement of penetration depth lambda(T) in YBa2Cu3O(7-delta) thin film
[DE93-014587] 02 p0810 N94-14122
Collisions and separations in 2D hydrodynamical code
[ITN-93-85225] 02 p0639 N94-14503
The motion of a conical shaped liner driven by explosive load
[ITN-93-85215] 02 p0585 N94-14507
X-SAR: The X-band synthetic aperture radar on board the Space Shuttle 03 p0990 N94-15891
Slidesurfaces with adaptive new definitions (SAND) for transient analysis
[DE93-014909] 03 p1059 N94-15983
SAND contact in DYNA3D
[DE93-016451] 04 p1340 N94-18113
The effect of crystallographic orientation on the performance of single crystal tungsten subscale penetrators
[AD-A268988] 04 p1597 N94-18468
Three-dimensional shock wave physics simulations with MIMD PAGOSA on massively parallel computers
[DE93-011682] 04 p1455 N94-18829
Earth Penetration Radar Imaging System (EPRIS)
[DE93-019890] 04 p1391 N94-19542
The influence of the target strength model on computed perforation
[DE93-018659] 04 p1460 N94-19543
Determination of parameters for hypervelocity dust grains encountered in near-Earth space
05 p2084 N94-20817
Penetrating nature of very collimated high-energy shower-clusters of hadrons and gamma rays
07 p3113 N94-25631
Users manual for CATNIP: A Computer Analysis Tool for Normal Impact Penetration
[DE94-003671] 07 p2962 N94-26371
Finite element analysis of axisymmetric deformations of thick thermoviscoplastic targets
08 p3320 N94-29688
Tearing resistance of a thin shell against projectile penetration: Material property effects
[DE94-007466] 09 p3733 N94-31316
Low dispersion of the muon precession frequency in HTSC samples YBa2Cu3O(x) and EuBa2Cu3O(x)
[DE94-608388] 09 p3896 N94-31395
PENETRATION BALLISTICS
U TERMINAL BALLISTICS
PENETROMETERS
Penetrometer compatible, fiber-optic sensor for continuous monitoring of chlorinated hydrocarbons: Field test results
[DE93-017974] 04 p1352 N94-19266
PENNING EFFECT
Quantum non demolition measurement of cyclotron excitations in a Penning trap 01 p0376 N94-10578
Radiative properties of molecular nitrogen ions produced by helium Penning ionization and argon effects
[NASA-CR-195126] 06 p2534 N94-24487
PENTABORANES
A proposed mechanism for the pyrolysis of diborane
[DE93-014275] 03 p0947 N94-15977
PENTACHLORIDES
U CHLORIDES
PENTAERYTHRITOL TETRANITRATE
U PETN
PENTANES
Synthesis of potential high-energy fuels
[AD-A267508] 03 p0975 N94-17073
PEPTIDES
NT POLYPEPTIDES
Development of bioelastic materials for the prevention of adhesions: Polypenta- and polytetrapeptides
[AD-A264851] 01 p0088 N94-10863
Probability of alamethicin conductance states varies with nonlamellar tendency of bilayer phospholipids
[AD-A264957] 01 p0301 N94-11648
Solitons and 1/f noise in molecular chains
[DE93-622898] 02 p0778 N94-12879
The evolution of energy-transducing systems: Studies with archaebacteria
[NASA-CR-194130] 02 p0728 N94-13562
Neuropeptide-Y (NPY) increases total blood flow in the tail, and reduces cutaneous microvascular blood flow in the tail and foot of the rat
[AD-A266839] 03 p1115 N94-14918
Bioorganic models for protein ion channels
[AD-A266365] 03 p1117 N94-16441
Vectorial electron transfer in spatially ordered arrays
[DE93-018150] 03 p1185 N94-16971
Enhancement of wound healing by biosynthetic growth factor
[AD-A272517] 05 p1892 N94-21415
Gamma-aminobutyric acid (GABA) and neuropeptides in neural areas mediating motion-induced emesis
05 p1886 N94-21902
The evolution of energy-transducing systems. Studies with archaebacteria
[NASA-CR-195129] 06 p2422 N94-24811
Capillary electrophoresis of biomolecules: Theory, instrumentation and applications
[ETN-94-95297] 06 p2236 N94-25233
Effect of PGE2 receptor agonists butaprost, M and B 28767 and an antagonist AH 6809 on the BK response of visceral polymodal receptors
07 p2906 N94-27494
PERCENTAGE
U RATIOS
PERCEPTION
NT AUDITORY PERCEPTION
NT BINAURAL HEARING
NT CONSCIOUSNESS
NT KINESTHESIA
NT MOTION PERCEPTION
NT PAIN
NT PAIN SENSITIVITY
NT PROPRIOCEPTION
NT SENSORY PERCEPTION
NT SOUND LOCALIZATION
NT SPACE PERCEPTION
NT TACTILE DISCRIMINATION
NT TASTE
NT TOUCH
NT VISUAL DISCRIMINATION
NT VISUAL PERCEPTION
Perception for outdoor navigation
[AD-A266867] 03 p0863 N94-14919
Transfer of perceptual adaptation to space sickness: What enhances an individual's ability to adapt?
[NASA-CR-188256] 06 p2427 N94-24227
Perceptions of organizational support and affectivity as predictors of job satisfaction
[DOT/FAA/AM-94/2] 06 p2429 N94-25442
CRC customer versus rater octane number requirement program (1990)
[AD-A273997] 07 p2758 N94-25901
The role of emotion in believable agents
[AD-A278952] 11 p4312 N94-35656
PERCEPTRONS
U SELF ORGANIZING SYSTEMS
PERCEPTUAL ERRORS
Perception of lightness and brightness in complex patterns
[AD-A268435] 03 p1134 N94-17513
Perception in flight: Shape and motion perception, space perception, spatial orientation, and visual vestibular interaction 06 p2429 N94-23979
Night vision goggle illusions and visual training
06 p2432 N94-23984
Mechanisms of eye-hand coordination
[AD-A273687] 06 p2428 N94-25437
DCT quantization matrices visually optimized for individual images 06 p2442 N94-25509
PERCEPTUAL TIME CONSTANT
The effects of Above Real-Time Training (ARTT) in an F-16 simulator 09 p3591 N94-32474
PERCHLORATES
NT AMMONIUM PERCHLORATES
NT POTASSIUM PERCHLORATES
Infrared spectroelectrochemical study of cyanide adsorption and reactions at platinum electrodes in aqueous perchlorate electrolyte
[AD-A276402] 09 p3631 N94-31238
PERCHLORIC ACID
Charge-dependent atomic-scale structures of high-index and (110) gold electrode surfaces as revealed by scanning tunneling microscopy
[AD-A276782] 09 p3869 N94-32170
PERCOLATION
Study of multicomponent diffusion and transport phenomena
[DE93-015095] 02 p0804 N94-13005
Ventilated oscillatory boundary layers
[AD-A266226] 03 p1023 N94-16110
Computerized simulations with cellular automates for cloud formation
[GKSS-92/E/22] 05 p1867 N94-21312
The Fermi paradox: An approach based on percolation theory 07 p2687 N94-27370
PERCUSSION
Effects of slot on rock surface for percussive rock excavation: Water jet assisted percussive rock excavation 07 p2871 N94-28155
PERFECT GAS
U IDEAL GAS
PERFLUORO COMPOUNDS
The properties of perfluoropolyethers used for space applications
[NASA-TM-106275] 01 p0088 N94-10864
Polyimides containing amide and perfluoroisopropylidene connecting groups
[NASA-CASE-LAR-14608-1] 05 p1702 N94-20374
Perfluoropolyalkylether decomposition on catalytic aluminas
[NASA-TM-106547] 09 p3617 N94-33021
Development and preliminary evaluation of aryl ester boundary additives for perfluoropolyethers
[NASA-TM-106603] 09 p3663 N94-33024
Halon 1211 replacement agent evaluation-perfluorohexane and halotron I
[AD-A278194] 10 p4031 N94-33385
Perfluorodiethoxymethane on nickel and nickel oxide surfaces
[DE94-011200] 12 p4426 N94-37712
PERFORATED PLATES
Perforated plates for thin-walled structures
01 p0063 N94-10056
Performance of the X-/Ka/KABLE-band dichroic plate in the DSS-13 beam waveguide antenna
06 p2291 N94-23261
Three-dimensional elastic stress concentration factors: Plain or countersunk hole in a wide plate subjected to tension, bending, or pin loading
[ESDU-93030] 07 p2845 N94-28143
X-/Ka-band dichroic plate design and grating lobe study 08 p3247 N94-29616

PERFORATING
An analysis of the dynamic response of the Space Station Freedom due to a module perforation by an orbital debris particle impact
[TABES PAPER 93-653] 03 p0899 N94-16154
A fresh look at crater scaling laws for normal and oblique hypervelocity impacts 05 p1666 N94-20864

PERFORMANCE
From red tape to results: Creating a government that works better and costs less 01 p0422 N94-11351
From red tape to results: Creating a government that works better and costs less. Executive summary 01 p0422 N94-11353
Defining the performance gap: Conducting a self-assessment 02 p0666 N94-13155
Performance of the upgraded Orroral laser ranging system 03 p0877 N94-15602

PERFORMANCE PREDICTION
Hydrostatic testing of thick laminated composite cylinders for performance model validation
[DE93-012728] 01 p0184 N94-10264
Characterization of a scannerless LADAR system
[DE93-011582] 01 p0174 N94-10959
Accelerated screening methods for predicting lubricant performance in refrigerant compressors
[DE93-014773] 01 p0089 N94-11146
A comparison between numerically modelled and experimentally measured loss mechanisms in wave rotors
[NASA-TM-106279] 01 p0029 N94-11255
Applying reliability models to the maintenance of Space Shuttle software 01 p0330 N94-11434
Criteria for assessing problem solving and decision making in complex environments 01 p0314 N94-11532
HF-OTH radar performance results
[AD-A266106] 01 p0138 N94-11655
The identification of ability requirements and selection instruments for fighter pilot training
[AD-A266340] 02 p0735 N94-13582
Stochastic performance modeling and evaluation of obstacle detectability with imaging range sensors
[NASA-CR-194510] 02 p0605 N94-13946
A performance prediction model for a fault-tolerant computer during recovery and restoration
[NASA-CR-194490] 02 p0741 N94-14136
Aeropropulsion test and evaluation methods 02 p0506 N94-14165
Development of Japanese Earth Resources Satellite-1 (JERS-1; FUYO-1) and it's operational results
[NASDA-SPP-930001] 03 p0884 N94-15001
Rotary engine performance computer program (RCEMAP and RCEMAPPC): User's guide
[NASA-CR-191192] 03 p0869 N94-15192
Concepts on measuring the benefits of software process improvements
[AD-A266994] 03 p1144 N94-15215
Comparison of RADARC high-frequency radar performance prediction model and ROTHR Amchitka data
[AD-A267077] 03 p0987 N94-15540
GLRS-R 2-colour retroreflector target design and predicted performance 03 p0921 N94-15615
A rapid computational model for estimating the performance of compliant airfoils in cascades
[AD-A266275] 03 p0857 N94-16471
Predicting radiation induced performance decrements of AH-1 helicopter crews. Volume 1: Predicted veersus actual performance of AH-1 crews induced with symptoms simulating radiation sickness
[AD-A268376] 03 p1138 N94-17460
Space Station Freedom electrical performance model
[NASA-TM-106395] 03 p0929 N94-17483
System performance modeling and analysis of a fault-tolerant, real time parallel processor
[AD-A268070] 03 p1162 N94-17551
Take-off performance monitoring system algorithm and display development
[NLR-TP-91395-U] 04 p1317 N94-17734
A study of the automatic generating system. 3: Improvement of the total system performance 04 p1429 N94-18040
RADARC HF ionospheric prediction program for OTH radar
[AD-A269557] 04 p1385 N94-18291
Prediction of the high-lift performance of multi-element aerofoils using an unstructured Navier-Stokes solver 04 p1307 N94-18427
Turbulence modeling in aircraft icing 04 p1412 N94-18555
Toward a high performance distributed memory climate model
[DE93-019156] 04 p1494 N94-19298
FNAS/summer faculty fellowship research continuation program. Task 6: Integrated model development for liquid fueled rocket propulsion systems. Task 9: Aspects of model-based rocket engine condition monitoring and control
[NASA-CR-194574] 04 p1338 N94-19706
System performance predictions for Space Station Freedom's electric power system
[NASA-TM-106396] 05 p1667 N94-20062
Signal processing in the linear statistical model
[AD-A272114] 05 p1736 N94-20570
Mathcad computer applications predicting antenna parameters from antenna physical dimensions and ground characteristics
[AD-A272987] 05 p1740 N94-21264
Problem reporting management system performance simulation 05 p1931 N94-21328
Compatibility evaluation and research on the Computerized Adaptive Screening Test (CAST): User and programmer's guide
[AD-A273112] 05 p1894 N94-21510
Proof test of the computer program BUCKY for plasticity problems
[NASA-TP-3444] 06 p2374 N94-22960
Foil bearing research at Penn State 06 p2215 N94-23058
Computational fluid dynamic modelling of cavitation 06 p2215 N94-23060
Mathematical modeling of MCFC cells/stacks and networks
[DE94-001914] 06 p2390 N94-23212
Optical subnet concepts for the deep space network 06 p2292 N94-23269
Investigation of time and intensity effects in operator workload and performance
[CTN-94-60927] 06 p2433 N94-24171
Pilot evaluation system 06 p2158 N94-24266
Aerodynamic models for performance calculations of modern technology propellers 06 p2161 N94-24285
CFD simulation of coaxial injectors 06 p2342 N94-24430
Space Shuttle Main Engine performance analysis 06 p2222 N94-24444
Tokamak Physics Experiment (TPX) cost and performance trade studies using supercode
[DE94-002720] 06 p2553 N94-24628
Design and implementation of a distributed version of the NASA Engine Performance Program
[NASA-CR-194475] 06 p2462 N94-25179
Transputer benchmarks and performance comparisons with other computing machines
[RR-467] 06 p2446 N94-25312
Relationship between the structure and performance of identified nonlinear polynomial models
[RR-474] 06 p2492 N94-25320
State-of-the-art engineering aeroprediction methods with emphasis on new semiempirical techniques for predicting nonlinear aerodynamics on complete missile configurations
[AD-A273680] 06 p2171 N94-25411
Predicting antenna parameters from antenna physical dimensions
[AD-A273893] 07 p3012 N94-25655
Program to develop a performance and heat load prediction system for multistage turbines
[NASA-CR-195223] 07 p2674 N94-26588
Early real-time performance measurements on the Columbus processor system 07 p2952 N94-26736
Integrated model development for liquid fueled rocket propulsion systems
[NASA-CR-195253] 07 p2702 N94-27166
Interdisciplinary technology 07 p2686 N94-27363
Rocket engine numerical simulation 07 p2688 N94-27375
Transient model applications. 3: Transient engine simulation and analysis of an ice ingestion test 07 p2829 N94-28050
Ejectors and jet pumps: Computer program for design and performance for liquid flow
[ESDU-93022] 07 p2832 N94-28093
Performance model of a recirculating stack nickel hydrogen cell 07 p2861 N94-28112
A340 testing 07 p2662 N94-28242
Development of the integrated environmental control model: Performance models of selective catalytic reduction NO(x) control systems
[DE94-002151] 08 p3341 N94-28465
BAG: A code for predicting the performance of a gas bag impact attenuation system for the Pathfinder lander
[DE94-003688] 08 p3165 N94-28477
Simulation Networking/Training Requirements Relational Database: User's guide
[AD-A275634] 08 p3528 N94-28637
Effects of workload on communication processes in decision making teams
[AD-A275894] 08 p3527 N94-28796
Role of microstructure on the fatigue durability of aluminum aircraft alloys
[AD-A275814] 08 p3202 N94-28830
GLRS-R 2-colour retroreflector target design and predicted performance
[REPT-932-440-106] 08 p3246 N94-29542
Performance evaluation of intelligent network services
[PB94-149564] 08 p3438 N94-30373
Performance predictions for composite materials
[AD-A276451] 09 p3618 N94-31261
Predicting antenna parameters from antenna physical dimensions
[AD-A276442] 09 p3672 N94-31300
An analysis of the maintenance performance measurement system for LAMPS MK 3 helicopter squadrons
[AD-A276421] 09 p3565 N94-31332
Communications networks in stressed environments
[AD-A275967] 09 p3672 N94-31384
Compiler techniques for managing data motion
[AD-A276514] 09 p3918 N94-31930
Civil tiltrotor market penetration: Effects on Northeast corridor airport delay
[AD-A277534] 09 p3576 N94-32955
Photonic fast packet switching using optically processed control
[AD-A278195] 10 p4038 N94-33386
Airframe systems studies review 10 p3970 N94-33453
Validity of the air traffic control specialist nonradar screen as a predictor of performance in radar-based air traffic control training
[AD-A279754] 10 p4098 N94-34210
A test system of pose repeatability precision of multi-path robot 10 p4067 N94-34341

PERFORMANCE TESTS
An approach to high precision antenna structures by a CFRP core sandwich concept 01 p0057 N94-10008
The electron beam furnace: A new facility for materials science research 01 p0109 N94-10126
Particle image velocimetry technique: Calibration tests 01 p0111 N94-10137
Hydrostatic testing of thick laminated composite cylinders for performance model validation
[DE93-012728] 01 p0184 N94-10264
Space nuclear thermal propulsion nuclear element tests at Sandia National Laboratories
[DE93-002301] 01 p0045 N94-10282
Demonstration prototype gamma-ray hodoscope alternative to CARGOSCAN for rocket stage monitoring
[DE93-006908] 01 p0169 N94-10326
AGBT advanced counter-rotating gearbox detailed design report
[NASA-CR-180883] 01 p0179 N94-10400
Static internal performance of a single expansion ramp nozzle with multiaxis thrust vectoring capability
[NASA-TM-4450] 01 p0012 N94-10675
Characterization of in-flight performance of ion propulsion systems
[NASA-TM-106283] 01 p0046 N94-10761
Vehicular fleet operation on natural gas and propane: An overview
[PB93-194603] 01 p0098 N94-10844
In-orbit performance tests and tele-command systems of the umbrella test satellite (DEBUT)
[NAL-TR-1165] 01 p0043 N94-10859
Performance and rotor loads measurements of the Lynx XZ170 helicopter with rectangular blades
[NASA-TM-104000] 01 p0001 N94-10936
Landing Craft Air Cushion (LCAC) crew selection system manual
[AD-A265158] 01 p0313 N94-11098
Pre-operation analysis of ERS-1 tracking and operation, part 2-F
[NASDA-CNT-930002-PT-2-F] 01 p0230 N94-11130
Accelerated screening methods for predicting lubricant performance in refrigerant compressors
[DE93-014773] 01 p0089 N94-11146
Development and application of an acceptance testing model 01 p0330 N94-11432
Monitoring cognitive function and need with the automated neuropsychological assessment metrics in Decompression Sickness (DCS) research 01 p0314 N94-11533
Electric and hybrid vehicle site operators program: Thinking of the future
[DE93-011231] 01 p0144 N94-11609
Theory of elementary particles and accelerator theory. Task C: Experimental high energy physics
[DE93-013139] 01 p0368 N94-11696
Basic attributes test (BAT): Operational pre-implementation analysis and score equating
[AD-A265885] 01 p0314 N94-12276
FR/GE/US radar receiver pulse compression ratio
[AD-A265391] 01 p0138 N94-12409

Digital sound: The selection of critical programme material and preparation of recordings for CCIR tests on low bit-rate codecs
[BBC-RD-1993/1] 02 p0598 N94-12925
Digital sound: Subjective tests on commentary-quality codecs
[BBC-RD-1993/2] 02 p0598 N94-12926
Evaluation for membrane components of water recycling system
[NAL-TM-646] 02 p0737 N94-13388
Arc-heating tests of thermal protection system materials for the H-2 rocket fairing
[NAL-TR-1181] 02 p0551 N94-13455
Selection of behavioral tasks and development of software for evaluation of rhesus monkey behavior during spaceflight
[NASA-CR-194176] 02 p0728 N94-13865
The Large Area Pulsed Solar Simulator (LAPSS)
[NASA-CR-194507] 02 p0703 N94-13940
Stochastic performance modeling and evaluation of obstacle detectability with imaging range sensors
[NASA-CR-194510] 02 p0605 N94-13946
Battery testing at Argonne National Laboratory
[DE93-011761] 02 p0624 N94-14012
Aerodynamic and aerothermal facilities 2: Continuous flow high enthalpy facilities 02 p0506 N94-14160
Aeropropulsion test and evaluation methods
02 p0506 N94-14165
Qualification test of the Ross Double Planetary Mixer
[NASA-CR-192600] 02 p0652 N94-14497
Control structural interaction testbed: A model for multiple flexible body verification
02 p0544 N94-14649
Performance evaluation of the honeywell GG1308 miniature ring laser gyroscope
[AD-A266694] 02 p0653 N94-14782
Performance comparison of high speed microchannel plate photomultiplier tubes 03 p0922 N94-15624
Development of the OMPAT neuropsychological/psychomotor performance evaluation and OMPAT data and timing support programs
[AD-A266954] 03 p1122 N94-15759
Recent advances in outdoor performance evaluation of PV systems
[DE93-015031] 03 p1091 N94-15994
Test plan for the evaluation of the initial capability of the National Satellite Test Bed: Phase 1D
[DOT/FAA/RD-93/20] 03 p0876 N94-16025
Cost-effective test methods for Shuttle payloads
[TABES PAPER 93-651] 03 p0883 N94-16151
Lithium D-cell study
[NASA-CR-192705] 03 p1011 N94-16505
ALS engine propellant effector system
[NASA-CR-194650] 03 p0926 N94-16590
TIMS performance evaluation summary
03 p1063 N94-16596
Cycle performance testing of nonazeotropic mixtures of HFC-142A/HCFC-124 and HFC-32/HCFC-124 with enhanced surface heat exchangers
[DE93-015215] 03 p1024 N94-16808
Category (CAT) 3B level 1 test plan for Global Positioning System (GPS)
[DOT/FAA/RD-93/21] 03 p0864 N94-16835
CALS test network handbook
[AD-A267587] 03 p1160 N94-17209
A ten year review of performance of photovoltaic systems
[DE93-015649] 03 p1093 N94-17217
Measurements of microlens performance
03 p1197 N94-17355
Radar transmitter procedures
[AD-A268274] 03 p1005 N94-17523
Optimisation and specification of Auger electron spectrometers for signal-to-noise ratio performance
[NPL-DMM(A)-101] 03 p1006 N94-17549
Test methods for acceptance testing of telescopes
[AD-A268316] 03 p1237 N94-17568
The stability and utility of the ESPRIT project, MUSiC, performance-based indicators of usability and tools: An evaluation of the usability of the NPL iSDX telephone system
[NPL-DITC-213/92] 04 p1613 N94-17925
Electric measurement of Lavet motors
04 p1408 N94-18022
Reliability control for wrist watches and their casements 04 p1427 N94-18030
Studies of dynamic contact of ceramics and alloys for advanced heat engines
[DE93-016366] 04 p1368 N94-18110
Performance evaluations of demountable electrical connections
[DE93-017399] 04 p1396 N94-18135
Adaptations to micropep and rocket to allow performance evaluation of multiple grain and/or airbreathing motors
[AD-A268798] 04 p1337 N94-18202
First on-sun test of NaK pool-boiler solar receiver
[DE93-015003] 04 p1466 N94-18208
Magnetic field measurements of a superconducting undulator for a Harmonic Generation FEL experiment at the NSLS
[DE93-017621] 04 p1438 N94-18504
Research on stable, high-efficiency amorphous silicon multijunction modules
[DE93-010046] 04 p1467 N94-18518
Testing and evaluation of large-area heliostats for solar thermal applications
[DE93-018509] 04 p1467 N94-18520
Characterization of the Facility for Atmospheric Corrosion Testing (FACT) at Sandia
[DE93-018510] 04 p1474 N94-18521
Evaluation of aftermarket LPG conversion kits in light-duty vehicle applications
[DE93-010035] 04 p1377 N94-18617
Building a joint-service classification research roadmap: Criterion-related issues
[AD-A269735] 04 p1512 N94-18754
Laboratory test and evaluation report of the essex model 60C-0037-2 molecular sieve oxygen generating system
[AD-A269967] 04 p1445 N94-18778
Technology test bed
[NASA-TM-109354] 04 p1322 N94-18953
Metallurgical evaluation of SRAM 2/SRAM A program mer base plates
[DE93-018689] 04 p1364 N94-19100
Development of a quartz digital accelerometer for environmental sensing and navigation applications
[DE93-018503] 04 p1433 N94-19243
On-line test methods of microprocessor based systems
[ETN-93-95008] 04 p1530 N94-19498
Design verification and acceptance tests of the ASST-A helium refrigeration system
[DE93-019746] 04 p1381 N94-19540
Human integration evaluation of three helmet systems
[AD-A271320] 04 p1513 N94-19570
Electro-optics display research, test, and evaluation laboratory program
[AD-A270947] 04 p1408 N94-19751
TCP performance analysis for wide area networks
[DE94-000449] 05 p1928 N94-19858
Night vision goggle model F4949 preflight adjustment/assessment procedures
[AD-A271079] 05 p1895 N94-19935
Efficient chip signature checking for diagnosing boundary scan systems
[RR-901-I] 05 p1749 N94-20166
Multiport solid-state imager characterization at variable pixel rates
[DE93-018366] 05 p1808 N94-20287
Performance evaluation of the JPL TOPSAR system: An across-track interferometric SAR system for topographic mapping 05 p1732 N94-20461
The One-Day Workshop on Batteries, Stepping Motors, and Electronic Clock Displays
[ETN-93-94632] 05 p1752 N94-20628
Battery tests 05 p1752 N94-20631
LCD display tests 05 p1752 N94-20635
Development and demonstration of a personal monitoring system for exposure to hydrogen fluoride
[DE93-041273] 05 p1891 N94-20935
Operational test and evaluation of electronic combat systems
[AD-A273093] 05 p1647 N94-21500
Mirror velocity sampling errors in a Michelson interferometer
[AD-A273105] 05 p1809 N94-21508
Performance evaluation of video on ethernet
[DE93-040696] 05 p1936 N94-21749
Surface acoustic wave sensing of VOC's in harsh chemical environments
[DE93-040721] 05 p1968 N94-21751
Electric and hybrid vehicles program
[DE93-040664] 06 p2352 N94-22881
A field evaluation of remote sensor measurements of wind, temperature, and moisture for ARM integrated sounding system research
[DE94-000565] 06 p2381 N94-23001
Contribution to the evaluation of efficiency of a microprocessor functional test
[ETN-94-95176] 06 p2445 N94-23153
Results of the Mojave tests of the Mars 96 rover
06 p2370 N94-23416
Performance evaluation of the Russian SPT-100 thruster at NASA LeRC
[NASA-TM-106401] 06 p2219 N94-23630
In-vacuum performance of Fomblin Z25-lubricated, 52100 steel bearings with TiC-coated balls
06 p2358 N94-24011
Data relay system satellite: The development of an antenna pointing mechanism for the inter-orbit link antenna 06 p2359 N94-24015
Development of gears for space use
06 p2360 N94-24021
Design and performances of electromagnetic initiators for space mechanisms: An alternative to pyrotechnic system 06 p2315 N94-24037
BLAST, a new lubricant screening tester for space oils and greases 06 p2362 N94-24042
Roles, uses, and benefits of general aviation aircraft in aerospace engineering education
[NASA-TM-106463] 06 p2153 N94-24100
Experimental verification of an acoustic telemetry link between an Aurora and CFAV quest
[DREA-TC-93-304] 06 p2202 N94-24121
The effects of spatially displaced visual feedback on remote manipulator performance
06 p2436 N94-24201
Analog communication transmitter and receiver test procedures
[AD-A273423] 06 p2300 N94-24687
Hubble Space Telescope high speed photometer science verification test report
[NASA-CR-189322] 06 p2205 N94-24710
Lightning tests and analyses of tunnel bond straps and shielded cables on the Space Shuttle solid rocket booster
[NASA-CR-193921] 06 p2200 N94-24801
Design and simulation of EVA tools for first servicing mission of HST
[NASA-CR-194784] 06 p2439 N94-24857
Performance measurements of the multimedia testbed on Mach 3.0: Experience writing real-time device drivers, servers, and applications
[AD-A273600] 06 p2460 N94-24932
Power electronics development for the SPT-100 thruster
[NASA-TM-106488] 06 p2221 N94-25189
The evaluation of ASOS for the Kennedy Space Center's Shuttle Landing Facility
[NASA-CR-195685] 06 p2416 N94-25271
Investigation of hand capabilities under a variety of performance conditions and an attempt to explain performance differences 06 p2444 N94-25354
Hydride thermodynamic machines
[VTT-JULK-768] 06 p2571 N94-25416
Evaluation of image quality 06 p2443 N94-25514
A test of the theory of reasoned action at the group level of analysis
[AD-A273965] 07 p2937 N94-25897
Mitsubishi 3-5 micrometers IR imager for machine-vision/ATA applications
[AD-A273812] 07 p3034 N94-25940
Investigation of plasma etch induced damage in compound semiconductor devices
[DE94-002849] 07 p3052 N94-25989
Digital Altimeter Setting Indicator (DASI) Operational Test and Evaluation (OT/E) operational test procedures
[AD-A274100] 07 p2672 N94-26030
Rewarming methodologies in the field
[AD-A274744] 07 p2909 N94-26173
Differential global positioning system for the surface-towed ordnance locating system: Testing, results, and user's guide
[DE94-002980] 07 p2664 N94-26309
Hadron gas ionization calorimeters
[DE93-634186] 07 p2810 N94-26397
Study on the compensated lead hadron calorimeter characteristics by means of hadron and electron beams
[DE93-634176] 07 p2810 N94-26439
Investigation of the aerodynamic environment for an advanced lightweight rotor in forward flight. Volume 4: Laser velocimeter wake data, advance ratio of 0.037
[NASA-TM-109040-VOL-4] 07 p2645 N94-26483
Effects of repeating resistance testing on firing ability of igniter EP360-3
[AD-A274814] 07 p2759 N94-26486
Investigation of the aerodynamic environment for an advanced lightweight rotor in forward flight. Volume 1: Laser velocimeter inflow data, advance ratio of 0.37, thrust coefficient of 0.0081 and hover tip speed of 603 feet/second
[NASA-TM-109040-VOL-1] 07 p2645 N94-26489
Investigation of the aerodynamic environment for an advanced lightweight rotor in forward flight. Volume 2: Laser velocimeter inflow data, advance ratio of 0.37, thrust coefficient of 0.0064 and hover tip speed of 710 feet/second
[NASA-TM-109040-VOL-2] 07 p2645 N94-26492
Investigation of the aerodynamic environment for an advanced lightweight rotor in forward flight. Volume 3: Laser velocimeter inflow data, advance ratio of 0.37, thrust coefficient of 0.0064 and hover tip speed of 603 feet/second
[NASA-TM-109040-VOL-3] 07 p2645 N94-26497

A comparison of sleep scored from electroencephalography to sleep scored by wrist actigraphy
[AD-A273739] 07 p2910 N94-26748
The PLVCR 500 and HCPC, tests and results
[DLR-MITT-93-04] 07 p2858 N94-26813
SP industry calorimeter for rate of heat release measurements up to 10MW
[PB94-124211] 07 p2811 N94-27044
Development of a performance evaluation tool (MMSOFE) for detection of failures with Multiple Model Adaptive Estimation (MMAE)
[AD-A274218] 07 p2685 N94-27071
Orbital transfer vehicle engine technology high velocity ratio diffusing crossover
[AD-A277180] 07 p2703 N94-27212
The OPAL vertex detector
[ISBN-0-315-51152-4] 07 p2812 N94-27257
Design and implementation of a DBMS performance assessment tool
[CWI-CS-R9270] 07 p2972 N94-27576
Test and evaluation of the Litton (Canada) Canadian strapdown gyroscope (CSG-2) Performance Evaluation Unit (PEU)
[DREO-1010] 07 p2813 N94-27597
A fully integrated 16 channel digitally trimmed pulse shaping amplifier
[DE94-004555] 07 p2787 N94-27618
Communication on the Paragon
[DE94-003103] 07 p2983 N94-27713
Extra-Vehicular Activity (EVA) glove evaluation test protocol
[NASA-TM-108442] 07 p2943 N94-27952
Transient model applications. 3: Transient engine simulation and analysis of an ice ingestion test
07 p2829 N94-28050
Cooling towers for combined cycles: Design philosophy, performance testing, and operating problems
07 p2832 N94-28087
Ni-H2 cell characterization for INTELSAT programs
07 p2861 N94-28109
Performance test results of ETS-6 Ni-Cd cells
07 p2863 N94-28121
AF Ni-Cd cell qualification program
07 p2863 N94-28122
Some observations on battery charge control
07 p2863 N94-28125
Construction of temperature compensated constant voltage (VT) curves for super Ni-Cd (tm) cells
07 p2863 N94-28126
A comparison of spectral decorrelation techniques and performance evaluation metrics for a wavelet-based, multispectral data compression algorithm
07 p2946 N94-28258
Fibrous ceramic candle filter for particle removal in pressurized fluidized bed combustion
[PB94-133089] 07 p2876 N94-28383
Thermal protective performance and instrumented mannequin evaluation of multi-layer garment systems
08 p3381 N94-28433
Rewarming methodologies in the field
08 p3382 N94-28441
Environmental characterization for target acquisition. Analysis of thermal and visible imagery
[AD-A275414] 08 p3242 N94-28862
Performance evaluation of a 22.5/30 kW 270 volts direct current generator system
[AD-A275106] 08 p3263 N94-28913
Stress and ergonomic design and evaluation of person-machine systems
[AD-A275156] 08 p3400 N94-29034
Some problems of scramjet propulsion for aerospace planes. Part 2: Scramjet: Development and test problems 08 p3152 N94-29301
Software testing practices and their evolution for the 1990's 08 p3415 N94-29335
A disciplined approach to software test and evaluation
08 p3416 N94-29339
Development of electromagnetic compatibility tests
[REPT-932-430-110] 08 p3245 N94-29421
A portable X-band front-end test package for beam-waveguide antenna performance evaluation. Part 2: Tests on the antenna 08 p3247 N94-29620
The use of screening tests in spacecraft lubricant evaluation 08 p3162 N94-29641
A study of the relationship between the performance and dependability of a fault-tolerant computer
[NASA-CR-195758] 08 p3406 N94-29695
Remote observatory access via the advanced communications technology satellite
08 p3253 N94-29894
Scanning and monitoring performance: Effects of the reinforcement values of the events being monitored
[DOT/FAA/AM-94/8] 08 p3398 N94-29918
A newly developed snow vehicle (SM100S) for Antarctica. Part 5: Result of general performance tests
08 p3314 N94-29985
A user's guide to the Software Testpilot
[CWI-CS-R9343] 08 p3426 N94-30435
NATO SOCMET trials 08 p3258 N94-30503
A performance analysis method for distributed real-time robotic systems: A case study of remote teleoperation
[AIAA PAPER 94-1212-CP] 08 p3445 N94-30563
Status of frequency and time support for NASA systems 08 p3468 N94-30640
Testing Operational Flight Programs (OFP's)
[AD-A276361] 09 p3578 N94-31387
Technical evaluation of the UH-60Q: Medical oxygen system
[AD-A276983] 09 p3579 N94-32242
Performance of the Sony lithium-ion rechargeable battery
[AD-A277076] 09 p3693 N94-32303
A low-cost, CCD solid state star tracker
[NASA-CR-192722] 09 p3882 N94-32417
Aircrew Eye/Respiratory Protection (AERP): 16-hour extended wear evaluation of chemical protective equipment
[AD-A277288] 09 p3804 N94-32609
The relative performance of FeS2 and CoS in long-life thermal-battery applications
[DE94-006145] 09 p3695 N94-32663
Design and evaluation of coils for a 50 mm diameter induction coilgun launcher
[DE94-005244] 09 p3603 N94-32671
Temperature-humidity-bias aging technique to identify defective surface mount capacitors
[DE94-005354] 09 p3660 N94-32727
A 10 GHz bandwidth, single transient, digitized oscilloscope with 20 GHz capability
[DE94-005400] 09 p3713 N94-32728
Polymer electrolyte fuel cells
[DE94-007558] 09 p3761 N94-32762
EDD-7 Electric Charge Point Meter test results
[DE94-008515] 09 p3696 N94-32828
Enhancement of mixing in a rectangular jet by mechanical tabs
[NASA-CR-185207] 09 p3709 N94-32872
Operational experience and evaluation of a dual-element stretched-membrane heliostat
[DE94-008827] 09 p3763 N94-32965
Two-axis antenna positioning mechanism
09 p3605 N94-33308
A human factors evaluation using tools for automated knowledge engineering 10 p4101 N94-33628
The US Navy/Canadian DCIEM research initiative on pressure breathing physiology 10 p4101 N94-33636
Evaluation of a liquid cooling garment as a component of the Launch and Entry Suit (LES)
10 p4101 N94-33653
Comparative performance of a modified Space Shuttle Reentry Anti-G Suit (REAGS) with and without pressure socks 10 p4101 N94-33655
Intelligent vehicle control: Opportunities for terrestrial-space system integration
10 p4127 N94-34038
Marshall Space Flight Center head development program
[NASA-CR-193944] 10 p4056 N94-34073
Minipilot solar system: Design/operation of system and results of non-solar testing at MRI
[PB94-152238] 10 p4079 N94-34165
The effective use of animation in simulation model validation
[AD-A278500] 10 p4109 N94-34291
A microcomputer measuring-controlling system for the performance test of fogging nozzles
10 p4032 N94-34362
Design and aerodynamic performance evaluation of a high-work mixed flow turbine stage
10 p4003 N94-34459
Techniques for aerodynamic characterization and performance evaluation at high angle of attack
10 p3991 N94-34614
Performance evaluation of digital phase-locked loops for advanced deep space transponders
11 p4254 N94-35558
Concept for an algorithm testing and evaluation program at NIST
[PB94-163029] 11 p4304 N94-35740
Carbon-carbon piston development
[NASA-CR-4595] 11 p4233 N94-35947
A solid oxide fuel cell power system: 1992-1993 field operation
[DE94-010383] 11 p4283 N94-36109
Flight test certification of a 480 gallon composite fuel tank on CF-18 11 p4196 N94-36340
In-flight refueling: Dassault Aviation research on the Rafale aircraft 11 p4196 N94-36341
CC-130H(T) tactical aerial refuelling tanker development flight test programme 11 p4198 N94-36347
Receiver design, performance analysis, and evaluation for space-borne laser altimeters and space-to-space laser ranging systems
[NASA-CR-194747] 12 p4397 N94-36988
Long-range mesoscale modeling of pollutant transport for the European Tracer EXperiment (ETEX)
[DE94-010820] 12 p4465 N94-37093
Role of burn-in during qualification testing
[DE94-007864] 12 p4439 N94-37513
The integrated performance evaluation program quality assurance guidance in support of EM environmental sampling and analysis activities
[DE94-013043] 12 p4468 N94-37731
Civil use of night vision devices: Evaluation pilot's guide, part 1
[SCT-91RR-43] 12 p4487 N94-37741
Assessment of night vision goggle workload: Flight test engineer's guide
[SCT-91RR-45] 12 p4487 N94-37743
Advanced Turbine Technology Applications Project (ATTAP)
[NASA-CR-195367] 12 p4452 N94-37763

PERFUSION
U DIFFUSION

PERICLASE
Correlated petrographic, electron microprobe, and ion microprobe studies of selected primitive and processed phase assemblages in meteorites
[NASA-CR-194827] 06 p2601 N94-23499
Microstructure and chemistry of MgO- and CoO-doped nickel-titanate spinels
[DE94-012741] 12 p4537 N94-37382

PERIDOTITE
First results from analysis of coordinated AVIRIS, TIMS, and ISM (French) data for the Ronda (Spain) and Beni Bousera (Morocco) peridotites 03 p1067 N94-16675
Euhedral metallic-Fe-Ni grains in extraterrestrial samples 05 p1697 N94-20724
Basaltic magmatism on the Moon. A perspective from volcanic picritic glasses 05 p2114 N94-20758
Primary differentiation in the early Earth: Nd and Sr isotopic evidence from diamondiferous eclogites for both old depleted and old enriched mantle, Yakutia, Siberia
05 p1862 N94-20776
The carbon components in SNC meteorites of feldspathic harzburgite composition
05 p2086 N94-20885
Studies in Jurassic and Cretaceous North American apparent polar wander 08 p3362 N94-29940
Geochemical and fluid dynamic investigations into the nature of chemical variability in the Earth's mantle
08 p3367 N94-30917

PERIGEES
High Earth orbit design for lunar assisted small Explorer class missions 11 p4202 N94-35608

PERIHELIONS
Dust grain resonant capture: A statistical study
03 p1245 N94-16384

PERIOD DOUBLING
To the theory of irregular auto modulation in electron beam-backward electromagnetic wave dynamic system
[DE93-620982] 01 p0133 N94-11030
Transition induced by fixed and freely convecting spherical particles in laminar boundary layers
[AD-A267757] 03 p1028 N94-17276
Extracavity frequency doubling study of a pulsed photodissociation iodine laser
[AD-A267893] 03 p1042 N94-17394
Bifurcation theory: Chaos and patterns
04 p1607 N94-18237

PERIOD EQUATIONS
U PERIODIC FUNCTIONS

PERIODIC FUNCTIONS
NT COSINE SERIES
NT SINE SERIES
NT TRIGONOMETRIC FUNCTIONS
Stoermer-Cowell and related methods for the numerical solution of second order periodic initial value problems for ODE's 2: Numerical characteristics of the methods
[MEMO-1082] 05 p1953 N94-21075
On the Daubechies-based wavelet differentiation matrix
[NASA-CR-191583] 06 p2479 N94-23090
Temporal aggregation in a periodically integrated autoregressive process
[PB93-230480] 06 p2479 N94-23122
Periodic nonlinear Schroedinger equation and invariant measures
[PB93-238012] 06 p2487 N94-23775
Cauchy problem for periodic KDV-type equations
[PB93-238020] 06 p2487 N94-23776
Representation, prediction and identification of cyclostationary processes: A state-space approach
[REPT-93-041] 09 p3850 N94-31191

Remarks on a result of LAV Carvalho
[AD-A276404] 09 p3841 N94-31360
New proof and extension of Sarkovskii's theorem
[AD-A278347] 10 p4129 N94-34004
Cauchy and invariant measure problem for the periodic Zakharov system
[PB94-167707] 11 p4317 N94-35760

PERIODIC ORBITS
U ORBITS

PERIODIC PROCESSES
U CYCLES

PERIODIC VARIATIONS
NT ANNUAL VARIATIONS
NT DIURNAL VARIATIONS
NT NOCTURNAL VARIATIONS
NT SECULAR VARIATIONS
A grid generation method to calculate the flow field in a three-dimensional cascade of blades
[NAL-TR-1158] 01 p0147 N94-10364
Large amplitude shape oscillations in a mercury drop using a drop tower
[DE93-767972] 01 p0125 N94-10730
Space and time variability of the Gulf Stream using ERS-1 ALT-OPR02 data 01 p0242 N94-11769
Proceedings of the PORSEC 1992 in Okinawa: Conference for Pacific Ocean Environments and Probing, volume 1
[JTN-93-80418] 01 p0191 N94-11894
Acoustic Doppler current profiling of the Kuroshio over the East China Sea shelf slope 01 p0194 N94-11914
Sea surface heat flux in the beginning of the Kuroshio 01 p0195 N94-11923
Seasonal variation of the surface mixed layer in the subtropical re-circulation area of the North Pacific during OMLET 01 p0195 N94-11924
The Kyucho events in Sukumo Bay induced by Kuroshio front disturbances 01 p0198 N94-11939
Current variability on the shelf break northeast of Taiwan 01 p0219 N94-12708
Variations common to the interplanetary magnetic field, the zonal atmospheric circulation and the Earth's rotation
[COMMUNICATIONS-SER-B-157] 02 p0837 N94-13504
Maximum entropy spectral analysis of the geological time series of the oxygen isotope record from deep-sea cores
[INPE-5465-PRE/1773] 02 p0725 N94-13728
AMIP: Diagnostic subproject on the variability in the tropics: Synoptic to intraseasonal time scales
[DE93-009287] 02 p0721 N94-13914
On the space-time ocean current variability and its effects on the length-of-day
[ISBN-0-315-59510-8] 02 p0726 N94-14205
ROSAT observations of the binary Be-star/radio pulsar PSR1259-63
[NASA-CR-194394] 02 p0832 N94-14357
Structural change of graphite during electron irradiation
[DE93-015961] 02 p0582 N94-14531
Nonlinear acoustics: Periodic waveguide, scattering of sound by sound, three-layer fluid, finite amplitude sound in a medium having a distribution of relaxation processes, and production of an isolated negative pulse in water
[AD-A267145] 03 p1177 N94-15732
Research into the influence of spatial variability and scale on the parameterization of hydrological processes
[NASA-CR-194610] 03 p1082 N94-16026
Similarity and scale in catchment storm response
[PAPER-89RG01615] 03 p1083 N94-16028
Observations of comets with the IUE
[NASA-CR-193652] 04 p1624 N94-17843
Active control of periodic noise with time-varying frequency
[REPT-93-012] 04 p1562 N94-17934
Global zones of particle precipitation as observed EXOS-C
[AD-A268758] 04 p1481 N94-18467
The effects of magnetic storm phases on F-layer irregularities from auroral to equatorial latitudes
[AD-A272685] 05 p1857 N94-21189
Forced vibrations of a non-viscous drop
[MPIS-24/1992] 06 p2318 N94-23198
Theoretical investigation of variable periodicity (graded) multilayers for hard x ray applications
[NASA-CR-193913] 06 p2543 N94-23502
Correlations in the actions of periodic orbits derived from quantum chaos
[DE93-616866] 06 p2571 N94-25340
Modal control of a satellite in an unstable periodic orbit about the Earth-Sun interior Lagrange point
[AD-A273707] 07 p2694 N94-25776
Modulating terrestrial impacts from Oort cloud comets by the adiabatically changing galactic tides 07 p2890 N94-28305
Long term variations of radio auroral activity 08 p3359 N94-29237
Extended horizon lifting for periodic gain adjustment in control systems, and for equalization of communication channels
[NASA-CASE-NPO-19166-1-CU] 08 p3246 N94-29495
On observing neutron star oscillations 08 p3538 N94-29795
Interannual-decadal variability in tropical climate systems: Stable isotope records and general circulation model experiments 08 p3373 N94-29962
Satellite estimation of the global distribution and interannual variability of photosynthetically active radiation 08 p3334 N94-29970
Oscillations in piston-driven shear flow of a non-Newtonian fluid
[AD-A276472] 09 p3701 N94-31245
ENSO forced variations of the sea surface temperature and adjusted sea level along the west coast of the United States
[AD-A277306] 09 p3789 N94-32327
Dependence of x ray absorption magnetic circular dichroism on layer periodicity in iron-platinum multilayers
[DE94-008786] 09 p3647 N94-32892
EOF characterization of Atlantic SST fields using AVHRR data
[INPE-5535-TDI/523] 10 p4093 N94-34203
Iterative regression analysis of periodicities in Be-10 and C-14 atmospheric cosmonuclides variations
[INPE-5547-TDI/533] 10 p4087 N94-34228
Periodicity and peculiarity in 120 first and second row diatomic molecules
[AD-A278836] 11 p4323 N94-35793

PERIODICALS
NASA STI program database: Journal coverage (1990-1992)
[NASA-TM-109720] 06 p2593 N94-25168
TRADOC library and information network (TRALINET). Union list of periodicals (TULIP)
[AD-A275263] 08 p3529 N94-28903
TILDA for Windows: A system for registration of journals in the library at NDRE NBC-Defence
[PB94-149168] 10 p4158 N94-34161
Electronic journals 12 p4544 N94-37342

PERIODICITY
U PERIODIC VARIATIONS

PERIODICITY (BIOLOGY)
U RHYTHM (BIOLOGY)

PERIPHERAL CIRCULATION
Automated strain gauge plethysmograph
[AD-A267323] 03 p1035 N94-17002
Effect of prostaglandin E1 on the relationship between skin sympathetic nerve activity and reduction in skin blood flow 07 p2929 N94-27524
Difference in skin blood flow reduction depending on activating maneuver of skin sympathetic nerve activity 07 p2929 N94-27525
Effect of L-dopa on hemodynamic functions in humans 07 p2929 N94-27526

PERIPHERAL EQUIPMENT (COMPUTERS)
NT REMOTE CONSOLES
Development of a MIL-STD-1750 microprocessor system for space applications 07 p2949 N94-26715
Pen-based computers: Computers without keys 09 p3808 N94-32434
THE VERTICAL 09 p3806 N94-32435
Development of large area, tiled, liquid crystal display
[AD-A277564] 10 p4039 N94-33588
Architectural constructs of Ampex DST 10 p4153 N94-33805

PERIPHERAL VISION
The effects of luminance boundaries on color perception
[AD-A268398] 03 p1133 N94-17397
Controlling telerobots with video data and compensating for time-delayed video using Omniview 10 p4127 N94-34031

PERIPHERIES
U BOUNDARIES

PERISCOPES
Atmospheric propagation analysis program
[AD-A268231] 03 p1006 N94-17565
Periscope mechanism for SWAN instrument 06 p2357 N94-24000

PERMAFROST
Ground movements associated with gas hydrate production
[DE93-019887] 04 p1486 N94-19018
Proceedings: International Symposium on Thermal Engineering and Science for Cold Regions
[AD-A270636] 04 p1487 N94-19529
Calderas produced by hydromagmatic eruptions through permafrost in northwest Alaska 05 p2089 N94-20385
Possible occurrence and origin of massive ice in Utopia Planitia 05 p2090 N94-20390
Cryoplanation terraces of interior and western Alaska 05 p2091 N94-20396
A formational model for the polygonal terrains of Mars: Taking a crack at the genesis of the Martian polygons 05 p2091 N94-20400
Interferometric detection of freeze-thaw displacements of Alaskan permafrost using ERS-1 data 05 p1732 N94-20460
Growth condition of an ice layer in freezing soils under applied loads. Part 1: Experiment
[AD-A275215] 08 p3357 N94-29070
On the temperature distribution near a cold surface
[AD-A275162] 08 p3332 N94-29288
Thermal and hydraulic considerations regarding the fate of water discharged by the outflow channels to the Martian northern plains 09 p3946 N94-33202
Temporal changes in the geographic distribution, elevation, and potential origin of the Martian outflow channels 09 p3951 N94-33235
A model of the CO2 exchanges between biosphere and atmosphere in the tundra
[NASA-CR-196008] 11 p4289 N94-35389

PERMALLOYS (TRADEMARK)
Atlas of formability: Permalloy - 80 flow stress curves
[AD-A268263] 04 p1356 N94-17801

PERMANENT MAGNETS
Lightweight linear alternators with and without capacitive tuning
[NASA-CR-185273] 01 p0140 N94-10505
Improvement of azimuthal homogeneity in permanent-magnet bearing rotors
[DE93-009954] 01 p0144 N94-11607
Suggestion for extended Viking magnetic properties experiment on future Mars missions 03 p1285 N94-16375
Electrodynamic forces of the cross-connected figure-eight null-flux coil suspension system
[DE93-015139] 03 p1048 N94-16969
Measurement and correction of magnetic fields in pulsed slotted-tube microwigglers
[DE93-040100] 05 p1815 N94-20272
Variable-field permanent magnet dipole
[DE94-000800] 05 p1820 N94-22020
Finite element based electric motor design optimization 06 p2315 N94-24411
Design and application of electromechanical actuators for deep space missions
[NASA-CR-195134] 06 p2365 N94-24842
Comparative M-H characteristics of 1-5 and 2-17 type samarium-cobalt permanent magnets to 300 C
[NASA-CR-194440] 06 p2312 N94-24870
First principle calculation for magneto-crystalline anisotropy
[DE93-634653] 07 p3052 N94-26012
Correlation of experimental data and three-dimensional finite element modeling of a spinning quadrupole
[DE93-041173] 07 p3008 N94-26421
Selected applications of planar permanent magnet multipoles in FEL insertion device design
[DE94-009014] 09 p3721 N94-32845
Maglev crude oil pipeline 11 p4226 N94-35919
Permanent superconducting magnets for space applications
[NASA-CR-196293] 12 p4439 N94-37634
Recent progress of the Los Alamos advanced free electron laser
[DE94-011654] 12 p4449 N94-37733

PERMEABILITY
NT DIELECTRIC PERMEABILITY
Transport properties of disordered porous media from the microstructure
[DE93-016065] 02 p0806 N94-13152
Locally non-uniform finite-difference time domain with application to stealth, crosstalk, and narrow apertures
[DE93-013958] 02 p0601 N94-13696
Upgrading of raw natural gas using high-performance polymer membranes
[DE93-014041] 02 p0566 N94-14586
HyperVentilate: Decision-support software for soil vapor extraction technology application
[PB93-134880] 03 p1094 N94-15136
Verification of a two-dimensional infiltration model for the resin transfer molding process
[NASA-CR-194597] 03 p0964 N94-15656
Influence of fiber packing structure on permeability 03 p0938 N94-16857
Flight 20 (STS-45) polysulfide gas path investigation
[NASA-CR-193861] 03 p0928 N94-17213
Factors determining the release of nitric oxide --- Calcium/cadmium transport by renal cortical collectin duct cells
[AD-A266232] 03 p1118 N94-17224
Aerosol filtration with steel fiber filters
[DE93-016990] 04 p1380 N94-18710

High-resolution numerical methods for compressible multi-phase flow in hierarchical porous media
[DE94-000740] 05 p1799 N94-20351
Variable-permittivity linear inverse problem for the H(sub z)-polarized case 05 p1719 N94-20408
Study on alloy films for hydrogen separation 07 p2726 N94-25565
Space-R thermionic space nuclear power system: Design and technology demonstration
[DE94-001890] 07 p2699 N94-25929
Application of the Positron Annihilation Technique to the study of vapor absorption process in polyethylene (LDPE) and in imide polymer (6FDA-TMPD PI)
[DE94-602737] 07 p2720 N94-27998
Plane wave propagation in an anisotropic chiral medium with isotropic permittivity and permeability
[PB94-133097] 07 p2778 N94-28384
Green dyadic and dipole fields for a medium with anisotropic chirality
[PB94-132933] 07 p2779 N94-28391
Fire-resistant water vapour permeable buoyant insulation 08 p3380 N94-28431
Flow past a circular cylinder with a permeable wake splitter plate 08 p3275 N94-29764
Melt flow during alloy solidification: Dimensional analysis and model problems
[PB94-138625] 08 p3206 N94-29997
New polymer target-shell properties and characterizations
[DE94-008420] 09 p3890 N94-32415
Flooded cell permeation testing of elastomers
[AD-A277698] 10 p4026 N94-33438
Diffusion and sorption of 1,4-dioxane into polychloroprene
[AD-A277743] 10 p4026 N94-33446

PERMEATING
Hydrogen uptake into silicon from an ECR plasma
[DE94-003771] 07 p3050 N94-25815
Ion-driven permeation of deuterium in metals
[DE94-701104] 07 p2744 N94-27876
Prediction of hydrogen entry and permeation in metals and alloys
[AD-A276637] 09 p3642 N94-31995
Flooded cell permeation testing of elastomers
[AD-A277698] 10 p4026 N94-33438

PERMITTIVITY
Locally non-uniform finite-difference time domain with application to stealth, crosstalk, and narrow apertures
[DE93-013958] 02 p0601 N94-13696
Stress sensitivity of dielectric resonators
[AD-A266767] 03 p1009 N94-15825
Cyanoresin, cyanoresin/cellulose triacetate blends for thin film, dielectric capacitors
[NASA-CASE-NPO-18913-1-CU] 03 p0966 N94-15930
Temperature and pressure effects on capacitance probe cryogenic liquid level measurement accuracy
[NASA-CR-190763] 03 p1034 N94-16521
Low dielectric constant insulators and gold metallization for GHz multi-chip modules, part 2
[AD-A268590] 03 p1176 N94-17605
Numerical modelling of fringing fields and their use for complex permittivity measurements at high frequencies
[AD-A270198] 04 p1388 N94-18782
Polymer films with enhanced dielectric properties
[AD-A271148] 04 p1375 N94-19740
Theoretical and experimental studies of quantum wells
[AD-A271180] 04 p1606 N94-19741
Numerical modeling of fringing fields and their use for complex permittivity measurements at high frequencies
[AD-A270478] 05 p1966 N94-19917
Variable-permittivity linear inverse problem for the H(sub z)-polarized case 05 p1719 N94-20408
Relating ground truth collection to model sensitivity 05 p1719 N94-20409
The effect of dissipative inhomogeneous medium on the statistics of the wave intensity 05 p1726 N94-20440
The Brewster angle effect in SAR polarimetry 05 p1731 N94-20456
Polarizability of gyrotropic sphere
[PB93-225019] 06 p2524 N94-23131
Spectroscopic IR ellipsometry of 100 and 001 oriented YBa2Cu3O(7-delta) films
[PB93-201481] 06 p2561 N94-23445
Mueller matrix analysis of infrared ellipsometry
[PB93-201549] 06 p2544 N94-23629
Temperature dependent performance of Coplanar Waveguide (CPW) on substrates of various materials
[NASA-TM-106505] 06 p2313 N94-25170
A study of LPM suppression of bremsstrahlung at 25 GeV
[DE94-003457] 07 p3018 N94-26133
Refractive and dielectric properties of helium, argon and nitrogen gases
[PB94-123783] 07 p3008 N94-26851
Plane wave propagation in an anisotropic chiral medium with isotropic permittivity and permeability
[PB94-133097] 07 p2778 N94-28384
Green dyadic and dipole fields for a medium with anisotropic chirality
[PB94-132933] 07 p2779 N94-28391
Dielectric polarizability of sphere with arbitrary anisotropy
[PB94-133113] 07 p2779 N94-28397
Microwave dielectric behavior of soils. Report 1: Summary of related research and applications
[AD-A275980] 09 p3771 N94-31351
Microwave dielectric behavior of soils. Report 2: A unique coaxial measurement apparatus
[AD-A275982] 09 p3771 N94-31353
A study of areas of low radio-thermal emissivity on Venus 09 p3942 N94-31992
A reassessment of the in-situ dielectric constant of polar firn
[AD-A276999] 09 p3773 N94-32154
Electromagnetic probe technique for fluid flow measurements 09 p3711 N94-32455
Inorganic polymer engineering materials
[DE94-008519] 09 p3659 N94-32655
Dielectric properties of Mars' surface: Proposed measurement on a Mars lander 09 p3951 N94-33237
Development of low dielectric constant alumina-based ceramics for microelectronic substrates
[DE94-011360] 12 p4439 N94-37302
Fluorinated resins with low dielectric constant
[AD-D016303] 12 p4427 N94-37773

PERMUTATIONS
Nonparametric statistics: Weighted rankings analysis
[AD-A266607] 03 p1173 N94-16657
Non-blocking crossbar permutation engine with constant routing latency
[NASA-CASE-NPO-18864-1-CU] 03 p1161 N94-17328
Heap construction in the parallel comparison tree model
[TR-409] 04 p1538 N94-19512
Multi-channel Kondo necklace
[DE93-634754] 07 p3057 N94-26389
Fast parallel permutation algorithms
[CWI-CS-R9303] 07 p2982 N94-27579

PEROVSKITES
The stability of hibonite and other aluminous phases in silicate melts: Implications for the origin of hibonite-bearing inclusions 01 p0080 N94-12052
Experimental partitioning of Zr, Ti, and Nb between silicate liquid and a complex noble metal alloy and the partitioning of Ti between perovskite and platinum metal 03 p0962 N94-16287
An experimental study of trace element partitioning between perovskite, hibonite and melt: Equilibrium values 03 p0954 N94-16313
Ten GHz YBa2Cu3O(7-delta) superconducting ring resonators on NdGaO3 substrates 05 p1735 N94-20515
Fundamental study of NO(x) control in catalytic combustion
[PB94-112323] 06 p2398 N94-23818
Polar and chemical domain structures of lead scandium tantalate (PST)
[DE94-600760] 07 p3056 N94-26363
Electrical conductivity of perovskite-magnesiowuestite as a function of pressure and temperature
[DE94-002714] 07 p2880 N94-26806
Ferroelectric thin film microstructure development and related property enhancement
[DE94-002741] 07 p3061 N94-26856
Perovskite solid electrolytes for SOFC
[DE94-001923] 07 p2859 N94-27005
Energetics, bonding mechanism, and electronic structure of ceramic/ceramic and metal/ceramic interfaces
[DE94-008551] 09 p3659 N94-32656
X ray and gamma ray spectroscopy of solids under pressure
[DE94-011207] 11 p4238 N94-36203

PEROXIDES
NT HYDROGEN PEROXIDE
NT ORGANIC PEROXIDES
Measurement of HO2 and other trace gases in the stratosphere using a high resolution far-infrared spectrometer at 28 km
[NASA-CR-194175] 02 p0714 N94-13816
In situ detection of tropospheric OH, HO2, NO2, and NO by laser-induced fluorescence in detection chambers at reduced pressures
[NASA-CR-194810] 06 p2397 N94-23277
Measurement of HO2 and other trace gases in the stratosphere using a high resolution far-infrared spectrometer
[NASA-CR-195173] 06 p2404 N94-24738
In situ detection of tropospheric OH and HO2 by laser-induced fluorescence in a detection chamber at low pressure 08 p3342 N94-28589
Detection of tropospheric OH and HO2 by laser-induced fluorescence at low pressure using the 308nm excitation of OH 08 p3343 N94-28591
Harvard ER-2 OH laser-induced fluorescence instrument 08 p3343 N94-28592
Peroxy radical measurements with NCAR's chemical amplifier 08 p3345 N94-28603
An improved method of measuring tropospheric NO2, NO3, HO2, and RO2 by Matrix Isolation and Electronic Spin Resonance (MIESR) 08 p3345 N94-28605
Tropospheric HO2 determination by FAGE 08 p3345 N94-28606
Near-IR diode laser absorption for measurement of tropospheric HO2 08 p3345 N94-28607
HO2 detection by near infrared absorption using tunable diode lasers 08 p3346 N94-28608
Hydrogen peroxide electrodes based on electrical connection of redox centers of various peroxidases to electrodes through a three-dimensional electron relaying polymer network
[AD-A276543] 09 p3691 N94-32056

PERSIAN GULF
Overview of physical oceanographic measurements taken during the Mount Mitchell cruise to ROPME sea area
[DE93-018460] 04 p1497 N94-18494

PERSONAL COMPUTERS
NT IBM PERSONAL COMPUTERS
NT MACINTOSH PERSONAL COMPUTERS
Estimation of critical values and vibration characteristics on supersonic delta wings. Part 1: On-line time series analysis of stationary random response
[NAL-TR-1153] 01 p0002 N94-10363
Application of parallel processing to a surface patch/wire junction EFIE code
[AD-A264965] 01 p0336 N94-10488
A PC-PCL-based control system for the high-voltage pulsed-power operation of the Intense Diagnostic Neutral Beam (IDNB) Experiment
[DE93-014144] 02 p0797 N94-13100
Mass market computers for software development
[ERB-1035] 02 p0741 N94-13547
Development of an automated film-reading system for ballistic ranges
[NASA-CR-194398] 02 p0650 N94-13815
PC viruses: How do they do that?
[DE93-012581] 02 p0753 N94-14289
Some tools of the trade we've developed for our cross-section calculations
[DE93-013835] 02 p0786 N94-14569
ASTEC and MODEL: Controls software development at Goddard Space Flight Center 02 p0678 N94-14628
Applying paperless technology to achieve excellence in manufacturing operations
[TABES PAPER 93-630] 03 p1052 N94-16147
Systolic array IC for genetic computation 04 p1400 N94-18361
Downsizing a database platform for increased performance and decreased costs
[DE93-018687] 04 p1618 N94-19099
Two-dimensional particle-in-cell simulation on transputer arrays
[DE93-017977] 05 p1972 N94-20181
Probability of detection calculations using MATLAB
[AD-A271958] 05 p1736 N94-20578
Mathcad computer applications predicting antenna parameters from antenna physical dimensions and ground characteristics
[AD-A272987] 05 p1740 N94-21264
Application development in a PC/LAN environment 05 p1923 N94-22067
Crystal ball gazing 05 p1925 N94-22477
PCIPS 2.0: Powerful multiprofile image processing implemented on PCs 05 p1927 N94-22532
Some background information on perceptual color matching pertinent to computer applications
[PB93-200327] 06 p2445 N94-23788
High performance, low cost, self-contained, multipurpose PC based ground systems 06 p2516 N94-23943
Users guide for GRIKURV: A code for drawing graphs
[PB94-123593] 07 p2968 N94-27154
Development of an automatic fatigue-data acquisition system using commercial software
[NAL-TM-650] 07 p2842 N94-27207
Inverted pendulum control apparatus using transputers
[DE94-701224] 07 p2973 N94-27732
Evaluation of access/navigational features of a graphical-user interface installed on a portable maintenance aid
[AD-A275791] 08 p3136 N94-28744

A PC program to optimize system configuration for desired reliability at minimum cost
09 p3823 N94-32438
Multimedia as a desktop and classroom tool
[DE94-009118] 09 p3807 N94-32766
Computer virus information update CIAC-2301
[DE94-011916] 11 p4308 N94-36236
Portable color multimedia training systems based on monochrome laptop computers (CBT-in-a-briefcase), with spinoff implications for video uplink and downlink in spaceflight operations
[NASA-TM-108460] 12 p4496 N94-37556

PERSONALITY
An evaluation of personality testing and the five-factor model in the selection of landing craft air cushion vehicle crew members
[AD-A275869] 08 p3397 N94-28754

PERSONALITY TESTS
Basic attributes test (BAT): Operational pre-implementation analysis and score equating
[AD-A265885] 01 p0314 N94-12276
An evaluation of personality testing and the five-factor model in the selection of landing craft air cushion vehicle crew members
[AD-A275869] 08 p3397 N94-28754

PERSONNEL
NT AIR TRAFFIC CONTROLLERS (PERSONNEL)
NT AIRCRAFT PILOTS
NT ASTRONAUTS
NT COSMONAUTS
NT CREWS
NT ENGINEERS
NT FLIGHT CREWS
NT FLIGHT SURGEONS
NT FLYING PERSONNEL
NT GROUND CREWS
NT INSTRUCTORS
NT MEDICAL PERSONNEL
NT OPERATORS (PERSONNEL)
NT ORBITAL WORKERS
NT PHYSICIANS
NT PILOTS (PERSONNEL)
NT POLICE
NT PROGRAMMERS
NT SCIENTISTS
NT SPACECREWS
NT SURGEONS
NT TEST PILOTS
Department of Energy fundamentals handbook: Engineering symbology, prints, and drawings
[DE93-012181] 01 p0129 N94-11456
The 27th International Applied Military Psychology Symposium: A Focus on Decision Making Research
[AD-A265278] 01 p0313 N94-11701
Building a quality culture in the Office of Space Flight: Approach, lessons learned and implications for the future
02 p0667 N94-13164
Environmental awareness
[DE93-014192] 02 p0707 N94-13218
Information requirements of self-managing teams
[DE93-010319] 02 p0824 N94-14048
Sleep management user's guide for special operations personnel
[AD-A267746] 03 p1119 N94-14943
Return to flight 3, the journey continues
[NASA-TM-109651] 03 p1223 N94-15319
Permanent change of station: The NASA employee's guide to an easier move
[NHB-9760.1A] 03 p1223 N94-15931
The Senior Executive Service
[NHB-3100.6] 03 p1224 N94-15945
Proceedings of the 1992 Annual Meeting NASA Occupational Health Program
[NASA-CR-193462] 03 p1123 N94-16609
New health and safety initiatives at the Department of Energy (DOE) 03 p1124 N94-16610
The Langley Fitness Center 03 p1126 N94-16635
Carpal tunnel syndrome and other cumulative trauma disorders of the arm and hand and occupation in US Navy enlisted personnel
[AD-A267747] 03 p1129 N94-17374
Human reliability analysis application guide
[DE93-015361] 04 p1511 N94-18244
Building a joint-service classification research roadmap: Criterion-related issues
[AD-A269735] 04 p1512 N94-18754
Road march performance of special operations soldiers carrying various loads and load distributions
[AD-A269198] 04 p1512 N94-18882
Activities of National Inst. for Aviation Research
[NIAR-93-16] 05 p2151 N94-20150
Survival suit for submarine personnel: Summary of evaluation studies
[PB93-204634] 06 p2430 N94-23743
NASA/DOD Aerospace Knowledge Diffusion Research Project. Report number 21: US aerospace industry librarians and technical information specialists as information intermediaries: Results of the phase 2 survey
[AD-A276020] 06 p2593 N94-24709
Aircraft digital flight control technical review
06 p2163 N94-25106
Evaluation and improvement of the inquest system on work accidents (TOT)
[VTT-TIED-1418] 07 p2762 N94-26261
Human dimensions research team, operation restore hope
[AD-A274340] 07 p2939 N94-27056
How to make good use of international research collaboration, with emphasis on the evolving situation in Europe
[PB94-119690] 07 p3101 N94-27323
Defense force management: Challenges facing DOD as it continues to downsize its civilian work force. Report to the Chairman, Subcommittee on Federal Services, Post Office, and Civil Service, Committee on Governmental Affairs, US Senate
[GAO/NSIAD-93-123] 07 p3095 N94-28177
Recent Canadian advances in active thermal protection 08 p3384 N94-28451
Effects of workload on communication processes in decision making teams
[AD-A275894] 08 p3527 N94-28796
Report of the workshops: Automated generation of electronic technical manuals
[AD-A278046] 10 p4150 N94-33401
Flight controller alertness and performance during MOD shiftwork operations 10 p4098 N94-33624
Johnson Space Center (JSC) research and technology
[NASA-TM-104788] 10 p4187 N94-34677

PERSONNEL DEVELOPMENT
Program/project management resource lists
[NASA-TM-109268] 02 p0822 N94-13107
PET team
[NASA-TM-109599] 03 p1223 N94-15293
The Senior Executive Service
[NHB-3100.6] 03 p1224 N94-15945
Building a joint-service classification research roadmap: Criterion-related issues
[AD-A269735] 04 p1512 N94-18754
Center for neural engineering
[AD-A271164] 05 p1890 N94-20185
NCCDS configuration management process improvement 05 p1931 N94-21327
Information and decision structure in a Japanese type of management with respect to QCC and just-in-time systems 05 p2046 N94-22063
Women scientists and engineers employed in industry: Why so few? A report based on a conference
[ISBN-0-309-04991-1] 06 p2585 N94-24698
Development centres: Assessing or developing people
[PB94-138070] 08 p3536 N94-29144
European business confronted with the 21st century: Men, the essential risk
[ESA-SP-1167] 09 p3914 N94-31181
Aircraft communication and navigation systems and communication and navigation systems
[AD-A277309] 09 p3582 N94-32328
Women as a resource for the flexibility required for high technology innovation 11 p4348 N94-35966

PERSONNEL MANAGEMENT
Information requirements of self-managing teams
[DE93-010319] 02 p0824 N94-14048
NASA directives master list and index
[NHB-1410.13L] 03 p1229 N94-15414
Permanent change of station: The NASA employee's guide to an easier move
[NHB-9760.1A] 03 p1223 N94-15931
NASA security handbook
[NHB-1620.3C] 03 p1224 N94-15937
Industrial labor relations manual
[NHB-5200.1B] 03 p1224 N94-15939
The NASA competitive placement plan for positions GS-15 and below (including trades and labor positions)
[NHB-3335.1C] 03 p1224 N94-15944
The Senior Executive Service
[NHB-3100.6] 03 p1224 N94-15945
Medical surveillance and biological monitoring of lead exposed employees 03 p1124 N94-16615
Ongoing Recovery Basic Information Tool (ORBIT)
03 p1124 N94-16616
Programs and resources for control of job stress in the Federal workplace 03 p1124 N94-16617
The Goddard Space Flight Center ergonomics program 03 p1125 N94-16621
Efficient management of cardiovascular risk screening programs 03 p1125 N94-16622
Industrial Hygiene Laboratory accreditation: The JSC experience 03 p1125 N94-16623
Using controlled daylight exposure and sleep timing in the prevention of shift lag during night operations
[AD-A269304] 04 p1504 N94-17824
Computing professionals: Changing needs for the 1990's
[B-030] 04 p1515 N94-19401
Factors associated with continuance commitment to FAA matrix teams
[DOT/FAA/AM-93/18] 05 p2040 N94-21626
Women scientists and engineers employed in industry: Why so few? A report based on a conference
[ISBN-0-309-04991-1] 06 p2585 N94-24698
Concepts and methods of measuring productivity at the organization level
[AD-A273126] 07 p3094 N94-27180
An investigation of integrated product development implementation issues: A case study of Bosma Machine and Tool Corp.
[AD-A273917] 07 p2942 N94-27320
Defense force management: Challenges facing DOD as it continues to downsize its civilian work force. Report to the Chairman, Subcommittee on Federal Services, Post Office, and Civil Service, Committee on Governmental Affairs, US Senate
[GAO/NSIAD-93-123] 07 p3095 N94-28177
The management issues of implementing telecommuting: A case study
[AD-A275267] 08 p3527 N94-28905
European business confronted with the 21st century: Men, the essential risk
[ESA-SP-1167] 09 p3914 N94-31181
Drug-related problems in the workplace
[CRANFIELD-AERO-9306] 09 p3914 N94-31538
Flight controller alertness and performance during MOD shiftwork operations 10 p4098 N94-33624
Telecommuting (work-at-home) at NASA Lewis Research Center
[NASA-CR-195334] 11 p4347 N94-36396
Toward a new National Weather Service: National Weather Service employee feedback
12 p4474 N94-37467

PERSONNEL SELECTION
NT PILOT SELECTION
A comparison of high and low-impact reports of investigation on adjudicators' decision making: A pilot study
[AD-A265747] 01 p0416 N94-10298
Landing Craft Air Cushion (LCAC) crew selection system manual
[AD-A265158] 01 p0313 N94-11098
The 27th International Applied Military Psychology Symposium: A Focus on Decision Making Research
[AD-A265278] 01 p0313 N94-11701
Basic attributes test (BAT): Operational pre-implementation analysis and score equating
[AD-A265885] 01 p0314 N94-12276
Readiness to perform testing: A critical analysis of the concept and current practices
[DOT/FAA/AM-93/13] 02 p0732 N94-13193
Astronauts number 1 --- mercury project
[NASA-TM-109428] 03 p1131 N94-15499
The NASA competitive placement plan for positions GS-15 and below (including trades and labor positions)
[NHB-3335.1C] 03 p1224 N94-15944
The Senior Executive Service
[NHB-3100.6] 03 p1224 N94-15945
Computing professionals: Changing needs for the 1990's
[B-030] 04 p1515 N94-19401
Psychometric developments related to tests and selection
[AD-A272971] 05 p1894 N94-21262
Compatibility evaluation and research on the Computerized Adaptive Screening Test (CAST): User and programmer's guide
[AD-A273112] 05 p1894 N94-21510
Strategies for recruiting additional African Americans into the NASA JSC summer faculty fellows program
06 p2585 N94-25362
A comparison of two hardware implementations of a crew selection system
[AD-A274913] 07 p2937 N94-26346
Validation of the Federal Aviation Administration air traffic control specialist pre-training screen
[DOT/FAA/AM-94/4] 07 p2938 N94-26600
An evaluation of personality testing and the five-factor model in the selection of landing craft air cushion vehicle crew members
[AD-A275869] 08 p3397 N94-28754
Naval aviation vision standards research at the naval aerospace medical research laboratory: The long view
[AD-A275885] 08 p3388 N94-28756
Scanning and monitoring performance: Effects of the reinforcement values of the events being monitored
[DOT/FAA/AM-94/8] 08 p3398 N94-29918

A neural/expert based client server architecture for MITE ITS
[AD-A278330] 10 p4113 N94-33968
Validity of the air traffic control specialist nonradar screen as a predictor of performance in radar-based air traffic control training
[AD-A279754] 10 p4098 N94-34210

PERSPIRATION
Difference in skin blood flow reduction depending on activating maneuver of skin sympathetic nerve activity 07 p2929 N94-27525
Enhancement of skin sympathetic nerve activity in amyotrophic lateral sclerosis 07 p2930 N94-27532
Simulation of the effect of wind on clothing by measurements and calculations
[PB94-132269] 08 p3399 N94-28406

PERTURBATION
NT ORBIT PERTURBATION
NT SATELLITE PERTURBATION
A 3D gyrokinetic particle-in-cell simulation of fusion plasma microturbulence on parallel computers
[DE93-012503] 02 p0794 N94-12846
A classical instability for black strings and p-branes
[DE93-014577] 02 p0839 N94-14116
Further on the current algebra of WZNW models at and away from criticality
[DE93-624809] 04 p1545 N94-17686
Exchange front stability in packed-column chromatography
[DE93-017526] 04 p1346 N94-17997
Fundamental research in nonlinear random vibration for aerospace applications
[AD-A268929] 04 p1454 N94-18487
Resonance Raman and photophysical studies of transition metal complexes in solution and entrapped in zeolites
[DE93-019892] 04 p1363 N94-19019
Longitudinal instability of an induction linac with acceleration
[DE93-019249] 05 p1980 N94-20290
Direct simulation of shock-induced mixing layer
[DE93-040498] 05 p1803 N94-21531
Universality in blow-up for non linear heat equations
[PB93-215465] 05 p2038 N94-22095
Effects of magnetic field perturbations in the ATF torsatron
[DE94-000474] 05 p1999 N94-22568
Decoupling problems around a trajectory: From linearity to nonlinearity
[MEMO-1115] 06 p2469 N94-22703
Contribution to the study of HF converters radiated disturbances
[ECL-92-34] 06 p2313 N94-25421
Mix induced by single shock passage through a material interface
[DE93-019505] 07 p2792 N94-26427
Delta f Algorithm
[DE94-003120] 07 p2963 N94-26521
Normal forms for perturbations of the euler top
[PB94-125390] 07 p3009 N94-26968
An enhanced global spectral model
[PL-TR-92-2011] 07 p2898 N94-26223
Missile launch detection electric field perturbation experiment
[DE94-004224] 08 p3466 N94-30586
Vibration control and design of composite cantilevers taking into account structural uncertainties and damage 09 p3733 N94-31213
Gravitational effects of cosmic strings
[ISBN-0-315-75484-2] 09 p3934 N94-31789
Effective computational strategy for predicting the response of complex systems
[AD-A277452] 09 p3740 N94-33011
Meso-beta scale numerical simulation studies of terrain-induced jet streak mass and momentum perturbations
[NASA-CR-195863] 10 p4089 N94-33752
Maneuvering and control of flexible space robots 11 p4218 N94-35867
Air quality implications associated with the selection of power plants in the Pacific Northwest
[DE94-004783] 11 p4287 N94-36027
Scattering theory for the quantum envelope of a classical system
[DE94-008530] 12 p4539 N94-36508

PERTURBATION THEORY
Nonperturbative methods in the problem of multiphoton excitation of atom by squeezed light 01 p0376 N94-10575
Direct solution of the mathematical adjoint equations for an interface current nodal formulation
[DE93-009961] 01 p0346 N94-11608
Stability of subharmonics and escape phenomena in the twin-well potential duffing system 02 p0775 N94-13235
A hybrid Pade-Galerkin technique for differential equations
[NASA-CR-191494] 02 p0767 N94-13289
A classical instability for black strings and p-branes
[DE93-014577] 02 p0839 N94-14116
Radiation perturbation theory in gravity and quantum universe as a hydrogen atom
[DE93-626621] 02 p0849 N94-14889
Shielding from space radiations
[NASA-CR-194578] 03 p1180 N94-15715
Many-body quantum mechanical studies of molecular clusters
[AD-A266624] 03 p1180 N94-15727
Implementing a 50x50 gravity field model in an orbit determination system
[AD-A267548] 03 p0888 N94-17103
The renormalization of the axial anomaly in dimensional regularization
[NIKHEF-H/92-18] 03 p1220 N94-17618
Waveguide and resonator perturbation techniques for measuring chirality and non-reciprocity of biisotropic materials
[PB93-187243] 04 p1384 N94-18116
Stability of the face-centered-cubic phase of heavy rare gas solids
[DE93-019949] 05 p1679 N94-20319
A theoretical and numerical study of polarimetric scattering and emission from random rough surfaces with anisotropic directional spectrum 05 p1730 N94-20454
Theoretical particle physics
[DE94-000538] 05 p1973 N94-20938
A formulation of quantum statistical mechanics based on the Feynman path centroid density 1: Equilibrium properties
[AD-A272809] 05 p2037 N94-21171
One- and multi-component theories of mixtures
[DE93-040543] 05 p1966 N94-21511
Simulating the Euclidean time Schroedinger equations using an INTEL iPSC/860 hypercube: Application to the t-J model of high-T(sub c) superconductivity
[DE94-000489] 05 p2035 N94-22385
Turbulization of free shear flows: 3D perturbations 05 p2000 N94-22626
Time variation of MHD accretion onto a black hole 05 p2009 N94-22692
Spiral Alfven instability in accretion disks 05 p2010 N94-22698
Projectile transverse motion and stability in electromagnetic induction launchers
[DE94-001557] 06 p2198 N94-23210
Perturbation theory in electron diffraction
[PB93-201424] 06 p2533 N94-23505
Reactivity of ambident anions in the gas phase
[PB93-232189] 06 p2533 N94-23713
Approximate optimal guidance for the advanced launch system
[NASA-CR-4568] 06 p2198 N94-24752
A finite-element-based perturbation model for the rotordynamic analysis of shrouded pump impellers: Part 1: Model development and applications
[NASA-CR-193916] 06 p2366 N94-24998
A finite-element-based perturbation model for the rotordynamic analysis of shrouded pump impellers: Part 2: User's guide
[NASA-CR-193917] 06 p2366 N94-24999
On a new functional integral formalism for Hubbard model
[DE93-614017] 06 p2492 N94-25334
Experimental study of the near threshold pi(sup +)p yields (pi(sup +))(pi(sup +))(n) cross section and chiral symmetry
[DE94-601671] 07 p3014 N94-25840
On the estimation of matrix elements for optical transitions in semiconductors
[DE93-613550] 07 p3051 N94-25851
The modal solution to the Moon's orbit using canonical Floquet perturbation theory
[AD-A273732] 07 p2690 N94-26001
First principle calculation for magneto-crystalline anisotropy
[DE93-634653] 07 p3052 N94-26012
Generalized perturbation method expansions of the total energy of an alloy
[DE94-003865] 07 p3055 N94-26238
On the phi(sub 0)-stability of perturbed nonlinear differential systems
[DE93-634304] 07 p2993 N94-26441
Low-energy hadronic interactions beyond the current algebra approach
[DE94-602600] 07 p3022 N94-26900
Operator regularization and renormalization theory
[ISBN-0-315-49334-8] 07 p3007 N94-27264
Quasipotential in the fourth order of perturbation theory
[DE94-606299] 08 p3484 N94-28584
Decoupled flight control system design using the singular perturbation method 08 p3155 N94-29850
Physics, astronomy, and astrophysics: A numerical study of the black hole plus Brill wave spacetime 08 p3540 N94-29990
Reconstruction of spectra in the discrete quantum mechanics (new elements of the lattice quantum engineering)
[DE94-608075] 08 p3524 N94-30087
Dissipation in Hamiltonian systems: Decaying cnoidal waves
[MEMO-1151] 08 p3460 N94-30738
Development and implementation of a full-potential ASW method
[ETN-94-95757] 09 p3858 N94-31560
Perturbative aspects of lower-dimensional gauge theories
[ISBN-0-315-86269-6] 09 p3911 N94-31712
Electromagnetic wave reflection from irregular plasma layers
[AD-A276727] 09 p3678 N94-32161
Semianalytic Satellite Theory (SST): Mathematical algorithms
[AD-A276836] 09 p3610 N94-32208
A cell-cycle model revisited
[CWI-AM-R9305] 09 p3851 N94-32229
Quantum dynamics in dual spaces
[DE94-008303] 09 p3913 N94-32824
A locally analytic method for the Euler equations 10 p4042 N94-33363
Whiskered tori for integrable pde's: Chaotic behavior in near integrable pde's
[AD-A278390] 10 p4128 N94-33430
Meso-beta scale numerical simulation studies of terrain-induced jet streak mass and momentum perturbations
[NASA-CR-195863] 10 p4089 N94-33752
Trim calculation of tandem rotor helicopter using simplified rotor system mathematical model 10 p4008 N94-34337
Linear and nonlinear pattern selection in Rayleigh-Benard stability problems
[NASA-TM-104007] 11 p4263 N94-35371
High energy asymptotics of perturbative multi-color QCD
[DE94-001350] 11 p4327 N94-36238
Nonlinearity with disorder: Spatio-temporal complex behavior arising from length scales competition
[DE94-000675] 12 p4502 N94-36685

PERVEANCE
Novel electron beam cathode
[AD-A270106] 04 p1404 N94-18872

PESTICIDES
Compatibility and efficacy of biocides qualified under military specification MIL-S-53021
[AD-A271496] 05 p1712 N94-20551
Isothiazolone volatility study of a water bottom from fuel treated with Kathon (tm) FP1.5 biocide
[AD-A273165] 06 p2266 N94-24728
Modeling the atmospheric input of nutrients, heavy metals, and pesticides to the Great Lakes
[DE94-005481] 11 p4286 N94-36007

PETN
Crystal orientation dependence of elastic precursor strength in pentaerythritol tetranitrate
[DE93-018340] 05 p2034 N94-22035

PETRI NETS
Task planning with uncertainty for robotic systems
[NASA-CR-193253] 01 p0338 N94-10638
Parallelizing Timed Petri Net simulations
[NASA-CR-194278] 02 p0758 N94-12938
Simulator for heterogeneous dataflow architectures
[NASA-CR-191545] 02 p0622 N94-13797
TANGO: A notation for describing advanced transaction models
[REPT-93-014] 04 p1613 N94-17936
Sensitivity and uncertainty analysis of Markov reward models
[MEMO-INF-92-89] 04 p1559 N94-19386
Interval timed coloured petri nets and their analysis
[PB93-191732] 05 p1903 N94-19992
Total order assumption
[PB93-191740] 05 p1903 N94-19993
Dependability and performability analysis
[NASA-CR-191565] 05 p1965 N94-21463
System level modelling using Petri nets and VHDL 05 p1772 N94-22113
Modeling and analysis of secure communication protocols using Petri net formalism 05 p1784 N94-22194
How to handle 6GBytes a night and not get swamped 05 p2058 N94-22444
Automated parallelization of timed Petri-net simulations
[NASA-CR-191574] 06 p2451 N94-23341

Mean-value of product-form stochastic Petri net models of slotted-ring systems
[PB94-110871] 06 p2494 N94-23749
Operational characterisation of requirements and early validation environment for high demanding space systems 06 p2519 N94-23959
Systems engineering: A formal approach. Part 4: Analysis methods
[PB94-101417] 06 p2271 N94-24475
Systems engineering: A formal approach. Part 2: Frameworks
[PB94-101391] 06 p2489 N94-24615
Timed coloured Petri nets and their application to logistics
[ETN-94-95310] 06 p2522 N94-25293
A modular approach to evaluation cryptographic protocols using Petri nets
[ISBN-0-315-85354-9] 07 p2972 N94-27595
Sheaf semantics for Petri Nets
[PB94-132826] 07 p2983 N94-28354
On conceptual design of active databases 08 p3531 N94-29535
Performability modelling using DyQNtool+
[MEMO-INF-93-45] 09 p3812 N94-31659
Design Methods based On Nets: DEMON
[PB94-147493] 09 p3813 N94-31687
Models for asynchronous circuit behaviour with OR causality
[PB94-148897] 10 p4112 N94-34126
High level modelling and design of asynchronous interface logic
[PB94-167822] 11 p4258 N94-35534

PETROGRAPHY
Apollo 16 core 60013/14 as a product of path 1 and path 2 regolith evolution processes 01 p0440 N94-12050
Petrography and preliminary interpretations of the crystalline breccias from the Manson M-1 core 01 p0281 N94-12056
The great 8 MA event and the structure of the H-chondrite parent body 01 p0429 N94-12058
Trace-element abundances in several new ureilites 01 p0080 N94-12096
Distribution of vanadium and melting of opaque assemblages in Efremovka CAI's 01 p0282 N94-12141
Stalking the LREE-enriched component in ureilites 03 p1241 N94-16190
Grosnaja ABCs: Magnesium isotope compositions 03 p1241 N94-16191
Euromet Ureilite Consortium: A preliminary report on carbon and nitrogen geochemistry 03 p1241 N94-16192
Petrography, mineralogy, and Mg isotope composition of VICTA: A vigarano CaAl4O7-bearing type A inclusion 03 p1103 N94-16203
Pyroxene equilibration temperatures in metamorphosed ordinary chondrites 03 p1242 N94-16224
Angrite LEW87051: Are the olivines pheno's or xeno's? A continuing story 03 p1103 N94-16285
Cat Mountain: A meteoritic sample of an impact-melted chondritic asteroid 03 p1244 N94-16328
Classificational parameters for acapulcoites and lodranites: The cases of FRO 90011, EET 84302 and ALH A81187/84190 03 p1245 N94-16389
A hydrogen isotope study of CO3 type carbonaceous chondrites; comparison with type 3 ordinary chondrites 03 p1246 N94-16425
Twenty-Fourth Lunar and Planetary Science Conference. Part 3: N-Z
[NASA-CR-193149] 05 p2092 N94-20636
Petrography of shock features in the 1953 Manson 2-A drill core 05 p1862 N94-20767
Petrography and origin of refractory inclusions from the Murray and Murchison C2 chondrites 05 p2084 N94-20770
Evaluation of lunar rocks and soils for resource utilization: Detailed image analysis of raw materials and beneficiated products 05 p2126 N94-20820
Catalog of Apollo 17 rocks. Volume 1: Stations 2 and 3 (South Massif)
[NASA-CR-194854] 06 p2613 N94-24058
A dynamic melting model for the origin of Apollo 15 olivine-normative and quartz-normative mare basalts 06 p2615 N94-24371
Melt rock components in KREEPy breccia 15205: Petrography and mineral chemistry of KREEP basalts and quartz-normative mare basalts 06 p2616 N94-24372
A geochemical study of acapulcoite and lodranite meteorites 06 p2605 N94-25358
The Twenty-Fifth Lunar and Planetary Science Conference. Part 1: A-G
[NASA-CR-195743] 11 p4355 N94-35395
Lunar mineral feedstocks from rocks and soils: X-ray digital imaging in resource evaluation 11 p4358 N94-35415
Petrographic characterization of lunar soils: Application of x ray digital-imaging to quantitative and automated analysis 11 p4368 N94-36138
Shocked materials from the Dutch Peak diamictite, Utah 11 p4352 N94-36140
On the origin of enstatite chondrite chondrules based on their petrography and comparison with experimentally produced chondrules 11 p4353 N94-36158
Cr, Mn, and Ca distributions for olivine in angritic systems: Constraints on the origins of Cr-rich and Ca-poor core olivine in angrite LEW87051 11 p4353 N94-36162

PETROLEUM
U CRUDE OIL

PETROLEUM PRODUCTS
NT ASPHALT
NT DIESEL FUELS
NT GASOLINE
Immediate response to free product discovery
[PB93-182970] 01 p0265 N94-11015
Methodologies for estimating air emissions from three non-traditional source categories: Oil spills, petroleum vessel loading and unloading, and cooling towers
[PB93-181592] 01 p0266 N94-11471
Laser-induced fluorescence over optical fibers for real time in situ measurement of petroleum hydrocarbons in seawater
[AD-A265106] 02 p0790 N94-12863
The First Energy Conference: Israel and the Former USSR
[ISBN-965-229-098-X] 07 p2853 N94-26050
Feasibility study on introduction of transportation-use petroleum substitution energy
[DE94-725205] 07 p2759 N94-26905
Present situation of the development of petroleum substitution energy (France)
[DE94-725201] 07 p2760 N94-26914

PETROLOGY
NT PETROGRAPHY
Twenty-fourth Lunar and Planetary Science Conference. Part 1: A-F
[NASA-CR-193095] 01 p0435 N94-12015
Carbon in weathered ordinary chondrites from Roosevelt County 01 p0428 N94-12035
Nitrogen and noble gases in a glass sample from LEW88516 01 p0080 N94-12051
The great 8 MA event and the structure of the H-chondrite parent body 01 p0429 N94-12058
Th-230 - U-238 series disequilibrium of the Olkaria basalts Gregory Rift Valley, Kenya: Petrogenesis 01 p0281 N94-12074
Th-230 - U-238 series disequilibrium of the Olkaria rhyolites Gregory Rift Valley, Kenya: Petrogenesis 01 p0281 N94-12075
Mineralogy versus bulk composition of the carbonaceous chondrite clast Kaidun 2 01 p0429 N94-12101
A structural and petrographic investigation of the pretoria saltpan impact structure 01 p0282 N94-12102
Carbonaceous chondrite clasts in the Kapoeta howardite 01 p0282 N94-12104
LEW88516 and SNC meteorites 01 p0430 N94-12150
Flash melting of chondrule precursors in excess of 1600 C. Series 1: Type 2 (B1) chondrule composition experiments 01 p0431 N94-12177
Rhenium-osmium isotope systematics of Group 2A and Group 4A iron meteorites 01 p0431 N94-12182
Regional mantle upwelling on Venus: The Beta-Atla-Themis anomaly and correlation with global tectonic patterns 01 p0467 N94-12196
The granulite suite: Impact melts and metamorphic breccias of the early lunar crust 01 p0282 N94-12197
Compositional heterogeneity within a dumbbell-shaped Apollo 15 green glass: Evidence for simultaneous eruption of different magmas 01 p0470 N94-12209
Soret diffusion: A possible cause of compositional heterogeneity within tektites 01 p0432 N94-12211
Stalking the LREE-enriched component in ureilites 03 p1241 N94-16190
Euromet Ureilite Consortium: A preliminary report on carbon and nitrogen geochemistry 03 p1241 N94-16192
Petrologic constraints on the surface processes on asteroid 4 Vesta and on excavation depths of diogenite fragments 03 p1241 N94-16208
Petrologic models of 15388, a unique Apollo 15 mare basalt 03 p1264 N94-16258
Complex zoning behavior in pyroxene in FeO-rich chondrules in the Semarkona ordinary chondrite 03 p1243 N94-16284
Angrite LEW87051: Are the olivines pheno's or xeno's? A continuing story 03 p1103 N94-16285
Experimental segregation of iron-nickel metal, iron-sulfide, and olivine in a thermal gradient: Preliminary results 03 p1243 N94-16288
An initial perspective of S-asteroid subtypes within asteroid families 03 p1243 N94-16310
Manson impact structure, Iowa: First geochemical results for drill core M-1 03 p1103 N94-16322
The monzonorite-anorthosite connection: The petrogenesis of terrestrial KREEP 03 p1104 N94-16365
The dregs of crystallization in Zagami 03 p1245 N94-16390
The Nakhla parent melt: REE partition coefficients and clues to major element composition 03 p1245 N94-16399
Igneous fractionation and subsolidus equilibration of diogenite meteorites 03 p1245 N94-16413
The role of carbon and temperature in determining electrical conductivity of basins, crust and mantle
[DE93-015936] 03 p1101 N94-16840
Twenty-Fourth Lunar and Planetary Science Conference. Part 3: N-Z
[NASA-CR-193149] 05 p2092 N94-20636
REE and other trace lithophiles in MAC88177, LEW88280 and LEW88763 05 p2082 N94-20639
The Erevan howardite: Petrology of glassy clasts and mineral chemistry 05 p1684 N94-20640
Petrogenesis of Apollo 12 mare basalts. Part 1: Multiple melts and fractional crystallization to explain olivine and ilmenite basalt compositions 05 p1684 N94-20644
Petrogenesis of Apollo 12 mare basalts. Part 2: An open system model to explain the pigeonite basalt compositions 05 p1684 N94-20645
The Sm-(146,147)-Nd-(142,143) formation interval for the lunar mantle and implications for lunar evolution 05 p2097 N94-20663
Modelling the gravity and magnetic field anomalies of the Chicxulub crater 05 p1862 N94-20668
Orthopyroxenes as recorders of diogenite petrogenesis: Major and minor element systematics 05 p1684 N94-20670
Opaque-rich lithology in the Divnoe achondrite: Petrology and origin 05 p2082 N94-20680
U-Pb isotopic ages and characteristics of ancient (greater than 4.0 Ga) lunar highland rocks 05 p2104 N94-20700
Oxygen isotopic relationships between the LEW85332 carbonaceous chondrite and CR chondrites 05 p2083 N94-20708
Micrometeorite dynamic pyrometamorphism: Nonstoichiometric clinoenstatite (CLEN) 05 p2083 N94-20715
Lunar basalt meteorite EET 87521: Petrology of the clast population 05 p2083 N94-20752
Orthopyroxenes as recorders of diogenite petrogenesis: Trace element systematics 05 p1686 N94-20760
Geochronology and petrogenesis of the western highlands alkali suite: Radiogenic isotopic evidence from Apollo 14 05 p2118 N94-20778
Magnesian anorthosites from the western highlands of the Moon: Isotope geochemistry and petrogenesis 05 p2118 N94-20779
Petrology and geochemistry of VLT glasses from double drive tube 79001/2 05 p1687 N94-20870
Lewis Cliff 87057: A new metal-rich E3 chondrite with similarities to Mt. Egerton, Shallowater and Happy Canyon 05 p2086 N94-20901
Chemical composition of new Acapulcoites and Lodranites 05 p2086 N94-20905
Correlated petrographic, electron microprobe, and ion microprobe studies of selected primitive and processed phase assemblages in meteorites
[NASA-CR-194827] 06 p2601 N94-23499
Highland crust at the Apollo 14 site: A review 06 p2614 N94-24364
Whole rock major element chemistry of KREEP basalt clasts in lunar breccia 15205: Implications for the petrogenesis of volcanic KREEP basalts 06 p2614 N94-24365
Polytopic vector analysis in igneous petrology: Application to lunar petrogenesis 06 p2615 N94-24368
The western highland province at the Apollo 14 site 06 p2615 N94-24369
A dynamic melting model for the origin of Apollo 15 olivine-normative and quartz-normative mare basalts 06 p2615 N94-24371
Melt rock components in KREEPy breccia 15205: Petrography and mineral chemistry of KREEP basalts and quartz-normative mare basalts 06 p2616 N94-24372
Heterogeneity in small aliquots of Apollo 15 olivine-normative basalt: Implications for breccia clast studies 06 p2616 N94-24373
The Twenty-Fifth Lunar and Planetary Science Conference. Part 1: A-G
[NASA-CR-195743] 11 p4355 N94-35395

On the possible role of elemental carbon in the formation of reduced chondrules 11 p4351 N94-35421
The Twenty-Fifth Lunar and Planetary Science Conference. Part 3: P-Z
[NASA-CR-195745] 11 p4362 N94-35448
FeO and MgO in plagioclase of lunar anorthosites: Igneous or metamorphic? 11 p4351 N94-35449
More shock recovery experiments on mesosiderite analogs 11 p4351 N94-35455
The Twenty-Fifth Lunar and Planetary Science Conference. Part 2: H-O
[NASA-CR-195744] 11 p4367 N94-36136
Partial melting of the St. Severin (LL) and Lost City (H) ordinary chondrites: One step backwards and two steps forward 11 p4353 N94-36146
Synthetic and natural Nakhla pyroxenes: Parent melt composition and REE partition coefficients 11 p4353 N94-36161
Cr, Mn, and Ca distributions for olivine in angritic systems: Constraints on the origins of Cr-rich and Ca-poor core olivine in angrite LEW87051 11 p4353 N94-36162

PH
A survey of techniques for corrosion monitoring
[DE93-012131] 01 p0083 N94-11250
Promotion of geothermal energy development in 1991
[DE93-799058] 02 p0701 N94-13215
Canonical correlation of waste glass compositions and durability, including pH
[DE93-012754] 02 p0578 N94-13493
Factors determining the release of nitric oxide --- Calcium/cadmium transport by renal cortical collectin duct cells
[AD-A266232] 03 p1118 N94-17224
Analog/digital pH meter system I.C. 05 p1764 N94-21701
Fiber optic sensors for corrosion detection 07 p3040 N94-27923
Recovery of carboxylic acids at pH greater than pKa
[DE94-007030] 09 p3636 N94-32376
A fuzzy classifier system for process control 09 p3839 N94-32422
Studies of the fundamental nature of catalytic acidity, sites and intermediates
[DE94-006999] 09 p3646 N94-32805
The pH of Mars 09 p3950 N94-33225
Computation of iodine species concentrations in water 10 p4102 N94-33660
Methane production and consumption in grassland and boreal ecosystems
[NASA-CR-196085] 11 p4284 N94-35486
A dynamic model of a linear actuator based on polymer hydrogel
[DE94-010800] 12 p4408 N94-37091
Submicrometer fiber-optic chemical sensors: Measuring pH inside single cells
[DE94-004160] 12 p4525 N94-37532

PH FACTOR
Size dependence of chemical reactivity of gaseous metal clusters: A new mechanistic probe
[AD-A264690] 01 p0077 N94-11264
Coatings for SiO2 optical fibers
[AD-D016197] 11 p4334 N94-36363

PHARMACOLOGY
NT PSYCHOPHARMACOLOGY
Evaluation of putative neurochemical intermediaries in space/motion sickness
[NASA-CR-193607] 03 p1118 N94-17090
Physiologically based pharmacokinetic modelling of percutaneously absorbed dibromomethane utilizing multiple dermal sub-compartments
[AD-A271106] 05 p1889 N94-19981
Electrophoresis in open capillaries: Some fundamental aspects
[ETN-94-95290] 06 p2236 N94-25232
Cubanes: Super explosives and potential pharmaceutical intermediates 08 p3227 N94-30454
International Journal of Quantum Chemistry. Quantum Biology Symposium number 20. Proceedings of the International Symposium on the Application of Fundamental Theory to Problems of Biology and Pharmacology
[AD-A276294] 09 p3792 N94-31294
Review of pharmacological approach to improve cold tolerance 09 p3796 N94-31740
Effect of barbiturates and hyperoxia on lipid peroxidation in hypoxic neurons
[AD-A278467] 10 p4094 N94-33545

PHASE ANGLE
U PHASE SHIFT

PHASE CHANGE MATERIALS
Modeling void growth and movement with phase change in thermal energy storage canisters
[NASA-TM-106288] 01 p0163 N94-12576
Advanced cooling for high power electric actuators
[AD-A266984] 03 p0866 N94-15761
Shrinkage void formation and its effect on freeze and thaw processes of lithium and lithium-fluoride for space applications
[DE93-019303] 04 p1338 N94-19128
Liquid metal MHD research and development in Israel 07 p2854 N94-26055

PHASE COHERENCE
Coherent structure in near wall turbulence with riblets 01 p0165 N94-12628
Dynamics of a coupled solid state laser array 08 p3294 N94-29551
Incoherent imaging by Z-contrast stem: Towards 1 Angstrom resolution
[DE94-006551] 09 p3896 N94-31489
Evaluation of surface phase change on large zones 09 p3755 N94-32567
Techniques and applications of SAR interferometry for ERS-1 09 p3756 N94-32568

PHASE CONJUGATION
NT FOUR-WAVE MIXING
Limitations to the quality of optical phase conjugation by stimulated Brillouin scattering
[AD-A266006] 01 p0383 N94-12389
Phase conjugation and beam combination using stimulated brillouin scattering
[AD-A269899] 04 p1439 N94-18656
Spatiotemporal behavior and nonlinear dynamics in a phase conjugate resonator
[NASA-CR-4567] 06 p2543 N94-23529
Investigation of Raman beam cleanup and phase conjugation
[AD-A273157] 06 p2545 N94-24672
Quantum optical aspects of topological phases, such as Berry's phase
[AD-A273632] 06 p2570 N94-25028
Phase conjugation and pulse compression of high energy lasers: From nanoseconds to microseconds
[DE94-001061] 07 p2818 N94-26699
High-speed, high-density, coherent time-domain optical memory
[AD-A274249] 07 p3037 N94-27010
Phase conjugated lasers applied to commercial x ray lithography
[DE94-001529] 07 p2819 N94-27018
Predoctoral training grant in the area of physical sciences
[DE94-004406] 07 p3039 N94-27603
Estimation of geomagnetic conjugate points by using Pc5 pulsations 08 p3357 N94-29079
Methods for SBS threshold reduction
[AD-A276554] 09 p3717 N94-31936
High average power pulsed phase conjugate laser with birefringence correction
[DE94-006049] 09 p3719 N94-32659
Studies of optical beam phase conjugation and electromagnetic scattering process
[AD-A278389] 09 p3884 N94-33145

PHASE CONTRAST
Measurements of edge fluctuations by phase contrast imaging on DIII-D
[DE93-014018] 02 p0802 N94-14579
Optimal detector strategies for the phase contrast imaging for scanning transmission electron microscopes
[ETN-94-95747] 09 p3866 N94-31613

PHASE CONTROL
Proceedings of the 11th Space Surveillance Workshop, volume 1
[AD-A265120] 02 p0531 N94-13358
Ceramic fiber coatings development and demonstration
[AD-A267286] 03 p0972 N94-17242
Phase screens for the control of the focal irradiance of the Nova laser
[DE94-001067] 05 p1820 N94-22401
Time-scale modification of complex acoustic signals in noise
[AD-A277535] 10 p4133 N94-34157
Active control of vaneless diffuser rotating stall 10 p4062 N94-34178

PHASE DEMODULATORS
Localized and distributed fiber-optic strain sensors embedded in composite materials
[UTIAS-346] 01 p0073 N94-12013
Phase demodulation of interferometric fiber-optic sensors
[ISBN-0-315-83425-0] 05 p1991 N94-22581

PHASE DETECTORS
Synchronous sampling phase and amplitude detection method and apparatus
[NASA-CASE-LAR-14725-1] 03 p1050 N94-15870
An analysis of carrier phase jitter in an MPSK receiver utilizing map estimation
[NASA-CR-195806] 08 p3164 N94-29880

PHASE DEVIATION
Phase linearity of the 914H coupled-cavity traveling wave tube
[NASA-CR-191056] 06 p2290 N94-23087
Design and analysis of a low-loss linear analog phase modulator for deep space spacecraft X-band transponder applications 08 p3248 N94-29625

PHASE DIAGRAMS
Phase equilibria and volumetric properties for the system NaCl-CaCl2-H2O
[DE93-013590] 01 p0076 N94-11244
Synthesis and magnetic properties of novel La*2-x*M*x*CuO*4 equals y* compositions (La equals La, Pr, Nd, Sm, Eu, Cd; M equals Ca, Sr, Ba; O (less than or equal) x 0.2; -0.5 (less than or equal) y (less than or equal) 0.5)
[DE93-011359] 01 p0403 N94-12363
Multiphase equation of state for iron
[DE93-013956] 02 p0568 N94-12977
First-principles studies of phase stability and the structural and dynamical properties of hydrogen-metal systems
[DE93-016129] 02 p0570 N94-13374
How to read a phase equilibrium diagram for high-temperature ceramics material as main object
[DE93-512333] 02 p0582 N94-14513
Is K3C60 a line phase?
[DE93-016700] 02 p0813 N94-14517
Statics and kinetics of phase transformations in bcc Fe-Cr
[DE93-013839] 02 p0574 N94-14793
Influence of heat treatment on microstructure of Ti-35wt Al prepared by elemental powder metallurgy
[GKSS/92/E/27] 02 p0574 N94-14821
Silica-bearing objects in the Dengli H3.8 and Gorlovka H3-4 chondrites 03 p1242 N94-16265
A new multiphase equation of state for iron
[DE93-017629] 04 p1357 N94-17819
Calculation of the LiF-CeF3-BeF2 and LiF-PuF3-BeF2 ternary phase diagrams
[DE93-017437] 04 p1360 N94-18501
Realistic theories of heavy electron and other strongly correlated materials
[DE93-010350] 04 p1571 N94-19204
Theoretical phase diagrams for solid H(sub 2)
[DE94-001049] 05 p1684 N94-22395
First-principles pressure-temperature phase diagrams in metals
[DE94-001056] 05 p1696 N94-22398
Physics of iron
[DE94-002002] 06 p2402 N94-23721
Lattice dynamics of Ba(1-x)K(x)BiO3 as studied by neutron scattering and computer simulation
[DE93-617053] 06 p2567 N94-25424
Phase diagram of La2NiO(4 + delta) (0 less than or equal to delta less than or equal to 0.18). 1: Phases at room temperature and phase transition above delta equal to 0.15
[REPT-A-2661] 07 p3053 N94-26089
Zr-rich corner of the Zr-Sn-O diagram
[DE93-633764] 07 p2734 N94-26161
Phase portraits of quadratic systems with finite multiplicity three and one critical point of infinity
[REPT-93-41] 07 p2991 N94-26215
Zr-Sn-Nb alloys: Preliminary studies
[DE93-633767] 07 p2734 N94-26263
Liquid and solid solubility of Ag in Bi2Sr2CaCu2O8
[DE94-002829] 07 p2735 N94-26273
Eutectic transformation L in equilibrium to Zr6Fe23 + Fe(tau) in the Fe-Zr system
[DE93-633766] 07 p2735 N94-26295
Experimental determination of the CU-IN-PB ternary phase diagram
[DE94-003765] 07 p2735 N94-26349
A new materials data compilation can help in actinide phase-diagram research
[DE94-000797] 07 p3058 N94-26514
Correlated mean field Ansatz for the Kondo necklace
[DE94-603671] 07 p3067 N94-27634
Phase stability in the Cd-Mg system
[DE94-004976] 07 p2743 N94-27792
Crystal structure of La(2-x)Ba(x)CuO4
[DE94-707688] 08 p3511 N94-28750
Structure of ordinary ice I(sub h). Part 1: Ideal structure of ice
[AD-A275149] 08 p3486 N94-29021
Some results on the phase diagram of the antiferromagnetic Potts model in an external magnetic field
[DE94-608115] 08 p3468 N94-30110
Boundary-induced phase transitions in equilibrium and non-equilibrium systems
[DE94-608137] 08 p3199 N94-30111
Terfenol: A study of the phase equilibrium diagram and the solidification process
[DE94-004883] 08 p3209 N94-30690

Theoretical studies of solid-fluid phase equilibria
[DE94-006406] 08 p3226 N94-30708

Synthesis, characterization, phase diagrams and superconducting, and normal state magnetic properties of La(2-x)Sr(x)CuO4 (0 is less than or equal to x which is less than or equal to 0.08) and electrochemically oxidized La(2-x)Sr(x)CuO(4 + delta) (0 is less than or equal to x which is less than or equal to 0.33, 0 is less than or equal to delta which is less than or equal to 0.12)
[DE94-005260] 09 p3895 N94-31067

The new Metals and Alloys Indexes, search manual: A phase diagram research tool
[DE94-005371] 09 p3643 N94-32098

Phase behavior, structure, and properties of model block polymers
[AD-A277530] 09 p3662 N94-32954

C.A.D. representation of ternary and quaternary phase diagrams
[NASA-CR-195845] 10 p4025 N94-34170

A classical model for closed-loop diagrams of binary liquid mixtures
[DE94-011011] 11 p4237 N94-36033

Magnetic and structural instabilities of ferromagnetic and antiferromagnetic Fe/Cu(100)
[DE94-011504] 12 p4509 N94-37517

PHASE ERROR

The limit of frequency estimation
01 p0356 N94-11001

Ionospheric effects on a wide-bandwidth, polarimetric, space-based, synthetic-aperture radar
[DE93-015084] 02 p0612 N94-14512

The spatial variance of ionospherically-induced phase errors in SAR imagery
[DE93-015643] 04 p1385 N94-18232

Array Simulations Platform (ASP) predicts NASA Data Link Module (NDLM) performance
05 p1744 N94-21348

Effect of errors on the phase centre and pointing angle of phased array antennas 05 p1746 N94-22162

Numerical simulation of tomographic reconstruction for the study of turbulence using optical wavefront sensor measurements
[AD-A273851] 07 p2789 N94-25587

Feasibility study of a multiaperture telescope for deep-space Earth surveillance
[AD-A273903] 07 p3102 N94-25658

Automatic focus and registration of synthetic aperture radar images 08 p3246 N94-29536

Effects of low sampling rate in the digital data-transition tracking loop 08 p3251 N94-29669

An analysis of carrier phase jitter in an MPSK receiver utilizing map estimation
[NASA-CR-195806] 08 p3164 N94-29880

PHASE LOCK DEMODULATORS

Design and test of a regenerative satellite transmultiplexer
[ISBN-0-315-85280-1] 07 p2786 N94-27303

PHASE LOCKED SYSTEMS

Method of recertifying a loaded bearing member using a phase point
[NASA-CASE-LAR-14741-1] 01 p0185 N94-10671

Sea surface temperature forcing and phase locking of Nordeste precipitation
[DE93-011873] 02 p0723 N94-14426

Improvements to pulsed phase locked loop strain monitor
[NASA-CASE-LAR-14887-1] 03 p1033 N94-15877

Phase conjugation and beam combination using stimulated brillouin scattering
[AD-A269899] 04 p1439 N94-18656

A method for eliminating skew introduced by non-uniform buffer delay and wire lengths in clock distribution trees
[AD-A270649] 04 p1544 N94-19530

Optical frequency division using an optical parametric oscillator
[AD-A270847] 04 p1581 N94-19578

An optical ASK and FSK phase diversity transmission system
[EUT-92-E-268] 06 p2542 N94-23171

Method of implementing digital phase-locked loops
[NASA-CASE-NPO-18757-1-CU] 08 p3265 N94-29374

Dynamics of a coupled solid state laser array
08 p3294 N94-29551

Design and implementation of a hybrid digital phase-locked loop with a TMS320C25: An application to a transponder receiver breadboard
08 p3251 N94-29667

Precision frequency synthesizing sources with excellent time/frequency performances 08 p3473 N94-30671

Development, characterization, and applications of high temperature superconductor nanobridge Josephson junctions
[DE94-008113] 09 p3903 N94-32409

YBCO Josephson Junction arrays
[AD-A277426] 09 p3908 N94-33005

Performance evaluation of digital phase-locked loops for advanced deep space transponders
11 p4254 N94-35558

Phase-locked arrays of vertical-cavity surface-emitting lasers
[DE94-009279] 11 p4272 N94-36178

PHASE MATCHING

New challenges in optical materials development
[DE93-011889] 01 p0383 N94-11676

High-order sum and difference-frequency generation in helium
[DE94-001064] 06 p2348 N94-23181

Three-wave nonlinear interactions in KTiOPO4 (KTP) and KTP isomorphs
[AD-A274079] 07 p3052 N94-25993

Laser phase induced intensity noise in fiber-optic signal processing and sensing systems
[ITN-94-85234] 07 p2819 N94-27179

Spectral-domain optical processing techniques
[AD-A278371] 10 p4141 N94-33739

Frequency doubling of copper lasers using temperature-tuned ADP
[DE94-011542] 12 p4448 N94-37240

PHASE MODULATION

NT BINARY PHASE SHIFT KEYING
NT FM/PM (MODULATION)
NT PHASE SHIFT KEYING
NT QUADRATURE PHASE SHIFT KEYING

Trellis coding with Continuous Phase Modulation (CPM) for satellite-based land-mobile communications
[NASA-CR-191325] 02 p0604 N94-13909

The optimal numerical algorithm for processing of phase coded time signals for radio-clocks
04 p1426 N94-18018

Evaluation of a liquid crystal spatial light modulator capable of amplitude- and phase-modulating modes
[AD-A269252] 04 p1577 N94-18262

Alternating-phase focusing with amplitude modulation
[DE93-018618] 04 p1574 N94-18273

Nanostructured materials: Mind over matter
[DE93-017690] 04 p1597 N94-18480

Resolution in radar mapping
[AD-A269730] 04 p1462 N94-18753

Integrated Photonics Research: Post-deadline papers
[AD-A269232] 04 p1609 N94-18908

Material optimization for hard x ray Fresnel zone plates
[DE93-019569] 05 p1990 N94-21837

Effect of bandwidth on beam smoothing and frequency conversion at the third harmonic of the Nova laser
[DE93-019917] 05 p1819 N94-21920

Preliminary analysis of amplitude and phase fluctuations in the JAPE multiple tone data to distances of 500 meters 06 p2528 N94-24216

Structure of the modulated magnetic phase of Mn3Sn
[DE94-002788] 07 p2733 N94-26092

Longitudinal effects and intensity-phase coupling in distributed feedback semiconductor lasers
08 p3294 N94-29590

Design and analysis of a low-loss linear analog phase modulator for deep space spacecraft X-band transponder applications 08 p3248 N94-29625

Two-way satellite time transfer: Overview and recent developments 08 p3469 N94-30646

Advanced optical fiber communication systems
[AD-A276416] 09 p3878 N94-31330

High-performance GaAs/AlGaAs optical phase modulators for microwave/photonic integrated circuits
[DE94-006361] 09 p3688 N94-31483

Analysis of key performance parameters of phase sampling digital RF memories
[AD-A276019] 09 p3688 N94-31494

High-performance GaAs/AlGaAs optical phase modulators for microwave photonic integrated circuits
[DE94-007376] 09 p3696 N94-32809

Phase-only 128x128 spatial light modulator based on LASLM technology
[AD-A277901] 10 p4141 N94-33591

New light sources and concepts for electro-optic sampling
[AD-A278533] 10 p4141 N94-33672

Spacecraft-spacecraft radio-metric tracking: Signal acquisition requirements and application to Mars approach navigation 11 p4254 N94-35557

Fabrication and phase tuning of an optical waveguide device
[AD-D016215] 11 p4334 N94-36122

Final report on spectral broadening by cross-phase modulation in linearly birefringent optical fibers
[DE94-010406] 12 p4524 N94-37191

PHASE RESPONSE

U FREQUENCY RESPONSE
U PHASE SHIFT

PHASE RULE

Workshop on Formation of Supermolecular Structures in Composite Fluid: Phase Rule and Dynamics
[DE93-782887] 02 p0581 N94-14421

How to read a phase equilibrium diagram for high-temperature ceramics material as main object
[DE93-512333] 02 p0582 N94-14513

PHASE SEPARATION (MATERIALS)

Design of multisample, multistep phase partitioning apparatus for use on Space Shuttle Spacelab, and Spacelab missions 01 p0108 N94-10120

Appearance of convective instabilities caused by liquid-liquid phase separation under small buoyancy forces 01 p0120 N94-10221

Phase separation at gas-liquid critical points
01 p0122 N94-10233

Use of inert immiscible liquid for crystal separation out of its feeding solution in weightlessness
01 p0124 N94-10242

The Lindemann criterion of melting for pure and mixed ionic crystals
[ITN-93-85210] 02 p0814 N94-14554

Sounding Rocket Experiments in Fluid Science and Materials Sciences: TEXUS 25 to 27 and MASER 4, volume 3
[ESA-SP-1132-VOL-3] 03 p0943 N94-15157

Temperature propagation in near-critical fluids prior to and during separation 03 p0944 N94-15165

Phase separation and superconductivity in La2CuO(4 + delta): Effects of oxygen diffusion
[DE93-016610] 04 p1594 N94-17907

Phase separation and ordering process in Al-Li alloys studied by small-angle neutron scattering and neutron diffraction
[DE93-016750] 04 p1358 N94-17947

PHASE SHIFT

NT SAGNAC EFFECT

Interferometry with particles of non-zero rest mass
[DE93-613518] 01 p0409 N94-10501

Three-nucleon problem with phase equivalent potentials
[DE93-617731] 01 p0363 N94-10722

Characterization of a scannerless LADAR system
[DE93-011582] 01 p0174 N94-10959

FEFF5: An ab initio multiple scattering XAFS code
[DE93-011000] 01 p0367 N94-11470

The MRIS feasibility study
[NASA-TM-107763] 02 p0597 N94-12804

Non-scanned LADAR imaging and applications
[DE93-013772] 02 p0655 N94-13261

Advanced ballistic range technology
[NASA-CR-194530] 02 p0533 N94-14540

Adaptive beamforming with imperfect arrays: Pattern effects and their partial correction
[AD-A267079] 03 p0987 N94-15541

A study of the observed tidal residue vectors B versus oceanic tidal load vectors L 03 p1100 N94-15813

Interaction types and their like-polarization phase-angle difference signatures 03 p1079 N94-16756

Fundamental-mode RF design in e(+)e(-) storage ring factories
[DE93-015249] 03 p1183 N94-16809

Speckles statistics and decorrelation effects in complex ABCD optical systems
[AD-A267843] 03 p1193 N94-17012

Optical system storage design with diffractive optical elements 03 p1198 N94-17360

Arc detection and protection in high-power antenna systems
[DE93-013272] 04 p1382 N94-17695

Development and test of readout electronics for optical quadrature signals
[DLR-MITT-92-11] 04 p1395 N94-17920

Topographic slope from the SAR interferometric phase gradient 05 p1731 N94-20459

Four-channel HF receiving antenna array simulator
[AD-A271876] 05 p1732 N94-20471

Space applications of superconducting microwave electronics at NASA Lewis Research Center
05 p1671 N94-20513

The coherent backscattering opposition effect
05 p1991 N94-20646

Modulation characteristics of a high-power semiconductor Master Oscillator Power Amplifier (MOPA)
[NASA-TM-104577] 06 p2306 N94-23281

Develop advanced nonlinear signal analysis topographical mapping system
[NASA-CR-194785] 06 p2389 N94-24856

The phase response of nonlinear systems
[RR-458] 06 p2476 N94-25308

Unwrapping the phase response functions for nonlinear systems
[RR-465] 06 p2462 N94-25311

Ferrite phase shifters using stress insensitive materials
[AD-A274639] 07 p2708 N94-26895
Bulletin of the Institute for Chemical Reaction Science, Tohoku University, volume 2
[JTN-94-80602] 07 p2717 N94-27385
Four phase microwave pulse generator for pulsed EPR spectrometer 07 p2718 N94-27388
Interhemispheric phase relationship of alpha waves and cerebral dominance 07 p2927 N94-27518
Derivation of a Fokker-Planck equation for bunched beams
[DE94-004950] 08 p3483 N94-28565
Observation of the phase shift of the wave function of the neutron under total reflection
[DE94-608244] 08 p3489 N94-30096
Phase unwrapping problems in ISAR images
[TELECOM-93-D-008] 09 p3670 N94-31097
Field studies of raindrop oscillations with applications to radar meteorology 09 p3782 N94-31743
Fiber optic continuous true time-delay modulator
[AD-D016098] 09 p3883 N94-32720
High-performance GaAs/AlGaAs optical phase modulators for microwave photonic integrated circuits
[DE94-007376] 09 p3696 N94-32809
Effective computational strategy for predicting the response of complex systems
[AD-A277452] 09 p3740 N94-33011
Sputter process investigation: Material and environment interaction processes investigation
[NASA-CR-193946] 10 p4028 N94-34076
A three-body calculation of the O-16(d,p)O-17 reaction using a two-term separable potential for the s-wave nucleon-core interaction
[DE94-616652] 11 p4320 N94-35579
Elastic p(4)He scattering at intermediate energies
[DE94-618544] 11 p4328 N94-36287
Phase shifter for directly sampled bandpass signals
[AD-D016320] 12 p4440 N94-37840

PHASE SHIFT KEYING
NT BINARY PHASE SHIFT KEYING
NT QUADRATURE PHASE SHIFT KEYING
Telemetering and telecommunications research
[NASA-CR-193235] 01 p0042 N94-11297
Flexible high-speed CODEC
[NASA-CR-191169] 01 p0146 N94-12433
Envelope and instantaneous frequency estimation of narrowband modulated signals
[DREO-TN-92-3] 02 p0605 N94-14033
Multiple-symbol differential detection of DPSK with frequency offset
[DREO-TN-92-5] 02 p0606 N94-14063
Capacity comparison between direct sequence PSK and MFSK spread spectrum systems in CDMA applications 05 p1747 N94-22224
Asynchronous timing and Doppler recovery in DSP based DPSK modems for fixed and mobile satellite applications 06 p2285 N94-22805
Theoretical and simulated performance for a novel frequency estimation technique 06 p2285 N94-22808
Pseudo-coherent demodulation for mobile satellite systems 06 p2287 N94-22819
Coding for frequency hopped spread spectrum satellite communications
[ECE-91-1] 06 p2296 N94-24132
Simulation of adjacent channel interference in a UHF satellite system
[AD-A273147] 06 p2299 N94-24669
Coding for frequency hopped spread spectrum satellite communications
[ECE-92-1] 06 p2300 N94-24697
On the performance of trellis coded 8PSK with Reed Solomon codes
[ISBN-0-315-84289-X] 07 p2770 N94-26626
Short-block data detection techniques employing channel estimation for fading time-dispersive channels
[ISBN-0-315-58970-1] 07 p2777 N94-27806
An analysis of carrier phase jitter in an MPSK receiver utilizing map estimation
[NASA-CR-195806] 08 p3164 N94-29880
Partially coherent detection of PSK signals in Rician channels
[ISBN-0-315-85799-4] 08 p3254 N94-30031
Modulation and coding for the Gaussian channel, possibly affected by fluctuations
[TELECOM-93-E-009] 09 p3840 N94-31169
Advanced optical fiber communication systems
[AD-A276416] 09 p3878 N94-31330

PHASE STABILITY (MATERIALS)
Fluid-fluid interfacial instabilities induced by gravity 01 p0121 N94-10229
Electronic structure and phase stability properties in ternary substitutional alloys
[DE93-013648] 02 p0569 N94-13137
Mesons at finite temperature in the NJL model with gluon condensate
[DE93-626697] 03 p1185 N94-17310
Kinetics of silica-phase transitions
[DE93-016231] 03 p1217 N94-17659
Bench-scale screening tests for a boiling sodium-potassium alloy solar receiver
[DE93-018512] 04 p1469 N94-19040
Fabrication, properties, and microstructures of high (Tc) tapes and coils made from Ag-clad Bi-2223 superconductor
[DE93-017405] 04 p1602 N94-19122
Prediction of non-equilibrium solidification modes in austenitic stainless steel laser welds
[DE93-018457] 04 p1364 N94-19203
Stability of the face-centered-cubic phase of heavy rare gas solids
[DE93-019949] 05 p1679 N94-20319
Sintering silicon nitride
[NASA-CASE-LEW-15489-1] 05 p1703 N94-20529
Generalized perturbation method expansions of the total energy of an alloy
[DE94-003865] 07 p3055 N94-26238
Octahedral metallomesogens: Liquid crystallinity in low aspect ratio materials
[AD-A274830] 07 p3059 N94-26571
A tri-junction diffusion couple analysis of the Nb-Cr-Ti system at 950 C
[DE94-002637] 07 p2737 N94-26607
Interstitially stabilized phases in the zirconium-nickel system
[DE94-005561] 08 p3201 N94-28525
Structure, stability, and mechanical properties of intermetallic phases
[DE94-009178] 09 p3647 N94-32852
The distribution of Martian ground ice at other epochs 09 p3948 N94-33218
Phase relationships and stability of the (mu)- and (zeta)-phases in the Ag-Al-X (X=Zn, Ga, Ge) systems
[DE94-009391] 09 p3648 N94-33270
Electronic structure and stability of simple and complex phases in transition metals
[DE94-009090] 10 p4024 N94-33679
Calculation of phase stability in Zr-Nb-Ru using LMTO and the cluster variation method
[AD-A278556] 10 p4137 N94-33896
The effect of alternative fuels on the stability and lubricity of crankcase lubricants
[DE94-010353] 11 p4245 N94-36108
Process simulation and modeling for advanced intermetallic alloys
[AD-A280327] 12 p4416 N94-37030
Mechanical behavior and phase stability of NiAl-based shape memory alloys
[DE94-012336] 12 p4419 N94-37420

PHASE TRANSFORMATIONS
NT ARC MELTING
NT BOILING
NT COAL LIQUEFACTION
NT EVAPORATION
NT EVAPOTRANSPIRATION
NT FLASHING (VAPORIZING)
NT FREEZING
NT FUSION (MELTING)
NT LEIDENFROST PHENOMENON
NT LEVITATION MELTING
NT LIQUEFACTION
NT MARTENSITIC TRANSFORMATION
NT MELTING
NT NUCLEATE BOILING
NT SUBLIMATION
NT TRANSPIRATION
NT VACUUM MELTING
NT VAPORIZING
NT ZONE MELTING
Studies of critical point phenomena of fluids: Bulk fluids, fluids in pores, and at interfaces 01 p0080 N94-10228
Singularity spectrum of self-organized criticality
[DE93-613820] 01 p0348 N94-10404
Monte Carlo simulations of phase transformations in Fe-Cr alloys
[DE93-013847] 01 p0081 N94-10522
Non-gauge phase transformations in quantum transition amplitudes 01 p0378 N94-10596
Confinement of acoustical modes due to the electron-phonon interaction within 2D-electron gas
[DE93-613910] 01 p0396 N94-10800
Non-barrier tunneling in presence of dissipations
[DE93-621381] 01 p0412 N94-11086
Low temperature synthesis of monolithic transparent Ta2O5 gels from hydrolysis of metal alkoxide
[NASA-TM-106246] 01 p0089 N94-11204
Real-space formation and dissipation dynamics of hexagonal reconstruction on Au(100) in aqueous media as explored by potentiodynamic scanning tunneling microscopy
[AD-A266138] 01 p0368 N94-11658
Shock transformations in quartzite 01 p0097 N94-12040
Phase transitions and 2D spherical convection in a large icy satellite 01 p0433 N94-12265
Electrode potential-induced reconstruction of Au(100): Effect of chemisorption on nanoscale dynamics as probed by the in-situ scanning tunneling microscopy
[AD-A265900] 01 p0404 N94-12388
Recovery of materials impacted at high velocity
[DE93-014150] 02 p0576 N94-12885
Effect of pressure on order and stability in alloys: The case of Al-Ge
[DE93-013842] 02 p0567 N94-12899
First-principles studies of phase stability and the structural and dynamical properties of hydrogen-metal systems
[DE93-016129] 02 p0570 N94-13374
The microstructural response of near gamma-TiAl+W to heat treatment
[DSIS-93-00237] 02 p0571 N94-13840
Phase transition in polymer blends and structure of ionomers and copolymers
[DE93-016256] 02 p0579 N94-13978
Monte Carlo simulation of the OCP freezing transition
[DE93-013039] 02 p0811 N94-14313
Effect of spontaneous decay of superconductor quasiparticles in the tunneling density of states
[DE93-012681] 02 p0811 N94-14339
Workshop on Formation of Supermolecular Structures in Composite Fluid: Phase Rule and Dynamics
[DE93-782887] 02 p0581 N94-14421
Computational diagnostics for detecting phase transitions during nanoindentation
[DE93-016536] 02 p0813 N94-14439
Immiscible phase incorporation during directional solidification of hypermonotectics
[NASA-CR-194412] 02 p0565 N94-14480
Statics and kinetics of phase transformations in bcc Fe-Cr
[DE93-013839] 02 p0574 N94-14793
Phases and phase transitions of polymeric liquid crystals: A high resolution x ray diffraction and light scattering study
[ITN-93-85218] 02 p0816 N94-14826
Pressures of supercritical salt solutions 03 p0945 N94-15166
Unidirectional solidification of liquid-crystal material 03 p0945 N94-15167
Ternary alloying effects in polycrystalline (beta)-NiAl
[DE93-012675] 03 p0955 N94-15885
Dynamical Ising model simulations of nucleation and growth in copper-cobalt alloys
[DE93-015336] 03 p0957 N94-16015
Scaling, soil moisture and evapotranspiration in runoff models 03 p1084 N94-16034
Phase equilibria of the magnesium sulfate-water system to 4 kbars 03 p0953 N94-16247
Electrorheological fluid chemical processing
[AD-D015785] 03 p0948 N94-16532
Process for shaping articles from electrosetting compositions
[AD-D015787] 03 p0935 N94-16534
Encapsulation of hemoglobin in non-phospholipid vesicles
[AD-A266505] 03 p1128 N94-16785
Structural phase transition and superconductivity in La(2-x)Ba(x)CuO4
[DE93-015812] 03 p1212 N94-16868
Process of shaping an electrorheological solid
[AD-D015885] 03 p1012 N94-16914
Slip, twinning and transformation in Laves phases
[DE93-018164] 03 p0960 N94-16972
An investigation of the hydrolytic resistance of sodium-calcium plate glass with a layer of silica deposited on its surface
[IFTR-34/1991] 03 p0971 N94-17120
Anisotropic phase separation in amorphous Fe-Ge alloys
[DE93-015255] 03 p0961 N94-17251
A basic principles description of liquid vapor phase transitions
[AD-A268331] 03 p1178 N94-17581
Kinetics of silica-phase transitions
[DE93-016231] 03 p1217 N94-17659
Shear wave measurements in shock-induced, high-pressure phases
[DE93-016481] 03 p1062 N94-17664
On relation between Berry phase and one-dimensional models with long-range 1/r(sup 2)-interaction
[DE93-824967] 04 p1592 N94-17690

A new multiphase equation of state for iron
[DE93-017629] 04 p1357 N94-17819
Phase transitions and neutron scattering
[DE93-016748] 04 p1594 N94-17866
Structure, thermodynamics, and dynamical properties of supercooled liquids
[DE93-788387] 04 p1607 N94-18211
Phase structure of (phi(4))(sub 3) field theory at finite temperature
[DE93-629907] 04 p1608 N94-18267
Research activity on particle spin systems and related problems
[AD-A269456] 04 p1562 N94-18286
Competitive dynamics and self-organization in photorefractive systems
[AD-A269663] 04 p1430 N94-18569
Ionic and molecular environments in heterogeneous electrocatalysis: Studies by radioactive labeling and LEED/AUGER spectroscopy
[AD-A268850] 04 p1567 N94-18766
Deformation mechanisms in a Laves phase
[DE93-018331] 04 p1361 N94-18806
Toward a characterization of the debris cloud created in a hypervelocity impact on a thin plate
[AD-A269190] 04 p1455 N94-18864
Pressure induced metallization of the Mott Insulator 6(sub 2)
[DE93-018296] 04 p1600 N94-18969
A free energy simulation method based study of interfacial segregation
[DE93-019462] 04 p1364 N94-19032
The study of the phase structure of hadronic matter by searching for the deconfined quark-gluon phase transition using 2 TeV (bar-p)-p collisions, and by searching for critical phenomena in an exclusive study of multifragmentation using 1 GeV/nucleon heavy ion collisions
[DE93-018925] 04 p1570 N94-19103
Prediction of non-equilibrium solidification modes in austenitic stainless steel laser welds
[DE93-018457] 04 p1364 N94-19203
Effects of pressure on the orientational ordering and phase transitions in solid C(60) and C(70)
[DE93-018858] 04 p1603 N94-19347
Optical frequency doubling at adsorbates of silver(110) surface
[ETN-93-94837] 04 p1603 N94-19355
Melt spinning study
[NASA-CR-193823] 04 p1380 N94-19423
Metallization and charge-transfer gap closure of transition-metal iodides under pressure
[DE93-040301] 04 p1353 N94-19538
High resolution transmission electron microscopy of mesoporous MCM-41 type materials
[AD-A271271] 04 p1354 N94-19728
Cooperative formation of inorganic-organic interfaces in the synthesis of silicate mesostructures
[AD-A271196] 04 p1375 N94-19742
Crystallographic phase transitions in actinide metals as a function of pressure
[DE93-040138] 05 p2011 N94-19827
Problems related to conservation laws: Phase transitions and viscoelasticity
[AD-A271429] 05 p1698 N94-19840
General introduction to microstructural evolution under cascade damage conditions
[DE93-017443] 05 p2012 N94-19923
Kinetics of phase transformations in glass forming systems
[NASA-CR-194270] 05 p1701 N94-20347
The effect of fluctuations on the electrical transport behavior in YBa2Cu3O(7-x) 05 p1736 N94-20519
Thermal expansion of electronic highly correlated materials
[ETN-93-93605] 05 p2026 N94-21135
Examinations of composition and deformation behavior of intermetallic phases on the basis of Fe3(AlSi)
[GKSS-92/E/16] 05 p1692 N94-21311
Static ultra-high pressure study of lanthanide and actinide metals using a diamond-anvil cell
[DE94-000369] 05 p1693 N94-21656
Temperature dependence of magnetic order in single-crystalline UPdSn
[DE93-040153] 05 p2033 N94-21991
The effect of correlated and point defects on the vortex lattice melting transition in single crystal YBa2Cu3O(7-delta)
[DE93-040277] 05 p2033 N94-21997
Theoretical studies of structural phase transitions in actinide metals
[DE94-000796] 05 p1696 N94-22388
The elastic and electromechanical properties of BaTiO3 single crystal through the ferroelectric transition
[DE94-001437] 06 p2557 N94-22927
Bridgman's concern
[DE93-040900] 06 p2558 N94-22953
Phase transformations in Cu-Zr multilayers
[DE94-000393] 06 p2241 N94-23297
Processing of semicrystalline polymers
06 p2226 N94-24351
Thermal phase behavior of metal surfaces: X-ray scattering studies of Pt(001)
[DE94-002991] 06 p2245 N94-24612
Dynamic measurements of thermophysical properties of metals and alloys at high temperatures by subsecond pulse heating techniques 06 p2247 N94-25124
Center for Analysis of Heterogeneous and Nonlinear Media
[AD-A273515] 06 p2230 N94-25158
Phase structure of the two-dimensional phi(4) field theory within thermo-field dynamics
[DE93-616850] 06 p2570 N94-25337
Electronic structure and high pressure phase transition in LaSb and CeSb
[DE93-617051] 06 p2567 N94-25423
Study on computerized experiment of amorphous transformation process by solid phase reaction
07 p2726 N94-25564
Coherent state approach for the (Phi)(sup 6)-lattice model and phase transitions
[DE93-613053] 07 p3050 N94-25825
Out of equilibrium phase transitions and a toy model for disoriented chiral condensates
[DE94-601642] 07 p3013 N94-25839
Successive structural phase transitions in stoichiometric La2NiO4 observed by x ray diffraction
[REPT-A-2665] 07 p3051 N94-25921
Structure and phase transformations in uranium metal
[DE94-003892] 07 p2732 N94-26004
Oriented lead zirconate titanate thin films: Characterization of film crystallization
[DE94-003104] 07 p3053 N94-26025
Phase diagram of La2NiO(4 + delta) (0 less than or equal to delta less than or equal to 0.18). 1: Phases at room temperature and phase transition above delta equal to 0.15
[REPT-A-2661] 07 p3053 N94-26089
Se EXAFS study of the elevated wurtzite to rock salt structural phase transition in CdSe nanocrystals
[DE94-003247] 07 p3054 N94-26125
Diffusion of substitutional elements in Ti in its hcp phase
[DE93-633762] 07 p2733 N94-26160
Fermi-liquid to non-Fermi-liquid transition in a dynamical generalization of the CPA in a disordered Hubbard model
[DE94-601875] 07 p2714 N94-26169
Zr-Sn-Nb alloys: Preliminary studies
[DE93-633767] 07 p2734 N94-26263
Analysis of the effect on growth kinetics of gamma prima phase in Inconel 713C alloys
[DE93-633763] 07 p2735 N94-26294
Eutectic transformation L in equilibrium to Zr6Fe23 + Fe(tau) in the Fe-Zr system
[DE93-633766] 07 p2735 N94-26295
C-periodicity and the physical mass in the 3-state Potts model
[DE94-601551] 07 p3019 N94-26423
Electron microscopy of AlN-SiC interfaces and solid solutions
[DE94-002449] 07 p3059 N94-26765
Cosmological phase transitions
[DE94-003001] 07 p3104 N94-26786
Titanium 1992: Science and Technology, volume 1
[AD-A274798-VOL-1] 07 p2739 N94-26799
Ultrastructure processing of macromolecular materials
[AD-A274460] 07 p2754 N94-27086
Morphology transitions during non-equilibrium growth processes
[ITN-94-85236] 07 p3065 N94-27243
Localization properties of one-dimensional electrified chains
[DE94-603672] 07 p3067 N94-27635
Second-order phase transition in (g(phi)4)2 theory
[DE94-603677] 07 p3067 N94-27638
Construction and test of experiment hardware for a space experiment on Spacelab mission IML-2
[DLR-FB-93-23] 07 p2903 N94-27743
A numerical approach to Stefan problem
[IPPCZ-334] 07 p2844 N94-27841
The Science Reports of the Research Institutes, Tohoku University. Series A: Physics, Chemistry, and Metallurgy. Volume 38, No. 1: Amorphous Materials 14
[JTN-94-80610] 07 p2744 N94-28158
Differential scanning calorimetric study of solid state amorphization and crystallization in Zr/Co and Zr/Ni multilayers 07 p2745 N94-28161
Formation and crystallization of hydrogen-induced amorphous Ti3InH(4.5) alloy 07 p2745 N94-28163
Formation of glassy Pd-Ni-P alloys by mechanical alloying and their structure and thermal stability
07 p2746 N94-28168
Production of an amorphous Fe(75)Si(10)B(15) sheet by a metallic mold casting method and its properties
07 p2746 N94-28170
Directional solidification studies in Ni-Al alloys
[DE94-005562] 08 p3201 N94-28527
Experimental and theoretical studies of molecular solids
[AD-A275511] 08 p3485 N94-28668
Crystal structure of La(2-x)Ba(x)CuO4
[DE94-707688] 08 p3511 N94-28750
Structure of ordinary ice I(sub h). Part 1: Ideal structure of ice
[AD-A275149] 08 p3486 N94-29021
Differential Scanning Calorimetry (DSC) for planetary surface exploration 08 p3236 N94-29776
Boundary-induced phase transitions in equilibrium and non-equilibrium systems
[DE94-608137] 08 p3199 N94-30111
Investigation of the phase equilibria and phase transformations associated with the Bi2Sr2CaCu2O(y) superconductor
[DE94-004889] 08 p3519 N94-30691
Structure and dynamics of microemulsions in bulk, at interfaces, and in confined geometries
[DE94-006043] 09 p3633 N94-31526
Fermi surface instability at 0.4 K in a heavy-fermion YbBiPt: SDW?
[DE94-006224] 09 p3899 N94-31916
Amorphous/crystalline structure and phase transformations in metastable semiconducting Ge(1-x)Sn(x)
[DE94-006659] 09 p3901 N94-32115
The 10th International Conference on Internal Friction and Ultrasonic Attenuation in Solids (ICIFUAS)
[AD-A276849] 09 p3902 N94-32209
Fabrication, phase transformation studies and characterization of SiC-AlN-Al2OC ceramics
[DE94-008587] 09 p3659 N94-32657
Surface probes of porous toluene/water ices: Adsorption kinetics and annealing spectra measured by second harmonic generation
[DE94-007564] 09 p3637 N94-32743
Interface controlled amorphization of crystalline Ni/Ti multilayers
[DE94-008685] 09 p3906 N94-32884
Irradiation-induced phase transformations in zirconium alloys
[DE94-008484] 09 p3648 N94-32993
A tandem microscopic-electrochemical examination of a charge-induced surface phase sequence: Ordered Au(110) in aqueous iodide electrolytes as probed by potentiodynamic scanning tunneling microscopy
[AD-A276905] 09 p3875 N94-33277
Displacive transformation in ceramics
[AD-A278442] 10 p4026 N94-33539
Calculation of phase stability in Zr-Nb-Ru using LMTO and the cluster variation method
[AD-A278556] 10 p4137 N94-33896
Fabrication, phase transformation studies, and characterization of SiC-AlN-Al2OC ceramics
[DE94-009649] 10 p4028 N94-33919
Calorimetric thermometry of meteoritic troilite: Preliminary thermometer relationships
11 p4355 N94-35399
Mineralogy of artificially heated carbonaceous chondrites 11 p4352 N94-35477
The silent phase transition in mesonic bags and lattice theory
[DE94-616852] 11 p4321 N94-35583
An indigenously developed photoacoustic spectrometer for study of actinide spectroscopy
[DE94-616508] 11 p4235 N94-35592
Kinetics of phase transformations in glass forming systems
[NASA-CR-196082] 11 p4245 N94-35977
Twin spacing versus size of a monocrystal for the nonstoichiometric 1:2:3 superconductors
[DE94-615511] 11 p4340 N94-36029
Twin spacing and the structural phase transitions in 1:2:3 high-Tc superconductors
[DE94-615647] 11 p4340 N94-36041
The structural changes of water ice I during warmup
11 p4239 N94-36144
Calorimetric thermobarometry of experimentally shocked quartz 11 p4240 N94-36174
Irradiation-related amorphization and crystallization: In situ transmission electron microscope studies
[DE94-009823] 11 p4241 N94-36222
Electrical conductivity of hydrogen shocked to megabar pressures
[DE93-019632] 11 p4238 N94-36237
Phase transitions in crystalline solids 1
[DE94-619029] 12 p4532 N94-36542
Theory of metal insulator transition in strongly correlated electron systems
[DE94-013135] 12 p4438 N94-37295

Non-equilibrium evolution of the disoriented chiral condensate in heavy-ion collisions
[DE94-012897] 12 p4522 N94-37310
Analytical electron microscopy examination of solid reaction products in long-term test of SRL 200 waste glasses
[DE94-005482] 12 p4411 N94-37380
Studies of the III-V compounds in the megabar regime
[DE94-012488] 12 p4537 N94-37435
Laser probing of interfaces
[DE94-011300] 12 p4449 N94-37628

PHASE VELOCITY
Wave propagation characteristics of short-period crustal phases near ARCESS and NORESS
[AD-A265959] 01 p0275 N94-11102
The phase mixing of shear Alfven waves
[DE93-624920] 04 p1581 N94-17688
Modeling and new equipment definition for the vibration isolation box equipment system
[NASA-CR-193185] 04 p1379 N94-17763
Azo polymers for optical storage 3: Effect of film thickness on net phase retardation and writing speed
[AD-A272994] 05 p1705 N94-21267
Superluminous laser pulse in an active medium
[DE94-007110] 09 p3720 N94-32684

PHASE-SPACE INTEGRAL
Correlated states of a quantum oscillator acted by short pulses 01 p0380 N94-10609
Phase space representations and quantum probability theory
[DE93-629863] 04 p1556 N94-18154

PHASED ARRAYS
Electrical characterization of the JET A(sub 2) antenna: Comparison of model with measurements Wade, T.
[DE93-012964] 02 p0607 N94-14291
Direct electron heating and current drive with fast waves in D3-D
[DE93-013028] 02 p0801 N94-14293
Experimental instrumentation system for the Phased Array Mirror Extendible Large Aperture (PAMELA) test program
[NASA-CR-194421] 02 p0705 N94-14430
Overview of Enhanced Data Stream Array Processor (EDSAP)
[AD-A266986] 03 p1158 N94-15492
Experimental evaluation of an adaptive focusing algorithm for a microwave planar phased-array hyperthermia system at UCSF
[AD-A267004] 03 p1121 N94-15634
System architecture of optically controlled phased array radar
[AD-A267056] 03 p0988 N94-15667
Phased array antenna analysis using hybrid finite element methods
[AD-A267620] 03 p1002 N94-17196
True time delay optically controlled dual band transmitter
[AD-A267663] 03 p1003 N94-17228
Proceedings of the 1992 Antenna Applications Symposium, volume 1
[AD-A268167] 03 p1005 N94-17431
Power compensators for phased operation of antenna arrays on JET and D3-D
[DE93-013208] 04 p1581 N94-17694
Interinjection-locked quasioptical power combiners and phased arrays
[AD-A271178] 05 p2015 N94-20214
Quartz/fused silica chip carriers
[NASA-CR-194154] 05 p2016 N94-20340
Optical beam forming techniques for phased array antennas 05 p1727 N94-20442
Phased array antenna with couplers in spatial filter arrangement
[CA-PATENT-1,296,098] 05 p1737 N94-21031
Investigation of the effect of various oxide and fluoride additives on the microstructure, electronic properties, and phase shifting ability of Ba(1-x)Sr(x)TiO3
[AD-A271756] 05 p2027 N94-21303
Effect of errors on the phase centre and pointing angle of phased array antennas 05 p1746 N94-22162
AlGaAs laser diode FM spectrum: Phased array antenna application 05 p1746 N94-22196
Adaptive digital beamforming for a CDMA mobile communications payload 06 p2274 N94-22743
Calibration block for digital beam forming antenna
[PB93-204550] 06 p2294 N94-23773
Calibration network intended for phase-array antennas at 3 GHz
[PB93-204352] 06 p2297 N94-24530
Project PARAS: Phased array radio astronomy from space 07 p3081 N94-25703
Characterization of an LCD for use as a programmable phase shifter to produce a single-lobed far-field pattern in a phased array
[AD-A273883] 07 p3034 N94-25729
A current evaluation of the digital beamforming testbed at Rome Laboratory
[AD-A274311] 07 p3032 N94-26881
Design and control of phased ICRF antenna arrays
[DE94-002796] 07 p3046 N94-27261
Solid-state, active-phased arrays: Some aspects of receiver design
[AD-A275893] 08 p3527 N94-28779
Pointing mechanisms for the Shuttle Radar Laboratory 08 p3162 N94-29638
A combined electron beam/optical lithography process step for the fabrication of sub-half-micron-gate-length MMIC chips 08 p3240 N94-30445
The development of active integrated antennas and a design methodology
[ISBN-0-315-86119-3] 09 p3675 N94-31708
Proceedings of the 1993 Antenna Applications Symposium, volume 1
[AD-A277202] 09 p3676 N94-32049
Proceedings of the 1993 Antenna Applications Symposium, volume 2
[AD-A277203] 09 p3677 N94-32050
Processing and characterization of functionally gradient ceramic materials
[AD-A277154] 09 p3657 N94-32367
Processing, packaging, and characterization of electroceramic materials for phased array antennas
[AD-A280251] 12 p4432 N94-36743
Baseline antenna design for space exploration initiative
[NASA-CR-196298] 12 p4435 N94-37255

PHENOL FORMALDEHYDE
Primaset (tm): A safer material for aircraft interior applications 01 p0018 N94-10772
Advanced phenolic systems for aircraft interiors 01 p0018 N94-10776
Fire resistance and mechanical properties for phenolic prepregs 01 p0020 N94-10786

PHENOLIC RESINS
Primaset (tm): A safer material for aircraft interior applications 01 p0018 N94-10772
Advanced phenolic systems for aircraft interiors 01 p0018 N94-10776
Initial evaluation of burn characteristics of phenolic foam runway brake arrestor material
[DOT/FAA/CT-TN93/7] 06 p2253 N94-23335
Soft ground arresting system for airports
[DOT/FAA/CT-93/80] 07 p2680 N94-26202
Measurement and modelling of bolted joint stress relaxation in plastics
[PB94-124849] 08 p3318 N94-28841
Fireproof barrier system for composite structure
[AD-D016158] 10 p4019 N94-33763

PHENOLOGY
Analytical framework for modeling scale-related variabilities in remote sensing 02 p0685 N94-13592
Recent advances in radar remote sensing of forest 03 p0991 N94-15897

PHENOLS
NT BISPHENOLS
Preconversion catalytic deoxygenation of phenolic functional groups
[DE93-017034] 03 p0950 N94-16912
Interpenetrating polymer network acoustic damping material
[AD-D015889] 03 p0969 N94-16916
Proton transfer dynamics and cluster ion fragmentation in phenol/ammonia cLusters
[AD-A269133] 04 p1348 N94-18256
Water-enhanced solvation of organics
[DE93-040297] 05 p1683 N94-21947
Effects of p-chlorophenol on sulfate reduction in marine sediments 07 p2870 N94-28150
Journal of NIRE, Vol. 2, No. 2
[JTN-94-80552] 08 p3187 N94-28675
Methanol-mediated continuous extraction of phenolic compounds from coal liquid 08 p3188 N94-28679

PHENOMENOLOGY
Nonlinear analysis, scientific computation, and continuum mechanics applied to the science of materials
[AD-A266641] 02 p0817 N94-14680
Phenomenological explanation of elastic anomalies in superlattices
[DE93-017475] 04 p1594 N94-17871
Institute for Nuclear Theory
[DE93-017369] 04 p1568 N94-18824
Thermally activated low temperature creep and primary water stress corrosion cracking of NiCrFe alloys
[DE94-001756] 06 p2241 N94-23219
Harvard University High Energy Physics
[DE94-002406] 07 p3032 N94-26119
Research on elementary particle physics. Task P: Studies in theory and phenomenology of elementary physics
[DE94-004955] 08 p3483 N94-28566
Local instabilities and the transition to chaos of non-linear waves
[PB94-170578] 11 p4341 N94-36213
CP violation outside the standard model phenomenology for pedestrians
[DE94-002216] 12 p4511 N94-36512

PHENYLALANINE
Theoretical prediction of the UV adsorption and fluorescence spectra of tyrosine and phenylalanine
[AD-A266970] 03 p0943 N94-15111

PHENYLS
NT POLYCHLORINATED BIPHENYLS
NT POLYPHENYLS
The synthesis of photocrosslinkable chalcone-bearing polyphosphazenes
[AD-A264915] 01 p0092 N94-11849
The photophysics of poly(methylphenylphosphazene)
[AD-A267321] 03 p0970 N94-16949
Di(hydroxyphenyl)- 1,2,4-triazole monomers
[NASA-CASE-LAR-14440-2] 06 p2252 N94-23075
Metal-catalyzed alkynylation of (Bromophenyl)Oligophenylenes: A rapid route to thermoset precursors of high density monolithic glass-like carbon
[AD-A273219] 06 p2260 N94-24863
Planar poly(p-phenylene) derivatives: Ladder formation for maximization of extended conjugation
[AD-A273220] 06 p2260 N94-24922
A relaxation study of poled nonlinear optical polymers by infrared reflection-absorption spectroscopy
[AD-A277513] 09 p3663 N94-33054
Kinetics and mechanisms of reactions involving small aromatic reactive intermediates
[DE94-009475] 10 p4018 N94-33932

PHILIPPINES
Status of remote sensing and Geographic Information System (GIS) applications in the Environment and Natural Resources (ENR) sector 01 p0036 N94-10687
Philippine thrust on environmental research relating to global change 07 p2873 N94-28279
Forecasters handbook for the Philippine Islands and surrounding waters
[AD-A277993] 09 p3787 N94-33089

PHILOSOPHY
NT PARADOXES
Heidegger's thinking 02 p0736 N94-13442
Identity: Quarrelling with an unproblematic notion
[LP-93-04] 08 p3455 N94-30327

PHOBIAS
NT FEAR

PHOBOS
Interdisciplinary scientist participation in the Phobos mission
[NASA-CR-193715] 01 p0482 N94-12446
A simultaneous estimation of the mass of Mars and its natural satellites, Phobos and Deimos, from the orbital perturbations on the Mariner 9, Viking 1, and Viking 2 orbiters 03 p1279 N94-16347
A mission concept of Phobos/Deimos exploration 03 p1287 N94-16387
The spectrum of Phobos from Phobos 2 observations at 0.3-2.6 microns: Comparison to previous data and meteorite analogs 03 p1295 N94-16429
A mission to Mercury and a mission to the moons of Mars
[NASA-CR-195530] 06 p2195 N94-24619
Project APEX: Advanced manned exploration of the Martian moon Phobos 07 p3079 N94-25688
The surface and interior of Phobos 11 p4355 N94-35400
The mass of Mars, Phobos, and Deimos, from the analysis of the Mariner 9 and Viking Orbiter tracking data 11 p4364 N94-35461

PHONEMES
Speech synthesis with artificial neural networks 05 p1743 N94-20245
On the quality of synthetic speech evaluation and improvements
[ETN-94-95298] 06 p2304 N94-25234
Researches of the Electrotechnical Laboratory. No. 955: Speech recognition by description of acoustic characteristic variations
[JTN-94-80604] 07 p2775 N94-27249

PHONEMICS
Neural networks applied to the phonemic segmentation of speech 09 p3686 N94-33152
Segment-based acoustic models for continuous speech recognition
[AD-A280332] 12 p4434 N94-37032

PHONETICS
Subphonetic acoustic modeling for speaker-independent continuous speech recognition
[AD-A275217] 08 p3244 N94-29303

PHONOCARDIOGRAPHY
NT ECHOCARDIOGRAPHY

PHONONS
Energy transfer dynamics and impact sensitivity
[DE93-009551] 01 p0098 N94-11269
On the theory of phononiton in cubic semiconductors with a degenerate valence band
[DE93-613539] 01 p0402 N94-11660
Basic optical studies of high T(c) oxide superconductors
[AD-A268148] 03 p1014 N94-17428
Polaron tunneling in high-temperature superconductors
[DE93-016880] 04 p1593 N94-17754
Suppressed electron-phonon scattering in superlattices
[AD-A270834] 04 p1604 N94-19597
Solid-state dynamics in novel semiconductor nanostructures
[AD-A271249] 04 p1605 N94-19725
The multicomponent lineshape of the anharmonic A(1)(TO) phonon in PbTiO3
[DE93-018995] 05 p1970 N94-19971
Phonons and metastability in compressed nitrogen
[DE93-019913] 05 p2016 N94-20318
Solid-state dynamics and quantum transport in novel semiconductor nanostructures
[AD-A272955] 05 p2027 N94-21248
Inelastic neutron scattering of (gamma)-iron, and the determination of the elastic constants by lattice dynamics
[DE94-000694] 05 p1978 N94-22573
Energy transfer in solid explosives
[DE94-001523] 06 p2265 N94-23778
Lattice dynamics of Ba(1-x)K(x)BiO3 as studied by neutron scattering and computer simulation
[DE93-617053] 06 p2567 N94-25424
Strongly interacting fermion systems
[DE94-002674] 07 p3021 N94-26677
Effect of phonon dispersion on properties of exciton in magnetic field
[DE93-634756] 08 p3481 N94-28469
Vibrational properties of homopolar and heteropolar surfaces and interfaces of the CdTe/HgTe system
[DE94-608105] 08 p3516 N94-30069
Interband optical absorption in the Wannier-Stark ladder under the electron-LO-phonon resonance condition
[DE94-608097] 08 p3267 N94-30092
Procedures for basic inverse problems: Black body radiation problem and phonon density of states problem
[ISBN-0-315-85757-9] 08 p3525 N94-30244
Experimental investigation of phonon eigenvectors using x ray interference fields
[ETN-94-95751] 09 p3865 N94-31511
A rejection method for selection of scattered states
[DE94-012232] 12 p4517 N94-37209

PHOSGENE
Infrared absorption spectroscopy of the weakly bonded CO-Cl2 complex
[AD-A271757] 05 p2027 N94-21304

PHOSPHATES
NT ADENOSINE TRIPHOSPHATE
NT AMMONIUM PHOSPHATES
NT CALCIUM PHOSPHATES
NT CYCLIC AMP
NT INDIUM PHOSPHATES
NT POTASSIUM PHOSPHATES
Advanced zinc phosphate conversion and pre-ceramic polymetallosiloxane coatings for corrosion protection of steel and aluminum, and characteristics of polyphenyletheretherketone-based materials
[DE93-008717] 01 p0088 N94-10891
In situ secondary ion mass spectrometry analysis
[DE93-012185] 01 p0076 N94-11140
Radiation-induced aperiodicity in irradiated ceramics
[DE93-013335] 01 p0091 N94-11698
Tandem mass spectrometric analysis of phosphate esters
[AD-A265483] 01 p0078 N94-12009
Development of vanadium-phosphate catalysts for methanol production by selective oxidation of methane
[DE93-016850] 03 p0949 N94-16897
An ultraviolet faraday rotator glass
[AD-D015879] 04 p1371 N94-18529
Advanced civil engineering materials based on inorganic polymers
[AD-A270837] 04 p1374 N94-19600
Transient studies of low temperature catalysts for methane conversion
[DE93-041232] 05 p1680 N94-20934
Spectroscopic studies of magnetic transitions in TbPO4
[DE94-001274] 05 p2035 N94-22565
Infrared analysis of vapor phase deposited tricresylphosphate (TCP)
[NASA-TM-106423] 06 p2253 N94-23371
Auto-metasomatism of the western lunar highlands: Result of closed system fractionation and mobilization of a KREEPy trapped liquid 06 p2615 N94-24367
Zinc(2) oxide stability in alkaline sodium phosphate solutions at elevated temperatures
[DE94-003316] 07 p2715 N94-26320
Development of K(1-x)Na(x)TiOPO4 crystals for nonlinear applications
[AD-A274336] 07 p3063 N94-27055
Effect of different ions on the anodic behaviour of alloy 800 in chloride solutions at high temperature
[DE94-602982] 07 p2743 N94-27832
Growth of hydrocarbon-rich microalga Botryococcus braunii in secondarily treated sewage and its consumption of nitrate ion and phosphate ion
08 p3387 N94-29519
Structural analysis of amorphous phosphates using high performance liquid chromatography
[DE94-004791] 08 p3199 N94-30723
Development of vanadium-phosphate catalysts for methanol production by selective oxidation of methane
[DE94-006759] 09 p3759 N94-31272
Carbonates, surfates, phosphates, nitrates, and organic materials: Their association in a Martian meteorite
09 p3952 N94-33239
Polyurethane self-priming topcoats
[AD-D016160] 10 p4030 N94-34285
Capillary column GC-MS/MS confirmation of phosphate esters with a hybrid tandem mass spectrometer
[AD-A278748] 11 p4238 N94-36091
Isolated SO4-2 and PO4-3 anions do not exist
[AD-A278831] 12 p4512 N94-36521

PHOSPHAZENE
Ring-opening polymerization of phosphazenes
[AD-A265000] 01 p0090 N94-11292
Synthesis, characterization, and modification of poly(organophosphazenes), that bear both 2,2,2-trifluoroethoxy and phenoxy groups
[AD-A264913] 01 p0092 N94-11847
Radiation-induced modifications of allylamino-substituted polyphosphazenes
[AD-A264914] 01 p0092 N94-11848
The synthesis of photocrosslinkable chalcone-bearing polyphosphazenes
[AD-A264915] 01 p0092 N94-11849
Synthetic lubricants and high-performance functional fluids: Phosphazenes
[ARL-TR-45] 02 p0580 N94-14126
The photochemistry of poly(methylphenylphosphazene)
[AD-A267320] 03 p0970 N94-16948
The photophysics of poly(methylphenylphosphazene)
[AD-A267321] 03 p0970 N94-16949
A preliminary evaluation of the phosphazene resin PPZ
[AD-A273674] 06 p2263 N94-25410
Phosphazene-containing amine as curing agent for phthalonitrile-base polymer
[AD-D016029] 07 p2755 N94-27147
Inorganic polymer engineering materials
[DE94-008519] 09 p3659 N94-32655

PHOSPHIDES
NT GALLIUM PHOSPHIDES
NT INDIUM PHOSPHIDES
NT SCHREIBERSITE
Growth of new materials for solid state laser applications. The growth of ZnGeP2 by the vertical Bridgman method
[NASA-CR-194571] 03 p1038 N94-15530
Photoluminescence spectroscopy of zinc germanium diphosphide (ZnGeP2)
[AD-A270705] 05 p1678 N94-19953
Studies of high temperature ternary phases in mixed-metal-rich early transition metal sulfide and phosphide systems
[DE94-006034] 08 p3209 N94-30336

PHOSPHINES
Remote plasma enhanced chemical vapor deposition of GaP with in situ generation of phosphine precursors
01 p0399 N94-11440
Synthesis, reactivity, and characterization of (-hexacarbocyclic) manganese dicarbonyl complexes with sulfur and phosphorus ligands
[AD-A267592] 03 p0930 N94-17192
Photochemically induced transformations of transition complexes
[AD-A271112] 05 p2014 N94-19982
High efficiency InP solar cells from low toxicity tertiarybutylphosphine
[NASA-TM-106598] 10 p4039 N94-33611
Detection of the 267 GHz J = 1-0 rotational transition of PH3 in Saturn with a new Fourier transform spectrometer
[NASA-CR-194364] 10 p4162 N94-34718
Study on extraction behavior of TRPO with different composition
[DE94-620287] 12 p4412 N94-37534

PHOSPHONIUM COMPOUNDS
Development of immobilized ligands for actinide separations
[DE94-012714] 12 p4410 N94-37284

PHOSPHORESCENCE
Thermographic properties of eight blue-emitting phosphors
[DE93-011459] 01 p0078 N94-11622
The photophysics of poly(methylphenylphosphazene)
[AD-A267321] 03 p0970 N94-16949
Dynamics of metastable states in supersonic beams
[ITN-94-85232] 07 p3028 N94-27760

PHOSPHORIC ACID
Qualitative analysis of rare earth elements contained in the phosphogypsum
[DE93-614153] 07 p2716 N94-26518

PHOSPHORS
Thermographic properties of eight blue-emitting phosphors
[DE93-011459] 01 p0078 N94-11622
Preparation and investigation of improved low voltage electron excitable phosphors
[AD-A266852] 03 p0963 N94-14948
Fiber optic temperature sensor using a Y2O2S:Eu thermographic phosphor
[DE94-000331] 06 p2543 N94-23461
Single crystal faceplate evaluation
[AD-A277922] 10 p4038 N94-33399
High definition TV projection via single crystal faceplate technology
[AD-A277850] 10 p4034 N94-33768

PHOSPHORUS
NT PHOSPHORUS ISOTOPES
Machining aspects of nickel-phosphorus coatings
[DE93-013037] 02 p0580 N94-14311
Multicrystalline silicon solar cells: Gettering optimization and characterization
[DE93-015001] 02 p0705 N94-14861
Synthesis, reactivity, and characterization of (-hexacarbocyclic) manganese dicarbonyl complexes with sulfur and phosphorus ligands
[AD-A267592] 03 p0930 N94-17192
Core formation in the Moon: The mystery of the excess depletion of Mo, W and P 05 p2095 N94-20651
Polymeric nitrogen
[DE93-040544] 05 p1706 N94-21512
Refractive index behaviour of phosphorus-doped planar silica waveguides, appendix 7 05 p1989 N94-21601
Simplified high-efficiency silicon cell processing
[DE94-002683] 07 p2857 N94-26617
He(+) and H(+) microbeam damage, swelling and annealing in diamonds
[DE94-601912] 07 p3063 N94-26987
Electron microscopy studies of undoped and phosphorus doped Si:H and Si,C:H films
[DE94-004738] 07 p3069 N94-27757
Formation of glassy Pd-Ni-P alloys by mechanical alloying and their structure and thermal stability
07 p2746 N94-28168
Determination of BPSG thin-film properties using IR reflection spectroscopy of product wafers
[DE94-006591] 09 p3634 N94-32110

PHOSPHORUS COMPOUNDS
NT ADENOSINE TRIPHOSPHATE
NT AMMONIUM PHOSPHATES
NT CALCIUM PHOSPHATES
NT CYCLIC AMP
NT GALLIUM PHOSPHIDES
NT INDIUM PHOSPHATES
NT INDIUM PHOSPHIDES
NT ORGANIC PHOSPHORUS COMPOUNDS
NT PHOSPHATES
NT PHOSPHAZENE
NT PHOSPHIDES
NT PHOSPHINES
NT PHOSPHONIUM COMPOUNDS
NT PHOSPHORIC ACID
NT PHOSPHORUS POLYMERS
NT POTASSIUM PHOSPHATES
NT SCHREIBERSITE
Aluminum-phosphorus chemistry: Preparation and structural characterization of (Et2AlP(SiMe3)2)2, Et(Cl)2Al(dot)P(SiMe3)3, and i-Bu2(Cl)Al(dot)P(SiMe3)3
[AD-A265268] 01 p0078 N94-11683
The electrochemistry of the solvated electron: A study of its properties and of its applications
[ETN-94-95313] 06 p2236 N94-25296
Synthesis and molecular structures of R(Me3CCH2)2In-E(SiMe3) (R = Me3CCH2, E = P or As; R = Me, E = P)
[AD-A275020] 08 p3486 N94-29131
Adhesion of phospholipid monolayers to planar supports deposited with the Langmuir-Blodgett technique
[PB94-148699] 10 p4029 N94-34102
Highly fluorinated polymers
[NASA-CR-196270] 12 p4422 N94-37025

PHOSPHORUS ISOTOPES
A calibration of the production rate ratio P-21/P-26 by low energy secondry neutrons: Identification of Ne spallation components at the 10(exp 6) atoms/g level in terrestrial samples 03 p1187 N94-16194
PHOSPHORUS POLYMERS
Fire-resistant hydrolytically stable poly(arylene phosphine oxide) material systems 01 p0019 N94-10780
PHOSPHORYLATION
Activation by G protein beta gamma subunits of G protein-coupled receptor kinase 07 p2931 N94-27534
PHOTOABSORPTION
Photoabsorption and Compton scattering in ionization of helium at high photon energies
[DE94-000380] 05 p1974 N94-21658
Single and double ionization of helium by high-energy photon impact
[DE94-000381] 05 p1975 N94-21785
The effect of Compton scattering on the double to single ionization ratio in helium
[DE94-000884] 05 p1827 N94-22390
Identification of electronic transitions in polyacetylene by acoustic phonon spectroscopy
[DE94-009324] 10 p4138 N94-34383
PHOTOACOUSTIC MICROSCOPY
Atomic oxygen damage characterization by photothermal scanning 09 p3598 N94-31051
PHOTOACOUSTIC SPECTROSCOPY
Application of the infrared photoacoustic spectroscopy to the study of the cure mechanisms of structural epoxy adhesives 01 p0061 N94-10040
An electroacoustic transducer for purposes of photoacoustic spectroscopy
[IFTR-7/1992] 03 p1013 N94-17071
Modern photoacoustic spectroscopy problems. Theory and experiment (a review)
[IFTR-41/1993] 07 p2716 N94-26823
Identification of electronic transitions in polyacetylene by acoustic phonon spectroscopy
[DE94-009324] 10 p4138 N94-34383
An indigenously developed photoacoustic spectrometer for study of actinide spectroscopy
[DE94-616508] 11 p4235 N94-35592
PHOTOCATHODES
Interference photocathode
[AD-D015770] 01 p0132 N94-10382
Gamma-insensitive optical focal plane array
[DE93-013100] 02 p0792 N94-14317
Absolute detection efficiency of a micro-channel plate detector to x rays in the 1-100 KeV energy range
[DE93-012592] 02 p0789 N94-14460
Microchannel plate imaging detectors for the ultraviolet 03 p0901 N94-15037
RF phase stabilization for RF photocathode gun through electro-optical monitoring
[DE93-019059] 04 p1406 N94-19310
Performance of the high brightness linac for the Advanced Free Electron Laser Initiative at Los Alamos
[DE93-040141] 05 p1816 N94-20277
CsI and some new photocathodes
[DE93-019387] 05 p1750 N94-20314
Electron quantum yields from a barium photocathode illuminated with polarized light
[DE93-019232] 05 p1980 N94-20475
SLD results from the study of polarized Z(sup 0) produced at the SLC
[DE93-041020] 05 p1982 N94-21952
Low voltage electron beam lithography
[AD-A278204] 10 p4038 N94-33375
Streak tube photocathode development program
[DE94-009905] 11 p4270 N94-36350
PHOTOCHEMICAL REACTIONS
NT PHOTOCHROMISM
NT PHOTODECOMPOSITION
NT PHOTOLYSIS
NT PHOTOSYNTHESIS
NT RADIOLYSIS
Photoinitiated radical polymerization of liquid monomers in microgravity 01 p0124 N94-10246
Symmetry lowering in crystalline solid solutions: A study of cinnamamide-thienylacrylamide by x ray and neutron diffraction and solid-state photochemistry
[DE93-010871] 01 p0394 N94-10301
Photochemical modelling of Venus clouds using Pioneer Venus data
[NASA-CR-194108] 01 p0434 N94-10823
Dynamics of charge-transfer excited states relevant to photochemical energy conversion
[DE93-013981] 01 p0263 N94-11116
The synthesis of photocrosslinkable chalcone-bearing polyphosphazenes
[AD-A264915] 01 p0092 N94-11849
NRL review for 1993
[AD-A265666] 01 p0497 N94-12334
A novel photosensitive polyimide resist consisting of a soluble polyimide and a bis(perfluorophenyl azide) as a cross-linker
[AD-A265998] 01 p0093 N94-12353
Photogenerated base in polymer imaging. Synthesis and photopatterning of poly(2-cyano-2-(p-vinylphenyl) butanoic acid)
[AD-A265288] 01 p0095 N94-12585
Infrared absorption spectroscopy and chemical kinetics of free radicals
[DE93-015078] 02 p0562 N94-13004
Diagnostic studies of the HxOy-NxOy-O3 photochemical system using data from NASA GTE field expeditions
[NASA-CR-193672] 02 p0706 N94-13170
Modeling of the partitioning of reactive odd nitrogen in the lower stratosphere using aircraft measurements of NOy, NO, and other trace species
[NASA-CR-194305] 02 p0714 N94-13707
Chemistry and transport in a multi-dimensional model
[NASA-CR-194425] 02 p0716 N94-13969
Photochemical dynamics of surface oriented molecules
[DE93-016289] 02 p0784 N94-13983
Lawrence Berkeley Laboratory Chemical Sciences Division
[DE93-015260] 02 p0851 N94-14401
Design, synthesis and characterization of novel nonlinear optical polymers
[AD-A267035] 03 p0964 N94-15675
Organic polymeric electro-optic materials: Synthesis, processing, and device applications
[AD-A267133] 03 p0964 N94-15688
Photochemistry in thin polymeric films
[AD-A266716] 03 p0964 N94-15729
Molecular beam studies of reaction dynamics
[DE93-015035] 03 p1181 N94-15995
Binding of carbon dioxide to metal macrocycles: Toward a mechanistic understanding of electrochemical and photochemical carbon dioxide reduction
[DE93-016244] 03 p0949 N94-16870
The photochemistry of poly(methylphenylphosphazene)
[AD-A267320] 03 p0970 N94-16948
The photophysics of poly(methylphenylphosphazene)
[AD-A267321] 03 p0970 N94-16949
Optical studies of glasses embedded with inorganic ions and organic dyes
[AD-A268146] 03 p1199 N94-17455
Pulse radiolytic studies of electron transfer processes and applications to solar photochemistry
[DE93-018715] 04 p1464 N94-17781
Energy efficiency and the environment: Innovative ways to improve air quality in the Los Angeles Basin
[DE93-016964] 04 p1473 N94-18050
Research at the Notre Dame Radiation Laboratory
[DE93-018716] 04 p1566 N94-18165
Experimental and theoretical investigation of surface chemistry induced by direct and indirect electronic excitation
[AD-A268846] 04 p1348 N94-18221
Photo-induced and electrooptic properties of (Pb,La)(Zr,Ti)O3 films
[DE93-017496] 04 p1371 N94-18519
Vibrational dynamics in photoinduced electron transfer
[DE93-040874] 04 p1567 N94-18533
Photodissociation studies of polyatomic free radicals
[AD-A270084] 04 p1350 N94-18799
Summaries of FY 1993 research in the chemical sciences
[DE93-011855] 04 p1632 N94-18915
Oligomer and mixed-metal compounds, potential multielectron transfer catalysts
[DE93-019592] 04 p1350 N94-19017
Resonance Raman and photophysical studies of transition metal complexes in solution and entrapped in zeolites
[DE93-019892] 04 p1363 N94-19019
Kinetics programs for simulation of tropospheric photochemistry on the global scale
[DE93-019035] 04 p1476 N94-19104
The Mexico City 1991 lidar measurements campaign
[DE93-019960] 04 p1478 N94-19272
Laboratory studies of low temperature rate coefficients: The atmospheric chemistry of the outer planets
[NASA-CR-193485] 05 p1972 N94-20130
Recent developments in aromatic azo polymers research
[AD-A272966] 05 p1705 N94-21259
Polyimide-based electrooptic materials
[DE93-019416] 05 p1706 N94-21526
Requirements for the early atmosphere of Mars from nitrogen isotope ratios 05 p2144 N94-21669
Mars atmosphere loss and isotopic fractionation by solar-wind-induced sputtering and photochemical escape 05 p2144 N94-21672
Possible solutions to the problem of channel formation on early Mars 05 p2144 N94-21673
The young Sun and photochemistry of the primitive Martian atmosphere 05 p2145 N94-21679
Global emissions and models of photochemically active compounds
[DE93-040490] 05 p1852 N94-21969
Photochemical approaches to conversion of light to electricity or fuel
[DE94-001650] 05 p1849 N94-22048
Development of advanced cloud parameterizations to examine air quality, cloud properties, and cloud-radiation feedback in mesoscale models
[DE93-041164] 05 p1853 N94-22384
Infrared FEL photochemistry: Multiple-photon dissociation of freon gas
[DE94-000817] 05 p1820 N94-22585
Chemistry on the mesoscale: Modeling and measurement issues 06 p2413 N94-24390
Photoinduced charge separation in solid state and molecular systems
[DE94-001727] 06 p2563 N94-24537
Eddy mixing coefficient upper limit derived from the photochemical balance of O2 06 p2621 N94-24897
Translational-energy-resolved studies of photogenerated carrier-induced reactions on UHV semiconductor surfaces
[DE94-004169] 07 p3058 N94-26526
Mechanistic studies of opto-electronic materials and syntheses using multiple laser and surface diagnostics
[AD-A274528] 07 p3036 N94-26834
Numerical analysis of the photo-dissociation/radical oxidation of formaldehyde by ultraviolet light in a photolytic reactor
[AD-A274539] 07 p2868 N94-26843
Photochemical processes and the atmospheric airglow emissions of OH and Na in the mesospheric region
[INPE-5380-PUD/050] 07 p2882 N94-27334
How well was total ozone abundance inferred with Mariner 9? 07 p3108 N94-27891
The kinetics and dynamics of the coma of Halley's comet
[NASA-CR-194828] 07 p3105 N94-28184
Ozone production at a rural site in Georgia during the summer 1992 SOS campaign
[DE94-003989] 08 p3342 N94-28523
Laboratory studies of chemical and photochemical processes relevant to stratospheric ozone
[NASA-CR-189351] 08 p3347 N94-29549
Developing a diode array spectrometer for tropospheric chemistry studies 08 p3362 N94-29752
Photochemistry in constrained spaces: Zeolites and layered double metal hydroxides
[DE94-004958] 08 p3200 N94-30769
Proceedings of the Seventeenth DOE Solar Photochemistry Research Conference
[DE94-005552] 09 p3759 N94-31648
Photopolymerization of cyclohexene oxide: A visible light initiating system and mechanistic investigations
[AD-A277110] 09 p3654 N94-31981
Mechanical properties of acrylate networks formed by visible laser-induced polymerization. 2. Control of the mechanical properties
[AD-A277111] 09 p3655 N94-31982
A model of the ion chemistry of electrified convection 09 p3868 N94-31993
Mechanisms of laser induced reactions in opaque heterogeneous environments
[AD-A276642] 09 p3717 N94-31996
The Sixth Symposium on Unconventional Photoactive Solids. Abstracts
[AD-A277198] 09 p3655 N94-32016
A visible light initiating system for free radical promoted cationic polymerization
[AD-A277164] 09 p3655 N94-32069
Radiation and photochemistry section
[DE94-008880] 09 p3873 N94-32757
Structural studies of photoinduced intramolecular electron transfer in cyclopentadienylnickelnitrosyl
[DE94-008467] 09 p3874 N94-32876
Dry deposition of PAN to grassland vegetation
[DE94-005111] 09 p3768 N94-32894
Mars atmospheric loss and isotopic fractionation by solar-wind-induced sputtering and photochemical escape 09 p3947 N94-33208
How well was total ozone abundance inferred with Mariner 9 09 p3947 N94-33212
Escape of Mars atmospheric carbon through time by photochemical means 09 p3948 N94-33214
Model calculations of radiative transfer and tropospheric chemistry 10 p4084 N94-33361
Model capabilities, 2-D 10 p3971 N94-33459
CO2 impulse response curves for GWP calculations
[DE94-004277] 10 p4081 N94-33736

Concurrent stabilization and imaging of a novel polymer for second harmonic generation via in situ photopolymerization
[AD-A278912] 11 p4243 N94-35588

Uniqueness of a solution of a steady state photochemical problem: Applications to Mars 11 p4370 N94-36151

H2O-H2SO4 system in Venus' clouds and OCS, CO, and H2SO4 profiles in Venus' troposphere 11 p4370 N94-36152

An investigation of solar wind effects on the evolution of the Martian atmosphere
[NASA-CR-193424] 12 p4549 N94-37012

Photochemistry without protons. Radical cation chemistry in zeolites
[DE94-012631] 12 p4412 N94-37439

The 1st International Symposium on Organic Photochromism: Molecules and Systems
[PB94-179488] 12 p4399 N94-37531

PHOTOCHEMISTRY
U PHOTOCHEMICAL REACTIONS

PHOTOCHROMISM
The 1st International Symposium on Organic Photochromism: Molecules and Systems
[PB94-179488] 12 p4399 N94-37531

PHOTOCLINOMETRY
U PHOTOGRAMMETRY

PHOTOCONDUCTIVITY
A thermal ionization model for the sustaining phase of lock-on in GaAs
[DE93-011558] 01 p0144 N94-11624

Electrical and optical properties of multiple quantum well structures and their applications to infrared detectors
[FFI-92/7012] 02 p0809 N94-14010

Characterization of InTISb grown by low pressure metalorganic chemical vapor deposition on GaAs substrate
[AD-A266878] 03 p1206 N94-14922

Impurity conduction photoconductor detectors 03 p0902 N94-15046

Lead chalcogenides based IR photosensitive array detectors with coordinate addressing 03 p0903 N94-15053

Electrical conductivity of ion implanted ladder and semi-ladder polymers
[AD-A267432] 03 p0970 N94-16978

Surface flashover of semiconductors: A fundamental study
[AD-A267382] 03 p1012 N94-17023

OSA proceedings on Ultrafast Electronics and Optoelectronics, volume 14
[AD-A267972] 03 p1014 N94-17410

Process to fabricate thick coplanar microwave electrode structures
[AD-D015913] 05 p1748 N94-19892

Photoconductive Semiconductor Switches for pulsed power applications
[DE93-019411] 05 p1750 N94-20294

Optically controlled current filamentation in GaAs photoconductive semiconductor switches
[DE93-019427] 05 p2016 N94-20296

Transport in microstructures in the microwave and millimeter-wave regime
[AD-A271875] 05 p2017 N94-20470

Advanced far infrared detectors
[DE93-040289] 05 p1988 N94-21528

Determination of surface recombination velocity and bulk lifetime in detector grade silicon and germanium crystals
[DE94-003886] 07 p3053 N94-26094

Fast photoconductor CdTe detectors for synchrotron x ray studies
[DE94-001334] 07 p3054 N94-26139

The optical properties of high-T(c) superconductors grown by pulsed laser deposition
[ISBN-0-315-84917-7] 07 p3039 N94-27962

Anisotropy in the electrical, magnetic and optical properties of Pb2Sr2RCu3O8
[ISBN-0-315-84930-4] 07 p3070 N94-27974

Transport properties of epitaxial lift off films
[NASA-TM-106156] 08 p3264 N94-29209

Study of the ultraviolet absorption and photoconduction spectra of polyimide films fabricated at various curing temperatures
[ISBN-0-315-85923-7] 08 p3218 N94-30036

Multifunctional macromolecules
[AD-A277347] 09 p3656 N94-32246

Low temperature materials --- indium gallium arsenides
[AD-A278703] 12 p4533 N94-36755

PHOTOCONDUCTORS
GaAs PCSS: High gain switching and device reliability
[DE93-009851] 01 p0401 N94-11605

Nonstationary behaviour of low background photon detectors 03 p0902 N94-15049

Performance testing of doped-germanium photoconductors for the ISO long wavelength spectrometer 03 p0905 N94-15066

Non-linear effects in doped-germanium photoconductors for the ISO long wavelength spectrometer 03 p0905 N94-15067

Extrinsic photoconductor detectors for the wavelength range 2 microns to 240 microns 03 p0906 N94-15073

Ionising radiation-induced effects in doped germanium FIR photoconductors 03 p0907 N94-15077

Silicon gallium doped photoconductor development for the AROME balloon borne instrument 03 p0908 N94-15087

A monolithic PbTeCCD focal plane array for MWIR imaging 03 p0910 N94-15100

Photodetector array having high pixel density
[AD-D015859] 04 p1432 N94-18731

Advanced far infrared detectors
[DE93-040289] 05 p1988 N94-21528

Fast photoconductor CdTe detectors for synchrotron x ray studies
[DE94-001334] 07 p3054 N94-26139

InTISb for long-wavelength infrared photodetectors and arrays
[AD-A275079] 08 p3512 N94-28872

Photoconductive switching for high power microwave generation
[PB94-137460] 08 p3244 N94-29177

The Sixth Symposium on Unconventional Photoactive Solids. Abstracts
[AD-A277198] 09 p3655 N94-32016

Fast acting optical deflection
[AD-A276630] 09 p3879 N94-32037

Bias-field scaling of terahertz radiation from large aperture photoconductors
[DE94-007534] 10 p4034 N94-33839

InTISb for long-wavelength infrared photodetectors and arrays
[AD-A280207] 12 p4524 N94-37149

Time-dependent simulations of filament propagation in photoconducting switches
[DE94-012146] 12 p4438 N94-37213

PHOTOCURRENTS
U ELECTRIC CURRENT
U PHOTOELECTRIC EMISSION

PHOTODECOMPOSITION
High-energy chemical processes: Laser irradiation of aromatic hydrocarbons
[DE94-008107] 09 p3720 N94-32707

PHOTODETACHMENT
Photodetachment studies on few-electron atomic negative ions
[DE93-008474] 01 p0358 N94-10154

Atomic beam studies relevant to the space environment
[AD-A268628] 03 p1186 N94-17436

Anionic states of LiFLi
[AD-A278830] 11 p4322 N94-35678

Fast beam studies of free radical photodissociation
[DE94-011380] 12 p4521 N94-37720

PHOTODETECTORS
U PHOTOMETERS

PHOTODIODES
New challenges in optical materials development
[DE93-011889] 01 p0383 N94-11676

Development of the one-component diode-array velocimeter
[AD-A265552] 01 p0171 N94-12533

An acoustic charge transport imager for high definition television applications
[NASA-CR-194518] 02 p0650 N94-14029

Vacuum ultraviolet instrumentation for solar irradiance and thermospheric airglow
[NASA-CR-194525] 02 p0652 N94-14684

Advanced high performance CdHgTe multiplexed arrays 03 p0903 N94-15051

X-ray spectroscopy with silicon pin and avalanche photo diodes 03 p0906 N94-15072

Improved optical radiation detectors and their calibration: 200 nm - 30 microns 03 p0906 N94-15075

Applications for large area silicon drift detectors on x ray and gamma ray astronomy 03 p0909 N94-15090

Measuring atmospheric dispersion with WLRS in multiple wavelength mode 03 p0916 N94-15582

Two wavelength satellite laser ranging using SPAD 03 p0916 N94-15584

Frequency resolution of an acousto-optical spectrometer
[AD-A267822] 03 p1035 N94-17401

The quantum efficiency of HgCdTe photodiodes in relation to the direction of illumination and to their geometry 05 p1735 N94-20512

Micro pulse laser radar
[NASA-CASE-GSC-13493-1] 06 p2294 N94-23827

CsI(Tl)-photodiode detectors for spectroscopy at low radiation levels
[MPI-PHE/92-22] 06 p2314 N94-25457

Elastic backscattering lidar for a MSTI satellite
[DE94-002701] 07 p2816 N94-26126

The automated rotating shadowband spectroradiometer
[DE94-001878] 08 p3269 N94-28464

Broadband EUV survey spectrometer for short-timescale experiments
[DE94-005459] 08 p3498 N94-28534

UV laser long-path absorption spectroscopy 08 p3343 N94-28595

Modeling the total dose radiation effects of Hg(1-x)Cd(x)Te photodiodes using numerical device simulators
[AD-A275235] 08 p3263 N94-29028

Miniaturization in x ray and gamma ray spectroscopy 08 p3236 N94-29773

Analysis of the photodiode boundary layer transition indicator
[DE94-005311] 09 p3701 N94-31268

Fiber optic transceiver for interfacing digital superconducting electronics
[DE94-008284] 10 p4040 N94-33842

High-sensitivity receiver for increasing multiplicity of measurement axes of Zygo's Heterodyne interferometer
[DE94-009916] 11 p4333 N94-35818

PHOTODISSOCIATION
Application of synchrotron radiation in chemical dynamics
[DE93-015040] 02 p0563 N94-13411

Thermochemistry of transition metal clusters
[DE93-016201] 02 p0571 N94-13977

Lawrence Berkeley Laboratory Chemical Sciences Division
[DE93-015260] 02 p0851 N94-14401

Investigation of the feasibility of optical diagnostic measurements at the exit of the SSME
[NASA-CR-193832] 02 p0553 N94-14682

Molecular processes in comets
[NASA-CR-194148] 03 p1239 N94-15188

Molecular beam studies of reaction dynamics
[DE93-015035] 03 p1181 N94-15995

Design of a formaldehyde photodissociation process for carbon and oxygen isotope separation
[DE93-016435] 03 p1039 N94-16450

Studies of combustion reactions at the state-resolved differential cross section level
[DE93-017605] 03 p0948 N94-16462

Extracavity frequency doubling study of a pulsed photodissociation iodine laser
[AD-A267893] 03 p1042 N94-17394

Removing CFC's from the atmosphere with lasers: A second look
[DE93-017516] 04 p1473 N94-18101

Photodissociation studies of polyatomic free radicals
[AD-A270084] 04 p1350 N94-18799

Photodissociation dynamics of cluster ions
[AD-A270296] 04 p1568 N94-18814

Unimolecular photodissociation dynamics of ketene (CH2CO): The singlet/triplet branching ratio and experimental observation of the vibrational level thresholds of the transition-state
[DE93-019252] 04 p1352 N94-19304

Ultraviolet absorption cross-sections of some carbonyl compounds and their temperature dependence
[AERONAUTICA-ACTA-A-368-1993] 04 p1353 N94-19456

Temperature dependence of ultraviolet absorption cross-sections of alternative hydrochlorofluorocarbons
[AERONAUTICA-ACTA-A-369-1993] 04 p1353 N94-19459

Ionization of H2(+) in intense laser fields
[DE93-019160] 05 p1818 N94-21829

Infrared FEL photochemistry: Multiple-photon dissociation of freon gas
[DE94-000817] 05 p1820 N94-22585

Theoretical determination of chemical rate constants using novel time-dependent methods
[NASA-CR-195221] 07 p2714 N94-26205

Numerical analysis of the photo-dissociation/radical oxidation of formaldehyde by ultraviolet light in a photolytic reactor
[AD-A274539] 07 p2868 N94-26843

The kinetics and dynamics of the coma of Halley's comet
[NASA-CR-194828] 07 p3105 N94-28184

Radiation transport in cloudy and aerosol loaded atmospheres 08 p3368 N94-30805

Reactions and spectroscopy of excited nitrenes
[AD-A278475] 10 p4136 N94-33745

Vacuum ultraviolet studies of molecular dynamics
[AD-A278940] 11 p4321 N94-35657

Infrared multiphoton ignition and combustion enhancement of natural gas.
[PB94-165438] 11 p4236 N94-35755

Photodissociation and spectroscopy of gas phase bimetallic clusters
[DE94-012607] 12 p4419 N94-37438
Fast beam studies of free radical photodissociation
[DE94-011380] 12 p4521 N94-37720

PHOTOELASTIC ANALYSIS
Use of photostress and strain gages to analyze behavior of weldments and use of photostress and strain gages to analyze behavior of an aft skirt test specimen
[NASA-CR-194575] 03 p1058 N94-15716
Use of photostress to analyze behavior of an aft skirt test specimen
[NASA-CR-195850] 10 p4069 N94-34075

PHOTOELASTIC MATERIALS
Use of photostress and strain gages to analyze behavior of weldments and use of photostress and strain gages to analyze behavior of an aft skirt test specimen
[NASA-CR-194575] 03 p1058 N94-15716

PHOTOELASTIC STRESS MEASUREMENT
U PHOTOELASTIC ANALYSIS

PHOTOELASTICITY
Studies of the effect of microstructure on the dynamic behavior of granular and particulate media
[AD-A279012] 12 p4455 N94-36520

PHOTOELECTRIC CATHODES
U PHOTOCATHODES

PHOTOELECTRIC CELLS
NT PHOTOCONDUCTIVE CELLS
NT PHOTOVOLTAIC CELLS
NT SOLAR CELLS

PHOTOELECTRIC EFFECT
NT PHOTOCONDUCTIVITY
NT PHOTOELECTRIC EMISSION
NT PHOTOIONIZATION
NT PHOTOVOLTAIC EFFECT
Photoelectron diffraction and holography: Some new directions
[DE94-006297] 08 p3289 N94-30027
Imaging of surface structure with energy-dependent photoelectron diffraction
[DE94-009096] 09 p3907 N94-32934

PHOTOELECTRIC EMISSION
Highly anisotropic but nodeless gap from a valence-fluctuation pairing mechanism
[DE93-010738] 01 p0401 N94-11646
Canted magnetic moments at the Gd(0001) surface
[DE93-014327] 02 p0805 N94-13102
Spin polarized photoemission studies of interfacial and thin film magnetism
[DE93-014326] 02 p0580 N94-14142
Effect of spontaneous decay of superconductor quasiparticles in the tunneling density of states
[DE93-012681] 02 p0811 N94-14339
High-order harmonic generation with short-pulse lasers
[DE93-016532] 02 p0659 N94-14594
Photoemission study of diamond (100) surface
[DE93-015251] 03 p1208 N94-16062
Structural characterization of epitaxial layers for infrared detectors
[AD-A267875] 03 p0940 N94-17013
Low temperature deposition and characterization of n- and p-type silicon carbide thin films and associated ohmic and Schottky contacts
[AD-A267966] 03 p0973 N94-17490
In-situ electron and optical spectroscopies of translational and vibrational activated bond breaking and formation on semiconductors
[AD-A268192] 03 p1015 N94-17560
Dynamics of short-pulse excitation, ionization and harmonic conversion
[DE93-017220] 04 p1436 N94-17996
Photoemission studies of Zn, Co, and Gd substituted YBa2Cu3O(7-delta)
[DE93-017403] 04 p1597 N94-18498
Magnetic circular dichroism in x ray absorption and core-level photoemission
[DE93-019381] 05 p1688 N94-19986
Development of a numerical simulation model for a-Si:H solar cells and application to the analysis of experimentally obtained spectral characteristics
[ETN-93-95061] 05 p1846 N94-20151
Electron quantum yields from a barium photocathode illuminated with polarized light
[DE93-019232] 05 p1980 N94-20475
Photoemission and the electronic properties of heavy fermions: Limitations of the Kondo model
[DE93-040191] 05 p1974 N94-21553
Photoelectron holography of platinum (111)
[DE93-040856] 05 p1810 N94-21950
Limits on high-order harmonic generation from single-atom calculations
[DE93-019950] 06 p2531 N94-22869
Performance of inverse photoemission spectrometer with a new bandpass photon detector of narrow bandwidth and high sensitivity
[REPT-A-2659] 06 p2345 N94-24977
The in situ observation of epitaxial diamond thin film nucleation and growth using emission electron microscopy
[AD-A273698] 06 p2263 N94-25489
A study of LPM suppression of bremsstrahlung at 25 GeV
[DE94-003457] 07 p3018 N94-26133
Near-ultraviolet laser photoemission: Scanning microscopy, buried interfaces and image-potential states
08 p3294 N94-29531
A photoemission electron microscope investigation of chemical vapor deposition diamond films and diamond nucleation 08 p3215 N94-29745
Characteristics of secondary electron emission from CsI induced by x rays with energies up to 100 keV
[DE94-608422] 08 p3395 N94-30185
Influence of surface defects and local structure on oxygenate reaction pathways over metal oxide surfaces
[DE94-005680] 08 p3522 N94-30901
The 4f heavy fermion photoelectron spectra do not exhibit the Kondo scale
[DE94-006252] 09 p3898 N94-31631
Analysis of Dietz's single, rectangular pulse theory for the generation of radiation via photoelectrons
[DE94-006131] 09 p3681 N94-32661
Particle-In-Cell (PIC) code simulation results and comparison with theory scaling laws for photoelectron-generated radiation
[DE94-006132] 09 p3695 N94-32662
Strongly anisotropic s-wave versus d-wave gap in cuprate superconductors: Evidence and theory
[DE94-007579] 09 p3904 N94-32746
Investigation of superconductivity and magnetism in d and f-electron materials
[DE94-008535] 09 p3907 N94-32933
Resonant photoemission and magnetic x-ray circular dichroism in the M shell of ultrathin films of Fe
[DE94-007453] 10 p4029 N94-34120
Two-photon photoemission and the dynamics of electrons at interfaces
[DE94-011373] 11 p4324 N94-36058
Preliminary soft x ray studies of beta-SiC
[DE94-013023] 12 p4537 N94-37498
A photoemission study of Au, Ge, and O2 deposition on NH4F etched Si(111)
[DE94-013352] 12 p4519 N94-37553

PHOTOELECTRIC GENERATORS
NT PHOTOVOLTAIC CELLS
NT SOLAR CELLS

PHOTOELECTRIC PHOTOMETERS
U ELECTROPHOTOMETERS

PHOTOELECTRICITY
NT PHOTOCONDUCTIVITY
NT PHOTOELECTRIC EFFECT
NT PHOTOELECTRIC EMISSION
NT PHOTOIONIZATION
NT PHOTOVOLTAIC EFFECT

PHOTOELECTROCHEMICAL DEVICES
Surface science instrumentation for the study of important catalytic and electrochemical interfaces
[DE93-015068] 02 p0563 N94-13413
Photoinduced charge separation in solid state and molecular systems
[DE94-001727] 06 p2563 N94-24537

PHOTOELECTROCHEMISTRY
Surface science instrumentation for the study of important catalytic and electrochemical interfaces
[DE93-015068] 02 p0563 N94-13413
Proceedings of the Seventeenth DOE Solar Photochemistry Research Conference
[DE94-005552] 09 p3759 N94-31648

PHOTOELECTROMAGNETIC DETECTORS
U PHOTOELECTROMAGNETIC EFFECTS
U RADIATION MEASURING INSTRUMENTS

PHOTOELECTROMAGNETIC EFFECTS
Technical report of ISSP. Ser. A, no. 2672: Magneto-optical effects of excitons in BiI3 crystals under pulsed high magnetic fields. 3: Excitons confined around a stacking disorder formed by a bending stress
[JTN-94-80558] 07 p3065 N94-27240
Photoelectronic study of GaAs epilayers and In(x)Ga(1-x)As/GaAs quantum wells
[ISBN-0-315-85756-0] 08 p3518 N94-30239

PHOTOELECTRON SPECTROSCOPY
Surface and near-surface atom imaging with photoelectron holography
[DE93-013197] 01 p0169 N94-10526
Effect of surface cleanliness of bearing steel on adhesive strength and tribological properties of sputter-deposited gold films
[DE93-767974] 01 p0082 N94-10732
Tribological characteristics of hot-pressed self-lubricating composites
[NAL-TR-1160] 01 p0066 N94-10858
Analysis of samples of reflector materials which are multicoated and metal samples with oxide coatings which have been exposed the space environment in LDEF testing
[NASA-CR-193647] 02 p0575 N94-12789
Surface science instrumentation for the study of important catalytic and electrochemical interfaces
[DE93-015068] 02 p0563 N94-13413
Applications of surface science to solid lubricants
[SMC-TR-93-24] 02 p0579 N94-13903
Vacuum ultraviolet instrumentation for solar irradiance and thermospheric airglow
[NASA-CR-194525] 02 p0652 N94-14684
A sulfur segregation study of PWA 1480, NiCrAl, and NiAl alloys
[NASA-TM-106289] 03 p0956 N94-15992
Design and fabrication of a reflection far ultraviolet polarizer and retarder
[NASA-CR-194630] 03 p1191 N94-16023
Photoemission study of diamond (100) surface
[DE93-015251] 03 p1208 N94-16062
The interaction of HCN(DCN) with Si(111)-7x7 studied with HREELS, UPS, and XPS
[AD-A266237] 03 p1182 N94-16111
Electron spectroscopy analysis
[NASA-CR-193591] 03 p0951 N94-17039
Growth of dielectric thin films by irradiation of condensed molecular precursors with synchrotron radiation
[DE93-016161] 03 p0974 N94-17676
Guidelines for the expression of uncertainties in surface chemical analysis by Auger Electron Spectroscopy (AES) and X ray Photoelectron Spectroscopy (XPS)
[NPL-DMM(A)-99] 04 p1346 N94-17900
ALE project
[AD-A271080] 05 p2014 N94-19980
Photoelectron spectroscopy at model boundary surfaces of energy converter semiconductors/electrolyte contacts: Adsorption, coadsorption, and triadsorption of Br2, Na, and H2O on Van der Waals surfaces of metal chalocogenide semiconductors
[ETN-93-95063] 05 p2015 N94-20152
Applications and source development for high-repetition rate x ray lasers
[DE93-019547] 05 p1815 N94-20259
Temperature dependence of 4f PES features and hole occupancy in ytterbium heavy fermions
[DE93-040131] 05 p1691 N94-20321
Study of the utilization of thin oxides in indium phosphides for the realisation of electron components
[ECL-92-38] 05 p2018 N94-20593
Alumoxanes: Rationalization of black box materials
[AD-A272805] 05 p1704 N94-21170
Diffraction and holography of photoelectrons and fluorescent x rays
[DE93-019240] 05 p1808 N94-21441
Photoemission and the electronic properties of heavy fermions: Limitations of the Kondo model
[DE93-040191] 05 p1974 N94-21553
An analytical ultra-high vacuum tribometer for solid lubricant studies 06 p2361 N94-24033
LPCVD of InN on GaAs(110) using HN3 and TMIn: Comparison with Si(100) results
[AD-A273555] 06 p2235 N94-24917
Photoelectron spectroscopic studies of the electronic structure and bonding in TiC and TiN
[ATR-93(8361)-2] 07 p2746 N94-28185
Structure of ordinary ice I(sub h). Part 1: Ideal structure of ice
[AD-A275149] 08 p3486 N94-29021
XPS analysis of 440C steel surfaces lubricated with perfluoropolyethers under sliding conditions in high vacuum
[NASA-TM-106548] 08 p3218 N94-30177
Electron cyclotron resonance plasma oxidation studies of InP
[AD-A277431] 09 p3893 N94-33007
Resonant photoemission and magnetic x-ray circular dichroism in the M shell of ultrathin films of Fe
[DE94-007453] 10 p4029 N94-34120
Two-photon photoemission and the dynamics of electrons at interfaces
[DE94-011373] 11 p4324 N94-36058

PHOTOELECTRONICS
U ELECTRONICS

PHOTOELECTRONS
Photodetachment studies on few-electron atomic negative ions
[DE93-008474] 01 p0358 N94-10154
Surface and near-surface atom imaging with photoelectron holography
[DE93-013197] 01 p0169 N94-10526

Strange meson spectroscopy in K(omega) and K(phi) at 11 GeV/c and Cherenkov ring imaging at SLD
[DE93-013593] 01 p0363 N94-10748
Research in cosmic and gamma ray astrophysics: Cosmic physics portion
[NASA-CR-194127] 02 p0847 N94-13211
Surface science instrumentation for the study of important catalytic and electrochemical interfaces
[DE93-015068] 02 p0563 N94-13413
Many-body corrections in XAFS
[DE93-011002] 02 p0563 N94-13478
Results from a water-Cerenkov array
[DE93-012715] 02 p0849 N94-14461
Spin-integrated and spin-dependent photoelectron diffraction
[DE93-016546] 04 p1565 N94-17850
Dynamics of short-pulse excitation, ionization and harmonic conversion
[DE93-017220] 04 p1436 N94-17996
Ionospheric photoelectrons measured at geosynchronous orbit
[AD-A272431] 05 p1857 N94-21202
Diffraction and holography of photoelectrons and fluorescent x rays
[DE93-019240] 05 p1808 N94-21441
Photoelectron holography of platinum (111)
[DE93-040856] 05 p1810 N94-21950
A Monte Carlo study of the Sudbury Neutrino Observatory small test detector experiment
[ISBN-0-315-59056-4] 05 p1977 N94-22416
The 1024 scintillation hodoscope
[DE93-634183] 07 p2810 N94-26394
Solar and airglow measurements aboard the two suborbital flights NASA 36.098 and 36.107
[NASA-CR-195279] 07 p2882 N94-27380
Photoelectron diffraction and holography: Some new directions
[DE94-006297] 08 p3289 N94-30027
Photochemistry in constrained spaces: Zeolites and layered double metal hydroxides
[DE94-004958] 08 p3200 N94-30769
Photoelectron diffraction and holography: Present status and future prospects
[DE94-006298] 09 p3712 N94-31629
The 4f heavy fermion photoelectron spectra do not exhibit the Kondo scale
[DE94-006252] 09 p3898 N94-31631
A simple model for determining photoelectron-generated radiation scaling laws
[DE94-006130] 09 p3761 N94-32660
Analysis of Dietz's single, rectangular pulse theory for the generation of radiation via photoelectrons
[DE94-006131] 09 p3681 N94-32661
Particle-In-Cell (PIC) code simulation results and comparison with theory scaling laws for photoelectron-generated radiation
[DE94-006132] 09 p3695 N94-32662
Near edge x ray spectroscopy theory
[DE94-008179] 09 p3905 N94-32799
Imaging of surface structure with energy-dependent photoelectron diffraction
[DE94-009096] 09 p3907 N94-32934

PHOTOEMISSION
U PHOTOELECTRIC EMISSION

PHOTOEMISSIVITY
U EMISSIVITY
U PHOTOELECTRIC EMISSION

PHOTOEXCITATION
Femtosecond dynamics, photoexcitation, and ESR spectra of MX chain solids
[AD-A264689] 01 p0399 N94-11263
Atomic processes relevant to polarization plasma spectroscopy
[DE93-753240] 01 p0393 N94-11594
Polaronic charge separation in mixed-halide MX solids
[AD-A266073] 01 p0403 N94-12345
Ultrafast photoinduced electron transfer reactions in supramolecular arrays: Studies of electronic coupling and solvation
[DE93-012910] 02 p0782 N94-13484
Photochemical dynamics of surface oriented molecules
[DE93-016289] 02 p0784 N94-13983
The E2 N(yields)(Delta) transition from polarized Compton scattering
[DE93-012522] 02 p0785 N94-14363
X ray laser program
[AD-A267075] 03 p1038 N94-15628
Direct solar pumping of semiconductor lasers: A feasibility study
[NASA-CR-193760] 04 p1440 N94-18834
Photochemical approaches to conversion of light to electricity or fuel
[DE94-001650] 05 p1849 N94-22048
Technical report of ISSP. Ser. A, no. 2680: Determination of intervalley scattering time in germanium by subpicosecond time-resolved Raman spectroscopy
[JTN-94-80566] 07 p3064 N94-27176
Predissociation in N2(C'4, 1 Sigma u +) and other N2 states and its importance in the atmospheres of Titan and Triton
[NASA-CR-195727] 08 p3549 N94-28816
Infrared multiphoton ignition and combustion enhancement of natural gas.
[PB94-165438] 11 p4236 N94-35755
The E2/M1 mixing ratio in the excitation of the Delta from polarized photo-reactions
[DE94-004235] 12 p4510 N94-36442

PHOTOGEOLOGY
Estimation of age of Dali-Ganis rifting and associated volcanic activity, Venus 01 p0440 N94-12046
Regional geology of the Vega landing sites: Tentative results of photogeologic mapping 01 p0440 N94-12047
Regional geology of the Venera landing sites: Tentative results of photogeologic mapping 01 p0440 N94-12048
Geomorphic processes in the Argyre-Dorsa Argentea region of Mars 03 p1270 N94-16293
Preliminary results from Mariner 10: High resolution images of the Moon 05 p2107 N94-20719
Photogeological analysis of Europan tectonic features 05 p2129 N94-20838
A model geophysics program
[DE94-007415] 09 p3747 N94-32203
Evaluation of the IHS transformation use on the integration of geophysical (aeromagnetometry) and remote sensing (TM-Landsat) data for the geological investigation in the Pojuca area (Serra dos Carajas, PA)
[INPE-5532-TDI/521] 10 p4077 N94-34223
Noachian and Hesperian modification of the original Chryse impact basin topography 11 p4364 N94-35462

PHOTOGRAMMETRY
On resolution of underwater stereo photogrammetry 01 p0172 N94-11966
Photogrammetric methods for trajectory measurements
[NLR-TP-91166-U] 02 p0650 N94-13527
Obtaining digital regional planning information from aerial pictures
[REPT-228] 02 p0700 N94-14810
Robust photo-topography by fusing shape-from-shading and stereo
[NASA-CR-194697] 05 p1806 N94-19920
Discharge rates in Ma'adim Vallis, Mars 05 p2128 N94-20830
A photogrammetric solution to a particular problem
[NASA-TP-3415] 06 p2381 N94-22961
Quantitative assessment of human motion using video motion analysis 06 p2436 N94-24203
Reach performance while wearing the Space Shuttle launch and entry suit during exposure to launch accelerations 06 p2436 N94-24204
Image analysis technology applied to problems in crystallography
[AD-A273516] 06 p2566 N94-25288
Exploitation of stereophotogrammetrically derived 3-D wireframe models to produce urban simulations
[AD-A275459] 08 p3325 N94-28808
Feature mapping in a photogrammetric GIS
[AD-A275418] 08 p3325 N94-28863
The use of digital stereo photogrammetric methods in historical photo analysis
[AD-A275287] 08 p3288 N94-29437
Calibration of charge coupled device digital cameras
[ISBN-0-315-85539-8] 08 p3290 N94-30232
Apron heights around stepped massifs in the Cydonia Mensae region: Do they record the local paleobathymetry of Oceanus Borealis? 09 p3949 N94-33224

PHOTOGRAPH INTERPRETATION
U PHOTOINTERPRETATION

PHOTOGRAPHIC EMULSIONS
NT NUCLEAR EMULSIONS
Analysis of SOFCAL calibration data
[NASA-CR-193910] 06 p2345 N94-25000

PHOTOGRAPHIC EQUIPMENT
NT CAMERAS
NT FAINT OBJECT CAMERA
NT FRAMING CAMERAS
NT HIGH SPEED CAMERAS
NT MULTISPECTRAL BAND CAMERAS
NT PANORAMIC CAMERAS
NT PINHOLE CAMERAS
NT STREAK CAMERAS
NT TELEVISION CAMERAS
STS-30 crew photo in building 4
[NASA-TM-109573] 03 p1031 N94-15304
STS-27 crew photo training and habitation procedures
[NASA-TM-109553] 03 p1032 N94-15405
STS-35 payload specialists Durrance and Parise: 70mm photo training and cabin familiarization
[NASA-TM-109499] 03 p1032 N94-15463
Imaging devices for satellite remote sensing
[VTT-TIED-1517] 09 p3743 N94-31658

PHOTOGRAPHIC FILM
Development of an automated film-reading system for ballistic ranges
[NASA-CR-194398] 02 p0650 N94-13815
Optical computing
[AD-A267881] 03 p1141 N94-17015
The performance and survivability of dichromated poly (vinyl alcohol) holograms for space based photonic applications
[AD-A270974] 04 p1434 N94-19791

PHOTOGRAPHIC MEASUREMENT
NT PHOTOGRAMMETRY
Interferometric and optical tests of water window imaging x ray microscopes
[NASA-CR-193866] 01 p0375 N94-10506
Debris/ice/TPS assessment and integrated photographic analysis for Shuttle mission STS-58
[NASA-TM-109194] 06 p2200 N94-24577

PHOTOGRAPHIC PROCESSING
The trustworthy digital camera: Restoring credibility to the photographic image 09 p3714 N94-32470

PHOTOGRAPHIC RECORDING
Debris/Ice/TPS assessment and integrated photographic analysis for Shuttle Mission STS-61
[NASA-TM-109195] 06 p2199 N94-24059
Root gravitropism in maize and Arabidopsis
[NASA-CR-195710] 07 p2903 N94-27940
Debris/ice/TPS assessment and integrated photographic analysis for Shuttle mission STS-60
[NASA-TM-109193] 07 p2692 N94-27956

PHOTOGRAPHIC TRACKING
Trajectory computations for an improved cinetheodolite tracking system 05 p1791 N94-22236

PHOTOGRAPHS
NT CLOUD PHOTOGRAPHS
NT LUNAR PHOTOGRAPHS
NT MARS PHOTOGRAPHS
NT MICROPHOTOGRAPHS
NT MOTION PICTURES
NT PHOTOMICROGRAPHS
Characterization of spatial and temporal variability of phytoplankton blooms in coastal waters
[AD-A267102] 03 p1116 N94-15633
A mineralized zone in Western Candor Chasma, Mars 03 p1248 N94-16179
Image blur
[DE93-017944] 04 p1580 N94-19113
A comparison of some of the most current methods of image compression
[AD-A271841] 05 p1907 N94-20525
Debris/ice/TPS assessment and integrated photographic analysis for Shuttle Mission STS-51
[NASA-TM-109189] 05 p1656 N94-21884
SkICAT: A cataloging and analysis tool for wide field imaging surveys 05 p2049 N94-22546
A paraperspective factorization method for shape and motion recovery
[AD-A276513] 09 p3712 N94-31929
The trustworthy digital camera: Restoring credibility to the photographic image 09 p3714 N94-32470
Debris/ice/TPS assessment and integrated photographic analysis for Shuttle Mission STS-62
[NASA-TM-109201] 10 p4012 N94-33423
The measurement of three-dimensional geometric parameter 10 p4057 N94-34358

PHOTOGRAPHY
NT AERIAL PHOTOGRAPHY
NT ASTRONOMICAL PHOTOGRAPHY
NT AUTORADIOGRAPHY
NT CINEMATOGRAPHY
NT CLOUD PHOTOGRAPHY
NT COLOR PHOTOGRAPHY
NT ELECTRO-OPTICAL PHOTOGRAPHY
NT FRACTOGRAPHY
NT HIGH SPEED PHOTOGRAPHY
NT HOLOGRAPHY
NT INFRARED IMAGERY
NT INFRARED PHOTOGRAPHY
NT LUNAR PHOTOGRAPHY
NT MICROWAVE HOLOGRAPHY
NT MULTISPECTRAL PHOTOGRAPHY
NT PHOTOMICROGRAPHY
NT SATELLITE-BORNE PHOTOGRAPHY
NT SCHLIEREN PHOTOGRAPHY
NT SHADOWGRAPH PHOTOGRAPHY
NT SPACEBORNE PHOTOGRAPHY
NT STEREOPHOTOGRAPHY
NT STEREOSCOPY
NT ULTRAVIOLET PHOTOGRAPHY
NT ULTRAVIOLET PHOTOMETRY
NT UNDERWATER PHOTOGRAPHY

Image motion photography
[DE93-013962] 02 p0653 N94-14858
National Aero-Space Plane
[NASA-TM-109450] 03 p0865 N94-15323
National Aero-Space Plane resource reel
[NASA-TM-109451] 03 p0865 N94-15324
STS-34 onboard 16mm photography quick release
[NASA-TM-109460] 03 p0880 N94-15355
STS-27 crew photo training and habitation procedures
[NASA-TM-109553] 03 p1032 N94-15405
STS-41 crew training bailout in CCT, 16mm camera class EVA prep, habitation equipment procedures, and food tasting
[NASA-TM-109517] 03 p0876 N94-15517
Fast-ICCD photography and gated photon counting measurements of blackbody emission from particulates generated in the KrF-laser ablation of BN and YBC
[DE93-015491] 03 p1210 N94-16460
Optical computing
[AD-A267881] 03 p1141 N94-17015
High speed 512X512 camera system
[DE93-015871] 04 p1430 N94-18235
Image blur
[DE93-017944] 04 p1580 N94-19113
Synchrotron x ray diffraction analysis of photorefractive crystals and their gratings
[AD-A271176] 05 p2015 N94-20213
Close-up analysis of inflight ice accretion
[NASA-TM-106457] 06 p2172 N94-23523

PHOTOINTERPRETATION
Satellite inventory of Minnesota forest resources
[NASA-CR-193565] 01 p0231 N94-11521
Preparations for and first results of the calibration and interpretation of ERS-1 SAR imagery over land
[BCRS-92-13] 02 p0684 N94-13123
Evaluation of C-band SAR data from SAREX 1992: Tapajos study site 05 p1839 N94-20964
Integrated use of hydrological modelling and remote sensing in the province of Drenthe (The Netherlands): Possibilities and restrictions
[REPT-61] 06 p2382 N94-23148
Debris/ice/TPS assessment and integrated photographic analysis for Shuttle mission STS-60
[NASA-TM-109193] 07 p2692 N94-27956
The use of digital stereo photogrammetric methods in historical photo analysis
[AD-A275287] 08 p3288 N94-29437
Radar image classification by texture measurements
[ONERA-NT-1993-3] 09 p3673 N94-31419
Assessment of region-based methods for automated SAR/optical registration, attribute extraction, and classification 09 p3750 N94-32536
Almaz marine applications 09 p3751 N94-32544
Statistical analysis and mapping of cotton and food crop cultivation surfaces in the west of Burkina Faso: Contribution of combined SPOT P and XS data 09 p3757 N94-32575

PHOTOIONIZATION
Dynamics of dissociation versus ionization in strong laser fields
[DE93-009261] 01 p0173 N94-10287
High power z pinches as x ray laser photopumps
[DE93-012842] 01 p0173 N94-10746
New infrared photon absorption processes
[DE93-017017] 02 p0780 N94-13071
A search for strong-field direct two electron ionization using coincidence spectroscopy
[DE93-013435] 02 p0781 N94-13241
The reionization of the intergalactic medium 02 p0838 N94-13651
Was 49: Mirror for a hidden Seyfert 1 galaxy
[NASA-CR-194537] 02 p0840 N94-14685
Investigation of the interactions of radiation with matter
[AD-A266743] 03 p1181 N94-15774
Multiphoton ionization studies of WF6 and UF6
[DE93-016232] 03 p1181 N94-15863
Characterization of UV emissions resulting from electronic energy transfer in atmospheric molecules
[AD-A266244] 03 p1101 N94-16469
Femtosecond growth dynamics of an underdense ionization front measured by spectral blueshifting
[DE93-013582] 03 p1183 N94-16818
Sensitive detection of gas-phase nitro-containing energetic materials employing 226-nm radiation
[AD-A267633] 03 p0951 N94-17203
Laser photoionization time-of-flight mass spectrometry of nitrated polycyclic aromatic hydrocarbons and nitrated heterocyclic compounds
[AD-A268126] 03 p0952 N94-17520
A physical model for one-dimension and time-dependent ionosphere. Part 2: Results and discussions
[DE93-627959] 03 p1103 N94-17631
Production of dense vapor targets for laser-plasma interaction studies with intense, ultra-short pulses
[DE93-017175] 04 p1584 N94-17993
Dynamics of short-pulse excitation, ionization and harmonic conversion
[DE93-017220] 04 p1436 N94-17996
A physical model for one-dimension and time-dependent ionosphere. Part 1: Description of the model
[DE93-627958] 04 p1486 N94-19255
Harmonic generation at high intensities
[DE93-018632] 04 p1572 N94-19283
Ultraviolet observations of clusters of Wolf-Rayet stars in the SBm3 galaxy NGC 4214 and Ultraviolet and optical observations of LINER's
[NASA-CR-194307] 04 p1622 N94-19431
Angular distributions of high-order ATI
[DE93-019125] 05 p1972 N94-20230
Photopumped x ray laser research on Saturn
[DE93-019430] 05 p1816 N94-20298
Generation of intense ultrashort x ray pulses
[DE93-019607] 05 p1817 N94-21299
Photoabsorption and Compton scattering in ionization of helium at high photon energies
[DE94-000380] 05 p1974 N94-21658
Single and double ionization of helium by high-energy photon impact
[DE94-000381] 05 p1975 N94-21785
Ionization of H2(+) in intense laser fields
[DE93-019160] 05 p1818 N94-21829
Direct detection of atomic ions from molecular photofragmentation during nonresonant multiphoton ionization of sputtered species
[DE93-040886] 05 p1976 N94-21951
The effect of Compton scattering on the double to single ionization ratio in helium
[DE94-000884] 05 p1827 N94-22390
Limits on high-order harmonic generation from single-atom calculations
[DE93-019950] 06 p2531 N94-22869
High-resolution soft x ray photoionization studies of selected molecules
[DE94-000568] 06 p2532 N94-23002
SALI chemical analysis of provided samples
[NASA-CR-194138] 06 p2232 N94-23524
Three methods to measure RH bond energies
[DE94-003795] 07 p3013 N94-25816
Development of laser spectroscopic technology in nuclear industry
[DE93-633327] 07 p2714 N94-26158
Study on laser atomic spectroscopy
[DE93-633328] 07 p2817 N94-26402
Measurement of metastable population distribution in gadolinium atomic beam by laser resonance photoionization method
[DE94-701194] 07 p3029 N94-27820
Optical field ionization of atoms and ions using ultrashort laser pulses
[DE94-006643] 08 p3488 N94-29845
Optical depth effects in cluster cooling flows 08 p3541 N94-30800
Elimination of two atomic electrons by a single high energy photon
[DE94-006834] 09 p3864 N94-31320
Double photoionization of helium with synchrotron x rays: Proceedings
[DE94-006737] 09 p3866 N94-31668
High-energy chemical processes: Laser irradiation of aromatic hydrocarbons
[DE94-008107] 09 p3720 N94-32707
Magnetic field effect on selective photoionization
[DE94-611079] 11 p4334 N94-36180
Direct photoionization of excited helium
[DE94-618732] 12 p4516 N94-37097
Infrared spectroscopy of organic free radicals related to combustion processes
[DE94-012481] 12 p4409 N94-37168
Resonance photoionization of the excited helium
[DE94-618733] 12 p4517 N94-37173

PHOTOLITHOGRAPHY
Radiation-induced modifications of allylamino-substituted polyphosphazenes
[AD-A264914] 01 p0092 N94-11848
Field emitter array RF amplifier development project. Phase 1: Cathode technology development
[AD-A266346] 02 p0622 N94-13776
Scalar limitations of diffractive optical elements 03 p1194 N94-17336
Fabricating binary optics: An overview of binary optics process technology 03 p1195 N94-17343
Laser figuring for the generation of analog micro-optics and kineform surfaces 03 p1196 N94-17346
Diffractive optics fabricated by direct write methods with an electron beam 03 p1196 N94-17347
Phase holograms in PMMA with proximity effect correction 03 p1037 N94-17348
Curved grating fabrication techniques for concentric-circle grating, surface-emitting semiconductor lasers 03 p1045 N94-17349
Fabrication of micro-optical devices 03 p1197 N94-17351
SURPHEX (tm): New dry photopolymers for replication of surface relief diffractive optics 03 p1198 N94-17358
Predesign of diamond turned refractive/diffractive elements for IR objectives 03 p1198 N94-17359
Field emission cathode and vacuum microelectronic microwave amplifier development
[AD-A269526] 04 p1403 N94-18639
X ray reflection masks: Manufacturing, characterization and first tests
[BONN-IR-92-31] 05 p1986 N94-21043
Examination for optimization of synchrotron radiation spectrum for the x ray depth lithography
[BONN-IR-92-32] 05 p1987 N94-21148
Sum frequency generation using an optical parametric oscillator
[DE94-001827] 07 p3040 N94-28000
Nearly time-optimal feedback control of a magnetically levitated photolithography positioning system
[DE94-005288] 08 p3266 N94-30055
Neural network based time-optimal control of a magnetically levitated precision positioning system
[DE94-006573] 08 p3437 N94-30250
Materials for efficient high-flux magnetic bearing actuators 11 p4214 N94-35845

PHOTOLUMINESCENCE
NT X RAY FLUORESCENCE
GaAs PCSS: High gain switching and device reliability
[DE93-009851] 01 p0401 N94-11605
Thermographic properties of eight blue-emitting phosphors
[DE93-011459] 01 p0078 N94-11622
Free-exciton recombination in GaAs
[DE93-009843] 02 p0809 N94-14079
Structural investigation of electrochemically etched silicon
[DE93-015300] 03 p1207 N94-15827
Numerical studies of the photoluminescence spectrum of quantum Hall systems
[DE93-015822] 03 p1220 N94-16810
Electrical conductivity of ion implanted ladder and semi-ladder polymers
[AD-A267432] 03 p0970 N94-16978
Growth and doping of Al(x)Ga(1-x)N films by electron cyclotron resonance assisted molecular beam epitaxy
[AD-A267305] 03 p1212 N94-16992
Nitride semiconductors for ultraviolet detection
[AD-A267877] 03 p1012 N94-17040
Investigation of the optical, electronic, and structural properties of fiber optic glasses
[AD-A267645] 03 p0971 N94-17204
Lattice relaxation theory of localized excitations in quasi-one-dimensional systems
[DE93-624947] 03 p1215 N94-17437
Pressure sensitive paint technique 04 p1431 N94-18647
Study of GaAs substrates by ambient temperature photoluminescence imagery
[ECL-92-61] 04 p1603 N94-19357
Effect of exciton localization and delocalization on magnetic-field-dependent photoluminescence linewidths in semiconductors
[DE93-018860] 05 p1748 N94-19884
Photoluminescence spectroscopy of zinc germanium diphosphide (ZnGeP2)
[AD-A270705] 05 p1678 N94-19953
Optically controlled current filamentation in GaAs photoconductive semiconductor switches
[DE93-019427] 05 p2016 N94-20296
Dephasing processes in III-V semiconductors
[AD-A271677] 05 p2028 N94-21362
Growth, characterization and device development in monocrystalline diamond films
[AD-A273097] 05 p2028 N94-21506
Implantation of carbon in GaAs and compensating native defects
[DE93-040122] 05 p2030 N94-21763
Ultraviolet photosulfidation of III-V compound semiconductors for electronic passivation
[DE94-001417] 06 p2555 N94-22717
Ordering and phase separation in MOCVD InGaP alloys and unicompositional quantum wells
[DE94-004693] 07 p3056 N94-26352
Light emitting porous silicon
[AD-A274152] 07 p3038 N94-27137
ECR plasma synthesis of silicon nitride films on GaAs and InSb
[DE94-005575] 08 p3515 N94-30006
Fluorescence observations of LDEF exposed materials as an indicator of induced material reactions 09 p3593 N94-31025
Femtosecond probe-probe transmission studies of LT-grown GaAs near the band edge
[DE94-006660] 09 p3904 N94-32634

Material engineering of the novel semiconductor structures
[AD-A278386] 09 p3910 N94-33355
Luminescence and electroluminescence of Nd, Tm, and Yb doped GaAs and some II-VI compounds
[AD-A278413] 10 p4146 N94-33554
Visible and infrared (1.54 micrometers) LED based on Er-doped porous Si
[AD-A278528] 10 p4042 N94-34295
The excitation mechanism of praseodymium-doped semiconductors
[AD-A280687] 12 p4535 N94-37129

PHOTOLYSIS
Vibrational overtone activation of methylcyclopropene
[AD-A265588] 01 p0079 N94-12373
Photocatalysis for the treatment of waste water: Applications involving the removal of metals
[DE93-011669] 02 p0561 N94-12841
Application of synchrotron radiation in chemical dynamics
[DE93-015040] 02 p0563 N94-13411
Thermochemistry of transition metal clusters
[DE93-016201] 02 p0571 N94-13977
Photodegradation of polyimides. V1: Effect of donor-acceptor groups on the photooxidative stability of polyimides and model compounds
[AD-A267319] 03 p0970 N94-16947
The photophysics of poly(methylphenylphosphazene)
[AD-A267321] 03 p0970 N94-16949
Pulsed laser kinetic studies of liquids under high pressure
[DE93-017826] 03 p1041 N94-16998
Pulse radiolytic studies of electron transfer processes and applications to solar photochemistry
[DE93-018715] 04 p1464 N94-17781
Nitridation of GaAs(100) by laser-induced decomposition of HN3
[AD-A269147] 04 p1438 N94-18258
Vibrational dynamics in photoinduced electron transfer
[DE93-040874] 04 p1567 N94-18533
Unimolecular photodissociation dynamics of ketene (CH2CO): The singlet/triplet branching ratio and experimental observation of the vibrational level thresholds of the transition-state
[DE93-019252] 04 p1352 N94-19304
Excited atomic bromine energy transfer and quenching mechanisms
[AD-A270672] 04 p1572 N94-19607
Photochemically induced transformations of transition complexes
[AD-A271112] 05 p2014 N94-19982
Ultraviolet photosulfidation of III-V compound semiconductors for electronic passivation
[DE94-001417] 06 p2555 N94-22717
Infrared fluorescence studies of electronic-to-vibrational energy transfer in a Br2:NO system
[AD-A273727] 06 p2539 N94-25443
Numerical analysis of the photo-dissociation/radical oxidation of formaldehyde by ultraviolet light in a photolytic reactor
[AD-A274539] 07 p2868 N94-26843
Time-resolved infrared absorption studies applied to the study of radical plus molecule reactions
[DE94-005921] 09 p3863 N94-31202
Mechanisms of laser induced reactions in opaque heterogeneous environments
[AD-A276642] 09 p3717 N94-31996
Laser flash photolysis, EPR and Raman studies of liquids at elevated pressures
[DE94-008351] 09 p3718 N94-32413
Dry deposition of PAN to grassland vegetation
[DE94-005111] 09 p3768 N94-32894
Previous model comparisons
10 p3971 N94-33458
Reactions and spectroscopy of excited nitrenes
[AD-A278475] 10 p4136 N94-33745
Metal-carbon nanostructures
[DE94-009177] 12 p4400 N94-36509
Bond selective chemistry beyond the adiabatic approximation
[DE94-012486] 12 p4408 N94-37095

PHOTOMAGNETIC EFFECTS
Photo- and thermal-induced antiferromagnetic interlayer coupling in Fe/(Fe-Si) superlattices
[DE93-040822] 05 p2031 N94-21930

PHOTOMAPPING
Regional geology of the Vega landing sites: Tentative results of photogeologic mapping
01 p0440 N94-12047
Regional geology of the Venera landing sites: Tentative results of photogeologic mapping
01 p0440 N94-12048
Galileo imaging results from the second Earth-Moon flyby: Lunar Maria and related units
03 p1252 N94-16199
Lunar impact basins: New data for the nearside northern high latitudes and eastern limb from the second Galileo flyby
03 p1258 N94-16228
Enhanced image capture through fusion
06 p2346 N94-25502
Optical pattern recognition system utilizing resonator array
[AD-D016071] 07 p3040 N94-28224
A model geophysics program
[DE94-007415] 09 p3747 N94-32203
Ultra wide band radar holographic imaging of subsurface targets
[DE94-004271] 09 p3713 N94-32681
Subpixel resolution from multiple images
11 p4281 N94-35417
Noachian and Hesperian modification of the original Chryse impact basin topography
11 p4364 N94-35462
Lunar horizon glow and the Clementine mission
11 p4366 N94-35478

PHOTOMAPS
Evaluation of the IHS transformation use on the integration of geophysical (aeromagnetometry) and remote sensing (TM-Landsat) data for the geological investigation in the Pojuca area (Serra dos Carajas, PA)
[INPE-5532-TDI/521] 10 p4077 N94-34223

PHOTOMASKS
A novel photosensitive polyimide resist consisting of a soluble polyimide and a bis(perfluorophenyl azide) as a cross-linker
[AD-A265998] 01 p0093 N94-12353
Fabrication of micro-optical devices
03 p1197 N94-17351
Low cost paths to binary optics
03 p1197 N94-17353

PHOTOMETERS
NT ELECTROPHOTOMETERS
NT TOTAL OZONE MAPPING SPECTROMETER
NT ULTRAVIOLET SPECTROMETERS
Barium fluoride research and development at Lawrence Livermore National Laboratory
[DE93-014682] 02 p0807 N94-13405
Investigation of the feasibility of optical diagnostic measurements at the exit of the SSME
[NASA-CR-193832] 02 p0553 N94-14682
A novel solid-state optical temporal analyzer with picosecond resolution and picowatt sensitivity
[AD-A266804] 03 p0986 N94-14912
Visible light photon counters for astronomy
03 p0902 N94-15043
Photoconductors and arrays for the far-infrared
03 p0902 N94-15045
Impurity conduction photoconductor detectors
03 p0902 N94-15046
BIB photodetectors based on antimony doped silicon
03 p0902 N94-15047
Optimisation of FIR photoconductors for atmospheric spectroscopy
03 p0902 N94-15048
Nonstationary behaviour of low background photon detectors
03 p0902 N94-15049
A 12.5 micron infrared detector for Earth observation
03 p0903 N94-15052
Lead chalcogenides based IR photosensitive array detectors with coordinate addressing
03 p0903 N94-15053
Performance optimization of detector electronics for millimeter laser ranging
03 p0913 N94-15569
Tracking capabilities of SPADs for laser ranging
03 p0914 N94-15570
How to squeeze high quantum efficiency and high time resolution out of a SPAD
03 p0914 N94-15571
Streak camera based SLR receiver for two color atmospheric measurements
03 p0914 N94-15573
Two wavelength satellite laser ranging using SPAD
03 p0916 N94-15584
The new MTLRS-1 receiving system
03 p0877 N94-15611
Linear encoding device
[NASA-CASE-GSC-13562-1] 03 p1147 N94-15703
Mass of Saturn's A ring
03 p1263 N94-16252
Optical ionospheric instrumentation and research
[AD-A266403] 03 p1192 N94-16550
Acousto-optical classifier
[AD-D015894] 03 p1000 N94-16921
Fundamental theory of light for applications: Notes for five informal lectures
[DE93-016463] 03 p1192 N94-16953
Development of ultra-low noise, high performance 3-V Quantum Well Infrared Photodectors (QWIP's) for focal plane array staring image sensor systems
[AD-A267715] 03 p1214 N94-17272
An analog retina model for detecting dim moving objects against a bright moving background
04 p1399 N94-18350
Photodetector array having high pixel density
[AD-D015859] 04 p1432 N94-18731
Radiation induced darkening of the optical elements in the Startracker camera
[DE93-018907] 04 p1433 N94-19004
High Speed/High Frequency Optoelectronics
[AD-A271985] 05 p1751 N94-20580
Silicon retina for optical tracking systems
05 p1755 N94-21098
Bidirectional method for optical channel waveguide attenuation measurement by detectors integrated on the wafer, appendix 3
05 p1988 N94-21597
New concepts for HgI2 scintillator gamma ray spectroscopy
[NASA-CR-194819] 06 p2233 N94-24113
Hubble Space Telescope high speed photometer orbital verification
[NASA-CR-189333] 06 p2204 N94-24226
Hubble Space Telescope high speed photometer science verification test report
[NASA-CR-189322] 06 p2205 N94-24710
Investigation of a normal incidence high-performance p-type strained layer In(0.3)Ga(0.7)As / In(0.52)Al(0.48) as quantum well infrared photodetector
[AD-A274854] 07 p3055 N94-26188
Multichip module high speed testing
[AD-A274873] 07 p2782 N94-26343
The growth and characterization of GaN as a photodetector
[AD-A274570] 07 p3063 N94-26965
Development of ultra-low noise, high performance 3 -5 quantum well infrared photodetectors (QWIPs) for focal plane array staring image sensor systems
[AD-A275745] 08 p3511 N94-28734
MOCVD growth of GaN, AlN and AlGaN for UV photodetector applications
[AD-A275078] 08 p3512 N94-28871
InTlSb for long-wavelength infrared photodetectors and arrays
[AD-A275079] 08 p3512 N94-28872
Remote sensing of inner heliospheric plasmas
[AD-A275021] 08 p3550 N94-29132
Issues arising with the application of optical fiber transmission in class 1E systems in nuclear power plants
[DE94-004743] 08 p3500 N94-29928
Hydrogenated amorphous silicon (a-Si:H) based gamma camera: Monte Carlo simulations
[DE94-007042] 09 p3795 N94-31323
A 1-picosecond InGaAs photodetector for operation at 1300-1600 nm
[AD-A275959] 09 p3895 N94-31350
Advanced infrared photodetectors: Materials review
[AD-A277058] 09 p3879 N94-32013
High T(sub c) superconductor tunnel junctions for photon detectors
[DE94-007686] 09 p3904 N94-32602
Bioluminescence bathyphotometer
[AD-D016102] 09 p3790 N94-32959
Quantum well infrared photodetector FPA
[AD-A278010] 09 p3908 N94-33248
Instrumentation on the RAIDS experiment 2: Extreme ultraviolet spectrometer, photometer, and near IR spectrometer
[AD-A278543] 10 p4085 N94-33676
Method and device for improved IR detection with compensations for individual detector response
[AD-D016153] 10 p4141 N94-33760
Fiber optic transceiver for interfacing digital superconducting electronics
[DE94-008284] 10 p4040 N94-33842
Receiver design, performance analysis, and evaluation for space-borne laser altimeters and space-to-space laser ranging systems
[NASA-CR-195847] 10 p4058 N94-34066
High-sensitivity receiver for increasing multiplicity of measurement axes of Zygo's Heterodyne interferometer
[DE94-009916] 11 p4333 N94-35818
Catalog of Helios 90 deg photometer events
[PL-TR-94-2040] 11 p4375 N94-36264
Development of ultra-low noise, high performance 3 to 5 Quantum Well Infrared Photodetectors (QWIPs) for focal plane array staring image sensor systems
[AD-A278861] 11 p4342 N94-36385
InTlSb for long-wavelength infrared photodetectors and arrays
[AD-A280207] 12 p4524 N94-37149

PHOTOMETRY
NT ASTRONOMICAL PHOTOMETRY
NT INFRARED PHOTOMETRY
NT SPECTROPHOTOMETRY
NT STELLAR SPECTROPHOTOMETRY
NT ULTRAVIOLET PHOTOMETRY
Simulating the daylight performance of fenestration systems and spaces of arbitrary complexity: The IDC method
[DE93-015177] 02 p0704 N94-14333

Activities report of the National Electrotechnical Institute Galileo Ferraris
[ETN-93-94224] 02 p0627 N94-14812
Laser guide star measurements at Lawrence Livermore National Laboratory
[DE93-018081] 04 p1441 N94-19251
Sunphotometer network for monitoring aerosol properties in the Brazilian Amazon
05 p1839 N94-20961
PHOTCAL: The IRAF photometric calibration package
05 p1925 N94-22465
MOSAIC: Software for creating mosaics from collections of images 05 p1927 N94-22543
Multicolor photometry of barred spiral galaxies
08 p3541 N94-30270
Three-stage attenuation using Glan-Thompson prisms
[AD-A280481] 12 p4525 N94-37350

PHOTOMICROGRAPHS
Grain surface features of Apollo 17 orange and black glass 03 p1289 N94-16397
Long duration exposure facility experiment m0003 deintegration observation database
[AD-A267579] 03 p0951 N94-17207

PHOTOMICROGRAPHY
The effect of crystal tilt on high resolution micrographs of small metal particles
[DE93-013915] 02 p0574 N94-14795

PHOTOMULTIPLIER TUBES
Calibration of the receiver channel for the GOPEX precursor experiments 02 p0610 N94-14387
Absolute detection efficiency of a micro-channel plate detector to x rays in the 1-100 KeV energy range
[DE93-012592] 02 p0789 N94-14460
A new detector concept for energetic auroral x ray imaging 03 p0907 N94-15081
Performance optimization of detector electronics for millimeter laser ranging 03 p0913 N94-15569
Two color satellite laser ranging upgrades at Goddard's 1.2m telescope facility 03 p0915 N94-15581
Two wavelength satellite laser ranging using SPAD
03 p0916 N94-15584
Performance comparison of high speed microchannel plate photomultiplier tubes 03 p0922 N94-15624
A Monte Carlo study of the Sudbury Neutrino Observatory small test detector experiment
[ISBN-0-315-59056-4] 05 p1977 N94-22416
The CEBAF beam loss sensors
[CEBAF-PR-93-032] 06 p2540 N94-24662
Performance of inverse photoemission spectrometer with a new bandpass photon detector of narrow bandwidth and high sensitivity
[REPT-A-2659] 06 p2345 N94-24977
The 1024 scintillation hodoscope
[DE93-634183] 07 p2810 N94-26394
Photon counting spectroscopy as done with a Thomson scattering diagnostic
[DE94-005543] 08 p3503 N94-28515
On possibility to create the scintillation trigger for liquid-argon neutrino detector
[DE94-607844] 08 p3489 N94-30050
Hydrogenated amorphous silicon (a-Si:H) based gamma camera: Monte Carlo simulations
[DE94-007042] 09 p3795 N94-31323
Microelectronic photomultiplier device with integrated circuitry
[AD-D016176] 10 p4039 N94-33723
X-ray remote sensing and in-situ spectroscopy for planetary exploration missions and gamma-ray remote sensing and in-situ spectroscopy for planetary exploration missions
[NASA-CR-189352] 11 p4375 N94-35381
Ultrafast readout of scintillating fibers using upgraded position-sensitive photomultipliers
[DE94-010419] 11 p4269 N94-36095
Wide aperture scintillation hodoscope with FEU-143 photomultipliers
[DE94-618211] 12 p4515 N94-37075

PHOTON BEAMS
Target motion detecting impulse Doppler radar system
[AD-D015898] 05 p1717 N94-20198
Proceedings of the Fifth Users Meeting for the Advanced Photon Source
[DE93-040692] 06 p2531 N94-22948
Spectral and temporal correlations of multifrequency waves in the turbulent atmosphere
[ITN-94-85229] 07 p2774 N94-27233
Activity report of Synchrotron Radiation Laboratory 1992
[JTN-94-80600] 08 p3495 N94-29596
Proceedings of the 37th international symposium on electron, ion, and photon beams
[AD-A276478] 09 p3875 N94-31247
Support of hadroproduction of bottom using the 800 GeV/c primary photon beam at the Fermilab tevatron
[DE94-009411] 11 p4324 N94-36016

PHOTON-ELECTRON INTERACTION
Variance reduction unique to coupled electron/photon Monte Carlo transport
[DE93-014999] 02 p0782 N94-13409
Adiabatic and non adiabatic effects in Free Electron Laser (FEL) non linear interactions
[ITN-93-85224] 02 p0659 N94-14547
Ultrafast processes in tunneling microstructure devices
[AD-A266570] 03 p1210 N94-16720
Studies of clusters
[DE93-018961] 04 p1572 N94-19309
Photoabsorption and Compton scattering in ionization of helium at high photon energies
[DE94-000380] 05 p1974 N94-21658
Single and double ionization of helium by high-energy photon impact
[DE94-000381] 05 p1975 N94-21785
Theoretical and experimental studies of elementary physics
[DE94-002310] 07 p3008 N94-25988
Deciphering the quark-gluon structure of the photon in electron(gamma) collisions
[DE93-634386] 07 p3017 N94-26043
Quantum-mechanical suppression of bremsstrahlung
[DE94-005223] 08 p3497 N94-30712
Program EPICSHOW: A computer code to allow interactive viewing of the EPIC data libraries, version 94-1
[DE94-009263] 10 p4108 N94-34141
XAFS-like structure of resonant Raman scattering
[DE94-618410] 12 p4517 N94-37171

PHOTONIC PROPULSION
NT LASER PROPULSION

PHOTONIC SWITCHING
U OPTICAL SWITCHING

PHOTONICS
Semiconductor ring lasers
[DE93-012386] 01 p0174 N94-11005
Preliminary surface-emitting laser logic device evaluation
[AD-A266111] 01 p0383 N94-12416
Energy and technology review, March 1993
[DE93-013941] 02 p0849 N94-13019
Alternative optical architectures for multichannel adaptive optical processing
[AD-A267052] 03 p1189 N94-15664
Fabricating binary optics: An overview of binary optics process technology 03 p1195 N94-17343
The photonical, pure grid method
[NLR-TP-91478-U] 03 p1062 N94-17600
Integrated photonics research volume 10. Conference edition
[AD-A269298] 04 p1577 N94-18298
Optical computing. Organization of the 1993 Photonics Science Topical Meetings. Technical digest series, volume 7
[AD-A269025] 04 p1578 N94-18332
Optical design for photonics. Organization of the 1993 Photonics Science Topical Meetings. Technical digest series, volume 9
[AD-A269027] 04 p1578 N94-18396
Quantum Optoelectronics. Organization of the 1993 photonics science topical meetings. Technical digest series, volume 8
[AD-A269026] 04 p1578 N94-18488
Advanced Solid-State Lasers/Compact Blue-Green Lasers. 1993 technical digest series. Volume 2: Organization of the 1993 photonics science topical meetings
[AD-A269058] 04 p1438 N94-18492
Photonics in Switching: Organization of the 1993 photonics science topical meetings. Technical digest
[AD-A269024] 04 p1578 N94-18528
Soft X Ray Projection Lithography. Organization of the 1993 photonics science optical meetings
[AD-A269159] 04 p1579 N94-18693
Integrated Photonics Research: Post-deadline papers
[AD-A269232] 04 p1609 N94-18908
Ultrafast Electronics and Optoelectronics: Summaries of papers. Technical digest conference edition
[AD-A269233] 04 p1405 N94-18909
Silicon MCM substrates for integration of 3-5 photonic devices and CMOS IC's
[DE93-017894] 04 p1405 N94-19112
Optoelectronic packaging: A review
[DE93-040059] 04 p1515 N94-19535
Novel nonlinear laser diagnostic techniques
[AD-A270968] 04 p1442 N94-19788
The performance and survivability of dichromated poly (vinyl alcohol) holograms for space based photonic applications
[AD-A270974] 04 p1434 N94-19791
Photonics and nonlinear optics with molecular materials and polymers
[AD-A271747] 05 p1988 N94-21457
Photonic technology for implementation of generalizable neural networks: A synthetic approach
[AD-A273497] 06 p2474 N94-24622
Component characterization and development 2
[AD-A274002] 07 p2765 N94-25660
Diagnostics and microelectronics
[DE94-003016] 07 p2784 N94-26777
Center for space microelectronics technology
[NASA-CR-195282] 07 p2786 N94-27574
Photonic devices and systems for optical signal processing
[AD-A275818] 08 p3498 N94-28804
Optoelectronic packaging activities at Sandia National Laboratories
[DE94-005287] 08 p3501 N94-30261
Photonics at Sandia National Laboratories: From research to applications
[DE94-006463] 08 p3501 N94-30828
Photonic bandgaps in periodic dielectric structures
[ISBN-0-315-86902-X] 09 p3899 N94-31729
Photonic band gap materials
[DE94-005566] 09 p3677 N94-32101
Flexible manufacturing for photonics device assembly
09 p3669 N94-32449
Automated fiber pigtailing technology
[DE94-007072] 09 p3695 N94-32688
Sandia's photonic program and its changing national role
[DE94-008616] 09 p3883 N94-32878
Influence of an externally modulated photonic link on a microwave communications system
11 p4252 N94-35544
Field demonstration of X-band photonic antenna remoting in the Deep Space Network
11 p4252 N94-35545
Poly(p-phenylene) derivatives new high performance nonlinear optical polymers
[AD-A280248] 12 p4422 N94-37121

PHOTONS
Disturbance, the uncertainty principle and quantum optics 01 p0375 N94-10569
Photon number amplification/duplication through parametric conversion 01 p0376 N94-10572
Non classical effects in planar waveguides
01 p0376 N94-10574
Nonperturbative methods in the problem of multiphoton excitation of atom by squeezed light
01 p0376 N94-10575
Study of Einstein-Podolsky-Rosen state for space-time variables in a two photon interference experiment
01 p0370 N94-10582
Squeezed colour states in gluon jet
01 p0379 N94-10599
Wavelets and spacetime squeeze
01 p0379 N94-10604
Strange meson spectroscopy in K(omega) and K(phi) at 11 GeV/c and Cherenkov ring imaging at SLD
[DE93-013593] 01 p0363 N94-10748
A review of two photon production of jets at PEP and PETRA energies
[DE93-011742] 01 p0364 N94-10754
Non-Euclidean space for local hidden variables
[DE93-621341] 01 p0344 N94-11032
Investigation of optically generated electronic defects and protonic transport in hydrogen-bonded molecular solids: Isomorphs of potassium dihydrogen phosphate
[DE93-012498] 01 p0399 N94-11243
LCLS optics: Selected technological issues and scientific opportunities
[DE93-010953] 01 p0175 N94-11468
Applications of in-situ ellipsometry to microwave electron cyclotron resonance plasma processes
[AD-A265197] 01 p0373 N94-11880
Metal-semiconductor, composite radiation detectors
[DE93-013313] 02 p0619 N94-12994
New infrared photon absorption processes
[DE93-017017] 02 p0780 N94-13071
EGS (underscore) windows 2: An enhanced graphical interface to EGS
[DE93-010447] 02 p0746 N94-13382
Variance reduction unique to coupled electron/photon Monte Carlo transport
[DE93-014999] 02 p0782 N94-13409
A positron annihilation radiation telescope using Laue diffraction in a crystal lens
[DE93-012905] 02 p0848 N94-13483
ROSAT observations of the binary Be-star/radio pulsar PSR1259-63
[NASA-CR-194394] 02 p0832 N94-14357
The E2 N(yields)(Delta) transition from polarized Compton scattering
[DE93-012522] 02 p0785 N94-14363
Measurements of the spatial structure and directivity of 100 KeV photon sources in solar flares using PVO and ISEE-3 spacecraft
[NASA-CR-194080] 02 p0845 N94-14492

Multiple Schroedinger cats from multilevel atoms
[DE93-013412] 02 p0786 N94-14526
Laser lithography by photon scanning tunneling microscopy
[DE93-015962] 02 p0660 N94-14863
Proceedings of an ESA Symposium on Photon Detectors for Space Instrumentation
[ESA-SP-356] 03 p0899 N94-15025
A new approach to optical photon detection 03 p0899 N94-15028
Superconductive x ray photon detectors 03 p0900 N94-15031
Metastable superconductors as photon detectors 03 p0900 N94-15032
The MIC photon counting detector 03 p0901 N94-15039
CCDs and photon counting devices: Applications in space and from the ground 03 p0901 N94-15041
Visible light photon counters for astronomy 03 p0902 N94-15043
Outlook for hard x ray and gamma ray astronomy 03 p0904 N94-15057
Developments in extreme ultraviolet and x ray instrumentation 03 p0904 N94-15058
The TAUVEX experiment 03 p0905 N94-15064
The Rutherford Appleton Laboratory photon counting detector 03 p0910 N94-15096
Work at Graz on satellite signatures 03 p0898 N94-15558
Sensor modelling for the Cyclops focal plane detector array based technology demonstrator
[AD-A267172] 03 p1190 N94-15846
The cooling of confined ions driven by laser beams
[DE93-016612] 03 p1039 N94-16114
Ablation, surface activation, and electroless metallization of insulating materials by pulsed excimer laser irradiation
[DE93-015808] 03 p1040 N94-16664
Scintillation mechanism in stoichiometric cerium compounds
[DE93-015499] 03 p0948 N94-16771
Optical properties of water released in low Earth orbit
[AD-A266197] 03 p1192 N94-16936
Detecting small debris using a ground-based photon counting detector
[DE93-012623] 03 p0898 N94-17669
Space and time as outcome of decoherence in an expanding universe
[DE93-016199] 04 p1624 N94-18047
Criticality benchmark comparisons leading to cross-section upgrades
[DE93-017184] 04 p1556 N94-18073
Coherent transient systems evaluation
[AD-A268808] 04 p1576 N94-18204
Experimental and theoretical investigation of surface chemistry induced by direct and indirect electronic excitation
[AD-A268846] 04 p1348 N94-18221
Simulation of emittance dilution in electron storage ring from Compton backscattering
[DE93-017611] 04 p1386 N94-18503
Investigation of physical structures and interactions at high energy
[DE93-014444] 04 p1574 N94-18927
The study of the phase structure of hadronic matter by searching for the deconfined quark-gluon phase transition using 2 TeV (bar-p)-p collisions, and by searching for critical phenomena in an exclusive study of multifragmentation using 1 GeV/nucleon heavy ion collisions
[DE93-018925] 04 p1570 N94-19103
Harmonic generation at high intensities
[DE93-018632] 04 p1572 N94-19283
Target motion detecting impulse Doppler radar system
[AD-D015898] 05 p1717 N94-20198
Direct photon results from CDF
[DE93-019908] 05 p1980 N94-20317
Material optimization for hard x ray Fresnel zone plates
[DE93-019569] 05 p1990 N94-21837
Search for excited quarks in p(-p) collisions at the square root of s = 1.8 TeV
[DE93-019910] 05 p1975 N94-21840
Studies of the deuteron at high energy and momentum transfer
[DE93-041162] 05 p1976 N94-21941
Detector noise statistics in the non-linear regime 05 p1748 N94-22526
Low p(sub T) photon production in proton-nucleus collisions at 18 GeV/c
[DE94-001380] 06 p2532 N94-23007
Photon-photon collisions at the next linear collider: Theory
[DE93-041025] 06 p2534 N94-23803
Flux measurements using the BATSE spectroscopic detectors 06 p2580 N94-24435
Electro-weak, QCD and top physics at the Tevatron
[DE94-002304] 06 p2535 N94-24611
Quantum optical aspects of topological phases, such as Berry's phase
[AD-A273632] 06 p2570 N94-25028
Biexciton formation by two-photon absorption in quantum wells
[DE93-613551] 07 p3071 N94-25852
Theoretical and experimental studies of elementary physics
[DE94-002310] 07 p3008 N94-25988
Deciphering the quark-gluon structure of the photon in electron(gamma) collisions
[DE93-634386] 07 p3017 N94-26043
Radiation-Induced Structural Changes, 2
[DE93-520314] 07 p3054 N94-26109
Fast photoconductor CdTe detectors for synchrotron x ray studies
[DE94-001334] 07 p3054 N94-26139
Photon and hadron production of heavy flavors
[DE94-004655] 07 p3018 N94-26245
Measurements of the p (mu)d-molecule formation rate at different hydrogen temperature
[DE93-634636] 07 p3020 N94-26511
Aspects of perturbative corrections in quantum chromodynamics
[ISBN-0-315-63607-6] 07 p3074 N94-27398
Omega omega and rho+ rho- production in two photon interactions at ARGUS
[ISBN-0-315-63748-X] 07 p3026 N94-27399
Nonlinear transverse propagation of photons in a ultrarelativistically hot and magnetized electron-positron plasma: Coupling of Langmuir and electromagnetic solitons
[DE94-603667] 07 p3046 N94-27630
Pi plus pi minus gamma and K+ K- production in two photon collisions at ARGUS
[ISBN-0-315-63598-3] 07 p3027 N94-27684
Photon counting spectroscopy as done with a Thomson scattering diagnostic
[DE94-005543] 08 p3503 N94-28515
Properties of events containing a photon and several jets seen in p(bar p) collisions at (radical)s = 1.8 TeV
[DE94-005596] 08 p3482 N94-28531
Advanced diagnostics for reacting flows
[AD-A275057] 08 p3272 N94-29136
Physical conditions in classical H2 regions in the Magellanic Clouds 08 p3543 N94-29722
Inclusive jet and direct photon production at the D0 experiment
[DE94-006001] 08 p3488 N94-30049
Experimental setup for study of hadron and hard photon production in nucleus-nucleus collisions
[DE94-607849] 08 p3489 N94-30051
Experimental setups and methods to obtain new nuclear data at intermediate and high energies
[DE94-607850] 08 p3489 N94-30052
Quantum-mechanical suppression of bremsstrahlung
[DE94-005223] 08 p3497 N94-30712
Time-dependent behavior of active galactic nuclei with pair production 09 p3929 N94-31125
Elimination of two atomic electrons by a single high energy photon
[DE94-006834] 09 p3864 N94-31320
Transport properties of quark and gluon plasmas
[DE94-007043] 09 p3864 N94-31405
Novel failure analysis techniques using photon probing with a scanning optical microscope
[DE94-006594] 09 p3692 N94-32112
ITS version 3.0: Powerful, user-friendly software for radiation modelling
[DE94-006607] 09 p3678 N94-32113
A quest for a new superconducting state
[DE94-008439] 09 p3908 N94-32991
Morphological aspects of surface reactions
[DE94-010184] 11 p4236 N94-35685
First measurement of helium on Mars: Implications for the problem of radiogenic gases on the terrestrial planets 11 p4370 N94-36153
Primordial nucleosynthesis in conformal Weyl gravity
[DE94-003002] 11 p4327 N94-36241
T-odd, P-even photon-fermion interactions
[DE94-616869] 11 p4327 N94-36246
MCNP: Multigroup/adjoint capabilities
[DE94-010682] 12 p4506 N94-36449
The t(anti t)(gamma) background to pp (yields) W(gamma) + X at the SSC
[DE94-001386] 12 p4512 N94-36526
Summary of the extensions of the Standard Model working group
[DE94-002217] 12 p4512 N94-36527
Production of a positron and a bound electron by high-energy photon in a strong Coulomb field
[DE94-618501] 12 p4514 N94-36747
Direct photoionization of excited helium
[DE94-618732] 12 p4516 N94-37097
Activities of the Photon Factory
[DE94-748682] 12 p4522 N94-37236
Experimental particle physics at the University of Pittsburgh
[DE94-011636] 12 p4521 N94-37721
A freon-filled, holographic bubble chamber as a high energy photon burst spectrometer
[DE94-011645] 12 p4446 N94-37723

PHOTONUCLEAR REACTIONS
Some tools of the trade we've developed for our cross-section calculations
[DE93-013835] 02 p0786 N94-14569
Studies of the deuteron at high energy and momentum transfer
[DE93-041162] 05 p1976 N94-21941
Proceedings of the workshop on (pi), K, (eta)-nucleon interactions
[DE94-701314] 07 p3027 N94-27733
Heavy flavor production at fixed target photo- and hadroproduction
[DE94-004651] 08 p3491 N94-30719
NN-interaction in (1)S0-state: Virtual level or dibaryon resonance?
[DE94-606492] 09 p3869 N94-32097
J/psi absorption effects in the coherent production on nuclei
[DE94-616870] 11 p4326 N94-36129

PHOTOPRODUCTION
A review of two photon production of jets at PEP and PETRA energies
[DE93-011742] 01 p0364 N94-10754
Investigation of physical structures and interactions at high energy
[DE93-014444] 04 p1574 N94-18927
Research in high energy physics
[DE93-018031] 04 p1575 N94-19287
Direct photon results from CDF
[DE93-019908] 05 p1980 N94-20317
Proceedings of the 1993 DOE/NREL Hydrogen Program Review
[DE93-018207] 05 p1847 N94-21616
Low p(sub T) photon production in proton-nucleus collisions at 18 GeV/c
[DE94-001380] 06 p2532 N94-23007
Electro-weak, QCD and top physics at the Tevatron
[DE94-002304] 06 p2535 N94-24611
Electroweak and other interactions in medium-energy nuclear physics
[DE94-004161] 07 p3027 N94-27689
Proceedings of the workshop on (pi), K, (eta)-nucleon interactions
[DE94-701314] 07 p3027 N94-27733
A measurement of the LMP effect
[DE94-005225] 08 p3482 N94-28493
Elementary particle interactions
[DE94-004238] 08 p3482 N94-28504
Properties of events containing a photon and several jets seen in p(bar p) collisions at (radical)s = 1.8 TeV
[DE94-005596] 08 p3482 N94-28531
Inclusive jet and direct photon production at the D0 experiment
[DE94-006001] 08 p3488 N94-30049
Heavy flavor production at fixed target photo- and hadroproduction
[DE94-004651] 08 p3491 N94-30719
Results from the H1 experiment at HERA
[PB94-145174] 09 p3868 N94-32008
Chiral symmetry and the threshold gamma(p) yields pi(sup 0)p reaction
[DE94-008117] 09 p3873 N94-32710
The E2/M1 mixing ratio in the excitation of the Delta from polarized photo-reactions
[DE94-004235] 12 p4510 N94-36442
Direct photoproduction of jets in the k(T)-factorisation prescription
[PB94-171139] 12 p4513 N94-36549

PHOTORECEPTORS
Melatonin, the pineal gland, and circadian rhythms
[AD-A268200] 03 p1129 N94-17478
Nature's crucible: Manufacturing optical nonlinearities for high resolution, high sensitivity encoding in the compound eye of the fly, Musca domestica 05 p1755 N94-21095

PHOTORECONNAISSANCE
Objective image quality metrics: Applications for partially compensated images of space objects
[AD-A273837] 07 p2847 N94-25741

PHOTOREDUCTION
U PHOTOCHEMICAL REACTIONS

PHOTORESISTIVITY
U PHOTOCONDUCTIVITY

PHOTORESISTORS
U PHOTOCONDUCTORS

PHOTOSENSITIVITY
NT LIGHT ADAPTATION

A novel solid-state optical temporal analyzer with picosecond resolution and picowatt sensitivity
[AD-A266804] 03 p0986 N94-14912
Photo-induced and electrooptic properties of (Pb,La)(Zr,Ti)O3 films
[DE93-017496] 04 p1371 N94-18519
Calorimeter with WLS fibers and parallel to beam scintillators
[DE93-634188] 07 p2810 N94-26378
Physical characteristics of polymethylmethacrylate scintillator SOFG-120
[DE93-634184] 07 p2810 N94-26395

PHOTOSENSORS
U RADIATION MEASURING INSTRUMENTS

PHOTOSPHERE
NT SOLAR GRANULATION
Spectrophotometry of emission-line stars in the magellanic clouds
[NASA-CR-194082] 04 p1628 N94-19425
Solar imaging vector magnetograph
[NASA-CR-194729] 05 p1810 N94-21876
Large-scale structure of the solar plasma corona: An analysis of Yohkoh SXT images 05 p2004 N94-22657
The solar spectral irradiances from x ray to radio wavelengths
[NASA-CR-195203] 06 p2629 N94-25260
Environmental conditions responsible for solar activity
[AD-A274191] 07 p3111 N94-27099
The structure of solar magnetic fields and their associated electric currents 08 p3544 N94-29723
Observations of accretion and angular momentum regulation in young circumstellar disks and the implications for planetary formation 09 p3928 N94-31122

PHOTOSTRESSES
Use of photostress and strain gages to analyze behavior of weldments and use of photostress and strain gages to analyze behavior of an aft skirt test specimen
[NASA-CR-194575] 03 p1058 N94-15716
Use of photostress to characterize the mechanical behavior of weldments
[NASA-CR-195201] 06 p2378 N94-25267
Use of photostress to analyze behavior of an aft skirt test specimen
[NASA-CR-195850] 10 p4069 N94-34075

PHOTOSYNTHESIS
Estimating Photosynthetically Available Radiation (PAR) at the Earth's surface from satellite observations 01 p0230 N94-10955
Coprocessing of fossil fuels and biomass for CO2 emission reduction in the transportation sector
[PB93-194165] 01 p0267 N94-11845
Variation of the photosynthetic products in the regional upwelling area around the Izu Islands, Japan 01 p0211 N94-12661
Ultrafast photoinduced electron transfer reactions in supramolecular arrays: Studies of electronic coupling and solvation
[DE93-012910] 02 p0782 N94-13484
Gordon Research Conference on Chronobiology, 1991
[AD-A266354] 02 p0728 N94-13698
Characterization of Spirulina biomass for CELSS diet potential
[NASA-CR-194123] 02 p0729 N94-14097
Using AVIRIS images to measure temporal trends in abundance of photosynthetic and nonphotosynthetic canopy components 03 p1066 N94-16668
Multiple dataset water-quality analyses in the vicinity of an ocean wastewater plume 03 p1069 N94-16687
Atmospheric correction of AVIRIS data in ocean waters 03 p1070 N94-16690
Tracking photosynthetic efficiency with narrow-band spectroradiometry
[CIW-PUBL-1133] 03 p1072 N94-16698
The dynamics of hydroponic crops for simulation studies of the CELSS initial reference configurations
[NASA-CR-194654] 03 p1118 N94-17279
Photobiotechnology: Application of photosynthesis to the production of renewable fuels and chemicals
[DE93-015522] 04 p1466 N94-18247
Photosynthetic responses to the environment, volume 8
[AD-A269584] 04 p1502 N94-18305
Photosynthetic reaction centers as active molecular electronic components, phase 1
[AD-A271388] 04 p1503 N94-19757
Estimation of the net production of moss community at Langhovde, East Antarctica 08 p3358 N94-29081
Satellite estimation of the global distribution and interannual variability of photosynthetically active radiation 08 p3334 N94-29970
Spectral inhomogeneity of the bacterial light-harvesting antennae: Causes and consequences
[ETN-94-96020] 09 p3792 N94-31533
Light utilization and photoinhibition of photosynthesis in marine phytoplankton
[DE94-005505] 09 p3794 N94-32896
Femtosecond transient absorption studies of the light harvesting Chl a/b protein complex of Photosystem 2 in higher plants
[DE94-009684] 12 p4477 N94-36481
Solvent effects on the energetics and dynamics of ultrafast electron transfer in chlorophyll-porphyrin-acceptor triads
[DE94-009693] 12 p4477 N94-36554
Femtosecond transient grating studies of electron transfer in porphyrin and chlorophyll donor-acceptor molecules
[DE94-009694] 12 p4478 N94-36555
High resolution electron diffraction analysis of structural changes associated with the photocycle of bacteriorhodopsin
[DE94-011800] 12 p4479 N94-37156

PHOTOTHERMAL CONVERSION
High-flux testing of heat pipes for point-focus solar collector systems
[DE93-011581] 02 p0628 N94-12884
First on-sun test of NaK pool-boiler solar receiver
[DE93-015003] 04 p1466 N94-18208
Tehachapi solar thermal system
[DE93-018443] 04 p1468 N94-19014
Examination of charge carriers dynamics in silicon and silicon solar cells with photoinduced laser beam deflection
[ETN-93-95060] 04 p1470 N94-19654
Quality and efficiency of solar collectors in Sweden
[PB94-137486] 08 p3337 N94-28909

PHOTOTHERMOTROPISM
U ANISOTROPY
U TEMPERATURE EFFECTS

PHOTOTRANSISTORS
Preliminary surface-emitting laser logic device evaluation
[AD-A266111] 01 p0383 N94-12416
A tri-state optical switch for local area network communications 07 p2789 N94-27922
Reconfigurable optical switches with monolithic electrical-to-optical interfaces
[DE94-007745] 09 p3881 N94-32385
Time-dependent simulations of filament propagation in photoconducting switches
[DE94-012146] 12 p4438 N94-37213

PHOTOTUBES
NT PHOTOMULTIPLIER TUBES

PHOTOVOLTAGES
Adsorption and dissociation of disilane on Si(001) studied by STM
[AD-A265269] 01 p0402 N94-11684

PHOTOVOLTAIC CELLS
NT SOLAR CELLS
Flexible polycrystalline thin-film photovoltaics for space applications 01 p0050 N94-11393
Space Station Freedom advanced photovoltaics and battery technology development planning 01 p0052 N94-11401
Computation of photovoltaic parameters under lunar temperature variation 01 p0053 N94-11411
Photovoltaics: Contract lists, fiscal year 1992
[DE93-000093] 02 p0701 N94-12902
Photovoltaics: Program overview, fiscal year 1992
[DE93-000055] 02 p0701 N94-12914
A photovoltaic catenary-tent array for the Martian surface
[NASA-TM-106306] 02 p0621 N94-13194
Activities of the Basic Sciences Branch
[DE93-010012] 02 p0851 N94-14455
Recent advances in outdoor performance evaluation of PV systems
[DE93-015031] 03 p1091 N94-15994
Space systems environmental interaction studies
[AD-A267280] 03 p0897 N94-17240
Field investigation of the relationship between battery size and PV system performance
[DE93-016503] 03 p1016 N94-17671
SUNRAYCE 1993: Working safely with lead-acid batteries and photovoltaic power systems
[DE93-016553] 04 p1464 N94-17712
Development of large-area monolithically integrated silicon-film photovoltaic modules
[DE93-010037] 04 p1464 N94-17731
Research on stable, high-efficiency amorphous silicon multijunction modules
[DE93-010046] 04 p1467 N94-18518
System performance predictions for Space Station Freedom's electric power system
[NASA-TM-106396] 05 p1667 N94-20062
Fabrication of stable large-area thin-film CdTe photovoltaic modules
[DE93-018204] 05 p1845 N94-20095
Self-deploying photovoltaic power system
[NASA-CASE-LEW-15308-1] 05 p1846 N94-20196
Building integrated photovoltaic systems analysis
[DE93-018208] 05 p1846 N94-21298
Annual Report, Materials Science Branch, FY 1992
[DE94-000204] 05 p1849 N94-22015
Novel two-stage selenization methods for fabrication of thin-film CIS cells and submodules
[DE94-000220] 06 p2390 N94-23296
A solar photovoltaic power system for use in Antarctica
[NASA-TM-106417] 06 p2395 N94-24071
Overview of the status and progress in photovoltaics research in the United States
[DE94-000981] 06 p2395 N94-24512
Laser energized high voltage direct current power supply
[AD-D015977] 06 p2312 N94-25036
Effect of power system technology and mission requirements on high altitude long endurance aircraft
[NASA-CR-194455] 06 p2189 N94-25200
Overview of the Photovoltaic Manufacturing Technology (PVMaT) project
[DE93-018234] 07 p2856 N94-26426
Low-cost photovoltaic inverters incorporating application-specific integrated circuits
[DE94-003270] 07 p2856 N94-26463
Handbook of photovoltaic power generating design for introduction
[DE94-725199] 07 p2858 N94-26913
Solar collector manufacturing activity, 1992
[DE94-003401] 07 p2859 N94-27048
The viability of photovoltaics on the Martian surface
[NASA-TM-106478] 08 p3338 N94-30196
Large-area triple-junction a-Si alloy production scale up
[DE94-000249] 08 p3339 N94-30604
Solar photovoltaics for development applications
[DE94-006116] 08 p3340 N94-30843
Draft minutes of IAPG Mechanical Working Group meeting
[DE94-004954] 09 p3759 N94-31266
Solar lunar power 09 p3599 N94-31427
Field operation test of utility interactive load conditioner with photovoltaic cells at a demonstration house
[DE94-757271] 09 p3762 N94-32918

PHOTOVOLTAIC CONVERSION
Japan's Sunshine Project
[DE93-767980] 01 p0262 N94-10498
High efficiency direct thermal to electric energy conversion from radioisotope decay using selective emitters and spectrally tuned solar cells
[NASA-TM-106227] 01 p0047 N94-11307
Proceedings of the 12th Space Photovoltaic Research and Technology Conference (SPRAT 12)
[NASA-CP-3210] 01 p0048 N94-11380
Flexible polycrystalline thin-film photovoltaics for space applications 01 p0050 N94-11393
Space Station Freedom advanced photovoltaics and battery technology development planning 01 p0052 N94-11401
Workshop summary: Receivers for laser power beaming 01 p0054 N94-11419
The 1992 JSEE/JWEA Joint Conference
[DE93-793955] 02 p0700 N94-12822
Photovoltaic Subcontract Program
[DE93-000092] 02 p0700 N94-12868
Photovoltaics: Contract lists, fiscal year 1992
[DE93-000093] 02 p0701 N94-12902
Photovoltaics: Program overview, fiscal year 1992
[DE93-000055] 02 p0701 N94-12914
Low temperature metal-organic chemical vapor deposition growth processes for high efficiency solar cells
[DE92-010562] 02 p0702 N94-13386
Photovoltaic advanced research and development project: Solar radiation research
[DE92-016430] 02 p0704 N94-14350
Activities of the Basic Sciences Branch
[DE93-010012] 02 p0851 N94-14455
Futurepath 1 --- power systems
[NASA-TM-109431] 03 p0925 N94-15503
A ten year review of performance of photovoltaic systems
[DE93-015649] 03 p1093 N94-17217
Gallium arsenide-based ternary compounds and multi-band-gap solar cell research
[DE93-010049] 04 p1467 N94-18483
Development of high-efficiency CdTe solar cells
[DE93-018206] 05 p1845 N94-19925
Growth mechanisms and characterization of hydrogenated amorphous-silicon-alloy films
[DE93-018202] 05 p1699 N94-20047
Power transmission by laser beam from lunar-synchronous satellite
[NASA-TM-4496] 05 p1669 N94-20102

Building integrated photovoltaic systems analysis
[DE93-018208] 05 p1846 N94-21298
Stable, high-efficiency amorphous-silicon solar cells with low hydrogen content
[DE93-018214] 05 p1848 N94-21826
Thin-film CdTe and CuInSe2 photovoltaic technologies
[DE93-018217] 05 p1848 N94-21827
Investigation on the chemically fixing technique of carbon dioxide utilizing solar energy
[DE94-714886] 05 p1849 N94-22043
Photochemical approaches to conversion of light to electricity or fuel
[DE94-001650] 05 p1849 N94-22048
Surveys on specific patterns of facility intallation of photovoltaic power generating technologies for international cooperation
[DE94-714901] 05 p1850 N94-22092
Research on stable, high-efficiency amorphous silicon multijunction modules
[DE93-018220] 05 p1850 N94-22257
Polycrystalline thin film materials and devices
[DE93-018213] 06 p2389 N94-22862
Progress in phases 2 and 3 of the Photovoltaic Manufacturing Technology Project (PVMaT)
[DE94-000206] 06 p2389 N94-22888
Preliminary study concerning development of petroleum-substitution energy integration technology
[DE94-714902] 06 p2264 N94-23027
Amorphous silicon PVMaT, phase 2A
[DE93-018221] 06 p2390 N94-23295
Low power ground-based laser illumination for electric propulsion applications
[NASA-CR-194444] 06 p2219 N94-23555
A solar photovoltaic power system for use in Antarctica
[NASA-TM-106417] 06 p2395 N94-24071
Overview of the status and progress in photovoltaics research in the United States
[DE94-000981] 06 p2395 N94-24512
The state of the art of thin-film photovoltaics
[DE94-000224] 07 p2855 N94-26115
Hybrid power system for remote communications stations
[AD-A274963] 07 p2782 N94-26301
Solar resource-utility load matching assessment: NREL photovoltaic project summary
[DE94-000232] 07 p2856 N94-26480
Merging photovoltaic hardware development with hybrid applications in the USA
[DE94-002682] 07 p2857 N94-26612
Handbook of photovoltaic power generating design for introduction
[DE94-725199] 07 p2858 N94-26913
Fibrous emissive burners selective and broad band
[PB94-128329] 07 p2859 N94-27225
Advanced development of PV encapsulents
[DE94-000219] 08 p3336 N94-28500
Photovoltaic power without batteries for continuous cathodic protection 08 p3341 N94-30465
Photovoltaic performance and reliability workshop
[DE94-000236] 08 p3339 N94-30601
Large-area triple-junction a-Si alloy production scale up
[DE94-000249] 08 p3339 N94-30604
NREL Photovoltaic Program FY 1993 bibliography
[DE94-000272] 08 p3340 N94-30820
Solar photovoltaics for development applications
[DE94-006116] 08 p3340 N94-30843
Solar energy in China
[PB94-137502] 09 p3758 N94-31071
Photovoltaics: Program overview, fiscal year 1993
[DE94-000246] 09 p3758 N94-31235
Solar resource: Utility load-matching assessment
[DE94-000297] 09 p3758 N94-31264
Silicon-Film(tm) photovoltaic manufacturing technology
[DE94-000202] 09 p3760 N94-32143
Renewable energy technology development at Sandia National Laboratories
[DE94-007734] 09 p3761 N94-32383
Solar activities at Sandia National Laboratories
[DE94-007737] 09 p3761 N94-32648
Development of a computer model for polycrystalline thin-film CuInSe2 and CdTe solar cells
[DE94-006853] 09 p3762 N94-32763
Optimal planning of residential photovoltaic systems under various rate structure
[DE94-757272] 09 p3762 N94-32919

PHOTOVOLTAIC EFFECT
An overview of the Defence Research Agency photovoltaic programme 01 p0053 N94-11412
NASDA activities in space solar power system research, development and applications 01 p0054 N94-11413
Thin film solar cell workshop 01 p0054 N94-11415
Polaronic charge separation in mixed-halide MX solids
[AD-A266073] 01 p0403 N94-12345
Polythiophene derivative with a side chain chromophore as photovoltaic and photorefractive materials
[AD-A273245] 06 p2260 N94-24813
Impact of LDEF photovoltaic experiment findings upon spacecraft solar array design and development requirements 09 p3594 N94-31028
Small-angle x ray scattering studies of microvoids in amorphous-silicon-based semiconductors
[DE94-006931] 12 p4533 N94-36745

PHTHALATES
Growth and morphology of crystals: Theory and observations
[PB93-221166] 05 p2035 N94-22273

PHTHALOCYANIN
Fundamental study on new synthetic technology by phthalocyanine complexes 07 p2721 N94-25569

PHUGOID OSCILLATIONS
U OSCILLATIONS
U PITCH (INCLINATION)

PHYSICAL CHEMISTRY
NT QUANTUM CHEMISTRY
Proceedings of the 8th European Symposium on Materials and Fluid Sciences in Microgravity, volume 2
[ESA-SP-333-VOL-2] 01 p0112 N94-10171
Crystal-chemistry and partitioning of REE in whitlockite 01 p0408 N94-12174
Dissociation rates of diatomic molecules
[AD-A266464] 03 p1182 N94-16586
Energy Conversion and Storage Program
[DE93-018602] 04 p1469 N94-19098
Physical chemical studies of conducting polymers fundamental and applied
[AD-A270728] 04 p1374 N94-19574
A comparison of calculated and measured rheological properties of crystallising lavas in the field and in the laboratory 05 p1862 N94-20690
Crystal chemistry and self-lubricating properties of monochalcogenides gallium selenide and tin selenide
[DE93-041177] 07 p2751 N94-26422
Ultrastructure processing of macromolecular materials
[AD-A274460] 07 p2754 N94-27086
Physical chemistry of molecules and grains in space
[AD-A276037] 09 p3932 N94-31280
Studies in physico-chemical hydrodynamics of extended systems
[DE94-006752] 09 p3706 N94-32149
Mars aqueous chemistry experiment
[NASA-CR-196024] 11 p4354 N94-35263
Application of an alkylammonium method for characterization of phyllosilicates in CI chondrites 11 p4351 N94-35432
Activities of the Chemical Technology Division
[DE94-013050] 12 p4410 N94-37357

PHYSICAL CONSTANTS TESTING REACTOR
U NUCLEAR RESEARCH AND TEST REACTORS
U WATER COOLED REACTORS

PHYSICAL ENDURANCE
U PHYSICAL FITNESS

PHYSICAL EXAMINATIONS
Monograph of the aviation epidemiology data register for FY 1991
[AD-A266896] 03 p1119 N94-14952
Ames Fitness Program 03 p1126 N94-16632
Analysis of health status from preliminary physical examination of flight academy applicants
[AD-A267759] 05 p1889 N94-19962
Echocardiographic screening of aircrew candidates 06 p2424 N94-23319
Monograph of the aviation epidemiology data register for calendar year 1988
[AD-A274589] 07 p2911 N94-26985
Hydrogenated amorphous silicon (a-Si:H) based gamma camera: Monte Carlo simulations
[DE94-007042] 09 p3795 N94-31323

PHYSICAL EXERCISE
Exercise countermeasures for bed-rest deconditioning
[NASA-TM-103987] 01 p0300 N94-11191
Monitoring cognitive function and need with the automated neuropsychological assessment metrics in Decompression Sickness (DCS) research 01 p0314 N94-11533
Carotid-cardiac baroreflex: Relation with orthostatic hypotension following simulated microgravity and implications for development of countermeasures 01 p0308 N94-11992
Mechanistic studies on reduced exercise performance and cardiac deconditioning with simulated zero gravity 01 p0310 N94-12001
Modifications to an interactive model of the human body during exercise: With special emphasis on thermoregulation 01 p0317 N94-12368
Work/rest schedules and performance of F/A-18 aviators during Fleet Exercise 1992
[AD-A265826] 02 p0735 N94-12982
Metabolic rate measurements comparing supine with upright upper-body exercises
[NASA-CR-4549] 02 p0729 N94-14028
Variability of prediction of maximal oxygen concumption on the cycle ergometer using standard equations
[NASA-TP-3412] 02 p0729 N94-14032
GSFC Fun Run
[NASA-TM-109587] 03 p1120 N94-15271
Living well in space: Ensuring crew capability
[NASA-TM-109538] 03 p1120 N94-15369
STS-27 crew presentation clip
[NASA-TM-109551] 03 p0881 N94-15403
Ames Fitness Program 03 p1126 N94-16632
Johnson Space Center health related fitness program 03 p1126 N94-16633
Kennedy Space Center exercise program 03 p1126 N94-16634
The Langley Fitness Center 03 p1126 N94-16635
Physical Exercise Program 03 p1127 N94-16636
Metabolic monitoring of hypobaric subjects
[AD-A268221] 03 p1130 N94-17554
Physiological correlates of stress-induced decrements in human perceptual performance
[DOT/FAA/AM-93/19] 05 p1893 N94-20081
Exercise, exercise training, and the immune system. A compendium of research (1902-1991)
[NASA-TM-108778] 06 p2426 N94-23575
NASA project 1: Full-body dynamometer
[NASA-CR-195507] 06 p2438 N94-24331
Loading, electromyograph, and motion during exercise 06 p2427 N94-25359
The effect of platform motion on human energy expenditure during walking. An exploratory experiment
[AD-A273760] 07 p2940 N94-25724
Plasma volume shifts and exercise thermoregulation with water immersion and six-degree head-down tilt
[NASA-TM-108781] 07 p2901 N94-26093
Thermoregulatory effects of caffeine ingestion during rest and exercise in men
[NASA-TM-108783] 07 p2901 N94-26210
Sympathetic nerve activity during dynamic leg exercise 07 p2929 N94-27527
Workshop on Countering Space Adaptation with Exercise: Current Issues
[NASA-CP-3252] 07 p2934 N94-28361
Muscular activity and its relationship to biomechanics and human performance 07 p2934 N94-28362
Eccentric exercise testing and training 07 p2934 N94-28363
Exercise detraining: Applicability to microgravity 07 p2934 N94-28364
Exercise and osteoporosis: Methodological and practical considerations 07 p2935 N94-28370
The value of electrical stimulation as an exercise training modality 07 p2936 N94-28372
The use of biomechanics in the study of movement in microgravity 07 p2936 N94-28373
Psychophysiology in microgravity and the role of exercise 07 p2936 N94-28374
Effects of three hydration beverages on exercise performance during 60 hours of simulated desert exposure 08 p3383 N94-28448
Studies on water electrolyte metabolism and endocrine responses at rest and during submaximal exercise at 6,000 m simulated altitude 08 p3388 N94-28496
Effects of training at simulated altitude of 6,000 m on endocrine responses at rest and during exercise at the same altitude 08 p3388 N94-28497
Effects of endurance training on heat-exercise tolerance in men wearing NBC protective clothing
[AD-A275176] 08 p3391 N94-29049
Leg muscle volume during 30-day 6-degree head-down bed rest with isotonic and isokinetic exercise training
[NASA-TM-4580] 08 p3385 N94-29401
Dual-cycle ergometry as an exercise modality during prebreathe with 100 percent oxygen 10 p4096 N94-33638
Exercise with prebreathe appears to increase protection from decompression sickness: Preliminary findings 10 p4096 N94-33639
Modeling heat exchange characteristics of long term space operations: Role of skin wettedness and exercise 10 p4101 N94-33650
A model for predicting central nervous system toxicity from hyperbaric oxygen exposure in man: Effects of immersion, exercise, and old and new data
[AD-A278348] 10 p4095 N94-34005
Methodologies to determine forces on bones and muscles of body segments during exercise, employing compact sensors suitable for use in crowded space vehicles
[NASA-CR-196272] 12 p4487 N94-37458

PHYSICAL FACTORS
Review of mathematical and physical basis of two-phase flow modeling
[KFK-4759] 02 p0642 N94-14708

Particle simulations on massively parallel machines
[DE93-015644] 03 p1157 N94-14927
Mass extinctions: Persistent problems and new directions 07 p2889 N94-28302
Modeling data throughput on communication networks
[DE94-005077] 08 p3260 N94-30772
An electromagnetic finite difference time domain analog treatment of small signal acoustic interactions
[DE94-009978] 11 p4319 N94-35770
On the shape of x ray spectra excited by heavy ions
[DE94-618747] 12 p4519 N94-37651

PHYSICAL FITNESS
Improving physical performance by chemical stimulation
[DSIS-92-03763] 02 p0728 N94-13823
Monograph of the aviation epidemiology data register for FY 1991
[AD-A266896] 03 p1119 N94-14952
Living well in space: Ensuring crew capability
[NASA-TM-109538] 03 p1120 N94-15369
Proceedings of the 1992 Annual Meeting NASA Occupational Health Program
[NASA-CR-193462] 03 p1123 N94-16609
Physical fitness and the Healthy People 2000 goals
03 p1125 N94-16619
Physical fitness and health education program at NASA Headquarters 03 p1126 N94-16631
Physical Exercise Program 03 p1127 N94-16636
The behavioral toxicology of high-peak, low average power, pulsed microwave irradiation
[AD-A268392] 03 p1134 N94-17535
Maximum team lifting capacity as a function of team size
[AD-A271642] 05 p1892 N94-21036
Aeromedical issues related to positive pressure breathing for +Gz protection
[AD-A274717] 07 p2910 N94-26435
Female combat helicopter pilot selection criteria
[AD-A273935] 07 p2938 N94-26749

PHYSICAL OPTICS
Physical optics modelling of Soft X ray Projection Lithography (SXPL) imaging experiments
[DE93-011556] 01 p0374 N94-10339
PO/PTD diffraction synthesis of array-fed reflector antennas for satellite and radar applications
01 p0137 N94-11636
Detection of subsurface defects in machined silicon nitride ceramics by optical scattering methods
[DE93-015554] 03 p0968 N94-16658
Investigation of the optical, electronic, and structural properties of fiber optic glasses
[AD-A267645] 03 p0971 N94-17204
Study of electromagnetic wave scattering from characterized rough surfaces
[AD-A270931] 05 p1716 N94-19934
RCS Analysis of Plate Geometries, parts 1 and 2
[NASA-CR-194173] 05 p1717 N94-20269
High-frequency techniques for RCS prediction of plate geometries 05 p1717 N94-20270
FD-TD modeling of 2-D dielectric waveguides for propagation and scattering of femtosecond optical solitons 05 p1719 N94-20406
An optically-assisted 3-D cellular array machine
[AD-A272683] 05 p1987 N94-21163
High-frequency techniques for RCS prediction of plate geometries and a physical optics/equivalent currents model for the RCS of trihedral corner reflectors, parts 1 and 2
[NASA-CR-195140] 06 p2298 N94-24616
Feasibility study of a synthesis procedure for array feeds to improve radiation performance of large distorted reflector antennas
[NASA-CR-195167] 06 p2301 N94-25005
The Radar Image Generation (RIG) model
06 p2306 N94-25497
Gaussian beam and physical optics iteration technique for wideband beam waveguide feed design
08 p3248 N94-29624
A physical optics model for scattering of HF radiation by irregular terrain
[DE94-006187] 08 p3255 N94-30106
The conoscopic microscope
[TELECOM-93-E-017] 09 p3877 N94-31173
An approximate model for vertical polarization and surface roughness using the parabolic equation
[AD-A278091] 09 p3684 N94-33186
Comparison of numerical models for computing underwater light fields
[AD-A278256] 10 p4140 N94-33411
Use of the sampling theorem to speed up near-field physical optics scattering calculations
11 p4253 N94-35549

PHYSICAL PROPERTIES
Synthetic lubricants and high-performance functional fluids: Phosphazenes
[ARL-TR-45] 02 p0580 N94-14126
A new multiphase equation of state for iron
[DE93-017629] 04 p1357 N94-17819
Mass properties measurement system dynamics
06 p2368 N94-23235
Mass properties measurement system: Dynamics and statics measurements 06 p2368 N94-23236

PHYSICAL SCIENCES
Project TIMS (Teaching Integrated Math/Science)
[NASA-CR-194288] 01 p0416 N94-11599
Guide to programs, fiscal year 1993
[NSF-92-78] 04 p1633 N94-19620
The 7th Annual National Conference of Black Physics Students 06 p2524 N94-24583
The Seventh Annual National Conference of Black Physics Students
[NASA-CR-195735] 08 p3526 N94-28746

PHYSICAL WORK
Complex terrain wind model evaluation
[AD-A266467] 03 p1096 N94-16589
Apparatus and method for measuring subject work rate on an exercise device
[NASA-CASE-MSC-21752-1] 05 p1895 N94-20194

PHYSICIANS
Clinical aspects of telemedicine
01 p0306 N94-11795
Tuberculosis: A case for increased screening
03 p1126 N94-16627

PHYSICS
Event-driven simulation in SELMON: An overview of EDSE
[NASA-CR-194505] 02 p0749 N94-13784
Generic results of the space physics community survey
[NASA-CR-194538] 02 p0818 N94-13984
The 1982 to 1992 decade of research on the vacuum ultraviolet ring at National Synchrotron Light Source
[DE93-019469] 04 p1603 N94-19564
Fractal geometry in physics
[AD-A273271] 06 p2523 N94-24936
Proceedings of the LLNL Technical Women's Symposium
[DE94-006616] 11 p4379 N94-35997
Activities of National Institute of Radiological Sciences
[DE94-727636] 11 p4296 N94-36101
Cosmic rays: Physics and astrophysics. A research briefing
[NASA-CR-196118] 12 p4550 N94-36921
Beginning a dialogue on the changing environment for the physical and mathematical sciences
12 p4509 N94-36948

PHYSIOCHEMISTRY
Stability of premixed laminar flames in a stagnation point flow to general disturbances
[AD-A273429] 06 p2234 N94-24673
Proposed law of nature linking impacts, plume volcanism, and Milankovitch cycles to terrestrial vertebrate mass extinctions via greenhouse-embryo death coupling
07 p2876 N94-28307

PHYSIOGRAPHY
U GEOMORPHOLOGY

PHYSIOLOGICAL ACCELERATION
Evaluation of near-infrared spectrophotometric method for individual tolerance to +Gz acceleration
07 p2933 N94-27944
Portable Linear Sled (PLS) for biomedical research
08 p3163 N94-29648

PHYSIOLOGICAL DEFENSES
NT IMMUNE SYSTEMS

PHYSIOLOGICAL EFFECTS
NT HEMODYNAMIC RESPONSES
NT PHYSIOLOGICAL RESPONSES
Effects of CSF hormones and ionic composition on salt/water metabolism
[NASA-CR-193232] 01 p0300 N94-11045
Exercise countermeasures for bed-rest deconditioning
[NASA-TM-103987] 01 p0300 N94-11191
Calcitonin control of calcium metabolism during weightlessness
[NASA-CR-193622] 02 p0731 N94-12960
Physiological Anatomical Rodent Experiment (PARE) .04 Feasibility Test 1
[NASA-CR-194423] 02 p0728 N94-13473
The problem of the sonic boom for future high-speed transport aircraft
[ESA-TT-1286] 02 p0776 N94-13692
An evaluation of noise and its effects on shuttle crewmembers during STS-50/USML-1
[NASA-TM-104775] 02 p0735 N94-13961
Variability of prediction of maximal oxygen concumption on the cycle ergometer using standard equations
[NASA-TP-3412] 02 p0729 N94-14032
Physical countermeasures for long-term manned space flights
[ESA-SP-1160] 02 p0733 N94-14860
Thyroid alterations in porcine after prolonged exposure to cold or heat
[AD-A266840] 02 p0733 N94-14879
Evaluation of dried storage of platelets for transfusion: Physiologic integrity and hemostatic functionality
[AD-A266958] 03 p1120 N94-15180
Living well in space: Ensuring crew capability
[NASA-TM-109538] 03 p1120 N94-15369
Transcranial Doppler ultrasound studies of cerebral blood-flow in microgravity 03 p0981 N94-16095
Synaptic plasticity and memory formation
[AD-A267988] 03 p1133 N94-17453
Ontogenesis of mammals in microgravity
[NASA-TM-103978] 03 p1139 N94-17636
Using controlled daylight exposure and sleep timing in the prevention of shift lag during night operations
[AD-A269304] 04 p1504 N94-17824
Bibliography of scientific publications of the Naval Biodynamics Laboratory, 1980 - 1992
[AD-A268886] 04 p1505 N94-18226
Compilation of 1992 annual reports of the navy ELF communications system ecological monitoring program. Volume 3: Tabs G - I
[AD-A269727] 04 p1388 N94-18741
Space research with intact organisms: The role of Space Station Freedom 04 p1502 N94-19213
Space research on organs and tissues
04 p1503 N94-19214
Microgravity research in plant biological systems: Realizing the potential of molecular biology
04 p1503 N94-19216
Life: Origin and evolution on Earth--How can we escape? 04 p1503 N94-19217
Cosmos 2229
[NASA-CR-194734] 05 p1895 N94-20338
Extra-corporeal blood access, sensing, and radiation methods and apparatuses
[NASA-CASE-MSC-21775-1] 05 p1890 N94-20372
Studies of neural and cognitive function in subjects exposed to the marine-air interface, phases 1 and 2
[AD-A272282] 05 p1891 N94-20624
A proposed methodology for combustion toxicology testing of combined halon replacement agent/jet fuel interaction
[AD-A272695] 05 p1681 N94-21165
Physiological efficacy of a lightweight ambient air cooling unit for various applications
[AD-A272952] 05 p1896 N94-21247
Aeromedical disposition for coronary artery disease
06 p2423 N94-23316
Exercise, exercise training, and the immune system. A compendium of research (1902-1991)
[NASA-TM-108778] 06 p2426 N94-23575
Transfer of perceptual adaptation to space sickness: What enhances an individual's ability to adapt?
[NASA-CR-188256] 06 p2427 N94-24227
Annals of the Research Inst. of Environmental Medicine, Nagoya Univ., volume 44
[REPT-44-VOL-44] 07 p2911 N94-27442
Study on posture control and adaption mechanism under weightlessness: Results of second rehearsal for space experiment using carp 07 p2912 N94-27446
Study on posture control and adaption mechanism under weightlessness: Differences in weight and shape of utricular otolith of carp 07 p2912 N94-27448
Telescience testbedding for physiological experiments under hypobaric hypoxic conditions
07 p2913 N94-27449
Telescience testbedding under hypobaric hypoxic conditions: Evaluation by operation ability and recognition ability 07 p2913 N94-27450
The electrogastrogram during parabolic flight
07 p2913 N94-27452
Vertical gaze direction during parabolic flight
07 p2913 N94-27453
Heart rate change in normal and labyrinthectomized hamsters during parabolic flight
07 p2914 N94-27454
Frequency analysis of body sway induced by optokinetic stimulation 07 p2914 N94-27455
Cardiovascular function during thermoneutral head-out water immersion in the elderly 07 p2915 N94-27458
Effects of 40 C hot water immersion for an hour on thermoregulatory functions in humans: Comparison with 34 C thermoneutral immersion 07 p2915 N94-27459
Effects of bathing at 40 C on cardiovascular system in humans: Comparison with 34 C thermoneutral bathing
07 p2918 N94-27473
Effects of 41 C bathing for 20 minutes on cardiovascular and thermoregulatory functions in humans
07 p2918 N94-27474
Monthly variation of physiological and psychological responses under unsteady thermal conditions
07 p2918 N94-27475

Man's ability to adapt himself for the seasonal climatic changes: From viewpoint of anticipation and seasonable behavior 07 p2919 N94-27476
Symptoms of hypoxia at simulated altitude of 25,000 feet 07 p2933 N94-27945
The use of biomechanics in the study of movement in microgravity 07 p2936 N94-28373
Physiological investigations of the isolated rat's liver in hypothermia and hypoxia and their relevance in aircraft incidents above the sea 08 p3382 N94-28439
Japanese Journal of Aerospace and Environmental Medicine, vol. 30, no. 3
[JTN-94-80606] 08 p3387 N94-28495
Studies on water electrolyte metabolism and endocrine responses at rest and during submaximal exercise at 6,000 m simulated altitude 08 p3388 N94-28496
Effects of training at simulated altitude of 6,000 m on endocrine responses at rest and during exercise at the same altitude 08 p3388 N94-28497
Some issues on Japan's space food development and relating preliminary experimental study 08 p3388 N94-28498
Effects of pressure on membrane-associated receptors and effector elements
[AD-A275813] 08 p3384 N94-28829
Japanese Journal of Aerospace and Environmental Medicine, volume 30, no. 1
[JTN-94-80598] 08 p3389 N94-28850
Image technology and information analysis of bone change with gravitational exposure 08 p3389 N94-28851
Arterial oxygen saturation during +Gz acceleration by short-radius centrifuge 08 p3389 N94-28852
Effect of chronic centrifugation on in vitro fertilization and early development in mice ova 08 p3386 N94-28853
Disturbance of equilibrium on JAL flight crew 08 p3390 N94-28856
Equilibrium dysfunction in the clinical field 08 p3390 N94-28858
The MERSS 5th Symposium on Space Medicine: Medical and Physiological Experiment Utilizing Parabolic Flight
[JTN-94-80588] 08 p3392 N94-29709
Space movement of Trichinella spiralis under microgravity 08 p3387 N94-29711
Posture control of goldfishes under microgravity 08 p3387 N94-29712
Behavior and visual control of cyprinodonts under microgravity 08 p3387 N94-29713
A discussion of eye-head coordinative movement under microgravity during parabolic flight 08 p3393 N94-29715
Analysis of various biological activity parameters during parabolic flight 08 p3393 N94-29716
Hemodynamic measurement during parabolic flight 08 p3393 N94-29717
Motion sickness in parabolic flight: Possibility of electrogastrography as an objective index 08 p3393 N94-29718
Japanese Journal of Aerospace and Environmental Medicine, vol. 30, no. 2
[JTN-94-80599] 08 p3394 N94-29863
Effect of water immersion on muscle sympathetic nerve response during static muscle contraction 08 p3394 N94-29865
Shortening velocity and calcium sensitivity of single fibers from hindlimb suspended muscle in rats 08 p3387 N94-29866
Toxicity of carbon monoxide-hydrogen cyanide gas mixtures: Exposure concentration, time-to-incapacitation, carboxyhemoglobin, and blood cyanide parameters
[DOT/FAA/AM-94/7] 08 p3395 N94-29919
Physiological Anatomical Rodent Experiment (PARE) .04 feasibility test 2
[NASA-CR-195210] 08 p3385 N94-29968
Review of pharmacological approach to improve cold tolerance 09 p3796 N94-31740
Muscle disuse through tail-suspension: Etiology and therapeutics 09 p3796 N94-31746
Exposure assessment of JAVELIN missile combustion products
[AD-A278128] 09 p3616 N94-33059
Characterization and utilization of opiate-like hibernation factors
[AD-A278136] 09 p3794 N94-33098
Effect of barbiturates and hyperoxia on lipid peroxidation in hypoxic neurons
[AD-A278467] 10 p4094 N94-33545
A model for predicting central nervous system toxicity from hyperbaric oxygen exposure in man: Effects of immersion, exercise, and old and new data
[AD-A278348] 10 p4095 N94-34005
A database to evaluate acceleration (+Gz) induced loss of consciousness (G-LOC) in the human centrifuge
[AD-A278769] 11 p4299 N94-35707
Ground and space flight experiments of the effects of light, sound and/or temperature on animals
[NASA-CR-196102] 12 p4478 N94-36986
Behavioral performance in monkeys exposed to TEMPO high-peak-power microwave pulses at 3 GHz
[AD-A280551] 12 p4478 N94-37045
Blast overpressure studies with animals and man
[AD-A280240] 12 p4480 N94-37118
Homeostatic responses to prolonged cold exposure: Human cold acclimatization
[AD-A280234] 12 p4481 N94-37136
Melatonin, the pineal gland, and circadian rhythms
[AD-A280467] 12 p4481 N94-37140
Cerebral neurochemical mechanisms in stress and anxiety
[AD-A280473] 12 p4482 N94-37233

PHYSIOLOGICAL FACTORS
NT PHYSICAL FACTORS
JPRS report: Central Eurasia: Aviation and cosmonautics, no. 11, November 1992
[JPRS-UAC-93-005] 04 p1632 N94-19208
Psychophysiological study on the effects of co-existence of lines for detecting dot target 08 p3394 N94-29867
Extended range operations: A review of recent developments 11 p4195 N94-36337
Determinants of subjective fatigue for C-141 crews during Operation Desert Storm 11 p4196 N94-36338

PHYSIOLOGICAL RESPONSES
NT HEMODYNAMIC RESPONSES
Unsupervised splitting rules for neural tree classifiers
[AD-A264961] 01 p0338 N94-10487
Effect of double density caging during Space Shuttle transport of laboratory rats
[NASA-CR-193228] 01 p0300 N94-11180
Allowable exposure limits for carbon dioxide during extravehicular activity
[NASA-TM-103832] 01 p0315 N94-11375
A mechanism for the reduction in risk of decompression sickness in microgravity environment 01 p0312 N94-11545
Proceedings of the First Joint NASA Cardiopulmonary Workshop
[NASA-CP-10068] 01 p0308 N94-11991
Central circulatory hemodynamics as a function of gravitational stress 01 p0309 N94-11995
Glycerol-induced hyperhydration 01 p0309 N94-11996
Spectral analysis of resting cardiovascular variables and responses to oscillatory LBNP before and after 6 degree head dowm bedrest 01 p0309 N94-11997
Effect of prolonged LBNP and saline ingestion on plasma volume and orthostatic responses during bed rest 01 p0310 N94-11998
Fitness, autonomic regulation and orthostatic tolerance 01 p0310 N94-11999
Local fluid shifts and edema in humans during simulated microgravity 01 p0311 N94-12003
Autogenic-feedback training: A countermeasure for orthostatic intolerance 01 p0311 N94-12006
Gender differences in endocrine responses to posture and 7 days of 6 deg head down bed rest
[NASA-TM-103991] 02 p0731 N94-12972
Gravity as a probe for understanding pattern specification
[NASA-CR-194142] 02 p0713 N94-13418
Clinical physiology of bed rest
[NASA-TM-104010] 02 p0727 N94-13447
Physiological Anatomical Rodent Experiment (PARE) .04 Feasibility Test 1
[NASA-CR-194423] 02 p0728 N94-13473
Endocrine and metabolic changes in payload specialist (L-1) 02 p0591 N94-13758
Manual control in space research on perceptual-motor functions under zero gravity conditions (L-10) 02 p0593 N94-13767
Psychophysiological investigations of the biomedical problems of manned spaceflight
[NASA-CR-194107] 02 p0732 N94-13782
Renal function alterations during skeletal muscle disuse in simulated microgravity
[NASA-CR-194258] 02 p0733 N94-13824
Thyroid alterations in porcine after prolonged exposure to cold or heat
[AD-A266840] 02 p0733 N94-14879
Neuropeptide-Y (NPY) increases total blood flow in the tail, and reduces cutaneous microvascular blood flow in the tail and foot of the rat
[AD-A266839] 03 p1115 N94-14918
Autogenic-Feedback Training (AFT) as a preventive method for space motion sickness: Background and experimental design
[NASA-TM-108780] 03 p1120 N94-15537
Activity/rest patterns of instructor and rates student pilots during rapid transitions from daytime to nighttime duty hours at the Eastern Army Aviation Training site
[AD-A267038] 03 p1131 N94-15659
Reliability of autonomic responses and malaise across multiple motion sickness stimulation tests
[NASA-TM-108787] 03 p1121 N94-15711
Heart rate response to parabolic flight manoeuvres 03 p0961 N94-16098
AFRRI reports, first quarter 1993
[AD-A266380] 03 p1123 N94-16515
The nature of dynamic arteriolar vasoreactivity: A mini-review and A classification scheme
[AD-A266499] 03 p1128 N94-16783
Neurotoxicity of hemoglobin in cortical cell culture
[AD-A266506] 03 p1128 N94-16786
TransRapid TR-07 maglev-spectrum magnetic field effects on daily pineal indoleamine metabolic rhythms in rodents
[DE93-015143] 03 p1117 N94-16893
Synaptic plasticity and memory formation
[AD-A267988] 03 p1133 N94-17453
Evaluation of physiological and psychological impairment of human performance in cold stressed subjects
[AD-A268637] 04 p1506 N94-18632
Compilation of 1992 annual reports of the navy ELF communications system ecological monitoring program, volume 2
[AD-A269726] 04 p1388 N94-18751
Characterization of fluid physics effects on cardiovascular response to microgravity (G-572) 04 p1323 N94-19163
A scientific role for Space Station Freedom: Research at the cellular level 04 p1503 N94-19215
Microgravity research in plant biological systems: Realizing the potential of molecular biology 04 p1503 N94-19216
Human responses to exercise-heat stress
[AD-A272581] 05 p1892 N94-21209
Increasing accuracy in the assessment of motion sickness: A construct methodology
[NASA-TM-108797] 06 p2420 N94-23088
Cytokines and immune surveillance in humans
[NASA-CR-194801] 06 p2425 N94-23331
Physiological protection for aircrew at high altitudes: A review of the literature
[DCIEM-93-13] 06 p2432 N94-24114
ELF communications system ecological monitoring program
[AD-A273456] 06 p2299 N94-24676
The role of visual context in manual target localization 06 p2429 N94-25351
The effect of platform motion on human energy expenditure during walking. An exploratory experiment
[AD-A273760] 07 p2940 N94-25724
Thermoregulatory effects of caffeine ingestion during rest and exercise in men
[NASA-TM-108783] 07 p2901 N94-26210
Changes in circadian variations of urine excretion in tail-suspended rats 07 p2911 N94-27443
Endocrinological evaluations of muscle and bone atrophy in tail-suspended rats 07 p2903 N94-27444
Aerobic fitness and orthostatic tolerance: Evidence against an association 07 p2934 N94-28365
Exercise and osteoporosis: Methodological and practical considerations 07 p2935 N94-28370
Electrical stimulation in exercise training 07 p2935 N94-28371
Prediction of survival times on land in a cold climate 08 p3379 N94-28423
Treatment of mild immersion hypothermia by body-to-body and forced-air warming 08 p3380 N94-28428
Thermoregulation in the extreme cold environment 08 p3381 N94-28438
Rewarming methodologies in the field 08 p3382 N94-28441
A comparison of four methods of rewarming individuals cooled by immersion in cold water 08 p3382 N94-28442
Work conditions assessment in pilots and ground personnel under high weather temperatures 08 p3382 N94-28444
Effects of three hydration beverages on exercise performance during 60 hours of simulated desert exposure 08 p3383 N94-28448
Alleviation of thermal strain in the CF: Keeping our cool during the Gulf conflict 08 p3383 N94-28449
Relaxed tolerance following HSG, high sustained +Gz
[AD-A275204] 08 p3391 N94-28892
Physiological responses during shipboard firefighting
[AD-A275104] 08 p3391 N94-28912
Effect of water immersion on muscle sympathetic nerve response during static muscle contraction 08 p3394 N94-29865

Isolating strain parameters correlated to skeletal adaptation 09 p3797 N94-31960
Autogenic-feedback training as a treatment for airsickness in high-performance military aircraft: Two case studies
[NASA-TM-108810] 09 p3801 N94-33068
Autogenic-feedback training improves pilot performance during emergency flying conditions 10 p4098 N94-33622
Dual-cycle ergometry as an exercise modality during prebreathe with 100 percent oxygen 10 p4096 N94-33638
Prediction modeling of physiological responses and human performance in the heat with application to space operations 10 p4098 N94-33652
The effects of cold exposure on wet aircraft passengers: A review
[AD-280253] 10 p4100 N94-34389
US experiment flown on the Soviet biosatellite Cosmos 1667
[NASA-TM-108803] 10 p4102 N94-34951
Extended range operations: A review of recent developments 11 p4195 N94-36337
Investigation of exposure to Extremely Low Frequency (ELF) magnetic and electric fields: Ongoing animals studies
[DE94-011239] 12 p4480 N94-37625

PHYSIOLOGICAL TESTS
NT BODY SWAY TEST
NT ELECTRONYSTAGMOGRAPHY
NT VESTIBULAR TESTS
Validation of an inexpensive illuminant for aeromedical color vision screening
[DOT/FAA/AM-93/16] 02 p0736 N94-14854
STS-32 crew training for lower body negative pressure unit and AFE
[NASA-TM-109475] 03 p1120 N94-15381
Reliability of autonomic responses and malaise across multiple motion sickness stimulation tests
[NASA-TM-108787] 03 p1121 N94-15711
Cardiopulmonary Aspects in Aerospace Medicine
[AGARD-LS-189] 06 p2423 N94-23313
Aortic valve disease 06 p2424 N94-23322
Aeromedical implications of mitral valve prolapse 06 p2424 N94-23323
Evaluation of bioimpedance for the measurement of physiologic variables as related to hemodynamic studies in space flight 06 p2427 N94-25378
Mechanisms of eye-hand coordination
[AD-A273687] 06 p2428 N94-25437
Effects of methamphetamine on vigilance and tracking during extended wakefulness
[AD-A274896] 07 p2909 N94-26179
The use of EEG as a workload assessment tool in flight test
[AD-A274568] 07 p2910 N94-26847
On the development of motor chunks and concurrent processing in a structured continuous keypressing task
[AD-A274153] 07 p2939 N94-27138
Does training-induced orthostatic hypotension result from reduced carotid baroreflex responsiveness? 07 p2935 N94-28366
Tripping over obstacles: Biomechanical analyses of how young and old try to avoid it 09 p3803 N94-31954
Exposure assessment of JAVELIN missile combustion products
[AD-A278128] 09 p3616 N94-33059
Comparative performance of a modified Space Shuttle Reentry Anti-G Suit (REAGS) with and without pressure socks 10 p4101 N94-33655
Further studies of 60-Hz exposure effects on human function
[DE94-010192] 11 p4297 N94-36223
Behavioral performance in monkeys exposed to TEMPO high-peak-power microwave pulses at 3 GHz
[AD-A280551] 12 p4478 N94-37045
Postural strategies for the continuous control of static and dynamic balance in man
[PB94-184678] 12 p4487 N94-37812

PHYSIOLOGY
NT ELECTROPHYSIOLOGY
NT EXERCISE PHYSIOLOGY
NT GRAVITATIONAL PHYSIOLOGY
NT NEUROPHYSIOLOGY
NT PSYCHOPHYSIOLOGY
NT RESPIRATORY PHYSIOLOGY
NT UNDERWATER PHYSIOLOGY
Conversion of acetic acid to methane by thermophiles
[DE93-014433] 01 p0300 N94-10652
Motion and spatial disorientation systems: Special research capabilities
[AD-A265155] 01 p0303 N94-11097
Arterial gas emboli in altitude-induced decompression sickness 01 p0312 N94-11543
Physiological water model development 01 p0316 N94-12367
Validated environmental and physiological data from the CELSS Breadboard Projects Biomass Production Chamber. BWT931 (Wheat cv. Yecora Rojo)
[NASA-TM-109191] 02 p0738 N94-13979
USAF physiological studies of personal microclimate cooling: A review
[AD-A267203] 03 p1022 N94-15858
Studies of aural acoustic emmissions with the use of an original apparatus and investigative methodology
[IFTR-20/1992] 03 p1177 N94-16650
Evaluation of spatial productivity patterns in an annual grassland during an AVIRIS overflight
[CIW-PUBL-1134] 03 p1067 N94-16672
Multitemporal diurnal AVIRIS images of a forested ecosystem 03 p1074 N94-16709
Using controlled daylight exposure and sleep timing in the prevention of shift lag during night operations
[AD-A269304] 04 p1504 N94-17824
Evaluation of dried storage of platelets for transfusion: Physiologic integrity and hemostatic functionality
[AD-A270756] 04 p1507 N94-19593
Physiologically based pharmacokinetic modelling of percutaneously absorbed dibromomethane utilizing multiple dermal sub-compartments
[AD-A271106] 05 p1889 N94-19981
Physiological correlates of stress-induced decrements in human perceptual performance
[DOT/FAA/AM-93/19] 05 p1893 N94-20081
Wind chill: The temperature feeling caused by the wind velocity
[KNMI-TR-103A] 05 p1890 N94-20238
Studies of neural and cognitive function in subjects exposed to the marine-air interface, phases 1 and 2
[AD-A272282] 05 p1891 N94-20624
Visual Problems in Night Operations
[AGARD-LS-187] 06 p2431 N94-23976
Use of infrared telemetry as part of a nonintrusive inflight data collection system to collect human factors data 06 p2434 N94-24193
ELF communications system ecological monitoring program
[AD-A273456] 06 p2299 N94-24676
Aeromedical issues related to positive pressure breathing for +Gz protection
[AD-A274717] 07 p2910 N94-26435
Multivariate calibration applied to near-infrared spectroscopy for the quantitative analysis of dilute aqueous solutions
[DE94-003231] 07 p2716 N94-26794
Eccentric exercise testing and training 07 p2934 N94-28363
Thermoregulation in the extreme cold environment 08 p3381 N94-28438
Physiological investigations of the isolated rat's liver in hypothermia and hypoxia and their relevance in aircraft incidents above the sea 08 p3382 N94-28439
Physiological Anatomical Rodent Experiment (PARE).04 feasibility test 2
[NASA-CR-195210] 08 p3385 N94-29968
A fuzzy logic controller for hormone administration using an implantable pump 08 p3397 N94-30459
Recommendations for meteorological data collection during physiological field studies
[AD-A276834] 09 p3901 N94-32153
The US Navy/Canadian DCIEM research initiative on pressure breathing physiology 10 p4101 N94-33636
Personal cooling systems: Possibilities and limitations 10 p4101 N94-33649
Activities of National Institute of Radiological Sciences
[DE94-727636] 11 p4296 N94-36101

PHYTOPLANKTON
Seasonal changes of phytoplankton distributions in the Northwest Pacific detected by Coastal Zone Color Scanner 01 p0200 N94-11948
Particle dynamics in the western subarctic Pacific: Implications from CZCS imagery 01 p0200 N94-11950
Development of shipboard ocean lidar 01 p0140 N94-11965
The development of phytoplankton sensing system with optical fiber 01 p0203 N94-11967
The seasonal change of phytoplankton size distribution using optical fiber sensor 01 p0210 N94-12656
The phytoplankton bloom in the Kinu-ura Bay, Japan in the rainy season 01 p0211 N94-12660
Variation of the photosynthetic products in the regional upwelling area around the Izu Islands, Japan 01 p0211 N94-12661
Optimum selection of spectral channels in the problem of remote sensing of phytoplankton concentration in ocean water 01 p0223 N94-12726
High biological production of the tidal mixing zones on Japan Sea shelf 01 p0228 N94-12758
Nonlinear relationships between particulate absorption and chlorophyll: Detritus or pigment packaging?
[AD-A266806] 02 p0731 N94-14899
Characterization of spatial and temporal variability of phytoplankton blooms in coastal waters
[AD-A267102] 03 p1116 N94-15633
Seasonal and spatial variations in phytoplanktonic chlorophyll in eutrophic Mono Lake, California, measured with the Airborne Visible and Infrared Imaging Spectrometer (AVIRIS) 03 p1069 N94-16684
Factors affecting the identification of phytoplankton groups by means of remote sensing
[NASA-TM-108799] 06 p2387 N94-24403
Nutrients and light as factors controlling phytoplankton biomass on the Dutch continental shelf (North Sea), 1988-1990
[PB94-111143] 06 p2418 N94-24601
Changes in phytoplankton population in the Chao Phraya estuary, Thailand, during the eutrophication mechanisms studies 07 p2875 N94-28287
Interaction processes between the ocean and the atmosphere 09 p3777 N94-30987
Light utilization and photoinhibition of photosynthesis in marine phytoplankton
[DE94-005505] 09 p3794 N94-32896
Bioluminescence bathyphotometer
[AD-D016102] 09 p3790 N94-32959
Phytoplankton blooms and coastal physical processes
[AD-A280646] 12 p4475 N94-36761

PHYTOTRONS
Statistical analysis of environmental variability within the CELSS breadboard project's biomass production chamber
[NASA-TM-109188] 01 p0315 N94-11258
Seed viability detection using computerized false-color radiographic image enhancement 08 p3387 N94-30461

PI-ELECTRONS
Planar poly(p-phenylene) derivatives: Ladder formation for maximization of extended conjugation
[AD-A273220] 06 p2260 N94-24922

PICKOFFS
U SENSORS

PICKUPS
U SENSORS

PICOSECOND PULSES
Nd:YLF laser for airborne/spaceborne laser ranging 03 p0913 N94-15563
A study of high field transport in wide band gap electronic materials using a picosecond transient charge technique
[AD-A267098] 03 p1008 N94-15636
Tetravalent chromium (Cr(4+)) as laser-active ion for tunable solid-state lasers
[NASA-CR-194528] 04 p1441 N94-19394
Infrared FEL photochemistry: Multiple-photon dissociation of freon gas
[DE94-000817] 05 p1820 N94-22585
Pump-probe method for investigating laser ablation and optical damage threshold mechanisms in optical materials
[DE94-008291] 09 p3720 N94-32753
10-GW CO2 laser system at the Brookhaven Accelerator Test Facility
[DE94-009001] 10 p4058 N94-34374

PICTURE ELEMENTS
U PIXELS

PIDV (VELOCIMETRY)
U PARTICLE IMAGE VELOCIMETRY

PIERS
U WHARVES

PIEZOELECTRIC CERAMICS
NT LEAD ZIRCONATE TITANATES
Smart structures at Aastra Corporation 01 p0069 N94-11326
Recent developments in piezoelectric and electrostrictive sensors and actuators for smart structures 01 p0070 N94-11332
Ceramic actuators for smart materials
[AD-A265664] 01 p0093 N94-12331
Active control of acoustic pressure fields using smart material technologies
[NASA-CR-191480] 02 p0768 N94-13354
Experimental and analytical analysis of the response of a smart beam to rate feedback
[AD-A266544] 02 p0557 N94-13706
Modeling and characterization of mechanoelectric conversion piezoelectric generators through dynamical or quasi static uniaxial stress
[ISAL-92-0097] 04 p1406 N94-19490
A study on piezoelectric actuators and sensors for vibration control of flexible space structures
[AD-A274925] 07 p2695 N94-26532
GEC Ferranti piezo vibratory gyroscope 08 p3239 N94-29790
Damage identification in composites using built-in piezoelectrics 08 p3184 N94-30355
Passive vibration damping materials: Piezoelectric ceramic composites for vibration damping applications
[AD-A276550] 09 p3653 N94-31935

Study on active control of waveguide with piezoceramic actuator
10 p4042 N94-34349
Active vibration damping using smart material
11 p4221 N94-35886

PIEZOELECTRIC GAGES
Application of piezoelectric stress gauges to the measurement of fast-rise-time multimegampere electric currents
[DE93-017625] 04 p1429 N94-18102
Free flight experiment with a laminar wing glove
05 p1639 N94-22600
Damage identification in composites using built-in piezoelectrics
08 p3184 N94-30355

PIEZOELECTRIC TRANSDUCERS
NT PIEZOELECTRIC GAGES
Active vibration control of adaptive flexible structures using piezoelectric smart sensors and actuators
01 p0189 N94-11823
Nanocomposites for electronic applications, volume 1
[AD-A267070] 03 p1009 N94-15669
Nanocomposites for electronic applications, volume 3
[AD-A267073] 03 p1009 N94-15672
Nanocomposites for electronic applications, volume 2
[AD-A267074] 03 p1009 N94-15673
Mechanical and surface force nanoprobe
[AD-D015792] 03 p1034 N94-16536
Fabrication of piezoelectric ceramic/polymer composites by injection molding
[AD-A267302] 03 p0972 N94-17227
Application of piezoelectric stress gauges to the measurement of fast-rise-time multimegampere electric currents
[DE93-017625] 04 p1429 N94-18102
Monolithic low noise preamplifier for piezoelectric sensors
[AD-D015860] 04 p1563 N94-18734
PVDF pressure transducers for shock wave and explosives research
[AD-A277319] 09 p3712 N94-32051
Detection of delaminations in composite beams using piezoelectric sensors
[NASA-TM-106611] 12 p4403 N94-36956

PIEZOELECTRICITY
Recent developments in piezoelectric and electrostrictive sensors and actuators for smart structures
01 p0070 N94-11332
Structural analysis and optimization of adaptive structures by use of the finite element method
01 p0071 N94-11339
Active damping augmentation of elastomechanical systems using piezoelectric sensors and actuators
01 p0072 N94-11346
Ceramic actuators for smart materials
[AD-A265664] 01 p0093 N94-12331
An acoustic charge transport imager for high definition television applications
[NASA-CR-194518] 02 p0650 N94-14029
Nanocomposites for electronic applications, volume 1
[AD-A267070] 03 p1009 N94-15669
Nanocomposites for electronic applications, volume 3
[AD-A267073] 03 p1009 N94-15672
Nanocomposites for electronic applications, volume 2
[AD-A267074] 03 p1009 N94-15673
Fabrication of piezoelectric ceramic/polymer composites by injection molding
[AD-A267302] 03 p0972 N94-17227
Two-dimensional, high flow, precisely controlled monodisperse drop source
[AD-A267660] 03 p1028 N94-17250
PVDF measurement of soft x ray induced shock and filter debris impulse
[DE93-017633] 04 p1382 N94-17806
Piezo-electric motor: Perspectives and miniaturization
04 p1408 N94-18015
Application of piezoelectric stress gauges to the measurement of fast-rise-time multimegampere electric currents
[DE93-017625] 04 p1429 N94-18102
Office of Naval Research Publications/Patents /Presentations/Honors report, 1 October 1992 - 30 September 1993
[AD-A270037] 04 p1632 N94-18791
Experiments and analysis of lateral piezoresistance gauges
[DE93-017874] 04 p1433 N94-19111
Modeling and characterization of mechanoelectric conversion piezoelectric generators through dynamical or quasi static uniaxial stress
[ISAL-92-0097] 04 p1406 N94-19490
The electromechanical properties of tetragonal BaTiO3 and PbTiO3 single crystals
[DE93-019008] 04 p1603 N94-19550
Proceedings of the 8th International Symposium on Applications of Ferroelectrics
[AD-A270679] 05 p1749 N94-20012
Application of change detection to dynamic contact sensing
[AD-A270523] 05 p1939 N94-20105
Actively controlled shaft seals for aerospace applications
[NASA-CR-194759] 05 p1823 N94-20538
Theoretical studies of wave propagation in multilayered piezoelectric media
[DE93-040273] 06 p2371 N94-22872
Ferroelectric thin films 3
[AD-A273394] 06 p2565 N94-25027
Object imaging accomplished with an integrated circuit robotic tactile sensor incorporating a piezoelectric polyvinylidene fluoride thin film
[AD-A274038] 07 p2780 N94-25845
Piezoelectric measurements on impact loaded PZT ceramics
[NPL-DMM(A)-88] 07 p2752 N94-26652
High temperature sensor/microphone development for active noise control
[NASA-CR-195214] 07 p2812 N94-27214
Piezoelectric materials research in Europe
[AD-A276207] 09 p3648 N94-31059
Electric field-induced changes in odd-numbered nylons
[AD-A278003] 09 p3664 N94-33138
Energy absorption apparatus
[AD-D016163] 10 p4133 N94-33699
Coupled electromechanical response of composite beams with embedded piezoelectric sensors and actuators
[NASA-CR-195313] 10 p4019 N94-33899
Aeroservoelastic tailoring with piezoelectric materials: Actuator optimization studies
[AD-A278640] 11 p4199 N94-36384

PIEZORESISTIVE TRANSDUCERS
NT PIEZOELECTRIC GAGES
High accuracy die mechanical stress measurement with the ATC04 Assembly Test Chip
[DE93-019435] 05 p1830 N94-20477

PIGMENTS
NT CAROTENE
NT CHLOROPHYLLS
Formulating infrared coatings for defence applications
[MRL-RR-1-93] 01 p0090 N94-11302
Materials Research Society Symposium Proceedings, Volume 292: Biomolecular Materials
[AD-A265776] 03 p1116 N94-15138
Polyurethane self-priming topcoats
[AD-D015870] 04 p1367 N94-17719
Polyurethane self-priming topcoats
[AD-D016041] 07 p2755 N94-27111
Oxide pigments in water: The colloid-chemical point of view
[PB94-148616] 09 p3633 N94-31591
Evolution of upwelling fronts off the coast of Portugal
[NASA-CR-195692] 09 p3790 N94-33045
Polyurethane self-priming topcoats
[AD-D016131] 10 p4027 N94-33697
Polyurethane self-priming topcoats
[AD-D016160] 10 p4030 N94-34285

PIGS (SWINE)
U SWINE

PILOT ERROR
Altitude deviations: Breakdowns of an error-tolerant system
[NASA-TM-108788] 03 p0862 N94-15550
Aircraft accident report: Runway departure following landing American Airlines flight 102, McDonnell Douglas DC-10-30, N139AA, Dallas/Fort Worth International Airport, Texas, April 14, 1993
[PB94-910402] 07 p2660 N94-27766
Flight technical error for category B non-precision approaches and missed approaches using non-differential GPS for course guidance
[PB94-142734] 09 p3576 N94-31680
Autogenic-feedback training improves pilot performance during emergency flying conditions
10 p4098 N94-33622
Aircraft accident report: Controlled flight into terrain Federal Aviation Administration Beech Super King Air 300/F, N82, Front Royal, Virginia, 26 October 1993
[PB94-910405] 10 p3987 N94-34390
Safety study: A review of flightcrew-involved, major accidents of US air carriers, 1978 through 1990
[PB94-917001] 11 p4191 N94-35482
Aircraft accident report: Uncontrolled collision with terrain, American International Airways Flight 808, Douglas DC-8-61, N814CK, US Naval Air Station, Guantanamo Bay, Cuba, 18 August 1993
[PB94-910406] 11 p4192 N94-35521

PILOT INDUCED OSCILLATION
Aircraft digital flight control technical review
06 p2163 N94-25106
A handling qualities investigation of conventional, rate command and attitude hold, and attitude command and attitude hold response types in the probe and drogue air refueling task
[AD-A278464] 10 p4006 N94-33543

PILOT PERFORMANCE
Aviation accident risk for airmen with aphakia and artificial lens implants
[DOT/FAA/AM-93/11] 01 p0303 N94-10813
Quantitative EEG patterns of differential in-flight workload
01 p0317 N94-11528
Psychophysiological measures of cognitive workload in laboratory and flight
01 p0317 N94-11529
Criteria for assessing problem solving and decision making in complex environments
01 p0314 N94-11532
A comparison of head-up and head-down display formats during instrument flying tasks
[AD-A266140] 01 p0316 N94-11642
The aging military aviator: A review and annotated bibliography
[AD-A265341] 01 p0311 N94-12423
Cognitive engineering in aerospace application: Pilot interaction with cockpit automation
[NASA-CR-177617] 02 p0510 N94-13247
Piloting Vertical Flight Aircraft: A Conference on Flying Qualities and Human Factors
[NASA-CP-3220] 02 p0521 N94-13294
A perspective on the FAA approval process: Integrating rotorcraft displays, controls and workload
02 p0521 N94-13298
Improvements in hover display dynamics for a combat helicopter
02 p0523 N94-13310
Visual information for judging temporal range
02 p0524 N94-13314
Visual cueing considerations in Nap-of-the-Earth helicopter flight head-slaved helmet-mounted displays
02 p0524 N94-13315
Primary display latency criteria based on flying qualities and performance data
02 p0525 N94-13318
Human factor implications of the Eurocopter AS332L-1 Super Puma cockpit
02 p0525 N94-13319
Piloting considerations for terminal area operations of civil tiltwing and tiltrotor aircraft
02 p0525 N94-13320
The identification of ability requirements and selection instruments for fighter pilot training
[AD-A266340] 02 p0735 N94-13582
The influence of ATC message length and timing on pilot communication
[NASA-CR-177621] 02 p0512 N94-14744
Validity of FAA-approved color vision tests for class 2 and class 3 aeromedical screening
[DOT/FAA/AM-93/17] 02 p0735 N94-14846
An information processing classification of beyond-visual-range air intercepts
[AD-A266927] 03 p1131 N94-15108
Predicting radiation induced performance decrements of AH-1 helicopter crews. Volume 1: Predicted veersus actual performance of AH-1 crews induced with symptoms simulating radiation sickness
[AD-A268376] 03 p1138 N94-17460
Research on man-machine productivity in aviation at Human Engineering Institute of Hangzhou University
[AD-A269952] 04 p1512 N94-18673
VMC left turn curved approaches, test results --- (visual meteorological conditions)
[AD-A269476] 04 p1316 N94-18728
Integrated measurement of crew resource management and technical flying skills
[AD-A270512] 04 p1510 N94-19677
Perception/action: An holistic approach 2
[AD-A271822] 05 p1891 N94-20627
Modelling decision-making by pilots
[NASA-CR-194767] 05 p2040 N94-21821
Pilot-vehicle interface
[DOT/FAA/CT-92/21] 06 p2430 N94-23083
Pilot evaluation system
06 p2158 N94-24266
Combined 1991 and 1992 Robinson-22B (R-22) parking test results
[AD-A273550] 06 p2193 N94-24559
Extracting heading and temporal range from optic flow: Human performance issues
06 p2442 N94-25510
Sensor fusion display evaluation using information integration models in enhanced/synthetic vision applications
06 p2443 N94-25512
Quality metrics for sensor images
06 p2443 N94-25513
US Army aviation epidemiology data registry: Incidence and outcomes of aviator flying evaluation boards
[AD-A274711] 07 p2910 N94-26432
Piloted simulation study of an ILS approach of a twin-pusher business/commuter turboprop aircraft configuration
[NASA-TM-4516] 07 p2646 N94-26602

Task demand, workload, and performance
[PB94-123627] 07 p2942 N94-27155
Brain wave correlates of attentional states: Event related potentials and quantitative EEG analysis during performance of cognitive and perceptual tasks
07 p2940 N94-27901
The Reports of Aeromedical Laboratory, volume 33, number 4
[JTN-94-80586] 07 p2933 N94-27942
Comparison of performance in simulator flight among subjects with different simulator experiences
07 p2933 N94-27943
Evaluation of near-infrared spectrophotometric method for individual tolerance to +Gz acceleration
07 p2933 N94-27944
Symptoms of hypoxia at simulated altitude of 25,000 feet 07 p2933 N94-27945
Disturbance of equilibrium on JAL flight crew
08 p3390 N94-28856
Human pilot response during single- and multi-axis tracking tasks
[AD-A275080] 08 p3398 N94-28887
Information presentation for expert systems in future fighter aircraft
[AD-A275126] 08 p3149 N94-29005
Aircraft accident/incident summary report: In-flight loss of control, leading to forced landing and runway overrun, Continental Express, Inc., N24706 Embraer EMB-120 RT, Pine Bluff, Arkansas, 29 April 1993
[PB94-910404] 08 p3135 N94-29402
Japanese Journal of Aerospace and Environmental Medicine, vol. 30, no. 2
[JTN-94-80599] 08 p3394 N94-29863
Psychophysiological study on the effects of co-existence of lines for detecting dot target
08 p3394 N94-29867
Flight simulator evaluation of advanced MLS procedures
[AD-B174270] 08 p3143 N94-30915
Aircraft simulation and pilot proficiency: From surrogate flying towards effective training
[AD-B179300] 09 p3587 N94-31179
Situational awareness: A feasibility investigation of near-threshold skills development
[AD-A276467] 09 p3798 N94-31243
Flight technical error for category B non-precision approaches and missed approaches using non-differential GPS for course guidance
[PB94-142734] 09 p3576 N94-31680
Fuzzy logic application for modeling man-in-the-loop space shuttle proximity operations
[NASA-CR-188263] 09 p3835 N94-32359
The effects of Above Real-Time Training (ARTT) in an F-16 simulator 09 p3591 N94-32474
Pilot GPS/LORAN receiver programming performance: A laboratory evaluation
[AD-A278258] 10 p3988 N94-33412
Laboratory and in-flight experiments to evaluate 3-D audio display technology 10 p4038 N94-33618
Autogenic-feedback training improves pilot performance during emergency flying conditions
10 p4098 N94-33622
Expanding the pilot's envelope
10 p3994 N94-34627
Effects of checklist interface on non-verbal crew communications
[NASA-CR-177639] 10 p3987 N94-34915
Safety study: A review of flightcrew-involved, major accidents of US air carriers, 1978 through 1990
[PB94-917001] 11 p4191 N94-35482
Aircraft accident report: Uncontrolled collision with terrain, American International Airways Flight 808, Douglas DC-8-61, N814CK, US Naval Air Station, Guantanamo Bay, Cuba, 18 August 1993
[PB94-910406] 11 p4192 N94-35521
The prediction of pilot opinion ratings using optimal and sub-optimal pilot models
[AD-A278679] 11 p4298 N94-35692
Review of human factors problems related to long distance and long endurance operation of aircraft
11 p4195 N94-36336
The use of a tactile interface to convey position and motion perceptions 12 p4486 N94-37281
Human factors for flight deck certification personnel
[AD-A280477] 12 p4487 N94-37347
Composite helicopter accident profiles: Deficient crew/aircraft performance
[SCT-90RR-46] 12 p4365 N94-37604
Synthetic vision display evaluation studies
[NASA-CR-194963] 12 p4387 N94-37658

PILOT PLANTS
Statistical procedures for corrosion studies
[PB93-199412] 06 p2244 N94-23802
Liquid metal MHD research and development in Israel
07 p2854 N94-26055
NIPER Lab WARDEN: Descriptive panels and diagrams for NIPER Lab WARDEN software, volume 2
[DE94-000126] 12 p4493 N94-36699

PILOT SELECTION
Basic attributes test (BAT): Operational pre-implementation analysis and score equating
[AD-A265885] 01 p0314 N94-12276
The identification of ability requirements and selection instruments for fighter pilot training
[AD-A266340] 02 p0735 N94-13582
Cardiopulmonary Aspects in Aerospace Medicine
[AGARD-LS-189] 06 p2423 N94-23313
Screening for asymptomatic coronary heart disease
06 p2423 N94-23315
Aeromedical disposition for coronary artery disease
06 p2423 N94-23316
Echocardiographic screening of aircrew candidates
06 p2424 N94-23319
Aortic valve disease 06 p2424 N94-23322
Asthma in aircrew 06 p2425 N94-23327
Female combat helicopter pilot selection criteria
[AD-A273935] 07 p2938 N94-26749
Comparison of performance in simulator flight among subjects with different simulator experiences
07 p2933 N94-27943

PILOT TRAINING
Flight simulator experiment of the cockpit advisory system
[NAL-TR-1151] 01 p0033 N94-10733
Transfer of training for aerospace operations: How to measure, validate, and improve it
01 p0314 N94-11530
Criteria for assessing problem solving and decision making in complex environments
01 p0314 N94-11532
Basic attributes test (BAT): Operational pre-implementation analysis and score equating
[AD-A265885] 01 p0314 N94-12276
Cognitive engineering in aerospace application: Pilot interaction with cockpit automation
[NASA-CR-177617] 02 p0510 N94-13247
The identification of ability requirements and selection instruments for fighter pilot training
[AD-A266340] 02 p0735 N94-13582
Determination of Loran-C/GPS human factors issues
[AD-A266334] 02 p0514 N94-14563
Activity/rest patterns of instructor and rates student pilots during rapid transitions from daytime to nighttime duty hours at the Eastern Army Aviation Training site
[AD-A267038] 03 p1131 N94-15659
Modelling decision-making by pilots
[NASA-CR-194767] 05 p2040 N94-21821
Public-sector aviation issues: Graduate research award papers, 1991-1992
[PB93-206258] 05 p1642 N94-22055
Pilot evaluation system 06 p2158 N94-24266
A simulation study of control and display requirements for zero-experience general aviation pilots
06 p2163 N94-25102
Symptoms of hypoxia at simulated altitude of 25,000 feet 07 p2933 N94-27945
Aircraft simulation and pilot proficiency: From surrogate flying towards effective training
[AD-B179300] 09 p3587 N94-31179
Situational awareness: A feasibility investigation of near-threshold skills development
[AD-A276467] 09 p3798 N94-31243
The effects of Above Real-Time Training (ARTT) in an F-16 simulator 09 p3591 N94-32474
Autogenic-feedback training as a treatment for airsickness in high-performance military aircraft: Two case studies
[NASA-TM-108810] 09 p3801 N94-33068
Autogenic-feedback training improves pilot performance during emergency flying conditions
10 p4098 N94-33622
Operational agility assessment with the AM-X aircraft
10 p3994 N94-34626

PILOTED CENTRIFUGES
U HUMAN CENTRIFUGES

PILOTLESS AIRCRAFT
NT DRONE AIRCRAFT
NT FIREBEE 2 TARGET DRONE AIRCRAFT
NT TARGET DRONE AIRCRAFT
Low-cost, dual-use platforms for environmental sensing, phase 1
[AD-A272951] 05 p1646 N94-21246
A conceptual design of an unmanned test vehicle using an airbreathing propulsion system
[NASA-CR-195550] 06 p2189 N94-25085
An analysis of multiple sensor system payloads for unmanned aerial vehicles
[AD-A274905] 07 p2667 N94-26182
Payload central control for unmanned aircraft
08 p3155 N94-30284
Army scout/reconnaissance helicopters versus unmanned aerial vehicles
[AD-A276902] 09 p3579 N94-32232
Design and Monte Carlo analysis of an unmanned aerial vehicle
[AD-A277648] 09 p3580 N94-33056
Aerial robotic data acquisition system
[DE94-009114] 10 p4076 N94-33938
Technological challenges of High Altitude Long Endurance unmanned configurations
11 p4193 N94-36323
UAV's in climate research: The ARM Unmanned Aerospace Vehicle Program
[DE94-011753] 12 p4465 N94-37154

PILOTS
ATC/pilot voice communications: A survey of the literature
[DOT/FAA/AM-93/20] 05 p1738 N94-21201

PILOTS (PERSONNEL)
NT AIRCRAFT PILOTS
NT TEST PILOTS
Work conditions assessment in pilots and ground personnel under high weather temperatures
08 p3382 N94-28444
Human pilot response during single- and multi-axis tracking tasks
[AD-A275080] 08 p3398 N94-28887

PINCH EFFECT
NT PLASMA PINCH
NT REVERSE FIELD PINCH
NT THETA PINCH
NT ZETA PINCH
Plasma-puff initiation of high Coulomb transfer switches
[NASA-CR-193186] 04 p1591 N94-19441
Research on plasma-puff initiation of high Coulomb transfer switches
[NASA-CR-194371] 05 p1994 N94-21289
Plasma-puff initiation of high Coulomb transfer switches 05 p1994 N94-21290
Characteristics of plasma-puff trigger for a inverse-pinch plasma switch 05 p1995 N94-21291
Characteristics of switching plasma in an inverse-pinch switch 05 p1995 N94-21292
Comparative study of INPIStron and spark gap
05 p1995 N94-21293
Pinched propagation of high-power, pulsed electron beams for welding and materials processing applications
[AD-A276925] 09 p3726 N94-32236
Plasma physics applications to intense radiation sources, pulsed power and space physics. Short pulse ultra intense laser-plasma interaction experiment
[AD-A278440] 10 p4144 N94-33555

PINEAL GLAND
TransRapid TR-07 maglev-spectrum magnetic field effects on daily pineal indoleamine metabolic rhythms in rodents
[DE93-015143] 03 p1117 N94-16893
Melatonin, the pineal gland, and circadian rhythms
[AD-A268200] 03 p1129 N94-17478
Melatonin, the pineal gland, and circadian rhythms
[AD-A280467] 12 p4481 N94-37140

PINHOLE CAMERAS
High resolution time- and 2-dimensional space-resolved x ray imaging of plasmas at NOVA
[DE93-011892] 01 p0393 N94-11677

PINHOLES
Multisensor pinhole yawsonde
[AD-A271715] 05 p1808 N94-20930

PINNACLES
U PEAKS (LANDFORMS)

PINNING
NT FLUX PINNING
High frequency behavior of long and small junctions
[AD-A265670] 01 p0403 N94-12336
Relaxation of hysteresis loop in a single crystal of YBa2Cu4O8
[DE93-019519] 05 p2029 N94-21649
Microstructural development in low activation ferritic alloys irradiated to 200 dpa at 420 C
[DE94-004269] 07 p2731 N94-25803
The potential for large critical currents in the high T(sub c) oxides 07 p2854 N94-26058
Evaluation of APC NbTi superconductor in a model dipole magnet
[DE94-003258] 07 p3060 N94-26795
Processing, fabrication, and demonstration of HTS integrated microwave circuits, appendix A
[AD-A274600] 07 p2785 N94-26890
Effect of twin boundary density on the vortex melting transition in YBa2Cu3O(7-delta) single crystals
[DE94-007684] 09 p3904 N94-32601
Critical-state flux-density profiles in type-2 superconducting thin-film strips and disks
[DE94-011199] 12 p4535 N94-37166

PINS
Extensions of some guidelines for the mechanical design of coaxial compression pin seals
[DE93-012385] 01 p0177 N94-10348
Crystal chemistry and self-lubricating properties of monochalcogenides gallium selenide and tin selenide
[DE93-041177] 07 p2751 N94-26422
Guidelines for unlubricated sliding wear tests. Part 2: Procedures for pin-on-disc testing
[PB94-123270] 07 p2825 N94-27324
Pip pin reliability and design 09 p3605 N94-33305
PINTLES
Atomization characteristics of a prefilming airblast atomizer
[NAL-TM-644] 01 p0148 N94-10727
Inherent stability of central element coaxial liquid-liquid injectors 06 p2212 N94-23043
PION BEAMS
Relativistic heavy ion research
[DE93-013127] 01 p0367 N94-11373
Study on the compensated lead hadron calorimeter characteristics by means of hadron and electron beams
[DE93-634176] 07 p2810 N94-26439
BNL possibilities
[DE94-007179] 09 p3864 N94-31398
PIONEER PROJECT
NASA images 11
[NASA-TM-109287] 02 p0842 N94-13626
PIONEER SPACE PROBES
The 1978 highlights
[NASA-TM-109625] 03 p1302 N94-15411
The 1968 highlights --- NASA programs and research
[NASA-TM-109627] 03 p1302 N94-15413
The 1982 highlights
[NASA-TM-109671] 03 p1303 N94-15508
PIONEER VENUS ORBITER
U PIONEER VENUS 1 SPACECRAFT
PIONEER VENUS SPACECRAFT
NT PIONEER VENUS 1 SPACECRAFT
Pioneer-Venus press clip --- Solar System formation and extraterrestrial life
[NASA-TM-109425] 03 p1239 N94-15495
SO2 on Venus: A final cross-calibration with Pioneer Venus
[NASA-CR-195162] 06 p2599 N94-24988
Correlation studies of Pioneer Venus imagery obtained from PV experiments with near IR imagery obtained from ground-based observations during Venus inferior conjunction
[NASA-CR-195772] 08 p3550 N94-29892
Taxonomy of gamma ray burster data using a self-organizing neural network
[DE94-006480] 08 p3553 N94-30248
PIONEER VENUS 1 SPACECRAFT
Pioneer Venus data analysis for the retarding potential analyzer
[NASA-CR-194673] 03 p1297 N94-17292
PIONEER 12 SPACE PROBE
U PIONEER VENUS SPACECRAFT
PIONS
Strangeness production with protons and pions
[DE93-010879] 01 p0359 N94-10304
Crossing-odd spin effects in the dipole model of hadron scattering
[DE93-617692] 01 p0362 N94-10551
Coherence influence on the intensity of Bose-Einstein correlations and visible size of a source
[DE93-617697] 01 p0349 N94-10556
Pion correlations and calorimeter design for high energy heavy ion collisions
[DE93-013861] 01 p0373 N94-12607
Low energy response of the DO calorimeter and jet energy measurement
[DE93-013569] 02 p0781 N94-13350
Dynamics of pion-nucleus systems
[DE93-014449] 02 p0785 N94-14468
Experimental study of weak interactions by precision measurement by rare kaon decay
[DE93-016864] 03 p1182 N94-16117
A high sensitivity search for CP violating rare K(sub L) decays and precision measurement of the direct CP violation parameter (epsilon)(prime)/(epsilon) via the four K (yields) 2(pi) decay modes
[DE93-016866] 03 p1184 N94-16899
On the difference caused by CP violation in the energy spectra of pions in K(sup (+-))(yields)(pi)(+-)(pi)(+-)(pi)-+ decays
[DE93-624828] 04 p1564 N94-17687
Meson production in relativistic heavy-ion collisions at AGS energies
[DE93-016871] 04 p1565 N94-17984
Evaluation of the chemical composition of cosmic radiation in energy area of 10(exp 15) eV
[ETN-93-93682] 05 p2150 N94-21056
Qualitative and quantitative aspects of the QCD theory of elastic form factors
[DE93-040864] 05 p2038 N94-21513
Low p(sub T) phenomena observed in high energy nuclear collisions
[DE94-000825] 05 p1982 N94-21849
Pions and neutrinos as probes of the nucleon and nuclear few-body system
[DE93-040127] 06 p2531 N94-22928
Gauge invariance and the electromagnetic current of composite pions
[DE93-040869] 06 p2532 N94-22952
Low p(sub T) photon production in proton-nucleus collisions at 18 GeV/c
[DE94-001380] 06 p2532 N94-23007
Calculations of Bose-Einstein correlations from Relativistic Quantum Molecular Dynamics
[DE94-000794] 06 p2569 N94-23453
New evaluation of hadronic contributions to the anomalous magnetic moment of charged leptons
[DE93-634394] 06 p2536 N94-24844
On the hadron formation time in pion-nucleus interaction
[DE93-616879] 06 p2539 N94-25476
Theoretical and computational studies in intermediate energy nuclear physics
[DE94-004177] 07 p3012 N94-25800
Experimental study of the near threshold pi(sup +)p yields (pi(sup +))(pi(sup +))(n) cross section and chiral symmetry
[DE93-601671] 07 p3014 N94-25840
Meson X(1814) as a candidate for a hybrid state
[DE93-634447] 07 p3017 N94-26045
Pion-nucleus interactions and the STAR experiment at RHIC
[DE94-000658] 07 p3021 N94-26586
Low-energy hadronic interactions beyond the current algebra approach
[DE94-602600] 07 p3022 N94-26900
Study of the process (pi)(sup -)A(yields)(pi)(sup -)(eta)'(eta)A at the moment 36 GeV/c
[DE93-634530] 07 p3024 N94-27250
Pi plus pi minus gamma and K+ K- production in two photon collisions at ARGUS
[ISBN-0-315-63598-3] 07 p3027 N94-27684
Medium energy measurements of N-N parameters
[DE94-006067] 09 p3869 N94-32173
Chiral symmetry and the threshold gamma(p) yields pi(sup 0)p reaction
[DE94-008117] 09 p3873 N94-32710
Pion-nucleon interaction in nuclear matter above the Delta resonance energy
[DE94-727455] 10 p4137 N94-33994
Studies in intermediate energy nuclear physics
[DE94-007602] 10 p4140 N94-34381
Goldstone pion and other mesons using a scalar confining interaction
[DE94-010016] 11 p4321 N94-35649
Calculations on some properties of the pion in the framework of Schwinger-Dyson and Bethe-Salpeter equations
[DE94-611232] 11 p4322 N94-35786
Elastic charge form factors for K mesons
[DE94-010014] 11 p4325 N94-36086
Angular dependence of parton-parton scattering extracted from hadron pair production in pp collisions at radicals equal to 11.5 GeV
[DE94-611174] 12 p4511 N94-36504
Measurement and processing of gammas accompanying muon pairs in the reaction pi(-)C yields mu(+)mu(-) + gamma + X at 38 GeV
[DE94-617044] 12 p4512 N94-36523
Radiative and rare mu and pi decays
[DE94-618549] 12 p4515 N94-37066
Mass identified particle production and Bose Einstein correlations at 1800 GeV
[DE94-013418] 12 p4515 N94-37067
Kaon correlation systematics in E859
[DE94-011927] 12 p4516 N94-37158
Comparison of oxygen and silicon induced reactions at 14.6 A(GeV/C)
[DE94-011923] 12 p4518 N94-37364
PIPE FLOW
Flow development in a circular pipe in the UTIAS/RPI M = 8.3 gun tunnel 01 p0006 N94-10442
Suppression of the near wall burst process of a fully developed turbulent pipe flow
[AD-A265995] 01 p0161 N94-12352
Nonlinear stability calculations of pipe flow 01 p0163 N94-12612
Potential flow in in-line and staggered tube banks
[IME-CRE-TR-006] 02 p0637 N94-13862
On solving the compressible Navier-Stokes equations for unsteady flows at very low Mach numbers
[NASA-TM-106380] 03 p1027 N94-17128
Examinations of the friction behavior in nonstationary flow processes in pipes
[MITT-7] 04 p1423 N94-19730
Features of a SINDA/FLUINT model of a liquid oxygen supply line 06 p2322 N94-23649
Comparison of numerical simulation and experimental data for steam-in-place sterilization 06 p2326 N94-23669
Heat pipe vapor dynamics
[NASA-CR-194217] 06 p2327 N94-24096
Modeling dynamically coupled fluid-duct systems with finite line elements
[NASA-CR-193909] 06 p2376 N94-24359
Interactive control in turbulent shear layers
[AD-A273544] 06 p2336 N94-24793
Decay of swirl in turbulent pipe flows
[ETN-94-95353] 06 p2339 N94-25248
Experimental contribution to the study of secondary flows in centrifugal turbopump stator components
[ECL-92-35] 07 p2789 N94-25654
Development of buoyancy affected laminar flow in a heated pipe 08 p3128 N94-28988
Mutual similarity of developing laminar flows with secondary streams in ducts: Curved pipe flow and orthogonal rotating pipe flow 08 p3129 N94-28989
Two-phase power-law modeling of pipe flows displaying shear-thinning phenomena
[DE94-005115] 08 p3279 N94-30020
Controlling the material properties of in vitro collagen through directed orientation and cross-linking of fibrils 08 p3221 N94-30797
Fluid-structure interaction in case of water hammer with cavitation
[PB94-148277] 09 p3702 N94-31588
Incompressible viscous flow in tubes with occlusions
[ISBN-0-315-75467-2] 09 p3704 N94-31778
Electromagnetic probe technique for fluid flow measurements 09 p3711 N94-32455
PIPELINES
Upgrading of raw natural gas using high-performance polymer membranes
[DE93-014041] 02 p0566 N94-14586
Demonstration of polyscann ultrasonic butt-fusion inspection system for polyethylene pipes
[AD-A273279] 06 p2373 N94-24814
Proceedings of the 12th International Congress: Corrosion Control for Low-Cost Reliability. Volume 4: Oil/Gas Pipeline
[AD-A273665] 06 p2250 N94-25405
Maglev crude oil pipeline 11 p4226 N94-35919
Role of magma-water interaction in very large explosive eruptions
[DE94-002698] 11 p4291 N94-36103
First results from a prototype level-1 calorimeter trigger system for LHC, RD 27 (UK) collaboration
[PB94-167475] 12 p4436 N94-36532
The potential for control of carbon dioxide emissions from integrated gasification/combined-cycle systems
[DE94-012646] 12 p4465 N94-37100
Jumper connector analysis
[DE94-010373] 12 p4451 N94-37188
PIPELINING (COMPUTERS)
Cesar user library
[FFI-93/7021] 04 p1529 N94-19378
Avoiding and tolerating latency in large-scale next-generation shared-memory multiprocessors 05 p1753 N94-21081
Instruction set commutivity 05 p1766 N94-21719
Using stream interleaving to eliminate the need for interlocks in deeply pipelined processors 05 p1781 N94-22175
A fast Fourier transform radix-2 complex butterfly with built-in self-test
[ISBN-0-315-84139-7] 07 p2982 N94-27649
Investigation of modularly configured attached processors with intelligent memories
[AD-A278418] 09 p3839 N94-33330
Storage media pipelining: Making good use of fine-grained media 10 p4155 N94-33816
Adaptable binary programs
[AD-A280243] 12 p4494 N94-37119
PIPER AIRCRAFT
VSAERO analysis of a Piper Cub aircraft 02 p0516 N94-14616
PIPES (TUBES)
NT GAS PIPES
NT U BENDS
A new and efficient way to join composite pipes 01 p0063 N94-10054
Separation of gravitational effects on the flow of suspension in tubes by measurements in weightlessness 01 p0105 N94-10105
An investigation on the effectiveness of the piping interference removal system for STOL aircraft wind tunnel tests
[NAL-TM-647] 01 p0002 N94-10350

Fracture mechanics and full scale pipe break testing for the Department of Environment's New Production Reactor-Heavy Water Reactor
[DE93-005428] 01 p0187 N94-11169
Potential flow in in-line and staggered tube banks
[IME-CRE-TR-006] 02 p0637 N94-13862
Long baseline watertubes 03 p1037 N94-15803
Potential transients, transmission and electrochemical corrosion detection
[DE93-014055] 03 p0956 N94-15922
Investigation of two-phase flow and boiling heat transfer during quenching of a tube under microgravity 03 p0979 N94-16087
Summary of work on coatings and claddings for fossil energy applications
[DE93-017005] 04 p1367 N94-17881
Wideband electromagnetic scattering/analysis program: Far zone electromagnetic scattering from complex shapes using geometrical theory of diffraction
[AD-A268790] 04 p1384 N94-18187
Evaluation of the fabricability of advanced iron aluminide-clad austenitic stainless steel tubing
[DE93-040598] 05 p1693 N94-21771
Fabrication of whisker-toughened alumina tubes
[DE94-001012] 05 p1677 N94-22022
Characterization of the microstructure of Nb-1wt.%Zr-0.1wt.%C tubes as affected by thermomechanical processing
[NASA-TM-106381] 06 p2242 N94-23550
Statistical procedures for corrosion studies
[PB93-199412] 06 p2244 N94-23802
Weld joint concepts for on-orbit repair of Space Station Freedom fluid system tube assemblies 06 p2371 N94-24427
Method and apparatus for the non-invasive measurement of pressure inside pipes using a fiber optic interferometer sensor
[AD-D016013] 06 p2344 N94-24734
Strength and life of pressure vessels subjected to impacts and thermomechanical GFRP loading
[VTT-JULK-771] 06 p2379 N94-25418
Testing composite-to-metal tubular lap joints
[DE94-003225] 07 p2836 N94-26032
Growth of small fatigue cracks in Incoloy-908
[DE94-003406] 07 p2836 N94-26129
Development of detection technique for fatigue crack due to thermal stratification phenomena in RCS piping
[DE93-632968] 07 p2838 N94-26400
Template synthesis of metal microtubule ensembles utilizing chemical, electrochemical, and vacuum deposition techniques
[AD-A274676] 07 p2715 N94-26444
Dynamics of a flexible extendible beam
[ISBN-0-315-84278-4] 07 p2838 N94-26639
Fabrication and testing of plasma-spray formed MoSi2 and MoSi2 composite tubes
[DE94-004995] 08 p3175 N94-28581
The influence of wall conductivity of film condensation with integral fin tubes
[AD-A275503] 08 p3523 N94-28662
Similarity between turbulent flows through curved pipe and orthogonal rotating pipe 08 p3128 N94-28986
Two-phase power-law modeling of pipe flows displaying shear-thinning phenomena
[DE94-005115] 08 p3279 N94-30020
The universal applications of microtubes and microtube composites 08 p3186 N94-30452
Methodology for damage study of a tube-grill contact
[ECL-92-49] 09 p3734 N94-31562
Fluid-structure interaction in case of water hammer with cavitation
[PB94-148277] 09 p3702 N94-31588
Modeling of residual stress mitigation in austenitic stainless steel pipe girth weldment
[DE94-007184] 09 p3738 N94-32639
Atomic oxygen reactor having at least one sidearm conduit
[NASA-CASE-MSC-21487-4] 11 p4250 N94-35445
Mitigation of harmful effects of welds in zirconium alloy components
[DE94-619033] 12 p4414 N94-36543
Jumper connector analysis
[DE94-010373] 12 p4451 N94-37188

PISTON ENGINES
NT DIESEL ENGINES
NT FREE-PISTON ENGINES
NT STIRLING ENGINES
Piston engine intake and exhaust system design
[ISVR-TR-222] 02 p0663 N94-13874
Some single-piston closed-cycle machines and Peter Tailer's thermal lag engine
[DE93-015983] 03 p1049 N94-17675
Internal combustion engine with a central crankshaft and integral tandem annular pistons
[CA-PATENT-1-320-878] 06 p2363 N94-24055
The effect of high altitude pressure on the power and efficiency of an airborne two-stroke engine 06 p2155 N94-24253
Controllability of free-piston Stirling engine/linear alternator driving a dynamic load
[NASA-TM-106497] 06 p2521 N94-24302
The hydrogen hybrid option
[DE94-006733] 09 p3667 N94-32148
Unleaded AVGAS program
[AD-A278650] 11 p4247 N94-35795
The STRATO 2C propulsion system: A low cost approach for a High Altitude Long Endurance aircraft 11 p4195 N94-36335

PISTON THEORY
Nonlinear equations of motion for a panel subject to external loads
[AD-A273142] 06 p2170 N94-24773

PISTONS
Cooled spool piston compressor
[NASA-CASE-MSC-22020-1] 01 p0179 N94-10674
Instantaneous engine frictional torque: Its components and piston assembly friction
[DE93-011639] 01 p0182 N94-11625
Ceramics technology project database
[DE93-012431] 01 p0091 N94-11672
Double inlet pulse tube cryocooler theory
[AD-A266832] 02 p0597 N94-14877
Hydraulic pump with integral electric motor
[AD-D015782] 03 p1011 N94-16549
Design of non-sled setup to measure head injury criteria
[NIAR-92-20] 03 p0872 N94-17263
High temperature hydraulic seals
[AD-A268257] 03 p1048 N94-17433
Some single-piston closed-cycle machines and Peter Tailer's thermal lag engine
[DE93-015983] 03 p1049 N94-17675
Studies of dynamic contact of ceramics and alloys for advanced heat engines
[DE93-016366] 04 p1368 N94-18110
Acoustic propagation modeling using MATLAB
[AD-A270905] 04 p1564 N94-19750
The flow of gas across the piston-segments-cylinder interface
[ECL-92-40] 05 p1824 N94-20594
Vapor-delivered lubrication of steel-steel and steel-ceramic systems
[PB93-202364] 05 p1825 N94-21451
Carbon-carbon piston development
[NASA-CR-4595] 11 p4233 N94-35947

PITCH
On non-linear longitudinal stability of an aircraft in a dive in the presence of atmospheric disturbances 01 p0031 N94-11492
Segmentation and frequency domain ML pitch estimation of speech signals 05 p1747 N94-22212

PITCH (INCLINATION)
The free decay of coupled heave and pitch motions of a model frigate
[DRA/TM(AWMH)92340] 03 p1146 N94-15702
Effects of internal yaw-vectoring devices on the static performance of a pitch-vectoring nonaxisymmetric convergent-divergent nozzle
[NASA-TP-3369] 03 p0858 N94-16572
LDA measurements of the unsteady near wake behind an airfoil undergoing transient and periodic pitching motions
[ISL-CO-215/92] 06 p2165 N94-23161
The influence of elastic pitch variations on helicopter flight mechanics 06 p2161 N94-24286
Piloted simulation study of two tilt-wing flap control concepts, phase 2
[NASA-TM-108817] 10 p4006 N94-33998
Comparison of pitch rate history effects on dynamic stall 10 p3996 N94-34968
Effect of initial acceleration on the development of the flow field of an airfoil pitching at constant rate 10 p3987 N94-34989
Data reduction, analysis and results of LACV-30-07 air cushion vehicle tests, Fort Story, VA, August - September 1993
[AD-A278859] 11 p4190 N94-35826

PITCH ANGLES
U PITCH (INCLINATION)

PITCH ATTITUDE CONTROL
U LONGITUDINAL CONTROL

PITCHING MOMENTS
Unsteady flow past a NACA 0012 airfoil pitching at constant rates
[AD-A265159] 01 p0016 N94-11889
Numerical simulation of dynamic stall of NACA0012 airfoil oscillating near static stall angle using the Navier-Stokes equations
[DE93-767970] 02 p0505 N94-14061
Suppression of dynamic stall with a leading-edge slat on a VR-7 airfoil
[NASA-TP-3357] 03 p0856 N94-15657
Comparison between swept and delta canards on a model of a combat aircraft
[AD-A269561] 04 p1317 N94-17826
Aerodynamic characteristics of a helicopter rotor airfoil as affected by simulated ballistic damage
[AD-A269206] 04 p1311 N94-18413
Lift and pitching moment induced on jet STOVL aircraft hovering in ground effect
[AD-A269700] 04 p1317 N94-18577
Lift and pitching moment induced on jet STOVL aircraft by the ground vortex
[AD-A269816] 04 p1318 N94-18733
Compressibility effects on dynamic stall of airfoils undergoing rapid transient pitching motion
[NASA-TM-109681] 06 p2167 N94-23975
A numerical study of airplanes flying in proximity
[AD-A273373] 06 p2173 N94-24718
A numerical study of high-speed missile configurations using a block-structured parallel algorithm
[AD-A273776] 07 p2979 N94-25860
Reconfigurable aircraft stick control
[AD-D016043] 07 p2681 N94-27113
Wind tunnel investigation of propfan slipstream/wing interactions on a De Havilland air motor powered semispan model at Mach numbers 0.6 and 0.7 07 p2651 N94-28316
An experimental and theoretical study of the aerodynamic characteristics of some generic missile concepts at Mach numbers from 2 to 6.8
[NASA-TM-109110] 08 p3130 N94-29473
An examination of the aerodynamic moment on rotor blade tips using flight test data and analysis
[NASA-TM-104006] 10 p3985 N94-34948
Comparison of pitch rate history effects on dynamic stall 10 p3996 N94-34968
The unsteady pressure field and vorticity productiion at the suction surface of a pitching airfoil 10 p3986 N94-34972

PITOT TUBES
Free flight experiment with a laminar wing glove 05 p1639 N94-22600
Riblet boundary layer measurements of an A-310 fuselage with Pitot combs 05 p1640 N94-22605

PITS
Application of in situ scanning x ray fluorescence to study the concentration of metal ions in simulated pits
[DE93-014054] 03 p0956 N94-15921

PITTING
Plating under reduced pressure
[DE93-011896] 01 p0084 N94-11668
Crystallographic and metallurgical characterization of radiation detector grade cadmium telluride materials
[DE93-014335] 02 p0806 N94-13150
Use of scanning tunneling microscope in corrosion studies
[VTT-TIED-1416] 06 p2250 N94-25346
The electrochemical behavior of the Al3Fe intermetallic compound and localized corrosion of impure 1100 Al
[DE94-002037] 07 p2739 N94-26912
Effect of different ions on the anodic behaviour of alloy 800 in chloride solutions at high temperature
[DE94-602982] 07 p2743 N94-27832
Pitting corrosion of titanium
[AD-A274980] 08 p3203 N94-29089
Pit initiation on passivated metal surfaces: Crystallographic orientation and environmental effects
[ISBN-0-315-85433-2] 08 p3208 N94-30138

PITUITARY HORMONES
NT ADRENOCORTICOTROPIN (ACTH)

PIV (VELOCIMETRY)
U PARTICLE IMAGE VELOCIMETRY

PIVOTED WING AIRCRAFT
U TILT WING AIRCRAFT

PIVOTS
Tilt mechanism
[AD-D015780] 03 p1047 N94-16548
Bladder operated robotic joint
[NASA-CASE-MFS-28682-1] 05 p1701 N94-20359
Mars rover mechanisms designed for Rocky 4 08 p3161 N94-29630
High precision moving magnet chopper for variable operation conditions 09 p3605 N94-33307
An experimental study of pilot/vehicle dynamics using a tilt rotor flying machine
[AD-A277516] 09 p3805 N94-33349

PIX
U PLASMA INTERACTION EXPERIMENT

PIXELS
Optimal hemicube sampling
[DE93-010499] 01 p0334 N94-12591
Color image processing for flat panel visual display modeling
[NASA-CR-193660] 02 p0790 N94-12797

Two dimensional measurement and evaluation of point images at microscope objectives
[ETN-93-94397] 02 p0793 N94-14856
A monolithic PbTeCCD focal plane array for MWIR imaging 03 p0910 N94-15100
Massively parallel, adaptive, color image processing for autonomous road following
[AD-A266988] 03 p0864 N94-15498
Pixel-level fusion using interest images
[AD-A266640] 03 p1164 N94-15746
A task adaptive parallel graphics renderer
[DE93-017123] 03 p1149 N94-16119
Color palette considerations for digital map displays
[AD-A269991] 04 p1462 N94-18679
Photodetector array having high pixel density
[AD-D015859] 04 p1432 N94-18731
The roughness of the Martian surface: A scale dependent model 05 p2115 N94-20762
Objective determination of image end-members in spectral mixture analysis 05 p1686 N94-20831
Convex set and linear mixing model 05 p1844 N94-20888
Nature's crucible: Manufacturing optical nonlinearities for high resolution, high sensitivity encoding in the compound eye of the fly, Musca domestica 05 p1755 N94-21095
Progress on the design of a data push architecture for an array of optimized time tagging pixels
[DE93-041011] 06 p2307 N94-22955
Analysis of the influence of weather on infrared imagery
[FEL-92-A421] 07 p3036 N94-26649
An algorithm for stereo correspondence problems on the analogy of human vision
[NAL-TR-1185] 07 p2940 N94-27584
Image quality measures and their performance 07 p2946 N94-28257
A multiscale approach to image segmentation using Kohonen networks
[RUU-CS-93-06] 08 p3438 N94-30349
Dimensional measurement to subpixel value 10 p4110 N94-34353
Automatic cataloguing and characterization of Earth science data using SE-trees 10 p4124 N94-35058
Subpixel resolution from multiple images 11 p4281 N94-35417
The iWarp display module
[AD-A278610] 11 p4260 N94-36248

PLAINS
NT COASTAL PLAINS
NT FLOOD PLAINS
NT PLAYAS
NT TUNDRA
Modern shelf ice, equatorial Aeolis Quadrangle, Mars 01 p0450 N94-12100
Shallow crustal discontinuities and graben and scarp formation in the Tharsis region of Mars 01 p0469 N94-12203
Modes of formation of lunar light plains and the detection of cryptomaria deposits 03 p1259 N94-16231
Workshop on the Martian Northern Plains: Sedimentological, Periglacial, and Paleoclimatic Evolution
[NASA-CR-194831] 05 p2088 N94-20382
The fate of water deposited in the low-lying northern plains 05 p2089 N94-20387
Stratigraphy of the Martian northern plains 05 p2091 N94-20398
Geomorphic evidence for an eolian contribution to the formation of the Martian northern plains 05 p2092 N94-20402
Mars: New evidence for origin of some Valles Marineris layered deposits 05 p2112 N94-20748
Thermal and hydraulic considerations regarding the fate of water discharged by the outflow channels to the Martian northern plains 09 p3946 N94-33202
Workshop on the Martian Northern Plains: Sedimentological, periglacial, and paleoclimatic evolution
[NASA-CR-196134] 11 p4354 N94-35359

PLAN POSITION INDICATORS
Color-coded radar plan position indicator
[AD-D016200] 11 p4257 N94-36364

PLANAR STRUCTURES
Orientation of Planar Deformation Features (PDFs) in quartz 03 p1219 N94-16341
High temperature superconducting planar circuit structure for high frequency applications
[AD-A273083] 05 p2028 N94-21521
Geometric optimization
[DE93-040152] 05 p1917 N94-21764
Time-laplace-transform-domain analysis of wave propagation in planar waveguides
[PB93-215226] 05 p1960 N94-22096
Modifications to 8x8 dynamical theory: Polarizations redefined according to x ray diffraction convention
[DE94-001290] 06 p2560 N94-23187
Planar poly(p-phenylene) derivatives: Ladder formation for maximization of extended conjugation
[AD-A273220] 06 p2260 N94-24922
Printed circuit elements with applications to antennas, scattering, and circuits
[AD-A275512] 08 p3262 N94-28669

PLANCKS CONSTANT
Localizability and the Planck mass
[DE94-009183] 10 p4149 N94-33988

PLANE STRAIN
Autofrettage: Stress distribution under load and retained stresses after depressurization. A modified plane-strain case
[AD-A266320] 02 p0671 N94-13579
Solution of elastic-plastic stress analysis problems by the p-version of the finite element method
[NASA-CR-194267] 03 p1062 N94-17445
Numerical analysis of pressure meter tests: Application of parameter identification of soils behavior
[ECL-92-52] 04 p1487 N94-19380
Morphology of highly textured polyethylene/polyethylene- propylene semicrystalline diblock copolymers
[AD-A273683] 06 p2263 N94-25413
Plane strain finite element analysis of sheet forming operations including bending effects 08 p3322 N94-30354
An investigation of fatigue crack propagation under mode 1 and mixed mode 1/2 loadings 08 p3323 N94-30814
An energy method approach to the problem of elastic strip
[PB94-171014] 11 p4279 N94-36000
Experimental and finite-element simulation results for a plane-strain punch-test using isotropic and anisotropic materials
[DE94-011711] 12 p4457 N94-37670

PLANE STRESS
Analysis of the strengthening of aluminum alloy undergoing plastic deformation under conditions of a compound state of stress
[IFTR-21/1991] 03 p0960 N94-17093
Solution of elastic-plastic stress analysis problems by the p-version of the finite element method
[NASA-CR-194267] 03 p1062 N94-17445
Interfacial cracks in plates: A three-dimensional numerical investigation 04 p1456 N94-19116
Formulation and identification of the anisotropic laws for thin sheets drawing
[ECL-92-55] 04 p1365 N94-19400
Plane stress stable crack growth and J-integral/HRR field
[AD-A275761] 08 p3317 N94-28761
A modeling study of the effect of stress state on void linking during ductile fracture
[AD-A275505] 08 p3317 N94-28811
Approximate estimation of the effects of asymmetry on the testing of tensile specimens
[NPL-DMM(A)-117] 08 p3322 N94-30523
An investigation of fatigue crack propagation under mode 1 and mixed mode 1/2 loadings 08 p3323 N94-30814
Influences of pressure-sensitive yielding and non-singular stress on plane-stress elastic-plastic crack-tip fields 09 p3737 N94-31965
Nonlinear effects in interfacial fracture 09 p3737 N94-31974
BUCKY instruction manual, version 3.3
[NASA-TM-104793] 09 p3820 N94-32899
Micromechanical characterization of nonlinear behavior of advanced polymer matrix composites
[NASA-TM-109129] 10 p4025 N94-34397
An energy method approach to the problem of elastic strip
[PB94-171014] 11 p4279 N94-36000

PLANE WAVES
Squeezing in phase-conjugated resonance fluorescence 01 p0376 N94-10576
Effects of energetic particle events on VLF/LF propagation parameters/1989
[AD-A265266] 01 p0275 N94-11013
Computer code for scattering from impedance bodies of revolution. Part 3: Surface impedance with s and phi variation. Analytical and numerical results
[NASA-CR-193396] 02 p0599 N94-13264
Active control of fan-generated plane wave noise
[NASA-TM-109008] 02 p0777 N94-14481
Parametric resonant triad interactions in a free shear layer
[NASA-TM-106365] 03 p1021 N94-15751
Regular and irregular reflection of a wave from a slanting flat wall
[IFTR-13/1991] 03 p1193 N94-17049
The exact solution of the problem of diffraction of an electromagnetic plane wave by a conductive half-plane situated at an interface
[IFTR-3/91] 03 p1002 N94-17057
Development of parallel architectures for sensor array processing, volume 1
[AD-A270426] 04 p1534 N94-18507
A parallel and pipelined architecture for estimation of direction of arrival using a bilinear transformation method, volume 3
[AD-A270137] 04 p1389 N94-18897
Transmission of acoustic waves through strongly heterogeneous, two-dimensional velocity models
[REPT-93-09] 04 p1563 N94-19083
Variable-permittivity linear inverse problem for the H(sub z)-polarized case 05 p1719 N94-20408
The effect of dissipative inhomogeneous medium on the statistics of the wave intensity 05 p1726 N94-20440
Signal processing in the linear statistical model
[AD-A272114] 05 p1736 N94-20570
Proceedings of the 1993 Bi-Isotropics Workshop on Novel Microwave Materials
[PB93-224772] 06 p2290 N94-23225
LRAT: Lightning Radiative Transfer 06 p2416 N94-24443
Hydroacoustic wave-fields generated by different source types, a computational study
[PB94-123536] 07 p3010 N94-27037
Mach reflection of spherical detonation waves
[DE93-016604] 07 p2797 N94-27705
The propagation of spark-produced N waves through turbulence 07 p2650 N94-28193
Plane wave propagation and polarization properties in transversely bianisotropic uniaxial medium
[PB94-132883] 07 p2778 N94-28380
Eigenwaves in the general uniaxial bianisotropic medium with symmetric parameter dyadics
[PB94-132891] 07 p2778 N94-28381
Plane wave propagation in an anisotropic chiral medium with isotropic permittivity and permeability
[PB94-133097] 07 p2778 N94-28384
Green dyadic and dipole fields for a medium with anisotropic chirality
[PB94-132933] 07 p2779 N94-28391
On wave interactions of rotational and irrotational flows 09 p3700 N94-31219
Boundary control of scattering 09 p3861 N94-31899
Penetrable wedge analysis
[AD-A277219] 09 p3845 N94-32022
Sound scattering by cylinders of noncircular cross section
[AD-A276663] 09 p3861 N94-32089
Prediction of the plane wave beamformed acoustic arrival structure for the 1992 Barents Sea coastal tomography test
[AD-A276741] 09 p3788 N94-32181
Plane shock generator explosive lens: Shock characterization of 4340 and PH13-8Mo steels, C360 brass and PZT 65/35 ferro-electric ceramic
[DE94-009254] 11 p4266 N94-35979
Signal processing for the 1992 Barents Sea tomography experiment
[AD-A278580] 12 p4476 N94-36971
Scattering cross section of sound waves by the modal element method
[NASA-TM-106667] 12 p4510 N94-37308

PLANET ORIGINS
U PLANETARY EVOLUTION

PLANETARY ATMOSPHERES
NT JUPITER ATMOSPHERE
NT MARS ATMOSPHERE
NT NEPTUNE ATMOSPHERE
NT PLANETARY IONOSPHERES
NT PLUTO ATMOSPHERE
NT SATURN ATMOSPHERE
NT VENUS ATMOSPHERE
NT VENUS CLOUDS
Twenty-fourth Lunar and Planetary Science Conference. Part 1: A-F
[NASA-CR-193095] 01 p0435 N94-12015
Giant impact-induced atmospheric blow-off 01 p0435 N94-12019
An interferometric spectral mapper for the Cassini mission to Saturn and Titan
[NASA-CR-193805] 01 p0482 N94-12429
Twenty-Fourth Lunar and Planetary Science Conference. Part 2: G-M
[NASA-CR-193174] 03 p1247 N94-16173
Trapping of water vapor from an atmosphere by condensed silicate matter formed by high-temperature pulse vaporization 03 p1248 N94-16180
Laboratory studies of low temperature rate coefficients: The atmospheric chemistry of the outer planets
[NASA-CR-193485] 05 p1972 N94-20130

Remote sounding of tropospheric minor constituents [NASA-CR-194265] 05 p1855 N94-20132
Dynamics of large scale impacts on Venus and Earth 05 p2098 N94-20666
Low-energy ion implantation: Large mass fractionation of argon 05 p1685 N94-20697
Numerical modeling of impact erosion of atmospheres: Preliminary results 05 p2131 N94-20847
Core formation, wet early mantle, and H2O degassing on early Mars 05 p2145 N94-21674
The Pluto fast flyby mission: Completing the reconnaissance of the solar system 08 p3235 N94-29768
The far-infrared absorption spectrum of low temperature hydrogen gas [ISBN-0-315-85432-4] 08 p3199 N94-30137
A spectral atlas of the nu(sub 12) fundamental of (13)C(12)CH6 in the 12 micron region [NASA-TM-104601] 10 p4138 N94-34945

PLANETARY BASES

A modular gas-cooled cermet reactor system for planetary base power [DE93-013672] 02 p0550 N94-13351
Mars exploration study workshop 2 [NASA-CP-3243] 05 p2146 N94-21883
Preliminary design of a universal Martian lander [NASA-CR-195529] 06 p2206 N94-25007
Pax: A permanent base for human habitation of Mars 07 p2943 N94-25706

PLANETARY BOUNDARY LAYER

Evolution of the lower planetary boundary layer over strongly contrasting surfaces [DE93-010667] 02 p0717 N94-14424
Atmospheric turbulence and diffusion research [DE93-011842] 02 p0718 N94-14425
Phillips Laboratory global spectral numerical weather prediction model [AD-A267293] 03 p1107 N94-17244
Further development and testing of a second-order bulk boundary layer model [AD-A268071] 03 p1109 N94-17552
A new approach to the study of the turbulence layer [NASA-CR-194546] 04 p1487 N94-19397
Temperature/pressure and water vapor sounding with microwave spectroscopy 05 p1812 N94-22436
Incorporation of the planetary boundary layer in atmospheric models 06 p2413 N94-24388
Joint sessions on moisture processes and cumulus parameterization 06 p2414 N94-24393
Joint sessions on modeling of boundary layer and radiative transfer processes 06 p2414 N94-24396
Session on coupled atmospheric/chemistry coupled models 06 p2414 N94-24398
Vertical transport of water in the Martian boundary layer 06 p2622 N94-24902
An evaluation of the utility of ground-based high resolution interferometer (GB-HIS) soundings of the planetary boundary layer [DE94-000960] 07 p3106 N94-25981
The Martian atmospheric planetary boundary layer stability, fluxes, spectra, and similarity [NASA-CR-195711] 07 p3108 N94-27935
ULF waves in the low-latitude boundary layer and their relationship to magnetospheric pulsations: A multisatellite observation [AD-A278906] 11 p4289 N94-35587
Turbulent transfer in the marine planetary boundary layer [AD-A280549] 12 p4476 N94-37038

PLANETARY COMPOSITION

Marslink 01 p0438 N94-12034
Venus mountain-top mineralogy: Misconceptions about pyrite as the high radar-reflecting phase 01 p0455 N94-12129
Automatic definition of spectral units in the equatorial regions of Mars 01 p0432 N94-12234
Composition of the Martian aerosols through near-IR spectroscopy 01 p0475 N94-12235
Primitive SNC parent magmas and crystallization: Low PH2O experiments 01 p0433 N94-12264
Twenty-Fourth Lunar and Planetary Science Conference. Part 2: G-M [NASA-CR-193174] 03 p1247 N94-16173
A mineralized zone in Western Candor Chasma, Mars 03 p1248 N94-16179
Evolutionary implications of a steady-state water abundance on Venus 03 p1254 N94-16206
A Pluto thermal model 03 p1256 N94-16216
Modeling the reflectance of CO2 frost with new optical constants: Application to Martian south polar cap spectra 03 p1256 N94-16217
Nd-142/Nd-144 in bulk planetary reservoirs, the problem of incomplete mixing of interstellar components and significance of very high precision Nd-145/Nd-144 measurements 03 p1256 N94-16220
A Moessbauer spectrometer for the mineralogical analysis of the Mars surface: First temperature dependent tests of the detector and drive system 03 p1259 N94-16233
Explosive volcanism and the compositions of the cores of differentiated asteroids 03 p1243 N94-16306
Evolution of Triton's volatile budget 03 p1284 N94-16373
Mars brine formation experiment 03 p1293 N94-16419
Twenty-Fourth Lunar and Planetary Science Conference. Part 3: N-Z [NASA-CR-193149] 05 p2092 N94-20636
Detectability of crystalline ferric and ferrous minerals on Mars 05 p2110 N94-20730
Fine resolution chronology based on initial Sr-87/Sr-86 [CONTRIB-5230(794)] 05 p1686 N94-20794
Discovery Venera surface: Atmosphere geochemistry experiments mission concept 05 p2123 N94-20806
The x ray microprobe determination of chromium oxidation state in olivine from lunar basalt and kimberlitic diamonds 05 p1686 N94-20807
Geology and radiophysical properties of the Venera and Vega landing sites 05 p2135 N94-20867
A study of carbonates, sulfates, and phosphates using thermal emission spectroscopy 05 p1686 N94-20868
An attempt to comprehend Martian weathering conditions through the analysis of terrestrial palagonite samples 05 p2143 N94-21668
In situ identification of the Martian surface material and its interaction with the Martian atmosphere using DTA/GC 05 p1812 N94-22434
Magmatic volatiles and the weathering of Mars 09 p3946 N94-33201
The pH of Mars 09 p3950 N94-33225
The mineralogic evolution of the Martian surface through time: Implications from chemical reaction path modeling studies 09 p3950 N94-33226
The Twenty-Fifth Lunar and Planetary Science Conference. Part 1: A-G [NASA-CR-195743] 11 p4355 N94-35395
High resolution visible to short-wave near-infrared CCD spectra of Mars during 1990 11 p4356 N94-35403
Low encounter speed comet COMA sample return missions 11 p4202 N94-35607
The Twenty-Fifth Lunar and Planetary Science Conference. Part 2: H-O [NASA-CR-195744] 11 p4367 N94-36136

PLANETARY CORES

NT EARTH CORE
Was Martian mantle wet? A possible consequence of rapid core formation 03 p1277 N94-16335
Expectations for the Martian core magnetic field 05 p2120 N94-20792
Core formation by giant impacts: Conditions for intact melt region formation 05 p1863 N94-20833
The connection between Venus' free obliquity and its CMB oblateness 05 p2139 N94-20896
Core formation, wet early mantle, and H2O degassing on early Mars 05 p2145 N94-21674
Forced libration of Mercury and geodetic determination of a possible fluid core 09 p3774 N94-32493

PLANETARY CRATERS

NT MARS CRATERS
Twenty-fourth Lunar and Planetary Science Conference. Part 1: A-F [NASA-CR-193095] 01 p0435 N94-12015
Estimation of age of Dali-Ganis rifting and associated volcanic activity, Venus 01 p0440 N94-12046
Regional geology of the Vega landing sites: Tentative results of photogeologic mapping 01 p0440 N94-12047
Landscape and geomorphic survey of Zhamanshin area, Northern Kazakhstan: Preliminary report on 1992 field trip data 01 p0282 N94-12123
A two-stage (turbulent-drainage) mechanism for the emplacement of impact crater outflows on Venus 01 p0458 N94-12145
Cratering on Gaspra 01 p0459 N94-12147
Magellan: Principal Venus science findings 03 p0989 N94-15887
Twenty-Fourth Lunar and Planetary Science Conference. Part 2: G-M [NASA-CR-193174] 03 p1247 N94-16173
Fluvial erosion on Mars: Implications for paleoclimatic change 03 p1241 N94-16210
Confirmation of saturation equilibrium conditions in crater populations 03 p1103 N94-16222
Chemical differentiation, thermal evolution, and catastrophic overturn on Venus: Predictions and geologic observations 03 p1259 N94-16232
The three ages of Venus: A hypothesis based on the cratering record 03 p1261 N94-16239
Trace-element composition of Chicxulub crater melt rock, K/T tektites and Yucatan basement 03 p1242 N94-16245
The size of complex craters 03 p1262 N94-16249
The depths of the largest impact craters on Venus 03 p1264 N94-16261
A first-order model for impact crater degradation on Venus 03 p1265 N94-16268
Radar properties of several fluidized ejecta blankets on Venus 03 p1267 N94-16278
Implications of crater distributions on Venus 03 p1270 N94-16300
Manson impact structure, Iowa: First geochemical results for drill core M-1 03 p1103 N94-16322
Preliminary Ar-40/Ar-39 age spectrum and laser probe dating of the M1 core of the Manson Impact Structure, Iowa: A K-T boundary crater candidate 03 p1104 N94-16334
Tectonic resurfacing of Venus 03 p1285 N94-16380
Relief of some small landforms on Venus 03 p1293 N94-16418
Guide to Magellan image interpretation [NASA-CR-194340] 03 p1298 N94-17654
Twenty-Fourth Lunar and Planetary Science Conference. Part 3: N-Z [NASA-CR-193149] 05 p2092 N94-20636
Largest impact features on Venus: Non-preserved or non-recognizable? 05 p2096 N94-20657
Venus magmatic and tectonic evolution 05 p2101 N94-20683
Crater destruction on the Venusian highlands by tectonic processes 05 p2103 N94-20696
Kalkkop crater, Eastern Cape: A new impact crater in South Africa 05 p1862 N94-20714
The Manson impact crater: Estimation of the energy of formation, possible size of the impacting asteroid or comet, and ejecta volume and mass 05 p2083 N94-20721
Named Venusian craters 05 p2109 N94-20725
Venus' impact-crater database: Update to approximately 98 percent of the planet's surface 05 p2110 N94-20736
Searching for ancient Venus 05 p2111 N94-20743
The missing impact craters on Venus 05 p2119 N94-20782
Impact basins on Venus and some interplanetary comparisons 05 p2119 N94-20785
Parabolic features and the erosion rate on Venus 05 p2122 N94-20801
Discovery Venera surface: Atmosphere geochemistry experiments mission concept 05 p2123 N94-20806
Original size of the Vredefort structure, South Africa 05 p1863 N94-20825
Origin of the Vredefort structure, South Africa: Impact model 05 p1863 N94-20826
Core formation by giant impacts: Conditions for intact melt region formation 05 p1863 N94-20833
Is there uniformitarian or catastrophic tectonics on Venus? 05 p2129 N94-20839
Geology of Galileo Regio quadrangle, Ganymede 05 p2130 N94-20842
Elevation and igneous crater modification on Venus: Implications for magmatic volatile content 05 p2135 N94-20872
Large floor-fractured craters and isostatic crater modification: Implications for lithospheric thickness on Venus 05 p2135 N94-20873
Evolution of the global water cycle on Mars: The geological evidence 05 p2142 N94-21660
The early Martian environment: Clues from the cratered highlands and the Precambrian Earth 05 p2143 N94-21667
Cratering rates from lunar xenospherules [DE94-003481] 07 p3106 N94-27007
The tectonic and volcanic evolution of Venus: Catastrophic or gradual? 09 p3940 N94-31111
Keeping that youthful look --- impact cratering of Venus 09 p3941 N94-31112
A tectonic resurfacing model for Venus 09 p3941 N94-31113
The resurfacing controversy for Venus: An overview and a mechanistic perspective 09 p3941 N94-31114
The Twenty-Fifth Lunar and Planetary Science Conference. Part 1: A-G [NASA-CR-195743] 11 p4355 N94-35395
The Twenty-Fifth Lunar and Planetary Science Conference. Part 3: P-Z [NASA-CR-195745] 11 p4362 N94-35448
Rheology, tectonics, and the structure of the Venus lithosphere 11 p4367 N94-35479
Magellan collection of radar calibration results [NASA-CR-194753] 11 p4367 N94-35509
Mercury: Mid-infrared (7.3 - 13.5 microns) spectroscopic observations showing features characteristic of plagioclase 11 p4370 N94-36150

PLANETARY CRUSTS
NT EARTH CRUST
Venus' center of mass - center of figure displacement and implications 01 p0444 N94-12067
Can weak crust explain the correlation of geoid and topography on Venus? 01 p0453 N94-12118
Fault geometries and extension in the Valles Marineris, Marc 01 p0458 N94-12144
Mars: The initial emplacement of ground ice in response to the thermal evolution of its early crust 01 p0462 N94-12168
The role of the geothermal gradient in the emplacement and replenishment of ground ice on Mars 01 p0463 N94-12169
The thermodynamic case for a water-rich Mars 01 p0463 N94-12170
Porosity and the ecology of icy satellites 01 p0431 N94-12186
Noble gas evidence of an aqueous reservoir near the surface of Mars more recently than 1.3 Ga 01 p0473 N94-12228
Do large impact basins in the southern hemisphere of Mars control the distribution of polar structures and deposits? 01 p0481 N94-12266
Free-air and Bouguer gravity anomalies and the Martian crustal dichotomy 01 p0481 N94-12267
New Mars free-air and Bouguer gravity: Correlation with topography, geology and large impact basins 01 p0481 N94-12268
Spatially extensive uniform stress fields on Venus inferred from radial dike swarm geometries: The Aphrodite Terra example 03 p1254 N94-16207
Chemical differentiation, thermal evolution, and catastrophic overturn on Venus: Predictions and geologic observations 03 p1259 N94-16232
The depths of the largest impact craters on Venus 03 p1264 N94-16261
Tessera terrain on Venus: Global characterization from Magellan data 03 p1264 N94-16262
Density of impact craters on tessera, Venus 03 p1264 N94-16263
An inversion of geoid and topography for mantle and crustal structure on Mars 03 p1273 N94-16315
Models of thermal/chemical boundary layer convection: Potential application to Venus 03 p1279 N94-16348
Large-scale volcanism associated with coronae on Venus 03 p1285 N94-16376
Geophysical models of Western Aphrodite-Niobe region: Venus 03 p1286 N94-16382
Variations in the Fe mineralogy of bright Martian soil 03 p1295 N94-16431
Composition of weakly altered Martian crust 03 p1296 N94-16436
A geological and geophysical information system for Eurasia [AD-A267841] 03 p1232 N94-17036
JPRS report: Science and technology. Central Eurasia: Space [JPRS-USP-93-004] 04 p1323 N94-19146
Beta Regio rift system on Venus: Geologic interpretation of Magellan images 05 p2095 N94-20655
Formation and evolution of radial fracture systems on Venus 05 p2099 N94-20672
Mixing of a chemically buoyant layer at the top of a thermally convecting fluid: Implications for mantle dynamics with application to Venus 05 p2099 N94-20675
Ridge belt-related scarps and troughs: Compressional crustal bending on Venus 05 p2106 N94-20711
Geoid, topography, and convection-driven crustal deformation on Venus 05 p2116 N94-20769
Response of the topography and gravity field on Venus to mantle upwelling beneath a chemical boundary layer 05 p2117 N94-20775
Differentiation of magma oceans and the thickness of the depleted layer on Venus 05 p2118 N94-20780
Impact basins on Venus and some interplanetary comparisons 05 p2119 N94-20785
The parent magma of the Nakhla (SNC) meteorite: Reconciliation of composition estimates from magmatic inclusions and element partitioning 05 p2085 N94-20836
Morphologic classes of impact basins on Venus 05 p2137 N94-20883
Wrinkle ridges, reverse faulting, and the depth penetration of lithospheric stress in lunae planum, Mars 05 p2141 N94-20910
Possible flexural signatures around Olympus and Ascraeus Montes, Mars 05 p2142 N94-20911
The evolution of the early Martian climate and the initial emplacement of crustal H2O 05 p2143 N94-21665
The hydrologic response of Mars to the onset of a colder climate and to the thermal evolution of its early crust 05 p2143 N94-21666
Basaltic Volcanism and Ancient Planetary Crusts [NASA-CR-193151] 06 p2614 N94-24363
The geophysical signal of the martian global dichotomy 06 p2623 N94-24997
The tectonic and volcanic evolution of Venus: Catastrophic or gradual? 09 p3940 N94-31111
The resurfacing controversy for Venus: An overview and a mechanistic perspective 09 p3941 N94-31114
Plains tectonism on Venus: The deformation belts of Lavinia Planitia 09 p3941 N94-31115
Thermal and hydraulic considerations regarding the fate of water discharged by the outflow channels to the Martian northern plains 09 p3946 N94-33202
The Martian sources of the SNC meteorites (two, not one), and what can and can't be learned from the SNC meteorites 09 p3951 N94-33234
Temporal changes in the geographic distribution, elevation, and potential origin of the Martian outflow channels 09 p3951 N94-33235
Mars aqueous chemistry experiment [NASA-CR-196024] 11 p4354 N94-35263
The Twenty-Fifth Lunar and Planetary Science Conference. Part 1: A-G [NASA-CR-195743] 11 p4355 N94-35395
Quantifying shapes of volcanoes on Venus 11 p4361 N94-35429
Volcano morphometry and volume scaling on Venus 11 p4361 N94-35431
The parent magma of xenoliths in shergottite EETA79001: Bulk and trace element composition inferred from magmatic inclusions 11 p4352 N94-35467
Rheology, tectonics, and the structure of the Venus lithosphere 11 p4367 N94-35479

PLANETARY ENTRY
U ATMOSPHERIC ENTRY

PLANETARY ENVIRONMENTS
NT JUPITER ATMOSPHERE
NT MARS ATMOSPHERE
NT MARS ENVIRONMENT
NT NEPTUNE ATMOSPHERE
NT PLANETARY ATMOSPHERES
NT PLANETARY IONOSPHERES
NT PLANETARY MAGNETOSPHERES
NT PLANETARY MAGNETOTAILS
NT PLUTO ATMOSPHERE
NT SATURN ATMOSPHERE
NT VENUS ATMOSPHERE
NT VENUS CLOUDS
Directory of research projects: Planetary materials and geochemistry [NASA-TM-4484] 03 p1095 N94-15781
First results from a laboratory facility for measurement of emission spectra under simulated planetary conditions 03 p0954 N94-16372
Electronic payloads for Martian missions: A preliminary assessment of technologies 06 p2610 N94-23408

PLANETARY EVOLUTION
Columbus proto-planetesimal dust aggregation experiment 01 p0123 N94-10236
Giant impact-induced atmospheric blow-off 01 p0435 N94-12019
Metal-rich meteorites from the aubrite parent body 01 p0430 N94-12142
On high-temperature formation of iron-rich olivine in the early solar system 01 p0432 N94-12225
Recondensation of chondritic material in the early solar system: Results of thermodynamic simulation 01 p0432 N94-12226
Laboratory studies on the velocity of fragments from impact disruptions 01 p0189 N94-12359
Regional tectonic analysis of Venus as part of the Pioneer Venus guest investigator project [NASA-CR-194079] 02 p0842 N94-13561
Organic Geochemical and tectonic evolution of the Midcontinent Rift system [DE93-015093] 02 p0717 N94-14338
Pioneer-Venus press clip --- Solar System formation and extraterrestrial life [NASA-TM-109425] 03 p1239 N94-15495
Trapping of water vapor from an atmosphere by condensed silicate matter formed by high-temperature pulse vaporization 03 p1248 N94-16180
The formation and evolution of Alpha and Tellus tesserae on Venus 03 p1249 N94-16183
Tessera terrain on Venus: Implications of tessera flooding models and boundary characteristics for global distribution and mode of formation 03 p1258 N94-16226
Chemical differentiation, thermal evolution, and catastrophic overturn on Venus: Predictions and geologic observations 03 p1259 N94-16232
Potassium isotope cosmochemistry, volatile depletion and the origin of the Earth 03 p0953 N94-16259
Was Martian mantle wet? A possible consequence of rapid core formation 03 p1277 N94-16335
Evolution of Triton's volatile budget 03 p1284 N94-16373
Workshop on early Mars: How warm and how wet, part 2? [NASA-CR-193503] 03 p1297 N94-17637
Applications of Quaternary stratigraphic, soil-geomorphic, and quantitative geomorphic analyses to the evaluation of tectonic activity and landscape evolution in the Upper Coastal Plain, South Carolina [DE93-016269] 04 p1484 N94-18725
Twenty-Fourth Lunar and Planetary Science Conference. Part 3: N-Z [NASA-CR-193149] 05 p2092 N94-20636
Dynamics of large scale impacts on Venus and Earth 05 p2098 N94-20666
Mixing of a chemically buoyant layer at the top of a thermally convecting fluid: Implications for mantle dynamics with application to Venus 05 p2099 N94-20675
Venus magmatic and tectonic evolution 05 p2101 N94-20683
Low-energy ion implantation: Large mass fractionation of argon 05 p1685 N94-20697
Diffusive redistribution of water vapor in the solar nebula revisited 05 p2113 N94-20751
Recondensation in the early solar system: Physical conditions and source material 05 p2085 N94-20849
Variety in planetary systems 05 p2086 N94-20871
The hydrologic response of Mars to the onset of a colder climate and to the thermal evolution of its early crust 05 p2143 N94-21666
The early Martian environment: Clues from the cratered highlands and the Precambrian Earth 05 p2143 N94-21667
Basaltic Volcanism and Ancient Planetary Crusts [NASA-CR-193151] 06 p2614 N94-24363
Protoplanetary disks: Theory and observation by millimeter and sub-millimeter arrays [REPT-331] 06 p2603 N94-24983
The Nobeyama millimeter array survey for protoplanetary disks around protostar candidates and T Tauri stars in Taurus [REPT-336] 06 p2604 N94-24987
Tectonic Evolution of Mars [NASA-CR-194714] 06 p2623 N94-24996
Studies of extra-solar Oort Clouds and the Kuiper Disk [NASA-CR-195242] 07 p3103 N94-26789
New Developments Regarding the KT Event and Other Catastrophes in Earth History [NASA-CR-195169] 07 p2887 N94-28294
Some implications of large impact craters and basins on Venus for terrestrial ringed craters and planetary evolution 07 p2890 N94-28306
The thermal consequences of giant impacts in the early solar system 08 p3543 N94-29698
Tectonic History of the Terrestrial Planets [NASA-CR-195696] 09 p3939 N94-31105
The tectonic and volcanic evolution of Venus: Catastrophic or gradual? 09 p3940 N94-31111
Keeping that youthful look --- impact cratering of Venus 09 p3941 N94-31112
A tectonic resurfacing model for Venus 09 p3941 N94-31113
The resurfacing controversy for Venus: An overview and a mechanistic perspective 09 p3941 N94-31114
Plains tectonism on Venus: The deformation belts of Lavinia Planitia 09 p3941 N94-31115
Observations of accretion and angular momentum regulation in young circumstellar disks and the implications for planetary formation 09 p3928 N94-31122
Evolution of protoplanetary disks with dynamo magnetic fields 09 p3931 N94-31135
Theory of protostellar accretion disks 09 p3931 N94-31136
Planetesimal dynamics in the vicinity of a growing protoplanet 09 p3935 N94-31926
A model for the evolution of CO2 on Mars 09 p3946 N94-33205
The effect of polar caps on obliquity 09 p3948 N94-33213
The distribution of Martian ground ice at other epochs 09 p3948 N94-33218
The mineralogic evolution of the Martian surface through time: Implications from chemical reaction path modeling studies 09 p3950 N94-33226
Geologic controls of erosion and sedimentation on Mars 09 p3951 N94-33232
Non-equilibrium chemistry of the early solar system [NASA-CR-195691] 10 p4163 N94-33603
What initiated planetesimal formation? 11 p4351 N94-35422
The fretted terrain of the Nilosyrtis Mensae region of Mars: Clues to the timing of dichotomy formation and the emplacement of the northern plains 11 p4360 N94-35424

Noachian and Hesperian modification of the original Chryse impact basin topography
11 p4364 N94-35462
A quick look method of detecting water of hydration in small solar system bodies 11 p4352 N94-35470
Mars atmospheric escape and isotopic fractionation: Synthesis of data and models 11 p4369 N94-36143
An investigation of solar wind effects on the evolution of the Martian atmosphere
[NASA-CR-193424] 12 p4549 N94-37012

PLANETARY EXPLORATION
U SPACE EXPLORATION

PLANETARY GEOLOGY
NT MARS VOLCANOES
Radiogenic age and isotopic studies
[DE93-610548] 01 p0274 N94-10407
Physical studies of planetary and satellite surfaces
[NASA-CR-193545] 01 p0434 N94-10817
Evolution of steep Martian slopes
01 p0434 N94-11184
Analysis of gravity, magnetic, and seismic reflection data from Tibet and neighboring regions of China
[NASA-CR-193405] 01 p0278 N94-11886
Twenty-fourth Lunar and Planetary Science Conference. Part 1: A-F
[NASA-CR-193095] 01 p0435 N94-12015
Rates of fluvio-thermal erosion on Mars
01 p0435 N94-12018
Morphology of large impact craters and basins on Venus: Implications for ring formation 01 p0436 N94-12023
Lineament analysis and tectonic interpretation for the Tharsis region 01 p0437 N94-12031
Reconstruction of the dynamics of the 1800-1801 Hualalai eruption: Implications for planetary lava flows
01 p0281 N94-12041
Horizontal stresses induced by vertical processes in planetary lithospheres 01 p0281 N94-12042
Increased depth-diameter ratios in the Medusae Fossae Formation deposits of Mars 01 p0439 N94-12043
Estimation of age of Dali-Ganis rifting and associated volcanic activity, Venus 01 p0440 N94-12046
Regional geology of the Vega landing sites: Tentative results of photogeologic mapping
01 p0440 N94-12047
Regional geology of the Venera landing sites: Tentative results of photogeologic mapping
01 p0440 N94-12048
Changes in Hawaiian palagonite FE mineralogy associated with thermal alteration: Implications for Mars
01 p0281 N94-12055
Petrography and preliminary interpretations of the crystalline breccias from the Manson M-1 core
01 p0281 N94-12056
Thermal studies of Martian channels and valleys using Termoskan data 01 p0443 N94-12064
Spectral analysis of the gravity and topography of Mars 01 p0444 N94-12065
Global organization of tectonic deformation on Venus
01 p0444 N94-12066
Venus' center of mass - center of figure displacement and implications 01 p0444 N94-12067
Using high spectral resolution spectrophotometry to study broad mineral absorption features on Mars
01 p0446 N94-12077
Venus resurfacing rates: Constraints provided by 3-D Monte Carlo simulations 01 p0453 N94-12119
Scalloped margin domes: What are the processes responsible and how do they operate?
01 p0454 N94-12120
Yana ring structure, North-Eastern Siberia: A possible counterpart of coronae on Venus
01 p0282 N94-12121
Russia's contribution to regional geologic mapping of Venus 01 p0454 N94-12122
Chemical weathering on Mars: Rate of oxidation of iron dissolved in brines 01 p0455 N94-12128
Geology and surface characteristics of Bell Regio, Venus 01 p0457 N94-12136
Fault geometries and extension in the Valles Marineris, Mars 01 p0458 N94-12144
A two-stage (turbulent-drainage) mechanism for the emplacement of impact crater outflows on Venus
01 p0458 N94-12145
Mars: The initial emplacement of ground ice in response to the thermal evolution of its early crust
01 p0462 N94-12168
The thermodynamic case for a water-rich Mars
01 p0463 N94-12170
Geologic history of central Chryse Planitia and the Viking 1 landing site, Mars 01 p0465 N94-12180
Large volcanoes on Venus: Examples of geologic and structural characteristics from different classes
01 p0467 N94-12195
Regional mantle upwelling on Venus: The Beta-Atla-Themis anomaly and correlation with global tectonic patterns 01 p0467 N94-12196
Small volcanoes in Tempe Terra, Mars: Their detailed morphometry and inferred geologic significance
01 p0469 N94-12202
Shallow crustal discontinuities and graben and scarp formation in the Tharsis region of Mars
01 p0469 N94-12203
Characteristics of arachnoids from Magellan data
01 p0469 N94-12204
Soret diffusion: A possible cause of compositional heterogeneity within tektites 01 p0432 N94-12211
Isotopic and trace element characteristics of an unusual refractory inclusion from Essebi
01 p0471 N94-12212
Relation between ages and elevations of Martian channels 01 p0472 N94-12216
Automatic definition of spectral units in the equatorial regions of Mars 01 p0432 N94-12234
Giant radiating dyke swarms on Earth and Venus
01 p0283 N94-12236
Terrestrial case studies of ilmenite exploration and lunar implications 01 p0478 N94-12247
Transmantle flux tectonics 01 p0283 N94-12249
Do large impact basins in the southern hemisphere of Mars control the distribution of polar structures and deposits? 01 p0481 N94-12266
New Mars free-air and Bouguer gravity: Correlation with topography, geology and large impact basins
01 p0481 N94-12268
Interdisciplinary scientist participation in the Phobos mission
[NASA-CR-193715] 01 p0482 N94-12446
Planetary astronomy of Mars. Mars data reduction
[NASA-CR-193515] 01 p0424 N94-12768
Spectral analysis for automated exploration and sample acquisition
[NASA-CR-194095] 02 p0545 N94-13189
The nature and origin of periodically spaced tectonic features on Mars
[NASA-CR-193821] 02 p0842 N94-13199
Exploring Mars
[NASA-TM-109306] 02 p0842 N94-13613
Martian sedimentary deposits
[NASA-CR-193266] 02 p0842 N94-13855
Workshop on the Space Environment: The Effects on the Optical Properties of Airless Bodies
[NASA-CR-194417] 02 p0842 N94-14298
Impact melting and vaporization in planetary regoliths
02 p0843 N94-14299
Extrapolation of space weathering processes to other small solar system bodies 02 p0843 N94-14300
Magellan: Principal Venus science findings
03 p0989 N94-15887
Twenty-Fourth Lunar and Planetary Science Conference. Part 2: G-M
[NASA-CR-193174] 03 p1247 N94-16173
Morphometric comparison of Icelandic lava shield volcanoes versus selected Venusian edifices
03 p1248 N94-16178
A mineralized zone in Western Candor Chasma, Mars
03 p1248 N94-16179
Pargo Chasma and its relationship to global tectonics
03 p1249 N94-16181
The formation and evolution of Alpha and Tellus tesserae on Venus 03 p1249 N94-16183
Cretaceous-tertiary boundary spherules and Cenozoic microtektites: Similarities and differences
03 p1241 N94-16186
Rheology of water and ammonia-water ices
03 p0953 N94-16188
Sand transport on Mars: Preliminary results from models 03 p1252 N94-16198
Mars Analog Site Study (MASS)
03 p1252 N94-16200
Earth imaging results from Galileo's second encounter
03 p1252 N94-16201
Collisional and dynamical history of Gaspra
03 p1241 N94-16202
Explosive mafic volcanism on Earth and Mars
03 p1253 N94-16204
Evolutionary implications of a steady-state water abundance on Venus 03 p1254 N94-16206
Spatially extensive uniform stress fields on Venus inferred from radial dike swarm geometries: The Aphrodite Terra example 03 p1254 N94-16207
The Acraman impact structure: Estimation of the diameter by the ejecta layer thickness
03 p1103 N94-16211
The Karakul depression in Pamirs: The first impact structure in Central Asia 03 p1241 N94-16212
Ishtar deformed belts: Evidence for deformation from below? 03 p1256 N94-16218
Confirmation of saturation equilibrium conditions in crater populations 03 p1103 N94-16222
Lava flow-field morphological classification and interpretation: Examples from Venus
03 p1259 N94-16230
Chemical differentiation, thermal evolution, and catastrophic overturn on Venus: Predictions and geologic observations 03 p1259 N94-16232
Emplacement of multiple flow units on very shallow slopes, east Kawelu Planitia flow field, Venus
03 p1260 N94-16235
Thermal inertia and radar reflectivity of the Martian north polar ERG: Low-density aggregates
03 p1260 N94-16238
Tessera terrain on Venus: Global characterization from Magellan data 03 p1264 N94-16262
A first-order model for impact crater degradation on Venus 03 p1265 N94-16268
Fractal geometry of some Martian lava flow margins: Alba Patera 03 p1270 N94-16298
Tectonics of Neyterkob corona on Venus
03 p1270 N94-16299
Implications of crater distributions on Venus
03 p1270 N94-16300
Megaplumes on Venus 03 p1271 N94-16301
Preliminary analysis of Dione Regio, Venus: The final Magellan regional imaging gap 03 p1271 N94-16302
The distribution of large volcanoes on Venus as a function of height and altitude 03 p1271 N94-16303
Tidal interaction: A possible explanation for geysers and other fluid phenomena in the Neptune-Triton system
03 p1272 N94-16311
An inversion of geoid and topography for mantle and crustal structure on Mars 03 p1273 N94-16315
Global Magellan-image map of Venus at full resolution
03 p1274 N94-16319
Meander properties of Venusian channels
03 p1275 N94-16324
Cat Mountain: A meteoritic sample of an impact-melted chondritic asteroid 03 p1244 N94-16328
Spectral study of Venus global topography and geoid from Magellan and PVO data 03 p1276 N94-16332
Vertical structure models of the 1990 equatorial disturbance on Saturn 03 p1277 N94-16333
Sheet flow fields on Venus 03 p1278 N94-16338
Hellas basin, Mars: Formation by oblique impact
03 p1280 N94-16350
Sedimentation, volcanism, and ancestral lakes in the Valles Marineris: Clues from topography
03 p1283 N94-16369
Evolution of Triton's volatile budget
03 p1284 N94-16373
Suggestion for extended Viking magnetic properties experiment on future Mars missions
03 p1285 N94-16375
Large-scale volcanism associated with coronae on Venus 03 p1285 N94-16376
Tectonic resurfacing of Venus
03 p1285 N94-16380
Geophysical models of Western Aphrodite-Niobe region: Venus 03 p1286 N94-16382
The dregs of crystallization in Zagami
03 p1245 N94-16390
Aspects of modelling the tectonics of large volcanoes on the terrestrial planets 03 p1104 N94-16396
Deucalionis Regio, Mars: Evidence for a unique mineralogic endmember and a crusted surface
03 p1291 N94-16406
Analysis of pyroxene absorptions observed in Martian dark regions 03 p1292 N94-16411
Relief of some small landforms on Venus
03 p1293 N94-16418
Mars brine formation experiment
03 p1293 N94-16419
Bright soil units on Mars determined from ISM imaging spectrometer data 03 p1295 N94-16430
A geological and geophysical information system for Eurasia
[AD-A267841] 03 p1232 N94-17036
Guide to Magellan image interpretation
[NASA-CR-194340] 03 p1298 N94-17654
Applications of Quaternary stratigraphic, soil-geomorphic, and quantitative geomorphic analyses to the evaluation of tectonic activity and landscape evolution in the Upper Coastal Plain, South Carolina
[DE93-016269] 04 p1484 N94-18725
Magellan, Galileo, and Ulysses
[NASA-TM-109362] 04 p1628 N94-18958
JPRS report: Science and technology. Central Eurasia: Space
[JPRS-USP-93-004] 04 p1323 N94-19146
Workshop on the Martian Northern Plains: Sedimentological, Periglacial, and Paleoclimatic Evolution
[NASA-CR-194831] 05 p2088 N94-20382
A wet-geology and cold-climate Mars model: Punctuation of a slow dynamic approach to equilibrium
05 p2090 N94-20389
Possible occurrence and origin of massive ice in Utopia Planitia 05 p2090 N94-20390

Observed climatic activity pertaining to the evolution of the northern plains 05 p2090 N94-20392
The thumbprint terrain: What will Mars Observer tell us? 05 p2091 N94-20397
Stratigraphy of the Martian northern plains 05 p2091 N94-20398
Balloon exploration of the northern plains of Mars near and north of the Viking 2 landing site 05 p2092 N94-20401
Twenty-Fourth Lunar and Planetary Science Conference. Part 3: N-Z [NASA-CR-193149] 05 p2092 N94-20636
SO2 on Venus: IUE, HST and ground-based measurements, and the active volcanism connection 05 p2092 N94-20637
The Koshak section: Evidence for element fractionation and an oxidation event at the K/T boundary 05 p1862 N94-20641
Determination of cosmic bodies size-velocity distribution by observation of current impacts on Mars 05 p2082 N94-20648
Geologic mapping of Northern Atla Regio on Venus: Preliminary data 05 p2095 N94-20654
Beta Regio rift system on Venus: Geologic interpretation of Magellan images 05 p2095 N94-20655
Beta Regio - Phoebe Regio on Venus: Geologic mapping with the Magellan data 05 p2096 N94-20656
Largest impact features on Venus: Non-preserved or non-recognizable? 05 p2096 N94-20657
Dynamics of large scale impacts on Venus and Earth 05 p2098 N94-20666
Structural evidence for reorientation of Miranda about a paleo-pole 05 p2098 N94-20671
Formation and evolution of radial fracture systems on Venus 05 p2099 N94-20672
Thermal and rheological controls on magma migration in dikes: Examples from the east rift zone of Kilauea volcano, Hawaii 05 p1862 N94-20673
Constraints on the rate of discharge and duration of the Mangala Valles flood 05 p2099 N94-20674
Venus magmatic and tectonic evolution 05 p2101 N94-20683
Eruption history of the Tharsis shield volcanoes, Mars 05 p2102 N94-20692
Geology of Biblis Patera, Ulysses Patera, and Jovis Tholus, Mars 05 p2103 N94-20693
Crater destruction on the Venusian highlands by tectonic processes 05 p2103 N94-20696
Geologic mapping of Harmakhis and Reull Valles region, Mars: Evidence for multiple resurfacing and drainage events 05 p1844 N94-20705
Some deformation trends and topographic characteristics of tesserae on Venus 05 p2105 N94-20706
Studying Venus using a GIS database 05 p2105 N94-20707
Chocolate tablet aspects of cytherean Meshkenet Tessera 05 p2106 N94-20710
Ridge belt-related scarps and troughs: Compressional crustal bending on Venus 05 p2106 N94-20711
Detectability of crystalline ferric and ferrous minerals on Mars 05 p2110 N94-20730
Venus pancake dome formation: Morphologic effects of a cooling-induced variable viscosity during emplacement 05 p2110 N94-20732
Mars: New evidence for origin of some Valles Marineris layered deposits 05 p2112 N94-20748
Rifting at Devana Chasma, Venus: Structure and estimation of the effective thickness of the elastic lithosphere 05 p2113 N94-20754
Volcanic rises on Venus: Geology, formation, and sequence of evolution 05 p2113 N94-20755
The roughness of the Martian surface: A scale dependent model 05 p2115 N94-20762
GMM-1: A 50 degree and order gravitational field model for Mars 05 p2117 N94-20774
Differentiation of magma oceans and the thickness of the depleted layer on Venus 05 p2118 N94-20780
Impact basins on Venus and some interplanetary comparisons 05 p2119 N94-20785
Discovery Venera surface: Atmosphere geochemistry experiments mission concept 05 p2123 N94-20806
Extensional history of Mars' Tharsis Region 05 p2125 N94-20814
Complex structure of the Thaumasia region of Mars 05 p2125 N94-20815
Large, ancient, compressional structures on Mars 05 p2125 N94-20816
Tumuli and tubes: Teaching scientific techniques 05 p2039 N94-20818
Magellan Mission 05 p1652 N94-20829
Discharge rates in Ma'adim Vallis, Mars 05 p2128 N94-20830
Complex ridged terrain-related ridge belts on Venus: Global distribution and classification 05 p2129 N94-20835
Is there uniformitarian or catastrophic tectonics on Venus? 05 p2129 N94-20839
Geology of Galileo Regio quadrangle, Ganymede 05 p2130 N94-20842
Spectral analysis of chemisorbed CO2 on Mars analog materials 05 p2140 N94-20900
Comparison of flank modification on Ascraeus and Arsia Montes volcanoes, Mars 05 p2140 N94-20903
Evolution of the global water cycle on Mars: The geological evidence 05 p2142 N94-21660
Ancient Martian valley genesis and paleoclimatic inference: The present as a key to the past 05 p2142 N94-21661
A carbon dioxide/methane greenhouse atmosphere on early Mars 05 p2142 N94-21662
Oxidation of dissolved iron under warmer, wetter conditions on Mars: Transitions to present-day arid environments 05 p2143 N94-21663
Mars: Noachian hydrology by its statistics and topology 05 p2143 N94-21664
The evolution of the early Martian climate and the initial emplacement of crustal H2O 05 p2143 N94-21665
An attempt to comprehend Martian weathering conditions through the analysis of terrestrial palagonite samples 05 p2143 N94-21668
Fluvial valleys in the heavily cratered terrains of Mars: Evidence for paleoclimatic change? 05 p2144 N94-21670
Early Mars: The inextricable link between internal and external influences on valley network formation 05 p2146 N94-21681
The Martian valley networks: Origin by niveo-fluvial processes 05 p2146 N94-21682
Post-Palbozoic crustal responses to the contemporary stress field in the eastern United States [DE93-040604] 05 p1859 N94-22006
MSATT Workshop on Innovative Instrumentation for the In Situ Study of Atmosphere-Surface Interactions on Mars [NASA-CR-194584] 05 p1811 N94-22430
A Backscatter Moessbauer Spectrometer (BaMS) for use on Mars 05 p1811 N94-22431
Optical luminescence spectroscopy as a probe of the surface mineralogy of Mars 05 p1813 N94-22437
An improved gravity model for Mars: Goddard Mars Model-1 (GMM-1) [NASA-TM-104584] 06 p2401 N94-23282
Robotic exploration of Moon and Mars 06 p2606 N94-23379
The geophysical signal of the martian global dichotomy 06 p2623 N94-24997
A geological and geophysical information system for Eurasia [AD-A274818] 07 p3098 N94-26490
Some implications of large impact craters and basins on Venus for terrestrial ringed craters and planetary evolution 07 p2890 N94-28306
An extraterrestrial event at the tertiary-quaternary boundary 07 p2890 N94-28309
Were all extinction events caused by impacts? 07 p2891 N94-28311
Venus Data Analysis Program: Directory of Research Projects (1993-1994) [NASA-CR-195742] 08 p3549 N94-29102
The Pluto fast flyby mission: Completing the reconnaissance of the solar system 08 p3235 N94-29768
Tectonic History of the Terrestrial Planets [NASA-CR-195696] 09 p3939 N94-31105
Aspects of modelling the tectonics of large volcanoes on the terrestrial planets 09 p3940 N94-31107
State of stress, faulting, and eruption characteristics of large volcanoes on Mars 09 p3940 N94-31108
Origin and thermal evolution of Mars 09 p3940 N94-31109
Geoid-to-topography ratios on Venus: A global perspective 09 p3940 N94-31110
The tectonic and volcanic evolution of Venus: Catastrophic or gradual? 09 p3940 N94-31111
Keeping that youthful look --- impact cratering of Venus 09 p3941 N94-31112
A tectonic resurfacing model for Venus 09 p3941 N94-31113
The resurfacing controversy for Venus: An overview and a mechanistic perspective 09 p3941 N94-31114
Quantitative modeling of bottom morphology and subbottom properties [AD-A278142] 09 p3790 N94-33062
Fine and microstructure observations at Fieberlin g Guyot R/V new horizon cruise report [AD-A277917] 09 p3791 N94-33109
Mars: Past, Present, and Future. Results from the MSATT Program, part 1 [NASA-CR-194279] 09 p3943 N94-33190
Deposition rates of oxidized iron on Mars 09 p3945 N94-33198
Thermal and hydraulic considerations regarding the fate of water discharged by the outflow channels to the Martian northern plains 09 p3946 N94-33202
The Northern Plains MSATT Meeting, and a call for a field-oriented successor to MSATT 09 p3947 N94-33210
Mineralogical diversity (spectral reflectance and Moessbauer data) in compositionally similar impact melt rocks from Manicouagan Crater, Canada 09 p3948 N94-33219
Martian spectral units derived from ISM imaging spectrometer data 09 p3949 N94-33220
Apron heights around stepped massifs in the Cydonia Mensae region: Do they record the local paleobathymetry of Oceanus Borealis? 09 p3949 N94-33224
The mineralogic evolution of the Martian surface through time: Implications from chemical reaction path modeling studies 09 p3950 N94-33226
Martian deltas: Morphology and distribution 09 p3950 N94-33230
Geologic controls of erosion and sedimentation on Mars 09 p3951 N94-33232
The Martian sources of the SNC meteorites (two, not one), and what can and can't be learned from the SNC meteorites 09 p3951 N94-33234
Temporal changes in the geographic distribution, elevation, and potential origin of the Martian outflow channels 09 p3951 N94-33235
An ethnographic object-oriented analysis of explorer presence in a volcanic terrain environment: Claims and evidence [NASA-TM-108823] 10 p4099 N94-33608
Mars aqueous chemistry experiment [NASA-CR-196024] 11 p4354 N94-35263
Workshop on the Martian Northern Plains: Sedimentological, periglacial, and paleoclimatic evolution [NASA-CR-196134] 11 p4354 N94-35359
The Twenty-Fifth Lunar and Planetary Science Conference. Part 1: A-G [NASA-CR-195743] 11 p4355 N94-35395
What initiated planetesimal formation? 11 p4351 N94-35422
Exopaleontology and the search for a fossil record on Mars 11 p4360 N94-35425
The Twenty-Fifth Lunar and Planetary Science Conference. Part 3: P-Z [NASA-CR-195745] 11 p4362 N94-35448
The topography of Mars: A re-evaluation of current data 11 p4364 N94-35460
Noachian and Hesperian modification of the original Chryse impact basin topography 11 p4364 N94-35462
The parent magma of xenoliths in shergottite EETA79001: Bulk and trace element composition inferred from magmatic inclusions 11 p4352 N94-35467
Formation of fold and thrust belts on Venus due to horizontal shortening of a laterally heterogeneous lithosphere 11 p4367 N94-35480
The Twenty-Fifth Lunar and Planetary Science Conference. Part 2: H-O [NASA-CR-195744] 11 p4367 N94-36136
Mossbauer and spectral (visible and near-IR) data for Fe(3+)-substituted rutile 11 p4240 N94-36154

PLANETARY GRAVITATION

Spectral analysis of the gravity and topography of Mars 01 p0444 N94-12065
Venus gravity [NASA-CR-194077] 02 p0841 N94-12823
Largest impact features on Venus: Non-preserved or non-recognizable? 05 p2096 N94-20657
Magellan at Venus: Summary of science findings 05 p2110 N94-20734
Venus gravity: New Magellan low altitude data 05 p2117 N94-20772
Variety in planetary systems 05 p2086 N94-20871
Analysis of crustal structure of Venus utilizing residual Line-of-Sight (LOS) gravity acceleration and surface topography data. A trial of global modeling of Venus gravity field using harmonic spline method [NASA-CR-195799] 08 p3549 N94-29737
High degree gravitational sensitivity from Mars orbiters for the GMM-1 gravity model [NASA-TM-104604] 10 p4088 N94-34992

PLANETARY IONOSPHERES

Pioneer Venus data analysis for the retarding potential analyzer [NASA-CR-194673] 03 p1297 N94-17292
Nonthermal planetary radio emissions: Theories and observations 05 p2001 N94-22635
Venus Data Analysis Program: Directory of Research Projects (1993-1994) [NASA-CR-195742] 08 p3549 N94-29102
Plasma waves in the nightside ionosphere of Venus 10 p4164 N94-33431

PLANETARY LANDING
Past US studies and developments for planetary rovers 06 p2369 N94-23375
Planetary and asteroid missions. Getting there: Anchoring spacecraft to asteroids [NASA-CR-195493] 06 p2614 N94-24333
Autonomous hazard detection and avoidance [NASA-CR-188331] 11 p4309 N94-36439
PLANETARY LIMB
Altitude profile of aerosols on Mars from measurements of its thermal radiation on limb 03 p1294 N94-16423
PLANETARY MAGNETIC FIELDS
Interpretation of lunar and planetary electromagnetic scattering using the full wave solutions 01 p0440 N94-12049
On the unique structure of the magnetic fields of Uranus and Neptune 01 p0472 N94-12221
Precession of Uranus and Neptune and their magnetic field 01 p0473 N94-12222
Magnetic effects in Venus/solar wind interaction [NASA-CR-194666] 03 p1299 N94-17281
Expectations for the Martian core magnetic field 05 p2120 N94-20792
Analysis of energetic proton and electron data in Neptune's magnetosphere [NASA-CR-195707] 07 p3107 N94-27784
Plasma waves in the nightside ionosphere of Venus 10 p4164 N94-33431
Magnetic field waves at Uranus [NASA-CR-194807] 10 p4164 N94-34000
PLANETARY MAGNETOSPHERES
NT PLANETARY MAGNETOTAILS
Multispectral observations of the Jovian aurora [NASA-CR-193628] 03 p1297 N94-16884
Nonthermal planetary radio emissions: Theories and observations 05 p2001 N94-22635
Studies for Io's extended atmosphere and neutral clouds and their impact on the local satellite atmosphere and on the planetary magnetosphere [NASA-CR-195255] 07 p3106 N94-27406
Analysis of energetic proton and electron data in Neptune's magnetosphere [NASA-CR-195707] 07 p3107 N94-27784
Observation of Jovian auroral Ly-alpha line profile and emission variability with a sounding rocket and the IUE archives 08 p3550 N94-30798
Plasma and radio waves from Neptune: Source mechanisms and propagation [NASA-CR-195877] 09 p3943 N94-33103
PLANETARY MAGNETOTAILS
An investigation of the near Earth space environments [AD-A265295] 01 p0278 N94-11828
Linear and non-linear studies of Alfven waves in space. Stationary and dynamic processes in magnetospheric plasmas [NASA-CR-193585] 03 p1239 N94-16647
Experimental investigation of possible geomagnetic feedback from energetic (0.1 to 16 keV) terrestrial O(+) ions in the magnetotail current sheet [PAPER-93JA01991] 08 p3507 N94-30128
Planetary magnetotails: Magnetic configuration and nonthermal plasma 09 p3942 N94-32326
PLANETARY MANTLES
NT EARTH MANTLE
Can weak crust explain the correlation of geoid and topography on Venus? 01 p0453 N94-12118
Buoyant subduction on Venus: Implications for subduction around coronae 01 p0455 N94-12130
Regional mantle upwelling on Venus: The Beta-Atla-Themis anomaly and correlation with global tectonic patterns 01 p0467 N94-12196
Noble gas evidence of an aqueous reservoir near the surface of Mars more recently than 1.3 Ga 01 p0473 N94-12228
Morphotectonics of Venus 01 p0478 N94-12248
Transmantle flux tectonics 01 p0283 N94-12249
Regional tectonic analysis of Venus as part of the Pioneer Venus guest investigator project [NASA-CR-194079] 02 p0842 N94-13561
Experimental constraints on CO2 and H2O in the Martian mantle and primary magmas 03 p1262 N94-16248
Estimates of lithospheric thickness on Venus 03 p1267 N94-16277
An inversion of geoid and topography for mantle and crustal structure on Mars 03 p1273 N94-16315
Models of thermal/chemical boundary layer convection: Potential application to Venus 03 p1279 N94-16348
Geophysical models of Western Aphrodite-Niobe region: Venus 03 p1286 N94-16382
Effective elastic thickness of the Venusian lithosphere with lateral viscosity variations in the mantle 03 p1293 N94-16421
Differentiation of magma oceans and the thickness of the depleted layer on Venus 05 p2118 N94-20780
Arcuate and circular structures in the Tharsis region: Evidence of coronae on Mars 05 p2134 N94-20863
The connection between Venus' free obliquity and its CMB oblateness 05 p2139 N94-20896
Wrinkle ridges, reverse faulting, and the depth penetration of lithospheric stress in lunae planum, Mars 05 p2141 N94-20910
Wet inside and out? Constraints on water in the Martian mantle and on outgassed water, based on melt inclusions in SNC meteorites 05 p2145 N94-21678
PLANETARY MAPPING
Meteorological Satellite Center [MSC-TN-26] 01 p0190 N94-11079
Fine tuning of stretched-VISSR image mapping 01 p0190 N94-11080
Russia's contribution to regional geologic mapping of Venus 01 p0454 N94-12122
Geologic history of central Chryse Planitia and the Viking 1 landing site, Mars 01 p0465 N94-12180
Synthesis of global thematic mapping, Venus: Geologic correlations/questions for the Magellan gravity mission 01 p0467 N94-12194
Relation between ages and elevations of Martian channels 01 p0472 N94-12216
Free-air and Bouguer gravity anomalies and the Martian crustal dichotomy 01 p0481 N94-12267
Interdisciplinary scientist participation in the Phobos mission [NASA-CR-193715] 01 p0482 N94-12446
Pargo Chasma and its relationship to global tectonics 03 p1249 N94-16181
Earth imaging results from Galileo's second encounter 03 p1252 N94-16201
Separation of topographic and intrinsic backscatter variations in biscopic radar images: A magic airbrush 03 p1086 N94-16318
Global Magellan-image map of Venus at full resolution 03 p1274 N94-16319
The cartography of Venus with Magellan data 03 p1274 N94-16320
Hellas basin, Mars: Formation by oblique impact 03 p1280 N94-16350
Tectonic resurfacing of Venus 03 p1285 N94-16380
The use of TIMS for mapping different pahoehoe surfaces: Mauna Iki, Kilauea 03 p1065 N94-16606
Unmixing AVIRIS data to provide a method for vegetation fraction subtraction 03 p1066 N94-16669
Mapping the mineralogy and lithology of Canyonlands, Utah with imaging spectrometer data and the multiple spectral feature mapping algorithm 03 p1066 N94-16670
Stratigraphy of the Martian northern plains 05 p2091 N94-20398
Balloon exploration of the northern plains of Mars near and north of the Viking 2 landing site 05 p2092 N94-20401
Geologic mapping of Northern Atla Regio on Venus: Preliminary data 05 p2095 N94-20654
Beta Regio - Phoebe Regio on Venus: Geologic mapping with the Magellan data 05 p2096 N94-20656
MinMap: An imaging spectrometer for high resolution compositional mapping of the Moon 05 p1813 N94-20688
Geologic mapping of Harmakhis and Reull Valles region, Mars: Evidence for multiple resurfacing and drainage events 05 p1844 N94-20705
Chronology, eruption duration, and atmospheric contribution of Apollinaris Patera, Mars 05 p2108 N94-20720
Earth-based measurement of lunar topography using delayed radar interferometry 05 p2119 N94-20787
The role of CO2 in weathering reactions and the presence of S2 on Venus: Implications for the pyrite stability field 05 p2122 N94-20799
Complex structure of the Thaumasia region of Mars 05 p2125 N94-20815
Comparison of flank modification on Ascraeus and Arsia Montes volcanoes, Mars 05 p2140 N94-20903
Science strategy for Mars exploration 06 p2606 N94-23380
Evidence for dust transport in Viking IR thermal mapper opacity data 06 p2620 N94-24892
The Mars Aerial Platform (MAP) mission 06 p2622 N94-24903
Copernicus: Lunar surface mapper 07 p3081 N94-25702
The Pluto fast flyby mission: Completing the reconnaissance of the solar system 08 p3235 N94-29768
Geoid-to-topography ratios on Venus: A global perspective 09 p3940 N94-31110
Mars: Five views on what is known [NASA-TM-109751] 09 p3942 N94-31805
The Lunar Scout Program: An international program to survey the Moon from orbit for geochemistry, mineralogy, imagery, geodesy, and gravity [NASA-TM-104791] 09 p3943 N94-32923
Mars: Past, Present, and Future. Results from the MSATT Program, part 1 [NASA-CR-194279] 09 p3943 N94-33190
Thermal studies of Martian channels and valleys using Termoskan data: New results 09 p3944 N94-33194
Global color views of Mars 09 p3948 N94-33217
Apron heights around stepped massifs in the Cydonia Mensae region: Do they record the local paleobathymetry of Oceanus Borealis? 09 p3949 N94-33224
The fretted terrain of the Nilosyrtis Mensae region of Mars: Clues to the timing of dichotomy formation and the emplacement of the northern plains 11 p4360 N94-35424
Noachian and Hesperian modification of the original Chryse impact basin topography 11 p4364 N94-35462
PLANETARY MASS
A simultaneous estimation of the mass of Mars and its natural satellites, Phobos and Deimos, from the orbital perturbations on the Mariner 9, Viking 1, and Viking 2 orbiters 03 p1279 N94-16347
PLANETARY METEOROLOGY
Observed climatic activity pertaining to the evolution of the northern plains 05 p2090 N94-20392
Workshop on Atmospheric Transport on Mars [NASA-CR-194855] 06 p2616 N94-24871
The NASA/GISS Mars general circulation model: Preliminary experiments 06 p2616 N94-24872
Optimal gains for a single polar orbiting satellite 06 p2208 N94-24873
A diagnostic model to estimate winds and small-scale drag from Mars Observer PMIRR data 06 p2617 N94-24874
Eddy mixing coefficient values derived from simulations with the NASA Ames Mars GCM 06 p2617 N94-24875
Mars dust-driven tides and their impact on the thermosphere 06 p2617 N94-24876
Eddy transport of water vapor in the Martian atmosphere 09 p3949 N94-33221
Numerical simulation of thermally induced near-surface flows over Martian terrain 09 p3949 N94-33223
Controls on the CO2 seasonal cycle 09 p3950 N94-33227
The wavelength dependence of Martian atmospheric dust radiative properties 09 p3950 N94-33228
PLANETARY MOTION
U SOLAR ORBITS
PLANETARY NEBULAE
Midplane temperatures in the solar nebula 01 p0448 N94-12088
Chondrule formation by clumpy accretion onto the solar nebula 01 p0448 N94-12089
The experimental production of matrix lumps within chondrules: Evidence of post-formational processes 01 p0431 N94-12176
Anomalous REE patterns in unequilibrated enstatite chondrites: Evidence and implications 01 p0431 N94-12191
A survey of compact planetary nebulae at radio wavelengths [ISBN-0-315-61950-3] 02 p0829 N94-13371
Gas-grain energy transfer in solar nebula shock waves: Implications for the origin of chondrules 03 p1262 N94-16251
Evolution of Triton's volatile budget 03 p1284 N94-16373
On the delivery of planetesimals to a protoplanet in the solar nebula 03 p1245 N94-16379
Evaporation in equilibrium, in vacuum, and in hydrogen gas 05 p1684 N94-20638
AGB stars as a source of short-lived radioactive nuclei in the solar nebula 05 p2133 N94-20859
High spatial resolution observations of CO in CRL 618 [REPT-334] 06 p2604 N94-24986
Spatially resolved spectroscopy of AG Carinae, and direct evidence for stellar evolution: The central star of NGC 2392 [NASA-CR-189291] 08 p3545 N94-29871
Application of an alkylammonium method for characterization of phyllosilicates in CI chondrites 11 p4351 N94-35432
Far-infrared emission line spectroscopy of planetary nebulae from the KAO [NASA-CR-196289] 12 p4547 N94-37825
PLANETARY ORBITS
The effects of orbital and climatic variations on Martian surface heat flow 03 p1290 N94-16402
The distribution of Martian ground ice at other epochs 09 p3948 N94-33218
High degree gravitational sensitivity from Mars orbiters for the GMM-1 gravity model [NASA-TM-104604] 10 p4088 N94-34992

PLANETARY QUAKES
The seismic response of an aquifer to the propagation of an impact generated shock wave: A possible trigger of the Martian outflow channels?
03 p1281 N94-16354
Seismic-triggering history of the catastrophic outflows in the Chryse region of Mars 05 p2091 N94-20399
PLANETARY QUARANTINE
Planetary protection issues and future Mars missions
[NASA-CP-10086] 10 p4164 N94-33533
PLANETARY RADIATION
Altitude profile of aerosols on Mars from measurements of its thermal radiation on limb 03 p1294 N94-16423
Plasma and radio waves from Neptune: Source mechanisms and propagation
[NASA-CR-195877] 09 p3943 N94-33103
Plasma and radio waves from Neptune: Source mechanisms and propagation
[NASA-CR-196284] 12 p4550 N94-37251
PLANETARY RINGS
NT SATURN RINGS
Wave structure in planetary rings
01 p0434 N94-11185
Submission of Earth-based ring occultation observations to the NASA planetary data system rings discipline node
[NASA-CR-193469] 01 p0427 N94-12557
Voyager's last encounter
[NASA-TM-109361] 04 p1628 N94-18957
PLANETARY ROTATION
A method to determine asteroid poles
01 p0431 N94-12205
Neptune encounter highlights
[NASA-TM-109421] 03 p1246 N94-15240
The connection between Venus' free obliquity and its CMB oblateness 05 p2139 N94-20896
Planetesimal dynamics in the vicinity of a growing protoplanet 09 p3935 N94-31926
PLANETARY SATELLITES
U NATURAL SATELLITES
PLANETARY SPACE FLIGHT
U INTERPLANETARY FLIGHT
PLANETARY SPACECRAFT
U INTERPLANETARY SPACECRAFT
PLANETARY STRUCTURE
Marslink 01 p0438 N94-12034
Noble gas evidence of an aqueous reservoir near the surface of Mars more recently than 1.3 Ga
01 p0473 N94-12228
Experimental constraints on CO2 and H2O in the Martian mantle and primary magmas 03 p1262 N94-16248
Geophysical models of Western Aphrodite-Niobe region: Venus 03 p1286 N94-16382
The use of velocity spectra for stacking receiver functions with application to IRIS/IDA stations OBNINSK (OBN) and ARTI (ARU), Russia
[AD-A269087] 04 p1483 N94-18717
Differentiation of magma oceans and the thickness of the depleted layer on Venus 05 p2118 N94-20780
Large, ancient, compressional structures on Mars
05 p2125 N94-20816
Wet inside and out? Constraints on water in the Martian mantle and on outgassed water, based on melt inclusions in SNC meteorites 05 p2145 N94-21678
Underground structure in the eastern part of Kanagawa Prefecture inferred from explosion seismic observations
07 p2886 N94-27987
Forced libration of Mercury and geodetic determination of a possible fluid core 09 p3774 N94-32493
PLANETARY SURFACES
NT MARS SURFACE
NT MERCURY SURFACE
NT VENUS SURFACE
Physical studies of planetary and satellite surfaces
[NASA-CR-193545] 01 p0434 N94-10817
Yana ring structure, North-Eastern Siberia: A possible counterpart of coronae on Venus
01 p0282 N94-12121
Cratering on Gaspra 01 p0459 N94-12147
Thermal-infrared emission spectroscopy of natural surfaces: Application to coated surfaces
01 p0081 N94-12156
Transmantle flux tectonics 01 p0283 N94-12249
Spectral analysis for automated exploration and sample acquisition
[NASA-CR-194095] 02 p0545 N94-13189
Impact melting and vaporization in planetary regoliths
02 p0843 N94-14299
Extrapolation of space weathering processes to other small solar system bodies 02 p0843 N94-14300
Twenty-Fourth Lunar and Planetary Science Conference. Part 2: G-M
[NASA-CR-193174] 03 p1247 N94-16173
Rover mounted ground penetrating radar as a tool for investigating the near-surface of Mars and beyong
03 p1007 N94-16197
Lava flow-field morphological classification and interpretation: Examples from Venus
03 p1259 N94-16230
Near-surface temperature gradients and their effects on thermal-infrared emission spectra of particulate planetary surfaces 03 p1260 N94-16236
Guide to Magellan image interpretation
[NASA-CR-194340] 03 p1298 N94-17654
Advances in spaceborne radar remote sensing
05 p1723 N94-20424
Twenty-Fourth Lunar and Planetary Science Conference. Part 3: N-Z
[NASA-CR-193149] 05 p2092 N94-20636
Largest impact features on Venus: Non-preserved or non-recognizable? 05 p2096 N94-20657
Goniospectrometric properties of a white standard
05 p1684 N94-20664
Dynamics of large scale impacts on Venus and Earth
05 p2098 N94-20666
Comparative hypsometric analysis of both Earth and Venus topographic distributions
05 p2108 N94-20722
The Clementine Mission science return at the Moon and Geographos 05 p1652 N94-20850
The new family of JPL planetary surface vehicles
06 p2369 N94-23398
Automation technology for remote sample acquisition
06 p2369 N94-23407
Evolving directions in NASA's planetary rover requirements and technology 06 p2370 N94-23414
Towards real-time stereovision systems for planetary missions 06 p2370 N94-23422
A DTM-based path planning method for planetary rovers 06 p2370 N94-23423
Mobility analysis, simulation, and scale model testing for the design of wheeled planetary rovers
06 p2370 N94-23425
The transition from diapirism to dike intrusion: Implications for planetary volcanism
[NASA-CR-195133] 06 p2403 N94-24580
Hardware design of a spherical mini-rover
07 p2833 N94-25669
Planetary surface exploration MESUR/autonomous lunar rover 07 p2833 N94-25683
The thermal consequences of giant impacts in the early solar system 08 p3543 N94-29698
Differential Scanning Calorimetry (DSC) for planetary surface exploration 08 p3236 N94-29776
Tectonic History of the Terrestrial Planets
[NASA-CR-195696] 09 p3939 N94-31105
A mineralogical instrument for planetary applications
11 p4357 N94-35408
The Twenty-Fifth Lunar and Planetary Science Conference. Part 3: P-Z
[NASA-CR-195745] 11 p4362 N94-35448
The temperature of nitrogen on Pluto
11 p4365 N94-35468
The Twenty-Fifth Lunar and Planetary Science Conference. Part 2: H-O
[NASA-CR-195744] 11 p4367 N94-36136
PLANETARY SYSTEMS
NT SOLAR SYSTEM
Planetary system detection by POINTS
[NASA-CR-194361] 02 p0545 N94-13067
Teaching planetary sciences to elementary school teachers: Programs that work 03 p1222 N94-16346
Variety in planetary systems 05 p2086 N94-20871
Studies of extra-solar Oort Clouds and the Kuiper Disk
[NASA-CR-195242] 07 p3103 N94-26789
Evolution of protoplanetary disks with dynamo magnetic fields 09 p3931 N94-31135
PLANETARY TEMPERATURE
Regional tectonic analysis of Venus as part of the Pioneer Venus guest investigator project
[NASA-CR-194079] 02 p0842 N94-13561
The effects of orbital and climatic variations on Martian surface heat flow 03 p1290 N94-16402
Equatorial ground ice on Mars: Steady-state stability
03 p1290 N94-16403
Mars and the early Sun 05 p2146 N94-21683
Three-dimensional numerical simulation of near-surface flows over the Martian north polar cap
06 p2621 N94-24895
IRTM brightness temperature maps of the Martian south polar region during the polar night: The cold spots don't move 09 p3949 N94-33222
The temperature of nitrogen on Pluto
11 p4365 N94-35468
PLANETARY WAVES
Minimal modeling of the bimodality of extratropical atmospheric planetary waves 02 p0713 N94-13622
A global traveling wave on Venus
[NASA-CR-194356] 03 p1246 N94-15182
Ray tracing on topographic Rossby waves
[AD-A267014] 03 p1112 N94-15844
Real time system for practical acoustic monitoring of global ocean temperature
[AD-A267868] 03 p1113 N94-17391
Planetary plasma waves
[NASA-CR-194295] 04 p1629 N94-19094
Interactions of free modes, tides, and gravity waves in the middle atmosphere
[REPT-84] 05 p1855 N94-20155
Global acoustic mapping of ocean temperatures (GAMOT)
[AD-A273387] 06 p2418 N94-24719
Regarding tracer transport in Mars' winter atmosphere in the presence of nearly stationary, forced planetary waves 06 p2618 N94-24882
Two-dimensional modeling of thermal inversion layers in the middle atmosphere of Mars
06 p2622 N94-24900
Numerical procedure for planetary wave solution
[DE94-004280] 07 p2879 N94-26576
Global barotropic response to a tropical forcing
[NASA-CR-195256] 07 p2896 N94-27408
Papers in meteorology and geophysics, vol. 44, no.1
[JTN-94-80585] 08 p3324 N94-28693
On the linear stability of Verkley's modons
08 p3324 N94-28695
Generation mechanisms of quasi-stationary waves in the Southern Hemisphere 08 p3365 N94-30789
Magnetohydrodynamics of the Earth's core. 1: Steady, rotating magnetoconvection. 2: Magnetic Rossby waves
09 p3770 N94-31104
Stationary eddies in the Mars general circulation as simulated by the NASA-Ames GCM
09 p3944 N94-33192
Non-linear interaction of gravity waves with average jet flows, instabilities, and turbulence
[PB94-170586] 11 p4291 N94-36214
PLANETESIMALS
U PROTOPLANETS
PLANETOCENTRIC COORDINATES
NT GEOCENTRIC COORDINATES
PLANETOLOGY
Planetary astronomy of Mars. Mars data reduction
[NASA-CR-193515] 01 p0424 N94-12768
PLANETS
NT EARTH (PLANET)
NT GAS GIANT PLANETS
NT JUPITER (PLANET)
NT MARS (PLANET)
NT MERCURY (PLANET)
NT NEPTUNE (PLANET)
NT PLUTO (PLANET)
NT SATURN (PLANET)
NT TERRESTRIAL PLANETS
NT URANUS (PLANET)
NT VENUS (PLANET)
The planetary data system educational CD-ROM
03 p1234 N94-16209
PLANFORMS
NT DELTA WINGS
NT RECTANGULAR PANELS
NT RECTANGULAR PLATES
NT RECTANGULAR WINGS
NT SWEPT FORWARD WINGS
NT SWEPTBACK WINGS
NT VARIABLE SWEEP WINGS
NT WING PLANFORMS
Wind-tunnel investigation of aerodynamic efficiency of three planar elliptical wings with curvature of quarter-chord line
[NASA-TP-3359] 03 p0859 N94-16574
Numerical solution of inverse problem in aerodynamics 08 p3125 N94-28965
Low-speed longitudinal aerodynamic characteristics of a flat-plate planform model of an advanced fighter configuration
[NASA-TM-109045] 08 p3130 N94-29443
PLANIGRAPHY
U TOMOGRAPHY
PLANKTON
NT PHYTOPLANKTON
NT ZOOPLANKTON
Acoustic estimation of plankton biomass
01 p0218 N94-12699
A possibility to define the location of epipelagic fish concentrations with assistance of satellite sensing
01 p0228 N94-12757
Coupling of pelagic and benthic communities over a seamount in the Eastern North Pacific
[AD-A274750] 07 p2899 N94-26149
Light utilization and photoinhibition of photosynthesis in marine phytoplankton
[DE94-005505] 09 p3794 N94-32896
PLANKTON BLOOM
U PLANKTON

PLANNING
NT AIRPORT PLANNING
NT MANAGEMENT PLANNING
NT MISSION PLANNING
NT PRODUCTION PLANNING
NT PROJECT PLANNING
NT REGIONAL PLANNING
NT TASK PLANNING (ROBOTICS)
NT TRAJECTORY PLANNING
NT URBAN PLANNING
Information resources management long-range plan, FY1994
[DE93-013898] 01 p0420 N94-11588
Bias in planning and explanation-based learning
[AD-A269608] 04 p1610 N94-17746
PRACTICAL: Planning and resource allocation in C2-domains with time critical algorithms
[FEL-93-B029] 04 p1544 N94-19458
Statistical probabilities for planning
[TR-474] 04 p1559 N94-19511
Graphical interactive planning of robotic applications with support of integrated simulation
[ETN-93-93793] 05 p1944 N94-21057
Multicriteria optimisation problem in the agricultural modelling 05 p1844 N94-22073
Environmental benefits of different types of heat pumps, available and expected
[DE94-002440] 07 p2866 N94-26123
A time reasoning system based on the event calculus for scheduling in aeronautic maintenance
[REPT-932-710-101] 08 p3122 N94-29463
Interactive analysis and planning tools for air traffic and airspace management 08 p3139 N94-29573
On a formal approach to the methodology of information planning
[MEMO-INF-93-42] 09 p3917 N94-31415
Planning of air crew schedules
[ISBN-0-315-86506-7] 09 p3914 N94-32074
Utility-based planning
[NASA-CR-195878] 09 p3816 N94-32086
An algorithm for probabilistic, totally-ordered temporal projection
[AD-A277341] 09 p3817 N94-32257
Planning applications in image analysis 10 p4122 N94-35045
Prodigy planning algorithm
[AD-A278900] 11 p4303 N94-35574
Bootstrap planning: Theory and application
[DE94-006466] 12 p4501 N94-37425

PLANT DESIGN
Field of solar collectors: Effect of shadowing on the optimal field design
[ITN-93-85197] 02 p0702 N94-13570
Knowledge based systems: From process control to policy analysis
[DE93-014582] 02 p0765 N94-14117

PLANT ROOTS
Acetate concentrations and oxidation in salt marsh sediments 01 p0269 N94-12459
Root gravitropism in maize and Arabidopsis
[NASA-CR-195710] 07 p2903 N94-27940

PLANT STRESS
Effects of elevated atmospheric CO2 concentrations and water stress on field-grown maize
[DE94-009636] 10 p4082 N94-33915

PLANTING
Forest management for fixing and sequestering carbon
[DE93-013520] 02 p0707 N94-13486
The carbon dioxide emissions game: Playing the net
[DE93-017670] 04 p1471 N94-17821

PLANTS (BOTANY)
NT ALFALFA
NT ALGAE
NT AQUATIC PLANTS
NT BARLEY
NT BLUE GREEN ALGAE
NT BRYOPHYTES
NT CONIFERS
NT CORN
NT DECIDUOUS TREES
NT FUNGI
NT GRASSES
NT NEUROSPORA
NT PHYTOPLANKTON
NT POTATOES
NT RICE
NT SEA GRASSES
NT SOYBEANS
NT TOBACCO
NT TREES (PLANTS)
NT YEAST
Plant architecture, growth and radiative transfer for terrestrial and space environments
[NASA-CR-193476] 01 p0302 N94-12559
Role of Ca(++)/calmodulin in the regulation of microtubules in higher plants
[DE93-015885] 02 p0727 N94-12835
Gravity, chromosomes, and organized development in aseptically cultured plant cells 02 p0592 N94-13764
The first steps of chlorophyll synthesis: RNA involvement and regulation
[DE93-014398] 02 p0730 N94-14509
Plant research
[NASA-TM-109664] 03 p1116 N94-15235
The 1990-1991 NASA space biology accomplishments
[NASA-TM-4501] 03 p1118 N94-17257
Photosynthetic responses to the environment, volume 8
[AD-A269584] 04 p1502 N94-18305
Compilation of 1992 annual reports of the Navy ELF communications system ecological monitoring program, volume 1
[AD-A269569] 04 p1386 N94-18473
Compilation of 1992 annual reports of the navy ELF communications system ecological monitoring program, volume 2
[AD-A269726] 04 p1388 N94-18751
Microgravity research in plant biological systems: Realizing the potential of molecular biology 04 p1503 N94-19216
Health effects of global warming: Problems in assessment
[DE93-040323] 05 p1850 N94-19930
ELF communications system ecological monitoring program
[AD-A273456] 06 p2299 N94-24676
Generalized linear mixed models and their application in plant breeding research
[ETN-94-95335] 06 p2460 N94-25061
Report of National Institute for Resources and Environment. No. 5: Study on direct liquefaction of woody biomass
[JTN-94-80551] 07 p2859 N94-27204
Ninth International Workshop on Plant Membrane Biology
[DE94-005690] 09 p3794 N94-32769
Response of plants and ecosystems to CO2 and climate change
[DE94-011583] 12 p4466 N94-37376
Surface-layer response over shrub-steppe canopy during springtime
[DE94-011235] 12 p4468 N94-37624

PLANTS (INDUSTRIES)
U INDUSTRIAL PLANTS

PLASMA ACCELERATION
Dispersion of plasma waves in a finite magnetic field (omega(sub H) greater than omega(sub p))
[DE93-621654] 01 p0391 N94-11210
Investigation of dynamics of plasma fluxes generated by the quasi-stationary plasma accelerator P-50
[DE93-621665] 02 p0794 N94-12854
Numerical modeling of the temperature gradients and spectra of the plasma armature on Thunderbolt
[AD-A266414] 03 p0878 N94-16552
Observations of MeV electrons and scattered light from intense, subpicosecond laser-plasma interactions
[DE93-017153] 04 p1435 N94-17855
Magnetic insulation of secondary electrons in plasma source ion implantation
[DE93-040106] 05 p1997 N94-21988

PLASMA ACCELERATORS
Investigation of dynamics of plasma fluxes generated by the quasi-stationary plasma accelerator P-50
[DE93-621665] 02 p0794 N94-12854

PLASMA ANTENNAS
Plasma production by helicon waves
[DE93-788396] 04 p1586 N94-18213
Waves in space plasma dipole antenna subsystem 08 p3161 N94-29632

PLASMA ARC SPRAYING
U ARC SPRAYING

PLASMA ARC WELDING
The Marshall Automated Weld System (MAWS)
[TABES PAPER 93-602] 03 p1049 N94-16138
Plasma arc welding repair of space flight hardware
[TABES PAPER 93-603] 03 p1049 N94-16139
Robotic weld overlay coatings for erosion control
[DE93-016938] 03 p0970 N94-16959
Impact of copper vapour contamination on argon arcs 05 p1994 N94-21053
Plasma ARC keyhole welding of aluminum
[PB93-201606] 06 p2353 N94-23449
Robotic weld overlay coatings for erosion control
[DE94-002665] 06 p2258 N94-24749
UAH mathematical model of the variable polarity plasma ARC welding system calculation
[NASA-CR-193926] 07 p2824 N94-27221
Plasma arc welding torch having means for vortexing plasma for exiting the welding torch
[NASA-CASE-MFS-28828-1] 08 p3298 N94-29351
Chamber free fusion welding root side purging method and apparatus
[NASA-CASE-MFS-28832-1] 08 p3204 N94-29380
Ternary arc gas plasma welding torch
[NASA-CASE-MFS-28857-1] 08 p3303 N94-30173
Robotic weld overlay coatings for erosion control
[DE94-008004] 09 p3658 N94-32408
Development of an automated wire delivery system for robotic welding applications
[NASA-CR-194216] 09 p3727 N94-32479
Robotic weld overlay coatings for erosion control
[DE94-009703] 10 p4060 N94-33902
Plasma arc welding weld imaging
[NASA-CASE-MFS-28797-1] 11 p4273 N94-35367

PLASMA ARCS
U PLASMA JETS

PLASMA BUBBLES
Interaction of multiple spark-generated bubbles in a compressible liquid
[AD-A275037] 08 p3272 N94-29149

PLASMA CHEMISTRY
Excitation balances and transport in an inductively coupled plasma
[ETN-94-95330] 06 p2554 N94-25241
Direct measurement of the reactivity of NH and OH on a silicon nitride surface
[DE94-005286] 08 p3199 N94-30260
Feasibility study to evaluate plasma quench process for natural gas conversion applications
[DE94-000086] 09 p3758 N94-31234
Degenerate four-wave mixing as a diagnostic of plasma chemistry
[DE94-008588] 09 p3889 N94-31766

PLASMA CLOUDS
NT MAGNETIC CLOUDS
Artificial plasma experiments. Chemical release observations associated with the CRRES program
[NASA-CR-194871] 06 p2550 N94-23565
Experiments on the two-stage dense plasma heating on the GOL-3 device
[DE94-608356] 08 p3508 N94-30193
Theory, Image Simulation, and Data Analysis of Chemical Release Experiments
[NASA-CR-194865] 09 p3954 N94-31101
Computer modeling of active experiments in space plasmas 09 p3890 N94-31927
Catalog of Helios 90 deg photometer events
[PL-TR-94-2040] 11 p4375 N94-36264

PLASMA COMPOSITION
Physics and modelling of scrape-off layer transport
[DE93-010510] 01 p0385 N94-10289
Atomic and molecular data for H2O, CO and CO2 relevant to edge plasma impurities
[DE93-771423] 01 p0387 N94-10662
Electron temperature measurements of x ray laser plasmas
[DE93-011874] 01 p0389 N94-11074
Helium transport scaling law studies
[DE93-013487] 01 p0393 N94-11513
Giotto data analysis: Electron plasma and heavy ion composition measurements at Comet Halley
[NASA-CR-193587] 01 p0428 N94-12770
Highly charged ions in hot, dense plasmas
[DE93-013348] 02 p0795 N94-12995
Variation of divertor plasma parameters with divertor depth for H-mode discharges in D3-D
[DE93-015475] 02 p0801 N94-14347
Direct determination of alpha particle transport coefficients
[DE93-013488] 02 p0787 N94-14691
Transient thermal analysis of cryocondensation pump for JET
[DE93-040372] 05 p1992 N94-20003
Fusion plasma theory project summaries
[DE94-001712] 06 p2551 N94-23808
Study on development of chemical measurement method utilizing plasmas 07 p2728 N94-25576
International bulletin on atomic and molecular data for fusion. No. 42-45, Mar. 1991 - Dec. 1992
[DE94-601817] 07 p3045 N94-26946
Helium transport and exhaust studies of H-mode discharges in the D3-D tokamak
[DE94-004744] 07 p3048 N94-27785
A study of the formation and dynamics of the Earth's plasma sheet using ion composition data
[NASA-CR-195119] 08 p3507 N94-30126
Characterization of atomic and molecular impurity sources and transport at the tokamak edge
[DE94-007212] 09 p3891 N94-32619
Analysis of data from the plasma composition experiment on the International Sun-Earth Explorer (ISEE 1)
[NASA-CR-189353] 09 p3893 N94-33074

A role of neutral hydrogen in CHS plasmas with reheat and collapse and comparison with JIPPT-IIU tokamak plasmas
[DE94-718985] 12 p4530 N94-37384

PLASMA COMPRESSION
On MHD mode equations in toroidal plasmas
[PPL-139] 02 p0800 N94-13877
Q-profile flattening due to nonlinear development of resistive kink mode and ensuing fast crash in sawtooth oscillations
[DE94-727625] 12 p4526 N94-36472

PLASMA CONDUCTIVITY
Experimental measurement of the plasma conductivity of Z93 and Z93P thermal control paint
[NASA-TM-106284] 01 p0043 N94-10756
Stationary spectra of short-wave convective and magnetostatic fluctuations in a finite-pressure plasma and anomalous heat conductivity
[DE93-617852] 01 p0388 N94-10840
The relaxed state and entropy production due to the electric resistivity and viscosity of plasma
05 p2010 N94-22696
Resistive ballooning mode in a gas-dynamic trap
[DE94-608328] 08 p3508 N94-30171

PLASMA CONFINEMENT
U PLASMA CONTROL

PLASMA CONTROL
Transport mechanisms acting in toroidal devices: A theoretician's view
[DE93-013463] 01 p0385 N94-10310
Optimization of break-down conditions in tokamak TOTUS
[DE93-617863] 01 p0386 N94-10524
Reversed-field pinch studies in the Madison Symmetric Torus
[DE93-013464] 01 p0388 N94-10747
Calculation of Mercier stability criterium in stellarators
[DE93-621599] 01 p0389 N94-11091
Possibilities of magnetic diagnostics in stellarators
[DE93-621608] 01 p0389 N94-11092
Particle transport analysis in torsatron configurations
[DE93-621640] 01 p0390 N94-11120
Physics of tokamak scrape-off layer confinement
[DE93-011949] 01 p0390 N94-11125
Simulation study of dynamo structure in reversed field pinch
[DE93-771406] 01 p0390 N94-11128
Analytical description of the torsatron Uragan-2M magnetic configuration with account of plasma pressure and external correcting magnetic field
[DE93-620983] 01 p0391 N94-11174
Characteristics of ICR-produced peripheral plasma in the Uragan-3M torsatron
[DE93-621666] 01 p0392 N94-11214
The role of plasma rotation on MHD instabilities in tokamaks
[DE93-013486] 01 p0393 N94-11512
Results from the D3-D advanced divertor program
[DE93-015472] 01 p0393 N94-11514
Initial assessment of lower hybrid current drive in D3-D
[DE93-013310] 01 p0394 N94-12370
An emerging understanding of H-mode discharges in tokamaks
[DE93-012829] 01 p0394 N94-12544
Theory of field-reversed configurations
[DE93-015611] 02 p0794 N94-12862
Growth curve analysis for plasma profiles using smoothing splines
[DE93-015741] 02 p0795 N94-12984
Nonlinear evolution of tearing modes in inhomogeneous plasmas
[PPL-133] 02 p0798 N94-13564
Studies of non-inductive current drive in the CDX-U tokamak 02 p0799 N94-13680
Experiments on the current rampdown phase in the STOR-M tokamak for AC operation
[PPL-132] 02 p0799 N94-13835
Dependence of beta(tau) on plasma shape in D3-D
[DE93-015473] 02 p0800 N94-13900
Stability and confinement properties of small-aspect-ratio tokamak
[INPE-5463-PRE/1771] 02 p0801 N94-14024
Variation of divertor plasma parameters with divertor depth for H-mode discharges in D3-D
[DE93-015475] 02 p0801 N94-14347
D3-D research operations
[DE93-016729] 02 p0802 N94-14519
Review of the Procyon explosive pulsed power system
[DE93-016562] 02 p0802 N94-14532
Active density control in DIII-D H-mode plasmas
[DE93-015477] 02 p0802 N94-14570
Measurements of edge fluctuations by phase contrast imaging on DIII-D
[DE93-014018] 02 p0802 N94-14579
The role of electric field shear stabilization of turbulence in the H-mode to VH-mode transition in D3-D
[DE93-015474] 02 p0802 N94-14583
Toward a quasi-linear closure for compressible turbulence
[DE93-017185] 02 p0647 N94-14895
ITER-HARD Toroidal Field coil structural analysis
[DE93-014834] 03 p1201 N94-15981
Active probing of plasma edge turbulence and feedback studies on the Texas experimental tokamak (TEXT)
[DE93-015799] 03 p1202 N94-16162
High beta and confinement studies of TFTR
[DE93-016204] 03 p1202 N94-16446
Method and apparatus for forming an agile plasma mirror effective as a microwave reflector
[AD-D015788] 03 p0998 N94-16535
3D and r,z particle simulations of heavy ion fusion beams
[DE93-013417] 03 p1205 N94-17670
ITER EDA design confinement capability
[DE93-013729] 04 p1582 N94-17697
Limits on m = 2, n = 1 error field induced locked mode instability in TPX with typical sources of poloidal field coil error field and a proto type correction coil, C-coil
[DE93-014408] 04 p1582 N94-17702
Self-regulated shear flow turbulence in confined plasmas
[DE93-015823] 04 p1583 N94-17743
Analysis of the ITER H-mode confinement database
[DE93-016984] 04 p1585 N94-18056
Coupled MHD and transport analysis of improved confinement D3-D discharges
[DE93-016985] 04 p1585 N94-18057
Dependence of helium transport on plasma current and ELM frequency in H-mode discharges in D3-D
[DE93-016986] 04 p1585 N94-18058
Application of piezoelectric stress gauges to the measurement of fast-rise-time multimegampere electric currents
[DE93-017625] 04 p1429 N94-18102
Ion mobility and transport barriers in the tokamak plasmas
[DE93-040320] 04 p1587 N94-18524
Materials processing and manufacturing technologies for diamond substrates multichip modules
[AD-A268989] 04 p1599 N94-18764
Lower hybrid counter current drive for edge current density modification in D3-D
[DE93-019157] 04 p1589 N94-19073
Modelization, numerical simulation and optimal control of NET tokamak plasma configuration evolution for the future generation of fusion reactors
[ETN-93-95019] 04 p1591 N94-19364
Transverse beam combiner for ILSE
[DE93-019239] 04 p1591 N94-19559
Theoretical studies of turbulence and anomalous transport in toroidal confinement devices
[DE93-040684] 04 p1592 N94-19656
Effect of limiter end loss in finite Larmor radius theory
[DE93-040913] 05 p1992 N94-19887
Fast ion behavior during neutral beam injection in ATF
[DE93-040267] 05 p1992 N94-20058
Beta-limiting instabilities in D3-D discharges with large bootstrap current
[DE93-015476] 05 p1993 N94-20326
Shear flow generation by Reynolds stress and suppression of resistive g-modes
[DE93-040911] 05 p1995 N94-21514
Parametric instabilities in picosecond time scales
[DE94-000384] 05 p1966 N94-21958
Fusion Plasma Theory. Task 1: Magnetic confinement fusion plasma theory
[DE94-000778] 05 p1998 N94-22019
Enhanced confinement regimes and control technology in the DIII-D tokamak
[DE93-019004] 05 p1998 N94-22039
A spheromak ignition experiment reusing Mirror Fusion Test Facility (MFTF) equipment
[DE94-001856] 05 p2034 N94-22050
A two-dimensional kinetic model of the scrape-off layer
[DE94-001235] 05 p1999 N94-22562
Fluid simulations of Delta T(sub e)-driven turbulence and transport in boundary plasmas
[DE94-001304] 05 p1999 N94-22566
Effects of magnetic field perturbations in the ATF torsatron
[DE94-000474] 05 p1999 N94-22568
Physics of transport phenomena in magnetic confinement plasmas 05 p2000 N94-22628
Massachusetts Institute of Technology Plasma Fusion Center 1992-1993 report to the President
[DE94-001725] 06 p2548 N94-22721
Active probing of plasma edge turbulence and feedback studies on the Texas Experimental Tokamak (TEXT)
[DE94-001017] 06 p2548 N94-22945
Plasma research in the Madison Symmetric Torus (MST)
[DE94-002318] 06 p2549 N94-22976
Fluctuations and confinement in ATF
[DE94-000485] 06 p2549 N94-22998
Structural analysis of a superconducting central solenoid for the Tokamak Physics Experiment
[DE94-001536] 06 p2549 N94-23014
Overview of the ATF stellarator program
[DE94-000371] 06 p2550 N94-23462
The role of the radial electric field in confinement and transport in H-mode and VH-mode discharges in the DIII-D tokamak
[DE94-002746] 06 p2551 N94-23782
Fusion plasma theory project summaries
[DE94-001712] 06 p2551 N94-23808
IPP Prague Contributions to the IAEA Technical Committee Meeting on Research Using Small Tokamaks
[IPPCZ-329] 06 p2551 N94-24293
Temporal behavior of the electron density profile during limiter biasing in the HYBTOK-2 tokamak
[NIFS-257] 06 p2552 N94-24456
Proposal of Modular Heliotron: Advanced modular helical system compatible with closed helical divertor
[NIFS-261] 06 p2552 N94-24458
Computer modeling of plasma flow switches-high current switching on Procyon
[DE93-040189] 06 p2311 N94-24500
Stabilization of the external kink and other MHD issues
[DE94-001541] 06 p2552 N94-24502
Start-up simulations of the PULSAR pulsed tokamak reactor
[DE94-002634] 06 p2552 N94-24519
Design of central control system for Large Helical Device (LHD)
[NIFS-258] 06 p2553 N94-24623
High-speed repetitive pellet injector for plasma fueling of magnetic confinement fusion devices
[DE94-002792] 07 p3042 N94-26140
Scaling of sustained ZT-40 M reversed field pinches
[DE94-003318] 07 p3043 N94-26321
Probability of accessing the multiple saturated states in the resistive interchange instability
[DE94-000478] 07 p3044 N94-26694
Potential of commercial tokamak reactors with improved physics
[DE94-002794] 07 p3044 N94-26860
Role of core toroidal rotation shear on turbulence and transport in the improved confinement regimes of the D3-D tokamak
[DE94-001215] 07 p3045 N94-26950
High gas-efficiency hydrogen negative ion sources
[PB93-232163] 07 p3025 N94-27348
Researches of the Electrotechnical Laboratory. No. 51: Study of formation and sustainment of reversed field pinch by slow control of magnetic field
[JTN-94-80548] 07 p3046 N94-27350
TFTR experimental data analysis collaboration
[DE94-004166] 07 p3047 N94-27690
Helium transport and exhaust studies of H-mode discharges in the D3-D tokamak
[DE94-004744] 07 p3048 N94-27785
Fuel ion rotation measurement and its implications on H-mode theories
[DE94-004860] 07 p3048 N94-27791
On radio frequency wave induced radial transport and wave helicity
[IPPCZ-326] 07 p2777 N94-27838
On helicon wave induced radial plasma transport
[IPPCZ-333] 07 p3048 N94-27840
Determination of the plasma column shape in the Tokamak Novillo cross section by magnetic probes
[DE94-604986] 07 p3048 N94-27844
Modelling and control of plasma position in the STOR-M tokamak
[ISBN-0-315-58891-8] 07 p3049 N94-27949
Progress in Z-Pinch Research
[IPPCZ-321] 08 p3505 N94-29074
A 6MeV heavy ion beam probe for the Large Helical Device
[AD-B183695L] 08 p3505 N94-29397
The effect of magnetic field configuration on particle pinch velocity in Compact Helical System (CHS)
[AD-B183299L] 08 p3505 N94-29398
Formation and self-healing of magnetic islands in finite-beta helias equilibria
[AD-B183271L] 08 p3505 N94-29483
Magnetic field generation by circularly polarized laser light and inertial plasma confinement in a miniature magnetic bottle induced by circularly polarized laser light
[DE94-608353] 08 p3508 N94-30192
The impact of improved physics on commercial tokamak reactors
[DE94-006103] 08 p3509 N94-30760

Application of divertor cryopumping to H-mode density control in DIII-D
[DE94-004859] 08 p3510 N94-30832
L-H confinement mode dynamics in three-dimensional state space
[DE94-007113] 09 p3887 N94-31396
Toroidal pinch experiments
[DE94-005876] 09 p3887 N94-31558
Plasma confinement theory and transport simulation
[DE94-006065] 09 p3888 N94-31619
High beta tokamak research
[DE94-006513] 09 p3888 N94-31664
First-wall heat-flux measurements during ELMing H-mode plasma
[DE94-008310] 09 p3888 N94-31765
Collisional and chaotic transport of energetic particles in toroidal plasma
[DE94-006504] 09 p3889 N94-31787
FWCD and ECCD experiments on D3-D
[DE94-007371] 09 p3890 N94-32201
Experimental survey of the L-H transition conditions in the D3-D tokamak
[DE94-007428] 09 p3891 N94-32595
Recent VH-mode results on D3-D
[DE94-007429] 09 p3891 N94-32611
Overview of H-mode studies in D3-D
[DE94-007430] 09 p3891 N94-32612
Anomalous thermalization of fast ions in magnetized plasma
[DE94-007109] 09 p3891 N94-32631
Coaxial slow source
[DE94-008191] 09 p3892 N94-32800
Divertor pumping and other reactor application issues for H-mode
[DE94-007431] 09 p3892 N94-32810
Cooperative program on D3-D (FY 1993)
[DE94-008343] 09 p3892 N94-32820
Anomalous transport equations in toroidal plasmas
[DE94-009206] 09 p3893 N94-32922
Precision operation of the Nova laser for fusion experiments
[DE94-007073] 10 p4057 N94-33405
Summary of experimental progress and suggestions for future work
[DE94-008893] 10 p4145 N94-34012
Power balance and characterization of impurities in the Maryland Spheromak, part 2
[DE94-009603] 11 p4335 N94-35670
A triggering mechanism of fast crash in sawtooth oscillation
[DE94-718974] 11 p4336 N94-35772
Particle orbit analysis for LHD helical axis configurations
[DE94-718995] 11 p4336 N94-35773
Applications of non-resonant RF forces for improvement of tokamak reactor performances. Part 1: Application of ponderomotive force
[DE94-718994] 11 p4336 N94-35813
Potential formation and transport in open field line systems
[DE94-718910] 11 p4337 N94-35983
Design study of LHD helical divertor and high temperature divertor plasma operation
[DE94-718975] 11 p4338 N94-36352
Modelling of ELMs and dynamic responses of the H-mode
[DE94-718977] 11 p4339 N94-36353
MHD and confinement characteristics in the high-beta regime on the CHS low-aspect-ratio heliotron/torsatron
[DE94-718981] 11 p4339 N94-36357
The role of heating and current drive in ITER
[DE94-012679] 12 p4527 N94-37082
Confinement improvement in H-mode-like plasmas in helical systems
[DE94-727619] 12 p4528 N94-37231
Towards nuclear fusion reactors
[DE94-748680] 12 p4528 N94-37235
Inertial Electrostatic Confinement (IEC) devices
[DE94-013114] 12 p4529 N94-37316
ELMy-H mode as limit cycle and transient responses of H-modes in tokamaks
[DE94-727510] 12 p4529 N94-37358
Isotope scaling and eta(i) mode with impurities in tokamak plasmas
[DE94-012763] 12 p4529 N94-37361
A role of neutral hydrogen in CHS plasmas with reheat and collapse and comparison with JIPPT-IIU tokamak plasmas
[DE94-718985] 12 p4530 N94-37384
Recent DIII-D high power heating and current drive experiments
[DE94-012509] 12 p4530 N94-37436
Theory of anomalous transport in H-mode plasmas
[DE94-727546] 12 p4531 N94-37485

PLASMA COOLING
Peculiarities of heat transfer in the experiments of beam injection heating of a plasma at the GOL-3 device
[DE94-608357] 08 p3508 N94-30194

PLASMA CURRENTS
Efficiency of fast wave current drive for a weakly relativistic plasma
[DE93-012775] 01 p0385 N94-10159
Possibilities of magnetic diagnostics in stellarators
[DE93-621608] 01 p0389 N94-11092
Initial assessment of lower hybrid current drive in D3-D
[DE93-013310] 01 p0394 N94-12370
Studies of non-inductive current drive in the CDX-U tokamak 02 p0799 N94-13680
Experiments on the current rampdown phase in the STOR-M tokamak for AC operation
[PPL-132] 02 p0799 N94-13835
Numerical Studies of Collisionless Current Layers
[NASA-CR-194337] 02 p0800 N94-13854
Active density control in DIII-D H-mode plasmas
[DE93-015477] 02 p0802 N94-14570
Inductive effects during second harmonic current drive experiments on T-10
[DE93-014411] 03 p1202 N94-16803
Simulation of enhanced tokamak performance on D3-D using fast wave current drive
[DE93-014009] 03 p1203 N94-16823
Detailed analysis of low energy plasma data under the Voyager Uranus data analysis program
[NASA-CR-193668] 04 p1628 N94-17842
Filamentary magnetohydrodynamic plasmas
[DE93-015616] 04 p1583 N94-17945
Coupled MHD and transport analysis of improved confinement D3-D discharges
[DE93-016985] 04 p1585 N94-18057
Dependence of helium transport on plasma current and ELM frequency in H-mode discharges in D3-D
[DE93-016986] 04 p1585 N94-18058
Lower hybrid counter current drive for edge current density modification in D3-D
[DE93-019157] 04 p1589 N94-19073
Electron cyclotron resonance heating in the microwave tokamak experiment
[DE93-018083] 04 p1590 N94-19289
Modelization, numerical simulation and optimal control of NET tokamak plasma configuration evolution for the future generation of fusion reactors
[ETN-93-95019] 04 p1591 N94-19364
Radiation of plasma wave wings through an electrodynamic tether satellite system with any sharp angle geometry
[REPT-85] 05 p1993 N94-20156
Beta-limiting instabilities in D3-D discharges with large bootstrap current
[DE93-015476] 05 p1993 N94-20326
Plasma heating in toroidal systems
05 p2000 N94-22629
Consequences of chaotic particle motion for the stability of space plasma current sheets
05 p2001 N94-22636
Current loop coalescence studied by 3-D electromagnetic particle code 05 p2005 N94-22660
Formation of fast magnetosonic shock waves during two current loops collision in solar flare
05 p2005 N94-22662
Dynamics of physical state during two current loops collision 05 p2005 N94-22663
Active probing of plasma edge turbulence and feedback studies on the Texas Experimental Tokamak (TEXT)
[DE94-001017] 06 p2548 N94-22945
1993 annual report for the Phaedrus-T RF current drive experiments
[DE94-001369] 06 p2550 N94-23192
Computer modeling of plasma flow switches-high current switching on Procyon
[DE93-040189] 06 p2311 N94-24500
Plasma initiation in a tokamak with conducting superstructure: First results from Alcator C-MOD
[DE94-001565] 06 p2552 N94-24504
Start-up simulations of the PULSAR pulsed tokamak reactor
[DE94-002634] 06 p2552 N94-24519
LHCD (low hybrid current drive) experiment on the HT-6B tokamak
[DE93-613720] 06 p2555 N94-25331
Numerical simulation of plasma vertical position stabilization in ITER
[DE93-634586] 07 p3044 N94-26510
Ionosphere-magnetosphere coupling
[NASA-CR-195222] 07 p2881 N94-27237
On radio frequency wave induced radial transport and wave helicity
[IPPCZ-326] 07 p2777 N94-27838
On helicon wave induced radial plasma transport
[IPPCZ-333] 07 p3048 N94-27840
Theoretical reversed field pinch and tokamak studies
[DE94-005409] 08 p3503 N94-28490
Fluctuation and transport reduction in a reversed field pinch by inductive poloidal current drive
[DE94-005542] 08 p3503 N94-28514
Three-dimensional effects for radio frequency antenna modeling
[DE94-006102] 08 p3255 N94-30105
Advanced steady-state operating scenarios
[DE94-004810] 08 p3509 N94-30768
Application of divertor cryopumping to H-mode density control in DIII-D
[DE94-004859] 08 p3510 N94-30832
First-wall heat-flux measurements during ELMing H-mode plasma
[DE94-008310] 09 p3888 N94-31765
FWCD and ECCD experiments on D3-D
[DE94-007371] 09 p3890 N94-32201
The SAMPIE flight experimental final technical requirements document
[NASA-TM-106224] 10 p4015 N94-34729
On the interpretation of diamagnetic loop measurements for a current-carrying plasma column in a conducting chamber
[DE94-007107] 12 p4526 N94-36536
Motional Stark effect upgrades on D3-D
[DE94-013146] 12 p4528 N94-37297

PLASMA CYLINDERS
NT CYLINDRICAL PLASMAS

PLASMA DECAY
Studies on the parametric decay of waves in fusion plasmas
[VTT-PUBS-110] 03 p1200 N94-15204
On the decay of a dipole pump wave to half-harmonics 03 p1201 N94-15211

PLASMA DENSITY
Comparison of hydrodynamic and semi-kinetic treatments for plasma flow along closed field lines
[NASA-CR-193589] 01 p0387 N94-10641
Dispersion of plasma waves in a finite magnetic field (omega(sub H) greater than omega(sub p))
[DE93-621654] 01 p0391 N94-11210
Spreading of Bimodulated Ultra-relativistic Electron Beam (BUEB) in Atmospheric Plasma Channel (APCh)
[DE93-621658] 01 p0392 N94-11213
Initial assessment of lower hybrid current drive in D3-D
[DE93-013310] 01 p0394 N94-12370
Excitation of coupled waves in plasma periodic structures by relativistic electron beam and acceleration of charged particles
[DE93-621657] 02 p0794 N94-12853
Dimensionally similar discharges with central RF heating on the D3-D tokamak
[DE93-012776] 02 p0795 N94-12953
Growth curve analysis for plasma profiles using smoothing splines
[DE93-015741] 02 p0795 N94-12984
Active density control in DIII-D H-mode plasmas
[DE93-015477] 02 p0802 N94-14570
Measurements of edge fluctuations by phase contrast imaging on DIII-D
[DE93-014018] 02 p0802 N94-14579
Characterization of short pulse laser-produced plasmas at the Lawrence Livermore National Laboratory ultra short-pulse laser
[DE93-017191] 04 p1585 N94-18082
Plasma production by helicon waves
[DE93-788396] 04 p1586 N94-18213
An investigation of methods for updating ionospheric scintillation models using topside in-situ plasma density measurements
[AD-A269872] 04 p1483 N94-18655
Phase-space description of plasma waves: Linear and nonlinear theory
[IRF-SR-211] 04 p1587 N94-18860
The spherical probe Electric Field and Wave Experiment for the Cluster mission 04 p1328 N94-19624
WHISPER: A sounder and high-frequency wave analyser experiment 04 p1328 N94-19626
Measurement of mesospheric turbulence in the framework of the metal campaign and development of a sensor for static pressure free measurements of neutral and electron density
[BONN-IR-92-45] 05 p1857 N94-21149
On effects of a local plasma density growth due to ponderomotive forces at fast wave launching in tokamaks
[IPPCZ-328] 05 p1996 N94-21571
Enhanced confinement regimes and control technology in the DIII-D tokamak
[DE93-019004] 05 p1998 N94-22039
Effects of magnetic field perturbations in the ATF torsatron
[DE94-000474] 05 p1999 N94-22568

Initial operation of a large-scale plasma source ion implantation experiment
[DE94-000805] 05 p2036 N94-22583
Non-equilibrium ionization in an M class solar flare 05 p2004 N94-22653
Plasma structure in a plasma flow along a magnetic mirror field 05 p2005 N94-22664
On the nonlinear instability of thermal structures 05 p2006 N94-22668
Fluctuations and confinement in ATF
[DE94-000485] 06 p2549 N94-22998
Analysis and experiments of a whistler-wave plasma thruster
[DE94-001533] 06 p2209 N94-23012
Upper atmosphere neutral and plasma density modeling
[AD-A274768] 07 p2879 N94-26569
Experiments and numerical simulations of electromagnetic wave propagation in plasma varying rapidly in space and time
[AD-A274376] 07 p2772 N94-26975
Shine through measurements with hydrogen beam in JT-60
[DE94-701113] 07 p3047 N94-27699
Laser blow-off lithium beam probing with high temporal resolution for edge plasma diagnostics
[DE94-701176] 07 p2820 N94-27701
Wave generation by contaminant ions near a large spacecraft
[NASA-CR-195797] 08 p3169 N94-29917
Magnetic field generation by circularly polarized laser light and inertial plasma confinement in a miniature magnetic bottle induced by circularly polarized laser light
[DE94-608353] 08 p3508 N94-30192
Experiments on the two-stage dense plasma heating on the GOL-3 device
[DE94-608356] 08 p3508 N94-30193
Peculiarities of heat transfer in the experiments of beam injection heating of a plasma at the GOL-3 device
[DE94-608357] 08 p3508 N94-30194
Variations of electron fluxes, low-frequency radiations and plasma density during the geomagnetic storm on 9-12 March, 1979 according to data of the Interkosmos-19 satellites
[DE94-607323] 08 p3365 N94-30223
Application of divertor cryopumping to H-mode density control in DIII-D
[DE94-004859] 08 p3510 N94-30832
An edge density fluctuation diagnostic for D3-D using lithium beams
[DE94-008554] 09 p3890 N94-32519
Divertor pumping and other reactor application issues for H-mode
[DE94-007431] 09 p3892 N94-32810
Plasma physics applications to intense radiation sources, pulsed power and space physics. Short pulse ultra intense laser-plasma interaction experiment
[AD-A278440] 10 p4144 N94-33555
An investigation of methods for improving models of ionospheric plasma-density irregularities and radio-frequency scintillation
[AD-A278568] 10 p4033 N94-33703
LLE review, volume 57
[DE94-009186] 10 p4145 N94-33990
Contributions of the low-latitude boundary layer to the finite width magnetotail convection model
[NASA-CR-196116] 11 p4289 N94-35392
D-D fusion experiments using fast z-pinches
[DE94-010090] 12 p4526 N94-36448
Microwave reflectometry for fusion plasma diagnostics
[DE94-620118] 12 p4527 N94-36566
ELMy-H mode as limit cycle and transient responses of H-modes in tokamaks
[DE94-727510] 12 p4529 N94-37358

PLASMA DIAGNOSTICS

Optimization of a CO2 laser Thomson scattering alpha particle diagnostic
[DE93-012782] 01 p0173 N94-10160
Electron temperature measurements of x ray laser plasmas
[DE93-011874] 01 p0389 N94-11074
Possibilities of magnetic diagnostics in stellarators
[DE93-621608] 01 p0389 N94-11092
The possibility of using carbon-graphite materials for microwave plasma diagnostics in large fusion devices
[DE93-621609] 01 p0066 N94-11143
High resolution time- and 2-dimensional space-resolved x ray imaging of plasmas at NOVA
[DE93-011892] 01 p0393 N94-11677
Inexpensive capillary discharge x-ray laser driver
[AD-A265932] 01 p0176 N94-12382
Spectrum analysis in beam diagnostics
[DE93-013401] 01 p0373 N94-12601
Equilibrium reconstruction of the q-profile in tokamaks from motional Stark effect data
[DE93-015815] 02 p0796 N94-13046
A PC-PCL-based control system for the high-voltage pulsed-power operation of the Intense Diagnostic Neutral Beam (IDNB) Experiment
[DE93-014144] 02 p0797 N94-13100
Interferometric investigation methods of plasma spatial characteristics on stellarators and tokamaks in submillimeter region
[DE93-621606] 02 p0798 N94-13507
Plasma-etching science meets technology in the MDL
[DE93-012086] 02 p0800 N94-13908
Measuring opacity of shock generated argon plasmas
[DE93-013038] 02 p0801 N94-14312
D3-D research operations
[DE93-016729] 02 p0802 N94-14519
Measurements of edge fluctuations by phase contrast imaging on DIII-D
[DE93-014018] 02 p0802 N94-14579
The 8 to 11 keV x ray sources for imaging and absorption experiments
[DE93-015973] 02 p0803 N94-14865
Active probing of plasma edge turbulence and feedback studies on the Texas experimental tokamak (TEXT)
[DE93-015799] 03 p1202 N94-16162
Numerical modeling of the temperature gradients and spectra of the plasma armature on Thunderbolt
[AD-A266414] 03 p0878 N94-16552
Femtosecond growth dynamics of an underdense ionization front measured by spectral blueshifting
[DE93-013582] 03 p1183 N94-16818
The effects of radiation transport on line ratios used as temperature and density diagnostic
[DE93-016424] 03 p1205 N94-17663
Analysis of neon soft x ray spectra from short-pulse laser-produced plasmas
[DE93-014420] 04 p1582 N94-17708
Application of piezoelectric stress gauges to the measurement of fast-rise-time multimegampere electric currents
[DE93-017625] 04 p1429 N94-18102
Time-resolved probing of electron thermal conduction in femtosecond-laser-pulse-produced plasmas
[DE93-016996] 04 p1585 N94-18129
Development of short pulse soft x ray lasers
[DE93-017150] 04 p1437 N94-18131
Active neutral particle diagnostics for high temperature plasma
[DE93-788457] 04 p1586 N94-18214
Experiments on nonlinear absorption of ECH waves in MTX and a comparison with theory
[DE93-019158] 04 p1589 N94-19074
Electron cyclotron resonance heating in the microwave tokamak experiment
[DE93-018083] 04 p1590 N94-19289
Parametric variations of ion transport in TFTR
[DE93-012653] 05 p1991 N94-19883
Optical diagnostic instrument for monitoring etch uniformity during plasma etching of polysilicon in a chlorine-helium plasma
[DE93-019582] 05 p1993 N94-20261
Development and characterization of a time-, position- and energy-resolved x ray diagnostic for PBFA 2 target experiments
[DE93-019429] 05 p1808 N94-20297
Laser diagnostics of RF hydrogen plasma reactors: Application to the processing of III-V materials
[AD-A272659] 05 p1994 N94-21214
A new innovative instrument for space plasma instrumentation
[NASA-CR-194736] 05 p1666 N94-21780
On Plasma Edge Spectroscopy and Spectroscopic Studies of Impurity Densities and Impurity Transport
[IPF-92-2] 05 p1996 N94-21802
Plasma edge spectroscopy 05 p1996 N94-21803
Spectroscopic studies of impurity densities and impurity transport 05 p1997 N94-21804
Fusion Plasma Theory. Task 1: Magnetic confinement fusion plasma theory
[DE94-000778] 05 p1998 N94-22019
Massachusetts Institute of Technology Plasma Fusion Center 1992-1993 report to the President
[DE94-001725] 06 p2548 N94-22721
Prospects for very-high-resolution solar physics with the Simuris inteferometric mission 06 p2625 N94-22848
Characterization of heat transport and radiation hydrodynamics in collisional laser plasmas using collective Thomson scattering
[DE94-001502] 06 p2349 N94-23209
Some theoretical problems of magnetic diagnostics in tokamaks and stellarators
[NIFS-262] 06 p2551 N94-24306
Pellet ablation in the large helical device
[NIFS-260] 06 p2551 N94-24358
A study of non-ideal focus properties of 30 deg parallel plate energy analyzers
[NIFS-263] 06 p2311 N94-24457
Plasma initiation in a tokamak with conducting superstructure: First results from Alcator C-MOD
[DE94-001565] 06 p2552 N94-24504
The chemistry of particulate formation in fluorocarbon plasmas
[DE94-001500] 06 p2552 N94-24546
Measurement of electron temperature and density in the DIII-D neutral beam ion source arc chamber
[DE94-001099] 06 p2553 N94-24746
Study on development of chemical measurement method utilizing plasmas 07 p2728 N94-25578
Heavy neutral beam probe for edge plasma analysis in tokamaks
[DE94-003391] 07 p3041 N94-25846
Development of fusion technology
[DE93-633444] 07 p3042 N94-26159
New Thomson scattering laser control for D3-D
[DE94-002890] 07 p3043 N94-26274
Laboratory plasma studies
[AD-A274655] 07 p3043 N94-26356
Proceedings of the 16th Symposium on Plasma Physics and Technology
[DE94-604181] 07 p3047 N94-27698
Laser blow-off lithium beam probing with high temporal resolution for edge plasma diagnostics
[DE94-701176] 07 p2820 N94-27701
Advanced development of particle beam probe diagnostic system
[DE94-002316] 07 p3047 N94-27720
Passive stabilization of MHD instabilities at high (beta)n in the HBT-EP tokamak
[DE94-003317] 07 p3047 N94-27735
Fuel ion rotation measurement and its implications on H-mode theories
[DE94-004860] 07 p3048 N94-27791
Determination of the plasma column shape in the Tokamak Novillo cross section by magnetic probes
[DE94-604986] 07 p3048 N94-27844
New high temperature plasmas and sample introduction systems for analytical atomic emission and mass spectrometry
[DE94-004564] 08 p3503 N94-28458
Photon counting spectroscopy as done with a Thomson scattering diagnostic
[DE94-005543] 08 p3503 N94-28515
Broadband EUV survey spectrometer for short-timescale experiments
[DE94-005459] 08 p3498 N94-28534
Journal of NIRE, Vol. 2, No. 2
[JTN-94-80552] 08 p3187 N94-28675
A novel spectroscopic measurement method of RF plasma for temperature and electron density diagnoses 08 p3188 N94-28682
Transient internal probe
[AD-A275054] 08 p3505 N94-29134
Experiments on the two-stage dense plasma heating on the GOL-3 device
[DE94-608356] 08 p3508 N94-30193
Inertial confinement fusion
[DE94-005957] 08 p3510 N94-30875
Magnetic flux reconstruction methods for shaped tokamaks
[DE94-005827] 08 p3510 N94-30882
Spectroscopy and atomic physics in EBIT and SuperEBIT
[DE94-006050] 09 p3864 N94-31508
Plasma confinement theory and transport simulation
[DE94-006065] 09 p3888 N94-31619
Diagnostics of high-brightness short-pulse lasers and the plasmas they generate
[DE94-006165] 09 p3716 N94-31624
High beta tokamak research
[DE94-006513] 09 p3888 N94-31664
Degenerate four-wave mixing as a diagnostic of plasma chemistry
[DE94-008588] 09 p3889 N94-31766
An edge density fluctuation diagnostic for D3-D using lithium beams
[DE94-008554] 09 p3890 N94-32519
Characterization of atomic and molecular impurity sources and transport at the tokamak edge
[DE94-007212] 09 p3891 N94-32619
Measurement of ICF fuel ion temperature on Nova
[DE94-006150] 09 p3892 N94-32730
Performance of a quasi-steady, multi megawatt, coaxial plasma thruster
[NASA-CR-195311] 09 p3616 N94-32970
Ultrafast x ray sources
[AD-A277455] 09 p3721 N94-33012
Millstone Hill radar studies of plasma waves and turbulence
[AD-A278409] 09 p3684 N94-33172
New calculations of Fe spectra in high-temperature plasmas
[DE94-009919] 11 p4339 N94-36386

Feasibility study for a novel pulsed neutral beam diagnostics for tokamaks
[DE94-617129] 11 p4339 N94-36417
On the interpretation of diamagnetic loop measurements for a current-carrying plasma column in a conducting chamber
[DE94-007107] 12 p4526 N94-36536
Microwave reflectometry for fusion plasma diagnostics
[DE94-620118] 12 p4527 N94-36566
Conceptual design for a fast neutron ionization chamber for fusion reactor plasma diagnostics
[DE94-013396] 12 p4527 N94-37101
Initial studies of reflectometer for ITER
[DE94-012476] 12 p4528 N94-37167
Motional Stark effect upgrades on D3-D
[DE94-013146] 12 p4528 N94-37297
A fast spectroscopic diagnostic for the measurement of plasma impurity ion dynamics
[DE94-012985] 12 p4529 N94-37354
Research using small tokamaks
[DE94-621827] 12 p4531 N94-37493
A freon-filled, holographic bubble chamber as a high energy photon burst spectrometer
[DE94-011645] 12 p4446 N94-37723

PLASMA DIFFUSION

Numerical method of singular problems on singular integrals
[DE93-613654] 01 p0343 N94-10546
Plasma diffusion through multidipole magnetic fields
[INPE-5460-PRE/1768] 02 p0795 N94-12901
The resonance broadening theory revisited
[PPL-134] 02 p0798 N94-13563
Parametric variations of ion transport in TFTR
[DE93-012653] 05 p1991 N94-19883
Fluid simulations of Delta T(sub e)-driven turbulence and transport in boundary plasmas
[DE94-001304] 05 p1999 N94-22566
Double diffusion convection in a rotating spherical shell 05 p2006 N94-22666
The anomalous transport caused by particles transverse drift
[DE93-613685] 06 p2554 N94-25329
Anomalous transport equations in toroidal plasmas
[DE94-009206] 09 p3893 N94-32922
Dynamical nature of inviscid power law for two-dimensional turbulences and self-consistent spectrum and transport of plasma filaments
[DE94-009425] 10 p4144 N94-33913
The kinetics of inhomogeneous plasma
[DE94-611459] 11 p4336 N94-35788
Theory of anomalous transport in H-mode plasmas
[DE94-727546] 12 p4531 N94-37485

PLASMA DIODES

X ray simulator theory support
[AD-A273613] 06 p2553 N94-24949
Research in pulsed power plasma physics
[AD-A274323] 07 p3045 N94-27074
Controlling chaos in plasma filled diodes
[AD-A275525] 08 p3504 N94-28686

PLASMA DISCHARGES

U PLASMA JETS

PLASMA DISPERSION

U PLASMA DIFFUSION

PLASMA DRIFT

Observing and modelling F-region ionospheric dynamics using the (O2) 7320A emission
[AD-A265407] 01 p0279 N94-12419
On energy transport equations for turbulent magnetized plasma
[PPL-135] 02 p0800 N94-13850
Anomalous transport due to small scale electromagnetic and large scale electrostatic modes in tokamaks
[PPL-140] 02 p0801 N94-14206
Structure and damping of toroidal drift waves (and their implications for anomalous transport)
[DE93-014005] 03 p1203 N94-16822
Convection algorithms for magnetospheric particles
[AD-A270103] 04 p1493 N94-18871
Excitation balances and transport in an inductively coupled plasma
[ETN-94-95330] 06 p2554 N94-25241
The anomalous transport caused by particles transverse drift
[DE93-613685] 06 p2554 N94-25329
Modification in the kinetic solution for magnetized plasmas
[DE93-613687] 06 p2555 N94-25343
Shear flow generation from the interaction of neoclassical and drift wave transport processes
[DE94-003135] 07 p2791 N94-26096
Quiet-time intensifications along the poleward auroral boundary near midnight
[ATR-93(7248)-2] 07 p2877 N94-26201
Numerical simulation of plasma vertical position stabilization in ITER
[DE93-634588] 07 p3044 N94-26510
The dynamics of interacting nonlinearities governing long wavelength driftwave turbulence
[DE94-001785] 07 p2793 N94-26558
Space-time structure of the morning aurora inferred from coincident DMSP-F6, -F8, and Sondrestrom incoherent scatter radar observations
[AD-A275442] 08 p3356 N94-28869
Analysis of stochastic particle behavior in a magnetic island due to electrostatic drift waves
[DE94-727553] 10 p4137 N94-33869
Collisonless dynamics of the magnetosphere
[AD-A278886] 11 p4290 N94-35708
Thickness of the layer of strong radial electric field in JFT-2M H-mode plasmas
[DE94-718993] 11 p4336 N94-35812
Ionospheric plasma drift and structure studies at high and mid-latitudes
[AD-A279415] 11 p4291 N94-36116
Anomalous cross field flux in CHS
[DE94-727547] 12 p4529 N94-37359

PLASMA DYNAMICS

Characteristics of ICR-produced peripheral plasma in the Uragan-3M torsatron
[DE93-621666] 01 p0392 N94-11214
Investigation of dynamics of plasma fluxes generated by the quasi-stationary plasma accelerator P-50
[DE93-621665] 02 p0794 N94-12854
Electrodynamics of helical plasma structures
[DE93-620981] 02 p0797 N94-13240
The resonance broadening theory revisited
[PPL-134] 02 p0798 N94-13563
Nonlinear evolution of tearing modes in inhomogeneous plasmas
[PPL-133] 02 p0798 N94-13564
Analysis of leading edge and trailing edge cover glass samples before and after treatment with advanced satellite contamination removal techniques
[AD-A267055] 03 p0885 N94-15666
Spectroscopic and computer modeling investigations of a laser-sustained plasma
[IFTR-30/1991] 03 p1204 N94-17066
Granular fluctuations in plasma turbulence and their role in transport
[DE93-013465] 03 p1187 N94-17674
Filamentary magnetohydrodynamic plasmas
[DE93-015616] 04 p1583 N94-17945
Ion mobility and transport barriers in the tokamak plasmas
[DE93-040320] 04 p1587 N94-18524
RAPID: The imaging energetic particle spectrometer on Cluster 04 p1329 N94-19633
Performance potential of plasma thrusters: Arcjet and Hall thruster modeling
[AD-A271085] 05 p1667 N94-19847
Neoclassical kinetic theory near an X-point: Plateau regime
[DE93-019825] 05 p1951 N94-20224
Comparative study of INPIStron and spark gap 05 p1995 N94-21293
INPIStron switched pulsed power for dense plasma pinches 05 p1995 N94-21294
Evaluation of externally heated pulsed MPD thruster cathodes
[NASA-CR-191090] 05 p1670 N94-21565
MHD relaxation in magnetic loops 05 p2004 N94-22658
Chaos in plasma simulation and experiment
[DE94-001574] 06 p2549 N94-22963
Chaos and simple determinism in reversed field pinch plasmas: Nonlinear analysis of numerical simulation and experimental data
[DE94-001575] 06 p2550 N94-23211
Start-up simulations of the PULSAR pulsed tokamak reactor
[DE94-002634] 06 p2552 N94-24519
Coherent HF radar system for the study of natural and heater induced ionospheric irregularities
[AD-A273804] 07 p2876 N94-25752
An investigation of magnetic field effects on plume density and temperature profiles of an applied-field MPD thruster
[NASA-TM-106416] 07 p2700 N94-26090
Molecular dynamics simulations of dense plasmas
[DE94-005082] 08 p3509 N94-30752
Convection and electrodynamic signatures in the vicinity of a Sun-aligned arc: Results from the Polar Acceleration Regions and Convection Study (Polar ARCS) 09 p3954 N94-31102
L-H confinement mode dynamics in three-dimensional state space
[DE94-007113] 09 p3887 N94-31396
Plasma confinement theory and transport simulation
[DE94-006065] 09 p3888 N94-31619
Pulsed expansion of plasma in a magnetic thruster 09 p3889 N94-31776
Computer modeling of active experiments in space plasmas 09 p3890 N94-31927
Basic principles approach for studying nonlinear Alfven wave-alpha particle dynamics
[DE94-007112] 09 p3891 N94-32664
Analytic formulation for the ac electrical conductivity in two-temperature, strongly coupled, overdense plasma: FORTRAN subroutine
[DE94-009466] 09 p3893 N94-32915
Dynamical nature of inviscid power law for two-dimensional turbulences and self-consistent spectrum and transport of plasma filaments
[DE94-009425] 10 p4144 N94-33913
Studies on equatorial shock formation during plasmaspheric refilling
[NASA-CR-195864] 10 p4088 N94-34669
Collisonless dynamics of the magnetosphere
[AD-A278886] 11 p4290 N94-35708
The kinetics of inhomogeneous plasma
[DE94-611459] 11 p4336 N94-35788
Improved models of beta-limit, anomalous transport and radial electric field with loss cone loss in heliotron/torsatron
[DE94-718976] 11 p4324 N94-35984
Modelling of ELMs and dynamic responses of the H-mode
[DE94-718977] 11 p4339 N94-36353
Non-equilibrium evolution of the disoriented chiral condensate in heavy-ion collisions
[DE94-012897] 12 p4522 N94-37310
ELMy-H mode as limit cycle and transient responses of H-modes in tokamaks
[DE94-727510] 12 p4529 N94-37358
Bounce resonance heating and transport in a magnetic mirror
[DE94-727545] 12 p4531 N94-37466

PLASMA ELECTRODES

Evaluation of materials proposed for the construction of the Plasma Electrode Pockels Cell (PEPC) on beamlet
[DE93-016952] 04 p1584 N94-17988
Reduction of the anode fall in a coaxial plasma thruster with an applied magnetic nozzle
[DE94-000670] 06 p2218 N94-23283
Time resolved measurements of light produced by onset of plasma formation on electrodes of fast pulsed high voltage diodes
[AD-A277974] 09 p3894 N94-33264

PLASMA ENGINES

Electromagnetic propulsion for spacecraft
[NASA-CR-191186] 02 p0551 N94-13416
Plasma instabilities and transport in the MPD thruster
[AD-A268268] 03 p1204 N94-17575
Performance potential of plasma thrusters: Arcjet and Hall thruster modeling
[AD-A271085] 05 p1667 N94-19847
Optimization of energy transfer in microwave electrothermal thrusters 06 p2216 N94-23065
CFD modeling of microwave electrothermal thrusters 06 p2216 N94-23066
Advanced space propulsion concepts 06 p2216 N94-23067
Stationary plasma thruster plume characteristics
[NASA-CR-194454] 06 p2219 N94-24361
Power electronics development for the SPT-100 thruster
[NASA-TM-106488] 06 p2221 N94-25189
Stationary plasma thruster plume emissions
[NASA-CR-194471] 07 p2701 N94-26209
Pulsed expansion of plasma in a magnetic thruster 09 p3889 N94-31776
Performance evaluation and operating characteristics of a waveguide microwave applicator for space propulsion applications 09 p3614 N94-31908
Performance of a quasi-steady, multi megawatt, coaxial plasma thruster
[NASA-CR-195311] 09 p3616 N94-32970

PLASMA EQUILIBRIUM

Stationary spectra in a quasi neutral current-carrying plasma
[DE93-617849] 01 p0387 N94-10539
Theory of field-reversed configurations
[DE93-015611] 02 p0794 N94-12862
Stability and confinement properties of small-aspect-ratio tokamak
[INPE-5463-PRE/1771] 02 p0801 N94-14024
Active probing of plasma edge turbulence and feedback studies on the Texas experimental tokamak (TEXT)
[DE93-015799] 03 p1202 N94-16162
Profile stabilization of tilt mode in a field reversed configuration
[DE93-016770] 04 p1583 N94-17753
A free boundary eigenvaue problem
[IPP-6/310] 04 p1584 N94-17981

Nonparaxial MHD stabilizers for an axisymmetric magnetic mirror
[DE93-017996] 04 p1587 N94-18505
Finite beta plasma equilibrium in toroidally linked mirrors
[DE93-040318] 04 p1590 N94-19193
On neutral plasma oscillations
[DE93-040319] 04 p1590 N94-19194
Some theoretical problems of magnetic diagnostics in tokamaks and stellarators
[NIFS-262] 06 p2551 N94-24306
Transport properties of interacting magnetic islands in tokamak plasmas
[DE94-009208] 10 p4145 N94-34140

PLASMA ETCHING
Resist materials design: Base-catalyzed chemical amplification
[AD-A265286] 01 p0145 N94-11819
Plasma-etching science meets technology in the MDL
[DE93-012086] 02 p0800 N94-13908
Field emission cathode and vacuum microelectronic microwave amplifier development
[AD-A269526] 04 p1403 N94-18639
Optical diagnostic instrument for monitoring etch uniformity during plasma etching of polysilicon in a chlorine-helium plasma
[DE93-019582] 05 p1993 N94-20261
Particle behavior in an ECR plasma etch tool
[DE93-040343] 05 p1996 N94-21769
Dry etching process development for submicron and nanometer semiconductor devices
[PB94-133196] 07 p2788 N94-28357
Electron cyclotron resonance plasma oxidation studies of InP
[AD-A277431] 09 p3893 N94-33007

PLASMA FLOW
U MAGNETOHYDRODYNAMIC FLOW

PLASMA FOCUS
Research on plasma-puff initiation of high Coulomb transfer switches
[NASA-CR-194371] 05 p1994 N94-21289
Plasma-puff initiation of high Coulomb transfer switches 05 p1994 N94-21290
Characteristics of plasma-puff trigger for a inverse-pinch plasma switch 05 p1995 N94-21291
INPIStron switched pulsed power for dense plasma pinches 05 p1995 N94-21294
Plasma lens experiments at the Final Focus Test Beam
[DE93-041081] 05 p1981 N94-21688
Flowing DPF design for propulsion experiments
[AD-A274973] 07 p2701 N94-26537
Studies of the plasma triggering mechanism of inverse pinch switch
[AD-A276117] 09 p3887 N94-31530

PLASMA FREQUENCIES
Stationary spectra in a magnetized current-carrying plasma
[DE93-617847] 01 p0386 N94-10397
Spreading of Bimodulated Ultra-relativistic Electron Beam (BUEB) in Atmospheric Plasma Channel (APCh)
[DE93-621658] 01 p0392 N94-11213
Decay interaction of bulk and surface Langmuir waves
[DE93-617843] 01 p0393 N94-11477
Investigation of plasma instabilities in the Polar cusp
[NASA-CR-194283] 02 p0796 N94-13084
Implicit multi-fluid simulation of interpenetrating plasmas
[DE93-013351] 02 p0801 N94-14342
Double stimulated Brillouin scattering 03 p1200 N94-15205
Theory of leaked auroral kilometric radiation 05 p2003 N94-22649
Ionospheric modification by high power, obliquely propagated HF radio wave transmissions. Part 1: Experimental
[AD-A273746] 07 p2878 N94-26224
Practical applications of plasma surface modification
[DE94-004892] 08 p3349 N94-29932
The fine structure of Langmuir waves observed upstream of the bow shock at Venus
[NASA-CR-196123] 11 p4354 N94-35378

PLASMA GENERATION
U PLASMA GENERATORS

PLASMA GENERATORS
NT JOINT EUROPEAN TORUS
NT PLASMA GUNS
NT TOKAMAK DEVICES
Investigation of onset of plasma formation at anode of fast-pulsed high-voltage vacuum diode
[AD-A267214] 03 p1204 N94-16987
A dc Penning surface-plasma source
[DE93-040126] 05 p1997 N94-21989
Burning rate of double-base propellant in the presence of plasma 06 p2155 N94-24252
Research in pulsed power plasma physics
[AD-A274323] 07 p3045 N94-27074

PLASMA GUNS
Experimental investigation of wake field excitation in plasma by a periodic succession of relativistic particle clots
[DE93-621655] 01 p0391 N94-11211
Investigation of dynamics of plasma fluxes generated by the quasi-stationary plasma accelerator P-50
[DE93-621665] 02 p0794 N94-12854
Computational model of surface ablation from tokamak disruptions
[DE94-002204] 06 p2550 N94-23474
Modelling erosion damage from low-energy plasma gun simulations of disruptions
[DE94-005196] 08 p3509 N94-30697

PLASMA HEATING
NT ELECTRON CYCLOTRON HEATING
Efficiency of fast wave current drive for a weakly relativistic plasma
[DE93-012775] 01 p0385 N94-10159
Simulations of D3-D divertor biasing with the LEDGE code
[DE93-010500] 01 p0385 N94-10262
Multiple Antenna Implementation System (MAntIS)
[DE93-012515] 01 p0131 N94-10270
Characterization of high-power RF structures using time-domain field codes
[DE93-013416] 01 p0132 N94-10518
Reversed-field pinch studies in the Madison Symmetric Torus
[DE93-013464] 01 p0388 N94-10747
Kinetic effects in stochastic topologically nontrivial field
[DE93-621642] 01 p0391 N94-11207
Characteristics of ICR-produced peripheral plasma in the Uragan-3M torsatron
[DE93-621666] 01 p0392 N94-11214
Conversion of the four-strap array in D3-D to a tunable traveling wave antenna
[DE93-012085] 01 p0137 N94-11453
Statistical approach to LHCD modeling using the wave kinetic equation
[DE93-012831] 01 p0394 N94-12545
Dimensionally similar discharges with central RF heating on the D3-D tokamak
[DE93-012776] 02 p0795 N94-12953
Evolution of high-repetition-rate induction accelerators through advancements in switching
[DE93-012599] 02 p0654 N94-12963
Ion cyclotron heating experiments and plans for the Advanced Toroidal Facility (ATF)
[DE93-012965] 02 p0795 N94-13033
Effect on antenna structure of high power RF during plasma operation
[DE93-013278] 02 p0797 N94-13144
Predicted performance of a dc beam driven FEM oscillator designed for fusion applications at 200-250 GHz
[DE93-013414] 02 p0655 N94-13145
Instability heating of the HDZP
[DE93-012641] 02 p0798 N94-13513
Folded waveguide designs for tokamaks
[DE93-013274] 02 p0798 N94-13577
Studies on equatorial shock formation during plasmaspheric refilling
[NASA-CR-194392] 02 p0715 N94-13954
Electrical characterization of the JET A(sub 2) antenna: Comparison of model with measurements Wade, T.
[DE93-012964] 02 p0607 N94-14291
D3-D research operations
[DE93-016729] 02 p0802 N94-14519
Design of the ion cyclotron system for TPX
[DE93-012961] 02 p0803 N94-14770
High frequency Raman current drive 03 p1201 N94-15208
Current drive with free electron lasers in high and low temperature tokamaks 03 p1201 N94-15209
Simulations of wave-particle interactions in stimulated Raman forward scattering in a magnetized plasma
[PB94-170990] 03 p1201 N94-15210
Synthesis of ceramic oxide powders in a microwave plasma device
[DE93-012741] 03 p0965 N94-15920
Inductive effects during second harmonic current drive experiments on T-10
[DE93-014411] 03 p1202 N94-16803
Recent results from the 60 GHz inside launch ECH system on the D3-D tokamak
[DE93-013027] 03 p1203 N94-16816
Simulation of enhanced tokamak performance on D3-D using fast wave current drive
[DE93-014009] 03 p1203 N94-16823
Power compensators for phased operation of antenna arrays on JET and D3-D
[DE93-013208] 04 p1581 N94-17694
Arc detection and protection in high-power antenna systems
[DE93-013272] 04 p1382 N94-17695
ITER EDA design confinement capability
[DE93-013729] 04 p1582 N94-17697
Design of a tunable 4-MW free electron maser for heating fusion plasmas
[DE93-017172] 04 p1437 N94-18134
Plasma production by helicon waves
[DE93-788396] 04 p1586 N94-18213
Experiments on nonlinear absorption of ECH waves in MTX and a comparison with theory
[DE93-019158] 04 p1589 N94-19074
ICRF direct electron heating experiments in TFTR
[DE93-017857] 04 p1590 N94-19273
Electron cyclotron resonance heating in the microwave tokamak experiment
[DE93-018083] 04 p1590 N94-19289
Fusion plasma theory grant. Task 3: Auxiliary radiofrequency heating of tokamaks
[DE94-000779] 05 p1994 N94-20940
High resolution studies of the structure of the solar atmosphere
[AD-A273084] 05 p2147 N94-21522
The TST: A small steady-state tokamak for integrated divertor testing
[DE94-001016] 05 p1998 N94-22045
Opacity measurements in shock-generated argon plasmas
[DE94-001057] 05 p1998 N94-22399
Plasma heating in toroidal systems 05 p2000 N94-22629
Massachusetts Institute of Technology Plasma Fusion Center 1992-1993 report to the President
[DE94-001725] 06 p2548 N94-22721
Plasma research in the Madison Symmetric Torus (MST)
[DE94-002318] 06 p2549 N94-22976
Analysis and experiments of a whistler-wave plasma thruster
[DE94-001533] 06 p2209 N94-23012
Structural analysis of a superconducting central solenoid for the Tokamak Physics Experiment
[DE94-001536] 06 p2549 N94-23014
Overview of the ATF stellarator program
[DE94-000371] 06 p2550 N94-23462
Multi-ion, multi-event test of ion cyclotron resonance heating
[NASA-CR-194859] 06 p2540 N94-23495
Review of tokamak experiments on direct electron heating and current drive with fast waves
[DE94-004185] 07 p3041 N94-25801
Design of folded waveguide antenna for Alcator C-Mod
[DE94-003584] 07 p2767 N94-25924
RF modeling and design of a folded waveguide launcher for the Alcator C-Mod tokamak
[DE94-003588] 07 p3041 N94-25933
Development of fusion technology
[DE93-633444] 07 p3042 N94-26159
Ionospheric modification by high power, obliquely propagated HF radio wave transmissions. Part 1: Experimental
[AD-A273746] 07 p2878 N94-26224
Design and control of phased ICRF antenna arrays
[DE94-002796] 07 p3046 N94-27261
High gas-efficiency hydrogen negative ion sources
[PB93-232163] 07 p3025 N94-27348
Fast wave current drive technology development at ORNL
[DE94-004243] 07 p3046 N94-27568
Proceedings of the 16th Symposium on Plasma Physics and Technology
[DE94-604181] 07 p3047 N94-27698
Shine through measurements with hydrogen beam in JT-60
[DE94-701113] 07 p3047 N94-27699
The calculation for energy balance of heating plasmas by Alfven waves
[DE94-604994] 07 p3049 N94-27855
Analysis of density limit and efficiency in lower hybrid current drive
[DE94-604995] 07 p3049 N94-27856
Modelling and control of plasma position in the STOR-M tokamak
[ISBN-0-315-58891-8] 07 p3049 N94-27949
Electron beam irradiation experiments of monoblock divertor mock-up
[DE94-707497] 08 p3503 N94-28555
Experimental and analytical studies of high heat flux components for fusion experimental reactor
[DE94-707671] 08 p3504 N94-28556
TFTR Ion Cyclotron Range of Frequencies (ICRF) experimental data analysis collaboration
[DE94-004699] 08 p3504 N94-28575

Plasma heating for containerless and microgravity materials processing
[NASA-CASE-NPO-18819-1-CU] 08 p3229 N94-29371
Efficiencies of the ICRF minority heating in the CHS and LHD plasmas
[AD-B183300L] 08 p3506 N94-29499
Three-dimensional effects for radio frequency antenna modeling
[DE94-006102] 08 p3255 N94-30105
Experiments on the two-stage dense plasma heating on the GOL-3 device
[DE94-608356] 08 p3508 N94-30193
Peculiarities of heat transfer in the experiments of beam injection heating of a plasma at the GOL-3 device
[DE94-608357] 08 p3508 N94-30194
Instability heating of solid-fiber Z pinches
[DE94-007055] 09 p3889 N94-31809
Performance evaluation and operating characteristics of a waveguide microwave applicator for space propulsion applications 09 p3614 N94-31908
ICRF heating and current drive in TFTR supershot plasmas: Data analysis and interpretation of ICRF/edge interactions
[DE94-008586] 09 p3890 N94-32520
Experimental survey of the L-H transition conditions in the D3-D tokamak
[DE94-007426] 09 p3891 N94-32595
Anomalous thermalization of fast ions in magnetized plasma
[DE94-007109] 09 p3891 N94-32631
A comprehensive analysis of electron conical distributions from multi-satellite databases
[NASA-CR-195848] 09 p3953 N94-33047
Ionospheric plasma outflow in response to transverse ion heating: Self-consistent macroscopic treatment
[NASA-CR-195820] 09 p3893 N94-33048
Time resolved measurements of light produced by onset of plasma formation on electrodes of fast pulsed high voltage diodes
[AD-A277974] 09 p3894 N94-33264
A triggering mechanism of fast crash in sawtooth oscillation
[DE94-718974] 11 p4336 N94-35772
Heating experiments using neutral beams with variable injection angle and ICRF waves in CHS
[DE94-718982] 11 p4337 N94-35936
The role of heating and current drive in ITER
[DE94-012679] 12 p4527 N94-37082
A role of neutral hydrogen in CHS plasmas with reheat and collapse and comparison with JIPPT-IIU tokamak plasmas
[DE94-718985] 12 p4530 N94-37384
Recent DIII-D high power heating and current drive experiments
[DE94-012509] 12 p4530 N94-37436

PLASMA INSTABILITY
U MAGNETOHYDRODYNAMIC STABILITY

PLASMA INTERACTION EXPERIMENT
TROPIX: A solar electric propulsion flight experiment
[NASA-TM-106297] 02 p0534 N94-13028
Laboratory simulation of spacecraft charging in the plasma wake region
[FFI-93-7007] 02 p0542 N94-14107
The angular velocity spread of REB induced by magnetic field discontinuity
[IPPCZ-331] 05 p1996 N94-21573

PLASMA INTERACTIONS
NT LASER PLASMA INTERACTIONS
NT PLASMA-ELECTROMAGNETIC INTERACTION
NT PLASMA-PARTICLE INTERACTIONS
High heat flux components and plasma surface interactions
[DE93-008786] 01 p0385 N94-10253
Results from the D3-D advanced divertor program
[DE93-015472] 01 p0393 N94-11514
Applications of in-situ ellipsometry to microwave electron cyclotron resonance plasma processes
[AD-A265197] 01 p0373 N94-11880
Giotto data analysis: Electron plasma and heavy ion composition measurements at Comet Halley
[NASA-CR-193587] 01 p0428 N94-12770
Interactions between spacecraft and their environments
[NASA-TM-106115] 02 p0541 N94-13917
Studies on equatorial shock formation during plasmaspheric refilling
[NASA-CR-194392] 02 p0715 N94-13954
Ionospheric effects on a wide-bandwidth, polarimetric, space-based, synthetic-aperture radar
[DE93-015084] 02 p0612 N94-14512
Synthesis of ceramic oxide powders in a microwave plasma device
[DE93-012741] 03 p0965 N94-15920
Plasma contactor development for Space Station
[NASA-TM-106425] 04 p1587 N94-18861
The study of the phase structure of hadronic matter by searching for the deconfined quark-gluon phase transition using 2 TeV (bar-p)-p collisions, and by searching for critical phenomena in an exclusive study of multifragmentation using 1 GeV/nucleon heavy ion collisions
[DE93-018925] 04 p1570 N94-19103
Two-dimensional particle-in-cell simulation on transputer arrays
[DE93-017977] 05 p1972 N94-20181
Modeling of the coupled magnetospheric and neutral wind dynamos
[NASA-CR-194728] 05 p1856 N94-20537
TROPIX plasma interactions group report
[NASA-CR-191149] 05 p1666 N94-21864
Consequences of plasma-maser in plasma astrophysics 05 p2006 N94-22669
Proceedings of Japan-US Workshop P-196 on High Heat Flux Components and Plasma Surface Interactions for Next Devices
[DE94-701164] 08 p3503 N94-28513
Active electron and ion beam experiments in space
[AD-A275570] 08 p3504 N94-28828
High sensitivity and resolution decimetric spectroscope: Preliminary analysis of solar bursts
[INPE-5537-TDI/525] 09 p3954 N94-33080
Studies on equatorial shock formation during plasmaspheric refilling
[NASA-CR-195864] 10 p4088 N94-34669
The SAMPIE flight experimental final technical requirements document
[NASA-TM-106224] 10 p4015 N94-34729
Flank solar wind interaction
[NASA-CR-189327] 10 p4166 N94-35225
JPRS report: Science and technology. Central Eurasia
[JPRS-UST-94-008] 11 p4249 N94-35228

PLASMA JETS
NT RADIO JETS (ASTRONOMY)
Macroscopic behaviour and discrete dynamo of RFP plasma in high theta discharge
[DE93-771408] 01 p0392 N94-11239
Jet shapes in hadron and electron colliders
[DE93-019386] 05 p1979 N94-20216
Impact of copper vapour contamination on argon arcs 05 p1994 N94-21053
Numerical simulation of magnetic reconnection associated with emerging flux in the solar atmosphere 05 p2004 N94-22654
X ray jets in the solar corona: Observations with Yohkoh Soft X Ray Telescope 05 p2004 N94-22655
Three-dimensional simulations of cosmic jets employing the smoothed particle hydrodynamics technique 05 p2008 N94-22685
Helical kink instability of jets from young stellar objects 05 p2008 N94-22686
Massachusetts Institute of Technology Plasma Fusion Center 1992-1993 report to the President
[DE94-001725] 06 p2548 N94-22721
CAMAC throughput of a new RISC-based data acquisition computer at the DIII-D tokamak
[DE94-001113] 06 p2550 N94-23182
Mixing and unmixedness in plasma jets 1: Near-field analysis 06 p2323 N94-23655
Synthesis of diamond film assisted by an arcjet plasma source, part 2
[INPE-5527-PRP/178-PT-2] 07 p3066 N94-27329
Synthesis of diamond in a hydrogen plasma jet: Simulations of XRD patterns of diamond polytypes and boundary layer on a substrate 08 p3522 N94-29515
Development and application of a multimesh auto-adaptive finite element method for the calculation of an electric arc plasma
[ECL-89-03] 09 p3886 N94-31378
The measurement of the hadronic energy flow and jet production with the ZEUS calorimeter in deep inelastic scattering events at HERA
[ETN-94-96021] 09 p3865 N94-31534
Stark broadening of the 2S state of hydrogen and douterium in arc plasmas of low density
[ETN-94-95731] 09 p3888 N94-31572
Ultrahigh-current-density metal-ion implantation and diamondlike-hydrocarbon films for tribological applications
[DE94-008958] 09 p3906 N94-32843

PLASMA LAYERS
NT PLASMA SHEATHS
Simulations of D3-D divertor biasing with the LEDGE code
[DE93-010500] 01 p0385 N94-10262
Physics and modelling of scrape-off layer transport
[DE93-010510] 01 p0385 N94-10289
Nonlinear second harmonic generation by light wave-plasma interaction in oscillating magnetic field
[DE93-613723] 01 p0386 N94-10387
Physics of tokamak scrape-off layer confinement
[DE93-011949] 01 p0390 N94-11125
Results from the D3-D advanced divertor program
[DE93-015472] 01 p0393 N94-11514
Ion anisotropy driven waves in the Earth's magnetosheath and plasma depletion layer
[DE93-012751] 02 p0712 N94-12952
Variation of divertor plasma parameters with divertor depth for H-mode discharges in D3-D
[DE93-015475] 02 p0801 N94-14347
D3-D research operations
[DE93-016729] 02 p0802 N94-14519
The effect of process parameters on the surface finish of plasma polymers
[DE93-014112] 03 p0966 N94-15924
Method and apparatus for forming an agile plasma mirror effective as a microwave reflector
[AD-D015788] 03 p0998 N94-16535
Time-resolved probing of electron thermal conduction in femtosecond-laser-pulse-produced plasmas
[DE93-016996] 04 p1585 N94-18129
Radiative divertor modeling studies
[DE93-018092] 04 p1590 N94-19290
Behavior of the particle transport coefficients near the density limit in MTX
[DE93-019108] 04 p1591 N94-19311
Three-wave resonant interaction in a thin layer
[AD-A272331] 05 p1994 N94-21039
A moving finite element model of the tokamak scrapeoff layer
[DE94-000673] 05 p1997 N94-21965
A two-dimensional kinetic model of the scrape-off layer
[DE94-001235] 05 p1999 N94-22562
Fluid simulations of Delta T(sub e)-driven turbulence and transport in boundary plasmas
[DE94-001304] 05 p1999 N94-22566
Electron temperature gradient driven instability in the tokamak boundary plasma
[DE94-001307] 05 p1999 N94-22596
Configuration of the near-Earth plasma sheet
[NASA-CR-195271] 07 p2883 N94-27438
Laser blow-off lithium beam probing with high temporal resolution for edge plasma diagnostics
[DE94-701176] 07 p2820 N94-27701
Plasma sprayed ceramic thermal barrier coating for NiAl-based intermetallic alloys
[NASA-CASE-LEW-15535-1] 08 p3205 N94-29507
A study of the formation and dynamics of the Earth's plasma sheet using ion composition data
[NASA-CR-195119] 08 p3507 N94-30126
Tail lobe ion composition at energies of 0.1 to 16 keV/e: Evidence for mass-dependent density gradients
[PAPER-93JA03201] 08 p3507 N94-30127
Transport phenomena in the Earth's plasma sheet 09 p3772 N94-31970
Electromagnetic wave reflection from irregular plasma layers
[AD-A276727] 09 p3678 N94-32161
Planetary magnetotails: Magnetic configuration and nonthermal plasma 09 p3942 N94-32326
Analysis of data from the plasma composition experiment on the International Sun-Earth Explorer (ISEE 1)
[NASA-CR-189353] 09 p3893 N94-33074
Characteristics of ion flow in the quiet state of the inner plasma sheet
[AD-A277451] 09 p3894 N94-33106
Contributions of the low-latitude boundary layer to the finite width magnetotail convection model
[NASA-CR-196116] 11 p4289 N94-35392
Design study of LHD helical divertor and high temperature divertor plasma operation
[DE94-718975] 11 p4338 N94-36352
A role of neutral hydrogen in CHS plasmas with reheat and collapse and comparison with JIPPT-IIU tokamak plasmas
[DE94-718985] 12 p4530 N94-37384
Origins of energetic ions in the Earth's magnetosheath
[NASA-CR-189359] 12 p4471 N94-37703

PLASMA LOSS
ELMy-H mode as limit cycle and transient responses of H-modes in tokamaks
[DE94-727510] 12 p4529 N94-37358

PLASMA OSCILLATIONS
Spatial helicon-wave echo in an inhomogeneous magnetized plasma
[DE93-617845] 01 p0389 N94-10885
Ion shaking in the 200 MeV XLS-ring
[DE93-014057] 01 p0374 N94-12782
Double stimulated Brillouin scattering 03 p1200 N94-15205
On neutral plasma oscillations
[DE93-040319] 04 p1590 N94-19194
Temporal behavior of the electron density profile during limiter biasing in the HYBTOK-2 tokamak
[NIFS-257] 06 p2552 N94-24456

LHCD (low hybrid current drive) experiment on the HT-6B tokamak
[DE93-613720] 06 p2555 N94-25331
Effect of LHCD (low hybrid current drive) on tearing mode instability
[DE93-613700] 06 p2555 N94-25344
Shear flow generation from the interaction of neoclassical and drift wave transport processes
[DE94-003135] 07 p2791 N94-26096
Asymptotics for Kummer functions, Bose plasmas, and related special functions
[DE94-601853] 07 p3007 N94-26928
Discrete vacuum ultra violet reflective interference filter
[AD-D016059] 07 p2756 N94-27675
Resistive ballooning mode in a gas-dynamic trap
[DE94-608328] 08 p3508 N94-30171
Simultaneous excitation of parametric decay cascades and the OTSI in 1D numerical simulations based on Aakarov's equations
[AD-A278108] 09 p3893 N94-33042
The fine structure of Langmuir waves observed upstream of the bow shock at Venus
[NASA-CR-196123] 11 p4354 N94-35378
Modelling of ELMs and dynamic responses of the H-mode
[DE94-718977] 11 p4339 N94-36353
Time-step stability for self-consistent Monte Carlo device simulation
[DE94-012145] 12 p4528 N94-37207
ELMy-H mode as limit cycle and transient responses of H-modes in tokamaks
[DE94-727510] 12 p4529 N94-37358

PLASMA PERTURBATION
U PLASMA OSCILLATIONS

PLASMA PHYSICS
Two fluid plasmas in the vicinity of a Schwarzschild black hole
[DE93-610264] 01 p0385 N94-10284
Texas experimental tokamak
[DE93-013377] 01 p0386 N94-10321
A flexible modelling software for data acquisition
[DE93-612915] 01 p0322 N94-10484
Cosmological gamma-ray burst model
[NASA-CR-193368] 01 p0484 N94-10507
Numerical method of singular problems on singular integrals
[DE93-613654] 01 p0343 N94-10546
Distribution of charged particles near the plasma boundary in the presence of external electric field
[DE93-617862] 01 p0389 N94-10886
To the complexity of dynamic system problem
[DE93-621355] 01 p0134 N94-11037
VLBI and the detection of interstellar magnetohydrodynamic waves 01 p0135 N94-11066
Magnetic fusion computing: A personal retrospective view
[DE93-014147] 02 p0797 N94-13217
Metastable enhancement of C(+) and O(+) capture reactions
[DE93-015075] 02 p0807 N94-13373
The International Colloquium on Atomic Spectra and Oscillator Strengths for Astrophysical and Laboratory Plasmas
[NASA-TM-109255] 02 p0849 N94-13376
Activities of the University of Saskatchewan, Plasma Physics Laboratory
[CTN-93-60831] 02 p0798 N94-13518
The resonance broadening theory revisited
[PPL-134] 02 p0798 N94-13563
Numerical Studies of Collisionless Current Layers
[NASA-CR-194337] 02 p0800 N94-13854
Implicit multi-fluid simulation of interpenetrating plasmas
[DE93-013351] 02 p0801 N94-14342
Physics of gas breakdown for ion beam transport in gas
[DE93-015646] 02 p0801 N94-14349
Review of the Procyon explosive pulsed power system
[DE93-016562] 02 p0802 N94-14532
Direct drive foil implosion experiments on Pegasus 2
[DE93-012666] 03 p1202 N94-16776
Linear stability of stationary solutions of the Vlasov-Poisson system in three dimensions
[DE93-013873] 03 p1174 N94-16820
Nonlinear problems in fluid dynamics and inverse scattering
[AD-A266234] 03 p1026 N94-16927
Investigation of onset of plasma formation at anode of fast-pulsed high-voltage vacuum diode
[AD-A267214] 03 p1204 N94-16987
Plasma Science Committee (PLSC) and the Panel on Opportunities in Plasma Science and Technology (OPST)
[DE93-018142] 03 p1204 N94-16995
Application of group theory to integral-difference equations of plasma physics
[IFTR-23/1992] 03 p1204 N94-17067
Role and development of small satellite missions in space plasma physics 03 p0891 N94-17149
Granular fluctuations in plasma turbulence and their role in transport
[DE93-013465] 03 p1187 N94-17674
Problems related to stimulated electromagnetic emissions, strong turbulence and ionospheric modification
[IRF-SR-212] 04 p1480 N94-17720
Self-regulated shear flow turbulence in confined plasmas
[DE93-015823] 04 p1583 N94-17743
Plasma properties research: Task 3
[DE93-017087] 04 p1583 N94-17854
Center of Excellence in Theoretical Geoplasma Research
[AD-A270210] 04 p1588 N94-18902
Review Committee report on the conceptual design of the tokamak physics experiment
[DE93-018408] 04 p1588 N94-19012
Generalized energy principle for flute perturbations in axisymmetric mirror machines
[DE93-019399] 04 p1589 N94-19037
Laser propagation in underdense plasmas: Scaling arguments
[DE93-040439] 05 p1816 N94-20480
Fusion plasma theory grant. Task 3: Auxiliary radiofrequency heating of tokamaks
[DE94-000779] 05 p1994 N94-20940
Engineering design, fabrication, installation, operation, and maintenance services in support of research on laser plasma physics
[AD-A272249] 05 p1994 N94-20943
Shock compression of low-density foams
[DE93-040545] 05 p1707 N94-21546
Fusion Plasma Theory. Task 1: Magnetic confinement fusion plasma theory
[DE94-000778] 05 p1998 N94-22019
Continuum damping of ideal toroidal Alfven eigenmodes
[DE94-001233] 05 p1998 N94-22560
Theory and simulation of plasma sheath waves
[DE94-001305] 05 p1999 N94-22567
Fourth International Toki Conference on Plasma Physics and Controlled Nuclear Fusion
[ESA-SP-351] 05 p2000 N94-22624
Driven reconnection and self-organization
05 p2000 N94-22625
Physics of transport phenomena in magnetic confinement plasmas 05 p2000 N94-22628
Jets associated with active galactic nuclei
05 p2000 N94-22631
Physical properties of dense astrophysical plasmas
05 p2001 N94-22637
1993 annual report for the Phaedrus-T RF current drive experiments
[DE94-001369] 06 p2550 N94-23192
Fusion plasma theory project summaries
[DE94-001712] 06 p2551 N94-23808
IPP Prague Contributions to the IAEA Technical Committee Meeting on Research Using Small Tokamaks
[IPPCZ-329] 06 p2551 N94-24293
Modification in the kinetic solution for magnetized plasmas
[DE93-613687] 06 p2555 N94-25343
Maryland controlled fusion research program
[DE94-003533] 07 p3044 N94-26523
Auroral Tomography Workshop Proceedings
[PB94-123718] 07 p2881 N94-27040
Research in pulsed power plasma physics
[AD-A274323] 07 p3045 N94-27074
Proceedings of the 16th Symposium on Plasma Physics and Technology
[DE94-604181] 07 p3047 N94-27698
Passive stabilization of MHD instabilities at high (beta)n in the HBT-EP tokamak
[DE94-003317] 07 p3047 N94-27735
Controlling chaos in plasma filled diodes
[AD-A275525] 08 p3504 N94-28686
A 6MeV heavy ion beam probe for the Large Helical Device
[AD-B183695L] 08 p3505 N94-29397
The effect of magnetic field configuration on particle pinch velocity in Compact Helical System (CHS)
[AD-B183299L] 08 p3505 N94-29398
Nonlinear wave packet evolution in a dispersive plasma: Application to rotational discontinuities
08 p3506 N94-29822
ECR plasma synthesis of silicon nitride films on GaAs and InSb
[DE94-005575] 08 p3515 N94-30006
The investigation of electron-ion radiative and dielectronic recombination in high-temperature plasmas
[DE94-005150] 08 p3509 N94-30755
The impact of improved physics on commercial tokamak reactors
[DE94-006103] 08 p3509 N94-30760
Self-similar variables and the problem of nonlocal electron heat conductivity
[DE94-005826] 08 p3493 N94-30881
Laboratory and space experiments as a key to the plasma universe
[TRITA-ALP-1993-01] 09 p3885 N94-31088
The double probe electric field experiment on Freja: Description and first results
[TRITA-ALP-1993-02] 09 p3885 N94-31089
Studies of the plasma triggering mechanism of inverse pinch switch
[AD-A276117] 09 p3887 N94-31530
Stability and instability criteria for magnetohydrodynamics
[PB94-148475] 09 p3889 N94-31772
Workshop on Models for Plasma Spectroscopy
[AD-A276565] 09 p3890 N94-32031
Atomic and molecular data needs for fusion
[DE94-006555] 09 p3870 N94-32177
Analytic properties of the OCP and ionic mixtures in the strongly coupled fluid state
[DE94-008216] 09 p3637 N94-32801
Cooperative program on D3-D (FY 1993)
[DE94-008343] 09 p3892 N94-32820
The Numerical Tokamak Project (NTP) simulation of turbulent transport in the core plasma: A grand challenge in plasma physics
[DE94-008279] 09 p3892 N94-32838
Stability of tearing modes in tokamak plasmas
[DE94-009205] 09 p3892 N94-32911
Electron cyclotron resonance plasma oxidation studies of InP
[AD-A277431] 09 p3893 N94-33007
Simultaneous excitation of parametric decay cascades and the OTSI in 1D numerical simulations based on Aakarov's equations
[AD-A278108] 09 p3893 N94-33042
Plasma physics applications to intense radiation sources, pulsed power and space physics. Short pulse ultra intense laser-plasma interaction experiment
[AD-A278440] 10 p4144 N94-33555
Development of a preliminary solar wind transport magnetosheath forecast model
[AD-A278560] 10 p4165 N94-33785
High beta and second stability region transport and stability analysis
[DE94-009654] 10 p4145 N94-33920
Summary of experimental progress and suggestions for future work
[DE94-008893] 10 p4145 N94-34012
Simulation models for computational plasma physics: Concluding report
[DE94-009976] 11 p4335 N94-35647
NIFS Symposium: Toward the research of fusion burning plasmas, present status and future strategy
[DE94-727618] 11 p4336 N94-35775
Potential formation and transport in open field line systems
[DE94-718910] 11 p4337 N94-35983
Improved models of beta-limit, anomalous transport and radial electric field with loss cone loss in heliotron/torsatron
[DE94-718976] 11 p4324 N94-35984
Recovery of frozen flow losses in arcjets
[AD-A278739] 11 p4228 N94-36089
A survey of reflectometry techniques with applications to TFTR
[DE94-010202] 11 p4338 N94-36093
D-D fusion experiments using fast z-pinches
[DE94-010090] 12 p4526 N94-36448
High Altitude Plasma Instrument (HAPI) data analysis
[NASA-CR-189360] 12 p4469 N94-36949
Dynamics explorer data analysis
[NASA-CR-196141] 12 p4469 N94-37016
Propagation of radius-tailored laser pulses over extended distances in a uniform plasma
[AD-A280405] 12 p4528 N94-37182
Towards nuclear fusion reactors
[DE94-748680] 12 p4528 N94-37235
MARFE's in tokamak edge plasma: Pattern formation under nonlocal constraints
[DE94-012766] 12 p4529 N94-37309
A role of neutral hydrogen in CHS plasmas with reheat and collapse and comparison with JIPPT-IIU tokamak plasmas
[DE94-718985] 12 p4530 N94-37384

PLASMA PINCH
NT THETA PINCH
NT ZETA PINCH

High resolution time- and 2-dimensional space-resolved x ray imaging of plasmas at NOVA
[DE93-011892] 01 p0393 N94-11677
Collisional effects of trapped electrons on the anomalous particle and thermal pinches
[PPL-128] 02 p0800 N94-13853
Plasma-puff initiation of high Coulomb transfer switches
[NASA-CR-193186] 04 p1591 N94-19441
Research on plasma-puff initiation of high Coulomb transfer switches
[NASA-CR-194371] 05 p1994 N94-21289
Plasma-puff initiation of high Coulomb transfer switches 05 p1994 N94-21290
Characteristics of plasma-puff trigger for a inverse-pinch plasma switch 05 p1995 N94-21291
Characteristics of switching plasma in an inverse-pinch switch 05 p1995 N94-21292
Comparative study of INPIStron and spark gap 05 p1995 N94-21293
INPIStron switched pulsed power for dense plasma pinches 05 p1995 N94-21294
The relaxed state and entropy production due to the electric resistivity and viscosity of plasma 05 p2010 N94-22696
Researches of the Electrotechnical Laboratory. No. 51: Study of formation and sustainment of reversed field pinch by slow control of magnetic field
[JTN-94-80548] 07 p3046 N94-27350
Studies of the plasma triggering mechanism of inverse pinch switch
[AD-A276117] 09 p3887 N94-31530

PLASMA POTENTIALS
Electron runaway in RF discharges
[DE93-771407] 01 p0363 N94-10661
NASCAP programmer's reference manual
[NASA-CR-191044] 01 p0278 N94-11702
Plasma auto-biasing during Ohmic H-mode in the STOR-M tokamak
[PPL-136] 02 p0799 N94-13849
Studies on equatorial shock formation during plasmaspheric refilling
[NASA-CR-194392] 02 p0715 N94-13954
Plasma contactor development for Space Station
[NASA-TM-106425] 04 p1587 N94-18861
Plasma structure in a plasma flow along a magnetic mirror field 05 p2005 N94-22664
1993 annual report for the Phaedrus-T RF current drive experiments
[DE94-001369] 06 p2550 N94-23192
Stationary plasma thruster plume characteristics
[NASA-CR-194454] 06 p2219 N94-24361
Thickness of the layer of strong radial electric field in JFT-2M H-mode plasmas
[DE94-718993] 11 p4336 N94-35812
Potential formation and transport in open field line systems
[DE94-718910] 11 p4337 N94-35983

PLASMA POWER SOURCES
NT PLASMA ENGINES

PLASMA PRESSURE
Analytical description of the torsatron Uragan-2M magnetic configuration with account of plasma pressure and external correcting magnetic field
[DE93-620983] 01 p0391 N94-11174
Magnetic island suppression in torsatron configurations
[DE93-621681] 01 p0392 N94-11215
Nonlinear evolution of tearing modes in inhomogeneous plasmas
[PPL-133] 02 p0798 N94-13564
Formation of the stable auroral arc that intensifies at substorm onset
[NASA-CR-193637] 03 p1098 N94-15433
Finite beta plasma equilibrium in toroidally linked mirrors
[DE93-040318] 04 p1590 N94-19193
Investigation and application of microwave electron cyclotron resonance plasma physical vapour deposition
[DE93-613909] 06 p2555 N94-25333
Formation and self-healing of magnetic islands in finite-beta helias equilibria
[AD-B183271L] 08 p3505 N94-29483
Experiments on the two-stage dense plasma heating on the GOL-3 device
[DE94-608356] 08 p3508 N94-30193
Magnetless magnetic fusion
[DE94-007114] 09 p3891 N94-32686
Magnetic island effects, interactions in tokamaks
[DE94-009209] 10 p4145 N94-34221
Contributions of the low-latitude boundary layer to the finite width magnetotail convection model
[NASA-CR-196116] 11 p4289 N94-35392

PLASMA PROBES
NT ELECTROSTATIC PROBES
Temporal behavior of the electron density profile during limiter biasing in the HYBTOK-2 tokamak
[NIFS-257] 06 p2552 N94-24456
A study of non-ideal focus properties of 30 deg parallel plate energy analyzers
[NIFS-263] 06 p2311 N94-24457

PLASMA PROPULSION
Arcjet space thrusters
[NASA-CR-193191] 01 p0046 N94-10700
Low power pulsed MPD thruster system analysis and applications
[NASA-CR-191187] 02 p0550 N94-13415
Electromagnetic propulsion for spacecraft
[NASA-CR-191186] 02 p0551 N94-13416
Plasma contactor technology for Space Station Freedom
[NASA-TM-106291] 02 p0553 N94-14725
Plasma instabilities and transport in the MPD thruster
[AD-A268268] 03 p1204 N94-17575
Application of a NEPTUNE propulsion concept to a manned Mars excursion
[AD-A268053] 03 p0929 N94-17587
Evaluation of externally heated pulsed MPD thruster cathodes
[NASA-CR-191090] 05 p1670 N94-21565
Performance evaluation of the Russian SPT-100 thruster at NASA LeRC
[NASA-TM-106401] 06 p2219 N94-23630
Numerical simulation of cylindrical, self-field MPD thrusters with multiple propellants
[NASA-CR-194458] 06 p2220 N94-24714
Power electronics development for the SPT-100 thruster
[NASA-TM-106488] 06 p2221 N94-25189
The Lightcraft project: Flight technology for a hypersonic mass transit system 07 p2670 N94-25695
An investigation of magnetic field effects on plume density and temperature profiles of an applied-field MPD thruster
[NASA-TM-106416] 07 p2700 N94-26090
Flowing DPF design for propulsion experiments
[AD-A274973] 07 p2701 N94-26537
Performance evaluation and operating characteristics of a waveguide microwave applicator for space propulsion applications 09 p3614 N94-31908
Performance of a quasi-steady, multi megawatt, coaxial plasma thruster
[NASA-CR-195311] 09 p3616 N94-32970

PLASMA RADIATION
Advanced concepts theory annual report 1992
[AD-A266132] 01 p0393 N94-11474
Highly charged ions in hot, dense plasmas
[DE93-013348] 02 p0795 N94-12995
Comparative study of x ray and microwave emissions during solar flares
[NASA-CR-194532] 02 p0845 N94-14577
The 8 to 11 keV x ray sources for imaging and absorption experiments
[DE93-015973] 02 p0803 N94-14865
Application of piezoelectric stress gauges to the measurement of fast-rise-time multimegampere electric currents
[DE93-017625] 04 p1429 N94-18102
Substrate temperature measurement and control during thermal plasma CVD
[DE93-040305] 04 p1433 N94-19135
Method and apparatus for producing a thermal atomic oxygen beam
[NASA-CASE-LEW-15614-1] 06 p2534 N94-23825
X ray simulator theory support
[AD-A273613] 06 p2553 N94-24949
Experiment and research on materials irradiated by plasma radiation
[DE94-605011] 07 p2758 N94-27845
Radiation from an aperture into an anisotropic plasma half-space 09 p3885 N94-31205
Spacecraft environmental anomalies expert system
[AD-A277962] 09 p3612 N94-33262
MARFE's in tokamak edge plasma: Pattern formation under nonlocal constraints
[DE94-012766] 12 p4529 N94-37309

PLASMA RENIN ACTIVITY
U IMMUNOASSAY

PLASMA RESONANCE
Resonant absorption of Alfven waves near a neutral point
[DE93-628761] 04 p1586 N94-18172
Kinetic resonance damping rate of the toroidal ion temperature gradient mode
[DE94-001234] 05 p1998 N94-22561
Time domain spectroscopy for studying a monopole antenna immersed in a plasma
[ISBN-0-315-86526-1] 09 p3888 N94-31727

PLASMA RINGS
U TOROIDAL PLASMAS

PLASMA SHEATHS
Simulations of D3-D divertor biasing with the LEDGE code
[DE93-010500] 01 p0385 N94-10262
Physics of tokamak scrape-off layer confinement
[DE93-011949] 01 p0390 N94-11125
Gyrosheath near the tokamak edge
[DE93-012191] 01 p0390 N94-11142
Plasma diffusion through multidipole magnetic fields
[INPE-5460-PRE/1768] 02 p0795 N94-12901
Detailed analysis of low energy plasma data under the Voyager Uranus data analysis program
[NASA-CR-193668] 04 p1628 N94-17842
Theoretical and numerical studies in magnetic fusion
[DE94-000536] 05 p1993 N94-20937
Magnetic insulation of secondary electrons in plasma source ion implantation
[DE93-040106] 05 p1997 N94-21988
Theory and simulation of plasma sheath waves
[DE94-001305] 05 p1999 N94-22567
Initial operation of a large-scale plasma source ion implantation experiment
[DE94-000805] 05 p2036 N94-22583
Chaotic phenomena in plasma, 2
[DE93-508286] 06 p2549 N94-22964
Computational model of surface ablation from tokamak disruptions
[DE94-002204] 06 p2550 N94-23474
Time domain spectroscopy for studying a monopole antenna immersed in a plasma
[ISBN-0-315-86526-1] 09 p3888 N94-31727
Dispersion relations for a plasma-filled helix-loaded-waveguide
[DE94-006333] 09 p3675 N94-31781
ICRF heating and current drive in TFTR supershot plasmas: Data analysis and interpretation of ICRF/edge interactions
[DE94-008586] 09 p3890 N94-32520
The spatial development of the magnetospheric low-latitude boundary layer
[ISBN-0-315-77418-5] 09 p3776 N94-33111
Theoretical aspect of low pressure discharges in simple gasses
[AD-A278762] 11 p4335 N94-35493

PLASMA SLABS
Three-wave resonant interaction in a thin layer
[AD-A272331] 05 p1994 N94-21039
Fluid simulations of Delta T(sub e)-driven turbulence and transport in boundary plasmas
[DE94-001304] 05 p1999 N94-22566
Theory and simulation of plasma sheath waves
[DE94-001305] 05 p1999 N94-22567

PLASMA SOUND WAVES
U MAGNETOHYDRODYNAMIC WAVES
U PLASMA WAVES

PLASMA SPECTRA
Stationary spectra of short-wave convective and magnetostatic fluctuations in a finite-pressure plasma and anomalous heat conductivity
[DE93-617852] 01 p0388 N94-10840
Active probing of plasma edge turbulence and feedback studies on the Texas experimental tokamak (TEXT)
[DE93-015799] 03 p1202 N94-16162
Detailed analysis of low energy plasma data under the Voyager Uranus data analysis program
[NASA-CR-193668] 04 p1628 N94-17842
Coronal temperatures of unusually active K-dwarf binary systems
[NASA-CR-189335] 08 p3545 N94-29861
Workshop on Models for Plasma Spectroscopy
[AD-A276565] 09 p3890 N94-32031

PLASMA SPRAYING
Microstructural evolution of NARloy-Z at elevated temperatures
[NASA-TM-108419] 02 p0571 N94-13715
Krupp technical reports no. 2, English edition, October 1992
[ETN-93-94631] 03 p0984 N94-16000
Vacuum plasma spraying 03 p0975 N94-16002
Turntable mechanism
[NASA-CASE-MFS-28522-1] 05 p1823 N94-20380
Method of fabricating a rocket engine combustion chamber
[NASA-CASE-MFS-28569-1] 05 p1703 N94-20541
Surface modification for corrosion resistance
[DE93-017419] 05 p1693 N94-21825
Selective hydrogen separation by palladium-based composite membranes
[PB93-201671] 06 p2254 N94-23431
Characterization and durability testing of plasma-sprayed zirconia-yttria and hafnia-yttria thermal barrier coatings. Part 2: Effect of spray parameters on the performance of several hafnia-yttria and zirconia-yttria coatings
[NASA-TP-3296] 06 p2242 N94-23467

Plasma sprayed thermal barrier coatings: Production, characterization and testing
[ISBN-9-03-860082-8] 06 p2555 N94-25439
Study on film generation phenomena by particle deposition 07 p2728 N94-25575
Fabrication and testing of plasma-spray formed MoSi2 and MoSi2 composite tubes
[DE94-004995] 08 p3175 N94-28581
Plasma sprayed ceramic thermal barrier coating for NiAl-based intermetallic alloys
[NASA-CASE-LEW-15535-1] 08 p3205 N94-29507
Development and characterization of intermediary layers allowing the bond between a metal alloy and a plasma sprayed ceramic
[ECL-91-39] 09 p3619 N94-31377

PLASMA STABILITY
U MAGNETOHYDRODYNAMIC STABILITY

PLASMA TEMPERATURE
Growth curve analysis for plasma profiles using smoothing splines
[DE93-015741] 02 p0795 N94-12984
Two temperature modeling and experimental measurements of laser sustained hydrogen plasmas
[AD-A265750] 02 p0796 N94-13039
ARIES tokamak reactor study
[DE93-017059] 03 p1203 N94-16901
Characterization of short pulse laser-produced plasmas at the Lawrence Livermore National Laboratory ultra short-pulse laser
[DE93-017191] 04 p1585 N94-18082
Plasma heating in toroidal systems
05 p2000 N94-22629
On the nonlinear instability of thermal structures
05 p2006 N94-22668
Imaging XUV spectroscopy of a Z-pinch plasma in the former Soviet Union
[DE93-040849] 06 p2549 N94-22949
Resistive ballooning mode in a gas-dynamic trap
[DE94-608328] 08 p3508 N94-30171
Peculiarities of heat transfer in the experiments of beam injection heating of a plasma at the GOL-3 device
[DE94-608357] 08 p3508 N94-30194
Magnetic island effects, interactions in tokamaks
[DE94-009209] 10 p4145 N94-34221
On the interpretation of diamagnetic loop measurements for a current-carrying plasma column in a conducting chamber
[DE94-007107] 12 p4526 N94-36536

PLASMA THEORY
U PLASMA PHYSICS

PLASMA TORCHES
Plasma arc welding torch having means for vortexing plasma for exiting the welding torch
[NASA-CASE-MFS-28828-1] 08 p3298 N94-29351
Plasma heating for containerless and microgravity materials processing
[NASA-CASE-NPO-18819-1-CU]
08 p3229 N94-29371
Ternary arc gas plasma welding torch
[NASA-CASE-MFS-28857-1] 08 p3303 N94-30173
Stabilization method of A.C. arc plasma
[DE94-757268] 09 p3893 N94-32916

PLASMA TURBULENCE
NT LANGMUIR TURBULENCE
Transport mechanisms acting in toroidal devices: A theoretician's view
[DE93-013463] 01 p0385 N94-10310
Texas experimental tokamak
[DE93-013377] 01 p0386 N94-10321
Stationary spectra in a quasi neutral current-carrying plasma
[DE93-617849] 01 p0387 N94-10539
Stationary spectra in a sheared plasma (linear limit)
[DE93-617850] 01 p0387 N94-10540
VLBI and the detection of interstellar magnetohydrodynamic waves 01 p0135 N94-11066
Physics of tokamak scrape-off layer confinement
[DE93-011949] 01 p0390 N94-11125
Discrete vortex representation of magnetohydrodynamics
[DE93-012190] 01 p0393 N94-11669
A 3D gyrokinetic particle-in-cell simulation of fusion plasma microturbulence on parallel computers
[DE93-012503] 02 p0794 N94-12846
Plasma diffusion through multidipole magnetic fields
[INPE-5460-PRE/1768] 02 p0795 N94-12901
Instability heating of the HDZP
[DE93-012641] 02 p0798 N94-13513
The resonance broadening theory revisited
[PPL-134] 02 p0798 N94-13563
Collisional effects of trapped electrons on the anomalous particle and thermal pinches
[PPL-128] 02 p0800 N94-13853
The role of electric field shear stabilization of turbulence in the H-mode to VH-mode transition in D3-D
[DE93-015474] 02 p0802 N94-14583
Active probing of plasma edge turbulence and feedback studies on the Texas experimental tokamak (TEXT)
[DE93-015799] 03 p1202 N94-16162
Plasma instabilities and transport in the MPD thruster
[AD-A268268] 03 p1204 N94-17575
Granular fluctuations in plasma turbulence and their role in transport
[DE93-013465] 03 p1187 N94-17674
Problems related to stimulated electromagnetic emissions, strong turbulence and ionospheric modification
[IRF-SR-212] 04 p1480 N94-17720
Behavior of the particle transport coefficients near the density limit in MTX
[DE93-019108] 04 p1591 N94-19311
Radial evolution of the solar wind turbulence with application to charged particle transport
[NASA-CR-194081] 04 p1629 N94-19427
The Wave Experiment Consortium
04 p1328 N94-19623
Theoretical studies of turbulence and anomalous transport in toroidal confinement devices
[DE93-040684] 04 p1592 N94-19656
Multi-CPU plasma fluid turbulence calculations on a CRAY Y-MP C90
[DE93-015425] 05 p1801 N94-20562
Shear flow generation by Reynolds stress and suppression of resistive g-modes
[DE93-040911] 05 p1995 N94-21514
Fluid simulations of Delta T(sub e)-driven turbulence and transport in boundary plasmas
[DE94-001304] 05 p1999 N94-22566
Dynamo driven by weak plasma turbulence: The effect of differential rotation 05 p2005 N94-22665
The onset and spectra of a magnetized Langmuir turbulence 05 p2006 N94-22673
Active probing of plasma edge turbulence and feedback studies on the Texas Experimental Tokamak (TEXT)
[DE94-001017] 06 p2548 N94-22945
Chaos in plasma simulation and experiment
[DE94-001574] 06 p2549 N94-22963
Chaos and simple determinism in reversed field pinch plasmas: Nonlinear analysis of numerical simulation and experimental data
[DE94-001575] 06 p2550 N94-23211
Nonlinear ion-mixing-mode particle transport in the dissipative trapped electron regime
[DE94-000989] 06 p2533 N94-23435
Multi-ion, multi-event test of ion cyclotron resonance heating
[NASA-CR-194859] 06 p2540 N94-23495
The role of the radial electric field in confinement and transport in H-mode and VH-mode discharges in the DIII-D tokamak
[DE94-002746] 06 p2551 N94-23782
Shear flow generation from the interaction of neoclassical and drift wave transport processes
[DE94-003135] 07 p2791 N94-26096
Maryland controlled fusion research program
[DE94-003533] 07 p3044 N94-26523
Role of core toroidal rotation shear on turbulence and transport in the improved confinement regimes of the D3-D tokamak
[DE94-001215] 07 p3045 N94-26950
Fast H-alpha line broadening during the 100 ns REB injection into a plasma
[IPPCZ-322] 07 p3048 N94-27836
Acceleration of electrons and ions by strong lower-hybrid turbulence in solar flares
[NASA-TM-109723] 07 p3111 N94-27953
Plasma turbulent bremsstrahlung
[PPL-144] 08 p3507 N94-30157
Dynamics of flux tubes in accretion disks
09 p3932 N94-31142
Transport suppression by shear flow generation in multihelicity resistive-g turbulence
[DE94-007108] 09 p3886 N94-31366
L-H confinement mode dynamics in three-dimensional state space
[DE94-007113] 09 p3887 N94-31396
An edge density fluctuation diagnostic for D3-D using lithium beams
[DE94-008554] 09 p3890 N94-32519
Recent VH-mode results on D3-D
[DE94-007429] 09 p3891 N94-32611
The Numerical Tokamak Project (NTP) simulation of turbulent transport in the core plasma: A grand challenge in plasma physics
[DE94-008279] 09 p3892 N94-32838
Millstone Hill radar studies of plasma waves and turbulence
[AD-A278409] 09 p3684 N94-33172
Dynamical nature of inviscid power law for two-dimensional turbulences and self-consistent spectrum and transport of plasma filaments
[DE94-009425] 10 p4144 N94-33913
K-epsilon model of anomalous transport in resistive interchange turbulence
[DE94-718983] 11 p4337 N94-35937
Confinement improvement in H-mode-like plasmas in helical systems
[DE94-727619] 12 p4528 N94-37231
Momentum-energy transport from turbulence driven by parallel flow shear
[DE94-012765] 12 p4443 N94-37362
Theory of anomalous transport in H-mode plasmas
[DE94-727546] 12 p4531 N94-37485

PLASMA WAVES
NT ELECTROSTATIC WAVES
Two fluid plasmas in the vicinity of a Schwarzschild black hole
[DE93-610264] 01 p0385 N94-10284
General renormalized statistical approach with finite cross-field correlations
[DE93-617846] 01 p0386 N94-10396
Stationary spectra in a magnetized current-carrying plasma
[DE93-617847] 01 p0386 N94-10397
Stationary spectra in a finite-pressure current-carrying plasma
[DE93-617848] 01 p0387 N94-10538
Spatial helicon-wave echo in an inhomogeneous magnetized plasma
[DE93-617845] 01 p0389 N94-10885
The angular structure of second harmonic emission from laser-produced plasmas irradiated at moderate intensity
[DE93-013102] 01 p0389 N94-11114
Studies on the parametric decay of waves in fusion plasmas
[DE93-621659] 01 p0390 N94-11148
Dispersion of plasma waves in a finite magnetic field (omega(sub H) greater than omega(sub p))
[DE93-621654] 01 p0391 N94-11210
Experimental investigation of wake field excitation in plasma by a periodic succession of relativistic particle clots
[DE93-621655] 01 p0391 N94-11211
Negative viscosity and generation of dissipative solitons and zonal dissipative structures by drift waves
[DE93-621656] 01 p0392 N94-11212
Studies of electrostatic waves and VLF-wave particle interaction in the ionosphere
[AD-A266013] 01 p0278 N94-12392
Excitation of coupled waves in plasma periodic structures by relativistic electron beam and acceleration of charged particles
[DE93-621657] 02 p0794 N94-12853
Ion anisotropy driven waves in the Earth's magnetosheath and plasma depletion layer
[DE93-012751] 02 p0712 N94-12952
ICE/ISEE plasma wave data analysis
[NASA-CR-194375] 02 p0796 N94-13081
Investigations of transitions from order to chaos in dynamical systems
[DE93-014438] 02 p0818 N94-14738
Studies on the parametric decay of waves in fusion plasmas
[VTT-PUBS-110] 03 p1200 N94-15204
Double stimulated Brillouin scattering
03 p1200 N94-15205
Dynamics of douple stimulated Brillouin scattering
03 p1200 N94-15206
Soliton-like structures in double stimulated Brillouin scattering 03 p1200 N94-15207
High frequency Raman current drive
03 p1201 N94-15208
Current drive with free electron lasers in high and low temperature tokamaks 03 p1201 N94-15209
Simulations of wave-particle interactions in stimulated Raman forward scattering in a magnetized plasma
[PB94-170990] 03 p1201 N94-15210
On the decay of a dipole pump wave to half-harmonics 03 p1201 N94-15211
Structure and damping of toroidal drift waves (and their implications for anomalous transport)
[DE93-014005] 03 p1203 N94-16822
The phase mixing of shear Alfven waves
[DE93-624920] 04 p1581 N94-17688
Transformation of energy and momentum due to Landau damping in space
[DE93-624921] 04 p1581 N94-17689
Resonant absorption of Alfven waves near a neutral point
[DE93-628761] 04 p1586 N94-18172
Plasma production by helicon waves
[DE93-788396] 04 p1586 N94-18213
Phase-space description of plasma waves: Linear and nonlinear theory
[IRF-SR-211] 04 p1587 N94-18860
Planetary plasma waves
[NASA-CR-194295] 04 p1629 N94-19094

On neutral plasma oscillations
[DE93-040319] 04 p1590 N94-19194
The Wave Experiment Consortium 04 p1328 N94-19623
The spherical probe Electric Field and Wave Experiment for the Cluster mission 04 p1328 N94-19624
WHISPER: A sounder and high-frequency wave analyser experiment 04 p1328 N94-19626
The wideband plasma wave investigation 04 p1328 N94-19627
Implementation of the digital wave-processing experiment 04 p1329 N94-19628
A study of Saturn's E-ring particles using the Voyager 1 plasma wave instrument
[NASA-CR-194694] 05 p2088 N94-20048
Radiation of plasma wave wings through an electrodynamic tether satellite system with any sharp angle geometry
[REPT-85] 05 p1993 N94-20156
Kinetic resonance damping rate of the toroidal ion temperature gradient mode
[DE94-001234] 05 p1998 N94-22561
Theory and simulation of plasma sheath waves
[DE94-001305] 05 p1999 N94-22567
Active probing of plasma edge turbulence and feedback studies on the Texas Experimental Tokamak (TEXT)
[DE94-001017] 06 p2548 N94-22945
Chaotic phenomena in plasma, 2
[DE93-508286] 06 p2549 N94-22964
Multi-ion, multi-event test of ion cyclotron resonance heating
[NASA-CR-194859] 06 p2540 N94-23495
A relativistic theory on wave propagation in inhomogeneous magnetoplasmas
[ETN-94-95322] 06 p2554 N94-25285
Numerical simulation and analysis of experimental results on stimulated Raman scattering in laser-plasma Hohlraum targets
[DE93-613719] 06 p2554 N94-25330
LHCD (low hybrid current drive) experiment on the HT-6B tokamak
[DE93-613720] 06 p2555 N94-25331
Review of tokamak experiments on direct electron heating and current drive with fast waves
[DE94-004185] 07 p3041 N94-25801
Collisionless shock structures of Earth and other planets
[NASA-CR-195257] 07 p3104 N94-27407
Space Experiments with Particle Accelerators (SEPAC)
[NASA-CR-193935] 07 p2761 N94-27664
On radio frequency wave induced radial transport and wave helicity
[IPPCZ-326] 07 p2777 N94-27838
On helicon wave induced radial plasma transport
[IPPCZ-333] 07 p3048 N94-27840
Preliminary considerations on the diffraction (quasi-optical) grill in CASTOR tokamak
[IPPCZ-335] 07 p3048 N94-27842
Acceleration of electrons and ions by strong lower-hybrid turbulence in solar flares
[NASA-TM-109723] 07 p3111 N94-27953
Coulomb field effect on plasma focusing and wake field acceleration
[DE94-004937] 08 p3504 N94-28564
Towards experimental verification and device applications of current driven plasma instabilities in solid state systems
[AD-A275395] 08 p3504 N94-29055
Wave generation by contaminant ions near a large spacecraft
[NASA-CR-195797] 08 p3169 N94-29917
A relativistic solitary wave in electron positron plasma
[DE94-608107] 08 p3507 N94-30071
Plasma turbulent bremsstrahlung
[PPL-144] 08 p3507 N94-30157
Langmuir waves in the electron-positron plasma
[DE94-608330] 08 p3508 N94-30191
Collective acceleration in solar flares
[DE94-006288] 09 p3953 N94-31632
Time domain spectroscopy for studying a monopole antenna immersed in a plasma
[ISBN-0-315-86526-1] 09 p3886 N94-31727
Basic principles approach for studying nonlinear Alfven wave-alpha particle dynamics
[DE94-007112] 09 p3891 N94-32664
Simultaneous excitation of parametric decay cascades and the OTSI in 1D numerical simulations based on Aakarov's equations
[AD-A278108] 09 p3893 N94-33042
Plasma and radio waves from Neptune: Source mechanisms and propagation
[NASA-CR-195877] 09 p3943 N94-33103
Participation in the scientific activities of the Waves in Space Plasma (WISP) project
[NASA-CR-195903] 09 p3894 N94-33113
Millstone Hill radar studies of plasma waves and turbulence
[AD-A278409] 09 p3684 N94-33172
Plasma waves in the nightside ionosphere of Venus 10 p4164 N94-33431
Beat wave current drive experiment on the Davis Diverted Tokamak (DDT)
[DE94-009770] 10 p4144 N94-33879
Diffusion at the magnetopause: A theoretical perspective
[DE94-009356] 10 p4086 N94-33910
LLE review, volume 57
[DE94-009186] 10 p4145 N94-33990
Studies of ion acoustic decay
[DE94-009470] 10 p4138 N94-34168
Analysis of DE-1 PWI electric field data
[NASA-CR-195950] 10 p4036 N94-34280
Landau damping of auroral hiss 10 p4088 N94-34950
Flank solar wind interaction
[NASA-CR-189327] 10 p4166 N94-35225
The fine structure of Langmuir waves observed upstream of the bow shock at Venus
[NASA-CR-196123] 11 p4354 N94-35378
ULF waves in the low-latitude boundary layer and their relationship to magnetospheric pulsations: A multisatellite observation
[AD-A278906] 11 p4289 N94-35587
Self-similar regimes of subsonic Langmuir wave collapse
[DE94-611466] 11 p4335 N94-35750
The kinetics of inhomogeneous plasma
[DE94-611459] 11 p4336 N94-35788
Initial perturbations and Langmuir waves in electron-positron plasma
[DE94-617190] 11 p4338 N94-36097
The energy density of fluctuative electromagnetic field near the semi-bounded plasma
[DE94-617188] 11 p4256 N94-36099
Basic studies in plasma wave interactions
[AD-A280465] 12 p4527 N94-37139
Time-step stability for self-consistent Monte Carlo device simulation
[DE94-012145] 12 p4528 N94-37207
Plasma and radio waves from Neptune: Source mechamisms and propagation
[NASA-CR-196284] 12 p4550 N94-37251
Langmuir waves in the electron-positron plasma
[DE94-618779] 12 p4531 N94-37728

PLASMA-ELECTROMAGNETIC INTERACTION
NT LASER PLASMA INTERACTIONS
The Langevin's approach to the statistical theory of bounded plasma
[DE93-617842] 01 p0388 N94-10839
Distribution of charged particles near the plasma boundary in the presence of external electric field
[DE93-617862] 01 p0389 N94-10886
Studies on the parametric decay of waves in fusion plasmas
[DE93-621659] 01 p0390 N94-11148
Scattering of reflectometer signals from rippled surfaces
[PPL-138] 02 p0602 N94-13802
Femtosecond growth dynamics of an underdense ionization front measured by spectral blueshifting
[DE93-013582] 03 p1183 N94-16818
Limits on m = 2, n = 1 error field induced locked mode instability in TPX with typical sources of poloidal field coil error field and a proto type correction coil, C-coil
[DE93-014408] 04 p1582 N94-17702
Wake field in electron-positron plasmas
[DE93-624929] 04 p1584 N94-17955
Resonant absorption of Alfven waves near a neutral point
[DE93-628761] 04 p1586 N94-18172
Studies of enhanced radar backscatter
[AD-A269544] 04 p1385 N94-18288
Radiation of plasma wave wings through an electrodynamic tether satellite system with any sharp angle geometry
[REPT-85] 05 p1993 N94-20156
Three-wave resonant interaction in a thin layer
[AD-A272331] 05 p1994 N94-21039
Solar wind-magnetosphere interaction as simulated by a 3D, EM particle code 05 p2007 N94-22674
Basic studies in plasma wave interactions
[AD-A280465] 12 p4527 N94-37139

PLASMA-PARTICLE INTERACTIONS
Momentum and heat frictions between fast ions and thermal plasma species
[DE93-771240] 01 p0390 N94-11149
Excitation of coupled waves in plasma periodic structures by relativistic electron beam and acceleration of charged particles
[DE93-621657] 02 p0794 N94-12853
Electrodynamics of helical plasma structures
[DE93-620981] 02 p0797 N94-13240
Simulations of wave-particle interactions in stimulated Raman forward scattering in a magnetized plasma
[PB94-170990] 03 p1201 N94-15210
Advanced fusion diagnostics
[DE93-040085] 04 p1589 N94-19133
Current loop coalescence studied by 3-D electromagnetic particle code 05 p2005 N94-22660
Dynamics of physical state during two current loops collision 05 p2005 N94-22663
Consequences of plasma-maser in plasma astrophysics 05 p2006 N94-22669
Fast H-alpha line broadening during the 100 ns REB injection into a plasma
[IPPCZ-322] 07 p3048 N94-27836
A 6MeV heavy ion beam probe for the Large Helical Device
[AD-B183695L] 08 p3505 N94-29397
Participation in the definition, conduct, and analysis of particle accelerator experiments for the first Spacelab Mission
[NASA-CR-193974] 11 p4330 N94-35483

PLASMAGUIDES
On a theory of two-beam mechanisms of charged particle acceleration in electrodynamic structures
[DE94-003482] 07 p3032 N94-26330

PLASMAPAUSE
Detailed analysis case studies of trapped plasmas at the Earth's magnetic equator
[AD-A272497] 05 p1858 N94-21432

PLASMAS (PHYSICS)
NT ARGON PLASMA
NT BETA PARTICLES
NT BOUNDARY LAYER PLASMAS
NT COLD PLASMAS
NT COLLISIONAL PLASMAS
NT COLLISIONLESS PLASMAS
NT COSMIC PLASMA
NT CYLINDRICAL PLASMAS
NT DENSE PLASMAS
NT ELECTRON PLASMA
NT ELECTRON-POSITRON PLASMAS
NT HELIUM PLASMA
NT HIGH TEMPERATURE PLASMAS
NT HYDROGEN PLASMA
NT LASER PLASMAS
NT METALLIC PLASMAS
NT MICROPLASMAS
NT NITROGEN PLASMA
NT NONEQUILIBRIUM PLASMAS
NT NONUNIFORM PLASMAS
NT OXYGEN PLASMA
NT PLASMA FOCUS
NT RAREFIED PLASMAS
NT RELATIVISTIC PLASMAS
NT ROTATING PLASMAS
NT SOLAR WIND
NT SPACE PLASMAS
NT STELLAR WINDS
NT STRONGLY COUPLED PLASMAS
NT THERMAL PLASMAS
NT TOROIDAL PLASMAS
MHD simulation of deuterium-fiber-initiated Z-pinches with two-fluid effects
[DE93-012682] 01 p0384 N94-10158
Simulations of D3-D divertor biasing with the LEDGE code
[DE93-010500] 01 p0385 N94-10262
X ray production (approximately)130 (Angstrom) from laser-produced plasmas for projection x ray lithography applications
[DE93-009256] 01 p0385 N94-10286
An investigation of conducted and radiated emissions from a hollow-cathode plasma contactor
[NASA-CR-191172] 01 p0386 N94-10346
Stationary spectra in a magnetized current-carrying plasma
[DE93-617847] 01 p0386 N94-10397
Stationary spectra in a plasma with a shear (renormalized statistical approach with non-zero eigenfrequencies)
[DE93-617851] 01 p0386 N94-10523
Stationary spectra in a finite-pressure current-carrying plasma
[DE93-617848] 01 p0387 N94-10538
Stationary spectra in a quasi neutral current-carrying plasma
[DE93-617849] 01 p0387 N94-10539
Stationary spectra in a sheared plasma (linear limit)
[DE93-617850] 01 p0387 N94-10540
Atomic and molecular data for H2O, CO and CO2 relevant to edge plasma impurities
[DE93-771423] 01 p0387 N94-10662
The heat transfer by radiation between two media
[DE93-617820] 01 p0149 N94-10838

The Langevin's approach to the statistical theory of bounded plasma
[DE93-617842] 01 p0388 N94-10839
Magnetohydrodynamic computation of feedback stabilization of resistive-shell instabilities in the reversed field pinch
[DE93-013466] 01 p0388 N94-10852
Wave generation by contaminant ions
[NASA-CR-193558] 01 p0364 N94-10946
Calculation of Mercier stability criterium in stellarators
[DE93-621599] 01 p0389 N94-11091
Possibilities of magnetic diagnostics in stellarators
[DE93-621608] 01 p0389 N94-11092
The angular structure of second harmonic emission from laser-produced plasmas irradiated at moderate intensity
[DE93-013102] 01 p0389 N94-11114
Radiative properties of strongly magnetized plasmas
[DE93-014098] 01 p0389 N94-11118
Particle transport analysis in torsatron configurations
[DE93-621640] 01 p0390 N94-11120
Simulation study of dynamo structure in reversed field pinch
[DE93-771406] 01 p0390 N94-11128
Negative viscosity and generation of dissipative solitons and zonal dissipative structures by drift waves
[DE93-621656] 01 p0392 N94-11212
Spreading of Bimodulated Ultra-relativistic Electron Beam (BUEB) in Atmospheric Plasma Channel (APCh)
[DE93-621658] 01 p0392 N94-11213
Characteristics of ICR-produced peripheral plasma in the Uragan-3M torsatron
[DE93-621666] 01 p0392 N94-11214
Discrete vortex representation of magnetohydrodynamics
[DE93-012190] 01 p0393 N94-11669
An investigation of the near Earth space environments
[AD-A265295] 01 p0278 N94-11828
Two-dimensional simulations of foil implosion experiments on the Los Alamos capacitor bank
[DE93-012676] 02 p0794 N94-12814
A 3D gyrokinetic particle-in-cell simulation of fusion plasma microturbulence on parallel computers
[DE93-012503] 02 p0794 N94-12846
Inertial Confinement Fusion
[DE93-013303] 02 p0795 N94-13017
Comment of parameter excitation of Alfven and Heliicon waves in a magnetoactive compensated semiconductor by microwave radiation
[DE93-623203] 02 p0806 N94-13228
On energy transport equations for turbulent magnetized plasma
[PPL-135] 02 p0800 N94-13850
Dependence of beta(tau) on plasma shape in D3-D
[DE93-015473] 02 p0800 N94-13900
Oscillator-amplifier experiments in neon-like yttrium
[DE93-012577] 02 p0657 N94-13976
The interaction of intense femtosecond laser pulses with solid targets
[DE93-014415] 02 p0658 N94-14114
Monte Carlo simulation of the OCP freezing transition
[DE93-013039] 02 p0811 N94-14313
Variation of divertor plasma parameters with divertor depth for H-mode discharges in D3-D
[DE93-015475] 02 p0801 N94-14347
Direct determination of alpha particle transport coefficients
[DE93-013488] 02 p0787 N94-14691
Anomalous ion transport and feedback control
[DE93-018324] 02 p0803 N94-14874
PHENIX Conceptual Design Report
[DE93-015759] 03 p1182 N94-16161
Application of non-thermal plasmas to pollution control
[DE93-016432] 03 p1096 N94-16449
Numerical modeling of the temperature gradients and spectra of the plasma armature on Thunderbolt
[AD-A266414] 03 p0878 N94-16552
Linear and non-linear studies of Alfven waves in space. Stationary and dynamic processes in magnetospheric plasmas
[NASA-CR-193585] 03 p1239 N94-16647
Elemental impurity analysis of mercuric iodide by ICP/MS
[DE93-015531] 03 p0949 N94-16876
Hollow cathode heater development for the Space Station plasma contactor
[NASA-CR-191131] 03 p0926 N94-16880
ARIES tokamak reactor study
[DE93-017059] 03 p1203 N94-16901
Plasma Science Committee (PLSC) and the Panel on Opportunities in Plasma Science and Technology (OPST)
[DE93-018142] 03 p1204 N94-16995
A state-of-the-art plasma polymerization coater for ICF targets
[DE93-016452] 03 p1204 N94-17237
High power steady state MPD thrusters
[AD-A267277] 03 p0928 N94-17308
Plasma flow switch and foil implosion experiments on Pegasus 2
[DE93-016464] 03 p1013 N94-17318
Kinetic plasma processes occurring in the outer plasmasphere
[NASA-CR-193452] 03 p1300 N94-17524
Optimal pulse modulator design criteria for plasma source ion implanters
[DE93-016465] 03 p1205 N94-17645
3D and r,z particle simulations of heavy ion fusion beams
[DE93-013417] 03 p1205 N94-17670
Observations of MeV electrons and scattered light from intense, subpicosecond laser-plasma interactions
[DE93-017153] 04 p1435 N94-17855
Configuration interaction in LTE spectra of heavy elements
[DE93-017166] 04 p1584 N94-17990
Analysis of the ITER H-mode confinement database
[DE93-016984] 04 p1585 N94-18056
Coupled MHD and transport analysis of improved confinement D3-D discharges
[DE93-016985] 04 p1585 N94-18057
Dependence of helium transport on plasma current and ELM frequency in H-mode discharges in D3-D
[DE93-016986] 04 p1585 N94-18058
Characterization of short pulse laser-produced plasmas at the Lawrence Livermore National Laboratory ultra short-pulse laser
[DE93-017191] 04 p1585 N94-18082
AEOLUS-IT MHD simulation code based on a toroidally incompressible plasma model
[DE93-788461] 04 p1586 N94-18157
RF vacuum microelectronics
[AD-A269454] 04 p1396 N94-18284
Nonparaxial MHD stabilizers for an axisymmetric magnetic mirror
[DE93-017996] 04 p1587 N94-18505
Center of Excellence in Theoretical Geoplasma Research
[AD-A270210] 04 p1588 N94-18902
Viscosity in the edge of tokamak plasmas
[DE93-018039] 04 p1588 N94-18988
Experiments on nonlinear absorption of ECH waves in MTX and a comparison with theory
[DE93-019158] 04 p1589 N94-19074
Radiative divertor modeling studies
[DE93-018092] 04 p1590 N94-19290
Manufacturing technology
[DE93-019580] 04 p1381 N94-19480
Plasma chemical vapor deposition of halide glasses
[AD-D015933] 05 p1701 N94-20331
Interleaved bismaleimide composites
[AD-A272233] 05 p1674 N94-20574
On magnetodynamic effects initiated by a high-speed impact of a large cosmic body upon the Earth's surface 05 p2082 N94-20647
Engineering design, fabrication, installation, operation, and maintenance services in support of research on laser plasma physics
[AD-A272249] 05 p1994 N94-20943
Three-wave resonant interaction in a thin layer
[AD-A272331] 05 p1994 N94-21039
Characteristics of switching plasma in an inverse-pinch switch 05 p1995 N94-21292
Radial diffusion of toroidally trapped particles induced by lower hybrid and fast waves
[IPPCZ-327] 05 p1996 N94-21593
Results from long conduction time plasma opening switch experiments at Sandia National Laboratories
[DE93-019063] 05 p1762 N94-21632
Particle behavior in an ECR plasma etch tool
[DE93-040343] 05 p1996 N94-21769
Plasma-chemical conversion of hydrogen sulfide into hydrogen and sulfur
[DE93-041167] 05 p1682 N94-21789
Edge plasma experiments on CASTOR tokamak
[IPPCZ-332] 05 p1997 N94-21816
Time evolution of the quark-gluon plasma
[DE94-000804] 05 p1998 N94-22389
A two-dimensional kinetic model of the scrape-off layer
[DE94-001235] 05 p1999 N94-22562
Massachusetts Institute of Technology Plasma Fusion Center 1992-1993 report to the President
[DE94-001725] 06 p2548 N94-22721
Semiempirical studies of atomic structure
[DE94-001588] 06 p2531 N94-22937
The internal structure and dynamics of the railgun plasma armature between infinitely wide ablating rails
[DE94-001473] 06 p2198 N94-23208
Overview of the ATF stellarator program
[DE94-000371] 06 p2550 N94-23462
Artificial plasma experiments. Chemical release observations associated with the CRRES program
[NASA-CR-194871] 06 p2550 N94-23585
Stationary plasma thruster plume characteristics
[NASA-CR-194454] 06 p2219 N94-24361
The chemistry of particulate formation in fluorocarbon plasmas
[DE94-001500] 06 p2552 N94-24548
X ray simulator theory support
[AD-A273613] 06 p2553 N94-24949
Excitation balances and transport in an inductively coupled plasma
[ETN-94-95330] 06 p2554 N94-25241
The anomalous transport caused by particles transverse drift
[DE93-613685] 06 p2554 N94-25329
Behavior of the intermittency exponents and a quark-gluon plasma formation in the heavy ion collisions
[DE93-616869] 06 p2541 N94-25342
Effect of LHCD (low hybrid current drive) on tearing mode instability
[DE93-613700] 06 p2555 N94-25344
Excitation mechanisms for XUV and x ray lasers
[DE93-617006] 06 p2351 N94-25482
Diffusion in electronegative discharges with magnetic fields
[AD-A273826] 06 p2304 N94-25521
Design of folded waveguide antenna for Alcator C-Mod
[DE94-003584] 07 p2767 N94-25924
Investigation of plasma etch induced damage in compound semiconductor devices
[DE94-002849] 07 p3052 N94-25989
New Thomson scattering laser control for D3-D
[DE94-002890] 07 p3043 N94-26274
Microwave and pulsed power
[DE94-003019] 07 p2782 N94-26312
Laboratory plasma studies
[AD-A274655] 07 p3043 N94-26356
Kinetic equation identification from measurement of a particular solution
[DE93-634585] 07 p2995 N94-26768
Equivalent performance in different helical resonator plasma polymerization coater platforms
[DE94-001517] 07 p2753 N94-26933
Experimental investigations of strong interaction in the non-perturbative QCD region
[DE94-001178] 07 p3024 N94-26949
HPm-tubes: Literature survey comprising 1992
[PB94-123643] 07 p2785 N94-27038
Experimental and theoretical investigation of RF absorption and reflection from preformed plasmas
[AD-A274189] 07 p3046 N94-27098
Researches of the Electrotechnical Laboratory. No. 51: Study of formation and sustainment of reversed field pinch by slow control of magnetic field
[JTN-94-80548] 07 p3046 N94-27350
Numerical experiment on finite element method for matching data
[DE94-701208] 07 p3000 N94-27731
Nonlinear magnetohydrodynamics
[DE94-005654] 08 p3503 N94-28547
Experimental and analytical studies of high heat flux components for fusion experimental reactor
[DE94-707671] 08 p3504 N94-28556
A novel spectroscopic measurement method of RF plasma for temperature and electron density diagnoses 08 p3188 N94-28682
Development of large area RF induction plasma for cost effective diamond
[AD-A275888] 08 p3504 N94-28776
Advanced diagnostics for reacting flows
[AD-A275057] 08 p3272 N94-29136
Plasma arc welding torch having means for vortexing plasma for exiting the welding torch
[NASA-CASE-MFS-28828-1] 08 p3298 N94-29351
Chamber free fusion welding root side purging method and apparatus
[NASA-CASE-MFS-28832-1] 08 p3204 N94-29380
Preparation and structure of amorphous hydrogenated carbon film deposited with RF plasma CVD 08 p3223 N94-29518
Nonlinear wave packet evolution in a dispersive plasma: Application to rotational discontinuities 08 p3506 N94-29822
Practical applications of plasma surface modification
[DE94-004892] 08 p3349 N94-29932
Magnetic field generation by circularly polarized laser light and inertial plasma confinement in a miniature magnetic bottle induced by circularly polarized laser light
[DE94-608353] 08 p3508 N94-30192
Direct measurement of the reactivity of NH and OH on a silicon nitride surface
[DE94-005286] 08 p3199 N94-30260
Plasma treatment of polymer dielectric films to improve capacitive energy storage 08 p3223 N94-30479

Advanced steady-state operating scenarios
[DE94-004810] 08 p3509 N94-30768
Deexcitation processes in nuclear reactions: The study of hot hadronic matter
[DE94-003396] 08 p3492 N94-30836
Self-similar variables and the problem of nonlocal electron heat conductivity
[DE94-005826] 08 p3493 N94-30881
Dynamics of flux tubes in accretion disks 09 p3932 N94-31142
Radiation from an aperture into an anisotropic plasma half-space 09 p3885 N94-31205
Theoretical studies on ionospheric irregularities and ion diode performance
[AD-A277115] 09 p3772 N94-31984
Analytic properties of the OCP and ionic mixtures in the strongly coupled fluid state
[DE94-008216] 09 p3637 N94-32801
The 1994 International Sherwood Fusion Theory Conference
[DE94-008961] 09 p3877 N94-32844
Potential applications of fusion neutral beam facilities for advanced material processing
[DE94-009167] 09 p3647 N94-32851
Stabilization method of A.C. arc plasma
[DE94-757268] 09 p3893 N94-32916
Ultrafast x ray sources
[AD-A277455] 09 p3721 N94-33012
Time resolved measurements of light produced by onset of plasma formation on electrodes of fast pulsed high voltage diodes
[AD-A277974] 09 p3894 N94-33264
Precision operation of the Nova laser for fusion experiments
[DE94-007073] 10 p4057 N94-33405
Application of pulsed plasma NO(x) reduction to diesel engine exhaust
[DE94-007454] 10 p4080 N94-33692
Transport properties of interacting magnetic islands in tokamak plasmas
[DE94-009208] 10 p4145 N94-34140
Theoretical aspect of low pressure discharges in simple gasses
[AD-A278762] 11 p4335 N94-35493
Simulation models for computational plasma physics: Concluding report
[DE94-009976] 11 p4335 N94-35647
Analysis of current diffusive ballooning mode
[DE94-718992] 11 p4336 N94-35811
Applications of non-resonant RF forces for improvement of tokamak reactor performances. Part 1: Application of ponderomotive force
[DE94-718994] 11 p4336 N94-35813
Atomic physics and radiation processes in plasmas
[DE94-727617] 11 p4337 N94-35939
A survey of reflectometry techniques with applications to TFTR
[DE94-010202] 11 p4338 N94-36093
The pressure of fluctuative electromagnetic field in inhomogeneous medium
[DE94-617189] 11 p4256 N94-36096
The energy density of fluctuative electromagnetic field near the semi-bounded plasma
[DE94-617188] 11 p4256 N94-36099
Collective plasma corrections to the solar opacity
[PB94-170511] 11 p4375 N94-36210
The new features of Ion Bernstein Wave Heating in JIPP T-2U tokamak
[DE94-718978] 11 p4338 N94-36247
Catalog of Helios 90 deg photometer events
[PL-TR-94-2040] 11 p4375 N94-36264
Studies of the dayside boundary layer processes based on ground observations in the Svalbard area
[AD-A280715] 11 p4292 N94-36265
Experiments in diamond film fabrication in table-top plasma apparatus 11 p4231 N94-36411
New plasma source of hydrides for epitaxial growth
[DE94-006918] 12 p4533 N94-36744
The mathematical simulation of physical processes in ECR multicharged ions sources
[DE94-618343] 12 p4515 N94-37077
Design of the divertor Thomson scattering system on DIII-D
[DE94-012672] 12 p4527 N94-37081
Improvement study of the divertor configuration of the Steady State Tokamak Reactor (SSTR)
[DE94-718961] 12 p4531 N94-37484
Langmuir waves in the electron-positron plasma
[DE94-618779] 12 p4531 N94-37728
Fast electron generation and transport in a turbulent, magnetized plasma
[DE94-012986] 12 p4531 N94-37730
Three-dimensional gyrokinetic particle-in-cell simulation of plasmas on a massively parallel computer: LDRD Core Competency Project
[DE94-013367] 12 p4532 N94-37732
Characteristics of ions emitted from high-current hollow cathodes
[NASA-CR-195372] 12 p4398 N94-37764

PLASMASPHERE

Studies on equatorial shock formation during plasmaspheric refilling
[NASA-CR-194392] 02 p0715 N94-13954
The role of ionospheric plasma in the magnetosphere
[NASA-CR-194404] 02 p0716 N94-13967
Kinetic plasma processes occurring in the outer plasmasphere
[NASA-CR-193452] 03 p1300 N94-17524
Ionospheric photoelectrons measured at geosynchronous orbit
[AD-A272431] 05 p1857 N94-21202
The Far Ultraviolet (FUV) auroral imager for the Inner Magnetospheric Imager (IMI) mission: Options 06 p2209 N94-24453
Electron beams at geosynchronous orbit
[AD-A275471] 08 p3355 N94-28684
Studies on equatorial shock formation during plasmaspheric refilling
[NASA-CR-195864] 10 p4088 N94-34669

PLASMOIDS

U PLASMAS (PHYSICS)

PLASMONS

The surface plasmon spectroscopy as diagnostic technique in microgravity experiments 01 p0110 N94-10133
Experimental and theoretical investigation of surface chemistry induced by direct and indirect electronic excitation
[AD-A268846] 04 p1348 N94-18221
Metal Film Surface Plasmon Resonance (MFSPR) fibre couplers
[AD-A268871] 04 p1579 N94-18635
Formation of colloidal Ag precipitates in fused silica by MeV ion implantation
[DE93-040268] 05 p2012 N94-19869
Fragmentation of Ge(1-x) Sn(x) Se2 glasses
[DE94-603009] 07 p2758 N94-27837

PLASTERS

NT GYPSUM

PLASTIC AIRCRAFT STRUCTURES

New aircraft materials and structures
[MBB-LME-202-S-PUB-502-A] 04 p1319 N94-19496

PLASTIC ANISOTROPY

NT ELASTIC ANISOTROPY
Plastic anisotropy in MoSi2 single crystals
[DE93-012650] 04 p1594 N94-17874

PLASTIC COATINGS

Follow-up on the effects of the space environment on UHCRE thermal blankets 09 p3592 N94-31018
Evaluation of flame-sprayed polymer coatings for civil works navigation structures
[AD-A280507] 12 p4422 N94-37104

PLASTIC DEFORMATION

A simple model of melt fracture
[AD-A265311] 01 p0092 N94-11862
A benchmark bending test of a thick specimen, Part 1: Experiments
[ARL-RR-6-PT-1] 02 p0670 N94-12927
A benchmark bending test of a thick specimen. Part 2: Surface displacement measurements
[ARL-RR-6-PT-2] 02 p0670 N94-12928
Inelastic deformation mechanisms in SCS-6/Ti 15-3 MMC lamina under compression
[NASA-CR-191170] 02 p0555 N94-13378
A stochastic model for behavior analysis of fiber-reinforced quasi-brittle materials 02 p0672 N94-13594
Non-uniqueness in dynamic rate-independent non-associated plasticity
[AD-A266342] 02 p0769 N94-13731
Thermal gradient-induced deflection of a thick-walled cylinder with bending residual stresses
[AD-A266347] 02 p0673 N94-13777
Ploughing on gold using a Scanning Tunneling Microscope
[DE93-012632] 02 p0812 N94-14365
Elastic-plastic finite element analyses of an unidirectional, 9 vol percent tungsten fiber reinforced copper matrix composite
[NASA-TM-106304] 02 p0559 N94-14719
Systematology for elastic-plastic material equations by large deformations on the basis of the Cosserat-continuum model
[SCHRIFTENR-PHYSIKAL-ING-BD-23] 03 p1058 N94-15642
Anisotropic damage mechanics modeling in metal matrix composites
[AD-A266328] 03 p0934 N94-16440
Slip, twinning and transformation in Laves phases
[DE93-018164] 03 p0960 N94-16972
Studies of changes in the energy stored in metals as a result of subjecting them to a surface type technological process
[IFTR-25/1991] 03 p0960 N94-17063
Analysis of the strengthening of aluminum alloy undergoing plastic deformation under conditions of a compound state of stress
[IFTR-21/1991] 03 p0960 N94-17093
Modeling microstructural evolution and the mechanical response of superplastic materials
[DE93-014417] 04 p1355 N94-17711
A benchmark bending test of a thick specimen. Part 1: Experiments
[AD-A268730] 04 p1360 N94-18325
Dislocation-drag contribution to high-rate plastic deformation in shock-loaded tantalum
[DE93-018286] 04 p1361 N94-18802
Deformation mechanisms in a Laves phase
[DE93-018331] 04 p1361 N94-18806
Influence of peak pressure and temperature on the shock-loading response of tantalum
[DE93-018561] 04 p1457 N94-19279
The effect of composition on the mechanism of continuous recrystallization and superplastic response of aluminum-scandium alloys
[DE93-018594] 04 p1365 N94-19280
Ni-Al2O3 solid state binding: Elaboration, state of thermal constraints, mechanical behavior
[ECL-92-31] 04 p1366 N94-19436
Current capabilities for simulating the extreme distortion of thin structures subjected to severe impacts 04 p1459 N94-19474
Crashdynamics with DYNA3D: Capabilities and research directions 04 p1460 N94-19475
Finite element mesh generation and analysis of solder joints for fatigue life predictions
[AD-A271329] 05 p1829 N94-19937
Analysis of Alloy 600 and X-750 stress corrosion cracks
[DE94-001578] 06 p2238 N94-22936
Proof test of the computer program BUCKY for plasticity problems
[NASA-TP-3444] 06 p2374 N94-22960
Damage under monotonic or cyclic loads of new AlSiFe alloys prepared by the Osprey (tm) process
[ISAL-93-0008] 06 p2239 N94-22972
The plastic response of a cylindrical shell subjected to an internal blast wave with a finite width shock front 06 p2154 N94-24246
On the deformation kinetics constitutive law of plastic deformation: The rate equation 06 p2161 N94-24289
Procedures for determining MATMOD-4V material constants
[DE94-002638] 06 p2245 N94-24520
Study on variation of damage generation mechanism by fatigue on TiAl compounds due to different slip systems 07 p2729 N94-25579
Nanoscale plasticity in silica glass
[DE94-004212] 07 p2751 N94-26554
On experimental studies of yield surfaces of metals: A more general approach
[IFTR-42/1993] 07 p2739 N94-26824
Geometry changes in the elastic-plastic analysis of steel spatial skeletal structures
[IFTR-37/1993] 07 p2839 N94-26825
On the Lagrangian and updated Lagrangian nonlinear finite element formulations
[ISBN-0-315-61111-1] 07 p3001 N94-27948
Superplasticity in fine-grained ceramics
[AD-A275461] 08 p3212 N94-28733
Finite element analysis of axisymmetric deformations of thick thermoviscoplastic targets 08 p3320 N94-29688
The effect of various metallurgical parameters on the flow and fracture behavior of polycrystalline NiAl near the brittle-to-ductile transition
[NASA-TM-106534] 08 p3205 N94-29758
Higher order asymptotic crack tip fields in a power-law hardening material 08 p3321 N94-29829
Nanodislocation structures generated in shocked crystals 08 p3514 N94-29915
The role of plastic deformation in brittle and near-brittle cracking behavior 08 p3322 N94-30226
Inelastic deformation of metal matrix composites 09 p3618 N94-31285
Toughening mechanisms in the high strain rate deformation of rubber-modified polymer glasses 09 p3653 N94-31942
High-temperature deformation and fracture toughness of duplex ceramic microstructures 09 p3653 N94-31945
A state variable material model for superplastic titanium-6 percent Al-4 percent V 09 p3644 N94-32498

Literature review and preliminary studies of fretting and fretting fatigue including special applications to aircraft joints
[AD-A280310] 12 p4456 N94-37125
Defect initiation/growth and energy dissipation induced by deformation and fracture
[AD-A280411] 12 p4424 N94-37184

PLASTIC FILMS
U POLYMERIC FILMS

PLASTIC FLOW
NT TRESCA FLOW
A simple model of melt fracture
[AD-A265311] 01 p0092 N94-11862
An experimental study on the effect of die geometry on swell and sag in the parison extrusion stage
[IMI-93RT-42400-1476-G] 02 p0597 N94-14070
Interdisciplinary research on wear of materials
[AD-A268190] 04 p1443 N94-17730
Dislocation-drag contribution to high-rate plastic deformation in shock-loaded tantalum
[DE93-018286] 04 p1361 N94-18802
HEMP 3D: A finite difference program for calculating elastic-plastic flow, appendix B
[AD-A269171] 04 p1418 N94-18878

PLASTIC PROPERTIES
NT ELASTOPLASTICITY
NT SUPERPLASTICITY
NT THERMOPLASTICITY
NT VISCOPLASTICITY
NT YIELD POINT
Design evaluation of GLARE laminate lay-ups
01 p0063 N94-10051
A benchmark bending test of a thick specimen, Part 1: Experiments
[ARL-RR-6-PT-1] 02 p0670 N94-12927
A benchmark bending test of a thick specimen. Part 2: Surface displacement measurements
[ARL-RR-6-PT-2] 02 p0670 N94-12928
Modeling the impact behavior of AD85 ceramic under multi-axial loading
[AD-A265877] 02 p0576 N94-12932
Investigation of criteria for ductile fracture under fully-plastic conditions 02 p0672 N94-13593
Non-uniqueness in dynamic rate-independent non-associated plasticity
[AD-A266342] 02 p0769 N94-13731
Elastic-plastic finite element analyses of an unidirectional, 9 vol percent tungsten fiber reinforced copper matrix composite
[NASA-TM-106304] 02 p0559 N94-14719
Characterization of the cyclic plasticity of polycrystalline aluminum in the 90-300K domain: Use of the ultrasonic wave coupling technique - low frequency restraint
[ISAL-92-0083] 03 p0954 N94-14930
Anisotropic damage mechanics modeling in metal matrix composites
[AD-A266328] 03 p0934 N94-16440
Quantitative assessment of the accuracy of constitutive laws for plasticity with an emphasis on cyclic deformation
[AD-A267562] 03 p0961 N94-17109
Solution of elastic-plastic stress analysis problems by the p-version of the finite element method
[NASA-CR-194267] 03 p1062 N94-17445
Computational strategies for composite structures
[PB93-195097] 04 p1452 N94-18079
Several fundamental issues in the mechanics of inelastic behavior
[AD-A269455] 04 p1453 N94-18285
HEMP 3D: A finite difference program for calculating elastic-plastic flow, appendix B
[AD-A269171] 04 p1418 N94-18878
A constitutive theory for rigid polyurethane foam
[DE93-011596] 04 p1372 N94-19059
Plastic mechanism analysis of T-joints in RHS subject to combined bending and concentrated force
[PB93-195774] 04 p1456 N94-19061
Formulation and identification of the anisotropic laws for thin sheets drawing
[ECL-92-55] 04 p1365 N94-19400
CTH: A software family for multi-dimensional shock physics analysis
[DE93-019428] 05 p1904 N94-20052
Development of bioelastic material for aspects of wound repair
[AD-A272000] 05 p1892 N94-21503
Gas-pressure forming of superplastic ceramic sheet
[DE94-001520] 06 p2252 N94-22930
Texture gradient effects in tantalum
[DE94-000689] 06 p2240 N94-23021
Mean stress models for low cycle fatigue of a nickel-base superalloy 06 p2159 N94-24276
The nanometer-scale mechanics of gold films
[AD-A273307] 06 p2565 N94-25086
Deviatoric stresses and plastic strain rates in strong shock waves for six metals
[DE94-002964] 07 p2733 N94-26022
Grain by grain study of the mechanisms of crack propagation during iodine SCC of Zry-4
[DE93-633765] 07 p2734 N94-26162
A study on the development of high-T(c) superconducting wire
[DE93-632438] 07 p2783 N94-26546
Nanoscale plasticity in silica glass
[DE94-004212] 07 p2751 N94-26554
A constitutive model for layered wire mesh and aramid cloth fabric
[DE94-003275] 07 p2708 N94-26796
On experimental studies of yield surfaces of metals: A more general approach
[IFTR-42/1993] 07 p2739 N94-26824
Geometry changes in the elastic-plastic analysis of steel spatial skeletal structures
[IFTR-37/1993] 07 p2839 N94-26825
Deformation, constitutive behavior, and damage of advanced structural materials under multiaxial loading
[AD-A274165] 07 p2709 N94-27142
Toughening mechanisms in ultrahigh-strength steels
[AD-A275439] 08 p3202 N94-28867
Preliminary evaluation of hybrid titanium composite laminates
[NASA-TM-109095] 08 p3180 N94-29472
On the mechanics of microballoon-reinforced metal matrix composites
[AD-A277928] 09 p3630 N94-33178
Aspects of robust computational modeling for plain and reinforced concrete
[PB94-169240] 11 p4251 N94-35820
Transformation plasticity in ductile solids
[DE94-010420] 11 p4240 N94-35953
Ability of the total strain version of strainrange partitioning to characterize thermomechanical fatigue behavior
[NASA-TM-4556] 12 p4455 N94-37102

PLASTIC YIELDING
U PLASTIC DEFORMATION

PLASTICITY
U PLASTIC PROPERTIES

PLASTICIZERS
Development of novel switchable protein surfaces
[AD-A275510] 08 p3384 N94-28667
Enhanced ion dissociation of LiCF3SO3 by new carbonate plasticizers: Raman and IR studies
[DE94-005448] 08 p3485 N94-28741
High elongation elastomers 08 p3223 N94-30477
Electrostrictive response of elastomeric polymers
[AD-A277983] 09 p3664 N94-33247
Diffusion and sorption of 1,4-dioxane into polychloroprene
[AD-A277743] 10 p4026 N94-33446
Diffusion and sorption of 1,4-dioxane into polychloroprene
[ARL-TR-338] 11 p4229 N94-35361

PLASTICS
NT ACRYLIC RESINS
NT ADDITION RESINS
NT CARBON FIBER REINFORCED PLASTICS
NT CARBON-PHENOLIC COMPOSITES
NT EPOXY RESINS
NT GLASS FIBER REINFORCED PLASTICS
NT KEVLAR (TRADEMARK)
NT NYLON (TRADEMARK)
NT PEEK
NT PHENOLIC RESINS
NT POLYAMIDE RESINS
NT POLYBUTADIENE
NT POLYESTER RESINS
NT POLYETHER RESINS
NT POLYETHYLENE TEREPHTHALATE
NT POLYETHYLENES
NT POLYMETHYL METHACRYLATE
NT POLYPROPYLENE
NT POLYSTYRENE
NT POLYTETRAFLUOROETHYLENE
NT POLYVINYL ALCOHOL
NT POLYVINYL CHLORIDE
NT POLYVINYL FLUORIDE
NT REINFORCED PLASTICS
NT TEFLON (TRADEMARK)
NT THERMOPLASTIC FILMS
NT THERMOPLASTIC RESINS
NT THERMOSETTING RESINS
NT VINYL COPOLYMERS
Modelling of creep data for plastics
[NPL-DMM(A)-92] 03 p1057 N94-15017
Dry stripping as a surface treatment method
[VTT-TIED-1348] 03 p0985 N94-17544
Sputtered TiN coatings in plastic
04 p1367 N94-18011
Ageing in Processed Polymers: Programme, summary, and abstracts discussion meeting
[AD-A268931] 04 p1370 N94-18448
Simulation of the impact of a plastic flyer on an aluminum block using the hydrocode AUTODYNE
[PML-1992-26] 04 p1458 N94-19444
Mold bolt and means for achieving close tolerances between bolts and bolt holes
[NASA-CASE-MFS-28720-1] 05 p1823 N94-20379
Technique to predict the curing behaviour of unsaturated polyester materials
[PB94-124856] 07 p2748 N94-25892
Modelling the inhibition cure behaviour of unsaturated polyester moulding materials
[PB94-124864] 07 p2748 N94-25893
Stress relaxation in dough moulding compounds
[PB94-124872] 07 p2748 N94-25894
Resonant holographic measurements of laser ablation plume expansion in vacuum and argon gas backgrounds
[DE94-001407] 07 p2813 N94-27615
Compatibility of refrigerants and lubricants with engineering plastics
[DE94-004959] 07 p2756 N94-27692
Ballistic performance of polycarbonate/polyester and polycarbonate/styrene- acrylonitrile microlayer sheets
[AD-A275462] 08 p3177 N94-28735
Laminated thermoplastic composite material from recycled high density polyethylene
11 p4230 N94-36403
Opportunities for innovation: Biotechnology
[PB94-157831] 12 p4478 N94-36720
Structural composite construction materials manufactured from municipal solid waste
[AD-A280635] 12 p4403 N94-36730
Gas microstrip detectors on resistive plastic substrates
[DE94-011336] 12 p4426 N94-37714
Fluorinated resins with low dielectric constant
[AD-D016303] 12 p4427 N94-37773

PLASTISOLS
NT SMOKE

PLATE (METAL)
U METAL PLATES

PLATE THEORY
Boundary element method for eigenvalue problems of thin plates
[ITN-93-85199] 01 p0343 N94-10392
Nonlinear vibrations of thick composite plates: Higher-order shear deformation plate theory
02 p0556 N94-13558
Finite element analysis of composite plates by use of modified complementary energy principle
02 p0672 N94-13596
Improvements to a method for the geometrically nonlinear analysis of compressively loaded stiffened composite panels
[NASA-CR-194715] 05 p1832 N94-21814
Vectorization and parallelization of the finite strip method for dynamic Mindlin plate problems
06 p2483 N94-23679
Nonlinear analysis using a modal based reduction technique 06 p2161 N94-24288
Nonlinear equations of motion for a panel subject to external loads
[AD-A273142] 06 p2170 N94-24773
An efficient higher order theory for laminated composite plates and a finite element implementation
09 p3617 N94-31215
Scaling, elasticity, and CLPT
12 p4458 N94-37800

PLATEAUS
NT MESAS
A mineralized zone in Western Candor Chasma, Mars
03 p1248 N94-16179
Electron energy dependence of amorphization in Zr3Fe
[DE94-008459] 09 p3906 N94-32875
Fluvial processes in Ma'adim Vallis and the potential of Gusev crater as a high priority site
11 p4358 N94-35414
Short-tower sigma(theta) measurements in the Colorado Plateaus region
[DE94-007478] 12 p4463 N94-36478

PLATELETS
Evaluation of dried storage of platelets for transfusion: Physiologic integrity and hemostatic functionality
[AD-A266958] 03 p1120 N94-15180
Evaluation of dried storage of platelets for transfusion: Physiologic integrity and hemostatic functionality
[AD-A270756] 04 p1507 N94-19593
Evaluation of dried storage of platelets for transfusion: Physiologic integrity and hemostatic functionality
[AD-A280665] 12 p4480 N94-36764

PLATENS
Neural network based time-optimal control of a magnetically levitated precision positioning system
[DE94-006573] 08 p3437 N94-30250

PLATES
Experimental measurement of local heat transfer coefficients over discrete roughened plates using infrared thermography 02 p0635 N94-13652
Response of a cantilevered plate in supersonic flow
[AD-A277487] 09 p3580 N94-33107

PLATES (STRUCTURAL MEMBERS)
NT ANISOTROPIC PLATES
NT ANNULAR PLATES
NT CIRCULAR PLATES
NT CORRUGATED PLATES
NT ELASTIC PLATES
NT METAL PLATES
NT ORTHOTROPIC PLATES
NT PERFORATED PLATES
NT POROUS PLATES
NT RECTANGULAR PLATES
NT REINFORCED PLATES
Development tests for a high stability optical bench 01 p0062 N94-10047
Finite element analysis of composite plates by use of modified complementary energy principle 02 p0672 N94-13596
Probabilistic micromechanics for high-temperature composites
[NASA-CR-191150] 02 p0676 N94-14408
A posteriori error estimation for hierarchic models of elliptic boundary value problems on thin domains
[AD-A267714] 03 p1168 N94-14939
Stress analysis of laminated composites with preformed holes. Part 1: Single plies with embedded material discontinuities
[AD-A266524] 03 p0936 N94-16795
Development of a finite element method program for the analysis of laminated composite plates using first-order shear deformation theory
[AD-A270318] 04 p1342 N94-18700
Three point lead screw positioning apparatus for a cavity tuning plate
[NASA-CASE-LEW-15216-1] 05 p1822 N94-20375
Hydro-elastic analysis using a selection of commercial analysis programs
[PB94-118734] 06 p2376 N94-24478
Responses of a finite baffled plate subject to turbulent and mean flow excitations
[NASA-CR-191570] 06 p2334 N94-24605
The free vibration of plates, shallow shells and solids
[ISBN-0-315-83931-7] 07 p2838 N94-26622
Response of structures to impact loads using elastic and plastic analysis
[ISBN-0-315-84647-X] 07 p2842 N94-27309
The experimental behavior of spinning pretwisted laminated composite plates
[NASA-CR-195220] 07 p2711 N94-27352
Finite element analysis of damped vibrations of laminated composite plates
[ISBN-0-315-84928-2] 07 p2843 N94-27585
On the Lagrangian and updated Lagrangian nonlinear finite element formulations
[ISBN-0-315-61111-1] 07 p3001 N94-27948
An efficient higher order theory for laminated composite plates and a finite element implementation 09 p3617 N94-31215
Random vibrations of composite beams and plates 09 p3735 N94-31777
QUAD4 seminar
[AD-A277366] 09 p3818 N94-32330
Effective computational strategy for predicting the response of complex systems
[AD-A277452] 09 p3740 N94-33011
Shape control of composite plates and shells using embedded actuators 10 p4018 N94-33532
Design oriented structural analysis
[NASA-TM-109124] 10 p4073 N94-34722
Angle interferometer cross axis errors
[DE94-006190] 12 p4446 N94-37388

PLATES (TECTONICS)
A model for the subduction mechanics of flexible lithosphere and its viscous coupling to the mantle using power-law rheologies 01 p0277 N94-11585
Horizontal stresses induced by vertical processes in planetary lithospheres 01 p0281 N94-12042
Buoyant subduction on Venus: Implications for subduction around coronae 01 p0455 N94-12130
Morphotectonics of Venus 01 p0478 N94-12248
Regional tectonic analysis of Venus as part of the Pioneer Venus guest investigator project
[NASA-CR-194079] 02 p0842 N94-13561
Tectonic deformation in southern California
[NASA-CR-194621] 03 p1101 N94-16021
Chemical differentiation, thermal evolution, and catastrophic overturn on Venus: Predictions and geologic observations 03 p1259 N94-16232
On the relationship between tectonic plates and thermal mantle plume morphology 03 p1104 N94-16349
Current (1985-1988) seismic activity in Belgium: Comparison with historical and instrumental seismic data 04 p1482 N94-18624
What can gravimetry contribute to recent and current tectonics in Belgium? 04 p1482 N94-18626
Seafloor characterization/Galapagos propagating rift
[AD-A272001] 05 p1882 N94-20581
Response of the topography and gravity field on Venus to mantle upwelling beneath a chemical boundary layer 05 p2117 N94-20775
Post-Palbozoic crustal responses to the contemporary stress field in the eastern United States
[DE93-040604] 05 p1859 N94-22006
The tectonic and volcanic evolution of Venus: Catastrophic or gradual? 09 p3940 N94-31111
Mantle melting and crustal recycling in subduction zones 10 p4084 N94-33368

PLATING
NT ELECTROPLATING
NT ION PLATING
NT NICKEL PLATE
Plating under reduced pressure
[DE93-011896] 01 p0084 N94-11668
Process to fabricate thick coplanar microwave electrode structures
[AD-D015913] 05 p1748 N94-19892
Investigate zero-stress replicated optics
[NASA-CR-193889] 06 p2545 N94-24665
An improved plating process 08 p3223 N94-30451
The electrical conductivities of candidate beam-waveguide antenna shroud materials 11 p4252 N94-35546

PLATINUM
Site dependence of the apparent shape of a molecule in STM images: Benzene on Pt(111)
[AD-A263488] 01 p0365 N94-11093
A model of elementary chemistry and fluid mechanics in the combustion of hydrogen on platinum surfaces
[DE93-012767] 01 p0077 N94-11370
Low energy electron diffraction and cyclic voltammetry studies of flame-annealed platinum single crystals
[AD-A263566] 01 p0401 N94-11518
Shock induced reaction in Chicxulub target materials (CaSO4 and SiO2) and their relation to extinctions 01 p0282 N94-12149
The effects of organic adsorbates on the underpotential deposition of silver on Pt(111) electrodes
[AD-A265623] 01 p0404 N94-12376
Electrocatalysis issues in polymer electrolyte fuel cells
[DE93-014450] 02 p0702 N94-13402
Stability of reference masses 1: Evidence for posiible variations in the mass of reference kilograms arising from mercury contamination
[NPL-DMM(A)-86] 02 p0708 N94-13667
Photochemical dynamics of surface oriented molecules
[DE93-016289] 02 p0784 N94-13983
Experimental partitioning of Zr, Ti, and Nb between silicate liquid and a complex noble metal alloy and the partitioning of Ti between perovskite and platinum metal 03 p0962 N94-16287
Potential dependent structural changes of underpotentially deposited copper on an iodine treated platinum surface determined in situ by surface EXAFS and its polarization dependence
[AD-A269890] 04 p1360 N94-18687
Oxidation-reduction induced roughening of platinum (111) surface
[DE93-017408] 05 p1687 N94-19922
Guanidine based vehicle/binders for use with oxides, metals, and ceramics
[NASA-CASE-LEW-15314-1] 05 p1700 N94-20195
Observation of x ray absorption magnetic circular dichroism in well-characterized iron-cobalt-platinum multilayers
[DE94-000303] 05 p1694 N94-21944
Photoelectron holography of platinum (111)
[DE93-040856] 05 p1810 N94-21950
High power density proton exchange membrane fuel cells 06 p2393 N94-23359
Fundamental and experimental studies on the catalytic combustion of methane
[PB94-112661] 06 p2233 N94-23736
Thermal phase behavior of metal surfaces: X-ray scattering studies of Pt(001)
[DE94-002991] 06 p2245 N94-24612
The structure and catalytic properties of supported platinum catalysts
[ETN-94-95357] 06 p2236 N94-25250
A mimic model of Pt-Rh catalyst prepared by electrochemical deposition of Rh on Pt (100) surface
[REPT-A-2664] 07 p2715 N94-26476
Geometric structures of thin film: Pt on Pd(110) and NiO on Ni(100)
[DE94-005564] 08 p3211 N94-28530
Realtime structural electrochemistry of platinum clusters using dispersive XAFS
[DE94-005093] 08 p3208 N94-30101
Infrared spectroelectrochemical study of cyanide adsorption and reactions at platinum electrodes in aqueous perchlorate electrolyte
[AD-A276402] 09 p3631 N94-31238
Lowering the Schottky barrier at metal or silicide/Si interfaces to extend the range of infrared detectors
[AD-A277253] 09 p3903 N94-32322
Induced adsorption of chloride and bromide by submonolayer amounts of copper underpotentially deposited on Pt(111)
[AD-A278023] 09 p3648 N94-33182
Scanning tunneling microscopy and infrared spectroscopy as combined in-situ probes of electrochemical adlayer structure: Cyanide on Pt(111)
[AD-A276715] 09 p3909 N94-33274
The underpotential deposition of copper on Pt(311): Site selective deposition and anion effects
[AD-A278022] 10 p4023 N94-33436
Oxidation performance of platinum-clad Mo-47Re alloy
[NASA-TM-4559] 10 p4025 N94-34398
High temperature sorbents for oxygen
[NASA-CASE-NPO-18409-1-CU] 11 p4235 N94-35255
A novel method for depositing precious metal films on difficult surfaces
[NASA-TM-106607] 11 p4243 N94-35260
Multicomponent glass surfaces: Structure and adsorption
[DE94-010516] 11 p4246 N94-36283
The hydrogenolysis and isomerization of light hydrocarbons over Pt catalysts
[DE94-013142] 12 p4410 N94-37296

PLATINUM ALLOYS
Surface science and modeling studies of endothermic fuels catalysis
[AD-A272850] 05 p1712 N94-21192
Magnetic instability of Kondo insulators
[DE93-040064] 05 p1768 N94-21762
Reduction of nitric oxide over platinum, rhodium and platinum-rhodium single crystal surfaces
[PB93-230092] 06 p2232 N94-23482
The origins of ordering in CuPt
[DE94-003864] 07 p2736 N94-26351
A mimic model of Pt-Rh catalyst prepared by electrochemical deposition of Rh on Pt (100) surface
[REPT-A-2664] 07 p2715 N94-26476
The electrocatalytic oxidation of ethylene and methane, and reduction of oxygen on gas-diffusion electrodes made of amorphous nickel-valve metal-platinum group metal alloys 07 p2722 N94-28165
Fermi surface instability at 0.4 K in a heavy-fermion YbBiPt: SDW?
[DE94-006224] 09 p3899 N94-31916
Methanol electrooxidation on well-characterized Pt-Ru alloys
[DE94-009640] 10 p4022 N94-33918

PLATINUM COMPOUNDS
NT PLATINUM OXIDES
Synthesis of novel composite Platinum-DNA films by way of wet-spinning
[AD-A278763] 11 p4243 N94-35494

PLATINUM OXIDES
PEM regenerative fuel cells 06 p2392 N94-23358

PLAYAS
Mapping a dynamic playa surface using multitemporal ERS-1 SAR data: First results 01 p0246 N94-12474
Briny lakes on early Mars? Terrestrial intracrater playas and Martian candidates 05 p2145 N94-21675

PLAYBACKS
Noise reduction techniques for the restoration of musical recordings
[TELECOM-93-E-019] 08 p3291 N94-30979
An experimental compact Hi-Vision VCR using metal evaporated tape
[NHK-LABS-NOTE-423] 09 p3683 N94-33081

PLETHYSMOGRAPHY
Validation of respiratory inductive plethysmography for measuring exercise tidal volumes
[AD-A266883] 03 p1119 N94-14923
Automated strain gauge plethysmograph
[AD-A267323] 03 p1035 N94-17002

PLEXIGLASS (TRADEMARK)
U POLYMETHYL METHACRYLATE

PLOTTERS
FORTRAN graphics routines for the Macintosh
[DE93-013092] 02 p0742 N94-12864

Post-experimental plots for high speed data acquisition program
[DE94-000956] 05 p1918 N94-22011
IRMA: A program for three-dimensional color display of data
[AD-A273811] 07 p2959 N94-25879

PLOTTING
FORTRAN graphics routines for the Macintosh
[DE93-013092] 02 p0742 N94-12864
Computer codes for checking, plotting and processing of neutron cross-section covariance data and their application
[DE93-018459] 04 p1570 N94-19129
The IDL astronomy user's library
05 p2048 N94-22500
VTGRAPH:Computer graphics program using ReGIS mode
[DE94-600342] 06 p2448 N94-23024
IRMA: A program for three-dimensional color display of data
[AD-A273811] 07 p2959 N94-25879
Description of a package for the analysis and display of the results of numerical simulations
[AD-A276285] 09 p3841 N94-31252

PLOTTING INSTRUMENTS
U PLOTTERS

PLOWED FIELDS
U FARMLANDS

PLSS
U PORTABLE LIFE SUPPORT SYSTEMS

PLUG NOZZLES
Hot-gas-side heat transfer characteristics of subscale, plug-nozzle rocket calorimeter chamber
[NASA-TP-3380] 01 p0055 N94-12569

PLUGS
Disengagable adapter for an optical fiber connector
[AD-D015959] 05 p1822 N94-20356

PLUMBANE
U LEAD COMPOUNDS
U METAL HYDRIDES

PLUMES
NT ROCKET EXHAUST
User's manual for the plume visibility model PLUVUE 2 (revised)
[PB93-188233] 01 p0265 N94-11016
Ultraviolet plume instrument description and plume data reduction methodology
[AD-A266141] 01 p0054 N94-11643
Tectonics on Triton 01 p0466 N94-12187
The 1991 version of the plume impingement computer program. Volume 2: User's input guide
[NASA-CR-194191] 01 p0166 N94-12774
The 1991 version of the plume impingement computer program. Volume 1: Description
[NASA-CR-194192] 01 p0166 N94-12775
UV and IR laser ablation for inductively coupled plasma mass spectrometry
[DE93-017124] 02 p0658 N94-14415
The MADONA experiments (Meteorology and Diffusion Over Non-uniform Areas): High-resolution in-plume concentration fluctuations measurements using lidar remote sensing technique
[AD-A267711] 03 p1105 N94-14938
Rocket Motor Plume Technology
[AGARD-LS-188] 03 p0923 N94-15217
Propulsion 03 p0924 N94-15219
Nuclear rocket plume studies
[AD-A267154] 03 p0925 N94-15837
Megaplumes on Venus 03 p1271 N94-16301
On the relationship between tectonic plates and thermal mantle plume morphology 03 p1104 N94-16349
Venusian pancake domes: Insights from terrestrial voluminous silicic lavas and thermal modeling
03 p1286 N94-16381
The use of TIMS data to estimate the SO2 concentrations of volcanic plumes: A case study at Mount Etna, Sicily 03 p1065 N94-16608
High power steady state MPD thrusters
[AD-A267277] 03 p0928 N94-17308
Low power arcjet system spacecraft impacts
[NASA-TM-106307] 04 p1336 N94-17856
A Bayesian approach to contaminant plume delineation
[DE93-012909] 04 p1472 N94-17890
UVPI imaging from the LACE satellite: The Nihka rocket plume
[AD-A268456] 04 p1334 N94-18149
Characterization of vapor plume species and deposition residues resulting from pulsed laser ablation of a graphite/epoxy composite
[AD-A270101] 04 p1343 N94-18869
Forward scattering of a pulsed continuous wave signal through laminar and turbulent thermal plumes
[AD-A271210] 04 p1564 N94-19723
UVPI imaging from the LACE satellite: The Strypi rocket plume
[AD-A270967] 04 p1335 N94-19787
Experimental investigation of nozzle/plume aerodynamics at hypersonic speeds
[NASA-CR-194628] 05 p1636 N94-20014
UVPI imaging from the LACE satellite: The Starbird rocket plume
[AD-A271981] 05 p1658 N94-20617
Are Plinian type eruptions possible on Venus?
05 p2123 N94-20803
Iterative electromagnetic Born inversion applied to earth conductivity imaging
[DE93-040668] 05 p1859 N94-21928
Molecular gas dynamics applied to low-thrust propulsion 06 p2214 N94-23053
Contamination control and plume assessment of low-energy thrusters
[NASA-TM-104585] 06 p2218 N94-23343
Diagnostic budgets of analyzed and modelled tropical plumes
[NASA-CR-194853] 06 p2409 N94-23621
Stationary plasma thruster plume characteristics
[NASA-CR-194454] 06 p2219 N94-24361
Optimal Space Station solar array gimbal angle determination via radial basis function neural networks
[NASA-TM-106482] 06 p2195 N94-24482
Analysis and effects of the advanced solid rocket motor on the Space Shuttle elements
[NASA-CR-193879] 06 p2200 N94-24664
An investigation of magnetic field effects on plume density and temperature profiles of an applied-field MPD thruster
[NASA-TM-106416] 07 p2700 N94-26090
A large high vacuum, high pumping speed space simulation chamber for electric propulsion
[NASA-TM-106453] 07 p2690 N94-26142
Enhanced tracking of airborne targets using forward looking infrared and laser return measurements
[AD-A274181] 07 p3037 N94-27102
Uncertainties in the characterization of the thermal environment of a solid rocket propellant fire
[DE94-002023] 07 p2760 N94-27719
First experimental assessment of RCS plume-flow field interaction on Hermes leading edge thruster configuration 07 p2703 N94-28032
SOCRATES simulation of the emission at wavelength 6300 A generated by the interaction between the atmosphere and the Space Shuttle exhaust
[AD-A275567] 08 p3164 N94-28827
A laboratory simulation of urban heat-island-induced circulation in a stratified environment
08 p3367 N94-30921
NASA/LaRC jet plume research
10 p3972 N94-33468
Instrumentation for in-flight SSME rocket engine plume spectroscopy
[NASA-TM-106596] 11 p4268 N94-35268
Radiative signals from impact of Shoemaker-Levy on Jupiter 11 p4355 N94-35396
UVPI imaging from the LACE satellite: The Low Cost Launch Vehicle (LCLV) rocket plume
[AD-A278785] 12 p4398 N94-36445
Experimental investigation of nozzle/plume aerodynamics at hypersonic speeds
[NASA-CR-195829] 12 p4382 N94-36687
NASA reload program
[NASA-CR-193972] 12 p4429 N94-37446
Program GAUSSPLYM: A tool in Windows environment for studying continuous releases
[PB94-184603] 12 p4468 N94-37856

PLUNGERS
Check valve with poppet dashpot/frictional damping mechanism
[NASA-CASE-MSC-21950-1] 01 p0179 N94-10658

PLUTO (PLANET)
A Pluto thermal model 03 p1256 N94-16216
Mapping the stability region of the 3:2 Neptune-Pluto resonance 03 p1280 N94-16351
The Pluto fast flyby mission: Completing the reconnaissance of the solar system
08 p3235 N94-29768
The temperature of nitrogen on Pluto
11 p4365 N94-35468

PLUTO ATMOSPHERE
A Pluto thermal model 03 p1256 N94-16216

PLUTONIUM
NT PLUTONIUM 238
Reduction of Pu(6) with hydrogen peroxide: Effects of plutonium, peroxide, and iron concentrations and of reaction time
[DE93-013598] 02 p0564 N94-13487
A model for fuel fire duration and application to the B-1B bomber
[DE93-013000] 02 p0512 N94-14292
Crystallographic phase transitions in actinide metals as a function of pressure
[DE93-040138] 05 p2011 N94-19827
A weighted least-squares lump correction algorithm for transmission-corrected gamma ray nondestructive assay
[DE93-018474] 05 p1904 N94-20049
A survey of metallurgical research on several actinides
[DE94-002643] 06 p2245 N94-24747
Effect of nitrocarburizing on shape of titanium alloy parts
[DE94-004040] 07 p2732 N94-25822
Nature of dissolution of binary tantalum-titanium alloys by molten plutonium
[DE94-005090] 08 p3210 N94-30776

PLUTONIUM COMPOUNDS
NT PLUTONIUM FLUORIDES

PLUTONIUM FLUORIDES
Calculation of the LiF-CeF3-BeF2 and LiF-PuF3-BeF2 ternary phase diagrams
[DE93-017437] 04 p1360 N94-18501

PLUTONIUM ISOTOPES
NT PLUTONIUM 238

PLUTONIUM 238
Calorimeter measurements of low wattage items
[DE93-018473] 05 p1807 N94-20115

PLUVIOGRAPHS
U RAIN GAGES

PLY ORIENTATION
Buckling analysis of laminated thin shells in a hot environment
[NASA-TM-106302] 02 p0683 N94-14776
Optimization of laminate orientation to enhance failure properties
[ISBN-0-315-83539-7] 06 p2227 N94-22892
Analysis of local delaminations caused by angle ply matrix cracks
[NASA-TM-109052] 06 p2228 N94-24083
Microstructure/property relationships for SCS6/Timetal 21-S composite
[AD-A275056] 08 p3178 N94-29135
Free edge and size effects on failure initiation and ultimate strength of laminates containing a center hole
08 p3181 N94-29735

PNEUMATIC CONTROL
Pneumatic management of blunted-forebody flow asymmetry for high-angle-of-attack directional control
07 p2679 N94-28028
The reduction of takeoff ground roll by the application of a nose gear jump strut
[NASA-TM-108822] 11 p4198 N94-36380

PNEUMATIC EQUIPMENT
NT GAS VALVES
NT PNEUMATIC PROBES
Friction drive position transducer
[AD-D015851] 04 p1424 N94-17717
A finite strain ring dynamical model for pneumatic tires
[AD-A269286] 04 p1444 N94-18266
Study and modeling of compressible flows of flapper nozzle type potentiometric systems
[ETN-93-95012] 04 p1421 N94-19495
Tipjet 80-inch model rotor hover test: Test no. 1198
[AD-A279680] 11 p4191 N94-36261

PNEUMATIC PROBES
The 3D pneumatic and 2D dynamic probes: Their development and subsequent use in a transonic fan
[RAE-TM-AERO/PROP-22] 02 p0653 N94-14827
Laser Doppler velocimetry in a low speed multistage compressor
[AD-A274836] 07 p2818 N94-26498

PNEUMATIC RESET
U PNEUMATIC CONTROL

PNEUMATICS
Lift enhancement of a wing/strake using pneumatic blowing
[AD-A265074] 01 p0026 N94-11872
Laser Doppler velocimetry in a low speed multistage compressor
[AD-A274836] 07 p2818 N94-26498
Pneumatic management of blunted-forebody flow asymmetry for high-angle-of-attack directional control
07 p2679 N94-28028
Controlling hazardous energy sources (lockout/tagout)
[NASA-TM-105290] 09 p3669 N94-32861

PNEUMOTHORAX
Spontaneous pneumothorax, cysts and bullae
06 p2425 N94-23326

POCKELS EFFECT
U BIREFRINGENCE

PODS (EXTERNAL STORES)
Spare parts analysis of the MK.32B-751 AAR pod
[DSIS-93-00737] 02 p0774 N94-13549
Techniques for the evaluation of outgassing from polymeric wafer pods
[DE94-008427] 10 p4028 N94-33926
Aerial refueling interoperability from a receiver flying qualities perspective 11 p4197 N94-36343

POINCARE PROBLEM
Chaos, entropy, and reversibility: A simple example
01 p0031 N94-11495
POINT DEFECTS
NT FRENKEL DEFECTS
NT VACANCIES (CRYSTAL DEFECTS)
Electronic characterization of defects in narrow gap semiconductors
[NASA-CR-193568] 01 p0397 N94-10819
The influence of irradiation conditions, type, and concentration of impurities on radiation defects characteristics in indium antimonide under electron irradiation
[DE93-617201] 01 p0397 N94-10843
A method of influence regions in the theory of vacancy swelling of metals
[DE93-620579] 01 p0083 N94-11363
Bulk and defect properties of ordered intermetallics: A first-principles total-energy investigation
[DE93-015492] 03 p0959 N94-16873
Lattice damage in ion-implanted compound semiconductors and its effect on electrical activation
[DE93-015907] 04 p1593 N94-17845
The effect of correlated and point defects on the vortex lattice melting transition in single crystal YBa2Cu3O(7-delta)
[DE93-040277] 05 p2033 N94-21997
Modeling defect production in high energy collision cascades
[DE94-003810] 07 p3017 N94-26049
Influence of point defects on grain boundary diffusion in oxides
[DE94-003164] 07 p3060 N94-26782
Indium-vacancy complexes in mercury cadmium telluride
[AD-A276177] 09 p3894 N94-31055
Defect-solute interactions near irradiation grain boundaries
[DE94-006215] 09 p3641 N94-31627
IR materials producibility
[AD-A277028] 09 p3879 N94-32006
The 10th International Conference on Internal Friction and Ultrasonic Attenuation in Solids (ICIFUAS)
[AD-A276849] 09 p3902 N94-32209
Intra-cascade surface recombination of point defects during ion bombardment of Ge(001)
[DE94-007740] 09 p3903 N94-32384
Structure, stability, and mechanical properties of intermetallic phases
[DE94-009178] 09 p3647 N94-32852
Defect structure of semiconducting and insulating epitaxial oxides
[DE94-009650] 10 p4146 N94-33845
Characterization of defects in Si and SiO2-Si using positrons
[DE94-009044] 10 p4147 N94-33877
Study of point defect mobilities in zirconium during electron irradiation in a HVEM
[DE94-619028] 11 p4242 N94-36289
POINT IMPACT
Detection of dust impacts by the Voyager planetary radio astronomy experiment
[NASA-CR-193281] 01 p0423 N94-11305
Point-contact and point-impact dynamics for multibody chains
[ISBN-0-315-87056-7] 09 p3734 N94-31737
POINT MATCHING METHOD (MATHEMATICS)
U BOUNDARY VALUE PROBLEMS
POINT SOURCES
The searchlight problem for neutrons in a semi-infinite medium
[DE93-010796] 01 p0365 N94-10952
About excitation of round waveguide by a point current source
[DE93-621352] 01 p0133 N94-11034
Search for UHE point-source emission over various time scales
[DE93-012718] 02 p0846 N94-12922
Search for continuous and single day emission from ultra-high-energy sources
[DE93-012724] 02 p0846 N94-12947
Localization from near-source quasi-static electromagnetic fields
[DE93-040390] 05 p1732 N94-20479
SkiCAT: A cataloging and analysis tool for wide field imaging surveys 05 p2049 N94-22546
Static image method for computing the electric potential due to sources in a layered sphere
[PB93-224970] 06 p2308 N94-23105
Electromagnetic scattering by inhomogeneous objects. Solution methods based upon reciprocity theorems of time-convolution and time-correlation type
[PB94-111010] 06 p2294 N94-23729
Characterization and calibration of the Agema 880+ imaging radiometer
[AD-A274417] 07 p3036 N94-26981
Hydroacoustic wave-fields generated by different source types, a computational study
[PB94-123536] 07 p3010 N94-27037
Thermal conductivity of liquid carboxylic acids
[ESDU-93017] 07 p2721 N94-28138
Image theory for DC problems involving a conducting half space bounded by the general anisotropic impedance surface
[PB94-132917] 07 p2779 N94-28390
A study of the convergence of spherical harmonic expansions of gravity using distributed point-mass Earth models 08 p3362 N94-29909
POINT SPREAD FUNCTIONS
Measurements of microlens performance
03 p1197 N94-17355
Telescope image modelling software in STSDAS
05 p1926 N94-22483
Deconvolution of Hubble Space Telescope images using simulated point spread functions
05 p2048 N94-22497
SPECFOCUS: An IRAF task for focusing spectrographs 05 p1965 N94-22540
Aberrated point-spread functions and beam quality for optical systems with annular pupils
[AD-A275311] 08 p3499 N94-28875
Calculation of turbulence degraded point spread function of an imaging system 08 p3260 N94-30514
POINT TO POINT COMMUNICATION
NT NASCOM NETWORK
MITS architecture V1.0
[PB93-201762] 06 p2452 N94-23451
The design of a standard message passing interface for distributed memory concurrent computers
[DE94-002536] 06 p2446 N94-24538
Laser-based communication link
[FFI-93/7023] 07 p2817 N94-26203
POINTERS
U DIALS
POINTING CONTROL SYSTEMS
NT ANNULAR SUSPENSION AND POINTING SYSTEM
Simulator study of uncoupled control functions. Use of manual pointing modes when aiming at ground targets and oncoming airborne target
[FFA-TN-1992-18] 02 p0528 N94-13588
Telescope pointing for GOPEX
02 p0610 N94-14389
Wavefront sensing, control, and pointing
02 p0546 N94-14833
Performance of the upgraded Orroral laser ranging system 03 p0877 N94-15602
The star identification, pointing and tracking system of UVSTAR, an attached payload instrument system for the Shuttle Hitchhiker-M platform 04 p1326 N94-19179
Pointing control design for autonomous space vehicle applications
[DE93-019943] 05 p1657 N94-19863
Ultra-clean high-precision mechanisms for the SUMER EUV spectrometer on SOHO 06 p2356 N94-23999
Data relay system satellite: The development of an antenna pointing mechanism for the inter-orbit link antenna 06 p2359 N94-24015
Inter orbit link antenna pointing mechanisms design using standard actuators 06 p2359 N94-24016
Design of a new high-performance pointing controller for the Hubble Space Telescope
[NASA-CR-193891] 06 p2364 N94-24088
Optimal Space Station solar array gimbal angle determination via radial basis function neural networks
[NASA-TM-106482] 06 p2195 N94-24482
Lasercom system architecture with reduced complexity
[NASA-CASE-NPO-19069-1-CU] 08 p3293 N94-29493
The 27th Aerospace Mechanisms Symposium
[NASA-CP-3205] 08 p3160 N94-29627
Design and control of active vision based mechanisms for intelligent robots
[AIAA PAPER 94-1196-CP] 08 p3442 N94-30547
Pointing and tracking space mechanism for laser communication 09 p3606 N94-33310
Rotating unbalanced mass proof-of-concept
[NASA-TM-109814] 10 p4141 N94-33720
Design and implementation of a beam-waveguide mirror control system for vernier pointing of the DSS-13 antenna 11 p4253 N94-35548
Overview of the Miniature Sensor Technology Integration (MSTI) spacecraft attitude control system
11 p4206 N94-35627
Input shaping for three-dimensional slew maneuvers of a precision pointing flexible spacecraft
[DE94-008937] 11 p4226 N94-36001
Estimation with multisensor/multiscan detection fusion
[AD-A278753] 11 p4256 N94-36092
Pointing and Tracking Systems
[AGARD-CP-539] 12 p4392 N94-36616
Pointing and tracking concept for a high energy laser weapon application 12 p4393 N94-36619
Inertial pseudo star reference unit
12 p4394 N94-36625
Aeroservoelastic stabilization considerations for pointing and tracking systems 12 p4394 N94-36627
Neural network for positioning Space Station solar arrays
[NASA-TM-106656] 12 p4431 N94-36943
Large angle magnetic suspension test fixture
[NASA-CR-196138] 12 p4390 N94-37450
POINTS (MATHEMATICS)
NT FIXED POINTS (MATHEMATICS)
Interior-point methodology for linear programming: Duality, sensitivity analysis and computational aspects
[PB94-149663] 04 p1525 N94-19143
Kaplan-Meier estimators of interpoint distance distributions for spatial point processes
[CWI-BS-R9315] 09 p3846 N94-32107
POISEUILLE FLOW
U LAMINAR FLOW
POISONING (TOXICOLOGY)
U TOXIC DISEASES
POISONS
NT PESTICIDES
NT PHOSGENE
NT URETHANES
Air transport of samples containing chemical warfare agents
[FFI-93/6005] 05 p1851 N94-21455
POISSON DENSITY FUNCTIONS
Poisson filtering of laser ranging data
03 p0917 N94-15593
JSEP fellowship: Fractal noise processes
[AD-A268841] 04 p1557 N94-18540
On estimation and testing in Poisson regression models with over-dispersion
[MEMO-1083] 05 p1963 N94-21076
Trends in software reliability modeling
05 p1788 N94-22214
Loss probabilities in batch-arrival bulk-service queues with finite capacity
[MEMO-1106] 06 p2493 N94-22724
Probabilistic methods in problems of applied analysis
[PB94-110681] 06 p2495 N94-24571
Photon counting spectroscopy as done with a Thomson scattering diagnostic
[DE94-005543] 08 p3503 N94-28515
Modelling of multiparticle production by dynamical semigroup method
[DE94-608132] 08 p3490 N94-30120
An intrinsic Hamiltonian formulation of the dynamics of LC-circuits
[MEMO-1154] 08 p3462 N94-30964
The Laplace functional and Palm measure of a quasi-Cox process which is driven by a Markov chain
[REPT-93-82] 09 p3851 N94-31699
Light-traffic analysis for queues with spatially distributed arrivals
[MEMO-1150] 09 p3832 N94-31826
Kaplan-Meier estimators of interpoint distance distributions for spatial point processes
[CWI-BS-R9315] 09 p3846 N94-32107
A new association-model for binary VLE of alcohol/hydrocarbon and amine/hydrocarbon mixtures
[DE94-011012] 11 p4248 N94-36034
POISSON EQUATION
Looking for O(N) Navier-Stokes solutions on non-structured meshes
[NASA-CR-191472] 01 p0345 N94-11277
Numerical simulation and analysis of electrical and optical properties of Al(x)Ga(1-x)As / GaAs
[ETN-93-94387] 02 p0703 N94-13997
Implicit multi-fluid simulation of interpenetrating plasmas
[DE93-013351] 02 p0801 N94-14342
Linear stability of stationary solutions of the Vlasov-Poisson system in three dimensions
[DE93-013873] 03 p1174 N94-16820
Calculation of turbulent boundary layer wall pressure spectra
[AD-A269549] 04 p1416 N94-18642
Solution of the Poisson equation with application to radar imaging
[PB93-195865] 04 p1389 N94-18950
F2D users manual: A two-dimensional compressible gas flow code
[DE94-000653] 05 p1805 N94-22386
A mixed method Poisson solver for three-dimensional self-gravitating astrophysical fluid dynamical systems
06 p2484 N94-23684
Comparison of time integration methods for the evolution of galaxies
[PB94-111671] 06 p2602 N94-24522

Triangular spectral elements for incompressible fluid flow
[AD-A276838] 06 p2490 N94-24914
On Poisson brackets and symplectic structures for the classical and quantum Zitterbewegung
[DE93-634305] 07 p2992 N94-26267
Grid-independent convergence based on preconditioning techniques
[PB94-125358] 07 p2997 N94-27000
Recent advances in the spectral element method 07 p2657 N94-28348
The upsilon-q method and the psi-q method for incompressible flows 08 p3126 N94-28971
A note on the Poisson brackets associated with Lax operators
[MATHS-REPT-A-195] 08 p3464 N94-29482
An efficient three-dimensional Poisson solver for SIMD high-performance-computing architectures 09 p3823 N94-31120
Eta percent-superconvergence in the interior of locally refined meshes of quadrilaterals: Superconvergence of the gradient in finite element solutions of Laplace's and Poisson's equations
[AD-A277242] 09 p3848 N94-32331
Study of superconvergence by a computer-based approach: Superconvergence of the gradient in finite element solutions of Laplace's and Poisson's equations
[AD-A277537] 10 p4129 N94-34158

POISSON PROCESS
U POISSON DENSITY FUNCTIONS
U STOCHASTIC PROCESSES

POISSON RATIO
Quantitative mapping of pore fraction variations in silicon nitride using an ultrasonic contact scan technique
[NASA-TP-3377] 02 p0665 N94-13056
Theory of the electronic and structural properties of solid state oxides
[DE93-016051] 02 p0811 N94-14296
Molecular dynamics modeling of the mechanical behavior of metallic multilayers
[DE93-019947] 05 p1694 N94-21921
Humidity effects on soluble core mechanical and thermal properties (polyvinyl alcohol/microballoon composite) type CG extendospheres, volume 2
[NASA-CR-193893] 06 p2229 N94-24224
An ultrasonic testing technique for monitoring the cure and mechanical properties of polymeric materials
[AD-A274536] 07 p2753 N94-26842
Experimental determination of orthotropic elastic constants
[FFA-TN-1991-35] 08 p3215 N94-29424
Ceramic Technology Project database
[DE94-008494] 09 p3659 N94-32632
Indentability of conventional and negative Poisson's ratio foams 09 p3629 N94-33131
Shoemaker-Levy 9 and the tidal disruption of comets 11 p4351 N94-35406

POLAR AURORAS
U AURORAS

POLAR CAP ABSORPTION
Performance statistics bulletin. High latitude metor scatter propagation, February, March, April, May 1992
[AD-A276667] 09 p3677 N94-32083
Performance statistics bulletin. High latitude meteor scatter propagation February, March, April, May 1991
[AD-A276723] 09 p3678 N94-32158
Performance statistics bulletin. High latitude meteor scatter propagation October, November, December 1991, January 1992
[AD-A276724] 09 p3678 N94-32159
Performance statistics bulletin. High latitude meteor scatter propagation, November and December 1989, and January 1990
[AD-A276688] 09 p3680 N94-32297
Performance statistics bulletin. High latitude meteor scatter propagation
[AD-A276694] 09 p3680 N94-32298
Performance statistics bulletin. High latitude meteor scatter propagation
[AD-A276695] 09 p3680 N94-32299
Performance statistics bulletin. High latitude meteor scatter propagation
[AD-A276696] 09 p3680 N94-32300
Performance statistics bulletin. High latitude meteor scatter propagation, June, July, August, September 1992
[AD-A277508] 09 p3685 N94-33347

POLAR CAPS
Spatial variation in the seasonal south polar cap of Mars as observed by Mariner 7 01 p0456 N94-12134
A new data collection system for ionospheric modelling and related topics
[AD-A265893] 01 p0278 N94-12277
The role of ionospheric plasma in the magnetosphere
[NASA-CR-194404] 02 p0716 N94-13967
Global auroral imaging: Dynamics of Explorer Miss ion
[NASA-CR-194284] 03 p1097 N94-15003
A Pluto thermal model 03 p1256 N94-16216
Balloon exploration of the northern plains of Mars near and north of the Viking 2 landing site 05 p2092 N94-20401
Geology of the southern hemisphere of Triton: No polar cap 05 p2111 N94-20739
Impact of the CO2 and H2O clouds of the Martian polar hood on the polar energy balance 06 p2618 N94-24880
High latitude cusp signature observations for southward IMF B sub Z
[AD-A273801] 06 p2406 N94-25536
Why is the north polar cap on Mars different than the south polar cap? 07 p3107 N94-27889
On observing neutron star oscillations 08 p3538 N94-29795
A reassessment of the in-situ dielectric constant of polar firn
[AD-A276999] 09 p3773 N94-32154
The effect of polar caps on obliquity 09 p3948 N94-33213
Studies of the dayside boundary layer processes based on ground observations in the Svalbard area
[AD-A280715] 11 p4292 N94-36265

POLAR COORDINATES
Polar processing project
[AD-A271583] 05 p1739 N94-21235

POLAR CUSPS
ULF waves and magnetic field characteristics in the polar cusp observed at Godhavn 08 p3361 N94-29244

POLAR IONOSPHERE BEACON
U BEACON SATELLITES

POLAR METEOROLOGY
Studies of dynamical processes affecting the distribution of stratospheric ozone
[NASA-CR-193477] 01 p0279 N94-12560
Arctic ozone expedition
[NASA-TM-109301] 02 p0708 N94-13602
Laboratory studies of chemical and photochemical processes relevant to stratospheric ozone
[NASA-CR-189351] 08 p3347 N94-29549

POLAR ORBITS
Exploration planning in the context of human exploration and development of the Moon 01 p0474 N94-12229
Earth observation from low-inclination orbit as a necessary complement to polar missions 02 p0694 N94-14248
Small launchers (current and future projects in the world) 03 p0878 N94-17137
Mission planning for an Earth observation low Earth orbiter: ERS-1 06 p2503 N94-23868
Ulysses: A solar odyssey
[NASA-TM-109820] 10 p4010 N94-33574

POLAR REGIONS
NT ANTARCTIC REGIONS
NT ARCTIC REGIONS
NT MCMURDO SOUND
NT ROSS ICE SHELF
Sea ice: A climate component 01 p0232 N94-11705
Analysis of ERS-1 altimeter data over the polar ice sheets 01 p0237 N94-11738
Geomorphology of Triton's polar materials 01 p0466 N94-12185
A first assessment of the value of ERS-1 scatterometer winds for meteorological studies in the polar regions 01 p0250 N94-12501
Polar mesospheric waves and structure
[AD-A265360] 01 p0279 N94-12561
Imaging radar studies of polar ice 03 p0991 N94-15899
TOPSAT: Global space topographic mission 03 p0992 N94-15905
Compositional diversity of the lunar North Pole: Preliminary analyses of Galileo SSI data 05 p2101 N94-20686
Linear structures on the small inner satellites of Saturn 05 p2121 N94-20797
Three-dimensional numerical simulation of near-surface flows over the Martian north polar cap 06 p2621 N94-24895
The role of atmospheric heat transport in the seasonal carbon dioxide cycle 06 p2621 N94-24896
Norwegian ionospheric satellite experiment: High latitude, low Earth orbit plasma measurements
[FFI-93/7025] 07 p2876 N94-25807
Comparative investigation of high-latitude ionospheric structure and effects near solar maximum
[AD-A273799] 07 p2877 N94-25877
Upper atmosphere neutral and plasma density modeling
[AD-A274768] 07 p2879 N94-26569
Kiruna geophysical data. Data summary 93/4-6, April-June 1993
[PB94-123700] 07 p2881 N94-27039
Kiruna geophysical data. Data summary 93/1-3, January-March, 1993
[PB94-123791] 07 p2881 N94-27043
Cooling the Martian atmosphere: The spectral overlap of the C02 15 micrometers band and dust 07 p3107 N94-27886
Why is the north polar cap on Mars different than the south polar cap? 07 p3107 N94-27889
The effects of magnetic storm phases on F-layer irregularities from auroral to equatorial latitudes
[AD-A275203] 08 p3356 N94-28891
Hydrodynamics of convection under winter polar leads
[AD-A275182] 08 p3369 N94-29067
Signatures of dayside solar wind/magnetosphere/ionosphere coupling as revealed by the pace HF radars and associated experiments 08 p3359 N94-29236
ULF waves and magnetic field characteristics in the polar cusp observed at Godhavn 08 p3361 N94-29244
Laboratory studies of chemical and photochemical processes relevant to stratospheric ozone
[NASA-CR-189351] 08 p3347 N94-29549
A study of the thermospheric dynamics of the high-latitude E region using a spectral thermospheric general circulation model 08 p3362 N94-29743
Cryosphere and climate 08 p3352 N94-30632
Convection and electrodynamic signatures in the vicinity of a Sun-aligned arc: Results from the Polar Acceleration Regions and Convection Study (Polar ARCS) 09 p3954 N94-31102
Radar scattering from the summer polar mesosphere: Theory and observations 09 p3772 N94-32077
IRTM brightness temperature maps of the Martian south polar region during the polar night: The cold spots don't move 09 p3949 N94-33222
Polar sediment accumulation: Role of surface winds at the two poles 09 p3951 N94-33233
Obliquity variation in a Mars climate evolution model 09 p3951 N94-33236
Analytic model of aurorally coupled magnetospheric and ionospheric electrostatic potentials
[NASA-CR-196130] 11 p4288 N94-35358
The effects of cloud inhomogeneities upon radiative fluxes, and the supply of a cloud truth validation dataset
[NASA-CR-196080] 11 p4293 N94-35391
Ionospheric plasma drift and structure studies at high and mid-latitudes
[AD-A279415] 11 p4291 N94-36116
High Altitude Plasma Instrument (HAPI) data analysis
[NASA-CR-189360] 12 p4469 N94-36949

POLAR SUBSTORMS
A correlative comparison of geomagnetic storms and auroral substorms using geomagnetic indeces
[AD-A268081] 03 p1102 N94-17512

POLAR WANDERING (GEOLOGY)
Nontidal gravity changes observed with a superconducting gravimeter 03 p1100 N94-15808
Estimability of polar motion using range observations to satellites
[PB93-219319] 05 p1842 N94-22265

POLARIMETERS
The intra-atomic motion of bound electrons as a possible source of a systematic error in electron beam polarization measurements by means of a Moeller polarimeter
[DE93-620984] 01 p0364 N94-10875
Localized and distributed fiber-optic strain sensors embedded in composite materials
[UTIAS-346] 01 p0073 N94-12013
Seeing the Black Forest by ERS-1 and AIRSAR: A comparison 01 p0249 N94-12495
Measurement of the spin of a particle using undulator radiation
[DE93-014334] 02 p0780 N94-13149
Ultraviolet spectrometer and polarimeter (UVSP) catalog of observations. Volume 1: Experiments 1-30719, February 1980 - April 1985
[NASA-CR-4529-VOL-1] 03 p1298 N94-15023
Ultraviolet spectrometer and polarimeter (UVSP) catalog of observations. Volume 2: Experiments 30720-63057, April 1985 - February 1988
[NASA-CR-4529-VOL-2] 03 p1298 N94-15024
Mass of Saturn's A ring 03 p1263 N94-16252
Earth observing scanning polarimeter 05 p1844 N94-21645
The polarization sensitivity of the liquid xenon imaging telescope 05 p2056 N94-22282
Stellar x ray polarimeter polarizer development and calibration at LEA/LLNL
[DE94-006400] 09 p3712 N94-31783

POLARIMETRY
NT ASTRONOMICAL POLARIMETRY
Enhancement effects in polarimetric radar returns: Phase difference statistics
[NASA-CR-193408] 01 p0231 N94-11309

Ionospheric effects on a wide-bandwidth, polarimetric, space-based, synthetic-aperture radar
[DE93-015084] 02 p0612 N94-14512
Application of Cloude's target decomposition theorem to polarimetric imaging radar data
03 p0991 N94-15901
Comparison of JPL-AIRSAR and DLR E-SAR images from the MAC Europe 1991 campaign over testsite Oberpfaffenhofen: Frequency and polarization dependent backscatter variations from agricultural fields
03 p1075 N94-16733
Characterization of wetland, forest, and agricultural ecosystems in Belize with airborne radar (AIRSAR)
03 p1076 N94-16738
Supervised fully polarimetric classification of the Black Forest test site: From MAESTROI to MAC Europe
03 p1076 N94-16740
Processing of polarimetric SAR data for soil moisture estimation over Mahantango watershed area
03 p1079 N94-16754
Polarimetric statistics of electromagnetic waves scattered by distributed targets
[PB93-195907] 04 p1389 N94-18951
A general rough-surface inversion algorithm: Theory and application to SAR data 05 p1719 N94-20407
Comparison of remote sensing measurements with a two-scale polarimetric emission and scattering model for sea surfaces 05 p1721 N94-20415
Advances in spaceborne radar remote sensing
05 p1723 N94-20424
Polarimetric backscattering from sea ice
05 p1723 N94-20426
On evaluating the accuracy of SAR sea-ice classification using multifrequency polarimetric AIRSAR data
05 p1724 N94-20428
Application of Cloude's target decomposition theorem to polarimetric imaging radar data
05 p1724 N94-20429
Retrieval of ice thickness from polarimetric SAR data
05 p1724 N94-20432
Radar backscattering from snow facies of the Greenland ice sheet: Results from the AIRSAR 1991 campaign
05 p1725 N94-20434
Polarimetric thermal emission from rough surfaces
05 p1727 N94-20441
Polarimetric thermal emission from periodic water surfaces 05 p1728 N94-20445
Symmetry in polarimetric remote sensing
05 p1729 N94-20449
Mapping of taiga forest units using AIRSAR data and/or optical data, and retrieval of forest parameters
05 p1729 N94-20452
Application of the target decomposition theorem to a polarimetric random media model
05 p1730 N94-20453
A theoretical and numerical study of polarimetric scattering and emission from random rough surfaces with anisotropic directional spectrum
05 p1730 N94-20454
Application of neural network to remote sensing of soil moisture using theoretical polarimetric backscattering coefficients 05 p1730 N94-20455
The Brewster angle effect in SAR polarimetry
05 p1731 N94-20456
Use of microwave polarimetry to enhance SAR images of the ocean surface
[AD-A271911] 05 p1882 N94-20489
Magellan vertical polarization radar observations
05 p1744 N94-20691
Earth observing scanning polarimeter
05 p1844 N94-21645
White-light, pressure, and temperature interferopolarimetric sensor featuring optical fibers
[PB93-199792] 06 p2545 N94-24631
Use of microwave polarimetry to enhance SAR images of the ocean surface
[AD-A273568] 06 p2419 N94-24944
Liquidus temperature and optical properties measurement by containerless techniques
06 p2247 N94-25126
Optical properties and emissivities of liquid metals and alloys 06 p2248 N94-25129
Polarimetric investigation of edge scattering by mono- and bistatic microwave imaging
[ESA-TT-1284] 07 p2768 N94-26317
Processing of wide-angle synthetic aperture radar signals for target detection
[AD-A274225] 07 p2773 N94-27073
Spectral and polarimetric analysis of hyperspectral data collected by an acousto-optic tunable filter system
[AD-A275076] 08 p3329 N94-29095
Transient internal probe
[AD-A275054] 08 p3505 N94-29134
Frequency dependence of polarization phase difference
[NASA-TM-109737] 08 p3254 N94-30094
Polarimetric backscatter measurements of natural surfaces at millimeter wavelengths
08 p3259 N94-30509
Multiple scattering of polarized radiation in planetary atmospheres
[ETN-94-96018] 09 p3674 N94-31551

POLARITONS

NT PLASMONS
On the theory of phonoriton in cubic semiconductors with a degenerate valence band
[DE93-613539] 01 p0402 N94-11660
Dephasing processes in III-V semiconductors
[AD-A271677] 05 p2028 N94-21362
Decay of non-equilibrium polariton condensate in semiconductors
[DE94-604016] 07 p3068 N94-27678

POLARITY

Polarity reversals and tilt of the Earth's magnetic dipole 01 p0283 N94-12219
Direct probing of chromatography columns by laser-induced fluorescence
[DE93-015208] 02 p0654 N94-13022
Observation of reflected waves on the SABRE positive polarity inductive adder MITL
[DE93-019413] 05 p1980 N94-20295
Two-polarity magnetization in the Manson impact breccia 05 p1863 N94-20789
Reverse polarity magnetized melt rocks from the Chicxulub impact structure, Yucatan Peninsula, Mexico
05 p1863 N94-20843
Observation of non-centrosymmetry and determination of polarity in III-V semiconductors
[PB93-201416] 06 p2561 N94-23503
Correlation of experimental data and three-dimensional finite element modeling of a spinning quadrupole
[DE93-041173] 07 p3008 N94-26421
UAH mathematical model of the variable polarity plasma ARC welding system calculation
[NASA-CR-193926] 07 p2824 N94-27221

POLARIZATION

Polarization and color transparency
[DE93-014319] 02 p0780 N94-13101
Polarization and variability of active galaxies and quasars 02 p0837 N94-13550
Polarized thin films from dye-substituted polymers containing hydrophobically terminated stilbazolium radicals
[AD-D015873] 04 p1367 N94-17706

POLARIZATION (CHARGE SEPARATION)

NT DIELECTRIC POLARIZATION
Gyrosheath near the tokamak edge
[DE93-012191] 01 p0390 N94-11142
Macroscopic electric charge separation during hypervelocity impacts: Potential implications for planetary paleomagnetism 01 p0431 N94-12181
Polaronic charge separation in mixed-halide MX solids
[AD-A266073] 01 p0403 N94-12345
Ultrafast photoinduced electron transfer reactions in supramolecular arrays: Studies of electronic coupling and solvation
[DE93-012910] 02 p0782 N94-13484
Charge storage and switching phenomena with molecular assemblies of metal complexes
[AD-A266673] 02 p0787 N94-14778
Relaxation of polar orientational order in nonlinear optical polymers by second harmonic generation
[AD-A269059] 04 p1370 N94-18515
Femtosecond Raman-induced Kerr effect study of polar solvent dynamics: Amides
[DE93-017563] 05 p1678 N94-19924
Charge collectors for the omega upgrade
[DE93-019684] 05 p1972 N94-20264
Photoinduced charge separation in solid state and molecular systems
[DE94-001727] 06 p2563 N94-24537
Effects of Class 3 antiarrhythmic agents, E-4031 and MS-551 on ventricular repolarization in isolated rabbit hearts 07 p2907 N94-27508
Intramolecular energy transfer reactions in polymetallic complexes
[DE94-010114] 11 p4326 N94-36126

POLARIZATION (SPIN ALIGNMENT)

Top quark polarization and T-odd spin correlations as tools for testing (non) Standard Model predictions
[DE93-622956] 02 p0778 N94-12847
The evolution of tensor polarization
[DE93-017209] 02 p0790 N94-14897
Measuring the sea quark polarization
[DE93-015792] 04 p1566 N94-18234
Polarized structure functions of the nucleon in the resonance region
[CEBAF-PR-94-001] 06 p2540 N94-24663
Spin-polarized atomic hydrogen: Devices and phenomena
[ETN-94-95342] 07 p3016 N94-26002
Calculation of electron-potassium scattering
[DE94-601812] 07 p3023 N94-26942
One-loop QCD mass effects in the production of polarized bottom and top quarks
[PB94-138104] 08 p3487 N94-29145
Improved QCD sum rule estimates of the higher twist contributions to polarised and unpolarised nucleon structure functions
[PB94-138112] 08 p3487 N94-29161
Hyperon polarization and magnetic moments
[DE94-006041] 09 p3864 N94-31507
Fusion with highly spin polarized HD and D2
[DE94-006209] 09 p3876 N94-32731
Hyperon polarization, crystal channeling, and E781 at Fermilab
[DE94-008224] 09 p3877 N94-32802
Relaxation of the density matrix for an arbitrary spin in random external fields
[DE94-618457] 12 p4509 N94-37078
Polarization phenomena in quantum chromodynamics
[DE94-010663] 12 p4539 N94-37543

POLARIZATION (WAVES)

NT CIRCULAR POLARIZATION
NT CROSS POLARIZATION
NT ELLIPTICAL POLARIZATION
NT LINEAR POLARIZATION
Method and apparatus for polarization-maintaining fiber optical amplification with orthogonal polarization output
[AD-D015756] 01 p0374 N94-10372
Polarisation of backscattering radiation at remote sensing of ocean with impulse laser beam
01 p0177 N94-12722
Non-image visible polarization remote sensing of the ocean 01 p0229 N94-12762
The E2 N(yields)(Delta) transition from polarized Compton scattering
[DE93-012522] 02 p0785 N94-14363
Multilayer thin film design for far ultraviolet polarizers using an induced transmission and absorption technique
[NASA-CR-194631] 03 p1190 N94-15869
Crystal optics of high energy gamma-beams
[DE93-630228] 04 p1577 N94-18217
Potential dependent structural changes of underpotentially deposited copper on an iodine treated platinum surface determined in situ by surface EXAFS and its polarization dependence
[AD-A269890] 04 p1360 N94-18687
A comparison of single-station backazimuth estimates with regional event locations in the Central Appalachians
[AD-A269897] 04 p1483 N94-18690
Polarimetric statistics of electromagnetic waves scattered by distributed targets
[PB93-195907] 04 p1389 N94-18951
Fiber optic Michelson sensor and arrays with passive elimination of polarization fading and source feedback isolation
[AD-D015944] 05 p1984 N94-20065
The polarization sensitivity of the liquid xenon imaging telescope 05 p2056 N94-22282
Laser manipulation of metastable neon atoms
[ETN-94-95344] 07 p2817 N94-26225
Refractive and dielectric properties of helium, argon and nitrogen gases
[PB94-123783] 07 p3008 N94-26851
Evaluation of dual polarization attenuation of millimeter frequencies through a meteorological radar
08 p3256 N94-30496
Structure estimation of phase objects from the diffraction near field: Microwave and model calculations
[ETN-94-95737] 09 p3674 N94-31608
An approximate model for vertical polarization and surface roughness using the parabolic equation
[AD-A278091] 09 p3684 N94-33186
Chilbolton Advanced Meteorological Radar: A tool for multi-disciplinary atmospheric research
[PB94-167467] 12 p4432 N94-36567

POLARIZATION CHARACTERISTICS

Polarisation of backscattering radiation at remote sensing of ocean with impulse laser beam
01 p0177 N94-12722
Interaction types and their like-polarization phase-angle difference signatures 03 p1079 N94-16756
The influence of an electric field on the kinetics of nucleation
[IFTR-2/91] 03 p1213 N94-17046
Potential dependent structural changes of underpotentially deposited copper on an iodine treated platinum surface determined in situ by surface EXAFS and its polarization dependence
[AD-A269890] 04 p1360 N94-18687
Optical properties and emissivities of liquid metals and alloys 06 p2248 N94-25129
Spin-polarized atomic hydrogen: Devices and phenomena
[ETN-94-95342] 07 p3016 N94-26002

Calculation of total cross sections for electron and positron scattering on sodium and potassium
[DE94-601814] 07 p3023 N94-26944
International bulletin on atomic and molecular data for fusion. No. 42-45, Mar. 1991 - Dec. 1992
[DE94-601817] 07 p3045 N94-26946
Polarizability matrix of layered chiral sphere
[PB94-132834] 07 p2778 N94-28355
Electromagnetic modeling of bi-isotropic media
[PB94-132909] 07 p2778 N94-28382
On the relation between SMMR 37-GHz polarization difference and the rainfall over Africa and Australia
[NASA-TM-104598] 08 p3370 N94-29408
Synthesis of novel composite Platinum-DNA films by way of wet-spinning
[AD-A278763] 11 p4243 N94-35494
Center for seismic studies
[AD-A278682] 11 p4290 N94-35693
Modelling of the structure and physical properties of simple disordered systems
[DE94-617087] 11 p4329 N94-36311
First-principles determination of the polarizabilities of carbon tubules as a function of length
[DE94-013015] 12 p4537 N94-37356

POLARIZATION CHARTS
U GRAPHS (CHARTS)
U POLARIZATION (WAVES)

POLARIZED ELECTROMAGNETIC RADIATION
NT POLARIZED LIGHT
NT SYNCHROTRON RADIATION
Remote identification of rain and hail with a polarization diversity radar
[ISBN-0-315-55623-4] 02 p0720 N94-13516
Magellan vertical polarization radar observations
05 p1744 N94-20691
On the relation between SMMR 37-GHz polarization difference and the rainfall over Africa and Australia
[NASA-TM-104598] 08 p3370 N94-29408
Radar cross sections of ground clutter at 95 GHz for summer and fall conditions 08 p3259 N94-30512

POLARIZED LIGHT
New tests of the equivalence principle using non-metric couplings of electromagnetism and gravitation
01 p0413 N94-11821
Non-image visible polarization remote sensing of the ocean 01 p0229 N94-12762
Polarization effects in optical fiber current sensors based on Sagnac interferometers with 3 by 3 couplers
[DE93-012665] 02 p0792 N94-14367
Display system employing acousto-optic tunable filter
[NASA-CASE-NPO-18736-1-CU]
03 p1190 N94-15933
A test of the applicability of independent scattering to high albedo planetary regoliths
03 p1250 N94-16187
Polarized optical emission due to decay or recombination of spin-polarized injected carriers
[AD-D015907] 04 p1408 N94-19763
Circular polarizing mirrors for high power lasers
[AD-A267820] 05 p1815 N94-19965
Photonic electromagnetic field sensor apparatus
[AD-D015938] 05 p1717 N94-20333
Photonic electromagnetic field sensor apparatus
[AD-D015939] 05 p1718 N94-20334
Intensity and polarization of light scattered by size distributions of randomly oriented nonspherical particles
05 p1721 N94-20416
Electron quantum yields from a barium photocathode illuminated with polarized light
[DE93-019232] 05 p1980 N94-20475
Efficiency of reversible optical storage in azo polymers
[AD-A272923] 05 p1705 N94-21223
Technical report of ISSP. Ser. A, no. 2684: Wavelength dependence of nonsequential double ionization in He
[JTN-94-80570] 07 p3025 N94-27338
Report of the National Research Institute for Earth Science and Disaster Prevention, No. 51
[JTN-94-80509] 07 p2886 N94-27985
Detection of water on road surface by the polarized light 07 p2886 N94-27989
One-loop QCD mass effects in the production of polarized bottom and top quarks
[PB94-138104] 08 p3487 N94-29145
Post-calibration correction for rotating-analyzer ellipsometer with optical fiber bundle detection system
[AD-A277329] 09 p3881 N94-32280
Microreflectance infrared study of electron-molecular vibrational coupling and lattice softness in BEDT-TTF salts
[DE94-008490] 09 p3907 N94-32989
Coherent processes in atom in strong radiation fields
[AD-A278388] 09 p3874 N94-33144
Magnetic field effect on selective photoionization
[DE94-611079] 11 p4334 N94-36180

POLARIZED RADIATION
NT POLARIZED ELECTROMAGNETIC RADIATION
NT POLARIZED LIGHT
NT SYNCHROTRON RADIATION
Atomic processes relevant to polarization plasma spectroscopy
[DE93-753240] 01 p0393 N94-11594
The continuum emission of active galactic nuclei
[ITN-93-85208] 02 p0847 N94-13232
Current drive with free electron lasers in high and low temperature tokamaks 03 p1201 N94-15209
The coherent backscattering opposition effect
05 p1991 N94-20646
Multiple scattering of polarized radiation in planetary atmospheres
[ETN-94-96018] 09 p3674 N94-31551
RHIC spin physics
[DE94-005452] 09 p3876 N94-32099

POLARIZERS
Multilayer thin film design for far ultraviolet polarizers using an induced transmission and absorption technique
[NASA-CR-194631] 03 p1190 N94-15869
Design and fabrication of a reflection far ultraviolet polarizer and retarder
[NASA-CR-194630] 03 p1191 N94-16023
Mesoepitaxy: A universal route to oriented materials
[AD-A270437] 04 p1598 N94-18511
X ray, extreme and far ultraviolet optical thin films for space applications
[NASA-CR-194635] 05 p1984 N94-20128
Miniature color display, phase 4
[AD-A272920] 05 p1760 N94-21221
Mueller matrix analysis of infrared ellipsometry
[PB93-201549] 06 p2544 N94-23629
GOLF mechanisms 06 p2357 N94-24003
Large-area conditioning of optics for high-power laser systems
[DE94-007028] 09 p3716 N94-31636
Stellar x ray polarimeter polarizer development and calibration at LEA/LLNL
[DE94-006400] 09 p3712 N94-31783
Three-stage attenuation using Glan-Thompson prisms
[AD-A280481] 12 p4525 N94-37350

POLARONS
Femtosecond dynamics, photoexcitation, and ESR spectra of MX chain solids
[AD-A264689] 01 p0399 N94-11263
Polaronic charge separation in mixed-halide MX solids
[AD-A266073] 01 p0403 N94-12345
Small polaron conduction in Y2Ti2O7
[ITN-93-85221] 02 p0814 N94-14557
New organic materials for nonlinear optics applications
[AD-A266451] 03 p1192 N94-16563
Lattice relaxation theory of localized excitations in quasi-one-dimensional systems
[DE93-624947] 03 p1215 N94-17437
Polaron tunneling in high-temperature superconductors
[DE93-016880] 04 p1593 N94-17754
Spin-polaron theory of high-(Tc) superconductivity. 1: Spin polarons and high (Tc) pairing
[DE93-019196] 05 p2014 N94-20002
Spin-polaron theory of high-T(c) superconductivity. 2: Electronic structure of the CuO2 planes
[DE93-019197] 06 p2556 N94-22919
Disorder effects on small-polaron formation and hopping
[DE94-001205] 06 p2534 N94-23804
Holes in a two-dimensional quantum antiferromagnet
[DE93-634753] 07 p3057 N94-26388
All-coupling polaron ground state energy in D-dimension
[DE94-603666] 07 p3027 N94-27629
Interband optical absorption in the Wannier-Stark ladder under the electron-LO-phonon resonance condition
[DE94-608097] 08 p3267 N94-30092
Theoretical studies of electron transfer and optical spectroscopy
[DE94-006985] 09 p3871 N94-32375

POLICE
Using satellite communications for a mobile computer network 06 p2280 N94-22777

POLICIES
NT ENERGY POLICY
NT PATENT POLICY
NT PROCUREMENT POLICY
National Aero-Space Plane: A need for program direction and funding decisions
[GAO/NSIAD-93-207] 01 p0416 N94-10910
NASA procurement: Proposed changes to the Jet Propulsion Laboratory contract. Report to Congressional Requesters
[GAO/NSIAD-93-178] 01 p0416 N94-10941
The Department of Clinical Investigation, reports control symbol MED-300(R-1)
[AD-A264969] 01 p0304 N94-11649
Planetary protection implementation on future Mars lander missions
[NASA-CP-3216] 02 p0841 N94-13183
An examination of utility emissions contributions to elevated ozone concentrations in the Chicago area
[DE93-012852] 02 p0708 N94-13495
Preliminary nuclear safety assessment of the NEPST (Topaz 2) space reactor program
[DE93-012853] 02 p0551 N94-13514
Science, technology, and the federal government: National goals for a new era 02 p0827 N94-14115
Mission management aircraft operations manual
[NHB-7900.3] 03 p1225 N94-16729
Aircraft operations management manual
[NHB-7900.3(V1)] 03 p1225 N94-16730
Equipment Management Manual
[NHB-4200.1D] 03 p1225 N94-16799
The Megascience Forum
[DE93-014445] 03 p1303 N94-16804
Computer Science and Telecommunications Board activities
[DE93-018141] 03 p1000 N94-17000
Abstracts of manuscripts submitted in 1992 for publication
[AD-A267963] 03 p1113 N94-17383
Setting the global thermostat with an exhaustible tradeable permit system
[DE93-012911] 04 p1472 N94-17891
Coastal Ocean Modeling Workshop
[AD-A268955] 04 p1497 N94-18393
Land-use related sources of CO2, CH4 and N2O: Current global emissions and projections for the period 1990-2100
[PB93-194819] 04 p1475 N94-18949
Finding optimal policies for Markov decision chains: A unifying framework for mean-variance-tradeoffs
[PB93-191930] 04 p1559 N94-19555
Use of economic models in Finnish economic policy
05 p2053 N94-22085
Electronic publishing and intelligent information retrieval 05 p2047 N94-22479
Proceedings of the Third International Mobile Satellite Conference (IMSC 1993)
[NASA-CR-194516] 06 p2273 N94-22735
US domestic and international regulatory issues
06 p2275 N94-22748
Use of negotiated rulemaking in developing technical rules for low-Earth orbit mobile satellite systems
06 p2276 N94-22750
NASA printing, duplicating, and copying management handbook
[NASA-NHB-1490.5] 06 p2590 N94-23971
Proceedings of Technology and Governance in the 1990's
[PB93-192904] 06 p2597 N94-24312
Orbital debris and near-Earth environmental management: A chronology
[NASA-RP-1320] 06 p2598 N94-24644
How to make good use of international research collaboration, with emphasis on the evolving situation in Europe
[PB94-119690] 07 p3101 N94-27323
The 1993 Federal Aviation Administration plan for research, engineering and development
[AD-A279037] 07 p2643 N94-27960
Fuel cycle evaluations of biomass-ethanol and reformulated gasoline
[DE94-000227] 08 p3226 N94-30818
Europe at the crossroads: The future of its satellite communications industry
[ESA-SP-1166] 09 p3670 N94-31182
Satellite communications industry
[AD-A276685] 09 p3610 N94-32039
Interagency Advanced Power Group: Steering Group meeting minutes
[DE94-007951] 09 p3761 N94-32701
National US public policy on global warming derived from optimization of energy use and environmental impact studies
[DE94-004606] 09 p3768 N94-32790
NASA/DOD Aerospace Knowledge Diffusion Research Project. Paper 18: Scientific and Technical Information (STI) policy and the competitive position of the US aerospace industry
[NASA-TM-109782] 09 p3921 N94-32833
Current policies of the major countries coping with the global warming problem and-the energy demand and supply
[DE94-757291] 09 p3769 N94-32920
Opinion polls and the US civil space program
[NASA-TM-109700] 09 p3914 N94-33066
Space history, space policy, and executive leadership
[NASA-TM-109787] 09 p3924 N94-33067

Partners in space. International cooperation in space: Strategies for the new century
[ISBN-0-9629930-2-6] 11 p4348 N94-35901
JPRS report: Science and technology. Central Eurasia: Space
[JPRS-USP-93-005] 11 p4201 N94-36011
Science priorities for the human dimensions of global change 12 p4464 N94-36987
JPRS report: Science and technology. Central Eurasia: Space
[JPRS-USP-94-004] 12 p4391 N94-37002
Comparative alternative/clean fuels provisions of the Clean Air Act Amendments of 1990 and the Energy Policy Act of 1992
[DE94-006887] 12 p4429 N94-37426

POLISHING
Zerodur polishing process for high surface quality and high efficiency
[DE93-012596] 01 p0087 N94-10271
Field emitter array RF amplifier development project. Phase 1: Cathode technology development
[AD-A266346] 02 p0622 N94-13776
Polished substrate surface and cleaning study for coated optic quality
[DE93-014116] 03 p1190 N94-15975
Surface modification of sapphire for IR window application
[DE93-019168] 04 p1602 N94-19075
Synchrotron/crystal sample preparation
[NASA-CR-193837] 04 p1603 N94-19513
Precision machining and polishing of scintillating crystals for large calorimeters and hodoscopes
[DE93-018663] 04 p1381 N94-19544
Ge-Au eutectic bonding of Ge (100) single crystals
[DE94-002281] 06 p2564 N94-24657
Calculations of material removal, removal rate, and Preston coefficient in continuous lapping/polishing machines
[DE94-002619] 07 p2763 N94-26804
Analysis of cost: CVD diamond deposition and finishing --- Quarterly report
[AD-A275586] 08 p3212 N94-28725
Float polishing studies of fused silica
[AD-A275001] 08 p3213 N94-28886
Neutral ion sources in precision manufacturing
09 p3875 N94-32447

POLITICS
Where no flag has gone before: Political and technical aspects of placing a flag on the Moon
[NASA-CR-188251] 02 p0827 N94-12800
NASA/DOD Aerospace Knowledge Diffusion Research Project. Paper 37: The impact of political control on technical communications: A comparative study of Russian and US aerospace engineers and scientists
[NASA-TM-109329] 02 p0826 N94-14488
The strategic environmental research and development program: A new paradigm for space, the environment, and national security
[AD-A266222] 03 p1174 N94-16109
Space and the American imagination
[NASA-CR-196131] 11 p4376 N94-35356

POLLEN
Backscatter and transmission of aerosol at UV through middle IR wavelengths
[AD-A277127] 09 p3718 N94-32305

POLLUTANTS
U CONTAMINANTS

POLLUTION
NT AIR POLLUTION
NT ENVIRONMENT POLLUTION
NT GLOBAL AIR POLLUTION
NT INDOOR AIR POLLUTION
NT NOISE POLLUTION
NT OIL POLLUTION
NT WATER POLLUTION
Soil pollution at former industrial sites, the heritage of 150 years of industrial development in Noord-Brabant, The Netherlands
[ISBN-9-09-005758-7] 08 p2400 N94-25223

POLLUTION CONTROL
Environmental Protection Agency's life cycle methodology: Guidelines for use in development of packaging
[PB93-194199] 01 p0265 N94-10841
Summary of implementation and demonstration projects in bays and estuaries
[PB93-194637] 01 p0265 N94-10846
Immediate response to free product discovery
[PB93-182970] 01 p0265 N94-11015
Gulf of Mexico sales 147 and 150: Central and western planning areas. Draft environmental impact statement. Volume 1: Sections 1 through 4.C
[PB93-190304] 01 p0265 N94-11018
Control of jet noise
[NASA-CR-193612] 01 p0358 N94-11176
Application of jet-shear-layer mixing and effervescent atomization to the development of a low-NO(x) combustor
[NASA-TM-105888] 01 p0028 N94-11234
Catalytic oxidation of organics in vapor streams at remediation sites
[PB93-182962] 01 p0266 N94-11472
A review of the global emissions, transport, and effects of heavy metals in the environment
[DE93-013507] 02 p0706 N94-12937
AQUIS: A PC-based source information manager
[DE93-012893] 02 p0707 N94-13383
Pollution prevention through total quality
[DE93-013814] 02 p0707 N94-13390
TABES 1993: 9th Annual Technical and Business Exhibition and Symposium 03 p1050 N94-16129
Emerging technologies for the changing global market
[TABES PAPER 93-612] 03 p0930 N94-16144
Application of non-thermal plasmas to pollution control
[DE93-016432] 03 p1096 N94-16449
Biomass energy: State of the technology present obstacles and future potential
[DE93-016295] 03 p1092 N94-16766
The 11th annual report of accomplishments under the airport improvement program: Fiscal year 1992
[AD-A268328] 03 p0865 N94-17458
Title 1 implementation: Status report on nonattainment areas
[DE93-017677] 04 p1471 N94-17777
The carbon dioxide emissions game: Playing the net
[DE93-017670] 04 p1471 N94-17821
Cost effective energy strategies for the reduction of CO2 emissions in the United States: Country report for ETSAP Annex 4
[DE93-016842] 04 p1472 N94-17852
A comparison of wet and dry scrubbing systems for control of metals and dioxin/furan emissions from incinerators
[DE93-017446] 04 p1474 N94-18502
Land-use related sources of CO2, CH4 and N2O: Current global emissions and projections for the period 1990-2100
[PB93-194819] 04 p1475 N94-18949
Organic carbonyl compounds in Albuquerque, New Mexico, air: A preliminary study of the effects of oxygenated fuel use
[DE93-017748] 04 p1476 N94-19045
Valuation of temporary and future greenhouse gas reductions
[DE93-018876] 04 p1478 N94-19319
Advanced batteries for electric vehicle applications: Nontechnical summary
[DE93-019007] 05 p1748 N94-19885
Alternative refrigerants and refrigeration cycles for domestic refrigerators
[DE93-040481] 05 p1714 N94-20099
Survey on evaluation of energy technology contributing to preservation of the global environment. 2
[DE94-714884] 05 p1853 N94-22051
Investigations on trends in global environment adaptive industrial technologies
[DE94-714888] 05 p1853 N94-22258
Economics of electron beam and electrical discharge processing for post-combustion NO(x) control in internal combustion engines
[DE93-019574] 06 p2351 N94-22865
Fundamental limitations of non-thermal plasma processing for internal combustion engine NO(x) control
[DE93-019622] 06 p2351 N94-22866
Reduction of nitric oxide over platinum, rhodium and platinum-rhodium single crystal surfaces
[PB93-230092] 06 p2232 N94-23482
Analysis and development of an F-5 pollution prevention management program with recommendations for creation of similar programs for other aircraft
[AD-A274016] 07 p2865 N94-25755
SIHTI 2: Energy and environmental technology
[DE94-702061] 07 p2867 N94-26241
Compilation of air pollutant emission factors. Volume 1: Stationary point and area sources. Supplement F
[PB94-121431] 07 p2867 N94-26757
Numerical analysis of the photo-dissociation/radical oxidation of formaldehyde by ultraviolet light in a photolytic reactor
[AD-A274539] 07 p2868 N94-26843
Optimising BMW four-cylinder two-valve engines
[PB94-125101] 07 p2824 N94-27254
Gas turbine combustion and emission control
07 p2831 N94-28082
Speciation in Water and Soil: A literature review
[PB94-132388] 08 p3341 N94-28412
Reduction of NO(x) by fuel-staging in gas turbine engines: A commitment to the future
08 p3194 N94-29272
Chambers of turboreactors with variable geometry: A response to the matrix of pollution in cycles at high temperature, high pressure 08 p3194 N94-29273
Ventilation cost and air cleaning
08 p3232 N94-29605
A study of low emissions gas turbine combustions
[NASA-CR-195763] 08 p3152 N94-29860
Technology 2003: The Fourth National Technology Transfer Conference and Exposition, volume 1
[NASA-CP-3249-VOL-1] 08 p3555 N94-30440
International Energy and Environmental Congress: Proceedings
[DE93-040609] 08 p3353 N94-30715
Biological conversion of synthesis gas
[DE94-005815] 08 p3340 N94-30879
Information resources for US Department of Energy pollution prevention programs
[DE94-006677] 09 p3763 N94-31582
Control and monitoring of heavy metal emissions
[VTT-TIED-1508] 09 p3765 N94-31657
Carbon dioxide abatement as a differential game
[DE94-722023] 09 p3765 N94-32590
Removal of CO2 from flue gases by algae
[DE94-008039] 09 p3766 N94-32703
Identification of research relating to the critical loads concept and its potential application to the regulation of acidic deposition
[DE94-008234] 09 p3767 N94-32752
Evaluation of the Hughes conversion coating touch-up pen
[AD-A278398] 09 p3664 N94-33166
First Annual High-Speed Research Workshop, part 2
[NASA-CP-10087-PT-2] 10 p3972 N94-33462
A NASA Lewis comparative propulsion system assessment for the High-Speed Civil Transport
10 p3974 N94-33477
Low emissions combustor technology for high-speed civil transport engines 10 p3974 N94-33481
Application of pulsed plasma NO(x) reduction to diesel engine exhaust
[DE94-007454] 10 p4080 N94-33692
Air quality assessment and control
[DE94-000046] 10 p4081 N94-33725
Emission control technology for diesel trucks (draft)
[PB94-150455] 10 p4082 N94-34116
Hynol: An economic process for methanol production from biomass and natural gas with reduced CO2 emission
[DE94-008872] 10 p4079 N94-34139
Trends in working on the Framework Convention on Climate Change in industrialized countries in Europe and America
[DE94-757292] 10 p4082 N94-34222
Low emission combustor technology for small aircraft gas turbines 10 p4003 N94-34454
How to develop a long term CO2 reduction plan
[DE94-009559] 11 p4284 N94-35668
Final regulatory impact analysis: Refueling emission regulations for light duty vehicles and trucks and heavy duty vehicles
[PB94-164027] 11 p4285 N94-35754
Dual cure low-VOC coating process
[DE94-009346] 11 p4245 N94-35809
Design and operation of a medium speed 12-cylinder coal-fueled diesel engine. Phase 2: Improvements
[DE94-009547] 11 p4275 N94-35815
Methanol fuel additive demonstration
[PB94-156668] 11 p4247 N94-35941
Treatment of toxic gases SO2 and NO(x) by electron beam irradiation
[DE94-615424] 11 p4330 N94-36028
Opportunities for innovation: Biotechnology
[PB94-157831] 12 p4478 N94-36720
Potential benefits of oxygen-enriched intake air in a vehicle powered by a spark-ignition engine
[DE94-013452] 12 p4451 N94-37070
Evaluation of flame-sprayed polymer coatings for civil works navigation structures
[AD-A280507] 12 p4422 N94-37104
Processing solid propellants for recycling
[DE94-011433] 12 p4428 N94-37202
Bibliography of work on the photocatalytic removal of hazardous compounds from water and air
[DE94-006906] 12 p4467 N94-37405
Comparative alternative/clean fuels provisions of the Clean Air Act Amendments of 1990 and the Energy Policy Act of 1992
[DE94-006887] 12 p4429 N94-37426
Biological determinants of photobioreactor design
[DE94-011665] 12 p4468 N94-37740

POLLUTION MONITORING
International Space Year in China
01 p0036 N94-10680
Remote surface water monitoring radio based telemetry system
[DE93-009643] 01 p0041 N94-11282

Methodologies for estimating air emissions from three non-traditional source categories: Oil spills, petroleum vessel loading and unloading, and cooling towers
[PB93-181592] 01 p0266 N94-11471
Satellite observations of red tide events: Plans for EESI 01 p0191 N94-11899
An algorithm for the detection of mucilage (green slime) in the Adriatic Sea 01 p0191 N94-11900
A study of pollution courses of spilled oil floatation in the outer ocean 01 p0205 N94-11983
Information capability of NOAA-AVHRR data for monitoring oceanographic and atmospheric pollution 01 p0214 N94-12677
Novel mass spectrometric instrument for gaseous and particulate characterization and monitoring
[DE93-014093] 01 p0272 N94-12783
Laser-induced fluorescence over optical fibers for real time in situ measurement of petroleum hydrocarbons in seawater
[AD-A265106] 02 p0790 N94-12863
Gathering and exchange information on atmospheric chemistry and polluted atmospheres
[DE93-009940] 02 p0705 N94-12869
The North Atlantic Regional Experiment (NARE)
[DE93-010126] 02 p0706 N94-13054
AQUIS: A PC-based source information manager
[DE93-012893] 02 p0707 N94-13383
Spatial and temporal variability of precipitation and chemistry: Case studies from the frontal boundary study
[DE93-007883] 02 p0708 N94-13910
Study of the consequences of the Chernobyl accident and technogenic activity in the Republic Belarus using aerospace methods 02 p0693 N94-14246
New York MARKAL: An evaluation of carbon dioxide emission control strategies in New York State
[DE93-013149] 03 p1095 N94-15999
Statement on global climate change before the Subcommittee on Energy and Power, United States House of Representatives
[DE93-013163] 03 p1095 N94-16006
Utility emissions associated with electric and hybrid vehicle (EHV) charging
[DE93-013734] 03 p1011 N94-16459
On-line monitoring of incinerator emissions
[DE93-017406] 04 p1474 N94-18499
Organic carbonyl compounds in Albuquerque, New Mexico, air: A preliminary study of the effects of oxygenated fuel use
[DE93-017748] 04 p1476 N94-19045
Novel mass spectrometric instrument for gaseous and particulate characterization and monitoring
[DE93-019992] 04 p1433 N94-19054
Spatiotemporal variability of non-urban ozone concentrations over the eastern United States and its potential replication by satellite data
[PB93-191328] 04 p1476 N94-19065
Advances in passive-remote and extractive Fourier transform infrared systems
[DE93-017402] 04 p1478 N94-19241
Manual of DRANC (release 1.1): A computer program for the Dutch risk assessment of new chemical substances
[PB93-194827] 05 p1851 N94-19998
The use of lidar for the evaluation of traffic-related urban pollution
[DE94-000704] 05 p1852 N94-22017
Estimation of delays and emissions at four-way junctions with different forms of regulation, principally four-way mandatory stop
[PB94-105236] 06 p2398 N94-23813
EPA's survey of in-use driving patterns: Implications for mobile source emission inventories
[PB94-118502] 06 p2399 N94-24525
Manual on measurement of methane and nitrous oxide emissions from agriculture
[DE93-616429] 06 p2399 N94-25167
An observational study of air pollution transport over a large urban complex
[REPT-6] 07 p2867 N94-26474
Advances in passive-remote and extractive Fourier transform infrared spectroscopic systems
[DE94-001424] 07 p2868 N94-26952
Determination of lead isotope ratios in seawater by purge and trap GC/MS after ethylation 07 p2870 N94-28152
Environmental management and audit 07 p2870 N94-28153
Intermedia transfer factors for fifteen toxic pollutants released to air basins in California
[DE94-005699] 08 p3349 N94-30044
Novel mass spectrometric instrument for gaseous and particulate characterization and monitoring
[DE94-005896] 08 p3349 N94-30047
Computerized in vitro test for chemical toxicity based on tetrahymena swimming patterns 08 p3354 N94-30463
Granulometry in environments with very small particle concentrations 08 p3259 N94-30511
Control and monitoring of heavy metal emissions
[VTT-TIED-1508] 09 p3765 N94-31657
NORSMAP 1989: Norwegian remote sensing spectroscopy for mapping and monitoring or algal blooms and pollution 09 p3744 N94-31856
Evaluation of Fluorescence Line Imager (FLI) airborne imaging spectrometer data for roadside tree damage assessment 09 p3745 N94-31866
Focused feasibility study final field sampling plan
[AD-A277445] 09 p3769 N94-33105
Minipilot solar system: Design/operation of system and results of non-solar testing at MRI
[PB94-152238] 10 p4079 N94-34165
Analysis of ambient monitoring data in the vicinity of open tire fires
[PB94-156197] 10 p4083 N94-34402
Aerosol optical depth derived from solar radiometry observations at northern mid-latitude sites
[DE94-007476] 11 p4287 N94-36053
UK methane emissions inventory: A scoping study on the use of ambient measurements to reduce uncertainties
[PB94-167855] 12 p4463 N94-36533
Mexico City air quality research initiative, volume 4
[DE94-013201] 12 p4466 N94-37299
Gaseous effluent monitoring and identification using an imaging Fourier transform spectrometer
[DE94-012627] 12 p4467 N94-37428
Program GAUSSPLYM: A tool in Windows environment for studying continuous releases
[PB94-184603] 12 p4468 N94-37856

POLLUTION TRANSPORT
A study of pollution courses of spilled oil floatation in the outer ocean 01 p0205 N94-11983
The North Atlantic Regional Experiment (NARE)
[DE93-010126] 02 p0706 N94-13054
Diagnostic studies of the HxOy-NxOy-O3 photochemical system using data from NASA GTE field expeditions
[NASA-CR-193672] 02 p0706 N94-13170
Importance of sprays for long range transport of harmful substances in the troposphere
[MITT-81] 02 p0711 N94-14723
A review of wind field models for atmospheric transport
[DE93-016085] 04 p1488 N94-17895
International Symposium on the Ecological Effects of Arctic Airborne Contaminants --- abstracts
[AD-A269955] 04 p1475 N94-18775
Inclusion of a three-dimensional washout coefficient in ADPIC
[DE93-018499] 04 p1476 N94-19038
Application of an atmospheric dispersion model to simulated pollutant releases in the Colorado Front range
[DE93-017118] 04 p1480 N94-19732
Analysis of wind observation from towers in the period 1977-1991
[KNMI-TR-148] 05 p1865 N94-20239
An economic analysis of transboundary air pollution between Finland and the Soviet Union
[ETLA-DISCUSSION-PAPER-335] 05 p1854 N94-22072
Carbon and hydrogen isotope composition and C-14 concentration in methane from sources and from the atmosphere: Implications for a global methane budget
[NASA-CR-195166] 06 p2399 N94-25092
Collection and evaluation of numerical models with the aim to investigate the impact of aircraft emissions
[DLR-MITT-93-06] 06 p2400 N94-25414
Air pollution transport modeling
[AD-A273863] 07 p2865 N94-25609
A positive finite-difference advection scheme applied on locally refined grids
[CWI-NM-R9309] 07 p2867 N94-26216
An observational study of air pollution transport over a large urban complex
[REPT-6] 07 p2867 N94-26474
Intermedia transfer factors for fifteen toxic pollutants released to air basins in California
[DE94-005699] 08 p3349 N94-30044
Evaluation of discretization schemes for advection-diffusion equations
[CWI-NM-R9311] 08 p3461 N94-30751
Temporal and spatial mapping of atmospheric dust opacity and surface albedo on Mars 09 p3947 N94-33211
Previous model comparisons 10 p3971 N94-33458
Model capabilities, 2-D 10 p3971 N94-33459
Atmospheric and dispersion modeling in areas of highly complex terrain employing a four-dimensional data assimilation technique
[DE94-004041] 11 p4285 N94-35823
Modeling the atmospheric input of nutrients, heavy metals, and pesticides to the Great Lakes
[DE94-005481] 11 p4286 N94-36007
Long-range mesoscale modeling of pollutant transport for the European Tracer EXperiment (ETEX)
[DE94-010820] 12 p4465 N94-37093
Modeling of trace constituent transport with the University of Wisconsin global isentropic-sigma model
[DE94-012729] 12 p4466 N94-37288
Evaluation of parameterizations for pollutant transport and dispersion in an urban street canyon using a three-dimensional dynamic flow model
[DE94-012641] 12 p4467 N94-37429
Modeling atmospheric concentrations and deposition of Hg
[DE94-012633] 12 p4467 N94-37440
Program GAUSSPLYM: A tool in Windows environment for studying continuous releases
[PB94-184603] 12 p4468 N94-37856

POLOIDAL FLUX
Neoclassical kinetic theory near an X-point: Plateau regime
[DE93-019825] 05 p1951 N94-20224

POLONIUM
NT POLONIUM ISOTOPES

POLONIUM ISOTOPES
Study of the atmospheric chemistry of radon progeny in laboratory and real indoor atmospheres
[DE93-012236] 01 p0266 N94-11671

POLYACETYLENE
Identification of electronic transitions in polyacetylene by acoustic phonon spectroscopy
[DE94-009324] 10 p4138 N94-34383
Syntheses and studies of acetylenic polymers
[DE94-011201] 11 p4245 N94-36057
Pressure dependence of the conductivity and magnetoconductance in oriented iodine-doped polyacetylene
[PB94-184488] 12 p4427 N94-37854

POLYACRYLATES
U ACRYLIC RESINS

POLYACRYLONITRILE
A new FR water resistant acoustic insulation material for aircraft 01 p0018 N94-10773
Preparation of carbon monoliths having tailored pore structure from porous polymer precursors
[DE93-011576] 01 p0089 N94-10958
Characterization of the lithium/pan-based polymer electrolytes interface
[AD-A268401] 03 p0973 N94-17434
Advances in preparing and characterizing low density pan-carbon microcellular foam
[DE94-002278] 07 p2748 N94-25932
Preparation of graphite fibers from polyimide 08 p3223 N94-29517
Sodium-23 NMR and complex impedance studies of gel electrolytes based on poly(acrylonitrile)
[AD-A280330] 12 p4408 N94-37031
The development of short, high surface area activated carbon fibers
[AD-A280509] 12 p4404 N94-37105
Basic solutions to carbon/carbon oxidation: Science and technology
[AD-A280447] 12 p4404 N94-37232

POLYAMIDE RESINS
NT KEVLAR (TRADEMARK)
NT NYLON (TRADEMARK)
Highly fluorinated polymers
[NASA-CR-194147] 02 p0579 N94-13964
Pore-size-distribution of cationic polyacrylamide hydrogels
[DE93-015218] 02 p0581 N94-14400
Mechanical properties and impact damage resistance of composites fabricated by low cost, vacuum assisted, resin transfer molding
[AD-A270361] 04 p1342 N94-18702
Polyimide-based electrooptic materials
[DE93-019416] 05 p1706 N94-21526
Polyimide processing additives
[NASA-CASE-LAR-13669-2] 06 p2252 N94-23079
Reaction of isocyanates with carboxylic acids and its application to polymer synthesis
[PB94-118858] 06 p2254 N94-23763

POLYATOMIC GASES
NT DIATOMIC GASES

POLYATOMIC MOLECULES
NT DIATOMIC MOLECULES
NT TRIATOMIC MOLECULES
Molecular dynamics simulation of electronically excited polyatomic molecules
[DE93-623045] 02 p0781 N94-13225
Selective excitation, relaxation, and energy channeling in molecular systems
[DE93-018819] 02 p0785 N94-14420

Geochemistry and cosmochemistry of fullerenes 3: Reaction of C60 and C70 with ozone
03 p0953 N94-16243
Spectroscopic investigations of nonambient systems with millimeter and submillimeter probes
[AD-A266537] 03 p0968 N94-16796
Photodissociation studies of polyatomic free radicals
[AD-A270084] 04 p1350 N94-18799
Ab initio potential energy surface for the H + OCS reaction
[AD-A270577] 05 p1696 N94-19947
Three methods to measure RH bond energies
[DE94-003795] 07 p3013 N94-25816
Chemical dynamics studies of reactions in energetic materials
[AD-A275607] 08 p3224 N94-28769
Theoretical investigation of gas-surface interactions
[NASA-CR-195755] 08 p3272 N94-29378
Spectroscopic and dynamical studies of highly energized small polyatomic molecules
[DE94-006509] 08 p3489 N94-30061
Energy transfer properties and mechanisms
[DE94-007403] 09 p3636 N94-32594
Wave packet studies of the vibrational predissociation of three and four-atom van der Waals complexes
[DE94-007623] 09 p3871 N94-32598

POLYBENZIMIDAZOLE
Di(hydroxyphenyl)- benzimidazole monomers
[NASA-CASE-LAR-14643-2] 06 p2253 N94-23305

POLYBLENDS
U POLYMER BLENDS

POLYBUTADIENE
Investigation of the reason for the softening behaviour of filled polymers 01 p0063 N94-10058
Interfacial modification through end group complexation in polymer blends
[AD-A265887] 01 p0093 N94-12340
Microstructure of styrene methyl methacrylate copolymers grafted onto polybutadiene seeds
[ETN-94-95360] 06 p2262 N94-25225
Cryogenic size reduction of solid propellant
[AD-A274844] 07 p2759 N94-26800
Correlation of cookoff behavior of rocket propellants with thermomechanical and thermochemical properties
[AD-A274983] 08 p3224 N94-29092
A newly developed snow vehicle (SM100S) for Antarctica. Part 4: Low temperature properties of crawler belt 08 p3314 N94-29984
Solventless, curable fluid oligomeric systems for high performance microwave, acoustical and mechanical applications 08 p3223 N94-30478
Basic solutions to carbon/carbon oxidation: Science and technology
[AD-A280447] 12 p4404 N94-37232

POLYCARBONATES
A non-halogenated, flame retarded polycarbonate
01 p0019 N94-10781
Sequestering carbon dioxide in industrial polymers: Building materials for the 21st century
[DE93-016087] 02 p0580 N94-14297
Optical studies of glasses embedded with inorganic ions and organic dyes
[AD-A268146] 03 p1199 N94-17455
Structure and properties of polycarbonate alloys
[ETN-93-95071] 04 p1375 N94-19611
Techniques for producing free-standing thin films on frames
[DE93-041144] 05 p1708 N94-21954
A preliminary evaluation of the phosphazene resin PPZ
[AD-A273674] 06 p2263 N94-25410
Birdstrike resistant crew enclosure program
[AD-A273700] 06 p2463 N94-25453
Ballistic performance of polycarbonate/polyester and polycarbonate/styrene- acrylonitrile microlayer sheets
[AD-A275462] 08 p3177 N94-28735
Surface energy changes produced by ultraviolet-ozone irradiation of poly(methylmethacrylate), polycarbone and polytetrafluoroethylene
[NASA-TM-106460] 08 p3213 N94-28922
Ablation of polymers by ultraviolet pulsed laser
[DE94-608100] 08 p3218 N94-30066
Improved construction materials for polar regions using microcellular thermoplastic foams
08 p3223 N94-30483
Advances in rapid prototyping
[DE94-010075] 12 p4430 N94-36447
Development of high sensitivity techniques for characterizing outgassing of polymeric construction materials for microenvironments
[DE94-012068] 12 p4424 N94-37204

POLYCARBOSILANES
Chain propagation/step propagation polymerization chemistry. The preparation of solvent resistant well phase-separated thermoplastic elastomers
[AD-A271128] 05 p1699 N94-20016
Conversion of polymers of methyl- and vinylsilane to Si-C ceramics
[NASA-TM-106554] 09 p3662 N94-32945

POLYCHLORINATED BIPHENYLS
Procurement and execution of PCB analyses: Customer-analyst interactions
[DE93-009964] 02 p0566 N94-14694

POLYCRYSTALS
Flexible polycrystalline thin-film photovoltaics for space applications 01 p0050 N94-11393
Grain boundary creep in copper
[DE93-610974] 01 p0084 N94-12361
Photovoltaic Subcontract Program
[DE93-000092] 02 p0700 N94-12868
Activities of the Basic Sciences Branch
[DE93-010012] 02 p0851 N94-14455
Quenching and annealing effects on the specific heat of YBa2Cu3O(7-delta)
[DE93-016483] 02 p0816 N94-14868
Ternary alloying effects in polycrystalline (beta)-NiAl
[DE93-012675] 03 p0955 N94-15885
Powder diffraction studies using anomalous dispersion
[DE93-012531] 03 p1210 N94-16775
Development of large-area monolithically integrated silicon-film photovoltaic modules
[DE93-010037] 04 p1464 N94-17731
Phase separation and ordering process in Al-Li alloys studied by small-angle neutron scattering and neutron diffraction
[DE93-016750] 04 p1358 N94-17947
Self-organized criticality and the Barkhausen effect in amorphous and polycrystalline metals
[AD-A269817] 04 p1361 N94-18735
Growth, characterization and device development in monocrystalline diamond films
[AD-A270074] 04 p1599 N94-18797
Polycrystalline thin-film cadmium telluride solar cells fabricated by electrodeposition
[DE93-018201] 04 p1468 N94-18944
Defect behavior of polycrystalline solar cell silicon
[DE93-018490] 04 p1468 N94-19016
Tribological studies of silicon for magnetic recording applications (Invited)
[AD-A270878] 04 p1447 N94-19784
Neutral copper cluster sputtering yields: Ne(+), Ar(+) and Xe(+) bombardment
[DE93-019010] 05 p1690 N94-20288
Temperature-dependent ion beam mixing
[DE93-040281] 05 p2033 N94-21999
Interface science of controlled metal/metal and metal/ceramic interfaces prepared using ultrahigh vacuum diffusion bonding
[DE94-001066] 05 p1696 N94-22025
Polycrystalline thin film materials and devices
[DE93-018213] 06 p2389 N94-22862
Chromate-free talc chemical conversion coatings for aluminum alloys
[DE94-001567] 06 p2238 N94-22932
Orientation imaging microscopy: New possibilities for microstructural investigations using automated BKD analysis
[DE94-000777] 06 p2557 N94-22938
Research on polycrystalline thin-film CuInGaSe2 solar cells
[DE94-000203] 06 p2560 N94-23205
Defects in electro-optically active polymer solids
06 p2223 N94-24342
Study on elucidation of damage generation process by electron beam lithography 07 p2729 N94-25581
The reactivity of lithium toward non-aqueous solvents of relevance to energy storage applications as studied by surface analytical techniques
[DE94-003483] 07 p2856 N94-26464
A model of electric breakdown in polycrystalline semiconductors with highly nonlinear I - V characteristics
[DE94-601537] 07 p3063 N94-27017
Deformation, constitutive behavior, and damage of advanced structural materials under multiaxial loading
[AD-A274165] 07 p2709 N94-27142
An improved method of measuring tropospheric NO2, NO3, HO2, and RO2 by Matrix Isolation and Electronic Spin Resonance (MIESR) 08 p3345 N94-28605
The effect of various metallurgical parameters on the flow and fracture behavior of polycrystalline NiAl near the brittle-to-ductile transition
[NASA-TM-106534] 08 p3205 N94-29758
The bases for the development of high-temperature integrated SQUID-systems
[DE94-607901] 08 p3267 N94-30073
Plasma enhanced chemical vapor deposition of ZrO2 thin films
[DE94-006031] 08 p3218 N94-30104
Electrooptical and optical evaluation of Pb(Zr,Ti)O3 thin films using waveguide refractometry
[DE94-006374] 08 p3518 N94-30247
Piezoelectric materials research in Europe
[AD-A276207] 09 p3648 N94-31059
Synthesis, characterization, phase diagrams and superconducting, and normal state magnetic properties of La(2-x)Sr(x)CuO4 (0 is less than or equal to x which is less than or equal to 0.08) and electrochemically oxidized La(2-x)Sr(x)CuO(4 + delta) (0 is less than or equal to x which is less than or equal to 0.33, 0 is less than or equal to delta which is less than or equal to 0.12)
[DE94-005260] 09 p3895 N94-31067
Role of polycrystallinity in CdTe and CuInSe2 photovoltaic cells
[DE94-000293] 09 p3758 N94-31236
A scanning defect mapping system for semiconductor characterization 09 p3885 N94-32446
Attempts to model the generation of new grain boundaries during the deformation of polycrystals
[DE94-007527] 09 p3903 N94-32597
Development of a computer model for polycrystalline thin-film CuInSe2 and CdTe solar cells
[DE94-006853] 09 p3762 N94-32763
Isothermal sintering, microstructure, and superconducting properties of Y1Ba2Cu3O(7-x) compound
[DE94-008132] 09 p3905 N94-32779
Nucleation and growth of cubic boron nitride films produced by ion-assisted pulsed laser deposition
[DE94-007295] 09 p3661 N94-32796
The path for long range conduction in high J(sub c) TlBa2Ca2Cu3O(8+x) spray-pyrolyzed deposits
[DE94-007211] 09 p3909 N94-33271
Method for forming aligned superconducting Bi-SR-CA-CU-O
[AD-D016192] 10 p4148 N94-34405
Modelling irradiation creep of zirconium alloys
[DE94-619055] 12 p4414 N94-36544
Diamond deposition and defect chemistry studied via solid state NMR
[AD-A280609] 12 p4533 N94-36727
Effect of thermal annealing on grain boundary chemistry of polycrystalline TlBa2Ca2Cu3O(y) films
[DE94-011464] 12 p4538 N94-37569

POLYCYCLIC AROMATIC HYDROCARBONS
Measurement of polycyclic aromatic hydrocarbon (PAHs) in interplanetary dust particles
01 p0431 N94-12167

POLYESTER RESINS
Polymer technology publication. Series no. 14, 1993
[PB93-195964] 04 p1372 N94-19052
Ultrasonic measurement technique to determine the state of cure in thermosetting materials
[PB94-124328] 07 p2756 N94-27217

POLYESTERS
Highly fluorinated polymers
[NASA-CR-194147] 02 p0579 N94-13964
Mechanical properties and impact damage resistance of composites fabricated by low cost, vacuum assisted, resin transfer molding
[AD-A270361] 04 p1342 N94-18702
Outgassing rate of Reemay Spunbonded Polyester and DuPont Double Aluminized Mylar
[DE93-040015] 05 p1699 N94-19973
Technique to predict the curing behaviour of unsaturated polyester materials
[PB94-124856] 07 p2748 N94-25892
Modelling the inhibition cure behaviour of unsaturated polyester moulding materials
[PB94-124864] 07 p2748 N94-25893
Stress relaxation in dough moulding compounds
[PB94-124872] 07 p2748 N94-25894
Trifluoromethyl-substituted polymers
[NASA-CR-195217] 07 p2751 N94-26641
The polymerization of epsilon-caprolactone with stannous catalyst and lactide/epsilon-caprolactone (LA/epsilon-CL) and lactide/glycolide (LA/GA) copolymers. Polymer technology publication series no. 15
[PB94-137551] 08 p3220 N94-30713
Improved resealing procedures for the second deseal/reseal program in RAAF F111 aircraft fuel tanks
[AD-A277069] 09 p3580 N94-32378
Highly fluorinated polymers
[NASA-CR-196270] 12 p4422 N94-37025

POLYETHER RESINS
NT PEEK
NT POLYMETHYL METHACRYLATE
Highly fluorinated polymers
[NASA-CR-194147] 02 p0579 N94-13964
Properties of perfluoropolyethers for space applications
[NASA-TM-106616] 12 p4426 N94-37520

POLYETHERETHERKETONES
U PEEK

POLYETHYLENE TEREPHTHALATE
Processing of semicrystalline polymers
06 p2226 N94-24351

A preliminary evaluation of the phosphazene resin PPZ
[AD-A273674] 06 p2263 N94-25410
Ablation of polymers by ultraviolet pulsed laser
[DE94-608100] 08 p3218 N94-30066
Electrical properties of double layer dielectric structures for space technology
[ISBN-0-315-86547-4] 09 p3610 N94-31910

POLYETHYLENES
NT POLYETHYLENE TEREPHTHALATE
Determination of concentration profiles at interfaces and surfaces of partially miscible polymer blends
[DE93-013140] 01 p0089 N94-11007
Development of plastic capsule for research reactor irradiation
[DE93-753186] 01 p0372 N94-11591
Effect of stabilization on the recycling of polyolefins in blow moulding
[IMI-93RT-42400-1477-G] 02 p0596 N94-13684
Thin composite solid electrolyte film for lithium batteries
[NASA-CASE-NPO-18694-1-CU] 03 p1014 N94-17325
Computer simulation of macromolecular crystals and their defects
[DE93-015213] 04 p1596 N94-18192
Mesoepitaxy: A universal route to oriented materials
[AD-A270437] 04 p1598 N94-18511
Polymer gels as precursors to high-performance materials
[AD-A270937] 05 p1699 N94-20046
Spatial organization of polymer chains in a crystallizable diblock polyethylene and polystyrene
[AD-A271862] 05 p1702 N94-20463
Development and demonstration of a personal monitoring system for exposure to hydrogen fluoride
[DE93-041273] 05 p1891 N94-20935
Mechanical properties and reliability of semi-crystalline polymers
[AD-A271591] 05 p1704 N94-20946
Column chromatographic separation of Y(3+) from Sr(2+) by polymeric ionizable crown ether resins
[DE94-000935] 05 p1683 N94-22021
Demonstration of polyscann ultrasonic butt-fusion inspection system for polyethylene pipes
[AD-A273279] 06 p2373 N94-24814
In situ spectroscopic applications to the study of rechargeable lithium batteries
[DE94-003478] 07 p2782 N94-26328
Failure behaviour of high density polyethylene with an embrittled surface layer due to weathering
[PB94-126406] 07 p2840 N94-26960
Application of the Positron Annihilation Technique to the study of vapor absorption process in polyethylene (LDPE) and in imide polymer (6FDA-TMPD PI)
[DE94-602737] 07 p2720 N94-27998
Temperature depencence of the far infrared optical constants of polyethylene
[PB94-124336] 08 p3213 N94-28795
Analysis of infrared radiation heating process considering chemical reaction of material to be heated
[DE94-744116] 08 p3199 N94-30267
Development of radiation resistant electrical cable insulations 08 p3223 N94-30480
Development of radiation resistant electrical cable insulations
[DE94-005189] 08 p3222 N94-30906
A comparison of atomic oxygen erosion yields of carbon and selected polymers exposed in ground based facilities and in low Earth orbit
[NASA-TM-106622] 11 p4243 N94-35243
Laminated thermoplastic composite material from recycled high density polyethylene 11 p4230 N94-36403
Microscale synthesis and characterization of polystyrene: NSF-POLYED scholars project 11 p4231 N94-36408
LET spectra of fragmented 600-MeV/A iron beam on aluminum and polyethylene: A preliminary analysis
[NASA-TP-3436] 12 p4416 N94-36993

POLYGONS
NT RECTANGLES
NT SQUARES (MATHEMATICS)
NT TETRAGONS
NT TRAPEZOIDS
NT TRIANGLES
Finding a covering triangulation whose maximum angle is provably small
[DE93-010691] 01 p0334 N94-12593
Extremal polygon containment problems and other issues in parametric searching
[ITN-93-85214] 02 p0771 N94-14506
Fast data parallel polygon rendering
[DE93-040157] 05 p1929 N94-20279
A model for the origin of Martian polygonal terrain 05 p2090 N94-20393
A formational model for the polygonal terrains of Mars: Taking a crack at the genesis of the Martian polygons 05 p2091 N94-20400
Geometric optimization
[DE93-040152] 05 p1917 N94-21764
An algorithm for the interference detection among polygonal surfaces 05 p1791 N94-22239
Strategy for motion of a moving body of quasi-polygonal form within a polygonal space 05 p1792 N94-22240
Number of moduli of families of curves on toric surfaces
[PB93-230381] 06 p2479 N94-23121
Tools for visualizing landscape pattern for large geographic areas
[DE94-001121] 06 p2388 N94-24757
An algorithm to find the intersection of two convex polygons
[AD-A274722] 07 p2961 N94-26148
Shape from diameter: Negative results
[RUU-CS-93-16] 08 p3458 N94-30407
Shape from diameter: Positive results
[RUU-CS-93-17] 08 p3458 N94-30408
Rectilinear decompositions with low stabbing number
[RUU-CS-93-25] 08 p3459 N94-30425

POLYHEDRONS
NT CUBES (MATHEMATICS)
NT ICOSAHEDRONS
NT PYRAMIDS
NT RHOMBOHEDRONS
NT TETRAHEDRONS
Applications of cut polyhedra
[CWI-BS-R9221] 01 p0347 N94-10354
Model-based recognition of 3-D objects by geometric hashing technique
[DE93-612916] 01 p0322 N94-10410
Extracting projective information from single views of 3D point sets
[OUEL-1973/93] 06 p2464 N94-25471
Polyhedral characterization of the economic lot-sizing problem with start-up costs
[MEMO-COSOR-92-46] 07 p2969 N94-27396
Representations of dynamical systems described by behavioral inequalities
[AD-B173649] 08 p3458 N94-30402
Polyhedric object recognition by indexing in a model base
[ETN-94-95913] 09 p3812 N94-31542
Efficient contact determination between geometric models
[AD-A280244] 12 p4494 N94-37120

POLYIMIDE RESINS
Research on radiation resistance properties of structural materials for space use 02 p0529 N94-13271
A process for preparing an assembly of an article and a soluble polyimide which resists dimensional change, delamination, and debonding when exposed to changes in temperature
[NASA-CASE-LAR-14763-1] 05 p1702 N94-20373
Tribological behaviour of fluorinated resins and polyimide resins sliding over a metallic surface in liquid nitrogen 06 p2355 N94-23991
Property enchancement of polyimide films by way of the incorporation of lanthanide metal ions 07 p2758 N94-27926
Low dielectric polyimide fibers
[NASA-CASE-LAR-14526-1] 08 p3214 N94-29359
Irradiation polymerization of bismaleimide resins
[REPT-932-430-105] 08 p3215 N94-29441
Addition polyimides with enhanced processability
[NASA-CASE-LEW-15043-1] 11 p4242 N94-35234
Tough high performance composite matrix
[NASA-CASE-LAR-14239-2] 11 p4232 N94-35372

POLYIMIDES
NT BISMALEIMIDE
NT KAPTON (TRADEMARK)
Polyimide foam insulation systems: A major weight reduction and improvement in fire resistance of sidewall systems 01 p0017 N94-10769
A polyimide foam for advanced fire resistant aircraft applications 01 p0017 N94-10770
Semiconductor ring lasers
[DE93-012386] 01 p0174 N94-11005
A novel photosensitive polyimide resist consisting of a soluble polyimide and a bis(perfluorophenyl azide) as a cross-linker
[AD-A265998] 01 p0093 N94-12353
Protective coatings for high-temperature polymer matrix composites
[NASA-TM-106276] 01 p0074 N94-12431
Research on radiation resistance properties of structural materials for space use 02 p0529 N94-13271
Photodegradation of polyimides. V1: Effect of donor-acceptor groups on the photooxidative stability of polyimides and model compounds
[AD-A267319] 03 p0970 N94-16947
Low dielectric polyimides
[NASA-CASE-LAR-14987-2] 03 p0974 N94-17559
Excimer laser induced permanent electrical conductivity and nanostructures in polymers
[DE93-015965] 04 p1368 N94-17946
Elastic properties of a polyimide film determined by Brillouin scattering and mechanical techniques
[DE93-017404] 04 p1368 N94-18098
A process for preparing an assembly of an article and a soluble polyimide which resists dimensional change, delamination, and debonding when exposed to changes in temperature
[NASA-CASE-LAR-14763-1] 05 p1702 N94-20373
Polyimides containing amide and perfluoroisopropylidene connecting groups
[NASA-CASE-LAR-14608-1] 05 p1702 N94-20374
Simulated space environmental effects on some experimental high performance polymers 05 p1662 N94-21385
Polyimide-based electrooptic materials
[DE93-019416] 05 p1706 N94-21526
Polyimide processing additives
[NASA-CASE-LAR-13669-2] 06 p2252 N94-23079
Polyimide/inorganic composite-interpenetrating polymer network for stable second-order nonlinear optics
[AD-A274646] 07 p2709 N94-27107
Outgas and vacuum seal characteristics of irradiated polyimide O-ring
[DE94-701200] 07 p2757 N94-27812
New monomers for high performance polymers 07 p2758 N94-27904
Property enchancement of polyimide films by way of the incorporation of lanthanide metal ions 07 p2758 N94-27926
Application of the Positron Annihilation Technique to the study of vapor absorption process in polyethylene (LDPE) and in imide polymer (6FDA-TMPD PI)
[DE94-602737] 07 p2720 N94-27998
Breakdown testing of wiring insulation 08 p3166 N94-28713
High temperature polymer dielectric film insulation 08 p3167 N94-28715
Low dielectric polyimide fibers
[NASA-CASE-LAR-14526-1] 08 p3214 N94-29359
Composite flexible blanket insulation
[NASA-CASE-ARC-11955-1-CU] 08 p3180 N94-29509
Preparation of graphite fibers from polyimide 08 p3223 N94-29517
Polyimides containing the penta fluoro sulfanyl benzene moiety
[NASA-CASE-LAR-15082-1] 08 p3175 N94-29554
Polyimides containing pendent siloxane groups
[NASA-CASE-LAR-14638-1] 08 p3215 N94-29555
Study of the ultraviolet absorption and photoconduction spectra of polyimide films fabricated at various curing temperatures
[ISBN-0-315-85923-7] 08 p3218 N94-30036
Performance of selected polymeric materials on LDEF 09 p3593 N94-31023
Reliability of multilayer copper/polyimide
[AD-A276228] 09 p3650 N94-31284
Molecular interactions at metal/polyimide interfaces: A correlation with adhesion and bond durability
[AD-A276301] 09 p3650 N94-31297
Electrical properties of double layer dielectric structures for space technology
[ISBN-0-315-86547-4] 09 p3610 N94-31910
Characterization of thermally stable dye-doped polyimide based electrooptic materials
[DE94-005309] 09 p3882 N94-32674
Characterization of crosslinked electrooptic polyimides
[DE94-007934] 09 p3661 N94-32819
Low pressure process for continuous fiber reinforced polyamic acid resin matrix composite laminates
[NASA-CASE-LAR-14954-1] 10 p4020 N94-35075
Tough, processable semi-interpenetrating polymer networks from monomer reactants
[NASA-CASE-LAR-14838-1] 11 p4242 N94-35233
Tough high performance composite matrix
[NASA-CASE-LAR-14239-2] 11 p4232 N94-35372
Residual Gas Analysis (RGA) and shear strength characteristics of a silver-filled epoxy and polyimide under long-term, high-temperature storage conditions
[DE94-010106] 11 p4244 N94-35705
Liquid crystalline thermosetting polyimides
[DE94-009939] 11 p4244 N94-35768
Third European Technical Symposium on Polyimides and High Performance Polymers: STEPI 3
[PB94-148491] 11 p4246 N94-36177

POLYISOPRENES
A newly developed snow vehicle (SM100S) for Antarctica. Part 4: Low temperature properties of crawler belt 08 p3314 N94-29984

POLYMER ALLOYS
U POLYMER BLENDS
POLYMER BLENDS
Determination of concentration profiles at interfaces and surfaces of partially miscible polymer blends
[DE93-013140] 01 p0089 N94-11007
Interfacial modification through end group complexation in polymer blends
[AD-A265887] 01 p0093 N94-12340
Phase transition in polymer blends and structure of ionomers and copolymers
[DE93-016256] 02 p0579 N94-13978
Polymer Infiltration Studies
[NASA-CR-194494] 03 p0932 N94-15275
Cyanoresin, cyanoresin/cellulose triacetate blends for thin film, dielectric capacitors
[NASA-CASE-NPO-18913-1-CU] 03 p0966 N94-15930
Polymer technology publication. Series no. 14, 1993
[PB93-195964] 04 p1372 N94-19052
Structure and properties of polycarbonate alloys
[ETN-93-95071] 04 p1375 N94-19611
Polymer films with enhanced dielectric properties
[AD-A271148] 04 p1375 N94-19740
Surface and interfacial properties of polymer blends. A literature survey
[PB93-230191] 06 p2254 N94-23561
Electric field-mediated processing of polymer blend solutions 06 p2223 N94-24341
Processing of semicrystalline polymers 06 p2226 N94-24351
Ultrastructure processing of macromolecular materials
[AD-A273413] 06 p2258 N94-24782
Center for advanced electrical and structural polymers
[AD-A273415] 06 p2259 N94-24783
Simulation studies for surfaces and materials strength
[NASA-CR-195185] 06 p2565 N94-25093
Ultrastructure processing of macromolecular materials
[AD-A274460] 07 p2754 N94-27086
Ballistic performance of polycarbonate/polyester and polycarbonate/styrene- acrylonitrile microlayer sheets
[AD-A275462] 08 p3177 N94-28735
Recent developments in polymeric charge transfer complexes
[AD-A277108] 09 p3654 N94-31979
Solvent diffusion coefficient concentration dependence in polymer solutions
[AD-A277023] 09 p3655 N94-32005
Compatibility studies of some azo polymer blends
[AD-A277141] 09 p3657 N94-32365
Intelligent processing of materials, technical activities, 1993 (NAS-NRC Assessment Panel, April 21-22 1994)
[PB94-164183] 11 p4251 N94-35737
Thermal cis-trans isomerization rates of azobenzenes bound in the side chain of some copolymers and blends
[AD-A280451] 12 p4424 N94-37227
POLYMER CHEMISTRY
New aromatic activated dihalides and bisphenol monomers for the preparation of novel poly(arylene ethers)
[NASA-CR-193190] 01 p0055 N94-10513
Ring-opening polymerization of phosphazenes
[AD-A265000] 01 p0090 N94-11292
Polymer-polymer interactions
[AD-A265304] 01 p0091 N94-11830
Molecular properties of polymeric materials for space applications
[NASA-CR-194370] 01 p0094 N94-12450
Photogenerated base in polymer imaging. Synthesis and photopatterning of poly(2-cyano-2-(p-vinylphenyl) butanoic acid)
[AD-A265288] 01 p0095 N94-12585
Effect of stabilization on the recycling of polyolefins in blow moulding
[IMI-93RT-42400-1477-G] 02 p0596 N94-13684
Office of Naval Research/DARPA publications: Composite materials with improved properties in compression
[AD-A265509] 02 p0560 N94-14794
Intramolecular versus intermolecular condensation rates in the acidic polymerization of octaethoxytrisiloxane
[AD-A266982] 03 p0963 N94-15490
Electrical conductivity of ion implanted ladder and semi-ladder polymers
[AD-A267432] 03 p0970 N94-16978
Soluble precursor route to polyanilines
[AD-A268015] 03 p0973 N94-17494
Royal Society of Chemistry, Heterocyclic Chemistry Group, Lakeland Heterocyclic Symposium
[AD-A270374] 04 p1338 N94-18703
Molecular and polymeric ceramic precursors
[DE93-040364] 04 p1372 N94-18891
Physical chemical studies of conducting polymers fundamental and applied
[AD-A270728] 04 p1374 N94-19574
The modification of polymer surfaces and the fabrication of submicron-scale functionalized structures by deep-UV and electron beam lithography
[AD-A265956] 05 p1700 N94-20328
Reaction of isocyanates with carboxylic acids and its application to polymer synthesis
[PB94-118858] 06 p2254 N94-23763
Synthesis of molecular wires by a novel divergent/convergent approach
[AD-A273332] 06 p2537 N94-25087
Influence of test configuration on the combustion characteristics of polymers as ignition sources 06 p2238 N94-25365
The x ray holographic microscopy using the atomic-force microscope
[DE94-004003] 07 p2814 N94-27779
Cellular and molecular approaches to polymer synthesis by bacteria
[AD-A275501] 08 p3212 N94-28661
High temperature arc-track resistant aerospace insulation 08 p3167 N94-28716
Polymer Technology Seminar, 1993. Kem-100.600
[PB94-137593] 08 p3213 N94-29031
Polymer technology publication series no. 16
[PB94-135522] 08 p3214 N94-29157
Polyimides containing the penta fluoro sulfanyl benzene moiety
[NASA-CASE-LAR-15082-1] 08 p3175 N94-29554
Polyimides containing pendent siloxane groups
[NASA-CASE-LAR-14638-1] 08 p3215 N94-29555
Solventless, curable fluid oligomeric systems for high performance microwave, acoustical and mechanical applications 08 p3223 N94-30478
The polymerization of epsilon-caprolactone with stannous catalyst and lactide/epsilon-caprolactone (LA/epsilon-CL) and lactide/glycolide (LA/GA) copolymers. Polymer technology publication series no. 15
[PB94-137551] 08 p3220 N94-30713
Crosslinking and surface reactions in macromolecules: Spectroscopic FT-IR studies 08 p3221 N94-30812
Reactions of electrophilic maleic anhydride and epoxy groups with nucleophilic functionalities such as carboxyl, hydroxyl, and amine groups. Polymer Technology Publication series no. 16
[PB94-135589] 09 p3648 N94-31069
Novel electroactive polymers and block copolymers
[AD-A276119] 09 p3650 N94-31509
Competition between crystallization and mixing/demixing in polymer mixture
[ETN-94-95753] 09 p3651 N94-31513
Mechanical properties of acrylate networks formed by visible laser-induced polymerization. 2. Control of the mechanical properties
[AD-A277111] 09 p3655 N94-31982
Multifunctional macromolecules
[AD-A277347] 09 p3656 N94-32246
Nonlinear optical polymers derived from organic/inorganic composites
[AD-A277408] 09 p3659 N94-32610
Nonlinear optical properties of rigid-rod polymers
[NASA-CR-191349] 09 p3882 N94-32702
Novel precursor approached for CMC derived by polymer pyrolysis
[AD-A278383] 09 p3665 N94-33352
Differential equations and continuum mechanics
[AD-A278341] 10 p4131 N94-34001
Syntheses and studies of acetylenic polymers
[DE94-011201] 11 p4245 N94-36057
Highly fluorinated polymers
[NASA-CR-196270] 12 p4422 N94-37025
Tert-butylalumoxanes: Synthetic analogs for methylalumoxane (MAO) and new catalytic routes to polyolefins and polyketones
[AD-A280532] 12 p4399 N94-37650
POLYMER MATRIX COMPOSITES
NT CARBON FIBER REINFORCED PLASTICS
NT CARBON-PHENOLIC COMPOSITES
NT EPOXY MATRIX COMPOSITES
NT GLASS FIBER REINFORCED PLASTICS
NT GRAPHITE-POLYIMIDE COMPOSITES
NT REINFORCED PLASTICS
Vectra insulative support structures within spacecraft 01 p0062 N94-10050
The Netherlands innovation oriented research programme on polymer composites and special polymers 1985-1993 01 p0065 N94-10067
Fibre reinforced polymer matrix composites: Microstructure and mechanical properties
[DLR-FB-92-28] 01 p0066 N94-11085
Protective coatings for high-temperature polymer matrix composites
[NASA-TM-106276] 01 p0074 N94-12431
The Second Workshop on Deployment and Assembly Experiment of Large Space Structure on Orbit
[NASDA-CON-930003] 02 p0529 N94-13268
Research on radiation resistance properties of structural materials for space use 02 p0529 N94-13271
Characterization of composite materials for aerospace structures
[ESA-TT-1260] 02 p0557 N94-13804
Prediction of thermal cycling induced cracking in polymer matrix composites
[NASA-CR-194677] 03 p0941 N94-17295
Molecular composites from liquid crystalline polymers and liquid crystalline thermosets
[DE93-016608] 04 p1368 N94-18096
Nondestructive inspection of graphite-epoxy laminates for heat damage using DRIFT and LPF spectroscopies
[DE93-017228] 04 p1343 N94-18761
Interleaved bismaleimide composites
[AD-A272233] 05 p1674 N94-20574
Composite materials with improved properties in compression
[AD-A272837] 05 p1675 N94-21176
Space environmental effects on polymer matrix composites: The UTIAS/LDEF experiment 05 p1660 N94-21373
Thermal stress analysis of composites in the space environment 05 p1661 N94-21379
Computational Methods for Failure Analysis and Life Prediction
[NASA-CP-3230] 05 p1833 N94-22608
Projections on structures and material strength in the computational context 05 p1834 N94-22610
An overview of computational simulation methods for composite structures failure and life analysis 05 p1835 N94-22617
Materials Science and Engineering
[DE94-003018] 06 p2228 N94-23493
Prediction of thermal cycling induced cracking in polmer matrix composites
[NASA-CR-195135] 06 p2229 N94-24579
Design and test of postbuckled stiffened curved plates: A literature survey
[PB94-126521] 07 p2840 N94-26961
Polyimide/inorganic composite-interpenetrating polymer network for stable second-order nonlinear optics
[AD-A274646] 07 p2709 N94-27107
Finite element analysis of damped vibrations of laminated composite plates
[ISBN-0-315-84928-2] 07 p2843 N94-27585
Effects of physical aging on long-term behavior of composites 07 p2712 N94-27897
Apparatus for providing a uniform, consolidated, unidirectional, continuous, fiber-reinforced polymeric material and method relating thereto
[NASA-CASE-LAR-15173-1-CU] 08 p3180 N94-29496
Effects of physical aging on long-term creep of polymers and polymer matrix composites
[NASA-TM-109081] 08 p3181 N94-29541
Standardisation requirements for ultrasonic C-scanning of polymer matrix composites: An initial assessment
[PB94-139318] 08 p3184 N94-30438
High elongation elastomers 08 p3223 N94-30477
Generalized Eulerian-Lagrangian formulations in free and moving boundary problems: Processing of viscoelastic polymers and fiber suspensions 08 p3283 N94-30955
Thermal-vacuum response of polymer matrix composites in space 09 p3595 N94-31033
Space environmental effects on polymer composites: Research needs and opportunities 09 p3595 N94-31035
Characterization of polymer decomposition products by laser desorption mass spectrometry 09 p3597 N94-31046
Space hypervelocity microparticle impact damage in polymer matrix composites
[ISBN-0-315-87057-5] 09 p3652 N94-31692
Briefing and review meeting implementation of the military handbook 17 for polymer matrix and metal matrix composites
[AD-A277446] 09 p3663 N94-33010
The effects of physical aging at elevated temperatures on the viscoelastic creep on IM7/K3B
[NASA-TM-109114] 10 p4025 N94-34396
Micromechanical characterization of nonlinear behavior of advanced polymer matrix composites
[NASA-TM-109129] 10 p4025 N94-34397
Implementation of the military handbook 17 for polymer matrix composites and metal matrix composites
[AD-A278795] 11 p4244 N94-35757
Report on the Workshop on Manufacturing Polymer Composites by Liquid Molding
[PB94-160066] 11 p4234 N94-36004
Continuous unidirectional fiber reinforced composites: Fabrication and testing 11 p4229 N94-36400
Advanced manufacturing technology for polymer composite structures in Japan 12 p4422 N94-36968

POLYMER PHYSICS
A simple model of melt fracture
[AD-A265311] 01 p0092 N94-11862
Theoretical treatment of the bulk and surface properties of fluids containing long, flexible molecules
[DE93-015560] 02 p0575 N94-12861
Modelling and predicting properties of polymers in the amorphous glassy state
[ETN-94-95345] 07 p2752 N94-26645
Organic materials that respond to molecules
[AD-A275392] 08 p3174 N94-29307
Competition between crystallization and mixing/demixing in polymer mixture
[ETN-94-95753] 09 p3651 N94-31513
Influence of trace components on the viscoelastic properties of a polymer solution
[AD-A277171] 09 p3656 N94-32253
Stable second-order nonlinear optical materials based on interpenetrating polymer networks
[AD-A277410] 09 p3658 N94-32579
Conjugated polymer fluorescence: Interplay of correlations and alternation
[DE94-005587] 09 p3660 N94-32729
Differential equations and continuum mechanics
[AD-A278341] 10 p4131 N94-34001

POLYMERIC FILMS
NT KAPTON (TRADEMARK)
NT MYLAR (TRADEMARK)
Sensing glass transitions in thin polymer films on acoustic wave microsensors
[DE93-010805] 01 p0087 N94-10295
The fire properties of insulation bags, as installed and after aircraft operations 01 p0019 N94-10778
Glucose electrodes based on cross-linked (Os(bpy)2Cl)(sup +/2+) complexed poly(1-vinylimidazole) films
[AD-A265404] 01 p0094 N94-12425
Preparation of stable photopatternable polymeric materials for non-linear optics
[AD-A265359] 01 p0095 N94-12577
Performance aspects of de Laval spray-forming nozzles
[DE93-013671] 01 p0163 N94-12604
Amorphous sol-gel insulating films
[DE93-012859] 02 p0576 N94-12866
Poling of thin polymer films in electro optic applications
[AD-A266562] 02 p0579 N94-13584
The use of polarised neutron reflection for unique density profile determination in thin films
[PB93-187136] 02 p0579 N94-13783
Impedance-power effects on plasma polymer surface finish using a helical resonator discharge
[DE93-016454] 02 p0803 N94-14590
Organic polymeric electro-optic materials: Synthesis, processing, and device applications
[AD-A267133] 03 p0964 N94-15688
Photochemistry in thin polymeric films
[AD-A266716] 03 p0964 N94-15729
The effect of process parameters on the surface finish of plasma polymers
[DE93-014112] 03 p0966 N94-15924
Cyanoresin, cyanoresin/cellulose triacetate blends for thin film, dielectric capacitors
[NASA-CASE-NPO-18913-1-CU] 03 p0966 N94-15930
Synthesis of novel electrically conducting polymers: Potential conducting Langmuir-Blodgett films and conducting polymers on defined surfaces
[NASA-CR-194651] 03 p0972 N94-17297
Polarized thin films from dye-substituted polymers containing hydrophobically terminated stilbazolium radicals
[AD-D015873] 04 p1367 N94-17706
Elastic properties of a polyimide film determined by Brillouin scattering and mechanical techniques
[DE93-017404] 04 p1368 N94-18098
Polymer films with enhanced dielectric properties
[AD-A271148] 04 p1375 N94-19740
Phthalonitrile prepolymer as high temperature sizing material for composite fibers
[AD-D015912] 05 p1672 N94-20010
Theoretical and experimental study of the winding of a thin plastic film: The role of aerodynamic effects
[ECL-93-04] 05 p1703 N94-20599
Electrochemical synthesis of ultrathin film composite membranes
[AD-A272721] 05 p1681 N94-21168
Chemically sensitive interfaces on SAW devices
[DE94-001832] 06 p2526 N94-23718
Ordered organic thin films self-assembled from the vapor phase 06 p2223 N94-24339
Electric field-mediated processing of polymer blend solutions 06 p2223 N94-24341
Low-gravity electrodeposition and growth of polymer thin films with large third-order optical nonlinearities by electrochemical processes for devices: Thiophene-based polymers 06 p2225 N94-24346
Nonlinear optical thin films 06 p2225 N94-24349
Proceedings of the 12th International Congress: Corrosion Control for Low-Cost Reliability. Volume 1: Coatings
[AD-A273661] 06 p2251 N94-25448
Micropyrolysis of polymer thin films for ceramics
[ECL-92-62] 07 p2750 N94-26088
Mechanical properties of polyaniline prepared by polymerization in an organized monolayer
[AD-A274350] 07 p2753 N94-26925
Ferroelectricity in a Langmuir-Blodgett multilayer film of a liquid crystalline side-chain polymer
[AD-A274477] 07 p2754 N94-27033
Liquid crystalline side-chain polysiloxanes with 4-amino-4'-stilbene-carboxylic ester mesogens
[AD-A274510] 07 p2754 N94-27036
Research and development within nonlinear optics for protection of optical sensors against laser irradiation on of optical sensors against laser irradiation. Quarterannual report 1 (april 1993))
[PB94-124245] 07 p3037 N94-27046
Langmuir-Blodgett and STM investigations of conducting polymer thin films
[AD-A274512] 07 p2755 N94-27087
Chemical polymerization and Langmuir-Blodgett techniques. 2: The polymerization of monolayers of 3-substituted pyrroles
[AD-A274478] 07 p2755 N94-27163
Molecular aspects of transport in thin films of controlled architecture
[DE94-004552] 08 p3211 N94-28457
High temperature polymer dielectric film insulation 08 p3167 N94-28715
A 3M high temperature dielectric film 08 p3167 N94-28717
Polyaniline membranes for gas and liquid separation
[AD-A275851] 08 p3408 N94-28790
Corrosion inhibition by electrodeposited conductive-polymer film
[AD-A275456] 08 p3213 N94-28806
Composite flexible blanket insulation
[NASA-CASE-ARC-11955-1-CU] 08 p3180 N94-29509
Study of nonlinear optical polymers and their applications in optical waveguides 08 p3216 N94-29807
Ablation of polymers by ultraviolet pulsed laser
[DE94-608100] 08 p3218 N94-30066
Plasma treatment of polymer dielectric films to improve capacitive energy storage 08 p3223 N94-30479
Fluorescence observations of LDEF exposed materials as an indicator of induced material reactions 09 p3593 N94-31025
On the linearity of fast atomic oxygen effects 09 p3594 N94-31027
Adsorption of water to the metal/polymer interface studied by neutron and x ray reflectivity
[DE94-005578] 09 p3651 N94-31649
Chemical interactions between protein molecules and polymer membrane materials
[DE94-006987] 09 p3651 N94-31672
Reversible optical storage in azo polymers
[AD-A277109] 09 p3654 N94-31980
Electrical communication between glucose oxidase and electrodes based on poly(vinylimidazole) complex of Os(bpy)2Cl2
[AD-A276585] 09 p3635 N94-32231
New developments in second-order nonlinear optical polymeric materials
[AD-A277409] 09 p3658 N94-32578
Stable second-order nonlinear optical materials based on interpenetrating polymer networks
[AD-A277410] 09 p3658 N94-32579
Electrostrictive response of elastomeric polymers
[AD-A277983] 09 p3664 N94-33247
Mechanical properties of crosslinked polymer coatings 11 p4231 N94-36410

POLYMERIZATION
NT COPOLYMERIZATION
NT DIMERIZATION
Heat and mass transfer mechanisms of the polymerization under terrestrial and microgravity conditions 01 p0103 N94-10092
Photoinitiated radical polymerization of liquid monomers in microgravity 01 p0124 N94-10246
Fire-resistant hydrolytically stable poly(arylene phosphine oxide) material systems 01 p0019 N94-10780
Polymeric nitrogen
[DE93-012600] 01 p0089 N94-11151
Ring-opening polymerization of phosphazenes
[AD-A265000] 01 p0090 N94-11292
Radiation-induced modifications of allylamino-substituted polyphosphazenes
[AD-A264914] 01 p0092 N94-11848
Synthesis and polymerization of oligomeric multiple aromatic ether-containing phthalonitriles
[AD-D015729] 01 p0094 N94-12399
NMR characterization of polymers formed in diazotizing mixtures of luminol and 3-amino-L-tyrosine
[AD-A266093] 01 p0094 N94-12536
Unexpectedly rapid hydrosilation polymerization of the diallyl derivative of bisphenol A and 2,6-diallylphenol
[AD-A265832] 02 p0577 N94-12986
Reverse micelle synthesis of nanoscale metal containing catalysts
[DE93-012869] 02 p0572 N94-14184
Impedance-power effects on plasma polymer surface finish using a helical resonator discharge
[DE93-016454] 02 p0803 N94-14590
Intramolecular versus intermolecular condensation rates in the acidic polymerization of octaethoxytrisiloxane
[AD-A266982] 03 p0963 N94-15490
Analysis of leading edge and trailing edge cover glass samples before and after treatment with advanced satellite contamination removal techniques
[AD-A267055] 03 p0885 N94-15666
Thermochemistry of silicate speciation in aqueous sodium silicate solutions: Ionization and polymerization of small silicate ion
[AD-A266825] 03 p0964 N94-15683
Photochemistry in thin polymeric films
[AD-A266716] 03 p0964 N94-15729
Effects of aging time on V205 sol-gel coatings
[AD-A266824] 03 p0965 N94-15843
Use of microgravity in the synthesis of ceramics using sol gel techniques 03 p0979 N94-16088
Interpenetrating polymer network acoustic damping material
[AD-D015889] 03 p0969 N94-16916
Synthetic and mechanistic investigation of olefin polymerization catalyzed by early transition metal compounds
[DE93-018301] 03 p0970 N94-16963
A state-of-the-art plasma polymerization coater for ICF targets
[DE93-016452] 03 p1204 N94-17237
Synthesis, characterization, and polymerization of new ferrocene-fluorene complexes. A novel high-molecular weight conjugated polymer with pendant ferrocene groups
[AD-A267717] 03 p0972 N94-17273
Soluble precursor route to polyanilines
[AD-A268015] 03 p0973 N94-17494
Detonation reaction steps frozen by free expansion and analyzed by mass spectrometry
[DE93-012734] 04 p1376 N94-17813
Polymerizable lipids in the development of controlled release carriers
[AD-D015789] 04 p1368 N94-17982
Morphology of polymerized membranes on an amorphous substrate at molecular resolution by AFM
[AD-A268760] 04 p1370 N94-18403
Strained ring energetic binders
[AD-A269056] 04 p1377 N94-18491
Cooperative formation of inorganic-organic interfaces in the synthesis of silicate mesostructures
[AD-A271196] 04 p1375 N94-19742
Chain propagation/step propagation polymerization chemistry. The preparation of solvent resistant well phase-separated thermoplastic elastomers
[AD-A271128] 05 p1699 N94-20016
Rotational isomers of Mo(VI) alkylidene complexes and Cis/trans polymer structure: Investigations in ring-opening metathesis polymerization
[AD-A272647] 05 p1704 N94-21184
Polymerization of enantiomerically pure 2,3-dicarboalkoxy norbornadienes and 5,6-disubstituted norbornenes by well-characterized molybdenum ROMP catalysts
[AD-A272649] 05 p1704 N94-21186
Techniques for producing free-standing thin films on frames
[DE93-041144] 05 p1708 N94-21954
Photochemical approaches to conversion of light to electricity or fuel
[DE94-001650] 05 p1849 N94-22048
Surface and interfacial properties of polymer blends. A literature survey
[PB93-230191] 06 p2254 N94-23561
Reaction of isocyanates with carboxylic acids and its application to polymer synthesis
[PB94-118858] 06 p2254 N94-23763
Prediction of nonlinear optical properties of organic materials. General theoretical considerations 06 p2224 N94-24343
Polydiacetylene thin films for nonlinear optical applications 06 p2225 N94-24347

Feasibility study: Monodisperse polymer particles containing laser-excitable dyes
06 p2225 N94-24350
Convective instabilities in traveling fronts of addition polymerization
06 p2226 N94-24352
Synthesis of soluble halogenated polyphenylenes: Mechanism for the coupling halogenated lithiobenzenes
[AD-A273547] 06 p2257 N94-24558
STM studies of LB deposited alkyl substituted polyaniline and its corresponding monomer
[AD-A273553] 06 p2257 N94-24562
Curing phthalonitrile resins with acid and amine
[AD-D016021] 06 p2258 N94-24721
Electrochemically mediated polymerization of 2-pentadecylaniline confined to a planar liquid-liquid interface
[AD-A273541] 06 p2259 N94-24792
The 2-D polymerized Langmuir-Blodgett films studied by STM
[AD-A273542] 06 p2261 N94-24930
Synthesis of molecular wires by a novel divergent/convergent approach
[AD-A273332] 06 p2537 N94-25087
Particle nucleation and growth in butadiene emulsion polymerization
[ETN-94-95300] 06 p2262 N94-25236
Controlled synthesis of polyenes by catalytic methods
[DE94-004168] 07 p2749 N94-25973
Trifluoromethyl-substituted polymers
[NASA-CR-195217] 07 p2751 N94-26641
Mechanical properties of polyaniline prepared by polymerization in an organized monolayer
[AD-A274350] 07 p2753 N94-26925
Equivalent performance in different helical resonator plasma polymerization coater platforms
[DE94-001517] 07 p2753 N94-26933
Kinetics of 2-pentadecylaniline polymerizations in monolayers: Relationships between experimental data and a new theoretical model
[AD-A274419] 07 p2754 N94-27080
Chemical polymerization and Langmuir-Blodgett techniques. 2: The polymerization of monolayers of 3-substituted pyrroles
[AD-A274478] 07 p2755 N94-27163
Alkylene-bridged polygerm- and polygermsilsesqui-oxanes: New hybrid organic-inorganic materials
[DE94-005096] 08 p3174 N94-28557
Cellular and molecular approaches to polymer synthesis by bacteria
[AD-A275501] 08 p3212 N94-28661
Polymer Technology Seminar, 1993. Kem-100.600
[PB94-137593] 08 p3213 N94-29031
Polymer technology publication series no. 16
[PB94-135522] 08 p3214 N94-29157
Irradiation polymerization of bismaleimide resins
[REPT-932-430-105] 08 p3215 N94-29441
Polyimides containing the penta fluoro sulfanyl benzene moiety
[NASA-CASE-LAR-15082-1] 08 p3175 N94-29554
Polyimides containing pendent siloxane groups
[NASA-CASE-LAR-14638-1] 08 p3215 N94-29555
Photopolymerization of cyclohexene oxide: A visible light initiating system and mechanistic investigations
[AD-A277110] 09 p3654 N94-31981
Mechanical properties of acrylate networks formed by visible laser-induced polymerization. 2. Control of the mechanical properties
[AD-A277111] 09 p3655 N94-31982
Isomeric poly(benzophenone)s: Synthesis of highly crystalline poly (4, 4 foot-benzophenone) and amorphous poly (2, 5-benzophenone), a soluble poly (p-phenylene) derivative
[AD-A277261] 09 p3655 N94-32017
A visible light initiating system for free radical promoted cationic polymerization
[AD-A277164] 09 p3655 N94-32069
Multifunctional macromolecules
[AD-A277347] 09 p3656 N94-32246
Intramolecular charge transfer complexes as fluorescence probes for UV and visible light induced acrylate polymerization
[AD-A277129] 09 p3657 N94-32381
Structure-property relationships of carbon aerogels
[DE94-007120] 09 p3660 N94-32687
Metal ion complexation by ionizable crown ethers
[DE94-008301] 09 p3661 N94-32847
Interpenetrating polymer network acoustic damping material
[AD-D016141] 09 p3663 N94-32975
Novel polydiacetylenes as materials for second and third order nonlinear optics
[AD-A277512] 09 p3664 N94-33082
Symposium on Inorganic and Organometallic Polymers
[AD-A277860] 10 p4027 N94-33772
Spirobislactone acrylate polymers
[AD-D016190] 10 p4030 N94-34403
Polymers of BIS (Ethynylstyryl) benzene and related monomers
[AD-D016194] 10 p4030 N94-34407
Addition polyimides with enhanced processability
[NASA-CASE-LEW-15043-1] 11 p4242 N94-35234
Concurrent stabilization and imaging of a novel polymer for second harmonic generation via in situ photopolymerization
[AD-A278912] 11 p4243 N94-35588
Novel catalysts for methane activation
[DE94-009705] 11 p4237 N94-35778
Syntheses and studies of acetylenic polymers
[DE94-011201] 11 p4245 N94-36057
Nonlinear optical composites of metal cluster laden polymers
[AD-D016217] 11 p4234 N94-36124
Third European Technical Symposium on Polyimides and High Performance Polymers: STEPI 3
[PB94-148491] 11 p4246 N94-36177
Microscale synthesis and characterization of polystyrene: NSF-POLYED scholars project
11 p4231 N94-36408
Highly fluorinated polymers
[NASA-CR-196270] 12 p4422 N94-37025
Scoping economics for the commercial manufacture of metallocene catalysts
[DE94-011526] 12 p4422 N94-37055
Tert-butylalumoxanes: Synthetic analogs for methylalumoxane (MAO) and new catalytic routes to polyolefins and polyketones
[AD-A280511] 12 p4399 N94-37106
Organic NLO polymers. 2: Main-chain and guest-host Chi(2)NLO polymers: NLO-phore structure versus poling
[AD-A280230] 12 p4423 N94-37133
Organic NLO polymers. 5: Homopolymerization of indole based NLO-phore: A heterocycle Chi(2)NLO main-chain polymer
[AD-A280229] 12 p4423 N94-37151
Organometallic NLO polymers. 4: Organometallic main-chain, side-chain, and guest-host polymers: A study of their orientation and relaxation using second harmonic generation
[AD-A280347] 12 p4423 N94-37179
Carborane-siloxane or silane-unsaturated hydrocarbon based polymers
[AD-D016220] 12 p4425 N94-37482
Fluorinated resins with low dielectric constant
[AD-D016303] 12 p4427 N94-37773
Synthesis of phthalonitrile resins containing ether and imide linkages with aromatic diamine curing agent
[AD-D016309] 12 p4427 N94-37778

POLYMERS

The Netherlands innovation oriented research programme on polymer composites and special polymers 1985-1993
01 p0065 N94-10067
Physical properties of injection molded liquid crystal polymers and high temperature engineering polymers
[AD-A264912] 01 p0087 N94-10508
Preparation of carbon monoliths having tailored pore structure from porous polymer precursors
[DE93-011576] 01 p0089 N94-10958
Polymeric nitrogen
[DE93-012600] 01 p0089 N94-11151
A new decomposition strategy for parallel bonded molecular dynamics
[DE93-009839] 01 p0366 N94-11284
Vacuum stability requirements of polymeric material for spacecraft application
[NASA-TM-109216] 01 p0091 N94-11350
Fracture behavior of ionomers and ionomeric blends
[AD-A265379] 01 p0094 N94-12407
NMR characterization of polymers formed in diazotizing mixtures of luminol and 3-amino-L-tyrosine
[AD-A266093] 01 p0094 N94-12536
Photogenerated base in polymer imaging. Synthesis and photopatterning of poly(2-cyano-2-(p-vinylphenyl) butanoic acid)
[AD-A265288] 01 p0095 N94-12585
Electrocatalysis issues in polymer electrolyte fuel cells
[DE93-014450] 02 p0702 N94-13402
Sequestering carbon dioxide in industrial polymers: Building materials for the 21st century
[DE93-016087] 02 p0580 N94-14297
Direct simulation of polymer drag reduction in free shear flows and vortex dipoles
02 p0644 N94-14755
Detection and dosimetry of chemical contaminants in polymeric materials
[AD-A266605] 03 p0968 N94-16727
Main chain chromophoric polymers with second order nonlinear optical properties
[AD-D015893] 03 p0969 N94-16920
Electrical conductivity of ion implanted ladder and semi-ladder polymers
[AD-A267432] 03 p0970 N94-16978
SURPHEX (tm): New dry photopolymers for replication of surface relief diffractive optics
03 p1198 N94-17358
NMR studies of enriched species at interfaces
[AD-A264703] 04 p1367 N94-17878
Mechanical-property changes of structural composite materials after low-temperature proton irradiation: Implications for use in SSC magnet systems
[DE93-016735] 04 p1343 N94-18763
Aragatz project samples experiment/MAPOL (polymer materials) experiment: Postflight expert evaluation
05 p1660 N94-21376
Simulated space environmental effects on some experimental high performance polymers
05 p1662 N94-21385
Polymeric nitrogen
[DE93-040544] 05 p1706 N94-21512
Modeling of polymer electrolyte fuel cell systems
[DE93-041187] 05 p1847 N94-21774
Method of determining shear stress employing a monomer-polymer laminate structure
[NASA-CASE-LAR-14654-2] 06 p2375 N94-23308
Selection of polymer binders and fabrication of SiC fiber-reinforced reaction-bonded silicon nitride matrix composites
[NASA-CR-194874] 06 p2255 N94-24223
Microgravity Studies of Organic and Polymeric Materials
[NASA-CP-3250] 06 p2223 N94-24338
Planar poly(p-phenylene) derivatives: Ladder formation for maximization of extended conjugation
[AD-A273220] 06 p2260 N94-24922
Reference electrodes for solid polymer electrolytes
[DE94-004583] 07 p2780 N94-25806
Morphological analysis of ionomers
[DE94-003660] 07 p2749 N94-26005
Alkylene-bridged polygerm- and polygermsilsesqui-oxanes: New hybrid organic-inorganic materials
[DE94-005096] 08 p3174 N94-28557
High temperature arc-track resistant aerospace insulation
08 p3167 N94-28716
Polymer Technology Seminar, 1993. Kem-100.600
[PB94-137593] 08 p3213 N94-29031
Measurement of bulk longitudinal modulus and correction for edge effects
[DE94-005581] 08 p3222 N94-30900
Performance of selected polymeric materials on LDEF
09 p3593 N94-31023
Molecular/polymeric magnetism
[DE94-005888] 09 p3649 N94-31201
Nonlinear optical properties of rigid-rod polymers
[NASA-CR-191349] 09 p3882 N94-32702
Low loss second-order nonlinear optical polymers based on all organic sol-gel materials
[AD-A277482] 09 p3663 N94-32985
Fundamental studies in crack initiation
[AD-A278387] 09 p3741 N94-33356
Energetic polymer
[AD-D016156] 10 p4027 N94-33762
Atomic oxygen protective coating with resistance to undercutting at defect sites
[NASA-CASE-LEW-15306-1] 11 p4243 N94-35502
Intelligent processing of materials, technical activities, 1993 (NAS-NRC Assessment Panel, April 21-22 1994)
[PB94-164183] 11 p4251 N94-35737
Replacement of silicone polymer A with silicone polymer B and the subsequent characterization of the new cellular silicone materials
[DE94-010105] 12 p4421 N94-36474
Flame resistant fibrous structures development
[NASA-CR-185700] 12 p4421 N94-36641
Highly fluorinated polymers
[NASA-CR-196270] 12 p4422 N94-37025
Poly(p-phenylene) derivatives new high performance nonlinear optical polymers
[AD-A280248] 12 p4422 N94-37121
Organic NLO polymers. 2: Main-chain and guest-host Chi(2)NLO polymers: NLO-phore structure versus poling
[AD-A280230] 12 p4423 N94-37133
Holographic grating relaxation studies of probe diffusion in amorphous polymers
[AD-A280496] 12 p4423 N94-37144
Solution characterization of poly(isobornyl methacrylate) in tetrahydrofuran
[AD-A280497] 12 p4409 N94-37145
Optically induced high efficiency gratings in azo polymer films
[AD-A280505] 12 p4423 N94-37147
Organic nonlinear optical (NLO) polymers. 4: Thermally stable NLO polymers
[AD-A280196] 12 p4423 N94-37148
Organic NLO polymers. 5: Homopolymerization of indole based NLO-phore: A heterocycle Chi(2)NLO main-chain polymer
[AD-A280229] 12 p4423 N94-37151

Azobenzene-containing polymers: Some optoelectronic properties
[AD-A280448] 12 p4424 N94-37185
Substituted silyl-terminated compounds and polymers thereof
[AD-D016310] 12 p4427 N94-37779

POLYMETHYL METHACRYLATE
A relaxation study of poled nonlinear optical polymers by infrared reflection-absorption spectroscopy
[AD-A265797] 01 p0093 N94-12380
Progress in the modeling of the shock response and mitigation of thick composite shells
[AD-A267009] 03 p1057 N94-15524
Contained liquids in microgravity, part 2
03 p0979 N94-16085
Phase holograms in PMMA with proximity effect correction 03 p1037 N94-17348
Structure and properties of polycarbonate alloys
[ETN-93-95071] 04 p1375 N94-19611
Millimeter-wave imaging of composite materials
[DE93-041160] 05 p1677 N94-21940
Extinguishment of combustible porous solids by water droplets
[PB93-198893] 06 p2270 N94-23740
Physical characteristics of polymethylmethacrylate scintillator SOFG-120
[DE93-634184] 07 p2810 N94-26395
Surface energy changes produced by ultraviolet-ozone irradiation of poly(methylmethacrylate), polycarbone and polytetrafluoroethylene
[NASA-TM-106460] 08 p3213 N94-28922
Ablation of polymers by ultraviolet pulsed laser
[DE94-608100] 08 p3218 N94-30066
Compatibility studies of some azo polymer blends
[AD-A277141] 09 p3657 N94-32365
A relaxation study of poled nonlinear optical polymers by infrared reflection-absorption spectroscopy
[AD-A277513] 09 p3663 N94-33054

POLYMORPHISM
Hydrogen-bond polymorphs of guanidinium 4-biphenylsulfonate
[AD-A265294] 01 p0402 N94-11827
C++ as a language for object-oriented numerics
[DE93-015027] 03 p1148 N94-15985
Are types needed for natural language?
[PB93-191831] 05 p1949 N94-19997
System at the cross-roads of functional and logic programming
[PB93-191823] 05 p1928 N94-20009
Nominalization, prediction and type containment
[PB93-191799] 05 p1898 N94-20082
A type declarative system for PROLOG
[ETN-94-95178] 06 p2449 N94-23155
A critique of type systems for global overloading
[AD-A278800] 11 p4304 N94-35676
The structural changes of water ice I during warmup
11 p4239 N94-36144

POLYNOMIALS
NT BINOMIALS
NT DYADICS
NT HERMITIAN POLYNOMIAL
A reliable stability test for exponential polynomials
[MEMO-COSOR-92-48] 01 p0341 N94-10168
An exactly solvable model of an oscillator with nonlinear coupling and zeros of Bessel functions
01 p0349 N94-10573
On convexity and Schoenberg's variation diminishing splines
[DE93-619673] 01 p0346 N94-11632
Robust stability of diamond families of polynomials with complex coefficients
[NASA-CR-194132] 02 p0768 N94-13421
Formally biorthogonal polynomials and a look-ahead Levinson algorithm for general Toeplitz systems
[NASA-CR-194297] 02 p0748 N94-13586
The Chebyshev-Legendre method: Implementing Legendre methods on Chebyshev points
[NASA-CR-191497] 02 p0769 N94-13725
Exploiting structure: Introduction and motivation
[NASA-CR-194199] 02 p0750 N94-13828
On a difference equation for generalizations of Charlier polynomials
[REPT-92-101] 02 p0770 N94-14150
Adaptive wavelet collocation methods for initial value boundary problems of nonlinear PDE's
[NASA-CR-191507] 03 p1169 N94-15833
Reductions to sets of low information content
[TR-417] 03 p1150 N94-16579
Fast algorithms for polynomial interpolation, integration and differentiation
[AD-A267505] 03 p1154 N94-17370
An extension of Wolovich's definition of equivalence of linear systems
[MATHS-REPT-A-183] 04 p1547 N94-18069
Introduction to spectral methods: Application to the Stokes problem 04 p1413 N94-18566
Active control of a multivariable system by way of polynomial neural networks: Computer simulation evaluations and laboratory experimental results
[AD-A270033] 04 p1541 N94-18790
Difference equations for generalized Meixner polynomials
[REPT-93-17] 04 p1550 N94-19082
A polynomial primal-dual Dikin-type algorithm for linear programming
[REPT-93-36] 04 p1525 N94-19156
On polynomials orthogonal with respect to an inner product involving differences (the general case)
[REPT-93-32] 04 p1551 N94-19285
Notes on multi-step ahead prediction based on the principle of concatenation
[MATHS-REPT-A-189] 04 p1544 N94-19410
Affine and non-affine blossoms
[RR-913-M] 05 p1950 N94-20200
Polynomial interpolation of real functions 1: Interpolation in an interval
[AD-A272330] 05 p1951 N94-20527
Graph minors: Structure theory and algorithms
[AD-A271851] 05 p1952 N94-20613
Orthogonal pairs and zeros of Sobolev-type orthogonal polynomials
[REPT-92-46] 05 p1953 N94-21059
Explicit results on gl(lambda) and sl(lambda)
[MEMO-1075] 05 p1953 N94-21072
Hilbert 90 for polynomial matrices
[CWI-AM-R9211] 05 p1954 N94-21159
Fast fourier transforms for nonequispaced data
[AD-A272687] 05 p1954 N94-21164
Computing solutions uniquely collapses the polynomial hierarchy
[TR-467] 05 p1954 N94-21314
Toward a new method of decoding algebraic codes using Groebner bases
[AD-A273089] 05 p1959 N94-21524
Operational equations for the five-point rectangle
[DE94-000366] 05 p1959 N94-21655
A mean field neural network for hierarchical module placement 05 p1766 N94-21720
The accuracy-through-order and the equivalence properties in the algebraic approximant
[DE93-040188] 05 p1960 N94-21946
Column reduced rational matrix functions with given null-pole data in the complex plane
[PB93-220531] 05 p1960 N94-22099
On the Daubechies-based wavelet differentiation matrix
[NASA-CR-191583] 06 p2479 N94-23090
Mathematical addenda to Hopper's model of plane stokes flow driven by capillarity on a free surface
[PB93-237691] 06 p2480 N94-23438
Adaptive nonlinear polynomial neural networks for control of boundary layer/structural interaction
[NASA-CR-189645] 06 p2525 N94-23698
Systematic construction of trigonometric neural networks
[PB93-200228] 06 p2474 N94-24544
Polynomials orthogonal with respect to an inner product involving differences
[PB94-110731] 06 p2489 N94-24572
On BRST quantization of constrained systems
[ETN-94-95386] 06 p2570 N94-25258
Relationship between the structure and performance of identified nonlinear polynomial models
[RR-474] 06 p2492 N94-25320
A reachability test for systems over polynomial rings using Groebner bases
[MEMO-COSOR-92-38] 06 p2493 N94-25527
Approximate solution of the fourth order initial value problem using deficient spline polynomials
[DE93-613023] 07 p2991 N94-25880
Classification of linear differential operators with an invariant subspace in monomials
[PB94-126620] 07 p2996 N94-26915
Fast methods for computation with algebraic numbers
[ISBN-0-315-57888-2] 07 p2998 N94-27269
Polyhedral characterization of the economic lot-sizing problem with start-up costs
[MEMO-COSOR-92-46] 07 p2969 N94-27396
Thermal conductivity of liquid carboxylic acids
[ESDU-93017] 07 p2721 N94-28138
Upwind method using local interpolation
08 p3128 N94-28982
Splines and ocean wave modelling
[PB94-139409] 08 p3378 N94-30002
Polynomial modeling of analog-to-digital converters
[DE94-005579] 08 p3406 N94-30008
Homogeneous Poisson structures
[DE94-608112] 08 p3453 N94-30119
Derivation lengths in term rewriting from interpretations in the naturals
[RUU-CS-92-43] 08 p3455 N94-30346
A note on the complexity of local search problems
[CT-93-02] 08 p3456 N94-30370
A polynomial representation of the valence orbital ionization potentials
[USIP-93-06] 09 p3640 N94-31083
A fully two-dimensional, non-oscillatory advection scheme for momentum and scalar transport equations
[DM-66] 09 p3700 N94-31221
Identification of polynomial and rational NARMAX models
[RR-483] 09 p3842 N94-31413
Penetrable wedge analysis
[AD-A277219] 09 p3845 N94-32022
On interpolating random fields using a finite number of observations
[CWI-BS-R9314] 09 p3847 N94-32194
On constructing multi-variate orthonormal polynomials associated with spectral distribution functions
[CWI-BS-R9310] 09 p3851 N94-32225
Polynomial interpolation and approximation of real functions. 2: Symmetrical interpolation for the triangle
[AD-A277345] 09 p3848 N94-32245
Least squares approximation by G1 piecewise parametric cubes
[AD-A277978] 09 p3850 N94-33265
A method available for processing the signal of thermocouples by computer 10 p4057 N94-34360
Cramer-von Mises variance estimators for simulations
[AD-A278799] 11 p4316 N94-35675
Inverse problem for symmetric tridiagonal matrices. Calculation of discrete orthogonal polynomial system with arbitrary weight
[DE94-612434] 11 p4315 N94-35789
Priorities and nonmonotonic reasoning
[PB94-171170] 11 p4346 N94-35959
Gauss elimination by segments and multivariate polynomial interpolation
[AD-A278646] 11 p4315 N94-36012

POLYORGANOSILOXANES
U POLYSILOXANES

POLYPEPTIDES
Polaron tunneling in high-temperature superconductors
[DE93-016880] 04 p1593 N94-17754
Development of bioelastic material for aspects of wound repair
[AD-A267832] 05 p1673 N94-20208
The molecular matching problem
07 p3030 N94-27910
Enzymology and molecular biology of cell wall biosynthesis
[DE94-008585] 10 p4094 N94-34008
Recombinant protein production and insect cell culture and process
[NASA-CASE-MSC-22336-1] 12 p4478 N94-36751

POLYPHENYLS
The photochemistry of poly(methylphenylphosphazene)
[AD-A267320] 03 p0970 N94-16948
Synthesis of soluble halogenated polyphenylenes: Mechanism for the coupling halogenated lithiobenzenes
[AD-A273547] 06 p2257 N94-24558
Metal-catalyzed alkynylation of brominated polyphenylenes: Thermoset precursors of high density monolithic glassy carbon
[AD-A273232] 06 p2259 N94-24789
Synthesis of polyphenylenes via Bergman cyclization of enediyne monomers
[AD-A273298] 06 p2260 N94-24924
Addition polyimides with enhanced processability
[NASA-CASE-LEW-15043-1] 11 p4242 N94-35234
Organic nonlinear optical (NLO) polymers. 4: Thermally stable NLO polymers
[AD-A280196] 12 p4423 N94-37148

POLYPROPYLENE
New technology for effective control of flammability in polyolefin fiber/textiles 01 p0018 N94-10774
Effect of stabilization on the recycling of polyolefins in blow moulding
[IMI-93RT-42400-1477-G] 02 p0596 N94-13684
Development and demonstration of a personal monitoring system for exposure to hydrogen fluoride
[DE93-041273] 05 p1891 N94-20935
Dendrite preventing separator for secondary lithium batteries
[NASA-CASE-NPO-18585-1-CU] 08 p3265 N94-29411
Scoping economics for the commercial manufacture of metallocene catalysts
[DE94-011526] 12 p4422 N94-37055

POLYSACCHARIDES
NT CELLULOSE
NT DEXTRANS
NT GLYCOGENS
NT STARCHES

Improving reservoir conformance using gelled polymer systems
[DE93-014532] 01 p0088 N94-10749
CarbBank: A structural and bibliographic database for complex carbohydrates
[DE93-015582] 02 p0827 N94-14803
Enzymology and molecular biology of cell wall biosynthesis
[DE94-008585] 10 p4094 N94-34008

POLYSILANES
Temperature dependence of the exciton-exciton annihilation rate constant in poly(di-n-hexylsilane)
[DE94-005584] 09 p3655 N94-32102
Conversion of polymers of methyl- and vinylsilane to Si-C ceramics
[NASA-TM-106554] 09 p3662 N94-32945
Symposium on Inorganic and Organometallic Polymers
[AD-A277860] 10 p4027 N94-33772
Carborane-(silane or siloxane)-unsaturated hydrocarbon based thermosetting polymers
[AD-D016311] 12 p4427 N94-37818

POLYSILOXANES
NT METHYL POLYSILOXANES
Phases and phase transitions of polymeric liquid crystals: A high resolution x ray diffraction and light scattering study
[ITN-93-85218] 02 p0816 N94-14826
Ferroelectricity in a Langmuir-Blodgett multilayer film of a liquid crystalline side-chain polymer
[AD-A274477] 07 p2754 N94-27033
Liquid crystalline side-chain polysiloxanes with 4-amino-4'-stilbene-carboxylic ester mesogens
[AD-A274510] 07 p2754 N94-27036
Metal-ion spin-on glasses: Novel materials for active waveguides
[DE94-007738] 09 p3882 N94-32649
Carborane-(silane or siloxane)-unsaturated hydrocarbon based thermosetting polymers
[AD-D016311] 12 p4427 N94-37818

POLYSTYRENE
Polymer-polymer interactions
[AD-A265304] 01 p0091 N94-11830
Polymers for microelectronics
[AD-A266036] 01 p0094 N94-12396
Soluble precursor route to polyanilines
[AD-A268015] 03 p0973 N94-17494
Expanded polystyrene protective barricade full-scale fire exposure test
[AD-A271450] 05 p1698 N94-19938
Spatial organization of polymer chains in a crystallizable diblock polyethylene and polystyrene
[AD-A271862] 05 p1702 N94-20463
Feasibility study: Monodisperse polymer particles containing laser-excitable dyes
06 p2225 N94-24350
Morphological analysis of ionomers
[DE94-003660] 07 p2749 N94-26005
Study on the compensated lead hadron calorimeter characteristics by means of hadron and electron beams
[DE93-634176] 07 p2810 N94-26439
Microspheres for laser velocimetry in high temperature wind tunnel 07 p2682 N94-27903
Ablation of polymers by ultraviolet pulsed laser
[DE94-608100] 08 p3218 N94-30066
Improved construction materials for polar regions using microcellular thermoplastic foams
08 p3223 N94-30483
Performance of selected polymeric materials on LDEF
09 p3593 N94-31023
Toughening mechanisms in the high strain rate deformation of rubber-modified polymer glasses
09 p3653 N94-31942
Solvent diffusion coefficient concentration dependence in polymer solutions
[AD-A277023] 09 p3655 N94-32005
New polymer target-shell properties and characterizations
[DE94-008420] 09 p3890 N94-32415
Microscale synthesis and characterization of polystyrene: NSF-POLYED scholars project
11 p4231 N94-36408

POLYSULFIDES
Thermal stability of sealants for military aircraft: Modification of polysulfide prepolymers with ether and thioether monomers
[AD-A264079] 01 p0089 N94-11107
Flight 20 (STS-45) polysulfide gas path investigation
[NASA-CR-193861] 03 p0928 N94-17213
Improved resealing procedures for the second deseal/reseal program in RAAF F111 aircraft fuel tanks
[AD-A277069] 09 p3580 N94-32378

POLYTETRAFLUOROETHYLENE
NT TEFLON (TRADEMARK)
Wide angle, single screen, gridded square-loop frequency selective surface for diplexing two closely separated frequency bands
[NASA-CASE-NPO-18664-1-CU]
03 p1237 N94-17438
Mesoepitaxy: A universal route to oriented materials
[AD-A270437] 04 p1598 N94-18511
Surface energy changes produced by ultraviolet-ozone irradiation of poly(methylmethacrylate), polycarbone and polytetrafluoroethylene
[NASA-TM-106460] 08 p3213 N94-28922
Custom uniform source system
[NASA-CR-189332] 09 p3711 N94-31492
Evaluation of pyrolysis and arc tracking on candidate wire insulation designs for space applications
[NASA-CR-195332] 09 p3731 N94-32901

POLYTOPES
Applications of cut polyhedra
[CWI-BS-R9221] 01 p0347 N94-10354
A simplicial approach to integer programming
[REPT-93-06] 01 p0322 N94-10355
Finding optimal policies for Markov decision chains: A unifying framework for mean-variance-tradeoffs
[PB93-191930] 04 p1559 N94-19555
Determining the distance to the perfect matching polytope of a bipartite graph
[RR-895-M] 05 p1950 N94-20161
Number of moduli of families of curves on toric surfaces
[PB93-230381] 06 p2479 N94-23121
Polytopic vector analysis in igneous petrology: Application to lunar petrogenesis
06 p2615 N94-24368
A simplicial approach to integer programming, part 2
[REPT-93-47-PT-2] 07 p2958 N94-25764

POLYURETHANE FOAM
A constitutive theory for rigid polyurethane foam
[DE93-011596] 04 p1372 N94-19059

POLYURETHANE RESINS
A multiphase model for shock-induced flow in low density foam
[DE93-013767] 02 p0632 N94-13397
Photodegradation of MDI based polyurethane/urea elastomers
[AD-A267308] 03 p0971 N94-16994
Polyurethane self-priming topcoats
[AD-D015870] 04 p1367 N94-17719
Characterization studies of lower and non-TDI polyurethane encapsulants
[DE93-041129] 05 p1698 N94-19857
Graphite/polyurethane flexible composites: Mechanical and vibration damping properties
[AD-A271608] 05 p1674 N94-20950
Reaction of isocyanates with carboxylic acids and its application to polymer synthesis
[PB94-118858] 06 p2254 N94-23763
Morphological analysis of ionomers
[DE94-003660] 07 p2749 N94-26005
Biomedical polyurethane networks
[ETN-94-95391] 07 p2750 N94-26211
Polyurethane self-priming topcoats
[AD-D016041] 07 p2755 N94-27111
Corrosion resistant coatings from conducting polymers
[DE94-003959] 07 p2757 N94-27747
Development of a unique polyurethane primer/topcoat
08 p3223 N94-30476
Fluorescence observations of LDEF exposed materials as an indicator of induced material reactions
09 p3593 N94-31025
Laser-induced fluorescence of space-exposed polyurethane 09 p3593 N94-31026
Mass-loaded coating for reducing the resonant frequency of a ceramic disc
[AD-D016095] 09 p3660 N94-32739
Acoustic window
[AD-D016171] 09 p3862 N94-33017
Electrostrictive response of elastomeric polymers
[AD-A277983] 09 p3664 N94-33247
Polyurethane self-priming topcoats
[AD-D016131] 10 p4027 N94-33697
Polyurethane self-priming topcoats
[AD-D016160] 10 p4030 N94-34285
Concurrent stabilization and imaging of a novel polymer for second harmonic generation via in situ photopolymerization
[AD-A278912] 11 p4243 N94-35588

POLYVINYL ALCOHOL
The performance and survivability of dichromated poly (vinyl alcohol) holograms for space based photonic applications
[AD-A270974] 04 p1434 N94-19791
A new material for removing heavy metals from water
08 p3354 N94-30471

POLYVINYL CHLORIDE
A model for non-linear creep and physical ageing in PVC
[NPL-DMM(A)-91] 03 p1057 N94-15016
A study of relaxation transitions in the polymers under the influence of magnetic fields
[AD-A263878] 03 p0963 N94-15133
The effect of temperature on creep and physical ageing of PVC
[NPL-DMM(A)-93] 08 p3217 N94-29885
Creep and physical aging of PVC: Dependence on stress and temperature
[NPL-DMM(A)-115] 08 p3217 N94-29886
Improved construction materials for polar regions using microcellular thermoplastic foams
08 p3223 N94-30483

POLYVINYL FLUORIDE
PVDF measurement of soft x ray induced shock and filter debris impulse
[DE93-017633] 04 p1382 N94-17806

POMERONS
Crossing-odd spin effects in the dipole model of hadron scattering
[DE93-617692] 01 p0362 N94-10551
Model for the pomeron
[DE93-617693] 01 p0362 N94-10552
Logarithmically rising cross section and the ratio sigma(sub el)/sigma(sub t)
[DE93-617694] 01 p0362 N94-10553
Detecting the odderon
[DE93-617695] 01 p0362 N94-10554
Fine structure of the Pomeron and the real part of the elastic scattering amplitude
[DE93-617696] 01 p0362 N94-10555
Parton-parton elastic scattering and rapidity gaps at Tevatron energies
[DE93-041024] 05 p1974 N94-21515
High energy parton-parton elastic scattering in QCD
[DE94-003432] 07 p3028 N94-27736
High energy asymptotics of perturbative multi-color QCD
[DE94-001350] 11 p4327 N94-36238
The Pomeron and Quantum Chromodynamics (QCD) with many light quarks
[DE94-001351] 12 p4513 N94-36538

PONDEROMOTIVE FORCES
Adiabatic and non adiabatic effects in Free Electron Laser (FEL) non linear interactions
[ITN-93-85224] 02 p0659 N94-14547
On effects of a local plasma density growth due to ponderomotive forces at fast wave launching in tokamaks
[IPPCZ-328] 05 p1996 N94-21571
Applications of non-resonant RF forces for improvement of tokamak reactor performances. Part 1: Application of ponderomotive force
[DE94-718994] 11 p4336 N94-35813
The pressure of fluctuative electromagnetic field in inhomogeneous medium
[DE94-617189] 11 p4256 N94-36096
Quantum and quasi-classical analyses of high order emission processes
[DE93-041348] 12 p4513 N94-36697

PONDS
Application of remote sensing for coastal management in the north coast of Java 01 p0218 N94-12701

PONTRYAGIN PRINCIPLE
A combined algorithm for minimum time slewing of flexible spacecraft 11 p4220 N94-35881

POPULATION INVERSION
X ray laser program
[AD-A267075] 03 p1038 N94-15628

POPULATION THEORY
Chaos and microbial systems
[DE93-016814] 02 p0730 N94-14596
Bifurcation and deterministic chaos in dynamic systems
[REPT-93-047] 09 p3911 N94-31893
On the reciprocal relationship between life histories and population dynamics
[CWI-AM-R9302] 09 p3793 N94-32226

POPULATIONS
Automatic classification system for zooplankton
01 p0203 N94-11969
Adaptively resizing populations: Algorithm, analysis, and first results
[NASA-CR-194277] 02 p0742 N94-12808
Coherent excitation of autoionizing resonances by electron impact
[DE93-018169] 02 p0785 N94-14419
Public census data on CD-ROM at Lawrence Berkeley Laboratory
[DE93-015273] 02 p0825 N94-14433
Development of pattern recognition techniques for the evaluation of toxicant impacts to multispecies systems
[AD-A267197] 03 p1095 N94-15790

Confirmation of saturation equilibrium conditions in crater populations 03 p1103 N94-16222
Resolving LDEF's flux distribution: Orbital (debris?) and natural meteoroid populations 03 p1245 N94-16391
Biofilm structure and diversity
[AD-A267254] 03 p1118 N94-16989
Uncertainty versus interindividual variability
[DE93-018105] 04 p1559 N94-19549
Extracting galactic structure parameters from multivariated density estimation 05 p1964 N94-22458
Aeromedical disposition for coronary artery disease 06 p2423 N94-23316
Primary prevention of coronary heart disease 06 p2423 N94-23317
Aeromedical implications of mitral valve prolapse 06 p2424 N94-23323
Sarcoidosis and the aviator 06 p2425 N94-23325
Subset selection for the best of two populations: Tables of the expected subset size
[PB93-237857] 06 p2494 N94-23546
Subset selection with a generalized selection goal based on a loss function
[PB94-111192] 06 p2494 N94-23798
Some generalized subset selection procedures
[PB94-111655] 06 p2487 N94-23799
Factors affecting the identification of phytoplankton groups by means of remote sensing
[NASA-TM-108799] 06 p2387 N94-24403
Efficiency of subset selection of an epsilon-best uniform population relative to selection of the best one
[PB93-237741] 06 p2490 N94-24763
An exploratory stochastic model for toxic effects on cells
[AD-A273438] 06 p2422 N94-25146
Solving the ranking and selection indifference-zone formulation for normal distributions using computer software
[AD-A273821] 06 p2496 N94-25518
Methane emissions from natural wetlands
[DE93-040796] 07 p2865 N94-25790
Calculations of population transfer during intense laser pulses
[DE94-001060] 07 p2818 N94-26698
Reproduction in the Japanese anchovy (Engraulis japonica) as related to population fluctuation 08 p3235 N94-29708
Seasons and chaos in population dynamics 09 p3912 N94-31897
On the reciprocal relationship between life histories and population dynamics
[CWI-AM-R9302] 09 p3793 N94-32226
Food security in the context of global environmental change
[DE94-007481] 09 p3768 N94-32812
Sonic boom predictions using a modified Euler code 10 p3973 N94-33474
Transnational environmental degradation
[AD-A278469] 10 p4080 N94-33546

PORES
U POROSITY

POROSITY
NT MICROPOROSITY
Improving reservoir conformance using gelled polymer systems
[DE93-014532] 01 p0088 N94-10749
Inverting ultrasonic data on solid/fluid mixtures for Biot-Gassmann parameters
[DE93-011952] 01 p0150 N94-11026
Plating under reduced pressure
[DE93-011896] 01 p0084 N94-11668
Porosity and the ecology of icy satellites 01 p0431 N94-12186
Transport properties of disordered porous media from the microstructure
[DE93-016065] 02 p0806 N94-13152
A multiphase model for shock-induced flow in low density foam
[DE93-013767] 02 p0632 N94-13397
The method of Laplace Transform MultiQuadrics (LTMQ) for the solution of the groundwater flow equation
[DE93-010408] 02 p0637 N94-14053
Pore-size-distribution of cationic polyacrylamide hydrogels
[DE93-015218] 02 p0581 N94-14400
Structural investigation of electrochemically etched silicon
[DE93-015300] 03 p1207 N94-15827
Gas separations using ceramic membranes
[DE93-000278] 03 p0947 N94-15861
Selective formation of porous silicon
[NASA-CASE-NPO-18735-1-CU] 03 p0966 N94-15960
Mechanical properties of magnesium ammonium phosphate cements and their zeolite composites
[DE93-015155] 03 p0934 N94-16057
The cooling rates of pahoehoe flows: The importance of lava porosity 03 p1103 N94-16282
Superconducting ceramics: Selected properties and methods of production
[IFTR-23/1991] 03 p0969 N94-16924
Investigation of the effects of polyelectrolyte coatings on colloid transport in porous media
[DE93-018300] 03 p0970 N94-16973
Influence of the loading rate on the endurance and deformability of cement matrix composites
[IFTR-1/1992] 03 p1060 N94-17052
Micromechanics modeling and analysis of Haversian compact bone tissues as a fiber reinforced composite material
[AD-A268250] 03 p1129 N94-17456
X ray computed tomography for casting demonstration
[AD-A268084] 03 p1056 N94-17596
Process relationship as influenced by carbonization rate
[AD-A269680] 04 p1341 N94-18572
Hydrolysis reaction and positronium decay in silica gels
[AD-A270028] 04 p1371 N94-18713
Development of the microstructure based stochastic life prediction model
[AD-A269742] 04 p1361 N94-18742
Numerical simulation of fluid dynamics and combustion for ram accelerator projectile/obturator interaction
[AD-A269715] 04 p1320 N94-18748
Modeling of the formation of microporosity in alloys
[DE93-017733] 04 p1364 N94-19044
Microstructure of the interfacial zone around aggregate particles in concrete
[PB93-195790] 04 p1380 N94-19322
High resolution transmission electron microscopy of mesoporous MCM-41 type materials
[AD-A271271] 04 p1354 N94-19728
High-resolution numerical methods for compressible multi-phase flow in hierarchical porous media
[DE94-000740] 05 p1799 N94-20351
Embedded microclusters in zeolites and cluster beam sputtering: Simulation on parallel computers
[DE94-000741] 05 p1701 N94-20352
Dynamic response of multiphase porous media
[AD-A272915] 05 p1831 N94-21219
Fabrication of porous ceramics by freeze-casting/freeze-drying
[PB93-202513] 05 p1705 N94-21425
Symposium on Microscopy and Image Analysis of Building Materials
[VTT-SYMP-136] 05 p1707 N94-21890
Optical air pore analysis 05 p1708 N94-21892
Determination of pore structure of concrete from thin sections by image analysis 05 p1708 N94-21895
Fabrication of whisker-toughened alumina tubes
[DE94-001012] 05 p1677 N94-22022
Influence of sintering atmospheres on the aluminum sintering characteristics
[DE93-632412] 06 p2239 N94-22965
Modelling the ignition of boron/titanium particles 06 p2159 N94-24273
Method of fabricating a receptor-based sensor
[AD-D016026] 06 p2344 N94-24723
Laser-deposited biocompatible films and methods and apparatuses for producing same
[AD-D016017] 06 p2350 N94-24952
Advances in preparing and characterizing low density pan-carbon microcellular foam
[DE94-002278] 07 p2748 N94-25932
Double layer capacitance of carbon foam electrodes
[DE94-002651] 07 p2780 N94-25975
CEN-VAMAS round robin on grain size measurement for advanced technical ceramics
[VAMAS-TR-12] 07 p2752 N94-26654
Computational methods in continuum mechanics
[AD-A275560] 08 p3451 N94-28792
Microfocus radioscopy, a high resolution means of inspecting composite materials
[REPT-932-430-109] 08 p3179 N94-29454
Non-chromate talc conversion coatings for aluminum
[DE94-005281] 08 p3207 N94-30053
Surface probes of porous toluene/water ices: Adsorption kinetics and annealing spectra measured by second harmonic generation
[DE94-007564] 09 p3637 N94-32743
Characterization of nanoparticles and nanophase materials
[DE94-008348] 09 p3907 N94-32990
A geoacoustic model for fine-grained, unconsolidated calcareous sediments (ARSRP natural laboratory)
[AD-A277830] 10 p4092 N94-33831
Porosity in plasma sprayed alumina coatings
[DE94-008874] 10 p4028 N94-34011
Method for producing closed cell spherical porosity in spray formed metals
[AD-D016126] 10 p4025 N94-34152
NMR imaging of components and materials for DOE application
[DE94-010664] 11 p4238 N94-36084
A mixture model for shock compression of porous multi-component reactive materials
[DE93-017638] 12 p4400 N94-36456
Investigation of ultrasonic surface wave interaction with porous saturated rocks
[DE94-013378] 12 p4469 N94-37177

POROUS AIRFOILS
U POROUS BOUNDARY LAYER CONTROL

POROUS BOUNDARY LAYER CONTROL
The transient behavior of a boundary layer exposed to uniform suction
[ITN-93-85205] 02 p0630 N94-13197
Boundary layer control device for duct silencers
[NASA-CASE-ARC-12030-1] 08 p3478 N94-29362

POROUS MATERIALS
Preparation of carbon monoliths having tailored pore structure from porous polymer precursors
[DE93-011576] 01 p0089 N94-10958
Electrophoretic and electrolytic deposition of ceramic particles on porous substrates
[AD-A265141] 02 p0575 N94-12812
Transport properties of disordered porous media from the microstructure
[DE93-016065] 02 p0806 N94-13152
The method of Laplace Transform MultiQuadrics (LTMQ) for the solution of the groundwater flow equation
[DE93-010408] 02 p0637 N94-14053
Theoretical studies of breakdown in random media
[DE93-018107] 02 p0558 N94-14418
Structural investigation of electrochemically etched silicon
[DE93-015300] 03 p1207 N94-15827
Structural studies of sol-gel glasses
[AD-A266277] 03 p0967 N94-16472
Porous silicon for pumping solid-state lasers
[AD-A266293] 03 p1039 N94-16474
Operator overloading as an enabling technology for automatic differentiation
[DE93-012899] 03 p1170 N94-16778
Investigation of the effects of polyelectrolyte coatings on colloid transport in porous media
[DE93-018300] 03 p0970 N94-16973
Buried porous silicon-germanium layers in monocrystalline silicon lattices and method of producing
[NASA-CASE-NPO-18836-1-CU] 03 p1215 N94-17327
The Aerocapacitor: A carbon aerogel based supercapacitor
[DE93-016537] 04 p1395 N94-17849
Characterization of short pulse laser-produced plasmas at the Lawrence Livermore National Laboratory ultra short-pulse laser
[DE93-017191] 04 p1585 N94-18082
Time-resolved shock compression of porous rutile: Wave dispersion in porous solids
[DE93-018848] 05 p1829 N94-19927
Shock response of porous Al-2 + Fe2O3 powder mixtures
[DE93-018851] 05 p1688 N94-19944
Silver lined ceramic vessel
[AD-D015917] 05 p1700 N94-20057
Antipodal fragment velocities for porous and weak targets at catastrophic impacts 05 p1836 N94-20891
Two-dimensional finite element analysis of porous media at multikilobar stress levels
[AD-A271540] 05 p1831 N94-20916
Dynamic response of multiphase porous media
[AD-A272915] 05 p1831 N94-21219
Fabrication of porous ceramics by freeze-casting/freeze-drying
[PB93-202513] 05 p1705 N94-21425
A note on singularities caused by the hydrodynamic dispersion tensor
[CWI-NM-R9302] 05 p1803 N94-21575
Local uniform grid refinement and brine transport in porous media with inhomogeneities
[CWI-NM-R9224] 05 p1803 N94-21609
Carbon aerogels: An update on structure, properties, and applications
[DE94-001528] 06 p2252 N94-22931
Extinguishment of combustible porous solids by water droplets
[PB93-198893] 06 p2270 N94-23740
Investigations on detonation shock dynamics and related topics
[DE94-002570] 06 p2326 N94-23809
Applications of the homogenization method to flow and transport in porous media
[BER-9110] 06 p2340 N94-25467
Structure of ionic fluids in equilibrium with a microporous ionic matrix
[DE94-600563] 07 p2715 N94-26391

A thermodynamically consistent constitutive theory for a rigid solid-stokesian fluid mixture
[DE93-633202] 07 p2792 N94-26401
Low cost, radial flow, solid oxide fuel cell
[DE94-002982] 07 p2858 N94-26785
Light emitting porous silicon
[AD-A274152] 07 p3038 N94-27137
Researches of the Electrotechnical Laboratory. No. 52: Studies of externally pressurized porous gas bearings
[JTN-94-80549] 07 p2825 N94-27351
Porous vycor glass tube joined to borosilicate glass 07 p2718 N94-27392
The sol-gel-xerogel transition
[AD-A276647] 09 p3616 N94-32038
High-resolution numerical methods for compressible multi-phase flow in hierarchical porous media
[DE94-008261] 09 p3707 N94-32410
Bottom backscatter from trapped bubbles
[AD-A277583] 10 p4132 N94-33425
Generalized syntheses of periodic surfactant and inorganic composite materials
[AD-A278001] 10 p4019 N94-34160
Microporous structure with layered interstitial surface treatment, and method and apparatus for preparation thereof
[NASA-CASE-MSC-21487-3] 11 p4235 N94-35229
Theoretical and experimental study of air and hydrogen electrodes
[DE94-763308] 11 p4283 N94-36060
A mixture model for shock compression of porous multi-component reactive materials
[DE93-017638] 12 p4400 N94-36456
DDT modeling and shock compression experiments of porous or damaged energetic materials
[DE94-011419] 12 p4428 N94-37052
The problems of the minimal surface and minimal lineal measure in three dimensions
[DE94-013002] 12 p4479 N94-37355
Effects of two-phase flow on the deflagration of porous energetic materials
[DE94-011423] 12 p4411 N94-37412

POROUS PLATES
Boundary layer control device for duct silencers
[NASA-CASE-ARC-12030-1] 08 p3478 N94-29362

POROUS WALLS
Wall interference studies: Revisited 02 p0640 N94-14604
A method for the modelling of porous and solid wind tunnel walls in computational fluid dynamics codes
[NASA-CR-195699] 08 p3270 N94-28724

PORPHYRINS
NT CHLOROPHYLLS
Pulse radiolytic studies of electron transfer processes and applications to solar photochemistry
[DE93-018715] 04 p1464 N94-17781
The coordination and atom transfer chemistry of titanium porphyrin complexes
[DE94-003091] 07 p2704 N94-26779
Photochemistry in constrained spaces: Zeolites and layered double metal hydroxides
[DE94-004958] 08 p3200 N94-30769
Solvent effects on the energetics and dynamics of ultrafast electron transfer in chlorophyll-porphyrin-acceptor triads
[DE94-009693] 12 p4477 N94-36554
Femtosecond transient grating studies of electron transfer in porphyrin and chlorophyll donor-acceptor molecules
[DE94-009694] 12 p4478 N94-36555

PORTABLE EQUIPMENT
A portable controller for unmanned ground vehicles
[AD-A264963] 01 p0181 N94-11290
DISTERM: A shipboard data system for satellite monitoring of ocean and atmosphere 01 p0226 N94-12749
Development of a portable multispectral thermal infrared camera
[NASA-CR-191340] 02 p0648 N94-13176
Portable acoustic wave sensor systems for real-time monitoring of volatile organic compounds
[DE93-013753] 02 p0582 N94-14511
Experience and results of the 1991 MTLRS-1 USSR campaign 03 p0914 N94-15575
Experience with disconnected operation in a mobile computing environment
[AD-A267524] 03 p1141 N94-17115
MAGSS-14: Medium Altitude Global Mobile Satellite System with enhanced regional coverage 03 p0893 N94-17164
Portable, solid state, fiber optic coupled Doppler interferometer system for detonation and shock diagnostics
[DE93-013917] 04 p1423 N94-17700
The First International Conference on PCTE
[FEL-92-A134] 04 p1518 N94-17965
Downlink acquisition and tracking procedures for the ASCAMP satellite communications terminal
[AD-A272912] 05 p1739 N94-21244
Physiological efficacy of a lightweight ambient air cooling unit for various applications
[AD-A272952] 05 p1896 N94-21247
Compact free electron lasers for medical applications
[AD-A273609] 06 p2350 N94-24934
Portable Habitat for Antarctic Scientific Research (PHASR) 07 p2943 N94-25681
System design analysis of a lightweight laser satellite terminal
[AD-A274033] 07 p2690 N94-25769
Status report for the development of the Antarctic penetrator: 1990-year program 07 p2885 N94-27973
Evaluation of access/navigational features of a graphical-user interface installed on a portable maintenance aid
[AD-A275791] 08 p3136 N94-28744
Radiation transport and focusing systems for power industrial lasers
[DE94-606817] 08 p3293 N94-28786
Portable electronically based method for the nondestructive remote sensing of crevice corrosion
[AD-A275403] 08 p3318 N94-29057
Portable Linear Sled (PLS) for biomedical research 08 p3163 N94-29648
Portable color multimedia training systems based on monochrome laptop computers (CBT-in-a-briefcase), with spinoff implications for video uplink and downlink in spaceflight operations
[NASA-TM-108460] 12 p4496 N94-37556

PORTABLE LIFE SUPPORT SYSTEMS
Portable ventilatory resuscitation systems
[AD-A274984] 08 p3401 N94-29093
Lunar surface operations. Volume 1: Lunar surface emergency shelter
[NASA-CR-195551] 08 p3299 N94-29354
Metal hydride heat pump engineering demonstration and evaluation model
[NASA-CR-188286] 09 p3669 N94-32857
The US Navy/Canadian DCIEM research initiative on pressure breathing physiology 10 p4101 N94-33636

PORTUGAL
Evolution of upwelling fronts off the coast of Portugal
[NASA-CR-195692] 09 p3790 N94-33045

POSEIDON SATELLITE
Topex/Poseidon: A United States/France mission. Oceanography from space: The oceans and climate
[NASA-TM-108253] 01 p0043 N94-10699
Analysis of TOPEX laser retroreflector array characteristics 03 p0915 N94-15578
TOPEX/Poseidon precision orbit determination production and expert system 06 p2196 N94-23920
TOPEX/Poseidon battery performance during the first year of operation 07 p2862 N94-28119
TOPEX/POSEIDON operational orbit determination results using global positioning satellites 08 p3160 N94-29666
Lessons learned from selecting and testing spaceflight potentiometers 09 p3607 N94-33318
Compatibility of TOPEX/Poseidon trajectory propagation with JPL and GSFC/FDF operational software 11 p4204 N94-35619
Improved solution accuracy for TDRSS-based TOPEX/Poseidon orbit determination 11 p4205 N94-35620
Tracking system options for future altimeter satellite missions 11 p4205 N94-35622

POSITION (LOCATION)
NT SOLAR POSITION
Visual encoding of spatial relations
[AD-A266049] 01 p0313 N94-10909
Analysis of IRAS solar system dust data
[NASA-CR-193704] 01 p0483 N94-10949
Joint pain and Doppler-detectable bubbles in altitude (Hypobaric) decompression 01 p0312 N94-11542
The Magellan volcanic and magmatic feature catalog 01 p0467 N94-12193
Design and performance of an automated video-based laser beam alignment system
[DE93-012571] 02 p0656 N94-13481
Simulated annealing for the problem of multiresource location on graph
[REPT-93-033] 02 p0770 N94-13809
Computational issues in optimal tuning and placement of passive dampers 02 p0681 N94-14647
Satellite sound broadcast propagation measurements 03 p0996 N94-16047
Intentionally Short Range Communications (ISRC)
[AD-A268788] 04 p1384 N94-18216
Constructing a reference event list for ARCESS
[AD-A269288] 04 p1481 N94-18297
Historical seismicity of Hainaut, Flanders and Artois 04 p1482 N94-18623
A program for passively tracking a target using an array of sensors
[DE93-019554] 04 p1390 N94-19306
Localization from near-source quasi-static electromagnetic fields
[DE93-040390] 05 p1732 N94-20479
Optimization of a satellite localization and message sending system
[ETN-93-94448] 05 p1737 N94-20592
Characterization of the Marquez Dome buried impact crater using gravity and magnetic data 05 p1863 N94-20882
Joint Acoustic Propagation Experiment (JAPE) 06 p2527 N94-24208
Worldwide vessel locating and tracking system, volume 1
[PB93-193217] 06 p2175 N94-24474
The role of visual context in manual target localization 06 p2429 N94-25351
Mechanisms of eye-hand coordination
[AD-A273687] 06 p2428 N94-25437
Differential global positioning system for the surface-towed ordnance locating system: Testing, results, and user's guide
[DE94-002980] 07 p2664 N94-26309
Short-range cloud amount forecasting with model output statistics
[AD-A274769] 07 p2895 N94-26798
Technical report of ISSP. Ser. A, no. 2671: Quasi-localization of light waves in Fibonacci dielectric multilayers
[JTN-94-80557] 07 p3064 N94-27231
Technical report of ISSP. Ser. A, no. 2675: High-field cyclotron resonance and valence-band structure in semiconducting diamond
[JTN-94-80561] 07 p3065 N94-27245
BATSE burst location accuracy and constraints on the fraction of repeating GRB sources
[DE94-004981] 07 p3116 N94-27714
An integrated approach to seismic event location: 1. Evaluating how method of location affects the volume of groups of hypocenters
[PL-TR-92-2323] 07 p2887 N94-28214
Testing for a signal with unknown location and scale in a stationary Gaussian random field
[AD-A275320] 08 p3464 N94-28876
Stability properties of inclusive connectivity for graphs
[AD-A275360] 08 p3452 N94-29016
Development of an accurate transmission line fault locator using the global positioning system satellites 08 p3144 N94-30652
Placing registration marks
[RUU-CS-93-21] 08 p3427 N94-30725
Computing the precision of localization in a plane using projective invariants
[TELECOM-93-D-005] 09 p3840 N94-31095
Shiptrack database analysis
[AD-A277228] 09 p3746 N94-32025
Selection of climate station data using clustering and triangulated irregular network techniques
[AD-A276658] 09 p3784 N94-32046
MODIS. Volume 2: MODIS level 1 geolocation, characterization and calibration algorithm theoretical basis document, version 1
[NASA-TM-104594-VOL-2] 09 p3613 N94-33289
A theory and experiments for detecting shock locations
[NASA-TM-106634] 10 p4056 N94-33952
Mesoscale roughness of Venus 11 p4361 N94-35430
Transformation plasticity in ductile solids
[DE94-010420] 11 p4240 N94-35953
Analysis of mid-tropospheric carbon monoxide data using a three-dimensional global atmospheric chemistry numerical model
[DE94-004782] 11 p4286 N94-36026
Extrapolating storm location using the Integrated Terminal Weather System (ITWS) storm motion algorithm
[AD-A278611] 11 p4295 N94-36249
Computational methods for material failure processes
[AD-A278716] 11 p4278 N94-36292
Aerial refueling interoperability from a receiver flying qualities perspective 11 p4197 N94-36343
Short-tower sigma(theta) measurements in the Colorado Plateaus region
[DE94-007478] 12 p4463 N94-36478

POSITION (TITLE)
The Senior Executive Service
[NHB-3100.6] 03 p1224 N94-15945

POSITION ERRORS
NT BORESIGHT ERROR
Force reflection with compliance control
[NASA-CASE-NPO-18668-1-CU] 01 p0179 N94-10654

Thermal error compensation feasibility study using artificial intelligence
[AD-A266084] 01 p0340 N94-12411
Position error determination for the speedometer and altimeter of the NAL QSTOL experimental aircraft ASKA
[NAL-TR-1144] 02 p0517 N94-13451
GPS satellite sky distribution: Impact on the propagation of some important errors in precise relative positioning
[ISBN-0-315-51838-3] 02 p0513 N94-13541
Orbit determination error analysis based on the requirements of ADEOS mission
[NASDA-CNT-930008] 02 p0532 N94-13644
Laser ranging data analysis
[NASA-CR-193547] 03 p1041 N94-16719
Category (CAT) 3B level 1 test plan for Global Positioning System (GPS)
[DOT/FAA/RD-93/21] 03 p0864 N94-16835
Limits on m = 2, n = 1 error field induced locked mode instability in TPX with typical sources of poloidal field coil error field and a proto type correction coil, C-coil
[DE93-014408] 04 p1582 N94-17702
Flight demonstration of image fix-taking with SAR
[DE93-016499] 04 p1382 N94-17861
About the accuracy of an image-based navigation system during the runway approach
[DLR-MITT-93-01] 04 p1316 N94-18146
Silicon retina for optical tracking systems
05 p1755 N94-21098
A motion extraction method for synthetic aperture radars
[DLR-FB-92-31] 05 p1742 N94-22279
A review of GPS-based tracking techniques for TDRS orbit determination 06 p2196 N94-23257
Accuracy analysis of multi-axis machines
[ETN-94-95341] 07 p3002 N94-26000
Ground station siting considerations for DGPS
07 p2642 N94-27293
Differential GPS methods and performance for marine applications
[DREP-93-09] 07 p2665 N94-27667
A simulation of GPS and differential GPS sensors
07 p2666 N94-27918
Time and position accuracy using codeless GPS
08 p3144 N94-30650
Error analysis of real-time and post-processed orbit determination for the Geosat Follow-On altimetric satellite using GPS tracking 09 p3576 N94-31845
In-flight scale/distortion calibration of the Hubble Space Telescope fixed-head star trackers
11 p4203 N94-35613
A more exact analysis of Sandia Laser Tracker data
[DE94-011411] 12 p4447 N94-37051
Operator gaze position control interfaces: Investigation of psychophysical and operational parameters
12 p4485 N94-37273

POSITION INDICATORS
NT PLAN POSITION INDICATORS
NT RADIO DIRECTION FINDERS
NT SPACECRAFT POSITION INDICATORS
Double-driven shield capacitive type proximity sensor
[NASA-CASE-GSC-13541-1] 03 p1165 N94-15946
Evaluation of site effects on a high frequency direction finding single site location system
[AD-A267465] 03 p1001 N94-17035
EUTELTRACS: The European experience on mobile satellite services 06 p2281 N94-22781
Lightning studies using LDAR and LLP data
06 p2416 N94-23238
Interchangeable end effector tools utilized on the PFMA
[NASA-CR-193925] 07 p2823 N94-27149
A comparison of two examples of magnetic tracker systems 12 p4485 N94-37275

POSITION SENSING
Performance evaluation tests of the GPS/DGPS navigation system installed in the NAL Dornier 228: Preliminary ground test results
[NAL-TM-649] 02 p0513 N94-13346
Close range 3-D position sensing using stereo vision and point-of-correspondance through mathematical morphology
[ISBN-0-315-61012-3] 02 p0763 N94-13515
Development of a tactile and vision integrated system, and object identification techniques for SPDM applications
[DSIS-93-00153] 02 p0764 N94-13842
Capaciflector camera
[NASA-CASE-GSC-13564-1] 03 p1033 N94-15872
Double-driven shield capacitive type proximity sensor
[NASA-CASE-GSC-13541-1] 03 p1165 N94-15946
Rotary encoding device using polygonal mirror with diffraction gratings on each facet
[NASA-CASE-GSC-13543-1] 05 p1985 N94-20240
Silicon retina for optical tracking systems
05 p1755 N94-21098
A 3-D vision method for estimating workspace occupancy of a power-line maintenance robot
05 p1770 N94-22105
Sensor integration and data fusion for object localization in robotic workcells 05 p1774 N94-22130
Charge integrating optical position sensor
05 p1778 N94-22152
An approach to the estimation of ground structure and aircraft motion from aerial image sequences
05 p1789 N94-22226
Wideband source location in two-dimensional array processing 05 p1747 N94-22250
Mobile robot perception in unknown and unstructured dynamic voxel environments
[ISBN-0-315-83951-1] 05 p1947 N94-22591
Sensing and modelling concepts for autonomous and remote mobile robot control 06 p2370 N94-23421
Autonomous Space Processor for Orbital Debris (ASPOD)
[NASA-CR-195521] 06 p2204 N94-24621
Interchangeable end effector tools utilized on the PFMA
[NASA-CR-193925] 07 p2823 N94-27149
Stripline monitor electronics for the bundle position determination in AmPS
[DIGEL-1993-8] 08 p3495 N94-29888
Computer Assisted Medical Interventions: Application to Conformal Radiotherapy
[RR-912-I] 08 p3395 N94-30028
Conformal external radiotherapy of prostatic carcinoma: Requirements and preliminary results
08 p3395 N94-30029
Pre- and intra-radiotherapy multimodal image registration: Principles and first experiments
08 p3395 N94-30030
Encoding technique for automated guided vehicle POSE recovery in a structured environment
08 p3144 N94-30286
Hydrogenated amorphous silicon (a-Si:H) based gamma camera: Monte Carlo simulations
[DE94-007042] 09 p3795 N94-31323
Digit-Eyes: Vision-based human hand tracking
[NASA-CR-195913] 09 p3803 N94-31447
CAD-based off-line planning for an active-vision system
[ISBN-0-315-86317-X] 09 p3813 N94-31713
The resolvability ellipsoid for sensor based manipulation
[AD-A277898] 10 p4055 N94-33549
Integration of magnetic bearings in the design of advanced gas turbine engines 11 p4223 N94-35903
Optical position measurement for a large gap magnetic suspension system: Design and performance analysis
[NASA-TP-3438] 12 p4447 N94-36946

POSITIONING
Determination of the viscous acoustic field for liquid drop positioning/forcing in an acoustic levitation chamber in microgravity 01 p0110 N94-10131
Thermal error compensation feasibility study using artificial intelligence
[AD-A266084] 01 p0340 N94-12411
GPS satellite sky distribution: Impact on the propagation of some important errors in precise relative positioning
[ISBN-0-315-51838-3] 02 p0513 N94-13541
Wide-area Differential Global Positioning System (WDGPS)/Wide-area Integrity Broadcast (WIB) alternatives analysis
[DOT/FAA/SE-93/3] 03 p0864 N94-16906
Radiocommunication problems of a position reporting and bidirectional messagery system using VHF/UHF with low-Earth orbit satellites 03 p0889 N94-17136
Adequation of mini satellites to oceanic altimetry missions 03 p0891 N94-17152
The ORBCOMM system 03 p0893 N94-17163
Six degree of freedom fine motion positioning stage based on magnetic levitation
[DE93-017651] 04 p1446 N94-19547
Absolute positioning by collecting Global Positioning System (GPS) data along short baselines
[AD-A271324] 04 p1317 N94-19572
The data acquisition system for the Anglo-Australian Observatory 2-degree field project
05 p2048 N94-22529
CNES organization for station positioning of geostationary satellites 06 p2501 N94-23857
MERCATOR: Methods and Realization for Control of the Attitude and the Orbit of spacecraft
06 p2202 N94-23925
HISPASAT launch and early operations phases: Computation and monitoring of geostationary satellite positioning 06 p2514 N94-23928
Differential GPS for air transport: Status
06 p2162 N94-25100
Modelling and stability of a shape memory alloy position control system
[ISBN-0-315-84467-1] 07 p2740 N94-27304
Status report for the development of the Antarctic penetrator: 1990-year program 07 p2885 N94-27973
Synchronization, positioning, and communication in multistatic radar systems for air defence
[PB94-137478] 08 p3243 N94-28908
Position control of a flexible beam with active damping of vibrations
[ISBN-0-315-85841-9] 08 p3321 N94-30033
Nearly time-optimal feedback control of a magnetically levitated photolithography positioning system
[DE94-005288] 08 p3266 N94-30055
Neural network based time-optimal control of a magnetically levitated precision positioning system
[DE94-006573] 08 p3437 N94-30250
The resolvability ellipsoid for sensor based manipulation
[AD-A277898] 10 p4055 N94-33549
Materials for efficient high-flux magnetic bearing actuators 11 p4214 N94-35845
Magnetically suspended stepping motors for clean room and vacuum environments 11 p4225 N94-35915
Six degree of freedom fine motion positioning stage based on magnetic levitation 11 p4225 N94-35916
Analysis of achievable disturbance attenuation in a precision magnetically-suspended motion control system
11 p4225 N94-35917

POSITIONING DEVICES (MACHINERY)
NT BOOMS (EQUIPMENT)
NT CAMS
Counter-balanced, multiple cable construction crane
[NASA-CASE-LAR-14565-1-CU]
05 p1822 N94-20369
Three point lead screw positioning apparatus for a cavity tuning plate
[NASA-CASE-LEW-15216-1] 05 p1822 N94-20375
Turntable mechanism
[NASA-CASE-MFS-28522-1] 05 p1823 N94-20380
Precision Displacement Mechanism (PDM)
06 p2360 N94-24026
System for automatic transportation of aircraft on the ground
[CA-PATENT-1-322-361] 06 p2193 N94-24785
Three methods to improve the accuracy of a PUMA 560 robot 08 p3307 N94-30290
Two-axis antenna positioning mechanism
09 p3605 N94-33308
Fuzzy self-learning control for magnetic servo system
11 p4215 N94-35852

POSITIVE FEEDBACK
A study on piezoelectric actuators and sensors for vibration control of flexible space structures
[AD-A274925] 07 p2695 N94-26532
Sensitivity and feedbacks associated with vegetation-related land surface parameters in a general circulation model 08 p3348 N94-29800
Modeling studies of frontogenesis in the upper and middle troposphere 08 p3375 N94-30868

POSITIVE IONS
NT CATIONS
NT HYDRONIUM IONS
Role of Ca(++)/calmodulin in the regulation of microtubules in higher plants
[DE93-015885] 02 p0727 N94-12835
Indirect processes in electron impact ionization of Kr(24+) and Kr(25+)
[DE93-014129] 02 p0784 N94-14140
Investigation of the effects of polyelectrolyte coatings on colloid transport in porous media
[DE93-018300] 03 p0970 N94-16973
Novel electrochemical materials prepared by sol-gel chemistry
[AD-A269060] 04 p1578 N94-18405
Low emittance 0.8A K(+) ion source for the LBL Induction Linac System Experiment (ILSE)
[DE93-019237] 05 p1981 N94-21439
Ion implantation of diamond: Damage, doping, and lift-off
[DE94-001133] 07 p3054 N94-26137
Structure of ionic fluids in equilibrium with a microporous ionic matrix
[DE94-600563] 07 p2715 N94-26391
Performance of an ion trap inductively coupled plasma mass spectrometer
[DE94-007470] 09 p3713 N94-32811

POSITRON ANNIHILATION
A window least squares algorithm for statistical noise smoothing of 2D-ACAR data
[DE93-613828] 01 p0395 N94-10537
A positron annihilation radiation telescope using Laue diffraction in a crystal lens
[DE93-012905] 02 p0848 N94-13483
Effects of additional isoscalar vector bosons in e(sup +)e)(sup -)(yields)ff-bar processes at the TRISTAN and LEP energies
[DE93-621451] 02 p0783 N94-13506

Positron annihilation study of Sr Doping in La(2-x)Sr(x)CuO4
[DE94-000307] 05 p2036 N94-22594
Window least squares method applied to statistical noise smoothing of positron annihilation data
[DE93-634665] 07 p3003 N94-26385
A jet calculus approach including coherence effects and the associated problem of moment inversion
[ISBN-0-315-51715-8] 07 p3025 N94-27266
Axial anomaly in e(+)e(-) yields gamma gamma and anyon superconductivity
[DE94-606406] 07 p3070 N94-27859
Fermi surface ridge at second and third Umklapp positron annihilations in Y Ba2Cu3O(7-delta)
[DE93-634760] 07 p3070 N94-27995
Application of the Positron Annihilation Technique to the study of vapor absorption process in polyethylene (LDPE) and in imide polymer (6FDA-TMPD PI)
[DE94-602737] 07 p2720 N94-27998
Influence of doping on the electronic structure of (La, Sr)2CuO4
[DE94-006383] 08 p3516 N94-30054
Experiment studies of electron-positron interactions at the Stanford Linear Accelerator Center
[DE94-005877] 08 p3491 N94-30702
A constraint on the pair-density ratio (Z+) in an electron-positron pair wind 09 p3930 N94-31132
High energy physics program at the University of Alabama
[DE94-006544] 09 p3875 N94-31488
Production of charginos and neutralinos for the reaction positron electron yields Z' boson yields chargino(+) (sub i) chargino(-) (sub j) or neutralino (sub i) neutralino (sub j) in SU(2) (sub L) x SU(2) (sub R) x U(1) (sub B-L)
[ISBN-0-315-87316-7] 09 p3867 N94-31832
Positron-molecule interactions
[AD-A276542] 09 p3869 N94-32082
Characterization of defects in Si and SiO2-Si using positrons
[DE94-009044] 10 p4147 N94-33877
T-odd, P-even photon-fermion interactions
[DE94-616869] 11 p4327 N94-36246
Positron implantation in solids
[DE94-013029] 12 p4537 N94-37499

POSITRONIUM
Hydrolysis reaction and positronium decay in silica gels
[AD-A270028] 04 p1371 N94-18713
Proof of stability of the hydrogen molecule
[PB93-221026] 05 p1977 N94-22271
Hyperfine structure of positronium energy levels in a crystal
[DE94-603898] 07 p3068 N94-27729
Logarithmic corrections of the two-body QED problem
[DE94-611157] 11 p4322 N94-35783

POSITRONS
Acceleration of positrons in supernova shocks
[NASA-CR-193713] 01 p0425 N94-10511
EGS (underscore) windows 2: An enhanced graphical interface to EGS
[DE93-010447] 02 p0746 N94-13382
A positron annihilation radiation telescope using Laue diffraction in a crystal lens
[DE93-012905] 02 p0848 N94-13483
Rare muon processes
[DE93-012646] 02 p0785 N94-14366
Experimental study of weak interactions by precision measurement by rare kaon decay
[DE93-016864] 03 p1182 N94-16117
The Intense Slow Positron Source concept: A theoretical perspective on a proposed INEL Facility
[DE93-013675] 04 p1564 N94-17738
An ab initio Monte Carlo study of low energy positron and electron implantation in elemental metals and multilayers
[DE93-019847] 04 p1603 N94-19541
Harvard University High Energy Physics
[DE94-002406] 07 p3032 N94-26119
Fast photoconductor CdTe detectors for synchrotron x ray studies
[DE94-001334] 07 p3054 N94-26139
Calculation of total cross sections for electron and positron scattering on sodium and potassium
[DE94-601814] 07 p3023 N94-26944
Langmuir waves in the electron-positron plasma
[DE94-606330] 08 p3508 N94-30191
Positron-molecule interactions
[AD-A276542] 09 p3869 N94-32082
Isothermal sintering, microstructure, and superconducting properties of Y1Ba2Cu3O(7-x) compound
[DE94-006132] 09 p3905 N94-32779
Characterization of defects in Si and SiO2-Si using positrons
[DE94-009044] 10 p4147 N94-33877
Convergent close-coupling calculations of low-energy positron-atomic-hydrogen scattering
[DE94-609858] 10 p4137 N94-33882
Precise measurement of the left-right cross section asymmetry in Z boson production by electron-positron collisions
[DE94-010751] 11 p4326 N94-36198
Older muons are wiser: Using time information in (mu)LCR spectroscopy
[DE93-018556] 12 p4511 N94-36457
Production of a positron and a bound electron by high-energy photon in a strong Coulomb field
[DE94-618501] 12 p4514 N94-36747
Precise determination of the weak mixing angle from a measurement of ALR in e(+)e(-) yields Z0
[DE94-013355] 12 p4515 N94-37085
Five-lepton decay modes of muon and tau mesons
[DE94-621636] 12 p4516 N94-37099
A freon-filled, holographic bubble chamber as a high energy photon burst spectrometer
[DE94-011645] 12 p4446 N94-37723

POSTFLIGHT ANALYSIS
Debris/ice/TPS assessment and integrated photographic analysis for Shuttle Mission STS-57
[NASA-TM-107562] 01 p0040 N94-10805
Promethazine and its use as a treatment for space motion sickness 01 p0312 N94-11550
STS-53 Space Shuttle mission report
[NASA-CR-193101] 02 p0535 N94-13934
STS-54 Space Shuttle mission report
[NASA-CR-194116] 02 p0535 N94-13935
Long duration exposure facility experiment m0003 deintegration observation database
[AD-A267579] 03 p0951 N94-17207
Postflight hardware evaluation 360T026 (RSRM-26, STS-47)
[NASA-CR-192559] 03 p0882 N94-17656
Conversion of LDEF experiment M0003 sample observation database to MS-DOS formats
[AD-A272945] 05 p1681 N94-21226
Postflight hardware evaluation RSRM-29 (STS-54). Appendix D: Nozzle postfire data
[NASA-CR-193898] 06 p2199 N94-24057
Postflight hardware evaluation RSRM-29 (STS-54). Appendix C: Nozzle PFORs
[NASA-CR-193894] 06 p2219 N94-24064
Final postflight hardware evaluation report RSRM-32 (STS-57)
[NASA-CR-193903] 06 p2200 N94-24065
Postflight hardware evaluation RSRM-29 (STS-54). Appendix E: Insulation postfire data
[NASA-CR-193897] 06 p2200 N94-24067
Final postflight hardware evaluation report RSRM-28 (STS-53)
[NASA-CR-193902] 06 p2200 N94-24112
Postflight hardware evaluation (RSRM-29, STS-54)
[NASA-CR-193895] 06 p2201 N94-24802
Postflight hardware evaluation 360T021 (RSRM-21, STS-45), revision A
[NASA-CR-193896] 06 p2201 N94-24965
Postflight hardware evaluation RSRM-29 (STS-54). Case, seals, and joints PFORs, appendix B
[NASA-CR-193899] 06 p2367 N94-25020

POSTLAUNCH REPORTS
Flight data analysis of Japanese Earth Resources Satellite-1 (JERS-1)
[NASDA-CNT-930004] 01 p0245 N94-12279
Debris/ice/TPS assessment and integrated photographic analysis for Shuttle Mission STS-51
[NASA-TM-109189] 05 p1656 N94-21884
Final postflight hardware evaluation report RSRM-32 (STS-57)
[NASA-CR-193903] 06 p2200 N94-24065
Debris/ice/TPS assessment and integrated photographic analysis for Shuttle Mission STS-59
[NASA-TM-109203] 11 p4211 N94-35523

POSTMISSION ANALYSIS (SPACECRAFT)
Debris/ice/TPS assessment and integrated photographic analysis for Shuttle Mission STS-57
[NASA-TM-107562] 01 p0040 N94-10805
STS-53 Space Shuttle mission report
[NASA-CR-193101] 02 p0535 N94-13934
STS-54 Space Shuttle mission report
[NASA-CR-194116] 02 p0535 N94-13935
Debris/Ice/TPS assessment and integrated photographic analysis for Shuttle Mission STS-61
[NASA-TM-109195] 06 p2199 N94-24059
Postflight hardware evaluation (RSRM-29, STS-54)
[NASA-CR-193895] 06 p2201 N94-24802
STS-58 Space Shuttle Mission Report
[NASA-TM-109867] 11 p4211 N94-35251
STS-51 Space Shuttle Mission Report
[NASA-TM-109866] 11 p4211 N94-35252

POSTULATES
U AXIOMS

POSTURE
Gender differences in endocrine responses to posture and 7 days of 6 deg head down bed rest
[NASA-TM-103991] 02 p0731 N94-12972
Neurophysiological study on visuo-vestibular control of posture and movement in fish during adaptation to weightlessness 02 p0591 N94-13759
The effect of body orientation on the perception of vertical and horizontal distance in an outdoor setting 07 p2915 N94-27461
Postural strategies for the continuous control of static and dynamic balance in man
[PB94-184678] 12 p4487 N94-37812

POTABLE LIQUIDS
NT BEVERAGES
NT POTABLE WATER

POTABLE WATER
Atmospheric moisture collection device
[AD-D015935] 05 p1865 N94-20332
Statistical procedures for corrosion studies
[PB93-199412] 06 p2244 N94-23802
Continuous monitoring of bacterial attachment 10 p4094 N94-33658
Characterization of spacecraft humidity condensate 10 p4102 N94-33659
Computation of iodine species concentrations in water 10 p4102 N94-33660
Determination of copper in tap water using solid-phase spectrophotometry
[NASA-TM-106480] 12 p4408 N94-36537

POTASSIUM
NT POTASSIUM ISOTOPES
NT POTASSIUM 40
Is K3C60 a line phase?
[DE93-016700] 02 p0813 N94-14517
Potassium-Rankine power conversion subsystem modeling for nuclear electric propulsion
[NASA-CR-191134] 04 p1468 N94-18821
K, U, and Th behavior in Martian environmental conditions 05 p2141 N94-20908
Low emittance 0.8A K(+) ion source for the LBL Induction Linac System Experiment (ILSE)
[DE93-019237] 05 p1981 N94-21439
Calculation of electron-potassium scattering
[DE94-601812] 07 p3023 N94-26942
Calculation of total cross sections for electron and positron scattering on sodium and potassium
[DE94-601814] 07 p3023 N94-26944
Silicone grease as a precursor to a pseudo crown-ether ligand: Crystal structure of (K(+)K(Me2SiO)7(+)) (HIn(CH2CMe3)3(-))4)
[AD-A276343] 09 p3895 N94-31327

POTASSIUM ALLOYS
First on-sun test of NaK pool-boiler solar receiver
[DE93-015003] 04 p1466 N94-18208
Bench-scale screening tests for a boiling sodium-potassium alloy solar receiver
[DE93-018512] 04 p1469 N94-19040
Thermodynamics of molten K-TE alloys
[DE94-608095] 08 p3208 N94-30090
Electrooptic crystal growth and properties
[AD-A276023] 09 p3896 N94-31439
Structural ordering in liquid K-Te alloys
[DE94-008477] 09 p3645 N94-32514

POTASSIUM COMPOUNDS
NT NEPHELINE
NT POTASSIUM HYDROXIDES
NT POTASSIUM NITRATES
NT POTASSIUM OXIDES
NT POTASSIUM PERCHLORATES
NT POTASSIUM PHOSPHATES
NT POTASSIUM SILICATES
Development of K(1-x)Na(x)TiOPO4 crystals for nonlinear applications
[AD-A274336] 07 p3063 N94-27055
Experimental and theoretical studies of molecular solids
[AD-A275511] 08 p3485 N94-28668
Displacive transformation in ceramics
[AD-A278442] 10 p4026 N94-33539

POTASSIUM HYDROXIDES
NASA Lewis advanced IPV nickel-hydrogen technology 06 p2392 N94-23356
Freon recovery from nitrogen tetroxide and freon solutions
[PL-TR-92-3051] 07 p2721 N94-28215
Development of nickel and metal hydride secondary battery
[DE94-757270] 09 p3697 N94-32917

POTASSIUM ISOTOPES
NT POTASSIUM 40
Radiogenic age and isotopic studies
[DE93-610548] 01 p0274 N94-10407
Potassium isotope cosmochemistry, volatile depletion and the origin of the Earth 03 p0953 N94-16259

POTASSIUM OXIDES
The de Haas-van Alphen measurements in Ba(0.6)K(0.4)BiO3
[DE93-041169] 06 p2556 N94-22920
High T(sub c) superconductor tunnel junctions for photon detectors
[DE94-007686] 09 p3904 N94-32602
POTASSIUM PERCHLORATES
A low cost igniter utilizing an SCB and titanium sub-hydride potassium perchlorate pyrotechnic
[DE94-006467] 09 p3666 N94-31827
POTASSIUM PHOSPHATES
Three-wave nonlinear interactions in KTiOPO4 (KTP) and KTP isomorphs
[AD-A274079] 07 p3052 N94-25993
Optical properties of lanthanide-doped RbTiOAsO4 and transition metal-doped KTiOPO4
[DE94-008433] 09 p3907 N94-32963
POTASSIUM SILICATES
Thermal history effects on electrical relaxation and conductivity for potassium silicate glass with low alkali concentrations
[NASA-TM-106324] 02 p0583 N94-14845
POTASSIUM 40
Geological Dating by Ar-40 - Ar-39 method
[DE94-601975] 07 p2880 N94-26874
POTATOES
Studies on the application of radiation for genetic transformation in higher plants
[DE93-632656] 07 p2901 N94-26470
Development of a sparging technique for volatile emissions from potato (Solanum tuberosum)
[NASA-TM-109199] 07 p2903 N94-27412
POTENTIAL ENERGY
NT BIOELECTRIC POTENTIAL
NT CONTACT POTENTIALS
NT COULOMB POTENTIAL
NT ELECTRIC POTENTIAL
NT GEOPOTENTIAL HEIGHT
NT IONIZATION POTENTIALS
NT LOW VOLTAGE
NT NUCLEAR POTENTIAL
NT OPEN CIRCUIT VOLTAGE
NT PHOTOEXCITATION
NT PHOTOVOLTAGES
NT PLASMA POTENTIALS
NT QUANTUM WELLS
NT THRESHOLD VOLTAGE
Non-empirical interatomic potentials for transition metals
[DE93-013705] 01 p0365 N94-11011
Demonstration designs for optical-field-ionized plasma x-ray lasers
[DE93-009227] 01 p0175 N94-11266
The global potential energy surfaces of the lowest two 1A' states of the ozone molecule: Theoretical determination and analysis 01 p0267 N94-12269
Incomplete melting of the Au(100) surface
[DE93-623192] 02 p0569 N94-13227
Predicting the vibrations of a spinning inflated membrane
[DE93-010690] 02 p0676 N94-14456
Molecular processes in comets
[NASA-CR-194148] 03 p1239 N94-15188
Impending motion direction of contacting rigid bodies
[AD-A266814] 03 p1164 N94-15756
A molecular dynamics simulator for optimal control of molecular motion
[AD-A266572] 03 p1183 N94-16722
Seasonal variability of wind electric potential in the US
[DE93-018182] 04 p1493 N94-19051
Ab initio potential energy surface for the H + OCS reaction
[AD-A270577] 05 p1698 N94-19947
Computed potential energy surfaces for chemical reactions
[NASA-CR-194600] 05 p1679 N94-20169
Mechanical and thermal buckling analysis of sandwich panels under different edge conditions
[NASA-TM-4535] 06 p2228 N94-23514
CAPE for CaPE 06 p2416 N94-24409
The torsion space nucleic acids molecular mechanics program DUPLEX: Surveying conformation space by potential energy minimization
[DE94-002441] 06 p2563 N94-24567
Free energy profiles for Li(+) and I(-) ions approaching Pt(100) surface: A molecular dynamics study
[AD-A273455] 06 p2536 N94-24675
Interaction of water with metal surfaces
[AD-A276260] 09 p3632 N94-31293
Chemisorbed-molecule potential-energy surfaces and electronically-stimulated processes
[DE94-007932] 09 p3719 N94-32603
Computed potential energy surfaces for chemical reactions
[NASA-CR-195835] 09 p3639 N94-33036
The asymptotics of matrix elements of Gaussian potential between the basis functions of three-dimensional harmonic oscillator
[DE94-618467] 12 p4539 N94-37079
Solving the two-dimensional Schroedinger equation in self-consistent basis
[DE94-621535] 12 p4504 N94-37174
POTENTIAL FIELDS
The general gravitational potential field of a homogeneous cylinder rotating about its axis
[DE93-622853] 02 p0775 N94-13508
Energy potential analysis of zero velocity curves in the restricted three-body problem
[AD-A267512] 03 p1170 N94-17076
Path planning for robotic truss assembly
[NASA-CR-194652] 03 p0897 N94-17280
Comparison of time integration methods for the evolution of galaxies
[PB94-111671] 06 p2602 N94-24522
Self-similar regimes of subsonic Langmuir wave collapse
[DE94-611466] 11 p4335 N94-35750
POTENTIAL FLOW
NT EQUIPOTENTIALS
Solving the inverse problem for incompressible potential flow through two-dimensional cascades
[NAL-TR-1162] 01 p0147 N94-10365
A robust quasi-simultaneous interaction method for a full potential flow with a boundary layer with application to wing/body configurations
[NLR-TP-91397-U] 02 p0503 N94-13531
Potential flow in in-line and staggered tube banks
[IME-CRE-TR-006] 02 p0637 N94-13862
Modal element method for potential flow in non-uniform ducts: Combining closed form analysis with CFD
[NASA-TM-106347] 03 p1169 N94-15799
Modelling stalled airfoils
[ISBN-0-315-59525-6] 05 p1639 N94-22382
Computational fluid dynamic modelling of cavitation 06 p2215 N94-23060
A dual reciprocal boundary element formulation for viscous flows 06 p2325 N94-23666
Doppler global velocimetry: Development of a flight research instrumentation system for application to non-intrusive measurements of the flow field
[NASA-CR-191490] 06 p2344 N94-24360
Calculation of unsteady incompressible inviscid flow about wings and bodies using CANAERO-T panel model 07 p2655 N94-28334
A residual correction method applied to 2D multi-point airfoil design and 3D single-point wing design
[NLR-TP-92524-U] 08 p3134 N94-30493
Prediction of transonic potential flow with slipstreams around configurations
[FFA-TN-1992-15] 09 p3568 N94-31220
A novel potential/viscous flow coupling technique for computing helicopter flow fields
[NASA-CR-193272] 09 p3571 N94-32476
POTENTIAL THEORY
Quasipotential in the fourth order of perturbation theory
[DE94-606299] 08 p3484 N94-28584
A general stochastic Liouville theory for sequential and superexchange electron-transfer reactions involving three Marcus potential surfaces
[DE94-007695] 09 p3869 N94-32141
The nucleon-nucleon potential in the chromodielectric soliton model
[DE94-004646] 11 p4329 N94-36305
Navier-Stokes and potential theory solutions for ahelicopter fuselage and comparison with experiment
[NASA-TM-4566] 12 p4383 N94-36966
POTENTIOMETERS
Lessons learned from selecting and testing spaceflight potentiometers 09 p3607 N94-33318
POTTING COMPOUNDS
NMR imaging of components and materials for DOE application
[DE94-010664] 11 p4238 N94-36084
POURING
Solidification modeling of a spiral casting to determine material fluidity
[DE94-002212] 07 p2739 N94-26935
POWDER (PARTICLES)
NT FINES
NT METAL POWDER
NT POWDERED ALUMINUM
Development of commercially viable high-T(sub c) Bi-2223 superconductor tapes
[DE93-009966] 01 p0142 N94-10951
Production of reactive sintered nickel aluminide
[DE93-014434] 01 p0083 N94-11127
Processing, properties, and wear resistance of aluminides
[DE93-012186] 01 p0083 N94-11141
Effect of powder processing on slip casting parameters and sintering of Si3N4-Y2O3-SiO2
[AD-A264474] 01 p0083 N94-11445
Apical Cu-O bond in YBa2Cu3O(7-delta) superconductors by XAFS
[DE93-010861] 01 p0400 N94-11458
Simulation of possible regolith optical alteration effects on carbonaceous chondrite meteorites 01 p0430 N94-12163
Dynamic high-pressure shock compaction of diamond powders
[AD-A266004] 01 p0093 N94-12354
Flamespreading in granular solid propellant: Design of an experiment
[AD-A266009] 02 p0583 N94-12987
Gas atomized Er3Ni powder for cryocooler applications
[DE93-011564] 02 p0568 N94-13000
Destruction of waste energetic materials using base hydrolysis
[DE93-012738] 02 p0584 N94-13491
Measurement of strain in individual phases of composites before, during, and after mechanical loading
[DE93-014585] 02 p0558 N94-14119
Reverse micelle synthesis of nanoscale metal containing catalysts
[DE93-012869] 02 p0572 N94-14184
Polymer infiltration studies
[NASA-CR-194521] 02 p0582 N94-14539
Shielded open-circuited sample holders for dielectric and magnetic measurements of liquids and powders
[PB93-198851] 02 p0652 N94-14687
Fine-powder Al2O3 and SiO2 for preparation of multielement standards for rare-earth elements analysis
[DE93-625118] 02 p0567 N94-14884
Polymer Infiltration Studies
[NASA-CR-194494] 03 p0932 N94-15275
Synthesis of ceramic oxide powders in a microwave plasma device
[DE93-012741] 03 p0965 N94-15920
The physical mechanism of comet outbursts: An experiment 03 p1242 N94-16221
Comparison of reflectance spectra of C asteroids and unique C chondrites Y86720, Y82162, and B7904 03 p1242 N94-16246
Powder diffraction studies using anomalous dispersion
[DE93-012531] 03 p1210 N94-16775
Characterization of nanoscale oxide and oxyhydroxide powders using EXAFS spectroscopy
[DE93-015683] 03 p0940 N94-17235
Process for applying high application-temperature coating to heat-sensitive aluminum alloys
[AD-D015823] 04 p1368 N94-17905
Equipment for investigation of cryogenic compaction of nanosize silicon nitride powders
[DE93-018740] 04 p1340 N94-18180
Fabrication and microstructural development of Ag-clad TlBa2Ca2Cu3O(x) tapes
[DE93-017407] 04 p1597 N94-18500
Fabrication and characterization of high-T(sub c) tapes and coils made from Ag-clad Bi-2223 superconductors
[DE93-018615] 04 p1601 N94-18993
Sol-spray preparation, particulate characteristics, and sintering of alumina powders
[DE93-018577] 05 p1690 N94-20183
Improvement of the stability of the process for synthesizing chemically prepared varistor powder
[DE94-000345] 05 p1763 N94-21654
Sulfur-bonded thiophenes in organometallic rhenium complexes and adsorption of isocyanides on gold
[DE93-041126] 05 p1694 N94-21937
Effect of powder characteristics on gas-pressure sintering of Si3N4 with rare earth additives
[DE94-000330] 05 p1694 N94-21945
Characteristics of shock-compressed configuration of Ti and Si powder mixtures
[DE93-018857] 05 p1713 N94-22033
Development of silicon nitride composites with continuous fiber reinforcement
[DE94-001996] 06 p2227 N94-23022
Theoretical considerations for Reaction-Formed Silicon Carbide (RFSC) formation by molten silicon infiltration into slurry-derived preforms
[NASA-TM-106414] 06 p2222 N94-23500
Magnetic power piston fluid compressor
[NASA-CASE-GSC-13565-1] 06 p2354 N94-23831
Modelling the ignition of boron/titanium particles 06 p2159 N94-24273
Experimental investigation of ignition of boron/titanium composite particles 06 p2159 N94-24275
Thermomechanical processing of Ag-clad Bi2Sr2CaCu2O(x) superconductors
[DE94-002347] 06 p2563 N94-24624
Debye-Waller factors of the light actinide metals
[DE94-000685] 07 p2733 N94-26069

Liquid and solid solubility of Ag in Bi2Sr2CaCu2O8
[DE94-002829] 07 p2735 N94-26273
Processing of LaCrO3 for solid oxide fuel cell applications
[DE94-002981] 07 p2857 N94-26747
Electro-optic materials by solid source MOCVD
[DE94-005120] 07 p2757 N94-27716
Bench-scale synthesis of nanoscale materials
[DE94-004787] 07 p2742 N94-27786
Characterization of ZnS-GaP naon-composites
[DE94-004888] 07 p2712 N94-27813
Synthesis and neutron diffraction study of Na3WN3 and Na3MoN3
[AD-A275158] 08 p3203 N94-29043
Bench-scale synthesis of nanoscale materials 08 p3240 N94-30473
Properties of chemical vapor infiltration diamond deposited in a diamond powder matrix
[DE94-005429] 08 p3220 N94-30591
Effect of surface forces on the rheology of particle-liquid systems and the consolidation of ceramic powders
[AD-A277092] 09 p3657 N94-32391
SUNY beamline facilities at the National Synchrotron Light Source
[DE94-006343] 09 p3905 N94-32770
Isothermal sintering, microstructure, and superconducting properties of Y1Ba2Cu3O(7-x) compound
[DE94-008132] 09 p3905 N94-32779
Deuterium absorption and material phase characteristics of SAES St198 Zr-Fe alloy
[DE94-008275] 09 p3646 N94-32781
X ray absorption study of pulsed laser deposited boron nitride films
[DE94-008295] 09 p3662 N94-32855
Optical properties of lanthanide-doped RbTiOAsO4 and transition metal-doped KTiOPO4
[DE94-008433] 09 p3907 N94-32963
Characterization of nanoparticles and nanophase materials
[DE94-008348] 09 p3907 N94-32990
Method for forming aligned superconducting BI-SR-CA-CU-O
[AD-D016192] 10 p4148 N94-34405
Structures and properties of materials recovered from high shock pressures
[DE94-010057] 11 p4232 N94-35696
Properties and applications of powder-filled evacuated-panel superinsulations
[DE94-009169] 11 p4233 N94-35932
A mixture model for shock compression of porous multi-component reactive materials
[DE93-017638] 12 p4400 N94-36456
Characterization and processing of sintered products from nano-crystalline powders generated by the RTDS method
[DE94-004765] 12 p4415 N94-36553

POWDER METALLURGY
Bibliography on Hot Isostatic Pressing (HIP) technology
[AD-A265668] 01 p0081 N94-10297
Application of powder metallurgy techniques to produce improved bearing elements for liquid rocket engines
[NASA-CR-193731] 01 p0082 N94-10804
A history of tungsten- and molybdenum-base alloys
[DE93-010283] 01 p0082 N94-11108
Production of reactive sintered nickel aluminide
[DE93-014434] 01 p0083 N94-11127
Effect of powder processing on slip casting parameters and sintering of Si3N4-Y2O3-SiO2
[AD-A264474] 01 p0083 N94-11445
The effect of processing on the microstructure and tensile properties of a (gamma)-TiAl based alloy
[DE93-013221] 01 p0084 N94-11488
Preparation of particle-dispersion alloys (M-6) 02 p0587 N94-13738
Study on the mechanism of liquid phase sintering (M-12) 02 p0588 N94-13744
Gas-evaporation in low-gravity field (cogelation mechanism of metal vapors) (M-14) 02 p0588 N94-13746
Army P/M research and development overview
[AD-A266921] 03 p0954 N94-15104
The effect of oxygen, grain size, and strain rate on the mechanical behavior of forged P/M tantalum
[DE93-011251] 03 p0959 N94-16764
Solid state synthesis of Fe-B-Si alloys
[VTT-PUBS-118] 06 p2250 N94-25316
The mechanical property data base from an Air Force/Industry Cooperative Test Program on advanced aluminum alloys (7064 and CW67)
[AD-A273741] 06 p2251 N94-25531
Crystallization and microstructural control of ferroelectric thin-films and glass-ceramics
[AD-A273767] 07 p2748 N94-25854
The processing of powder metallurgically produced near gamma-titanium aluminide
[ISBN-0-315-84018-8] 07 p2738 N94-26633
Powder synthesis, fabrication, and transport properties of long-length Ag clad Bi-2223 conductors
[DE94-002376] 07 p2740 N94-26957
Material optimization and manufacturing development of reduced cost powder metal titanium alloy components for gas turbine engine application, phase 2
[AD-A274410] 07 p2709 N94-26978
Characterization of ZnS-GaP naon-composites
[DE94-004888] 07 p2712 N94-27813
Study on the production of flaky amorphous alloy powders by impact flattening of atomized liquid droplets on a rapidly rotating wheel 07 p2746 N94-28169
Powder metallurgical processing of fibre reinforced aluminium composites
[PB94-148285] 09 p3620 N94-31688
Pressureless sintering of ceramic composites
[AD-A277274] 09 p3657 N94-32404
On the formation of muon- and zeta-phases in Ag-Al system by mechanical alloying
[DE94-007125] 09 p3645 N94-32636
Method for producing closed cell spherical porosity in spray formed metals
[AD-D016126] 10 p4025 N94-34152
NiAl-base composite containing high volume fraction of AlN for advanced engines
[NASA-CASE-LEW-15818-1] 12 p4403 N94-36752
The control of cleanness in powder metallurgy materials for turbine disks 12 p4421 N94-37325
Defects and their effects on the integrity of nickel based aeroengine discs 12 p4421 N94-37328
Substantiating powder metal life methodologies for engines 12 p4455 N94-37330

POWDERED ALUMINUM
PM technology and mechanical properties of metallic foams 01 p0064 N94-10059
Aluminum powder/water reaction ignited by electrical pulsed power
[AD-A269223] 04 p1376 N94-17840
Powdered aluminum and oxygen rocket propellants: Subscale combustion experiments
[NASA-TM-106439] 05 p1713 N94-21760
Influence of sintering atmospheres on the aluminum sintering characteristics
[DE93-632412] 06 p2239 N94-22965
On the formation of muon- and zeta-phases in Ag-Al system by mechanical alloying
[DE94-007125] 09 p3645 N94-32636

POWDERED METALS
U METAL POWDER

POWER AMPLIFIERS
Low cost high efficiency GaAs monolithic RF module for SARSAT distress beacons
[NASA-CR-194235] 01 p0146 N94-12773
Inertial confinement fusion program
[DE93-013372] 02 p0796 N94-13047
Design and performance of the terawatt Cr:LiSrAlF6 laser system
[DE93-014678] 02 p0657 N94-13882
High efficiency low cost monolithic module for SARSAT distress beacons
[NASA-CR-194234] 04 p1315 N94-18852
Simulation of the ALS longitudinal multibunch feedback system
[DE93-019227] 04 p1575 N94-19152
Laser amplifier developments at Mercury
[DE93-040103] 05 p1814 N94-19867
Method for remotely powering a device such as a lunar rover
[NASA-CASE-LAR-14789-1] 05 p1824 N94-20587
Heterojunction bipolar transistor technology for data acquisition and communication 05 p1763 N94-21697
Broadband linearisation of high-efficiency power amplifiers 06 p2275 N94-22747
Modulation characteristics of a high-power semiconductor Master Oscillator Power Amplifier (MOPA)
[NASA-TM-104577] 06 p2308 N94-23281
Design and testing of ubitron amplifier tubes
[AD-A273297] 06 p2311 N94-24818
Bounds and simulation results of 32-ary and 64-ary quadrature amplitude modulation for broadband-ISDN via satellite
[NASA-TM-106484] 06 p2202 N94-25095
Phase conjugation and pulse compression of high energy lasers: From nanoseconds to microseconds
[DE94-001061] 07 p2818 N94-26699
Design and control of phased ICRF antenna arrays
[DE94-002796] 07 p3046 N94-27261
NASA satellite communications application research. Phase 2: Efficient high power, solid state amplifier for EFH communications
[NASA-CR-195713] 07 p2776 N94-27669
Micro-electron deflector
[AD-D016055] 07 p2787 N94-27672
NASA satellite communications application research, phase 2 addendum. Efficient high power, solid state amplifier for EHF communications
[NASA-CR-195712] 07 p2777 N94-27946
Miniaturization in x ray and gamma ray spectroscopy 08 p3236 N94-29773
Communications technology for unattended sensors
[DE94-005685] 08 p3254 N94-30043
Design of a high power x-band magnicon amplifier
[AD-A277001] 09 p3692 N94-32199
Design, characterization and control of the Unique Mobility Corporation robot 09 p3603 N94-33296
Single-shot intensity and phase measurements of detuning and saturation effects in an ultrashort XeCl amplifier
[DE94-007535] 10 p4058 N94-33860
High power diode laser Master Oscillator-Power Amplifier (MOPA)
[NASA-CR-196095] 11 p4271 N94-35488
A 32-GHz solid-state power amplifier for deep space communications 11 p4255 N94-35562
Chirped-pulse amplification with flashlamp-pumped Ti:Sapphire amplifiers
[DE94-010055] 11 p4272 N94-35695
Radially combined 30 W, 14-16 GHz amplifier
[DE94-010078] 12 p4432 N94-36471
Field emitter array RF amplifier development project phase one, cathode technology development
[AD-A280334] 12 p4437 N94-37033
Field emitter array RF amplifier development project. Phase 1, option 1
[AD-A280377] 12 p4437 N94-37035
High average power pulsed phase conjugate laser with birefringence correction
[DE94-012062] 12 p4447 N94-37160
Single event mirroring and sense amplifier designs for enhanced SE tolerance of DRAMs
[DE94-010397] 12 p4438 N94-37190

POWER BEAMING
NT LASER POWER BEAMING
NT MICROWAVE POWER BEAMING
NT SATELLITE POWER TRANSMISSION
Two temperature modeling and experimental measurements of laser sustained hydrogen plasmas
[AD-A265750] 02 p0796 N94-13039
Power beaming to space using a nuclear reactor-pumped laser
[DE94-001208] 06 p2348 N94-23185

POWER CONDITIONING
Experimental and theoretical investigations of Cs-Ba vapor tacitron inverter for power conditioning in space power systems
[DE93-012971] 01 p0048 N94-11372
High flux heat exchanger
[AD-A266341] 02 p0636 N94-13730
Overview of the solar dynamic ground test demonstration program
[NASA-TM-106296] 03 p0928 N94-17256
Analysis of superconducting magnetic energy storage applications at a proposed wind farm site near Browning, Montana
[DE93-018793] 04 p1466 N94-18276
Power conditioning system modelling for nuclear electric propulsion
[NASA-CR-191136] 05 p1846 N94-21179
Development of a power electronics unit for the Space Station plasma contactor
[NASA-TM-106486] 06 p2222 N94-25201
Parallel processing methods for space based power systems 06 p2222 N94-25352
Non-isolated 30 kW class arcjet PCU
[NASA-CR-189148] 08 p3173 N94-29444
Optimal adaptive estimation algorithm for harmonic current reduction using power limited active line conditioners
[AD-A277354] 09 p3693 N94-32336
Universal signal conditioning amplifier 09 p3699 N94-32460
The constant current loop: A new paradigm for resistance signal conditioning 09 p3685 N94-32461
Field operation test of utility interactive load conditioner with photovoltaic cells at a demonstration house
[DE94-757271] 09 p3762 N94-32918

POWER CONVERTERS
Power converters for the 120 V bus supply control
[CNES-NT-134] 02 p0622 N94-13552
Operation of high power converters in parallel
[NASA-CR-191096] 02 p0622 N94-13786
Multi-output flyback converter with ultrafast current protection
[CNES-NT-133] 02 p0625 N94-14138
SPDE/SPRE final summary report
[NASA-CR-187086] 03 p0924 N94-15482

Forback DC-to-DC converter
[NASA-CASE-GSC-13404-1] 03 p1010 N94-15874
Overview of the solar dynamic ground test demonstration program
[NASA-TM-106296] 03 p0928 N94-17256
Potassium-Rankine power conversion subsystem modeling for nuclear electric propulsion
[NASA-CR-191134] 04 p1468 N94-18821
AC to DC power converter with regulated bi-polar outputs
[AD-D016032] 07 p2786 N94-27145
Real time simulation model for designing converter regulation
[ETN-94-95735] 09 p3689 N94-31576
Microprocessor control of multiple peak power tracking DC/DC converters for use with solar cell arrays
[NASA-CASE-GSC-13450-2] 11 p4282 N94-35540

POWER DENSITY (ELECTROMAGNETIC)
U RADIANT FLUX DENSITY

POWER EFFICIENCY
InGaAs concentrator cells for laser power converters and tandem cells 01 p0050 N94-11394
A high specific power solar array for low to mid-power spacecraft 01 p0051 N94-11399
Electromagnetic propulsion for spacecraft
[NASA-CR-191186] 02 p0551 N94-13416
Fuel cell systems program plan, fiscal year 1993
[DE93-017828] 04 p1466 N94-18103
National Program Plan Fuel Cells in Transportation
[DE93-017557] 04 p1469 N94-19346
Optical fiber sensor having an active core
[NASA-CASE-LAR-14607-1-SB] 05 p1986 N94-20586
Mixed voltage VLSI design 05 p1756 N94-21104
Second law analysis of a conventional steam power plant 06 p2322 N94-23646
The effect of high altitude pressure on the power and efficiency of an airborne two-stroke engine 06 p2155 N94-24253
Investigation on application of genetic algorithms to optimal reactive power dispatch of power systems
[MATHS-REPT-A-197] 08 p3266 N94-29527
Optimal reactive power dispatch of power systems using nonlinear programming
[MATHS-REPT-A-209] 09 p3808 N94-31164

POWER FACTOR CONTROLLERS
Technical manual PCDU MT 254
[FFI-92/7020] 05 p1751 N94-20553

POWER GAIN
Design of a matching network for dipole antennas
[AD-A265115] 01 p0136 N94-11158
Windshear radar calibration, 1992 flights: Transmitter power and receiver gain stability
[NASA-TM-108997] 03 p0986 N94-15140
Sodium-mercury excimer laser, phase 1
[AD-A267728] 03 p1042 N94-17230
Recent activities in printed Antennas at LeRC 05 p1722 N94-20422
Design and testing of ubitron amplifier tubes
[AD-A273297] 06 p2311 N94-24818

POWER GENERATORS
U ELECTRIC GENERATORS

POWER LINES
Potential techniques for non-destructive evaluation of cable materials
[DE93-008350] 01 p0183 N94-11586
Operation of digital systems in severe electromagnetic environments
[AD-A267176] 03 p0988 N94-15693
Response of transmission line systems to pulse excitation by radiation and injection methods
[DE93-015112] 04 p1384 N94-18210
Effects of harmonics on EMI/RFI filters operating under nonlinear loading conditions
[AD-A269559] 04 p1388 N94-18769
Mitigation of EMI/RFI produced by a 1.2 kW uninterruptible power supply
[AD-A273149] 06 p2299 N94-24670
Electric power lines: Questions and answers on research into health effects
[DE94-005637] 08 p3353 N94-30757
Optimal adaptive estimation algorithm for harmonic current reduction using power limited active line conditioners
[AD-A277354] 09 p3693 N94-32336
On optimal placement of spacers in bundled conductors 11 p4258 N94-35354
CABPRO: An expert system for process planning multiwire cables
[DE94-010213] 11 p4312 N94-35810
National Maglev initiative: California line electric utility power system requirements 11 p4215 N94-35850

POWER LOSS
Effects of a vibrating wire carrying DC current on a moving type 2 superconducting slab of arbitrary thickness
[DE93-617136] 06 p2566 N94-25391

POWER PLANTS
Design considerations for a fiber optic communications network for power systems
[DE93-018404] 05 p1984 N94-20179
Second law analysis of a conventional steam power plant 06 p2322 N94-23646
Knowledge organization in intelligent tutoring systems for diagnostic problem solving in complex dynamic domains
[AD-A273986] 07 p2984 N94-25899
Parametric analysis of the space power plants on the base of criterion of specific mass in generalized design variants
[DE93-634153] 07 p2701 N94-26166
Air quality implications associated with the selection of power plants in the Pacific Northwest
[DE94-004783] 11 p4287 N94-36027

POWER PROCESSING SYSTEMS
U POWER CONDITIONING

POWER REACTORS
Advanced steady-state operating scenarios
[DE94-004810] 08 p3509 N94-30768
Guidelines for design and development of computer/microprocessor based systems in research and power reactors
[DE94-616271] 11 p4300 N94-35570

POWER SERIES
NT TAYLOR SERIES
Deviations from the straight line: Bumps (and grinds) in the collisionally evolved size distribution of asteroids 01 p0431 N94-12201
Confirmation of saturation equilibrium conditions in crater populations 03 p1103 N94-16222
Method of Chabauty-Coleman and the second case of Fermat's last theorem for regular primes
[PB94-138187] 08 p3467 N94-29162

POWER SPECTRA
Polar mesospheric waves and structure
[AD-A265360] 01 p0279 N94-12561
Maximum entropy spectral analysis of the geological time series of the oxygen isotope record from deep-sea cores
[INPE-5465-PRE/1773] 02 p0725 N94-13728
Segmenting textured 3D surfaces using the space/frequency representation
[AD-A266960] 03 p1163 N94-14968
Self-organized criticality and the Barkhausen effect in amorphous and polycrystalline metals
[AD-A269817] 04 p1361 N94-18735
Signal processing in the linear statistical model
[AD-A272114] 05 p1736 N94-20570
A motion extraction method for synthetic aperture radars
[DLR-FB-92-31] 05 p1742 N94-22279
Time variations of x rays from black hole candidates: Canonical time variations in high and low intensity states 05 p2009 N94-22690
Propagation model for the Land Mobile Satellite channel in urban environments 06 p2283 N94-22796
Laser linewidth measurement in the presence of RIN and using the recirculating self heterodyne method
[EUT-92-E-262] 06 p2347 N94-22874
Continuous gust response and sensitivity derivatives using state-space models 06 p2161 N94-24287
PROPWR: A versatile tool for 1/3 octave processing and narrowband line tracking
[DREA-TC-93-303] 06 p2297 N94-24298
Composite sequences for rapid acquisition of direct-sequence spread spectrum signals
[CTN-94-60901] 06 p2300 N94-24696
Choice of filters for the detection of gravitational waves from coalescing binaries. 2: Detection in coloured noise
[DE93-616844] 06 p2604 N94-25211
The deterministic power-spectral-density method
[AD-B175894] 07 p2678 N94-27395
The deterministic power-spectral-density-method for nonlinear systems
[AD-B179687] 07 p3001 N94-28353
Parameter identification of the rotordynamic coefficients of high-Reynolds-number hydrostatic bearings 08 p3311 N94-30792
Theory and observations of horizontal and vertical structure of gravity wave perturbations in the middle atmosphere 08 p3366 N94-30802
Analysis using bi-spectral related technique
[AD-A276017] 09 p3672 N94-31386
Atmospheric structure simulation: An autoregressive model for smooth geophysical power spectra with known autocorrelation function
[AD-A276691] 09 p3773 N94-32118
Note on the variance of autospectral density processed using Welch's method
[DE94-005352] 09 p3849 N94-32675
In-flight estimation of gyro noise on the Upper Atmosphere Research Satellite (UARS) and Extreme Ultraviolet Explorer (EUVE) missions 11 p4204 N94-35616
Measuring attitude with a gradiometer 11 p4206 N94-35630
Atmospheric structure simulation: An ARMA model for smooth isotropic two-dimensional geophysical power spectra
[AD-A280476] 12 p4470 N94-37649

POWER SUPPLIES
Power generation technology options for a Mars mission
[NASA-TM-106451] 06 p2220 N94-24681
Investigation on application of genetic algorithms to optimal reactive power dispatch of power systems
[MATHS-REPT-A-197] 08 p3266 N94-29527

POWER SUPPLY CIRCUITS
A soft-start circuit for arcjet ignition
[NASA-TM-106287] 01 p0180 N94-10760
Circle diagram approach for self excited induction generators
[DE93-010031] 03 p1010 N94-15971
A power system for a microsatellite 03 p0895 N94-17176
Smart Power: New power integrated circuit technologies and their applications
[VTT-TIED-1358] 03 p1015 N94-17546
Techniques for low consumption circuits 04 p1428 N94-18032
A study of the automatic generating system. 3: Improvement of the total system performance 04 p1429 N94-18040
Design of power electronics for TVC EMA systems
[NASA-CR-193839] 04 p1407 N94-19642
Control and readout of the extraction septum of AmPS
[DIGEL-1993-2] 05 p1979 N94-20117
Power electronics development for the SPT-100 thruster
[NASA-TM-106488] 06 p2221 N94-25189
Selection of the Space Station Freedom (SSF) Flat Collector Circuit (FCC) insulation material 08 p3165 N94-28701
Electric power system test and verification program
[NASA-TM-106405] 08 p3169 N94-30123

POWER TRANSMISSION
Flex-gear electrical power transmission
[NASA-CR-194422] 02 p0661 N94-13445
Communications and control for electric power systems: Power flow classification for static security assessment
[NASA-CR-194512] 02 p0624 N94-13948
Fluid dynamometer having fluid characteristic power absorption adjustment capability
[AD-D015820] 04 p1424 N94-17904
Vibrational power transmission analysis of machinery installations in ships with the objective of noise reduction
[ISVR-TR-216] 06 p2363 N94-24076
High-temperature superconducting transformer performance, cost, and market evaluation
[DE94-005494] 09 p3687 N94-31152
Roll ring assemblies for the Space Station 09 p3603 N94-33294

POWER TRANSMISSION (LASERS)
U LASER POWER BEAMING

POWER TRANSMISSION (MICROWAVE)
U MICROWAVE POWER BEAMING

POWERED LIFT AIRCRAFT
Design criteria for integrated flight/propulsion control systems for STOVL fighter aircraft 02 p0521 N94-13297
Numerical simulation of a powered-lift landing, tracking flow features using overset grids, and simulation of high lift devices on a fighter-lift-and-control wing
[NASA-CR-194260] 02 p0527 N94-14322
The lift-fan powered-lift aircraft concept: Lessons learned
[NASA-CR-177616] 03 p0866 N94-15718
Design, development, and flight evaluation of the Boeing YC-14 USB powered lift aircraft 04 p1310 N94-18444
Survey of lift-fan aerodynamic technology
[NASA-CR-177615] 05 p1646 N94-21592
Summary of lift and lift/cruise fan powered lift concept technology
[NASA-CR-177619] 06 p2176 N94-23489
Powered lift facility at NASA Lewis Research Center's Aeroacoustic Propulsion Laboratory
[NASA-TM-106577] 10 p4009 N94-33604
STOVL
[NASA-TM-109845] 10 p3989 N94-33790

PPI (POSITION INDICATORS)
U PLAN POSITION INDICATORS

PPM (MODULATION)
U PULSE POSITION MODULATION
PRACTICES
U PROCEDURES
PRAIRIES
U GRASSLANDS
PRANDTL NUMBER
Instability of thermocapillary convection in floating zones 01 p0101 N94-10076
High Prandtl number fluids in a multilayered system under 1-g or micro-g environment 01 p0104 N94-10096
Experimental investigation of turbulent Prandtl number and Reynolds analogy in transitional and post-transitional boundary layers
[AD-A270092] 04 p1418 N94-18867
Low Reynolds-number turbulent boundary layers
[AD-A272011] 05 p1803 N94-21459
Computational fluid mechanics
[NASA-CR-194765] 06 p2337 N94-24859
PRASEODYMIUM
Synthesis of organic ligands for f-element separations
[DE93-012915] 02 p0554 N94-14290
Local environment about O atoms in Pr-Y-Ba-Cu-O films studied by O K-edge XAFS
[DE93-016218] 03 p1209 N94-16447
The excitation mechanism of praseodymium-doped semiconductors
[AD-A280687] 12 p4535 N94-37129
PRASEODYMIUM COMPOUNDS
Synthesis and characterization of charge-substituted garnets YCaLnGa5O12 (Ln = Ce, Pr, Tb)
[DE93-040227] 05 p2033 N94-21992
Quadrupolar effects in PrCu2Si2
[DE94-011509] 12 p4534 N94-37054
PRE-MAIN SEQUENCE STARS
NT T TAURI STARS
Detection of accreting circumstellar gas around weak emission-line Herbig Ae/Be stars
[NASA-TM-108256] 01 p0424 N94-11306
The evidence for clumpy accretion in the Herbig Ae star HR 5999
[NASA-CR-189314] 02 p0828 N94-12915
Search for x ray emitting young stars outside of massive molecular clouds
[NASA-CR-193609] 02 p0830 N94-13462
Millimeter and infrared studies of young stellar objects in dark cloud L1641 02 p0838 N94-13648
Pre-main sequence stars in the Chamaeleon cloud and pre-main sequence stars in the Rho Ophiuchi cloud core
[NASA-CR-194713] 05 p2080 N94-20337
The circumstellar environments of intermediate mass main sequence stars
[NASA-CR-189311] 05 p2055 N94-21498
The formation of massive stars: A 30 Mo case study
[ISBN-0-315-83944-9] 05 p2081 N94-22593
Circumstellar material around young stars in Orion 09 p3930 N94-31133
Double-lined pre-main-sequence binaries: A test of pre-main-sequence evolutionary theory 09 p3933 N94-31497
Radio emission from pre-main-sequence stars 09 p3955 N94-31890
IUE observations of new A star candidate proto-planetary systems
[NASA-CR-189355] 10 p4162 N94-34267
PREAMPLIFIERS
Discrete CMT infrared detectors for space application, from ISSR to second generation Meteosat and MIPAS 03 p0905 N94-15065
A RFI measurement system for field sites
[AD-A269340] 04 p1385 N94-18301
Monolithic low noise preamplifier for piezoelectric sensors
[AD-D015860] 04 p1563 N94-18734
New preamplifiers for the SEM scanner
[DIGEL-1993-3] 05 p1979 N94-20118
Bundle profile monitor for AmPS
[DIGEL-1992-8] 05 p1979 N94-20123
A high rate, low noise, x ray silicon strip detector system
[DE94-004557] 08 p3268 N94-30717
A low noise silicon detector preamplifier system for room temperature x ray spectroscopy
[REPT-93-058] 08 p3291 N94-30930
Processing, fabrication, and demonstration of HTS integrated microwave circuits
[AD-A277684] 10 p4040 N94-33893
Influence of an externally modulated photonic link on a microwave communications system 11 p4252 N94-35544
Sensitivity and signal to noise ratio improvement of a one micron lidar system incorporating a neodymium doped optical fiber preamplifier. Laser radar testbed
[AD-A280235] 12 p4447 N94-37137
PREBURNERS
STS-55 pad abort: Engine 2011 oxidizer preburner augmented spark igniter check valve leak
[NASA-CR-193830] 02 p0533 N94-12806
Simulation of preburner sprays, volume 1
[NASA-CR-193844] 02 p0647 N94-14906
SSME fuel preburner injector characterization 06 p2211 N94-23037
CFD simulation of coaxial injectors 06 p2342 N94-24430
Hotfire testing of a SSME HPOTP with an annular hydrostatic bearing 10 p4065 N94-34196
PRECAMBRIAN PERIOD
Assimilation of solids during ascent of magmas from the Bartoy Field of the Baikal Region, Siberia 03 p1103 N94-16214
Tidal regime of intact planetoid capture model for the Earth-Moon system: Does it relate to the archean sedimentary rock record? 03 p1245 N94-16378
Ozone control of biological activity during Earth's history, including the KT catastrophe 07 p2876 N94-28312
PRECAUTIONS
U ACCIDENT PREVENTION
PRECESSION
NT QUENCHING (ATOMIC PHYSICS)
Precession of Uranus and Neptune and their magnetic field 01 p0473 N94-12222
State-of-the-art satellite laser range modeling for geodetic and oceanographic applications 03 p0916 N94-15586
On relativity principle violation in local measurements of spin precession of moving particles
[DE94-608067] 08 p3489 N94-30085
A twisted disk equation that describes warped galaxy disks 09 p3928 N94-31118
The dynamical settling of warped disks and angular momentum transport in galaxies 09 p3928 N94-31121
Hyperon polarization, crystal channeling, and E781 at Fermilab
[DE94-008224] 09 p3877 N94-32802
PRECIOUS METALS
U NOBLE METALS
PRECIPITATES
Effect of microstructure on passive film formation and breakdown on Al alloys
[AD-A265339] 02 p0569 N94-13050
Effects of processing and prolonged high temperature exposure on the microstructure of Nb-1Zr-C sheet
[NASA-TM-106370] 03 p0959 N94-16883
Formation of colloidal Ag precipitates in fused silica by MeV ion implantation
[DE93-040268] 05 p2012 N94-19869
Microstructural stability of wrought, laser and electron beam glazed NARloy-Z alloy at elevated temperatures
[NASA-TM-108431] 05 p1689 N94-20100
Relationship of microstructure and mechanical properties for V-Cr-Ti alloys
[DE94-001431] 06 p2238 N94-22718
Potent solvents for C60 and their utility for the rapid acquisition of 13CNMR data for fullerenes
[AD-A273349] 06 p2235 N94-24925
An atom probe investigation of the influence of trace impurities on the mechanical behavior of NiAl
[DE94-002797] 07 p2734 N94-26272
Study of precipitation and recrystallization in Al alloy 2519 by backscattered electron imaging methods
[AD-A274919] 07 p2736 N94-26533
Effect of precipitate structure on hot deformation of Al-Mg-Mn alloys
[DE94-004596] 07 p2741 N94-27622
A transmission electron microscope study of Ni4W precipitates in a Ni-37 wt. percent W alloy
[ISBN-0-315-59932-4] 07 p2743 N94-27803
Indium-vacancy complexes in mercury cadmium telluride
[AD-A276177] 09 p3894 N94-31055
Irradiation-induced phase transformations in zirconium alloys
[DE94-008484] 09 p3648 N94-32993
Formation and stability of Fe-rich precipitates in dilute Zr(Fe) single-crystal alloys
[DE94-619027] 11 p4242 N94-36288
Precipitation in Zr-2.5 Nb enhanced by proton irradiation
[DE94-619056] 12 p4415 N94-36563
PRECIPITATION (CHEMISTRY)
Interfacial precipitation, segregation and deformation in alloy 600: Implications on primary-side IGSCC
[DE93-013161] 02 p0568 N94-13035
Some superhigh-frequency and magnetic properties of chemically precipitated films
[AD-A266195] 04 p1351 N94-19110
Preparation of catalyst particles using methods of colloid chemistry. Part 1: Preparation of silica particles from alcohol solutions
[PB94-135597] 09 p3634 N94-31679
PRECIPITATION (METEOROLOGY)
NT ACID RAIN
NT HAIL
NT RAIN
NT SNOW
NT SNOW COVER
Design of a global soil moisture initialization procedure for the simple biosphere model
[NASA-TM-104590] 01 p0284 N94-10940
The impact of horizontal resolution on moist processes in the ECMWF model
[DE93-011718] 01 p0276 N94-11227
Activities relating to understanding the initiation, organization and structure of moist convection in the Southeast environment
[NASA-CR-193829] 01 p0285 N94-11598
Modeling present and future river runoff using global atmospheric models
[AD-A265274] 01 p0285 N94-11685
Evaporation and thermal/hydrologic balance in the Pacific 01 p0195 N94-11919
Measurements of ocean cross-section with a side-looking airborne radar 01 p0201 N94-11954
A basic consideration for remote sensing using microwave radars on a satellite 01 p0212 N94-12665
Measuring surface fluxes in CAPE
[NASA-CR-193664] 02 p0711 N94-12788
Precipitation verification LAM
[KNMI-TR-143] 02 p0722 N94-13991
A verification of the Euroguidance: A guidance forecast for transportation and tourism
[KNMI-TR-145] 02 p0722 N94-13993
Circulation and rainfall climatology of a 10-year (1979 - 1988) integration with the Goddard Laboratory for atmospheres general circulation model
[NASA-TM-104591] 02 p0723 N94-14074
The standardized precipitation index and its use in the western contiguous United States
[AD-A267547] 03 p1107 N94-17102
Phillips Laboratory global spectral numerical weather prediction model
[AD-A267293] 03 p1107 N94-17244
Effect of spatial resolution on the simulation of regional precipitation in China in a global climate model
[DE93-013433] 04 p1489 N94-18053
Station climatic summaries: North America. Volume 1: The contiguous United States
[AD-A269567] 04 p1490 N94-18303
Global zones of particle precipitation as observed EXOS-C
[AD-A268758] 04 p1481 N94-18467
Station climatic summaries, North America. Volume 2: Alaska, Canada and Greenland
[AD-A269793] 04 p1493 N94-18732
Investigations of a coherent vector radar technique for the observation of the atmosphere near 10 GHz
[KFK-5068] 04 p1494 N94-19616
Snow cover measurements and areal assessment of precipitation and soil moisture
[WMO-749] 05 p1841 N94-21068
Remote sensing for hydrology progress and prospects
[WMO-773] 05 p1841 N94-21069
A documentation of icing relevant cloud physical parameters on horizontal soundings of stratiform clouds (continuation)
[DLR-MITT-92-10] 05 p1871 N94-22280
NOAA Federal/State Cooperative Program in Atmospheric Modification Research. Collected publication titles and abstracts
[PB93-198125] 06 p2396 N94-22913
Scientific investigations of atmospheric processes
[NASA-CR-194805] 06 p2401 N94-23271
Precipitation measurement using SIR-C: A feasibility study
[NASA-CR-195104] 06 p2409 N94-24048
Water cycle research associated with the CaPE hydrometeorology project (CHymP 06 p2416 N94-24414
Observational and modeling studies of heat, moisture, precipitation and global-scale circulation patterns
[NASA-CR-195148] 06 p2415 N94-24485
Observational case studies and diagnostic analyses of long-lived large-amplitude inertia-gravity waves
[AD-A273545] 06 p2404 N94-24794
Numerical modelling of precipitation over complex terrain
[ISBN-0-315-84327-6] 07 p2894 N94-26628
Meteorological data at the Nagaoka Institute of Snow and Ice Studies
[REPT-158] 07 p2896 N94-27169

Examination of micro- and macro-physical structures and processes in hailstorms with respect to their modification
[DLR-FB-93-25] 07 p2897 N94-27751
Sensitivity and feedbacks associated with vegetation-related land surface parameters in a general circulation model 08 p3348 N94-29800
The incorporation and initialization of cloud water/ice in an operational forecast model 08 p3373 N94-29814
A study of precipitation in the coastal area of Antarctica as observed at Syowa Station using a vertical pointing radar 08 p3363 N94-29979
Some aspects of the drought in North Africa and in the Mediterranean basin 09 p3778 N94-30989
Tropical squall lines 09 p3778 N94-30992
The ocean-atmosphere interactions in the Mediterranean Sea 09 p3779 N94-30995
The Global Climatology Network precipitation data
[DE93-019199] 09 p3764 N94-31596
Diagnostic studies of climate variability
[DE94-003629] 09 p3767 N94-32711
Effects of elevated atmospheric CO2 concentrations and water stress on field-grown maize
[DE94-009636] 10 p4082 N94-33915
Production of long-term global water vapor and liquid water data set using ultra-fast methods to assimilate multi-satellite and radiosonde observations
[NASA-CR-196044] 11 p4292 N94-35355
Modeling of trace constituent transport with the University of Wisconsin global isentropic-sigma model
[DE94-012729] 12 p4466 N94-37288
NASA ER-2 Doppler radar reflectivity calibration for the CAMEX project
[NASA-TM-104611] 12 p4475 N94-37790

PRECIPITATION HARDENING
On problem about nature of Portevin-Le Chatelier effect in irradiated aluminium alloys
[DE93-617200] 01 p0082 N94-10842
Microstructural mechanisms that enhance electromigration resistance in Al-Cu thin films
[DE93-013770] 02 p0812 N94-14345
Ternary alloying effects in polycrystalline (beta)-NiAl
[DE93-012675] 03 p0955 N94-15885
Morphology, deformation, and defect structures of TiCr2 in Ti-Cr alloys
[DE93-018332] 04 p1361 N94-18807
Alloying effects on mechanical and metallurgical properties of NiAl
[DE93-040814] 05 p1694 N94-21948
Effect of irradiation on the stress corrosion cracking behavior of Alloy X-750 and Alloy 625
[DE94-001759] 06 p2244 N94-23792
Study on the mechanism of titanium alloy toughness and the improvement of properties 07 p2726 N94-25566
Toughening mechanisms in ultrahigh-strength steels
[AD-A275439] 08 p3202 N94-28867
Continuous measurement of aging response in aluminum alloys by eddy current methods
[AD-A277233] 09 p3644 N94-32371
Experimental studies on the effect of coherency strains on coarsening kinetics: Current status and future outlook
[DE94-008480] 09 p3647 N94-32964
The effect of thermomechanical processing on mechanical properties of a cast 6061 aluminum metal matrix composite
[AD-A277995] 10 p4019 N94-34220
Substantiating powder metal life methodologies for engines 12 p4455 N94-37330

PRECIPITATION PARTICLE MEASUREMENT
Drop size distributions and related properties of fog for five locations measured from aircraft
[NASA-CR-4585] 09 p3787 N94-33065

PRECIPITATORS
NT ELECTROSTATIC PRECIPITATORS

PRECISION
The precision of today's satellite laser ranging systems 03 p0912 N94-15559
Evaluation of a scanning Hartmann device for single point turning applications
[DE93-019204] 05 p1821 N94-19891
Calorimeter measurements of low wattage items
[DE93-018473] 05 p1807 N94-20115
Precision drive and speed reduction device
[AD-D016004] 06 p2367 N94-25046
Design of gas bearing systems for precision applications
[ISBN-9-03-860112-3] 06 p2367 N94-25249
An Earth observation telescope refocusing mechanism
[REPT-932-440-103] 08 p3332 N94-29417
Precision and manufacturing at the Lawrence Livermore National Laboratory 08 p3240 N94-30449
Time and position accuracy using codeless GPS 08 p3144 N94-30650
Computing the precision of localization in a plane using projective invariants
[TELECOM-93-D-005] 09 p3840 N94-31095
Precision operation of the Nova laser for fusion experiments
[DE94-007073] 10 p4057 N94-33405
A test system of pose repeatability precision of multi-path robot 10 p4067 N94-34341

PRECONDITIONING
Topics on spatially high-order accurate methods and pre-conditioning for the Navier-Stokes equations with finite-rate chemistry 02 p0633 N94-13572
Preconditioning and the limit to the incompressible flow equations
[NASA-CR-191500] 02 p0769 N94-13717
On solving the compressible Navier-Stokes equations for unsteady flows at very low Mach numbers
[NASA-TM-106380] 03 p1027 N94-17128
Pseudo-compressibility methods for the incompressible flow equations
[NASA-CR-191533] 04 p1551 N94-19315
Butcher-Kuntzmann methods for nonstiff problems on parallel computers
[CWI-NM-R9305] 05 p1935 N94-21493
An implicit numerical scheme for the simulation of internal viscous flows on unstructured grids
[NASA-TM-106437] 06 p2481 N94-23554
Preconditioning in parallel Runge-Kutta methods for stiff initial value problems
[CWI-NM-R9310] 07 p2991 N94-26217
Semantics, orderings and recursion in the weakest precondition calculus
[CWI-CS-R9267] 07 p2995 N94-26776
Grid-independent convergence based on preconditioning techniques
[PB94-125358] 07 p2997 N94-27000
Preconditioned time-difference methods for advection-diffusion-reaction equations
[DE94-006472] 09 p3638 N94-32840
Preconditioned implicit solvers for the Navier-Stokes equations on distributed-memory machines
[NASA-TM-106449] 12 p4502 N94-36647
Research in parallel computing
[NASA-CR-196267] 12 p4442 N94-36960

PREDATORS
Qualitative properties of two-dimensional predator-prey systems
[REPT-93-75] 09 p3844 N94-31644
A predator-prey model with Ivlev's functional response
[REPT-93-79] 09 p3844 N94-31696

PREDICATE CALCULUS
Useful lambda notation
[PB93-191856] 04 p1524 N94-19066
Commutative Lambek categorial grammars
[ML-93-01] 08 p3457 N94-30395
Modal quantification over structured domains
[ML-93-02] 08 p3457 N94-30396
Isomorphisms between predicate and state transformers
[CWI-CS-R9338] 08 p3459 N94-30430
Relating state transformation semantics and predicate transformer semantics for parallel programs
[CWI-CS-R9339] 08 p3433 N94-30431

PREDICATE LOGIC
A path-oriented matrix-based knowledge representation system
[NASA-CR-4539] 02 p0744 N94-13065
Design and specification of a generic task model for solving boolean constraint satisfaction problems
[PB94-118841] 06 p2486 N94-23762
Interrogatives and adverbs of quantification
[LP-92-14] 08 p3456 N94-30372
The Vanilla meta-interpreter for definite logic programs and ambivalent syntax
[CT-93-01] 08 p3424 N94-30386
Commutative Lambek categorial grammars
[ML-93-01] 08 p3457 N94-30395
Modal quantification over structured domains
[ML-93-02] 08 p3457 N94-30396
Isomorphisms between predicate and state transformers
[RUU-CS-93-09] 08 p3458 N94-30403
Isomorphisms between predicate and state transformers
[CWI-CS-R9338] 08 p3459 N94-30430
Relating state transformation semantics and predicate transformer semantics for parallel programs
[CWI-CS-R9339] 08 p3433 N94-30431
Bisimulations and predicate logic
[CWI-CS-R9333] 08 p3460 N94-30735
Updates in dynamic semantics
[LP-93-06] 09 p3856 N94-31450
Weaks vs. strong readings of donkey sentences and monotonicity inference in a dynamic setting
[LP-93-10] 09 p3856 N94-31468

PREDICTION ANALYSIS TECHNIQUES
Parametric analysis of atmospheric processes
[NASA-CR-192523] 01 p0347 N94-10757
Failure prediction of thin beryllium sheets used in spacecraft structures
[NASA-CR-194164] 01 p0187 N94-11190
A comparison between numerically modelled and experimentally measured loss mechanisms in wave rotors
[NASA-TM-106279] 01 p0029 N94-11255
A research program for improving heat transfer prediction for the laminar to turbulent transition region of turbine vanes/blades
[NASA-TM-106278] 01 p0151 N94-11256
Computational mechanics needs study
[NASA-CR-193712] 01 p0327 N94-11279
Chaotic time series analysis 01 p0031 N94-11490
Boundary layer transition: Prediction and wind tunnel simulation 01 p0032 N94-11498
Further studies using matched filter theory and stochastic simulation for gust loads prediction
[NASA-TM-109010] 01 p0026 N94-11587
Problem of climate change predictability and satellite radiation budget observations 01 p0229 N94-12766
A method of predicting quasi-steady aerodynamics for flutter analysis of high speed vehicles using steady CFD calculations
[NASA-TM-109009] 02 p0514 N94-12850
Improved aeroprediction code. Part 1: Summary of new methods and comparison with experiment
[AD-A266015] 02 p0500 N94-12989
Transition prediction and control in subsonic flow over a hump
[NASA-CR-4543] 02 p0629 N94-13066
Research on chemical vapor deposition processes for advanced ceramic coatings
[NASA-CR-193613] 02 p0577 N94-13089
Methods for evaluating the predictive accuracy of structural dynamic models
[NASA-CR-191337] 02 p0671 N94-13124
Simulation of orbital debris impacts on bumper shields
[DE93-013773] 02 p0540 N94-13398
Piston engine intake and exhaust system design
[ISVR-TR-222] 02 p0663 N94-13874
Transition of building energy consumption using multi-input, single-output dynamic model
[VTT-PUBS-116] 02 p0597 N94-14055
Extrapolation of ground test data to flight 02 p0507 N94-14170
Boundary-layer transition 02 p0507 N94-14171
Electromagnetic wave test 02 p0508 N94-14173
Nonlinear wave predictions in ceramics
[DE93-016516] 02 p0582 N94-14436
Predicting the vibrations of a spinning inflated membrane
[DE93-010690] 02 p0676 N94-14456
Long duration measurements of fading on a low elevation angle, 11-GHz satellite path 02 p0613 N94-14661
Coastal scour problems and methods for prediction of maximum scour
[AD-A266658] 02 p0726 N94-14775
Measurements of crystal growth kinetics at extreme deviations from equilibrium
[DE93-014526] 02 p0815 N94-14798
A computer program to calculate growth rates for cracks at notches in regions of residual stress
[RAE-TM-MAT/STR-1207] 02 p0683 N94-14818
On the accuracy of ERS-1 orbit predictions 03 p0874 N94-15589
Compensation for the distortion in satellite laser range predictions due to varying pulse travel times 03 p0917 N94-15590
Incorporation of boundary layer heating predictive methodology into NSWCDD aeroprediction code
[AD-A267000] 03 p1020 N94-15632
Multiaxial deformation and life prediction model and experimental data for advanced silicon nitride ceramics
[DE93-015450] 03 p0967 N94-16067
A fuzzy method for preliminary design random access memory failure rate prediction
[AD-A267948] 03 p1055 N94-17044
Recirculation in forward roll coating
[VKI-TM-48] 04 p1409 N94-17901
The performance of drag relations in the WAQUA storm surge model
[KNMI-TR-149] 04 p1496 N94-17923
Development of the microstructure based stochastic life prediction models
[AD-A269880] 04 p1454 N94-18683
Development of the microstructure based stochastic life prediction models
[AD-A270453] 04 p1455 N94-18714
On the use of semi-Lagrangian methods for accurate predictions of gravity waves
[DM-61] 04 p1562 N94-18859

Adsorption analysis of ammonia in an aqueous solution
[DE93-019512] 04 p1353 N94-19552
Numerical modeling of fringing fields and their use for complex permittivity measurements at high frequencies
[AD-A270478] 05 p1966 N94-19917
Statistical analysis of a reciprocal translocations data base
[RR-900-I] 05 p1963 N94-20165
Offshore decision support system: ERS-1 pilot project WAVEWATCH
[BCRS-92-09] 05 p1865 N94-20532
The flow of gas across the piston-segments-cylinder interface
[ECL-92-40] 05 p1824 N94-20594
Psychometric developments related to tests and selection
[AD-A272971] 05 p1894 N94-21262
Columbus PMP Critical Technologies Program: Approach for materials life time prediction
05 p1664 N94-21402
Survey of lift-fan aerodynamic technology
[NASA-CR-177615] 05 p1646 N94-21592
Brief summary of the evolution of high-temperature creep-fatigue life prediction models for crack initiation
05 p1834 N94-22613
Life prediction systems for critical rotating components
05 p1835 N94-22615
Analysis of thermal mechanical fatigue in titanium matrix composites 05 p1835 N94-22618
A high temperature fatigue life prediction computer code based on the total strain version of StrainRange Partitioning (SRP) 05 p1835 N94-22620
Electromagnetic field strength prediction in an urban environment: A useful tool for the planning of LMSS
06 p2283 N94-22795
Fatigue life and crack growth prediction methodology
[NASA-TM-109044] 06 p2228 N94-23279
Physical modeling and dynamic simulation of planet vehicles: Application to the motion prediction
06 p2371 N94-23426
Transient Ejector Analysis (TEA) code user's guide
[NASA-TM-106310] 06 p2186 N94-23466
Development of an analytical-numerical model to predict radiant emission or absorption
[NASA-CR-194860] 06 p2453 N94-23624
Examples of data assimilation in mesoscale models
06 p2412 N94-24384
Predictive head movement tracking using innovations generated by Kalman filters
[ISBN-0-315-83371-8] 06 p2427 N94-24467
Further studies to extend and test the area-time-integral technique applied to satellite data
[NASA-CR-195132] 06 p2415 N94-24705
The hydrodynamics of a moving fluid-liquid contact line
[ETN-94-95352] 06 p2339 N94-25247
Kernels of anti-causal operators and the multivariable generalized predictive control problem
[MATHS-REPT-A-191] 06 p2476 N94-25428
Advances in generalized and constrained generalized predictive control with application to a dynamometer model
[MATHS-REPT-A-192] 06 p2476 N94-25429
Fault detection in HVAC systems using fuzzy models
[OUEL-1977/93] 06 p2373 N94-25475
Development and testing of the Coupled Ocean/Atmosphere Mesoscale Prediction System (COAMPS)
[AD-A273925] 07 p2892 N94-25793
Image segmentation by a combination of edge detection and region growing
[ETN-94-95032] 07 p2960 N94-26106
Predictive modeling of particle-laden, turbulent flows
[DE94-003298] 07 p2792 N94-26319
Proceedings of the Non-Linear Aero Prediction Requirements Workshop
[NASA-CP-10138] 07 p2670 N94-27439
Uncertainties in the characterization of the thermal environment of a solid rocket propellant fire
[DE94-002023] 07 p2760 N94-27719
Methodology development of forecasting inter-regional air transport demand in China
[DLR-FB-93-24] 07 p2660 N94-27746
Understanding and development of a prediction method of transonic limit cycle oscillation characteristics of fighter aircraft
[NLR-TP-92210-U] 07 p2679 N94-27798
Predictions of momentum and scalar fields in a jet in cross-flow using first and second order turbulence closures 07 p2803 N94-28025
Landscape dynamics of northeastern forests
[NASA-CR-195272] 07 p2852 N94-28070
Calculation methods for steadily loaded central circumferential groove hydrodynamic journal bearings (guide to use of computer program A9304)
[ESDU-93004] 07 p2830 N94-28073
Calculation methods for steadily loaded axial groove hydrodynamic journal bearings (guide to use of computer program A9305)
[ESDU-93005] 07 p2830 N94-28074
Variability of measured sonic boom signatures
07 p2651 N94-28197
A general theory of impacts and mass extinctions, and the consequences of large-body impact on the Earth
07 p2891 N94-28310
Modeling turbulence in flows with a strong rotational component
[DE94-003577] 08 p3270 N94-28475
BAG: A code for predicting the performance of a gas bag impact attenuation system for the Pathfinder lander
[DE94-003688] 08 p3165 N94-28477
Role of microstructure on the fatigue durability of aluminum aircraft alloys
[AD-A275814] 08 p3202 N94-28830
Decompression sickness risk versus time and altitude
[AD-A275261] 08 p3391 N94-29071
Spray combustion experiments and numerical predictions 08 p3195 N94-29277
Free edge and size effects on failure initiation and ultimate strength of laminates containing a center hole
08 p3181 N94-29735
Theoretical prediction of the influence coefficients on damped simple flexible rotors using the transfer matrix method
[IMR-TM-TR-002] 08 p3321 N94-30018
Development of a method to predict transonic limit cycle oscillation characteristics of fighter aircraft (continued)
[NLR-TP-92156-U] 08 p3148 N94-30342
Comparison of RCS prediction techniques, computations and measurements
[PB94-125515] 08 p3256 N94-30392
Predictive sufficiency and the use of stored internal state
[AIAA PAPER 94-1213-CP] 08 p3445 N94-30564
A real-time prediction of UTC
08 p3470 N94-30654
Numerical simulation and prediction of implosion phenomena
[GKSS-92/E/99] 08 p3284 N94-30968
Feasibility and stability results for constrained stable generalized predictive control
[MATHS-REPT-A-203] 09 p3828 N94-31158
Prediction of transonic potential flow with slipstreams around configurations
[FFA-TN-1992-15] 09 p3568 N94-31220
Development of a three-dimensional icing model for predicting ice accretion on aircraft
[ONERA-NT-1993-5] 09 p3574 N94-31230
Analysis of ionospheric parameters in Europe and creation of the prediction algorithm
[AD-A276342] 09 p3771 N94-31326
The prediction of convective transfer on the thermal insulation of a solid-propellant rocket motor
[ONERA-NT-1993-15] 09 p3614 N94-31423
Viscoelastic fracture characterization of polymeric solids 09 p3652 N94-31745
Computer modelling of cyclic deformation of high-temperature materials
[AD-A277056] 09 p3623 N94-32012
Fracture and fatigue strength evaluation of multiple site damaged aircraft fuselages - curved panel testing and analysis
[PB94-152808] 09 p3579 N94-32015
Aircraft weight prediction capability. Volume 1: Weight study and results
[AD-A277206] 09 p3579 N94-32062
Exploring phase space concepts in the forecasting of time series with artificial neural networks
[DE94-005810] 09 p3834 N94-32127
Analysis of Dietz's single, rectangular pulse theory for the generation of radiation via photoelectrons
[DE94-006131] 09 p3681 N94-32661
Aspects of modeling uncertainty and prediction
[DE94-007565] 09 p3852 N94-32744
User's guide for a flat wake rotor inflow/wake velocity prediction code, DOWN
[NASA-TM-104139] 09 p3572 N94-32873
Development and testing of improved techniques for modeling the hydrologic cycle in a mesoscale weather prediction system
[AD-A277416] 09 p3786 N94-32921
Effective computational strategy for predicting the response of complex systems
[AD-A277452] 09 p3740 N94-33011
Reciprocity-based experimental determination of dynamic forces and moments: A feasibility study
[NASA-CR-194905] 09 p3862 N94-33023
Statistical characteristics of bistatic surface scatter and mean bistatic surface scattering strengths
[AD-A278155] 09 p3862 N94-33096
HSCT noise reduction technology development at GE Aircraft Engines 10 p3972 N94-33466
Sonic boom prediction and minimization using computational fluid dynamics 10 p3973 N94-33472
Task network models in the prediction of workload imposed by extravehicular activities during the Hubble Space Telescope servicing mission
10 p4101 N94-33627
An Assessment of Fatigue Damage and Crack Growth Prediction Techniques
[AD-280273] 10 p4071 N94-34581
Miner's rule revisited 10 p4071 N94-34582
Fatigue life and crack growth prediction methodology
10 p4071 N94-34583
Crack growth predictions using a crack closure model
10 p4071 N94-34584
An assessment of fatigue crack growth prediction models for aerospace structures
10 p4071 N94-34586
A combined approach to buffet response analyses and fatigue life prediction 10 p4072 N94-34587
Space environment laboratory in review, 1993
[PB94-153004] 10 p4187 N94-34946
The development and application of composite complexity models and a relative complexity metric in a software maintenance environment
11 p4255 N94-35559
An empirical comparison of a dynamic software testability metric to static cyclomatic complexity
12 p4491 N94-36498
Characterisation of Fibre Reinforced Titanium Matrix Composites
[AGARD-R-796] 12 p4400 N94-36649
Vibration signature analysis of a faulted gear transmission system
[NASA-TM-106623] 12 p4450 N94-36953
United States Air Force Summer Research Program, 1993. Volume 3: Phillips Laboratory
[AD-A278694] 12 p4550 N94-36979
Bond selective chemistry beyond the adiabatic approximation
[DE94-012486] 12 p4408 N94-37095
Ability of the total strain version of strainrange partitioning to characterize thermomechanical fatigue behavior
[NASA-TM-4556] 12 p4455 N94-37102
Embedded chaotic time series: Applications in prediction and spatio-temporal classification
[AD-A280690] 12 p4508 N94-37130
Substantiating powder metal life methodologies for engines 12 p4455 N94-37330
Predicting defect behaviour 12 p4455 N94-37331
Fatigue case study and loading spectra for wind turbines
[DE94-010798] 12 p4457 N94-37622

PREDICTIONS

NT FLOOD PREDICTIONS
NT IMPACT PREDICTION
NT LINEAR PREDICTION
NT NOISE PREDICTION
NT NOISE PREDICTION (AIRCRAFT)
NT PERFORMANCE PREDICTION
Predicted and real development in the aviation in the period 1961-1991 03 p0853 N94-15122
On predicting the person-in-water drift for search and rescue
[AD-A268083] 03 p1055 N94-17514
Development of the microstructure based stochastic life prediction model
[AD-A269742] 04 p1361 N94-18742
Statistical learning theory and algorithms
[AD-A270209] 04 p1523 N94-18901
Psychometric developments related to tests and selection
[AD-A272971] 05 p1894 N94-21262
Mathcad computer applications predicting antenna parameters from antenna physical dimensions and ground characteristics
[AD-A272987] 05 p1740 N94-21264
Predicting scheduling success
05 p1932 N94-21334
The program system for the diagnostics of strains and fracture prediction of solids 05 p1836 N94-22065
NASA Langley developments in response calculations needed for failure and life prediction
05 p1836 N94-22621
Screening for asymptomatic coronary heart disease
06 p2423 N94-23315
The ignition temperature of solid explosives exposed to a fire
[DE94-001047] 06 p2265 N94-23436
Stability questions in predictive control
[OUEL-1970/93] 06 p2477 N94-25469

Adaptive predictive control of the benchmark plant
[OUEL-1972/93] 06 p2477 N94-25470
Parameter estimation by genetic algorithms
[DE94-002924] 07 p2961 N94-26146
Effects of historical and predictive information on ability of transport pilot to predict an alert
[NASA-TM-4547] 07 p2673 N94-27864
Experimental studies of loudness and annoyance response to sonic booms 07 p2651 N94-28195
Comparison of methods of predicting community response to impulsive and nonimpulsive noise 07 p2651 N94-28196
Significant figures and Lyapunov exponents in chaos and constrained divergence of chaotic orbits 08 p3467 N94-29910
A real-time prediction of UTC 08 p3470 N94-30654
Contribution to the study of multiaxial fatigue under periodic or random stresses
[ISAL-92-0004] 09 p3734 N94-31544
Degradation of radiant ceramic structures in combustion atmospheres
[PB94-157849] 10 p4030 N94-34601
The computation of cloud base height from paired whole-sky imaging cameras
[DE94-009868] 11 p4294 N94-35767
Process/composite concurrent tailoring of SiC/Ti composites 12 p4402 N94-36663

PREDICTOR-CORRECTOR METHODS
Parallel methods for dynamic simulation of multiple manipulator systems 02 p0680 N94-14637
Stoermer-Cowell and related methods for the numerical solution of second order periodic initial value problems for ODE's 2: Numerical characteristics of the methods
[MEMO-1082] 05 p1953 N94-21075
Users manual for the NASA Lewis three-dimensional ice accretion code (LEWICE 3D)
[NASA-TM-105974] 05 p1642 N94-21590
Extended range modified gradient technique for profile inversion (extended version of report Et/Em-1992-8)
[PB93-215242] 05 p1742 N94-22346
F2D users manual: A two-dimensional compressible gas flow code
[DE94-000653] 05 p1805 N94-22386
An adaptive streamline diffusion finite element method for hyperbolic systems in gas dynamics
[PREPRINT-688] 06 p2340 N94-25466
Research on primal-dual interior point algorithms for mathematical programming
[DE94-003982] 07 p2959 N94-25821
Effective computational strategy for predicting the response of complex systems
[AD-A277452] 09 p3740 N94-33011
A predictor-corrector scheme for vortex identification
[AD-A279751] 10 p4043 N94-33433
Description and use of LSODE, the Livermore Solver for Ordinary Differential Equations
[NASA-RP-1327] 11 p4313 N94-35259
Theory and computation of optimal low- and medium-thrust transfers
[NASA-CR-196077] 11 p4202 N94-35487
Vortex tubes in turbulent flows: Identification, representation, reconstruction
[AD-A280504] 11 p4267 N94-35992

PREDICTORS
U PREDICTIONS

PREFLIGHT OPERATIONS
Kennedy Space Center processing of Shuttle small payloads 04 p1326 N94-19177
Constraint-based scheduling 06 p2510 N94-23904
STS-56, RSRM-031, 360L031 KSC processing configuration and data report
[NASA-CR-193922] 07 p2691 N94-26135
STS-51, RSRM-033, 360T033 KSC processing configuration and data report
[NASA-CR-193923] 07 p2691 N94-26153
Report of the Shuttle Processing Review Team
[NASA-TM-109728] 07 p2692 N94-28178

PREFORMS
Design and manufacturing of CFRP rings by RTM 01 p0059 N94-10025
Optimization of the processing parameters of high temperature superconducting glass-ceramics: Center Director's discretionary fund final report
[NASA-TM-108421] 02 p0808 N94-13938
Graphite fiber textile preform/copper matrix composites
[NASA-CR-193797] 02 p0558 N94-14050
Verification of a two-dimensional infiltration model for the resin transfer molding process
[NASA-CR-194597] 03 p0964 N94-15656
An overview of the NASA textile composites program 03 p0937 N94-16846
Design and cost drivers in 2-D braiding 03 p0937 N94-16849
Weaving multi-layer fabrics for reinforcement of engineering components 03 p0937 N94-16850
Textile composite processing science 03 p0938 N94-16856
Process relationship as influenced by carbonization rate
[AD-A269680] 04 p1341 N94-18572
Transducers and method for making same
[AD-D015949] 04 p1408 N94-19759
Composite fiber structures for catalysts and electrodes 06 p2393 N94-23364
Theoretical considerations for Reaction-Formed Silicon Carbide (RFSC) formation by molten silicon infiltration into slurry-derived preforms
[NASA-TM-106414] 06 p2222 N94-23500
Lunar preform manufacturing 07 p2765 N94-25677
3-D braided, continuous fiber ceramic composites produced by chemical vapor infiltration
[AD-A275192] 08 p3178 N94-29024
Microwave assisted chemical vapor infiltration
[DE94-005005] 08 p3185 N94-30771
Second NASA Advanced Composites Technology Conference
[NASA-CP-3154] 09 p3627 N94-33121
Recent progress in NASA Langley Research Center textile reinforced composites program 09 p3629 N94-33134
Advanced textile applications for primary aircraft structures 09 p3629 N94-33135
Comparison of resin film infusion, resin transfer molding, and consolidation of textile preforms for primary aircraft structure 09 p3630 N94-33136
Method for producing closed cell spherical porosity in spray formed metals
[AD-D016126] 10 p4025 N94-34152
A review of radial forging technology including preform design for process optimization
[AD-A278770] 11 p4250 N94-35711
SCS-6 (tm) fiber reinforced titanium 12 p4400 N94-36652

PREGNANCY
Physiological Anatomical Rodent Experiment (PARE).04 Feasibility Test 1
[NASA-CR-194423] 02 p0728 N94-13473
Physiological Anatomical Rodent Experiment (PARE).04 feasibility test 2
[NASA-CR-195210] 08 p3385 N94-29968

PREHEATERS
U HEATING EQUIPMENT

PREHEATING
U HEATING

PRELAUNCH SUMMARIES
Galileo probe spacecraft mission to Jupiter
[NASA-TM-109646] 03 p1247 N94-16070
Space Shuttle Mission STS-61: Hubble Space Telescope servicing mission-01
[NASA-TM-109344] 05 p1653 N94-20192

PRELAUNCH TESTS
A facility for testing 10- to 100-kWe space power reactors
[DE92-040420] 01 p0372 N94-11296
Constraint-based scheduling 06 p2510 N94-23904
Electric power system test and verification program
[NASA-TM-106405] 08 p3169 N94-30123

PRELOADING
U PRESTRESSING

PREMIXED FLAMES
Influence of gravity and ambient pressure variations on the behavior of buoyant laminar diffusion flames 01 p0123 N94-10240
The evolution equation for the flame surface density in turbulent premixed combustion 01 p0081 N94-12316
Generation of two-dimensional vortices in a cross-flow 01 p0160 N94-12318
Why does preferential diffusion strongly affect premixed turbulent combustion? 01 p0081 N94-12319
A coherent flame model of premixed turbulent combustion in a counterflow geometry
[CUED/A-THERMO/TR.60] 02 p0562 N94-13085
DNS and modeling of the interaction between turbulent premixed flames and walls 02 p0646 N94-14763
The evolution equation for the flame surface density in turbulent premixed combustion 02 p0567 N94-14764
Numerical simulations of turbulent premixed H2/O2/N2 flames with complex chemistry 02 p0567 N94-14765
Mechanisms of combustion limits in premixed gas flames at microgravity
[NASA-CR-194557] 03 p0946 N94-15713
A comparison of one and two dimensional flame quenching: Heat transfer results
[DE93-015196] 03 p0947 N94-16060
Studies of premixed laminar and turbulent flames at microgravity
[NASA-CR-194656] 03 p0951 N94-17125
Studies on high pressure and unsteady flame phenomena: Revision
[AD-A269138] 04 p1348 N94-18257
Flame structure studies of a lean 20-torr H2/N2O/Ar flame employing molecular beam mass spectrometry
[AD-A268889] 04 p1349 N94-18456
Mathematical problems in combustion
[AD-A270147] 04 p1349 N94-18776
Detailed structure study of an H2/N2O/Ar flame employing molecular beam mass spectrometry, laser spectroscopy, and modeling
[AD-A270720] 05 p1679 N94-20111
Mechanism and enhancement of flame stabilization
[DE94-002181] 06 p2232 N94-23023
Stretch-induced quenching in flame-vortex interactions 06 p2237 N94-24156
The production of premixed flame surface area in turbulent shear flow 06 p2237 N94-24158
Experimental investigation of ignition of boron/titanium composite particles 06 p2159 N94-24275
Stability of premixed laminar flames in a stagnation point flow to general disturbances
[AD-A273429] 06 p2234 N94-24673
Modelling of premixed laminar flames
[ETN-94-95317] 06 p2236 N94-25284
Prediction of prompt NO(x) in hydrocarbon air flames 08 p3190 N94-29250
Simulation of pollutant formation in turbulent combustors using an extended coherent flame model 08 p3190 N94-29251
Ducted kerosene spray flames 08 p3195 N94-29276
Turbulence structure of a premixed flame in a coaxial free air jet in the presence or absence of a base flow
[ISBN-0-315-78739-2] 09 p3633 N94-31471
Rich methane/air flames: Burning velocities, extinction limits, and flammability limit
[DE94-004340] 12 p4407 N94-36462
Rich flammability limits in CH3OH/CO/diluent mixtures
[DE94-004341] 12 p4407 N94-36482
Some effects of heat release in premixed flames
[DE94-011346] 12 p4409 N94-37199

PREMIXING
Application of jet-shear-layer mixing and effervescent atomization to the development of a low-NO(x) combustor
[NASA-TM-105888] 01 p0028 N94-11234
Mechanisms of combustion limits in premixed gas flames at microgravity
[NASA-CR-194557] 03 p0946 N94-15713
Studies on high pressure and unsteady flame phenomena: Revision
[AD-A269138] 04 p1348 N94-18257
Research activity on particle spin systems and related problems
[AD-A269456] 04 p1562 N94-18286
Metal slurry droplet and spray combustion
[AD-A269648] 04 p1349 N94-18736
Focused Schlieren flow visualization studies of multiple venturi fuel injectors in a high pressure combustor
[NASA-TM-106479] 07 p2674 N94-26573
The effect of incomplete fuel-air mixing on the lean limit and emissions characteristics of a Lean Prevaporized Premixed (LPP) combustor 08 p3193 N94-29265
Effects of hydrogen addition on pollutant emissions in a gas turbine combustor 08 p3195 N94-29275
Numerical prediction of mixing process in a methane-fueled engine 08 p3304 N94-30230
LeRC in-house experimental research 10 p3975 N94-33484

PREPARATION
NT PRECONDITIONING
NT PRESTRESSING
NT PRETREATMENT
Food for space
[NASA-TM-109668] 03 p1136 N94-15435
Preparation of concrete specimens for microstructural image analysis studies 05 p1707 N94-21891
Preparation and properties of translucent gamma-aluminium oxynitride
[ETN-94-95305] 06 p2263 N94-25281

PREPOLYMERS
NT DIMERS
NT TRIMERS
Thermal stability of sealants for military aircraft: Modification of polysulfide prepolymers with ether and thioether monomers
[AD-A264079] 01 p0089 N94-11107
Preparation of homogeneous aluminosilicate gels by sol/gel techniques
[AD-A266823] 03 p0962 N94-14914

Single source precursors for the OMCVD of 3/5 compound semiconductors
[AD-A271147] 04 p1606 N94-19739
Phthalonitrile prepolymer as high temperature sizing material for composite fibers
[AD-D015912] 05 p1672 N94-20010
High temperature adhesive
[AD-D016019] 06 p2258 N94-24737
Curing phthalonitriles with acid
[AD-D015996] 06 p2261 N94-25054
Polymer from DIIMIDO-DI-PHTHALONITRILE
[AD-D016189] 10 p4030 N94-34682

PREPREGS
Hybrid materials for use at elevated temperatures
01 p0057 N94-10013
Advanced phenolic systems for aircraft interiors
01 p0018 N94-10776
Fire resistance and mechanical properties for phenolic prepregs 01 p0020 N94-10786
Polymer infiltration studies
[NASA-CR-194521] 02 p0582 N94-14539
Machine development 03 p0932 N94-15258
Polymer Infiltration Studies
[NASA-CR-194494] 03 p0932 N94-15275
A new NASA LaRC Multi-Purpose Prepregging Unit
03 p0932 N94-15276
Process for preparing thermoplastic composites
[AD-D015864] 04 p1339 N94-18074
Phthalonitrile prepolymer as high temperature sizing material for composite fibers
[AD-D015912] 05 p1672 N94-20010
Preparing polymeric matrix composites using an aqueous slurry technique
[NASA-CASE-LAR-14771-1] 06 p2252 N94-23076
Composite material impregnation unit
[NASA-TM-107751] 06 p2254 N94-23486
Polymer infiltration studies
[NASA-CR-195729] 08 p3213 N94-28748
Non-rectangular towpreg architectures
[NASA-CASE-LAR-14863-1-CU]
08 p3180 N94-29485
Apparatus for providing a uniform, consolidated, unidirectional, continuous, fiber-reinforced polymeric material and method relating thereto
[NASA-CASE-LAR-15173-1-CU]
08 p3180 N94-29496
Empirical optimization of the consolidation of thermoplastic prepregs
[ISBN-0-315-86455-9] 09 p3652 N94-31722
Low pressure process for continuous fiber reinforced polyamic acid resin matrix composite laminates
[NASA-CASE-LAR-14954-1] 10 p4020 N94-35075
Through-the-thickness tensile strength of textile composites
[NASA-TM-109115] 11 p4233 N94-35946

PREPROCESSING
The TREES project: Pre-processing and generation of terrain data for inclusion in an ERS-1 SAR classification scheme 01 p0249 N94-12496
The 1991 version of the plume impingement computer program. Volume 1: Description
[NASA-CR-194192] 01 p0166 N94-12775
Preprocessing data collected with the ACTS propagation terminal 02 p0616 N94-14676
Adaptive median filtering for preprocessing of time series measurements 03 p0912 N94-15561
Application of the robust estimate in SLR data preprocessing 03 p0918 N94-15597
Data acquisition, preprocessing and analysis for the Virginia Tech OLYMPUS experiment
03 p0995 N94-16038
Segmented operations for sparse matrix computation on vector multiprocessors
[AD-A270601] 05 p1928 N94-19950
An optically-assisted 3-D cellular array machine
[AD-A272683] 05 p1987 N94-21163
Color image segmentation
[AD-A274027] 07 p2984 N94-25759
Extension of the LUSTRE language and application to circuit design: The LUSTRE V4 language and the POLLUX system
[ETN-94-95918] 09 p3812 N94-31543
Inflight calibration, preprocessing, and data evaluation of GER 2 imaging spectrometry data
09 p3744 N94-31858
CMS Preprocessing Subsystem user's guide: Software version 2.0
[DE94-005327] 09 p3816 N94-32145
CMS Distribution Subsystem user's guide
[DE94-005328] 09 p3816 N94-32146
An analog preprocessing architecture for high-speed analog-to-digital conversion
[AD-A276737] 09 p3807 N94-32163
A novel optoelectronic system for distortion-invariant ATR
[AD-A277985] 09 p3884 N94-33087
ML partial evaluation using set-based analysis
[AD-A278955] 11 p4304 N94-35718
Experience with automatic, dynamic load balancing and adaptive finite element computation
[DE94-001422] 12 p4498 N94-37487

PRESBYOPIA
Vision impairment and corrective considerations of civil airmen
[DOT/FAA/AM-93/21] 06 p2426 N94-23623

PRESELECTORS
U PREAMPLIFIERS

PRESERVING
Preserving electronic records: Not the easiest task
10 p4152 N94-33800

PRESIDENTIAL REPORTS
From red tape to results: Creating a government that works better and costs less 01 p0422 N94-11351
From red tape to results: Creating a government that works better and costs less. Executive summary
01 p0422 N94-11353
Advanced nuclear thermal propulsion concepts
06 p2217 N94-23068
Aeronautics and space report of the President: Fiscal year 1993 activities 09 p3966 N94-32854

PRESINTERING
U SINTERING

PRESSES
Investigation of materials processing technology
[AD-A277588] 10 p4031 N94-33428

PRESSING (FORMING)
Cost effectiveness of structural applications of fibre reinforced thermoplastics 01 p0060 N94-10032
Generalized Eulerian-Lagrangian formulations in free and moving boundary problems: Processing of viscoelastic polymers and fiber suspensions
08 p3283 N94-30955

PRESSURE
NT ATMOSPHERIC PRESSURE
NT BASE PRESSURE
NT BLOOD PRESSURE
NT CRITICAL PRESSURE
NT DENSIFICATION
NT DIASTOLIC PRESSURE
NT DIFFERENTIAL PRESSURE
NT DYNAMIC PRESSURE
NT FLUID PRESSURE
NT GAS PRESSURE
NT HIGH ALTITUDE PRESSURE
NT HIGH PRESSURE
NT HIGH VACUUM
NT HYDROSTATIC PRESSURE
NT HYPERTENSION
NT HYPOTENSION
NT ILLUMINANCE
NT INLET PRESSURE
NT INTERNAL PRESSURE
NT ISOSTATIC PRESSURE
NT LOW PRESSURE
NT LOWER BODY NEGATIVE PRESSURE
NT LUMINANCE
NT LUMINOUS INTENSITY
NT OVERPRESSURE
NT OXYGEN TENSION
NT PARTIAL PRESSURE
NT PLASMA PRESSURE
NT RADIATION PRESSURE
NT SOUND PRESSURE
NT STAGNATION PRESSURE
NT STATIC PRESSURE
NT SUPERCRITICAL PRESSURES
NT SYSTOLIC PRESSURE
NT TRANSIENT PRESSURES
NT TRANSITION PRESSURE
NT ULTRAHIGH VACUUM
NT VACUUM
NT VAPOR PRESSURE
NT WALL PRESSURE
NT WATER PRESSURE
Test and evaluation methods
02 p0506 N94-14163
The motion of a conical shaped liner driven by explosive load
[ITN-93-85215] 02 p0585 N94-14507
Hypersonic shock wave boundary layer interactions over simplified deflected control surface configurations
03 p1018 N94-15203
First results from a laboratory facility for measurement of emission spectra under simulated planetary conditions
03 p0954 N94-16372
Computational prediction of isolated performance of an axisymmetric nozzle at Mach number 0.90
[NASA-TM-4506] 07 p2646 N94-26547
Scaling in heavy-fermion systems
[DE94-005002] 08 p3492 N94-30775
Experimental measurements and analytical analysis related to gas turbine heat transfer. Part 1: Time-averaged heat-flux and surface-pressure measurements on the vanes and blades of the SSME fuel-side turbine and comparison with prediction. Part 2: Phase-resolved surface-pressure and heat-flux measurements on the first blade of the SSME fuel-side turbine
[NASA-CR-196296] 12 p4442 N94-36969

PRESSURE BREATHING
Hypobaric decompression prebreathe requirements and breathing environment 01 p0317 N94-11541
In-flight measurement of aircrew breathing in Navy aircraft
[AD-A271811] 05 p1896 N94-21154
Aeromedical issues related to positive pressure breathing for +Gz protection
[AD-A274717] 07 p2910 N94-26435
Comparative centrifuge evaluation of the Air Force Advanced Technology Anti-G Suit (ATAGS) and the Navy Enhanced Anti-G Lower Ensemble (EAGLE)
[AD-A275348] 08 p3400 N94-28996
The US Navy/Canadian DCIEM research initiative on pressure breathing physiology 10 p4101 N94-33636

PRESSURE BROADENING
The pressure broadening of HDO by O2, N2, H2, and He between 100 K and 600 K
[AD-A267118] 03 p0946 N94-15684
The young Sun and photochemistry of the primitive Martian atmosphere 05 p2145 N94-21679
High resolution molecular spectroscopy of atmospheric species
[AD-A278382] 09 p3776 N94-33351

PRESSURE CABINS
U PRESSURIZED CABINS

PRESSURE CHAMBERS
NT HYPERBARIC CHAMBERS
NT VACUUM CHAMBERS
Combustion-induced crack/debond propagation in solid propellants 02 p0584 N94-13560
Simulation of collisional fragmentation with explosives
03 p1063 N94-16254
Numerical simulation and prediction of implosion phenomena
[GKSS-92/E/99] 08 p3284 N94-30968

PRESSURE DEPENDENCE
The effect of pressure and quadrupolar interactions on the nematic-isotropic transition properties: Numerical results for a system of prolate ellipsoids including second and fourth rank orientational order parameters
[DE93-613540] 01 p0410 N94-10536
Phase equilibria and volumetric properties for the system NaCl-CaCl2-H2O
[DE93-013590] 01 p0076 N94-11244
Orientation of Planar Deformation Features (PDFs) in quartz 03 p1219 N94-16341
The low-temperature specific heat of CeCu2Ge2 at 0 and 9.5 kbar
[DE93-014914] 04 p1360 N94-18398
Role of pressure in the study of fullerenes
[DE93-018839] 04 p1602 N94-19340
Effects of pressure on the orientational ordering and phase transitions in solid C(60) and C(70)
[DE93-018858] 04 p1603 N94-19347
Metallization and charge-transfer gap closure of transition-metal iodides under pressure
[DE93-040301] 04 p1353 N94-19538
Electron reactions in nonpolar liquids: Pressure effects
[DE93-040328] 05 p1970 N94-19931
Magnetism in CeRu2Ge2 and CeRh2Ge2 and its pressure dependence
[DE93-040061] 05 p2032 N94-21987
High oxygen pressure synthesis of new copper oxide superconductors
[DE93-040278] 05 p2033 N94-21998
First-principles pressure-temperature phase diagrams in metals
[DE94-001056] 05 p1696 N94-22398
Anisotropic uniaxial pressure effects in YBa2Cu3O(7-delta)
[DE94-001456] 06 p2557 N94-22929
Bridgman's concern
[DE93-040900] 06 p2558 N94-22953
Physics of iron
[DE94-002002] 06 p2402 N94-23721
The effect of high altitude pressure on the power and efficiency of an airborne two-stroke engine
06 p2155 N94-24253
Grain boundary degradation of YBCO superconductors sintered in CO2-containing atmospheres
[DE94-003206] 07 p3053 N94-26029
Iron: What is melt?
[DE94-003373] 07 p2735 N94-26322
Influence of point defects on grain boundary diffusion in oxides
[DE94-003164] 07 p3060 N94-26782

Electrical conductivity of perovskite-magnesiowuestite as a function of pressure and temperature
[DE94-002714] 07 p2880 N94-26806
An improvement in the modified finite element procedure for underwater shock analysis
[DE94-004451] 07 p2797 N94-27617
Dislocation theory of melting for iron, revisited
[DE94-002715] 08 p3355 N94-28538
Crystal structure of La(2-x)Ba(x)CuO4
[DE94-707688] 08 p3511 N94-28750
Synthesis and neutron diffraction study of Na3WN3 and Na3MoN3
[AD-A275158] 08 p3203 N94-29043
Scaling in heavy-fermion systems
[DE94-005002] 08 p3492 N94-30775
Studies of interfaces and vapors with Optical Second Harmonic Generation
[DE94-006295] 08 p3476 N94-30841
High pressure experiments on the Y-Ba-Cu-O superconductors: A major role for holes
[ETN-94-96013] 09 p3897 N94-31547
Pressure dependence of the conductivity and magnetoconductance in oriented iodine-doped polyacetylene
[PB94-184488] 12 p4427 N94-37854

PRESSURE DISTRIBUTION

Schlieren photographs and internal pressure distributions for three-dimensional sidewall-compression scramjet inlets at a Mach number of 6 in CF4
[NASA-TM-4479] 01 p0148 N94-10644
Results of wind tunnel tests of an ASRM configured 0.03 scale Space Shuttle integrated vehicle model (47-OTS) in the AEDC 16-foot transonic wind tunnel, volume 2
[NASA-CR-185697] 02 p0534 N94-12965
Exploratory study of in-plane streamline curvature effects on a turbulent boundary layer at a Mach number of 3
[NASA-CR-193673] 02 p0501 N94-13292
Numerical simulations of unsteady flows in turbomachines 02 p0633 N94-13569
Flow-field interference produced by an asymmetrical support strut
[IAR-AN-75] 02 p0504 N94-14031
The motion of a conical shaped liner driven by explosive load
[ITN-93-85215] 02 p0585 N94-14507
VSAERO analysis of a Piper Cub aircraft 02 p0516 N94-14616
Vortex-induced disturbance field in a compressible shear layer 02 p0645 N94-14760
Laser Doppler velocimetry measurements across a normal shock in transonic flow
[AD-A267240] 03 p0855 N94-14973
Wind tunnel investigation of three axisymmetric cowls of different lengths at Mach numbers from 0.60 to 0.92
[NASA-TM-4488] 03 p0856 N94-15681
Recirculation in forward roll coating
[VKI-TM-48] 04 p1409 N94-17901
In-flight pressure distributions and skin-friction measurements on a subsonic transport high-lift wing section 04 p1308 N94-18435
Preliminary design of a water cooled avionics cooling rack
[AD-A268826] 04 p1320 N94-18536
A comparative study of turbulence models in predicting hypersonic inlet flows 04 p1314 N94-18553
Finite beta plasma equilibrium in toroidally linked mirrors
[DE93-040318] 04 p1590 N94-19193
Semi-span model testing in the National Transonic Facility
[NASA-CR-194479] 04 p1312 N94-19388
Numerical investigation of the incompressible flow around a wing with a fixed spoiler
[ISL-R-109/91] 04 p1313 N94-19524
Variable-permittivity linear inverse problem for the H(sub z)-polarized case 05 p1719 N94-20408
A study of the compressible flow through a diffusing S-duct
[NASA-TM-106411] 05 p1638 N94-21591
Modelling stalled airfoils
[ISBN-0-315-59525-6] 05 p1639 N94-22382
Computational fluid dynamic modelling of cavitation 06 p2215 N94-23060
An experimental study of the flow field surrounding a subsonic jet in a cross flow
[NASA-CR-194770] 06 p2317 N94-23072
Probe systems for measuring static pressure and turbulence intensity in fluid streams
[NASA-CASE-ARC-11935-1] 06 p2319 N94-23306
Experimental investigation of generic three-dimensional sidewall-compression scramjet inlets at Mach 6 in tetrafluoromethane
[NASA-TM-4497] 06 p2319 N94-23339
The 3-D CFD modeling of gas turbine combustor-integral bleed flow interaction 06 p2189 N94-23658
FAS multigrid calculations of three dimensional flow using non-staggered grids 06 p2341 N94-23675
Evaluation of turbulence models in the PARC code for transonic diffuser flows
[NASA-TM-106391] 06 p2168 N94-24084
CFD simulation of coaxial injectors 06 p2342 N94-24430
Aerodynamic characteristics and pressure distributions for an executive-jet baseline airfoil section
[NASA-TM-4529] 06 p2169 N94-24586
Eddy mixing coefficient upper limit derived from the photochemical balance of O2 06 p2621 N94-24897
Three-dimensional numerical simulation of thermal tides in the Martian atmosphere 06 p2622 N94-24901
Low-speed pressure distribution measurements over the aft-fuselage, fins, and stabilators of a 1/9th scale F/A-18 wind-tunnel model
[AD-A274870] 07 p2644 N94-26342
Pressure distributions on a 0.02-scale Space Shuttle orbiter nose at Mach 21.5 in helium
[NASA-TM-4495] 07 p2646 N94-26592
Numerical studies on the dynamics of bubble, turbulent, free shear flows: Effect of the inter-phase coupling on the global flow evolution
[AD-A274521] 07 p2794 N94-26832
New variational techniques for acoustic radiation and scattering from elastic shell structures
[AD-A274599] 07 p3010 N94-26889
Aircraft wheel life assessment
[AD-A274378] 07 p2823 N94-26976
Verification of thermal analysis codes for modeling solid rocket nozzles
[NASA-CR-195248] 07 p2702 N94-27150
Streamwise vorticity in a turbine rotor with conical endwalls
[DLR-FB-93-13] 07 p2826 N94-27591
Experimental and theoretical investigations of the influence of the jet on the flow around a bypass-engine
[DLR-FB-93-17] 07 p2675 N94-27593
An improvement in the modified finite element procedure for underwater shock analysis
[DE94-004451] 07 p2797 N94-27617
Flat rectangular orthotropic plates under uniformly distributed normal pressure. Elastic stresses and deflections for various forms of edge restraint
[ESDU-93011] 07 p2845 N94-28061
Simulation: A tool for steam plant dynamic analysis 07 p2831 N94-28084
Examples of excrescence drag prediction for typical wing components of a subsonic transport aircraft at the cruise condition
[ESDU-93032] 07 p2649 N94-28144
Effect of surface finish on turbine airfoil cascade losses 07 p2652 N94-28320
The effect of axial velocity ratio, turbulence intensity, incidence, and leading edge geometry on the midspan performance of a turbine cascade 07 p2652 N94-28321
Measurements of steady and dynamic pressure on an F/A-18 wind tunnel model at high angles of attack 07 p2653 N94-28323
Fluid dynamic noise in a centrifugal pump
[AD-A275264] 08 p3477 N94-28904
Quadruplet expansion of the acoustic pressure field in a wedge shaped ocean
[AD-A275121] 08 p3477 N94-29003
Wall pressure fluctuations in the reattachment region of a supersonic free shear layer
[NASA-CR-195790] 08 p3132 N94-29920
Computation of wind tunnel wall effects for complex models using a low-order panel method
[NASA-TM-104019] 08 p3132 N94-30151
An interactive, design and educational tool for supersonic external-compression inlets
[NASA-TM-106581] 08 p3421 N94-30174
Three-dimensional flow characteristics downstream of a blade endwall corner 08 p3280 N94-30229
Calculus of variations applied to 2D multi-point airfoil design
[PB94-125457] 08 p3133 N94-30401
Sensitivity analysis of the static aeroelastic response of a wing 08 p3134 N94-30525
Design of a variable-conductance vacuum insulation
[DE94-000270] 08 p3268 N94-30819
Dynamics of flux tubes in accretion disks 09 p3932 N94-31142
Rotordynamic effects driven by fluid forces from a geometrically imperfect labyrinth
[AD-A276424] 09 p3722 N94-31333
Shock impingement near mild hypersonic expansion corners 09 p3569 N94-31879
Design of a two dimensional planer pressurized air labyrinth seal test rig
[AD-A277232] 09 p3726 N94-32370
In flight measurement of steady and unsteady blade surface pressure of a single rotation large scale advanced prop-fan installed on the PTA aircraft
[NASA-CR-187096] 09 p3584 N94-32859
Cylinder drag experiment: An upgraded laboratory
[AD-A277841] 10 p3982 N94-33835
Inverse design of radial flow impellers with prescribed velocity at hub and shroud 10 p4002 N94-34448
Control of leading-edge separation on a cambered delta wing 10 p3992 N94-34616
Combined LAURA-UPS solution procedure for chemically-reacting flows
[NASA-TM-107964] 10 p4049 N94-34721
The unsteady pressure field and vorticity productiion at the suction surface of a pitching airfoil 10 p3986 N94-34972
Mechanisms of flow control with the unsteady bleed technique 10 p3986 N94-34987
A supersonic tunnel for laser and flow-seeding techniques
[NASA-TM-106588] 11 p4265 N94-35945
Expansion effects on supersonic turbulent boundary layers
[AD-A278989] 11 p4190 N94-35950
Propellant stress relief groove for the Titan 4 SRMU
[AD-A278628] 11 p4228 N94-36254
Controlling forebody asymmetries in flight: Experience with boundary layer transition strips
[NASA-TM-4595] 12 p4383 N94-36944
Pressure-sensing performance of upright cylinders in a Mach 10 boundary-layer
[NASA-TM-4633] 12 p4383 N94-37395
Aerodynamic characteristics of the National Launch System (NLS) 1 1/2 stage launch vehicle
[NASA-TP-3488] 12 p4384 N94-37577

PRESSURE DRAG

NT SUPERSONIC DRAG
NT WAVE DRAG
Computational prediction of isolated performance of an axisymmetric nozzle at Mach number 0.90
[NASA-TM-4506] 07 p2646 N94-26547

PRESSURE DROP

Prediction of pressure drop in fluid tuned mounts using analytical and computational techniques 06 p2321 N94-23643
Solution of mixed convection heat transfer from isothermal in-line fins 06 p2321 N94-23644
Design of a refueling tanker delivering liquid hydrogen 07 p2671 N94-25717

PRESSURE EFFECTS

Influence of gravity and ambient pressure variations on the behavior of buoyant laminar diffusion flames 01 p0123 N94-10240
The effect of pressure and quadrupolar interactions on the nematic-isotropic transition properties: Numerical results for a system of prolate ellipsoids including second and fourth rank orientational order parameters
[DE93-613540] 01 p0410 N94-10536
Phase equilibria and volumetric properties for the system NaCl-CaCl2-H2O
[DE93-013590] 01 p0076 N94-11244
Thermodynamics of lunar ilmenite reduction 01 p0415 N94-12028
Shock transformations in quartzite 01 p0097 N94-12040
The effects of atmospheric pressure on infrared reflectance spectra of Martian analogs 01 p0445 N94-12071
Methanol pan fires in an enclosed space: Effect of pressure and oxygen concentration
[AD-A266108] 01 p0079 N94-12415
Effect of pressure on order and stability in alloys: The case of Al-Ge
[DE93-013842] 02 p0567 N94-12899
A multiphase model for shock-induced flow in low density foam
[DE93-013767] 02 p0632 N94-13397
Temperature and pressure effects on capacitance probe cryogenic liquid level measurement accuracy
[NASA-CR-190763] 03 p1034 N94-16521
Structural phase transition and superconductivity in La(2-x)Ba(x)CuO4
[DE93-015812] 03 p1212 N94-16868
The low-temperature specific heat of CeCu2Ge2 at 0 and 9.5 kbar
[DE93-014914] 04 p1360 N94-18398
Growth, characterization and device development in monocrystalline diamond films
[AD-A270074] 04 p1599 N94-18797
Research on Earth's rotation and the effect of atmospheric pressure on vertical deformation and sea level variability
[NASA-CR-194300] 04 p1484 N94-18838
Influence of peak pressure and temperature on the shock-loading response of tantalum
[DE93-018561] 04 p1457 N94-19279

Role of pressure in the study of fullerenes
[DE93-018839] 04 p1602 N94-19340
Effects of pressure on the orientational ordering and phase transitions in solid C(60) and C(70)
[DE93-018858] 04 p1603 N94-19347
Pressure and temperature effects on the kinetics and quality of diamond films
[AD-A270876] 04 p1606 N94-19771
Electron reactions in nonpolar liquids: Pressure effects
[DE93-040328] 05 p1970 N94-19931
Lamellar olivine in the Divnoe achondrite: Evidence for high-pressure exsolution? 05 p1685 N94-20679
Pressure versus drag effects on crater size 05 p1862 N94-20742
Adhesive bonded joint with improved cyclic fatigue life for alumina-ceramic cylinders and hemispheres: Fourth generation housings
[AD-A273061] 05 p1831 N94-21310
First-principles pressure-temperature phase diagrams in metals
[DE94-001056] 05 p1696 N94-22398
Anisotropic uniaxial pressure effects in YBa2Cu3O(7-delta)
[DE94-001456] 06 p2557 N94-22929
Performance evaluation of the Russian SPT-100 thruster at NASA LeRC
[NASA-TM-106401] 06 p2219 N94-23630
Squeeze casting: A literature review
[PB94-124575] 07 p2741 N94-27326
Technical report of ISSP. Ser. A, no. 2682: Pressure dependence of Sm:YAG fluorescence to 50 GPa: A new calibration as a high pressure scale
[JTN-94-80568] 07 p3066 N94-27354
A rapid-pressure correlation representation consistent with the Taylor-Proudman theorem materially-frame-indifferent in the 2D limit
[AD-A277582] 07 p2796 N94-27435
Examples of excrescence drag prediction for typical wing components of a subsonic transport aircraft at the cruise condition
[ESDU-93032] 07 p2649 N94-28144
Dislocation theory of melting for iron, revisited
[DE94-002715] 08 p3355 N94-28538
Effects of pressure on membrane-associated receptors and effector elements
[AD-A275813] 08 p3384 N94-28829
Pollutant emissions from and within a model gas turbine combustor at elevated pressures and temperatures 08 p3194 N94-29271
Formation and self-healing of magnetic islands in finite-beta helias equilibria
[AD-B183271L] 08 p3505 N94-29483
The effect of pressure gradient on the structure of an equilibrium turbulent boundary layer 08 p3282 N94-30807
Computational study of single-expansion-ramp nozzles with external burning
[NASA-TM-106550] 09 p3700 N94-31229
A model of the ion chemistry of electrified convection 09 p3868 N94-31993
Advanced thermally stable jet fuels
[DE94-006760] 09 p3667 N94-32150
Simulation of low-density nozzle plumes in non-zero ambient pressures
[NASA-TM-106501] 09 p3615 N94-32742
Composite fuselage shell structures research at NASA Langley Research Center 09 p3628 N94-33124
The influence of thermal inertia on Mars' seasonal pressure variation and the effect of the weather component 09 p3952 N94-33238
Effect of barbiturates and hyperoxia on lipid peroxidation in hypoxic neurons
[AD-A278467] 10 p4094 N94-33545
Effect of pressure on arsenic diffusion in germanium
[DE94-009451] 10 p4147 N94-33914
Effect of pressure gradient on first mode of instability in high-speed boundary layers
[AD-280579] 10 p4048 N94-34130
Integral pressure sensor
[AD-D016188] 10 p4056 N94-34681
X ray and gamma ray spectroscopy of solids under pressure
[DE94-011207] 11 p4238 N94-36203

PRESSURE FIELDS
U PRESSURE DISTRIBUTION

PRESSURE GAGES
NT BAROMETERS
NT IONIZATION GAGES
NT PIEZOELECTRIC GAGES
Analysis of Hopkinson bar pressure gage
[AD-A262366] 01 p0171 N94-12362
Determination of equivalent circuit for PVDF shock-pressure gauges
[DE93-016492] 03 p1034 N94-16452
Integral pressure sensor
[AD-D016188] 10 p4056 N94-34681

PRESSURE GRADIENTS
Underwing compression vortex attenuation device
[NASA-CASE-LAR-14744-1] 01 p0012 N94-10673
A Galilean and tensorial invariant k-epsilon model for near wall turbulence
[NASA-TM-106263] 01 p0151 N94-11192
The role of the geothermal gradient in the emplacement and replenishment of ground ice on Mars 01 p0463 N94-12169
Large eddy simulations of time-dependent and buoyancy-driven channel flows 01 p0155 N94-12287
Progress in modeling hypersonic turbulent boundary layers 01 p0157 N94-12300
Fluctuations of the Kuroshio extension detected by the GEOSAT altimetry data 01 p0209 N94-12649
Thermal gravitational modelling and scaling of two-phase heat transport systems: Similarity considerations and useful equations predictions versus experimental results
[NLR-TP-91477-U] 02 p0632 N94-13533
A three-dimensional supersonic turbulent boundary layer generated by an isentropic compression 02 p0503 N94-13556
Interaction of two glancing, crossing shock waves with a turbulent boundary-layer at various Mach numbers
[NASA-TM-103740] 02 p0509 N94-14780
Orographic microbursts in a severe winter windstorm
[AD-A267651] 03 p1108 N94-17247
Low Reynolds-number turbulent boundary layers
[AD-A272011] 05 p1803 N94-21459
Heat transfer and flow structure in end-wall boundary layers
[AD-A273470] 06 p2335 N94-24689
Fluid velocity and electromagnetic forces measured by a rotating Langmuir probe in the scrape off layer of JFT-2M
[OUEL-1968/92] 06 p2554 N94-25327
An enhanced global spectral model
[PL-TR-92-2011] 07 p2898 N94-28223
The effect of pressure gradient on the structure of an equilibrium turbulent boundary layer 08 p3282 N94-30807
Atmospheric turbulence within and above a coniferous forest
[ISBN-0-315-75468-0] 08 p3375 N94-30870
Modification of the MML turbulence model for adverse pressure gradient flows
[NASA-TM-106544] 09 p3709 N94-32947
Effect of pressure gradient on first mode of instability in high-speed boundary layers
[AD-280579] 10 p4048 N94-34130
The effect of crossflow on Goertler vortices
[AD-280361] 10 p4049 N94-34680

PRESSURE HEADS
Evaluation of a distributed catchment scale water balance model
[PAPER-93WR00398] 03 p1083 N94-16031

PRESSURE ICE
Observation of pressure ridges in SAR images of sea ice: Scattering theory and comparison with observations 05 p1723 N94-20427

PRESSURE MEASUREMENT
Microgravity combustion of dust suspension in a spherical chamber 01 p0080 N94-10248
An experimental investigation of high-speed water-entry for full-size and scale-model pointed nose vehicles
[DE93-008491] 01 p0147 N94-10252
Pressure and force measurements on models set in hypersonic flows: A review 01 p0005 N94-10435
Flow development in a circular pipe in the UTIAS/RPI M = 8.3 gun tunnel 01 p0006 N94-10442
Experimental and computational comparisons of Mach 6 high Reynolds number heat transfer and skin friction 01 p0006 N94-10443
Some experimental study and numerical simulation in wind tunnel flow 01 p0008 N94-10457
Wall interference correction based on interface measurements in subsonic wind tunnel testing 01 p0015 N94-11154
A laboratory model of a hydrogen/oxygen engine for combustion and nozzle studies
[NASA-TM-106281] 01 p0047 N94-11252
Overview of the 1989 Wind Tunnel Calibration Workshop
[NASA-TP-3393] 01 p0034 N94-11869
Analysis of Hopkinson bar pressure gage
[AD-A262366] 01 p0171 N94-12362
Results of experimental investigations to determine external tank protuberance loads using a 0.03-scale model of the Space Shuttle launch configuration (model 47-OTS) in the NASA/ARC unitary plan wind tunnel, volume 1
[NASA-CR-167690] 02 p0534 N94-12810
A wall interference assessment/correction system
[NASA-CR-194174] 02 p0500 N94-13076
NASA metrology and calibration, 1993
[NASA-TM-109280] 02 p0597 N94-14410
Interaction of two glancing, crossing shock waves with a turbulent boundary-layer at various Mach numbers
[NASA-TM-103740] 02 p0509 N94-14780
Measurements of Interfacial Tension: MITE 03 p0943 N94-15158
Pressures of supercritical salt solutions 03 p0945 N94-15166
Mechanical and surface force nanoprobe
[AD-D015792] 03 p1034 N94-16536
An experimental investigation of the effects of leading edge geometry on the dynamics of blunt fin-induced shock wave turbulent boundary layer interaction
[AD-A267656] 03 p0860 N94-17221
Experimental study of vortex and aerodynamic characteristics of stack wings with sideslip
[AD-A267722] 03 p0860 N94-17274
An experimental study of fluctuating wall pressures in a highly swept, sharp fin-induced, Mach 5 shock wave/turbulent boundary layer interaction
[AD-A268394] 03 p0861 N94-17461
Instrumented experiments aboard the frigate WOLF. Wolf 2: Measurement results of the 5.5 kg TNT in the crew aft sleeping compartment
[PML-1992-12] 04 p1451 N94-17931
Measurement Techniques
[VKI-LS-1993-05] 04 p1430 N94-18643
Static pressure measurements for near isentropic flows using laser induced iodine fluorescence 04 p1431 N94-18646
Pressure sensitive paint technique 04 p1431 N94-18647
Construction and evaluation of an environmental chamber for calibration of temperature and pressure sensors for laser interferometers
[PB93-197838] 04 p1322 N94-19332
Numerical analysis of pressure meter tests: Application of parameter identification of soils behavior
[ECL-92-52] 04 p1487 N94-19380
Shock response of porous Al-2 + Fe2O3 powder mixtures
[DE93-018851] 05 p1688 N94-19944
Description and assessment of a new Optical Pressure Measurement System (OPMS) demonstrated in the high speed wind tunnel in Goettingen (Germany)
[DLR-FB-92-24] 05 p1651 N94-21280
Measurement Technology for Flight Tests
[ILR-MITT-256(1991)] 05 p1639 N94-22597
Free flight experiment with a laminar wing glove 05 p1639 N94-22600
Riblet boundary layer measurements of an A-310 fuselage with Pitot combs 05 p1640 N94-22605
Experimental Methods in Separated Flows
[ILR-MITT-260(1991)] 06 p2315 N94-22852
Pressure oscillation measurements in turbulent flows 06 p2316 N94-22855
The use of near-wall hot-wire probes for time-resolved skin-friction measurements 06 p2316 N94-22857
Probe shapes that measure time-averaged streamwise momentum and cross-stream turbulence intensity
[NASA-CASE-ARC-11934-1] 06 p2317 N94-23077
Probe systems for measuring static pressure and turbulence intensity in fluid streams
[NASA-CASE-ARC-11935-1] 06 p2319 N94-23306
Calibration of HYPULSE for hypervelocity air flows corresponding to flight Mach numbers 13.5, 15, and 17
[NASA-CR-191578] 06 p2192 N94-23564
Improved pressure measurement system for calibration of the NASA LeRC 10x10 supersonic wind tunnel
[NASA-TM-106470] 06 p2344 N94-24362
Experimental cavity pressure measurements at subsonic and transonic speeds. Static-pressure results
[NASA-TP-3358] 06 p2169 N94-24464
White-light, pressure, and temperature interferopolarimetric sensor featuring optical fibers
[PB93-199792] 06 p2545 N94-24631
Method and apparatus for the non-invasive measurement of pressure inside pipes using a fiber optic interferometer sensor
[AD-D016013] 06 p2344 N94-24734
Analysis of the effects of wake passage on heat transfer in a linear turbine cascade
[AD-A273729] 06 p2339 N94-25446
Theoretical and experimental investigation of converging cylindrical shock waves propagating in narrow cylindrical chambers
[ISBN-0-315-84694-1] 07 p2795 N94-27313
The cryogenic tunnel Cologne at DLR
[DLR-MITT-93-10] 07 p2681 N94-27587
Steady pressure measurements on an Aeroelastic Research Wing (ARW-2)
[NASA-TM-109046] 08 p3122 N94-28658
Micro-sensors for in-situ meteorological measurements 08 p3236 N94-29777

Analysis of fluctuating static pressure measurements in a large high Reynolds number transonic cryogenic wind tunnel 08 p3158 N94-30788

The execution of wind energy projects 1986 - 1992 between China Aerodynamics Research and Development Centre (CARDC) and The Aeronautical Research Institute of Sweden (FFA)
[FFA-TN-1993-19] 08 p3340 N94-30945

Research in marine boundary layer intermittency
[AD-A276076] 09 p3701 N94-31460

Development of a cascade simulation of fan-passage flow
[AD-A277234] 09 p3584 N94-32026

In flight measurement of steady and unsteady blade surface pressure of a single rotation large scale advanced prop-fan installed on the PTA aircraft
[NASA-CR-187096] 09 p3584 N94-32859

Simultaneous pressure measurement and high-speed photography study of cavitation in a dynamically loaded journal bearing
[NASA-TM-106456] 09 p3728 N94-32893

Measurement of the coolant channel temperatures and pressures of a cooled radial-inflow turbine
[NASA-TM-106594] 10 p3997 N94-33706

Guide to the measurement of the transient performance of aircraft turbine engines and components
[AD-280272] 10 p3997 N94-33874

Integral pressure sensor
[AD-D016188] 10 p4056 N94-34681

Flow quality studies of the NASA Lewis Research Center Icing Research Tunnel
[NASA-TM-106545] 10 p4010 N94-34919

Method for making a dynamic pressure sensor and a pressure sensor made according to the method
[NASA-CASE-LAR-14029-1] 11 p4269 N94-35369

Flight testing of a luminescent surface pressure sensor
[NASA-TM-103970] 11 p4189 N94-35394

Determination of extensional viscosity from capillary rheometer entrance pressure drop measurements using a numerical simulation of contraction flow
[PB94-171154] 11 p4263 N94-35603

Portable high precision pressure transducer system
[DE94-010137] 11 p4270 N94-36389

Experimental measurements and analytical analysis related to gas turbine heat transfer. Part 1: Time-averaged heat-flux and surface-pressure measurements on the vanes and blades of the SSME fuel-side turbine and comparison with prediction. Part 2: Phase-resolved surface-pressure and heat-flux measurements on the first blade of the SSME fuel-side turbine
[NASA-CR-196296] 12 p4442 N94-36969

Measurement uncertainty and feasibility study of a flush airdata system for a hypersonic flight experiment
[NASA-TM-4627] 12 p4383 N94-37378

Pressure-sensing performance of upright cylinders in a Mach 10 boundary-layer
[NASA-TM-4633] 12 p4383 N94-37395

PRESSURE MODULATOR RADIOMETERS

Modeling and data assimilation for Mars Observer 06 p2620 N94-24889

Optical Chopper Assembly for the Mars Observer 08 p3162 N94-29639

PRESSURE OSCILLATIONS

Establishing baseline data for an experimental appratus that measures heat transfer under conditions of oscillating pressure and flow
[NASA-CR-193772] 01 p0413 N94-12343

Calculation of turbulent boundary layer wall pressure spectra
[AD-A269549] 04 p1416 N94-18642

Correlation of incoming boundary layer pitot pressure fluctuations with the unsteadiness of fin-induced shock wave turbulent boundary layer interactions
[AD-A270059] 04 p1417 N94-18796

Relation between the fluctuating wall pressure and the turbulent structure of a boundary layer on a cylinder in axial flow
[AD-A270242] 04 p1418 N94-18906

Stability curves for a thermoacoustic prime mover
[AD-A272607] 05 p1968 N94-21422

Shear flow generation by Reynolds stress and suppression of resistive g-modes
[DE93-040911] 05 p1995 N94-21514

Pressure oscillation measurements in turbulent flows 06 p2316 N94-22855

Three-dimensional numerical simulation of thermal tides in the Martian atmosphere 06 p2622 N94-24901

Compressibility effects on rotor forces in the leakage path between a shrouded pump impeller and its housing 07 p2796 N94-27379

Flowfield dynamics in blunt fin-induced shock wave/turbulent boundary layer interactions
[NASA-CR-195170] 07 p2798 N94-27802

Wall pressure fluctuations in the reattachment region of a supersonic free shear layer
[NASA-CR-195790] 08 p3132 N94-29920

Shock impingement near mild hypersonic expansion corners 09 p3569 N94-31879

Vibrations of structures with cyclic symmetry: Application to the case of turbine engines 10 p4004 N94-34463

PRESSURE PROBES

U PRESSURE SENSORS

PRESSURE PULSES

Acousto-optical confirmation of the localized wave phenomena
[DE93-016425] 03 p1177 N94-16448

A probability method of fracture mechanics analysis for HFIR vessel
[DE93-015510] 04 p1453 N94-18246

Stress pulse phenomena
[DE93-019064] 04 p1456 N94-19078

Magnetic power piston fluid compressor
[NASA-CASE-GSC-13565-1] 06 p2354 N94-23831

PRESSURE RATIO

Rotordynamic and leakage characteristics of a 4-stage brush seal
[AD-A266012] 02 p0660 N94-12988

A comparison of computational and experimental data for a subscale high speed propulsive nozzle at low mach numbers
[AD-A266543] 02 p0504 N94-13705

Vane optimization for maximum efficiency using Design Of Experiments (DOX)
[AD-A270270] 04 p1320 N94-18907

Internal performance of a nonaxisymmetric nozzle with a rotating upper flap and a center-pivoted lower flap
[NASA-TP-3385] 05 p1637 N94-21569

Wake passage effects on the losses in a linear turbine cascade
[AD-A273794] 07 p2790 N94-25874

Influence of headwind on hot gas reingestion and consideration of pressure ratio scaling 07 p2675 N94-28018

Transitional flight characteristics of a geometrically simplified STOVL model 07 p2672 N94-28035

Evaluation of flip-flop jet nozzles for use as practical excitation devices
[NASA-TM-106377] 08 p3135 N94-30949

Advanced concepts for next generation small gas turbine engine compressors 10 p4001 N94-34443

Advanced small high pressure ratio centrifugal compressor 10 p4001 N94-34444

The centrifugal compressor, an essential component of small and medium power engines 10 p4001 N94-34445

Flow field analysis in a high pressure ratio centrifugal compressor 10 p4001 N94-34447

PRESSURE RECOVERY

Improving diffusing S-duct performance by secondary flow control
[NASA-TM-106492] 06 p2170 N94-25182

Results of a preliminary investigation of inlet unstart on a high-speed civil transport airplane concept 10 p3978 N94-33508

PRESSURE REDUCTION

Hypobaric decompression prebreathe requirements and breathing environment 01 p0317 N94-11541

Joint pain and Doppler-detectable bubbles in altitude (Hypobaric) decompression 01 p0312 N94-11542

Arterial gas emboli in altitude-induced decompression sickness 01 p0312 N94-11543

Transcranial Doppler ultrasound and the etiology of neurologic decompression sickness during altitude decompression 01 p0312 N94-11544

Risk of decompression sickness in the presence of circulating microbubbles 01 p0312 N94-11546

Strategies and methodologies to develop techniques for computer-assisted analysis of gas phase formation during altitude decompression 01 p0312 N94-11547

Autofrettage: Stress distribution under load and retained stresses after depressurization. A modified plane-strain case
[AD-A266320] 02 p0671 N94-13579

Effects of rotation on coolant passage heat transfer. Volume 2: Coolant passages with trips normal and skewed to the flow
[NASA-CR-4396-VOL-2] 03 p1023 N94-15991

Temperature lowering in cryogenic chemical-synthesis techniques and system
[DE93-018348] 04 p1562 N94-18810

Experimental and analytical study of cryogenic propellant boiloff to develop and verify alternate pressurization concepts for Space Shuttle external tank using a scaled down tank 06 p2266 N94-23657

Effects of crenulations on three dimensional losses in a linear compressor cascade
[AD-A273778] 07 p2790 N94-25862

Gravity dependence or pressure drop and heat transfer in straight two-phase heat transport system condenser ducts
[NLR-TP-92167-U] 07 p2798 N94-27853

Experimental investigation of jet-induced mixing of a large liquid hydrogen storage tank
[NASA-TM-106629] 10 p4044 N94-33607

Exercise with prebreathe appears to increase protection from decompression sickness: Preliminary findings 10 p4096 N94-33639

Determination of extensional viscosity from capillary rheometer entrance pressure drop measurements using a numerical simulation of contraction flow
[PB94-171154] 11 p4263 N94-35603

Cardiac pressure changes with venous gas embolism and decompression
[AD-A280412] 12 p4481 N94-37224

PRESSURE REGULATORS

A comparison between numerically modelled and experimentally measured loss mechanisms in wave rotors
[NASA-TM-106279] 01 p0029 N94-11255

A novel scheme to handle highly pulsed loads with a standard helium refrigerator
[DE93-019617] 05 p1799 N94-20263

Computer control of an electro-mechancial regulator for providing positive pressure breathing and an electronic G-valve for human +Gz research
[DCIEM-93-05] 06 p2437 N94-24299

The pressure loaded volumetric ceramic receiver 500 kW version design and construction
[DLR-MITT-93-02] 06 p2396 N94-25479

Determination of pressure response times for gaseous flow in a tube
[AD-A275274] 08 p3272 N94-29435

Measurand transient signal suppressor
[NASA-CASE-MSC-22027-1] 08 p3435 N94-29466

Dual valve plate two-way pressure relief valve
[AD-D016293] 12 p4452 N94-37766

PRESSURE RIDGES

U PRESSURE ICE

PRESSURE SENSORS

Combustion-induced crack propagation process in a solid-propellant crack cavity 01 p0098 N94-10901

A laboratory model of a hydrogen/oxygen engine for combustion and nozzle studies
[NASA-TM-106281] 01 p0047 N94-11252

Calculation of turbulent boundary layer wall pressure spectra
[AD-A269549] 04 p1416 N94-18642

Recent developments in fast response aerodynamic probe technology 04 p1431 N94-18645

Construction and evaluation of an environmental chamber for calibration of temperature and pressure sensors for laser interferometers
[PB93-197838] 04 p1322 N94-19332

Simulation of the behavior of micro-electronic capacitive pressure sensors
[LAAS-93190] 04 p1434 N94-19659

Description and assessment of a new Optical Pressure Measurement System (OPMS) demonstrated in the high speed wind tunnel in Goettingen (Germany)
[DLR-FB-92-24] 05 p1651 N94-21280

Experimental evaluation of oxygen-enriched air and emulsified fuels in a six-cylinder diesel engine
[DE94-000907] 05 p1811 N94-22391

Probe shapes that measure time-averaged streamwise momentum and cross-stream turbulence intensity
[NASA-CASE-ARC-11934-1] 06 p2317 N94-23077

Probe systems for measuring static pressure and turbulence intensity in fluid streams
[NASA-CASE-ARC-11935-1] 06 p2319 N94-23306

White-light, pressure, and temperature interferopolarimetric sensor featuring optical fibers
[PB93-199792] 06 p2545 N94-24631

Digital Altimeter Setting Indicator (DASI) Operational Test and Evaluation (OT/E) operational test procedures
[AD-A274100] 07 p2672 N94-26030

PVDF pressure transducers for shock wave and explosives research
[AD-A277319] 09 p3712 N94-32051

Measurement of the coolant channel temperatures and pressures of a cooled radial-inflow turbine
[NASA-TM-106594] 10 p3997 N94-33706

Bottom boundary layer stress measurements with BASS tripods: Data report STRESS 1988-1989
[AD-A277864] 10 p4092 N94-33775

Integral pressure sensor
[AD-D016188] 10 p4056 N94-34681

Method for making a dynamic pressure sensor and a pressure sensor made according to the method
[NASA-CASE-LAR-14029-1] 11 p4269 N94-35369

Flight testing of a luminescent surface pressure sensor
[NASA-TM-103970] 11 p4189 N94-35394

Portable high precision pressure transducer system
[DE94-010137] 11 p4270 N94-36389

PRESSURE SUITS
NT EXTRAVEHICULAR MOBILITY UNITS
NT SPACE SUITS
Motion and spatial disorientation systems: Special research capabilities
[AD-A265155] 01 p0303 N94-11097
Hypobaric decompression prebreathe requirements and breathing environment 01 p0317 N94-11541
Evaluation of the Retrograde Inflation Anti-G Suit (RIAGS)
[AD-A265884] 02 p0736 N94-12935
Aircrew/groundcrew life support systems research. Volume 1: CLIN 0001 research requirements
[AD-A268229] 03 p1139 N94-17563
Aircrew/groundcrew life support systems research. Volume 2: CLIN 0002 task order requirements
[AD-A268230] 03 p1139 N94-17564
System test results of the Advanced Technology Anti-G Suit (ATAGS)
[AD-A271535] 05 p1896 N94-20914
Aeromedical issues related to positive pressure breathing for +Gz protection
[AD-A274717] 07 p2910 N94-26435
A reliable and repeatable method for volume calculation of pressurized garments
[AD-A275600] 08 p3399 N94-28766
Comparative centrifuge evaluation of the Air Force Advanced Technology Anti-G Suit (ATAGS) and the Navy Enhanced Anti-G Lower Ensemble (EAGLE)
[AD-A275348] 08 p3400 N94-28996
Procedures and metrics for anti-G suit evaluations
[AD-A275349] 08 p3400 N94-28997
Decompression sickness risk versus time and altitude
[AD-A275261] 08 p3391 N94-29071
EVA glove evaluation methodology and test protocol
08 p3401 N94-29729
The US Navy/Canadian DCIEM research initiative on pressure breathing physiology 10 p4101 N94-33636
Evaluation of a liquid cooling garment as a component of the Launch and Entry Suit (LES)
10 p4101 N94-33653
Comparative performance of a modified Space Shuttle Reentry Anti-G Suit (REAGS) with and without pressure socks 10 p4101 N94-33655
Current and future issues in USAF full pressure suit research and development 10 p4102 N94-33656

PRESSURE TRANSDUCERS
U PRESSURE SENSORS

PRESSURE VESSEL DESIGN
A new and efficient way to join composite pipes
01 p0063 N94-10054

PRESSURE VESSELS
NT PREBURNERS
Design with high strength steel: A case of failure and its implications 01 p0058 N94-10017
Spin-rolling, welding, and heat treatment of aluminium 2219 for Ariane 5 GAM high pressure vessel liners
01 p0062 N94-10045
Heavy-section steel technology program
[DE93-009222] 01 p0184 N94-10155
Potential change in flaw geometry during pressurized-thermal-shock transients
[DE93-009709] 01 p0184 N94-10288
Autofrettage: Stress distribution under load and retained stresses after depressurization. A modified plane-strain case
[AD-A266320] 02 p0671 N94-13579
Fatigue design curves for 6061-T6 aluminum
[DE93-011849] 02 p0571 N94-14021
Estimation of strain in 1-kW primary containment vessels by microstructural examination
[DE93-013053] 02 p0573 N94-14316
Heavy section steel irradiation experiment
[DE93-015517] 02 p0573 N94-14537
Design of a cruciform bend specimen for determination of out-of-plane biaxial tensile stress effects on fracture toughness for shallow cracks
[DE93-015455] 03 p1059 N94-16104
Design of a fluid elastic actuator with application to structure control
[AD-A267649] 03 p0897 N94-17246
Effects of irradiation temperature on embrittlement of nuclear pressure vessel steels
[DE93-015428] 04 p1359 N94-18245
A probability method of fracture mechanics analysis for HFIR vessel
[DE93-015510] 04 p1453 N94-18246
Fluid-structure-interaction analyses of reactor vessel using improved hybrid Lagrangian Eulerian code ALICE-II
[DE93-015536] 04 p1409 N94-18248
Mechanism-dependent fractal character of fracture surfaces in high strength and toughness ASTM A723 steels
[AD-A268956] 04 p1360 N94-18542
Effects of irradiation temperature on Charpy and tensile properties of high-copper, low upper-shelf, submerged-arc welds
[DE93-017858] 04 p1445 N94-19047
Atom probe field ion microscopy characterizations of VVER steels
[DE93-017864] 05 p1689 N94-20180
A pressurized thermogravimetric analyzer for use in studies of gas/solid systems
[DE94-001224] 06 p2342 N94-22989
Dispersion of fire suppression agents discharged from high pressure vessels: Establishing initial/boundary conditions for the flow outside the vessel
[PB94-103660] 06 p2172 N94-23810
J-integral patch for finite element analysis of dynamic fracture due to impact of pressure vessels
06 p2381 N94-24429
Plasma initiation in a tokamak with conducting superstructure: First results from Alcator C-MOD
[DE94-001565] 06 p2552 N94-24504
Metal hydride storage
[VTT-JULK-769] 06 p2396 N94-25417
Strength and life of pressure vessels subjected to impacts and thermomechanical GFRP loading
[VTT-JULK-771] 06 p2379 N94-25418
Fracture Toughness Round Robin Test International in pressure tube materials
[DE93-634140] 07 p2837 N94-26265
The role of point defect clusters in reactor pressure vessel embrittlement
[DE94-001122] 07 p2739 N94-26931
A laboratory test on construction of ice domes and their load-carrying capacity 07 p2884 N94-27966
Single specimen fracture toughness determination procedure using instrumented impact test
[PB94-132040] 08 p3316 N94-28402
Experimental and analytical comparison of constraint effects due to biaxial loading and shallow-flaws
[DE94-004794] 08 p3323 N94-30689
Development of high-pressure diaphragms for the AEDC impulse tunnel
[AD-A277053] 09 p3588 N94-32009
Reactor pressure vessel structural integrity research in the US Nuclear Regulatory Commission HSST and HSSI Programs
[DE94-006550] 09 p3739 N94-32771
Integral pressure sensor
[AD-D016188] 10 p4056 N94-34681
Data compatibility for various Charpy-tests
[DE94-617534] 12 p4416 N94-37074

PRESSURE WAVES
U ELASTIC WAVES

PRESSURE WELDING
NT COLD WELDING
NT DIFFUSION WELDING

PRESSURIZED CABINS
Pressure wall patch
[NASA-CASE-MFS-28724-1] 06 p2203 N94-23824
Pressurized Lunar Rover (PLR)
07 p2833 N94-25704
Impact tests on fibre metal laminates under a tensile load
[PB94-126570] 07 p2710 N94-27201

PRESSURIZED WATER REACTORS
Potential change in flaw geometry during pressurized-thermal-shock transients
[DE93-009709] 01 p0184 N94-10288
Hydrogen pickup and redistribution in alpha-annealed zircaloy-4
[DE93-018050] 05 p1689 N94-20182

PRESSURIZING
NT FUEL TANK PRESSURIZATION
A finite strain ring dynamical model for pneumatic tires
[AD-A269286] 04 p1444 N94-18266
Thermodynamic models for bounding pressurant mass requirements of cryogenic tanks
[NASA-TM-106476] 06 p2346 N94-25202
Control experiments in liquid metal combustion
[AD-A276918] 09 p3635 N94-32234

PRESTON TUBES
U PITOT TUBES
U SPEED INDICATORS

PRESTRAINING
U PRESTRESSING

PRESTRESSING
Interpretation of warm prestress-induced fracture toughness based on crack-tip constraint
[DE93-015967] 04 p1451 N94-17913
Process and apparatus for the release of a prestress initially applied to a mechanism such as a bearing on board a space vehicle
[CA-PATENT-APPL-SN-2,020,909]
05 p1824 N94-21142
Jumper connector analysis
[DE94-010373] 12 p4451 N94-37188

PRETESTS
U TESTS

PRETREATMENT
NT PRESTRESSING
Microbiological test results using three urine pretreatment regimes with 316L stainless steel
[NASA-CR-192568] 01 p0299 N94-10360
Assessment of chromate and non-chromate conversion coatings for Al alloys using electrochemical impedance spectroscopy
[AD-A267205] 03 p0965 N94-15859
Wound healing after laser injury to skin: The effect of occlusion and vitamin E
[AD-A266473] 03 p1128 N94-16779
The c-jun gene expression in human cells exposed to either ionizing radiation or hydrogen peroxide
[DE93-017436] 04 p1502 N94-18476
Monocrystalline germanium film on sapphire
[AD-D015925] 05 p2017 N94-20348
Technology development for iron Fischer-Tropsch catalysts
[DE94-008723] 09 p3638 N94-32889
Evaluation of the Hughes conversion coating touch-up pen
[AD-A278398] 09 p3664 N94-33166
Thermal-oxidative pretreatment and evaluation of poly (hexafluoropropene oxide) fluids
[NASA-TM-106659] 12 p4424 N94-37300

PRETWISTING
U PRESTRESSING

PREVENTION
NT ACCIDENT PREVENTION
NT CORROSION PREVENTION
NT FIRE PREVENTION
NT ICE PREVENTION
A tentative plan on China and Asian-Pacific satellite system for disaster reduction 02 p0693 N94-14247
Legionella: An overview 03 p1126 N94-16629
Primary prevention of coronary heart disease
06 p2423 N94-23317
Waste minimization/pollution prevention at R/D facilities: A cradle-to-grave tracking and information system that will be implemented at Sandia National Laboratories
[DE93-040330] 06 p2591 N94-24607
Application of remote sensing in prevention of disasters 08 p3332 N94-29230
Occurrence of sub-synchronous vibration in a multistage turbine pump and its prevention
10 p4064 N94-34189

PRIMARY BATTERIES
NT ALKALINE BATTERIES
NT METAL AIR BATTERIES
NT NICKEL ZINC BATTERIES
NT SODIUM SULFUR BATTERIES
NT THERMAL BATTERIES

PRIMARY COSMIC RAYS
NT SOLAR COSMIC RAYS
Investigation of the relative abundance of heavy versus light nuclei in primary cosmic rays using underground muon bundles
[DE93-017601] 04 p1630 N94-17818
Measurement of the energy of horizontal cosmic ray muons
[KFK-5163] 04 p1631 N94-19505

PRIMATES
NT BABOONS
NT HUMAN BEINGS
NT MONKEYS
Localization of figure background segregation mechanisms in primate visual cortex
[PB93-187961] 04 p1508 N94-18121
Cortical substrate of haptic representation
[AD-A269583] 04 p1508 N94-18304

PRIMERS
Polyurethane self-priming topcoats
[AD-D016160] 10 p4030 N94-34285

PRIMERS (COATINGS)
Evaluation of inorganic zinc-rich primers using Electrochemical Impedance Spectroscopy (EIS)
06 p2237 N94-23233
Development of a unique polyurethane primer/topcoat
08 p3223 N94-30476
Dual cure low-VOC coating process
[DE94-009346] 11 p4245 N94-35809

PRIMITIVE EARTH ATMOSPHERE
Earth's partial pressure of CO2 over the past 100-500 Ma; evidence from Ce anomalies in mostly shallow seas (less than 200 m) as recorded in carbonate sediments, 2
03 p1104 N94-16360

PRIMITIVE EQUATIONS
An efficient data assimilation algorithm with a gaussian covariance structure
[AD-A273152] 06 p2418 N94-24671
A diagnostic model to estimate winds and small-scale drag from Mars Observer PMIRR data
06 p2617 N94-24874
The influence of orography on the transport of atmospheric constituents 06 p2619 N94-24886
Modeling studies of frontogenesis in the upper and middle troposphere 08 p3375 N94-30868
PRINCIPAL COMPONENTS ANALYSIS
A consideration on principal component analysis of satellite IR data 01 p0193 N94-11909
Fourier domain target transformation analysis in the thermal infrared 01 p0258 N94-12030
Spatiotemporal variability of non-urban ozone concentrations over the eastern United States and its potential replication by satellite data
[PB93-191328] 04 p1476 N94-19065
Nonlinear PCA: Algorithms and applications
[PB94-137544] 08 p3419 N94-29680
Principal component analysis with missing data and its application to object modeling
[AD-A276644] 09 p3845 N94-31939
Airborne SAR as a complement to SPOT HRV in land-cover classification: The use of normalization and principal components analysis 09 p3750 N94-32539
Statistical intercomparison of global climate models: A common principal component approach
[DE94-008671] 09 p3768 N94-32882
Evaluation of the IHS transformation use on the integration of geophysical (aeromagnetometry) and remote sensing (TM-Landsat) data for the geological investigation in the Pojuca area (Serra dos Carajas, PA)
[INPE-5532-TDI/521] 10 p4077 N94-34223
PRINTED CIRCUITS
Radiation hardness of Mo/Si multilayers designed for use in a soft x ray projection lithography system
[DE93-011879] 01 p0143 N94-11273
Solderability of surface mount devices
[AD-A265751] 02 p0620 N94-13040
Rigid-flexible printed wiring boards
[DE93-013938] 02 p0620 N94-13094
Development of alternatives to lead-bearing solders
[DE93-016509] 04 p1357 N94-17862
Solderability perservative coatings: Electroless tin versus organic azoles
[DE93-017634] 04 p1370 N94-18477
Solder technology in the manufacturing of electronic products
[DE93-018842] 05 p1699 N94-19960
A comparative study between shielded and open coplanar waveguide discontinuities
05 p1733 N94-20501
Computer-Aided Test Equipment Graphics System (CATEGS)
[DE94-000383] 05 p1915 N94-21561
Process characterization and control of hand-soldered printed wiring assemblies
[DE93-041290] 05 p1763 N94-21652
CADBIT 2: Computer-aided design for built-in test, volume 1
[AD-A273702] 06 p2463 N94-25455
CADBIT 2: Computer-aided design for built-in test, volume 2
[AD-A273703] 06 p2463 N94-25456
Aspects of the circuit board thermal design
[VTT-PUBS-132] 07 p2779 N94-25644
Test methods and custom hardware for functional testing of a high speed GaAs DRAM
[AD-A274859] 07 p2781 N94-26175
Phase conjugated lasers applied to commercial x ray lithography
[DE94-001529] 07 p2819 N94-27018
Baseline for a Nordtest method. Reliability stress screening of components. A guide for component users
[PB94-123775] 07 p2835 N94-27042
Printed circuit elements with applications to antennas, scattering, and circuits
[AD-A275512] 08 p3262 N94-28669
Screening of flexible cables by nonlinear resistance measurements
[AD-A275193] 08 p3264 N94-29289
Controlled thermal expansion printed wiring boards based on liquid crystal polymer dielectrics
[NASA-CR-189338] 08 p3287 N94-29400
From display and PWB to MCMs: Large panel manufacturing
[DE94-007855] 09 p3693 N94-32386
An electrical test system for conductor formation process analysis
[DE94-007291] 09 p3696 N94-32786
Space flight printed wiring board measling investigation
[NASA-TM-104602] 09 p3732 N94-33101
SpaceHab 1 maintenance experiment
10 p4015 N94-33669
Manufacturing feasibility of several lead-free solders for electronic assembly
[DE94-007732] 11 p4258 N94-35564
Ionic contamination detection
[DE94-010212] 11 p4258 N94-35686
Capillary flow solderability test for printed wiring boards
[DE94-010321] 11 p4259 N94-36094
Laser drilling of printed wiring boards: Sandia LDRD program
[DE94-011004] 12 p4448 N94-37198
Selected case studies in modeling and simulation applied to environmentally conscious design and manufacturing
[DE94-007556] 12 p4466 N94-37389
PRINTERS
Human factors involvement in bringing the power of AI to a heterogeneous user population
10 p4110 N94-33633
PRINTING
NT LITHOGRAPHY
NT PHOTOLITHOGRAPHY
Electronic publishing and intelligent information retrieval 05 p2047 N94-22479
NASA printing, duplicating, and copying management handbook
[NASA-NHB-1490.5] 06 p2590 N94-23971
Development of an industrial CO2 laser for mask marking
[DE93-632901] 07 p2816 N94-26184
Fundamentals of printing technology
[PB94-132602] 08 p3530 N94-29141
Electronic document interchange
12 p4541 N94-36848
PRIORITIES
Chairmanship of the Neptune/Pluto outer planets science working group
[NASA-CR-194625] 03 p1297 N94-16832
A real-time executive implementing priority inheritance protocols 07 p2952 N94-26733
Risk-based prioritization: A comparison of approaches
[DE94-003368] 08 p3526 N94-28474
Probabilities and priorities in timed CSP
[PB94-169216] 11 p4316 N94-35536
Priorities and nonmonotonic reasoning
[PB94-171170] 11 p4346 N94-35959
Science priorities for the human dimensions of global change 12 p4464 N94-36987
Standards for data and document interchange
12 p4543 N94-37337
PRISMS
Three short articles from Japanese laser journal
[AD-A268249] 03 p1042 N94-17415
Metal Film Surface Plasmon Resonance (MFSPR) fibre couplers
[AD-A268871] 04 p1579 N94-18635
Precision prism coupling setup applied to measure planar silica films on silicon, appendix 9
05 p1989 N94-21603
Three-stage attenuation using Glan-Thompson prisms
[AD-A280481] 12 p4525 N94-37350
PRIVACY
NASA security handbook
[NHB-1620.3C] 03 p1224 N94-15937
Securing electronic mail: The risks and future of electronic mail
[DE93-017187] 04 p1383 N94-17994
Management of PEM public key certificates using X.500 directory service: Some problems and solutions
[DE94-004200] 08 p3431 N94-29952
PEM public key certificate cache server
[DE94-006404] 09 p3675 N94-31784
PRIVATE AIRCRAFT
U GENERAL AVIATION AIRCRAFT
PROBABILITY
U PROBABILITY THEORY
PROBABILITY DENSITY FUNCTIONS
NT NORMAL DENSITY FUNCTIONS
NT PEARSON DISTRIBUTIONS
NT RAYLEIGH DISTRIBUTION
NT WEIBULL DENSITY FUNCTIONS
Probabilistic evaluation of uncertainties and risks in aerospace components
[NASA-TM-105603] 01 p0185 N94-10361
Probability density distribution of velocity differences at high Reynolds numbers 01 p0158 N94-12304
PDF approach for turbulent scalar field: Some recent developments 01 p0160 N94-12315
Numerical studies of spray combustion in liquid-fueled engines 02 p0564 N94-13685
A new method for generating Bayes classifiers assuming mixtures of Gaussian densities
[FFI-91/4029] 03 p1172 N94-15298
On the use of the noncentral chi-square density function for the distribution of helicopter spectral estimates
[NASA-CR-191546] 03 p1176 N94-15487
Expansions of cumulative distribution functions directly from characteristic functions
[AD-A267727] 03 p1173 N94-17372
A Bayesian approach to contaminant plume delineation
[DE93-012909] 04 p1472 N94-17890
Polarimetric statistics of electromagnetic waves scattered by distributed targets
[PB93-195907] 04 p1389 N94-18951
Quantification of uncertainties in the performance of smart composite structures
[NASA-TM-106335] 05 p1830 N94-20171
Interpolative modeling of GaAs FET S-parameter data bases for use in Monte Carlo simulations
05 p1767 N94-21723
Evaluation of a nonlinear method for the enhancement of tonal signal detection
[NASA-CR-191562] 05 p1968 N94-21741
Numerical solutions of the complete Navier-Stokes equations
[NASA-CR-194780] 06 p2337 N94-24858
Probabilistic assessment of smart composite structures
[NASA-TM-106358] 06 p2378 N94-25188
The deterministic power-spectral-density method
[AD-B175894] 07 p2678 N94-27395
Estimators for the Cauchy distribution
[DE94-004990] 07 p3005 N94-27816
Ten new checks to assess the statistical quality of Monte Carlo solutions in MCNP
[DE94-006137] 08 p3465 N94-30366
Detection of a chi-square fluctuating target in Gaussian noise
[AD-A276078] 09 p3850 N94-31462
Mixture model simulating reactive turbulent flows: Testing of Eulerian-Lagrangian probabilistic models
[ONERA-NT-1993-13] 09 p3702 N94-31477
Diagonal band probability distributions
[REPT-93-80] 09 p3851 N94-31697
A non-local model for prediction of the probability density function of turbulent fluctuations in boundary-layer flows
09 p3706 N94-32076
High-performance speech recognition using consistency modeling
[AD-A276775] 09 p3679 N94-32185
Comparison of PDF and moment closure methods in the modeling of turbulent reacting flows
[NASA-TM-106614] 11 p4265 N94-35948
PROBABILITY DISTRIBUTION FUNCTIONS
Bayesian reliability analysis with imprecise prior probabilities
[MEMO-COSOR-92-50] 01 p0183 N94-10170
Probabilistic evaluation of uncertainties and risks in aerospace components
[NASA-TM-105603] 01 p0185 N94-10361
Imprecise highest density regions related to intervals of measures
[MEMO-COSOR-92-54] 01 p0347 N94-10876
Stochastic bounds for a polling system
[CWI-BS-R9230] 02 p0765 N94-14361
Distributional inferences for a location parameter
[W-9219] 02 p0774 N94-14545
The distribution of a sum of binomial random variables
[AD-A266969] 03 p1172 N94-15002
Expansions of cumulative distribution functions directly from characteristic functions
[AD-A267727] 03 p1173 N94-17372
EDF tests for normality in linear models after a Box-Cox transformation
[AD-A269068] 04 p1557 N94-18517
Learning control of large-scale systems
[MATHS-REPT-A-186] 04 p1544 N94-19408
Current directions in the vulnerability/lethality process structure
[AD-A272836] 05 p1964 N94-21175
Detailed analysis case studies of trapped plasmas at the Earth's magnetic equator
[AD-A272497] 05 p1858 N94-21432
Mobile robot perception in unknown and unstructured dynamic voxel environments
[ISBN-0-315-83951-1] 05 p1947 N94-22591
Characterizations of shift-invariant distributions based on summation modulo one
[PB93-237824] 06 p2481 N94-23442
Simulation approaches for calculations in directed graphical models
[AD-A274825] 07 p3003 N94-26494
A comparison of Probability Of Detection (POD) data determined using different statistical methods
[LTR-ST-1947] 07 p2835 N94-26644
A moment plotting method for characterizing aircraft fatigue data population distributions
[AD-A275500] 08 p3145 N94-28660

A family of joint probability models for cost and schedule uncertainties
[AD-A275513] 08 p3463 N94-28670
A method for the probabilistic design assessment of composite structures
[NASA-TM-106384] 08 p3319 N94-29384
Rocket engine system reliability analyses using probabilistic and fuzzy logic techniques
[NASA-TM-106519] 08 p3173 N94-29403
Pearl's belief propagation: The proofs
[RUU-CS-92-47] 08 p3456 N94-30378
Diagonal band probability distributions
[REPT-93-80] 09 p3851 N94-31697
Probability distributions with given marginals and given correlation that have maximal entropy
[REPT-93-81] 09 p3851 N94-31698
On the relationship between generalization error, hypothesis complexity, and sample complexity for radial basis functions
[AD-A276802] 09 p3851 N94-32142
The use of L-moments to fit the generalized lambda distribution to sample data
[AD-A278549] 10 p4130 N94-33678

PROBABILITY THEORY
Applications of cut polyhedra
[CWI-BS-R9221] 01 p0347 N94-10354
Singularity spectrum of self-organized criticality
[DE93-613820] 01 p0348 N94-10404
Positive phase space distributions and uncertainty relations 01 p0379 N94-10598
Wavelets and spacetime squeeze 01 p0379 N94-10604
Wave and pseudo-diffusion equations from squeezed states 01 p0347 N94-10607
Probability of particle trapping/detrapping in torsatrons
[DE93-621641] 01 p0390 N94-11121
Probability of alamethicin conductance states varies with nonlamellar tendency of bilayer phospholipids
[AD-A264957] 01 p0301 N94-11648
Applications of multivariate analysis
[AD-A265250] 01 p0347 N94-11882
Collisions of small Spacewatch asteroids with the Earth 01 p0430 N94-12157
Efficient dynamic optimization of logic programs
[NASA-TM-109251] 02 p0761 N94-12889
Rare attributes in finite universe: Hypotheses testing specification and exact randomized upper confidence bounds
[DE93-012783] 02 p0775 N94-12955
A probabilistic method for the buckling assessment of stiffened composite shells
[NASA-TM-106286] 02 p0671 N94-13379
An improved approach for flight readiness certification: Methodology for failure risk assessment and application examples, volume 1
[NASA-CR-194498] 02 p0542 N94-14076
An improved approach for flight readiness certification: Methodology for failure risk assessment and application examples. Volume 2: Software documentation
[NASA-CR-194499] 02 p0542 N94-14077
An improved approach for flight readiness certification: Methodology for failure risk assessment and application examples. Volume 3: Structure and listing of programs
[NASA-CR-194500] 02 p0542 N94-14078
Computational problems with the binomial failure rate model and incomplete common cause failure reliability data
[DE93-014346] 02 p0669 N94-14143
A model for fuel fire duration and application to the B-1B bomber
[DE93-013000] 02 p0512 N94-14292
Self organized criticality
[DE93-013182] 02 p0773 N94-14320
Probabilistic micromechanics for high-temperature composites
[NASA-CR-191150] 02 p0676 N94-14408
Distributional inferences for a location parameter
[W-9219] 02 p0774 N94-14545
An improved approach for flight readiness certification: Probabilistic models for flaw propagation and turbine blade failure. Volume 1: Methodology and applications
[NASA-CR-194496] 02 p0519 N94-14841
An improved approach for flight readiness certification: Probabilistic models for flaw propagation and turbine blade failure. Volume 2: Software documentation
[NASA-CR-194497] 02 p0519 N94-14842
Statistical computation of tolerance limits
[NASA-TM-108424] 03 p1172 N94-15535
Logarithmic asymptotics for steady-state tail probabilities in a single-server queue
[AD-A266746] 03 p1165 N94-15775
The cooling of confined ions driven by laser beams
[DE93-016612] 03 p1039 N94-16114
Combinatorial semantics
[TR-444] 03 p1149 N94-16575
Set-based Bayesianism
[TR-407] 03 p1170 N94-16582
Discovering sequence similarity by the algorithmic significance method
[DE93-015556] 03 p1150 N94-16659
Nonlinear methods for communications
[AD-A267376] 03 p1001 N94-17019
Statistics of the half-integer stopband
[DE93-016101] 03 p1173 N94-17236
High order nonlinear estimation with signal processing applications
[AD-A268407] 03 p1005 N94-17463
Mathematical Sciences Division 1992 programs
[AD-A268586] 03 p1140 N94-17623
Kinetic growth of random-like and ballistic-like deposition models
[DE93-624946] 04 p1595 N94-17956
An empirical evaluation of five circular error probable estimation techniques and a method for improving them
[AD-A266528] 04 p1556 N94-18397
Software reliability: Estimation and prediction
[AD-A268895] 04 p1521 N94-18458
The rank of the present excursion
[REPT-93-22] 04 p1558 N94-19137
A simple calculus of finite probabilistic processes
[MEMO-INF-93-08] 04 p1558 N94-19195
Bahadur-Kiefer theorem beyond the largest observation
[PB93-197473] 04 p1558 N94-19325
Bounds for expected loss in Bayesian decision theory with imprecise prior probabilities
[PB93-197507] 04 p1558 N94-19327
A language of finite probabilistic processes and its interleaving semantics
[MEMO-INF-93-24] 04 p1558 N94-19354
Adaptive uniformization
[MEMO-INF-92-88] 04 p1558 N94-19385
Fault-tolerance and complexity
[TR-450] 04 p1530 N94-19483
Statistical probabilities for planning
[TR-474] 04 p1559 N94-19511
Uncertainty versus interindividual variability
[DE93-018105] 04 p1559 N94-19549
Problems in probability, statistics and reliability
[AD-A270830] 04 p1559 N94-19595
Equivalence and reduction of hidden Markov models
[AD-A270762] 04 p1560 N94-19768
Some topics in regenerative steady-state simulation
[AD-A271145] 05 p1902 N94-19855
Worldwide frequency of temperatures at selected altitudes
[AD-A271111] 05 p1864 N94-19908
SIMBAT theoretical manual
[AD-A271063] 05 p1882 N94-19979
Multi-disciplinary coupling effects for integrated design of propulsion systems
[NASA-TM-106349] 05 p1830 N94-20170
Quantification of uncertainties in the performance of smart composite structures
[NASA-TM-106335] 05 p1830 N94-20171
Electronic neural network for solving traveling salesman and similar global optimization problems
[NASA-CASE-NPO-17807-2-CU] 05 p1942 N94-20360
Believing in the basis of the evidence
[TR-438] 05 p2039 N94-20364
The effect of dissipative inhomogeneous medium on the statistics of the wave intensity 05 p1726 N94-20440
Development and testing of a reliability performance index for modular robotic systems
[AD-A271901] 05 p1942 N94-20488
The quantum efficiency of HgCdTe photodiodes in relation to the direction of illumination and to their geometry 05 p1735 N94-20512
Closure properties of stochastic languages
[TR-441] 05 p1907 N94-20521
Explanation closure, action closure, and the Sandewall test suite for reasoning about change
[TR-440] 05 p1907 N94-20522
Signal processing in the linear statistical model
[AD-A272114] 05 p1736 N94-20570
Probability of detection calculations using MATLAB
[AD-A271958] 05 p1736 N94-20578
Current directions in the vulnerability/lethality process structure
[AD-A272836] 05 p1964 N94-21175
Space-efficient deterministic simulation of probabilistic automata
[TR-463] 05 p1900 N94-21281
Threshold computation and cryptographic security
[TR-461] 05 p1912 N94-21285
Promises and fault-tolerant database access
[TR-447] 05 p2043 N94-21287
Computing with Bayesian multi-networks
[AD-A273106] 05 p1914 N94-21501
A methodology for quantifying uncertainty in models
[DE93-040154] 05 p1916 N94-21747
Probabilistic assessment of composite structures
[NASA-TM-106368] 05 p1832 N94-21757
A simulation model for probabilistic analysis of Space Shuttle abort modes
[NASA-TM-108432] 05 p1656 N94-21859
On some approximately balanced combinatorial cooperative games
[MEMO-1113] 06 p2493 N94-22702
Probabilistic analysis of mechanical systems
[DE93-041145] 06 p2371 N94-22918
Simple calculus of finite probabilistic processes
[PB93-223782] 06 p2493 N94-23108
Application of maximum entropy and irreducible cluster integrals to joint probability distributions for x ray structure determination
[PB93-224152] 06 p2559 N94-23109
On non-informativeness in a classical Bayesian inference problem
[MEMO-COSOR-92-35] 06 p2494 N94-23143
Review of the probabilistic failure analysis methodology and other probabilistic approaches for application in aerospace structural design
[NASA-TP-3434] 06 p2376 N94-23342
Bayesian decision theory with imprecise prior probabilities applied to replacement problems
[PB93-237634] 06 p2481 N94-23456
Development and application of an empirical probability distribution for the prediction error of re-entry body maximum dynamic pressure 06 p2207 N94-23653
Mean-value of product-form stochastic Petri net models of slotted-ring systems
[PB94-110871] 06 p2494 N94-23749
Logarithm of probability measures and infinite divisibility of sub-stable random vectors
[PB94-118627] 06 p2486 N94-23758
Decision making with imprecise probabilities
[PB94-111622] 06 p2494 N94-23772
Asymptotic confidence intervals for the length of the shortt under random censoring
[PB93-237816] 06 p2494 N94-23774
Subset selection with a generalized selection goal based on a loss function
[PB94-111192] 06 p2494 N94-23798
Some generalized subset selection procedures
[PB94-111655] 06 p2487 N94-23799
Specifying design conservatism: Worst case versus probabilistic analysis 06 p2374 N94-23939
Probabilistic simulation of concurrent engineering of propulsion systems 06 p2177 N94-24317
Uniform limit theorems for marked point processes
[PB94-118726] 06 p2488 N94-24526
Integral equations for the microstructures of supercritical fluids
[DE94-002460] 06 p2535 N94-24569
Probabilistic methods in problems of applied analysis
[PB94-110681] 06 p2495 N94-24571
Mitigation of EMI/RFI produced by a 1.2 kW uninterruptible power supply
[AD-A273149] 06 p2299 N94-24670
Topics in probability and dynamics
[AD-A273543] 06 p2496 N94-24931
Infinitely divisible processes and their nonlinear functionals; a study of their structural, statistical and sample path properties and their prediction problems
[AD-A273468] 06 p2496 N94-25147
Solving the ranking and selection indifference-zone formulation for normal distributions using computer software
[AD-A273821] 06 p2496 N94-25518
Proficiency scaling based on conditional probability functions for attributes
[AD-A273816] 07 p3002 N94-25962
Multiple model adaptive estimation applied to the LAMBDA URV for failure detection and identification
[AD-A274078] 07 p3002 N94-25992
A doubly logarithmic communication algorithm for the Completely Connected Optical Communication Parallel Computer
[DE93-019408] 07 p2980 N94-26473
Probabilistic methods for image generation and encoding
[AD-A274294] 07 p2964 N94-26682
Probability of accessing the multiple saturated states in the resistive interchange instability
[DE94-000478] 07 p3044 N94-26694
Short-range cloud amount forecasting with model output statistics
[AD-A274769] 07 p2895 N94-26798
Topological conditions for the existence of invariant measures for unimodal maps
[PB94-123296] 07 p2849 N94-26866
Modeling systems by probabilistic process algebra: An event structures approach
[PB94-125259] 07 p3004 N94-26867

Recursive bundle event structures
[PB94-125275] 07 p3004 N94-26870
Blurred focal elements generalization of dempster's rule
[PB94-124278] 07 p2986 N94-26992
A superprocess with a disappearing self-interaction
[AD-A274647] 07 p3009 N94-27108
Interdisciplinary technology 07 p2686 N94-27363
The Fermi paradox: An approach based on percolation theory 07 p2687 N94-27370
Is probability of frequency too narrow?
[DE94-000687] 07 p3004 N94-27612
Estimators for the Cauchy distribution
[DE94-004990] 07 p3005 N94-27816
Risk-based prioritization: A comparison of approaches
[DE94-003368] 08 p3526 N94-28474
Identification of components to optimize improvement in system reliability
[DE94-001601] 08 p3315 N94-28503
A family of joint probability models for cost and schedule uncertainties
[AD-A275513] 08 p3463 N94-28670
Markov chains for random urinalysis 3: Daily model and drug kinetics
[AD-A275540] 08 p3389 N94-28797
The effects of molecular orientation geometry and surface anisotropy upon etching
[AD-A275154] 08 p3486 N94-29032
Stability of dynamical systems in the presence of noise
[AD-A275383] 08 p3243 N94-29072
Boundary layer coherent structures
[AD-A275007] 08 p3272 N94-29195
A method for the probabilistic design assessment of composite structures
[NASA-TM-106384] 08 p3319 N94-29384
Conditional dependence in probabilistic networks
[RUU-CS-92-34] 08 p3464 N94-29450
Reliability of composite material structures. Application: High pressure spherical coded tanks
[REPT-932-430-103] 08 p3180 N94-29478
Comparison of Savannah River Site's meteorological databases
[DE94-001751] 08 p3373 N94-29817
Risk measures in living probabilistic safety assessment
[VTT-PUBS-146] 08 p3465 N94-30154
Vulnerability of manned spacecraft to crew loss from orbital debris penetration
[NASA-TM-108452] 08 p3169 N94-30161
Bayesian belief networks and conditional independencies
[RUU-CS-92-36] 08 p3465 N94-30376
A probabilistic approach to motion planning for car-like robots
[RUU-CS-93-18] 08 p3438 N94-30410
Modeling systems by probabilistic process algebra: An event structures approach
[MEMO-INF-93-29-REV] 08 p3425 N94-30416
Thermodynamics of computation and information distance
[CWI-CS-R9341] 08 p3526 N94-30433
A probabilistic view of Datalog parallelization
[TELECOM-93-D-021] 09 p3824 N94-31183
Study of B(0) - bar-B(0) mixing in D0
[DE94-006000] 09 p3897 N94-31506
The Laplace functional and Palm measure of a quasi-Cox process which is driven by a Markov chain
[REPT-93-82] 09 p3851 N94-31699
Performance metrics for low probability of intercept-communication system
[AD-A277346] 09 p3677 N94-32073
High-performance speech recognition using consistency modeling
[AD-A276775] 09 p3679 N94-32185
Multiserver queues with impatient customers
[CWI-BS-R9319] 09 p3835 N94-32198
An algorithm for probabilistic, totally-ordered temporal projection
[AD-A277341] 09 p3817 N94-32257
Structural probability concepts adapted to electrical engineering
[NASA-TM-106499] 09 p3739 N94-32735
Aspects of modeling uncertainty and prediction
[DE94-007565] 09 p3852 N94-32744
Visual processing of object velocity and acceleration
[AD-A277425] 09 p3801 N94-32998
Resonance capture in unbalanced dual-spin spacecraft
[AD-A278501] 10 p4015 N94-34292
Identification of mechanical systems using probabilistic neural networks
[DE94-007555] 10 p4114 N94-34296
Assessment of in-service aircraft fatigue monitoring process 10 p3996 N94-34593
Probabilities and priorities in timed CSP
[PB94-169216] 11 p4316 N94-35536
Point and interval estimation of series system reliability using small data sets
[AD-A278647] 11 p4316 N94-35575
Integral characteristics of the magnetic bremsstrahlung
[DE94-616788] 11 p4256 N94-36078
High energy
[DE94-009477] 11 p4331 N94-36428
Probability-based inference in cognitive diagnosis
[AD-A280553] 12 p4506 N94-36732
Virtual representation of IID observations in Bayesian belief networks
[AD-A280552] 12 p4507 N94-37046
Statistical characterization of rare events 12 p4454 N94-37327
Probability techniques for reliability analysis of composite materials
[NASA-CR-195294] 12 p4406 N94-37633
Probabilistic assessment of space nuclear propulsion system nozzle
[NASA-TM-106539] 12 p4457 N94-37704

PROBES
Numerical modeling of fringing fields and their use for complex permittivity measurements at high frequencies
[AD-A270478] 05 p1966 N94-19917
Laser probing of interfaces
[DE94-011300] 12 p4449 N94-37628

PROBLEM SOLVING
NT ALTERNATING DIRECTION IMPLICIT METHODS
NT ASYMPTOTIC METHODS
NT ITERATIVE SOLUTION
NT THEOREM PROVING
A real-time spoken-language system for interactive problem solving
[AD-A266046] 01 p0324 N94-11104
Criteria for assessing problem solving and decision making in complex environments 01 p0314 N94-11532
Design, development, and testing of an automated knowledge-acquisition tool to aid problem solving, decision making, and planning
[DE93-010239] 01 p0417 N94-11661
Problem specific environments for parallel systems
[AD-A266129] 01 p0337 N94-12540
The effects of evaluation and production blocking on the performance of brainstorming groups
[AD-A265495] 02 p0734 N94-12929
Application of symbolic and algebraic manipulation software in solving applied mechanics problems
[NASA-CR-4544] 02 p0596 N94-13798
An experimental analysis of bottleneck-centered opportunistic scheduling
[AD-A266643] 02 p0820 N94-14796
Generating knight's tours without backtracking from errors
[AD-A266807] 02 p0772 N94-14900
HSTS: Integrating planning and scheduling
[AD-A266991] 03 p1222 N94-15213
Representation in incremental learning
[NASA-CR-194595] 03 p1221 N94-15719
Module interconnection frameworks for a real-time spreadsheet
[AD-A267317] 03 p1153 N94-17220
Design and diagnosis problem solving with multifunctional technical knowledge bases
[AD-A268375] 03 p1234 N94-17419
A method for cognitive task analysis
[IZF-1992-B5] 04 p1508 N94-17967
Why are human-computer interfaces difficult to design and implement?
[AD-A268843] 04 p1514 N94-18317
On masking effect
[AD-A269593] 04 p1541 N94-18462
Towards versatile and practical knowledge acquisition
[AD-A269596] 04 p1615 N94-18464
Efficient domain-independent experimentation
[AD-A269530] 04 p1557 N94-18640
Putting knowledge to use: The acquisition and transfer of knowledge in situated problem solving environments
[AD-A269746] 04 p1509 N94-18744
Automatically generating abstractions for planning
[AD-A269772] 04 p1541 N94-18759
Neutral networks: An NRL perspective
[AD-A269122] 04 p1541 N94-18773
Adaptive uniformization
[MEMO-INF-92-88] 04 p1558 N94-19385
Problems in probability, statistics and reliability
[AD-A270830] 04 p1559 N94-19595
A real-time spoken-language system for interactive problem-solving, combining linguistic and statistical technology for improved spoken language understanding
[AD-A270901] 04 p1392 N94-19749
Electronic neural network for solving traveling salesman and similar global optimization problems
[NASA-CASE-NPO-17807-2-CU] 05 p1942 N94-20360
Neural network studies
[AD-A271593] 05 p1943 N94-20947
An NP set with no co-DP sparse subset
[TR-475] 05 p1954 N94-21199
The combinatorial algorithms for large scale discrete optimization problems 05 p1923 N94-22079
On the discovery of approximate arithmetic relations by backpropagation networks 05 p1782 N94-22181
Framework for interactive solving of meta-constraint satisfaction problems
[PB94-118825] 06 p2585 N94-23761
Design and specification of a generic task model for solving boolean constraint satisfaction problems
[PB94-118841] 06 p2486 N94-23762
Two applications of a generic task model for solving boolean constraint satisfaction problems
[PB94-119047] 06 p2487 N94-23765
Egalitarian non-average contribution method for cooperative games
[PB94-111705] 06 p2497 N94-23800
Non-brittleness of a DESIRE-model for an office assignment task
[PB94-119021] 06 p2489 N94-24643
Introduction to a behavioral approach for continuous time systems
[ETN-94-95301] 06 p2492 N94-25277
Knowledge organization in intelligent tutoring systems for diagnostic problem solving in complex dynamic domains
[AD-A273986] 07 p2984 N94-25899
Long term learning: Integration of knowledge acquisition and knowledge compilation
[AD-A274775] 07 p3098 N94-26570
Parallel computational geometry on analog Hopfield networks
[ISBN-0-315-84093-5] 07 p2980 N94-26635
Design and evaluation of fault tolerance in opto-electronic computing
[AD-A274281] 07 p2954 N94-27016
A cognitive model of decision making: Chunking and the radar detection device
[AD-A275185] 08 p3242 N94-28859
Incorporating geometric constraints into rule-based systems using nonlinear optimization
[AD-A275093] 08 p3452 N94-29063
Propagation of evidence through fuzzy rules
[AD-A275071] 08 p3411 N94-29180
Neural network solutions to logic programs with geometric constraints
[AD-A275419] 08 p3435 N94-29198
More problems on rewriting
[CWI-CS-R9332] 08 p3428 N94-30734
The (n squared)-hard problems in computational geometry
[RUU-CS-93-15] 08 p3461 N94-30747
On the use of genetic algorithms to solve the time-table problem
[REPT-90-060-REV] 09 p3829 N94-31176
Techniques for increasing the robustness of iterative algorithms for multi-resources location problems
[REPT-93-037] 09 p3809 N94-31188
Exact solution of the single machine scheduling problem with earliness and flow time penalties
[REPT-93-038] 09 p3809 N94-31189
A hypertext system that learns from user feedback 09 p3923 N94-32428
Reminding-based learning
[AD-A277424] 09 p3801 N94-32997
Assembly of a neural analog computer, phase 2
[AD-A278192] 10 p4103 N94-33402
Human factors involvement in bringing the power of AI to a heterogeneous user population 10 p4110 N94-33633
Assessing design activity in complex CMOS circuit design
[AD-A277620] 10 p4040 N94-33854
The Stanford how things work project 10 p4160 N94-34041
Recursive heuristic classification 10 p4160 N94-34058
Intelligent resources for satellite ground control operations 10 p4125 N94-35062
The weakest failure detector for solving Consensus
[NASA-CR-190545] 11 p4300 N94-35365
Prodigy planning algorithm
[AD-A278900] 11 p4303 N94-35574
Case based reasoning in engineering design
[AD-A278943] 11 p4305 N94-36006
Can we break intractability using randomization or the average case setting?
[AD-A278598] 11 p4316 N94-36425

Searching for plans using a hierarchy of learned macros and selective reuse
[AD-A280594] 12 p4499 N94-36722
A scalable parallel algorithm for multiple objective linear programs
[NASA-CR-194920] 12 p4495 N94-37539

PROCEDURES
NT BOUNDARY INTEGRAL METHOD
NT CREW PROCEDURES (INFLIGHT)
NT CREW PROCEDURES (PREFLIGHT)
NT FINITE ELEMENT METHOD
NT FINITE VOLUME METHOD
NT OPTICAL CORRECTION PROCEDURE
NT PANEL METHOD (FLUID DYNAMICS)
Insights into software development in Japan
01 p0330 N94-11435
Study on improvement of flammability, odor and offgassing tests for materials
[NASDA-CNT-930009] 02 p0563 N94-13471
A TRALINET guide to the Internet
[AD-A266946] 03 p1229 N94-15178
Safety-routines and guidelines for work in the clean room at the Epitek-Laboratory, Kjeller (Norway)
[FFI-93/7012] 04 p1322 N94-17735
Air transport of samples containing chemical warfare agents
[FFI-93/6005] 05 p1851 N94-21455
An analysis of traditional operational testing to project how testing will be conducted in the future
[AD-A273189] 06 p2372 N94-24553
Aircraft digital flight control technical review
06 p2163 N94-25106
Digital Altimeter Setting Indicator (DASI) Operational Test and Evaluation (OT/E) operational test procedures
[AD-A274100] 07 p2672 N94-26030
Environmental Compliance Assessment System (ECAS) --- Japan supplement
[AD-A275549] 08 p3346 N94-28722
Cleanroom engineering handbook. Volume 4. Specification team practices
[AD-A275861] 08 p3156 N94-28753
Tuning of AmPS
[NIKHEF-K-AMPS-93-01] 08 p3494 N94-29422
A graphic view of Geometric Dimensioning and Tolerancing
[DE94-011478] 12 p4435 N94-37736

PROCEEDINGS
U CONFERENCES
U CONGRESSIONAL REPORTS

PROCESS CONTROL (INDUSTRY)
Pollution prevention through total quality
[DE93-013814] 02 p0707 N94-13390
Contribution to the elaboration of some adaptive control algorithms for fermentation processes monitoring
[LAAS-92513] 03 p1116 N94-15643
A software process framework for the SEI capability maturity model: Repeatable level
[AD-A268059] 03 p1157 N94-17588
A structured approach for modeling, analyzing and simulating real-time control systems
[REPT-93-044] 04 p1539 N94-17916
The intelligent processing of materials
[AD-A269250] 04 p1362 N94-18923
Process characterization and control of hand-soldered printed wiring assemblies
[DE93-041290] 05 p1763 N94-21652
Improvement of the stability of the process for synthesizing chemically prepared varistor powder
[DE94-000345] 05 p1763 N94-21654
Application of the structures query language of APROS for specification of industrial processes
05 p1923 N94-22078
Tool sharing: An application of max-algebra, part 2
[MEMO-1122] 06 p2478 N94-22710
Sensors for process control Focus Team report
[DE93-040897] 06 p2560 N94-23204
Intelligent control of chemical vapor deposition processes
[AD-A273356] 06 p2261 N94-24937
Production control and demand management in capacitated flow process industries
[ISBN-9-03-860211-1] 06 p2586 N94-25235
MIMO system identification for H(infinity) robust control: A frequency domain approach with minimum error bounds
[ETN-94-95354] 06 p2476 N94-25262
Safety analysis in conceptual design of process control
[VTT-PUBS-117] 07 p2762 N94-25641
Advances in preparing and characterizing low density pan-carbon microcellular foam
[DE94-002278] 07 p2748 N94-25932
Statistical quality management
[MEMO-COSOR-92-43] 07 p2834 N94-26008
Distributed Nd:YAG laser welding and process control in inert glove boxes
[DE94-002629] 07 p2818 N94-26605
Simplified high-efficiency silicon cell processing
[DE94-002683] 07 p2857 N94-26617
Multiple weight stepwise regression
[DE94-001602] 07 p3000 N94-27564
Dry etching process development for submicron and nanometer semiconductor devices
[PB94-133196] 07 p2788 N94-28357
The development and demonstration of the metric assessment tool
[AD-A275788] 08 p3230 N94-28742
Effect of non-metallic inclusions on the machinability of steel
[PB93-230233] 08 p3204 N94-29387
Formal specification and verification of real-time sequential control systems
[AD-A275776] 08 p3419 N94-29678
Yield and variability optimization of integrated circuits: Principles and practical solutions
08 p3266 N94-29805
Managing customer order driven engineering. An interdisciplinary and design oriented approach
[PB94-145083] 09 p3917 N94-31583
The future of open architecture process control systems
[DE94-006163] 09 p3830 N94-31623
Powder metallurgical processing of fibre reinforced aluminium composites
[PB94-148285] 09 p3620 N94-31688
A fuzzy classifier system for process control
09 p3839 N94-32422
Application of statistical process control and process capability analysis procedures in orbiter processing activities at the Kennedy Space Center
10 p4068 N94-33626
Robust requirements specifications for safety-critical systems
[PB94-167806] 11 p4250 N94-35532
AICD: Advanced Industrial Concepts Division Biological and Chemical Technologies Research Program
[DE94-006854] 11 p4283 N94-36051
Process capability determination of new and existing equipment 11 p4230 N94-36406
Maintaining constant standards during the forging process 12 p4421 N94-37326

PROCESS HEAT
Department of Energy solar process heat program: FY 1991 solar process heat prefeasibility studies activity
[DE93-010010] 01 p0262 N94-10258
Calculation of the thermoneutral potential of NiCd and NiH2 cells 07 p2861 N94-28111

PROCESSORS (COMPUTERS)
U CENTRAL PROCESSING UNITS

PROCUREMENT
NT GOVERNMENT PROCUREMENT
Johnson Space Center procurement: Controls over payments to contractors should be strengthened
[AD-A265722] 02 p0819 N94-13060
Procurement and execution of PCB analyses: Customer-analyst interactions
[DE93-009964] 02 p0566 N94-14694
Software reliability management through metrics
[AD-A267129] 03 p1146 N94-15687
CALS test network handbook
[AD-A267587] 03 p1160 N94-17209
An evolutionary approach to space launch commercialization
[AD-A269861] 04 p1331 N94-18411
Audit report. Navy's aircraft structural life surveillance program data recorders
[AD-A270391] 05 p1645 N94-20040
Using electronic data interchange to report product quality
[AD-A271843] 05 p1828 N94-20468
NASA procurement report, FY 1993
[NASA-TM-109393] 05 p2040 N94-21625
Reference model for project support environments, version 2.0
[AD-A275191] 08 p3410 N94-29068
Estimating the impact of crashworthiness standards on mortality and morbidity events in the US Army rotary-wing aircraft mishaps
[AD-A277121] 09 p3575 N94-32363
Machine Translation Project 12 p4541 N94-36846
A guide to tenders and contracts alerting services
[AGARD-R-799] 12 p4540 N94-37447

PROCUREMENT MANAGEMENT
Facilities maintenance handbook
[NHB-8831.2] 03 p1224 N94-15934
NASA information resources management handbook
[NHB-2410.1E] 03 p1230 N94-15941
Equipment Management Manual
[NHB-4200.1D] 03 p1225 N94-16799
Materials inventory management manual
[NHB-4100.1C] 03 p1225 N94-16830
Implementation of electronic data interchange in the department of defense: Lessons learned from private industry
[AD-A269532] 04 p1534 N94-18768
Activities of National Inst. for Aviation Research
[NIAR-93-16] 05 p2151 N94-20150
NASA procurement: Planning for pilot test of new procurement procedures is adequate. Report to the Chairman, Committee on Governmental Affairs, US Senate
[GAO/NSIAD-94-67] 05 p2039 N94-20236
Implementing Electronic Data Interchange (EDI) with small business suppliers in the pre-award acquisition process
[AD-A271767] 05 p1945 N94-21305
Operational test and evaluation of electronic combat systems
[AD-A273093] 05 p1647 N94-21500
NASA procurement report, FY 1992
[NASA-TM-109390] 05 p2040 N94-21623
Summary data on all NASA procurement actions
[NASA-TM-109392] 05 p2040 N94-21638
Statement by Bill D. Colvin, Inspector General
[NASA-TM-109793] 11 p4348 N94-35446
Budget estimates, fiscal year 1995. Volume 1: Agency summary, human space flight, and science, aeronautics and technology
[NASA-TM-109791] 11 p4347 N94-35899
Budget estimates, fiscal year 1995. Volume 2: Mission support and Inspector General
[NASA-TM-109792] 11 p4348 N94-35900

PROCUREMENT POLICY
Equipment management user's handbook for property custodians
[NHB-4200.2A] 03 p1224 N94-15957
Small business innovation research program solicitation
[NASA-TM-109695] 07 p3094 N94-27661

PRODUCT DEVELOPMENT
NT WEAPONS DEVELOPMENT
Solving the essentials of an innovative tennis racket product: Functionality, simplicity, and super-lightweight technology 01 p0065 N94-10068
Future material development trends for commercial airplane interiors 01 p0021 N94-10792
Rigid-flexible printed wiring boards
[DE93-013938] 02 p0620 N94-13094
Molten carbonate fuel cell product development test environmental assessment/protection plan
[DE93-000288] 02 p0702 N94-13380
Production Technology for Components from Nonmetallic Fiber Reinforced Materials
[ETN-93-94607] 03 p0931 N94-15254
Production process 03 p0931 N94-15257
Prioritization methodology for chemical replacement
[NASA-TP-3421] 03 p0976 N94-15723
Research and development: Engine of innovation at Krupp 03 p0984 N94-16001
Government/contractor development teams
[TABES PAPER 93-460] 03 p1050 N94-16134
Status of molten carbonate fuel cell technology development
[DE93-015666] 03 p1092 N94-16715
Small satellite product assurance
03 p0896 N94-17188
Key trends of the small satellite market
03 p0897 N94-17191
X ray computed tomography for failure analysis investigations
[AD-A268086] 03 p1055 N94-17515
The development of flexible software for the Italian/Dutch satellite SAX: Advantages and disadvantages of the use of CASE tools
[NLR-TP-91288-U] 03 p1157 N94-17626
Cut and paste based modeling with boundary features
[PB93-187250] 04 p1520 N94-18117
Reference model for project support environments, version 1.0
[AD-A269110] 04 p1520 N94-18251
Engineering research, development and technology thrust area report, FY92
[DE93-016334] 04 p1632 N94-18856
Technology benefits model user manual, version 01.00.04
[AD-A270637] 04 p1620 N94-19777
Activities Report of the Institute of Applied Physics
[ETN-93-93749] 05 p1966 N94-21798
Electronic locking system 05 p1796 N94-21801
Multidisciplinary specification and design of microelectronics in products
[EUT-93-E-269] 06 p2308 N94-23136
Rolls-Royce in perspective: Past, present and future
[PNR-90882] 06 p2187 N94-23519

The RB211: The first 25 years
[PNR-90977] 06 p2187 N94-23570
Overview of molten carbonate fuel cell technology development
[DE94-001911] 06 p2394 N94-23781
Training: Plugging the information gaps 06 p2429 N94-23934
Roles, uses, and benefits of general aviation aircraft in aerospace engineering education
[NASA-TM-106463] 06 p2153 N94-24100
Early manufacturing considerations in design 06 p2177 N94-24315
Frameworks for integrated airframe design 06 p2178 N94-24318
Characteristics of products generated by selective sintering and stereolithography rapid prototyping processes 06 p2264 N94-24412
High-order technology: Applying technical excellence to new airplane development 06 p2185 N94-25069
Reuse-Driven Software Processes Guidebook, version 02.00.03
[AD-A273644] 06 p2461 N94-25148
New Technologies for Space Avionics, 1993
[NASA-CR-188272] 06 p2272 N94-25193
Appendix B: Rapid development approaches for system engineering and design 06 p2272 N94-25195
Appendix C: Rapid development approaches for system engineering and design 06 p2272 N94-25196
A multimedia adult literacy program: Combining NASA technology, instructional design theory, and authentic literacy concepts 06 p2585 N94-25384
The MUSA design methodology
[CWI-CS-R9265] 07 p3097 N94-26220
Business process redesign: Design the improved process
[AD-A274947] 07 p3093 N94-26299
Flash unit for high speed photography
[PML-1992-91] 07 p2811 N94-26647
Future of aerospace
[PB94-120185] 07 p2669 N94-26906
An investigation of integrated product development implementation issues: A case study of Bosma Machine and Tool Corp.
[AD-A273917] 07 p2942 N94-27320
The 1993 Federal Aviation Administration plan for research, engineering and development
[AD-A279037] 07 p2643 N94-27960
Software assurance standard
[NASA-TM-109705] 07 p2975 N94-27992
Development of the gas turbine. Part 1: Design philosophy and performance 07 p2831 N94-28080
Development of the gas turbine. Part 2: Manufacturing, commissioning, and operation 07 p2831 N94-28081
Systematic safety consideration in product design
[PB94-132354] 08 p3229 N94-28410
A conceptual framework for software technology transition
[AD-A275637] 08 p3407 N94-28639
Cleanroom engineering handbook. Volume 2: Organization and project formation in the cleanroom environment
[AD-A275809] 08 p3156 N94-28772
Comparative centrifuge evaluation of the Air Force Advanced Technology Anti-G Suit (ATAGS) and the Navy Enhanced Anti-G Lower Ensemble (EAGLE)
[AD-A275348] 08 p3400 N94-28996
The UNICON approach to through-life support and evolution of software-intensive systems 08 p3416 N94-29340
The discipline of defining the software product 08 p3416 N94-29343
A common approach for an aerospace software environment 08 p3417 N94-29346
A comparison of product realization frameworks
[AD-A275992] 09 p3810 N94-31357
An application reference model for layered manufacturing
[DE94-006368] 09 p3811 N94-31484
Concept, construction and testing of a high resolution QCLAM electron spectrometer with large solid angle and high impulse acceptance for the electron accelerator S-DALINAC
[ETN-94-95755] 09 p3711 N94-31515
Managing customer order driven engineering. An interdisciplinary and design oriented approach
[PB94-145083] 09 p3917 N94-31583
Effective information modelling support
[PB94-148236] 09 p3917 N94-31586
Case studies of software process improvement methods
[AD-A277289] 09 p3818 N94-32508
NASA/DOD Aerospace Knowledge Diffusion Research Project. Paper 24: A general approach to measuring the value of aerospace information products and services
[NASA-TM-109775] 10 p4150 N94-33371
Framework for modelling evolving requirements
[PB94-148855] 10 p4107 N94-33979
Designing aluminum sealing glasses for manufacturability
[DE94-010081] 11 p4244 N94-35699
Proceedings of the Eighteenth Annual Software Engineering Workshop
[NASA-CR-189348] 12 p4489 N94-36484
The maturing of the quality improvement paradigm in the SEL 12 p4489 N94-36485
Process improvement as an investment: Measuring its worth 12 p4489 N94-36486
Software quality: Process or people 12 p4492 N94-36499
MCFC product development test
[DE94-002005] 12 p4463 N94-37488

PRODUCTION COSTS
NT AIRCRAFT PRODUCTION COSTS
Space transportation alternatives for large space programs: The International Space University Summer Session, 1992
[NASA-TM-106271] 01 p0040 N94-10811
Space Solar Power Program
[DE93-011750] 01 p0055 N94-11675
Analysis of the economics of DC arc CVD diamond
[AD-A265688] 01 p0403 N94-12339
Spacecraft COst REduction Team (SCORE): TQM/CI on a massive scale 02 p0667 N94-13160
Status and future opportunities for conversion of synthesis gas to liquid energy fuels
[DE93-010025] 02 p0584 N94-14089
Continuous roll-to-roll a-Si photovoltaic manufacturing technology
[DE93-010006] 02 p0704 N94-14109
Production process 03 p0931 N94-15257
Development of a computer supported instrumentation for economic planning and evaluation of production facilities for fiber reinforced composites elements 03 p0932 N94-15260
Conflict Resolution (CORE) for software quality factors
[AD-A267248] 03 p1151 N94-16941
Integrated circuits: Resistless processing simplifies production and cuts costs
[DE93-018069] 04 p1405 N94-18941
A novel VLSI processor architecture for supercomputing arrays 05 p1758 N94-21115
Self assembly: An approach to terascale integration
[DE93-040104] 05 p1769 N94-21846
An assessment of the cost of microwave sintering ceramic tiles for armor applications
[DE94-000978] 05 p1693 N94-21850
Investigation on construction of the database system for research and development of the global environment industry technology
[DE94-714890] 05 p1853 N94-22090
Amorphous silicon PVMaT, phase 2A
[DE93-018221] 06 p2390 N94-23295
New Ways Of Doing Business (NWODB) cost quantification analysis
[NASA-CR-195186] 06 p2586 N94-25197
Large-area triple-junction a-Si alloy production scale up
[DE94-000249] 08 p3339 N94-30604
Budget allocation and monopolistic pricing in a multiproduct firm
[REPT-93-86] 09 p3924 N94-31617
Recovery of carboxylic acids at pH greater than pKa
[DE94-007030] 09 p3636 N94-32376
Leveraging metal matrix composites to reduce costs in space mechanisms 09 p3604 N94-33301

PRODUCTION ENGINEERING
NT PRODUCTION PLANNING
Object recognition in industrial environment by means of tactile sensor
[ITN-93-85200] 01 p0178 N94-10393
Rigid-flexible printed wiring boards
[DE93-013938] 02 p0620 N94-13094
Government/contractor development teams
[TABES PAPER 93-460] 03 p1050 N94-16134
Design of a formaldehyde photodissociation process for carbon and oxygen isotope separation
[DE93-016435] 03 p1039 N94-16450
The intelligent processing of materials
[AD-A269250] 04 p1362 N94-18923
Integrated circuits: Resistless processing simplifies production and cuts costs
[DE93-018069] 04 p1405 N94-18941
MODIL cryocooler producibility demonstration project results
[DE93-017981] 04 p1335 N94-19275
Feature-based tolerancing for intelligent inspection process definition
[DE93-017984] 05 p1906 N94-20311
Modeling of glass fabrication 05 p1711 N94-21800
Microdynamic model of reproduction: Taxation and currency issue as regulators of economy 05 p2053 N94-22084
Making tomorrow's mistakes today: Evolutionary prototyping for risk reduction and shorter development time 06 p2197 N94-23902
Tool sharing, part 3
[PB94-111697] 06 p2467 N94-24524
What makes industries believe in formal methods
[PB94-110848] 06 p2272 N94-24648
The increase of the controllability of production organizations
[ISBN-9-03-860161-1] 06 p2586 N94-25076
Throughput time control and due date reliability in tool and die shops
[ISBN-9-03-860182-4] 06 p2587 N94-25283
Continuous fiber reinforced thermoplastic composites: Literature survey
[VTT-TIED-1422] 07 p2704 N94-25651
Concepts and methods of measuring productivity at the organization level
[AD-A273126] 07 p3094 N94-27180
Microcomputer-based protective functions in industrial production systems: Assessment method
[PB94-137817] 08 p3411 N94-29159
Managing customer order driven engineering. An interdisciplinary and design oriented approach
[PB94-145083] 09 p3917 N94-31583
Fractional-factorial process development techniques
[DE94-005580] 09 p3690 N94-31593
Flexible manufacturing for photonics device assembly 09 p3669 N94-32449
Continuous fiber ceramic composite program, phase 1
[DE94-009180] 10 p4026 N94-33408

PRODUCTION MANAGEMENT
Ninth Annual NASA/Contractors Conference on Quality and Productivity. World Class Excellence: The Journey Continues. Keynote presentations
[NASA-CR-194513] 02 p0665 N94-13148
The power of cross-functional teams in driving total quality 02 p0666 N94-13159
The application of automated operations at the Institutional Processing Center 06 p2509 N94-23901
The integration of design and manufacturing processes at Alenia DVD 06 p2179 N94-24325
The increase of the controllability of production organizations
[ISBN-9-03-860161-1] 06 p2586 N94-25076
New Ways Of Doing Business (NWODB) cost quantification analysis
[NASA-CR-195186] 06 p2586 N94-25197
Production control and demand management in capacitated flow process industries
[ISBN-9-03-860211-1] 06 p2586 N94-25235
Open communication in manufacturing automation
[PB94-132479] 07 p2976 N94-28377
Technology transfer initiatives
[NASA-CR-195151] 08 p3537 N94-29410
An application reference model for layered manufacturing
[DE94-006368] 09 p3811 N94-31484
Managing customer order driven engineering. An interdisciplinary and design oriented approach
[PB94-145083] 09 p3917 N94-31583
Process mapping: A user-friendly tool for process improvement
[DE94-004357] 09 p3730 N94-31605
Assessing efficiency of software production for NASA-SEL data 12 p4490 N94-36490

PRODUCTION METHODS
U PRODUCTION ENGINEERING

PRODUCTION PLANNING
Miniature mechanism assembly
[DE93-015595] 02 p0624 N94-13928
Decision support for material planners
[ISBN-9-03-860201-4] 02 p0819 N94-14449
Production Technology for Components from Nonmetallic Fiber Reinforced Materials
[ETN-93-94607] 03 p0931 N94-15254
Development of a computer supported instrumentation for economic planning and evaluation of production facilities for fiber reinforced composites elements 03 p0932 N94-15260
Class of strong valid inequalities for the discrete lot-sizing and scheduling problem
[PB93-237774] 06 p2459 N94-24765
Production control and demand management in capacitated flow process industries
[ISBN-9-03-860211-1] 06 p2586 N94-25235

PRODUCTIVITY
Measuring human performance on NASA's microgravity aircraft 01 p0317 N94-11537
High biological production of the tidal mixing zones on Japan Sea shelf 01 p0228 N94-12758

Ninth Annual NASA/Contractors Conference on Quality and Productivity. World Class Excellence: The Journey Continues. Keynote presentations
[NASA-CR-194513] 02 p0665 N94-13148
Ninth Annual NASA/Contractors Conference on Quality and Productivity. World Class Excellence: The Journey Continues. Conference presentations
[NASA-CR-194514] 02 p0665 N94-13153
Measuring quality progress 02 p0666 N94-13154
Object-oriented productivity metrics 02 p0667 N94-13161
Miniature mechanism assembly
[DE93-015595] 02 p0624 N94-13928
Land evaluation for agricultural productivity in North-East Thailand using LANDSAT TM data and geographic information 02 p0693 N94-14242
PET team
[NASA-TM-109599] 03 p1223 N94-15293
The Langley Fitness Center 03 p1126 N94-16635
Evaluation of spatial productivity patterns in an annual grassland during an AVIRIS overflight
[CIW-PUBL-1134] 03 p1067 N94-16672
The effectiveness of AMT investment in UK metal component manufacture
[IND-MANU-SCI-TECH-REPT-3] 07 p2762 N94-25775
Concepts and methods of measuring productivity at the organization level
[AD-A273126] 07 p3094 N94-27180
Realizing the productivity potential of expeditious operations
[PB94-135555] 08 p3230 N94-29188
Triple Diagonal modeling: A mechanism to focus productivity improvement for business success
[DE94-004309] 08 p3527 N94-30041
An analysis of the records management process to determine the impact of automation on productivity
[AD-A275923] 09 p3916 N94-31344
Drug-related problems in the workplace
[CRANFIELD-AERO-9306] 09 p3914 N94-31538
Implementing bright light treatment for MSFC payload operations shiftworkers 10 p4098 N94-33623
A practical guide to the technology and adoption of software process automation
[AD-A278719] 11 p4308 N94-36294

PRODUCTS
NT ASPHALT
NT DIESEL FUELS
NT GASOLINE
NT GREASES
NT GROSS NATIONAL PRODUCT
NT PETROLEUM PRODUCTS
NT REACTION PRODUCTS

PROFICIENCY
U ABILITIES

PROFILOMETERS
Confocal profilometer with nanometric vertical resolution
[DE93-622698] 02 p0653 N94-12857
The determination of surface roughness from reflected step edges
[AD-A273987] 07 p2984 N94-25900
Measuring the upper profile of sea ice in the Bay of Bothnia with a laser profilometer
[PB94-184561] 12 p4477 N94-37855

PROGRAM MANAGEMENT
U PROJECT MANAGEMENT

PROGRAM RELIABILITY (COMPUTERS)
U SOFTWARE RELIABILITY

PROGRAM VERIFICATION (COMPUTERS)
A formally verified algorithm for interactive consistency under a hybrid fault model
[NASA-CR-4527] 01 p0326 N94-11188
Development and application of an acceptance testing model 01 p0330 N94-11432
A recent Cleanroom success story: The Redwing project 01 p0039 N94-11433
The 1991 version of the plume impingement computer program. Volume 1: Description
[NASA-CR-194192] 01 p0166 N94-12775
Demonstration and acceptance test plan for real-time excision software on the Adaptive Signal Processing Testbed
[DSIS-93-00275] 02 p0751 N94-13990
EVES: An overview
[DSIS-93-00238] 02 p0752 N94-14088
ORGBUG: A Windows-based combinatorial geometry debugger
[DE93-016640] 02 p0755 N94-14515
Verification of critical software by statistical testing
[LAAS-93006] 02 p0756 N94-14714
Toward a verifiable approach to the design of concurrent computations
[DE93-012908] 02 p0756 N94-14844
Army Software Test and Evaluation Panel (STEP) software metrics initiatives report
[AD-A266889] 03 p1142 N94-14924
Lecture notes on engineering measurement for software engineers
[AD-A266959] 03 p1142 N94-14967
Evaluation of ALSYS 037 Ada Compiler
[AD-A266972] 03 p1143 N94-15110
Safety-critical software: Status report and annotated bibliography
[AD-A266993] 03 p1144 N94-15214
Concepts on measuring the benefits of software process improvements
[AD-A266994] 03 p1144 N94-15215
An expert system shell for inferring vegetation characteristics: Atmospheric techniques (Task G)
[NASA-CR-194570] 03 p1082 N94-15531
An elementary tutorial on formal specification and verification using PVS
[NASA-TM-108991] 03 p1158 N94-15536
Process-centered development environments: An exploration of issues
[AD-A266997] 03 p1145 N94-15630
Integrated trusted systems development environment
[AD-A267029] 03 p1146 N94-15674
Mechanistic models of soot formation
[AD-A267806] 03 p0950 N94-17008
Effects of inspection error on optimal inspection policies and software fault detection models
[AD-A267511] 03 p1153 N94-17075
Progress in computational unsteady aerodynamics
[NASA-CR-177630] 03 p0860 N94-17081
Causality-preserving timestamps in distributed programs
[AD-A267534] 03 p1153 N94-17118
Establishing a software measurement process
[AD-A267896] 03 p1154 N94-17396
A protocol validator for the SCM and CFSM models
[AD-A268523] 03 p1156 N94-17541
Verification of VALISYS cad based CMM software at LLNL
[DE93-013854] 04 p1517 N94-17911
A verification logic representation of indeterministic signal states 04 p1401 N94-18372
A case study in software maintenance
[AD-A269923] 04 p1521 N94-18659
UUGM code development
[AD-A269945] 04 p1416 N94-18671
Initial Graphics Exchange Specification (IGES)
[AD-A270049] 04 p1522 N94-18794
How to apply the IEEE standards to software testing
[DE93-018514] 04 p1527 N94-19245
Software quality in test and measurment equipment
[PB93-197846] 04 p1528 N94-19333
A research program in empirical computer science
[NASA-CR-194069] 04 p1530 N94-19429
On-line test methods of microprocessor based systems
[ETN-93-95008] 04 p1530 N94-19498
Model checking, abstraction, and compositional verification
[AD-A270552] 05 p1902 N94-19919
Set based analysis of ML programs
[AD-A270597] 05 p1902 N94-19948
A methodology for formal hardware verification, with application to microprocessors
[AD-A270550] 05 p1898 N94-20085
PREVAIL-DM: A framework-based environment for formal hardware verification
[RR-899] 05 p1905 N94-20164
Test and evaluation: DOD has been slow in improving testing of software-intensive systems
[AD-A271541] 05 p1908 N94-20917
An assessment of the statistical and editorial output of text analysis programs
[AD-A272185] 05 p2042 N94-20924
Synthesis algorithm of VLSI multipliers for ASIC 05 p1758 N94-21116
Automated synthesis and verification of configurable DRAM blocks for ASIC's 05 p1759 N94-21123
The readiness growth model: A quantitative analysis of software risk
[AD-A272383] 05 p1910 N94-21144
Two visually meaningful correlation measures for comparing calculated and measured response histories
[AD-A273044] 05 p1964 N94-21322
MAYGEN: A symbolic debugger generation system
[AD-A272512] 05 p1913 N94-21413
Tests of logic spaces: A new strategy for certifying the accuracy of programs 05 p1772 N94-22116
Modeling software systems for data flow testing 05 p1772 N94-22117
Formal methods in the design of critical software systems 05 p1779 N94-22158
SPPTOOLS: Programming tools for the IRAF SPP language 05 p1925 N94-22474
Verification of the PROS timing analysis package 05 p1926 N94-22508
Definition and realization of a formal verification tool of LUSTRE programs: The LESAR system
[ETN-94-95164] 06 p2447 N94-22882
Proof test of the computer program BUCKY for plasticity problems
[NASA-TP-3444] 06 p2374 N94-22960
Formal methods and digital systems validation for airborne systems
[NASA-CR-4551] 06 p2466 N94-23293
Micro SIL-1 simulator
[PB94-110889] 06 p2454 N94-23750
Towards the formal verification of the requirements and design of a processor interface unit
[NASA-CR-4522] 06 p2467 N94-24075
Verification and validation of models
[PB94-110566] 06 p2456 N94-24507
Validation activities for LOTOS based on static data flow analysis
[PB94-110863] 06 p2459 N94-24758
Analyzing the properties of user interface software
[AD-A273601] 06 p2460 N94-24933
DARPA DICE manufacturing optimization
[AD-A273345] 06 p2461 N94-25156
Computerized testing system software conversion and development: Identifying software and hardware portability issues and solutions
[AD-A273489] 06 p2462 N94-25287
Software Error Estimation Program (SWEEP), version 02.00.00 user manual
[AD-A274697] 07 p2962 N94-26373
Verification and validation of the on-board software real time requirements 07 p2953 N94-26739
Formal methods for dependable real-time systems 07 p2953 N94-26740
Vcalc: A 3-space vector calculator
[AD-A274520] 07 p2965 N94-26831
Freeness analysis for logic programs-and correctness
[PB94-126703] 07 p2966 N94-26956
Memory subsystem performance of programs with intensive heap allocation
[AD-A274122] 07 p2967 N94-27063
Deferred compilation: The automation of run-time code generation
[AD-A274124] 07 p2967 N94-27065
Alternative architectures for domain-oriented application composition and generation systems
[AD-A274180] 07 p2968 N94-27128
Research in improved assessment of software reliability
[AD-A274161] 07 p2968 N94-27140
Validation tests of TOPSIM 4
[ESA-STM-249] 07 p2972 N94-27582
Software assurance standard
[NASA-TM-109705] 07 p2975 N94-27992
Using formal specification in the Guidance and Control Software (GCS) experiment. Formal design and verification technology for life critical systems
[NASA-CR-194884] 07 p2956 N94-28267
Software Technology for Adaptable, Reliable Systems (STARS) program
[AD-A275675] 08 p3407 N94-28664
Reasoning about programs by exploiting the environment
[AD-A275852] 08 p3408 N94-28794
Microcomputer-based protective functions in industrial production systems: Assessment method
[PB94-137817] 08 p3411 N94-29159
Program derivation by proof transformation
[AD-A275260] 08 p3453 N94-29304
Object versus functional oriented design 08 p3413 N94-29321
Software testing practices and their evolution for the 1990's 08 p3415 N94-29335
Validation and test of complex weapon systems 08 p3150 N94-29336
Integrated formal verification and validation of safety critical software 08 p3416 N94-29338
Animators and error reporters for generated programming environments
[CWI-CS-R9253] 08 p3418 N94-29503
Formal specification and verification of real-time sequential control systems
[AD-A275776] 08 p3419 N94-29678
Electric power system test and verification program
[NASA-TM-106405] 08 p3169 N94-30123
GNU debugger internal architecture
[DE94-006665] 08 p3422 N94-30251
Isomorphisms between predicate and state transformers
[CWI-CS-R9338] 08 p3459 N94-30430
A user's guide to the Software Testpilot
[CWI-CS-R9343] 08 p3426 N94-30435

The MACS-TSA applied in the ISO and SAX spacecraft projects
[PB94-126257] 08 p3170 N94-30857
Cleanroom engineering handbook. Volume 6: Certification team practices
[AD-A275951] 09 p3587 N94-31346
The maintenance of operational flight program
[AD-A276363] 09 p3565 N94-31367
Testing Operational Flight Programs (OFP's)
[AD-A276361] 09 p3578 N94-31387
Consistency checks for SCR-style requirements specifications
[AD-A276077] 09 p3811 N94-31461
An epistemic proof system for parallel processes
[TR-93-17] 09 p3826 N94-32291
SynRGen: An extensible file reference generator
[AD-A277678] 09 p3821 N94-33030
Faultless software project
[AD-A278161] 09 p3822 N94-33188
Ada support for the mathematical foundations of software engineering
[AD-A278031] 09 p3822 N94-33284
Projection in temporal logic programming
[PB94-148814] 10 p4108 N94-34123
Verification and benchmark testing of the NUFT computer code
[DE94-005650] 10 p4048 N94-34138
Data structure extraction, conversion, and display tool
[AD-D016129] 10 p4108 N94-34284
Developing interpretable models with optimized set reduction for identifying high risk software components
11 p4301 N94-35435
Symbolic debugging of globally optimized code: Data value problems and their solutions
[AD-A278898] 11 p4302 N94-35572
Concept for an algorithm testing and evaluation program at NIST
[PB94-163029] 11 p4304 N94-35740
Analysis of a successful inspection program
12 p4490 N94-36492
Software quality: Process or people
12 p4492 N94-36499
An arbitrary grid CFD algorithm for configuration aerodynamics analysis. Volume 1: Theory and validations
[NASA-CR-195918] 12 p4493 N94-36914
A survey of commonly applied methods for software process improvement
[AD-A278595] 12 p4493 N94-36974
Adaptable binary programs
[AD-A280243] 12 p4494 N94-37119
Proto code generation techniques
[AD-A280275] 12 p4494 N94-37123
SACS: A cache simulator incorporating timing analysis with buffer and memory management
[AD-A280472] 12 p4494 N94-37230

PROGRAMMABLE LOGIC DEVICES
Programmable logic devices
[DE93-013117] 01 p0144 N94-11479
Motorola MC68040 high-speed design using Altera EPM5000 erasable programmable logic devices
[DE93-017635] 04 p1523 N94-19006
Logic synthesis on programmable networks
[ETN-94-95174] 06 p2449 N94-23151
A/GATECH DOSP fabrication --- optical programmable logic array
[AD-A275848] 08 p3430 N94-28781
Extension of the LUSTRE language and application to circuit design: The LUSTRE V4 language and the POLLUX system
[ETN-94-95918] 09 p3812 N94-31543
Application of programmable logic controller to pump regulation system for supplying water
10 p4067 N94-34344

PROGRAMMED INSTRUCTION
NT COMPUTER ASSISTED INSTRUCTION

PROGRAMMERS
Insights into software development in Japan
01 p0330 N94-11435
Analysis and guidelines for reusable Ada software
[AD-A264918] 01 p0332 N94-11850
Process-centered development environments: An exploration of issues
[AD-A266997] 03 p1145 N94-15630
ACE: Lessons learned, volume 1
[AD-A267979] 03 p1155 N94-17411
A case study in software maintenance
[AD-A269923] 04 p1521 N94-18659
The development of a course sequence in real-time systems design
[AD-A269459] 04 p1522 N94-18726
Performance and scalability aspects of directory-based cache coherence in shared-memory multiprocessors
[DE93-016442] 04 p1536 N94-19115
Computing professionals: Changing needs for the 1990's
[B-030] 04 p1515 N94-19401
Security evaluation of Unix networks
[AD-A273076] 05 p1945 N94-21520
SPIKE: Application for ASTRO-D mission planning
05 p1926 N94-22486
Designers' models of the human-computer interface
06 p2433 N94-24188
Introduction of the UNIX International Performance Management Work Group 10 p4154 N94-33810

PROGRAMMING (SCHEDULING)
Scheduling for locality in shared-memory multiprocessors
[AD-A272948] 05 p1930 N94-21228
Modular approach to project management
[PB94-118833] 06 p2586 N94-24528

PROGRAMMING ENVIRONMENTS
Reuse: A knowledge-based approach
01 p0329 N94-11430
A recent Cleanroom success story: The Redwing project 01 p0039 N94-11433
Problem specific environments for parallel systems
[AD-A266129] 01 p0337 N94-12540
Common lisp framework
[AD-A265878] 02 p0742 N94-12933
The KASE approach to domain-specific software systems 02 p0745 N94-13357
A measurement and evaluation process model applied to software engineering environments
[INPE-5345-PUD/048] 02 p0746 N94-13428
Caesy: A software tool for computer-aided engineering
02 p0678 N94-14627
Open environments to support systems engineering tool integration: A study using the Portable Common Tool Environment (PCTE)
[NASA-TM-4489] 03 p1144 N94-15486
Visual parallel programming with determinacy: A language specification, an analysis technique, and a programming tool
[AD-A267560] 03 p1153 N94-17107
Process evolution for the MARVEL environment
[AD-A267813] 03 p1155 N94-17398
Concurrency control in rule-based software development environments
[AD-A267829] 03 p1155 N94-17404
Language-based document processing
[INRIA-RR-1731] 03 p1234 N94-17529
An object-oriented environment for computer vision and pattern recognition
[DE93-017098] 04 p1517 N94-17867
Reference model for project support environments, version 1.0
[AD-A269110] 04 p1520 N94-18251
The evolution of the PVM concurrent computing system
[DE93-017764] 04 p1534 N94-18482
Software engineering for effective utilization of parallel processing computing system
[AD-A269191] 04 p1535 N94-18865
Case studies of software development tools for parallel architectures
[AD-A269193] 04 p1535 N94-18866
Early experiences with the IBM SP-1
[DE93-018398] 04 p1535 N94-19010
Cesar user library
[FFI-93/7021] 04 p1529 N94-19378
A proposed research program in information processing
[NASA-CR-194271] 05 p2041 N94-20134
Advanced software development workstation: Knowledge base methodology: Methodology for first Engineering Script Language (ESL) knowledge base
[NASA-CR-193643] 05 p1930 N94-21065
An investigation into the state of the practice of CASE tool integration
[AD-A272441] 05 p1912 N94-21205
The transition to massively parallel computing within a production environment at a DOE access center
[DE93-019155] 05 p1936 N94-21828
Development of the FITS tools package for multiple software environments 05 p1927 N94-22516
IRAF in the nineties 05 p2048 N94-22535
MITS architecture V1.0
[PB93-201762] 06 p2452 N94-23451
A programming environment for distributed complex computing. An overview of the Framework for Interdisciplinary Design Optimization (FIDO) project. NASA Langley TOPS exhibit H120b
[NASA-TM-109058] 06 p2457 N94-24603
Using database technology to support domain-oriented application composition systems
[AD-A274091] 07 p3096 N94-26024
Software redesign for usability: A case study
[DE94-003704] 07 p2960 N94-26048
Multimedia in Views
[CWI-CS-R9263] 07 p2961 N94-26218
Development of a MIL-STD-1750 microprocessor system for space applications 07 p2949 N94-26715
An object model for multimedia programming
[CWI-CS-R9327] 07 p2971 N94-27552
Guide to the Environmental-Language
[AD-A275849] 08 p3408 N94-28784
SDE's for the year 2000 and beyond: An EF perspective 08 p3417 N94-29344
A common approach for an aerospace software environment 08 p3417 N94-29346
A distributed object-based environment in Ada
08 p3417 N94-29347
DSSA-ADAGE: An environment for architecture-based avionics development 08 p3150 N94-29348
Entreprise 2: A PCTE integrated project support environment 08 p3417 N94-29349
The ABC structure editor: Structure-based editing for the ABC programming environment
[CWI-CS-R9256] 08 p3418 N94-29487
Animators and error reporters for generated programming environments
[CWI-CS-R9253] 08 p3418 N94-29503
Considerations on graphical user interfaces for intelligent ATM support systems 08 p3139 N94-29572
Programming aspects of Views: An open-architecture application environment
[CWI-CS-R9259] 08 p3422 N94-30321
Modelling interaction tools in the Views architecture
[CWI-CS-R9261] 08 p3423 N94-30323
Maintaining presentation invariants in the Views system
[CWI-CS-R9262] 08 p3423 N94-30324
E-L user's manual
[AD-A276378] 09 p3810 N94-31370
LORE and reason maintenance
[REPT-93-88] 09 p3812 N94-31522
Automatic generation of context-sensitive textual help
[REPT-93-68] 09 p3812 N94-31646
Incremental recompilation for Standard ML of New Jersey
[AD-A276522] 09 p3815 N94-32080
Integrated Trusted System Development Environment Process
[AD-A276414] 09 p3816 N94-32131
MULTIGRAPH: An architecture for model-based programming. Model-based program synthesis for parallel computing. PREMOS: Programming environment for model-based program synthesis, version 01.00.00
[AD-A276949] 09 p3817 N94-32219
Evolving software reengineering technology for the emerging innovative-competitive era
09 p3823 N94-32439
MADE: A Multiple Application Development Environment
[CWI-CS-R9360] 09 p3822 N94-33097
Pursuit: Visual programming in a visual domain
[AD-A277567] 10 p4104 N94-33394
Parallel programming methodologies for non-uniform structured problems in materials science
[AD-A277868] 10 p4111 N94-33777
Symbolic debugging of globally optimized code: Data value problems and their solutions
[AD-A278898] 11 p4302 N94-35572
Environment/tool integrator for software development, version 1.2
[AD-A278965] 11 p4303 N94-35660
An object-oriented implementation of a graphical-programming system
[DE94-009298] 11 p4304 N94-35808
An environment for visualization, reliability, and knowledge acquisition in equational programming
[AD-A278639] 11 p4308 N94-36258
Lessons learned applying CASE methods/tools to Ada software development projects
12 p4491 N94-36493
Standards for data and document interchange
12 p4543 N94-37337
The distributed development environment for SDSS software
[DE94-013238] 12 p4547 N94-37555

PROGRAMMING LANGUAGES
NT ADA (PROGRAMMING LANGUAGE)
NT ALGOL
NT APL (PROGRAMMING LANGUAGE)
NT ASSEMBLY LANGUAGE
NT C (PROGRAMMING LANGUAGE)
NT C++ (PROGRAMMING LANGUAGE)
NT CONTEXT FREE LANGUAGES
NT FORTRAN
NT HIGH LEVEL LANGUAGES
NT LISP (PROGRAMMING LANGUAGE)
NT NATURAL LANGUAGE (COMPUTERS)
NT PASCAL (PROGRAMMING LANGUAGE)
NT PROLOG (PROGRAMMING LANGUAGE)

Bundle event structures: A non-interleaving semantics for LOTOS
[MEMO-INF-92-73] 01 p0320 N94-10164
An object-oriented model for extensible concurrent systems: The composition-filters approach
[MEMO-INF-92-87] 01 p0320 N94-10166
Techniques, processes, and measures for software safety and reliability
[DE93-012379] 01 p0322 N94-10347
Flexible language constructs for large parallel programs
[NASA-CR-191478] 01 p0326 N94-11196
The instrumentation of the multimodel and multilingual user interface
[AD-A265444] 01 p0333 N94-12332
Simplification-driven automated partial evaluation
[DE93-012890] 02 p0768 N94-13391
The 8th Workshop on the Mathematical Foundations of Programming Semantics
[AD-A266436] 02 p0749 N94-13700
Execution methods, and parallel virtual machines for distributed implementation of the LCS parallel programming language
[LAAS-93032] 02 p0761 N94-14716
VDM specification of the MD4 message digest algorithm
[NPL-DITC-204/92] 03 p1142 N94-14944
A CENTAUR tutorial
[INRIA-RT-140] 03 p1142 N94-14978
The CAML numbers reference manual
[INRIA-RT-141] 03 p1142 N94-14979
Applicability of the session and the presentation layers for the support of high speed applications
[INRIA-RT-144] 03 p1158 N94-14980
The use of formal methods in data security standards
[NPL-DITC-205/92] 03 p1142 N94-15008
RAISE specification of the MD4 message digest algorithm
[NPL-DITC-206/92] 03 p1142 N94-15010
The application of programming languages to the production of reference implementations
[NPL-DITC-209/92] 03 p1143 N94-15012
Testability of data security standards
[NPL-DITC-217/93] 03 p1143 N94-15022
ACM SIGPLAN Workshop on ML and Its Applications
[AD-A266617] 03 p1147 N94-15725
Models for reactivity
[AD-A266419] 03 p1149 N94-16554
Monads and comonads in intensional semantics
[AD-A266522] 03 p1151 N94-16790
Design and implementation of an object-oriented interface for the multi-model/multi-lingual database system
[AD-A267413] 03 p1232 N94-16977
Sequential functions on indexed domains and full abstraction for a sub-language of PCF
[AD-A267838] 03 p1152 N94-17009
Networked workstations and parallel processing utilizing functional languages
[AD-A267464] 03 p1160 N94-17034
Visual parallel programming with determinacy: A language specification, an analysis technique, and a programming tool
[AD-A267560] 03 p1153 N94-17107
Automatic translation of database integrity constraints into compensating production rules
[REPT-92-055] 03 p1234 N94-17502
Language-based document processing
[INRIA-RR-1731] 03 p1234 N94-17529
PostScript: A study in conformity
[NPL-DITC-214/93] 04 p1517 N94-17917
Multistack languages and grammars
[REPT-93-018] 04 p1518 N94-17926
TANGO: A notation for describing advanced transaction models
[REPT-93-014] 04 p1613 N94-17936
PARX: Architecture of an operating system for parallel machines
[ETN-93-94401] 04 p1533 N94-18068
APLAC: An object-oriented analog circuit simulator and design tool. 6.1 reference manual
[PB93-187193] 04 p1396 N94-18091
Portable parallel ray tracing algorithms
[AD-A268984] 04 p1522 N94-18698
Connection machine software conversion of a Navy oceans model
[AD-A269876] 04 p1535 N94-18772
Software engineering for effective utilization of parallel processing computing system
[AD-A269191] 04 p1535 N94-18865
A teaching tool for linear programming
[AD-A270240] 04 p1523 N94-18905
Asynchronous rendezvous in the presence of backtracking
[PB93-197739] 04 p1524 N94-19062
DataTypeLog: A deductive object oriented query language
[MEMO-INF-92-79] 04 p1526 N94-19221
The TM typing rules
[MEMO-INF-92-80] 04 p1526 N94-19222
The TM manual version 1.3 working document
[MEMO-INF-93-06] 04 p1527 N94-19229
Advances in architectural concepts to support distributed systems design
[MEMO-INF-93-17] 04 p1527 N94-19261
Stochastic grammars: Theory and applications
[PB94-149556] 04 p1528 N94-19262
A language of finite probabilistic processes and its interleaving semantics
[MEMO-INF-93-24] 04 p1558 N94-19354
A comparison of data-parallel algorithms for connected components
[AD-A270551] 05 p1902 N94-19918
Implementation of a portable nested data-parallel language
[AD-A270524] 05 p1902 N94-19932
Set based analysis of ML programs
[AD-A270597] 05 p1902 N94-19948
Programming logic for F omega
[PB93-191781] 05 p1928 N94-19996
Nominalization, prediction and type containment
[PB93-191799] 05 p1898 N94-20082
Closure properties of stochastic languages
[TR-441] 05 p1907 N94-20521
GWB: Manual for the Grammar WorkBench version 1.5
[TR-92-14] 05 p1909 N94-21061
A simplified token bus protocol specified using LOTOS
[TR-92-15] 05 p1910 N94-21062
Advanced software development workstation: Knowledge base methodology: Methodology for first Engineering Script Language (ESL) knowledge base
[NASA-CR-193643] 05 p1930 N94-21065
MINIFOLD: A kernel for a MANIFOLD-like coordination language
[CWI-CS-R9252] 05 p1915 N94-21534
Changing preferences
[CWI-CS-R9310] 05 p1915 N94-21551
SPPTOOLS: Programming tools for the IRAF SPP language 05 p1925 N94-22474
The IDL astronomy user's library 05 p2048 N94-22500
DECONV-TOOL: An IDL based deconvolution software package 05 p1927 N94-22542
Parallel functional programming in SISAL: Fictions, facts, and future
[DE93-040486] 05 p1937 N94-22558
Definition and realization of a formal verification tool of LUSTRE programs: The LESAR system
[ETN-94-95164] 06 p2447 N94-22882
Asynchronous rendezvous in distributed logic programming
[PB93-220614] 06 p2448 N94-23096
Tools reference manual for a Requirements Specification Language (RSL), version 2.0
[NASA-CR-191461] 06 p2445 N94-23125
PROGRIL: A language for the definition of protocol grammars
[EUT-93-E-270] 06 p2449 N94-23172
Arc consistency problem: An exercise in parallel programming with shared objects
[PB94-110590] 06 p2466 N94-23706
Transition system specifications in stalk format with bisimulation as a congruence
[PB94-110608] 06 p2453 N94-23707
Object distribution in orca using compile-time and run-time techniques
[PB94-110574] 06 p2453 N94-23745
Mission and science activity scheduling language 06 p2515 N94-23938
Tensoral for post-processing users and simulation authors 06 p2333 N94-24169
Sequential composition, action prefixes and process prefix
[PB94-101433] 06 p2488 N94-24539
Correct and efficient interface for logical query languages with complex objects
[PB93-211175] 06 p2593 N94-24743
Software redesign for usability: A case study
[DE94-003704] 07 p2960 N94-26048
Development of a MIL-STD-1750 microprocessor system for space applications 07 p2949 N94-26715
A formalization of objects using equational dynamic logic
[PB94-125218] 07 p2965 N94-26852
Implementation and performance of a domain decomposition algorithm in Sisal
[DE94-002012] 07 p2981 N94-27092
Users guide for GRIKURV: A code for drawing graphs
[PB94-123593] 07 p2968 N94-27154
Proceedings of the Third Workshop Computersystems: Research Forum on Design, Realization and Use of Computersystems
[ISBN-90-6144-995-2] 07 p2954 N94-27191
DALIA: A language for the description and analysis of digital systems 07 p2954 N94-27192
Efficient implementation of high-level parallel symbolic languages 07 p2955 N94-27196
Semantics of MANIFOLD: Specification in ASF+SDF and extension
[CWI-CS-R9269] 07 p2971 N94-27575
ARM: Abstract Rewriting Machine
[CWI-CS-R9330] 07 p2974 N94-27794
Guide to the Environmental-Language
[AD-A275849] 08 p3408 N94-28784
Summer intern program
[AD-A275194] 08 p3466 N94-28888
Tinkertoy(tm) transactions
[AD-A275271] 08 p3410 N94-29006
Advanced languages for systems software
[AD-A275272] 08 p3410 N94-29007
North American jumelage 'type systems'
[AD-A275342] 08 p3411 N94-29214
Constrained objects
[AD-A275273] 08 p3418 N94-29434
Graphics for ABC
[CWI-CS-R9255] 08 p3418 N94-29449
The ABC structure editor: Structure-based editing for the ABC programming environment
[CWI-CS-R9256] 08 p3418 N94-29487
Proceedings: SISAL 1993
[DE94-006641] 08 p3420 N94-30056
Programming aspects of Views: An open-architecture application environment
[CWI-CS-R9259] 08 p3422 N94-30321
A conceptual language for the description and manipulation of complex information models
[TR-92-34] 08 p3423 N94-30344
On blocks: Locality and asynchronous communication (extended abstract)
[RUU-CS-92-44] 08 p3424 N94-30347
A note on the Smyth powerdomain construction
[RUU-CS-93-02] 08 p3457 N94-30393
Algebraic domains, chain completion, and the Plotkin powerdomain construction
[RUU-CS-93-03] 08 p3457 N94-30394
Modeling systems by probabilistic process algebra: An event structures approach
[MEMO-INF-93-29-REV] 08 p3425 N94-30416
Three metric domains of processes for bisimulation
[CWI-CS-R9335] 08 p3459 N94-30427
MANIFOLD version 1.0 programming: Programs and problems
[CWI-CS-R9334] 08 p3425 N94-30428
Manray: A replicated workers program in MANIFOLD
[CWI-CS-R9337] 08 p3433 N94-30429
Topological models for higher order control flow
[CWI-CS-R9340] 08 p3425 N94-30432
Comparative semantics for linear arrays of communicating processes
[CWI-CS-R9336] 08 p3426 N94-30491
A streamlined software environment for situated skills
[AIAA PAPER 94-1205-CP] 08 p3444 N94-30556
On the relation between Unity properties and sequences of states
[RUU-CS-93-07] 08 p3433 N94-30720
Parallel language constructs for paradigm integration and deterministic computations
[DE94-005119] 08 p3428 N94-30754
A new programming methodology for lazy functional languages
[MEMO-INF-93-44] 08 p3429 N94-30765
Federal grammars and modular compilers
[REPT-93-054] 08 p3429 N94-30928
LORE and reason maintenance
[REPT-93-88] 09 p3812 N94-31522
Extension of the LUSTRE language and application to circuit design: The LUSTRE V4 language and the POLLUX system
[ETN-94-95918] 09 p3812 N94-31543
Methods for parallelizing search paths in phrasing
[AD-A276876] 09 p3817 N94-32212
Translucent procedures, abstraction without opacity
[AD-A276877] 09 p3817 N94-32213
Information disclosure in evolving information systems: Taking a shot at a moving target
[TR-93-22] 09 p3919 N94-32506
Machine assisted implementation of complex algorithms and labor intensive software, closing report
[AD-A277662] 09 p3821 N94-33027
Pursuit: Visual programming in a visual domain
[AD-A277567] 10 p4104 N94-33394
Negation by default for framing in temporal logic programming
[PB94-148848] 10 p4107 N94-33978

An overview of the Opus language and runtime system
[AD-A281616] 10 p4108 N94-34206
Probabilities and priorities in timed CSP
[PB94-169216] 11 p4316 N94-35536
A lower bound for the intersection of regular forests
[AD-A278653] 11 p4303 N94-35576
A critique of type systems for global overloading
[AD-A278800] 11 p4304 N94-35676
Task networks for controlling continuous processes
[AD-A278683] 11 p4312 N94-35710
Software engineering with application-specific languages 12 p4491 N94-36494
Design, implementaion and evaluation of a declarative object-oriented programming language
[PB94-169208] 12 p4492 N94-36546

PROGRAMS
NT APOLLO PROJECT
NT APOLLO SOYUZ TEST PROJECT
NT AUSTRALIAN SPACE PROGRAM
NT CANADIAN SPACE PROGRAM
NT CHINESE SPACE PROGRAM
NT DEFENSE PROGRAM
NT EUROPEAN SPACE PROGRAMS
NT FIRE (CLIMATOLOGY)
NT FRENCH SPACE PROGRAM
NT GALILEO PROJECT
NT GERMAN SPACE PROGRAM
NT INDIAN SPACE PROGRAM
NT INDONESIAN SPACE PROGRAM
NT ISCCP PROJECT
NT ITALIAN SPACE PROGRAM
NT JAPANESE SPACE PROGRAM
NT LUNAR PROGRAMS
NT MAGELLAN PROJECT (NASA)
NT MARINER-MERCURY 1973
NT MERCURY PROJECT
NT NASA PROGRAMS
NT NASA SPACE PROGRAMS
NT NATIONAL AEROSPACE PLANE PROGRAM
NT NATIONAL LAUNCH VEHICLE PROGRAM
NT NETHERLANDS SPACE PROGRAM
NT PAKISTAN SPACE PROGRAM
NT PIONEER PROJECT
NT PROJECT SETI
NT RUSSIAN SPACE PROGRAM
NT SCOUT PROJECT
NT SPACE PROGRAMS
NT SPANISH SPACE PROGRAM
NT SUPERSONIC CRUISE AIRCRAFT RESEARCH
NT SURVEYOR PROJECT
NT SWEDISH SPACE PROGRAM
NT TILT ROTOR RESEARCH AIRCRAFT PROGRAM
NT U.S.S.R. SPACE PROGRAM
NT UNIVERSITY PROGRAM
NT VIKING MARS PROGRAM
NT VOYAGER PROJECT

PROJECT MANAGEMENT
Analysis of the cost evaluation of ESA programmes and comparable national and international programmes
[GTS-92063] 01 p0416 N94-10145
The 40 kWe S-PRIME Thermionic Design and Technology Demonstration Program
[DE93-004738] 01 p0040 N94-10147
Summary of implementation and demonstration projects in bays and estuaries
[PB93-194637] 01 p0265 N94-10846
Engineering performance metrics
[DE93-012084] 01 p0128 N94-11028
Development and application of an acceptance testing model 01 p0330 N94-11432
STGT program: Ada coding and architecture lessons learned 01 p0330 N94-11437
Software management guide
[DE93-012034] 01 p0330 N94-11452
Research and development of post-classical management tools for government program offices, volume 2
[DE93-010236] 01 p0417 N94-11600
Quality assurance in basic research and R/D
[DE93-010825] 01 p0183 N94-11647
The Department of Clinical Investigation, reports control symbol MED-300(R-1)
[AD-A264969] 01 p0304 N94-11649
The requirement for global training programmes to meet the new remote sensing technology 01 p0196 N94-11929
Program/project management resource lists
[NASA-TM-109268] 02 p0822 N94-13107
Spacecraft COst REduction Team (SCORE): TQM/CI on a massive scale 02 p0667 N94-13160
NASA/contractor partnership on the second TDRSS ground terminal program: Breaking barriers 02 p0668 N94-13168
Creating a strategic plan for configuration management using computer aided software engineering (CASE) tools
[DE93-013663] 02 p0746 N94-13394
Information requirements of self-managing teams
[DE93-010319] 02 p0824 N94-14048
Program operations plan
[DE93-012765] 02 p0710 N94-14182
NREL solar radiation resource assessment project: Status and outlook
[DE93-010034] 02 p0704 N94-14422
Advanced Communications Technology Satellite (ACTS) program: ACTS project update 02 p0815 N94-14673
Cohen program management briefing
[NASA-TM-109536] 03 p1223 N94-15367
An analysis of SEI software process assessment results: 1987-1991
[AD-A266996] 03 p1145 N94-15629
Creating and maintaining a visionary quality program
[DE93-015122] 03 p1050 N94-16055
Scientific use of Space Station Freedom 03 p0977 N94-16072
Design Quality Task Force survey comments
[AD-A266283] 03 p1225 N94-16473
Physical fitness and health education program at NASA Headquarters 03 p1126 N94-16631
Chairmanship of the Neptune/Pluto outer planets science working group
[NASA-CR-194625] 03 p1297 N94-16832
Cost drivers: Why do conventional satellites cost so much? 03 p0897 N94-17190
An object-oriented dynamic software process model
[AD-A267726] 03 p1154 N94-17371
Software Capability Evaluation (SCE) version 1.5 method description. Software capability evaluation project
[AD-A267895] 03 p1154 N94-17395
Establishing a software measurement process
[AD-A267896] 03 p1154 N94-17396
Lightweight materials for transportation: Program plan
[DE93-017381] 04 p1340 N94-18087
Safeguarding our energy future
[DE93-016001] 04 p1466 N94-18109
Reference model for project support environments, version 1.0
[AD-A269110] 04 p1520 N94-18251
Knowledge sources for an intelligent MCM analyzer
[AD-A269224] 04 p1542 N94-18887
Review Committee report on the conceptual design of the tokamak physics experiment
[DE93-018408] 04 p1588 N94-19012
Pantex Plant Meteorological Monitoring Program
[DE93-018495] 04 p1493 N94-19127
Networks Technology Conference
[NASA-CP-3241] 05 p1931 N94-21323
The NCC project: A quality management perspective 05 p1828 N94-21324
Let your fingers do the walking: The projects most invaluable tool 05 p1922 N94-21325
NCCDS configuration management process improvement 05 p1931 N94-21327
The automated ground network system 05 p1932 N94-21330
Issues in NASA program and project management. Special Report: 1993 conference
[NASA-SP-6101(07)] 05 p2039 N94-21497
Issues in NASA program and project management
[NASA-SP-6101(06)] 05 p2040 N94-21499
Factors associated with continuance commitment to FAA matrix teams
[DOT/FAA/AM-93/18] 05 p2040 N94-21626
Progress in phases 2 and 3 of the Photovoltaic Manufacturing Technology Project (PVMaT)
[DE94-000206] 06 p2389 N94-22888
Flexible framework for contingent information systems modelling
[PB93-220549] 06 p2589 N94-23095
A framework for SFC/DC system data analysis 06 p2523 N94-23234
Framework for interactive solving of meta-constraint satisfaction problems
[PB94-118825] 06 p2585 N94-23761
Mission engineering 06 p2505 N94-23881
Manned Space-laboratories Control Center (MSCC) operations concept 06 p2505 N94-23882
An approach to the design of operations systems 06 p2506 N94-23884
Mission operations and command assurance: Instilling quality into flight operations 06 p2374 N94-23932
Frameworks for integrated airframe design 06 p2178 N94-24318
Risk identification and reduction in integrated product teams 06 p2497 N94-24407
Spatial interpretation of NASA's Marshall Space Flight Center Payload Operations Control Center using virtual reality technology 06 p2198 N94-24432
Extension of the critical path method
[PB94-118817] 06 p2488 N94-24527
Modular approach to project management
[PB94-118833] 06 p2586 N94-24528
A methodology for software cost estimation using machine learning techniques
[AD-A273158] 06 p2459 N94-24775
New Ways Of Doing Business (NWODB) cost quantification analysis
[NASA-CR-195186] 06 p2586 N94-25197
Feasibility study on introduction of the bio-fuel power generation in tropical regions
[DE94-725203] 07 p2858 N94-26838
Aerospace safety advisory panel
[NASA-TM-109692] 07 p3118 N94-27381
Space projects: Astrophysics facility program contains cost and technical risks. Report to Congressional Requesters
[GAO/NSIAD-94-80] 07 p2696 N94-27382
Training on assessment and mapping of deforestation: WFW conference, Brazil
[INPE-5482-PRE/1781] 07 p2850 N94-27384
University program management information system, FY 1993
[NASA-TM-109719] 07 p3100 N94-27413
NASA: Major challenges for management. Testimony before the Legislation and National Security Subcommittee, Committee on Government Operations, House of Representatives
[GAO/T-NSIAD-94-18] 07 p3095 N94-28176
Activities of Remote Sensing Technology Center of Japan (RESTEC) 07 p2853 N94-28274
NASA Parts Program Office responsibilities 08 p3165 N94-28702
NAVAIR aircraft wiring standardization and qualification program 08 p3166 N94-28704
Cleanroom engineering handbook. Volume 2: Organization and project formation in the cleanroom environment
[AD-A275809] 08 p3156 N94-28772
Application of information management methodologies for project quality improvement in a changing environment 08 p3416 N94-29342
SDE's for the year 2000 and beyond: An EF perspective 08 p3417 N94-29344
The 1993 Federal Aviation Administration Aviation System Capital Investment Plan
[AD-A279036] 08 p3136 N94-29445
Crystalline-silicon solar cell development sponsored by the US Department of Energy
[DE94-003783] 08 p3340 N94-30609
Benchmarking for cost improvement
[DE94-002276] 08 p3528 N94-30824
An active computer supported medium for distributed planning in enterprises
[ETN-94-95738] 09 p3829 N94-31372
Evaluating success levels of mega-projects 09 p3599 N94-31432
Mission operations and command assurance: Flight operations quality improvements 10 p4150 N94-33616
National facilities study. Volume 2A: Facility Study Office on the National Wind Tunnel Complex
[NASA-TM-109856] 10 p4009 N94-34634
Software Management Environment (SME): Components and algorithms
[NASA-CR-189346] 10 p4109 N94-34996
Apollo 11 at twenty-five, version 1.0
[NASA-CR-193380] 11 p4376 N94-35363
Statement by Bill D. Colvin, Inspector General
[NASA-TM-109793] 11 p4348 N94-35446
Earth Observing System (EOS) Advanced Microwave Sounding Unit-A (AMSU-A) schedule plan
[NASA-CR-194856] 11 p4281 N94-35734
The maturing of the quality improvement paradigm in the SEL 12 p4489 N94-36485
The Engineering Review Board 12 p4540 N94-36843
JPRS report: Science and technology. Central Eurasia: Space
[JPRS-USP-94-004] 12 p4391 N94-37002

PROJECT PLANNING
Canada's longterm space plan and ISY activities 01 p0037 N94-10692
National Aero-Space Plane: A need for program direction and funding decisions
[GAO/NSIAD-93-207] 01 p0416 N94-10910
Lunar-Ultraviolet Telescope Experiment (LUTE) integrated program plan
[NASA-CR-193267] 01 p0424 N94-11356
The requirement for global training programmes to meet the new remote sensing technology 01 p0196 N94-11929
Devices related for thermal control systems used in microgravity 01 p0162 N94-12553
Organization and management policy for two phase fluid experiment in space environment 01 p0162 N94-12556

METEOSAT second generation programme SEVIRI: An enhanced visible and IR radiometer for meteorology
01 p0212 N94-12667
The North Atlantic Regional Experiment (NARE)
[DE93-010126] 02 p0706 N94-13054
Present status of JEM utilization projects
02 p0530 N94-13273
Heat and seed recovery technology project
[DE93-009203] 02 p0800 N94-13913
Program operations plan
[DE93-012765] 02 p0710 N94-14182
Space transportation systems within ESA programmes: Current status and perspectives
02 p0537 N94-14275
Information Technology Resources Assessment
[DE93-013899] 03 p1230 N94-16010
Creating and maintaining a visionary quality program
[DE93-015122] 03 p1050 N94-16055
Lightweight materials for transportation: Program plan
[DE93-017381] 04 p1340 N94-18087
Report to Congress: Comprehensive Program Plan for Advanced Turbine Systems
[DE93-016718] 04 p1467 N94-18475
Automatically generating abstractions for planning
[AD-A269772] 04 p1541 N94-18759
Manned Space-laboratories Control Center (MSCC) operations concept 06 p2505 N94-23882
Component characterization and development 2
[AD-A274002] 07 p2765 N94-25660
The 1993 Federal Aviation Administration plan for research, engineering and development
[AD-A279037] 07 p2643 N94-27960
Asia-Pacific Seminar on Global Change Research Cooperation
[JTN-94-80517] 07 p2871 N94-28268
NASDA contribution plan to Asian countries
07 p2853 N94-28273
The Environmental Research and Training Centre
07 p2873 N94-28280
Global Change and Terrestrial Ecosystems (GCTE): Progress report and prospects for Asian contributions
07 p2874 N94-28281
Global change: A research strategy for Australia 1992-1996 07 p2874 N94-28282
A progress report on global change studies in China
07 p2874 N94-28283
Intelligent automated process planning and code generation for computer-controlled inspection
[AD-A275346] 08 p3409 N94-28920
EOS project and ASTER (ITIR)
08 p3331 N94-29226
Earth-observation plan in Europe
08 p3331 N94-29227
Japan's Earth observation satellite programs
08 p3332 N94-29232
Artificial intelligence technology program at Rome Laboratory 08 p3414 N94-29328
An Operational Control Segment (OCS) update on GPS constellation status and future program directions
08 p3144 N94-30643
Development status of the Communications and Broadcasting Engineering Test Satellite (COMETS)
[JTN-94-80545] 08 p3169 N94-30811
NASA's space platform technology program and planning 09 p3597 N94-31044
NASCOM system development plan: System description, capabilities, and plans, FY 94-2
[NASA-TM-109744] 09 p3674 N94-31503
Reuse strategy model: Planning aid for reuse-based projects
[AD-A277641] 10 p4106 N94-33891
Automated documentation generator for advanced protein crystal growth
[NASA-CR-193955] 10 p4147 N94-34072
Lunar Ultraviolet Telescope Experiment (LUTE), phase A
[NASA-TM-4594] 10 p4162 N94-34920
Software Management Environment (SME): Components and algorithms
[NASA-CR-189346] 10 p4109 N94-34996
Cost and schedule estimation study report
[NASA-CR-189344] 11 p4300 N94-35256
Budget estimates, fiscal year 1995. Volume 2: Mission support and Inspector General
[NASA-TM-109792] 11 p4348 N94-35900
NASA STI Program Coordinating Council Eleventh Meeting: NASA STI Modernization Plan
[NASA-TM-109415] 12 p4540 N94-36841
NASA STI modernization plan
12 p4540 N94-36842
The Engineering Review Board
12 p4540 N94-36843
Network upgrades 12 p4541 N94-36851

PROJECT SETI
Preparing for the initial observations of the Targeted Search and the Sky Survey systems
[NASA-CR-193644] 01 p0318 N94-10865
Search for extraterrestrial intelligence/high resolution microwave survey team member
[NASA-CR-194177] 02 p0739 N94-13086
Search for Extraterrestrial Intelligence (SETI)
03 p1125 N94-16620
Efficient computational methods to study new and innovative signal detection techniques in SETI
[NASA-CR-193602] 03 p0998 N94-16649
SETI: Search for extraterrestrial intelligence. An international interdisciplinary seminar, star days
[PB93-230597] 06 p2444 N94-23754
The Telecommunications and Data Acquisition Report
[NASA-CR-195694] 08 p3246 N94-29613
The quest for contact
[NASA-TM-109778] 09 p3806 N94-32389

PROJECTILE CRATERING
A two-stage (turbulent-drainage) mechanism for the emplacement of impact crater outflows on Venus
01 p0458 N94-12145
Projectile-target mixing in melted ejecta formed during a hypervelocity impact cratering event
01 p0432 N94-12241
The Manson impact crater: Estimation of the energy of formation, possible size of the impacting asteroid or comet, and ejecta volume and mass
05 p2083 N94-20721
Pressure versus drag effects on crater size
05 p1862 N94-20742
Impactor control of central peak and peak-ring formation 05 p1862 N94-20744
Delimitation of terrestrial impact craters by way of pseudotachylytic rock distribution
05 p1863 N94-20783
Parabolic features and the erosion rate on Venus
05 p2122 N94-20801
Triton's cratering record and its time of capture
05 p2122 N94-20802
Hypervelocity impact
[AD-A272957] 05 p1831 N94-21249
Craters in aluminum 1100 targets using glass projectiles at 1-7 km/s 11 p4280 N94-35407
Impact basins in Southern Daedalia, Mars: Evidence for clustered impactors? 11 p4360 N94-35426
Distribution of siderophile and other trace elements in melt rock at the Chicxulub impact structure
11 p4352 N94-35456
Experimental impacts into Teflon targets and LDEF thermal blankets 11 p4352 N94-36141

PROJECTILE PENETRATION
U TERMINAL BALLISTICS

PROJECTILES
NT HYPERVELOCITY PROJECTILES
NT SABOT PROJECTILES
A computational study of the base region flow field for the M865 projectile
[ARL-TR-109] 02 p0504 N94-13795
Development of test techniques to simulate high-frequency mechanical shock on weapon components
[KCP-613-4998] 02 p0675 N94-13907
Collisions and separations in 2D hydrodynamical code
[ITN-93-85225] 02 p0639 N94-14503
An electronic imaging system for the Aeroballistic Research Facility
[AD-A267157] 03 p1033 N94-15826
The physical mechanism of comet outbursts: An experiment 03 p1242 N94-16221
Feasibility study for a measuring system velocity projectile
[FEL-91-A368] 04 p1434 N94-19797
Absolute total and one and two electron transfer cross sections for Ar(8+) on Ar as a function of energy
[DE93-040283] 05 p1970 N94-19870
Numerical modeling of impact erosion of atmospheres: Preliminary results 05 p2131 N94-20847
Geometrical analysis of the microcraters found on LDEF samples 05 p1666 N94-20890
Antipodal fragment velocities for porous and weak targets at catastrophic impacts
05 p1836 N94-20891
Multisensor pinhole yawsonde
[AD-A271715] 05 p1808 N94-20930
Projectile transverse motion and stability in electromagnetic induction launchers
[DE94-001557] 06 p2198 N94-23210
A comparison of in-bore projectile motion from an electromagnetic railgun versus that of a conventional cannon barrel
[AD-A273473] 06 p2198 N94-24690
Users manual for CATNIP: A Computer Analysis Tool for Normal Impact Penetration
[DE94-003671] 07 p2962 N94-26371
Tearing resistance of a thin shell against projectile penetration: Material property effects
[DE94-007466] 09 p3733 N94-31316
Using Monte Carlo techniques and parallel processing for debris hazard analysis of rocket systems
[DE94-007250] 09 p3609 N94-31382
Eureka! Aerogel capture of meteoroids in space
11 p4351 N94-35412
Energy partitioning in high speed impact of analog solid rocket motors
[AD-A278771] 11 p4228 N94-35825

PROJECTION
On geometric and algebraic aspects of 3D affine and projective structures from perspective 2D views
[AD-A270520] 05 p1983 N94-19968
Projection techniques for iterative solution of A(bar x) equals (bar b) with successive right-hand sides
[NASA-CR-191571] 06 p2490 N94-24836

PROJECTIVE GEOMETRY
VLSI architectures for geometrical mapping problems in high-definition image processing
04 p1398 N94-18345
On geometric and algebraic aspects of 3D affine and projective structures from perspective 2D views
[AD-A270520] 05 p1983 N94-19968
Orbit spaces over commutative rings and projectives as semi-isomorphisms
[DE93-616822] 06 p2493 N94-25473
Computing the precision of localization in a plane using projective invariants
[TELECOM-93-D-005] 09 p3840 N94-31095
Algebraic functions for recognition
[AD-A276803] 09 p3846 N94-32167
Projective and object space geometry for monocular building extraction
[AD-A277586] 10 p4075 N94-33426

PROJECTORS
Display of dynamic, volume graphic images by holographic voxel projection: Initial investigation
[AD-A267622] 03 p1035 N94-17197
A full-color, high-resolution laser projector for a flight simulator visual display
[AD-A270578] 05 p1651 N94-20108
A paraperspective factorization method for shape and motion recovery
[AD-A276513] 09 p3712 N94-31929
Display projector technology by way of single crystal faceplate technology
[AD-A277800] 10 p4038 N94-33398

PROJECTS
NT APOLLO PROJECT
NT APOLLO SOYUZ TEST PROJECT
NT FIRE (CLIMATOLOGY)
NT GALILEO PROJECT
NT ISCCP PROJECT
NT MAGELLAN PROJECT (NASA)
NT MERCURY PROJECT
NT PIONEER PROJECT
NT PROJECT SETI
NT SCOUT PROJECT
NT SURVEYOR PROJECT
NT VOYAGER PROJECT

PROKARYOTES
Light utilization and photoinhibition of photosynthesis in marine phytoplankton
[DE94-005505] 09 p3794 N94-32896

PROLATE SPHEROIDS
Mathematical problems in combustion
[AD-A270147] 04 p1349 N94-18776
Intensity and polarization of light scattered by size distributions of randomly oriented nonspherical particles
05 p1721 N94-20416
Electrostatic image solution for the conducting prolate spheroid
[PB94-133154] 07 p2778 N94-28387
Three-dimensional velocity measurements on a 6:1 prolate spheroid at 10 deg angle of attack
[AD-A276485] 09 p3702 N94-31476

PROLATENESS
The effect of pressure and quadrupolar interactions on the nematic-isotropic transition properties: Numerical results for a system of prolate ellipsoids including second and fourth rank orientational order parameters
[DE93-613540] 01 p0410 N94-10536
Anisotropic phase separation in amorphous Fe-Ge alloys
[DE93-015255] 03 p0961 N94-17251
Resonance capture in unbalanced dual-spin spacecraft
[AD-A278501] 10 p4015 N94-34292

PROLOG (PROGRAMMING LANGUAGE)
Computational Russian morphological generation on Prolog: Noun, pronoun, and adjective
02 p0747 N94-13436
On the occur-check free PROLOG programs
[CWI-CS-R9238] 02 p0748 N94-13524

Proving run-time properties of general programs w.r.t. constructive negation
[CWI-CS-R9245] 05 p1909 N94-21025
A declarative approach for first-order built-in's of PROLOG
[CWI-CS-R9246] 05 p1909 N94-21026
A type declarative system for PROLOG
[ETN-94-95178] 06 p2449 N94-23155
A parallel PROLOG system for distributed memory multiprocessor
[ETN-94-95173] 06 p2465 N94-23167
Applications of the Aurora parallel PROLOG system to computational molecular biology
[DE93-041166] 06 p2420 N94-23468
Declarative Object Manipulation Environment (DOME): Alpha version
[AD-A273233] 06 p2460 N94-24935
Automatic test case generation using PROLOG
[NPL-DITC-215/93] 07 p2964 N94-26655
Modular termination proofs for logic and pure PROLOG programs
[CWI-CS-R9316] 07 p2970 N94-27544
On the unification free PROLOG programs
[CWI-CS-R9331] 08 p3427 N94-30733

PROMETHAZINE
Promethazine and its use as a treatment for space motion sickness 01 p0312 N94-11550
Update on the incidence and treatment of space motion sickness 01 p0312 N94-11551

PROMINENCES
NT SOLAR PROMINENCES

PRONY SERIES
Advances in the identification of transfer function models using Prony analysis
[DE93-017980] 04 p1548 N94-18094
An iterative extension of Prony's method for ARMA signal modeling
[AD-A278841] 11 p4319 N94-35800

PROOFS
U PROVING

PROP-FAN TECHNOLOGY
AGBT advanced counter-rotating gearbox detailed design report
[NASA-CR-180883] 01 p0179 N94-10400
Laser velocimeter measurements of the flow field generated by a forward-swept propfan during flutter
[NASA-TM-106195] 01 p0014 N94-10892
Back to propellers
[NASA-TM-109445] 03 p0869 N94-15344
The 1982 highlights
[NASA-TM-109671] 03 p1303 N94-15508
Holographic testing of composite propfans for a cruise missile wind tunnel model
[NASA-TM-105271] 06 p2187 N94-23545
Aerodynamic models for performance calculations of modern technology propellers 06 p2161 N94-24285
Dumbo heavy lifter aircraft
[NASA-CR-195500] 06 p2182 N94-24915
A review of recent aeroelastic analysis methods for propulsion at NASA Lewis Research Center
[NASA-TP-3406] 07 p2846 N94-28227
Investigation of advanced counterrotation blade configuration concepts for high speed turboprop systems. Task 2: Unsteady ducted propfan analysis computer program users manual
[NASA-CR-187105] 08 p3152 N94-29438
In flight measurement of steady and unsteady blade surface pressure of a single rotation large scale advanced prop-fan installed on the PTA aircraft
[NASA-CR-187096] 09 p3584 N94-32859

PROPAGATION (EXTENSION)
NT CRACK PROPAGATION
NT FLAME PROPAGATION

PROPAGATION MODES
NT WHISPERING GALLERY MODES
Combustion-induced crack/debond propagation in solid propellants 02 p0584 N94-13560
Theoretical, experimental, and computational evaluation of disk-loaded circular wave guides
[NASA-TM-106640] 10 p4041 N94-33944

PROPAGATION VELOCITY
A Kirchhoff approach to seismic modeling and prestack depth migration
[AD-A271010] 05 p1854 N94-19820
Normal zone propagation and thermal hydraulic quenchback in a cable-in-conduit superconductor
[DE94-002457] 06 p2271 N94-24568
Arbitrary-order numerical schemes for linear hyperbolic systems
[CRANFIELD-AERO-9211] 06 p2523 N94-25480
Superluminous laser pulse in an active medium
[DE94-007110] 09 p3720 N94-32684

PROPANE
Vehicular fleet operation on natural gas and propane: An overview
[PB93-194603] 01 p0098 N94-10844
Conversion of ethane and of propane to higher olefin hydrocarbons
[DE93-015282] 04 p1347 N94-18194
Evaluation of aftermarket LPG conversion kits in light-duty vehicle applications
[DE93-010035] 04 p1377 N94-18617
Measurements and predictions of the combustion characteristics of enclosed swirl-stabilized propane flames
[IECE-CFE-TR-001] 08 p3198 N94-30017
Volatiles combustion in fluidized beds
[DE94-008382] 09 p3636 N94-32414
The reaction of hydroperoxy-propyl radicals with molecular oxygen
[DE94-006392] 11 p4239 N94-36319
Alternative fuel information: Facts about CNG and LPG conversion
[DE94-006888] 12 p4429 N94-37402
Probing flame chemistry with MBMS, theory, and modeling
[DE94-011224] 12 p4413 N94-37623

PROPARGYL GROUPS
Infrared absorption spectroscopy and chemical kinetics of free radicals
[DE93-015078] 02 p0562 N94-13004

PROPELLANT ADDITIVES
NT PROPELLANT BINDERS
Damage evolution in filled elastomers
[AD-A268067] 03 p1062 N94-17507
A study of low emissions gas turbine combustions
[NASA-CR-195763] 08 p3152 N94-29860
A compatibility study of FEFO with various containment materials
[DE94-005753] 09 p3649 N94-31198

PROPELLANT BINDERS
Strained ring energetic binders
[AD-A269056] 04 p1377 N94-18491
Energetic polymer
[AD-D016156] 10 p4027 N94-33762

PROPELLANT CHEMISTRY
Spectral studies of solid propellant combustion 4: Absorption and burn rate results for M43, XM39, and M10 propellants
[AD-A267119] 03 p0946 N94-15685
Space Shuttle solid rocket motor exposure monitoring 03 p0976 N94-16624
A proposed methodology for combustion toxicology testing of combined halon replacement agent/jet fuel interaction
[AD-A272695] 05 p1681 N94-21165
Chemistry of the burning surface
[AD-A272725] 05 p1681 N94-21181
Fuels combustion research
[AD-A275122] 08 p3189 N94-29004
Superior energetic materials that contain carbocations and anions. Energetic materials restricted in composition to C, H, N, and O atoms
[AD-A275449] 08 p3225 N94-29310
NASA reload program
[NASA-CR-193972] 12 p4429 N94-37446

PROPELLANT COMBUSTION
NT SOLID PROPELLANT COMBUSTION
NT SOLID PROPELLANT IGNITION
A computer model for liquid jet atomization in rocket thrust chambers
[NASA-CR-194194] 02 p0627 N94-12803
Chemical reactions in scramjet engines: Reduced kinetic models for ignition, combustion and nozzle flow
[NAL-TR-1184] 02 p0563 N94-13458
Numerical studies of spray combustion in liquid-fueled engines 02 p0564 N94-13685
Closed-chamber analysis of M5 propellant lot RAD-64597
[AD-A266321] 02 p0585 N94-14145
Droplet-turbulence interactions in sprays exposed to supercritical environmental conditions
[NASA-CR-194408] 02 p0638 N94-14308
Aluminum powder/water reaction ignited by electrical pulsed power
[AD-A269223] 04 p1376 N94-17840
Investigation of flame driving and flow turning in axial solid rocket instabilities
[AD-A271066] 05 p1667 N94-20015
Chemistry of the burning surface
[AD-A272725] 05 p1681 N94-21181
Electronically metastable molecules of high symmetry
[AD-A272015] 05 p1974 N94-21461
A theoretical evaluation of aluminum gel propellant two-phase flow losses on vehicle performance 06 p2210 N94-23031
Laser diagnostics for small rockets 06 p2210 N94-23032
CFD analyses of combustor and nozzle flowfields 06 p2210 N94-23033
LOX droplet vaporization in a supercritical forced convective environment 06 p2211 N94-23034
Development of a computational testbed for numerical simulation of combustion instability 06 p2213 N94-23046
Numerical investigation of two- and three-dimensional heat transfer in expander cycle engines 06 p2213 N94-23048
Two stage turbine for rockets 06 p2215 N94-23059
The Jet Propulsion Laboratory space exploration: Past, present and future 06 p2153 N94-24242
Burning rate of double-base propellant in the presence of plasma 06 p2155 N94-24252
Ignition and combustion characteristics of metallized propellants, phase 2
[NASA-CR-195107] 06 p2266 N94-24700
Fuel-rich catalytic combustion of a high density fuel
[NASA-TP-3281] 08 p3197 N94-29356
Liquid-oxygen droplet vaporization and combustion: Analysis of transcritical behavior and application to liquid-rocket combustion instability 08 p3197 N94-29592
Photothermal laser deflection, an innovative technique to measure particles in exhausts
[AD-A277151] 09 p3718 N94-32366
Validation and implementation of optical diagnostics for particle sizing in rocket motors
[AD-A278581] 12 p4428 N94-36972
A fully coupled thermal, chemical, mechanical cookoff model
[DE94-011432] 12 p4428 N94-37201

PROPELLANT GRAINS
Combustion-induced crack propagation process in a solid-propellant crack cavity 01 p0098 N94-10901
New test method to determine modulus of elasticity of rocket grain material
[AD-A269758] 04 p1377 N94-18758
Design considerations of hybrid rockets 06 p2156 N94-24254
Condensed-phase processes during solid propellant combustion. 3: Preliminary depth-profiling studies on XM39, JA2, M9, M30, and HMX2
[AD-A276595] 09 p3635 N94-32124

PROPELLANT MASS RATIO
Proceedings of the High Energy Density Matter (HEDM) Contractor's Conference
[AD-A274452] 07 p3033 N94-27083

PROPELLANT OXIDIZERS
U ROCKET OXIDIZERS

PROPELLANT PROPERTIES
NT PROPELLANT SENSITIVITY
NT PROPELLANT STORABILITY
Advanced fuel properties: A computer program for estimating property values
[AD-A275248] 08 p3224 N94-28901
Correlation of cookoff behavior of rocket propellants with thermomechanical and thermochemical properties
[AD-A274983] 08 p3224 N94-29092

PROPELLANT SENSITIVITY
Densifying and stabilizing ingredient
[AD-D015751] 03 p0975 N94-16934
Cryogenic size reduction of solid propellant
[AD-A274844] 07 p2759 N94-26800
Insensitive energetic materials: The importance of physical properties and molecular structure
[AD-A275393] 08 p3225 N94-29308

PROPELLANT SPRAYS
Computational analysis of Variable Thrust Engine (VTE) performance
[NASA-CR-193852] 03 p0928 N94-17442
Combustion instability phenomena of importance to liquid propellant engines
[AD-A268800] 04 p1348 N94-18389
A coupled implicit solution method for turbulent spray combustion in propulsion systems 04 p1411 N94-18549

PROPELLANT STORABILITY
A compatibility study of FEFO with various containment materials
[DE94-005753] 09 p3649 N94-31198

PROPELLANT STORAGE
New methane chemistry synthesis of materials for reversible uptake and useful functionalization of methane
[PB94-112786] 06 p2233 N94-23801
Design of a lunar propellant processing facility. NASA/USRA advanced program
[NASA-CR-195502] 06 p2266 N94-24618
Large scale cryogenic fluid systems testing
[NASA-TM-109735] 08 p3157 N94-29904
A compatibility study of FEFO with various containment materials
[DE94-005753] 09 p3649 N94-31198
Cryogenic fluid management technologies for space transportation. Zero G thermodynamic vent system
[NASA-CR-193981] 12 p4430 N94-36806

PROPELLANT TANKS
Spinforming characteristics of a net shape forming process 01 p0056 N94-10004
Power Reactant Storage Assembly (PRSA) (Space Shuttle). PRSA hydrogen and oxygen DVT tank refurbishment
[NASA-CR-188262] 03 p0926 N94-16922
Large scale cryogenic fluid systems testing
[NASA-TM-109735] 08 p3157 N94-29904
Experimental results of hydrogen slosh in a 62 cubic foot (1750 liter) tank
[NASA-TM-106625] 11 p4263 N94-35250

PROPELLANT TESTS
On the combustion of a laminar spray
[NASA-TM-106210] 01 p0028 N94-11238
Supersonic Combustion Research Laboratory. Volume 1: Design and fabrication
[AD-A267667] 03 p0943 N94-14962
Correlation of cookoff behavior of rocket propellants with thermomechanical and thermochemical properties
[AD-A274983] 08 p3224 N94-29092

PROPELLANT TRANSFER
Propellant management in surface tension tanks 01 p0106 N94-10110
On-orbit refueling 01 p0038 N94-11566
Development and testing of the Automated Fluid Interface System 08 p3161 N94-29636

PROPELLANTS
NT COLLOIDAL PROPELLANTS
NT COMPOSITE PROPELLANTS
NT CRYOGENIC ROCKET PROPELLANTS
NT DOUBLE BASE PROPELLANTS
NT DOUBLE BASE ROCKET PROPELLANTS
NT GASEOUS ROCKET PROPELLANTS
NT GELLED ROCKET PROPELLANTS
NT GUN PROPELLANTS
NT HIGH ENERGY PROPELLANTS
NT HMX
NT HTPB PROPELLANTS
NT HYBRID PROPELLANTS
NT LIQUID ROCKET PROPELLANTS
NT METAL PROPELLANTS
NT MONOPROPELLANTS
NT NITRAMINE PROPELLANTS
NT RDX
NT ROCKET PROPELLANTS
NT SLURRY PROPELLANTS
NT SLUSH HYDROGEN
NT SOLID PROPELLANTS
NT SOLID ROCKET PROPELLANTS
NT STORABLE PROPELLANTS
NT TAGN
NT TATB
Destruction of waste energetic materials using base hydrolysis
[DE93-012738] 02 p0584 N94-13491
Densifying and stabilizing ingredient
[AD-D015751] 03 p0975 N94-16934
Shock compression properties of silicon carbide
[DE93-019927] 04 p1373 N94-19271
Electronically metastable molecules of high symmetry
[AD-A272015] 05 p1974 N94-21461
Experimental and analytical study of cryogenic propellant boiloff to develop and verify alternate pressurization concepts for Space Shuttle external tank using a scaled down tank 06 p2266 N94-23657
Numerical simulation of cylindrical, self-field MPD thrusters with multiple propellants
[NASA-CR-194458] 06 p2220 N94-24714
Inertial electrostatic confinement as a power source for electric propulsion 07 p2688 N94-27373
Superior energetic materials that contain carbocations and anions. Energetic materials restricted in composition to C, H, N, and O atoms
[AD-A275449] 08 p3225 N94-29310
One fantastic ride
[NASA-TM-109828] 10 p4016 N94-33582
The thermochemistry and reaction mechanisms in the decomposition of energetic materials
[DE94-011420] 11 p4248 N94-36376

PROPELLER BLADES
Cruise noise measurements of a scale model advanced ducted propulsor
[NASA-TM-105808] 03 p1176 N94-15115
Counterrotating aircraft propulsor blades
[CA-PATENT-1-319-357] 06 p2186 N94-23255
Wing mounted unducted fan engine
[CA-PATENT-1323353] 06 p2188 N94-24180
Aerodynamic models for performance calculations of modern technology propellers 06 p2161 N94-24285
Aircraft accident report: In-flight loss of propeller blade and uncontrolled collision with terrain Mitsubishi MU-2B-60, N86SD, Zwingle, Iowa, 19 April 1993
[PB93-910409] 06 p2174 N94-25175
The experimental behavior of spinning pretwisted laminated composite plates
[NASA-CR-195220] 07 p2711 N94-27352
In flight measurement of steady and unsteady blade surface pressure of a single rotation large scale advanced prop-fan installed on the PTA aircraft
[NASA-CR-187096] 09 p3584 N94-32859

PROPELLER DRIVE
NT HELICOPTER PROPELLER DRIVE

PROPELLER EFFICIENCY
Aerodynamic models for performance calculations of modern technology propellers 06 p2161 N94-24285

PROPELLER FANS
Back to propellers
[NASA-TM-109445] 03 p0869 N94-15344
The 1982 highlights
[NASA-TM-109671] 03 p1303 N94-15508
Holographic testing of composite propfans for a cruise missile wind tunnel model
[NASA-TM-105271] 06 p2187 N94-23545
A review of recent aeroelastic analysis methods for propulsion at NASA Lewis Research Center
[NASA-TP-3406] 07 p2846 N94-28227
In flight measurement of steady and unsteady blade surface pressure of a single rotation large scale advanced prop-fan installed on the PTA aircraft
[NASA-CR-187096] 09 p3584 N94-32859

PROPELLER NOISE
An experimental investigation of the sources of propeller noise due to turbulence ingestion 01 p0358 N94-11057
Cruise noise measurements of a scale model advanced ducted propulsor
[NASA-TM-105808] 03 p1176 N94-15115
A pilot study of comfort criteria and sound quality metrics for sound inside cabins of propeller-driven aircraft
[CTH-F-93-03] 09 p3859 N94-31090
Experimental and computational studies on propeller noise due to inflow distortion 09 p3860 N94-31846

PROPELLER SLIPSTREAMS
An experimental investigation of the sources of propeller noise due to turbulence ingestion 01 p0358 N94-11057
Wind tunnel investigation of propfan slipstream/wing interactions on a De Havilland air motor powered semispan model at Mach numbers 0.6 and 0.7 07 p2651 N94-28316
Flow field investigation in the near slipstream of an 8-bladed propfan on the De Havilland WTEJ half-model at Mach numbers 0.6 and 0.7 07 p2651 N94-28317
Aerodynamic characteristics of a propeller-powered high-lift semispan wing
[NASA-TM-4541] 08 p3132 N94-29937
Aerodynamic analysis of slipstream/wing/nacelle interference for preliminary design of aircraft configurations
[AD-B173651] 08 p3135 N94-30916

PROPELLERS
NT CONTRAROTATING PROPELLERS
NT PROPELLER FANS
NT SHROUDED PROPELLERS
NT VARIABLE PITCH PROPELLERS
On the use of the method of matched asymptotic expansions in propeller aerodynamics and acoustics
[NLR-TP-91307-U] 02 p0503 N94-13528
Cruise noise measurements of a scale model advanced ducted propulsor
[NASA-TM-105808] 03 p1176 N94-15115
Aerodynamic models for performance calculations of modern technology propellers 06 p2161 N94-24285
Hydro-elastic analysis using a selection of commercial analysis programs
[PB94-118734] 06 p2376 N94-24478
Propeller off-axis loads due to thrust axis incidence and nacelle magnus force 07 p2652 N94-28319
Aerodynamic characteristics of a propeller-powered high-lift semispan wing
[NASA-TM-4541] 08 p3132 N94-29937
Experimental and computational studies on propeller noise due to inflow distortion 09 p3860 N94-31846

PROPFAN TECHNOLOGY
U PROP-FAN TECHNOLOGY

PROPHYLAXIS
Update on the incidence and treatment of space motion sickness 01 p0312 N94-11551
The role of hyperbaric oxygen as a prophylaxis for radiation enteritis
[AD-A274974] 07 p2901 N94-26517

PROPIONIC ACID
Water-enhanced solvation of organics
[DE93-040297] 05 p1683 N94-21947

PROPORTIONAL CONTROL
Real-time implementation of neural network learning control of a flexible space manipulator
[AD-A266962] 03 p1045 N94-14970
Optimal tuning of heavy equipment motion controllers
[AD-A267873] 03 p1167 N94-17392
Proceedings of the Twentieth Annual Technologyfest 05 p1645 N94-20188
A study on piezoelectric actuators and sensors for vibration control of flexible space structures
[AD-A274925] 07 p2695 N94-26532
Advanced control of a flexible spherical wrist
[ISBN-0-315-84424-8] 07 p2826 N94-27652
Development of a reconfigurable helicopter flight control system
[ISBN-0-315-87218-7] 09 p3585 N94-31837

PROPORTIONAL COUNTERS
Analysis and interpretation of high energy cosmic rays measured on Spacelab-2
[NASA-CR-193586] 01 p0485 N94-12771
The imaging microstrip proportional counter: Features of a practical design 03 p0900 N94-15030
The high pressure gas scintillation proportional counter for SAX 03 p0906 N94-15076
Performance of the position-sensitive proportional counters of the Yohkoh Bragg crystal spectrometer 03 p0909 N94-15094
The formation process of the He I lambda 10830 line in cool giant stars
[NASA-CR-194648] 03 p1240 N94-17094
Monte Carlo simulation of the microstrip gas counter
[NIKHEF-H/93-07] 03 p1035 N94-17619
Measurements of cosmic ray muons with multi-wire proportional chambers with a prototype setup for KASCADE
[KFK-5173] 04 p1631 N94-19506
The laser and its applications on environment and biotechnology research
[DE94-000376] 05 p1820 N94-21957
VETA x ray data acquisition and control system 05 p2047 N94-22455
SPIKE: Application for ASTRO-D mission planning 05 p1926 N94-22486
An x ray archive on your desk: The Einstein CD-ROM's 05 p2048 N94-22519
Cosmic x ray physics
[NASA-CR-195225] 07 p3115 N94-27236
Cosmic x ray physics
[NASA-CR-195218] 07 p3115 N94-27419
Experimental characterisation of gas microstrip detectors. Part 2: Counting rate characteristics
[PB94-167095] 11 p4269 N94-36061

PROPORTIONAL LIMIT
Crystal orientation dependence of elastic precursor strength in pentaerythritol tetranitrate
[DE93-018340] 05 p2034 N94-22035

PROPOSALS
Research interests and broad agency announcement 94-1 of the Air Force Office of Scientific Research
[AD-A273410] 06 p2632 N94-25075
Advanced gas turbine systems research
[DE94-005303] 08 p3297 N94-28485
Hubble Space Telescope cycle 5. Phase 1: Proposal instructions, version 4.0
[NASA-CR-189364] 12 p4547 N94-36963

PROPRIOCEPTION
Proprioceptive isokinetic exercise test
[NASA-TM-104015] 07 p2902 N94-27227

PROPRIOCEPTORS
Proprioceptive isokinetic exercise test
[NASA-TM-104015] 07 p2902 N94-27227

PROPULSION
NT AUXILIARY PROPULSION
NT CHEMICAL PROPULSION
NT ELECTRIC PROPULSION
NT ELECTROMAGNETIC PROPULSION
NT HYBRID PROPULSION
NT ION PROPULSION
NT JET PROPULSION
NT LASER PROPULSION
NT LOW THRUST PROPULSION
NT MARINE PROPULSION
NT MATTER-ANTIMATTER PROPULSION
NT NUCLEAR ELECTRIC PROPULSION
NT NUCLEAR PROPULSION
NT PLASMA PROPULSION
NT SOLAR ELECTRIC PROPULSION
NT SOLAR PROPULSION
NT SPACECRAFT PROPULSION
Propulsion 03 p0924 N94-15219
KINETIC: A system code for analyzing Nuclear thermal propulsion rocket engine transients
[DE93-016825] 04 p1337 N94-17884
Multi-disciplinary coupling effects for integrated design of propulsion systems
[NASA-TM-106349] 05 p1830 N94-20170
Modeling of polymer electrolyte fuel cell systems
[DE93-041187] 05 p1847 N94-21774

The 1993 NASA/ASEE Summer Faculty Fellowship Program
[NASA-CR-193862] 06 p2574 N94-24405
Design and flight test of the Propulsion Controlled Aircraft (PCA) flight control system on the NASA F-15 test aircraft
[NASA-CR-186028] 07 p2674 N94-27432
Institute for Computational Mechanics in Propulsion (ICOMP)
[NASA-TM-106542] 09 p3710 N94-32969
AFOSR Contractors Propulsion Meeting
[AD-A279028] 11 p4198 N94-35746

PROPULSION SYSTEM CONFIGURATIONS

Distributed simulation using a real-time shared memory network
[NASA-TM-106239] 01 p0319 N94-10724
Nuclear propulsion systems engineering
[DE93-010791] 02 p0548 N94-12870
Mirror fusion propulsion system: A performance comparison with alternate propulsion systems for the manned Mars Mission
[NASA-TM-109248] 02 p0550 N94-13147
Recent testing of 30 kW hydrogen arcjet thrusters
[NASA-TM-106214] 02 p0551 N94-13430
Gas core nuclear thermal rocket engine research and development in the former USSR
[DE93-012165] 02 p0552 N94-14013
Hypersonic propulsion characterization 02 p0505 N94-14156
Aeropropulsion facilities 02 p0506 N94-14161
Propulsion integration 02 p0508 N94-14174
Active control of fan-generated plane wave noise
[NASA-TM-109008] 02 p0777 N94-14481
NASA Operational Environment Team (NOET): NASA's key to environmental technology
[TABES PAPER 93-611] 03 p1052 N94-16143
Emerging technologies for the changing global market
[TABES PAPER 93-612] 03 p0930 N94-16144
Space Propulsion Synergy Group ETO technology assessments
[TABES PAPER 93-641] 03 p0929 N94-16149
Lunar lander and return propulsion system trade study
[NASA-TP-3388] 03 p0925 N94-16496
Advanced transportation system studies technical area 3: Alternate propulsion subsystem concepts, volume 2
[NASA-CR-193863] 03 p0927 N94-17096
Advanced transportation system studies technical area 3: Alternate propulsion subsystem concepts, volume 3
[NASA-CR-193864] 03 p0927 N94-17097
Advanced transportation system studies technical area 3: Alternate propulsion system concepts. SSME upper stage use
[NASA-CR-193865] 03 p0927 N94-17098
The ANL electric vehicle battery R&D program for DOE-EHP
[DE93-017414] 04 p1394 N94-17750
Mission needs and system commonality for space nuclear power and propulsion
[DE93-016557] 04 p1337 N94-17863
National Program Plan Fuel Cells in Transportation
[DE93-017557] 04 p1469 N94-19346
Overview of STOVL aircraft propulsion research offtakes and vertical lift systems
[NASA-TM-106387] 04 p1321 N94-19353
Initiation and modification of reaction by energy addition: Kinetic and transport phenomena
[AD-A271315] 05 p1797 N94-19936
Thrust expansion engine
[AD-D015896] 05 p1669 N94-20121
Entry velocities at Mars and Earth for short transit times
[AD-A272591] 05 p1665 N94-21420
Thrust augmentation options for the Beta 2 two-stage-to-orbit vehicle
[NASA-TM-106448] 05 p1648 N94-21563
Modeling of polymer electrolyte fuel cell systems
[DE93-041187] 05 p1847 N94-21774
Navy GTE seal development activity 05 p1655 N94-21794
Specialized data analysis for the Space Shuttle Main Engine and diagnostic evaluation of advanced propulsion system components
[NASA-CR-194720] 05 p1656 N94-21813
Brayton power conversion system parametric design modelling for nuclear electric propulsion
[NASA-CR-191135] 05 p1671 N94-21874
On the estimation algorithm used in adaptive performance optimization of turbofan engines
[NASA-TM-4551] 05 p1649 N94-21879
Grid generation requirements at Marshall Space Flight Center 05 p1919 N94-22354
Analysis and experiments of a whistler-wave plasma thruster
[DE94-001533] 06 p2209 N94-23012
Efficiency and reliability enhancements in propulsion flowfield modeling 06 p2215 N94-23055
Performance assessment of low pressure nuclear thermal propulsion 06 p2217 N94-23070
Lewis Research Center R and D Facilities
[NASA-TM-109400] 06 p2630 N94-23135
Assessment of an SP-100 bi-modal propulsion and power system
[DE94-000889] 06 p2218 N94-23433
Heat pipe cooled heat rejection subsystem modelling for nuclear electric propulsion
[NASA-CR-191132] 06 p2219 N94-24061
Probabilistic simulation of concurrent engineering of propulsion systems 06 p2177 N94-24317
Multi-disciplinary coupling for integrated design of propulsion systems 06 p2179 N94-24326
Center for modeling of turbulence and transition: Research briefs, 1993
[NASA-TM-106383] 06 p2333 N94-24336
VLCT-13: A commercial transport for the 21st Century
[NASA-CR-195492] 06 p2181 N94-24803
The Blue Emu
[NASA-CR-195535] 06 p2182 N94-24817
Extended duration lunar lander
[NASA-CR-195527] 06 p2206 N94-24916
Space transfer vehicle concepts and requirements. Volume 4: Summary of special studies
[NASA-CR-193918] 06 p2201 N94-24970
Effect of aeroelastic-propulsive interactions on flight dynamics of a hypersonic vehicle 06 p2164 N94-25113
Shielded Coil Electrodynamic Propulsion (SCEP). A feasibility study
[AD-A273824] 06 p2314 N94-25539
Proceedings of the 8th Annual Summer Conference: NASA/USRA Advanced Design Program
[NASA-CR-195118] 07 p3075 N94-25665
Systematic Propulsion Optimization Tools (SPOT) 07 p2976 N94-25666
Extraterrestrial surface propulsion systems 07 p2833 N94-25691
Eagle RTS: A design of a regional transport 07 p2671 N94-25709
Project Ares 3 07 p2671 N94-25712
Tesseract supersonic business transport 07 p2671 N94-25713
The design of four hypersonic reconnaissance aircraft 07 p2671 N94-25716
Nuclear electric propulsion for future NASA space science missions
[DE93-019086] 07 p2700 N94-25969
Interdisciplinary technology 07 p2686 N94-27363
A parametric sensitivity study for single-stage-to-orbit hypersonic vehicles using trajectory optimization
[NASA-CR-195703] 07 p2697 N94-27789
A numerical study of mixing and combustion in hypervelocity flows through a scramjet combustor model 07 p2808 N94-27911
A review of recent aeroelastic analysis methods for propulsion at NASA Lewis Research Center
[NASA-TP-3406] 07 p2846 N94-28227
Nuclear electric propulsion: A better, safer, cheaper transportation system for human exploration of Mars
[NASA-TM-106406] 08 p3171 N94-28833
Research and Development of Ram/Scramjets and Turboramjets in Russia
[AD-A275588] 08 p3151 N94-29291
Turboramjet engines: Types and performances 08 p3151 N94-29293
Fission-activated laser as primary power for CW laser propulsion
[DE94-006138] 08 p3295 N94-30367
Futurepath 3
[NASA-TM-109762] 09 p3735 N94-31819
First Annual High-Speed Research Workshop, part 2
[NASA-CP-10087-PT-2] 10 p3972 N94-33462
The NASA sponsored HSCT propulsion studies 10 p3974 N94-33476
P and W/GE propulsion systems studies introduction 10 p3974 N94-33478
Results of GEAE HSCT propulsion system studies 10 p3974 N94-33479
P and W propulsion systems studies results/status 10 p3974 N94-33480
First Annual High-Speed Research Workshop, part 3
[NASA-CP-10087-PT-3] 10 p3975 N94-33487
Enabling propulsion materials for high-speed civil transport engines 10 p3978 N94-33511
One fantastic ride
[NASA-TM-109828] 10 p4016 N94-33582
Advanced transportation system study: Manned launch vehicle concepts for two way transportation system payloads to LEO. Program cost estimates document
[NASA-CR-193953] 10 p4013 N94-34912
The 30th JANNAF Combustion Subcommittee Meeting, volume 2
[AD-A276794] 11 p4247 N94-35656
Technological challenges of High Altitude Long Endurance unmanned configurations 11 p4193 N94-36323
Propulsion system selection for a High Altitude Long Endurance aircraft 11 p4195 N94-36333
Propulsion system technologies for long range and long endurance aircraft 11 p4195 N94-36334
The STRATO 2C propulsion system: A low cost approach for a High Altitude Long Endurance aircraft 11 p4195 N94-36335

PROPULSION SYSTEM PERFORMANCE

Space nuclear thermal propulsion nuclear element tests at Sandia National Laboratories
[DE93-002301] 01 p0045 N94-10282
Arcjet space thrusters
[NASA-CR-193191] 01 p0046 N94-10700
Characterization of in-flight performance of ion propulsion systems
[NASA-TM-106283] 01 p0046 N94-10761
Space Storable Rocket Technology program (SSRT). Option 1 program
[NASA-CR-191171] 01 p0046 N94-10938
A distributed version of the NASA Engine Performance Program
[NASA-TM-106208] 01 p0327 N94-11231
Nuclear propulsion systems engineering
[DE93-010791] 02 p0548 N94-12870
Effects of hydrogen addition on combustion performance of a LOX/kerosene rocket
[NAL-TR-1177] 02 p0548 N94-12945
Propulsion simulator for magnetically-suspended wind tunnel models
[NASA-CR-189560] 02 p0527 N94-13127
Mirror fusion propulsion system: A performance comparison with alternate propulsion systems for the manned Mars Mission
[NASA-TM-109248] 02 p0550 N94-13147
Electromagnetic propulsion for spacecraft
[NASA-CR-191186] 02 p0551 N94-13416
Piston engine intake and exhaust system design
[ISVR-TR-222] 02 p0663 N94-13874
Gas core nuclear thermal rocket engine research and development in the former USSR
[DE93-012165] 02 p0552 N94-14013
Closed-chamber analysis of M5 propellant lot RAD-64597
[AD-A266321] 02 p0585 N94-14145
Hypersonic propulsion characterization 02 p0505 N94-14156
Aeropropulsion test and evaluation methods 02 p0506 N94-14165
Hypersonic flight test. Part 1: Propulsion flight testing 02 p0507 N94-14168
Development of Japanese Earth Resources Satellite-1 (JERS-1; FUYO-1) and it's operational results
[NASDA-SPP-930001] 03 p0884 N94-15001
Research in robust control for hypersonic aircraft
[NASA-CR-194106] 03 p0870 N94-15416
NASA Operational Environment Team (NOET): NASA's key to environmental technology
[TABES PAPER 93-611] 03 p1052 N94-16143
Emerging technologies for the changing global market
[TABES PAPER 93-612] 03 p0930 N94-16144
Space Propulsion Synergy Group ETO technology assessments
[TABES PAPER 93-641] 03 p0929 N94-16149
Lunar lander and return propulsion system trade study
[NASA-TP-3388] 03 p0925 N94-16496
Comparisons of selected laser beam power missions to conventionally powered missions
[NASA-TM-106110] 03 p1040 N94-16522
Effects of internal yaw-vectoring devices on the static performance of a pitch-vectoring nonaxisymmetric convergent-divergent nozzle
[NASA-TP-3369] 03 p0858 N94-16572
ALS engine propellant effector system
[NASA-CR-194650] 03 p0926 N94-16590
Space Shuttle main engine. NASA has not evaluated the alternate fuel turbopump costs and benefits. Report to the Administrator of the National Aeronautics and Space Administration
[GAO/NSIAD-94-54] 03 p0926 N94-16834
The ANL electric vehicle battery R&D program for DOE-EHP
[DE93-017414] 04 p1394 N94-17750
Mission needs and system commonality for space nuclear power and propulsion
[DE93-016557] 04 p1337 N94-17863
Adaptations to micropep and rocket to allow performance evaluation of multiple grain and/or airbreathing motors
[AD-A268798] 04 p1337 N94-18202
Evaluation of aftermarket LPG conversion kits in light-duty vehicle applications
[DE93-010035] 04 p1377 N94-18617

Technology test bed
[NASA-TM-109354] 04 p1322 N94-18953
National Program Plan Fuel Cells in Transportation
[DE93-017557] 04 p1469 N94-19346
Initiation and modification of reaction by energy addition: Kinetic and transport phenomena
[AD-A271315] 05 p1797 N94-19936
Multi-disciplinary coupling effects for integrated design of propulsion systems
[NASA-TM-106349] 05 p1830 N94-20170
Formulation of a next-generation interior ballistic code
[AD-A271539] 05 p1801 N94-20915
Entry velocities at Mars and Earth for short transit times
[AD-A272591] 05 p1665 N94-21420
Options for thrust augmentation for the Beta 2 two-stage-to-orbit launch vehicle
[NASA-TM-106418] 05 p1649 N94-21759
Modeling of polymer electrolyte fuel cell systems
[DE93-041187] 05 p1847 N94-21774
Navy GTE seal development activity
05 p1655 N94-21794
Specialized data analysis for the Space Shuttle Main Engine and diagnostic evaluation of advanced propulsion system components
[NASA-CR-194720] 05 p1656 N94-21813
Brayton power conversion system parametric design modelling for nuclear electric propulsion
[NASA-CR-191135] 05 p1671 N94-21874
On the estimation algorithm used in adaptive performance optimization of turbofan engines
[NASA-TM-4551] 05 p1649 N94-21879
Advanced Turbine Systems (ATS). Phase 1: System scoping and feasibility studies
[DE93-041130] 05 p1826 N94-21938
Analysis and experiments of a whistler-wave plasma thruster
[DE94-001533] 06 p2209 N94-23012
Small rocket research and technology
06 p2211 N94-23038
Performance assessment of low pressure nuclear thermal propulsion 06 p2217 N94-23070
Assessment of an SP-100 bi-modal propulsion and power system
[DE94-000889] 06 p2218 N94-23433
Performance evaluation of the Russian SPT-100 thruster at NASA LeRC
[NASA-TM-106401] 06 p2219 N94-23630
Center for modeling of turbulence and transition: Research briefs, 1993
[NASA-TM-106383] 06 p2333 N94-24336
A minimum cost tolerance allocation method for rocket engines and robust rocket engine design
06 p2222 N94-24419
Space Shuttle Main Engine performance analysis
06 p2222 N94-24444
Ignition and combustion characteristics of metallized propellants, phase 2
[NASA-CR-195107] 06 p2266 N94-24700
Performance of the NASA cm ion thruster
[NASA-TM-106426] 06 p2221 N94-24770
A conceptual design of an unmanned test vehicle using an airbreathing propulsion system
[NASA-CR-195550] 06 p2189 N94-25085
Effect of aeroelastic-propulsive interactions on flight dynamics of a hypersonic vehicle
06 p2164 N94-25113
Shielded Coil Electrodynamic Propulsion (SCEP). A feasibility study
[AD-A273824] 06 p2314 N94-25539
Extraterrestrial surface propulsion systems
07 p2833 N94-25691
Asteroid exploration and utilization
07 p3080 N94-25697
Nuclear electric propulsion for future NASA space science missions
[DE93-019086] 07 p2700 N94-25969
Interdisciplinary technology 07 p2686 N94-27363
Inertial electrostatic confinement as a power source for electric propulsion 07 p2668 N94-27373
Rocket engine numerical simulation
07 p2688 N94-27375
A parametric sensitivity study for single-stage-to-orbit hypersonic vehicles using trajectory optimization
[NASA-CR-195703] 07 p2697 N94-27789
A numerical study of mixing and combustion in hypervelocity flows through a scramjet combustor model
07 p2808 N94-27911
A review of recent aeroelastic analysis methods for propulsion at NASA Lewis Research Center
[NASA-TP-3406] 07 p2846 N94-28227
Nuclear electric propulsion: A better, safer, cheaper transportation system for human exploration of Mars
[NASA-TM-106406] 08 p3171 N94-28833
Fuels combustion research
[AD-A275122] 08 p3189 N94-29004
Orbital applications of electrodynamic propulsion
[AD-A275413] 08 p3173 N94-29216
Combustion for future supersonic transport propulsion
08 p3190 N94-29249
Research and Development of Ram/Scramjets and Turboramjets in Russia
[AD-A275588] 08 p3151 N94-29291
Turboramjet engines: Types and performances
08 p3151 N94-29293
Some problems of scramjet propulsion for aerospace planes. Part 1: Scramjet: Aims and features
08 p3151 N94-29295
CIAM experimental turboramjets
08 p3152 N94-29299
Some problems of scramjet propulsion for aerospace planes. Part 2: Scramjet: Development and test problems 08 p3152 N94-29301
Aspects of model-based rocket engine condition monitoring and control
[NASA-CR-195116] 08 p3173 N94-29848
Futurepath 3
[NASA-TM-109762] 09 p3735 N94-31819
Performance of a quasi-steady, multi megawatt, coaxial plasma thruster
[NASA-CR-195311] 09 p3616 N94-32970
First Annual High-Speed Research Workshop, part 2
[NASA-CP-10087-PT-2] 10 p3972 N94-33462
A NASA Lewis comparative propulsion system assessment for the High-Speed Civil Transport
10 p3974 N94-33477
P and W/GE propulsion systems studies introduction
10 p3974 N94-33478
Results of GEAE HSCT propulsion system studies
10 p3974 N94-33479
P and W propulsion systems studies results/status
10 p3974 N94-33480
One fantastic ride
[NASA-TM-109828] 10 p4016 N94-33582
Operating characteristics of the Russian D-55 thruster with anode layer
[NASA-TM-106610] 10 p4016 N94-33606
A versatile rocket engine hot gas facility
[NASA-CR-195339] 10 p4011 N94-34131
Compact diffusers for small transonic compressors
10 p4002 N94-34449
Effect of tip clearance on the performance of a highly loaded turbine stage 10 p4003 N94-34458
Design and aerodynamic performance evaluation of a high-work mixed flow turbine stage
10 p4003 N94-34459
USAF/AEDC aerodynamic and propulsion ground test and evaluation techniques for highly maneuverable aircraft: Capabilities and challenges 10 p3990 N94-34606
Engine characteristics for agile aircraft
10 p3991 N94-34608
The 30th JANNAF Combustion Subcommittee Meeting, volume 2
[AD-A278794] 11 p4247 N94-35656
Recent Advances in Long Range and Long Endurance Operation of Aircraft
[AGARD-CP-547] 11 p4193 N94-36321
Technological challenges of High Altitude Long Endurance unmanned configurations
11 p4193 N94-36323
Hot dynamic test rig for measuring hypersonic engine seal flow and durability
[NASA-TM-106507] 12 p4450 N94-36645
Possibilities and pitfalls in aerospace applications of titanium matrix composites 12 p4400 N94-36650
Characteristics of ions emitted from high-current hollow cathodes
[NASA-CR-195372] 12 p4398 N94-37764

PROPULSIVE EFFICIENCY
NT PROPELLER EFFICIENCY
Propulsion integration 02 p0508 N94-14174
Plasma instabilities and transport in the MPD thruster
[AD-A268268] 03 p1204 N94-17575
Fuel cell systems program plan, fiscal year 1993
[DE93-017828] 04 p1466 N94-18103
National Program Plan Fuel Cells in Transportation
[DE93-017557] 04 p1469 N94-19346
Thrust augmentation options for the Beta 2 two-stage-to-orbit vehicle
[NASA-TM-106448] 05 p1648 N94-21563
Pulsed expansion of plasma in a magnetic thruster
09 p3889 N94-31776
Operating characteristics of the Russian D-55 thruster with anode layer
[NASA-TM-106610] 10 p4016 N94-33606

PROPYL COMPOUNDS
The reaction of hydroperoxy-propyl radicals with molecular oxygen
[DE94-006392] 11 p4239 N94-36319

PROPYLENE
Determination of concentration profiles at interfaces and surfaces of partially miscible polymer blends
[DE93-013140] 01 p0089 N94-11007
Surface characterization of LDEF materials
[NASA-CR-194519] 02 p0543 N94-14683
Synthesis of potential high-energy fuels
[AD-A267508] 03 p0975 N94-17073
Morphology of highly textured polyethylene/polyethylene- propylene semicrystalline diblock copolymers
[AD-A273683] 06 p2263 N94-25413
Enhanced ion dissociation of LiCF3SO3 by new carbonate plasticizers: Raman and IR studies
[DE94-005448] 08 p3485 N94-28741
An investigation of molybdenum and molybdenum oxide catalyzed hydrocarbon formation reactions
[DE94-013700] 12 p4409 N94-37132

PROSPECTING
U EXPLORATION

PROSTAGLANDINS
Effect of PGE2 receptor agonists butaprost, M and B 28767 and an antagonist AH 6809 on the BK response of visceral polymodal receptors
07 p2906 N94-27494
Effect of prostaglandin E1 on the relationship between skin sympathetic nerve activity and reduction in skin blood flow 07 p2929 N94-27524
The polymodal receptor 07 p2908 N94-27539

PROSTATE GLAND
Screening for prostate cancer
03 p1126 N94-16630
Conformal external radiotherapy of prostatic carcinoma: Requirements and preliminary results
08 p3395 N94-30029

PROSTHETIC DEVICES
New prosthetic devices
[NASA-TM-109304] 02 p0737 N94-13611
Automatic locking orthotic knee device
[NASA-CASE-MFS-28633-1] 05 p1896 N94-20493
Image remapping strategies applied as protheses for the visually impaired 06 p2444 N94-25363
Application of dexterous space robotics technology to myoelectric prostheses 09 p3729 N94-32450
Prosthetic elbow joint
[NASA-CASE-MFS-28707-1] 10 p4100 N94-35115
Selectively lockable knee brace
[NASA-CASE-MFS-28991-1] 12 p4486 N94-36838
Channel in hip implant stem
[NASA-CASE-MFS-28987-1] 12 p4486 N94-36840

PROTEASE
Cellular mechanism of turnover of the stress induced protein HSP 70
[AD-A265723] 02 p0732 N94-13061
Regulation of attached bacterial growth by adsorbed proteins
[AD-A267756] 03 p1118 N94-17275
Enhancement of wound healing by biosynthetic growth factor
[AD-A272517] 05 p1892 N94-21415
Evaluation of ovostatin and ovostatin assay
06 p2422 N94-24437
Studies on bacterial spore ultraviolet light resistance and regulation of the activity of a spore protease
[AD-A275448] 08 p3384 N94-28884

PROTECTION
NT ACCELERATION PROTECTION
NT CIRCUIT PROTECTION
NT CORROSION PREVENTION
NT ENVIRONMENT PROTECTION
NT EYE PROTECTION
NT METEOROID PROTECTION
NT RADIATION PROTECTION
NT RADIATION SHIELDING
NT SOLAR RADIATION SHIELDING
NT THERMAL PROTECTION
An assessment of the potential for neck injury due to padding of aircraft interior walls for head impact protection
[DOT/FAA/AM-93/14] 02 p0738 N94-13972
NASA security handbook
[NHB-1620.3C] 03 p1224 N94-15937
The effect of surface treatment and gaseous rust protection paper on the atmospheric corrosion stability of aluminium alloy
[DE93-623326] 04 p1355 N94-17679
Lightning studies using LDAR and LLP data
06 p2416 N94-23238
Development of a new chemical warfare agent protective material 08 p3381 N94-28432
Controlling hazardous energy sources (lockout/tagout)
[NASA-TM-105290] 09 p3669 N94-32861
Magnetic field sources and their threat to magnetic media 10 p4151 N94-33794
Evaluation of pulsed Doppler bubble detection
[AD-A277920] 10 p4095 N94-34695

Blast overpressure studies with animals and man
[AD-A280240] 12 p4480 N94-37118

PROTECTIVE CLOTHING
NT EXTRAVEHICULAR MOBILITY UNITS
NT HELMETS
NT PRESSURE SUITS
NT SPACE SUITS
NT VAPOR BARRIER CLOTHING

Aerospace medicine and biology: A continuing bibliography with indexes (supplement 375)
[NASA-SP-7011(375)] 01 p0303 N94-10398

Aerospace medicine and biology: A continuing bibliography with indexes (supplement 376)
[NASA-SP-7011(376)] 01 p0303 N94-10399

Aerospace medicine and biology: A continuing bibliography with indexes (supplement 374)
[NASA-SP-7011(374)] 01 p0304 N94-11689

Flammability of clothing, volume 2
[DSIS-93-00036-VOL-2] 02 p0564 N94-13819

Review of test methods for material flammability
[DSIS-93-00480] 02 p0564 N94-13942

Aerospace medicine and biology: A continuing bibliography with indexes (supplement 379)
[NASA-SP-7011(379)] 02 p0733 N94-14412

Firefighters breathing system
[NASA-TM-109611] 03 p1135 N94-15362

STS-29 crew bailout in WETF
[NASA-TM-109548] 03 p1136 N94-15385

Investigation of the effects of extravehicular activity (EVA) gloves on performance
[NASA-TP-3401] 03 p1137 N94-15717

USAF physiological studies of personal microclimate cooling: A review
[AD-A267203] 03 p1022 N94-15858

Aerospace medicine and biology: A continuing bibliography with indexes (supplement 378)
[NASA-SP-7011(378)] 03 p1122 N94-16478

Aerospace medicine and biology: A continuing bibliography with indexes (supplement 380)
[NASA-SP-7011(380)] 03 p1122 N94-16479

Conductive garments to prevent Radio-Frequency (RF) burns
[AD-D015832] 04 p1512 N94-18730

Aerospace medicine and biology: A continuing bibliography with indexes (supplement 382)
[NASA-SP-7011(382)] 04 p1507 N94-18936

Aerospace medicine and biology: A continuing bibliography with indexes (supplement 381)
[NASA-SP-7011(381)] 04 p1507 N94-19069

Cold-start minidiesel engine development
[AD-A271064] 05 p1823 N94-20567

Aerospace medicine and biology: A continuing bibliography with indexes (supplement 383)
[NASA-SP-7011(383)] 05 p1892 N94-21288

Survival suit for submarine personnel: Summary of evaluation studies
[PB93-204634] 06 p2430 N94-23743

Operation Friction: Development and introduction of personal cooling for CH124 Sea King aircrew
[DCIEM-93-06] 06 p2433 N94-24119

Control panel dimensions for gloved operation study 2: Toggle switches minimum spacing required between toggle
[AD-A274518] 07 p2942 N94-27089

Aerospace medicine and biology: A continuing bibliography with indexes (supplement 386)
[NASA-SP-7011(386)] 07 p2933 N94-28208

Aerospace medicine and biology: A continuing bibliography with indexes (supplement 387)
[NASA-SP-7011(387)] 07 p2933 N94-28213

The Support of Air Operations under Extreme Hot and Cold Weather Conditions
[AGARD-CP-540] 08 p3379 N94-28420

Evaluation of life support equipment during an unsupported North Pole expedition
08 p3379 N94-28422

The potential of new textiles in improving survival prospects
08 p3380 N94-28430

Fire-resistant water vapour permeable buoyant insulation
08 p3380 N94-28431

Thermal protective performance and instrumented mannequin evaluation of multi-layer garment systems
08 p3381 N94-28433

Effectiveness of protection clothing for cold weather conditions after ejection over sea: A case report
08 p3381 N94-28435

Advanced integrated cold protection for aircrew
08 p3381 N94-28436

Thermal strain generated by an enhanced anti-G protection system in a hot climate
08 p3383 N94-28445

Implications of climatic extremes in aircrew NBC operations
08 p3383 N94-28446

Test of a new protection suit in a climatic chamber
08 p3384 N94-28452

A reliable and repeatable method for volume calculation of pressurized garments
[AD-A275600] 08 p3399 N94-28766

Comparison of two cool vests on heat-strain reduction while wearing a firefighting ensemble in a hot/humid environment
[AD-A275103] 08 p3400 N94-28902

Physiological responses during shipboard firefighting
[AD-A275104] 08 p3391 N94-28912

Comparative centrifuge evaluation of the Air Force Advanced Technology Anti-G Suit (ATAGS) and the Navy Enhanced Anti-G Lower Ensemble (EAGLE)
[AD-A275348] 08 p3400 N94-28996

Procedures and metrics for anti-G suit evaluations
[AD-A275349] 08 p3400 N94-28997

Effects of endurance training on heat-exercise tolerance in men wearing NBC protective clothing
[AD-A275176] 08 p3391 N94-29049

Insulative properties of two thermo-metal neoprenes
[AD-A275209] 08 p3401 N94-29302

A review of microclimate cooling systems in the chemical, biological, radiological environment
[AD-A276446] 09 p3802 N94-31302

Proceedings of the DCIEM Diver Thermal Protection Workshop
[DCIEM-92-10] 09 p3795 N94-31738

Thermotropic liquid crystals: A variable Clo material
09 p3796 N94-31739

Validation and sensitivity analysis of Texas human thermal model predictions during cold water immersion
[AD-A275240] 09 p3797 N94-32156

Aerospace medicine and biology: A continuing bibliography with indexes (supplement 389)
[NASA-SP-7011(389)] 09 p3797 N94-32347

Aerospace medicine and biology: A continuing bibliography with indexes (supplement 385)
[NASA-SP-7011(385)] 09 p3797 N94-32348

Aircrew Eye/Respiratory Protection (AERP): 16-hour extended wear evaluation of chemical protective equipment
[AD-A277288] 09 p3804 N94-32609

Personal cooling systems: Possibilities and limitations
10 p4101 N94-33649

Advanced integrated life support system update
10 p4102 N94-33657

Effects of heat acclimation on heat-exercise tolerance in untrained and endurance-trained men wearing NBC protective clothing
[AD-A277522] 10 p4099 N94-33707

Aerospace medicine and biology: A continuing bibliography with indexes (supplement 391)
[NASA-SP-7011(391)] 11 p4297 N94-35345

Aerospace medicine and biology: A continuing bibliography with indexes (supplement 392)
[NASA-SP-7011(392)] 12 p4482 N94-37445

PROTECTIVE COATINGS
NT ANODIC COATINGS
NT CERAMIC COATINGS
NT PRIMERS (COATINGS)
NT REFRACTORY COATINGS

Selectively strippable paint schemes
01 p0128 N94-10629

Advanced zinc phosphate conversion and pre-ceramic polymetallosiloxane coatings for corrosion protection of steel and aluminum, and characteristics of polyphenyletheretherketone-based materials
[DE93-008717] 01 p0088 N94-10891

Understanding cracking failures of coatings: A fracture mechanics approach
01 p0187 N94-11218

Field evaluation of six protective coatings applied to T-56 turbine blades after 2500 hours of engine use
[ARL-TR-27] 01 p0090 N94-11311

High-temperature corrosion of ceramic-ceramic composites in a waste incinerator environment
[DE93-012430] 01 p0072 N94-11368

Weld overlay coatings for erosion control
[DE93-013592] 01 p0084 N94-11816

Protective coatings for high-temperature polymer matrix composites
[NASA-TM-106276] 01 p0074 N94-12431

Corrosion and passivation of high temperature superconductors
[AD-A265402] 01 p0405 N94-12586

High-temperature corrosion and protection of materials
[DE93-011072] 02 p0568 N94-12998

Dry film lubricant evaluation
[DE93-013114] 02 p0578 N94-13118

The effect of TiN coatings on the rolling contact fatique behavior of M50 bearing steel
[ARL-TR-40] 02 p0662 N94-13794

JPRS report: Science and technology. Central Eurasia: Materials science
[JPRS-UMS-93-006] 02 p0558 N94-14573

JPRS report: Science and technology. Central Eurasia: Materials science
[JPRS-UMS-93-005] 02 p0559 N94-14575

Restoring Miss Liberty --- inorganic coatings
[NASA-TM-109605] 03 p0963 N94-15313

Assessment of chromate and non-chromate conversion coatings for Al alloys using electrochemical impedance spectroscopy
[AD-A267205] 03 p0965 N94-15859

Krupp technical reports no. 2, English edition, October 1992
[ETN-93-94631] 03 p0984 N94-16000

Vacuum plasma spraying 03 p0975 N94-16002

Chemical vapor deposition of Ta2O5 corrosion resistant coatings
[DE93-015488] 03 p0969 N94-16889

Robotic weld overlay coatings for erosion control
[DE93-016938] 03 p0970 N94-16959

Evaluation of hybrid reinforcement (fiber-reinforced-plastic rod with steel core)
[AD-A268009] 03 p0941 N94-17473

Titanium carbon-hydrogen layers on decorative surfaces 04 p1375 N94-18010

Sputtered TiN coatings in plastic
04 p1367 N94-18011

Gold-copper-zinc coatings as an alternative to gold-copper-cadmium 04 p1367 N94-18012

NSWCWODET participation in Space Shuttle mission STS-46
[AD-A268875] 04 p1332 N94-18321

Solderability perservative coatings: Electroless tin versus organic azoles
[DE93-017634] 04 p1370 N94-18477

Carbon/carbon composites coated with SiC by chemical vapor deposition
[AD-A269934] 04 p1341 N94-18544

Joining and Adhesion of Advanced Inorganic Materials Symposium
[AD-A269748] 04 p1342 N94-18720

JPRS report: Science and technology. Central Eurasia: Materials science
[JPRS-UMS-93-002] 04 p1339 N94-18833

Thermal analysis of coatings and substrate materials during a disruption in fusion reactors
[DE93-017688] 04 p1588 N94-18971

Contribution to the tribological study of magnetic-tape head contact
[ECL-92-57] 04 p1434 N94-19414

Testing of protective coatings in hydrogen
[DE93-040326] 04 p1375 N94-19651

Tribological studies of silicon for magnetic recording applications (Invited)
[AD-A270878] 04 p1447 N94-19784

Oxidation resistant protective coating system for gas turbine components and process for penetration thereof
[CA-PATENT-1,294,155] 05 p1704 N94-21143

Fifth International Symposium on Materials in a Space Environment
[ISBN-2-85-428293-0] 05 p1659 N94-21367

Aragatz project samples experiment/MAPOL (polymer materials) experiment: Postflight expert evaluation
05 p1660 N94-21376

The implications of the LDEF results on Space Station Freedom power system materials
05 p1660 N94-21377

Evaluation of plasma-deposited protective coatings for spacecraft applications 05 p1663 N94-21394

Forecasting technique of variations of the optical absorptivity of thermal control coatings under different simultaneous radiations 05 p1664 N94-21399

Thermal control coatings 05 p1664 N94-21400

Study of space factors effect on materials for spacecraft external surfaces in NPO Energia programs
05 p1664 N94-21401

Review of corrosion behavior of ceramic heat exchanger materals: Corrosion characteristics of silicon carbide and silicon nitride
[DE93-041307] 05 p1706 N94-21516

Performance of carbon-based hot frit substrates
[DE94-000509] 05 p1676 N94-21754

Surface modification for corrosion resistance
[DE93-017419] 05 p1693 N94-21825

Surface modification of Ti3Al for improved oxidation resistance
[DE93-018297] 05 p1696 N94-22034

Advanced research and technology development of MCFCs
[DE94-001918] 06 p2389 N94-22723

Chromate-free talc chemical conversion coatings for aluminum alloys
[DE94-001567] 06 p2238 N94-22932

Advanced materials for radiation-cooled rockets
06 p2214 N94-23052

Counterrotating aircraft propulsor blades
[CA-PATENT-1-319-357] 06 p2186 N94-23255

Fiber optic temperature sensor using a Y2O2S:Eu thermographic phosphor
[DE94-000331] 06 p2543 N94-23461
Characterization and durability testing of plasma-sprayed zirconia-yttria and hafnia-yttria thermal barrier coatings. Part 2: Effect of spray parameters on the performance of several hafnia-yttria and zirconia-yttria coatings
[NASA-TP-3296] 06 p2242 N94-23467
Diffuse panel studies: Conclusions
06 p2384 N94-23606
New tribocoating combination for vacuum operation
06 p2355 N94-23990
Tribological characteristics of ball bearings lubricated with a sputtered molybdenum disulphide film in a vacuum under a high thrust load 06 p2355 N94-23992
In-vacuum performance of Fomblin Z25-lubricated, 52100 steel bearings with TiC-coated balls
06 p2358 N94-24011
Structural characterization and thermal cycling behaviour of EB-PVD thermal barrier coating systems
[ISBN-0-315-83365-3] 06 p2257 N94-24468
Robotic weld overlay coatings for erosion control
[DE94-002665] 06 p2258 N94-24749
The reaction mechanism of W-CVD in Si
[ETN-94-95329] 06 p2261 N94-25084
Proceedings of the 12th International Congress: Corrosion Control for Low-Cost Reliability. Volume 4: Oil/Gas Pipeline
[AD-A273665] 06 p2250 N94-25405
Proceedings of the 12th International Congress: Corrosion Control for Low-Cost Reliability. Volume 5A: Corrosion: General issues
[AD-A273666] 06 p2250 N94-25406
A preliminary evaluation of the phosphazene resin PPZ
[AD-A273674] 06 p2263 N94-25410
Proceedings of the 12th International Congress: Corrosion Control for Low-Cost Reliability. Volume 1: Coatings
[AD-A273661] 06 p2251 N94-25448
Proceedings of the 12th International Congress: Corrosion Control for Low-Cost Reliability. Volume 2: Process Industries Plant Operations
[AD-A273662] 06 p2251 N94-25449
Proceedings of the 12th International Congress: Corrosion Control for Low-Cost Reliability. Volume 3B: Corrosion: Specific issues
[AD-A273664] 06 p2251 N94-25451
R and D for creation, measurement, application of ultra-high vacuum 07 p2723 N94-25549
Hydrogen trapping with Pd coated alloy films
07 p2723 N94-25551
Issues for conversion coating of aluminum alloys with hydrotalcite
[DE94-003804] 07 p2732 N94-25819
Cracking of textured zinc coating during forming process
[DE94-003414] 07 p2750 N94-26085
Ceramic technology project
[DE94-003782] 07 p2750 N94-26332
Titanium 1992: Volume 3: Science and technology
[AD-A274800] 07 p2735 N94-26337
Polyurethane self-priming topcoats
[AD-D016041] 07 p2755 N94-27111
Corrosion resistant coatings from conducting polymers
[DE94-003959] 07 p2757 N94-27747
Selection of the Space Station Freedom (SSF) Flat Collector Circuit (FCC) insulation material
08 p3165 N94-28701
Corrosion inhibition by electrodeposited conductive-polymer film
[AD-A275456] 08 p3213 N94-28806
Heat flux instrumentation for Hyflite thermal protection system
[NASA-CR-195731] 08 p3286 N94-28824
Low Earth orbit durability evaluation of protected silicone for advanced refractive photovoltaic concentrator arrays
[NASA-TM-106543] 08 p3172 N94-28999
Evaluation of oxide-coated iridium-rhenium chambers
[NASA-TM-106442] 08 p3172 N94-29097
Electrochemical behavior and surface chemistry of nonequilibrium aluminum alloys: Passivity mechanism and fabrication methods
[AD-A275401] 08 p3204 N94-29196
Insulative properties of two thermo-metal neoprenes
[AD-A275209] 08 p3401 N94-29302
Thick thermal barrier coatings for diesel components
[NASA-CR-187111] 08 p3537 N94-29350
Rules and definition of the range of paints applied on aeronautical structrural composites
[REPT-932-600-106] 08 p3215 N94-29459
Plasma sprayed ceramic thermal barrier coating for NiAl-based intermetallic alloys
[NASA-CASE-LEW-15535-1] 08 p3205 N94-29507
Polyimides containing pendent siloxane groups
[NASA-CASE-LAR-14638-1] 08 p3215 N94-29555
Performance of CVD and CVR coated carbon-carbon in high temperature hydrogen
[DE94-005451] 08 p3487 N94-29841
Non-chromate talc conversion coatings for aluminum
[DE94-005281] 08 p3207 N94-30053
Evaluation of corrosion protecting properties of modern aircraft paint systems
[AD-B179388] 08 p3220 N94-30420
Deposition of tantalum carbide coatings on graphite by laser interactions 08 p3223 N94-30475
Development of a unique polyurethane primer/topcoat
08 p3223 N94-30476
Four advances in carbon-carbon materials technology
08 p3186 N94-30481
The performance of gloss meters on curving surfaces
[NPL-DMM(A)-111] 08 p3501 N94-30522
Atomic oxygen interaction at defect sights in protective coatings on polymers flown on LDEF
09 p3593 N94-31024
Low-Earth orbit effects on organic composite materials flown on LDEF 09 p3595 N94-31036
Evaluation of corrosion protective organic coatings for steel structures in fresh water
[PB94-138484] 09 p3649 N94-31072
Sol-gel metal oxide and metal oxide/polymer multilayers applied by meniscus coating
[DE94-005813] 09 p3649 N94-31199
Electrostatic reduction of particulates for laser resistant hafnia coatings
[DE94-005824] 09 p3651 N94-31557
Processing boron and boron carbide thin films for protective coatings and device fabrication
[AD-A277266] 09 p3900 N94-32041
Compilation of diamond-like carbon properties for barriers and hard coatings
[DE94-008231] 09 p3661 N94-32803
Method and apparatus for inhibiting the disbonding of a paint from metal surfaces
[AD-D016106] 09 p3663 N94-32960
Interface engineering in oxide fiber/oxide matrix composites
[AD-A277672] 09 p3627 N94-33029
Evaluation of the Hughes conversion coating touch-up pen
[AD-A278398] 09 p3664 N94-33166
Polyurethane self-priming topcoats
[AD-D016131] 10 p4027 N94-33697
A new tape product for optical data storage
10 p4152 N94-33796
Thermal cyclic oxidation behavior of the developed compositionally gradient graphite material of SiC and C in air environment
[DE94-727591] 10 p4027 N94-33872
Robotic weld overlay coatings for erosion control
[DE94-009703] 10 p4060 N94-33902
Proceedings of the 57th National Congress of Japan Thermal Spraying Society
[DE94-731734] 10 p4029 N94-34133
Polyurethane self-priming topcoats
[AD-D016160] 10 p4030 N94-34285
Oxidation performance of platinum-clad Mo-47Re alloy
[NASA-TM-4559] 10 p4025 N94-34398
Analysis of the Shuttle Orbiter reinforced carbon-carbon oxidation protection system
[NASA-TM-104792] 11 p4262 N94-35245
Atomic oxygen protective coating with resistance to undercutting at defect sites
[NASA-CASE-LEW-15306-1] 11 p4243 N94-35502
Coatings for SiO2 optical fibers
[AD-D016197] 11 p4334 N94-36363
Atomic oxygen treatment for non-contact removal of organic protective coatings from painting surfaces
[NASA-TM-106650] 12 p4421 N94-36952
Robotic weld overlay coatings for erosion control
[DE94-013477] 12 p4417 N94-37116
Interfaces of high-protection performance polyaryls-coated zinc phosphated steels
[DE94-011732] 12 p4417 N94-37153
Compilation of diamond-like carbon properties for barriers and hard coatings
[DE94-012139] 12 p4427 N94-37725

PROTECTORS
NT EAR PROTECTORS

PROTEIN CRYSTAL GROWTH
Advanced protein, crystallization facility and associated new developments 01 p0039 N94-10119
Effects of a microgravity environment on the crystallization of biological macromolecules
01 p0117 N94-10198
Breadboard activities for advanced protein crystal growth
[NASA-CR-193559] 02 p0803 N94-12796
Advanced protein crystal growth programmatic sensitivity study
[NASA-CR-193827] 02 p0804 N94-12934
Protein crystal growth 02 p0591 N94-13756
Crystal growth of enzymes in low gravity (L-5)
02 p0592 N94-13762
STS-26 protein growth (PCG) experiment
[NASA-TM-109533] 03 p0976 N94-15395
Convective flow effects on protein crystal growth
[NASA-CR-194560] 03 p1206 N94-15476
Solution behaviour in microgravity: Considerations for protein crystal growth 03 p0982 N94-16102
The roles of fluid motion and other transport phenomena in the morphology of materials
[NASA-CR-194665] 03 p1028 N94-17298
Method for controlling protein crystallization
[NASA-CASE-MFS-28688-1] 05 p2017 N94-20528
Microgravity sciences application visiting scientist program
[NASA-CR-194804] 06 p2267 N94-23287
Modeling of PCG fluid dynamics: Salient results
06 p2224 N94-24345
Stiffening of deployable space booms: Automated Protein Crystal Growth Facility
[NASA-CR-195547] 06 p2196 N94-24820
Survey report of JSUP Space Environment Utilization Research Committee in fiscal year 1992: Protein Crystal Growth Session
[JTN-94-80584] 08 p3158 N94-28583
Overview of space environment utilization science
[JTN-94-80581] 08 p3227 N94-28938
Protein crystal growth in microgravity
08 p3228 N94-28943
Thermal enclosure system functional simulation user's manual
[NASA-TM-109094] 08 p3466 N94-29489
Convective flow effects on protein crystal growth
[NASA-CR-195785] 08 p3515 N94-30015

PROTEIN METABOLISM
NT LIPID METABOLISM
Space research on organs and tissues
04 p1503 N94-19214
Skeletal muscle metabolism in hypokinetic rats
[NASA-CR-195082] 06 p2420 N94-24124

PROTEIN SYNTHESIS
Cellular mechanism of turnover of the stress induced protein HSP 70
[AD-A265723] 02 p0732 N94-13061
The first steps of chlorophyll synthesis: RNA involvement and regulation
[DE93-014398] 02 p0730 N94-14509
Cellular and molecular level responses after radiofrequency radiation exposure, alone or in combination with x rays or chemicals
[AD-A268189] 04 p1501 N94-17729
A complex systems approach to computational molecular biology
[DE93-040062] 05 p1884 N94-19866
Stress and brain protein synthesis
[PB94-170750] 11 p4296 N94-35601

PROTEINS
NT ALBUMINS
NT ALDOLASE
NT CALMODULIN
NT CARBOXYHEMOGLOBIN
NT ELASTIN
NT ENZYMES
NT GLOBULINS
NT HEMOGLOBIN
NT LYSOZYME
NT MYOGLOBIN
NT OXIDASE
NT PROTEASE
NT TRYPSIN
Electrohydrodynamic effects in continuous flow electrophoresis observations on Earth and in microgravity 01 p0122 N94-10234
HRTEM in protein crystallography
[DE93-610322] 01 p0395 N94-10406
Amperometric biosensors based on 3-dimensional hydrogel-forming epoxy networks
[AD-A265528] 01 p0087 N94-10510
Aluminum and membrane channels
[AD-A265241] 01 p0300 N94-11020
A new decomposition strategy for parallel bonded molecular dynamics
[DE93-009839] 01 p0366 N94-11284
Probability of alamethicin conductance states varies with nonlamellar tendency of bilayer phospholipids
[AD-A264957] 01 p0301 N94-11648
The phytoplankton bloom in the Kinu-ura Bay, Japan in the rainy season 01 p0211 N94-12660
Solitons and 1/f noise in molecular chains
[DE93-622898] 02 p0778 N94-12879

Cellular mechanism of turnover of the stress induced protein HSP 70
[AD-A265723] 02 p0732 N94-13061
Protein crystal growth 02 p0591 N94-13756
Characterization of Spirulina biomass for CELSS diet potential
[NASA-CR-194123] 02 p0729 N94-14097
The surface-located YopN protein is involved in calcium signal transduction in Yersinia pseudotuberculosis
[FOA-B-40416-4.4] 02 p0729 N94-14128
Selective excitation, relaxation, and energy channeling in molecular systems
[DE93-018819] 02 p0785 N94-14420
The first steps of chlorophyll synthesis: RNA involvement and regulation
[DE93-014398] 02 p0730 N94-14509
Biomimetic methane oxidation
[DE93-013196] 02 p0705 N94-14510
Materials Research Society Symposium Proceedings, Volume 292: Biomolecular Materials
[AD-A265776] 03 p1116 N94-15138
The relationship of metallothionein induction to the heat shock response
[AD-A266634] 03 p1122 N94-15741
Study of protein-H2O interactions by multidimensional NMR spectroscopy
[AD-A266955] 03 p0946 N94-15760
Bioorganic models for protein ion channels
[AD-A266365] 03 p1117 N94-16441
Heat shock protein induction in human cells by CO2 laser irradiation
[AD-A266430] 03 p1117 N94-16545
Hemoglobin
[AD-A266455] 03 p1123 N94-16566
Release of iron from hemoglobin
[AD-A266503] 03 p1128 N94-16784
Regulation of attached bacterial growth by adsorbed proteins
[AD-A267756] 03 p1118 N94-17275
In vivo animal models of body composition in aging
[DE93-012527] 04 p1501 N94-17889
X ray absorption spectroscopic studies of the active sites of nickel- and copper-containing metalloproteins
[DE93-017142] 04 p1347 N94-18059
The c-jun gene expression in human cells exposed to either ionizing radiation or hydrogen peroxide
[DE93-017436] 04 p1502 N94-18476
High resolution electron crystallography of protein molecules
[DE93-040114] 05 p1884 N94-19826
Quinoa: An emerging new crop with potential for CELSS
[NASA-TP-3422] 05 p1895 N94-20137
Microgravity sciences application visiting scientist program
[NASA-CR-194804] 06 p2267 N94-23287
Microinjection of the Yersinia YopE cytotoxin in mammalian cells induces actin microfilament disruption
[FOA-B-40418-4.4] 06 p2421 N94-24290
Evaluation of ovostatin and ovostatin assay
06 p2422 N94-24437
In vitro system for studying metabolism of environmental chemicals in human cells
[AD-A273427] 06 p2421 N94-24688
Molecular biological studies on the human radioresistance and drug resistance
[DE93-632682] 07 p2910 N94-26549
Neutron and x ray scattering studies of the interactions between Ca(2+)-binding proteins and their regulatory targets: Comparisons of troponin C and calmodulin
[DE94-002706] 07 p2901 N94-26623
Cloning of rat RXR alpha cDNA and the expression of its mRNA in regenerating liver and primary cultured hepatocytes 07 p2905 N94-27479
Cloning of a novel POU family gene by RT-PCR method 07 p2905 N94-27480
Expression analysis of Thyroxine-Binding Globulin Complete Deficiency in Japanese (TBG-CDJ)
07 p2905 N94-27482
Activation by G protein beta gamma subunits of G protein-coupled receptor kinase
07 p2931 N94-27534
The molecular matching problem
07 p3030 N94-27910
Barley cell culture as a producer of heterologous protein
[PB94-132339] 08 p3379 N94-28408
Survey report of JSUP Space Environment Utilization Research Committee in fiscal year 1992: Protein Crystal Growth Session
[JTN-94-80584] 08 p3158 N94-28583
Development of novel switchable protein surfaces
[AD-A275510] 08 p3384 N94-28667
Protein crystal growth in microgravity
08 p3228 N94-28943
Employment of a porous gold actuator in ISFET-based coulometric sensor-actuator systems with application to protein characterization
[ISBN-9-09-005887-7] 09 p3689 N94-31536
Chemical interactions between protein molecules and polymer membrane materials
[DE94-006987] 09 p3651 N94-31672
Neural network definitions of highly predictable protein secondary structure classes
[DE94-006234] 09 p3834 N94-32175
A genetic algorithm based method for docking flexible molecules
[DE94-007525] 09 p3793 N94-32269
Development and application of photosensitive device systems to studies of biological and organic materials
[DE94-008503] 09 p3793 N94-32516
The magnesium chelation step in chlorophyll biosynthesis
[DE94-008727] 09 p3794 N94-32890
Phase-sensitive flow cytometry: New technology for analyzing biochemical, functional, and structural features in fluorochrome-labeled cells and particles
[DE94-003960] 10 p4094 N94-33734
Stress and brain protein synthesis
[PB94-170750] 11 p4296 N94-35601
A low temperature scanning force microscope for biological samples
[DE94-011357] 11 p4297 N94-36269
Femtosecond transient absorption studies of the light harvesting Chl a/b protein complex of Photosystem 2 in higher plants
[DE94-009684] 12 p4477 N94-36481
Recombinant protein production and insect cell culture and process
[NASA-CASE-MSC-22336-1] 12 p4478 N94-36751
Chemical and structural characterization of nitroaromatic adducts with hemoglobins
[AD-A280533] 12 p4480 N94-37089
High resolution electron diffraction analysis of structural changes associated with the photocycle of bacteriorhodopsin
[DE94-011800] 12 p4479 N94-37156
Status review and accomplishments of the Materials Research Center at the University of Pittsburgh
[AD-A280422] 12 p4399 N94-37214
Crystallographic studies of nitrogenase and hydrogenase
[DE94-011972] 12 p4538 N94-37677

PROTIUM
U LIGHT WATER

PROTOCOL (COMPUTERS)
An efficient medium access control strategy for high speed WDM multiaccess networks
[MEMO-INF-92-74] 01 p0131 N94-10165
Asynchronous Transfer Mode (ATM) technology: An overview
[AD-A266087] 01 p0383 N94-12413
Mobile host internetworking using IP loose source routing
[AD-A265713] 02 p0759 N94-13052
On the end-to-end communication problem in unreliable networks
[ITN-93-85188] 02 p0598 N94-13195
Kerberos: A UNIX-TCP/IP network authentication system
[DE93-011677] 02 p0760 N94-14011
Overview of the Scalable Coherent Interface, IEEE STD 1596 (SCI)
[DE93-015247] 02 p0761 N94-14476
Applicability of the session and the presentation layers for the support of high speed applications
[INRIA-RT-144] 03 p1158 N94-14980
The Third Annual NASA Science Internet User Working Group Conference
[NASA-CP-3170] 03 p1228 N94-15116
A formal protocol test procedure for the Survivable Adaptable Fiber Optic Embedded Network (SAFENET)
[AD-A267410] 03 p1192 N94-16975
Isochronets: A high-speed network switching architecture
[AD-A267811] 03 p1161 N94-17409
NASA Lewis Meshed VSAT Workshop meeting summary
[NASA-TM-106332] 03 p0883 N94-17487
A protocol validator for the SCM and CFSM models
[AD-A268523] 03 p1156 N94-17541
An internetwork authentication architecture
[AD-A268579] 03 p1162 N94-17622
PARX: Architecture of an operating system for parallel machines
[ETN-93-94401] 04 p1533 N94-18068
Specification and analysis of a high speed transport protocol
[AD-A268941] 04 p1386 N94-18449
On asynchronous testing
[MEMO-INF-93-03] 04 p1543 N94-19226
Specification and verification of a dynamic leader election protocol in a broadcast network
[MEMO-INF-93-05] 04 p1558 N94-19228
Vectorized presentation-level services for scientific distributed applications
[DE93-018091] 04 p1537 N94-19253
Specifying and proving communication closedness in protocols
[PB94-149515] 04 p1390 N94-19267
Protocol service decomposition for high-performance networking
[AD-A270613] 04 p1538 N94-19533
TCP performance analysis for wide area networks
[DE94-000449] 05 p1928 N94-19858
Robust, high-speed network design for large-scale multiprocessing
[AD-A271003] 05 p1716 N94-19977
Total order assumption
[PB93-191740] 05 p1903 N94-19993
Design considerations for a fiber optic communications network for power systems
[DE93-018404] 05 p1984 N94-20179
Distributed Virtual System (DIVIRS) project
[NASA-CR-194360] 05 p1905 N94-20228
Understanding Open Systems Interconnection (OSI)
[AD-A271877] 05 p1929 N94-20472
Standard ML signatures for a protocol stack
[AD-A272060] 05 p1908 N94-20622
A semi-Markov model of a home network access protocol
[MEMO-INF-92-71] 05 p1909 N94-21045
A simplified token bus protocol specified using LOTOS
[TR-92-15] 05 p1910 N94-21062
Government Open Systems Interconnection Profile (GOSIP) transition strategy
[AD-A273005] 05 p1740 N94-21308
Using manufacturing message specification for monitor and control at Venus 05 p1932 N94-21333
Distributed intelligent control and status networking
05 p1932 N94-21335
A packet switched communications system for GRO
05 p1744 N94-21345
A lower bound on wait-free counting
[CWI-CS-R9307] 05 p1915 N94-21537
Uniform self-stabilizing leader election. Part 1: Complete graph protocols
[CWI-CS-R9308-PT-1] 05 p1935 N94-21549
A mechanized process algebra for verification of device synchronization protocols 05 p1766 N94-21716
Performance evaluation of video on ethernet
[DE93-040696] 05 p1936 N94-21749
IAS telecommunication infrastructure and value added network services provided by IASNET
05 p1744 N94-22069
The conformance testing methodology to CTRON (communication and central TRON) extended OS
05 p1772 N94-22118
CREIR: A multiaccess protocol for on-board processing satellite systems 05 p1780 N94-22168
Throughput, blocking, and interference in packet radio networks 05 p1746 N94-22190
Specification and formal verification of the safety criterion in the alternating bit protocol
05 p1784 N94-22193
Modeling and analysis of secure communication protocols using Petri net formalism
05 p1784 N94-22194
File transfer performance in LAN interconnection through a satellite channel 05 p1746 N94-22209
Everything you might want to know about the Internet but are afraid to ask!
[DE93-041118] 05 p2046 N94-22413
A structured data transfer protocol
05 p2047 N94-22450
The HEASARC graphical user interface
05 p1926 N94-22487
A generic archive protocol and an implementation
05 p2047 N94-22493
The Keck Task Library (KTL)
05 p2048 N94-22504
Land mobile satellite propagation measurements in Japan using ETS-V satellite 06 p2282 N94-22790
A protocol for satellite access via use of spot-beams
06 p2286 N94-22811
System services and architecture of the TMI satellite mobile data system 06 p2286 N94-22817
Representation and specification of architectures for heterogeneous internetworking: Using a knowledge based approach
[LAAS-93088] 06 p2445 N94-22903
Generation of modules for control communication circuits: A design study used in the framework of the safe vehicle PROMETHEUS
[ETN-94-95171] 06 p2308 N94-23165

PROGRIL: A language for the definition of protocol grammars
[EUT-93-E-270] 06 p2449 N94-23172
Code generation for the attribute evaluator of the protocol engine grammar processor unit
[EUT-93-E-271] 06 p2450 N94-23173
MITS architecture V1.0
[PB93-201762] 06 p2452 N94-23451
Command/telemetry bus general specification for the NOAA-OPQ polar orbiting environmental satellites and EUMETSAT polar satellite systems
[NASA-TM-109407] 06 p2208 N94-23479
Low rate data bus general specification for the NOAA-OPQ polar orbiting environmental satellites and EUMETSAT polar satellite systems
[NASA-TM-109408] 06 p2208 N94-23480
High-rate data link general specification for the NOAA-OPQ polar orbiting environmental satellites and EUMETSAT satellite systems
[NASA-TM-109384] 06 p2208 N94-23481
Source spacing in B-ISDN
[PB93-201747] 06 p2293 N94-23508
Radar stimulator interface protocol, preliminary interface design and Doppler Beam Sharpening implementation
[DE94-002567] 06 p2453 N94-23701
Design and implementation issues of end-to-end protocols in high-speed networks
[PB94-110905] 06 p2467 N94-23752
A reference model for space data system interconnection services 06 p2305 N94-23847
Reliable transfer of data from ground to space 06 p2305 N94-23908
The EURECA telecommanding chain: Experience with packet telecommand and telemetry systems 06 p2305 N94-23909
Verification of technical elements of the advanced spacecraft based upon the CCSDS recommendation 06 p2207 N94-23910
Real-time process logic
[PB94-101441] 06 p2446 N94-24540
Optimizing parallelization
[AD-A273565] 06 p2467 N94-24692
Validation activities for LOTOS based on static data flow analysis
[PB94-110863] 06 p2459 N94-24758
HORACE: Presentation-level protocol standard for digital transmission of monochrome television images
[AD-A273395] 06 p2197 N94-25064
Models of trace theory systems
[ETN-94-95361] 06 p2468 N94-25226
Failure detection and recovery in the assembly/contingency subsystem 06 p2306 N94-25360
Interface technical specification of the V.25 bis emulator
[AD-A273754] 07 p2948 N94-25720
Weapon system integration for the AFIT virtual cockpit
[AD-A274058] 07 p2667 N94-25772
Object-oriented design and implementation of a parallel Ada simulation system
[AD-A274119] 07 p2979 N94-25906
A VHDL register transfer level model of the linear token passing multiplex data bus protocol for the high speed data bus
[AD-A273734] 07 p2980 N94-26009
Design and specification of the Xpress transfer high-speed protocol
[AD-A274941] 07 p3097 N94-26297
Modeling and simulation of a fiber distributed data interface local area network
[AD-A274838] 07 p3098 N94-26500
Automatic test case generation using PROLOG
[NPL-DITC-215/93] 07 p2964 N94-26655
A real-time executive implementing priority inheritance protocols 07 p2952 N94-26733
Example of the EXPANSE signalling protocol
[PB94-125283] 07 p2771 N94-26872
Hard real-time reliable multicast in the DEDOS system
[PB94-126745] 07 p2966 N94-26920
Binary snapshots
[CWI-CS-R9319] 07 p2955 N94-27547
An efficient off-line electronic cash system based on the representation problem
[CWI-CS-R9323] 07 p2776 N94-27551
A modular approach to evaluation cryptographic protocols using Petri nets
[ISBN-0-315-85354-9] 07 p2972 N94-27595
Simulating fail-stop in asynchronous distributed systems
[AD-A278101] 07 p2974 N94-27767
Refinement for fault-tolerance: An aircraft hand-off protocol
[AD-A278004] 07 p2666 N94-27768
Design of parallel systems for signal processing
[AD-A275490] 08 p3430 N94-28659
Preliminary analysis of Asynchronous Transfer Mode (ATM) over microwave channels
[AD-A275214] 08 p3243 N94-29069
Model-oriented analysis of a communications protocol
[PB94-138146] 08 p3244 N94-29109
Invariants, frames and postconditions: A comparison of two formal specification notations
[PB94-138153] 08 p3405 N94-29110
NPSNET: Integration of Distributed Interactive Simulation (DIS) protocol for communication architecture and information interchange
[AD-A275061] 08 p3530 N94-29139
Space reclamation for uncoordinated checkpointing in message-passing systems
[NASA-CR-195761] 08 p3420 N94-29906
Performance issues of signalling protocols for broadband ISDN
[PB94-150380] 08 p3255 N94-30374
End-to-end delay reduction in narrow bandwidth real-time multimedia tele-education applications
[AD-B179614] 08 p3260 N94-30518
Design and analysis of dynamic leader election protocols in broadcast networks
[MEMO-INF-93-43] 08 p3260 N94-30520
The NIST Internet time service 08 p3475 N94-30678
Validation experiments with an Ethernet model using the simulation tool 'PROMISE'
[AD-B174795] 08 p3429 N94-30912
An UIO-based method for protocol conformance testing
[REPT-93-060] 08 p3429 N94-30931
Communications networks in stressed environments
[AD-A275967] 09 p3672 N94-31384
Using atomic actions in replica groups to simplify the replication implementation
[REPT-93-78] 09 p3813 N94-31695
The FELICIA bulletin board system and the IRBIS anonymous FTP server: Computer security information sources for the DOE community
[DE94-008219] 09 p3825 N94-31920
The use of service limits for efficient operation of multi-station single-medium communication systems
[CWI-BS-R9312] 09 p3677 N94-32085
IRIG J asynchronous ASCII time code formats
[AD-A277244] 09 p3681 N94-32332
Voice and video transmission using XTP and FDDI 09 p3685 N94-32468
Multicast communication with guaranteed quality of service
[AD-A277650] 09 p3682 N94-33025
Software fault tolerance: Dynamic combination of dependability and efficiency
[PB94-148830] 10 p4106 N94-33977
Design and implementation of Voltan fault-tolerant nodes for distributed systems
[PB94-148863] 10 p4107 N94-33980
Simple authentication
[PB94-148871] 10 p4108 N94-34124
Building fault-tolerant distributed computing systems using standard components
[PB94-148889] 10 p4112 N94-34125
Analysis of optimistic window-based synchronization
[AD-280468] 10 p4102 N94-34918
Group-oriented coordination models for distributed client-server computing 10 p4126 N94-35068
A distributed computing model for telemetry data processing 10 p4013 N94-35069
Asynchronous optimistic rollback recovery using secure distributed time
[AD-A278978] 11 p4344 N94-35526
The rel/REL: A family of reliable multicast protocols for distributed real-time systems
[PB94-167830] 11 p4310 N94-35535
Probabilities and priorities in timed CSP
[PB94-169216] 11 p4316 N94-35536
Mathematical theory of synchronous communication
[PB94-169224] 11 p4252 N94-35537
The development and application of composite complexity models and a relative complexity metric in a software maintenance environment 11 p4255 N94-35559
Large granularity cache coherence for intermittent connectivity
[AD-A278897] 11 p4345 N94-35571
Synthesis of asynchronous systems from data flow specifications
[AD-A278687] 11 p4303 N94-35662
SandiaXTP, an object-oriented implementation of XTP 3.7
[DE94-011752] 11 p4257 N94-36354
Analysis of end-to-end encryption and traffic flow confidentiality options
[AD-A278612] 12 p4433 N94-36754
OSI and TCP/IP 12 p4542 N94-36855
Research in parallel computing
[NASA-CR-196267] 12 p4442 N94-36960
An error-resistant linguistic protocol for air traffic control
[NASA-CR-196098] 12 p4385 N94-37013
Global information networks: How they work 12 p4543 N94-37335
Policies for implementing network firewalls
[DE94-011030] 12 p4495 N94-37430
Advanced information processing system: Authentication protocols for network communication
[NASA-CR-194923] 12 p4498 N94-37500

PROTON BEAMS

Possibility of a crossed-beam experiment involving slow-neutron capture by unstable nuclei rapid-process-tron
[DE93-754288] 01 p0363 N94-10720
Experimental particle physics at the University of Pittsburgh
[DE93-013326] 01 p0369 N94-12546
Measurement of H zero excited states produced by foil stripping of 800-MeV H(-) ions
[DE93-014391] 02 p0788 N94-13103
Recent study of beam stability in the PSR
[DE93-014473] 02 p0780 N94-13173
Nuclear fusion of protons with ions of boron
[DE93-014284] 02 p0781 N94-13219
Beam halo in high-intensity beams
[DE93-014565] 02 p0789 N94-13328
Double semi-leptonic charm decay in HELIOS-I 450 GeV/c p-Be data
[DE93-013493] 02 p0781 N94-13348
Proton-proton scattering contribution to emittance growth
[DE93-016090] 02 p0787 N94-14588
Microstructure of Zr3Al after 2 MeV proton bombardment
[DE93-015331] 03 p1211 N94-16814
Effects of transverse coupling on transverse beam size, simulation and measurements
[DE93-017804] 04 p1574 N94-18972
A high-intensity He-jet production source for radioactive beams
[DE93-040247] 05 p1981 N94-21767
On radiation defects in strip detectors
[DE93-616646] 07 p3015 N94-25916
Spin effects in hard interactions (interest in accelerated polarized beam)
[DE93-634398] 07 p3031 N94-26044
Regrouping of the beam in the IHEP PS for the UNK p-p programs
[DE93-634021] 07 p3032 N94-26164
Longitudinal diffusion of a proton bunch under external noise
[DE93-634022] 07 p3032 N94-26165
Physics at HERA
[DE94-005117] 08 p3483 N94-28569
Search for heavy neutrinos at the IHEP-JINR neutrino detector
[DE94-608175] 08 p3489 N94-30095
RHIC spin physics
[DE94-005452] 09 p3876 N94-32099
H(-) injection simulation for a 5 MW spallation neutron source
[DE94-009003] 10 p4140 N94-33983
Spin dynamics in storage rings and linear accelerators
[DE94-010320] 11 p4330 N94-36106
The effects of proton-beam quality on the production of gamma rays for nuclear resonance absorption in nitrogen
[DE94-011609] 12 p4523 N94-37629

PROTON BELTS

Self-consistent effects of magnetospheric hydromagnetic waves on ring current ions
[AD-A277406] 09 p3774 N94-32346

PROTON DENSITY (CONCENTRATION)

Variations of electron fluxes, low-frequency radiations and plasma density during the geomagnetic storm on 9-12 March, 1979 according to data of the Interkosmos-19 satellites
[DE94-607323] 08 p3365 N94-30223

PROTON ENERGY

The LAHET code system: Introduction, development, and benchmarking
[DE93-012657] 02 p0787 N94-14804
CRRES high energy proton flux map
[AD-A274803] 07 p2878 N94-26338
Modeling the DMSP and CRRES dosimeters using the path length distribution method
[RXR-93051] 07 p2698 N94-28200
The PROTEL contamination code
[RXR-93071] 07 p3040 N94-28202
Proton switches
[AD-A275150] 08 p3167 N94-29022

PROTON FLUX DENSITY
The SCR Ne-21 and Ar-38 in lunar rock 68815: The solar proton energy spectrum over the past 2 MYR
03 p1248 N94-16177
PROTON IMPACT
Double excitation of He and H(-) by fast proton and anti-proton impact
[DE94-004581] 07 p3026 N94-27620
PROTON IRRADIATION
Investigation of the radiation resistance of triple-junction a-Si:H alloy solar cells irradiated with 1.00 MeV protons
01 p0050 N94-11391
Diffusion length damage coefficient and annealing studies in proton-irradiated InP
[NASA-TM-106262] 01 p0404 N94-12430
The 1.00 MeV proton radiation resistance studies of amorphous silicon-based alloy solar cells
02 p0703 N94-13639
Mechanical-property changes of structural composite materials after low-temperature proton irradiation: Implications for use in SSC magnet systems
[DE93-016735] 04 p1343 N94-18763
On modelling nuclear reactions in meteorites
05 p2085 N94-20844
Proton radiation testing of an 18 bit A/D converter
05 p1755 N94-21096
On the origin of 1/f noise in epitaxial GaAs
[ISBN-9-09-006067-7] 06 p2566 N94-25297
Radiation hardening effects on localized deformation and stress corrosion cracking of stainless steels
[DE94-004308] 07 p2731 N94-25804
Proton irradiation on materials
07 p3030 N94-27898
Precipitation in Zr-2.5 Nb enhanced by proton irradiation
[DE94-619056] 12 p4415 N94-36563
PROTON PRECIPITATION
Proton aurora and substorm intensifications
[ATR-93(7248)-1] 07 p2887 N94-28218
PROTON SCATTERING
Indication on the existence of the bound state in the p anti p-system
[DE92-641575] 01 p0361 N94-10532
Medium energy hadron-nucleus scattering in the 1/N expansion formalism
[DE93-622957] 02 p0778 N94-12848
Relativistic proton-nucleus scattering and one-boson-exchange models 02 p0786 N94-14550
Proton-proton scattering contribution to emittance growth
[DE93-016090] 02 p0787 N94-14588
The pp elastic scattering experiment at RHIC and polarization studies in the Coulomb Nuclear Interference region
[DE93-015391] 03 p1187 N94-16829
An antiproton-proton partial-wave analysis
[DE94-002690] 07 p3021 N94-26620
First observation of neutral current proton electron scattering at the square root of s = 300 GeV
[DE94-701107] 07 p3030 N94-27877
PROTON TELESCOPES
U PARTICLE TELESCOPES
PROTON-PROTON REACTIONS
Strangeness production with protons and pions
[DE93-010879] 01 p0359 N94-10304
Polarization and color transparency
[DE93-014319] 02 p0780 N94-13101
The PAPAGENO Partonic Monte-Carlo Program
[DE93-018524] 04 p1571 N94-19247
Research on elementary particle physics, part 2
[DE94-004956] 07 p3029 N94-27815
Analysis of the high energy behavior of the forward scattering parameters - sigma(tot), rho and B
[DE94-006537] 09 p3864 N94-31310
PROTONS
NT SOLAR PROTONS
Indication on the existence of the bound state in the p anti p-system
[DE92-641575] 01 p0361 N94-10532
Experiments to measure the gluon helicity distribution in protons
[DE93-011756] 01 p0368 N94-11613
Solid-state structures of guanidinium methane, ethane, and trifluoromethanesulfonate
[AD-A265293] 01 p0402 N94-11654
Ion anisotropy driven waves in the Earth's magnetosheath and plasma depletion layer
[DE93-012751] 02 p0712 N94-12952
Measurement of H zero excited states produced by foil stripping of 800-MeV H(-) ions
[DE93-014391] 02 p0788 N94-13103
Measurement of the spin of a particle using undulator radiation
[DE93-014334] 02 p0780 N94-13149
The E2 N(yields)(Delta) transition from polarized Compton scattering
[DE93-012522] 02 p0785 N94-14363
Primary and secondary electrical space power based on advanced PEM systems
[DE93-012643] 02 p0553 N94-14689
The LAHET code system: Introduction, development, and benchmarking
[DE93-012657] 02 p0787 N94-14804
Study of the rare decays K(sub L)(sup 0) yields (mu)e, K(sub L)(sup 0) yields ee, and K(sub L)(sup 0) yields (mu)(mu) at KEK
[DE93-753247] 03 p1180 N94-15135
Nuclear fusion of protons with ions of boron
[DE93-015399] 03 p1202 N94-16019
Energy-loss cross sections for inclusive charge-exchange reactions at intermediate energies
[NASA-TM-4522] 03 p1188 N94-17018
Search for the top quark from (e(mu)) and (e,e) events in the D0 detector in p(bar-p) collisions at the square root of s = 1.8 TeV
[DE93-016350] 03 p1186 N94-17662
Proton transfer dynamics and cluster ion fragmentation in phenol/ammonia cLusters
[AD-A269133] 04 p1348 N94-18256
Global zones of particle precipitation as observed EXOS-C
[AD-A268758] 04 p1481 N94-18467
Charmonium physics from (bar p)p interactions
[DE93-017809] 04 p1569 N94-18973
A study of events with the highest total transverse energy in CDF
[DE93-019904] 05 p1978 N94-19972
The cross section for the production of b(bar-b) pairs in p(bar p) collisions at the square root of s equals 1.8 TeV
[DE93-019900] 05 p1972 N94-20225
STRV RADMON: An integrated high-energy particle detector 05 p1666 N94-21086
SLAC measurement of the neutron spin structure function
[DE93-040998] 05 p1975 N94-21788
Toward a QCD analysis of jet rates in deep-inelastic Muon-Proton scattering
[DE94-000618] 05 p1976 N94-21962
A novel method for determination of transport parameters of H2 and O2 in PEMFCs
[DE94-001492] 06 p2389 N94-22962
Low p(sub T) photon production in proton-nucleus collisions at 18 GeV/c
[DE94-001380] 06 p2532 N94-23007
Primary and secondary electrical space power based on advanced PEM systems 06 p2392 N94-23357
PEM regenerative fuel cells 06 p2392 N94-23358
High power density proton exchange membrane fuel cells 06 p2393 N94-23359
A high performance H2-Cl2 fuel cell for space power applications 06 p2394 N94-23366
Investigation of evolution-related aspects of bacterial rhodopsins
[NASA-CR-194826] 06 p2420 N94-23501
Low mass muon pair production in 450 GeV p-Be collisions
[PB94-110699] 06 p2533 N94-23746
Momentum loss in proton-nucleus and nucleus-nucleus collisions
[NASA-TP-3405] 06 p2540 N94-24305
Polarized structure functions of the nucleon in the resonance region
[CEBAF-PR-94-001] 06 p2540 N94-24663
Activities of Academia Sinica
[DE93-614529] 06 p2541 N94-25335
Proton spin: The role of quark-gluon and hadron degrees of freedom
[DE93-616867] 06 p2538 N94-25341
Spin effects in hard interactions (interest in accelerated polarized beam)
[DE93-634398] 07 p3031 N94-26044
CRRES high energy proton flux map
[AD-A274803] 07 p2878 N94-26338
An antiproton-proton partial-wave analysis
[DE94-002690] 07 p3021 N94-26620
Double excitation of He and H(-) by fast proton and anti-proton impact
[DE94-004581] 07 p3026 N94-27620
Proton electromagnetic form factor near the proton-antiproton threshold and quasinuclear bound state
[DE94-606458] 07 p3027 N94-27681
Analysis of energetic proton and electron data in Neptune's magnetosphere
[NASA-CR-195707] 07 p3107 N94-27784
Modeling the DMSP and CRRES dosimeters using the path length distribution method
[RXR-93051] 07 p2698 N94-28200
The PROTEL contamination code
[RXR-93071] 07 p3040 N94-28202
Properties of W + jet events in proton-antiproton collisions at 1.8 TeV
[DE94-004002] 08 p3482 N94-28524
Results on structure functions from fixed-target experiments
[DE94-005233] 08 p3482 N94-28541
Proton switches
[AD-A275150] 08 p3167 N94-29022
Inclusive jet and direct photon production at the D0 experiment
[DE94-006001] 08 p3488 N94-30049
A search for rapidity gap events in p(bar p) collisions at D(0)
[DE94-004654] 08 p3491 N94-30722
State of hadron collider physics
[DE94-005279] 09 p3863 N94-31147
F0-975, A0-980 as eye-witnesses of confinement
[PB94-147105] 09 p3868 N94-31923
NN-interaction in (1)S0-state: Virtual level or dibaryon resonance?
[DE94-606492] 09 p3869 N94-32097
Self-consistent effects of magnetospheric hydromagnetic waves on ring current ions
[AD-A277406] 09 p3774 N94-32348
Studies of jet production with the D0 detector
[DE94-008271] 09 p3873 N94-32780
LDEF satellite radiation study
[NASA-CR-193948] 10 p4015 N94-34147
Electron and Proton Wide-Angle Spectrometer (EPAS) on the CRRES spacecraft
[AD-A278630] 11 p4227 N94-35362
Particle orbit analysis for LHD helical axis configurations
[DE94-718995] 11 p4336 N94-35773
Dynamic aperture and transverse proton diffusion in HERA
[DE94-010309] 11 p4331 N94-36224
The E2/M1 mixing ratio in the excitation of the Delta from polarized photo-reactions
[DE94-004235] 12 p4510 N94-36442
Deep inelastic scattering results from the first year of HERA operation
[DE94-004578] 12 p4511 N94-36483
Angular dependence of parton-parton scattering extracted from hadron pair production in pp collisions at radicals equal to 11.5 GeV
[DE94-611174] 12 p4511 N94-36504
Mass identified particle production and Bose Einstein correlations at 1800 GeV
[DE94-013418] 12 p4515 N94-37067
Physics with primary beams of the KEK-PS
[DE94-748635] 12 p4522 N94-37234
AEM and AES of radiation-induced segregation in proton-irradiated stainless steels
[DE94-012734] 12 p4418 N94-37398
PROTOPLANETS
Columbus proto-planetesimal dust aggregation experiment 01 p0123 N94-10236
Giant impact-induced atmospheric blow-off
01 p0435 N94-12019
Recondensation of chondritic material in the early solar system: Results of thermodynamic simulation
01 p0432 N94-12226
Physical properties of gas disks around shell stars with and without dust
[NASA-CR-193655] 02 p0835 N94-13239
Petrologic constraints on the surface processes on asteroid 4 Vesta and on excavation depths of diogenite fragments 03 p1241 N94-16208
I-Xe structure of ILAFEGH 009 and shallowater: Evidence for early formation and rapid cooling of impact-derived enstatite meteorites
03 p1243 N94-16305
An initial perspective of S-asteroid subtypes within asteroid families 03 p1243 N94-16310
On the delivery of planetesimals to a protoplanet in the solar nebula 03 p1245 N94-16379
Structuration processes in protoplanetary accretion disks
[MPE-243] 04 p1628 N94-19519
Diffusive redistribution of water vapor in the solar nebula revisited 05 p2113 N94-20751
FE-60 and the evolution of eucrites
05 p2083 N94-20768
Volatile loss from accreting icy protoplanets
05 p2084 N94-20793
The Sm-Nd systematics of silicate inclusions in iron meteorites: Results from Caddo (IAB)
[CONTRIB-5241(804)] 05 p2084 N94-20795
Triton's cratering record and its time of capture
05 p2122 N94-20802
Recondensation in the early solar system: Physical conditions and source material
05 p2085 N94-20849

Protoplanetary disks: Theory and observation by millimeter and sub-millimeter arrays
[REPT-331] 06 p2603 N94-24983
The Nobeyama millimeter array survey for protoplanetary disks around protostar candidates and T Tauri stars in Taurus
[REPT-336] 06 p2604 N94-24987
Observational studies of the clearing phase in proto-planetary disk systems
[NASA-CR-195182] 06 p2604 N94-25265
Investigations of the dynamical evolution of protoplanetary nebulae
[NASA-CR-195278] 07 p3105 N94-27428
Observations of accretion and angular momentum regulation in young circumstellar disks and the implications for planetary formation 09 p3928 N94-31122
Evolution of protoplanetary disks with dynamo magnetic fields 09 p3931 N94-31135
Multiwavelength search for protoplanetary disks 09 p3599 N94-31430
Planetesimal dynamics in the vicinity of a growing protoplanet 09 p3935 N94-31926
What initiated planetesimal formation? 11 p4351 N94-35422

PROTOPLASTS
Effects of freezing and cold acclimation on the plasma membrane of isolated protoplasts
[DE94-012487] 12 p4479 N94-37248

PROTOSTARS
NT PRE-MAIN SEQUENCE STARS
NT T TAURI STARS
Initiating solar system formation through stellar shock waves 01 p0448 N94-12090
The physical and chemical evolution of protostellar disks. The growth of protostellar disks: Progress to date
[NASA-CR-194111] 02 p0836 N94-13423
Millimeter and infrared studies of young stellar objects in dark cloud L1641 02 p0838 N94-13648
The 1 to 5 micron imaging of deeply embedded young stellar objects 02 p0831 N94-13657
The molecular environment of S106 IR
[MPE-PREPRINT-241] 04 p1622 N94-19417
Helical kink instability of jets from young stellar objects 05 p2008 N94-22686
Theory of protostellar accretion disks 09 p3931 N94-31136
Gravitational instabilities in protostellar disks 09 p3932 N94-31140
Near and far infrared observations of protostars and dark clouds 09 p3926 N94-31969

PROTOTYPES
Characterization of a scannerless LADAR system
[DE93-011582] 01 p0174 N94-10959
A prototype urine collection device for female aircrew 01 p0317 N94-11549
Progress in the concentrator initiative program
[DE93-015006] 03 p1091 N94-15984
Center of Excellence in Laser Medicine
[DE93-016541] 03 p1122 N94-16113
Prototype instrumentation and design studies
[AD-A266402] 03 p0882 N94-16530
ACE: Lessons learned, volume 1
[AD-A267979] 03 p1155 N94-17411
Developmental testing of a prototype all-reflection Michelson interferometer
[AD-A269064] 04 p1430 N94-18406
Tunneling spectroscopy of ultrasmall clusters and grains
[AD-A268840] 04 p1598 N94-18539
ARPA/CSTO rapid VLSI implementation
[AD-A269170] 04 p1403 N94-18695
Computer-Aided Prototyping System (CAPS) within the software acquisition process. A case study
[AD-A268705] 04 p1522 N94-18786
Fiber optic Raman spectrograph for in situ environmental monitoring
[DE93-019466] 04 p1478 N94-19305
Direct broadcast satellite-radio, receiver development 06 p2273 N94-22739
The Automated Instrumentation and Monitoring System (AIMS) reference manual
[NASA-TM-108795] 06 p2452 N94-23510
Harmonisation of man-machine interface experiments in the context of the development of PHARE advanced tools
[PB93-204725] 06 p2430 N94-23744
Making tomorrow's mistakes today: Evolutionary prototyping for risk reduction and shorter development time 06 p2197 N94-23902
Performing speech recognition research with hypercard 06 p2306 N94-24194
Characteristics of products generated by selective sintering and stereolithography rapid prototyping processes 06 p2264 N94-24412
Integration and evaluation of a simulator designed to be used within a dynamic prototyping environment 06 p2198 N94-24436
A prototype to automate the video subsystem routing for the video distribution subsystem of Space Station Freedom 06 p2306 N94-25353
Software redesign for usability: A case study
[DE94-003704] 07 p2960 N94-26048
Rapid prototyping of application specific signal processors (RASSP)
[AD-A274324] 07 p2772 N94-26884
An optoelectronic graphics display processor
[AD-A274401] 07 p3037 N94-26990
The OPAL vertex detector
[ISBN-0-315-51152-4] 07 p2812 N94-27257
Automated interface for retrieving reusable software components
[AD-A275004] 08 p3409 N94-28896
Fundamental studies on the corrosion behavior of weldments in marine microbial environments
[AD-A275247] 08 p3203 N94-28900
Mars rover mechanisms designed for Rocky 4 08 p3161 N94-29630
Test of prototype liquid-water-content meter for aircraft use
[NASA-CR-189304] 08 p3374 N94-30187
Results of real-time testing and demonstration of the US Army Corps of Engineers real-time on-the-fly positioning system
[AD-A276160] 09 p3576 N94-31080
Model borne data management system for wind tunnel testing, phase 2
[AD-A276296] 09 p3587 N94-31295
Study of virtual prototyping of aircraft instruments
[CMC-0687-1090] 09 p3581 N94-31903
Parallel methods for synthesizing whole-hand grasps from generalized prototypes
[AD-A276798] 09 p3726 N94-32166
Technical evaluation of the UH-60Q: Aircraft in typical aeromedical evacuation missions
[AD-A276944] 09 p3586 N94-32217
Airborne Trailblazer: Two decades with NASA Langley's 737 flying laboratory
[NASA-SP-4216] 09 p3566 N94-32793
Design, development, and testing of a lightweight optical sensor cover system 09 p3604 N94-33302
Solid Freeform Fabrication Symposium Proceedings
[AD-A277718] 10 p4032 N94-33441
Digital mapping, charting, and geodesy analysis program technical review of Urban Vector Smart Map (UV(sub Map)) prototype 1
[AD-A277831] 10 p4076 N94-33832
Applying observations of work activity in designing prototype data analysis tools
[DE94-010206] 11 p4347 N94-36297
Advances in rapid prototyping
[DE94-010075] 12 p4430 N94-36447
First results from a prototype level-1 calorimeter trigger system for LHC, RD 27 (UK) collaboration
[PB94-167475] 12 p4436 N94-36532
Solid state fluorometer: Prototype development
[AD-A280321] 12 p4534 N94-37027

PROTOZOA
NT PARAMECIA
Chaos and microbial systems
[DE93-016814] 02 p0730 N94-14596

PROTUBERANCES
Results of experimental investigations to determine external tank protuberance loads using a 0.03-scale model of the Space Shuttle launch configuration (model 47-OTS) in the NASA/ARC unitary plan wind tunnel, volume 1
[NASA-CR-167690] 02 p0534 N94-12810
Results of experimental investigations to determine external tank protuberance loads using a 0.03-scale model of the Space Shuttle launch configuration (Model 47-OTS) in the NASA/ARC unitary plan wind tunnel, volume 2
[NASA-CR-167691] 02 p0536 N94-14047

PROVING
NT THEOREM PROVING
Validation of directional wave spectra from the ERS-1 during the ESA CAL/VAL campaign 01 p0232 N94-11707
The Grand Banks ERS-1 SAR wave spectra validation experiment 01 p0232 N94-11708
Validation of ERS-1 wind and wave data by use of operational forecast models 01 p0233 N94-11710
Validation test system for sea surface temperature detected by satellites in Mutsu Bay 01 p0213 N94-12670
Evaluation of the method of geostrophic flow using NOAA-AVHRR data 01 p0213 N94-12673
Further study of the Non-Regression-Coefficient SST retrieval method 01 p0213 N94-12674
A knowledge-based expert system to coordinate CAD/CAE with integration and test
[NASA-CR-191394] 02 p0745 N94-13130
Methods for calibration/validation of AVNIR 02 p0689 N94-14216
Verification of 3I retrievals vis-a-vis radiosonde observations
[KNMI-TR-150] 04 p1488 N94-17924
Stochastic optimization by simulation: Convergence proofs for the G1/G/1 queue in steady-state
[AD-A271141] 05 p1962 N94-19999
Formal hardware verification in Maple 05 p1771 N94-22112
Formal verification of an ALU 05 p1772 N94-22114
Tests of logic spaces: A new strategy for certifying the accuracy of programs 05 p1772 N94-22116
Modeling software systems for data flow testing 05 p1772 N94-22117
The conformance testing methodology to CTRON (communication and central TRON) extended OS 05 p1772 N94-22118
Satellite validation of GCM-simulated annual cycle of the Earth radiation budget and cloud forcing 05 p1860 N94-22287
Use of satellite data for validation of operational forecast models and operational analyses 05 p1861 N94-22291
Validating identified nonlinear models with chaotic dynamics
[RR-469] 06 p2523 N94-25314
Trace-based compositional proof theory for fault tolerant distributed systems
[PB94-126737] 07 p2966 N94-26971
Capillary column GC-MS/MS confirmation of phosphate esters with a hybrid tandem mass spectrometer
[AD-A278748] 11 p4238 N94-36091

PROXIMITY
Steering capaciflector sensor
[NASA-CASE-GSC-13489-1] 03 p1164 N94-15704

PROXIMITY EFFECT (ELECTRICITY)
Thin film studies of the proximity Josephson effect
[AD-A270129] 04 p1600 N94-18876

PRUSSIC ACID
U HYDROCYANIC ACID

PSEUDOMONAS
Continuous monitoring of bacterial attachment 10 p4094 N94-33658

PSEUDONOISE
Acquisition time analysis of noncoherent PN sequence acquisition schemes
[AD-A275017] 08 p3244 N94-29094
Measured channel parameters for the disturbed wide-bandwidth HF channel
[AD-A277877] 10 p4034 N94-33778
Spacecraft-spacecraft radio-metric tracking: Signal acquisition requirements and application to Mars approach navigation 11 p4254 N94-35557

PSEUDOPOTENTIALS
First-principles studies of phase stability and the structural and dynamical properties of hydrogen-metal systems
[DE93-016129] 02 p0570 N94-13374
First principles pseudopotential calculations on aluminum and aluminum alloys
[DE94-004890] 08 p3206 N94-29931
Theoretical studies of electron transfer and optical spectroscopy
[DE94-006985] 09 p3871 N94-32375

PSEUDORANDOM SEQUENCES
Production and test of pseudo random elements
[ETN-93-95070] 04 p1559 N94-19610

PSYCHIATRY
Practice patterns of US Army medical department psychiatrists and psychologists
[AD-A274787] 07 p2909 N94-26360

PSYCHOACOUSTICS
Signal feature analysis using neural networks and psychoacoustics
[AD-A266048] 01 p0340 N94-12398
On the auditory discrimination of spectral shape
[ETN-94-95306] 06 p2530 N94-25289
Subjective response to sonic booms having different shapes, rise times, and durations
[NASA-TM-109090] 08 p3479 N94-29464
Quality of sound in large rooms: Alteration of room impulse responses
[CTH-E-93-02] 09 p3859 N94-31077
Complex auditory signals
[AD-A278391] 09 p3862 N94-33146
Dose-response relationships derived from data collected at Grand Canyon, Haleakala and Hawaii Volcanoes National Parks
[PB94-151941] 10 p4134 N94-34380

PSYCHOLINGUISTICS
Modeling the human mental lexicon with self-organizing feature maps 05 p1743 N94-20244
An exploration of clause boundary effects in SRN representations 05 p1937 N94-20253

PSYCHOLOGICAL EFFECTS
NT DESYNCHRONIZATION (BIOLOGY)
NT ILLUSIONS
NT JET LAG
An evaluation of noise and its effects on shuttle crewmembers during STS-50/USML-1
[NASA-TM-104775] 02 p0735 N94-13961
Scuba-diving, anxiety and task performance
03 p1132 N94-15938
Incongruity, incongruity resolution, and mental states: The measure and modification of situational awareness and control
[NASA-CR-194568] 05 p1893 N94-20168
Transfer of perceptual adaptation to space sickness: What enhances an individual's ability to adapt?
[NASA-CR-188256] 06 p2427 N94-24227
Monthly variation of physiological and psychological responses under unsteady thermal conditions
07 p2918 N94-27475
Man's ability to adapt himself for the seasonal climatic changes: From viewpoint of anticipation and seasonable behavior 07 p2919 N94-27476
A study of psychological factors affecting an extremely isolated environment 07 p2927 N94-27517
Some issues on Japan's space food development and relating preliminary experimental study
08 p3388 N94-28498
La Chalupa-30: Lessons learned from a 30-day subsea mission analogue 10 p4098 N94-33654
Crisis and disaster research: A review
[PB94-149234] 10 p4097 N94-34108
PSYCHOLOGICAL FACTORS
Incongruity, incongruity resolution, and mental states: The measure and modification of situational awareness and control
[NASA-CR-194568] 05 p1893 N94-20168
Development of stimulus-seeking scale for expecting individual differences against confinement stress
07 p2915 N94-27460
The effect of body orientation on the perception of vertical and horizontal distance in an outdoor setting
07 p2915 N94-27461
Eye-head coordination and swinging of the visual scene when wearing visually up-down reversing mirror for 14 days 07 p2915 N94-27462
Comparative measurement of visual stability in cosmic space: Onboard experiment and pre-flight activities
07 p2916 N94-27463
A study of psychological factors affecting an extremely isolated environment 07 p2927 N94-27517
The management issues of implementing telecommuting: A case study
[AD-A275267] 08 p3527 N94-28905
Creative inventive design and research
[NASA-TM-104607] 10 p4032 N94-33719
Extended range operations: A review of recent developments 11 p4195 N94-36337
Determinants of subjective fatigue for C-141 crews during Operation Desert Storm
11 p4196 N94-36338
PSYCHOLOGICAL INDEXES
U PSYCHOLOGICAL TESTS
PSYCHOLOGICAL TESTS
Basic attributes test (BAT): Operational pre-implementation analysis and score equating
[AD-A265885] 01 p0314 N94-12276
Work/rest schedules and performance of S-3 aviators during fleet exercise
[AD-A265807] 02 p0734 N94-12975
Work/rest schedules and performance of F/A-18 aviators during Fleet Exercise 1992
[AD-A265826] 02 p0735 N94-12982
A description of psychological type at the Defense Systems Management College, 1993 edition
[AD-A271612] 05 p1894 N94-21237
Psychometric developments related to tests and selection
[AD-A272971] 05 p1894 N94-21262
Extracting information from wrong answers in computerized adaptive testing
[AD-A272832] 05 p1894 N94-21434
Practice patterns of US Army medical department psychiatrists and psychologists
[AD-A274787] 07 p2909 N94-26360
Validation of the Federal Aviation Administration air traffic control specialist pre-training screen
[DOT/FAA/AM-94/4] 07 p2938 N94-26600
A study of psychological factors affecting an extremely isolated environment 07 p2927 N94-27517
Autogenic-feedback training improves pilot performance during emergency flying conditions
10 p4098 N94-33622
La Chalupa-30: Lessons learned from a 30-day subsea mission analogue 10 p4098 N94-33654
PSYCHOLOGY
NT AVIATION PSYCHOLOGY
NT COGNITIVE PSYCHOLOGY
NT MILITARY PSYCHOLOGY
NT PSYCHOACOUSTICS
NT PSYCHOPHYSICS
NT SPACE PSYCHOLOGY
The effects of evaluation and production blocking on the performance of brainstorming groups
[AD-A265495] 02 p0734 N94-12929
Development of the OMPAT neuropsychological/psychomotor performance evaluation and OMPAT data and timing support programs
[AD-A266954] 03 p1122 N94-15759
Interdisciplinary training in life science (FY 1991 ASSERT)
[AD-A269220] 04 p1512 N94-18886
Proficiency scaling based on conditional probability functions for attributes
[AD-A273816] 07 p3002 N94-25962
Pacing visual attention: Temporal structure effects
[AD-A273859] 07 p2937 N94-25965
PSYCHOMETRICS
Development of the UTC-PAB normative database
[AD-A271319] 05 p1893 N94-20023
A description of psychological type at the Defense Systems Management College, 1993 edition
[AD-A271612] 05 p1894 N94-21237
Psychometric developments related to tests and selection
[AD-A272971] 05 p1894 N94-21262
Extracting information from wrong answers in computerized adaptive testing
[AD-A272832] 05 p1894 N94-21434
EEG and chaos: Description of underlying dynamics and its relation to dissociative states
[NASA-CR-195171] 06 p2428 N94-24799
Extending the rule space model to a semantically-rich domain: Diagnostic assessment in architecture
[AD-A273789] 07 p2948 N94-25864
A diagnostic classification model for document processing skills
[AD-A273790] 07 p3096 N94-25925
Dealing with uncertainty about item parameters: Expected response functions
[AD-A280610] 12 p4506 N94-36728
PSYCHOMOTOR PERFORMANCE
Landing Craft Air Cushion (LCAC) crew selection system manual
[AD-A265158] 01 p0313 N94-11098
Measuring human performance on NASA's microgravity aircraft 01 p0317 N94-11537
Development of the OMPAT neuropsychological/psychomotor performance evaluation and OMPAT data and timing support programs
[AD-A266954] 03 p1122 N94-15759
Evaluation of physiological and psychological impairment of human performance in cold stressed subjects
[AD-A268637] 04 p1506 N94-18632
Effects of practice in selecting and executing keypressing sequences
[IZF-1992-B-10] 04 p1509 N94-19420
A forthcoming key press can be selected while earlier ones are executed
[IZF-1993-B-2] 04 p1509 N94-19422
Development of the UTC-PAB normative database
[AD-A271319] 05 p1893 N94-20023
Experimental evaluation of two systems of individual air-conditioning 08 p3384 N94-28450
An evaluation of personality testing and the five-factor model in the selection of landing craft air cushion vehicle crew members
[AD-A275869] 08 p3397 N94-28754
Some solutions to reduce the human effects of extended operation times 11 p4196 N94-36339
PSYCHOPHARMACOLOGY
Some solutions to reduce the human effects of extended operation times 11 p4196 N94-36339
PSYCHOPHYSICS
NT PSYCHOACOUSTICS
Visual encoding of spatial relations
[AD-A266049] 01 p0313 N94-10909
Visual psychophysics of egomotion
[AD-A265253] 01 p0304 N94-11681
The 12th Annual Carmel Conference, distinctiveness and Memory: Cognitive Psychophysiological and Physiological Considerations
[AD-A267181] 03 p1131 N94-15148
Context-related scaling of human judgement in the multiplicative AHP, SMART and ELECTRE
[REPT-93-38] 04 p1611 N94-19158
Physical aspects of the visual stimulus
06 p2431 N94-23978
Luminance-brightness mapping: The missing decades
[ETN-94-95351] 06 p2428 N94-25298
Extracting heading and temporal range from optic flow: Human performance issues 06 p2442 N94-25510
Top down influences on bottom-up processing
[AD-A274220] 07 p2939 N94-27072
Sensory sensitivities and discriminations and their roles in aviation
[AD-A277312] 09 p3800 N94-32276
Visual encoding of spatial relations
[AD-A277400] 09 p3800 N94-32344
Workshop on Visual Perception: Computation and Psychophysics
[AD-A278412] 09 p3802 N94-33326
Psychophysics of complex auditory and speech stimuli
[AD-A277605] 10 p4035 N94-33848
PSYCHOPHYSIOLOGY
Psychophysiological measures of cognitive workload in laboratory and flight 01 p0317 N94-11529
Psychophysiological investigations of the biomedical problems of manned spaceflight
[NASA-CR-194107] 02 p0732 N94-13782
The 12th Annual Carmel Conference, distinctiveness and Memory: Cognitive Psychophysiological and Physiological Considerations
[AD-A267181] 03 p1131 N94-15148
Activity/rest patterns of instructor and rates student pilots during rapid transitions from daytime to nighttime duty hours at the Eastern Army Aviation Training site
[AD-A267038] 03 p1131 N94-15859
Perception of lightness and brightness in complex patterns
[AD-A268435] 03 p1134 N94-17513
Psychophysical analyses of perceptual representations
[AD-A268711] 04 p1508 N94-18313
EEG and chaos: Description of underlying dynamics and its relation to dissociative states
[NASA-CR-195171] 06 p2428 N94-24799
Top down influences on bottom-up processing
[AD-A274220] 07 p2939 N94-27072
Psychophysiology in microgravity and the role of exercise 07 p2936 N94-28374
Psychophysiological study on the effects of co-existence of lines for detecting dot target
08 p3394 N94-29867
Determination of multiple sound sources
[AD-A277379] 09 p3799 N94-32096
From animals to animats
[AD-A277427] 09 p3802 N94-33241
Seventh Annual Workshop on Space Operations Applications and Research (SOAR 1993), volume 1
[NASA-CP-3240-VOL-1] 10 p4179 N94-34019
PUBLIC HEALTH
Technical Conference on Tropical Urban Climates: Extended Abstracts
[WMO/TD-538] 01 p0283 N94-10561
International Telemedicine/Disaster Medicine Conference: Papers and Presentations
[NASA-NP-207] 01 p0304 N94-11787
The Canadian experience: Using telemedicine for the support of medical care at remote sites
01 p0305 N94-11789
Applications of the INTELSAT system to remote health care 01 p0306 N94-11794
Clinical aspects of telemedicine
01 p0306 N94-11795
Commercial applications of telemedicine
01 p0306 N94-11798
Space technology in remote health care
01 p0306 N94-11799
The National Disaster Medical System
01 p0307 N94-11801
Satellite, environmental, and medical information applied to epidemiological monitoring 01 p0307 N94-11802
A telemedicine health care delivery system
01 p0307 N94-11803
Use of satellite telecommunications for telemedicine
01 p0308 N94-11807
US-USSR telemedicine consultation spacebridge to Armenia and Ufa 01 p0308 N94-11809
The revitalization of health and education in Rural America Act of 1992 01 p0308 N94-11810
An assessment of acid fog
[DE93-009347] 03 p1095 N94-15940
Physical fitness and the Healthy People 2000 goals
03 p1125 N94-16619
International Symposium on the Ecological Effects of Arctic Airborne Contaminants — abstracts
[AD-A269955] 04 p1475 N94-18775
Health effects of global warming: Problems in assessment
[DE93-040323] 05 p1850 N94-19930
Systems for the monitoring of working conditions relating to health and safety: Extensive description. Norway
[PB94-138542] 09 p3803 N94-31839
Transnational environmental degradation
[AD-A278469] 10 p4080 N94-33548

Proceedings of the 6th International Congress on Noise as a Public Health Problem, volume 1
[AD-A278259] 10 p4133 N94-33961
Proceedings of the 6th International Congress on Noise as a Public Health Problem, volume 2
[AD-A278217] 10 p4134 N94-34290
Proceedings of the Sixth International Congress on Noise as a Public Health Problem, volume 3
[AD-A278218] 11 p4319 N94-36176

PUBLIC LAW
NT LEGAL LIABILITY
Report of the defense science board task force on aircraft assessment
[AD-A274531] 07 p2669 N94-26835
Loran-C time management 08 p3144 N94-30644
Alternative fuel information: State alternative fuel laws and incentives
[DE94-006892] 12 p4429 N94-37404
Comparative alternative/clean fuels provisions of the Clean Air Act Amendments of 1990 and the Energy Policy Act of 1992
[DE94-006887] 12 p4429 N94-37426

PUBLIC RELATIONS
Military space programs in the press: An analysis for change
[AD-A267799] 03 p0874 N94-17306
Space technology: A study of the significance of recognition for innovators of spinoff technologies. 1993 activities/1994, 1995 plans
[NASA-CR-194836] 06 p2596 N94-23526

PUBLIC SPEAKING
An exploratory study of neuro linguistic programming and communication anxiety
[AD-A277756] 09 p3682 N94-32986

PUBLICATIONS
U DOCUMENTS

PULLING
Analysis of pultrusion processing for long fiber reinforced thermoplastic composite system
[NASA-CR-194504] 04 p1339 N94-17766

PULMONARY FUNCTIONS
Project ARGO: Gas phase formation in simulated microgravity
[NASA-TM-104762] 01 p0125 N94-11235
Proceedings of the First Joint NASA Cardiopulmonary Workshop
[NASA-CP-10068] 01 p0308 N94-11991
Pulmonary function in microgravity: KC-135 experience 01 p0309 N94-11994
Medical problems in high mountain environments. A handbook for medical officers
[AD-A278095] 09 p3798 N94-33268

PULSAR MAGNETOSPHERES
Interstellar scattering and the pulsar studies with space VLBI 01 p0135 N94-11065
Particle acceleration on the Alfven surface of a plasma ejecting axisymmetric rotator 05 p2008 N94-22681
GRO: Studies of high energy pulsars with EGRET
[NASA-CR-196003] 11 p4349 N94-35516

PULSARS
Pulsar astrometry by using VLBI (PSR0329 between Kashima 26mPhi and Usuda 64mPhi) 01 p0351 N94-10968
An ensemble pulsar time 01 p0351 N94-10969
Search for ultra-high energy emission from Geminga and five unidentified EGRET sources
[DE93-012717] 02 p0846 N94-12816
High time resolution studies of binary x ray pulsars
[NASA-CR-194395] 02 p0832 N94-13894
ROSAT observations of the binary Be-star/radio pulsar PSR1259-63
[NASA-CR-194394] 02 p0832 N94-14357
Multiwavelength observations of unidentified high energy gamma ray sources
[NASA-CR-194536] 02 p0840 N94-14688
Fast pulsars, compact stars, and the strange matter hypothesis
[DE93-015039] 03 p1239 N94-16052
Pulse-timing studies of x ray pulsars
[NASA-CR-193778] 04 p1621 N94-18611
Eclipsing cataclysmic variables. Deep eclipses in H0928+501. YY Draconis, the whirling dervish. New x ray pulsar candidates from HEAO-1
[NASA-CR-194027] 04 p1621 N94-18855
Computational astrophysics: Pulsating stars
[DE93-018389] 04 p1627 N94-18857
High-energy astrophysics: A theoretical analysis of thermal radiation from neutron stars
[NASA-CR-194806] 05 p2055 N94-20952
Verification of the PROS timing analysis package 05 p1926 N94-22508
Gamma ray burst as a result of the explosive instability in the magnetosphere of old neutron star 05 p2007 N94-22675
Structure of accretion plasmas of x ray binary pulsars in MHD turbulence 05 p2007 N94-22679
VHE gamma ray generation by radio pulsars 05 p2007 N94-22680
An April 1991 outburst from 4U0115+63 observed by BATSE
[DE94-007093] 07 p3116 N94-27440
Fusion reactor systems studies
[DE94-003162] 07 p3046 N94-27686
Equation of state of neutron star matter, limiting rotational periods of fast pulsars, and the properties of strange stars
[DE94-005214] 08 p3542 N94-28480
A study of recycled pulsars in globular clusters 08 p3539 N94-29825
Evolution of vaporizing pulsars 09 p3929 N94-31128
A study of angular momentum loss in binaries using the free Lagrange method 09 p3931 N94-31134
A search for 100 TeV gamma ray emission from the x ray binary pulsar 4U 0115+63 using the CYGNUS extensive air-shower array 09 p3955 N94-31900
The evolutionary status of PSR 1259-63
[DE94-007094] 09 p3938 N94-32503
GRO: Studies of high energy pulsars with EGRET
[NASA-CR-196003] 11 p4349 N94-35516
Absolute limit on rotation of gravitationally bound stars
[DE94-011367] 12 p4548 N94-37049

PULSATING FLOW
U UNSTEADY FLOW

PULSE (CARDIOVASCULAR)
U HEART RATE

PULSE AMPLITUDE
Conversion of ADC pulse heights into MIP units: NUMASS test data, September 1991
[USIP-93-03] 04 p1432 N94-18846
Pulse waveform and transcranial Doppler analysis during lower body negative pressure
[AD-A274516] 07 p2911 N94-27088
Coronal temperatures of unusually active K-dwarf binary systems
[NASA-CR-189335] 08 p3545 N94-29861
Pulse height response of Si surface barrier detectors 08 p3497 N94-30221
A miniaturized ASIC-based multichannel scaler instrument
[DE94-007222] 09 p3807 N94-32783

PULSE CODE MODULATION
NT DELTA MODULATION
NT DIFFERENTIAL PULSE CODE MODULATION
An adaptive, lossless data compression algorithm and VLSI implementations 05 p1753 N94-21080
Image detection using edge extraction algorithms
[AD-A272439] 05 p1911 N94-21203

PULSE COMMUNICATION
NT DIGITAL SPACECRAFT TELEVISION
Study on color video pictures transmission by digital acoustic signal 01 p0139 N94-11917
DSP software development environments for the Adaptive Signal Processing Testbed
[DSIS-93-00347] 02 p0607 N94-14066
Space communications technology research in CRL 02 p0618 N94-14285
NTT's activities in satellite communications technology development 02 p0618 N94-14286
Future outlook on international satellite communications in Asia Pacific region 02 p0618 N94-14287
Technological development for broadcasting satellites in NHK Laboratories 02 p0618 N94-14288
Operation of digital systems in severe electromagnetic environments
[AD-A267176] 03 p0988 N94-15693
Signal processing in impulsive electromagnetic interference
[AD-A266425] 03 p0998 N94-16557
Four Frequency-Shift Keying (4-FSK) spread spectrum modulator and demodulator
[AD-A267433] 03 p1000 N94-16979
A study on an experimental communication system using microsatellites 03 p0892 N94-17160
VHF air/ground communications for air traffic control. Volume 1: A decision tree approach to system innovations
[AD-A268485] 04 p1316 N94-18384
Initial Graphics Exchange Specification (IGES)
[AD-A270049] 04 p1522 N94-18794
Nonlinear acoustics: Periodic waveguide, finite-amplitude propagation in a medium having a distribution of relaxation processes, and production of an isolated negative pulse in water
[AD-A270530] 05 p1967 N94-19894
Worldwide survey of direct-to-listener digital audio delivery systems development since WARC-1992 06 p2273 N94-22736
Direct broadcast satellite-radio, receiver development 06 p2273 N94-22739
Utilizing a TDRS satellite for direct broadcast satellite-radio propagation experiments and demonstrations 06 p2274 N94-22740
Adaptive digital beamforming for a CDMA mobile communications payload 06 p2274 N94-22743
Transparent data service with multiple wireless access 06 p2276 N94-22754
APLAC: An object-oriented analog circuit simulator and design tool. 6.1 system simulations manual
[PB93-224871] 06 p2450 N94-23226
Source spacing in B-ISDN
[PB93-201747] 06 p2293 N94-23508
Improved performance of hybrid error control techniques for real-time digital communications over noisy channels
[ISBN-0-315-84281-4] 07 p2770 N94-26625
Short-block data detection techniques employing channel estimation for fading time-dispersive channels
[ISBN-0-315-58970-1] 07 p2777 N94-27806
Receiving antennas for electromagnetic pulses and transients
[ISBN-0-315-62312-8] 07 p2777 N94-27871
1.8 gigahertz (GHz) digital Low Density Radio Communications Link (LDRCL) Operational Test and Evaluation (OT&E) integration and OT&E operational final test report
[AD-A275800] 08 p3241 N94-28771
Channel equalization for block transmission systems
[TELECOM-93-D-002] 09 p3670 N94-31093
Kalman filtering approach to blind equalization
[AD-A276320] 09 p3671 N94-31299
The effects of a multipath channel and interference on coherent M-PSK digital communication systems
[AD-A278158] 09 p3684 N94-33254

PULSE COMPRESSION
One-dimensional calculation of high-power microwave pulse compression by the earth's ionosphere
[DE93-009517] 01 p0137 N94-11466
FR/GE/US radar receiver pulse compression ratio
[AD-A265391] 01 p0138 N94-12409
Lower bounds on time of arrival estimation of pulse compression waveforms
[ITN-93-85189] 02 p0599 N94-13196
A combined analogue and digital pulse compression system using large time bandwidth product signals for use in synthetic aperture radar
[ISBN-0-315-54373-6] 02 p0600 N94-13489
Design and performance of the terawatt Cr:LiSrAlF6 laser system
[DE93-014678] 02 p0657 N94-13882
Independent adjustment of the higher order frequency dependent phase in chirped pulse amplification systems
[DE93-017106] 02 p0625 N94-14522
Simultaneous compression of the passively mode-locked pulsewidth and pulse train 03 p0913 N94-15566
Resolution in radar mapping
[AD-A269730] 04 p1462 N94-18753
Applications of correlator chips in radio science 05 p1763 N94-21695
Microwave excitation of pulsed high pressure gas discharge lasers
[DLR-FB-93-12] 06 p2351 N94-25304
Direct-conversion-to-baseband for a nonlinear FM signal
[AD-A274861] 07 p2768 N94-26189
Phase conjugation and pulse compression of high energy lasers: From nanoseconds to microseconds
[DE94-001061] 07 p2818 N94-26699
Digital pulse compression and its application in reducing radar interference
[ISBN-0-315-85767-6] 08 p3255 N94-30240
New light sources and concepts for electro-optic sampling
[AD-A278533] 10 p4141 N94-33672
Signal processing for the 1992 Barents Sea tomography experiment
[AD-A278580] 12 p4476 N94-36971

PULSE DOPPLER RADAR
NT MONOPULSE RADAR
Designing clutter rejection filters with complex coefficients for airborne pulsed Doppler weather radar
[NASA-CR-4550] 03 p0862 N94-15444
Description and availability of airborne Doppler radar data 05 p1722 N94-20419
CFAR processing for airborne pulse-Doppler radars 05 p1745 N94-22142
Space-based radar for moving target detection 05 p1745 N94-22143
Theory and application of a Radio-Acoustic Sounding System (RASS) 08 p3367 N94-30869

PULSE DURATION
Response of silicon solar cell to pulsed laser illumination 01 p0051 N94-11396
Design and performance of the terawatt Cr:LiSrAlF6 laser system
[DE93-014678] 02 p0657 N94-13882

Tetravalent chromium (Cr(4+)) as laser-active ion for tunable solid-state lasers
[NASA-CR-194527] 02 p0659 N94-14576
Dynamics of douple stimulated Brillouin scattering
03 p1200 N94-15206
Simultaneous compression of the passively mode-locked pulsewidth and pulse train
03 p0913 N94-15566
Optimum wavelengths for two color ranging
03 p0915 N94-15580
Pulse response based control for minimum time maneuver of flexible spacecraft
[AD-A266186] 03 p0886 N94-16455
Development of short pulse soft x ray lasers
[DE93-017150] 04 p1437 N94-18131
Resolution in radar mapping
[AD-A269730] 04 p1462 N94-18753
Spice modeling of a FET-switched induction accelerator cell
[DE93-018662] 04 p1575 N94-18996
Effects of stimulated Raman scattering on light beam properties during high-power laser beam long-path propagation
[AD-A273109] 05 p1818 N94-21509
Bundle Intensity and Beamgate Length recorder (BIBL)
[DIGEL-1993-7] 07 p3031 N94-25619
Development of surgical CW Nd:YAG laser with optical fiber delivery system
[DE93-632902] 07 p2817 N94-26185
Development of high average power industrial Nd:YAG laser with peak power of 10 kW class
[DE93-633201] 07 p2818 N94-26520
Calculations of population transfer during intense laser pulses
[DE94-001060] 07 p2818 N94-26698
Pulse control method and its characteristics
[DE94-701187] 07 p2989 N94-27809
Limiting vibration in systems with constant amplitude actuators through command preshaping
[NASA-CR-188284] 09 p3739 N94-32907
Advanced laser driver for soft x-ray projection lithography
[DE94-011643] 12 p4449 N94-37722

PULSE DURATION MODULATION
Design of power electronics for TVC EMA systems
[NASA-CR-193839] 04 p1407 N94-19642
Development of real-time pulse shaping technology in solid-state lasers
[DE93-633438] 07 p2817 N94-26403
Real time simulation model for designing converter regulation
[ETN-94-95735] 09 p3689 N94-31576
Examination of fast semiconductor diodes (recovery) with respect to switching valves in PWM and resonance devices
[ETN-94-95740] 09 p3690 N94-31609
Design, characterization and control of the Unique Mobility Corporation robot 09 p3603 N94-33296
Efficiency consideration of DC link soft-switching inverters for motor drive applications
[DE94-003604] 10 p4039 N94-33732
Microprocessor control of multiple peak power tracking DC/DC converters for use with solar cell arrays
[NASA-CASE-GSC-13450-2] 11 p4282 N94-35540

PULSE GENERATORS
Characterization of the pulse transformer
[AD-A263414] 01 p0143 N94-11298
Advanced concepts theory annual report 1992
[AD-A266132] 01 p0393 N94-11474
A PC-PCL-based control system for the high-voltage pulsed-power operation of the Intense Diagnostic Neutral Beam (IDNB) Experiment
[DE93-014144] 02 p0797 N94-13100
Review of the Procyon explosive pulsed power system
[DE93-016562] 02 p0802 N94-14532
A high-precision direct current measuring device over a kiloampere range
[DE93-626409] 02 p0627 N94-14885
User manual and program description of the data acquisition system of PML-pulse physics
[AD-A266752] 03 p1147 N94-15776
A microsecond-pulsewidth, intense, light-ion beam accelerator
[DE93-016455] 03 p1202 N94-16451
Digital laser range finder emulator
[AD-D015811] 03 p1040 N94-16540
Multi-frame x ray imaging with a large area 40ps camera
[DE93-017179] 03 p1035 N94-16960
Characterization of electromagnetic fields in an extended chamber at the Short Pulse Experimental Electron Device (SPEED) simulator
[AD-A265955] 05 p1717 N94-20329
Compact lightweight CO2 laser for SDIO application
[AD-A273010] 05 p1817 N94-21284
Results from long conduction time plasma opening switch experiments at Sandia National Laboratories
[DE93-019063] 05 p1762 N94-21632
Ultrafast gas switching experiments
[DE93-019071] 05 p1762 N94-21634
A FET-switched induction accelerator cell
[DE93-019604] 05 p1769 N94-21838
Safety guidelines for the operation of the DREO 10 m EMP simulator DREMPS
[DREO-TN-93-5] 06 p2193 N94-24117
TEM cell safety report
[DREO-TN-93-9] 06 p2193 N94-24123
Computer modeling of plasma flow switches-high current switching on Procyon
[DE93-040189] 06 p2311 N94-24500
Study of a system for producing a pulsed magnetic field (B 2T) with a frequency of 50 Hz
[ISL-N-601/92] 06 p2314 N94-25460
Development of an industrial CO2 laser for mask marking
[DE93-632901] 07 p2816 N94-26184
Microwave and pulsed power
[DE94-003019] 07 p2782 N94-26312
Development of real-time pulse shaping technology in solid-state lasers
[DE93-633438] 07 p2817 N94-26403
Pulse transformer characterization
[PML-1992-73] 07 p2784 N94-26646
Research in pulsed power plasma physics
[AD-A274323] 07 p3045 N94-27074
Bulletin of the Institute for Chemical Reaction Science, Tohoku University, volume 2
[JTN-94-80602] 07 p2717 N94-27385
Four phase microwave pulse generator for pulsed EPR spectrometer 07 p2718 N94-27388
High repetition rate, mode locked, figure eight laser with extracavity feedback
[AD-D016053] 07 p2820 N94-27670
Waveform generation for ultra-wideband radar system
[AD-A276352] 09 p3673 N94-31401
A noncritically phase matched femtosecond optical parametric oscillator near 3 microns
[DE94-008050] 09 p3720 N94-32704
Arbitrary waveform generator
[AD-D016123] 10 p4041 N94-34149
Analysis of recent agile mirror data
[AD-A278758] 11 p4318 N94-36427

PULSE HEATING
Experiments on nonlinear absorption of ECH waves in MTX and a comparison with theory
[DE93-019158] 04 p1589 N94-19074
Dynamic measurements of thermophysical properties of metals and alloys at high temperatures by subsecond pulse heating techniques 06 p2247 N94-25124

PULSE HEIGHT
U PULSE AMPLITUDE

PULSE MODULATION
NT DELTA MODULATION
NT DIFFERENTIAL PULSE CODE MODULATION
NT PULSE CODE MODULATION
NT PULSE DURATION MODULATION
NT PULSE POSITION MODULATION
A 27 channels, 1 MHz fibre-optic measuring system
[AD-A266943] 03 p1003 N94-17307
Enhanced acceleration in a self-modulated-laser wakefield accelerator
[AD-A268452] 04 p1586 N94-18148
Measurement of the frequency stability of responders in aircraft 08 p3261 N94-30673
Workshop on Commercialization of Pulsed Power Science and Technology Proceedings
[AD-A276987] 09 p3692 N94-32258
Propagation of radius-tailored laser pulses over extended distances in a uniform plasma
[AD-A280405] 12 p4528 N94-37182

PULSE POSITION MODULATION
Integration and test of high-speed transmitter electronics for free-space laser communications
[NASA-TM-106295] 06 p2295 N94-24101

PULSE RADAR
NT MONOPULSE RADAR
NT PULSE DOPPLER RADAR
Target detection by way of Kalman filtering
[AD-A267314] 03 p1000 N94-16945
The accuracy of monostatic and bistatic radar imaging by range-Doppler-processing with and without motion compensation
[DLR-FB-93-07] 04 p1384 N94-18071
Missile antenna pattern coordinate system and data formats
[AD-A269153] 04 p1385 N94-18260
Analysis of Ku-band cross section at low incidence angles 05 p1720 N94-20414
Real-time step frequency radar
[ISBN-0-315-83588-5] 05 p1743 N94-22576
Digital pulse compression and its application in reducing radar interference
[ISBN-0-315-85767-6] 08 p3255 N94-30240
Initial studies of reflectometer for ITER
[DE94-012476] 12 p4528 N94-37167

PULSE RATE
NT PULSE REPETITION RATE
Evolution of high-repetition-rate induction accelerators through advancements in switching
[DE93-012599] 02 p0654 N94-12963
Spice modeling of a FET-switched induction accelerator cell
[DE93-018662] 04 p1575 N94-18996

PULSE RECORDERS
U COUNTERS

PULSE REPETITION RATE
First and second order Stokes generation by SRS in methane: Influence of rep-rate, beam quality and astigmatism
[FEL-92-A125] 04 p1441 N94-19426
Development of an industrial CO2 laser for mask marking
[DE93-632901] 07 p2816 N94-26184

PULSE TIME MODULATION
NT PULSE DURATION MODULATION
NT PULSE POSITION MODULATION

PULSE WIDTH
U PULSE DURATION

PULSE WIDTH MODULATION
U PULSE DURATION MODULATION

PULSED JET ENGINES
Low power pulsed MPD thruster system analysis and applications
[NASA-CR-191187] 02 p0550 N94-13415
Pulsed expansion of plasma in a magnetic thruster
09 p3889 N94-31776

PULSED LASER DEPOSITION
In-situ crystallization of silicate glass films deposited on alpha- Al2O3
[DE93-012969] 01 p0095 N94-12596
Laser assisted CVD growth of AlN and GaN
[AD-A267150] 03 p1206 N94-15764
Pulsed laser deposition of metastable Ca(1-x)Sr(x)CuO2 thin films
[DE93-015804] 03 p1040 N94-16863
Imaging and blackbody emission spectra of hot particulates generated during laser ablation
[DE93-015818] 04 p1439 N94-18724
Particles on surfaces of laser ablated Y1Ba2Cu3O(7-delta) films
[DE93-040269] 05 p2013 N94-19929
Laser-deposited biocompatible films and methods and apparatuses for producing same
[AD-D016017] 06 p2350 N94-24952
Soft x ray optics by pulsed laser deposition
[NASA-CR-195139] 06 p2546 N94-24967
Laser ablation and deposition of metals
[ETN-94-95311] 06 p2351 N94-25294
In-situ TEM crystallization of anorthite-glass films on (alpha)-Al2O3
[DE94-006317] 09 p3652 N94-31780
Properties of doped and undoped (Ca,Sr)CuO2 thin films
[DE94-007230] 09 p3905 N94-32785
Nucleation and growth of cubic boron nitride films produced by ion-assisted pulsed laser deposition
[DE94-007295] 09 p3661 N94-32796
X ray absorption study of pulsed laser deposited boron nitride films
[DE94-008295] 09 p3662 N94-32855
Residual stress and Raman spectra of laser deposited highly-tetrahedral-coordinated-amorphous-carbon films
[DE94-012067] 12 p4426 N94-37537

PULSED LASERS
NT Q SWITCHED LASERS
NT ULTRASHORT PULSED LASERS
NT ULTRAVIOLET LASERS
Progress in zirconium resonance ionization spectroscopy
[DE93-011881] 01 p0076 N94-11075
Thermal-optical switching of a silicon based interference filter
[AD-A265152] 01 p0174 N94-11095
The efficiency of photovoltaic cells exposed to pulsed laser light 01 p0050 N94-11395
Response of silicon solar cell to pulsed laser illumination 01 p0051 N94-11396
Approaches to solar cell design for pulsed laser power receivers 01 p0051 N94-11397
Short pulse lasers for generation of fields exceeding 100 MG
[DE93-013346] 01 p0369 N94-11815
Submicrosecond, synchronizable x ray source
[AD-D015745] 01 p0176 N94-12337

Damage threshold study of ion beam sputtered coatings for a visible high-repetition laser at LLNL
[DE93-013430] 01 p0095 N94-12602
Inertial confinement fusion program
[DE93-013372] 02 p0796 N94-13047
New infrared photon absorption processes
[DE93-017017] 02 p0780 N94-13071
Imaging microscopy with x ray lasers at Lawrence Livermore National Laboratory
[DE93-013419] 02 p0655 N94-13258
Shock-free acceleration of laser driven targets
[DE93-008050] 02 p0655 N94-13387
Excimer laser surface processing of titanium
[DE93-012633] 02 p0570 N94-13512
Theoretical investigation of scattering by homogeneous or coated dielectric spheres illuminated with a steady state or pulsed laser beam 02 p0657 N94-13624
Single event effects and laser simulation studies
[NASA-CR-194506] 02 p0657 N94-13812
The interaction of intense femtosecond laser pulses with solid targets
[DE93-014415] 02 p0658 N94-14114
A laser-based technique to continuously monitor metal aerosol emissions
[DE93-012836] 02 p0710 N94-14183
Effects of depositon rate on Bi2Sr2CaCu2O(8+x) and Bi2Sr(1.6)La(0.4)CuO(6+x) epitaxial thin film growth by pulsed-laser ablation
[DE93-015797] 02 p0812 N94-14362
Data analysis for GOPEX image frames
02 p0810 N94-14388
Independent adjustment of the higher order frequency dependent phase in chirped pulse amplification systems
[DE93-017106] 02 p0625 N94-14522
High-order harmonic generation with short-pulse lasers
[DE93-016532] 02 p0659 N94-14594
The 8 to 11 keV x ray sources for imaging and absorption experiments
[DE93-015973] 02 p0803 N94-14865
Channel of the system for pulse charged particle beam diagnostics
[DE93-623867] 03 p1179 N94-14931
Prelaunch optical characterization of the Laser Geodynamic Satellite (LAGEOS 2)
[NASA-TP-3400] 03 p0884 N94-15193
Nd:YLF laser for airborne/spaceborne laser ranging
03 p0913 N94-15563
New methods of generation of ultrashort laser pulses for ranging 03 p0913 N94-15565
An improved light source for laser ranging
03 p0913 N94-15567
The solid state detector technology for picosecond laser ranging 03 p0914 N94-15572
Streak camera based SLR receiver for two color atmospheric measurements 03 p0914 N94-15573
Test results from LAGEOS-2 optical characterization using pulsed lasers 03 p0915 N94-15577
Bench checkout equipment for spaceborne laser altimeter systems 03 p0921 N94-15618
Multi-beam laser altimeter 03 p0921 N94-15620
X ray laser program
[AD-A267075] 03 p1038 N94-15628
Experimental investigations of superconductivity in quasi-two-dimensional epitaxial copper oxide superlattices and trilayers
[DE93-015306] 03 p1207 N94-15829
Laser-shock damage of iron-based materials
[AD-A267196] 03 p1038 N94-15852
Laser with optically driven Q-switch
[NASA-CASE-NPO-18470-1-CU]
03 p1038 N94-15932
Ablation, surface activation, and electroless metallization of insulating materials by pulsed excimer laser irradiation
[DE93-015808] 03 p1040 N94-16664
Observation of nonsequential ionization of helium and its impact on intensity monitoring
[DE93-017174] 03 p0949 N94-16904
Pulsed laser kinetic studies of liquids under high pressure
[DE93-017826] 03 p1041 N94-16998
Pulsed hydrogen fluoride overtone chemical laser studies
[AD-A267597] 03 p1041 N94-17193
Sensitive detection of gas-phase nitro-containing energetic materials employing 226-nm radiation
[AD-A267633] 03 p0951 N94-17203
Extracavity frequency doubling study of a pulsed photodissociation iodine laser
[AD-A267893] 03 p1042 N94-17394
Basic studies of the liquid state of matter: Electrical properties and laser interactions
[AD-A268311] 03 p1042 N94-17567
The copper-pumped dye laser system at Lawrence Livermore National Laboratory
[DE93-014429] 04 p1435 N94-17723
Pulse radiolytic studies of electron transfer processes and applications to solar photochemistry
[DE93-018715] 04 p1464 N94-17781
Observations of MeV electrons and scattered light from intense, subpicosecond laser-plasma interactions
[DE93-017153] 04 p1435 N94-17855
Pulsed LASER for testing silicon strip detectors
[DE93-017816] 04 p1436 N94-17883
Limitations on the fidelity of 100 fs pulses produced by chirped pulse amplification
[DE93-017167] 04 p1396 N94-17991
Production of dense vapor targets for laser-plasma interaction studies with intense, ultra-short pulses
[DE93-017175] 04 p1584 N94-17993
Dynamics of short-pulse excitation, ionization and harmonic conversion
[DE93-017220] 04 p1436 N94-17996
Ultra-shallow box-like profiles fabricated by pulsed UV-laser doping process
[DE93-017221] 04 p1437 N94-18083
Development of short pulse soft x ray lasers
[DE93-017150] 04 p1437 N94-18131
Enhanced acceleration in a self-modulated-laser wakefield accelerator
[AD-A268452] 04 p1586 N94-18148
Integrated photonics research volume 10. Conference edition
[AD-A269298] 04 p1577 N94-18298
Nonlinear Thomson scattering of intense laser pulse from beams and plasmas
[AD-A269556] 04 p1438 N94-18460
Quantum Optoelectronics. Organization of the 1993 photonics science topical meetings. Technical digest series, volume 8
[AD-A269026] 04 p1578 N94-18488
Advanced Solid-State Lasers/Compact Blue-Green Lasers. 1993 technical digest series. Volume 2: Organization of the 1993 photonics science topical meetings
[AD-A269058] 04 p1438 N94-18492
Photonics in Switching: Organization of the 1993 photonics science topical meetings. Technical digest
[AD-A269024] 04 p1578 N94-18528
High spatial resolution, range gated, underwater imaging method and apparatus
[AD-D015882] 04 p1430 N94-18530
Single-transverse-mode, narrow-bandwidth pulsed tunable dye laser with hollow circular intracavity dielectric waveguide
[AD-A270022] 04 p1439 N94-18614
Characterization of vapor plume species and deposition residues resulting from pulsed laser ablation of a graphite/epoxy composite
[AD-A270101] 04 p1343 N94-18869
Multi-terrawatt, 100 fsec laser system using flashlamp-pumped, dye-converted Ti:sapphire as an amplifier
[DE93-017190] 04 p1440 N94-18889
Ultrafast Electronics and Optoelectronics: Summaries of papers. Technical digest conference edition
[AD-A269233] 04 p1405 N94-18909
Growth of epitaxial semiconductor alloys and superlattices with continuously variable composition by pulsed-laser ablation
[DE93-018726] 04 p1601 N94-18998
Electron cyclotron resonance heating in the microwave tokamak experiment
[DE93-018083] 04 p1590 N94-19289
Tetravalent chromium (Cr(4+)) as laser-active ion for tunable solid-state lasers
[NASA-CR-194528] 04 p1441 N94-19394
Spectrally and temporally resolved laser emission from vertical cavity surface emitting lasers
[DE93-019410] 04 p1442 N94-19563
PVDF gauge characterization of hypervelocity-impact-generated debris clouds
[DE93-018831] 05 p1829 N94-19943
Applications and source development for high-repetition rate x ray lasers
[DE93-019547] 05 p1815 N94-20259
Ocular damage induced by ultrashort laser pulses
[AD-A271859] 05 p1890 N94-20462
Low-altitude cross-wind velocity measurements using pulsed visible fringe-type laser anemometry
[ISL-CO-216/92] 05 p1866 N94-20557
A theory for optical wavelength control in short pulse free electron laser oscillators
[AD-A271706] 05 p1817 N94-21353
Simulations of spectral broadening by cross-phase modulation (XPM) with chaotic light pulses
[DE93-019623] 05 p1819 N94-21872
Parametric instabilities in picosecond time scales
[DE94-000384] 05 p1966 N94-21978
Micro pulse laser radar
[NASA-CASE-GSC-13493-1] 06 p2294 N94-23827
Excimer laser study: Discharge and magnetic switching systems
[PB93-199768] 06 p2349 N94-24629
Laser-deposited biocompatible films and methods and apparatuses for producing same
[AD-D016017] 06 p2350 N94-24952
Microwave excitation of pulsed high pressure gas discharge lasers
[DLR-FB-93-12] 06 p2351 N94-25304
Imaging with x ray lasers
[DE94-002844] 07 p2816 N94-26020
Fast photoconductor CdTe detectors for synchrotron x ray studies
[DE94-001334] 07 p3054 N94-26139
Laser altimetry simulator. Version 3.0: User's guide
[NASA-TM-104588] 07 p2877 N94-26152
Development of an industrial CO2 laser for mask marking
[DE93-632901] 07 p2816 N94-26184
Development of surgical CW Nd:YAG laser with optical fiber delivery system
[DE93-632902] 07 p2817 N94-26185
Theoretical determination of chemical rate constants using novel time-dependent methods
[NASA-CR-195221] 07 p2714 N94-26205
Compact, solid-state femtosecond source
[AD-A273932] 07 p2817 N94-26271
New Thomson scattering laser control for D3-D
[DE94-002890] 07 p3043 N94-26274
Development of real-time pulse shaping technology in solid-state lasers
[DE93-633438] 07 p2817 N94-26403
Development of high average power industrial Nd:YAG laser with peak power of 10 kW class
[DE93-633201] 07 p2818 N94-26520
Calculations of population transfer during intense laser pulses
[DE94-001060] 07 p2818 N94-26698
Development of lasers optimized for pumping Ti:Al2O3 lasers
[NASA-CR-4573] 07 p2818 N94-26705
High repetition rate, mode locked, figure eight laser with extracavity feedback
[AD-D016053] 07 p2820 N94-27670
Design and testing of the LITE Variable Field Stop mechanism 08 p3161 N94-29633
Optical field ionization of atoms and ions using ultrashort laser pulses
[DE94-006643] 08 p3488 N94-29845
Optical techniques for time and frequency transfer
08 p3469 N94-30647
Time-resolved infrared absorption studies applied to the study of radical plus molecule reactions
[DE94-005921] 09 p3863 N94-31202
Workshop on Commercialization of Pulsed Power Science and Technology Proceedings
[AD-A276987] 09 p3692 N94-32258
Ti:sapphire based ultrafast pump-probe laser source in the violet and ultraviolet
[DE94-007542] 09 p3718 N94-32270
High average power pulsed phase conjugate laser with birefringence correction
[DE94-006049] 09 p3719 N94-32659
Superluminous laser pulse in an active medium
[DE94-007110] 09 p3720 N94-32684
Repetitively pulsed Cr:LiSAF laser for lidar applications
[DE94-007546] 09 p3720 N94-32761
Progress in understanding and improving x ray lasers
[DE94-006048] 09 p3720 N94-32794
A reliable low-maintenance flashlamp-pumped Ti:sapphire laser operating at 120 PPS
[DE94-009030] 09 p3721 N94-32848
X ray absorption study of pulsed laser deposited boron nitride films
[DE94-008295] 09 p3662 N94-32855
Ultrafast x ray sources
[AD-A277455] 09 p3721 N94-33012
Basic study of the pumping of a gamma ray laser
[AD-A278537] 10 p4057 N94-33673
Electron acceleration by laser fields in a gas
[DE94-008345] 10 p4139 N94-33924
Laser/lidar analysis and testing
[NASA-CR-193954] 10 p4058 N94-34136
10-GW CO2 laser system at the Brookhaven Accelerator Test Facility
[DE94-009001] 10 p4058 N94-34374
Molecular systems for ultrafast optical switching: Controlling electron transfer reactions with femtosecond laser pulses
[DE94-009695] 11 p4332 N94-35671
Chirped-pulse amplification with flashlamp-pumped Ti:Sapphire amplifiers
[DE94-010055] 11 p4272 N94-35695

An externally heated copper vapour laser
[DE94-619484] 12 p4447 N94-36565
High average power pulsed phase conjugate laser with birefringence correction
[DE94-012062] 12 p4447 N94-37160
Propagation of radius-tailored laser pulses over extended distances in a uniform plasma
[AD-A280405] 12 p4528 N94-37182
Time-resolved probing of electron thermal transport in plasma produced by femtosecond laser pulses
[DE94-012061] 12 p4530 N94-37392

PULSED RADIATION
NT ELECTROMAGNETIC PULSES
NT SYSTEM GENERATED ELECTROMAGNETIC PULSES
Laser Synchrotron Source (LSS)
[AD-D015755] 01 p0173 N94-10371
Propagation of light pulses through a three-layer medium (cloud, pure air, and ocean water) 01 p0222 N94-12725
Two-dimensional simulations of foil implosion experiments on the Los Alamos capacitor bank
[DE93-012676] 02 p0794 N94-12814
The Large Area Pulsed Solar Simulator (LAPSS)
[NASA-CR-194507] 02 p0703 N94-13940
A review of some dynamics models in six-dimensional phase space and their suitable conditions of motion equation
[DE93-623741] 03 p1175 N94-17317
The behavioral toxicology of high-peak, low average power, pulsed microwave irradiation
[AD-A268392] 03 p1134 N94-17535
Characteristics and pulsed radiation response of non-ideal quartz shock stress gauges
[DE93-017628] 04 p1424 N94-17999
A study of the effects of high power pulsed 2450 MHz microwaves, ELF modulated microwaves, and ELF fields on human lymphocytes and selected cell lines
[AD-A269070] 04 p1505 N94-18294
First and second order Stokes generation by SRS in methane: Influence of rep-rate, beam quality and astigmatism
[FEL-92-A125] 04 p1441 N94-19426
Rough surface scattering from moving ocean surfaces as an indicator of scattering mechanisms 05 p1726 N94-20439
Tuning of AmPS
[NIKHEF-K-AMPS-93-01] 08 p3494 N94-29422
Free electrons as a versatile source of coherent radiation
[ETN-94-96011] 09 p3715 N94-31545
Design and characterization of a pulsed x ray source for fluorescent lifetime measurements
[DE94-007495] 09 p3880 N94-32138
A historical perspective on fifteen years of laser damage thresholds at LLNL
[DE94-007930] 09 p3719 N94-32613
The use of pulsed neutron diffraction to measure strain in composites
[DE94-007536] 10 p4019 N94-33693
Time-of-flight diffraction at pulsed neutron sources: An introduction to the symposium
[DE94-010442] 11 p4327 N94-36225

PULSES
NT ELECTRIC PULSES
NT ELECTROMAGNETIC PULSES
NT GEOMAGNETIC PULSATIONS
NT PICOSECOND PULSES
NT PRESSURE PULSES
NT SYSTEM GENERATED ELECTROMAGNETIC PULSES
Propagation of light pulses through a three-layer medium (cloud, pure air, and ocean water) 01 p0222 N94-12725
Flue gas cleaning by pulse corona streamer
[EUT-93-E-272] 06 p2268 N94-23174

PULTRUSION
Analysis of pultrusion processing for long fiber reinforced thermoplastic composite system
[NASA-CR-194504] 04 p1339 N94-17766
Composites and textile reinforcement
[VTT-TIED-1424] 06 p2231 N94-25420
Lunar preform manufacturing 07 p2765 N94-25677
Fatigue behavior of unidirectional pultruded composite materials
[ISBN-0-315-86425-7] 09 p3621 N94-31719
Advanced manufacturing technology for polymer composite structures in Japan 12 p4422 N94-36968

PULVERIZING
U GRINDING (COMMINUTION)

PUMP IMPELLERS
Computational Fluid Dynamics (CFD) applications in rocket propulsion analysis and design 06 p2214 N94-23054
A finite-element-based perturbation model for the rotordynamic analysis of shrouded pump impellers: Part 1: Model development and applications
[NASA-CR-193916] 06 p2366 N94-24998
A finite-element-based perturbation model for the rotordynamic analysis of shrouded pump impellers: Part 2: User's guide
[NASA-CR-193917] 06 p2366 N94-24999
The high Reynolds number flow through an axial-flow pump
[AD-A273844] 07 p2789 N94-25604
Pump CFD code validation tests
[NASA-CR-193939] 07 p2822 N94-26597
Bulk-Flow Analysis, part A
[NASA-CR-193911-PT-A] 07 p2796 N94-27377
Compressibility effects on rotor forces in the leakage path between a shrouded pump impellier and its housing 07 p2796 N94-27379
Experiments on the aerodynamic generation of noise in centrifugal turbomachinery 08 p3480 N94-30804

PUMP SEALS
An experimental study on the static and dynamic characteristics of pump annular seals with two phase flow 10 p4062 N94-34179
Hotfire testing of a SSME HPOTP with an annular hydrostatic bearing 10 p4065 N94-34196

PUMPS
NT AXIAL FLOW PUMPS
NT BLOOD PUMPS
NT CENTRIFUGAL PUMPS
NT DIFFUSION PUMPS
NT ELECTROMAGNETIC PUMPS
NT FUEL PUMPS
NT JET PUMPS
NT TURBINE PUMPS
NT VACUUM PUMPS
NT WINDPOWERED PUMPS
New insulin pump
[NASA-TM-109642] 03 p1120 N94-15253
Electro-rheological disk pump
[AD-D015783] 03 p1047 N94-16531
Hydraulic pump with integral electric motor
[AD-D015782] 03 p1011 N94-16549
High pressure pump for electro-rheological fluids
[AD-D015888] 03 p1048 N94-16915
Application of thermal spray and ceramic coatings and reinforced epoxy for cavitation damage repair of hydroelectric turbines and pumps
[AD-A267624] 03 p0971 N94-17198
Sensorless, brushless motor to drive a sealed freon-ammonia pump 06 p2315 N94-24036
Argon frost continuous cryopump for fusion applications
[DE94-004478] 08 p3230 N94-29017
Low power, constant-flow air pump systems
[DE94-007463] 09 p3727 N94-32758
A review of vibration problems in power station boiler feed pumps 10 p4064 N94-34190
Application of programmable logic controller to pump regulation system for supplying water 10 p4067 N94-34344

PUPILS
Analysis of various biological activity parameters during parabolic flight 08 p3393 N94-29716

PURGING
Chamber free fusion welding root side purging method and apparatus
[NASA-CASE-MFS-28832-1] 08 p3204 N94-29380

PURIFICATION
NT AIR PURIFICATION
Electrohydrodynamic effects in continuous flow electrophoresis observations on Earth and in microgravity 01 p0122 N94-10234
Photochemically induced transformations of transition complexes
[AD-A271112] 05 p2014 N94-19982
Physics with chemically and isotopically pure semiconductors
[DE93-040120] 06 p2557 N94-22926
New method for increasing machine service-life, phase 2
[PB93-200707] 06 p2354 N94-23533
Study on utilization of super clean, high vacuum space 07 p2682 N94-25586
Development of liquid membrane separation processes 07 p2717 N94-27386
Development of novel switchable protein surfaces
[AD-A275510] 08 p3384 N94-28667
Fossil energy biotechnology: A research needs assessment
[DE94-004239] 08 p3338 N94-29953
Gas stream purifier 08 p3354 N94-30469
A new material for removing heavy metals from water 08 p3354 N94-30471

PURIFIERS
U PURIFICATION

PURINES
NT CAFFEINE
NT XANTHINES

PURITY
Production of electronic grade lunar silicon by disproportionation of silicon difluoride 01 p0435 N94-12017
Method of test for cleanness assessment of metal alloys: The preparation of button specimens by electron beam melting and the characterisation of recovered inclusions
[NPL-DMM(A)-130] 08 p3210 N94-30796
Purity and cleanness of aerogel as a cosmic dust capture medium 11 p4247 N94-35469

PURSUIT TRACKING
A piloted simulation investigation of the normal load factor and longitudinal thrust required for air-to-air acquisition and tracking 02 p0522 N94-13301
Analysis of pursuit tracking eye movements in pilots and nonfliers
[AD-A276597] 09 p3799 N94-32035
Two-axis camera platform for machine vision 12 p4394 N94-36628

PUSHBROOM SENSOR MODES
Airborne SAR as a complement to SPOT HRV in land-cover classification: The use of normalization and principal components analysis 09 p3750 N94-32539

PUSHING
Particle Engulfment and Pushing by Solidifying Interfaces (PEPSI)
[NASA-CR-193856] 03 p0960 N94-17079

PWM (MODULATION)
U PULSE DURATION MODULATION

PYLONS
Aircraft accident report: In-flight engine separation. Japan Airlines, Inc., flight 46E, Boeing 747-121, N473EV, Anchorage, Alaska, 31 March 1993
[PB93-410407] 06 p2173 N94-24062

PYRAMIDS
A pyramid neural network architecture for stereo fusion 05 p1785 N94-22201

PYRANOMETERS
Determination of sunshine duration from radiation intensity pyranometric measurements of global and sky radiation
[BER-181] 03 p1105 N94-15302

PYRENES
Synthesis and catalytic properties of metal and semiconductor nanoclusters
[DE93-019418] 05 p2028 N94-21541
Computer simulation of molecular interactions in supercritical solvents
[AD-A274977] 08 p3486 N94-29087
Photochemistry in constrained spaces: Zeolites and layered double metal hydroxides
[DE94-004958] 08 p3200 N94-30769

PYREX (TRADEMARK)
U BOROSILICATE GLASS

PYRIDINES
Pulsed laser kinetic studies of liquids under high pressure
[DE93-017826] 03 p1041 N94-16998
The direct synthesis of organic and organometallic-containing MICA-type aluminosilicates
[DE93-019001] 04 p1373 N94-19321
Dynamics of adsorbed, swollen block copolymers
[AD-A272013] 05 p1706 N94-21460
Hydrogen peroxide electrodes based on electrical connection of redox centers of various peroxidases to electrodes through a three-dimensional electron relaying polymer network
[AD-A276543] 09 p3691 N94-32056
Dynamics of block poly(styrene-co-vinylpyridine) (SVP) in solution and on silica
[AD-A277139] 09 p3657 N94-32364
Laser flash photolysis, EPR and Raman studies of liquids at elevated pressures
[DE94-008351] 09 p3718 N94-32413

PYRITES
The rate of chemical weathering of pyrite on the surface of Venus 01 p0477 N94-12246
The role of CO2 in weathering reactions and the presence of S2 on Venus: Implications for the pyrite stability field 05 p2122 N94-20799

PYROELECTRICITY
Proceedings of the 8th International Symposium on Applications of Ferroelectrics
[AD-A270679] 05 p1749 N94-20012
Pyroelectric sensors in copolymer integrated on silicon
[LAAS-93044] 06 p2342 N94-22902
Photopyroelectric spectroscopy as a non-intrusive technique for the determination of the optical absorption spectra of multiple quantum well samples
[ISBN-0-315-87164-4] 09 p3833 N94-31875

PYROGRAPHALLOY
U COMPOSITE MATERIALS
U PYROLYTIC GRAPHITE
U REFRACTORY MATERIALS

PYROLYSIS
Fibre-reinforced ceramic components by filament winding for intermediate temperature applications
01 p0061 N94-10041
Applications of a model to predict flame spread over interior finish materials in a compartment
01 p0019 N94-10783
Preparation of carbon monoliths having tailored pore structure from porous polymer precursors
[DE93-011576] 01 p0089 N94-10958
Nitrogen and noble gases in a glass sample from LEW88516 01 p0080 N94-12051
Separation of spallation and terrestrial C-14 in chondrites 01 p0431 N94-12183
Synthesis of ceramic oxide powders in a microwave plasma device
[DE93-012741] 03 p0965 N94-15920
A proposed mechanism for the pyrolysis of diborane
[DE93-014275] 03 p0947 N94-15977
Nitrogen isotopic signatures in agglutinates from breccia 79035 03 p0954 N94-16314
Advanced thermally stable jet fuels
[DE93-017711] 03 p0975 N94-16996
Characterization of vapor plume species and deposition residues resulting from pulsed laser ablation of a graphite/epoxy composite
[AD-A270101] 04 p1343 N94-18869
Molecular and polymeric ceramic precursors
[DE93-040364] 04 p1372 N94-18891
Accelerated screening methods for determining chemical and thermal stability of refrigerant-lubricant mixtures. Part 1: Method assessment
[DE93-040215] 04 p1351 N94-19136
Direct aromatization of methane
[DE93-040631] 05 p1678 N94-19890
Are the C delta light nitrogen and noble gases located in the same carrier? 05 p2085 N94-20846
High temperature size selective membranes
[DE93-019865] 05 p1709 N94-21982
Mass spectrometer-pyrolysis experiment for atmospheric and soil sample analysis on the surface of Mars 05 p1812 N94-22435
Atomic probes of surface structure and dynamics
[DE94-001651] 06 p2530 N94-22720
Ceramic silicon-boron-carbon fibers from organic silicon-boron-polymers
[NASA-CASE-ARC-11956-1-SB] 06 p2253 N94-23311
CMC design consequences 06 p2256 N94-24238
Investigating pyrolysis/incineration as a method of resource recovery from solid waste
06 p2444 N94-25375
Double layer capacitance of carbon foam electrodes
[DE94-002651] 07 p2780 N94-25975
Micropyrolysis of polymer thin films for ceramics
[ECL-92-62] 07 p2750 N94-26088
Emissions of nitrogen oxides (NO(x) and N2O) in pressurized fluidized bed combustion
[PB94-133071] 07 p2876 N94-28395
Gas phase thermochemistry of organogermanium compounds
[DE94-004885] 08 p3187 N94-28561
Evaluation of pyrolysis and arc tracking on candidate wire insulation designs for space applications
08 p3166 N94-28711
Hypervelocity impact induced arcing and Kapton pyrolization in a plasma environment
[NASA-TM-106528] 08 p3167 N94-28814
A study of solid propellants using a microprobe mass spectrometer system
[AD-A275325] 08 p3224 N94-28879
Endothermic fuels for hypersonic aviation
08 p3197 N94-29285
The intramolecular cyclization of bis-2,5-dimethylene-2,5-dihydrofurans and bis-2,5-dimethylene-2,5-dihydrothiophenes: An approach to macrocycles
[DE94-007060] 09 p3657 N94-32377
Improved oxidation resistance of 3-D carbon/carbon composites
[AD-A277349] 09 p3625 N94-32624
Structure-property relationships of carbon aerogels
[DE94-007120] 09 p3660 N94-32687
Direct aromatization of methane
[DE94-008719] 09 p3638 N94-32888
Evaluation of pyrolysis and arc tracking on candidate wire insulation designs for space applications
[NASA-CR-195332] 09 p3731 N94-32901
Conversion of polymers of methyl- and vinylsilane to Si-C ceramics
[NASA-TM-106554] 09 p3662 N94-32945
Novel precursor approached for CMC derived by polymer pyrolysis
[AD-A278383] 09 p3665 N94-33352
Basic solutions to carbon/carbon oxidation: Science and technology
[AD-A280447] 12 p4404 N94-37232

PYROLYTIC GRAPHITE
The optical constants and spectral specular reflectivity of Highly Oriented Pyrolytic Graphite (HOPG)
[DE93-011894] 02 p0790 N94-12865
Structural change of graphite during electron irradiation
[DE93-015961] 02 p0582 N94-14531
Solvational barriers to interfacial electron transfer: Minimization by way of valence delocalization
[AD-A267371] 03 p0950 N94-17006
Tunneling spectroscopy of ultrasmall clusters and grains
[AD-A268840] 04 p1598 N94-18539
Atomic-scale friction and microfriction of graphite and diamond using friction force microscopy
[AD-A270952] 04 p1605 N94-19679
The optical constants and spectral specular reflectivity of Highly Oriented Pyrolytic Graphite (HOPG)
[DE93-040546] 05 p1709 N94-21970
Wear reduction in ceramic bearings by surface generated pyrolytic carbon continuously replenished by ethylene gas
[AD-A278264] 06 p2364 N94-24090

PYROLYTIC MATERIALS
NT PYROLYTIC GRAPHITE

PYROMETERS
NT RADIATION PYROMETERS
Development of a multi-point two-color pyrometer for tube and wall temperature and emissivity measurement at the CFFF
[DE93-014716] 04 p1429 N94-18207

PYROMETRY
U TEMPERATURE MEASUREMENT

PYROPHORIC MATERIALS
Ignition delays, heats of combustion, and reaction rates of aluminum alkyl derivatives used as ignition and combustion enhancers for supersonic combustion
[NASA-CR-189581] 09 p3638 N94-32868

PYROTECHNICS
NT HMX
Destruction of waste energetic materials using base hydrolysis
[DE93-012738] 02 p0584 N94-13491
Densifying and stabilizing ingredient
[AD-D015751] 03 p0975 N94-16934
Structural analysis of a frangible nut used on the NASA Space Shuttle
[DE94-003672] 07 p2821 N94-25811
Radiometric, spectral, and effectiveness equipment
[AD-A274208] 07 p3037 N94-27066
Pyrotechnic shock: Devices in pyrotechnic environment qualification logic
[REPT-932-430-108] 08 p3225 N94-29429
The 27th Aerospace Mechanisms Symposium
[NASA-CP-3205] 08 p3160 N94-29627
Integration of pyrotechnics into aerospace systems
08 p3161 N94-29634
A low cost igniter utilizing an SCB and titanium sub-hydride potassium perchlorate pyrotechnic
[DE94-006467] 09 p3666 N94-31827

PYROXENES
NT ENSTATITE
The Fe2(+)-Mg interdiffusion in orthopyroxene: Constraints from cation ordering and structural data and implications for cooling rates of meteorites
03 p1241 N94-16175
Stalking the LREE-enriched component in ureilites
03 p1241 N94-16190
Pyroxene equilibration temperatures in metamorphosed ordinary chondrites 03 p1242 N94-16224
Complex zoning behavior in pyroxene in FeO-rich chondrules in the Semarkona ordinary chondrite
03 p1243 N94-16284
Water in Earth's mantle: Hydrogen analysis of mantle olivine, pyroxenes and garnet using the SIMS
03 p1104 N94-16336
Mixing model analysis of telescopic lunar spectra
03 p1284 N94-16371
Analysis of pyroxene absorptions observed in Martian dark regions 03 p1292 N94-16411
Zaoyang chondrite cooling history from pyroxene Fe(2+)-Mg intracrystalline ordering and exolutions
03 p1246 N94-16417
Composition of weakly altered Martian crust
03 p1296 N94-16436
Petrogenesis of Apollo 12 mare basalts. Part 1: Multiple melts and fractional crystallization to explain olivine and ilmenite basalt compositions 05 p1684 N94-20644
Petrogenesis of Apollo 12 mare basalts. Part 2: An open system model to explain the pigeonite basalt compositions 05 p1684 N94-20645
Orthopyroxenes as recorders of diogenite petrogenesis: Major and minor element systematics
05 p1684 N94-20670
Post-igneous redistribution of components in eucrites
05 p1685 N94-20684
Primary differentiation in the early Earth: Nd and Sr isotopic evidence from diamondiferous eclogites for both old depleted and old enriched mantle, Yakutia, Siberia
05 p1862 N94-20776
The U-Th-Pb, Sm-Nd, and Ar-Ar isotopic systematics of lunar meteorite Yamato-793169
05 p2084 N94-20834
Rare Earth elements in individual minerals in Shergottites 05 p1686 N94-20852
Diffuse reflectance spectra of orthopyroxene, olivine, and plagioclase as a function of composition and structure 05 p2087 N94-20906
Evidence for ultramafic lavas on Syrtis Major
09 p3950 N94-33229
Reduction of lunar mare soil and pyroclastic glass
11 p4355 N94-35398
Partial melting of the St. Severin (LL) and Lost City (H) ordinary chondrites: One step backwards and two steps forward 11 p4353 N94-36146
Synthetic and natural Nakhla pyroxenes: Parent melt composition and REE partition coefficients
11 p4353 N94-36161
Hematite formed from pyroxene on Mars by meteoritic impact 11 p4372 N94-36165

PYROXYLIN
U CELLULOSE NITRATE

PYRRHOTITE
NT TROILITE

PYRROLES
NT INDOLES
NT TRYPTOPHAN
A simple chemical procedure for extending the conductive state of polypyrrole to more negative potentials
[AD-A266235] 03 p0969 N94-16928
LB-Deposited, side-chain substituted polyaniline, polypyrrole and the corresponding monomers, studied by STM
[AD-A274405] 07 p2754 N94-26977
Langmuir-Blodgett and STM investigations of conducting polymer thin films
[AD-A274512] 07 p2755 N94-27087
Chemical polymerization and Langmuir-Blodgett techniques. 2: The polymerization of monolayers of 3-substituted pyrroles
[AD-A274478] 07 p2755 N94-27163

PYRUVATES
Preparation, characterization, and thermal behaviour study of lanthanides (3) and yttrium (3) 4-methoxy benzylidene pyruvate in solid state
[DE94-604079] 07 p3068 N94-27697

P3V AIRCRAFT
U P-3 AIRCRAFT

Q

Q FACTORS
Quality factors and local adaption (with applications in Eulerian hydrodynamics)
[DE93-010502] 01 p0151 N94-11272
H2S data reduction
[NASA-CR-193389] 02 p0617 N94-14743
Structural investigation of electrochemically etched silicon
[DE93-015300] 03 p1207 N94-15827
Effective conductivity of wire mesh reflectors for space deployable antenna systems
[NASA-CR-191605] 07 p2788 N94-27770
Aperture excitation of electrically large, lossy cavities
[PB94-145711] 09 p3675 N94-31683

Q SWITCHED LASERS
Novel Co:MgF2 lidar for aerosol profiler
[NASA-CR-191525] 02 p0654 N94-13091
Development of the Mars Observer Laser Altimeter (MOLA) 03 p0921 N94-15617
Laser with optically driven Q-switch
[NASA-CASE-NPO-18470-1-CU] 03 p1038 N94-15932
Pulsed laser kinetic studies of liquids under high pressure
[DE93-017826] 03 p1041 N94-16998
Optics survivability support, volume 1
[DE93-019616] 05 p1985 N94-20262
The development of Cr, Tm, Ho:YAG lasers for airborne lidar
[AD-A274895] 07 p2816 N94-26178

Development of lasers optimized for pumping Ti:Al2O3 lasers
[NASA-CR-4573] 07 p2818 N94-26705
Development of high time-resolution laser flash equipment for thermal diffusivity measurements using miniature-size specimens
[AD-B183270L] 08 p3295 N94-30186
Repetitively pulsed Cr:LiSAF laser for lidar applications
[DE94-007546] 09 p3720 N94-32761
Chirped-pulse amplification with flashlamp-pumped Ti:Sapphire amplifiers
[DE94-010055] 11 p4272 N94-35695
Greater than 100 watt average power at 0.53 micron with 25 ns, 2.5 kHz repetition rate pulses from a single power oscillator
[DE94-011641] 12 p4447 N94-37114
The 250 watt average power electro-quality Q-switched diode pumped power oscillator
[DE94-011644] 12 p4449 N94-37737

Q VALUES
Q-profile flattening due to nonlinear development of resistive kink mode and ensuing fast crash in sawtooth oscillations
[DE94-727625] 12 p4526 N94-36472

QAM (MODULATION)
U QUADRATURE AMPLITUDE MODULATION

QCD
U QUANTUM CHROMODYNAMICS

QPSK
U QUADRATURE PHASE SHIFT KEYING

QSO (RADIO SOURCES)
U QUASARS

QUADRANTS
Some practicable applications of quadtree data structures/representation in astronomy
05 p1927 N94-22515

QUADRATIC EQUATIONS
Phase portraits of quadratic systems with finite multiplicity three and one critical point of infinity
[REPT-93-41] 07 p2991 N94-26215
Convolutional encoding of self-dual codes
08 p3250 N94-29662
L(sub)p optimal d dimensional triangulations for piecewise linear interpolation: A new result on data dependent triangulations
[RUU-CS-93-13] 08 p3458 N94-30406
Recent progress in irrational conformal field theory
[DE94-011908] 11 p4317 N94-36234

QUADRATIC PROGRAMMING
Impending motion direction of contacting rigid bodies
[AD-A266814] 03 p1164 N94-15756
A sequential quadratic programming algorithm using an incomplete solution of the subproblem
[DE93-017439] 03 p1149 N94-16120
Large-scale shape optimization: Numerical methods, parallel algorithms, and applications to aerodynamic design
09 p3815 N94-31966
Application of sequential quadratic programming to large-scale structural design problems
[AD-A278574] 11 p4307 N94-36185

QUADRATURE AMPLITUDE MODULATION
Exploitation of cyclostationarity for signal-parameter estimation and system identification
[AD-A267137] 03 p0988 N94-15690
Coded 64QAM using a binary convolutional code
05 p1747 N94-22223
Bounds and simulation results of 32-ary and 64-ary quadrature amplitude modulation for broadband-ISDN via satellite
[NASA-TM-106484] 06 p2202 N94-25095

QUADRATURE APPROXIMATION
U QUADRATURES

QUADRATURE PHASE SHIFT KEYING
Development and test of readout electronics for optical quadrature signals
[DLR-MITT-92-11] 04 p1395 N94-17920
Advanced coding and modulation schemes for TDRSS
05 p1744 N94-21350
The influence of lowpass filtering and the effects of fading on the group demodulation of QPSK signals
05 p1746 N94-22170
Quadrature biorthogonal modulation
05 p1747 N94-22232
A comparison between coherent and noncoherent mobile systems in large Doppler shift, delay spread, and C/I environment
06 p2287 N94-22818
Detection and analysis of unbalanced QPSK in Gaussian noise, version 1.0
[DREO-12-020.1] 06 p2296 N94-24131

QUADRATURES
Numerical method of singular problems on singular integrals
[DE93-613654] 01 p0343 N94-10546
Quantum noise and squeezing in optical parametric oscillator with arbitrary output coupling
01 p0375 N94-10568
One dimensional representations in quantum optics
01 p0375 N94-10570
Comparison of multiresolution techniques for digital signal processing
[AD-A265364] 01 p0138 N94-12406
A new formulation of longitudinal coherent instabilities
[DE93-014288] 02 p0789 N94-13220
I/Q demodulation of radar signals with calibration and filtering
[DREO-RN-1119] 02 p0606 N94-14064
High resolution radar profiling using higher-order statistics
[AD-D015891] 03 p1000 N94-16918
Linear characteristic spatial quadrature for discrete ordinates neutral particle transport on arbitrary triangles
[AD-A267485] 03 p1185 N94-17365
Exponential characteristic spatial quadrature for discrete ordinates neutral particle transport in two-dimensional cartesian coordinates
[AD-A270458] 04 p1554 N94-19671
Use of switched capacitor filters to implement the discrete wavelet transform 05 p1755 N94-21097
Generalized Gaussian quadrature rules for systems of arbitrary functions
[AD-A273610] 06 p2491 N94-24947
Correlation function estimator performance in non-Gaussian spherically invariant random processes
[AD-A273498] 06 p2496 N94-24951
A current evaluation of the digital beamforming testbed at Rome Laboratory
[AD-A274311] 07 p3032 N94-26881
A survey of numerical cubature over triangles
[DE94-006810] 09 p3841 N94-31274
Correlator data analysis for the array feed compensation system 11 p4253 N94-35553
Multiquadric collocation methods in the numerical solution of Volterra integral equations with weakly singular kernels
[DE94-013000] 12 p4505 N94-37497

QUADRIPHASE SHIFT KEYING
U QUADRATURE PHASE SHIFT KEYING

QUADRUPOLE LENSES
U MAGNETIC LENSES

QUADRUPOLES
Fabrication and test of a superconducting RFQ
[DE93-010860] 01 p0140 N94-10300
The effect of pressure and quadrupolar interactions on the nematic-isotropic transition properties: Numerical results for a system of prolate ellipsoids including second and fourth rank orientational order parameters
[DE93-613540] 01 p0410 N94-10536
Performance characteristics of the INS 25.5-MHz split coaxial RFQ
[DE93-753168] 01 p0144 N94-11508
On the unique structure of the magnetic fields of Uranus and Neptune 01 p0472 N94-12221
Operational characteristics of a 100-mA, 2-MeV radio-frequency quadrupole
[DE93-014474] 01 p0374 N94-12786
Magnetic effects in anomalous dispersion
[DE93-014291] 03 p1175 N94-15978
Emittance and beam size distortion due to linear coupling
[DE93-015402] 03 p1184 N94-16886
Statistics of the half-integer stopband
[DE93-016101] 03 p1173 N94-17236
Heavy Ion Fusion Injector Program
[DE93-018706] 04 p1575 N94-18997
Space-charge dominated beam transport in magnetic quadrupoles with large aperture ratios
[DE93-040443] 05 p1992 N94-20004
High current injector for heavy ion fusion
[DE93-019241] 05 p1979 N94-20289
Study of possible energy upgrade for the ALS and modeling of the real lattice for the diagnosis of lattice problems
[DE93-040286] 05 p2016 N94-20323
Simulation studies of space-charge-dominated beam transport in large aperture ratio quadrupoles
[DE93-019238] 05 p1981 N94-21440
Focusing properties of a three-element quadrupole lens system and its stigmatic focusing behaviour
[DE93-616534] 07 p2766 N94-25915
Correlation of experimental data and three-dimensional finite element modeling of a spinning quadrupole
[DE93-041173] 07 p3008 N94-26421
Hyperfine structure of positronium energy levels in a crystal
[DE94-603898] 07 p3068 N94-27729
Image theory for DC problems involving a conducting half space bounded by the general anisotropic impedance surface
[PB94-132917] 07 p2779 N94-28390
Magnetic properties of a quantum transverse spin-1 Blume-Emery-Griffiths model
[DE94-608114] 08 p3517 N94-30109
General-relativistic celestial mechanics. 4: Theory of satellite motion
[PB94-147782] 09 p3601 N94-31769
RHIC chromatic correction system
[DE94-008532] 09 p3883 N94-32994
Hot-ion plasma in the quadrupole trap
[DE94-617216] 11 p4337 N94-36082
Method of N-15 analysis by mass-spectroscopy on ion implanter MPB-200
[DE94-618203] 12 p4407 N94-36529
Quadrupolar effects in PrCu2Si2
[DE94-011509] 12 p4534 N94-37054
Tune modulation due to gradient ripple and the dynamic aperture
[DE94-011922] 12 p4524 N94-37157

QUALIFICATIONS
Design, qualification and operation of nuclear rockets for safe Mars missions
[DE93-010792] 02 p0549 N94-12996
The Senior Executive Service
[NHB-3100.6] 03 p1224 N94-15945
Qualifying codes under software quality assurance: Two examples as guidelines for codes that are existing or under development
[DE93-040452] 05 p1904 N94-20097
Advanced qualification techniques
[DE94-003709] 07 p2780 N94-25812
NAVAIR aircraft wiring standardization and qualification program 08 p3166 N94-28704
Organized wiring systems 08 p3166 N94-28705
Pyrotechnic shock: Devices in pyrotechnic environment qualification logic
[REPT-932-430-108] 08 p3225 N94-29429
Fire behavior of aeronautical materials
[REPT-932-600-105] 08 p3197 N94-29457
Logistics for the implementation of lead-free solders on electronic assemblies
[DE94-004800] 08 p3206 N94-29936
Utilizing a Russian space nuclear reactor for a United States space mission: Flight qualification issues
[DE94-004674] 09 p3613 N94-31265

QUALITATIVE ANALYSIS
Field evaluation of six protective coatings applied to T-56 turbine blades after 2500 hours of engine use
[ARL-TR-27] 01 p0090 N94-11311
Molecular surface electrostatic potentials in the analysis of non-hydrogen-bonding noncovalent interactions
[AD-A274612] 07 p3022 N94-26894
Knowledge based system for identification of gamma sources
[PB94-137742] 08 p3487 N94-29683
Tetraalkyldiarsines as potential precursors for electronic materials: Synthesis and characterization of various iso-propyl arsenic compounds
[AD-A277003] 09 p3900 N94-32001
Modelling and optimal control of Pb-Sn continuous crystallization process 10 p4118 N94-34345
United States Air Force Summer Research Program, 1993. Volume 16: Arnold Engineering Development Center, Frank J. Seiler Research Laboratory and Wilford Hall Medical Center
[AD-A278658] 12 p4550 N94-36978
SAW chemical sensor arrays using new thin-film materials
[DE94-011940] 12 p4411 N94-37365

QUALITY
NT AIR QUALITY
NT ENVIRONMENTAL QUALITY
NT RIDING QUALITY
NT WATER QUALITY
The experience factory: Can it make you a 5? or what is its relationship to other quality and improvement concepts? 01 p0328 N94-11424
Digital sound: The selection of critical programme material and preparation of recordings for CCIR tests on low bit-rate codecs
[BBC-RD-1993/1] 02 p0598 N94-12925
Digital sound: Subjective tests on commentary-quality codecs
[BBC-RD-1993/2] 02 p0598 N94-12926
Ninth Annual NASA/Contractors Conference on Quality and Productivity. World Class Excellence: The Journey Continues. Keynote presentations
[NASA-CR-194513] 02 p0665 N94-13148
The airline quality report 1993
[NIAR-93-11] 03 p0863 N94-17262
Measurement of laboratory quality
[VTT-TIED-1427] 07 p2679 N94-25652
Quality of sound in large rooms: Alteration of room impulse responses
[CTH-E-93-02] 09 p3859 N94-31077

QUALITY CONTROL
NT TOTAL QUALITY MANAGEMENT
Software process assessments
01 p0329 N94-11427

Large array SQUID magnetometer for NDE
[AD-A264799] 01 p0304 N94-11449
Quality assurance in basic research and R/D
[DE93-010825] 01 p0183 N94-11647
An integrated approach to total end-to-end quality control of ocean data in the real-time environment
01 p0211 N94-12662
Quality assurance for environmental chemistry: 1991, volume 2
[DE93-011792] 01 p0272 N94-12780
Project AIRSTREAM: Trace gas
[DE93-008849] 02 p0706 N94-12904
Johnson Space Center procurement: Controls over payments to contractors should be strengthened
[AD-A265722] 02 p0819 N94-13060
NASA Johnson Space Center: Total quality partnership 02 p0668 N94-13165
Teamwork for Oversight of Processes and Systems (TOPS). Implementation guide for TOPS version 2.0, 10 August 1992 02 p0668 N94-13167
George M. Low Trophy: NASA's quality and excellence award. 1992 recipients: Honeywell Clearwater, IBM Houston
[NASA-TM-109265] 02 p0669 N94-13396
The Large Area Pulsed Solar Simulator (LAPSS)
[NASA-CR-194507] 02 p0703 N94-13940
Quality assurance for environmental chemistry, 1991, volume 1
[DE93-011791] 02 p0709 N94-14020
An improved approach for flight readiness certification: Methodology for failure risk assessment and application examples, volume 1
[NASA-CR-194498] 02 p0542 N94-14076
An improved approach for flight readiness certification: Methodology for failure risk assessment and application examples. Volume 2: Software documentation
[NASA-CR-194499] 02 p0542 N94-14077
An improved approach for flight readiness certification: Methodology for failure risk assessment and application examples. Volume 3: Structure and listing of programs
[NASA-CR-194500] 02 p0542 N94-14078
Knowledge based systems: From process control to policy analysis
[DE93-014582] 02 p0765 N94-14117
Procurement and execution of PCB analyses: Customer-analyst interactions
[DE93-009964] 02 p0566 N94-14694
An improved approach for flight readiness certification: Probabilistic models for flaw propagation and turbine blade failure. Volume 1: Methodology and applications
[NASA-CR-194496] 02 p0519 N94-14841
An improved approach for flight readiness certification: Probabilistic models for flaw propagation and turbine blade failure. Volume 2: Software documentation
[NASA-CR-194497] 02 p0519 N94-14842
Geometric tolerance assessment
[NPL-DITC-210/92] 03 p1049 N94-15013
Component testing and quality assurance
03 p0932 N94-15259
IG nuts and bolts
[NASA-TM-109652] 03 p1049 N94-15320
Statistical computation of tolerance limits
[NASA-TM-108424] 03 p1172 N94-15535
An analysis of SEI software process assessment results: 1987-1991
[AD-A266996] 03 p1145 N94-15629
Prioritization methodology for chemical replacement
[NASA-TP-3421] 03 p0976 N94-15723
TAFVER 2 users manual
[AD-A266850] 03 p1106 N94-15757
Krupp technical reports no. 2, English edition, October 1992
[ETN-93-94631] 03 p0984 N94-16000
RELMA: On-line quality control in the rubber mixing room using laser analysis 03 p0984 N94-16005
Design Quality Task Force survey comments
[AD-A266283] 03 p1225 N94-16473
Mission management aircraft operations manual
[NHB-7900.3] 03 p1225 N94-16729
Conflict Resolution (CORE) for software quality factors
[AD-A267248] 03 p1151 N94-16941
Simulation reduction using the Taguchi method
[NASA-CR-4542] 03 p1055 N94-17082
Small satellite product assurance
03 p0896 N94-17188
Software Capability Evaluation (SCE) version 1.5 method description. Software capability evaluation project
[AD-A267895] 03 p1154 N94-17395
Establishing a software measurement process
[AD-A267896] 03 p1154 N94-17396
Verification of VALISYS cad based CMM software at LLNL
[DE93-013854] 04 p1517 N94-17911
Process and quality on-line control in laser welding
04 p1426 N94-18020
Testing and evaluation of large-area heliostats for solar thermal applications
[DE93-018509] 04 p1467 N94-18520
Metallurgical evaluation of SRAM 2/SRAM A program mer base plates
[DE93-018689] 04 p1364 N94-19100
Image blur
[DE93-017944] 04 p1580 N94-19113
Pantex Plant Meteorological Monitoring Program
[DE93-018495] 04 p1493 N94-19127
Incology 908 database report: On process-structure-property relationship
[DE93-017616] 04 p1366 N94-19546
Qualifying codes under software quality assurance: Two examples as guidelines for codes that are existing or under development
[DE93-040452] 05 p1904 N94-20097
Using electronic data interchange to report product quality
[AD-A271843] 05 p1828 N94-20468
Correct CMOS IC defect models for quality testing
05 p1755 N94-21093
Software metrics: The key to quality software on the NCC project 05 p1922 N94-21326
Factors associated with continuance commitment to FAA matrix teams
[DOT/FAA/AM-93/18] 05 p2040 N94-21626
Process characterization and control of hand-soldered printed wiring assemblies
[DE93-041290] 05 p1763 N94-21652
Information and decision structure in a Japanese type of management with respect to QCC and just-in-time systems 05 p2046 N94-22063
Formal methods in the design of critical software systems 05 p1779 N94-22158
A robust quality control system for GPS navigation and kinematic positioning
[ISBN-0-315-83148-0] 05 p1644 N94-22427
Quality control of EUVE databases
05 p2047 N94-22490
SIMBAD quality-control 05 p2048 N94-22502
Tests of a simple data merging algorithm for the GONG project 05 p1927 N94-22549
Quality data validation: Comprehensive approach to environmental data validation
[DE94-000925] 06 p2589 N94-22944
Sensors for process control Focus Team report
[DE93-040897] 06 p2560 N94-23204
The use of design automation software by government-contracted architect/engineer firms: A status report
[AD-A273181] 06 p2459 N94-24812
Demonstration of polyscann ultrasonic butt-fusion inspection system for polyethylene pipes
[AD-A273279] 06 p2373 N94-24814
New Ways Of Doing Business (NWODB) cost quantification analysis
[NASA-CR-195186] 06 p2586 N94-25197
Software engineering methodologies and tools
06 p2465 N94-25382
Package integrity measurement technology and quality assurance
[AD-A273881] 07 p2834 N94-25727
Objective image quality metrics: Applications for partially compensated images of space objects
[AD-A273837] 07 p2847 N94-25741
An exploratory survey of methods used to develop measures of performance
[AD-A273945] 07 p2834 N94-25896
Digital control and data acquisition for high-value GTA welding
[DE94-000885] 07 p2821 N94-25980
The use of on-line ion chromatography for high temperature and high pressure reaction studies
[DE94-002525] 07 p2713 N94-26075
Business process redesign: Design the improved process
[AD-A274947] 07 p3093 N94-26299
Analytical study of beam handling and emittance control
[AD-A274412] 07 p3033 N94-27078
Quality assurance for fracture mechanical finite element analyses (appendix 3/1) 07 p2841 N94-27189
An investigation of integrated product development implementation issues: A case study of Bosma Machine and Tool Corp.
[AD-A273917] 07 p2942 N94-27320
Development of a 2f optical performance measurement system
[DE94-003489] 07 p3039 N94-27721
Software assurance standard
[NASA-TM-109705] 07 p2975 N94-27992
Report of the Shuttle Processing Review Team
[NASA-TM-109728] 07 p2692 N94-28178
Testing laboratories as notified bodies
[PB94-132396] 08 p3160 N94-28413
NAVAIR aircraft wiring standardization and qualification program 08 p3166 N94-28704
Organized wiring systems 08 p3166 N94-28705
Cleanroom engineering handbook. Volume 3: Project execution in the cleanroom environment
[AD-A275860] 08 p3156 N94-28752
A reliable and repeatable method for volume calculation of pressurized garments
[AD-A275600] 08 p3399 N94-28766
Screening of flexible cables by nonlinear resistance measurements
[AD-A275193] 08 p3264 N94-29289
Application of information management methodologies for project quality improvement in a changing environment 08 p3416 N94-29342
The discipline of defining the software product
08 p3416 N94-29343
A normative frame of reference for the metrology function
[REPT-932-430-102] 08 p3231 N94-29477
The 1992 report on the next generation ultra clean technology for advanced microfabrication
[DE94-744171] 08 p3157 N94-30268
A user's guide to the Software Testpilot
[CWI-CS-R9343] 08 p3426 N94-30435
Evaluation of nondestructive inspection techniques for quality control of alumina-ceramic housing components
[AD-A276220] 09 p3730 N94-31065
Guide to software quality assurance
[ESA-PSS-05-11-ISSUE-1] 09 p3809 N94-31223
Cleanroom engineering handbook. Volume 6: Certification team practices
[AD-A275951] 09 p3587 N94-31346
Determination of BPSG thin-film properties using IR reflection spectroscopy of product wafers
[DE94-006591] 09 p3634 N94-32110
Management of government quality assurance functions for NASA contracts
[NHB-5300.4(2B-2)] 09 p3731 N94-32387
A facilitated mentoring process for engineers
[DE94-005823] 09 p3914 N94-32677
Pip pin reliability and design 09 p3605 N94-33305
Upper-air quality control: A comparison study
[AD-A277884] 10 p4080 N94-33553
Activities of the NASA centers
[NASA-TM-109836] 10 p4068 N94-33721
Air quality assessment and control
[DE94-000046] 10 p4081 N94-33725
Framework for modelling evolving requirements
[PB94-148855] 10 p4107 N94-33979
Differential GPS positioning: DGPS modelling using pseudo range observations
[PB94-149697] 10 p3988 N94-34113
A quality control package for the Digisonde Drift Analysis (DDA)
[AD-A278663] 11 p4289 N94-35578
Using experimental design modules for process characterization in manufacturing/materials processes laboratories 11 p4230 N94-36405
The maturing of the quality improvement paradigm in the SEL 12 p4489 N94-36485
Process improvement as an investment: Measuring its worth 12 p4489 N94-36486
Recent SEL experiments and studies
12 p4490 N94-36487
Software quality: Process or people
12 p4492 N94-36499
Impact of Materials Defects on Engine Structures Integrity
[AGARD-R-790] 12 p4453 N94-37321
The control of cleanness in powder metallurgy materials for turbine disks 12 p4421 N94-37325
Maintaining constant standards during the forging process 12 p4421 N94-37326
NASA Lewis wind tunnel model systems criteria
[NASA-TM-106565] 12 p4390 N94-37522
The integrated performance evaluation program quality assurance guidance in support of EM environmental sampling and analysis activities
[DE94-013043] 12 p4468 N94-37731

QUALITY FACTORS
U Q FACTORS

QUANTILES
Bahadur-Kiefer theorem beyond the largest observation
[PB93-197473] 04 p1558 N94-19325

QUANTITATIVE ANALYSIS
Quantitative EEG patterns of differential in-flight workload 01 p0317 N94-11528
Novel mass spectrometric instrument for gaseous and particulate characterization and monitoring
[DE93-014093] 01 p0272 N94-12783
Procedures for analysis of debris relative to Space Shuttle systems
[NASA-TM-109190] 02 p0534 N94-12900

A quantitative analysis of TIMS data obtained on the Learjet 23 at various altitudes 03 p1063 N94-16597
Elemental impurity analysis of mercuric iodide by ICP/MS
[DE93-015531] 03 p0949 N94-16876
Analysis of deposit precursors in jet fuels using Fourier transform infrared spectroscopy
[AD-A269035] 04 p1377 N94-18489
Integrated test plan for the demonstration of a commercial Fourier Transform Infrared instrument
[DE93-018518] 04 p1433 N94-19041
Novel mass spectrometric instrument for gaseous and particulate characterization and monitoring
[DE93-019992] 04 p1433 N94-19054
Quantitative evaluation of material composition of composites using x ray energy-dispersive NDE technique
[DE93-041157] 05 p1672 N94-19888
The readiness growth model: A quantitative analysis of software risk
[AD-A272383] 05 p1910 N94-21144
Quantitative analysis of scanning tunneling microscopy images for surface structure determination: Sulfur on Re(0001)
[DE93-019235] 05 p2034 N94-22041
Generic microelectronic smart sensor platform for detection of toxic, hazardous, and flammable gases
[DE93-017626] 06 p2343 N94-23200
FTIR quantification of industrial hydraulic fluids in perchloroethylene 06 p2264 N94-23243
Interpretation of discrepancies in mass spectroscopy data obtained from different experimental configurations 06 p2237 N94-23245
Quantitative analysis in the Al-Mg-Si system with small amounts of Mg and Si
[PB93-201499] 06 p2241 N94-23446
Real-time holographic endoscopy
[ISL-CO-203/92] 06 p2343 N94-24054
Study on analyzing method establishment for metallic material development 07 p2729 N94-25578
Hydrogen uptake into silicon from an ECR plasma
[DE94-003771] 07 p3050 N94-25815
Analytical method for estimation of the total amount of aromatic and poly aromatic compounds in diesel fuel
[PB94-123692] 07 p2759 N94-25907
Radiochemistry Division annual progress report : 1991
[DE94-600652] 07 p2715 N94-26392
New FORTRAN computer programs to acquire and process isotopic mass spectrometric data: Operator's manual
[DE94-003174] 07 p2965 N94-26784
Multivariate calibration applied to near-infrared spectroscopy for the quantitative analysis of dilute aqueous solutions
[DE94-003231] 07 p2716 N94-26794
Gordon Research Conference on the Physics and Chemistry of Laser Diagnostics in Combustion
[AD-A274609] 07 p2716 N94-26893
Preparation, characterization, and thermal behaviour study of lanthanides (3) and yttrium (3) 4-methoxy benzylidene pyruvate in solid state
[DE94-604079] 07 p3068 N94-27697
Development of sample charge compensation for characterization of impurities in semiconductor materials
[AD-A277113] 09 p3899 N94-31983
Rate coefficient for the reaction H + O2 yields OH + O: Results from 2000 to 5300 K
[DE94-008105] 09 p3871 N94-32615
Molten metal analysis by laser produced plasmas
[DE94-007014] 09 p3646 N94-32782
Modelling and optimal control of Pb-Sn continuous crystallization process 10 p4118 N94-34345
Study on contaminants on flight and other critical surfaces
[NASA-CR-193975] 11 p4235 N94-35447
Petrographic characterization of lunar soils: Application of x ray digital-imaging to quantitative and automated analysis 11 p4368 N94-36138
Method of N-15 analysis by mass-spectroscopy on ion implanter MPB-200
[DE94-618203] 12 p4407 N94-36529
Development of high sensitivity techniques for characterizing outgassing of polymeric construction materials for microenvironments
[DE94-012068] 12 p4424 N94-37204

QUANTIZATION
U MEASUREMENT

QUANTIZER
U COUNTERS

QUANTUM AMPLIFIERS
Photon number amplification/duplication through parametric conversion 01 p0376 N94-10572

QUANTUM CHEMISTRY
Ab initio potential energy surface for the H + OCS reaction
[AD-A270577] 05 p1698 N94-19947
International journal of quantum chemistry. Quantum Chemistry Symposium Number 27: Proceedings of the International Symposium on Atomic, Molecular, and Condensed Matter Theory and Computational Methods
[AD-A274352] 07 p3023 N94-26926
International Journal of Quantum Chemistry. Quantum Biology Symposium number 20. Proceedings of the International Symposium on the Application of Fundamental Theory to Problems of Biology and Pharmacology
[AD-A276294] 09 p3792 N94-31294
A combined experimental and theoretical study of the neutral, cationic and anionic Si3N cluster molecule
[AD-A278834] 11 p4323 N94-35792
New anionic states of the lithium trimer
[AD-A278832] 11 p4323 N94-35797
Isolated SO4-2 and PO4-3 anions do not exist
[AD-A278831] 12 p4512 N94-36521

QUANTUM CHROMODYNAMICS
Some new/old approaches to QCD
[DE93-010451] 01 p0408 N94-10261
Squeezed colour states in gluon jet 01 p0379 N94-10599
Spontaneous symmetry breaking in QCD
[DE93-753080] 01 p0396 N94-10645
Experiments to measure the gluon helicity distribution in protons
[DE93-011756] 01 p0368 N94-11613
Quenched chiral logarithms
[DE93-010195] 01 p0346 N94-11663
Top quark search in D(O) from the lepton + jets mode
[DE93-014027] 01 p0370 N94-12781
Quark and lepton masses
[DE93-012308] 01 p0370 N94-12787
Top quark polarization and T-odd spin correlations as tools for testing (non) Standard Model predictions
[DE93-622956] 02 p0778 N94-12847
Polarization and color transparency
[DE93-014319] 02 p0780 N94-13101
Quark and gluon jets at CDF
[DE93-014919] 02 p0783 N94-13884
The theory of relativistic heavy ion collisions
[DE93-015934] 02 p0784 N94-13952
Research in theoretical nuclear physics
[DE93-015096] 02 p0839 N94-14330
Top quark search: Results and prospects at Fermilab
[DE93-013016] 02 p0786 N94-14524
The off shell (rho)-(omega) mixing in the QCD sum rules
[DE93-014845] 02 p0786 N94-14527
Iteration scheme for the multiparameter nonlinear boundary value problem with the additional conditions and its application to some field models
[DE93-626638] 03 p1168 N94-14933
The quantum mass shift of the soliton in Skyrme model
[ITN-93-85219] 03 p1180 N94-15283
PHENIX Conceptual Design Report
[DE93-015759] 03 p1182 N94-16161
Theoretical high energy physics
[DE93-015884] 03 p1187 N94-16170
Quark-loop effects in high energy spin-flip processes
[DE93-626692] 03 p1188 N94-17313
The three-loop QCD beta-function and anomalous dimensions
[NIKHEF-H/92-17] 03 p1186 N94-17617
The renormalization of the axial anomaly in dimensional regularization
[NIKHEF-H/92-18] 03 p1220 N94-17618
Measuring the sea quark polarization
[DE93-015792] 04 p1566 N94-18234
Institute for Nuclear Theory
[DE93-017369] 04 p1568 N94-18824
Charmonium physics from (bar p)p interactions
[DE93-017809] 04 p1569 N94-18973
Investigations in gauge theories, topological solitons, and string theories
[DE93-015029] 04 p1609 N94-19250
A study of events with the highest total transverse energy in CDF
[DE93-019904] 05 p1978 N94-19972
The two-jet differential cross-section at CDF
[DE93-019905] 05 p1978 N94-19983
Jet shapes in hadron and electron colliders
[DE93-019386] 05 p1979 N94-20216
The cross section for the production of b(bar-b) pairs in p(bar p) collisions at the square root of s equals 1.8 TeV
[DE93-019900] 05 p1972 N94-20225
Theoretical particle physics
[DE94-000538] 05 p1973 N94-20938
Qualitative and quantitative aspects of the QCD theory of elastic form factors
[DE93-040864] 05 p2038 N94-21513
Hadronic molecules and scattering amplitudes from the nonrelativistic quark model
[DE94-000377] 05 p1974 N94-21657
Measurement of the inclusive jet cross section in p(bar-p) collisions at CDF
[DE94-000581] 05 p1982 N94-21866
New perspectives in quantum chromodynamics
[DE93-041021] 05 p2038 N94-21935
Toward a QCD analysis of jet rates in deep-inelastic Muon-Proton scattering
[DE94-000618] 05 p1976 N94-21962
The status of glueballs
[DE93-040040] 06 p2531 N94-22923
Momentum and coordinate space three-nucleon potentials
[DE93-040868] 06 p2531 N94-22951
Strong interactions studies with medium energy probes
[DE94-001446] 06 p2540 N94-23791
Photon-photon collisions at the next linear collider: Theory
[DE93-041025] 06 p2534 N94-23803
Electro-weak, QCD and top physics at the Tevatron
[DE94-002304] 06 p2535 N94-24611
New evaluation of hadronic contributions to the anomalous magnetic moment of charged leptons
[DE93-634394] 06 p2536 N94-24844
Relativistic hadrons in an external field
[ETN-94-95387] 06 p2538 N94-25259
A quark structure of hadrons and nuclei
[DE93-616872] 06 p2539 N94-25474
On the transverse size of a fast moving nucleon
[DE93-616891] 06 p2539 N94-25481
Out of equilibrium phase transitions and a toy model for disoriented chiral condensates
[DE94-601642] 07 p3013 N94-25839
Unravelling the structure of matter on high-performance computers
[DE94-601620] 07 p3015 N94-25891
Nucleon-nucleon scattering lengths in QCD sum rules
[DE93-520239] 07 p3015 N94-25922
Heavy quark production and spectroscopy
[DE94-003619] 07 p3015 N94-25935
Monte Carlo event generators for hadron-hadron collisions
[DE94-003212] 07 p3015 N94-25955
A dependence of exclusive vector meson production in muon-nucleus scattering
[DE94-003363] 07 p3016 N94-25957
Deciphering the quark-gluon structure of the photon in electron(gamma) collisions
[DE93-634386] 07 p3017 N94-26043
Spin effects in hard interactions (interest in accelerated polarized beam)
[DE93-634398] 07 p3031 N94-26044
The STAR experiment at the Relativistic Heavy Ion Collider
[DE94-003409] 07 p3017 N94-26083
The delta (1232) resonance transition form factor
[DE94-003442] 07 p3017 N94-26101
Photon and hadron production of heavy flavors
[DE94-004655] 07 p3018 N94-26245
Nuclear Theory Group, University of Washington recent and planned research
[DE94-002729] 07 p3022 N94-26809
Experimental investigations of strong interaction in the non-perturbative QCD region
[DE94-001178] 07 p3024 N94-26949
The challenges of exclusive processes in QCD
[DE94-003429] 07 p3024 N94-27050
Charmonium physics at a tau-charm factory
[PB94-124344] 07 p3024 N94-27199
QCD corrections to inclusive B - S processes in the standard model
[ISBN-0-315-54572-0] 07 p3073 N94-27263
A relativistic quark model
[ISBN-0-315-60926-5] 07 p3025 N94-27333
Aspects of perturbative corrections in quantum chromodynamics
[ISBN-0-315-63607-6] 07 p3074 N94-27398
Quantum chromodynamics and nuclear physics at extreme energy density
[DE94-004418] 07 p3026 N94-27604
Electroweak and other interactions in medium-energy nuclear physics
[DE94-004161] 07 p3027 N94-27889
High energy parton-parton elastic scattering in QCD
[DE94-003432] 07 p3028 N94-27736
Report of the subgroup on the top quark
[DE94-004624] 08 p3481 N94-28462
Properties of W + jet events in proton-antiproton collisions at 1.8 TeV
[DE94-004002] 08 p3482 N94-28524
Properties of events containing a photon and several jets seen in p(bar p) collisions at (radical)s = 1.8 TeV
[DE94-005596] 08 p3482 N94-28531

Proceedings of the workshop on quark and lepton mass matrices
[DE94-707692] 08 p3485 N94-28624
One-loop QCD mass effects in the production of polarized bottom and top quarks
[PB94-138104] 08 p3487 N94-29145
Improved QCD sum rule estimates of the higher twist contributions to polarised and unpolarised nucleon structure functions
[PB94-138112] 08 p3487 N94-29161
A pot-pourri of results in QCD from large lattice simulations on the CM5
[DE94-005084] 08 p3514 N94-29818
Inclusive jet and direct photon production at the D0 experiment
[DE94-006001] 08 p3488 N94-30049
Gluon and fermion damping in hot QCD
[ISBN-0-315-85982-2] 08 p3490 N94-30141
Direct anti-b b production in anti-pp collisions at the square root of s = 1.8 TeV
[DE94-006167] 08 p3491 N94-30369
Problems in particle theory
[DE94-003665] 08 p3491 N94-30685
Theory of ultra dense matter and the dynamics of high energy interactions involving nuclei
[DE94-004178] 08 p3491 N94-30686
Heavy flavor production at fixed target photo- and hadroproduction
[DE94-004651] 08 p3491 N94-30719
Research in elementary particle physics
[DE94-001657] 08 p3491 N94-30762
Theoretical studies in hadronic and nuclear physics
[DE94-003524] 08 p3492 N94-30838
Computing at the leading edge: Research in the energy sciences
[DE94-006121] 08 p3563 N94-30844
The measurement of the hadronic energy flow and jet production with the ZEUS calorimeter in deep inelastic scattering events at HERA
[ETN-94-96021] 09 p3865 N94-31534
Non-equilibrium electrodynamics in the large N expansion
[DE94-006156] 09 p3911 N94-31760
New QCD results from string theory
[DE94-005226] 09 p3911 N94-31823
F0-975, A0-980 as eye-witnesses of confinement
[PB94-147105] 09 p3868 N94-31923
Research in theoretical high-energy physics
[DE94-008388] 09 p3876 N94-32407
Jet physics and QCD tests at the Tevatron collider
[DE94-006987] 09 p3871 N94-32587
The form factors of the nucleons
[DE94-007096] 09 p3872 N94-32630
Chromogravity explains strong gravity
[DE94-009184] 10 p4149 N94-33989
Proceedings of 2nd Working meeting: Physics at VLEPP, volume 1
[DE94-616200] 11 p4320 N94-35569
Leptonic decay constants of heavy quarkonia in effective QCD sum rules
[DE94-611160] 11 p4322 N94-35784
Proceedings of 2nd Working Meeting on Physics at VLEPP, volume 2
[DE94-616167] 11 p4326 N94-36182
High energy asymptotics of perturbative multi-color QCD
[DE94-001350] 11 p4327 N94-36238
Summary: Hadron dynamics sessions
[DE94-003011] 11 p4328 N94-36303
Collapse of flux tubes
[DE94-004645] 11 p4328 N94-36304
The nucleon-nucleon potential in the chromodielectric soliton model
[DE94-004646] 11 p4329 N94-36305
Angular dependence of parton-parton scattering extracted from hadron pair production in pp collisions at radicals equal to 11.5 GeV
[DE94-611174] 12 p4511 N94-36504
The Pomeron and Quantum Chromodynamics (QCD) with many light quarks
[DE94-001351] 12 p4513 N94-36538
Effective Lagrangian for gluons and Higgs pseudoscalars
[DE94-001381] 12 p4513 N94-36539
High Energy Physics Division of research activities
[DE93-019681] 12 p4521 N94-36694
Methods of calculation of higher power corrections in QCD
[DE94-618511] 12 p4521 N94-36748
Introduction to the heavy quark effective theory, part 1
[DE94-618512] 12 p4514 N94-36749
Relativistic di-quark model of p p-bar yields K(+)K(-) reaction
[DE94-618519] 12 p4514 N94-37063
Sum rules for 1/m corrections to the form factors of semileptonic B decays
[DE94-618548] 12 p4514 N94-37065
A study of jet handedness in hadronic Z0 decays
[DE94-013358] 12 p4515 N94-37087
Polarization phenomena in quantum chromodynamics
[DE94-010663] 12 p4539 N94-37543
Strangeness and the quark-gluon plasma: An experimenter's perspective
[DE94-011377] 12 p4519 N94-37558
Pre-equilibrium parton dynamics: Proceedings
[DE94-011347] 12 p4520 N94-37716

QUANTUM COUNTERS
Quantum groups, non-commutative differential geometry and applications
[DE94-011358] 11 p4315 N94-36270

QUANTUM EFFICIENCY
Development of ultra-low noise, high sensitivity planar metal grating coupled 3 to 5 multiquantum well infrared detectors for focal plane array staring IR sensor systems
[AD-A265599] 01 p0404 N94-12375
The 1.00 MeV proton radiation resistance studies of amorphous silicon-based alloy solar cells 02 p0703 N94-13639
Numerical simulation and analysis of electrical and optical properties of Al(x)Ga(1-x)As / GaAs
[ETN-93-94367] 02 p0703 N94-13997
Gamma-insensitive optical focal plane array
[DE93-013100] 02 p0792 N94-14317
CCDs and photon counting devices: Applications in space and from the ground 03 p0901 N94-15041
Visible light photon counters for astronomy 03 p0902 N94-15043
How to squeeze high quantum efficiency and high time resolution out of a SPAD 03 p0914 N94-15571
Porous silicon for pumping solid-state lasers
[AD-A266293] 03 p1039 N94-16474
Development of ultra-low noise, high performance 3-V Quantum Well Infrared Photodectors (QWIP's) for focal plane array staring image sensor systems
[AD-A267715] 03 p1214 N94-17272
Simplified processing for 23 percent-efficient silicon concentrator solar cells
[DE93-015018] 04 p1464 N94-17787
CsI and some new photocathodes
[DE93-019387] 05 p1750 N94-20314
The quantum efficiency of HgCdTe photodiodes in relation to the direction of illumination and to their geometry 05 p1735 N94-20512
Stable, high-efficiency amorphous-silicon solar cells with low hydrogen content
[DE93-018214] 05 p1848 N94-21826
Quantum well infrared photodetector FPA
[AD-A278010] 09 p3908 N94-33248
Visible and infrared (1.54 micrometers) LED based on Er-doped porous Si
[AD-A278528] 10 p4042 N94-34295

QUANTUM ELECTRODYNAMICS
The legacy of uncertainty 01 p0376 N94-10577
Non-gauge phase transformations in quantum transition amplitudes 01 p0378 N94-10596
Squeezed colour states in gluon jet 01 p0379 N94-10599
Non-stationary and non-linear dispersive medium as external field which generates the squeezed states 01 p0380 N94-10605
Quantized conic sections; quantum gravity
[DE93-010950] 01 p0411 N94-10956
Studies in quantum field theory
[DE93-017201] 02 p0818 N94-14896
Fundamental theory of light for applications: Notes for five informal lectures
[DE93-016463] 03 p1192 N94-16953
Multipolar-like form of nonabelian gauge theories
[DE93-626690] 03 p1171 N94-17314
Quantum optoelectronics technical digest, 1993. Voolume 8: Postconference edition
[AD-A268209] 04 p1576 N94-17887
Detection of single molecules in microspheres
[DE93-017776] 04 p1567 N94-18493
Relativistic configuration interaction calculation of the correlation energies of heliumlike ions
[DE93-018093] 04 p1571 N94-19201
Dynamics of vortices in superconductors
[DE93-019535] 05 p2011 N94-19808
Back-reaction beyond the mean field approximation
[DE94-003936] 07 p3012 N94-25612
Theoretical and experimental studies of elementary physics
[DE94-002310] 07 p3008 N94-25988
Spinor and isospinor structure of relativistic particle propagators
[DE94-601552] 07 p3019 N94-26424
A variational approach to the quantum field theoretic bound-state problem
[ISBN-0-315-60960-5] 07 p3074 N94-27401
Relativistic two-body system in 1+1-dimensional QED. 1: On the circle S1
[DE94-603716] 07 p3067 N94-27647
Excited Landau levels, orbital angular momentum and axial anomaly
[DE94-606407] 07 p3068 N94-27679
Enhancement of the rate of radiative processes in the field of a magnetic monopole
[DE94-603717] 07 p3074 N94-27696
The proper field of charges and gauge-invariant variables in electrodynamics
[DE94-606405] 08 p3523 N94-28751
Curved-space quantization, and Dirac versus reduced quantization of Poincare gauge theories
[ISBN-0-315-85990-3] 08 p3525 N94-30142
Spectroscopy and atomic physics in EBIT and SuperEBIT
[DE94-006050] 09 p3864 N94-31508
Perturbative aspects of lower-dimensional gauge theories
[ISBN-0-315-86269-6] 09 p3911 N94-31712
Non-equilibrium electrodynamics in the large N expansion
[DE94-006156] 09 p3911 N94-31760
Logarithmic corrections of the two-body QED problem
[DE94-611157] 11 p4322 N94-35783

QUANTUM ELECTRONICS
The response of an electron in a biased double well to a strong laser: Delocalization and low frequency generation
[AD-A265169] 01 p0366 N94-11100
High frequency behavior of long and small junctions
[AD-A265670] 01 p0403 N94-12336
Electronic and atomic structure of semiconductors and of high-temperature superconductors
[AD-A266805] 03 p1205 N94-14913
Spectroscopic investigations of nonambient systems with millimeter and submillimeter probes
[AD-A266537] 03 p0968 N94-16796
Activities of the Research Laboratory of Electronics
[AD-A266730] 03 p1304 N94-17651
Spatial light modulators and applications: Summaries of papers presented at the Spatial Light Modulators and Applications Topical Meeting
[AD-A269452] 04 p1577 N94-18283
Quantum Optoelectronics. Organization of the 1993 photonics science topical meetings. Technical digest series, volume 8
[AD-A269026] 04 p1578 N94-18488
Advanced Solid-State Lasers/Compact Blue-Green Lasers. 1993 technical digest series. Volume 2: Organization of the 1993 photonics science topical meetings
[AD-A269058] 04 p1438 N94-18492
Photonics in Switching: Organization of the 1993 photonics science topical meetings. Technical digest
[AD-A269024] 04 p1578 N94-18528
Joint services electronics program
[AD-A269383] 04 p1403 N94-18638
Ultrafast Electronics and Optoelectronics: Summaries of papers. Technical digest conference edition
[AD-A269233] 04 p1405 N94-18909
Theoretical and experimental studies of quantum wells
[AD-A271180] 04 p1606 N94-19741
Optical and transport properties of metallic and semiconductor nanostructures
[AD-A271716] 05 p2018 N94-20554
Solid-state dynamics and quantum transport in novel semiconductor nanostructures
[AD-A272955] 05 p2027 N94-21248
Quantum tunneling transport of electrons in double-barrier heterostructures: Theory and modeling
[ETN-94-95332] 06 p2565 N94-25059
Solid state research
[AD-A274063] 07 p3049 N94-25645
Frontiers of science and measurement: Report on a seminar jointly organized by the National Physical Laboratory and the Institute of Physics
[PB94-124310] 07 p3009 N94-27131
An electronic switch based on quantum interference
[ISBN-0-315-84609-7] 07 p2787 N94-27650
The effects of propagational factors on quantum wires in close parallel proximity
[ISBN-0-315-86157-6] 08 p3254 N94-30035
Electronic structure of Zn-based quantum wells
[DE94-608104] 08 p3516 N94-30068
Novel growth technologies for in situ formation of semiconductor quantum wire structures
[AD-A277188] 09 p3902 N94-32255

QUANTUM MECHANICS
NT QUANTUM ELECTRODYNAMICS
Some new/old approaches to QCD
[DE93-010451] 01 p0408 N94-10261

Wave function collapse: An unnecessary condition for the dynamical description of the Zeno and partial Zeno effect
[DE93-612970] 01 p0132 N94-10401

A group-theoretic approach to the study of small oscillations of a dynamical system with a known symmetry
[DE93-612971] 01 p0409 N94-10402

Standard model status (in search of new physics)
[DE93-013288] 01 p0410 N94-10528

Bound states of the N-dimensional Klein-Gordon equation with vector and scalar Coulomb potentials
[DE93-617650] 01 p0349 N94-10547

The Second International Workshop on Squeezed States and Uncertainty Relations
[NASA-CP-3219] 01 p0375 N94-10564

One dimensional representations in quantum optics
01 p0375 N94-10570

Harmonic oscillator interaction with squeezed radiation
01 p0376 N94-10571

Non classical effects in planar waveguides
01 p0376 N94-10574

Phasing operator for two oscillators in classical field
01 p0370 N94-10579

On a Lagrange-Hamilton formalism describing position and momentum uncertainties 01 p0349 N94-10583

Dissipation in a squeezed-state environment
01 p0370 N94-10584

Squeezed spin states: Squeezing the spin uncertainty relations 01 p0377 N94-10585

Observables, measurements and phase operators from a Bohmian perspective 01 p0378 N94-10589

Uncertainty relations, zero point energy and the linear canonical group 01 p0378 N94-10590

Information entrophy via Glauber's Q-representation
01 p0378 N94-10592

Squeezed states of electrons and transitions of the density of states 01 p0370 N94-10593

Quantum mechanical effects of topological origin
01 p0378 N94-10594

Collision-induced squeezing in a harmonic oscillator
01 p0379 N94-10597

Positive phase space distributions and uncertainty relations 01 p0379 N94-10598

The uncertainty principle and quantum chaos
01 p0379 N94-10602

Relation of squeezed states between damped harmonic and simple harmonic oscillators
01 p0380 N94-10606

Infinite-mode squeezed coherent states and non-equilibrium statistical mechanics (phase-space-picture approach)
[LBL-32695] 01 p0380 N94-10608

Correlated states of a quantum oscillator acted by short pulses 01 p0380 N94-10609

Floquet operator as integral of motion
01 p0380 N94-10610

Exact solutions of a many-anyon problem
[DE93-617646] 01 p0411 N94-10832

Quantum dynamics of helium clusters
[AD-A266060] 01 p0411 N94-10874

Superfield description of N = 2 extended one-dimensional supersymmetric quantum mechanics
[DE93-621420] 01 p0412 N94-11087

Three-dimensional N = 4 extended supersymmetrical quantum mechanics
[DE93-621421] 01 p0412 N94-11164

Absorption spectrum calculations using mixed quantum-gaussian wave packet dynamics
[AD-A265179] 01 p0413 N94-11877

Quaternions and the heuristic role of mathematical structures in physics
[DE93-622865] 02 p0816 N94-12844

Electromagnetic deflection of spinning particles
[DE93-622866] 02 p0778 N94-12858

The geometric phase in quantum physics
[DE93-011121] 02 p0817 N94-13479

Selective excitation, relaxation, and energy channeling in molecular systems
[DE93-018819] 02 p0785 N94-14420

Multiple Schroedinger cats from multilevel atoms
[DE93-013412] 02 p0786 N94-14526

The fractional quantum Hall effect and the spherical shell model
[DE93-014553] 02 p0818 N94-14740

Tests of non-local interferences in kaon physics at asymmetric phi-factories
[DE93-013905] 02 p0787 N94-14857

Studies in quantum field theory
[DE93-017201] 02 p0818 N94-14896

Molecular processes in comets
[NASA-CR-194148] 03 p1239 N94-15188

Electronic structure and enthalpy of hydrogen and helium mixtures
[DE93-014128] 03 p1208 N94-15976

Theoretical high energy physics research at the University of Chicago
[DE93-016863] 03 p1187 N94-16116

Bulk and defect properties of ordered intermetallics: A first-principles total-energy investigation
[DE93-015492] 03 p0959 N94-16873

Stochastic chaos: An analog of quantum chaos
[DE93-016619] 03 p1220 N94-16956

SUSY in the sky
[NIKHEF-H/93-04] 03 p1240 N94-17603

Quantum phase fluctuations in the Jaynes-Cummings model: Effects of cavity damping
[DE93-627984] 03 p1186 N94-17612

The renormalization of the axial anomaly in dimensional regularization
[NIKHEF-H/92-18] 03 p1220 N94-17618

Tensorial structure of a q-deformed sp(4,R) superalgebra
[DE93-624808] 04 p1545 N94-17685

On relation between Berry phase and one-dimensional models with long-range 1/r(sup 2)-interaction
[DE93-624967] 04 p1592 N94-17690

A zeta function approach to the semiclassical quantization of maps
[DE93-624774] 04 p1547 N94-17949

Space and time as outcome of decoherence in an expanding universe
[DE93-016199] 04 p1624 N94-18047

Advanced Solid-State Lasers/Compact Blue-Green Lasers. 1993 technical digest series. Volume 2: Organization of the 1993 photonics science topical meetings
[AD-A269058] 04 p1438 N94-18492

Space and time from quantum mechanics
[DE93-015263] 04 p1609 N94-18629

The quantum dynamics of electronically nonadiabatic chemical reactions
[NASA-CR-194309] 04 p1568 N94-18837

On the theory of morphology-dependent resonances: Shape resonances, width formulas, and graphical representations
[AD-A272279] 05 p2037 N94-20945

A formulation of quantum statistical mechanics based on the Feynman path centroid density 2 dynamical properties
[AD-A272698] 05 p2037 N94-21166

A formulation of quantum statistical mechanics based on the Feynman path centroid density 1: Equilibrium properties
[AD-A272809] 05 p2037 N94-21171

Solid-state dynamics and quantum transport in novel semiconductor nanostructures
[AD-A272955] 05 p2027 N94-21248

The quantum structure of matter grand challenge project: Large-scale 3-D solutions in relativistic quantum dynamics
[DE94-000328] 05 p1960 N94-21955

On the correspondence limit of relativistic quantum mechanics
[DE93-040939] 05 p2038 N94-21971

Restoring locality with faster-than-light velocities
[DE93-040926] 05 p2038 N94-22010

Proof of stability of the hydrogen molecule
[PB93-221026] 05 p1977 N94-22271

Quantum mechanics, locality and realism
[MEMO-1117] 06 p2568 N94-22709

Limits on high-order harmonic generation from single-atom calculations
[DE93-019950] 06 p2531 N94-22869

The torsion space nucleic acids molecular mechanics program DUPLEX: Surveying conformation space by potential energy minimization
[DE94-002441] 06 p2563 N94-24567

An attempt at a macrorealistic quantum worldview
[DE93-616821] 06 p2570 N94-25206

Intramultiplet mixing for Ne(**)(3p)+He at superthermal energies
[ETN-94-95327] 06 p2538 N94-25240

Applications of supersymmetric quantum mechanics
[ETN-94-95385] 06 p2570 N94-25257

Correlations in the actions of periodic orbits derived from quantum chaos
[DE93-616866] 06 p2571 N94-25340

Coherent state approach for the (Phi)(sup 6)-lattice model and phase transitions
[DE93-613053] 07 p3050 N94-25825

Quantizable configurations of the relativistic string
[DE93-634346] 07 p3072 N94-26036

Holes in a two-dimensional quantum antiferromagnet
[DE93-634753] 07 p3057 N94-26388

Finite dimensional representations of the quantum superalgebra U(sub q)(gl(3/2))
[DE93-634303] 07 p2993 N94-26440

Quantum Hamiltonian differential geometry: How does quantization affect space?
[DE93-634306] 07 p2993 N94-26442

Quantum group and Manin plane related to a colored braid group representation
[DE94-601509] 07 p3072 N94-26461

How to build analogues of the Bessel-Clifford expansions for the sum of the repulsive Coulomb potential and central potential decreasing more rapidly than the centrifugal one?
[DE93-634308] 07 p3007 N94-26472

Stochastic solution to quantum dynamics
[NASA-TP-3408] 07 p3114 N94-26550

Wigner quantum oscillators
[DE94-601508] 07 p3073 N94-26758

Quantum statistical inference for density estimation
[DE94-002625] 07 p3073 N94-26805

Length-scale dependent ensemble-averaged conductance of a 1D disordered conductor: Conductance minimum
[DE94-602732] 07 p3062 N94-26902

Pigs in cyberspace 07 p2689 N94-27376

Decay of non-equilibrium polariton condensate in semiconductors
[DE94-604016] 07 p3068 N94-27678

The gl(n/m) and related q-identitiesematics and computer science ends in nuclear and related q-identities
[DE94-603653] 07 p3001 N94-27839

Miln equation for the calculation of the phases and amplitudes of wave functions for continuum spectrum of Coulomb two-center problem
[DE94-606292] 08 p3522 N94-28616

Dissipative quantum dynamics and nonlinear sigma-model
[DE94-606295] 08 p3523 N94-28617

Classical interpretation of quantum mechanics
[DE94-606304] 08 p3523 N94-28719

Electronic structure and mechanical properties of grain boundaries
[AD-A275198] 08 p3512 N94-28890

Existence of quantum characteristic exponents
[PB94-138161] 08 p3523 N94-29146

Coherent states of SU(l,1) groups
[DE94-603654] 08 p3524 N94-29498

Nonadiabatic effects in the quantum Hall regime
08 p3513 N94-29530

Quantum interference phenomena and novel switching in split gate high electron mobility transistors
08 p3266 N94-29734

A semiclassical study of quantum maps
08 p3524 N94-29987

The MSRC ab initio methods benchmark suite: A measurement of hardware and software performance in the area of electronic structure methods
[DE94-006428] 08 p3514 N94-30001

On chaos in quantum mechanics: The two meanings of sensitive dependence
[DE94-608069] 08 p3524 N94-30086

Reconstruction of spectra in the discrete quantum mechanics (new elements of the lattice quantum engineering)
[DE94-608075] 08 p3524 N94-30087

Quantum-mechanical suppression of bremsstrahlung
[DE94-005223] 08 p3497 N94-30712

Molecular dynamics simulations of dense plasmas
[DE94-005082] 08 p3509 N94-30752

Non-Markovian quantum Brownian motion of a harmonic oscillator
[DE94-005922] 08 p3477 N94-30873

Non-commutative geometry
[PB94-139342] 08 p3462 N94-30889

Modern integral equation techniques for quantum reactive scattering theory
[DE94-007039] 09 p3857 N94-31639

Cometary molecules 09 p3935 N94-31869

Research program in particle physics
[DE94-008449] 09 p3871 N94-32512

Quantum dynamics in dual spaces
[DE94-008303] 09 p3913 N94-32624

Computed potential energy surfaces for chemical reactions
[NASA-CR-195835] 09 p3639 N94-33036

Stapp's quantum dualism: The James and Heisenberg model of consciousness
[DE94-009028] 10 p4148 N94-33929

Decoherence, determinism and chaos
[DE94-009018] 10 p4149 N94-33984

Decoherence, chaos, the quantum and the classical
[DE94-009317] 10 p4149 N94-34099

Identity for propagator in four-fermion theory
[DE94-611104] 11 p4342 N94-35781

Inverse problem for symmetric tridiagonal matrices. Calculation of discrete orthogonal polynomial system with arbitrary weight
[DE94-612434] 11 p4315 N94-35789

Quantum mechanics and thermodynamics of particles with distance dependent statistics
[DE94-616820] 11 p4343 N94-36072

Exact multiplicities in the three-anion spectrum
[DE94-616768] 11 p4325 N94-36075
Boson spectra and correlations in thermal locally equilibrium systems
[DE94-616799] 11 p4325 N94-36079
Quantum groups, non-commutative differential geometry and applications
[DE94-011358] 11 p4315 N94-36270
Scattering theory for the quantum envelope of a classical system
[DE94-008530] 12 p4539 N94-36508
Testing violation of CPT and quantum mechanics in the K(0) - bar-K(0) system
[DE94-012057] 12 p4539 N94-37366
The angular and energy distributions of ejected electrons in electron-impact ionization of helium
[DE94-618748] 12 p4519 N94-37528

QUANTUM NUMBERS

Quantized conic sections; quantum gravity
[DE93-010950] 01 p0411 N94-10956
Clusterization of quantum states in the Hartmann model
[DE93-626624] 03 p1220 N94-17315
Evaluation of uranium transitions for isotopically-selective laser induced fluorescence with diode lasers (technical report for ST064)
[DE94-002000] 06 p2347 N94-22974
Proton electromagnetic form factor near the proton-antiproton threshold and quasinuclear bound state
[DE94-606458] 07 p3027 N94-27681
Baryogenesis from a primordial lepton asymmetry
[PB94-145166] 09 p3868 N94-31921
Periodicity and peculiarity in 120 first and second row diatomic molecules
[AD-A278836] 11 p4323 N94-35793
The asymptotics of matrix elements of Gaussian potential between the basis functions of three-dimensional harmonic oscillator
[DE94-618467] 12 p4539 N94-37079

QUANTUM OPTICS

The Second International Workshop on Squeezed States and Uncertainty Relations
[NASA-CP-3219] 01 p0375 N94-10564
A phaseonium magnetometer: A new optical magnetometer based on index enhanced media
01 p0375 N94-10565
Smoothly deformed light 01 p0375 N94-10566
Nonclassical states of the second optical harmonic in the presence of self-action 01 p0375 N94-10567
Quantum noise and squeezing in optical parametric oscillator with arbitrary output coupling
01 p0375 N94-10568
Disturbance, the uncertainty principle and quantum optics 01 p0375 N94-10569
One dimensional representations in quantum optics
01 p0375 N94-10570
Photon number amplification/duplication through parametric conversion 01 p0376 N94-10572
Non classical effects in planar waveguides
01 p0376 N94-10574
Completeness properties of the minimum uncertainty states 01 p0349 N94-10581
Uncertainty relations, zero point energy and the linear canonical group 01 p0378 N94-10590
Information entrophy via Glauber's Q-representation
01 p0378 N94-10592
Positive phase space distributions and uncertainty relations 01 p0379 N94-10598
Wavelets and spacetime squeeze
01 p0379 N94-10604
Quantum phase fluctuations in the Jaynes-Cummings model: Effects of cavity damping
[DE93-627984] 03 p1186 N94-17612
A microscopic theory of quantum optics and new photon-locked bistable states
[AD-A271250] 05 p1983 N94-19901
Quantum optical aspects of topological phases, such as Berry's phase
[AD-A273632] 06 p2570 N94-25028

QUANTUM STATISTICS

Coherence influence on the intensity of Bose-Einstein correlations and visible size of a source
[DE93-617697] 01 p0349 N94-10556
Relation of squeezed states between damped harmonic and simple harmonic oscillators
01 p0380 N94-10606
Infinite-mode squeezed coherent states and non-equilibrium statistical mechanics (phase-space-picture approach)
[LBL-32695] 01 p0380 N94-10608
On the statistical theory of the even-even nucleons levels' density
[DE93-623990] 02 p0788 N94-14875
Calculations of Bose-Einstein correlations from Relativistic Quantum Molecular Dynamics
[DE94-000794] 06 p2569 N94-23453
Ultracold atoms in traps and fountains
[ETN-94-95325] 06 p2537 N94-25239
Equation of state of stellar plasmas
[DE94-004186] 08 p3542 N94-28526
Exact multiplicities in the three-anion spectrum
[DE94-616768] 11 p4325 N94-36075
Mass identified particle production and Bose Einstein correlations at 1800 GeV
[DE94-013418] 12 p4515 N94-37067
Kaon correlation systematics in E859
[DE94-011927] 12 p4516 N94-37158

QUANTUM THEORY

Discrete space-time symmetries
[DE93-010199] 01 p0341 N94-10259
The structure of Hilbert flag varieties
[MEMO-1095] 01 p0348 N94-10272
Standard model status (in search of new physics)
[DE93-013288] 01 p0410 N94-10528
From the Weyl theory to a theory of locally anisotropic space-time
[DE92-644734] 01 p0410 N94-10535
The Second International Workshop on Squeezed States and Uncertainty Relations
[NASA-CP-3219] 01 p0375 N94-10564
A phaseonium magnetometer: A new optical magnetometer based on index enhanced media
01 p0375 N94-10565
Nonclassical states of the second optical harmonic in the presence of self-action 01 p0375 N94-10567
Disturbance, the uncertainty principle and quantum optics 01 p0375 N94-10569
Generalised squeezing and information theory approach to quantum entanglement 01 p0377 N94-10580
Study of Einstein-Podolsky-Rosen state for space-time variables in a two photon interference experiment
01 p0370 N94-10582
Dissipation in a squeezed-state environment
01 p0370 N94-10584
Squeezed spin states: Squeezing the spin uncertainty relations 01 p0377 N94-10585
Quantum entropy and uncertainty for two-mode squeezed, coherent and intelligent spin states
01 p0377 N94-10586
Geometric aspects of uncertainty and correlation
01 p0349 N94-10588
Nonunitary and unitary approach to Eigenvalue problem of Boson operators and squeezed coherent states
01 p0350 N94-10595
Non-gauge phase transformations in quantum transition amplitudes 01 p0378 N94-10596
Exact and quasi-classical density matrix and Wigner functions for a particle in the box and half space
01 p0350 N94-10600
New squeezed landau states
01 p0379 N94-10601
The uncertainty principle and quantum chaos
01 p0379 N94-10602
Wigner functions for nonclassical states of a collection of two-level atoms 01 p0379 N94-10603
Infinite-mode squeezed coherent states and non-equilibrium statistical mechanics (phase-space-picture approach)
[LBL-32695] 01 p0380 N94-10608
Quantum processes in resonators with moving walls
01 p0380 N94-10612
Limitation and suppression of hot electron fluctuations in submicron semiconductor structures
[DE93-613911] 01 p0396 N94-10801
Quantum solitons with cylindrical symmetry
[DE93-617659] 01 p0344 N94-10881
Proceedings of the Workshop on New Aspects of Quantum Field Theories
[DE93-754136] 01 p0411 N94-10887
Dissipative phase transitions in field theory models with spontaneous symmetry violation
[DE93-621382] 01 p0412 N94-11039
Creation and annihilation of solitons in nonlinear integrable systems
[DE93-621379] 01 p0365 N94-11078
Non-barrier tunneling in presence of dissipations
[DE93-621381] 01 p0412 N94-11086
Green-Schwarz superstrings in the generalized harmonical Newmann-Penrose formalism
[DE93-621422] 01 p0412 N94-11088
A theoretical kinematical study of the gradient of any cosmic scalar field
[DE92-644731] 01 p0425 N94-11136
One-loop quantum gravity on de Sitter space
[DE92-641349] 01 p0425 N94-11152
Characterization of the Si/SiO2 interfere morphology from quantum oscillations in Fowler-Nordheim tunneling currents
[AD-A265149] 01 p0143 N94-11160
Divergences in the moduli space integral and accumulating handles in the infinite-genus limit
[DE93-619722] 01 p0346 N94-11693
Duality twisted boundary conditions in n-sta te Potts models
[DE93-619724] 01 p0346 N94-11811
Explorations in quantum gravity: From one loop effective actions to two-dimensional theories
01 p0413 N94-11822
Superfluid turbulence 01 p0158 N94-12307
Gauging the octonion algebra
[DE93-622864] 02 p0775 N94-12843
Measurements on two-dimensional arrays of mesoscopic Josephson junctions
[AD-A265129] 02 p0807 N94-13359
Dilaton quantum cosmology in two dimensions
[DE93-621377] 02 p0836 N94-13361
Mathematics and string theory
[DE93-017903] 02 p0817 N94-14417
Electronic states in systems of reduced dimensionality
[DE93-014440] 02 p0815 N94-14739
Radiation perturbation theory in gravity and quantum universe as a hydrogen atom
[DE93-626621] 02 p0849 N94-14889
Studies in quantum field theory
[DE93-017201] 02 p0818 N94-14896
Fundamental theory of light for applications: Notes for five informal lectures
[DE93-016463] 03 p1192 N94-16953
The universality of the shift of the Chern-Simons parameter for a general class of BRS invariant regularizations
[NIKHEF-H/93-03] 03 p1220 N94-17602
Quantum Heisenberg groups and Sklyanin algebras
[DE93-628590] 03 p1175 N94-17643
On a conformal perfect fluid in the classical vacuum
[DE93-624797] 04 p1480 N94-17682
Infinite Grassmannian and moduli space of G-bundles
[DE93-624798] 04 p1545 N94-17683
International Centre for Theoretical Physics, Trieste Scientific activities in 1991
[DE93-624757] 04 p1606 N94-17792
Avoiding degenerate coframes in an affine gauge approach to quantum gravity
[DE93-013146] 04 p1607 N94-17892
Phase space representations and quantum probability theory
[DE93-629863] 04 p1556 N94-18154
Four-fermion interactions
[DE93-629905] 04 p1566 N94-18199
Optical and transport properties of metallic and semiconductor nanostructures
[AD-A270009] 04 p1598 N94-18609
Space and time from quantum mechanics
[DE93-015263] 04 p1609 N94-18629
Investigations in gauge theories, topological solitons, and string theories
[DE93-015029] 04 p1609 N94-19250
Essential shift: Scientific revolution in the 20th century
[AD-A270810] 04 p1610 N94-19663
Schroedinger's hope
[AD-A270988] 04 p1581 N94-19772
F-spin concept and g-bosons in the interceding boson model
[ETN-93-93607] 05 p1973 N94-21136
A formulation of quantum statistical mechanics based on the Feynman path centroid density 2 dynamical properties
[AD-A272698] 05 p2037 N94-21166
Restoring locality with faster-than-light velocities
[DE93-040926] 05 p2038 N94-22010
Non commutative geometry and physics
[PB93-215499] 05 p1961 N94-22264
Quantum mechanics, locality and realism
[MEMO-1117] 06 p2568 N94-22709
On spontaneous symmetry breaking mechanism in light-front quantized field theory
[DE93-633211] 06 p2568 N94-22968
Flavor changing strings and domain walls
[DE93-633217] 06 p2532 N94-22970
Coadjoint orbits and conformal field theory
[DE94-002285] 06 p2523 N94-24658
Quantum optical aspects of topological phases, such as Berry's phase
[AD-A273632] 06 p2570 N94-25028
On the connection of classical mechanics, physical kinetics and quantum theory
[DE93-616823] 06 p2570 N94-25207
Applications of supersymmetric quantum mechanics
[ETN-94-95385] 06 p2570 N94-25257
Duality for multiparametric quantum GL(n) and for a Lorentz quantum group
[DE93-613048] 07 p3005 N94-25868
Topological amplitudes in string theory
[DE94-601561] 07 p3071 N94-25882

On string theory interacting with two-dimensional gravity
[DE94-601562] 07 p3071 N94-25883
The algebra of non-local charges in non-linear sigma models
[DE94-601563] 07 p2991 N94-25884
A research program in experimental and theoretical high energy physics
[DE94-002156] 07 p3031 N94-25931
Studies in nonlinear numerical analysis
[AD-A273911] 07 p2959 N94-25968
The massless representations of the conformal quantum algebra
[DE94-601555] 07 p3006 N94-26413
Affine algebras on the torus
[DE94-601556] 07 p3006 N94-26414
Higher spin extensions of the Virasoro algebra, area-preserving algebras and the matrix algebra a-bar(sub (infinity))
[DE94-601557] 07 p3006 N94-26415
Differential regularization of a non-relativistic anyon model
[DE94-601558] 07 p3019 N94-26416
Vortices in curved spacetime
[DE94-601559] 07 p3072 N94-26417
Orthodox gravity
[DE94-601560] 07 p2878 N94-26418
Gauging of Chern-Simons p-Barnes
[DE94-601553] 07 p2993 N94-26425
Quantum subgroups and quantum co-set spaces and differential calculi on them
[DE94-602520] 07 p3073 N94-26876
Improved numerical methods for quantum field theory (Outstanding Junior Investigator Award)
[DE94-001793] 07 p3073 N94-27002
Operator regularization and renormalization theory
[ISBN-0-315-49334-8] 07 p3007 N94-27264
Quantum chromodynamics and nuclear physics at extreme energy density
[DE94-004418] 07 p3026 N94-27604
Second-order phase transition in (g(phi)4)2 theory
[DE94-603677] 07 p3067 N94-27638
Stochastic space-time, confinement potential and particle propagator
[DE94-606415] 07 p3074 N94-27680
A method for obtaining quantum doubles from the Yang-Baxter R-matrices
[DE94-606300] 07 p3001 N94-27846
The (j,0) + (0,j) representation space: Dirac-like construct
[DE94-005011] 08 p3522 N94-28572
On invariant measures for some infinite-dimensional dynamical systems
[DE94-606342] 08 p3522 N94-28609
Anomalous algebraic structures in quantum field theories 08 p3524 N94-29911
A Tevatron collider beauty factory
[DE94-004879] 08 p3488 N94-29930
Discrete symmetries, strong CP problem and gravity
[DE94-608091] 08 p3524 N94-30089
Modelling of multiparticle production by dynamical semigroup method
[DE94-608132] 08 p3490 N94-30120
A theory approach for creation of the matter of universe
[DE94-608109] 08 p3548 N94-30163
GL(sub q)(N)-covariant quantum algebras and covariant differential calculus
[DE94-608072] 08 p3460 N94-30726
Space-time symmetries: P and CP violation
[DE94-005012] 08 p3526 N94-30750
Non-commutative geometry
[PB94-139342] 08 p3462 N94-30889
Dynamical entropy of generalized quantum Markov chains
[PB94-148483] 09 p3850 N94-31590
Multiparameter quantum groups and multiparameter R-matrices
[CWI-AM-R9307] 09 p3846 N94-32106
Quantum homogeneous spaces, duality, and quantum 2-spheres
[CWI-AM-R9309] 09 p3857 N94-32192
Research in theoretical high-energy physics
[DE94-008388] 09 p3876 N94-32407
Research program in particle physics
[DE94-008449] 09 p3871 N94-32512
Quantum fluctuations of vortices in Josephson-coupled superconductors
[DE94-007609] 09 p3905 N94-32747
Localizability and the Planck mass
[DE94-009183] 10 p4149 N94-33988
This non-axiomatizable quantum theory. From Hilbert's sixth problem to the recent viewpoint of Gell-mann and Hartle
[PB94-167715] 11 p4342 N94-35761
The 2+1-dimensional integrable generalization of the Sine-Gordon equation
[DE94-611074] 11 p4315 N94-36100
Quantum groups, non-commutative differential geometry and applications
[DE94-011358] 11 p4315 N94-36270
N = 4 supersymmetry from the quantum affine algebra U(sub q)(A-circumflex(sup 1)(sub 3))
[DE94-611145] 11 p4317 N94-36307
On quantization of time-dependent systems with constraints
[DE94-611114] 11 p4343 N94-36351
Wick-Cutkovsky model: An introduction
[DE94-618365] 12 p4504 N94-37170

QUANTUM WELL LASERS

Ion doped quantum well lasers
[AD-A267198] 03 p1038 N94-15853
Quantum optoelectronics technical digest, 1993. Voolume 8: Postconference edition
[AD-A268209] 04 p1576 N94-17887
Direct solar pumping of semiconductor lasers: A feasibility study
[NASA-CR-193760] 04 p1440 N94-18834
High Speed/High Frequency Optoelectronics
[AD-A271985] 05 p1751 N94-20580
The n-p(p(+))-n Al(yGa)(1-y) As-GaAs-In(x)Ga(1-x) as quantum well laser with p(+)-n(+)GaAs-InGaAs tunnel contact on n GaAs
[AD-A271292] 05 p2030 N94-21805
Development of intermetallic compounds for high performance luminescence elements 07 p2722 N94-25545
High speed, strained layer, multiquantum well, GaInAsP and GaAs lasers and heterostructures
[AD-A277287] 09 p3719 N94-32608
High power diode laser Master Oscillator-Power Amplifier (MOPA)
[NASA-CR-196095] 11 p4271 N94-35488

QUANTUM WELLS

NT PHOTOEXCITATION
Non-gauge phase transformations in quantum transition amplitudes 01 p0378 N94-10596
Effect of effective mass differences on the tunneling current-voltage behaviour of a resonant diode in the presence of space charge build-up
[DE93-613817] 01 p0142 N94-10799
The response of an electron in a biased double well to a strong laser: Delocalization and low frequency generation
[AD-A265169] 01 p0366 N94-11100
The additional contribution caused by Coulomb interaction to the exciton dispersion in multiple quantum wells and superlattices for direct band gap cubic semiconductors
[DE93-613538] 01 p0402 N94-11659
Development of ultra-low noise, high sensitivity planar metal grating coupled 3 to 5 multiquantum well infrared detectors for focal plane array staring IR sensor systems
[AD-A265599] 01 p0404 N94-12375
Theoretical investigation of some novel phenomenal in artificially structured semiconductors
[AD-A266142] 01 p0405 N94-12587
Nonlinear laser spectroscopy studies of semiconductor heterostructures
[AD-A265728] 02 p0805 N94-13037
Surfaces and interfaces of ceramics and metals
[DE93-014959] 02 p0578 N94-13408
Electrical and optical properties of multiple quantum well structures and their applications to infrared detectors
[FFI-92/7012] 02 p0809 N94-14010
Spin polarized photoemission studies of interfacial and thin film magnetism
[DE93-014326] 02 p0580 N94-14142
Optoelectronics based on SiGe/Si heterostructures
[AD-A267178] 03 p1190 N94-15848
JSEP fellowship
[AD-A266568] 03 p1211 N94-16800
Structural characterization of epitaxial layers for infrared detectors
[AD-A267875] 03 p0940 N94-17013
Development of ultra-low noise, high performance 3-V Quantum Well Infrared Photodectors (QWIP's) for focal plane array staring image sensor systems
[AD-A267715] 03 p1214 N94-17272
High-speed nonlinear switching mechanisms and devices for multi-gigabit data processing
[AD-A267753] 03 p1014 N94-17375
Kinetic aspects of lattice mismatch in molecular beam epitaxial growth on planar and patterned substrates
[AD-A270424] 04 p1597 N94-18506
Fundamental properties and device applications of Ge(x)Si(1-x)/Si superlattices (supplemental)
[AD-A269212] 04 p1600 N94-18884
Suppressed electron-phonon scattering in superlattices
[AD-A270834] 04 p1604 N94-19597
Solid-state dynamics in novel semiconductor nanostructures
[AD-A271249] 04 p1605 N94-19725
Theoretical and experimental studies of quantum wells
[AD-A271180] 04 p1606 N94-19741
Investigation of quantum effects in heterostructures
[AD-A270938] 05 p2011 N94-19817
Theory of energy-assisted epitaxy; theory of ordered semiconductor alloys: In(1-x)Tl(x)Sb as a long-wave infrared material
[AD-A271007] 05 p2012 N94-19835
Common Themes and Mechanisms of Epitaxial Growth, volume 312 — Materials Research Society symposium proceedings
[AD-A270513] 05 p2013 N94-19967
Center for the integration of optical computing
[AD-A271874] 05 p1899 N94-20469
An x-band peeled HEMT amplifier 05 p1732 N94-20498
Optical and transport properties of metallic and semiconductor nanostructures
[AD-A271716] 05 p2018 N94-20554
Investigation of heterojunctions and multiple quantum well structures using crystalline organic semiconductors
[AD-A272113] 05 p2018 N94-20569
Optical amplification and threshold behavior on InGaAs/InGaAsP multiquantum well structures
[ETN-93-94181] 05 p2026 N94-21151
Synthesis and properties of mismatched heterojunction/substrate interfaces
[AD-A272904] 05 p1760 N94-21229
Manufacturing and characterization of GaAs/AlGaAs multiple quantumwell ridge waveguide lasers
[EUT-92-E-265] 06 p2348 N94-23168
Characterization of nonlinear effects in optically pumped vertical cavity surface emitting lasers
[AD-A273840] 07 p2815 N94-25744
Biexciton formation by two-photon absorption in quantum wells
[DE93-613551] 07 p3071 N94-25852
Instantaneous amplitude and frequency dynamics of coherent wave mixing in semiconductor quantum wells
[DE94-003262] 07 p3054 N94-26128
Investigation of a normal incidence high-performance p-type strained layer In(0.3)Ga(0.7)As / In(0.52)Al(0.48) as quantum well infrared photodetector
[AD-A274854] 07 p3055 N94-26188
Ordering and phase separation in MOCVD InGaP alloys and unicompositional quantum wells
[DE94-004693] 07 p3056 N94-26352
Development of ultra-low noise, high performance 3 -5 quantum well infrared photodetectors (QWIPs) for focal plane array staring image sensor systems
[AD-A275745] 08 p3511 N94-28734
Photonic devices and systems for optical signal processing
[AD-A275818] 08 p3498 N94-28804
Carrier collection and scattering in quantum well and superlattice devices
[AD-A275443] 08 p3512 N94-28880
Visible vertical cavity surface emitting lasers
[AD-A275334] 08 p3293 N94-28919
Spatial light modulators with arbitrary quantum wells profiles
[AD-A275023] 08 p3499 N94-29114
The effects of propagational factors on quantum wires in close parallel proximity
[ISBN-0-315-86157-6] 08 p3254 N94-30035
Electronic structure of Zn-based quantum wells
[DE94-608104] 08 p3516 N94-30068
Photoelectronic study of GaAs epilayers and In(x)Ga(1-x)As/GaAs quantum wells
[ISBN-0-315-85756-0] 08 p3518 N94-30239
Nonlinear optics response of semiconductor quantum wells under high magnetic fields
[DE94-003244] 08 p3520 N94-30835
Photopyroelectric spectroscopy as a non-intrusive technique for the determination of the optical absorption spectra of multiple quantum well samples
[ISBN-0-315-87164-4] 09 p3833 N94-31875
Cooling and trapping of neutral atoms
[AD-A276957] 09 p3870 N94-32360
High speed, strained layer, multiquantum well, GaInAsP and GaAs lasers and heterostructures
[AD-A277287] 09 p3719 N94-32608
The 6th International Conference on Modulated Semiconductor Structures
[AD-A276815] 09 p3906 N94-32908
Large-diameter InGaAs/AlGaAs vertical-cavity surface-emitting lasers with low threshold current density fabricated using a simple chemical etch process
[AD-A277733] 09 p3721 N94-33003
Research in the optical sciences
[AD-A278271] 09 p3884 N94-33140
Quantum well infrared photodetector FPA
[AD-A278010] 09 p3908 N94-33248

Material engineering of the novel semiconductor structures
[AD-A276386] 09 p3910 N94-33355
Spectral-domain optical processing techniques
[AD-A278371] 10 p4141 N94-33739
Infrared detectors based on Si/SiGe superlattices and silicide/SiGe Schotty barriers operating beyond 12 micrometers
[AD-A277900] 10 p4147 N94-34082
Activities of the optoelectronics laboratory
[PB94-171196] 11 p4334 N94-36190
Development of ultra-low noise, high performance 3 to 5 Quantum Well Infrared Photodetectors (QWIPs) for focal plane array staring image sensor systems
[AD-A278861] 11 p4342 N94-36385

QUARK MODELS
NT QUARK PARTON MODEL
Quenched chiral logarithms
[DE93-010195] 01 p0346 N94-11663
Measuring strangeness in the nucleon
[DE93-014861] 02 p0785 N94-14471
Production of D-mesons in pp-collisions and quark-gluon string model
[DE93-626721] 03 p1185 N94-17312
The three-loop QCD beta-function and anomalous dimensions
[NIKHEF-H/92-17] 03 p1186 N94-17617
The renormalization of the axial anomaly in dimensional regularization
[NIKHEF-H/92-18] 03 p1220 N94-17618
Search for top quark with D0 detector
[DE93-040170] 04 p1572 N94-19536
Hadronic molecules and scattering amplitudes from the nonrelativistic quark model
[DE94-000377] 05 p1974 N94-21657
A relativistic constituent quark model
[DE93-041085] 05 p1946 N94-21689
Gauge invariance and the electromagnetic current of composite pions
[DE93-040869] 06 p2532 N94-22952
A measurement of the forward-backward asymmetry and sin(sup 2)(theta)(sub W) from the process Z(sup 0) (yields) (mu)(sup +)(mu)(sup (minus)) at (radical)s = 1.8 TeV
[DE94-001908] 06 p2532 N94-23018
A quark structure of hadrons and nuclei
[DE93-616872] 06 p2539 N94-25474
On the hadron formation time in pion-nucleus interaction
[DE93-616879] 06 p2539 N94-25476
Lepton masses in an SU(3)(sub L) x U(1)(sub N) gauge model
[DE93-634366] 07 p3016 N94-26040
Spin effects in hard interactions (interest in accelerated polarized beam)
[DE93-634398] 07 p3031 N94-26044
Dibaryon-induced instability of neutron stars
[DE93-634453] 07 p3103 N94-26046
Measuring the time dependence of B(sub s)(sup 0) meson - anti B(sub s)(sup 0) meson oscillations
[ISBN-0-315-84367-5] 07 p3021 N94-26665
Low-energy hadronic interactions beyond the current algebra approach
[DE94-602600] 07 p3022 N94-26900
Spectroscopy and strong decays of baryons
[ISBN-0-315-49073-X] 07 p3024 N94-27258
Finding the missing pieces of the standard model
[ISBN-0-315-57174-8] 07 p3024 N94-27259
QCD corrections to inclusive B - S processes in the standard model
[ISBN-0-315-54572-0] 07 p3073 N94-27263
A relativistic quark model
[ISBN-0-315-60926-5] 07 p3025 N94-27333
Aspects of perturbative corrections in quantum chromodynamics
[ISBN-0-315-63607-6] 07 p3074 N94-27398
Search for excited quarks in p(bar p) collisions at the square root of s = 1.8 TeV
[DE94-004658] 08 p3484 N94-28573
Semileptonic heavy-to-light decays of baryons
[DE94-606481] 08 p3487 N94-29502
Polarized lepton-nucleon scattering
[DE94-009027] 09 p3875 N94-33278
About G-parity violation in tau yields nu pi eta decay
[DE94-611146] 10 p4136 N94-33863
Baryonic currents and their correlators in the heavy quark effective theory
[DE94-612496] 11 p4320 N94-35567
The silent phase transition in mesonic bags and lattice theory
[DE94-616852] 11 p4321 N94-35583
A quark model of bar Lambda production in bar Rho interactions
[DE94-008071] 11 p4324 N94-35824
Collapse of flux tubes
[DE94-004645] 11 p4328 N94-36304
The E2/M1 mixing ratio in the excitation of the Delta from polarized photo-reactions
[DE94-004235] 12 p4510 N94-36442
Relativistic di-quark model of p p-bar yields K(+)K(-) reaction
[DE94-618519] 12 p4514 N94-37063
Sum rules for 1/m corrections to the form factors of semileptonic B decays
[DE94-618548] 12 p4514 N94-37065
The form factors of the nucleons
[DE94-013357] 12 p4515 N94-37086

QUARK PARTON MODEL
High energy parton-parton elastic scattering in QCD
[DE94-003432] 07 p3028 N94-27736
Determination of the neutron spin-structure function
[DE94-005234] 08 p3483 N94-28542
Spin-structure function of the neutron He-3: SLAC results
[DE94-008927] 09 p3875 N94-33189
QCD parametrizations of the parton distribution of deep inelastic scattering
[DE94-616660] 11 p4325 N94-36074

QUARKS
Top and Higgs masses in a composite boson model
[DE93-010874] 01 p0359 N94-10302
Production of strange clusters in relativistic heavy ion collisions
[DE93-010876] 01 p0359 N94-10303
Searches for strangelets and other exotics at the AGS
[DE93-013341] 01 p0359 N94-10308
On the relativistic string size at finite temperature
[DE93-617658] 01 p0409 N94-10394
S(sup 1) x S(sup 2) as a bag membrane and its Einstein-Weyl geometry
[DE93-613149] 01 p0410 N94-10635
Proceedings of the third workshop on light quark meson spectroscopy
[DE93-754138] 01 p0363 N94-10696
Filamentation instability of hot quark-gluon plasma with hard jet
[DE93-617679] 01 p0388 N94-10882
Gluon gas viscosity in nonperturbative region
[DE93-617680] 01 p0397 N94-10883
Relativistic heavy-ion collisions
[DE93-014844] 01 p0366 N94-11147
Experiments to measure the gluon helicity distribution in protons
[DE93-011756] 01 p0368 N94-11613
Quenched chiral logarithms
[DE93-010195] 01 p0346 N94-11663
Top quark search in D(O) from the lepton + jets mode
[DE93-014027] 01 p0370 N94-12781
Quark and lepton masses
[DE93-012308] 01 p0370 N94-12787
Measurements of transverse energy and forward energy in high-energy nuclear collisions
[DE93-012755] 02 p0788 N94-12817
Top quark polarization and T-odd spin correlations as tools for testing (non) Standard Model predictions
[DE93-622956] 02 p0778 N94-12847
No-lost theorem for parity violating nucleon-nucleon scattering experiments
[DE93-012737] 02 p0779 N94-12949
A search for scalar leptoquarks in D0
[DE93-012780] 02 p0779 N94-12954
Inclusive single muons at DO
[DE93-012779] 02 p0783 N94-13494
Quark and gluon jets at CDF
[DE93-014919] 02 p0783 N94-13884
Top quark search: Results and prospects at Fermilab
[DE93-013016] 02 p0786 N94-14524
Early baryon and meson spectroscopy culminating in the discovery of the Omega minus SU(3) and quarks
[DE93-014321] 02 p0787 N94-14580
On the nature of mirror particles
[DE93-626670] 03 p1179 N94-14934
Astronomy and astrophysics 03 p1239 N94-15970
PHENIX Conceptual Design Report
[DE93-015759] 03 p1182 N94-16161
Calorimeter based detectors for high energy hadron colliders
[DE93-017055] 03 p1188 N94-16900
Heavy ion physics research at Creighton University
[DE93-016809] 03 p1185 N94-16957
Mesons at finite temperature in the NJL model with gluon condensate
[DE93-626697] 03 p1185 N94-17310
Quark-loop effects in high energy spin-flip processes
[DE93-626692] 03 p1188 N94-17313
Search for the top quark from (e(mu)) and (e,e) events in the D0 detector in p(bar-p) collisions at the square root of s = 1.8 TeV
[DE93-016350] 03 p1186 N94-17662
Beauty without charm in B-meson decays
[PREPRINT-732] 04 p1565 N94-17972
Measuring the sea quark polarization
[DE93-015792] 04 p1566 N94-18234
Charmonium physics from (bar p)p interactions
[DE93-017809] 04 p1569 N94-18973
Search for top quark with D0 detector
[DE93-040170] 04 p1572 N94-19536
Top search at the TEVATRON
[DE93-019392] 05 p1978 N94-19988
Jet shapes in hadron and electron colliders
[DE93-019386] 05 p1979 N94-20216
Measurement of the strange quark distribution function in W(+) charm quark events
[DE93-018267] 05 p1973 N94-20474
Theoretical particle physics
[DE94-000538] 05 p1973 N94-20938
Recent results on top, bottom and exotic physics at the Tevatron
[DE94-000578] 05 p1975 N94-21786
Measurement of the B meson and b quark cross-section in (-p)p collisions at the square root of s = 1.8 TeV using the exclusive decays B(+) and B(exp 0) yields J/psiK*(exp 0)
[DE93-019907] 05 p1975 N94-21806
Search for excited quarks in p(-p) collisions at the square root of s = 1.8 TeV
[DE93-019910] 05 p1975 N94-21840
New perspectives in quantum chromodynamics
[DE93-041021] 05 p2038 N94-21935
Time evolution of the quark-gluon plasma
[DE94-000804] 05 p1998 N94-22389
The status of glueballs
[DE93-040040] 06 p2531 N94-22923
Towards a theory of quark and lepton masses
[DE94-001726] 06 p2533 N94-23218
Progress report for the UCSD experimental HEP group
[DE94-001357] 06 p2533 N94-23699
Strong interactions studies with medium energy probes
[DE94-001446] 06 p2540 N94-23791
B-quark production at hadron colliders
[DE94-001459] 06 p2534 N94-23806
Search for the top quark and other new particles at D0
[DE94-001220] 06 p2535 N94-24515
Stitching the Yukawa quilt
[PB93-204477] 06 p2569 N94-24532
Electro-weak, QCD and top physics at the Tevatron
[DE94-002304] 06 p2535 N94-24611
The determination of the branching ratios of the Z(zero) boson into heavy quarks using neural networks
[ETN-94-95381] 06 p2538 N94-25246
Bottom quark production at the Z resonance
[ISBN-9-09-006217-3] 06 p2538 N94-25255
A scalar-vector model of quark-antiquark interaction under linear confinement
[DE93-616871] 06 p2538 N94-25317
The Casimir energy of the rigid string with massive ends
[DE93-616851] 06 p2492 N94-25338
Proton spin: The role of quark-gluon and hadron degrees of freedom
[DE93-616867] 06 p2538 N94-25341
Heavy flavour physics at LEP
[NIKHEF-H/92-19] 06 p2539 N94-25465
A quark structure of hadrons and nuclei
[DE93-616872] 06 p2539 N94-25474
On the hadron formation time in pion-nucleus interaction
[DE93-616879] 06 p2539 N94-25476
Quark-antiquark bound states
[DE93-613054] 07 p3013 N94-25826
A possible way of connecting the Grassmann variables and the number of generation
[DE94-601624] 07 p2990 N94-25838
Out of equilibrium phase transitions and a toy model for disoriented chiral condensates
[DE94-601642] 07 p3013 N94-25839
Structure functions of sea quarks, Kogut-Susskind pole and dynamics of pp- and pp-bar-interactions at high energies
[DE93-613184] 07 p3031 N94-25870
Heavy quark production and spectroscopy
[DE94-003619] 07 p3015 N94-25935
Pseudoscalar glueball in the composite interpolating fields approach
[DE93-634374] 07 p3016 N94-26042
Deciphering the quark-gluon structure of the photon in electron(gamma) collisions
[DE93-634386] 07 p3017 N94-26043
The STAR experiment at the Relativistic Heavy Ion Collider
[DE94-003409] 07 p3017 N94-26083
JLC-1
[DE93-520380] 07 p3031 N94-26113
Why is the Higgs doublet light?
[DE94-601711] 07 p3018 N94-26333

Mesons and diquarks in a NJL-model at finite temperature and chemical potential
[DE93-634375] 07 p3020 N94-26505
Measuring the time dependence of B(sub s)(sup 0) meson - anti B(sub s)(sup 0) meson oscillations
[ISBN-0-315-84367-5] 07 p3021 N94-26665
Light-quark, heavy-quark systems: An update
[DE94-002298] 07 p3021 N94-26759
Strange Dibaryons
[DE94-003005] 07 p3022 N94-26769
Low-energy hadronic interactions beyond the current algebra approach
[DE94-602600] 07 p3022 N94-26900
D0 results on searches for the top quark
[DE94-003361] 07 p3023 N94-26938
Experimental investigations of strong interaction in the non-perturbative QCD region
[DE94-001178] 07 p3024 N94-26949
Finding the missing pieces of the standard model
[ISBN-0-315-57174-8] 07 p3024 N94-27259
A relativistic quark model
[ISBN-0-315-60926-5] 07 p3025 N94-27333
Quantum chromodynamics and nuclear physics at extreme energy density
[DE94-004418] 07 p3026 N94-27604
Search for the top quark in the single lepton + jets channel at D0
[DE94-004660] 07 p3028 N94-27749
Report of the subgroup on the top quark
[DE94-004624] 08 p3481 N94-28462
Discrete quark-lepton symmetry need not pose a cosmological domain wall problem
[DE94-601606] 08 p3481 N94-28471
Properties of W + jet events in proton-antiproton collisions at 1.8 TeV
[DE94-004002] 08 p3482 N94-28524
Research on elementary particle physics. Task P: Studies in theory and phenomenology of elementary physics
[DE94-004955] 08 p3483 N94-28566
Search for excited quarks in p(bar p) collisions at the square root of s = 1.8 TeV
[DE94-004658] 08 p3484 N94-28573
Masses and mixing of leptons and quarks (Dirac particles)
[DE94-606446] 08 p3484 N94-28611
Proceedings of the workshop on quark and lepton mass matrices
[DE94-707692] 08 p3485 N94-28624
The small-x behaviour of parton distribution functions
[DE94-606414] 08 p3485 N94-28758
One-loop QCD mass effects in the production of polarized bottom and top quarks
[PB94-138104] 08 p3487 N94-29145
Semileptonic heavy-to-light decays of baryons
[DE94-606481] 08 p3487 N94-29502
Statistical description of hot and dense clustering matter
[DE94-608155] 08 p3490 N94-30112
Direct anti-b b production in anti-pp collisions at the square root of s = 1.8 TeV
[DE94-006167] 08 p3491 N94-30369
Operator analysis for quark and lepton masses in SO(10)
[DE94-005201] 08 p3491 N94-30709
Search for the top quark in the electron-electron and electron-muon channels at D0
[DE94-006174] 08 p3492 N94-30779
Theoretical studies in hadronic and nuclear physics
[DE94-003524] 08 p3492 N94-30838
Charmonium and bottomonium in (-p)p interactions
[DE94-006173] 08 p3493 N94-30886
Transport properties of quark and gluon plasmas
[DE94-007043] 09 p3864 N94-31405
F0-975, A0-980 as eye-witnesses of confinement
[PB94-147105] 09 p3868 N94-31923
The form factors of the nucleons
[DE94-007096] 09 p3872 N94-32630
CP violation and the top quark
[DE94-008930] 09 p3874 N94-32841
Nuclear physics and astrophysics
[DE94-007168] 09 p3939 N94-33147
Measurement of the ratio R = (sigma x B(p(bar p) yields W(sup (+-)) yields e(sup(+-))(nu))))/(sigma x B(p(bar p) yields Z(sup 0) yields e(sup +e(sup -)) in p(bar p) collisions at the square root of s = 1,800 GeV
[DE94-006846] 10 p4138 N94-35073
Goldstone pion and other mesons using a scalar confining interaction
[DE94-010016] 11 p4321 N94-35649
Leptonic decay constants of heavy quarkonia in effective QCD sum rules
[DE94-611160] 11 p4322 N94-35784
Calculations on some properties of the pion in the framework of Schwinger-Dyson and Bethe-Salpeter equations
[DE94-611232] 11 p4322 N94-35786
A quark model of bar Lambda production in bar Rho interactions
[DE94-008071] 11 p4324 N94-35824
Spin effects in high energy quark-quark scattering
[DE94-616800] 11 p4330 N94-36080
CDF electroweak studies and the search for the top quark
[DE94-010333] 11 p4326 N94-36107
Top dilepton search at CDF
[DE94-002302] 11 p4327 N94-36266
Collapse of flux tubes
[DE94-004645] 11 p4328 N94-36304
Top quark search at CDF
[DE94-003643] 12 p4511 N94-36459
A search for first generation scalar leptoquarks at radical s equal to 1.8 TeV with the D0 detector
[DE94-008846] 12 p4511 N94-36506
The t(anti t)(gamma) background to pp (yields) W(gamma) + X at the SSC
[DE94-001386] 12 p4512 N94-36526
Summary of the extensions of the Standard Model working group
[DE94-002217] 12 p4512 N94-36527
The Pomeron and Quantum Chromodynamics (QCD) with many light quarks
[DE94-001351] 12 p4513 N94-36538
B quark production cross sections and the b- (bar b) correlated production cross section at CDF
[DE94-000620] 12 p4514 N94-36700
Methods of calculation of higher power corrections in QCD
[DE94-618511] 12 p4521 N94-36748
Introduction to the heavy quark effective theory, part 1
[DE94-618512] 12 p4514 N94-36749
A study of jet handedness in hadronic Z0 decays
[DE94-013358] 12 p4515 N94-37087
Numerical solution to the boundary-value problem for the Bethe-Salpeter equation with quadratically rising potential
[DE94-621606] 12 p4504 N94-37175
Non-equilibrium evolution of the disoriented chiral condensate in heavy-ion collisions
[DE94-012897] 12 p4522 N94-37310
The Mesozoic Era of relativistic heavy ion physics and beyond
[DE94-011341] 12 p4548 N94-37557
Strangeness and the quark-gluon plasma: An experimenter's perspective
[DE94-011377] 12 p4519 N94-37558
Pre-equilibrium parton dynamics: Proceedings
[DE94-011347] 12 p4520 N94-37716

QUARRIES
U MINES (EXCAVATIONS)

QUARTIC EQUATIONS
Enumerative geometry of Del Pezzo Surfaces
[DE93-624768] 04 p1546 N94-17816

QUARTZ
NT STISHOVITE
Dynamic studies of crystal growth using the AFM
[DE93-009549] 01 p0399 N94-11268
Si-29 NMR spectroscopy of naturally-shocked quartz from Meteor Crater, Arizona: Correlation to Kieffer's classification scheme 01 p0080 N94-12087
Recovery of materials impacted at high velocity
[DE93-014150] 02 p0576 N94-12885
Theory of the electronic and structural properties of solid state oxides
[DE93-016051] 02 p0811 N94-14296
A calibration of the production rate ratio P-21/P-26 by low energy secondry neutrons: Identification of Ne spallation components at the 10(exp 6) atoms/g level in terrestrial samples 03 p1187 N94-16194
Orientation of Planar Deformation Features (PDFs) in quartz 03 p1219 N94-16341
Investigation of the effects of polyelectrolyte coatings on colloid transport in porous media
[DE93-018300] 03 p0970 N94-16973
SRB thermal curtain design support
[NASA-CR-193857] 03 p0927 N94-17123
SRB thermal curtain design support
[NASA-CR-193858] 03 p0928 N94-17124
Quartz crystal resonators and oscillators for frequency control and timing applications: A tutorial, revision 6.1
[AD-A268205] 03 p1216 N94-17480
Kinetics of silica-phase transitions
[DE93-016231] 03 p1217 N94-17659
The Lever oscillator for use in high resistance resonator applications
[DE93-017652] 04 p1404 N94-18827
Development of a quartz digital accelerometer for environmental sensing and navigation applications
[DE93-018503] 04 p1433 N94-19243
Characterization of amorphous material in shocked quartz by NMR spectroscopy
[DE93-019069] 05 p1679 N94-20307
Shock attenuation at the Slate Islands revisited 05 p1863 N94-20887
A dynamic melting model for the origin of Apollo 15 olivine-normative and quartz-normative mare basalts 06 p2615 N94-24371
NMR characterization of shocked quartz
[DE94-007733] 09 p3774 N94-32816
Calorimetric thermobarometry of experimentally shocked quartz 11 p4240 N94-36174
Assess progress being made for the KTeV electromagnetic calorimeter crystal order in France
[DE94-009396] 12 p4533 N94-36746

QUARTZ CRYSTALS
The laser ablation of gold films at the electrode surface of a quartz crystal microbalance
[AD-A265535] 01 p0175 N94-12012
NMR spectroscopy of experimentally shocked single crystal quartz: A reexamination of the NMR shock barometer 01 p0081 N94-12258
A novel test method for fuel thermal stability
[AD-A265853] 01 p0099 N94-12275
Quartz crystal resonators and oscillators for frequency control and timing applications: A tutorial, revision 6.1
[AD-A268205] 03 p1216 N94-17480
Proceedings of the 4th European Congress on Chronometry
[ETN-93-94633] 04 p1424 N94-18006
Simulation of a quartz-clockwork 04 p1426 N94-18019
Simulation of quartz resonators 04 p1426 N94-18021
Quartz analog watch with perpetual calendar 04 p1429 N94-18042
Atomic oxygen fluence detector for Bremsat: Scientific and technical description 05 p1663 N94-21396
Application of an electrochemical quartz crystal microbalance to the study of electrocatalytic films
[DE93-041124] 05 p2029 N94-21691
Pre-flight testing of Thermoelectric Quartz Crystal Microbalances (TQCM) for midcourse space experiment (MSX) spacecraft
[AD-A277054] 09 p3610 N94-32010

QUARTZ LAMPS
An analysis of the radiation field beneath a bank of tubular quartz lamps
[NASA-CR-191551] 03 p1024 N94-16542

QUARTZITE
Shock transformations in quartzite 01 p0097 N94-12040
Mercury: Mid-infrared (7.3 - 13.5 microns) spectroscopic observations showing features characteristic of plagioclase 11 p4370 N94-36150

QUASARS
Polarization and variability of active galaxies and quasars 02 p0837 N94-13550
The extent and content of low-ionization gas in galaxies 02 p0837 N94-13551
A long-term space astrophysics research program: The evolution of the quasar continuum
[NASA-CR-193714] 02 p0839 N94-14404
The theory of QSO absorption line systems and their relationship to the galaxies
[NASA-CR-194596] 03 p1236 N94-15679
Complex QSO absorbers: High-redshift clusters of galaxies?
[NASA-CR-194617] 03 p1237 N94-16833
EGRET Mission and Data Analysis
[MPE-PREPRINT-223] 04 p1622 N94-19462
EGRET observations of 3 C 273 04 p1623 N94-19464
Automated investigation of quasars at a galactic latitude of -45 deg
[ISBN-0-315-57576-X] 05 p2056 N94-22415
Adaptive filtering of Echelle spectra of distant Quasars 05 p2072 N94-22520
100 GHz map of 3C 446
[PB94-104882] 06 p2599 N94-23705
Sloan Digital Sky Survey
[DE94-004662] 07 p3103 N94-27750
Weak bump quasars
[NASA-CR-195267] 07 p3103 N94-27933
Infrared properties of obscuring dust tori in active galactic nuclei 08 p3545 N94-29832
High redshift QSOs and the x ray background
[NASA-CR-195112] 08 p3540 N94-29957
Broad H alpha profiles of radio-loud active galactic nuclei and rapid profile variability in Seyfert and radio galaxies 08 p3552 N94-29989
Are there two engines at the center of 3C286?
[PB94-149218] 10 p4162 N94-34379

The BL LAC phenomenon: X-ray observations of transition objects and determination of the x-ray spectrum of a complete sample of flat-spectrum radio sources
[NASA-CR-195951] 12 p4546 N94-36688
Ultraviolet spectropolarimetry of high redshift quasars with the Hubble Space Telescope
[NASA-CR-196014] 12 p4546 N94-36690
Correlated radio and optical variations in a sample of AGN. A simultaneous radio-optical flare in BL lacertae
[PB94-179181] 12 p4548 N94-37834

QUASI-PARTICLES
U ELEMENTARY EXCITATIONS

QUASI-STEADY STATES
Time resolved measurement of electron temperatures of exploding foil x ray laser plasmas
[DE93-017161] 02 p0803 N94-14894
The temperature at the phase boundary during quasi-static motions of a two-phase thermoelastic bar
[AD-A268769] 04 p1596 N94-18388
Scaling of sustained ZT-40 M reversed field pinches
[DE94-003318] 07 p3043 N94-26321

QUASI-STELLAR RADIO SOURCES
U QUASARS

QUASILINEARITY
U NONLINEARITY

QUATERNARY ALLOYS
Electronic and total energy properties of ternary and quaternary semiconductor compounds, alloys and superlattices
[NASA-CR-192905] 01 p0405 N94-12570

QUATERNIONS
Derivation of three closed loop kinematic velocity models using normalized quaternion feedback for an autonomous redundant manipulator with application to inverse kinematics
[DE93-012823] 01 p0340 N94-12543
Quaternions and the heuristic role of mathematical structures in physics
[DE93-622865] 02 p0816 N94-12844
Robust control of nonlinear flexible multibody systems using quaternion feedback and dissipative compensation
[NASA-TM-109099] 10 p4014 N94-34103
Modelling and control of a rotor supported by magnetic bearings 11 p4216 N94-35858

QUENCHING
Quenching and annealing effects on the specific heat of YBa2Cu3O(7-delta)
[DE93-016483] 02 p0816 N94-14868

QUENCHING (ATOMIC PHYSICS)
Vibrational energy transfer within the B 3Pi (O(+) sub u) state of 79BR2 upon collision with N2, O2, NO, and SF6
[AD-A273905] 07 p3011 N94-25589
Quenching of the excited state of hydrated Europium(3) ions by electron transfer
[DE94-005553] 08 p3482 N94-28518

QUENCHING (COOLING)
AGF (Automatic Gradient Furnace): A proposed microgravity facility 01 p0112 N94-10141
EUSO-D2-experiment: Unidirectional solidification with quenching of an AlSi11 alloy 01 p0086 N94-10199
A comparison of one and two dimensional flame quenching: Heat transfer results
[DE93-015196] 03 p0947 N94-16060
Investigation of two-phase flow and boiling heat transfer during quenching of a tube under microgravity 03 p0979 N94-16087
Ageing in Processed Polymers: Programme, summary, and abstracts discussion meeting
[AD-A268931] 04 p1370 N94-18448
Stretch-induced quenching in flame-vortex interactions 06 p2237 N94-24156
Study on the production of flaky amorphous alloy powders by impact flattening of atomized liquid droplets on a rapidly rotating wheel 07 p2746 N94-28169
Formation and high mechanical strength of Al-based alloys containing a nanoscale icosahedral phase as a main constituent 07 p2746 N94-28171

QUERY LANGUAGES
A correct and efficient interface for logical query languages with complex objects
[MEMO-INF-93-01] 01 p0320 N94-10167
The relational-to-object-oriented cross-model accessing capability in a multi-model and multi-lingual database system
[AD-A264911] 01 p0420 N94-11846
EDMS: Engineering data management system. User's reference
[PB93-187391] 04 p1614 N94-18119
Learning database abstractions for query reformulation
[AD-A269531] 04 p1616 N94-18641
DataTypeLog: A deductive object oriented query language
[MEMO-INF-92-79] 04 p1526 N94-19221
Working visit to the University of L'Aquila, Italy
[FEL-93-B020] 04 p1618 N94-19452
Application of the structures query language of APROS for specification of industrial processes 05 p1923 N94-22078
Intelligent text retrieval in the NASA astrophysics data system 05 p2048 N94-22499
Multi-set extended relational algebra: A formal approach to a practical issue
[PB94-110830] 06 p2486 N94-23725
The ESIS query environment pilot project 06 p2518 N94-23952
Correct and efficient interface for logical query languages with complex objects
[PB93-211175] 06 p2593 N94-24743
A comparison of Boolean-based retrieval to the WAIS system for retrieval of aeronautical information
[NASA-CR-4569] 06 p2594 N94-25487
Design and implementation of a query editor for the Amadeus system
[AD-A274955] 07 p3097 N94-26300
Automated interface for retrieving reusable software components
[AD-A275004] 08 p3409 N94-28896
DTL: A deductive and typed object-oriented language
[MEMO-INF-93-41] 08 p3425 N94-30417
A probabilistic view of Datalog parallelization
[TELECOM-93-D-021] 09 p3824 N94-31183
The meaning of duplicates in the relational database model
[CT-93-04] 09 p3916 N94-31392
A simulation of uncertain reasoning on parametric databases using data-dependency derived inference nets 09 p3919 N94-32499
Information disclosure in evolving information systems: Taking a shot at a moving target
[TR-93-22] 09 p3919 N94-32506

QUESTOL AIRCRAFT
An investigation on the effectiveness of the piping interference removal system for STOL aircraft wind tunnel tests
[NAL-TM-647] 01 p0002 N94-10350
Aerodynamic model identification of quiet STOL experimental aircraft ASKA from dynamic flight test data
[DE93-767967] 01 p0025 N94-10728
Flight simulator experiment of the cockpit advisory system
[NAL-TR-1151] 01 p0033 N94-10733

QUEUEING THEORY
Complex functions in queueing theory
[CWI-BS-R9219] 01 p0342 N94-10352
Scalable spin locks for multiprogrammed systems
[AD-A265007] 01 p0337 N94-11650
Stochastic scheduling games with Markov decision arrival processes
[CWI-BS-R9231] 02 p0773 N94-14005
Stochastic bounds for a polling system
[CWI-BS-R9230] 02 p0765 N94-14361
Stochastic scheduling in in-forest networks
[INRIA-RR-1719] 03 p1164 N94-15695
Logarithmic asymptotics for steady-state tail probabilities in a single-server queue
[AD-A266746] 03 p1165 N94-15775
A comparison of queueing, cluster and distributed computing systems
[NASA-TM-109025] 03 p1160 N94-16878
Stochastic scheduling in a multiclass G/G/1 queue
[INRIA-RR-1746] 03 p1162 N94-17537
Efficient simulation of DEDS by means of standard clock techniques: Queueing and integrated radio network examples
[AD-A269878] 04 p1432 N94-18681
Polling systems: Moment stability of station times and central limit theorems
[PB93-191955] 04 p1560 N94-18990
On asynchronous testing
[MEMO-INF-93-03] 04 p1543 N94-19226
Tandem queues with deterministic service times
[PB93-197465] 04 p1543 N94-19324
Compensation approach for three or more dimensional random walks
[PB93-197499] 04 p1543 N94-19326
Control of integrated voice/data multi-hop radio networks via reduced-load approximations
[AD-A270661] 04 p1393 N94-19779
Stochastic optimization by simulation: Numerical experiments with M/M/1 queue in steady-state
[AD-A271143] 05 p1949 N94-19854
Large deviations behavior of counting processes and their inverses
[AD-A271142] 05 p1939 N94-19909
Memory contention in scalable cache-coherent multiprocessors
[TR-448] 05 p1929 N94-20144
Time warp operating system version 2.7 internals manual
[NASA-CR-194798] 05 p1899 N94-20549
The correlated M/G/1 queue
[CWI-BS-R9303] 05 p1943 N94-21032
On the optimality of FCFS for networks of multi-server queues
[CWI-BS-R9235] 05 p1944 N94-21160
Optimization of static traffic allocation policies
[CWI-BS-R9302] 05 p1930 N94-21161
N parallel queueing systems with server breakdown and repair
[CWI-BS-R9236] 05 p1944 N94-21232
Optimization of fixed time polling schemes
[CWI-BS-R9237] 05 p1945 N94-21233
Tandem queues with deterministic service times
[CWI-BS-R9238] 05 p1946 N94-21577
Algorithms for Markov decision chains with partial information
[PB93-220085] 05 p1918 N94-22098
Loss probabilities in batch-arrival bulk-service queues with finite capacity
[MEMO-1106] 06 p2493 N94-22724
Uniform limit theorems for marked point processes
[PB94-118726] 06 p2488 N94-24526
Fast simulation of packet loss rates in a shared buffer communications switch
[NASA-CR-191556] 06 p2457 N94-24638
Data structures and amortized complexity in a functional setting
[ETN-94-95307] 06 p2476 N94-25290
Product forms as a solution base for queueing systems
[MEMO-COSOR-92-37] 06 p2477 N94-25526
Single-server queues with spatially distributed arrivals
[PB94-126638] 07 p2986 N94-26916
M-interference queue analysis by decomposition method
[ISBN-0-315-85795-1] 08 p3453 N94-30139
Performance evaluation of intelligent network services
[PB94-149564] 08 p3438 N94-30373
Customer creation and combination in queueing networks
[MEMO-INF-93-35] 08 p3438 N94-30375
Performability modelling using DyQNtool+
[MEMO-INF-93-45] 09 p3812 N94-31659
Light-traffic analysis for queues with spatially distributed arrivals
[MEMO-1150] 09 p3832 N94-31826
The use of service limits for efficient operation of multi-station single-medium communication systems
[CWI-BS-R9312] 09 p3677 N94-32085
A polling system with a dormant server
[CWI-BS-R9313] 09 p3835 N94-32193
Multiserver queues with impatient customers
[CWI-BS-R9319] 09 p3835 N94-32198
Undiscounted Markov decision chains with partial information; an algorithm for computing a locally optimal periodic policy
[TW-93-10] 09 p3851 N94-32205
An RSM study of the effects of simulation work and metamodel specification on the statistical quality of metamodel estimates
[AD-A278551] 10 p4130 N94-33783
A mean value analysis heuristic for analysis of aircraft sortie generation
[AD-A278578] 12 p4507 N94-36970

QUINONES
Femtosecond transient grating studies of electron transfer in porphyrin and chlorophyll donor-acceptor molecules
[DE94-009694] 12 p4478 N94-36555

QUOTIENTS
Finding minimum-quotient cuts in planar graphs
[DE93-011675] 01 p0344 N94-10961

R

R CORONAE BOREALIS STARS
Dust production in the envelopes of carbon stars: R Coronae Borealis
[ETN-93-94389] 02 p0839 N94-14075

RABBITS
Ocular damage induced by ultrashort laser pulses
[AD-A271859] 05 p1890 N94-20462

RACKS (GEARS)
Metal band drives in spacecraft mechanisms 06 p2355 N94-23987
Metal band drives in spacecraft mechanisms 08 p3162 N94-29637

RACON BEACONS
U RADAR BEACONS

RADAR
NT AIRBORNE RADAR
NT AIRBORNE SURVEILLANCE RADAR
NT COHERENT RADAR
NT CONTINUOUS WAVE RADAR
NT DIFFERENTIAL ABSORPTION LIDAR
NT DOPPLER RADAR
NT IMAGING RADAR
NT INCOHERENT SCATTER RADAR
NT INFRARED RADAR
NT LANDING RADAR
NT METEOROLOGICAL RADAR
NT MONOPULSE RADAR
NT MOVING TARGET INDICATORS
NT MULTISPECTRAL RADAR
NT MULTISTATIC RADAR
NT OPTICAL RADAR
NT OVER-THE-HORIZON RADAR
NT PULSE DOPPLER RADAR
NT PULSE RADAR
NT RADAR MEASUREMENT
NT RANGE AND RANGE RATE TRACKING
NT SATELLITE-BORNE RADAR
NT SEARCH RADAR
NT SECONDARY RADAR
NT SIDE-LOOKING RADAR
NT SPACE BASED RADAR
NT SURVEILLANCE RADAR
NT SYNTHETIC APERTURE RADAR
NT TRACKING RADAR

Multiparameter airborne rain radar development for TRMM validation and TRMM-follow-on study
02 p0690 N94-14226

Notes on the use of Dempster-Shafer and fuzzy reasoning to fuse identity attribute data
[AD-A267426] 03 p1004 N94-17309

Image processing for flight crew enhanced situation awareness 06 p2442 N94-25508

System analysis of ultra-wideband instrumentation radars: Impulse versus stepped-chirp approaches
[AD-A276624] 09 p3677 N94-32087

RADAR ALTIMETERS
U RADIO ALTIMETERS

RADAR ANTENNAS
System architecture of optically controlled phased array radar
[AD-A267056] 03 p0988 N94-15667

Advanced antennas for SAR spacecraft
03 p0993 N94-15912

Manufacturing tolerance requirements for frequency selective surfaces
[AD-A266541] 03 p0999 N94-16797

C-band PARC manual
[FEL-92-B159] 04 p1383 N94-18070

Modeling a Yagi array antenna for VHF radar use
[AD-A268973] 04 p1387 N94-18525

Probe compensation in cylindrical near-field scanning: A novel simulation methodology
05 p1718 N94-20404

Two microstrip arrays for interferometric SAR applications 05 p1722 N94-20421

Target angular motion and its effects on simulated SSAR ship images 05 p1745 N94-22161

Calibration block for digital beam forming antenna
[PB93-204550] 06 p2294 N94-23773

The down, release, and deployment of the RADARSAT SAR antenna 06 p2305 N94-23986

Calibration network intended for phase-array antennas at 3 GHz
[PB93-204352] 06 p2297 N94-24530

Cloud liquid water content measurement tests using dual-wavelength radar
[PB94-125960] 07 p2896 N94-26959

Printed circuit elements with applications to antennas, scattering, and circuits
[AD-A275512] 08 p3262 N94-28669

Orbital debris radar instrumentation
08 p3248 N94-29626

Radar estimations of atmospheric winds in the troposphere and lower stratosphere
08 p3370 N94-29697

Proceedings of the 1993 Antenna Applications Symposium, volume 1
[AD-A277202] 09 p3676 N94-32049

Proceedings of the 1993 Antenna Applications Symposium, volume 2
[AD-A277203] 09 p3677 N94-32050

Development of a frequency-domain electromagnetic scattering measurement system
[AD-A276738] 09 p3678 N94-32179

Generation of the ambiguity function for ultra wideband radar waveforms
[AD-A277913] 09 p3684 N94-33261

RADAR APPROACH CONTROL
SATORI: Situation Assessment Through the Re-creation of Incidents
[DOT/FAA/AM-93/12] 01 p0038 N94-12567

Terminal area forecasts, FY 1993-2005
[AD-A269855] 04 p1316 N94-18336

Design of Center-TRACON Automation System
08 p3138 N94-29568

Development of precision runway monitor system for increasing capacity of parallel runway operations
08 p3142 N94-29587

RADAR ASTRONOMY
The Telecommunications and Data Acquisition Report
[NASA-CR-195694] 08 p3246 N94-29613

The Telecommunications and Data Acquisition Report
[NASA-CR-196117] 11 p4252 N94-35542

The real-time display of interferometry data for Goldstone radar astronomy data acquisition
11 p4255 N94-35560

A new presentation of complex voltage data for Goldstone radar astronomy 11 p4255 N94-35561

RADAR ATTENUATION
Cloud liquid water content measurement tests using dual-wavelength radar
[PB94-125960] 07 p2896 N94-26959

Low altitude near-the-horizon propagation: A comparison between RPO and M-layer
[AD-A277358] 09 p3679 N94-32282

RADAR BEACONS
ATCRBS reply environment at Memphis International Airport
[AD-A266322] 03 p0864 N94-16439

Missile antenna pattern coordinate system and data formats
[AD-A269153] 04 p1385 N94-18260

RADAR BEAMS
System architecture of optically controlled phased array radar
[AD-A267056] 03 p0988 N94-15667

Resolution in radar mapping
[AD-A269730] 04 p1462 N94-18753

Method and apparatus of generating sum or difference signals corresponding to an apparent beam in a monopulse radar system
[AD-D015998] 06 p2302 N94-25056

Theoretical aspects of the agile mirror
[AD-A274890] 07 p2767 N94-26177

Subspace estimation without eigenvectors for adaptive beamforming
[AD-A276287] 09 p3671 N94-31254

RADAR CORNER REFLECTORS
An experiment for the radiometric calibration of the ERS-1 SAR 01 p0236 N94-11733

Prelaunch optical characterization of the Laser Geodynamic Satellite (LAGEOS 2)
[NASA-TP-3400] 03 p0884 N94-15193

Laser ranging application to time transfer using geodetic satellite and to other Japanese space programs
03 p0911 N94-15555

Evaluation of the TOPSAR performance by using passive and active calibrators 03 p1078 N94-16750

External calibration of polarimetric radar images using distributed targets 03 p1079 N94-16753

RCS Analysis of Plate Geometries, parts 1 and 2
[NASA-CR-194173] 05 p1717 N94-20269

A physical optics/equivalent currents model for the RCS of trihedral corner reflectors 05 p1717 N94-20271

Modifications to the three-component classification algorithm for SAR data 05 p1719 N94-20410

Radar backscattering from snow facies of the Greenland ice sheet: Results from the AIRSAR 1991 campaign
05 p1725 N94-20434

High-frequency techniques for RCS prediction of plate geometries and a physical optics/equivalent currents model for the RCS of trihedral corner reflectors, parts 1 and 2
[NASA-CR-195140] 06 p2298 N94-24616

RADAR CROSS SECTIONS
Theoretical studies of the radar properties of the icy Galilean moons of Jupiter
[NASA-CR-193407] 01 p0434 N94-11361

ERS-1 scatterometer data characteristics and wind retrieval skill 01 p0233 N94-11709

A preliminary C-band scatterometer model function for the ERS-1 AMI instrument 01 p0233 N94-11715

Ocean wave detection by SAR
01 p0197 N94-11932

Measurements of ocean cross-section with a side-looking airborne radar 01 p0201 N94-11954

Fundamental studies of radar scattering from water surfaces: The Lake Washington experiment
[NASA-CR-194030] 01 p0139 N94-12778

Scattering by a groove in an impedance plane
[NASA-CR-193362] 02 p0602 N94-13720

Analysis of microstrip patch antennas with nonzero surface resistance
[NASA-TP-3362] 02 p0604 N94-13916

Analysis of electromagnetic scattering from irregularly shaped, thin, metallic flat plates
[NASA-TP-3361] 03 p0998 N94-16655

Measurements of the radar cross section and Inverse Synthetic Aperture Radar (ISAR) images of a Piper Navajo at 9.5 GHz and 49 GHz
[AD-A267570] 03 p1002 N94-17110

Statistical description of the bistatic radar cross section distributions for a right circular cylinder
[AD-A270001] 04 p1387 N94-18666

RCS Analysis of Plate Geometries, parts 1 and 2
[NASA-CR-194173] 05 p1717 N94-20269

High-frequency techniques for RCS prediction of plate geometries 05 p1717 N94-20270

A physical optics/equivalent currents model for the RCS of trihedral corner reflectors 05 p1717 N94-20271

Massively parallel computation of RCS with finite elements 05 p1726 N94-20437

RCS of ships and aircraft at HF frequencies
05 p1745 N94-22128

High-frequency techniques for RCS prediction of plate geometries and a physical optics/equivalent currents model for the RCS of trihedral corner reflectors, parts 1 and 2
[NASA-CR-195140] 06 p2298 N94-24616

Extension of On-Surface Radiation Condition (OSRC) theory to full-vector electromagnetic wave scattering by three-dimensional conducting, dielectric, and coated targets
[AD-A274023] 07 p2766 N94-25757

A study of two dimensional tapered periodic edge treatments to reduce wideband edge diffraction
[AD-A274054] 07 p2766 N94-25824

Radar cross section visualization using sample buffer progressive refinement volume rendering
[AD-A274179] 07 p2773 N94-27127

Printed circuit elements with applications to antennas, scattering, and circuits
[AD-A275512] 08 p3262 N94-28669

RL/ERCT automated swept-angle bistatic measurement system
[AD-A275763] 08 p3241 N94-28763

Comparison of RCS prediction techniques, computations and measurements
[PB94-125515] 08 p3256 N94-30392

The influence of the evaporation duct on the angle of arrival and amplitude of the backscattered signal from targets low above the sea 08 p3256 N94-30498

Polarimetric backscatter measurements of natural surfaces at millimeter wavelengths
08 p3259 N94-30509

Radar cross sections of ground clutter at 95 GHz for summer and fall conditions 08 p3259 N94-30512

Development of a frequency-domain electromagnetic scattering measurement system
[AD-A276738] 09 p3678 N94-32179

MOM3D method of moments code theory manual
[NASA-CR-189594] 09 p3682 N94-32897

Bistatic clutter RCS simulation using scale model surfaces with two scale roughness
[AD-A277604] 10 p4035 N94-33847

Numerical computation and measurement of radar cross section for impulse radar
[PB94-149200] 10 p4036 N94-34096

RADAR DATA
Groundwave HF ocean surface radar
01 p0139 N94-11906

Volcanism in southern Guinevere Planitia, Venus: Regional volcanic history and morphology of volcanic domes 01 p0467 N94-12190

Synthesis of global thematic mapping, Venus: Geologic correlations/questions for the Magellan gravity mission
01 p0467 N94-12194

SATORI: Situation Assessment Through the Re-creation of Incidents
[DOT/FAA/AM-93/12] 01 p0038 N94-12567

Fundamental studies of radar scattering from water surfaces: The Lake Washington experiment
[NASA-CR-194030] 01 p0139 N94-12778

Sensitivity testing of a single-Doppler temperature retrieval and forecast system
[AD-A267278] 03 p1105 N94-14958

Proceedings of the Third Spaceborne Imaging Radar Symposium
[NASA-CR-194104] 03 p0989 N94-15886

Recent advances in radar remote sensing of forest
03 p0991 N94-15897

Imaging radar studies of polar ice
03 p0991 N94-15899

Application of Cloude's target decomposition theorem to polarimetric imaging radar data
03 p0991 N94-15901

Recent advances and plans in processing and geocoding of SAR data at the DFD
03 p0992 N94-15909
Data distribution 03 p0993 N94-15910
International collaboration in SAR ground data systems 03 p0993 N94-15917
Morphology and models for the evolution of eastern Hecate Chasma, Venus 03 p1256 N94-16215
Separation of topographic and intrinsic backscatter variations in biscopic radar images: A magic airbrush
03 p1086 N94-16318
SAR backscatter from coniferous forest gaps
03 p1076 N94-16736
Characterization of wetland, forest, and agricultural ecosystems in Belize with airborne radar (AIRSAR)
03 p1076 N94-16738
Supervised fully polarimetric classification of the Black Forest test site: From MAESTROI to MAC Europe
03 p1076 N94-16740
Extraction of quantitative surface characteristics from AIRSAR data for Death Valley, California
03 p1078 N94-16748
Opposing mesoscale flows in a broken midlatitude squall line
[AD-A268011] 03 p1109 N94-17492
Environmental characterization for target acquisition. Report 3: New concepts for evaluating low-grazing angle radar measurements
[AD-A269956] 04 p1388 N94-18777
Polarimetric statistics of electromagnetic waves scattered by distributed targets
[PB93-195907] 04 p1389 N94-18951
Moments of ambient Doppler spectra
[DE93-017948] 04 p1390 N94-19114
Modifications to the three-component classification algorithm for SAR data 05 p1719 N94-20410
Determination of noise equivalent sigma(0) using highly correlated repeat-pass SAR images
05 p1720 N94-20411
On evaluating the accuracy of SAR sea-ice classification using multifrequency polarimetric AIRSAR data
05 p1724 N94-20428
Application of Cloude's target decomposition theorem to polarimetric imaging radar data
05 p1724 N94-20429
Direction angle sensitivity of agricultural field backscatter with AIRSAR data 05 p1724 N94-20430
Mapping of taiga forest units using AIRSAR data and/or optical data, and retrieval of forest parameters
05 p1729 N94-20452
NAVSPASUR sensor system digital signal processing receiver. Volume 1: Hardware and software overview
[AD-A272899] 05 p1738 N94-21198
NAVSPASUR sensor system digital signal processing receiver. Volume 2: Function and capabilities of hardware and software components
[AD-A272900] 05 p1739 N94-21218
Interpretation of Ground Penetrating Radar data at the Hanford Site, Richland, Washington
[DE93-040409] 05 p1743 N94-22557
Further studies to extend and test the area-time-integral technique applied to satellite data
[NASA-CR-195132] 06 p2415 N94-24705
Radar detection of low-altitude targets in a maritime environment. Volume 2: Meteorological and radar data
[AD-A274658] 07 p2768 N94-26335
Leadex environmental phenomena and effects observed by DMSP, NOAA, and ERS-1 satellites
[AD-A274596] 07 p2868 N94-26888
Radar measurements 09 p3685 N94-31002
Patterns of deformation and volcanic flows associated with lithospheric loading by large volcanoes on Venus
09 p3776 N94-31106
A numerical study of thunderstorm electrification
[AD-A277531] 10 p4089 N94-33709
Alaska SAR Facility mass storage, current system
10 p4156 N94-33823
Radar detection of low-altitude targets in a maritime environment. Volume 1: Final analysis
[AD-A278493] 10 p4037 N94-34376
NAVSPACECOM space surveillance sensor system digital signal processing receiver. Volume 3: Operating system functions
[AD-A278839] 11 p4212 N94-35799
NAVSPACECOM space surveillance sensor system digital signal processing receiver. Volume 4: Hardware interfaces
[AD-A278845] 11 p4212 N94-35801

RADAR DETECTION
Improved Many-On-Many ROUTE software description
[DE93-013961] 01 p0334 N94-12608
Digital quadrature demodulation for radar ESM applications
[DREO-TN-92-10] 02 p0603 N94-13838
Survey of subsurface geophysical exploration technologies adaptable to an airborne platform
[DE93-015080] 02 p0717 N94-14294
Adaptive interference canceller
[CA-PATENT-1-310-709] 03 p0988 N94-15698
Windshear detection radar signal processing studies
[NASA-CR-194615] 03 p0994 N94-16022
Enhanced down-range profiles of complex targets using wideband radar echo returns
[AD-A266508] 03 p0999 N94-16788
Target detection by way of Kalman filtering
[AD-A267314] 03 p1000 N94-16945
Signal detection in correlated Gaussian and non-Gaussian radar clutter
[AD-A267453] 03 p1001 N94-17033
Intelligent use of CFAR algorithms
[AD-A267755] 03 p1003 N94-17206
Remote sensing of precipitation and electrification with a dual-polarization, coherent, wideband radar system
[AD-A267479] 03 p1004 N94-17364
Tomographic mathematical ideas applied to radar detection
[AD-A268789] 04 p1384 N94-18186
Space debris detection
[AD-A269254] 04 p1334 N94-18264
Low-noise oscillators for airborne radar applications, revision 1
[AD-A269372] 04 p1403 N94-18471
A comparison between several computer codes for calculations on microwave propagation
[FEL-92-A435] 04 p1390 N94-19449
Earth Penetration Radar Imaging System (EPRIS)
[DE93-019890] 04 p1391 N94-19542
Target motion detecting impulse Doppler radar system
[AD-D015898] 05 p1717 N94-20198
Analysis of Ku-band cross section at low incidence angles 05 p1720 N94-20414
Probability of detection calculations using MATLAB
[AD-A271958] 05 p1736 N94-20578
Mars subsurface sounding with a ground penetrating radar 06 p2608 N94-23393
ASR-9 microburst detection algorithm
[AD-A273591] 06 p2415 N94-24850
Radar E-O image fusion 06 p2306 N94-25503
Machine intelligent gust front algorithm
[AD-A273695] 07 p2680 N94-26196
Radar detection of low-altitude targets in a maritime environment. Volume 2: Meteorological and radar data
[AD-A274658] 07 p2768 N94-26335
Processing of wide-angle synthetic aperture radar signals for target detection
[AD-A274225] 07 p2773 N94-27073
Radar returns from a low-flying target over a rough sea surface under multipath and clutter conditions
08 p3253 N94-29882
An electromagnetic noncontacting sensor for thickness measurement in a dispersive medium
[AIAA PAPER 94-1200-CP] 08 p3443 N94-30551
Peak detection of Swerling type targets. Part 1: Detection probabilities in white noise
[AD-A276217] 09 p3670 N94-31062
Proceedings of the 4th Tunnel Detection Symposium on Subsurface Exploration Technology
[AD-A276372] 09 p3771 N94-31369
Waveform generation for ultra-wideband radar system
[AD-A276352] 09 p3673 N94-31401
The development and testing of a backscatter absorption gas imaging (BAGI) system designed to image at a range of 300 m
[DE94-006192] 09 p3675 N94-31761
Some problems of applied algebra
[CWI-AM-R9306] 09 p3847 N94-32204
Radar detection of low-altitude targets in a maritime environment. Volume 1: Final analysis
[AD-A278493] 10 p4037 N94-34376
Terminal Doppler Weather Radar (TDWR) Low Level Wind Shear Alert System 3 (LLWAS 3) integration studies at Orlando International Airport
[AD-A278957] 11 p4294 N94-35807

RADAR DIRECTION FINDERS
U RADIO DIRECTION FINDERS

RADAR DISPLAYS
U RADARSCOPES

RADAR ECHOES
NT CLUTTER
NT LUNAR RADAR ECHOES
NT VENUS RADAR ECHOES
Statistical study of HF ocean radar echo
01 p0139 N94-11905
Measurements of ocean cross-section with a side-looking airborne radar 01 p0201 N94-11954
Development of shipboard ocean lidar
01 p0140 N94-11965
Fundamental studies of radar scattering from water surfaces: The Lake Washington experiment
[NASA-CR-194030] 01 p0139 N94-12778
Enhanced down-range profiles of complex targets using wideband radar echo returns
[AD-A266508] 03 p0999 N94-16788
Magellan vertical polarization radar observations
05 p1744 N94-20691
On the analysis of clear air radar echoes severely contaminated by clutter 06 p2306 N94-24423
Analyzing adaptive beamformer performance in a stable multipath environment
[AD-A274029] 07 p2766 N94-25766
Investigation of a normal incidence high-performance p-type strained layer In(0.3)Ga(0.7)As / In(0.52)Al(0.48) as quantum well infrared photodetector
[AD-A274854] 07 p3055 N94-26188
Long term variations of radio auroral activity
08 p3359 N94-29237
New-type echoes observed with the 50 MHz auroral Doppler radar at Showa Station
08 p3360 N94-29238
Radar scattering from the summer polar mesosphere: Theory and observations 09 p3772 N94-32077

RADAR EQUIPMENT
NT PLAN POSITION INDICATORS
NT RADAR ANTENNAS
NT RADAR BEACONS
NT RADAR CORNER REFLECTORS
NT RADAR FILTERS
NT RADAR RECEIVERS
NT RADAR REFLECTORS
NT RADAR TRANSMITTERS
NT RADARSCOPES
NT RETROREFLECTORS
The radar eye blinded: The USAF and electronic warfare, 1945-1955
[AD-A265494] 01 p0132 N94-10497
HF ocean radar system at Okinawa Radio Observatory 01 p0139 N94-11902
Resistivity and radar void detectors for tunneling machines 01 p0140 N94-12706
High resolution SAR applications and instrument design 03 p0993 N94-15913
Space debris detection
[AD-A269254] 04 p1334 N94-18264
Orbital debris radar instrumentation
08 p3248 N94-29626
Modular Simulator System (MSS). System/segment specification for the generic modular simulator system-radar module, volume 8
[AD-A276975] 09 p3589 N94-32314
Assembly flow simulation of a radar
09 p3823 N94-32431
Nonlinear frequency conversion optical filter
[AD-D016127] 10 p4036 N94-34283

RADAR FILTERS
Adaptive interference canceller
[CA-PATENT-1-310-709] 03 p0988 N94-15698

RADAR GEOLOGY
Geologic remote sensing with radar
03 p0991 N94-15900
Summaries of the Third Annual JPL Airborne Geoscience Workshop. Volume 3: AIRSAR Workshop
[NASA-CR-194542] 03 p1075 N94-16731
A snow wetness retrieval algorithm for SAR
03 p1075 N94-16732
Interpretation of Ground Penetrating Radar data at the Hanford Site, Richland, Washington
[DE93-040409] 05 p1743 N94-22557

RADAR HOMING MISSILES
Enhanced down-range profiles of complex targets using wideband radar echo returns
[AD-A266508] 03 p0999 N94-16788

RADAR IMAGERY
Validation of directional wave spectra from the ERS-1 during the ESA CAL/VAL campaign
01 p0232 N94-11707
Wind and surface features in SAR images: The Canadian program 01 p0234 N94-11718
Coastal ocean studies with ERS-1 SAR during NORCSEX 1991 01 p0234 N94-11720
SAR imaging of dynamical features in the English Channel 01 p0234 N94-11721
SAR ocean imaging in the Gulf of Alaska
01 p0235 N94-11723
Preliminary results of the experiment I-7
01 p0235 N94-11728
Calibration of the ERS-1 SAR fast-delivery images
01 p0236 N94-11730
The use of active devices in the ERS-1 radiometric calibration 01 p0236 N94-11732
Techniques and applications of SAR interferometry for ERS-1: Topographic mapping, change detection, and slope measurement 01 p0236 N94-11734
SAR interferometry experiments with ERS-1
01 p0237 N94-11735
SAR-interferometry applying ERS-1: Some preliminary test results 01 p0237 N94-11736

Monitoring of the Greenland Ice Sheet using ERS-1 synthetic aperture radar imagery
01 p0237 N94-11741
Use of ERS-1 SAR to measure ice flux in the East Greenland current 01 p0238 N94-11746
Validation of ERS-1 SAR measurements of sea ice during ARCTIC-1991 01 p0238 N94-11747
Ocean circulation revealed by ice floe tracking
01 p0240 N94-11759
Evaluating ERS-1 ice motion and classification products 01 p0241 N94-11763
A stochastic-deterministic approach as an alternative to classical cross-over techniques in small ocean basins
01 p0242 N94-11767
An analysis of the gravity field in the Norwegian Sea and mapping of the ice cap of Greenland using ERS-1 altimeter measurements 01 p0242 N94-11768
Proceedings of the PORSEC 1992 in Okinawa: Conference for Pacific Ocean Environments and Probing, volume 1
[JTN-93-80418] 01 p0191 N94-11894
Ocean-ice interaction study of waves and mesoscale features 01 p0197 N94-11935
The microwave backscattering from wind waves
01 p0201 N94-11959
Venus small volcano classification and description
01 p0438 N94-12037
A pattern recognition system for locating small volvanoes in Magellan SAR images of Venus
01 p0455 N94-12126
Using lunar sounder imagery to distinguish surface from subsurface reflectors in lunar highlands areas
01 p0464 N94-12179
Volcanism in southern Guinevere Planitia, Venus: Regional volcanic history and morphology of volcanic domes 01 p0467 N94-12190
The Magellan volcanic and magmatic feature catalog
01 p0467 N94-12193
Characteristics of arachnoids from Magellan data
01 p0469 N94-12204
ISAR motion compensation using the burst derivative measure as a focal quality indicator
[AD-A265647] 01 p0138 N94-12440
Methodological considerations for use of ERS-1 imagery for the delineation of river networks in tropical forest areas 01 p0247 N94-12484
Per-field filtering and classification of multitemporal ERS-1 SAR imagery 01 p0247 N94-12485
Extraction of plant and soil parameters from multitemporal ERS-1 SLC data of the Freiburg test site
01 p0248 N94-12491
The TREES project: Pre-processing and generation of terrain data for inclusion in an ERS-1 SAR classification scheme 01 p0249 N94-12496
TREES project: A suite of tools for information extraction from ERS-1 SAR data 01 p0250 N94-12498
ERS-1 and Almaz SAR ocean wave imaging over the Gulf Stream and the Grand Banks
01 p0251 N94-12505
Real time processing wave spectra from satellite SAR
01 p0251 N94-12506
A statistical analysis of sea state surface ERS-1 SAR-wave mode imagettes 01 p0251 N94-12507
A new model for Synthetic Aperture Radar (SAR) images from ocean scatter 01 p0251 N94-12508
On the extraction of ocean wave spectra from ERS-1 SAR wave mode image spectra
01 p0251 N94-12509
Tide-generated nonlinear internal wave packets in the Strait of Gibraltar observed by the synthetic aperture radar aboard the ERS-1 satellite 01 p0252 N94-12510
Cloud studies using ATSR data
01 p0253 N94-12517
Artificial oil pollution detection and wave observation in the sea adjacent to Japan by ERS-1 SAR
01 p0253 N94-12520
Ship traffic monitoring using the ERS-1 SAR
01 p0253 N94-12521
Pilot project PPF12. Coastal and fluvial environment in French Guiana: First results of ERS-1 SAR data analysis
01 p0254 N94-12523
Coastal morphodynamics and energetic characteristics of swell studied with ERS-1 SAR
01 p0254 N94-12524
Mapping of sea bottom topography with ERS-1 C-band SAR 01 p0254 N94-12525
ERS-1 imaging radar over the Waddensea-North Netherlands 01 p0254 N94-12526
SAR imaging of geology and bathymetry: Kent coastal area - southern North Sea 01 p0254 N94-12527
Comparison of ERS-1 SAR images of the Western Mediterranean to in situ oceanographic data: PRIM-1 Cruise (May 1992) 01 p0255 N94-12529
Ice studies in the Barents Sea by ERS-1 during SIZEX 1992 01 p0210 N94-12653
A basic consideration for remote sensing using microwave radars on a satellite
01 p0212 N94-12665
Remote sensing of light scattering coefficient of sea water vertical distribution by the means of airborne lidar
01 p0224 N94-12736
Spatial variability of the ocean underwater dynamic noise from satellite radar sensing data
01 p0225 N94-12740
Wind-wave and foam dynamics from optical and radar airborne observations 01 p0226 N94-12745
Observations of surface signatures in the north-west Pacific Ocean with the spaceborne SAR
01 p0226 N94-12746
Radar observation of internal waves field in the north-west Pacific 01 p0226 N94-12747
Preparations for and first results of the calibration and interpretation of ERS-1 SAR imagery over land
[BCRS-92-13] 02 p0684 N94-13123
EOS workstation
[NASA-CR-191326] 02 p0736 N94-13132
Radar imaging of sub-mesoscale ocean phenomena
[AD-A266339] 02 p0725 N94-13581
Feature discovery on segmented objects in SAR imagery using self-organizing neural networks
[DE93-010685] 02 p0686 N94-14056
An exact processing algorithm for wide beam spaceborne SAR data 02 p0689 N94-14213
Proceedings of the Third Spaceborne Imaging Radar Symposium
[NASA-CR-194104] 03 p0989 N94-15886
Almaz 03 p0898 N94-15889
Recent advances in radar remote sensing of forest
03 p0991 N94-15897
Imaging radar studies of polar ice
03 p0991 N94-15899
Geologic remote sensing with radar
03 p0991 N94-15900
Multifrequency observations 03 p0992 N94-15902
Spaceborne radar for geoscientific applications in North China 03 p0993 N94-15915
Primary studies of Chinese spaceborne SAR
03 p0993 N94-15916
Rover mounted ground penetrating radar as a tool for investigating the near-surface of Mars and beyong
03 p1007 N94-16197
Radar properties of several fluidized ejecta blankets on Venus 03 p1267 N94-16278
Separation of topographic and intrinsic backscatter variations in biscopic radar images: A magic airbrush
03 p1086 N94-16318
The cartography of Venus with Magellan data
03 p1274 N94-16320
Resolving topographic detail on Venus by modeling complex Magellan altimetry echoes
03 p1283 N94-16368
Relief of some small landforms on Venus
03 p1293 N94-16418
Comparison of JPL-AIRSAR and DLR E-SAR images from the MAC Europe 1991 campaign over testsite Oberpfaffenhofen: Frequency and polarization dependent backscatter variations from agricultural fields
03 p1075 N94-16733
Monitoring environmental state of Alaskan forests with AIRSAR 03 p1075 N94-16734
Comparison of modeled backscatter with SAR data at P-band 03 p1076 N94-16735
Characterization of wetland, forest, and agricultural ecosystems in Belize with airborne radar (AIRSAR)
03 p1076 N94-16738
SAR observations in the Gulf of Mexico
03 p1077 N94-16742
Investigation of AIRSAR signatures of the Gulf Stream
03 p1077 N94-16743
Mapping of sea bottom topography
03 p1077 N94-16744
Sea bottom topography imaging with SAR
03 p1077 N94-16745
Preliminary results of polarization signatures for glacial moraines in the Mono Basin, Eastern Sierra Nevada
03 p1078 N94-16746
Fitting a three-component scattering model to polarimetric SAR data 03 p1079 N94-16751
External calibration of polarimetric radar images using distributed targets 03 p1079 N94-16753
Processing of polarimetric SAR data for soil moisture estimation over Mahantango watershed area
03 p1079 N94-16754
Evaluation of polarimetric SAR parameters for soil moisture retrieval 03 p1079 N94-16755
Interaction types and their like-polarization phase-angle difference signatures 03 p1079 N94-16756
Radar Analysis and Visualization Environment (RAVEN): Software for polarimetric radar analysis
03 p1080 N94-16758
Measuring ocean coherence time with dual-baseline interferometry 03 p1080 N94-16759
Comparison of edges detected at different polarisations in MAESTRO data 03 p1080 N94-16761
Moving target indicator using higher order statistics
[AD-D015890] 03 p1000 N94-16917
High resolution radar profiling using higher-order statistics
[AD-D015891] 03 p1000 N94-16918
Measurements of the radar cross section and Inverse Synthetic Aperture Radar (ISAR) images of a Piper Navajo at 9.5 GHz and 49 GHz
[AD-A267570] 03 p1002 N94-17110
Developing automated analysis methods for sea ice imagery: A status report with recommendations
[AD-A267284] 03 p1113 N94-17241
Arctic cyclones and Marginal Ice Zone (MIZ) variability
[AD-A268610] 03 p1108 N94-17465
Guide to Magellan image interpretation
[NASA-CR-194340] 03 p1298 N94-17654
The accuracy of monostatic and bistatic radar imaging by range-Doppler-processing with and without motion compensation
[DLR-FB-93-07] 04 p1384 N94-18071
Tomographic mathematical ideas applied to radar detection
[AD-A268789] 04 p1384 N94-18186
The spatial variance of ionospherically-induced phase errors in SAR imagery
[DE93-015643] 04 p1385 N94-18232
Laser imaging radar system
[AD-A270436] 04 p1387 N94-18510
Application of Fourier-based features for classification of synthetic aperture radar imagery
[AD-A270450] 04 p1387 N94-18513
Resolution in radar mapping
[AD-A269730] 04 p1462 N94-18753
Solution of the Poisson equation with application to radar imaging
[PB93-195865] 04 p1389 N94-18950
Modeling of current features in Gulf Stream SAR imagery
[AD-A270734] 04 p1499 N94-19609
Remote sensing of Earth terrain
[NASA-CR-194598] 04 p1464 N94-19681
SeaTrack: Ground station orbit prediction and planning software for sea-viewing satellites
[NASA-RP-1331] 04 p1532 N94-19761
Determination of noise equivalent sigma(0) using highly correlated repeat-pass SAR images
05 p1720 N94-20411
Topographic mapping using a monopulse SAR system
05 p1721 N94-20417
Observation of pressure ridges in SAR images of sea ice: Scattering theory and comparison with observations
05 p1723 N94-20427
On evaluating the accuracy of SAR sea-ice classification using multifrequency polarimetric AIRSAR data
05 p1724 N94-20428
Use of microwave polarimetry to enhance SAR images of the ocean surface
[AD-A271911] 05 p1882 N94-20489
Beta Regio rift system on Venus: Geologic interpretation of Magellan images 05 p2095 N94-20655
Beta Regio - Phoebe Regio on Venus: Geologic mapping with the Magellan data 05 p2096 N94-20656
Magellan at Venus: Summary of science findings
05 p2110 N94-20734
Magellan Mission 05 p1652 N94-20829
Neural network studies
[AD-A271593] 05 p1943 N94-20947
Evaluation of C-band SAR data from SAREX 1992: Tapajos study site 05 p1839 N94-20964
An overview of synthetic aperture radar signal processing techniques 05 p1745 N94-22159
Target angular motion and its effects on simulated SSAR ship images 05 p1745 N94-22161
Radar imaging of moving targets
05 p1747 N94-22238
STAR-1 SAR road extraction using texture analysis and mathematical morphology
[ISBN-0-315-83255-X] 05 p1843 N94-22429
Mission planning for Shuttle Imaging Radar-C (SIR-C) with a real-time interactive planning software
06 p2305 N94-23842
Free-surface/vorticity interaction
[AD-A273263] 06 p2335 N94-24686
Use of microwave polarimetry to enhance SAR images of the ocean surface
[AD-A273568] 06 p2419 N94-24944
Edge detection using a complex wavelet
[AD-A273699] 06 p2493 N94-25452
Synthetic vision system flight test results and lessons learned 06 p2429 N94-25492
The Radar Image Generation (RIG) model
06 p2306 N94-25497

Radar E-O image fusion 06 p2306 N94-25503
Response of an airborne synthetic aperture radar to sea ice in the marginal ice zone
[ISBN-0-315-84243-1] 07 p2849 N94-26668
Encoding approaches for data link transmission of weather graphics
[AD-A274497] 07 p2772 N94-26963
Processing of wide-angle synthetic aperture radar signals for target detection
[AD-A274225] 07 p2773 N94-27073
Method of correcting rotational motion error in SAR and ISAR imagery
[AD-D016033] 07 p2773 N94-27146
Image quality analysis of compressed synthetic aperture radar imagery
[AD-A273399] 07 p2774 N94-27170
Non-adaptive robust filters for speckle noise reduction
[INPE-5519-PRE/1794] 07 p2776 N94-27335
Perceptual compression of magnitude-detected synthetic aperture radar imagery 07 p2946 N94-28260
Some implications of large impact craters and basins on Venus for terrestrial ringed craters and planetary evolution 07 p2890 N94-28306
Fusion of range and luminance data from laser radar systems
[AD-A275608] 08 p3292 N94-28770
SAR-related stress variability in the Marine Atmospheric Boundary Layer (MABL)
[AD-A275275] 08 p3377 N94-29436
Automatic focus and registration of synthetic aperture radar images 08 p3246 N94-29536
Pointing mechanisms for the Shuttle Radar Laboratory 08 p3162 N94-29638
Application of remote sensing techniques for the seismo-tectonic study of Nahanni earthquake area
[ISBN-0-315-85942-3] 08 p3334 N94-30037
Frequency dependence of polarization phase difference
[NASA-TM-109737] 08 p3254 N94-30094
Phase unwrapping problems in ISAR images
[TELECOM-93-D-008] 09 p3670 N94-31097
Patterns of deformation and volcanic flows associated with lithospheric loading by large volcanoes on Venus 09 p3776 N94-31106
Radar image classification by texture measurements
[ONERA-NT-1993-3] 09 p3673 N94-31419
Real time character recognition for F-111C video tape records
[AD-A277061] 09 p3580 N94-32263
Validation support of the ERIM ocean model
[AD-A277364] 09 p3788 N94-32284
Restoration of interferometric, polarimetric, radiometric, and textural information in SAR images 09 p3750 N94-32535
Fusion of multispectral (XS) and Panchromatic (P) SPOT images and radar images 09 p3750 N94-32541
Almaz marine applications 09 p3751 N94-32544
Structural study in an alteritic region: Contribution of ERS-1 SAR data of the Mauges Plateau (Loire Atlantique, France)
[BRGM-93032] 09 p3752 N94-32551
Synergy of thermal infrared and microwave remote sensing for evaporation estimation 09 p3754 N94-32559
European MARS project: The potential integration of SPOT and air- and satellite-borne radar data over two pilot areas for agricultural statistics. PROSPER programme and ERS-1 pilot project
[BRGM-93035] 09 p3754 N94-32561
Land cover change detection with ERS-1 data and data from other remote sensing satellites. Example: The delta of the River Ebro (Spain) 09 p3755 N94-32564
The processing technology and some applications of Almaz-1 data 09 p3756 N94-32573
Synthetic vision technology demonstration. Volume 1: Executive summary
[AD-280564] 09 p3582 N94-33076
Synthetic vision technology demonstration. Volume 2: Sensor tower testing
[DOT/FAA/RD-93/40-VOL-2] 09 p3582 N94-33077
Synthetic vision technology demonstration. Volume 3: Flight tests
[AD-A281051] 09 p3582 N94-33078
Synthetic vision technology demonstration. Volume 4: Appendices
[AD-A281052] 09 p3583 N94-33079
A foundation for fusion
[AD-A277521] 10 p4074 N94-33372
Alaska SAR Facility mass storage, current system 10 p4156 N94-33823
Quantifying shapes of volcanoes on Venus 11 p4361 N94-35429
Magellan collection of radar calibration results
[NASA-CR-194753] 11 p4367 N94-35509
The polygon-ellipse method of data compression of weather maps
[AD-A278958] 11 p4293 N94-35719

RADAR MAPS
Mapping of the East Australian current with the ERS-1 SAR and shipborne studies 01 p0234 N94-11717
Radarmap of Germany: First mosaic and classification 01 p0246 N94-12477
Combined analysis of ERS-1 SAR and visible/infrared remote sensing data for land cover/land use mapping in a tropical zone: A case study in Guinea 01 p0246 N94-12478
Example of SPOT/ERS-1 complementarity 01 p0247 N94-12479
The use of ERS-1 SAR data to study surface states 01 p0247 N94-12480
Application of ERS-1 SAR data to snow mapping 01 p0247 N94-12483
The TOPSAR interferometric radar topographic mapping instrument 03 p1078 N94-16749
Resolution in radar mapping
[AD-A269730] 04 p1462 N94-18753
Performance evaluation of the JPL TOPSAR system: An across-track interferometric SAR system for topographic mapping 05 p1732 N94-20461
Beta Regio - Phoebe Regio on Venus: Geologic mapping with the Magellan data 05 p2096 N94-20656
The polygon-ellipse method of data compression of weather maps
[AD-A278958] 11 p4293 N94-35719

RADAR MEASUREMENT
Using transponders with the ERS-1 altimeter to measure orbit altitude to +/- 3 cm 01 p0244 N94-11785
Measurement of wave parameters by HF ocean radar 01 p0192 N94-11903
Kuroshio observations by the HF ocean radar 01 p0192 N94-11904
Experiment and results of the Italian activity in the field of ocean microwave backscattering 01 p0200 N94-11953
Air-sea interaction: Fluxes, a review 01 p0201 N94-11955
Polar mesospheric waves and structure
[AD-A265360] 01 p0279 N94-12561
Remote sensing of light scattering coefficient of sea water vertical distribution by the means of airborne lidar 01 p0224 N94-12736
Remote identification of rain and hail with a polarization diversity radar
[ISBN-0-315-55623-4] 02 p0720 N94-13516
TRMM radar 03 p0990 N94-15894
Application of Cloude's target decomposition theorem to polarimetric imaging radar data 03 p0991 N94-15901
Calibration: Practical experience with ERS-1 03 p0992 N94-15907
Spatial and frequency diversity in lidar systems
[AD-A266192] 03 p1039 N94-16124
A snow wetness retrieval algorithm for SAR 03 p1075 N94-16732
Fitting a three-component scattering model to polarimetric SAR data 03 p1079 N94-16751
Flight demonstration of image fix-taking with SAR
[DE93-016499] 04 p1382 N94-17861
Environmental characterization for target acquisition. Report 3: New concepts for evaluating low-grazing angle radar measurements
[AD-A269956] 04 p1388 N94-18777
The Mexico City 1991 lidar measurements campaign
[DE93-019960] 04 p1478 N94-19272
Investigations of a coherent vector radar technique for the observation of the atmosphere near 10 GHz
[KFK-5068] 04 p1494 N94-19616
Radar backscatter measurements from simulated sea ice during CRRELEX 1990
[AD-A271034] 05 p1715 N94-19823
Multiple scattering effects on the Linear Depolarization Ratio (LDR) measured during CaPE by a Ka-band air-borne radar 05 p1728 N94-20446
Application of the target decomposition theorem to a polarimetric random media model 05 p1730 N94-20453
Magellan at Venus: Summary of science findings 05 p2110 N94-20734
Geology and radiophysical properties of the Venera and Vega landing sites 05 p2135 N94-20867
Obtaining surface optical properties from space-based lidar systems
[AD-A272831] 05 p1987 N94-21172
Lidar and radar derived cirrus microphysical properties for the 26 November 1991 case study 05 p1873 N94-22305
Dynamical characteristics of cirrus clouds from aircraft and radar measurements 05 p1878 N94-22332
Mars subsurface sounding with a ground penetrating radar 06 p2608 N94-23393
HERACLITUS, phase 1. Harbour Entrance of Rotterdam Radar based Current Related Information for Traffic Guidance of Ships: Feasibility of deriving current profile data from sea surface observations in the Rotterdam (Netherlands) port entrance
[BCRS-93-04] 06 p2417 N94-24107
Mesospheric and lower thermospheric winds, temperatures densities, and volume emission rates
[NASA-CR-195147] 06 p2403 N94-24486
Cloud liquid water content measurement tests using dual-wavelength radar
[PB94-125960] 07 p2896 N94-26959
RL/ERCT automated swept-angle bistatic measurement system
[AD-A275763] 08 p3241 N94-28763
New-type echoes observed with the 50 MHz auroral Doppler radar at Showa Station 08 p3360 N94-29238
Radar estimations of atmospheric winds in the troposphere and lower stratosphere 08 p3370 N94-29697
Antarctic Record, vol. 36, no. 3
[REPT-108] 08 p3363 N94-29978
Radar measurements 09 p3685 N94-31002
Microwave dielectric behavior of soils. Report 1: Summary of related research and applications
[AD-A275980] 09 p3771 N94-31351
Satellite radar altimetry over the continental ice sheets 09 p3742 N94-31570
Radar rainfall measurements from space 09 p3782 N94-31889
High-resolution synthetic aperture radar observations of the Moon 09 p3676 N94-31952
A reassessment of the in-situ dielectric constant of polar firn
[AD-A276999] 09 p3773 N94-32154
Gyrotrons and free electron lasers for atmospheric sensing
[AD-A277281] 09 p3718 N94-32406
The use of ERS images for mapping 09 p3749 N94-32531
Radio wave refractivity deduced from lidar measurements
[AD-D016147] 10 p4034 N94-33780
Numerical computation and measurement of radar cross section for impulse radar
[PB94-149200] 10 p4036 N94-34096
Use of wind profiler data in short-range forcasting
[AD-A279482] 11 p4295 N94-36228
Groundwater penetrating radar and high resolution seismic for locating shallow faults in unconsolidated sediments
[DE94-007284] 11 p4257 N94-36366

RADAR NAVIGATION
Ground independent landing system 08 p3137 N94-29564
ARC2000: Automatic radar control 08 p3141 N94-29583

RADAR NETWORKS
A feasibility study on bird classification with neural network
[AD-A273753] 07 p2659 N94-25780
A novel near-range radar network for airport surface control 08 p3142 N94-29586
A simulator for multi-radar analysis for realistic traffic
[AD-B179099] 08 p3142 N94-30439

RADAR OBSERVATION
U RADAR TRACKING

RADAR RANGE
Improved Many-On-Many ROUTE software description
[DE93-013961] 01 p0334 N94-12608
Development of a lidar for integration with the Naval Postgraduate School Infrared Search and Target Designation (NPS-IRSTD) system
[AD-A271847] 05 p1817 N94-20611
New binary integration strategies and corresponding R90 calculations
[AD-A274786] 07 p2769 N94-26359
Retarded distances and the Doppler effect
[DE94-606296] 08 p3523 N94-28618
Orbital debris radar instrumentation 08 p3248 N94-29626
Method for ambiguity resolution in range-Doppler measurements
[NASA-CASE-GSC-13542-1] 08 p3252 N94-29739
The real-time display of interferometry data for Goldstone radar astronomy data acquisition 11 p4255 N94-35560

RADAR RECEIVERS
FR/GE/US radar receiver pulse compression ratio
[AD-A265391] 01 p0138 N94-12409
Radome depolarization effects on monopulse receiver tracking performance
[AD-A267446] 03 p1001 N94-17031

Signal detection in correlated Gaussian and non-Gaussian radar clutter
[AD-A267453] 03 p1001 N94-17033
Synchronization in multistatic radar
[PB94-136975] 08 p3242 N94-28885
Ground independent landing system
08 p3137 N94-29564
An evaluation of three GPS receivers for use in the GPS sounder
[AD-A278157] 09 p3577 N94-33253
Generation of the ambiguity function for ultra wideband radar waveforms
[AD-A277913] 09 p3684 N94-33261
Investigation and simulation of nonlinear processors for spread spectrum receivers, volume 1
[AD-A278025] 10 p4037 N94-34288
Investigation and simulation of nonlinear processors for spread spectrum receivers. Volume 2: Users manual
[AD-A278026] 10 p4037 N94-34289
NAVSPACECOM space surveillance sensor system digital signal processing receiver. Volume 3: Operating system functions
[AD-A278839] 11 p4212 N94-35799
NAVSPACECOM space surveillance sensor system digital signal processing receiver. Volume 4: Hardware interfaces
[AD-A278845] 11 p4212 N94-35801
An analysis of operational suitability for test and evaluation of highly reliable systems
[AD-A278573] 11 p4192 N94-36184

RADAR REFLECTIONS
U RADAR ECHOES

RADAR REFLECTORS
NT RADAR CORNER REFLECTORS
Method and apparatus for forming an agile plasma mirror effective as a microwave reflector
[AD-D015788] 03 p0998 N94-16535
All-weather precision landing system for aircraft in remote areas
[AD-D015924] 05 p1643 N94-20197
On the estimation of the correlation dimension and its application to radar reflector discrimination
[NASA-CR-4564] 06 p2309 N94-23304

RADAR RESOLUTION
A SAR image-formation algorithm that compensates for the spatially-variant effects of antenna motion
[DE94-008456] 10 p4078 N94-34382

RADAR SCANNING
Multichannel dual angle approach for sea surface temperature retrieval in context of ERS-1 scenario
01 p0252 N94-12512
Validation of ATSR-1 using aircraft radiometer measurements over the South Atlantic
01 p0252 N94-12515
Cloud studies using ATSR data
01 p0253 N94-12517
A comparison of ATSR and shipboard radiometer SST measurements along transects between the UK and the Antarctic 01 p0253 N94-12518
Preliminary validation of ATSR sea surface temperatures near the Faeroes 01 p0253 N94-12519
The development of an in-motion radiography system for large area aircraft scanning
[DREP-TM-93-53] 07 p2670 N94-27666

RADAR SCATTERING
Theoretical studies of the radar properties of the icy Galilean moons of Jupiter
[NASA-CR-193407] 01 p0434 N94-11361
Development of shipboard ocean lidar
01 p0140 N94-11965
Remote sensing of subsurface water temperature profile and backscattering coefficient in the China Sea by Ocean Lidar (OLIDAR) 01 p0203 N94-11970
Polarisation of backscattering radiation at remote sensing of ocean with impulse laser beam
01 p0177 N94-12722
Fundamental studies of radar scattering from water surfaces: The Lake Washington experiment
[NASA-CR-194030] 01 p0139 N94-12778
Scattering by a groove in an impedance plane
[NASA-CR-193362] 02 p0602 N94-13720
Radar response of vegetation: An overview
03 p0991 N94-15898
Relating multifrequency radar backscattering to forest biomass: Modeling and AIRSAR measurement
03 p1077 N94-16741
Evaluation of polarimetric SAR parameters for soil moisture retrieval 03 p1079 N94-16755
What is the radar tracking Glint problem and can it be solved?
[AD-A266509] 03 p0999 N94-16789
The split-step algorithm for microwave propagation modeling above a conducting surface
[FEL-92-A430] 04 p1390 N94-19447
A comparison between several computer codes for calculations on microwave propagation
[FEL-92-A435] 04 p1390 N94-19449
Classification of simple vegetation types using POLSAR image data 05 p1722 N94-20420
Observation of pressure ridges in SAR images of sea ice: Scattering theory and comparison with observations
05 p1723 N94-20427
Application of Cloude's target decomposition theorem to polarimetric imaging radar data
05 p1724 N94-20429
Direction angle sensitivity of agricultural field backscatter with AIRSAR data 05 p1724 N94-20430
Studies of Greenland using the SEASAT scatterometer 05 p1725 N94-20433
Radar backscattering from snow facies of the Greenland ice sheet: Results from the AIRSAR 1991 campaign
05 p1725 N94-20434
C-band radar backscatter of sea ice in the Weddell Sea, Antarctica during the austral winter of 1992
05 p1725 N94-20435
Massively parallel computation of RCS with finite elements 05 p1726 N94-20437
Rough surface scattering from moving ocean surfaces as an indicator of scattering mechanisms
05 p1726 N94-20439
Application of the target decomposition theorem to a polarimetric random media model
05 p1730 N94-20453
Magellan vertical polarization radar observations
05 p1744 N94-20691
Low-power millimeter-wave radar observations of the atmosphere
[NASA-CR-194738] 05 p1858 N94-21811
RCS of ships and aircraft at HF frequencies
05 p1745 N94-22128
Printed circuit elements with applications to antennas, scattering, and circuits
[AD-A275512] 08 p3262 N94-28669
Radar returns from a low-flying target over a rough sea surface under multipath and clutter conditions
08 p3253 N94-29882
Radar scattering from the summer polar mesosphere: Theory and observations 09 p3772 N94-32077
Millstone Hill radar studies of plasma waves and turbulence
[AD-A278409] 09 p3684 N94-33172
Numerical computation and measurement of radar cross section for impulse radar
[PB94-149200] 10 p4036 N94-34096

RADAR SIGNATURES
The theory for, and demonstration of, information theory applied to radar target identification
[DE93-006393] 01 p0132 N94-10315
Signatures of Antarctic firn by means of ERS-1 AMI and by field measurements 01 p0237 N94-11737
Experiences from the Swedish sea ice programme during BEERS-1992 01 p0239 N94-11751
Air-sea-ice interactions in the Weddell Sea
01 p0239 N94-11753
Arctic sea ice microwave signature and geophysical processes study 01 p0240 N94-11754
C-band SAR backscatter from ice on shallow tundra lakes: Observations and modelling
01 p0240 N94-11755
Sea ice radar signatures from ERS-1 SAR during late Summer and Fall in the Beaufort and Chukchi Seas
01 p0240 N94-11756
I/Q demodulation of radar signals with calibration and filtering
[DREO-RN-1119] 02 p0606 N94-14064
Investigation of AIRSAR signatures of the Gulf Stream
03 p1077 N94-16743
Lithological and textural controls on radar and diurnal thermal signatures of weathered volcanic deposits, Lunar Crater region, Nevada 03 p1080 N94-16762
Environmental characterization for target acquisition. Report 3: New concepts for evaluating low-grazing angle radar measurements
[AD-A269956] 04 p1388 N94-18777
Polarimetric backscattering from sea ice
05 p1723 N94-20426
Use of the Weiss-Weinstein bound to compare the direction-finding performance of sparse arrays
[AD-A272582] 05 p1738 N94-21210
Progress in interpreting CO2 lidar signatures to obtain cirrus microphysical and optical properties
05 p1874 N94-22308
Radar signature related radome techniques for flush-mounted HF-, VHF- and, UHF communication antennas
[PB93-204618] 06 p2294 N94-23742
High latitude cusp signature observations for southward IMF B sub Z
[AD-A273801] 06 p2406 N94-25536
Radar jet engine health monitoring project
[ASSGI-301] 08 p3153 N94-30130
Precision and level of artefacts in the computation of digital terrain models by interferometry
09 p3756 N94-32571
Multiparameter radar and aircraft based studies of microphysical, kinematic, and electrical structure of convective clouds during CaPE
[AD-A278544] 10 p4085 N94-33677

RADAR TARGETS
The theory for, and demonstration of, information theory applied to radar target identification
[DE93-006393] 01 p0132 N94-10315
ISAR motion compensation using the burst derivative measure as a focal quality indicator
[AD-A265647] 01 p0138 N94-12440
Enhanced down-range profiles of complex targets using wideband radar echo returns
[AD-A266508] 03 p0999 N94-16788
Moving target indicator using higher order statistics
[AD-D015890] 03 p1000 N94-16917
High resolution radar profiling using higher-order statistics
[AD-D015891] 03 p1000 N94-16918
Target detection by way of Kalman filtering
[AD-A267314] 03 p1000 N94-16945
Radome depolarization effects on monopulse receiver tracking performance
[AD-A267446] 03 p1001 N94-17031
Measurements of the radar cross section and Inverse Synthetic Aperture Radar (ISAR) images of a Piper Navajo at 9.5 GHz and 49 GHz
[AD-A267570] 03 p1002 N94-17110
The accuracy of monostatic and bistatic radar imaging by range-Doppler-processing with and without motion compensation
[DLR-FB-93-07] 04 p1384 N94-18071
Millimeter wave reflectivity measurement system
[AD-A270008] 04 p1387 N94-18601
Target motion detecting impulse Doppler radar system
[AD-D015898] 05 p1717 N94-20198
Application of Cloude's target decomposition theorem to polarimetric imaging radar data
05 p1724 N94-20429
Calculation of a diffracted electric field with the aid of the Method of Equivalent Currents (MEC)
05 p1745 N94-22127
RCS of ships and aircraft at HF frequencies
05 p1745 N94-22128
Radar target discrimination by spectrum analysis
[AD-D015982] 06 p2301 N94-25040
Radar target discrimination systems using artificial neural network topology
[AD-D015984] 06 p2301 N94-25041
Radar detection of low-altitude targets in a maritime environment. Volume 2: Meteorological and radar data
[AD-A274658] 07 p2768 N94-26335
New binary integration strategies and corresponding R90 calculations
[AD-A274786] 07 p2769 N94-26359
Processing of wide-angle synthetic aperture radar signals for target detection
[AD-A274225] 07 p2773 N94-27073
RL/ERCT automated swept-angle bistatic measurement system
[AD-A275763] 08 p3241 N94-28763
Method for ambiguity resolution in range-Doppler measurements
[NASA-CASE-GSC-13542-1] 08 p3252 N94-29739
Ultra wide band radar holographic imaging of subsurface targets
[DE94-004271] 09 p3713 N94-32681
Adaptive estimation and approximation of continuously varying spectral density functions to airborne radar
[AD-A277532] 10 p4033 N94-33710
The real-time display of interferometry data for Goldstone radar astronomy data acquisition
11 p4255 N94-35560
Estimation with multisensor/multiscan detection fusion
[AD-A278753] 11 p4256 N94-36092
Color-coded radar plan position indicator
[AD-D016200] 11 p4257 N94-36364
Imaging targets embedded in a lossy half space with Synthetic Aperture Radar
[DE94-010807] 12 p4435 N94-37391

RADAR TRACKING
Mid-latitude ionospheric response to active experiments
[NASA-CR-193549] 01 p0280 N94-12583
Improved Many-On-Many ROUTE software description
[DE93-013961] 01 p0334 N94-12608
Venus gravity
[NASA-CR-194077] 02 p0841 N94-12823
Reasoning with uncertain and incomplete information in aerospace applications
[NLR-TP-91366-U] 02 p0763 N94-13529

MUSIC and maximum likelihood using a refined propagation model: Performance comparison for radar low-angle tracking
[DREO-RN-1122] 02 p0603 N94-13832
Sea ice motions in the central arctic ice central arctic pack ice as inferred from AVHRR imagery
[NASA-CR-194572] 03 p1112 N94-15701
Radar diagnostic parameters as indicators of severe weather in central Florida
[PB93-183507] 03 p1106 N94-16465
What is the radar tracking Glint problem and can it be solved?
[AD-A266509] 03 p0999 N94-16789
Range safety transponder catalog
[AD-A270882] 04 p1323 N94-19581
New algorithm of ground track processing in high-frequency skywave over-the-horizon-B radar
[AD-A267821] 05 p1717 N94-20207
Probability of detection calculations using MATLAB
[AD-A271958] 05 p1736 N94-20578
Magellan vertical polarization radar observations 05 p1744 N94-20691
GMM-1: A 50 degree and order gravitational field model for Mars 05 p2117 N94-20774
NAVSPASUR sensor system digital signal processing receiver. Volume 1: Hardware and software overview
[AD-A272899] 05 p1738 N94-21198
NAVSPASUR sensor system digital signal processing receiver. Volume 2: Function and capabilities of hardware and software components
[AD-A272900] 05 p1739 N94-21218
Radar imaging of moving targets 05 p1747 N94-22238
Remote sensing of multilevel clouds during FIRE IFO 2 05 p1844 N94-22303
An improved gravity model for Mars: Goddard Mars Model-1 (GMM-1)
[NASA-TM-104584] 06 p2401 N94-23282
Method and apparatus for determining target elevation angle, altitude and range, and the like in a monopulse radar system with reduced multipath errors
[AD-D016005] 06 p2302 N94-25058
IRIG radar calibration catalog. Version 2: The IRIG error model reference for radar calibrations
[AD-A273344] 06 p2303 N94-25155
Methods for improving low-angle, low-altitude radar tracking accuracy
[AD-A274914] 07 p2768 N94-26347
Combatting inherent vulnerabilities of CFAR algorithms and a new robust CFAR design
[AD-A274918] 07 p2770 N94-26751
Processing of wide-angle synthetic aperture radar signals for target detection
[AD-A274225] 07 p2773 N94-27073
Laser beam steering with semiconductor waveguide
[AD-A275775] 08 p3292 N94-28765
Numerical simulations of a mountain thunderstorm. A comparison with Doppler radar observations
[AD-A275296] 08 p3369 N94-28873
Synchronization, positioning, and communication in multistatic radar systems for air defence
[PB94-137478] 08 p3243 N94-28908
Simulation of fully automated air traffic control concepts 08 p3139 N94-29569
Orbital debris radar instrumentation 08 p3248 N94-29626
A simulator for multi-radar analysis for realistic traffic
[AD-B179099] 08 p3142 N94-30439
Systematic error estimation in multisensor fusion systems
[AD-B179298] 08 p3428 N94-30764
CRAD Signal and Information Processing Working Group Workshop on Neural networks, volume 1
[DREA-TC-93-305-VOL-1] 09 p3836 N94-33149
The application of a radial basis function neural network for radar tracking over the sea 09 p3686 N94-33150
Some neural computing approaches to target tracking 09 p3837 N94-33151
A heuristic multiple target tracker 09 p3686 N94-33346
Adaptive estimation and approximation of continuously varying spectral density functions to airborne radar
[AD-A277532] 10 p4033 N94-33710
Compression of a radar track of a near Earth satellite into an Earth centered inertial state vector using least squares differential correction
[AD-A278498] 10 p4037 N94-34302
High degree gravitational sensitivity from Mars orbiters for the GMM-1 gravity model
[NASA-TM-104604] 10 p4088 N94-34992
Pointing and Tracking Systems
[AGARD-CP-539] 12 p4392 N94-36616
Multitarget track initiation using a modified Hough transform 12 p4395 N94-36630
Radar tracking in multipath: Techniques for improved performance 12 p4395 N94-36631
Contact level fusion of radar and IRST contacts on almost electromagnetically silent platform 12 p4395 N94-36634

RADAR TRANSMISSION

HF-OTH radar performance results
[AD-A266106] 01 p0138 N94-11655
MUSIC and maximum likelihood using a refined propagation model: Performance comparison for radar low-angle tracking
[DREO-RN-1122] 02 p0603 N94-13832
Comparison of RADARC high-frequency radar performance prediction model and ROTHR Amchitka data
[AD-A267077] 03 p0987 N94-15540
Forecasting the ducting of electromagnetic waves on the mesoscale
[AD-A268101] 03 p1109 N94-17571
Over-the-horizon propagation measurements at six radar-frequency bands at the Atlantic Ocean Coast
[AD-A274151] 07 p2773 N94-27136
Atmospheric Propagation Effects Through Natural and Man-Made Obscurants for Visible to MM-Wave Radiation
[AD-A276919] 08 p3256 N94-30495
The influence of the evaporation duct on the angle of arrival and amplitude of the backscattered signal from targets low above the sea 08 p3256 N94-30498
Waveform generation for ultra-wideband radar system
[AD-A276352] 09 p3673 N94-31401
Low altitude near-the-horizon propagation: A comparison between RPO and M-layer
[AD-A277358] 09 p3679 N94-32282
A new tool for signal processing
[AD-A278385] 09 p3685 N94-33354
Channel probe measurements for the American Sector Clutter Experiment, January 1994
[DE94-013086] 12 p4469 N94-37314
MTI compatible coherent sidelobe canceller
[AD-D016300] 12 p4435 N94-37771

RADAR TRANSMITTERS

Radar transmitter procedures
[AD-A268274] 03 p1005 N94-17523
S-76 high intensity radiated fields, volume 3
[AD-A274416] 07 p2772 N94-26980
Ground independent landing system 08 p3137 N94-29564
The CF-18 diagnostic and maintenance expert system project 09 p3567 N94-33338

RADARSAT

RADARSAT program 03 p0898 N94-15893
The down, release, and deployment of the RADARSAT SAR antenna 06 p2305 N94-23986

RADARSCOPES

NT PLAN POSITION INDICATORS

Designing for performance: A cognitive systems engineering approach to modifying an AWACS human computer interface
[AD-A275187] 08 p3399 N94-28861
Final-Approach Spacing Aids (FASA) evaluation for terminal-area, time-based air traffic control
[NASA-TP-3399] 11 p4192 N94-36048

RADIAL DISTRIBUTION

Effects of levitated dust on astronomical observations from the lunar surface 03 p1239 N94-16433
A radial transmission line material measurement apparatus
[DE93-018508] 04 p1394 N94-17780
Optical diagnostic instrument for monitoring etch uniformity during plasma etching of polysilicon in a chlorine-helium plasma
[DE93-019582] 05 p1993 N94-20261
C2, CN and dust in Comet Wilson (1987VII) 05 p2083 N94-20746
Shock attenuation at the Slate Islands revisited 05 p1863 N94-20887
Impact of copper vapour contamination on argon arcs 05 p1994 N94-21053
Structural ordering in liquid K-Te alloys
[DE94-008477] 09 p3645 N94-32514
Improved models of beta-limit, anomalous transport and radial electric field with loss cone loss in heliotron/torsatron
[DE94-718976] 11 p4324 N94-35984

RADIAL DRAINAGE PATTERNS

U DRAINAGE PATTERNS

RADIAL FLOW

Development of passive superconducting bearings. Phase 3
[AD-A266050] 01 p0180 N94-10706
Simulation study of dynamo structure in reversed field pinch
[DE93-771406] 01 p0390 N94-11128
Large volcanoes on Venus: Examples of geologic and structural characteristics from different classes 01 p0467 N94-12195
Formation and evolution of radial fracture systems on Venus 05 p2099 N94-20672
Two-dimensional Navier-Stokes computations of subsonic and supersonic flows through turbine cascades
[PB93-226223] 06 p2317 N94-23114
Low cost, radial flow, solid oxide fuel cell
[DE94-002982] 07 p2858 N94-26785
On helicon wave induced radial plasma transport
[IPPCZ-333] 07 p3048 N94-27840
Fluid dynamic noise in a centrifugal pump
[AD-A275264] 08 p3477 N94-28904
Near-critical spherically symmetric accretion by neutron stars 08 p3546 N94-29991
Inverse design of radial flow impellers with prescribed velocity at hub and shroud 10 p4002 N94-34448
Turbine blade dynamics and blade-vane interaction in a radial inflow turbine 10 p4004 N94-34461
An air bearing system for small high speed gas turbines 10 p4004 N94-34466

RADIAL VELOCITY

Photometry and spectroscopy in the open cluster Alpha Persei, 2
[NASA-CR-193397] 02 p0833 N94-14358
The IRAF radial velocity analysis package 05 p1925 N94-22475
Convective turbulence and transport in stars 08 p3546 N94-29913
Pushing the limit: Precision radial velocities, techniques, and applications 08 p3542 N94-30861

RADIANCE

A statistical method to determine aerosol path radiance and its application to atmospheric correction for CZCS imagery 01 p0191 N94-11897
Distribution of mineral aerosols over the North Pacific 01 p0204 N94-11976
The evaluation of radiative process in the atmosphere-ground system by Monte Carlo method 01 p0205 N94-11980
Seasonal variability of surface ocean color in the Omura Bay using multitemporal LANDSAT-5 TM data 01 p0218 N94-12698
Optimum selection of spectral channels in the problem of remote sensing of phytoplankton concentration in ocean water 01 p0223 N94-12726
Trajectory curving in underwater propagation of light 01 p0226 N94-12748
Recent results from material processing studies on new generation lasers
[DE93-013841] 02 p0653 N94-12898
Infrared transmission and path radiance through dust and fog
[AD-A265825] 02 p0791 N94-12979
Volume 14: The first SeaWiFS intercalibration round-robin experiment, SIRREX-1, July 1992
[NASA-TM-104566-VOL-14] 02 p0725 N94-14090
Unmixing AVIRIS data to provide a method for vegetation fraction subtraction 03 p1066 N94-16669
Hyperspectral modeling for extracting aerosols from aircraft/satellite data 03 p1067 N94-16673
A field measure of the shade fraction 03 p1068 N94-16677
Seasonal and spatial variations in phytoplanktonic chlorophyll in eutrophic Mono Lake, California, measured with the Airborne Visible and Infrared Imaging Spectrometer (AVIRIS) 03 p1069 N94-16684
Multiple dataset water-quality analyses in the vicinity of an ocean wastewater plume 03 p1069 N94-16687
Atmospheric correction of AVIRIS data in ocean waters 03 p1070 N94-16690
Simulation of AVHRR-K band ratios with AVIRIS 03 p1075 N94-16714
Spectral radiance measurements on a bluff body stabilized flame: Characterization of the IR signature
[PB93-195899] 04 p1347 N94-18081
Work plan for the Marine Aerosol Properties and the Thermal Imager Performance Trial (MAPTIP)
[AD-A270026] 04 p1483 N94-18712
Cutting and drilling studies using high power visible lasers
[DE93-019149] 04 p1441 N94-19294
Scientific studies in association with the Shuttle Solar Backscatter Ultraviolet (SSBUV) project
[NASA-CR-193404] 04 p1630 N94-19437
Marine-modified LOWTRAN: The contribution of sun glint
[AD-A269547] 04 p1500 N94-19762
UVPI imaging from the LACE satellite: The Starbird rocket plume
[AD-A271981] 05 p1658 N94-20617
Goniospectrometric properties of a white standard 05 p1684 N94-20664
Wavelength dependence of limb-darkening of Mars from visible and near-IR telescopic spectral imaging 05 p2101 N94-20685

Measurement of evapotranspiration with combined reflective and thermal infrared radiance observations
[NASA-CR-194802] 05 p1837 N94-20951
Intercomparison of MAS, AVIRIS, and HIS data from FIRE cirrus 2 05 p1872 N94-22298
Development of methods for inferring cloud thickness and cloud-base height from satellite radiance data 05 p1872 N94-22301
Atmospheric parameterization schemes for satellite cloud property retrieval during FIRE IFO 2 05 p1874 N94-22312
Spectral emissivity of cirrus clouds 05 p1876 N94-22322
Calibration of radiation codes in climate models: Comparison of calculations with observations from the SPECtral Radiation Experiment (SPECTRE) 05 p1879 N94-22337
SSH-2 measurements of cirrus at 18-28 micrometers from the King Air during FIRE 2 05 p1880 N94-22338
Investigation of the effects of the macrophysical and microphysical properties of cirrus clouds on the retrieval of optical properties: Results for FIRE 2 05 p1880 N94-22339
Algorithm-development activities
[NASA-CR-193225] 06 p2420 N94-23538
VNIR and SWIR transfer radiometers developed at NRLM for preflight laboratory cross-calibration 06 p2385 N94-23610
Modelling TOVS radiances of synoptic systems
[NASA-CR-194847] 06 p2408 N94-23620
Evaluation of visual acuity with Gen 3 night vision goggles
[NASA-TM-108792] 06 p2431 N94-23974
The IRGen infrared data base modeler 06 p2440 N94-25496
MODIS airborne simulator visible and near-infrared calibration, 1992 ASTEX field experiment. Calibration version: ASTEX King 1.0
[NASA-TM-104599] 07 p2897 N94-28179
CBSD: The celestial background scene descriptor
[AD-A275521] 08 p3538 N94-28671
SHARC, a model for calculating atmospheric and infrared radiation under non-equilibrium conditions
[AD-A275207] 08 p3357 N94-28893
Custom uniform source system
[NASA-CR-189332] 09 p3711 N94-31492
Development of a statistical method for estimating the downward longwave radiation at the surface from satellite observations 09 p3742 N94-31553
SeaWiFS technical report series. Volume 16: The second SeaWiFS Intercalibration Round-Robin Experiment, SIRREX-2, June 1993
[NASA-TM-104566-VOL-16] 10 p4093 N94-34412

RADIANT COOLING
X ray emission from dynamical shock models in hot-star winds
[NASA-CR-194093] 02 p0847 N94-13288
Recent testing of 30 kW hydrogen arcjet thrusters
[NASA-TM-106214] 02 p0551 N94-13430
Investigate wave-mean flow interaction and transport in the extratropical winter stratosphere
[NASA-CR-194555] 03 p1098 N94-15639
An improved patch for radiative coolers
[NASA-CASE-GSC-13503-1] 05 p1822 N94-20127
Numerical simulation of radiative heat loss in an experimental burner
[DE94-002016] 08 p3277 N94-29923
Thermal conductivities, electrical resistivities, and Seebeck coefficients of YBa2Cu3O(7-x) superconductors from 80 to 300 K
[DE94-004796] 08 p3520 N94-30724

RADIANT ENERGY
U RADIATION

RADIANT FLUX DENSITY
NT ELECTRON FLUX DENSITY
NT ILLUMINANCE
NT IRRADIANCE
NT LUMINANCE
NT LUMINOUS INTENSITY
NT NEUTRON FLUX DENSITY
NT PARTICLE FLUX DENSITY
NT PROTON FLUX DENSITY
NT RADIANCE
NT SOLAR FLUX DENSITY
Retrieval of radiation budgets in the Arctic from satellite measurements 01 p0229 N94-10714
Radiation hardness of Mo/Si multilayers designed for use in a soft x ray projection lithography system
[DE93-011879] 01 p0143 N94-11273
EOL performance comparison of GaAs/Ge and Si BSF/R solar arrays 01 p0051 N94-11398
The 1 to 5 micron imaging of deeply embedded young stellar objects 02 p0831 N94-13657
Observation of nonsequential ionization of helium and its impact on intensity monitoring
[DE93-017174] 03 p0949 N94-16904
Spectroscopic and computer modeling investigations of a laser-sustained plasma
[IFTR-30/1991] 03 p1204 N94-17066
High temperature co-axial winding transformers
[NASA-CR-194580] 04 p1407 N94-19643
UVPI imaging from the LACE satellite: The Strypi rocket plume
[AD-A270967] 04 p1335 N94-19787
RADCAL: A narrow-band model for radiation calculations in a combustion environment
[PB93-200889] 05 p1682 N94-21448
Miyun 232 MHz survey 1: Fields centered at: alpha:00(h)41(m), delta:41 deg 12 min and alpha: 07(h)00(m),delta:35 deg 00 min 05 p2080 N94-22554
Physical aspects of the visual stimulus 06 p2431 N94-23978
An extended laser flash technique for thermal diffusivity measurement of high-temperature materials 06 p2238 N94-25132
UVPI imaging from the LACE satellite: The Low Cost Launch Vehicle (LCLV) rocket plume
[AD-A278785] 12 p4398 N94-36445

RADIANT HEATING
Measuring surface fluxes in CAPE
[NASA-CR-193664] 02 p0711 N94-12788
Investigation of radiative interaction in laminar flows using Monte Carlo simulation
[NASA-CR-194604] 03 p1021 N94-15795
An analysis of the radiation field beneath a bank of tubular quartz lamps
[NASA-CR-191551] 03 p1024 N94-16542
Wavefront sensors for optical diagnostics in fluid mechanics: Application to heated flow, turbulence, and droplet evaporation
[DE93-040060] 05 p1797 N94-19974
The young Sun and photochemistry of the primitive Martian atmosphere 05 p2145 N94-21679
Strain gage measurement errors in the transient heating of structural components
[NASA-TM-104274] 06 p2376 N94-23487
Numerical and experimental analyses of the radiant heat flux produced by quartz heating systems
[NASA-TP-3387] 07 p3011 N94-27659
Analysis of infrared radiation heating process considering chemical reaction of material to be heated
[DE94-744116] 08 p3199 N94-30267
Optical processing for semiconductor device fabrication 09 p3885 N94-32445

RADIANT INTENSITY
U RADIANT FLUX DENSITY

RADIATION
Global climate study
[NASA-TM-109612] 03 p1098 N94-15363
Radiation and scattering from printed antennas on cylindrically conformal platforms
[NASA-CR-194703] 05 p1741 N94-21885

RADIATION ABSORPTION
NT AURORAL ABSORPTION
NT ELECTROMAGNETIC ABSORPTION
NT GAMMA RAY ABSORPTION
NT INFRARED ABSORPTION
NT MICROWAVE ABSORPTION
NT MOLECULAR ABSORPTION
NT MULTIPHOTON ABSORPTION
NT PHOTOABSORPTION
NT POLAR CAP ABSORPTION
NT SELF ABSORPTION
NT ULTRAVIOLET ABSORPTION
NT X RAY ABSORPTION
Spectroscopic and computer modeling investigations of a laser-sustained plasma
[IFTR-30/1991] 03 p1204 N94-17066
Work plan for the Marine Aerosol Properties and the Thermal Imager Performance Trial (MAPTIP)
[AD-A270026] 04 p1483 N94-18712
Evaluation of fiber optic performance in the ACRR
[DE93-018515] 04 p1580 N94-18970
Radiation induced darkening of the optical elements in the Startracker camera
[DE93-018907] 04 p1433 N94-19004
Optics survivability support, volume 2
[DE93-040310] 05 p1985 N94-20283
Extra-corporeal blood access, sensing, and radiation methods and apparatuses
[NASA-CASE-MSC-21775-1] 05 p1890 N94-20372
The quantum efficiency of HgCdTe photodiodes in relation to the direction of illumination and to their geometry 05 p1735 N94-20512
Examination for optimization of synchrotron radiation spectrum for the x ray depth lithography
[BONN-IR-92-32] 05 p1987 N94-21148
Radiation applications of physical chemistry 07 p2854 N94-26054
Evanescent field infrared spectroscopy using chalcogenide glass fiber
[ITN-94-85233] 07 p3038 N94-27178
TFTR Ion Cyclotron Range of Frequencies (ICRF) experimental data analysis collaboration
[DE94-004699] 08 p3504 N94-28575
A comprehensive analysis of electron conical distributions from multi-satellite databases
[NASA-CR-195848] 09 p3953 N94-33047
The effects of proton-beam quality on the production of gamma rays for nuclear resonance absorption in nitrogen
[DE94-011609] 12 p4523 N94-37629

RADIATION BELTS
NT INNER RADIATION BELT
NT PROTON BELTS
Proton transport methods for satellite shield modeling
[DE93-013602] 01 p0042 N94-10520
Analysis of geophysical measurements and spacecraft interactions
[AD-A266064] 01 p0043 N94-10944
Potential health effects of space radiation 01 p0312 N94-11558
Force-free magnetic fields, curl eigenfunctions, and the sphere in transform space, with applications to fluid dynamics and electromagnetic theory
[AD-A265805] 02 p0834 N94-12971
Stormtime transport of ring current and radiation belt ions
[NASA-CR-194416] 02 p0714 N94-13793
Dynamical model for the distribution of geomagnetically trapped anomalous-component ions
[ATR-91(9558)-6] 02 p0784 N94-13936
Penetrating radiation environment and effects study
[AD-A270126] 04 p1485 N94-18874
Solar flares and magnetospheric particles: Investigations based upon the ONR-602 and ONR-604 experiments
[AD-A273639] 06 p2628 N94-25031
The CRRES time history data base: All sensors
[AD-A273737] 06 p2207 N94-25542
Analysis of energetic proton and electron data in Neptune's magnetosphere
[NASA-CR-195707] 07 p3107 N94-27784
Identification of an unexpected space radiation hazard
[AD-A275170] 08 p3552 N94-29046
Lightning-induced coupling of the radiation belts to geomagnetically conjugate ionospheric regions 09 p3772 N94-31773
Self-consistent effects of magnetospheric hydromagnetic waves on ring current ions
[AD-A277406] 09 p3774 N94-32346
Gyroresonant scattering of radiation belt electrons by oblique whistler waves 10 p4166 N94-33357
Global changes of radiation situation at heights less than 1000 km
[DE94-610504] 11 p4290 N94-35780

RADIATION CHEMISTRY
NT PHOTODECOMPOSITION
NT PHOTODISSOCIATION
NT PHOTOLYSIS
NT RADIOLYSIS
Research at the Notre Dame Radiation Laboratory
[DE93-018716] 04 p1566 N94-18165
Summaries of FY 1993 research in the chemical sciences
[DE93-011855] 04 p1632 N94-18915
Chemistry and materials science
[DE94-001449] 05 p2152 N94-21858
The First Energy Conference: Israel and the Former USSR
[ISBN-965-229-098-X] 07 p2853 N94-26050
Radiation applications of physical chemistry 07 p2854 N94-26054
Radiation and photochemistry section
[DE94-008880] 09 p3873 N94-32757
Physics with primary beams of the KEK-PS
[DE94-748635] 12 p4522 N94-37234

RADIATION COUNTERS
NT CERENKOV COUNTERS
NT ELECTRON COUNTERS
NT NEUTRON COUNTERS
NT NEUTRON SPECTROMETERS
NT PARTICLE TELESCOPES
NT PROPORTIONAL COUNTERS
NT QUANTUM COUNTERS
NT SCINTILLATION COUNTERS
Silicon-based elementary particle tracking system: Materials science and mechanical engineering design
[DE93-012630] 01 p0065 N94-10740
Effects of energetic particle events on VLF/LF propagation parameters/1989
[AD-A265266] 01 p0275 N94-11013

Conceptual design report for the SDC barrel and intermediate muon detectors based on a jet-type drift chamber
[DE93-753173] 01 p0367 N94-11510
Experimental particle physics at the University of Pittsburgh
[DE93-013326] 01 p0369 N94-12546
Search for UHE point-source emission over various time scales
[DE93-012718] 02 p0846 N94-12922
A program of correlated observations using the EGRET instrument on GRO and the IMB neutrino detector
[NASA-CR-194367] 02 p0783 N94-13856
Radiation effects on optoelectronic analog link for particle detectors
[DE93-015794] 02 p0793 N94-14529
The MIC photon counting detector
03 p0901 N94-15039
CCDs and photon counting devices: Applications in space and from the ground 03 p0901 N94-15041
Visible light photon counters for astronomy
03 p0902 N94-15043
The TAUVEX experiment 03 p0905 N94-15064
The Rutherford Appleton Laboratory photon counting detector 03 p0910 N94-15096
The 3D-Flow processor for a programmable level-1 trigger (feasibility study)
[DE93-016045] 03 p1159 N94-16172
Calorimeter based detectors for high energy hadron colliders
[DE93-017055] 03 p1188 N94-16900
Electroweak results from D0
[DE93-014926] 03 p1185 N94-16968
Astrophysics with MILAGRO
[DE93-012722] 03 p1240 N94-17657
Detecting small debris using a ground-based photon counting detector
[DE93-012623] 03 p0898 N94-17669
A bit serial first level calorimeter trigger for an LHC detector
[USIP-92-08] 04 p1574 N94-18845
Research in high energy physics
[DE93-018031] 04 p1575 N94-19287
A programmable systolic trigger processor for FERA-bus data
[USIP-92-04] 04 p1405 N94-19292
Search for top quark with D0 detector
[DE93-040170] 04 p1572 N94-19536
Thermal information regarding the cooldown and operation of liquid argon calorimeters
[DE93-019391] 05 p1807 N94-19987
The GEM Silicon Tracking System
[DE93-040133] 05 p2016 N94-20322
STRV RADMON: An integrated high-energy particle detector 05 p1666 N94-21086
A High Resolution Liquid Xenon Imaging Telescope for 0.3-10 MeV Gamma Ray Astrophysics: Construction and Initial Balloon Flights
[NASA-CR-194709] 05 p2056 N94-22281
A measurement of the forward-backward asymmetry and sin(sup 2)(theta)(sub W) from the process Z(sup 0) (yields) (mu)(sup +)(mu)(sup (minus)) at (radical)s = 1.8 TeV
[DE94-001908] 06 p2532 N94-23018
Examination of the response capacity of a silicon pixel detector for ions and molecules in the energy area 100 to 300 keV
[MPE-241] 06 p2346 N94-25415
Use of parallel counters for triggering
[DE93-616656] 07 p2979 N94-25918
Harvard University High Energy Physics
[DE94-002406] 07 p3032 N94-26119
Hadron gas ionization calorimeters
[DE93-634186] 07 p2810 N94-26397
Measuring the time dependence of B(sub s)(sup 0) meson - anti B(sub s)(sup 0) meson oscillations
[ISBN-0-315-84367-5] 07 p3021 N94-26665
The OPAL vertex detector
[ISBN-0-315-51152-4] 07 p2812 N94-27257
Elementary particle interactions
[DE94-004238] 08 p3482 N94-28504
Adaption of the bubble detector for use as a LET spectrometer 08 p3291 N94-30216
A bipolar analog front-end integrated circuit for the SDC silicon tracker
[DE94-005203] 08 p3267 N94-30711
Research in elementary particle physics
[DE94-001657] 08 p3491 N94-30762
The D0 upgrade
[DE94-006953] 09 p3867 N94-31671
Gamma Large Area Silicon Telescope (GLAST)
[DE94-006439] 09 p3925 N94-31786
Studies of jet production with the D0 detector
[DE94-008271] 09 p3873 N94-32780
Using neural networks as an event trigger in elementary particle physics experiments
[DE94-006316] 10 p4136 N94-33716
Relaxation of radiation damages in silicon planar detectors
[DE94-009084] 10 p4148 N94-34166
Beam tests of a prototype level-1 calorimeter trigger for LHC experiments
[PB94-170495] 11 p4269 N94-35599
Determination of the Fermi level position for neutron irradiated high resistivity silicon detectors and materials using the Transient Charge Technique (TChT)
[DE94-009107] 11 p4260 N94-36221
Testing new technology for the heavy ion experiment at CERN
[DE94-004747] 12 p4521 N94-37220
Particle physics
[DE94-012944] 12 p4518 N94-37312
Experimental particle physics at the University of Pittsburgh
[DE94-011636] 12 p4521 N94-37721

RADIATION DAMAGE
NT LASER DAMAGE
Proton transport methods for satellite shield modeling
[DE93-013602] 01 p0042 N94-10520
EOL performance comparison of GaAs/Ge and Si BSF/R solar arrays 01 p0051 N94-11398
Results of thermal vacuum tests for the PASP+ flight modules 01 p0053 N94-11410
Multi-band gap and new solar cell options workshop
01 p0054 N94-11418
Potential health effects of space radiation
01 p0312 N94-11558
Diffusion length damage coefficient and annealing studies in proton-irradiated InP
[NASA-TM-106262] 01 p0404 N94-12430
About the influence of inert gas ion implantation on metal corrosion stability
[DE93-620574] 02 p0569 N94-13360
Growth of samarskite crystal under microgravity conditions (M-20) 02 p0590 N94-13752
Radiation effects on optoelectronic analog link for particle detectors
[DE93-015794] 02 p0793 N94-14529
Radiation hardening of a CCD technology through process and design modifications
03 p0906 N94-15071
Report of the 1991 Workshop on Particle-Material Interactions for Fusion Research
[DE93-788393] 04 p1573 N94-18156
Studies of deep levels in high resistivity silicon detectors irradiated by high fluence fast neutrons using a thermally stimulated current spectrometer
[DE93-016133] 04 p1602 N94-19258
General introduction to microstructural evolution under cascade damage conditions
[DE93-017443] 05 p2012 N94-19923
Tensile and shear fracture behavior of fiber reinforced plastics at 77K irradiated by various radiation sources
[DE93-040280] 05 p1706 N94-21542
Tensile strength of fiber reinforced plastics at 77K irradiated by various radiation sources
[DE93-040826] 05 p1709 N94-22008
Irradiation damage behavior of low alloy steel wrought and weld materials
[DE94-000519] 06 p2239 N94-22999
Temperature dependence of the radiation induced change of depletion voltage in silicon PIN detectors
[DE94-002705] 07 p3052 N94-25972
Temperature dependence of static RAM volatility
[DE93-040345] 07 p2948 N94-26111
Experimental and numerical investigation of shock wave propagation through complex geometry, gas continuous, two-phase media
[DE94-001408] 07 p2791 N94-26121
Disturbed neuronal migration in the cerebral cortex of mice by low-dose gamma radiation
07 p2904 N94-27470
Distribution of GABA immunoreactive neurons in the brain of rolling mouse Nagoya and gamma-irradiated mouse 07 p2904 N94-27471
Effects of gamma ray radiation on the developing mouse cerebellum: Apoptotic cell death and induction of tissue transglutaminase 07 p2904 N94-27472
Influence of lattice damage on retention and transport of deuterium in beta silicon carbide
[DE94-005206] 07 p3068 N94-27693
Damage growth in MgAl2O4 crystals by Xe ion irradiations
[DE94-005009] 07 p3069 N94-27828
Proceedings of Japan-US Workshop P-196 on High Heat Flux Components and Plasma Surface Interactions for Next Devices
[DE94-701164] 08 p3503 N94-28513
Analysis of data by long-time mechanical properties of 08KH18N10T steel irradiated by neutrons
[DE94-605337] 08 p3202 N94-28551
Electron beam irradiation experiments of monoblock divertor mock-up
[DE94-707497] 08 p3503 N94-28555
Dislocation loops in spinel crystals irradiated successively with deep and shallow ion implants
[DE94-005083] 08 p3517 N94-30201
Irradiation-induced structure and property changes in tokamak plasma-facing, carbon-carbon composites
[DE94-006046] 08 p3508 N94-30365
Ion damage studies in GaAs/Al(0.6)Ga(0.4)As/GaAs heterostructures
[DE94-005384] 08 p3521 N94-30894
Atomic oxygen damage characterization by photothermal scanning 09 p3598 N94-31051
The threshold energy for defect production in SiC: A molecular dynamic study
[DE94-007123] 09 p3896 N94-31499
Effect of irradiation damage and helium on the swelling and structure of vanadium-base alloys
[DE94-006540] 09 p3641 N94-31666
Experimental investigations and molecular dynamics simulations of radiation induced surface damage
[AD-A277323] 09 p3871 N94-32621
Vulnerability assessment of a space based weapon platform electronic system exposed to a thermonuclear weapon detonation
[DE94-007229] 09 p3611 N94-32667
Irradiation-induced phase transformations in zirconium alloys
[DE94-008484] 09 p3648 N94-32993
The impact of ASIC devices on the SEU vulnerability of space-borne computers
[AD-A278134] 09 p3808 N94-33252
Relaxation of radiation damages in silicon planar detectors
[DE94-009084] 10 p4148 N94-34166
Irradiation assisted stress corrosion cracking of HTH Alloy X-750 and Alloy 625
[DE94-012667] 12 p4416 N94-37080
Thermodynamics of minerals stable near the Earth's surface
[DE94-012479] 12 p4539 N94-37094
Estimates of cellular mutagenesis from cosmic rays
[NASA-TP-3453] 12 p4481 N94-37282

RADIATION DETECTORS
NT DOSIMETERS
NT GOLAY DETECTOR CELLS
NT SILICON RADIATION DETECTORS
Analysis and interpretation of high energy cosmic rays measured on Spacelab-2
[NASA-CR-193586] 01 p0485 N94-12771
Crystallographic and metallurgical characterization of radiation detector grade cadmium telluride materials
[DE93-014335] 02 p0806 N94-13150
Absolute detection efficiency of a micro-channel plate detector to x rays in the 1-100 KeV energy range
[DE93-012592] 02 p0789 N94-14460
Results from a water-Cerenkov array
[DE93-012715] 02 p0849 N94-14461
Measuring parity violation using the neutron capture reaction
[DE93-016629] 02 p0786 N94-14514
Radiation effects on optoelectronic analog link for particle detectors
[DE93-015794] 02 p0793 N94-14529
Metastable superconductors as photon detectors
03 p0900 N94-15032
Thinned, backside illuminated, area CCD imager for electron detection 03 p0901 N94-15036
Outlook for hard x ray and gamma ray astronomy
03 p0904 N94-15057
Work at Graz on satellite signatures
03 p0898 N94-15558
The solid state detector technology for picosecond laser ranging 03 p0914 N94-15572
Electroweak physics from D0
[DE93-015041] 03 p1181 N94-16053
ALEXIS and HETE: Two small, low cost, scientific satellite systems 03 p0896 N94-17185
Contained (nu) events observed in Soudan 2
[DE93-015548] 03 p1300 N94-17233
Detecting small debris using a ground-based photon counting detector
[DE93-012623] 03 p0898 N94-17669
New room temperature high resolution solid-state detector (CdZnTe) for hard x rays and gamma rays
04 p1324 N94-19165
The GAMCIT gamma ray burst detector
04 p1324 N94-19168
High rate resistive plate chambers: An inexpensive, fast, large area detector of energetic charged particles for accelerator and non-accelerator applications
[DE93-018664] 04 p1572 N94-19545
The NRL LACE program
[AD-A270861] 05 p1657 N94-19896

Top search at the TEVATRON
[DE93-019392] 05 p1978 N94-19988
B production at D0
[DE93-019250] 05 p1972 N94-20291
STRV RADMON: An integrated high-energy particle detector 05 p1666 N94-21086
Advanced far infrared detectors
[DE93-040289] 05 p1988 N94-21528
The lepton charge asymmetry in the decay of W bosons produced in p(bar p) collisions at (radical)s = 1.8 TeV
[DE93-019903] 05 p1976 N94-21847
VETA x ray data acquisition and control system 05 p2047 N94-22455
Electro-weak, QCD and top physics at the Tevatron
[DE94-002304] 06 p2535 N94-24611
To perform a proof-of-concept study on the use of superheated drop detectors for the measurement of LET spectra in space environments
[BTI-92/3-31] 06 p2629 N94-24695
High energy gamma astronomy above 200 GeV
[MPI-PHE/93-04] 06 p2600 N94-25458
JLC-1
[DE93-520380] 07 p3031 N94-26113
Auxiliary controller for time-to-digital converter module readout
[DE93-634172] 07 p2948 N94-26266
Exploration of GaAs structures for solid-state detectors
[DE93-634191] 07 p3056 N94-26379
The 12-channel flash-ADC FASTBUS module
[DE93-634229] 07 p2783 N94-26380
Separation and reconstruction of electron neutrino interaction in the IHEP-JINR neutrino detector and BARS detector
[DE93-634182] 07 p3019 N94-26393
Proceedings of the Second EGS4 User's Meeting in Japan
[DE93-520383] 07 p3032 N94-26543
The response of an hyperpure Ge detector to ionizing radiation
[ISBN-0-315-83968-6] 07 p2811 N94-26662
Channel to energy calibration results for the BATSE large area detectors 07 p3115 N94-26690
Advances in gamma ray field instrumentation at Los Alamos
[DE93-040264] 07 p2813 N94-27624
The status of the solar neutrino problem
[DE94-003934] 07 p3111 N94-27742
Performance of a 14-MeV neutron generator as an in situ calibration source for TFTR
[DE94-004993] 07 p3048 N94-27825
Proton switches
[AD-A275150] 08 p3167 N94-29022
Backscatter haze device for measurement of haze in aircraft transparencies
[AD-A275127] 08 p3146 N94-29042
A Tevatron collider beauty factory
[DE94-004879] 08 p3488 N94-29930
Deexcitation processes in nuclear reactions: The study of hot hadronic matter
[DE94-003396] 08 p3492 N94-30836
Implementation of instruments and facilities at the SGP CART site
[DE94-006839] 09 p3781 N94-31322
High energy physics program at the University of Alabama
[DE94-006544] 09 p3875 N94-31488
Minimax: Multiparticle physics at the Tevatron collider
[DE94-007095] 09 p3873 N94-32689
Studies of jet production with the D0 detector
[DE94-008271] 09 p3873 N94-32780
A teleoperated system for remote site characterization 10 p4066 N94-34029
Measurement of the ratio R = (sigma x B(p(bar p) yields W(sup (+-)) yields e(sup(+-))(nu)))/(sigma x B(p(bar p) yields Z(sup 0) yields e(sup + e(sup -)) in p(bar p) collisions at the square root of s = 1,800 GeV
[DE94-006846] 10 p4138 N94-35073
Multiwavelength pyrometer for gray and non-gray surfaces in the presence of interfering radiation
[NASA-CASE-LEW-15250-1] 11 p4269 N94-35383
High Energy Physics Division of research activities
[DE93-019681] 12 p4521 N94-36694
LET spectra of fragmented 600-MeV/A iron beam on aluminum and polyethylene: A preliminary analysis
[NASA-TP-3436] 12 p4416 N94-36993
BMAP dipole magnetic field analysis and orbit tracking/calculations of energy deposition in GaAs WHEBY detectors
[DE94-012080] 12 p4522 N94-37303
The 24/36/48 Cathode Strip Chamber layout for SSC GEM detector muon subsystem
[DE94-012676] 12 p4439 N94-37306
Gas microstrip detectors on resistive plastic substrates
[DE94-011336] 12 p4426 N94-37714

RADIATION DISTRIBUTION
NT ANTENNA RADIATION PATTERNS
NT DIFFRACTION PATTERNS
NT SIDELOBES
A modeling perspective on cloud radiative forcing
[DE93-012383] 01 p0276 N94-11241
On possibility of diamond formations in radiation process 01 p0433 N94-12254
Study of the consequences of the Chernobyl accident and technogenic activity in the Republic Belarus using aerospace methods 02 p0693 N94-14246
Meteorological data, new series A monographs. Volume 6, no. 3: Estimation of influence of high clouds in the radiation field and the climat by analysis of NOAA AVHRR data
[ETN-93-94170] 02 p0723 N94-14707
An analysis of the radiation field beneath a bank of tubular quartz lamps
[NASA-CR-191551] 03 p1024 N94-16542
Extra-corporeal blood access, sensing, and radiation methods and apparatuses
[NASA-CASE-MSC-21775-1] 05 p1890 N94-20372
Monte Carlo calculation of multi-electron effects on synchrotron radiation
[DE94-001259] 05 p1982 N94-21974
Caesium-137 in a boreal forest ecosystem: Aspects on the long-term behavior
[PB94-137809] 08 p3347 N94-29158
A study of physical conditions, radiative transfer and shocks in the interstellar medium 09 p3937 N94-31963
Basic study of the pumping of a gamma ray laser
[AD-A278537] 10 p4057 N94-33673
Effects of isotope selection on solution convergence in HZE transport
[NASA-TP-3445] 10 p4167 N94-33686
Body-wave radiation patterns and AVO in transversely isotropic media
[DE94-009214] 10 p4036 N94-34162
Coherent multiple-foil x-ray transition radiation
[DE93-040831] 12 p4525 N94-37486

RADIATION DOSAGE
Proton transport methods for satellite shield modeling
[DE93-013602] 01 p0042 N94-10520
A window least squares algorithm for statistical noise smoothing of 2D-ACAR data
[DE93-613828] 01 p0395 N94-10537
On problem about nature of Portevin-Le Chatelier effect in irradiated aluminium alloys
[DE93-617200] 01 p0082 N94-10842
Radiation defect production in InAs crystals under electron irradiation
[DE93-617202] 01 p0397 N94-10845
A proposed performance index for galactic cosmic ray shielding materials
[NASA-TM-4444] 01 p0484 N94-11278
Activation energy and capture cross section of majority carrier traps in Zn doped InP 01 p0049 N94-11386
Potential health effects of space radiation 01 p0312 N94-11558
Radiation considerations for interplanetary missions 01 p0045 N94-11559
Longitudinal study of astronaut health: Mortality in the years 1959-1991 01 p0312 N94-11560
Operational radiological support for the US manned space program 01 p0318 N94-11561
Lessons learned from the Long Duration Exposure Facility
[AD-A266026] 01 p0044 N94-12394
Experimental particle physics at the University of Pittsburgh
[DE93-013326] 01 p0369 N94-12546
Temperature dependence of diffusivities, preliminary definition phase
[NASA-CR-192613] 02 p0648 N94-13326
Genetic effects of HZE and cosmic radiation (L-9) 02 p0593 N94-13766
Development and application of the automated Monte Carlo biasing procedure in SAS4
[DE93-015205] 02 p0774 N94-14334
Exposure fluctuations of astronauts due to orientation
[NASA-TP-3364] 03 p1300 N94-15816
Aberration correction of unstable resonators
[NASA-CASE-NPO-18791-1-CU] 03 p1034 N94-15987
Quantifying lifetime exposure to ultraviolet radiation in the epidemiology of cutaneous malignant melanoma: A pilot study
[DE93-015274] 03 p1128 N94-16812
The determination of the Young moduli of a material after exposure to laser light and delineation of the zone of laser alterations
[IFTR-37/1991] 03 p1061 N94-17058
Bioeffects of radiofrequency radiation on cell growth and differentation. Volume 1: Engineering considerations
[AD-A267754] 03 p1118 N94-17232
Predicting radiation induced performance decrements of AH-1 helicopter crews. Volume 1: Predicted veersus actual performance of AH-1 crews induced with symptoms simulating radiation sickness
[AD-A268376] 03 p1138 N94-17460
Energy deposition fluctuations induced by ions in microvolumes and nanovolumes: An analytic approach. 1: Theory
[AD-A267959] 03 p1173 N94-17495
Cellular and molecular level responses after radiofrequency radiation exposure, alone or in combination with x rays or chemicals
[AD-A268189] 04 p1501 N94-17729
High dose effects in neutron irradiated face-centered cubic metals
[DE93-017671] 04 p1364 N94-19043
Effect of EMP fields on cell membrane potentials
[DE93-015819] 04 p1503 N94-19341
Focused-ion-beam material removal rates
[AD-A270852] 05 p1713 N94-19834
Extra-corporeal blood access, sensing, and radiation methods and apparatuses
[NASA-CASE-MSC-21775-1] 05 p1890 N94-20372
Radiometry in commercial aircraft
[GSF-41/91] 05 p1892 N94-21141
Spaceflight Radiation Health program at the Lyndon B. Johnson Space Center
[NASA-TM-104782] 05 p1893 N94-21863
Tensile strength of fiber reinforced plastics at 77K irradiated by various radiation sources
[DE93-040826] 05 p1709 N94-22008
Microstructural development in low activation ferritic alloys irradiated to 200 dpa at 420 C
[DE94-004269] 07 p2731 N94-25803
Advanced qualification techniques
[DE94-003709] 07 p2780 N94-25812
Window least squares method applied to statistical noise smoothing of positron annihilation data
[DE93-634665] 07 p3003 N94-26385
Studies on the application of radiation for genetic transformation in higher plants
[DE93-632656] 07 p2901 N94-26470
The role of hyperbaric oxygen as a prophylaxis for radiation enteritis
[AD-A274974] 07 p2901 N94-26517
Conceptual design of the tokamak radiation shielding for the Tokamak Physics Experiment (TPX)
[DE94-002791] 07 p3044 N94-26858
Effect of temperature and recoil-energy spectra on irradiation-induced amorphization in Ca2La8(SiO4)6O2
[DE94-004371] 07 p3067 N94-27602
Modeling the DMSP and CRRES dosimeters using the path length distribution method
[RXR-93051] 07 p2698 N94-28200
Develop and fabricate a radiation dose measurement system for satellites
[PL-TR-93-2161] 07 p2698 N94-28210
Develop and fabricate a radiation dose measurement system for satellites
[PL-TR-93-2099] 07 p2698 N94-28217
Modeling the total dose radiation effects of Hg(1-x)Cd(x)Te photodiodes using numerical device simulators
[AD-A275235] 08 p3263 N94-29028
Recent results from testing fast ADCs
[DE94-005565] 08 p3406 N94-30004
Model of spacecraft atomic oxygen and solar exposure microenvironments 09 p3593 N94-31021
Ionizing radiation effects on silicon test structures
[DE94-006060] 09 p3865 N94-31607
Neutron measurements at the commercial aircraft altitudes
[ISBN-0-315-86201-7] 09 p3955 N94-31709
Ion-irradiation-induced densification of zirconia sol-gel thin films
[DE94-006248] 09 p3656 N94-32103
Complete model description of an electron beam using ACCEPT Monte Carlo simulation code
[DE94-007063] 09 p3872 N94-32628
Vulnerability assessment of a space based weapon platform electronic system exposed to a thermonuclear weapon detonation
[DE94-007229] 09 p3611 N94-32667
An investigation of the radiolytic stability of a resorcinol-formaldehyde ion exchange resin
[DE94-007971] 09 p3660 N94-32698
Controlling hazardous energy sources (lockout/tagout)
[NASA-TM-105290] 09 p3669 N94-32861
Electron energy dependence of amorphization in Zr3Fe
[DE94-008459] 09 p3906 N94-32875
Spacecraft environmental anomalies expert system
[AD-A277962] 09 p3612 N94-33262
Stopping power of charged particles from 10 eV/amu to 10 GeV/amu
[DE94-719024] 12 p4518 N94-37387

Two-dimensional over-all neutronics analysis of the ITER device
[DE94-718963] 12 p4530 N94-37464
RADIATION EFFECTS
NT LASER DAMAGE
NT RADIATION DAMAGE
NT RADIATION INJURIES
NT RADIOLYSIS
NT SINGLE EVENT UPSETS
Radiation hardened nonvolatile memory for space and strategic applications
[DE93-000746] 01 p0319 N94-10146
High heat flux components and plasma surface interactions
[DE93-008786] 01 p0385 N94-10253
Workshop on NN Bremsstrahlung and Polarization Observables
[DE93-010181] 01 p0361 N94-10334
Investigation of soft errors in MOS RAM under influence of heavy ions
[DE92-644554] 01 p0484 N94-10534
Szilard-Chalmers effect in solid HIO4.2H2O by neutron irradiation
[DE93-617173] 01 p0397 N94-10830
On problem about nature of Portevin-Le Chatelier effect in irradiated aluminium alloys
[DE93-617200] 01 p0082 N94-10842
The influence of irradiation conditions, type, and concentration of impurities on radiation defects characteristics in indium antimonide under electron irradiation
[DE93-617201] 01 p0397 N94-10843
Radiation defect production in InAs crystals under electron irradiation
[DE93-617202] 01 p0397 N94-10845
Proceedings of the Symposium on Radiation Research in Life Science
[DE93-754137] 01 p0300 N94-10888
Combustion chamber analysis code
[NASA-CR-192585] 01 p0046 N94-10934
Welding tritium aged stainless steel
[DE93-011782] 01 p0181 N94-11228
Effect of switched-bias bakes on the postirradiation electrical response of MOS devices
[DE93-009629] 01 p0143 N94-11271
Proceedings of the 12th Space Photovoltaic Research and Technology Conference (SPRAT 12)
[NASA-CP-3210] 01 p0048 N94-11380
Radiation effects in heteroepitaxial InP solar cells
01 p0048 N94-11383
Results of some initial space qualification testing on triple junction a-Si and CuInSe2 thin film solar cells
01 p0050 N94-11392
Radiation effects in Ga(0.47)In(0.53)As solar cells
01 p0052 N94-11404
The UoSAT-5 solar cell experiment: First year in orbit
01 p0053 N94-11409
Potential health effects of space radiation
01 p0312 N94-11558
Potential techniques for non-destructive evaluation of cable materials
[DE93-008350] 01 p0183 N94-11586
Radiation-induced aperiodicity in irradiated ceramics
[DE93-013335] 01 p0091 N94-11698
The upwelling radiation at the top of the atmosphere in coastal region 01 p0205 N94-11981
On possibility of diamond formations in radiation process 01 p0433 N94-12254
Chemical release and radiation effects (CRRES) data directory
[NASA-CR-192551] 01 p0279 N94-12581
Project proposal for partial computational physics support for Survivability of Coatings program
[DE93-013788] 02 p0576 N94-12939
Annealing study of main electron irradiation-induced defects (H4 and H5) in P-InP using DLTS technique
[DE93-623204] 02 p0806 N94-13213
Comment of parameter excitation of Alfven and Helicon waves in a magnetoactive compensated semiconductor by microwave radiation
[DE93-623203] 02 p0806 N94-13228
About the influence of inert gas ion implantation on metal corrosion stability
[DE93-620574] 02 p0569 N94-13360
Cellular track model for study of heavy ion beams
[NASA-TP-3351] 02 p0732 N94-13714
Genetic effects of HZE and cosmic radiation (L-9)
02 p0593 N94-13766
Study on the biological effect of cosmic radiation and the development of radiation protection technology (L-11) 02 p0593 N94-13768
Interactions between spacecraft and their environments
[NASA-TM-106115] 02 p0541 N94-13917
Radiation hardening and radiation-induced chromium depletion effects on intergranular stress corrosion cracking of austenitic stainless steels
[DE93-011602] 02 p0572 N94-14058
Radiation effects on optoelectronic analog link for particle detectors
[DE93-015794] 02 p0793 N94-14529
Structural change of graphite during electron irradiation
[DE93-015961] 02 p0582 N94-14531
JPRS report: Science and technology. Central Eurasia: Materials science
[JPRS-UMS-93-004] 02 p0559 N94-14574
AlGaAs diode laser blue shift resulting from fast neutron irradiation
[AD-A266642] 02 p0659 N94-14681
Investigations of low-temperature neutron embrittlement of ferritic steels
[DE93-015460] 02 p0573 N94-14700
Quantitative luminescence imaging system
[DE93-015691] 02 p0793 N94-14702
Theoretical studies relating to the interaction of radiation with matter
[AD-A266894] 03 p1179 N94-14949
Merged beam studies of laser stimulated radiative recombination
[AD-A267186] 03 p1037 N94-15145
Plume radiation 03 p0924 N94-15223
Fault handling schemes in electronic systems with specific application to radiation tolerance and VLSI design
[NASA-CR-194559] 03 p1008 N94-15640
Long Duration Exposure Facility experiment M0003 deintegration/findings and impacts
[AD-A267140] 03 p0885 N94-15749
Investigation of radiative interaction in laminar flows using Monte Carlo simulation
[NASA-CR-194604] 03 p1021 N94-15795
Exposure fluctuations of astronauts due to orientation
[NASA-TP-3364] 03 p1300 N94-15816
PHENIX Conceptual Design Report
[DE93-015759] 03 p1182 N94-16161
The effect of irradiation on the mechanical properties of 6061-T651 aluminum
[DE93-015825] 03 p0958 N94-16168
AFRRI reports, first quarter 1993
[AD-A266380] 03 p1123 N94-16515
Ergonomics in the office environment
03 p1124 N94-16612
Evolution of microstructure in face centered cubic metals during irradiation: A review
[DE93-015682] 03 p0958 N94-16662
The role of constitutive and inducible processes in the response of human squamous cell carcinoma cell lines to ionizing radiation
[DE93-015150] 03 p1129 N94-16970
L-shell binning and display of sensor data from the CRRES spacecraft
[AD-A267256] 03 p0888 N94-16990
The determination of the Young moduli of a material after exposure to laser light and delineation of the zone of laser alterations
[IFTR-37/1991] 03 p1061 N94-17058
Studies of premixed laminar and turbulent flames at microgravity
[NASA-CR-194656] 03 p0951 N94-17125
Bioeffects of radiofrequency radiation on cell growth and differentation. Volume 1: Engineering considerations
[AD-A267754] 03 p1118 N94-17232
Predicting radiation induced performance decrements of AH-1 helicopter crews. Volume 1: Predicted veersus actual performance of AH-1 crews induced with symptoms simulating radiation sickness
[AD-A268376] 03 p1138 N94-17460
Quartz crystal resonators and oscillators for frequency control and timing applications: A tutorial, revision 6.1
[AD-A268205] 03 p1216 N94-17480
Energy deposition fluctuations induced by ions in microvolumes and nanovolumes: An analytic approach. 1: Theory
[AD-A267959] 03 p1173 N94-17495
The behavioral toxicology of high-peak, low average power, pulsed microwave irradiation
[AD-A268392] 03 p1134 N94-17535
Basic studies of the liquid state of matter: Electrical properties and laser interactions
[AD-A268311] 03 p1042 N94-17567
Growth of dielectric thin films by irradiation of condensed molecular precursors with synchrotron radiation
[DE93-016161] 03 p0974 N94-17676
Air pollution effects field research facility. 3: UV-B exposure and monitoring system
[DE93-013098] 04 p1470 N94-17773
PVDF measurement of soft x ray induced shock and filter debris impulse
[DE93-017633] 04 p1382 N94-17806
Using controlled daylight exposure and sleep timing in the prevention of shift lag during night operations
[AD-A269304] 04 p1504 N94-17824
Charpy impact toughness of martensitic steels irradiated in FFTF: Effect of heat treatment
[DE93-015960] 04 p1450 N94-17848
Characteristics and pulsed radiation response of non-ideal quartz shock stress gauges
[DE93-017628] 04 p1424 N94-17999
Report of the 1991 Workshop on Particle-Material Interactions for Fusion Research
[DE93-788393] 04 p1573 N94-18156
Study on radiation-induced deterioration of grease at high temperature, 3
[DE93-788368] 04 p1369 N94-18220
Effects of irradiation temperature on embrittlement of nuclear pressure vessel steels
[DE93-015428] 04 p1359 N94-18245
A study of the effects of high power pulsed 2450 MHz microwaves, ELF modulated microwaves, and ELF fields on human lymphocytes and selected cell lines
[AD-A269070] 04 p1505 N94-18294
Experience with custom processors in space flight applications 04 p1336 N94-18338
Upper atmospheric effects of the HF Active Auroral Research Program Ionospheric Research Instrument (HAARP IRI)
[AD-A268948] 04 p1481 N94-18451
Compilation of 1992 annual reports of the Navy ELF communications system ecological monitoring program, volume 1
[AD-A269569] 04 p1386 N94-18473
The c-jun gene expression in human cells exposed to either ionizing radiation or hydrogen peroxide
[DE93-017436] 04 p1502 N94-18476
Electromagnetic environmental effects compendium
[AD-A270441] 04 p1387 N94-18512
The LET spectrum and its uncertainty during the CRRES mission
[AD-A269977] 04 p1630 N94-18676
Mechanical-property changes of structural composite materials after low-temperature proton irradiation: Implications for use in SSC magnet systems
[DE93-016735] 04 p1343 N94-18763
Penetrating radiation environment and effects study
[AD-A270126] 04 p1485 N94-18874
Development of robust multilayer optics for use in high-peak power radiation environments
[DE93-018557] 04 p1580 N94-18931
Neutron-induced collision cascade mixing in Nb/V superlattices
[DE93-018575] 04 p1600 N94-18933
Evaluation of fiber optic performance in the ACRR
[DE93-018515] 04 p1580 N94-18970
Radiation induced darkening of the optical elements in the Startracker camera
[DE93-018907] 04 p1433 N94-19004
High dose effects in neutron irradiated face-centered cubic metals
[DE93-017671] 04 p1364 N94-19043
Effects of irradiation temperature on Charpy and tensile properties of high-copper, low upper-shelf, submerged-arc welds
[DE93-017858] 04 p1445 N94-19047
Static Computer Memory Integrity Testing (SCMIT): An experiment flown on STS-40 as part of GAS payload G-616 04 p1325 N94-19169
Overlay welding irradiated stainless steel
[DE93-018767] 04 p1446 N94-19334
Effect of EMP fields on cell membrane potentials
[DE93-015819] 04 p1503 N94-19341
The performance and survivability of dichromated poly (vinyl alcohol) holograms for space based photonic applications
[AD-A270974] 04 p1434 N94-19791
General introduction to microstructural evolution under cascade damage conditions
[DE93-017443] 05 p2012 N94-19923
Hydrogen pickup and redistribution in alpha-annealed zircaloy-4
[DE93-018050] 05 p1689 N94-20182
Single-event upset testing of the performance semiconductor 1750A CMOS/SOS chip set
[AD-A271158] 05 p2015 N94-20184
Optics survivability support, volume 1
[DE93-019616] 05 p1985 N94-20262
Optics survivability support, volume 2
[DE93-040310] 05 p1985 N94-20283
High energy ionization in liquids: The free ion yield
[DE93-040329] 05 p1973 N94-20324
Extra-corporeal blood access, sensing, and radiation methods and apparatuses
[NASA-CASE-MSC-21775-1] 05 p1890 N94-20372
Effects of hydrodynamics and thermal radiation in the atmosphere after comet impacts
05 p1862 N94-20649

The Fifth NASA Symposium on VLSI Design
[NASA-CR-194644] 05 p1753 N94-21079
Rad-hard computer elements for space applications
05 p1753 N94-21082
Design of CMOS logic gates for TID radiation
05 p1754 N94-21083
Evaluation of radiation effects in re-oxidized nitrided oxide devices by hot carrier stressing at 77 K
05 p1754 N94-21084
Space qualified high speed Reed Solomon encoder
05 p1754 N94-21088
Proton radiation testing of an 18 bit A/D converter
05 p1755 N94-21096
Automated radiation hard ASIC design tool
05 p1759 N94-21126
Simulated space environmental effects on some experimental high performance polymers
05 p1662 N94-21385
Evaluation of electroconductivity of two surface paints for spacecraft
[AD-A273063] 05 p1706 N94-21437
Tensile and shear fracture behavior of fiber reinforced plastics at 77K irradiated by various radiation sources
[DE93-040280] 05 p1706 N94-21542
Temperature-dependent ion beam mixing
[DE93-040281] 05 p2033 N94-21999
Tensile strength of fiber reinforced plastics at 77K irradiated by various radiation sources
[DE93-040826] 05 p1709 N94-22008
Microstructural evolution of neutron-irradiated Fe-Cr-Ni ternary alloys at high helium generation rates
[DE93-018786] 05 p1696 N94-22037
Miniaturized disk-bend testing, nano-indentation, and the microstructure of ion-irradiated titanium aluminides
[DE93-040600] 05 p1697 N94-22559
Report of the Joint Seminar on Solid State Physics, Atomic and Molecular Physics, and Materials Science in the Energy Region of Tandem Accelerators
[DE93-508268] 06 p2548 N94-22924
Low temperature diffusion of hydrogenic species in oxide crystals: Radiation induced diffusion
[DE94-000374] 06 p2558 N94-22957
A new automatic design method to develop multilayer thin film devices for high power laser applications
[DE93-632490] 06 p2347 N94-22967
Effects of neutron irradiation and hydrogen on ductile-brittle transition temperatures of V-Cr-Ti alloys
[DE94-001466] 06 p2240 N94-23009
Advanced materials for radiation-cooled rockets
06 p2214 N94-23052
Development of small punch testing technique and its application to evaluation of mechanical properties degradation
[DE94-001193] 06 p2375 N94-23184
Generalized melting criterion for beam-induced amorphization
[DE94-001333] 06 p2560 N94-23189
Grain-boundary microchemistry and intergranular cracking of irradiated austenitic stainless steel
[DE94-000466] 06 p2242 N94-23457
Surface modification of sapphire for enhanced infrared window performance
[DE94-000333] 06 p2543 N94-23458
Research for electric energy systems
[DE94-001839] 06 p2293 N94-23719
Effect of irradiation on the stress corrosion cracking behavior of Alloy X-750 and Alloy 625
[DE94-001759] 06 p2244 N94-23792
The role of radiation in mesoscale flows: Physics, parameterizations, codes 06 p2413 N94-24389
Effects of ionizing radiation on modern ion exchange materials
[DE94-001569] 06 p2535 N94-24505
Highly-reliable fly-by-light/power-by-wire technology
06 p2162 N94-25099
The CRRES time history data base: All sensors
[AD-A273737] 06 p2207 N94-25542
A review of carbide fuel corrosion for nuclear thermal propulsion applications
[DE94-003938] 07 p2699 N94-25613
Microstructural development in low activation ferritic alloys irradiated to 200 dpa at 420 C
[DE94-004269] 07 p2731 N94-25803
Advanced qualification techniques
[DE94-003709] 07 p2780 N94-25812
Electrical properties of p-type GaInP2
[AD-A273771] 07 p3051 N94-25856
On radiation defects in strip detectors
[DE93-616646] 07 p3015 N94-25916
Temperature dependence of the radiation induced change of depletion voltage in silicon PIN detectors
[DE94-002705] 07 p3052 N94-25972
Radiation-Induced Structural Changes, 2
[DE93-520314] 07 p3054 N94-26109
Temperature dependence of static RAM volatility
[DE93-040345] 07 p2948 N94-26111
Regrowth zones in laser annealed radiation damaged diamond
[DE94-600821] 07 p3056 N94-26364
Radiochemistry Division annual progress report : 1991
[DE94-600652] 07 p2715 N94-26392
Studies on the application of radiation for genetic transformation in higher plants
[DE93-632656] 07 p2901 N94-26470
The role of hyperbaric oxygen as a prophylaxis for radiation enteritis
[AD-A274974] 07 p2901 N94-26517
Molecular biological studies on the human radioresistance and drug resistance
[DE93-632682] 07 p2910 N94-26549
Microstructural development in irradiated vanadium alloys
[DE94-004307] 07 p2737 N94-26556
Influence of helium generation rate and temperature history on mechanical properties of model Fe-Cr-Ni alloys irradiated in FFTF at relatively low displacement rates
[DE94-004264] 07 p2737 N94-26575
Suppression of thermal grain growth in nickel by prior electron irradiation
[DE94-004602] 07 p2737 N94-26587
Disintegration of (C60) by Xe ion irradiation
[DE94-601913] 07 p3023 N94-26929
The role of point defect clusters in reactor pressure vessel embrittlement
[DE94-001122] 07 p2739 N94-26931
Initial ultraviolet-B intensity data at Lawrence Livermore National Laboratory
[DE94-004279] 07 p2869 N94-27267
The radiation design handbook
[ESA-PSS-01-609-ISSUE-1] 07 p2696 N94-27397
Annals of the Research Inst. of Environmental Medicine, Nagoya Univ., volume 44
[REPT-44-VOL-44] 07 p2911 N94-27442
Disturbed neuronal migration in the cerebral cortex of mice by low-dose gamma radiation
07 p2904 N94-27470
Distribution of GABA immunoreactive neurons in the brain of rolling mouse Nagoya and gamma-irradiated mouse 07 p2904 N94-27471
Effects of gamma ray radiation on the developing mouse cerebellum: Apoptotic cell death and induction of tissue transglutaminase 07 p2904 N94-27472
Grain boundary chromium concentration effects on the IGSCC and IASCC of austenitic stainless steels
[DE94-004268] 07 p2741 N94-27570
Effect of temperature and recoil-energy spectra on irradiation-induced amorphization in Ca2La8(SiO4)6O2
[DE94-004371] 07 p3067 N94-27602
Fusion reactor systems studies
[DE94-003162] 07 p3046 N94-27686
Ion implantation in silicate glasses
[DE94-003785] 07 p2757 N94-27726
Outgas and vacuum seal characteristics of irradiated polyimide O-ring
[DE94-701200] 07 p2757 N94-27812
Damage growth in MgAl2O4 crystals by Xe ion irradiations
[DE94-005009] 07 p3069 N94-27828
Experiment and research on materials irradiated by plasma radiation
[DE94-605011] 07 p2758 N94-27845
Proton irradiation on materials
07 p3030 N94-27898
Sonic booms and marine mammals: Informational status and recommendations 07 p2651 N94-28198
Relationship between swelling and irradiation creep in cold-worked PCA stainless steel irradiated to approximately 178 dpa at approximately 400 C
[DE94-004368] 08 p3201 N94-28456
Radiation effects in beryllium used for plasma protection
[DE94-004599] 08 p3201 N94-28460
Response of GaAs charge storage devices to transient ionizing radiation
[DE94-005273] 08 p3510 N94-28484
Proceedings of Japan-US Workshop P-196 on High Heat Flux Components and Plasma Surface Interactions for Next Devices
[DE94-701164] 08 p3503 N94-28513
Analysis of data by long-time mechanical properties of 08KH18N10T steel irradiated by neutrons
[DE94-605337] 08 p3202 N94-28551
Modeling the total dose radiation effects of Hg(1-x)Cd(x)Te photodiodes using numerical device simulators
[AD-A275235] 08 p3263 N94-29028
Identification of an unexpected space radiation hazard
[AD-A275170] 08 p3552 N94-29046
Charge trapping and breakdown in N2O oxides
[DE94-003775] 08 p3266 N94-30040
Research laboratories annual report 1992
[DE94-608124] 08 p3555 N94-30168
Dislocation loops in spinel crystals irradiated successively with deep and shallow ion implants
[DE94-005083] 08 p3517 N94-30201
Computer simulation of the interaction of fast hydrogen atoms with a molybdenum containing sorbed hydrogen
[DE94-608419] 08 p3209 N94-30253
Role of x ray-induced transcripts in adaptive responses following x rays
[DE94-005412] 08 p3386 N94-30895
Development of radiation resistant electrical cable insulations
[DE94-005189] 08 p3222 N94-30906
Investigations into ultraviolet matrix-assisted laser desorption
[DE94-005265] 08 p3296 N94-30908
Model of spacecraft atomic oxygen and solar exposure microenvironments 09 p3593 N94-31021
Performance of selected polymeric materials on LDEF
09 p3593 N94-31023
Fluorescence observations of LDEF exposed materials as an indicator of induced material reactions
09 p3593 N94-31025
Laser-induced fluorescence of space-exposed polyurethane 09 p3593 N94-31026
Degradation of optical components in space
09 p3594 N94-31029
Physical properties of glasses exposed to Earth-facing and trailing-side environments on LDEF
09 p3594 N94-31030
Space environmental effects on polymer composites: Research needs and opportunities
09 p3595 N94-31035
Spacecraft materials: Comparison between flight results obtained on LDEF and MIR 09 p3597 N94-31045
Transient radiation-induced absorption in the materials for a GSGG laser
[DE94-005316] 09 p3714 N94-31148
Analysis of beam-on-target interaction in a neutron-source test facility
[DE94-005392] 09 p3863 N94-31151
The role of defects in laser damage of multilayer coatings
[DE94-006731] 09 p3714 N94-31269
Ion-beam-driven amorphization of Ca2La8(Si4)6O2 single crystals
[DE94-006219] 09 p3895 N94-31307
Mitigation of adverse environmental effects on lunar-based astronomical instruments
09 p3598 N94-31426
The threshold energy for defect production in SiC: A molecular dynamic study
[DE94-007123] 09 p3896 N94-31499
Ionizing radiation effects on silicon test structures
[DE94-006060] 09 p3865 N94-31607
The influence of transmutation, void swelling, and flux/spectra uncertainties on the electrical properties of copper and copper alloys
[DE94-006213] 09 p3641 N94-31626
Defect-solute interactions near irradiation grain boundaries
[DE94-006215] 09 p3641 N94-31627
Design of new polymers to improve radiation stability of plastic scintillators
[DE94-008220] 09 p3652 N94-31764
ITS version 3.0: Powerful, user-friendly software for radiation modelling
[DE94-006607] 09 p3678 N94-32113
A comparison between two Monte Carlo codes on determination of transient chemical yields
[DE94-007224] 09 p3636 N94-32251
Analytical solutions of minimum ionization particle induced current shapes of silicon detectors and simulation of charge collection properties
[DE94-007523] 09 p3870 N94-32355
Intra-cascade surface recombination of point defects during ion bombardment of Ge(001)
[DE94-007740] 09 p3903 N94-32384
Point defect production, geometry, and stability in silicon: A molecular dynamics simulation study
[DE94-008292] 09 p3903 N94-32411
Vulnerability assessment of a space based weapon platform electronic system exposed to a thermonuclear weapon detonation
[DE94-007229] 09 p3611 N94-32667
Electron energy dependence of amorphization in Zr3Fe
[DE94-008459] 09 p3906 N94-32875
Irradiation-induced phase transformations in zirconium alloys
[DE94-008484] 09 p3648 N94-32993
Spacecraft environmental anomalies expert system
[AD-A277962] 09 p3612 N94-33262
Implementing bright light treatment for MSFC payload operations shiftworkers 10 p4098 N94-33623

Development of high temperature property database for Alloy 800H
[DE94-727589] 10 p4024 N94-33870
Relaxation of radiation damages in silicon planar detectors
[DE94-009084] 10 p4148 N94-34166
Solar radiation effects on glasses
[NASA-CR-195900] 10 p4029 N94-34232
Measuring track densities in lunar grains using image analysis 11 p4357 N94-35409
Improved performance of degraded solar arrays at non-zero sun incidence angles
[AD-A278905] 11 p4282 N94-35804
Irradiation-related amorphization and crystallization: in situ transmission electron microscope studies
[DE94-009823] 11 p4241 N94-36222
Enhanced charge trapping in bipolar spacer oxides during low-dose-rate irradiation
[DE94-007863] 11 p4260 N94-36268
On the effects of transforming the vibrational spectra of molecular systems under microwave radiation
[DE94-617057] 11 p4329 N94-36310
Hardness variability in commercial and hardened technologies
[DE94-007270] 11 p4261 N94-36362
Estimating low-dose rate irradiation response of MOSFETs
[DE94-007292] 11 p4342 N94-36367
Bounding the total-dose response of modern bipolar transistors
[DE94-007742] 11 p4261 N94-36371
A critical examination of charge funneling and its impact on single-event upset in Si devices
[DE94-007868] 11 p4261 N94-36373
Correlation of hot-carrier stress and ionization induced degradation in bipolar transistors
[DE94-007289] 12 p4532 N94-36540
Modelling irradiation creep of zirconium alloys
[DE94-619055] 12 p4414 N94-36544
Precipitation in Zr-2.5 Nb enhanced by proton irradiation
[DE94-619056] 12 p4415 N94-36563
Irradiation effects in Fe-30 percent Ni alloy during Ar ion implantation
[DE94-619057] 12 p4415 N94-36564
Ground and space flight experiments of the effects of light, sound and/or temperature on animals
[NASA-CR-196102] 12 p4478 N94-36986
Behavioral performance in monkeys exposed to TEMPO high-peak-power microwave pulses at 3 GHz
[AD-A280551] 12 p4478 N94-37045
Data compatibility for various Charpy-tests
[DE94-617534] 12 p4416 N94-37074
Irradiation assisted stress corrosion cracking of HTH Alloy X-750 and Alloy 625
[DE94-012667] 12 p4416 N94-37080
AEM and AES of radiation-induced segregation in proton-irradiated stainless steels
[DE94-012734] 12 p4418 N94-37398
Characterization of mechanical properties degradation using small punch testing technique
[DE94-011202] 12 p4418 N94-37410
Role of burn-in during qualification testing
[DE94-007864] 12 p4439 N94-37513
Studying of ion implantation effect on the biology in China
[DE94-620692] 12 p4479 N94-37535
Characterization of nuclear transmutations in materials irradiated test facilities
[DE94-013309] 12 p4420 N94-37552
Investigation of exposure to Extremely Low Frequency (ELF) magnetic and electric fields: Ongoing animals studies
[DE94-011239] 12 p4480 N94-37625

RADIATION EMISSION
U RADIATION

RADIATION EXPOSURE
U RADIATION DOSAGE

RADIATION FIELDS
U RADIATION DISTRIBUTION

RADIATION HARDENING
Radiation hardened nonvolatile memory for space and strategic applications
[DE93-000746] 01 p0319 N94-10146
Specification and testing for power by wire aircraft
[NASA-TM-106232] 01 p0046 N94-10765
Effect of switched-bias bakes on the postirradiation electrical response of MOS devices
[DE93-009629] 01 p0143 N94-11271
1/f noise and oxide traps in MOSFETs
[DE93-007581] 02 p0619 N94-12942
Mongoose ASIC microcontroller programming guide
[NASA-RP-1319] 02 p0623 N94-13671
Radiation hardening and radiation-induced chromium depletion effects on intergranular stress corrosion cracking of austenitic stainless steels
[DE93-011602] 02 p0572 N94-14058
Impurity conduction photoconductor detectors 03 p0902 N94-15046
Radiation hardening of a CCD technology through process and design modifications 03 p0906 N94-15071
SONOS technology for commercial and military nonvolatile memory applications
[DE93-015647] 03 p1011 N94-16661
Technology, design, simulation, and evaluation for SEP-hardened circuits 04 p1399 N94-18352
Radiation hardened microprocessor for small payloads 04 p1327 N94-19184
CMOS gate array characterization procedures
[AD-A269943] 05 p2014 N94-20029
Optics survivability support, volume 1
[DE93-019616] 05 p1985 N94-20262
Mongoose: Creation of a Rad-Hard MIPS R3000 05 p1754 N94-21090
Fully-depleted silicon-on-sapphire and its application to advanced VLSI design 05 p1765 N94-21709
Design and test of field programmable gate arrays in space applications 05 p1765 N94-21710
A qualified radiation hardened nonvolatile memory for space and tactical weapons applications
[DE94-001211] 06 p2559 N94-23186
Microstructural development in low activation ferritic alloys irradiated to 200 dpa at 420 C
[DE94-004269] 07 p2731 N94-25803
Radiation hardening effects on localized deformation and stress corrosion cracking of stainless steels
[DE94-004308] 07 p2731 N94-25804
Advanced qualification techniques
[DE94-003709] 07 p2780 N94-25812
Elementary particle interactions
[DE94-004238] 08 p3482 N94-28504
Recent results from testing fast ADCs
[DE94-005565] 08 p3406 N94-30004
Development of radiation resistant electrical cable insulations 08 p3223 N94-30480
Silica scintillating materials prepared by sol-gel methods
[DE94-005123] 08 p3220 N94-30778
Development of radiation resistant electrical cable insulations
[DE94-005189] 08 p3222 N94-30906
Radiation tolerant, high speed, low power, gallium arsenide logic
[AD-A277293] 09 p3694 N94-32509
Spacecraft environmental anomalies expert system
[AD-A277962] 09 p3612 N94-33262
Proposal to produce novel, transparent radiation hard low refractive index
[AD-A278476] 10 p4029 N94-34087
Relaxation of radiation damages in silicon planar detectors
[DE94-009084] 10 p4148 N94-34166
Rapid and accurate timing simulation of radiation-hardened digital microelectronics using VHDL
[AD-A278644] 11 p4261 N94-36361
Hardness variability in commercial and hardened technologies
[DE94-007270] 11 p4261 N94-36362
A critical examination of charge funneling and its impact on single-event upset in Si devices
[DE94-007868] 11 p4261 N94-36373
Single event mirroring and sense amplifier designs for enhanced SE tolerance of DRAMs
[DE94-010397] 12 p4438 N94-37190
A proposed SEU tolerant DRAM cell
[DE94-010758] 12 p4438 N94-37196
Role of burn-in during qualification testing
[DE94-007864] 12 p4439 N94-37513

RADIATION HAZARDS
Fully coupled neutronic and hydrodynamic analysis of space nuclear reactor reentry accidents
[DE93-005459] 01 p0372 N94-10890
Radiation considerations for interplanetary missions 01 p0045 N94-11559
Hazard calculations of diffuse reflected laser radiation for the SELENE program
[NASA-TM-4520] 03 p1042 N94-17285
VLF Harold E. Holt RADHAZ measurements
[AD-A272018] 05 p1737 N94-20620
Magnetic insulation of secondary electrons in plasma source ion implantation
[DE93-040106] 05 p1997 N94-21988
Risk perspectives for Topaz 2 flight mission
[DE94-003229] 07 p2700 N94-25956
Vacuum-UV-effects on E. coli plasmid pUC19: Inactivation, strand break induction and mutation induction
[DLR-FB-93-26] 07 p2903 N94-27754
Identification of an unexpected space radiation hazard
[AD-A275170] 08 p3552 N94-29046
Caesium-137 in a boreal forest ecosystem: Aspects on the long-term behavior
[PB94-137809] 08 p3347 N94-29158
Laser safety manual for DREO
[AD-A276288] 09 p3714 N94-31255
High peak power microwaves: A health hazard
[AD-A277168] 09 p3681 N94-32576
Independent safety assessment of the Topaz-2 space nuclear reactor power system
[DE94-008653] 09 p3877 N94-32879

RADIATION HEATING
U RADIANT HEATING

RADIATION INJURIES
Wound healing after laser injury to skin: The effect of occlusion and vitamin E
[AD-A266473] 03 p1128 N94-16779
Conductive garments to prevent Radio-Frequency (RF) burns
[AD-D015832] 04 p1512 N94-18730
Disturbed neuronal migration in the cerebral cortex of mice by low-dose gamma radiation 07 p2904 N94-27470
Distribution of GABA immunoreactive neurons in the brain of rolling mouse Nagoya and gamma-irradiated mouse 07 p2904 N94-27471
Effects of gamma ray radiation on the developing mouse cerebellum: Apoptotic cell death and induction of tissue transglutaminase 07 p2904 N94-27472
High peak power microwaves: A health hazard
[AD-A277168] 09 p3681 N94-32576

RADIATION INTENSITY
U RADIANT FLUX DENSITY

RADIATION LAWS
NT KIRCHHOFF LAW OF RADIATION
NT STEFAN-BOLTZMANN LAW
A simple model for determining photoelectron-generated radiation scaling laws
[DE94-006130] 09 p3761 N94-32660

RADIATION MEASUREMENT
An intercomparison of the radium mass standards of the UK and the USSR: 2
[NPL-RSA(EXT)-34] 01 p0359 N94-10266
Demonstration prototype gamma-ray hodoscope alternative to CARGOSCAN for rocket stage monitoring
[DE93-006908] 01 p0169 N94-10326
Measuring surface fluxes in CAPE
[NASA-CR-193664] 02 p0711 N94-12788
Evolution of the lower planetary boundary layer over strongly contrasting surfaces
[DE93-010667] 02 p0717 N94-14424
Real time radiation measurements in space 03 p0980 N94-16092
Development and evaluation of alternative radioanalytical methods, including mass spectrometry for marine materials
[DE93-625117] 04 p1345 N94-17691
Planetary plasma waves
[NASA-CR-194295] 04 p1629 N94-19094
Thermal infrared remote sensing and Kirchhoff's law: 1. Laboratory measurements 05 p1685 N94-20733
Areally averaged estimates of surface heat flux from ARM field studies
[DE93-018569] 05 p1859 N94-22036
Applications of planar near-field measurements to electromagnetic radiation and interference problems 05 p1747 N94-22252
Proceedings of the Workshop on New Generation of Radiation Budget Measurements From Space and Their Use in Climate Modelling and Diagnostic Studies
[MPIM-90] 05 p1860 N94-22283
Satellite measurements of radiation budget parameters 05 p1860 N94-22284
Optical properties of cirrus derived from airborne measurements during FIRE IFO 2 05 p1872 N94-22297
Ground-based passive remote sensing during FIRE IFO 2 05 p1844 N94-22319
Atmospheric Radiation Measurement (ARM)/CART site 06 p2411 N94-24379
Testbed model and data assimilation for ARM
[DE94-000432] 07 p2893 N94-26082
Develop and fabricate a radiation dose measurement system for satellites
[PL-TR-93-2161] 07 p2698 N94-28210
Develop and fabricate a radiation dose measurement system for satellites
[PL-TR-93-2099] 07 p2698 N94-28217
The automated rotating shadowband spectroradiometer
[DE94-001878] 08 p3269 N94-28464
Measurement basis of near fields in spherical coordinates in the 100 MHz to 6 GHz band
[REPT-932-430-107] 08 p3255 N94-30153

Determination of photon fluence spectra from the NPL Mobaltron Co-60 unit
[PB94-149150] 08 p3492 N94-30795
Solar neutrino experiments: An update
[DE94-006061] 08 p3551 N94-30884
Neutron measurements at the commercial aircraft altitudes
[ISBN-0-315-86201-7] 09 p3955 N94-31709
Investigation of scintillator and fibre light in plastic scintillation dosimetry
[ISBN-0-315-87190-3] 09 p3879 N94-31877
System for monitoring and analyzing field energy exposure
[AD-D016115] 09 p3681 N94-32625
Water vapor from sunradiometry in comparison with microwave and balloon-sonde measurements at the Southern Great Plains ARM Site
[DE94-007479] 09 p3786 N94-32759
Radiometry spot measurement system
[NASA-TM-106561] 09 p3883 N94-32777
User interface development and metadata considerations for the Atmospheric Radiation Measurement (ARM) archive 10 p4157 N94-33827
Single-shot intensity and phase measurements of detuning and saturation effects in an ultrashort XeCl amplifier
[DE94-007535] 10 p4058 N94-33860
The Atmospheric Radiation Measurement Program and interfaces with external data sources
[DE94-003699] 11 p4286 N94-36024
ARM: A climate process observatory
[DE94-007473] 12 p4463 N94-36477
Two-channel microwave radiometer for observations of total column precipitable water vapor and cloud liquid water path
[DE94-007480] 12 p4471 N94-36479
Site Scientific Mission Plan for the Southern Great Plains CART site, January - June 1994
[DE94-012114] 12 p4474 N94-37394
Proceedings of the Third Atmospheric Radiation Measurement (ARM) Science Team Meeting
[DE94-011194] 12 p4467 N94-37454

RADIATION MEASURING INSTRUMENTS
NT ADVANCED VERY HIGH RESOLUTION RADIOMETER
NT BOLOMETERS
NT CERENKOV COUNTERS
NT DICKE RADIOMETERS
NT DOSIMETERS
NT EBERT SPECTROMETERS
NT ELECTRON COUNTERS
NT ELECTROPHOTOMETERS
NT ELECTROSTATIC PROBES
NT FABRY-PEROT SPECTROMETERS
NT FLIR DETECTORS
NT GOLAY DETECTOR CELLS
NT HODOSCOPES
NT INFRARED DETECTORS
NT INFRARED INSTRUMENTS
NT INFRARED RADIOMETERS
NT INFRARED SCANNERS
NT INFRARED SPECTROMETERS
NT INFRARED SPECTROPHOTOMETERS
NT MICROWAVE RADIOMETERS
NT NEUTRON COUNTERS
NT NEUTRON SPECTROMETERS
NT PARTICLE TELESCOPES
NT PHOTOMETERS
NT PRESSURE MODULATOR RADIOMETERS
NT PROPORTIONAL COUNTERS
NT PYRANOMETERS
NT QUANTUM COUNTERS
NT RADIATION COUNTERS
NT RADIATION DETECTORS
NT RADIOMETERS
NT RIOMETERS
NT SCINTILLATION COUNTERS
NT SILICON RADIATION DETECTORS
NT SOLAR SPECTROMETERS
NT SPECTROHELIOGRAPHS
NT SPECTROPHOTOMETERS
NT SPECTRORADIOMETERS
NT TOTAL OZONE MAPPING SPECTROMETER
NT ULTRAVIOLET DETECTORS
NT ULTRAVIOLET SPECTROMETERS
NT X RAY DETECTORS

A Fourier transform microscope for x ray and/or gamma ray imaging
[AD-D015742] 02 p0791 N94-13664
Proceedings of an ESA Symposium on Photon Detectors for Space Instrumentation
[ESA-SP-356] 03 p0899 N94-15025
Outlook for hard x ray and gamma ray astronomy 03 p0904 N94-15057
Nb-based SJTJ for nuclear detection: Preliminary results with alpha radiation 03 p0905 N94-15068
Improved optical radiation detectors and their calibration: 200 nm - 30 microns 03 p0906 N94-15075
In orbit adiabatic demagnetization refrigeration for bolometric and microcalorimetric detectors 03 p0907 N94-15079
Silicon radiation sensor systems for gamma and x ray detection at SI 03 p0909 N94-15095
The space technology research vehicle: Development status 03 p0896 N94-17183
Contributions to the 23rd ICRC from emulsion chamber experiments at Mt. Chacaltaya and Pamirs
[ICRR-REPT-295-93-7] 07 p3112 N94-25624
Observation of characteristics of cosmic-ray hadron interactions in uniform-type thick lead chambers at Pamir, 1 07 p3112 N94-25628
Observation of characteristics of cosmic-ray hadron interactions in uniform-type thick lead chambers at Pamir, 2 07 p3113 N94-25629
Solar neutrino experiments: An update
[DE94-006061] 08 p3551 N94-30884
Evidence of solar oscillations in Rayleigh-scattered light 09 p3952 N94-31214

RADIATION MEDICINE
U NUCLEAR MEDICINE

RADIATION METERS
U RADIATION MEASURING INSTRUMENTS

RADIATION NOISE
U ELECTROMAGNETIC NOISE

RADIATION PRESSURE
NT ILLUMINANCE
NT LUMINANCE
NT LUMINOUS INTENSITY
NT SOUND PRESSURE

Using solar flare track densities to determine the origin of interplanetary dust particles 01 p0429 N94-12078
Improved treatment of global positioning system force parameters in precise orbit determination applications 02 p0514 N94-14371
Contribution to the study of HF converters radiated disturbances
[ECL-92-34] 06 p2313 N94-25421
Infrared properties of obscuring dust tori in active galactic nuclei 08 p3545 N94-29832
The Earth Satellite Program (ESP), version 2.0
[AD-A278860] 11 p4201 N94-35827

RADIATION PROTECTION
NT RADIATION SHIELDING
NT SOLAR RADIATION SHIELDING

Report on Subgroup on Data Banks for Risk Assessment
[DE93-012150] 01 p0418 N94-10646
A proposed performance index for galactic cosmic ray shielding materials
[NASA-TM-4444] 01 p0484 N94-11278
A photovoltaic catenary-tent array for the Martian surface
[NASA-TM-106306] 02 p0621 N94-13194
Beta/gamma test problems for ITS
[DE93-013522] 02 p0781 N94-13349
Preliminary nuclear safety assessment of the NEPST (Topaz 2) space reactor program
[DE93-012853] 02 p0551 N94-13514
CRRES to blaze new trails in orbit
[NASA-TM-109314] 02 p0713 N94-13620
Study on the biological effect of cosmic radiation and the development of radiation protection technology (L-11) 02 p0593 N94-13768
Exposure fluctuations of astronauts due to orientation
[NASA-TP-3364] 03 p1300 N94-15816
Towards a new radiation protection organization
[FOA-C-40304-4.3] 06 p2437 N94-24292
Proceedings of the Second EGS4 User's Meeting in Japan
[DE93-520383] 07 p3032 N94-26543
Conceptual design of the tokamak radiation shielding for the Tokamak Physics Experiment (TPX)
[DE94-002791] 07 p3044 N94-26858
Research and development within nonlinear optics for protection of optical sensors against laser irradiation on of optical sensors against laser irradiation. Quarterannual report 1 (april 1993))
[PB94-124245] 07 p3037 N94-27046
Nuclear energy related research
[DE94-606286] 08 p3494 N94-28623
Selection of the Space Station Freedom (SSF) Flat Collector Circuit (FCC) insulation material 08 p3165 N94-28701
Design of new polymers to improve radiation stability of plastic scintillators
[DE94-008220] 09 p3652 N94-31764
Integrated safety program for the Nuclear Electric Propulsion Space Test Program
[DE94-004670] 09 p3615 N94-32669

RADIATION PYROMETERS
Correction-free pyrometry in radiant wall furnaces
[NASA-CASE-NPO-18655-1-CU] 10 p4056 N94-35114
Multiwavelength pyrometer for gray and non-gray surfaces in the presence of interfering radiation
[NASA-CASE-LEW-15250-1] 11 p4269 N94-35383

RADIATION RESISTANCE
U RADIATION TOLERANCE

RADIATION SHIELDING
NT SOLAR RADIATION SHIELDING
Proton transport methods for satellite shield modeling
[DE93-013602] 01 p0042 N94-10520
Development of deterministic transport methods for low energy neutrons for shielding in space
[NASA-CR-194172] 01 p0366 N94-11199
A proposed performance index for galactic cosmic ray shielding materials
[NASA-TM-4444] 01 p0484 N94-11278
Radiation considerations for interplanetary missions 01 p0045 N94-11559
Effects of radiobiological uncertainty on vehicle and habitat shield design for missions to the moon and Mars
[NASA-TP-3312] 02 p0846 N94-12875
Semiempirical fragmentation models on galactic cosmic ray transport calculations with hydrogen target
[NASA-TP-3350] 02 p0847 N94-13263
Development and application of the automated Monte Carlo biasing procedure in SAS4
[DE93-015205] 02 p0774 N94-14334
Measuring parity violation using the neutron capture reaction
[DE93-016629] 02 p0786 N94-14514
Engineering Physics and Mathematics Division progress report, period ending 31 December 1992
[DE93-015118] 03 p1301 N94-14926
Shielding from space radiations
[NASA-CR-194578] 03 p1180 N94-15715
Exposure fluctuations of astronauts due to orientation
[NASA-TP-3364] 03 p1300 N94-15816
Approximate Green's function methods for HZE transport in multilayered materials
[NASA-TM-4519] 03 p1300 N94-17084
Shielding from space radiations
[NASA-CR-194664] 03 p1301 N94-17255
Calculations of cosmic-ray helium transport in shielding materials
[NASA-TP-3354] 03 p1301 N94-17666
Exponential characteristic spatial quadrature for discrete ordinates neutral particle transport in two-dimensional cartesian coordinates
[AD-A270458] 04 p1554 N94-19671
Transient thermal analysis of cryocondensation pump for JET
[DE93-040372] 05 p1992 N94-20003
Shielding from space radiations
[NASA-CR-194683] 05 p1895 N94-20063
Improved approximate formulas for flux from cylindrical and rectangular sources
[DE93-011390] 05 p1742 N94-22268
GOLF mechanisms 06 p2357 N94-24003
Magnetic shielding of interplanetary spacecraft against solar flare radiation
[NASA-CR-195539] 06 p2204 N94-24334
The 1991-1992 project summaries 07 p2943 N94-25698
Experimental and numerical investigation of shock wave propagation through complex geometry, gas continuous, two-phase media
[DE94-001408] 07 p2791 N94-26121
A robust helium-cooled shield/blanket design for ITER
[DE94-003402] 07 p3043 N94-26323
Conceptual design of the tokamak radiation shielding for the Tokamak Physics Experiment (TPX)
[DE94-002791] 07 p3044 N94-26858
A widely adaptable habitat construction system utilizing space resources 07 p2688 N94-27374
Monte Carlo calculations of low background detector response
[DE94-004593] 07 p3116 N94-27621
Fusion reactor systems studies
[DE94-003162] 07 p3046 N94-27686
Mitigation of adverse environmental effects on lunar-based astronomical instruments 09 p3598 N94-31426
Complete model description of an electron beam using ACCEPT Monte Carlo simulation code
[DE94-007063] 09 p3872 N94-32628
Implementation and display of Computer Aided Design (CAD) models in Monte Carlo radiation transport and shielding applications
[DE94-007221] 09 p3819 N94-32641
Multi-group helium and hydrogen production cross section libraries for fusion neutronics design
[DE94-727627] 10 p4140 N94-33934

Estimates of cellular mutagenesis from cosmic rays
[NASA-TP-3453] 12 p4481 N94-37282
The logic behind thick, liquid-walled, fusion concepts
[DE94-012678] 12 p4528 N94-37307
Stopping power of charged particles from 10 eV/amu to 10 GeV/amu
[DE94-719024] 12 p4518 N94-37387
Two-dimensional over-all neutronics analysis of the ITER device
[DE94-718963] 12 p4530 N94-37464

RADIATION SICKNESS
Predicting radiation induced performance decrements of AH-1 helicopter crews. Volume 1: Predicted veersus actual performance of AH-1 crews induced with symptoms simulating radiation sickness
[AD-A268376] 03 p1138 N94-17460

RADIATION SOURCES
NT MONOCHROMATORS
NT NEUTRON SOURCES
NT POINT SOURCES
Intense neutron sources for fusion materials studies
[DE93-009782] 01 p0391 N94-11171
Advanced concepts theory annual report 1992
[AD-A266132] 01 p0393 N94-11474
Two-dimensional simulations of foil implosion experiments on the Los Alamos capacitor bank
[DE93-012676] 02 p0794 N94-12814
Powder diffraction studies using anomalous dispersion
[DE93-012531] 03 p1210 N94-16775
Conical geometry for sagittal focusing as applied to x rays from synchrotrons
[DE93-017238] 04 p1593 N94-17760
General geometry PIC for MIMD computers
[AD-A269085] 04 p1534 N94-18767
Harmonic generation at high intensities
[DE93-018632] 04 p1572 N94-19283
Electrical analysis of wideband and distributed windows using time-dependent field codes
[DE94-002987] 07 p2768 N94-26310
Monte Carlo calculations of low background detector response
[DE94-004593] 07 p3116 N94-27621
Determination of photon fluence spectra from the NPL Mobaltron Co-60 unit
[PB94-149150] 08 p3492 N94-30795
Plasma physics applications to intense radiation sources, pulsed power and space physics. Short pulse ultra intense laser-plasma interaction experiment
[AD-A278440] 10 p4144 N94-33555

RADIATION SPECTRA
NT ABSORPTION SPECTRA
NT BALMER SERIES
NT D LINES
NT ELECTROMAGNETIC SPECTRA
NT ELECTRONIC SPECTRA
NT EMISSION SPECTRA
NT FRAUNHOFER LINES
NT GAMMA RAY SPECTRA
NT H ALPHA LINE
NT H LINES
NT INFRARED SPECTRA
NT K LINES
NT LINE SPECTRA
NT LYMAN SPECTRA
NT MICROWAVE SPECTRA
NT RADIO SPECTRA
NT RAMAN SPECTRA
NT RYDBERG SERIES
NT SOLAR SPECTRA
NT STELLAR SPECTRA
NT UBV SPECTRA
NT ULTRAVIOLET SPECTRA
NT VIBRATIONAL SPECTRA
NT VISIBLE SPECTRUM
NT X RAY SPECTRA
Operational test of the airborne data acquisition system: SADA, the Bara Bonita experiment
[INPE-5451-NTC/305] 02 p0685 N94-13610
Earth observational research using multistage EOS-like data
[NASA-CR-194626] 03 p1084 N94-16831
Development of robust multilayer optics for use in high-peak power radiation environments
[DE93-018557] 04 p1580 N94-18931
EGRET Mission and Data Analysis
[MPE-PREPRINT-223] 04 p1622 N94-19462
Suitability of infrared spectroscopy for remote sensing of tropospheric trace gases
[KFK-5183] 04 p1479 N94-19507
The NRL LACE program
[AD-A270861] 05 p1657 N94-19896
Diffuse reflectance spectra of orthopyroxene, olivine, and plagioclase as a function of composition and structure 05 p2087 N94-20906
Examination for optimization of synchrotron radiation spectrum for the x ray depth lithography
[BONN-IR-92-32] 05 p1987 N94-21148
A double arm time-of-flight spectrometer based on position-sensitive parallel-grid avalanche counters
[DE93-616665] 07 p3012 N94-25750
Remote pumping of solid state lasers with nuclear driven fluorescers
[DE94-004846] 08 p3296 N94-30614
Determination of photon fluence spectra from the NPL Mobaltron Co-60 unit
[PB94-149150] 08 p3492 N94-30795

RADIATION THERAPY
The role of constitutive and inducible processes in the response of human squamous cell carcinoma cell lines to ionizing radiation
[DE93-015150] 03 p1129 N94-16970
Numerical modeling for an electric-field hyperthermia applicator 05 p1729 N94-20451
The role of hyperbaric oxygen as a prophylaxis for radiation enteritis
[AD-A274974] 07 p2901 N94-26517
Computer Assisted Medical Interventions: Application to Conformal Radiotherapy
[RR-912-I] 08 p3395 N94-30028
Conformal external radiotherapy of prostatic carcinoma: Requirements and preliminary results 08 p3395 N94-30029
Pre- and intra-radiotherapy multimodal image registration: Principles and first experiments 08 p3395 N94-30030
Laboratory Directed Research & Development Program
[DE94-005928] 09 p3956 N94-31523

RADIATION TOLERANCE
A detailed study of the photo-injection annealing of thermally diffused InP solar cells 01 p0048 N94-11381
High temperature annealing of minority carrier traps in irradiated MOCVD n(+)p InP solar cell junctions 01 p0048 N94-11382
Radiation effects in heteroepitaxial InP solar cells 01 p0048 N94-11383
Progress in p(+)n InP solar cells fabricated by thermal diffusion 01 p0048 N94-11384
Electrochemical characterization of p(+)n and n(+)p diffused InP structures 01 p0049 N94-11385
Investigation of the radiation resistance of triple-junction a-Si:H alloy solar cells irradiated with 1.00 MeV protons 01 p0050 N94-11391
Results of some initial space qualification testing on triple junction a-Si and CuInSe2 thin film solar cells 01 p0050 N94-11392
Radiation effects in Ga(0.47)In(0.53)As solar cells 01 p0052 N94-11404
The UoSAT-5 solar cell experiment: First year in orbit 01 p0053 N94-11409
An overview of the Defence Research Agency photovoltaic programme 01 p0053 N94-11412
Workshop on Heteroepitaxial InP Solar Cells 01 p0054 N94-11414
Development of plastic capsule for research reactor irradiation
[DE93-753186] 01 p0372 N94-11591
The Second Workshop on Deployment and Assembly Experiment of Large Space Structure on Orbit
[NASDA-CON-930003] 02 p0529 N94-13268
Research on radiation resistance properties of structural materials for space use 02 p0529 N94-13271
The 1.00 MeV proton radiation resistance studies of amorphous silicon-based alloy solar cells 02 p0703 N94-13639
Fault handling schemes in electronic systems with specific application to radiation tolerance and VLSI design
[NASA-CR-194559] 03 p1008 N94-15640
The role of constitutive and inducible processes in the response of human squamous cell carcinoma cell lines to ionizing radiation
[DE93-015150] 03 p1129 N94-16970
Experience with custom processors in space flight applications 04 p1336 N94-18338
Radiation hardened microprocessor for small payloads 04 p1327 N94-19184
A method of measuring the thermoradiative properties of ceramic materials in a space environment 05 p1665 N94-21405
Single crystal diamond films
[AD-A266759] 05 p2028 N94-21517
Issues related to mechanical properties of neutron-irradiated ceramics
[DE93-040262] 05 p1707 N94-21560
Spaceflight Radiation Health program at the Lyndon B. Johnson Space Center
[NASA-TM-104782] 05 p1893 N94-21863
Effects of ionizing radiation on modern ion exchange materials
[DE94-001569] 06 p2535 N94-24505
Molecular biological studies on the human radioresistance and drug resistance
[DE93-632682] 07 p2910 N94-26549
The radiation design handbook
[ESA-PSS-01-609-ISSUE-1] 07 p2696 N94-27397
Studies on bacterial spore ultraviolet light resistance and regulation of the activity of a spore protease
[AD-A275448] 08 p3384 N94-28884
Development of radiation resistant electrical cable insulations
[DE94-005189] 08 p3222 N94-30906

RADIATION TRANSPORT
A new method to assess Monte Carlo convergence
[DE93-012667] 02 p0772 N94-12919
Three dimensional time-dependent hydrodynamic and propagation modeling of x ray laser emission
[DE93-012575] 02 p0654 N94-12962
MCNP benchmark analyses of critical experiments for the Space Nuclear Thermal Propulsion program
[DE93-014046] 02 p0548 N94-12981
Semiempirical fragmentation models on galactic cosmic ray transport calculations with hydrogen target
[NASA-TP-3350] 02 p0847 N94-13263
Beta/gamma test problems for ITS
[DE93-013522] 02 p0781 N94-13349
Distributed processor Monte Carlo: MCNP results on a 16-node IBM cluster
[DE93-012639] 02 p0752 N94-14176
Development and application of the automated Monte Carlo biasing procedure in SAS4
[DE93-015205] 02 p0774 N94-14334
The LAHET code system: Introduction, development, and benchmarking
[DE93-012657] 02 p0787 N94-14804
Engineering Physics and Mathematics Division progress report, period ending 31 December 1992
[DE93-015118] 03 p1301 N94-14926
The effects of radiation transport on line ratios used as temperature and density diagnostic
[DE93-016424] 03 p1205 N94-17663
Computational model of surface ablation from tokamak disruptions
[DE94-002204] 06 p2550 N94-23474
Improved gas core propulsion model
[DE94-000929] 06 p2220 N94-24511
Proton irradiation on materials 07 p3030 N94-27898
Performance of MCNP4A on seven computing platforms
[DE93-040101] 08 p3419 N94-29816
Radiative flux calculations at UV and visible wavelengths
[DE94-004278] 08 p3350 N94-30613
Modelling erosion damage from low-energy plasma gun simulations of disruptions
[DE94-005196] 08 p3509 N94-30697
Radiation transport in cloudy and aerosol loaded atmospheres 08 p3366 N94-30805
ITS version 3.0: Powerful, user-friendly software for radiation modelling
[DE94-006607] 09 p3678 N94-32113
Implementation and display of Computer Aided Design (CAD) models in Monte Carlo radiation transport and shielding applications
[DE94-007221] 09 p3819 N94-32641
The 2D deterministic radiation transport with the discontinuous finite element method
[DE94-004687] 09 p3849 N94-32670
Recursive recovery of Markov transition probabilities from boundary value data
[DE94-011914] 11 p4317 N94-36235
Data simulation for the Associated Particle Imaging system
[DE94-012664] 12 p4518 N94-37305
User's manual for SNL-SAND-2 code
[DE94-011744] 12 p4496 N94-37673

RADIATIVE HEAT TRANSFER
The cloud radiative feedback of a midlatitude squall line system and implication for climate study
[DE93-010511] 01 p0283 N94-10290
The heat transfer by radiation between two media
[DE93-617820] 01 p0149 N94-10838
Meteorological Satellite Center
[MSC-TN-26] 01 p0190 N94-11079
Why convective heat transport in the solar nebula was inefficient 01 p0458 N94-12143
Chemistry and transport in a multi-dimensional model
[NASA-CR-194425] 02 p0716 N94-13969
The accuracy of approximating radiative heat transfer using a temperature dependent thermal conductivity
[DE93-013105] 02 p0638 N94-14318

Study of multi-dimensional radiative energy transfer in molecular gases
[NASA-CR-194613] 03 p1181 N94-15752
The cooling rates of pahoehoe flows: The importance of lava porosity 03 p1103 N94-16282
Studies on nonequilibrium phenomena in supersonic chemically reacting flows
[NASA-CR-194662] 03 p1027 N94-17215
Heat transfer quantitative characterization: Passive and active methods 04 p1431 N94-18650
Total hemispherical emittance of Niobium-1 percent zirconium fuel cladding for the SP-100 space reactor
[AD-A270456] 04 p1576 N94-19589
RADCAL: A narrow-band model for radiation calculations in a combustion environment
[PB93-200889] 05 p1682 N94-21448
Flames in dusty mixtures: Their structure and stability
[NASA-CR-191567] 06 p2317 N94-23089
Fully coupled nonlinear thermomechanical analysis including general contact in PALM2D
[DE94-001661] 06 p2568 N94-23216
Accuracy control in Monte Carlo radiative calculations 06 p2321 N94-23639
Ignition and combustion characteristics of metallized propellants, phase 2
[NASA-CR-195107] 06 p2266 N94-24700
ARM Fourier transform spectrometer data analysis tools
[DE94-000865] 07 p2895 N94-26697
Researches of the Electrotechnical Laboratory. No. 53: Spectral emission from combustion gas containing scattering media
[JTN-94-80603] 07 p2717 N94-27246
Numerical and experimental analyses of the radiant heat flux produced by quartz heating systems
[NASA-TP-3387] 07 p3011 N94-27659
Numerical simulation of radiative heat loss in an experimental burner
[DE94-002016] 08 p3277 N94-29923
Measurements and predictions of the combustion characteristics of enclosed swirl-stabilized propane flames
[IECE-CFE-TR-001] 08 p3198 N94-30017
Thermal conductivities, electrical resistivities, and Seebeck coefficients of YBa2Cu3O(7-x) superconductors from 80 to 300 K
[DE94-004796] 08 p3520 N94-30724
Computational radiative heat transfer in homogeneous and nonhomogeneous nonscattering media 09 p3702 N94-31563
Chemical vapor deposition fluid flow simulation modelling tool
[NASA-CR-189648] 09 p3707 N94-32480
An evaluation of RAMS radiation schemes by field measurements
[DE94-008053] 09 p3767 N94-32750
JPRS report: Science and technology. Central Eurasia
[JPRS-UST-94-008] 11 p4249 N94-35228
Selected translated abstracts of Russian-language climate-change publications. 2: Clouds
[DE94-011465] 11 p4295 N94-36244
Hypersonic, nonequilibrium flow over the FIRE 2 forebody at 1634 sec
[NASA-TM-109141] 12 p4444 N94-37455
Factors influencing the parameterization of anvil clouds within GCMs
[DE94-010794] 12 p4475 N94-37621

RADIATIVE LIFETIME

Scintillation mechanism in stoichiometric cerium compounds
[DE93-015499] 03 p0948 N94-16771
B lifetimes at CDF
[DE94-006850] 09 p3866 N94-31669

RADIATIVE RECOMBINATION

Time-resolved optical studies of charge relaxation and charge transfer at electrode interfaces
[DE93-013985] 01 p0398 N94-11117
Atomic processes relevant to polarization plasma spectroscopy
[DE93-753240] 01 p0393 N94-11594
Merged beam studies of laser stimulated radiative recombination
[AD-A267186] 03 p1037 N94-15145
The investigation of electron-ion radiative and dielectronic recombination in high-temperature plasmas
[DE94-005150] 08 p3509 N94-30755
Material engineering of the novel semiconductor structures
[AD-A278386] 09 p3910 N94-33355

RADIATIVE TRANSFER

NT RADIATIVE HEAT TRANSFER
Conductive-radiative model for predicting the shape of HgI2 crystal grown in the LTVG furnace 01 p0117 N94-10201
Retrieval of radiation budgets in the Arctic from satellite measurements 01 p0229 N94-10714
Studies of the net surface radiative flux from satellite radiances during FIFE
[NASA-CR-193150] 01 p0230 N94-10953
Simulation of images of water vapor channel and infrared split channel 01 p0190 N94-11081
Effects of satellite spectral resolution and atmospheric water vapor on retrieval of near-ground temperatures
[AD-A264920] 01 p0245 N94-11851
Remote sensing for numerical modelling of radiative transfer processes in ocean environment 01 p0204 N94-11973
The evaluation of radiative process in the atmosphere-ground system by Monte Carlo method 01 p0205 N94-11980
An observational search for CO2 ice clouds on Mars 01 p0441 N94-12054
Multichannel dual angle approach for sea surface temperature retrieval in context of ERS-1 scenario 01 p0252 N94-12512
Optimal hemicube sampling
[DE93-010499] 01 p0334 N94-12591
Verification of the atmosphere-ocean radiative transfer parametric models 01 p0225 N94-12738
DMSP F11 SSM/T-2 calibration and validation
[AD-A265817] 02 p0719 N94-12978
The continuum emission of active galactic nuclei
[ITN-93-85208] 02 p0847 N94-13232
Basic research in solar physics
[NASA-CR-193632] 02 p0844 N94-13234
Radiative transfer in the dynamic atmospheres of Mira-type variables
[NASA-CR-193324] 02 p0829 N94-13287
ADP study of gamma-ray bursts
[NASA-CR-194311] 02 p0848 N94-13708
Water-vapour, total water and rainrate from passive microwave satellite data over ocean
[DLR-FB-92-37] 02 p0723 N94-14189
Ground truth spectrometry and imagery of eruption clouds to maximize utility of satellite imagery
[NASA-CR-194358] 03 p1081 N94-15181
Study of multi-dimensional radiative energy transfer in molecular gases
[NASA-CR-194613] 03 p1181 N94-15752
The vertical distribution of heating in the tropical atmosphere
[AD-A270452] 04 p1490 N94-18514
Physical retrieval of precipitation water contents from Special Sensor Microwave/Imager (SSM/I) data. Part 1: A cloud ensemble/radiative parameterization for sensor response (report version) 04 p1491 N94-18604
Computational astrophysics: Pulsating stars
[DE93-018369] 04 p1627 N94-18857
Radiosity algorithms using higher order finite element methods
[DE93-018098] 04 p1531 N94-19548
Remote sensing of Earth terrain
[NASA-CR-194598] 04 p1464 N94-19681
Relating ground truth collection to model sensitivity 05 p1719 N94-20409
Simulated retrieval of land surface parameters using multichannel satellite microwave radiometry 05 p1727 N94-20443
Second order distorted born approximation for backscattering from a layer of discrete random medium 05 p1728 N94-20448
Effects of hydrodynamics and thermal radiation in the atmosphere after comet impacts 05 p1862 N94-20649
A retrieval error analysis technique for passive infrared atmospheric sounders
[AD-A272618] 05 p1867 N94-21212
Cirrus properties deduced from CO2 lidar observations of zenith-enhanced backscatter from oriented crystals 05 p1871 N94-22295
Bi-directional reflectance and other radiation parameters of cirrus from ER-2 observations 05 p1871 N94-22296
Lidar and radar derived cirrus microphysical properties for the 26 November 1991 case study 05 p1873 N94-22305
Comparisons of downwelling radiation to model predictions based on groundbased measurements during FIRE 1991 05 p1876 N94-22320
A comparison of small and larger mesoscale latent heat and radiative fluxes: December 6 case study 05 p1879 N94-22335
Investigation of the effects of the macrophysical and microphysical properties of cirrus clouds on the retrieval of optical properties: Results for FIRE 2 05 p1880 N94-22339
Extinction efficiencies from DDA calculations solved for finite circular cylinders and disks 05 p1880 N94-22340
Remote sensing estimates of cirrus particle size for tropical and midlatitude cirrus: Hexagonal crystals and ice spheres 05 p1880 N94-22342
An overview of the radiation component of the NASA TOGA-COARE experiment 05 p1881 N94-22344
Modelling TOVS radiances of synoptic systems
[NASA-CR-194847] 06 p2408 N94-23620
Development of an analytical-numerical model to predict radiant emission or absorption
[NASA-CR-194860] 06 p2453 N94-23624
Thermal analysis of combinatorial solid geometry models using SINDA 06 p2323 N94-23650
Radiative forcing calculations for SF6 and CH4 using a correlated k-distribution transmission model
[DE94-001855] 06 p2397 N94-23700
Participation in TOMS missions
[NASA-CR-195110] 06 p2398 N94-24078
Atmospheric Radiation Measurement (ARM)/CART site 06 p2411 N94-24379
Session on modeling of radiative transfer processes 06 p2414 N94-24397
LRAT: Lightning Radiative Transfer 06 p2416 N94-24443
The annual pressure cycle on Mars: Results from the LMD Martian atmospheric general circulation model 06 p2619 N94-24884
Temporal and spatial mapping of surface albedo and atmospheric dust opacity on Mars 06 p2619 N94-24887
A research program on radiative transfer model development in support of the ARM program
[DE94-001146] 07 p2767 N94-25950
Interactions between a tropical mixed boundary layer and cumulus convection in a radiative-convective model
[DE94-000848] 07 p2877 N94-25979
A numerical solution to the one and two dimensional line radiative transfer equation
[ISBN-0-315-84258-X] 07 p2994 N94-26640
Cooling the Martian atmosphere: The spectral overlap of the C02 15 micrometers band and dust 07 p3107 N94-27886
Martian atmospheric radiation budget 07 p3107 N94-27887
How well was total ozone abundance inferred with Mariner 9? 07 p3108 N94-27891
Lead detection and mapping with reference to relationships between scale, sensor characteristics, surface conditions and atmospheric properties
[AD-A275321] 08 p3377 N94-28877
Infrared properties of obscuring dust tori in active galactic nuclei 08 p3545 N94-29832
Radiative flux calculations at UV and visible wavelengths
[DE94-004278] 08 p3350 N94-30613
Optical depth effects in cluster cooling flows 08 p3541 N94-30800
Tropospheric radiative forcing of O3 for the 1994 IPCC report
[DE94-005698] 08 p3367 N94-30876
Thermal continua of AGN accretion disks 09 p3931 N94-31137
Three-dimensional radiative transfer calculations on an SIMD machine applied to accretion disks 09 p3932 N94-31141
A study of physical conditions, radiative transfer and shocks in the interstellar medium 09 p3937 N94-31963
Sensitivity analysis of the AVHRR infrared cirrus model
[AD-A276690] 09 p3784 N94-32117
Temporal and spatial mapping of atmospheric dust opacity and surface albedo on Mars 09 p3947 N94-33211
How well was total ozone abundance inferred with Mariner 9 09 p3947 N94-33212
The wavelength dependence of Martian atmospheric dust radiative properties 09 p3950 N94-33228
Model calculations of radiative transfer and tropospheric chemistry 10 p4084 N94-33361
Arctic radiative fluxes modeled from the ISCCP-C2 data set, 1983 - 1986 10 p4084 N94-33369
Development of a radiative cloud parameterization scheme of stratocumulus and stratus clouds which includes the impact of CCN on cloud albedo
[DE94-005476] 10 p4081 N94-33714
Venus climate stability and volcanic resurfacing rates 11 p4358 N94-35413
First measurement of helium on Mars: Implications for the problem of radiogenic gases on the terrestrial planets 11 p4370 N94-36153
Two-channel microwave radiometer for observations of total column precipitable water vapor and cloud liquid water path
[DE94-007480] 12 p4471 N94-36479
Accelerated line-by-line calculations for the radiative transfer of trace gases related to climate studies
[DE94-004404] 12 p4464 N94-36552

Proceedings of the Third Atmospheric Radiation Measurement (ARM) Science Team Meeting
[DE94-011194] 12 p4467 N94-37454
Tropospheric radiative forcing of CH4
[DE94-011628] 12 p4468 N94-37631

RADIATORS
Optically-switched submillimeter-wave oscillator and radiator
[NASA-CASE-NPO-18547-1-CU] 03 p1014 N94-17324

RADICALS
NT AMINO RADICAL
NT FREE RADICALS
NT HYDROXYL RADICALS
NT VINYL RADICAL
Application of synchrotron radiation in chemical dynamics
[DE93-015040] 02 p0563 N94-13411
Synthesis, characterization, and polymerization of new ferrocene-fluorene complexes. A novel high-molecular weight conjugated polymer with pendant ferrocene groups
[AD-A267717] 03 p0972 N94-17273
Photochemically induced transformations of transition complexes
[AD-A271112] 05 p2014 N94-19982
Physical chemistry of energetic nitrogen compounds
[AD-A271819] 05 p1712 N94-20625
Polymerization of enantiomerically pure 2,3-dicarboalkoxy norbornadienes and 5,6-disubstituted norbornenes by well-characterized molybdenum ROMP catalysts
[AD-A272649] 05 p1704 N94-21186
Potent solvents for C60 and their utility for the rapid acquisition of 13CNMR data for fullerenes
[AD-A273349] 06 p2235 N94-24925
Dispersion of Rh/Cu in a sol-gel matrix. Highly chemo- and stereoselective catalyst for the reduction of alkynes to Z-alkenes
[AD-A273306] 06 p2262 N94-25145
Three methods to measure RH bond energies
[DE94-003795] 07 p3013 N94-25816
Bulletin of the Institute for Chemical Reaction Science, Tohoku University, volume 2
[JTN-94-80602] 07 p2717 N94-27385
Reactivity of nitrate radical (NO3) toward organic compounds 07 p2704 N94-27387
The addition of molecular oxygen to hydroperoxy-propyl radicals
[DE94-003662] 07 p2760 N94-27725
Peroxy radical measurements with NCAR's chemical amplifier 08 p3345 N94-28603
The radical amplifier 08 p3345 N94-28604
An improved method of measuring tropospheric NO2, NO3, HO2, and RO2 by Matrix Isolation and Electronic Spin Resonance (MIESR) 08 p3345 N94-28605
HO2 detection by near infrared absorption using tunable diode lasers 08 p3346 N94-28608
Direct measurement of the reactivity of NH and OH on a silicon nitride surface
[DE94-005286] 08 p3199 N94-30260
Time-resolved infrared absorption studies applied to the study of radical plus molecule reactions
[DE94-005921] 09 p3863 N94-31202
A comparison between two Monte Carlo codes on determination of transient chemical yields
[DE94-007224] 09 p3636 N94-32251
The reaction of hydroperoxy-propyl radicals with molecular oxygen
[DE94-006392] 11 p4239 N94-36319

RADII
NT LARMOR RADIUS

RADIO ALTIMETERS
Topex/Poseidon: A United States/France mission. Oceanography from space: The oceans and climate
[NASA-TM-108253] 01 p0043 N94-10699
Proceedings of First ERS-1 Symposium on Space at the Service of Our Environment, volume 1
[ESA-SP-359-VOL-1] 01 p0232 N94-11704
Effects of wave nonlinearity on ERS-1 radar altimeter returns: A preliminary investigation 01 p0235 N94-11722
The height calibration of the ERS-1 radar altimeter 01 p0241 N94-11764
Separation of geoid and sea surface topography in shallow water regions: A first ERS-1 radar altimeter data evaluation 01 p0242 N94-11766
Operational ERS-1 orbit determination at D-PAF 01 p0243 N94-11774
Validating the UK-PAF land ice product surface elevation 01 p0244 N94-11780
Surface roughness variations across the Iceland-Faroes frontal region observed by the GEOSAT altimeter and NOAA AVHRR 01 p0201 N94-11958
On the variability of wind speeds in the North Western Pacific observed by altimeter/GEOSAT and SSM/I/DMSP 01 p0201 N94-11960
Observation of wind and waves by GEOSAT altimeter 01 p0202 N94-11961
Topography of the Western Mediterranean from the ERS-1 altimeter 01 p0255 N94-12531
Ionospheric calibration for single frequency altimeter measurements
[NASA-CR-194262] 02 p0716 N94-14049
High performance multi-mode radar altimeter for future spaceborne application 02 p0548 N94-14214
The cartography of Venus with Magellan data 03 p1274 N94-16320
Resolving topographic detail on Venus by modeling complex Magellan altimetry echoes 03 p1283 N94-16368
Analysis of Ku-band cross section at low incidence angles 05 p1720 N94-20414
C-band radar backscatter of sea ice in the Weddell Sea, Antarctica during the austral winter of 1992 05 p1725 N94-20435
Synthesis of passive microwave and radar altimeter data for estimating accumulation rates of polar snow
[NASA-CR-194864] 06 p2382 N94-23573
Ionospheric calibration for single frequency altimeter measurements
[NASA-CR-195709] 07 p2883 N94-27883
Altimeter data processing from sea surface topography to horizontal eddy momentum fluxes
[PB94-147550] 08 p3378 N94-30714
Minimum performance standards: Airborne low-range radar altimeters
[RTCA-DO-155] 11 p4198 N94-35344
Mesoscale roughness of Venus 11 p4361 N94-35430

RADIO ANTENNAS
NT HORN ANTENNAS
NT MICROWAVE ANTENNAS
Multiple Antenna Implementation System (MAntIS)
[DE93-012515] 01 p0131 N94-10270
A review of OPEX activities and measurement results 03 p0994 N94-16036
The analysis of low-profile, broadband, monopole, vehicle antennas and matching network synthesis
[AD-A268340] 03 p1006 N94-17582
Meteor burst communications improvement study
[AD-A270866] 04 p1393 N94-19793
The MSAT spacecraft of Telesat Mobile Inc. 06 p2207 N94-22742
Very low frequency and low frequency transmitting antenna parameter monitoring system
[AD-D015989] 06 p2302 N94-25049
Fast wave current drive technology development at ORNL
[DE94-004243] 07 p3046 N94-27568
Active antennas, a review
[PB94-137445] 08 p3243 N94-28907
Three-dimensional effects for radio frequency antenna modeling
[DE94-006102] 08 p3255 N94-30105
Broadband, high-power, 2-30 MHz, twin-whip antenna. Computer and 1/10-scale model design study
[AD-A277619] 09 p3682 N94-32971
Switched-beam radiometer front-end network analysis
[NASA-CR-194922] 11 p4252 N94-35247

RADIO ASTRONOMY
Interstellar scattering and the selection of extragalactic radiosources with highly compact components 01 p0134 N94-11063
Interstellar scattering and the pulsar studies with space VLBI 01 p0135 N94-11065
The possibility of image restoration under observation in a regime of strong scattering 01 p0136 N94-11068
Detection of dust impacts by the Voyager planetary radio astronomy experiment
[NASA-CR-193281] 01 p0423 N94-11305
Models of Neptune's smooth recurrent radio emission
[NASA-CR-193283] 01 p0484 N94-11312
Neptune high-latitude emission: Dependence of angle on frequency
[NASA-CR-193280] 02 p0848 N94-13476
Theoretical molecular studies of astrophysical interest
[NASA-CR-193300] 02 p0838 N94-13781
The next century astrophysics program 02 p0546 N94-14832
Preparation and properties of Nb/Al SIS and SIN junctions for millimeter and submillimeter radioastronomical receivers 03 p0907 N94-15078
Activities of the Research Laboratory of Electronics
[AD-A266730] 03 p1304 N94-17651
Berne (Switzerland) solar observations: Data for April 1991 - August 1992
[REPT-59] 05 p2147 N94-21150
Applications of correlator chips in radio science 05 p1763 N94-21695
NASA SERC digital correlator projects 05 p1765 N94-21708
A 1 GHz sample rate, 256-channel, 1-bit quantization, CMOS, digital correlator chip 05 p1768 N94-21732
Circumstellar environments of Be stars at infra-red and radio wavelengths
[ISBN-0-315-83135-9] 05 p2081 N94-22426
Programmability in AIPS++ 05 p1926 N94-22482
Preliminary results of observations of solar flares with Nobeyama Radioheliograph 05 p2001 N94-22633
Molecular abundances in the envelopes around evolved stars
[PB94-104916] 06 p2602 N94-23812
Voyager planetary radio astronomy studies
[NASA-CR-194776] 06 p2614 N94-24328
Infrared and SiO maser observations of OH/IR stars
[PB94-104890] 06 p2599 N94-24780
Investigation relative to the Roentgen Satellite (ROSAT)
[NASA-CR-195192] 06 p2600 N94-25269
The Telecommunications and Data Acquisition Report
[NASA-CR-195694] 08 p3246 N94-29613
Radio science ground data system for the Voyager-Neptune encounter, part 1 08 p3248 N94-29623
A multi wavelength observational study of the Cartwheel ring galaxy 08 p3539 N94-29821
A study of recycled pulsars in globular clusters 08 p3539 N94-29825
Plasma and radio waves from Neptune: Source mechanisms and propagation
[NASA-CR-195877] 09 p3943 N94-33103
Catalog and atlas from a sensitive 1.5 GHz radio survey around the North Ecliptic Pole
[AD-A277705] 10 p4085 N94-33440
Utility of interplanetary scintillation maps in forecasting geomagnetic activity: A study based on single-station data from Cambridge, United Kingdom
[PB94-156775] 10 p4087 N94-34600
The Telecommunications and Data Acquisition Report
[NASA-CR-196117] 11 p4252 N94-35542
Plasma and radio waves from Neptune: Source mechamisms and propagation
[NASA-CR-196284] 12 p4550 N94-37251
Correlated radio and optical variations in a sample of AGN. A simultaneous radio-optical flare in BL lacertae
[PB94-179181] 12 p4548 N94-37834

RADIO ATTENUATION
Statistical results from the Virginia Tech propagation experiment using the Olympus 12, 20, and 30 GHz satellite beacons 02 p0613 N94-14658
Long duration measurements of fading on a low elevation angle, 11-GHz satellite path 02 p0613 N94-14661
Large-scale rainfall diversity for ACTS 02 p0613 N94-14662
Rain-rate data base development and rain-rate climate analysis 02 p0614 N94-14664
Propagation issues for emerging mobile and portable communications: A systems perspective 02 p0614 N94-14667
Power attenuation characteristics as switch-over criterion in personal satellite mobile communications 06 p2277 N94-22756
Adaptive power control as a fade countermeasure on satellite links 08 p3253 N94-29897

RADIO AURORAS
Preliminary results of observations of solar flares with Nobeyama Radioheliograph 05 p2001 N94-22633

RADIO BEACONS
Low cost high efficiency GaAs monolithic RF module for SARSAT distress beacons
[NASA-CR-194235] 01 p0146 N94-12773
Olympus propagation measurement results at Virginia Tech 03 p0995 N94-16037
Data acquisition, preprocessing and analysis for the Virginia Tech OLYMPUS experiment 03 p0995 N94-16038
Propagation measurements in Alaska using ACTS beacons 03 p0995 N94-16040
Comparison of OLYMPUS beacon and radiometric attenuation measurements at Blacksburg, Virginia 03 p0996 N94-16046
High efficiency low cost monolithic module for SARSAT distress beacons
[NASA-CR-194234] 04 p1315 N94-18852
Marker beacon case
[AD-D016322] 12 p4385 N94-37830
System for broadcasting marker beacon signals and processing responses from seeking entities
[AD-D016313] 12 p4385 N94-37839

RADIO BROADCASTING
U BROADCASTING

RADIO BURSTS
NT SOLAR RADIO BURSTS
Electron acceleration in and radio emission from SN1987A 05 p2007 N94-22677
An April 1991 outburst from 4U0115+63 observed by BATSE
[DE94-007093] 07 p3116 N94-27440
RADIO COMMUNICATION
NT CODE DIVISION MULTIPLE ACCESS
NT RADIO RELAY SYSTEMS
NT RADIO TELEMETRY
NT TELEPHONY
NT TIME DIVISION MULTIPLE ACCESS
Disturbance Impact Assessment System (DIAS), version 2.0. System design document
[AD-A265251] 01 p0138 N94-11883
Measurement of wave propagation for VHF/UHF and a comparison between measured and predicted values
[FFI/RAPPORT-92/7024] 02 p0605 N94-13968
The developments of satellite communications of China 02 p0618 N94-14282
The current situation, trends, international cooperation of space communication technological development in the Republic of Korea 02 p0699 N94-14283
Space communications technology research in CRL 02 p0618 N94-14285
Future outlook on international satellite communications in Asia Pacific region 02 p0618 N94-14287
Technological development for broadcasting satellites in NHK Laboratories 02 p0618 N94-14288
Proceedings of the Seventeenth NASA Propagation Experimenters Meeting (NAPEX 17) and the Advanced Communications Technology Satellite (ACTS) Propagation Studies Miniworkshop
[NASA-CR-194096] 02 p0612 N94-14654
Opening remarks: Current and future activities 02 p0612 N94-14655
New challenges in propagation research in the US 02 p0612 N94-14656
Statistical results from the Virginia Tech propagation experiment using the Olympus 12, 20, and 30 GHz satellite beacons 02 p0613 N94-14658
Long duration measurements of fading on a low elevation angle, 11-GHz satellite path 02 p0613 N94-14661
A database for propagation models 02 p0614 N94-14665
Contribution towards a draft revision of recommendations 681: Propagation data required for the design of Earth-space land mobile telecommunications systems 02 p0614 N94-14666
Propagation considerations in the American Mobile Satellite system design 02 p0614 N94-14668
Coverage aspects of a single frequency network designed for digital audio broadcasting
[BBC-RD-1993/3] 02 p0616 N94-14742
The ACTS propagation program 03 p0995 N94-16039
Four Frequency-Shift Keying (4-FSK) spread spectrum modulator and demodulator
[AD-A267433] 03 p1000 N94-16979
Ground wave emergency network final operational capability: Environmental assessment for central Wyoming relay node, site number RN 8C928WY
[AD-A267842] 03 p1001 N94-17011
Small Satellites Systems and Services
[ISBN-2-85-428327-9] 03 p0888 N94-17131
Radiocommunication problems of a position reporting and bidirectional messagery system using VHF/UHF with low-Earth orbit satellites 03 p0889 N94-17136
Ground wave emergency network final operational capability: Environmental assessment for central Nevada relay node, site number RN 8W917NV
[AD-A267630] 03 p1002 N94-17200
Ground wave emergency network environmental assessment for northwestern Colorado relay node site number RN 8C924CO
[AD-A267654] 03 p1003 N94-17249
Ground wave emergency network final operational capability. Environmental assessment for southern Arkansas relay node site no. RN 8C912AR
[AD-A268001] 03 p1004 N94-17376
Swatch Pager 04 p1428 N94-18039
Control of integrated voice/data multi-hop radio networks via reduced-load approximations
[AD-A270661] 04 p1393 N94-19779
Ground wave emergency network. Final operational capability. Environmental assessment for south central Montana relay node, site no. RN8C925MT
[AD-A267795] 05 p1716 N94-19964
Four-channel HF receiving antenna array simulator
[AD-A271875] 05 p1732 N94-20471
High Frequency (HF) and meteor burst communications in a polar environment
[AD-A271604] 05 p1737 N94-20949
ATC/pilot voice communications: A survey of the literature
[DOT/FAA/AM-93/20] 05 p1738 N94-21201
Inclined orbits and interference to stationary service and to stationary service by satellite 05 p1653 N94-22188
The MSAT spacecraft of Telesat Mobile Inc. 06 p2207 N94-22742
Power attenuation characteristics as switch-over criterion in personal satellite mobile communications 06 p2277 N94-22756
Evolution of INMARSAT systems and applications: The land mobile experience 06 p2280 N94-22779
EUTELTRACS: The European experience on mobile satellite services 06 p2281 N94-22781
System services and architecture of the TMI satellite mobile data system 06 p2286 N94-22817
Pseudo-coherent demodulation for mobile satellite systems 06 p2287 N94-22819
Handover aspects for a Low Earth Orbit (LEO) CDMA Land Mobile Satellite (LMS) system 06 p2288 N94-22824
Radio communication and wave propagation. A visit to the Netherlands in December 1992
[PB93-204360] 06 p2297 N94-24531
Conceptual communications system design in the 25.25-27.5 and 37.0-40.5 GHz frequency bands 06 p2306 N94-25379
Meteor Burst Communications (MBC) throughput improvement tests
[AD-A273941] 07 p2767 N94-25990
Technical description of the Vulcano software library
[FFI-93/7024] 07 p2767 N94-26105
Packet radio data link applications in the NASA Langley Research Center Transport Systems Research Vehicle
[NASA-TM-109071] 07 p2665 N94-27423
1.8 gigahertz (GHz) digital Low Density Radio Communications Link (LDRCL) Operational Test and Evaluation (OT&E) integration and OT&E operational final test report
[AD-A275800] 08 p3241 N94-28771
Acquisition time analysis of noncoherent PN sequence acquisition schemes
[AD-A275017] 08 p3244 N94-29094
Optimizing the Galileo space communication link 08 p3250 N94-29663
Simulation of interference between Earth stations and Earth-orbiting satellites 08 p3252 N94-29673
Fast autodidactic adaptive equalization algorithms
[TELECOM-93-E-018] 09 p3670 N94-31174
Atmospheric effects assessment program: Ionospheric sounding
[AD-A276447] 09 p3770 N94-31303
Analysis of ionospheric parameters in Europe and creation of the prediction algorithm
[AD-A276342] 09 p3771 N94-31326
A multichannel architecture for Naval Task Force Communication
[AD-A276230] 09 p3673 N94-31446
Performance statistics bulletin. High latitude meteor scatter propagation October, November, December 1990, January 1991
[AD-A276693] 09 p3676 N94-31998
Design, development, and testing of a Network Frequency Selection Service (NFSS)
[AD-A277362] 09 p3680 N94-32283
High frequence and automatic link establishment (HF and ALE) radio propagation test to Antarctica
[AD-A277730] 09 p3682 N94-33001
An analysis of cellular telephone and INMARSAT systems for providing radio data link computer communications for US Navy vessels
[AD-A278143] 09 p3684 N94-33160
High temperature superconducting Josephson junction array systems, phase 1
[AD-A277937] 09 p3908 N94-33246
Antarctic meteor scatter test, December 1992
[AD-A277894] 10 p4033 N94-33547
Ground vehicle control at NIST: From teleoperation to autonomy 10 p4127 N94-34037
The Mars Observer Ka-band link experiment 11 p4255 N94-35563
VHF adaptive antenna development task
[AD-A280320] 12 p4434 N94-37127
ELF Communications System ecological monitoring program: Electromagnetic field measurements and engineering support
[AD-A280489] 12 p4481 N94-37353
RADIO CONTROL
NASA advanced design program. Design and analysis of a radio-controlled flying wing aircraft
[NASA-CR-195515] 06 p2180 N94-24589
Remote robot manipulator coupled with remote-controlled guide vehicle for soil sampling in hazardous waste sites 09 p3723 N94-31569
RADIO DETECTION AND RANGING
U RADAR
RADIO DIRECTION FINDERS
Portable multipath measurement system
[DSIS-93-00177] 02 p0603 N94-13843
Sporadic-E observations during LoVHF transionospheric direction finder measurements
[AD-A270619] 05 p1716 N94-19951
Algorithms for a digital radio direction finding system in the HF band
[PB94-149176] 10 p3988 N94-34093
RADIO ECHOES
A study of meteor scatter communications
[DSIS-93-00151] 02 p0603 N94-13841
RADIO ELECTRONICS
Spaceborne Imaging Radar-C instrument 03 p0990 N94-15890
RADIO EMISSION
NT HYDROXYL EMISSION
NT RADIO BURSTS
NT SOLAR RADIO BURSTS
NT SOLAR RADIO EMISSION
Models of Neptune's smooth recurrent radio emission
[NASA-CR-193283] 01 p0484 N94-11312
Neptune high-latitude emission: Dependence of angle on frequency
[NASA-CR-193280] 02 p0848 N94-13476
Radio and optical emission: Spectral shapes and breaks in GRB
[NASA-CR-194763] 05 p2150 N94-21781
Circumstellar environments of Be stars at infra-red and radio wavelengths
[ISBN-0-315-83135-9] 05 p2081 N94-22426
Radiation from solar flares 05 p2001 N94-22634
Nonthermal planetary radio emissions: Theories and observations 05 p2001 N94-22635
Electron acceleration in and radio emission from SN1987A 05 p2007 N94-22677
Langmuir microstructures and pulsar radio emission 05 p2007 N94-22678
Voyager planetary radio astronomy studies
[NASA-CR-194776] 06 p2614 N94-24328
Phasing the Very Large Array on Galileo in the presence of Jupiter's strong radio emission 08 p3164 N94-29621
On observing neutron star oscillations 08 p3538 N94-29795
Radio emission from pre-main-sequence stars 09 p3955 N94-31890
Plasma and radio waves from Neptune: Source mechanisms and propagation
[NASA-CR-195877] 09 p3943 N94-33103
Plasma and radio waves from Neptune: Source mechamisms and propagation
[NASA-CR-196284] 12 p4550 N94-37251
RADIO EQUIPMENT
NT HORN ANTENNAS
NT IONOSONDES
NT MICROWAVE ANTENNAS
NT RADIO ANTENNAS
NT RADIO BEACONS
NT RADIO FILTERS
NT RADIO RECEIVERS
NT RADIO TELESCOPES
NT RADIO TRANSMITTERS
NT RADIOSONDES
NT RADIOTELEPHONES
NT RAWINSONDES
NT RECEPTION DIVERSITY
NT RECTENNAS
NT SONOBUOYS
NT SPACECRAFT ANTENNAS
NT SUPERHETERODYNE RECEIVERS
NT TRANSMITTER RECEIVERS
NT TRANSPONDERS
NT VERY HIGH FREQUENCY RADIO EQUIPMENT
NT VERY LARGE ARRAY (VLA)
NT VERY LONG BASELINE ARRAY (VLBA)
Preparing for the initial observations of the Targeted Search and the Sky Survey systems
[NASA-CR-193644] 01 p0318 N94-10865
Development of UHF spark-switched L-C Oscillators
[DE93-015019] 02 p0623 N94-13892
Ground wave emergency network final operational capability: Environmental assessment for central Nevada relay node, site number RN 8W917NV
[AD-A267630] 03 p1002 N94-17200
Ground wave emergency network final operational capability: Environmental assessment for southern Nevada relay node site number RN 8W918NV
[AD-A267647] 03 p1002 N94-17205
Ground wave emergency network final operational capability: Environmental assessment for central Utah relay node, site number RN 8C920UT
[AD-A267628] 03 p1003 N94-17211

Ground wave emergency network final operational capability: Environmental assessment for northwestern Nebraska relay node, site number RN 8C930NE
[AD-A267629] 03 p1003 N94-17212
Environmental assessment for northwestern Indiana relay node site no. RN 8C902IN
[AD-A267849] 03 p1004 N94-17406
Radio wave propagation in structured ionization for satellite and radar applications
[AD-A268457] 04 p1382 N94-17844
Intentionally Short Range Communications (ISRC)
[AD-A268788] 04 p1384 N94-18216
Efficient simulation of DEDS by means of standard clock techniques: Queueing and integrated radio network examples
[AD-A269878] 04 p1432 N94-18681
Control of integrated voice/data multi-hop radio networks via reduced-load approximations
[AD-A270661] 04 p1393 N94-19779
Optical signal processing
[AD-A271036] 05 p1983 N94-20013
Mitigation of EMI/RFI produced by a 1.2 kW uninterruptible power supply
[AD-A273149] 06 p2299 N94-24670
ELF communications system ecological monitoring program
[AD-A273456] 06 p2299 N94-24676
1.8 gigahertz (GHz) digital Low Density Radio Communications Link (LDRCL) Operational Test and Evaluation (OT&E) integration and OT&E operational final test report
[AD-A275800] 08 p3241 N94-28771
Communications technology for unattended sensors
[DE94-005685] 08 p3254 N94-30043
Low sidelobe reflector antenna design for communications
[AD-A276079] 09 p3673 N94-31463
High frequence and automatic link establishment (HF and ALE) radio propagation test to Antarctica
[AD-A277730] 09 p3682 N94-33001
Minimum performance standards: Airborne low-range radar altimeters
[RTCA-DO-155] 11 p4198 N94-35344
VHF adaptive antenna development task
[AD-A280320] 12 p4434 N94-37127
Design and analysis of a mode B and mode JD satellite Earth station
[AD-A280417] 12 p4391 N94-37225

RADIO FILTERS
Direct-conversion-to-baseband for a nonlinear FM signal
[AD-A274861] 07 p2768 N94-26189
KONRAD: Wide band digital HF receiver
[PB94-184686] 12 p4435 N94-37813

RADIO FREQUENCIES
NT C BAND
NT EXTREMELY HIGH FREQUENCIES
NT EXTREMELY LOW RADIO FREQUENCIES
NT HIGH FREQUENCIES
NT LOW FREQUENCIES
NT LOW FREQUENCY BANDS
NT MICROWAVE FREQUENCIES
NT P BAND
NT SUPERHIGH FREQUENCIES
NT ULTRAHIGH FREQUENCIES
NT VERY HIGH FREQUENCIES
NT VERY LOW FREQUENCIES
Multiple Antenna Implementation System (MAntIS)
[DE93-012515] 01 p0131 N94-10270
Characterization of high-power RF structures using time-domain field codes
[DE93-013416] 01 p0132 N94-10518
Electron runaway in RF discharges
[DE93-771407] 01 p0363 N94-10661
RF vacuum microelectronics
[AD-A266066] 01 p0142 N94-10818
Journal of Research of the National Institute of Standards and Technology, volume 98, number 2, March - April 1993
[PB93-196228] 01 p0485 N94-10850
DILUTE: A code for studying beam evolution under RF noise
[DE93-011605] 01 p0133 N94-10960
Initial assessment of lower hybrid current drive in D3-D
[DE93-013310] 01 p0394 N94-12370
Operational characteristics of a 100-mA, 2-MeV radio-frequency quadrupole
[DE93-014474] 01 p0374 N94-12786
Dimensionally similar discharges with central RF heating on the D3-D tokamak
[DE93-012776] 02 p0795 N94-12953
Design for low beam loss in accelerators for intense neutron source applications
[DE93-014557] 02 p0789 N94-13327
Electron beam probe measurements of electric fields in rf discharges 02 p0601 N94-13661
Field emitter array RF amplifier development project. Phase 1: Cathode technology development
[AD-A266346] 02 p0622 N94-13776
Plasma-etching science meets technology in the MDL
[DE93-012086] 02 p0800 N94-13908
Ionospheric calibration for single frequency altimeter measurements
[NASA-CR-194282] 02 p0716 N94-14049
Velocity matched millimeterwave electro-optic modulator
[AD-A267264] 03 p1188 N94-14957
Display system employing acousto-optic tunable filter
[NASA-CASE-NPO-18736-1-CU] 03 p1190 N94-15933
Satellite sound broadcast propagation measurements 03 p0996 N94-16047
Measurements of the operation of the SINUS-6/BWO system
[AD-A266423] 03 p1011 N94-16556
Fundamental-mode RF design in e(+)e(-) storage ring factories
[DE93-015249] 03 p1183 N94-16809
Cortical adaptive filtering in bioacoustic signal classification
[AD-A266229] 03 p1177 N94-16939
Radiocommunication problems of a position reporting and bidirectional messagery system using VHF/UHF with low-Earth orbit satellites 03 p0889 N94-17136
RF vacuum microelectronics
[AD-A268399] 03 p1014 N94-17423
Field-emitter arrays for RF vacuum microelectronics
[AD-A268397] 03 p1015 N94-17526
Field emitter arrays for RF vacuum microelectronics
[AD-A268595] 03 p1015 N94-17608
Power compensators for phased operation of antenna arrays on JET and D3-D
[DE93-013208] 04 p1581 N94-17694
Synchrotron beam-loading stability with a higher RF harmonic
[DE93-014549] 04 p1573 N94-17726
RF vacuum microelectronics
[AD-A269454] 04 p1396 N94-18284
Broadband RF spectrum from electrostatic discharges on spacecraft
[AD-A269543] 04 p1385 N94-18287
Field emitter array RF amplifier development project, phase 1, option 1
[AD-A268687] 04 p1396 N94-18293
Magnetostatic waves-based integrated optic bragg cell modules with applications to RF signal processing
[AD-A269115] 04 p1577 N94-18295
Millimeter wave reflectivity measurement system
[AD-A270008] 04 p1387 N94-18601
RF vacuum microelectronics
[AD-A270003] 04 p1403 N94-18667
Conductive garments to prevent Radio-Frequency (RF) burns
[AD-D015832] 04 p1512 N94-18730
Experiments on nonlinear absorption of ECH waves in MTX and a comparison with theory
[DE93-019158] 04 p1589 N94-19074
Advanced fusion diagnostics
[DE93-040085] 04 p1589 N94-19133
RF phase stabilization for RF photocathode gun through electro-optical monitoring
[DE93-019059] 04 p1406 N94-19310
Study of coupled-bunch collective effects in the ALS
[DE93-019235] 04 p1575 N94-19558
Study of coupled-bunch collective effects in the PEP-2 B-Factory
[DE93-040117] 05 p1979 N94-20274
Field emitter array RF amplifier development project, phase 1, option 1
[AD-A272567] 05 p1740 N94-21361
Hybrid finite element/waveguide mode analysis of passive RF devices
[AD-A273074] 05 p1740 N94-21518
Simulation and compensation of multibunch energy variation in NLC
[DE93-041057] 05 p1981 N94-21687
Particle behavior in an ECR plasma etch tool
[DE93-040343] 05 p1996 N94-21769
The preservation of low emittance flat beams
[DE93-040964] 05 p1981 N94-21773
Verification of frequency scaling laws for capacitive rf discharges using two-dimensional simulations
[DE94-001306] 05 p1999 N94-22595
Aeronautical audio broadcasting via satellite 06 p2274 N94-22741
The MSAT spacecraft of Telesat Mobile Inc. 06 p2207 N94-22742
Direct digital RF synthesis and modulation for MSAT mobile applications 06 p2285 N94-22804
Separable concatenated codes with iterative map decoding for Rician fading channels 06 p2286 N94-22815
1993 annual report for the Phaedrus-T RF current drive experiments
[DE94-001369] 06 p2550 N94-23192
Two dimensional self-consistent fluid simulation of RF inductive sources
[DE94-003635] 07 p2767 N94-25937
Low noise measurements in an RF environment
[AD-A273813] 07 p2767 N94-25960
MIMO recursive least squares control algorithm for the AN/FPN-44A Loran-C transmitter
[AD-A274820] 07 p2664 N94-26493
Investigation of ACC/CCI tunnel diodes
[AD-A274549] 07 p2785 N94-26845
Ferrite phase shifters using stress insensitive materials
[AD-A274639] 07 p2708 N94-26895
An analysis of FM jamming and noise quality measures
[AD-A274349] 07 p2772 N94-26924
Technical report of ISSP. Ser. A, no. 2688: Suppression of higher-order modes in an RF cavity by resistive material
[JTN-94-80574] 07 p2787 N94-27606
On radio frequency wave induced radial transport and wave helicity
[IPPCZ-326] 07 p2777 N94-27838
A space-based classification system for RF transients
[DE94-003933] 08 p3240 N94-28522
Derivation of a Fokker-Planck equation for bunched beams
[DE94-004950] 08 p3483 N94-28565
A novel spectroscopic measurement method of RF plasma for temperature and electron density diagnoses 08 p3188 N94-28682
Development of large area RF induction plasma for cost effective diamond
[AD-A275888] 08 p3504 N94-28776
RF vacuum microelectronics
[AD-A275221] 08 p3263 N94-28915
Preliminary analysis of Asynchronous Transfer Mode (ATM) over microwave channels
[AD-A275214] 08 p3243 N94-29069
Waves in space plasma dipole antenna subsystem 08 p3161 N94-29632
Communications technology for unattended sensors
[DE94-005685] 08 p3254 N94-30043
Three-dimensional effects for radio frequency antenna modeling
[DE94-006102] 08 p3255 N94-30105
RF and microwave dielectric measurements upon layered materials using reflectometric coaxial sensor
[NPL-DES-125] 08 p3476 N94-30781
Noninductive current drive experiments on D3-D, and future plans
[DE94-007373] 09 p3886 N94-31324
Advanced optical fiber communication systems
[AD-A276416] 09 p3878 N94-31330
RF vacuum microelectronics
[AD-A276512] 09 p3691 N94-31928
High frequency active auroral research program (HAARP) imager
[AD-A277469] 09 p3775 N94-32999
Applications of non-resonant RF forces for improvement of tokamak reactor performances. Part 1: Application of ponderomotive force
[DE94-718994] 11 p4336 N94-35813
The mathematical simulation of physical processes in ECR multicharged ions sources
[DE94-618343] 12 p4515 N94-37077
Field emitter array RF amplifier development project. Phase 1, option 1
[AD-A280513] 12 p4437 N94-37107
Field emitter array RF amplifier development project. Cathode technology development. Phase 1
[AD-A280515] 12 p4437 N94-37108

RADIO FREQUENCY HEATING
Conversion of the four-strap array in D3-D to a tunable traveling wave antenna
[DE93-012085] 01 p0137 N94-11453
Ion cyclotron heating experiments and plans for the Advanced Toroidal Facility (ATF)
[DE93-012965] 02 p0795 N94-13033
Effect on antenna structure of high power RF during plasma operation
[DE93-013278] 02 p0797 N94-13144
Electrical characterization of the JET A(sub 2) antenna: Comparison of model with measurements Wade, T.
[DE93-012964] 02 p0607 N94-14291
Microwave sintering of large alumina bodies
[DE93-012752] 02 p0581 N94-14340
Design of the ion cyclotron system for TPX
[DE93-012961] 02 p0803 N94-14770

Anomalous ion transport and feedback control
[DE93-018324] 02 p0803 N94-14874
ICRF direct electron heating experiments in TFTR
[DE93-017857] 04 p1590 N94-19273
Numerical modeling for an electric-field hyperthermia applicator 05 p1729 N94-20451
Fusion plasma theory grant. Task 3: Auxiliary radiofrequency heating of tokamaks
[DE94-000779] 05 p1994 N94-20940
Design of folded waveguide antenna for Alcator C-Mod
[DE94-003584] 07 p2767 N94-25924
RF modeling and design of a folded waveguide launcher for the Alcator C-Mod tokamak
[DE94-003588] 07 p3041 N94-25933
Excitation of Earth-ionosphere waveguide in the ELF and lower VLF bands by modulated ionospheric current
[AD-A274969] 07 p2878 N94-26304
Critical survey of plasma processing
[AD-A274233] 07 p3044 N94-26820
Design and control of phased ICRF antenna arrays
[DE94-002796] 07 p3046 N94-27261
Fast wave current drive technology development at ORNL
[DE94-004243] 07 p3046 N94-27568
The calculation for energy balance of heating plasmas by Alfven waves
[DE94-604994] 07 p3049 N94-27855
TFTR Ion Cyclotron Range of Frequencies (ICRF) experimental data analysis collaboration
[DE94-004699] 08 p3504 N94-28575
Efficiencies of the ICRF minority heating in the CHS and LHD plasmas
[AD-B183300L] 08 p3506 N94-29499
FWCD and ECCD experiments on D3-D
[DE94-007371] 09 p3890 N94-32201
ICRF heating and current drive in TFTR supershot plasmas: Data analysis and interpretation of ICRF/edge interactions
[DE94-008586] 09 p3890 N94-32520
Experimental observations of thermal spikes in microwave processing of ceramic oxide fibers
[DE94-009348] 10 p4027 N94-33683
Bounce resonance heating and transport in a magnetic mirror
[DE94-727545] 12 p4531 N94-37466

RADIO FREQUENCY INTERFERENCE
NT ATMOSPHERICS
NT CHIRP
NT CHIRP SIGNALS
NT COSMIC NOISE
NT DAWN CHORUS
NT ELECTROMAGNETIC NOISE
NT HISS
NT IONOSPHERIC NOISE
NT IONOSPHERICS
NT SHOT NOISE
NT THERMAL NOISE
NT WHISTLERS
NT WHITE NOISE
A simulation study of the performance of the NASA (2,1,6) convolutional code on RFI/burst channels 03 p0997 N94-16508
Studies of enhanced radar backscatter
[AD-A269544] 04 p1385 N94-18288
A RFI measurement system for field sites
[AD-A269340] 04 p1385 N94-18301
Communication in the presence of unknown interference
[AD-A271146] 04 p1392 N94-19738
The Composite Analytic and Simulation Package or RFI (CASPR) on a coded channel 05 p1744 N94-21339
The Automated Conflict Resolution System (ACRS) 05 p1744 N94-21341
Advanced coding and modulation schemes for TDRSS 05 p1744 N94-21350
Interference reduction using neural networks 05 p1783 N94-22186
Inclined orbits and interference to stationary service and to stationary service by satellite 05 p1653 N94-22188
Throughput, blocking, and interference in packet radio networks 05 p1746 N94-22190
Diversity reception for advanced multi-satellite networks: A CDMA approach 06 p2286 N94-22816
Development of a multilayer interference simulation program for MSS systems 06 p2287 N94-22823
A method for interference mitigation in space communications scheduling 06 p2305 N94-23918
Analysis and surveillance performance at Chicago O'Hare Airport
[DOT/FAA/RD-92/29] 06 p2175 N94-24127
Error coding simulations 06 p2306 N94-24439
Simulation of adjacent channel interference in a UHF satellite system
[AD-A273147] 06 p2299 N94-24669
Evaluation of an Acoustic Charge Transport (ACT) device for adaptive interference suppression in spread spectrum communications systems
[AD-A274073] 07 p2765 N94-25647
Characteristics of 30-MHz interference noises observed by riometers 07 p2884 N94-27965
Simulation of interference between Earth stations and Earth-orbiting satellites 08 p3252 N94-29673
Aperture excitation of electrically large, lossy cavities
[PB94-145711] 09 p3675 N94-31683
The effects of a multipath channel and interference on coherent M-PSK digital communication systems
[AD-A278158] 09 p3684 N94-33254
VHF adaptive antenna development task
[AD-A280320] 12 p4434 N94-37127

RADIO FREQUENCY NOISE
U ELECTROMAGNETIC NOISE

RADIO FREQUENCY RADIATION
U RADIO WAVES

RADIO FREQUENCY SHIELDING
Aperture excitation of electrically large, lossy cavities
[PB94-145711] 09 p3675 N94-31683

RADIO GALAXIES
The morphologies of distant radio galaxies 01 p0426 N94-11597
ROSAT observations of clusters with wide-angle tailed radio sources
[NASA-CR-193784] 02 p0833 N94-14405
Radio galaxies and their environment
[DE93-040851] 05 p2150 N94-22397
CCD surface photometry of galaxies 05 p2058 N94-22445
The kinematics of molecular gas and dust in the nearby galaxies Centaurus A and M82 08 p3544 N94-29738
Broad H alpha profiles of radio-loud active galactic nuclei and rapid profile variability in Seyfert and radio galaxies 08 p3552 N94-29989
The BL LAC phenomenon: X-ray observations of transition objects and determination of the x-ray spectrum of a complete sample of flat-spectrum radio sources
[NASA-CR-195951] 12 p4546 N94-36688

RADIO HORIZONS
Johnson-Gierhart program predictions of excess propagation loss for super-high frequency air-to-ground paths. Volume 2: Appendices
[AD-A267021] 03 p0987 N94-15527
Radar detection of low-altitude targets in a maritime environment. Volume 2: Meteorological and radar data
[AD-A274658] 07 p2768 N94-26335
Low altitude near-the-horizon propagation: A comparison between RPO and M-layer
[AD-A277358] 09 p3679 N94-32282
Radar detection of low-altitude targets in a maritime environment. Volume 1: Final analysis
[AD-A278493] 10 p4037 N94-34376

RADIO INTERFERENCE
U RADIO FREQUENCY INTERFERENCE

RADIO INTERFEROMETERS
The influence of the propagation medium on the sensitivity and resolution of meter wavelength aperture synthesis systems 01 p0134 N94-11062
Elimination of the influence of the atmosphere on the accuracy of solutions to astrometric problems by means of a ground-space VLBI network 01 p0136 N94-11071

RADIO JETS (ASTRONOMY)
Jets associated with active galactic nuclei 05 p2000 N94-22631
The 1404+286: A non-ideal calibrator for VLBI observations
[PB94-104908] 06 p2599 N94-24521
Are there two engines at the center of 3C286?
[PB94-149218] 10 p4162 N94-34379

RADIO METEOROLOGY
Field studies of raindrop oscillations with applications to radar meteorology 09 p3782 N94-31743

RADIO METEORS
Meteor forward scatter studies
[DSIS-93-00382] 02 p0602 N94-13801
A study of meteor scatter communications
[DSIS-93-00151] 02 p0603 N94-13841
Meteor burst communications improvement study
[AD-A270866] 04 p1393 N94-19793

RADIO NAVIGATION
NT LORAN C
Environmental projects. Volume 15: Environmental assessment: Proposed 1-megawatt radar transmitter at the Mars site
[NASA-CR-194098] 02 p0598 N94-13090
FM interference in radio navigation receivers 05 p1645 N94-22219
A robust quality control system for GPS navigation and kinematic positioning
[ISBN-0-315-83148-0] 05 p1644 N94-22427
The Telecommunications and Data Acquisition Report
[NASA-CR-195694] 08 p3246 N94-29613
The Telecommunications and Data Acquisition Report
[NASA-CR-195689] 08 p3249 N94-29652
The use of low cost differential mode GPS receivers in unmanned vehicles 08 p3144 N94-30285
An Operational Control Segment (OCS) update on GPS constellation status and future program directions 08 p3144 N94-30643
The Telecommunications and Data Acquisition Report
[NASA-CR-196117] 11 p4252 N94-35542

RADIO OBSERVATION
HF ocean radar system at Okinawa Radio Observatory 01 p0139 N94-11902
Reduction and analysis of seasons 15 and 16 (1991 - 1992) Pioneer Venus radio occultation data and correlative studies with observations of the near-infrared emission of Venus
[NASA-CR-194128] 02 p0841 N94-13083
CO-to-H2 conversion factor in dwarf irregular galaxies
[REPT-333] 06 p2603 N94-24985
High spatial resolution observations of CO in CRL 618
[REPT-334] 06 p2604 N94-24986
The Nobeyama millimeter array survey for protoplanetary disks around protostar candidates and T Tauri stars in Taurus
[REPT-336] 06 p2604 N94-24987
Solar-geophysical data number 590, October 1993. Part 1: (Prompt reports). Data for September, August 1993, and late data
[PB94-125903] 07 p3110 N94-27053

RADIO OCCULTATION
Reduction and analysis of seasons 15 and 16 (1991 - 1992) Pioneer Venus radio occultation data and correlative studies with observations of the near-infrared emission of Venus
[NASA-CR-194128] 02 p0841 N94-13083

RADIO PROBING
Theory and application of a Radio-Acoustic Sounding System (RASS) 08 p3367 N94-30869

RADIO PROPAGATION
U RADIO TRANSMISSION

RADIO RANGES
U RADIO BEACONS

RADIO RECEIVERS
NT SUPERHETERODYNE RECEIVERS
NT TRANSMITTER RECEIVERS
Coordinated Radio, Electron, and Waves Experiment (CREWE) for the NASA Comet Rendezvous and Asteroid Flyby (CRAF) instrument
[NASA-CR-194376] 01 p0427 N94-12566
Theoretical SIS mixer research
[AD-A266323] 02 p0807 N94-13580
Results from a study of scintillation behavior at 12, 20, and 30 GHz using the results from the Virginia Tech Olympus receivers 02 p0613 N94-14659
On-board spatial scientific experiment project on small satellites 03 p0896 N94-17184
Swatch Pager 04 p1428 N94-18039
Millimeter wave imaging technology
[AD-A271257] 05 p1715 N94-19912
NHK Science and Technical Research Laboratories 05 p2151 N94-20342
Digital receiver for on-board FM/FSK-FM/BPSK demodulation 05 p1744 N94-21091
Direct broadcast satellite-radio, space-segment/receiver tradeoffs 06 p2273 N94-22738
Direct broadcast satellite-radio, receiver development 06 p2273 N94-22739
Measurements on the satellite-mobile channel at L and S bands 06 p2282 N94-22791
A study of satellite motion-induced multipath phenomena 06 p2283 N94-22794
A comparison between coherent and noncoherent mobile systems in large Doppler shift, delay spread, and C/I environment 06 p2287 N94-22818
A low noise 665 GHz SIS quasi-particle waveguide receiver
[NASA-CR-194735] 06 p2296 N94-24105
Northern Exposure 1992: An investigation of transauroral HF radio skywave propagation
[AD-A273363] 06 p2303 N94-25089
Analysis and simulation of a GPS receiver design using combined delay-lock and modified tanlock loops
[AD-A274037] 07 p2664 N94-25810
Acquisition time analysis of noncoherent PN sequence acquisition schemes
[AD-A275017] 08 p3244 N94-29094
Design and implementation of a hybrid digital phase-locked loop with a TMS320C25: An application to a transponder receiver breadboard 08 p3251 N94-29667
Effects of low sampling rate in the digital data-transition tracking loop 08 p3251 N94-29669

Communications technology for unattended sensors
[DE94-005685] 08 p3254 N94-30043
Towards 10(exp 9) GPS geodesy: Vector baselines, Earth rotation and reference frames
[NASA-CR-195768] 08 p3142 N94-30243
The use of low cost differential mode GPS receivers in unmanned vehicles 08 p3144 N94-30285
Design, performance, and test standards for flight termination receivers/decoders. Volume 1: Design and performance requirements
[AD-A277245] 09 p3602 N94-32333
Spacecraft-spacecraft radio-metric tracking: Signal acquisition requirements and application to Mars approach navigation 11 p4254 N94-35557
KONRAD: Wide band digital HF receiver
[PB94-184686] 12 p4435 N94-37813

RADIO REFLECTION
U RADIO ECHOES

RADIO RELAY SYSTEMS
NT CODE DIVISION MULTIPLE ACCESS
NT TIME DIVISION MULTIPLE ACCESS
Ground wave emergency network final operational capability: Environmental assessment for central Wyoming relay node, site number RN 8C928WY
[AD-A267842] 03 p1001 N94-17011
Ground wave emergency network final operational capability: Environmental assessment for central Nevada relay node, site number RN 8W917NV
[AD-A267630] 03 p1002 N94-17200
Ground wave emergency network final operational capability: Environmental assessment for southern Nevada relay node site number RN 8W918NV
[AD-A267647] 03 p1002 N94-17205
Ground wave emergency network final operational capability: Environmental assessment for central Utah relay node, site number RN 8C920UT
[AD-A267628] 03 p1003 N94-17211
Ground wave emergency network final operational capability: Environmental assessment for northwestern Nebraska relay node, site number RN 8C930NE
[AD-A267629] 03 p1003 N94-17212
Ground wave emergency network. Final operational capability. Environmental assessment for southeastern Idaho relay node, site no. RN8W927ID
[AD-A267796] 03 p1003 N94-17304
Ground wave emergency network final operational capability. Environmental assessment for southern Arkansas relay node site no. RN 8C912AR
[AD-A268001] 03 p1004 N94-17376
Environmental assessment for northwestern Indiana relay node site no. RN 8C902IN
[AD-A267849] 03 p1004 N94-17406
Visibility considerations in frequency sharing with low Earth orbit satellites 05 p1746 N94-22187
Satellite communications system
[CA-PATENT-APPL-SN-2053597] 06 p2297 N94-24183
Hybrid power system for remote communications stations
[AD-A274963] 07 p2782 N94-26301
Annex report FEL-92-A163: Description of the Link and BER Test Analysis System (LIBERTAS) for the frequency band V (14.5 - 15.3 GHz)
[FEL-92-A442] 07 p2770 N94-26650

RADIO SCATTERING
Antarctic meteor scatter test, December 1992
[AD-A277894] 10 p4033 N94-33547

RADIO SIGNAL ATTENUATION
U RADIO ATTENUATION

RADIO SIGNAL PROPAGATION
U RADIO TRANSMISSION

RADIO SIGNALS
Elimination of the influence of the atmosphere on the accuracy of solutions to astrometric problems by means of a ground-space VLBI network 01 p0136 N94-11071
Coverage aspects of a single frequency network designed for digital audio broadcasting
[BBC-RD-1993/3] 02 p0616 N94-14742
A RFI measurement system for field sites
[AD-A269340] 04 p1385 N94-18301
Sporadic-E observations during LoVHF transionospheric direction finder measurements
[AD-A270619] 05 p1716 N94-19951
Four-channel HF receiving antenna array simulator
[AD-A271876] 05 p1732 N94-20471
The VLBA correlator: Real-time in the distributed era 05 p2049 N94-22547
Mitigation of EMI/RFI produced by a 1.2 kW uninterruptible power supply
[AD-A273149] 06 p2299 N94-24670
Direct-conversion-to-baseband for a nonlinear FM signal
[AD-A274861] 07 p2768 N94-26189
Enhanced adaptive statistical filter providing improved performance for target motion analysis noise discrimination statement of government interest
[AD-D016039] 07 p2786 N94-27109
Spurs in digital radio frequency memory and applications of DRFM
[AD-A275013] 08 p3243 N94-28897
Detection methods for stealth radio signals: A literature survey
[PB94-137452] 08 p3244 N94-29176
Performance statistics bulletin. High latitude meteor scatter propagation, February, March, April, May 1992
[AD-A276667] 09 p3677 N94-32083
Performance statistics bulletin. High latitude meteor scatter propagation February, March, April, May 1991
[AD-A276723] 09 p3678 N94-32158
Performance statistics bulletin. High latitude meteor scatter propagation October, November, December 1991, January 1992
[AD-A276724] 09 p3678 N94-32159
Performance statistics bulletin. High latitude meteor scatter propagation, November and December 1989, and January 1990
[AD-A276688] 09 p3680 N94-32297
Performance statistics bulletin. High latitude meteor scatter propagation
[AD-A276694] 09 p3680 N94-32298
Performance statistics bulletin. High latitude meteor scatter propagation
[AD-A276695] 09 p3680 N94-32299
Performance statistics bulletin. High latitude meteor scatter propagation
[AD-A276696] 09 p3680 N94-32300
Automatic modulation recognition 09 p3686 N94-33153
VHF adaptive antenna development task
[AD-A280320] 12 p4434 N94-37127
Wavefront simulator for evaluating RF communication array signal processors
[AD-D016281] 12 p4436 N94-37835

RADIO SOURCES (ASTRONOMY)
NT EXTRAGALACTIC RADIO SOURCES
NT PULSARS
NT QUASARS
NT RADIO GALAXIES
NT RADIO JETS (ASTRONOMY)
Tropospheric and ionospheric effects on differential astrometry with a ground-space based VLBI array 01 p0136 N94-11070
Models of Neptune's smooth recurrent radio emission
[NASA-CR-193283] 01 p0484 N94-11312
A survey of compact planetary nebulae at radio wavelengths
[ISBN-0-315-61950-3] 02 p0829 N94-13371
100 GHz map of 3C 446
[PB94-104882] 06 p2599 N94-23705
The 1404+286: A non-ideal calibrator for VLBI observations
[PB94-104908] 06 p2599 N94-24521
Catalog and atlas from a sensitive 1.5 GHz radio survey around the North Ecliptic Pole
[AD-A277705] 10 p4085 N94-33440
Are there two engines at the center of 3C286?
[PB94-149218] 10 p4162 N94-34379
Utility of interplanetary scintillation maps in forecasting geomagnetic activity: A study based on single-station data from Cambridge, United Kingdom
[PB94-156775] 10 p4087 N94-34600
Correlated radio and optical variations in a sample of AGN. A simultaneous radio-optical flare in BL lacertae
[PB94-179181] 12 p4548 N94-37834

RADIO SPECTRA
NT MICROWAVE SPECTRA

RADIO SPECTROSCOPY
High sensitivity and resolution decimetric spectroscope: Preliminary analysis of solar bursts
[INPE-5537-TDI/525] 09 p3954 N94-33080

RADIO STARS
NT PULSARS

RADIO TELEMETRY
The 17th Transducer Workshop
[AD-A265526] 01 p0141 N94-10509
Remote surface water monitoring radio based telemetry system
[DE93-009643] 01 p0041 N94-11282
Characteristics of the amateur radio means of the Arsene satellite
[CNES-NT-131] 02 p0605 N94-13950
An in-depth analysis and modelling of the Shuttle to MILA S-band telemetry link 05 p1657 N94-21340
The advanced orbiting systems testbed program: Results to date 06 p2197 N94-23907
Experimental verification of an acoustic telemetry link between an Aurora and CFAV quest
[DREA-TC-93-304] 06 p2202 N94-24121
The Mars Observer Ka-band link experiment 11 p4255 N94-35563

RADIO TELESCOPES
NT VERY LARGE ARRAY (VLA)
NT VERY LONG BASELINE ARRAY (VLBA)
Search for Extraterrestrial Intelligence (SETI) 03 p1125 N94-16620
Solar Electro-Optical Network (SEON) upgrade/replacement program. Phase 1: Qualification operational test and evaluation plan
[AD-A266364] 03 p1237 N94-17225
Miyun 232 MHz survey 1: Fields centered at: alpha:00(h)41(m), delta:41 deg 12 min and alpha: 07(h)00(m),delta:35 deg 00 min 05 p2080 N94-22554
Radioastron flight operations 06 p2502 N94-23861
Project PARAS: Phased array radio astronomy from space 07 p3081 N94-25703
Phasing the Very Large Array on Galileo in the presence of Jupiter's strong radio emission 08 p3164 N94-29621
Providing hydrogen maser timing stability to orbiting VLBI radio telescope observations by post-measurement compensation of linked frequency standard imperfections 08 p3297 N94-30670
The quest for contact
[NASA-TM-109778] 09 p3806 N94-32389

RADIO TRACKING
High-resolution robot tracking and direction finding for space station environment 08 p3168 N94-29896

RADIO TRANSMISSION
NT DOUBLE SIDEBAND TRANSMISSION
NT IONOSPHERIC PROPAGATION
NT MICROWAVE ATTENUATION
NT MICROWAVE TRANSMISSION
NT MULTIPATH TRANSMISSION
NT SHORT WAVE RADIO TRANSMISSION
NT SINGLE SIDEBAND TRANSMISSION
NT SPREAD SPECTRUM TRANSMISSION
Building penetration loss measurements for DAB signals at 211 MHz
[BBC-RD-1992/14] 01 p0133 N94-11024
Propagation Effects in Space VLBI 01 p0134 N94-11060
Radiowaves propagation through inhomogeneous interstellar plasma 01 p0134 N94-11061
Interstellar scattering and the selection of extragalactic radiosources with highly compact components 01 p0134 N94-11063
Intraday variability and the compactness of extragalactic radio sources 01 p0135 N94-11064
Measurement of wave propagation for VHF/UHF and a comparison between measured and predicted values
[FFI/RAPPORT-92/7024] 02 p0605 N94-13968
Johnson-Gierhart program predictions of excess propagation loss for super-high frequency air-to-ground paths. Volume 2: Appendices
[AD-A267021] 03 p0987 N94-15527
Proceedings of the Fifteenth NASA Propagation Experimenters Meeting (NAPEX 15) and the Advanced Communications Technology Satellite (ACTS) Propagation Studies Miniworkshop
[NASA-CR-194539] 03 p0994 N94-16035
A review of OPEX activities and measurement results 03 p0994 N94-16036
An overview of the text propagation effects for land-mobile-satellite systems: Experimental and modeling results 03 p0996 N94-16048
Database for propagation models 03 p0996 N94-16049
A CCIR-based prediction model for Earth-Space propagation 03 p0997 N94-16050
Radio wave propagation in structured ionization for satellite and radar applications
[AD-A268457] 04 p1382 N94-17844
Studies of enhanced radar backscatter
[AD-A269544] 04 p1385 N94-18283
Morphology and characteristics of disturbed HF skywave channels
[AD-A269755] 04 p1388 N94-18722
Compilation of 1992 annual reports of the navy ELF communications system ecological monitoring program. Volume 3: Tabs G - I
[AD-A269727] 04 p1388 N94-18741
Compilation of 1992 annual reports of the navy ELF communications system ecological monitoring program, volume 2
[AD-A269726] 04 p1388 N94-18751
Quasi-optical transponder using FET's and patch antennas
[AD-A271339] 04 p1407 N94-19584
Communication in the presence of unknown interference
[AD-A271146] 04 p1392 N94-19738

Meteor burst communications improvement study
[AD-A270866] 04 p1393 N94-19793
High Frequency (HF) and meteor burst communications in a polar environment
[AD-A271604] 05 p1737 N94-20949
Throughput, blocking, and interference in packet radio networks 05 p1746 N94-22190
An introduction to digital modulation and OFDM techniques
[BBC-RD-1993/10] 06 p2295 N94-24086
Radio communication and wave propagation. A visit to the Netherlands in December 1992
[PB93-204360] 06 p2297 N94-24531
Comparison of HF groundwave propagation models
[AD-A273146] 06 p2299 N94-24668
Mitigation of EMI/RFI produced by a 1.2 kW uninterruptible power supply
[AD-A273149] 06 p2299 N94-24670
Northern Exposure 1992: An investigation of transauroral HF radio skywave propagation
[AD-A273363] 06 p2303 N94-25089
Conceptual communications system design in the 25.25-27.5 and 37.0-40.5 GHz frequency bands 06 p2306 N94-25379
Ionospheric modification by high power, obliquely propagated HF radio wave transmissions. Part 1: Experimental
[AD-A273746] 07 p2878 N94-26224
Optical communications for transport aircraft 07 p2643 N94-27298
The Sixteenth Symposium on Coordinated Observations of the Ionosphere and the Magnetosphere in the Polar Regions: Program and abstracts
[JTN-94-80601] 07 p2882 N94-27300
Antarctic Record, Vol. 36, No. 2
[REPT-107] 07 p2883 N94-27963
Characteristics of 30-MHz interference noises observed by riometers 07 p2884 N94-27965
Data transfer system using a multi-ID ARGOS transmitter for the Antarctic polar patrol balloon experiment 08 p3363 N94-29980
Discrete-event-dynamic-system-based approaches for scheduling transmissions in multihop packet radio networks
[AD-A276566] 09 p3679 N94-32230
High frequence and automatic link establishment (HF and ALE) radio propagation test to Antarctica
[AD-A277730] 09 p3682 N94-33001
A comparison of rough surface parabolic equation models
[AD-A278090] 09 p3791 N94-33185
An approximate model for vertical polarization and surface roughness using the parabolic equation
[AD-A278091] 09 p3684 N94-33186
An investigation of methods for improving models of ionospheric plasma-density irregularities and radio-frequency scintillation
[AD-A278568] 10 p4033 N94-33703
Detection of possible burst transmissions in a dense signal environment
[PB94-149259] 10 p4036 N94-34109
Wavefront simulator for evaluating RF communication array signal processors
[AD-D016281] 12 p4436 N94-37835

RADIO TRANSMITTERS
NT IONOSONDES
NT RADIO BEACONS
NT RADIOSONDES
NT RADIOTELEPHONES
NT RAWINSONDES
NT SONOBUOYS
NT TRANSMITTER RECEIVERS
In-orbit performance tests and tele-command systems of the umbrella test satellite (DEBUT)
[NAL-TR-1165] 01 p0043 N94-10859
Low cost high efficiency GaAs monolithic RF module for SARSAT distress beacons
[NASA-CR-194235] 01 p0146 N94-12773
Ground wave emergency network environmental assessment for northwestern Colorado relay node site number RN 8C924CO
[AD-A267654] 03 p1003 N94-17249
An electromagnetic interference study of potential transmitter sites for the HF Active Auroral Research Program (HAARP)
[AD-A267743] 03 p1004 N94-17373
The optimal numerical algorithm for processing of phase coded time signals for radio-clocks 04 p1426 N94-18018
Compilation of 1992 annual reports of the Navy ELF communications system ecological monitoring program, volume 1
[AD-A269569] 04 p1386 N94-18473
Aircraft fire sentry. Volume 1: Summary
[AD-A270087] 04 p1315 N94-18822
Aircraft fire sentry. Volume 2: Appendices A, B, C and D
[AD-A270088] 04 p1315 N94-18823
Spread spectrum random access networks
[AD-A272280] 05 p1737 N94-20585
VLF Harold E. Holt RADHAZ measurements
[AD-A272018] 05 p1737 N94-20620
ELF communications system ecological monitoring program
[AD-A272507] 05 p1740 N94-21412
ELF communications system ecological monitoring program
[AD-A273456] 06 p2299 N94-24676
MIMO recursive least squares control algorithm for the AN/FPN-44A Loran-C transmitter
[AD-A274820] 07 p2664 N94-26493
High-power microwave-tube transmitters
[DE94-005340] 09 p3686 N94-31150
ELF Communications System ecological monitoring program: Electromagnetic field measurements and engineering support
[AD-A280489] 12 p4481 N94-37353
NRL HF propagation measurements between Guadeloupe and Providenciales during the CRRES exercises
[DE94-012078] 12 p4435 N94-37393

RADIO WAVE REFRACTION
Marine boundary layer model evaluation by using a height gain measurement technique in the interference region 05 p1777 N94-22145

RADIO WAVES
NT EXTRATERRESTRIAL RADIO WAVES
NT GALACTIC RADIO WAVES
NT HYDROXYL EMISSION
NT LONG WAVE RADIATION
NT MICROWAVE EMISSION
NT MICROWAVES
NT MILLIMETER WAVES
NT RADIO BURSTS
NT RADIO EMISSION
NT SHORT WAVE RADIATION
NT SKY WAVES
NT SOLAR RADIO BURSTS
NT SOLAR RADIO EMISSION
NT SUBMILLIMETER WAVES
NT WHISTLERS
Proceedings of the Seventeenth NASA Propagation Experimenters Meeting (NAPEX 17) and the Advanced Communications Technology Satellite (ACTS) Propagation Studies Miniworkshop
[NASA-CR-194096] 02 p0612 N94-14654
Opening remarks: Current and future activities 02 p0612 N94-14655
Proceedings of the Fifteenth NASA Propagation Experimenters Meeting (NAPEX 15) and the Advanced Communications Technology Satellite (ACTS) Propagation Studies Miniworkshop
[NASA-CR-194539] 03 p0994 N94-16035
A review of OPEX activities and measurement results 03 p0994 N94-16036
Propagation measurements in Alaska using ACTS beacons 03 p0995 N94-16040
Planned LMSS propagation experiment using ACTS: Preliminary antenna pointing results during mobile operations 03 p0995 N94-16041
A comparison of cloud attenuation models using measured cloud data 03 p0996 N94-16044
Comparison of OLYMPUS beacon and radiometric attenuation measurements at Blacksburg, Virginia 03 p0996 N94-16046
Satellite sound broadcast propagation measurements 03 p0996 N94-16047
An overview of the text propagation effects for land-mobile-satellite systems: Experimental and modeling results 03 p0996 N94-16048
Database for propagation models 03 p0996 N94-16049
A CCIR-based prediction model for Earth-Space propagation 03 p0997 N94-16050
A study of land mobile satellite service multipath effects using SATLAB software 03 p0997 N94-16051
Ground wave emergency network final operational capability: Environmental assessment for central Utah relay node, site number RN 8C920UT
[AD-A267628] 03 p1003 N94-17211
Effect of powerful oblique HF waves on ionospheric D-layer absorption
[AD-A268443] 03 p1102 N94-17499
Radio wave propagation in structured ionization for satellite and radar applications
[AD-A268457] 04 p1382 N94-17844
Studies of enhanced radar backscatter
[AD-A269544] 04 p1385 N94-18288
VLF Harold E. Holt RADHAZ measurements
[AD-A272018] 05 p1737 N94-20620
Comparison of HF groundwave propagation models
[AD-A273146] 06 p2299 N94-24668
Ionospheric modification by high power, obliquely propagated HF radio wave transmissions. Part 1: Experimental
[AD-A273746] 07 p2878 N94-26224
Correlation analysis on optical and radio light curves for a large sample of active galactic nuclei 08 p3546 N94-29992
Low altitude near-the-horizon propagation: A comparison between RPO and M-layer
[AD-A277358] 09 p3679 N94-32282
Radio wave refractivity deduced from lidar measurements
[AD-D016147] 10 p4034 N94-33780
Intensity of waves diffracted from symmetrical profile lamellar gratings
[DE94-611101] 12 p4433 N94-36753

RADIOACTIVE AGE DETERMINATION
Radiogenic age and isotopic studies
[DE93-610548] 01 p0274 N94-10407
Dispersion of the ratios of cosmogenic isotopes of noble gases in chondrites of different cosmic-ray exposure ages 01 p0428 N94-12020
Peculiarities of distributions of the cosmic-ray exposure ages of H chondrite falls and finds 01 p0428 N94-12021
Search for effects of a supernova explosion 30 to 40 thousand years ago in chondrites 01 p0428 N94-12022
Re-Os dating of 3AB iron meteorites 01 p0432 N94-12237
The Xe-Q in lodranites and a hint for Xe-L. FRO90011 another lodranite? 01 p0432 N94-12239
On the origin of (4)He and (40)Ar in natural gold 01 p0087 N94-12240
Dating native gold by noble gas analyses 05 p1684 N94-20652
Exposure ages of carbonaceous chondrites, 1 05 p2082 N94-20658
LREE variability in CM matrices: Another look at meteorite compaction ages 05 p2086 N94-20884

RADIOACTIVE CONTAMINANTS
A review of wind field models for atmospheric transport
[DE93-016085] 04 p1488 N94-17895
Inclusion of a three-dimensional washout coefficient in ADPIC
[DE93-018499] 04 p1476 N94-19038

RADIOACTIVE DATING
U RADIOACTIVE AGE DETERMINATION

RADIOACTIVE DECAY
NT ALPHA DECAY
NT NEUTRON EMISSION
Nuclear astrophysics
[DE93-010569] 01 p0425 N94-10292
The effect of a scalar boson coupled to neutrinos on the behavior of the tritium beta decay spectrum near the end point
[DE93-012655] 01 p0361 N94-10349
On parity conservation and the question of the missing, right-handed neutrino
[DE93-613092] 01 p0361 N94-10414
High efficiency direct thermal to electric energy conversion from radioisotope decay using selective emitters and spectrally tuned solar cells
[NASA-TM-106227] 01 p0047 N94-11307
Tau physics
[DE93-010956] 01 p0367 N94-11469
Double semi-leptonic charm decay in HELIOS-I 450 GeV/c p-Be data
[DE93-013493] 02 p0781 N94-13348
The beta(+) decay and cosmic-ray half-life of Mn-54
[DE93-013913] 02 p0848 N94-13695
Are there atmospheric neutrino oscillations?
[DE93-015550] 02 p0783 N94-13890
Charge-exchange reactions and weak interaction rates for Type 2 supernovae
[DE93-015104] 02 p0783 N94-13893
The (mu)(+) yields e(+)gamma
[DE93-012750] 02 p0785 N94-14181
Rare muon processes
[DE93-012646] 02 p0785 N94-14366
E789 and P865: High-rate fixed-target studies of charm and beauty
[DE93-017223] 02 p0788 N94-14898
On the 17-keV neutrino
[DE93-012638] 03 p1181 N94-15974
Electroweak physics from D0
[DE93-015041] 03 p1181 N94-16053
Experimental study of weak interactions by precision measurement by rare kaon decay
[DE93-016864] 03 p1182 N94-16117
Neutrino mass and mixing: Summary of the neutrino sessions
[DE93-014342] 03 p1183 N94-16801

A high sensitivity search for CP violating rare K(sub L) decays and precision measurement of the direct CP violation parameter (epsilon)(prime)/(epsilon) via the four K (yields) 2(pi) decay modes
[DE93-016866] 03 p1184 N94-16899
Neutral-current detection in the Sudbury Neutrino Observatory
[DE93-014481] 03 p1185 N94-16951
Search for the top quark from (e(mu)) and (e,e) events in the D0 detector in p(bar-p) collisions at the square root of s = 1.8 TeV
[DE93-016350] 03 p1186 N94-17662
Investigation of the relative abundance of heavy versus light nuclei in primary cosmic rays using underground muon bundles
[DE93-017601] 04 p1630 N94-17818
Beauty without charm in B-meson decays
[PREPRINT-732] 04 p1565 N94-17972
Neutrino mass
[DE93-018467] 04 p1567 N94-18269
Research in particle physics
[DE93-040875] 04 p1567 N94-18534
Inverse neutrinoless double (beta)-decay at the NLC?
[DE93-017397] 04 p1568 N94-18825
Experimental research in high energy physics
[DE93-011912] 04 p1574 N94-18916
High energy physics at Tufts University
[DE93-018299] 04 p1575 N94-19023
Simulating supersymmetry with ISAJET 7.0/ISASUSY 1.0
[DE93-018266] 05 p1969 N94-19804
A search for new gauge bosons in (bar p)p collisions at square root of s equals 1.8 TeV in the dielectron decay mode
[DE93-019901] 05 p1969 N94-19813
Measurement of the B(+) and B(0) lifetimes
[DE93-019906] 05 p1969 N94-19814
B production at D0
[DE93-019250] 05 p1972 N94-20291
Measurement of the B meson and b quark cross-section in (-p)p collisions at the square root of s = 1.8 TeV using the exclusive decays B(+) and B(exp 0) yields J/psiK*(exp 0)
[DE93-019907] 05 p1975 N94-21806
Low p(sub T) photon production in proton-nucleus collisions at 18 GeV/c
[DE94-001380] 06 p2532 N94-23007
Heavy flavour physics at LEP
[NIKHEF-H/92-19] 06 p2539 N94-25465
Weak interactions in a bilocal chiral theory
[DE93-616887] 06 p2539 N94-25477
Vector meson exchanges and CP asymmetry in K(sup +/-) yields pi(sup +/-)pi(sup 0)
[DE94-601605] 07 p3014 N94-25887
CP violation in Higgs decays
[DE94-601607] 07 p3014 N94-25888
Unravelling the structure of matter on high-performance computers
[DE94-601620] 07 p3015 N94-25891
Fast vertex search (in plane)
[DE93-616655] 07 p2959 N94-25917
Algorithms of the vertex coordinate reconstruction for straight tracks of short-lived particles
[DE93-616661] 07 p3015 N94-25919
Pseudoscalar glueball in the composite interpolating fields approach
[DE93-634374] 07 p3016 N94-26042
Meson X(1814) as a candidate for a hybrid state
[DE93-634447] 07 p3017 N94-26045
Measurement of tau lepton branching fractions
[DE94-003423] 07 p3018 N94-26325
Chance to use W-decay lepton channels for width determination
[DE93-634438] 07 p3020 N94-26507
Light-quark, heavy-quark systems: An update
[DE94-002298] 07 p3021 N94-26759
Leptonic decay constants of heavy mesons in QCD
[DE93-634426] 07 p3022 N94-26767
Low-energy hadronic interactions beyond the current algebra approach
[DE94-602600] 07 p3022 N94-26900
Study of the process (pi)(sup -)A(yields)(pi)(sup -)(eta)'(eta)A at the moment 36 GeV/c
[DE93-634530] 07 p3024 N94-27250
Spectroscopy and strong decays of baryons
[ISBN-0-315-49073-X] 07 p3024 N94-27258
QCD corrections to inclusive B - S processes in the standard model
[ISBN-0-315-54572-0] 07 p3073 N94-27263
An analysis of monojet data in p(bar-p) collisions at square root of s equal to 1.8 TEV
[DE94-001822] 07 p3026 N94-27565
Decay of non-equilibrium polariton condensate in semiconductors
[DE94-604016] 07 p3068 N94-27678
Research on elementary particle physics, part 2
[DE94-004956] 07 p3029 N94-27815
Decay constants of heavy mesons in the relativistic potential model with velocity dependent corrections
[DE94-606495] 07 p3030 N94-27860
Report of the subgroup on the top quark
[DE94-004624] 08 p3481 N94-28462
Weak decays of charged K-mesons and charm particles
[PB94-138062] 08 p3486 N94-29143
Search for heavy neutrinos at the IHEP-JINR neutrino detector
[DE94-608175] 08 p3489 N94-30095
Measurement of the W mass in the D0 detector
[DE94-006002] 08 p3490 N94-30103
Collective and quasiparticle excitations in light Pb isotopes
[ETN-94-96014] 09 p3865 N94-31548
About G-parity violation in tau yields nu pi eta decay
[DE94-611146] 10 p4136 N94-33863
GRACE manual
[DE94-727456] 10 p4105 N94-33867
Measurement of the decay rate of the SiH feature as a function of temperature 11 p4318 N94-36171
Determination of the upsilon(1s) leptonic width
[DE94-618534] 12 p4516 N94-37096
Five-lepton decay modes of muon and tau mesons
[DE94-621636] 12 p4516 N94-37099

RADIOACTIVE ELEMENTS
U RADIOACTIVE ISOTOPES

RADIOACTIVE ISOTOPES
NT AMERICIUM
NT BERYLLIUM 10
NT CALIFORNIUM
NT CALIFORNIUM ISOTOPES
NT CARBON 14
NT CESIUM 137
NT COBALT 60
NT CURIUM
NT INDIUM ISOTOPES
NT NEPTUNIUM
NT PLUTONIUM
NT PLUTONIUM 238
NT POTASSIUM 40
NT TRANSURANIUM ELEMENTS
NT TRITIUM
NT URANIUM 238
Spin characteristics of ion beams during the motion of electromagnetic elements
[DE93-617448] 01 p0364 N94-10848
Project AIRSTREAM: Trace gas
[DE93-008849] 02 p0706 N94-12904
Research in cosmic and gamma ray astrophysics: Cosmic physics portion
[NASA-CR-194127] 02 p0847 N94-13211
Study of the consequences of the Chernobyl accident and technogenic activity in the Republic Belarus using aerospace methods 02 p0693 N94-14246
The LAHET code system: Introduction, development, and benchmarking
[DE93-012657] 02 p0787 N94-14804
Development and evaluation of alternative radioanalytical methods, inciuding mass spectrometry for marine materials
[DE93-625117] 04 p1345 N94-17691
Gamma scattering in condensed matter with high intensity Moessbauer radiation
[DE93-019461] 04 p1601 N94-19031
Studies of clusters
[DE93-018961] 04 p1572 N94-19309
Dating native gold by noble gas analyses 05 p1684 N94-20652
Exposure ages of carbonaceous chondrites, 1 05 p2082 N94-20658
Geochronology and petrogenesis of the western highlands alkali suite: Radiogenic isotopic evidence from Apollo 14 05 p2118 N94-20778
AGB stars as a source of short-lived radioactive nuclei in the solar nebula 05 p2133 N94-20859
Column chromatographic separation of Y(3+) from Sr(2+) by polymeric ionizable crown ether resins
[DE94-000935] 05 p1683 N94-22021
A double arm time-of-flight spectrometer based on position-sensitive parallel-grid avalanche counters
[DE93-616665] 07 p3012 N94-25750
Simulations of terrestrial in-situ cosmogenic-nuclide production
[DE94-004999] 07 p3117 N94-27826
Production rates of terrestrial in-situ-produced cosmogenic nuclides
[DE94-005156] 08 p3543 N94-28545
Caesium-137 in a boreal forest ecosystem: Aspects on the long-term behavior
[PB94-137809] 08 p3347 N94-29158
Knowledge based system for identification of gamma sources
[PB94-137742] 08 p3487 N94-29683
Intercomparison of theoretical calculations of important activation cross sections for fusion reactor technology
[DE94-002642] 08 p3497 N94-30825
The long-range transport of aerosol particles over the North Atlantic Ocean 08 p3366 N94-30867
Solar proton produced neon in shergottite meteorites 11 p4351 N94-35428
Isotopic and geochemical precursors of earthquakes and volcanic eruptions
[DE94-615824] 11 p4289 N94-35568

RADIOACTIVE MATERIALS
Wind system documentation
[DE93-010381] 01 p0285 N94-11664
Moessbauer spectrometer for mineralogical analysis of the Mars surface: Moessbauer source considerations 01 p0476 N94-12242
Research in cosmic and gamma ray astrophysics: Cosmic physics portion
[NASA-CR-194127] 02 p0847 N94-13211
Nuclear rocket plume studies
[AD-A267154] 03 p0925 N94-15837
Monte Carlo calculations of low background detector response
[DE94-004593] 07 p3116 N94-27621

RADIOACTIVE NUCLIDES
U RADIOACTIVE ISOTOPES

RADIOACTIVE WASTES
Computer models used to support cleanup decision-making at hazardous and radioactive waste sites
[PB93-183333] 01 p0274 N94-10698
Canonical correlation of waste glass compositions and durability, including pH
[DE93-012754] 02 p0578 N94-13493
Environmental radioactivity intercomparison 1992
[NPL-RSA(EXT)-37] 02 p0708 N94-13880
Camera calibration in a hazardous environment performed in situ with automated analysis and verification
[DE93-010274] 02 p0651 N94-14046
Relationship between borosilicate glass composition, structure, and durability test response (SRS)
[DE93-013578] 02 p0581 N94-14343
Modeling surface area to volume effects on borosilicate glass dissolution
[DE93-011891] 02 p0581 N94-14432
Dynamic soil pressures on rigid cylindrical vaults
[DE93-013930] 02 p0676 N94-14585
A study of hydrogen effects on fracture behavior of radioactive waste storage tanks
[DE93-018171] 02 p0574 N94-14873
Rapid analysis of mixed waste samples via the optical emission from laser initiated microplasmas
[DE93-014563] 04 p1582 N94-17727
Rapid geophysical surveyor
[DE93-016637] 04 p1461 N94-17851
Stochastic simulation for imaging spatial uncertainty: Comparison and evaluation of available algorithms
[DE93-040058] 05 p1916 N94-21761
Interpretation of Ground Penetrating Radar data at the Hanford Site, Richland, Washington
[DE93-040409] 05 p1743 N94-22557
Development of laser spectroscopic technology in nuclear industry
[DE93-633327] 07 p2714 N94-26158
Recent ASCOT experiments in multi-layered flows
[DE94-002360] 07 p2880 N94-26762
Nuclear energy related research
[DE94-606286] 08 p3494 N94-28623
Novel mass spectrometric instrument for gaseous and particulate characterization and monitoring
[DE94-005896] 08 p3349 N94-30047
A modular approach for automated sample preparation and chemical analysis 08 p3354 N94-30464
Design reuse experience of space and hazardous operations robots
[AIAA PAPER 94-1220-CP] 08 p3445 N94-30568
Surface chemistry and durability of borosilicate glass
[DE94-006734] 09 p3656 N94-32116
Development and demonstration of a telerobotic excavation system 10 p4066 N94-34028
A teleoperated system for remote site characterization 10 p4066 N94-34029
Decision and systems analysis for underground storage tank waste retrieval systems and tank waste remediation system
[SAND94-0065] 11 p4286 N94-35957
Paleoclimate validation of a numerical climate model
[DE94-009287] 12 p4463 N94-36470
Activities of the Chemical Technology Division
[DE94-013050] 12 p4410 N94-37357

Analytical electron microscopy examination of solid reaction products in long-term test of SRL 200 waste glasses
[DE94-005482] 12 p4411 N94-37380

RADIOACTIVITY

Al-26-Mg-26 ages of iron meteorites
03 p1242 N94-16240

Operator overloading as an enabling technology for automatic differentiation
[DE93-012899] 03 p1170 N94-16778

Development and evaluation of alternative radioanalytical methods, including mass spectrometry for marine materials
[DE93-625117] 04 p1345 N94-17691

A high-intensity He-jet production source for radioactive beams
[DE93-040247] 05 p1981 N94-21767

Gamma ray spectrometry of LDEF samples: Results of 1992 analyses
[DE94-001177] 05 p1684 N94-22046

Comparison of 14 MeV isomer production of Hf-178m1 and Hf-179m2 using Feshbach-Kerman-Koonin and exciton preequilibrium models
[DE94-002640] 08 p3488 N94-30039

Conceptual study of moderately coupled plasmas and experimental comparison of laboratory x ray sources
[DE94-005828] 08 p3506 N94-30045

Complex source rate estimation for atmospheric transport and dispersion models
[DE94-000958] 08 p3354 N94-30822

RADIOBIOLOGY

Effects of radiobiological uncertainty on vehicle and habitat shield design for missions to the moon and Mars
[NASA-TP-3312] 02 p0846 N94-12875

AFRRI reports, first quarter 1993
[AD-A266380] 03 p1123 N94-16515

Extra-corporeal blood access, sensing, and radiation methods and apparatuses
[NASA-CASE-MSC-21775-1] 05 p1890 N94-20372

Molecular biological studies on the human radioresistance and drug resistance
[DE93-632682] 07 p2910 N94-26549

RADIOCHEMISTRY

Ionic and molecular environments in heterogeneous electrocatalysis: Studies by radioactive labeling and LEED/AUGER spectroscopy
[AD-A268850] 04 p1567 N94-18766

Research program activities of the ORNL Analytical Chemistry Division
[DE93-017938] 04 p1339 N94-19117

Fifty years of continuous improvement: What has DOE done for analytical chemistry?
[DE94-002539] 06 p2234 N94-24548

Radiochemistry Division annual progress report : 1991
[DE94-600652] 07 p2715 N94-26392

Research laboratories annual report 1992
[DE94-608124] 08 p3555 N94-30168

Recent results from SAGE
[DE94-006229] 08 p3551 N94-30845

RADIOGENIC MATERIALS

The Lathrop Wells Volcanic Center: Status of field and geochronology studies
[DE93-008917] 01 p0273 N94-10285

Radiogenic age and isotopic studies
[DE93-610548] 01 p0274 N94-10407

Noble gases in LEW88516 shergottite: Evidence for exposure age pairing with ALH77005
01 p0080 N94-12082

Studies of the release of radiogenic Xe-129 from Bjurboele: Evidence against simple diffusion models
01 p0430 N94-12125

Isotopic signatures and distribution of nitrogen and trapped and radiogenic xenon in the Acapulco and FRO90011 meteorites 03 p1243 N94-16317

Dating native gold by noble gas analyses
05 p1684 N94-20652

Geochronology and petrogenesis of the western highlands alkali suite: Radiogenic isotopic evidence from Apollo 14 05 p2118 N94-20778

Magnesian anorthosites from the western highlands of the Moon: Isotope geochemistry and petrogenesis
05 p2118 N94-20779

First measurement of helium on Mars: Implications for the problem of radiogenic gases on the terrestrial planets 11 p4370 N94-36153

RADIOGONIOMETERS

Energy Dispersive X ray Diffraction (EDXD) apparatus for liquids at high temperature 07 p2721 N94-28159

RADIOGRAPHY

NT ANGIOGRAPHY
NT AUTORADIOGRAPHY
NT COMPUTER AIDED TOMOGRAPHY
NT NEUTRON RADIOGRAPHY
NT TOMOGRAPHY

Design of inspection and acceptance test methodology for TIG welded aluminum-alloy bracket for camera housings for IRS-1A space craft and executing it
01 p0061 N94-10037

New x ray scanning topographic approaches to nondestructive evaluation of composites
01 p0061 N94-10039

Real time radiography of Titan 4 booster
[DE93-012450] 02 p0548 N94-12911

Laser weld repair of tantalum sheet
[DE93-016417] 03 p1041 N94-16871

Single sided tomography of extremely large dense objects
[DE93-017993] 04 p1580 N94-19268

PVDF gauge characterization of hypervelocity-impact-generated debris clouds
[DE93-018831] 05 p1829 N94-19943

Experimental and numerical studies of high-velocity impact fragmentation
[DE93-040205] 05 p1832 N94-21557

Measurement of intact-core length of atomizing liquid jets by image deconvolution 06 p2210 N94-23029

An evaluation of Compton scatter imaging using COMSCAN
[DREP-TM-93-38] 06 p2372 N94-24136

The development of an in-motion radiography system for large area aircraft scanning
[DREP-TM-93-53] 07 p2670 N94-27666

Upset welding process for 21-6-9 spherical vessels
[DE93-018194] 07 p2832 N94-28229

Microfocus radioscopy, a high resolution means of inspecting composite materials
[REPT-932-430-109] 08 p3179 N94-29454

Characteristics of secondary electron emission from CsI induced by x rays with energies up to 100 keV
[DE94-608422] 08 p3395 N94-30185

An inverse kinematics algorithm for the DREP/Philips real-time radiographic manipulator system
08 p3307 N94-30292

Seed viability detection using computerized false-color radiographic image enhancement
08 p3387 N94-30461

X ray radiographic imaging of hydrodynamic phenomena in radiation driven materials: Shock propagation and shear flow
[DE94-010891] 11 p4318 N94-36201

RADIOISOTOPE BATTERIES

Development testing of the two-watt RTG heat source and Hastelloy-S/T-111 alloy compatibility studies
[DE94-002875] 06 p2243 N94-23784

Preliminary reentry safety assessment of the General Purpose Heat Source module for the Cassini mission: Aerospace Nuclear Safety Program
[DE94-001646] 07 p2699 N94-25926

GPHS-RTGs in support of the Cassini mission
[DE94-009994] 11 p4212 N94-35648

RADIOLOGY

Operational radiological support for the US manned space program 01 p0318 N94-11561

Development and evaluation of alternative radioanalytical methods, including mass spectrometry for marine materials
[DE93-625117] 04 p1345 N94-17691

A teleoperated system for remote site characterization
10 p4066 N94-34029

Activities of National Institute of Radiological Sciences
[DE94-727636] 11 p4296 N94-36101

The integrated performance evaluation program quality assurance guidance in support of EM environmental sampling and analysis activities
[DE94-013043] 12 p4468 N94-37731

RADIOLYSIS

Pulse radiolytic studies of electron transfer processes and applications to solar photochemistry
[DE93-018715] 04 p1464 N94-17781

The effects of radiolysis on the corrosion and stress corrosion behavior of 316 stainless steels
[DE93-019933] 04 p1363 N94-19021

Radiation-Induced Structural Changes, 2
[DE93-520314] 07 p3054 N94-26109

A comparison between two Monte Carlo codes on determination of transient chemical yields
[DE94-007224] 09 p3636 N94-32251

An investigation of the radiolytic stability of a resorcinol-formaldehyde ion exchange resin
[DE94-007971] 09 p3660 N94-32698

High-energy chemical processes: Laser irradiation of aromatic hydrocarbons
[DE94-008107] 09 p3720 N94-32707

RADIOMETERS

NT ADVANCED VERY HIGH RESOLUTION RADIOMETER
NT DICKE RADIOMETERS
NT INFRARED DETECTORS
NT INFRARED RADIOMETERS
NT INFRARED SCANNERS
NT MICROWAVE RADIOMETERS
NT PRESSURE MODULATOR RADIOMETERS
NT SPECTRORADIOMETERS

Development of a balloon-borne stabilized platform for measuring radiative flux profiles in the atmospheric boundary layer
[DE93-013186] 01 p0274 N94-10323

Coherence effects in radiometry and in spectroscopy
[DE93-013437] 01 p0075 N94-10519

Progress in multidisciplinary design optimization at NASA Langley
[NASA-TM-107754] 01 p0318 N94-10814

Atmospheric correction plans for SeaWiFS
01 p0204 N94-11975

Radiometer offsets and count conversion coefficients for the Earth Radiation Budget Experiment (ERBE) spacecraft for the years 1987, 1988, and 1989
[NASA-CR-191489] 01 p0286 N94-12772

Nimbus-7 Earth radiation budget calibration history. Part 1: The solar channels
[NASA-RP-1316] 02 p0844 N94-13963

Volume 14: The first SeaWiFS intercalibration round-robin experiment, SIRREX-1, July 1992
[NASA-TM-104566-VOL-14] 02 p0725 N94-14090

Earth Observation Center Annual Report on Research and Development, Fiscal Year 1992
[EOC-92-01-0007] 02 p0687 N94-14091

Earth observation experiment data analysis
02 p0687 N94-14093

ADEOS project
02 p0687 N94-14094

A calibration procedure for radiation budget radiometers and its influence on interpretation of measured values
[MITT-82] 02 p0651 N94-14149

Clouds and the Earth's Radiant Energy System (CERES) on the Tropical Rainfall Measuring Mission (TRMM)
02 p0690 N94-14223

Absolute Radiometric Measurements in Space: ARMS
03 p0908 N94-15085

The laboratory performance of the short wavelength instrument for the Along Track Scanning Radiometer ATSR-2 (initial results) 03 p0908 N94-15088

Absolute, Extreme-Ultraviolet Solar Spectral Irradiance Monitor (AESSIM)
[AD-A267045] 03 p1299 N94-15836

ERS-1: 18 months in orbit 03 p0990 N94-15888

Olympus propagation measurement results at Virginia Tech 03 p0995 N94-16037

Data acquisition, preprocessing and analysis for the Virginia Tech OLYMPUS experiment
03 p0995 N94-16038

Brightness temperature and attenuation statistics at 20.6 and 31.65 GHz 03 p0996 N94-16045

Comparison of preliminary results from Airborne Aster Simulator (AAS) with TIMS data
03 p1064 N94-16600

In-flight calibration of the spectral and radiometric characteristics of AVIRIS in 1991
03 p1037 N94-16667

Simulation of ASTER data using AVIRIS images
03 p1071 N94-16693

The Earth radiation budget experiment: Overview of data-processing and error sources
[KNMI-TR-146] 04 p1481 N94-18142

Broadband IF matching for quasioptical mixers
[MPE-PREPRINT-240] 04 p1390 N94-19416

Low power, CMOS digital autocorrelator spectrometer for spaceborne applications 05 p1666 N94-21733

Satellite measurements of radiation budget parameters 05 p1860 N94-22284

ScaRaB and its subsystems 05 p1860 N94-22285

Bi-directional reflectance and other radiation parameters of cirrus from ER-2 observations
05 p1871 N94-22296

Eos cross-calibration radiometers
06 p2383 N94-23601

Flight solar calibrations using the Mirror Attenuator Mosaic (MAM): Low scattering mirror
06 p2384 N94-23602

Infrared calibration 06 p2384 N94-23608

VNIR and SWIR transfer radiometers developed at NRLM for preflight laboratory cross-calibration
06 p2385 N94-23610

In-flight cross-calibration of ASTER/TIR and MODIS-N
06 p2385 N94-23611

ASTER, a multinational Earth observing concept
06 p2389 N94-23840

High resolution encoder-motor used in the orbital spin scan radiometer, GOES VAS satellites
06 p2209 N94-24038

Evidence for dust transport in Viking IR thermal mapper opacity data 06 p2620 N94-24892

An AVHRR cloud classification database typed by experts
[AD-A273560] 06 p2416 N94-25162

Advanced radiometric and interferometric milimeter-wave scene simulations
06 p2306 N94-25498
Hyperspectral analysis of space objects: Signal to noise evaluation
[AD-A273882] 07 p2765 N94-25728
Characterization and calibration of the Agema 880+ imaging radiometer
[AD-A274417] 07 p3036 N94-26981
Radiometric, spectral, and effectiveness equipment
[AD-A274208] 07 p3037 N94-27066
Initial ultraviolet-B intensity data at Lawrence Livermore National Laboratory
[DE94-004279] 07 p2869 N94-27267
The validation of ATSR measurements with in situ sea temperatures
[DE94-003195] 07 p2852 N94-27875
Observations by ERS-1 start
08 p3327 N94-28933
Principles and application tendency of remote sensing: Its principle, function and utilization
08 p3328 N94-29037
Observatory system of Earth Resources Satellite-1
08 p3330 N94-29221
Application of JERS-1 data to geologic analyses
08 p3330 N94-29222
EOS project and ASTER (ITIR)
08 p3331 N94-29226
An absolute measurement of the cosmic background radiation temperature at 1.4 GHz
08 p3553 N94-30351
A study of areas of low radio-thermal emissivity on Venus
09 p3942 N94-31992
NOAA-9 Earth Radiation Budget Experiment (ERBE) scanner offsets determination
[NASA-TM-109086] 09 p3785 N94-32737
Radiometry spot measurement system
[NASA-TM-106561] 09 p3883 N94-32777
Studies of atmospheric dust from Viking IR thermal mapper data
09 p3948 N94-33216
SeaWiFS technical report series. Volume 16: The second SeaWiFS Intercalibration Round-Robin Experiment, SIRREX-2, June 1993
[NASA-TM-104566-VOL-16] 10 p4093 N94-34412
Switched-beam radiometer front-end network analysis
[NASA-CR-194922] 11 p4252 N94-35247
Controller for the Electronically Scanned Thinned Array Radiometer (ESTAR) instrument
[NASA-TM-104608] 11 p4259 N94-36049
Absolute, Extreme Ultraviolet Solar Spectral Irradiance Monitor (AESSIM)
[AD-A278709] 11 p4227 N94-36189
Astronomy in the region between 1 mm and 0.1 mm wavelength
[NASA-CR-196020] 11 p4349 N94-36419
Scientific and technical support for the Galileo net flux radiometer experiment
[NASA-CR-196009] 12 p4549 N94-36689
NOAA polar satellite calibration: A system description
[NOAA-TR-NESDIS-77] 12 p4396 N94-37009

RADIOMETRIC CORRECTION
Analytical framework for modeling scale-related variabilities in remote sensing
02 p0685 N94-13592
Radio metric errors due to mismatch and offset between a DSN antenna beam and the beam of a troposphere calibration instrument
02 p0607 N94-14370
Topographic mapping using a monopulse SAR system
05 p1721 N94-20417
European Imaging Spectroscopy Aircraft Campaign
[ESA-SP-360] 09 p3743 N94-31853
The European Imaging Spectroscopy Airborne Campaign (EISAC). Data takes and evaluation programme: An overview
09 p3743 N94-31854
Ground based radiometric and atmospheric measurements
09 p3744 N94-31855
Investigation on correction models for airborne imaging spectrometry data from the EISAC-campaign for geoscientific purposes
09 p3745 N94-31861
Extraction of agricultural parameters from imaging-spectrometry data and simulated MERIS data through red edge analysis
09 p3745 N94-31865
Restoration of interferometric, polarimetric, radiometric, and textural information in SAR images
09 p3750 N94-32535
Modelling topographic effects on digital remotely sensed data
10 p4074 N94-33360
Reduction procedures for accurate analysis of MSX surveillance experiment data
11 p4203 N94-35611

RADIOMETRIC RECTIFICATION
U RADIOMETRIC CORRECTION

RADIOMETRIC RESOLUTION
Preliminary results of the experiment I-7
01 p0235 N94-11728
Calibration of the ERS-1 SAR fast-delivery images
01 p0236 N94-11730
The use of active devices in the ERS-1 radiometric calibration
01 p0236 N94-11732
An experiment for the radiometric calibration of the ERS-1 SAR
01 p0236 N94-11733
Improved optical radiation detectors and their calibration: 200 nm - 30 microns
03 p0906 N94-15075
A motion extraction method for synthetic aperture radars
[DLR-FB-92-31] 05 p1742 N94-22279
Calibration of SAR systems
[DLR-FB-93-18] 07 p2777 N94-27738

RADIONUCLIDES
U RADIOACTIVE ISOTOPES

RADIOSENSITIVITY
U RADIATION TOLERANCE

RADIOSONDES
NT IONOSONDES
NT RAWINSONDES
Cloud liquid water content over the Pacific Ocean tropical zone derived from ship microwave radiometric measurement
01 p0225 N94-12743
DMSP F11 SSM/T-2 calibration and validation
[AD-A265817] 02 p0719 N94-12978
Verification of 3I retrievals vis-a-vis radiosonde observations
[KNMI-TR-150] 04 p1488 N94-17924
Radiosonde data collected on the ERS-1 validation cruise RRS Charles Darwin Cruise 62A, Iceland Faeroes region
[IOS-297-1992] 04 p1461 N94-18137
Intercomparison of remote and balloon-borne sensors operated at JAPE-91
06 p2527 N94-24210
Observed and Navy operational global model climatologies of synoptic disturbances over the tropical western Pacific during winter 1991-1992
[AD-A273400] 06 p2416 N94-25071
A nighttime structure model of atmospheric optical turbulence, c2(n), derived from thermosonde and high resolution rawinsonde measurements
[AD-A273803] 06 p2406 N94-25537
Coastal boundary layer and refractivity measurements using the ground-based high resolution interferometer sounder (GB-HIS)
[AD-A277980] 09 p3683 N94-33159
Production of long-term global water vapor and liquid water data set using ultra-fast methods to assimilate multi-satellite and radiosonde observations
[NASA-CR-196044] 11 p4292 N94-35355
Production of long-term global water vapor and liquid water data set using ultra-fast methods to assimilate multi-satellite and radiosonde observations
[NASA-CR-195981] 11 p4293 N94-35499

RADIOTELEPHONES
An analysis of cellular telephone and INMARSAT systems for providing radio data link computer communications for US Navy vessels
[AD-A278143] 09 p3684 N94-33160

RADIOTHERAPY
U RADIATION THERAPY

RADIUM
NT RADIUM ISOTOPES

RADIUM ISOTOPES
An intercomparison of the radium mass standards of the UK and the USSR: 2
[NPL-RSA(EXT)-34] 01 p0359 N94-10266

RADOME MATERIALS
Radar signature related radome techniques for flush-mounted HF-, VHF- and, UHF communication antennas
[PB93-204618] 06 p2294 N94-23742

RADOMES
Antenna gain loss and pattern degradation due to transmission through dielectric radomes
[AD-A267242] 03 p0986 N94-14974
Manufacturing tolerance requirements for frequency selective surfaces
[AD-A266541] 03 p0999 N94-16797
Radome depolarization effects on monopulse receiver tracking performance
[AD-A267446] 03 p1001 N94-17031
Radome having integral heating and impedance matching elements
[CA-PATENT-APPL-SN-2,026,855]
05 p1738 N94-21049
Radar signature related radome techniques for flush-mounted HF-, VHF- and, UHF communication antennas
[PB93-204618] 06 p2294 N94-23742
Analyzing adaptive beamformer performance in a stable multipath environment
[AD-A274029] 07 p2766 N94-25766
A study of two dimensional tapered periodic edge treatments to reduce wideband edge diffraction
[AD-A274054] 07 p2766 N94-25824

RADON
NT RADON ISOTOPES
Study of the atmospheric chemistry of radon progeny in laboratory and real indoor atmospheres
[DE93-012236] 01 p0266 N94-11671
Indoor environment program
[DE93-018601] 04 p1513 N94-18935
Brief summary of accomplishments since our DOE-sponsored radon project commenced
[DE94-004643] 08 p3348 N94-29926
The long-range transport of aerosol particles over the North Atlantic Ocean
08 p3366 N94-30867
California residential indoor air quality study. Volume 1: Methodology and descriptive statistics
[PB94-166048] 12 p4464 N94-36994

RADON ISOTOPES
Isotopic and geochemical precursors of earthquakes and volcanic eruptions
[DE94-615824] 11 p4289 N94-35568

RAFTS
NT LIFE RAFTS

RAIL TRANSPORTATION
Safety of high speed ground transportation systems: X2000 US demonstration vehicle dynamics trials, preliminary test report, October 1992 - January 1993
[PB93-194645] 01 p0422 N94-10736
Experiment on a high Reynolds number turbulent boundary layer
01 p0164 N94-12617
On the wake behind a high speed train
01 p0164 N94-12618
Activities of Bombardier, Inc.
[ISBN-2-921393-11-5] 02 p0499 N94-13520
Adaptation of model parameters of a rail model at measured rail compliances
[ILR-MITT-274(1992)] 05 p1831 N94-21153
Vehicle/guideway interaction and ride comfort in maglev systems
[DE94-001319] 06 p2352 N94-22991
Performance analysis of the combined EDS maglev propulsion, levitation, and guidance system
[DE94-001346] 06 p2352 N94-22996
Rail Corrugations
[ILR-BER-59] 06 p2269 N94-23581
A rail corrugation theory which allows for contact patch size
06 p2269 N94-23582
A rail joint: The possible initiator of corrugation?
06 p2269 N94-23583
A linear model for corrugation and its limit of validity
06 p2269 N94-23584
Lateral high frequency oscillations and stability of a wheel rolling on a flexible track
06 p2269 N94-23585
Wear characteristics of technical dry rolling/sliding systems with relations to corrugation problems
06 p2269 N94-23586
Surface analysis of corrugated rail treads
06 p2270 N94-23587
Surface observations of stick-slip oscillations in tightly conformal wheel/rail contacts
06 p2270 N94-23588
Contact analysis of rough rail surfaces
06 p2270 N94-23589
Electrical engineering and industrial electronics education days: Control of asynchronous generators
[PB94-135514] 08 p3266 N94-29523
Theoretical principles for designing long stator/linear motors with iron
[ETN-94-95741] 09 p3688 N94-31374
Applicable dimensioning and measure and technological examination of long stator-linear motors for magnetic high-speed railways
[ETN-94-95734] 09 p3689 N94-31575
System concept definition of the Grumman superconducting Electromagnetic Suspension (EMS) Maglev design
11 p4213 N94-35840
Transrapid (the first high-speed Maglev train system certified ready for application): Development status and prospects for deployment
11 p4213 N94-35841
Control of maglev vehicles with aerodynamic and guideway disturbances
11 p4213 N94-35842
Fault tolerant computer control for a Maglev transportation system
11 p4215 N94-35848
Superconducting Electromagnetic Suspension (EMS) system for Grumman Maglev concept
11 p4215 N94-35849
National Maglev initiative: California line electric utility power system requirements
11 p4215 N94-35850
Study of Japanese electrodynamic-suspension maglev systems
[DE94-011486] 12 p4452 N94-37515

RAILGUN ACCELERATORS
Investigation of multiphase railgun systems
01 p0040 N94-11637
Numerical modeling of the temperature gradients and spectra of the plasma armature on Thunderbolt
[AD-A266414] 03 p0878 N94-16552
The internal structure and dynamics of the railgun plasma armature between infinitely wide ablating rails
[DE94-001473] 06 p2198 N94-23208

A comparison of in-bore projectile motion from an electromagnetic railgun versus that of a conventional cannon barrel
[AD-A273473] 06 p2198 N94-24690
Interaction between a high density-low temperature plasma and a frozen hydrogen pellet in a railgun injector
[DE94-000846] 07 p3041 N94-25949
Application of railgun principle to high-velocity hydrogen pellet injection for magnetic fusion reactor fueling
[DE94-004411] 07 p3044 N94-26579
The 100 kA, 5000 V solid-state opening switch for inductive energy storage
[AD-A274993] 08 p3263 N94-28994
Microwave Michelson interferometer system report of first use on a railgun, Green Farm, San Diego, CA
[DE94-005294] 08 p3289 N94-30059
Design of an electromagnetic accelerator for turbulent hydrodynamic mix studies
[DE94-005821] 08 p3281 N94-30600
Design and evaluation of coils for a 50 mm diameter induction coilgun launcher
[DE94-005244] 09 p3603 N94-32671

RAILROADS
U RAIL TRANSPORTATION

RAILS
Rail Corrugations
[ILR-BER-59] 06 p2269 N94-23581
A rail corrugation theory which allows for contact patch size 06 p2269 N94-23582
A rail joint: The possible initiator of corrugation? 06 p2269 N94-23583
A linear model for corrugation and its limit of validity 06 p2269 N94-23584
Lateral high frequency oscillations and stability of a wheel rolling on a flexible track 06 p2269 N94-23585
Wear characteristics of technical dry rolling/sliding systems with relations to corrugation problems 06 p2269 N94-23586
Surface analysis of corrugated rail treads 06 p2270 N94-23587
Surface observations of stick-slip oscillations in tightly conformal wheel/rail contacts 06 p2270 N94-23588
Contact analysis of rough rail surfaces 06 p2270 N94-23589
The railway track response function
[REPT-93-40] 07 p2837 N94-26214
A non-linear mathematical model or finite, periodic rail corrugations
[REPT-93-49] 07 p2996 N94-26967
Considering ties elasticities in high frequency rail dynamics
[ILR-MITT-281(1993)] 09 p3733 N94-31375
Testing of the fracture resistance of rails 11 p4279 N94-35353

RAIN
NT ACID RAIN
The effect of rain on ERS-1 altimeter data 01 p0243 N94-11773
Flood monitoring in northern part of Central Java by remote sensing technique. Case study: The flooding of Semarang in January, 1990 01 p0206 N94-11989
Rainfall-runoff estimation using digital radar
[AD-A265390] 01 p0286 N94-12408
The phytoplankton bloom in the Kinu-ura Bay, Japan in the rainy season 01 p0211 N94-12660
Worldwide map of rainfall amount over the ocean derived from passive microwave radiometer 01 p0211 N94-12663
Remote identification of rain and hail with a polarization diversity radar
[ISBN-0-315-55623-4] 02 p0720 N94-13516
Spatial and temporal variability of precipitation and chemistry: Case studies from the frontal boundary study
[DE93-007883] 02 p0708 N94-13910
Water-vapour, total water and rainrate from passive microwave satellite data over ocean
[DLR-FB-92-37] 02 p0723 N94-14189
TRMM system overview and status in the United States 02 p0690 N94-14221
TRMM Project in Japan: Overview and status 02 p0690 N94-14222
TRMM precipitation radar algorithm 02 p0690 N94-14224
Estimate of sampling errors of TRMM rainfall observation by using radar-AMeDAS composite data 02 p0690 N94-14225
Multiparameter airborne rain radar development for TRMM validation and TRMM-follow-on study 02 p0690 N94-14226
Future TRMM follow-on mission 02 p0691 N94-14228
Large-scale rainfall diversity for ACTS 02 p0613 N94-14662
Rain rate duration statistics derived from the Mid-Atlantic coast rain gauge network 02 p0614 N94-14663
Rain-rate data base development and rain-rate climate analysis 02 p0614 N94-14664
Wind shear and heavy rain --- effects on flight stability
[NASA-TM-109453] 03 p1105 N94-15326
TRMM radar 03 p0990 N94-15894
Recent scientific advances in the use of radar in scientific hydrology 03 p0991 N94-15895
Some thoughts on future rain mapping missions (TRMM follow-on) 03 p0992 N94-15906
Similarity and scale in catchment storm response
[PAPER-89RG01615] 03 p1083 N94-16028
Olympus propagation measurement results at Virginia Tech 03 p0995 N94-16037
A CCIR-based prediction model for Earth-Space propagation 03 p0997 N94-16050
Validation and analysis of microwave-derived rainfall over the tropics
[AD-A267785] 03 p1108 N94-17303
Initialization and assimilation of cloud and rainwater in a regional model 04 p1492 N94-18608
Inclusion of a three-dimensional washout coefficient in ADPIC
[DE93-018499] 04 p1476 N94-19038
Modeling of interactions between biosphere and atmosphere on the global scale
[NASA-CR-193423] 05 p1837 N94-20205
Schools of the Pacific rainfall climate experiment 05 p1881 N94-20699
A laboratory system for the investigation of rain fade compensation techniques for Ka-band satellites
[NASA-CR-191200] 05 p1762 N94-21566
Presenting the Rain-Sea Interaction Facility
[NASA-RP-1322] 05 p1884 N94-21628
Evolution of the global water cycle on Mars: The geological evidence 05 p2142 N94-21660
The evolution of the early Martian climate and the initial emplacement of crustal H2O 05 p2143 N94-21665
Observations of multi-layered clouds using K-band radar 05 p1874 N94-22311
Adaptive data rate control TDMA systems as a rain attenuation compensation technique 06 p2287 N94-22821
An analytic study of a two-phase laminar airfoil in simulated heavy rain 06 p2171 N94-23661
Estimation of the rain signal in the presence of large surface clutter
[NASA-CR-195105] 06 p2409 N94-24087
Precipitation measurement using SIR-C: A feasibility study. Investigation at nadir
[NASA-CR-195103] 06 p2410 N94-24126
CAPE for CaPE 06 p2416 N94-24409
Water cycle research associated with the CaPE hydrometeorology project (CHymP 06 p2416 N94-24414
Further studies to extend and test the area-time-integral technique applied to satellite data
[NASA-CR-195132] 06 p2415 N94-24705
Worst case analysis: Earth sensor assembly for the tropical rainfall measuring mission observatory
[NASA-CR-189320] 06 p2311 N94-24754
Human impacts on soil carbon dynamics of deep-rooted Amazonian forests
[NASA-CR-195127] 06 p2399 N94-24861
A synoptic study on periods of deficiency over Rio Grande do Sul/Brazil
[INPE-5456-TDI/498] 07 p2896 N94-27422
Physical processes in snowpacks during rain or melt events
[AD-A275445] 08 p3325 N94-28881
On the relation between SMMR 37-GHz polarization difference and the rainfall over Africa and Australia
[NASA-TM-104598] 08 p3370 N94-29408
GCM studies of the influence of vegetation on the general circulation: The role of albedo in modulating climate change 08 p3348 N94-29749
Evaluation of dual polarization attenuation of millimeter frequencies through a meteorological radar 08 p3256 N94-30496
Numerical simulations of monsoon rainfall with the NRL/NCSU regional nested grid model 09 p3782 N94-31791
Radar rainfall measurements from space 09 p3782 N94-31889
Estimation and analysis of climate-scale rainfall over the Tropical Pacific 09 p3783 N94-32030
Simulation of a precipitation event in the western United States
[DE94-004835] 09 p3786 N94-32791
TRMM-related research: Tropical rainfall and energy analysis experiment
[NASA-CR-195834] 09 p3787 N94-33288

RAIN EROSION
Evaluating the spread of red soil with LANDSAT TM data in coral reefs of Okinawa main island, southwestern Japan 01 p0212 N94-12668

RAIN FORESTS
TREES project: A suite of tools for information extraction from ERS-1 SAR data 01 p0250 N94-12498
Modeling of biosphere-atmosphere interaction for forest and pastureland in the Amazon
[INPE-5454-TDI/496] 02 p0707 N94-13330
Spatial variability of throughfall chemistry in a tropical rainforest (Central Amazonia, Brazil)
[INPE-5431-PRE/1765] 02 p0720 N94-13429
Estimations of temperature and humidity of the canopy in Amazon Forest using microwave data from SMMR sensor of Nimbus-7 satellite
[INPE-5444-TDI/490] 02 p0720 N94-13614
Application of symmetry properties to polarimetric remote sensing with JPL AIRSAR data 03 p1079 N94-16752
Change detection on land use and rainforest cover at Paragominas region, Brazilian Amazon 05 p1838 N94-20957
Evaluation of C-band SAR data from SAREX 1992: Tapajos study site 05 p1839 N94-20964
Assessment of tropical forests using satellite data
[SILVA-CARELICA-21] 07 p2850 N94-27182
Global tropical forest cover assessments using satellite imagery 07 p2850 N94-27183
Mapping closed tropical forest cover in West Africa using NOAA/AVHRR-LAC data 07 p2850 N94-27184
Training on assessment and mapping of deforestation: WFW conference, Brazil
[INPE-5482-PRE/1781] 07 p2850 N94-27384
Behavior and dynamics of tropical forests and savannas 09 p3757 N94-31004
The forest inventory project at the Tapajos National Forest, volume 1
[INPE-5423-PRP/171] 10 p4033 N94-33434
Completing below-ground carbon budgets for pastures, recovering forests, and mature forests of Amazonia
[NASA-CR-195959] 10 p4076 N94-33948
Study of the energy partition in complex terrains (deforested and forested areas)
[INPE-5522-TDI/519] 10 p4083 N94-34225

RAIN GAGES
Rain rate duration statistics derived from the Mid-Atlantic coast rain gauge network 02 p0614 N94-14663

RAINDROPS
A laboratory system for the investigation of rain fade compensation techniques for Ka-band satellites
[NASA-CR-191200] 05 p1762 N94-21566
The appearance of the Sun and Moon seen through clouds
[AD-A275336] 08 p3551 N94-29212
Field studies of raindrop oscillations with applications to radar meteorology 09 p3782 N94-31743

RAINSTORMS
NT THUNDERSTORMS
Wind shear and heavy rain --- effects on flight stability
[NASA-TM-109453] 03 p1105 N94-15326

RAM ACCELERATORS
Numerical simulation of fluid dynamics and combustion for ram accelerator projectile/obturator interaction
[AD-A269715] 04 p1320 N94-18748
Basic and applied studies of the ram accelerator as a hypervelocity projectile launcher
[AD-A277392] 09 p3602 N94-32288

RAMAN EFFECT
U RAMAN SPECTRA

RAMAN LASERS
Theory and modeling of stimulated Raman scattering
[AD-A273755] 07 p3033 N94-25721
Specification for the TITANIA krF laser system
[PB94-167103] 11 p4272 N94-36062

RAMAN SCATTERING
U RAMAN SPECTRA

RAMAN SPECTRA
Surface-enhanced raman spectroscopy of electroactive films of C60 and an Ir-C60 complex on gold: Symmetry lowering, electron localization, and counteraction effects
[AD-A265934] 01 p0396 N94-10705
Characterization of gas-aerosol interaction kinetics using morphology dependent stimulated Raman scattering
[DE93-012324] 01 p0077 N94-11359
Ecological application of Surface Enhanced Raman Spectroscopy 01 p0227 N94-12756
Inertial Confinement Fusion
[DE93-013303] 02 p0795 N94-13017
Resonant x ray Raman scattering from atoms and molecules
[DE93-015158] 02 p0784 N94-13896
Brillouin scattering from fluctuations produced by stimulated Raman scattering
[DE93-016531] 02 p0792 N94-14438
Investigation of the feasibility of optical diagnostic measurements at the exit of the SSME
[NASA-CR-193832] 02 p0553 N94-14682

Studies on the parametric decay of waves in fusion plasmas
[VTT-PUBS-110] 03 p1200 N94-15204
High frequency Raman current drive
03 p1201 N94-15208
Current drive with free electron lasers in high and low temperature tokamaks 03 p1201 N94-15209
Simulations of wave-particle interactions in stimulated Raman forward scattering in a magnetized plasma
[PB94-170990] 03 p1201 N94-15210
New methods of generation of ultrashort laser pulses for ranging 03 p0913 N94-15565
Investigation of the optical, electronic, and structural properties of fiber optic glasses
[AD-A267645] 03 p0971 N94-17204
BACKSCAT lidar simulation version 3.0: Technical documentation and users guide
[AD-A267296] 03 p1003 N94-17268
Applications of nonlinear optic effects in new specialty fibers
[AD-A268890] 04 p1578 N94-18457
Resonance Raman and photophysical studies of transition metal complexes in solution and entrapped in zeolites
[DE93-019892] 04 p1363 N94-19019
First and second order Stokes generation by SRS in methane: Influence of rep-rate, beam quality and astigmatism
[FEL-92-A125] 04 p1441 N94-19426
Femtosecond Raman-induced Kerr effect study of polar solvent dynamics: Amides
[DE93-017563] 05 p1678 N94-19924
The multicomponent lineshape of the anharmonic A(1)(TO) phonon in PbTiO3
[DE93-018995] 05 p1970 N94-19971
Phonons and metastability in compressed nitrogen
[DE93-019913] 05 p2016 N94-20018
Examinations of a thallium atomic vapor filter for a Raman temperature lidar
[GKSS-92/E/13] 05 p1857 N94-21044
Effects of stimulated Raman scattering on light beam properties during high-power laser beam long-path propagation
[AD-A273109] 05 p1818 N94-21509
Parametric instabilities in picosecond time scales
[DE94-000384] 05 p1966 N94-21958
Numerical simulation and analysis of experimental results on stimulated Raman scattering in laser-plasma Hohlraum targets
[DE93-613719] 06 p2554 N94-25330
Measurement of the volume mass by spontaneous Raman scattering. Study of turbulent fluctuations of mixing in a subsonic free jet. Measurements in supersonic wind tunnels
[ISL-R-102/92] 06 p2339 N94-25462
Theory and modeling of stimulated Raman scattering
[AD-A273755] 07 p3033 N94-25721
Gaseous hydrogen/oxygen injector performance characterization
[NASA-CR-194464] 07 p2701 N94-26208
High definition Raman microscopic imaging
[DE94-003158] 07 p2716 N94-26781
Technical report of ISSP. Ser. A, no. 2680: Determination of intervalley scattering time in germanium by subpicosecond time-resolved Raman spectroscopy
[JTN-94-80566] 07 p3064 N94-27176
Stimulated Cerenkov-radiation processes in dusty AGN
[DE94-009639] 10 p4163 N94-33917
Implementation of Raman lidar for profiling of atmospheric water vapor and aerosols at the SGP CART site
[DE94-011754] 11 p4295 N94-36285
XAFS-like structure of resonant Raman scattering
[DE94-618410] 12 p4517 N94-37171
Final report on spectral broadening by cross-phase modulation in linearly birefringent optical fibers
[DE94-010406] 12 p4524 N94-37191
Raman scattering of variable bandwidth KrF radiation in long air paths
[DE94-012912] 12 p4449 N94-37495
Residual stress and Raman spectra of laser deposited highly-tetrahedral-coordinated-amorphous-carbon films
[DE94-012067] 12 p4426 N94-37537
Optical spectroscopy of a nitrogen-hydrogen complex in ZnSe
[DE94-011622] 12 p4413 N94-37630

RAMAN SPECTROSCOPY
Surface-enhanced raman spectroscopy of electroactive films of C60 and an Ir-C60 complex on gold: Symmetry lowering, electron localization, and counteraction effects
[AD-A265934] 01 p0396 N94-10705
Scanning tunneling microscopy studies of diamond films and optoelectronic materials
[NASA-CR-194363] 02 p0578 N94-13246
In situ Raman spectroscopy of lithium electrode surface in ambient temperature lithium secondary battery
[DE93-015238] 03 p1010 N94-16061
Femtosecond Fourier-transform spectroscopy of low-frequency intermolecular motions in weakly interacting liquids
[DE93-017312] 04 p1566 N94-18085
Remote cure monitoring of polymeric resins by laser Raman spectroscopy
[DE93-016445] 04 p1369 N94-18112
Fiber optic Raman spectrograph for in situ environmental monitoring
[DE93-019466] 04 p1478 N94-19305
Growth, characterization and device development in monocrystalline diamond films
[AD-A273097] 05 p2028 N94-21506
Materials Science and Engineering
[DE93-040497] 05 p1675 N94-21530
Laser Raman and x ray scattering studies of corrosion films on metals
[DE93-040243] 05 p1692 N94-21558
Femtosecond dynamics in hydrogen-bonded solvents
[DE93-019937] 05 p1683 N94-21842
Materials Science and Engineering
[DE94-003018] 06 p2228 N94-23493
Total light loss optic spectroscopy: Progress towards a fiber optic Raman organic vapor sensor
[DE94-002545] 06 p2234 N94-24549
Nondestructive evaluations
[DE94-003020] 06 p2373 N94-24613
Investigation of Raman beam cleanup and phase conjugation
[AD-A273157] 06 p2545 N94-24672
Study of the homogeneity of InP wafers
[AD-A273658] 07 p3055 N94-26194
High definition Raman microscopic imaging
[DE94-003158] 07 p2716 N94-26781
Spectroscopy Division
[DE94-604074] 07 p2717 N94-26988
Enhanced ion dissociation of LiCF3SO3 by new carbonate plasticizers: Raman and IR studies
[DE94-005448] 08 p3485 N94-28741
Vibrational spectroscopy at metal-solution interfaces: Some perspectives and prospects for electrochemical surface science
[AD-A276781] 09 p3644 N94-32169
Raman scattering of variable bandwidth KrF radiation in long air paths
[DE94-012912] 12 p4449 N94-37495
Optical spectroscopy of a nitrogen-hydrogen complex in ZnSe
[DE94-011622] 12 p4413 N94-37630

RAMJET ENGINES
NT INTEGRAL ROCKET RAMJETS
NT SUPERSONIC COMBUSTION RAMJET ENGINES
NT TURBORAMJET ENGINES
Equations of motion of a hinged body over a spherical earth
[AD-A268408] 03 p0868 N94-17435
Development of hypersonic engine seals: Flow effects of preload and engine pressures
[NASA-TM-106333] 07 p2826 N94-27599
Research and development of ramjets/ramrockets. Part 1: Integral solid propellant ramrockets
08 p3151 N94-29294
Research and development of ramjets/ramrockets. Part 2: Integral liquid fuel ramjets 08 p3152 N94-29297
Research and development of ramjets/ramrockets. Part 3: The study of gaseous hydrogen ram combustors
08 p3152 N94-29298
CIAM experimental turboramjets
08 p3152 N94-29299
Potential of the ramjet engine for hypersonic flight speeds 08 p3153 N94-30935

RAMJET-IN-TUBE ACCELERATORS
U RAM ACCELERATORS

RAMPS (STRUCTURES)
Numerical simulation of unsteady aerodynamic heating induced by shock reflections 08 p3123 N94-28952

RANDOM ACCESS
VHF air/ground communications for air traffic control. Volume 1: A decision tree approach to system innovations
[AD-A268485] 04 p1316 N94-18384
Communication in the presence of unknown interference
[AD-A271146] 04 p1392 N94-19738
M-dimensional computer memory with M-1 dimensional hyperplane access
[AD-D015960] 05 p1898 N94-20357
Spread spectrum random access networks
[AD-A272280] 05 p1737 N94-20585
Dynamic microsets for RAMs
[RUU-CS-93-22] 08 p3406 N94-30727
Data structure extraction, conversion, and display tool
[AD-D016129] 10 p4108 N94-34284

RANDOM ACCESS MEMORY
NT CORE STORAGE
Investigation of soft errors in MOS RAM under influence of heavy ions
[DE92-644554] 01 p0484 N94-10534
Gallium arsenide dynamic random access memory support circuitry
[AD-A265176] 01 p0320 N94-11875
Hashing and rehashing in emulated shared memory
[CWI-CS-R9240] 02 p0740 N94-13525
Single event effects and laser simulation studies
[NASA-CR-194506] 02 p0657 N94-13812
Paradigms for very fast parallel algorithms
[ITN-93-85212] 02 p0755 N94-14556
A fuzzy method for preliminary design random access memory failure rate prediction
[AD-A267948] 03 p1055 N94-17044
Performance of defect-tolerant set-associative cache memories 04 p1398 N94-18346
VLSI for high-speed digital signal processing
[AD-A270406] 04 p1404 N94-18706
Proceedings of the 8th International Symposium on Applications of Ferroelectrics
[AD-A270679] 05 p1749 N94-20012
M-dimensional computer memory with M-1 dimensional hyperplane access
[AD-D015960] 05 p1898 N94-20357
Light update notification mechanism for shared data structures
[AD-D015967] 05 p2043 N94-21276
A DRAM compiler algorithm for high performance VLSI embedded memories 05 p1767 N94-21729
Crosstie random access memory element having associated read/write circuitry
[AD-D016027] 06 p2446 N94-24724
Temperature dependence of static RAM volatility
[DE93-040345] 07 p2948 N94-26111
Test methods and custom hardware for functional testing of a high speed GaAs DRAM
[AD-A274859] 07 p2781 N94-26175
Ferroelectric fluoride memory FET development
[AD-A274341] 07 p2785 N94-27057
Advantages of the LBL 88-inch cyclotron ion beam for SEP studies
[AD-A275142] 08 p3494 N94-29065
Multiple single event upsets in CMOS static rams
08 p3496 N94-30215
Using Cf-252 for single event upset testing
08 p3496 N94-30219
Charge collection spectroscopy applied to MOS RAM's 08 p3201 N94-30220
Design of free space interconnected signal processor
[AD-A278129] 09 p3683 N94-33093
A proposed SEU tolerant DRAM cell
[DE94-010758] 12 p4438 N94-37196

RANDOM DISTRIBUTIONS
U STATISTICAL DISTRIBUTIONS

RANDOM ERRORS
An extended Reed Solomon decoder design
04 p1398 N94-18348
A comparative study of clock rate and drift estimation
08 p3473 N94-30669
Regional sources of error growth in the National Meteorological Center's medium-range forecast model
09 p3781 N94-31554
Bounds on least-squares four-parameter sine-fit errors due to harmonic distortion and noise
[DE94-007859] 09 p3849 N94-32653

RANDOM LOADS
NT GUST LOADS
A simplistic look at limit stresses from random loading
[NASA-TM-108427] 03 p1058 N94-15710
Random vibrations of composite beams and plates
09 p3735 N94-31777
Frequency domain analysis of the random loading of cracked panels
[NASA-CR-196021] 11 p4279 N94-35974

RANDOM NOISE
A simulation study of the performance of the NASA (2,1,6) convolutional code on RFI/burst channels
03 p0997 N94-16508
Analysis of temporal symmetry in non-gaussian random fields
[AD-A266496] 03 p0999 N94-16794
High resolution radar profiling using higher-order statistics
[AD-D015891] 03 p1000 N94-16918
High order nonlinear estimation with signal processing applications
[AD-A268407] 03 p1005 N94-17463
Fundamental research in nonlinear random vibration for aerospace applications
[AD-A268929] 04 p1454 N94-18487
JSEP fellowship: Fractal noise processes
[AD-A268841] 04 p1557 N94-18540

Analytic approximations of an integral in remote sensing
[AD-A270085] 04 p1463 N94-18800
Noise filtering using multilayer feedforward neural network 05 p1770 N94-22104
Applications of a two-dimensional nonlinear filters to image restoration 05 p1789 N94-22225
Asynchronous timing and Doppler recovery in DSP based DPSK modems for fixed and mobile satellite applications 06 p2285 N94-22805
Separable concatenated codes with iterative map decoding for Rician fading channels 06 p2286 N94-22815
A mixed map/variable structure observer for target tracking 06 p2157 N94-24263
An analysis of gamma ray burst time histories
[NASA-CR-195191] 06 p2629 N94-25199
White noise theory of robust nonlinear filtering with correlated state and observation noises
[PB94-126661] 07 p3004 N94-27211
Testing for a signal with unknown location and scale in a stationary Gaussian random field
[AD-A275320] 08 p3464 N94-28876
Modulation and coding for the Gaussian channel, possibly affected by fluctuations
[TELECOM-93-E-009] 09 p3840 N94-31169
An adaptive Kalman filter excisor for suppressing narrowband interference
[AD-A276286] 09 p3671 N94-31253
Analysis using bi-spectral related technique
[AD-A276017] 09 p3672 N94-31386
Detection of a chi-square fluctuating target in Gaussian noise
[AD-A276078] 09 p3850 N94-31462
Control of a random walk with noisy delayed information
[CWI-BS-R9316] 09 p3846 N94-32108
Stochastic realization of a Gaussian stochastic control system
[CWI-BS-R9320] 09 p3852 N94-32350
The effects of a multipath channel and interference on coherent M-PSK digital communication systems
[AD-A278158] 09 p3684 N94-33254
Nonlocal methods for signal detection and estimation in the dependent nonstationary environment
[AD-A278472] 10 p4033 N94-33594
Effects of noise variance model on optimal feedback design and actuator placement 11 p4220 N94-35883
Relaxation of the density matrix for an arbitrary spin in random external fields
[DE94-618457] 12 p4509 N94-37078

RANDOM NUMBERS
Production and test of pseudo random elements
[ETN-93-95070] 04 p1559 N94-19610
Stochastic optimization by simulation: Convergence proofs for the G1/G/1 queue in steady-state
[AD-A271141] 05 p1962 N94-19999
On a proposed symbolic dynamics for the Henon map
[AD-A272514] 05 p1955 N94-21359
Two-stage versus sequential sample-size determination in regression analysis of simulation experiments
[PB94-110558] 06 p2495 N94-24634

RANDOM PROCESSES
NT RANDOM WALK
Intermittency following a Hopf bifurcation
[W-9301] 01 p0344 N94-10907
Search for structures in the cosmic microwave background radiation
[INPE-5491-TDI/508] 01 p0484 N94-12357
Investigation for improving Global Positioning System (GPS) orbits using a discrete sequential estimator and stochastic models of selected physical processes
[NASA-CR-194167] 02 p0512 N94-13082
Implications of crater distributions on Venus 03 p1270 N94-16300
Towards dynamic randomized algorithms in computational geometry
[INRIA-RR-1727] 03 p1156 N94-17528
Non Linear Dynamics and Chaos
[AGARD-LS-191] 04 p1607 N94-18236
Generalized multichannel signal detection
[AD-A271385] 04 p1391 N94-19587
Logarithm of probability measures and infinite divisibility of sub-stable random vectors
[PB94-118627] 06 p2486 N94-23758
Correlation function estimator performance in non-Gaussian spherically invariant random processes
[AD-A273498] 06 p2496 N94-24951
Data on parity violation in the compound nucleus and its interpretation
[DE94-003965] 07 p3013 N94-25820
Polynomial modeling of analog-to-digital converters
[DE94-005579] 08 p3406 N94-30008
Thermodynamics of computation and information distance
[CWI-CS-R9341] 08 p3526 N94-30433
The Boltzmann entropy and randomness tests
[CWI-CS-R9342] 08 p3426 N94-30434
On interpolating random fields using a finite number of observations
[CWI-BS-R9314] 09 p3847 N94-32194
Area-interaction point processes
[CWI-BS-R9318] 09 p3847 N94-32197
Robust multisource classification method using the Markov random field methods 09 p3750 N94-32537
Nonlocal methods for signal detection and estimation in the dependent nonstationary environment
[AD-A278472] 10 p4033 N94-33594
Decoherence, chaos, the quantum and the classical
[DE94-009317] 10 p4149 N94-34099

RANDOM SAMPLING
A CM chondrite cluster and CM streams 01 p0432 N94-12215
Rare attributes in finite universe: Hypotheses testing specification and exact randomized upper confidence bounds
[DE93-012783] 02 p0775 N94-12955
Fast simulation of steady-state availability in non-Markovian highly dependable systems
[AD-A266747] 03 p1174 N94-15823
Rao-Blackwell theorem in stereology and some counterexamples
[PB94-111713] 06 p2496 N94-24639
Aspects of goodness-of-fit
[AD-A274826] 07 p3003 N94-26495
U-statistics of random-size samples and limit theorems for systems of Markovian particles with non-Poisson initial distributions
[AD-A275018] 08 p3464 N94-29129

RANDOM VARIABLES
Parametric analysis of atmospheric processes
[NASA-CR-192523] 01 p0347 N94-10757
Monte Carlo algorithms in simulation of 2beta-decay and penetration of electrons through matter
[DE93-617741] 01 p0364 N94-10837
A new method to assess Monte Carlo convergence
[DE93-012667] 02 p0772 N94-12919
The distribution of a sum of binomial random variables
[AD-A266969] 03 p1172 N94-15002
Bounds on inconsistent inferences for sequences of trials with varying probabilities
[AD-A267146] 03 p1172 N94-15733
Performance of coded coherent FSK lightwave system with noncoherent detection
[AD-A267442] 03 p1193 N94-17028
Closed form characteristic function for general complex second-order form in correlated complex Gaussian random variables
[AD-A267883] 03 p1171 N94-17393
Bahadur-Kiefer theorem beyond the largest observation
[PB93-197473] 04 p1558 N94-19325
Sensitivity and uncertainty analysis of Markov reward models
[MEMO-INF-92-89] 04 p1559 N94-19386
A methodology for quantifying uncertainty in models
[DE93-040154] 05 p1916 N94-21747
On the asymptotically uniform distribution modulo 1 of extreme order statistics
[MEMO-COSOR-91-38-REV] 06 p2493 N94-23142
Limiting distribution of fractional parts of extreme order statistics
[PB93-237733] 06 p2494 N94-23440
Characterizations of shift-invariant distributions based on summation modulo one
[PB93-237824] 06 p2481 N94-23442
Subset selection for the best of two populations: Tables of the expected subset size
[PB93-237857] 06 p2494 N94-23546
Subset selection with a generalized selection goal based on a loss function
[PB94-111192] 06 p2494 N94-23798
Some generalized subset selection procedures
[PB94-111655] 06 p2487 N94-23799
Infinite divisible and stable distributions modulo 1
[PB94-110640] 06 p2495 N94-23815
A comparison of approximate interval estimators for the Bernoulli parameter
[AD-A276322] 06 p2458 N94-24680
Efficiency of subset selection of an epsilon-best uniform population relative to selection of the best one
[PB93-237741] 06 p2490 N94-24763
Topics in probability and dynamics
[AD-A273543] 06 p2496 N94-24931
Simulation approaches for calculations in directed graphical models
[AD-A274825] 07 p3003 N94-26494
Central dynamic share scheduling in distributed systems
[REPT-93-48] 07 p2966 N94-26966
U-statistics of random-size samples and limit theorems for systems of Markovian particles with non-Poisson initial distributions
[AD-A275018] 08 p3464 N94-29129
Probability distributions with given marginals and given correlation that have maximal entropy
[REPT-93-81] 09 p3851 N94-31698
On the minimum of independent geometrically distributed random variables
[AD-A279629] 09 p3821 N94-33075
Nonlocal methods for signal detection and estimation in the dependent nonstationary environment
[AD-A278472] 10 p4033 N94-33594

RANDOM VIBRATION
Development of a fatigue analysis approach for CFRP structures under acoustic loading 01 p0058 N94-10018
Sine and random vibration program evaluation on vibration control systems
[DE93-011974] 01 p0188 N94-11460
Estimation of critical values and vibration characteristics on supersonic delta wings. Part 2: Locally-stationary time series analysis of nonstationary random responses
[NAL-TR-1179] 02 p0502 N94-13345
Low-noise oscillators for airborne radar applications, revision 1
[AD-A269372] 04 p1403 N94-18471
Fundamental research in nonlinear random vibration for aerospace applications
[AD-A268929] 04 p1454 N94-18487
Microwelding due to random vibration 06 p2359 N94-24019
Space Station Freedom NiH2 cell testing program 07 p2861 N94-28108
Root-sum-square structural strength verification approach
[NASA-TM-108453] 08 p3322 N94-30206
Random vibrations of composite beams and plates 09 p3735 N94-31777
A user's manual for the program TRES4: Random vibration analysis of vertical-axis wind turbines in turbulent winds
[DE94-009012] 10 p4079 N94-34078

RANDOM WALK
On a class of two-dimensional nearest neighboring random walks
[CWI-BS-R9220] 01 p0347 N94-10353
Cosmological gamma-ray burst model
[NASA-CR-193368] 01 p0484 N94-10507
The limit of frequency estimation 01 p0356 N94-11001
Deterministic growth-dispersal models and branching random walk
[REPT-93-14] 04 p1550 N94-19088
Compensation approach for three or more dimensional random walks
[PB93-197499] 04 p1543 N94-19326
Coherence lost? Not-so-fast escapes from the in-phase attractor of a set of globally coupled nonlinear oscillators
[DE94-000799] 06 p2557 N94-22940
Accuracy metrics for judging time scale algorithms 08 p3471 N94-30656
Control of a random walk with noisy delayed information
[CWI-BS-R9316] 09 p3846 N94-32108
Recursive recovery of Markov transition probabilities from boundary value data
[DE94-011914] 11 p4317 N94-36235

RANGE (EXTREMES)
NT DYNAMIC RANGE
NT FREQUENCY RANGES
NT OCTAVES
NT PROPORTIONAL LIMIT
NT ROCHE LIMIT
Robust stability of diamond families of polynomials with complex coefficients
[NASA-CR-194132] 02 p0768 N94-13421

RANGE AND RANGE RATE TRACKING
Real-time 3-D pose estimation using a high-speed range sensor
[AD-A273873] 07 p2809 N94-25967

RANGE CONTROL
U TRAJECTORY CONTROL

RANGE ERRORS
Comparison of c.t.s. based prediction of store trajectory with flight test data 06 p2158 N94-24268
A simulation of GPS and differential GPS sensors 07 p2666 N94-27918

RANGE FINDERS
NT LASER RANGE FINDERS
NT OPTICAL RANGE FINDERS
CMU very fast range-imaging system
[AD-A272057] 05 p1761 N94-21282

Expansion-based passive ranging
06 p2176 N94-25504
Flexible range finding applied to 3D surface synthesis: A pseudo-trinocular approach
[ISBN-0-315-84616-X] 07 p2813 N94-27651

RANGE INDICATORS
U RANGE FINDERS

RANGE MEASUREMENT
U RANGEFINDING

RANGE SAFETY
Range safety transponder catalog
[AD-A270682] 04 p1323 N94-19581
Advanced silver zinc battery development for the SRB and ET range safety subsystems
07 p2865 N94-28136
Design, performance, and test standards for flight termination receivers/decoders. Volume 1: Design and performance requirements
[AD-A277245] 09 p3602 N94-32333
Integrated safety program for the Nuclear Electric Propulsion Space Test Program
[DE94-004670] 09 p3615 N94-32669
Independent safety assessment of the Topaz-2 space nuclear reactor power system
[DE94-008653] 09 p3877 N94-32879

RANGEFINDING
NT LUNAR RANGEFINDING
NT SOUND RANGING
Sequential ranging: How it works
[NASA-CR-194508] 02 p0532 N94-13796
Eighth International Workshop on Laser Ranging Instrumentation
[NASA-CP-3214] 03 p0911 N94-15552
Laser tracking for vertical control
03 p0911 N94-15553
Laser ranging network performance and routine orbit determination at D-PAF 03 p0911 N94-15554
Laser ranging application to time transfer using geodetic satellite and to other Japanese space programs
03 p0911 N94-15555
Satellite signatures in SLR observations
03 p0912 N94-15557
Work at Graz on satellite signatures
03 p0898 N94-15558
The precision of today's satellite laser ranging systems 03 p0912 N94-15559
SLR data screening; location of peak of data distribution 03 p0912 N94-15560
Adaptive median filtering for preprocessing of time series measurements 03 p0912 N94-15561
SATCOP mission planning software package
03 p0912 N94-15562
Nd:YLF laser for airborne/spaceborne laser ranging
03 p0913 N94-15563
Alternative wavelengths for laser ranging
03 p0913 N94-15564
New methods of generation of ultrashort laser pulses for ranging 03 p0913 N94-15565
An improved light source for laser ranging
03 p0913 N94-15567
Preliminary results from the portable standard satellite laser ranging intercomparison with MOBLAS-7
03 p0913 N94-15568
Performance optimization of detector electronics for millimeter laser ranging 03 p0913 N94-15569
Tracking capabilities of SPADs for laser ranging
03 p0914 N94-15570
The solid state detector technology for picosecond laser ranging 03 p0914 N94-15572
Streak camera based SLR receiver for two color atmospheric measurements 03 p0914 N94-15573
The first satellite laser echoes recorded on the streak camera 03 p0914 N94-15574
Experience and results of the 1991 MTLRS-1 USSR campaign 03 p0914 N94-15575
Test results from LAGEOS-2 optical characterization using pulsed lasers 03 p0915 N94-15577
Historical MOBLAS system characterization
03 p0915 N94-15579
Optimum wavelengths for two color ranging
03 p0915 N94-15580
Two color satellite laser ranging upgrades at Goddard's 1.2m telescope facility 03 p0915 N94-15581
Measuring atmospheric dispersion with WLRS in multiple wavelength mode 03 p0916 N94-15582
Millimeter accuracy satellites for two color ranging
03 p0916 N94-15583
Two wavelength satellite laser ranging using SPAD
03 p0916 N94-15584
New perspectives for high accuracy SLR with second generation geodesic satellites 03 p0916 N94-15585
State-of-the-art satellite laser range modeling for geodetic and oceanographic applications
03 p0916 N94-15586
Geometric analysis of satellite laser ranging data
03 p0917 N94-15587
Improvement of SLR accuracy, a possible new step
03 p0917 N94-15588
Compensation for the distortion in satellite laser range predictions due to varying pulse travel times
03 p0917 N94-15590
Timebias corrections to predictions
03 p0875 N94-15591
Formation of on-site normal points
03 p0917 N94-15592
Poisson filtering of laser ranging data
03 p0917 N94-15593
Computer networking at SLR stations
03 p0917 N94-15594
Upgrading NASA/DOSE laser ranging system control computers 03 p0918 N94-15595
HP upgrade operational streamlining
03 p0918 N94-15596
Application of the robust estimate in SLR data preprocessing 03 p0918 N94-15597
A computer-controlled x-y offset guiding stage for the MLRS 03 p0918 N94-15598
LLR: Activities in Wettzell 03 p0876 N94-15600
Matera Laser Ranging Observatory (MLRO): An overview 03 p0877 N94-15601
Sub-cm ranging and other improvements in Graz
03 p0919 N94-15603
Upgrading of the Borowiec laser station
03 p0877 N94-15604
Development of Shanghai satellite laser ranging station 03 p0877 N94-15605
WLRS --- Wettzell Laser Ranging System (WLRS)
03 p0877 N94-15606
New progress of ranging technology at Wuhan Satellite Laser Ranging Station 03 p0877 N94-15608
TLRS-3 system upgrades 03 p0877 N94-15609
Results of the MTLRS-1 upgrade
03 p0877 N94-15610
The new MTLRS-1 receiving system
03 p0877 N94-15611
The new MTLRS transmitting system
03 p0877 N94-15612
Airborne 2 color ranging experiment
03 p0920 N94-15614
GLRS-R 2-colour retroreflector target design and predicted performance 03 p0921 N94-15615
Effects of turbulence on the geodynamic laser ranging system 03 p0921 N94-15616
Mars laser altimeter based on a single photon ranging technique 03 p0921 N94-15619
Satellite laser station Helwan status 1992
03 p0877 N94-15621
Optical attenuation mechanism upgrades, MOBLAS, and TLRS systems 03 p0922 N94-15622
The third generation SLR station Potsdam no. 7836
03 p0877 N94-15623
Performance comparison of high speed microchannel plate photomultiplier tubes 03 p0922 N94-15624
Station report on the Goddard Space Flight Center (GSFC) 1.2 meter telescope facility
03 p0922 N94-15625
Clementine: Anticipated scientific datasets from the Moon and Geographos 03 p1288 N94-16392
Digital laser range finder emulator
[AD-D015811] 03 p1040 N94-16540
Atomic beam studies relevant to the space environment
[AD-A268628] 03 p1186 N94-17436
Data fusion through simulated annealing of registered range and reflectance images
[DE93-015910] 04 p1612 N94-17858
Flight demonstration of image fix-taking with SAR
[DE93-016499] 04 p1382 N94-17861
Survey of collision avoidance and ranging sensors for mobile robots, revision 1
[AD-A269846] 04 p1541 N94-18474
Absolute positioning by collecting Global Positioning System (GPS) data along short baselines
[AD-A271324] 04 p1317 N94-19572
Development of a lidar for integration with the Naval Postgraduate School Infrared Search and Target Designation (NPS-IRSTD) system
[AD-A271847] 05 p1817 N94-20611
CMU very fast range-imaging system
[AD-A272057] 05 p1761 N94-21282
Estimability of polar motion using range observations to satellites
[PB93-219319] 05 p1842 N94-22265
A feasibility study of a parallax-based passive missile approach warning system
[ISBN-0-315-60640-1] 05 p1743 N94-22410
EUTELTRACS: The European experience on mobile satellite services 06 p2281 N94-22781
Lightning studies using LDAR and LLP data
06 p2416 N94-23238
Object recognition through image understanding for an autonomous mobile robot
[AD-A273206] 06 p2475 N94-24862
Method and apparatus for determining target elevation angle, altitude and range, and the like in a monopulse radar system with reduced multipath errors
[AD-D016005] 06 p2302 N94-25058
Expansion-based passive ranging
06 p2176 N94-25504
Multiple-camera/motion stereoscopy for range estimation in helicopter flight 06 p2441 N94-25505
Validation of vision-based range estimation algorithms using helicopter flight data 06 p2442 N94-25506
A simulation of GPS and differential GPS sensors
07 p2666 N94-27918
Simulation of fully automated air traffic control concepts 08 p3139 N94-29569
Orbital debris radar instrumentation
08 p3248 N94-29626
Method for ambiguity resolution in range-Doppler measurements
[NASA-CASE-GSC-13542-1] 08 p3252 N94-29739
The Mars Observer differential one-way range demonstration 11 p4210 N94-35543
Spacecraft-spacecraft radio-metric tracking: Signal acquisition requirements and application to Mars approach navigation 11 p4254 N94-35557
The real-time display of interferometry data for Goldstone radar astronomy data acquisition
11 p4255 N94-35560
The Mars Observer Ka-band link experiment
11 p4255 N94-35563
Application of a Monte Carlo accuracy assessment tool to TDRS and GPS 11 p4207 N94-35635
Nondestructive Inspection (NDI) of reduced strength bonds
[AD-A278745] 11 p4278 N94-36090
A more exact analysis of Sandia Laser Tracker data
[DE94-011411] 12 p4447 N94-37051

RANGELANDS
Using AVIRIS images to measure temporal trends in abundance of photosynthetic and nonphotosynthetic canopy components 03 p1066 N94-16668

RANGES (FACILITIES)
NT BALLISTIC RANGES
NT MISSILE RANGES
NT TEST RANGES

RANGING
U RANGEFINDING

RANK TESTS
Statistical analysis of the m rankings problem: Kendall's prototype and the grouping estimate method based on normal scores
[DSIS-93-00139] 02 p0773 N94-13848
The rank of the present excursion
[REPT-93-22] 04 p1558 N94-19137

RANKINE CYCLE
Potassium-Rankine power conversion subsystem modeling for nuclear electric propulsion
[NASA-CR-191134] 04 p1468 N94-18821
Utilization of recently developed codes for high power Brayton and Rankine cycle power systems
06 p2222 N94-23641
Limitations of power conversion systems under transient loads and impact on the pulsed tokamak power reactor
[DE94-003404] 07 p3043 N94-26324

RANKING
Statistical analysis of the m rankings problem: Kendall's prototype and the grouping estimate method based on normal scores
[DSIS-93-00139] 02 p0773 N94-13848
Nonparametric statistics: Weighted rankings analysis
[AD-A266607] 03 p1173 N94-16657
Solving the ranking and selection indifference-zone formulation for normal distributions using computer software
[AD-A273821] 06 p2496 N94-25518
Ranking alternatives using fuzzy numbers: A computational approach short communication
[INPE-5483-PRE/1782] 07 p2974 N94-27835
Evaluating the analytic hierarchy process and recommended modifications for its use in multi-attribute decision making
[AD-A275065] 08 p3527 N94-29153
List ranking and list scan on the CRAY C-90
[AD-A276411] 09 p3824 N94-31259

RAPCON (CONTROL)
U RADAR APPROACH CONTROL

RAPID QUENCHING (METALLURGY)
Structure and properties of an RS Al-Si-Ni-Mn-Zr alloy for high temperature applications
01 p0064 N94-10063
Measurements of crystal growth kinetics at extreme deviations from equilibrium
[DE93-014526] 02 p0815 N94-14798

Melt spinning study
[NASA-CR-193823] 04 p1380 N94-19423
Recent advances in high density tungsten composite processing
[AD-A270764] 04 p1344 N94-19576
Investigation of cracking and erratic behavior of the uranium-titanium alloy
[DE93-018591] 05 p1688 N94-19957
Study on solidification of non-homogeneous melting/solidification materials 07 p2728 N94-25573
Near-net-shape manufacturing: Spray-formed metal matrix composites and tooling 08 p3186 N94-30447
Solidification structure synthesis in undercooled liquids
[AD-A276166] 09 p3910 N94-31054
Microstructures and mechanical properties of Al3Ti-based alloys: Analysis in single phase and multiphase systems
[ONERA-NT-1993-6] 09 p3640 N94-31420

RAPID SOLIDIFICATION
U RAPID QUENCHING (METALLURGY)
U SOLIDIFICATION

RAPID TRANSIT SYSTEMS
Safety of high speed ground transportation systems: X2000 US demonstration vehicle dynamics trials, preliminary test report, October 1992 - January 1993
[PB93-194645] 01 p0422 N94-10736
Electrical engineering and industrial electronics education days: Control of asynchronous generators
[PB94-135514] 08 p3266 N94-29523
Applicable dimensioning and measure and technological examination of long stator-linear motors for magnetic high-speed railways
[ETN-94-95734] 09 p3689 N94-31575
First Annual High-Speed Research Workshop, part 4
[NASA-CP-10087-PT-4] 10 p3979 N94-33517
Overview of NASA HSR high-lift program
10 p3979 N94-33518
Status of LaRC HSCT high-lift research
10 p3979 N94-33519
Status of CFD for LaRC's HSR high-lift program
10 p3980 N94-33520
HSR high lift research program: Status and plans
10 p3980 N94-33521
HSCT high-lift technology requirements
10 p3980 N94-33523
NASA F-16XL supersonic laminar flow control program overview 10 p3980 N94-33525

RARE EARTH ALLOYS
NT GADOLINIUM ALLOYS
NT LANTHANUM ALLOYS
NT NEODYMIUM ALLOYS
Bibliography on silicides
[AD-A270516] 04 p1374 N94-19532
Magnetostriction and magnetostrictive materials
[VTT-TIED-1434] 07 p3058 N94-26545
Formation and high mechanical strength of Al-based alloys containing a nanoscale icosahedral phase as a main constituent 07 p2746 N94-28171

RARE EARTH COMPOUNDS
NT CERIUM COMPOUNDS
NT CERIUM OXIDES
NT DYSPROSIUM COMPOUNDS
NT ERBIUM COMPOUNDS
NT EUROPIUM COMPOUNDS
NT NEODYMIUM COMPOUNDS
NT PRASEODYMIUM COMPOUNDS
NT SAMARIUM COMPOUNDS
NT SCANDIUM COMPOUNDS
NT SCANDIUM OXIDES
NT TERBIUM COMPOUNDS
NT YTTERBIUM COMPOUNDS
Fine-powder Al2O3 and SiO2 for preparation of multielement standards for rare-earth elements analysis
[DE93-625118] 02 p0567 N94-14884
Microstructural modeling and toughening of Si3N4 ceramics for high temperature engine applications
[AD-A272897] 05 p1704 N94-21197
Preparation, characterization, and thermal behaviour study of lanthanides (3) and yttrium (3) 4-methoxy benzylidene pyruvate in solid state
[DE94-604079] 07 p3068 N94-27697
Hypersensitive transition spectrum of f-element and coordination structure
[DE94-604133] 07 p3070 N94-27843
The optical properties of high-T(c) superconductors grown by pulsed laser deposition
[ISBN-0-315-84917-7] 07 p3039 N94-27962
Anisotropy in the electrical, magnetic and optical properties of Pb2Sr2RCu3O8
[ISBN-0-315-84930-4] 07 p3070 N94-27974
Normal state resistivity of MBa2Cu3O(7-x) ceramics
[DE94-608456] 08 p3220 N94-30745
Conductivity measurements of ceria-based solid electrolytes using AC impedance
[DE94-007380] 09 p3694 N94-32593

RARE EARTH ELEMENTS
NT CERIUM
NT DYSPROSIUM
NT ERBIUM
NT EUROPIUM
NT GADOLINIUM
NT HOLMIUM
NT LANTHANUM
NT LANTHANUM ISOTOPES
NT NEODYMIUM
NT NEODYMIUM ISOTOPES
NT PRASEODYMIUM
NT SAMARIUM
NT SAMARIUM ISOTOPES
NT SCANDIUM
NT TERBIUM
NT THULIUM
NT THULIUM ISOTOPES
NT YTTERBIUM
NT YTTRIUM
Minor and trace element composition and age of Yukon probable-microtektites 01 p0429 N94-12094
Crystal-chemistry and partitioning of REE in whitlockite
01 p0408 N94-12174
Anomalous REE patterns in unequilibrated enstatite chondrites: Evidence and implications
01 p0431 N94-12191
Fine-powder Al2O3 and SiO2 for preparation of multielement standards for rare-earth elements analysis
[DE93-625118] 02 p0567 N94-14884
An experimental study of trace element partitioning between perovskite, hibonite and melt: Equilibrium values 03 p0954 N94-16313
AVIRIS as a tool for carbonatite exploration: Comparison of SPAM and Mbandmap data analysis methods
03 p1073 N94-16703
Theoretical studies of the crystal structure of rare earths and actinides at zero temperature
[DE93-016488] 03 p1214 N94-17301
Rare Earth elements in individual minerals in Shergottites 05 p1686 N94-20852
The formation of FeO-rich pyroxene and enstatite in unequilibrated enstatite chondrites: A petrologic-trace element (SIMS) study 05 p2086 N94-20866
LREE variability in CM matrices: Another look at meteorite compaction ages 05 p2086 N94-20884
Static ultra-high pressure study of lanthanide and actinide metals using a diamond-anvil cell
[DE94-000369] 05 p1693 N94-21656
Theoretical studies of structural phase transitions in actinide metals
[DE94-000796] 05 p1696 N94-22388
Development of infrared sensors using energy transfer/energy upconversion processes: Study of laser excited fluorescence in rare Earth ion doped crystals
[NASA-TM-108437] 06 p2233 N94-24073
Qualitative analysis of rare earth elements contained in the phosphogypsum
[DE93-614153] 07 p2716 N94-26518
Property enchancement of polyimide films by way of the incorporation of lanthanide metal ions
07 p2758 N94-27926
Preparation of monodispersed fine particles containing rare metals and rare earths 08 p3201 N94-29514
Metal-ion spin-on glasses: Novel materials for active waveguides
[DE94-007738] 09 p3682 N94-32649
Rare Earth Doped Semiconductors and Materials Research Society Symposium Proceedings, Volume 301
[AD-A277517] 09 p3908 N94-33055
Consequences of competing hybridization for magnetic ordering in correlated-electron lattices
[DE94-011648] 12 p4534 N94-37057

RARE GAS-HALIDE LASERS
NT KRYPTON FLUORIDE LASERS
NT XENON CHLORIDE LASERS

RARE GASES
NT ARGON
NT ARGON ISOTOPES
NT HELIUM
NT HELIUM ISOTOPES
NT KRYPTON
NT LIQUID HELIUM
NT LIQUID HELIUM 2
NT NEON
NT NEON ISOTOPES
NT RADON
NT RADON ISOTOPES
NT XENON
NT XENON ISOTOPES
NT XENON 129
Joint pain and Doppler-detectable bubbles in altitude (Hypobaric) decompression 01 p0312 N94-11542
Nitrogen and noble gases in a glass sample from LEW88516 01 p0080 N94-12051
Noble gases in LEW88516 shergottite: Evidence for exposure age pairing with ALH77005
01 p0080 N94-12082
Noble gas evidence of an aqueous reservoir near the surface of Mars more recently than 1.3 Ga
01 p0473 N94-12228
The fractionation of noble gases in diamonds of CV3 Efremovka chondrite 01 p0081 N94-12256
Measurements of scattering processes in negative ion-atom collisions
[DE93-013863] 02 p0779 N94-12940
About the influence of inert gas ion implantation on metal corrosion stability
[DE93-620574] 02 p0569 N94-13360
Al-26-Mg-26 ages of iron meteorites
03 p1242 N94-16240
First investigation of noble gases in the Dengli H3.8 chondrite 03 p0953 N94-16264
Transition metals in superheat melts
03 p0962 N94-16273
A search for noble-gas evidence for presolar oxide grains 03 p0954 N94-16353
Noble gases in twenty Yamato H-chondrites: Comparison with Allan Hills chondrites and modern falls
03 p1244 N94-16361
Nitrogen and light noble gases in Parsa enstatite chondrite 03 p1246 N94-16435
Structure, thermodynamics, and dynamical properties of supercooled liquids
[DE93-788387] 04 p1607 N94-18211
Excited atomic bromine energy transfer and quenching mechanisms
[AD-A270672] 04 p1572 N94-19607
Design aspects and parametric characterisation of a neutral rare gas laser
[AD-A271100] 05 p1814 N94-19850
Stability of the face-centered-cubic phase of heavy rare gas solids
[DE93-019949] 05 p1679 N94-20319
On demand, non-halon, fire extinguishing systems
[AD-D015957] 05 p1714 N94-20355
Dating native gold by noble gas analyses
05 p1684 N94-20652
A carbon and nitrogen isotope study of carbonaceous vein material in ureilite meteorites
05 p2083 N94-20726
The chondrite Mihonoseki: New observed fall
05 p2083 N94-20764
Are the C delta light nitrogen and noble gases located in the same carrier? 05 p2085 N94-20846
A long-term change of the AR/KR/XE fractionation in the solar corpuscular radiation 05 p2136 N94-20875
Evolution of the Martian atmosphere
05 p2146 N94-21680
The laser and its applications on environment and biotechnology research
[DE94-000376] 05 p1820 N94-21957
Spectroscopic and vibrational energy transfer studies in molecular bromine
[AD-A273795] 07 p3014 N94-25875
Chamber free fusion welding root side purging method and apparatus
[NASA-CASE-MFS-28832-1] 08 p3204 N94-29380
Metal cluster-rare gas van der Waals complexes: Microscopic models of physisorption
[DE94-008134] 09 p3873 N94-32797
Anatomy of a cluster IDP. Part 2: Noble gas abundances, trace element geochemistry, isotopic abundances, and trace organic chemistry of several fragments from L2008#5 11 p4352 N94-35465
Hypobaric decompression sickness model development. Part 1: Diffusion of inert gas from a viscoelastic fluid (blood) into an expanding gas phase
[AD-A280298] 12 p4481 N94-37124

RAREFACTION
DSMC simulations of Mach 20 nitrogen flows about a 70 degree blunted cone and its wake
[NASA-TM-107762] 03 p1018 N94-15291
Control jets in interaction with hypersonic rarefied flow
07 p2698 N94-28020

RAREFACTION WAVES
U ELASTIC WAVES

RAREFIED GAS DYNAMICS
Three-dimensional hypersonic rarefied flow calculations using direct simulation Monte Carlo method
01 p0007 N94-10449
Techniques for estimating Space Station aerodynamic characteristics
[NASA-CR-193394] 02 p0541 N94-13955
Particle kinetic simulation of high altitude hypervelocity flight
[NASA-CR-194599] 03 p0856 N94-15678
Particle simulation of hypersonic flow
[AD-A267185] 03 p0857 N94-15787

To extend the thirteen-moment theory and its application to problems in rarefied hypersonic flow
[AD-A267384] 03 p0859 N94-17021
Modelling of ionisation reactions and of the resulting electric fields in one-dimensional hypersonic shock waves with the direct simulation Monte Carlo method
[IC-AERO-92-01] 07 p2644 N94-26248
Control jets in interaction with hypersonic rarefied flow 07 p2698 N94-28020
Surface boundary conditions and related technical issues concerning Burnett equations for 2-D hypersonic flow
[AD-A277322] 09 p3706 N94-32256
Analysis and computation for vortex dynamics and rarefied gases
[AD-A277415] 09 p3708 N94-32581
Simulation of CO2 release at 800 km altitude
[AD-A276692] 09 p3776 N94-33272

RAREFIED GASES
NT COSMIC GASES
NT INTERSTELLAR GAS
Electronic spectroscopy of the gas-phase OH-Kr van der Waals complex
[AD-A266891] 03 p0942 N94-14946
Interferometry in rarefied gas flows
[ISL-CO-207/92] 06 p2318 N94-23160
Mix induced by single shock passage through a material interface
[DE93-019505] 07 p2792 N94-26427
Monte Carlo simulation or normal shock wave. Part 2: VHS model and VSS model 08 p3123 N94-28948
The maximum entropy approach applied to energy exchange, chemical reactions and ionisation in the direct simulation Monte Carlo method for rarefied hypersonic flows
[IC-AERO-93-01] 08 p3524 N94-29481
Analysis and computation for vortex dynamics and rarefied gases
[AD-A277415] 09 p3708 N94-32581

RAREFIED PLASMAS
Nonlinear second harmonic generation by light wave-plasma interaction in oscillating magnetic field
[DE93-613723] 01 p0386 N94-10387

RASERS
U MASERS

RASTER SCANNING
Confocal profilometer with nanometric vertical resolution
[DE93-622698] 02 p0653 N94-12857
Krupp technical reports no. 2, English edition, October 1992
[ETN-93-94631] 03 p0984 N94-16000
RELMA: On-line quality control in the rubber mixing room using laser analysis 03 p0984 N94-16005
Three dimensional ultrasonic imaging
[DE93-040549] 05 p1968 N94-22003
Results of a laboratory experiment that tests rotating unbalanced-mass devices for scanning gimbaled payloads and free-flying spacecraft
[NASA-TP-3458] 06 p2269 N94-23574
Optimal detector strategies for the phase contrast imaging for scanning transmission electron microscopes
[ETN-94-95747] 09 p3866 N94-31613
Differential phase acoustic microscope for micro-NDE
[NASA-CR-189617] 09 p3731 N94-32481

RATE METERS
U MEASURING INSTRUMENTS

RATES (PER TIME)
NT ACCELERATION (PHYSICS)
NT ACOUSTIC VELOCITY
NT AIRSPEED
NT ANGULAR ACCELERATION
NT ANGULAR VELOCITY
NT ARRHYTHMIA
NT BIT ERROR RATE
NT BURNING RATE
NT COLLISION PARAMETERS
NT COLLISION RATES
NT CRITICAL VELOCITY
NT CURRENT DENSITY
NT DECAY RATES
NT DECELERATION
NT DRIFT RATE
NT ELECTRON ACCELERATION
NT ELECTRON FLUX DENSITY
NT ESCAPE VELOCITY
NT EVAPORATION RATE
NT EXHAUST VELOCITY
NT FLOW VELOCITY
NT FLUX (RATE)
NT FLUX DENSITY
NT GROUP VELOCITY
NT HEART RATE
NT HEAT FLUX
NT HIGH ACCELERATION
NT HIGH GRAVITY ENVIRONMENTS
NT HIGH SPEED
NT HYPERSONIC SPEED
NT ILLUMINANCE
NT IMPACT ACCELERATION
NT IRRADIANCE
NT LIGHT SPEED
NT LOADING RATE
NT LOW SPEED
NT LUMINANCE
NT LUMINOUS INTENSITY
NT MAGNETIC FLUX
NT MASS FLOW RATE
NT NEUTRON FLUX DENSITY
NT ORBITAL VELOCITY
NT PARTICLE ACCELERATION
NT PARTICLE FLUX DENSITY
NT PHASE VELOCITY
NT PHYSIOLOGICAL ACCELERATION
NT PLASMA ACCELERATION
NT PROPAGATION VELOCITY
NT PROTON FLUX DENSITY
NT PULSE RATE
NT PULSE REPETITION RATE
NT RADIAL VELOCITY
NT RADIANCE
NT RADIANT FLUX DENSITY
NT RELATIVISTIC VELOCITY
NT RESPIRATORY RATE
NT ROTOR SPEED
NT SOLAR FLUX
NT SOLAR FLUX DENSITY
NT SOLAR WIND VELOCITY
NT SOUND INTENSITY
NT SPIN REDUCTION
NT STRAIN ENERGY RELEASE RATE
NT STRAIN RATE
NT SUBSONIC SPEED
NT SUPERSONIC SPEED
NT SYSTOLE
NT TERMINAL VELOCITY
NT TIP SPEED
NT TRANSMISSION RATE (COMMUNICATIONS)
NT TRANSONIC SPEED
NT TRANSVERSE ACCELERATION
NT WIND VELOCITY
NT ZERO SOUND
Rates of fluvio-thermal erosion on Mars 01 p0435 N94-12018
Adaptive Signal Processing Testbed
[DSIS-93-00258] 02 p0604 N94-13869
Template based low data rate speech encoder
[AD-A270900] 04 p1392 N94-19748
Complex source rate estimation for atmospheric transport and dispersion models
[DE94-000958] 08 p3354 N94-30822

RATINGS
The airline quality report 1993
[NIAR-93-11] 03 p0863 N94-17262
A critical analysis of workload predictions generated by multiple resource theory during early crewstation design
[AD-A274804] 07 p2941 N94-26339

RATIOMETERS
The laser and its applications on environment and biotechnology research
[DE94-000376] 05 p1820 N94-21957

RATIONAL FUNCTIONS
Rational trigonometric approximations using Fourier series partial sums
[NASA-CR-191535] 05 p1959 N94-21568
Column reduced rational matrix functions with given null-pole data in the complex plane
[PB93-220531] 05 p1960 N94-22099
A rational elliptic surface related to the question of expressing squares as sum of consecutive squares
[W-9305] 06 p2479 N94-23139
Mathematical addenda to Hopper's model of plane stokes flow driven by capillarity on a free surface
[PB93-237691] 06 p2480 N94-23438
Approximation to nonlinear equations using nonlinear rational models
[RR-448] 06 p2492 N94-25306
Chebyshev-Markov rational functions over several intervals
[PB94-125333] 07 p2998 N94-27116
Frequency-domain analysis of nonlinear microwave circuits
[PB94-132024] 08 p3261 N94-28400
Trace formulas and dynamical zeta functions in the Nielsen theory
[PB94-138195] 08 p3467 N94-29163

RATIONS
Nutrition and hydration status of aircrew members consuming an improved survival ration during a simulated survival scenario 08 p3380 N94-28429

RATIOS
NT ASPECT RATIO
NT COMPRESSION RATIO
NT FIBER VOLUME FRACTION
NT FROUDE NUMBER
NT FUEL-AIR RATIO
NT GRASHOF NUMBER
NT HARTMANN NUMBER
NT HIGH ASPECT RATIO
NT HIGH REYNOLDS NUMBER
NT INDEXES (RATIOS)
NT KP INDEX
NT LEAF AREA INDEX
NT LIFT DRAG RATIO
NT LOW ASPECT RATIO
NT LOW REYNOLDS NUMBER
NT MACH NUMBER
NT MASS RATIOS
NT MIXING RATIOS
NT NUSSELT NUMBER
NT PAYLOAD MASS RATIO
NT PERVEANCE
NT POISSON RATIO
NT PRANDTL NUMBER
NT PRESSURE RATIO
NT PROPELLANT MASS RATIO
NT RAYLEIGH NUMBER
NT REYNOLDS NUMBER
NT RICHARDSON NUMBER
NT SCALE (RATIO)
NT SCHMIDT NUMBER
NT SIGNAL TO NOISE RATIOS
NT SIMILARITY NUMBERS
NT STANDING WAVE RATIOS
NT STANTON NUMBER
NT STRESS RATIO
NT STROUHAL NUMBER
NT THRUST-WEIGHT RATIO
NT VOID RATIO
Damping measurements for ultra-high carbon steel/brass laminates
[DE93-011886] 01 p0082 N94-11076
A calibration of the production rate ratio P-21/P-26 by low energy secondry neutrons: Identification of Ne spallation components at the 10(exp 6) atoms/g level in terrestrial samples 03 p1187 N94-16194
Encapsulation of hemoglobin in non-phospholipid vesicles
[AD-A266505] 03 p1128 N94-16785
The computation of R(sub 0) for discrete-time epidemic models with dynamic heterogeneity
[CWI-AM-R9301] 06 p2420 N94-23521

RATS
Toxicity study of dimethylethoxysilane (DMSES), the waterproofing agent for the Orbiter heat protective system 01 p0318 N94-11554
Mechanistic studies on reduced exercise performance and cardiac deconditioning with simulated zero gravity 01 p0310 N94-12001
Fluid compartment and renal function alterations in the rat during 7 and 14 day head down tilt 01 p0310 N94-12002
The organization of the suprachiasmatic circadian pacemaker of the rat and its regulation by neurotransmitters and modulators
[AD-A266113] 01 p0301 N94-12417
Physiological Anatomical Rodent Experiment (PARE).04 Feasibility Test 1
[NASA-CR-194423] 02 p0728 N94-13473
Improving physical performance by chemical stimulation
[DSIS-92-03763] 02 p0728 N94-13823
Neuropeptide-Y (NPY) increases total blood flow in the tail, and reduces cutaneous microvascular blood flow in the tail and foot of the rat
[AD-A266839] 03 p1115 N94-14918
TransRapid TR-07 maglev-spectrum magnetic field effects on daily pineal indoleamine metabolic rhythms in rodents
[DE93-015143] 03 p1117 N94-16893
The behavioral toxicology of high-peak, low average power, pulsed microwave irradiation
[AD-A268392] 03 p1134 N94-17535
Intracellular physiology of the rat suprachiasmatic nucleus: Electrical properties, neurotransmission and effects of neuromodulators
[AD-A268829] 04 p1505 N94-18538
A study of the effect of hydrocarbon structure on the induction of male rat nephropathy and metabolic structure
[AD-A270969] 04 p1504 N94-19789
Relationship of area postrema to three putative measures of motion sickness 05 p1885 N94-21900
Conditioned taste aversion induced by motion is prevented by selective vagotomy in the rat 05 p1887 N94-21908

Experimental studies of gastric dysfunction in motion sickness: The effect of gastric and vestibular stimulation on the vagal and splanchnic gastric efferents
05 p1888 N94-21911
Role of the area postrema in three putative measures of motion sickness in the rat
05 p1888 N94-21912
Electrophysiology of the rat nucleus accumbens: Local circuitry, neuromodulation and synaptic plasticity
[PB93-232254] 06 p2420 N94-23454
Skeletal muscle metabolism in hypokinetic rats
[NASA-CR-195082] 06 p2420 N94-24124
In vitro system for studying metabolism of environmental chemicals in human cells
[AD-A273427] 06 p2421 N94-24688
Cortical mechanisms of attention, discrimination, and motor response to somesthetic stimuli
[AD-A274163] 07 p2940 N94-27141
Development of inbred strains from Japanese wild rats (Rattus norvegicus)
07 p2906 N94-27492
Physiological investigations of the isolated rat's liver in hypothermia and hypoxia and their relevance in aircraft incidents above the sea
08 p3382 N94-28439
Shortening velocity and calcium sensitivity of single fibers from hindlimb suspended muscle in rats
08 p3387 N94-29866
Stress and brain protein synthesis
[PB94-170750] 11 p4296 N94-35601
Ground and space flight experiments of the effects of light, sound and/or temperature on animals
[NASA-CR-196102] 12 p4478 N94-36986

RAWINSONDES

Atmospheric soundings during the Washita 1992 campaign
[NASA-CR-194383] 02 p0712 N94-13212
Empirical relationships among atmospheric variables from rawinsonde and field data as surrogates for AVIRIS measurements: Estimation of regional land surface evapotranspiration
03 p1074 N94-16712
Overview of microphysical and state parameter measurements from FIRE 2
05 p1871 N94-22293
Cloud fields derived from satellite and surface data during FIRE cirrus phase 2
05 p1872 N94-22302
Breaking Kelvin-Helmholtz waves and cloud-top entrainment as revealed by K-band Doppler radar
05 p1874 N94-22310
Meteorological analysis of the December 4-6 FIRE cirrus-2 case
05 p1875 N94-22314
Meteorological analysis of the November 25 FIRE cirrus-2 case: A well-defined ridge-crest cirrus system over Oklahoma
05 p1877 N94-22328
A nighttime structure model of atmospheric optical turbulence, c2(n), derived from thermosonde and high resolution rawinsonde measurements
[AD-A273803] 06 p2406 N94-25537
A preliminary method for atmospheric soundings in real time using satellite and ground-based remotely sensed data
[AD-A274381] 07 p2880 N94-26828
Development and testing of improved techniques for modeling the hydrologic cycle in a mesoscale weather prediction system
[AD-A277416] 09 p3786 N94-32921
Upper-air quality control: A comparison study
[AD-A277884] 10 p4080 N94-33553

RAY ACOUSTICS

U GEOMETRICAL ACOUSTICS

RAY OPTICS

U GEOMETRICAL OPTICS

RAY TRACING

Source to detector spectrum transformation and its inverse for the Pegasus Z-pinch
[DE93-012674] 01 p0384 N94-10157
Implementation and use of a computational ray-tracing program for the design and analysis of complex optical systems
[AD-A265075] 01 p0382 N94-11653
Optimal hemicube sampling
[DE93-010499] 01 p0334 N94-12591
The propagation characteristics and instability properties of low-frequency electromagnetic waves in the Io plasma torus
02 p0601 N94-13650
A data distributed parallel algorithm for ray-traced volume rendering
[NASA-CR-191520] 02 p0749 N94-13721
AXAF FITS standard for ray trace interchange
[NASA-CR-194025] 02 p0832 N94-14305
The three-dimensional ray trajectories of the WKB optical fiber modes
[AD-A267167] 03 p1189 N94-15739
Ray tracing on topographic Rossby waves
[AD-A267014] 03 p1112 N94-15844
A ray trace model for propagation loss
[AD-A266314] 03 p0997 N94-16467
Portable parallel ray tracing algorithms
[AD-A268984] 04 p1522 N94-18698
A general purpose ionospheric ray tracing procedure
[AD-A271058] 05 p1854 N94-19860
Feedback controlled optics with wavefront compensation
[NASA-CASE-NPO-18194-1-CU]
05 p1985 N94-20305
Validation of the design of a high resolution all-reflection Michelson interferometer for atmospheric spectroscopy
[AD-A272505] 05 p1987 N94-21410
A data distributed, parallel algorithm for ray-traced volume rendering
[DE93-040150] 05 p1935 N94-21622
Telescope image modelling software in STSDAS
05 p1926 N94-22483
Electromagnetic field strength prediction in an urban environment: A useful tool for the planning of LMSS
06 p2283 N94-22795
Proposed additions to the SHADOW ray-tracing code for general-asymmetric perfect-crystal optics
[DE94-001291] 06 p2560 N94-23188
Refraction of high frequency noise in an arbitrary jet flow
[NASA-TM-106465] 06 p2525 N94-23464
Theoretical investigation of variable periodicity (graded) multilayers for hard x ray applications
[NASA-CR-193913] 06 p2543 N94-23502
Dynamic ray tracing and its application in triangulated media
[DE94-000875] 06 p2402 N94-23516
Accuracy control in Monte Carlo radiative calculations
06 p2321 N94-23639
Efficient modeling in transversely isotropic inhomogeneous media
[DE94-003394] 07 p2877 N94-25847
Ionospheric modification by high power, obliquely propagated HF radio wave transmissions. Part 1: Experimental
[AD-A273746] 07 p2878 N94-26224
Dynamic and kinematic P wave tracing for a three-dimensional elastic inhomogeneous media by the asymptotic ray theory and application
[ITN-94-85239] 07 p2775 N94-27244
Synthetic image generator model; application of view angle dependent reflectivity components and performance evaluation in the visible region
[AD-A275365] 08 p3499 N94-29009
Optimizing ray tracing with visual coherence
[AD-A275218] 08 p3499 N94-29059
The High-Frequency Benchmark propagation program
[AD-A276323] 09 p3672 N94-31334
Ultrasonic tomography in fiber-reinforced composite materials
09 p3620 N94-31565
Prediction of the plane wave beamformed acoustic arrival structure for the 1992 Barents Sea coastal tomography test
[AD-A276741] 09 p3788 N94-32181
Landau damping of auroral hiss
10 p4088 N94-34950
Correction-free pyrometry in radiant wall furnaces
[NASA-CASE-NPO-18655-1-CU]
10 p4056 N94-35114

RAYLEIGH DISTRIBUTION

Ocean wave height transformation model using surface roller theory
[AD-A272610] 05 p1883 N94-21423
Control algorithms for effective operation of variable-speed wind turbines
[DE94-002607] 06 p2394 N94-23704

RAYLEIGH NUMBER

Stability measurements of Rayleigh-Benard convection near the critical state using a spectral model
[MPIS-15/1992] 04 p1422 N94-19520
A parametric study of heat transfer within a planar thermosyphon
[DE93-019546] 05 p1799 N94-20258
Expectations for the Martian core magnetic field
05 p2120 N94-20792
Linear and nonlinear pattern selection in Rayleigh-Benard stability problems
[NASA-TM-104007] 11 p4263 N94-35371

RAYLEIGH SCATTERING

The structure of turbulent boundary layers and shock wave boundary layer interactions
[AD-A266240] 03 p1026 N94-16929
Development of a technique to determine the morphology and dynamics of agglomerates in chemically reacting flows
[AD-A271160] 05 p1678 N94-20000
New relativistic S-matrix results for scattering -- beyond the usual anomalous factors/beyond impulse approximation
[DE93-019148] 05 p1971 N94-20096
Multiple scattering effects on the Linear Depolarization Ratio (LDR) measured during CaPE by a Ka-band air-borne radar
05 p1728 N94-20446
RADCAL: A narrow-band model for radiation calculations in a combustion environment
[PB93-200889] 05 p1682 N94-21448
Laser guide star adaptive optics: Present and future
[DE93-018642] 05 p1989 N94-21619
Data analysis and interpretation of lunar dust exosphere
06 p2623 N94-25349
Polarizability matrix of layered chiral sphere
[PB94-132834] 07 p2778 N94-28355
Considerations in the modelling of seafloor acoustic backscatter
[AD-A275404] 08 p3478 N94-29206
Evidence of solar oscillations in Rayleigh-scattered light
09 p3952 N94-31214

RAYLEIGH WAVES

On the secondary instability of the most dangerous Goertler vortex
[NASA-CR-191504] 02 p0636 N94-13785
High resolution geological site characterization utilizing ground motion data
[AD-A268926] 04 p1481 N94-18485
Experimental investigation of wave and fracture phenomena in impacted ceramics: Experiments on sapphire
[AD-A270040] 04 p1372 N94-18792
Surface wave group velocity tomography of East Asia, part 1
[AD-A270100] 04 p1484 N94-18868
Elastic properties of amorphous thin films studied by Rayleigh waves
[DE93-018375] 04 p1372 N94-19202
A preliminary shear velocity model for Central Asia
[AD-A274972] 07 p2880 N94-26752
Problems in nonlinear acoustics: Rayleigh waves, pulsed sound beams, and waveguides
[AD-A274587] 07 p3010 N94-26983
Acoustical-optical fracture analysis
[PB94-170602] 11 p4279 N94-36216

RAYLEIGH-BENARD CONVECTION

NT BENARD CELLS

Evaporation under microgravity conditions
01 p0102 N94-10086
Benard and Marangoni convection in multiple liquid layers
01 p0105 N94-10100
Marangoni-driven solitary waves
01 p0119 N94-10214
Transient effects in the Benard instabilities: Coupling between capillary and gravity effects
01 p0119 N94-10216
Numerical investigations on Marangoni-Benard instability in multi layer systems
01 p0120 N94-10217
Appearance of convective instabilities caused by liquid-liquid phase separation under small buoyancy forces
01 p0120 N94-10221
Large eddy simulations of time-dependent and buoyancy-driven channel flows
01 p0155 N94-12287
Convective and dynamic instability in meridional trenches
01 p0225 N94-12739
Stability measurements of Rayleigh-Benard convection near the critical state using a spectral model
[MPIS-15/1992] 04 p1422 N94-19520
Linear and nonlinear pattern selection in Rayleigh-Benard stability problems
[NASA-TM-104007] 11 p4263 N94-35371
Spatio-temporal properties of centrifugal instabilities: Abstracts of 8th Couette-Taylor Meeting
[PB94-150240] 11 p4266 N94-35981
Coupled Marangoni-Benard/Rayleigh-Benard instability with temperature dependent viscosity
[NASA-TM-106646] 12 p4444 N94-37507

RAYLEIGH-RITZ METHOD

A robust multilevel simultaneous eigenvalue solver
[NASA-CR-191491] 02 p0767 N94-13202
Mechanical and thermal buckling analysis of sandwich panels under different edge conditions
[NASA-TM-4535] 06 p2228 N94-23514
Response of structures to impact loads using elastic and plastic analysis
[ISBN-0-315-84647-X] 07 p2842 N94-27309
Mechanical and thermal buckling analysis of rectangular sandwich panels under different edge conditions
[NASA-TM-4585] 10 p4069 N94-33704

RAYON

The development of short, high surface area activated carbon fibers
[AD-A280509] 12 p4404 N94-37105

RB-50 AIRCRAFT

U B-50 AIRCRAFT

RBE

U RELATIVE BIOLOGICAL EFFECTIVENESS (RBE)

RC CIRCUITS

Computation of signal delays in RC networks
05 p1744 N94-21102

Carbon supercapacitors
[DE94-002652] 06 p2311 N94-24748
RC NETWORKS
U RC CIRCUITS
RCB STARS
U R CORONAE BOREALIS STARS
RDX
Laser ignition of solid propellants: 1. Ignition delays
[AD-A268454] 03 p0976 N94-17538
The minimum detection limits of RDX and TNT deposited on various surfaces as determined by ion mobility spectroscopy
[DE93-018521] 04 p1378 N94-19042
Evaluation of pre-extraction analytical holding times for nitroaromatic and nitramine explosives in water
[AD-A271547] 05 p1712 N94-20927
Chemistry of the burning surface
[AD-A272725] 05 p1681 N94-21181
Chemical dynamics studies of reactions in energetic materials
[AD-A275607] 08 p3224 N94-28769
Correlation of cookoff behavior of rocket propellants with thermomechanical and thermochemical properties
[AD-A274983] 08 p3224 N94-29092
Insensitive energetic materials: The importance of physical properties and molecular structure
[AD-A275393] 08 p3225 N94-29308
Condensed-phase processes during solid propellant combustion. 3: Preliminary depth-profiling studies on XM39, JA2, M9, M30, and HMX2
[AD-A276595] 09 p3635 N94-32124
A fully coupled thermal, chemical, mechanical cookoff model
[DE94-011432] 12 p4428 N94-37201
Thermal decomposition reactions of HMX and RDX and their importance in predicting cookoff hazards
[DE94-011430] 12 p4429 N94-37413
REACTANCE AMPLIFIERS
U PARAMETRIC AMPLIFIERS
REACTING FLOW
NT COMBUSTIBLE FLOW
CFD analysis of hypersonic, chemically reacting flow fields 01 p0002 N94-10422
Stability of hypersonic boundary-layer flows with chemistry 01 p0007 N94-10451
Nonequilibrium hypersonic flow in a wind-tunnel nozzle 01 p0008 N94-10456
Some experimental study and numerical simulation in wind tunnel flow 01 p0008 N94-10457
Hypersonic multi block flow simulations around space vehicles including non-equilibrium chemistry 01 p0009 N94-10460
Thermal and chemical non equilibrium hypersonic flow computations 01 p0010 N94-10465
Combustion chamber analysis code
[NASA-CR-192585] 01 p0046 N94-10934
CRESLAF. Version 4.0: A Fortran program for modeling laminar, chemically reacting, boundary-layer flow in cylindrical or planar channels
[DE93-012835] 01 p0152 N94-11371
PDF approach for turbulent scalar field: Some recent developments 01 p0160 N94-12315
Theories of turbulent combustion in high speed flows
[AD-A265735] 01 p0079 N94-12403
A time-accurate numerical method for chemically reacting flows at all Mach numbers 02 p0500 N94-13198
Topics on spatially high-order accurate methods and pre-conditioning for the Navier-Stokes equations with finite-rate chemistry 02 p0633 N94-13572
Hypersonic overview 02 p0505 N94-14154
Computation of nonequilibrium flows using PNS equations 02 p0641 N94-14610
Simulation of hypersonic, reacting flow around reentry bodies: Comparisons of numerical and experimental results
[MBB-LME-211-S-PUB-507] 02 p0509 N94-14710
Studying Turbulence Using Numerical Simulation Databases. 4: Proceedings of the 1992 Summer Program
[NASA-CR-194556] 02 p0643 N94-14745
DNS and modeling of the interaction between turbulent premixed flames and walls 02 p0646 N94-14763
The evolution equation for the flame surface density in turbulent premixed combustion 02 p0567 N94-14764
Effect of finite-rate chemistry and unequal Schmidt numbers on turbulent non-premixed flames modeled with single-step chemistry 02 p0567 N94-14766
Stochastic modeling of turbulent reacting flows 02 p0647 N94-14768
Reaction and diffusion in turbulent combustion
[DE93-017085] 03 p0943 N94-15146
Large eddy simulation and direct numerical simulation of high speed turbulent reacting flows
[NASA-CR-193131] 03 p1018 N94-15427
Fundamental studies of rocket combustion chemistry and combustion instability
[AD-A266248] 03 p0925 N94-16482
Studies in turbulence and turbulence control
[AD-A266318] 03 p1026 N94-16950
Studies on nonequilibrium phenomena in supersonic chemically reacting flows
[NASA-CR-194662] 03 p1027 N94-17215
Chemical reactions in turbulent mixing flows
[AD-A268287] 03 p0861 N94-17580
Chemical reactions in turbulent mixing flows
[AD-A269377] 04 p1410 N94-18472
A coupled implicit solution method for turbulent spray combustion in propulsion systems 04 p1411 N94-18549
Numerical investigation of complex, transitional, and chemically reacting flows 04 p1411 N94-18550
Analysis of supersonic flows using k-epsilon model and the RPLUS code: Progress towards high speed combustor analysis 04 p1411 N94-18551
Numerical simulation of turbulent mixing and combustion near the inlet of a burner
[DE93-017960] 04 p1350 N94-18987
Numerical simulation of viscous flows in chemical nonequilibrium
[MBB-LME-211-S-PUB-506] 04 p1421 N94-19497
Development of a technique to determine the morphology and dynamics of agglomerates in chemically reacting flows
[AD-A271160] 05 p1678 N94-20000
Reaction zone models for vortex simulation of turbulent combustion
[AD-A272723] 05 p1681 N94-21213
Establishing the basis for validated predictions of highly non-equilibrium flows (with 9 attachments)
[AD-A272918] 05 p1802 N94-21220
Instantaneous velocity field imaging instrument for supersonic reacting flows
[NASA-CR-191162] 05 p1809 N94-21607
Comparison of mixing calculations for reacting and non-reacting flows in a cylindrical duct
[NASA-TM-106435] 05 p1649 N94-21758
Simulations of diffusion-reaction equations with implications to turbulent combustion modeling
[NASA-CR-191536] 05 p1804 N94-21861
Numerical parametric studies of spray combustion instability 06 p2212 N94-23041
A random distribution reacting mixing layer model
[NASA-CR-194445] 06 p2187 N94-23552
Upwind MacCormack Euler solver with non-equilibrium chemistry 06 p2326 N94-23672
Fundamental and experimental studies on the catalytic combustion of methane
[PB94-112661] 06 p2233 N94-23736
A large eddy simulation scheme for turbulent reacting flows 06 p2330 N94-24154
The combustion program at CTR 06 p2237 N94-24155
A transport equation for the scalar dissipation in reacting flows with variable density: First results 06 p2331 N94-24157
Workshop on Computational Turbulence Modeling
[NASA-CP-10130] 06 p2333 N94-24460
Conservation equations for reacting gas flow
[PB94-111168] 06 p2334 N94-24574
Numerical solutions of the complete Navier-Stokes equations
[NASA-CR-194780] 06 p2337 N94-24858
LES, DNS and RANS for the analysis of high-speed turbulent reacting flows
[NASA-CR-195196] 06 p2337 N94-25094
Modelling of ionisation reactions and of the resulting electric fields in one-dimensional hypersonic shock waves with the direct simulation Monte Carlo method
[IC-AERO-92-01] 07 p2644 N94-26248
High resolution measurements of mixing and reaction processes in turbulent flows
[AD-A274970] 07 p2793 N94-26534
Direct simulation Monte-Carlo of near continuum hypersonic flow with chemical reactions
[DLR-FB-93-01] 07 p2797 N94-27588
TVD flux-difference split methods for high-speed thermochemical nonequilibrium flows with strong shocks
[UTIAS-350] 07 p2799 N94-27880
A random distribution reacting mixing layer model
[NASA-TM-106517] 08 p3150 N94-28923
On approximate Riemann solvers: Improvement of HLLEM scheme and its generalization for chemically reacting flows 08 p3126 N94-28973
Advanced diagnostics for reacting flows
[AD-A275057] 08 p3272 N94-29136
A vorticity transport closure method for turbulent reacting flows 08 p3274 N94-29761
An evaluation of explicit pseudo-steady-state approximation schemes for stiff ODE systems from chemical kinetics
[CWI-NM-R9312] 08 p3353 N94-30729
Mixture model simulating reactive turbulent flows: Testing of Eulerian-Lagrangian probabilistic models
[ONERA-NT-1993-13] 09 p3702 N94-31477
Reactive flows in compact objects 09 p3934 N94-31567
A numerical method for mixing/chemically reacting compressible flow with finite rate chemistry 09 p3634 N94-31824
Computed potential energy surfaces for chemical reactions
[NASA-CR-195835] 09 p3639 N94-33036
Turbulent reacting flows and supersonic combustion
[AD-A277462] 09 p3639 N94-33242
Combined LAURA-UPS solution procedure for chemically-reacting flows
[NASA-TM-107964] 10 p4049 N94-34721
Comparison of PDF and moment closure methods in the modeling of turbulent reacting flows
[NASA-TM-106614] 11 p4265 N94-35948
A flux splitting scheme with high-resolution and robustness for discontinuities
[NASA-TM-106452] 12 p4441 N94-36646
REACTION BONDING
High-temperature corrosion of ceramic-ceramic composites in a waste incinerator environment
[DE93-012430] 01 p0072 N94-11368
NMR and theoretical investigation of cation binding with sol-gel silicates
[AD-A266999] 03 p0963 N94-15631
Selection of polymer binders and fabrication of SiC fiber-reinforced reaction-bonded silicon nitride matrix composites
[NASA-CR-194874] 06 p2255 N94-24223
Chemical reactions of chlorine on a vicinal Si(100) surface studied by ESDIAD
[AD-A279059] 11 p4236 N94-35731
REACTION CONTROL
First experimental assessment of RCS plume-flow field interaction on Hermes leading edge thruster configuration 07 p2703 N94-28032
REACTION JETS
U JET FLOW
U JET THRUST
REACTION KINETICS
Chemical pattern formation under microgravity 01 p0121 N94-10227
The reaction between titanium carbide and aluminium carbide in liquid aluminium; a microgravity study 01 p0123 N94-10238
Report of the Workshop on Light Particle-Induced Reactions
[DE93-752300] 01 p0360 N94-10317
The intensity of knock in an internal combustion engine: An experimental and modeling study
[DE93-013089] 01 p0177 N94-10322
Comparison of computation and experiment for a high enthalpy, heated-driver, shock-tube environment 01 p0007 N94-10447
Review of SHARC 2.0 O3 kinetics and spectroscopy
[AD-A265481] 01 p0274 N94-10496
Kinetics of high concentration arsenic deactivation at moderate to low temperatures
[DE93-013349] 01 p0395 N94-10516
A lattice gas model for enzyme kinetics with next-nearest neighbor interactions
[DE93-613026] 01 p0410 N94-10631
Szilard-Chalmers effect in solid HIO4.2H2O by neutron irradiation
[DE93-617173] 01 p0397 N94-10830
Journal of Research of the National Institute of Standards and Technology, volume 98, number 2, March - April 1993
[PB93-196228] 01 p0485 N94-10850
KIVA-3: A KIVA program with block-structured mesh for complex geometries
[DE93-011986] 01 p0077 N94-11249
Synthesis and thermal evolution of structure in alkoxide-derived niobium pentoxide gels
[NASA-TM-106259] 01 p0090 N94-11257
Characterization of gas-aerosol interaction kinetics using morphology dependent stimulated Raman scattering
[DE93-012324] 01 p0077 N94-11359
A model of elementary chemistry and fluid mechanics in the combustion of hydrogen on platinum surfaces
[DE93-012767] 01 p0077 N94-11370
CRESLAF. Version 4.0: A Fortran program for modeling laminar, chemically reacting, boundary-layer flow in cylindrical or planar channels
[DE93-012835] 01 p0152 N94-11371
The evolution equation for the flame surface density in turbulent premixed combustion 01 p0081 N94-12316

Study and modeling of finite rate chemistry effects in turbulent non-premixed flames 01 p0081 N94-12317
Solvent dynamical effects in electron transfer: Molecular dynamics simulations of reactions in methanol
[AD-A266061] 01 p0369 N94-12420
Molecular solvent-dynamical effects on activated electron-transfer kinetics: How important is solvent friction?
[AD-A265886] 02 p0779 N94-12894
Modeling ignition chemistry
[DE93-012340] 02 p0561 N94-12910
Conversion of light hydrocarbon gases to metal carbides for production of liquid fuels and chemicals
[DE93-014962] 02 p0583 N94-13002
Infrared absorption spectroscopy and chemical kinetics of free radicals
[DE93-015078] 02 p0562 N94-13004
Fifteenth Combustion Research Conference
[DE93-015758] 02 p0562 N94-13045
A coherent flame model of premixed turbulent combustion in a counterflow geometry
[CUED/A-THERMO/TR.60] 02 p0562 N94-13085
Research on chemical vapor deposition processes for advanced ceramic coatings
[NASA-CR-193613] 02 p0577 N94-13089
Absorption and damage thresholds of low defect density hafnia deposited with activated oxygen
[DE93-013853] 02 p0655 N94-13243
Low temperature metal-organic chemical vapor deposition growth processes for high efficiency solar cells
[DE92-010562] 02 p0702 N94-13386
Application of synchrotron radiation in chemical dynamics
[DE93-015040] 02 p0563 N94-13411
Chemical reactions in scramjet engines: Reduced kinetic models for ignition, combustion and nozzle flow
[NAL-TR-1184] 02 p0563 N94-13458
Reduction of Pu(6) with hydrogen peroxide: Effects of plutonium, peroxide, and iron concentrations and of reaction time
[DE93-013598] 02 p0564 N94-13487
Chemistry and transport in a multi-dimensional model
[NASA-CR-194425] 02 p0716 N94-13969
Hypersonic overview 02 p0505 N94-14154
Hydrogen peroxide safety issues
[DE93-013895] 02 p0565 N94-14346
Modeling surface area to volume effects on borosilicate glass dissolution
[DE93-011891] 02 p0581 N94-14432
Numerical simulation of velocity-coupled combustion response of solid rocket propellants
02 p0585 N94-14490
Numerical simulations of turbulent premixed H2/O2/N2 flames with complex chemistry
02 p0567 N94-14765
Study of chemical reactions under the influence of ultrasound
[DE93-016458] 02 p0778 N94-14867
Comparative ignition of hexane and octane isomers in a shock tube
[DE93-016535] 02 p0566 N94-14869
Reactions of chemiluminescence induced by singlet oxygen with metals
[ONERA-NT-1992-13] 03 p0955 N94-15149
Intramolecular versus intermolecular condensation rates in the acidic polymerization of octaethoxytrisiloxane
[AD-A266982] 03 p0963 N94-15490
Particle simulation of hypersonic flow
[AD-A267185] 03 p0857 N94-15787
A proposed mechanism for the pyrolysis of diborane
[DE93-014275] 03 p0947 N94-15977
Molecular beam studies of reaction dynamics
[DE93-015035] 03 p1181 N94-15995
A comparison of one and two dimensional flame quenching: Heat transfer results
[DE93-015196] 03 p0947 N94-16060
Corrosion kinetics and mechanisms for nuclear grade graphites
[DE93-015462] 03 p0947 N94-16105
Single-collision studies of energy transfer and chemical reaction
[DE93-017603] 03 p1182 N94-16121
Evaporation kinetics of Mg2SiO4 crystals and melts from molecular dynamics simulations
03 p1219 N94-16331
Studies of combustion reactions at the state-resolved differential cross section level
[DE93-017605] 03 p0948 N94-16462
Structural effects in electron transfer reactions: Comparative interfacial electrochemical kinetics for cis- versus trans-dioxorhenium (V) (bi)pyridine oxidation
[AD-A266307] 03 p1182 N94-16466
Tritium diffusion and desorption in single crystal LiAlO2
[DE93-015140] 03 p1211 N94-16805
Emissions of volatile organic compounds from stationary combustion sources: Numerical modeling capabilities
[DE93-014123] 03 p1096 N94-16825
Modeling study to evaluate the ionic mechanism of soot formation in flames
[AD-A266242] 03 p0950 N94-16930
Materials processing and manufacturing technologies for diamond substrate multichip modules (DSMCM)
[AD-A267316] 03 p0969 N94-16946
Advanced thermally stable jet fuels
[DE93-017711] 03 p0975 N94-16996
Pulsed laser kinetic studies of liquids under high pressure
[DE93-017826] 03 p1041 N94-16998
Solvational barriers to interfacial electron transfer: Minimization by way of valence delocalization
[AD-A267371] 03 p0950 N94-17006
The influence of an electric field on the kinetics of nucleation
[IFTR-2/91] 03 p1213 N94-17046
Surface reactivity of combustion generated soot particles
[AD-A268017] 03 p0952 N94-17532
Cathode sheath charge transfer effects
[AD-A268393] 03 p1186 N94-17536
Laser ignition of solid propellants: 1. Ignition delays
[AD-A268454] 03 p0976 N94-17538
Coefficients for calculating thermodynamic and transport properties of individual species
[NASA-TM-4513] 03 p1220 N94-17624
Kinetics of silica-phase transitions
[DE93-016231] 03 p1217 N94-17659
Fundamental studies of the mechanism of catalytic reactions with catalysts effective in the gasification of carbon solids and the oxidative coupling of methane
[DE93-015262] 04 p1347 N94-18193
Applications of scanning tunneling microscopy to electrochemistry
[AD-A269129] 04 p1348 N94-18255
Temperature, kinetic energy, and rotational temperature dependences for the reactions of Ar(+)(2)P3/2 with O2 and CO
[AD-A268974] 04 p1567 N94-18526
Numerical investigation of complex, transitional, and chemically reacting flows 04 p1411 N94-18550
Wettability and reaction kinetics in metal matrix composites
[AD-A270377] 04 p1342 N94-18704
Transport phenomena and interfacial kinetics in multiphase combustion systems
[AD-A270202] 04 p1349 N94-18785
The Fourteenth Symposium on Molecular Beams
[AD-A268721] 04 p1568 N94-18787
LX-17 chemical kinetic material model for Chemical TOPAZ2D
[DE93-014363] 04 p1377 N94-18893
Surface phases and their influence on metal-oxide interfaces
[DE93-019931] 04 p1601 N94-19020
Chemical dynamics in time and energy space
[DE93-018595] 04 p1350 N94-19097
Kinetics programs for simulation of tropospheric photochemistry on the global scale
[DE93-019035] 04 p1476 N94-19104
Environmental Research Program
[DE93-019101] 04 p1477 N94-19105
Single source precursors for the OMCVD of 3/5 compound semiconductors
[AD-A271147] 04 p1606 N94-19739
Pressure and temperature effects on the kinetics and quality of diamond films
[AD-A270876] 04 p1606 N94-19771
Collaborative research on combustion diagnostics and modeling between Rolls-Royce, Inc. and the United States Air Force Wright Laboratory
[AD-A270660] 04 p1354 N94-19778
Materials processing and manufacturing technologies for Diamond Substrate MultiChip Modules (DSMCM)
[AD-A271011] 05 p2011 N94-19821
Segregation of Si to the surface of Fe-29Ni-17Co alloy
[DE93-040053] 05 p1687 N94-19864
Initiation and modification of reaction by energy addition: Kinetic and transport phenomena
[AD-A271315] 05 p1797 N94-19936
Ab initio potential energy surfaces for the H + OCS reaction
[AD-A270577] 05 p1698 N94-19947
Encounters of H and D atoms with O2 in water: Relative diffusion and reaction rates
[DE93-018587] 05 p1970 N94-19956
Common Themes and Mechanisms of Epitaxial Growth, volume 312 --- Materials Research Society symposium proceedings
[AD-A270513] 05 p2013 N94-19967
High performance heavy alloys by alloying and process control
[AD-A271129] 05 p1689 N94-20019
Laboratory studies of low temperature rate coefficients: The atmospheric chemistry of the outer planets
[NASA-CR-193485] 05 p1972 N94-20130
Computed potential energy surfaces for chemical reactions
[NASA-CR-194600] 05 p1679 N94-20169
Surface science and modeling studies of endothermic fuels catalysis
[AD-A272850] 05 p1712 N94-21192
Reaction zone models for vortex simulation of turbulent combustion
[AD-A272723] 05 p1681 N94-21213
Electronically metastable molecules of high symmetry
[AD-A272015] 05 p1974 N94-21461
A project on parameter identification in reaction kinetics
[CWI-NM-R9301] 05 p1682 N94-21574
Modeling of outgassing and matrix decomposition in carbon-phenolic composites
[NASA-CR-194741] 05 p1676 N94-21743
Simulations of diffusion-reaction equations with implications to turbulent combustion modeling
[NASA-CR-191536] 05 p1804 N94-21861
Study of improved methods for predicting chemical equilibria
[DE94-001647] 06 p2568 N94-22719
A novel method for determination of transport parameters of H2 and O2 in PEMFCs
[DE94-001492] 06 p2389 N94-22962
Integrated hydrometallurgical jarosite treatment
[PB93-217990] 06 p2232 N94-22983
Reburning rich-lean kinetics
[PB93-220887] 06 p2232 N94-23100
Modelling of solid polymer and direct methanol fuel cells: Phenomenological equations and analytical solutions
[PB93-224897] 06 p2390 N94-23102
Alloys for hydrogen storage in nickel/hydrogen and nickel/metal hydride batteries 06 p2391 N94-23353
Reaction of isocyanates with carboxylic acids and its application to polymer synthesis
[PB94-118858] 06 p2254 N94-23763
Selection of polymer binders and fabrication of SiC fiber-reinforced reaction-bonded silicon nitride matrix composites
[NASA-CR-194874] 06 p2255 N94-24223
Fracture kinetics analysis of empirical and semi-empirical corrosion fatigue relations 06 p2159 N94-24277
Adsorption, desorption, and decomposition of HCl and HBr on Ge(100): Competitive pairingand near-first-order desorption kinetics
[AD-A273504] 06 p2235 N94-24790
Eddy mixing coefficient upper limit derived from the photochemical balance of O2 06 p2621 N94-24897
Reactive trace metals as indicators of subduction and ventilation processes in the ocean
[AD-A273585] 06 p2419 N94-25164
Development and implementation of a scramjet cycle analysis code with a finite-rate-chemistry combustion model for use on a personal computer
[AD-A273834] 07 p2673 N94-25617
Three methods to measure RH bond energies
[DE94-003795] 07 p3013 N94-25816
Technique to predict the curing behaviour of unsaturated polyester materials
[PB94-124856] 07 p2748 N94-25892
Oxygen reduction at a YSZ interface with cathode materials La(1-x)(Ca or Sr)(x)MnO3(1-x)CaMnO3
[DE94-002954] 07 p3054 N94-26147
The importance of vibrationally excited nitrogen in silicon nitride deposition systems
[AD-A274874] 07 p2750 N94-26167
Theoretical determination of chemical rate constants using novel time-dependent methods
[NASA-CR-195221] 07 p2714 N94-26205
Chemical and vibrational nonequilibrium viscous flows: Modelling, internal and external flow applications
[ESA-TT-1274] 07 p2791 N94-26316
In situ spectroscopic applications to the study of rechargeable lithium batteries
[DE94-003478] 07 p2782 N94-26328
High resolution measurements of mixing and reaction processes in turbulent flows
[AD-A274970] 07 p2793 N94-26534
A semiclassical reactive flux method for the calculation of condensed phase activated rate constants
[AD-A274850] 07 p3020 N94-26562
Design of gasifiers to optimize fuel cell systems
[DE94-000010] 07 p2856 N94-26581
An investigation of the effect of surface impurities on the adsorption kinetics of hydrogen chemisorbed onto iron
[NASA-CR-195213] 07 p2716 N94-26643

Mechanistic studies of opto-electronic materials and syntheses using multiple laser and surface diagnostics
[AD-A274528] 07 p3036 N94-26834
Kinetics of 2-pentadecylaniline polymerizations in monolayers: Relationships between experimental data and a new theoretical model
[AD-A274419] 07 p2754 N94-27080
Laser probes of natural gas ignition chemistry
[PB94-128345] 07 p2717 N94-27226
Basic research on natural gas combustion phenomena
[PB94-129046] 07 p2717 N94-27256
Reactivity of nitrate radical (NO3) toward organic compounds 07 p2704 N94-27387
Thermogravimetric study of oxidation of a PdCr alloy used for high-temperature sensors
[NASA-TM-106473] 07 p2741 N94-27426
High temperature grain growth and oxidation of Fe-29Ni-17Co (Kovar (tm)) alloy leads
[DE94-004691] 07 p3069 N94-27753
Kinetic parameters from thermogravimetric analysis 07 p2721 N94-27909
CO2 methanation catalysts prepared from amorphous Ni-valve metal alloys containing platinum group elements 07 p2745 N94-28166
SAFSIM theory manual: A computer program for the engineering simulation of flow systems
[DE94-005381] 08 p3270 N94-28488
Ozone production at a rural site in Georgia during the summer 1992 SOS campaign
[DE94-003989] 08 p3342 N94-28523
Ion-assisted tropospheric OH measurement technique 08 p3344 N94-28601
Chemical dynamics studies of reactions in energetic materials
[AD-A275607] 08 p3224 N94-28769
High temperature resistant jet fuels 08 p3192 N94-29260
Development of global/chemistry model for jet-fuel thermal stability based on observations from static and flowing experiments 08 p3192 N94-29262
Application of semiclassical methods to reaction rate theory
[DE94-007041] 08 p3199 N94-30266
XCHEM-1D: A heat transfer/chemical kinetics computer program for multilayered reactive materials
[DE94-005072] 08 p3226 N94-30615
An evaluation of explicit pseudo-steady-state approximation schemes for stiff ODE systems from chemical kinetics
[CWI-NM-R9312] 08 p3353 N94-30729
Lattice gas simulations of replicating domains
[DE94-005006] 08 p3200 N94-30748
Theory for electron-transfer reactions involving two Marcus surfaces with a different force constant
[DE94-005925] 08 p3493 N94-30874
Reinterpretation of rate data for the reaction of ClF and F2
[DE94-005819] 08 p3200 N94-30880
Role of x ray-induced transcripts in adaptive responses following x rays
[DE94-005412] 08 p3386 N94-30895
Surface chemistry of boron-doped SiO2 CVD: Enhanced uptake of tetraethyl orthosilicate by hydroxyl groups bonded to boron
[DE94-005428] 08 p3221 N94-30896
Influence of surface defects and local structure on oxygenate reaction pathways over metal oxide surfaces
[DE94-005680] 08 p3522 N94-30901
High-temperature study of O+H2CO yields OH+HCO
[DE94-006837] 09 p3864 N94-31321
Combustion-related studies using weakly-bonded complexes
[DE94-006632] 09 p3633 N94-31493
Cloud studies seen from a physical chemist's perspective
[DE94-006059] 09 p3771 N94-31527
Modern integral equation techniques for quantum reactive scattering theory
[DE94-007039] 09 p3857 N94-31639
A numerical method for mixing/chemically reacting compressible flow with finite rate chemistry 09 p3634 N94-31824
Analysis of forward and inverse problems in chemical dynamics and spectroscopy
[DE94-007607] 09 p3635 N94-32140
Stability and precipitation kinetics in Si(1-y)C(y)/Si and Si(1-x-y)Ge(x)C(y)/Si heterostructures prepared by solid phase epitaxy
[DE94-006589] 09 p3902 N94-32296
Chemical structure and kinetics at liquid/solid interfaces
[AD-A277112] 09 p3636 N94-32304
Time-resolved IR spectroscopy, energy transfer, and state-to-state collision dynamics of atmospheric species
[AD-A277372] 09 p3773 N94-32338
Volatiles combustion in fluidized beds
[DE94-008382] 09 p3636 N94-32414
Chemical vapor deposition fluid flow simulation modelling tool
[NASA-CR-189648] 09 p3707 N94-32480
Formation mechanism and yield of molecules ejected from ZnS, CdS, and FeS2 during ion bombardment
[DE94-008487] 09 p3871 N94-32515
Molecular Science Research Center
[DE94-007464] 09 p3871 N94-32605
Rate coefficient for the reaction H + O2 yields OH + O: Results from 2000 to 5300 K
[DE94-008105] 09 p3871 N94-32615
Time-resolved analytical methods for liquid/solid interfaces
[DE94-008352] 09 p3637 N94-32826
Ignition delays, heats of combustion, and reaction rates of aluminum alkyl derivatives used as ignition and combustion enhancers for supersonic combustion
[NASA-CR-189581] 09 p3638 N94-32868
Experimental studies on the effect of coherency strains on coarsening kinetics: Current status and future outlook
[DE94-008480] 09 p3647 N94-32964
Computed potential energy surfaces for chemical reactions
[NASA-CR-195835] 09 p3639 N94-33036
Theoretical study of thermodynamic properties and reaction rates of importance in the high-speed research program 10 p3974 N94-33482
The kinetics of heterogeneous electron transfer reactions in polar solvents
[AD-A278459] 10 p4136 N94-33540
Reactions and spectroscopy of excited nitrenes
[AD-A278475] 10 p4136 N94-33745
Kinetics and mechanisms of reactions involving small aromatic reactive intermediates
[DE94-009475] 10 p4018 N94-33932
A two-dimensional model for collisional energy transfer in bimolecular ion-molecule dynamics
[AD-A278913] 11 p4321 N94-35589
Ultrafast chemical dynamics of reactions in beams
[AD-A278939] 11 p4323 N94-35805
Comparison of PDF and moment closure methods in the modeling of turbulent reacting flows
[NASA-TM-106614] 11 p4265 N94-35948
NEQPAK, the AEDC thermochemical nonequilibrium package: Theory and use
[AD-A279005] 11 p4266 N94-35951
CSTL technical activities, 1991
[PB94-160769] 11 p4318 N94-36003
Heterogeneous reaction mechanisms and kinetics relevant to the CVD of semiconductor materials
[DE94-011001] 11 p4340 N94-36032
Tritiated ammonia formation
[DE94-011170] 11 p4237 N94-36056
Kinetics studies following state-selective laser excitation
[DE94-010305] 11 p4330 N94-36105
Neutron detectors for fusion reaction-rate measurements
[DE94-010407] 11 p4330 N94-36114
A new comprehensive reaction mechanism for combustion of hydrocarbon fuels
[DE94-008288] 11 p4238 N94-36205
The thermochemistry and reaction mechanisms in the decomposition of energetic materials
[DE94-011420] 11 p4248 N94-36376
Effects of natural gas composition on ignition delay under diesel conditions
[DE94-006405] 11 p4276 N94-36378
Rich methane/air flames: Burning velocities, extinction limits, and flammability limit
[DE94-004340] 12 p4407 N94-36462
Bond selective chemistry beyond the adiabatic approximation
[DE94-012486] 12 p4408 N94-37095
Thermomechanical studies of tungsten heavy alloys
[AD-A280250] 12 p4417 N94-37122
A fully coupled thermal, chemical, mechanical cookoff model
[DE94-011432] 12 p4428 N94-37201
Influences of flame-vortex interactions on formation of oxides of nitrogen in curved methane-air diffusion flamelets
[DE94-005105] 12 p4409 N94-37221
Thermodynamic and kinetic aspects of surface acidity
[DE94-012351] 12 p4411 N94-37372
Effect of temperature on the electron attachment and detachment properties of c-C4F6
[DE94-012750] 12 p4518 N94-37383
Electron-transfer reactions involving two harmonic potentials with a different force constant: The Zusman approach versus the spin-boson model
[DE94-013306] 12 p4519 N94-37550
Probing flame chemistry with MBMS, theory, and modeling
[DE94-011224] 12 p4413 N94-37623
Effects of molecular transport on turbulence-chemistry interactions in a hydrogen-argon-air jet diffusion flame
[DE93-005107] 12 p4413 N94-37711

REACTION PRODUCTS

Geochemistry and cosmochemistry of fullerenes 3: Reaction of C60 and C70 with ozone 03 p0953 N94-16243
Studies of combustion reactions at the state-resolved differential cross section level
[DE93-017605] 03 p0948 N94-16462
Penetrometer compatible, fiber-optic sensor for continuous monitoring of chlorinated hydrocarbons: Field test results
[DE93-017974] 04 p1352 N94-19266
Condensed-phase thermal decomposition of TATB investigated by Atomic Force Microscopy (AFM) and Simultaneous Thermogravimetric Modulated Beam Mass Spectrometry (STMBMS)
[DE94-000396] 06 p2232 N94-23298
Metal-mullite reactions
[DE94-002038] 06 p2244 N94-23811
Dynamic response of ceramics
[AD-A275396] 08 p3214 N94-29203
Ground-based simulation of LEO environment: Investigations of a select LDEF material: FEP Teflon (trademark) 09 p3596 N94-31039
Stellar alchemy: The origin of the chemical elements
[DE94-011903] 11 p4350 N94-36229
Analytical electron microscopy examination of solid reaction products in long-term test of SRL 200 waste glasses
[DE94-005482] 12 p4411 N94-37380

REACTION RATE

U REACTION KINETICS

REACTION TIME

Evaluation of the C/EC/KC-135 ground collision avoidance system (GCAS), Study 2
[AD-A265193] 01 p0024 N94-11879
Reduction of Pu(6) with hydrogen peroxide: Effects of plutonium, peroxide, and iron concentrations and of reaction time
[DE93-013598] 02 p0564 N94-13487
A novel solid-state optical temporal analyzer with picosecond resolution and picowatt sensitivity
[AD-A266804] 03 p0986 N94-14912
Apparatus for and a method of growing thin films of elemental semiconductors
[AD-D015813] 03 p1210 N94-16487
Automated system function allocation and display format: Task information processing requirements 06 p2434 N94-24189
Endogeneous and exogenous control of visual selection: A review of the literature
[AD-A273761] 07 p2908 N94-25871
On the development of motor chunks and concurrent processing in a structured continuous keypressing task
[AD-A274153] 07 p2939 N94-27138
Strategies to sustain and enhance performance in stressful environments
[AD-A275223] 08 p3398 N94-29027

REACTION WHEELS

Low cost attitude control system reaction wheel development
[NASA-CR-191332] 02 p0540 N94-13140
A combined Earth scanner and momentum wheel for attitude determination and control of small spacecraft 06 p2208 N94-24022
The low noise momentum wheel MW-X: EM design and predicted properties 06 p2360 N94-24024
Reactive thrust cruise for a geosynchronous satellite with minimum fuel consumption 06 p2158 N94-24271
Momentum management and torque distribution 06 p2159 N94-24272
Suspension system for gimbal supported scanning payloads
[NASA-CASE-MFS-28817-1] 08 p3287 N94-29358
A gimbaled low noise momentum wheel 08 p3162 N94-29640
Overview of the Miniature Sensor Technology Integration (MSTI) spacecraft attitude control system 11 p4206 N94-35627
The control of satellites with microgravity constraints: The COMET Control System 11 p4207 N94-35632

REACTIVITY

Applications of surface science to solid lubricants
[SMC-TR-93-24] 02 p0579 N94-13903
Metastability of yttrium-oxides
[DE93-016548] 02 p0813 N94-14440
Models for reactivity
[AD-A266419] 03 p1149 N94-16554

Synthesis, reactivity, and characterization of (-hexacarbocyclic) manganese dicarbonyl complexes with sulfur and phosphorus ligands
[AD-A267592] 03 p0930 N94-17192
Surface reactivity of combustion generated soot particles
[AD-A268017] 03 p0952 N94-17532
Temperature, kinetic energy, and rotational temperature dependences for the reactions of Ar(+)(2)P3/2 with O2 and CO
[AD-A268974] 04 p1567 N94-18526
Photodissociation dynamics of cluster ions
[AD-A270296] 04 p1568 N94-18814
Application of the reactive flux formalism to study water hydrogen bond dynamics
[AD-A271824] 05 p1680 N94-20560
Surface electrochemistry of metals
[AD-A272913] 05 p1691 N94-21245
Melt-spin processing of high (Tc) oxide superconductors
[DE94-000696] 05 p2036 N94-22582
Reburning rich-lean kinetics
[PB93-220887] 06 p2232 N94-23100
Reactivity of ambident anions in the gas phase
[PB93-232189] 06 p2533 N94-23713
Fundamental and experimental studies on the catalytic combustion of methane
[PB94-112661] 06 p2233 N94-23736
Chemically sensitive interfacial force microscopy: Contact potential measurements of self-assembling monolayer films
[AD-A273135] 06 p2234 N94-24772
Reactive trace metals as indicators of subduction and ventilation processes in the ocean
[AD-A273585] 06 p2419 N94-25164
In situ spectroscopic applications to the study of rechargeable lithium batteries
[DE94-003478] 07 p2782 N94-26328
The reactivity of lithium toward non-aqueous solvents of relevance to energy storage applications as studied by surface analytical techniques
[DE94-003483] 07 p2856 N94-26464
A semiclassical reactive flux method for the calculation of condensed phase activated rate constants
[AD-A274850] 07 p3020 N94-26562
The coordination and atom transfer chemistry of titanium porphyrin complexes
[DE94-003091] 07 p2704 N94-26779
Reactivity of nitrate radical (NO3) toward organic compounds 07 p2704 N94-27387
Observation of stimulated emission from an MBE grown GaN film on sapphire
[DE94-003638] 07 p3068 N94-27724
SAFSIM theory manual: A computer program for the engineering simulation of flow systems
[DE94-005381] 08 p3270 N94-28488
Dendrite preventing separator for secondary lithium batteries
[NASA-CASE-NPO-18585-1-CU] 08 p3265 N94-29411
Direct measurement of the reactivity of NH and OH on a silicon nitride surface
[DE94-005286] 08 p3199 N94-30260
XCHEM-1D: A heat transfer/chemical kinetics computer program for multilayered reactive materials
[DE94-005072] 08 p3226 N94-30615
An overview of the Evaluation of Oxygen Interaction with Materials-third phase (EOIM-3) experiment: Space Shuttle Mission 46 09 p3596 N94-31040
Process parameter-growth environment-film property relationships for reactive sputter deposited metal (V, Nb, Zr, Y, Au) oxide, nitride, and oxynitride films
[AD-A276382] 09 p3640 N94-31258
Cloud studies seen from a physical chemist's perspective
[DE94-006059] 09 p3771 N94-31527
Phenylethynyl endcapping reagents and reactive diluents
[NASA-CASE-LAR-14796-1] 10 p4023 N94-35077
Evaluation of Oxygen Interactions with Materials 3: Mission and induced environments
[NASA-TM-109349] 11 p4236 N94-35680
Chemical reactions of chlorine on a vicinal Si(100) surface studied by ESDIAD
[AD-A279059] 11 p4236 N94-35731
Metal cluster alloys and oxides: Elucidating structural and electronic effects in governing the reactivity and catalytic role of matter in finite dimensions
[DE94-010224] 11 p4328 N94-36298
A coarse-mesh nodal method-diffusive-mesh finite difference method
[DE94-010809] 12 p4502 N94-36455
A mixture model for shock compression of porous multi-component reactive materials
[DE93-017638] 12 p4400 N94-36456
DDT modeling and shock compression experiments of porous or damaged energetic materials
[DE94-011419] 12 p4428 N94-37052
Chemical and structural characterization of nitroaromatic adducts with hemoglobins
[AD-A280533] 12 p4480 N94-37089
The effect of reactive elements on the segregation behavior and microstructure of alpha-Al2O3 scales on beta-NiAl
[DE94-012739] 12 p4418 N94-37399

REACTOR CHEMISTRY

U RADIOCHEMISTRY

REACTOR CORES

Facility for stress corrosion cracking test of irradiated material in high temperature water
[DE93-753189] 01 p0084 N94-11593
Heavy section steel irradiation experiment
[DE93-015517] 02 p0573 N94-14537
Hydrogen pickup and redistribution in alpha-annealed zircaloy-4
[DE93-018050] 05 p1689 N94-20182
A review of carbide fuel corrosion for nuclear thermal propulsion applications
[DE94-003938] 07 p2699 N94-25613
Consolidation of zircaloy-4 end crops by induction melting
[DE94-010031] 11 p4240 N94-35650
A coarse-mesh nodal method-diffusive-mesh finite difference method
[DE94-010809] 12 p4502 N94-36455

REACTOR DESIGN

A critical assembly designed to measure neutronic benchmarks in support of the Space Nuclear Thermal Propulsion program
[DE92-040974] 01 p0371 N94-10529
Looking beyond ITER: Toroidal concept improvement
[DE93-012762] 01 p0388 N94-10744
Applying design principles to fusion reactor configurations for propulsion in space
[NASA-TM-108247] 01 p0047 N94-11053
Experimental approach to the physics of the high density divertor
[DE93-009149] 01 p0391 N94-11170
Laboratory microfusion capability study
[DE93-014373] 04 p1583 N94-17912
Review Committee report on the conceptual design of the tokamak physics experiment
[DE93-018408] 04 p1588 N94-19012
Thermo-hydraulic analysis of superconducting toroidal-field magnets for the Tokamak Physics Experiment
[DE93-018096] 04 p1590 N94-19269
Materials processing and manufacturing technologies for diamond substrate multichip modules
[AD-A271484] 05 p2027 N94-21319
SPACE-R Thermionic Space Nuclear Power System: Design and Technology Demonstration Program
[DE93-013969] 05 p1670 N94-21824
A spheromak ignition experiment reusing Mirror Fusion Test Facility (MFTF) equipment
[DE94-001856] 05 p2034 N94-22050
Design and testing of a unique randomized gravity, continuous flow bioreactor 06 p2423 N94-25368
Small low mass advanced PBR's for bi-modal operation
[DE94-003201] 07 p2699 N94-25798
A robust helium-cooled shield/blanket design for ITER
[DE94-003402] 07 p3043 N94-26323
Limitations of power conversion systems under transient loads and impact on the pulsed tokamak power reactor
[DE94-003404] 07 p3043 N94-26324
The organometallic chemical vapor deposition of transition metal carbides: The use of homoleptic alkyls
[DE94-005577] 08 p3206 N94-30007
Small low mass advanced PBR's for propulsion
[DE94-005142] 08 p3497 N94-30588
Summary of particle bed reactor designs for the Space Nuclear Thermal Propulsion Program
[DE94-007434] 09 p3615 N94-32266
Overview of H-mode studies in D3-D
[DE94-007430] 09 p3891 N94-32612
Conceptual design: TFE verification program
[DE94-012469] 12 p4398 N94-37433
Two-dimensional over-all neutronics analysis of the ITER device
[DE94-718963] 12 p4530 N94-37464
TFE verification program
[DE94-009870] 12 p4398 N94-37514

REACTOR FUELS

U NUCLEAR FUELS

REACTOR MATERIALS

High heat flux components and plasma surface interactions
[DE93-008786] 01 p0385 N94-10253
The possibility of using carbon-graphite materials for microwave plasma diagnostics in large fusion devices
[DE93-621609] 01 p0066 N94-11143
Intense neutron sources for fusion materials studies
[DE93-009782] 01 p0391 N94-11171
A data base for aging of structural materials
[DE93-009714] 02 p0824 N94-13915
Estimation of strain in 1-kW primary containment vessels by microstructural examination
[DE93-013053] 02 p0573 N94-14316
Investigations of low-temperature neutron embrittlement of ferritic steels
[DE93-015460] 02 p0573 N94-14700
Space exploration initiative fuels, materials and related nuclear propulsion technologies panel
[NASA-TM-105706] 03 p0923 N94-15118
The effect of irradiation on the mechanical properties of 6061-T651 aluminum
[DE93-015825] 03 p0958 N94-16168
Using the Tritium Plasma Experiment to evaluate ITER PFC safety
[DE93-016614] 04 p1582 N94-17713
Report of the 1991 Workshop on Particle-Material Interactions for Fusion Research
[DE93-788393] 04 p1573 N94-18156
Effects of irradiation temperature on embrittlement of nuclear pressure vessel steels
[DE93-015428] 04 p1359 N94-18245
A probability method of fracture mechanics analysis for HFIR vessel
[DE93-015510] 04 p1453 N94-18246
Thermal analysis of coatings and substrate materials during a disruption in fusion reactors
[DE93-017688] 04 p1588 N94-18971
The effects of radiolysis on the corrosion and stress corrosion behavior of 316 stainless steels
[DE93-019933] 04 p1363 N94-19021
Beryllium processing technology review for applications in plasma-facing components
[DE93-018396] 04 p1363 N94-19028
Overlay welding irradiated stainless steel
[DE93-018767] 04 p1446 N94-19334
Silver lined ceramic vessel
[AD-D015917] 05 p1700 N94-20057
Hydrogen pickup and redistribution in alpha-annealed zircaloy-4
[DE93-018050] 05 p1689 N94-20182
Tensile and shear fracture behavior of fiber reinforced plastics at 77K irradiated by various radiation sources
[DE93-040280] 05 p1706 N94-21542
Issues related to mechanical properties of neutron-irradiated ceramics
[DE93-040262] 05 p1707 N94-21560
SPACE-R Thermionic Space Nuclear Power System: Design and Technology Demonstration Program
[DE93-013969] 05 p1670 N94-21824
Effects of neutron irradiation and hydrogen on ductile-brittle transition temperatures of V-Cr-Ti alloys
[DE94-001466] 06 p2240 N94-23009
Performance assessment of low pressure nuclear thermal propulsion 06 p2217 N94-23070
A review of carbide fuel corrosion for nuclear thermal propulsion applications
[DE94-003938] 07 p2699 N94-25613
Toroidal plasma beta-FLR limit in a toroidally linked mirror system
[DE94-003119] 07 p3041 N94-25792
Space-R thermionic space nuclear power system: Design and technology demonstration
[DE94-001890] 07 p2699 N94-25929
Effect of loading mode on the fracture toughness of a reduced activation ferritic/martensitic stainless steel
[DE94-004290] 07 p2732 N94-25987
Fusion Energy Advisory Committee: Advice and recommendations to the US Department of Energy in response to the charge letter of September 1, 1992
[DE93-019842] 07 p3043 N94-26428
Microstructural development in irradiated vanadium alloys
[DE94-004307] 07 p2737 N94-26556
The effect of Ti conduit on the critical current in (Nb, Ti)3Sn cable-in-conduit conductors
[DE94-701204] 07 p2788 N94-27817
Experiment and research on materials irradiated by plasma radiation
[DE94-605011] 07 p2758 N94-27845
Relationship between swelling and irradiation creep in cold-worked PCA stainless steel irradiated to approximately 178 dpa at approximately 400 C
[DE94-004368] 08 p3201 N94-28456
Radiation effects in beryllium used for plasma protection
[DE94-004599] 08 p3201 N94-28460

Proceedings of Japan-US Workshop P-196 on High Heat Flux Components and Plasma Surface Interactions for Next Devices
[DE94-701164] 08 p3503 N94-28513
Analysis of data by long-time mechanical properties of 08KH18N10T steel irradiated by neutrons
[DE94-605337] 08 p3202 N94-28551
Fatigue of carbon and low-alloy steels in LWR environments
[DE94-005116] 08 p3207 N94-30021
Development of evaluated data bank of physical properties of perspective nuclear engineering steels and alloys
[DE94-607999] 08 p3207 N94-30076
Irradiation-induced structure and property changes in tokamak plasma-facing, carbon-carbon composites
[DE94-006046] 08 p3508 N94-30365
Development of radiation resistant electrical cable insulations 08 p3223 N94-30480
Modelling erosion damage from low-energy plasma gun simulations of disruptions
[DE94-005196] 08 p3509 N94-30697
Neutronics of a D-Li neutron source: An overview
[DE94-005372] 08 p3493 N94-30893
Analysis of beam-on-target interaction in a neutron-source test facility
[DE94-005392] 09 p3863 N94-31151
Creep properties of vanadium-base alloys
[DE94-006541] 09 p3641 N94-31486
The influence of transmutation, void swelling, and flux/spectra uncertainties on the electrical properties of copper and copper alloys
[DE94-006213] 09 p3641 N94-31626
Effect of irradiation damage and helium on the swelling and structure of vanadium-base alloys
[DE94-006540] 09 p3641 N94-31666
Creep-fatigue criteria and inelastic behavior of modified 9Cr-1Mo steel at elevated temperatures
[DE94-007915] 09 p3642 N94-31918
Irradiation-assisted stress corrosion cracking of materials from commercial BWRs: Role of grain-boundary microchemistry
[DE94-006542] 09 p3643 N94-32109
Development of high temperature property database for Alloy 800H
[DE94-727589] 10 p4024 N94-33870
Weldability of Ni-Cr-W superalloy manufactured on industrial scale
[DE94-727593] 10 p4059 N94-33873
Multi-group helium and hydrogen production cross section libraries for fusion neutronics design
[DE94-727627] 10 p4140 N94-33934
Towards nuclear fusion reactors
[DE94-748680] 12 p4528 N94-37235
Examination of weldability of Ni-Cr-W superalloys
[DE94-719014] 12 p4418 N94-37385
Material and design considerations for the carbon armored ITER divertor
[DE94-737854] 12 p4530 N94-37415
Creep-fatigue interaction property of a nickel-base heat-resistant alloy Hastelloy XR in simulated HTGR helium gas environment
[DE94-737934] 12 p4418 N94-37416
Transient thermal and dynamic stresses in strongback-design blankets
[DE94-012639] 12 p4530 N94-37441
Development of intermetallic coatings for fusion power applications
[DE94-012647] 12 p4419 N94-37442
Creep properties with short period excessive loadings on a nickel-base heat-resistant alloy Hastelloy XR
[DE94-718965] 12 p4419 N94-37465
Characterization of nuclear transmutations in materials irradiated test facilities
[DE94-013309] 12 p4420 N94-37552

REACTOR PHYSICS
A critical assembly designed to measure neutronic benchmarks in support of the Space Nuclear Thermal Propulsion program
[DE92-040974] 01 p0371 N94-10529
Pre-orbital criticality safety for the NEPSTP mission
[DE94-002600] 07 p3005 N94-26802
An overview of the current status of resonance theory in reactor physics applications
[DE94-010465] 12 p4521 N94-37194

REACTOR SAFETY
Techniques, processes, and measures for software safety and reliability
[DE93-012379] 01 p0322 N94-10347
Proceedings of the Second Technical Meeting on High Temperature Gas-Cooled Reactors
[DE93-754285] 01 p0371 N94-10719
Fracture mechanics and full scale pipe break testing for the Department of Environment's New Production Reactor-Heavy Water Reactor
[DE93-005428] 01 p0187 N94-11169
GRISET certification package
[DE93-011783] 01 p0327 N94-11246
Preliminary nuclear safety assessment of the NEPST (Topaz 2) space reactor program
[DE93-012853] 02 p0551 N94-13514
A data base for aging of structural materials
[DE93-009714] 02 p0824 N94-13915
SHEAN (Simplified Human Error Analysis code) and automated THERP
[DE93-014904] 02 p0738 N94-14451
System performance modeling and analysis of a fault-tolerant, real time parallel processor
[AD-A268070] 03 p1162 N94-17551
Using the Tritium Plasma Experiment to evaluate ITER PFC safety
[DE93-016614] 04 p1582 N94-17713
Safety approaches for high power modular laser operation
[DE93-017213] 04 p1435 N94-17759
A probability method of fracture mechanics analysis for HFIR vessel
[DE93-015510] 04 p1453 N94-18246
Fluid-structure-interaction analyses of reactor vessel using improved hybrid Lagrangian Eulerian code ALICE-II
[DE93-015536] 04 p1409 N94-18248
Review Committee report on the conceptual design of the tokamak physics experiment
[DE93-018408] 04 p1588 N94-19012
HDR reactor containment fire modeling with BRI2
[VTT-PUBS-113] 07 p3031 N94-25621
Preliminary reentry safety assessment of the General Purpose Heat Source module for the Cassini mission: Aerospace Nuclear Safety Program
[DE94-001646] 07 p2699 N94-25926
Risk perspectives for Topaz 2 flight mission
[DE94-003229] 07 p2700 N94-25956
Fusion Energy Advisory Committee: Advice and recommendations to the US Department of Energy in response to the charge letter of September 1, 1992
[DE93-019842] 07 p3043 N94-26428
Mesoscale meteorological measurements characterizing complex flows
[DE94-002359] 07 p2895 N94-26761
Pre-orbital criticality safety for the NEPSTP mission
[DE94-002600] 07 p3005 N94-26802
Single specimen fracture toughness determination procedure using instrumented impact test
[PB94-132040] 08 p3316 N94-28402
Nuclear energy related research
[DE94-606286] 08 p3494 N94-28623
Risk measures in living probabilistic safety assessment
[VTT-PUBS-146] 08 p3465 N94-30154
The TOPAZ 2 space reactor response under accident conditions
[DE94-004998] 08 p3498 N94-30847
Quench detection and instrumentation for the Tokamak Physics Experiment magnets
[DE94-006656] 09 p3888 N94-31667
Integrated safety program for the Nuclear Electric Propulsion Space Test Program
[DE94-004670] 09 p3615 N94-32669
Independent safety assessment of the Topaz-2 space nuclear reactor power system
[DE94-008653] 09 p3877 N94-32879
HFE safety reviews of advanced nuclear power plant control rooms 10 p4100 N94-33613
An overview of the current status of resonance theory in reactor physics applications
[DE94-010465] 12 p4521 N94-37194
Towards nuclear fusion reactors
[DE94-748680] 12 p4528 N94-37235

REACTOR TECHNOLOGY
A critical assembly designed to measure neutronic benchmarks in support of the Space Nuclear Thermal Propulsion program
[DE92-040974] 01 p0371 N94-10529
Intense neutron sources for fusion materials studies
[DE93-009782] 01 p0391 N94-11171
Development of plastic capsule for research reactor irradiation
[DE93-753186] 01 p0372 N94-11591
Research results
[DE93-753403] 01 p0372 N94-11595
Test apparatus for ITER blanket cooling water distribution design
[DE93-753157] 02 p0795 N94-12944
Space exploration initiative fuels, materials and related nuclear propulsion technologies panel
[NASA-TM-105706] 03 p0923 N94-15118
Beryllium processing technology review for applications in plasma-facing components
[DE93-018396] 04 p1363 N94-19028
Start-up simulations of the PULSAR pulsed tokamak reactor
[DE94-002634] 06 p2552 N94-24519
Small low mass advanced PBR's for bi-modal operation
[DE94-003201] 07 p2699 N94-25798
Experimental and numerical investigation of shock wave propagation through complex geometry, gas continuous, two-phase media
[DE94-001408] 07 p2791 N94-26121
Nuclear energy related research
[DE94-606286] 08 p3494 N94-28623
Development of evaluated data bank of physical properties of perspective nuclear engineering steels and alloys
[DE94-607999] 08 p3207 N94-30076
Intercomparison of theoretical calculations of important activation cross sections for fusion reactor technology
[DE94-002642] 08 p3497 N94-30825
Data visualization for ONEDANT and TWODANT discrete ordinates codes
[DE94-005087] 10 p4105 N94-33713
Development of the static analyzer ANALYSIS/EX for FORTRAN programs
[DE94-727537] 10 p4105 N94-33868

READ-ONLY MEMORY DEVICES
NT CD-ROM
Radiation hardened nonvolatile memory for space and strategic applications
[DE93-000746] 01 p0319 N94-10146
A high speed CMOS A/D converter 05 p1767 N94-21726

READERS
Development of an automated film-reading system for ballistic ranges
[NASA-CR-194398] 02 p0650 N94-13815
The impact of report of investigation writing style on the assessment times, impressions, perceptions and preferences of adjudicators
[AD-A265748] 03 p1223 N94-15682
Harmonisation of man-machine interface experiments in the context of the development of PHARE advanced tools
[PB93-204725] 06 p2430 N94-23744

READING
Enhancing sight
[NASA-TM-109637] 03 p1221 N94-15248
The impact of report of investigation writing style on the assessment times, impressions, perceptions and preferences of adjudicators
[AD-A265748] 03 p1223 N94-15682
A multimedia adult literacy program: Combining NASA technology, instructional design theory, and authentic literacy concepts 06 p2585 N94-25384
Literacity: A multimedia adult literacy package combining NASA technology, recursive ID theory, and authentic instruction theory 09 p3924 N94-32462
Reading: Interaction with memory
[AD-A277547] 09 p3801 N94-32956

READING MACHINES
U READERS

READOUT
Method for producing a hybridization of detector array and integrated circuit for readout
[NASA-CASE-NPO-18062-1-CU] 01 p0141 N94-10656
Cryogenic readout electronics for astronomical applications 03 p0910 N94-15099
Development and test of readout electronics for optical quadrature signals
[DLR-MITT-92-11] 04 p1395 N94-17920
Progress on the design of a data push architecture for an array of optimized time tagging pixels
[DE93-041011] 06 p2307 N94-22955
Looking at Earth from space: Direct readout from environmental satellites
[NASA-EP-300] 10 p4078 N94-34268

REAGENTS
Unexpectedly rapid hydrosilation polymerization of the diallyl derivative of bisphenol A and 2,6-diallylphenol
[AD-A265832] 02 p0577 N94-12986
A commercialized, continuous flow fiber optic sensor for trichloroethylene and haloforms 08 p3502 N94-30462
Time-resolved analytical methods for liquid/solid interfaces
[DE94-008352] 09 p3637 N94-32826

REAL GASES
Issues and approach to develop validated analysis tools for hypersonic flows: One perspective 01 p0007 N94-10446
Real gas and surface transpiration effects upon swept leading edge high speed flow including transition 01 p0008 N94-10452
On the accuracy and efficiency of CFD methods in real gas hypersonics 01 p0009 N94-10462

An efficient numerical method for three-dimensional hypersonic flow
[AD-A272506] 05 p1637 N94-21411
Application of maximum entropy and irreducible cluster integrals to joint probability distributions for x ray structure determination
[PB93-224152] 06 p2559 N94-23109

REAL NUMBERS

NT INTEGERS
Bounding the Vapnik-Chervonenkis dimension of concept classes parameterized by real numbers
[DE93-011600] 01 p0331 N94-11611
Winding numbers in homotopy theory from integers to reals
[DE94-601510] 07 p2992 N94-26367

REAL TIME OPERATION

Towards real time numerical stimulation of Marangoni convection: A help for telescience microgravity experiments 01 p0102 N94-10087
Virtual sound for virtual reality
[DE93-010519] 01 p0321 N94-10291
A flexible modelling software for data acquisition
[DE93-612915] 01 p0322 N94-10484
Application of normalized gray-scale correlation
[DE93-013765] 01 p0141 N94-10521
Distributed simulation using a real-time shared memory network
[NASA-TM-106239] 01 p0319 N94-10724
Report of the IAEA Consultants' Meeting on Real-Time Nondestructive Monitoring of Wear and Corrosion Using the Thin Layer Activation Technique
[DE93-617422] 01 p0183 N94-10847
RighTime: A real time clock correcting program for MS-DOS-based computer systems 01 p0334 N94-10986
A real-time spoken-language system for interactive problem solving
[AD-A266046] 01 p0324 N94-11104
Effective software reuse in an embedded realtime system
[AD-A264993] 01 p0326 N94-11220
Application of the airborne ocean color imager for commercial fishing
[NASA-TM-103986] 01 p0231 N94-11378
Spatial light rebroadcaster architecture study
[AD-A266102] 01 p0382 N94-11421
A combustion products analyzer for contingency use during thermodegradation events on spacecraft 01 p0318 N94-11555
Teaching high-performance skills using above-real-time training
[NASA-CR-4528] 01 p0315 N94-11627
Parametric study of diffusion-enhancement networks for spatiotemporal grouping in real-time artificial vision
[AD-A265065] 01 p0331 N94-11652
Real-time tomography mooring
[AD-A264923] 01 p0289 N94-11854
Distributed real-time system design: Theoretical concepts and applications
[AD-A265199] 01 p0337 N94-11881
ISAR motion compensation using the burst derivative measure as a focal quality indicator
[AD-A265647] 01 p0138 N94-12440
Real time processing wave spectra from satellite SAR 01 p0251 N94-12506
A user appraisal of ATSR near-real-time products 01 p0252 N94-12516
Networks of real-time processes
[DE93-013049] 01 p0338 N94-12597
An integrated approach to total end-to-end quality control of ocean data in the real-time environment 01 p0211 N94-12662
Novel mass spectrometric instrument for gaseous and particulate characterization and monitoring
[DE93-014093] 01 p0272 N94-12783
Laser-induced fluorescence over optical fibers for real time in situ measurement of petroleum hydrocarbons in seawater
[AD-A265106] 02 p0790 N94-12863
Real time radiography of Titan 4 booster
[DE93-012450] 02 p0548 N94-12911
Development of a portable multispectral thermal infrared camera
[NASA-CR-191340] 02 p0648 N94-13176
Thermal Expert System (TEXSYS): Systems automony demonstration project, volume 1. Overview
[NASA-TM-102877-VOL-1] 02 p0538 N94-13201
Error analysis of real time and post processed or bit determination of GFO using GPS tracking
[NASA-CR-193646] 02 p0512 N94-13238
The silent step in time
[CWI-CS-R9221] 02 p0768 N94-13496
Weather forecasting support for AASE-2
[NASA-CR-194342] 02 p0721 N94-13675
Communications and control for electric power systems: Power flow classification for static security assessment
[NASA-CR-194512] 02 p0624 N94-13948
Portable acoustic wave sensor systems for real-time monitoring of volatile organic compounds
[DE93-013753] 02 p0582 N94-14511
Real-time dynamic simulation of the Cassini spacecraft using DARTS. Part 2: Parallel/vectorized real-time implementation 02 p0680 N94-14639
Design and control of a macro-micro robot for precise force applications 02 p0682 N94-14651
Identification of continuous-time dynamical systems: Neural network based algorithms and parallel implementation
[DE93-014427] 02 p0766 N94-14737
Mathematic methods and algorithms for real-time applications
[AD-A266776] 02 p0771 N94-14789
The MADONA experiments (Meteorology and Diffusion Over Non-uniform Areas): High-resolution in-plume concentration fluctuations measurements using lidar remote sensing technique
[AD-A267711] 03 p1105 N94-14938
Fuzzy inverse kinematic mapping: Rule generation, efficiency, and implementation
[AD-A266967] 03 p1163 N94-14954
Visualization of solidification front phenomena
[NASA-CR-193838] 03 p0976 N94-15006
Evaluation of ALSYS 037 Ada Compiler
[AD-A266972] 03 p1143 N94-15110
Short term weather forecasting in real time in a base weather station setting
[AD-A266872] 03 p1105 N94-15142
Overview of Enhanced Data Stream Array Processor (EDSAP)
[AD-A266986] 03 p1158 N94-15492
Hidden Markov model approach to skill learning and its application to telerobotics
[AD-A266989] 03 p1164 N94-15502
Upgrading NASA/DOSE laser ranging system control computers 03 p0918 N94-15595
HP upgrade operational streamlining 03 p0918 N94-15596
Complexity analysis of real-time reinforcement learning applied to finding shortest paths in deterministic domains
[AD-A266636] 03 p1131 N94-15742
Adaptive weld control for high-integrity welding applications
[TABES PAPER 93-604] 03 p1049 N94-16140
Real-time adaptive neural network data processing
[TABES PAPER 93-660] 03 p1054 N94-16155
Visually guided touching and manual tracking
[TR-412] 03 p1166 N94-16581
Efficient scheduling of real-time compute-intensive periodic graphs on large grain data flow multiprocessor
[AD-A267444] 03 p1141 N94-17030
Causality-preserving timestamps in distributed programs
[AD-A267534] 03 p1153 N94-17118
ARPA unmanned ground vehicle stereo vision program at Teleos Research
[AD-A267632] 03 p1167 N94-17202
Module interconnection frameworks for a real-time spreadsheet
[AD-A267317] 03 p1153 N94-17220
Module interconnection frameworks for a real-time spreadsheet
[AD-A267752] 03 p1153 N94-17231
Image accuracy and representational enhancement through low-level, multi-sensor integration techniques
[DE93-014888] 03 p1167 N94-17287
Estimating task execution delay in a real-time system via static source code analysis
[AD-A267496] 03 p1161 N94-17367
Real time system for practical acoustic monitoring of global ocean temperature
[AD-A267868] 03 p1113 N94-17391
Femtosecond carrier processes in compound semiconductors and real time signal processing
[AD-A268122] 03 p1005 N94-17519
System performance modeling and analysis of a fault-tolerant, real time parallel processor
[AD-A268070] 03 p1162 N94-17551
Magnetostrictive actuators for human sensory feedback
[AD-A269266] 04 p1511 N94-17841
An object-oriented environment for computer vision and pattern recognition
[DE93-017098] 04 p1517 N94-17867
A structured approach for modeling, analyzing and simulating real-time control systems
[REPT-93-044] 04 p1539 N94-17916
Single phase dynamic CMOS PLA using charge sharing technique 04 p1397 N94-18341
VHF air/ground communications for air traffic control: A decision tree approach to system innovations, volume 2
[AD-A268632] 04 p1386 N94-18495
Distributed Computing Design System (DCDS)
[AD-A270435] 04 p1534 N94-18509
SERCAA cloud analysis integration: Design concepts and interaction with cloud forecast models
[AD-A269104] 04 p1492 N94-18637
The development of a course sequence in real-time systems design
[AD-A269459] 04 p1522 N94-18726
Atlas of SSM/I satellite ice concentration interpolated to operational ice model domains of the Arctic for 1992
[AD-A270306] 04 p1499 N94-18727
ControlShell: A real-time software framework
[AD-A269172] 04 p1523 N94-18879
Adaptive path planning: Algorithm and analysis
[DE93-008348] 04 p1523 N94-18926
Template based low data rate speech encoder
[AD-A270900] 04 p1392 N94-19748
A real-time spoken-language system for interactive problem-solving, combining linguistic and statistical technology for improved spoken language understanding
[AD-A270901] 04 p1392 N94-19749
Improved HF data network simulator, software user's manual, volume 2
[AD-A270954] 04 p1393 N94-19753
A software architecture for the construction and management of real-time virtual worlds
[AD-A271465] 05 p1904 N94-20091
Simulated real-time intercomparison of hydrological models
[WMO-779] 05 p1867 N94-21070
An optically-assisted 3-D cellular array machine
[AD-A272683] 05 p1987 N94-21163
A formulation of quantum statistical mechanics based on the Feynman path centroid density 2 dynamical properties
[AD-A272698] 05 p2037 N94-21166
Fault tolerant real-time systems
[AD-A272878] 05 p1899 N94-21195
Real-time fault tolerant computer systems
[AD-A272909] 05 p1899 N94-21230
Developing a space network interface simulator: The NTS approach 05 p1933 N94-21343
Analysis of multigrid methods on massively parallel computers: Architectural implications 05 p1938 N94-21468
A VLSI implementation of DCT using pass transistor technology 05 p1767 N94-21725
A real time correlator architecture using distributed arithmetic principles 05 p1768 N94-21734
Particle image velocimetry
[DE93-040657] 05 p1804 N94-21748
Optimization and control of a small angle ion source using an adaptive neural network controller
[DE93-040063] 05 p1946 N94-21845
The Board on Earth sciences and resources
[DE94-000745] 05 p1859 N94-22018
A neural network approach to the maximum flow problem 05 p1783 N94-22183
A Hopfield neural net for discrete Fourier transform calculation 05 p1783 N94-22184
A real-time infrared image processing testbed 05 p1790 N94-22227
Second Annual Conference on Astronomical Data Analysis Software and Systems. Abstracts
[NASA-TM-108245] 05 p2057 N94-22438
How to handle 6GBytes a night and not get swamped 05 p2058 N94-22444
VETA x ray data acquisition and control system 05 p2047 N94-22455
The data acquisition system for the Anglo-Australian Observatory 2-degree field project 05 p2048 N94-22529
The VLBA correlator: Real-time in the distributed era 05 p2049 N94-22547
Solar full-disk magnetic field image receiving system and observation software 05 p2079 N94-22552
A novel process monitoring and control system based on a neural manufacturing concept
[DE94-001516] 06 p2471 N94-23011
Urban/rural application of weather radar for flow forecasting. Proceedings of the Informal CEc -Workshop
[PB93-220135] 06 p2407 N94-23129
CAMAC throughput of a new RISC-based data acquisition computer at the DIII-D tokamak
[DE94-001113] 06 p2550 N94-23182
Towards real-time stereovision systems for planetary missions 06 p2370 N94-23422
Mission planning for Shuttle Imaging Radar-C (SIR-C) with a real-time interactive planning software 06 p2305 N94-23842
SAMPEX payload operation control center implementation 06 p2197 N94-23843

PILOT: An intelligent distributed operations support system 06 p2508 N94-23895
Combining real-time monitoring and knowledge-based analysis in MARVEL 06 p2477 N94-23900
Real-time on-board orbit determination with DORIS 06 p2196 N94-23919
A real-time navigation monitoring expert system for the Space Shuttle Mission Control Center 06 p2202 N94-23921
XRTD: An X-Windows based, real-time radiometric display and analysis system 06 p2305 N94-23922
Kalman filtering applied to real-time monitoring of apogee maneuvers 06 p2196 N94-23923
SIMSAT: An object oriented architecture for real-time satellite simulation 06 p2197 N94-23940
Real-time holographic endoscopy [ISL-CO-203/92] 06 p2343 N94-24054
Making intelligent systems team players: Additional case studies [NASA-TM-104786] 06 p2473 N94-24068
Doppler global velocimetry: Development of a flight research instrumentation system for application to non-intrusive measurements of the flow field [NASA-CR-191490] 06 p2344 N94-24360
Real-time process logic [PB94-101441] 06 p2446 N94-24540
ASR-9 microburst detection algorithm [AD-A273591] 06 p2415 N94-24850
Performance measurements of the multimedia testbed on Mach 3.0: Experience writing real-time device drivers, servers, and applications [AD-A273600] 06 p2460 N94-24932
Reengineering real-time software systems [AD-A273408] 06 p2461 N94-25074
On chain coding of line drawings [ISBN-9-06-275778-2] 06 p2462 N94-25252
Non-invasive optical detection of glucose in cell culture nutrient medium 06 p2422 N94-25357
Proceedings of the 12th International Congress: Corrosion Control for Low-Cost Reliability. Volume 6: Electric Power Industry [AD-A273668] 06 p2250 N94-25408
Expert system rule-base evaluation using real-time parallel processing [AD-A273701] 06 p2469 N94-25454
Module interconnection frameworks for a real-time spreadsheet [AD-A273653] 07 p2956 N94-25588
Distributing functionality in the drift scan camera system [DE94-003640] 07 p2809 N94-25599
Characteristics and control response of the TOPAZ 2 reactor system real-time dynamic simulator [DE94-003788] 07 p2699 N94-25600
Design of dynamically reconfigurable real-time software using port-based objects [NASA-CR-195178] 07 p2958 N94-25777
The use of ASN.1 and XDR for data representation in real-time distributed systems [AD-A273769] 07 p2959 N94-25855
Real-time 3-D pose estimation using a high-speed range sensor [AD-A273873] 07 p2809 N94-25967
Real-time tracking with a 3D-flow processor array [DE94-003981] 07 p2980 N94-25984
Coordinated scheduling for dynamic real-time systems [NASA-CR-195231] 07 p3093 N94-26206
Studies of thin-film growth, adsorption, and oxidation by in situ, real-time, and ex situ ion beam analysis [DE94-002907] 07 p3055 N94-26275
A multitasking behavioral control system for the Robotic All-Terrain Lunar Exploration Rover (RATLER) 07 p2685 N94-26292
NPSNET-4: A real-time, 3D distributed interactive virtual world [AD-A274942] 07 p2961 N94-26298
Differential global positioning system for the surface-towed ordnance locating system: Testing, results, and user's guide [DE94-002980] 07 p2664 N94-26309
Development of real-time pulse shaping technology in solid-state lasers [DE93-633438] 07 p2817 N94-26403
Automated system for gas detectors providing with binary mixtures [DE93-634192] 07 p2715 N94-26406
Adaptive path planning in changing environments [DE94-003269] 07 p2985 N94-26462
Real-Time Embedded Processing for Space Applications [ISBN-2-85428-335-X] 07 p2948 N94-26713
Real time avionics constraints: Silicon solutions 07 p2949 N94-26717
Fault tolerant real-time processing system for space use 07 p2949 N94-26720
A complete version of the Ada tasking coprocessor 07 p2950 N94-26721
The Ariane 5 data management system 07 p2950 N94-26724
PRONAOS flight software: A real-time application for a balloonborne scientific gondola 07 p2950 N94-26725
MATRA Marconi Space: The Silex on-board processor and on-board software 07 p2950 N94-26726
Scheduling tasks with unpredictable timing parameters in hard real-time systems 07 p2951 N94-26728
Standardize Ada hard real-time services? 07 p2951 N94-26729
Ada multiple-programming for hard real time applications in space systems 07 p2951 N94-26730
Implementing hard real-time systems: A case study 07 p2951 N94-26731
Tool for performance analysis and off-line prediction of timing behaviour 07 p2952 N94-26732
A real-time executive implementing priority inheritance protocols 07 p2952 N94-26733
Scheduling approaches with Ada 07 p2952 N94-26734
Fault-tolerant scheduling in distributed critical real-time systems 07 p2952 N94-26735
Early real-time performance measurements on the Columbus processor system 07 p2952 N94-26736
Test of onboard real time applications (LICE (tm)) 07 p2952 N94-26737
Verification and validation of the on-board software real time requirements 07 p2953 N94-26739
Formal methods for dependable real-time systems 07 p2953 N94-26740
Developing with Ada using HOOD design methodology 07 p2953 N94-26741
Use of HOOD coupled to real time monitors 07 p2953 N94-26742
Specification performance optimization and executive generation for onboard multiprocessor real time application with SynDEx 07 p2954 N94-26745
A preliminary method for atmospheric soundings in real time using satellite and ground-based remotely sensed data [AD-A274381] 07 p2880 N94-26828
Hard real-time reliable multicast in the DEDOS system [PB94-126745] 07 p2966 N94-26920
Interactive control of a parallel simulation from a remote graphics workstation [AD-A274217] 07 p2981 N94-27070
Technology transition push. Part 1: A case study of rate monotonic analysis [AD-A275616] 08 p3407 N94-28633
The bootstrapped algorithm: A fast algorithm for blind signal separation [AD-A275759] 08 p3408 N94-28760
Information presentation for expert systems in future fighter aircraft [AD-A275126] 08 p3149 N94-29005
NPSNET: Integration of Distributed Interactive Simulation (DIS) protocol for communication architecture and information interchange [AD-A275061] 08 p3530 N94-29139
A common Ada run-time system for avionics software 08 p3150 N94-29331
Design of a thinwire real-time multiprocessor operating system 08 p3415 N94-29333
Validation and test of complex weapon systems 08 p3150 N94-29336
GPS/GNSS for ATM 08 p3138 N94-29565
ACCS Surveillance Exploratory Prototype (ASEP) 08 p3138 N94-29566
Formal specification and verification of real-time sequential control systems [AD-A275776] 08 p3419 N94-29678
Hypra/TR: A tuple oriented recovery method for a continuously available distributed DBMS on a shared nothing multi-computer [PB94-141264] 08 p3533 N94-29921
Novel mass spectrometric instrument for gaseous and particulate characterization and monitoring [DE94-005896] 08 p3349 N94-30047
Computational balance in real-time cyclic spectral analysis [DE94-005091] 08 p3432 N94-30100
Common spaceborne multicomputer operating system and development environment [NASA-TM-109092] 08 p3422 N94-30197
Sensing the gas metal arc welding process 08 p3314 N94-30444
ARK: Autonomous mobile robot in an industrial environment [AIAA PAPER 94-1177-CP] 08 p3439 N94-30529
A performance analysis method for distributed real-time robotic systems: A case study of remote teleoperation [AIAA PAPER 94-1212-CP] 08 p3445 N94-30563
Predictive sufficiency and the use of stored internal state [AIAA PAPER 94-1213-CP] 08 p3445 N94-30564
The use of the AOA TTR-4P GPS receiver in operation at the BIPM for real-time restitution of GPS time 08 p3144 N94-30651
A real-time prediction of UTC 08 p3470 N94-30654
'Real time' and the NLR aerodynamic facilities [AD-B173626] 08 p3158 N94-30856
Results of real-time testing and demonstration of the US Army Corps of Engineers real-time on-the-fly positioning system [AD-A276160] 09 p3576 N94-31080
Scheduling techniques for multiple processor systems in real-time environments [AD-A276149] 09 p3824 N94-31249
New and emerging techniques for imaging surfaces [AD-A276497] 09 p3878 N94-31262
Algorithms and structures for real-time signal processing [AD-A276101] 09 p3810 N94-31277
ControlShell: A real-time software framework [AD-A276481] 09 p3811 N94-31475
A neural network methodology for engineering applications: The learning control of robotic systems [RR-480] 09 p3830 N94-31500
The future of open architecture process control systems [DE94-006163] 09 p3830 N94-31623
The development and testing of a backscatter absorption gas imaging (BAGI) system designed to image at a range of 300 m [DE94-006192] 09 p3675 N94-31761
A theory of distributed time [AD-A276631] 09 p3815 N94-31994
Theoretical basis for state vector comparison, relative position display, and relative position/rendezvous prediction [AD-A277216] 09 p3608 N94-32020
Gamma-ray optical counterpart search experiment (GROCSE) [DE94-007124] 09 p3955 N94-32129
Real time character recognition for F-111C video tape records [AD-A277061] 09 p3580 N94-32263
Communication networks for autonomous mobile robot computer architectures and distributed real-time computing 09 p3680 N94-32310
Photothermal laser deflection, an innovative technique to measure particles in exhausts [AD-A277151] 09 p3718 N94-32366
Empirical modeling for intelligent, real-time manufacture control 09 p3839 N94-32424
New approaches for real time decision support systems 09 p3915 N94-32426
Construction of a parallel processor for simulating manipulators and other mechanical systems [NASA-CR-191327] 09 p3826 N94-32482
Model-based reconfiguration: Diagnosis and recovery [NASA-CR-4596] 09 p3820 N94-32776
A multitasking behavioral control system for the Robotic All Terrain Lunar Exploration Rover (RATLER) [DE94-007293] 09 p3835 N94-32787
High frequency active auroral research program (HAARP) imager [AD-A277469] 09 p3775 N94-32999
Theory and application of image enhancement [AD-A277896] 09 p3821 N94-33031
Real-time centimeter positioning with GPS: A system developed by the US Army Corps of Engineers [AD-A278152] 09 p3577 N94-33095
Real-time sensor data validation [NASA-CR-195295] 09 p3616 N94-33099
An experimental study of pilot/vehicle dynamics using a tilt rotor flying machine [AD-A277516] 09 p3805 N94-33349
The StarLite Project: Prototyping real-time software [AD-A278201] 10 p4103 N94-33374
Assembly of a neural analog computer, phase 2 [AD-A278192] 10 p4103 N94-33402
Ultraviolet Absorption Spectrometry (UVAS) and Liquid Atomic Emission Spectrometry (LAES) for oceanographic analysis systems [AD-A278263] 10 p4091 N94-33413
Systems design factors: The essential ingredients of system design, version 0.4 [AD-A277702] 10 p4031 N94-33439
Using task analysis to understand the Data System Operations Team 10 p4159 N94-33614
Fusion interfaces for tactical environments: An application of virtual reality technology 10 p4100 N94-33619
Quantitative 3-D imaging topogrammetry for telemedicine applications 10 p4096 N94-33645

The Portable Dynamic Fundus Instrument: Uses in telemedicine and research 10 p4096 N94-33647
A volatile organic analyzer for Space Station: Description and evaluation of a gas chromatography/ ion mobility 10 p4102 N94-33661
A self-organizing neural network architecture for auditory and speech perception with applications to acoustic and other temporal prediction problems
[AD-A277526] 10 p4095 N94-33708
Predictable and adaptable complex real-time systems
[AD-A277827] 10 p4105 N94-33830
A CMOS VLSI IC for real-time opto-electronic two-dimensional histogram generation
[AD-A277910] 10 p4040 N94-33921
Ground vehicle control at NIST: From teleoperation to autonomy 10 p4127 N94-34037
Acting to gain information: Real-time reasoning meets real-time perception 10 p4160 N94-34042
Filtering as a reasoning-control strategy: An experimental assessment 10 p4127 N94-34053
Development of a machine vision fire detection system
[AD-A278208] 10 p4032 N94-34084
Constraints and system primitives in achieving multilevel security in real time distributed system environment
[AD-A278407] 10 p4107 N94-34086
Projection in temporal logic programming
[PB94-148814] 10 p4108 N94-34123
The design and realization of a real-time multitasking control system by using AMX multitasking executive 10 p4118 N94-34343
Dimensional measurement to subpixel value 10 p4110 N94-34353
A real-time 2-D composite damage monitoring system employing neural network 10 p4074 N94-34355
A method available for processing the signal of thermocouples by computer 10 p4057 N94-34360
A format for storing and managing multiple level of detail terrain for simulated environments
[AD-A278497] 10 p4159 N94-34377
Space environment laboratory in review, 1993
[PB94-153004] 10 p4187 N94-34946
Modeling heterogeneous processor scheduling for real time systems 10 p4124 N94-35053
Vista goes online: Decision-analytic systems for real-time decision-making in mission control 10 p4125 N94-35063
ISTAR: Intelligent System for Telemetry Analysis in Real-time 10 p4013 N94-35070
Adjustable control station with movable monitors and cameras for viewing systems in robotics and teleoperations
[NASA-CASE-NPO-17837-1-CU] 11 p4332 N94-35384
Software architecture standard for simulation virtual machine, version 2.0
[NASA-CR-188291] 11 p4301 N94-35443
The rel/REL: A family of reliable multicast protocols for distributed real-time systems
[PB94-167830] 11 p4310 N94-35535
Correlator data analysis for the array feed compensation system 11 p4253 N94-35553
The real-time display of interferometry data for Goldstone radar astronomy data acquisition 11 p4255 N94-35560
A new presentation of complex voltage data for Goldstone radar astronomy 11 p4255 N94-35561
Operational support for Upper Atmosphere Research Satellite (UARS) attitude sensors 11 p4204 N94-35617
TDRSS Onboard Navigation System (TONS) flight qualification experiment 11 p4206 N94-35625
Advantages of estimating rate corrections during dynamic propagation of spacecraft rates: Applications to real-time attitude determination of SAMPEX 11 p4209 N94-35642
Task allocation for parallel real-time execution
[AD-A278789] 11 p4310 N94-35653
A determinizable class of timed automata
[AD-A278858] 11 p4317 N94-35743
A taxonomy of coordination mechanisms used in real-time software based on domain analysis
[AD-A279014] 11 p4304 N94-35794
NAVSPACECOM space surveillance sensor system digital signal processing receiver. Volume 3: Operating system functions
[AD-A278839] 11 p4212 N94-35799
NAVSPACECOM space surveillance sensor system digital signal processing receiver. Volume 4: Hardware interfaces
[AD-A278845] 11 p4212 N94-35801
Task and environment-sensitive tracking
[AD-A278846] 11 p4312 N94-35802
Doppler weather radar studies of precipitation systems
[AD-A279417] 11 p4295 N94-36262
Interfacing the RAP system to real-time control, version 1
[AD-A278725] 11 p4312 N94-36295
Subgrouped real time recurrent learning neural networks
[AD-A280618] 12 p4500 N94-37043
Design of the divertor Thomson scattering system on D3-D
[DE94-012672] 12 p4527 N94-37081
Long-range mesoscale modeling of pollutant transport for the European Tracer EXperiment (ETEX)
[DE94-010820] 12 p4465 N94-37093
Efficient contact determination between geometric models
[AD-A280244] 12 p4494 N94-37120
VHF adaptive antenna development task
[AD-A280320] 12 p4434 N94-37127
Interaction effects of cracks, flaws and damage in ceramic
[AD-A280368] 12 p4423 N94-37181
Time-of-flight pulsed ion beam surface analysis as a means of in situ, real-time characterization of the growth of ferro-electric and conductive oxide heterostructures
[DE94-012628] 12 p4517 N94-37249
Interactive large screen: A multi-mode dialogue tool for future cockpits 12 p4484 N94-37266
A non-intrusive way to measure point-of-gaze 12 p4484 N94-37272
Operator gaze position control interfaces: Investigation of psychophysical and operational parameters 12 p4485 N94-37273
Low cost software-based rendering and stereoscopic interfaces for teleoperation and virtual reality 12 p4486 N94-37279
Chemical recognition software
[DE94-012918] 12 p4495 N94-37496
Advanced information processing system: Authentication protocols for network communication
[NASA-CR-194923] 12 p4498 N94-37500
Techniques for real-time parallel processing: Sensor processing case studies
[AD-A280633] 12 p4499 N94-37760

REAL VARIABLES

NT ABEL FUNCTION
NT ASYMPTOTES
NT ASYMPTOTIC SERIES
NT BESSEL FUNCTIONS
NT BETHE-SALPETER EQUATION
NT BIHARMONIC EQUATIONS
NT BINARY INTEGRATION
NT BLASIUS EQUATION
NT BURGER EQUATION
NT CALCULUS OF VARIATIONS
NT CAUCHY-RIEMANN EQUATIONS
NT COMPOSITE FUNCTIONS
NT COSINE SERIES
NT CUBIC EQUATIONS
NT DELTA FUNCTION
NT DIFFERENTIAL EQUATIONS
NT DUFFING DIFFERENTIAL EQUATION
NT EINSTEIN EQUATIONS
NT ELLIPTIC DIFFERENTIAL EQUATIONS
NT EXISTENCE THEOREMS
NT FALKNER-SKAN EQUATION
NT FOKKER-PLANCK EQUATION
NT FOURIER SERIES
NT FOURIER-BESSEL TRANSFORMATIONS
NT FUNCTIONAL INTEGRATION
NT GAUSS EQUATION
NT GREEN'S FUNCTIONS
NT HANKEL FUNCTIONS
NT HELMHOLTZ VORTICITY EQUATION
NT HYPERBOLIC DIFFERENTIAL EQUATIONS
NT HYPERBOLIC FUNCTIONS
NT HYPERPLANES
NT INTEGRAL CALCULUS
NT J INTEGRAL
NT JACOBI INTEGRAL
NT JACOBI MATRIX METHOD
NT KERNEL FUNCTIONS
NT LEBESGUE THEOREM
NT LIAPUNOV FUNCTIONS
NT LIMITS (MATHEMATICS)
NT LINEAR EQUATIONS
NT LINEAR EVOLUTION EQUATIONS
NT LIOUVILLE EQUATIONS
NT LIPSCHITZ CONDITION
NT MAXIMA
NT MEASURE AND INTEGRATION
NT MINIMA
NT NEUMANN PROBLEM
NT NONLINEAR EQUATIONS
NT NONLINEAR EVOLUTION EQUATIONS
NT NUMERICAL INTEGRATION
NT PADE APPROXIMATION
NT PARABOLIC DIFFERENTIAL EQUATIONS
NT PARTIAL DIFFERENTIAL EQUATIONS
NT PERIODIC FUNCTIONS
NT POISSON EQUATION
NT POWER SERIES
NT PRONY SERIES
NT QUADRATIC EQUATIONS
NT QUARTIC EQUATIONS
NT RICCATI EQUATION
NT RUNGE-KUTTA METHOD
NT SERIES (MATHEMATICS)
NT SINE SERIES
NT STIELTJES INTEGRAL
NT TAYLOR SERIES
NT TRIGONOMETRIC FUNCTIONS
NT VECTOR ANALYSIS
NT VLASOV EQUATIONS
NT VORTICITY
NT VORTICITY EQUATIONS
NT WEIERSTRASS FUNCTIONS
NT WEIGHTING FUNCTIONS

REARWARD FACING STEPS

U BACKWARD FACING STEPS

REATTACHED FLOW

A comparative study of computational solutions to flow over a backward-facing step 06 p2326 N94-23670
Computation of turbulent flows over backward and forward-facing steps using a near-wall Reynolds stress model 06 p2172 N94-24145
An experimental study of the flowfield on a semispan rectangular wing with a simulated glaze ice accretion 08 p3130 N94-29674

REB

U RELATIVISTIC ELECTRON BEAMS

RECEIVERS

NT RADAR RECEIVERS
NT RADIO RECEIVERS
NT RADIOTELEPHONES
NT SUPERHETERODYNE RECEIVERS
NT TRANSMITTER RECEIVERS
Diagnostic complex for the space-time analysis of energy and current of pulsed relativistic particles
[DE93-620980] 01 p0362 N94-10649
Progress on GPS standardization 01 p0024 N94-10965
Workshop summary: Receivers for laser power beaming 01 p0054 N94-11419
Airborne optical tracking control system design study
[DE93-009515] 01 p0382 N94-11662
Studies of electrostatic waves and VLF-wave particle interaction in the ionosphere
[AD-A266013] 01 p0278 N94-12392
Adaptive Signal Processing Testbed
[DSIS-93-00258] 02 p0604 N94-13869
Calibration of the receiver channel for the GOPEX precursor experiments 02 p0610 N94-14387
Preparation and properties of Nb/Al SIS and SIN junctions for millimeter and submillimeter radioastronomical receivers 03 p0907 N94-15078
Streak camera based SLR receiver for two color atmospheric measurements 03 p0914 N94-15573
The new MTLRS-1 receiving system 03 p0877 N94-15611
Optical attenuation mechanism upgrades, MOBLAS, and TLRS systems 03 p0922 N94-15622
The third generation SLR station Potsdam no. 7836 03 p0877 N94-15623
Planned LMSS propagation experiment using ACTS: Preliminary antenna pointing results during mobile operations 03 p0995 N94-16041
OETC optical backplane bus testbed. IBM tasks: Receiver OEIC and link simulation tools and analysis
[AD-A266198] 03 p1191 N94-16128
Notes on the use of Dempster-Shafer and fuzzy reasoning to fuse identity attribute data
[AD-A267426] 03 p1004 N94-17309
Development of a selective volumetric receiver for central receiver systems: Investigation of parameters and exergetic evaluation
[DLR-FB-93-05] 04 p1465 N94-18089
Advanced optical fiber communication systems
[AD-A269120] 04 p1577 N94-18254
Photorefractive receiver study
[AD-A269352] 04 p1577 N94-18302
Testing and evaluation of large-area heliostats for solar thermal applications
[DE93-018509] 04 p1467 N94-18520
The use of velocity spectra for stacking receiver functions with application to IRIS/IDA stations OBNINSK (OBN) and ARTI (ARU), Russia
[AD-A269087] 04 p1483 N94-18717
Quasi-optical transponder using FET's and patch antennas
[AD-A271339] 04 p1407 N94-19584

An investigation into the integration of meter-level range and millimeter-level phase data using a multimode stimulation for optimal filter estimation software package
[AD-A267955] 05 p1751 N94-20483
Spread spectrum random access networks
[AD-A272280] 05 p1737 N94-20585
QPPM receiver for free-space laser communications
[NASA-TM-106424] 05 p1741 N94-21567
Transient acoustic wave modeling: Higher-order WKBJ asymptotics and symbolical manipulation (revised)
[PB93-215432] 05 p1969 N94-22262
Solar full-disk magnetic field image receiving system and observation software 05 p2079 N94-22552
Systems implications of L-band fade data statistics for LEO mobile systems 06 p2284 N94-22799
Low cost coherent demodulation for mobile satellite terminals 06 p2284 N94-22803
An optical ASK and FSK phase diversity transmission system
[EUT-92-E-268] 06 p2542 N94-23171
Integration and test of high-speed transmitter electronics for free-space laser communications
[NASA-TM-106295] 06 p2295 N94-24101
Effects of atmospheric variations on acoustic system performance 06 p2527 N94-24211
Comparison of measured and predicted pure tone propagation levels from JAPE-1: An evaluation of the performance of ASOPRAT 06 p2527 N94-24212
Simulation of adjacent channel interference in a UHF satellite system
[AD-A273147] 06 p2299 N94-24669
Measurements and modeling of multitone, low-frequency acoustic data from the Arraial do Cabo range
[AD-A273406] 06 p2530 N94-25073
A current evaluation of the digital beamforming testbed at Rome Laboratory
[AD-A274311] 07 p3032 N94-26881
A compact 150 GHz SIS receiver cooled by 4 K GM refrigerator
[REPT-36] 07 p2776 N94-27340
A simulation of GPS and differential GPS sensors 07 p2666 N94-27918
Output statistics of the SALFAS FM normalizer Smoothing/Prediction function
[AD-A275758] 08 p3463 N94-28759
Performance and durability of high emittance heat receiver surfaces for solar dynamic power systems
[NASA-TM-106549] 08 p3172 N94-28834
An analysis of carrier phase jitter in an MPSK receiver utilizing map estimation
[NASA-CR-195806] 08 p3164 N94-29880
An absolute measurement of the cosmic background radiation temperature at 1.4 GHz 08 p3553 N94-30351
Time and position accuracy using codeless GPS 08 p3144 N94-30650
The use of the AOA TTR-4P GPS receiver in operation at the BIPM for real-time restitution of GPS time 08 p3144 N94-30651
Development of a frequency-domain electromagnetic scattering measurement system
[AD-A276738] 09 p3678 N94-32179
Operational experience and evaluation of a dual-element stretched-membrane heliostat
[DE94-008827] 09 p3763 N94-32965
Pilot GPS/LORAN receiver programming performance: A laboratory evaluation
[AD-A278258] 10 p3988 N94-33412
Processing, fabrication, and demonstration of HTS integrated microwave circuits
[AD-A277684] 10 p4040 N94-33893
Detail design of a 10.4-m stretched-membrane dish
[DE94-009462] 10 p4079 N94-34167
A quality control package for the Digisonde Drift Analysis (DDA)
[AD-A278663] 11 p4289 N94-35578
High-sensitivity receiver for increasing multiplicity of measurement axes of Zygo's Heterodyne interferometer
[DE94-009916] 11 p4333 N94-35818
Receiver design, performance analysis, and evaluation for space-borne laser altimeters and space-to-space laser ranging systems
[NASA-CR-194747] 12 p4397 N94-36988
NRL HF propagation measurements between Guadeloupe and Providenciales during the CRRES exercises
[DE94-012078] 12 p4435 N94-37393
Study on the measurement uncertainty of noise properties of a millimeter wave amplifier
[PB94-170917] 12 p4510 N94-37632

RECEIVING SYSTEMS
U RECEIVERS

RECEPTACLES (CONTAINERS)
U CONTAINERS

RECEPTION DIVERSITY
Spatial and frequency diversity in lidar systems
[AD-A266192] 03 p1039 N94-16124
Variable-permittivity linear inverse problem for the H(sub z)-polarized case 05 p1719 N94-20408
Diversity reception for advanced multi-satellite networks: A CDMA approach 06 p2286 N94-22816
Isolated and coupled superquadric loop antennas for mobile communications applications 06 p2289 N94-22834

RECEPTORS (PHYSIOLOGY)
NT BARORECEPTORS
NT CHEMORECEPTORS
NT OTOLITH ORGANS
NT PHOTORECEPTORS
NT PROPRIOCEPTORS
Probability of alamethicin conductance states varies with nonlamellar tendency of bilayer phospholipids
[AD-A264957] 01 p0301 N94-11648
Modified aequorin shows increased bioluminescence activity
[AD-A268774] 04 p1347 N94-18185
Intracellular physiology of the rat suprachiasmatic nucleus: Electrical properties, neurotransmission and effects of neuromodulators
[AD-A268829] 04 p1505 N94-18538
Annals of the Research Inst. of Environmental Medicine, Nagoya Univ., volume 44
[REPT-44-VOL-44] 07 p2911 N94-27442
Effect of PGE2 receptor agonists butaprost, M and B 28767 and an antagonist AH 6809 on the BK response of visceral polymodal receptors 07 p2906 N94-27494
Excitation of cutaneous polymodal receptor induced by sympathetic stimulation in adjuvant-induced arthritis rats 07 p2906 N94-27495
Influence of mechanical stimulation on inflammatory edema 07 p2906 N94-27497
The effect of naloxone on sleeping time in adjuvant arthritic rats 07 p2906 N94-27498
Effects of capsaicin on freshly dissociated rat dorsal root ganglion cells 07 p2906 N94-27499
Contribution of muscle spindle afferent activity to transient pause in EMG during voluntary tonic contraction 07 p2928 N94-27522
Activation by G protein beta gamma subunits of G protein-coupled receptor kinase 07 p2931 N94-27534
Mechanism for regulation of myocardial contractility by autonomic drugs: Pathophysiological relevance in congestive heart failure 07 p2931 N94-27536
The polymodal receptor 07 p2908 N94-27539
The role of beta-adrenoceptor stimulation in the progression of chronic heart failure 07 p2932 N94-27541
Effects of pressure on membrane-associated receptors and effector elements
[AD-A275813] 08 p3384 N94-28829

RECESSES
Portable electronically based method for the nondestructive remote sensing of crevice corrosion
[AD-A275403] 08 p3318 N94-29057

RECESSION
Rates of fluvio-thermal erosion on Mars 01 p0435 N94-12018
Air traffic in recession 07 p2662 N94-28240

RECHARGING
Anode for rechargeable ambient temperature lithium cells
[NASA-CASE-NPO-18580-1-CU] 08 p3265 N94-29505

RECIPROCATING ENGINES
U PISTON ENGINES

RECIPROCATION
Performance analysis of reciprocating regenerative magnetic heat pumping
[DE94-009488] 11 p4264 N94-35683

RECIPROCITY THEOREM
Electromagnetic scattering by inhomogeneous objects. Solution methods based upon reciprocity theorems of time-convolution and time-correlation type
[PB94-111010] 06 p2294 N94-23729

RECIRCULATION
U CIRCULATION

RECIRCULATIVE FLUID FLOW
Recirculation in forward roll coating
[VKI-TM-48] 04 p1409 N94-17901
A comparative study of computational solutions to flow over a backward-facing step 06 p2326 N94-23670
Experiments into the scaling parameters required for exhaust gas ingestion testing of vertical landing aircraft 07 p2671 N94-28017
Influence of headwind on hot gas reingestion and consideration of pressure ratio scaling 07 p2675 N94-28018
Unsteady aspects of hot gas reingestion and statistical analysis 07 p2676 N94-28019
A new Eulerian model for turbulent evaporating sprays in recirculating flows 08 p3195 N94-29279
An experimental study of the flowfield on a semispan rectangular wing with a simulated glaze ice accretion 08 p3130 N94-29674
Computational study of simultaneous heat and mass transfer in turbulent separated flows 09 p3704 N94-31843
An experimental study of the flowfield on a semispan rectangular wing with a simulated glaze ice accretion
[NASA-CR-195301] 09 p3571 N94-32475

RECLAMATION
NT GAS RECOVERY
NT MATERIALS RECOVERY
NT WATER RECLAMATION
Rapid geophysical surveyor
[DE93-016637] 04 p1461 N94-17851
Freon recovery from nitrogen tetroxide and freon solutions
[PL-TR-92-3051] 07 p2721 N94-28215

RECOGNITION
NT CHARACTER RECOGNITION
NT PATTERN RECOGNITION
NT SPEECH RECOGNITION
NT TARGET RECOGNITION
NT TIMBER IDENTIFICATION
On geometric and algebraic aspects of 3D affine and projective structures from perspective 2D views
[AD-A270520] 05 p1983 N94-19968
Sensor integration and data fusion for object localization in robotic workcells 05 p1774 N94-22130
High-resolution subsurface imaging and neural network recognition
[DE94-009546] 11 p4290 N94-35666

RECOIL ATOMS
Optical spin polarization and state-sensitive detection of a cesium atomic beam
[ATR-92(8436)-1] 06 p2534 N94-24077

RECOIL IONS
Experimental study of interactions of highly charged ions with atoms at keV energies
[DE93-040222] 04 p1571 N94-19257

RECOMBINATION REACTIONS
NT ATOMIC RECOMBINATION
NT ELECTRON RECOMBINATION
NT ELECTRON-ION RECOMBINATION
NT HYDROGEN RECOMBINATIONS
NT ION RECOMBINATION
NT RADIATIVE RECOMBINATION
Surface passivation of InP solar cells with InAlAs layers 01 p0049 N94-11389
Merged beam studies of laser stimulated radiative recombination
[AD-A267186] 03 p1037 N94-15145
OSA proceedings on Ultrafast Electronics and Optoelectronics, volume 14
[AD-A267972] 03 p1014 N94-17410
A physical model for one-dimension and time-dependent ionosphere. Part 1: Description of the model
[DE93-627958] 04 p1486 N94-19255
Reinterpretation of rate data for the reaction of ClF and F2
[DE94-005819] 08 p3200 N94-30880
High-temperature study of O+H2CO yields OH+HCO
[DE94-006837] 09 p3864 N94-31321
Material engineering of the novel semiconductor structures
[AD-A278386] 09 p3910 N94-33355
Studies of the effect of image degradation and recombination
[AD-A278343] 10 p4142 N94-34002

RECOMMENDATIONS
Guidelines for the expression of uncertainties in surface chemical analysis by Auger Electron Spectroscopy (AES) and X ray Photoelectron Spectroscopy (XPS)
[NPL-DMM(A)-99] 04 p1346 N94-17900
Ultraviolet, visible, and gravity astrophysics: A plan for the 1990's
[NASA-NP-152] 06 p2603 N94-24973
Partners in space. International cooperation in space: Strategies for the new century
[ISBN-0-9629930-2-6] 11 p4348 N94-35901

RECOMPRESSION
U COMPRESSING

RECONNAISSANCE
NT AERIAL RECONNAISSANCE
NT PHOTORECONNAISSANCE
NT SPECTRAL RECONNAISSANCE
Integrating the services' imagery architectures
[AD-A265487] 01 p0171 N94-12335
Space countersurveillance: A requisite for theater defense planning
[AD-A266871] 03 p0884 N94-15147

Design project: LONGBOW supersonic interceptor
[NASA-CR-195510] 06 p2180 N94-24581
The Pluto fast flyby mission: Completing the reconnaissance of the solar system
08 p3235 N94-29768
JPRS report: Central Eurasia. Aviation and cosmonautics, no. 3, March 1993
[JPRS-UAC-94-002] 10 p4011 N94-35116

RECONNAISSANCE AIRCRAFT
NT F-5 AIRCRAFT
NT SR-71 AIRCRAFT
NT U-2 AIRCRAFT
Design and pilot evaluation of the RAH-66 Comanche Core AFCS 02 p0525 N94-13321
Design and pilot evaluation of the RAH-66 Comanche selectable control modes 02 p0525 N94-13322
An analysis of helicopter attrition using a low level combat simulation
[DSIS-93-00282] 02 p0515 N94-13839
UAV current technology and future trends
06 p2154 N94-24245
S-2E Tracker maritime patrol aircraft re-engine and system upgrade program 06 p2158 N94-24270
The design of four hypersonic reconnaissance aircraft
07 p2671 N94-25716
Army scout/reconnaissance helicopters versus unmanned aerial vehicles
[AD-A276902] 09 p3579 N94-32232

RECONNAISSANCE SPACECRAFT
Space countersurveillance: A requisite for theater defense planning
[AD-A266871] 03 p0884 N94-15147

RECONSTRUCTION
NT WAVE FRONT RECONSTRUCTION
Unitary plan wind tunnel landmark dedication and revitalization
[NASA-TM-109649] 03 p1302 N94-15434
ENO schemes on unstructured meshes
04 p1412 N94-18561
The renewing of the test section of the NAL transonic wind tunnel. Part 1: Reconstruction of the 1st corner turning vanes and aerodynamic stress measurement
[NAL-TM-651] 07 p2681 N94-27247

RECORDING
NT DATA RECORDING
NT DATA SMOOTHING
NT MAGNETIC RECORDING
NT PHOTOGRAPHIC RECORDING
Noise reduction techniques for the restoration of musical recordings
[TELECOM-93-E-019] 08 p3291 N94-30979

RECORDING HEADS
Contribution to the tribological study of magnetic-tape head contact
[ECL-92-57] 04 p1434 N94-19414

RECORDING INSTRUMENTS
NT BATHYTHERMOGRAPHS
NT FLIGHT LOAD RECORDERS
NT FLIGHT RECORDERS
NT LUNAR SEISMOGRAPHS
NT OSCILLOGRAPHS
NT PLOTTERS
NT SEISMOGRAPHS
NT TAPE RECORDERS
NT VIDEO TAPE RECORDERS

RECORDS
Monitoring history
[NASA-TM-109640] 03 p1229 N94-15251
A concise introduction to MARC
12 p4542 N94-36856

RECORDS MANAGEMENT
Making the connection between information modeling and implementation
[DE93-011588] 02 p0820 N94-12907
Monitoring history
[NASA-TM-109640] 03 p1229 N94-15251
NASA security handbook
[NHB-1620.3C] 03 p1224 N94-15937
Managing information as a corporate asset: Key strategies for information professionals to remain competitive
[DE93-015515] 03 p1232 N94-16875
Document control and conduct of operations
[DE93-016555] 04 p1613 N94-17880
Networked MS windows 3.1 based classified document control system (CDOCS)
[DE93-017880] 04 p1617 N94-18984
A comparison Air Force data systems --- Comments on IDA Paper P-2863
[AD-A270662] 04 p1619 N94-19780
Project Records Information System (PRIS): User's manual
[DE94-001548] 05 p2045 N94-22047
Fact-based enterprise information management using NIAM
[DE93-041135] 06 p2591 N94-24501
The evolution of information management
[DE94-004173] 08 p3535 N94-30179
An analysis of the records management process to determine the impact of automation on productivity
[AD-A275923] 09 p3916 N94-31344
Developing a personal-computer-based records retention system using Paradox(tm)
[DE94-007984] 09 p3819 N94-32749
Data considerations for modelbases
[DE94-004614] 10 p4151 N94-33711
Virtual file system for PSDS 10 p4153 N94-33806

RECOVERABLE LAUNCH VEHICLES
HOPE conceptual design in FY 1991
[NASDA-CNT-930017] 02 p0535 N94-13600
Conceptual design on H-2 Orbiting Plane (HOPE)
[NASDA-CNT-930018] 02 p0535 N94-13656
The concept study of the space transportation system HOPE in FY 1991
[NASDA-CNT-930016] 02 p0536 N94-14100

RECOVERABLE SPACECRAFT
NT AEROSPACE PLANES
NT APOLLO LUNAR EXPERIMENT MODULE
NT BURAN SPACE SHUTTLE
NT CHALLENGER (ORBITER)
NT COLUMBIA (ORBITER)
NT DISCOVERY (ORBITER)
NT FRIENDSHIP 7
NT HERMES MANNED SPACEPLANE
NT MERCURY SPACECRAFT
NT REUSABLE SPACECRAFT
NT SPACE SHUTTLE ORBITERS
NT SPACE SHUTTLES
NT X-30 VEHICLE

RECOVERY
Galileo spacecraft anomaly and safing recovery
06 p2207 N94-23864

RECOVERY PARACHUTES
Regulated drag area parachute
[AD-D015992] 06 p2170 N94-25051
Further development and flight test of an autonomous precision landing system using a parafoil
[NASA-TM-4599] 10 p3983 N94-33995

RECREATION
GSFC Fun Run
[NASA-TM-109587] 03 p1120 N94-15271

RECRYSTALLIZATION
Petrography and preliminary interpretations of the crystalline breccias from the Manson M-1 core
01 p0281 N94-12056
Simulation of possible regolith optical alteration effects on carbonaceous chondrite meteorites
01 p0430 N94-12163
Thin Ni silicide formation by low temperature-induced metal atom reaction with ion implanted amorphous silicon
[DE93-015449] 03 p1209 N94-16066
Isotopic signatures and distribution of nitrogen and trapped and radiogenic xenon in the Acapulco and FRO90011 meteorites 03 p1243 N94-16317
Tensile and stress-rupture behavior of hafnium carbide dispersed molybdenum and tungsten base alloy wires
[NASA-TM-106350] 03 p0962 N94-17652
Atlas of formability: Nickelvac C-276
[AD-A268264] 04 p1357 N94-17802
Atlas of formability: ALLVAC 718
[AD-A268304] 04 p1357 N94-17804
The effect of composition on the mechanism of continuous recrystallization and superplastic response of aluminum-scandium alloys
[DE93-018594] 04 p1365 N94-19280
Fragments of ancient lunar crust: Ferroan noritic anorthosites from the descartes region of the Moon
05 p2096 N94-20660
Post-igneous redistribution of components in eucrites
05 p1685 N94-20684
Fine resolution chronology based on initial Sr-87/Sr-86
[CONTRIB-5230(794)] 05 p1686 N94-20794
Characterization of 3-D particle distributions and effects on recrystallization studied by computer simulation
[PB93-201408] 06 p2562 N94-23535
Influence of grain structure and solute composition on the work hardening behavior of aluminium at cryogenic temperatures
[DE94-003415] 07 p2733 N94-26087
Study of precipitation and recrystallization in Al alloy 2519 by backscattered electron imaging methods
[AD-A274919] 07 p2736 N94-26533
Effect of precipitate structure on hot deformation of Al-Mg-Mn alloys
[DE94-004596] 07 p2741 N94-27622
On the prediction of HAZ grain size using Monte Carlo simulation
[DE94-005465] 08 p3511 N94-28535
Failures to model the development of a cube texture during the high temperature compression of Al-Mg alloys
[DE94-005013] 08 p3201 N94-28544
Work hardening behavior in aluminum alloy 2090
[DE94-007036] 09 p3643 N94-32064
Attempts to model the generation of new grain boundaries during the deformation of polycrystals
[DE94-007527] 09 p3903 N94-32597
Materials processing apparatus development for fluoride glass
[NASA-CR-193963] 10 p4030 N94-34388
Thermomechanical studies of tungsten heavy alloys
[AD-A280250] 12 p4417 N94-37122

RECTANGLES
Fully developed turbulent flow in rectangular interrupted-plate ducts
[ISBN-0-315-63594-0] 02 p0632 N94-13474
Operational equations for the five-point rectangle
[DE94-000366] 05 p1959 N94-21655
Rectilinear decompositions with low stabbing number
[RUU-CS-93-25] 08 p3459 N94-30425
Cost-effective computations with boundary interface operators in elliptic problems
[DE94-621506] 12 p4503 N94-37098

RECTANGULAR BEAMS
A simplistic look at limit stresses from random loading
[NASA-TM-108427] 03 p1058 N94-15710

RECTANGULAR COORDINATES
U CARTESIAN COORDINATES

RECTANGULAR DRAINAGE
U DRAINAGE PATTERNS

RECTANGULAR PANELS
Nonlinear equations of motion for a panel subject to external loads
[AD-A273142] 06 p2170 N94-24773
Response of a cantilevered plate in supersonic flow
[AD-A277487] 09 p3580 N94-33107

RECTANGULAR PLANFORMS
NT RECTANGULAR PANELS
NT RECTANGULAR PLATES
NT RECTANGULAR WINGS

RECTANGULAR PLATES
Measuring methods for CFRP laminates' bending and torsion rigidities characteristics
02 p0529 N94-13272
High-frequency techniques for RCS prediction of plate geometries 05 p1717 N94-20270
Further investigation of curve veering phenomena
08 p3460 N94-30515
Nonlinear vibration analysis of laminated plates on linear and nonlinear elastic foundations
09 p3737 N94-32079
The dynamic flexibility method in structural dynamics: Application to nonuniform beams and plates and to cavity-backed plates 10 p4068 N94-33370

RECTANGULAR WAVEGUIDES
Nonlinear instability of a laminar flow in a rectangular duct and generation of the turbulent secondary flow
01 p0164 N94-12622
Formulation for numerical solution of radiation and transmission from arbitrary apertures
05 p1745 N94-22140
Computer program for numerical evaluation of the performance of an overmoded TM01 circular to TE10 rectangular waveguide mode converter
[AD-A274548] 07 p2771 N94-26844
Performance evaluation and operating characteristics of a waveguide microwave applicator for space propulsion applications 09 p3614 N94-31908
A novel transition between rectangular waveguide and layered ridge dielectric waveguide
[NASA-TM-106661] 12 p4433 N94-36955

RECTANGULAR WINGS
Viscous-inviscid calculation of high-lift separated compressible flows over airfoils and wings
04 p1309 N94-18440
An experimental study of wing tip vortex in the near wake of a rectangular wing
[AD-A275389] 08 p3129 N94-29306
An experimental study of the flowfield on a semispan rectangular wing with a simulated glaze ice accretion
08 p3130 N94-29674
An experimental study of the flowfield on a semispan rectangular wing with a simulated glaze ice accretion
[NASA-CR-195301] 09 p3571 N94-32475

RECTENNAS
Construction and testing of a space ready rectenna
[NASA-CR-193310] 01 p0137 N94-11357
Dual polarization microstrip array antenna
[CA-PATENT-1-307-842] 03 p0994 N94-15986

RECTIFICATION
NT GEOMETRIC RECTIFICATION (IMAGERY)
Plasma-etching science meets technology in the MDL
[DE93-012086] 02 p0800 N94-13908

A direct current rectification scheme for microwave space power conversion using traveling wave electron acceleration 07 p2687 N94-27371
RECTIFIER ANTENNAS
U RECTENNAS
RECTIFIERS
NT AVALANCHE DIODES
NT IGNITRONS
NT SILICON CONTROLLED RECTIFIERS
NT THYRATRONS
NT THYRISTORS
RECUPERATORS
U REGENERATORS
RECURSION FORMULAS
U RECURSIVE FUNCTIONS
RECURSIVE FUNCTIONS
Deformations and recursion operators for evolution equations
[MEMO-1104] 01 p0341 N94-10163
Spatially-varying IIR filter banks for image coding
[NASA-CR-193727] 02 p0619 N94-12897
Recursive time-varying filter banks for subband image coding
[NASA-CR-193726] 02 p0598 N94-12920
Using geometric techniques to improve dynamic programming algorithms for the economic lot-sizing problem and extensions
[PB93-197556] 04 p1528 N94-19330
Time dependent identification of nonlinear structures
[ECL-92-64] 04 p1457 N94-19403
Notes on multi-step ahead prediction based on the principle of concatenation
[MATHS-REPT-A-189] 04 p1544 N94-19410
Efficient and correct translation of strict applicative programming languages
[ETN-93-95056] 05 p1903 N94-20020
Cascaded recursive artificial neural networks
05 p1780 N94-22167
Experiments with recursive estimation in astronomical image processing 05 p2047 N94-22457
Mean-value of product-form stochastic Petri net models of slotted-ring systems
[PB94-110871] 06 p2494 N94-23749
The Adam language: Ada extended with support for multiway activities
[NASA-CR-4565] 06 p2456 N94-24480
MIMO recursive least squares control algorithm for the AN/FPN-44A Loran-C transmitter
[AD-A274820] 07 p2664 N94-26493
Simulation dynamics of a multibody chain: Recursion based on chain modal coordinates
[ISBN-0-315-83555-9] 07 p2994 N94-26659
Congruence theorem for structured operational semantics with predicates and negative premises
[PB94-126729] 07 p2966 N94-26970
Categorial generalization of algebraic recursion theory
[ML-93-06] 08 p3456 N94-30382
Development and validation of a linear recursive order-N algorithm for the simulation of flexible space manipulators dynamics
[AD-B173557] 08 p3311 N94-30391
Higher order recursive program schemes are Turing incomplete
[CWI-CS-R9348] 08 p3425 N94-30414
Formal verification of systolic multipliers with the Boyer-Moore theorem prover
[RR-897-M] 09 p3839 N94-31082
RECYCLING
Environmental Protection Agency's life cycle methodology: Guidelines for use in development of packaging
[PB93-194199] 01 p0265 N94-10841
Some environmental aspects of the application of fibre reinforced plastics in structures
[LM-998] 01 p0088 N94-10877
Evaluation for membrane components of water recycling system
[NAL-TM-646] 02 p0737 N94-13388
Survey and study on Environmental Control and Life Support (ECLS) technologies, part 2
[NASDA-CNT-930012-PT-2] 02 p0737 N94-13472
Recycling in space
[NASA-TM-109307] 02 p0737 N94-13615
Effect of stabilization on the recycling of polyolefins in blow moulding
[IMI-93RT-42400-1477-G] 02 p0596 N94-13684
Fourteenth National Industrial Energy Technology Conference: Proceedings
[DE93-016698] 02 p0710 N94-14516
User's guide: Hot-mix recycling of asphalt concrete pavements
[AD-A266939] 03 p0983 N94-15177
Investigations into the recovery of waste sulfuric acid with concentrated solar radiation
[DLR-FB-93-11] 03 p0952 N94-17594
Current status of environmental, health, and safety issues of nickel metal-hydride batteries for electric vehicles
[DE93-017079] 05 p1748 N94-19902
Resonantly pumped, erbium-doped, GSGG, 2.8 micron, solid state laser with energy recycling and high slope efficiency
[AD-D015920] 05 p1815 N94-20060
Feasibility study on a CO2 global recycling system using natural energy
[DE94-714889] 06 p2397 N94-23026
Feasibility study for the recycling of nickel metal hydride electric vehicle batteries
[DE94-000268] 09 p3690 N94-31598
Engineering design knowledge recycling in near-real-time 10 p4160 N94-34061
Hynol: An economic process for methanol production from biomass and natural gas with reduced CO2 emission
[DE94-008872] 10 p4079 N94-34139
Laminated thermoplastic composite material from recycled high density polyethylene
11 p4230 N94-36403
Microscale synthesis and characterization of polystyrene: NSF-POLYED scholars project
11 p4231 N94-36408
Structural composite construction materials manufactured from municipal solid waste
[AD-A280635] 12 p4403 N94-36730
Processing solid propellants for recycling
[DE94-011433] 12 p4428 N94-37202
RED BLOOD CELLS
U ERYTHROCYTES
RED DWARF STARS
In search of Nemesis 07 p2888 N94-28297
RED GIANT STARS
NT CARBON STARS
Abundance patterns in red-giant CH stars
08 p3539 N94-29820
RED SEA
Optical properties of the Red Sea
[AD-A266466] 03 p1113 N94-16588
RED SHIFT
Redshift distortions of galaxy correlation functions
[DE93-014007] 02 p0834 N94-12980
A photometric and morphological study of compact groups of galaxies and their environments
[ISBN-0-315-59601-5] 02 p0829 N94-13370
The flight performance of the Galileo orbiter USO
02 p0611 N94-14398
A long-term space astrophysics research program: The evolution of the quasar continuum
[NASA-CR-193714] 02 p0839 N94-14404
Brillouin scattering from fluctuations produced by stimulated Raman scattering
[DE93-016531] 02 p0792 N94-14438
Complex QSO absorbers: High-redshift clusters of galaxies?
[NASA-CR-194617] 03 p1237 N94-16833
The universe at moderate redshift
[NASA-CR-193771] 04 p1627 N94-19093
Radio galaxies and their environment
[DE93-040851] 05 p2150 N94-22397
Visualizing the universe, part 2
05 p2063 N94-22472
Using contour maps to search for red-shifted 511 keV features in BATSE GRB spectra
06 p2585 N94-24455
High redshift QSOs and the x ray background
[NASA-CR-195112] 08 p3540 N94-29957
Broad H alpha profiles of radio-loud active galactic nuclei and rapid profile variability in Seyfert and radio galaxies
08 p3552 N94-29989
A constraint on the pair-density ratio (Z+) in an electron-positron pair wind 09 p3930 N94-31132
The kinematics of dense clusters of galaxies
09 p3937 N94-32029
GRO: Studies of high energy pulsars with EGRET
[NASA-CR-196003] 11 p4349 N94-35516
RED TIDE
Satellite observations of red tide events: Plans for EESI 01 p0191 N94-11899
REDOX CELLS
Technical Update: Johnson Space Center system using a solid electrolytic cell in a remote location to measure oxygen fugacities in CO/CO2 controlled-atmosphere furnaces
[NASA-TM-104774] 01 p0423 N94-11183
Solvational barriers to interfacial electron transfer: Minimization by way of valence delocalization
[AD-A267371] 03 p0950 N94-17006
REDUCED GRAVITY
U MICROGRAVITY
Proceedings of the 8th European Symposium on Materials and Fluid Sciences in Microgravity, volume 1
[ESA-SP-333-VOL-1] 01 p0099 N94-10070
Experimental study of axisymmetric thermocapillary flows 01 p0100 N94-10072
The use of magnetic fields for damping unsteady Marangoni convection in GaAs floating zones under microgravity 01 p0100 N94-10073
Transient three-dimensional numerical simulation of Marangoni flow in a liquid column under microgravity
01 p0101 N94-10079
Effect of rotation on microgravity floating-zone crystal growth 01 p0101 N94-10080
On shape of single crystals grown by FZM in microgravity 01 p0102 N94-10084
Liquid bridges and floating zones
01 p0102 N94-10085
Model of convective motion under low gravity
01 p0103 N94-10088
Gas-liquid jets under reduced gravity conditions
01 p0103 N94-10091
Heat and mass transfer mechanisms of the polymerization under terrestrial and microgravity conditions 01 p0103 N94-10092
High Prandtl number fluids in a multilayered system under 1-g or micro-g environment
01 p0104 N94-10096
Bubbles and drops behaviour under low-gravity: A space experiment for the IML-2 mission
01 p0104 N94-10098
Space and temporal behavior and control of the residual convection in microgravity 01 p0104 N94-10099
Measurement of the thermal conductivity of molten InSb in a drop shaft 01 p0105 N94-10102
The effect of gravity modulation on thermosolutal convection 01 p0105 N94-10103
Separation of gravitational effects on the flow of suspension in tubes by measurements in weightlessness
01 p0105 N94-10105
Numerical simulation of Marangoni convection around gas bubbles in a liquid matrix 01 p0106 N94-10107
Propellant management in surface tension tanks
01 p0106 N94-10110
CdTe crystal growth in the Soviet facility zona 4
01 p0106 N94-10111
The pyrene laser induced fluorescence technique as a diagnostic tool for combustion thermometry in microgravity 01 p0107 N94-10113
A new method for hysteresis measurements developed for C(sub v) measurements at the critical point during the D2-mission 01 p0107 N94-10114
CdTe crystal growth by THM with a rotating magnetic field 01 p0107 N94-10116
Advanced protein, crystallization facility and associated new developments 01 p0039 N94-10119
Design of multisample, multistep phase partitioning apparatus for use on Space Shuttle Spacelab, and Spacelab missions 01 p0108 N94-10120
Calibration of accelerometers on drop tower Bremen
01 p0108 N94-10121
Gas film levitator for containerless processing of glasses in microgravity conditions: Early concept and technology demonstration 01 p0108 N94-10122
Holographic interferometry for microgravity applications 01 p0108 N94-10123
The High Precision Thermostat HPT-HYDRA
01 p0109 N94-10124
TEMPUS: An electromagnetic levitation facility for containerless processing under micro-g in Spacelab
01 p0109 N94-10125
The electron beam furnace: A new facility for materials science research 01 p0109 N94-10126
Design of a CVD reactor for the deposition of diamond in a microgravity environment 01 p0109 N94-10127
Microgravity Applications Furnace Facility (MAFF) for parabolic flights 01 p0109 N94-10128
Force and power efficiency of micro-g electromagnetic levitation coils 01 p0110 N94-10129
High temperature processing and diagnostic technologies for microgravity applications
01 p0110 N94-10130
Determination of the viscous acoustic field for liquid drop positioning/forcing in an acoustic levitation chamber in microgravity 01 p0110 N94-10131
MUZO: The programmable multi zone furnace for gas payloads and sounding rockets
01 p0110 N94-10132
The surface plasmon spectroscopy as diagnostic technique in microgravity experiments
01 p0110 N94-10133
TOLS (Telescience On-Line Simulator): An essential instrument for micro-gravity interactive experiment
01 p0039 N94-10134
Laser beam deflection: A diagnostic tool for vapour growth experiments in microgravity
01 p0111 N94-10135
The advanced fluid physics module: How to achieve scientific goals for Spacelab D2
01 p0039 N94-10136

Results of mission preparation support to microgravity experiments on board of Eureca 1
01 p0111 N94-10138
AGF (Automatic Gradient Furnace): A proposed microgravity facility 01 p0112 N94-10141
Microgravity experiments using TR-1A rocket
01 p0112 N94-10142
Proceedings of the 8th European Symposium on Materials and Fluid Sciences in Microgravity, volume 2 [ESA-SP-333-VOL-2] 01 p0112 N94-10171
Thermocapillary convection instability in microgravity crystal growth 01 p0112 N94-10172
STARDUST: A simulation experiment of cosmic dust analogues production in microgravity conditions
01 p0113 N94-10175
Solidification from supercooled melt under microgravity 01 p0113 N94-10176
Scientific specifications for an automated facility for growing large semiconducting crystals from the melt in space 01 p0114 N94-10180
Results of crystal growth experiments by FZM on Zona facilities in microgravity 01 p0116 N94-10193
Effects of a microgravity environment on the crystallization of biological macromolecules
01 p0117 N94-10198
Solidification and metastable phase formation of highly undercooled Fe-Cr-Ni alloy melts
01 p0087 N94-10204
Containerless processing of equiatomic Mn50Bi50 in a drop tube 01 p0118 N94-10205
Liquid phase sintering of tungsten composites under microgravity. Effect of matrix composition
01 p0118 N94-10207
Crystallization of zeolites in the microgravity environment of space 01 p0119 N94-10210
A study of the quasibinary Al-W-Mo system. Part 1: Preliminary investigations and preparation for microgravity experiments 01 p0119 N94-10211
Instability of thermocapillary convection in multiple superposed immiscible liquid layers
01 p0120 N94-10218
Influence of neutral particles concentration on flame propagation in methane-air mixtures at zero and normal gravity conditions 01 p0121 N94-10224
Surface tension and adsorption kinetics in immiscible liquid systems at microgravity 01 p0121 N94-10225
Gravity and electric field effects on pool boiling heat transfer 01 p0121 N94-10226
Chemical pattern formation under microgravity
01 p0121 N94-10227
Transport of heat and mass in near-critical fluids
01 p0122 N94-10230
Study of vapor bubble growth in a supersaturated liquid 01 p0122 N94-10232
Phase separation at gas-liquid critical points
01 p0122 N94-10233
Electrohydrodynamic effects in continuous flow electrophoresis observations on Earth and in microgravity 01 p0122 N94-10234
Interface reactions of (Ni3Al) ribbons/Al-MMC in ground preparation as preliminary test for microgravity experiments 01 p0123 N94-10237
The reaction between titanium carbide and aluminium carbide in liquid aluminium; a microgravity study
01 p0123 N94-10238
Laser cooling and trapping of atoms in microgravity: Ultracold atoms collisions 01 p0124 N94-10241
Single bubble experiments in pool boiling: Results from TEXUS 26 01 p0124 N94-10243
Some aspects of combustion modelling by low and normal gravity 01 p0124 N94-10244
Photoinitiated radical polymerization of liquid monomers in microgravity 01 p0124 N94-10246
A method for determination of the elongational viscosity of viscoelastic fluids without body forces
01 p0124 N94-10247
Microgravity combustion of dust suspension in a spherical chamber 01 p0080 N94-10248
The International Microgravity Laboratory, a Spacelab for materials and life sciences 01 p0125 N94-10249
Large amplitude shape oscillations in a mercury drop using a drop tower
[DE93-767972] 01 p0125 N94-10730
Effects of CSF hormones and ionic composition on salt/water metabolism
[NASA-CR-193232] 01 p0300 N94-11045
Measuring human performance on NASA's microgravity aircraft 01 p0317 N94-11537
A mechanism for the reduction in risk of decompression sickness in microgravity environment
01 p0312 N94-11545
Comprehensive analysis of airborne contaminants from recent Spacelab missions 01 p0318 N94-11553
Carotid-cardiac baroreflex: Relation with orthostatic hypotension following simulated microgravity and implications for development of countermeasures
01 p0308 N94-11992
Pulmonary function in microgravity: KC-135 experience
01 p0309 N94-11994
Central circulatory hemodynamics as a function of gravitational stress 01 p0309 N94-11995
Autogenic-feedback training: A countermeasure for orthostatic intolerance 01 p0311 N94-12006

REDUCED ORDER FILTERS
Failure modes of reduced-order orbit determination filters and their remedies 02 p0532 N94-14373
A component modes projection and assembly model reduction methodology for articulated, multi-flexible body structures 02 p0677 N94-14622
Enhanced orbit determination filter sensitivity analysis: Error budget development 08 p3159 N94-29655
Enhanced orbit determination filter: Inclusion of ground system errors as filter parameters
08 p3159 N94-29656

REDUCTION
Perpetual reductions and strong normalization in orthogonal term rewriting systems
[CWI-CS-R9345] 08 p3426 N94-30437

REDUCTION (CHEMISTRY)
NT DEOXIDIZING
NT HYDROGENATION
Effects of microscopic iron metal on the reflectance spectra of glass and minerals 01 p0436 N94-12024
Thermodynamics of lunar ilmenite reduction
01 p0415 N94-12028
The spectral effects of subsolidus reduction of olivine and pyroxene 01 p0081 N94-12110
Oxidation state of the Earth's upper mantle during the last 3800 million years: Implications for the origin of life
01 p0283 N94-12210
In situ studies of passive film chemistry using x ray absorption spectroscopy
[DE93-014023] 03 p0947 N94-16011
Oxygen reduction at a stabilized zirconia interface with Y(1-x)Ca(x)MnO3 or La(1-x)Sr(x)MnO3 cathode materials
[DE93-015681] 04 p1593 N94-17747
Catalytic hydrogenation of carbon monoxide
[DE94-000881] 05 p1678 N94-20103
Dispersion of Rh/Cu in a sol-gel matrix. Highly chemo- and stereoselective catalyst for the reduction of alkynes to Z-alkenes
[AD-A273306] 06 p2262 N94-25145
The electrochemistry of the solvated electron: A study of its properties and of its applications
[ETN-94-95313] 06 p2236 N94-25296
Journal of NIRE, volume 2, number 4
[JTN-94-80554] 07 p2869 N94-28147
Effects of p-chlorophenol on sulfate reduction in marine sediments 07 p2870 N94-28150
The electrocatalytic oxidation of ethylene and methane, and reduction of oxygen on gas-diffusion electrodes made of amorphous nickel-valve metal-platinum group metal alloys 07 p2722 N94-28165
Reduction of lunar mare soil and pyroclastic glass
11 p4355 N94-35398

REDUCTION (MATHEMATICS)
U OPTIMIZATION

REDUNDANCY
Exploiting the cannibalistic traits of Reed-Solomon codes 02 p0609 N94-14378
Computation of large numbers and VLSI: Application to GCD, to stretched GCD and at euclidian distance
[ETN-93-95009] 04 p1552 N94-19499
Real-time fault tolerant computer systems
[AD-A272909] 05 p1899 N94-21230
Links between N-modular redundancy and the theory of error-correcting codes 05 p1765 N94-21713
New mixed integer algorithm for classification and placement of measurements in process flow networks
[PB94-126752] 07 p2966 N94-26921
Local performance optimization for a class of redundant eight-degree-of-freedom manipulators
[NASA-TP-3417] 07 p2989 N94-27773
Algorithms for treating redundancy in repairable and non-repairable systems
[DE94-005289] 08 p3315 N94-29020
Kinematic functions for redundancy resolution using configuration control
[NASA-CASE-NPO-18608-1-CU]
08 p3436 N94-29504
A PC program to optimize system configuration for desired reliability at minimum cost
09 p3823 N94-32438
A new solution method for the inverse kinematic joint velocity calculations of redundant manipulators
[DE94-004427] 09 p3727 N94-32682
Improvement of control system reliability with analytical redundancy technique 10 p4118 N94-34340

REDUNDANCY ENCODING
System performance modeling and analysis of a fault-tolerant, real time parallel processor
[AD-A268070] 03 p1162 N94-17551
Fault tolerant sequential circuits using sequence invariant state machines 04 p1398 N94-18344
A partitioning and redundancy model for wafer-scale integrated circuits 07 p2955 N94-27195
Software engineering methods in the Hermes on-board software 08 p3414 N94-29326
Checkpoint-based forward recovery using lookahead execution and rollback validation in parallel and distributed systems
[NASA-CR-195760] 08 p3431 N94-29869
Object-oriented construction of fault-tolerant software
[PB94-148806] 10 p4108 N94-34122

REDUNDANT COMPONENTS
Generalized impedance control of a redundant manipulator 02 p0661 N94-13575
Synthesis techniques and analysis tool for on-chip fault-tolerance
[AD-A269148] 04 p1521 N94-18259
Reliable redundant device for mechanisms
06 p2361 N94-24030
Reliability analysis of a repairable dependent parallel system
[ETN-94-95312] 06 p2373 N94-25295
Redundant disk arrays in transaction processing systems
[NASA-CR-195759] 08 p3418 N94-29404
An algorithm for the Italian atomic time scale
08 p3473 N94-30668
A PC program to optimize system configuration for desired reliability at minimum cost
09 p3823 N94-32438
Hierarchical modeling for reliability analysis using Markov models
[NASA-CR-188288] 09 p3731 N94-32862
Fault detection and isolation for the Bluebird test bed aircraft
[AD-A277979] 09 p3586 N94-33086

REDUNDANT STRUCTURES
U REDUNDANT COMPONENTS

REED-SOLOMON CODES
An investigation of error characteristics and coding performance
[NASA-CR-193620] 01 p0324 N94-10932
Exploiting the cannibalistic traits of Reed-Solomon codes 02 p0609 N94-14378
Enhanced decoding for the Galileo S-band mission
02 p0609 N94-14380
Compact disk error measurements
03 p1227 N94-14988
An extended Reed Solomon decoder design
04 p1398 N94-18348
Arithmetic in !arge GF(2(exp n))
05 p1760 N94-21131
The Composite Analytic and Simulation Package or RFI (CASPR) on a coded channel 05 p1744 N94-21339
Advanced coding and modulation schemes for TDRSS
05 p1744 N94-21350
Schematic driven layout of Reed Solomon encoders
05 p1766 N94-21722
Performance of RS codes in lognormally shadowed Rician channels 05 p1792 N94-22244
Box codes of lengths 48 and 72
06 p2292 N94-23265
Improved performance of hybrid error control techniques for real-time digital communications over noisy channels
[ISBN-0-315-84281-4] 07 p2770 N94-26625
On the performance of trellis coded 8PSK with Reed Solomon codes
[ISBN-0-315-84289-X] 07 p2770 N94-26626
Coded communications with nonideal interleaving
[ITN-94-85235] 07 p2774 N94-27242
Optimizing the Galileo space communication link
08 p3250 N94-29663
Decoder synchronization for deep space missions
08 p3250 N94-29664
Modulation and coding for the Gaussian channel, possibly affected by fluctuations
[TELECOM-93-E-009] 09 p3840 N94-31169
Trace-shortened Reed-Solomon codes
11 p4254 N94-35554

REELS
An experimental study of tether reel system: A laboratory model
[NAL-TR-1176T] 02 p0539 N94-12943
Nearly uniform deployment/retrieval strategy for space tether systems 06 p2156 N94-24256

REENTRY
NT HYPERSONIC REENTRY
NT MANNED REENTRY
NT SPACECRAFT REENTRY
NT UNCONTROLLED REENTRY (SPACECRAFT)

First experimental assessment of RCS plume-flow field interaction on Hermes leading edge thruster configuration 07 p2703 N94-28032
REENTRY BODIES
U REENTRY VEHICLES
REENTRY BREAKUP
U SPACECRAFT BREAKUP
REENTRY EFFECTS
Analysis and effects of the advanced solid rocket motor on the Space Shuttle elements
[NASA-CR-193879] 06 p2200 N94-24664
REENTRY GLIDERS
U LIFTING REENTRY VEHICLES
REENTRY PHYSICS
A survey of uncontrolled satellite reentry and impact prediction
[AD-A274903] 07 p2695 N94-26750
REENTRY SHIELDING
Compilation of reinforced carbon-carbon transatlantic abort landing arc jet test results
[NASA-TM-104778] 05 p1676 N94-21834
High-temperature behavior of advanced spacecraft TPS
[NASA-CR-195832] 10 p4014 N94-34063
REENTRY TRAJECTORIES
Aerodynamic and aerothermal challenges for the design of the Hermes spaceplane 01 p0003 N94-10423
START user manual version 2.1
[LR-726] 04 p1335 N94-19614
Effects of thrust vector control on the performance of the aerobang orbital plane change maneuver
[AD-A272532] 05 p1646 N94-21418
A survey of uncontrolled satellite reentry and impact prediction
[AD-A274903] 07 p2695 N94-26750
REENTRY VEHICLES
NT AEROSPACE PLANES
NT APOLLO LUNAR EXPERIMENT MODULE
NT BURAN SPACE SHUTTLE
NT CHALLENGER (ORBITER)
NT COLUMBIA (ORBITER)
NT DISCOVERY (ORBITER)
NT FRIENDSHIP 7
NT HERMES MANNED SPACEPLANE
NT HL-10 REENTRY VEHICLE
NT LIFTING REENTRY VEHICLES
NT MERCURY SPACECRAFT
NT REUSABLE SPACECRAFT
NT SINGLE STAGE TO ORBIT VEHICLES
NT SPACE SHUTTLE ORBITERS
NT SPACE SHUTTLES
NT X-30 VEHICLE
Planetary entry vehicle design for planned and potential ESA missions to Titan, Mars, and Earth return (FGE TN 51/92) 01 p0004 N94-10428
Synthesis of the Workshop on Hypersonic Flows for ReEntry Problems 01 p0005 N94-10440
Local aerothermal problems during Hermes re-entry 01 p0010 N94-10464
Progress in modeling hypersonic turbulent boundary layers 01 p0157 N94-12300
High temperature electromagnetic characterization of thermal protection system tile materials
[NASA-CR-189687] 02 p0578 N94-13431
Simulation of hypersonic, reacting flow around reentry bodies: Comparisons of numerical and experimental results
[MBB-LME-211-S-PUB-507] 02 p0509 N94-14710
Tetrahedral lander
[NASA-CASE-MSC-22082-1] 05 p1658 N94-20590
Reentry vehicle adaptive telemetry
[DE94-001168] 05 p1656 N94-21852
Development and application of an empirical probability distribution for the prediction error of re-entry body maximum dynamic pressure 06 p2207 N94-23653
Chemical and vibrational nonequilibrium viscous flows: Modelling, internal and external flow applications
[ESA-TT-1274] 07 p2791 N94-26316
REFERENCE STARS
Optical propagation through atmospheric turbulence. Model analysis of anisoplanatism and application to adaptive optics
[ONERA-P-1992-4] 02 p0716 N94-14192
Design of pulse stretching cell for a sodium guide star optical system
[DE93-016436] 03 p1236 N94-14929
Tip-tilt compensation: Resolution limits for ground-based telescopes using laser guide star adaptive optics
[DE93-016426] 03 p1237 N94-16872
Design and early results of the sodium-layer laser guide star adaptive optics experiment at the Lawrence Livermore National Laboratory
[DE94-006653] 09 p3926 N94-32189
Performance of adaptive optics at Lick Observatory
[DE94-009382] 10 p4142 N94-33911
REFERENCE SYSTEMS
Toward 10(exp 9) GPS geodesy: Vector baselines, Earth rotation and reference frames
[NASA-CR-193184] 01 p0229 N94-10702
The Keck keyword layer 05 p1925 N94-22460
REFERENCES (STANDARDS)
U STANDARDS
REFILLING
Studies on equatorial shock formation during plasmaspheric refilling
[NASA-CR-194392] 02 p0715 N94-13954
Kinetic plasma processes occurring in the outer plasmasphere
[NASA-CR-193452] 03 p1300 N94-17524
REFINING
NT ELECTROSLAG REFINING
Highly anisotropic but nodeless gap from a valence-fluctuation pairing mechanism
[DE93-010738] 01 p0401 N94-11646
Proceedings of the 12th International Congress: Corrosion Control for Low-Cost Reliability. Volume 4: Oil/Gas Pipeline
[AD-A273665] 06 p2250 N94-25405
Bulletin of the Institute for Chemical Reaction Science, Tohoku University, volume 2
[JTN-94-80602] 07 p2717 N94-27385
Development of liquid membrane separation processes 07 p2717 N94-27386
Near-net-shape manufacturing: Spray-formed metal matrix composites and tooling 08 p3186 N94-30447
Alternate melting and refining routes 12 p4421 N94-37323
REFLECTANCE
NT BIDIRECTIONAL REFLECTANCE
NT SPECTRAL REFLECTANCE
Effects of energetic particle events on VLF/LF propagation parameters/1989
[AD-A265266] 01 p0275 N94-11013
An expert system shell for inferring vegetation characteristics: Prototype help system (Task 1)
[NASA-CR-193411] 01 p0231 N94-11236
Needs for super-smooth surfaces
[DE93-012482] 01 p0382 N94-11242
Formulating infrared coatings for defence applications
[MRL-RR-1-93] 01 p0090 N94-11302
On the coupling of electromagnetic radiation into cavities
[DE93-011406] 01 p0137 N94-11621
Feature association without a motion estimate
[AD-A265162] 01 p0138 N94-11891
Effects of microscopic iron metal on the reflectance spectra of glass and minerals 01 p0436 N94-12024
Simulation of possible regolith optical alteration effects on carbonaceous chondrite meteorites 01 p0430 N94-12163
Reflective coatings for solar applications
[DE93-010026] 02 p0702 N94-13381
Optimization of transparent and reflecting electrodes for amorphous silicon solar cells
[DE93-010009] 02 p0704 N94-14110
Determination of the surface cleanliness of metals by FT-IR spectroscopy
[DE93-013252] 02 p0565 N94-14525
Shielded open-circuited sample holders for dielectric and magnetic measurements of liquids and powders
[PB93-198851] 02 p0652 N94-14687
An expert system shell for inferring vegetation characteristics: Atmospheric techniques (Task G)
[NASA-CR-194570] 03 p1082 N94-15531
ETALON-1,-2 center of mass correction and array reflectivity 03 p0915 N94-15576
Engineering design of sub-micron topographies for simultaneously adherent and reflective metal-polymer interfaces
[NASA-CR-194573] 03 p0964 N94-15700
Laboratory for x ray optics
[AD-A267149] 03 p1189 N94-15735
Multilayer thin film design for far ultraviolet polarizers using an induced transmission and absorption technique
[NASA-CR-194631] 03 p1190 N94-15869
Modeling the reflectance of CO2 frost with new optical constants: Application to Martian south polar cap spectra 03 p1256 N94-16217
Thermal inertia and radar reflectivity of the Martian north polar ERG: Low-density aggregates 03 p1260 N94-16238
Iron oxide bands in the visible and near-infrared reflectance spectra of primitive asteroids 03 p1242 N94-16274
Radar properties of several fluidized ejecta blankets on Venus 03 p1267 N94-16278
VUV thin films, chapter 7
[NASA-CR-194634] 03 p0967 N94-16494
Unmixing AVIRIS data to provide a method for vegetation fraction subtraction 03 p1066 N94-16669
Ground-truthing AVIRIS mineral mapping at Cuprite, Nevada 03 p1069 N94-16682
MAC Europe 1991: Evaluation of AVIRIS, GER imaging spectrometry data for the land application testsite Oberpfaffenhofen 03 p1070 N94-16688
Simulation of ASTER data using AVIRIS images 03 p1071 N94-16693
Investigation of the optical, electronic, and structural properties of fiber optic glasses
[AD-A267645] 03 p0971 N94-17204
Data fusion through simulated annealing of registered range and reflectance images
[DE93-015910] 04 p1612 N94-17858
Time-resolved probing of electron thermal conduction in femtosecond-laser-pulse-produced plasmas
[DE93-016996] 04 p1585 N94-18129
Studies of enhanced radar backscatter
[AD-A269544] 04 p1385 N94-18288
Testing and evaluation of large-area heliostats for solar thermal applications
[DE93-018509] 04 p1467 N94-18520
Millimeter wave reflectivity measurement system
[AD-A270008] 04 p1387 N94-18601
High efficiency epitaxial optical reflector solar cells
[DE93-017115] 05 p1845 N94-19805
An expert system shell for inferring vegetation characteristics
[NASA-CR-189318] 05 p1837 N94-20284
A theoretical and numerical study of polarimetric scattering and emission from random rough surfaces with anisotropic directional spectrum 05 p1730 N94-20454
The coherent backscattering opposition effect 05 p1991 N94-20646
The role of CO2 in weathering reactions and the presence of S2 on Venus: Implications for the pyrite stability field 05 p2122 N94-20799
The stability of oxyamphiboles: Existence of Ferric-bearing minerals under the reducing conditions on the surface of Venus 05 p2122 N94-20800
A new Antarctic meteorite with chromite, orthopyroxene and metal with reference to a formation model of S asteroids 05 p2084 N94-20813
Objective determination of image end-members in spectral mixture analysis 05 p1686 N94-20831
Diffuse reflectance spectra of orthopyroxene, olivine, and plagioclase as a function of composition and structure 05 p2087 N94-20906
X ray reflection masks: Manufacturing, characterization and first tests
[BONN-IR-92-31] 05 p1986 N94-21043
Long-range laser imaging
[AD-A273020] 05 p1817 N94-21253
Forecasting technique of variations of the optical absorptivity of thermal control coatings under different simultaneous radiations 05 p1664 N94-21399
Role of surface characteristics in urban meteorology and air quality
[DE93-040929] 05 p1851 N94-21740
The optical constants and spectral specular reflectivity of Highly Oriented Pyrolytic Graphite (HOPG)
[DE93-040546] 05 p1709 N94-21970
X ray characterization of a three-element condenser system for soft x ray projection lithography
[DE93-019916] 05 p1990 N94-21985
A motion extraction method for synthetic aperture radars
[DLR-FB-92-31] 05 p1742 N94-22279
Bi-directional reflectance and other radiation parameters of cirrus from ER-2 observations 05 p1871 N94-22296
Estimation of cirrus cloud particle fallspeeds from vertically pointing Doppler radar 05 p1879 N94-22333
Surface-induced brightness temperature variations and their effects on detecting thin cirrus clouds using IR emission channels in the 8-12 micrometer region 05 p1880 N94-22341
Remote sensing estimates of cirrus particle size for tropical and midlatitude cirrus: Hexagonal crystals and ice spheres 05 p1880 N94-22342
Spatial and temporal variability of soil temperature, moisture and surface soil properties
[NASA-CR-194109] 06 p2401 N94-23337
Theoretical investigation of variable periodicity (graded) multilayers for hard x ray applications
[NASA-CR-193913] 06 p2543 N94-23502
Nimbus-7 Total Ozone Mapping Spectrometer (TOMS) data products user's guide
[NASA-RP-1323] 06 p2410 N94-24355
Neutron reflection interferometry
[DE94-601876] 07 p2714 N94-26170
Sulfur dioxide in the atmosphere of Venus 1 sounding rocket observations
[NASA-CR-195224] 07 p3106 N94-26237

Sound, speed, reflectivity, absorption, and thermal diffusivity measurements in Arctic ice in 1990
[AD-A274326] 07 p2899 N94-26886
Discrete vacuum ultra violet reflective interference filter
[AD-D016059] 07 p2756 N94-27675
Reflectometer employing an integrating sphere and lens-mirror concentrator
[AD-D016061] 07 p3039 N94-27676
Synthetic image generator model; application of view angle dependent reflectivity components and performance evaluation in the visible region
[AD-A275365] 08 p3499 N94-29009
Satellite estimation of the global distribution and interannual variability of photosynthetically active radiation 08 p3334 N94-29970
Electrooptical and optical evaluation of Pb(Zr,Ti)O3 thin films using waveguide refractometry
[DE94-006374] 08 p3518 N94-30247
Characterization of thermally annealed Sb implanted fused silica
[DE94-005464] 08 p3219 N94-30335
The performance of gloss meters on curving surfaces
[NPL-DMM(A)-111] 08 p3501 N94-30522
Modeling the interaction between solar radiation and terrestrial surfaces 09 p3779 N94-30999
Shiptrack database analysis
[AD-A277228] 09 p3746 N94-32025
Electromagnetic wave reflection from irregular plasma layers
[AD-A276727] 09 p3678 N94-32161
Research and applications of a canopy reflectance model 09 p3747 N94-32492
A quest for a new superconducting state
[DE94-008439] 09 p3908 N94-32991
Ocean surface roughness from infrared measurements: A failure of shape from reflection
[AD-A278008] 10 p4091 N94-33435
Body-wave radiation patterns and AVO in transversely isotropic media
[DE94-009214] 10 p4036 N94-34162
Multiwavelength pyrometer for gray and non-gray surfaces in the presence of interfering radiation
[NASA-CASE-LEW-15250-1] 11 p4269 N94-35383
New prospects for analyzing lunar pyroclastic glass 11 p4355 N94-35397
High Resolution Transmission Electron Microscopy (HRTEM) of nanophase ferric oxides 11 p4239 N94-35433
The nature of agglutinitic glass in the fine-size fraction of lunar soil 10084 11 p4369 N94-36148
Mercury: Mid-infrared (7.3 - 13.5 microns) spectroscopic observations showing features characteristic of plagioclase 11 p4370 N94-36150
NASA ER-2 Doppler radar reflectivity calibration for the CAMEX project
[NASA-TM-104611] 12 p4475 N94-37790

REFLECTED RADIATION
U REFLECTED WAVES

REFLECTED RAYS
U REFLECTED WAVES

REFLECTED WAVES
Retrieval of radiation budgets in the Arctic from satellite measurements 01 p0229 N94-10714
Regular and irregular reflection of a wave from a slanting flat wall
[IFTR-13/1991] 03 p1193 N94-17049
Observation of reflected waves on the SABRE positive polarity inductive adder MITL
[DE93-019413] 05 p1980 N94-20295
System and method for cancelling expansion waves in a wave rotor
[NASA-CASE-LEW-15218-1] 05 p1801 N94-20588
The coherent backscattering opposition effect 05 p1991 N94-20646
Neutron reflection interferometry
[DE94-601876] 07 p2714 N94-26170
Mix induced by single shock passage through a material interface
[DE93-019505] 07 p2792 N94-26427
Method for cancelling expansion waves in a wave rotor
[NASA-CASE-LEW-15218-2] 08 p3274 N94-29740

REFLECTING TELESCOPES
Holographic optical elements correcting the off-axis aberrations of a parabolic mirror
[ISBN-0-315-57581-6] 05 p1990 N94-22411
Issues in the design and optimization of adaptive optics and laser guide stars for the Keck Telescopes
[DE94-009384] 11 p4349 N94-35565

REFLECTION
NT INFRARED REFLECTION
NT MACH REFLECTION
NT OPTICAL REFLECTION
NT RETROREFLECTION
NT SIGNAL REFLECTION
NT SPECULAR REFLECTION
NT SPREAD REFLECTION
NT ULTRAVIOLET REFLECTION
NT WAVE REFLECTION
The 24 GHz measurements of 2.2 lambda conical horn antennas illuminating a conducting sheet
[NASA-TM-109002] 02 p0598 N94-12811
Composite refraction-reflection stack sections: Tracing faults in the Atlantic coastal plain sediments
[DE93-013581] 03 p1112 N94-16009
High-resolution seismic reflection survey at the Manson crater, Iowa 03 p1103 N94-16307
ATCRBS reply environment at Memphis International Airport
[AD-A266322] 03 p0864 N94-16439
Modifications to the three-component classification algorithm for SAR data 05 p1719 N94-20410
The Brewster angle effect in SAR polarimetry 05 p1731 N94-20456
Dynamics of surface thermal expansion and diffusivity using two-color reflection transient gratings
[DE93-040547] 05 p1990 N94-22002
An Earth albedo model: A mathematical model for the radiant energy input to an orbiting spacecraft due to the diffuse reflectance of solar radiation from the Earth below
[NASA-TM-104596] 06 p2195 N94-24497
The Radar Image Generation (RIG) model 06 p2306 N94-25497
Development and evaluation of a near infrared reflecting and low visibility paint scheme for RAAF P-3C Orion aircraft
[AD-A274881] 07 p2669 N94-26864
Experimental and theoretical investigation of RF absorption and reflection from preformed plasmas
[AD-A274189] 07 p3046 N94-27098
Discrete vacuum ultra violet reflective interference filter
[AD-D016059] 07 p2756 N94-27675
Observation of the phase shift of the wave function of the neutron under total reflection
[DE94-608244] 08 p3489 N94-30096
Hybrid optics for space applications
[ESA-CP-1158] 08 p3501 N94-30418

REFLECTION COEFFICIENT
U REFLECTANCE

REFLECTIVITY
U REFLECTANCE

REFLECTOMETERS
NT MICROWAVE REFLECTOMETERS
Ocean measuring experiments using optical fiber distributed temperature sensor 01 p0172 N94-11968
Center for X-Ray Optics, 1992
[DE94-000726] 05 p1990 N94-21868
In situ x ray reflectivity measurements of thin film structural evolution
[DE94-002289] 07 p3051 N94-25944
Surface physics with cold and thermal neutron reflectometry
[DE94-001447] 07 p2733 N94-26070
Time domain reflectometry for measuring bulk soil electrical conductivity and comparison with the Em38 instrument
[PB94-125432] 07 p2881 N94-27052
Reflectometer employing an integrating sphere and lens-mirror concentrator
[AD-D016061] 07 p3039 N94-27676
VHF impedance measurement: A review
[PB94-138682] 08 p3267 N94-30115
RF and microwave dielectric measurements upon layered materials using reflectometric coaxial sensor
[NPL-DES-125] 08 p3476 N94-30781
A distributed optical fiber strain sensor for monitoring structural deformations 10 p4057 N94-34361
Initial studies of reflectometer for ITER
[DE94-012476] 12 p4528 N94-37167

REFLECTOR ANTENNAS
NT PARABOLIC ANTENNAS
PO/PTD diffraction synthesis of array-fed reflector antennas for satellite and radar applications 01 p0137 N94-11636
An initial study of using the 34-m antenna for lunar mission support 02 p0611 N94-14396
Feasibility study of a synthesis procedure for array feeds to improve radiation performance of large distorted reflector antennas
[NASA-CR-194491] 02 p0612 N94-14501
Proceedings of the 1992 Antenna Applications Symposium, volume 2
[AD-A266916] 03 p0986 N94-14998
Proceedings of the 1992 Antenna Applications Symposium, volume 1
[AD-A268167] 03 p1005 N94-17431
Multi-band reflector antenna with double-ring element frequency selective subreflector 05 p1728 N94-20447
Mobile terminal antennas for helicopters 05 p1731 N94-20458
A compact, portable EHF/SHF antenna for advanced SCAMP
[AD-A272614] 05 p1739 N94-21211
Performance of a simple circular polarization selective surface 05 p1746 N94-22198
Electrical performance of wire mesh for spacecraft deployable reflector antennas 06 p2275 N94-22744
K- and Ka-band mobile-vehicular satellite-tracking reflector antenna system for the NASA ACTS mobile terminal 06 p2289 N94-22831
Integrated reflector antenna design and analysis
[NASA-CR-195164] 06 p2300 N94-24678
Feasibility study of a synthesis procedure for array feeds to improve radiation performance of large distorted reflector antennas
[NASA-CR-195167] 06 p2301 N94-25005
Effective conductivity of wire mesh reflectors for space deployable antenna systems
[NASA-CR-191605] 07 p2788 N94-27770
Defocussing characteristics of the ACTS, T1-VSAT Earth terminal antennas
[NASA-TM-106420] 08 p3242 N94-28826
Beam scanning offset Cassegrain reflector antennas by subreflector movement
[NASA-CR-191604] 08 p3160 N94-28836
GLRS-R 2-colour retroreflector target design and predicted performance
[REPT-932-440-106] 08 p3246 N94-29542
Low sidelobe reflector antenna design for communications
[AD-A276079] 09 p3673 N94-31463
Proceedings of the 1993 Antenna Applications Symposium, volume 1
[AD-A277202] 09 p3676 N94-32049
Proceedings of the 1993 Antenna Applications Symposium, volume 2
[AD-A277203] 09 p3677 N94-32050
INSAT-2A and 2B development mechanisms 09 p3603 N94-33293
Special test equipment and fixturing for MSAT reflector assembly alignment 09 p3606 N94-33316
Baseline antenna design for space exploration initiative
[NASA-CR-196298] 12 p4435 N94-37255

REFLECTOR SATELLITES
U PASSIVE SATELLITES

REFLECTORS
NT FRESNEL REFLECTORS
NT PARABOLIC REFLECTORS
NT PARABOLOID MIRRORS
NT RADAR CORNER REFLECTORS
NT RADAR REFLECTORS
NT RETROREFLECTORS
NT SOLAR COLLECTORS
NT SOLAR REFLECTORS
NT WIGGLER MAGNETS
Universal adjustable mould for antenna reflectors 01 p0059 N94-10027
Damage thresholds of fluoride multilayers at 355 nm
[DE93-009523] 01 p0090 N94-11230
Feature association without a motion estimate
[AD-A265162] 01 p0138 N94-11891
Using lunar sounder imagery to distinguish surface from subsurface reflectors in lunar highlands areas 01 p0464 N94-12179
Spatial light modulator having photosensitive and ferroelectric layers
[AD-D015731] 01 p0404 N94-12400
Analysis of samples of reflector materials which are multicoated and metal samples with oxide coatings which have been exposed the space environment in LDEF testing
[NASA-CR-193647] 02 p0575 N94-12789
Fundamentals and techniques of nonimaging optics
[DE93-013145] 02 p0791 N94-13015
Research on inflatable structure for space use 02 p0530 N94-13275
Reflective coatings for solar applications
[DE93-010026] 02 p0702 N94-13381
An improved patch for radiative coolers
[NASA-CASE-GSC-13503-1] 05 p1822 N94-20127
Goniospectrometric properties of a white standard 05 p1684 N94-20664
X ray characterization of a three-element condenser system for soft x ray projection lithography
[DE93-019916] 05 p1990 N94-21985
Surface physics with cold and thermal neutron reflectometry
[DE94-001447] 07 p2733 N94-26070
Joint services electronics program
[AD-A274643] 07 p2785 N94-27027
Deployable reflector structure
[NASA-CASE-LAR-14513-1-SB] 08 p3245 N94-29360

Optical Chopper Assembly for the Mars Observer
08 p3162 N94-29639
Overview of shielding analyses for the MHTGR from 1986 to 1991
[DE94-002448] 08 p3495 N94-29924
Nonlinear absorption in high reflector multilayers
[DE94-005818] 08 p3295 N94-30598
Sol-gel metal oxide and metal oxide/polymer multilayers applied by meniscus coating
[DE94-005813] 09 p3649 N94-31199
Electromagnetic wave reflection from irregular plasma layers
[AD-A276727] 09 p3678 N94-32161
Special test equipment and fixturing for MSAT reflector assembly alignment 09 p3606 N94-33316
An amorphous fluoropolymer: Next generation optical coating candidate
[DE94-012386] 12 p4425 N94-37422

REFLEXES
NT CONDITIONED REFLEXES
NT COUGH
NT VESTIBULAR NYSTAGMUS
Carotid-cardiac baroreflex: Relation with orthostatic hypotension following simulated microgravity and implications for development of countermeasures
01 p0308 N94-11992
Area postrema ablations in cats: Evidence for separate neural routes for motion- and xylazine-induced CTA and emesis 05 p1887 N94-21906
Role of the area postrema in three putative measures of motion sickness in the rat 05 p1888 N94-21912
Muscle sympathetic nerve activity in humans
07 p2932 N94-27538
Analysis of pursuit tracking eye movements in pilots and nonfliers
[AD-A276597] 09 p3799 N94-32035
Cellular analysis of the startle reflex
[AD-A278243] 10 p4094 N94-33380
Response to graded Lower Body Negative Pressure (LBNP) after space flight 10 p4096 N94-33637
Relation of motion sickness susceptibility to vestibular and behavioral measures of orientation
[NASA-CR-196121] 12 p4480 N94-37005
Gaze orientation under G(z)-load. Methodological aspects: Preliminary results 12 p4485 N94-37274

REFORESTATION
Woody biomass density in the Tendelti area of the central Sudan 07 p2850 N94-27185

REFRACTED RADIATION
U REFRACTED WAVES

REFRACTED RAYS
U REFRACTED WAVES

REFRACTED WAVES
Ocean acoustic propagation measurements and wave propagation in random media
[AD-A276165] 09 p3787 N94-31053

REFRACTION
NT ATMOSPHERIC REFRACTION
NT BIREFRINGENCE
NT RADIO WAVE REFRACTION
Optimization study of x ray laser coherence in Ni-like Ta
[DE93-016419] 02 p0660 N94-14888
Composite refraction-reflection stack sections: Tracing faults in the Atlantic coastal plain sediments
[DE93-013581] 03 p1112 N94-16009
Using computerized tomography to determine ionospheric structures
[DE93-018904] 04 p1485 N94-19002
Synchrotron x ray diffraction analysis of photorefractive crystals and their gratings
[AD-A271176] 05 p2015 N94-20213
Optical fibers and Fluorosensors having improved power efficiency and methods of producing same
[NASA-CASE-LAR-14525-1-CU]
05 p1986 N94-20378
Refraction of high frequency noise in an arbitrary jet flow
[NASA-TM-106465] 06 p2525 N94-23464
Long Duration Exposure Facility space optics handbook
[AD-A274831] 07 p3035 N94-26572
Wave propagation in the shallow regions of the earth's crust and the borehole vicinity
[ITN-94-85237] 07 p2882 N94-27330
Optical parametric oscillator modeling with diffraction, depletion, and double refraction
[DE94-001504] 07 p3040 N94-27999
Hybrid optics for space applications
[ESA-CP-1158] 08 p3501 N94-30418

REFRACTIVE INDEX
U REFRACTIVITY

REFRACTIVITY
The sensitivity of an optical fiber holographic interferometer 01 p0107 N94-10117
Demonstration designs for optical-field-ionized plasma x-ray lasers
[DE93-009227] 01 p0175 N94-11266
Laser photoheterodyne interferometers for oceanographic investigations 01 p0177 N94-12732
The optical constants and spectral specular reflectivity of Highly Oriented Pyrolytic Graphite (HOPG)
[DE93-011894] 02 p0790 N94-12865
Optical properties of CO2 ice and CO2 snow in the ultraviolet, visible, and infrared
[NASA-CR-194110] 02 p0686 N94-14081
Manufacturing and examination of integrated optical waveguide components in silicon
[ETN-93-94393] 02 p0793 N94-14704
Determination of average refractive index of spin coated DCG films for HOE fabrication 03 p1036 N94-14992
A test of the applicability of independent scattering to high albedo planetary regoliths
03 p1250 N94-16187
A ray trace model for propagation loss
[AD-A266314] 03 p0997 N94-16467
Characterization of voids formed during liquid impregnation of nonwoven multifilament glass networks as related to composite processing
03 p0939 N94-16858
BACKSCAT lidar simulation version 3.0: Technical documentation and users guide
[AD-A267296] 03 p1003 N94-17268
Review of rigorous coupled-wave analysis and of homogeneous effective medium approximations for high spatial-frequency surface-relief gratings
03 p1194 N94-17335
Diffractive optical elements for generating arbitrary line foci 03 p1195 N94-17338
Applications of advanced diffractive optical elements
03 p1197 N94-17356
Predesign of diamond turned refractive/diffractive elements for IR objectives 03 p1198 N94-17359
Photorefractive receiver study
[AD-A269352] 04 p1577 N94-18302
Apparatus and method for varying a Bragg wavelength of a Bragg grating formed in an optical fiber
[AD-D015876] 04 p1579 N94-18743
A comparison between several computer codes for calculations on microwave propagation
[FEL-92-A435] 04 p1390 N94-19449
Optical switch evaluation support
[AD-A270948] 04 p1581 N94-19601
Refractive index structure in the lower atmosphere
[AD-A270935] 05 p1854 N94-19899
Refractive index behaviour of phosphorus-doped planar silica waveguides, appendix 7 05 p1989 N94-21601
Precision prism coupling setup applied to measure planar silica films on silicon, appendix 9
05 p1989 N94-21603
The optical constants and spectral specular reflectivity of Highly Oriented Pyrolytic Graphite (HOPG)
[DE93-040546] 05 p1709 N94-21970
Extended range modified gradient technique for profile inversion (extended version of report Et/Em-1992-8)
[PB93-215242] 05 p1742 N94-22346
Design refinement of multilayer optical thin film devices with two optimization techniques
[DE93-634228] 06 p2542 N94-22979
Dimensional analysis of acoustically propagated signals 06 p2528 N94-24217
Conformal method of fabricating and optical waveguide on a semiconductor substrate
[AD-D015988] 06 p2546 N94-25043
Liquidus temperature and optical properties measurement by containerless techniques
06 p2247 N94-25126
Optical properties and emissivities of liquid metals and alloys 06 p2248 N94-25129
Microtubules for nonlinear optical limiting
[AD-A273940] 07 p3035 N94-25941
Peculiarities and application perspectives of metal-ion implants in glasses
[DE94-004671] 07 p3035 N94-26246
Radar detection of low-altitude targets in a maritime environment. Volume 2: Meteorological and radar data
[AD-A274658] 07 p2768 N94-26335
Modelling atmospheric turbulence effects on ground-based telescope systems
[DE94-004211] 07 p3102 N94-26528
Refractive and dielectric properties of helium, argon and nitrogen gases
[PB94-123783] 07 p3008 N94-26851
Optical characterization and guided wave loss measurements for end-capped 6F-polybenzoxazole
[AD-A274586] 07 p3036 N94-26982
Research and development within nonlinear optics for protection of optical sensors against laser irradiation on of optical sensors against laser irradiation. Quarterannual report 1 (april 1993))
[PB94-124245] 07 p3037 N94-27046
Theoretical and experimental analysis of the spatial and temporal behaviour of the intensity of an electro-magnetic wave reflected from a diffuse target after passing through a turbulent atmosphere
[ITN-94-85230] 07 p2774 N94-27234
Ion implantation in silicate glasses
[DE94-003785] 07 p2757 N94-27726
High damage threshold anti-reflectors by physical vapor deposited amorphous fluoropolymer
[DE94-004865] 08 p3212 N94-28560
Electrooptical and optical evaluation of Pb(Zr,Ti)O3 thin films using waveguide refractometry
[DE94-006374] 08 p3518 N94-30247
Characterization of thermally annealed Sb implanted fused silica
[DE94-005464] 08 p3219 N94-30335
Ocean acoustic propagation measurements and wave propagation in random media
[AD-A276165] 09 p3787 N94-31053
Multifunctional macromolecules
[AD-A277347] 09 p3656 N94-32246
Coastal boundary layer and refractivity measurements using the ground-based high resolution interferometer sounder (GB-HIS)
[AD-A277980] 09 p3683 N94-33159
Radio wave refractivity deduced from lidar measurements
[AD-D016147] 10 p4034 N94-33780
A theory and experiments for detecting shock locations
[NASA-TM-106634] 10 p4056 N94-33952
Proposal to produce novel, transparent radiation hard low refractive index
[AD-A278476] 10 p4029 N94-34087
Method and apparatus for removing unwanted reflections from an interferometer
[NASA-CASE-NPO-18478-1-CU]
11 p4333 N94-35749
Determining the refractive index of a lambda/4 thin film on a thick substrate from a transmittance measurement
[DE93-019584] 12 p4523 N94-36693
An amorphous fluoropolymer: Next generation optical coating candidate
[DE94-012386] 12 p4425 N94-37422

REFRACTORIES
How to read a phase equilibrium diagram for high-temperature ceramics material as main object
[DE93-512333] 02 p0582 N94-14513
Refractory precursor components in an Allende ferromagnesian chondrule 03 p1245 N94-16412
Tambo Quemado: Extraordinary concentrations of REE and refractory trace elements caused by artificial heating
05 p1684 N94-20667
High temperature materials technology research for advanced thermionic systems
[DE94-008341] 09 p3646 N94-32825

REFRACTORY COATINGS
Research on chemical vapor deposition processes for advanced ceramic coatings
[NASA-CR-193613] 02 p0577 N94-13089
Performance of carbon-based hot frit substrates
[DE94-000509] 05 p1676 N94-21754
Compilation of reinforced carbon-carbon transatlantic abort landing arc jet test results
[NASA-TM-104778] 05 p1676 N94-21834
Molten salt reactor for potentiostatic electroplating
[AD-D016020] 06 p2258 N94-24720
A novel approach to the fabrication of SiC structures of arbitrary shape
[AD-A275475] 08 p3214 N94-29073
The development of CVR coatings for PBR fuels
[DE94-004233] 09 p3875 N94-31480
Composite matrix experimental combustor
[AD-280344] 10 p4005 N94-34679

REFRACTORY MATERIALS
NT CHROMIUM
NT IRIDIUM
NT MOLYBDENUM
NT MOLYBDENUM ALLOYS
NT NIOBIUM
NT NIOBIUM ALLOYS
NT OSMIUM
NT OSMIUM ISOTOPES
NT REFRACTORIES
NT REFRACTORY METAL ALLOYS
NT REFRACTORY METALS
NT RHENIUM
NT RHENIUM ALLOYS
NT RHENIUM ISOTOPES
NT TANTALUM
NT TANTALUM ALLOYS
NT TUNGSTEN
NT TUNGSTEN ALLOYS
High temperature materials for hypersonic transport
01 p0056 N94-10003

Distortions and stresses in thin shells due to anisotropic thermal expansion 01 p0057 N94-10014
An ultralight carbon-carbon composite with amorphous matrix 01 p0061 N94-10042
Ceramic matrix composites: High performance materials for space application 01 p0062 N94-10044
Joints between dissimilar metallic and ceramic materials 01 p0063 N94-10052
Advanced methods of permanently joining carbon materials 01 p0063 N94-10057
High temperature composites in Aerospatiale activities 01 p0064 N94-10062
Structure and properties of an RS Al-Si-Ni-Mn-Zr alloy for high temperature applications 01 p0064 N94-10063
Fibre reinforced structures with glass matrix 01 p0064 N94-10064
STARDUST: A simulation experiment of cosmic dust analogues production in microgravity conditions 01 p0113 N94-10175
Space Storable Rocket Technology program (SSRT). Option 1 program
[NASA-CR-191171] 01 p0046 N94-10938
Thermal stability of sealants for military aircraft: Modification of polysulfide prepolymers with ether and thioether monomers
[AD-A264079] 01 p0089 N94-11107
The giant impact produced a precipitated Moon 01 p0430 N94-12135
Ceramics formed by pyrolysis of either linear or thermosetting carborane (siloxane or silane) acetylene based precursor polymers
[AD-D015747] 01 p0093 N94-12330
Synthesis and polymerization of oligomeric multiple aromatic ether-containing phthalonitriles
[AD-D015729] 01 p0094 N94-12399
High-temperature corrosion and protection of materials
[DE93-011072] 02 p0568 N94-12998
How to read a phase equilibrium diagram for high-temperature ceramics material as main object
[DE93-512333] 02 p0582 N94-14513
Processing and protection of high temperature structural materials
[AD-A267292] 03 p0954 N94-14961
High temperature advanced structural composites. Volume 2: Ceramic matrix composites, fiber processiing and properties, and interfaces
[AD-A267023] 03 p0933 N94-15528
High temperature advanced structural composites. Volume 1: Executive summary and intermetallic compounds
[AD-A267022] 03 p0933 N94-15835
Techniques for preparation of ingot metallurgical discontinuous composites
[AD-D015748] 03 p0940 N94-16933
Plastic anisotropy in MoSi2 single crystals
[DE93-012650] 04 p1594 N94-17874
The 6th Japan-U.S. conference on composite materials
[AD-A268535] 04 p1341 N94-18630
Developing and understanding the high temperature behavior of niobium aluminides and niobium aluminide composites
[AD-A268874] 04 p1341 N94-18636
Phthalonitrile prepolymer as high temperature sizing material for composite fibers
[AD-D015912] 05 p1672 N94-20010
Development of improved processing and evaluation methods for high reliability structural ceramics for advanced heat engine applications, phase 1
[DE93-040528] 05 p1702 N94-20481
Petrography and origin of refractory inclusions from the Murray and Murchison C2 chondrites 05 p2084 N94-20770
Trace element compositions of spinel-rich refractory inclusions from the Murchison meteorite 05 p2086 N94-20897
Polyimide-based electrooptic materials
[DE93-019416] 05 p1706 N94-21526
Evaluation of A5Si3Z(x) intermetallics for use as high temperature structural materials
[DE93-041127] 06 p2227 N94-22977
Small rocket research and technology 06 p2211 N94-23038
Advanced materials for radiation-cooled rockets 06 p2214 N94-23052
Vaporization behavior of non-stoichiometric refractory carbide materials and direct observations of the vapor phase using laser diagnostics
[DE93-040094] 06 p2348 N94-23203
Preceedings of the 12th International Congress: Corrosion Control for Low-Cost Reliability. Volume 2: Process Industries Plant Operations
[AD-A273662] 06 p2251 N94-25449
Preceedings of the 12th International Congress: Corrosion Control for Low-Cost Reliability. Volume 3A: Corrosion: Specific issues
[AD-A273663] 06 p2251 N94-25450
Computer modelling of cyclic deformation of high-temperature materials
[AD-A273852] 07 p2704 N94-25608
Optical characterization and guided wave loss measurements for end-capped 6F-polybenzoxazole
[AD-A274586] 07 p3036 N94-26982
Computer modelling of cyclic deformation of high-temperature materials
[AD-A274504] 07 p2840 N94-27034
High temperature sensor/microphone development for active noise control
[NASA-CR-195214] 07 p2812 N94-27214
Fibrous emissive burners selective and broad band
[PB94-128329] 07 p2859 N94-27225
Thermal expansion and elastic anisotropy in single crystal Al2O3 and SiC reinforcements
[NASA-TM-106516] 08 p3214 N94-29105
Method of producing a ceramic fiber-reinforced glass-ceramic matrix composite
[NASA-CASE-LEW-15264-2] 08 p3180 N94-29508
Surface fatigue life of high temperature gear materials
[NASA-TM-106562] 08 p3303 N94-30227
High temperature NASP engine seal development
[NASA-TM-109750] 09 p3725 N94-31804
Computer modelling of cyclic deformation of high-temperature materials
[AD-A277056] 09 p3623 N94-32012
High temperature materials technology research for advanced thermionic systems
[DE94-008341] 09 p3646 N94-32825
Research on high reliability refractory ohmic contacts for GaAs FETs and MODFETs
[AD-A276848] 09 p3697 N94-33034
Enabling propulsion materials for high-speed civil transport engines 10 p3978 N94-33511
Combustor materials requirements and status of ceramic matrix composites 10 p3978 N94-33512
HSCT airframe materials: The Boeing perspective 10 p3979 N94-33515
High Temperature Materials Laboratory sixth annual report, October 1992 - September 1993
[DE94-009840] 10 p4027 N94-33881
Expendable gas turbine engine technology advances 10 p4000 N94-34438
Tough, processable semi-interpenetrating polymer networks from monomer reactants
[NASA-CASE-LAR-14838-1] 11 p4242 N94-35233
Tough high performance composite matrix
[NASA-CASE-LAR-14239-2] 11 p4232 N94-35372
Carbon-carbon piston development
[NASA-CR-4595] 11 p4233 N94-35947
Advanced composites in Japan 11 p4234 N94-36045
Possibilities and pitfalls in aerospace applications of titanium matrix composites 12 p4400 N94-36650
Mechanical behavior of MoSi2 and MoSi2 composites
[DE94-013116] 12 p4405 N94-37289
Development of durable high-temperature catalysts for natural gas combustion: Catalytic materials (CATMAT (trade name)) properties database
[PB94-171824] 12 p4412 N94-37462
Development of processing techniques for advanced thermal protection materials
[NASA-CR-196261] 12 p4426 N94-37510
Substituted silyl-terminated compounds and polymers thereof
[AD-D016310] 12 p4427 N94-37779

REFRACTORY METAL ALLOYS

NT MOLYBDENUM ALLOYS
NT NIOBIUM ALLOYS
NT RHENIUM ALLOYS
NT TANTALUM ALLOYS
NT TUNGSTEN ALLOYS

Structural material, manufacture, and design requirements for high-temperature fasteners for space plane technologies 01 p0063 N94-10055
Constitutive laws for describing the service relevant creep behaviour of metallic materials 01 p0064 N94-10060
JPRS report: Science and technology. Central Eurasia: Materials science
[JPRS-UMS-93-006] 02 p0558 N94-14573
High temperature materials technology research for advanced thermionic systems
[DE93-018302] 03 p0960 N94-16964
Fundamental concepts relating local atomic arrangements, deformation, and fracture of intermetallic alloys
[AD-A268745] 04 p1361 N94-18788
Strengthening and toughening in refractory metal alloys
[DE93-019942] 05 p1695 N94-21986
An extended laser flash technique for thermal diffusivity measurement of high-temperature materials 06 p2238 N94-25132
Recent advances and developments in refractory alloys
[DE94-007929] 09 p3644 N94-32374
High temperature materials technology research for advanced thermionic systems
[DE94-008444] 09 p3644 N94-32416
High temperature materials technology research for advanced thermionic systems
[DE94-008341] 09 p3646 N94-32825
High Temperature Silicides and Refractory Alloys Symposium, volume 322
[AD-A278373] 10 p4024 N94-33741

REFRACTORY METALS

NT CHROMIUM
NT IRIDIUM
NT MOLYBDENUM
NT NIOBIUM
NT OSMIUM
NT OSMIUM ISOTOPES
NT RHENIUM
NT RHENIUM ISOTOPES
NT TANTALUM
NT TUNGSTEN

Chemical Vapor Deposition of Refractory Metals and Ceramics 2. Materials Research Society Symposium proceedings
[AD-A265072] 01 p0092 N94-11866
Isotopic and trace element characteristics of an unusual refractory inclusion from Essebi 01 p0471 N94-12212
Thermal spray forming of refractory sample ampoule cartridges for single crystal growth space furnaces
[TABES PAPER 93-605] 03 p1051 N94-16141
Experimental partitioning of Zr, Ti, and Nb between silicate liquid and a complex noble metal alloy and the partitioning of Ti between perovskite and platinum metal 03 p0962 N94-16287
Properties of thin films for high temperature flow sensors
[NASA-CR-191526] 03 p0967 N94-16541
Effects of processing history on the creep strength of Nb-1Zr
[DE93-015905] 05 p1689 N94-20093
New extensions in the development of deformation processed metal-metal matrix composites
[DE94-000692] 06 p2227 N94-23004
The effects of texture and strain on the r-va lue of heavy gauge tantalum plate
[DE94-000690] 06 p2242 N94-23541
Growth, characterization and device development in monocrystalline diamond films
[AD-A274245] 07 p3060 N94-26839
List of papers published by the members of Institute for Materials Research, Tohoku University 1992
[JTN-94-80608] 07 p3118 N94-27355
Recent advances and developments in refractory alloys
[DE94-007929] 09 p3644 N94-32374
High temperature materials technology research for advanced thermionic systems
[DE94-008341] 09 p3646 N94-32825

REFRASIL (TRADEMARK)

U FIBERS
U SILICON DIOXIDE

REFRIGERANTS

Theoretical evaluation of R22 and R502 alternatives
[DE93-014767] 01 p0411 N94-10853
Measurement of viscosity, density and gas solubility of refrigerant blends
[DE93-014772] 01 p0089 N94-11145
Accelerated screening methods for predicting lubricant performance in refrigerant compressors
[DE93-014773] 01 p0089 N94-11146
ARTI Refrigerant Database
[DE93-014774] 02 p0595 N94-13021
Miscibility of lubricants with refrigerants, phase 1
[DE93-014766-PHASE-1] 02 p0596 N94-13407
Compatibility of refrigerants and lubricants with motor materials
[DE93-014768] 02 p0583 N94-14801
Cycle performance testing of nonazeotropic mixtures of HFC-142A/HCFC-124 and HFC-32/HCFC-124 with enhanced surface heat exchangers
[DE93-015215] 03 p1024 N94-16808
Malone refrigeration
[DE93-014468] 04 p1379 N94-17725
Compatibility of refrigerants and lubricants with motor materials, volume 1
[DE93-040216] 04 p1350 N94-18895
Compatibility of refrigerants and lubricants with motor materials, volume 2
[DE93-040217] 04 p1350 N94-18896

Measurement of viscosity, density, and gas solubility of refrigerant blends in selected synthetic lubricants
[DE93-040221] 04 p1350 N94-18977
Thermophysical properties
[DE93-040219] 04 p1351 N94-19134
Accelerated screening methods for determining chemical and thermal stability of refrigerant-lubricant mixtures. Part 1: Method assessment
[DE93-040215] 04 p1351 N94-19136
Compatibility of refrigerants and lubricants with motor materials, volume 3
[DE93-040218] 04 p1352 N94-19191
Absorption heat pump for space applications
[NASA-CR-194693] 05 p1845 N94-20066
Alternative refrigerants and refrigeration cycles for domestic refrigerators
[DE93-040481] 05 p1714 N94-20099
EHD enhancement of pool and in-tube boiling of alternate refrigerants
[DE94-000787] 05 p1798 N94-20101
The laser and its applications on environment and biotechnology research
[DE94-000376] 05 p1820 N94-21957
US Department of Energy phaseout of CFC-refrigerants
[DE94-001668] 06 p2397 N94-23016
Measurement of viscosity, density, and gas solubility of refrigerant blends in selected synthetic lubricants
[DE94-003609] 07 p2713 N94-25934
Accelerated screening methods for determining chemical and thermal stability of refrigerant-lubricant mixtures. Part 2: Experimental comparison and verification of methods
[DE94-003664] 07 p2749 N94-26007
Thermophysical properties of HFC-143a and HFC-152a
[DE94-004236] 07 p2719 N94-27567
Compatibility of refrigerants and lubricants with engineering plastics
[DE94-004959] 07 p2756 N94-27692
Thermophysical properties of refrigerant R-134a (1,1,1,2-tetrafluoroethane)
[ESDU-93001] 07 p2720 N94-27959
Solubility, viscosity, and density of refrigerant/lubricant mixtures
[DE94-004237] 07 p2721 N94-28069
ARTI Refrigerant Database
[DE94-004906] 08 p3230 N94-28563
An experimental investigation of flow patterns and liquid entrainment in a horizontal-tube evaporator
08 p3277 N94-29899
Large heat pumps using CO2 refrigerant
[PB94-138773] 08 p3279 N94-29999
Materials compatibility and lubricants research on CFC-refrigerant substitutes
[DE94-004905] 08 p3220 N94-30692
Application of natural refrigerants: A rational solution to a pressing problem
[PB94-138781] 09 p3668 N94-31073
Measurement of viscosity, density, and gas solubility of refrigerant blends in selected synthetic lubricants
[DE94-007723] 09 p3653 N94-31917
Compatibility of refrigerants and lubricants with elastomers
[DE94-008552] 09 p3658 N94-32518
Measurement of viscosity, density, and gas solubility of refrigerant blends in selected synthetic lubricants
[DE94-010426] 11 p4244 N94-35687
Solubility, viscosity and density of refrigerant/lubricant mixtures
[DE94-009996] 11 p4245 N94-35771
Thermophysical properties of HFC-143a and HFC-152a
[DE94-009995] 11 p4251 N94-36008
Research update: Materials Compatibility and Lubricant Research (MCLR) program
[DE94-010001] 11 p4247 N94-36387
Sealed tube comparisons of the compatibility of desiccants with refrigerants and lubricants
[DE94-010002] 11 p4251 N94-36388
Materials Compatibility and Lubricant Research on CFC-refrigerant substitutes
[DE94-012352] 12 p4425 N94-37373
Sealed tube comparisons of the compatibility of desiccants with refrigerants and lubricants
[DE94-012371] 12 p4425 N94-37421
Information on alternative refrigerants and lubricants: The ARTI refrigerant database
[DE94-009997] 12 p4426 N94-37490

REFRIGERATING
ARTI Refrigerant Database
[DE93-014774] 02 p0595 N94-13021
Double inlet pulse tube cryocooler theory
[AD-A266832] 02 p0597 N94-14877
Space Station thermal storage/refrigeration system research and development
[NASA-CR-193841] 03 p0879 N94-15191
Proceedings of the 7th International Cryocooler Conference, part 1
[AD-A268448] 03 p0985 N94-17482
Proceedings of the 7th International Cryocooler Conference, part 2
[AD-A268449] 03 p0985 N94-17484
Proceedings of the 7th International Cryocooler Conference, part 3
[AD-A268450] 03 p0985 N94-17485
Malone refrigeration
[DE93-014468] 04 p1379 N94-17725
The 7th International Cryocooler Conference
[AD-A268451] 04 p1379 N94-18147
Regenerator optimization for Stirling cycle refrigeration
[DE93-018468] 04 p1380 N94-18818
Design verification and acceptance tests of the ASST-A helium refrigeration system
[DE93-019746] 04 p1381 N94-19540
Alternative refrigerants and refrigeration cycles for domestic refrigerators
[DE93-040481] 05 p1714 N94-20099
EHD enhancement of pool and in-tube boiling of alternate refrigerants
[DE94-000787] 05 p1798 N94-20101
A novel scheme to handle highly pulsed loads with a standard helium refrigerator
[DE93-019617] 05 p1799 N94-20263
US Department of Energy phaseout of CFC-refrigerants
[DE94-001668] 06 p2397 N94-23016
Evaluation of high temperature superconductive thermal bridges for space-borne cryogenic infrared detectors
07 p2815 N94-27921
ARTI Refrigerant Database
[DE94-004906] 08 p3230 N94-28563
Application of natural refrigerants: A rational solution to a pressing problem
[PB94-138781] 09 p3668 N94-31073
Research update: Materials Compatibility and Lubricant Research (MCLR) program
[DE94-010001] 11 p4247 N94-36387
Sealed tube comparisons of the compatibility of desiccants with refrigerants and lubricants
[DE94-010002] 11 p4251 N94-36388
Miniature thermoacoustic refrigerator
[AD-A280326] 12 p4431 N94-37029
Refrigeration and Air-Conditioning Technology Workshop
[DE94-010813] 12 p4431 N94-37452

REFRIGERATING MACHINERY
NT REFRIGERATORS
Accelerated screening methods for predicting lubricant performance in refrigerant compressors
[DE93-014773] 01 p0089 N94-11146

REFRIGERATORS
The superfluid Stirling refrigerator, a new method for cooling below 0.5 K
[DE93-012672] 01 p0128 N94-11161
The Second Workshop on Refrigerating System Utilization Onboard the JEM
[NASDA-CON-930001] 01 p0129 N94-11831
Summary of the pre-AO of the JEM onboard scientific and engineering experiments for refrigerator utilization
01 p0129 N94-11832
Development of space refrigerator
01 p0129 N94-11833
Studies on refrigerator sensors and cooling section interface 01 p0129 N94-11834
Trend of miniature refrigerator utilization in earth observation area 01 p0130 N94-11835
Satellite observation of atmospheric tracer components: JEM/POP 01 p0130 N94-11836
Submillimeter wave observation experiment of Earth atmosphere with SIS mixer 01 p0130 N94-11837
Refrigerator utilization in infrared astronomy
01 p0130 N94-11838
Study on various cryogenic refrigeration cycles using all purpose refrigerators 01 p0130 N94-11839
Development test on 2 K cooling systems
01 p0130 N94-11840
Generation of superfluid He by G-M cycle cryogenic refrigerator 01 p0130 N94-11841
Development of 4 K refrigerator using highly efficient heat accumulating reservoir 01 p0130 N94-11842
Utilization of superconductivity in the area of space
01 p0131 N94-11843
Three-stage linear, split-Stirling cryocooler for 1 to 2K magnetic cold stage
[NASA-CR-4538] 02 p0776 N94-13897
A recuperative superfluid Stirling refrigerator
[DE93-016521] 02 p0597 N94-14592
Double inlet pulse tube cryocooler theory
[AD-A266832] 02 p0597 N94-14877
An adiabatic demagnetisation refrigerator with a mechanical pre-cooler for space applications
03 p0906 N94-15070
In orbit adiabatic demagnetization refrigeration for bolometric and microcalorimetric detectors
03 p0907 N94-15079
Proceedings of the 7th International Cryocooler Conference, part 1
[AD-A268448] 03 p0985 N94-17482
Proceedings of the 7th International Cryocooler Conference, part 2
[AD-A268449] 03 p0985 N94-17484
Proceedings of the 7th International Cryocooler Conference, part 3
[AD-A268450] 03 p0985 N94-17485
The 7th International Cryocooler Conference
[AD-A268451] 04 p1379 N94-18147
Design verification and acceptance tests of the ASST-A helium refrigeration system
[DE93-019746] 04 p1381 N94-19540
Alternative refrigerants and refrigeration cycles for domestic refrigerators
[DE93-040481] 05 p1714 N94-20099
A novel scheme to handle highly pulsed loads with a standard helium refrigerator
[DE93-019617] 05 p1799 N94-20263
A study of element interaction in thermoacoustic engines
[AD-A273228] 06 p2569 N94-24777
A compact 150 GHz SIS receiver cooled by 4 K GM refrigerator
[REPT-36] 07 p2776 N94-27340
Annual summary of basic research thermoacoustic heat transport, 1993
[AD-A275751] 08 p3230 N94-28644
Properties and applications of powder-filled evacuated-panel superinsulations
[DE94-009169] 11 p4233 N94-35932
MODIL cryocooler producibility demonstration project results
[DE93-019213] 12 p4430 N94-36444
Miniature thermoacoustic refrigerator
[AD-A280326] 12 p4431 N94-37029
Fundamentals studies of radial wave thermoacoustic engines
[AD-A280534] 12 p4431 N94-37090

REFUELING
NT AIR TO AIR REFUELING
Vehicular fleet operation on natural gas and propane: An overview
[PB93-194603] 01 p0098 N94-10844
Business fleet refueling assessment
[PB93-189892] 01 p0098 N94-11017
On-orbit refueling 01 p0038 N94-11565
On-orbit refueling 01 p0038 N94-11566
Preliminary analysis of the benefits derived to US Air Force spacecraft from on-orbit refueling
01 p0038 N94-11567
Mechanically refuelable zinc/air electric vehicle cells
[DE93-016446] 04 p1394 N94-17770
High-speed repetitive pellet injector for plasma fueling of magnetic confinement fusion devices
[DE94-002792] 07 p3042 N94-26140
Application of railgun principle to high-velocity hydrogen pellet injection for magnetic fusion reactor fueling
[DE94-004411] 07 p3044 N94-26579
Development and testing of the Automated Fluid Interface System 08 p3161 N94-29636
Autonomous Robotic Refueling System (ARRS) for rapid aircraft turnaround 08 p3305 N94-30279
Robotic technologies of the Flight Telerobotic Servicer (FTS) including fault tolerance 10 p4067 N94-34034
Final regulatory impact analysis: Refueling emission regulations for light duty vehicles and trucks and heavy duty vehicles
[PB94-164027] 11 p4285 N94-35754
LNG vehicle technology, economics, and safety assessment
[PB94-165487] 12 p4450 N94-36721

REGENERATION (ENGINEERING)
Regeneration of near-wall turbulence structures
01 p0158 N94-12308
Destruction of problematic airborne contaminants by hydrogen reduction using a Catalytically Active, Regenerable Sorbent (CARS)
[NASA-CR-194354] 02 p0709 N94-14103
Performance calculations and research direction for a water enhanced regenerative gas turbine cycle
[DE93-019866] 05 p1826 N94-21983

REGENERATION (PHYSIOLOGY)
Validated environmental and physiological data from the CELSS Breadboard Projects Biomass Production Chamber. BWT931 (Wheat cv. Yecora Rojo)
[NASA-TM-109191] 02 p0738 N94-13979
Bioregenerative system components for microgravity
07 p2903 N94-25673

REGENERATIVE COOLING
Recent testing of 30 kW hydrogen arcjet thrusters
[NASA-TM-106214] 02 p0551 N94-13430
Proceedings of the 7th International Cryocooler Conference, part 1
[AD-A268448] 03 p0985 N94-17482
Proceedings of the 7th International Cryocooler Conference, part 2
[AD-A268449] 03 p0985 N94-17484
Proceedings of the 7th International Cryocooler Conference, part 3
[AD-A268450] 03 p0985 N94-17485
Flow visualization study in high aspect ratio cooling channels for rocket engines 06 p2213 N94-23049
Effect of hydrogen exposure on a Cu-8 Cr-4 Nb alloy
[NASA-TM-106429] 06 p2243 N94-23556
Heat transfer in rocket engine combustion chambers and regeneratively cooled nozzles
[NASA-CR-193949] 06 p2220 N94-24471
Experimental analysis of heat transfer characteristics and pressure drop through screen regenerative heat exchangers
[AD-A273902] 07 p2790 N94-25657
The 4 K Stirling cryocooler demonstration
[NASA-CR-191792] 09 p3669 N94-32484
Active cooling from the sixties to NASP
[NASA-TM-109079] 12 p4456 N94-37541
REGENERATIVE CYCLES
U REGENERATION (ENGINEERING)
REGENERATIVE FEEDBACK
U POSITIVE FEEDBACK
REGENERATIVE FUEL CELLS
Computation of photovoltaic parameters under lunar temperature variation 01 p0053 N94-11411
Primary and secondary electrical space power based on advanced PEM systems
[DE93-012643] 02 p0553 N94-14689
Regenerative fuel cells for High Altitude Long Endurance Solar Powered Aircraft
[DE93-016991] 04 p1465 N94-17853
Primary and secondary electrical space power based on advanced PEM systems 06 p2392 N94-23357
PEM regenerative fuel cells 06 p2392 N94-23358
Effect of power system technology and mission requirements on high altitude long endurance aircraft
[NASA-CR-194455] 06 p2189 N94-25200
REGENERATORS
NT THERMOSIPHONS
The 7th International Cryocooler Conference
[AD-A268451] 04 p1379 N94-18147
Regenerator optimization for Stirling cycle refrigeration
[DE93-018468] 04 p1380 N94-18818
A low cost alternative to high performance PCM bit synchronizers 05 p1813 N94-21347
Performance calculations and research direction for a water enhanced regenerative gas turbine cycle
[DE93-019866] 05 p1826 N94-21983
The 4 K Stirling cryocooler demonstration
[NASA-CR-191792] 09 p3669 N94-32484
REGGE POLES
Model for the pomeron
[DE93-617693] 01 p0362 N94-10552
Alternating series fit to the total cross sections
[DE94-616888] 11 p4326 N94-36132
High energy asymptotics of perturbative multi-color QCD
[DE94-001350] 11 p4327 N94-36238
REGIONAL PLANNING
NT URBAN PLANNING
Summary of implementation and demonstration projects in bays and estuaries
[PB93-194637] 01 p0265 N94-10846
Obtaining digital regional planning information from aerial pictures
[REPT-228] 02 p0700 N94-14810
The 7th Brazilian Remote Sensing Symposium, volume 1 05 p1838 N94-20953
Application of SPOT to GIS/LIS in land capability evaluation for regional planning of JAICO semi-arid region of Piaui, Brazil 05 p1838 N94-20955
The advantages of the location Germany must not be jeopardized in air traffic 07 p2661 N94-28236
Geomorphological map of the region of the Paraiba Valley and the northern coastal zone of Sao Paulo State
[INPE-5531-PRP/179] 10 p4077 N94-34226
National Maglev initiative: California line electric utility power system requirements 11 p4215 N94-35850
REGIONS
NT AMAZON REGION (SOUTH AMERICA)
NT ANTARCTIC REGIONS
NT ARCTIC REGIONS
NT AURORAL ZONES
NT BRILLOUIN ZONES
NT D REGION
NT E REGION
NT EQUATORIAL REGIONS
NT F REGION
NT F 2 REGION
NT FRESNEL REGION
NT HABITATS
NT INTERTROPICAL CONVERGENT ZONES
NT M REGION
NT MCMURDO SOUND
NT POLAR REGIONS
NT REMOTE REGIONS
NT ROSS ICE SHELF
NT SPORADIC E LAYER
NT SUBARCTIC REGIONS
NT TEMPERATE REGIONS
NT TROPICAL REGIONS
Eastern Europe: A climatological study
[AD-A269200] 04 p1493 N94-18883
Image segmentation by a combination of edge detection and region growing
[ETN-94-95032] 07 p2960 N94-26106
Non-local sub-characteristic zones of influence in unsteady interactive boundary-layers
10 p4053 N94-34982
REGISTERS (COMPUTERS)
Simulation of a parallel computer
[NAL-TR-1154] 01 p0335 N94-10368
Wait-free linearization with an assertional proof
[CS-9208] 01 p0323 N94-10878
A 20 MHz CMOS reorder buffer for a superscalar microprocessor 05 p1764 N94-21700
REGOLITH
Cold press sintering of simulated lunar basalt
01 p0131 N94-12026
Apollo 16 core 60013/14 as a product of path 1 and path 2 regolith evolution processes
01 p0440 N94-12050
The spectral effects of subsolidus reduction of olivine and pyroxene 01 p0081 N94-12110
Impact comminution of glasses: Implications for lunar regolith evolution 01 p0461 N94-12159
Simulation of possible regolith optical alteration effects on carbonaceous chondrite meteorites
01 p0430 N94-12163
Porosity and the ecology of icy satellites
01 p0431 N94-12186
Workshop on the Space Environment: The Effects on the Optical Properties of Airless Bodies
[NASA-CR-194417] 02 p0842 N94-14298
Impact melting and vaporization in planetary regoliths
02 p0843 N94-14299
Extrapolation of space weathering processes to other small solar system bodies 02 p0843 N94-14300
Laboratory simulations of lunar darkening processes
02 p0843 N94-14301
Deposition of impact-generated vapors in the lunar regolith 02 p0843 N94-14302
The state of Fe in the lunar regolith and its relationship to the spectral reflectance properties of the moon
02 p0843 N94-14303
A test of the applicability of independent scattering to high albedo planetary regoliths
03 p1250 N94-16187
Nitrates in SNCs: Implications for the nitrogen cycle on Mars 03 p1251 N94-16193
Why is the Moon dark? 03 p1256 N94-16219
The physical mechanism of comet outbursts: An experiment 03 p1242 N94-16221
JSC-1: A new lunar regolith simulant
03 p1289 N94-16398
Equatorial ground ice on Mars: Steady-state stability
03 p1290 N94-16403
Mars brine formation experiment
03 p1293 N94-16419
Helium-3 inventory of lunar samples: A potential future energy resource for mankind? 03 p1295 N94-16428
The distribution of ground ice on Mars
05 p2090 N94-20394
The Erevan howardite: Petrology of glassy clasts and mineral chemistry 05 p1684 N94-20640
The coherent backscattering opposition effect
05 p1991 N94-20646
Characterization of Minnesota lunar simulant for plant growth 05 p1897 N94-20665
Abundance and composition of solar KR in the H3-H6 chondrite ACFER111 05 p1684 N94-20676
Evaluation of lunar rocks and soils for resource utilization: Detailed image analysis of raw materials and beneficiated products 05 p2126 N94-20820
Regolith breccia consisting of H and LL chondrite mixture 05 p2080 N94-20892
Oxidation of dissolved iron under warmer, wetter conditions on Mars: Transitions to present-day arid environments 05 p2143 N94-21663
Early Mars: The inextricable link between internal and external influences on valley network formation
05 p2146 N94-21681
Determination of Martian soil mineralogy and water content using the Thermal Analyzer for Planetary Soils (TAPS) 05 p1812 N94-22433
Whole rock major element chemistry of KREEP basalt clasts in lunar breccia 15205: Implications for the petrogenesis of volcanic KREEP basalts
06 p2614 N94-24365
Design of a lunar propellant processing facility. NASA/USRA advanced program
[NASA-CR-195502] 06 p2266 N94-24618
Vertical transport of water in the Martian boundary layer 06 p2622 N94-24902
The pH of Mars 09 p3950 N94-33225
Temporal changes in the geographic distribution, elevation, and potential origin of the Martian outflow channels 09 p3951 N94-33235
Simultaneous laboratory measurements of CO2 and H2O adsorption on palagonite: Implications for the Martian climate and volatile reservoir 09 p3952 N94-33240
Mars aqueous chemistry experiment
[NASA-CR-196024] 11 p4354 N94-35263
Grain rims on ilmenite in the lunar regolith: Comparison to vapor deposits on regolith silicates
11 p4359 N94-35418
Luna 24 regolith breccias: A possible source of the fine size material of the Luna 24 regolith
11 p4362 N94-35450
REGRESSION (STATISTICS)
U REGRESSION ANALYSIS
REGRESSION ANALYSIS
NT REGRESSION COEFFICIENTS
Applicability of satellite infrared data for the monitoring of coastal environments 01 p0220 N94-12714
Exploratory data analysis: Past, present and future
[AD-A266775] 02 p0774 N94-14788
Generalized smooth models
[DE93-013045] 02 p0756 N94-14864
Efficiency effects of variation in controlled experimental variables
[DE93-014345] 03 p1169 N94-15979
A linear spectral matching technique for retrieving equivalent water thickness and biochemical constituents of green vegetation 03 p1068 N94-16678
Computing science and statistics. Volume 24: Graphics and visualization
[AD-A266571] 03 p1150 N94-16721
Ensemble forecasting techniques in medium-range forecasting
[AD-A267443] 03 p1107 N94-17029
Linear parameter identification methods for ARMA models with periodic coefficients
[REPT-92-070] 04 p1556 N94-17938
EDF tests for normality in linear models after a Box-Cox transformation
[AD-A269068] 04 p1557 N94-18517
Modeling of driver behavior: Information perception, rule and control strategies in experiments and simulations
[ETN-93-95053] 04 p1510 N94-19649
Generalized regression trees: Function estimation via recursive partitioning and maximum likelihood
[AD-A271259] 04 p1560 N94-19726
Statistical analysis of a reciprocal translocations data base
[RR-900-I] 05 p1963 N94-20165
On estimation and testing in Poisson regression models with over-dispersion
[MEMO-1083] 05 p1963 N94-21076
An evaluation of artificial neural network modeling for manpower analysis
[AD-A273001] 05 p1945 N94-21269
The European Southern Observatory-MIDAS table file system 05 p2048 N94-22518
Atmospheric moisture fields derived by satellite observations over the tropical Pacific Ocean
[NASA-CR-194852] 06 p2408 N94-23542
Maximal type test statistics based on conditional processes
[PB94-111614] 06 p2494 N94-23771
First order conditions for the maximum likelihood estimation of an exact ARMA model
[PB94-110533] 06 p2495 N94-23814
Verification and validation of models
[PB94-110566] 06 p2456 N94-24507
Two-stage versus sequential sample-size determination in regression analysis of simulation experiments
[PB94-110558] 06 p2495 N94-24634
Generalized linear mixed models and their application in plant breeding research
[ETN-94-95335] 06 p2460 N94-25061
Parameter estimation for ARMA models with infinite variance innovations
[AD-A274654] 07 p3003 N94-26355
Three dimensional object recognition using a complex autoregressive model
[AD-A274388] 07 p2995 N94-26829

The Hough transform algorithm for sea ice lead analysis: An evaluation
[AD-A274535] 07 p2899 N94-26853
Multiple weight stepwise regression
[DE94-001602] 07 p3000 N94-27564
Least-squares determination of burst-point coordinates
[AD-A275423] 08 p3452 N94-28864
Atmospheric moisture fields derived by satellite observations over the tropical Pacific Ocean
08 p3375 N94-30863
Representation, prediction and identification of cyclostationary processes: A state-space approach
[REPT-93-041] 09 p3850 N94-31191
A review of sensitivity analysis techniques
[DE94-007192] 09 p3842 N94-31399
Diagonal band probability distributions
[REPT-93-80] 09 p3851 N94-31697
Multiple regression and measurement errors: Relative efficiency of two models, the standard model and Fuller's model, for estimating structural relationships
[ISBN-0-315-86834-1] 09 p3845 N94-31755
Feasibility evaluation of new data interpretation approaches for vegetation analysis from airborne imaging spectroscopy 09 p3745 N94-31862
Hierarchical mixtures of experts and the EM algorithm
[AD-A276516] 09 p3814 N94-31932
Proceedings of the NIPS 1993 Postconference Workshop on Pulling It All Together: Methods for Combining Neural Networks
[AD-A277507] 09 p3836 N94-33014
Iterative regression analysis of periodicities in Be-10 and C-14 atmospheric cosmonuclides variations
[INPE-5547-TDI/533] 10 p4087 N94-34228
A comparison of variable selection criteria for multiple linear regression: A THIRD simulation study
[AD-A278678] 11 p4316 N94-35691
Scaling laws for TEXT plasma profiles
[DE94-010832] 11 p4338 N94-36200
Graphing techniques for materials laboratory using Excel 11 p4232 N94-36414
United States Air Force Summer Research Program, 1993. Volume 3: Phillips Laboratory
[AD-A278694] 12 p4550 N94-36979
Feature and model selection in feedforward neural networks
[AD-A280709] 12 p4501 N94-37526
Atmospheric structure simulation: An ARMA model for smooth isotropic two-dimensional geophysical power spectra
[AD-A280476] 12 p4470 N94-37649

REGRESSION COEFFICIENTS
Space Shuttle Main Engine performance analysis
06 p2222 N94-24444
Estimation of the net production of moss community at Langhovde, East Antarctica 08 p3358 N94-29081

REGULARITY
On a class of singular quasilinear elliptic equations with general structure and distribution data
[DE93-628585] 03 p1171 N94-17613
Serial pattern complexity: Irregularity and hierarchy
[PB93-191914] 04 p1509 N94-19348
Large deviations behavior of counting processes and their inverses
[AD-A271142] 05 p1939 N94-19909

REGULATIONS
Aircraft material fire testing and the creation of an international working group 01 p0021 N94-10790
Development of a hypermedia knowledge base of aircraft fire safety regulations 01 p0021 N94-10793
The future of aircraft cabin fire safety
01 p0022 N94-10797
Toxic chemical release inventory reporting Form R and instructions. Revised 1992 version. Section 313 of the Emergency Planning and Community Right-to-Know Act
[PB93-194140] 01 p0264 N94-10836
Environmental awareness
[DE93-014192] 02 p0707 N94-13218
Fourteenth National Industrial Energy Technology Conference: Proceedings
[DE93-016698] 02 p0710 N94-14516
Permanent change of station: The NASA employee's guide to an easier move
[NHB-9760.1A] 03 p1223 N94-15931
Incorporating global warming risks in power sector planning. Volume 1: A case study of the New England region
[DE93-015241] 03 p1096 N94-17289
Safeguarding our energy future
[DE93-016001] 04 p1466 N94-18109
Airport activity statistics of certificated route air carriers, 1992
[AD-A269042] 04 p1315 N94-18490
US domestic and international regulatory issues
06 p2275 N94-22748
Use of negotiated rulemaking in developing technical rules for low-Earth orbit mobile satellite systems
06 p2276 N94-22750
NASA printing, duplicating, and copying management handbook
[NASA-NHB-1490.5] 06 p2590 N94-23971
Coastal Zone Management Act and related legislation, revision 3
[DE94-004180] 07 p2869 N94-27691
Technical Report of National Research Institute of Fisheries Engineering: Fishing Boat and Instrument, No. 12
[JTN-94-80595] 07 p2764 N94-27976
Recent trend of domestic and international regulations on intact stability of ships for safety
07 p2764 N94-27977
Journal of NIRE, volume 2, number 4
[JTN-94-80554] 07 p2869 N94-28147
Recent legal movement on water quality regulation in Japan 07 p2869 N94-28148
Lufthansa Yearbook 1992
[DSK-9734-H-92] 07 p2660 N94-28230
The single European market and air traffic chances and risks 07 p2660 N94-28231
Air traffic of the European Community with European neighbors 07 p2661 N94-28233
Air traffic administration enroute to Europe
07 p2661 N94-28238
Effects of repair on structural integrity
[PB94-143336] 08 p3145 N94-28647
Environmental Compliance Assessment System (ECAS) --- Japan supplement
[AD-A275549] 08 p3346 N94-28722
Environmental Compliance Assessment And Management System Program (ECAMP). US Air Force European Economic Community (EEC)
[AD-A275593] 08 p3346 N94-28727
Environmental Review Guide for Operations (ERGO)
[AD-A275611] 08 p3346 N94-28774
Crashworthiness analysis of commuter aircraft seats
[AD-A275889] 08 p3135 N94-28799
Evaluation of monitoring audiometry in the United States Air Force Hearing Conservation Program
[AD-A275309] 08 p3391 N94-29211
Non-aqueous cleaning solvent substitution
[DE94-005339] 08 p3219 N94-30245
Non-aqueous cleaning solvent substitution
08 p3354 N94-30466
TCM exemptions to promote alternative-fuel vehicles: The good, the bad, and the ugly
[DE94-005924] 08 p3311 N94-30703
Federal aviation regulations. Part 91: General operating and flight rules, change 4
[PB94-159944] 10 p3987 N94-34401
Federal aviation regulations. Part 91: General operating and flight rules, change 3
[PB94-159910] 10 p3987 N94-34410

REGULATORS
NT AUTOMATIC FREQUENCY CONTROL
NT CURRENT REGULATORS
NT FLOW REGULATORS
NT FREQUENCY CONTROL
NT PRESSURE REGULATORS
NT RELIEF VALVES
NT THERMOSTATS
NT VOLTAGE REGULATORS
Regulated emergency oxygen system
[AD-A266228] 03 p1138 N94-16983
Optimal control of the tip of a flexible arm
05 p1794 N94-22256
Non-isolated 30 kW class arcjet PCU
[NASA-CR-189148] 08 p3173 N94-29444

REGULATORY MECHANISMS (BIOLOGY)
The organization of the suprachiasmatic circadian pacemaker of the rat and its regulation by neurotransmitters and modulators
[AD-A266113] 01 p0301 N94-12417
Thyroid hormone action in cultured human skin fibroblasts: Evaluation using spheroid culture
07 p2919 N94-27478
Japanese Journal of Aerospace and Environmental Medicine, vol. 30, no. 2
[JTN-94-80599] 08 p3394 N94-29863
Effects of make-up on the heat transfer from the head in hyperthermic conditions 08 p3394 N94-29864

REHEATING
U HEATING

REIGNITION
U IGNITION

REINFORCED PLASTICS
NT CARBON FIBER REINFORCED PLASTICS
NT GLASS FIBER REINFORCED PLASTICS
Advanced Materials for Lightweight Structures
[ESA-SP-336] 01 p0056 N94-10001
Applications of continuous fiber reinforced thermoplastics in aircraft interiors
01 p0018 N94-10775
Evaluation of hybrid reinforcement (fiber-reinforced-plastic rod with steel core)
[AD-A268009] 03 p0941 N94-17473
The calculation methods of a cracked plastic composite laminate: A literature survey
[VTT-TIED-1362] 04 p1339 N94-17958
A study of the structural stability of an unbalanced sandwich composite configuration
[AD-A272496] 05 p1675 N94-21431
Tensile and shear fracture behavior of fiber reinforced plastics at 77K irradiated by various radiation sources
[DE93-040280] 05 p1706 N94-21542
Tensile strength of fiber reinforced plastics at 77K irradiated by various radiation sources
[DE93-040826] 05 p1709 N94-22008
Fire-resistant barriers for composite materials
[AD-D016014] 06 p2230 N94-24735
Composites and textile reinforcement
[VTT-TIED-1424] 06 p2231 N94-25420
Continuous fiber reinforced thermoplastic composites: Literature survey
[VTT-TIED-1422] 07 p2704 N94-25651
Design and life-time of polymer matrix composite structures: Summary
[VTT-TIED-1415] 07 p2707 N94-26260

REINFORCED PLATES
Dynamic behavior of fiber and particle reinforced composites
[AD-A266905] 03 p0930 N94-15143
Out of plane gradients in laminated composites
[NASA-CR-194875] 06 p2228 N94-23566
Post buckling behaviour of stiffened composite panels loaded in cyclic compression and shear
06 p2157 N94-24260
Super finite elements for nonlinear static and dynamic analysis of stiffened plate structures
[ISBN-0-315-63903-2] 07 p2844 N94-27808
Vibrational and acoustic response of ribbed plates
09 p3736 N94-31955

REINFORCED SHELLS
Post buckling behaviour of stiffened composite panels loaded in cyclic compression and shear
06 p2157 N94-24260
CORSS: Cylinder Optimization of Rings, Skin, and Stringers
[NASA-TP-3457] 06 p2490 N94-24727
Influence of an asymmetric ring on the modeling of an orthogonally stiffened cylindrical shell
[NASA-CR-195953] 10 p4070 N94-34262

REINFORCEMENT (PSYCHOLOGY)
Computer software and hardware to determine contrast sensitivity using three methods: Tracking, limits, and constant stimuli
[AD-A265168] 01 p0324 N94-11099

REINFORCEMENT (STRUCTURES)
Three-dimensional finite element analysis of explosive safety facilities: A technology assessment
[AD-A265700] 01 p0035 N94-12562
Evaluation of hybrid reinforcement (fiber-reinforced-plastic rod with steel core)
[AD-A268009] 03 p0941 N94-17473
Thermally activated retainer means utilizing shape memory alloy
[NASA-CASE-MSC-21793-1] 05 p1654 N94-20304
Investigation of the bond strength of a discrete skin-stiffener interface
[NLR-TP-92183-U] 07 p2670 N94-27796
Test and analysis results for composite transport fuselage and wing structures 09 p3628 N94-33129

REINFORCEMENT RINGS
CORSS: Cylinder Optimization of Rings, Skin, and Stringers
[NASA-TP-3457] 06 p2490 N94-24727
Influence of an asymmetric ring on the modeling of an orthogonally stiffened cylindrical shell
[NASA-CR-195953] 10 p4070 N94-34262

REINFORCING FIBERS
NT ARAMID FIBERS
NT CARBON FIBERS
Design concepts for load-carrying hot structures for reentry bodies 01 p0057 N94-10012
Damping mechanisms in chemically vapor deposited SiC fibers
[NASA-TM-106334] 01 p0066 N94-11135
An analysis of fiber-matrix interface failure stresses for a range of ply stress states
[NASA-TM-108999] 01 p0067 N94-11276
Mechanical interaction between synthetic fiber and cement base matrix in FRC composites
[AD-A265310] 01 p0073 N94-11686

Electronic and total energy properties of ternary and quaternary semiconductor compounds, alloys and superlattices
[NASA-CR-192905] 01 p0405 N94-12570
Characterization of composite materials for aerospace structures
[ESA-TT-1260] 02 p0557 N94-13804
Thermal shock resistance of ceramic matrix composites
[NASA-CR-189136] 02 p0557 N94-13920
Construction, testing, and representation of resin and fiber reinforced materials 03 p0931 N94-15255
Production process 03 p0931 N94-15257
Sound radiation from infinite laminated composite shell with periodic rib stiffening
[DRA/TM(USGR)92326] 03 p0933 N94-15699
NEXTEL(trademark)/SiC composites using forced chemical vapor infiltration
[DE93-013532] 03 p0934 N94-16008
Overview of chemical vapor infiltration
[DE93-015440] 03 p0934 N94-16065
Environmental effects on elevated temperature subcritical crack growth of SiC/SiC composites
[DE93-015688] 03 p0934 N94-16158
Continuous fabrication of SiC fiber tows by chemical vapor deposition
[AD-A266460] 03 p0936 N94-16569
Interfacial shear behavior and its influence on fiber damage in sapphire-reinforced gamma titanium aluminide composites
[AD-A267943] 03 p1060 N94-17043
Fiber strength utilization in carbon/carbon composites
[AD-A267713] 03 p0940 N94-17271
Direct observation of fracture of CAS-glass/SiC composites and processing of toughened alumina
[AD-A268275] 03 p0941 N94-17457
A comprehensive study of matrix fracture mechanisms in fiber-reinforced ceramic matrix composites
[AD-A268809] 04 p1340 N94-18205
Bibliography on ceramic matrix composites and reinforcing whiskers, platelets, and fibers, 1970-1990
[AD-A270139] 04 p1371 N94-18750
Biotechnology and composite materials
[AD-A264278] 05 p1673 N94-20327
Fiber reinforced thermosetting resin composition with coated fibers for improved toughness
[CA-PATENT-1,306,320] 05 p1674 N94-21040
Tensile and shear fracture behavior of fiber reinforced plastics at 77K irradiated by various radiation sources
[DE93-040280] 05 p1706 N94-21542
Tensile strength of fiber reinforced plastics at 77K irradiated by various radiation sources
[DE93-040826] 05 p1709 N94-22008
Creep deformation characteristics of ductile discontinuous fiber reinforced composites
[DE94-000697] 06 p2227 N94-23005
Development of silicon nitride composites with continuous fiber reinforcement
[DE94-001996] 06 p2227 N94-23022
Determination of fiber-matrix interface failure parameters from off-axis tests
[NASA-TM-109043] 06 p2241 N94-23274
Interface evaluation in ceramic composites 06 p2255 N94-24231
CMC design consequences 06 p2256 N94-24238
Constitutive modelling of fiber-reinforced concrete under uniaxial tensile loading
[VTT-JULK-774] 06 p2379 N94-25385
Alternatives for reinforcement: Fiber composites
[VTT-TIED-1412] 06 p2230 N94-25386
The pressure loaded volumetric ceramic receiver 500 kW version design and construction
[DLR-MITT-93-02] 06 p2396 N94-25479
Inner fiber observation for metal matrix composites under the stress load condition utilizing Synchrotron Orbital Radiation (SR) by X-ray CT 07 p2724 N94-25553
Continuous fiber reinforced thermoplastic composites: Literature survey
[VTT-TIED-1422] 07 p2704 N94-25651
Characterization of fatigue damage in a metal matrix composite (SCS-6/Ti-15-3) at elevated temperature
[AD-A273797] 07 p2706 N94-25876
High performance fibers
[AD-A274693] 07 p2707 N94-26450
Investigation of forced and isothermal chemical vapor infiltrated SiC/SiC ceramic matrix composites
[DE94-004544] 07 p2708 N94-26557
Innovative processing of composites for ultra-high temperature applications, book 1
[AD-A275597] 08 p3176 N94-28729
Thermal expansion and elastic anisotropy in single crystal Al2O3 and SiC reinforcements
[NASA-TM-106516] 08 p3214 N94-29105
Damage meso-modeling of 3D evolutive composites
[REPT-932-430-106] 08 p3179 N94-29442
Method of producing a ceramic fiber-reinforced glass-ceramic matrix composite
[NASA-CASE-LEW-15264-2] 08 p3180 N94-29508
On the mechanics of stress analysis of fiber-reinforced composites 09 p3619 N94-31481
Toughening mechanisms in fiber-reinforced ceramic-matrix composites 09 p3622 N94-31943
Mechanics of the single fiber pullout problem with several interface conditions 09 p3623 N94-32078
The effect of ductile phase (Nb) reinforcement morphology on the mechanical behavior of an intermetallic matrix (MoSi2) 09 p3615 N94-32500
Engineering scale development of the Vapor-Liquid-Solid (VLS) process for the production of silicon carbide fibrils
[DE94-007132] 09 p3659 N94-32618
Comparison of resin film infusion, resin transfer molding, and consolidation of textile preforms for primary aircraft structure 09 p3630 N94-33136
Contingency airfield construction: Mechanical stabilization using monofilament and fibrillated fibers
[AD-A277732] 10 p4008 N94-33444
SCS-6 (tm) fiber reinforced titanium 12 p4400 N94-36652
Properties of TMC processed by fibre coating and hiping 12 p4401 N94-36656
A simple evaluation of thermally-induced streses in the vicinity of the stitch in a through-thickness reinforced cross-ply laminate
[NASA-CR-196317] 12 p4406 N94-37653

REINFORCING MATERIALS
Continuous fabrication of SiC fiber tows by chemical vapor deposition
[AD-A266460] 03 p0936 N94-16569
Strength and toughness improvement of silicide intermetallics by nanophase and microphase reinforcements
[AD-A272914] 05 p1692 N94-21320
Technology base enhancement program. Metal matrix composites
[AD-A275531] 08 p3176 N94-28688
Controlled thermal expansion printed wiring boards based on liquid crystal polymer dielectrics
[NASA-CR-189338] 08 p3287 N94-29400
Thermodynamic analysis of chemical compatibility of several compounds with Fe-Cr-Al alloys
[NASA-CR-191166] 08 p3181 N94-29684
A review of mechanical test methods for ceramic matrix composites
[PB94-147576] 08 p3184 N94-30524
Leveraging metal matrix composites to reduce costs in space mechanisms 09 p3604 N94-33301
Using nonequilibrium alloying techniques for corrosion inhibition in Gr/Al and Gr/Mg metal matrix composites
[AD-A280529] 12 p4404 N94-37088

RELATIVE BIOLOGICAL EFFECTIVENESS (RBE)
Potential health effects of space radiation 01 p0312 N94-11558

RELATIVISTIC EFFECTS
Efficiency of fast wave current drive for a weakly relativistic plasma
[DE93-012775] 01 p0385 N94-10159
Electron momentum spectroscopy of atoms, molecules and solids
[DE93-610148] 01 p0360 N94-10332
On the relativistic string size at finite temperature
[DE93-617658] 01 p0409 N94-10394
Quasi-relativistic effects in barrier-penetration processes
[DE93-617730] 01 p0410 N94-10721
Investigation of the interactions of radiation with matter
[AD-A266743] 03 p1181 N94-15774
Acoustic travel time perturbations due to an internal tide and internal wave field in the Barents Sea
[AD-A270879] 04 p1499 N94-19580
The quantum structure of matter grand challenge project: Large-scale 3-D solutions in relativistic quantum dynamics
[DE94-000328] 05 p1960 N94-21955
Rydberg states in multiply charged ions
[DE94-002335] 07 p3021 N94-26760
Decay constants of heavy mesons in the relativistic potential model with velocity dependent corrections
[DE94-606495] 07 p3030 N94-27860
Apparent unambiguousness of relativistic time dilation
[DE94-606328] 08 p3522 N94-28586
On a direct experimental verification of the elongation formula
[DE94-606329] 08 p3523 N94-28721
Theoretical investigation of gas-surface interactions
[NASA-CR-195755] 08 p3272 N94-29378
Large amplitude Langmuir and ion-acoustic waves in a relativistic two-fluid plasma
[AD-B183694L] 08 p3506 N94-29547
General-relativistic celestial mechanics. 4: Theory of satellite motion
[PB94-147782] 09 p3601 N94-31769
Variational method in relativistic two-body problem
[DE94-612462] 11 p4315 N94-36416

RELATIVISTIC ELECTRON BEAMS
An experimental program for collective acceleration of ions using intense relativistic electron beams
[DE93-612205] 01 p0371 N94-10316
Scattering of modulated Ultra-Relativistic Electron Beam (UREB) by atmospheric plasma
[DE93-620987] 01 p0387 N94-10558
Excitation of coupled waves in plasma periodic structures by relativistic electron beam and acceleration of charged particles
[DE93-621657] 02 p0794 N94-12853
Stripping efficiencies for 277 MeV/amu gold beam on copper foils
[DE93-014306] 02 p0569 N94-13221
Interaction of intense lasers and relativistic electron beams with solids, gases and plasmas
[AD-A269655] 04 p1439 N94-18737
The angular velocity spread of REB induced by magnetic field discontinuity
[IPPCZ-331] 05 p1996 N94-21573
Acceleration of solar-flare particles as viewed from their chemical composition 05 p2006 N94-22672
On a theory of two-beam mechanisms of charged particle acceleration in electrodynamic structures
[DE94-003482] 07 p3032 N94-26330
Implementation of a compact magnetic electron energy spectrometer for intense relativistic electron beams
[AD-A274451] 07 p3033 N94-27082
Computer simulations of radiation generation from relativistic electron beams
[AD-A274139] 07 p3024 N94-27133
Fast H-alpha line broadening during the 100 ns REB injection into a plasma
[IPPCZ-322] 07 p3048 N94-27836
Experiments on the two-stage dense plasma heating on the GOL-3 device
[DE94-608356] 08 p3508 N94-30193
Peculiarities of heat transfer in the experiments of beam injection heating of a plasma at the GOL-3 device
[DE94-608357] 08 p3508 N94-30194
Pinched propagation of high-power, pulsed electron beams for welding and materials processing applications
[AD-A276925] 09 p3726 N94-32236
Gyroresonant scattering of radiation belt electrons by oblique whistler waves 10 p4166 N94-33357
State of the art in high-power microwaves: An overview
[DE94-007075] 11 p4272 N94-35978
Coherent multiple-foil x-ray transition radiation
[DE93-040831] 12 p4525 N94-37486

RELATIVISTIC PARTICLES
NT RELATIVISTIC ELECTRON BEAMS
Diagnostic complex for the space-time analysis of energy and current of pulsed relativistic particles
[DE93-620980] 01 p0362 N94-10649
Quantized conic sections; quantum gravity
[DE93-010950] 01 p0411 N94-10956
Relativistic heavy-ion collisions
[DE93-014844] 01 p0366 N94-11147
Experimental investigation of wake field excitation in plasma by a periodic succession of relativistic particle clots
[DE93-621655] 01 p0391 N94-11211
Investigation of plasma instabilities in the Polar cusp
[NASA-CR-194283] 02 p0796 N94-13084
The theory of relativistic heavy ion collisions
[DE93-015934] 02 p0784 N94-13952
Meson production in relativistic heavy-ion collisions at AGS energies
[DE93-016871] 04 p1565 N94-17984
Relativistic configuration interaction calculation of the correlation energies of heliumlike ions
[DE93-018093] 04 p1571 N94-19201
A field-based technique for the longitudinal profiling of ultrarelativistic electron or positron bunches down to lengths of less than or equal to 10 microns
[DE93-040954] 05 p1978 N94-19873
Relativistic shock spectra: A prediction
[NASA-CR-194764] 05 p2150 N94-21782
On the correspondence limit of relativistic quantum mechanics
[DE93-040939] 05 p2038 N94-21971
VHE gamma ray generation by radio pulsars 05 p2007 N94-22680
Relativistic hadrons in an external field
[ETN-94-95387] 06 p2538 N94-25259
Weak interactions in a bilocal chiral theory
[DE93-613097] 07 p3013 N94-25836
Relativistic heavy ion physics
[DE94-003161] 07 p3031 N94-26097

Spinor and isospinor structure of relativistic particle propagators
[DE94-601552] 07 p3019 N94-26424
Spin from isospin: The model of superparticle in a non-Grassmannian approach
[DE93-634341] 07 p3019 N94-26454
Investigation of plasma instabilities in the polar cusp
[NASA-CR-195212] 07 p2879 N94-26599
Computer simulations of radiation generation from relativistic electron beams
[AD-A274139] 07 p3024 N94-27133
Stopping powers and cross sections due to two-photon processes in relativistic nucleus-nucleus collisions
[NASA-CR-4574] 07 p3033 N94-27646
On the model of the relativistic particle with curvature and torsion
[DE94-606330] 07 p3029 N94-27848
Correlations in inelastic collisions of relativistic nuclei with emulsion at (4.1 - 4.5) A GeV/c
[DE93-634526] 07 p3030 N94-27994
The effects of relativistic neutrons on nonthermal models of active galactic nuclei 08 p3547 N94-29993
On relativity principle violation in local measurements of spin precession of moving particles
[DE94-608067] 08 p3489 N94-30085
Perturbative and nonperturbative EM lepton pair production in relativistic heavy-ion collisions
[DE94-006315] 09 p3867 N94-31779
High baryon density from relativistic heavy ion collisions
[DE94-003894] 12 p4511 N94-36460
The Mesozoic Era of relativistic heavy ion physics and beyond
[DE94-011341] 12 p4548 N94-37557
Strangeness and the quark-gluon plasma: An experimenter's perspective
[DE94-011377] 12 p4519 N94-37558

RELATIVISTIC PLASMAS
Efficiency of fast wave current drive for a weakly relativistic plasma
[DE93-012775] 01 p0385 N94-10159
Collective acceleration of ions in near-anode plasma of a strong-current relativistic diode
[DE93-620977] 01 p0387 N94-10541
Filamentation instability of hot quark-gluon plasma with hard jet
[DE93-617679] 01 p0388 N94-10882
Enhanced acceleration in a self-modulated-laser wakefield accelerator
[AD-A268452] 04 p1586 N94-18148
General relativistic winds in a black hole magnetosphere 05 p2002 N94-22644
Relativistically expanding pair plasmas as bursting sources of cosmic gamma rays 05 p2003 N94-22646
Langmuir microstructures and pulsar radio emission 05 p2007 N94-22678
Asymptotic structure of magnetically driven MHD wind 05 p2008 N94-22682
A relativistic theory on wave propagation in inhomogeneous magnetoplasmas
[ETN-94-95322] 06 p2554 N94-25285
Back-reaction beyond the mean field approximation
[DE94-003936] 07 p3012 N94-25612
Nonlinear transverse propagation of photons in a ultrarelativistically hot and magnetized electron-positron plasma: Coupling of Langmuir and electromagnetic solitons
[DE94-603667] 07 p3046 N94-27630
Large amplitude Langmuir and ion-acoustic waves in a relativistic two-fluid plasma
[AD-B183694L] 08 p3506 N94-29547
A relativistic solitary wave in electron positron plasma
[DE94-608107] 08 p3507 N94-30071
Transport properties of quark and gluon plasmas
[DE94-007043] 09 p3864 N94-31405
Non-equilibrium electrodynamics in the large N expansion
[DE94-006156] 09 p3911 N94-31760

RELATIVISTIC THEORY
Two fluid plasmas in the vicinity of a Schwarzschild black hole
[DE93-610264] 01 p0385 N94-10284
From the Weyl theory to a theory of locally anisotropic space-time
[DE92-644734] 01 p0410 N94-10535
On the doubling of hydrodynamic theorems in relativistic theory of superfluidity
[DE93-617895] 01 p0148 N94-10717
The electric field of a current-carrying conductor
[DE93-626637] 02 p0617 N94-14892
Relativistic mean-field calculations of lambda and sigma hypernuclei
[DE93-015269] 03 p1181 N94-16013
Lunar LIGO: A new concept in gravitational wave astronomy 03 p1277 N94-16337
Relativistic dynamics of spin in strong external fields
[NIKHEF-H/93-06] 03 p1240 N94-17604
Meson production in relativistic heavy-ion collisions at AGS energies
[DE93-016871] 04 p1565 N94-17984
Relativistic calculations of the superheavy nucleus (sup 298)114
[KVI-969] 05 p1971 N94-20119
Relativistic shock spectra: A prediction
[NASA-CR-194764] 05 p2150 N94-21782
On the correspondence limit of relativistic quantum mechanics
[DE93-040939] 05 p2038 N94-21971
A relativistic theory on wave propagation in inhomogeneous magnetoplasmas
[ETN-94-95322] 06 p2554 N94-25285
Dynamical group of relativistic straight-line string
[DE93-634347] 07 p3072 N94-26037
Gravitational field of a point mass in the Lobachevskij space
[DE93-634333] 07 p3072 N94-26503
The solving of the relativistic two-body problem with a nonlinear dependence upon a spectrum parameter
[DE94-606343] 08 p3451 N94-28783
Relativistic theory for picosecond time transfer in the vicinity of Earth 08 p3470 N94-30653
General-relativistic celestial mechanics. 4: Theory of satellite motion
[PB94-147782] 09 p3601 N94-31769
Ives-Stilwell experiment and relativistic length
[DE94-611076] 10 p4142 N94-33903
Decoherence, determinism and chaos
[DE94-009018] 10 p4149 N94-33984
The relativistic invariant and the Galilean mass of bodies
[DE94-616615] 11 p4318 N94-35956
First, second and fourth sound in relativistic superfluidity theory with account for dissipative effects
[DE94-617393] 11 p4267 N94-36314
The form factors of the nucleons
[DE94-013357] 12 p4515 N94-37086
Activities of the Tandem Accelerator Center, University of Tsukuba
[DE94-748687] 12 p4522 N94-37237

RELATIVISTIC VELOCITY
Restoring locality with faster-than-light velocities
[DE93-040926] 05 p2038 N94-22010

RELATIVITY
Standard model status (in search of new physics)
[DE93-013288] 01 p0410 N94-10528
From the Weyl theory to a theory of locally anisotropic space-time
[DE92-644734] 01 p0410 N94-10535
The uncertainty principle in resonant gravitational wave antennae and quantum non-demolition measurement schemes 01 p0378 N94-10587
Dimensional transition of the space-time at the minimum action near the planck scale
[DE93-754192] 01 p0410 N94-10718
Explorations in quantum gravity: From one loop effective actions to two-dimensional theories 01 p0413 N94-11822
Maximal hypersurfaces in asymptotically stationary spacetimes
[MPA-708] 04 p1621 N94-18141
Tensor-scalar cosmological models and their relaxation toward general relativity
[PB93-220796] 06 p2601 N94-23099
On BRST quantization of constrained systems
[ETN-94-95386] 06 p2570 N94-25258
Quark-antiquark bound states
[DE93-613054] 07 p3013 N94-25826
The gravity equations in the Lobachevskij space
[DE93-634334] 07 p2879 N94-26504
A relativistic quark model
[ISBN-0-315-60926-5] 07 p3025 N94-27333
Apparent unambiguousness of relativistic time dilation
[DE94-606328] 08 p3522 N94-28586
Retarded distances and the Doppler effect
[DE94-606296] 08 p3523 N94-28618
On the importance of the Michelson-Morley experiment
[DE94-606298] 08 p3523 N94-28620
Three forms of relativity
[DE94-606338] 08 p3523 N94-28782
On dyonic black holes and cosmic censorship 08 p3548 N94-29912
On relativity principle violation in local measurements of spin precession of moving particles
[DE94-608067] 08 p3489 N94-30085
Lattice geometrodynamics 09 p3857 N94-31825
Classical time machine
[DE94-616616] 11 p4342 N94-36070

RELAXATION (MECHANICS)
NT SPIN-LATTICE RELAXATION
NT STRESS RELAXATION
Viscous relaxation of the Moho under large lunar basins 01 p0452 N94-12113
Muon spin relaxation studies of heavy fermion superconductors
[DE93-014576] 02 p0815 N94-14773
Thermal history effects on electrical relaxation and conductivity for potassium silicate glass with low alkali concentrations
[NASA-TM-106324] 02 p0583 N94-14845
Structure and energetics of high index Fe, Al, Cu and Ni surfaces using equivalent crystal theory
[NASA-TM-106408] 06 p2249 N94-25171
Strain relaxation and surface roughness as a function of growth temperature in linearly graded In(x)Al(1-x)As (x = 0.05 to 0.25) buffers
[DE94-005430] 08 p3519 N94-30592
Viscoelastic fracture characterization of polymeric solids 09 p3652 N94-31745
The study of the local magnetic field in the oxide alpha-Bi2O3 by the mu SR-technique
[DE94-612636] 11 p4322 N94-35751

RELAXATION METHOD (MATHEMATICS)
A new heuristic for set covering problems
[INPE-5471-TDI/502] 01 p0333 N94-12358
Aspects of applying a relaxation method to computing sea surface velocities from sea surface temperature images 01 p0214 N94-12679
Theory for iterative solution of large dynamical systems using parallel computation
[TKK-MAT-A304] 02 p0760 N94-14187
Shop problems with two machines and time lags
[REPT-93-020] 04 p1518 N94-17927
Optimal convolution SOR acceleration of waveform relaxation with application to semiconductor device simulation 05 p1922 N94-21475
A multigrid method for steady Euler equations on unstructured adaptive grids 05 p1957 N94-21476
Multigrid solution of the Navier-Stokes equations on highly stretched grids with defect correction 05 p1806 N94-21481
Mapping robust parallel multigrid algorithms to scalable memory architectures 05 p1922 N94-21483
Parallelizing a highly vectorized multigrid code with zebra relaxation
[CWI-NM-R9225] 05 p1935 N94-21610
Numerical multigrid software (MGD5M): A parallel multigrid code with a twisted ILLU-relaxation
[CWI-NM-R9226] 05 p1916 N94-21611
Relaxation schemes for Chebyshev spectral multigrid methods 06 p2484 N94-23688
One machine scheduling with delayed precedence constraints
[PB93-237626] 07 p3094 N94-26314
Numerical analysis of two dimensional/axisymmetric non-equilibrium hypersonic flow 08 p3125 N94-28963
An implicit upwind scheme for the three-dimensional Euler equations using a pointwise relaxation method 08 p3128 N94-28983
Numerical solution of the two-dimensional time-dependent incompressible Euler equations
[NASA-CR-195775] 08 p3277 N94-29859
Exact solution of the single machine scheduling problem with earliness and flow time penalties
[REPT-93-038] 09 p3809 N94-31189
A note on windowing for the waveform relaxation
[AD-A280999] 10 p4130 N94-34922

RELAXATION OSCILLATORS
The stability and dynamics of elastic structures and fluid flows
[AD-A267990] 03 p1029 N94-17414

RELAXATION TIME
Relaxation of polar orientational order in nonlinear optical polymers by second harmonic generation
[AD-A269059] 04 p1370 N94-18515
Dipolar relaxation in a second-order nonlinear optical interpenetrating polymer network
[AD-A273626] 06 p2258 N94-24732

RELAY SATELLITES
The Olympus PAX, measurement of mechanism induced vibration 06 p2362 N94-24041

RELIABILITY
NT AIRCRAFT RELIABILITY
NT CIRCUIT RELIABILITY
NT COMPONENT RELIABILITY
NT COMPUTER PROGRAM INTEGRITY
NT SOFTWARE RELIABILITY
NT SPACECRAFT RELIABILITY
NT STRUCTURAL RELIABILITY
A reliable stability test for exponential polynomials
[MEMO-COSOR-92-48] 01 p0341 N94-10168
RAMCAD (reliability, availability, and maintainability in computer-aided design)
[AD-A265143] 01 p0331 N94-11679

Computational problems with the binomial failure rate model and incomplete common cause failure reliability data
[DE93-014346] 02 p0669 N94-14143
Statistical computation of tolerance limits
[NASA-TM-108424] 03 p1172 N94-15535
Reliability characterization of digital microcircuits: Investigation of an in-process oxide reliability screening method
[AD-A267053] 03 p1008 N94-15665
Reliability of autonomic responses and malaise across multiple motion sickness stimulation tests
[NASA-TM-108787] 03 p1121 N94-15711
Fast simulation of steady-state availability in non-Markovian highly dependable systems
[AD-A266747] 03 p1174 N94-15823
General Monte Carlo reliability simulation code including common mode failures and HARP fault/error-handling
[NASA-CR-187587] 03 p1150 N94-16594
The 1987 Goddard Space Flight Center Battery Workshop
[NASA-CP-3236] 03 p1012 N94-17062
A ten year review of performance of photovoltaic systems
[DE93-015649] 03 p1093 N94-17217
X ray computed tomography for failure analysis investigations
[AD-A268086] 03 p1055 N94-17515
Reliability and maintainability of modular robot systems: A roadmap for design
[AD-A268104] 03 p1168 N94-17517
Development of a new concept diver's watch 04 p1429 N94-18041
Laser materials processing applications at Lawrence Livermore National Laboratory
[DE93-017976] 04 p1437 N94-18093
Performance evaluations of demountable electrical connections
[DE93-017399] 04 p1396 N94-18135
Problems in probability, statistics and reliability
[AD-A270830] 04 p1559 N94-19595
Increasing mission reliability using open-loop control
[AD-A271208] 04 p1545 N94-19721
Development and testing of a reliability performance index for modular robotic systems
[AD-A271901] 05 p1942 N94-20488
Lithium batteries: Future batteries 05 p1752 N94-20630
Army aircraft fire-detection systems operation and reliability
[AD-A271327] 05 p1641 N94-20912
Automated synthesis and verification of configurable DRAM blocks for ASIC's 05 p1759 N94-21123
N parallel queueing systems with server breakdown and repair
[CWI-BS-R9236] 05 p1944 N94-21232
Efficiency and reliability enhancements in propulsion flowfield modeling 06 p2215 N94-23055
Connector mechanisms in compliance with extreme space conditions 06 p2360 N94-24025
Embodiment design for a multipropellant resistojet
[NASA-CR-195505] 06 p2221 N94-24834
On the reliability of a window least squares algorithm
[DE93-634666] 07 p2962 N94-26386
Practical problems in aggregating expert opinions
[DE94-002623] 07 p3094 N94-27707
Silicon device performance measurements to support temperature range enhancement
[NASA-CR-195265] 07 p2844 N94-27824
Comparative analysis of different configurations of PLC-based safety systems from reliability point of view 07 p2836 N94-27925
Controls, monitoring and performance measurements 07 p2831 N94-28086
Summary of NASA Aerospace Flight Battery Systems Program activities 07 p2860 N94-28101
SAFT nickel hydrogen cell cycling status 07 p2861 N94-28110
Identification of components to optimize improvement in system reliability
[DE94-001601] 08 p3315 N94-28503
Rocket engine system reliability analyses using probabilistic and fuzzy logic techniques
[NASA-TM-106519] 08 p3173 N94-29403
ASSIST internals reference manual
[NASA-TM-109102] 08 p3431 N94-29494
Issues arising with the application of optical fiber transmission in class 1E systems in nuclear power plants
[DE94-004743] 08 p3500 N94-29928
Reliability of multilayer copper/polyimide
[AD-A276228] 09 p3650 N94-31284
Validation of the Environmentally Conscious Manufacturing Integrated Demonstration hardware
[DE94-003824] 09 p3765 N94-32144
Effect of surface forces on the rheology of particle-liquid systems and the consolidation of ceramic powders
[AD-A277092] 09 p3657 N94-32391
A PC program to optimize system configuration for desired reliability at minimum cost 09 p3823 N94-32438
Space flight risk data collection and analysis project: Risk and reliability database
[NASA-CR-195879] 09 p3603 N94-32494
Temperature-humidity-bias aging technique to identify defective surface mount capacitors
[DE94-005354] 09 p3660 N94-32727
Implementing software safety in the NASA environment
[NASA-TM-106597] 09 p3731 N94-33032
Pip pin reliability and design 09 p3605 N94-33305
Certification of ICI 1012 optical data storage tape 10 p4152 N94-33797
The development of an auxiliary power unit for a fighter aircraft 10 p4001 N94-34442
Point and interval estimation of series system reliability using small data sets
[AD-A278647] 11 p4316 N94-35575

RELIABILITY ANALYSIS

Bayesian reliability analysis with imprecise prior probabilities
[MEMO-COSOR-92-50] 01 p0183 N94-10170
Investigation of alternate power source for Space Shuttle Orbiter hydraulic system
[NASA-CR-193229] 01 p0046 N94-10911
Applying reliability models to the maintenance of Space Shuttle software 01 p0330 N94-11434
Reliability analysis for FDDI dual homing networks
[AD-A266133] 01 p0337 N94-11475
Chip-level testability requirements guidelines
[AD-A262583] 02 p0619 N94-12967
Switchover software reliability estimate for Paducah freezer/sublimer computer systems
[DE93-013844] 02 p0756 N94-14696
Verification of critical software by statistical testing
[LAAS-93006] 02 p0756 N94-14714
Software reliability through fault-avoidance and fault-tolerance
[NASA-CR-194353] 03 p1143 N94-15114
Safety-critical software: Status report and annotated bibliography
[AD-A266993] 03 p1144 N94-15214
Concepts on measuring the benefits of software process improvements
[AD-A266994] 03 p1144 N94-15215
Technology transfers and reliable oxides
[AD-A266948] 03 p1175 N94-15758
NASA trend analysis procedures
[NASA-RP-1290] 03 p1223 N94-15782
General Monte Carlo reliability simulation code including common mode failures and HARP fault/error-handling
[NASA-CR-187587] 03 p1150 N94-16594
Reducing data dimension to lower signal processing computational requirements and maximize performance
[AD-A266606] 03 p0999 N94-16728
Reliability analysis of Surface Mount Technology (SMT)
[AD-A267598] 03 p1055 N94-17194
Tutorial: Advanced fault tree applications using HARP
[NASA-TM-102747] 03 p1155 N94-17447
FAROW: A tool for fatigue and reliability of wind turbines
[DE93-017639] 04 p1465 N94-18001
Human reliability analysis application guide
[DE93-015361] 04 p1511 N94-18244
Software reliability: Estimation and prediction
[AD-A268895] 04 p1521 N94-18458
Knowledge sources for an intelligent MCM analyzer
[AD-A269224] 04 p1542 N94-18887
Handbook. Volume 3: Digital systems validation book plan
[DOT/FAA/CT-93/16-VOL-3] 05 p1647 N94-20053
Development and testing of a reliability performance index for modular robotic systems
[AD-A271901] 05 p1942 N94-20488
Trends in software reliability modeling 05 p1788 N94-22214
Recent advances in computational structural reliability analysis methods 05 p1828 N94-22616
Time-dependent reliability analysis of ceramic engine components 05 p1828 N94-22619
Phased-mission system analysis using Boolean algebraic methods
[NASA-CR-191564] 06 p2451 N94-23340
Specifying design conservatism: Worst case versus probabilistic analysis 06 p2374 N94-23939
Aviation system safety risk management tool analysis. Volume 2: Appendices
[AD-A273502] 06 p2173 N94-24864
Reliability analysis of a repairable dependent parallel system
[ETN-94-95312] 06 p2373 N94-25295
Calculation of a 3-D pose of a known object in a single perspective view
[VTT-PUBS-122] 07 p2957 N94-25642
An approach to studying the reliability of microgravity experiments
[NASA-TM-106489] 07 p2834 N94-26199
Simulation modeling for long duration spacecraft control systems 07 p2684 N94-26288
Modeling systems by probabilistic process algebra: An event structures approach
[PB94-125259] 07 p3004 N94-26867
Baseline for a Nordtest method. Reliability stress screening of components. A guide for component users
[PB94-123775] 07 p2835 N94-27042
Access to space study
[NASA-TM-109693] 07 p2685 N94-27151
Hardware and software reliability estimation using simulations
[NASA-CR-187588] 07 p2973 N94-27663
Identification of components to optimize improvement in system reliability
[DE94-001601] 08 p3315 N94-28503
Statistical Modeling and Estimation of Reliability Functions for Software (SMERFS) user's guide, revision 3
[AD-A275390] 08 p3411 N94-29202
Statistical Modeling and Estimation of Reliability Functions for Software (SMERFS) library access guide, revision 3
[AD-A275405] 08 p3411 N94-29207
Rocket engine system reliability analyses using probabilistic and fuzzy logic techniques
[NASA-TM-106519] 08 p3173 N94-29403
Reliability of composite material structures. Application: High pressure spherical coded tanks
[REPT-932-430-103] 08 p3180 N94-29478
ASSIST internals reference manual
[NASA-TM-109102] 08 p3431 N94-29494
Dependability analysis of parallel systems using a simulation-based approach
[NASA-CR-195762] 08 p3431 N94-29846
Estimation of Weibull modulus from dynamic and static fatigue experiments
[PB94-138641] 08 p3322 N94-30114
TOTAL user manual
[NASA-TM-109101] 08 p3432 N94-30160
Modeling systems by probabilistic process algebra: An event structures approach
[MEMO-INF-93-29-REV] 08 p3425 N94-30416
A survey of NASA and military standards on fault tolerance and reliability applied to robotics
[AIAA PAPER 94-1211-CP] 08 p3445 N94-30562
Photovoltaic performance and reliability workshop
[DE94-000236] 08 p3339 N94-30601
An evaluation of aircraft maintenance performance factors in the objective wing
[AD-A276010] 09 p3565 N94-31362
Reliability analysis of structural ceramics subjected to biaxial flexure 09 p3650 N94-31454
Statistical inference for coherent systems from partial information and in resampling techniques in survival analysis
[AD-A277382] 09 p3852 N94-32339
A PC program to optimize system configuration for desired reliability at minimum cost 09 p3823 N94-32438
Automatic contact in DYNA3D for vehicle crashworthiness
[DE94-007143] 09 p3738 N94-32637
Hierarchical modeling for reliability analysis using Markov models
[NASA-CR-188288] 09 p3731 N94-32862
Stochastic models in reliability theory
[AD-A277529] 09 p3731 N94-32953
Spur, helical, and spiral bevel transmission life modeling
[NASA-TM-106552] 09 p3728 N94-32979
Accelerated reliability testing utilizing design of experiments
[AD-A277989] 09 p3732 N94-33088
Advanced release technologies program 09 p3607 N94-33322
Assessing the vulnerability of multi-commodity networks with failing components
[AD-A278434] 09 p3684 N94-33334
Developing interpretable models with optimized set reduction for identifying high risk software components 11 p4301 N94-35435
Robust requirements specifications for safety-critical systems
[PB94-167806] 11 p4250 N94-35532
Possibilities and pitfalls in aerospace applications of titanium matrix composites 12 p4400 N94-36650

Network survivability performance
[AD-A278746] 12 p4433 N94-36756
Network survivability performance (computer diskette)
[AD-M000332] 12 p4433 N94-36757
Evaluating plastic assembly processes for high reliability applications using HAST and Assembly Test Chips
[DE94-010750] 12 p4439 N94-37363
Probability techniques for reliability analysis of composite materials
[NASA-CR-195294] 12 p4406 N94-37633
Probabilistic assessment of space nuclear propulsion system nozzle
[NASA-TM-106539] 12 p4457 N94-37704

RELIABILITY CONTROL
U QUALITY CONTROL
U RELIABILITY ENGINEERING

RELIABILITY ENGINEERING
A Recommended Methodology for Quantifying NDE/NDI Based on Aircraft Engine Experience
[AGARD-LS-190] 01 p0028 N94-11022
Defining the performance gap: Conducting a self-assessment 02 p0666 N94-13155
On the end-to-end communication problem in unreliable networks
[ITN-93-85188] 02 p0598 N94-13195
Study of the intermateability of Cannon and Souriau subminiature connectors
[CNES-NT-132] 02 p0624 N94-13951
Computational problems with the binomial failure rate model and incomplete common cause failure reliability data
[DE93-014346] 02 p0669 N94-14143
An improved approach for flight readiness certification: Probabilistic models for flaw propagation and turbine blade failure. Volume 1: Methodology and applications
[NASA-CR-194496] 02 p0519 N94-14841
An improved approach for flight readiness certification: Probabilistic models for flaw propagation and turbine blade failure. Volume 2: Software documentation
[NASA-CR-194497] 02 p0519 N94-14842
Concepts on measuring the benefits of software process improvements
[AD-A266994] 03 p1144 N94-15215
Small satellite product assurance 03 p0896 N94-17188
Reliability control for wrist watches and their casements 04 p1427 N94-18030
Mutrometre: Construction for fast water proof measurements under low pressure and air suppression 04 p1427 N94-18031
Handbook. Volume 3: Digital systems validation book plan
[DOT/FAA/CT-93/16-VOL-3] 05 p1647 N94-20053
Intervention strategies for the management of human error
[NASA-CR-4547] 05 p1642 N94-22373
Reliability enhancement of Navier-Stokes codes through convergence enhancement 06 p2216 N94-23064
Contribution to the evaluation of efficiency of a microprocessor functional test
[ETN-94-95176] 06 p2445 N94-23153
Aviation system safety risk management tool analysis. Volume 2: Appendices
[AD-A273502] 06 p2173 N94-24864
Preceedings of the 12th International Congress: Corrosion Control for Low-Cost Reliability. Volume 3A: Corrosion: Specific issues
[AD-A273663] 06 p2251 N94-25450
Fault detection in HVAC systems using fuzzy models
[OUEL-1977/93] 06 p2373 N94-25475
The 1991-1992 walking robot design 07 p2833 N94-25686
Hierarchical test development and design-for-testability for (a)synchronous semi-custom ASIC's
[ISBN-9-09-005928-8] 07 p2834 N94-26003
Development of a MIL-STD-1750 microprocessor system for space applications 07 p2949 N94-26715
Advanced languages for systems software
[AD-A275272] 08 p3410 N94-29007
Satellites: Reliability and operation security
[REPT-932-440-108] 08 p3168 N94-29419
A survey of NASA and military standards on fault tolerance and reliability applied to robotics
[AIAA PAPER 94-1211-CP] 08 p3445 N94-30562
Engineering of damage in ion implanted silicon
[ISBN-9-09-005097-3] 09 p3897 N94-31521
Improvement of control system reliability with analytical redundancy technique 10 p4118 N94-34340
Robust requirements specifications for safety-critical systems
[PB94-167806] 11 p4250 N94-35532
On the use of fuzzy logic assessment for high consequence implementation risk analysis
[DE94-011417] 12 p4507 N94-37564

RELIEF MAPS
The extraction of bottom characteristics and mapping in Kin Bay, Okinawa Main Island, Japan, using LANDSAT-5/TM and SPOT-1/HRV data 01 p0197 N94-11931
An ancient inner lake in Maadim Vallis 01 p0456 N94-12133
Separation of topographic and intrinsic backscatter variations in biscopic radar images: A magic airbrush 03 p1086 N94-16318
Topographic mapping using a monopulse SAR system 05 p1721 N94-20417
Topographic slope from the SAR interferometric phase gradient 05 p1731 N94-20459
Chronology, eruption duration, and atmospheric contribution of Apollinaris Patera, Mars 05 p2108 N94-20720
Linear structures on the small inner satellites of Saturn 05 p2121 N94-20797
Detecting topographical regions in digital terrain maps
[AD-A272889] 05 p1841 N94-21453
Using contour maps to search for red-shifted 511 keV features in BATSE GRB spectra 06 p2585 N94-24455
Geometric correction of SPOT images with use of digital elevation models
[ETN-94-95033] 07 p2847 N94-26107
Optimization of Vector Product Format (VPF) data for map background display in army tactical systems
[AD-A274687] 07 p2848 N94-26446
Multivariate spectral analysis to extract materials from multispectral data
[AD-A274142] 07 p2709 N94-27135
The Image Digitizing System (IDS)
[AD-A275341] 08 p3329 N94-29213
SPOT imagery for updating land cover information of 1:50,000 numerical topographic maps 09 p3749 N94-32532
Example of SPOT/ERS-1 complementarity 09 p3749 N94-32533
Geomorphological map of the region of the Paraiba Valley and the northern coastal zone of Sao Paulo State
[INPE-5531-PRP/179] 10 p4077 N94-34226

RELIEF VALVES
Dual valve plate two-way pressure relief valve
[AD-D016293] 12 p4452 N94-37766

RELIEVING
NT STRESS RELIEVING

RELOCATION
Permanent change of station: The NASA employee's guide to an easier move
[NHB-9760.1A] 03 p1223 N94-15931

REMAGNETIZATION
U MAGNETIZATION

REMANENCE
Reverse polarity magnetized melt rocks from the Chicxulub impact structure, Yucatan Peninsula, Mexico 05 p1863 N94-20843
Photo-induced antiferromagnetic interlayer coupling in Fe superlattices with iron silicide spacers
[DE94-001345] 06 p2559 N94-22995
Comparative M-H characteristics of 1-5 and 2-17 type samarium-cobalt permanent magnets to 300 C
[NASA-CR-194440] 06 p2312 N94-24870
Shape, size, and distribution of magnetic particles in Bjurbole chondrules 11 p4353 N94-36167

REMELTING
U MELTING

REMOTE CONSOLES
The warm eddy detection from NOAA/AVHRR thermal images using the Hough transformation 01 p0220 N94-12713
Relationships between access and use in information systems: Remote access to and browsing of online catalogs 09 p3919 N94-32488

REMOTE CONTROL
NT RADIO CONTROL
Towards real time numerical stimulation of Marangoni convection: A help for telescience microgravity experiments 01 p0102 N94-10087
TOLS (Telescience On-Line Simulator): An essential instrument for micro-gravity interactive experiment 01 p0039 N94-10134
Analysis of the alignment of a Schlieren system for tele-operation 01 p0111 N94-10140
A portable controller for unmanned ground vehicles
[AD-A264963] 01 p0181 N94-11290
Heavy section steel irradiation experiment
[DE93-015517] 02 p0573 N94-14537
Infrared remote activity transceiver universal model
[AD-A266965] 03 p1188 N94-15144
Remote tire pressure sensing technique
[NASA-CASE-LAR-14160-1] 03 p1033 N94-15884
Krupp technical reports no. 2, English edition, October 1992
[ETN-93-94631] 03 p0984 N94-16000
Remote diagnosis as used for mechanized parking systems 03 p0984 N94-16004
The ESA telescience program 03 p0977 N94-16073
MAXUS: The new sounding rocket program for long duration microgravity flight 03 p0978 N94-16079
Magnetostrictive actuators for human sensory feedback
[AD-A269266] 04 p1511 N94-17841
A wind tunnel model control surface actuator interface
[AD-A268729] 04 p1322 N94-18324
Design considerations for remotely operated welding in space: Task definition and visual weld monitoring experiment
[AD-A268752] 04 p1445 N94-18634
VPU(tm) demonstration mission vicinity processor unit(tm) overview 04 p1325 N94-19171
Digital wireless control system
[DE93-040211] 05 p1714 N94-19946
Teleoperation with virtual force feedback
[DE93-019406] 05 p1942 N94-20293
Control vane guidance for a ducted-fan unmanned air vehicle
[AD-A271957] 05 p1645 N94-20561
Automating the control of robotic systems in unstructured environments
[DE93-040753] 05 p1946 N94-21929
Mars 96 rover: Science, instrumentation, and control 06 p2369 N94-23395
The remote-operated autonomous-robot concept: From deep sea to outer space applications 06 p2370 N94-23413
Sensing and modelling concepts for autonomous and remote mobile robot control 06 p2370 N94-23421
The European Space Agency standard for space packet utilisation 06 p2203 N94-23954
Crew interface analysis: Selected articles on space human factors research, 1987 - 1991
[NASA-TM-104756] 06 p2433 N94-24185
UAV current technology and future trends 06 p2154 N94-24245
Generic drone control system
[AD-D015993] 06 p2184 N94-25052
An artificial reality environment for remote factory control and monitoring 07 p2687 N94-27369
Telescience testbedding for physiological experiments under hypobaric hypoxic conditions 07 p2913 N94-27449
Telescience testbedding under hypobaric hypoxic conditions: Evaluation by operation ability and recognition ability 07 p2913 N94-27450
Telescience testbedding for physiological experiments under hypobaric hypoxic conditions: Development and evaluation in CNV measuring 07 p2913 N94-27451
Telecommand decoder specification
[ESA-PSS-04-151-ISSUE-1] 07 p2693 N94-27583
Remote control of transcranial Doppler (TCD) probe during centrifuge exposures up to 9 +Gz
[AD-A275253] 08 p3400 N94-29029
An emergency response mobile robot for operations in combustible atmospheres
[NASA-CASE-NPO-19020-1-CU] 08 p3299 N94-29420
Simplified and symmetrical five-bar linkage driver for manipulating a six-degree-of-freedom parallel minimanipulator with three inextensible limbs
[NASA-CASE-GSC-13485-2] 08 p3301 N94-29556
Remote observatory access via the advanced communications technology satellite 08 p3253 N94-29894
Aspects of the operator interface for military robotic applications in unstructured environments 08 p3309 N94-30304
A multiplexed two-way solid communications link for teleoperated robots 08 p3310 N94-30310
Task automation in a successful industrial telerobot
[AIAA PAPER 94-1189-CP] 08 p3441 N94-30539
Object-based task-level control: A hierarchical control architecture for remote operation of space robots
[AIAA PAPER 94-1209-CP] 08 p3444 N94-30560
A performance analysis method for distributed real-time robotic systems: A case study of remote teleoperation
[AIAA PAPER 94-1212-CP] 08 p3445 N94-30563
A multi-mode manipulator display system for controlling remote robotic systems
[AIAA PAPER 94-0888-CP] 08 p3446 N94-30569
Development of a frequency-domain electromagnetic scattering measurement system
[AD-A276738] 09 p3678 N94-32179
A low-cost, CCD solid state star tracker
[NASA-CR-192722] 09 p3882 N94-32417
Applying robotics to HAZMAT 09 p3729 N94-32452
Technology transfer of operator-in-the-loop simulation 09 p3802 N94-32472

Perseus: Global watcher
[NASA-TM-109813] 10 p3989 N94-33565
IMIS: An intelligence microscope imaging system 10 p4127 N94-33646
Technical parameters for specifying imagery requirements 10 p4144 N94-33648
The expanded role of software in a control system
[DE94-007524] 10 p4113 N94-33838
A teleoperated system for remote site characterization 10 p4066 N94-34029
EVA-SCRAM operations 10 p4102 N94-34035
An electronic interface for a fiber optic tethered unmanned underwater vehicle
[AD-A279046] 11 p4333 N94-35747
Remote use of distributed robotics resources to enhance technology development and insertion
[DE94-009285] 12 p4502 N94-37785

REMOTE HANDLING
STS-41 VCS training with mission specialist Bruce Melnick and Bill Shepard
[NASA-TM-109513] 03 p1046 N94-15459
Automating the control of robotic systems in unstructured environments
[DE93-040753] 05 p1946 N94-21929
System for automatic transportation of aircraft on the ground
[CA-PATENT-1-322-361] 06 p2193 N94-24785
Telescience testbedding under hypobaric hypoxic conditions: Evaluation by operation ability and recognition ability 07 p2913 N94-27450
Telescience testbedding for physiological experiments under hypobaric hypoxic conditions: Development and evaluation in CNV measuring 07 p2913 N94-27451
A multiplexed two-way solid communications link for teleoperated robots 08 p3310 N94-30310
Aiding the operator in the manual control of a space manipulator
[PB94-125549] 08 p3402 N94-30390
Bilateral control to coordinate operators with supporting systems by force sensed grips 10 p4067 N94-34335

REMOTE MANIPULATOR SYSTEM
Momentum management in redundant manipulators for vibration suppression
[NASA-CR-194112] 01 p0180 N94-10821
Application of intelligently adaptable structure and robot to large space structure 02 p0530 N94-13277
Space Station Common Berthing Mechanism, a multi-body simulation application 02 p0544 N94-14640
STS-26 EVA rescue training
[NASA-TM-109563] 03 p0875 N94-15333
Space Station/Orbiter berthing dynamics during an assembly flight
[NASA-TM-109049] 03 p1062 N94-17451
Robotics
[NASA-TM-109351] 04 p1332 N94-18920
Illumination requirements for operating a space remote manipulator 06 p2435 N94-24195
Programmable display pushbuttons on the Space Station's telerobot control panel 06 p2435 N94-24198
The effects of spatially displaced visual feedback on remote manipulator performance 06 p2436 N94-24201
Admittance model for the shuttle remote manipulator system in four configurations
[NASA-CR-4555] 06 p2474 N94-24635
Modelling the Shuttle Remote Manipulator System: Another flexible model 06 p2371 N94-25350
Direct model reference adaptive control of robotic arms 07 p2683 N94-26282
Berthing of Space Station Freedom using the shuttle remote manipulator system 07 p2684 N94-26284
Status report of RMS active damping augmentation 07 p2684 N94-26285
A multi-mode manipulator display system for controlling remote robotic systems
[AIAA PAPER 94-0888-CP] 08 p3446 N94-30569
End effector monitoring system: An illustrated case of operational prototyping 10 p4109 N94-33631
Hardware interface for isolation of vibrations in flexible manipulators: Development and applications 10 p4067 N94-34036
Robotics Demo Peer Group review
[NASA-TM-109849] 10 p4061 N94-34117
Real-time RMS active damping augmentation: Heavy and very light payload evaluations
[NASA-TM-109134] 10 p4015 N94-34386
International Space Station alpha remote manipulator system workstation controls test report
[NASA-TM-104796] 11 p4274 N94-35481
Dynamic analysis of Space Shuttle/RMS configuration using continuum approach 11 p4221 N94-35887

REMOTE REGIONS
NT ANTARCTIC REGIONS
NT ARCTIC REGIONS
Space technology in remote health care 01 p0306 N94-11799

REMOTE SENSING
Space Activities in the Asia Pacific Region
[JTN-93-80421] 01 p0035 N94-10676
Current status of space activities in Asia Pacific region 01 p0035 N94-10677
Considerations for future regional space cooperation 01 p0035 N94-10678
Space research and remote sensing programmes in Bangladesh 01 p0035 N94-10679
Space program in Indonesia 01 p0036 N94-10681
Space programme in Malaysia 01 p0036 N94-10685
National space programmes and application of the remote sensing data in Mongolia 01 p0036 N94-10686
Status of remote sensing and Geographic Information System (GIS) applications in the Environment and Natural Resources (ENR) sector 01 p0036 N94-10687
Russian space system for the Earth remote sensing 01 p0037 N94-10688
Sun-synchronous and geo-synchronous satellite data utilization for environmental studies 01 p0037 N94-10689
Thailand ISY activities 01 p0037 N94-10690
National space program in Australia 01 p0037 N94-10691
Panel discussion: Role of space program in the Asia Pacific Region 01 p0037 N94-10694
Topex/Poseidon: A United States/France mission. Oceanography from space: The oceans and climate
[NASA-TM-108253] 01 p0043 N94-10699
A browse facility for Earth science remote sensing data: Center director's discretionary fund final report
[NASA-TM-108413] 01 p0419 N94-10723
Meteorological Satellite Center
[MSC-TN-26] 01 p0190 N94-11079
An expert system shell for inferring vegetation characteristics: Prototype help system (Task 1)
[NASA-CR-193411] 01 p0231 N94-11236
Remote surface water monitoring radio based telemetry system
[DE93-009643] 01 p0041 N94-11282
Atmospheric correction of AVIRIS data in ocean waters
[AD-A264931] 01 p0288 N94-11287
Enhancement effects in polarimetric radar returns: Phase difference statistics
[NASA-CR-193408] 01 p0231 N94-11309
Extended ecosystem signatures with application to Eos synergism requirements
[NASA-CR-193398] 01 p0266 N94-11374
Application of the airborne ocean color imager for commercial fishing
[NASA-TM-103986] 01 p0231 N94-11378
Satellite inventory of Minnesota forest resources
[NASA-CR-193565] 01 p0231 N94-11521
Landsat as a commercial enterprise
[INPE-5477-TAE/019] 01 p0232 N94-11524
More sense for less cents: Cost effective servicing of remote sensing satellites 01 p0348 N94-11572
Activities relating to understanding the initiation, organization and structure of moist convection in the Southeast environment
[NASA-CR-193829] 01 p0285 N94-11598
Proceedings of First ERS-1 Symposium on Space at the Service of Our Environment, volume 1
[ESA-SP-359-VOL-1] 01 p0232 N94-11704
Sea ice: A climate component 01 p0232 N94-11705
Calibration and validation of the ERS-1 wind scatterometer 01 p0232 N94-11706
Validation of directional wave spectra from the ERS-1 during the ESA CAL/VAL campaign 01 p0232 N94-11707
The Grand Banks ERS-1 SAR wave spectra validation experiment 01 p0232 N94-11708
ERS-1 scatterometer data characteristics and wind retrieval skill 01 p0233 N94-11709
Validation of ERS-1 wind and wave data by use of operational forecast models 01 p0233 N94-11710
A C-band wind scatterometer model derived from the data obtained during the ERS-1 calibration/validation campaign 01 p0233 N94-11711
ERS-1 studies at the Department of Oceanography from Space, IFREMER/Brest (France) 01 p0233 N94-11712
The activity of the ERS-1 Venice (Italy) group on scatterometry 01 p0233 N94-11713
Use of ERS-1 data at Saclant Undersea Research Centre 01 p0233 N94-11714
A preliminary C-band scatterometer model function for the ERS-1 AMI instrument 01 p0233 N94-11715
Mapping of the East Australian current with the ERS-1 SAR and shipborne studies 01 p0234 N94-11717
Wind and surface features in SAR images: The Canadian program 01 p0234 N94-11718
Preliminary analysis of circulations over the Indian Ocean and adjoining regions using ERS-1 surface winds in the NCMRWF data assimilation system 01 p0234 N94-11719
Coastal ocean studies with ERS-1 SAR during NORCSEX 1991 01 p0234 N94-11720
SAR imaging of dynamical features in the English Channel 01 p0234 N94-11721
Effects of wave nonlinearity on ERS-1 radar altimeter returns: A preliminary investigation 01 p0235 N94-11722
SAR ocean imaging in the Gulf of Alaska 01 p0235 N94-11723
Evaluation of two January - June 1992 ERS-1 AMI wind vector data sets 01 p0235 N94-11724
Comparisons of ERS-1 altimeter height data and the Fine Resolution Antarctic Model (FRAM) 01 p0235 N94-11725
Calibration results for the ERS-1, AIRSAR, and PHARS 01 p0236 N94-11731
Techniques and applications of SAR interferometry for ERS-1: Topographic mapping, change detection, and slope measurement 01 p0236 N94-11734
SAR interferometry experiments with ERS-1 01 p0237 N94-11735
SAR-interferometry applying ERS-1: Some preliminary test results 01 p0237 N94-11736
Signatures of Antarctic firn by means of ERS-1 AMI and by field measurements 01 p0237 N94-11737
Analysis of ERS-1 altimeter data over the polar ice sheets 01 p0237 N94-11738
Some results of the derivation of ice sheet elevations in Antarctica from ERS-1 altimeter data 01 p0237 N94-11739
Utilisation of ERS-1 data for mapping of Antarctica 01 p0237 N94-11740
Monitoring of the Greenland Ice Sheet using ERS-1 synthetic aperture radar imagery 01 p0237 N94-11741
Preliminary evaluation of ERS-1 altimetry over Filchner-Ronne Ice Shelf, Antarctica 01 p0238 N94-11742
Investigations of Arctic ice-sheets and glaciers using ERS-1 SAR 01 p0238 N94-11743
Spatial patterns in backscatter strength across the Greenland Ice Sheet 01 p0238 N94-11744
Ice studies in the Barents Sea by ERS-1 SAR during SIZEX 92 01 p0238 N94-11745
Use of ERS-1 SAR to measure ice flux in the East Greenland current 01 p0238 N94-11746
Validation of ERS-1 SAR measurements of sea ice during ARCTIC-1991 01 p0238 N94-11747
Arctic coastal polynya observations with ERS-1 SAR and DMSP SSM/I 01 p0239 N94-11748
Sea ice deformation observed with ERS-1 SAR 01 p0239 N94-11749
Finnish ERS-1 Baltic Sea ice experiment in Winter 1992 01 p0239 N94-11750
Experiences from the Swedish sea ice programme during BEERS-1992 01 p0239 N94-11751
Greenland Sea observations 01 p0239 N94-11752
Air-sea-ice interactions in the Weddell Sea 01 p0239 N94-11753
Arctic sea ice microwave signature and geophysical processes study 01 p0240 N94-11754
C-band SAR backscatter from ice on shallow tundra lakes: Observations and modelling 01 p0240 N94-11755
Sea ice radar signatures from ERS-1 SAR during late Summer and Fall in the Beaufort and Chukchi Seas 01 p0240 N94-11756
Waves and mesoscale features in the marginal ice zone 01 p0240 N94-11757
The seasonal Sea Ice Monitoring and Modelling Site (SIMMS): Using ERS-1 in climate research 01 p0240 N94-11758
Ocean circulation revealed by ice floe tracking 01 p0240 N94-11759
Preliminary evaluation of ERS-1 SAR data for operational use in the Canadian sea ice monitoring program 01 p0241 N94-11760
Sea ice feature and type identification in merged ERS-1 SAR and LANDSAT Thematic Mapper imagery 01 p0241 N94-11761
Summer Arctic ice concentrations and characteristics from SAR and SSM/I data 01 p0241 N94-11762
Evaluating ERS-1 ice motion and classification products 01 p0241 N94-11763
First results for the simultaneous estimation of the geoid and the sea surface topography by ERS-1 altimeter data 01 p0241 N94-11765
Quick-look monitoring of the sea surface with ERS-1 fast delivery altimeter data 01 p0243 N94-11777

Satellite, environmental, and medical information applied to epidemiological monitoring 01 p0307 N94-11802
Satellite observation of atmospheric tracer components: JEM/POP 01 p0130 N94-11836
Effects of satellite spectral resolution and atmospheric water vapor on retrieval of near-ground temperatures [AD-A264920] 01 p0245 N94-11851
Effect of species structure and dielectric constant on C-band forest backscatter [NASA-TM-109219] 01 p0245 N94-11885
Proceedings of the PORSEC 1992 in Okinawa: Conference for Pacific Ocean Environments and Probing, volume 1 [JTN-93-80418] 01 p0191 N94-11894
Remote sensing and global environment 01 p0191 N94-11895
Remote sensing and the air-sea boundary layers 01 p0191 N94-11896
Effects of wind-roughened sea surface on ocean color remote sensing: Noise derived from reflected light and whitecaps 01 p0191 N94-11898
Satellite observations of red tide events: Plans for EESI 01 p0191 N94-11899
An algorithm for the detection of mucilage (green slime) in the Adriatic Sea 01 p0191 N94-11900
Remote sensing of the suspended matter distribution with high concentration in China Sea 01 p0192 N94-11901
Kuroshio observations by the HF ocean radar 01 p0192 N94-11904
Statistical study of HF ocean radar echo 01 p0139 N94-11905
Satellite derived sea surface temperature applications for Indian Ocean resources development 01 p0193 N94-11907
Exchange of bay water with ocean current monitored by the NOAA satellite 01 p0193 N94-11908
A consideration on principal component analysis of satellite IR data 01 p0193 N94-11909
Current structures in the western equatorial Pacific during JAPACS cruises 01 p0193 N94-11911
Acoustic waveguide characteristics of the Indian Ocean north of equator 01 p0193 N94-11912
Evaporation and thermal/hydrologic balance in the Pacific 01 p0195 N94-11919
The use of remote sensing data for coastal zone management and environment in Indonesia 01 p0196 N94-11927
Shoreline change detection using remote sensing and GIS in Vietnam 01 p0196 N94-11928
The requirement for global training programmes to meet the new remote sensing technology 01 p0196 N94-11929
Analysis of the characteristic and mechanism of suspended matter transportation in Huanghe delta sea area using remote sensing techniques 01 p0197 N94-11930
The extraction of bottom characteristics and mapping in Kin Bay, Okinawa Main Island, Japan, using LANDSAT-5/TM and SPOT-1/HRV data 01 p0197 N94-11931
Ocean wave detection by SAR 01 p0197 N94-11932
On the determination of the SAR ocean surface scattering patch size 01 p0197 N94-11933
The optical/computer hybrid processing of extracting ocean wave directional spectrum by airborne photograph 01 p0197 N94-11934
Ocean-ice interaction study of waves and mesoscale features 01 p0197 N94-11935
Appearance, behavior, and oceanic structures of warm streamers in the Kuroshio Oyashio frontal region 01 p0198 N94-11937
Warm streamers extended from Warm Core Rings (WCRs) and their role on fish migration and fishing ground formation 01 p0198 N94-11938
The Kyucho events in Sukumo Bay induced by Kuroshio front disturbances 01 p0198 N94-11939
The coherent structure in the oceanic turbulence around Japan Islands Chain forced by an air, sea, and solid Earth interaction 01 p0198 N94-11940
Westward propagation of sea surface anomalies in the western North Pacific as seen by the altimeter and radiometer 01 p0198 N94-11941
Characteristic scales and vortex features of mesoscale vortices observed by the satellites during the winter 01 p0199 N94-11943
The use of CZCS for primary production estimate in the Pacific 01 p0199 N94-11946
CZCS derived chlorophyll distribution in Antarctic water during austral summer 01 p0199 N94-11947
Seasonal changes of phytoplankton distributions in the Northwest Pacific detected by Coastal Zone Color Scanner 01 p0200 N94-11948
Satellite-derived oceanic features 01 p0200 N94-11949
Particle dynamics in the western subarctic Pacific: Implications from CZCS imagery 01 p0200 N94-11950
High-reflectance water mass in Off-Sanriku area observed by CZCS 01 p0200 N94-11951
Physical processes of microwave backscattering from laboratory wind-wave surfaces 01 p0200 N94-11952
Experiment and results of the Italian activity in the field of ocean microwave backscattering 01 p0200 N94-11953
Measurements of ocean cross-section with a side-looking airborne radar 01 p0201 N94-11954
Air-sea interaction: Fluxes, a review 01 p0201 N94-11955
Scatterometer observations: Review 01 p0201 N94-11956
Dependence of oceanic microwave emission on wind direction 01 p0201 N94-11957
Surface roughness variations across the Iceland-Faroes frontal region observed by the GEOSAT altimeter and NOAA AVHRR 01 p0201 N94-11958
The microwave backscattering from wind waves 01 p0201 N94-11959
On the variability of wind speeds in the North Western Pacific observed by altimeter/GEOSAT and SSM/I/DMSP 01 p0201 N94-11960
Observation of wind and waves by GEOSAT altimeter 01 p0202 N94-11961
Wind field estimate by using one hour GMS data 01 p0202 N94-11963
The Pacific responses exhibited by an OGCM to various wind fields 01 p0202 N94-11964
Development of shipboard ocean lidar 01 p0140 N94-11965
Remote sensing of subsurface water temperature profile and backscattering coefficient in the China Sea by Ocean Lidar (OLIDAR) 01 p0203 N94-11970
Bi-directional reflectance by oceanic waters studied via Monte-Carlo simulations 01 p0203 N94-11971
Optical characteristics in Tokyo Bay 01 p0204 N94-11972
Atmospheric correction plans for SeaWiFS 01 p0204 N94-11975
Distribution of mineral aerosols over the North Pacific 01 p0204 N94-11976
Implications of aerosol retrieval and atmospheric correction in remote sensing 01 p0205 N94-11978
Overwater atmospheric dispersion of volcanic smokes from Mt. Sakurajima observed in NOAA-AVHRR data 01 p0205 N94-11979
Incident shortwave and longwave radiations over the western North Pacific and the Sea of Okhotsk derived from GMS-WEFAX images 01 p0205 N94-11982
A study of pollution courses of spilled oil floatation in the outer ocean 01 p0205 N94-11983
Observations of the fractal properties of the Japan sea surface temperature patterns 01 p0205 N94-11984
Flood monitoring in northern part of Central Java by remote sensing technique. Case study: The flooding of Semarang in January, 1990 01 p0206 N94-11989
Fourier domain target transformation analysis in the thermal infrared 01 p0258 N94-12030
Compositional and textural information from the dual inversion of visible, near and thermal infrared remotely sensed data 01 p0258 N94-12097
Remote sensing x ray fluorescence spectrometry for future lunar exploration missions 01 p0462 N94-12165
Automatic definition of spectral units in the equatorial regions of Mars 01 p0432 N94-12234
Observing and modelling F-region ionospheric dynamics using the (O2) 7320A emission [AD-A265407] 01 p0279 N94-12419
Sampling and position effects in the Electronically Steered Thinned Array Radiometer (ESTAR) [NASA-TM-108998] 01 p0245 N94-12432
Interdisciplinary scientist participation in the Phobos mission [NASA-CR-193715] 01 p0482 N94-12446
Emissions of sulfur gases from marine and freshwater wetlands of the Florida Everglades: Rates and extrapolation using remote sensing 01 p0269 N94-12457
Effects of inorganic sulfur addition on fluxes of volatile sulfur compounds in Sphagnum peatlands 01 p0270 N94-12461
Proceedings of 1st ERS-1 Symposium on Space at the Service of Our Environment, Volume 2 [ESA-SP-359-VOL-2] 01 p0245 N94-12471
ERS-1 altimetry of inland water and land 01 p0246 N94-12475
Combined analysis of ERS-1 SAR and visible/infrared remote sensing data for land cover/land use mapping in a tropical zone: A case study in Guinea 01 p0246 N94-12478
Example of SPOT/ERS-1 complementarity 01 p0247 N94-12479
The use of ERS-1 SAR data to study surface states 01 p0247 N94-12480
Snow and glacier investigations by ERS-1 SAR: First results 01 p0247 N94-12481
Monitoring of snowcover in high mountain terrain with ERS-1 SAR 01 p0247 N94-12482
Application of ERS-1 SAR data to snow mapping 01 p0247 N94-12483
Preliminary ERS-1 assessment for Canadian agriculture and forestry applications 01 p0248 N94-12486
Segmentation and change detection in ERS-1 images over East Anglia 01 p0248 N94-12487
ERS-1 SAR crop monitoring experiment in East Anglia, UK 01 p0248 N94-12488
Geoecological monitoring of an agricultural area 01 p0248 N94-12489
Integration of ERS-1 data into the European project of agriculture statistics 01 p0248 N94-12490
Extraction of plant and soil parameters from multitemporal ERS-1 SLC data of the Freiburg test site 01 p0248 N94-12491
Assessment of ERS-1 SAR data for soil moisture estimation 01 p0249 N94-12492
Temporal monitoring of soil moisture using ERS-1 SAR data 01 p0249 N94-12493
Observations of ERS-1 SAR sensitivities to changes in aboveground biomass in young loblolly pine forests 01 p0249 N94-12494
Seeing the Black Forest by ERS-1 and AIRSAR: A comparison 01 p0249 N94-12495
The TREES project: Pre-processing and generation of terrain data for inclusion in an ERS-1 SAR classification scheme 01 p0249 N94-12496
TREES project: A case study on the use of multi-temporal ERS-1 SAR data and SPOT data for monitoring tropical ecosystems 01 p0249 N94-12497
TREES project: Overview and status of the ERS-1 SAR contribution 01 p0250 N94-12499
Impact of ERS-1 wind/wave/ice data on operational ocean forecasting 01 p0250 N94-12500
A first assessment of the value of ERS-1 scatterometer winds for meteorological studies in the polar regions 01 p0250 N94-12501
Use of SAR-wave, altimeter, and wind-scatterometer data in an operational swell forecasting system 01 p0250 N94-12503
Use of ERS-1 scatterometer winds in Canadian forecast centres 01 p0250 N94-12504
ERS-1 and Almaz SAR ocean wave imaging over the Gulf Stream and the Grand Banks 01 p0251 N94-12505
Real time processing wave spectra from satellite SAR 01 p0251 N94-12506
A statistical analysis of sea state surface ERS-1 SAR-wave mode imagettes 01 p0251 N94-12507
A new model for Synthetic Aperture Radar (SAR) images from ocean scatter 01 p0251 N94-12508
On the extraction of ocean wave spectra from ERS-1 SAR wave mode image spectra 01 p0251 N94-12509
Tide-generated nonlinear internal wave packets in the Strait of Gibraltar observed by the synthetic aperture radar aboard the ERS-1 satellite 01 p0252 N94-12510
Validation of the ATSR/M microwave radiometer data 01 p0252 N94-12511
Multichannel dual angle approach for sea surface temperature retrieval in context of ERS-1 scenario 01 p0252 N94-12512
Estimations of the surface fluxes from satellite observations of boundary layer and the surface 01 p0252 N94-12513
ATSR correlative skin measurements of sea surface temperature 01 p0252 N94-12514
Validation of ATSR-1 using aircraft radiometer measurements over the South Atlantic 01 p0252 N94-12515
A comparison of ATSR and shipboard radiometer SST measurements along transects between the UK and the Antarctic 01 p0253 N94-12518
Artificial oil pollution detection and wave observation in the sea adjacent to Japan by ERS-1 SAR 01 p0253 N94-12520
Ship traffic monitoring using the ERS-1 SAR 01 p0253 N94-12521
Oil spill detection using satellite-based SAR: Experience from a field experiment 01 p0253 N94-12522
Coastal morphodynamics and energetic characteristics of swell studied with ERS-1 SAR 01 p0254 N94-12524
SAR imaging of geology and bathymetry: Kent coastal area - southern North Sea 01 p0254 N94-12527

Proceedings of the PORSEC 1992 in Okinawa: Conference for Pacific Ocean Environments and Probing, volume 2
[JTN-93-80419] 01 p0207 N94-12635
Analysis of GEOSAT wind data
01 p0207 N94-12636
SSMI wind speed variability over the Pacific Ocean
01 p0207 N94-12637
Observation of wave crests by satellite remote sensed data 01 p0207 N94-12638
Observations of eddy fields in the Northwest Pacific by GEOSAT altimetry 01 p0207 N94-12639
Variability of sea level and sea surface temperature anomalies in the equatorial Pacific
01 p0208 N94-12640
Theory and oceanographic applications of satellite altimeter measurements 01 p0208 N94-12641
Analysis of collinear passes of satellite altimeter data
01 p0208 N94-12642
Surface eddy fluxes from the GEOSAT satellite altimeter 01 p0208 N94-12643
Comparison of GEOSAT sea surface height and model-simulated surface dynamic height
01 p0208 N94-12644
Pseudo magnetic anomaly derived from satellite altimetry and its application to the tectonics in the North Fuji Basin 01 p0208 N94-12645
Principal oscillation pattern analysis of sea level variations in the tropical Pacific measured by the GEOSAT altimeter 01 p0209 N94-12646
Measurement of eddy structure and movement in the north-east Pacific with the GEOSAT altimeter
01 p0209 N94-12647
Preliminary results from a satellite altimetric data assimilation using a Kalman filter and smoother
01 p0209 N94-12648
Fluctuations of the Kuroshio extension detected by the GEOSAT altimetry data 01 p0209 N94-12649
Mean flow and variability in the Kuroshio extension from GEOSAT altimetry data 01 p0209 N94-12650
Pacific rim sea ice as observed with the NIMBUS-7 SMMR 01 p0210 N94-12651
ice studies in the Barents Sea by ERS-1 during SIZEX 1992 01 p0210 N94-12653
Disintegrating ice front of Shirase Glacier, East Antarctica 01 p0210 N94-12654
Microwave radiometry of ice cover in polar regions
01 p0210 N94-12655
The seasonal change of phytoplankton size distribution using optical fiber sensor 01 p0210 N94-12656
Worldwide map of rainfall amount over the ocean derived from passive microwave radiometer
01 p0211 N94-12663
Study on diffusion phenomena of river effluents issued into sea around Japan with satellite remote sensing data
01 p0212 N94-12664
A basic consideration for remote sensing using microwave radars on a satellite
01 p0212 N94-12665
Migration of operational ice analysis and forecasting to a workstation platform at the Joint Ice Center
01 p0212 N94-12666
Evaluating the spread of red soil with LANDSAT TM data in coral reefs of Okinawa main island, southwestern Japan 01 p0212 N94-12668
Simple and low cost image processing system for satellite remote sensing data 01 p0212 N94-12669
Validation test system for sea surface temperature detected by satellites in Mutsu Bay
01 p0213 N94-12670
Sea surface temperature images of Geostationary Meteorological Satellite (GMS) and sea truth data from ferry boats 01 p0213 N94-12671
Measurement of the sea surface emissivity
01 p0213 N94-12672
Evaluation of the method of geostrophic flow using NOAA-AVHRR data 01 p0213 N94-12673
Further study of the Non-Regression-Coefficient SST retrieval method 01 p0213 N94-12674
Delineation of mesoscale features of ocean on satellite IR image 01 p0214 N94-12675
Observation of warm current at the boundary from north equatorial current to Kuroshio by NOAA/AVHRR
01 p0214 N94-12676
Information capability of NOAA-AVHRR data for monitoring oceanographic and atmospheric pollution
01 p0214 N94-12677
Satellite observations of the northeast monsoon coastal current 01 p0214 N94-12678
Aspects of applying a relaxation method to computing sea surface velocities from sea surface temperature images 01 p0214 N94-12679
Sea surface temperature difference between NOAA/AVHRR and in-situ observation
01 p0215 N94-12680
Application of NOAA AVHRR data to fisheries
01 p0215 N94-12681
Statistical features of mesoscale eddies at the Kuroshio front 01 p0215 N94-12682
Intrusion of Kuroshio warm water into Sagami Bay
01 p0215 N94-12683
A study of front dynamics off northeastern Taiwan based on the NOAA-AVHRR satellite remote sensing data
01 p0215 N94-12684
Satellite thermal variations of Kuroshio in relation to storm floods 01 p0215 N94-12685
ADCP evidence for upper layer circulation in northeast of the South China Sea 01 p0215 N94-12686
Frontal zones in Pacific Ocean: Satellite and ship data analysis 01 p0216 N94-12687
Swordfish (Xiphias gladius) catch distributions relative to environmental features observed from satellites off Coquimbo, Chile (30 deg S) 01 p0216 N94-12688
Observation of cold coastal water with high turbidity around the southwestern tip of Korean Peninsula
01 p0216 N94-12689
On the error characteristics of the sea surface temperature observed by satellite
01 p0216 N94-12690
The WOCE/TOGA Surface Velocity Programme (SVP)
01 p0216 N94-12691
Remote sensing of polluting focal points and coastal disturbances in the Gulf of Arauco and adjacent bays, central Chile 01 p0217 N94-12695
Role of remote sensing and its cost effectiveness in site selection for coastal aquaculture
01 p0217 N94-12697
Seasonal variability of surface ocean color in the Omura Bay using multitemporal LANDSAT-5 TM data
01 p0218 N94-12698
Acoustic estimation of plankton biomass
01 p0218 N94-12699
Properties of spectral reflectance of crown and crown structure of mangrove species in Okinawa
01 p0218 N94-12700
Application of remote sensing for coastal management in the north coast of Java 01 p0218 N94-12701
Study of growing processes of a tombolo using an air photograph 01 p0218 N94-12702
Estimation of areal evapotranspiration using LANDSAT TM data: Kitami City, Hokkaido, Japan
01 p0219 N94-12703
Land use/land cover mapping of central water shed of Iran area based on satellite data interpretation
01 p0219 N94-12704
A method to minimize reference data in classifying satellite remote sensing data into land cover classes
01 p0219 N94-12705
The circulation near Luzon 01 p0219 N94-12707
Current variability on the shelf break northeast of Taiwan 01 p0219 N94-12708
Study on air-sea interactions in the OMLET (Ocean Mixed Layer Experiment) area using satellite remote sensing 01 p0220 N94-12710
Investigation of meso-scale fronts, eddies and upwellings in China Seas with AVHRR data
01 p0220 N94-12711
Coastal upwelling monitored by satellite data: Methodologies and results 01 p0220 N94-12712
Applicability of satellite infrared data for the monitoring of coastal environments 01 p0220 N94-12714
Satellite and moored buoy observations of polar frontal system over the Yamato Rise in the Japan Sea
01 p0221 N94-12715
The relationship between skin and bulk sea surface temperatures 01 p0221 N94-12716
Variability of the Kuroshio observed from satellite thermal imagery 01 p0221 N94-12717
Variability of the mixed layer depth in the North Pacific Ocean as calculated by a 3-D semi-analytical mixed layer remote sensing model 01 p0221 N94-12718
SST assimilation: Eastern Mediterranean case study
01 p0221 N94-12719
Mapping of high density area of benthic diatom in Ariake Sea 01 p0222 N94-12720
Advective surface velocity in the north west Pacific derived from NOAA AVHRR images
01 p0222 N94-12721
Polarisation of backscattering radiation at remote sensing of ocean with impulse laser beam
01 p0177 N94-12722
The method of investigation of the horizontal structure of the thermal fronts 01 p0222 N94-12723
On a nonstationary dynamics of the north-west Pacific Ocean 01 p0222 N94-12724
Optimum selection of spectral channels in the problem of remote sensing of phytoplankton concentration in ocean water 01 p0223 N94-12726
Field research of wind wave spectrum variability
01 p0223 N94-12727
The acoustic arrangement for measuring vertical structure of sea current 01 p0223 N94-12729
Turbulence generation in the Pacific undercurrent by shear 01 p0223 N94-12730
The Pacific Subarctic Frontal Zone: Structure and dynamics 01 p0223 N94-12731
Laser photoheterodyne interferometers for oceanographic investigations 01 p0177 N94-12732
A detailed investigation of the benthic regime in the Clarion-Clipperton province of the Pacific and a forecast of consequences of manganese nodule mining
01 p0224 N94-12733
Bottom currents and possibilities for near bottom layer environmental investigations in the Pacific by means of self contained bottom stations 01 p0224 N94-12734
Remote sensing of light scattering coefficient of sea water vertical distribution by the means of airborne lidar
01 p0224 N94-12736
Influence of the Kuroshio warm-core rings on hydrographic and fishery conditions off southern Kuril Islands 01 p0224 N94-12737
Verification of the atmosphere-ocean radiative transfer parametric models 01 p0225 N94-12738
Spatial variability of the ocean underwater dynamic noise from satellite radar sensing data
01 p0225 N94-12740
Observations of film slicks and internal waves with Ka-band scatterometer 01 p0225 N94-12741
Optical transfer operator of the atmosphere-ocean system 01 p0225 N94-12742
Cloud liquid water content over the Pacific Ocean tropical zone derived from ship microwave radiometric measurement 01 p0225 N94-12743
Variability of spectral reflectance in coastal waters near the river plumes 01 p0226 N94-12744
Wind-wave and foam dynamics from optical and radar airborne observations 01 p0226 N94-12745
Observations of surface signatures in the north-west Pacific Ocean with the spaceborne SAR
01 p0226 N94-12746
Radar observation of internal waves field in the north-west Pacific 01 p0226 N94-12747
Trajectory curving in underwater propagation of light
01 p0226 N94-12748
DISTERM: A shipboard data system for satellite monitoring of ocean and atmosphere
01 p0226 N94-12749
Atmospheric correction for determination of average SST fields based on AVHRR data
01 p0227 N94-12750
Complex (hydrodynamic, satellite) monitoring of dynamic structures in the western Pacific with the aim of forecasting the marine ecosystems behaviour
01 p0227 N94-12753
Mesoscale dynamic structures of the Subarctic Frontal Zone in the Pacific Ocean 01 p0227 N94-12754
Laser fluorescent monitoring of dissolved organic matter in natural water 01 p0177 N94-12755
Ecological application of Surface Enhanced Raman Spectroscopy 01 p0227 N94-12756
A possibility to define the location of epipelagic fish concentrations with assistance of satellite sensing
01 p0228 N94-12757
High biological production of the tidal mixing zones on Japan Sea shelf 01 p0228 N94-12758
Study of the admixture diffusion in the sea using remote techniques 01 p0228 N94-12759
The algorithm of primary production determination
01 p0228 N94-12761
Non-image visible polarization remote sensing of the ocean 01 p0229 N94-12762
Problem of climate change predictability and satellite radiation budget observations 01 p0229 N94-12766
Knowledge-based oceanographic image compression
[AD-A265752] 02 p0821 N94-13041
Linkage of anthropogenic aerosol to clouds and climate
[DE93-016434] 02 p0719 N94-13080
Novel Co:MgF2 lidar for aerosol profiler
[NASA-CR-191525] 02 p0654 N94-13091
Development of a portable multispectral thermal infrared camera
[NASA-CR-191340] 02 p0648 N94-13176
Design of partially supervised classifiers for multispectral image data
[NASA-CR-194299] 02 p0823 N94-13192
Dendrometric variables estimation in homogeneous forests using LANDSAT TM data
[INPE-5455-TDI/497] 02 p0684 N94-13331
Spectral reflectance of soils from Sao Paulo State
[INPE-5424-PRP/172] 02 p0684 N94-13377
Remote sensing of aquatic system
[INPE-5271-PRP/159] 02 p0684 N94-13426

Net radiation mapping of mountainous terrain using Landsat-5 thematic mapper imagery and digital terrain data
[ISBN-0-315-57755-X] 02 p0685 N94-13475
Remote identification of rain and hail with a polarization diversity radar
[ISBN-0-315-55623-4] 02 p0720 N94-13516
A knowledge-based model for the integration of remote sensing into a mineral exploration program
[ISBN-0-315-58982-5] 02 p0685 N94-13523
Analytical framework for modeling scale-related variabilities in remote sensing 02 p0685 N94-13592
A review and analysis of neural networks for classification of remotely sensed multispectral imagery
[NASA-CR-194291] 02 p0763 N94-13603
Operational test of the airborne data acquisition system: SADA, the Bara Bonita experiment
[INPE-5451-NTC/305] 02 p0685 N94-13610
Estimations of temperature and humidity of the canopy in Amazon Forest using microwave data from SMMR sensor of Nimbus-7 satellite
[INPE-5444-TDI/490] 02 p0720 N94-13614
Study on TRMM data utilization for meteorology
[NASDA-CNT-930007] 02 p0721 N94-13643
Advanced solid-state array spectroradiometer data collection during HAPEX-2 Sahel
[NASA-CR-194144] 02 p0808 N94-13875
Wind erosion in semiarid landscapes: Predictive models and remote sensing methods for the influence of vegetation
[NASA-CR-194029] 02 p0715 N94-13956
Activities report of the Netherlands Remote Sensing Board
[ETN-93-93880] 02 p0686 N94-14073
Intelligent environment for interpretation tasks of remotely sensed images
[INPE-5466-PRE/1774] 02 p0687 N94-14082
Volume 14: The first SeaWiFS intercalibration round-robin experiment, SIRREX-1, July 1992
[NASA-TM-104566-VOL-14] 02 p0725 N94-14090
Minutes of the Sixth CEOS Plenary Meeting
[NASA-TM-108252] 02 p0542 N94-14112
Integration of remotely sensed data and cadastral ownership boundaries for land inventory purposes
[BCRS-92-16] 02 p0687 N94-14127
Multisensor remote sensing data and GIS techniques for monitoring preservation areas: A case study
[INPE-5317-PRE/1714] 02 p0688 N94-14131
An algorithm for the remote sensing of fog using satellite data and additional information
[DLR-FB-92-23] 02 p0688 N94-14135
Water-vapour, total water and rainrate from passive microwave satellite data over ocean
[DLR-FB-92-37] 02 p0723 N94-14189
Asia-Pacific ISY Conference, volume 2
[NASDA-CM-199-VOL-2] 02 p0688 N94-14209
Artificial oil pollution detection and wave observation in the sea adjacent to Japan by ERS-1 SAR
02 p0688 N94-14212
High performance multi-mode radar altimeter for future spaceborne application 02 p0548 N94-14214
IMG: Interferometric monitor for greenhouse gases
02 p0689 N94-14217
Spectroscopic method and data reduction algorithm for laser long-path absorption measurements using RIS
02 p0689 N94-14218
Image processing and analysis of airborne POLDER data 02 p0689 N94-14219
Overview of the ILAS operational data processing system 02 p0690 N94-14220
TRMM system overview and status in the United States 02 p0690 N94-14221
TRMM Project in Japan: Overview and status
02 p0690 N94-14222
Clouds and the Earth's Radiant Energy System (CERES) on the Tropical Rainfall Measuring Mission (TRMM)
02 p0690 N94-14223
TRMM precipitation radar algorithm
02 p0690 N94-14224
Estimate of sampling errors of TRMM rainfall observation by using radar-AMeDAS composite data
02 p0690 N94-14225
Space measurements for determining the Earth's energy and water cycles 02 p0690 N94-14227
Future TRMM follow-on mission
02 p0691 N94-14228
Remote sensing of low level cloud optical characteristics 02 p0691 N94-14229
The effects of anthropogenic aerosols on optical thickness and particle size of clouds. Part 1: Retrieval algorithm 02 p0691 N94-14230
Climate products from NOAA operational satellites
02 p0691 N94-14231
Seasonal change of the land-surface temperature over Asian Continent derived from GAC data on NOAA-11 AVHRR 02 p0691 N94-14232
Earth radiation budget, cloud, and aerosol parameters derived from AVHRR and TOVS measurements
02 p0691 N94-14233
Some potentials of the Indonesian region for Earth observation 02 p0692 N94-14237
Application of satellite remote sensing technology in disaster mitigation: A case study of Bangladesh
02 p0692 N94-14238
Integration of remote sensing and mathematical modelling in disaster mitigation
02 p0692 N94-14239
Soil erosion mapping using remote sensing and GIS techniques 02 p0692 N94-14240
Detecting land cover changes in Chiang-Mai area in Thailand 02 p0693 N94-14241
Land evaluation for agricultural productivity in North-East Thailand using LANDSAT TM data and geographic information 02 p0693 N94-14242
Effects of typhoon on TOMS data
02 p0693 N94-14243
Satellite remote sensing for disaster mitigation
02 p0693 N94-14244
A concept for the world environment and disaster observation system 02 p0693 N94-14245
Study of the consequences of the Chernobyl accident and technogenic activity in the Republic Belarus using aerospace methods 02 p0693 N94-14246
A tentative plan on China and Asian-Pacific satellite system for disaster reduction 02 p0693 N94-14247
Earth observation from low-inclination orbit as a necessary complement to polar missions
02 p0694 N94-14248
Development of a remote sensing geographic information system for land cover changes and assessment of risk due to natural and man made hazards covering the area of the inner delta of the Yellow River
02 p0694 N94-14249
The role of the dynamics for the deviation of the total ozone from the long-term mean at the edge of the polar vortex 02 p0694 N94-14250
The European Arctic ozone experiment: An investigation of Northern Hemisphere ozone depletion
02 p0694 N94-14251
Space-based activities: SAM 2 and SAGE 2
02 p0694 N94-14252
New evidences supported the Wei hypothesis about the formation of the Antarctic ozone hole
02 p0694 N94-14253
Multi-source national forest inventory of Finland
02 p0694 N94-14254
Global assessment of human activities
02 p0695 N94-14255
The Swedish ISY contribution
02 p0695 N94-14256
Vegetation mapping of Indo-China Peninsula using MOS-1 MESSR and NOAA AVHRR
02 p0695 N94-14257
Remote sensing for monitoring tropical moist forests in the Indo-Chinese region 02 p0695 N94-14258
Estimation of vegetation damage due to ash fall in Mt. Pinatubo area using MOS-1 data
02 p0695 N94-14259
Mangrove afforestation monitoring using remote sensing 02 p0695 N94-14260
Outline of ISY sea surface temperature data sets
02 p0696 N94-14261
Integration of SST data sets using MOS-1 satellite data: For validation and monitoring 02 p0696 N94-14262
Geophysical validation of ATSR sea surface temperatures 02 p0696 N94-14263
Accuracy validation test of estimated sea surface temperature by satellite data 02 p0696 N94-14264
Sea surface effect on the sea surface temperature estimation by satellite data 02 p0696 N94-14265
On the sea truth data of the Kuroshio meander and cold eddy movement 02 p0696 N94-14266
Tracking of change of a warm-core ring structure
02 p0696 N94-14267
Outline of ISY Kuroshio observation experiment
02 p0697 N94-14268
A method for estimation of partial cloud cover within a pixel and its effect 02 p0697 N94-14269
Warm streamers extended from Warm Core Rings (WCR's) and their role on fish migration and fishing ground formation 02 p0697 N94-14270
Atmospheric correction for sea surface temperature by application of microwave dual-channel technique to VTIR data 02 p0697 N94-14271
Some thoughts on the space programs in the Asia Pacific regions 02 p0697 N94-14272
China's devotion to space science and applications
02 p0532 N94-14273
Survey of subsurface geophysical exploration technologies adaptable to an airborne platform
[DE93-015080] 02 p0717 N94-14294
Workshop on the Space Environment: The Effects on the Optical Properties of Airless Bodies
[NASA-CR-194417] 02 p0842 N94-14298
ERS-1 system
[ESA-SP-1146] 02 p0699 N94-14353
Supervised classification of remotely sensed images
[DLR-FB-92-07] 02 p0700 N94-14428
Educational module for the Higher Agricultural Education. Part 2: Eutrophication observed by remote sensing: An educational approach to water quality monitoring
[BCRS-92-11B] 02 p0818 N94-14462
Determination of the surface cleanliness of metals by FT-IR spectroscopy
[DE93-013252] 02 p0565 N94-14525
The National Remote Sensing Program (NRSP-2 1991 - 2000): The 1992 annual plan of the Netherlands Remote Sensing Board
[BCRS-92-22] 02 p0700 N94-14544
Computer vision and sensor fusion for detecting buried objects
[DE93-012605] 02 p0700 N94-14566
Educational module for the higher agricultural education. Part 1: Land use classification using satellite pictures
[BCRS-92-11A] 02 p0819 N94-14809
Obtaining digital regional planning information from aerial pictures
[REPT-228] 02 p0700 N94-14810
Signal and reference wavelengths for the elimination of SO2 cross sensitivity in remote measurements of tropospheric ozone with lidar
[GKSS/92/E/24] 02 p0617 N94-14819
The MADONA experiments (Meteorology and Diffusion Over Non-uniform Areas): High-resolution in-plume concentration fluctuations measurements using lidar remote sensing technique
[AD-A267711] 03 p1105 N94-14938
Views from space
[NASA-TM-109634] 03 p1081 N94-15245
Combating malaria
[NASA-TM-109609] 03 p1081 N94-15297
Heterodyne efficiency for a coherent laser radar with diffuse or aerosol targets
[NASA-CR-194563] 03 p1038 N94-1 477
SeaWiFS technical report series. Volume 12, SeaWiFS technical report series cumulative index: Volumes 1-11
[NASA-TM-104566-VOL-12] 03 p1111 N94-15529
An expert system shell for inferring vegetation characteristics: Atmospheric techniques (Task G)
[NASA-CR-194570] 03 p1082 N94-15531
Steering capaciflector sensor
[NASA-CASE-GSC-13489-1] 03 p1164 N94-15704
Workshop on advanced technologies for planetary instruments
[NASA-CR-194585] 03 p1032 N94-15797
Environmental characterization for target acquisition. Report 1: Site descriptions and measurements
[AD-A267192] 03 p1106 N94-15851
Proceedings of the Third Spaceborne Imaging Radar Symposium
[NASA-CR-194104] 03 p0989 N94-15886
ERS-1: 18 months in orbit 03 p0990 N94-15888
X-SAR: The X-band synthetic aperture radar on board the Space Shuttle 03 p0990 N94-15891
ENVISAT ASAR 03 p0898 N94-15892
TRMM radar 03 p0990 N94-15894
Driving terrestrial ecosystem models from space
03 p0991 N94-15896
Recent advances in radar remote sensing of forest
03 p0991 N94-15897
Radar response of vegetation: An overview
03 p0991 N94-15898
Geologic remote sensing with radar
03 p0991 N94-15900
SIR-C/X-SAR free flyer concept
03 p0898 N94-15903
EOS SAR: A new approach 03 p0992 N94-15904
A summary of microwave remote sensing investigations planned for BOREAS 03 p0993 N94-15914
Primary studies of Chinese spaceborne SAR
03 p0993 N94-15916
AIRSAR South American deployment: Operation plan, version 3.0 03 p0994 N94-15919
Spatial and frequency diversity in lidar systems
[AD-A266192] 03 p1039 N94-16124
Earth imaging results from Galileo's second encounter
03 p1252 N94-16201
Remote sensing studies of the northeastern portion of the lunar nearside 03 p1258 N94-16225
Far-infrared spectra of CO2 clathrate hydrate frosts
03 p0954 N94-16340
Martian lavas: Three complementary remote sensing techniques to derive flow properties
03 p1283 N94-16366
The Clementine instrument complement
03 p1086 N94-16370

A mission concept of Phobos/Deimos exploration
03 p1287 N94-16387
Remote visual detection of impacts on the lunar surface 03 p1290 N94-16404
Do it yourself remote sensing: Generating an inexpensive, high tech, real science lake mapping project for the classroom 03 p1086 N94-16407
A quantitative analysis of TIMS data obtained on the Learjet 23 at various altitudes 03 p1063 N94-16597
Comparison of preliminary results from Airborne Aster Simulator (AAS) with TIMS data
03 p1064 N94-16600
An algorithm for the estimation of bounds on the emissivity and temperatures from thermal multispectral airborne remotely sensed data 03 p1064 N94-16603
Multi-resolution processing for fractal analysis of airborne remotely sensed data 03 p1065 N94-16604
Ejecta patterns of Meteor Crater, Arizona derived from the linear un-mixing of TIMS data and laboratory thermal emission spectra 03 p1065 N94-16607
Using AVIRIS images to measure temporal trends in abundance of photosynthetic and nonphotosynthetic canopy components 03 p1066 N94-16668
Mapping the mineralogy and lithology of Canyonlands, Utah with imaging spectrometer data and the multiple spectral feature mapping algorithm
03 p1066 N94-16670
Hyperspectral modeling for extracting aerosols from aircraft/satellite data 03 p1067 N94-16673
AVIRIS study of Death Valley evaporite deposits using least-squares band-fitting methods
03 p1067 N94-16676
A field measure of the shade fraction
03 p1068 N94-16677
A linear spectral matching technique for retrieving equivalent water thickness and biochemical constituents of green vegetation 03 p1068 N94-16678
Mapping the spectral variability in photosynthetic and non-photosynthetic vegetation, soils, and shade using AVIRIS 03 p1068 N94-16679
Exploring the remote sensing of foliar biochemical concentrations with AVIRIS data
03 p1069 N94-16683
AVIRIS calibration and application in coastal oceanic environments 03 p1069 N94-16685
Mapping vegetation types with the multiple spectral feature mapping algorithm in both emission and absorption 03 p1069 N94-16686
Multiple dataset water-quality analyses in the vicinity of an ocean wastewater plume 03 p1069 N94-16687
Using endmembers in AVIRIS images to estimate changes in vegetative biomass
03 p1070 N94-16689
The 1991 AVIRIS/POLDER experiment in Camargue, France 03 p1070 N94-16691
JPL activities on development of acousto-optic tunable filter imaging spectrometer 03 p1037 N94-16696
Measuring dry plant residues in grasslands: A case study using AVIRIS 03 p1072 N94-16697
Tracking photosynthetic efficiency with narrow-band spectroradiometry
[CIW-PUBL-1133] 03 p1072 N94-16698
Integrating remote sensing techniques at Cuprite, Nevada: AVIRIS, Thematic Mapper, and field spectroscopy 03 p1072 N94-16701
Oregon transect: Comparison of leaf-level reflectance with canopy-level and modelled reflectance
03 p1073 N94-16702
Expert system-based mineral mapping using AVIRIS
03 p1073 N94-16704
AVIRIS data and neural networks applied to an urban ecosystem 03 p1073 N94-16705
Temporal variation in spectral detection thresholds of substrate and vegetation in AVIRIS images
03 p1073 N94-16706
A comparison of LOWTRAN-7 corrected Airborne Visible/Infrared Imaging Spectrometer (AVIRIS) data with ground spectral measurements
03 p1074 N94-16710
Discrimination among semi-arid landscape endmembers using the Spectral Angle Mapper (SAM) algorithm
03 p1074 N94-16711
Empirical relationships among atmospheric variables from rawinsonde and field data as surrogates for AVIRIS measurements: Estimation of regional land surface evapotranspiration 03 p1074 N94-16712
Retrieval of pine forest biomass using JPL AIRSAR data 03 p1076 N94-16737
Characterization of wetland, forest, and agricultural ecosystems in Belize with airborne radar (AIRSAR)
03 p1076 N94-16738
Strategies for detection of floodplain inundation with multi-frequency polarimetric SAR
03 p1076 N94-16739
Supervised fully polarimetric classification of the Black Forest test site: From MAESTROI to MAC Europe
03 p1076 N94-16740
Relating multifrequency radar backscattering to forest biomass: Modeling and AIRSAR measurement
03 p1077 N94-16741
Mapping of sea bottom topography
03 p1077 N94-16744
Preliminary results of polarization signatures for glacial moraines in the Mono Basin, Eastern Sierra Nevada
03 p1078 N94-16746
Extraction of quantitative surface characteristics from AIRSAR data for Death Valley, California
03 p1078 N94-16748
Application of symmetry properties to polarimetric remote sensing with JPL AIRSAR data
03 p1079 N94-16752
Processing of polarimetric SAR data for soil moisture estimation over Mahantango watershed area
03 p1079 N94-16754
Soil conservation applications with C-band SAR
03 p1080 N94-16760
Earth observational research using multistage EOS-like data
[NASA-CR-194626] 03 p1084 N94-16831
Remote sensing of precipitation and electrification with a dual-polarization, coherent, wideband radar system
[AD-A267479] 03 p1004 N94-17364
Arctic cyclones and Marginal Ice Zone (MIZ) variability
[AD-A268610] 03 p1108 N94-17465
An investigation of the Ground-Based High-Resolution Interferometer Sounder (GB-HIS) in a costal marine environment
[AD-A268052] 03 p1114 N94-17503
An analysis of simulated and actual DMSP SSM/T-2 brightness temperatures
[AD-A268103] 03 p1109 N94-17573
Packaging, deployment, and panel design concepts for a truss-stiffened 7-panel precision deployable reflector with feed boom
[NASA-TM-109000] 04 p1333 N94-17765
A mobile remote sensing laboratory for water vapor, trace gas, aerosol, and wind speed measurements
[DE93-017158] 04 p1489 N94-18132
Arctic ice studies
[AD-A268608] 04 p1497 N94-18277
A RFI measurement system for field sites
[AD-A269340] 04 p1385 N94-18301
Microwave (SSM/I) Estimates of the Precipitation Rate to Improve Numerical Atmospheric Model Forecasts
[NASA-CR-193566] 04 p1491 N94-18602
Physical retrieval of precipitation water contents from Special Sensor Microwave/Imager (SSM/I) data. Part 1: A cloud ensemble/radiative parameterization for sensor response (report version) 04 p1491 N94-18604
Physical retrieval of precipitation water contents from Special Sensor Microwave/Imager (SSM/I) data. Part 2: Retrieval method and applications (report version)
04 p1491 N94-18605
Forecast model applications of retrieved three dimensional liquid water fields 04 p1492 N94-18606
Current positioning possibilities by spatial techniques and the Royal Oservatory of Belgium program
04 p1483 N94-18627
Atlas of SSM/I satellite ice concentration interpolated to operational ice model domains of the Arctic for 1992
[AD-A270306] 04 p1499 N94-18727
Analytic approximations of an integral in remote sensing
[AD-A270085] 04 p1463 N94-18800
Engineering research, development and technology thrust area report, FY92
[DE93-016334] 04 p1632 N94-18856
Spatiotemporal variability of non-urban ozone concentrations over the eastern United States and its potential replication by satellite data
[PB93-191328] 04 p1476 N94-19065
Development of ISY data set, part 2
[NASDA-CNT-930006-PT-2] 04 p1463 N94-19384
Suitability of infrared spectroscopy for remote sensing of tropospheric trace gases
[KFK-5183] 04 p1479 N94-19507
Airborne studies of ocean-particle-cloud interactions in the Arctic
[AD-A270752] 04 p1479 N94-19575
Footprint size of a helicopter-borne electromagnetic induction sounding system versus antenna altitude
[AD-A270468] 04 p1463 N94-19672
Remote sensing of Earth terrain
[NASA-CR-194598] 04 p1464 N94-19681
Radar backscatter measurements from simulated sea ice during CRRELEX 1990
[AD-A271034] 05 p1715 N94-19823
Ionospheric tomography using the FORTE satellite
[DE93-018545] 05 p1854 N94-19955
Global and regional comparative performance of linear and nonlinear satellite multichannel sea surface temperature algorithms
[AD-A270475] 05 p1837 N94-20028
Remote sounding of tropospheric minor constituents
[NASA-CR-194265] 05 p1855 N94-20132
Dynamics Explorer 2: Continued FPI and NACS instrument data analysis and associated scientific activity at the University of Michigan
[NASA-CR-194689] 05 p1657 N94-20173
The future of remote sensing from space: Civilian satellite systems and applications
[OTA-ISC-558] 05 p1837 N94-20209
An expert system shell for inferring vegetation characteristics
[NASA-CR-189318] 05 p1837 N94-20284
Milankovitch insulation forcing and cyclic formation of large-scale glacial, fluvial, and eolian landforms in central Alaska 05 p2089 N94-20386
Comparison of remote sensing measurements with a two-scale polarimetric emission and scattering model for sea surfaces 05 p1721 N94-20415
Integrated display of multi-sensor geophysical and electromagnetic flight data 05 p1721 N94-20418
Advances in spaceborne radar remote sensing
05 p1723 N94-20424
Observation of pressure ridges in SAR images of sea ice: Scattering theory and comparison with observations
05 p1723 N94-20427
On evaluating the accuracy of SAR sea-ice classification using multifrequency polarimetric AIRSAR data
05 p1724 N94-20428
Application of Cloude's target decomposition theorem to polarimetric imaging radar data
05 p1724 N94-20429
Direction angle sensitivity of agricultural field backscatter with AIRSAR data 05 p1724 N94-20430
Studies of Greenland using the SEASAT scatterometer 05 p1725 N94-20433
Radar backscattering from snow facies of the Greenland ice sheet: Results from the AIRSAR 1991 campaign
05 p1725 N94-20434
C-band radar backscatter of sea ice in the Weddell Sea, Antarctica during the austral winter of 1992
05 p1725 N94-20435
Near grazing scattering from non-Gaussian ocean surfaces 05 p1726 N94-20438
Rough surface scattering from moving ocean surfaces as an indicator of scattering mechanisms
05 p1726 N94-20439
Polarimetric thermal emission from rough surfaces
05 p1727 N94-20441
Simulated retrieval of land surface parameters using multichannel satellite microwave radiometry
05 p1727 N94-20443
Symmetry in polarimetric remote sensing
05 p1729 N94-20449
Mapping of taiga forest units using AIRSAR data and/or optical data, and retrieval of forest parameters
05 p1729 N94-20452
A theoretical and numerical study of polarimetric scattering and emission from random rough surfaces with anisotropic directional spectrum
05 p1730 N94-20454
Application of neural network to remote sensing of soil moisture using theoretical polarimetric backscattering coefficients 05 p1730 N94-20455
Four-dimensional remote sensing of the marine boundary layer with a digital beamforming radar wind profiler
[AD-A270627] 05 p1882 N94-20564
The application of spaceborne synthetic aperture radar in the maritime environment
[DRA-TM(AWE)-91013] 05 p1737 N94-20596
Goniospectrometric properties of a white standard
05 p1684 N94-20664
Visible-infrared properties of controlled laboratory soils
05 p1685 N94-20689
Thermal infrared remote sensing and Kirchhoff's law: 1. Laboratory measurements 05 p1685 N94-20733
Convex set and linear mixing model
05 p1844 N94-20888
The 7th Brazilian Remote Sensing Symposium, volume 1 05 p1838 N94-20953
The use of satellite images in Amazonian archaeology: A case study in the Upper Rio Negro Basin
05 p1838 N94-20954
Application of SPOT to GIS/LIS in land capability evaluation for regional planning of JAICO semi-arid region of Piaui, Brazil 05 p1838 N94-20955
The 7th Brazilian Remote Sensing Symposium, volume 2 05 p1838 N94-20956
The 7th Brazilian Remote Sensing Symposium, volume 3 05 p1839 N94-20960

Sunphotometer network for monitoring aerosol properties in the Brazilian Amazon
05 p1839 N94-20961
On the origin and evolution of circular forms observed in remote sensing images of the Rio de Janeiro State, Brazil 05 p1839 N94-20963
Evaluation of C-band SAR data from SAREX 1992: Tapajos study site 05 p1839 N94-20964
The 7th Brazilian Remote Sensing Symposium, volume4 05 p1840 N94-20965
SIMA: An integrated environmental monitoring system
05 p1840 N94-20967
The development of remote sensing in Brazil and Canada: Comparative case studies
05 p1840 N94-20968
Rapid estimates of crop production using remote sensing: European experience 05 p1840 N94-20969
Using NDVI/AVHRR data for crop monitoring and forecasting in South Italy 05 p1841 N94-20970
Mobility of salt domes
[BCRS-92-08] 05 p1857 N94-21016
Ocean mapping using satellite radar altimetry
[ETN-93-93470] 05 p1841 N94-21017
Snow cover measurements and areal assessment of precipitation and soil moisture
[WMO-749] 05 p1841 N94-21068
Remote sensing for hydrology progress and prospects
[WMO-773] 05 p1841 N94-21069
Obtaining surface optical properties from space-based lidar systems
[AD-A272831] 05 p1987 N94-21172
Data format standards for civilian remote sensing satellites
[PB93-192920] 05 p1841 N94-21446
Earth observing scanning polarimeter
05 p1844 N94-21645
Orbit and sampling requirements: TRMM experience
05 p1870 N94-21647
Multiorder etalon sounder (MOES) development and test for balloon experiment
[NASA-CR-194730] 05 p1859 N94-22026
Remote sensing of multilevel clouds during FIRE IFO 2 05 p1844 N94-22303
Microphysical properties of the November 26 cirrus cloud retrieved by Doppler radar/IR radiometer technique
05 p1873 N94-22304
CIMSS FIRE research activities
05 p1873 N94-22307
Atmospheric parameterization schemes for satellite cloud property retrieval during FIRE IFO 2
05 p1874 N94-22312
Cloud boundaries during FIRE 2
05 p1876 N94-22318
Ground-based passive remote sensing during FIRE IFO 2 05 p1844 N94-22319
Surface-induced brightness temperature variations and their effects on detecting thin cirrus clouds using IR emission channels in the 8-12 micrometer region
05 p1880 N94-22341
Remote sensing estimates of cirrus particle size for tropical and midlatitude cirrus: Hexagonal crystals and ice spheres 05 p1880 N94-22342
Studies in remotely sensed geophysical parameter retrieval and analysis
[NASA-CR-193914] 05 p1842 N94-22374
Chromaticity analysis of LANDSAT multispectral scanner and thematic mapper imagery of Chilko Lake, British Columbia, using a theoretical optical water quality model
[ISBN-0-315-63832-X] 05 p1843 N94-22422
The AGRHYMET data communications project
06 p2280 N94-22776
A field evaluation of remote sensor measurements of wind, temperature, and moisture for ARM integrated sounding system research
[DE94-000565] 06 p2381 N94-23001
Integrated use of hydrological modelling and remote sensing in the province of Drenthe (The Netherlands): Possibilities and restrictions
[REPT-61] 06 p2382 N94-23148
Literature study on: Remote Fraunhofer luminescence detection of algal bloom in marine environments
[BCRS-92-25] 06 p2417 N94-23176
Optical component MAC Europe ground truth report: Flevoland 1991 (Netherlands)
[BCRS-92-27] 06 p2382 N94-23177
Application of ERS-1 active microwave instrumentation data to remote sensing of snow
[PB93-224756] 06 p2382 N94-23224
SeaWiFS technical report series. Volume 9: The simulated SeaWiFS data set, version 1
[NASA-TM-104566-VOL-9] 06 p2417 N94-23291
SeaWiFS technical report series. Volume 11: Analysis of selected orbit propagation models for the SeaWiFS mission
[NASA-TM-104566-VOL-11] 06 p2417 N94-23338
Rover in the Mars 96 mission
06 p2609 N94-23397
Lunar exploration rover program developments
[DE93-040759] 06 p2613 N94-23469
Remote sensing, imaging, and signal engineering
[DE94-003021] 06 p2382 N94-23494
The Fifth Calibration/Data Product Validation Panel Meeting
[NASA-TM-108270] 06 p2383 N94-23595
ASTER TIR subsystem and calibration
06 p2385 N94-23612
Methodology for the assessment of surface resistance and soil water storage variability at mesoscale based on remote sensing measurements. A case study with HAPEX-EFEDA data. UNESCO-International Hydrological Program 4
[PB94-111721] 06 p2386 N94-23734
NASDA's view of ground control in mission operations
06 p2305 N94-23835
SPOT satellite family: Past, present, and future of the operations in the mission and control center
06 p2500 N94-23846
SPOT4 Operational Control Center (CMP)
06 p2197 N94-23856
Mission planning for an Earth observation low Earth orbiter: ERS-1 06 p2503 N94-23868
MAMS data for the Convection and Moisture Experiment (CAMEX)
[NASA-TM-108435] 06 p2409 N94-24080
Estimation of the rain signal in the presence of large surface clutter
[NASA-CR-195105] 06 p2409 N94-24087
Roles, uses, and benefits of general aviation aircraft in aerospace engineering education
[NASA-TM-106463] 06 p2153 N94-24100
Intercomparison of remote and balloon-borne sensors operated at JAPE-91 06 p2527 N94-24210
Preliminary analysis of the JAPE ground vehicle test data with an artificial neural network classifier
06 p2529 N94-24222
Optimization of microscopic and macroscopic second order optical nonlinearities 06 p2226 N94-24354
Mapping Tomorrow's Resources: A symposium on the uses of remote sensing, Geographic Information Systems (GIS), and Global Positioning Systems (GPS) for natural resources management 06 p2387 N94-24357
Factors affecting the identification of phytoplankton groups by means of remote sensing
[NASA-TM-108799] 06 p2387 N94-24403
The measurement and analysis of leaf spectral reflectance of two stands of loblolly pine populations
06 p2389 N94-24442
An investigation of current and future satellite and in-situ data for the remote sensing of the land surface energy balance
[NASA-CR-195138] 06 p2387 N94-24596
Nondestructive evaluations
[DE94-003020] 06 p2373 N94-24613
Hyperspectral imagery classification using a backpropagation neural network
[AD-A273615] 06 p2545 N94-24730
Method for selection of wavelength bands for multispectral classification
[PB93-204378] 06 p2388 N94-24741
Evaluation of the use of remote-sensing data to identify crop types and estimate irrigated acreage, Uvalde and Medina Counties, Texas, 1989
[PB93-193159] 06 p2388 N94-24809
Investigation of passive atmospheric sounding using millimeter and submillimeter wavelength channels
[NASA-CR-194858] 06 p2404 N94-24843
Feasibility study of a synthesis procedure for array feeds to improve radiation performance of large distorted reflector antennas
[NASA-CR-195167] 06 p2301 N94-25005
Remote vibration measurements at a sud aviation alouette 3 helicopter with a CW CO2-laser system
[AD-A273818] 06 p2190 N94-25516
The potential for the Department of Defense to use space-based remote sensing to support DOD and other government agencies' environmental programs
[AD-A273895] 07 p2847 N94-25656
Real-time 3-D pose estimation using a high-speed range sensor
[AD-A273873] 07 p2809 N94-25967
Zernike moments and rotation invariant object recognition. A neural network oriented case study
[AD-A273749] 07 p2767 N94-26011
Remote sensing and GIS for the management and investigation of the Wadden Sea
[BCRS-92-20] 07 p2847 N94-26228
Remote Earth Sciences data collection using ACTS
[NASA-CR-195227] 07 p2848 N94-26236
Application of Space Shuttle Project Hercules imagery in the investigation of ship cloud tracks
[AD-A274923] 07 p2692 N94-26529
Mapping coastal habitats using an imaging spectrometer
[ISBN-0-315-84362-4] 07 p2848 N94-26664
An evaluation of an airborne remote sensing system used to determine ice thickness and geometry of a first year sea ice ridge located in the Beaufort Sea
[ISBN-0-315-84383-7] 07 p2849 N94-26667
ARM Fourier transform spectrometer data analysis tools
[DE94-000865] 07 p2895 N94-26697
Digital filter design for sensor simulation: Application to the Brazilian remote sensing satellite
[INPE-5523-RPQ/665] 07 p2849 N94-26827
A preliminary method for atmospheric soundings in real time using satellite and ground-based remotely sensed data
[AD-A274381] 07 p2880 N94-26828
The Hough transform algorithm for sea ice lead analysis: An evaluation
[AD-A274535] 07 p2899 N94-26853
Leadex environmental phenomena and effects observed by DMSP, NOAA, and ERS-1 satellites
[AD-A274596] 07 p2868 N94-26888
Assessment of tropical forests using satellite data
[SILVA-CARELICA-21] 07 p2850 N94-27182
Global tropical forest cover assessments using satellite imagery 07 p2850 N94-27183
Training on assessment and mapping of deforestation: WFW conference, Brazil
[INPE-5482-PRE/1781] 07 p2850 N94-27384
Global change research related to the Earth's energy and hydrologic cycle
[NASA-CR-195270] 07 p2869 N94-27430
Calibration of SAR systems
[DLR-FB-93-18] 07 p2777 N94-27738
Remote sensing of global snowpack energy and mass balance: In-situ measurements on the snow of interior and Arctic Alaska
[NASA-CR-195704] 07 p2851 N94-27787
Multispectral and textural classifications of a SPOT HRV-1 image, region of Sherbrooke, Quebec, Canada
[ISBN-0-315-84978-9] 07 p2851 N94-27863
Fractals and their applications to remote sensing and digital mapping
[ISBN-0-315-59469-1] 07 p2852 N94-27870
Mapping of soil humidity using C-band radar images
[ISBN-0-315-85076-0] 07 p2852 N94-27878
In situ Mars ozone detector 07 p3108 N94-27892
Role of remote sensing in energy, water, and carbon cycle studies over the Amazon
[INPE-5486-PRE/1786] 07 p2852 N94-27957
Landscape dynamics of northeastern forests
[NASA-CR-195272] 07 p2852 N94-28070
MODIS airborne simulator visible and near-infrared calibration, 1991 FIRE-Cirrus field experiment. Calibration version: FIRE King 1.1
[NASA-TM-104600] 07 p2897 N94-28182
Persistence of auroral electron flux events from DMSP/F9 electron measurements
[RXR-92012] 07 p2887 N94-28206
A comparative study of SAR data compression schemes 07 p2946 N94-28259
Asia-Pacific Seminar on Global Change Research Cooperation
[JTN-94-80517] 07 p2871 N94-28268
Role and activity of STA on Asian Pacific regional cooperation 07 p2853 N94-28269
Cooperative research projects on satellite remote sensing for the hydrological subjects
07 p2853 N94-28270
Research activities on the meteorology over the Asia-Pacific region 07 p2853 N94-28271
An oceanographical observation in the Western Pacific and international cooperations 07 p2872 N94-28272
NASDA contribution plan to Asian countries
07 p2853 N94-28273
Activities of Remote Sensing Technology Center of Japan (RESTEC) 07 p2853 N94-28274
Global concern on research cooperation for environment 07 p2872 N94-28275
Progress in the study of global change in China
07 p2873 N94-28276
Research and observation programmes on global changes in Indonesia 07 p2873 N94-28277
Country report on global change research for the Republic of Korea 07 p2873 N94-28278
Philippine thrust on environmental research relating to global change 07 p2873 N94-28279
Study on environment monitoring over whole China using NDVI from AVHRR data and future project
07 p2875 N94-28289
Utilization of remote sensing data for global climate change research in Malaysia 07 p2875 N94-28290
Thailand satellite ground receiving station in global change research cooperation 07 p2875 N94-28291

Utilization of remote sensing data for global change research 07 p2875 N94-28292
Contribution of satellite observation to global change research 07 p2876 N94-28293
Laboratory of Space Technology
[PB94-133204] 07 p2689 N94-28358
Objective analysis of a coastal ocean eddy using satellite AVHRR and in situ hydrographic data
[AD-A275715] 08 p3376 N94-28642
Proceedings of the International Symposium on Remote Sensing
[JTN-94-80578] 08 p3325 N94-28925
Keynote address --- Japanese Earth Resources Satellite 1 (JERS-1) and future remote sensing projects 08 p3326 N94-28926
Synthetic aperture radar applications: Now and in the future 08 p3260 N94-28927
Research trends on remote sensing at research facilities in Japan: The priority area programme on better understanding of earth environment via satellite 08 p3326 N94-28928
Evaluation of simulated JERS-1 data for geologic mapping at Drum Mountains, Utah, Silver Bell, Arizona, and Wind River, Wyoming under the GEOSAT-ERSDAC/JAPEX/JGI/RESTEC joint studies 08 p3326 N94-28929
Image processing for hyperspectral data 08 p3326 N94-28930
JERS-1 data and information system for resources exploration 08 p3327 N94-28932
Observations by ERS-1 start 08 p3327 N94-28933
Sea ice and oceans applications of SAR 08 p3327 N94-28934
Amazonia: Remote sensing test site and survey 08 p3327 N94-28935
Utilization of remote sensing data in Southeast Asia 08 p3327 N94-28936
Remote sensing and global management 08 p3328 N94-28937
Synthetic image generator model; application of view angle dependent reflectivity components and performance evaluation in the visible region
[AD-A275365] 08 p3499 N94-29009
Proceedings of the 15th Earth Observation Symposium
[JTN-94-80607] 08 p3328 N94-29036
Principles and application tendency of remote sensing: Its principle, function and utilization 08 p3328 N94-29037
Status and tendency of earth observation system 08 p3328 N94-29038
Perspectives of earth observing techniques: Expectation of earth observation in space development history 08 p3328 N94-29039
Oceanic survey utilizing satellites 08 p3328 N94-29040
Tohoku district observed by artificial satellites 08 p3328 N94-29041
Portable electronically based method for the nondestructive remote sensing of crevice corrosion
[AD-A275403] 08 p3318 N94-29057
Activities of the wintering party at Showa Station by the 31st Japanese Antarctic Research Expedition in 1990 08 p3358 N94-29083
Role of satellite observations of sea-surface temperature in the detection of global change
[PB94-138120] 08 p3329 N94-29107
Remote sensing of inner heliospheric plasmas
[AD-A275021] 08 p3550 N94-29132
Proceedings of the 3rd International Symposium: JERS-1 and Remote Sensing in the Future
[JTN-94-80597] 08 p3329 N94-29217
Remote sensing and the Earth 08 p3329 N94-29218
A new information system: Satellite observation 08 p3330 N94-29219
Application of optical sensor data to resource survey 08 p3330 N94-29223
Radar applications at the Canada Centre for Remote Sensing 08 p3331 N94-29224
Earth-observation plan in Europe 08 p3331 N94-29227
Rock identification using thermal infrared data 08 p3331 N94-29228
JERS-1 and future remote sensing: Application of remote sensing data to agroecological problems 08 p3331 N94-29229
Application of remote sensing in prevention of disasters 08 p3332 N94-29230
Future expectation of remote sensing technology 08 p3332 N94-29231
Japan's Earth observation satellite programs 08 p3332 N94-29232
Imaging spectrometry of the Earth and other solar system bodies 08 p3237 N94-29779
Evolution of miniature detectors and focal plane arrays for infrared sensors 08 p3237 N94-29781
Frequency dependence of polarization phase difference
[NASA-TM-109737] 08 p3254 N94-30094
The extraction and representation of forest inventory information using continuous density surfaces
[ISBN-0-315-85658-0] 08 p3334 N94-30236
Cloud and aerosol characterization for the ARM central facility: Multiple remote sensor techniques development
[DE94-003523] 08 p3365 N94-30608
FAME: A Forest Assessment and Monitoring Environment scenario
[AD-B179106] 08 p3335 N94-30759
Multitemporal analysis of a braiding river: The advanced study of 1992
[NLR-TP-93100-U] 08 p3335 N94-30942
Subtropical Climates and Their Evolution: From Space-Based Observation to Modelling
[ISBN-2-85-428333-3] 09 p3776 N94-30981
Radiation/remote sensing: Review of the principal definitions 09 p3757 N94-30996
Modeling the interaction between solar radiation and terrestrial surfaces 09 p3779 N94-30999
Radar measurements 09 p3685 N94-31002
Airborne instruments 09 p3757 N94-31006
Global change research and NASA's Earth Observing System
[PB94-126992] 09 p3741 N94-31068
Chamber optics for testing passive remote sensing vapor detectors
[AD-A275909] 09 p3878 N94-31340
Gas hydrate detection and mapping on the US east coast
[DE94-005959] 09 p3742 N94-31504
Development of a statistical method for estimating the downward longwave radiation at the surface from satellite observations 09 p3742 N94-31553
Imaging devices for satellite remote sensing
[VTT-TIED-1517] 09 p3743 N94-31658
The development and testing of a backscatter absorption gas imaging (BAGI) system designed to image at a range of 300 m
[DE94-006192] 09 p3675 N94-31761
European Imaging Spectroscopy Aircraft Campaign
[ESA-SP-360] 09 p3743 N94-31853
The European Imaging Spectroscopy Airborne Campaign (EISAC). Data takes and evaluation programme: An overview 09 p3743 N94-31854
NORSMAP 1989: Norwegian remote sensing spectroscopy for mapping and monitoring or algal blooms and pollution 09 p3744 N94-31856
Analysis of GER imaging spectrometry data for the identification of soil and vegetation parameters in land degradation studies 09 p3744 N94-31857
Inflight calibration, preprocessing, and data evaluation of GER 2 imaging spectrometry data 09 p3744 N94-31858
Possibilities of GER data for soil surface characteristics in the Almaden area 09 p3744 N94-31859
The effects of vegetation on the ability to map soils using GERIS data 09 p3744 N94-31860
Investigation on correction models for airborne imaging spectrometry data from the EISAC-campaign for geoscientific purposes 09 p3745 N94-31861
Feasibility evaluation of new data interpretation approaches for vegetation analysis from airborne imaging spectroscopy 09 p3745 N94-31862
Monitoring fertilizer application by imaging spectrometry (Somerset Levels test site) 09 p3745 N94-31863
High resolution spectroscopy in agriculture: Results of the EISAC 1989 campaign 09 p3745 N94-31864
Extraction of agricultural parameters from imaging-spectrometry data and simulated MERIS data through red edge analysis 09 p3745 N94-31865
Remote infrared vapor detection of volatile organic compounds
[AD-A276982] 09 p3746 N94-31999
Estimation and analysis of climate-scale rainfall over the Tropical Pacific 09 p3783 N94-32030
Gyrotrons and free electron lasers for atmospheric sensing
[AD-A277281] 09 p3718 N94-32406
Remote sensing for urban planning 09 p3758 N94-32465
Remote sensing and the Mississippi high accuracy reference network 09 p3758 N94-32466
Assessment of region-based methods for automated SAR/optical registration, attribute extraction, and classification 09 p3750 N94-32536
Ship traffic monitoring and oil spill detection using the ERS-1 SAR 09 p3751 N94-32542
SAR image feature extraction system: A pre-operational application of ERS-1 SAR 09 p3751 N94-32543
Almaz marine applications 09 p3751 N94-32544
Evaluation of the potential of SAR data for mapping of landslide risks
[BRGM-93033] 09 p3753 N94-32552
A case study comparing multi-temporal ERS-1 SAR data and SPOT data for tropical forest mapping 09 p3753 N94-32556
Synergy of thermal infrared and microwave remote sensing for evaporation estimation 09 p3754 N94-32559
Monitoring landsurface characteristics in Niger using complementary SPOT and ERS-1 SAR data 09 p3754 N94-32560
European MARS project: The potential integration of SPOT and air- and satellite-borne radar data over two pilot areas for agricultural statistics. PROSPER programme and ERS-1 pilot project
[BRGM-93035] 09 p3754 N94-32561
Evaluation of surface phase change on large zones 09 p3755 N94-32567
Quantitative analysis of woody vegetation in Soudano-Sahalian region. Textural approach (application to a Burkina Faso region) 09 p3757 N94-32574
Statistical analysis and mapping of cotton and food crop cultivation surfaces in the west of Burkina Faso: Contribution of combined SPOT P and XS data 09 p3757 N94-32575
An integrated cloud observation and modeling investigation in support of the ARM program
[DE94-003160] 09 p3785 N94-32716
Water vapor from sunradiometry in comparison with microwave and balloon-sonde measurements at the Southern Great Plains ARM Site
[DE94-007479] 09 p3786 N94-32759
Repetitively pulsed Cr:LiSAF laser for lidar applcations
[DE94-007546] 09 p3720 N94-32761
Evolution of diurnal surface winds and surface currents for Monterey Bay
[AD-A277649] 09 p3790 N94-33057
Assisting wine growers
[NASA-TM-109812] 10 p4094 N94-33564
Refocusing space technology
[NASA-TM-109833] 10 p4161 N94-33569
A collection of The Movies
[NASA-TM-109806] 10 p4075 N94-33598
Technical parameters for specifying imagery requirements 10 p4144 N94-33648
Characterization of tidal currents in Monterey Bay from remote and in-situ measurements
[AD-A277844] 10 p4092 N94-33767
Distributed Active Archive Center 10 p4157 N94-33826
The Payload Advisory Panel and the Data and Information System Advisory Panel of the Investigators Working Group of the Earth Observing System: A joint report
[NASA-TM-109847] 10 p4076 N94-34018
Remote sensing of hydrologic variables in boreal areas, phase 1
[NASA-CR-189354] 10 p4077 N94-34134
The modelling of the ocean surface image in optical remote sensing 10 p4078 N94-34369
SeaWiFS technical report series. Volume 16: The second SeaWiFS Intercalibration Round-Robin Experiment, SIRREX-2, June 1993
[NASA-TM-104566-VOL-16] 10 p4093 N94-34412
Automatic cataloguing and characterization of Earth science data using SE-trees 10 p4124 N94-35058
VEG: An intelligent workbench for analysing spectral reflectance data 10 p4125 N94-35059
Remote geochemical experiment package for Discovery class missions 11 p4350 N94-35420
Insight to global change: EOS/SAR mission
[NASA-CR-196133] 11 p4284 N94-35503
Obtaining coincident image observations for Mission to Planet Earth science data return 11 p4202 N94-35609
A precise passive narrow-beam filter infrared radiometer and its use with LIDAR in the ARM program
[DE94-004167] 11 p4269 N94-36085
Selected translated abstracts of Russian-language climate-change publications. 2: Clouds
[DE94-011465] 11 p4295 N94-36244
Molecular nitrogen fluorescence lidar for remote sensing of the auroral ionosphere
[AD-A280716] 11 p4291 N94-36263
SeaWiFS technical report series. Volume 20: The SeaWiFS bio-optical archive and storage system (SeaBASS), part 1
[NASA-TM-104566-VOL-20-PT-1] 12 p4475 N94-36958
Airborne ROWS data report for the high resolution experiment, June 1993
[NASA-TM-104609] 12 p4477 N94-37397
Gaseous effluent monitoring and identification using an imaging Fourier transform spectrometer
[DE94-012627] 12 p4467 N94-37426

Chemical recognition software
[DE94-012918] 12 p4495 N94-37496
Laser probing of interfaces
[DE94-011300] 12 p4449 N94-37628
Measuring the upper profile of sea ice in the Bay of Bothnia with a laser profilometer
[PB94-184561] 12 p4477 N94-37855

REMOTE SENSORS
NT THEMATIC MAPPERS (LANDSAT)
Enhanced Damage-Resistant Optics for Spaceflight Laser Systems: Workshop findings and recommendations
[NASA-TM-109243] 01 p0381 N94-11054
Activities relating to understanding the initiation, organization and structure of moist convection in the Southeast environment
[NASA-CR-193829] 01 p0285 N94-11598
Trend of miniature refrigerator utilization in earth observation area 01 p0130 N94-11835
Development test on 2 K cooling systems 01 p0130 N94-11840
HF ocean radar system at Okinawa Radio Observatory 01 p0139 N94-11902
Measurement of wave parameters by HF ocean radar 01 p0192 N94-11903
Groundwave HF ocean surface radar 01 p0139 N94-11906
Trouble areas in the IRT measurement of the Earth surface temperature 01 p0193 N94-11910
Acoustic characteristics of side scan sonar and sub-bottom profiler for 10,000 m class ROV 01 p0172 N94-11916
Atmospheric correction plans for SeaWiFS 01 p0204 N94-11975
Project of an attitude control system (three axis) of a satellite using the LQG/LTR methodology
[INPE-5473-TDI/504] 01 p0044 N94-12356
METEOSAT second generation programme SEVIRI: An enhanced visible and IR radiometer for meteorology 01 p0212 N94-12667
Resistivity and radar void detectors for tunneling machines 01 p0140 N94-12706
Autonomous self contained bottom pop-up stations for study of the benthic layer and seismicity of the ocean's bottom 01 p0224 N94-12735
The structure of hydrophysical measuring systems of vertical sounding and self-contained stations 01 p0227 N94-12751
Buoy experiments to obtain the sea-truth data for OCTS/NSCAT, part 1
[NASDA-CNT-930005-PT-1] 02 p0725 N94-13653
Microgravity acceleration measurement environment characterization 02 p0590 N94-13755
Evaluation of the Shuttle remote manipulator
[NASA-CR-194351] 02 p0662 N94-13800
Earth Observation Center Annual Report on Research and Development, Fiscal Year 1992
[EOC-92-01-0007] 02 p0687 N94-14091
Calibration and in-house validation results of JERS-1 data 02 p0687 N94-14092
Earth observation experiment data analysis 02 p0687 N94-14093
ADEOS project 02 p0687 N94-14094
Asia-Pacific ISY Conference, volume 2
[NASDA-CM-199-VOL-2] 02 p0688 N94-14209
Results from ERS-1 and JERS-1 SAR calibration experiments and data analysis 02 p0688 N94-14210
Geologic application of JERS-1 SAR data 02 p0688 N94-14211
High performance multi-mode radar altimeter for future spaceborne application 02 p0548 N94-14214
Sensor operation of Advanced Earth Observing Satellite (ADEOS) 02 p0689 N94-14215
Methods for calibration/validation of AVNIR 02 p0689 N94-14216
Overview of the ILAS operational data processing system 02 p0690 N94-14220
Clouds and the Earth's Radiant Energy System (CERES) on the Tropical Rainfall Measuring Mission (TRMM) 02 p0690 N94-14223
Multiparameter airborne rain radar development for TRMM validation and TRMM-follow-on study 02 p0690 N94-14226
Hardware design for the Autonomous Visibility Monitoring (AVM) observatory 02 p0533 N94-14394
The laboratory performance of the short wavelength instrument for the Along Track Scanning Radiometer ATSR-2 (initial results) 03 p0908 N94-15088
IR detectors and subsystems for space applications 03 p0909 N94-15091
ENVISAT ASAR 03 p0898 N94-15892
Advances in spaceborne radar remote sensing 05 p1723 N94-20424
Predicting LANDSAT MSS endmember signatures from corresponding higher resolution TM fraction images 05 p1839 N94-20962
Observations of multi-layered clouds using K-band radar 05 p1874 N94-22311
A field evaluation of remote sensor measurements of wind, temperature, and moisture for ARM integrated sounding system research
[DE94-000565] 06 p2381 N94-23001
PULSAUR 2
[NASA-CR-194832] 06 p2209 N94-23484
MODIS calibration 06 p2383 N94-23600
Eos cross-calibration radiometers 06 p2383 N94-23601
Activities of NIST (National Inst. of Standards and Technology) 06 p2384 N94-23605
A fifteen years lifetime mechanism for an infrared Earth sensor 06 p2362 N94-24040
Intercomparison of remote and balloon-borne sensors operated at JAPE-91 06 p2527 N94-24210
An analysis of multiple sensor system payloads for unmanned aerial vehicles
[AD-A274905] 07 p2667 N94-26182
Beam scanning offset Cassegrain reflector antennas by subreflector movement
[NASA-CR-191604] 08 p3160 N94-28836
Proceedings of the International Symposium on Remote Sensing
[JTN-94-80578] 08 p3325 N94-28925
Conceptual radiometer design studies for Earth observations from low Earth orbit
[NASA-CR-4588] 08 p3329 N94-29098
Proceedings of the 3rd International Symposium: JERS-1 and Remote Sensing in the Future
[JTN-94-80597] 08 p3329 N94-29217
Outline of JERS-1 system 08 p3330 N94-29220
Observatory system of Earth Resources Satellite-1 08 p3330 N94-29221
Application of JERS-1 data to geologic analyses 08 p3330 N94-29222
Rock identification using thermal infrared data 08 p3331 N94-29228
Remote sensor observations during WISP91: The use of microwave radiometers, RASS, and lidar ceilometers for detection of aircraft icing conditions
[PB94-142106] 08 p3136 N94-30890
Space equipment for Earth observations 09 p3613 N94-30997
Airborne instruments 09 p3757 N94-31006
Imaging devices for satellite remote sensing
[VTT-TIED-1517] 09 p3743 N94-31658
The processing technology and some applications of Almaz-1 data 09 p3756 N94-32573
Aerial robotic data acquisition system
[DE94-009114] 10 p4076 N94-33938
X-ray remote sensing and in-situ spectroscopy for planetary exploration missions and gamma-ray remote sensing and in-situ spectroscopy for planetary exploration missions
[NASA-CR-189352] 11 p4375 N94-35381
Gaseous effluent monitoring and identification using an imaging Fourier transform spectrometer
[DE94-012627] 12 p4467 N94-37428

REMOTELY PILOTED VEHICLES
A portable controller for unmanned ground vehicles
[AD-A264963] 01 p0181 N94-11290
Non-lethal Unmanned Aerial Vehicles (UAVs)
[AD-A267139] 03 p0866 N94-15692
Control vane guidance for a ducted-fan unmanned air vehicle
[AD-A271957] 05 p1645 N94-20561
Design, fabrication and test of a vertical attitude takeoff and landing unmanned air vehicle
[AD-A273003] 05 p1646 N94-21283
Low-cost Unmanned Air Vehicle (UAV) for oceanographic research
[AD-A273103] 05 p1646 N94-21507
Data link development for the archytas vertical takeoff and landing transitional flight unmanned aerial vehicle
[AD-A272499] 05 p1646 N94-21548
Decentralized autonomous attitude determination using an inertially stabilized payload 06 p2157 N94-24264
Overall system concepts in mission planning 06 p2521 N94-25009
Generic drone control system
[AD-D015993] 06 p2184 N94-25052
Design study to simulate the development of a commercial freight transportation system 07 p2671 N94-25715
Solar powered multipurpose remotely powered aircraft 07 p2671 N94-25719
An analysis of multiple sensor system payloads for unmanned aerial vehicles
[AD-A274905] 07 p2667 N94-26182
Acquisition, design modification, assembly, and ground test of NPS Hummingbird remotely piloted helicopter
[AD-A275546] 08 p3146 N94-28837
A non-linear simulation for an autonomous unmanned air vehicle
[AD-A275062] 08 p3146 N94-29200
Navigation of military and space unmanned ground vehicles in unstructured terrains 08 p3144 N94-30282
A generic semi-autonomous ground vehicle control system 08 p3306 N94-30283
The use of low cost differential mode GPS receivers in unmanned vehicles 08 p3144 N94-30285
HATT-X: A high performance flying laboratory for autonomous unmanned aircraft research and development 08 p3149 N94-30293
Unmanned Air Vehicle/Remotely Piloted Vehicle analysis for lethal UAV/RPV
[AD-A276052] 09 p3578 N94-31442
A model geophysics program
[DE94-007415] 09 p3747 N94-32203
Army scout/reconnaissance helicopters versus unmanned aerial vehicles
[AD-A276902] 09 p3579 N94-32232
Undersea applications of dexterous robotics 10 p4067 N94-34033

REMOVAL
Environmentally Safe and Effective Processes for Paint Removal
[AGARD-R-791] 01 p0126 N94-10613
Paint removal activities in the US Navy 01 p0126 N94-10614
Paint removal activities in Canada 01 p0126 N94-10615
Procedures without danger to the environment and efficiency (PSDEE) for the removal of paint. Point on the French activities concerning the removal of paint 01 p0126 N94-10616
Paint removal activities in Germany 01 p0126 N94-10617
The development of alternative paint removal techniques in the RAF 01 p0126 N94-10618
Operational aspects of F.16 plastic media blasting, as carried out by Fokker Aircraft Services 01 p0126 N94-10619
Use of robots for aircraft dry stripping via plastic media blasting 01 p0127 N94-10620
German Air Forces experiences with plastic media blasting and future requirements 01 p0127 N94-10621
Plastic media blasting activities at Hill Air Force Base 01 p0127 N94-10622
Large Aircraft Robotic Paint Stripping (LARPS) system and the high pressure water process 01 p0127 N94-10623
Automated Laser Paint Stripping (ALPS) update 01 p0127 N94-10624
Aquastrip (tm): An innovative paint removal technology 01 p0127 N94-10625
Paint removal and surface cleaning using ice particles 01 p0128 N94-10626
Paint removal using wheat starch blast media 01 p0128 N94-10627
IATA taskforce: Paintstripping 01 p0128 N94-10628
Selectively strippable paint schemes 01 p0128 N94-10629
Dry stripping as a surface treatment method
[VTT-TIED-1348] 03 p0985 N94-17544
Focused-ion-beam material removal rates
[AD-A270852] 05 p1713 N94-19834
Atomic oxygen treatment for non-contact removal of organic protective coatings from painting surfaces
[NASA-TM-106650] 12 p4421 N94-36952

RENAL CALCULI
U CALCULI

RENAL FUNCTION
Proceedings of the First Joint NASA Cardiopulmonary Workshop
[NASA-CP-10068] 01 p0308 N94-11991
Fluid compartment and renal function alterations in the rat during 7 and 14 day head down tilt 01 p0310 N94-12002
Physiological water model development 01 p0316 N94-12367
Renal function alterations during skeletal muscle disuse in simulated microgravity
[NASA-CR-194258] 02 p0733 N94-13824

RENDEZVOUS
NT EARTH ORBITAL RENDEZVOUS
NT ORBITAL RENDEZVOUS
NT SPACE RENDEZVOUS

RENDEZVOUS GUIDANCE
A guidance and navigation system for two spacecraft rendezvous in translunar halo orbit
[AD-A267498] 03 p0898 N94-17368

Theoretical basis for state vector comparison, relative position display, and relative position/rendezvous prediction
[AD-A277216] 09 p3608 N94-32020
Global Positioning System Synchronized Active Light Autonomous Docking System
[NASA-CASE-MFS-28853-1] 12 p4395 N94-36825
Evaluation of GPS position and attitude determination for automated rendezvous and docking missions
[NASA-CR-4614] 12 p4397 N94-37506

RENDEZVOUS SPACECRAFT
A guidance and navigation system for two spacecraft rendezvous in translunar halo orbit
08 p3142 N94-29837

RENDEZVOUS TRAJECTORIES
A mission concept of Phobos/Deimos exploration
03 p1287 N94-16387
Automated rendezvous and capture demonstration study
[NASA-CR-192587] 04 p1331 N94-19366
A six degree of freedom, plume-fuel optimal trajectory planner for spacecraft proximity operations using an A* node search
[NASA-CR-188285] 09 p3601 N94-32388

RENORMALIZATION GROUP METHODS
On renormalization group flow in matrix model
[DE93-613050] 01 p0409 N94-10413
Development of a recursion RNG-based turbulence model
[NASA-CR-191511] 02 p0636 N94-13718
Large-Eddy Simulations (LES) of flows and turbulence distribution
[AD-A267182] 03 p1016 N94-15151
Computation of confined coflow jets with three turbulence models
[NASA-TM-106378] 03 p1025 N94-16879
Renormalizations in supersymmetric and nonsupersymmetric non-abelian Chern-Simons field theories with matter
[DE93-626646] 04 p1593 N94-17748
Development and validation of RNG methodology for compressible turbulence
[AD-A273469] 06 p2337 N94-24929
The renormalization group for flag manifolds
[DE93-616846] 06 p2491 N94-25213
Performance of renormalization group algebraic turbulence model on boundary layer transition simulation
[NASA-CR-194466] 07 p2644 N94-26131
Differential regularization of a non-relativistic anyon model
[DE94-601558] 07 p3019 N94-26416
On kinetic expansion in scalar field theory
[DE93-634338] 07 p3072 N94-26553
Limit theorems for functionals of Markov processes and renormalizable stable fields
[AD-A274645] 07 p3004 N94-27106
Operator regularization and renormalization theory
[ISBN-0-315-49334-8] 07 p3007 N94-27264
Study of modeling of turbulence of renormalization group analysis 08 p3126 N94-28970
Renormalization group theory of Bolgiano scaling in Boussinesq turbulence
[NASA-TM-106602] 09 p3710 N94-33070
Infrared troubles of differential renormalization
[DE94-611119] 10 p4142 N94-33862

REPAIRING
U MAINTENANCE

REPEATERS
Development of analog watch with minute repeater
04 p1429 N94-18043
Advanced satellite communication system
[NASA-CR-194211] 09 p3681 N94-32477

REPETITION
Two-stage versus sequential sample-size determination in regression analysis of simulation experiments
[PB94-110558] 06 p2495 N94-24634
Effects of repeating resistance testing on firing ability of igniter EP360-3
[AD-A274814] 07 p2759 N94-26486

REPLACING
On-line upgrade of program modules using AdaPT
[NASA-CR-194331] 02 p0754 N94-14472
Alumina ceramic: A cost effective replacement for titanium in deep submergence pressure housings
[AD-A275640] 08 p3212 N94-28641
Technology transfer initiatives
[NASA-CR-195151] 08 p3537 N94-29410
Enhanced thermal capacity aerogels summary report, FY 1993
[DE94-008888] 09 p3639 N94-33260
Sealed tube comparisons of the compatibility of desiccants with refrigerants and lubricants
[DE94-010002] 11 p4251 N94-36388

REPLENISHMENT
The role of the geothermal gradient in the emplacement and replenishment of ground ice on Mars
01 p0463 N94-12169

REPORT GENERATORS
TILDA for Windows: A system for registration of journals in the library at NDRE NBC-Defence
[PB94-149168] 10 p4158 N94-34161

REPORTS
NT CONGRESSIONAL REPORTS
NT POSTLAUNCH REPORTS
NT PRESIDENTIAL REPORTS
A comparison of high and low-impact reports of investigation on adjudicators' decision making: A pilot study
[AD-A265747] 01 p0416 N94-10298
NASA/DOD Aerospace Knowledge Diffusion Research Project. Paper 34: Users and uses of DOD technical reports: A report from the field
[NASA-TM-109327] 02 p0825 N94-14485
AFOSR technical report summaries, January - March 1993
[AD-A267187] 03 p1230 N94-15850
List of the scientific and personal papers of Sir George Deacon, FRS
[IOS-301-1992] 03 p1114 N94-17518
Activities report of the Rutherford Appleton Laboratory
[ETN-93-94555] 04 p1631 N94-17968
Listing of approved recurring information requirements
[AD-A271673] 05 p2042 N94-20919
Activities report to NATO
[ETN-94-95047] 06 p2318 N94-23227
Fiscal year 1993 scientific and technical reports, articles, papers, and presentations
[NASA-TM-108423] 06 p2590 N94-24079
NASA/DOD Aerospace Knowledge Diffusion Research Project. Report number 21: US aerospace industry librarians and technical information specialists as information intermediaries: Results of the phase 2 survey
[AD-A276020] 06 p2593 N94-24709
NASA/DOD Aerospace Knowledge Diffusion Research Project. Paper 11: The voice of the user: How US aerospace engineers and scientists view DOD technical reports
[NASA-TM-109348] 09 p3921 N94-32834
NASA/DOD Aerospace Knowledge Diffusion Research Project. Report 25: The technical communications practices of British aerospace engineers and scientists: Results of the phase 4 RAeS mail survey
[NASA-TM-109098] 09 p3922 N94-32836
NASA/DOD Aerospace Knowledge Diffusion Research Project. Report 24: The technical communications practices of US aerospace engineers and scientists: Results of the phase 1 SAE mail survey
[NASA-TM-109088] 09 p3922 N94-32837
Space Sciences Laboratory publications and presentations, 1 January - 31 December, 1993
[NASA-TM-108450] 10 p4158 N94-34173
NASA/DOD Aerospace Knowledge Diffusion Research Project. Paper 35: The US government technical report and aerospace knowledge diffusion: Results of an on-going investigation
[NASA-TM-109861] 10 p4159 N94-34603

REPRESENTATIONS
Representation of spoken words in a self-organizing neural net
05 p1940 N94-20243
Representation of idioms in connectionist models
05 p1940 N94-20247
A connectionist representation for phrase structures
05 p1941 N94-20249
An exploration of clause boundary effects in SRN representations
05 p1937 N94-20253

REPRODUCTION (BIOLOGY)
Opportunities and questions for the fundamental biological sciences in space 04 p1502 N94-19212
Cloning of rat RXR alpha cDNA and the expression of its mRNA in regenerating liver and primary cultured hepatocytes 07 p2905 N94-27479
Cloning of a novel POU family gene by RT-PCR method 07 p2905 N94-27480
Expression analysis of Thyroxine-Binding Globulin Complete Deficiency in Japanese (TBG-CDJ)
07 p2905 N94-27482
Electron microscopic analysis of meiotic chromosome pairing in male house musk shrew, Suncus murinus
07 p2906 N94-27493
Reproduction in the Japanese anchovy (Engraulis japonica) as related to population fluctuation
08 p3235 N94-29708
The legacy of Kermack and McKendrick
[CWI-AM-R9304] 09 p3793 N94-32228

REPRODUCTION (COPYING)
Design and implementation of an object-oriented interface for the multi-model/multi-lingual database system
[AD-A267413] 03 p1232 N94-16977
Theory of dispersive microlenses
03 p1198 N94-17361
Color test chart for facsimile
[AD-A269754] 04 p1387 N94-18721
NASA printing, duplicating, and copying management handbook
[NASA-NHB-1490.5] 06 p2590 N94-23971
Fundamentals of printing technology
[PB94-132602] 08 p3530 N94-29141

REPRODUCTIVE SYSTEMS
NT PROSTATE GLAND

REPUBLIC MILITARY AIRCRAFT
U MILITARY AIRCRAFT

REPUBLIC OF CHINA
U TAIWAN

REPUBLIC OF KOREA
U SOUTH KOREA

REPUBLIC OF SOUTH AFRICA
A structural and petrographic investigation of the pretoria saltpan impact structure 01 p0282 N94-12102
Geophysical signature of the Pretoria saltpan impact structure and a possible satellite crater
01 p0282 N94-12103
The South African Astronomical Observatory
[SAAO-17] 04 p1623 N94-19657
The age of the Pretoria Saltpan impact crater, South Africa 05 p1863 N94-20798

REPUBLIC OF VIETNAM
U VIETNAM

REQUIREMENTS
An environment for requirement reuse
[REPT-92-082] 04 p1613 N94-17939
Secure open systems: An investigation of current standardisation efforts for security in open systems
[FEL-92-B225] 04 p1618 N94-19450
Reference manual for a Requirements Specification Language (RSL), version 2.0
[NASA-CR-191460] 05 p1898 N94-20039
Listing of approved recurring information requirements
[AD-A271673] 05 p2042 N94-20919
The next Japanese solar satellite
06 p2625 N94-22846
Requirements for future solar-physics missions that include UV instrumentation 06 p2625 N94-22851
Tools reference manual for a Requirements Specification Language (RSL), version 2.0
[NASA-CR-191461] 06 p2445 N94-23125
Rover requirements for the planet surface segment of the space exploration initiative 06 p2369 N94-23377
Electronic payloads for Martian missions: A preliminary assessment of technologies 06 p2610 N94-23408
An approach to the design of operations systems
06 p2506 N94-23884
The Columbus logistics support at the APMC: Requirements and implementation aspects
06 p2515 N94-23935
CRC customer versus rater octane number requirement program (1990)
[AD-A273997] 07 p2758 N94-25901
Computing in space: Issues and answers
07 p2948 N94-26714
High performance flight computer developed for deep space applications 07 p2949 N94-26718
MATRA Marconi Space: The Silex on-board processor and on-board software 07 p2950 N94-26726
Verification and validation of the on-board software real time requirements 07 p2953 N94-26739
Steam plant: Steam turbines for combined cycles
07 p2831 N94-28085
Development of electromagnetic compatibility tests
[REPT-932-430-110] 08 p3245 N94-29421
MODIS. Volume 1: MODIS level 1A software baseline requirements
[NASA-TM-104594-VOL-1] 09 p3823 N94-33287
Robust requirements specifications for safety-critical systems
[PB94-167806] 11 p4250 N94-35532

RESCUE OPERATIONS
STS-26 EVA rescue training
[NASA-TM-109563] 03 p0875 N94-15333
Life saving satellites
[NASA-TM-109616] 03 p0862 N94-15426
Inflatable rescue device
[NASA-CASE-MSC-22244-1] 03 p1137 N94-15883
Technical urban search and rescue, System To Locate Survivors (STOLS) units: Operator's manual
[AD-A266317] 03 p0862 N94-16438
Evaluation of Night Vision Goggles (NVG) for maritime search and rescue (HH-3/HH-60) comparison report
[AD-A266493] 03 p1138 N94-16793

On predicting the person-in-water drift for search and rescue
[AD-A268083] 03 p1055 N94-17514
AN/APS-137 Forward Looking Airborne Radar (FLAR) evaluation Spring 1992 experiment
[AD-A268899] 04 p1384 N94-18228
Effectiveness of protection clothing for cold weather conditions after ejection over sea: A case report 06 p3381 N94-28435
SATCOM feasibility study for search and rescue aircraft
[DSIS-94-01083] 09 p3575 N94-31902
The ALEXIS mission recovery
[DE94-007549] 09 p3611 N94-32813
Forward-looking infrared: Capabilities for search and rescue
[AD-A277895] 10 p4141 N94-33548
Performance demonstration: UH-60Q external rescue hoist and cargo loadmeter
[AD-A277533] 10 p3989 N94-34080
Self-rescue strategies for EVA crewmembers equipped with the SAFER backpack 11 p4207 N94-35633
EH101: A new helicopter capable of long range missions 11 p4194 N94-36330

RESEARCH
NT DYNAMIC PROGRAMMING
NT HIGH TEMPERATURE RESEARCH
NT LINEAR PROGRAMMING
NT MARKET RESEARCH
NT NONLINEAR PROGRAMMING
NT NUCLEAR RESEARCH
NT QUADRATIC PROGRAMMING
NASA Space Engineering Research Center for VLSI System Design
[NASA-CR-194587] 03 p1008 N94-15547
White House technology reinvestment project: Briefing and transcripts
[PB93-169829] 04 p1611 N94-18090
Research activities, Faculty of Civil Engineering, Delft University of Technology, 1990 - 1991
[PB93-195022] 04 p1380 N94-19254
A foundation for the 21st Century: A progressive framework for the National Science Foundation. Report of the National Science Board Commission on the future of the National Science Foundation
[NSB-92-196] 04 p1611 N94-19618
The national geomagnetic initiative
[LC-93-85739] 06 p2401 N94-23344
Bibliography of Lewis Research Center technical publications announced in 1992
[NASA-TM-106035] 06 p2590 N94-23562
Index to FAA Office of Aviation Medicine Reports: 1961 through 1993
[AD-A275913] 06 p2426 N94-24093
RIACS/USRA
[NASA-CR-195117] 06 p2631 N94-25003
Research interests and broad agency announcement 94-1 of the Air Force Office of Scientific Research
[AD-A273410] 06 p2632 N94-25075
National Aeronautics and Space Administration (NASA)/American Society for Engineering Education (ASEE) Summer Faculty Fellowship Program, 1993, volume 2
[NASA-CR-188271-VOL-2] 06 p2636 N94-25367
Proceedings of the symposium on current concepts and approaches on animal test alternatives
[AD-A273926] 07 p2900 N94-25593
Highlights 1993 --- Lawrence Berkeley Laboratory
[DE94-002270] 07 p3118 N94-26937
Microbiology research at some research institutes in the former Soviet Union: A survey of scientific publications
[PB94-123320] 07 p2902 N94-27171
Data analysis and data fusion for intelligence analysis and decision support. Research plan 1993-2000
[PB94-123569] 07 p3005 N94-27173
The 1993 NASA-ODU American Society for Engineering Education (ASEE) Summer Faculty Fellowship Program
[NASA-CR-191544] 07 p3085 N94-27893
Science beyond the atmosphere: The history of space research in Europe
[ESA-HSR-SPECIAL] 07 p2689 N94-28207
Atmospheric science research in Malaysia: Perspectives on international cooperation 07 p2874 N94-28285
Laboratory of Space Technology
[PB94-133204] 07 p2689 N94-28358
Venus Data Analysis Program: Directory of Research Projects (1993-1994)
[NASA-CR-195742] 08 p3549 N94-29102
Basic research in computer science
[AD-A275184] 08 p3405 N94-29181
Activities report of the International Meteorological Institute
[ETN-94-95524] 08 p3370 N94-29423
Antarctic Record, vol. 36, no. 3
[REPT-108] 08 p3363 N94-29978
Activities of the wintering party at Syowa Station by the 32nd Japanese Antarctic Research Expedition in 1991 08 p3364 N94-29986
Aviation human factors research in US universities: Potential contributions to national needs
[NASA-TM-108814] 09 p3575 N94-32927
Oceanography in the next decade: Building new partnerships
[NASA-CR-195926] 10 p4093 N94-34265
Introduction to USRA
[NASA-CR-195980] 11 p4376 N94-35590
Activities of the optoelectronics laboratory
[PB94-171196] 11 p4334 N94-36190
Beginning a dialogue on the changing environment for the physical and mathematical sciences 12 p4509 N94-36948
UAV's in climate research: The ARM Unmanned Aerospace Vehicle Program
[DE94-011753] 12 p4465 N94-37154
Catalog of data bases and reports
[DE94-012230] 12 p4466 N94-37208
Activities of the Laboratory of Physics, Helsinki University of Technology
[PB94-175247] 12 p4509 N94-37301

RESEARCH AIRCRAFT
NT B-70 AIRCRAFT
NT FIREBEE 2 TARGET DRONE AIRCRAFT
NT QUESTOL AIRCRAFT
NT ROTOR SYSTEMS RESEARCH AIRCRAFT
NT U-2 AIRCRAFT
NT X-14 AIRCRAFT
NT X-15 AIRCRAFT
NT X-31 AIRCRAFT
NT XV-5 AIRCRAFT
Measuring human performance on NASA's microgravity aircraft 01 p0317 N94-11537
Preliminary design features of the RASCAL: A NASA /Army rotorcraft in-flight simulator 02 p0526 N94-13325
Performance evaluation tests of the GPS/DGPS navigation system installed in the NAL Dornier 228: Preliminary ground test results
[NAL-TM-649] 02 p0513 N94-13346
Position error determination for the speedometer and altimeter of the NAL QSTOL experimental aircraft ASKA
[NAL-TR-1144] 02 p0517 N94-13451
Theoretical support for the Airborne Antarctic Ozone Experiment
[NASA-CR-193669] 02 p0713 N94-13465
Flight validation of a pulsed smoke flow visualization system
[NASA-CR-186026] 02 p0516 N94-14106
Canadian microgravity experiments flown in 1989-1990 03 p0977 N94-16075
The vibro-acoustic mapping of low gravity trajectories on a Learjet aircraft 03 p0978 N94-16078
Ozone hole
[NASA-TM-109368] 04 p1476 N94-18960
X-29: Research aircraft
[NASA-TM-109370] 04 p1318 N94-18962
The world's largest wind tunnel
[NASA-TM-109371] 04 p1322 N94-18963
Experiments with a fluid deicing system for cleaning laminar wings 05 p1640 N94-22601
Close-up analysis of inflight ice accretion
[NASA-TM-106457] 06 p2172 N94-23523
A conceptual design of an unmanned test vehicle using an airbreathing propulsion system
[NASA-CR-195550] 06 p2189 N94-25085
X-31 aerodynamic characteristics determined from flight data 06 p2164 N94-25109
Nonlinear aerodynamic modeling using multivariate orthogonal functions 06 p2164 N94-25110
Multiple model adaptive estimation applied to the LAMBDA URV for failure detection and identification
[AD-A274078] 07 p3002 N94-25992
Description of the Experimental Avionics Systems Integration Laboratory (EASILY)
[NASA-TM-109072] 07 p2681 N94-27425
The radiocarbon hydroxyl technique 08 p3344 N94-28600
Design and construction of the Aerobot Robotic Manipulator (ARM)
[AD-A275362] 08 p3298 N94-28894
HATT-X: A high performance flying laboratory for autonomous unmanned aircraft research and development 08 p3149 N94-30293
Fault detection and isolation for the Bluebird test bed aircraft
[AD-A277979] 09 p3586 N94-33086
Ground vibration test of the XV-15 Tiltrotor Research Aircraft and pretest predictions 11 p4200 N94-35972
The reduction of takeoff ground roll by the application of a nose gear jump strut
[NASA-TM-108822] 11 p4198 N94-36380
Predicting the effects of unmodeled dynamics on an aircraft flight control system design using eigenspace assignment
[NASA-TM-4548] 12 p4388 N94-37059

RESEARCH AND DEVELOPMENT
Advanced Materials for Lightweight Structures
[ESA-SP-336] 01 p0056 N94-10001
The EUREKA project portfolio in new materials 01 p0056 N94-10002
Investigations on aluminium-lithium alloys for damage tolerant application 01 p0059 N94-10023
Fibre optic strain and temperature measurement in composite materials: A review of the OSTIC programme 01 p0065 N94-10066
The Netherlands innovation oriented research programme on polymer composites and special polymers 1985-1993 01 p0065 N94-10067
Protein, glass, aerosol research, containerless processing and diagnostics technology for microgravity application 01 p0106 N94-10112
The NASA Lewis Research Center SBIR program: An assessment
[NASA-TM-106205] 01 p0485 N94-10356
Recommendations for future research in hypersonic instrumentation 01 p0004 N94-10433
Future material development trends for commercial airplane interiors 01 p0021 N94-10792
Advanced aircraft materials research and development plan 01 p0022 N94-10796
The future of aircraft cabin fire safety 01 p0022 N94-10797
National patterns of R and D resources, 1992
[NSF-92-330] 01 p0422 N94-11186
NASDA activities in space solar power system research, development and applications 01 p0054 N94-11413
Quality assurance in basic research and R/D
[DE93-010825] 01 p0183 N94-11647
The 27th International Applied Military Psychology Symposium: A Focus on Decision Making Research
[AD-A265278] 01 p0313 N94-11701
AGARD highlights 92/2, September 1992
[AGARD-HIGHLIGHTS-92/2] 01 p0497 N94-11820
Integrating the services' imagery architectures
[AD-A265487] 01 p0171 N94-12335
National SBIR Phase 3 Commercialization Conference
[AD-A266083] 01 p0417 N94-12410
Elementary particle physics and high energy phenomena
[DE93-013971] 01 p0370 N94-12609
National atmospheric sciences program, fiscal years 1987-1990
[NSF-92-16] 02 p0711 N94-12794
Here's the beef: A case study in organizational transformation 02 p0667 N94-13163
JPRS report: Science and technology. Central Eurasia: Space
[JPRS-USP-93-003] 02 p0828 N94-13182
Publications of the Jet Propulsion Laboratory: 1990 and 1991
[NASA-CR-193287] 02 p0823 N94-13461
Artificial intelligence in Canada: A description by the members of the ACAI
[NRC-31789] 02 p0763 N94-13517
Highlights, 1981
[NASA-TM-109305] 02 p0850 N94-13612
Artificial intelligence in Canada: A description by the members of the ACAI
[CNR-31790] 02 p0764 N94-13820
Research and technology highlights, 1992
[NASA-TM-4452] 02 p0850 N94-13962
Selected data on academic science and engineering R and D expenditures: Fiscal Year 1991
[NSF-92-329] 02 p0819 N94-13982
Science, technology, and the federal government: National goals for a new era 02 p0827 N94-14115
Activities of Institute for Microstructural Sciences
[NRC-32815] 02 p0810 N94-14198
Activities of Institute for Microstructural Sciences
[CNR-32815] 02 p0810 N94-14199
Storage systems for national information assets
[DE93-015101] 02 p0825 N94-14331
NASA/DOD Aerospace Knowledge Diffusion Research Project. Paper 36: Technical uncertainty as a correlate of information use by US industry-affiliated aerospace engineers and scientists
[NASA-TM-109328] 02 p0825 N94-14486
The 1991 research and technology report, Goddard Space Flight Center
[NASA-TM-108738] 02 p0851 N94-14791
Infrared detectors and coolers for space instrumentation: Summary and concluding remarks 03 p0904 N94-15059
Expectations for the future of military aviation 03 p0854 N94-15128
Expectations for the future of the National Aerospace Laboratory 03 p0854 N94-15129

Expectations for the future of the Faculty of Aeronautics and Astronautics of the Technical University of Delft
03 p0854 N94-15131
Return to flight 1
[NASA-TM-109663] 03 p1223 N94-15234
The 1969 highlights
[NASA-TM-109630] 03 p1301 N94-15241
The 1972 highlights
[NASA-TM-109631] 03 p1301 N94-15242
The 1965 highlights --- NASA programs
[NASA-TM-109632] 03 p1301 N94-15243
NASA images 6
[NASA-TM-109437] 03 p0862 N94-15336
Student researchers
[NASA-TM-109441] 03 p1221 N94-15340
Back to propellers
[NASA-TM-109445] 03 p0869 N94-15344
Annual historical report, calendar year 1992
[AD-A267050] 03 p1121 N94-15663
Report on computing and networking in the Space Science Laboratory by the SSL Computer Committee
[NASA-TM-108422] 03 p1147 N94-15721
AFOSR technical report summaries, January - March 1993
[AD-A267187] 03 p1230 N94-15850
Research and development: Engine of innovation at Krupp
03 p0984 N94-16001
Modeling and simulation: A key to future defense technology
[TABES PAPER 93-654] 03 p1054 N94-16153
Looking at science on board Eureca
[ESA-BR-80] 03 p0874 N94-16584
The early activities of the COPERS and the drafting of the ESRO Convention (1961/62)
[ESA-HSR-4] 03 p1225 N94-16593
Resources and activities of the European Space Agency
03 p1303 N94-16792
The Megascience Forum
[DE93-014445] 03 p1303 N94-16804
Research grant handbook
[NHB-5800.1C] 03 p1225 N94-16907
Plasma Science Committee (PLSC) and the Panel on Opportunities in Plasma Science and Technology (OPST)
[DE93-018142] 03 p1204 N94-16995
Computer Science and Telecommunications Board activities
[DE93-018141] 03 p1000 N94-17000
Technology in action
[NASA-TM-109345] 03 p1235 N94-17294
ONRASIA scientific information bulletin, volume 18, number 2
[AD-A267798] 03 p1304 N94-17305
Mechanical Systems Technology Branch research summary, 1985 - 1992
[AD-A276450] 03 p1049 N94-17583
Satellite communications systems and technology. Executive summary
[NASA-TM-109346] 03 p1006 N94-17661
The ANL electric vehicle battery R&D program for DOE-EHP
[DE93-017414] 04 p1394 N94-17750
Activities report of the Rutherford Appleton Laboratory
[ETN-93-94555] 04 p1631 N94-17968
Lightweight materials for transportation: Program plan
[DE93-017381] 04 p1340 N94-18087
White House technology reinvestment project: Briefing and transcripts
[PB93-169829] 04 p1611 N94-18090
Trends in Information Management at Department of Energy Headquarters
[DE93-017197] 04 p1615 N94-18496
The 1994 NASA authorization, volume 2
[GPO-71-510] 04 p1620 N94-18842
The FAA Technical Center Human Factors Laboratory information guide
[AD-A269343] 04 p1513 N94-18992
Research and design activities and the economic balance of MBB
[ETN-93-94909] 04 p1310 N94-19383
Report on the activities of Space Science Department, 1990 - mid 1992
[ESA-SP-1161] 04 p1633 N94-19404
Program descriptions
[NSF-92-123] 04 p1531 N94-19619
NASA's Education Program
[NASA-EP-297] 05 p2038 N94-20129
Documents on the history of aeronautical and space research in Germany, 1900 - 1970
[DLR-MITT-92-08] 05 p2152 N94-20543
High energy physics program at Texas A/M University
[DE93-041089] 05 p1980 N94-20933
Aerospace: Facts and figures, 1992-1993
[AD-A272571] 05 p1635 N94-21419
Index to 1992 NASA Tech Briefs, volume 16, numbers 1-12
[NASA-TM-109377] 05 p2053 N94-21736
Index to 1991 NASA Tech Briefs, volume 15, numbers 1-12
[NASA-TM-109376] 05 p2053 N94-21737
Cumulative index to NASA Tech Briefs, 1986-1990, volumes 10-14
[NASA-TM-109378] 05 p2054 N94-21738
Application development in a PC/LAN environment
05 p1923 N94-22067
NASA Propulsion Engineering Research Center, volume 1
[NASA-CR-194721-VOL-1] 05 p1671 N94-22428
Progress in phases 2 and 3 of the Photovoltaic Manufacturing Technology Project (PVMaT)
[DE94-000206] 06 p2389 N94-22888
JPRS report: Science and technology. Central Eurasia: Space
[JPRS-USP-93-006] 06 p2194 N94-23015
NASA Propulsion Engineering Research Center, volume 2
[NASA-CR-194719-VOL-2] 06 p2209 N94-23028
Activities report to NATO
[ETN-94-95047] 06 p2318 N94-23227
Bibliography of Lewis Research Center technical publications announced in 1992
[NASA-TM-106035] 06 p2590 N94-23562
The RB211: The first 25 years
[PNR-90977] 06 p2187 N94-23570
Contributions of DOE weapons labs and NIST to semicondutor technology
[OTA-ITE-585] 06 p2630 N94-23572
Satellite communications systems and technology. Volume 1: Analytical chapters
[NASA-TM-109398] 06 p2293 N94-23627
Fiscal year 1993 scientific and technical reports, articles, papers, and presentations
[NASA-TM-108423] 06 p2590 N94-24079
Proceedings of Technology and Governance in the 1990's
[PB93-192904] 06 p2597 N94-24312
NASA high performance computing and communications program
[NASA-TM-4554] 06 p2591 N94-24337
Radio communication and wave propagation. A visit to the Netherlands in December 1992
[PB93-204360] 06 p2297 N94-24531
Structural dynamics division research and technology accomplishments for FY 1993 and plans for FY 1994
[NASA-TM-109036] 06 p2169 N94-24576
Nondestructive evaluations
[DE94-003020] 06 p2373 N94-24613
NASA/DOD Aerospace Knowledge Diffusion Research Project. Report number 20: The use of selected information products and services by US aerospace engineers and scientists: Results of two surveys
[AD-A276068] 06 p2592 N94-24649
NADA/DOD Aerospace Knowledge Diffusion Research Project. Report number 19: The US government technical report and the transfer of federally funded aerospace R/D: An analysis of five studies
[AD-A276146] 06 p2592 N94-24660
Research interests and broad agency announcement 94-1 of the Air Force Office of Scientific Research
[AD-A273410] 06 p2632 N94-25075
National Aeronautics and Space Administration (NASA)/American Society for Engineering Education (ASEE) Summer Faculty Fellowship Program, 1993, volume 1
[NASA-CR-188271-VOL-1] 06 p2632 N94-25348
Technical and scientific research for aeronautics and astronautics
[ETN-94-95392] 07 p2641 N94-26212
Technology development in space projects
[VTT-TIED-1438] 07 p2682 N94-26249
Preparation and characterization of high temperature superconductor film surfaces
[AD-A274293] 07 p3059 N94-26681
Ferrite phase shifters using stress insensitive materials
[AD-A274639] 07 p2708 N94-26895
Frontiers of science and measurement: Report on a seminar jointly organized by the National Physical Laboratory and the Institute of Physics
[PB94-124310] 07 p3009 N94-27131
Robotics handbook. Version 1: For the interested party and professional
[NASA-TM-109690] 07 p2824 N94-27238
Basic research on natural gas combustion phenomena
[PB94-129046] 07 p2717 N94-27256
How to make good use of international research collaboration, with emphasis on the evolving situation in Europe
[PB94-119690] 07 p3101 N94-27323
Vision 21: Interdisciplinary Science and Engineering in the Era of Cyberspace
[NASA-CP-10129] 07 p2685 N94-27358
Small business innovation research program solicitation
[NASA-TM-109695] 07 p3094 N94-27661
NASA SBIR abstracts of 1992, phase 1 projects
[NASA-TM-109694] 07 p3094 N94-27772
The 1993 Federal Aviation Administration plan for research, engineering and development
[AD-A279037] 07 p2643 N94-27960
Research and Development Annual Report, 1992
[NASA-TM-104777] 07 p3119 N94-27993
Development of the gas turbine. Part 1: Design philosophy and performance 07 p2831 N94-28080
Development of the gas turbine. Part 2: Manufacturing, commissioning, and operation 07 p2831 N94-28081
Selected data on Federal support to universities and colleges: FY 1991
[NSF-93-320] 07 p3101 N94-28201
Visit to CERMA: Centre d'Etudes et de Recherches de Medecine Aerospatiale, Centre for Studies and Research in Aviation and Space Medicine, Bretigny sur Orge, France, November 16-18, 1992
[PB94-132990] 07 p2937 N94-28392
Glass-ceramic matrix composites
[REPT-932-430-112] 08 p3179 N94-29413
Journal of NIRE, vol. 2, no. 3
[JTN-94-80553] 08 p3553 N94-29512
Activity report of Synchrotron Radiation Laboratory 1992
[JTN-94-80600] 08 p3495 N94-29596
Proceedings: SISAL 1993
[DE94-006641] 08 p3420 N94-30056
NASA/DOD Aerospace Knowledge Diffusion Research Project. Report 23: The communications practices of US aerospace engineering faculty and students: Results of the phase 3 survey
[NASA-TM-109085] 08 p3534 N94-30149
NASA/DOD Aerospace Knowledge Diffusion Research Project. Report 22: US academic librarians and technical information specialists as information intermediaries: Results of the phase 3 survey
[NASA-TM-109067] 08 p3534 N94-30150
Proceedings of the 3rd Conference on Military Robotic Applications
[DRES-SP-149] 08 p3304 N94-30275
Intelligent robotics can boost America's economic growth
[AIAA PAPER 94-1301-CP] 08 p3439 N94-30527
Geothermal direct-heat utilization assistance
[DE94-005831] 08 p3340 N94-30700
Photonics at Sandia National Laboratories: From research to applications
[DE94-006463] 08 p3501 N94-30828
Naval Surface Warfare Center Dahlgren Division Technical Digest: Advanced materials technology
[AD-A276448] 09 p3668 N94-31364
Laboratory Directed Research & Development Program
[DE94-005928] 09 p3956 N94-31523
The contribution of aeronautics and astronautics to the quality of life on Earth
[ILR-MITT-283(1993)] 09 p3764 N94-31611
Aerospace test facilities at NASA LERC Plumbrook
[NASA-TM-109755] 09 p3602 N94-31814
Division of Microwave Technology
[PB94-148079] 09 p3676 N94-31925
Advances in MOVPE compound semiconductor epitaxy manufacturing technology: From high throughput large area reactors to cluster tools
[DE94-006367] 09 p3901 N94-32104
X ray optics for science and technology
[AD-A277369] 09 p3880 N94-32155
The future of high energy physics in the US statement for the Science Subcommittee of the House Science, Space and Technology Committee
[DE94-008986] 09 p3876 N94-32586
The future of high-energy physics in the US: Statement for the 1994 HEPAP Subpanel
[DE94-008994] 09 p3876 N94-32588
Research on stable, high-efficiency amorphous silicon multijunction modules
[DE94-000298] 09 p3695 N94-32680
NASA/DOD Aerospace Knowledge Diffusion Research Project. Paper 5: Aerospace librarians and technical information specialists as information intermediaries: A report of phase 2 activities of the NASA/DOD Aerospace Knowledge Diffusion Research Project
[NASA-TM-109777] 09 p3921 N94-32829
NASA/DOD Aerospace Knowledge Diffusion Research Project. Paper 10: The NASA/DOD Aerospace Knowledge Diffusion Research Project
[NASA-TM-109769] 09 p3921 N94-32831

NASA/DOD Aerospace Knowledge Diffusion Research Project. Paper 12: The diffusion of federally funded aerospace research and development (R/D) and the information seeking behavior of US aerospace engineers and scientists
[NASA-TM-109404] 09 p3921 N94-32832
NASA/DOD Aerospace Knowledge Diffusion Research Project. Paper 18: Scientific and Technical Information (STI) policy and the competitive position of the US aerospace industry
[NASA-TM-109782] 09 p3921 N94-32833
NASA/DOD Aerospace Knowledge Diffusion Research Project. Paper 1: The value of scientific and technical information (STI), its relationship to Research and Development (R/D), and its use by US aerospace engineers and scientists
[NASA-TM-109774] 09 p3922 N94-32835
LLNL casting technology
[DE94-008282] 09 p3669 N94-32839
Sandia's photonic program and its changing national role
[DE94-008616] 09 p3883 N94-32878
Research and Technology Objectives and Plans Summary (RTOPS)
[NASA-TM-105441] 09 p3966 N94-32885
Aerospace sponsored research
[ATR-93(8498)-1] 09 p3966 N94-32949
Novel sol-gel deposition for repair of conducting paths in polyceramic systems
[AD-A278381] 09 p3664 N94-33350
An assessment of research and development leadership in advanced batteries for electric vehicles
[DE94-009253] 10 p4041 N94-34068
National Facilities study
[NASA-TM-109851] 10 p4009 N94-34071
Science and engineering indicators, 1993
[NSB-93-1] 10 p4149 N94-34169
Technology for small spacecraft
[NASA-CR-196041] 10 p4015 N94-34411
National facilities study. Volume 2: Task group on aeronautical research and development facilities report
[NASA-TM-109855] 10 p4009 N94-34633
National facilities study. Volume 3: Mission and requirements model report
[NASA-TM-109857] 10 p4009 N94-34635
National facilities study. Volume 4: Space operations facilities task group
[NASA-TM-109858] 10 p4010 N94-34636
National facilities study. Volume 5: Space research and development facilities task group
[NASA-TM-109859] 10 p4010 N94-34637
Johnson Space Center (JSC) research and technology
[NASA-TM-104788] 10 p4187 N94-34677
NASA/DOD Aerospace Knowledge Diffusion Research Project. Paper 42: An analysis of the transfer of Scientific and Technical Information (STI) in the US aerospace industry
[NASA-TM-109863] 10 p4159 N94-34730
ICF program
[DE94-008281] 10 p4145 N94-35079
JPRS report: Science and technology. Central Eurasia: Physics and mathematics
[JPRS-UPM-93-003] 10 p4132 N94-35118
The Federal Aviation Administration plan for research, engineering and development 11 p4376 N94-35262
JPRS report: Science and technology. Central Eurasia
[JPRS-UST-94-001] 11 p4229 N94-35340
JPRS report: Science and technology. Central Eurasia
[JPRS-UST-94-004] 11 p4249 N94-35341
JPRS report: Science and technology. Central Eurasia
[JPRS-UST-94-005] 11 p4249 N94-35342
Director's discretionary fund
[NASA-TM-103997] 11 p4376 N94-35370
JPRS report: Science and technology. Central Eurasia
[JPRS-UST-94-010] 11 p4250 N94-35385
JPRS report: Science and technology. Central Eurasia
[JPRS-UST-94-011] 11 p4250 N94-35386
JPRS report: Science and technology. Central Eurasia
[JPRS-UST-94-012] 11 p4250 N94-35387
AGARD highlights 93/2
[AGARD-HIGHLIGHTS-93/2] 11 p4376 N94-35444
JPRS report: Science and technology. Central Eurasia: Space
[JPRS-USP-94-003] 11 p4201 N94-35520
Challenging the Future - Journey to Excellence. Aeropropulsion strategic plan for the 1990's
[NASA-TM-109250] 11 p4226 N94-35591
Budget estimates, fiscal year 1995. Volume 1: Agency summary, human space flight, and science, aeronautics and technology
[NASA-TM-109791] 11 p4347 N94-35899
CSTL technical activities, 1991
[PB94-160769] 11 p4318 N94-36003
JPRS report: Science and technology. Central Eurasia: Space
[JPRS-USP-93-005] 11 p4201 N94-36011
Earthquake Engineering Research Center: 25th anniversy edition
[PB94-160645] 11 p4291 N94-36019
JTEC/WTEC report and program summary 11 p4379 N94-36042
Research and technology, 1993
[NASA-TM-108816] 11 p4380 N94-36117
Research and development of Proton-Exchange Membrane (PEM) fuel cell system for transportation applications: Initial conceptual design report
[DE94-010576] 11 p4283 N94-36243
Activities of the Laser and Plasma Technology Division
[DE94-617113] 11 p4273 N94-36393
National Educators' Workshop: Update 1993. Standard Experiments in Engineering Materials Science and Technology
[NASA-CP-3259] 11 p4229 N94-36398
Solid state research
[AD-A280573] 12 p4533 N94-36734
NASA-UVA Light Aerospace Alloy and Structures Technology Program (LA2ST)
[NASA-CR-196290] 12 p4415 N94-36809
United States Air Force Summer Research Program, 1993. Volume 13: Phillips Laboratory
[AD-A278657] 12 p4550 N94-36977
United States Air Force Summer Research Program, 1993. Volume 16: Arnold Engineering Development Center, Frank J. Seiler Research Laboratory and Wilford Hall Medical Center
[AD-A278658] 12 p4550 N94-36978
United States Air Force Summer Research Program, 1993. Volume 3: Phillips Laboratory
[AD-A278694] 12 p4550 N94-36979
United States Air Force Summer Research Program, 1993. Volume 4: Rome Laboratory
[AD-A278695] 12 p4551 N94-36980
United States Air Force Summer Research Program, 1993. Volume 5A: Wright Laboratory
[AD-A278696] 12 p4551 N94-36981
United States Air Force Summer Research Program, 1993. Volume 6: Arnold Engineering Development Center, Frank J. Seiler Research Laboratory and Wilford Hall Medical Center
[AD-A278697] 12 p4551 N94-36982
United States Air Force Summer Research Program, 1993. Volume 8: Phillips Laboratory
[AD-A278698] 12 p4551 N94-36983
United States Air Force Summer Research Program, 1993. Volume 9: Rome Laboratory
[AD-A278699] 12 p4551 N94-36984
JPRS report: Science and technology. Central Eurasia: Space
[JPRS-USP-94-004] 12 p4391 N94-37002
JPRS report: Science and technology. Central Eurasia: Space 12 p4391 N94-37003
JPRS report: Science and technology. Central Eurasia
[JPRS-UST-94-013] 12 p4509 N94-37006
JPRS report: Science and technology. Central Eurasia: Materials science
[JPRS-UMS-93-008] 12 p4404 N94-37010
ORNL superconducting technology program for electric power systems
[DE94-011471] 12 p4438 N94-37239
Hydrogen storage for vehicular applications: Technology status and key development areas
[DE94-011626] 12 p4428 N94-37243
The Canadian network for the advancement of research, industry and education (CANARIE) 12 p4543 N94-37336
Materials Compatibility and Lubricant Research on CFC-refrigerant substitutes
[DE94-012352] 12 p4425 N94-37373
JPRS report: Science and technology. Central Eurasia: Engineering and equipment
[JPRS-UEQ-93-007] 12 p4431 N94-37523
JPRS report: Science and technology. Central Eurasia: Engineering and equipment
[JPRS-UEQ-93-008] 12 p4432 N94-37524
JPRS report: Science and technology. Central Eurasia: Engineering and equipment
[JPRS-UEQ-93-005] 12 p4432 N94-37538
NASA commercial technology. Agenda for change
[NASA-TM-109898] 12 p4546 N94-37765

RESEARCH FACILITIES

Proceedings of the 8th European Symposium on Materials and Fluid Sciences in Microgravity, volume 1
[ESA-SP-333-VOL-1] 01 p0099 N94-10070
Description of the liquid structure facility architecture and experimental demonstration of the diagnostic capabilities 01 p0039 N94-10118
The electron beam furnace: A new facility for materials science research 01 p0109 N94-10126
Microgravity Applications Furnace Facility (MAFF) for parabolic flights 01 p0109 N94-10128
Laser beam deflection: A diagnostic tool for vapour growth experiments in microgravity 01 p0111 N94-10135
The advanced fluid physics module: How to achieve scientific goals for Spacelab D2 01 p0039 N94-10136
Scientific specifications for an automated facility for growing large semiconducting crystals from the melt in space 01 p0114 N94-10180
Crystal growth in the Zone Melting Facility (ZMF) 01 p0119 N94-10213
The critical facility on IML-1 01 p0044 N94-10250
Numerical wind tunnel project and computational fluid dynamics at National Aerospace Laboratory, Japan
[NAL-TM-648T] 01 p0149 N94-10861
Motion and spatial disorientation systems: Special research capabilities
[AD-A265155] 01 p0303 N94-11097
Five biomedical experiments flown in an Earth orbiting laboratory: Lessons learned from developing these experiments on the first international microgravity mission from concept to landing 01 p0302 N94-11556
Quality assurance in basic research and R/D
[DE93-010825] 01 p0183 N94-11647
Vertical motion simulator familiarization guide
[NASA-TM-103923] 02 p0527 N94-13008
Technology parks and the cooperation among universities and firms: The cases of Campinas, Sao Jose dos Campos e Sao Carlos
[INPE-5251-TAE/04] 02 p0818 N94-13427
Activities of Institute for Aerospace Research, Flight Research Laboratory
[CTN-93-60832] 02 p0850 N94-13519
Cray Y-MP
[NASA-TM-109303] 02 p0741 N94-13609
A future view of computational science in aircraft
[NASA-TM-109284] 02 p0504 N94-13621
A history of the Defence Research Establishment, Ottawa
[CTN-93-60737] 02 p0850 N94-14060
DCIEM: The first fifty years, 1939-1989
[CTN-93-60767] 02 p0733 N94-14141
Uniform user and group IDs on a large network
[DE93-013047] 02 p0760 N94-14315
Current titles --- National Center for Electron Microscopy
[DE93-015859] 02 p0851 N94-14587
A guide to the DRA 13 ft x 9 ft Low Speed Wind Tunnel Facility
[AD-A267739] 02 p0528 N94-14876
Supersonic Combustion Research Laboratory. Volume 1: Design and fabrication
[AD-A267667] 03 p0943 N94-14962
Expectations for the future of the National Aerospace Laboratory 03 p0854 N94-15129
GFSC-TV demo tape
[NASA-TM-109586] 03 p0875 N94-15270
Stock footage of Goddard Space Flight Center and Headquarters
[NASA-TM-109589] 03 p0875 N94-15273
Manned vehicle systems research facility
[NASA-TM-109650] 03 p0875 N94-15318
NASA images 6
[NASA-TM-109437] 03 p0862 N94-15336
Building 46 grand opening
[NASA-TM-109524] 03 p0875 N94-15386
Lunar Curatorial Facility resource
[NASA-TM-109531] 03 p0875 N94-15393
Johnson Space Center and downtown Houston, Texas aerials
[NASA-TM-109522] 03 p1032 N94-15472
Commitment to challenge
[NASA-TM-109523] 03 p0876 N94-15473
Heat transfer and aerodynamics of a 3D design nozzle guide vane tested in the Pyestock isentropic light piston facility
[RAE-TM-AERO/PROP-19] 03 p0856 N94-15696
Facilities maintenance handbook
[NHB-8831.2] 03 p1224 N94-15934
Scientific use of Space Station Freedom 03 p0977 N94-16072
New findings and instrumentation from the NASA Lewis Microgravity Facility 03 p0977 N94-16076
QUESTS: A microgravity research facility for materials science experiments 03 p0978 N94-16082
First results from a laboratory facility for measurement of emission spectra under simulated planetary conditions 03 p0954 N94-16372
An electromagnetic interference study of potential transmitter sites for the HF Active Auroral Research Program (HAARP)
[AD-A267743] 03 p1004 N94-17373
Design of an experiment hardware for the ESA space facility BIOPAN
[DLR-FB-93-06] 03 p0876 N94-17548

Activities report of the Rutherford Appleton Laboratory
[ETN-93-94555] 04 p1631 N94-17968
The world's most powerful computer
[NASA-TM-109369] 04 p1514 N94-18961
The world's largest wind tunnel
[NASA-TM-109371] 04 p1322 N94-18963
The FAA Technical Center Human Factors Laboratory information guide
[AD-A269343] 04 p1513 N94-18992
Activities of National Inst. for Aviation Research
[NIAR-93-16] 05 p2151 N94-20150
Center for neural engineering
[AD-A271164] 05 p1890 N94-20185
National Synchrotron Light Source user's manual: Guide to the VUV and x ray beamlines
[DE93-019564] 05 p2015 N94-20260
The National High Magnetic Field Laboratory, a user facility in support of research in high magnetic fields
[DE93-040145] 05 p1714 N94-20278
Hypervelocity impact studies at CEG: Experimental and numerical capabilities 05 p1664 N94-21397
A FET-switched induction accelerator cell
[DE93-019604] 05 p1769 N94-21838
Chemistry and materials science
[DE94-001449] 05 p2152 N94-21858
Satellite communications systems and technology. Volume 2: Site reports
[NASA-TM-109399] 06 p2293 N94-23628
Suddenly, tomorrow came... A history of the Johnson Space Center
[NASA-SP-4307] 06 p2631 N94-24584
Advanced ballistic range technology
[NASA-CR-195198] 06 p2165 N94-25169
Activities of Academia Sinica
[DE93-614529] 06 p2541 N94-25335
Automatic pressure control system for the Wright Laboratory Compressor Research Facility
[AD-A273827] 06 p2194 N94-25522
Technical and scientific research for aeronautics and astronautics
[ETN-94-95392] 07 p2641 N94-26212
Research and test facilities
[NASA-TM-109685] 07 p2681 N94-26684
Selected data on Federal support to universities and colleges: FY 1991
[NSF-93-320] 07 p3101 N94-28201
JSC almanac
[NASA-TM-109702] 07 p3119 N94-28204
Physics at HERA
[DE94-005117] 08 p3483 N94-28569
Antarctic Record, volume 36, no. 1
[REPT-106-VOL-36-NO-1] 08 p3357 N94-29078
Fishermans Bend: A centre of Australian aviation
[AD-A274981] 08 p3121 N94-29090
Joint research activities with CCMRI (China) 08 p3240 N94-29521
Portable Linear Sled (PLS) for biomedical research 08 p3163 N94-29648
Research and technology, 1992
[NASA-TM-103996] 08 p3555 N94-29891
Energy and Technology Review
[DE94-004472] 08 p3338 N94-29955
On the (mu)SR activity at LNP JINR phasotron
[DE94-608385] 08 p3517 N94-30195
Microgravity fluid science research in Europe
[AD-B179178] 08 p3229 N94-30409
BNL possibilities
[DE94-007179] 09 p3864 N94-31398
Free electrons as a versatile source of coherent radiation
[ETN-94-96011] 09 p3715 N94-31545
Aerospace test facilities at NASA LERC Plumbrook
[NASA-TM-109755] 09 p3602 N94-31814
Airborne Trailblazer: Two decades with NASA Langley's 737 flying laboratory
[NASA-SP-4216] 09 p3566 N94-32793
John C. Stennis Space Center overview
[NASA-TM-109816] 10 p4011 N94-33567
Activities of the NASA centers
[NASA-TM-109836] 10 p4068 N94-33721
National Facilities study
[NASA-TM-109851] 10 p4009 N94-34071
A versatile rocket engine hot gas facility
[NASA-CR-195339] 10 p4011 N94-34131
National facilities study. Volume 1: Facilities inventory
[NASA-TM-109854] 10 p4009 N94-34632
National facilities study. Volume 2: Task group on aeronautical research and development facilities report
[NASA-TM-109855] 10 p4009 N94-34633
National facilities study. Volume 3: Mission and requirements model report
[NASA-TM-109857] 10 p4009 N94-34635
National facilities study. Volume 4: Space operations facilities task group
[NASA-TM-109858] 10 p4010 N94-34636
National facilities study. Volume 5: Space research and development facilities task group
[NASA-TM-109859] 10 p4010 N94-34637
Data acquisition systems
[DE94-009848] 11 p4345 N94-35817
A guide to research facilities at the National Renewable Energy Laboratory
[DE94-006857] 11 p4283 N94-36052
Environmental resource document for the Idaho National Engineering Laboratory, volume 1
[DE94-008522] 11 p4287 N94-36207
Environmental resource document for the Idaho National Engineering Laboratory, volume 2
[DE94-008523] 11 p4287 N94-36208
High Energy Physics Division of research activities
[DE93-019681] 12 p4521 N94-36694
Design and development of experimental facilities for short duration, low-gravity combustion and fire experiments
[NASA-CR-196107] 12 p4389 N94-36967
Engineering directorate technical facilities catalog
[NASA-TM-109895] 12 p4390 N94-37443

RESEARCH MANAGEMENT

Canada's longterm space plan and ISY activities 01 p0037 N94-10692
National Institute of Health Almanac, 1992
[PB93-183556] 01 p0303 N94-10828
Low-expansion ceramics initiative
[DE93-011860] 01 p0089 N94-11106
Quality assurance in basic research and R/D
[DE93-010825] 01 p0183 N94-11647
The Department of Clinical Investigation, reports control symbol MED-300(R-1)
[AD-A264969] 01 p0304 N94-11649
Selected data on academic science and engineering R and D expenditures: Fiscal Year 1991
[NSF-92-329] 02 p0819 N94-13982
The National Remote Sensing Program (NRSP-2 1991 - 2000): The 1992 annual plan of the Netherlands Remote Sensing Board
[BCRS-92-22] 02 p0700 N94-14544
Army Software Test and Evaluation Panel (STEP) software metrics initiatives report
[AD-A266889] 03 p1142 N94-14924
NASA information resources management handbook
[NHB-2410.1E] 03 p1230 N94-15941
Krupp technical reports no. 2, English edition, October 1992
[ETN-93-94631] 03 p0984 N94-16000
Research and development: Engine of innovation at Krupp 03 p0984 N94-16001
Mathematical Sciences Division 1992 programs
[AD-A268586] 03 p1140 N94-17623
Activities report of the Rutherford Appleton Laboratory
[ETN-93-94555] 04 p1631 N94-17968
A foundation for the 21st Century: A progressive framework for the National Science Foundation. Report of the National Science Board Commission on the future of the National Science Foundation
[NSB-92-196] 04 p1611 N94-19618
Neural network studies
[AD-A271593] 05 p1943 N94-20947
Satellite communications systems and technology. Volume 2: Site reports
[NASA-TM-109399] 06 p2293 N94-23628
Collaborating with our customers: NIST building and fire research laboratory
[PB94-110194] 06 p2272 N94-24955
Joint services electronics program
[AD-A274692] 07 p2783 N94-26449
Joint services electronics program
[AD-A274643] 07 p2785 N94-27027
Frontiers of science and measurement: Report on a seminar jointly organized by the National Physical Laboratory and the Institute of Physics
[PB94-124310] 07 p3009 N94-27131
NCVS, volume 5
[AD-A274975] 07 p2902 N94-27165
How to make good use of international research collaboration, with emphasis on the evolving situation in Europe
[PB94-119690] 07 p3101 N94-27323
Spin-off companies as agents of technology transfer: An empirical study of the spin-off companies of the Technical Research Centre of Finland
[PB94-132248] 08 p3537 N94-28405
Fundamental studies on the corrosion behavior of weldments in marine microbial environments
[AD-A275247] 08 p3203 N94-28900
Basic research in computer science
[AD-A275222] 08 p3405 N94-28916
Construction of visual representations and time-space organization of resources in astronomy
[ISBN-0-315-86694-2] 09 p3925 N94-31914
Advances in MOVPE compound semiconductor epitaxy manufacturing technology: From high throughput large area reactors to cluster tools
[DE94-006367] 09 p3901 N94-32104
Research and Technology Objectives and Plans Summary (RTOPS)
[NASA-TM-105441] 09 p3966 N94-32885
Aviation human factors research in US universities: Potential contributions to national needs
[NASA-TM-108814] 09 p3575 N94-32927
NASA historical data book. Volume 4: NASA resources 1969-1978
[NASA-SP-4012-VOL-4] 10 p4179 N94-33949
National facilities study. Volume 5: Space research and development facilities task group
[NASA-TM-109859] 10 p4010 N94-34637
The Federal Aviation Administration plan for research, engineering and development 11 p4376 N94-35262

RESEARCH PROJECTS

The EUREKA project portfolio in new materials 01 p0056 N94-10002
The Netherlands innovation oriented research programme on polymer composites and special polymers 1985-1993 01 p0065 N94-10067
Pakistan Space and Upper Atmosphere Research Commission 01 p0037 N94-10693
Low-expansion ceramics initiative
[DE93-011860] 01 p0089 N94-11106
Facts about the US Antarctic program
[NSF-92-134] 01 p0279 N94-12568
Earth system dynamics: The interrelation of atmospheric, ocean and solid earth dynamics
[NASA-CR-193487] 03 p1081 N94-17444
Research at the Notre Dame Radiation Laboratory
[DE93-018716] 04 p1566 N94-18165
Where is high-lift today? A review of past UK research programmes 04 p1305 N94-18416
The GARTEUR high lift research programme 04 p1307 N94-18430
Langley's 50th year
[NASA-TM-109365] 04 p1632 N94-18980
Report on the activities of Space Science Department, 1990 - mid 1992
[ESA-SP-1161] 04 p1633 N94-19404
Guide to programs, fiscal year 1993
[NSF-92-78] 04 p1633 N94-19620
Fiscal year 1993 scientific and technical reports, articles, papers, and presentations
[NASA-TM-108423] 06 p2590 N94-24079
GRYPHON: Air launched space booster
[NASA-CR-195497] 06 p2199 N94-25022
National Aeronautics and Space Administration (NASA)/American Society for Engineering Education (ASEE) Summer Faculty Fellowship Program, 1993, volume 2
[NASA-CR-188271-VOL-2] 06 p2636 N94-25367
FAA/NASA Joint University Program for Air Transportation Research, 1992-1993
[NASA-CP-3246] 07 p2641 N94-27284
University program management information system, FY 1993
[NASA-TM-109719] 07 p3100 N94-27413
NASA SBIR abstracts of 1992, phase 1 projects
[NASA-TM-109694] 07 p3094 N94-27772
Global concern on research cooperation for environment 07 p2872 N94-28275
Advanced gas turbine systems research
[DE94-005303] 08 p3297 N94-28485
US/Japan cooperation in high energy physics
[DE94-005376] 08 p3494 N94-28486
Summaries of FY 1993 geosciences research
[DE94-004710] 08 p3355 N94-28558
Relativistic heavy ion research
[DE94-004701] 08 p3484 N94-28576
Annual summary of basic research thermoacoustic heat transport, 1993
[AD-A275751] 08 p3230 N94-28644
The Norwegian seismic array (NORSAR), phase 3
[AD-A275440] 08 p3356 N94-28868
Annual report and summaries of FY 1993 activities: Division of Energy Biosciences
[DE94-001723] 08 p3386 N94-30607
Crystalline-silicon solar cell development sponsored by the US Department of Energy
[DE94-003783] 08 p3340 N94-30609
State of hadron collider physics
[DE94-005279] 09 p3863 N94-31147
Aerospace test facilities at NASA LERC Plumbrook
[NASA-TM-109755] 09 p3602 N94-31814
NASA HSR phase 1 low noise nozzle technology program overview 10 p3972 N94-33463
HSCT nozzle source noise programs at Pratt and Whitney 10 p3972 N94-33465
NASA Ames Fluid Mechanics Laboratory research briefs
[NASA-TM-108818] 10 p3983 N94-33997

Director's discretionary fund
[NASA-TM-103997] 11 p4376 N94-35370
United States Air Force Summer Research Program, 1993. Volume 6: Arnold Engineering Development Center, Frank J. Seiler Research Laboratory and Wilford Hall Medical Center
[AD-A278697] 12 p4551 N94-36982

RESEARCH VEHICLES
NT B-70 AIRCRAFT
NT FIREBEE 2 TARGET DRONE AIRCRAFT
NT QUESTOL AIRCRAFT
NT RESEARCH AIRCRAFT
NT ROTOR SYSTEMS RESEARCH AIRCRAFT
NT U-2 AIRCRAFT
NT UNDERWATER RESEARCH LABORATORIES
NT X-14 AIRCRAFT
NT X-15 AIRCRAFT
NT X-30 VEHICLE
NT X-31 AIRCRAFT
NT XV-5 AIRCRAFT
Development of a shuttle AUV for oceanographic measurement 01 p0217 N94-12692
Configuration development study of the OSU 1 hypersonic research vehicle
[NASA-CR-195522] 06 p2181 N94-24591
Design of a wheeled articulating land rover
[NASA-CR-195520] 06 p2365 N94-24806
Design of a flight controller for an unmanned research vehicle with control surface failures using quantitative feedback theory
[AD-A274049] 07 p2677 N94-25833
Multiple model adaptive estimation applied to the LAMBDA URV for failure detection and identification
[AD-A274078] 07 p3002 N94-25992
Prediction of leading-edge transition and relaminarization phenomena on a subsonic multi-element high-lift system 07 p2659 N94-27929
Benchmarking of the state-of-the-art in nondestructive testing/evaluation for applicability in the Composite Armored Vehicle (CAV) Advanced Technology Demonstrator (ATD) program, phase 1
[AD-A276660] 09 p3730 N94-32088
Airborne Trailblazer: Two decades with NASA Langley's 737 flying laboratory
[NASA-SP-4216] 09 p3566 N94-32793
Installed F/A-18 inlet flow calculations at 30 degrees angle-of-attack: A comparative study
[NASA-CR-195297] 09 p3573 N94-33119
An automatic planetary vehicle for exploring Mars 11 p4354 N94-35336
The reduction of takeoff ground roll by the application of a nose gear jump strut
[NASA-TM-108822] 11 p4198 N94-36380

RESERVOIRS
BOAST 2 for the IBM 3090 and RISC 6000
[DE93-000138] 02 p0638 N94-14351
Numerical modelling of an active direct nonpotable hot water heating system making use of the energy of solar radiation
[IFTR-38/1991] 03 p1093 N94-17070
High-resolution numerical methods for compressible multi-phase flow in hierarchical porous media
[DE94-000740] 05 p1799 N94-20351
Current situation in developing petroleum substituting energy (the United Kingdom)
[DE94-714897] 05 p1713 N94-22091
Near-surface seismic imaging
[PB94-119096] 06 p2404 N94-24647
Fiscal 1990 geothermal development promotion survey
[DE94-732333] 08 p3337 N94-28628
SNC meteorites and their implications for reservoirs of Martian volatiles 09 p3947 N94-33209

RESIDENTIAL AREAS
Remote sensing for urban planning 09 p3758 N94-32465

RESIDUAL GAS
Outgassing rate of Reemay Spunbonded Polyester and DuPont Double Aluminized Mylar
[DE93-040015] 05 p1699 N94-19973
Residual atmosphere in the FRECOPA experiment and degassing of materials 05 p1660 N94-21374
Hot hydrogen testing of metallic turbo pump materials
[NASA-CR-193880] 06 p2244 N94-24066
Residual Gas Analysis (RGA) and shear strength characteristics of a silver-filled epoxy and polyimide under long-term, high-temperature storage conditions
[DE94-010106] 11 p4244 N94-35705

RESIDUAL STRENGTH
Fatigue and residual strength characteristics of fiber metal laminates subjected to incidental damage
[LR-708] 02 p0674 N94-13803
The development of inspection and repair methods for the C-17 aft cargo door
[LR-704] 02 p0499 N94-13904
Low and high velocity impact response of thick hybrid composites 03 p0936 N94-16837
Residual strength predictions for fibre metal laminates: The R-curves approach
[LR-717] 04 p1344 N94-19666
Full-scale testing and analysis of curved aircraft fuselage panels
[AD-A275666] 08 p3145 N94-28657
Fatigue and residual strength behaviour of ARALL3 panels with bonded-on doublers
[AD-B181062] 11 p4279 N94-36226
A methodology to predict damage initiation, damage growth and residual strength in titanium matrix composites
[NASA-TM-109135] 12 p4405 N94-37320
Impact force as a scaling parameter 12 p4460 N94-37811

RESIDUAL STRESS
Extensions of some guidelines for the mechanical design of coaxial compression pin seals
[DE93-012385] 01 p0177 N94-10348
Fracture behavior of surface-modified ceramics
[DE93-013707] 01 p0088 N94-10710
Sensitivities of calculated residual stress to separation distances of two simultaneous events
[DE92-019571] 01 p0098 N94-10751
Computational simulation of hot composite structures
[NASA-TM-106200] 01 p0186 N94-10762
Analytical models for describing the mechanical behavior of fiber reinforced composites
[AD-A265906] 01 p0074 N94-12347
Measurement of residual strain in composites by means of time-of-flight neutron diffraction
[DE93-012939] 02 p0555 N94-13248
Residual contact restraints in cryogenics
[ETN-93-94375] 02 p0671 N94-13501
Thermal gradient-induced deflection of a thick-walled cylinder with bending residual stresses
[AD-A266347] 02 p0673 N94-13777
Hierarchical nonlinear behavior of hot composite structures
[NASA-TM-106229] 02 p0676 N94-14041
Optimal synthesis of hot composite laminates with interphase layers
[NASA-TM-106326] 02 p0557 N94-14042
Finite element analytical techniques for ceramic production in microgravity: A hypoelastic model 03 p0981 N94-16099
Evaluation of the interfacial mechanical properties in fiber-reinforced ceramic composites
[DE93-015494] 03 p0935 N94-16461
Thermal stress effects in intermetallic matrix composites
[NASA-CR-191191] 03 p1054 N94-16518
The processing and mechanical properties of high temperature/high performance composites. Book 5: Processing and miscellaneous properties
[AD-A266398] 03 p0935 N94-16529
Interfacial shear behavior and its influence on fiber damage in sapphire-reinforced gamma titanium aluminide composites
[AD-A267943] 03 p1060 N94-17043
Measurement and theory of the dependence of hardness on residual stress
[AD-A267553] 03 p1061 N94-17105
Evaluation of interfacial properties of fiber-reinforced ceramic composites using fiber push-in tests
[DE93-015427] 03 p0972 N94-17253
Aspects of high temperature damage in fiber reinforced titanium metal matrix composites
[AD-A267907] 03 p0941 N94-17379
Low dielectric constant insulators and gold metallization for GHz multi-chip modules, part 2
[AD-A268590] 03 p1176 N94-17605
Residual strain measurement on the production-grade class 4 flextensional transducer shell
[AD-A268828] 04 p1430 N94-18537
Fatigue resistant Ti3Al composites
[AD-A270305] 04 p1341 N94-18692
Analytical and experimental evaluation of joining silicon nitride to metal and silicon carbide to metal for advanced heat engine applications
[DE93-018128] 04 p1446 N94-19291
Ni-Al2O3 solid state binding: Elaboration, state of thermal constraints, mechanical behavior
[ECL-92-31] 04 p1366 N94-19436
Strengthening of NiAl matrix composites
[AD-A271491] 05 p1674 N94-20550
Benefits of thread rolling process to the stress corrosion cracking and fatigue resistance of high strength fasteners
[DE93-040438] 05 p1833 N94-22001
Analysis of thermal mechanical fatigue in titanium matrix composites 05 p1835 N94-22618
Control of the internal stresses in plane elasticity
[PB93-225514] 06 p2374 N94-23112
Analysis of local delaminations caused by angle ply matrix cracks
[NASA-TM-109052] 06 p2228 N94-24083
Dynamic localization and second-order subgrid-scale models in large eddy simulations of channel flow 06 p2329 N94-24149
Feasibility study of shot-peening modeling
[CTN-94-60926] 06 p2244 N94-24170
Birdstrike resistant crew enclosure program
[AD-A273700] 06 p2463 N94-25453
Study on film generation phenomena by particle deposition 07 p2728 N94-25575
The fracture behavior of a CVD crystalline Si3N4/amorphous Si3N4 composite
[DE94-002646] 07 p2750 N94-26124
Grain by grain study of the mechanisms of crack propagation during iodine SCC of Zry-4
[DE93-633765] 07 p2734 N94-26162
High intensity x ray instrumentation for residual strain measurements in composites and textured materials
[ISBN-0-315-85169-4] 07 p2842 N94-27278
Implementation of thermal residual stresses in the analysis of fiber bridged matrix crack growth in titanium matrix composites
[NASA-TM-109082] 07 p2711 N94-27658
Prediction of stress-strain response of SCS-6/Timetal-21S subjected to a hypersonic flight profile
[NASA-TM-109026] 08 p3177 N94-28823
Multiple Concentric Cylinder Model (MCCM) user's guide
[NASA-CR-195299] 08 p3183 N94-30125
Processing of novel nanoparticle dispersion strengthened ceramics for improved mechanical performance
[AD-A275965] 09 p3649 N94-31276
Inelastic deformation of metal matrix composites 09 p3618 N94-31285
Effect of vibratory stress relief during welding of thick stainless steel plate
[DE94-006557] 09 p3733 N94-31312
Feasibility study of cold expansion processes modelling
[DSIS-94-01186] 09 p3735 N94-31849
Mechanics of failure of high temperature metal matrix composites
[AD-A277397] 09 p3624 N94-32342
Modeling of residual stress mitigation in austenitic stainless steel pipe girth weldment
[DE94-007184] 09 p3738 N94-32639
Mapping of residual strains of a ceramic-to-metal joint using x ray diffraction
[DE94-007421] 10 p4069 N94-33691
Optimization of residual stresses in MMC's using compensating/compliant interfacial layers. Part 2: OPTCOMP user's guide
[NASA-CR-195337] 11 p4278 N94-35239
Testing of the fracture resistance of rails 11 p4279 N94-35353
Mitigation of harmful effects of welds in zirconium alloy components
[DE94-619033] 12 p4414 N94-36543
Micromechanical modeling of damage growth in titanium based metal-matrix composites 12 p4402 N94-36664
Material and design considerations for the carbon armored ITER divertor
[DE94-737854] 12 p4530 N94-37415
Residual stress and Raman spectra of laser deposited highly-tetrahedral-coordinated-amorphous-carbon films
[DE94-012067] 12 p4426 N94-37537
Residual stresses in a multi-pass weld in an austenitic stainless steel plate before and after thermal stress relief
[DE94-013278] 12 p4420 N94-37548

RESIDUES
Mineralogy of chondritic interplanetary dust particle impact residues from LDEF 01 p0080 N94-12045
Composition and modal frequencies of hypervelocity particles less than 1 millimeter in diameter in low-Earth orbit 01 p0429 N94-12063
Promotion of geothermal energy development in 1991
[DE93-799058] 02 p0701 N94-13215
Analysis of deposit precursors in jet fuels using Fourier transform infrared spectroscopy
[AD-A269035] 04 p1377 N94-18489
The use of post detonation analysis of stable isotope ratios to determine the type and production process of the explosive involved
[DE93-018497] 04 p1378 N94-19242
Bits and relative order from residues, space efficiently
[TR-464] 04 p1530 N94-19482
Low-latency digital frequency synthesizer using the residue number system 05 p1759 N94-21121
Chemical characterization of some aerobic liquids in CELSS 06 p2422 N94-23241

Analysis of impactor residues in tray clamps from the Long Duration Exposure Facility. Part 2: Clamps from Bay B of the satellite
[NASA-TM-104784] 06 p2386 N94-24095
Interferometric JFTOT tube deposit measuring device
[AD-D016295] 12 p4430 N94-37768

RESILIENCE
Filamentation, current profiles and transport in a tokamak
[DE93-016768] 04 p1584 N94-17948

RESIN BONDING
Polymer infiltration studies
[NASA-CR-194521] 02 p0582 N94-14539

RESIN MATRIX COMPOSITES
NT CARBON-PHENOLIC COMPOSITES
NT GRAPHITE-EPOXY COMPOSITES
Deformation mechanisms of continuous fibre-reinforced thermoplastic composites during manufacturing: A probabilistic approach 01 p0060 N94-10030
Heat analysis of thermoplastic components during the initial stages of manufacturing: A probabilistic approach 01 p0060 N94-10031
Application of advanced thermoplastics 01 p0060 N94-10033
Low cost thermoplastic composites for structural applications: Design concepts using new materials and processes 01 p0060 N94-10034
Tape winding of thermoplastic composites 01 p0060 N94-10035
Silicon-based elementary particle tracking system: Materials science and mechanical engineering design
[DE93-012630] 01 p0065 N94-10740
Dry in-line thermoplastic matrix impregnation, phase 1
[AD-A265016] 01 p0067 N94-11221
An analysis of fiber-matrix interface failure stresses for a range of ply stress states
[NASA-TM-108999] 01 p0067 N94-11276
Construction, testing, and representation of resin and fiber reinforced materials 03 p0931 N94-15255
Polymer Infiltration Studies
[NASA-CR-194494] 03 p0932 N94-15275
Analysis of pultrusion processing for long fiber reinforced thermoplastic composite system
[NASA-CR-194504] 04 p1339 N94-17766
A study of graphite peek composite with central elliptical holes under tension
[AD-A273779] 07 p2705 N94-25863
Thermoplastic or thermosetting composites in aircrafts
[PB94-123809] 07 p2710 N94-27253
Polymer infiltration studies
[NASA-CR-195729] 08 p3213 N94-28748
On the dynamic mechanical behavior of 3-D integrated fabric reinforced composites
[AD-A275424] 08 p3177 N94-28865
Low pressure process for continuous fiber reinforced polyamic acid resin matrix composite laminates
[NASA-CASE-LAR-14954-1] 10 p4020 N94-35075
Processing and properties of high temperature metal/fiber-reinforced-thermoplastic laminates
[AD-A278791] 11 p4232 N94-35654
Structural composite construction materials manufactured from municipal solid waste
[AD-A280635] 12 p4403 N94-36730

RESIN TRANSFER MOLDING
Design and manufacturing of CFRP rings by RTM 01 p0059 N94-10025
Resin transfer molding of textile composites
[NASA-CR-191505] 02 p0554 N94-12833
An overview of the NASA textile composites program 03 p0937 N94-16846
Textile composite processing science 03 p0938 N94-16856
Mechanical properties and impact damage resistance of composites fabricated by low cost, vacuum assisted, resin transfer molding
[AD-A270361] 04 p1342 N94-18702
Composites and textile reinforcement
[VTT-TIED-1424] 06 p2231 N94-25420
Development of stitched/RTM composite primary structures 09 p3628 N94-33127
Resin transfer molding for advanced composite primary wing and fuselage structures 09 p3628 N94-33128
Test and analysis results for composite transport fuselage and wing structures 09 p3628 N94-33129
Composite fuselage crown panel manufacturing technology 09 p3629 N94-33133
Advanced textile applications for primary aircraft structures 09 p3629 N94-33135
Comparison of resin film infusion, resin transfer molding, and consolidation of textile preforms for primary aircraft structure 09 p3630 N94-33136

RESINS
NT ACRYLIC RESINS
NT ADDITION RESINS
NT EPOXY RESINS
NT ION EXCHANGE RESINS
NT KEVLAR (TRADEMARK)
NT NYLON (TRADEMARK)
NT PEEK
NT PHENOLIC RESINS
NT POLYAMIDE RESINS
NT POLYESTER RESINS
NT POLYETHER RESINS
NT POLYIMIDE RESINS
NT POLYMETHYL METHACRYLATE
NT POLYURETHANE RESINS
NT THERMOPLASTIC FILMS
NT THERMOPLASTIC RESINS
NT THERMOSETTING RESINS
NT VINYL COPOLYMERS
Polymer infiltration studies
[NASA-CR-194521] 02 p0582 N94-14539
Construction, testing, and representation of resin and fiber reinforced materials 03 p0931 N94-15255
Cyanoresin, cyanoresin/celluiose triacetate blends for thin film, dielectric capacitors
[NASA-CASE-NPO-18913-1-CU] 03 p0966 N94-15930
Column chromatographic separation of Y(3+) from Sr(2+) by polymeric ionizable crown ether resins
[DE94-000935] 05 p1683 N94-22021
Curing phthalonitrile resins with acid and amine
[AD-D016021] 06 p2258 N94-24721
Chemically modified polymeric resins for separation of cations, organic acids, and small polar molecules by high performance liquid chromatography
[DE94-005548] 08 p3211 N94-28516
Electroset Technology: On the forefront of manufacturing
[AD-A275166] 08 p3263 N94-29045
Development of stitched/RTM composite primary structures 09 p3628 N94-33127
Third European Technical Symposium on Polyimides and High Performance Polymers: STEPI 3
[PB94-148491] 11 p4246 N94-36177
Fluorinated resins with low dielectric constant
[AD-D016303] 12 p4427 N94-37773

RESISTANCE
Photogenerated base in polymer imaging. Synthesis and photopatterning of poly(2-cyano-2-(p-vinylphenyl) butanoic acid)
[AD-A265288] 01 p0095 N94-12585

RESISTANCE COEFFICIENTS
U RESISTANCE

RESISTANCE HEATING
Crystal growth in the Zone Melting Facility (ZMF) 01 p0119 N94-10213
Ohmic heating of composite candidate graphite-fiber/coating combinations
[NASA-TM-4491] 02 p0554 N94-12871
Instability heating of the HDZP
[DE93-012641] 02 p0798 N94-13513
Heating of lubricant with an electric resistance heater
[VTT-TIED-1359] 03 p0974 N94-17547
A spheromak ignition experiment reusing Mirror Fusion Test Facility (MFTF) equipment
[DE94-001856] 05 p2034 N94-22050
Modelling and control of plasma position in the STOR-M tokamak
[ISBN-0-315-58891-8] 07 p3049 N94-27949
Solid-state resistance upset welding: A process with unique advantages for advanced materials
[DE94-005941] 09 p3723 N94-31524
Time-resolved analytical methods for liquid/solid interfaces
[DE94-008352] 09 p3637 N94-32826
Scaling laws for TEXT plasma profiles
[DE94-010832] 11 p4338 N94-36200

RESISTIVITY
U ELECTRICAL RESISTIVITY

RESISTOJET ENGINES
Strategy for the reduction of total integrated fluid logistics to the Space Station Freedom
[NASA-TM-107744] 03 p1138 N94-17452
Embodiment design for a multipropellant resistojet
[NASA-CR-195505] 06 p2221 N94-24834
Design of a resistojet for Space Station Freedom
[NASA-CR-195506] 06 p2221 N94-24979

RESISTOJETS
U RESISTOJET ENGINES

RESISTORS
NT THERMISTORS
Stray insensitive switched capacitor composite operational amplifiers
[AD-A267412] 03 p1012 N94-16976
Models for interpreting interstrand resistance measurements in Rutherford cables
[DE94-010844] 11 p4259 N94-36194

RESOLUTION
NT ANGULAR RESOLUTION
NT HIGH RESOLUTION
NT IMAGE RESOLUTION
NT RADAR RESOLUTION
NT RADIOMETRIC RESOLUTION
NT SPATIAL RESOLUTION
NT SPECTRAL RESOLUTION
NT TEMPORAL RESOLUTION
A guide to resolving disputes over contractor delay entitlements
[AD-A272022] 05 p2039 N94-21444
Kinematic functions for redundancy resolution using configuration control
[NASA-CASE-NPO-18608-1-CU] 08 p3436 N94-29504
Method for ambiguity resolution in range-Doppler measurements
[NASA-CASE-GSC-13542-1] 08 p3252 N94-29739
Measurement of scanning electron microscope resolution
[DE94-012661] 12 p4525 N94-37374

RESOLVERS
Multi-speed multi-phase resolver converter
[NASA-CASE-MFS-28855-1] 08 p3264 N94-29372

RESOLVING POWER
U RESOLUTION

RESONANCE
NT BARYON RESONANCE
NT CYCLOTRON RESONANCE
NT ELECTRON PARAMAGNETIC RESONANCE
NT FERROMAGNETIC RESONANCE
NT MAGNETIC RESONANCE
NT MAGNETOSONIC RESONANCE
NT MESON RESONANCE
NT MICROWAVE RESONANCE
NT NUCLEAR MAGNETIC RESONANCE
NT NUCLEAR QUADRUPOLE RESONANCE
NT OPTICAL RESONANCE
NT ORBITAL RESONANCES (CELESTIAL MECHANICS)
NT PLASMA RESONANCE
NT RESONANT VIBRATION
NT SPIN RESONANCE
Progress in zirconium resonance ionization spectroscopy
[DE93-011881] 01 p0076 N94-11075
The IR properties of ringed galaxies and the IRAS database
[NASA-CR-194286] 01 p0426 N94-11590
Nonlinear resonance: Noise-assisted information processing in physical and neurophysiological systems
[AD-A265161] 01 p0313 N94-11890
Stability of subharmonics and escape phenomena in the twin-well potential duffing system 02 p0775 N94-13235
Resonances in the Sigma NN system
[DE93-014353] 02 p0785 N94-14144
Measuring parity violation using the neutron capture reaction
[DE93-016629] 02 p0786 N94-14514
Magnetic effects in anomalous dispersion
[DE93-014291] 03 p1175 N94-15978
Orbital evolution of dust from comet Schwassmann-Wachmann 1: A case of one-to-one resonance trapping 03 p1242 N94-16270
Processing of resonance parameter covariance files
[DE93-015506] 03 p1231 N94-16874
An automated system for ultrasound measurements of liquids by the resonance (Eggers) method
[IFTR-17/1992] 03 p1178 N94-17087
Metal Film Surface Plasmon Resonance (MFSPR) fibre couplers
[AD-A268871] 04 p1579 N94-18635
Resonance Raman and photophysical studies of transition metal complexes in solution and entrapped in zeolites
[DE93-019892] 04 p1363 N94-19019
Contribution to the modelling and the identification of nonlinear mechanical systems
[ECL-92-32] 04 p1529 N94-19409
Rotational spectrum of a dark state in 2-fluoroethanol using microwave/radiofrequency-infrared multiple resonance
[AD-A272101] 05 p1817 N94-20583
On the theory of morphology-dependent resonances: Shape resonances, width formulas, and graphical representations
[AD-A272279] 05 p2037 N94-20945
Three-wave resonant interaction in a thin layer
[AD-A272331] 05 p1994 N94-21039
Search for excited quarks in p(-p) collisions at the square root of s = 1.8 TeV
[DE93-019910] 05 p1975 N94-21840
Low p(sub T) phenomena observed in high energy nuclear collisions
[DE94-000825] 05 p1982 N94-21849
Analysis and experiments of a whistler-wave plasma thruster
[DE94-001533] 06 p2209 N94-23012

An active antenna for ELF magnetic fields
06 p2303 N94-25192
Bottom quark production at the Z resonance
[ISBN-9-09-006217-3] 06 p2538 N94-25255
Stochastic resonance in a periodic potential system under a constant force
[DE93-616817] 07 p3008 N94-25831
Kinetic resonance damping rate of the toroidal ion temperature gradient mode
[DE94-003511] 07 p3041 N94-25923
Meson X(1814) as a candidate for a hybrid state
[DE93-634447] 07 p3017 N94-26045
Signatures for hybrids
[DE94-004244] 07 p3020 N94-26574
Pion-nucleus interactions and the STAR experiment at RHIC
[DE94-000658] 07 p3021 N94-26586
Bifurcation sequences at 1:4 resonance: An inventory
[PB94-125408] 07 p2997 N94-27028
Geometrical resonances in the nyquist noise spectrum for ballistic conductors
[DE94-603668] 07 p3027 N94-27631
A measurement of the tau polarization at the resonance with the DELPHI detector at LEP
[DE94-005557] 08 p3482 N94-28520
Overlap of metal clusters and nuclear structure physics
[DE94-606387] 08 p3517 N94-30183
Multiple weather regimes and baroclinically forced spherical resonance
[DM-65] 08 p3376 N94-30966
Resonance capture in unbalanced dual-spin spacecraft
[AD-A278501] 10 p4015 N94-34292
On the effects of transforming the vibrational spectra of molecular systems under microwave radiation
[DE94-617057] 11 p4329 N94-36310
Notes on possible S-wave resonances in relativistic two-particle systems
[DE94-616889] 11 p4329 N94-36392
Older muons are wiser: Using time information in (mu)LCR spectroscopy
[DE93-018556] 12 p4511 N94-36457
Determination of the upsilon(1s) leptonic width
[DE94-618534] 12 p4516 N94-37096
Resonance photoionization of the excited helium
[DE94-618733] 12 p4517 N94-37173
An overview of the current status of resonance theory in reactor physics applications
[DE94-010465] 12 p4521 N94-37194

RESONANCE FLUORESCENCE
Squeezing in phase-conjugated resonance fluorescence 01 p0376 N94-10576
Activity report of Synchrotron Radiation Laboratory 1992
[JTN-94-80600] 08 p3495 N94-29596
Particle-In-Cell (PIC) code simulation results and comparison with theory scaling laws for photoelectron-generated radiation
[DE94-006132] 09 p3695 N94-32662

RESONANCE LINES
Electron impact excitation of copper atoms
[DE93-017995] 04 p1363 N94-18939
Semiempirical studies of atomic structure
[DE94-001588] 06 p2531 N94-22937
The resonance lines of MG2 as diagnostics of the upper solar chromosphere
[NASA-CR-195084] 06 p2627 N94-24300
The investigation of electron-ion radiative and dielectronic recombination in high-temperature plasmas
[DE94-005150] 08 p3509 N94-30755

RESONANCE PROBES
WHISPER: A sounder and high-frequency wave analyser experiment 04 p1328 N94-19626

RESONANCE RADIATION
U RESONANCE FLUORESCENCE

RESONANCE SCATTERING
Linear antenna of an arbitrary orientation and position in cylindric screen
[DE93-621353] 01 p0134 N94-11035
Resonant x ray Raman scattering from atoms and molecules
[DE93-015158] 02 p0784 N94-13896
Suppression of charge scattering in Moessbauer experiments using synchrotron radiation
[DE93-015406] 03 p1212 N94-16887
On the theory of morphology-dependent resonances: Shape resonances, width formulas, and graphical representations
[AD-A272279] 05 p2037 N94-20945

RESONANT CAVITIES
U CAVITY RESONATORS

RESONANT FREQUENCIES
Laboratory study on the natural modes of a rotating two-phase fluid system subject to axial excitation
01 p0106 N94-10106
Boundary element method for eigenvalue problems of thin plates
[ITN-93-85199] 01 p0343 N94-10392
On the stability of stationary regimes in a distributed autovibration system with external feedback
[DE93-620979] 01 p0141 N94-10543
Quantum non demolition measurement of cyclotron excitations in a Penning trap 01 p0376 N94-10578
Magnetic Earth Ionosphere Resonant Frequencies (MEIRF) project
[NASA-CR-193182] 01 p0276 N94-11355
The laser second threshold: Its exact analytical dependence on detuning and relaxation rates
[DE93-619706] 01 p0175 N94-11633
Nonlinear effects in ferrite tuned cavities
[DE93-014136] 01 p0374 N94-12785
Predicting the vibrations of a spinning inflated membrane
[DE93-010690] 02 p0676 N94-14456
Applications of computer algebra to distributed parameter systems 02 p0677 N94-14623
Parametric study of a finite element model of the Sidewinder missile
[AD-A267245] 03 p0865 N94-14976
Resonant frequencies of irregularly shaped microstrip antennas using method of moments
[NASA-TP-3386] 03 p0989 N94-15767
Digital reverberation time measurement system
[AD-D015892] 03 p1177 N94-16919
Wide angle, single screen, gridded square-loop frequency selective surface for diplexing two closely separated frequency bands
[NASA-CASE-NPO-18664-1-CU]
03 p1237 N94-17438
Predicted structural response of the lightweight-interceptor technology demonstration vehicle
[DE93-014676] 04 p1333 N94-17782
The Lever oscillator for use in high resistance resonator applications
[DE93-017652] 04 p1404 N94-18827
Free fall liquid column dynamics in a droptower
[LRT-WE-9-FB-6-1992] 04 p1379 N94-19491
Transient response of a viscous and anchored liquid bridge to an axial pulse
[LRT-WE-9-FB-7-1992] 04 p1379 N94-19492
Measuring liquid properties with smooth and textured-surface resonators
[DE93-019433] 05 p1749 N94-20054
Coplanar waveguide radial line stub
05 p1733 N94-20503
Probabilistic assessment of composite structures
[NASA-TM-106368] 05 p1832 N94-21757
A vibration model for centrifugal contactors
[DE93-040645] 05 p1833 N94-21927
Improvement of the performance of IMPATT oscillators through appropriate modification of resonant-cap activity
05 p1782 N94-22179
Study of TE(1-delta) mode in open dielectric resonators by a finite difference time domain method
05 p1747 N94-22253
Aperture coupling of circular cylindrical dielectric resonator antenna
[ISBN-0-315-60632-0] 05 p1743 N94-22409
Liquid oscillations in a spherical system with sliding edges boundary by two conical solid surfaces in zero-gravity
[LRT-WE-9-FB-5-1992] 06 p2318 N94-23197
Vibrations of variable cross section Timoshenko beams 06 p2160 N94-24279
The H(sub infinity) optimal controller design and reduction for the inertial hold mode of the attitude control system of the XTE spacecraft
[NASA-CR-195137] 06 p2366 N94-24846
Magnetic Earth Ionosphere Resonant Frequencies
[NASA-CR-195131] 06 p2303 N94-25191
An active antenna for ELF magnetic fields
06 p2303 N94-25192
Characterization of acoustic effects on flame structures by beam deflection technique
[DE94-003240] 07 p2714 N94-26122
Parameter estimation by genetic algorithms
[DE94-002924] 07 p2961 N94-26146
Shake test results of the MDHC test stand in the 40-by 80-foot wind tunnel
[NASA-TM-108801] 07 p2641 N94-26596
Practical design of resonant cavity for a RF free electron laser
[AD-A274306] 07 p2819 N94-26941
Extraction of modal parameters from an operating HAWT using the Natural Excitation Technique (NExT)
[DE94-001831] 07 p2859 N94-27004
Influence of impeller shroud forces on turbopump rotor dynamics 07 p2796 N94-27378
Effective conductivity of wire mesh reflectors for space deployable antenna systems
[NASA-CR-191605] 07 p2788 N94-27770
Parameter estimation of linear systems from frequency response measurements (computer program)
[ESDU-93016] 07 p2976 N94-28137
Acoustic bubble sizing, using active and passive techniques to compare ambient and entrained populations
[ISVR-TR-229] 07 p2807 N94-28172
Rotor instability induced by dead band clearance in bearing supports 08 p3312 N94-30809
A series resonant converter in half bridge circuits with combined serial and parallel charge coupling and several output circuits
[ETN-94-95739] 09 p3687 N94-31373
Considering ties elasticities in high frequency rail dynamics
[ILR-MITT-281(1993)] 09 p3733 N94-31375
Vibration localization in dual-span axially moving elastic systems 09 p3736 N94-31964
Mass-loaded coating for reducing the resonant frequency of a ceramic disc
[AD-D016095] 09 p3660 N94-32739
Applying transfer matrix method to the estimation of the modal characteristics of the NASA Mini-Mass Truss
11 p4218 N94-35870
Rotor dynamic behaviour of a high-speed oil-free motor compressor with a rigid coupling supported on four radial magnetic bearings 11 p4224 N94-35911
Laminated thin shell structures subjected to free vibration in a hygrothermal environment
[NASA-TM-106600] 12 p4456 N94-37456
Magnetic Earth Ionosphere Resonant Frequencies (NASA-MEIRF Project)
[NASA-CR-196303] 12 p4435 N94-37461

RESONANT TUNNELING
Effect of effective mass differences on the tunneling current-voltage behaviour of a resonant diode in the presence of space charge build-up
[DE93-613817] 01 p0142 N94-10799
Metal Film Surface Plasmon Resonance (MFSPR) fibre couplers
[AD-A268871] 04 p1579 N94-18635
Theoretical and experimental studies of quantum wells
[AD-A271180] 04 p1606 N94-19741
Investigation of quantum effects in heterostructures
[AD-A270938] 05 p2011 N94-19817
Interinjection-locked quasioptical power combiners and phased arrays
[AD-A271178] 05 p2015 N94-20214
Transport in microstructures in the microwave and millimeter-wave regime
[AD-A271875] 05 p2017 N94-20470
Quantum tunneling transport of electrons in double-barrier heterostructures: Theory and modeling
[ETN-94-95332] 06 p2565 N94-25059
Strong overlap and transmission in triple barrier resonant structures
[DE94-608103] 08 p3516 N94-30067

RESONANT VIBRATION
Adiabatic and non adiabatic effects in Free Electron Laser (FEL) non linear interactions
[ITN-93-85224] 02 p0659 N94-14547
Time dependent identification of nonlinear structures
[ECL-92-64] 04 p1457 N94-19403
Blade and hub loads of ballistically damaged helicopter rotors
[AD-A270663] 04 p1319 N94-19781
On the theory of morphology-dependent resonances: Shape resonances, width formulas, and graphical representations
[AD-A272279] 05 p2037 N94-20945
A review of vibration problems in power station boiler feed pumps 10 p4064 N94-34190

RESONATORS
NT CAVITY RESONATORS
NT HELMHOLTZ RESONATORS
NT MULTIMODE RESONATORS
NT OPTICAL RESONATORS
NT SUPERCONDUCTING CAVITY RESONATORS
Quantum processes in resonators with moving walls
01 p0380 N94-10612
Dielectric resonator
[US-PATENT-4,580,116] 01 p0141 N94-10668
Conversion of the four-strap array in D3-D to a tunable traveling wave antenna
[DE93-012085] 01 p0137 N94-11453
Measurement electronics of industrial microwave resonator sensors
[TKK-S-RAD-S194] 02 p0625 N94-14096
H2S data reduction
[NASA-CR-193389] 02 p0617 N94-14743
Stress sensitivity of dielectric resonators
[AD-A266767] 03 p1009 N94-15825
Aberration correction of unstable resonators
[NASA-CASE-NPO-18791-1-CU]
03 p1034 N94-15987

Quartz crystal resonators and oscillators for frequency control and timing applications: A tutorial, revision 6.1
[AD-A268205] 03 p1216 N94-17480
Simulation of quartz resonators
04 p1426 N94-18021
The Lever oscillator for use in high resistance resonator applications
[DE93-017652] 04 p1404 N94-18827
Measuring liquid properties with smooth and textured-surface resonators
[DE93-019433] 05 p1749 N94-20054
TlCaBaCuO high Tc superconducting microstrip ring resonators designed for 12 GHz
05 p1735 N94-20516
Study of TE(1-delta) mode in open dielectric resonators by a finite difference time domain method
05 p1747 N94-22253
Spatiotemporal behavior and nonlinear dynamics in a phase conjugate resonator
[NASA-CR-4567] 06 p2543 N94-23529
Internally folded scalable laser
[AD-D015978] 06 p2350 N94-25216
Effective conductivity of wire mesh reflectors for space deployable antenna systems
[NASA-CR-191605] 07 p2788 N94-27770
Fundamentals studies of radial wave thermoacoustic engines
[AD-A280534] 12 p4431 N94-37090

RESOURCE ALLOCATION
ACARA user's manual
[NASA-TM-106277] 01 p0183 N94-11167
PC4CAST: A tool for DSN load forecasting and capacity planning 02 p0610 N94-14384
Applicability of computer spreadsheet simulation for solving resource allocation problems
[AD-A267436] 03 p1152 N94-17027
Satellite communications systems and technology. Executive summary
[NASA-TM-109346] 03 p1006 N94-17661
An annealing approach to multi-facility location problems in euclidean spaces
[REPT-93-022] 04 p1547 N94-17928
Annealing algorithms for multiresource absolute location problems on graph
[REPT-93-028] 04 p1520 N94-18145
PRACTICAL: Planning and resource allocation in C2-domains with time critical algorithms
[FEL-93-B029] 04 p1544 N94-19458
Optimal repairman assignment in two maintenance models which are equivalent to routing models with early decisions
[CWI-BS-R9301] 05 p1930 N94-21234
Generating and evaluating alternate schedules
05 p1933 N94-21336
Computer-aided design system for objects location and reservoir with dispersed resource evolution investigation
05 p1923 N94-22064
Resource allocation planning with international components 06 p2520 N94-23963
NEMO: Advanced energy systems and technologies
[DE94-721996] 09 p3760 N94-31767
Construction of visual representations and time-space organization of resources in astronomy
[ISBN-0-315-86694-2] 09 p3925 N94-31914
Task allocation and scheduling for high level synthesis
[AD-A277570] 10 p4110 N94-33395

RESOURCES
NT AQUIFERS
NT COAL
NT CRUDE OIL
NT EARTH RESOURCES
NT EXTRATERRESTRIAL RESOURCES
NT FORESTS
NT FOSSIL FUELS
NT GEOTHERMAL RESOURCES
NT GEYSERS
NT GLACIERS
NT ICEBERGS
NT LAND ICE
NT LUNAR RESOURCES
NT MARINE RESOURCES
NT NATURAL GAS
NT OIL FIELDS
NT PEAT
NT RAIN FORESTS
NT SPRINGS (WATER)
NT UNDERWATER RESOURCES
NT WATER RESOURCES

RESOURCES MANAGEMENT
NT FOREST MANAGEMENT
NT LAND MANAGEMENT
NT REFORESTATION
Current status of space activities in Asia Pacific region
01 p0035 N94-10677
Summary of implementation and demonstration projects in bays and estuaries
[PB93-194637] 01 p0265 N94-10846
Information resources management long-range plan, FY1994
[DE93-013898] 01 p0420 N94-11588
Data management strategy for the Tampa Bay National Estuary Program: Recommendations and implementation plan
[PB93-191633] 01 p0267 N94-11864
The use of remote sensing data for coastal zone management and environment in Indonesia
01 p0196 N94-11927
The requirement for global training programmes to meet the new remote sensing technology
01 p0196 N94-11929
Integrating the services' imagery architectures
[AD-A265487] 01 p0171 N94-12335
Quality assurance for environmental chemistry: 1991, volume 2
[DE93-011792] 01 p0272 N94-12780
Hot Dry Rock energy
[DE93-014452] 02 p0702 N94-13403
Quality assurance for environmental chemistry, 1991, volume 1
[DE93-011791] 02 p0709 N94-14020
An evaluation of ZIM and entity-relational models in managing databases for decision support systems
[ERB-1034] 02 p0824 N94-14202
Sequestering carbon dioxide in industrial polymers: Building materials for the 21st century
[DE93-016087] 02 p0580 N94-14297
Fourteenth National Industrial Energy Technology Conference: Proceedings
[DE93-016698] 02 p0710 N94-14516
Pattern and Process in Landscape Ecology: Eighth Annual US Landscape Ecology Symposium
[DE93-014032] 02 p0711 N94-14859
Applicability of computer spreadsheet simulation for solving resource allocation problems
[AD-A267436] 03 p1152 N94-17027
Trends in Information Management at Department of Energy Headquarters
[DE93-017197] 04 p1615 N94-18496
The ecological and environmental impacts of manmade marshes
[AD-A269213] 04 p1475 N94-18885
Integrated measurement of crew resource management and technical flying skills
[AD-A270512] 04 p1510 N94-19677
Planning: Management of predictability and uncertainty and keeping abreast of developments
06 p2520 N94-23967
Mapping Tomorrow's Resources: A symposium on the uses of remote sensing, Geographic Information Systems (GIS), and Global Positioning Systems (GPS) for natural resources management 06 p2387 N94-24357
A biological survey for the nation
[LC-93-85920] 06 p2421 N94-24704
The HEC NexGen software development project
[AD-A273512] 06 p2460 N94-24822
Investigating pyrolysis/incineration as a method of resource recovery from solid waste
06 p2444 N94-25375
Environmental benefits of different types of heat pumps, available and expected
[DE94-002440] 07 p2866 N94-26123
Coordinated scheduling for dynamic real-time systems
[NASA-CR-195231] 07 p3093 N94-26206
ADP Analysis project for the Human Resources Management Division 07 p2978 N94-27927
HDGEC activity in Asia Pacific region
07 p2874 N94-28286
On United States-Japan Conference on Development and Utilization of Natural Resources: Report of the 14th Joint Meeting of U. S. and Japan Marine Mining Panel
08 p3188 N94-28683
Remote sensing and global management
08 p3328 N94-28937
Remote sensing and the Earth
08 p3329 N94-29218
Future expectation of remote sensing technology
08 p3332 N94-29231
Research report on the potential of ocean development suitable for area characteristics
[JTN-94-80587] 08 p3377 N94-29595
Techniques for increasing the robustness of iterative algorithms for multi-resources location problems
[REPT-93-037] 09 p3809 N94-31188
Common property resources and low-level flying in Labrador: Flight, fight or fancy?
[ISBN-0-315-87318-3] 09 p3924 N94-31732
Food security in the context of global environmental change
[DE94-007481] 09 p3768 N94-32812
EOCAP: Commercial Earth observations program
[NASA-TM-109798] 10 p4075 N94-33748

RESPIRATION
NT HIGH ALTITUDE BREATHING
NT PRESSURE BREATHING
Toxicity study of dimethylethoxysilane (DMSES), the waterproofing agent for the Orbiter heat protective system 01 p0318 N94-11554
Validation of respiratory inductive plethysmography for measuring exercise tidal volumes
[AD-A266883] 03 p1119 N94-14923
Interaction between endogenous opioid and Cholecystokinin (CCK) in modulating respiratory responses induced by thin-fiber muscular afferents
07 p2906 N94-27502
Effects of combined breathing impediments on diver's respiratory performance
[AD-A277437] 09 p3805 N94-33084
Characterization and utilization of opiate-like hibernation factors
[AD-A278136] 09 p3794 N94-33098

RESPIRATORS
Respiratory Protection Program medical clearance for respirator use 03 p1127 N94-16642
Portable ventilatory resuscitation systems
[AD-A274984] 08 p3401 N94-29093

RESPIRATORY DISEASES
NT ASTHMA
NT EMPHYSEMA
NT TUBERCULOSIS
Allowable exposure limits for carbon dioxide during extravehicular activity
[NASA-TM-103832] 01 p0315 N94-11375
Respiratory Protection Program medical clearance for respirator use 03 p1127 N94-16642

RESPIRATORY PHYSIOLOGY
Validation of respiratory inductive plethysmography for measuring exercise tidal volumes
[AD-A266883] 03 p1119 N94-14923

RESPIRATORY RATE
Evaluation of physiological and psychological impairment of human performance in cold stressed subjects
[AD-A268637] 04 p1506 N94-18632
Interaction between endogenous opioid and Cholecystokinin (CCK) in modulating respiratory responses induced by thin-fiber muscular afferents
07 p2906 N94-27502
Estimation of the net production of moss community at Langhovde, East Antarctica 08 p3358 N94-29081

RESPIRATORY REFLEXES
NT COUGH

RESPIRATORY SYSTEM
NT ALVEOLI
NT BRONCHI
NT LARYNX
NT LUNGS
Respiratory Protection Program medical clearance for respirator use 03 p1127 N94-16642
Chronic obstructive pulmonary disease
06 p2425 N94-23324
Aeromedical issues related to positive pressure breathing for +Gz protection
[AD-A274717] 07 p2910 N94-26435
Blast overpressure studies with animals and man
[AD-A275038] 08 p3391 N94-29150

RESPIROMETERS
Validation of respiratory inductive plethysmography for measuring exercise tidal volumes
[AD-A266883] 03 p1119 N94-14923

RESPONDERS
U TRANSPONDERS

RESPONSE TIME (COMPUTERS)
Analysis and effects of the number of nests of DO loops during vector supercomputing
[NAL-TR-1146] 02 p0748 N94-13453
A design methodology for portable software on parallel computers
[NASA-CR-194181] 02 p0752 N94-14139
Conception and analysis of numerical parallel algorithms: Realization on the Connection Machine
[ETN-93-95005] 04 p1531 N94-19517
A conceptual database design and performance analysis of the MILSATCOM requirements database
[AD-A272672] 05 p1658 N94-21217
Query optimization strategies for browsing sessions
[CWI-CS-R9268] 07 p3100 N94-27394

RESPONSES
NT DYNAMIC RESPONSE
NT HEMODYNAMIC RESPONSES
NT MODAL RESPONSE
NT PHYSIOLOGICAL RESPONSES
NT TRANSIENT RESPONSE

REST
NT BED REST

Thermoregulatory effects of caffeine ingestion during rest and exercise in men
[NASA-TM-108783] 07 p2901 N94-26210

RESTARTABLE ROCKET ENGINES
Advanced transportation system studies technical area 3: Alternate propulsion system concepts. SSME upper stage use
[NASA-CR-193865] 03 p0927 N94-17098

RESTORATION
Summary of implementation and demonstration projects in bays and estuaries
[PB93-194637] 01 p0265 N94-10846
Integrated, flexible, and rapid geophysical surveying
[DE93-009989] 02 p0712 N94-12906
Restoring Miss Liberty --- inorganic coatings
[NASA-TM-109605] 03 p0963 N94-15313
Computing and Information Sciences
[DE93-017149] 03 p1151 N94-16902
Restoration of an 18th century English clock
04 p1427 N94-18026
Environmental restoration and waste management five-year plan, fiscal years 1994-1998. Volume 3: Public concerns
[DOE/S-00097P-VOL-3] 04 p1475 N94-18835
Fiber optic Raman spectrograph for in situ environmental monitoring
[DE93-019466] 04 p1478 N94-19305
Restoration of HST images with missing data
05 p2057 N94-22439
HST image restoration: A comparison of pre- and post-servicing mission results 05 p1925 N94-22478
First MEM task IRMEO in IRAF
05 p1928 N94-22551
Development and implementation of a scrub habitat compensation plan for Kennedy Space Center
[NASA-TM-109202] 08 p3347 N94-29099
Benchmarking for cost improvement
[DE94-002276] 08 p3528 N94-30824
Projective and object space geometry for monocular building extraction
[AD-A277586] 10 p4075 N94-33426
The integrated performance evaluation program quality assurance guidance in support of EM environmental sampling and analysis activities
[DE94-013043] 12 p4468 N94-37731

RESTRAINTS
U CONSTRAINTS

RESTRICTIONS
U CONSTRICTIONS

RESUSCITATION
Evaluation of medical treatments to increase survival of ebullism in guinea pigs 01 p0302 N94-11548
A mathematical model for the study of hemorrhagic shock and fluid resuscitation: Transcapillary exchange
[AD-A266427] 03 p1123 N94-16544
A mathematical model for the study of hemorrhagic shock and fluid resuscitation: Exchange of fluid and solutes between vascular, interstitial, and tissue cell compartments
[AD-A266426] 03 p1123 N94-16558
Increased vascular resistance with hemoglobin-based oxygen carriers
[AD-A266454] 03 p1123 N94-16565
The nature of dynamic arteriolar vasoreactivity: A mini-review and A classification scheme
[AD-A266499] 03 p1128 N94-16783
Portable ventilatory resuscitation systems
[AD-A274984] 08 p3401 N94-29093

RETARDANTS
NT FLAME RETARDANTS

RETARDING
Magnetic insulation of secondary electrons in plasma source ion implantation
[DE93-040106] 05 p1997 N94-21988

RETARDING ION MASS SPECTROMETERS
U MASS SPECTROMETERS

RETENTION (PSYCHOLOGY)
SONOS technology for commercial and military nonvolatile memory applications
[DE93-015647] 03 p1011 N94-16661
Comparing performance on implicit memory tests
[AD-A269900] 04 p1508 N94-18657
Key cognitive issues in the design of electronic displays of instrument approach procedure charts
[AD-A275647] 08 p3399 N94-28649

RETICLES
Test methods for acceptance testing of telescopes
[AD-A268316] 03 p1237 N94-17568
Application of the modified voltage-dividing potentiometer to overlay metrology in a CMOS/bulk process
[DE94-007937] 09 p3695 N94-32700

RETINA
NT FOVEA
Parametric study of diffusion-enhancement networks for spatiotemporal grouping in real-time artificial vision
[AD-A265065] 01 p0331 N94-11652
Reference frames in vision
[AD-A266174] 03 p1132 N94-16925
Localization of figure background segregation mechanisms in primate visual cortex
[PB93-187961] 04 p1508 N94-18121
An analog retina model for detecting dim moving objects against a bright moving background
04 p1399 N94-18350
Physical aspects of the visual stimulus
06 p2431 N94-23978
Digital tracking and control of retinal images
[AD-A275469] 08 p3389 N94-28810
High peak power microwaves: A health hazard
[AD-A277168] 09 p3681 N94-32576

RETINAL ADAPTATION
NT LIGHT ADAPTATION

RETINAL IMAGES
Visual psychophysics of egomotion
[AD-A265253] 01 p0304 N94-11681
Digital tracking and control of retinal images
[AD-A275469] 08 p3389 N94-28810
The Portable Dynamic Fundus Instrument: Uses in telemedicine and research 10 p4096 N94-33647
Visual accommodation to virtual image displays when knowledge of object distance conflicts with optical distance 12 p4485 N94-37278

RETINENE
Inductive differentiation of nerve cells in mouse embryonic ectoderm at early primitive streak stage by retinoic acid 07 p2905 N94-27488
Anorectal malformations induced by intraperitoneal injection of all-trans retinoic acid in suncus
07 p2905 N94-27489

RETRACTABLE EQUIPMENT
In-orbit performance tests and tele-command systems of the umbrella test satellite (DEBUT)
[NAL-TR-1165] 01 p0043 N94-10859
Deployable and retractable telescoping tubular structure development 09 p3607 N94-33317
Attitude stability of a spinning spacecraft during appendage deployment/retraction
11 p4208 N94-35639

RETRACTABLE LANDING GEAR
U LANDING GEAR
U RETRACTABLE EQUIPMENT

RETRIEVAL
NT DATA RETRIEVAL
NT INFORMATION RETRIEVAL
NT PAYLOAD RETRIEVAL (STS)
EVA retriever demonstration
[NASA-TM-109510] 03 p1046 N94-15456
Nearly uniform deployment/retrieval strategy for space tether systems 06 p2156 N94-24256

RETROREFLECTION
Reduction of parasitic lasing
[NASA-CASE-LAR-14645-1-SB]
03 p1039 N94-15942
Transient internal probe
[AD-A275054] 08 p3505 N94-29134
New perspectives for high accuracy SLR with second generation geodesic satellites
[REPT-932-440-105] 08 p3336 N94-30965

RETROREFLECTORS
Galileo EM-2 contributions to the lunar control network 01 p0468 N94-12198
Work at Graz on satellite signatures
03 p0898 N94-15558
Alternative wavelengths for laser ranging
03 p0913 N94-15564
ETALON-1,-2 center of mass correction and array reflectivity 03 p0915 N94-15576
Analysis of TOPEX laser retroreflector array characteristics 03 p0915 N94-15578
Millimeter accuracy satellites for two color ranging
03 p0916 N94-15583
New perspectives for high accuracy SLR with second generation geodesic satellites 03 p0916 N94-15585
A computer-controlled x-y offset guiding stage for the MLRS 03 p0918 N94-15598
GLRS-R 2-colour retroreflector target design and predicted performance 03 p0921 N94-15615
Effects of turbulence on the geodynamic laser ranging system 03 p0921 N94-15616
Reduction of parasitic lasing
[NASA-CASE-LAR-14645-1-SB]
03 p1039 N94-15942

RETURN TO EARTH SPACE FLIGHT
HOPE real time flight operations analyses for return to earth phase, part B
[NASDA-CNT-930011] 02 p0535 N94-13599
HOPE real time flight operations analyses for return to earth phase, part A
[NASDA-CNT-930010-PT-A] 02 p0535 N94-13645
Assured crew return vehicle post landing configuration design and test 07 p2697 N94-25671

REUSABLE HEAT SHIELDING
High temperature electromagnetic characterization of thermal protection system tile materials
[NASA-CR-189687] 02 p0578 N94-13431
Thermally activated retainer means utilizing shape memory alloy
[NASA-CASE-MSC-21793-1] 05 p1654 N94-20304

REUSABLE LAUNCH VEHICLES
NT SINGLE STAGE TO ORBIT VEHICLES
HOPE conceptual design in FY 1991
[NASDA-CNT-930017] 02 p0535 N94-13600
Conceptual design on H-2 Orbiting Plane (HOPE)
[NASDA-CNT-930018] 02 p0535 N94-13656
The concept study of the space transportation system HOPE in FY 1991
[NASDA-CNT-930016] 02 p0536 N94-14100
Research and development of space transportation systems in ISAS 02 p0537 N94-14277
Contributions of winged re-entry vehicle to space activities 02 p0537 N94-14278

REUSABLE ROCKET ENGINES
The conceptual study on future space transportation systems. Part A: Conceptual study of flyback booster
[NASDA-CNT-930013] 02 p0536 N94-14099

REUSABLE SPACECRAFT
NT AEROSPACE PLANES
NT BURAN SPACE SHUTTLE
NT CHALLENGER (ORBITER)
NT COLUMBIA (ORBITER)
NT DISCOVERY (ORBITER)
NT HERMES MANNED SPACEPLANE
NT SINGLE STAGE TO ORBIT VEHICLES
NT SPACE SHUTTLE ORBITERS
NT SPACE SHUTTLES
NT X-30 VEHICLE
The concept study of the space transportation system HOPE in FY 1991
[NASDA-CNT-930016] 02 p0536 N94-14100
An assessment of solid lubricant films for use in high temperature space applications
06 p2363 N94-24044
Conceptual design of a two stage to orbit spacecraft
[NASA-CR-195536] 06 p2204 N94-24620

REUSE
NT SOFTWARE REUSE
Case based reasoning in engineering design
[AD-A278943] 11 p4305 N94-36006

REVENUE
Survey to determine the value of DYNA
[DE93-012390] 01 p0321 N94-10267
Federal Aviation Administration aviation forecasts
[AD-A265611] 01 p0002 N94-12578

REVERBERATION
Digital reverberation time measurement system
[AD-D015892] 03 p1177 N94-16919
Modelling the late part of room impulse responses using adaptive filtering: On the recreation of reality
[CTH-E-93-01] 09 p3859 N94-31076
Quality of sound in large rooms: Alteration of room impulse responses
[CTH-E-93-02] 09 p3859 N94-31077
Surface forward-scattered acoustic measurements and analysis
[AD-A276998] 09 p3788 N94-32000
Survey method for determining sound power levels under reverberant conditions in situ: A pilot study. Nordtest project 1064-92
[PB94-149143] 10 p4133 N94-34145

REVERSE ENGINEERING
Reuse: A knowledge-based approach
01 p0329 N94-11430
Myths and realities: Defining re-engineering for a large organization 01 p0330 N94-11436
Integrating interface slicing into software engineering processes
[NASA-CR-192761] 02 p0754 N94-14368
A proposal for reverse engineering CASE tools to support new software development
[DE93-040207] 05 p1906 N94-20281
Update of GRASP/Ada reverse engineering tools for Ada
[NASA-CR-193890] 06 p2455 N94-24111
Information systems criteria for applying software reengineering: Guidelines for identifying information systems for software reengineering
[AD-A274699] 07 p3097 N94-26375
Spiral Survey Expedition: A proposal to organize for the Survey, exploration and eventual colonization of the Milky Way Galaxy 07 p2686 N94-27366
The UNICON approach to through-life support and evolution of software-intensive systems
08 p3416 N94-29340
Applying formal methods and object-oriented analysis to existing flight software 12 p4491 N94-36495

REVERSE FIELD PINCH
Reversed-field pinch studies in the Madison Symmetric Torus
[DE93-013464] 01 p0388 N94-10747
Magnetohydrodynamic computation of feedback stabilization of resistive-shell instabilities in the reversed field pinch
[DE93-013466] 01 p0388 N94-10852
Simulation study of dynamo structure in reversed field pinch
[DE93-771406] 01 p0390 N94-11128
Macroscopic behaviour and discrete dynamo of RFP plasma in high theta discharge
[DE93-771408] 01 p0392 N94-11239
Theory of field-reversed configurations
[DE93-015611] 02 p0794 N94-12862
Profile stabilization of tilt mode in a field reversed configuration
[DE93-016770] 04 p1583 N94-17753
Chaos in plasma simulation and experiment
[DE94-001574] 06 p2549 N94-22963
Plasma research in the Madison Symmetric Torus (MST)
[DE94-002318] 06 p2549 N94-22976
Chaos and simple determinism in reversed field pinch plasmas: Nonlinear analysis of numerical simulation and experimental data
[DE94-001575] 06 p2550 N94-23211
Measurement of magnetic fluctuation induced energy transport
[DE94-003846] 07 p3042 N94-26132
Scaling of sustained ZT-40 M reversed field pinches
[DE94-003318] 07 p3043 N94-26321
Researches of the Electrotechnical Laboratory. No. 51: Study of formation and sustainment of reversed field pinch by slow control of magnetic field
[JTN-94-80548] 07 p3046 N94-27350
Theoretical reversed field pinch and tokamak studies
[DE94-005409] 08 p3503 N94-28490
Fluctuation and transport reduction in a reversed field pinch by inductive poloidal current drive
[DE94-005542] 08 p3503 N94-28514
The effect of magnetic field configuration on particle pinch velocity in Compact Helical System (CHS)
[AD-B183299L] 08 p3505 N94-29398
Toroidal pinch experiments
[DE94-005876] 09 p3887 N94-31558
Coaxial slow source
[DE94-008191] 09 p3892 N94-32800

REVERSE OSMOSIS
Evaluation for membrane components of water recycling system
[NAL-TM-646] 02 p0737 N94-13388

REVERSE TIME
U REACTION TIME

REVERSING
Eye-head coordination and swinging of the visual scene when wearing visually up-down reversing mirror for 14 days 07 p2915 N94-27462
Granular bases for heavily loaded pavements
[AD-A275171] 08 p3156 N94-29047

REVIEWING
Research on two phase flow in microgravity 01 p0162 N94-12554

REYNOLDS EQUATION
Proteus three-dimensional Navier-Stokes computer code, version 1.0. Volume 3: Programmer's reference
[NASA-TM-106341] 03 p1022 N94-15865
Unsteady fluid and optical simulation of transonic aero-windows
[AIAA PAPER 93-3017] 03 p0858 N94-16512
Computation of a controlled store separation from a cavity 03 p0858 N94-16513
New concepts for Reynolds stress transport equation modeling of inhomogeneous flows 06 p2171 N94-24143
Carrying the mass flux terms exactly in the first and second moment equations of compressible turbulence
[AD-A276346] 06 p2335 N94-24712
Development of advanced Navier-Stokes solver
[NASA-CR-195094] 12 p4504 N94-37449

REYNOLDS LAW
U REYNOLDS EQUATION

REYNOLDS NUMBER
NT HIGH REYNOLDS NUMBER
NT LOW REYNOLDS NUMBER
Numerical calculation of scramjet inlet flow
[NAL-TR-1174T] 01 p0027 N94-10370
Regeneration of near-wall turbulence structures 01 p0158 N94-12308
A solution algorithm for the prediction of compressible laminar and turbulent shear flows 02 p0634 N94-13635
Boundary-layer transition 02 p0507 N94-14171
The structure of laminar flow in a three-dimensional driven cavity 02 p0640 N94-14601
The structure of intense vorticity in homogeneous isotropic turbulence 02 p0643 N94-14747
Transmission of light through a turbulent mixing layer
[AD-A267266] 03 p1193 N94-17264
Lifted turbulent jet flames
[AD-A267911] 03 p0952 N94-17381
Error propagation equations and tables for estimating the uncertainty in high-speed wind tunnel test results
[DE93-018685] 04 p1311 N94-18275
An experimental investigation of attachment-line transition on the slat of a combat aircraft model 04 p1308 N94-18432
Semi-span model testing in the National Transonic Facility
[NASA-CR-194479] 04 p1312 N94-19388
Numerical prediction of transition of the F-16 wing at supersonic speeds
[NASA-CR-194407] 04 p1312 N94-19433
Numerical investigation of the incompressible flow around a wing with a fixed spoiler
[ISL-R-109/91] 04 p1313 N94-19524
An investigation of low Marangoni number fluid flow in a cold corner
[AD-A271317] 04 p1422 N94-19569
A method to simulate viscous diffusion of vorticity by convective transport of vortices at a non-solenoidal velocity
[DE94-001777] 06 p2318 N94-23220
Unstructured grid large eddy simulation of wall bounded turbulent flows 06 p2329 N94-24151
Energy transfer and constrained simulations in isotropic turbulence 06 p2330 N94-24153
Stagnation region heat transfer: The influence of turbulence parameters, Reynolds number and body shape
[NASA-TM-106504] 06 p2334 N94-24481
Interactive control in turbulent shear layers
[AD-A273544] 06 p2336 N94-24793
Active control of oscillatory lift forces on a circular cylinder
[AD-A273243] 06 p2338 N94-25140
Wake passage effects on the losses in a linear turbine cascade
[AD-A273794] 07 p2790 N94-25874
Nominally 2-dimensional flow about a normal flat plate
[AD-A274472] 07 p2794 N94-27026
The cryogenic tunnel Cologne at DLR
[DLR-MITT-93-10] 07 p2681 N94-27587
A parallel multigrid algorithm for solving the Navier-Stokes equations on a transputer system
[PREPRINT-699] 07 p2807 N94-28099
Forced convection heat transfer in straight tubes. Part 2: Laminar and transitional flow
[ESDU-93018-PT-2] 07 p2807 N94-28139
Direct and large-eddy simulations of turbulent flow in a square duct 08 p3275 N94-29809
The h-p adaptive methods for incompressible viscous flow problems 08 p3275 N94-29836
Local heat transfer in an enclosed corotating disk with axial throughflow 08 p3276 N94-29849
A modernised HST of NLR
[AD-B179220] 08 p3158 N94-30423
Hypervelocity Tunnel 9 Mach 10/14 Calibration
[AD-A275960] 09 p3587 N94-31318
Heat transfer studies on a rectangular channel with offset plate fins
[AD-A277300] 09 p3912 N94-32043
Design of a two dimensional planer pressurized air labyrinth seal test rig
[AD-A277232] 09 p3726 N94-32370
Visualization of secondary flow development in high aspect ratio channels with curvature
[NASA-TM-106658] 10 p4046 N94-33941
Eccentricity effects upon the flow field inside a whirling annular seal 10 p4062 N94-34181
F/A-18 forebody vortex control. Volume 2: Rotary-balance tests
[NASA-CR-4582-VOL-2] 10 p3984 N94-34430
Direct simulation of a self-similar plane wake
[NASA-TM-108815] 10 p4050 N94-34917
Experimental studies of very-high Mach number hydrodynamics
[AD-A278761] 11 p4263 N94-35492
Numerical investigation of multi-element airfoils
[NASA-CR-194592] 11 p4191 N94-36394
Subsonic aerodynamic characteristic of semispan commercial transport model with wing-mounted advanced ducted propeller operating in reverse thrust --- conducted in the Langley 14 by 22 foot subsonic wind tunnel
[NASA-TP-3427] 12 p4384 N94-37505

REYNOLDS STRESS
A local dynamic model for large eddy simulation 01 p0155 N94-12285
Parameterization of subgrid-scale stress by the velocity gradient tensor 01 p0155 N94-12286
A normal stress subgrid-scale eddy viscosity model in large eddy simulation 01 p0155 N94-12288
Application of a dynamic subgrid-scale model to turbulent recirculating flows 01 p0156 N94-12290
Direct numerical simulation of turbulent flow over a backward-facing step 01 p0156 N94-12296
Reynolds stress closure modeling in wall-bounded flows 01 p0157 N94-12298
Application of a Reynolds stress model to separating boundary layers 01 p0157 N94-12299
Sub-grid scale modeling for large eddy simulations in analysis of shock-turbulence interactions
[DE93-013425] 02 p0631 N94-13250
Development of a recursion RNG-based turbulence model
[NASA-CR-191511] 02 p0636 N94-13718
Vortex-induced disturbance field in a compressible shear layer 02 p0645 N94-14760
Computation of confined coflow jets with three turbulence models
[NASA-TM-106378] 03 p1025 N94-16879
Three-dimensional turbulent boundary layer
[AD-A266261] 03 p1025 N94-16908
Structure of high Reynolds number turbulent boundary layer
[AD-A267476] 03 p0860 N94-17099
Investigation of high-speed free shear flows using improved pressure-strain correlated Reynolds stress turbulence model
[NASA-CR-194661] 03 p1027 N94-17127
Structure of turbulence in three-dimensional boundary layers
[NASA-CR-194655] 03 p1027 N94-17130
Self-regulated shear flow turbulence in confined plasmas
[DE93-015823] 04 p1583 N94-17743
On memory effects in turbulence
[DLR-FB-93-03] 04 p1409 N94-18124
Assessment and development of second order turbulence models 04 p1411 N94-18548
Numerical implementation and performance of Reynolds-stress closures in finite-volume computations of recirculating and strongly swirling flows 04 p1415 N94-18589
Modelling engineering flows with Reynolds stress turbulence closure 04 p1415 N94-18591
Shear flow generation by Reynolds stress and suppression of resistive g-modes
[DE93-040911] 05 p1995 N94-21514
New results on the realizability of Reynolds stress turbulence closures
[NASA-CR-191548] 05 p1804 N94-21875
Turbulence sensors for separated flows: Current capabilities, future requirements 06 p2315 N94-22853
Computation of flows in a turn-around duct and a turbine cascade using advanced turbulence models 06 p2216 N94-23062
A representation for the turbulent mass flux contribution to Reynolds-stress and two-equation closures for compressible turbulence
[NASA-CR-191569] 06 p2319 N94-23302
Reliability in second moment turbulence closures revisited
[NASA-TM-106469] 06 p2326 N94-24063
Toward modeling wingtip vortices 06 p2171 N94-24142
New concepts for Reynolds stress transport equation modeling of inhomogeneous flows 06 p2171 N94-24143
Turbulence modeling for non-equilibrium flows 06 p2328 N94-24144
Computation of turbulent flows over backward and forward-facing steps using a near-wall Reynolds stress model 06 p2172 N94-24145
Dynamic localization and second-order subgrid-scale models in large eddy simulations of channel flow 06 p2329 N94-24149
Sound radiation due to boundary layer transition 06 p2332 N94-24163
Effects of shock strength on shock turbulence interaction 06 p2332 N94-24165
Local isotropy in distorted turbulent boundary layers at high Reynolds number 06 p2332 N94-24166
Implementation of the Baldwin-Barth turbulence model into the ZETA code and its diagnosis
[NASA-CR-194795] 06 p2335 N94-24640
Carrying the mass flux terms exactly in the first and second moment equations of compressible turbulence
[AD-A276346] 06 p2335 N94-24712
Shear flow generation from the interaction of neoclassical and drift wave transport processes
[DE94-003135] 07 p2791 N94-26096
Potential capabilities of Reynolds stress turbulence model in the COMMIX-RSM code
[DE94-003716] 07 p2792 N94-26331

On prediction of equilibrium states in homogeneous compressible turbulence
[NASA-CR-4570] 07 p2792 N94-26467
A rapid-pressure correlation representation consistent with the Taylor-Proudman theorem materially-frame-indifferent in the 2D limit
[AD-A277582] 07 p2796 N94-27435
Calculation of single and multiple jets in cross-flow with and without impingement using Reynolds-stress-transport closure 07 p2803 N94-28024
Modeling turbulence in flows with a strong rotational component
[DE94-003577] 08 p3270 N94-28475
Potential capabilities of Reynolds stress turbulence model in the COMMIX-RSM code 08 p3285 N94-30450
Transport suppression by shear flow generation in multihelicity resistive-g turbulence
[DE94-007108] 09 p3886 N94-31386
Three-dimensional velocity measurements on a 6:1 prolate spheroid at 10 deg angle of attack
[AD-A276485] 09 p3702 N94-31476
A critical evaluation of the Reynolds stress turbulence closure for the flow of a turbulent free-stream over a turbulent boundary layer
[ISBN-0-315-75792-2] 09 p3707 N94-32497
Backward-facing step measurements at low Reynolds number, Re(sub h) = 5000
[NASA-TM-108807] 09 p3711 N94-33290
Turbulence structure associated with intercomponent and interscale energy transfer and modification by forcing
[AD-A278269] 10 p4043 N94-33414
Direct simulation of a self-similar plane wake
[NASA-TM-108815] 10 p4050 N94-34917
Turbulence modelling for unsteady separated flows 10 p4053 N94-34984
The alternative faces of turbulent flow
[TM-5-94] 12 p4442 N94-36934
Momentum-energy transport from turbulence driven by parallel flow shear
[DE94-012765] 12 p4443 N94-37362

RH-2 HELICOPTER
U UH-1 HELICOPTER

RHENIUM
NT RHENIUM ISOTOPES
Space Storable Rocket Technology program (SSRT). Option 1 program
[NASA-CR-191171] 01 p0046 N94-10938
Osmium isotopes in Ivory Coast tektites: Confirmation of a meteoritic component and rhenium depletion 03 p1244 N94-16321
Structural effects in electron transfer reactions: Comparative interfacial electrochemical kinetics for cis- versus trans-dioxorhenium (V) (bi)pyridine oxidation
[AD-A266307] 03 p1182 N94-16466
Sulfur-bonded thiophenes in organometallic rhenium complexes and adsorption of isocyanides on gold
[DE93-041126] 05 p1694 N94-21937
Advanced materials for radiation-cooled rockets 06 p2214 N94-23052
Surface compositional variations of Mo-47Re alloy as a function of temperature
[NASA-TP-3402] 06 p2245 N94-25117
Evaluation of oxide-coated iridium-rhenium chambers
[NASA-TM-106442] 08 p3172 N94-29097

RHENIUM ALLOYS
Toward insulating quasicrystalline alloy in Al-Pd-Re icosahedral phase
[REPT-A-2666] 07 p2736 N94-26477

RHENIUM COMPOUNDS
High-valent oxo, methoxorhenium complexes: Models for intermediates and transition states in proton-coupled multi-electron transfer reactions
[AD-A266492] 03 p1211 N94-16782
Photochemical approaches to conversion of light to electricity or fuel
[DE94-001650] 05 p1849 N94-22048
Novel approaches to the production of higher alcohols from synthesis gas
[DE94-006770] 09 p3666 N94-32132
Ligand intermediates in metal-catalyzed reactions
[DE94-008713] 09 p3638 N94-32887

RHENIUM ISOTOPES
Rhenium-osmium isotope systematics of Group 2A and Group 4A iron meteorites 01 p0431 N94-12182
Re-Os dating of 3AB iron meteorites 01 p0432 N94-12237

RHEOLOGY
Improving reservoir conformance using gelled polymer systems
[DE93-014532] 01 p0088 N94-10749
A model for the subduction mechanics of flexible lithosphere and its viscous coupling to the mantle using power-law rheologies 01 p0277 N94-11585
Quantifying the effect of rheology on plan-view shapes of lava flows 01 p0282 N94-12116
Numerical simulation of the non-Newtonian mixing layer 01 p0159 N94-12314
Workshop on Formation of Supermolecular Structures in Composite Fluid: Phase Rule and Dynamics
[DE93-782887] 02 p0581 N94-14421
Rheology and microstructure of concentrated zirconia-alumina suspensions for gelcasting composites
[DE93-015339] 03 p0966 N94-16016
Rheology of water and ammonia-water ices 03 p0953 N94-16188
The rheology and composition of cryovolcanic flows on icy satellites 03 p1243 N94-16294
Geophysical models of Western Aphrodite-Niobe region: Venus 03 p1286 N94-16382
Electro-rheological disk pump
[AD-D015783] 03 p1047 N94-16531
Some problems in the rheological characterisation of composite rocket propellants
[AD-A268806] 04 p1376 N94-18203
Numerical analysis of pressure meter tests: Application of parameter identification of soils behavior
[ECL-92-52] 04 p1487 N94-19380
Microscopic modeling of tribological and interfacial phenomena
[AD-A271864] 05 p1823 N94-20464
Thermal and rheological controls on magma migration in dikes: Examples from the east rift zone of Kilauea volcano, Hawaii 05 p1862 N94-20673
A comparison of calculated and measured rheological properties of crystallising lavas in the field and in the laboratory 05 p1862 N94-20690
Electro-rheology fluids and liquid fuel flow
[AD-A273640] 06 p2337 N94-25032
Constraining proposed combinations of ice history and Earth rheology using VLBI determined baseline length rates in North America 06 p2405 N94-25205
Nonlinear hysteresis in an endochronic solid
[AD-A274594] 07 p2880 N94-26855
Synthesis, rheology, and forming of Y-Ba-Cu-O ceramics
[DE94-005558] 07 p2757 N94-27695
Lubricant rheology at high shear rates 08 p3217 N94-29967
The role of sea ice dynamics in global climate change 08 p3350 N94-30620
Influence of trace components on the viscoelastic properties of a polymer solution
[AD-A277171] 09 p3656 N94-32253
Effect of surface forces on the rheology of particle-liquid systems and the consolidation of ceramic powders
[AD-A277092] 09 p3657 N94-32391
Rheology, tectonics, and the structure of the Venus lithosphere 11 p4367 N94-35479
Patterns of brittle deformation under extension on Venus 11 p4373 N94-36168

RHEOMETERS
Some problems in the rheological characterisation of composite rocket propellants
[AD-A268806] 04 p1376 N94-18203
Lubricant rheology at high shear rates 08 p3217 N94-29967
Determination of extensional viscosity from capillary rheometer entrance pressure drop measurements using a numerical simulation of contraction flow
[PB94-171154] 11 p4263 N94-35603

RHO-MESONS
Omega omega and rho + rho- production in two photon interactions at ARGUS
[ISBN-0-315-63748-X] 07 p3026 N94-27399

RHODAMINE
Fluorescence detection of single molecules using pulsed near-field optical excitation and time correlated photon counting
[DE94-007553] 11 p4320 N94-35376

RHODIUM
Dispersion of Rh/Cu in a sol-gel matrix. Highly chemo- and stereoselective catalyst for the reduction of alkynes to Z-alkenes
[AD-A273306] 06 p2262 N94-25145
Polymer-bound rhodium hydroformylation catalysts
[ETN-94-95388] 07 p2712 N94-25747
A mimic model of Pt-Rh catalyst prepared by electrochemical deposition of Rh on Pt (100) surface
[REPT-A-2664] 07 p2715 N94-26476
Morphological aspects of surface reactions
[DE94-011208] 12 p4413 N94-37713

RHODIUM ALLOYS
Magnetism in CeRu2Ge2 and CeRh2Ge2 and its pressure dependence
[DE93-040061] 05 p2032 N94-21987
Reduction of nitric oxide over platinum, rhodium and platinum-rhodium single crystal surfaces
[PB93-230092] 06 p2232 N94-23482

RHODIUM COMPOUNDS
Novel approaches to the production of higher alcohols from synthesis gas
[DE94-006770] 09 p3666 N94-32132

RHOMBOHEDRONS
X ray absorption study of pulsed laser deposited boron nitride films
[DE94-008295] 09 p3662 N94-32855

RHYOLITE
Stable isotope analyses of the peralkaline volcanics Gregory Rift Valley, Kenya 01 p0281 N94-12072
Th-230 - U-238 series disequilibrium of the Olkaria rhyolites Gregory Rift Valley, Kenya: Petrogenesis 01 p0281 N94-12075
Th-230 - U-238 series disequilibrium of the Olkaria rhyolites Gregory Rift Valley, Kenya: Residence times 01 p0281 N94-12076
Venusian pancake domes: Insights from terrestrial voluminous silicic lavas and thermal modeling 03 p1286 N94-16381
Venus pancake dome formation: Morphologic effects of a cooling-induced variable viscosity during emplacement 05 p2110 N94-20732

RHYTHM (BIOLOGY)
NT CIRCADIAN RHYTHMS
The 2nd Annual Meeting of the Society for Research on Biological Rhythms
[AD-A264869] 01 p0303 N94-10872
Gordon Research Conference on Chronobiology, 1991
[AD-A266354] 02 p0728 N94-13698

RIBBONS
Polymer infiltration studies
[NASA-CR-194521] 02 p0582 N94-14539
Polymer Infiltration Studies
[NASA-CR-194494] 03 p0932 N94-15275
Non-rectangular towpreg architectures
[NASA-CASE-LAR-14863-1-CU] 08 p3180 N94-29485
Theoretical studies of the solar atmosphere and interstellar pickup ions
[NASA-CR-195846] 10 p4166 N94-34716

RIBLETS
Coherent structure in near wall turbulence with riblets 01 p0165 N94-12628
Riblets: New speed technology
[NASA-TM-109641] 03 p1018 N94-15252
Active turbulence control in wall bounded flows using direct numerical simulation
[AD-A267261] 03 p1028 N94-17286
The effect of fine surface riblets on the flow around an inclined axially symmetrical body
[MPIS-105/1993] 04 p1420 N94-19356
Measurement Technology for Flight Tests
[ILR-MITT-256(1991)] 05 p1639 N94-22597
Riblet boundary layer measurements of an A-310 fuselage with Pitot combs 05 p1640 N94-22605
Coherent structures over grooved surfaces
[ETN-94-95308] 06 p2339 N94-25291
Flight test results of riblets at supersonic speeds
[NASA-TM-4387] 09 p3572 N94-32880

RIBONUCLEIC ACIDS
Evolution of catalytic RNA in the laboratory
[NASA-CR-194124] 02 p0727 N94-13210
Analysis of the V antigen lcrGVH-yopBD operon of Yersinia pseudotuberculosis: Evidence for a regulatory role of LcrH and LcrV
[FOA-B-40417-4.4] 02 p0729 N94-14129
The first steps of chlorophyll synthesis: RNA involvement and regulation
[DE93-014398] 02 p0730 N94-14509
Biofilm structure and diversity
[AD-A267254] 03 p1118 N94-16989
The torsion space nucleic acids molecular mechanics program DUPLEX: Surveying conformation space by potential energy minimization
[DE94-002441] 06 p2563 N94-24567
Molecular biological studies on the human radioresistance and drug resistance
[DE93-632682] 07 p2910 N94-26549
Cloning of a novel POU family gene by RT-PCR method 07 p2905 N94-27480
Effect of sera from patients treated with long-term hemodialysis on mRNA's for collagenase, stromelysin, and tissue inhibitor of metalloprotease in cultured human synovial cells 07 p2920 N94-27481
Stable RNA sequences as a tool for DNA probes and phylogenetic studies
[PB94-135423] 08 p3385 N94-29156
Employment of a porous gold actuator in ISFET-based coulometric sensor-actuator systems with application to protein characterization
[ISBN-9-09-005887-7] 09 p3689 N94-31536
Phase-sensitive flow cytometry: New technology for analyzing biochemical, functional, and structural features in fluorochrome-labeled cells and particles
[DE94-003960] 10 p4094 N94-33734

A low temperature scanning force microscope for biological samples
[DE94-011357] 11 p4297 N94-36269

RIBS (SUPPORTS)
Turbulent drag reduction of a d-type rough wall boundary layer with longitudinal ribs placed within the grooves
01 p0165 N94-12627
Sound radiation from infinite laminated composite shell with periodic rib stiffening
[DRA/TM(USGR)92326] 03 p0933 N94-15699
Orbit transfer rocket engine technology program enhanced heat transfer combustor technology
[AD-A277123] 07 p2700 N94-26156
Vibrational and acoustic response of ribbed plates
09 p3736 N94-31955

RICCATI EQUATION
A new approach to the I/N-expansion for the Dirac equation
[DE93-617647] 01 p0349 N94-10833
Kalman filter input estimation
[NAL-TR-1182] 02 p0649 N94-13456
On the geometry of external spectral factors and the Riccati inequality
[CWI-BS-R9227] 02 p0770 N94-14002
The optimal projection equations for finite-dimensional fixed-order H2-optimal control of infinite-dimensional discrete-time systems
[REPT-93-11] 04 p1542 N94-19085
The fixed, finite-order L(sup 2)-optimal control of infinite-dimensional time-varying discrete-time systems
[REPT-93-23] 04 p1542 N94-19138
Discrete-time infinity control problem with measurement feedback
[PB93-197523] 04 p1543 N94-19329
A mixed H2/H(infinity) function for a discrete time system
[MEMO-COSOR-92-36] 06 p2480 N94-23144
Coordinate-free interpretations of the optimal costs for Lq problems subject to implicit systems
[PB94-118700] 06 p2473 N94-23760
Control of nonlinear systems represented in quasilinear form
[NASA-CR-194840] 06 p2475 N94-24760
Necessary and sufficient conditions for the existence of the stabilizing solution of the Riccati equation in a Hilbert space: A Popov function approach
[PB94-125341] 07 p2997 N94-26999
Digital state-feedback H(infinity) control of Pritchard-Salamon systems: A Popov function approach
[REPT-93-69] 09 p3830 N94-31647
A Hyland-Bernstein approach to the digital control of Pritchard-Salamon systems
[REPT-93-76] 09 p3844 N94-31693
Feedback stabilization of matrix second-order systems by solving Riccati equation 10 p4115 N94-34315
A note on the regularity of solutions of infinite dimensional Riccati equations
[NASA-CR-194898] 12 p4502 N94-36562

RICE
Rice cultivation and methane emission: Documentation of distributed geographic data sets
[NASA-TM-104595] 06 p2381 N94-24800

RICHARDSON NUMBER
Lifted turbulent jet flames
[AD-A267911] 03 p0952 N94-17381
Nominally 2-dimensional flow about a normal flat plate
[AD-A274472] 07 p2794 N94-27026

RICHARDSON-DUSHMAN EQUATION
U TEMPERATURE EFFECTS
U THERMIONIC EMISSION

RIDING QUALITY
Active landing gear control for improved ride quality during ground roll 01 p0027 N94-11345
Examples of flight path optimisation using a multivariate gradient-search method
[ESDU-93021] 07 p2670 N94-28092
Lufthansa long range services: More simplicity
07 p2663 N94-28246
Control of maglev vehicles with aerodynamic and guideway disturbances 11 p4213 N94-35842
Fault tolerant computer control for a Maglev transportation system 11 p4215 N94-35848

RIEMANN INTEGRAL
U MEASURE AND INTEGRATION

RIEMANN MANIFOLD
From the Weyl theory to a theory of locally anisotropic space-time
[DE92-644734] 01 p0410 N94-10535
Scalar curvature and spherical-type Riemannian manifolds
[DE93-622852] 02 p0767 N94-12895
Heat flows and harmonic maps with a free boundary
[DE93-622856] 02 p0632 N94-13509
A hydrogen atom in the curved space: Orthogonality of radial wave functions with respect to the critical momentum
[DE93-626623] 02 p0788 N94-14891
Differential geometry of CR-submanifolds of a normal almost para contact manifold
[DE93-624764] 04 p1545 N94-17793
Unbounded components in parameter space of rational maps
[DE93-628621] 04 p1548 N94-18170
Contact 3-manifolds, integrable Hamiltonian systems and exotic symplectic structures in R(sup 4)
[DE93-624767] 04 p1551 N94-19248
Vanishing theorem on arithmetic surfaces
[PB93-215481] 05 p1961 N94-22263
Non commutative geometry and physics
[PB93-215499] 05 p1961 N94-22264
Lacunary series as quadratic differentials in conformal dynamics
[PB93-238061] 06 p2481 N94-23547
Applications of supersymmetric quantum mechanics
[ETN-94-95385] 06 p2570 N94-25257
Deviation equations of Synge and Schild in spaces with affine connection and metric, and equations for gravitational waves detectors
[DE93-616852] 06 p2571 N94-25339
On the first integrals of geodesics
[DE93-612974] 07 p3007 N94-25603
A note on Riemannian 2-space
[DE94-602560] 07 p3073 N94-27024
Approximate Riemann solvers: Improvement of the HLLEM scheme and its generalization for chemically reacting flows
[NAL-TR-1189] 07 p2795 N94-27205
The Einstein tensor characterizing some Riemann spaces
[DE94-603663] 07 p3074 N94-27626
The super Weierstrass (zeta)-function and operator product expansions in 2D-induced supergravity on the supertorus
[DE94-603664] 07 p3074 N94-27627
Proton electromagnetic form factor near the proton-antiproton threshold and quasinuclear bound state
[DE94-606458] 07 p3027 N94-27681
SU(2) WZNW model at higher genera from gauge field functional integral
[PB94-148467] 09 p3857 N94-31589
Conformal field theory and geometry of strings
[PB94-148442] 09 p3857 N94-31770
Moduli space of monopoles and some invariants of 3-manifolds
[PB94-167756] 11 p4314 N94-35764
Some theorems on a class of harmonic manifolds
[DE94-611102] 11 p4315 N94-35934
Zero modes of the two-dimensional Dirac operator on a noncompact Riemann surface in an external magnetic field
[DE94-616618] 11 p4343 N94-36071

RIEMANN PROBLEM
U CAUCHY PROBLEM

RIEMANN SPACE
U RIEMANN MANIFOLD

RIEMANN SPHERE
U RIEMANN MANIFOLD

RIEMANN WAVES
Full Riemann solution of the one- and two-dimensional Euler equations
[DLR-FB-92-34] 02 p0638 N94-14188
Approximate Riemann solvers: Improvement of the HLLEM scheme and its generalization for chemically reacting flows
[NAL-TR-1189] 07 p2795 N94-27205
An approximate Riemann solver for magnetohydrodynamics (that works in more than one dimension)
[AD-280296] 09 p3849 N94-33033

RIFLES
Thermal Weapon Sight (TWS) AN/PAS-13 diffractive optics designed for producibility
03 p1197 N94-17354

RIFT VALLEYS
U VALLEYS

RIFTS
U GEOLOGICAL FAULTS

RIGID BODIES
U RIGID STRUCTURES

RIGID ROTOR HELICOPTERS
Numerical analysis of airfoil for helicopter blade at high angle of attack using Navier-Stokes code
08 p3124 N94-28958

RIGID ROTORS (PLASMA PHYSICS)
NT PLASMA PHYSICS

RIGID STRUCTURES
Determination of position and orientation of rigid bodies from image segments
[FFI-92-4005] 02 p0752 N94-14039
Predicting the vibrations of a spinning inflated membrane
[DE93-010690] 02 p0676 N94-14456
Animation of multi-flexible body systems and its use in control system design 02 p0678 N94-14629
Nonrecursive formulations of multibody dynamics and concurrent multiprocessing 02 p0679 N94-14632
Parallel O(log n) algorithms for open- and closed-chain rigid multibody systems based on a new mass matrix factorization technique 02 p0679 N94-14636
Real-time dynamics simulation of the Cassini spacecraft using DARTS. Part 1: Functional capabilities and the spatial algebra algorithm 02 p0680 N94-14638
Computational Control Workstation: Users' perspectives 02 p0681 N94-14648
Impending motion direction of contacting rigid bodies
[AD-A266814] 03 p1164 N94-15756
Computation of a controlled store separation from a cavity 03 p0858 N94-16513
Equations of motion of a hinged body over a spherical earth
[AD-A268408] 03 p0868 N94-17435
Crashdynamics with DYNA3D: Capabilities and research directions 04 p1460 N94-19475
Estimability of polar motion using range observations to satellites
[PB93-219319] 05 p1842 N94-22265
A structural design decomposition method utilizing substructuring
[NASA-TM-107750] 06 p2376 N94-23368
Pressure wall patch
[NASA-CASE-MFS-28724-1] 06 p2203 N94-23824
Numerical analysis of the motion of a rigid body with an attached spring-mass-damper
[AD-A273825] 06 p2379 N94-25520
A comparison of three approximate mathematical models for the gravity gradient stabilized satellite
[AD-A273832] 07 p2694 N94-25615
Balancing of a planar bouncing object
[AD-A273805] 07 p2821 N94-25878
Normal forms for perturbations of the euler top
[PB94-125390] 07 p3009 N94-26968
Collapsible mechanical joint
[NASA-CASE-MFS-28765-1] 08 p3299 N94-29367
Stiffness-generated rigid-body mode shapes for Lanczos eigensolution with SUPORT DOF by way of a MSC/NASTRAN DMAP alter
[NASA-TM-106537] 08 p3319 N94-29406
Computation of vibration mode elastic-rigid and effective weight coefficients from finite-element computer program output 08 p3247 N94-29615
Theory of fundamental interactions
[DE94-608126] 08 p3525 N94-30169
Determination of acceleration field parameters with linear accelerometers
[PB94-125606] 08 p3290 N94-30742
Applying transfer matrix method to the estimation of the modal characteristics of the NASA Mini-Mass Truss
11 p4218 N94-35870
Robust tracking control of a magnetically suspended rigid body 11 p4225 N94-35913
Predicting the effects of unmodeled dynamics on an aircraft flight control system design using eigenspace assignment
[NASA-TM-4548] 12 p4388 N94-37059
A new technique for dynamic load distribution when two manipulators mutually lift a rigid object, part 2
[DE94-010126] 12 p4501 N94-37735

RILLS
U VALLEYS

RIMS
Characterization of the Marquez Dome buried impact crater using gravity and magnetic data
05 p1863 N94-20882
Alteration and formation of rims on the CM parent body 11 p4357 N94-35411

RING CURRENTS
The interplanetary origins and the main-phase development of moderate geomagnetic storms (1978 - 1979)
[INPE-5445-TDI/491] 02 p0835 N94-13174
Stormtime transport of ring current and radiation belt ions
[NASA-CR-194416] 02 p0714 N94-13793
Energetic neutral atoms: Imaging the magnetospheric ring current
[NASA-CR-194339] 02 p0715 N94-13826
Terrestrial magnetospheric imaging: Numerical modeling of low energy neutral atoms
[DE93-014561] 02 p0717 N94-14328
Penetrating radiation environment and effects study
[AD-A270126] 04 p1485 N94-18874

Dynamics explorer interdisciplinary scientist investigations
[NASA-CR-195226] 07 p2878 N94-26204

RING GALAXIES
The IR properties of ringed galaxies and the IRAS database
[NASA-CR-194286] 01 p0426 N94-11590
A multi wavelength observational study of the Cartwheel ring galaxy 08 p3539 N94-29821
Stellar and gas dynamics of interacting ring galaxies 08 p3548 N94-30340

RING LASERS
Semiconductor ring lasers
[DE93-012386] 01 p0174 N94-11005
Performance evaluation of the honeywell GG1308 miniature ring laser gyroscope
[AD-A266694] 02 p0653 N94-14782
On the application of Allan variance method for Ring Laser Gyro performance characterization
[DE94-003880] 07 p2810 N94-26525
High-speed, high-density, coherent time-domain optical memory
[AD-A274249] 07 p3037 N94-27010
Fiber laser amplifiers and oscillators
[AD-A274231] 07 p2820 N94-28068
High-power CW diode-laser-array-pumped solid-state lasers and efficient nonlinear optical frequency conversion
[AD-A276126] 09 p3714 N94-31278
An investigation of airborne GPS/INS for high accuracy position and velocity determination
[DE94-006139] 09 p3576 N94-31306
Spectrally-selective fiber transmission filter system
[AD-D016133] 10 p4141 N94-33698

RING STRUCTURES
NT REINFORCEMENT RINGS
NT RING WINGS
Design and manufacturing of CFRP rings by RTM 01 p0059 N94-10025
The ring structure of chiral operators for minimal models coupled to 2D gravity
[DE93-013119] 01 p0409 N94-10500
Morphology of large impact craters and basins on Venus: Implications for ring formation 01 p0436 N94-12023
Yana ring structure, North-Eastern Siberia: A possible counterpart of coronae on Venus 01 p0282 N94-12121
Morphologic classes of impact basins on Venus 05 p2137 N94-20883
Roll ring assemblies for the Space Station 09 p3603 N94-33294
International Space Station Alpha's bearing, motor, and roll ring module developmental testing and results 09 p3603 N94-33295

RING WINGS
Simulated wake characteristics of tapered annular wings by a discrete vortex method
[NAL-TR-1156] 01 p0013 N94-10855
Simulated and experimental aerodynamic characteristics of tapered annular wings
[NAL-TR-1157] 01 p0013 N94-10856

RINGS
The IRAF Fabry-Perot analysis package: Ring fitting 05 p2048 N94-22527
Matrix near rings and pseudo distributivity
[DE94-601505] 07 p2992 N94-26366

RINGS (MATHEMATICS)
Modal ring method for the scattering of sound
[NASA-TM-106342] 03 p1177 N94-16497
Distributively generated matrix near rings
[DE93-628588] 03 p1175 N94-17641
Stabilization of time-delay systems: An overview of the algebraic approach
[PB93-191989] 04 p1553 N94-19556
Orbit spaces over commutative rings and projectives as semi-isomorphisms
[DE93-616822] 06 p2493 N94-25473
Remarks on Galois symmetry in RCFT
[PB94-138179] 08 p3467 N94-29147
Hierarchical structures and asymmetric stochastic processes on p-adics and adeles
[PB94-138203] 08 p3464 N94-29178

RIOMETERS
Development of imaging riometers 07 p2884 N94-27967
Quick-look system of auroral absorption images by imaging riometer 07 p2884 N94-27968
Initial observation results with imaging riometer at NY-Alesund (L is equal to 16) 08 p3360 N94-29239

RIPPLES
Tune modulation due to gradient ripple and the dynamic aperture
[DE94-011922] 12 p4524 N94-37157

RISK
Report on Subgroup on Data Banks for Risk Assessment
[DE93-012150] 01 p0418 N94-10646
Efficient management of cardiovascular risk screening programs 03 p1125 N94-16622
A handbook of cost risk analysis methods
[AD-A267253] 03 p1235 N94-16988
X ray computed tomography for failure analysis investigations
[AD-A268086] 03 p1055 N94-17515
Indoor environment program
[DE93-018601] 04 p1513 N94-18935
Uncertainty versus interindividual variability
[DE93-018105] 04 p1559 N94-19549
Manual of DRANC (release 1.1): A computer program for the Dutch risk assessment of new chemical substances
[PB93-194827] 05 p1851 N94-19998
Meteoroids and debris impact risk assessment on Columbus and Hermes using a realistic geometrical analysis tool 05 p1662 N94-21388
MLS signal-in-space category 3 landing hazard analysis 05 p1644 N94-22134
Aeromedical disposition for coronary artery disease 06 p2423 N94-23316
Arterial hypertension and the aviator 06 p2425 N94-23328
Risk identification and reduction in integrated product teams 06 p2497 N94-24407
In vitro system for studying metabolism of environmental chemicals in human cells
[AD-A273427] 06 p2421 N94-24688
A statistical analysis of recent Naval Experimental Diving Unit (NEDU) single-depth human exposures to 100 percent oxygen at pressure
[AD-A273488] 06 p2427 N94-24950
Integrated risk management 06 p2588 N94-25361
Risk perspectives for Topaz 2 flight mission
[DE94-003229] 07 p2700 N94-25956
Space projects: Astrophysics facility program contains cost and technical risks. Report to Congressional Requesters
[GAO/NSIAD-94-80] 07 p2696 N94-27382
Space radiation health research, 1991-1992
[NASA-TM-109721] 07 p2932 N94-27556
Is probability of frequency too narrow?
[DE94-000687] 07 p3004 N94-27612
Practical problems in aggregating expert opinions
[DE94-002623] 07 p3094 N94-27707
Risk-based prioritization: A comparison of approaches
[DE94-003368] 08 p3526 N94-28474
Identification of components to optimize improvement in system reliability
[DE94-001601] 08 p3315 N94-28503
Risk measures in living probabilistic safety assessment
[VTT-PUBS-146] 08 p3465 N94-30154
Fuzzy-algebra uncertainty analysis for abnormal-environment safety assessment
[DE94-006257] 08 p3462 N94-30849
Space flight risk data collection and analysis project: Risk and reliability database
[NASA-CR-195879] 09 p3603 N94-32494
Evaluation of the potential of SAR data for mapping of landslide risks
[BRGM-93033] 09 p3753 N94-32552
Risk analysis of the C-141 WS405 inner-to-outer wing joint 10 p3996 N94-34592
Modeling and managing risk early in software development 11 p4301 N94-35436
CAirTOX: A compartment model for assessing the fate of and human exposure to toxic-chemical emissions to air
[DE94-010084] 11 p4284 N94-35700
Residual Gas Analysis (RGA) and shear strength characteristics of a silver-filled epoxy and polyimide under long-term, high-temperature storage conditions
[DE94-010106] 11 p4244 N94-35705
Analysis spectral shapes from California and central United States ground motion
[DE94-010041] 12 p4469 N94-36758
Environmental risk management
[DE94-620987] 12 p4467 N94-37492
On the use of fuzzy logic assessment for high consequence implementation risk analysis
[DE94-011417] 12 p4507 N94-37564

RIVER BASINS
Modeling present and future river runoff using global atmospheric models
[AD-A265274] 01 p0285 N94-11685
Simultaneous 3D turbulent large-scale structures in a flood flow by multi-channels measuring system 01 p0165 N94-12624

RIVERS
NT MISSISSIPPI RIVER (US)
Shoreline change detection using remote sensing and GIS in Vietnam 01 p0196 N94-11928
Analysis of the characteristic and mechanism of suspended matter transportation in Huanghe delta sea area using remote sensing techniques 01 p0197 N94-11930
Methodological considerations for use of ERS-1 imagery for the delineation of river networks in tropical forest areas 01 p0247 N94-12484
Study on diffusion phenomena of river effluents issued into sea around Japan with satellite remote sensing data 01 p0212 N94-12664
Variability of spectral reflectance in coastal waters near the river plumes 01 p0226 N94-12744
The ecological and environmental impacts of manmade marshes
[AD-A269213] 04 p1475 N94-18885
Hydraulics and morphology of mountain rivers: A literature survey. Communications on hydraulic and geotechnical engineering
[PB94-110772] 06 p2388 N94-24636
Glaciohydrologic and glaciohydraulic effects on runoff and sediment yield in glacierized basins
[AD-A275134] 08 p3361 N94-29286
Dewatering of contaminated river sediments 08 p3354 N94-30472
Multitemporal analysis of a braiding river: The advanced study of 1992
[NLR-TP-93100-U] 08 p3335 N94-30942

RIVETED JOINTS
Fatigue crack initiation in riveted lap joints and in pressurized fuselages
[LR-725] 04 p1461 N94-19669
Multiple-site damage in aircraft fuselage structures
[LR-729] 09 p3578 N94-31675

RIVETS
Mechanically fastened composite laminates subjected to combined bearing-bypass and shear loading 07 p2712 N94-27914
Full-scale testing and analysis of curved aircraft fuselage panels
[AD-A275666] 08 p3145 N94-28657

RL CIRCUITS
NT RLC CIRCUITS

RL-10 ENGINES
Extended duration lunar lander
[NASA-CR-195527] 06 p2206 N94-24916

RLC CIRCUITS
Study of a system for producing a pulsed magnetic field (B 2T) with a frequency of 50 Hz
[ISL-N-601/92] 06 p2314 N94-25460
Broadband, high-power, 2-30 MHz, twin-whip antenna. Computer and 1/10-scale model design study
[AD-A277619] 09 p3682 N94-32971

RLC NETWORKS
U RLC CIRCUITS

RNA
U RIBONUCLEIC ACIDS

ROADS
NT HIGHWAYS
Stochastic performance modeling and evaluation of obstacle detectability with imaging range sensors
[NASA-CR-194510] 02 p0605 N94-13946
YARF: An open-ended framework for robot road following
[AD-A266788] 03 p1163 N94-14910
Massively parallel, adaptive, color image processing for autonomous road following
[AD-A266988] 03 p0864 N94-15498
Traffic noise in a roundabout way 05 p1966 N94-21799
STAR-1 SAR road extraction using texture analysis and mathematical morphology
[ISBN-0-315-83255-X] 05 p1843 N94-22429
Estimation of delays and emissions at four-way junctions with different forms of regulation, principally four-way mandatory stop
[PB94-105236] 06 p2398 N94-23813
Unscreened low tension cables scrape abrasion testing
[PB94-123767] 07 p2823 N94-26849
Report of the National Research Institute for Earth Science and Disaster Prevention, No. 51
[JTN-94-80509] 07 p2886 N94-27985
Detection of water on road surface by the polarized light 07 p2886 N94-27989
Development of a method for predicting snowfall intensity and compacted snow on roads 07 p2853 N94-27990
Conception of snow information network system in Yamagata Prefecture 07 p2853 N94-27991
The road plan model: Information model for planning road building activities
[AIAA PAPER 94-1219-CP] 08 p3445 N94-30567
Tracking roads in an aerial image by Kalman filtering
[TELECOM-93-D-007] 09 p3711 N94-31096

The contribution of satellite data in communication infrastructure projects 09 p3749 N94-32530

ROBOT ARMS

Payload sensitivity in coupled bending and torsional vibrations in flexible beams
[MEMO-1102] 01 p0184 N94-10161

Force reflection with compliance control
[NASA-CASE-NPO-18668-1-CU] 01 p0179 N94-10654

Telerobot control system
[NASA-CASE-NPO-18116-1-CU] 01 p0179 N94-10670

Momentum management in redundant manipulators for vibration suppression
[NASA-CR-194112] 01 p0180 N94-10821

An adaptive and robust control for motion coordination of two-cooperating robot manipulators 01 p0340 N94-11825

Roller-gear drives for robotic manipulators design, fabrication and test
[NASA-CR-194248] 02 p0660 N94-12802

Control algorithm implementation for a redundant degree of freedom manipulator
[NASA-CR-191339] 02 p0762 N94-13131

Modelling robotic systems with DADS 02 p0678 N94-14625

Fuzzy inverse kinematic mapping: Rule generation, efficiency, and implementation
[AD-A266967] 03 p1163 N94-14954

Contextually dependent control strategies for manipulation
[TR-416] 03 p1165 N94-16580

Visually guided touching and manual tracking
[TR-412] 03 p1166 N94-16581

Three axis force override rate control of a PUMA 560 manipulator
[AD-A267313] 03 p1048 N94-16944

Research in lightweight elastic robotic arms
[AD-A270846] 05 p1821 N94-19833

Interactive simulation package for coupled bending and torsional vibrations in flexible robot arms
[MEMO-1089] 05 p1944 N94-21140

Optimal control of the tip of a flexible arm 05 p1794 N94-22256

Control of a serpentine manipulator with collision avoidance 06 p2368 N94-23232

Telerobotic rendezvous and docking vision system architecture
[NASA-CR-191329] 06 p2204 N94-23828

HERA (Hermes robot arm) overview 06 p2357 N94-24005

The development of the HERA Test Facility (HTF) 06 p2197 N94-24020

Robust stability of second-order systems
[NASA-CR-195175] 06 p2488 N94-24564

Autonomous Space Processor for Orbital Debris (ASPOD)
[NASA-CR-195521] 06 p2204 N94-24621

Human-like robots for space and hazardous environments
[NASA-CR-195549] 06 p2365 N94-24703

Research experience for undergraduates in robotics and materials
[AD-A273659] 06 p2368 N94-25436

Autonomous space processor for orbital debris advanced design project in support of solar system exploration 07 p2697 N94-25667

Inertial-space disturbance rejection for space-based manipulators 07 p2683 N94-26281

Direct model reference adaptive control of robotic arms 07 p2683 N94-26282

Motion planning for serial manipulators with many degrees of freedom: Implementation of a sequential search strategy
[ISBN-0-315-83682-2] 07 p2822 N94-26642

Generalized finite element dynamic modelling and simulation for flexible robot manipulators
[ISBN-0-315-84623-2] 07 p2825 N94-27343

Dynamic control of kinematically redundant manipulators
[ISBN-0-315-84627-5] 07 p2825 N94-27344

Design and construction of the Aerobot Robotic Manipulator (ARM)
[AD-A275362] 08 p3298 N94-28894

Experimental evaluation of fuzzy logic control of a flexible arm manipulator
[AD-A275375] 08 p3434 N94-29013

Feedback control of a three-link planar under-actuated manipulator using a surge velocity
[AD-A275159] 08 p3435 N94-29044

High level language-based robotic control system
[NASA-CASE-NPO-17918-2-CU] 08 p3435 N94-29465

Simplified and symmetrical five-bar linkage driver for manipulating a six-degree-of-freedom parallel minimanipulator with three inextensible limbs
[NASA-CASE-GSC-13485-2] 08 p3301 N94-29556

Kinematic representations, workspace analysis, and grasp stability in robot arms and multi-fingered hands 08 p3301 N94-29847

Three methods to improve the accuracy of a PUMA 560 robot 08 p3307 N94-30290

Aiding the operator in the manual control of a space manipulator
[PB94-125549] 08 p3402 N94-30390

The use of interactive computer vision and robot hand controllers for enhancing manufacturing safety 08 p3314 N94-30442

ODYSSEUS autonomous walking robot: The leg/arm design
[AIAA PAPER 94-1180-CP] 08 p3439 N94-30531

A highly redundant robot system for inspection
[AIAA PAPER 94-1194-CP] 08 p3442 N94-30545

An intelligent robotic aid system for human services
[AIAA PAPER 94-1232-CP] 08 p3447 N94-30580

Kinematic analysis of platform-type robotic manipulators
[ISBN-0-315-78703-1] 08 p3311 N94-30793

Robust adaptive control of a mechanical manipulator 08 p3449 N94-30806

Integrated structure/control design of nonrigid robot arms for high-speed manipulation 08 p3312 N94-30866

Kinematics and force analysis of a robot hand based on an artificial biological control scheme 08 p3313 N94-30957

A high-performance multi-arm environment: Theoretical aspects and practical implementation
[RR-479] 09 p3722 N94-31379

Control of a flexible space robot tracking a moving target 09 p3722 N94-31469

Point-contact and point-impact dynamics for multibody chains
[ISBN-0-315-87056-7] 09 p3734 N94-31737

Trajectory learning with a direct drive robotic manipulator 09 p3831 N94-31794

Model identification of a reconfigurable robot manipulator
[ISBN-0-315-87109-1] 09 p3725 N94-31874

Control of a flexible-link robotic arm manipulating an unknown dynamic payload 09 p3725 N94-31973

Parallel methods for synthesizing whole-hand grasps from generalized prototypes
[AD-A276798] 09 p3726 N94-32166

Information theory for arm visuo-motor coordination 09 p3800 N94-32495

Design, characterization and control of the Unique Mobility Corporation robot 09 p3603 N94-33296

Force override rate control for robotic manipulators 10 p4066 N94-33665

Graphical programming: A systems approach for telerobotic servicing of space assets 10 p4066 N94-33666

Dexterous end effector flight demonstration 10 p4067 N94-34032

Hardware interface for isolation of vibrations in flexible manipulators: Development and applications 10 p4067 N94-34036

Robotics Demo Peer Group review
[NASA-TM-109849] 10 p4061 N94-34117

Bilateral control to coordinate operators with supporting systems by force sensed grips 10 p4067 N94-34335

Computer aided design of robotic control systems 10 p4110 N94-34336

Technology demonstration of space intravehicular automation and robotics
[NASA-TM-109138] 12 p4501 N94-37589

ROBOT CONTROL

Position and force control of a vehicle with two or more steerable drive wheels
[DE93-012512] 01 p0177 N94-10269

Force reflection with compliance control
[NASA-CASE-NPO-18668-1-CU] 01 p0179 N94-10654

Telerobot control system
[NASA-CASE-NPO-18116-1-CU] 01 p0179 N94-10670

Sensor abstractions to support many-robot systems
[AD-A265907] 01 p0180 N94-10803

Momentum management in redundant manipulators for vibration suppression
[NASA-CR-194112] 01 p0180 N94-10821

The development of an interactive synthesis tool for intelligent controllers of modular, reconfigurable robots 01 p0339 N94-10898

Basic experiment on an ultrasonic method of localization
[DE93-754295] 01 p0358 N94-11042

Development and evaluation of a predictive algorithm for telerobotic task complexity 01 p0341 N94-11562

The rational behavior model: A multi-paradigm, tri-level software architecture for the control of autonomous vehicles
[AD-A265175] 01 p0332 N94-11874

Derivation of three closed loop kinematic velocity models using normalized quaternion feedback for an autonomous redundant manipulator with application to inverse kinematics
[DE93-012823] 01 p0340 N94-12543

Experiments in mobile robot navigation and range imaging
[DE93-013280] 01 p0341 N94-12598

Roller-gear drives for robotic manipulators design, fabrication and test
[NASA-CR-194248] 02 p0660 N94-12802

Application of intelligently adaptable structure and robot to large space structure 02 p0530 N94-13277

Robot programming, natural computation and conceptual graphs
[ITN-93-85193] 02 p0748 N94-13539

Robot-task compliance: The energy criterion
[ITN-93-85196] 02 p0763 N94-13568

Goddard Space Flight Center robotics demo
[NASA-TM-109302] 02 p0662 N94-13604

A capacifiector-based robotic system
[NASA-CR-193783] 02 p0833 N94-14359

Inverse dynamics: Simultaneous trajectory tracking and vibration reduction with distributed actuators 02 p0678 N94-14624

A neural-network approach to robotic control 02 p0679 N94-14634

Design and control of a macro-micro robot for precise force applications 02 p0682 N94-14651

Tactile sensing and control in humans and robotic/teleoperated systems
[AD-A267710] 03 p1163 N94-14937

Fuzzy inverse kinematic mapping: Rule generation, efficiency, and implementation
[AD-A266967] 03 p1163 N94-14954

Real-time implementation of neural network learning control of a flexible space manipulator
[AD-A266962] 03 p1045 N94-14970

Infrared remote activity transceiver universal model
[AD-A266965] 03 p1188 N94-15144

Contextually dependent control strategies for manipulation
[TR-416] 03 p1165 N94-16580

Visually guided touching and manual tracking
[TR-412] 03 p1166 N94-16581

A modular control architecture for real-time synchronous and asynchronous systems
[DE93-015439] 03 p1166 N94-16888

Development of a prototype kinestatic platform for application to space and ground servicing tasks. Phase 1: Concept Modeling
[NASA-CR-194036] 03 p0887 N94-16905

Three axis force override rate control of a PUMA 560 manipulator
[AD-A267313] 03 p1048 N94-16944

An object-oriented program specification for a mobile robot motion control language
[AD-A267213] 03 p1166 N94-16986

End-effector: Joint conjugates for robotic assembly of large truss structures in space: Extended concepts
[NASA-CR-193576] 03 p1048 N94-17088

Path planning for robotic truss assembly
[NASA-CR-194652] 03 p0897 N94-17280

Efficient dynamic modeling of manipulators containing closed kinematic loops
[REPT-92-083] 04 p1444 N94-17940

Autonomous neural network controllers for adaptive material handling
[AD-A268908] 04 p1540 N94-18331

Flexible integration of path-planning capabilities
[AD-A269594] 04 p1541 N94-18463

MART: An overview of the Mobile Autonomous Robot Twente project
[MEMO-INF-93-12] 04 p1543 N94-19199

Robot navigation in unknown terrains: Introductory survey of non-heuristic algorithms
[DE93-019221] 04 p1316 N94-19300

Research in lightweight elastic robotic arms
[AD-A270846] 05 p1821 N94-19833

Robot skill learning and the effects of basis function choice
[TR-437] 05 p1939 N94-20135

Self-organization via active exploration in robotic applications. Phase 2: Hybrid hardware prototype
[NASA-CR-194723] 05 p1939 N94-20212

Climbing robot --- caterpillar design
[NASA-CASE-GSC-13442-1] 05 p1823 N94-20494

Internal camera calibration using rotation and geometric shapes
[AD-A272718] 05 p1808 N94-21167

Automating the control of robotic systems in unstructured environments
[DE93-040753] 05 p1946 N94-21929
An adaptive control to enable a robot to follow Cartesian trajectories 05 p1790 N94-22229
A robust adaptive control design for flexible joint manipulators 05 p1790 N94-22230
An algorithm for the interference detection among polygonal surfaces 05 p1791 N94-22239
Analytical representation of working articulation space of a plane manipulator in an encumbered environment 05 p1792 N94-22241
Control of multiple robot manipulators with optimal force distribution 05 p1794 N94-22255
Optimal control of the tip of a flexible arm 05 p1794 N94-22256
Robot link and contact surface dynamic interaction: An experimental study of contact instability
[ISBN-0-315-83439-0] 05 p1827 N94-22578
Normal forms of kinematic singularities of 3R robot manipulators
[MEMO-1124] 06 p2469 N94-22712
Control of a serpentine manipulator with collision avoidance 06 p2368 N94-23232
Rack Insertion End Effector (RIEE) automation 06 p2368 N94-23242
The robotic Mars rover 06 p2608 N94-23390
Sensing and modelling concepts for autonomous and remote mobile robot control 06 p2370 N94-23421
Bond graph modeling, simulation, and reflex control of the Mars planetary automatic vehicle 06 p2370 N94-23424
Experiments with a small behaviour controlled planetary rover 06 p2371 N94-23427
Telerobotic rendezvous and docking vision system architecture
[NASA-CR-191329] 06 p2204 N94-23828
Ground operation of robotics on Space Station Freedom 06 p2371 N94-23841
Development of a force feedback anthropomorphic teleoperation input device for control of robot hands
[NASA-CR-195109] 06 p2437 N94-24329
Autonomous Space Processor for Orbital Debris (ASPOD)
[NASA-CR-195521] 06 p2204 N94-24621
Human-like robots for space and hazardous environments
[NASA-CR-195549] 06 p2365 N94-24703
Preliminary results on time-varying feedback stabilization of a nonholonomic car-like mobile robot
[INRIA-RR-1512] 06 p2475 N94-24963
Advanced control structures: A transputer-based multi-robot system
[RR-468] 06 p2446 N94-25313
The 1991-1992 walking robot design 07 p2833 N94-25686
Graphical programming at Sandia National Laboratories
[DE94-003803] 07 p2958 N94-25818
Application of the CIRSSE cooperating robot path planner to the NASA Langley truss assembly problem 07 p2683 N94-26280
Performance measures from the explorer platform berthing experiment 07 p2683 N94-26283
Computer visualizations in engineering applications
[DE94-003589] 07 p2822 N94-26465
On-board computer for control subsystem of satellite 07 p2949 N94-26716
Sensor-based navigation of a mobile robot using automatically constructed fuzzy rules
[DE94-001137] 07 p2986 N94-26948
Robotics handbook. Version 1: For the interested party and professional
[NASA-TM-109690] 07 p2824 N94-27238
The universal robot 07 p2686 N94-27361
Design, implementation and experimental results of robotic environment input into the Robot Controller Test Station (RCTS)
[ISBN-0-315-85355-7] 07 p2826 N94-27596
The state transition diagram with path priority and it's applications
[AD-A275524] 08 p3434 N94-28672
Experimental evaluation of fuzzy logic control of a flexible arm manipulator
[AD-A275375] 08 p3434 N94-29013
High level language-based robotic control system
[NASA-CASE-NPO-17918-2-CU] 08 p3435 N94-29465
Integration of a path generation algorithm into off-line programming of airbus panels
[REPT-932-600-103] 08 p3435 N94-29480
Robotic hand-eye motor learning 08 p3436 N94-29835
Collision avoidance and control of multiple revolute manipulators 08 p3302 N94-29884
A study of the flexible space platform based deployable manipulator
[ISBN-0-315-85410-3] 08 p3303 N94-30135
DREV activities related to military vehicles robotization 08 p3305 N94-30278
The NRC mobile robot project 08 p3305 N94-30280
A generic semi-autonomous ground vehicle control system 08 p3306 N94-30283
An optimal obstacle avoidance path planning algorithm for the Excalibur robot 08 p3306 N94-30287
Maestro: An open system architecture for multi-robot control 08 p3306 N94-30288
Coordinated control of multiple robot manipulators 08 p3306 N94-30289
An inverse kinematics algorithm for the DREP/Philips real-time radiographic manipulator system 08 p3307 N94-30292
Simulation of lightweight robots and their controllers 08 p3307 N94-30294
Elements of supervisory control for military robotic applications 08 p3309 N94-30303
Supervised autonomous control for Space Station Special Purpose Dextrous Manipulator (SPDM) robot 08 p3309 N94-30305
A testbed for the development of ground-based control of space-based manipulators 08 p3309 N94-30306
Achieving robot autonomy 08 p3310 N94-30307
Improving the execution speed of robot control computations: An allocation scheme for heterogeneous multiprocessors 08 p3310 N94-30308
Motion control of mobile robots 08 p3310 N94-30309
Control system design for A and R supported microgravity experiments: An experiment payload control development
[AD-B179107] 08 p3229 N94-30421
A force-controllable macro-micro manipulator and its application to medical robots 08 p3314 N94-30441
The use of interactive computer vision and robot hand controllers for enhancing manufacturing safety 08 p3314 N94-30442
Programmable Automated Welding System (PAWS): Control of welding through software and hardware 08 p3314 N94-30443
Conference on Intelligent Robotics in Field, Factory, Service, and Space (CIRFFSS 1994), volume 1
[NASA-CP-3251] 08 p3439 N94-30526
ARK: Autonomous mobile robot in an industrial environment
[AIAA PAPER 94-1177-CP] 08 p3439 N94-30529
Integration of vision and robotic workcell
[AIAA PAPER 94-1186-CP] 08 p3440 N94-30536
Meeting the challenges of installing a mobile robotic system
[AIAA PAPER 94-1187-CP] 08 p3440 N94-30537
Controlling multiple security robots in a warehouse environment
[AIAA PAPER 94-1300-CP] 08 p3441 N94-30540
A Space Station robot walker and its shared control software
[AIAA PAPER 94-1192-CP] 08 p3442 N94-30543
Perception system and functions for autonomous navigation in a natural environment
[AIAA PAPER 94-1201-CP] 08 p3443 N94-30552
A streamlined software environment for situated skills
[AIAA PAPER 94-1205-CP] 08 p3444 N94-30556
Object-based task-level control: A hierarchical control architecture for remote operation of space robots
[AIAA PAPER 94-1209-CP] 08 p3444 N94-30560
Task-level control for autonomous robots
[AIAA PAPER 94-1210-CP] 08 p3444 N94-30561
A performance analysis method for distributed real-time robotic systems: A case study of remote teleoperation
[AIAA PAPER 94-1212-CP] 08 p3445 N94-30563
Using generic tool kits to build intelligent systems
[AIAA PAPER 94-1214-CP] 08 p3445 N94-30565
A reactive system for open terrain navigation: Performance and limitations
[AIAA PAPER 94-1218-CP] 08 p3445 N94-30566
The road plan model: Information model for planning road building activities
[AIAA PAPER 94-1219-CP] 08 p3445 N94-30567
Programmable Automated Welding System (PAWS)
[AIAA PAPER 94-1221-CP] 08 p3446 N94-30570
Robotic NDE inspection of advanced solid rocket motor casings
[AIAA PAPER 94-1222-CP] 08 p3446 N94-30571
Piecewise linear paths among convex obstacles
[RUU-CS-93-20] 08 p3460 N94-30721
Robust adaptive control of a mechanical manipulator 08 p3449 N94-30806
ELF: Learning incomplete fuzzy rule sets for an autonomous robot
[REPT-93-043] 08 p3449 N94-30923
Kinematics and force analysis of a robot hand based on an artificial biological control scheme 08 p3313 N94-30957
Iterative removal of boundary minima of harmonic potential function for mobile robot navigation
[REPT-93-059] 08 p3449 N94-30962
Robust control of robots via linear estimated state-feedback
[MEMO-1153] 08 p3449 N94-30963
Camera-space manipulation with natural visual information 09 p3829 N94-31207
A high-performance multi-arm environment: Theoretical aspects and practical implementation
[RR-479] 09 p3722 N94-31379
Control of a flexible space robot tracking a moving target 09 p3722 N94-31469
ControlShell: A real-time software framework
[AD-A276481] 09 p3811 N94-31475
Contingency-tolerant robot motion planning and control 09 p3830 N94-31482
A neural network methodology for engineering applications: The learning control of robotic systems
[RR-480] 09 p3830 N94-31500
Motion and force control of coordinated robots
[ISBN-0-315-86323-4] 09 p3724 N94-31714
Strategy for tracking and grabbing a moving object with the aid of a decouplable manipulator with six degrees of freedom general architecture, guided by a vision system
[ISBN-0-315-86864-3] 09 p3831 N94-31757
Trajectory learning with a direct drive robotic manipulator 09 p3831 N94-31794
Adaptive control of a robot in Cartesian coordinates: Analysis and implementation
[ISBN-0-315-86493-1] 09 p3831 N94-31798
Development of a feedforward controller for a flexible manipulator
[ISBN-0-315-86515-6] 09 p3832 N94-31801
Real-time control and application to robotics: Hardware and software architectures
[ISBN-0-315-87192-X] 09 p3833 N94-31876
High-speed path constrained manipulator operation using optimal-feedback combined controller 09 p3833 N94-31962
Control of a flexible-link robotic arm manipulating an unknown dynamic payload 09 p3725 N94-31973
Parallel methods for synthesizing whole-hand grasps from generalized prototypes
[AD-A276798] 09 p3726 N94-32166
An experimental testbed for a free-floating manipulator
[AD-A277350] 09 p3726 N94-32334
Applying robotics to HAZMAT 09 p3729 N94-32452
Information theory for arm visuo-motor coordination 09 p3800 N94-32495
A multitasking behavioral control system for the Robotic All Terrain Lunar Exploration Rover (RATLER)
[DE94-007293] 09 p3835 N94-32787
Identification and control of structures in space
[NASA-CR-195910] 09 p3612 N94-33115
Design, characterization and control of the Unique Mobility Corporation robot 09 p3603 N94-33296
Experiments in autonomous navigation and control of multi-manipulator, free-flying space robots 10 p4013 N94-33383
End effector monitoring system: An illustrated case of operational prototyping 10 p4109 N94-33631
Force override rate control for robotic manipulators 10 p4066 N94-33665
Vehicle development of Lunar/Mars exploration 10 p4067 N94-34030
Controlling telerobots with video data and compensating for time-delayed video using Omniview 10 p4127 N94-34031
Dexterous end effector flight demonstration 10 p4067 N94-34032
Undersea applications of dexterous robotics 10 p4067 N94-34033
Robotic technologies of the Flight Telerobotic Servicer (FTS) including fault tolerance 10 p4067 N94-34034
Robotic vehicle mobility and task performance: A flexible control modality for manned systems 10 p4067 N94-34040
Robust control of nonlinear flexible multibody systems using quaternion feedback and dissipative compensation
[NASA-TM-109099] 10 p4014 N94-34103
Computer aided design of robotic control systems 10 p4110 N94-34336
A test system of pose repeatability precision of multi-path robot 10 p4067 N94-34341
A linguistic geometry for space applications 10 p4123 N94-35050
Multiresolutional schemata for unsupervised learning of autonomous robots for 3D space operation 10 p4123 N94-35051

A genetic technique for planning a control sequence to navigate the state space with a quasi-minimum-cost output trajectory for a non-linear multi-dimnensional system 10 p4123 N94-35052
Adjustable control station with movable monitors and cameras for viewing systems in robotics and teleoperations [NASA-CASE-NPO-17837-1-CU] 11 p4332 N94-35384
Interfacing the RAP system to real-time control, version 1 [AD-A278725] 11 p4312 N94-36295
Robust stability of second-order systems [NASA-CR-196384] 12 p4501 N94-37590
What is an open architecture robot controller? [DE94-007854] 12 p4501 N94-37783

ROBOT DYNAMICS
The development of an interactive synthesis tool for intelligent controllers of modular, reconfigurable robots 01 p0339 N94-10898
Trajectory pattern inverse dynamics and control of nonlinear dynamics systems with application to flexible structures 01 p0181 N94-11219
Space Station maintenance studies using plaid graphics 01 p0335 N94-11578
Robotic servicing on Earth orbiting satellites 01 p0045 N94-11579
An adaptive and robust control for motion coordination of two-cooperating robot manipulators 01 p0340 N94-11825
Derivation of three closed loop kinematic velocity models using normalized quaternion feedback for an autonomous redundant manipulator with application to inverse kinematics [DE93-012823] 01 p0340 N94-12543
Dynamics and design of nonholonomic robotic mechanical systems [ISBN-0-315-72009-3] 02 p0662 N94-13597
Inverse dynamics: Simultaneous trajectory tracking and vibration reduction with distributed actuators 02 p0678 N94-14624
Modelling robotic systems with DADS 02 p0678 N94-14625
A neural-network approach to robotic control 02 p0679 N94-14634
Parallel methods for dynamic simulation of multiple manipulator systems 02 p0680 N94-14637
Design and control of a macro-micro robot for precise force applications 02 p0682 N94-14651
An experimental comparison of CLOS and C(++) implementations of an object-oriented graphical simulation of walking robot kinematics [AD-A267168] 03 p1165 N94-15855
Temporal segmentation of tasks from human hand motion [AD-A266596] 03 p1166 N94-16725
Development of a prototype kinestatic platform for application to space and ground servicing tasks. Phase 1: Concept Modeling [NASA-CR-194036] 03 p0887 N94-16905
Reference frames in vision [AD-A266174] 03 p1132 N94-16925
An object-oriented program specification for a mobile robot motion control language [AD-A267213] 03 p1166 N94-16986
Joint stiffness estimation based on force sensor measurements in industrial manipulators [REPT-92-053] 04 p1443 N94-17937
Direct kinematics solution architectures for industrial robot manipulators: Bit-serial versus parallel 04 p1399 N94-18358
Survey of collision avoidance and ranging sensors for mobile robots, revision 1 [AD-A269846] 04 p1541 N94-18474
Robot skill learning and the effects of basis function choice [TR-437] 05 p1939 N94-20135
Climbing robot --- caterpillar design [NASA-CASE-GSC-13442-1] 05 p1823 N94-20494
Model-based automatic generation of grasping regions [NASA-TM-104785] 05 p1946 N94-21550
An adaptive control to enable a robot to follow Cartesian trajectories 05 p1790 N94-22229
Normal forms of kinematic singularities of 3R robot manipulators [MEMO-1124] 06 p2469 N94-22712
Motion planning for a non-holonomic mobile in a dynamic workspace [ETN-94-95180] 06 p2470 N94-22898
Contribution to geometric and dynamic modeling of parallel robots [LAAS-93089] 06 p2470 N94-22904
An architecture for teleprogramming autonomous mobile robots at task level [LAAS-93107] 06 p2470 N94-22906
Perception and 3D environment modeling for mobile robot autonomous navigation [LAAS-93117] 06 p2471 N94-22908
Walking, jumping, and tumbling: More than one way to get around Mars 06 p2370 N94-23419
Perspective of creation of means for collecting information concerning transport situation 06 p2370 N94-23420
Sensing and modelling concepts for autonomous and remote mobile robot control 06 p2370 N94-23421
Physical modeling and dynamic simulation of planet vehicles: Application to the motion prediction 06 p2371 N94-23426
Human-like robots for space and hazardous environments [NASA-CR-195549] 06 p2365 N94-24703
Preliminary results on time-varying feedback stabilization of a nonholonomic car-like mobile robot [INRIA-RR-1512] 06 p2475 N94-24963
Advanced control structures: A transputer-based multi-robot system [RR-468] 06 p2446 N94-25313
Genetic-based motion planning for articulated robotic manipulators [RR-476] 06 p2368 N94-25322
A biologically-inspired autonomous robot [AD-A273909] 07 p2821 N94-25782
Robotics handbook. Version 1: For the interested party and professional [NASA-TM-109690] 07 p2824 N94-27238
Generalized finite element dynamic modelling and simulation for flexible robot manipulators [ISBN-0-315-84623-2] 07 p2825 N94-27343
Dynamic control of kinematically redundant manipulators [ISBN-0-315-84627-5] 07 p2825 N94-27344
Integration of a path generation algorithm into off-line programming of airbus panels [REPT-932-600-103] 08 p3435 N94-29480
Kinematic representations, workspace analysis, and grasp stability in robot arms and multi-fingered hands 08 p3301 N94-29847
Motion control of mobile robots 08 p3310 N94-30309
Development and validation of a linear recursive order-N algorithm for the simulation of flexible space manipulators dynamics [AD-B173557] 08 p3311 N94-30391
A probabilistic approach to motion planning for car-like robots [RUU-CS-93-18] 08 p3438 N94-30410
Biologically-inspired hexapod robot design and simulation [AIAA PAPER 94-1178-CP] 08 p3439 N94-30530
ODYSSEUS autonomous walking robot: The leg/arm design [AIAA PAPER 94-1180-CP] 08 p3439 N94-30531
Free-floating dual-arm robots for space assembly [AIAA PAPER 94-1195-CP] 08 p3442 N94-30546
Aspects of vision and planning in a dynamic, uncertain environment 08 p3448 N94-30803
Integrated structure/control design of nonrigid robot arms for high-speed manipulation 08 p3312 N94-30866
Kinematics and force analysis of a robot hand based on an artificial biological control scheme 08 p3313 N94-30957
Camera-space manipulation with natural visual information 09 p3829 N94-31207
A high-performance multi-arm environment: Theoretical aspects and practical implementation [RR-479] 09 p3722 N94-31379
Control of a flexible space robot tracking a moving target 09 p3722 N94-31469
Kinematic synthesis and analysis of a novel class of six-DOF parallel minimanipulators 09 p3723 N94-31568
Remote robot manipulator coupled with remote-controlled guide vehicle for soil sampling in hazardous waste sites 09 p3723 N94-31569
Penetration distances and their applications to path planning 09 p3858 N94-31725
Point-contact and point-impact dynamics for multibody chains [ISBN-0-315-87056-7] 09 p3734 N94-31737
Application of contact mechanics for the validation of robotized operations of grasping objects subjected to static and dynamic force fields [ISBN-0-315-86831-7] 09 p3725 N94-31754
Trajectory learning with a direct drive robotic manipulator 09 p3831 N94-31794
Study of a path planning and tracking system for an articulated mobile robot [ISBN-0-315-86502-4] 09 p3831 N94-31800
Automatic analysis of force distribution in multi-fingered articulated hands [ISBN-0-315-87205-5] 09 p3725 N94-31878
Hierarchical mixtures of experts and the EM algorithm [AD-A276516] 09 p3814 N94-31932
High-speed path constrained manipulator operation using optimal-feedback combined controller 09 p3833 N94-31962
Robot motion vision by fixation 09 p3833 N94-31991
An experimental testbed for a free-floating manipulator [AD-A277350] 09 p3726 N94-32334
Construction of a parallel processor for simulating manipulators and other mechanical systems [NASA-CR-191327] 09 p3826 N94-32482
Dynamic error compensation in robotic trusses 09 p3738 N94-32486
Identification and control of structures in space [NASA-CR-195910] 09 p3612 N94-33115
Task and environment-sensitive tracking [AD-A278846] 11 p4312 N94-35802
Robot trajectory planning via dynamic programming [DE94-008424] 12 p4501 N94-37529
Robust stability of second-order systems [NASA-CR-196384] 12 p4501 N94-37590

ROBOT FINGERS
U END EFFECTORS

ROBOT HANDS
U END EFFECTORS

ROBOT MOTION
U ROBOT DYNAMICS

ROBOT SENSORS
NT TACTILE SENSORS (ROBOTICS)
Experiments in mobile robot navigation and range imaging [DE93-013280] 01 p0341 N94-12598
A capacitector-based robotic system [NASA-CR-193783] 02 p0833 N94-14359
Panacea: An active sensor controller for the ALVINN autonomous driving system [AD-A266964] 03 p0864 N94-14972
Programmable Remapper project [NASA-TM-109508] 03 p1164 N94-15515
MART: An overview of the Mobile Autonomous Robot Twente project [MEMO-INF-93-12] 04 p1543 N94-19199
Automated rendezvous and capture demonstration study [NASA-CR-192587] 04 p1331 N94-19366
Head-centered orientation strategies in animate vision [TR-442] 05 p1894 N94-20520
Sensor integration and data fusion for object localization in robotic workcells 05 p1774 N94-22130
Ultrasonic sensor vision in robotics 05 p1775 N94-22131
An evaluation of three-dimensional sensors for the extravehicular activity helper/retriever 06 p2444 N94-25369
Object imaging accomplished with an integrated circuit robotic tactile sensor incorporating a piezoelectric polyvinylidene fluoride thin film [AD-A274038] 07 p2780 N94-25845
DREV activities related to military vehicles robotization 08 p3305 N94-30278
The NRC mobile robot project 08 p3305 N94-30280
Thermal imaging for a mobile robot 08 p3308 N94-30300
Sonar sensing and obstable detection 08 p3309 N94-30301
Conference on Intelligent Robotics in Field, Factory, Service, and Space (CIRFFSS 1994), volume 1 [NASA-CP-3251] 0[illegible]3439 N94-30526
TRC research products: components for service robots [AIAA PAPER 94-1227-CP] 08 p3447 N94-30576
Synchronized laser scanning three dimensional acquisition system [ISBN-0-315-86848-1] 09 p3879 N94-31756
Undergraduate robotics projects in support of research on neural networks [AD-A277331] 09 p3835 N94-32281
The resolvability ellipsoid for [illegible]or based manipulation [AD-A277898] 10 p4055 N94-33549
Adaptive multisensor fusion for the perception and interpretation of outdoor robot scenes [PB94-170719] 12 p4499 N94-36535

ROBOTICS
NT TELEROBOTICS
Lightweight CFRP frame structures for a Rotex-derived manipulator system 01 p0056 N94-10005
Position and force control of a vehicle with two or more steerable drive wheels [DE93-012512] 01 p0177 N94-10269

Preliminary system design of a Three Arm Capture Mechanism (TACM) flight demonstration article
[NASA-CR-192573] 01 p0177 N94-10341
Task planning with uncertainty for robotic systems
[NASA-CR-193253] 01 p0338 N94-10638
Sensor abstractions to support many-robot systems
[AD-A265907] 01 p0180 N94-10803
Mechanical analysis of parallel manipulators with simulation, design, and control applications
[ISBN-0-315-72013-1] 01 p0181 N94-11156
Sixth Annual Workshop on Space Operations Applications and Research (SOAR 1992), volume 2
[NASA-CP-3187-VOL-2] 01 p0486 N94-11527
Space Station maintenance studies using plaid graphics 01 p0335 N94-11578
Robotic servicing on Earth orbiting satellites 01 p0045 N94-11579
The rational behavior model: A multi-paradigm, tri-level software architecture for the control of autonomous vehicles
[AD-A265175] 01 p0332 N94-11874
Roller-gear drives for robotic manipulators design, fabrication and test
[NASA-CR-194248] 02 p0660 N94-12802
Advancing automation and robotics technology for the Space Station Freedom and for the U.S. economy
[NASA-TM-104024] 02 p0739 N94-12838
Flex-gear electrical power transmission
[NASA-CR-194422] 02 p0661 N94-13445
Robot programming, natural computation and conceptual graphs
[ITN-93-85193] 02 p0748 N94-13539
Dynamics and design of nonholonomic robotic mechanical systems
[ISBN-0-315-72009-3] 02 p0662 N94-13597
Goddard Space Flight Center robotics demo
[NASA-TM-109302] 02 p0662 N94-13604
New prosthetic devices
[NASA-TM-109304] 02 p0737 N94-13611
Development of a tactile and vision integrated system, and object identification techniques for SPDM applications
[DSIS-93-00153] 02 p0764 N94-13842
Activities of Institute for Information Technology
[CNR-35024] 02 p0824 N94-14069
Knowledge based systems: From process control to policy analysis
[DE93-014582] 02 p0765 N94-14117
A capacitflector-based robotic system
[NASA-CR-193783] 02 p0833 N94-14359
Large space structures and systems in the space station era: A bibliography with indexes (supplement 05)
[NASA-SP-7085(05)] 02 p0543 N94-14411
Proceedings of the Fifth NASA/NSF/DOD Workshop on Aerospace Computational Control
[NASA-CR-194515] 02 p0677 N94-14618
Modelling robotic systems with DADS 02 p0678 N94-14625
Spatial operator algebra for flexible multibody dynamics 02 p0679 N94-14631
A neural-network approach to robotic control 02 p0679 N94-14634
Design and control of a macro-micro robot for precise force applications 02 p0682 N94-14651
The further development and refinement of an expert-systems approach to the creative design of mechanisms and mechanical systems
[AD-A266812] 02 p0665 N94-14901
Tactile sensing and control in humans and robotic/teleoperated systems
[AD-A267710] 03 p1163 N94-14937
Fuzzy control and fuzzy kinematic mapping for a redundant space robot
[AD-A266866] 03 p1163 N94-14950
Infrared remote activity transceiver universal model
[AD-A266965] 03 p1188 N94-15144
Robotics for Space Station tape 2
[NASA-TM-109578] 03 p1045 N94-15263
Robotics in space
[NASA-TM-109584] 03 p1045 N94-15268
Robotics for Space Station, tape 1
[NASA-TM-109588] 03 p1045 N94-15272
Future of robotics
[NASA-TM-109592] 03 p1045 N94-15284
Plasma arc welding repair of space flight hardware
[TABES PAPER 93-603] 03 p1049 N94-16139
Contextually dependent control strategies for manipulation
[TR-416] 03 p1165 N94-16580
Visually guided touching and manual tracking
[TR-412] 03 p1166 N94-16581
Temporal segmentation of tasks from human hand motion
[AD-A266596] 03 p1166 N94-16725
A modular control architecture for real-time synchronous and asynchronous systems
[DE93-015439] 03 p1166 N94-16888
End-effector: Joint conjugates for robotic assembly of large truss structures in space: Extended concepts
[NASA-CR-193576] 03 p1048 N94-17088
Path planning for robotic truss assembly
[NASA-CR-194652] 03 p0897 N94-17280
Reliability and maintainability of modular robot systems: A roadmap for design
[AD-A268104] 03 p1168 N94-17517
Environmental use of a Laser Range Finder and the Advanced Visualization System
[DE93-016163] 03 p1043 N94-17677
Magnetostrictive actuators for human sensory feedback
[AD-A269266] 04 p1511 N94-17841
Joint stiffness estimation based on force sensor measurements in industrial manipulators
[REPT-92-053] 04 p1443 N94-17937
Autonomous neural network controllers for adaptive material handling
[AD-A268908] 04 p1540 N94-18331
Survey of collision avoidance and ranging sensors for mobile robots, revision 1
[AD-A269846] 04 p1541 N94-18474
Robotics
[NASA-TM-109351] 04 p1332 N94-18920
Research in lightweight elastic robotic arms
[AD-A270846] 05 p1821 N94-19833
Robot skill learning and the effects of basis function choice
[TR-437] 05 p1939 N94-20135
Aviation safety research at the National Institute for Aviation Research, Wichita State University
[NIAR-93-4] 05 p1641 N94-20189
Self-organization via active exploration in robotic applications. Phase 2: Hybrid hardware prototype
[NASA-CR-194723] 05 p1939 N94-20212
Bladder operated robotic joint
[NASA-CASE-MFS-28682-1] 05 p1701 N94-20359
Development and testing of a reliability performance index for modular robotic systems
[AD-A271901] 05 p1942 N94-20488
Head-centered orientation strategies in animate vision
[TR-442] 05 p1894 N94-20520
Visual tracking
[AD-A271686] 05 p1943 N94-20920
Graphical interactive planning of robotic applications with support of integrated simulation
[ETN-93-93793] 05 p1944 N94;21057
Simulation of tripod gaits for a hexapod underwater walking machine
[AD-A271719] 05 p1945 N94-21355
NEP Early Flight program: System performance and development considerations
[NASA-TM-106415] 05 p1654 N94-21570
Robotic concepts for operation in barren terrain
[DE93-040539] 05 p1946 N94-21925
Automating the control of robotic systems in unstructured environments
[DE93-040753] 05 p1946 N94-21929
Canadian Conference on Electrical and Computer Engineering, volumes 1 and 2
[ISBN-0-9694170-2-0] 05 p1770 N94-22101
Optimal object modelling for an active-vision system 05 p1771 N94-22107
Ultrasonic sensor vision in robotics 05 p1775 N94-22131
Dynamic analyses of flexible robotic manipulators
[ISBN-0-315-59251-6] 05 p1827 N94-22421
Mobile robot perception in unknown and unstructured dynamic voxel environments
[ISBN-0-315-83951-1] 05 p1947 N94-22591
Normal forms of kinematic singularities of 3R robot manipulators
[MEMO-1124] 06 p2469 N94-22712
Motion planning for a non-holonomic mobile in a dynamic workspace
[ETN-94-95180] 06 p2470 N94-22898
Contribution to geometric and dynamic modeling of parallel robots
[LAAS-93089] 06 p2470 N94-22904
Plan generation for flexible assembly systems
[PB93-217974] 06 p2267 N94-22981
Spline screw multiple rotations mechanism
[NASA-CASE-GSC-13452-1] 06 p2352 N94-23078
Split spline screw
[NASA-CASE-GSC-13434-1] 06 p2352 N94-23082
NASA/ASEE Summer Faculty Fellowship Program
[NASA-CR-194678] 06 p2571 N94-23230
Rack Insertion End Effector (RIEE) automation 06 p2368 N94-23242
Missions, Technologies, and Design of Planetary Mobile Vehicles
[ISBN-2-85428-331-7] 06 p2605 N94-23373
The study of the mobile lunar explorer 06 p2607 N94-23389
The robotic Mars rover 06 p2608 N94-23390
Electrical power technology for robotic planetary rovers 06 p2314 N94-23401
Mechanical design of a planetary rover 06 p2369 N94-23403
Conceptual design and architecture of hexapod robotic vehicles for the (L)OVLA project 06 p2369 N94-23405
Automation technology for remote sample acquisition 06 p2369 N94-23407
Evolving directions in NASA's planetary rover requirements and technology 06 p2370 N94-23414
Towards real-time stereovision systems for planetary missions 06 p2370 N94-23422
Mobility analysis, simulation, and scale model testing for the design of wheeled planetary rovers 06 p2370 N94-23425
Lunar exploration rover program developments
[DE93-040759] 06 p2613 N94-23469
The instant sequencing task: Toward constraint-checking a complex spacecraft command sequence interactively 06 p2504 N94-23875
The Fifth European Space Mechanisms and Tribology Symposium
[ESA-SP-334] 06 p2355 N94-23985
Multipurpose clamping device with electrical connector for in orbit attachment of payloads 06 p2361 N94-24035
Human-like robots for space and hazardous environments
[NASA-CR-195549] 06 p2365 N94-24703
Design of a wheeled articulating land rover
[NASA-CR-195520] 06 p2365 N94-24806
Object recognition through image understanding for an autonomous mobile robot
[AD-A273206] 06 p2475 N94-24862
Design of a walking robot
[NASA-CR-195200] 06 p2367 N94-25274
Advanced control structures: A transputer-based multi-robot system
[RR-468] 06 p2446 N94-25313
An evaluation of three-dimensional sensors for the extravehicular activity helper/retreiver 06 p2444 N94-25369
Robotics in a controlled, ecological life support system 06 p2444 N94-25371
Research experience for undergraduates in robotics and materials
[AD-A273659] 06 p2368 N94-25436
The 1991-1992 walking robot design 07 p2833 N94-25686
Design of dynamically reconfigurable real-time software using port-based objects
[NASA-CR-195178] 07 p2958 N94-25777
Graphical programming at Sandia National Laboratories
[DE94-003803] 07 p2958 N94-25818
Balancing of a planar bouncing object
[AD-A273805] 07 p2821 N94-25878
Recent developments in the Robotic All Terrain Lunar Exploration Rover (RATLER) program
[DE93-040342] 07 p2821 N94-26110
Modeling and experimental verification of single event upsets 07 p2684 N94-26287
Early lunar rover mission studies 07 p2684 N94-26290
The Robotic All-Terrain Lunar Exploration Rover (RATLER): Increased mobility through simplicity 07 p2685 N94-26291
A multitasking behavioral control system for the Robotic All-Terrain Lunar Exploration Rover (RATLER) 07 p2685 N94-26292
Computer visualizations in engineering applications
[DE94-003589] 07 p2822 N94-26465
Automated in-situ inspection systems for underground storage tanks
[AD-A274644] 07 p2764 N94-27144
Robotics handbook. Version 1: For the interested party and professional
[NASA-TM-109690] 07 p2824 N94-27238
Dynamic control of kinematically redundant manipulators
[ISBN-0-315-84627-5] 07 p2825 N94-27344
Vision 21: Interdisciplinary Science and Engineering in the Era of Cyberspace
[NASA-CP-10129] 07 p2685 N94-27358
Utility fog: A universal physical substance 07 p2687 N94-27367
Design, implementation and experimental results of robotic environment input into the Robot Controller Test Station (RCTS)
[ISBN-0-315-85355-7] 07 p2826 N94-27596

Local performance optimization for a class of redundant eight-degree-of-freedom manipulators
[NASA-TP-3417] 07 p2989 N94-27773
Comparison of dynamic analysis of a Schilling hydraulic manipulator with experimental results
[DE94-004597] 07 p2827 N94-27780
Automation life-cycle cost model
[NASA-CR-195695] 07 p3095 N94-27866
Artemis common lunar lander. Phase 2: Study results for external review
[NASA-TM-109699] 07 p2692 N94-28205
Design and construction of the Aerobot Robotic Manipulator (ARM)
[AD-A275362] 08 p3298 N94-28894
High level language-based robotic control system
[NASA-CASE-NPO-17918-2-CU] 08 p3435 N94-29465
The 27th Aerospace Mechanisms Symposium
[NASA-CP-3205] 08 p3160 N94-29627
A compact roller-gear pitch-yaw joint module: Design and control issues 08 p3161 N94-29629
Kinematic representations, workspace analysis, and grasp stability in robot arms and multi-fingered hands 08 p3301 N94-29847
Collision avoidance and control of multiple revolute manipulators 08 p3302 N94-29884
Robotics and the battlefield of the future 08 p3304 N94-30277
DREV activities related to military vehicles robotization 08 p3305 N94-30278
A generic semi-autonomous ground vehicle control system 08 p3306 N94-30283
An inverse kinematics algorithm for the DREP/Philips real-time radiographic manipulator system 08 p3307 N94-30292
Sonar sensing and obstable detection 08 p3309 N94-30301
Shape from diameter: Negative results
[RUU-CS-93-16] 08 p3458 N94-30407
Shape from diameter: Positive results
[RUU-CS-93-17] 08 p3458 N94-30408
Control system design for A and R supported microgravity experiments: An experiment payload control development
[AD-B179107] 08 p3229 N94-30421
A force-controllable macro-micro manipulator and its application to medical robots 08 p3314 N94-30441
The use of interactive computer vision and robot hand controllers for enhancing manufacturing safety 08 p3314 N94-30442
Programmable Automated Welding System (PAWS): Control of welding through software and hardware 08 p3314 N94-30443
Conference on Intelligent Robotics in Field, Factory, Service, and Space (CIRFFSS 1994), volume 1
[NASA-CP-3251] 08 p3439 N94-30526
Intelligent robotics can boost America's economic growth
[AIAA PAPER 94-1301-CP] 08 p3439 N94-30527
Teleoperated systems for nuclear reactors: Inspection and maintenance
[AIAA PAPER 94-1176-CP] 08 p3439 N94-30528
A highly redundant robot system for inspection
[AIAA PAPER 94-1194-CP] 08 p3442 N94-30545
Microwave vision for robots
[AIAA PAPER 94-0887-CP] 08 p3443 N94-30550
Fuzzy logic based robotic controller
[AIAA PAPER 94-1202-CP] 08 p3443 N94-30553
The real-world navigator
[AIAA PAPER 94-1204-CP] 08 p3443 N94-30555
Autonomous mobile robot teams
[AIAA PAPER 94-1207-CP] 08 p3444 N94-30558
A survey of NASA and military standards on fault tolerance and reliability applied to robotics
[AIAA PAPER 94-1211-CP] 08 p3445 N94-30562
Design reuse experience of space and hazardous operations robots
[AIAA PAPER 94-1220-CP] 08 p3445 N94-30568
A multi-mode manipulator display system for controlling remote robotic systems
[AIAA PAPER 94-0888-CP] 08 p3446 N94-30569
Robotic NDE inspection of advanced solid rocket motor casings
[AIAA PAPER 94-1222-CP] 08 p3446 N94-30571
Automation for nondestructive inspection of aircraft
[AIAA PAPER 94-1223-CP] 08 p3446 N94-30572
The Automated Aircraft Rework System (AARS): A system integration approach
[AIAA PAPER 94-1225-CP] 08 p3446 N94-30574
A robotic wheelchair
[AIAA PAPER 94-1229-CP] 08 p3447 N94-30578
An intelligent robotic aid system for human services
[AIAA PAPER 94-1232-CP] 08 p3447 N94-30580
On-orbit spacecraft servicing: An element in the evolution of space robotics applications
[AIAA PAPER 94-1236-CP] 08 p3448 N94-30583
Kinematic analysis of platform-type robotic manipulators
[ISBN-0-315-78703-1] 08 p3311 N94-30793
Integrated structure/control design of nonrigid robot arms for high-speed manipulation 08 p3312 N94-30866
Kinematics and force analysis of a robot hand based on an artificial biological control scheme 08 p3313 N94-30957
ControlShell: A real-time software framework
[AD-A276481] 09 p3811 N94-31475
Kinematic synthesis and analysis of a novel class of six-DOF parallel minimanipulators 09 p3723 N94-31568
A contribution to the representation and identification of semi-flexible robots
[ISBN-0-315-86450-8] 09 p3724 N94-31721
Robot grasping: Stability and optimization issues 09 p3724 N94-31724
Real-time control and application to robotics: Hardware and software architectures
[ISBN-0-315-87192-X] 09 p3833 N94-31876
Adaptive control of telerobotic systems worn by humans
[AD-A276608] 09 p3834 N94-32036
Parallel methods for synthesizing whole-hand grasps from generalized prototypes
[AD-A276798] 09 p3726 N94-32166
Undergraduate robotics projects in support of research on neural networks
[AD-A277331] 09 p3835 N94-32281
Application of dexterous space robotics technology to myoelectric prostheses 09 p3729 N94-32450
Navy Omni-Directional Vehicle (ODV) development program 09 p3729 N94-32451
Development of an automated wire delivery system for robotic welding applications
[NASA-CR-194216] 09 p3727 N94-32479
Dynamic error compensation in robotic trusses 09 p3738 N94-32486
A new solution method for the inverse kinematic joint velocity calculations of redundant manipulators
[DE94-004427] 09 p3727 N94-32682
A multitasking behavioral control system for the Robotic All Terrain Lunar Exploration Rover (RATLER)
[DE94-007293] 09 p3835 N94-32787
Identification and control of structures in space
[NASA-CR-195910] 09 p3612 N94-33115
The 28th Aerospace Mechanisms Symposium
[NASA-CP-3260] 09 p3603 N94-33291
Innovative mechanism for measuring the mass properties of an object 09 p3604 N94-33299
Experiments in autonomous navigation and control of multi-manipulator, free-flying space robots 10 p4013 N94-33383
The resolvability ellipsoid for sensor based manipulation
[AD-A277898] 10 p4055 N94-33549
NASA report to education, volume 6
[NASA-TM-109818] 10 p4167 N94-33573
Seventh Annual Workshop on Space Operations Applications and Research (SOAR 1993), volume 2
[AD-A278178] 10 p4167 N94-33612
Aerial robotic data acquisition system
[DE94-009114] 10 p4076 N94-33938
Automated cleaning of electronic components
[DE94-008742] 10 p4082 N94-34009
Seventh Annual Workshop on Space Operations Applications and Research (SOAR 1993), volume 1
[NASA-CP-3240-VOL-1] 10 p4179 N94-34019
Design of the MESUR/pathfinder microrover 10 p4066 N94-34021
Air Force construction automation/robotics 10 p4066 N94-34022
Vehicle development of Lunar/Mars exploration 10 p4067 N94-34030
EVA-SCRAM operations 10 p4102 N94-34035
Intelligent vehicle control: Opportunities for terrestrial-space system integration 10 p4127 N94-34038
The servicing aid tool: A teleoperated robotics system for space applications 10 p4067 N94-34039
Robotic vehicle mobility and task performance: A flexible control modality for manned systems 10 p4067 N94-34040
Proceedings of the Asia-Pacific Conference on Control and Measurement (APCCM 1993), volume 10, no. 1 10 p4114 N94-34308
Computer aided design of robotic control systems 10 p4110 N94-34336
A linguistic geometry for space applications 10 p4123 N94-35050
Robot friendly probe and socket assembly
[NASA-CASE-MSC-22028-1] 11 p4274 N94-35374
Adjustable control station with movable monitors and cameras for viewing systems in robotics and teleoperations
[NASA-CASE-NPO-17837-1-CU] 11 p4332 N94-35384
Space robotics in Japan 11 p4278 N94-36046
Beyond intelligent vacuum cleaners
[AD-A280565] 12 p4500 N94-37039
Efficient contact determination between geometric models
[AD-A280244] 12 p4494 N94-37120
Bootstrap planning: Theory and application
[DE94-006486] 12 p4501 N94-37425
Technology demonstration of space intravehicular automation and robotics
[NASA-TM-109138] 12 p4501 N94-37589
Interactive Collaborative Environments (ICE): Platform independent X application sharing and multi-media over wide area networks
[DE94-008868] 12 p4502 N94-37784
Remote use of distributed robotics resources to enhance technology development and insertion
[DE94-009285] 12 p4502 N94-37785

ROBOTS

Position and force control of a vehicle with two or more steerable drive wheels
[DE93-012512] 01 p0177 N94-10269
Operational aspects of F.16 plastic media blasting, as carried out by Fokker Aircraft Services 01 p0126 N94-10619
Use of robots for aircraft dry stripping via plastic media blasting 01 p0127 N94-10620
Plastic media blasting activities at Hill Air Force Base 01 p0127 N94-10622
Large Aircraft Robotic Paint Stripping (LARPS) system and the high pressure water process 01 p0127 N94-10623
Telerobot control system
[NASA-CASE-NPO-18116-1-CU] 01 p0179 N94-10670
Sensor abstractions to support many-robot systems
[AD-A265907] 01 p0180 N94-10803
Development and evaluation of a predictive algorithm for telerobotic task complexity 01 p0341 N94-11562
Supervised autonomous control, shared control, and teleoperation for space servicing 01 p0183 N94-11577
Robotic servicing on Earth orbiting satellites 01 p0045 N94-11579
Application of intelligently adaptable structure and robot to large space structure 02 p0530 N94-13277
Robot-task compliance: The energy criterion
[ITN-93-85196] 02 p0763 N94-13568
The BIRIS server: Integration of a three-dimensional range sensor into a harmony-based realtime architecture
[ERB-1036] 02 p0765 N94-14201
Design and control of a macro-micro robot for precise force applications 02 p0682 N94-14651
Perception for outdoor navigation
[AD-A266867] 03 p0863 N94-14919
Engineering Physics and Mathematics Division progress report, period ending 31 December 1992
[DE93-015118] 03 p1301 N94-14926
Hidden Markov model approach to skill learning and its application to telerobotics
[AD-A266989] 03 p1164 N94-15502
Opportunity for early science return by the Artemis Program 03 p1291 N94-16408
Exploiting world structure to efficiently search for objects
[TR-434] 03 p1231 N94-16576
Integrating reactive and deliberative planning for agents
[AD-A267631] 03 p1166 N94-17201
Reliability and maintainability of modular robot systems: A roadmap for design
[AD-A268104] 03 p1168 N94-17517
An object-oriented environment for computer vision and pattern recognition
[DE93-017098] 04 p1517 N94-17867
Joint stiffness estimation based on force sensor measurements in industrial manipulators
[REPT-92-053] 04 p1443 N94-17937
Flexible integration of path-planning capabilities
[AD-A269594] 04 p1541 N94-18463
Survey of collision avoidance and ranging sensors for mobile robots, revision 1
[AD-A269846] 04 p1541 N94-18474
Robotics
[NASA-TM-109351] 04 p1332 N94-18920
Adaptive path planning: Algorithm and analysis
[DE93-008348] 04 p1523 N94-18926
Geometrical pattern learning
[DE93-017641] 04 p1542 N94-19007

MART: An overview of the Mobile Autonomous Robot Twente project
[MEMO-INF-93-12] 04 p1543 N94-19199
Robot navigation in unknown terrains: Introductory survey of non-heuristic algorithms
[DE93-019221] 04 p1316 N94-19300
Robot skill learning and the effects of basis function choice
[TR-437] 05 p1939 N94-20135
Climbing robot --- caterpillar design
[NASA-CASE-GSC-13442-1] 05 p1823 N94-20494
Internal camera calibration using rotation and geometric shapes
[AD-A272718] 05 p1808 N94-21167
High dimension action spaces in robot skill learning
[TR-458] 05 p1945 N94-21317
Simulation of tripod gaits for a hexapod underwater walking machine
[AD-A271719] 05 p1945 N94-21355
Low energy CMOS for space applications 05 p1768 N94-21735
Determining the 3-D structure and motion of objects using a scanning laser range sensor
[NASA-CR-194745] 05 p1818 N94-21817
Robotic concepts for operation in barren terrain
[DE93-040539] 05 p1946 N94-21925
Sensor integration and data fusion for object localization in robotic workcells 05 p1774 N94-22130
An adaptive control to enable a robot to follow Cartesian trajectories 05 p1790 N94-22229
Control of multiple robot manipulators with optimal force distribution 05 p1794 N94-22255
Optimal control of the tip of a flexible arm 05 p1794 N94-22256
Robot link and contact surface dynamic interaction: An experimental study of contact instability
[ISBN-0-315-83439-0] 05 p1827 N94-22578
Mobile robot perception in unknown and unstructured dynamic voxel environments
[ISBN-0-315-83951-1] 05 p1947 N94-22591
Normal forms of kinematic singularities of 3R robot manipulators
[MEMO-1124] 06 p2469 N94-22712
Plan generation for flexible assembly systems
[PB93-217974] 06 p2267 N94-22981
Graphical programming: A systems approach for telerobotic servicing of space assets
[DE93-019016] 06 p2472 N94-23201
Missions, Technologies, and Design of Planetary Mobile Vehicles
[ISBN-2-85428-331-7] 06 p2605 N94-23373
Lunar science strategy: Exploring the Moon with humans and machines 06 p2605 N94-23376
Robotic exploration of Moon and Mars 06 p2606 N94-23379
Mission and system concepts for Mars robotic precursor missions 06 p2608 N94-23391
Planetary rover locomotion mechanisms 06 p2369 N94-23404
The remote-operated autonomous-robot concept: From deep sea to outer space applications 06 p2370 N94-23413
Walking, jumping, and tumbling: More than one way to get around Mars 06 p2370 N94-23419
Sensing and modelling concepts for autonomous and remote mobile robot control 06 p2370 N94-23421
Experiments with a small behaviour controlled planetary rover 06 p2371 N94-23427
Human-like robots for space and hazardous environments
[NASA-CR-195549] 06 p2365 N94-24703
Design of a wheeled articulating land rover
[NASA-CR-195520] 06 p2365 N94-24806
Object recognition through image understanding for an autonomous mobile robot
[AD-A273206] 06 p2475 N94-24862
Preliminary results on time-varying feedback stabilization of a nonholonomic car-like mobile robot
[INRIA-RR-1512] 06 p2475 N94-24963
Design of a walking robot
[NASA-CR-195200] 06 p2367 N94-25274
A soft robot interface
[OUEL-1948/92] 06 p2463 N94-25468
The 1991-1992 walking robot design 07 p2833 N94-25686
A biologically-inspired autonomous robot
[AD-A273909] 07 p2821 N94-25782
Balancing of a planar bouncing object
[AD-A273805] 07 p2821 N94-25878
The television as robot servant
[AD-A273985] 07 p2984 N94-25898
The determination of surface roughness from reflected step edges
[AD-A273987] 07 p2984 N94-25900
Rational handling of multiple goals for mobile robots
[NASA-CR-195177] 07 p2985 N94-26006
A global approach to kinematic path planning to robots with holonomic and nonholonomic constraints 07 p2683 N94-26279
Application of the CIRSSE cooperating robot path planner to the NASA Langley truss assembly problem 07 p2683 N94-26280
Adaptive path planning in changing environments
[DE94-003269] 07 p2985 N94-26462
Computer visualizations in engineering applications
[DE94-003589] 07 p2822 N94-26465
Implementation of integral manifold control on a two degree of freedom flexible joint manipulator: Theory and experiments
[ISBN-0-315-83572-9] 07 p2823 N94-26658
Sensor-based navigation of a mobile robot using automatically constructed fuzzy rules
[DE94-001137] 07 p2986 N94-26948
Automated in-situ inspection systems for underground storage tanks
[AD-A274644] 07 p2764 N94-27144
Ir-fibers in a laser threat warning system and robot shot warning system
[PB94-124476] 07 p3038 N94-27209
The universal robot 07 p2686 N94-27361
Parallel algorithm for dominant points correspondences in robot binocular stereo vision 07 p2686 N94-27364
Utility fog: A universal physical substance 07 p2687 N94-27367
Pigs in cyberspace 07 p2689 N94-27376
Design, implementation and experimental results of robotic environment input into the Robot Controller Test Station (RCTS)
[ISBN-0-315-85355-7] 07 p2826 N94-27596
Advanced control of a flexible spherical wrist
[ISBN-0-315-84424-8] 07 p2826 N94-27652
Feedback control of a three-link planar under-actuated manipulator using a surge velocity
[AD-A275159] 08 p3435 N94-29044
An emergency response mobile robot for operations in combustible atmospheres
[NASA-CASE-NPO-19020-1-CU] 08 p3299 N94-29420
Robotic hand-eye motor learning 08 p3436 N94-29835
High-resolution robot tracking and direction finding for space station environment 08 p3168 N94-29896
Proceedings of the 3rd Conference on Military Robotic Applications
[DRES-SP-149] 08 p3304 N94-30275
Autonomous intelligent military robots: Army ants, killer bees, and cybernetic soldiers 08 p3304 N94-30276
Autonomous Robotic Refueling System (ARRS) for rapid aircraft turnaround 08 p3305 N94-30279
The NRC mobile robot project 08 p3305 N94-30280
An optimal obstacle avoidance path planning algorithm for the Excalibur robot 08 p3306 N94-30287
Maestro: An open system architecture for multi-robot control 08 p3306 N94-30288
Coordinated control of multiple robot manipulators 08 p3306 N94-30289
Three methods to improve the accuracy of a PUMA 560 robot 08 p3307 N94-30290
Force control techniques for robot manipulators and their military applications 08 p3307 N94-30291
Simulation of lightweight robots and their controllers 08 p3307 N94-30294
Thermal imaging for a mobile robot 08 p3308 N94-30300
Aspects of the operator interface for military robotic applications in unstructured environments 08 p3309 N94-30304
Achieving robot autonomy 08 p3310 N94-30307
Improving the execution speed of robot control computations: An allocation scheme for heterogeneous multiprocessors 08 p3310 N94-30308
Motion control of mobile robots 08 p3310 N94-30309
Electrochemical Power Source (EPS) selection for Energetically Independent Robots (EIR): A systematic approach 08 p3269 N94-30312
Conference on Intelligent Robotics in Field, Factory, Service, and Space (CIRFFSS 1994), volume 1
[NASA-CP-3251] 08 p3439 N94-30526
ARK: Autonomous mobile robot in an industrial environment
[AIAA PAPER 94-1177-CP] 08 p3439 N94-30529
Biologically-inspired hexapod robot design and simulation
[AIAA PAPER 94-1178-CP] 08 p3439 N94-30530
ODYSSEUS autonomous walking robot: The leg/arm design
[AIAA PAPER 94-1180-CP] 08 p3439 N94-30531
VAS: A Vision Advisor System combining agents and object-oriented databases
[AIAA PAPER 94-1181-CP] 08 p3440 N94-30532
Application of the Modular Automated Reconfigurable Assembly System (MARAS) concept to adaptable vision gauging and parts feeding
[AIAA PAPER 94-1182-CP] 08 p3440 N94-30533
Confessions of a robot lobotomist
[AIAA PAPER 94-1185-CP] 08 p3440 N94-30535
Integration of vision and robotic workcell
[AIAA PAPER 94-1186-CP] 08 p3440 N94-30536
Meeting the challenges of installing a mobile robotic system
[AIAA PAPER 94-1187-CP] 08 p3440 N94-30537
Design of an autonomous exterior security robot
[AIAA PAPER 94-1188-CP] 08 p3441 N94-30538
Task automation in a successful industrial telerobot
[AIAA PAPER 94-1189-CP] 08 p3441 N94-30539
Free-floating dual-arm robots for space assembly
[AIAA PAPER 94-1195-CP] 08 p3442 N94-30546
Vision based object pose estimation for mobile robots
[AIAA PAPER 94-1197-CP] 08 p3442 N94-30548
Microwave vision for robots
[AIAA PAPER 94-0887-CP] 08 p3443 N94-30550
Perception system and functions for autonomous navigation in a natural environment
[AIAA PAPER 94-1201-CP] 08 p3443 N94-30552
Fuzzy logic based robotic controller
[AIAA PAPER 94-1202-CP] 08 p3443 N94-30553
The real-world navigator
[AIAA PAPER 94-1204-CP] 08 p3443 N94-30555
A streamlined software environment for situated skills
[AIAA PAPER 94-1205-CP] 08 p3444 N94-30556
Situational reaction and planning
[AIAA PAPER 94-1206-CP] 08 p3444 N94-30557
Autonomous mobile robot teams
[AIAA PAPER 94-1207-CP] 08 p3444 N94-30558
Building brains for bodies
[AIAA PAPER 94-1208-CP] 08 p3444 N94-30559
Object-based task-level control: A hierarchical control architecture for remote operation of space robots
[AIAA PAPER 94-1209-CP] 08 p3444 N94-30560
Task-level control for autonomous robots
[AIAA PAPER 94-1210-CP] 08 p3444 N94-30561
A survey of NASA and military standards on fault tolerance and reliability applied to robotics
[AIAA PAPER 94-1211-CP] 08 p3445 N94-30562
Using generic tool kits to build intelligent systems
[AIAA PAPER 94-1214-CP] 08 p3445 N94-30565
The road plan model: Information model for planning road building activities
[AIAA PAPER 94-1219-CP] 08 p3445 N94-30567
Design reuse experience of space and hazardous operations robots
[AIAA PAPER 94-1220-CP] 08 p3445 N94-30568
Automation for nondestructive inspection of aircraft
[AIAA PAPER 94-1223-CP] 08 p3446 N94-30572
Graphical simulation for aerospace manufacturing
[AIAA PAPER 94-1224-CP] 08 p3446 N94-30573
TRC research products: Components for service robots
[AIAA PAPER 94-1227-CP] 08 p3447 N94-30576
An update on Lab Rover: A hospital material transporter
[AIAA PAPER 94-1228-CP] 08 p3447 N94-30577
An intelligent robot for helping astronauts
[AIAA PAPER 94-1233-CP] 08 p3447 N94-30581
On-orbit spacecraft servicing: An element in the evolution of space robotics applications
[AIAA PAPER 94-1236-CP] 08 p3448 N94-30583
Aspects of vision and planning in a dynamic, uncertain environment 08 p3448 N94-30803
ELF: Learning incomplete fuzzy rule sets for an autonomous robot
[REPT-93-043] 08 p3449 N94-30923
Iterative removal of boundary minima of harmonic potential function for mobile robot navigation
[REPT-93-059] 08 p3449 N94-30962
Concepts and environment
[REPT-93-032] 09 p3829 N94-31186
A high-performance multi-arm environment: Theoretical aspects and practical implementation
[RR-479] 09 p3722 N94-31379
Control of a flexible space robot tracking a moving target 09 p3722 N94-31469
Remote robot manipulator coupled with remote-controlled guide vehicle for soil sampling in hazardous waste sites 09 p3723 N94-31569
CAD-based off-line planning for an active-vision system
[ISBN-0-315-86317-X] 09 p3813 N94-31713
Motion and force control of coordinated robots
[ISBN-0-315-86323-4] 09 p3724 N94-31714
A contribution to the representation and identification of semi-flexible robots
[ISBN-0-315-86450-8] 09 p3724 N94-31721

Development of a robotic simulator for studying interference and contact problems
[ISBN-0-315-86705-1] 09 p3588 N94-31747
Application of contact mechanics for the validation of robotized operations of grasping objects subjected to static and dynamic force fields
[ISBN-0-315-86831-7] 09 p3725 N94-31754
Adaptive control of a robot in Cartesian coordinates: Analysis and implementation
[ISBN-0-315-86493-1] 09 p3831 N94-31798
Study of a path planning and tracking system for an articulated mobile robot
[ISBN-0-315-86502-4] 09 p3831 N94-31800
Development of a feedforward controller for a flexible manipulator
[ISBN-0-315-86515-6] 09 p3832 N94-31801
Control of a flexible-link robotic arm manipulating an unknown dynamic payload 09 p3725 N94-31973
Communication networks for autonomous mobile robot computer architectures and distributed real-time computing 09 p3680 N94-32310
An experimental testbed for a free-floating manipulator
[AD-A277350] 09 p3726 N94-32334
Applying robotics to HAZMAT 09 p3729 N94-32452
Identification and control of structures in space
[NASA-CR-195910] 09 p3612 N94-33115
From animals to animats
[AD-A277427] 09 p3802 N94-33241
Experiments in autonomous navigation and control of multi-manipulator, free-flying space robots 10 p4013 N94-33383
Force override rate control for robotic manipulators 10 p4066 N94-33665
Graphical programming: A systems approach for telerobotic servicing of space assets 10 p4066 N94-33666
Controlling telerobots with video data and compensating for time-delayed video using Omniview 10 p4127 N94-34031
Undersea applications of dexterous robotics 10 p4067 N94-34033
A test system of pose repeatability precision of multi-path robot 10 p4067 N94-34341
Multiresolutional schemata for unsupervised learning of autonomous robots for 3D space operation 10 p4123 N94-35051
Robot friendly probe and socket assembly
[NASA-CASE-MSC-22028-1] 11 p4274 N94-35374
Genetic algorithms
[PB94-171048] 11 p4303 N94-35602
Task and environment-sensitive tracking
[AD-A278846] 11 p4312 N94-35802
Maneuvering and control of flexible space robots 11 p4218 N94-35867
Space robotics in Japan 11 p4278 N94-36046
Adaptive multisensor fusion for the perception and interpretation of outdoor robot scenes
[PB94-170719] 12 p4499 N94-36535
Beyond intelligent vacuum cleaners
[AD-A280565] 12 p4500 N94-37039
Adaptive learning of multi-sensor integration techniques with genetic algorithms
[DE94-012744] 12 p4500 N94-37083
Robot trajectory planning via dynamic programming
[DE94-008424] 12 p4501 N94-37529
Remote use of distributed robotics resources to enhance technology development and insertion
[DE94-009285] 12 p4502 N94-37785

ROBUSTNESS (MATHEMATICS)
RAMCAD (reliability, availability, and maintainability in computer-aided design)
[AD-A265143] 01 p0331 N94-11679
A robust multilevel simultaneous eigenvalue solver
[NASA-CR-191491] 02 p0767 N94-13202
Robust stability of diamond families of polynomials with complex coefficients
[NASA-CR-194132] 02 p0768 N94-13421
Robust synthesis of discrete-time multivariable control systems with induced delays 02 p0662 N94-13642
Exploiting structure: Introduction and motivation
[NASA-CR-194199] 02 p0750 N94-13828
A review of robust detection
[DSIS-93-00400] 02 p0603 N94-13829
Robust estimators and tests in one-sample location problem with particular consideration on modified maximum likelihood process
[ETN-93-94391] 02 p0774 N94-14703
Research in robust control for hypersonic aircraft
[NASA-CR-194106] 03 p0870 N94-15416
Application of the robust estimate in SLR data preprocessing 03 p0918 N94-15597
The design and analysis of robust feedback systems
[AD-A267152] 03 p1165 N94-15778
An overview of the SAFSIM computer program
[DE93-017657] 04 p1519 N94-18002
Non Linear Dynamics and Chaos
[AGARD-LS-191] 04 p1607 N94-18236
Robustness and efficiency of generalized predictive control algorithms with guaranteed stability
[MATHS-REPT-A-190] 04 p1530 N94-19412
Fault-tolerance and complexity
[TR-450] 04 p1530 N94-19483
Use of shape memory alloys in the robust control of smart structures
[AD-A270827] 04 p1366 N94-19594
A learning autopilot for automatically controlled robust regulation
[ETN-93-95075] 04 p1321 N94-19711
A real-time spoken-language system for interactive problem-solving, combining linguistic and statistical technology for improved spoken language understanding
[AD-A270901] 04 p1392 N94-19749
Asymptotics of the GLRT for the disorder problem in diffusion processes
[INRIA-RR-1735] 05 p1951 N94-20227
Time-domain analysis of planar microstrip devices using a generalized Yee-algorithm based on unstructured grids 05 p1724 N94-20431
Numerical study of a multigrid method with four smoothing methods for the incompressible Navier-Stokes equations in general coordinates 05 p1806 N94-21487
A comparative robustness evaluation of feedforward neurofilters
[NASA-TM-106440] 05 p1650 N94-21742
A robust adaptive control design for flexible joint manipulators 05 p1790 N94-22230
Robust unstructured grid generation with VGRID 05 p1919 N94-22359
An advancing-front Delaunay-triangulation algorithm designed for robustness 05 p1920 N94-22362
A robust quality control system for GPS navigation and kinematic positioning
[ISBN-0-315-83148-0] 05 p1644 N94-22427
Nonlinear state space H(sub infinity) control theory
[MEMO-1119] 06 p2469 N94-22706
Identification for robust control using an H(sub infinity) norm
[EUT-92-E-261] 06 p2470 N94-22873
A reliable algorithm for optimal control synthesis
[NASA-CR-194809] 06 p2472 N94-23332
Descent and landing phase: Vision based robust spacecraft motion estimation and elevation modeling 06 p2608 N94-23394
Failure-proof estimation under conditions of lack of information 06 p2158 N94-24267
Parametric uncertainty reduction in robust multivariable control
[AD-A273412] 06 p2460 N94-24927
Parametric uncertainty modeling for application to robust control 06 p2163 N94-25103
Robust, nonlinear, high angle-of-attack control design for a supermaneuverable vehicle 06 p2164 N94-25108
Practical evaluation of robust control for a class of nonlinear mechanical dynamic systems
[ISBN-9-03-860092-5] 06 p2475 N94-25224
Distributing functionality in the drift scan camera system
[DE94-003640] 07 p2809 N94-25599
On the robustness of a multiple semi-coarsened grid method
[REPT-93-51] 07 p2992 N94-26252
Fuzzy robust statistics for application to the fuzzy c-means clustering algorithm
[AD-A274719] 07 p3003 N94-26436
Designing robust control laws using genetic algorithms 07 p2643 N94-27295
Dynamics and robust control for uncertain flexible space systems
[INPE-5510-TAE/020] 07 p2696 N94-27357
Tools for quantitative stability robustness analysis
[ISBN-0-315-59950-2] 07 p2988 N94-27641
Track filtering by robust neural network
[DE94-606067] 08 p3434 N94-28613
A design methodology for synthesizing low-order robust controllers for flexible structures 08 p3302 N94-29870
Robust adaptive control and filtering 08 p3437 N94-29895
Robust adaptive control of a mechanical manipulator 08 p3449 N94-30806
Robust multisource classification method using the Markov random field methods 09 p3750 N94-32537
Limiting vibration in systems with constant amplitude actuators through command preshaping
[NASA-CR-188284] 09 p3739 N94-32907
Fuzzy logic, neural networks, and soft computing 10 p4127 N94-34048
Theoretical and experimental studies of auditory processing
[AD-A278505] 10 p4134 N94-34293
Revisiting the connection problem of identification and control 10 p4114 N94-34311
A continuously tuned adaptive robust controller 10 p4115 N94-34317
H infinity/LTR state feedback control 10 p4115 N94-34320
Robust stabilization of nonlinear systems with a class of unmatched uncertainties 10 p4115 N94-34322
Robust variable structure flight control system 10 p4007 N94-34327
A new robust adaptive algorithm based on intelligent integrators 10 p4122 N94-34371
Forced unsteady deceleration of a turbulent boundary layer from a temporal perspective 10 p4053 N94-34983
Robust requirements specifications for safety-critical systems
[PB94-167806] 11 p4250 N94-35532
Aspects of robust computational modeling for plain and reinforced concrete
[PB94-169240] 11 p4251 N94-35820
Robustness properties of LQG optimized compensators for collocated rate sensors 11 p4221 N94-35890
Semigroup approximation and robust stabilization of distributed parameter systems 11 p4222 N94-35894
Robust tracking control of a magnetically suspended rigid body 11 p4225 N94-35913
A flux splitting scheme with high-resolution and robustness for discontinuities
[NASA-TM-106452] 12 p4441 N94-36646
H infinity control for nonlinear and linear systems
[AD-A280450] 12 p4494 N94-37226
Optimization for minimum sensitivity to uncertain parameters
[NASA-TM-109139] 12 p4386 N94-37256

ROCHE LIMIT
Evolution of vaporizing pulsars 09 p3929 N94-31128

ROCK INTRUSIONS
Giant radiating dyke swarms on Earth and Venus 01 p0283 N94-12236
Spatially extensive uniform stress fields on Venus inferred from radial dike swarm geometries: The Aphrodite Terra example 03 p1254 N94-16207
Mode of emplacement of lunar mare volcanic deposits: Graben formation due to near surface deformation accompanying dike emplacement at Rima Parry 5 03 p1258 N94-16227
Geomorphic processes in the Argyre-Dorsa Argentea region of Mars 03 p1270 N94-16293
The monzonorite-anorthosite connection: The petrogenesis of terrestrial KREEP 03 p1104 N94-16365
Preliminary analysis of thermal-infrared multispectral scanner data of the Iron Hill, Colorado carbonatite-alkalic rock complex 03 p1065 N94-16605
Thermal and rheological controls on magma migration in dikes: Examples from the east rift zone of Kilauea volcano, Hawaii 05 p1862 N94-20673
The transition from diapirism to dike intrusion: Implications for planetary volcanism
[NASA-CR-195133] 06 p2403 N94-24580
Studies in Jurassic and Cretaceous North American apparent polar wander 08 p3362 N94-29940
Vent processes during the 1912 eruption at Novarupta, Katmai National Park, Alaska
[DE94-010740] 12 p4468 N94-36451

ROCK MECHANICS
Ground movements associated with gas hydrate production
[DE93-019887] 04 p1486 N94-19018
Nonlinear hysteresis in an endochronic solid
[AD-A274594] 07 p2880 N94-26855

ROCK SALT
U HALITES

ROCKET BOOSTERS
U BOOSTER ROCKET ENGINES

ROCKET CHAMBERS
U THRUST CHAMBERS

ROCKET ENGINE CASES
Impact damage in filament wound composite bottles 06 p2231 N94-24421
Evaluation of advanced materials through experimental mechanics and modelling 06 p2374 N94-24454
Assessment of impact damage of composite rocket motor cases
[NASA-CR-195143] 06 p2220 N94-24595
Lightning tests and analyses of tunnel bond straps and shielded cables on the Space Shuttle solid rocket booster
[NASA-CR-193921] 06 p2200 N94-24801

Study on contaminants on flight and other critical surfaces
[NASA-CR-193975] 11 p4235 N94-35447

ROCKET ENGINE CONTROL
FNAS/summer faculty fellowship research continuation program. Task 6: Integrated model development for liquid fueled rocket propulsion systems. Task 9: Aspects of model-based rocket engine condition monitoring and control
[NASA-CR-194574] 04 p1338 N94-19706

ROCKET ENGINE DESIGN
In-reactor testing of the closed cycle gas core reactor: The Nuclear Light Bulb concept
[DE93-004053] 01 p0370 N94-10149
Space Storable Rocket Technology program (SSRT). Option 1 program
[NASA-CR-191171] 01 p0046 N94-10938
Applying design principles to fusion reactor configurations for propulsion in space
[NASA-TM-108247] 01 p0047 N94-11053
The conceptual study on future space transportation systems. Part A: Conceptual study of flyback booster
[NASDA-CNT-930013] 02 p0536 N94-14099
ALS engine controller system
[NASA-CR-194647] 03 p0926 N94-16654
Development and analysis of startup strategies for particle bed nuclear rocket engine
[AD-A267949] 03 p0927 N94-17053
Advanced transportation system studies technical area 3: Alternate propulsion system concepts. SSME upper stage use
[NASA-CR-193865] 03 p0927 N94-17098
Computational analysis of Variable Thrust Engine (VTE) performance
[NASA-CR-193852] 03 p0928 N94-17442
CPIA/M5 liquid propellant engine manual
[AD-A268062] 03 p0929 N94-17589
Future technical directions 05 p1668 N94-20072
The Vulcain cryogenic engine 05 p1668 N94-20077
Dynamics of face seals for high speed turbomachinery 05 p1655 N94-21796
Dual-bell altitude compensating nozzles 06 p2215 N94-23057
Liquid rocket propulsion: Retrospective and prospects 06 p2154 N94-24243
A minimum cost tolerance allocation method for rocket engines and robust rocket engine design 06 p2222 N94-24419
Performance of the NASA cm ion thruster
[NASA-TM-106426] 06 p2221 N94-24770
Rocket engine numerical simulation 07 p2688 N94-27375
The 7.5K lbf thrust engine preliminary design for Orbit Transfer Vehicle
[AD-A277519] 09 p3614 N94-31618
Performance evaluation and operating characteristics of a waveguide microwave applicator for space propulsion applications 09 p3614 N94-31908
Design of a cold-flow test facility for the high pressure fuel turbopump turbine of the Space Shuttle main engine
[AD-A276743] 09 p3615 N94-32182
Summary of particle bed reactor designs for the Space Nuclear Thermal Propulsion Program
[DE94-007434] 09 p3615 N94-32266
Structurally compliant rocket engine combustion chamber: Experimental and analytical validation
[NASA-TP-3431] 10 p4017 N94-34392

ROCKET ENGINES
NT ADVANCED SOLID ROCKET MOTOR (STS)
NT ARC JET ENGINES
NT BOOSTER ROCKET ENGINES
NT DUCTED ROCKET ENGINES
NT ELECTRIC ROCKET ENGINES
NT ELECTROSTATIC ENGINES
NT HYBRID PROPELLANT ROCKET ENGINES
NT HYDRAZINE ENGINES
NT HYDROGEN OXYGEN ENGINES
NT ION ENGINES
NT J-2 ENGINE
NT LIQUID PROPELLANT ROCKET ENGINES
NT NUCLEAR ENGINE FOR ROCKET VEHICLES
NT NUCLEAR LIGHTBULB ENGINES
NT NUCLEAR ROCKET ENGINES
NT RESISTOJET ENGINES
NT RESTARTABLE ROCKET ENGINES
NT REUSABLE ROCKET ENGINES
NT RL-10 ENGINES
NT SOLID PROPELLANT ROCKET ENGINES
NT SPACE SHUTTLE BOOSTERS
NT SPACE SHUTTLE MAIN ENGINE
NT UPPER STAGE ROCKET ENGINES
Durability of a carbon segmented circumferential seal for a liquid oxygen turbopump
[NAL-TR-1155] 01 p0178 N94-10369
Hot-gas-side heat transfer characteristics of subscale, plug-nozzle rocket calorimeter chamber
[NASA-TP-3380] 01 p0055 N94-12569
Low thrust space propulsion
[NASA-TM-109286] 02 p0552 N94-13625
Nuclear thermal propulsion engine based on particle bed reactor using light water steam as a propellant
[DE93-014336] 02 p0552 N94-14111
The problem of traveling in outer space: The rocket motor
[NASA-TT-10002] 02 p0552 N94-14463
Coaxial airblast atomizers
[NASA-CR-193845] 03 p1016 N94-15109
TABES 1993: 9th Annual Technical and Business Exhibition and Symposium 03 p1050 N94-16129
ALS engine controller system
[NASA-CR-194647] 03 p0926 N94-16654
Heat transfer parametric system identification
[AD-A268525] 03 p0929 N94-17543
KINETIC: A system code for analyzing Nuclear thermal propulsion rocket engine transients
[DE93-016825] 04 p1337 N94-17884
Adaptations to micropep and rocket to allow performance evaluation of multiple grain and/or airbreathing motors
[AD-A268798] 04 p1337 N94-18202
Spacecraft Propulsion
[VKI-LS-1993-01] 05 p1667 N94-20068
Cryogenic propellant rocket engine problems 05 p1668 N94-20076
Liquid fuel injection elements for rocket engines
[NASA-CASE-MFS-28547-1] 05 p1669 N94-20370
UVPI imaging from the LACE satellite: The Starbird rocket plume
[AD-A271981] 05 p1658 N94-20617
Dynamics of face seals for high speed turbomachinery 05 p1655 N94-21796
Small rocket research and technology 06 p2211 N94-23038
An experimental study of characteristic combustion-driven flows for CFD validation 06 p2212 N94-23040
Efficiency and reliability enhancements in propulsion flowfield modeling 06 p2215 N94-23055
Brush seals for cryogenic applications 06 p2216 N94-23063
Reduction of the anode fall in a coaxial plasma thruster with an applied magnetic nozzle
[DE94-000670] 06 p2218 N94-23283
An overview on the main available ceramic composites and their processing routes 06 p2255 N94-24229
The 33rd Israel Annual Conference on Aviation and Astronautics
[ITN-94-85227] 06 p2153 N94-24241
A minimum cost tolerance allocation method for rocket engines and robust rocket engine design 06 p2222 N94-24419
Controller modeling and evaluation for PCV electro-mechanical actuator 06 p2371 N94-24441
Conceptual design of a two stage to orbit spacecraft
[NASA-CR-195536] 06 p2204 N94-24620
Evaluation of moderate angle of attack roll of a dual engine, thrust vectoring aircraft using quantitative feedback theory
[AD-A274118] 07 p2667 N94-25905
Orbit transfer rocket engine technology program enhanced heat transfer combustor technology
[AD-A277123] 07 p2700 N94-26156
An ultrasonic testing technique for monitoring the cure and mechanical properties of polymeric materials
[AD-A274536] 07 p2753 N94-26842
Rocket engine numerical simulation 07 p2688 N94-27375
Rocket engine system reliability analyses using probabilistic and fuzzy logic techniques
[NASA-TM-106519] 08 p3173 N94-29403
Method of reducing hydraulic instability
[NASA-CASE-LEW-15463-1] 08 p3273 N94-29539
CFD analyses for advanced pump design
[NASA-CR-193969] 08 p3300 N94-29550
Aspects of model-based rocket engine condition monitoring and control
[NASA-CR-195116] 08 p3173 N94-29848
Using Monte Carlo techniques and parallel processing for debris hazard analysis of rocket systems
[DE94-007250] 09 p3609 N94-31382
Operating characteristics of the Russian D-55 thruster with anode layer
[NASA-TM-106610] 10 p4016 N94-33606
A versatile rocket engine hot gas facility
[NASA-CR-195339] 10 p4011 N94-34131
Structurally compliant rocket engine combustion chamber: Experimental and analytical validation
[NASA-TP-3431] 10 p4017 N94-34392
UVPI imaging from the LACE satellite: The Low Cost Launch Vehicle (LCLV) rocket plume
[AD-A278785] 12 p4398 N94-36445
Validation and implementation of optical diagnostics for particle sizing in rocket motors
[AD-A278581] 12 p4428 N94-36972

ROCKET EXHAUST
Ultraviolet plume instrument description and plume data reduction methodology
[AD-A266141] 01 p0054 N94-11643
The 1991 version of the plume impingement computer program. Volume 2: User's input guide
[NASA-CR-194191] 01 p0166 N94-12774
The 1991 version of the plume impingement computer program. Volume 1: Description
[NASA-CR-194192] 01 p0166 N94-12775
Analysis of reacting flowfields in low-thrust rocket engines and plumes 02 p0552 N94-14491
Investigation of the feasibility of optical diagnostic measurements at the exit of the SSME
[NASA-CR-193832] 02 p0553 N94-14682
Low altitude plume impingement handbook
[NASA-CR-194193] 02 p0643 N94-14741
Rocket Motor Plume Technology
[AGARD-LS-188] 03 p0923 N94-15217
Plume primary smoke 03 p0923 N94-15218
Propulsion 03 p0924 N94-15219
Secondary smoke 03 p0924 N94-15220
Rocket motor plume flowfields: Phenomenology and simulation 03 p0924 N94-15221
Microwave properties and systems overview 03 p0924 N94-15222
Plume radiation 03 p0924 N94-15223
Fundamental studies of rocket combustion chemistry and combustion instability
[AD-A266248] 03 p0925 N94-16482
UVPI imaging from the LACE satellite: The Nihka rocket plume
[AD-A268456] 04 p1334 N94-18149
Ultraviolet plume instrument calibration and sensor assessment
[AD-A269687] 04 p1337 N94-18574
JPRS report: Science and technology. Central Eurasia: Earth Sciences
[JPRS-UES-93-004] 04 p1461 N94-19209
The NRL LACE program
[AD-A270861] 05 p1657 N94-19896
Parameters affecting hydrogen chloride measurements
[AD-A271326] 05 p1851 N94-20025
Dual-beam multiple wavelength light transmittance measurement for particle sizing in rocket motor plumes
[AD-A272491] 05 p1670 N94-21208
Flame trench analysis of NLS vehicles 06 p2199 N94-23249
Development of an analytical-numerical model to predict radiant emission or absorption
[NASA-CR-194860] 06 p2453 N94-23624
Using neural networks to assist in OPAD data analysis 06 p2477 N94-24452
Preliminary far-field plume sputtering characterization of the Stationary Plasma Thruster (SPT-100)
[NASA-TM-106464] 06 p2221 N94-24766
Stationary plasma thruster plume emissions
[NASA-CR-194471] 07 p2701 N94-26209
SOCRATES simulation of the emission at wavelength 6300 A generated by the interaction between the atmosphere and the Space Shuttle exhaust
[AD-A275567] 08 p3164 N94-28827
A six degree of freedom, plume-fuel optimal trajectory planner for spacecraft proximity operations using an A* node search
[NASA-CR-188285] 09 p3601 N94-32388
Simulation of low-density nozzle plumes in non-zero ambient pressures
[NASA-TM-106501] 09 p3615 N94-32742
Possible effect of the chlorine oxide dimer on transient ozone loss in rocket plumes
[AD-A278135] 09 p3616 N94-33094

ROCKET LAUNCHERS
The launch of ELDO
[ESA-HSR-7] 03 p0886 N94-16501
Feasibility study of superconducting LSM rocket launcher system 11 p4225 N94-35914

ROCKET LAUNCHING
NT LUNAR LAUNCH
NT ORBITAL LAUNCHING
The launch of ELDO
[ESA-HSR-7] 03 p0886 N94-16501

ROCKET MOTOR CASES
U ROCKET ENGINE CASES

ROCKET NOSE CONES
Arc-heating tests of thermal protection system materials for the H-2 rocket fairing
[NAL-TR-1181] 02 p0551 N94-13455

ROCKET NOZZLES
NT DUAL THRUST NOZZLES

Development of a high specific 1.5 to 5 kW thermal arcjet
[NASA-CR-193133] 01 p0047 N94-11354
Qualification test of the Ross Double Planetary Mixer
[NASA-CR-192600] 02 p0652 N94-14497
ASRM nozzle thermal analysis
[NASA-CR-194672] 03 p0928 N94-17277
Postflight hardware evaluation 360T026 (RSRM-26, STS-47)
[NASA-CR-192559] 03 p0882 N94-17656
Analysis of film cooling in rocket nozzles
[NASA-CR-194674] 04 p1338 N94-19438
A tutorial on the aero/thermodynamical design of liquid-propellant rocket engine nozzles
05 p1668 N94-20074
Two stage turbine for rockets
06 p2215 N94-23059
Postflight hardware evaluation RSRM-29 (STS-54). Appendix D: Nozzle postfire data
[NASA-CR-193898] 06 p2199 N94-24057
Postflight hardware evaluation RSRM-29 (STS-54). Appendix C: Nozzle PFORs
[NASA-CR-193894] 06 p2219 N94-24064
Final postflight hardware evaluation report RSRM-32 (STS-57)
[NASA-CR-193903] 06 p2200 N94-24065
Postflight hardware evaluation RSRM-29 (STS-54). Appendix E: Insulation postfire data
[NASA-CR-193897] 06 p2200 N94-24067
Properties and processing characteristics of low density carbon cloth phenolic composites
06 p2231 N94-24450
Postflight hardware evaluation 360T021 (RSRM-21, STS-45), revision A
[NASA-CR-193896] 06 p2201 N94-24965
Ablation of solid-propellant rocket-motor nozzle materials
[ESA-TT-1289] 07 p2699 N94-25638
Verification of thermal analysis codes for modeling solid rocket nozzles
[NASA-CR-195248] 07 p2702 N94-27150
Materials characterization on efforts for ablative materials
[NASA-CR-193929] 07 p2756 N94-27230
NASA reload program
[NASA-CR-193972] 12 p4429 N94-37446

ROCKET OXIDIZERS
NT TAGN
STS-55 pad abort: Engine 2011 oxidizer preburner augmented spark igniter check valve leak
[NASA-CR-193830] 02 p0533 N94-12806
Effects of hydrogen addition on combustion performance of a LOX/kerosene rocket
[NAL-TR-1177] 02 p0548 N94-12945
Aluminum powder/water reaction ignited by electrical pulsed power
[AD-A269223] 04 p1376 N94-17840
Chemistry of the burning surface
[AD-A272725] 05 p1681 N94-21181

ROCKET PLANES
NT X-15 AIRCRAFT

ROCKET PROPELLANT TANKS
U PROPELLANT TANKS

ROCKET PROPELLANTS
NT CRYOGENIC ROCKET PROPELLANTS
NT DOUBLE BASE ROCKET PROPELLANTS
NT GASEOUS ROCKET PROPELLANTS
NT GELLED ROCKET PROPELLANTS
NT LIQUID ROCKET PROPELLANTS
NT METAL PROPELLANTS
NT MONOPROPELLANTS
NT NITRAMINE PROPELLANTS
NT SLURRY PROPELLANTS
NT SLUSH HYDROGEN
NT SOLID ROCKET PROPELLANTS
NT TAGN
NT TATB
Some problems in the rheological characterisation of composite rocket propellants
[AD-A268806] 04 p1376 N94-18203
New test method to determine modulus of elasticity of rocket grain material
[AD-A269758] 04 p1377 N94-18758
Design of a lunar propellant processing facility. NASA/USRA advanced program
[NASA-CR-195502] 06 p2266 N94-24618
Embodiment design for a multipropellant resistojet
[NASA-CR-195505] 06 p2221 N94-24834
Laser and Fourier transform spectroscopy of novel propellant molecules
[AD-A277506] 09 p3667 N94-33013

ROCKET SONDES
U SOUNDING ROCKETS

ROCKET SOUNDING
The 1980 highlights
[NASA-TM-109672] 03 p1303 N94-15509
Principal investigators data package for Project Initiation Conference (PIC): EUVS sounding rocket no. 36.117CL. Target: Venus
[NASA-CR-194663] 03 p0923 N94-17126
Time series comparisons of satellite and rocketsonde temperatures in 1978-1979
[NASA-TP-3409] 08 p3370 N94-29455
A sounding rocket program in extreme and far ultraviolet interferometry
[NASA-CR-195114] 08 p3289 N94-29907
Three flights into thunderstorms with the revised Rocket Electric Field Sounding (REFS) payload
[AD-A280424] 12 p4473 N94-37217

ROCKET TEST FACILITIES
ASRM testing at Stennis Space Center (proposed)
[NASA-TM-109795] 10 p4016 N94-33557

ROCKET THRUST
In-reactor testing of the closed cycle gas core reactor: The Nuclear Light Bulb concept
[DE93-004053] 01 p0370 N94-10149
Liquid rocket propulsion. Theory
05 p1667 N94-20069
Space Shuttle Main Engine. Overview
05 p1667 N94-20070

ROCKET VEHICLES
NT ARIANE LAUNCH VEHICLE
NT ATLAS LAUNCH VEHICLES
NT BLACK BRANT SOUNDING ROCKETS
NT BLUE STREAK LAUNCH VEHICLE
NT CENTAUR LAUNCH VEHICLE
NT ELDO LAUNCH VEHICLE
NT MULTISTAGE ROCKET VEHICLES
NT PEGASUS AIR-LAUNCHED BOOSTER
NT SATURN 5 LAUNCH VEHICLES
NT SCOUT LAUNCH VEHICLE
NT SINGLE STAGE ROCKET VEHICLES
NT SOUNDING ROCKETS
NT TITAN LAUNCH VEHICLES
NT TITAN 4 LAUNCH VEHICLE
NT X-15 AIRCRAFT
Rockets: Physical science teacher's guide with activities
[NASA-EP-291] 05 p1669 N94-20226

ROCKET-BORNE INSTRUMENTS
A rocket-borne lidar for studies of the middle atmosphere
[FFI/RAPPORT-92/7034] 02 p0715 N94-13949

ROCKETS
The problem of traveling in outer space: The rocket motor
[NASA-TT-10002] 02 p0552 N94-14463

ROCKS
NT ANDESITE
NT ANORTHOSITE
NT BASALT
NT BEDROCK
NT BRECCIA
NT COAL
NT FELSITE
NT GABBRO
NT GRANITE
NT IGNEOUS ROCKS
NT KREEP
NT LIMESTONE
NT LUNAR ROCKS
NT METAMORPHIC ROCKS
NT PERIDOTITE
NT QUARTZITE
NT REGOLITH
NT RHYOLITE
NT SANDSTONES
NT SEDIMENTARY ROCKS
NT SHALES
NT SHATTER CONES
NT TRACHYTE
Oxygen isotopes as tracers of tektite source rocks: An example from the Ivory Coast tektites and Lake Bosumtwi Crater 01 p0430 N94-12146
Hot Dry Rock energy
[DE93-014452] 02 p0702 N94-13403
BOAST 2 for the IBM 3090 and RISC 6000
[DE93-000138] 02 p0638 N94-14351
Temperature measurements 03 p1037 N94-15804
Stalking the LREE-enriched component in ureilites
03 p1241 N94-16190
Mars Analog Site Study (MASS)
03 p1252 N94-16200
Near-surface temperature gradients and their effects on thermal-infrared emission spectra of particulate planetary surfaces 03 p1260 N94-16236
Trace-element composition of Chicxulub crater melt rock, K/T tektites and Yucatan basement
03 p1242 N94-16245
From minerals to rocks: Toward modeling lithologies with remote sensing 03 p1086 N94-16437
AVIRIS as a tool for carbonatite exploration: Comparison of SPAM and Mbandmap data analysis methods
03 p1073 N94-16703
Thermal conductivity measurements of particulate materials under Martian conditions
05 p1685 N94-20703
Reverse polarity magnetized melt rocks from the Chicxulub impact structure, Yucatan Peninsula, Mexico
05 p1863 N94-20843
Dynamic response of multiphase porous media
[AD-A272915] 05 p1831 N94-21219
Post-Palbozoic crustal responses to the contemporary stress field in the eastern United States
[DE93-040604] 05 p1859 N94-22006
Nonlinear hysteresis in an endochronic solid
[AD-A274594] 07 p2880 N94-26855
Speciation in Water and Soil: A literature review
[PB94-132388] 08 p3341 N94-28412
Nonlocal theory for fracturing of quasibrittle materials
[AD-A278283] 09 p3740 N94-33143
Distribution of siderophile and other trace elements in melt rock at the Chicxulub impact structure
11 p4352 N94-35456
Investigation of ultrasonic surface wave interaction with porous saturated rocks
[DE94-013378] 12 p4469 N94-37177
A computational model for three-dimensional jointed media with a single joint set
[DE94-007582] 12 p4470 N94-37527

ROCKWELL HARDNESS
Measurement and theory of the dependence of hardness on residual stress
[AD-A267553] 03 p1061 N94-17105
Thermal insulation of wet shielded metal arc welds
[AD-A268697] 04 p1445 N94-18465

ROCKY MOUNTAINS (NORTH AMERICA)
Large eddy simulations of the atmospheric boundary layer east of the Colorado Rockies
01 p0277 N94-11465

RODENTS
NT GUINEA PIGS
NT MICE
NT RABBITS
NT RATS
Cross-sectional anatomy of day 30 suncus fetuses
07 p2905 N94-27490

RODS
NT CONTROL RODS
Evaluation of hybrid reinforcement (fiber-reinforced-plastic rod with steel core)
[AD-A268009] 03 p0941 N94-17473
A finite strain ring dynamical model for pneumatic tires
[AD-A269286] 04 p1444 N94-18266
The influence of the target strength model on computed perforation
[DE93-018659] 04 p1460 N94-19543
Dynamic, multiaxial impact response of confined and unconfined ceramic rods
[DE93-040057] 05 p1829 N94-19824
Inverse dynamics of a rigid rod system as a simplified model of flexible beam 06 p2160 N94-24281
Lunar preform manufacturing
07 p2765 N94-25677
Chirped-pulse amplification with flashlamp-pumped Ti:Sapphire amplifiers
[DE94-010055] 11 p4272 N94-35695

ROENTGEN SATELLITE
U ROSAT MISSION

ROGALLO WINGS
U FLEXIBLE WINGS
U FOLDING STRUCTURES

ROLL
Investigation of the effects of bandwidth and time delay on helicopter roll-axis handling qualities
02 p0522 N94-13300
Equations of motion of a hinged body over a spherical earth
[AD-A268408] 03 p0868 N94-17435
A study of roll attractor and wing rock of delta wings at high angles of attack 06 p2164 N94-25111
Evaluation of moderate angle of attack roll of a dual engine, thrust vectoring aircraft using quantitative feedback theory
[AD-A274118] 07 p2667 N94-25905
Phase-lock roll control of inertially pointing spacecraft
09 p3609 N94-31470
Study findings on the influence of maneuverability and agility on helicopter handling qualities
10 p3993 N94-34624
Data reduction, analysis and results of LACV-30-07 air cushion vehicle tests, Fort Story, VA, August - September 1993
[AD-A278859] 11 p4190 N94-35826
The reduction of takeoff ground roll by the application of a nose gear jump strut
[NASA-TM-108822] 11 p4198 N94-36380

ROLL CONTROL
U LATERAL CONTROL

ROLL FORMING
Weld cladding of hard surfaces
[PB93-201598] 06 p2353 N94-23448
Lubrication in cold rolling: Numerical simulation using multigrid techniques
[ISBN-9-09-005313-1] 06 p2262 N94-25230
Development of thermoplastic composite aircraft structures
[NASA-CR-189593] 09 p3626 N94-32860

ROLLER BEARINGS
The effect of TiN coatings on the rolling contact fatigue behavior of M50 bearing steel
[ARL-TR-40] 02 p0662 N94-13794
Computer program for analysis of high speed, single row, angular contact, spherical roller bearing, SASHBEAN. Volume 1: User's guide
[NASA-CR-191183] 02 p0663 N94-14445
Computer program for analysis of high speed, single row, angular contact, spherical roller bearing, SASHBEAN. Volume 2: Mathematical formulation and analysis
[AD-A276235] 02 p0664 N94-14446
Mechanical Systems Technology Branch research summary, 1985 - 1992
[AD-A276450] 03 p1049 N94-17583
NASA/Army rotorcraft transmission research, a review of recent significant accomplishments
[NASA-TM-106508] 06 p2367 N94-25181
Development of long-life, low-noise linear bearings for atmospheric interferometry 09 p3606 N94-33312

ROLLERS
Roller-gear drives for robotic manipulators design, fabrication and test
[NASA-CR-194248] 02 p0660 N94-12802
Modelling of the temperature distribution in a copper roll for the design of a system of cooled rolls adapted to vertical strip casting
[IMI-93RT-21200-1436-G] 02 p0557 N94-13866
Electrostatic fiber spreader including a corona discharge device
[AD-D015793] 03 p0936 N94-16537
Electromagnetic brake/clutch device
[NASA-CASE-GSC-13502-1] 06 p2354 N94-23969
Contact stress in disc cams with roller followers
[ESDU-93001] 07 p2829 N94-28055
Blending profiles of disc cams with radial translating roller followers. Part 2: To incorporate an intermediate precision point or a constant velocity component
[ESDU-93002-PT-2] 07 p2830 N94-28056

ROLLING CONTACT LOADS
The effect of TiN coatings on the rolling contact fatigue behavior of M50 bearing steel
[ARL-TR-40] 02 p0662 N94-13794
Measuring methods for evaluation of dynamic tyre properties
[ETN-93-95054] 04 p1381 N94-19650
The causes of contact noise
[REPT-92-100] 05 p1822 N94-20157
Rail Corrugations
[ILR-BER-59] 06 p2269 N94-23581
A rail corrugation theory which allows for contact patch size 06 p2269 N94-23582
A rail joint: The possible initiator of corrugation? 06 p2269 N94-23583
A linear model for corrugation and its limit of validity 06 p2269 N94-23584
Lateral high frequency oscillations and stability of a wheel rolling on a flexible track 06 p2269 N94-23585
Wear characteristics of technical dry rolling/sliding systems with relations to corrugation problems 06 p2269 N94-23586
Surface observations of stick-slip oscillations in tightly conformal wheel/rail contacts 06 p2270 N94-23588
Contact analysis of rough rail surfaces 06 p2270 N94-23589

ROLLING MOMENTS
Rolling moment control in the NAL 10 cm x 10 cm magnetic suspension and balance system
[NAL-TR-1164] 02 p0526 N94-13347
A mechanical system damping measurement technique using a one-degree-of-freedom (1DOF) cylindrical gas bearing
[AD-A268402] 03 p1048 N94-17462
Wear characteristics of technical dry rolling/sliding systems with relations to corrugation problems 06 p2269 N94-23586
Contribution of body-mounted fins and tailplanes to lateral derivatives due to sideslip at subsonic speeds for general body width to height ratio
[ESDU-93007] 07 p2648 N94-28057
Yaw control by tangential forebody blowing 10 p3992 N94-34615

ROLLUP SOLAR ARRAYS
U SOLAR ARRAYS

ROM DEVICES
U READ-ONLY MEMORY DEVICES

RONCHI TEST
Design of a surface deformation measuring instrument for the Surface Tension Driven Convection Experiment (STDCE-2)
[NASA-CR-194758] 06 p2343 N94-23285

ROOFS
Rooftop emergency heliports
[AD-A278872] 08 p3157 N94-29754

ROOM TEMPERATURE
Room temperature degradation of YBa2Cu3O(7-x) superconductors in varying relative humidity environments
[NASA-TP-3368] 02 p0813 N94-14409
Technology transfers and reliable oxides
[AD-A266948] 03 p1175 N94-15758
New room temperature high resolution solid-state detector (CdZnTe) for hard x rays and gamma rays 04 p1324 N94-19165
Static ultra-high pressure study of lanthanide and actinide metals using a diamond-anvil cell
[DE94-000369] 05 p1693 N94-21656
Test results of two high temperature superconducting sample coils
[DE94-000496] 05 p2035 N94-22570
Selective hydrogen separation by palladium-based composite membranes
[PB93-201671] 06 p2254 N94-23431
Laser-deposited biocompatible films and methods and apparatuses for producing same
[AD-D016017] 06 p2350 N94-24952
Failure mechanisms of high temperature semiconductor lasers
[AD-A273833] 07 p2815 N94-25616
Investigation of tension-compression fatigue behavior of a cross-ply metal matrix composite at room and elevated temperatures
[AD-A273731] 07 p2706 N94-25999
Deformation, constitutive behavior, and damage of advanced structural materials under multiaxial loading
[AD-A274165] 07 p2709 N94-27142
Observation of stimulated emission from an MBE grown GaN film on sapphire
[DE94-003638] 07 p3068 N94-27724
Anode for rechargeable ambient temperature lithium cells
[NASA-CASE-NPO-18580-1-CU] 08 p3265 N94-29505
Molecular/polymeric magnetism
[DE94-005888] 09 p3649 N94-31201
Room temperature molten salts for advanced energy conversion and storage
[AD-A277777] 09 p3763 N94-33015

ROOMS
NT CLEAN ROOMS

ROOT-MEAN-SQUARE ERRORS
Sub-cm ranging and other improvements in Graz 03 p0919 N94-15603
Orbit and sampling requirements: TRMM experience 05 p1870 N94-21647
Integer cosine transform compression for Galileo at Jupiter: A preliminary look 06 p2292 N94-23266
Development and validation of RNG methodology for compressible turbulence
[AD-A273469] 06 p2337 N94-24929
Estimators for the Cauchy distribution
[DE94-004990] 07 p3005 N94-27816
Error growth in poor ECMWF forecasts over the contiguous United States
[AD-A275297] 08 p3369 N94-29183
Development of a statistical method for estimating the downward longwave radiation at the surface from satellite observations 09 p3742 N94-31553

ROOTS OF EQUATIONS
A theorem regarding roots of the zero-order Bessel function of the first kind 06 p2325 N94-23667

ROSAT MISSION
ROSAT: X ray survey of compact groups
[NASA-CR-193297] 02 p0829 N94-13181
X ray observations of late-type stars using the ROSAT all-sky survey
[NASA-CR-193716] 02 p0832 N94-14146
ROSAT-IUE observations of symbiotic stars. The x ray morphology of high latitude associations
[NASA-CR-194616] 03 p1236 N94-16492
Participation in the north ecliptic pole sky survey
[NASA-CR-191933] 03 p1059 N94-16815
The formation process of the He I lambda 10830 line in cool giant stars
[NASA-CR-194648] 03 p1240 N94-17094
Variability of the Seyfert galaxy MKN 766 in the Rosat all sky survey
[MPE-PREPRINT-221] 03 p1240 N94-17591
Rosat and optical observations of two X-ray transients: MX 0836-42 and GS 0834-430
[MPE-PREPRINT-237] 04 p1622 N94-19451
ROSAT and IRAS observations
[MPE-PREPRINT-231] 04 p1623 N94-19526
ROSAT X ray observation of the 30 Dor giant HII region 04 p1623 N94-19527
IRAS galaxies observed in the ROSAT survey: Starbursts or central activity 04 p1623 N94-19528
Particle induced background by Roentgen satellites
[MPE-242] 04 p1631 N94-19714
Stellar coronae at the end of the main sequence: A Rosat survey of the late M dwarfs
[NASA-CR-194700] 04 p1628 N94-19794
A deep x ray survey in the Lockman hole and the soft x ray log N - log S
[NASA-CR-194698] 05 p2054 N94-20174
X ray archeology in the Coma cluster
[NASA-CR-194799] 05 p2054 N94-20175
The x ray halo of Cen X-3
[NASA-CR-189309] 05 p2055 N94-21295
ROSAT implementation of a proposed multi-mission x ray data format 05 p2047 N94-22462
ROSAT data analysis with EXSAS 05 p2080 N94-22555
Results from ROSAT 05 p2000 N94-22630
Shocked clouds in the Cygnus Loop
[NASA-CR-195190] 06 p2600 N94-25178
ROSAT observations of the x ray binary HD 154791
[NASA-CR-195189] 06 p2600 N94-25198
Investigation relative to the Roentgen Satellite (ROSAT)
[NASA-CR-195192] 06 p2600 N94-25269
ROSAT mission planning using artificial intelligence methods
[DLR-FB-93-14] 06 p2476 N94-25345
Coronal temperatures of unusually active K-dwarf binary systems
[NASA-CR-189335] 08 p3545 N94-29861
Multiwavelength search for protoplanetary disks 09 p3599 N94-31430
ROSAT/XRT-PSPC observations and the ionizing continuum of Seyfert 1 galaxy Mkn 478
[PB94-167053] 11 p4350 N94-35530

ROSS ICE SHELF
A reassessment of the in-situ dielectric constant of polar firn
[AD-A276999] 09 p3773 N94-32154

ROSSBY REGIMES
Global barotropic response to a tropical forcing
[NASA-CR-195256] 07 p2896 N94-27408
Rotational effects in turbulence driven by convection 09 p3930 N94-31131

ROSSBY WAVES
U PLANETARY WAVES

ROTARY DRIVES
U MECHANICAL DRIVES

ROTARY ENGINES
Rotary engine performance computer program (RCEMAP and RCEMAPPC): User's guide
[NASA-CR-191192] 03 p0869 N94-15192
Stratified charge rotary engine critical technology enablement, volume 1
[NASA-CR-189106-VOL-1] 10 p3999 N94-34231
Stratified charge rotary engine critical technology enablement. Volume 2: Appendixes
[NASA-CR-189106-VOL-2] 10 p3999 N94-34233

ROTARY GYROSCOPES
Emerging technologies in microguidance and control 08 p3144 N94-29788

ROTARY STABILITY
NT GYROSCOPIC STABILITY
Rotor instability induced by dead band clearance in bearing supports 08 p3312 N94-30809
Occurrence of sub-synchronous vibration in a multistage turbine pump and its prevention 10 p4064 N94-34189
A waved journal bearing concept with improved steady-state and dynamic performance 10 p4065 N94-34200
F/A-18 forebody vortex control. Volume 2: Rotary-balance tests
[NASA-CR-4582-VOL-2] 10 p3984 N94-34430

ROTARY WING AIRCRAFT
NT AH-1G HELICOPTER
NT AH-64 HELICOPTER
NT H-53 HELICOPTER
NT H-60 HELICOPTER
NT HELICOPTERS
NT LIGHT HELICOPTERS
NT MILITARY HELICOPTERS
NT OH-6 HELICOPTER
NT RIGID ROTOR HELICOPTERS
NT ROTOR SYSTEMS RESEARCH AIRCRAFT
NT SH-3 HELICOPTER
NT TANDEM ROTOR HELICOPTERS

NT TILT ROTOR AIRCRAFT
NT UH-1 HELICOPTER
NT UH-60A HELICOPTER
NT V-22 AIRCRAFT
NT XV-15 AIRCRAFT
Smart materials for helicopter rotor active control
01 p0027 N94-11321
MIL-H-8501B: Application to shipboard terminal operations 02 p0521 N94-13296
A perspective on the FAA approval process: Integrating rotorcraft displays, controls and workload
02 p0521 N94-13298
Some lessons learned in three years with ADS-33C --- rotorcraft handling qualities specification
02 p0521 N94-13299
A model for rotorcraft flying qualities studies
02 p0523 N94-13308
Visual cueing aids for rotorcraft landings
02 p0524 N94-13313
Effects of simulator motion and visual characteristics on rotorcraft handling qualities evaluations
02 p0524 N94-13317
Flight testing and frequency domain analysis for rotorcraft handling qualities characteristics
02 p0526 N94-13324
Preliminary design features of the RASCAL: A NASA /Army rotorcraft in-flight simulator
02 p0526 N94-13325
Rotorcraft research
[NASA-TM-109452] 03 p0871 N94-15325
Center for Rotorcraft Education and Research progress report, 1987 - 1992
[AD-A266760] 03 p0857 N94-15824
Rotorcraft noise: Status and recent developments
[NASA-CR-194761] 05 p1967 N94-20523
The future of rotary-wing aircraft
06 p2185 N94-25070
NASA/Army rotorcraft transmission research, a review of recent significant accomplishments
[NASA-TM-106508] 06 p2367 N94-25181
Investigation of the aerodynamic environment for an advanced lightweight rotor in forward flight. Volume 4: Laser velocimeter wake data, advance ratio of 0.037
[NASA-TM-109040-VOL-4] 07 p2645 N94-26483
Investigation of the aerodynamic environment for an advanced lightweight rotor in forward flight. Volume 1: Laser velocimeter inflow data, advance ratio of 0.37, thrust coefficient of 0.0081 and hover tip speed of 603 feet/second
[NASA-TM-109040-VOL-1] 07 p2645 N94-26489
Investigation of the aerodynamic environment for an advanced lightweight rotor in forward flight. Volume 2: Laser velocimeter inflow data, advance ratio of 0.37, thrust coefficient of 0.0064 and hover tip speed of 710 feet/second
[NASA-TM-109040-VOL-2] 07 p2645 N94-26492
Investigation of the aerodynamic environment for an advanced lightweight rotor in forward flight. Volume 3: Laser velocimeter inflow data, advance ratio of 0.37, thrust coefficient of 0.0064 and hover tip speed of 603 feet/second
[NASA-TM-109040-VOL-3] 07 p2645 N94-26497
S-76 high intensity radiated fields, volume 2
[AD-A274572] 07 p2771 N94-26836
S-76 high intensity radiated fields, volume 1
[AD-A274571] 07 p2771 N94-26854
Future of aerospace
[PB94-120185] 07 p2669 N94-26906
Nonlinear multibody formulation for rotorcraft analysis
08 p3149 N94-30787
Controls design with crossfeeds for hovering rotorcraft using quantitative feedback theory
[NASA-CR-195765] 09 p3585 N94-31203
Rotorcraft ditchings and water-related impacts that occurred from 1982 - 1989, phase 2
[AD-A276473] 09 p3574 N94-31246
Rotorcraft fatigue life-prediction: Past, present, and future 10 p4072 N94-34590
Rotorwash analysis handbook. Volume 1: Development and analysis
[SCT-93RR-17-VOL-1] 12 p4381 N94-36466
Rotorwash analysis handbook. Volume 2: Appendixes
[SCT-93RR-17-VOL-2] 12 p4382 N94-36467
TRENDS: A flight test relational database user's guide and reference manual
[NASA-TM-108806] 12 p4381 N94-37332
Advanced distributed simulation technology advanced rotary wing aircraft. Software programmer's manual visual system module
[AD-A280260] 12 p4390 N94-37755
Advanced distributed simulation technology advanced rotary wing aircraft. System/segment specification. Volume 4: Simulation system module RAH-66 Kit
[AD-A280261] 12 p4391 N94-37756

ROTARY WINGS
NT LIFTING ROTORS
NT TILTING ROTORS
NT X WING ROTORS
Quantifying disbond area 01 p0061 N94-10038
Determining XV-15 aeroelastic modes from flight data with frequency-domain methods
[NASA-TP-3330] 01 p0025 N94-10935
Performance and rotor loads measurements of the Lynx XZ170 helicopter with rectangular blades
[NASA-TM-104000] 01 p0001 N94-10936
Smart materials for helicopter rotor active control
01 p0027 N94-11321
Free-wake computation of helicopter rotor flowfield for general flight regimes
[AD-A266692] 02 p0509 N94-14781
A new treatment of periodic systems with applications to helicopter rotor blade dynamics
[AD-A266770] 02 p0510 N94-14784
Center of excellence in rotary wing technology
[AD-A266655] 02 p0510 N94-14799
Aerodynamic characteristics of a helicopter rotor airfoil as affected by simulated ballistic damage
[AD-A269206] 04 p1311 N94-18413
Blade and hub loads of ballistically damaged helicopter rotors
[AD-A270663] 04 p1319 N94-19781
An experimental investigation of the drag mechanisms of a helicopter rotor in hovering flight
[AD-A270201] 05 p1636 N94-20486
Rotorcraft noise: Status and recent developments
[NASA-CR-194761] 05 p1967 N94-20523
The modern rotor aerodynamic limits survey: A report and data survey
[NASA-TM-4446] 05 p1635 N94-21490
Bent-tip blade for aircraft rotary-wing
[CA-PATENT-1-315-259] 06 p2176 N94-23254
An overview of a model rotor icing test in the NASA Lewis Icing Research Tunnel
[NASA-TM-106471] 06 p2166 N94-23299
The influence of elastic pitch variations on helicopter flight mechanics 06 p2161 N94-24286
Validation of the ROTAC code for the rotor noise prediction
[PB93-204311] 06 p2529 N94-24514
Wind tunnel test of a variable-diameter tiltrotor (VDTR) model
[NASA-CR-177629] 06 p2181 N94-24796
Dynamic analysis of pretwisted elastically-coupled rotor blades
[NASA-TM-109070] 06 p2378 N94-24839
Study of the blade/vortex interaction: Acoustics, aerodynamics and models
[ISL-R-104/92] 06 p2340 N94-25463
Correlation of airloads on a two-bladed helicopter rotor
[NASA-TM-103982] 07 p2644 N94-26143
Investigation of the aerodynamic environment for an advanced lightweight rotor in forward flight. Volume 4: Laser velocimeter wake data, advance ratio of 0.037
[NASA-TM-109040-VOL-4] 07 p2645 N94-26483
Investigation of the aerodynamic environment for an advanced lightweight rotor in forward flight. Volume 1: Laser velocimeter inflow data, advance ratio of 0.37, thrust coefficient of 0.0081 and hover tip speed of 603 feet/second
[NASA-TM-109040-VOL-1] 07 p2645 N94-26489
Investigation of the aerodynamic environment for an advanced lightweight rotor in forward flight. Volume 2: Laser velocimeter inflow data, advance ratio of 0.37, thrust coefficient of 0.0064 and hover tip speed of 710 feet/second
[NASA-TM-109040-VOL-2] 07 p2645 N94-26492
Investigation of the aerodynamic environment for an advanced lightweight rotor in forward flight. Volume 3: Laser velocimeter inflow data, advance ratio of 0.37, thrust coefficient of 0.0064 and hover tip speed of 603 feet/second
[NASA-TM-109040-VOL-3] 07 p2645 N94-26497
Computer code for interactive rotorcraft preliminary design using a harmonic balance method for rotor trim
[AD-A274924] 07 p2668 N94-26531
A finite wake theory for two-dimensional rotary wing unsteady aerodynamics
[AD-A274921] 07 p2645 N94-26535
Boundary layers induced by three-dimensional vortex loops
[AD-A275678] 08 p3270 N94-28665
A free-wake Euler and Navier-Stokes CFD method and its application to helicopter rotors including dynamic stall
[AD-A275416] 08 p3129 N94-29197
Helicopter mission and rotor performance optimization with quasi-linear inflow theory 08 p3147 N94-29594
Numerical study of the trailing vortex of a wing with wing-tip blowing
[NASA-CR-195803] 08 p3130 N94-29760
Computational analysis of high resolution unsteady airloads for rotor aeroacoustics
[NASA-CR-194894] 08 p3480 N94-30274
Nonlinear multibody formulation for rotorcraft analysis
08 p3149 N94-30787
Experimental and numerical simulation of helicopter rotor fuselage interaction
[ONERA-NT-1993-8] 09 p3568 N94-31421
A critical assessment of UH-60 main rotor blade airfoil data
[NASA-TM-103985] 09 p3571 N94-32063
User's guide for a flat wake rotor inflow/wake velocity prediction code, DOWN
[NASA-TM-104139] 09 p3572 N94-32873
The analysis of wake-induced unsteady aerodynamics related to higher harmonic control
[AD-A277914] 09 p3573 N94-33108
Multilevel decomposition approach to integrated aerodynamic/dynamic/structural optimization of helicopter rotor blades
[NASA-TM-109084] 10 p3989 N94-33900
Sensitivity of lag-damping correlations to structural and aerodynamic approximations of isolated experimental rotors in forward flight
[NASA-CR-195822] 10 p3983 N94-33991
A free-wake Euler and Navier-Stokes CFD method and its application to helicopter rotors including dynamic stall
[AD-A278000] 10 p3983 N94-34159
Trim calculation of tandem rotor helicopter using simplified rotor system mathematical model
10 p4008 N94-34337
An examination of the aerodynamic moment on rotor blade tips using flight test data and analysis
[NASA-TM-104006] 10 p3985 N94-34948
Unsteady separation experiments on 2-D airfoils, 3-D wings, and model helicopter rotors
10 p3986 N94-34967
Prediction of unsteady airfoil flows at large angles of incidence 10 p3986 N94-34978
Departure solutions of the unsteady thin-layer and full Navier-Stokes equations solved using streamline curvature based iteration techniques 10 p4052 N94-34980
The quest for stall-free dynamic lift
10 p3986 N94-34986
Selected topics on the active control of helicopter aeromechanical and vibration problems
11 p4200 N94-35874
Computation of helicopter rotor acoustics in forward flight
[NASA-CR-196132] 11 p4319 N94-36031
Forward sweep, low noise rotor blade
[NASA-CASE-LAR-14569-1] 12 p4386 N94-36767

ROTATING
U ROTATION

ROTATING BODIES
NT COMPRESSOR ROTORS
NT FLYWHEELS
NT IMPELLERS
NT LIFTING ROTORS
NT PUMP IMPELLERS
NT ROTARY WINGS
NT ROTATING CYLINDERS
NT ROTATING DISKS
NT ROTATING SPHERES
NT ROTORS
NT TAIL ROTORS
NT TILTING ROTORS
NT TIP VANES
NT TURBINE WHEELS
NT X WING ROTORS
Reduced gravity multibody dynamics testing
[NASA-CR-192589] 01 p0125 N94-11483
The magnetic field of rotating bodies
[DE93-619769] 01 p0427 N94-11812
Laboratory studies on the velocity of fragments from impact disruptions 01 p0189 N94-12359
Criteria for onset of boundary-layer transition on spinning bodies 01 p0164 N94-12620
On curve veering and flutter of rotating blades
[NASA-TM-106282] 02 p0670 N94-12872
Flex-gear electrical power transmission
[NASA-CR-194422] 02 p0661 N94-13445
Applications of neural networks in fault detection of rotating machinery
[AD-A270755] 04 p1448 N94-19766
Normal forms for perturbations of the euler top
[PB94-125390] 07 p3009 N94-26968
Trajectories of ballistic impact ejecta on a rotating Earth 07 p2887 N94-28295
Flow and heat transfer in a rotating square sectioned U-bend 08 p3128 N94-28984
Rotating unbalanced mass proof-of-concept
[NASA-TM-109814] 10 p4141 N94-33720

Attenuating the disorienting effects of head movement during whole-body rotation using a visual reference: Further tests of a predictive hypothesis
12 p4482 N94-37276

ROTATING CYLINDERS
The three-dimensional flow past a rapidly rotating circular cylinder
[NASA-CR-191512] 02 p0630 N94-13075
The general gravitational potential field of a homogeneous cylinder rotating about its axis
[DE93-622853] 02 p0775 N94-13508
In-flight investigation of a rotating cylinder-based structural excitation system for flutter testing
[NASA-TM-4512] 03 p0867 N94-15783
Numerical study of compressible boundary-level transition between two concentric cylinders
[NASA-CR-194622] 03 p1025 N94-16842
Simulation of rotary-drum and repose tests for frictional spheres and rigid sphere clusters
[DE94-008094] 10 p4044 N94-33841
Toward the optimization of control of unsteady separation 10 p4053 N94-34985

ROTATING DISKS
Local heat transfer in an enclosed corotating disk with axial throughflow 08 p3276 N94-29849

ROTATING ENVIRONMENTS
Apparatus and method for producing an artificial gravitational field
[NASA-CASE-MSC-22021-1] 03 p0886 N94-15935
Autogenic-feedback training as a treatment for airsickness in high-performance military aircraft: Two case studies
[NASA-TM-108810] 09 p3801 N94-33068

ROTATING FLUIDS
NT ROTATING LIQUIDS
Laboratory study on the natural modes of a rotating two-phase fluid system subject to axial excitation
01 p0106 N94-10106
SWIRL as a means of liquid management in low gravity
[NASA-CR-4545] 01 p0412 N94-11523
Acoustic and optical investigations of superfluid He-3
[PB93-224889] 06 p2523 N94-23101
Investigation of the asymptotic state of rotating turbulence using large-eddy simulation
06 p2330 N94-24152
Transient flows occurring during the accelerated crucible rotation technique
[DE93-617049] 06 p2567 N94-25422
Numerical simulation of turbulent free jet by TFKE model 07 p2871 N94-28157
Modeling turbulence in flows with a strong rotational component
[DE94-003577] 08 p3270 N94-28475
Acoustic and optical investigations of superfluid (3)He
[PB94-135415] 08 p3477 N94-29186
Forced generation of solitary waves in a rotating fluid and their stability 08 p3274 N94-29689
Magnetohydrodynamics of the Earth's core. 1: Steady, rotating magnetoconvection. 2: Magnetic Rossby waves
09 p3770 N94-31104
On the structure and stability of slender viscous vortices 09 p3700 N94-31218
Eccentricity effects upon the flow field inside a whirling annular seal 10 p4062 N94-34181

ROTATING GENERATORS
NT DYNAMOMETERS
NT HOMOPOLAR GENERATORS
Modeling of the coupled magnetospheric and neutral wind dynamos
[NASA-CR-194728] 05 p1856 N94-20537

ROTATING LIQUIDS
Use of rotation to suppress thermosolutal convection in directionally solidified binary alloys
[NASA-CR-196372] 12 p4415 N94-36811

ROTATING PLASMAS
Kinetic approach to long wave length modes in rotating plasmas
[DE93-771286] 01 p0388 N94-10807
The role of plasma rotation on MHD instabilities in tokamaks
[DE93-013486] 01 p0393 N94-11512
Finite Larmor radius flute mode theory with end loss
[DE93-040914] 05 p1991 N94-19872
Neoclassical kinetic theory near an X-point: Plateau regime
[DE93-019825] 05 p1951 N94-20224
Gravitational instability of magnetized filamentary clouds. 2: Rotation 05 p2009 N94-22689
Magnetic island effects, interactions in tokamaks
[DE94-009209] 10 p4145 N94-34221
Thickness of the layer of strong radial electric field in JFT-2M H-mode plasmas
[DE94-718993] 11 p4336 N94-35812
Anomalous cross field flux in CHS
[DE94-727547] 12 p4529 N94-37359

ROTATING SHAFTS
NT TURBOSHAFTS
Rotary encoding device
[NASA-CASE-GSC-13556-1] 03 p1148 N94-15943
Fluid dynamometer having fluid characteristic power absorption adjustment capability
[AD-D015820] 04 p1424 N94-17904
Rotary encoding device using polygonal mirror with diffraction gratings on each facet
[NASA-CASE-GSC-13543-1] 05 p1985 N94-20240
Shaft mount for data coupler system
[NASA-CASE-LAR-13805-1] 05 p1822 N94-20365
Viscous rotary damper 06 p2361 N94-24031
A novel rotary actuator for spacecraft
06 p2361 N94-24034
A new method for torsional critical speed calculation of practical industrial rotors
[IMR-T&M-TR-001] 07 p2828 N94-28041
Propeller off-axis loads due to thrust axis incidence and nacelle magnus force 07 p2652 N94-28319
Rotary actuator
[NASA-CASE-MFS-28581-1] 08 p3205 N94-29447
Adaptive automatic balancing of magnetic bearing systems 10 p4067 N94-34338
Planar rotational magnetic micromotors with integrated shaft encoder and magnetic rotor levitation
11 p4224 N94-35907

ROTATING SPHERES
On the motion through a viscous fluid of a spherical particle touching a plane wall: Slip boundary conditions
[DE93-012540] 02 p0628 N94-12961
Double diffusion convection in a rotating spherical shell 05 p2006 N94-22666

ROTATING STALLS
Analysis and characteristics of compressor stall precursor signals in forward and AFT swept high speed compressor
[AD-A273820] 06 p2171 N94-25517
An investigation of the surge behavior of a high-speed ten-stage axial flow compressor
[AD-A274910] 07 p2674 N94-26345
Active control of vaneless diffuser rotating stall
10 p4062 N94-34178

ROTATING VEHICLES
U ROTATING BODIES
U VEHICLES

ROTATION
NT AUTOROTATION
NT COROTATION
NT COUNTER ROTATION
NT EARTH ROTATION
NT MOLECULAR ROTATION
NT MUON SPIN ROTATION
NT PLANETARY ROTATION
NT SATELLITE ROTATION
NT STELLAR ROTATION
Effect of rotation on microgravity floating-zone crystal growth 01 p0101 N94-10080
Analytical description of the torsatron Uragan-2M magnetic configuration with account of plasma pressure and external correcting magnetic field
[DE93-620983] 01 p0391 N94-11174
Laboratory studies on the velocity of fragments from impact disruptions 01 p0189 N94-12359
On the motion through a viscous fluid of a spherical particle touching a plane wall: Slip boundary conditions
[DE93-012540] 02 p0628 N94-12961
Theoretical study and modelling of homogeneous turbulence under rotation for implantation in a code for solving Navier-Stokes equations
[ECL-93-05] 04 p1420 N94-19381
Cognitive ability and whole-body rotation
[IZF-1993-B-4] 04 p1510 N94-19440
Turntable mechanism
[NASA-CASE-MFS-28522-1] 05 p1823 N94-20380
Liquid-phase circulation and mixing in multicomponent droplets vaporizing in a laminar convective environment
[AD-A272851] 05 p1802 N94-21193
Method for design rotation
[AD-A272440] 05 p1911 N94-21204
Relationship of area postrema to three putative measures of motion sickness 05 p1885 N94-21900
Motion sickness elicited by passive rotation in squirrel monkeys 05 p1887 N94-21905
Gravitational instability of magnetized filamentary clouds. 2: Rotation 05 p2009 N94-22689
Spline screw multiple rotations mechanism
[NASA-CASE-GSC-13452-1] 06 p2352 N94-23078
Projectile transverse motion and stability in electromagnetic induction launchers
[DE94-001557] 06 p2198 N94-23210
Results of a laboratory experiment that tests rotating unbalanced-mass devices for scanning gimbaled payloads and free-flying spacecraft
[NASA-TP-3458] 06 p2269 N94-23574
Satellite attitude determination using linear combination of models
[AD-A274082] 07 p2694 N94-25996
Method of correcting rotational motion error in SAR and ISAR imagery
[AD-D016033] 07 p2773 N94-27146
Translation and rotation invariant pattern recognition
[PB94-123676] 07 p2968 N94-27157
Fuel ion rotation measurement and its implications on H-mode theories
[DE94-004860] 07 p3048 N94-27791
Spin-up in a rectangular cylinder
[AD-A275465] 08 p3271 N94-28738
Similarity between turbulent flows through curved pipe and orthogonal rotating pipe 08 p3128 N94-28986
Mutual similarity of developing laminar flows with secondary streams in ducts: Curved pipe flow and orthogonal rotating pipe flow 08 p3129 N94-28989
Suspension system for gimbal supported scanning payloads
[NASA-CASE-MFS-28817-1] 08 p3287 N94-29358
Dynamic modeling of multibody flexible structures
08 p3323 N94-30813
Theory of protostellar accretion disks
09 p3931 N94-31136
Optical flow from 1D correlation: Application to a simple time-to-crash detector
[AD-A276777] 09 p3880 N94-32186
Unit specific crew rest strategies: Phase 1 evaluation of the 1/212th Aviation Battalion during shiftwork transitions
[AD-A277122] 09 p3804 N94-32379
Modelling and control of a rotor supported by magnetic bearings 11 p4216 N94-35858

ROTATIONAL FLOW
U FLUID FLOW
U VORTICES

ROTATIONAL SPECTRA
Molecular processes in comets
[NASA-CR-194148] 03 p1239 N94-15188
Laboratory detection of C5S by pulsed-discharge-nozzle Fourier-transform microwave spectroscopy
[JTN-94-80519] 06 p2235 N94-24984
CO-to-H2 conversion factor in dwarf irregular galaxies
[REPT-333] 06 p2603 N94-24985
The Nobeyama millimeter array survey for protoplanetary disks around protostar candidates and T Tauri stars in Taurus
[REPT-336] 06 p2604 N94-24987
Degenerate four-wave mixing as a diagnostic of plasma chemistry
[DE94-008588] 09 p3889 N94-31766

ROTATIONAL STATES
High resolution infrared spectroscopy of formamide and deuterated formamide in a molecular beam
[AD-A271986] 05 p1973 N94-20618
Radiative properties of molecular nitrogen ions produced by helium Penning ionization and argon effects
[NASA-CR-195126] 06 p2534 N94-24487
Detection of the 267 GHz J = 1-0 rotational transition of PH3 in Saturn with a new Fourier transform spectrometer
[NASA-CR-194364] 10 p4162 N94-34718

ROTOR AERODYNAMICS
A grid generation method to calculate the flow field in a three-dimensional cascade of blades
[NAL-TR-1158] 01 p0147 N94-10364
Solving the inverse problem for incompressible potential flow through two-dimensional cascades
[NAL-TR-1162] 01 p0147 N94-10365
On the use of the method of matched asymptotic expansions in propeller aerodynamics and acoustics
[NLR-TP-91307-U] 02 p0503 N94-13528
New vortex dynamics methods for rotor free wake analysis
[AD-A266656] 02 p0509 N94-14774
Free-wake computation of helicopter rotor flowfield for general flight regimes
[AD-A266692] 02 p0509 N94-14781
Center for Rotorcraft Education and Research progress report, 1987 - 1992
[AD-A266760] 03 p0857 N94-15824
Jet engine performance enhancement through use of a wave-rotor topping cycle
[NASA-TM-4486] 03 p0870 N94-17470
The fluid mechanics of vortex cutting by a blade
[AD-A270932] 05 p1636 N94-20043
An experimental investigation of the drag mechanisms of a helicopter rotor in hovering flight
[AD-A270201] 05 p1636 N94-20486
Computation of the loads on the AH-1/OLS model rotor in forward flight and comparison with wind tunnel tests
[ISL-CO-230/92] 06 p2176 N94-23146
The influence of elastic pitch variations on helicopter flight mechanics 06 p2161 N94-24286

Validation of the ROTAC code for the rotor noise prediction
[PB93-204311] 06 p2529 N94-24514
A parametric study of harmonic rotor hub loads
[NASA-CR-4558] 06 p2181 N94-24726
Two-dimensional CFD modeling of wave rotor flow dynamics
[NASA-TM-106261] 06 p2189 N94-25185
Study of the blade/vortex interaction: Acoustics, aerodynamics and models
[ISL-R-104/92] 06 p2340 N94-25463
A design of third-generation airfoils for helicopter rotor blades using Navier-Stokes 08 p3124 N94-28957
Numerical analysis of airfoil for helicopter blade at high angle of attack using Navier-Stokes code 08 p3124 N94-28958
Verification of a three-dimensional viscous flow analysis for a single stage compressor 08 p3127 N94-28976
International collaborative research in wind turbine rotor aerodynamics
[DE94-000244] 08 p3339 N94-30602
An adaptive finite element method for unsteady compressible rotor airfoil aerodynamics 09 p3567 N94-31204
Experimental and numerical simulation of helicopter rotor fuselage interaction
[ONERA-NT-1993-8] 09 p3568 N94-31421
Multilevel decomposition approach to integrated aerodynamic/dynamic/structural optimization of helicopter rotor blades
[NASA-TM-109084] 10 p3989 N94-33900
Coupled 2-dimensional cascade theory for noise and unsteady aerodynamics of blade row interaction in turbofans. Volume 1: Theory development and parametric studies
[NASA-CR-4506-VOL-1] 10 p3998 N94-34146
Trim calculation of tandem rotor helicopter using simplified rotor system mathematical model 10 p4008 N94-34337
Aerodynamic design and investigation of a mixed flow compressor stage 10 p4002 N94-34450
An examination of the aerodynamic moment on rotor blade tips using flight test data and analysis
[NASA-TM-104006] 10 p3985 N94-34948
Ground vibration test of the XV-15 Tiltrotor Research Aircraft and pretest predictions 11 p4200 N94-35972
Computation of helicopter rotor acoustics in forward flight
[NASA-CR-196132] 11 p4319 N94-36031

ROTOR BLADES

The fluid mechanics of vortex cutting by a blade
[AD-A270932] 05 p1636 N94-20043
The influence of elastic pitch variations on helicopter flight mechanics 06 p2161 N94-24286
Dynamic analysis of pretwisted elastically-coupled rotor blades
[NASA-TM-109070] 06 p2378 N94-24839
Numerical study of the trailing vortex of a wing with wing-tip blowing
[NASA-CR-195803] 08 p3130 N94-29760

ROTOR BLADES (TURBOMACHINERY)

A grid generation method to calculate the flow field in a three-dimensional cascade of blades
[NAL-TR-1158] 01 p0147 N94-10364
Solving the inverse problem for incompressible potential flow through two-dimensional cascades
[NAL-TR-1162] 01 p0147 N94-10365
Viscous analysis of three-dimensional rotor flows using a multigrid method
[NASA-TM-106266] 01 p0152 N94-11481
Development of a high-speed mechanical drive system for oscillating an annular blade row in the bending mode
[NAL-TR-1170] 02 p0502 N94-13342
A rapid computational model for estimating the performance of compliant airfoils in cascades
[AD-A266275] 03 p0857 N94-16471
Experimental and computational investigation of the NASA low-speed centrifugal compressor flow field
[NASA-TM-4481] 03 p0869 N94-17386
Near wake measurements on a rotor model with Mie-vanes in the Delft open jet tunnel
[PB93-215382] 05 p1638 N94-22260
Simulation of unsteady flows through stator and rotor blades of a gas turbine using the Chimera method 06 p2323 N94-23652
Fluid dynamic noise in a centrifugal pump
[AD-A275264] 08 p3477 N94-28904
Verification of a three-dimensional viscous flow analysis for a single stage compressor 08 p3127 N94-28976
Tuned mass damper for integrally bladed turbine rotor
[NASA-CASE-MFS-28697-1] 08 p3298 N94-29353
Development of a cascade simulation of fan-passage flow
[AD-A277234] 09 p3584 N94-32026
Experimental investigation of turbine blade-tip excitation forces 10 p4062 N94-34177

ROTOR BODY INTERACTIONS

An analytic modeling and system identification study of rotor/fuselage dynamics at hover 02 p0524 N94-13312
Influence of backup bearings and support structure dynamics on the behavior of rotors with active supports
[NASA-CR-195106] 06 p2365 N94-24751
An analytical study of unsteady rotor/fuselage interaction in hover and forward flight 08 p3131 N94-29826
Experimental and numerical simulation of helicopter rotor fuselage interaction
[ONERA-NT-1993-8] 09 p3568 N94-31421
Coupled 2-dimensional cascade theory for noise and unsteady aerodynamics of blade row interaction in turbofans. Volume 1: Theory development and parametric studies
[NASA-CR-4506-VOL-1] 10 p3998 N94-34146

ROTOR DISKS

U TURBINE WHEELS

ROTOR DYNAMICS

Cryogenic fluid film bearing tester development study
[NASA-CR-192586] 02 p0660 N94-12791
Rotordynamic and leakage characteristics of a 4-stage brush seal
[AD-A266012] 02 p0660 N94-12988
An analytic modeling and system identification study of rotor/fuselage dynamics at hover 02 p0524 N94-13312
A new treatment of periodic systems with applications to helicopter rotor blade dynamics
[AD-A266770] 02 p0510 N94-14784
Center for Rotorcraft Education and Research progress report, 1987 - 1992
[AD-A266760] 03 p0857 N94-15824
A technique to measure rotordynamic coefficients in hydrostatic bearings 06 p2215 N94-23061
A parametric study of harmonic rotor hub loads
[NASA-CR-4558] 06 p2181 N94-24726
Influence of backup bearings and support structure dynamics on the behavior of rotors with active supports
[NASA-CR-195106] 06 p2365 N94-24751
Aeroelastic response and stability of tiltrotors with elastically-coupled composite rotor blades
[NASA-TM-108758] 06 p2182 N94-24953
A finite-element-based perturbation model for the rotordynamic analysis of shrouded pump impellers: Part 1: Model development and applications
[NASA-CR-193916] 06 p2366 N94-24998
A finite-element-based perturbation model for the rotordynamic analysis of shrouded pump impellers: Part 2: User's guide
[NASA-CR-193917] 06 p2366 N94-24999
Computer code for interactive rotorcraft preliminary design using a harmonic balance method for rotor trim
[AD-A274924] 07 p2668 N94-26531
Bulk-Flow Analysis, part A
[NASA-CR-193911-PT-A] 07 p2796 N94-27377
Influence of impeller shroud forces on turbopump rotor dynamics 07 p2796 N94-27378
Enhanced simulation software for rocket turbopump, turbulent, annular liquid seals
[NASA-CR-195239] 07 p2825 N94-27383
Rotordynamic analysis of annular honeycomb-stator turbulent gas seals using a new friction-factor model based on flat plate tests 08 p3302 N94-29916
Theoretical prediction of the influence coefficients on damped simple flexible rotors using the transfer matrix method
[IMR-TM-TR-002] 08 p3321 N94-30018
Parameter identification of the rotordynamic coefficients of high-Reynolds-number hydrostatic bearings 08 p3311 N94-30792
Rotor instability induced by dead band clearance in bearing supports 08 p3312 N94-30809
Rotordynamic effects driven by fluid forces from a geometrically imperfect labyrinth
[AD-A276424] 09 p3722 N94-31333
Multilevel decomposition approach to integrated aerodynamic/dynamic/structural optimization of helicopter rotor blades
[NASA-TM-109084] 10 p3989 N94-33900
Rotordynamic Instability Problems in High-Performance Turbomachinery, 1993
[NASA-CP-3239] 10 p4061 N94-34176
Experimental investigation of turbine blade-tip excitation forces 10 p4062 N94-34177
Test results for rotordynamic coefficients of anti-swirl self-injection seals 10 p4062 N94-34180
A 3D-CFD code for accurate prediction of fluid flows and fluid forces in seals 10 p4063 N94-34183
Rotordynamic forces in labyrinth seals: Theory and experiment 10 p4063 N94-34186
Calculation and measurement of the influence of flow parameters on rotordynamic coefficients in labyrinth seals 10 p4063 N94-34187
An experimental study of dynamic characteristics of labyrinth seal 10 p4064 N94-34188
Occurrence of sub-synchronous vibration in a multistage turbine pump and its prevention 10 p4064 N94-34189
Experimental and analytical study on fluid whirl and fluid whip modes 10 p4054 N94-34191
An investigation of angular stiffness and damping coefficients of an axial spline coupling in high-speed rotating machinery 10 p4064 N94-34192
Stability and stability degree of a cracked flexible rotor supported on journal bearings 10 p4064 N94-34193
A test apparatus and facility to identify the rotordynamic coefficients of high-speed hydrostatic bearings 10 p4065 N94-34199
Active magnetic bearing control loop modeling for a finite element rotordynamics code 11 p4216 N94-35857
Rotor dynamic behaviour of a high-speed oil-free motor compressor with a rigid coupling supported on four radial magnetic bearings 11 p4224 N94-35911

ROTOR HUBS

U HUBS
U ROTORS

ROTOR LIFT

A design of third-generation airfoils for helicopter rotor blades using Navier-Stokes 08 p3124 N94-28957
The quest for stall-free dynamic lift 10 p3986 N94-34986

ROTOR SPEED

An overview of a model rotor icing test in the NASA Lewis Icing Research Tunnel
[NASA-TM-106471] 06 p2166 N94-23299
A new method for torsional critical speed calculation of practical industrial rotors
[IMR-T&M-TR-001] 07 p2828 N94-28041

ROTOR SYSTEMS RESEARCH AIRCRAFT

The 1982 highlights
[NASA-TM-109671] 03 p1303 N94-15508
The 1980 highlights
[NASA-TM-109672] 03 p1303 N94-15509

ROTORCRAFT

U ROTARY WING AIRCRAFT

ROTORDYNAMICS

U ROTOR DYNAMICS

ROTORS

NT COMPRESSOR ROTORS
NT FLYWHEELS
NT IMPELLERS
NT LIFTING ROTORS
NT PUMP IMPELLERS
NT ROTARY WINGS
NT TAIL ROTORS
NT TILTING ROTORS
NT TIP VANES
NT TURBINE WHEELS
NT X WING ROTORS

Dynamic tester for rotor seals and bearings
[NASA-CASE-MFS-28493-1] 01 p0033 N94-10669
Development of passive superconducting bearings. Phase 3
[AD-A266050] 01 p0180 N94-10706
A comparison between numerically modelled and experimentally measured loss mechanisms in wave rotors
[NASA-TM-106279] 01 p0029 N94-11255
Rotor stator CGI
[NASA-TM-109313] 02 p0518 N94-13608
Helicopter structures: A review of loads, fatigue design techniques, and usage monitoring
[AD-A267115] 03 p0866 N94-15651
Jet engine performance enhancement through use of a wave-rotor topping cycle
[NASA-TM-4486] 03 p0870 N94-17470
A survey on technical problems in designing high-speed rotors with developing materials
[DE93-788519] 04 p1444 N94-18159
Some problems in the rheological characterisation of composite rocket propellants
[AD-A268806] 04 p1376 N94-18203
System and method for cancelling expansion waves in a wave rotor
[NASA-CASE-LEW-15218-1] 05 p1801 N94-20588
An application of the Cerebellar Model Articulation Controller for a switched reluctance rotor position estimator
[AD-A271769] 05 p1943 N94-20926
Brush seal bristle flexure and hard-rub characteristics 05 p1654 N94-21791
Operation of a test bed axial-gap brushless dc rotor with a superconducting stator
[DE93-019167] 05 p1769 N94-21830
Sensorless, brushless motor to drive a sealed freon-ammonia pump 06 p2315 N94-24036

Influence of backup bearings and support structure dynamics on the behavior of rotors with active supports
[NASA-CR-195106] 06 p2365 N94-24751
Two-dimensional CFD modeling of wave rotor flow dynamics
[NASA-TM-106261] 06 p2189 N94-25185
Analysis and characteristics of compressor stall precursor signals in forward and AFT swept high speed compressor
[AD-A273820] 06 p2171 N94-25517
Laser Doppler velocimetry in a low speed multistage compressor
[AD-A274836] 07 p2818 N94-26498
A finite wake theory for two-dimensional rotary wing unsteady aerodynamics
[AD-A274921] 07 p2645 N94-26535
Gas fired advanced turbine system
[DE94-003193] 07 p2827 N94-27874
A new method for torsional critical speed calculation of practical industrial rotors
[IMR-T&M-TR-001] 07 p2828 N94-28041
Acquisition, design modification, assembly, and ground test of NPS Hummingbird remotely piloted helicopter
[AD-A275546] 08 p3146 N94-28837
Rotary blood pump
[NASA-CASE-MSC-22424-1] 08 p3299 N94-29370
Method for cancelling expansion waves in a wave rotor
[NASA-CASE-LEW-15218-2] 08 p3274 N94-29740
Theoretical prediction of the influence coefficients on damped simple flexible rotors using the transfer matrix method
[IMR-TM-TR-002] 08 p3321 N94-30018
Use of magnetic compression to support turbine engine rotors 08 p3314 N94-30484
Rotor instability induced by dead band clearance in bearing supports 08 p3312 N94-30809
Rotordynamic effects driven by fluid forces from a geometrically imperfect labyrinth
[AD-A276424] 09 p3722 N94-31333
Eccentricity effects upon the flow field inside a whirling annular seal 10 p4062 N94-34181
Experimental and analytical study on fluid whirl and fluid whip modes 10 p4054 N94-34191
An investigation of angular stiffness and damping coefficients of an axial spline coupling in high-speed rotating machinery 10 p4064 N94-34192
Stability and stability degree of a cracked flexible rotor supported on journal bearings 10 p4064 N94-34193
Parameter identification of a rotor supported in a pressurized bearing lubricated with water 10 p4065 N94-34197
Advanced concepts for next generation small gas turbine engine compressors 10 p4001 N94-34443
Data reduction procedures for laser velocimeter measurements in turbomachinery rotors
[NASA-CR-195343] 10 p4057 N94-35224
Influence of backup bearings and support structure dynamics on the behavior of rotors with active supports
[NASA-CR-196119] 11 p4274 N94-35500
Design, construction, and testing of a five active axes magnetic bearing system 11 p4214 N94-35846
Third order LPF type compensator for flexible rotor suspension 11 p4217 N94-35863
Electromechanical simulation and test of rotating systems with magnetic bearing or piezoelectric actuator active vibration control 11 p4223 N94-35905
Planar rotational magnetic micromotors with integrated shaft encoder and magnetic rotor levitation 11 p4224 N94-35907
Rotor dynamic behaviour of a high-speed oil-free motor compressor with a rigid coupling supported on four radial magnetic bearings 11 p4224 N94-35911
Magnetically suspended stepping motors for clean room and vacuum environments 11 p4225 N94-35915
Tipjet 80-inch model rotor hover test: Test no. 1198
[AD-A279680] 11 p4191 N94-36261

ROUGHNESS
NT SEA ROUGHNESS
NT SURFACE ROUGHNESS

ROUTES
Federal Aviation Administration aviation forecasts
[AD-A265611] 01 p0002 N94-12578
Strategic planning for aircraft noise route impact analysis: A three dimensional approach
[NASA-CR-191484] 03 p1178 N94-17278
Airport activity statistics of certificated route air carriers, 1992
[AD-A269042] 04 p1315 N94-18490
A distributed reinforcement learning scheme for network routing
[AD-A270600] 05 p1938 N94-19845
Next Generation Weather Radar (NEXRAD) Principal User Processor (PUP) Operational Test and Evaluation (OT/E)
[AD-A273075] 05 p1868 N94-21519
Genetic algorithms applied to a mission routing problem
[AD-A274130] 07 p2968 N94-27120

ROVING VEHICLES
NT LUNAR ROVING VEHICLES
NT LUNOKHOD LUNAR ROVING VEHICLES
Conceptual studies report on lunar and planetary exploration
[NASDA-TK-SS0438] 01 p0481 N94-12323
Exploring Mars
[NASA-TM-109306] 02 p0842 N94-13613
Rover mounted ground penetrating radar as a tool for investigating the near-surface of Mars and beyong 03 p1007 N94-16197
International testing of a Mars rover prototype 03 p1273 N94-16312
Robotic concepts for operation in barren terrain
[DE93-040539] 05 p1946 N94-21925
Missions, Technologies, and Design of Planetary Mobile Vehicles
[ISBN-2-85428-331-7] 06 p2605 N94-23373
Soviet developments of planet rovers in period of 1964 - 1990 06 p2369 N94-23374
Rover requirements for the planet surface segment of the space exploration initiative 06 p2369 N94-23377
Robotic exploration of Moon and Mars 06 p2606 N94-23379
Science strategy for Mars exploration 06 p2606 N94-23380
Mars 96 small rover: Mission strategy 06 p2606 N94-23381
A reference Martian mission for a long range rover 06 p2606 N94-23382
Science objectives for short-range rovers on Mars 06 p2606 N94-23383
Prospects for using mobile vehicles in missions to Mars and other planets 06 p2607 N94-23384
The robotic Mars rover 06 p2608 N94-23390
Mission and system design of a long range rover mission 06 p2608 N94-23392
Mars 96 rover: Science, instrumentation, and control 06 p2369 N94-23395
Rover in the Mars 96 mission 06 p2609 N94-23397
The new family of JPL planetary surface vehicles 06 p2369 N94-23398
Feasibility study of an automatic vehicle for planetary exploration 06 p2369 N94-23399
Rover: Autonomous concepts for Mars exploration 06 p2369 N94-23400
Electrical power technology for robotic planetary rovers 06 p2314 N94-23401
Development/drilling test of auger boring machine on board Mars rover for Mars exploration 06 p2369 N94-23402
Mechanical design of a planetary rover 06 p2369 N94-23403
Planetary rover locomotion mechanisms 06 p2369 N94-23404
Carbon monoxide fuel cells as a source for Mars rover electric power 06 p2314 N94-23409
The mass of massive rover software 06 p2464 N94-23410
Machines for moving in soil 06 p2369 N94-23411
Evolving directions in NASA's planetary rover requirements and technology 06 p2370 N94-23414
Dual rover concept for Mars exploration 06 p2370 N94-23415
Results of the Mojave tests of the Mars 96 rover 06 p2370 N94-23416
Mars 96 rover: Technical vision and navigation 06 p2370 N94-23417
Marsohkod movement control 06 p2370 N94-23418
Walking, jumping, and tumbling: More than one way to get around Mars 06 p2370 N94-23419
Perspective of creation of means for collecting information concerning transport situation 06 p2370 N94-23420
Sensing and modelling concepts for autonomous and remote mobile robot control 06 p2370 N94-23421
Towards real-time stereovision systems for planetary missions 06 p2370 N94-23422
A DTM-based path planning method for planetary rovers 06 p2370 N94-23423
Bond graph modeling, simulation, and reflex control of the Mars planetary automatic vehicle 06 p2370 N94-23424
Mobility analysis, simulation, and scale model testing for the design of wheeled planetary rovers 06 p2370 N94-23425
Physical modeling and dynamic simulation of planet vehicles: Application to the motion prediction 06 p2371 N94-23426
Experiments with a small behaviour controlled planetary rover 06 p2371 N94-23427
Operations concepts for Mars missions with multiple mobile spacecraft 06 p2501 N94-23852
Human-like robots for space and hazardous environments
[NASA-CR-195549] 06 p2365 N94-24703
Design of a wheeled articulating land rover
[NASA-CR-195520] 06 p2365 N94-24806
Hardware design of a spherical mini-rover 07 p2833 N94-25669
The 1991-1992 project summaries 07 p2943 N94-25698
Project Ares 3 07 p2671 N94-25712
Mars rover mechanisms designed for Rocky 4 08 p3161 N94-29630
Smart focal-plane technology fof micro-instruments and micro-rovers 08 p3237 N94-29780
Navigation of military and space unmanned ground vehicles in unstructured terrains 08 p3144 N94-30282
Microrover research at JPL 10 p4066 N94-34020
Design of the MESUR/pathfinder microrover 10 p4066 N94-34021
Vehicle development of Lunar/Mars exploration 10 p4067 N94-34030
An automatic planetary vehicle for exploring Mars 11 p4354 N94-35336
Planetary Rover Program
[NASA-CR-196108] 11 p4201 N94-35511

ROWLAND CIRCLES
Vacuum ultraviolet instrumentation for solar irradiance and thermospheric airglow
[NASA-CR-194525] 02 p0652 N94-14684

RPV
U REMOTELY PILOTED VEHICLES

RS CODES
U REED-SOLOMON CODES

RTM (COMPOSITE MATERIALS)
U RESIN TRANSFER MOLDING

RUBBER
NT ADIPRENE (TRADEMARK)
NT CHLOROPRENE RESINS
NT ELASTOMERS
NT SILICONE RUBBER
NT SYNTHETIC RUBBERS
NT VITON RUBBER (TRADEMARK)
XPS analysis of Al/EPDM bondlines from IUS SRM-1 polar bosses
[AD-A266851] 03 p1056 N94-14945
RELMA: On-line quality control in the rubber mixing room using laser analysis 03 p0984 N94-16005
Synthesis and evaluation of polymeric materials
[AD-A267809] 03 p0973 N94-17408
Damage evolution in filled elastomers
[AD-A268067] 03 p1062 N94-17507
Stress-induced cracking of fluorocarbon rubber MTL-0002 after exposure to DS-2
[AD-A271753] 05 p1705 N94-21302
The simulation of action of some space environment factors on Teflon and on rubber materials 05 p1661 N94-21380
New rubber qualification for the igniter adapter
[NASA-CR-193936] 07 p2752 N94-26708
SAG compensated vibration isolation mount
[AD-D016040] 07 p2841 N94-27110
A newly developed snow vehicle (SM100S) for Antarctica. Part 4: Low temperature properties of crawler belt 08 p3314 N94-29984
Novel techniques applied to polymer lifetime predictions
[DE94-005095] 08 p3218 N94-30102
Toughening mechanisms in the high strain rate deformation of rubber-modified polymer glasses 09 p3653 N94-31942

RUBIDIUM
Disciplined rubidium oscillator with GPS selective availability 01 p0353 N94-10977
Matter-wave interferometry with laser cooled atoms
[AD-A273249] 06 p2536 N94-24717
Diode-laser-pumped, gas-cell atomic clocks
[AD-A274812] 07 p3008 N94-26484
Time and frequency technology at NIST 08 p3468 N94-30641
Optical properties of lanthanide-doped RbTiOAsO4 and transition metal-doped KTiOPO4
[DE94-008433] 09 p3907 N94-32963
X ray and gamma ray spectroscopy of solids under pressure
[DE94-011207] 11 p4238 N94-36203

RUBIDIUM COMPOUNDS
Fullerene derivatives and fullerene superconductors
[DE93-019568] 05 p2031 N94-21871
Inorganic materials for anomalous-dispersion phase-matched second harmonic generation: Rubidium titanyl arsenate isomorphs, Rb(Ti(1-2x)Ln(x)Nb(x))OAsO4
[DE94-006141] 09 p3899 N94-31847

Advances and applications of dynamic-angle spinning nuclear magnetic resonance
[DE94-007031] 09 p3870 N94-32250
Extended-range order in glasses
[DE94-008135] 09 p3661 N94-32798

RUBY
A dual-cavity ruby maser for the Ka-band link experiment 08 p3250 N94-29658

RUBY LASERS
A reliable low-maintenance flashlamp-pumped Ti:sapphire laser operating at 120 PPS
[DE94-009030] 09 p3721 N94-32848

RUDDERS
Cockpit control system conceptual design
[NASA-CR-195543] 06 p2190 N94-24551

RULES
NT FLIGHT RULES
NT INSTRUMENT FLIGHT RULES
NT PHASE RULE
NT SUM RULES
NT VISUAL FLIGHT RULES
An expert system class library for Audition
[IME-MET-TR-008] 02 p0824 N94-14196
Generating knight's tours without backtracking from errors
[AD-A266807] 02 p0772 N94-14900
Automatic generation of production rules for integrity maintenance
[REPT-92-054] 03 p1156 N94-17501
Better termination analysis for active databases
[REPT-93-026] 04 p1614 N94-18144
ELF: Learning incomplete fuzzy rule sets for an autonomous robot
[REPT-93-043] 08 p3449 N94-30923

RUN TIME (COMPUTERS)
Massively parallel hydrodynamics on unstructured grids
[DE93-007325] 01 p0153 N94-11601
Proving run-time properties of general programs w.r.t. constructive negation
[CWI-CS-R9245] 05 p1909 N94-21025
Linear time algorithm to schedule trees with communication delays optimally on two machines
[PB93-237782] 06 p2451 N94-23441
Object distribution in orca using compile-time and run-time techniques
[PB94-110574] 06 p2453 N94-23745
Runtime support and compilation methods for user-specified data distributions
[AD-A276326] 06 p2458 N94-24679
Tool for performance analysis and off-line prediction of timing behaviour 07 p2952 N94-26732
Efficient rebalancing of tree-type main memory dictionaries
[PB94-133105] 07 p3100 N94-28396
A++ and P++ array classes for architecture independent finite difference computations
[DE94-009321] 10 p4106 N94-33906
An overview of the Opus language and runtime system
[AD-A281616] 10 p4108 N94-34206
Runtime support for data parallel tasks
[AD-A280899] 11 p4300 N94-35240
Parallel Spectral Transform Shallow Water Model: A runtime-tunable parallel benchmark code
[DE94-011460] 12 p4498 N94-37568

RUNGE-KUTTA METHOD
Analysis of reacting flowfields in low-thrust rocket engines and plumes 02 p0552 N94-14491
A vertex-based finite-volume algorithm for the Navier-Stokes equations 02 p0639 N94-14599
Navier-Stokes simulation of transonic vortex flow over a delta wing 02 p0640 N94-14606
A new treatment of periodic systems with applications to helicopter rotor blade dynamics
[AD-A266770] 02 p0510 N94-14784
Multigrid time-accurate integration of Navier-Stokes equations
[NASA-TM-106373] 03 p1028 N94-17258
Numerically solving a transient heat conduction problem with convection and radiation
[AD-A268521] 03 p1220 N94-17540
Numerical calculations of high lift flows using structured and unstructured methods 04 p1307 N94-18428
An algebraic turbulence model for turbomachinery 04 p1411 N94-18554
Adaptive grids for quasilinear parabolic systems in one space dimension
[ETN-93-93611] 05 p1954 N94-21137
Butcher-Kuntzmann methods for nonstiff problems on parallel computers
[CWI-NM-R9305] 05 p1935 N94-21493
Users manual for the NASA Lewis three-dimensional ice accretion code (LEWICE 3D)
[NASA-TM-105974] 05 p1642 N94-21590
Modelling short bent, graded index dielectric slab waveguides
[PB93-215283] 05 p1742 N94-22349
A multigrid multiblock solver for compressible turbulent flow
[MEMO-1125] 06 p2315 N94-22713
Computation of propulsion-related flowfields using unstructured adaptive meshes 06 p2215 N94-23056
Reliability enhancement of Navier-Stokes codes through convergence enhancement 06 p2216 N94-23064
The theoretical accuracy of Runge-Kutta time discretizations for the initial boundary value problem: A careful study of the boundary error
[NASA-CR-191561] 06 p2480 N94-23272
Differential algebraic equations
[PB93-237618] 06 p2481 N94-23455
Compressible turbulent flow simulation with a multigrid multiblock method 06 p2342 N94-23694
Preconditioning in parallel Runge-Kutta methods for stiff initial value problems
[CWI-NM-R9310] 07 p2991 N94-26217
On the error committed by stopping the Newton iteration in implicit Runge-Kutta methods
[TW-93-02] 07 p2992 N94-26229
Parallel implicit unstructured grid Euler solvers
[AD-A277581] 07 p2999 N94-27434
High-lift system analysis method using unstructured meshes
[NLR-TP-92351-U] 07 p2647 N94-27554
Time-step enlargement and optimal smoothing in Runge-Kutta time-integration algorithms by implicit and explicit smoothing
[NLR-TP-92221-U] 07 p2798 N94-27799
Formulas of the Runge-Kutta-Nystroem type
[ISBN-0-315-85774-9] 08 p3454 N94-30241
Parallel iteration across the steps of high order Runge-Kutta methods for nonstiff initial value problems
[CWI-NM-R9313] 08 p3433 N94-30730
Eigenvalue analysis of the convergence behaviour of an Euler method
[PB94-1255722-U] 08 p3281 N94-30743
Symplectic Runge-Kutta schemes 3: Canonical elementary differentials
[MATHS-REPT-A-204] 09 p3840 N94-31159
Symbolic derivation of Runge-Kutta methods
[MATHS-REPT-A-205] 09 p3840 N94-31160
A brief introduction to symplectic integrators and recent results
[DE94-006225] 09 p3845 N94-31763
Solution of the average-passage equations for the incompressible flow through multiple-blade-row turbomachinery
[AD-A276515] 09 p3583 N94-31931
On the error committed by stopping the Newton iteration in Runge-Kutta methods and linear multistep methods
[TW-93-13] 09 p3847 N94-32206
Fourth-order 2N-storage Runge-Kutta schemes
[NASA-TM-109112] 09 p3573 N94-32950
Third-order 2N-storage Runge-Kutta schemes with error control
[NASA-TM-109111] 10 p3984 N94-34204

RUNOFFS
U DRAINAGE

RUNWAY CONDITIONS
The 94 GHz MMW imaging radar system 06 p2306 N94-25493

RUNWAY LIGHTS
Improved taxiway exit identification system
[AD-A277892] 10 p4008 N94-33538

RUNWAYS
The Memphis Precision Runway Monitor Program Instrument Landing System final approach study
[AD-A266035] 01 p0023 N94-11103
Evaluation of infrared sensors for autonomous landing guidance
[AD-A266450] 02 p0513 N94-13703
The 1971 highlights --- NASA programs and research
[NASA-TM-109629] 03 p1302 N94-15417
Notes on Antarctic aviation
[AD-A273018] 05 p1651 N94-21239
Parallel runway requirement analysis study. Volume 1: The analysis
[NASA-CR-191549-VOL-1] 05 p1644 N94-22277
Parallel runway requirement analysis study. Volume 2: Simulation manual
[NASA-CR-191549-VOL-2] 05 p1644 N94-22278
Performance of prefabricated geocomposite subdrainage system in an airport runway
[DOT/FAA/RD-93/23] 06 p2192 N94-23303
Airport pavement test machine design and cost study
[DOT/FAA/CT-93/51] 06 p2192 N94-24072
Soft ground arresting system for airports
[DOT/FAA/CT-93/80] 07 p2680 N94-26202
Tests of highly loaded skids on a concrete runway
[NASA-TP-3435] 07 p2669 N94-26608
Methods for experimentally determining commercial jet aircraft landing parameters from video image data
[AD-A274207] 07 p2669 N94-27105
Aircraft accident report: Runway departure following landing American Airlines flight 102, McDonnell Douglas DC-10-30, N139AA, Dallas/Fort Worth International Airport, Texas, April 14, 1993
[PB94-910402] 07 p2660 N94-27766
Contributions of DLR to air traffic capacity enhancement within a terminal area 08 p3138 N94-29567
Determining the bearing capacity of flexible airfield pavements using a heavy weight deflectometer
[ISBN-0-315-86210-6] 09 p3587 N94-31710
Evaluation for the development of taxiway lighting intensity standards
[AD-A276706] 09 p3588 N94-32120
Improved taxiway exit identification system
[AD-A277892] 10 p4008 N94-33538
A model-based approach for detection of runways and other objects in image sequences acquired using an on-board camera
[NASA-CR-196424] 12 p4446 N94-36812

RUPTURING
Residual contact restraints in cryogenics
[ETN-93-94375] 02 p0671 N94-13501
Head-on collision of drops: A numerical investigation
[NASA-TM-106394] 05 p1798 N94-20167
Mechanical behavior of CMCs: Crack growth resistance and creep aspects 06 p2256 N94-24235
Ceramic matrix composite parts design 06 p2256 N94-24237

RURAL AREAS
The Canadian experience: Using telemedicine for the support of medical care at remote sites 01 p0305 N94-11789
The revitalization of health and education in Rural America Act of 1992 01 p0308 N94-11810
Spatiotemporal variability of non-urban ozone concentrations over the eastern United States and its potential replication by satellite data
[PB93-191328] 04 p1476 N94-19065
Urban/rural application of weather radar for flow forecasting. Proceedings of the Informal CEc -Workshop
[PB93-220135] 06 p2407 N94-23129
Report of feasibility study on international-cooperation in high efficient energy conversion technology
[DE94-732340] 08 p3337 N94-28631

RURAL LAND USE
Educational module for the higher agricultural education. Part 1: Land use classification using satellite pictures
[BCRS-92-11A] 02 p0819 N94-14809
Obtaining digital regional planning information from aerial pictures
[REPT-228] 02 p0700 N94-14810
Common property resources and low-level flying in Labrador: Flight, fight or fancy?
[ISBN-0-315-87318-3] 09 p3924 N94-31732

RUSSIA
U RUSSIAN FEDERATION

RUSSIAN FEDERATION
Space nuclear technology
[DE93-010184] 01 p0045 N94-10299
JPRS report: Science and technology. Central Eurasia: Space
[JPRS-USP-93-003] 02 p0828 N94-13182
Computational Russian morphological generation on Prolog: Noun, pronoun, and adjective 02 p0747 N94-13436
NASA/DOD Aerospace Knowledge Diffusion Research Project. Paper 37: The impact of political control on technical communications: A comparative study of Russian and US aerospace engineers and scientists
[NASA-TM-109329] 02 p0826 N94-14488
Commonwealth of Independent States aerospace science and technology, 1992: A bibliography with indexes
[NASA-SP-7106] 03 p0854 N94-16481
Satellite communications systems and technology. Executive Summary
[NASA-TM-109388] 06 p2293 N94-23622
Satellite communications systems and technology. Volume 1: Analytical chapters
[NASA-TM-109398] 06 p2293 N94-23627
Research and Development of Ram/Scramjets and Turboramjets in Russia
[AD-A275588] 08 p3151 N94-29291
Russian national time scale long-term stability 08 p3475 N94-30679
Station climatic summaries: China, the former USSR, and Mongolia
[AD-A276548] 09 p3784 N94-32057
Information systems to enhance technology exchange
[DE94-007744] 09 p3920 N94-32808
Utilizing a Russian space nuclear reactor for a US space mission: Systems integration issues
[DE94-005585] 10 p4017 N94-34137

JPRS Report: Science and Technology. Central Eurasia: Space. Russian federation law on space
[JPRS-USP-94-002] 11 p4348 N94-35519
JTEC/WTEC report and program summary 11 p4379 N94-36042
Information and communication technology 11 p4257 N94-36043
JPRS report: Central Eurasia. Aviation and cosmonautics, No. 4, April 1993
[JPRS-UAC-94-003] 12 p4391 N94-36999
JPRS report: Science and technology. Central Eurasia: Space
[JPRS-USP-94-004] 12 p4391 N94-37002
JPRS report: Science and technology. Central Eurasia: Space 12 p4391 N94-37003
JPRS report: Science and technology. Central Eurasia
[JPRS-UST-94-013] 12 p4509 N94-37006
JPRS report: Science and technology. Central Eurasia: Materials science
[JPRS-UMS-93-008] 12 p4404 N94-37010
Space Station: Impact of the expanded Russian role on funding and research. Report to the Ranking Minority Member, Subcommittee on Oversight of Government Management, Committee on Governmental Affairs, US Senate
[GAO/NSIAD-94-220] 12 p4396 N94-37257
Problems of international exchange of scientific and technical information for a Russian aerospace research institute 12 p4544 N94-37339

RUSSIAN SPACE PROGRAM
Space Nuclear Facility test capability at the Baikal-1 and IGR sites Semipalatinsk-21, Kazakhstan
[DE93-011662] 03 p0926 N94-16773
Advanced display technologies in Russia, Ukraine, and Belarus. Viewgraphs 06 p2630 N94-22893
Satellite communications systems and technology. Volume 2: Site reports
[NASA-TM-109399] 06 p2293 N94-23628
Utilizing a Russian space nuclear reactor for a US space mission: Systems integration issues
[DE94-005585] 10 p4017 N94-34137
JPRS Report: Science and Technology. Central Eurasia: Space. Russian federation law on space
[JPRS-USP-94-002] 11 p4348 N94-35519

RUSTING
Effect of surface cleanliness of bearing steel on adhesive strength and tribological properties of sputter-deposited gold films
[DE93-767974] 01 p0082 N94-10732

RUTHENIUM
The structure and mechanical properties of Ru-Cu and Ru-Ti nanolayer composites
[DE93-014453] 02 p0558 N94-14469
Photochemically induced transformations of transition complexes
[AD-A271112] 05 p2014 N94-19982

RUTHENIUM ALLOYS
Magnetism in CeRu2Ge2 and CeRh2Ge2 and its pressure dependence
[DE93-040061] 05 p2032 N94-21987
Methanol electrooxidation on well-characterized Pt-Ru alloys
[DE94-009640] 10 p4022 N94-33918

RUTHERFORDIUM
On-line gas chromatographic studies of Rutherfordium (element 104), hahnium (element 105), and homologs
[DE93-013890] 03 p0948 N94-16821

RUTILE
Prism-film coupling in anisotropic planar waveguides of epitaxial (101) rutile thin films
[DE93-012912] 02 p0811 N94-14304
Time-resolved shock compression of porous rutile: Wave dispersion in porous solids
[DE93-018848] 05 p1829 N94-19927
Electronic structure of a single oxygen vacancy in rutile TiO2
[DE94-602717] 07 p3062 N94-26901
Mossbauer and spectral (visible and near-IR) data for Fe(3+)-substituted rutile 11 p4240 N94-36154

RYAN AIRCRAFT
NT FIREBEE 2 TARGET DRONE AIRCRAFT
NT XV-5 AIRCRAFT

RYDBERG SERIES
Rydberg states in multiply charged ions
[DE94-002335] 07 p3021 N94-26760
Diamagnetism in helium Rydberg atoms
[ETN-94-96015] 09 p3865 N94-31549

S

S BAND
U SUPERHIGH FREQUENCIES
U ULTRAHIGH FREQUENCIES

S GLASS
Hydrostatic testing of thick laminated composite cylinders for performance model validation
[DE93-012728] 01 p0184 N94-10264
SRB thermal curtain design support
[NASA-CR-193857] 03 p0927 N94-17123
SRB thermal curtain design support
[NASA-CR-193858] 03 p0928 N94-17124

S MATRIX THEORY
Recent developments in multiple-scattering calculations of XAFS and XANES
[DE93-010999] 02 p0563 N94-13477
Convergence of the multiple scattering expansion in XAFS and XANES
[DE93-011001] 03 p0948 N94-16772
Polarimetric statistics of electromagnetic waves scattered by distributed targets
[PB93-195907] 04 p1389 N94-18951
New relativistic S-matrix results for scattering -- beyond the usual anomalous factors/beyond impulse approximation
[DE93-019148] 05 p1971 N94-20096
Mapping between the Sinh-Gordon and Ising models
[DE94-601535] 07 p2998 N94-27162
Single scattering of light by ensembles of particles with various shapes
[ETN-94-96016] 09 p3878 N94-31550

S WAVES
NT SH WAVES
Wave propagation characteristics of short-period crustal phases near ARCESS and NORESS
[AD-A265959] 01 p0275 N94-11102
Shear wave measurements in shock-induced, high-pressure phases
[DE93-016461] 03 p1062 N94-17664
The phase mixing of shear Alfven waves
[DE93-624920] 04 p1581 N94-17688
Constraints on crustal structure from long period pressure and displacement measurements on the deep seafloor
[AD-A269931] 04 p1498 N94-18663
Seismic studies of the geologic structure and physical properties of the seabed
[AD-A270895] 04 p1500 N94-19747
Measurements and modeling of multitone, low-frequency acoustic data from the Arraial do Cabo range
[AD-A273406] 06 p2530 N94-25073
Downward extrapolation of multi-component seismic data
[ISBN-9-09-005213-5] 06 p2405 N94-25229
Decomposition of multi-component measurements into P and S waves
[ISBN-9-09-005197-X] 06 p2405 N94-25251
Parametric and nonparametric discriminants for regional earthquakes and explosions
[AD-A273807] 06 p2406 N94-25538
Elastic scattering by a spherical inclusion
[AD-A274713] 07 p2878 N94-26433
A preliminary shear velocity model for Central Asia
[AD-A274972] 07 p2880 N94-26752
Analysis of S-wave seismogram envelope of deep earthquakes and estimation of random inhomogeneities in the Kanto-Tokai area 07 p2886 N94-27988
Initial wave-type identification with neural networks and its contribution to automated processing in IMS version 3.0
[AD-A275058] 08 p3359 N94-29137
On wave interactions of rotational and irrotational flows 09 p3700 N94-31219
A geoacoustic model for fine-grained, unconsolidated calcareous sediments (ARSRP natural laboratory)
[AD-A277830] 10 p4092 N94-33831
Body-wave radiation patterns and AVO in transversely isotropic media
[DE94-009214] 10 p4036 N94-34162
A three-body calculation of the O-16(d,p)O-17 reaction using a two-term separable potential for the s-wave nucleon-core interaction
[DE94-616652] 11 p4320 N94-35579
Notes on possible S-wave resonances in relativistic two-particle systems
[DE94-616689] 11 p4329 N94-36392

S-A-W DEVICES
U SURFACE ACOUSTIC WAVE DEVICES

S-N DIAGRAMS
Development of a fatigue analysis approach for CFRP structures under acoustic loading 01 p0058 N94-10018
Factors which affect fatigue strength of fasteners
[DE93-017272] 04 p1453 N94-18084
Pre-standardisation work on fatigue and fracture testing of titanium matrix composites 12 p4402 N94-36667

S-18 SATELLITE
U OAO

S-2 AIRCRAFT
S-2E Tracker maritime patrol aircraft re-engine and system upgrade program 06 p2158 N94-24270

S-3 AIRCRAFT
Work/rest schedules and performance of S-3 aviators during fleet exercise
[AD-A265807] 02 p0734 N94-12975

SABOT PROJECTILES
Transient internal probe
[AD-A275054] 08 p3505 N94-29134

SABRELINER AIRCRAFT
U T-39 AIRCRAFT

SACCADIC EYE MOVEMENTS
Comparative measurement of visual stability in cosmic space: Onboard experiment and pre-flight activities 07 p2916 N94-27463
Function of selective attention intrinsic to the saccade system: Does the voluntary control override the stimulus driven control? 07 p2928 N94-27523
Eye movements and visual information processing
[AD-A278364] 10 p4097 N94-33700

SACCHARIDES
U CARBOHYDRATES

SADDLE POINTS
Ab initio potential energy surface for the H + OCS reaction
[AD-A270577] 05 p1698 N94-19947
The cusp horseshoe and its bifurcations in the unfolding of an inclination-flip homoclinic orbit
[W-9307] 06 p2480 N94-23141
Magnetic field-induced saddle point in GaAs/AlGaAs short period superlattices
[REPT-A-2656] 06 p2568 N94-25515
Phase portraits of quadratic systems with finite multiplicity three and one critical point of infinity
[REPT-93-41] 07 p2991 N94-26215
Heteroclinic attractors: Time averages and moduli of topological conjugacy
[W-9318] 09 p3844 N94-31690
Steepest descent paths for integrals defining the modified Bessel functions of imaginary order
[CWI-AM-R9303] 09 p3848 N94-32227

SADDLES
The cusp horseshoe and its bifurcations in the unfolding of an inclination-flip homoclinic orbit
[W-9307] 06 p2480 N94-23141

SAFETY
NT AEROSPACE SAFETY
NT AIRCRAFT SAFETY
NT FLIGHT SAFETY
NT INDUSTRIAL SAFETY
NT RANGE SAFETY
NT REACTOR SAFETY
Safety of high speed ground transportation systems: X2000 US demonstration vehicle dynamics trials, preliminary test report, October 1992 - January 1993
[PB93-194645] 01 p0422 N94-10736
Hydrogen peroxide safety issues
[DE93-013895] 02 p0565 N94-14346
Americans with Disabilities Act considerations for the practice of occupational medicine 03 p1124 N94-16611
Programs and resources for control of job stress in the Federal workplace 03 p1124 N94-16617
Industrial Hygiene Laboratory accreditation: The JSC experience 03 p1125 N94-16623
Space Shuttle main engine. NASA has not evaluated the alternate fuel turbopump costs and benefits. Report to the Administrator of the National Aeronautics and Space Administration
[GAO/NSIAD-94-54] 03 p0926 N94-16834
The 1987 Goddard Space Flight Center Battery Workshop
[NASA-CP-3236] 03 p1012 N94-17062
SUNRAYCE 1993: Working safely with lead-acid batteries and photovoltaic power systems
[DE93-016553] 04 p1464 N94-17712
Safety-routines and guidelines for work in the clean room at the Epitek-Laboratory, Kjeller (Norway)
[FFI-93/7012] 04 p1322 N94-17735
Laboratory test and evaluation report of the essex model 60C-0037-2 molecular sieve oxygen generating system
[AD-A269967] 04 p1445 N94-18778
Current status of environmental, health, and safety issues of nickel metal-hydride batteries for electric vehicles
[DE93-017079] 05 p1748 N94-19902
Female security as a general mobility condition
[ISBN-3-79-831536-1] 05 p2039 N94-20153
The FY1992 survey on commercialization of Stirling engine utilization equipment
[DE94-707416] 05 p1849 N94-22029
GPHS-RTG's in support of the Cassini mission
[DE94-001445] 06 p2218 N94-23459

Impacts: NIST Building and Fire Research Laboratory (technical and societal)
[PB94-113420] 06 p2270 N94-23737
An automated tool to facilitate code translation for software fault tree analysis
[AD-A273205] 06 p2457 N94-24556
Waste minimization/pollution prevention at R/D facilities: A cradle-to-grave tracking and information system that will be implemented at Sandia National Laboratories
[DE93-040330] 06 p2591 N94-24607
Project Columbiad: Reestablishment of human presence on the Moon 07 p2689 N94-25687
The structural behaviour of the steel or composite concrete and steel frames and the connections of frame members during the fire: A literature review
[VTT-TIED-1437] 07 p2837 N94-26307
Comparative analysis of different configurations of PLC-based safety systems from reliability point of view 07 p2836 N94-27925
Technical Report of National Research Institute of Fisheries Engineering: Fishing Boat and Instrument, No. 12
[JTN-94-80595] 07 p2764 N94-27976
Recent trend of domestic and international regulations on intact stability of ships for safety 07 p2764 N94-27977
Propellants and explosives in ballistic missiles
[UCRL-LR-113578] 07 p2760 N94-28222
Safety enhancement of composites via periodic proof testing
[AD-A275662] 08 p3176 N94-28655
Non-aqueous cleaning solvent substitution
[DE94-005339] 08 p3219 N94-30245
Non-aqueous cleaning solvent substitution 08 p3354 N94-30466
Fuzzy-algebra uncertainty analysis for abnormal-environment safety assessment
[DE94-006257] 08 p3462 N94-30849
Laser safety manual for DREO
[AD-A276288] 09 p3714 N94-31255
Scientific basis for safety science
[PB94-138534] 09 p3668 N94-31838
Systems for the monitoring of working conditions relating to health and safety: Extensive description. Norway
[PB94-138542] 09 p3803 N94-31839
Controlling hazardous energy sources (lockout/tagout)
[NASA-TM-105290] 09 p3669 N94-32861
Implementing software safety in the NASA environment
[NASA-TM-106597] 09 p3731 N94-33032
Safety concerns for first entry operations of orbiting spacecraft 10 p4102 N94-33662
Crystal growth furnace safety system validation
[NASA-CR-193964] 10 p4056 N94-34266
Robust requirements specifications for safety-critical systems
[PB94-167806] 11 p4250 N94-35532
Information on alternative refrigerants and lubricants: The ARTI refrigerant database
[DE94-009997] 12 p4426 N94-37490

SAFETY DEVICES
NT ABORT APPARATUS
NT AIR BAG RESTRAINT DEVICES
NT ARRESTING GEAR
NT EJECTION SEATS
NT HELMETS
NT SEAT BELTS
Respiratory Protection Program medical clearance for respirator use 03 p1127 N94-16642
Regulated emergency oxygen system
[AD-A266228] 03 p1138 N94-16983
Solid-state, resistive hydrogen sensors for safety monitoring
[DE93-017769] 04 p1424 N94-17778
Army Cockpit Delethalization Program (CDP)
[AD-A268990] 04 p1512 N94-18765
Plasma contactor development for Space Station
[NASA-TM-106425] 04 p1587 N94-18861
Evaluation of head injury criteria
[NIAR-93-2] 05 p1890 N94-20190
Composite material impregnation unit
[NASA-TM-107751] 06 p2254 N94-23486
Reach performance while wearing the Space Shuttle launch and entry suit during exposure to launch accelerations 06 p2436 N94-24204
Studies of Shuttle orbiter arrestment system
[NASA-TP-3370] 06 p2177 N94-24304
The 1991-1992 project summaries 07 p2943 N94-25698
Annual conference on fire research, 1993: Book of abstracts
[PB94-121324] 07 p2717 N94-26907
Comparison of two cool vests on heat-strain reduction while wearing a firefighting ensemble in a hot/humid environment
[AD-A275103] 08 p3400 N94-28902
Microcomputer-based protective functions in industrial production systems: Assessment method
[PB94-137817] 08 p3411 N94-29159
The use of interactive computer vision and robot hand controllers for enhancing manufacturing safety 08 p3314 N94-30442
Advanced eye or sensor protection and high speed variable optical attenuation system
[AD-D016150] 10 p4099 N94-33781
Aircraft command in emergency situations prototype development users manual
[DOT/FAA/CT-94/24] 12 p4385 N94-37706

SAFETY FACTORS
Structural design/margin assessment
[NASA-TP-3410] 02 p0669 N94-12831
Effects of radiobiological uncertainty on vehicle and habitat shield design for missions to the moon and Mars
[NASA-TP-3312] 02 p0846 N94-12875
Design, qualification and operation of nuclear rockets for safe Mars missions
[DE93-010792] 02 p0549 N94-12996
Early detection of insulation failure in electric motors
[PB93-198208] 02 p0626 N94-14686
Safety-critical software: Status report and annotated bibliography
[AD-A266993] 03 p1144 N94-15214
ASRM nozzle thermal analysis
[NASA-CR-194672] 03 p0928 N94-17277
Specifying design conservatism: Worst case versus probabilistic analysis 06 p2374 N94-23939
Safety analysis in conceptual design of process control
[VTT-PUBS-117] 07 p2762 N94-25641
Technology drivers for flight telerobotic system software 07 p2684 N94-26289
Structural design feasibility study of Space Station long spacer truss
[NASA-TM-106346] 07 p2843 N94-27559
Technical Report of National Research Institute of Fisheries Engineering: Fishing Boat and Instrument, No. 12
[JTN-94-80595] 07 p2764 N94-27976
Recent trend of domestic and international regulations on intact stability of ships for safety 07 p2764 N94-27977
Systematic safety consideration in product design
[PB94-132354] 08 p3229 N94-28410
NASA wiring program: Survey of NASA experiences in wiring system safety 08 p3165 N94-28700
Advanced steady-state operating scenarios
[DE94-004810] 08 p3509 N94-30768

SAFETY MANAGEMENT
Achievements and challenges of Space Station Freedom's safety review process
[NASA-TM-106199] 01 p0040 N94-10640
Health and safety issues for aerospace workers in the use of advanced materials 01 p0021 N94-10795
The future of aircraft cabin fire safety 01 p0022 N94-10797
NASA directives master list and index
[NHB-1410.13L] 03 p1229 N94-15414
New health and safety initiatives at the Department of Energy (DOE) 03 p1124 N94-16610
Safety approaches for high power modular laser operation
[DE93-017213] 04 p1435 N94-17759
Human reliability analysis application guide
[DE93-015361] 04 p1511 N94-18244
Safety guidelines for the operation of the DREO 10 m EMP simulator DREMPS
[DREO-TN-93-5] 06 p2193 N94-24117
TEM cell safety report
[DREO-TN-93-9] 06 p2193 N94-24123
Collaborating with our customers: NIST building and fire research laboratory
[PB94-110194] 06 p2272 N94-24955
Evaluation and improvement of the inquest system on work accidents (TOT)
[VTT-TIED-1418] 07 p2762 N94-26261
Proceedings of the Second EGS4 User's Meeting in Japan
[DE93-520383] 07 p3032 N94-26543
Aerospace safety advisory panel
[NASA-TM-109692] 07 p3118 N94-27381
Report of the Shuttle Processing Review Team
[NASA-TM-109728] 07 p2692 N94-28178
Evaluation of monitoring audiometry in the United States Air Force Hearing Conservation Program
[AD-A275309] 08 p3391 N94-29211
Joint research activities with CCMRI (China) 08 p3240 N94-29521
Risk measures in living probabilistic safety assessment
[VTT-PUBS-146] 08 p3465 N94-30154
Scientific basis for safety science
[PB94-138534] 09 p3668 N94-31838
Integrated safety program for the Nuclear Electric Propulsion Space Test Program
[DE94-004670] 09 p3615 N94-32669
Independent safety assessment of the Topaz-2 space nuclear reactor power system
[DE94-008653] 09 p3877 N94-32879
HFE safety reviews of advanced nuclear power plant control rooms 10 p4100 N94-33613
Impact of weather on flight operations at a major airport
[PB94-127990] 10 p4090 N94-34408
Aerospace Safety Advisory Panel
[NASA-TM-109840] 11 p4201 N94-35390
Implementation of a Computerized Maintenance Management System 11 p4343 N94-35970
Space Shuttle: Incomplete data and funding approach increase cost risk for upgrade program. Report to Congressional Requesters
[GAO/NSIAD-94-23] 12 p4392 N94-37026
NASA Lewis wind tunnel model systems criteria
[NASA-TM-106585] 12 p4390 N94-37522

SAGE SATELLITE
Present status of SAGE
[DE93-014350] 02 p0781 N94-13205
Stratospheric Aerosol and Gas Experiment (SAGE 3) 05 p1869 N94-21644

SAGNAC EFFECT
Interferometry with particles of non-zero rest mass
[DE93-613518] 01 p0409 N94-10501
Polarization effects in optical fiber current sensors based on Sagnac interferometers with 3 by 3 couplers
[DE93-012665] 02 p0792 N94-14367

SAILPLANES
U GLIDERS

SALINITY
Shear, strain and thermohaline vertical fine structure in the upper ocean
[AD-A265961] 01 p0289 N94-12348
Preliminary results on the hydrological measurements in the Aegean Sea off Crete: Cruise, Georgia, 1989
[PREPRINT-736] 02 p0725 N94-13500
Phase aligner for the Electronically Scanned Thinned Array Radiometer (ESTAR) instrument
[NASA-TM-4518] 02 p0623 N94-13878
CTD and XBT data collected on ERS-1 validation cruise RRS Charles Darwin Cruise 62A, Iceland-Faeroes region
[IOS-294-1992] 04 p1461 N94-18063
SeaSoar and CTD sections across the Iceland-Faeroes Front and Faeroe Shetland Channel, August 1990
[IOS-295-1992] 04 p1496 N94-18064
SeaSoar CTD, fluorescence and scalar irradiance data from RRS Charles Darwin Cruises 58/59, NE Atlantic, Vivaldi 1991
[IOS-299-1992] 04 p1496 N94-18066
Synoptic ocean prediction experiment. EN216 CTD section data report
[AD-A268903] 04 p1497 N94-18230
Overview of physical oceanographic measurements taken during the Mount Mitchell cruise to ROPME sea area
[DE93-018460] 04 p1497 N94-18494
On the sources of North Atlantic deep water
[AD-A270854] 05 p1881 N94-19895
Briny lakes on early Mars? Terrestrial intracrater playas and Martian candidates 05 p2145 N94-21675
A two-dimensional dispersion module for the TOUGH2 simulator
[DE94-002262] 06 p2335 N94-24655
Examination of the physical, electrical, and microwave evolution of water into young sea ice
[AD-A273559] 06 p2418 N94-24918
Cryosphere and climate 08 p3352 N94-30632

SALMONELLA
Compatibility tests for biological specimens to on-board experiments in the Space Shuttle flight
[NASDA-CNT-930003] 01 p0301 N94-12278

SALT BEDS
Mobility of salt domes
[BCRS-92-08] 05 p1857 N94-21016

SALTS
Aluminum and membrane channels
[AD-A265241] 01 p0300 N94-11020
Modeling void growth and movement with phase change in thermal energy storage canisters
[NASA-TM-106288] 01 p0163 N94-12576
Mechanical modeling of the growth of salt structures
[DE93-015342] 04 p1596 N94-18243

SAMARITAN AIRCRAFT
U C-131 AIRCRAFT

SAMARIUM
NT SAMARIUM ISOTOPES
Comparative M-H characteristics of 1-5 and 2-17 type samarium-cobalt permanent magnets to 300 C
[NASA-CR-194440] 06 p2312 N94-24870

Technical report of ISSP. Ser. A, no. 2682: Pressure dependence of Sm:YAG fluorescence to 50 GPa: A new calibration as a high pressure scale
[JTN-94-80568] 07 p3066 N94-27354
Study on the formation of ultrafine particles of Sm-Co intermetallic compounds using RF thermal plasma
08 p3211 N94-29516

SAMARIUM COMPOUNDS
Study on the formation of ultrafine particles of Sm-Co intermetallic compounds using RF thermal plasma
08 p3211 N94-29516
Magnetotransport measurements in magnetic fields up to 50T in SmB6 and FeSi
[DE94-006227] 08 p3520 N94-30848

SAMARIUM ISOTOPES
Radiogenic age and isotopic studies
[DE93-610548] 01 p0274 N94-10407
Nd-142/Nd-144 in bulk planetary reservoirs, the problem of incomplete mixing of interstellar components and significance of very high precision Nd-145/Nd-144 measurements 03 p1256 N94-16220
Constraints on the differentiation of the Earth from the coupled Sm-146,147-Nd-142,143 systematics
03 p1103 N94-16271
Examination of low level magnetic dipole intensities in the transition nuclei Sm-148, Sm-150, Sm-152 and Sm-154, with inelastic photon scattering at S-DALINAC
[ETN-93-95069] 05 p1971 N94-20030
The Sm-(146,147)-Nd-(142,143) formation interval for the lunar mantle and implications for lunar evolution
05 p2097 N94-20663
Magnesian anorthosites from the western highlands of the Moon: Isotope geochemistry and petrogenesis
05 p2118 N94-20779
The Sm-Nd systematics of silicate inclusions in iron meteorites: Results from Caddo (IAB)
[CONTRIB-5241(804)] 05 p2084 N94-20795
New data supporting a Sm-146,147-Nd-142,143 formation interval for the lunar mantle
11 p4374 N94-36173

SAMPLED DATA SYSTEMS
The design and analysis of robust feedback systems
[AD-A267152] 03 p1165 N94-15778
Discrete sliding mode control for nonlinear sampled data systems
[AD-A267500] 03 p1167 N94-17369
High accuracy switched-current circuits using an improved dynamic mirror 04 p1401 N94-18368
An 18 bit 50 kHz ADC for low earth orbit
05 p1764 N94-21702
Operator theoretic methods in the control of distributed and nonlinear systems
[AD-A274160] 07 p2988 N94-27139
Investigation of spectral analysis techniques for randomly sampled velocimetry data
07 p3009 N94-27924

SAMPLERS
Analytical method for water vapor collection and analysis in aircraft cabin fires
[DOT/FAA/CT-TN93/33] 01 p0022 N94-12575
Maximum likelihood estimation for constrained or missing data models
[AD-A266563] 02 p0773 N94-13585
Methods to obtain blood samples periodically during exercise research studies while subjects are immersed in water or otherwise inaccessible
[AD-A268227] 03 p1130 N94-17562
Novel mass spectrometric instrument for gaseous and particulate characterization and monitoring
[DE93-019992] 04 p1433 N94-19054
Passive Cryogenic Sampler
[DE94-000918] 05 p1811 N94-22392
Automation technology for remote sample acquisition
06 p2369 N94-23407
Comet nucleus and asteroid sample return missions
07 p2689 N94-25692
Simulation approaches for calculations in directed graphical models
[AD-A274825] 07 p3003 N94-26494
California residential indoor air quality study. Volume 1: Methodology and descriptive statistics. Appendix
[PB94-166055] 12 p4464 N94-36995

SAMPLES
NT MARS SURFACE SAMPLES
Practical reporting times for environmental samples
[DE93-013461] 04 p1472 N94-17910
Vapor-fortified QA/QC samples for the analysis of volatile organic compounds
[AD-A278712] 11 p4229 N94-35776

SAMPLING
NT AIR SAMPLING
NT CORE SAMPLING
NT DATA SAMPLING
NT PARTICULATE SAMPLING
NT RANDOM SAMPLING
Analytical method for water vapor collection and analysis in aircraft cabin fires
[DOT/FAA/CT-TN93/33] 01 p0022 N94-12575
Optimal hemicube sampling
[DE93-010499] 01 p0334 N94-12591
Sampling of globular clusters and the distance to the galactic center
[INPE-5446-TDI/492] 02 p0837 N94-13449
A mission concept of Phobos/Deimos exploration
03 p1287 N94-16387
Exploring the remote sensing of foliar biochemical concentrations with AVIRIS data
03 p1069 N94-16683
Gas Analysis System
[DE93-014617] 03 p0949 N94-16891
Practical reporting times for environmental samples
[DE93-013461] 04 p1472 N94-17910
Bayesian analysis of ARMA processes: Complete sampling based inference under full likelihoods
[AD-A269168] 04 p1557 N94-18694
Ultrafast Electronics and Optoelectronics: Summaries of papers. Technical digest conference edition
[AD-A269233] 04 p1405 N94-18909
A weighted least-squares lump correction algorithm for transmission-corrected gamma ray nondestructive assay
[DE93-018474] 05 p1904 N94-20049
Development and demonstration of a personal monitoring system for exposure to hydrogen fluoride
[DE93-041273] 05 p1891 N94-20935
Green Sheet project: Dye sheet evolution
[AD-A272019] 05 p1883 N94-21443
Orbit and sampling requirements: TRMM experience
05 p1870 N94-21647
Subset selection with a generalized selection goal based on a loss function
[PB94-111192] 06 p2494 N94-23798
Verification and validation of models
[PB94-110566] 06 p2456 N94-24507
Two-stage versus sequential sample-size determination in regression analysis of simulation experiments
[PB94-110558] 06 p2495 N94-24634
The use of on-line ion chromatography for high temperature and high pressure reaction studies
[DE94-002525] 07 p2713 N94-26075
Macrobenthic fauna in the dutch sector of the north sea in 1991
[PB94-126414] 07 p2868 N94-27200
Fiscal 1991 geothermal development promotion energy
[DE94-732332] 08 p3337 N94-28627
Acceptance sampling methods for sample results verification
[DE94-002882] 08 p3465 N94-29925
Sampling behaviour in a four instrument monitoring task: Effects of signal bandwidth and number of events per signal
[AD-B179613] 08 p3402 N94-30422
Prediction and standard error estimation for a finite universe total when a stratum is not sampled
[DE94-004929] 08 p3465 N94-30696
Analysis of key performance parameters of phase sampling digital RF memories
[AD-A276019] 09 p3688 N94-31494
The effects of altimeter sampling characteristics: Some Geosat examples
[AD-A276899] 09 p3747 N94-32214
Focused feasibility study final field sampling plan
[AD-A277445] 09 p3769 N94-33105
The application of the bi-phase coding in the serial transfer 10 p4110 N94-34357
Use of the sampling theorem to speed up near-field physical optics scattering calculations
11 p4253 N94-35549

SAMPLING DEVICES
U SAMPLERS

SAN ANDREAS FAULT
Heterogeneous slip and rupture models of the San Andreas fault zone based upon three-dimensional earthquake tomography
[DE93-015037] 04 p1480 N94-17898
Analysis of regional deformation and strain accumulation data adjacent to the San Andreas fault
[NASA-CR-194072] 04 p1487 N94-19428

SAN MARCO SATELLITES
Mission San Marco
[NASA-TM-109442] 03 p0878 N94-15341

SAND DUNES
U DUNES

SANDS
Coastal processes due to nearshore current around an upheaving island 01 p0199 N94-11942
A simple model of clastic sediments on Mars
01 p0460 N94-12155
Soil erosion rates caused by wind and saltating sand stresses in a wind tunnel
[DE93-009154] 02 p0706 N94-12905
Sand transport on Mars: Preliminary results from models 03 p1252 N94-16198
Experimental study of nonassociated flow and instability of frictional materials
[AD-A266421] 03 p1024 N94-16555
Centrifuge modeling of explosion-induced craters in unsaturated sand
[AD-A270194] 04 p1417 N94-18780
Analysis of a sandstorm weather process-translation
[AD-A272959] 05 p1867 N94-21250
The microstructural response of granular soil under uniaxial strain
[AD-A274808] 07 p2763 N94-26341
Windblown sand on Mars: The effect of saltation threshold on drift potentials derived from Mars GCM
11 p4366 N94-35474
Geophysical data fusion for subsurface imaging
[DE94-000056] 12 p4469 N94-36738

SANDSTONES
Inverting ultrasonic data on solid/fluid mixtures for Biot-Gassmann parameters
[DE93-011952] 01 p0150 N94-11026
In situ secondary ion mass spectrometry analysis
[DE93-012185] 01 p0076 N94-11140
Si-29 NMR spectroscopy of naturally-shocked quartz from Meteor Crater, Arizona: Correlation to Kieffer's classification scheme 01 p0080 N94-12087
The estimation of pre-stress by deformation rate analysis and suggestion of a mechanism from the elast-plastical theory 07 p2871 N94-28156
NMR characterization of shocked quartz
[DE94-007733] 09 p3774 N94-32816

SANDWICH CONSTRUCTION
U SANDWICH STRUCTURES

SANDWICH STRUCTURES
Low cost and thermally stable sandwich design for FIRST 01 p0057 N94-10009
Design and manufacturing of filament wound thrust cylinder 01 p0057 N94-10010
Development tests for a high stability optical bench
01 p0062 N94-10047
Adaptive structure design employing shape memory actuators 01 p0070 N94-11331
System integration and demonstration of adhesive bonded high temperature aluminum alloys for aerospace structure, phase 2
[NASA-CR-191459] 02 p0575 N94-12792
Structural investigation of a damaged GRP/foam sandwich composite using x ray computed tomography
02 p0669 N94-13857
Multilayer thin film design for far ultraviolet polarizers using an induced transmission and absorption technique
[NASA-CR-194631] 03 p1190 N94-15869
Effect of Impact Damage and Open Hole on Compressive Strength of Hybrid Composite Laminates
[NASA-CR-194603] 03 p0936 N94-16836
Research in textile composites at KU, Leuven
03 p0937 N94-16848
Packaging, deployment, and panel design concepts for a truss-stiffened 7-panel precision deployable reflector with feed boom
[NASA-TM-109000] 04 p1333 N94-17765
A study of the structural stability of an unbalanced sandwich composite configuration
[AD-A272496] 05 p1675 N94-21431
Mechanical and thermal buckling analysis of sandwich panels under different edge conditions
[NASA-TM-4535] 06 p2228 N94-23514
Effect of impact face damage on strength of sandwich composites
[VTT-PUBS-128] 07 p2704 N94-25734
Damage tolerance aspects of a full composite airplane fuselage: Requirements, modelling, predictions, experiments
[LR-728] 09 p3578 N94-31674
Honeycomb sandwich structures: Vented versus unvented designs for space systems
[AD-A276713] 09 p3624 N94-32122
Mechanical and thermal buckling analysis of rectangular sandwich panels under different edge conditions
[NASA-TM-4585] 10 p4069 N94-33704

SANITATION
Research activities, Faculty of Civil Engineering, Delft University of Technology, 1990 - 1991
[PB93-195022] 04 p1380 N94-19254

SAPPHIRE
Arcjet exploratory tests of ARC optical window design for the AFE vehicle
[NASA-CR-192655] 01 p0034 N94-10930
Ion mixing of thin ZrO2 films on sapphire
[DE93-015214] 03 p1206 N94-14925
The processing and mechanical properties of high temperature/high performance composites. Book 5: Processing and miscellaneous properties
[AD-A266398] 03 p0935 N94-16529

Growth and doping of Al(x)Ga(1-x)N films by electron cyclotron resonance assisted molecular beam epitaxy
[AD-A267305] 03 p1212 N94-16992
Nitride semiconductors for ultraviolet detection
[AD-A267877] 03 p1012 N94-17040
Interfacial shear behavior and its influence on fiber damage in sapphire-reinforced gamma titanium aluminide composites
[AD-A267943] 03 p1060 N94-17043
Experimental investigation of wave and fracture phenomena in impacted ceramics: Experiments on sapphire
[AD-A270040] 04 p1372 N94-18792
Multi-terrawatt, 100 fsec laser system using flashlamp-pumped, dye-converted Ti:sapphire as an amplifier
[DE93-017190] 04 p1440 N94-18889
Surface modification of sapphire for IR window application
[DE93-019168] 04 p1602 N94-19075
High pressure Hugoniot of sapphire
[DE94-001048] 06 p2558 N94-22946
Surface modification of sapphire for enhanced infrared window performance
[DE94-000333] 06 p2543 N94-23458
Collaborative research on ion implantation of ceramics
[DE93-019177] 07 p2749 N94-26080
Demonstration of monolithic co-fabrication of Y1Ba2Cu3O7-Sigma and CMOS devices on the same sapphire substrate
[AD-A274757] 07 p3059 N94-26566
Technical report of ISSP. Ser. A, no. 2685: ASE-free terawatt KrF/Ti : sapphire hybrid laser system
[JTN-94-80571] 07 p2820 N94-27339
Adsorption and desorption studies of cesium on sapphire surfaces
[DE94-003798] 07 p3070 N94-28067
MOCVD growth of GaN, AlN and AlGaN for UV photodetector applications
[AD-A275078] 08 p3512 N94-28871
Thermal expansion and elastic anisotropy in single crystal Al2O3 and SiC reinforcements
[NASA-TM-106516] 08 p3214 N94-29105

SARCOMA
U CANCER

SARSAT
Low cost high efficiency GaAs monolithic RF module for SARSAT distress beacons
[NASA-CR-194235] 01 p0146 N94-12773
Life saving satellites
[NASA-TM-109616] 03 p0862 N94-15426
High efficiency low cost monolithic module for SARSAT distress beacons
[NASA-CR-194234] 04 p1315 N94-18852
The space operations at CNES
06 p2498 N94-23837
A neural network application to search and rescue satellite aided tracking (SARSAT)
09 p3613 N94-33345

SAS
SkICAT: A cataloging and analysis tool for wide field imaging surveys 05 p2049 N94-22546

SAS-D
U IUE

SATAN (SENSOR)
U TERRAIN ANALYSIS

SATELLITE ALTIMETRY
Topex/Poseidon: A United States/France mission. Oceanography from space: The oceans and climate
[NASA-TM-108253] 01 p0043 N94-10699
Proceedings of First ERS-1 Symposium on Space at the Service of Our Environment, volume 1
[ESA-SP-359-VOL-1] 01 p0232 N94-11704
Calibration of ERS-1 altimetry over the North Sea
01 p0234 N94-11716
Effects of wave nonlinearity on ERS-1 radar altimeter returns: A preliminary investigation
01 p0235 N94-11722
Comparisons of ERS-1 altimeter height data and the Fine Resolution Antarctic Model (FRAM)
01 p0235 N94-11725
Analysis of ERS-1 altimeter data over the polar ice sheets 01 p0237 N94-11738
Some results of the derivation of ice sheet elevations in Antarctica from ERS-1 altimeter data
01 p0237 N94-11739
Preliminary evaluation of ERS-1 altimetry over Filchner-Ronne Ice Shelf, Antarctica
01 p0238 N94-11742
The height calibration of the ERS-1 radar altimeter
01 p0241 N94-11764
First results for the simultaneous estimation of the geoid and the sea surface topography by ERS-1 altimeter data
01 p0241 N94-11765
Separation of geoid and sea surface topography in shallow water regions: A first ERS-1 radar altimeter data evaluation 01 p0242 N94-11766
A stochastic-deterministic approach as an alternative to classical cross-over techniques in small ocean basins
01 p0242 N94-11767
An analysis of the gravity field in the Norwegian Sea and mapping of the ice cap of Greenland using ERS-1 altimeter measurements 01 p0242 N94-11768
Space and time variability of the Gulf Stream using ERS-1 ALT-OPR02 data 01 p0242 N94-11769
ERS-1 radar altimetry over the North Atlantic
01 p0242 N94-11772
The effect of rain on ERS-1 altimeter data
01 p0243 N94-11773
Preliminary geophysical investigation with ERS-1 35-day altimeter data 01 p0243 N94-11775
Arctic geodynamics: Continental shelf and deep ocean geophysics. ERS-1 satellite altimetry: A first look
01 p0243 N94-11776
Quick-look monitoring of the sea surface with ERS-1 fast delivery altimeter data 01 p0243 N94-11777
The Earth's gravity model for the ERS-1 commissioning phase 01 p0243 N94-11778
Global wave height climatologies from ERS-1 altimeter data, and comparisons with those from GEOSAT
01 p0244 N94-11781
The 1992 El Nino viewed by ERS-1 altimetry
01 p0244 N94-11784
Using transponders with the ERS-1 altimeter to measure orbit altitude to +/- 3 cm 01 p0244 N94-11785
Ocean circulation revealed by altimeter data
01 p0245 N94-11786
Westward propagation of sea surface anomalies in the western North Pacific as seen by the altimeter and radiometer 01 p0198 N94-11941
Surface roughness variations across the Iceland-Faroes frontal region observed by the GEOSAT altimeter and NOAA AVHRR 01 p0201 N94-11958
On the variability of wind speeds in the North Western Pacific observed by altimeter/GEOSAT and SSM/I/DMSP 01 p0201 N94-11960
Observation of wind and waves by GEOSAT altimeter
01 p0202 N94-11961
ERS-1 altimetry of inland water and land
01 p0246 N94-12475
Use of ERS-1 wind and wave products in operational meteorology 01 p0250 N94-12502
Comparison of ERS-1 SAR images of the Western Mediterranean to in situ oceanographic data: PRIM-1 Cruise (May 1992) 01 p0255 N94-12529
Topography of the Western Mediterranean from the ERS-1 altimeter 01 p0255 N94-12531
Observations of eddy fields in the Northwest Pacific by GEOSAT altimetry 01 p0207 N94-12639
Variability of sea level and sea surface temperature anomalies in the equatorial Pacific
01 p0208 N94-12640
Theory and oceanographic applications of satellite altimeter measurements 01 p0208 N94-12641
Analysis of collinear passes of satellite altimeter data
01 p0208 N94-12642
Surface eddy fluxes from the GEOSAT satellite altimeter 01 p0208 N94-12643
Comparison of GEOSAT sea surface height and model-simulated surface dynamic height
01 p0208 N94-12644
Pseudo magnetic anomaly derived from satellite altimetry and its application to the tectonics in the North Fuji Basin 01 p0208 N94-12645
Principal oscillation pattern analysis of sea level variations in the tropical Pacific measured by the GEOSAT altimeter 01 p0209 N94-12646
Measurement of eddy structure and movement in the north-east Pacific with the GEOSAT altimeter
01 p0209 N94-12647
Preliminary results from a satellite altimetric data assimilation using a Kalman filter and smoother
01 p0209 N94-12648
Fluctuations of the Kuroshio extension detected by the GEOSAT altimetry data 01 p0209 N94-12649
Mean flow and variability in the Kuroshio extension from GEOSAT altimetry data 01 p0209 N94-12650
On the space-time ocean current variability and its effects on the length-of-day
[ISBN-0-315-59510-8] 02 p0726 N94-14205
The depths of the largest impact craters on Venus
03 p1264 N94-16261
Resolving topographic detail on Venus by modeling complex Magellan altimetry echoes
03 p1283 N94-16368
TAOS (S80): A (LEO-MSS) system for position reporting and telemanagement services 03 p0893 N94-17162
Developing automated analysis methods for sea ice imagery: A status report with recommendations
[AD-A267284] 03 p1113 N94-17241
Scattering by Venus' surface
05 p2117 N94-20771
Geology and radiophysical properties of the Venera and Vega landing sites 05 p2135 N94-20867
Ocean mapping using satellite radar altimetry
[ETN-93-93470] 05 p1841 N94-21017
Estimating the rotation rate of mesoscale ocean rings from satellite altimetry
[AD-A272922] 05 p1883 N94-21222
Comparison of satellite-derived velocity fields in the coastal transition zone
[AD-A272565] 05 p1883 N94-21360
Influence of geoid model uncertainty on the determination of ocean circulation with satellite altimetry
[PB93-219301] 05 p1842 N94-22097
Modes of ocean variability in the tropical Pacific as derived from Geosat altimetry
[MPIM-103] 06 p2382 N94-23158
The effect of sub-surface volume scattering on the accuracy of ice-sheet altimeter retracking algorithms
[NASA-CR-194825] 06 p2386 N94-24060
Laser altimetry simulator. Version 3.0: User's guide
[NASA-TM-104588] 07 p2877 N94-26152
The effects of altimeter sampling characteristics: Some Geosat examples
[AD-A275225] 08 p3357 N94-29062
Filtering of satellite altimetry data with optimal smoothing cubic splines to compute geoid heights, along-tract geoid and gravity gradients in the Indonesian waters and its surroundings
[PB94-147527] 09 p3741 N94-31074
Application of radon transformation for improved analysis of sparsely sampled data: A feasibility study
[PB94-147535] 09 p3741 N94-31075
Satellite radar altimetry over the continental ice sheets
09 p3742 N94-31570
Error analysis of real-time and post-processed orbit determination for the Geosat Follow-On altimetric satellite using GPS tracking 09 p3576 N94-31845
The effects of altimeter sampling characteristics: Some Geosat examples
[AD-A276899] 09 p3747 N94-32214
Fields of experiments in ERS-1 SAR interferometry in Bonn and Naples 09 p3756 N94-32572
Normal matrix in gravity field determination with satellite methods. Its stabilization, its information content and its use in error propagation
[PB94-149705] 10 p4076 N94-34114
Some aspects of simultaneously flying Topex Follow-On in a Topex orbit with Geosat Follow-On in a Geosat orbit
[NASA-CR-196075] 10 p4077 N94-34214
Mesoscale roughness of Venus
11 p4361 N94-35430

SATELLITE ANTENNAS
The Second Workshop on Deployment and Assembly Experiment of Large Space Structure on Orbit
[NASDA-CON-930003] 02 p0529 N94-13268
Structural design of hexa-link truss deployable antenna 02 p0529 N94-13269
Thermal distortion measurement of TETRUS type thermal test model of large deployable antenna for mobile communications satellite 02 p0529 N94-13270
Development of modular cable mesh deployable antenna 02 p0530 N94-13274
Trial manufacture model and in-space verification method of deployable antenna 02 p0530 N94-13278
Proceedings of the 1992 Antenna Applications Symposium, volume 2
[AD-A266916] 03 p0986 N94-14998
Small satellite constellation system: Optimization criteria 03 p0888 N94-17132
Proceedings of the 1992 Antenna Applications Symposium, volume 1
[AD-A268167] 03 p1005 N94-17431
Missile antenna pattern coordinate system and data formats
[AD-A269153] 04 p1385 N94-18260
Investigations into deployment complications of the ERS-1 SAR antenna 06 p2305 N94-23996
Data relay system satellite: The development of an antenna pointing mechanism for the inter-orbit link antenna 06 p2359 N94-24015
Screening of flexible cables by nonlinear resistance measurements
[AD-A275193] 08 p3264 N94-29289
Proceedings of the 1993 Antenna Applications Symposium, volume 1
[AD-A277202] 09 p3676 N94-32049
Proceedings of the 1993 Antenna Applications Symposium, volume 2
[AD-A277203] 09 p3677 N94-32050
Two-axis antenna positioning mechanism
09 p3605 N94-33308
Special test equipment and fixturing for MSAT reflector assembly alignment 09 p3606 N94-33316

SATELLITE ATMOSPHERES
NT LUNAR ATMOSPHERE
Sources of Na for the Io atmosphere
01 p0455 N94-12127
Geomorphology of Triton's polar materials
01 p0466 N94-12185
Studies for Io's extended atmosphere and neutral clouds and their impact on the local satellite atmosphere and on the planetary magnetosphere
[NASA-CR-195255] 07 p3106 N94-27406
Studies for the loss of atomic and molecular species from Io
[NASA-CR-195702] 07 p3108 N94-27941
Predissociation in N2(C'4, 1 Sigma u +) and other N2 states and its importance in the atmospheres of Titan and Triton
[NASA-CR-195727] 08 p3549 N94-28816
Infrared spectroscopy of Jupiter and Saturn
[NASA-CR-196294] 12 p4549 N94-36961

SATELLITE ATTITUDE CONTROL
Project of an attitude control system (three axis) of a satellite using the LQG/LTR methodology
[INPE-5473-TDI/504] 01 p0044 N94-12356
Low cost attitude control system reaction wheel development
[NASA-CR-191332] 02 p0540 N94-13140
Transmission zeros of spacecraft attitude control system
[NAL-TR-1166] 02 p0540 N94-13339
MINISAT programme 03 p0896 N94-17182
The development of flexible software for the Italian/Dutch satellite SAX: Advantages and disadvantages of the use of CASE tools
[NLR-TP-91288-U] 03 p1157 N94-17626
The star identification, pointing and tracking system of UVSTAR, an attached payload instrument system for the Shuttle Hitchhiker-M platform 04 p1326 N94-19179
Method of orienting a synchronous satellite
[CA-PATENT-1,305,772] 05 p1658 N94-21041
A combined Earth scanner and momentum wheel for attitude determination and control of small spacecraft
06 p2208 N94-24022
Reactive thrust cruise for a geosynchronous satellite with minimum fuel consumption
06 p2158 N94-24271
Momentum management and torque distribution
06 p2159 N94-24272
The H(sub infinity) optimal controller design and reduction for the inertial hold mode of the attitude control system of the XTE spacecraft
[NASA-CR-195137] 06 p2366 N94-24846
High temperature superconducting infrared imaging satellite 07 p2698 N94-25700
On-board computer for control subsystem of satellite
07 p2949 N94-26716
The development procedures and tools applied for the attitude control software of the Italian satellite SAX
08 p3170 N94-29324
The influence of appendage vibration on the attitude dynamics of a dual-spin satellite
08 p3168 N94-29828
The MACS-TSA applied in the ISO and SAX spacecraft projects
[PB94-126257] 08 p3170 N94-30857
Chaotic attitude motion of satellites in the central gravitational field
[ISBN-0-315-78768-6] 09 p3610 N94-31723
Trajectory planning for space manipulators
[AD-A277229] 09 p3611 N94-32369
Performance analysis of an integrated GPS/inertial attitude determination system
[NASA-CR-188269] 09 p3577 N94-32864
Spacecraft attitude determination accuracy from mission experience 11 p4204 N94-35618
MME-based attitude dynamics identification and estimation for SAMPEX 11 p4209 N94-35643
A simple suboptimal least-squares algorithm for attitude determination with multiple sensors
11 p4210 N94-35645

SATELLITE ATTITUDE DISTURBANCE
U ATTITUDE STABILITY
U SPACECRAFT STABILITY

SATELLITE BREAKUP
U SPACECRAFT BREAKUP

SATELLITE CAPTURE
U SPACECRAFT RECOVERY

SATELLITE CLUSTERS
U SATELLITE CONSTELLATIONS

SATELLITE COMMUNICATION
Potential markets for advanced satellite communications
[NASA-CR-191145] 01 p0041 N94-10512
Space Activities in the Asia Pacific Region
[JTN-93-80421] 01 p0035 N94-10676
Current status of space activities in Asia Pacific region
01 p0035 N94-10677
Space programme in Malaysia
01 p0036 N94-10685
National space program in Australia
01 p0037 N94-10691
PARTNERS 01 p0038 N94-10695
The 24th Annual Precise Time and Time Interval (PTTI) Applications and Planning Meeting
[NASA-CP-3218] 01 p0350 N94-10963
Two way time transfer results at NRL and USNO
01 p0353 N94-10983
New technology applied to telemedicine
01 p0306 N94-11796
Space technology in remote health care
01 p0306 N94-11799
Use of satellite telecommunications for telemedicine
01 p0308 N94-11807
Use of low orbital satellite communications systems for humanitarian programs 01 p0308 N94-11808
Destination-directed, packet-switched architecture for a geostationary communications satellite network
[NASA-TP-3379] 02 p0538 N94-13111
Fine time uplink synchronization for frequency-hopped spread spectrum satellite communication system
[ISBN-0-315-54370-1] 02 p0600 N94-13488
Trellis coding with Continuous Phase Modulation (CPM) for satellite-based land-mobile communications
[NASA-CR-191325] 02 p0604 N94-13909
SCAILET: An intelligent assistant for satellite ground terminal operations
[NASA-TM-105879] 02 p0538 N94-13918
Simulation of downlink synchronization for a frequency-hopped satellite communication system
[DSIS-93-00477] 02 p0605 N94-13941
ALFIS: Astronomical Low Frequency Interferometry Satellites. A feasibility study
[LR-699] 02 p0542 N94-13988
Multiple-symbol differential detection of DPSK with frequency offset
[DREO-TN-92-5] 02 p0606 N94-14063
Asia-Pacific ISY Conference, volume 2
[NASDA-CM-199-VOL-2] 02 p0688 N94-14209
The developments of satellite communications of China 02 p0618 N94-14282
The current situation, trends, international cooperation of space communication technological development in the Republic of Korea 02 p0699 N94-14283
Joint experiments using ETS-5
02 p0618 N94-14284
Space communications technology research in CRL
02 p0618 N94-14285
NTT's activities in satellite communications technology development 02 p0618 N94-14286
Future outlook on international satellite communications in Asia Pacific region 02 p0618 N94-14287
Technological development for broadcasting satellites in NHK Laboratories 02 p0618 N94-14288
New challenges in propagation research in the US
02 p0612 N94-14656
User needs for propagation data
02 p0613 N94-14657
Statistical results from the Virginia Tech propagation experiment using the Olympus 12, 20, and 30 GHz satellite beacons 02 p0613 N94-14658
Results from a study of scintillation behavior at 12, 20, and 30 GHz using the results from the Virginia Tech Olympus receivers 02 p0613 N94-14659
Large-scale rainfall diversity for ACTS
02 p0613 N94-14662
Contribution towards a draft revision of recommendations 681: Propagation data required for the design of Earth-space land mobile telecommunications systems 02 p0614 N94-14666
Propagation issues for emerging mobile and portable communications: A systems perspective
02 p0614 N94-14667
Characterisation of the LMS propagation channel at L- and S-bands: Narrowband experimental data and channel modelling 02 p0615 N94-14669
Results of multiband (L, S, Ku band) propagation measurements and model for high elevation angle land mobile satellite channel 02 p0615 N94-14670
Effects of the equatorial ionosphere on L-band Earth-space transmissions 02 p0615 N94-14671
Tree attenuation at 20 GHz: Foliage effects
02 p0615 N94-14672
Preprocessing data collected with the ACTS propagation terminal 02 p0616 N94-14676
ACTS data center 02 p0616 N94-14677
NASA images 8
[NASA-TM-109416] 02 p0544 N94-14783
The 1991 research and technology report, Goddard Space Flight Center
[NASA-TM-108738] 02 p0851 N94-14791
Development of Japanese Earth Resources Satellite-1 (JERS-1; FUYO-1) and it's operational results
[NASDA-SPP-930001] 03 p0884 N94-15001
TDRS video clip
[NASA-TM-109585] 03 p0884 N94-15269
Activities of Canadian Satellite Communications, Inc.
[CTN-93-60864] 03 p0994 N94-15959
Data acquisition, preprocessing and analysis for the Virginia Tech OLYMPUS experiment
03 p0995 N94-16038
The ACTS propagation program
03 p0995 N94-16039
Propagation measurements in Alaska using ACTS beacons 03 p0995 N94-16040
Planned LMSS propagation experiment using ACTS: Preliminary antenna pointing results during mobile operations 03 p0995 N94-16041
Propagation-related AMT design aspects and supporting experiments 03 p0995 N94-16042
Propagation research in Japan
03 p0996 N94-16043
Low-Complexity, High-Performance Bandwidth Efficient Coding and Coded Modulation Techniques for Satellite and Space Communications
[NASA-CR-194623] 03 p0997 N94-16506
Satellite communications installation plan
[AD-A266303] 03 p1000 N94-16965
Four Frequency-Shift Keying (4-FSK) spread spectrum modulator and demodulator
[AD-A267433] 03 p1000 N94-16979
On-board B-ISDN fast packet switching architectures. Phase 1: Study
[NASA-CR-191143] 03 p0883 N94-17111
Small Satellites Systems and Services
[ISBN-2-85-428327-9] 03 p0888 N94-17131
Low Earth orbit constellations: Orbit control or not
03 p0875 N94-17134
Data processing system for ARSENE ground station: A tool for small satellite control and development
03 p0878 N94-17157
A study on an experimental communication system using microsatellites 03 p0892 N94-17160
LEOCOM-SPES: Low cost message communications
03 p0892 N94-17161
TAOS (S80): A (LEO-MSS) system for position reporting and telemanagement services 03 p0893 N94-17162
S 80/T: A micro satellite system combining high performances and limited resources
03 p0893 N94-17166
The ELLIPSO (tm) system: Elliptical low orbits for mobile communications 03 p0893 N94-17167
Solar Electro-Optical Network (SEON) upgrade/replacement program. Phase 1: Qualification operational test and evaluation plan
[AD-A266364] 03 p1237 N94-17225
NASA Lewis Meshed VSAT Workshop meeting summary
[NASA-TM-106332] 03 p0883 N94-17487
Satellite communications systems and technology. Executive summary
[NASA-TM-109346] 03 p1006 N94-17661
Radio wave propagation in structured ionization for satellite and radar applications
[AD-A268457] 04 p1382 N94-17844
Direct solar pumping of semiconductor lasers: A feasibility study
[NASA-CR-193760] 04 p1440 N94-18834
Oceanic in situ Fraunhofer-line characteristics: Fraunhofer-line underwater experiment (FLUX)
[AD-A270659] 05 p1881 N94-19952
Optimization of a satellite localization and message sending system
[ETN-93-94448] 05 p1737 N94-20592
A compact, portable EHF/SHF antenna for advanced SCAMP
[AD-A272614] 05 p1739 N94-21211
Mission Operations Support Area (MOSA) for ground network support 05 p1932 N94-21331
Space network scheduling benchmark: A proof-of-concept process for technology transfer
05 p1932 N94-21332
The Automated Conflict Resolution System (ACRS)
05 p1744 N94-21341
Satellite Communication Hardware Emulation System (SCHES) 05 p1744 N94-21344
Military satellite communications decision support system requirements analysis and user interface design
[AD-A273047] 05 p1740 N94-21436
A laboratory system for the investigation of rain fade compensation techniques for Ka-band satellites
[NASA-CR-191200] 05 p1762 N94-21566
CREIR: A multiaccess protocol for on-board processing satellite systems 05 p1780 N94-22168
Timing recovery in the channel processor of a digital group demodulator 05 p1780 N94-22169
TDMA satellite communication systems for ISDN services 05 p1746 N94-22171
A consideration of the integration of terrestrial and satellite mobile systems 05 p1746 N94-22172

Visibility considerations in frequency sharing with low Earth orbit satellites 05 p1746 N94-22187
Inclined orbits and interference to stationary service and to stationary service by satellite 05 p1653 N94-22188
File transfer performance in LAN interconnection through a satellite channel 05 p1746 N94-22209
ESA personal communications and digital audio broadcasting systems based on non-geostationary satellites 06 p2273 N94-22737
Direct broadcast satellite-radio, space-segment/receiver tradeoffs 06 p2273 N94-22738
Electrical performance of wire mesh for spacecraft deployable reflector antennas 06 p2275 N94-22744
US domestic and international regulatory issues 06 p2275 N94-22748
International organizations to enable world-wide mobile satellite services 06 p2275 N94-22749
The possibilities for mobile and fixed services in the 20/30 GHz frequency bands 06 p2276 N94-22752
Use of the 30/20 GHz band by multipurpose satellite systems 06 p2276 N94-22753
Interworking and integration of the Inmarsat Standard-M with Pan-European GSM system 06 p2277 N94-22759
MSAT and cellular hybrid networking 06 p2278 N94-22762
Trends in mobile satellite communication 06 p2278 N94-22763
Optimizing space constellations for mobile satellite systems 06 p2278 N94-22764
Geostationary payload concepts for personal satellite communications 06 p2278 N94-22765
Applicability of different onboard routing and processing techniques to mobile satellite systems 06 p2278 N94-22767
Study of LEO-SAT microwave link for broad-band mobile satellite communication system 06 p2279 N94-22769
ROCSAT-1 telecommunication experiments 06 p2279 N94-22770
ACTS broadband aeronautical experiment 06 p2279 N94-22771
The FAA satellite communications program 06 p2279 N94-22772
ACTS mobile SATCOM experiments 06 p2280 N94-22774
Cockpit weather graphics using mobile satellite communications 06 p2280 N94-22775
Using satellite communications for a mobile computer network 06 p2280 N94-22777
Evolution of INMARSAT systems and applications: The land mobile experience 06 p2280 N94-22779
ACTS advanced system concepts and experimentation 06 p2280 N94-22780
EUTELTRACS: The European experience on mobile satellite services 06 p2281 N94-22781
The ORBCOMM data communications system 06 p2281 N94-22782
Implementation of a system to provide mobile satellite services in North America 06 p2281 N94-22784
The Iridium (tm) system: Personal communications anytime, anyplace 06 p2281 N94-22785
The Globalstar mobile satellite system for worldwide personal communications 06 p2282 N94-22786
Odyssey personal communications satellite system 06 p2282 N94-22787
INMARSAT's personal communicator system 06 p2282 N94-22788
The European Mobile System (EMS) 06 p2282 N94-22789
Land mobile satellite propagation measurements in Japan using ETS-V satellite 06 p2282 N94-22790
Measurements on the satellite-mobile channel at L and S bands 06 p2282 N94-22791
K-band mobile propagation measurements using ACTS 06 p2283 N94-22792
Measurement of multipath delay profile in land mobile satellite channels 06 p2283 N94-22793
A study of satellite motion-induced multipath phenomena 06 p2283 N94-22794
Electromagnetic field strength prediction in an urban environment: A useful tool for the planning of LMSS 06 p2283 N94-22795
Propagation model for the Land Mobile Satellite channel in urban environments 06 p2283 N94-22796
The Westinghouse Series 1000 Mobile Phone: Technology and applications 06 p2284 N94-22800
First satellite mobile communication trials using BLQS-CDMA 06 p2284 N94-22801
Channel and terminal description of the ACTS mobile terminal 06 p2284 N94-22802
Low cost coherent demodulation for mobile satellite terminals 06 p2284 N94-22803
Asynchronous timing and Doppler recovery in DSP based DPSK modems for fixed and mobile satellite applications 06 p2285 N94-22805
Improved frame synchronization schemes for INMARSAT-B/M SCPC and TDM channels 06 p2285 N94-22806
Estimation of frequency offset in mobile satellite modems 06 p2285 N94-22807
A pattern jitter free AFC scheme for mobile satellite systems 06 p2285 N94-22809
A CDMA synchronisation scheme 06 p2285 N94-22810
A protocol for satellite access via use of spot-beams 06 p2286 N94-22811
A high quality voice coder with integrated echo canceller and voice activity detector for mobile satellite applications 06 p2286 N94-22812
Performance of the unique-word-reverse-modulation type demodulator for mobile satellite communications 06 p2286 N94-22813
Transmission over EHF mobile satellite channels 06 p2287 N94-22820
Adaptive data rate control TDMA systems as a rain attenuation compensation technique 06 p2287 N94-22821
Development of a multilayer interference simulation program for MSS systems 06 p2287 N94-22823
Study on networking issues of medium earth orbit satellite communications systems 06 p2288 N94-22825
The design and networking of dynamic satellite constellations for global mobile communication systems 06 p2288 N94-22826
Low earth orbit satellite/terrestrial mobile service compatibility 06 p2288 N94-22827
A practical system for regional mobile satellite services 06 p2288 N94-22828
Supercomputer networking for space science applications [NASA-CR-194876] 06 p2465 N94-23085
Phase linearity of the 914H coupled-cavity traveling wave tube [NASA-CR-191056] 06 p2290 N94-23087
Satellite communications systems and technology. Executive Summary [NASA-TM-109388] 06 p2293 N94-23622
Satellite communications systems and technology. Volume 1: Analytical chapters [NASA-TM-109398] 06 p2293 N94-23627
Satellite communications systems and technology. Volume 2: Site reports [NASA-TM-109399] 06 p2293 N94-23628
Advanced technology for a satellite multichannel demultiplexer/demodulator [NASA-CR-194435] 06 p2202 N94-23631
Multi-access laser communications terminal [NASA-CR-191251] 06 p2295 N94-23830
Commonality of flight control systems for support of European telecommunications missions 06 p2304 N94-23834
The European Space Agency standard for space packet utilisation 06 p2203 N94-23954
Generalized three-dimensional simulation of ferruled coupled-cavity traveling-wave-tube dispersion and impedance characteristics [NASA-TP-3389] 06 p2310 N94-24056
Satellite communications system [CA-PATENT-APPL-SN-2053597] 06 p2297 N94-24183
The 33rd Israel Annual Conference on Aviation and Astronautics [ITN-94-85227] 06 p2153 N94-24241
Error coding simulations 06 p2306 N94-24439
Comparison of HF groundwave propagation models [AD-A273146] 06 p2299 N94-24668
Simulation of adjacent channel interference in a UHF satellite system [AD-A273147] 06 p2299 N94-24669
Bounds and simulation results of 32-ary and 64-ary quadrature amplitude modulation for broadband-ISDN via satellite [NASA-TM-106484] 06 p2202 N94-25095
Conceptual communications system design in the 25.25-27.5 and 37.0-40.5 GHz frequency bands 06 p2306 N94-25379
Modeling of the ground-to-SSFMB link networking features using SPW 06 p2306 N94-25381
Development of satellite telecommunications during the period 1990 - 2005 [CRANFIELD-AERO-9301] 07 p2765 N94-25639
Low Earth orbit communications satellite 07 p2698 N94-25701
System design analysis of a lightweight laser satellite terminal [AD-A274033] 07 p2690 N94-25769
Remote Earth Sciences data collection using ACTS [NASA-CR-195227] 07 p2848 N94-26236
Analysis of linear combining and its application to frequency-hopped signals [ISBN-0-315-84007-2] 07 p2770 N94-26624
The Communication Link and Error ANalysis (CLEAN) simulator [NASA-CR-195243] 07 p2968 N94-27168
Equalization and cancellation of nonlinear intersymbol interference in a dispersive satellite communication channel [ISBN-0-315-85147-3] 07 p2775 N94-27274
A GPS coverage model 07 p2642 N94-27292
Design and test of a regenerative satellite transmultiplexer [ISBN-0-315-85280-1] 07 p2786 N94-27303
Analysis of a multiaccess/switching technique for multibeam satellites in a prioritized ISDN environment [ISBN-0-315-84632-1] 07 p2776 N94-27345
The telemedicine spacebridge project: A joint US/Russian venture in long distance medicine via satellite [NASA-TM-106523] 07 p2693 N94-27427
NASA satellite communications application research. Phase 2: Efficient high power, solid state amplifier for EFH communications [NASA-CR-195713] 07 p2776 N94-27669
Communications subsystem for the Petite Amateur Navy Satellite (PANSAT) [AD-A275532] 08 p3242 N94-28812
Microvibrations on a GEO telecommunication satellite [REPT-932-440-101] 08 p3168 N94-29415
Simulation of interference between Earth stations and Earth-orbiting satellites 08 p3252 N94-29673
Remote observatory access via the advanced communications technology satellite 08 p3253 N94-29894
Adaptive power control as a fade countermeasure on satellite links 08 p3253 N94-29897
Communications technology for unattended sensors [DE94-005685] 08 p3254 N94-30043
Radial microstrip slotline feed network for circular mobile communications array [NASA-TM-106540] 08 p3267 N94-30198
The two-way time synchronization system via a satellite voice channel 08 p3471 N94-30658
Providing hydrogen maser timing stability to orbiting VLBI radio telescope observations by post-measurement compensation of linked frequency standard imperfections 08 p3297 N94-30670
Europe at the crossroads: The future of its satellite communications industry [ESA-SP-1166] 09 p3670 N94-31182
Channel and terminal description of the ACTS mobile terminal 09 p3599 N94-31428
Hubless satellite communications networks 09 p3600 N94-31433
Multisatellite constellation configuration selection for multiregional highly elliptical orbit constellations 09 p3600 N94-31437
SATCOM feasibility study for search and rescue aircraft [DSIS-94-01083] 09 p3575 N94-31902
Satellite communications industry [AD-A276685] 09 p3610 N94-32039
CIM in space: Corporate Information Management (CIM) implications for space-based information systems [AD-A276882] 09 p3600 N94-32126
Advanced satellite communication system [NASA-CR-194211] 09 p3681 N94-32477
COVICS: A covert video communications system [DE94-007568] 09 p3682 N94-32745
Aerospace sponsored research [ATR-93(8498)-1] 09 p3966 N94-32949
Pointing and tracking space mechanism for laser communication 09 p3606 N94-33310
An advanced communications synthesizer [AD-A277832] 10 p4034 N94-33833
Multichannel demultiplexer-demodulator [NASA-CR-191201] 10 p4013 N94-34215
An adaptive technique to maximize lossless image data compression of satellite images 10 p4124 N94-35057
Optimum satellite relay positions with application to a TDRS-1 Indian Ocean relay 11 p4205 N94-35624
Application of a Monte Carlo accuracy assessment tool to TDRS and GPS 11 p4207 N94-35635
North American ISDN Users' Forum agreements on Integrated Services Digital Network [PB94-162559] 11 p4305 N94-35940
Information and communication technology 11 p4257 N94-36043
Preliminary PANSAT ground station software design and use of an expert system to analyze telemetry [AD-A280600] 12 p4392 N94-36726

Error control techniques for satellite and space communications
[NASA-CR-196302] 12 p4433 N94-36931

SATELLITE CONFIGURATIONS

ALFIS: Astronomical Low Frequency Interferometry Satellites. A feasibility study
[LR-699] 02 p0542 N94-13988
Development of Japanese Earth Resources Satellite-1 (JERS-1; FUYO-1) and it's operational results
[NASDA-SPP-930001] 03 p0884 N94-15001
The EXOSAT operational experience
[ESA-STM-248] 05 p1657 N94-20235
Mobilesat (tm): A world first 06 p2281 N94-22783

SATELLITE CONSTELLATIONS

Small satellite constellation system: Optimization criteria 03 p0888 N94-17132
AMIGAU: A prototype tool aimed at mission analysis for satellites and satellite constellations 03 p0888 N94-17133
Low Earth orbit constellations: Orbit control or not 03 p0875 N94-17134
Impact of launching uncertainties on the visibility of communication satellite constellations without orbit control 03 p0889 N94-17135
Small satellite constellation deployment strategies 03 p0878 N94-17138
Adequation of mini satellites to oceanic altimetry missions 03 p0891 N94-17152
STARSYS: A view after WARC-92 --- satellite position and messaging system 03 p0893 N94-17168
Key trends of the small satellite market 03 p0897 N94-17191
Optimizing space constellations for mobile satellite systems 06 p2278 N94-22764
The design and networking of dynamic satellite constellations for global mobile communication systems 06 p2288 N94-22826
Low Earth orbit communications satellite 07 p2698 N94-25701
A virtual environment for satellite modeling and orbital analysis in a distributed interactive simulation
[AD-A274114] 07 p2694 N94-25904
An Operational Control Segment (OCS) update on GPS constellation status and future program directions 08 p3144 N94-30643
Multisatellite constellation configuration selection for multiregional highly elliptical orbit constellations 09 p3600 N94-31437
Obtaining coincident image observations for Mission to Planet Earth science data return 11 p4202 N94-35609
The Earth Satellite Program (ESP), version 2.0
[AD-A278860] 11 p4201 N94-35827

SATELLITE CONTROL

NT SATELLITE ATTITUDE CONTROL
Pre-operation analysis of ERS-1 tracking and operation, part 2-A
[NASDA-CNT-930001-PT-2-A] 01 p0230 N94-11129
Pre-operation analysis of ERS-1 tracking and operation, part 2-F
[NASDA-CNT-930002-PT-2-F] 01 p0230 N94-11130
Flight data analysis of Japanese Earth Resources Satellite-1 (JERS-1)
[NASDA-CNT-930004] 01 p0245 N94-12279
Development of Japanese Earth Resources Satellite-1 (JERS-1; FUYO-1) and it's operational results
[NASDA-SPP-930001] 03 p0884 N94-15001
Low Earth orbit constellations: Orbit control or not 03 p0875 N94-17134
Impact of launching uncertainties on the visibility of communication satellite constellations without orbit control 03 p0889 N94-17135
Data processing system for ARSENE ground station: A tool for small satellite control and development 03 p0878 N94-17157
Satellite control: A comprehensive approach 03 p0878 N94-17158
TAOS (S80): A (LEO-MSS) system for position reporting and telemanagement services 03 p0893 N94-17162
S 80/T: A micro satellite system combining high performances and limited resources 03 p0893 N94-17166
CONTACT: An Air Force technical report on military satellite control technology
[AD-A269375] 04 p1334 N94-18408
Corporate Information Management (CIM) report on the simulation processes, version 2.0
[AD-A269119] 04 p1617 N94-18770
Analysis of the TDRS multiple access system for possible use as an attitude control system sensor 05 p1666 N94-21338
Commonality of flight control systems for support of European telecommunications missions 06 p2304 N94-23834
SPOT4 Operational Control Center (CMP) 06 p2197 N94-23856
A quick uplink, expandable executable for the NSSC-1 of the Hubble Space Telescope 06 p2305 N94-23859
NASDA knowledge-based network planning system 06 p2508 N94-23898
Kalman filtering applied to real-time monitoring of apogee maneuvers 06 p2196 N94-23923
MERCATOR: Methods and Realization for Control of the Attitude and the Orbit of spacecraft 06 p2202 N94-23925
The geo-control system for station keeping and colocation of geostationary satellites 06 p2464 N94-23927
Operational training for the mission operations at the Brazilian National Institute for Space Research (INPE) 06 p2429 N94-23933
GenSAA: A tool for advancing satellite monitoring with graphical expert systems 06 p2516 N94-23945
Iowa satellite project ISAT-1
[NASA-CR-195517] 06 p2206 N94-24838
A comparison of three approximate mathematical models for the gravity gradient stabilized satellite
[AD-A273832] 07 p2694 N94-25615
Dynamics and control of tethered satellite systems 08 p3170 N94-30864
Aerospace sponsored research
[ATR-93(8498)-1] 09 p3966 N94-32949
Intelligent command and control systems for satellite ground operations
[NASA-CR-195852] 10 p4130 N94-34064
Definition of ground test for verification of large space structure control
[NASA-CR-193945] 10 p4014 N94-34074

SATELLITE DEFENSE

U SPACECRAFT DEFENSE

SATELLITE DESIGN

Design and development of a CFRP central cylinder for satellites 01 p0056 N94-10007
Japanese space activities 01 p0036 N94-10682
Overview of KITSAT 01 p0036 N94-10683
Korea space program 01 p0036 N94-10684
Space transportation alternatives for large space programs: The International Space University Summer Session, 1992
[NASA-TM-106271] 01 p0040 N94-10811
Earth Observation Center Annual Report on Research and Development, Fiscal Year 1992
[EOC-92-01-0007] 02 p0687 N94-14091
ADEOS project 02 p0687 N94-14094
Propagation considerations in the American Mobile Satellite system design 02 p0614 N94-14668
Pre-phase a study report of lunar polar orbiter
[NASDA-TK-SS0440] 03 p0873 N94-15000
Development of Japanese Earth Resources Satellite-1 (JERS-1; FUYO-1) and it's operational results
[NASDA-SPP-930001] 03 p0884 N94-15001
Small Satellites Systems and Services
[ISBN-2-85-428327-9] 03 p0888 N94-17131
Small missions for space science 03 p0874 N94-17142
UoSAT: A decade of experience pioneering microsatellites 03 p0894 N94-17169
A mini satellite called Arsene: The way to make it at a minimum cost 03 p0895 N94-17179
The space technology research vehicle: Development status 03 p0896 N94-17183
On-board spatial scientific experiment project on small satellites 03 p0896 N94-17184
Big results with small space systems: What small systems are doing today 03 p0896 N94-17187
Environment tests for mini satellites 03 p0896 N94-17189
Cost drivers: Why do conventional satellites cost so much? 03 p0897 N94-17190
A conceptual design study for a two-dimensional, electronically scanned thinned array radiometer
[NASA-TM-109051] 03 p1085 N94-17665
Aeronautical audio broadcasting via satellite 06 p2274 N94-22741
A system architecture for an advanced Canadian wideband mobile satellite system 06 p2278 N94-22766
GPHS-RTG's in support of the Cassini mission
[DE94-001445] 06 p2218 N94-23459
An engineering database management system for spacecraft operations 06 p2517 N94-23951
A combined Earth scanner and momentum wheel for attitude determination and control of small spacecraft 06 p2208 N94-24022
The Submillimeter Wave Astronomy Satellite (SWAS) solar array system 06 p2361 N94-24029
The 33rd Israel Annual Conference on Aviation and Astronautics
[ITN-94-85227] 06 p2153 N94-24241
NPS alternate techsat satellite, design project for AE-4871
[NASA-CR-195512] 06 p2204 N94-24590
A small satellite design for deep space network testing and training
[NASA-CR-195526] 06 p2205 N94-24702
Iowa satellite project ISAT-1
[NASA-CR-195517] 06 p2206 N94-24838
Preliminary design of a satellite observation system for Space Station Freedom
[NASA-CR-195514] 06 p2209 N94-24840
High temperature superconducting infrared imaging satellite 07 p2698 N94-25700
Copernicus: Lunar surface mapper 07 p3081 N94-25702
A simple satellite system to locate gamma ray bursters using scintillating fiber technology
[DE94-601287] 07 p3117 N94-27996
NSWC Crane Aerospace Cell Test History Database 07 p2860 N94-28102
Outline of JERS-1 system 08 p3330 N94-29220
Development status of the Communications and Broadcasting Engineering Test Satellite (COMETS)
[JTN-94-80545] 08 p3169 N94-30811
Development status of COMETS missions
[JTN-94-80544] 08 p3170 N94-30932
New perspectives for high accuracy SLR with second generation geodesic satellites
[REPT-932-440-105] 08 p3336 N94-30965
Automated detection of ship tracks in multispectral satellite data
[AD-A276697] 09 p3746 N94-32119
Design and performance of the telescope and detector covers on the Extreme Ultraviolet Explorer satellite 09 p3605 N94-33309
Pointing and tracking space mechanism for laser communication 09 p3606 N94-33310
MSAT boom joint testing and load absorber design 09 p3606 N94-33315
Natural orbital environment definition guidelines for use in aerospace vehicle development
[NASA-TM-4527] 11 p4291 N94-36175
Computer graphics tools for the visualization of spacecraft dynamics
[AD-A278615] 11 p4226 N94-36251

SATELLITE DOPPLER POSITIONING

STARSYS: A view after WARC-92 --- satellite position and messaging system 03 p0893 N94-17168
Mars 1994/1996: The French navigation tasks 06 p2195 N94-23924
Navigation of space VLBI missions: Radioastron and VSOP 06 p2513 N94-23926
A neural network application to search and rescue satellite aided tracking (SARSAT) 09 p3613 N94-33345

SATELLITE DRAG

Evaluation of semiempirical atmospheric density models for orbit determination applications 11 p4208 N94-35636

SATELLITE FRAGMENTATION

U SPACECRAFT BREAKUP

SATELLITE GROUND SUPPORT

Pre-operation analysis of ERS-1 tracking and operation, part 2-A
[NASDA-CNT-930001-PT-2-A] 01 p0230 N94-11129
Pre-operation analysis of ERS-1 tracking and operation, part 2-F
[NASDA-CNT-930002-PT-2-F] 01 p0230 N94-11130
A European mobile satellite system concept exploiting CDMA and OBP 06 p2279 N94-22768
Kalman filtering applied to real-time monitoring of apogee maneuvers 06 p2196 N94-23923
The European Space Agency standard for space packet utilisation 06 p2203 N94-23954
Site comparison for optical visibility statistics in southern California 08 p3247 N94-29617

SATELLITE GROUND TRACKS

Some aspects of simultaneously flying Topex Follow-On in a Topex orbit with Geosat Follow-On in a Geosat orbit
[NASA-CR-196075] 10 p4077 N94-34214
The Earth Satellite Program (ESP), version 2.0
[AD-A278860] 11 p4201 N94-35827

SATELLITE GUIDANCE

Pre-operation analysis of ERS-1 tracking and operation, part 2-A
[NASDA-CNT-930001-PT-2-A] 01 p0230 N94-11129
Pre-operation analysis of ERS-1 tracking and operation, part 2-F
[NASDA-CNT-930002-PT-2-F] 01 p0230 N94-11130
Development of Japanese Earth Resources Satellite-1 (JERS-1; FUYO-1) and it's operational results
[NASDA-SPP-930001] 03 p0884 N94-15001
Real-time on-board orbit determination with DORIS 06 p2196 N94-23919
TOPEX/Poseidon precision orbit determination production and expert system 06 p2196 N94-23920

The ALEXIS mission recovery
[DE94-007549] 09 p3611 N94-32813

SATELLITE IMAGERY

Space research and remote sensing programmes in Bangladesh 01 p0035 N94-10679
Space program in Indonesia 01 p0036 N94-10681
Panel discussion: Role of space program in the Asia Pacific Region 01 p0037 N94-10694
Statistical study on the regional and seasonal distribution of fog in the far east region by using GMS imagery 01 p0190 N94-11082
TOVS soundings: Impact on the synoptic analysis over the south and southeast regions of Brazil from March 18 to March 19, 1991
[INPE-5497-TDI/512] 01 p0230 N94-11179
Bayesian model for pictorial data fusion of satellite image
[INPE-5457-TDI/499] 01 p0345 N94-11193
Satellite inventory of Minnesota forest resources
[NASA-CR-193565] 01 p0231 N94-11521
Validation of directional wave spectra from the ERS-1 during the ESA CAL/VAL campaign 01 p0232 N94-11707
Coastal ocean studies with ERS-1 SAR during NORCSEX 1991 01 p0234 N94-11720
SAR imaging of dynamical features in the English Channel 01 p0234 N94-11721
SAR ocean imaging in the Gulf of Alaska 01 p0235 N94-11723
ERS-1 SAR calibration strategy 01 p0235 N94-11726
Calibration of the ERS-1 SAR fast-delivery images 01 p0236 N94-11730
The use of active devices in the ERS-1 radiometric calibration 01 p0236 N94-11732
An experiment for the radiometric calibration of the ERS-1 SAR 01 p0236 N94-11733
Techniques and applications of SAR interferometry for ERS-1: Topographic mapping, change detection, and slope measurement 01 p0236 N94-11734
SAR interferometry experiments with ERS-1 01 p0237 N94-11735
SAR-interferometry applying ERS-1: Some preliminary test results 01 p0237 N94-11736
Monitoring of the Greenland Ice Sheet using ERS-1 synthetic aperture radar imagery 01 p0237 N94-11741
Investigations of Arctic ice-sheets and glaciers using ERS-1 SAR 01 p0238 N94-11743
Ice studies in the Barents Sea by ERS-1 SAR during SIZEX 92 01 p0238 N94-11745
Arctic coastal polynya observations with ERS-1 SAR and DMSP SSM/I 01 p0239 N94-11748
Sea ice deformation observed with ERS-1 SAR 01 p0239 N94-11749
Finnish ERS-1 Baltic Sea ice experiment in Winter 1992 01 p0239 N94-11750
C-band SAR backscatter from ice on shallow tundra lakes: Observations and modelling 01 p0240 N94-11755
Sea ice radar signatures from ERS-1 SAR during late Summer and Fall in the Beaufort and Chukchi Seas 01 p0240 N94-11756
Sea ice feature and type identification in merged ERS-1 SAR and LANDSAT Thematic Mapper imagery 01 p0241 N94-11761
An analysis of the gravity field in the Norwegian Sea and mapping of the ice cap of Greenland using ERS-1 altimeter measurements 01 p0242 N94-11768
The Earth's gravity model for the ERS-1 commissioning phase 01 p0243 N94-11778
Proceedings of the PORSEC 1992 in Okinawa: Conference for Pacific Ocean Environments and Probing, volume 1
[JTN-93-80418] 01 p0191 N94-11894
A statistical method to determine aerosol path radiance and its application to atmospheric correction for CZCS imagery 01 p0191 N94-11897
Satellite observations of red tide events: Plans for EESI 01 p0191 N94-11899
Satellite derived sea surface temperature applications for Indian Ocean resources development 01 p0193 N94-11907
Exchange of bay water with ocean current monitored by the NOAA satellite 01 p0193 N94-11908
A consideration on principal component analysis of satellite IR data 01 p0193 N94-11909
The use of remote sensing data for coastal zone management and environment in Indonesia 01 p0196 N94-11927
Shoreline change detection using remote sensing and GIS in Vietnam 01 p0196 N94-11928
The requirement for global training programmes to meet the new remote sensing technology 01 p0196 N94-11929
Analysis of the characteristic and mechanism of suspended matter transportation in Huanghe delta sea area using remote sensing techniques 01 p0197 N94-11930
The extraction of bottom characteristics and mapping in Kin Bay, Okinawa Main Island, Japan, using LANDSAT-5/TM and SPOT-1/HRV data 01 p0197 N94-11931
Ocean-ice interaction study of waves and mesoscale features 01 p0197 N94-11935
Warm streamers extended from Warm Core Rings (WCRs) and their role on fish migration and fishing ground formation 01 p0198 N94-11938
The Kyucho events in Sukumo Bay induced by Kuroshio front disturbances 01 p0198 N94-11939
The coherent structure in the oceanic turbulence around Japan Islands Chain forced by an air, sea, and solid Earth interaction 01 p0198 N94-11940
Westward propagation of sea surface anomalies in the western North Pacific as seen by the altimeter and radiometer 01 p0198 N94-11941
Characteristic scales and vortex features of mesoscale vortices observed by the satellites during the winter 01 p0199 N94-11943
The use of CZCS for primary production estimate in the Pacific 01 p0199 N94-11946
CZCS derived chlorophyll distribution in Antarctic water during austral summer 01 p0199 N94-11947
Seasonal changes of phytoplankton distributions in the Northwest Pacific detected by Coastal Zone Color Scanner 01 p0200 N94-11948
Satellite-derived oceanic features 01 p0200 N94-11949
Particle dynamics in the western subarctic Pacific: Implications from CZCS imagery 01 p0200 N94-11950
High-reflectance water mass in Off-Sanriku area observed by CZCS 01 p0200 N94-11951
Dependence of oceanic microwave emission on wind direction 01 p0201 N94-11957
Surface roughness variations across the Iceland-Faroes frontal region observed by the GEOSAT altimeter and NOAA AVHRR 01 p0201 N94-11958
On the variability of wind speeds in the North Western Pacific observed by altimeter/GEOSAT and SSM/I/DMSP 01 p0201 N94-11960
Wind field estimate by using one hour GMS data 01 p0202 N94-11963
Atmospheric correction plans for SeaWiFS 01 p0204 N94-11975
Overwater atmospheric dispersion of volcanic smokes from Mt. Sakurajima observed in NOAA-AVHRR data 01 p0205 N94-11979
Incident shortwave and longwave radiations over the western North Pacific and the Sea of Okhotsk derived from GMS-WEFAX images 01 p0205 N94-11982
Observations of the fractal properties of the Japan sea surface temperature patterns 01 p0205 N94-11984
Flood monitoring in northern part of Central Java by remote sensing technique. Case study: The flooding of Semarang in January, 1990 01 p0206 N94-11989
Preliminary report of lunar observations by the Near-Infrared Mapping Spectrometer (NIMS) during the second Galileo Earth-Moon encounter 01 p0425 N94-12140
Galileo EM-2 contributions to the lunar control network 01 p0468 N94-12198
Proceedings of 1st ERS-1 Symposium on Space at the Service of Our Environment, Volume 2
[ESA-SP-359-VOL-2] 01 p0245 N94-12471
Methodological considerations for use of ERS-1 imagery for the delineation of river networks in tropical forest areas 01 p0247 N94-12484
Per-field filtering and classification of multitemporal ERS-1 SAR imagery 01 p0247 N94-12485
Preliminary ERS-1 assessment for Canadian agriculture and forestry applications 01 p0248 N94-12486
Segmentation and change detection in ERS-1 images over East Anglia 01 p0248 N94-12487
ERS-1 SAR crop monitoring experiment in East Anglia, UK 01 p0248 N94-12488
The TREES project: Pre-processing and generation of terrain data for inclusion in an ERS-1 SAR classification scheme 01 p0249 N94-12496
ERS-1 and Almaz SAR ocean wave imaging over the Gulf Stream and the Grand Banks 01 p0251 N94-12505
Oil spill detection using satellite-based SAR: Experience from a field experiment 01 p0253 N94-12522
ERS-1 imaging radar over the Waddensea-North Netherlands 01 p0254 N94-12526
Comparison of ERS-1 SAR images of the Western Mediterranean to in situ oceanographic data: PRIM-1 Cruise (May 1992) 01 p0255 N94-12529
Proceedings of the PORSEC 1992 in Okinawa: Conference for Pacific Ocean Environments and Probing, volume 2
[JTN-93-80419] 01 p0207 N94-12635
Analysis of GEOSAT wind data 01 p0207 N94-12636
Observation of wave crests by satellite remote sensed data 01 p0207 N94-12638
Variability of sea level and sea surface temperature anomalies in the equatorial Pacific 01 p0208 N94-12640
Pacific rim sea ice as observed with the NIMBUS-7 SMMR 01 p0210 N94-12651
Disintegrating ice front of Shirase Glacier, East Antarctica 01 p0210 N94-12654
Worldwide map of rainfall amount over the ocean derived from passive microwave radiometer 01 p0211 N94-12663
Study on diffusion phenomena of river effluents issued into sea around Japan with satellite remote sensing data 01 p0212 N94-12664
A basic consideration for remote sensing using microwave radars on a satellite 01 p0212 N94-12665
Migration of operational ice analysis and forecasting to a workstation platform at the Joint Ice Center 01 p0212 N94-12666
Evaluating the spread of red soil with LANDSAT TM data in coral reefs of Okinawa main island, southwestern Japan 01 p0212 N94-12668
Simple and low cost image processing system for satellite remote sensing data 01 p0212 N94-12669
Validation test system for sea surface temperature detected by satellites in Mutsu Bay 01 p0213 N94-12670
Sea surface temperature images of Geostationary Meteorological Satellite (GMS) and sea truth data from ferry boats 01 p0213 N94-12671
Evaluation of the method of geostrophic flow using NOAA-AVHRR data 01 p0213 N94-12673
Further study of the Non-Regression-Coefficient SST retrieval method 01 p0213 N94-12674
Delineation of mesoscale features of ocean on satellite IR image 01 p0214 N94-12675
Observation of warm current at the boundary from north equatorial current to Kuroshio by NOAA/AVHRR 01 p0214 N94-12676
Information capability of NOAA-AVHRR data for monitoring oceanographic and atmospheric pollution 01 p0214 N94-12677
Satellite observations of the northeast monsoon coastal current 01 p0214 N94-12678
Aspects of applying a relaxation method to computing sea surface velocities from sea surface temperature images 01 p0214 N94-12679
Sea surface temperature difference between NOAA/AVHRR and in-situ observation 01 p0215 N94-12680
Application of NOAA AVHRR data to fisheries 01 p0215 N94-12681
Statistical features of mesoscale eddies at the Kuroshio front 01 p0215 N94-12682
Intrusion of Kuroshio warm water into Sagami Bay 01 p0215 N94-12683
A study of front dynamics off northeastern Taiwan based on the NOAA-AVHRR satellite remote sensing data 01 p0215 N94-12684
Satellite thermal variations of Kuroshio in relation to storm floods 01 p0215 N94-12685
Frontal zones in Pacific Ocean: Satellite and ship data analysis 01 p0216 N94-12687
Swordfish (Xiphias gladius) catch distributions relative to environmental features observed from satellites off Coquimbo, Chile (30 deg S) 01 p0216 N94-12688
Observation of cold coastal water with high turbidity around the southwestern tip of Korean Peninsula 01 p0216 N94-12689
On the error characteristics of the sea surface temperature observed by satellite 01 p0216 N94-12690
Remote sensing of polluting focal points and coastal disturbances in the Gulf of Arauco and adjacent bays, central Chile 01 p0217 N94-12695
Role of remote sensing and its cost effectiveness in site selection for coastal aquaculture 01 p0217 N94-12697
Application of remote sensing for coastal management in the north coast of Java 01 p0218 N94-12701
Estimation of areal evapotranspiration using LANDSAT TM data: Kitami City, Hokkaido, Japan 01 p0219 N94-12703
Land use/land cover mapping of central water shed of Iran area based on satellite data interpretation 01 p0219 N94-12704

A method to minimize reference data in classifying satellite remote sensing data into land cover classes
01 p0219 N94-12705
Study on air-sea interactions in the OMLET (Ocean Mixed Layer Experiment) area using satellite remote sensing 01 p0220 N94-12710
Investigation of meso-scale fronts, eddies and upwellings in China Seas with AVHRR data
01 p0220 N94-12711
Coastal upwelling monitored by satellite data: Methodologies and results 01 p0220 N94-12712
The warm eddy detection from NOAA/AVHRR thermal images using the Hough transformation
01 p0220 N94-12713
Applicability of satellite infrared data for the monitoring of coastal environments 01 p0220 N94-12714
Satellite and moored buoy observations of polar frontal system over the Yamato Rise in the Japan Sea
01 p0221 N94-12715
Variability of the Kuroshio observed from satellite thermal imagery 01 p0221 N94-12717
SST assimilation: Eastern Mediterranean case study
01 p0221 N94-12719
Mapping of high density area of benthic diatom in Ariake Sea 01 p0222 N94-12720
Advective surface velocity in the north west Pacific derived from NOAA AVHRR images
01 p0222 N94-12721
On a nonstationary dynamics of the north-west Pacific Ocean 01 p0222 N94-12724
Influence of the Kuroshio warm-core rings on hydrographic and fishery conditions off southern Kuril Islands 01 p0224 N94-12737
Verification of the atmosphere-ocean radiative transfer parametric models 01 p0225 N94-12738
Optical transfer operator of the atmosphere-ocean system 01 p0225 N94-12742
Atmospheric correction for determination of average SST fields based on AVHRR data
01 p0227 N94-12750
The application of VAS satellite imagery to thunderstorm forecasting at Cape Canaveral
[NASA-CR-193563] 02 p0718 N94-12839
Knowledge-based oceanographic image compression
[AD-A265752] 02 p0821 N94-13041
EOS workstation
[NASA-CR-191326] 02 p0736 N94-13132
Dendrometric variables estimation in homogeneous forests using LANDSAT TM data
[INPE-5455-TDI/497] 02 p0684 N94-13331
Net radiation mapping of mountainous terrain using Landsat-5 thematic mapper imagery and digital terrain data
[ISBN-0-315-57755-X] 02 p0685 N94-13475
Satellite imagery and exogenous data integration by neural network in automation land-cover classification
[INPE-5480-PRE/1778] 02 p0686 N94-13729
Nonlinear aspects of data integration for land-cover classification in a neural network environment
[INPE-5479-PRE/1778] 02 p0686 N94-13789
Integration of remotely sensed data and cadastral ownership boundaries for land inventory purposes
[BCRS-92-16] 02 p0687 N94-14127
Asia-Pacific ISY Conference, volume 2
[NASDA-CM-199-VOL-2] 02 p0688 N94-14209
Artificial oil pollution detection and wave observation in the sea adjacent to Japan by ERS-1 SAR
02 p0688 N94-14212
Seasonal change of the land-surface temperature over Asian Continent derived from GAC data on NOAA-11 AVHRR 02 p0691 N94-14232
Detecting land cover changes in Chiang-Mai area in Thailand 02 p0693 N94-14241
Land evaluation for agricultural productivity in North-East Thailand using LANDSAT TM data and geographic information 02 p0693 N94-14242
Effects of typhoon on TOMS data
02 p0693 N94-14243
Multi-source national forest inventory of Finland
02 p0694 N94-14254
Global assessment of human activities
02 p0695 N94-14255
Remote sensing for monitoring tropical moist forests in the Indo-Chinese region 02 p0695 N94-14258
Estimation of vegetation damage due to ash fall in Mt. Pinatubo area using MOS-1 data
02 p0695 N94-14259
Outline of ISY sea surface temperature data sets
02 p0696 N94-14261
Integration of SST data sets using MOS-1 satellite data: For validation and monitoring 02 p0696 N94-14262
Geophysical validation of ATSR sea surface temperatures 02 p0696 N94-14263
Accuracy validation test of estimated sea surface temperature by satellite data 02 p0696 N94-14264
Tracking of change of a warm-core ring structure
02 p0696 N94-14267
A method for estimation of partial cloud cover within a pixel and its effect 02 p0697 N94-14269
Warm streamers extended from Warm Core Rings (WCR's) and their role on fish migration and fishing ground formation 02 p0697 N94-14270
Atmospheric correction for sea surface temperature by application of microwave dual-channel technique to VTIR data 02 p0697 N94-14271
Meteorological data, new series A monographs. Volume 6, no. 3: Estimation of influence of high clouds in the radiation field and the climat by analysis of NOAA AVHRR data
[ETN-93-94170] 02 p0723 N94-14707
NASA images 8
[NASA-TM-109416] 02 p0544 N94-14783
Assessment of TDI operation of a frame transfer CCD for high resolution imaging from a fast spinning spacecraft 03 p0910 N94-15097
Ground truth spectrometry and imagery of eruption clouds to maximize utility of satellite imagery
[NASA-CR-194358] 03 p1081 N94-15181
Sea ice motions in the central arctic ice central arctic pack ice as inferred from AVHRR imagery
[NASA-CR-194572] 03 p1112 N94-15701
ERS-1: 18 months in orbit 03 p0990 N94-15888
Almaz 03 p0898 N94-15889
EUVE observations of the Moon
03 p1250 N94-16185
Remote sensing studies of the northeastern portion of the lunar nearside 03 p1258 N94-16225
A geological and geophysical information system for Eurasia
[AD-A267841] 03 p1232 N94-17036
Developing automated analysis methods for sea ice imagery: A status report with recommendations
[AD-A267284] 03 p1113 N94-17241
Nowcasting methods for satellite imagery
[AD-A267294] 03 p1108 N94-17267
Three dimensional visualization of GOES cloud data using OCTRESS
[AD-A268102] 03 p1109 N94-17572
An empirical study of tropical cloud clusters using special sensor microwave imager data
[AD-A268072] 03 p1110 N94-17595
The Central American cold surge: An observational analysis of the deep southward penetration of North American cold fronts
[AD-A268592] 03 p1110 N94-17607
Ship-produced cloud line of 13 July 1991
[DE93-016879] 04 p1472 N94-17986
Application of fractal methods to estimate the aerosol-optical depth for atmospheric correction of high resolution satellite data
[DLR-FB-93-04] 04 p1480 N94-18088
Three-dimensional cloud visualization based on satellite imagery
[AD-A269318] 04 p1490 N94-18300
The Navy tessellated spheroid map projection system: A comprehensive definition
[AD-A269989] 04 p1462 N94-18677
Ozone hole
[NASA-TM-109368] 04 p1476 N94-18960
Mathematical modeling of the free surface hydrodynamic and of transport in suspensions of non cohesive sediments: Aid to the interpretation of spatial images
[ETN-93-95011] 04 p1421 N94-19502
The analysis of global cloud and radiation data for the study of cloud-climate interactions
[NASA-CR-193388] 05 p1865 N94-20535
Optical climatology of the Northeast Pacific Ocean
[AD-A271671] 05 p1866 N94-20559
Geology and radiophysical properties of the Venera and Vega landing sites 05 p2135 N94-20867
The 7th Brazilian Remote Sensing Symposium, volume 1 05 p1838 N94-20953
The use of satellite images in Amazonian archaeology: A case study in the Upper Rio Negro Basin
05 p1838 N94-20954
Change detection on land use and rainforest cover at Paragominas region, Brazilian Amazon
05 p1838 N94-20957
Linear mixing model applied to AVHRR LAC data
05 p1838 N94-20958
The 7th Brazilian Remote Sensing Symposium, volume 3 05 p1839 N94-20960
Predicting LANDSAT MSS endmember signatures from corresponding higher resolution TM fraction images
05 p1839 N94-20962
Evaluation of C-band SAR data from SAREX 1992: Tapajos study site 05 p1839 N94-20964
Comparison of radiation and cloud parameters derived from satellite and aircraft measurements during FIRE 2 cirrus IFO 05 p1872 N94-22299
Managing an archive of weather satellite images
05 p2048 N94-22525
The AGRHYMET data communications project
06 p2280 N94-22776
Computer assisted analysis of auroral images obtained from high altitude polar satellites
[NASA-CR-194873] 06 p2400 N94-23084
Application of ERS-1 active microwave instrumentation data to remote sensing of snow
[PB93-224756] 06 p2382 N94-23224
SeaWiFS technical report series. Volume 11: Analysis of selected orbit propagation models for the SeaWiFS mission
[NASA-TM-104566-VOL-11] 06 p2417 N94-23338
Image pattern recognition supporting interactive analysis and graphical visualization
[NASA-CR-194878] 06 p2451 N94-23369
The Far Ultraviolet (FUV) auroral imager for the Inner Magnetospheric Imager (IMI) mission: Options
06 p2209 N94-24453
An AVHRR cloud classification database typed by experts
[AD-A273560] 06 p2416 N94-25162
Human visual system enhancement of reconstructed satellite images
[AD-A273867] 07 p2693 N94-25595
Objective image quality metrics: Applications for partially compensated images of space objects
[AD-A273837] 07 p2847 N94-25741
Geometric correction of SPOT images with use of digital elevation models
[ETN-94-95033] 07 p2847 N94-26107
Solid estimation feature based correlation method for measuring control points required for correcting satellite images
[VTT-JULK-772] 07 p2848 N94-26253
A geological and geophysical information system for Eurasia
[AD-A274818] 07 p3098 N94-26490
Application of Space Shuttle Project Hercules imagery in the investigation of ship cloud tracks
[AD-A274923] 07 p2692 N94-26529
The Hough transform algorithm for sea ice lead analysis: An evaluation
[AD-A274535] 07 p2899 N94-26853
Assessment of tropical forests using satellite data
[SILVA-CARELICA-21] 07 p2850 N94-27182
Global tropical forest cover assessments using satellite imagery 07 p2850 N94-27183
Woody biomass density in the Tendelti area of the central Sudan 07 p2850 N94-27185
Morphodynamics of inter-tidal areas: The Wadden Sea
[NLR-TP-92356-U] 07 p2851 N94-27555
Role of remote sensing in energy, water, and carbon cycle studies over the Amazon
[INPE-5486-PRE/1786] 07 p2852 N94-27957
An image assessment study of image acceptability of the Galileo low gain antenna mission
07 p2945 N94-28252
Image compression software for the SOHO LASCO and EIT experiments 07 p2945 N94-28253
Compression of multispectral Landsat imagery using the Embedded Zerotree Wavelet (EZW) algorithm
07 p2947 N94-28261
Vector quantizer designs for joint compression and terrain categorization of multispectral imagery
07 p2947 N94-28262
Study on environment monitoring over whole China using NDVI from AVHRR data and future project
07 p2875 N94-28289
Utilization of remote sensing data for global climate change research in Malaysia 07 p2875 N94-28290
Far ultraviolet images of the nighttime ionosphere
[AD-A275083] 08 p3356 N94-28843
Lead detection and mapping with reference to relationships between scale, sensor characteristics, surface conditions and atmospheric properties
[AD-A275321] 08 p3377 N94-28877
Proceedings of the International Symposium on Remote Sensing
[JTN-94-80578] 08 p3325 N94-28925
Synthetic aperture radar applications: Now and in the future 08 p3260 N94-28927
Evaluation of simulated JERS-1 data for geologic mapping at Drum Mountains, Utah, Silver Bell, Arizona, and Wind River, Wyoming under the GEOSAT-ERSDAC/JAPEX/JGI/RESTEC joint studies
08 p3326 N94-28929
Image processing for hyperspectral data
08 p3326 N94-28930
JERS-1 data acquisition and distribution
08 p3326 N94-28931
JERS-1 data and information system for resources exploration 08 p3327 N94-28932
Observations by ERS-1 start
08 p3327 N94-28933

Sea ice and oceans applications of SAR
08 p3327 N94-28934
Amazonia: Remote sensing test site and survey
08 p3327 N94-28935
Utilization of remote sensing data in Southeast Asia
08 p3327 N94-28936
Remote sensing and global management
08 p3328 N94-28937
Proceedings of the 15th Earth Observation Symposium
[JTN-94-80607] 08 p3328 N94-29036
Principles and application tendency of remote sensing: Its principle, function and utilization
08 p3328 N94-29037
Oceanic survey utilizing satellites
08 p3328 N94-29040
Proceedings of the 3rd International Symposium: JERS-1 and Remote Sensing in the Future
[JTN-94-80597] 08 p3329 N94-29217
A new information system: Satellite observation
08 p3330 N94-29219
Observatory system of Earth Resources Satellite-1
08 p3330 N94-29221
Application of JERS-1 data to geologic analyses
08 p3330 N94-29222
Application of optical sensor data to resource survey
08 p3330 N94-29223
Radar applications at the Canada Centre for Remote Sensing 08 p3331 N94-29224
Application of remote sensing techniques in petroleum exploration: The Indonesian experience
08 p3331 N94-29225
JERS-1 and future remote sensing: Application of remote sensing data to agroecological problems
08 p3331 N94-29229
Application of remote sensing in prevention of disasters 08 p3332 N94-29230
Future expectation of remote sensing technology
08 p3332 N94-29231
Japan's Earth observation satellite programs
08 p3332 N94-29232
Extrapolation of point data for resource mapping
08 p3334 N94-29959
Application of remote sensing techniques for the seismo-tectonic study of Nahanni earthquake area
[ISBN-0-315-85942-3] 08 p3334 N94-30037
Estimation of transmittance from satellite imagery
08 p3257 N94-30500
Statistical analysis of a satellite imagery time series: Implications for the study of coastal and estuarine circulation 08 p3335 N94-30919
Multitemporal analysis of a braiding river: The advanced study of 1992
[NLR-TP-93100-U] 08 p3335 N94-30942
Desert aerosols: Sources, transports, and impacts determined by remote sensing 09 p3770 N94-31003
Automatic extraction of cartographic objects by fusion of data extracted from satellite images
[TELECOM-93-E-001] 09 p3742 N94-31165
Estimation of visible and near-infrared reflectivity for Peyto Glacier Basin using satellite data
[ISBN-0-315-87039-7] 09 p3743 N94-31733
The basement fracture pattern of southern Ontario: A tectonic interpretation based on Landsat TM imagery, airphotos and field data
[ISBN-0-315-87086-9] 09 p3772 N94-31834
Shiptrack database analysis
[AD-A277228] 09 p3746 N94-32025
Sensitivity analysis of the AVHRR infrared cirrus model
[AD-A276690] 09 p3784 N94-32117
Automated detection of ship tracks in multispectral satellite data
[AD-A276697] 09 p3746 N94-32119
Research and applications of a canopy reflectance model 09 p3747 N94-32492
From Optics to Radar, SPOT and ERS Applications
[ISBN-2-85428-345-7] 09 p3747 N94-32523
Monitoring land cover and crop types in Denmark using ERS-1 SAR and optical satellite images
09 p3748 N94-32528
Optics and radar: Cohabitation, rivality or happy marriage. Towards new planning tools
09 p3748 N94-32529
The contribution of satellite data in communication infrastructure projects 09 p3749 N94-32530
The use of ERS images for mapping
09 p3749 N94-32531
SPOT imagery for updating land cover information of 1:50,000 numerical topographic maps
09 p3749 N94-32532
Example of SPOT/ERS-1 complementarity
09 p3749 N94-32533
The use of SPOT, and the contribution of ERS-1, in the assessment of urban pressure on agriculture land in Greater Tunis (Tunisia) 09 p3749 N94-32534
Restoration of interferometric, polarimetric, radiometric, and textural information in SAR images
09 p3750 N94-32535
Assessment of region-based methods for automated SAR/optical registration, attribute extraction, and classification 09 p3750 N94-32536
Technique of ERS-1 image processing in association with SPOT data 09 p3750 N94-32538
Production of terrain data: Optical radar complementarity 09 p3750 N94-32540
Fusion of multispectral (XS) and Panchromatic (P) SPOT images and radar images 09 p3750 N94-32541
Integration of ERS-1 images into the European Agriculture Statistics project Action 4: Thematic aspect
09 p3753 N94-32554
Rapid estimates of crop acreage and production at European scale using high resolution imagery
09 p3754 N94-32557
Differential interferometry study of an earthquake
09 p3756 N94-32570
Quantitative analysis of woody vegetation in Soudano-Sahalian region. Textural approach (application to a Burkina Faso region) 09 p3757 N94-32574
Evolution of upwelling fronts off the coast of Portugal
[NASA-CR-195692] 09 p3790 N94-33045
Modelling topographic effects on digital remotely sensed data 10 p4074 N94-33360
Comparison of standard multispectral and map-assisted classification methods with a new layered approach
10 p4075 N94-33422
The forest inventory project at the Tapajos National Forest, volume 1
[INPE-5423-PRP/171] 10 p4033 N94-33434
Refocusing space technology
[NASA-TM-109833] 10 p4161 N94-33569
A collection of The Movies
[NASA-TM-109806] 10 p4075 N94-33598
Stratification of deforested areas by vegetation types in Amazonia, using geographic information systems: Study of case at SB20 Purus map
[INPE-5541-TDI/529] 10 p4077 N94-34230
An adaptive technique to maximize lossless image data compression of satellite images
10 p4124 N94-35057
Automatic cataloguing and characterization of Earth science data using SE-trees 10 p4124 N94-35058
A statistical inference approach for the retrieval of the atmospheric ozone profile from simulated satellite measurements of solar backscattered ultraviolet radiation 10 p4083 N94-35060
Preliminary study of satellite attitude determination for the LANDSAT 7 spacecraft
[AD-A278876] 11 p4212 N94-35585
Theoretical and experimental studies relevant to interpretation of auroral emissions
[NASA-CR-196032] 11 p4376 N94-36421
Variability of the California Current System off Point Sur, California from April 1988 to December 1990
[AD-A278579] 12 p4476 N94-36985

SATELLITE INSTRUMENTS

NASA airborne satellite instrumentation calibrator (NASIC) technical reference
[NASA-RP-1315] 02 p0545 N94-13713
ALFIS: Astronomical Low Frequency Interferometry Satellites. A feasibility study
[LR-699] 02 p0542 N94-13988
ECS: Eighth year in orbit
[ESA-BR-82] 02 p0543 N94-14352
Development of Japanese Earth Resources Satellite-1 (JERS-1; FUYO-1) and it's operational results
[NASDA-SPP-930001] 03 p0884 N94-15001
Eighth International Workshop on Laser Ranging Instrumentation
[NASA-CP-3214] 03 p0911 N94-15552
Laser ranging application to time transfer using geodetic satellite and to other Japanese space programs
03 p0911 N94-15555
Applications of SLR 03 p0911 N94-15556
The precision of today's satellite laser ranging systems 03 p0912 N94-15559
New methods of generation of ultrashort laser pulses for ranging 03 p0913 N94-15565
Preliminary results from the portable standard satellite laser ranging intercomparison with MOBLAS-7
03 p0913 N94-15568
Test results from LAGEOS-2 optical characterization using pulsed lasers 03 p0915 N94-15577
Two wavelength satellite laser ranging using SPAD
03 p0916 N94-15584
State-of-the-art satellite laser range modeling for geodetic and oceanographic applications
03 p0916 N94-15586
Improvement of SLR accuracy, a possible new step
03 p0917 N94-15588
Poisson filtering of laser ranging data
03 p0917 N94-15593
Results of the MTLRS-1 upgrade
03 p0877 N94-15610
Satellite laser station Helwan status 1992
03 p0877 N94-15621
Optical attenuation mechanism upgrades, MOBLAS, and TLRS systems 03 p0922 N94-15622
The third generation SLR station Potsdam no. 7836
03 p0877 N94-15623
Station report on the Goddard Space Flight Center (GSFC) 1.2 meter telescope facility
03 p0922 N94-15625
ENVISAT ASAR 03 p0898 N94-15892
Tectonic deformation in southern California
[NASA-CR-194621] 03 p1101 N94-16021
L-shell binning and display of sensor data from the CRRES spacecraft
[AD-A267256] 03 p0888 N94-16990
Big results with small space systems: What small systems are doing today 03 p0896 N94-17187
Experience with custom processors in space flight applications 04 p1336 N94-18338
Ultraviolet plume instrument calibration and sensor assessment
[AD-A269687] 04 p1337 N94-18574
Oceanic in situ Fraunhofer-line characteristics: Fraunhofer-line underwater experiment (FLUX)
[AD-A270659] 05 p1881 N94-19952
The EXOSAT operational experience
[ESA-STM-248] 05 p1657 N94-20235
Comparison of radiation and cloud parameters derived from satellite and aircraft measurements during FIRE 2 cirrus IFO 05 p1872 N94-22299
Instrument interface description for NOAA 2000 instruments with European morning spacecraft and/or NOAA-OPO spacecraft
[NASA-TM-109406] 06 p2208 N94-23478
Command/telemetry bus general specification for the NOAA-OPQ polar orbiting environmental satellites and EUMETSAT polar satellite systems
[NASA-TM-109407] 06 p2208 N94-23479
Low rate data bus general specification for the NOAA-OPQ polar orbiting environmental satellites and EUMETSAT polar satellite systems
[NASA-TM-109408] 06 p2208 N94-23480
Mission planning for an Earth observation low Earth orbiter: ERS-1 06 p2503 N94-23868
Science planning and sequencing for Cassini
06 p2504 N94-23871
Connecting science and operations: The operations coordinator 06 p2504 N94-23874
A combined Earth scanner and momentum wheel for attitude determination and control of small spacecraft
06 p2208 N94-24022
Hubble Space Telescope high speed photometer science verification test report
[NASA-CR-189322] 06 p2205 N94-24710
High energy collimating fine grids for HESP program
[NASA-CR-189317] 06 p2209 N94-24767
A space fiber-optic x ray burst detector
[DE94-002722] 07 p2696 N94-26808
Nimbus-7 Earth radiation budget calibration history. Part 2: The Earth flux channels
[NASA-RP-1335-PT-2] 07 p2814 N94-27981
A simple satellite system to locate gamma ray bursters using scintillating fiber technology
[DE94-601287] 07 p3117 N94-27996
Develop and fabricate a radiation dose measurement system for satellites
[PL-TR-93-2161] 07 p2698 N94-28210
Develop and fabricate a radiation dose measurement system for satellites
[PL-TR-93-2099] 07 p2698 N94-28217
EOS project and ASTER (ITIR)
08 p3331 N94-29226
The 25th Annual Precise Time and Time Interval (PTTI) Applications and Planning Meeting
[AD-A280955] 08 p3468 N94-30639
Development status of the Communications and Broadcasting Engineering Test Satellite (COMETS)
[JTN-94-80545] 08 p3169 N94-30811
MODIS. Volume 1: MODIS level 1A software baseline requirements
[NASA-TM-104594-VOL-1] 09 p3823 N94-33287
Instrumentation on the RAIDS experiment 2: Extreme ultraviolet spectrometer, photometer, and near IR spectrometer
[AD-A278543] 10 p4085 N94-33676
Earth Observing System (EOS) Advanced Microwave Sounding Unit-A (AMSU-A) schedule plan
[NASA-CR-194856] 11 p4281 N94-35734

SATELLITE LAUNCHING

U SPACECRAFT LAUNCHING

SATELLITE LIFETIME

Satellite situation report, volume 33, no. 3
[NASA-TM-109278] 03 p0885 N94-15712

Satellite control: A comprehensive approach
03 p0878 N94-17158

SATELLITE MANEUVERS
U SPACECRAFT MANEUVERS

SATELLITE NAVIGATION SYSTEMS
NT GLONASS
Comparison of GPS and GLONASS common-view time transfers 01 p0024 N94-10967
BRIDGE: A small scientific satellite for geodesy
03 p0890 N94-17146
Satellite autonomous navigation and orbit determination using magnetometers 06 p2156 N94-24258
Differential GPS for air transport: Status
06 p2162 N94-25100
Satellite navigation system GPS: A review of principles and performance and developments in general
[PB94-124534] 07 p2665 N94-27210
Differential GPS methods and performance for marine applications
[DREP-93-09] 07 p2665 N94-27667
Use of GPS in automated air traffic control
08 p3137 N94-29563
An Operational Control Segment (OCS) update on GPS constellation status and future program directions
08 p3144 N94-30643
A review of the status and capabilities of Navstar GPS
[AD-B174629] 08 p3143 N94-30854

SATELLITE NETWORKS
NT ARGOS SYSTEM
NT SATELLITE CONSTELLATIONS
NT VSAT (NETWORK)
Use of low orbital satellite communications systems for humanitarian programs 01 p0308 N94-11808
The 1991 research and technology report, Goddard Space Flight Center
[NASA-TM-108738] 02 p0851 N94-14791
Laser ranging network performance and routine orbit determination at D-PAF 03 p0911 N94-15554
SATCOP mission planning software package
03 p0912 N94-15562
ECS: Ninth year in orbit
[ESA-BR-91] 03 p0987 N94-15644
On-board B-ISDN fast packet switching architectures. Phase 1: Study
[NASA-CR-191143] 03 p0883 N94-17111
Small Satellites Systems and Services
[ISBN-2-85-428327-9] 03 p0888 N94-17131
Small satellite constellation system: Optimization criteria 03 p0888 N94-17132
AMIGAU: A prototype tool aimed at mission analysis for satellites and satellite constellations
03 p0888 N94-17133
Low Earth orbit constellations: Orbit control or not
03 p0875 N94-17134
Impact of launching uncertainties on the visibility of communication satellite constellations without orbit control 03 p0889 N94-17135
Small satellite constellation deployment strategies
03 p0878 N94-17138
Delta launch vehicle: Accommodations for small satellites 03 p0878 N94-17139
Adequation of mini satellites to oceanic altimetry missions 03 p0891 N94-17152
Regulation of low Earth orbit satellites
03 p0892 N94-17159
LEOCOM-SPES: Low cost message communications
03 p0892 N94-17161
TAOS (S80): A (LEO-MSS) system for position reporting and telemanagement services 03 p0893 N94-17162
The ORBCOMM system 03 p0893 N94-17163
MAGSS-14: Medium Altitude Global Mobile Satellite System with enhanced regional coverage
03 p0893 N94-17164
Feasibility study of a personal communications system IRIDIUM-like 03 p0893 N94-17165
The ELLIPSO (tm) system: Elliptical low orbits for mobile communications 03 p0893 N94-17167
STARSYS: A view after WARC-92 — satellite position and messaging system 03 p0893 N94-17168
S-80: A satellite for less than 50 MF
03 p0894 N94-17172
Key trends of the small satellite market
03 p0897 N94-17191
Solar Electro-Optical Network (SEON) upgrade/replacement program. Phase 1: Qualification operational test and evaluation plan
[AD-A266364] 03 p1237 N94-17225
CONTACT: An Air Force technical report on military satellite control technology
[AD-A269375] 04 p1334 N94-18408
The NCC project: A quality management perspective
05 p1828 N94-21324
Software metrics: The key to quality software on the NCC project 05 p1922 N94-21326
The Test Analysis Retrieval System (TARS): Meeting the challenges of the network's test processes
05 p1933 N94-21337
On-board closed-loop congestion control for satellite based packet switching networks
[NASA-TM-106446] 05 p1656 N94-21581
Visibility considerations in frequency sharing with low Earth orbit satellites 05 p1746 N94-22187
Internetworking satellite and local exchange networks for personal communications applications
06 p2276 N94-22755
Integration of mobile satellite and cellular systems
06 p2277 N94-22757
Interworking evolution of mobile satellite and terrestrial networks 06 p2277 N94-22758
Interworking and integration of the Inmarsat Standard-M with Pan-European GSM system
06 p2277 N94-22759
Architectures and protocols for an integrated satellite-terrestrial mobile system
06 p2277 N94-22760
Handover procedures in integrated satellite and terrestrial mobile systems 06 p2277 N94-22761
Optimizing space constellations for mobile satellite systems 06 p2278 N94-22764
A system architecture for an advanced Canadian wideband mobile satellite system
06 p2278 N94-22766
Applicability of different onboard routing and processing techniques to mobile satellite systems
06 p2278 N94-22767
The ORBCOMM data communications system
06 p2281 N94-22782
Implementation of a system to provide mobile satellite services in North America 06 p2281 N94-22784
The Iridium (tm) system: Personal communications anytime, anyplace 06 p2281 N94-22785
The Globalstar mobile satellite system for worldwide personal communications 06 p2282 N94-22786
The European Mobile System (EMS)
06 p2282 N94-22789
Global coverage Mobile Satellite Systems: System availability versus channel propagation impairments
06 p2284 N94-22798
First satellite mobile communication trials using BLOS-CDMA 06 p2284 N94-22801
Improved frame synchronization schemes for INMARSAT-B/M SCPC and TDM channels
06 p2285 N94-22806
Diversity reception for advanced multi-satellite networks: A CDMA approach 06 p2286 N94-22816
Development of a multilayer interference simulation program for MSS systems 06 p2287 N94-22823
Handover aspects for a Low Earth Orbit (LEO) CDMA Land Mobile Satellite (LMS) system
06 p2288 N94-22824
Study on networking issues of medium earth orbit satellite communications systems
06 p2288 N94-22825
The design and networking of dynamic satellite constellations for global mobile communication systems
06 p2288 N94-22826
Low earth orbit satellite/terrestrial mobile service compatibility 06 p2288 N94-22827
A practical system for regional mobile satellite services 06 p2288 N94-22828
Multi-access laser communications terminal
[NASA-CR-191251] 06 p2295 N94-23830
The Second Annual International Space University Alumni Conference
[NASA-CP-3253] 09 p3598 N94-31425
North American ISDN Users' Forum agreements on Integrated Services Digital Network
[PB94-162559] 11 p4305 N94-35940

SATELLITE OBSERVATION
Space Activities in the Asia Pacific Region
[JTN-93-80421] 01 p0035 N94-10676
Space research and remote sensing programmes in Bangladesh 01 p0035 N94-10679
Space program in Indonesia 01 p0036 N94-10681
Space programme in Malaysia
01 p0036 N94-10685
National space programmes and application of the remote sensing data in Mongolia
01 p0036 N94-10686
Russian space system for the Earth remote sensing
01 p0037 N94-10688
Sun-synchronous and geo-synchronous satellite data utilization for environmental studies
01 p0037 N94-10689
Thailand ISY activities 01 p0037 N94-10690
National space program in Australia
01 p0037 N94-10691
Panel discussion: Role of space program in the Asia Pacific Region 01 p0037 N94-10694
Retrieval of radiation budgets in the Arctic from satellite measurements 01 p0229 N94-10714
Satellite-derived photosynthetically available and total solar irradiance at the surface during FIFE's intensive field campaigns 01 p0230 N94-10954
Estimating Photosynthetically Available Radiation (PAR) at the Earth's surface from satellite observations
01 p0230 N94-10955
Ultraviolet plume instrument description and plume data reduction methodology
[AD-A266141] 01 p0054 N94-11643
Utilisation of ERS-1 data for mapping of Antarctica
01 p0237 N94-11740
A stochastic-deterministic approach as an alternative to classical cross-over techniques in small ocean basins
01 p0242 N94-11767
The Earth's gravity model for the ERS-1 commissioning phase 01 p0243 N94-11778
Using transponders with the ERS-1 altimeter to measure orbit altitude to +/- 3 cm 01 p0244 N94-11785
Satellite observation of atmospheric tracer components: JEM/POP 01 p0130 N94-11836
Submillimeter wave observation experiment of Earth atmosphere with SIS mixer 01 p0130 N94-11837
Satellite observations of red tide events: Plans for EESI 01 p0191 N94-11899
An algorithm for the detection of mucilage (green slime) in the Adriatic Sea 01 p0191 N94-11900
Remote sensing of the suspended matter distribution with high concentration in China Sea
01 p0192 N94-11901
Scatterometer observations: Review
01 p0201 N94-11956
Overwater atmospheric dispersion of volcanic smokes from Mt. Sakurajima observed in NOAA-AVHRR data
01 p0205 N94-11979
Integration of ERS-1 data into the European project of agriculture statistics 01 p0248 N94-12490
Assessment of ERS-1 SAR data for soil moisture estimation 01 p0249 N94-12492
Temporal monitoring of soil moisture using ERS-1 SAR data 01 p0249 N94-12493
Observations of ERS-1 SAR sensitivities to changes in aboveground biomass in young loblolly pine forests
01 p0249 N94-12494
Seeing the Black Forest by ERS-1 and AIRSAR: A comparison 01 p0249 N94-12495
TREES project: A case study on the use of multi-temporal ERS-1 SAR data and SPOT data for monitoring tropical ecosystems 01 p0249 N94-12497
Studies of dynamical processes affecting the distribution of stratospheric ozone
[NASA-CR-193477] 01 p0279 N94-12560
Proceedings of the PORSEC 1992 in Okinawa: Conference for Pacific Ocean Environments and Probing, volume 2
[JTN-93-80419] 01 p0207 N94-12635
Observations of surface signatures in the north-west Pacific Ocean with the spaceborne SAR
01 p0226 N94-12746
Radar observation of internal waves field in the north-west Pacific 01 p0226 N94-12747
Complex (hydrodynamic, satellite) monitoring of dynamic structures in the western Pacific with the aim of forecasting the marine ecosystems behaviour
01 p0227 N94-12753
Mesoscale dynamic structures of the Subarctic Frontal Zone in the Pacific Ocean 01 p0227 N94-12754
The algorithm of primary production determination
01 p0228 N94-12761
Non-image visible polarization remote sensing of the ocean 01 p0229 N94-12762
Problem of climate change predictability and satellite radiation budget observations 01 p0229 N94-12766
Radiometer offsets and count conversion coefficients for the Earth Radiation Budget Experiment (ERBE) spacecraft for the years 1987, 1988, and 1989
[NASA-CR-191489] 01 p0286 N94-12772
Circulation model experiments of the Gulf Stream using satellite-derived fields
[AD-A266067] 02 p0725 N94-12990
Degradation of the visible and near-infrared channels of the advanced very high resolution radiometer on the NOAA-9 spacecraft: Assessment and recommendations for corrections
[NOAA-TR-NESDIS-70] 02 p0544 N94-13029
Study on TRMM data utilization for meteorology
[NASDA-CNT-930007] 02 p0721 N94-13643
Activities report of the Netherlands Remote Sensing Board
[ETN-93-93880] 02 p0686 N94-14073
Calibration and in-house validation results of JERS-1 data 02 p0687 N94-14092
Earth observation experiment data analysis
02 p0687 N94-14093

Asia-Pacific ISY conference, volume 1
[NASDA-CM-199-1] 02 p0532 N94-14098
Asia-Pacific ISY Conference, volume 2
[NASDA-CM-199-VOL-2] 02 p0688 N94-14209
Artificial oil pollution detection and wave observation in the sea adjacent to Japan by ERS-1 SAR
02 p0688 N94-14212
IMG: Interferometric monitor for greenhouse gases
02 p0689 N94-14217
Spectroscopic method and data reduction algorithm for laser long-path absorption measurements using RIS
02 p0689 N94-14218
TRMM system overview and status in the United States 02 p0690 N94-14221
TRMM Project in Japan: Overview and status
02 p0690 N94-14222
Clouds and the Earth's Radiant Energy System (CERES) on the Tropical Rainfall Measuring Mission (TRMM)
02 p0690 N94-14223
TRMM precipitation radar algorithm
02 p0690 N94-14224
Estimate of sampling errors of TRMM rainfall observation by using radar-AMeDAS composite data
02 p0690 N94-14225
Space measurements for determining the Earth's energy and water cycles 02 p0690 N94-14227
Future TRMM follow-on mission
02 p0691 N94-14228
The effects of anthropogenic aerosols on optical thickness and particle size of clouds. Part 1: Retrieval algorithm 02 p0691 N94-14230
Climate products from NOAA operational satellites
02 p0691 N94-14231
Seasonal change of the land-surface temperature over Asian Continent derived from GAC data on NOAA-11 AVHRR 02 p0691 N94-14232
Earth radiation budget, cloud, and aerosol parameters derived from AVHRR and TOVS measurements
02 p0691 N94-14233
The development and implementation of an interactive retrieval/analysis/forecast algorithm
02 p0692 N94-14234
Satellite technology for environmental monitoring in developing countries 02 p0692 N94-14236
Some potentials of the Indonesian region for Earth observation 02 p0692 N94-14237
Application of satellite remote sensing technology in disaster mitigation: A case study of Bangladesh
02 p0692 N94-14238
Integration of remote sensing and mathematical modelling in disaster mitigation
02 p0692 N94-14239
Soil erosion mapping using remote sensing and GIS techniques 02 p0692 N94-14240
Detecting land cover changes in Chiang-Mai area in Thailand 02 p0693 N94-14241
Land evaluation for agricultural productivity in North-East Thailand using LANDSAT TM data and geographic information 02 p0693 N94-14242
Effects of typhoon on TOMS data
02 p0693 N94-14243
Satellite remote sensing for disaster mitigation
02 p0693 N94-14244
A concept for the world environment and disaster observation system 02 p0693 N94-14245
Study of the consequences of the Chernobyl accident and technogenic activity in the Republic Belarus using aerospace methods 02 p0693 N94-14246
A tentative plan on China and Asian-Pacific satellite system for disaster reduction 02 p0693 N94-14247
Earth observation from low-inclination orbit as a necessary complement to polar missions
02 p0694 N94-14248
Development of a remote sensing geographic information system for land cover changes and assessment of risk due to natural and man made hazards covering the area of the inner delta of the Yellow River
02 p0694 N94-14249
The role of the dynamics for the deviation of the total ozone from the long-term mean at the edge of the polar vortex 02 p0694 N94-14250
The European Arctic ozone experiment: An investigation of Northern Hemisphere ozone depletion
02 p0694 N94-14251
Space-based activities: SAM 2 and SAGE 2
02 p0694 N94-14252
New evidences supported the Wei hypothesis about the formation of the Antarctic ozone hole
02 p0694 N94-14253
Multi-source national forest inventory of Finland
02 p0694 N94-14254
Global assessment of human activities
02 p0695 N94-14255
The Swedish ISY contribution
02 p0695 N94-14256
Vegetation mapping of Indo-China Peninsula using MOS-1 MESSR and NOAA AVHRR
02 p0695 N94-14257
Remote sensing for monitoring tropical moist forests in the Indo-Chinese region 02 p0695 N94-14258
Estimation of vegetation damage due to ash fall in Mt. Pinatubo area using MOS-1 data
02 p0695 N94-14259
Mangrove afforestation monitoring using remote sensing 02 p0695 N94-14260
Outline of ISY sea surface temperature data sets
02 p0696 N94-14261
Integration of SST data sets using MOS-1 satellite data: For validation and monitoring 02 p0696 N94-14262
Geophysical validation of ATSR sea surface temperatures 02 p0696 N94-14263
Accuracy validation test of estimated sea surface temperature by satellite data 02 p0696 N94-14264
Tracking of change of a warm-core ring structure
02 p0696 N94-14267
Outline of ISY Kuroshio observation experiment
02 p0697 N94-14268
A method for estimation of partial cloud cover within a pixel and its effect 02 p0697 N94-14269
Warm streamers extended from Warm Core Rings (WCR's) and their role on fish migration and fishing ground formation 02 p0697 N94-14270
Atmospheric correction for sea surface temperature by application of microwave dual-channel technique to VTIR data 02 p0697 N94-14271
Some thoughts on the space programs in the Asia Pacific regions 02 p0697 N94-14272
Summary of the NOAA/NESDIS Workshop on Development of a Global Satellite/In Situ Environmental Database
[NOAA-TR-NESDIS-72] 02 p0826 N94-14498
Educational module for the higher agricultural education. Part 1: Land use classification using satellite pictures
[BCRS-92-11A] 02 p0819 N94-14809
Finding fish from above --- remote sensing
[NASA-TM-109602] 03 p1081 N94-15310
ATLAS-2 and UARS correlative measurement opportunities during Space Shuttle mission on April 8-17, 1993
[NASA-TM-109020] 03 p1105 N94-15480
SeaWiFS technical report series. Volume 12, SeaWiFS technical report series cumulative index: Volumes 1-11
[NASA-TM-104566-VOL-12] 03 p1111 N94-15529
ERS-1: 18 months in orbit 03 p0990 N94-15888
ENVISAT ASAR 03 p0898 N94-15892
Some thoughts on future rain mapping missions (TRMM follow-on) 03 p0992 N94-15906
EUVE observations of the Moon
03 p1250 N94-16185
Galileo photometry of Apollo landing sites
03 p1259 N94-16234
Big results with small space systems: What small systems are doing today 03 p0896 N94-17187
Developing automated analysis methods for sea ice imagery: A status report with recommendations
[AD-A267284] 03 p1113 N94-17241
Arctic and Antarctic sea ice, 1978-1987: Satellite passive-microwave observations and analysis
[NASA-SP-511] 03 p1114 N94-17439
Optimization of satellite coverage in observing cause and effect changes in the ionosphere, magnetosphere, and solar wind
[AD-A267956] 03 p1102 N94-17493
An analysis of simulated and actual DMSP SSM/T-2 brightness temperatures
[AD-A268103] 03 p1109 N94-17573
Current positioning possibilities by spatial techniques and the Royal Oservatory of Belgium program
04 p1483 N94-18627
Modifications of airborne oceanographic lidar for the long range P-3 missions
[NASA-CR-194682] 04 p1499 N94-18819
Development of ISY data set, part 2
[NASDA-CNT-930006-PT-2] 04 p1463 N94-19384
SeaTrack: Ground station orbit prediction and planning software for sea-viewing satellites
[NASA-RP-1331] 04 p1532 N94-19761
Ionospheric tomography using the FORTE satellite
[DE93-018545] 05 p1854 N94-19955
Global and regional comparative performance of linear and nonlinear satellite multichannel sea surface temperature algorithms
[AD-A270475] 05 p1837 N94-20028
The future of remote sensing from space: Civilian satellite systems and applications
[OTA-ISC-558] 05 p1837 N94-20209
Studies of Greenland using the SEASAT scatterometer 05 p1725 N94-20433
Interferometric detection of freeze-thaw displacements of Alaskan permafrost using ERS-1 data
05 p1732 N94-20460
Spatial and temporal variations of satellite microwave measurements of latent heat release in tropic cyclones due to environmental forcing obtained from a numerical model
[AD-A267947] 05 p1865 N94-20482
The analysis of global cloud and radiation data for the study of cloud-climate interactions
[NASA-CR-193388] 05 p1865 N94-20535
Comparison of satellite-derived velocity fields in the coastal transition zone
[AD-A272565] 05 p1883 N94-21360
Long-Term Monitoring of Global Climate Forcings and Feedbacks
[NASA-CP-3234] 05 p1868 N94-21639
Climsat rationale 05 p1869 N94-21643
Stratospheric Aerosol and Gas Experiment (SAGE 3)
05 p1869 N94-21644
Earth observing scanning polarimeter
05 p1844 N94-21645
Orbit and sampling requirements: TRMM experience
05 p1870 N94-21647
Satellite orbit and data sampling requirements
05 p1870 N94-21648
Urban applications of satellite remote sensing and GIS analysis
[PB93-202174] 05 p1842 N94-21855
Estimability of polar motion using range observations to satellites
[PB93-219319] 05 p1842 N94-22265
Proceedings of the Workshop on New Generation of Radiation Budget Measurements From Space and Their Use in Climate Modelling and Diagnostic Studies
[MPIM-90] 05 p1860 N94-22283
Satellite measurements of radiation budget parameters 05 p1860 N94-22284
ScaRaB and its subsystems 05 p1860 N94-22285
Use of satellite data for validation of the ECHAM models 05 p1861 N94-22289
Simulation of clear-sky outgoing longwave radiation over the oceans using operational analysis
05 p1861 N94-22290
Use of satellite data for validation of operational forecast models and operational analyses
05 p1861 N94-22291
Cloud fields derived from satellite and surface data during FIRE cirrus phase 2 05 p1872 N94-22302
Remote sensing of multilevel clouds during FIRE IFO 2 05 p1844 N94-22303
Comparison of cloud microphysical parameters derived from surface and satellite measurements during FIRE phase 2 05 p1873 N94-22306
CIMSS FIRE research activities
05 p1873 N94-22307
Automated cloud classification with a fuzzy logic expert system 05 p1875 N94-22313
The AGRHYMET data communications project
06 p2280 N94-22776
Land mobile satellite propagation measurements in Japan using ETS-V satellite 06 p2282 N94-22790
SeaWiFS technical report series. Volume 9: The simulated SeaWiFS data set, version 1
[NASA-TM-104566-VOL-9] 06 p2417 N94-23291
Atmospheric moisture fields derived by satellite observations over the tropical Pacific Ocean
[NASA-CR-194852] 06 p2408 N94-23542
Evaluating NOAA satellite products for global climate monitoring 06 p2384 N94-23604
Validating a large geophysical data set: Experiences with satellite-derived cloud parameters
06 p2385 N94-23615
Experience of the JPL Exploratory Data Analysis Team at validating HIRS2/MSU cloud parameters
06 p2385 N94-23616
An overview of the UARS data validation effort
06 p2386 N94-23617
SPOT4 Operational Control Center (CMP)
06 p2197 N94-23856
AGENDA: A task organizer and scheduler
06 p2504 N94-23876
The effect of sub-surface volume scattering on the accuracy of ice-sheet altimeter retracking algorithms
[NASA-CR-194825] 06 p2386 N94-24060
Factors affecting the identification of phytoplankton groups by means of remote sensing
[NASA-TM-108799] 06 p2387 N94-24403
Further studies to extend and test the area-time-integral technique applied to satellite data
[NASA-CR-195132] 06 p2415 N94-24705
Optimal gains for a single polar orbiting satellite
06 p2208 N94-24873
High temperature superconducting infrared imaging satellite 07 p2698 N94-25700
Digital filter design for sensor simulation: Application to the Brazilian remote sensing satellite
[INPE-5523-RPQ/665] 07 p2849 N94-26827

A preliminary method for atmospheric soundings in real time using satellite and ground-based remotely sensed data
[AD-A274381] 07 p2880 N94-26828
Nimbus-7 Earth radiation budget calibration history. Part 2: The Earth flux channels
[NASA-RP-1335-PT-2] 07 p2814 N94-27981
MODIS airborne simulator visible and near-infrared calibration, 1991 FIRE-Cirrus field experiment. Calibration version: FIRE King 1.1
[NASA-TM-104600] 07 p2897 N94-28182
Asia-Pacific Seminar on Global Change Research Cooperation
[JTN-94-80517] 07 p2871 N94-28268
Role and activity of STA on Asian Pacific regional cooperation 07 p2853 N94-28269
Cooperative research projects on satellite remote sensing for the hydrological subjects 07 p2853 N94-28270
Research activities on the meteorology over the Asia-Pacific region 07 p2853 N94-28271
NASDA contribution plan to Asian countries 07 p2853 N94-28273
Thailand satellite ground receiving station in global change research cooperation 07 p2875 N94-28291
Utilization of remote sensing data for global change research 07 p2875 N94-28292
Contribution of satellite observation to global change research 07 p2876 N94-28293
Lead detection and mapping with reference to relationships between scale, sensor characteristics, surface conditions and atmospheric properties
[AD-A275321] 08 p3377 N94-28877
Proceedings of the International Symposium on Remote Sensing
[JTN-94-80578] 08 p3325 N94-28925
Keynote address --- Japanese Earth Resources Satellite 1 (JERS-1) and future remote sensing projects 08 p3326 N94-28926
Synthetic aperture radar applications: Now and in the future 08 p3260 N94-28927
Research trends on remote sensing at research facilities in Japan: The priority area programme on better understanding of earth environment via satellite 08 p3326 N94-28928
Evaluation of simulated JERS-1 data for geologic mapping at Drum Mountains, Utah, Silver Bell, Arizona, and Wind River, Wyoming under the GEOSAT-ERSDAC/JAPEX/JGI/RESTEC joint studies 08 p3326 N94-28929
JERS-1 data acquisition and distribution 08 p3326 N94-28931
Observations by ERS-1 start 08 p3327 N94-28933
Sea ice and oceans applications of SAR 08 p3327 N94-28934
Amazonia: Remote sensing test site and survey 08 p3327 N94-28935
Utilization of remote sensing data in Southeast Asia 08 p3327 N94-28936
Remote sensing and global management 08 p3328 N94-28937
Proceedings of the 15th Earth Observation Symposium
[JTN-94-80607] 08 p3328 N94-29036
Principles and application tendency of remote sensing: Its principle, function and utilization 08 p3328 N94-29037
Status and tendency of earth observation system 08 p3328 N94-29038
Perspectives of earth observing techniques: Expectation of earth observation in space development history 08 p3328 N94-29039
Oceanic survey utilizing satellites 08 p3328 N94-29040
Tohoku district observed by artificial satellites 08 p3328 N94-29041
Antarctic Record, volume 36, no. 1
[REPT-106-VOL-36-NO-1] 08 p3357 N94-29078
Activities of the wintering party at Showa Station by the 31st Japanese Antarctic Research Expedition in 1990 08 p3358 N94-29083
Conceptual radiometer design studies for Earth observations from low Earth orbit
[NASA-CR-4588] 08 p3329 N94-29098
Role of satellite observations of sea-surface temperature in the detection of global change
[PB94-138120] 08 p3329 N94-29107
Proceedings of the 3rd International Symposium: JERS-1 and Remote Sensing in the Future
[JTN-94-80597] 08 p3329 N94-29217
Remote sensing and the Earth 08 p3329 N94-29218
A new information system: Satellite observation 08 p3330 N94-29219
Outline of JERS-1 system 08 p3330 N94-29220
Application of JERS-1 data to geologic analyses 08 p3330 N94-29222
Application of optical sensor data to resource survey 08 p3330 N94-29223
Radar applications at the Canada Centre for Remote Sensing 08 p3331 N94-29224
Application of remote sensing techniques in petroleum exploration: The Indonesian experience 08 p3331 N94-29225
EOS project and ASTER (ITIR) 08 p3331 N94-29226
Earth-observation plan in Europe 08 p3331 N94-29227
Rock identification using thermal infrared data 08 p3331 N94-29228
JERS-1 and future remote sensing: Application of remote sensing data to agroecological problems 08 p3331 N94-29229
Application of remote sensing in prevention of disasters 08 p3332 N94-29230
Future expectation of remote sensing technology 08 p3332 N94-29231
Japan's Earth observation satellite programs 08 p3332 N94-29232
On the relation between SMMR 37-GHz polarization difference and the rainfall over Africa and Australia
[NASA-TM-104598] 08 p3370 N94-29408
A simulation study of high degree and order geopotential determination using satellite gravity gradiometry 08 p3333 N94-29762
Satellite estimation of the global distribution and interannual variability of photosynthetically active radiation 08 p3334 N94-29970
Estimation of transmittance from satellite imagery 08 p3257 N94-30500
Altimeter data processing from sea surface topography to horizontal eddy momentum fluxes
[PB94-147550] 08 p3378 N94-30714
FAME: A Forest Assessment and Monitoring Environment scenario
[AD-B179106] 08 p3335 N94-30759
Atmospheric moisture fields derived by satellite observations over the tropical Pacific Ocean 08 p3375 N94-30863
Multitemporal analysis of a braiding river: The advanced study of 1992
[NLR-TP-93100-U] 08 p3335 N94-30942
Subtropical Climates and Their Evolution: From Space-Based Observation to Modelling
[ISBN-2-85-428333-3] 09 p3776 N94-30981
Space equipment for Earth observations 09 p3613 N94-30997
The use of meteorological satellite data for studying tropical atmospheric phenomena 09 p3779 N94-31000
The surface parameters: Remote sensing observations and climatology applications 09 p3779 N94-31001
Desert aerosols: Sources, transports, and impacts determined by remote sensing 09 p3770 N94-31003
Airborne instruments 09 p3757 N94-31006
Development of a statistical method for estimating the downward longwave radiation at the surface from satellite observations 09 p3742 N94-31553
Imaging devices for satellite remote sensing
[VTT-TIED-1517] 09 p3743 N94-31658
Radar rainfall measurements from space 09 p3782 N94-31889
Sensitivity analysis of the AVHRR infrared cirrus model
[AD-A276690] 09 p3784 N94-32117
Remote sensing and the Mississippi high accuracy reference network 09 p3758 N94-32466
Research and applications of a canopy reflectance model 09 p3747 N94-32492
From Optics to Radar, SPOT and ERS Applications
[ISBN-2-85428-345-7] 09 p3747 N94-32523
The complementary nature of the SPOT and ERS-1 systems and their place in major international programmes 09 p3748 N94-32524
From optics to radar: Environmental problems and the SPOT/ERS systems 09 p3748 N94-32525
Feasibility in the use of satellite remote sensing data as a fast reaction tool for natural disaster relief 09 p3748 N94-32526
Contribution of SAR ERS1 data to study the French Guiana tropical coast environment
[BRGM-93034] 09 p3748 N94-32527
Monitoring land cover and crop types in Denmark using ERS-1 SAR and optical satellite images 09 p3748 N94-32528
Optics and radar: Cohabitation, rivality or happy marriage. Towards new planning tools 09 p3748 N94-32529
The contribution of satellite data in communication infrastructure projects 09 p3749 N94-32530
The use of ERS images for mapping 09 p3749 N94-32531
SPOT imagery for updating land cover information of 1:50,000 numerical topographic maps 09 p3749 N94-32532
Example of SPOT/ERS-1 complementarity 09 p3749 N94-32533
The use of SPOT, and the contribution of ERS-1, in the assessment of urban pressure on agriculture land in Greater Tunis (Tunisia) 09 p3749 N94-32534
Almaz marine applications 09 p3751 N94-32544
The use of SPOT and ERS-1 images to map the eruption of Nevado Sabancaya (Province of Arequipa, South Peru) and evaluate associated risks 09 p3751 N94-32546
A case study comparing multi-temporal ERS-1 SAR data and SPOT data for tropical forest mapping 09 p3753 N94-32556
Land cover change detection with ERS-1 data and data from other remote sensing satellites. Example: The delta of the River Ebro (Spain) 09 p3755 N94-32564
ERS-1 SAR and optical data for land use/land cover mapping: A case study in a savannah zone of Guinea 09 p3755 N94-32565
Statistical analysis and mapping of cotton and food crop cultivation surfaces in the west of Burkina Faso: Contribution of combined SPOT P and XS data 09 p3757 N94-32575
Parameterizing atmosphere-land surface exchange for climate models with satellite data: A case study for the Southern Great Plains CART site
[DE94-005109] 09 p3775 N94-32874
Evolution of upwelling fronts off the coast of Portugal
[NASA-CR-195692] 09 p3790 N94-33045
Stationary eddies in the Mars general circulation as simulated by the NASA-Ames GCM 09 p3944 N94-33192
TRMM-related research: Tropical rainfall and energy analysis experiment
[NASA-CR-195834] 09 p3787 N94-33288
MODIS. Volume 2: MODIS level 1 geolocation, characterization and calibration algorithm theoretical basis document, version 1
[NASA-TM-104594-VOL-2] 09 p3613 N94-33289
Arctic radiative fluxes modeled from the ISCCP-C2 data set, 1983 - 1986 10 p4084 N94-33369
Application of remote sensing and GIS techniques for environmental geologic investigation, Northeast Iowa 10 p4075 N94-33420
Comparison of standard multispectral and map-assisted classification methods with a new layered approach 10 p4075 N94-33422
Instrumentation on the RAIDS experiment 2: Extreme ultraviolet spectrometer, photometer, and near IR spectrometer
[AD-A278543] 10 p4085 N94-33676
Typhoon monitoring using passive satellite observations
[AD-A277859] 10 p4089 N94-33769
CDAW-9 analysis of magnetospheric events on 3 May 1986: Event C
[AD-A277610] 10 p4086 N94-33851
Error analysis of the step drag-free system with respect to gravity field determination
[PB94-149804] 10 p4076 N94-34115
SeaWiFS technical report series. Volume 17: Ocean color in the 21st century. A strategy for a 20-year time series
[NASA-TM-104566-VOL-17] 10 p4093 N94-34209
Looking at Earth from space: Direct readout from environmental satellites
[NASA-EP-300] 10 p4078 N94-34268
Detection and analysis of fog at night using GOES multispectral infrared imagery
[NOAA-TR-NESDIS-75] 10 p4143 N94-34913
A statistical inference approach for the retrieval of the atmospheric ozone profile from simulated satellite measurements of solar backscattered ultraviolet radiation 10 p4083 N94-35060
CATLAC: Calibration and validation analysis tool of local area coverage for the SeaWiFS mission
[NASA-TM-104603] 11 p4211 N94-35269
Production of long-term global water vapor and liquid water data set using ultra-fast methods to assimilate multi-satellite and radiosonde observations
[NASA-CR-196044] 11 p4292 N94-35355
The Mars Observer differential one-way range demonstration 11 p4210 N94-35543
Obtaining coincident image observations for Mission to Planet Earth science data return 11 p4202 N94-35609
Estimation with multisensor/multiscan detection fusion
[AD-A278753] 11 p4256 N94-36092

SeaWiFS technical report series. Volume 20: The SeaWiFS bio-optical archive and storage system (SeaBASS), part 1
[NASA-TM-104566-VOL-20-PT-1] 12 p4475 N94-36958

SATELLITE ORBIT CALCULATION
U ORBIT CALCULATION

SATELLITE ORBITS
NT GEOSYNCHRONOUS ORBITS
NT PARKING ORBITS
NT POLAR ORBITS
Satellite situation report, volume 32, no. 1
[NASA-TM-109233] 01 p0042 N94-10562
Satellite situation report, volume 32, no. 2
[NASA-TM-109234] 01 p0042 N94-10563
Satellite situation report, volume 31, no. 4
[NASA-TM-109232] 01 p0039 N94-10659
ERS-1 precise orbit determination 01 p0244 N94-11779
Orbital simulations of satellite escape/capture and the origin of satellites such as Triton 01 p0429 N94-12057
Regional orbit precision in the Mediterranean area 01 p0039 N94-12530
Orbit determination error analysis based on the requirements of ADEOS mission
[NASDA-CNT-930008] 02 p0532 N94-13644
Development of Japanese Earth Resources Satellite-1 (JERS-1; FUYO-1) and it's operational results
[NASDA-SPP-930001] 03 p0884 N94-15001
Satellite situation report, volume 33, no. 3
[NASA-TM-109278] 03 p0885 N94-15712
ERS-1: 18 months in orbit 03 p0990 N94-15888
On the delivery of planetesimals to a protoplanet in the solar nebula 03 p1245 N94-16379
Low Earth orbit constellations: Orbit control or not 03 p0875 N94-17134
Impact of launching uncertainties on the visibility of communication satellite constellations without orbit control 03 p0889 N94-17135
Delta launch vehicle: Accommodations for small satellites 03 p0878 N94-17139
CERISE microsatellite system 03 p0894 N94-17170
Satellite orbit and data sampling requirements 05 p1870 N94-21648
Estimability of polar motion using range observations to satellites
[PB93-219319] 05 p1842 N94-22265
The design and networking of dynamic satellite constellations for global mobile communication systems 06 p2288 N94-22826
Low earth orbit satellite/terrestrial mobile service compatibility 06 p2288 N94-22827
Improved thermal force modeling for GPS satellites 06 p2207 N94-23259
Real-time on-board orbit determination with DORIS 06 p2196 N94-23919
Low Earth orbit communications satellite 07 p2698 N94-25701
Modal control of a satellite in an unstable periodic orbit about the Earth-Sun interior Lagrange point
[AD-A273707] 07 p2694 N94-25776
Hill equations for satellite orbit determination
[ETN-94-95374] 07 p2690 N94-25787
A virtual environment for satellite modeling and orbital analysis in a distributed interactive simulation
[AD-A274114] 07 p2694 N94-25904
A GPS coverage model 07 p2642 N94-27292
TOPEX/POSEIDON operational orbit determination results using global positioning satellites 08 p3160 N94-29666
Application of extended Lagrange series to the precise determination of Global Positioning Satellite orbits
[ISBN-0-315-85724-2] 08 p3159 N94-30237
Towards 10(exp 9) GPS geodesy: Vector baselines, Earth rotation and reference frames
[NASA-CR-195768] 08 p3142 N94-30243
Multisatellite constellation configuration selection for multiregional highly elliptical orbit constellations 09 p3600 N94-31437
Possible improvements of satellite ephemeris programs used in geodesy
[PB94-148681] 09 p3743 N94-31592
General-relativistic celestial mechanics. 4: Theory of satellite motion
[PB94-147782] 09 p3601 N94-31769
Testing for preferred-frame effects in gravity with artificial Earth satellites
[PB94-148459] 09 p3610 N94-31771
Semianalytic Satellite Theory (SST): Mathematical algorithms
[AD-A276836] 09 p3610 N94-32208
High degree gravitational sensitivity from Mars orbiters for the GMM-1 gravity model
[NASA-TM-104604] 10 p4088 N94-34992
Evaluation of semiempirical atmospheric density models for orbit determination applications 11 p4208 N94-35636
Filter parameter tuning analysis for operational orbit determination support 11 p4208 N94-35637
The Earth Satellite Program (ESP), version 2.0
[AD-A278860] 11 p4201 N94-35827

SATELLITE ORIENTATION
Estimation of the attitude motion of the small satellite ORIZURU
[NAL-TR-1145] 01 p0042 N94-10366
Self-tuning control techniques for multivariable systems
[INPE-5449-TDI/495] 02 p0765 N94-14084
ETALON-1,-2 center of mass correction and array reflectivity 03 p0915 N94-15576
Method of orienting a synchronous satellite
[CA-PATENT-1,305,772] 05 p1658 N94-21041
Momentum management and torque distribution 06 p2159 N94-24272
Satellite attitude determination using linear combination of models
[AD-A274082] 07 p2694 N94-25996
Towards 10(exp 9) GPS geodesy: Vector baselines, Earth rotation and reference frames
[NASA-CR-195768] 08 p3142 N94-30243
Time transfer using geostationary satellites: Implementation of a Kalman filter 08 p3471 N94-30657
The ALEXIS mission recovery
[DE94-007549] 09 p3611 N94-32813
Performance analysis of an integrated GPS/inertial attitude determination system
[NASA-CR-188289] 09 p3577 N94-32864
Resonance capture in unbalanced dual-spin spacecraft
[AD-A278501] 10 p4015 N94-34292
Propagating orientation constraints for the Hubble Space Telescope 10 p4123 N94-35049
Flight Mechanics/Estimation Theory Symposium, 1994
[NASA-CP-3265] 11 p4202 N94-35605
Fixed-head star tracker attitude updates on the Hubble Space Telescope 11 p4203 N94-35612
Comparison of Kalman filter and optimal smoother estimates of spacecraft attitude 11 p4208 N94-35638
Application of star identification using pattern matching to space ground systems at GSFC 11 p4209 N94-35640
Advantages of estimating rate corrections during dynamic propagation of spacecraft rates: Applications to real-time attitude determination of SAMPEX 11 p4209 N94-35642
MME-based attitude dynamics identification and estimation for SAMPEX 11 p4209 N94-35643
A new algorithm for attitude-independent magnetometer calibration 11 p4209 N94-35644
A simple suboptimal least-squares algorithm for attitude determination with multiple sensors 11 p4210 N94-35645
Motion models in attitude estimation 11 p4210 N94-35646

SATELLITE PERTURBATION
SeaWiFS technical report series. Volume 11: Analysis of selected orbit propagation models for the SeaWiFS mission
[NASA-TM-104566-VOL-11] 06 p2417 N94-23338
Numerical simulation of Ulysses nutation 06 p2207 N94-24017
Spacecraft vibrations due to mechanisms; measurements from Olympus on-station 06 p2207 N94-24018
The influence of appendage vibration on the attitude dynamics of a dual-spin satellite 08 p3168 N94-29828
Application of extended Lagrange series to the precise determination of Global Positioning Satellite orbits
[ISBN-0-315-85724-2] 08 p3159 N94-30237
Semianalytic Satellite Theory (SST): Mathematical algorithms
[AD-A276836] 09 p3610 N94-32208

SATELLITE POWER TRANSMISSION
Space transportation alternatives for large space programs: The International Space University Summer Session, 1992
[NASA-TM-106271] 01 p0040 N94-10811
Construction and testing of a space ready rectenna
[NASA-CR-193310] 01 p0137 N94-11357
Small scale adaptive optics experiment systems engineering
[NASA-CR-194419] 02 p0793 N94-14548
Power transmission by laser beam from lunar-synchronous satellite
[NASA-TM-4496] 05 p1669 N94-20102
Method for remotely powering a device such as a lunar rover
[NASA-CASE-LAR-14789-1] 05 p1824 N94-20587
WISPER: Wirless Space Power Experiment
[NASA-CR-195538] 06 p2396 N94-24701
Iowa satellite project ISAT-1
[NASA-CR-195517] 06 p2206 N94-24838
Reactor-pumped laser facility at DOE's Nevada Test Site
[DE94-006371] 08 p3295 N94-30265

SATELLITE RENDEZVOUS
U ORBITAL RENDEZVOUS

SATELLITE REPAIR
U ORBITAL SERVICING

SATELLITE ROTATION
Momentum management and torque distribution 06 p2159 N94-24272
The Solar Anomalous and Magnetospheric Particle Explorer (SAMPEX) yo-yo despin and solar array deployment mechanism 08 p3163 N94-29645
Attitude stability of a spinning spacecraft during appendage deployment/retraction 11 p4208 N94-35639
Advantages of estimating rate corrections during dynamic propagation of spacecraft rates: Applications to real-time attitude determination of SAMPEX 11 p4209 N94-35642
MME-based attitude dynamics identification and estimation for SAMPEX 11 p4209 N94-35643
A simple suboptimal least-squares algorithm for attitude determination with multiple sensors 11 p4210 N94-35645
Motion models in attitude estimation 11 p4210 N94-35646

SATELLITE SOLAR ENERGY CONVERSION
A direct current rectification scheme for microwave space power conversion using traveling wave electron acceleration 07 p2687 N94-27371

SATELLITE SOLAR POWER STATIONS
Space transportation alternatives for large space programs: The International Space University Summer Session, 1992
[NASA-TM-106271] 01 p0040 N94-10811

SATELLITE SOUNDING
Space Activities in the Asia Pacific Region
[JTN-93-80421] 01 p0035 N94-10676
Panel discussion: Role of space program in the Asia Pacific Region 01 p0037 N94-10694
TOVS soundings: Impact on the synoptic analysis over the south and southeast regions of Brazil from March 18 to March 19, 1991
[INPE-5497-TDI/512] 01 p0230 N94-11179
Satellite observation of atmospheric tracer components: JEM/POP 01 p0130 N94-11836
Submillimeter wave observation experiment of Earth atmosphere with SIS mixer 01 p0130 N94-11837
Effects of satellite spectral resolution and atmospheric water vapor on retrieval of near-ground temperatures
[AD-A264920] 01 p0245 N94-11851
The extraction of bottom characteristics and mapping in Kin Bay, Okinawa Main Island, Japan, using LANDSAT-5/TM and SPOT-1/HRV data 01 p0197 N94-11931
The application of VAS satellite imagery to thunderstorm forecasting at Cape Canaveral
[NASA-CR-193563] 02 p0718 N94-12839
EOS Laser Atmosphere Wind Sounder (LAWS) investigation
[NASA-CR-193445] 03 p1109 N94-17525
Verification of 3I retrievals vis-a-vis radiosonde observations
[KNMI-TR-150] 04 p1488 N94-17924
Some potential errors in satellite wind estimates using the geostrophic approximation and the thermal wind
[AD-A269784] 04 p1491 N94-18599
Remote sensing of multilevel clouds during FIRE IFO 2 05 p1844 N94-22303
Comparison of cloud microphysical parameters derived from surface and satellite measurements during FIRE phase 2 05 p1873 N94-22306
Atmospheric parameterization schemes for satellite cloud property retrieval during FIRE IFO 2 05 p1874 N94-22312
Atmospheric moisture fields derived by satellite observations over the tropical Pacific Ocean
[NASA-CR-194852] 06 p2408 N94-23542
Uncertainties in climate data sets
[NASA-CR-194848] 06 p2408 N94-23577
TOVS Pathfinder product validation and intercomparison 06 p2384 N94-23603
Experience of the JPL Exploratory Data Analysis Team at validating HIRS2/MSU cloud parameters 06 p2385 N94-23616
Convective organization in the Pacific ITCZ: Merging OLR, TOVS, and SSM/I information
[NASA-CR-194850] 06 p2408 N94-23619

Cloud-free aerosol optical depth determination over oceans from satellite radiometry
[DE94-001897] 06 p2386 N94-23779
Implementation of a state of the art automated system for the production of cloud/water vapor motion winds from geostationary satellites
[NASA-CR-195087] 06 p2410 N94-24125
Objective analysis of a coastal ocean eddy using satellite AVHRR and in situ hydrographic data
[AD-A275715] 08 p3376 N94-28642
Far ultraviolet images of the nighttime ionosphere
[AD-A275083] 08 p3356 N94-28843
Proceedings of the 15th Earth Observation Symposium
[JTN-94-80607] 08 p3328 N94-29036
Principles and application tendency of remote sensing: Its principle, function and utilization 08 p3328 N94-29037
Status and tendency of earth observation system 08 p3328 N94-29038
The use of meteorological satellite data for studying tropical atmospheric phenomena 09 p3779 N94-31000
Development of a statistical method for estimating the downward longwave radiation at the surface from satellite observations 09 p3742 N94-31553
Production of long-term global water vapor and liquid water data set using ultra-fast methods to assimilate multi-satellite and radiosonde observations
[NASA-CR-195981] 11 p4293 N94-35499

SATELLITE SURFACES
NT LUNAR SURFACE
Physical studies of planetary and satellite surfaces
[NASA-CR-193545] 01 p0434 N94-10817
A structural origin for the cantaloupe terrain of Triton 01 p0449 N94-12095
Sources of Na for the Io atmosphere 01 p0455 N94-12127
Interdisciplinary scientist participation in the Phobos mission
[NASA-CR-193715] 01 p0482 N94-12446
Crustal structure and igneous processes in a chondritic Io 03 p1243 N94-16292
The rheology and composition of cryovolcanic flows on icy satellites 03 p1243 N94-16294
The spectrum of Phobos from Phobos 2 observations at 0.3-2.6 microns: Comparison to previous data and meteorite analogs 03 p1295 N94-16429
Diapirs and cantaloupes: Layering and overturn of Triton's crust 05 p2111 N94-20738
Geology of Galileo Regio quadrangle, Ganymede 05 p2130 N94-20842
Results from LDEF experiment A0114: The interaction of atomic oxygen with materials surfaces at orbital altitudes
[NASA-CR-196016] 11 p4235 N94-35388

SATELLITE TRACKING
NT SATELLITE-TO-SATELLITE TRACKING
Toward 10(exp 9) GPS geodesy: Vector baselines, Earth rotation and reference frames
[NASA-CR-193184] 01 p0229 N94-10702
Operational ERS-1 orbit determination at D-PAF 01 p0243 N94-11774
ERS-1 precise orbit determination 01 p0244 N94-11779
Regional orbit precision in the Mediterranean area 01 p0039 N94-12530
NASA images 8
[NASA-TM-109416] 02 p0544 N94-14783
Development of Japanese Earth Resources Satellite-1 (JERS-1; FUYO-1) and it's operational results
[NASDA-SPP-930001] 03 p0884 N94-15001
Eighth International Workshop on Laser Ranging Instrumentation
[NASA-CP-3214] 03 p0911 N94-15552
Laser ranging network performance and routine orbit determination at D-PAF 03 p0911 N94-15554
Satellite signatures in SLR observations 03 p0912 N94-15557
Work at Graz on satellite signatures 03 p0898 N94-15558
The precision of today's satellite laser ranging systems 03 p0912 N94-15559
SLR data screening; location of peak of data distribution 03 p0912 N94-15560
Adaptive median filtering for preprocessing of time series measurements 03 p0912 N94-15561
SATCOP mission planning software package 03 p0912 N94-15562
Preliminary results from the portable standard satellite laser ranging intercomparison with MOBLAS-7 03 p0913 N94-15568
Tracking capabilities of SPADs for laser ranging 03 p0914 N94-15570
Streak camera based SLR receiver for two color atmospheric measurements 03 p0914 N94-15573
The first satellite laser echoes recorded on the streak camera 03 p0914 N94-15574
ETALON-1,-2 center of mass correction and array reflectivity 03 p0915 N94-15576
Test results from LAGEOS-2 optical characterization using pulsed lasers 03 p0915 N94-15577
Analysis of TOPEX laser retroreflector array characteristics 03 p0915 N94-15578
Two color satellite laser ranging upgrades at Goddard's 1.2m telescope facility 03 p0915 N94-15581
Measuring atmospheric dispersion with WLRS in multiple wavelength mode 03 p0916 N94-15582
Two wavelength satellite laser ranging using SPAD 03 p0916 N94-15584
New perspectives for high accuracy SLR with second generation geodesic satellites 03 p0916 N94-15585
State-of-the-art satellite laser range modeling for geodetic and oceanographic applications 03 p0916 N94-15586
Geometric analysis of satellite laser ranging data 03 p0917 N94-15587
Improvement of SLR accuracy, a possible new step 03 p0917 N94-15588
On the accuracy of ERS-1 orbit predictions 03 p0874 N94-15589
Compensation for the distortion in satellite laser range predictions due to varying pulse travel times 03 p0917 N94-15590
Timebias corrections to predictions 03 p0875 N94-15591
Formation of on-site normal points 03 p0917 N94-15592
Poisson filtering of laser ranging data 03 p0917 N94-15593
Computer networking at SLR stations 03 p0917 N94-15594
HP upgrade operational streamlining 03 p0918 N94-15596
Application of the robust estimate in SLR data preprocessing 03 p0918 N94-15597
A computer-controlled x-y offset guiding stage for the MLRS 03 p0918 N94-15598
Lunar laser ranging data processing in a Unix/X windows environment 03 p0918 N94-15599
LLR: Activities in Wettzell 03 p0876 N94-15600
Upgrading of the Borowiec laser station 03 p0877 N94-15604
Development of Shanghai satellite laser ranging station 03 p0877 N94-15605
WLRS --- Wettzell Laser Ranging System (WLRS) 03 p0877 N94-15606
Ground based laser ranging for satellite location 03 p0919 N94-15607
New progress of ranging technology at Wuhan Satellite Laser Ranging Station 03 p0877 N94-15608
Results of the MTLRS-1 upgrade 03 p0877 N94-15610
The new MTLRS-1 receiving system 03 p0877 N94-15611
The new MTLRS transmitting system 03 p0877 N94-15612
Transputer based control system for MTLRS 03 p0877 N94-15613
Optical attenuation mechanism upgrades, MOBLAS, and TLRS systems 03 p0922 N94-15622
Station report on the Goddard Space Flight Center (GSFC) 1.2 meter telescope facility 03 p0922 N94-15625
Satellite control: A comprehensive approach 03 p0878 N94-17158
CONTACT: An Air Force technical report on military satellite control technology
[AD-A269375] 04 p1334 N94-18408
Parallelization of the Air Force Space Command (AFSPACECOM) satellite motion models
[AD-A269327] 04 p1334 N94-18470
Downlink acquisition and tracking procedures for the ASCAMP satellite communications terminal
[AD-A272912] 05 p1739 N94-21244
Mathematician Wang Ju
[AD-A267882] 05 p1912 N94-21255
Enhanced networks operations using the X Window System 05 p1932 N94-21329
K- and Ka-band mobile-vehicular satellite-tracking reflector antenna system for the NASA ACTS mobile terminal 06 p2289 N94-22831
Microstrip monopulse antenna for land mobile communications 06 p2289 N94-22833
Aeronautical satellite antenna steering using magnetic field sensors 06 p2289 N94-22836
The Telecommunications and Data Acquisition Report
[NASA-CR-194766] 06 p2290 N94-23256
A review of GPS-based tracking techniques for TDRS orbit determination 06 p2196 N94-23257
New approaches for tracking earth orbiters using modified GPS ground receivers 06 p2196 N94-23258
Beam-waveguide antenna servo design issues for tracking low earth-orbiting satellites 06 p2292 N94-23268
Ground data system for Space Flyer Unit (SFU) 06 p2207 N94-23860
Radioastron flight operations 06 p2502 N94-23861
Navigation of space VLBI missions: Radioastron and VSOP 06 p2513 N94-23926
Worldwide vessel locating and tracking system, volume 1
[PB93-193217] 06 p2175 N94-24474
The velocity field in the Northeast Atlantic from satellite-tracked drifting buoys
[AD-A275704] 08 p3376 N94-28690
Towards 10(exp 9) GPS geodesy: Vector baselines, Earth rotation and reference frames
[NASA-CR-195768] 08 p3142 N94-30243
A comparison of GPS broadcast and DMA precise ephemerides 08 p3145 N94-30660
Air Force Space Command satellite orbit predictor using parallel virtual machines
[AD-A276316] 09 p3601 N94-31298
Compression of a radar track of a near Earth satellite into an Earth centered inertial state vector using least squares differential correction
[AD-A278498] 10 p4037 N94-34302
CATLAC: Calibration and validation analysis tool of local area coverage for the SeaWiFS mission
[NASA-TM-104603] 11 p4211 N94-35269
Flight Mechanics/Estimation Theory Symposium, 1994
[NASA-CP-3265] 11 p4202 N94-35605
Improved solution accuracy for TDRSS-based TOPEX/Poseidon orbit determination 11 p4205 N94-35620
A genetic algorithm approach to automating satellite range scheduling
[AD-A278577] 11 p4226 N94-36188
Design and analysis of a mode B and mode JD satellite Earth station
[AD-A280417] 12 p4391 N94-37225

SATELLITE TRACKING AND DATA ACQ NETWORK
U STDN (NETWORK)

SATELLITE TRANSMISSION
The developments of satellite communications of China 02 p0618 N94-14282
The current situation, trends, international cooperation of space communication technological development in the Republic of Korea 02 p0699 N94-14283
Joint experiments using ETS-5 02 p0618 N94-14284
Space communications technology research in CRL 02 p0618 N94-14285
NTT's activities in satellite communications technology development 02 p0618 N94-14286
Future outlook on international satellite communications in Asia Pacific region 02 p0618 N94-14287
Technological development for broadcasting satellites in NHK Laboratories 02 p0618 N94-14288
Effects of the equatorial ionosphere on L-band Earth-space transmissions 02 p0615 N94-14671
Almaz 03 p0898 N94-15889
BRIDGE: A small scientific satellite for geodesy 03 p0890 N94-17146
NHK Science and Technical Research Laboratories 05 p2151 N94-20342
Advanced coding and modulation schemes for TDRSS 05 p1744 N94-21350
Network command processing system overview 05 p1935 N94-21351
Comparison of theoretical and simulated performance results for sloppy-slotted Aloha signaling 05 p1746 N94-22204
Design and implementation considerations of a MSAT packet data network 06 p2280 N94-22778
The ORBCOMM data communications system 06 p2281 N94-22782
The Iridium (tm) system: Personal communications anytime, anyplace 06 p2281 N94-22785
K-band mobile propagation measurements using ACTS 06 p2283 N94-22792
Measurement of multipath delay profile in land mobile satellite channels 06 p2283 N94-22793
A study of satellite motion-induced multipath phenomena 06 p2283 N94-22794
Electromagnetic field strength prediction in an urban environment: A useful tool for the planning of LMSS 06 p2283 N94-22795
Iowa satellite project ISAT-1
[NASA-CR-195517] 06 p2206 N94-24838
A new information system: Satellite observation 08 p3330 N94-29219

Data transfer system using a multi-ID ARGOS transmitter for the Antarctic polar patrol balloon experiment
08 p3363 N94-29980

SATELLITE-BORNE INSTRUMENTS
NT ADVANCED VERY HIGH RESOLUTION RADIOMETER
NT TOTAL OZONE MAPPING SPECTROMETER
Imaging of magnetospheric dynamics using low energy neutral atom detection
[DE93-012656] 01 p0275 N94-10742
Calibration and validation of the ERS-1 wind scatterometer 01 p0232 N94-11706
A preliminary C-band scatterometer model function for the ERS-1 AMI instrument 01 p0233 N94-11715
Calibration of ERS-1 altimetry over the North Sea
01 p0234 N94-11716
Preliminary results of the experiment I-7
01 p0235 N94-11728
The ERS-1/CV 580 SAR cross-calibration experiment: Sault Ste Marie, October 26 - November 2, 1991
01 p0236 N94-11729
Calibration results for the ERS-1, AIRSAR, and PHARS 01 p0236 N94-11731
An experiment for the radiometric calibration of the ERS-1 SAR 01 p0236 N94-11733
NASA airborne satellite instrumentation calibrator (NASIC) technical reference
[NASA-RP-1315] 02 p0545 N94-13713
Methods for calibration/validation of AVNIR
02 p0689 N94-14216
IMG: Interferometric monitor for greenhouse gases
02 p0689 N94-14217
Spectroscopic method and data reduction algorithm for laser long-path absorption measurements using RIS
02 p0689 N94-14218
Overview of the ILAS operational data processing system 02 p0690 N94-14220
Multiparameter airborne rain radar development for TRMM validation and TRMM-follow-on study
02 p0690 N94-14226
Wavefront sensing, control, and pointing
02 p0546 N94-14833
The XMM pn-CCD detector system: First results
03 p0900 N94-15034
Prospects for high pressure imaging gas scintillation drift chambers 03 p0901 N94-15040
Development of an ultra violet auroral imager for the Freja project 03 p0904 N94-15060
The high pressure gas scintillation proportional counter for SAX 03 p0906 N94-15076
A new detector concept for energetic auroral x ray imaging 03 p0907 N94-15081
The laboratory performance of the short wavelength instrument for the Along Track Scanning Radiometer ATSR-2 (initial results) 03 p0908 N94-15088
ENVISAT ASAR 03 p0898 N94-15892
Transparent conductive coatings in the far ultraviolet
[NASA-CR-194632] 03 p1191 N94-16024
Strategy for a small satellite program and a proposal for a first mission 03 p0874 N94-17143
Cosmic dust and space debris measurements on board the small satellites HITEN and BREM-SAT
03 p0890 N94-17147
Environment tests for mini satellites
03 p0896 N94-17189
Atomic oxygen fluence detector for Bremsat: Scientific and technical description 05 p1663 N94-21396
Single event phenomena: Testing and prediction
05 p1763 N94-21696
Low power, CMOS digital autocorrelator spectrometer for spaceborne applications 05 p1666 N94-21733
ScaRaB and its subsystems 05 p1860 N94-22285
ASpect: A new spectrum and line analysis package for IRAF 05 p1926 N94-22485
The application of artificial intelligence to astronomical scheduling problems 05 p1949 N94-22492
Prospects for improved instrumentation on future solar space missions 06 p2624 N94-22843
The next Japanese solar satellite
06 p2625 N94-22846
Interferometer scan unit mechanism definition
06 p2358 N94-24012
CRRES high energy proton flux map
[AD-A274803] 07 p2878 N94-26338
Space equipment for Earth observations
09 p3613 N94-30997
Imaging devices for satellite remote sensing
[VTT-TIED-1517] 09 p3743 N94-31658
Development of POINTS as a planetology instrument
[NASA-CR-196026] 11 p4354 N94-35265
Theoretical and experimental studies relevant to interpretation of auroral emissions
[NASA-CR-196032] 11 p4376 N94-36421
Characterization of spacecraft and environmental disturbances on a SmallSat
[NASA-CR-194915] 12 p4396 N94-36990
NOAA polar satellite calibration: A system description
[NOAA-TR-NESDIS-77] 12 p4396 N94-37009

SATELLITE-BORNE PHOTOGRAPHY
Mangrove afforestation monitoring using remote sensing 02 p0695 N94-14260
JPRS report: Central Eurasia. Aviation and cosmonautics, no. 1, January 1993
[JPRS-UAC-93-007] 04 p1632 N94-19147
Far ultraviolet images of the nighttime ionosphere
[AD-A275083] 08 p3356 N94-28843
Lunar horizon glow and the Clementine mission
11 p4366 N94-35478

SATELLITE-BORNE RADAR
Utilisation of ERS-1 data for mapping of Antarctica
01 p0237 N94-11740
Monitoring of the Greenland Ice Sheet using ERS-1 synthetic aperture radar imagery
01 p0237 N94-11741
A calibration procedure for radiation budget radiometers and its influence on interpretation of measured values
[MITT-82] 02 p0651 N94-14149
An exact processing algorithm for wide beam spaceborne SAR data 02 p0689 N94-14213
High performance multi-mode radar altimeter for future spaceborne application 02 p0548 N94-14214
Almaz 03 p0898 N94-15889
Ocean mapping using satellite radar altimetry
[ETN-93-93470] 05 p1841 N94-21017

SATELLITE-TO-SATELLITE TRACKING
Pointing and tracking space mechanism for laser communication 09 p3606 N94-33310

SATURATED HYDROCARBONS
U ALKANES

SATURATION
Evaluation of a distributed catchment scale water balance model
[PAPER-93WR00398] 03 p1083 N94-16031

SATURATION (CHEMISTRY)
Probability of accessing the multiple saturated states in the resistive interchange instability
[DE94-000478] 07 p3044 N94-26694
Arterial oxygen saturation during +Gz acceleration by short-radius centrifuge 08 p3389 N94-28852

SATURN (PLANET)
Disk-resolved spectral characteristics of Saturn's medium-sized satellites 01 p0471 N94-12213
NASA images 12 --- Voyager encounters
[NASA-TM-109417] 03 p1247 N94-15511
Life and the solar system: The CRAF and Cassini missions
[NASA-TM-109422] 03 p1247 N94-15513
Science planning and sequencing for Cassini
06 p2504 N94-23871
The Jet Propulsion Laboratory space exploration: Past, present and future 06 p2153 N94-24242

SATURN ATMOSPHERE
Vertical structure models of the 1990 equatorial disturbance on Saturn 03 p1277 N94-16333
Detection of the 267 GHz J = 1-0 rotational transition of PH3 in Saturn with a new Fourier transform spectrometer
[NASA-CR-194364] 10 p4162 N94-34718

SATURN LAUNCH VEHICLES
NT SATURN 5 LAUNCH VEHICLES

SATURN RINGS
Voyager encounter highlights
[NASA-TM-109420] 03 p1246 N94-15239
Mass of Saturn's A ring 03 p1263 N94-16252
A study of Saturn's E-ring particles using the Voyager 1 plasma wave instrument
[NASA-CR-194694] 05 p2088 N94-20048

SATURN SATELLITES
NT TITAN
Disk-resolved spectral characteristics of Saturn's medium-sized satellites 01 p0471 N94-12213
Linear structures on the small inner satellites of Saturn 05 p2121 N94-20797

SATURN 5 LAUNCH VEHICLES
Technology test bed
[NASA-TM-109354] 04 p1322 N94-18953

SAUDI ARABIA
Martian crater degradation by eolian processes: Analogy with the Rio Cuarto Crater Field, Argentina
03 p1251 N94-16196
Scientific and technical information transfer: Promoting information acquisition in the Saudi Arabian industrial sector 08 p3532 N94-29803

SAVANNAHS
U GRASSLANDS

SAWTOOTH WAVEFORMS
LHCD (low hybrid current drive) experiment on the HT-6B tokamak
[DE93-613720] 06 p2555 N94-25331

SCALARS
The effect of a scalar boson coupled to neutrinos on the behavior of the tritium beta decay spectrum near the end point
[DE93-012655] 01 p0361 N94-10349
Bound states of the N-dimensional Klein-Gordon equation with vector and scalar Coulomb potentials
[DE93-617650] 01 p0349 N94-10547
A new approach to the I/N-expansion for the Dirac equation
[DE93-617647] 01 p0349 N94-10833
Exact solution of the N-dimensional generalized Dirac-Coulomb equation
[DE93-617649] 01 p0411 N94-10834
A theoretical kinematical study of the gradient of any cosmic scalar field
[DE92-644731] 01 p0425 N94-11136
PDF approach for turbulent scalar field: Some recent developments 01 p0160 N94-12315
Scalar curvature and spherical-type Riemannian manifolds
[DE93-622852] 02 p0767 N94-12895
A search for scalar leptoquarks in D0
[DE93-012780] 02 p0779 N94-12954
On a nonminimal gauge interaction of a scalar field in D=2+1 Chern-Simons-Maxwell theory
[DE93-621380] 02 p0621 N94-13224
Scalar limitations of diffractive optical elements
03 p1194 N94-17336
On a conformal perfect fluid in the classical vacuum
[DE93-624797] 04 p1480 N94-17682
Texture splats for 3D vector and scalar field visualization
[DE93-017104] 04 p1520 N94-18130
A transport equation for the scalar dissipation in reacting flows with variable density: First results
06 p2331 N94-24157
On kinetic expansion in scalar field theory
[DE93-634338] 07 p3072 N94-26553
Predictions of momentum and scalar fields in a jet in cross-flow using first and second order turbulence closures 07 p2803 N94-28025
Fields and potentials in general uniaxial bianisotropic media I. Axial sources
[PB94-132875] 07 p2778 N94-28379
Numerical modelling of turbine combustion chambers
08 p3154 N94-29254
Notes on the Langevin model for turbulent diffusion of marked particles
[DE94-007847] 09 p3708 N94-32652
Effective Lagrangian for gluons and Higgs pseudoscalars
[DE94-001381] 12 p4513 N94-36539

SCALE (CORROSION)
Effects of alloying and temperature on the high-temperature oxidation of Cr-Cr2Nb
[DE93-015800] 03 p0957 N94-16163

SCALE (RATIO)
Analytical framework for modeling scale-related variabilities in remote sensing 02 p0685 N94-13592

SCALE EFFECT
Planck scale effects on the Majoron
[DE93-613120] 01 p0410 N94-10545
An experimental investigation of attachment-line transition on the slat of a combat aircraft model
04 p1308 N94-18432
Multiple size scale structures in silica/siloxane composites studied by small-angle scattering
[DE94-007300] 09 p3625 N94-32642
Workshop on Scaling Effects in Composite Materials and Structures
[NASA-CP-3271] 12 p4457 N94-37796
Experimental observations of scale effects on bonded and bolted joints in composite structures
12 p4458 N94-37801
The effects of specimen scale on the compression strength of composite materials
12 p4459 N94-37802
On nature's scaling effects 12 p4459 N94-37803
Damage and strength of composite materials: Trends, predictions, and challenges 12 p4459 N94-37805
Scaling effects of defects in fiber-reinforced composites 12 p4459 N94-37807
Size effect in composite materials and structures: Basic concepts and design considerations
12 p4460 N94-37808
Statistical scaling relationships and size effects in the strength and creep rupture of fibrous composites
12 p4460 N94-37809

SCALE HEIGHT
Determining the solar-flare photospheric scale height from SMM gamma-ray measurements
[NASA-CR-194084] 02 p0844 N94-13671
The influence of orography on the transport of atmospheric constituents 06 p2619 N94-24886

Data analysis and interpretation of lunar dust exosphere 06 p2623 N94-25349

SCALE MODELS

An experimental investigation of high-speed water-entry for full-size and scale-model pointed nose vehicles [DE93-008491] 01 p0147 N94-10252

Application of normalized gray-scale correlation [DE93-013765] 01 p0141 N94-10521

Characterization of a scannerless LADAR system [DE93-011582] 01 p0174 N94-10959

A four-dimensional, mesoscale, non-gaussian multispectral smoke model. Phase 1: Feasibility study [AD-A264805] 01 p0152 N94-11519

Results of experimental investigations to determine external tank protuberance loads using a 0.03-scale model of the Space Shuttle launch configuration (model 47-OTS) in the NASA/ARC unitary plan wind tunnel, volume 1 [NASA-CR-167690] 02 p0534 N94-12810

Results of wind tunnel tests of an ASRM configured 0.03 scale Space Shuttle integrated vehicle model (47-OTS) in the AEDC 16-foot transonic wind tunnel, volume 2 [NASA-CR-185697] 02 p0534 N94-12965

Results of wind tunnel tests of an ASRM configured 0.03 scale Space Shuttle integrated vehicle model (47-OTS) in the AEDC 16-foot Transonic wind tunnel (IA613A), volume 1 [NASA-CR-185696] 02 p0534 N94-13191

Surfactant studies for bench-scale operation [NASA-CR-194511] 02 p0564 N94-13947

Results of experimental investigations to determine external tank protuberance loads using a 0.03-scale model of the Space Shuttle launch configuration (Model 47-OTS) in the NASA/ARC unitary plan wind tunnel, volume 2 [NASA-CR-167691] 02 p0536 N94-14047

Design and evaluation of single and dual flow thrust vector nozzles with post exit vanes [NASA-CR-193393] 02 p0638 N94-14086

Simulating the daylight performance of fenestration systems and spaces of arbitrary complexity: The IDC method [DE93-015177] 02 p0704 N94-14333

Effect of size, shape, and end condition of test specimen on compressive strength of high-strength concrete [DE93-500412] 02 p0682 N94-14653

Cruise noise measurements of a scale model advanced ducted propulsor [NASA-TM-105808] 03 p1176 N94-15115

Evaluation of a distributed catchment scale water balance model [PAPER-93WR00398] 03 p1083 N94-16031

A detailed model for simulation of catchment scale subsurface hydrologic processes [PAPER-92WR02333] 03 p1084 N94-16032

Scaling, soil moisture and evapotranspiration in runoff models 03 p1084 N94-16034

The application of nondestructive techniques to the testing of a wind turbine blade [DE93-016731] 04 p1447 N94-18128

A study of the use of half-models in high-lift wind-tunnel testing 04 p1308 N94-18434

Development and operation of the F/A-18 model control surface actuators [AD-A271330] 05 p1645 N94-19914

Structural similitude and design of scaled down laminated models [NASA-CR-194687] 05 p1673 N94-20172

Improved ceramic slip casting technique --- application to aircraft model fabrication [NASA-CASE-LAR-14471-1] 05 p1702 N94-20377

The roughness of the Martian surface: A scale dependent model 05 p2115 N94-20762

Extinguishment of enclosed gas fires with water sprays [PB93-201663] 06 p2268 N94-23430

Experimental investigation of advanced hub and pylon fairing configurations to reduce helicopter drag [NASA-TM-4540] 07 p2668 N94-26604

Catalytic fabric filtration for simultaneous NO(x) and particulate control [DE94-001660] 08 p3341 N94-28463

Bistatic clutter RCS simulation using scale model surfaces with two scale roughness [AD-A277604] 10 p4035 N94-33847

Conceptual design and analysis of a dynamic scale model of the Space Station Freedom [NASA-CR-4598] 10 p4070 N94-34236

Yaw control by tangential forebody blowing 10 p3992 N94-34615

Design of scaled down structural models 12 p4457 N94-37797

Sub-ply level scaling approach investigated for graphite-epoxy composite beam columns 12 p4458 N94-37798

Effects of scale in predicting global structural response 12 p4458 N94-37799

SCALERS

A miniaturized ASIC-based multichannel scaler instrument [DE94-007222] 09 p3807 N94-32783

SCALING LAWS

Dimensional scaling for impact cratering and perforation [NASA-CR-188259] 01 p0042 N94-10665

Helium transport scaling law studies [DE93-013487] 01 p0393 N94-11513

Power-law confusion: You say incremental, I say differential 01 p0347 N94-12175

Thermal gravitational modelling and scaling of two-phase heat transport systems: Similarity considerations and useful equations predictions versus experimental results [NLR-TP-91477-U] 02 p0632 N94-13533

Anomalous ion transport and feedback control [DE93-018324] 02 p0803 N94-14874

Swept shock/boundary-layer interactions: Scaling laws, flowfield structure, and experimental methods 03 p1017 N94-15197

The size of complex craters 03 p1262 N94-16249

Evolution of hadron beams under intrabeam scattering [DE93-014330] 03 p1184 N94-16826

Scaling laws for diffraction loading by air blast [PML-1991-54] 04 p1452 N94-17941

Analysis of the ITER H-mode confinement database [DE93-016984] 04 p1585 N94-18056

Scaling laws for diamond chemical vapor deposition. 2: Atomic hydrogen transport [AD-A269842] 04 p1371 N94-18740

Scaling laws for diamond chemical vapor deposition. Diamond surface chemistry [AD-A269874] 04 p1599 N94-18745

Centrifuge modeling of explosion-induced craters in unsaturated sand [AD-A270194] 04 p1417 N94-18780

Structural similitude and design of scaled down laminated models [NASA-CR-194687] 05 p1673 N94-20172

A fresh look at crater scaling laws for normal and oblique hypervelocity impacts 05 p1666 N94-20864

Verification of frequency scaling laws for capacitive rf discharges using two-dimensional simulations [DE94-001306] 05 p1999 N94-22595

Strong interactions studies with medium energy probes [DE94-001446] 06 p2540 N94-23791

Rime-, mixed- and glaze-ice evaluations of three scaling laws [NASA-TM-106461] 06 p2173 N94-24047

Hydrodynamics, acoustics and scaling of traveling bubble cavitation [AD-A273846] 07 p2789 N94-25605

Violation of Feynman scaling law in the forward region 07 p3113 N94-25633

Scaling of sustained ZT-40 M reversed field pinches [DE94-003318] 07 p3043 N94-26321

On the aging of sonic booms 07 p2650 N94-28194

Butterfly and scaling law in YBa2Cu4O8 [DE94-006037] 08 p3519 N94-30338

Experiments and theoretical considerations regarding the allowable roughness height in laminar flow [PB94-125556] 08 p3133 N94-30389

Scaling in heavy-fermion systems [DE94-005002] 08 p3492 N94-30775

Computer modelling of cyclic deformation of high-temperature materials [AD-A277056] 09 p3623 N94-32012

Electromagnetic wave reflection from irregular plasma layers [AD-A276727] 09 p3678 N94-32161

A simple model for determining photoelectron-generated radiation scaling laws [DE94-006130] 09 p3761 N94-32660

Analysis of Dietz's single, rectangular pulse theory for the generation of radiation via photoelectrons [DE94-006131] 09 p3681 N94-32661

Particle-In-Cell (PIC) code simulation results and comparison with theory scaling laws for photoelectron-generated radiation [DE94-006132] 09 p3695 N94-32662

Experimental studies of very-high Mach number hydrodynamics [AD-A278761] 11 p4263 N94-35492

Leptonic decay constants of heavy quarkonia in effective QCD sum rules [DE94-611160] 11 p4322 N94-35784

Scaling laws for TEXT plasma profiles [DE94-010832] 11 p4338 N94-36200

Nonlinearity with disorder: Spatio-temporal complex behavior arising from length scales competition [DE94-000675] 12 p4502 N94-36685

The role of heating and current drive in ITER [DE94-012679] 12 p4527 N94-37082

Isotope scaling and eta(i) mode with impurities in tokamak plasmas [DE94-012763] 12 p4529 N94-37361

Workshop on Scaling Effects in Composite Materials and Structures [NASA-CP-3271] 12 p4457 N94-37796

Design of scaled down structural models 12 p4457 N94-37797

Scaling, elasticity, and CLPT 12 p4458 N94-37800

Statistical scaling relationships and size effects in the strength and creep rupture of fibrous composites 12 p4460 N94-37809

Scaling of impact damage in fiber composites 12 p4460 N94-37810

Impact force as a scaling parameter 12 p4460 N94-37811

SCANDIUM

Crystallographic phase transitions in actinide metals as a function of pressure [DE93-040138] 05 p2011 N94-19827

SCANDIUM COMPOUNDS

NT SCANDIUM OXIDES

Non-fermi liquid and spin-glass behavior of the Sc(1-x)U(x)Pd3 system [DE93-040134] 05 p2016 N94-20335

NNN-Ising model simulation of nanodomain textures in relaxor-type lead scandium tantalate [DE94-601884] 07 p2748 N94-25844

Polar and chemical domain structures of lead scandium tantalate (PST) [DE94-600760] 07 p3056 N94-26363

Technical report of ISSP. Ser. A, no. 2670: Electronic structure of light transition metal compounds studied by photoemission [JTN-94-80556] 07 p3065 N94-27239

Study of the hyperfine magnetic field at Ta-181 site in the Heusler Co2ScSn, Co2ScGa, and Co2HfSn alloys [DE94-603989] 07 p3067 N94-27623

SCANDIUM OXIDES

Properties of E-beam interactive oxide films for nanometer scale structures [AD-A272848] 05 p1675 N94-21191

SCANNERS

NT COASTAL ZONE COLOR SCANNER
NT HORIZON SCANNERS
NT INFRARED SCANNERS
NT MULTISPECTRAL BAND SCANNERS
NT OCEAN COLOR SCANNER
NT OPTICAL SCANNERS
NT THEMATIC MAPPERS (LANDSAT)
NT ULTRASONIC SCANNERS

Calorimetric thermometry of meteoritic troilite: A feasibility study 01 p0428 N94-12025

Display system employing acousto-optic tunable filter [NASA-CASE-NPO-18736-1-CU] 03 p1190 N94-15933

Laser beam steering device 03 p1045 N94-17357

Environmental use of a Laser Range Finder and the Advanced Visualization System [DE93-016163] 03 p1043 N94-17677

Three dimensional ultrasonic imaging [DE93-040549] 05 p1968 N94-22003

Results of a laboratory experiment that tests rotating unbalanced-mass devices for scanning gimbaled payloads and free-flying spacecraft [NASA-TP-3458] 06 p2269 N94-23574

Interferometer scan unit mechanism definition 06 p2358 N94-24012

High precision double four bar linkage mechanism for interferometric linear scanning 06 p2359 N94-24013

Distributing functionality in the drift scan camera system [DE94-003640] 07 p2809 N94-25599

Color head down display program [AD-A274807] 07 p2672 N94-26340

The Hough transform algorithm for sea ice lead analysis: An evaluation [AD-A274535] 07 p2899 N94-26853

The development of an in-motion radiography system for large area aircraft scanning [DREP-TM-93-53] 07 p2670 N94-27666

Beam scanning offset Cassegrain reflector antennas by subreflector movement [NASA-CR-191604] 08 p3160 N94-28836

Suspension system for gimbal supported scanning payloads [NASA-CASE-MFS-28817-1] 08 p3287 N94-29358

MODIS technical report series. Volume 3: MODIS airborne simulator level 1B data user's guide [NASA-TM-104594-VOL-3] 08 p3231 N94-29385

Millimeter wave, high-resolution, holographic surveillance system [DE94-004289] 09 p3712 N94-31831

COVICS: A covert video communications system
[DE94-007568] 09 p3682 N94-32745
PSIDD: A Post-Scan Interactive Data Display system for ultrasonic scans
[NASA-TM-4545] 09 p3732 N94-33038
Rotating unbalanced mass proof-of-concept
[NASA-TM-109814] 10 p4141 N94-33720
Design and implementation of a beam-waveguide mirror control system for vernier pointing of the DSS-13 antenna 11 p4253 N94-35548
Overview of the MSTI 2 on-orbit alignment 11 p4206 N94-35629
A low temperature scanning force microscope for biological samples
[DE94-011357] 11 p4297 N94-36269
A new, optical-lever based atomic force microscope
[AD-A280524] 12 p4524 N94-37110
Poly(p-phenylene) derivatives new high performance nonlinear optical polymers
[AD-A280248] 12 p4422 N94-37121

SCANNING
NT CONICAL SCANNING
NT FREQUENCY SCANNING
NT RADAR SCANNING
NT RASTER SCANNING
Medical imaging
[NASA-TM-109675] 03 p1229 N94-15520
Feasibility study of a synthesis procedure for array feeds to improve radiation performance of large distorted reflector antennas
[NASA-CR-195167] 06 p2301 N94-25005
Unsteady wake structures in transverse jets 07 p2800 N94-28006
Three methods to improve the accuracy of a PUMA 560 robot 08 p3307 N94-30290
Standardisation requirements for ultrasonic C-scanning of polymer matrix composites: An initial assessment
[PB94-139318] 08 p3184 N94-30438
Sequencing items in multiple-item displays on online public access catalogs 10 p4150 N94-33419

SCANNING DEVICES
U SCANNERS

SCANNING ELECTRON MICROSCOPY
Fractography handbook of spaceflight metals
[NASA-RP-1291] 01 p0081 N94-10504
Measurement of the minority carrier diffusion length and edge surface-recombination velocity in InP 01 p0049 N94-11388
Atomic-scale imaging of surfaces and interfaces. Materials Research Society Symposium Proceedings, volume 295
[AD-A265674] 01 p0369 N94-12379
Crystallographic phase identification in the scanning electron microscope: Backscattered electron Kikuchi patterns
[DE93-011574] 02 p0804 N94-12813
Procedures for analysis of debris relative to Space Shuttle systems
[NASA-TM-109190] 02 p0534 N94-12900
High-resolution Z-contrast imaging and hole concentration mapping of YBCO thin films
[DE93-015803] 02 p0808 N94-13930
Room temperature degradation of YBa2Cu3O(7-x) superconductors in varying relative humidity environments
[NASA-TP-3368] 02 p0813 N94-14409
Application of Z-contrast imaging to obtain column-by-column spectroscopic analysis of materials
[DE93-015333] 03 p0947 N94-16014
Insights into semiconducting materials and growth phenomena through Z-contrast STEM
[DE93-015964] 03 p1212 N94-16841
UHV-stem studies on nucleation and growth of thin metal silicide films on silicon
[DE93-017604] 03 p1212 N94-16961
Applications of scanning tunneling microscopy to electrochemistry
[AD-A269129] 04 p1348 N94-18255
Thin film studies of the proximity Josephson effect
[AD-A270129] 04 p1600 N94-18876
Atomic resolution electron energy loss spectroscopy in the scanning transmission electron microscope
[DE93-015334] 04 p1352 N94-19239
Microtribology of magnetic media
[AD-A271209] 04 p1407 N94-19722
Asbestos characterization using scanning electron microscopy/light element x ray spectrometry
[AD-A271611] 05 p1681 N94-21241
The use of backscattered electron imaging mode to assess the effect of fine dispersions on development of superplastic microstructure in Al-Mg alloys
[AD-A272426] 05 p1691 N94-21258
Some experiments on using backscattered electron and energy dispersive x ray imaging in determination of portland cement clinker phase composition 05 p1708 N94-21893
A quantitative S.E.M. image analysis of cement paste microstructure 05 p1708 N94-21894
Influence of sintering atmospheres on the aluminum sintering characteristics
[DE93-632412] 06 p2239 N94-22965
Microstructural analysis of the 2195 aluminum-lithium alloy welds 06 p2251 N94-24448
LPCVD of InN on GaAs(110) using HN3 and TMIn: Comparison with Si(100) results
[AD-A273555] 06 p2235 N94-24917
Scanning probe surface modification
[AD-A273178] 06 p2346 N94-25151
Analysis of the effect on growth kinetics of gamma prima phase in Inconel 713C alloys
[DE93-633763] 07 p2735 N94-26294
Developments in crystallographic phase analysis in the SEM: Backscattered electron Kikuchi patterns
[DE93-040755] 07 p3057 N94-26420
The 27th Annual Meeting of the Israel Society for Microscopy and the 12th Annual Meeting of the Israel Society for Histochemistry and Cytochemistry
[DE93-632416] 07 p2716 N94-26519
Electron microscopy: Metal alloy x ray microanalysis
[REPT-932-600-101] 08 p3205 N94-29525
A sub-cm micromachined electron microscope 08 p3236 N94-29775
Atomic-scale structure and chemistry of interfaces by Z-contrast imaging and electron energy loss spectroscopy in the STEM
[DE94-006563] 08 p3516 N94-30064
Optimal detector strategies for the phase contrast imaging for scanning transmission electron microscopes
[ETN-94-95747] 09 p3866 N94-31613
Deuterium absorption and material phase characteristics of SAES St198 Zr-Fe alloy
[DE94-008275] 09 p3646 N94-32781
Computer image analysis of etched tracks from ionizing radiation
[NASA-CR-196025] 11 p4319 N94-35264
High-resolution imaging using Z-contrast Scanning Transmission Electron Microscopy
[DE94-008510] 11 p4333 N94-36055
Processing, packaging, and characterization of electroceramic materials for phased array antennas
[AD-A280251] 12 p4432 N94-36743
Determination of interface structure and bonding at atomic resolution in the stem
[DE94-011466] 12 p4517 N94-37238
Measurement of scanning electron microscope resolution
[DE94-012661] 12 p4525 N94-37374
Atomic resolution characterization of a SrTiO3 grain boundary in the STEM
[DE94-011469] 12 p4538 N94-37545
The application of maximum entropy to Z-contrast imaging in a stem
[DE94-011470] 12 p4412 N94-37546

SCANNING LASER ACOUSTIC MICROSCOPE (SLAM)
U ACOUSTIC MICROSCOPES

SCANNING TUNNELING MICROSCOPY
Site dependence of the apparent shape of a molecule in STM images: Benzene on Pt(111)
[AD-A263488] 01 p0365 N94-11093
Dynamic studies of crystal growth using the AFM
[DE93-009549] 01 p0399 N94-11268
Real-space formation and dissipation dynamics of hexagonal reconstruction on Au(100) in aqueous media as explored by potentiodynamic scanning tunneling microscopy
[AD-A266138] 01 p0368 N94-11658
Adsorption and dissociation of disilane on Si(001) studied by STM
[AD-A265269] 01 p0402 N94-11684
Atomic-scale imaging of surfaces and interfaces. Materials Research Society Symposium Proceedings, volume 295
[AD-A265674] 01 p0369 N94-12379
Electrode potential-induced reconstruction of Au(100): Effect of chemisorption on nanoscale dynamics as probed by the in-situ scanning tunneling microscopy
[AD-A265900] 01 p0404 N94-12388
Scanning tunneling microscopy studies of diamond films and optoelectronic materials
[NASA-CR-194363] 02 p0578 N94-13246
Ploughing on gold using a Scanning Tunneling Microscope
[DE93-012632] 02 p0812 N94-14365
Laser lithography by photon scanning tunneling microscopy
[DE93-015962] 02 p0660 N94-14863
Method and apparatus for performing scanning tunneling optical absorption spectroscopy
[AD-D015796] 03 p0948 N94-16539
Methods of tunneling spectroscopy with the STM
[AD-A266507] 03 p0948 N94-16787
Applications of scanning tunneling microscopy to electrochemistry
[AD-A269129] 04 p1348 N94-18255
Tunneling spectroscopy of ultrasmall clusters and grains
[AD-A268840] 04 p1598 N94-18539
Thin film studies of the proximity Josephson effect
[AD-A270129] 04 p1600 N94-18876
Scanning tunneling microscopy investigations of metal dichalcogenide materials
[AD-A272910] 05 p2027 N94-21242
Quantitative analysis of scanning tunneling microscopy images for surface structure determination: Sulfur on Re(0001)
[DE93-019235] 05 p2034 N94-22041
JOVE NASA-FIT program: Microgravity and aeronomy projects
[NASA-CR-195121] 06 p2631 N94-24493
The 2-D polymerized Langmuir-Blodgett films studied by STM
[AD-A273542] 06 p2261 N94-24930
Scanning probe lithography. 2: Selective chemical vapor deposition of copper into scanning tunneling microscope-defined patterns
[AD-A273304] 06 p2547 N94-25144
Use of scanning tunneling microscope in corrosion studies
[VTT-TIED-1416] 06 p2250 N94-25346
Observation on metal surface in aqueous solution using an electrochemical Scanning Tunneling Microscope (STM) 07 p2724 N94-25554
Halogen chemisorption on silver(111): Scanning tunneling microscopy of coadsorbed halogen atoms
[AD-A275219] 08 p3486 N94-29060
Studying transient mobility and energy loss using scanning tunneling microscopy
[AD-A276292] 09 p3877 N94-31256
Analytical applications of scanning tunneling microscopy
[AD-A276066] 09 p3711 N94-31283
The adsorption of sulfate on gold(111) in acidic aqueous media: Adlayer structural inferences from infrared spectroscopy and scanning tunneling microscopy
[AD-A276643] 09 p3642 N94-31997
Vibrational spectroscopy at metal-solution interfaces: Some perspectives and prospects for electrochemical surface science
[AD-A276781] 09 p3644 N94-32169
Charge-dependent atomic-scale structures of high-index and (110) gold electrode surfaces as revealed by scanning tunneling microscopy
[AD-A276782] 09 p3869 N94-32170
The 14th Annual West Coast Theoretical Chemistry/Statistical Mechanics Conference
[AD-A276942] 09 p3656 N94-32239
Sensitivity of electrochemical adlayer structure to the metal crystallographic orientation: Potential-independent iodide adsorption on Au(100) in comparison with other low-index surfaces
[AD-A276714] 09 p3909 N94-33273
Scanning tunneling microscopy and infrared spectroscopy as combined in-situ probes of electrochemical adlayer structure: Cyanide on Pt(111)
[AD-A276715] 09 p3909 N94-33274
Nanoscale structural changes upon electrooxidation of Au(111) as probed by potentiodynamic scanning tunneling microscopy
[AD-A276780] 09 p3909 N94-33275

SCAR PROGRAM
U SUPERSONIC CRUISE AIRCRAFT RESEARCH

SCARPS
U ESCARPMENTS

SCARS (GEOLOGY)
U EROSION

SCAT
U SUPERSONIC COMMERCIAL AIR TRANSPORT

SCATTER PROPAGATION
Meteor forward scatter studies
[DSIS-93-00382] 02 p0602 N94-13801
A study of meteor scatter communications
[DSIS-93-00151] 02 p0603 N94-13841
BACKSCATTER.FOR: A program to calculate the backscattering strength of an inhomogeneous seabed
[AD-A269235] 04 p1499 N94-18910
Performance statistics bulletin: High altitude meteor scatter propagation, August, September, October 1989
[AD-A274455] 07 p2773 N94-27085
Performance statistics bulletin. High latitude meteor scatter propagation October, November, December 1990, January 1991
[AD-A276693] 09 p3676 N94-31998
Performance statistics bulletin. High latitude meteor scatter propagation, February, March, April, May 1992
[AD-A276667] 09 p3677 N94-32083

Performance statistics bulletin. High latitude meteor scatter propagation February, March, April, May 1991
[AD-A276723] 09 p3678 N94-32158
Performance statistics bulletin. High latitude meteor scatter propagation October, November, December 1991, January 1992
[AD-A276724] 09 p3678 N94-32159
Performance statistics bulletin. High latitude meteor scatter propagation, November and December 1989, and January 1990
[AD-A276688] 09 p3680 N94-32297
Performance statistics bulletin. High latitude meteor scatter propagation
[AD-A276694] 09 p3680 N94-32298
Performance statistics bulletin. High latitude meteor scatter propagation
[AD-A276695] 09 p3680 N94-32299
Performance statistics bulletin. High latitude meteor scatter propagation
[AD-A276696] 09 p3680 N94-32300
Performance statistics bulletin. High latitude meteor scatter propagation, June, July, August, September 1992
[AD-A277508] 09 p3685 N94-33347
Antarctic meteor scatter test, December 1992
[AD-A277894] 10 p4033 N94-33547

SCATTERERS
U SCATTERING

SCATTERING
NT ACOUSTIC SCATTERING
NT ATMOSPHERIC SCATTERING
NT BACKSCATTERING
NT COHERENT SCATTERING
NT COMPTON EFFECT
NT ELASTIC SCATTERING
NT ELECTROMAGNETIC SCATTERING
NT ELECTRON SCATTERING
NT FORWARD SCATTERING
NT HALOS
NT INCOHERENT SCATTERING
NT INELASTIC SCATTERING
NT INVERSE SCATTERING
NT ION SCATTERING
NT LIGHT SCATTERING
NT MICROWAVE SCATTERING
NT MIE SCATTERING
NT NEUTRON SCATTERING
NT NUCLEAR SCATTERING
NT NUCLEON-NUCLEON SCATTERING
NT PROTON SCATTERING
NT RADAR SCATTERING
NT RAMAN SPECTRA
NT RAYLEIGH SCATTERING
NT RESONANCE SCATTERING
NT REVERBERATION
NT THOMSON SCATTERING
NT TROPOSPHERIC SCATTERING
NT WAVE SCATTERING
NT X RAY SCATTERING

Preliminary results on backscattering strength from a wind generated bubbly ocean surface
[AD-A265006] 01 p0287 N94-10490
Coherence effects in radiometry and in spectroscopy
[DE93-013437] 01 p0075 N94-10519
Scattering of modulated Ultra-Relativistic Electron Beam (UREB) by atmospheric plasma
[DE93-620987] 01 p0387 N94-10558
Interstellar scattering and the selection of extragalactic radiosources with highly compact components
01 p0134 N94-11083
Radiation and scattering by cavity-backed antennas on a circular cylinder
[NASA-CR-193409] 01 p0136 N94-11084
Grain-boundary electronic states by multiple-scattering theory
[DE93-013198] 02 p0805 N94-13010
ADP study of gamma-ray bursts
[NASA-CR-194311] 02 p0848 N94-13708
Theoretical molecular studies of astrophysical interest
[NASA-CR-193300] 02 p0838 N94-13781
Dynamics of pion-nucleus systems
[DE93-014449] 02 p0785 N94-14468
Effects of spin-orbit coupling on disordered mesoscopic systems
[ITN-93-85220] 03 p1180 N94-15288
Interfacial structure of lattice mismatched bcc(110)/bcc(110) transition metal superlattices
[DE93-015162] 03 p1208 N94-16058
Application of symmetry properties to polarimetric remote sensing with JPL AIRSAR data
03 p1079 N94-16752
External calibration of polarimetric radar images using distributed targets 03 p1079 N94-16753
Convergence of the multiple scattering expansion in XAFS and XANES
[DE93-011001] 03 p0948 N94-16772
Evolution of hadron beams under intrabeam scattering
[DE93-014330] 03 p1184 N94-16826
Diffuse scattering and image contrast of tweed in superconducting oxides: A simulation and interpretation
[DE93-016131] 03 p1212 N94-16844
Optical properties of redispersed iron fibers measured at 94 GHz
[AD-A269739] 04 p1342 N94-18756
Analytic approximations of an integral in remote sensing
[AD-A270085] 04 p1463 N94-18800
Research in high energy physics
[DE93-018031] 04 p1575 N94-19287
A new conformal absorbing boundary condition for finite element meshes and parallelization of FEMATS
[NASA-CR-194740] 05 p1950 N94-20034
A comparative study of an ABC and an artificial absorber for truncating finite element meshes
[NASA-CR-194275] 05 p1716 N94-20160
Modifications to the three-component classification algorithm for SAR data 05 p1719 N94-20410
The effect of dissipative inhomogeneous medium on the statistics of the wave intensity 05 p1726 N94-20440
A theoretical and numerical study of polarimetric scattering and emission from random rough surfaces with anisotropic directional spectrum
05 p1730 N94-20454
Single and double ionization of helium by high-energy photon impact
[DE94-000381] 05 p1975 N94-21785
Radiation and scattering from printed antennas on cylindrically conformal platforms
[NASA-CR-194703] 05 p1741 N94-21885
Scattering by cavity-backed antennas on a circular cylinder 05 p1741 N94-21886
Conductors with small Fermi energies and small gap energies
[DE93-040887] 06 p2561 N94-23432
Momentum loss in proton-nucleus and nucleus-nucleus collisions
[NASA-TP-3405] 06 p2540 N94-24305
Integral equations for the microstructures of supercritical fluids
[DE94-002460] 06 p2535 N94-24569
Behavior of the intermittency exponents and a quark-gluon plasma formation in the heavy ion collisions
[DE93-616869] 06 p2541 N94-25342
Back-reaction beyond the mean field approximation
[DE94-003936] 07 p3012 N94-25612
Two dimensional self-consistent fluid simulation of RF inductive sources
[DE94-003635] 07 p2767 N94-25937
Harvard University High Energy Physics
[DE94-002406] 07 p3032 N94-26119
Rescattering and energy loss of fast partons in nuclear matter
[DE94-002918] 07 p3018 N94-26145
Experimental measurement of local displacement and chemical pair correlations in crystalline solid solutions
[DE94-001124] 07 p3065 N94-27251
Decay of non-equilibrium polariton condensate in semiconductors
[DE94-604016] 07 p3068 N94-27678
Neutron-neutron scattering: Possibility of in-beam experiment
[DE94-606459] 07 p3027 N94-27682
Printed circuit elements with applications to antennas, scattering, and circuits
[AD-A275512] 08 p3262 N94-28669
Carrier collection and scattering in quantum well and superlattice devices
[AD-A275443] 08 p3512 N94-28880
A physical optics model for scattering of HF radiation by irregular terrain
[DE94-006187] 08 p3255 N94-30106
Impurities and conductivity in a D-wave superconductor
[DE94-006222] 09 p3898 N94-31628
Modern integral equation techniques for quantum reactive scattering theory
[DE94-007039] 09 p3857 N94-31639
Stellar x ray polarimeter polarizer development and calibration at LEA/LLNL
[DE94-006400] 09 p3712 N94-31783
Penetrable wedge analysis
[AD-A277219] 09 p3845 N94-32022
The multiple scattering contributions in the strong fluctuation theory to the microwave brightness temperature
[AD-A277721] 10 p4075 N94-33442
The temperature of nitrogen on Pluto
11 p4365 N94-35468
Use of the sampling theorem to speed up near-field physical optics scattering calculations
11 p4253 N94-35549
Magnetoresistance of films and strips with the diffuse surface scattering
[DE94-611100] 11 p4340 N94-35933
X ray and gamma ray spectroscopy of solids under pressure
[DE94-011207] 11 p4238 N94-36203
Scattering theory for the quantum envelope of a classical system
[DE94-008530] 12 p4539 N94-36508
Dipole forbidden vibrational modes for NO and CO on Cu observed in the far IR
[DE94-003199] 12 p4408 N94-36559
A rejection method for selection of scattered states
[DE94-012232] 12 p4517 N94-37209

SCATTERING AMPLITUDE
Indication on the existence of the bound state in the p anti p-system
[DE92-641575] 01 p0361 N94-10532
P-matrix description of the two-particle interaction
[DE93-617690] 01 p0361 N94-10549
Crossing-odd spin effects in the dipole model of hadron scattering
[DE93-617692] 01 p0362 N94-10551
Model for the pomeron
[DE93-617693] 01 p0362 N94-10552
Fine structure of the Pomeron and the real part of the elastic scattering amplitude
[DE93-617696] 01 p0362 N94-10555
On the possible unobservability of the Wu-Yang phase factor in curved space
[DE93-617645] 01 p0411 N94-10831
FEFF5: An ab initio multiple scattering XAFS code
[DE93-011000] 01 p0367 N94-11470
Fermion-boson scattering in ladder approximation
[DE93-613111] 01 p0368 N94-11581
The E2 N(yields)(Delta) transition from polarized Compton scattering
[DE93-012522] 02 p0785 N94-14363
Scattering calculations and confining interactions
[NASA-CR-194242] 02 p0786 N94-14549
Relativistic proton-nucleus scattering and one-boson-exchange models 02 p0786 N94-14550
Convergence of the multiple scattering expansion in XAFS and XANES
[DE93-011001] 03 p0948 N94-16772
Quark-loop effects in high energy spin-flip processes
[DE93-626692] 03 p1188 N94-17313
Lectures of Fermi liquid theory
[DE93-016630] 04 p1592 N94-17714
First and second order Stokes generation by SRS in methane: Influence of rep-rate, beam quality and astigmatism
[FEL-92-A125] 04 p1441 N94-19426
Hadronic molecules and scattering amplitudes from the nonrelativistic quark model
[DE94-000377] 05 p1974 N94-21657
Momentum and coordinate space three-nucleon potentials
[DE93-040868] 06 p2531 N94-22951
Application and development of the Schwinger multichannel scattering theory and the partial differential equation theory of electron-molecule scattering
[NASA-CR-194774] 06 p2536 N94-24798
The amplitude of the elastic hadron-hadron scattering in the coulombic range of transfer momenta
[DE93-613183] 07 p3014 N94-25869
The challenges of exclusive processes in QCD
[DE94-003429] 07 p3024 N94-27050
Proton electromagnetic form factor near the proton-antiproton threshold and quasinuclear bound state
[DE94-606458] 07 p3027 N94-27681
GRACE manual
[DE94-727456] 10 p4105 N94-33867
Convergent close-coupling calculations of low-energy positron-atomic-hydrogen scattering
[DE94-609858] 10 p4137 N94-33882
Medium energy measurements of N-N parameters
[DE94-008340] 10 p4137 N94-33923
On a generalized bootstrap principle
[DE94-727517] 11 p4314 N94-35774
Low energy theorems from the effective Lagrangian with vector mesons
[DE94-611173] 11 p4322 N94-35785
Q-deformations of the Veneziano model
[DE94-616769] 11 p4315 N94-36076
Spin effects in high energy quark-quark scattering
[DE94-616800] 11 p4330 N94-36080
T-odd, P-even photon-fermion interactions
[DE94-616869] 11 p4327 N94-36246
Elastic p(4)He scattering at intermediate energies
[DE94-618544] 11 p4328 N94-36287

SCATTERING COEFFICIENTS
Polarisation of backscattering radiation at remote sensing of ocean with impulse laser beam
01 p0177 N94-12722

Remote sensing of light scattering coefficient of sea water vertical distribution by the means of airborne lidar
01 p0224 N94-12736
Radar response of vegetation: An overview
03 p0991 N94-15898
Multifrequency observations 03 p0992 N94-15902
Application of symmetry properties to polarimetric remote sensing with JPL AIRSAR data
03 p1079 N94-16752
Analysis of meteorological conditions during AGASP-4: 30 March - 23 April 1992
[PB93-190205] 04 p1489 N94-18126
Symmetry in polarimetric remote sensing
05 p1729 N94-20449
Application of neural network to remote sensing of soil moisture using theoretical polarimetric backscattering coefficients 05 p1730 N94-20455
A simplified method for S-parameter calculations of metal septum waveguide filters
05 p1782 N94-22180
Backscatter and transmission of aerosol at UV through middle IR wavelengths
[AD-A277127] 09 p3718 N94-32305

SCATTERING CROSS SECTIONS
Convergent close-coupling calculations of electron-hydrogen scattering
[DE93-610049] 01 p0360 N94-10328
Distorted-wave calculation of He(e,2e) including core-exchange
[DE93-610072] 01 p0360 N94-10330
Logarithmically rising cross section and the ratio sigma(sub el)/sigma(sub t)
[DE93-617694] 01 p0362 N94-10553
Detecting the odderon
[DE93-617695] 01 p0362 N94-10554
Interpretation of lunar and planetary electromagnetic scattering using the full wave solutions
01 p0440 N94-12049
Low voltage electron beam lithography
[AD-A265358] 01 p0145 N94-12405
Final state interactions and inclusive nuclear collisions
[NASA-TP-3353] 01 p0373 N94-12435
Calculation of electron-lithium scattering using the coupled-channel optical method
[DE93-623049] 02 p0806 N94-13226
Recent developments in multiple-scattering calculations of XAFS and XANES
[DE93-010999] 02 p0563 N94-13477
Measurement of the Fe-56(n,p)Mn-56, Al-27(n,p)Mg-27 and Al-27(n,alpha)Na-24 cross sections at 16.0, 17.0 and 18.3 MeV
[NPL-RSA(EXT)-38] 02 p0783 N94-13883
The quantum mass shift of the soliton in Skyrme model
[ITN-93-85219] 03 p1180 N94-15283
Criticality benchmark comparisons leading to cross-section upgrades
[DE93-017184] 04 p1556 N94-18073
New relativistic S-matrix results for scattering -- beyond the usual anomalous factors/beyond impulse approximation
[DE93-019148] 05 p1971 N94-20096
Near grazing scattering from non-Gaussian ocean surfaces 05 p1726 N94-20438
Parton-parton elastic scattering and rapidity gaps at Tevatron energies
[DE93-041024] 05 p1974 N94-21515
Inelastic electron scattering from surfaces
[DE94-001738] 05 p1977 N94-22049
Inelastic electron scattering from surfaces
[DE94-001368] 06 p2531 N94-22733
Pions and neutrinos as probes of the nucleon and nuclear few-body system
[DE93-040127] 06 p2531 N94-22928
B-quark production at hadron colliders
[DE94-001459] 06 p2534 N94-23806
Optical spin polarization and state-sensitive detection of a cesium atomic beam
[ATR-92(8436)-1] 06 p2534 N94-24077
The delta (1232) resonance transition form factor
[DE94-003442] 07 p3017 N94-26101
Elastic scattering by a spherical inclusion
[AD-A274713] 07 p2878 N94-26433
Relativistic collision rate calculations for electron-air interactions
[DE94-004204] 07 p3020 N94-26527
Calculation of electron-potassium scattering
[DE94-601812] 07 p3023 N94-26942
Spin asymmetry in resonant electron-hydrogen elastic scattering
[DE94-601813] 07 p3023 N94-26943
Calculation of total cross sections for electron and positron scattering on sodium and potassium
[DE94-601814] 07 p3023 N94-26944
Jet production in muon scattering at Fermilab E665
[DE94-004663] 07 p3028 N94-27752
Muon transfer rates in collisions of hydrogen isotope mesic atoms on bare nuclei: Multichannel adiabatic approach
[DE94-606752] 07 p3030 N94-27861
Radiation transport in cloudy and aerosol loaded atmospheres 08 p3366 N94-30805
Production of charginos and neutralinos for the reaction positron electron yields Z' boson yields chargino(+) (sub i) chargino(-) (sub j) or neutralino (sub i) neutralino (sub j) in SU(2) (sub L) x SU(2) (sub R) x U(1) (sub B-L)
[ISBN-0-315-87316-7] 09 p3867 N94-31832
Scatterometer wind-speed exponents: A review and SAXON 35-GHz measurements
[AD-A276568] 09 p3783 N94-31937
Development of a frequency-domain electromagnetic scattering measurement system
[AD-A276738] 09 p3678 N94-32179
Time-resolved IR spectroscopy, energy transfer, and state-to-state collision dynamics of atmospheric species
[AD-A277372] 09 p3773 N94-32338
Quantum dynamics in dual spaces
[DE94-008303] 09 p3913 N94-32824
Bistatic clutter RCS simulation using scale model surfaces with two scale roughness
[AD-A277604] 10 p4035 N94-33847
Medium energy measurements of N-N parameters
[DE94-008340] 10 p4137 N94-33923
Pion-nucleon interaction in nuclear matter above the Delta resonance energy
[DE94-727455] 10 p4137 N94-33994
SCATTER program of cross section calculation of the hadron and lepton interactions with nuclei
[DE94-617006] 11 p4326 N94-36134
Measurement of the elastic, total and diffraction cross sections at tevatron energies
[DE94-004659] 12 p4511 N94-36463
Scattering cross section of sound waves by the modal element method
[NASA-TM-106667] 12 p4510 N94-37308
Neutrino-nucleon scattering
[DE94-011720] 12 p4520 N94-37671

SCATTERING FUNCTIONS
Forward scattering of a pulsed continuous wave signal through laminar and turbulent thermal plumes
[AD-A271210] 04 p1564 N94-19723
Analytical evaluation of a surface integral expressing the coupling between interior and exterior volumes in a FE-IE approach 05 p1722 N94-20423
Scattering by Venus' surface
05 p2117 N94-20771
Documentation for PCDIST, a FORTRAN subroutine to calculate Pollack-Cuzzi scattering
[AD-A273070] 05 p1988 N94-21491
Propagation model for the Land Mobile Satellite channel in urban environments 06 p2283 N94-22796
Elastic scattering by a spherical inclusion
[AD-A274713] 07 p2878 N94-26433
Single scattering of light by ensembles of particles with various shapes
[ETN-94-96016] 09 p3878 N94-31550
Recursive analysis of matrix scattering functions
[AD-A277264] 09 p3845 N94-32018
Comparison of numerical models for computing underwater light fields
[AD-A278256] 10 p4140 N94-33411
Measured channel parameters for the disturbed wide-bandwidth HF channel
[AD-A277877] 10 p4034 N94-33778
Convergent close-coupling calculations of low-energy positron-atomic-hydrogen scattering
[DE94-609858] 10 p4137 N94-33882

SCATTERING MATRIX
U S MATRIX THEORY

SCATTEROMETERS
Calibration and validation of the ERS-1 wind scatterometer 01 p0232 N94-11706
ERS-1 scatterometer data characteristics and wind retrieval skill 01 p0233 N94-11709
Validation of ERS-1 wind and wave data by use of operational forecast models 01 p0233 N94-11710
A C-band wind scatterometer model derived from the data obtained during the ERS-1 calibration/validation campaign 01 p0233 N94-11711
ERS-1 studies at the Department of Oceanography from Space, IFREMER/Brest (France)
01 p0233 N94-11712
The activity of the ERS-1 Venice (Italy) group on scatterometry 01 p0233 N94-11713
Use of ERS-1 data at Saclant Undersea Research Centre 01 p0233 N94-11714
A preliminary C-band scatterometer model function for the ERS-1 AMI instrument 01 p0233 N94-11715
Preliminary analysis of circulations over the Indian Ocean and adjoining regions using ERS-1 surface winds in the NCMRWF data assimilation system
01 p0234 N94-11719
Evaluation of two January - June 1992 ERS-1 AMI wind vector data sets 01 p0235 N94-11724
Scatterometer observations: Review
01 p0201 N94-11956
The microwave backscattering from wind waves
01 p0201 N94-11959
A first assessment of the value of ERS-1 scatterometer winds for meteorological studies in the polar regions
01 p0250 N94-12501
Use of ERS-1 wind and wave products in operational meteorology 01 p0250 N94-12502
Use of ERS-1 scatterometer winds in Canadian forecast centres 01 p0250 N94-12504
Earth Observation Center Annual Report on Research and Development, Fiscal Year 1992
[EOC-92-01-0007] 02 p0687 N94-14091
ADEOS project 02 p0687 N94-14094
Theoretical and experimental research on coherent microwave backscatter from the ocean
[AD-A271276] 04 p1500 N94-19743
Probe compensation in cylindrical near-field scanning: A novel simulation methodology
05 p1718 N94-20404
ERS-1 and Seasat scatterometer measurements of ocean winds: Model functions and the directional distribution of short waves 05 p1720 N94-20412
Ku-band ocean radar backscatter observations during SWADE 05 p1720 N94-20413
Direction angle sensitivity of agricultural field backscatter with AIRSAR data 05 p1724 N94-20430
Observations by ERS-1 start
08 p3327 N94-28933
Scatterometer wind-speed exponents: A review and SAXON 35-GHz measurements
[AD-A276568] 09 p3783 N94-31937

SCAVENGING
In-cylinder gas velocity measurements comparing crankcase and blower scavenging in a fired two-stroke cycle engine
[DE94-005752] 08 p3311 N94-30596

SCENE ANALYSIS
Retrieval of radiation budgets in the Arctic from satellite measurements 01 p0229 N94-10714
A summary of image segmentation techniques
[NASA-TM-104022] 01 p0327 N94-11274
Determination of position and orientation of rigid bodies from image segments
[FFI-92-4005] 02 p0752 N94-14039
Passive recovery of scene geometry for an unmanned ground vehicle
[AD-A266670] 02 p0766 N94-14777
Extracting heading and temporal range from optic flow: Human performance issues 06 p2442 N94-25510
Optical information in landing scenes
06 p2442 N94-25511
Science support for the Earth radiation budget experiment
[NASA-CR-191600] 07 p2894 N94-26506
Synthetic image generator model; application of view angle dependent reflectivity components and performance evaluation in the visible region
[AD-A275365] 08 p3499 N94-29009
Unmanned vehicle mobility: Limits of autonomous navigation 08 p3310 N94-30311
Vision based object pose estimation for mobile robots
[AIAA PAPER 94-1197-CP] 08 p3442 N94-30548
Multi-sensor data fusion and the use of artificial intelligence
[PB94-126216] 08 p3448 N94-30741
Automatic extraction of cartographic objects by fusion of data extracted from satellite images
[TELECOM-93-E-001] 09 p3742 N94-31165
Volumetric modelling of three dimensional scenes by octree decomposition of geometric models
[ISBN-0-315-86866-X] 09 p3814 N94-31728
A neural network model for the visual perception of the depth of a scene from stereoscopy and shading
[ISBN-0-315-86753-1] 09 p3831 N94-31750
Safe navigation and active vision for autonomous vehicles: A purposive and direct solution
09 p3832 N94-31842
Neural models of spatial orientation in novel environments
[AD-A277383] 09 p3835 N94-32340
Adaptive multisensor fusion for the perception and interpretation of outdoor robot scenes
[PB94-170719] 12 p4499 N94-36535

SCF
U SELF CONSISTENT FIELDS

SCHEDULES
National Aero-Space Plane: A need for program direction and funding decisions
[GAO/NSIAD-93-207] 01 p0416 N94-10910
Avoidance and suppression of compensation code in a trace scheduling compiler
[AD-A265812] 01 p0333 N94-12439

Coordinated Radio, Electron, and Waves Experiment (CREWE) for the NASA Comet Rendezvous and Asteroid Flyby (CRAF) instrument
[NASA-CR-194376] 01 p0427 N94-12566
Work/rest schedules and performance of S-3 aviators during fleet exercise
[AD-A265807] 02 p0734 N94-12975
Work/rest schedules and performance of F/A-18 aviators during Fleet Exercise 1992
[AD-A265826] 02 p0735 N94-12982
Sleep management user's guide for special operations personnel
[AD-A267746] 03 p1119 N94-14943
HSTS: Integrating planning and scheduling
[AD-A266991] 03 p1222 N94-15213
Activity/rest patterns of instructor and rates student pilots during rapid transitions from daytime to nighttime duty hours at the Eastern Army Aviation Training site
[AD-A267038] 03 p1131 N94-15659
AIRSAR South American deployment: Operation plan, version 3.0 03 p0994 N94-15919
Establishing a software measurement process
[AD-A267896] 03 p1154 N94-17396
Using controlled daylight exposure and sleep timing in the prevention of shift lag during night operations
[AD-A269304] 04 p1504 N94-17824
Predicting scheduling success 05 p1932 N94-21334
Generating and evaluating alternate schedules 05 p1933 N94-21336
Linear time algorithm to schedule trees with communication delays optimally on two machines
[PB93-237782] 06 p2451 N94-23441
Preemptive scheduling in a two-stage multiprocessor flow shop is Np-hard
[PB94-111648] 06 p2467 N94-23756
Three, four, five, six or the complexity of scheduling with communication delays
[PB94-111630] 06 p2467 N94-23767
The mission events graphic generator software: A small tool with big results 06 p2464 N94-23893
ESSOPE: Towards S/C operations with reactive schedule planning 06 p2508 N94-23896
Panel to review EOSDIS plans
[NASA-CR-195088] 06 p2387 N94-24303
Analysis of cost and schedule growth on sole source and competitive Air Force contracts
[AD-A273920] 07 p3094 N94-26814
A family of joint probability models for cost and schedule uncertainties
[AD-A275513] 08 p3463 N94-28670
Circadian countermeasures for shiftworkers during USMP-2: A report to mission management
[NASA-CR-195260] 08 p3402 N94-30188
Unit specific crew rest strategies: Phase 1 evaluation of the 1/212th Aviation Battalion during shiftwork transitions
[AD-A277122] 09 p3804 N94-32379
Earth Observing System (EOS) Advanced Microwave Sounding Unit-A (AMSU-A) schedule plan
[NASA-CR-194856] 11 p4281 N94-35734
Recent SEL experiments and studies 12 p4490 N94-36487

SCHEDULING
NT PREDICTION ANALYSIS TECHNIQUES
ACARA user's manual
[NASA-TM-106277] 01 p0183 N94-11167
Distributed real-time system design: Theoretical concepts and applications
[AD-A265199] 01 p0337 N94-11881
Avoidance and suppression of compensation code in a trace scheduling compiler
[AD-A265612] 01 p0333 N94-12439
Present status of JEM utilization projects 02 p0530 N94-13273
Three, four, five, six or the complexity of scheduling with communication delays
[CWI-BS-R9229] 02 p0751 N94-14004
Stochastic scheduling games with Markov decision arrival processes
[CWI-BS-R9231] 02 p0773 N94-14005
An experimental analysis of bottleneck-centered opportunistic scheduling
[AD-A266643] 02 p0820 N94-14796
HSTS: Integrating planning and scheduling
[AD-A266991] 03 p1222 N94-15213
Stochastic scheduling in in-forest networks
[INRIA-RR-1719] 03 p1164 N94-15695
Fast interrupt priority management in operating system kernels
[AD-A266638] 03 p1140 N94-15744
Processor capacity reserves for multimedia operating systems
[AD-A266639] 03 p1158 N94-15745
Efficient scheduling of real-time compute-intensive periodic graphs on large grain data flow multiprocessor
[AD-A267444] 03 p1141 N94-17030
Stochastic scheduling in a multiclass G/G/1 queue
[INRIA-RR-1746] 03 p1162 N94-17537
Shop problems with two machines and time lags
[REPT-93-020] 04 p1518 N94-17927
PRACTICAL: Planning and resource allocation in C2-domains with time critical algorithms
[FEL-93-B029] 04 p1544 N94-19458
Exploiting the parallelism exposed by partial evaluation
[AD-A270678] 05 p1928 N94-19877
Multilist scheduling: A new parallel programming model
[AD-A270549] 05 p1929 N94-20084
Fault tolerant real-time systems
[AD-A272878] 05 p1899 N94-21195
Space network scheduling benchmark: A proof-of-concept process for technology transfer 05 p1932 N94-21332
Predicting scheduling success 05 p1932 N94-21334
Generating and evaluating alternate schedules 05 p1933 N94-21336
The Automated Conflict Resolution System (ACRS) 05 p1744 N94-21341
Heuristic-based scheduling algorithm for high level synthesis 05 p1764 N94-21704
A statistical-based scheduling algorithm in automated data path synthesis 05 p1764 N94-21706
Instruction set commutivity 05 p1766 N94-21719
The EUVE proposal database and scheduling system 05 p2047 N94-22459
SPIKE: Application for ASTRO-D mission planning 05 p1926 N94-22486
The application of artificial intelligence to astronomical scheduling problems 05 p1949 N94-22492
Personnel shift assignment: Existence conditions and network models
[MEMO-1116] 06 p2585 N94-22704
Using genetic algorithms for scheduling data flow graphs
[EUT-92-E-266] 06 p2449 N94-23169
Linear time algorithm to schedule trees with communication delays optimally on two machines
[PB93-237782] 06 p2451 N94-23441
Preemptive scheduling in a two-stage multiprocessor flow shop is Np-hard
[PB94-111648] 06 p2467 N94-23756
Framework for interactive solving of meta-constraint satisfaction problems
[PB94-118825] 06 p2585 N94-23761
Three, four, five, six or the complexity of scheduling with communication delays
[PB94-111630] 06 p2467 N94-23767
Mission planning for an Earth observation low Earth orbiter: ERS-1 06 p2503 N94-23868
Integrating payload design, planning, and control in the Dutch Utilisation Centre 06 p2207 N94-23869
Techniques and software for optimum and efficient mission science sequence development 06 p2504 N94-23872
Connecting science and operations: The operations coordinator 06 p2504 N94-23874
AGENDA: A task organizer and scheduler 06 p2504 N94-23876
NASDA knowledge-based network planning system 06 p2508 N94-23898
Constraint-based scheduling 06 p2510 N94-23904
A method for interference mitigation in space communications scheduling 06 p2305 N94-23918
Mission and science activity scheduling language 06 p2515 N94-23938
An intelligent planning and scheduling system for the HST servicing missions 06 p2520 N94-23964
Scheduling the future NASA Space Network: Experiences with a flexible scheduling prototype 06 p2520 N94-23965
Software reuse in spacecraft planning and scheduling systems 06 p2520 N94-23966
Planning: Management of predictability and uncertainty and keeping abreast of developments 06 p2520 N94-23967
Design and specification of a centralized manufacturing data management and scheduling system 06 p2577 N94-24416
Compositional architecture for simple design formally specified in DESIRE
[PB94-119013] 06 p2474 N94-24543
Sensitivity analysis of list scheduling heuristics
[PB93-237766] 06 p2468 N94-24764
Class of strong valid inequalities for the discrete lot-sizing and scheduling problem
[PB93-237774] 06 p2459 N94-24765
Multiprocessor scheduling with communication delays
[ETN-94-95346] 06 p2468 N94-25221
Conflict-free trajectory planning for air traffic control automation
[NASA-TM-108790] 06 p2174 N94-25272
ROSAT mission planning using artificial intelligence methods
[DLR-FB-93-14] 06 p2476 N94-25345
Automating satellite range scheduling
[AD-A273829] 07 p2694 N94-25738
Coordinated scheduling for dynamic real-time systems
[NASA-CR-195231] 07 p3093 N94-26206
The general pickup and delivery problem
[MEMO-COSOR-92-44] 07 p2992 N94-26226
A linear description of the discrete lot-sizing and scheduling problem
[MEMO-COSOR-92-47] 07 p2992 N94-26227
One machine scheduling with delayed precedence constraints
[PB93-237626] 07 p3094 N94-26314
Real-Time Embedded Processing for Space Applications
[ISBN-2-85428-335-X] 07 p2948 N94-26713
Scheduling tasks with unpredictable timing parameters in hard real-time systems 07 p2951 N94-26728
Ada multiple-programming for hard real time applications in space systems 07 p2951 N94-26730
Implementing hard real-time systems: A case study 07 p2951 N94-26731
A real-time executive implementing priority inheritance protocols 07 p2952 N94-26733
Scheduling approaches with Ada 07 p2952 N94-26734
Fault-tolerant scheduling in distributed critical real-time systems 07 p2952 N94-26735
Central dynamic share scheduling in distributed systems
[REPT-93-48] 07 p2966 N94-26966
Artificial Intelligence Research Branch future plans
[NASA-TM-109733] 07 p2989 N94-28065
Technology transition push. Part 1: A case study of rate monotonic analysis
[AD-A275616] 08 p3407 N94-28633
Artificial intelligence technology program at Rome Laboratory 08 p3414 N94-29328
A time reasoning system based on the event calculus for scheduling in aeronautic maintenance
[REPT-932-710-101] 08 p3122 N94-29463
On the use of genetic algorithms to solve the time-table problem
[REPT-90-060-REV] 09 p3829 N94-31176
Exact solution of the single machine scheduling problem with earliness and flow time penalties
[REPT-93-038] 09 p3809 N94-31189
Scheduling techniques for multiple processor systems in real-time environments
[AD-A276149] 09 p3824 N94-31249
A model and algorithms for a software evolution control system
[AD-A276431] 09 p3811 N94-31449
Planning of air crew schedules
[ISBN-0-315-86506-7] 09 p3914 N94-32074
Discrete-event-dynamic-system-based approaches for scheduling transmissions in multihop packet radio networks
[AD-A276566] 09 p3679 N94-32230
Scheduling fighter missions using an expert system with an operations research module 09 p3853 N94-33337
The StarLite Project: Prototyping real-time software
[AD-A278201] 10 p4103 N94-33374
Task allocation and scheduling for high level synthesis
[AD-A277570] 10 p4110 N94-33395
Predictable and adaptable complex real-time systems
[AD-A277827] 10 p4105 N94-33830
A neural/expert based client server architecture for MITE ITS
[AD-A278330] 10 p4113 N94-33968
Reinforcement learning in scheduling 10 p4099 N94-34045
Constraint-based integration of planning and scheduling for space-based observatory management 10 p4150 N94-34046
Advanced timeline systems
[NASA-CR-193958] 10 p4131 N94-34281
On-board emergent scheduling of autonomous spacecraft payload operations 10 p4123 N94-35047
A criterion autoscheduler for long range planning 10 p4123 N94-35048
Modeling heterogeneous processor scheduling for real time systems 10 p4124 N94-35053
Cost and schedule estimation study report
[NASA-CR-189344] 11 p4300 N94-35256
A genetic algorithm approach to automating satellite range scheduling
[AD-A278577] 11 p4226 N94-36188

Planning German Army helicopter maintenance and mission assignment
[AD-A280483] 12 p4381 N94-37352

SCHEMATICS
U CIRCUIT DIAGRAMS

SCHIFF BASES
U IMINES

SCHLIEREN PHOTOGRAPHY
Analysis of the alignment of a Schlieren system for tele-operation 01 p0111 N94-10140
Evaluation of dual flow thrust vectored nozzles with exhaust stream impingement
[NASA-CR-193292] 01 p0150 N94-10912
Fundamental study of shock wave/turbulent boundary layer interactions with passive control in transonic flows
[ESA-TT-1278] 02 p0630 N94-13117
Images constructed from computed flow fields
[NASA-CR-194397] 02 p0650 N94-13814
Advanced ballistic range technology
[NASA-CR-194396] 02 p0532 N94-14068
Advanced ballistic range technology
[NASA-CR-194530] 02 p0533 N94-14540
Supersonic flow visualization of a nacelle in close proximity to a simulated wing
[NASA-CR-194675] 03 p0860 N94-17260
An experimental study of the flow field surrounding a subsonic jet in a cross flow
[NASA-CR-194770] 06 p2317 N94-23072
Focused Schlieren flow visualization studies of multiple venturi fuel injectors in a high pressure combustor
[NASA-TM-106479] 07 p2674 N94-26573
Effects of free-stream turbulence on a jet in a cross flow 07 p2805 N94-28036
Noninvasive spectral analysis and beam mapping of focused ultrasound, part 1
[AD-A276211] 09 p3859 N94-31060
A supersonic tunnel for laser and flow-seeding techniques
[NASA-TM-106588] 11 p4265 N94-35945

SCHMIDT NUMBER
Combustion in turbulent jets and buoyant flames
[PB93-202372] 05 p1682 N94-21452
A random distribution reacting mixing layer model
[NASA-CR-194445] 06 p2187 N94-23552
The instantaneous concentration field in the self-similar region of a high Schmidt number round jet 08 p3278 N94-29976

SCHMIDT TELESCOPES
Hardware design for the Autonomous Visibility Monitoring (AVM) observatory 02 p0533 N94-14394

SCHOOLS
A summer program in mathematics and computer science for academically oriented student
[AD-A263467] 01 p0415 N94-11517
Career Information in the Mathematical Sciences (CIMS)
[DE93-013780] 01 p0318 N94-11817
Workshop for coordinating South Carolina's pre-college systemic initiatives in science and mathematics
[DE93-012263] 02 p0818 N94-13216
Developments in the Higher Technical Aerospace Education 03 p0854 N94-15130
From the Moons of Jupiter to the Milky Way
[NASA-CR-194649] 03 p1240 N94-17059
Undergraduate origins of recent science and engineering doctorate recipients
[NSF-92-332] 04 p1610 N94-19389
Undergraduate course and curriculum development program and calculus and the bridge to calculus program: 1992 awards
[NSF-93-24] 04 p1610 N94-19446
Schools of the Pacific rainfall climate experiment 05 p1881 N94-20699
Sparking young minds with Moon rocks and meteorites 05 p2039 N94-20819
An evaluation of techniques for ranking academic information systems journals
[AD-A275179] 08 p3529 N94-29066
Building on the foundation for an engineering career 11 p4343 N94-35973

SCHOOLS (FISH)
A predictive parametric model for volume scattering strength in the deep ocean with an application to nighttime near-surface scattering in the North Sargasso Sea below 16 kHz
[AD-A277902] 10 p4091 N94-33592

SCHOTTKY BARRIER DIODES
U SCHOTTKY DIODES

SCHOTTKY DIODES
Activation energy and capture cross section of majority carrier traps in Zn doped InP 01 p0049 N94-11386
Annealing study of main electron irradiation-induced defects (H4 and H5) in P-InP using DLTS technique
[DE93-623204] 02 p0806 N94-13213
Schottky barrier focal plane arrays for SWIR and MWIR 03 p0903 N94-15050
Study of mechanisms for long wavelength Schottky-barrier infrared detectors
[AD-A270538] 05 p1971 N94-20083
Study of the utilization of thin oxides in indium phosphides for the realisation of electron components
[ECL-92-38] 05 p2018 N94-20593
Modification of semiconductor surface properties with chemically bound molecular films
[AD-A276162] 09 p3895 N94-31081
Lowering the Schottky barrier at metal or silicide/Si interfaces to extend the range of infrared detectors
[AD-A277253] 09 p3903 N94-32322

SCHOTTKY EFFECT
U WORK FUNCTIONS

SCHREIBERSITE
Tambo Quemado: Extraordinary concentrations of REE and refractory trace elements caused by artificial heating 05 p1684 N94-20667

SCHROEDINGER EQUATION
P-matrix description of the two-particle interaction
[DE93-617690] 01 p0361 N94-10549
Studies of P-matrix formalism on the basis of the potential description of two-particle interaction
[DE93-617691] 01 p0362 N94-10550
Completeness properties of the minimum uncertainty states 01 p0349 N94-10581
Uncertainty relations, zero point energy and the linear canonical group 01 p0378 N94-10590
Positive phase space distributions and uncertainty relations 01 p0379 N94-10598
Coherent states and uncertainty relations for the damped harmonic oscillator with time-dependent frequency 01 p0380 N94-10611
Quasi-relativistic effects in barrier-penetration processes
[DE93-617730] 01 p0410 N94-10721
Exact solutions of a many-anyon problem
[DE93-617646] 01 p0411 N94-10832
Grain-boundary electronic states by multiple-scattering theory
[DE93-013198] 02 p0805 N94-13010
Multiple Schroedinger cats from multilevel atoms
[DE93-013412] 02 p0786 N94-14526
Soliton equations and self-dual gauge fields
[DE93-626620] 02 p0818 N94-14887
Many-body quantum mechanical studies of molecular clusters
[AD-A266624] 03 p1180 N94-15727
Variable time-step integration for intense field effects
[DE93-013296] 04 p1382 N94-17909
Impulsive moving mirror model in a Schroedinger picture with impulse effect in a Banach space
[DE93-629864] 04 p1561 N94-18155
Asymptotic behaviour of the solutions of Schroedinger equation with impulse effect in a Banach space
[DE93-629865] 04 p1548 N94-18195
Impulsive moving mirror model and the stability of Schroedinger equation with impulse effect in a Banach space
[DE93-629866] 04 p1548 N94-18196
Impulsive moving mirror model and impulsive differential equations in Banach space
[DE93-629867] 04 p1549 N94-18197
A hydrogen atom in the curved space. Expansion over free solutions on the three-dimensional sphere
[DE93-629868] 04 p1549 N94-18198
The rise of accuracy for the multichannel scattering problem solving
[DE93-630145] 04 p1608 N94-18253
Schroedinger's hope
[AD-A270988] 04 p1581 N94-19772
Two-dimensional nonlinear Schrodinger equations and their properties
[AD-A272184] 05 p1952 N94-20923
Ionization of H2(+) in intense laser fields
[DE93-019160] 05 p1818 N94-21829
Simulating the Euclidean time Schroedinger equations using an INTEL iPSC/860 hypercube: Application to the t-J model of high-T(sub c) superconductivity
[DE94-000489] 05 p2035 N94-22385
Periodic nonlinear Schroedinger equation and invariant measures
[PB93-238012] 06 p2487 N94-23775
On the connection of classical mechanics, physical kinetics and quantum theory
[DE93-616823] 06 p2570 N94-25207
Calculations of population transfer during intense laser pulses
[DE94-001060] 07 p2818 N94-26698
The three-dimensional hydrogen atom in crossed magnetic and electric fields
[DE94-606301] 07 p3029 N94-27847
Calculation of eigenvalues of Schroedinger operators for arbitrary coupling
[DE94-606302] 08 p3522 N94-28582
Miln equation for the calculation of the phases and amplitudes of wave functions for continuum spectrum of Coulomb two-center problem
[DE94-606292] 08 p3522 N94-28616
Dissipative quantum dynamics and nonlinear sigma-model
[DE94-606295] 08 p3523 N94-28617
Numerical solution of the multichannel scattering problem
[DE94-606297] 08 p3484 N94-28619
Variational calculation of the eigenpotential for H(sup -)-system
[DE94-606269] 08 p3407 N94-28622
The solving of the relativistic two-body problem with a nonlinear dependence upon a spectrum parameter
[DE94-606343] 08 p3451 N94-28783
Reconstruction of spectra in the discrete quantum mechanics (new elements of the lattice quantum engineering)
[DE94-608075] 08 p3524 N94-30087
Graded Froelicher-Nijenhuis brackets and the theory of recursion operators for super differential equations
[MEMO-1147] 08 p3460 N94-30736
Coherent processes in atom in strong radiation fields
[AD-A278388] 09 p3874 N94-33144
Whiskered tori for integrable pde's: Chaotic behavior in near integrable pde's
[AD-A278390] 10 p4128 N94-33430
Self-similar regimes of subsonic Langmuir wave collapse
[DE94-611466] 11 p4335 N94-35750
Coherent states versus de Broglie-wavelets
[DE94-611075] 11 p4343 N94-36381
Nonlinearity with disorder: Spatio-temporal complex behavior arising from length scales competition
[DE94-000675] 12 p4502 N94-36685
Solving the two-dimensional Schroedinger equation in self-consistent basis
[DE94-621535] 12 p4504 N94-37174
Final report on spectral broadening by cross-phase modulation in linearly birefringent optical fibers
[DE94-010406] 12 p4524 N94-37191
The angular and energy distributions of ejected electrons in electron-impact ionization of helium
[DE94-618748] 12 p4519 N94-37528

SCHUMANN-RUNGE BANDS
Determination of spectroscopic properties of atmospheric molecules from high resolution vacuum ultraviolet cross section and wavelength measurements
[NASA-CR-194024] 02 p0712 N94-13092

SCHWARZSCHILD METRIC
Physics, astronomy, and astrophysics: A numerical study of the black hole plus Brill wave spacetime 08 p3540 N94-29990

SCHWASSMANN-WACHMANN COMET
Orbital evolution of dust from comet Schwassmann-Wachmann 1: A case of one-to-one resonance trapping 03 p1242 N94-16270
Infrared observations of cometary dust by COBE 08 p3541 N94-29994

SCIENCE
Project TIMS (Teaching Integrated Math/Science)
[NASA-CR-194288] 01 p0416 N94-11599
Selected data on academic science and engineering R and D expenditures: Fiscal Year 1991
[NSF-92-329] 02 p0819 N94-13982
Science, technology, and the federal government: National goals for a new era 02 p0827 N94-14115
From the Moons of Jupiter to the Milky Way
[NASA-CR-194649] 03 p1240 N94-17059
A foundation for the 21st Century: A progressive framework for the National Science Foundation. Report of the National Science Board Commission on the future of the National Science Foundation
[NSB-92-196] 04 p1611 N94-19618
Selected data on Federal support to universities and colleges: FY 1991
[NSF-93-320] 07 p3101 N94-28201
OPTIONS for systemic change in mathematics, science, and technology education: Scientist/teacher partnerships
[DE94-007472] 09 p3914 N94-32910
Science and engineering indicators, 1993
[NSB-93-1] 10 p4149 N94-34169
Proceedings of the LLNL Technical Women's Symposium
[DE94-006616] 11 p4379 N94-35997

SCIENTIFIC INSTRUMENT MODULES
U SIM

SCIENTIFIC SATELLITES
NT AMPTE (SATELLITES)
NT ASTRONOMICAL SATELLITES
NT COSMIC BACKGROUND EXPLORER SATELLITE
NT CRRES (SATELLITE)
NT DYNAMICS EXPLORER SATELLITES
NT ENVIRONMENTAL RESEARCH SATELLITES

NT EXOS-C SATELLITE
NT EXOSAT SATELLITE
NT EXPLORER SATELLITES
NT EXPLORER 2 SATELLITE
NT EXTREME ULTRAVIOLET EXPLORER SATELLITE
NT GAMMA RAY OBSERVATORY
NT GINGA SATELLITE
NT HUBBLE SPACE TELESCOPE
NT IMP
NT INTERNATIONAL SUN EARTH EXPLORER 1
NT INTERNATIONAL SUN EARTH EXPLORER 3
NT LONG DURATION EXPOSURE FACILITY
NT SMALL SCIENTIFIC SATELLITES
NT SPACE INFRARED TELESCOPE FACILITY
NT UPPER ATMOSPHERE RESEARCH SATELLITE (UARS)
NT X RAY ASTROPHYSICS FACILITY
NT X RAY TIMING EXPLORER

ESRO's first scientific satellite programme, 1961 - 1966
[ESA-HSR-2] 01 p0044 N94-11462

The definition of a scientific policy: ESRO's satellite programme in 1969-1973
[ESA-HSR-6] 03 p1303 N94-16500

Choosing ESRO's first scientific satellites
[ESA-HSR-3] 03 p0887 N94-16523

Optical measurements of NASA/USAF CRRES high altitude rocket borne chemical release experiments in conjunction with the USAF airborne ionospheric observatory aircraft
[AD-A266404] 03 p1101 N94-16551

Space debris detection
[AD-A269254] 04 p1334 N94-18264

Data analysis support for the SPREE instruments on the TSS-1 shuttle flight
[AD-A272445] 05 p1654 N94-21429

Connecting science and operations: The operations coordinator 06 p2504 N94-23874

Mission engineering 06 p2505 N94-23881

The development procedures and tools applied for the attitude control software of the Italian satellite SAX 08 p3170 N94-29324

MSFC orbital spacecraft development emphases for this decade 09 p3598 N94-31048

Odin aeronomy science: A phase-A report by the Aeronomy Science Working Group for the Odin satellite
[AP-31] 09 p3770 N94-31222

SCIENTIFIC VISUALIZATION

The Air Force Interactive Meteorological System: A research tool for satellite meteorology
[AD-A265957] 01 p0284 N94-11113

Computing science and statistics, Volume 24: Graphics and visualization
[AD-A265181] 01 p0332 N94-11878

ULTRA 2 user's manual for ULTRA 2 revision 3.0
[DE93-015970] 02 p0744 N94-13120

SCORE user's manual
[DE93-015987] 02 p0822 N94-13121

Charged-particle evaluation methodology at Lawrence Livermore National Laboratory
[DE93-013429] 02 p0781 N94-13251

A perspective on AVS in an engineering sciences environment
[DE93-015011] 02 p0596 N94-13889

Visualization techniques to aid in the analysis of multi-spectral astrophysical data sets
[NASA-CR-194489] 02 p0840 N94-14482

Earth science and application
[NASA-CR-184381] 02 p0683 N94-14484

An overview of parallel scientific visualization
[DE93-017105] 02 p0755 N94-14521

The 1989 computational fluid dynamics highlights
[NASA-TM-109635] 03 p1018 N94-15246

The 1988 computational fluid dynamics highlights
[NASA-TM-109645] 03 p1019 N94-15431

Computing science and statistics, Volume 24: Graphics and visualization
[AD-A266571] 03 p1150 N94-16721

Theoretical crystallography with the Advanced Visualization System
[DE93-015692] 03 p1215 N94-17319

TDNOVA interactive graphics
[AD-A268000] 03 p1156 N94-17530

Texture splats for 3D vector and scalar field visualization
[DE93-017104] 04 p1520 N94-18130

An evolving infrastructure for scientific computing and the integration of new graphics technology
[DE93-017164] 04 p1520 N94-18133

Three-dimensional cloud visualization based on satellite imagery
[AD-A269318] 04 p1490 N94-18300

VHDL simulation with access to transistor models 04 p1402 N94-18381

3D composite grids using Bezier curves and surfaces in component adaptive methods
[AD-A269188] 04 p1549 N94-18863

A visualization environment for supercomputing-based applications in computational mechanics
[DE93-015024] 04 p1537 N94-19249

Volume rendering of 3D scalar and vector fields at Lawrence Livermore National Laboratory
[DE93-018000] 04 p1528 N94-19276

Fast data parallel polygon rendering
[DE93-040157] 05 p1929 N94-20279

A data distributed, parallel algorithm for ray-traced volume rendering
[DE93-040150] 05 p1935 N94-21622

Geometric optimization
[DE93-040152] 05 p1917 N94-21764

PROS: An IRAF based system for analysis of x ray data 05 p1925 N94-22461

The IDL astronomy user's library 05 p2048 N94-22500

GRO/EGRET data analysis software: An integrated system of custom and commercial software using standard interfaces 05 p1926 N94-22501

SKYMAP: Exploring the Universe in software 05 p1927 N94-22511

The European Southern Observatory-MIDAS table file system 05 p2048 N94-22518

Software for scientific visualization: State of the art and experiences
[PB93-225183] 06 p2449 N94-23111

Visualization of results from meteorological simulations on CRAY
[PB93-201358] 06 p2451 N94-23443

GLview user's guide
[PB93-201366] 06 p2452 N94-23444

A knowledge based system for scientific data visualization
[NASA-CR-194879] 06 p2452 N94-23507

Simultaneous simulation and visualization using DGL
[PB93-201341] 06 p2453 N94-23534

Multimission image processing and science data visualization 06 p2518 N94-23955

A white paper: NASA virtual environment research, applications, and technology
[NASA-TM-109682] 06 p2428 N94-24855

IRMA: A program for three-dimensional color display of data
[AD-A273811] 07 p2959 N94-25879

Center for computation and visualization of geometric structures
[DE94-001882] 07 p2991 N94-25928

Radar cross section visualization using sample buffer progressive refinement volume rendering
[AD-A274179] 07 p2773 N94-27127

Sculpting in cyberspace: Parallel processing the development of new software 07 p2686 N94-27365

Thirteen ways to say nothing with scientific visualization
[NASA-CR-195280] 07 p2970 N94-27542

RIAD visual imaging branch assessment 07 p2815 N94-27895

Visualization techniques to aid in the analysis of multispectral astrophysical data sets
[NASA-CR-195268] 07 p3105 N94-27932

Analytic rendering of curvilinear volume data
[DE94-004934] 08 p3407 N94-28506

Using stereoscopic imaging for visualization applications
[DE94-006247] 08 p3536 N94-30706

Applications of data compression to 3-D scalar field visualization 09 p3817 N94-32294

Virtual reality in medical education and assessment 09 p3798 N94-32471

On the use of computers for teaching fluid mechanics
[NASA-TM-106587] 09 p3820 N94-32773

Comet impact 1994 animation reel
[NASA-TM-109810] 10 p4163 N94-33562

Data visualization for ONEDANT and TWODANT discrete ordinates codes
[DE94-005087] 10 p4105 N94-33713

Interactive archives of scientific data 10 p4122 N94-35044

RAVE: Rapid Visualization Environment 10 p4122 N94-35046

Representing spatial information in a computational model for network management
[NASA-CR-191669] 11 p4306 N94-36040

EM-ANIMATE: A computer program for displaying and animating electromagnetic near-field and surface-current solutions: Video supplement to NASA Technical Memorandum 4539
[NASA-TM-4539-VIDEO-SUPPL] 12 p4492 N94-36518

SCIENTISTS

The legacy of uncertainty 01 p0376 N94-10577

NASA/DOD Aerospace Knowledge Diffusion Research Project. Report 17: A comparison of the technical communication practices of Dutch and US aerospace engineers and scientists
[NASA-TM-108987] 01 p0419 N94-11352

NASA/DOD Aerospace Knowledge Diffusion Research Project. Report 18: A comparison of the technical communication practices of aerospace engineers and scientists in India and the United States
[NASA-TM-109006] 02 p0821 N94-13057

Generic results of the space physics community survey
[NASA-CR-194538] 02 p0818 N94-13984

NASA/DOD Aerospace Knowledge Diffusion Research Project. Paper 34: Users and uses of DOD technical reports: A report from the field
[NASA-TM-109327] 02 p0825 N94-14485

NASA/DOD Aerospace Knowledge Diffusion Research Project. Paper 36: Technical uncertainty as a correlate of information use by US industry-affiliated aerospace engineers and scientists
[NASA-TM-109328] 02 p0825 N94-14486

NASA/DOD Aerospace Knowledge Diffusion Research Project. Paper 39: The role of computer networks in aerospace engineering
[NASA-TM-109331] 02 p0825 N94-14487

NASA/DOD Aerospace Knowledge Diffusion Research Project. Paper 37: The impact of political control on technical communications: A comparative study of Russian and US aerospace engineers and scientists
[NASA-TM-109329] 02 p0826 N94-14488

NASA/DOD Aerospace Knowledge Diffusion Research Project. Paper 38: Computer Mediated Communication (CMC) and the communication of technical information in aerospace
[NASA-TM-109330] 02 p0826 N94-14489

Scientists, engineers, and technicians in nonmanufacturing industries: 1990. Detailed statistical tables
[NSF-92-334] 02 p0820 N94-14499

NASA/DOD Aerospace Knowledge Diffusion Research Project. Report 15: Technical uncertainty and project complexity as correlates of information use by US industry-affiliated aerospace engineers and scientists: Results of an exploratory investigation
[NASA-TM-107693] 03 p1233 N94-17291

Magnetic Fusion Energy Technology Fellowship: Report on survey of institutional coordinators
[DE93-014646] 04 p1583 N94-17739

Origins of solar activity. First year report, AASERT grant
[AD-A268848] 04 p1629 N94-18222

Computing professionals: Changing needs for the 1990's
[B-030] 04 p1515 N94-19401

Women scientists and engineers employed in industry: Why so few? A report based on a conference
[ISBN-0-309-04991-1] 06 p2585 N94-24698

General Motors Corporation and Pacific Northwest Laboratory staff exchange: Inspection of case hardened steels and metal-matrix composites
[DE94-003470] 07 p2706 N94-25982

Predoctoral training grant in the area of physical sciences
[DE94-004406] 07 p3039 N94-27603

Science observed: The mass-extinction debates 07 p2888 N94-28300

Construction of visual representations and time-space organization of resources in astronomy
[ISBN-0-315-86694-2] 09 p3925 N94-31914

NASA/DOD Aerospace Knowledge Diffusion Research Project. Paper 12: The diffusion of federally funded aerospace research and development (R/D) and the information seeking behavior of US aerospace engineers and scientists
[NASA-TM-109404] 09 p3921 N94-32832

NASA/DOD Aerospace Knowledge Diffusion Research Project. Paper 11: The voice of the user: How US aerospace engineers and scientists view DOD technical reports
[NASA-TM-109348] 09 p3921 N94-32834

NASA/DOD Aerospace Knowledge Diffusion Research Project. Paper 1: The value of scientific and technical information (STI), its relationship to Research and Development (R/D), and its use by US aerospace engineers and scientists
[NASA-TM-109774] 09 p3922 N94-32835

NASA/DOD Aerospace Knowledge Diffusion Research Project. Report 25: The technical communications practices of British aerospace engineers and scientists: Results of the phase 4 RAeS mail survey
[NASA-TM-109098] 09 p3922 N94-32836

NASA/DOD Aerospace Knowledge Diffusion Research Project. Report 24: The technical communications practices of US aerospace engineers and scientists: Results of the phase 1 SAE mail survey
[NASA-TM-109088] 09 p3922 N94-32837
Science and engineering indicators, 1993
[NSB-93-1] 10 p4149 N94-34169
NASA/DOD Aerospace Knowledge Diffusion Research Project. Paper 41: Technical communication practices of Dutch and US aerospace engineers and scientists: International perspective on aerospace
[NASA-TM-109862] 10 p4159 N94-34604
NASA/DOD Aerospace Knowledge Diffusion Research Project. Paper 42: An analysis of the transfer of Scientific and Technical Information (STI) in the US aerospace industry
[NASA-TM-109863] 10 p4159 N94-34730
Women as a resource for the flexibility required for high technology innovation 11 p4348 N94-35966

SCINTILLATING FIBERS
Gamma-insensitive optical focal plane array
[DE93-013100] 02 p0792 N94-14317
A space fiber-optic x ray burst detector
[DE94-002722] 07 p2696 N94-26808
A simple satellite system to locate gamma ray bursters using scintillating fiber technology
[DE94-601287] 07 p3117 N94-27996
Final results from the SDC dopant search for new green wavelength shifting (WLS) fibers, volume 1
[DE94-006744] 09 p3878 N94-31271
Investigation of scintillator and fibre light in plastic scintillation dosimetry
[ISBN-0-315-87190-3] 09 p3879 N94-31877
The first balloon flight and accelerator calibration of the scintillating optical fiber isotope experiment 10 p4167 N94-33389
Experimental and theoretical high energy physics research
[DE94-008339] 10 p4139 N94-33844
Ultrafast readout of scintillating fibers using upgraded position-sensitive photomultipliers
[DE94-010419] 11 p4269 N94-36095

SCINTILLATION
A new data collection system for ionospheric modelling and related topics
[AD-A265893] 01 p0278 N94-12277
Barium fluoride research and development at Lawrence Livermore National Laboratory
[DE93-014682] 02 p0807 N94-13405
Gamma-insensitive optical focal plane array
[DE93-013100] 02 p0792 N94-14317
Results from a study of scintillation behavior at 12, 20, and 30 GHz using the results from the Virginia Tech Olympus receivers 02 p0613 N94-14659
Effects of the equatorial ionosphere on L-band Earth-space transmissions 02 p0615 N94-14671
Optical ionospheric instrumentation and research
[AD-A266403] 03 p1192 N94-16550
Scintillation mechanism in stoichiometric cerium compounds
[DE93-015499] 03 p0948 N94-16771
Radio wave propagation in structured ionization for satellite and radar applications
[AD-A268457] 04 p1382 N94-17844
An investigation of methods for updating ionospheric scintillation models using topside in-situ plasma density measurements
[AD-A269872] 04 p1483 N94-18655
Precision machining and polishing of scintillating crystals for large calorimeters and hodoscopes
[DE93-018663] 04 p1381 N94-19544
The effects of magnetic storm phases on F-layer irregularities from auroral to equatorial latitudes
[AD-A272685] 05 p1857 N94-21189
Temperature dependence of CsI(Tl) gamma ray excited scintillation characteristics
[DE94-000636] 05 p2034 N94-22028
Calorimeter with WLS fibers and parallel to beam scintillators
[DE93-634188] 07 p2810 N94-26378
The 1024 scintillation hodoscope
[DE93-634183] 07 p2810 N94-26394
Physical characteristics of polymethylmethacrylate scintillator SOFG-120
[DE93-634184] 07 p2810 N94-26395
On possibility to create the scintillation trigger for liquid-argon neutrino detector
[DE94-607844] 08 p3489 N94-30050
Preliminary detector design ST862-prototype neutron detector
[DE94-004714] 08 p3491 N94-30695
Silica scintillating materials prepared by sol-gel methods
[DE94-005123] 08 p3220 N94-30778
Final results from the SDC dopant search for new green wavelength shifting (WLS) fibers, volume 1
[DE94-006744] 09 p3878 N94-31271
Design of new polymers to improve radiation stability of plastic scintillators
[DE94-008220] 09 p3652 N94-31764
Statistics of time averaged atmospheric scintillation
[DE94-006998] 09 p3747 N94-32249
Phase-only correction of scintillated laser beams: Downrange experimental results
[AD-A277778] 09 p3722 N94-33282
An investigation of methods for improving models of ionospheric plasma-density irregularities and radio-frequency scintillation
[AD-A278568] 10 p4033 N94-33703
Utility of interplanetary scintillation maps in forecasting geomagnetic activity: A study based on single-station data from Cambridge, United Kingdom
[PB94-156775] 10 p4087 N94-34600
Wide aperture scintillation hodoscope with FEU-143 photomultipliers
[DE94-618211] 12 p4515 N94-37075

SCINTILLATION COUNTERS
Experimental efforts and results in finding new heavy scintillators
[DE93-010406] 01 p0371 N94-10156
Conceptual design report for the SDC barrel and intermediate muon detectors based on a jet-type drift chamber
[DE93-753173] 01 p0367 N94-11510
Measurements of optical properties of waveshifting optical fiber for liquid scintillator hadron calorimetry
[DE93-012606] 02 p0791 N94-13482
Cosmic and solar gamma ray and neutron experiments
[NASA-CR-193359] 02 p0849 N94-13965
Absolute detection efficiency of a micro-channel plate detector to x rays in the 1-100 KeV energy range
[DE93-012592] 02 p0789 N94-14460
Results from a water-Cerenkov array
[DE93-012715] 02 p0849 N94-14461
Prospects for high pressure imaging gas scintillation drift chambers 03 p0901 N94-15040
The high pressure gas scintillation proportional counter for SAX 03 p0906 N94-15076
A new detector concept for energetic auroral x ray imaging 03 p0907 N94-15081
Applications for large area silicon drift detectors on x ray and gamma ray astronomy 03 p0909 N94-15090
Scintillation mechanism in stoichiometric cerium compounds
[DE93-015499] 03 p0948 N94-16771
An investigation of methods for updating ionospheric scintillation models using topside in-situ plasma density measurements
[AD-A269872] 04 p1483 N94-18655
Conversion of ADC pulse heights into MIP units: NUMASS test data, September 1991
[USIP-93-03] 04 p1432 N94-18846
SSC detector muon sub-system beam tests
[DE93-018415] 04 p1569 N94-19013
New room temperature high resolution solid-state detector (CdZnTe) for hard x rays and gamma rays 04 p1324 N94-19165
Telescope for x ray and gamma ray studies in astrophysics 04 p1324 N94-19166
New concepts for HgI2 scintillator gamma ray spectroscopy
[NASA-CR-194819] 06 p2233 N94-24113
The L3 visualization system and its use in the Z(zero) line shape analysis
[ETN-94-95382] 06 p2537 N94-25231
Bottom quark production at the Z resonance
[ISBN-9-09-006217-3] 06 p2538 N94-25255
The data-acquisition and second level trigger system for ZEUS calorimeter
[ETN-94-95384] 06 p2541 N94-25256
CsI(Tl)-photodiode detectors for spectroscopy at low radiation levels
[MPI-PHE/92-22] 06 p2314 N94-25457
An electromagnetic calorimeter with wavelength shifting fiber readout
[DE93-616664] 07 p2809 N94-25735
Calorimeter with WLS fibers and parallel to beam scintillators
[DE93-634188] 07 p2810 N94-26378
The 1024 scintillation hodoscope
[DE93-634183] 07 p2810 N94-26394
Physical characteristics of polymethylmethacrylate scintillator SOFG-120
[DE93-634184] 07 p2810 N94-26395
Unsegmented electromagnetic calorimeter prototype. Energy and coordinate resolution
[DE93-634185] 07 p2810 N94-26396
Study on the compensated lead hadron calorimeter characteristics by means of hadron and electron beams
[DE93-634176] 07 p2810 N94-26439
A space fiber-optic x ray burst detector
[DE94-002722] 07 p2696 N94-26808
First observation of neutral current proton electron scattering at the square root of s = 300 GeV
[DE94-701107] 07 p3030 N94-27877
A prototype presampler for the uranium-scintillator calorimeter in Zeus
[NIKHEF-H/93-11] 07 p2814 N94-28098
On possibility to create the scintillation trigger for liquid-argon neutrino detector
[DE94-607844] 08 p3489 N94-30050
Preliminary detector design ST862-prototype neutron detector
[DE94-004714] 08 p3491 N94-30695
Silica scintillating materials prepared by sol-gel methods
[DE94-005123] 08 p3220 N94-30778
Particle identification in a segmented calorimeter (NUMASS test data, September 1991)
[USIP-93-08] 09 p3711 N94-31085
Final results from the SDC dopant search for new green wavelength shifting (WLS) fibers, volume 1
[DE94-006744] 09 p3878 N94-31271
Mechanisms of formation and of de-excitation in the reaction Mg-24 + C-12 yields 9 alpha at 35MeV per nucleon
[ISBN-0-315-86746-9] 09 p3867 N94-31749
Design of new polymers to improve radiation stability of plastic scintillators
[DE94-008220] 09 p3652 N94-31764
Investigation of scintillator and fibre light in plastic scintillation dosimetry
[ISBN-0-315-87190-3] 09 p3879 N94-31877
The first balloon flight and accelerator calibration of the scintillating optical fiber isotope experiment 10 p4167 N94-33389
X-ray remote sensing and in-situ spectroscopy for planetary exploration missions and gamma-ray remote sensing and in-situ spectroscopy for planetary exploration missions
[NASA-CR-189352] 11 p4375 N94-35381
Electronics for the SND scintillation counter system
[DE94-616453] 11 p4259 N94-36104
Neutron detectors for fusion reaction-rate measurements
[DE94-010407] 11 p4330 N94-36114
High Energy Physics Division of research activities
[DE93-019681] 12 p4521 N94-36694
Simple and efficient method of secondary vertex searching
[DE94-618542] 12 p4514 N94-37064
Wide aperture scintillation hodoscope with FEU-143 photomultipliers
[DE94-618211] 12 p4515 N94-37075

SCINTILLATION FIBERS
U SCINTILLATING FIBERS

SCINTILLATORS
U SCINTILLATION COUNTERS

SCINTILLOMETERS
U SCINTILLATION COUNTERS

SCISSION
U CLEAVAGE

SCORING
Generalized smooth models
[DE93-013045] 02 p0756 N94-14864
Extracting information from wrong answers in computerized adaptive testing
[AD-A272832] 05 p1894 N94-21434

SCORPIO CONSTELLATION
U SCORPIUS CONSTELLATION

SCORPIUS CONSTELLATION
Mass of Saturn's A ring 03 p1263 N94-16252

SCOUT LAUNCH VEHICLE
Scout: The unsung hero of space
[NASA-TM-109289] 02 p0540 N94-13628
Nasa Langley Research Center seventy-fifth anniversary publications, 1992
[NASA-TM-109691] 07 p3118 N94-27431

SCOUT PROJECT
Scout: The unsung hero of space
[NASA-TM-109289] 02 p0540 N94-13628

SCPC TRANSMISSION
U SINGLE CHANNEL PER CARRIER TRANSMISSION

SCR (RECTIFIERS)
U SILICON CONTROLLED RECTIFIERS

SCRAMJET ENGINES
U SUPERSONIC COMBUSTION RAMJET ENGINES

SCRAMJETS
U SUPERSONIC COMBUSTION RAMJET ENGINES

SCREW DISLOCATIONS
Internal friction associated with dislocation relaxations in virgin martensite
[PB93-226280] 06 p2240 N94-23119

SCREWS
Three point lead screw positioning apparatus for a cavity tuning plate
[NASA-CASE-LEW-15216-1] 05 p1822 N94-20375
Self locking set screw
[AD-D015969] 05 p1824 N94-21277
Spline screw multiple rotations mechanism
[NASA-CASE-GSC-13452-1] 06 p2352 N94-23078
Split spline screw
[NASA-CASE-GSC-13434-1] 06 p2352 N94-23082
Kinematic analysis of platform-type robotic manipulators
[ISBN-0-315-78703-1] 08 p3311 N94-30793
An experimental and analytical investigation of a threaded fastener
[VTT-JULK-786] 09 p3724 N94-31654

SCRIBING
U SCORING

SCRUBBERS
Gas stream purifier 08 p3354 N94-30469

SCRUBBING
U WASHING

SDV
U SHUTTLE DERIVED VEHICLES

SEA BREEZE
A study of the Merritt Island, Florida sea breeze flow regimes and their effect on surface heat and moisture fluxes
[NASA-CR-4537] 01 p0286 N94-12580
Predicting lightning events in the KSC area: A feasibility study using single station data
[AD-A271440] 05 p1864 N94-20088
The sea breeze convergence zone and its relationship to fair weather electricity in east central Florida
[AD-A268511] 05 p1868 N94-21502
An observational and numerical study of sea/land-breeze circulations in an area of complex coastal heating 08 p3372 N94-29813
Evolution of diurnal surface winds and surface currents for Monterey Bay
[AD-A277649] 09 p3790 N94-33057
A comparison of modeled and observed ocean mixed layer behavior in a sea breeze influenced coastal region
[AD-A277911] 10 p4092 N94-33922

SEA FLOOR SPREADING
Constraints on crustal structure from long period pressure and displacement measurements on the deep seafloor
[AD-A269931] 04 p1498 N94-18663
Light in Thermal Environments (LITE) Workshop
[NASA-CR-195851] 09 p3790 N94-32981

SEA GRASSES
The role of certain infauna and vascular plants in the mediation of redox reactions in marine sediments 01 p0268 N94-12454

SEA ICE
NT ICE FLOES
NT ICEBERGS
NT PRESSURE ICE
AMIP: The Atmospheric Model Intercomparison Project
[DE93-007400] 01 p0273 N94-10151
AMIP: The Atmospheric Model Intercomparison Project
[DE93-007413] 01 p0273 N94-10152
Sea ice: A climate component 01 p0232 N94-11705
Monitoring of the Greenland Ice Sheet using ERS-1 synthetic aperture radar imagery 01 p0237 N94-11741
Investigations of Arctic ice-sheets and glaciers using ERS-1 SAR 01 p0238 N94-11743
Spatial patterns in backscatter strength across the Greenland Ice Sheet 01 p0238 N94-11744
Ice studies in the Barents Sea by ERS-1 SAR during SIZEX 92 01 p0238 N94-11745
Validation of ERS-1 SAR measurements of sea ice during ARCTIC-1991 01 p0238 N94-11747
Arctic coastal polynya observations with ERS-1 SAR and DMSP SSM/I 01 p0239 N94-11748
Sea ice deformation observed with ERS-1 SAR 01 p0239 N94-11749
Finnish ERS-1 Baltic Sea ice experiment in Winter 1992 01 p0239 N94-11750
Experiences from the Swedish sea ice programme during BEERS-1992 01 p0239 N94-11751
Greenland Sea observations 01 p0239 N94-11752
Arctic sea ice microwave signature and geophysical processes study 01 p0240 N94-11754
Sea ice radar signatures from ERS-1 SAR during late Summer and Fall in the Beaufort and Chukchi Seas 01 p0240 N94-11756
Waves and mesoscale features in the marginal ice zone 01 p0240 N94-11757
The seasonal Sea Ice Monitoring and Modelling Site (SIMMS): Using ERS-1 in climate research 01 p0240 N94-11758
Preliminary evaluation of ERS-1 SAR data for operational use in the Canadian sea ice monitoring program 01 p0241 N94-11760
Sea ice feature and type identification in merged ERS-1 SAR and LANDSAT Thematic Mapper imagery 01 p0241 N94-11761
Summer Arctic ice concentrations and characteristics from SAR and SSM/I data 01 p0241 N94-11762
Evaluating ERS-1 ice motion and classification products 01 p0241 N94-11763
Ocean-ice interaction study of waves and mesoscale features 01 p0197 N94-11935
Impact of ERS-1 wind/wave/ice data on operational ocean forecasting 01 p0250 N94-12500
Pacific rim sea ice as observed with the NIMBUS-7 SMMR 01 p0210 N94-12651
Microwave radiometry of ice cover in polar regions 01 p0210 N94-12655
Exploring the southern ocean response to climate change
[NASA-CR-194601] 03 p1112 N94-15680
Sea ice motions in the central arctic ice central arctic pack ice as inferred from AVHRR imagery
[NASA-CR-194572] 03 p1112 N94-15701
Imaging radar studies of polar ice 03 p0991 N94-15899
Developing automated analysis methods for sea ice imagery: A status report with recommendations
[AD-A267284] 03 p1113 N94-17241
Arctic and Antarctic sea ice, 1978-1987: Satellite passive-microwave observations and analysis
[NASA-SP-511] 03 p1114 N94-17439
Arctic cyclones and Marginal Ice Zone (MIZ) variability
[AD-A268610] 03 p1108 N94-17465
Atlas of SSM/I satellite ice concentration interpolated to operational ice model domains of the Arctic for 1992
[AD-A270306] 04 p1499 N94-18727
Method for extracting tidal and inertial motion from ARGOS ice buoys applied to the Barents Sea during CEAREX
[PB93-190213] 04 p1499 N94-19063
Oil spreading in surface waters with an ice cover
[PB93-190767] 04 p1476 N94-19064
Airborne studies of ocean-particle-cloud interactions in the Arctic
[AD-A270752] 04 p1479 N94-19575
Radar backscatter measurements from simulated sea ice during CRRELEX 1990
[AD-A271034] 05 p1715 N94-19823
Polarimetric backscattering from sea ice 05 p1723 N94-20426
Observation of pressure ridges in SAR images of sea ice: Scattering theory and comparison with observations 05 p1723 N94-20427
On evaluating the accuracy of SAR sea-ice classification using multifrequency polarimetric AIRSAR data 05 p1724 N94-20428
Retrieval of ice thickness from polarimetric SAR data 05 p1724 N94-20432
Studies of Greenland using the SEASAT scatterometer 05 p1725 N94-20433
Radar backscattering from snow facies of the Greenland ice sheet: Results from the AIRSAR 1991 campaign 05 p1725 N94-20434
C-band radar backscatter of sea ice in the Weddell Sea, Antarctica during the austral winter of 1992 05 p1725 N94-20435
The effect of sub-surface volume scattering on the accuracy of ice-sheet altimeter retracking algorithms
[NASA-CR-194825] 06 p2386 N94-24060
Examination of the physical, electrical, and microwave evolution of water into young sea ice
[AD-A273559] 06 p2418 N94-24918
National Academy of Sciences-Academy of Sciences of the USSR Workshop on the Mechanics of Ice and its Applications
[AD-A273338] 06 p2419 N94-25088
An evaluation of an airborne remote sensing system used to determine ice thickness and geometry of a first year sea ice ridge located in the Beaufort Sea
[ISBN-0-315-84383-7] 07 p2849 N94-26667
Response of an airborne synthetic aperture radar to sea ice in the marginal ice zone
[ISBN-0-315-84243-1] 07 p2849 N94-26668
The Hough transform algorithm for sea ice lead analysis: An evaluation
[AD-A274535] 07 p2899 N94-26853
Sound, speed, reflectivity, absorption, and thermal diffusivity measurements in Arctic ice in 1990
[AD-A274326] 07 p2899 N94-26886
The NOGAPS ten year AMIP integration
[AD-A274332] 07 p2900 N94-26887
Leadex environmental phenomena and effects observed by DMSP, NOAA, and ERS-1 satellites
[AD-A274596] 07 p2868 N94-26888
Ice surface temperature retrieval from AVHRR, ATSR, and passive microwave satellite data: Algorithm development and application
[NASA-CR-195276] 07 p2851 N94-27849
Extraterrestrial accretion and glacial cycles 07 p2890 N94-28308
Studies in ice mechanics
[PB94-133055] 07 p2900 N94-28393
Lead detection and mapping with reference to relationships between scale, sensor characteristics, surface conditions and atmospheric properties
[AD-A275321] 08 p3377 N94-28877
Sea ice and oceans applications of SAR 08 p3327 N94-28934
Dynamic constraints on CO2 uptake by an iron-fertilized Antarctic 08 p3350 N94-30619
The role of sea ice dynamics in global climate change 08 p3350 N94-30620
A toy model of sea ice growth 08 p3351 N94-30626
Cryosphere and climate 08 p3352 N94-30632
The use of ERS-1 within an operational ice monitoring program 09 p3751 N94-32545
The multiple scattering contributions in the strong fluctuation theory to the microwave brightness temperature
[AD-A277721] 10 p4075 N94-33442
Coupled ice-ocean model supporting winter navigation in the Baltic Sea. Part 1: Ice dynamics and water levels
[PB94-148780] 10 p4092 N94-34121
Operational Baltic Sea circulation model. Part 1: Baratropic version
[PB94-149101] 10 p4093 N94-34143
Environmental measurements in the Beaufort Sea, Spring 1993
[AD-A278718] 11 p4296 N94-36293
Measuring the upper profile of sea ice in the Bay of Bothnia with a laser profilometer
[PB94-184561] 12 p4477 N94-37855

SEA KING HELICOPTER
U SH-3 HELICOPTER

SEA LEVEL
Topex/Poseidon: A United States/France mission. Oceanography from space: The oceans and climate
[NASA-TM-108253] 01 p0043 N94-10699
Hypobaric decompression prebreathe requirements and breathing environment 01 p0317 N94-11541
Spatial scales of wave height 01 p0244 N94-11782
The 1992 El Nino viewed by ERS-1 altimetry 01 p0244 N94-11784
Observation of wind and waves by GEOSAT altimeter 01 p0202 N94-11961
Observations of eddy fields in the Northwest Pacific by GEOSAT altimetry 01 p0207 N94-12639
Variability of sea level and sea surface temperature anomalies in the equatorial Pacific 01 p0208 N94-12640
Theory and oceanographic applications of satellite altimeter measurements 01 p0208 N94-12641
Analysis of collinear passes of satellite altimeter data 01 p0208 N94-12642
Comparison of GEOSAT sea surface height and model-simulated surface dynamic height 01 p0208 N94-12644
Principal oscillation pattern analysis of sea level variations in the tropical Pacific measured by the GEOSAT altimeter 01 p0209 N94-12646
Measurement of eddy structure and movement in the north-east Pacific with the GEOSAT altimeter 01 p0209 N94-12647
Preliminary results from a satellite altimetric data assimilation using a Kalman filter and smoother 01 p0209 N94-12648
Fluctuations of the Kuroshio extension detected by the GEOSAT altimetry data 01 p0209 N94-12649
Mean flow and variability in the Kuroshio extension from GEOSAT altimetry data 01 p0209 N94-12650
The 1990 Western Pacific Geophysics meeting
[NASA-CR-193456] 02 p0712 N94-13334
Atmospheric transmittance between 1.0 and 2.0 micrometers
[AD-A267076] 03 p1098 N94-15539
The Central American cold surge: An observational analysis of the deep southward penetration of North American cold fronts
[AD-A268592] 03 p1110 N94-17607
Research on Earth's rotation and the effect of atmospheric pressure on vertical deformation and sea level variability
[NASA-CR-194300] 04 p1484 N94-18838
The WAQUA/CSM-16 model 04 p1494 N94-19700

Modes of ocean variability in the tropical Pacific as derived from Geosat altimetry
[MPIM-103] 06 p2382 N94-23158
Analysis of vulnerability to the impacts of sea level rise: A case study for The Netherlands
[PB94-111150] 06 p2399 N94-24573
Altimeter data processing from sea surface topography to horizontal eddy momentum fluxes
[PB94-147550] 08 p3378 N94-30714
World height system definition and implementation
[AD-A276725] 09 p3747 N94-32160
ENSO forced variations of the sea surface temperature and adjusted sea level along the west coast of the United States
[AD-A277306] 09 p3789 N94-32327
Characterization of tidal currents in Monterey Bay from remote and in-situ measurements
[AD-A277844] 10 p4092 N94-33767
Operational Baltic Sea circulation model. Part 1: Baratropic version
[PB94-149101] 10 p4093 N94-34143
Some aspects of simultaneously flying Topex Follow-On in a Topex orbit with Geosat Follow-On in a Geosat orbit
[NASA-CR-196075] 10 p4077 N94-34214

SEA OF JAPAN

High biological production of the tidal mixing zones on Japan Sea shelf 01 p0228 N94-12758
Generation of internal waves near the shelf boundary 01 p0229 N94-12763
Papers in meteorology and geophysics, vol. 44, no.1
[JTN-94-80585] 08 p3324 N94-28693
The Japan Sea proper water and water circulation in the Japan Sea 08 p3324 N94-28694

SEA ROUGHNESS

Proceedings of the PORSEC 1992 in Okinawa: Conference for Pacific Ocean Environments and Probing, volume 1
[JTN-93-80418] 01 p0191 N94-11894
Remote sensing and the air-sea boundary layers 01 p0191 N94-11896
Effects of wind-roughened sea surface on ocean color remote sensing: Noise derived from reflected light and whitecaps 01 p0191 N94-11898
HF ocean radar system at Okinawa Radio Observatory 01 p0139 N94-11902
Measurement of wave parameters by HF ocean radar 01 p0192 N94-11903
The coherent structure in the oceanic turbulence around Japan Islands Chain forced by an air, sea, and solid Earth interaction 01 p0198 N94-11940
Westward propagation of sea surface anomalies in the western North Pacific as seen by the altimeter and radiometer 01 p0198 N94-11941
Surface roughness variations across the Iceland-Faroes frontal region observed by the GEOSAT altimeter and NOAA AVHRR 01 p0201 N94-11958
Proceedings of the PORSEC 1992 in Okinawa: Conference for Pacific Ocean Environments and Probing, volume 2
[JTN-93-80419] 01 p0207 N94-12635
Spatial variability of the ocean underwater dynamic noise from satellite radar sensing data 01 p0225 N94-12740

SEA STATES

Effects of wave nonlinearity on ERS-1 radar altimeter returns: A preliminary investigation 01 p0235 N94-11722
Quick-look monitoring of the sea surface with ERS-1 fast delivery altimeter data 01 p0243 N94-11777
Proceedings of the PORSEC 1992 in Okinawa: Conference for Pacific Ocean Environments and Probing, volume 1
[JTN-93-80418] 01 p0191 N94-11894
Remote sensing and the air-sea boundary layers 01 p0191 N94-11896
Effects of wind-roughened sea surface on ocean color remote sensing: Noise derived from reflected light and whitecaps 01 p0191 N94-11898
Satellite observations of red tide events: Plans for EESI 01 p0191 N94-11899
HF ocean radar system at Okinawa Radio Observatory 01 p0139 N94-11902
Measurement of wave parameters by HF ocean radar 01 p0192 N94-11903
Ocean wave detection by SAR 01 p0197 N94-11932
On the determination of the SAR ocean surface scattering patch size 01 p0197 N94-11933
The coherent structure in the oceanic turbulence around Japan Islands Chain forced by an air, sea, and solid Earth interaction 01 p0198 N94-11940
Westward propagation of sea surface anomalies in the western North Pacific as seen by the altimeter and radiometer 01 p0198 N94-11941
Observations of the fractal properties of the Japan sea surface temperature patterns 01 p0205 N94-11984
Circulation of North Pacific Intermediate Water 01 p0206 N94-11985
SOFAR float tracking in the Shikoku basin 01 p0206 N94-11986
Use of SAR-wave, altimeter, and wind-scatterometer data in an operational swell forecasting system 01 p0250 N94-12503
Proceedings of the PORSEC 1992 in Okinawa: Conference for Pacific Ocean Environments and Probing, volume 2
[JTN-93-80419] 01 p0207 N94-12635
Variability of sea level and sea surface temperature anomalies in the equatorial Pacific 01 p0208 N94-12640
A numerical study of deep convection at high latitudes 01 p0210 N94-12652
The Pacific Subarctic Frontal Zone: Structure and dynamics 01 p0223 N94-12731
Laser photoheterodyne interferometers for oceanographic investigations 01 p0177 N94-12732
Spatial variability of the ocean underwater dynamic noise from satellite radar sensing data 01 p0225 N94-12740
Buoy experiments to obtain the sea-truth data for OCTS/NSCAT, part 1
[NASDA-CNT-930005-PT-1] 02 p0725 N94-13653
Sea surface effect on the sea surface temperature estimation by satellite data 02 p0696 N94-14265
The application of a radial basis function neural network for radar tracking over the sea 09 p3686 N94-33150
Airborne ROWS data report for the high resolution experiment, June 1993
[NASA-TM-104609] 12 p4477 N94-37397

SEA SURFACE TEMPERATURE

AMIP: The Atmospheric Model Intercomparison Project
[DE93-007400] 01 p0273 N94-10151
AMIP: The Atmospheric Model Intercomparison Project
[DE93-007413] 01 p0273 N94-10152
Preliminary results of the comparison of ATSR measurements with in situ sea temperatures
[DE93-013399] 01 p0287 N94-10517
A modeling perspective on cloud radiative forcing
[DE93-012383] 01 p0276 N94-11241
Central Equatorial Pacific Experiment (CEPEX)
[DE93-011656] 01 p0190 N94-11674
Latent and sensible heat flux estimated from ERS-1 data 01 p0244 N94-11783
The subduction experiment. Cruise report, R/V Oceanus, cruise number 250 legs 1 and 2. Subduction 2 mooring deployment and recovery cruise, 25 January-26 February 1992
[AD-A264922] 01 p0289 N94-11853
Satellite derived sea surface temperature applications for Indian Ocean resources development 01 p0193 N94-11907
Exchange of bay water with ocean current monitored by the NOAA satellite 01 p0193 N94-11908
A consideration on principal component analysis of satellite IR data 01 p0193 N94-11909
Trouble areas in the IRT measurement of the Earth surface temperature 01 p0193 N94-11910
Estimation of solar radiation at the sea surface with geostationary meteorological satellite data 01 p0196 N94-11926
The Kyucho events in Sukumo Bay induced by Kuroshio front disturbances 01 p0198 N94-11939
Satellite-derived oceanic features 01 p0200 N94-11949
Observations of the fractal properties of the Japan sea surface temperature patterns 01 p0205 N94-11984
Sea surface temperature anomalies in the Arabian Sea 01 p0206 N94-11988
Multichannel dual angle approach for sea surface temperature retrieval in context of ERS-1 scenario 01 p0252 N94-12512
ATSR correlative skin measurements of sea surface temperature 01 p0252 N94-12514
Validation of ATSR-1 using aircraft radiometer measurements over the South Atlantic 01 p0252 N94-12515
A user appraisal of ATSR near-real-time products 01 p0252 N94-12516
A comparison of ATSR and shipboard radiometer SST measurements along transects between the UK and the Antarctic 01 p0253 N94-12518
Preliminary validation of ATSR sea surface temperatures near the Faeroes 01 p0253 N94-12519
Comments on possible causes of recent global warming
[DE93-010501] 01 p0272 N94-12592
Variability of sea level and sea surface temperature anomalies in the equatorial Pacific 01 p0208 N94-12640
Validation test system for sea surface temperature detected by satellites in Mutsu Bay 01 p0213 N94-12670
Sea surface temperature images of Geostationary Meteorological Satellite (GMS) and sea truth data from ferry boats 01 p0213 N94-12671
Measurement of the sea surface emissivity 01 p0213 N94-12672
Evaluation of the method of geostrophic flow using NOAA-AVHRR data 01 p0213 N94-12673
Further study of the Non-Regression-Coefficient SST retrieval method 01 p0213 N94-12674
Delineation of mesoscale features of ocean on satellite IR image 01 p0214 N94-12675
Observation of warm current at the boundary from north equatorial current to Kuroshio by NOAA/AVHRR 01 p0214 N94-12676
Aspects of applying a relaxation method to computing sea surface velocities from sea surface temperature images 01 p0214 N94-12679
Sea surface temperature difference between NOAA/AVHRR and in-situ observation 01 p0215 N94-12680
Intrusion of Kuroshio warm water into Sagami Bay 01 p0215 N94-12683
Satellite thermal variations of Kuroshio in relation to storm floods 01 p0215 N94-12685
Swordfish (Xiphias gladius) catch distributions relative to environmental features observed from satellites off Coquimbo, Chile (30 deg S) 01 p0216 N94-12688
Observation of cold coastal water with high turbidity around the southwestern tip of Korean Peninsula 01 p0216 N94-12689
On the error characteristics of the sea surface temperature observed by satellite 01 p0216 N94-12690
The WOCE/TOGA Surface Velocity Programme (SVP) 01 p0216 N94-12691
Application of remote sensing for coastal management in the north coast of Java 01 p0218 N94-12701
Investigation of meso-scale fronts, eddies and upwellings in China Seas with AVHRR data 01 p0220 N94-12711
Coastal upwelling monitored by satellite data: Methodologies and results 01 p0220 N94-12712
Applicability of satellite infrared data for the monitoring of coastal environments 01 p0220 N94-12714
Satellite and moored buoy observations of polar frontal system over the Yamato Rise in the Japan Sea 01 p0221 N94-12715
The relationship between skin and bulk sea surface temperatures 01 p0221 N94-12716
Variability of the Kuroshio observed from satellite thermal imagery 01 p0221 N94-12717
SST assimilation: Eastern Mediterranean case study 01 p0221 N94-12719
The method of investigation of the horizontal structure of the thermal fronts 01 p0222 N94-12723
Atmospheric correction for determination of average SST fields based on AVHRR data 01 p0227 N94-12750
Outline of ISY sea surface temperature data sets 02 p0696 N94-14261
Integration of SST data sets using MOS-1 satellite data: For validation and monitoring 02 p0696 N94-14262
Geophysical validation of ATSR sea surface temperatures 02 p0696 N94-14263
Accuracy validation test of estimated sea surface temperature by satellite data 02 p0696 N94-14264
Sea surface effect on the sea surface temperature estimation by satellite data 02 p0696 N94-14265
On the sea truth data of the Kuroshio meander and cold eddy movement 02 p0696 N94-14266
A method for estimation of partial cloud cover within a pixel and its effect 02 p0697 N94-14269
Atmospheric correction for sea surface temperature by application of microwave dual-channel technique to VTIR data 02 p0697 N94-14271
Sea surface temperature forcing and phase locking of Nordeste precipitation
[DE93-011873] 02 p0723 N94-14426
The laboratory performance of the short wavelength instrument for the Along Track Scanning Radiometer ATSR-2 (initial results) 03 p0908 N94-15088
Effect of spatial resolution on the simulation of regional precipitation in China in a global climate model
[DE93-013433] 04 p1489 N94-18053
SeaSoar CTD, fluorescence and scalar irradiance data from RRS Charles Darwin Cruises 58/59, NE Atlantic, Vivaldi 1991
[IOS-299-1992] 04 p1496 N94-18066
Global and regional comparative performance of linear and nonlinear satellite multichannel sea surface temperature algorithms
[AD-A270475] 05 p1837 N94-20028

Use of satellite data for validation of the ECHAM models 05 p1861 N94-22289
Development and testing of the Coupled Ocean/Atmosphere Mesoscale Prediction System (COAMPS)
[AD-A273925] 07 p2892 N94-25793
The NOGAPS ten year AMIP integration
[AD-A274332] 07 p2900 N94-26887
Ice surface temperature retrieval from AVHRR, ATSR, and passive microwave satellite data: Algorithm development and application
[NASA-CR-195276] 07 p2851 N94-27849
The validation of ATSR measurements with in situ sea temperatures
[DE94-003195] 07 p2852 N94-27875
Role of satellite observations of sea-surface temperature in the detection of global change
[PB94-138120] 08 p3329 N94-29107
On the annual cycle of the tropical Pacific atmosphere and ocean 08 p3371 N94-29763
On interannual variability and climate change in the North Pacific 08 p3374 N94-29963
The validation of ocean surface heat fluxes in AMIP
[DE94-001539] 08 p3378 N94-30823
General ocean circulation 09 p3777 N94-30984
Low frequency variability observed in the tropical Atlantic Ocean 09 p3778 N94-30991
Air-sea interaction patterns in the equatorial Pacific
[AD-A277305] 09 p3788 N94-32072
ENSO forced variations of the sea surface temperature and adjusted sea level along the west coast of the United States
[AD-A277306] 09 p3789 N94-32327
Development of a radiative cloud parameterization scheme of stratocumulus and stratus clouds which includes the impact of CCN on cloud albedo
[DE94-005476] 10 p4081 N94-33714
EOF characterization of Atlantic SST fields using AVHRR data
[INPE-5535-TDI/523] 10 p4093 N94-34203
Long range forecasts of the Northern Hemisphere anomalies with antecedent sea surface temperature patterns
[NASA-CR-189358] 11 p4292 N94-35380
JPRS report: Science and technology. Central Eurasia: Space
[JPRS-USP-94-003] 11 p4201 N94-35520

SEA TRUTH
A comparison of ATSR and shipboard radiometer SST measurements along transects between the UK and the Antarctic 01 p0253 N94-12518
Preliminary validation of ATSR sea surface temperatures near the Faeroes 01 p0253 N94-12519
Oil spill detection using satellite-based SAR: Experience from a field experiment 01 p0253 N94-12522
Comparison of ERS-1 SAR images of the Western Mediterranean to in situ oceanographic data: PRIM-1 Cruise (May 1992) 01 p0255 N94-12529
A surface water monitoring system: A device for the sea-truth observations 01 p0210 N94-12657
Primary productivity in the Oyashio area in the spring and summer of 1990 01 p0211 N94-12658
Characterization of dissolved organic matter in the ocean by using the fluorescence excitation-emission matrix 01 p0211 N94-12659
Sea surface temperature images of Geostationary Meteorological Satellite (GMS) and sea truth data from ferry boats 01 p0213 N94-12671
Frontal zones in Pacific Ocean: Satellite and ship data analysis 01 p0216 N94-12687
The WOCE/TOGA Surface Velocity Programme (SVP) 01 p0216 N94-12691
The circulation near Luzon 01 p0219 N94-12707
Buoy experiments to obtain the sea-truth data for OCTS/NSCAT, part 1
[NASDA-CNT-930005-PT-1] 02 p0725 N94-13653
Sea surface effect on the sea surface temperature estimation by satellite data 02 p0696 N94-14265
On the sea truth data of the Kuroshio meander and cold eddy movement 02 p0696 N94-14266

SEA WALLS
U BREAKWATERS

SEA WATER
A new expression for the production rate of sea water droplets on the sea surface 01 p0195 N94-11920
The flow structure around a cylindrical pier for the flow of transcritical Reynolds number 01 p0169 N94-11944
An application of reduced gravity model to mesoscale eddies 01 p0199 N94-11945
Optical characteristics in Tokyo Bay 01 p0204 N94-11972
Remote sensing for numerical modelling of radiative transfer processes in ocean environment 01 p0204 N94-11973
A development on estimation method of undersea light 01 p0204 N94-11974
A surface water monitoring system: A device for the sea-truth observations 01 p0210 N94-12657
Primary productivity in the Oyashio area in the spring and summer of 1990 01 p0211 N94-12658
Characterization of dissolved organic matter in the ocean by using the fluorescence excitation-emission matrix 01 p0211 N94-12659
The phytoplankton bloom in the Kinu-ura Bay, Japan in the rainy season 01 p0211 N94-12660
Variation of the photosynthetic products in the regional upwelling area around the Izu Islands, Japan 01 p0211 N94-12661
Propagation of light pulses through a three-layer medium (cloud, pure air, and ocean water) 01 p0222 N94-12725
The Pacific Subarctic Frontal Zone: Structure and dynamics 01 p0223 N94-12731
Laser photoheterodyne interferometers for oceanographic investigations 01 p0177 N94-12732
Remote sensing of light scattering coefficient of sea water vertical distribution by the means of airborne lidar 01 p0224 N94-12736
Convective and dynamic instability in meridional trenches 01 p0225 N94-12739
Variability of spectral reflectance in coastal waters near the river plumes 01 p0226 N94-12744
Ecological application of Surface Enhanced Raman Spectroscopy 01 p0227 N94-12756
Experimental and theoretical investigation of undular bore formation upstream the bank 01 p0229 N94-12764
Laser-induced fluorescence over optical fibers for real time in situ measurement of petroleum hydrocarbons in seawater
[AD-A265106] 02 p0790 N94-12863
Preliminary results on the hydrological measurements in the Aegean Sea off Crete: Cruise, Georgia, 1989
[PREPRINT-736] 02 p0725 N94-13500
Open boundary conditions for incompletely parabolic systems
[FFI/RAPPORT-92/7029] 02 p0770 N94-13971
Earth's partial pressure of CO2 over the past 120 Ma; evidence from Ce anomalies in the deep (greater than 600 m) Pacific Ocean, 1 03 p1104 N94-16358
Regulation of attached bacterial growth by adsorbed proteins
[AD-A267756] C3 p1118 N94-17275
Chemical tracer studies at IOSDL. 3: The measurement of silicate, nitrate and phosphate in seawater
[IOS-302-1992] 03 p1114 N94-17489
The application of spaceborne synthetic aperture radar in the maritime environment
[DRA-TM(AWE)-91013] 05 p1737 N94-20596
Symbiosis in marine luminous bacteria
[AD-A273540] 06 p2422 N94-24791
Mapping of seawater intrusion into the coastal aquifer of Israel (the seawater-freshwater interface) by TDEM (Time Domain Electromagnetic) method
[ITN-94-85238] 07 p2850 N94-27331
Determination of lead isotope ratios in seawater by purge and trap GC/MS after ethylation 07 p2870 N94-28152
Investigation of carbon dioxide in the central South Pacific Ocean (WOCE Sections P-16C and P-17C) during the TUNES/2 expedition of the R/V Thomas Washington, July-August, 1991
[DE94-006638] 09 p3763 N94-31347
Magnetohydrodynamic boundary layer control system
[AD-D016120] 09 p3710 N94-32958
Ultraviolet Absorption Spectrometry (UVAS) and Liquid Atomic Emission Spectrometry (LAES) for oceanographic analysis systems
[AD-A278263] 10 p4091 N94-33413
Ocean magnetics
[PB94-149026] 10 p4092 N94-34142
Cooling of the West Spitzbergen Current: Wintertime observations west of Svalbard
[AD-A280648] 12 p4475 N94-36762

SEALANTS
U SEALERS

SEALERS
Thermal stability of sealants for military aircraft: Modification of polysulfide prepolymers with ether and thioether monomers
[AD-A264079] 01 p0089 N94-11107
Sealant research for solid oxide fuel cells
[DE94-000015] 07 p2857 N94-26584
Mechanical flexible joint design document
[NASA-CR-193941] 08 p3297 N94-28419
Improved resealing procedures for the second deseal/reseal program in RAAF F111 aircraft fuel tanks
[AD-A277069] 09 p3580 N94-32378
Compatibility of refrigerants and lubricants with elastomers
[DE94-008552] 09 p3658 N94-32518
Analysis of the Shuttle Orbiter reinforced carbon-carbon oxidation protection system
[NASA-TM-104792] 11 p4262 N94-35245

SEALING
Durability of a carbon segmented circumferential seal for a liquid oxygen turbopump
[NAL-TR-1155] 01 p0178 N94-10369
High temperature hydraulic seals
[AD-A268257] 03 p1048 N94-17433
Joining and Adhesion of Advanced Inorganic Materials Symposium
[AD-A269748] 04 p1342 N94-18720
Viscoelastic analysis of seals for extended service life 06 p2371 N94-24408
Sealant research for solid oxide fuel cells
[DE94-000015] 07 p2857 N94-26584
Development of a new seal for use on large openings of pressurized spacecraft
[NASA-TM-108444] 07 p2825 N94-27560
Compatibility of refrigerants and lubricants with elastomers
[DE94-008552] 09 p3658 N94-32518
Designing aluminum sealing glasses for manufacturability
[DE94-010081] 11 p4244 N94-35699

SEALS (STOPPERS)
NT BRUSH SEALS
NT GASKETS
NT HERMETIC SEALS
NT LABYRINTH SEALS
NT O RING SEALS
NT PLUGS
NT PUMP SEALS
Extensions of some guidelines for the mechanical design of coaxial compression pin seals
[DE93-012385] 01 p0177 N94-10348
Check valve with poppet damping mechanism
[NASA-CASE-MSC-21903-1] 01 p0175 N94-10655
Dynamic tester for rotor seals and bearings
[NASA-CASE-MFS-28493-1] 01 p0033 N94-10669
Compatibility testing of vacuum seal materials
[DE93-014366] 02 p0663 N94-14113
A hot dynamic seal rig for measuring hypersonic engine seal durability and flow performance
[NASA-TM-106294] 02 p0664 N94-14727
Development of braided fiber seals for engine applications 03 p0939 N94-16859
ASRM nozzle thermal analysis
[NASA-CR-194672] 03 p0928 N94-17277
High temperature hydraulic seals
[AD-A268257] 03 p1048 N94-17433
Actively controlled shaft seals for aerospace applications
[NASA-CR-194759] 05 p1823 N94-20538
The 1992 Seals Flow Code Development Workshop
[NASA-CP-10124] 05 p1654 N94-21790
Navy GTE seal development activity 05 p1655 N94-21794
Dynamics of face seals for high speed turbomachinery 05 p1655 N94-21796
An application of small-gap equations in sealing devices 06 p2325 N94-23668
Viscous rotary damper 06 p2361 N94-24031
Seal assembly
[CA-PATENT-1,312,888] 06 p2364 N94-24128
Simulation of cryogenic turbopump annular seals 06 p2371 N94-24440
Enhanced simulation software for rocket turbopump, turbulent, annular liquid seals
[NASA-CR-195239] 07 p2825 N94-27383
Development of a new seal for use on large openings of pressurized spacecraft
[NASA-TM-108444] 07 p2825 N94-27560
Development of hypersonic engine seals: Flow effects of preload and engine pressures
[NASA-TM-106333] 07 p2826 N94-27599
Development of braided rope engine seals
[NASA-TM-105902] 08 p3298 N94-28838
Rotordynamic analysis of annular honeycomb-stator turbulent gas seals using a new friction-factor model based on flat plate tests 08 p3302 N94-29916
High temperature NASP engine seal development
[NASA-TM-109750] 09 p3725 N94-31804
Engine seal technology requirements to meet NASA's advanced subsonic technology program goals
[NASA-TM-106582] 10 p4060 N94-33960
Rotordynamic Instability Problems in High-Performance Turbomachinery, 1993
[NASA-CP-3239] 10 p4061 N94-34176
Eccentricity effects upon the flow field inside a whirling annular seal 10 p4062 N94-34181

Application of an improved Nelson-Nguyen analysis to eccentric, arbitrary profile liquid annular seals
10 p4062 N94-34182
A 3D-CFD code for accurate prediction of fluid flows and fluid forces in seals 10 p4063 N94-34183
The effect of inlet swirl on the dynamics of long annular seals in centrifugal pumps 10 p4063 N94-34184
Whirl measurements on leakage flows in turbomachine models 10 p4054 N94-34185
High-temperature, bellows hybrid seal
[NASA-CASE-LEW-15570-1] 11 p4274 N94-35373
Rotor dynamic behaviour of a high-speed oil-free motor compressor with a rigid coupling supported on four radial magnetic bearings 11 p4224 N94-35911
Wear-resisting oxide films for 900 C
[DE94-010093] 11 p4246 N94-36306
Streak tube photocathode development program
[DE94-009905] 11 p4270 N94-36350
Hot dynamic test rig for measuring hypersonic engine seal flow and durability
[NASA-TM-106507] 12 p4450 N94-36645
Evaluation of seals and lubricants used on the Long Duration Exposure Facility
[NASA-CR-4604] 12 p4399 N94-37614

SEAMOUNTS
Coupling of pelagic and benthic communities over a seamount in the Eastern North Pacific
[AD-A274750] 07 p2899 N94-26149
Fine and microstructure observations at Fieberlin g Guyot R/V new horizon cruise report
[AD-A277917] 09 p3791 N94-33109

SEAMS (JOINTS)
Flight 20 (STS-45) polysulfide gas path investigation
[NASA-CR-193861] 03 p0928 N94-17213
Chamber free fusion welding root side purging method and apparatus
[NASA-CASE-MFS-28832-1] 08 p3204 N94-29380

SEARCH AND RESCUE SATELLITE
U SARSAT

SEARCH FOR EXTRATERRESTRIAL INTELLIGENCE
U PROJECT SETI

SEARCH PROFILES
Software Toolkit for Analysis Research (STAR)
[DE93-017368] 04 p1519 N94-18086
A comparison of Boolean-based retrieval to the WAIS system for retrieval of aeronautical information
[NASA-CR-4569] 06 p2594 N94-25487
What can we learn from genetic algorithms: A new perspective for search methods
[PB94-125234] 07 p2967 N94-26997
A unified framework for retrieval in image databases
08 p3533 N94-29811
Knowledge combination and data fusion with application to recognition systems 08 p3259 N94-30513
Methods for parallelizing search paths in phrasing
[AD-A276876] 09 p3817 N94-32212
Sequencing items in multiple-item displays on online public access catalogs 10 p4150 N94-33419

SEARCH RADAR
NT OVER-THE-HORIZON RADAR
Alternative optical architectures for multichannel adaptive optical processing
[AD-A267052] 03 p1189 N94-15664
Development of a lidar for integration with the Naval Postgraduate School Infrared Search and Target Designation (NPS-IRSTD) system
[AD-A271847] 05 p1817 N94-20611
Method and apparatus for determining target elevation angle, altitude and range, and the like in a monopulse radar system with reduced multipath errors
[AD-D016005] 06 p2302 N94-25058

SEARCHING
NT SEARCH PROFILES
Extremal polygon containment problems and other issues in parametric searching
[ITN-93-85214] 02 p0771 N94-14506
A browsing tool for the Internet Logical Library of the HPCC Software Exchange
[NASA-CR-194545] 03 p1143 N94-15189
Finding the strong components in a directed graph
[PB93-187342] 04 p1555 N94-19708
Using multiple searchers to locate a randomly moving target
[AD-A275602] 08 p3463 N94-28768
Enhancing performance of full-text retrieval systems using relevance feedback 08 p3532 N94-29806
A note on the complexity of local search problems
[CT-93-02] 08 p3456 N94-30370
Searching for plans using a hierarchy of learned macros and selective reuse
[AD-A280594] 12 p4499 N94-36722
Simple and efficient method of secondary vertex searching
[DE94-618542] 12 p4514 N94-37064

SEAS
NT ADRIATIC SEA
NT ARABIAN SEA
NT BALTIC SEA
NT BARENTS SEA
NT BEAUFORT SEA (NORTH AMERICA)
NT BLACK SEA
NT MEDITERRANEAN SEA
NT NORTH SEA
NT RED SEA
NT SEA OF JAPAN
An analysis of the gravity field in the Norwegian Sea and mapping of the ice cap of Greenland using ERS-1 altimeter measurements 01 p0242 N94-11768
On the application and evaluation of the relocatable diecast ocean circulation model in coastal and semi-enclosed seas
[AD-A266626] 03 p1112 N94-15771
Field observations of infragravity, sea and swell directional spectra
[AD-A266439] 03 p1113 N94-16561
An atlas of bathy-thermograph temperature cross-sections for Coral and Tasman Sea transects from 1960 to 1987
[AD-A268775] 04 p1497 N94-18329
Overview of physical oceanographic measurements taken during the Mount Mitchell cruise to ROPME sea area
[DE93-018460] 04 p1497 N94-18494
SeaTrack: Ground station orbit prediction and planning software for sea-viewing satellites
[NASA-RP-1331] 04 p1532 N94-19761
Survival suit for submarine personnel: Summary of evaluation studies
[PB93-204634] 06 p2430 N94-23743
Interpreting the implied meridional oceanic energy transport in AMIP
[DE94-001538] 07 p2898 N94-26072
The validation of ocean surface heat fluxes in AMIP
[DE94-001539] 08 p3378 N94-30823
Cooling of the West Spitzbergen Current: Wintertime observations west of Svalbard
[AD-A280648] 12 p4475 N94-36762

SEASAT SATELLITES
Variability of wind stress, and sensible and latent heat flux in the North Atlantic during SEASAT
01 p0194 N94-11918
ERS-1 and Seasat scatterometer measurements of ocean winds: Model functions and the directional distribution of short waves 05 p1720 N94-20412
Studies of Greenland using the SEASAT scatterometer 05 p1725 N94-20433
Comparison of SPOT, ERS-1, SEASAT, LANDSAT TM, and merged imagery for geological investigations
09 p3752 N94-32547
Evaluation of surface phase change on large zones
09 p3755 N94-32567

SEASONAL VARIATIONS
U ANNUAL VARIATIONS

SEASONS
NT SPRING (SEASON)
NT SUMMER
NT WINTER
Royal Belgium observatory calendar: 156th year
[ETN-93-94221] 02 p0833 N94-14811
Global and regional/seasonal color mosaics of Mars
03 p1288 N94-16393
CTD oxygen, tracer and nutrient data from RRS Charles Darwin Cruises 58/59 in the NE Atlantic as part of Vivaldi 1991
[IOS-296-1992] 04 p1496 N94-18065
Monthly variation of physiological and psychological responses under unsteady thermal conditions
07 p2918 N94-27475
Man's ability to adapt himself for the seasonal climatic changes: From viewpoint of anticipation and seasonable behavior 07 p2919 N94-27476

SEAT BELTS
Numerical simulation of vehicle crashworthiness and occupant protection 04 p1459 N94-19471
Efficiency and biofidelity of occupant simulations
04 p1459 N94-19473
Crashworthiness analysis of commuter aircraft seats
[AD-A275889] 08 p3135 N94-28799

SEATS
NT EJECTION SEATS
Analysis of differences between seating positions in simulators and orbiters
[NASA-TM-104776] 02 p0737 N94-13399
Basic principles of helicopter crashworthiness
[AD-A267099] 03 p0862 N94-15637
Ergonomics in the office environment
03 p1124 N94-16612
Analysis of seating and restraint limitations restricting total body weight for aircrew and passengers on US Army helicopters
[AD-A269117] 04 p1511 N94-18296
Army Cockpit Delethalization Program (CDP)
[AD-A268990] 04 p1512 N94-18765
Aviation safety research at the National Institute for Aviation Research, Wichita State University
[NIAR-93-4] 05 p1641 N94-20189
Design of a recumbent seating system
[NASA-CR-195503] 06 p2438 N94-24786
Full-scale fire testing of seat component materials
[AD-A273499] 06 p2174 N94-24941
Crashworthiness analysis of commuter aircraft seats
[AD-A275889] 08 p3135 N94-28799
An overview of Space Shuttle anthropometry and biomechanics research with emphasis on STS/Mir recumbent seat system design
10 p4101 N94-33629

SECONDARY BATTERIES
U STORAGE BATTERIES

SECONDARY EMISSION
Measurements of scattering processes in negative ion-atom collisions
[DE93-013863] 02 p0779 N94-12940
New preamplifiers for the SEM scanner
[DIGEL-1993-3] 05 p1979 N94-20118
Effect of geostationary environment constituents on secondary electron emission rates
05 p1661 N94-21382
Secondary electron emission from copper surface due to neodymium and gadolinium ion bombardment
[DE94-701115] 07 p3027 N94-27718
Characteristics of secondary electron emission from CsI induced by x rays with energies up to 100 keV
[DE94-608422] 08 p3395 N94-30185
Elimination of two atomic electrons by a single high energy photon
[DE94-006834] 09 p3864 N94-31320
Energy and angular distributions of secondary ions during electronic sputtering of nonconducting surfaces
[ETN-94-95756] 09 p3865 N94-31516

SECONDARY FLOW
Unsteady flow past a NACA 0012 airfoil pitching at constant rates
[AD-A265159] 01 p0016 N94-11889
Turbine blade tip film cooling measurements
[AD-A267686] 03 p0868 N94-14964
STREMR: Numerical model for depth-averaged incompressible flow
[AD-A269949] 04 p1417 N94-18672
Measurement and prediction of the flow through an annular turbine cascade
[AD-A272530] 05 p1803 N94-21417
CFD analyses of coolant channel flowfields
06 p2214 N94-23050
Improving diffusing S-duct performance by secondary flow control
[NASA-TM-106492] 06 p2170 N94-25182
Experimental contribution to the study of secondary flows in centrifugal turbopump stator components
[ECL-92-35] 07 p2789 N94-25654
Flow and heat transfer in a rotating square sectioned U-bend 08 p3128 N94-28984
Incorporating radial mixing in axisymmetric streamline curvature through-flow analysis
[AD-A277325] 09 p3706 N94-32279
Visualization of secondary flow development in high aspect ratio channels with curvature
[NASA-TM-106658] 10 p4046 N94-33941
The influence of the inlet boundary layers on the secondary losses of turbine stages
10 p4003 N94-34457
The aerodynamic and heat transfer effects of an endwall boundary layer fence in a 90 degree turning square duct
[AD-A278903] 11 p4265 N94-35803
Unsteady flow field of large-amplitude pitching airfoils
[AD-A280444] 12 p4383 N94-37219

SECONDARY ION MASS SPECTROMETRY
In situ secondary ion mass spectrometry analysis
[DE93-012185] 01 p0076 N94-11140
Solar wind-induced secondary ions and their relation to lunar surface composition 01 p0474 N94-12232
Ultra-shallow box-like profiles fabricated by pulsed UV-laser doping process
[DE93-017221] 04 p1437 N94-18083
Research program activities of the ORNL Analytical Chemistry Division
[DE93-017938] 04 p1339 N94-19117
Electric-field dependence of electroreflectance and photocurrent spectra at visible wavelengths in MOVPE-grown InAlGaP multiple strained quantum-well structures
[DE94-004692] 07 p2780 N94-25664

SECONDARY RADAR
Activities report of the Federal Administration for Flight Safety (Germany)
[ETN-93-94208] 02 p0511 N94-14008
Diffraction of microwaves at rectangular facades of buildings with and without ground reflections (Fresnel-Kirchhoff-Approximation)
[DLR-FB-92-35] 03 p0987 N94-15155
SECONDARY WAVES
U S WAVES
SECRETIONS
NT ADRENOCORTICOTROPIN (ACTH)
NT ENDOCRINE SECRETIONS
NT HORMONES
NT INSULIN
NT PROSTAGLANDINS
NT SWEAT
NT THYROXINE
SECULAR PERTURBATION
U LONG TERM EFFECTS
SECULAR VARIATIONS
Geomagnetic field models incorporating physical constraints on the secular variation
[NASA-CR-195165] 06 p2405 N94-24854
Electromagnetic core-mantle coupling 08 p3366 N94-30808
SECURITY
NT COMPUTER INFORMATION SECURITY
A comparison of high and low-impact reports of investigation on adjudicators' decision making: A pilot study
[AD-A265747] 01 p0416 N94-10298
Practical authorization in large heterogeneous distributed systems
[DE93-013192] 01 p0335 N94-10324
Classified information: Volume could be reduced by changing retention policy
[AD-A266938] 03 p1228 N94-15176
NASA security handbook
[NHB-1620.3C] 03 p1224 N94-15937
Military space programs in the press: An analysis for change
[AD-A267799] 03 p0874 N94-17306
Automated assistance for detecting malicious code
[DE93-018106] 04 p1523 N94-18943
Security evaluation of Unix networks
[AD-A273076] 05 p1945 N94-21520
Initial laboratory evaluation of color video cameras, phase 2
[DE93-040201] 05 p1809 N94-21556
Security aspects of computer supported collaborative work
[AD-A275638] 08 p3528 N94-28640
Design of an autonomous exterior security robot
[AIAA PAPER 94-1188-CP] 08 p3441 N94-30538
Controlling multiple security robots in a warehouse environment
[AIAA PAPER 94-1300-CP] 08 p3441 N94-30540
NATO contributions to European environmental security
[AD-A275918] 09 p3763 N94-31275
Millimeter wave, high-resolution, holographic surveillance system
[DE94-004269] 09 p3712 N94-31831
Economic espionage and information security
[DE94-003692] 10 p4161 N94-33733
Software use control
[DE94-008429] 12 p4489 N94-36480
Criminal Acts Against Civil Aviation, 1993
[AD-A280694] 12 p4384 N94-37131
The effects of proton-beam quality on the production of gamma rays for nuclear resonance absorption in nitrogen
[DE94-011609] 12 p4523 N94-37629
SEDIMENT TRANSPORT
Application of remote sensing for coastal management in the north coast of Java 01 p0218 N94-12701
Coastal scour problems and methods for prediction of maximum scour
[AD-A266658] 02 p0726 N94-14775
Louisiana delta study
[NASA-TM-109622] 03 p1095 N94-15408
Ventilated oscillatory boundary layers
[AD-A266226] 03 p1023 N94-16110
A Geographic Information System approach to modeling nutrient and sediment transport
[DE93-013747] 03 p1097 N94-17426
Mathematical modeling of the free surface hydrodynamic and of transport in suspensions of non cohesive sediments: Aid to the interpretation of spatial images
[ETN-93-95011] 04 p1421 N94-19502
Hydraulics and morphology of mountain rivers: A literature survey. Communications on hydraulic and geotechnical engineering
[PB94-110772] 06 p2388 N94-24636
Temporal and spatial mapping of surface albedo and atmospheric dust opacity on Mars 03 p2619 N94-24887
Glaciohydrologic and glaciohydraulic effects on runoff and sediment yield in glacierized basins
[AD-A275134] 08 p3361 N94-29286
Temporal and spatial mapping of atmospheric dust opacity and surface albedo on Mars 09 p3947 N94-33211
Fluid mechanical measurements within the bottom boundary layer over the Northern California continental shelf during stress
[AD-A277916] 09 p3791 N94-33243
Bottom boundary layer stress measurements with BASS tripods: Data report STRESS 1988-1989
[AD-A277864] 10 p4092 N94-33775
SEDIMENTARY ROCKS
NT COAL
NT LIMESTONE
NT SANDSTONES
NT SHALES
Stratigraphy and sedimentology of the K/T boundary deposit in Haiti 01 p0282 N94-12138
A simple model of clastic sediments on Mars 01 p0460 N94-12155
The Karakul depression in Pamirs: The first impact structure in Central Asia 03 p1241 N94-16212
Geomorphic processes in the Argyre-Dorsa Argentea region of Mars 03 p1270 N94-16293
Tidal regime of intact planetoid capture model for the Earth-Moon system: Does it relate to the archean sedimentary rock record? 03 p1245 N94-16378
Shock propagation in crustal rock
[AD-A270148] 04 p1485 N94-18899
Field guide to Cretaceous-tertiary boundary sections in northeastern Mexico
[NASA-CR-195719] 08 p3354 N94-28416
Analysis of deep seismic reflection and other data from the southern Washington Cascades
[DE94-005958] 09 p3771 N94-31525
Shocked materials from the Dutch Peak diamictite, Utah 11 p4352 N94-36140
Analysis of deep seismic reflection and other data from the Southern Washington Cascades
[DE94-004075] 12 p4470 N94-37489
SEDIMENTS
NT GRAVELS
NT MUD
NT SANDS
Acoustics of bubbly sediments
[AD-A263726] 01 p0288 N94-11299
Impact mineralogy and chemistry of the cretaceous-tertiary boundary at DSDP site 576 01 p0282 N94-12091
Minor and trace element composition and age of Yukon probable-microtektites 01 p0429 N94-12094
A simple model of clastic sediments on Mars 01 p0460 N94-12155
Iron and nickel isotopic mass fractionation in deep-sea spherules 01 p0282 N94-12199
The role of certain infauna and vascular plants in the mediation of redox reactions in marine sediments 01 p0268 N94-12454
Acetate concentrations and oxidation in salt marsh sediments 01 p0269 N94-12459
Coastal morphodynamics and energetic characteristics of swell studied with ERS-1 SAR 01 p0254 N94-12524
Application of remote sensing for coastal management in the north coast of Java 01 p0218 N94-12701
Sedimentation rates and particulate fluxes in the slope and deep sea areas off eastern Taiwan 01 p0220 N94-12709
Martian sedimentary deposits
[NASA-CR-193266] 02 p0842 N94-13855
Overview: Gas hydrate geology and geography
[DE93-014043] 02 p0688 N94-14151
Coastal scour problems and methods for prediction of maximum scour
[AD-A266658] 02 p0726 N94-14775
Efficacy of flocculating and other emergency water purification tablets
[AD-A266695] 03 p1148 N94-15840
Ventilated oscillatory boundary layers
[AD-A266226] 03 p1023 N94-16110
Martian crater degradation by eolian processes: Analogy with the Rio Cuarto Crater Field, Argentina 03 p1251 N94-16196
Sedimentation, volcanism, and ancestral lakes in the Valles Marineris: Clues from topography 03 p1283 N94-16369
Multiple dataset water-quality analyses in the vicinity of an ocean wastewater plume 03 p1069 N94-16687
A Geographic Information System approach to modeling nutrient and sediment transport
[DE93-013747] 03 p1097 N94-17426
Three-dimensional high-resolution seismic profiling on the New Jersey outer continental shelf
[AD-A269835] 04 p1498 N94-18600
Carbon Isotope Biogeochemistry of Methane from Anoxic Sediments
[NASA-CR-194620] 04 p1477 N94-19231
A carbon isotope mass balance for an anoxic marine sediment: Isotopic signatures of diagenesis 04 p1477 N94-19232
The carbon isotope biogeochemistry of (epsilon)CO2 production in a methanogenic marine sediment 04 p1477 N94-19233
The carbon isotope biogeochemistry of methane production in anoxic sediments. 1: Field observations 04 p1477 N94-19234
Factors that control the stable carbon isotopic composition of methane produced in an anoxic marine sediment 04 p1477 N94-19235
Gravity and the geoid in the Nepal Himalaya
[NASA-CR-194166] 04 p1463 N94-19430
Mathematical modeling of the free surface hydrodynamic and of transport in suspensions of non cohesive sediments: Aid to the interpretation of spatial images
[ETN-93-95011] 04 p1421 N94-19502
Faulted structure of the bottom simulating reflector on the Blake Ridge, western North Atlantic
[AD-A271289] 04 p1500 N94-19745
Workshop on the Martian Northern Plains: Sedimentological, Periglacial, and Paleoclimatic Evolution
[NASA-CR-194831] 05 p2088 N94-20382
A model for the origin of Martian polygonal terrain 05 p2090 N94-20393
Iridium in sediments containing large abundances of Australasian microtektites from DSDP hole 758B in the Eastern Indian Ocean and from DSDP hole 769A in the Sulu Sea 05 p2083 N94-20741
Mars: New evidence for origin of some Valles Marineris layered deposits 05 p2112 N94-20748
Early Mars: A regional assessment of denudation chronology 05 p2145 N94-21676
Hydraulics and morphology of mountain rivers: A literature survey. Communications on hydraulic and geotechnical engineering
[PB94-110772] 06 p2388 N94-24636
Macrobenthic fauna in the dutch sector of the north sea in 1991
[PB94-126414] 07 p2868 N94-27200
Journal of NIRE, volume 2, number 4
[JTN-94-80554] 07 p2869 N94-28147
Effects of p-chlorophenol on sulfate reduction in marine sediments 07 p2870 N94-28150
An evaluation of criteria that may be used to identify species surviving a mass extinction 07 p2889 N94-28304
Extraterrestrial accretion and glacial cycles 07 p2890 N94-28308
An extraterrestrial event at the tertiary-quaternary boundary 07 p2890 N94-28309
Glaciohydrologic and glaciohydraulic effects on runoff and sediment yield in glacierized basins
[AD-A275134] 08 p3361 N94-29286
The undrained shear strength characteristics of undisturbed soil from fishing port areas 08 p3234 N94-29704
Dewatering of contaminated river sediments 08 p3354 N94-30472
Gas hydrate detection and mapping on the US east coast
[DE94-005959] 09 p3742 N94-31504
Geologic controls of erosion and sedimentation on Mars 09 p3951 N94-33232
Polar sediment accumulation: Role of surface winds at the two poles 09 p3951 N94-33233
Fluid mechanical measurements within the bottom boundary layer over the Northern California continental shelf during stress
[AD-A277916] 09 p3791 N94-33243
Bottom backscatter from trapped bubbles
[AD-A277583] 10 p4132 N94-33425
Bottom boundary layer stress measurements with BASS tripods: Data report STRESS 1988-1989
[AD-A277864] 10 p4092 N94-33775
A geoacoustic model for fine-grained, unconsolidated calcareous sediments (ARSRP natural laboratory)
[AD-A277830] 10 p4092 N94-33831
Groundwater penetrating radar and high resolution seismic for locating shallow faults in unconsolidated sediments
[DE94-007284] 11 p4257 N94-36366
SEE (SOFTWARE ENGINEERING ENVIRONMENTS)
U PROGRAMMING ENVIRONMENTS
SEEBECK COEFFICIENT
U SEEBECK EFFECT

SEEBECK EFFECT
Thermal conductivities, electrical resistivities, and Seebeck coefficients of YBa2Cu3O(7-x) superconductors from 80 to 300 K
[DE94-004796] 08 p3520 N94-30724
SEEDING (INOCULATION)
U INOCULATION
SEEDS
Seed viability detection using computerized false-color radiographic image enhancement
08 p3387 N94-30461
SEEKERS
U HOMING DEVICES
SEGMENTS
Segmenting textured 3D surfaces using the space/frequency representation
[AD-A266960] 03 p1163 N94-14968
Segmented operations for sparse matrix computation on vector multiprocessors
[AD-A270601] 05 p1928 N94-19950
Segmented ion thruster
[NASA-CASE-NPO-18192-1-CU] 05 p1669 N94-20496
Image segmentation by a combination of edge detection and region growing
[ETN-94-95032] 07 p2960 N94-26106
SEGREGATION
U SEPARATION
SEISMIC ENERGY
Wave propagation characteristics of short-period crustal phases near ARCESS and NORESS
[AD-A265959] 01 p0275 N94-11102
NORSAR basic seismological research
[AD-A266193] 03 p1101 N94-16125
Analysis of regional bodywave phases from earthquakes in western China, part 2
[AD-A270125] 04 p1485 N94-18873
Proceedings of the 15th Annual Seismic Research Symposium
[AD-A271458] 05 p1855 N94-20090
A geological and geophysical information system for Eurasia
[AD-A274818] 07 p3098 N94-26490
Axial focusing of impact energy in the Earth's interior: Proof-of-principle tests of a new hypothesis
07 p2888 N94-28296
Finite-element modeling of the blockage and scattering of LG propagation
[AD-A277430] 09 p3775 N94-33006
SEISMIC WAVES
NT LOVE WAVES
NT MICROSEISMS
NT RAYLEIGH WAVES
Wave propagation characteristics of short-period crustal phases near ARCESS and NORESS
[AD-A265959] 01 p0275 N94-11102
The 1990 Western Pacific Geophysics meeting
[NASA-CR-193456] 02 p0712 N94-13334
Broadband teleseismic array recording in the Adirondack Mountains, New York State
[AD-A267290] 03 p1097 N94-14960
Generation of artificial helioseismic time-series
[NASA-CR-194612] 03 p1299 N94-15968
Composite refraction-reflection stack sections: Tracing faults in the Atlantic coastal plain sediments
[DE93-013581] 03 p1112 N94-16009
NORSAR basic seismological research
[AD-A266193] 03 p1101 N94-16125
A search for evidence of nonlinear elasticity in the earth
[DE93-015279] 03 p1102 N94-17252
Preliminary estimates of frequency-direction spectra derived from the SAMSON pressure gage array, November 1990 to May 1991
[AD-A267960] 03 p1114 N94-17497
Generalized seismic analysis
04 p1449 N94-17832
A comparison of single-station backazimuth estimates with regional event locations in the Central Appalachians
[AD-A269897] 04 p1483 N94-18690
Wave propagation near explosive sources
[AD-A270102] 04 p1418 N94-18870
Analysis of regional bodywave phases from earthquakes in western China, part 2
[AD-A270125] 04 p1485 N94-18873
Fast iterative solution of sparsely sampled seismic inverse problems
[REPT-93-16] 04 p1486 N94-19081
Transmission of acoustic waves through strongly heterogeneous, two-dimensional velocity models
[REPT-93-09] 04 p1563 N94-19083
Inverse scattering of surface waves: A new look at surface consistency
[REPT-93-25] 04 p1486 N94-19140
An iterative inverse scattering method for the removal of scattered surface waves
[REPT-93-18] 04 p1488 N94-19644
Analysis of data from Columbia Point Arena Ocean-Bottom Seismic Station (OBSS)
[AD-A271263] 04 p1500 N94-19727
A Kirchhoff approach to seismic modeling and prestack depth migration
[AD-A271010] 05 p1854 N94-19820
Proceedings of the 15th Annual Seismic Research Symposium
[AD-A271458] 05 p1855 N94-20090
Inversion of gravity and bathymetry in oceanic regions for long-wavelength variations in upper mantle temperature and composition
[NASA-CR-192272] 05 p1882 N94-20131
Analysis of the effects of eurasian crustal and upper mantel structure on regional phases using broadband seismic data
[AD-A272446] 05 p1858 N94-21206
The Board on Earth sciences and resources
[DE94-000745] 05 p1859 N94-22018
Transient acoustic wave modeling: Higher-order WKBJ asymptotics and symbolical manipulation (revised)
[PB93-215432] 05 p1969 N94-22262
Dynamic ray tracing and its application in triangulated media
[DE94-000875] 06 p2402 N94-23516
Near-surface seismic imaging
[PB94-119096] 06 p2404 N94-24647
Downward extrapolation of multi-component seismic data
[ISBN-9-09-005213-5] 06 p2405 N94-25229
Decomposition of multi-component measurements into P and S waves
[ISBN-9-09-005197-X] 06 p2405 N94-25251
Parametric and nonparametric discriminants for regional earthquakes and explosions
[AD-A273807] 06 p2406 N94-25538
Efficient modeling in transversely isotropic inhomogeneous media
[DE94-003394] 07 p2877 N94-25847
Emerging technologies
[DE94-003022] 07 p3102 N94-26023
Elastic scattering by a spherical inclusion
[AD-A274713] 07 p2878 N94-26433
A geological and geophysical information system for Eurasia
[AD-A274818] 07 p3098 N94-26490
Nonlinear hysteresis in an endochronic solid
[AD-A274594] 07 p2880 N94-26855
Elastic wave up/down decomposition in inhomogeneous and anisotropic media: An operator approach and its approximations
[PB94-126497] 07 p2881 N94-26880
Wave propagation in the shallow regions of the earth's crust and the borehole vicinity
[ITN-94-85237] 07 p2882 N94-27330
Underground structure in the eastern part of Kanagawa Prefecture inferred from explosion seismic observations
07 p2886 N94-27987
Analysis of S-wave seismogram envelope of deep earthquakes and estimation of random inhomogeneities in the Kanto-Tokai area 07 p2886 N94-27988
Axial focusing of impact energy in the Earth's interior: Proof-of-principle tests of a new hypothesis
07 p2888 N94-28296
Initial wave-type identification with neural networks and its contribution to automated processing in IMS version 3.0
[AD-A275058] 08 p3359 N94-29137
Statistical characterization of rugged propagation paths with application to Rg scattering study
[AD-A275237] 08 p3361 N94-29393
Effects and implications of fault zone heterogeneity and anisotropy on earthquake strong ground motion
08 p3363 N94-29941
The rupture process of large earthquakes along convergent margins: Cast studies from Alaska and Armenia 08 p3363 N94-29969
Extension of love wave transformation theory to laterally heterogeneous structures
[DE94-008098] 08 p3365 N94-30093
Finite-element modeling of the blockage and scattering of LG propagation
[AD-A277430] 09 p3775 N94-33006
Tomographic imaging of internal Earth structure: The core-mantle boundary and the trade-off between volumetric and topographic structure
10 p4083 N94-33358
Investigations on local seismic phases and modeling of seismic signals
[AD-A277891] 10 p4085 N94-33537
Processed seismic motion records from earthquakes, 1982-1993: Recorded at Scotty's Castle, California
[DE94-001371] 10 p4086 N94-33729
Application of the compound-matrix method to wave propagation in range-independent fluid-solid media
[PB94-149077] 10 p4129 N94-34105
Resolution of iterative inverses in seismic tomography
[DE94-008079] 10 p4087 N94-34132
Center for seismic studies
[AD-A278682] 11 p4290 N94-35693
Hydrodynamically induced loads on components submerged in high-level waste-storage tanks
[DE94-009663] 11 p4264 N94-35756
SEISMOGRAMS
NORSAR basic seismological research
[AD-A266193] 03 p1101 N94-16125
Analysis of regional bodywave phases from earthquakes in western China, part 2
[AD-A270125] 04 p1485 N94-18873
Dynamic ray tracing and its application in triangulated media
[DE94-000875] 06 p2402 N94-23516
A program for rapid computation of multioffset vertical seismic profile synthetic seismograms for layered media
[AD-A275464] 08 p3355 N94-28737
Effects and implications of fault zone heterogeneity and anisotropy on earthquake strong ground motion
08 p3363 N94-29941
Analysis of deep seismic reflection and other data from the Southern Washington Cascades
[DE94-004075] 12 p4470 N94-37489
SEISMOGRAPHS
NT LUNAR SEISMOGRAPHS
Preliminary analysis of the FLIP array data from the NOBS experiment
[AD-A265911] 01 p0289 N94-12349
Broadband teleseismic array recording in the Adirondack Mountains, New York State
[AD-A267290] 03 p1097 N94-14960
Analysis of regional bodywave phases from earthquakes in western China, part 2
[AD-A270125] 04 p1485 N94-18873
Antarctic Record, Vol. 36, No. 2
[REPT-107] 07 p2883 N94-27963
Status report for the development of the Antarctic penetrator: 1990-year program 07 p2885 N94-27973
Report of the National Research Institute for Earth Science and Disaster Prevention, No. 51
[JTN-94-80509] 07 p2886 N94-27985
Observation with STS seismometer at Nakaizu, central Japan: Observation system and comparison with tiltmeter 07 p2886 N94-27986
A broad-band microseismometer for planetary operations 08 p3237 N94-29778
Air-deployable geophysics package
[DE94-005651] 08 p3335 N94-30594
Long transect seafloor seismic array: A component of SAMSON (Sources of Ambient Micro Seismic Ocean ic Noise)
[AD-A277009] 09 p3789 N94-32401
Processed seismic motion records from earthquakes, 1982-1993: Recorded at Scotty's Castle, California
[DE94-001371] 10 p4086 N94-33729
SEISMOLOGY
NT HELIOSEISMOLOGY
Inverting ultrasonic data on solid/fluid mixtures for Biot-Gassmann parameters
[DE93-011952] 01 p0150 N94-11026
Wave propagation characteristics of short-period crustal phases near ARCESS and NORESS
[AD-A265959] 01 p0275 N94-11102
Autonomous self contained bottom pop-up stations for study of the benthic layer and seismicity of the ocean's bottom 01 p0224 N94-12735
Papers presented at the Eleventh International Symposium on Earth Tides
[COMMUNICATIONS-SER-B-158] 03 p1098 N94-15800
NORSAR basic seismological research
[AD-A266193] 03 p1101 N94-16125
High-resolution seismic reflection survey at the Manson crater, Iowa 03 p1103 N94-16307
The seismic response of an aquifer to the propagation of an impact generated shock wave: A possible trigger of the Martian outflow channels?
03 p1261 N94-16354
A geological and geophysical information system for Eurasia
[AD-A267841] 03 p1232 N94-17036
Generalized seismic analysis
04 p1449 N94-17832
Constructing a reference event list for ARCESS
[AD-A269288] 04 p1481 N94-18297
High resolution geological site characterization utilizing ground motion data
[AD-A268926] 04 p1481 N94-18485

Belgian Royal Observatory Communications, Series A, No. 104, Geophysics Series No. 175
[COMMUNICATIONS-SER-A-104] 04 p1482 N94-18622
Historical seismicity of Hainaut, Flanders and Artois 04 p1482 N94-18623
Current (1985-1988) seismic activity in Belgium: Comparison with historical and instrumental seismic data 04 p1482 N94-18624
Macroseismic study of the Dour (Belgium) earthquakes of 22 March 1987 and of Gulpen (Belgium) 17 October 1988 04 p1482 N94-18625
Current positioning possibilities by spatial techniques and the Royal Oservatory of Belgium program 04 p1483 N94-18627
The use of velocity spectra for stacking receiver functions with application to IRIS/IDA stations OBNINSK (OBN) and ARTI (ARU), Russia
[AD-A269087] 04 p1483 N94-18717
Analysis of regional deformation and strain accumulation data adjacent to the San Andreas fault
[NASA-CR-194072] 04 p1487 N94-19428
The interpretation of crustal dynamics data in terms of plate motions and regional deformation near plate boundaries
[NASA-CR-194302] 04 p1487 N94-19432
Seismic studies of the geologic structure and physical properties of the seabed
[AD-A270895] 04 p1500 N94-19747
A Kirchhoff approach to seismic modeling and prestack depth migration
[AD-A271010] 05 p1854 N94-19820
Proceedings of the 15th Annual Seismic Research Symposium
[AD-A271458] 05 p1855 N94-20090
Seafloor characterization/Galapagos propagating rift
[AD-A272001] 05 p1882 N94-20581
Modal combination in response spectrum modal dynamic analysis
[DE94-000339] 05 p1833 N94-21956
Post-Palbozoic crustal responses to the contemporary stress field in the eastern United States
[DE93-040604] 05 p1859 N94-22006
The Board on Earth sciences and resources
[DE94-000745] 05 p1859 N94-22018
Seafloor characterization/Galapagos propagating rift
[AD-A273586] 06 p2419 N94-25165
A geological and geophysical information system for Eurasia
[AD-A274818] 07 p3098 N94-26490
A preliminary shear velocity model for Central Asia
[AD-A274972] 07 p2880 N94-26752
An integrated approach to seismic event location: 1. Evaluating how method of location affects the volume of groups of hypocenters
[PL-TR-92-2323] 07 p2887 N94-28214
A program for rapid computation of multioffset vertical seismic profile synthetic seismograms for layered media
[AD-A275464] 08 p3355 N94-28737
The Norwegian seismic array (NORSAR), phase 3
[AD-A275440] 08 p3356 N94-28868
Initial wave-type identification with neural networks and its contribution to automated processing in IMS version 3.0
[AD-A275058] 08 p3359 N94-29137
Statistical characterization of rugged propagation paths with application to Rg scattering study
[AD-A275237] 08 p3361 N94-29393
A broad-band microseismometer for planetary operations 08 p3237 N94-29778
The rupture process of large earthquakes along convergent margins: Cast studies from Alaska and Armenia 08 p3363 N94-29969
Theoretical asteroseismology of white dwarf stars: The encyclopedia Seismologica 08 p3547 N94-30011
Application of remote sensing techniques for the seismo-tectonic study of Nahanni earthquake area
[ISBN-0-315-85942-3] 08 p3334 N94-30037
Proceedings of the 4th Tunnel Detection Symposium on Subsurface Exploration Technology
[AD-A276372] 09 p3771 N94-31369
Gas hydrate detection and mapping on the US east coast
[DE94-005959] 09 p3742 N94-31504
Differential interferometry study of an earthquake 09 p3756 N94-32570
Procedures for computing site seismicity
[AD-A277666] 09 p3775 N94-33028
Permanent GPS Geodetic Array in Southern California (PGGA) and GPS observations in Indonesia
[NASA-CR-195897] 10 p3988 N94-33534
Investigations on local seismic phases and modeling of seismic signals
[AD-A277891] 10 p4085 N94-33537
Environmental process tomography in the United States
[DE94-006402] 10 p4081 N94-33718
Seismic event interpretation using fuzzy logic and neural networks
[DE94-009469] 10 p4087 N94-33931
Center for seismic studies
[AD-A278682] 11 p4290 N94-35693
Activity report 1990-1992 and proceedings, volume 1
[DE94-610480] 11 p4290 N94-35830
Activity Report, 1990 - 1992 and proceedings, volume 2
[DE94-610481] 11 p4291 N94-36087
Groundwater penetrating radar and high resolution seismic for locating shallow faults in unconsolidated sediments
[DE94-007284] 11 p4257 N94-36366
Analysis spectral shapes from California and central United States ground motion
[DE94-010041] 12 p4469 N94-36758

SEISMOMETERS
U SEISMOGRAPHS

SEIZURES
Monitor for status epilepticus seizures 08 p3397 N94-30460

SELECTION
NT PERSONNEL SELECTION
NT PILOT SELECTION
NT SITE SELECTION
On the selection of indices in relational databases
[MEMO-INF-92-72] 05 p2043 N94-21071
Columbus: Materials for 30 years habitability in space 05 p1662 N94-21387
Some generalized subset selection procedures
[PB94-111655] 06 p2487 N94-23799
Solving the ranking and selection indifference-zone formulation for normal distributions using computer software
[AD-A273821] 06 p2496 N94-25518
Cooling towers for combined cycles: Design philosophy, performance testing, and operating problems 07 p2832 N94-28087
Unravelling nondeterminism: On having the ability to choose
[RUU-CS-93-30] 08 p3428 N94-30749

SELECTIVE DISSEMINATION OF INFORMATION
Classified information: Volume could be reduced by changing retention policy
[AD-A266938] 03 p1228 N94-15176
NASA security handbook
[NHB-1620.3C] 03 p1224 N94-15937
NASA Electronic Library System (NELS): The system impact of security
[NASA-CR-194614] 03 p1231 N94-16499
Military space programs in the press: An analysis for change
[AD-A267799] 03 p0874 N94-17306
NASA aeronautics: Protecting sensitive technology. Report to Congressional requesters
[GAO/NSIAD-93-201] 04 p1617 N94-18848
Inventory management plan for a research and development local area network
[DE93-018381] 04 p1617 N94-19026
Secure open systems: An investigation of current standardisation efforts for security in open systems
[FEL-92-B225] 04 p1618 N94-19450
Secure open systems: An investigation
[FEL-91-B293] 04 p1619 N94-19454
Computer security. Evolutions 1987 to 1992: Trends and perspectives
[RR-905-I] 04 p1532 N94-19713
Security management of electronic data interchange
[AD-A272962] 05 p1899 N94-21252
Data management for interdisciplinary field experiments: OTTER project support
[NASA-CR-4559] 05 p1842 N94-22345
A systems engineering approach to AIS accreditation
[DE94-009354] 10 p4158 N94-33909

SELECTIVE FADING
Measurement of multipath delay profile in land mobile satellite channels 06 p2283 N94-22793

SELECTIVE SURFACES
Manufacturing tolerance requirements for frequency selective surfaces
[AD-A266541] 03 p0999 N94-16797
Development of a selective volumetric receiver for central receiver systems: Investigation of parameters and exergetic evaluation
[DLR-FB-93-05] 04 p1465 N94-18089
Performance of a simple circular polarization selective surface 05 p1746 N94-22198
Radar signature related radome techniques for flush-mounted HF-, VHF- and, UHF communication antennas
[PB93-204618] 06 p2294 N94-23742
Solar energy utilization in the USSR 07 p2853 N94-26052

SELECTIVITY
Stimulus-driven capture and attentional set: Selective search for color and visual abrupt onsets
[IZF-1992-B-9] 04 p1509 N94-19419
Selectivity: Reductions, nondeterminism, and function classes
[TR-469] 05 p1912 N94-21273

SELECTORS
Crosspoint analog data selector
[AD-D016326] 12 p4440 N94-37832

SELENIDES
NT CADMIUM SELENIDES
NT COPPER SELENIDES
NT GALLIUM SELENIDES
NT ZINC SELENIDES
The state of the art of thin-film photovoltaics
[DE94-000224] 07 p2855 N94-26115
Fragmentation of Ge(1-x) Sn(x) Se2 glasses
[DE94-603009] 07 p2758 N94-27837
Studies of high temperature ternary phases in mixed-metal-rich early transition metal sulfide and phosphide systems
[DE94-006034] 08 p3209 N94-30336
NREL preprints for the 23rd IEEE Photovoltaic Specialists Conference
[DE93-010027] 10 p4078 N94-33724

SELENIUM
Selenium x ray laser line profile measurements
[DE93-012580] 02 p0658 N94-14175
Experimental measurements of selenium x-ray laser spectral line profiles
[DE93-016543] 02 p0659 N94-14595
The long-range transport of aerosol particles over the North Atlantic Ocean 08 p3366 N94-30867
Electrical characteristics of GaAs MESFET fabrication by ion implantation of Si or Se
[AD-A278416] 09 p3909 N94-33328
Air quality assessment and control
[DE94-000046] 10 p4081 N94-33725
New plasma source of hydrides for epitaxial growth
[DE94-006918] 12 p4533 N94-39744
Ionization balance and gain calculations for nec.-like selenium x-ray laser plasmas
[DE94-012590] 12 p4530 N94-37437

SELENIUM COMPOUNDS
NT CADMIUM SELENIDES
NT COPPER SELENIDES
NT GALLIUM SELENIDES
NT SELENIDES
NT SELENIUM OXIDES
NT ZINC SELENIDES

SELENIUM OXIDES
Experimental and theoretical studies of molecular solids
[AD-A275511] 08 p3485 N94-28668

SELENOLOGY
Mission to the Moon: An ESA study on future exploration 01 p0460 N94-12153
Differential scaling: Implications for central structures in large lunar craters 01 p0461 N94-12158
Exploration planning in the context of human exploration and development of the Moon 01 p0474 N94-12229
Mixing model analysis of telescopic lunar spectra 03 p1284 N94-16371
Tidal regime of intact planetoid capture model for the Earth-Moon system: Does it relate to the archean sedimentary rock record? 03 p1245 N94-16378
Contributions of the Clementine mission to our understanding of the processes and history of the Moon 05 p2119 N94-20784

SELF ABSORPTION
Time-resolved optical studies of charge relaxation and charge transfer at electrode interfaces
[DE93-013985] 01 p0398 N94-11117

SELF ADAPTIVE CONTROL SYSTEMS
Automatic, self-adaptive control of unfold transformations
[DE94-012455] 12 p4504 N94-37247

SELF ALIGNMENT
Neural-network-directed alignment of optical systems using the laser-beam spatial filter as an example
[NASA-TP-3372] 03 p1034 N94-15961

SELF CONSISTENT FIELDS
To the theory of triplet pairing in Fermi-liquid model
[DE93-821770] 02 p0816 N94-12855
Continuum solvent models for computational chemistry
[DE93-016329] 03 p0953 N94-17660
3D and r,z particle simulations of heavy ion fusion beams
[DE93-013417] 03 p1205 N94-17670
Granular fluctuations in plasma turbulence and their role in transport
[DE93-013465] 03 p1187 N94-17674

Polaron tunneling in high-temperature superconductors
[DE93-016880] 04 p1593 N94-17754
Overview of WARP: A particle code for heavy ion fusion
[DE93-018637] 04 p1588 N94-19034
An introduction to GUGA in the COLUMBUS Program System
[DE93-018994] 05 p1902 N94-19928
Theoretical studies of the structures and electronic properties of U(NH2)(sub 3) and Np(NH2)(sub 3)
[DE94-000768] 05 p2031 N94-21857
Asymptotic structure of magnetically driven MHD wind 05 p2008 N94-22682
On kinetic expansion in scalar field theory
[DE93-634338] 07 p3072 N94-26553
Molecular surface electrostatic potentials in the analysis of non-hydrogen-bonding noncovalent interactions
[AD-A274612] 07 p3022 N94-26894
New anionic states of the lithium trimer
[AD-A278832] 11 p4323 N94-35797
Anionic and neutral states of Li3O
[AD-A278833] 11 p4323 N94-35798

SELF DEPLOYING SPACE STATIONS
U SELF ERECTING DEVICES
U SPACE STATIONS

SELF ERECTING DEVICES
Self-deploying photovoltaic power system
[NASA-CASE-LEW-15308-1] 05 p1846 N94-20196

SELF FOCUSING
Kinetic simulations of ultra-intense laser plasma interactions
[DE93-014419] 02 p0802 N94-14564
Singularities and symmetries of nonlinear ordinary and partial differential equations
[DE93-040083] 04 p1550 N94-19190
Two-dimensional nonlinear Schrodinger equations and their properties
[AD-A272184] 05 p1952 N94-20923
Automatic focus and registration of synthetic aperture radar images 08 p3246 N94-29536
Effect of the stimulated Brillouin backscattering on self-focusing threshold
[DE94-008678] 12 p4510 N94-37536

SELF INDUCED VIBRATION
NT SUBSONIC FLUTTER
NT SUPERSONIC FLUTTER
NT TRANSONIC FLUTTER
Occurrence of sub-synchronous vibration in a multistage turbine pump and its prevention 10 p4064 N94-34189
A review of vibration problems in power station boiler feed pumps 10 p4064 N94-34190
Experimental and analytical study on fluid whirl and fluid whip modes 10 p4054 N94-34191

SELF LUBRICATING MATERIALS
Canadian Target Assembly (CTA) to Airborne Support Equipment (ASE) vibration test report
[IME-AMT-TR-001] 02 p0663 N94-14195
The effect of prolonged exposure to 750 C air on the tribological performance of PM212
[NASA-TM-106472] 09 p3617 N94-32941
Wear-resisting oxide films for 900 C
[DE94-010093] 11 p4246 N94-36306

SELF LUBRICATION
Torque characteristics of solid lubricated precision bearings during oscillatory motion
[AD-A278133] 09 p3728 N94-33061

SELF ORGANIZING SYSTEMS
Communications and control for electric power systems: Power flow classification for static security assessment
[NASA-CR-194512] 02 p0624 N94-13948
Self organized criticality
[DE93-013182] 02 p0773 N94-14320
Application of the network discriminant function to learning
[AD-A268793] 04 p1540 N94-18189
Competitive dynamics and self-organization in photorefractive systems
[AD-A269663] 04 p1430 N94-18569
Self-organization via active exploration in robotic applications. Phase 2: Hybrid hardware prototype
[NASA-CR-194723] 05 p1939 N94-20212
Representation of spoken words in a self-organizing neural net 05 p1940 N94-20243
Modeling the human mental lexicon with self-organizing feature maps 05 p1743 N94-20244
Retrieval of ice thickness from polarimetric SAR data 05 p1724 N94-20432
A framework of connectionist network toward speech waveform coding 05 p1746 N94-22211
Speaker-independent isolated-digit recognition using neural networks and hidden Markov model 05 p1747 N94-22213
The adaptive resonance theory network: (Clustering-) behaviour in relation with brainstem auditory evoked potential patterns
[EUT-92-E-264] 06 p2470 N94-22877
Evolving recurrent perceptrons
[AD-A273241] 06 p2496 N94-24778
Taxonomy of gamma ray burster data using a self-organizing neural network
[DE94-006480] 08 p3553 N94-30248
A lateral inhibition neural network that emulates a winner-takes-all algorithm
[RUU-CS-92-46] 08 p3438 N94-30334
A generic model for data acquisition: Connectionist methods of information processing
[TELECOM-93-E-003] 09 p3730 N94-31166
ART: Adaptive Resonance Theory
[TELECOM-93-D-020] 09 p3829 N94-31193
Numerical optimization techniques in neural network training 09 p3838 N94-33158
A Fortran based learning system using multilayer back-propagation neural network techniques
[AD-A278463] 10 p4112 N94-33542
Workshop on Self-Determination in Developing and Evolving systems
[AD-A278367] 10 p4097 N94-33737
A real-time 2-D composite damage monitoring system employing neural network 10 p4074 N94-34355

SELF OSCILLATION
Quasi-optical transponder using FET's and patch antennas
[AD-A271339] 04 p1407 N94-19584

SELF REGULATING
U AUTOMATIC CONTROL

SELF TESTS
Design automation tools for testable VLSI circuits
[ISBN-0-315-61461-7] 02 p0621 N94-13333
Module generation for self-testing integrated systems
[ISBN-9-09-004570-8] 09 p3688 N94-31520

SELSYNS (TRADEMARK)
U SERVOMOTORS

SEM (MICROSCOPY)
U SCANNING ELECTRON MICROSCOPY

SEMANTICS
Bundle event structures: A non-interleaving semantics for LOTOS
[MEMO-INF-92-73] 01 p0320 N94-10164
Automatic word categorization: An information-theoretic approach
[CS-9209] 01 p0419 N94-10903
The silent step in time
[CWI-CS-R9221] 02 p0768 N94-13496
On the foundations of final semantics: Non-standard sets, metric spaces, partial orders
[CWI-CS-R9241] 02 p0768 N94-13526
The 8th Workshop on the Mathematical Foundations of Programming Semantics
[AD-A266436] 02 p0749 N94-13700
Programming languages made in Italy
[REPT-93-002] 02 p0750 N94-13805
Combinatorial semantics
[TR-444] 03 p1149 N94-16575
Monads and comonads in intensional semantics
[AD-A266522] 03 p1151 N94-16790
Using semantic information for processing negation and disjunction in logic programs
[DE93-017412] 04 p1614 N94-18099
Navigation in hypermedia applications: Modelling and semantics
[REPT-93-034] 04 p1520 N94-18136
Asynchronous rendezvous in the presence of backtracking
[PB93-197739] 04 p1524 N94-19062
Axiomatization, declarative semantics and operational semantics of passive and active updates in logic databases
[PB93-195956] 04 p1618 N94-19067
The TM typing rules
[MEMO-INF-92-80] 04 p1526 N94-19222
Attribute evaluation during generalized parsing
[MEMO-INF-92-85] 04 p1526 N94-19224
Action systems and action refinement in the development of parallel systems: An algebraic approach
[MEMO-INF-93-14] 04 p1538 N94-19296
A language of finite probabilistic processes and its interleaving semantics
[MEMO-INF-93-24] 04 p1558 N94-19354
Non-well-foundedness and type freeness can unify the interpretation of functional application
[PB93-191849] 04 p1560 N94-19710
Semantic models for distributed data base management. Part 2: Development of an integral meta-model for data modeling and data base modeling
[REPT-93-08-PT-2] 04 p1620 N94-19795
Set based analysis of ML programs
[AD-A270597] 05 p1902 N94-19948
Total order assumption
[PB93-191740] 05 p1903 N94-19993
Bottom-up abstract interpretation of logic programs
[PB93-191773] 05 p1928 N94-19995
Programming logic for F omega
[PB93-191781] 05 p1928 N94-19996
Back and forth bisimulations on prime event structures
[RR-888-I-IMAG-124-LIFIA] 05 p1929 N94-20124
Causal reconstruction
[AD-A271692] 05 p1908 N94-20929
A declarative approach for first-order built-in's of PROLOG
[CWI-CS-R9246] 05 p1909 N94-21026
COCOLOG: A conditional observer and controller logic for finite machines
[INRIA-RR-1714] 05 p1910 N94-21063
Behavioural semantics of parallel functional programming languages
[MEMO-INF-92-66] 05 p1913 N94-21313
Procedural dynamic semantics, verb-phrase ellipsis, and presupposition
[CWI-CS-R9311] 05 p1914 N94-21495
MINIFOLD: A kernel for a MANIFOLD-like coordination language
[CWI-CS-R9252] 05 p1915 N94-21534
Fortran for the nineties 05 p1926 N94-22481
Formal verification of digital circuits described in VHDL
[ETN-94-95165] 06 p2306 N94-22883
Asynchronous rendezvous in distributed logic programming
[PB93-220614] 06 p2448 N94-23096
Transition system specifications in stalk format with bisimulation as a congruence
[PB94-110608] 06 p2453 N94-23707
Multi-set extended relational algebra: A formal approach to a practical issue
[PB94-110830] 06 p2486 N94-23725
Logic of capabilities
[PB94-110715] 06 p2473 N94-23747
Design and specification of a generic task model for solving boolean constraint satisfaction problems
[PB94-118841] 06 p2486 N94-23762
Semantics, orderings and recursion in the weakest precondition calculus
[CWI-CS-R9267] 07 p2995 N94-26776
Modeling systems by probabilistic process algebra: An event structures approach
[PB94-125259] 07 p3004 N94-26867
Combining logics
[PB94-125242] 07 p2965 N94-26908
Congruence theorem for structured operational semantics with predicates and negative premises
[PB94-126729] 07 p2966 N94-26970
Trace-based compositional proof theory for fault tolerant distributed systems
[PB94-126737] 07 p2966 N94-26971
Alternative architectures for domain-oriented application composition and generation systems
[AD-A274180] 07 p2968 N94-27128
A strategy for dynamic interpretation: A fragment and an implementation
[CWI-CS-R9317] 07 p2970 N94-27545
Semantics of MANIFOLD: Specification in ASF+SDF and extension
[CWI-CS-R9269] 07 p2971 N94-27575
Expressiveness results for process algebras
[CWI-CS-R9301] 07 p3000 N94-27577
A theory for simulator tools
[CWI-CS-R9302] 07 p2972 N94-27578
Sheaf semantics for Petri Nets
[PB94-132826] 07 p2983 N94-28354
Operation semantics with read and write frames
[PB94-138138] 08 p3529 N94-29108
North American jumelage 'type systems'
[AD-A275342] 08 p3411 N94-29214
Second-order algebraic specification of state semantics
[CWI-CS-R9254] 08 p3453 N94-29889
A smart child of Peano's
[ML-92-10] 08 p3455 N94-30325
Completeness of the Lambek calculus with respect to relativized relational semantics
[LP-93-03] 08 p3455 N94-30326
Identity: Quarrelling with an unproblematic notion
[LP-93-04] 08 p3455 N94-30327
On blocks: Locality and asynchronous communication (extended abstract)
[RUU-CS-92-44] 08 p3424 N94-30347
Index expression belief networks for information disclosure
[TR-92-23] 08 p3465 N94-30358
Parsing in ISBES
[TR-92-32] 08 p3432 N94-30363
Interrogatives and adverbs of quantification
[LP-92-14] 08 p3456 N94-30372

Bounded contraction and many-valued semantics
[ML-93-04] 08 p3456 N94-30380
Models of the untyped lambda-calculus in semi Cartesian closed categories
[ML-93-05] 08 p3456 N94-30381
Algorithmic problems concerning first-order definability of modal formulas on the class of all finite frames
[ML-93-07] 08 p3456 N94-30383
The Vanilla meta-interpreter for definite logic programs and ambivalent syntax
[CT-93-01] 08 p3424 N94-30386
A note on the Smyth powerdomain construction
[RUU-CS-93-02] 08 p3457 N94-30393
Algebraic domains, chain completion, and the Plotkin powerdomain construction
[RUU-CS-93-03] 08 p3457 N94-30394
Modal quantification over structured domains
[ML-93-02] 08 p3457 N94-30396
Isomorphisms between predicate and state transformers
[RUU-CS-93-09] 08 p3458 N94-30403
Modeling systems by probabilistic process algebra: An event structures approach
[MEMO-INF-93-29-REV] 08 p3425 N94-30416
Termination of term rewriting by semantic labelling
[RUU-CS-93-24] 08 p3459 N94-30424
Three metric domains of processes for bisimulation
[CWI-CS-R9335] 08 p3459 N94-30427
Isomorphisms between predicate and state transformers
[CWI-CS-R9338] 08 p3459 N94-30430
Relating state transformation semantics and predicate transformer semantics for parallel programs
[CWI-CS-R9339] 08 p3433 N94-30431
Topological models for higher order control flow
[CWI-CS-R9340] 08 p3425 N94-30432
Comparative semantics for linear arrays of communicating processes
[CWI-CS-R9336] 08 p3426 N94-30491
On the relation between Unity properties and sequences of states
[RUU-CS-93-07] 08 p3433 N94-30720
Bisimulations and predicate logic
[CWI-CS-R9333] 08 p3460 N94-30735
Unravelling nondeterminism: On having the ability to choose
[RUU-CS-93-30] 08 p3428 N94-30749
A structural co-induction theorem
[CWI-CS-R9346] 08 p3461 N94-30753
Termination of term rewriting by semantic labelling
[RUU-CS-92-38] 08 p3462 N94-30859
Inventory of fragments and exact models in intuitionistic proportional logic
[ML-93-11] 08 p3463 N94-30974
What comes first in dynamic semantics: A compositional, non-representational account of natural language presupposition
[LP-93-15] 09 p3855 N94-31389
The interpretation of free focus
[CL-93-01] 09 p3855 N94-31390
Resumptive quantifiers in exception sentences
[LP-93-11] 09 p3855 N94-31403
Binary quantifiers and relational semantics
[LP-93-13] 09 p3855 N94-31404
Sums and quantifiers
[LP-93-05] 09 p3856 N94-31411
Effective truth
[ML-93-15] 09 p3856 N94-31416
Correspondence theory for extended modal logics, version 3.0
[ML-93-16] 09 p3856 N94-31417
Updates in dynamic semantics
[LP-93-06] 09 p3856 N94-31450
Completeness and decidability of the mixed style of inference with composition
[LP-93-09] 09 p3842 N94-31453
Weaks vs. strong readings of donkey sentences and monotonicity inference in a dynamic setting
[LP-93-10] 09 p3856 N94-31468
Compositionality of application oriented structuring mechanisms for algebraic specification languages with initial semantics
[ETN-94-95736] 09 p3812 N94-31577
Report on implementing part relationships using VML metaclasses
[PB94-147485] 09 p3813 N94-31686
Translucent procedures, abstraction without opacity
[AD-A276877] 09 p3817 N94-32213
An epistemic proof system for parallel processes
[TR-93-17] 09 p3826 N94-32291
Multiple inheritance via intersection types
[TR-93-18] 09 p3848 N94-32292
Formal semantics for a subset of VHDL and its use in analysis of the FTPP scoreboard circuit
[NASA-CR-191577] 09 p3827 N94-32734
Negation by default for framing in temporal logic programming
[PB94-148848] 10 p4107 N94-33978
Finding accurate frontiers: A knowledge-intensive approach to relational learning 10 p4098 N94-34044
Probabilities and priorities in timed CSP
[PB94-169216] 11 p4316 N94-35536
Mathematical theory of synchronous communication
[PB94-169224] 11 p4252 N94-35537
Task networks for controlling continuous processes
[AD-A278683] 11 p4312 N94-35710

SEMICIRCULAR CANALS
Basic understanding of vertigo
08 p3390 N94-28855

SEMICONDUCTING FILMS
Growth, characterization and device development in monocrystalline diamond films
[AD-A268206] 03 p1216 N94-17553
Atomic layer epitaxy of group 4 materials: Surface processes, thin films, devices and their characterization
[AD-A274325] 07 p3061 N94-26885
Optical properties of cadmium sulfide, zinc selenide, and zinc manganese selenide semiconductor films
08 p3500 N94-29759

SEMICONDUCTOR DEVICES
NT ALUMINUM GALLIUM ARSENIDE LASERS
NT AVALANCHE DIODES
NT BIPOLAR TRANSISTORS
NT CHARGE COUPLED DEVICES
NT CHARGE FLOW DEVICES
NT CHARGE TRANSFER DEVICES
NT CMOS
NT FIELD EFFECT TRANSISTORS
NT GALLIUM ARSENIDE LASERS
NT HETEROJUNCTION DEVICES
NT HIGH ELECTRON MOBILITY TRANSISTORS
NT JFET
NT JUNCTION DIODES
NT JUNCTION TRANSISTORS
NT LIGHT EMITTING DIODES
NT METAL OXIDE SEMICONDUCTORS
NT MIS (SEMICONDUCTORS)
NT MODFETS
NT MSM (SEMICONDUCTORS)
NT PHOTODIODES
NT PHOTOTRANSISTORS
NT PHOTOVOLTAIC CELLS
NT QUANTUM WELL LASERS
NT SCHOTTKY DIODES
NT SEMICONDUCTOR LASERS
NT SILICON CONTROLLED RECTIFIERS
NT SILICON TRANSISTORS
NT SOI (SEMICONDUCTORS)
NT SOLAR CELLS
NT SOS (SEMICONDUCTORS)
NT THERMISTORS
NT THYRISTORS
NT TRANSISTOR AMPLIFIERS
NT TRANSISTORS
NT VARACTOR DIODES
NT VARISTORS
Continuous-time adaptive learning circuit
[AD-D015773] 01 p0140 N94-10384
Limitation and suppression of hot electron fluctuations in submicron semiconductor structures
[DE93-613911] 01 p0396 N94-10801
Review of betavoltaic energy conversion
01 p0053 N94-11407
GaAs PCSS: High gain switching and device reliability
[DE93-009851] 01 p0401 N94-11605
Multicomponent and multilayered thin films for advanced microtechnologies: Techniques, fundamentals, and devices
[AD-A265685] 01 p0405 N94-12442
Proceedings of the Workshop on Applications of Synchrotron Radiation to Trace Impurity Analysis for Advanced Silicon Processing
[DE93-013389] 02 p0805 N94-13020
Surfaces and interfaces of ceramics and metals
[DE93-014959] 02 p0578 N94-13408
Growth of Si spherical crystals and the surface oxidation (M-9) 02 p0587 N94-13741
Single Event Upset (SEU) testing of semiconductor components at the McMaster Accelerator Laboratory
[DSIS-93-00071] 02 p0623 N94-13834
Activities of Institute for Microstructural Sciences
[NRC-32815] 02 p0810 N94-14198
Activities of Institute for Microstructural Sciences
[CNR-32815] 02 p0810 N94-14199
NASA Space Engineering Research Center for VLSI systems design
[NASA-CR-194035] 02 p0625 N94-14325
Interface properties of wide bandgap semiconductor structures
[AD-A268269] 03 p1215 N94-17377
Smart Power: New power integrated circuit technologies and their applications
[VTT-TIED-1358] 03 p1015 N94-17546
Proceedings of the 6th International Conference on Narrow Gap Semiconductors
[AD-A268097] 03 p1015 N94-17570
Joint services electronics program
[AD-A269383] 04 p1403 N94-18638
Recent developments in fast response aerodynamic probe technology 04 p1431 N94-18645
Optoelectronic packaging: A review
[DE93-040059] 04 p1515 N94-19535
A comparison of iterative methods for a model coupled system of elliptic equations
[DE93-040482] 04 p1553 N94-19655
Method for anisotropic etching in the manufacture of semiconductor devices
[NASA-CASE-MSC-21631-1] 05 p1993 N94-20491
Solid-state dynamics and quantum transport in novel semiconductor nanostructures
[AD-A272955] 05 p2027 N94-21248
Some experiences of solving 1-D semiconductor device equations on a matrix coprocessor by a domain decomposition method
[CWI-NM-R9304] 05 p1935 N94-21492
Advanced far infrared detectors
[DE93-040289] 05 p1988 N94-21528
Defect motion as the origin of the 1/f conductance noise in solids
[EUT-92-E-259] 05 p2029 N94-21552
Semiconductor isotope engineering
[DE93-040119] 05 p2030 N94-21744
Particle behavior in an ECR plasma etch tool
[DE93-040343] 05 p1996 N94-21769
A qualified radiation hardened nonvolatile memory for space and tactical weapons applications
[DE94-001211] 06 p2559 N94-23186
Sensors for process control Focus Team report
[DE93-040897] 06 p2560 N94-23204
CRRES microelectronics package flight data analysis
[NASA-TP-3423] 06 p2540 N94-23273
A multigrid solver for the semiconductor equations
06 p2482 N94-23674
Advanced qualification techniques
[DE94-003709] 07 p2780 N94-25812
Temperature dependence of the radiation induced change of depletion voltage in silicon PIN detectors
[DE94-002705] 07 p3052 N94-25972
Investigation of plasma etch induced damage in compound semiconductor devices
[DE94-002849] 07 p3052 N94-25989
Lithium drifted silicon detector fabrication on gettered floating-zone silicon
[DE94-003890] 07 p3054 N94-26095
Temperature dependence of static RAM volatility
[DE93-040345] 07 p2948 N94-26111
Fast generator of program waveforms signals
[DE93-634230] 07 p2948 N94-26381
Modeling Group 4 elements with new transferable tight-binding models
[DE94-000770] 07 p3059 N94-26695
Diagnostics and microelectronics
[DE94-003016] 07 p2784 N94-26777
Bulletin of Precision and Intelligence Laboratory, No. 68
[JTN-94-80609] 07 p3010 N94-27282
Multiple weight stepwise regression
[DE94-001602] 07 p3000 N94-27564
Dry etching process development for submicron and nanometer semiconductor devices
[PB94-133196] 07 p2788 N94-28357
Investigation of advanced fault insertion and simulator methods
[NASA-CR-195241] 08 p3261 N94-28511
Innovative optoelectronic materials and structures using OMVPE
[AD-A275811] 08 p3511 N94-28773
Optoelectronic integrated circuits fabricated using atomic layer epitaxy
[AD-A275454] 08 p3262 N94-28805
Cryogenic probe station for use in automated microwave and noise figure measurements
[NASA-TM-106560] 08 p3286 N94-29000
Effects of oxide charge and surface recombination velocity on the excess base current of BJT's
[DE94-003711] 08 p3263 N94-29025
Towards experimental verification and device applications of current driven plasma instabilities in solid state systems
[AD-A275395] 08 p3504 N94-29055
Proceedings of the Workshop on Microtechnologies and Applications to Space Systems
[NASA-CR-195688] 08 p3235 N94-29767
Micro-opto-mechanical devices and systems using epitaxial lift off 08 p3239 N94-29793

Photonics at Sandia National Laboratories: From research to applications
[DE94-006463] 08 p3501 N94-30828
III-V compound semiconductor strip-loaded waveguide devices for PICs: Design for minimum crosstalk and high density
[DE94-006588] 09 p3897 N94-31502
Examination of fast semiconductor diodes (recovery) with respect to switching valves in PWM and resonance devices
[ETN-94-95740] 09 p3690 N94-31609
Advanced infrared photodetectors: Materials review
[AD-A277058] 09 p3879 N94-32013
Novel growth technologies for in situ formation of semiconductor quantum wire structures
[AD-A277188] 09 p3902 N94-32255
WOCSDICE 1993 --- 17th European Workshop on Compound Semiconductor Devices and Integrated Circuits
[AD-A276766] 09 p3693 N94-32307
Optical processing for semiconductor device fabrication 09 p3885 N94-32445
Sandia's photonic program and its changing national role
[DE94-008616] 09 p3883 N94-32878
The 6th International Conference on Modulated Semiconductor Structures
[AD-A276815] 09 p3906 N94-32908
Superconducting and semiconducting hybrids and advance memory concepts for superconducting electronics
[AD-A277766] 09 p3907 N94-32988
Optically switched submillimeter-wave oscillator
[AD-A278014] 09 p3698 N94-33249
Material engineering of the novel semiconductor structures
[AD-A278386] 09 p3910 N94-33355
Semiconductor single-electron digital devices and circuits
[AD-A278338] 10 p4147 N94-33969
Nanochannel glass matrix used in making mesoscopic structures
[AD-D016216] 11 p4234 N94-36123
A critical examination of charge funneling and its impact on single-event upset in Si devices
[DE94-007868] 11 p4261 N94-36373
A proposed SEU tolerant DRAM cell
[DE94-010758] 12 p4438 N94-37196
Time-step stability for self-consistent Monte Carlo device simulation
[DE94-012145] 12 p4528 N94-37207

SEMICONDUCTOR DIODES
NT AVALANCHE DIODES
NT JUNCTION DIODES
NT LIGHT EMITTING DIODES
NT PHOTODIODES
NT SCHOTTKY DIODES
NT TUNNEL DIODES
NT VARACTOR DIODES
Nonlinear Dynamics in Optical Systems. Postdeadline papers presented at the Optical Society of America Conference
[AD-A264958] 01 p0375 N94-10486
Lecture note on circuit technology for high energy physics experiment
[DE93-771422] 01 p0372 N94-11245
Infrared detector annealing and calibration with IR-laser diodes 03 p0909 N94-15092
Laser imaging radar system
[AD-A270436] 04 p1387 N94-18510
Interinjection-locked quasioptical power combiners and phased arrays
[AD-A271178] 05 p2015 N94-20214
High Speed/High Frequency Optoelectronics
[AD-A271985] 05 p1751 N94-20580
Investigation on the chemically fixing technique of carbon dioxide utilizing solar energy
[DE94-714886] 05 p1849 N94-22043
Tunable lasers pumped by visible laser diodes
[AD-D016000] 06 p2350 N94-25044
Ultra-high aggregate bandwidth two-dimensional multiple-wavelength diode laser arrays
[AD-A274018] 07 p2815 N94-25756
Examination of fast semiconductor diodes (recovery) with respect to switching valves in PWM and resonance devices
[ETN-94-95740] 09 p3690 N94-31609
High power diode lasers for solid-state laser pumps 09 p3722 N94-32448
Improved performance of high average power semiconductor arrays for applications in diode pumped solid state lasers
[DE94-009516] 11 p4271 N94-35665
System for end-pumping a solid state laser using a large aperture laser diode bar
[AD-D016213] 11 p4273 N94-36370

SEMICONDUCTOR INSULATOR SEMICONDUCTORS
U SIS (SEMICONDUCTORS)

SEMICONDUCTOR JUNCTIONS
NT HETEROJUNCTIONS
NT HOMOJUNCTIONS
NT P-I-N JUNCTIONS
NT P-N JUNCTIONS
NT SILICON JUNCTIONS
InGaAs concentrator cells for laser power converters and tandem cells 01 p0050 N94-11394
Review of betavoltaic energy conversion 01 p0053 N94-11407
A new approach to optical photon detection 03 p0899 N94-15028
Superconductive x ray photon detectors 03 p0900 N94-15031
Atomic layer epitaxy of boron nitride
[AD-A266260] 03 p1212 N94-16932
Ultra-shallow box-like profiles fabricated by pulsed UV-laser doping process
[DE93-017221] 04 p1437 N94-18083
Strong overlap and transmission in triple barrier resonant structures
[DE94-608103] 08 p3516 N94-30067
Lowering the Schottky barrier at metal or silicide/Si interfaces to extend the range of infrared detectors
[AD-A277253] 09 p3903 N94-32322

SEMICONDUCTOR LASERS
NT ALUMINUM GALLIUM ARSENIDE LASERS
NT GALLIUM ARSENIDE LASERS
NT QUANTUM WELL LASERS
NT YLF LASERS
Nonlinear Dynamics in Optical Systems. Postdeadline papers presented at the Optical Society of America Conference
[AD-A264958] 01 p0375 N94-10486
Rapid thermal processing for strained-layer semiconductor devices
[DE93-013754] 01 p0396 N94-10809
Characterization of a scannerless LADAR system
[DE93-011582] 01 p0174 N94-10959
Semiconductor ring lasers
[DE93-012386] 01 p0174 N94-11005
New challenges in optical materials development
[DE93-011889] 01 p0383 N94-11676
Gathering and exchange information on atmospheric chemistry and polluted atmospheres
[DE93-009940] 02 p0705 N94-12869
Non-scanned LADAR imaging and applications
[DE93-013772] 02 p0655 N94-13261
Characteristics of semiconductor lasers with optical feedback
[ISBN-0-315-55435-5] 02 p0656 N94-13522
Horizontal-cavity surface-emitting lasers, superluminescent LEDs, and amplifiers, and parabolic gain unstable resonator semiconductor lasers 02 p0656 N94-13573
Microchannel cooled heatsinks for high average power laser diode arrays
[DE93-016533] 02 p0658 N94-14442
AlGaAs diode laser blue shift resulting from fast neutron irradiation
[AD-A266642] 02 p0659 N94-14681
Infrared detector annealing and calibration with IR-laser diodes 03 p0909 N94-15092
Nd:YLF laser for airborne/spaceborne laser ranging 03 p0913 N94-15563
Development of the Mars Observer Laser Altimeter (MOLA) 03 p0921 N94-15617
Laser with optically driven Q-switch
[NASA-CASE-NPO-18470-1-CU] 03 p1038 N94-15932
Fundamental theory of light for applications: Notes for five informal lectures
[DE93-016463] 03 p1192 N94-16953
Curved grating fabrication techniques for concentric-circle grating, surface-emitting semiconductor lasers 03 p1045 N94-17349
Nonintrusive fast response oxygen monitoring system for high temperature flows
[NASA-CR-4553] 03 p1036 N94-17655
Pulsed LASER for testing silicon strip detectors
[DE93-017816] 04 p1436 N94-17883
Advanced optical fiber communication systems
[AD-A269120] 04 p1577 N94-18254
Laser imaging radar system
[AD-A270436] 04 p1387 N94-18510
Ultrafast Electronics and Optoelectronics: Summaries of papers. Technical digest conference edition
[AD-A269233] 04 p1405 N94-18909
Evaluation of laser diode based optical switches for optical processors
[AD-A270949] 04 p1581 N94-19602
Experimental examinations of semiconductor laser amplifiers for optical communication technology
[ETN-93-95050] 04 p1442 N94-19647
Spatial patterns in semiconductor lasers
[DE93-040056] 05 p1814 N94-19865
First results on InGaAsP separate confinement heterostructure diode lasers
[AD-A270849] 05 p1815 N94-19878
A full-color, high-resolution laser projector for a flight simulator visual display
[AD-A270578] 05 p1651 N94-20108
Optically controlled current filamentation in GaAs photoconductive semiconductor switches
[DE93-019427] 05 p2016 N94-20296
High Speed/High Frequency Optoelectronics
[AD-A271985] 05 p1751 N94-20580
Optical amplification and threshold behavior on InGaAs/InGaAsP multiquantum well structures
[ETN-93-94181] 05 p2026 N94-21151
SFOLDA: A semiconductor LDA for measurements in complex flows 06 p2316 N94-22856
Laser linewidth measurement in the presence of RIN and using the recirculating self heterodyne method
[EUT-92-E-262] 06 p2347 N94-22874
Evaluation of uranium transitions for isotopically-selective laser induced fluorescence with diode lasers (technical report for ST064)
[DE94-002000] 06 p2347 N94-22974
InGaAsP/InP based 1.3/1.55 micron vertical cavity surface emitting lasers for wavelength division multiplexed high speed distributed computing, phase 1
[AD-A271081] 06 p2348 N94-23123
Electrochemical sulfur passivation of visible (approximately 670nm) AlGaInP lasers
[DE94-002293] 06 p2350 N94-24659
Matter-wave interferometry with laser cooled atoms
[AD-A273249] 06 p2536 N94-24717
Tunable lasers pumped by visible laser diodes
[AD-D016000] 06 p2350 N94-25044
The effects of optical feedback on polarization of vertical cavity surface emitting lasers
[AD-A273728] 06 p2351 N94-25445
Characterization of an LCD for use as a programmable phase shifter to produce a single-lobed far-field pattern in a phased array
[AD-A273883] 07 p3034 N94-25729
Ultra-high aggregate bandwidth two-dimensional multiple-wavelength diode laser arrays
[AD-A274018] 07 p2815 N94-25756
System design analysis of a lightweight laser satellite terminal
[AD-A274033] 07 p2690 N94-25769
Design analysis of a combined optical/LADAR deep-space surveillance satellite
[AD-A274040] 07 p2694 N94-25832
Instantaneous amplitude and frequency dynamics of coherent wave mixing in semiconductor quantum wells
[DE94-003262] 07 p3054 N94-26128
Laser-based communication link
[FFI-93/7023] 07 p2817 N94-26203
Diode-laser-pumped, gas-cell atomic clocks
[AD-A274812] 07 p3008 N94-26484
Near-IR diode laser absorption for measurement of tropospheric HO2 08 p3345 N94-28607
HO2 detection by near infrared absorption using tunable diode lasers 08 p3346 N94-28608
Visible vertical cavity surface emitting lasers
[AD-A275334] 08 p3293 N94-28919
High-power CW diode-laser-array-pumped solid-state lasers and efficient nonlinear optical frequency
[AD-A275394] 08 p3293 N94-29309
Dynamics of a coupled solid state laser array 08 p3294 N94-29551
Longitudinal effects and intensity-phase coupling in distributed feedback semiconductor lasers 08 p3294 N94-29590
Time and frequency technology at NIST 08 p3468 N94-30641
Diode-pumped solid-state-laser drivers and the competitiveness of inertial fusion energy
[DE94-006654] 08 p3296 N94-30830
Laser Diode Ignition (LDI)
[DE94-006590] 09 p3666 N94-31579
Semiconductor microcavity lasers
[DE94-006143] 09 p3716 N94-31622
High conversion efficiency pumped-cavity second harmonic generation of a diode laser
[DE94-006805] 09 p3717 N94-32134
Control and reliability of optical networks in multiprocessors
[AD-A277385] 09 p3881 N94-32285
High power diode lasers for solid-state laser pumps 09 p3722 N94-32448
Flexible manufacturing for photonics device assembly 09 p3669 N94-32449
Rare Earth Doped Semiconductors and Materials Research Society Symposium Proceedings, Volume 301
[AD-A277517] 09 p3908 N94-33055

Research in the optical sciences
[AD-A278271] 09 p3884 N94-33140
Advanced release technologies program
09 p3607 N94-33322
Improved performance of high average power semiconductor arrays for applications in diode pumped solid state lasers
[DE94-009516] 11 p4271 N94-35665
The optimization of interfaces in InAsSb/InGaAs strained-layer superlattices grown by metal-organic chemical vapor deposition
[DE94-010070] 11 p4340 N94-35698
High-power CW operation of AlGaInP diode-laser arrays
[DE94-010409] 11 p4272 N94-36115
Phase-locked arrays of vertical-cavity surface-emitting lasers
[DE94-009279] 11 p4272 N94-36178
Activities of the optoelectronics laboratory
[PB94-171196] 11 p4334 N94-36190
System for end-pumping a solid state laser using a large aperture laser diode bar
[AD-D016213] 11 p4273 N94-36370
Diode array alternative to paint removal solid-state cw laser
[DE94-011482] 12 p4448 N94-37203
Advanced laser driver for soft x-ray projection lithography
[DE94-011643] 12 p4449 N94-37722

SEMICONDUCTORS (MATERIALS)
NT ACCEPTOR MATERIALS
NT AMORPHOUS SEMICONDUCTORS
NT AMORPHOUS SILICON
NT CMOS
NT DONOR MATERIALS
NT METAL OXIDE SEMICONDUCTORS
NT MIS (SEMICONDUCTORS)
NT N-TYPE SEMICONDUCTORS
NT ORGANIC SEMICONDUCTORS
NT P-TYPE SEMICONDUCTORS
NT PHOTOCONDUCTORS
NT SOS (SEMICONDUCTORS)
NT SUPERLATTICES
NT VYCOR
Measurement of the thermal conductivity of molten InSb in a drop shaft 01 p0105 N94-10102
Scientific specifications for an automated facility for growing large semiconducting crystals from the melt in space 01 p0114 N94-10180
THM-growth of III-V-semiconductors in the magnetic field 01 p0118 N94-10209
Photostimulated attenuation of hypersound in superlattice
[DE93-611231] 01 p0357 N94-10408
Structure of s - p bonded metal clusters with 8, 20 and 40 valence electrons
[DE93-613643] 01 p0361 N94-10503
Method for producing a hybridization of detector array and integrated circuit for readout
[NASA-CASE-NPO-18062-1-CU] 01 p0141 N94-10656
Crack suppression in GaInSb buffer layers initially under tensile stress
[DE93-012839] 01 p0396 N94-10745
Confinement of acoustical modes due to the electron-phonon interaction within 2D-electron gas
[DE93-613910] 01 p0396 N94-10800
Rapid thermal processing for strained-layer semiconductor devices
[DE93-013754] 01 p0396 N94-10809
Electronic characterization of defects in narrow gap semiconductors
[NASA-CR-193568] 01 p0397 N94-10819
Ellipsometry studies of semiconductors surface cleaning
[AD-A265150] 01 p0142 N94-11094
Time-resolved optical studies of charge relaxation and charge transfer at electrode interfaces
[DE93-013985] 01 p0398 N94-11117
Characterization of the Si/SiO2 interfere morphology from quantum oscillations in Fowler-Nordheim tunneling currents
[AD-A265149] 01 p0143 N94-11160
Memory effects in the organometallic chemical beam epitaxy of compound semiconductors
[NASA-CR-193106] 01 p0399 N94-11439
Remote plasma enhanced chemical vapor deposition of GaP with in situ generation of phosphine precursors 01 p0399 N94-11440
Lattice-matched heteroepitaxy of wide gap ternary compound semiconductors 01 p0400 N94-11441
Development of microstrip gas chambers with multi-chip technology
[DE93-753169] 01 p0367 N94-11509
Wide Band-Gap Semiconductors. 1991 Materials Research Society Symposium proceedings
[AD-A263418] 01 p0401 N94-11515
A thermal ionization model for the sustaining phase of lock-on in GaAs
[DE93-011558] 01 p0144 N94-11624
The additional contribution caused by Coulomb interaction to the exciton dispersion in multiple quantum wells and superlattices for direct band gap cubic semiconductors
[DE93-613538] 01 p0402 N94-11659
On the theory of phonoriton in cubic semiconductors with a degenerate valence band
[DE93-613539] 01 p0402 N94-11660
Adsorption and dissociation of disilane on Si(001) studied by STM
[AD-A265269] 01 p0402 N94-11684
Gallium arsenide dynamic random access memory support circuitry
[AD-A265176] 01 p0320 N94-11875
Production of electronic grade lunar silicon by disproportionation of silicon difluoride 01 p0435 N94-12017
Development of ultra-low noise, high sensitivity planar metal grating coupled 3 to 5 multiquantum well infrared detectors for focal plane array staring IR sensor systems
[AD-A265599] 01 p0404 N94-12375
Multicomponent and multilayered thin films for advanced microtechnologies: Techniques, fundamentals, and devices
[AD-A265685] 01 p0405 N94-12442
Synthesis and electronic properties of nanophase semiconductor materials
[AD-A265287] 01 p0146 N94-12584
Theoretical investigation of some novel phenomenal in artificially structured semiconductors
[AD-A266142] 01 p0405 N94-12587
Liquid phase epitaxy of gallium arsenide: A review
[DE93-622212] 02 p0804 N94-12893
Metal-semiconductor, composite radiation detectors
[DE93-013313] 02 p0619 N94-12994
Nonlinear laser spectroscopy studies of semiconductor heterostructures
[AD-A265728] 02 p0805 N94-13037
Crystallographic and metallurgical characterization of radiation detector grade cadmium telluride materials
[DE93-014335] 02 p0806 N94-13150
Comment of parameter excitation of Alfven and Helicon waves in a magnetoactive compensated semiconductor by microwave radiation
[DE93-623203] 02 p0806 N94-13228
Surfaces and interfaces of ceramics and metals
[DE93-014959] 02 p0578 N94-13408
Crystal growth of ZnSe and related ternary compound semiconductors by physical vapor transport
[NASA-CR-193834] 02 p0807 N94-13444
Spacelab J experiment descriptions
[NASA-TM-4517] 02 p0586 N94-13732
Growth experiment of narrow band-gap semiconductor PbSnTe single crystals in space (M-1) 02 p0586 N94-13733
Growth of PbSnTe single crystal by traveling-zone method in low gravity (M-2) 02 p0586 N94-13734
Growth of semiconductor compound single crystal InSb by floating zone method (M-3) 02 p0586 N94-13735
Crystal growth of compound semiconductors in a low-gravity environment (InGaAs crystals) (M-22) 02 p0590 N94-13754
Activities of the Basic Sciences Branch
[DE93-010012] 02 p0851 N94-14455
A sum-rule of luminescence spectrum
[ITN-93-85223] 02 p0814 N94-14559
Dynamic Jahn-Teller effect: Calculation of fine structure spectrum, isotope shift and Zeeman behavior at deep center Ni2+ in CdS
[ETN-93-94394] 02 p0815 N94-14705
Electronic and atomic structure of semiconductors and of high-temperature superconductors
[AD-A266805] 03 p1205 N94-14913
Transparent conductive coatings in the far ultraviolet
[NASA-CR-194632] 03 p1191 N94-16024
Thermal spray forming of refractory sample ampoule cartridges for single crystal growth space furnaces
[TABES PAPER 93-605] 03 p1051 N94-16141
Apparatus for and a method of growing thin films of elemental semiconductors
[AD-D015813] 03 p1210 N94-16487
Properties of thin films for high temperature flow sensors
[NASA-CR-191526] 03 p0967 N94-16541
SONOS technology for commercial and military nonvolatile memory applications
[DE93-015647] 03 p1011 N94-16661
Ultrafast processes in tunneling microstructure devices
[AD-A266570] 03 p1210 N94-16720
Methods of tunneling spectroscopy with the STM
[AD-A266507] 03 p0948 N94-16787
JSEP fellowship
[AD-A266568] 03 p1211 N94-16800
Insights into semiconducting materials and growth phenomena through Z-contrast STEM
[DE93-015964] 03 p1212 N94-16841
Activation and deactivation of high concentration arsenic with some evidence of precipitation
[DE93-016437] 03 p0950 N94-16952
Vectorial electron transfer in spatially ordered arrays
[DE93-018150] 03 p1185 N94-16971
Surface flashover of semiconductors: A fundamental study
[AD-A267382] 03 p1012 N94-17023
Nitride semiconductors for ultraviolet detection
[AD-A267877] 03 p1012 N94-17040
Photo-assisted epitaxial growth for III-V semiconductors
[AD-A267889] 03 p1213 N94-17042
Investigation of the optical, electronic, and structural properties of fiber optic glasses
[AD-A267645] 03 p0971 N94-17204
A state-of-the-art plasma polymerization coater for ICF targets
[DE93-016452] 03 p1204 N94-17237
A 27 channels, 1 MHz fibre-optic measuring system
[AD-A266943] 03 p1003 N94-17307
Subwavelength structured surfaces and their applications 03 p1194 N94-17337
Curved grating fabrication techniques for concentric-circle grating, surface-emitting semiconductor lasers 03 p1045 N94-17349
OSA proceedings on Ultrafast Electronics and Optoelectronics, volume 14
[AD-A267972] 03 p1014 N94-17410
Laser probing of the kinetics and dynamics of 3-5 semiconductor growth
[AD-A268388] 03 p1215 N94-17422
Mechanical properties and crystal growth studies of semiconductor alloys
[AD-A268144] 03 p1216 N94-17454
Femtosecond carrier processes in compound semiconductors and real time signal processing
[AD-A268122] 03 p1005 N94-17519
In-situ electron and optical spectroscopies of translational and vibrational activated bond breaking and formation on semiconductors
[AD-A268192] 03 p1015 N94-17560
Proceedings of the 6th International Conference on Narrow Gap Semiconductors
[AD-A268097] 03 p1015 N94-17570
Rare earth doped III-V semiconductors for optoelectronics
[AD-A268279] 03 p1216 N94-17577
Activities of the Research Laboratory of Electronics
[AD-A266730] 03 p1304 N94-17651
Design and test of a low jitter metal to metal contact solid dielectric switch
[DE93-016957] 04 p1394 N94-17755
Lattice damage in ion-implanted compound semiconductors and its effect on electrical activation
[DE93-015907] 04 p1593 N94-17845
Feasibility survey of thermoelectric conversion technology using semiconductors
[DE93-520882] 04 p1595 N94-18105
Experimental and theoretical investigation of surface chemistry induced by direct and indirect electronic excitation
[AD-A268846] 04 p1348 N94-18221
Superconducting/semiconducting hybrids and advance memory concepts for superconducting electronics
[AD-A268679] 04 p1397 N94-18312
Gallium arsenide-based ternary compounds and multi-band-gap solar cell research
[DE93-010049] 04 p1467 N94-18483
Optical and transport properties of metallic and semiconductor nanostructures
[AD-A270009] 04 p1598 N94-18609
In-situ growth monitoring of molecular beam epitaxy processes
[AD-A269287] 04 p1598 N94-18616
Integration of ferroelectric/semiconductor thin films for SLM and photorefractive applications
[AD-A268645] 04 p1598 N94-18633
Joint services electronics program
[AD-A269383] 04 p1403 N94-18638
Photodetector array having high pixel density
[AD-D015859] 04 p1432 N94-18731
Tunneling microscopy of semiconductors
[AD-A270232] 04 p1600 N94-18904
Ultrafast Electronics and Optoelectronics: Summaries of papers. Technical digest conference edition
[AD-A269233] 04 p1405 N94-18909

Growth of epitaxial semiconductor alloys and superlattices with continuously variable composition by pulsed-laser ablation
[DE93-018726] 04 p1601 N94-18998
X ray studies of microstructures in semiconductor and superconducting materials
[DE93-040690] 04 p1601 N94-19056
Radiation hardened microprocessor for small payloads
04 p1327 N94-19184
A comparison of iterative methods for a model coupled system of elliptic equations
[DE93-040482] 04 p1553 N94-19655
The deposition of electro-optic films on semiconductors
[AD-A270823] 04 p1605 N94-19664
Solid-state dynamics in novel semiconductor nanostructures
[AD-A271249] 04 p1605 N94-19725
Single source precursors for the OMCVD of 3/5 compound semiconductors
[AD-A271147] 04 p1606 N94-19739
Nanofabrication by focused ion beam
[AD-A271290] 04 p1345 N94-19746
Polarized optical emission due to decay or recombination of spin-polarized injected carriers
[AD-D015907] 04 p1408 N94-19763
MOCVD-grown InGaAsP heterostructure diode lasers
[AD-A270848] 04 p1606 N94-19769
Investigation of quantum effects in heterostructures
[AD-A270938] 05 p2011 N94-19817
Theory of energy-assisted epitaxy; theory of ordered semiconductor alloys: In(1-x)Tl(x)Sb as a long-wave infrared material
[AD-A271007] 05 p2012 N94-19835
Effect of exciton localization and delocalization on magnetic-field-dependent photoluminescence linewidths in semiconductors
[DE93-018860] 05 p1748 N94-19884
Development of high-efficiency CdTe solar cells
[DE93-018206] 05 p1845 N94-19925
Research on defects and transport in amorphous-silicon-based semiconductors
[DE93-017117] 05 p2013 N94-19939
Photoluminescence spectroscopy of zinc germanium diphosphide (ZnGeP2)
[AD-A270705] 05 p1678 N94-19953
ALE project
[AD-A271080] 05 p2014 N94-19980
Study of mechanisms for long wavelength Schottky-barrier infrared detectors
[AD-A270538] 05 p1971 N94-20083
Development of a numerical simulation model for a-Si:H solar cells and application to the analysis of experimentally obtained spectral characteristics
[ETN-93-95061] 05 p1846 N94-20151
Photoelectron spectroscopy at model boundary surfaces of energy converter semiconductors/electrolyte contacts: Adsorption, coadsorption, and triadsorption of Br2, Na, and H2O on Van der Waals surfaces of metal chalocogenide semiconductors
[ETN-93-95063] 05 p2015 N94-20152
Single-event upset testing of the performance semiconductor 1750A CMOS/SOS chip set
[AD-A271158] 05 p2015 N94-20184
Photoconductive Semiconductor Switches for pulsed power applications
[DE93-019411] 05 p1750 N94-20294
Optically controlled current filamentation in GaAs photoconductive semiconductor switches
[DE93-019427] 05 p2016 N94-20296
High current density contacts for photoconductive semiconductor switches
[DE93-018837] 05 p1750 N94-20312
Optical and transport properties of metallic and semiconductor nanostructures
[AD-A271716] 05 p2018 N94-20554
Fabrication and evaluation of superconducting and semiconducting materials
[AD-A271645] 05 p2018 N94-20558
High Speed/High Frequency Optoelectronics
[AD-A271985] 05 p1751 N94-20580
Laser diagnostics of RF hydrogen plasma reactors: Application to the processing of III-V materials
[AD-A272659] 05 p1994 N94-21214
Dephasing processes in III-V semiconductors
[AD-A271677] 05 p2028 N94-21362
Analysis of semi-insulating bulk GaAs using glow discharge mass spectrometry
[AD-A273032] 05 p1682 N94-21435
Semiconductors A(III)B(VI): Translation
[AD-A273064] 05 p2028 N94-21438
Single crystal diamond films
[AD-A266759] 05 p2028 N94-21517
Advanced far infrared detectors
[DE93-040289] 05 p1988 N94-21528
Synthesis and catalytic properties of metal and semiconductor nanoclusters
[DE93-019418] 05 p2028 N94-21541
Heterojunction bipolar transistor technology for data acquisition and communication
05 p1763 N94-21697
Semiconductor isotope engineering
[DE93-040119] 05 p2030 N94-21744
High power, electron-beam induced switching in diamond
[DE93-040535] 05 p1768 N94-21770
Characterization of convection related defects in II-VI compound semiconductors
[NASA-CR-194704] 05 p2030 N94-21778
Hydrogen in compound semiconductors
[DE93-040300] 05 p2031 N94-21922
Lattice damage during ion implantation of semiconductors
[DE94-000335] 05 p2034 N94-22016
Ultraviolet photosulfidation of III-V compound semiconductors for electronic passivation
[DE94-001417] 06 p2555 N94-22717
Report of the Joint Seminar on Solid State Physics, Atomic and Molecular Physics, and Materials Science in the Energy Region of Tandem Accelerators
[DE93-508268] 06 p2548 N94-22924
Physics with chemically and isotopically pure semiconductors
[DE93-040120] 06 p2557 N94-22926
Sensors for process control Focus Team report
[DE93-040897] 06 p2560 N94-23204
Modulation characteristics of a high-power semiconductor Master Oscillator Power Amplifier (MOPA)
[NASA-TM-104577] 06 p2308 N94-23281
Microgravity sciences application visiting scientist program
[NASA-CR-194804] 06 p2267 N94-23287
Observation of non-centrosymmetry and determination of polarity in III-V semiconductors
[PB93-201416] 06 p2561 N94-23503
Contributions of DOE weapons labs and NIST to semiconductor technology
[OTA-ITE-585] 06 p2630 N94-23572
A multigrid solver for the semiconductor equations
06 p2482 N94-23674
Magnetic resonance studies of 3d transition metal impurities in compound semiconductors
[PB93-232197] 06 p2243 N94-23714
Disorder effects on small-polaron formation and hopping
[DE94-001205] 06 p2534 N94-23804
Pulsed Ion Beam Surface Analysis (PIBSA) as a means of in-situ real-time analysis of thin films during growth
[DE94-001276] 06 p2562 N94-23805
Effects of thermal-solutal convection on temperature and solutal fields under various gravitational orientations
06 p2267 N94-24451
Ge-Au eutectic bonding of Ge (100) single crystals
[DE94-002281] 06 p2564 N94-24657
Electrochemical sulfur passivation of visible (approximately 670nm) AlGaInP lasers
[DE94-002293] 06 p2350 N94-24659
SEMATECH, a case study: Analysis of a government-industry partnership
[AD-A273166] 06 p2586 N94-24683
Method of fabricating a receptor-based sensor
[AD-D016026] 06 p2344 N94-24723
The 5th Engineering Foundation Conference: Advanced Heterostructure Transistors
[AD-A273508] 06 p2312 N94-24819
LPCVD of InN on GaAs(110) using HN3 and TMIn: Comparison with Si(100) results
[AD-A273555] 06 p2235 N94-24917
Conformal method of fabricating and optical waveguide on a semiconductor substrate
[AD-D015988] 06 p2546 N94-25043
An overview of the measurements of thermophysical properties and some results on molten superalloys and semiconductors 06 p2248 N94-25128
Effect of high frequency field on the transport properties of superlattice
[DE93-617047] 06 p2568 N94-25447
Bulletin of National Research Institute for Metals in Fiscal Year 1993, no. 14
[REPT-14] 07 p2722 N94-25544
Failure mechanisms of high temperature semiconductor lasers
[AD-A273833] 07 p2815 N94-25616
Hydrogen uptake into silicon from an ECR plasma
[DE94-003771] 07 p3050 N94-25815
On the estimation of matrix elements for optical transitions in semiconductors
[DE93-613550] 07 p3051 N94-25851
On radiation defects in strip detectors
[DE93-616646] 07 p3015 N94-25916
The AFIT multielectrode array for neural recording and simulation: Design, testing, and encapsulation
[AD-A274086] 07 p2909 N94-25943
Determination of surface recombination velocity and bulk lifetime in detector grade silicon and germanium crystals
[DE94-003886] 07 p3053 N94-26094
Lithium drifted silicon detector fabrication on gettered floating-zone silicon
[DE94-003890] 07 p3054 N94-26095
Se EXAFS study of the elevated wurtzite to rock salt structural phase transition in CdSe nanocrystals
[DE94-003247] 07 p3054 N94-26125
Instantaneous amplitude and frequency dynamics of coherent wave mixing in semiconductor quantum wells
[DE94-003262] 07 p3054 N94-26128
Studies of thin-film growth, adsorption, and oxidation by in situ, real-time, and ex situ ion beam analysis
[DE94-002907] 07 p3055 N94-26275
Exploration of GaAs structures for solid-state detectors
[DE93-634191] 07 p3056 N94-26379
On the electron mobility in slightly compensated heavily doped gallium arsenide at low temperatures
[DE93-634712] 07 p3057 N94-26387
Translational-energy-resolved studies of photogenerated carrier-induced reactions on UHV semiconductor surfaces
[DE94-004169] 07 p3058 N94-26526
Diagnostics and microelectronics
[DE94-003016] 07 p2784 N94-26777
Mechanistic studies of opto-electronic materials and syntheses using multiple laser and surface diagnostics
[AD-A274528] 07 p3036 N94-26834
Nitride semiconductors for ultraviolet detection
[AD-A274246] 07 p3060 N94-26840
Effect of impurity correlation on the density of states in slightly compensated heavily doped semiconductors
[DE94-602539] 07 p3061 N94-26879
A model of electric breakdown in polycrystalline semiconductors with highly nonlinear I - V characteristics
[DE94-601537] 07 p3063 N94-27017
AC to DC power converter with regulated bi-polar outputs
[AD-D016032] 07 p2786 N94-27145
Technical report of ISSP. Ser. A, no. 2674: High-field cyclotron resonance and impurity transition in n- and p-3C-SiC at magnetic fields up to 175 T
[JTN-94-80560] 07 p3064 N94-27232
Technical report of ISSP. Ser. A, no. 2675: High-field cyclotron resonance and valence-band structure in semiconducting diamond
[JTN-94-80561] 07 p3065 N94-27245
Optimising BMW four-cylinder two-valve engines
[PB94-125101] 07 p2824 N94-27254
Decay of non-equilibrium polariton condensate in semiconductors
[DE94-604016] 07 p3068 N94-27678
Laser beam steering with semiconductor waveguide
[AD-A275775] 08 p3292 N94-28765
Innovative optoelectronic materials and structures using OMVPE
[AD-A275811] 08 p3511 N94-28773
Electroset Technology: On the forefront of manufacturing
[AD-A275166] 08 p3263 N94-29045
High resistivity buffer layers by oxygen doping
[AD-A274986] 08 p3513 N94-29125
Preparation, characterization, and facile thermolysis of (X2GaP(SiMe3)2) (X = Br, I) and (Cl3Ga2P)n; new precursors to nanocrystalline gallium phosphide
[AD-A275019] 08 p3513 N94-29130
Monolithic in-based III-V compound semiconductor focal plane array cell with single stage CCD output
[NASA-CASE-NPO-18978-1-CU] 08 p3265 N94-29488
Epitaxial heterojunctions of oxide semiconductors and metals on high temperature superconductors
[NASA-CASE-NPO-18483-1-CU] 08 p3513 N94-29501
Near-ultraviolet laser photoemission: Scanning microscopy, buried interfaces and image-potential states
08 p3294 N94-29531
Optical properties of cadmium sulfide, zinc selenide, and zinc manganese selenide semiconductor films
08 p3500 N94-29759
Overview of microoptics: Past, present, and future
08 p3235 N94-29771
ECR plasma synthesis of silicon nitride films on GaAs and InSb
[DE94-005575] 08 p3515 N94-30006
Structural characterization of semiconductor heterostructures by atomic resolution Z-contrast imaging at 300 kV
[DE94-006561] 08 p3516 N94-30063

Vibrational properties of homopolar and heteropolar surfaces and interfaces of the CdTe/HgTe system
[DE94-608105] 08 p3516 N94-30069
II-VI wide band gap semiconductors under hydrostatic pressure
[DE94-608106] 08 p3516 N94-30070
Band structure of superlattice with (delta)-like potential
[DE94-608108] 08 p3516 N94-30072
Survey report of JSUP Space Environment Utilization Research Committee in fiscal year 1992: Functional New Materials Session
[JTN-94-80582] 08 p3159 N94-30162
The 1992 report on the next generation ultra clean technology for advanced microfabrication
[DE94-744171] 08 p3157 N94-30268
Nonlinear optics response of semiconductor quantum wells under high magnetic fields
[DE94-003244] 08 p3520 N94-30835
Nuclear magnetic relaxation studies of semiconductor nanocrystals and solids
[DE94-006301] 08 p3520 N94-30842
Rotator phases in narrow-gap semiconductors
[DE94-005472] 08 p3521 N94-30897
Indium-vacancy complexes in mercury cadmium telluride
[AD-A276177] 09 p3894 N94-31055
Passivation of III-V compound semiconductor based devices
[AD-A276178] 09 p3894 N94-31056
Electron-beam controlled semiconductor switches
[AD-A276198] 09 p3686 N94-31057
Modification of semiconductor surface properties with chemically bound molecular films
[AD-A276162] 09 p3895 N94-31081
Growth and characterization of III-V semiconductors with rare earth impurities for optoelectronic devices
[AD-A276021] 09 p3896 N94-31455
Semiconductor microcavity lasers
[DE94-006143] 09 p3716 N94-31622
A low cost igniter utilizing an SCB and titanium sub-hydride potassium perchlorate pyrotechnic
[DE94-006467] 09 p3666 N94-31827
Development of sample charge compensation for characterization of impurities in semiconductor materials
[AD-A277113] 09 p3899 N94-31983
IR materials producibility
[AD-A277028] 09 p3879 N94-32006
Advanced infrared photodetectors: Materials review
[AD-A277058] 09 p3879 N94-32013
Anomalous small angle x ray scattering studies of amorphous metal-germanium alloys
[DE94-007258] 09 p3900 N94-32065
Advances in MOVPE compound semiconductor epitaxy manufacturing technology: From high throughput large area reactors to cluster tools
[DE94-006367] 09 p3901 N94-32104
Amorphous/crystalline structure and phase transformations in metastable semiconducting Ge(1-x)Sn(x)
[DE94-006659] 09 p3901 N94-32115
The 10th International Conference on Internal Friction and Ultrasonic Attenuation in Solids (ICIFUAS)
[AD-A276849] 09 p3902 N94-32209
Novel growth technologies for in situ formation of semiconductor quantum wire structures
[AD-A277188] 09 p3902 N94-32255
Proceedings of the International Workshop on Computational Electronics
[AD-A277020] 09 p3692 N94-32259
WOCSDICE 1993 --- 17th European Workshop on Compound Semiconductor Devices and Integrated Circuits
[AD-A276766] 09 p3693 N94-32307
Theoretical studies of electron transfer and optical spectroscopy
[DE94-006985] 09 p3871 N94-32375
A scanning defect mapping system for semiconductor characterization 09 p3885 N94-32446
Ionization probes of molecular structure and chemistry
[DE94-007605] 09 p3872 N94-32643
Metal-ion spin-on glasses: Novel materials for active waveguides
[DE94-007738] 09 p3882 N94-32649
Research on stable, high-efficiency amorphous silicon multijunction modules
[DE94-000298] 09 p3695 N94-32680
Application of the modified voltage-dividing potentiometer to overlay metrology in a CMOS/bulk process
[DE94-007937] 09 p3695 N94-32700
The 6th International Conference on Modulated Semiconductor Structures
[AD-A276815] 09 p3906 N94-32908
Silicon-Based Optoelectronic Materials Symposium and Materials Research Society Proceedings, volume 298
[AD-A277518] 09 p3662 N94-32952
Rare Earth Doped Semiconductors and Materials Research Society Symposium Proceedings, Volume 301
[AD-A277517] 09 p3908 N94-33055
Spacecraft environmental anomalies expert system
[AD-A277962] 09 p3612 N94-33262
Electrical characteristics of GaAs MESFET fabrication by ion implantation of Si or Se
[AD-A278416] 09 p3909 N94-33328
Material engineering of the novel semiconductor structures
[AD-A278386] 09 p3910 N94-33355
Characterization of defects in Si and SiO2-Si using positrons
[DE94-009044] 10 p4147 N94-33877
Dynamics of supermatrix semiconductor growth
[AD-A278380] 10 p4147 N94-34085
Relaxation of radiation damages in silicon planar detectors
[DE94-009084] 10 p4148 N94-34166
InP solar cell with window layer
[NASA-CASE-LEW-15606-1] 11 p4281 N94-35230
The optimization of interfaces in InAsSb/InGaAs strained-layer superlattices grown by metal-organic chemical vapor deposition
[DE94-010070] 11 p4340 N94-35698
Heterogeneous reaction mechanisms and kinetics relevant to the CVD of semiconductor materials
[DE94-011001] 11 p4340 N94-36032
Activities of the optoelectronics laboratory
[PB94-171196] 11 p4334 N94-36190
High temperature heterojunction bipolar transistors
[AD-A278605] 11 p4261 N94-36360
Gas-Phase and Surface Chemistry in Electronic Materials Processing. Materials Research Society Symposium proceedings, volume 334
[AD-A280586] 12 p4408 N94-36735
Small-angle x ray scattering studies of microvoids in amorphous-silicon-based semiconductors
[DE94-006931] 12 p4533 N94-36745
Ampoule failure sensor time response testing: Experiments 2 and 3
[NASA-TM-108458] 12 p4446 N94-36822
The excitation mechanism of praseodymium-doped semiconductors
[AD-A280687] 12 p4535 N94-37129
Preliminary soft x ray studies of beta-SiC
[DE94-013023] 12 p4537 N94-37498
Theoretical studies of the transport properties in compound semiconductors
[NASA-CR-196109] 12 p4439 N94-37501
The application of maximum entropy to Z-contrast imaging in a stem
[DE94-011470] 12 p4412 N94-37546
Experimental particle physics at the University of Pittsburgh
[DE94-011636] 12 p4521 N94-37721
Comparison of gaseous and semiconductor detectors for medical imaging
[DE94-621344] 12 p4482 N94-37729
Implanting impurities in semiconductors and semiconductor implanted with impurities
[AD-D016298] 12 p4538 N94-37770

SEMIMETALS
U METALLOIDS

SEMISPAN MODELS
Semi-span model testing in the National Transonic Facility
[NASA-CR-194479] 04 p1312 N94-19388
Semi-span model testing in the national transonic facility
[NASA-CR-195952] 10 p4048 N94-34300

SENDERS
U TRANSMITTERS

SENSE ORGANS
NT BARORECEPTORS
NT CHEMORECEPTORS
NT COCHLEA
NT CORNEA
NT CORTI ORGAN
NT EYE (ANATOMY)
NT FOVEA
NT OCULOMOTOR NERVES
NT OTOLITH ORGANS
NT PHOTORECEPTORS
NT PROPRIOCEPTORS
NT PUPILS
NT RETINA
NT SEMICIRCULAR CANALS
NT VESTIBULES

SENSES
U SENSORY PERCEPTION

SENSIBILITY
U SENSITIVITY

SENSING
U DETECTION

SENSITIVITY
NT IMPACT RESISTANCE
NT LIGHT ADAPTATION
NT NOTCH SENSITIVITY
NT PAIN SENSITIVITY
NT PHOTOSENSITIVITY
NT PROPELLANT SENSITIVITY
NT RADIATION TOLERANCE
NT SPECTRAL SENSITIVITY
Computer software and hardware to determine contrast sensitivity using three methods: Tracking, limits, and constant stimuli
[AD-A265168] 01 p0324 N94-11099
Regional climatology sensitivity studies
[DE93-010712] 02 p0722 N94-14057
Decentralized control of uncertain systems via sensitivity models
[DE93-012963] 02 p0766 N94-14568
Differential Sensitivity Theory applied to the MESA code for high pressure interactions
[DE93-016460] 02 p0676 N94-14591
The role of constitutive and inducible processes in the response of human squamous cell carcinoma cell lines to ionizing radiation
[DE93-015150] 03 p1129 N94-16970
Scale sensitivity in the multiplicative AHP and SMART
[REPT-93-37] 04 p1611 N94-19157
Round robin experiments on the Explosive Components Water Gap Test (ECWGT)
[PML-1992-69] 04 p1378 N94-19445
Atmospheric sampling glow discharge ionization and triple quadrupole tandem mass spectrometry for explosives vapor detection
[DE93-040593] 05 p1852 N94-22004
A sensitivity equation approach to shape optimization in fluid flows
[AD-A278423] 07 p2999 N94-27415
Insensitive energetic materials: The importance of physical properties and molecular structure
[AD-A275393] 08 p3225 N94-29308
Sensitivity analysis of the static aeroelastic response of a wing 08 p3134 N94-30525
A review of sensitivity analysis techniques
[DE94-007192] 09 p3842 N94-31399
Sensitivity analysis of the AVHRR infrared cirrus model
[AD-A276690] 09 p3784 N94-32117
Sensitivity of electrochemical adlayer structure to the metal crystallographic orientation: Potential-independent iodide adsorption on Au(100) in comparison with other low-index surfaces
[AD-A276714] 09 p3909 N94-33273
Sensitivity of cloud forcing to the cloud cover parameterization in a GCM
[DE94-000678] 10 p4089 N94-33728
Collective plasma corrections to the solar opacity
[PB94-170511] 11 p4375 N94-36210
Use of formal calculation to automatically obtain adjoint programs
[PB94-170701] 11 p4308 N94-36259
Astronomy in the region between 1 mm and 0.1 mm wavelength
[NASA-CR-196020] 11 p4349 N94-36419
Molecular beam surface analysis
[DE94-010773] 12 p4406 N94-36453
Older muons are wiser: Using time information in (mu)LCR spectroscopy
[DE93-018556] 12 p4511 N94-36457
Optimization for minimum sensitivity to uncertain parameters
[NASA-TM-109139] 12 p4386 N94-37256

SENSORIMOTOR PERFORMANCE
NT PSYCHOMOTOR PERFORMANCE
Characteristics of aimed arm movements in humans under low gravity 03 p0980 N94-16093
Gamma-aminobutyric acid (GABA) and neuropeptides in neural areas mediating motion-induced emesis 05 p1886 N94-21902
The role of visual context in manual target localization 06 p2429 N94-25351
Mechanisms of eye-hand coordination
[AD-A273687] 06 p2428 N94-25437
On the development of motor chunks and concurrent processing in a structured continuous keypressing task
[AD-A274153] 07 p2939 N94-27138
Pigs in cyberspace 07 p2689 N94-27376
Deterioration of manual performance in cold and windy climates 08 p3381 N94-28434
Human pilot response during single- and multi-axis tracking tasks
[AD-A275080] 08 p3398 N94-28887
Concepts and environment
[REPT-93-032] 09 p3829 N94-31186
Situational awareness: A feasibility investigation of near-threshold skills development
[AD-A276467] 09 p3798 N94-31243

Tripping over obstacles: Biomechanical analyses of how young and old try to avoid it 09 p3803 N94-31954
Information theory for arm visuo-motor coordination 09 p3800 N94-32495

SENSORS
Passive tracking of a target using an array of sensors [DE93-015870] 03 p0997 N94-16169
Micro-optics technology and sensor systems applications 03 p1197 N94-17350
Solid-state, resistive hydrogen sensors for safety monitoring [DE93-017769] 04 p1424 N94-17778
Optical fibers and Fluorosensors having improved power efficiency and methods of producing same [NASA-CASE-LAR-14525-1-CU] 05 p1986 N94-20378
The application of micromachined sensors to manned space systems 08 p3171 N94-29791
Micro guidance and control synthesis: New components, architectures, and capabilities 08 p3144 N94-29792
Air-deployable geophysics package [DE94-005651] 08 p3335 N94-30594
Fiber optic chemical sensors on Mars [DE94-005251] 09 p3941 N94-31145
Three dimensional ICs intelligent sensors 10 p4057 N94-34354
A real-time 2-D composite damage monitoring system employing neural network 10 p4074 N94-34355
Intelligent processing of materials, technical activities, 1993 (NAS-NRC Assessment Panel, April 21-22 1994) [PB94-164183] 11 p4251 N94-35737
Ampoule failure sensor time response testing: Experiments 2 and 3 [NASA-TM-108458] 12 p4446 N94-36822
Detection of delaminations in composite beams using piezoelectric sensors [NASA-TM-106611] 12 p4403 N94-36956

SENSORY DISCRIMINATION
NT BRIGHTNESS DISCRIMINATION
NT TACTILE DISCRIMINATION
NT VISUAL DISCRIMINATION
Segment-based acoustic models for continuous speech recognition [AD-A271483] 05 p1736 N94-20547
Auditory spectro-temporal pattern analysis [AD-A273554] 06 p2427 N94-24865
On the auditory discrimination of spectral shape [ETN-94-95306] 06 p2530 N94-25289
Mechanisms of temporal pattern discrimination by human observers [AD-A277407] 09 p3801 N94-32577
Complex auditory signals [AD-A278391] 09 p3862 N94-33146

SENSORY FEEDBACK
Magnetostrictive actuators for human sensory feedback [AD-A269266] 04 p1511 N94-17841

SENSORY PERCEPTION
NT AUDITORY PERCEPTION
NT CONSCIOUSNESS
NT KINESTHESIA
NT PAIN
NT PAIN SENSITIVITY
NT PROPRIOCEPTION
NT SPACE PERCEPTION
NT TACTILE DISCRIMINATION
NT TASTE
NT TOUCH
NT VISUAL DISCRIMINATION
NT VISUAL PERCEPTION
The clocks and the perception of time in the 18th century society 04 p1424 N94-18007
About time 04 p1426 N94-18024
Somatosensory responsiveness in behaving monkeys and human subjects [AD-A268924] 04 p1501 N94-18231
Comparing performance on implicit memory tests [AD-A269900] 04 p1508 N94-18657
Interpretation of evolutive environment by a multisensory perception machine [LAAS-93111] 06 p2471 N94-22907
A white paper: NASA virtual environment research, applications, and technology [NASA-TM-109682] 06 p2428 N94-24855
Cortical mechanisms of attention, discrimination, and motor response to somesthetic stimuli [AD-A274163] 07 p2940 N94-27141
Annals of the Research Inst. of Environmental Medicine, Nagoya Univ., volume 44 [REPT-44-VOL-44] 07 p2911 N94-27442
Basic understanding of vertigo 08 p3390 N94-28855
Disturbance of equilibrium on JAL flight crew 08 p3390 N94-28856
Space and vertigo: In relation to space motion sickness 08 p3390 N94-28857
The cognitive, perceptual, and neural bases of skilled performance [AD-A277608] 10 p4097 N94-33849
On the feasibility of virtual environments in medicine 12 p4483 N94-37264
The use of a tactile interface to convey position and motion perceptions 12 p4486 N94-37281

SENSORY STIMULATION
States of awareness 1: Subliminal perception relationship to situational awareness [AD-A267249] 03 p1132 N94-16942
Effects of practice in selecting and executing keypressing sequences [IZF-1992-B-10] 04 p1509 N94-19420
Susceptibility of the squirrel monkey to different motion conditions 05 p1885 N94-21899
Changes in pain sensation induced by repetitive application of noxious heat pulses to the human skin 07 p2924 N94-27501
Visual-vestibular interaction [NASA-CR-196097] 11 p4297 N94-35379

SENTENCES
NT SYLLABLES
NT WORDS (LANGUAGE)
The impact of report of investigation writing style on the assessment times, impressions, perceptions and preferences of adjudicators [AD-A265748] 03 p1223 N94-15682
Segment-based acoustic models for continuous speech recognition [AD-A267138] 03 p0988 N94-15691
Non-well-foundedness and type freeness can unify the interpretation of functional application [PB93-191849] 04 p1560 N94-19710
Neural data oriented parsing 05 p1940 N94-20248
A connectionist representation for phrase structures 05 p1941 N94-20249
An architecturally-based theory of human sentence comprehension [AD-A275380] 08 p3398 N94-29313
Resumptive quantifiers in exception sentences [LP-93-11] 09 p3855 N94-31403
Sums and quantifiers [LP-93-05] 09 p3856 N94-31411
Updates in dynamic semantics [LP-93-06] 09 p3856 N94-31450
Completeness and decidability of the mixed style of inference with composition [LP-93-09] 09 p3842 N94-31453
Weaks vs. strong readings of donkey sentences and monotonicity inference in a dynamic setting [LP-93-10] 09 p3856 N94-31468

SEO (INDIAN SPACECRAFT)
U INDIAN SPACECRAFT

SEPAC (PAYLOAD)
Space Experiments with Particle Accelerators (SEPAC) [NASA-CR-193935] 07 p2761 N94-27664
Participation in the definition, conduct, and analysis of particle accelerator experiments for the first Spacelab Mission [NASA-CR-193974] 11 p4330 N94-35483

SEPARATED FLOW
NT BOUNDARY LAYER SEPARATION
A comparative study of full Navier-Stokes and Reduced Navier-Stokes analyses for separating flows within a diffusing inlet S-duct [NASA-TM-106250] 01 p0039 N94-10764
Unsteady flow past a NACA 0012 airfoil pitching at constant rates [AD-A265159] 01 p0016 N94-11889
A solution algorithm for the prediction of compressible laminar and turbulent shear flows 02 p0634 N94-13635
Numerical studies of spray combustion in liquid-fueled engines 02 p0564 N94-13685
Development of a recursion RNG-based turbulence model [NASA-CR-191511] 02 p0636 N94-13718
Measurements of wing and fin buffeting on the standard dynamics model [IAR-AN-76] 02 p0526 N94-13859
Numerical simulation of dynamic stall of NACA0012 airfoil oscillating near static stall angle using the Navier-Stokes equations [DE93-767970] 02 p0505 N94-14061
Unsteady separated flows: Empirical model and control [AD-A267282] 03 p0855 N94-14959
Unsteady phenomena in shock wave/boundary layer interaction 03 p1017 N94-15200
Hypersonic shock wave boundary layer interactions over simplified deflected control surface configurations 03 p1018 N94-15203
Study into the limits of an Euler equation method applied to leading-edge vortex flow [NLR-TP-91350-U] 03 p1031 N94-17627
Numerical solution of the Navier-Stokes equations for high-lift configurations on structured composite grids 04 p1306 N94-18423
A viscous-inviscid solver for high-lift incompressible flows over multi-element airfoils at deep separation conditions 04 p1306 N94-18425
Viscous-inviscid calculation of high-lift separated compressible flows over airfoils and wings 04 p1309 N94-18440
Correlation of incoming boundary layer pitot pressure fluctuations with the unsteadiness of fin-induced shock wave turbulent boundary layer interactions [AD-A270059] 04 p1417 N94-18796
Interferometric investigations of compressible dynamic stall over a transiently pitching airfoil [NASA-TM-109380] 04 p1312 N94-19119
Fluid dynamic mechanisms and interactions within separated flows [AD-A271037] 05 p1797 N94-19978
A theoretical investigation of unsteady separation phenomena related to dynamic stall [AD-A271865] 05 p1636 N94-20465
Computational and analytical methods in nonlinear fluid dynamics [AD-A272722] 05 p1802 N94-21169
Modelling stalled airfoils [ISBN-0-315-59525-6] 05 p1639 N94-22382
Experimental Methods in Separated Flows [ILR-MITT-260(1991)] 06 p2315 N94-22852
Turbulence sensors for separated flows: Current capabilities, future requirements 06 p2315 N94-22853
Measurement of kinematically unstationary separated flows 06 p2315 N94-22854
Pressure oscillation measurements in turbulent flows 06 p2316 N94-22855
Turbulent separated flows above an obstacle in an open channel 06 p2316 N94-22859
A method for recognition of frequency cells in a cylinder flow influenced by wall effects 06 p2316 N94-22860
Leading-edge votex-system details obtained on F-106B aircraft using a rotating vapor screen and surface techniques [NASA-TP-3374] 06 p2166 N94-23512
Computation of turbulent flows over backward and forward-facing steps using a near-wall Reynolds stress model 06 p2172 N94-24145
Large-eddy simulation of flow in a plane, asymmetric diffuser 06 p2328 N94-24147
Implementation of the Baldwin-Barth turbulence model into the ZETA code and its diagnosis [NASA-CR-194795] 06 p2335 N94-24640
A vorticity dynamics based model for the turbulent dissipation: Model development and validation [NASA-TM-106177] 06 p2336 N94-24713
Flow past a circular cylinder with a permeable wake splitter plate [AD-A273765] 07 p2790 N94-25872
Behaviour of separation bubbles in sharp-edged gaps of finite dimensions [ISBN-0-315-84113-3] 07 p2793 N94-26637
Control of leading-edge separation on an airfoil by localized excitation [DLR-FB-93-16] 07 p2647 N94-27592
Flowfield dynamics in blunt fin-induced shock wave/turbulent boundary layer interactions [NASA-CR-195170] 07 p2798 N94-27802
Investigation of aerodynamic design issues with regions of separated flow 07 p2658 N94-27902
Separated flow generated by a vectored jet in a crossflow 07 p2800 N94-28007
A numerical investigation of a subsonic jet in a crossflow 07 p2803 N94-28023
Theoretical and experimental investigation of a delta wing with turbulent leading-edge jets 07 p2659 N94-28029
Potential flow modelling of airfoil stall 07 p2654 N94-28332
Attached and separated trailing edge flow measurements with a triple-split hot-film probe 07 p2656 N94-28339
A study of blunt trailing edge airfoils using the Navier Stokes code: ARC2D 07 p2656 N94-28340
Thin-layer Navier-Stokes computations for multi-element airfoils 07 p2656 N94-28341
Role of computational fluid dynamics in aeronautical engineering. Part 10: Numerical analysis of flow around 2-D multi-element HLD 08 p3125 N94-28964
Aspects of the modeling and numerical simulation of leading-edge vortex flow [AD-B179108] 08 p3133 N94-30492

Development and application of particle image velocimetry in high-speed separated flow: Two-dimensional base cavities 08 p3282 N94-30791
Numerical simulation of leading-edge vortex flow [AD-B175154] 08 p3134 N94-30871
Computational study of simultaneous heat and mass transfer in turbulent separated flows 09 p3704 N94-31843
Computational prediction of stall flutter in spanwise-finite blade cascades 09 p3584 N94-31967
Control of low-speed turbulent separated flow over a backward-facing ramp [NASA-TM-109740] 09 p3573 N94-33071
Backward-facing step measurements at low Reynolds number, Re(sub h)=5000 [NASA-TM-108807] 09 p3711 N94-33290
Experimental studies of hypersonic transitional and turbulent boundary layers in hypersonic flow [AD-A278441] 10 p4044 N94-33556
Control of leading-edge separation on a cambered delta wing 10 p3992 N94-34616
Physics of Forced Unsteady Separation [NASA-CP-3144] 10 p4050 N94-34966
Unsteady separation experiments on 2-D airfoils, 3-D wings, and model helicopter rotors 10 p3986 N94-34967
Comparison of pitch rate history effects on dynamic stall 10 p3996 N94-34968
Unsteady flow past an airfoil pitched at constant rate 10 p3986 N94-34969
Unsteady separation process and vorticity balance on unsteady airfoils 10 p3986 N94-34970
The unsteady pressure field and vorticity productiion at the suction surface of a pitching airfoil 10 p3986 N94-34972
Investigation of mechanisms for vorticity generation and flow separation on bodies in unsteady motion 10 p4051 N94-34973
Characterization of dynamic stall phenomenon using two-dimensional unsteady Navier-Stokes equations 10 p3986 N94-34974
Will the real dynamic instability mechanism please be recognized! 10 p4052 N94-34976
Experiments on an unsteady, three-dimensional separation 10 p4052 N94-34981
Unsteady flow field of large-amplitude pitching airfoils [AD-A280444] 12 p4383 N94-37219

SEPARATION
Convection related radial segregation in an idealized horizontal Bridgman configuration 01 p0115 N94-10185
Electrophoresis visualisation 03 p0944 N94-15163
Vortex generators for control of shock-induced separation. Part 1: Introduction and aerodynamics [ESDU-93024-PT-1] 07 p2806 N94-28095
Vortex generators for control of shock-induced separation. Part 3: Examples of applications of vortex generators to aircraft [ESDU-93026-PT-3] 07 p2807 N94-28096
Development of immobilized ligands for actinide separations [DE94-012714] 12 p4410 N94-37284

SEPARATORS
NT AIR FILTERS
NT CLASSIFIERS
NT DRYING APPARATUS
NT DUST COLLECTORS
NT ELECTROSTATIC PRECIPITATORS
NT EVAPORATORS
NT FLUID FILTERS
NT SIEVES
NT SPIRALS (CONCENTRATORS)
Monochromator SP-017. The results of the first experiments [DE93-617463] 01 p0372 N94-10849
The bootstrapped algorithm: Fast algorithm for blind signal separation [AD-A266671] 03 p1147 N94-15772
Spiral fluid separator [NASA-CASE-MFS-28658-1] 05 p1800 N94-20361
Development of an electrochemical hydrogen separator [DE93-019877] 05 p1683 N94-21984
Capillary electrokinetic separations with optical detection [DE94-001639] 06 p2233 N94-23716
Systematic construction of trigonometric neural networks [PB93-200228] 06 p2474 N94-24544
A Shuttle mechanism for molten-electrolyte lithium batteries [DE94-002914] 07 p2781 N94-26144
Development of laser spectroscopic technology in nuclear industry [DE93-633327] 07 p2714 N94-26158
Performance model of a recirculating stack nickel hydrogen cell 07 p2861 N94-28112
Specialized data base management system for data processing in the experiments at low energies [DE94-606268] 08 p3485 N94-28621
Polyaniline membranes for gas and liquid separation [AD-A275851] 08 p3408 N94-28790
Dendrite preventing separator for secondary lithium batteries [NASA-CASE-NPO-18585-1-CU] 08 p3265 N94-29411
Electrostatic reduction of particulates for laser resistant hafnia coatings [DE94-005824] 09 p3651 N94-31557
Development of silver-zinc cells of improved cycle life and energy density [AD-A277311] 09 p3693 N94-32329
Fabrication, phase transformation studies and characterization of SiC-AlN-Al2OC ceramics [DE94-008587] 09 p3659 N94-32657
Separation tool for multipin electrical connectors [NASA-CASE-NPO-18786-1-CU] 11 p4274 N94-35375

SEPTUM
A simplified method for S-parameter calculations of metal septum waveguide filters 05 p1782 N94-22180
Aortic valve disease 06 p2424 N94-23322

SEQUENCING
Cellular mechanism of turnover of the stress induced protein HSP 70 [AD-A265723] 02 p0732 N94-13061
Temporal segmentation of tasks from human hand motion [AD-A266596] 03 p1166 N94-16725
FSM test: A functional test generation system for sequential circuits [REPT-93-017] 03 p1014 N94-17505
Shop problems with two machines and time lags [REPT-93-020] 04 p1518 N94-17927
Matrix- and substrate-assisted laser desorption for fast DNA sequencing [DE93-015332] 04 p1501 N94-18242
Model checking, abstraction, and compositional verification [AD-A270552] 05 p1902 N94-19919
Total order assumption [PB93-191740] 05 p1903 N94-19993
A methodology for formal hardware verification, with application to microprocessors [AD-A270550] 05 p1898 N94-20085
High-speed Viterbi decoding with overlapping code sequences 05 p1760 N94-21130
On the decomposition of synchronous state mechines using sequence invariant state machines 05 p1764 N94-21703
A shared buffer memory switch with maximum queue and minimum allocation 05 p1773 N94-22119
A one-shot access scheme for a multicast switch 05 p1773 N94-22120
Science planning and sequencing for Cassini 06 p2504 N94-23871
A packet-based concept for spacecraft command planning 06 p2504 N94-23873
The instant sequencing task: Toward constraint-checking a complex spacecraft command sequence interactively 06 p2504 N94-23875
AGENDA: A task organizer and scheduler 06 p2504 N94-23876
One machine scheduling with delayed precedence constraints [PB93-237626] 07 p3094 N94-26314
Stable RNA sequences as a tool for DNA probes and phylogenetic studies [PB94-135423] 08 p3385 N94-29156
A time reasoning system based on the event calculus for scheduling in aeronautic maintenance [REPT-932-710-101] 08 p3122 N94-29463
Sequencing items in multiple-item displays on online public access catalogs 10 p4150 N94-33419
Computer assisted multiplex sequencing [DE94-008549] 10 p4107 N94-34007
Synthesis of asynchronous systems from data flow specifications [AD-A278687] 11 p4303 N94-35662

SEQUENTIAL ANALYSIS
On the asymptotically uniform distribution modulo 1 of extreme order statistics [MEMO-COSOR-91-38-REV] 06 p2493 N94-23142
North American jumelage 'type systems' [AD-A275342] 08 p3411 N94-29214
Several modified goodness-of-fit tests for the cauchy distribution with unknown scale and location parameters [AD-A278496] 10 p4130 N94-34301

SEQUENTIAL COMPUTERS
A design methodology for portable software on parallel computers [NASA-CR-194181] 02 p0752 N94-14139
A method for the general simultaneous full decomposition of sequential machines: Algorithms and implementation [EUT-92-E-267] 06 p2445 N94-23170
Transputer benchmarks and performance comparisons with other computing machines [RR-467] 06 p2446 N94-25312

SEQUENTIAL CONTROL
Digital laser range finder emulator [AD-D015811] 03 p1040 N94-16540
Temporal segmentation of tasks from human hand motion [AD-A266596] 03 p1166 N94-16725
Motorola MC68040 high-speed design using Altera EPM5000 erasable programmable logic devices [DE93-017635] 04 p1523 N94-19006
High level language-based robotic control system [NASA-CASE-NPO-17918-2-CU] 08 p3435 N94-29465
Formal specification and verification of real-time sequential control systems [AD-A275776] 08 p3419 N94-29678
Topological models for higher order control flow [CWI-CS-R9340] 08 p3425 N94-30432
Novel failure analysis techniques using photon probing with a scanning optical microscope [DE94-006594] 09 p3692 N94-32112
A genetic technique for planning a control sequence to navigate the state space with a quasi-minimum-cost output trajectory for a non-linear multi-dimnensional system 10 p4123 N94-35052

SERIES (MATHEMATICS)
NT ASYMPTOTIC SERIES
NT COSINE SERIES
NT FOURIER SERIES
NT PADE APPROXIMATION
NT POWER SERIES
NT PRONY SERIES
NT SINE SERIES
NT TAYLOR SERIES
Detecting non-linearities in stationary time series [W-9223] 01 p0344 N94-10906
Time dependent identification of nonlinear structures [ECL-92-64] 04 p1457 N94-19403
Incomplete corrections in nonlinear problems [PB93-225746] 06 p2479 N94-23106

SERIES EXPANSION
Studies of P-matrix formalism on the basis of the potential description of two-particle interaction [DE93-617691] 01 p0362 N94-10550
A new approach to the I/N-expansion for the Dirac equation [DE93-617647] 01 p0349 N94-10833
Medium energy hadron-nucleus scattering in the 1/N expansion formalism [DE93-622957] 02 p0778 N94-12848
Magnetic interactions and disorder - phase transitions in dilute spin-glasses and high temperature superconductors [ITN-93-85217] 02 p0815 N94-14825
Analysis of an electromagnetic field in the vicinity of a caustic by asymptotic methods [IFTR-12/1991] 03 p0998 N94-16653
Convergence of the multiple scattering expansion in XAFS and XANES [DE93-011001] 03 p0948 N94-16772
Expansions of cumulative distribution functions directly from characteristic functions [AD-A267727] 03 p1173 N94-17372
Convection effects on radial segregation and crystal melt interface in vertical Bridgman growth [NASA-CR-191541] 03 p1029 N94-17387
Decomposition invariance of generalized steady-state of a 1-D diffusion system [REPT-93-26] 04 p1550 N94-19141
Asymptotic analysis: Basic concepts and definitions [DE94-001000] 05 p1961 N94-22393
Approximate optimal guidance for the advanced launch system [NASA-CR-4568] 06 p2198 N94-24752
Asymptotics for Kummer functions, Bose plasmas, and related special functions [DE94-601853] 07 p3007 N94-26928
Higher order asymptotic crack tip fields in a power-law hardening material 08 p3321 N94-29829
Symplectic Runge-Kutta schemes 3: Canonical elementary differentials [MATHS-REPT-A-204] 09 p3840 N94-31159
Stirling's formula and approximations for n(factorial) and the middle ratio [REPT-93-73] 09 p3843 N94-31642

Generalization of a theorem of Kusmin
[REPT-93-74] 09 p3844 N94-31643
Finite-part integrals and the Euler-Maclaurin expansion
[DE94-006539] 09 p3844 N94-31665
Probability distributions with given marginals and given correlation that have maximal entropy
[REPT-93-81] 09 p3851 N94-31698
Compression of a radar track of a near Earth satellite into an Earth centered inertial state vector using least squares differential correction
[AD-A278498] 10 p4037 N94-34302
SEROTONIN
Strategies for enhancing catecholamine-mediated neurotransmission
[NASA-CR-193807] 04 p1506 N94-18862
Abnormal development of serotonin nerve fibers in the cerebral cortex of young rats with methylazoxymethanol induced microcephaly 07 p2905 N94-27485
SERUMS
Non-invasive optical detection of glucose in cell culture nutrient medium 06 p2422 N94-25357
Strategies to sustain and enhance performance in stressful environments
[AD-A275223] 08 p3398 N94-29027
SERVICE LIFE
Characterization of in-flight performance of ion propulsion systems
[NASA-TM-106283] 01 p0046 N94-10761
Fatigue life prediction for wind turbines: A case study on loading spectra and parameter sensitivity
[DE93-011597] 01 p0263 N94-11173
GaAs PCSS: High gain switching and device reliability
[DE93-009851] 01 p0401 N94-11605
Battery testing at Argonne National Laboratory
[DE93-011761] 02 p0624 N94-14012
Inflow characteristics associated with high-blade-loading events in a wind farm
[DE93-010042] 02 p0704 N94-14423
Derated ion thruster development status
[NASA-TM-106292] 02 p0553 N94-14726
Field investigation of the relationship between battery size and PV system performance
[DE93-016503] 03 p1016 N94-17671
Ageing studies on a composite propellant containing a new organo-copper burn rate catalyst
[AD-A271060] 05 p1711 N94-19906
Photoconductive Semiconductor Switches for pulsed power applications
[DE93-019411] 05 p1750 N94-20294
The 1992 USAF structural integrity program conference
[AD-A272876] 05 p1635 N94-21194
Ceramic Technology Project
[DE94-001011] 05 p1707 N94-21822
Life prediction systems for critical rotating components 05 p1835 N94-22615
NASA Lewis advanced IPV nickel-hydrogen technology 06 p2392 N94-23356
New method for increasing machine service-life, phase 2
[PB93-200707] 06 p2354 N94-23533
Impacts: NIST Building and Fire Research Laboratory (technical and societal)
[PB94-113420] 06 p2270 N94-23737
Viscoelastic analysis of seals for extended service life 06 p2371 N94-24408
Performance of the NASA cm ion thruster
[NASA-TM-106426] 06 p2221 N94-24770
Embodiment design for a multipropellant resistojet
[NASA-CR-195505] 06 p2221 N94-24834
General aviation activity survey
[AD-A273284] 06 p2162 N94-24923
Reliability analysis of a repairable dependent parallel system
[ETN-94-95312] 06 p2373 N94-25295
Modelling early failures in Space Station Freedom 06 p2374 N94-25372
Proceedings of the 12th International Congress: Corrosion Control for Low-Cost Reliability. Volume 5B: Corrosion: General issues
[AD-A273667] 06 p2250 N94-25407
Computer modelling of cyclic deformation of high-temperature materials
[AD-A273852] 07 p2704 N94-25608
Stress relaxation in dough moulding compounds
[PB94-124872] 07 p2748 N94-25894
Aircraft wheel life assessment
[AD-A274378] 07 p2823 N94-26976
The development of stress intensity factors
[DRA-TR-93057] 07 p2845 N94-27954
Software assurance standard
[NASA-TM-109705] 07 p2975 N94-27992
SAFT nickel hydrogen cell cycling status 07 p2861 N94-28110
Cycle life versus depth of discharge update on modeling studies --- Nickel-Hydrogen Batteries 07 p2862 N94-28115
Orbital management and design considerations for NiCd satellite power systems 07 p2862 N94-28118
AF Ni-Cd cell qualification program 07 p2863 N94-28122
Discriminating performance parameters for 50 amp-hour and 60 amp-hour nickel-cadmium plates and battery cells 07 p2863 N94-28123
Ni-MH storage test and cycle life test 07 p2864 N94-28131
Advanced development of PV encapsulents
[DE94-000219] 08 p3336 N94-28500
Service life prediction of composite structures through fiber testing
[AD-A275661] 08 p3176 N94-28654
Aircraft age impacts on maintenance requirements
[AD-A275701] 08 p3121 N94-28666
Aircraft age impact on individual operating and support cost elements
[AD-A275739] 08 p3121 N94-28732
Performance and durability of high emittance heat receiver surfaces for solar dynamic power systems
[NASA-TM-106549] 08 p3172 N94-28834
Measurement and modelling of bolted joint stress relaxation in plastics
[PB94-124849] 08 p3318 N94-28841
An outdoor exposure testing program for optical materials used in solar thermal electric technologies
[DE94-000265] 08 p3500 N94-29799
Space flight manipulator technologies and requirements for the NASA Flight Telerobotic Servicer (FTS)
[AIAA PAPER 94-1191-CP] 08 p3441 N94-30542
Model of spacecraft atomic oxygen and solar exposure microenvironments 09 p3593 N94-31021
Design application and development of spacecraft in LEO utilizing LDEF results 09 p3597 N94-31047
Shearographic inspection of a DeHavilland DHC-7
[AD-A276716] 09 p3566 N94-32157
Development of silver-zinc cells of improved cycle life and energy density
[AD-A277311] 09 p3693 N94-32329
Spur, helical, and spiral bevel transmission life modeling
[NASA-TM-106552] 09 p3728 N94-32979
Analysis of intermediate level maintenance following F404-GE-400 engine component life reductions
[AD-A277918] 09 p3585 N94-33283
Design of a high-speed reliable ball bearing 09 p3606 N94-33314
The role of fatigue analysis for design of military aircraft 10 p3996 N94-34594
An overview of the F-16 service life approach 10 p3996 N94-34599
Mechanical failure probability of glasses in Earth orbit
[NASA-CR-195912] 10 p4031 N94-34947
On optimal placement of spacers in bundled conductors 11 p4258 N94-35354
Space Shuttle: Incomplete data and funding approach increase cost risk for upgrade program. Report to Congressional Requesters
[GAO/NSIAD-94-23] 12 p4392 N94-37026
Impact of Materials Defects on Engine Structures Integrity
[AGARD-R-790] 12 p4453 N94-37321
Alternate melting and refining routes 12 p4421 N94-37323
SERVICES
NT MEDICAL SERVICES
NT METEOROLOGICAL SERVICES
Passenger terminal level of service measurement: A utility theoretic approach
[ISBN-0-315-59037-8] 05 p1651 N94-22418
Service description of communication systems supporting multi-media multi-user applications
[PB94-110855] 06 p2299 N94-24650
Information retrieval services on wide area networks: A vision of the future 12 p4545 N94-37346
SERVOCONTROL
Increasing mission reliability using open-loop control
[AD-A271208] 04 p1545 N94-19721
The optohydraulic servovalve: A novel device for the precise optical control of hydraulic pressure
[ISBN-0-315-83580-X] 05 p1827 N94-22577
SERVOMECHANISMS
NT SERVOMOTORS
Dynamic testbed laboratory and micro-optics 03 p1199 N94-14986
A complete study of differential wax-wane focus servo technique 03 p1199 N94-14996
Optimal tuning of heavy equipment motion controllers
[AD-A267873] 03 p1167 N94-17392
Design of power electronics for TVC EMA systems
[NASA-CR-193839] 04 p1407 N94-19642
Long range fast tool servo
[AD-A271614] 05 p1761 N94-21257
The optohydraulic servovalve: A novel device for the precise optical control of hydraulic pressure
[ISBN-0-315-83580-X] 05 p1827 N94-22577
Plan generation for flexible assembly systems
[PB93-217974] 06 p2267 N94-22981
Beam-waveguide antenna servo design issues for tracking low earth-orbiting satellites 06 p2292 N94-23268
The Columbus solar array mechanisms 06 p2356 N94-23994
GOLF mechanisms 06 p2357 N94-24003
High precision double four bar linkage mechanism for interferometric linear scanning 06 p2359 N94-24013
Design, characterization and control of the Unique Mobility Corporation robot 09 p3603 N94-33296
Rotary hydraulic servo or throttle valve
[AD-D016134] 10 p4059 N94-33757
Design and implementation of a beam-waveguide mirror control system for vernier pointing of the DSS-13 antenna 11 p4253 N94-35548
Fuzzy self-learning control for magnetic servo system 11 p4215 N94-35852
High accuracy control algorithm application to a tracking turret 12 p4394 N94-36626
A dynamic model of a linear actuator based on polymer hydrogel
[DE94-010800] 12 p4408 N94-37091
SERVOMOTORS
Increasing mission reliability using open-loop control
[AD-A271208] 04 p1545 N94-19721
SERVOS
U SERVOMOTORS
SERVOSTABILITY CONTROL
U SERVOCONTROL
SES
U SURFACE EFFECT SHIPS
SES (SHUTTLE)
U SHUTTLE ENGINEERING SIMULATOR
SET THEORY
NT EQUIVALENCE
NT THRESHOLD LOGIC
An algebraic approach to incomparable families of formal languages
[MEMO-INF-92-82] 01 p0342 N94-10279
Boundary of Fatou sets of hyperbolic rational maps or degree two
[DE93-613031] 01 p0348 N94-10412
A surrogate heuristic for set covering problems
[INPE-5462-PRE/1770] 01 p0325 N94-11178
A new heuristic for set covering problems
[INPE-5471-TDI/502] 01 p0333 N94-12358
On the foundations of final semantics: Non-standard sets, metric spaces, partial orders
[CWI-CS-R9241] 02 p0768 N94-13526
Reductions to sets of low information content
[TR-417] 03 p1150 N94-16579
A fuzzy method for preliminary design random access memory failure rate prediction
[AD-A267948] 03 p1055 N94-17044
Fuzzy almost linear spaces
[DE93-624772] 04 p1545 N94-17680
Performance of defect-tolerant set-associative cache memories 04 p1398 N94-18346
Fuzzy hypergraphs and fuzzy intersection graphs
[AD-A270303] 04 p1549 N94-18815
Excursion theory of a finite set via resolvents
[REPT-93-19] 04 p1557 N94-19090
Excursions of stochastic processes, Cox-point processes, entrance behavior and resolvents
[PB93-197291] 04 p1558 N94-19323
On network representation of the solutions in combinatorial optimization
[RR-910-I] 04 p1552 N94-19392
A perfection-preserving operation
[RR-911-I] 04 p1552 N94-19393
Neighbourhood-perfect line graphs
[RR-915-I] 04 p1552 N94-19395
On Hamilton-connectedness of Cayley graphs 04 p1554 N94-19684
On Hamiltonian properties of 2-tough graphs 04 p1554 N94-19685
Toughness and the cycle structure of graphs 04 p1554 N94-19686
The Hopping Lemma 04 p1554 N94-19687
Two problems related to results of Chvatal-Erdoes 04 p1555 N94-19693
Non-well-foundedness and type freeness can unify the interpretation of functional application
[PB93-191849] 04 p1560 N94-19710
Set based analysis of ML programs
[AD-A270597] 05 p1902 N94-19948
Set theory and nominalisation, part 1
[PB93-191807-PT-1] 05 p1962 N94-20007

Set theory and nominalisation, part 2
[PB93-191815-PT-2] 05 p1962 N94-20008
Nominalization, prediction and type containment
[PB93-191799] 05 p1898 N94-20082
On multiflow problems
[RR-889-M] 05 p1950 N94-20125
Totally strong and strong graphs
[RR-902-I] 05 p1951 N94-20237
Half-integral flows in a planar graph with four holes
[RR-894-M] 05 p1951 N94-20302
Convex set and linear mixing model
05 p1844 N94-20888
The communication complexity of set intersection problems
[MEMO-1077] 05 p1738 N94-21073
The Robinson-Schensted and Schuetzenberger algorithms. Part 2: Geometric interpretations
[CWI-AM-R9209-PT-2] 05 p1911 N94-21157
An NP set with no co-DP sparse subset
[TR-475] 05 p1954 N94-21199
Advice from nonadaptive queries to NP
[TR-470] 05 p1911 N94-21200
Selectivity: Reductions, nondeterminism, and function classes
[TR-469] 05 p1912 N94-21273
Threshold computation and cryptographic security
[TR-461] 05 p1912 N94-21285
On the topological size of p-m-complete degrees
[TR-459] 05 p1965 N94-21286
Promises and fault-tolerant database access
[TR-447] 05 p2043 N94-21287
On the closure properties of #P in the context of PF of #P
[TR-445] 05 p1955 N94-21456
Modular interval spaces
[PB93-220663] 05 p1961 N94-22266
Generalized concavity in cooperative game theory: Characterizations in terms of the core
[MEMO-1121] 06 p2497 N94-22708
Making some issues of implicit knowledge explicit
[PB93-220606] 06 p2478 N94-22984
Median stabilization degree of a median algebra
[PB93-220010] 06 p2479 N94-23093
Characterization of measures with a convex range: A generalization of Lyapounov's theorem
[PB93-220523] 06 p2523 N94-23094
Linear algorithm for flattening list graphs
[PB93-220648] 06 p2448 N94-23097
How much integral action can a control system tolerate?
[OUEL-1923/92] 06 p2471 N94-23147
When an infinitely-renormalizable endomorphism of the interval can be smoothed
[PB93-238087] 06 p2481 N94-23548
Medians and steiner trees
[PB94-110616] 06 p2486 N94-23708
Relational algebra and equational proofs
[PB94-110822] 06 p2486 N94-23724
Multi-set extended relational algebra: A formal approach to a practical issue
[PB94-110830] 06 p2486 N94-23725
Subset selection with a generalized selection goal based on a loss function
[PB94-111192] 06 p2494 N94-23798
Some generalized subset selection procedures
[PB94-111655] 06 p2487 N94-23799
Infinite divisible and stable distributions modulo 1
[PB94-110640] 06 p2495 N94-23815
Reduced game properties of egalitarian division rules for cooperative games
[PB94-111689] 06 p2521 N94-24523
On the continuity of limit capacity of central Cantor sets
[DE93-613022] 06 p2523 N94-25328
The least energy critical set
[DE93-616820] 06 p2493 N94-25434
Set based analysis of arithmetic
[AD-A274112] 07 p3002 N94-25903
Some properties of graphs with local Ore conditions
[PB94-126612] 07 p2996 N94-26962
Graphs satisfying a local ore-type condition
[PB94-126679] 07 p3007 N94-27222
Ranking alternatives using fuzzy numbers: A computational approach short communication
[INPE-5483-PRE/1782] 07 p2974 N94-27835
On blocks: Locality and asynchronous communication (extended abstract)
[RUU-CS-92-44] 08 p3424 N94-30347
A note on the Smyth powerdomain construction
[RUU-CS-93-02] 08 p3457 N94-30393
Algebraic domains, chain completion, and the Plotkin powerdomain construction
[RUU-CS-93-03] 08 p3457 N94-30394
Commutative Lambek categorial grammars
[ML-93-01] 08 p3457 N94-30395
Representations of dynamical systems described by behavioral inequalities
[AD-B173649] 08 p3458 N94-30402
Isomorphisms between predicate and state transformers
[RUU-CS-93-09] 08 p3458 N94-30403
Isomorphisms between predicate and state transformers
[CWI-CS-R9338] 08 p3459 N94-30430
Dynamic microsets for RAMs
[RUU-CS-93-22] 08 p3406 N94-30727
Set games
[MEMO-1148] 08 p3466 N94-30737
Total termination of term rewriting
[RUU-CS-92-42] 08 p3460 N94-30744
A structural co-induction theorem
[CWI-CS-R9346] 08 p3461 N94-30753
Non-commutative geometry
[PB94-139342] 08 p3462 N94-30889
Remarks on uniformly finitely precomplete positive equivalences
[ML-93-12] 08 p3463 N94-30975
Triangular norms and conorms: A general tool for generating fuzzy mathematical morphologies
[TELECOM-93-D-001] 09 p3839 N94-31092
Frames and stable bases for shift-invariant subspaces of L(sub 2)(IR(sup d))
[AD-A276470] 09 p3843 N94-31474
Line transects, covariance functions and set approximation
[CWI-BS-R9311] 09 p3846 N94-32084
Multiple inheritance via intersection types
[TR-93-18] 09 p3848 N94-32292
A survey of fuzzy logic and applications
[AD-A278524] 10 p4037 N94-34378
Interactive calculator for use with multi-dimensional netCDF files
[DE94-007477] 12 p4545 N94-37348

SETI
U PROJECT SETI

SEWAGE
NT SOLID WASTES

SEWAGE TREATMENT
Growth of hydrocarbon-rich microalga Botryococcus braunii in secondarily treated sewage and its consumption of nitrate ion and phosphate ion
08 p3387 N94-29519

SEWING
Parachute having improved vent line stacking
[NASA-CASE-MFS-28508-1] 01 p0014 N94-11021
Variable speed controller 07 p2943 N94-25678
Development of stitched/RTM composite primary structures 09 p3628 N94-33127
Test and analysis results for composite transport fuselage and wing structures 09 p3628 N94-33129

SEX FACTOR
Gender differences in endocrine responses to posture and 7 days of 6 deg head down bed rest
[NASA-TM-103991] 02 p0731 N94-12972

SEX GLANDS
NT PROSTATE GLAND

SEYFERT GALAXIES
Polarization and variability of active galaxies and quasars 02 p0837 N94-13550
Ultraviolet observations of NGC 4395, the least luminous and nearest known Seyfert 1 nucleus
[NASA-CR-194304] 02 p0831 N94-13679
Was 49: Mirror for a hidden Seyfert 1 galaxy
[NASA-CR-194537] 02 p0840 N94-14685
Variability of the Seyfert galaxy MKN 766 in the Rosat all sky survey
[MPE-PREPRINT-221] 03 p1240 N94-17591
Spatial distribution of near infrared line radiation in galactic nuclei measured with Fabry-Perot spectrometer FAST
[MPE-239] 05 p2081 N94-21138
The 1404+286: A non-ideal calibrator for VLBI observations
[PB94-104908] 06 p2599 N94-24521
Infrared properties of obscuring dust tori in active galactic nuclei 08 p3545 N94-29832
Broad H alpha profiles of radio-loud active galactic nuclei and rapid profile variability in Seyfert and radio galaxies
08 p3552 N94-29989
UV spectroscopy of low-redshift active galaxies
[NASA-CR-189323] 10 p4161 N94-33904
ROSAT/XRT-PSPC observations and the ionizing continuum of Seyfert 1 galaxy Mkn 478
[PB94-167053] 11 p4350 N94-35530
Guaranteed time observations support for Faint Object Spectrograph (FOS) on HST
[NASA-CR-196305] 12 p4547 N94-37037

SFERICS
U ATMOSPHERICS

SGEMP
U SYSTEM GENERATED ELECTROMAGNETIC PULSES

SH WAVES
High resolution geological site characterization utilizing ground motion data
[AD-A268926] 04 p1481 N94-18485

SH-3 HELICOPTER
Evaluation of Night Vision Goggles (NVG) for maritime search and rescue (HH-3/HH-60) comparison report
[AD-A266493] 03 p1138 N94-16793

SHADOWGRAPH PHOTOGRAPHY
NT SCHLIEREN PHOTOGRAPHY
Flowfield structure of swept shock wave/turbulent boundary-layer interactions 01 p0149 N94-10899
Images constructed from computed flow fields
[NASA-CR-194397] 02 p0650 N94-13814
Development of an automated film-reading system for ballistic ranges
[NASA-CR-194398] 02 p0650 N94-13815
Advanced ballistic range technology
[NASA-CR-194396] 02 p0532 N94-14068
Advanced ballistic range technology
[NASA-CR-194530] 02 p0533 N94-14540
A shadowgraph study of Space Transportation System (STS): The Space Shuttle Launch Vehicle (SSLV)
[NASA-RP-1341] 12 p4382 N94-36741

SHADOWGRAPHS
U SHADOWGRAPH PHOTOGRAPHY

SHADOWS
NT LUNAR SHADOW
Field of solar collectors: Effect of shadowing on the optimal field design
[ITN-93-85197] 02 p0702 N94-13570
Cooperativity and 3-D representation
[AD-A267180] 03 p1131 N94-15694
A field measure of the shade fraction
03 p1068 N94-16677
Mapping the spectral variability in photosynthetic and non-photosynthetic vegetation, soils, and shade using AVIRIS 03 p1068 N94-16679
Multitemporal diurnal AVIRIS images of a forested ecosystem 03 p1074 N94-16709
Direct evidence of the interplanetary magnetic field effect on the cosmic-ray shadow by the sun
[ICRR-296-93-8] 07 p3116 N94-27607

SHAFTS (MACHINE ELEMENTS)
NT ROTATING SHAFTS
NT TURBOSHAFTS
Dynamic tester for rotor seals and bearings
[NASA-CASE-MFS-28493-1] 01 p0033 N94-10669
Rotordynamic and leakage characteristics of a 4-stage brush seal
[AD-A266012] 02 p0660 N94-12988
Friction drive position transducer
[AD-D015851] 04 p1424 N94-17717
Actively controlled shaft seals for aerospace applications
[NASA-CR-194759] 05 p1823 N94-20538
Acceleration-augmented LQG control of an active magnetic bearing 05 p1757 N94-21112
Compliant seal development
05 p1655 N94-21795
Modeling bristle lift-off in idealized brush seal configurations 05 p1655 N94-21797
A technique to measure rotordynamic coefficients in hydrostatic bearings 06 p2215 N94-23061
Spline screw multiple rotations mechanism
[NASA-CASE-GSC-13452-1] 06 p2352 N94-23078
An overview of a model rotor icing test in the NASA Lewis Icing Research Tunnel
[NASA-TM-106471] 06 p2166 N94-23299
Zone fire modeling with natural building flows and a zero order shaft model
[PB94-112166] 06 p2270 N94-23735
Electromagnetic brake/clutch device
[NASA-CASE-GSC-13502-1] 06 p2354 N94-23969
Opening mechanism for ISO/CVV cover release
06 p2357 N94-24001
Precision drive and speed reduction device
[AD-D016004] 06 p2367 N94-25046
Multi-speed multi-phase resolver converter
[NASA-CASE-MFS-28855-1] 08 p3264 N94-29372
Flexible drive shaft coupling
[AD-D016096] 09 p3727 N94-32718
The analysis of wake-induced unsteady aerodynamics related to higher harmonic control
[AD-A277914] 09 p3573 N94-33108
Superconducting Meissner effect bearings for cryogenic turbomachines, phase 2
[AD-A277865] 10 p4059 N94-33776
Experimental investigation and performance analysis of the turbojet engine T117 10 p4000 N94-34439
Robot friendly probe and socket assembly
[NASA-CASE-MSC-22028-1] 11 p4274 N94-35374

Rotor dynamic behaviour of a high-speed oil-free motor compressor with a rigid coupling supported on four radial magnetic bearings 11 p4224 N94-35911

SHAKERS

Root-sum-square structural strength verification approach
[NASA-TM-108453] 08 p3322 N94-30206

SHAKING

NT DITHERS

Shake test results of the MDHC test stand in the 40- by 80-foot wind tunnel
[NASA-TM-108801] 07 p2641 N94-26596

Monitor for status epilepticus seizures 08 p3397 N94-30460

Procedures for computing site seismicity
[AD-A277666] 09 p3775 N94-33028

SHALES

Petrography and preliminary interpretations of the crystalline breccias from the Manson M-1 core 01 p0281 N94-12056

Microtektite-like glass spherules in Late Devonian (367 MA) shales 01 p0461 N94-12160

Overview: Gas hydrate geology and geography
[DE93-014043] 02 p0688 N94-14151

SHALLOW SHELLS

The free vibration of plates, shallow shells and solids
[ISBN-0-315-83931-7] 07 p2838 N94-26622

Refined triangular plate and shell elements
[PB94-126356] 07 p2839 N94-26875

Theory of thick, laminated composite shallow shells 09 p3622 N94-31953

SHALLOW WATER

SAR imaging of geology and bathymetry: Kent coastal area - southern North Sea 01 p0254 N94-12527

Trajectory curving in underwater propagation of light 01 p0226 N94-12748

Coupled numerical model for altimetric data assimilation and velocity field analysis 01 p0227 N94-12752

Nonlinear wave forces on large ocean structures
[AD-A266820] 02 p0683 N94-14902

Comments on computational underwater acoustics
[DE93-013789] 04 p1562 N94-17873

DYNLET1 model formulation and user's guide
[AD-A269843] 04 p1498 N94-18723

A finite element scheme for shock capturing
[AD-A270182] 04 p1417 N94-18755

Seismic studies of the geologic structure and physical properties of the seabed
[AD-A270895] 04 p1500 N94-19747

A survey of the impact on acoustic propagation of warm core ocean eddys
[AD-A272188] 05 p1883 N94-20925

Measurements and modeling of multitone, low-frequency acoustic data from the Arraial do Cabo range
[AD-A273406] 06 p2530 N94-25073

Analysis of modal evolution caused by a weakly range-dependent seabed in shallow water and its application to inversion for geoacoustic properties
[AD-A273656] 06 p2419 N94-25435

Remote sensing and GIS for the management and investigation of the Wadden Sea
[BCRS-92-20] 07 p2847 N94-26228

Nonlinear ocean waves
[AD-A274651] 07 p2899 N94-26354

Broad geoacoustic assessment of some regional areas
[AD-A275504] 08 p3356 N94-28791

Storm evolution of directional seas in shallow water
[AD-A278541] 10 p4089 N94-33404

Three-parameter characterization of shallow-water directional wind wave spectra
[AD-A278532] 10 p4091 N94-33671

SHANKS

U JOINTS (JUNCTIONS)

SHANNON INFORMATION THEORY

U INFORMATION THEORY

SHAPE CONTROL

MIMO recursive least squares control algorithm for the AN/FPN-44A Loran-C transmitter
[AD-A274820] 07 p2664 N94-26493

Control of micromachined deformable mirrors 08 p3239 N94-29787

Shape control of composite plates and shells using embedded actuators 10 p4018 N94-33532

SHAPE FUNCTIONS

Boundary formulations for nonlinear design sensitivity analysis 02 p0672 N94-13669

Analysis of electromagnetic scattering from irregularly shaped, thin, metallic flat plates
[NASA-TP-3361] 03 p0998 N94-16655

The identification of inflow fluid dynamics parameters that can be used to scale fatigue loading spectra of wind turbine structural components
[DE94-000231] 07 p2791 N94-26117

SHAPE MEMORY ALLOYS

NT NITINOL ALLOYS

On the stability of shape memory materials and their properties in static and dynamic applications 01 p0069 N94-11329

Adaptive structure design employing shape memory actuators 01 p0070 N94-11331

Structural analysis and optimization of adaptive structures by use of the finite element method 01 p0071 N94-11339

Intelligent materials systems and structures. Part 4: The influence of thermomechanical loading on the life of shape memory alloys
[PB93-195923] 04 p1363 N94-18952

The applications of modified metals in the construction industry
[VTT-TIED-1329] 04 p1365 N94-19374

Use of shape memory alloys in the robust control of smart structures
[AD-A270827] 04 p1366 N94-19594

Damping in ferrous shape memory alloys
[AD-A271009] 04 p1366 N94-19775

Process and apparatus for the release of a prestress initially applied to a mechanism such as a bearing on board a space vehicle
[CA-PATENT-APPL-SN-2,020,909] 05 p1824 N94-21142

Shape memory metals
[DE94-001373] 05 p1695 N94-21976

Recharge mechanism based on shape memory alloy 06 p2362 N94-24039

SAG compensated vibration isolation mount
[AD-D016040] 07 p2841 N94-27110

Modelling and stability of a shape memory alloy position control system
[ISBN-0-315-84467-1] 07 p2740 N94-27304

Report on smart materials
[PB94-137528] 08 p3203 N94-29015

Research on the improvement of shape-memory and magnetostrictive materials
[AD-A275397] 08 p3203 N94-29056

Rotary actuator
[NASA-CASE-MFS-28581-1] 08 p3205 N94-29447

Transmissibility of nickel-titanium shape memory alloy springs
[AD-A276055] 09 p3640 N94-31456

Implementation of heaters on thermally actuated spacecraft mechanisms 09 p3607 N94-33320

Displacive transformation in ceramics
[AD-A278442] 10 p4026 N94-33539

A real-time 2-D composite damage monitoring system employing neural network 10 p4074 N94-34355

Mechanical behavior and phase stability of NiAl-based shape memory alloys
[DE94-012336] 12 p4419 N94-37420

SHAPED CHARGES

The motion of a conical shaped liner driven by explosive load
[ITN-93-85215] 02 p0585 N94-14507

Instrumented experiments aboard the frigate WOLF. Wolf 2: Measurement results of the 5.5 kg TNT in the crew aft sleeping compartment
[PML-1992-12] 04 p1451 N94-17931

PVDF gauge characterization of hypervelocity-impact-generated debris clouds
[DE93-018831] 05 p1829 N94-19943

SHAPES

NT CONVEXITY
NT ELLIPTICITY
NT FLATNESS
NT LINE SHAPE

Stability of liquid bridges between parallel plates 01 p0101 N94-10078

On shape of single crystals grown by FZM in microgravity 01 p0102 N94-10084

A preliminary study on ice shape tracing with a laser light sheet
[NASA-TM-105964] 01 p0174 N94-11132

Fractal dimensions of rampart impact craters on Mars 01 p0460 N94-12154

Effect of size, shape, and end condition of test specimen on compressive strength of high-strength concrete
[DE93-500412] 02 p0682 N94-14653

Segmenting textured 3D surfaces using the space/frequency representation
[AD-A266960] 03 p1163 N94-14968

Process for shaping articles from electrosetting compositions
[AD-D015787] 03 p0935 N94-16534

Wideband electromagnetic scattering/analysis program: Far zone electromagnetic scattering from complex shapes using geometrical theory of diffraction
[AD-A268790] 04 p1384 N94-18187

Jet shapes in hadron and electron colliders
[DE93-019386] 05 p1979 N94-20216

Linear structures on the small inner satellites of Saturn 05 p2121 N94-20797

Gas-pressure forming of superplastic ceramic sheet
[DE94-001520] 06 p2252 N94-22930

Perception in flight: Shape and motion perception, space perception, spatial orientation, and visual vestibular interaction 06 p2429 N94-23979

Polymer morphologh 06 p2226 N94-24353

Effect of nitrocarburizing on shape of titanium alloy parts
[DE94-004040] 07 p2732 N94-25822

Endogeneous and exogenous control of visual selection: A review of the literature
[AD-A273761] 07 p2908 N94-25871

Morphology transitions during non-equilibrium growth processes
[ITN-94-85236] 07 p3065 N94-27243

Interactive shape metamorphosis
[AD-A277572] 07 p2970 N94-27417

Mach reflection of spherical detonation waves
[DE93-016604] 07 p2797 N94-27705

Interactive reconstruction of anatomical structures with free-form surfaces
[TELECOM-93-E-002] 09 p3794 N94-31195

A paraperspective factorization method for shape and motion recovery
[AD-A276513] 09 p3712 N94-31929

Principal component analysis with missing data and its application to object modeling
[AD-A276644] 09 p3845 N94-31939

Large-scale shape optimization: Numerical methods, parallel algorithms, and applications to aerodynamic design 09 p3815 N94-31966

Visual encoding of spatial relations
[AD-A277400] 09 p3800 N94-32344

Visual neural development and chromatic aberration
[AD-A277402] 09 p3800 N94-32345

Computer image analysis of wear debris with its applications to machine wear diagnosis 10 p4067 N94-34366

Quantifying shapes of volcanoes on Venus 11 p4361 N94-35429

SHARP LEADING EDGES

Study into the limits of an Euler equation method applied to leading-edge vortex flow
[NLR-TP-91350-U] 03 p1031 N94-17627

Numerical investigation into high-angle-of-attack leading-edge vortex flow
[PB94-125564] 08 p3133 N94-30388

Aspects of the modeling and numerical simulation of leading-edge vortex flow
[AD-B179108] 08 p3133 N94-30492

Numerical simulation of leading-edge vortex flow
[AD-B175154] 08 p3134 N94-30871

SHATTER CONES

Shock attenuation at the Slate Islands revisited 05 p1863 N94-20887

SHATTERING

U FRAGMENTATION

SHEAR

Shear, strain and thermohaline vertical fine structure in the upper ocean
[AD-A265961] 01 p0289 N94-12348

Light scattering studies of an electrorheological fluid
[DE93-019419] 05 p1700 N94-20315

SHEAR DISTURBANCES

U S WAVES

SHEAR FATIGUE

U SHEAR STRESS

SHEAR FLOW

Transport mechanisms acting in toroidal devices: A theoretician's view
[DE93-013463] 01 p0385 N94-10310

The nonlinear evolution of modes on unstable stratified shear layers
[NASA-CR-191492] 01 p0149 N94-10810

High order accurate solutions of viscous problems
[NASA-TM-106267] 01 p0151 N94-11253

Shear flow control of gas jets in liquids
[AD-A264673] 01 p0152 N94-11448

Modelling quasi-two-dimensional turbulent shear flow 01 p0153 N94-11616

Vortex-induced forces on oscillating bluff cylinders
[AD-A265056] 01 p0154 N94-11865

Numerical simulation using vorticity-vector potential formulation 01 p0157 N94-12297

Local isotropy in high Reynolds number turbulent shear flows 01 p0157 N94-12302

Probability density distribution of velocity differences at high Reynolds numbers 01 p0158 N94-12304

Mixing in a stratified shear flow: Energetics and sampling 01 p0159 N94-12311

Numerical simulation of the non-Newtonian mixing layer 01 p0159 N94-12314

The thermodynamics of the nonlinear shear flows 01 p0169 N94-12728

Turbulence generation in the Pacific undercurrent by shear 01 p0223 N94-12730
Study of the admixture diffusion in the sea using remote techniques 01 p0228 N94-12759
Studies of turbulent shear flows and their control [NASA-CR-194114] 02 p0635 N94-13676
Turbulent diffusion in homogeneous shear flow with stable density stratification [DLR-FB-92-26] 02 p0639 N94-14443
Search for subgrid scale parameterization by projection pursuit regression 02 p0643 N94-14749
A study of the fine scale motions of incompressible time-developing mixing layers 02 p0644 N94-14751
Direct simulation of polymer drag reduction in free shear flows and vortex dipoles 02 p0644 N94-14755
Investigation of the dilatational dissipation in compressible homogeneous shear flow 02 p0645 N94-14758
The turbulent wall jet [AD-A267675] 03 p0855 N94-14963
Parametric resonant triad interactions in a free shear layer [NASA-TM-106365] 03 p1021 N94-15751
Turbulence and transition modeling for high-speed flows [AD-A266748] 03 p1022 N94-15953
Implementation of an anisotropic turbulence model in the COMMIX-1C/ATM computer code [DE93-015541] 03 p1023 N94-16444
Search for chaos in free shear flows [AD-A266245] 03 p1023 N94-16470
Investigation of high-speed free shear flows using improved pressure-strain correlated Reynolds stress turbulence model [NASA-CR-194661] 03 p1027 N94-17127
A numerical investigation of energy transfer and subgrid-scale eddy-viscosity in homogeneous, isotropic, and shear turbulence [AD-A267265] 03 p1029 N94-17363
Time dependent turbulence modeling and analytical theories of turbulence [NASA-TM-106379] 03 p1029 N94-17385
Self-regulated shear flow turbulence in confined plasmas [DE93-015823] 04 p1583 N94-17743
On memory effects in turbulence [DLR-FB-93-03] 04 p1409 N94-18124
Research on two equation models 04 p1411 N94-18547
Large-eddy simulation of turbulent diffusion in stably stratified shear flow 04 p1416 N94-18595
Research and training activities of the Joint Institute for Aeronautics and Acoustics [NASA-CR-194742] 04 p1421 N94-19493
The effects of initial conditions on the 3-D topology of temporally evolving wakes (ARI on 3-D bluff body wakes) [AD-A271008] 04 p1423 N94-19774
Development of phased twin flip-flop jets [NASA-TM-106404] 05 p1637 N94-20563
An analysis of pool surface deformation due to a plunging liquid jet [AD-A272970] 05 p1802 N94-21261
Shear flow generation by Reynolds stress and suppression of resistive g-modes [DE93-040911] 05 p1995 N94-21514
Coupling of smooth particle hydrodynamics with PRONTO [DE93-019080] 05 p1915 N94-21539
New results on the realizability of Reynolds stress turbulence closures [NASA-CR-191548] 05 p1804 N94-21875
The role of the radial electric field in confinement and transport in H-mode and VH-mode discharges in the DIII-D tokamak [DE94-002746] 06 p2551 N94-23782
The production of premixed flame surface area in turbulent shear flow 06 p2237 N94-24158
Numerical simulation of non-Newtonian free shear flows 06 p2331 N94-24160
Local isotropy in distorted turbulent boundary layers at high Reynolds number 06 p2332 N94-24166
A vorticity dynamics based model for the turbulent dissipation: Model development and validation [NASA-TM-106177] 06 p2336 N94-24713
Shear flow generation from the interaction of neoclassical and drift wave transport processes [DE94-003135] 07 p2791 N94-26096
The effects of three-dimensional imposed 3-d disturbances on bluff-body near wake flows [AD-A274845] 07 p2791 N94-26187
On prediction of equilibrium states in homogeneous compressible turbulence [NASA-CR-4570] 07 p2792 N94-26467
Numerical studies on the dynamics of bubble, turbulent, free shear flows: Effect of the inter-phase coupling on the global flow evolution [AD-A274521] 07 p2794 N94-26832
Surface roughness lengths [AD-A274550] 07 p2895 N94-26846
Numerical simulation of turbulent free jet by TFKE model 07 p2871 N94-28157
On the numerical analysis of shear flows 08 p3126 N94-28972
An alternative assessment of second-order closure models in turbulent shear flows [AD-A279072] 08 p3272 N94-29381
Lubricant rheology at high shear rates 08 p3217 N94-29967
Potential capabilities of Reynolds stress turbulence model in the COMMIX-RSM code 08 p3285 N94-30450
Evaluation of flip-flop jet nozzles for use as practical excitation devices [NASA-TM-106377] 08 p3135 N94-30949
On wave interactions of rotational and irrotational flows 09 p3700 N94-31219
Oscillations in piston-driven shear flow of a non-Newtonian fluid [AD-A276472] 09 p3701 N94-31245
Transport suppression by shear flow generation in multihelicity resistive-g turbulence [DE94-007108] 09 p3886 N94-31366
Shear flow control of cold and heated rectangular jets by mechanical tabs. Volume 1: Results and discussion [NASA-CR-182296-VOL-1] 09 p3708 N94-32867
Shear flow control of cold and heated rectangular jets by mechanical tabs. Volume 2: Tabulated data [NASA-CR-182296-VOL-2] 09 p3709 N94-32869
The structure of high Reynolds number turbulent boundary layers, part A [AD-A278392] 09 p3710 N94-33162
Turbulence structure associated with intercomponent and interscale energy transfer and modification by forcing [AD-A278269] 10 p4043 N94-33414
Real-time adaptive control of mixing in a plane shear layer [AD-A278379] 10 p4113 N94-33744
Direct simulation of a self-similar plane wake [NASA-TM-108815] 10 p4050 N94-34917
Dynamic and thermal turbulent time scale modelling for homogeneous shear flows [NASA-TM-106635] 11 p4263 N94-35253
X ray radiographic imaging of hydrodynamic phenomena in radiation driven materials: Shock propagation, material compression and shear flow [DE94-009515] 11 p4266 N94-35982
X ray radiographic imaging of hydrodynamic phenomena in radiation driven materials: Shock propagation and shear flow [DE94-010891] 11 p4318 N94-36201
Momentum-energy transport from turbulence driven by parallel flow shear [DE94-012765] 12 p4443 N94-37362
The stabilizing effect of compressibility in turbulent shear flow [NASA-CR-194932] 12 p4444 N94-37605
Towards enhancing and delaying disturbances in free shear flows [NASA-CR-194945] 12 p4445 N94-37606

SHEAR LAYERS

The nonlinear evolution of modes on unstable stratified shear layers [NASA-CR-191492] 01 p0149 N94-10810
Application of jet-shear-layer mixing and effervescent atomization to the development of a low-NO(x) combustor [NASA-TM-105888] 01 p0028 N94-11234
High order accurate solutions of viscous problems [NASA-TM-106267] 01 p0151 N94-11253
Receptivity in parallel flows: An adjoint approach 01 p0157 N94-12301
LIF measurements of scalar mixing in turbulent shear layers 01 p0159 N94-12312
Shear, strain and thermohaline vertical fine structure in the upper ocean [AD-A265961] 01 p0289 N94-12348
Aerodynamic sound due to interaction between a two-dimensional free shear layer and the leading edge of a parallel flat plate 01 p0163 N94-12615
Turbulence modeling of free shear layers for high-performance aircraft [NASA-CR-193659] 02 p0520 N94-12799
Linear instability of curved free shear layers [NASA-TM-106290] 02 p0642 N94-14729
A study of the fine scale motions of incompressible time-developing mixing layers 02 p0644 N94-14751
Vortex-induced disturbance field in a compressible shear layer 02 p0645 N94-14760
Parametric resonant triad interactions in a free shear layer [NASA-TM-106365] 03 p1021 N94-15751
Search for chaos in free shear flows [AD-A266245] 03 p1023 N94-16470
Selected computations of transonic cavity flows 03 p0858 N94-16511
Unsteady fluid and optical simulation of transonic aero-windows [AIAA PAPER 93-3017] 03 p0858 N94-16512
The structure of turbulent boundary layers and shock wave boundary layer interactions [AD-A266240] 03 p1026 N94-16929
Investigation of high-speed free shear flows using improved pressure-strain correlated Reynolds stress turbulence model [NASA-CR-194661] 03 p1027 N94-17127
Structure of turbulence in three-dimensional boundary layers [NASA-CR-194655] 03 p1027 N94-17130
Chemical reactions in turbulent mixing flows [AD-A268287] 03 p0861 N94-17580
Chemical reactions in turbulent mixing flows [AD-A269377] 04 p1410 N94-18472
A random distribution reacting mixing layer model [NASA-CR-194445] 06 p2187 N94-23552
Effect of initial droplet-size distributions on fuel-vapor profiles in a shear-layer flow 06 p2160 N94-24283
Interactive control in turbulent shear layers [AD-A273544] 06 p2336 N94-24793
The effects of profiles on supersonic jet noise [NASA-CR-195184] 06 p2530 N94-25177
Numerical studies on the dynamics of bubble, turbulent, free shear flows: Effect of the inter-phase coupling on the global flow evolution [AD-A274521] 07 p2794 N94-26832
Recent developments in the simulation of steady and transient transverse jet interactions for missile, rotorcraft, and propulsive applications 07 p2804 N94-28030
A random distribution reacting mixing layer model [NASA-TM-106517] 08 p3150 N94-28923
Wall pressure fluctuations in the reattachment region of a supersonic free shear layer [NASA-CR-195790] 08 p3132 N94-29920
The effect of a wavy boundary on turbulent flow 08 p3280 N94-30272
Numerical simulation of leading-edge vortex flow [AD-B175154] 08 p3134 N94-30871
An experimental study of nonlinear wave coupling and energy transfer characterizing the transition of a planar jet shear layer 08 p3282 N94-30953
Control of hypersonic aerodynamic forces with surface blowing 09 p3567 N94-31216
Real-time adaptive control of mixing in a plane shear layer [AD-A278379] 10 p4113 N94-33744
Physical description of boundary-layer transition: Experimental evidence 10 p4045 N94-33885
Asymptotic approaches to transition modelling 10 p4045 N94-33887
Controlling combustion and maximizing heat release in a reacting compressible free shear layer [AD-A278328] 10 p3982 N94-33966
Control of leading-edge vortices on a delta wing 10 p3986 N94-34971
Characterization of dynamic stall phenomenon using two-dimensional unsteady Navier-Stokes equations 10 p3986 N94-34974
An experimental investigation of active control of thrust vectoring nozzle flow fields [AD-A278702] 11 p4229 N94-36291
Turbulence modeling of free shear layers for high performance aircraft [NASA-CR-196137] 12 p4442 N94-36808
Holt film wall shear instrumentation for boundary layer transition research [NASA-CR-196040] 12 p4443 N94-37060

SHEAR PROPERTIES

NT SHEAR STRENGTH

Shear buckling of fiber metal laminates: Comparison between orthotropic and anisotropic plate models using finite element method [LTR-ST-1934] 02 p0671 N94-13565
Studies of momentum and energy transfer across wavy gas-liquid interfaces [AD-A266432] 02 p0635 N94-13699
An experimental study on the effect of die geometry on swell and sag in the parison extrusion stage [IMI-93RT-42400-1476-G] 02 p0597 N94-14070
Machining and grinding: High rate deformation in practice [DE93-010718] 02 p0664 N94-14457
Structures and shear response of lipid monolayers [DE93-015076] 02 p0730 N94-14802

The processing and mechanical properties of high temperature/high performance composites. Book 4: Coonstitutive laws and design
[AD-A266397] 03 p0935 N94-16528
Interfacial shear behavior and its influence on fiber damage in sapphire-reinforced gamma titanium aluminide composites
[AD-A267943] 03 p1060 N94-17043
Shear wave measurements in shock-induced, high-pressure phases
[DE93-016461] 03 p1062 N94-17664
Numerical integration of structural elements in NIKE3D and DYNA3D
[DE93-016325] 04 p1452 N94-18049
Chemical reactions in turbulent mixing flows
[AD-A269377] 04 p1410 N94-18472
Development of a finite element method program for the analysis of laminated composite plates using first-order shear deformation theory
[AD-A270318] 04 p1342 N94-18700
Elastic properties of amorphous thin films studied by Rayleigh waves
[DE93-018375] 04 p1372 N94-19202
Development and characterization of adiabatic shear prone tungsten heavy alloys
[AD-A270477] 04 p1366 N94-19673
Frequency and temperature dependence of high damping elastomers
[DE93-019539] 05 p1697 N94-19809
Shear flow generation by Reynolds stress and suppression of resistive g-modes
[DE93-040911] 05 p1995 N94-21514
Control of the internal stresses in plane elasticity
[PB93-225514] 06 p2374 N94-23112
Dynamic analysis of pretwisted elastically-coupled rotor blades
[NASA-TM-109070] 06 p2378 N94-24839
Test methods for composites: A status report. Volume 3: Shear test methods
[AD-A273561] 06 p2230 N94-25163
Aluminum alloy 8090-T8771 thick plate material characterization
[AD-A274146] 07 p2987 N94-27077
Experimental determination of orthotropic elastic constants
[FFA-TN-1991-35] 08 p3215 N94-29424
Performance of a higher-order triangular finite element for composite laminated structures
08 p3181 N94-29810
Lubricant rheology at high shear rates
08 p3217 N94-29967
Ceramic Technology Project database
[DE94-008494] 09 p3659 N94-32632
Analysis of new composite architectures
[NASA-CR-195303] 09 p3626 N94-32904
A mechanics mode for the compressive response of fiber reinforced composites
[AD-A278866] 11 p4233 N94-35715

SHEAR STRAIN

Computational procedures for determining parameters in Ramberg-Osgood elastoplastic model based on modulus and damping versus strain
[DE93-013309] 01 p0185 N94-10306
Damping measurements for ultra-high carbon steel/brass laminates
[DE93-011886] 01 p0082 N94-11076
Nonlinear vibrations of thick composite plates: Higher-order shear deformation plate theory
02 p0556 N94-13558
Computer program for analysis of high speed, single row, angular contact, spherical roller bearing, SASHBEAN. Volume 1: User's guide
[NASA-CR-191183] 02 p0663 N94-14445
Cyclic axial-torsional deformation behavior of a cobalt-base superalloy
[NASA-TM-106372] 08 p3203 N94-28921
Interlaminar fracture analysis for laminated composites under combined loading 08 p3182 N94-29964
Thin-walled orthotropic laminated beam theory
08 p3324 N94-30920
Non-linear numerical analysis of the losipescu specimen for composite materials
[NASA-CR-195934] 10 p4020 N94-34306

SHEAR STRENGTH

Design of inspection and acceptance test methodology for TIG welded aluminum-alloy bracket for camera housings for IRS-1A space craft and executing it
01 p0061 N94-10037
Computational procedures for determining parameters in Ramberg-Osgood elastoplastic model based on modulus and damping versus strain
[DE93-013309] 01 p0185 N94-10306
System integration and demonstration of adhesive bonded high temperature aluminum alloys for aerospace structure, phase 2
[NASA-CR-191459] 02 p0575 N94-12792
Evaluation of the production-grade class 4 flextensional transducer shell
[AD-A268796] 04 p1340 N94-18201
Coupling of smooth particle hydrodynamics with PRONTO
[DE93-019080] 05 p1915 N94-21539
Relationship of microstructure and mechanical properties for V-Cr-Ti alloys
[DE94-001431] 06 p2238 N94-22718
The mechanical property data base from an Air Force/Industry Cooperative Test Program on advanced aluminum alloys (7064 and CW67)
[AD-A273741] 06 p2251 N94-25531
The undrained shear strength characteristics of undisturbed soil from fishing port areas
08 p3234 N94-29704
Delamination growth in composites under cyclic loads
08 p3183 N94-30256
Four advances in carbon-carbon materials technology
08 p3186 N94-30481
Joining of alumina by vacuum brazing
[VTT-TIED-1495] 09 p3724 N94-31656
Contingency airfield construction: Mechanical stabilization using monofilament and fibrillated fibers
[AD-A277732] 10 p4008 N94-33444
Non-linear numerical analysis of the losipescu specimen for composite materials
[NASA-CR-195934] 10 p4020 N94-34306
Residual Gas Analysis (RGA) and shear strength characteristics of a silver-filled epoxy and polyimide under long-term, high-temperature storage conditions
[DE94-010106] 11 p4244 N94-35705
A comparison of graphite/epoxy tape laminates and 2-D braided composites mechanical properties
[NASA-CR-4610] 12 p4420 N94-37582

SHEAR STRESS

NT TORSIONAL STRESS
Design evaluation of GLARE laminate lay-ups
01 p0063 N94-10051
The effects of successive distortions on a turbulent boundary layer in a supersonic flow
01 p0014 N94-11058
Application of a Reynolds stress model to separating boundary layers 01 p0157 N94-12299
Colorimetric qualification of shear sensitive liquid crystal coatings
[NASA-CR-194126] 02 p0806 N94-13291
Finite element analysis of composite plates by use of modified complementary energy principle
02 p0672 N94-13596
Non-uniqueness in dynamic rate-independent non-associated plasticity
[AD-A266342] 02 p0769 N94-13731
Shock compression and quasielastic release in tantalum
[DE93-014566] 02 p0811 N94-14329
Computer program for analysis of high speed, single row, angular contact, spherical roller bearing, SASHBEAN. Volume 2: Mathematical formulation and analysis
[AD-A276235] 02 p0664 N94-14446
Vortex-induced disturbance field in a compressible shear layer 02 p0645 N94-14760
Thermal stresses of a trimaterial medium in a nonuniform temperature field
[AD-A267243] 03 p0930 N94-14975
Forced harmonic vibration of the generally orthotropic cylindrical shell with inner and outer fluid loading
[AD-A266985] 03 p1057 N94-15150
Theoretical study of laminar film condensation on horizontal ellipitical tubes under conditions of free and forced convection
[AD-A267161] 03 p1021 N94-15737
Adaptive algorithm for aircraft configuration in turbulent flow
[AD-A266188] 03 p0867 N94-16122
Evaluation of the interfacial mechanical properties in fiber-reinforced ceramic composites
[DE93-015494] 03 p0935 N94-16461
Structure of high Reynolds number turbulent boundary layer
[AD-A267476] 03 p0860 N94-17099
Convection effects on radial segregation and crystal melt interface in vertical Bridgman growth
[NASA-CR-191541] 03 p1029 N94-17387
Dislocation-drag contribution to high-rate plastic deformation in shock-loaded tantalum
[DE93-018286] 04 p1361 N94-18802
Stress pulse phenomena
[DE93-019064] 04 p1456 N94-19078
A comparative evaluation of in-plane shear test methods for laminated graphite-epoxy composites
[NASA-CR-193808] 04 p1456 N94-19095
Development of engineering models for calculation of failure loads and defect states of steel concrete beams and plates
[ETN-93-95052] 04 p1460 N94-19648
Collaborative research on combustion diagnostics and modeling between Rolls-Royce, Inc. and the United States Air Force Wright Laboratory
[AD-A270660] 04 p1354 N94-19778
Principles and applications of oil film interferometry for measuring wall friction fields in air flows
[ETN-93-95062] 05 p1798 N94-20147
Crystal orientation dependence of elastic precursor strength in pentaerythritol tetranitrate
[DE93-018340] 05 p2034 N94-22035
The use of near-wall hot-wire probes for time-resolved skin-friction measurements 06 p2316 N94-22857
Method of determining shear stress employing a monomer-polymer laminate structure
[NASA-CASE-LAR-14654-2] 06 p2375 N94-23308
Skin friction measurement in complex flows using thin oil film techniques
[NASA-CR-194872] 06 p2327 N94-24098
Role of interfaces on the cyclic fatigue behaviour of ceramic matrix composites 06 p2256 N94-24234
Post buckling behaviour of stiffened composite panels loaded in cyclic compression and shear
06 p2157 N94-24260
Evaluation of the fracture resistance and durability of adhesive bonded joints 06 p2160 N94-24278
Use of photostress to characterize the mechanical behavior of weldments
[NASA-CR-195201] 06 p2378 N94-25267
Formulae for the buckling of simply-supported corrugated panels of orthotropic material under shear load
[PB94-126547] 07 p2840 N94-26911
Experimental verification of tomographic reconstruction of turbulent air flow structure using optical wavefront measurements
[AD-A274392] 07 p2795 N94-27129
Implementation of thermal residual stresses in the analysis of fiber bridged matrix crack growth in titanium matrix composites
[NASA-TM-109082] 07 p2711 N94-27658
Cyclic axial-torsional deformation behavior of a cobalt-base superalloy
[NASA-TM-106372] 08 p3203 N94-28921
Granular bases for heavily loaded pavements
[AD-A275171] 08 p3156 N94-29047
Performance of a higher-order triangular finite element for composite laminated structures
08 p3181 N94-29810
Nanodislocation structures generated in shocked crystals 08 p3514 N94-29915
Vacuum chamber and adaptors for shearography and holography
[NASA-CR-192467] 08 p3157 N94-29956
On interannual variability and climate change in the North Pacific 08 p3374 N94-29963
An efficient higher order theory for laminated composite plates and a finite element implementation
09 p3617 N94-31215
Considering ties elasticities in high frequency rail dynamics
[ILR-MITT-281(1993)] 09 p3733 N94-31375
Fatigue in single crystal nickel superalloys
[AD-A276662] 09 p3643 N94-32047
Shearographic inspection of a DeHavilland DHC-7
[AD-A276716] 09 p3566 N94-32157
Non-linear numerical analysis of the losipescu specimen for composite materials
[NASA-CR-195934] 10 p4020 N94-34306
Active thermal isolation for temperature responsive sensors
[NASA-CASE-LAR-14612-1] 10 p4054 N94-35074
Fibre-matrix interface properties in Ti-matrix composites: Chemical compatibility and micromechanical behaviour
12 p4401 N94-36657

SHEAR WAVES

U S WAVES

SHEARING

A stochastic model for behavior analysis of fiber-reinforced quasi-brittle materials
02 p0672 N94-13594
Forced unsteady deceleration of a turbulent boundary layer from a temporal perspective
10 p4053 N94-34983

SHEARING STRESS

U SHEAR STRESS

SHEATHS

NT PLASMA SHEATHS
Cathode sheath charge transfer effects
[AD-A268393] 03 p1186 N94-17536
Fiber optic microcable produced with radiation cured composite
[AD-D016155] 10 p4142 N94-33761
High-temperature, bellows hybrid seal
[NASA-CASE-LEW-15570-1] 11 p4274 N94-35373

SHEEP
Blast overpressure studies with animals and man
[AD-A275038] 08 p3391 N94-29150
SHEET METAL
U METAL SHEETS
SHELL STABILITY
A survey of crack path stability criteria and their application to crack flapping phenomena in stiffened structures
[LR-681] 02 p0675 N94-13929
The effect of initial imperfections on shell stability: An updated review
[LR-695] 02 p0682 N94-14692
Comparison of level-1 and level-2 buckling and postbuckling solutions
[NASA-CR-194611] 03 p1057 N94-15154
A separation technique for asymptotic-numeric solution for general shells of revolution 09 p3736 N94-31961
SHELL STARS
Physical properties of gas disks around shell stars with and without dust
[NASA-CR-193655] 02 p0835 N94-13239
SHELL THEORY
Sound radiation from infinite laminated composite shell with periodic rib stiffening
[DRA/TM(USGR)92326] 03 p0933 N94-15699
Numerical integration of structural elements in NIKE3D and DYNA3D
[DE93-016325] 04 p1452 N94-18049
Energy estimates and asymptotic analysis in the theory of shells
[PB93-225738] 06 p2374 N94-23113
Electron energy loss spectroscopy in a crystalline environment using inner shell ionization
[DE94-601820] 07 p3018 N94-26334
Plane strain finite element analysis of sheet forming operations including bending effects 08 p3322 N94-30354
Theory of thick, laminated composite shallow shells 09 p3622 N94-31953
Development of an advanced continuum theory for composite laminates, volume 2
[AD-A277276] 09 p3625 N94-32592
Shape control of composite plates and shells using embedded actuators 10 p4018 N94-33532
SHELLS (STRUCTURAL FORMS)
NT ANISOTROPIC SHELLS
NT CONICAL SHELLS
NT CYLINDRICAL SHELLS
NT DOMES (STRUCTURAL FORMS)
NT ELASTIC SHELLS
NT FLUID FILLED SHELLS
NT LIQUID FILLED SHELLS
NT METAL SHELLS
NT ORTHOTROPIC SHELLS
NT RADOMES
NT REINFORCED SHELLS
NT SHALLOW SHELLS
NT SPHERICAL SHELLS
NT THIN WALLED SHELLS
Probabilistic micromechanics for high-temperature composites
[NASA-CR-191150] 02 p0676 N94-14408
Dynamic behavior of fiber and particle reinforced composites
[AD-A266905] 03 p0930 N94-15143
Comparison of level-1 and level-2 buckling and postbuckling solutions
[NASA-CR-194611] 03 p1057 N94-15154
Progress in the modeling of the shock response and mitigation of thick composite shells
[AD-A267009] 03 p1057 N94-15524
Evaluation of the production-grade class 4 flextensional transducer shell
[AD-A268796] 04 p1340 N94-18201
Residual strain measurement on the production-grade class 4 flextensional transducer shell
[AD-A268828] 04 p1430 N94-18537
Response statistics of shell structures with geometrical and material nonlinearities, volume 1
[ISBN-0-315-84006-4] 05 p1833 N94-22590
Counterrotating aircraft propulsor blades
[CA-PATENT-1-319-357] 06 p2186 N94-23255
A separation technique for asymptotic-numeric solution for general shells of revolution 09 p3736 N94-31961
Effective computational strategy for predicting the response of complex systems
[AD-A277452] 09 p3740 N94-33011
Shape control of composite plates and shells using embedded actuators 10 p4018 N94-33532
SHELTERS
NT LUNAR SHELTERS
Manned Mars mission on-orbit operations FTS capabilities assessment
[NASA-CR-189328] 06 p2430 N94-23080
Portable Habitat for Antarctic Scientific Research (PHASR) 07 p2943 N94-25681
Pax: A permanent base for human habitation of Mars 07 p2943 N94-25706
Safety standards for aircraft shelter
[FFI-92/4003] 07 p2680 N94-26305
Thermal performance of residential duct systems in basements
[LBL-33962] 11 p4250 N94-35364
SHERGOTTITES
Moessbauer spectroscopy of the SNC meteorite Zagami 01 p0428 N94-12016
Nitrogen and noble gases in a glass sample from LEW88516 01 p0080 N94-12051
Noble gases in LEW88516 shergottite: Evidence for exposure age pairing with ALH77005 01 p0080 N94-12082
LEW88516 and SNC meteorites 01 p0430 N94-12150
Noble gas evidence of an aqueous reservoir near the surface of Mars more recently than 1.3 Ga 01 p0473 N94-12228
Nitrates in SNCs: Implications for the nitrogen cycle on Mars 03 p1251 N94-16193
Potassium isotope cosmochemistry, volatile depletion and the origin of the Earth 03 p0953 N94-16259
Os isotopes in SNC meteorites and their implications to the early evolution of Mars and Earth 03 p1242 N94-16272
Martian carbon dioxide: Clues from isotopes in SNC meteorites 03 p1270 N94-16295
The dregs of crystallization in Zagami 03 p1245 N94-16390
Rare Earth elements in individual minerals in Shergottites 05 p1686 N94-20852
Equilibrium and fractional crystallization of a primitive Shergottite composition 05 p2085 N94-20861
Weathering features and secondary minerals in Antarctic Shergottites ALHA77005 and LEW88516 05 p2086 N94-20869
The carbon components in SNC meteorites of feldspathic harzburgite composition 05 p2086 N94-20885
Further carbon isotope measurements of LEW 88516 05 p2086 N94-20886
An attempt to comprehend Martian weathering conditions through the analysis of terrestrial palagonite samples 05 p2143 N94-21668
Cosmogenic C-14 in Antarctic and non-Antarctic meteorites and lunar samples
[NASA-CR-195795] 08 p3546 N94-29905
SNC meteorites and their implications for reservoirs of Martian volatiles 09 p3947 N94-33209
The Martian sources of the SNC meteorites (two, not one), and what can and can't be learned from the SNC meteorites 09 p3951 N94-33234
Solar proton produced neon in shergottite meteorites 11 p4351 N94-35428
The parent magma of xenoliths in shergottite EETA79001: Bulk and trace element composition inferred from magmatic inclusions 11 p4352 N94-35467
Pigeonholing planetary meteorites: The lessons of misclassification of EET87521 and ALH84001 11 p4353 N94-36157
SHIELDING
NT ELECTROMAGNETIC SHIELDING
NT HEAT SHIELDING
NT MAGNETIC SHIELDING
NT RADIATION SHIELDING
NT RADIO FREQUENCY SHIELDING
NT REENTRY SHIELDING
NT REUSABLE HEAT SHIELDING
NT SOLAR RADIATION SHIELDING
NT SPACECRAFT SHIELDING
Linear antenna of an arbitrary orientation and position in cylindric screen
[DE93-621353] 01 p0134 N94-11035
Overview of shielding analyses for the MHTGR from 1986 to 1991
[DE94-002448] 08 p3495 N94-29924
Method of N-15 analysis by mass-spectroscopy on ion implanter MPB-200
[DE94-618203] 12 p4407 N94-36529
SHIELDS (GEOLOGY)
U BEDROCK
SHIFT REGISTERS
Some problems of applied algebra
[CWI-AM-R9306] 09 p3847 N94-32204
SHIP HULLS
Microstructure-based fatigue life prediction methods for naval steel structures
[AD-A265429] 01 p0085 N94-12426
Advances in low carbon, high strength ferrous alloys
[AD-A265264] 01 p0085 N94-12532
Hydro-elastic analysis using a selection of commercial analysis programs
[PB94-118734] 06 p2376 N94-24478
Weldability aspects in the design and fabrication of aluminium structures subjected to fatigue loads. Part 1: Effect of welding on the structural integrity of joint types designed for repairing aluminium ship sections
[PB94-132487] 07 p2833 N94-28378
An improvement of the slender body theory for oscillating ships with finite forward speed 08 p3234 N94-29705
SHIP TERMINALS
Orbital applications of electrodynamic propulsion
[AD-A275413] 08 p3173 N94-29216
SHIP TO SHORE COMMUNICATION
An analysis of cellular telephone and INMARSAT systems for providing radio data link computer communications for US Navy vessels
[AD-A278143] 09 p3684 N94-33160
SHIPS
NT AIRCRAFT CARRIERS
NT SUBMARINES
NT SURFACE EFFECT SHIPS
DISTERM: A shipboard data system for satellite monitoring of ocean and atmosphere 01 p0226 N94-12749
The free decay of coupled heave and pitch motions of a model frigate
[DRA/TM(AWMH)92340] 03 p1146 N94-15702
Instrumented experiments aboard the frigate WOLF. Wolf 2: Measurement results of the 5.5 kg TNT in the crew aft sleeping compartment
[PML-1992-12] 04 p1451 N94-17931
Ship-produced cloud line of 13 July 1991
[DE93-016879] 04 p1472 N94-17986
HERACLITUS, phase 1. Harbour Entrance of Rotterdam Radar based Current Related Information for Traffic Guidance of Ships: Feasibility of deriving current profile data from sea surface observations in the Rotterdam (Netherlands) port entrance
[BCRS-93-04] 06 p2417 N94-24107
Free-surface/vorticity interaction
[AD-A273263] 06 p2335 N94-24686
Application of Space Shuttle Project Hercules imagery in the investigation of ship cloud tracks
[AD-A274923] 07 p2692 N94-26529
Technical Report of National Research Institute of Fisheries Engineering: Fishing Boat and Instrument, No. 12
[JTN-94-80595] 07 p2764 N94-27976
Recent trend of domestic and international regulations on intact stability of ships for safety 07 p2764 N94-27977
E. H. P. estimation of high speed fishing boats by some existing methods 07 p2764 N94-27978
Physiological responses during shipboard firefighting
[AD-A275104] 08 p3391 N94-28912
An improvement of the slender body theory for oscillating ships with finite forward speed 08 p3234 N94-29705
Shiptrack database analysis
[AD-A277228] 09 p3746 N94-32025
Automated detection of ship tracks in multispectral satellite data
[AD-A276697] 09 p3746 N94-32119
Ship traffic monitoring and oil spill detection using the ERS-1 SAR 09 p3751 N94-32542
Landing of an unmanned helicopter on a moving platform. High accuracy navigation and tracking 12 p4387 N94-36618
SHIVERING
NT DITHERS
Evaluation of physiological and psychological impairment of human performance in cold stressed subjects
[AD-A268637] 04 p1506 N94-18632
Fuelling shivering in humans during cold water immersion 08 p3379 N94-28426
Homeostatic responses to prolonged cold exposure: Human cold acclimatization
[AD-A280234] 12 p4481 N94-37136
SHOCK (PHYSIOLOGY)
A review of the efficacy of 7.5 percent NaCl/6 percent Dextran-70 (HSD) in experimental animals and humans
[AD-A266633] 03 p1122 N94-15740
A mathematical model for the study of hemorrhagic shock and fluid resuscitation: Transcapillary exchange
[AD-A266427] 03 p1123 N94-16544
A mathematical model for the study of hemorrhagic shock and fluid resuscitation: Exchange of fluid and solutes between vascular, interstitial, and tissue cell compartments
[AD-A266426] 03 p1123 N94-16558
Increased vascular resistance with hemoglobin-based oxygen carriers
[AD-A266454] 03 p1123 N94-16565

SHOCK ABSORBERS
Mechanical energy absorber
[NASA-CASE-MSC-22111-1] 03 p1047 N94-15966
Preloaded launch locking devices for SILEX
06 p2358 N94-24008
Landing gear with swivelling beam
[CA-PATENT-1323020] 06 p2176 N94-24181
Design of a recumbent seating system
[NASA-CR-195503] 06 p2438 N94-24786
Landing gear energy absorption system
[NASA-CASE-MSC-22277-1] 08 p3300 N94-29448
Identification of the damping ratio relationship of an autovehicle suspension
[REPT-93-063] 08 p3313 N94-30937
MSAT boom joint testing and load absorber design
09 p3606 N94-33315
Method and means for isolating equipment from shock loads
[AD-D016161] 10 p4070 N94-34286
SHOCK DIFFUSERS
U DIFFUSERS
SHOCK DISCONTINUITY
A second-order shock-adaptive Godunov scheme based on the generalized Lagrangian formulation
[ISBN-0-315-84549-X] 07 p2795 N94-27307
Techniques for accurately solving unsteady shock waves and contact discontinuities 07 p2656 N94-28342
An adaptive method for the exact resolution of shock waves and contact discontinuities
[ISBN-0-315-86498-2] 09 p3704 N94-31799
SHOCK FRONTS
Numerical simulations and experiments on physics of high Mach number shockwave: Turbulent flow interactions
[DE93-013424] 02 p0631 N94-13249
Shock compression and quasielastic release in tantalum
[DE93-014566] 02 p0811 N94-14329
Evolution of the shock front and turbulence structures in the shock/turbulence interaction
02 p0645 N94-14761
Dynamic testing and characterization of pre-fractured ceramic
[DE93-016457] 03 p0972 N94-17238
Velocity measurements in a boundary layer with a density gradient
[DE93-019627] 04 p1422 N94-19515
Shock induced condensation in fluids of high molar specific heat: Shock structure and relaxation
[MPIS-106/1993] 05 p1798 N94-20145
Photopumped x ray laser research on Saturn
[DE93-019430] 05 p1816 N94-20298
Original size of the Vredefort structure, South Africa
05 p1863 N94-20825
Computer simulation of molecular response at a shock front
[DE94-001050] 05 p1977 N94-22396
Energy transfer in solid explosives
[DE94-001523] 06 p2265 N94-23778
The plastic response of a cylindrical shell subjected to an internal blast wave with a finite width shock front
06 p2154 N94-24246
The scattering and collision of gravitational waves in Friedmann-Robertson-Walker open universes
[MATHS-REPT-A-193] 06 p2406 N94-25430
Experimental investigation of three-dimensional vortex-airfoil interaction in a supersonic stream
[AD-A275107] 08 p3122 N94-28899
Nanodislocation structures generated in shocked crystals 08 p3514 N94-29915
Flank solar wind interaction
[NASA-CR-189327] 10 p4166 N94-35225
SHOCK HEATING
Impact mineralogy and chemistry of the cretaceous-tertiary boundary at DSDP site 576
01 p0282 N94-12091
Primordial lightning: Evidence preserved in chondrites
01 p0432 N94-12230
X ray emission from dynamical shock models in hot-star winds
[NASA-CR-194093] 02 p0847 N94-13288
Boost-phase discrimination research
[NASA-TM-109347] 05 p1666 N94-19818
Reverse polarity magnetized melt rocks from the Chicxulub impact structure, Yucatan Peninsula, Mexico
05 p1863 N94-20843
Opacity measurements in shock-generated argon plasmas
[DE94-001057] 05 p1998 N94-22399
Numerical simulation of unsteady aerodynamic heating induced by shock reflections 08 p3123 N94-28952
A study of low emissions gas turbine combustions
[NASA-CR-195763] 08 p3152 N94-29860
SHOCK LAYERS
Experimental study of a shock accelerated thin gas layer
[DE93-018354] 05 p1799 N94-20286
Nonequilibrium radiation and chemistry models for aerocapture vehicle flowfields
[NASA-CR-195706] 07 p2648 N94-28071
Development of a cascade simulation of fan-passage flow
[AD-A277234] 09 p3584 N94-32026
SHOCK LOADS
NT BLAST LOADS
Vaporization by shock loading of albite, jadeite, and pyrex glass: Experimental study 01 p0097 N94-12039
Shock transformations in quartzite
01 p0097 N94-12040
Dynamic high-pressure shock compaction of diamond powders
[AD-A266004] 01 p0093 N94-12354
Micromechanical strength effects in shock compression of solids
[DE93-014425] 02 p0670 N94-12887
Shock compression and quasielastic release in tantalum
[DE93-014566] 02 p0811 N94-14329
Nonlinear wave predictions in ceramics
[DE93-016516] 02 p0582 N94-14436
Progress in the modeling of the shock response and mitigation of thick composite shells
[AD-A267009] 03 p1057 N94-15524
Design of a cruciform bend specimen for determination of out-of-plane biaxial tensile stress effects on fracture toughness for shallow cracks
[DE93-015455] 03 p1059 N94-16104
Orientation of Planar Deformation Features (PDFs) in quartz 03 p1219 N94-16341
Omega phase formation in shock-loaded zirconium
[DE93-018343] 04 p1595 N94-18162
Dislocation-drag contribution to high-rate plastic deformation in shock-loaded tantalum
[DE93-018286] 04 p1361 N94-18802
Effects of shock loading on a solid-solution strengthened superalloy
[DE93-018345] 04 p1362 N94-18809
Toward a characterization of the debris cloud created in a hypervelocity impact on a thin plate
[AD-A269190] 04 p1455 N94-18864
Shock-loading response of advanced materials
[DE93-018344] 04 p1455 N94-19033
Shock compression properties of silicon carbide
[DE93-019927] 04 p1373 N94-19271
Influence of peak pressure and temperature on the shock-loading response of tantalum
[DE93-018561] 04 p1457 N94-19279
Simulation of the impact of a plastic flyer on an aluminum block using the hydrocode AUTODYNE
[PML-1992-26] 04 p1458 N94-19444
An equation of state for shock in homogeneous materials and comparison to shock data
[AD-A271436] 05 p1829 N94-19881
Time-resolved shock compression of porous rutile: Wave dispersion in porous solids
[DE93-018848] 05 p1829 N94-19927
Shock response of porous Al-2 + Fe2O3 powder mixtures
[DE93-018851] 05 p1688 N94-19944
CTH: A software family for multi-dimensional shock physics analysis
[DE93-019428] 05 p1904 N94-20052
Characterization of amorphous material in shocked quartz by NMR spectroscopy
[DE93-019069] 05 p1679 N94-20307
Shock attenuation at the Slate Islands revisited
05 p1863 N94-20887
Shock compression of low-density foams
[DE93-040545] 05 p1707 N94-21546
Ductile-brittle transition behavior of tungsten under shock loading conditions
[DE93-019945] 05 p1693 N94-21843
Disks of YBa2Cu3O7 shocked to 10 GPa pressures
[DE94-000464] 05 p2031 N94-21931
Characteristics of shock-compressed configuration of Ti and Si powder mixtures
[DE93-018857] 05 p1713 N94-22033
Crystal orientation dependence of elastic precursor strength in pentaerythritol tetranitrate
[DE93-018340] 05 p2034 N94-22035
Bridgman's concern
[DE93-040900] 06 p2558 N94-22953
Bibliographic Retrieval System (BARS), Sandia Shock Compression (SSC) database Shock Physics Index
[DE94-001679] 06 p2589 N94-23126
Bibliographic Retrieval System (BARS). Sandia Shock Compression (SSC) database Shock Physics Index (SPHINX) database. Volume 1: UNIX version query guide customized application for INGRES
[DE94-001703] 06 p2589 N94-23127
Bibliographic Retrieval System (BARS), Sandia Shock Compression (SSC) database, Shock Physics Index (SPHINX) database, Volume 2: UNIX version user's guide
[DE94-001704] 06 p2589 N94-23128
Bibliographic Retrieval System (BARS) Sandia Shock Compression (SSC) database Shock Physics Index (SPHINX) database, volume 3
[DE94-001705] 07 p3099 N94-27022
Pyrotechnic shock: Devices in pyrotechnic environment qualification logic
[REPT-932-430-108] 08 p3225 N94-29429
Method and means for isolating equipment from shock loads
[AD-D016161] 10 p4070 N94-34286
Structures and properties of materials recovered from high shock pressures
[DE94-010057] 11 p4232 N94-35696
X ray radiographic imaging of hydrodynamic phenomena in radiation driven materials: Shock propagation, material compression and shear flow
[DE94-009515] 11 p4266 N94-35982
Shocked materials from the Dutch Peak diamictite, Utah 11 p4352 N94-36140
Calorimetric thermobarometry of experimentally shocked quartz 11 p4240 N94-36174
X ray radiographic imaging of hydrodynamic phenomena in radiation driven materials: Shock propagation and shear flow
[DE94-010891] 11 p4318 N94-36201
Electrical conductivity of hydrogen shocked to megabar pressures
[DE93-019632] 11 p4238 N94-36237
A mixture model for shock compression of porous multi-component reactive materials
[DE93-017638] 12 p4400 N94-36456
Fluids at high shock pressures and temperatures and some thoughts about future possibilities
[DE94-003625] 12 p4407 N94-36458
DDT modeling and shock compression experiments of porous or damaged energetic materials
[DE94-011419] 12 p4428 N94-37052
SHOCK MEASURING INSTRUMENTS
Determination of equivalent circuit for PVDF shock-pressure gauges
[DE93-016492] 03 p1034 N94-16452
SHOCK RESISTANCE
NT IMPACT RESISTANCE
Thermal shock resistance of ceramic matrix composites
[NASA-CR-189136] 02 p0557 N94-13920
Fabrication of whisker-toughened alumina tubes
[DE94-001012] 05 p1677 N94-22022
Method for improving electromagnetic shielding performance of composite materials by electropulsing
[AD-D016050] 07 p2709 N94-27076
Mechanical properties of vacuum-sintered yttria ceramics
[DE94-008138] 09 p3659 N94-32617
SHOCK SPECTRA
Computational methods for problems in aerodynamics using parallel and vector architectures
[AD-A265626] 01 p0016 N94-12377
Development of test techniques to simulate high-frequency mechanical shock on weapon components
[KCP-613-4998] 02 p0675 N94-13907
Relativistic shock spectra: A prediction
[NASA-CR-194764] 05 p2150 N94-21782
SHOCK TESTS
Start-up imprinting and shock dynamics in laser-target interaction
[DE93-008051] 01 p0172 N94-10150
Theoretical investigation of 3-D shock wave turbulent boundary layer interactions
[AD-A265275] 01 p0150 N94-11014
Dynamic loading in manufacturing and service: Australia's shock testing capability
[AD-A268334] 01 p0128 N94-11304
Shock-free acceleration of laser driven targets
[DE93-008050] 02 p0655 N94-13387
Development of test techniques to simulate high-frequency mechanical shock on weapon components
[KCP-613-4998] 02 p0675 N94-13907
Thermal shock resistance of ceramic matrix composites
[NASA-CR-189136] 02 p0557 N94-13920
CO2 production by impact in carbonates? An ATEM and stable isotope (C,O) study 03 p0954 N94-16383

Hydrodynamic compressibility of high-strength ceramics
[DE93-019424] 05 p1698 N94-19903
Method for simulating a vehicle shock test: Design and realization of the required implementation tools
[ECL-92-14] 06 p2352 N94-22685
Deviatoric stresses and plastic strain rates in strong shock waves for six metals
[DE94-002964] 07 p2733 N94-26022
A versatile rocket engine hot gas facility
[NASA-CR-195339] 10 p4011 N94-34131
More shock recovery experiments on mesosiderite analogs 11 p4351 N94-35455
Fluids at high shock pressures and temperatures and some thoughts about future possibilities
[DE94-003625] 12 p4407 N94-36458

SHOCK TUBES
NT SHOCK TUNNELS
Comparison of computation and experiment for a high enthalpy, heated-driver, shock-tube environment 01 p0007 N94-10447
New developments in the method of space-time conservation element and solution element: Applications to the Euler and Navier-Stokes equations
[NASA-TM-106226] 01 p0150 N94-10939
A multiphase model for shock-induced flow in low density foam
[DE93-013767] 02 p0632 N94-13397
Experimental investigation of the effects of blowing ratio parameter on heat transfer to a film-cooled flat plate
[AD-A266599] 02 p0636 N94-13780
Comparative ignition of hexane and octane isomers in a shock tube
[DE93-016535] 02 p0566 N94-14869
Mechanistic models of soot formation
[AD-A267806] 03 p0950 N94-17008
Film condensation in a shock wave
[MPIS-22/1992] 04 p1422 N94-19509
An investigation on a new technique to improve the performance of the shock tube/tunnel testing in the equilibrium interface condition 06 p2154 N94-24247
Basic research on natural gas combustion phenomena
[PB94-129046] 07 p2717 N94-27256
Development of high-pressure diaphragms for the AEDC impulse tunnel
[AD-A277053] 09 p3588 N94-32009
A shock tube study of aerodynamic heating of gaps in a cylinder subjected to supersonic cross flow
[AD-A278550] 10 p3982 N94-33782
Experimental investigation of nozzle/plume aerodynamics at hypersonic speeds
[NASA-CR-195829] 12 p4382 N94-36687

SHOCK TUNNELS
The high enthalpy facilities HEG and TH 2 in Germany 01 p0004 N94-10430
Numerical simulation of hypersonic flow for the design of the H-2 orbiting plane (HOPE), part 3
[NAL-TR-1168-PT-3] 02 p0499 N94-12948
Aerodynamic and aerothermal facilities 2. Part 1: Short-duration, high-enthalpy facilities 02 p0506 N94-14159
Experimental investigation of nozzle/plume aerodynamics at hypersonic speeds
[NASA-CR-194628] 05 p1636 N94-20014
Shock tunnel studies of scramjet phenomena, supplement 7
[NASA-CR-191572] 06 p2319 N94-23513
Shock tunnel studies of scramjet phenomena, supplement 8
[NASA-CR-191573] 06 p2320 N94-23532
An investigation on a new technique to improve the performance of the shock tube/tunnel testing in the equilibrium interface condition 06 p2154 N94-24247
A numerical study of mixing and combustion in hypervelocity flows through a scramjet combustor model 07 p2808 N94-27911
Experiments on interaction force of jets in hypervelocity cross-flow in a shock tunnel 07 p2659 N94-28022
Calibration and validation studies in the LENS facility
[AD-A278403] 09 p3591 N94-33167
Experimental investigation of nozzle/plume aerodynamics at hypersonic speeds
[NASA-CR-195829] 12 p4382 N94-36687

SHOCK WAVE GENERATORS
NT SHOCK TUBES
NT SHOCK TUNNELS
Plane shock generator explosive lens: Shock characterization of 4340 and PH13-8Mo steels, C360 brass and PZT 65/35 ferro-electric ceramic
[DE94-009254] 11 p4266 N94-35979

SHOCK WAVE INTERACTION
Experimental, analytical, and computational methods applied to hypersonic compression ramp flows 01 p0006 N94-10444
Development of a Delaunay-based adaption scheme with applications to complex three-dimensional rotational flows 01 p0149 N94-10824
Flowfield structure of swept shock wave/turbulent boundary-layer interactions 01 p0149 N94-10899
An improved material interface reconstruction algorithm for Eulerian codes
[DE93-011679] 01 p0326 N94-11226
Large eddy simulation of shock turbulence interaction 01 p0155 N94-12289
Fundamental study of shock wave/turbulent boundary layer interactions with passive control in transonic flows
[ESA-TT-1278] 02 p0630 N94-13117
Sub-grid scale modeling for large eddy simulations in analysis of shock-turbulence interactions
[DE93-013425] 02 p0631 N94-13250
Shock/boundary-layer/shock interactions 02 p0507 N94-14172
Multi-dimensional high order essentially non-oscillatory finite difference methods in generalized coordinates
[NASA-CR-194031] 02 p0770 N94-14429
Evolution of the shock front and turbulence structures in the shock/turbulence interaction 02 p0645 N94-14761
Interaction of two glancing, crossing shock waves with a turbulent boundary-layer at various Mach numbers
[NASA-TM-103740] 02 p0509 N94-14780
Laser Doppler velocimetry measurements across a normal shock in transonic flow
[AD-A267240] 03 p0855 N94-14973
Special course on Shock-Wave/Boundary-Layer Interactions in Supersonic and Hypersonic Flows
[AGARD-R-792] 03 p1017 N94-15196
Swept shock/boundary-layer interactions: Scaling laws, flowfield structure, and experimental methods 03 p1017 N94-15197
Swept shock wave/laminar boundary layer interactions, experimental, and numerical results 03 p1017 N94-15198
Numerical simulation of 3-D shock wave turbulent boundary layer interactions 03 p1017 N94-15199
Unsteady phenomena in shock wave/boundary layer interaction 03 p1017 N94-15200
Contribution of laser Doppler velocimetry to the physical description of shock wave/turbulent boundary layer interactions with incidence on turbulence modelling 03 p1018 N94-15201
Turbulence modelling for shock wave/boundary layer interactions specific issues and examples of applications 03 p1018 N94-15202
Hypersonic shock wave boundary layer interactions over simplified deflected control surface configurations 03 p1018 N94-15203
On the interaction between the shock wave attached to a wedge and freestream disturbances
[NASA-CR-191528] 03 p1019 N94-15478
The structure of turbulent boundary layers and shock wave boundary layer interactions
[AD-A266240] 03 p1026 N94-16929
An investigation of oblique shock/boundary layer interaction control
[AD-A268106] 03 p0861 N94-17574
Shock wave interactions with exothermic mixtures
[AD-A271149] 05 p1829 N94-19836
Experimental study of a shock accelerated thin gas layer
[DE93-018354] 05 p1799 N94-20286
The 2D and 3D hypersonic flows with unstructured meshes 05 p1920 N94-22365
Experimental investigation of generic three-dimensional sidewall-compression scramjet inlets at Mach 6 in tetrafluoromethane
[NASA-TM-4497] 06 p2319 N94-23339
Effects of shock strength on shock turbulence interaction 06 p2332 N94-24165
Shocked clouds in the Cygnus Loop
[NASA-CR-195190] 06 p2600 N94-25178
Two-dimensional CFD modeling of wave rotor flow dynamics
[NASA-TM-106261] 06 p2189 N94-25185
The scattering and collision of gravitational waves in Friedmann-Robertson-Walker open universes
[MATHS-REPT-A-193] 06 p2406 N94-25430
Shock wave interaction with L-shaped structures
[AD-A273774] 07 p2790 N94-25858
Flowfield dynamics in blunt fin-induced shock wave/turbulent boundary layer interactions
[NASA-CR-195170] 07 p2798 N94-27802
Vortex generators for control of shock-induced separation. Part 1: Introduction and aerodynamics
[ESDU-93024-PT-1] 07 p2806 N94-28095
Vortex generators for control of shock-induced separation. Part 3: Examples of applications of vortex generators to aircraft
[ESDU-93026-PT-3] 07 p2807 N94-28096
Interaction of the sonic boom with atmospheric turbulence 07 p2650 N94-28191
Experimental study on the shock wave interaction with a hypersonic boundary layer near a convex corner 07 p2654 N94-28328
Wall pressure fluctuations in the reattachment region of a supersonic free shear layer
[NASA-CR-195790] 08 p3132 N94-29920
Development of a cascade simulation of fan-passage flow
[AD-A277234] 09 p3584 N94-32026
Numerical analysis of transonic wing buffet 09 p3586 N94-32713
An analysis of supersonic flows with low-Reynolds number compressible two-equation turbulence models using LU finite volume implicit numerical techniques
[NASA-CR-195302] 09 p3572 N94-32926
Experimental studies of shock-wave/wall-jet interaction in hypersonic flow
[NASA-CR-195844] 10 p4048 N94-34171
Partial spreading of a laser beam into a light sheet by shock waves and its use as a shock detection technique
[NASA-CR-195329] 10 p4144 N94-34923
Experimental studies of shock-wave/wall-jet interaction in hypersonic flow, part A
[NASA-CR-195957] 10 p3985 N94-34964
Experimental studies of transpiration cooling with shock interaction in hypersonic flow, part B
[NASA-CR-195958] 10 p3985 N94-34965
Investigation of Burnett equations for two-dimensional hypersonic flow
[AD-A278942] 11 p4190 N94-35717
Analysis of high speed flow, thermal and structural interactions
[NASA-CR-196017] 11 p4268 N94-36420
Hypersonic shock/boundary-layer interaction database: New and corrected data
[NASA-CR-177638] 12 p4441 N94-36519

SHOCK WAVE PROFILES
Measurement and analysis of three 1.5-GPa shock-wave profiles in copper
[DE93-016559] 04 p1451 N94-17864
Wave structure induced by fluid dynamic limits in the Broadwell model
[AD-A268512] 04 p1410 N94-18385
A new flux vector splitting scheme 07 p2657 N94-28343
Numerical simulation of unsteady aerodynamic heating induced by shock reflections 08 p3123 N94-28952
Numerical simulation of steady Mach reflection by shock capturing schemes 08 p3123 N94-28953

SHOCK WAVE PROPAGATION
Flow visualization of shock propagation in baffle systems
[DE93-013312] 01 p0147 N94-10307
Giant impact-induced atmospheric blow-off 01 p0435 N94-12019
Modeling the impact behavior of AD85 ceramic under multi-axial loading
[AD-A265877] 02 p0576 N94-12932
MHD shocks in coronal mass ejections
[NASA-CR-193418] 02 p0828 N94-12970
Studies on equatorial shock formation during plasmaspheric refilling
[NASA-CR-194392] 02 p0715 N94-13954
Laser-shock damage of iron-based materials
[AD-A267196] 03 p1038 N94-15852
On possible Mn-53 heterogeneity in the early solar system 03 p1244 N94-16344
CTH: A software family for multi-dimensional shock physics analysis
[DE93-019428] 05 p1904 N94-20052
Photopumped x ray laser research on Saturn
[DE93-019430] 05 p1816 N94-20298
The scattering and collision of gravitational waves in Friedmann-Robertson-Walker open universes
[MATHS-REPT-A-193] 06 p2406 N94-25430
Experimental and numerical investigation of shock wave propagation through complex geometry, gas continuous, two-phase media
[DE94-001408] 07 p2791 N94-26121
Approximate Riemann solvers: Improvement of the HLLEM scheme and its generalization for chemically reacting flows
[NAL-TR-1189] 07 p2795 N94-27205
Theoretical and experimental investigation of converging cylindrical shock waves propagating in narrow cylindrical chambers
[ISBN-0-315-84694-1] 07 p2795 N94-27313
High-Speed Research: Sonic Boom, Volume 1
[NASA-CP-10132] 07 p2649 N94-28188
Progress in modeling atmospheric propagation of sonic booms 07 p2650 N94-28189
Techniques for accurately solving unsteady shock waves and contact discontinuities 07 p2656 N94-28342

Numerical simulation of steady Mach reflection by shock capturing schemes 08 p3123 N94-28953
Advanced CFD methodology for fast transients encountered in nonlinear combustion instability problems. Volume 1: Theory and validation
[NASA-CR-191351] 09 p3637 N94-32696
Convection in Type 2 supernovae
[DE94-009373] 09 p3938 N94-32914
New broadband shock noise model and computer code for ANOPP 10 p3975 N94-33489
Studies on equatorial shock formation during plasmaspheric refilling
[NASA-CR-195864] 10 p4088 N94-34669

SHOCK WAVES
NT DETONATION WAVES
NT NORMAL SHOCK WAVES
NT OBLIQUE SHOCK WAVES
NT RIEMANN WAVES
NT SONIC BOOMS

Problems in the validation of CFD codes through comparison with experiment 01 p0006 N94-10441
Aerodynamic characteristics analysis of Garabedian-Korn 75-06-12 airfoil
[PAPER-2D-8] 01 p0011 N94-10473
Exergy decrease in shock waves and boundary layers of space launch vehicles
[AD-A265272] 01 p0042 N94-10493
Acceleration of positrons in supernova shocks
[NASA-CR-193713] 01 p0425 N94-10511
Evaluation of dual flow thrust vectored nozzles with exhaust stream impingement
[NASA-CR-193292] 01 p0150 N94-10912
Theoretical investigation of 3-D shock wave turbulent boundary layer interactions
[AD-A265275] 01 p0150 N94-11014
A symmetrical form for equations of a nonlinear spiral magnetic
[DE93-621350] 01 p0344 N94-11033
Turbulent wall jet in blast wave precursor
[DE93-011955] 01 p0151 N94-11144
Nonlinear aspects of transonic aeroelasticity
[UTIAS-345] 01 p0015 N94-11857
Chondrule formation by clumpy accretion onto the solar nebula 01 p0448 N94-12089
Initiating solar system formation through stellar shock waves 01 p0448 N94-12090
NMR spectroscopy of experimentally shocked single crystal quartz: A reexamination of the NMR shock barometer 01 p0081 N94-12258
Large eddy simulation of shock turbulence interaction 01 p0155 N94-12289
Analysis of Hopkinson bar pressure gage
[AD-A262366] 01 p0171 N94-12362
Computational methods for problems in aerodynamics using parallel and vector architectures
[AD-A265626] 01 p0016 N94-12377
Recovery of materials impacted at high velocity
[DE93-014150] 02 p0576 N94-12885
Micromechanical strength effects in shock compression of solids
[DE93-014425] 02 p0670 N94-12887
The 3-D massively parallel impact simulations using PCTH
[DE93-011593] 02 p0670 N94-12908
MHD shocks in coronal mass ejections
[NASA-CR-193418] 02 p0828 N94-12970
Fundamental study of shock wave/turbulent boundary layer interactions with passive control in transonic flows
[ESA-TT-1278] 02 p0630 N94-13117
Numerical simulations and experiments on physics of high Mach number shockwave: Turbulent flow interactions
[DE93-013424] 02 p0631 N94-13249
Sub-grid scale modeling for large eddy simulations in analysis of shock-turbulence interactions
[DE93-013425] 02 p0631 N94-13250
A multiphase model for shock-induced flow in low density foam
[DE93-013767] 02 p0632 N94-13397
Measuring opacity of shock generated argon plasmas
[DE93-013038] 02 p0801 N94-14312
Nonlinear wave predictions in ceramics
[DE93-016516] 02 p0582 N94-14436
Atmospheric acoustic modeling
[DE93-016727] 02 p0718 N94-14518
Comparative ignition of hexane and octane isomers in a shock tube
[DE93-016535] 02 p0566 N94-14869
Adaptive algorithm for aircraft configuration in turbulent flow
[AD-A266188] 03 p0867 N94-16122
Gas-grain energy transfer in solar nebula shock waves: Implications for the origin of chondrules 03 p1262 N94-16251
Orientation of Planar Deformation Features (PDFs) in quartz 03 p1219 N94-16341
The seismic response of an aquifer to the propagation of an impact generated shock wave: A possible trigger of the Martian outflow channels? 03 p1281 N94-16354
The structure of turbulent boundary layers and shock wave boundary layer interactions
[AD-A266240] 03 p1026 N94-16929
The shock Hugoniot of 316 SS and sound velocity measurements
[DE93-016525] 03 p1178 N94-16955
An experimental investigation of the effects of leading edge geometry on the dynamics of blunt fin-induced shock wave turbulent boundary layer interaction
[AD-A267656] 03 p0860 N94-17221
Numerical solution of SUPG finite-element method for supersonic viscous flow
[AD-A267762] 03 p0860 N94-17222
Dynamic testing and characterization of pre-fractured ceramic
[DE93-016457] 03 p0972 N94-17238
Supersonic flow visualization of a nacelle in close proximity to a simulated wing
[NASA-CR-194675] 03 p0860 N94-17260
Experimental studies on a gas dynamic laser with narrow throat and high area-ratio grid nozzles
[AD-A267818] 03 p1042 N94-17400
An experimental study of fluctuating wall pressures in a highly swept, sharp fin-induced, Mach 5 shock wave/turbulent boundary layer interaction
[AD-A268394] 03 p0861 N94-17461
Design, development and characterization studies of a large aperture high power Nd: Glass rod amplifier stage
[DE93-624944] 03 p1042 N94-17630
Shear wave measurements in shock-induced, high-pressure phases
[DE93-016461] 03 p1062 N94-17664
PVDF measurement of soft x ray induced shock and filter debris impulse
[DE93-017633] 04 p1382 N94-17806
A new multiphase equation of state for iron
[DE93-017629] 04 p1357 N94-17819
Measurement and analysis of three 1.5-GPa shock-wave profiles in copper
[DE93-016559] 04 p1451 N94-17864
Modeling shock initiation in Composition B
[DE93-016544] 04 p1376 N94-18095
Wave structure induced by fluid dynamic limits in the Broadwell model
[AD-A268512] 04 p1410 N94-18385
Introduction to spectral methods for hyperbolic system of conservation laws 04 p1413 N94-18567
Correlation of incoming boundary layer pitot pressure fluctuations with the unsteadiness of fin-induced shock wave turbulent boundary layer interactions
[AD-A270059] 04 p1417 N94-18796
Three-dimensional shock wave physics simulations with MIMD PAGOSA on massively parallel computers
[DE93-011682] 04 p1455 N94-18829
Shock propagation in crustal rock
[AD-A270148] 04 p1485 N94-18899
The effects of reverberant impulse noise (blast waves) on hearing: Parametric studies
[AD-A269242] 04 p1506 N94-18911
Visualization for applications in shock physics
[DE93-012849] 04 p1418 N94-18918
The application of front tracking to the simulation of shock refractions and shock accelerated interface mixing
[DE93-018342] 04 p1419 N94-19025
Shock-loading response of advanced materials
[DE93-018344] 04 p1455 N94-19033
Air blast measurements at 20 and 40 km distance from detonating 10 and 20 ton high explosive charges
[PB93-195949] 04 p1419 N94-19068
Experiments and analysis of lateral piezoresistance gauges
[DE93-017874] 04 p1433 N94-19111
Liquid sound speeds at pressure from the optical analyzer technique
[DE93-018362] 04 p1563 N94-19151
Impact strength and indentation hardness of high-strength ceramics
[DE93-018833] 04 p1373 N94-19338
Simulation of the impact of a plastic flyer on an aluminum block using the hydrocode AUTODYNE
[PML-1992-26] 04 p1458 N94-19444
Velocity measurements in a boundary layer with a density gradient
[DE93-019627] 04 p1422 N94-19515
Locally adaptive remeshing scheme for calculating fluid instabilities
[DE93-019577] 04 p1422 N94-19568
Shock wave interactions with exothermic mixtures
[AD-A271149] 05 p1829 N94-19836
An equation of state for shock in homogeneous materials and comparison to shock data
[AD-A271436] 05 p1829 N94-19881
Unlike-pair interactions at high pressure and high temperature
[DE93-019948] 05 p1796 N94-19916
Time-resolved shock compression of porous rutile: Wave dispersion in porous solids
[DE93-018848] 05 p1829 N94-19927
Shock response of porous Al-2 + Fe2O3 powder mixtures
[DE93-018851] 05 p1688 N94-19944
CTH: A software family for multi-dimensional shock physics analysis
[DE93-019428] 05 p1904 N94-20052
Proceedings of the 15th Annual Seismic Research Symposium
[AD-A271458] 05 p1855 N94-20090
Shape optimization governed by the Euler equations using an adjoint method
[NASA-CR-191555] 05 p1950 N94-20092
Determination of cosmic bodies size-velocity distribution by observation of current impacts on Mars 05 p2082 N94-20648
Direct simulation of shock-induced mixing layer
[DE93-040498] 05 p1803 N94-21531
Shock compression of low-density foams
[DE93-040545] 05 p1707 N94-21546
Physics of magnetospheric boundary layers
[NASA-CR-194725] 05 p1858 N94-21836
Shock temperature measurements of iron to 350 GPa
[DE94-001058] 05 p1695 N94-22024
Computer simulation of molecular response at a shock front
[DE94-001050] 05 p1977 N94-22396
Transonic flow calculations: Integral method
[ISBN-0-315-83538-9] 05 p1639 N94-22586
Formation of fast magnetosonic shock waves during two current loops collision in solar flare 05 p2005 N94-22662
Magnetic superbubbles in the galactic disk and halo 05 p2009 N94-22694
Shock formation in magnetohydrodynamical accretion onto a black hole 05 p2010 N94-22699
High pressure Hugoniot of sapphire
[DE94-001048] 06 p2558 N94-22946
Bibliographic Retrieval System (BARS), Sandia Shock Compression (SSC) database Shock Physics Index
[DE94-001679] 06 p2589 N94-23126
Bibliographic Retrieval System (BARS). Sandia Shock Compression (SSC) database Shock Physics Index (SPHINX) database. Volume 1: UNIX version query guide customized application for INGRES
[DE94-001703] 06 p2589 N94-23127
Bibliographic Retrieval System (BARS), Sandia Shock Compression (SSC) database, Shock Physics Index (SPHINX) database, Volume 2: UNIX version user's guide
[DE94-001704] 06 p2589 N94-23128
Shock-induced turbulent flow in baffle systems
[DE94-001532] 06 p2319 N94-23470
Calibration of HYPULSE for hypervelocity air flows corresponding to flight Mach numbers 13.5, 15, and 17
[NASA-CR-191578] 06 p2192 N94-23564
Energy transfer in solid explosives
[DE94-001523] 06 p2265 N94-23778
Multiple shock initiation of LX-17
[DE94-001524] 06 p2265 N94-23807
Heat pipe vapor dynamics
[NASA-CR-194217] 06 p2327 N94-24096
Effects of shock strength on shock turbulence interaction 06 p2332 N94-24165
Scientific study in solar and plasma physics relative to rocket and balloon projects
[NASA-CR-193885] 06 p2627 N94-24461
Characteristic method for one-dimensional scalar hyperbolic conservation laws with stiff source terms
[PB93-237675] 06 p2491 N94-24954
A continuing search for a near-perfect numerical flux scheme. Part 1: AUSM+
[NASA-TM-106524] 06 p2338 N94-25180
Deviatoric stresses and plastic strain rates in strong shock waves for six metals
[DE94-002964] 07 p2733 N94-26022
Iron: What is melt?
[DE94-003373] 07 p2735 N94-26322
Mix induced by single shock passage through a material interface
[DE93-019505] 07 p2792 N94-26427
Numerical simulation of the reignition of detonation by reflected shocks
[AD-A274755] 07 p2795 N94-27252
A second-order shock-adaptive Godunov scheme based on the generalized Lagrangian formulation
[ISBN-0-315-84549-X] 07 p2795 N94-27307

Theoretical and experimental investigation of converging cylindrical shock waves propagating in narrow cylindrical chambers
[ISBN-0-315-84694-1] 07 p2795 N94-27313
Collisionless shock structures of Earth and other planets
[NASA-CR-195257] 07 p3104 N94-27407
An improvement in the modified finite element procedure for underwater shock analysis
[DE94-004451] 07 p2797 N94-27617
TVD flux-difference split methods for high-speed thermochemical nonequilibrium flows with strong shocks
[UTIAS-350] 07 p2799 N94-27880
Inclined air-jets used as vortex generators to suppress shock-induced separation 07 p2659 N94-28040
Nonequilibrium radiation and chemistry models for aerocapture vehicle flowfields
[NASA-CR-195706] 07 p2648 N94-28071
Computation of static pressure downstream of a normal shock for hypersonic flight (ambient temperature known)
[ESDU-93020] 07 p2649 N94-28091
Dislocation theory of melting for iron, revisited
[DE94-002715] 08 p3355 N94-28538
Acceleration in astrophysics
[DE94-004986] 08 p3552 N94-28580
Report of National Institute for Resources and Environment. No. 8: Research on blasting sound related to it's measurement, propagation prediction, control and evaluation
[JTN-94-80605] 08 p3479 N94-29597
A multiwavelength study of two prototypical supernova remnants 08 p3540 N94-29833
Wall pressure fluctuations in the reattachment region of a supersonic free shear layer
[NASA-CR-195790] 08 p3132 N94-29920
An interactive, design and educational tool for supersonic external-compression inlets
[NASA-TM-106581] 08 p3421 N94-30174
Control of hypersonic aerodynamic forces with surface blowing 09 p3567 N94-31216
Numerical simulation of interplanetary dynamics 09 p3933 N94-31566
An adaptive method for the exact resolution of shock waves and contact discontinuities
[ISBN-0-315-86498-2] 09 p3704 N94-31799
A new inverse method for generating high-speed aerodynamic flows with application to waverider design 09 p3569 N94-31828
Shock impingement near mild hypersonic expansion corners 09 p3569 N94-31879
A study of physical conditions, radiative transfer and shocks in the interstellar medium 09 p3937 N94-31963
PVDF pressure transducers for shock wave and explosives research
[AD-A277319] 09 p3712 N94-32051
Elastic as limit of viscoelastic response, in a context of self-similar viscous limits
[AD-A277043] 09 p3738 N94-32273
Overview of shock physics codes for armor analysis
[DE94-008948] 09 p3739 N94-32842
Analysis of data from the plasma composition experiment on the International Sun-Earth Explorer (ISEE 1)
[NASA-CR-189353] 09 p3893 N94-33074
Relaxation and turbulence effects on sonic boom signatures 10 p3976 N94-33496
The effect of turbulence and molecular relaxation on sonic boom signatures 10 p3976 N94-33497
A theory and experiments for detecting shock locations
[NASA-TM-106634] 10 p4056 N94-33952
Magnetic field waves at Uranus
[NASA-CR-194807] 10 p4164 N94-34000
Experimental studies of shock-wave/wall-jet interaction in hypersonic flow
[NASA-CR-195844] 10 p4048 N94-34171
Partial spreading of a laser beam into a light sheet by shock waves and its use as a shock detection technique
[NASA-CR-195329] 10 p4144 N94-34923
Experimental studies of shock-wave/wall-jet interaction in hypersonic flow, part A
[NASA-CR-195957] 10 p3985 N94-34964
The fine structure of Langmuir waves observed upstream of the bow shock at Venus
[NASA-CR-196123] 11 p4354 N94-35378
Experimental studies of very-high Mach number hydrodynamics
[AD-A278761] 11 p4263 N94-35492
Numerical simulation of shock interaction with above-ground structures
[AD-A278713] 11 p4279 N94-35949
Plane shock generator explosive lens: Shock characterization of 4340 and PH13-8Mo steels, C360 brass and PZT 65/35 ferro-electric ceramic
[DE94-009254] 11 p4266 N94-35979
X ray radiographic imaging of hydrodynamic phenomena in radiation driven materials: Shock propagation and shear flow
[DE94-010891] 11 p4318 N94-36201
High-order centered difference methods with sharp shock resolution
[NASA-CR-196374] 12 p4496 N94-37656
A nonconservative scheme for isentropic gas dynamics
[DE94-011488] 12 p4445 N94-37724

SHOEMAKER-LEVY 9 COMET
The crash of P/Shoemaker-Levy 9 into Jupiter and its implications for comet bombardment on Earth 07 p2891 N94-28313
Comet impact 1994 animation reel
[NASA-TM-109810] 10 p4163 N94-33562
Aeronautics and Space Reports number 267: Comet impacts Jupiter
[NASA-TM-109841] 10 p4163 N94-33601
Radiative signals from impact of Shoemaker-Levy on Jupiter 11 p4355 N94-35396
Shoemaker-Levy 9 and the tidal disruption of comets 11 p4351 N94-35406

SHORELINES
Shoreline change detection using remote sensing and GIS in Vietnam 01 p0196 N94-11928
Coastal processes due to nearshore current around an upheaving island 01 p0199 N94-11942
Study on sea water purification using a substratum of marine organisms 01 p0217 N94-12696
Study of growing processes of a tombolo using an air photograph 01 p0218 N94-12702
Ecological and environmental impacts of construction in the coastal zone
[AD-A269196] 04 p1475 N94-18881
A marine sedimentary model for the evolution of the northern plains 05 p2091 N94-20395
Mapping coastal habitats using an imaging spectrometer
[ISBN-0-315-84362-4] 07 p2848 N94-26664
Digital mapping, charting, and geodesy analysis program technical review of Urban Vector Smart Map (UV(sub Map)) prototype 1
[AD-A277831] 10 p4076 N94-33832

SHORT CIRCUITS
A device for testing cables
[NASA-CASE-LAR-14093-1] 03 p1010 N94-15988
Impedence calculation with recursive folding
[ETN-93-95049] 04 p1406 N94-19387
A new test method for the assessment of the arc tracking properties of wire insulation in air, oxygen enriched atmospheres and vacuum 08 p3167 N94-28714

SHORT CRACKS
Finite element calculation of stress-intensity factors for thumb-nail cracks in DEN specimens
[LTR-ST-1929] 02 p0850 N94-13548
Finite element calculation of stress-intensity factors for thru-thickness cracks in DEN specimens
[LTR-ST-1905] 02 p0675 N94-14035
The growth of short fatigue cracks in an aluminium alloy
[RAE-TR-92063] 02 p0574 N94-14828
Early stages in the development of stress corrosion cracks
[DE94-003867] 07 p2838 N94-26524
Fatigue propagation behaviour of short cracks (1-2 mm) in steels
[ESDU-93033] 07 p2845 N94-28145
Near tip stress and strain fields for short elastic cracks 10 p4068 N94-33418

SHORT HAUL AIRCRAFT
NT A-310 AIRCRAFT
NT EUROPEAN AIRBUS
The reduction of takeoff ground roll by the application of a nose gear jump strut
[NASA-TM-108822] 11 p4198 N94-36380

SHORT TAKEOFF & VERTICAL LANDING AIRCRAFT
U STOVL AIRCRAFT

SHORT TAKEOFF AIRCRAFT
NT QUESTOL AIRCRAFT
Position error determination for the speedometer and altimeter of the NAL QSTOL experimental aircraft ASKA
[NAL-TR-1144] 02 p0517 N94-13451
Flight path control for the approach and landing of the quiet STOL experimental aircraft ASKA
[NAL-TR-1183] 02 p0513 N94-13457
An experimental study of ASTOVL related jet flows to produce CFD code validation data. Phase 3: Results of experiments
[TT-9203] 03 p1020 N94-15645
Design, development, and flight evaluation of the Boeing YC-14 USB powered lift aircraft 04 p1310 N94-18444
Lift and pitching moment induced on jet STOVL aircraft by the ground vortex
[AD-A269816] 04 p1318 N94-18733
Aircraft digital flight control technical review 06 p2163 N94-25106
Wind tunnel investigation of an STOL aircraft model: An effect of engine nacelle shape
[NAL-TM-653] 07 p2647 N94-27235
A study of jet effect and ground effect interference on a STOL fighter 07 p2671 N94-28034
Results from the STOL and Maneuver Technology Demonstration program 10 p3991 N94-34611
Direct reduced order mixed H2/H infinity control for the Short Take-Off and Landing/Maneuver Technology Demonstrator (STOL/MTD)
[AD-A278675] 11 p4199 N94-35796
The reduction of takeoff ground roll by the application of a nose gear jump strut
[NASA-TM-108822] 11 p4198 N94-36380

SHORT WAVE RADIATION
NT MICROWAVE EMISSION
NT MICROWAVES
NT MILLIMETER WAVES
NT SUBMILLIMETER WAVES
Studies of the net surface radiative flux from satellite radiances during FIFE
[NASA-CR-193150] 01 p0230 N94-10953
The use of ERBE data for climate studies 05 p1860 N94-22286
Cloud-free aerosol optical depth determination over oceans from satellite radiometry
[DE94-001897] 06 p2386 N94-23779
A physical optics model for scattering of HF radiation by irregular terrain
[DE94-006187] 08 p3255 N94-30106

SHORT WAVE RADIO TRANSMISSION
Measurements of spatial and frequency coherence of an equatorial hf path during spread-F
[DE93-016615] 11 p4257 N94-36316

SHORTENING
U REDUCTION

SHOT NOISE
JSEP fellowship: Fractal noise processes
[AD-A268841] 04 p1557 N94-18540
Wavelet transform of fixed pattern noise in focal plane arrays
[AD-A276963] 09 p3712 N94-32393

SHOT PEENING
Feasibility study of shot-peening modeling
[CTN-94-60926] 06 p2244 N94-24170
Literature review and preliminary studies of fretting and fretting fatigue including special applications to aircraft joints
[AD-A280310] 12 p4456 N94-37125

SHOULDERS
Control of shoulder muscles during goal directed movements
[PB93-195139] 04 p1504 N94-18080

SHRINKAGE
Shrinkage void formation and its effect on freeze and thaw processes of lithium and lithium-fluoride for space applications
[DE93-019303] 04 p1338 N94-19128
The use of expanding monomers in carbon fibre composites
[ISBN-0-315-83550-8] 06 p2226 N94-22890
Drying deformable media: Kinetics, shrinkage and stresses
[ETN-94-95314] 06 p2236 N94-25302
Stress relaxation in dough moulding compounds
[PB94-124872] 07 p2748 N94-25894
Innovative processing of composites for ultra-high temperature applications, book 3
[AD-A275599] 08 p3177 N94-28731
Measurement and modelling of bolted joint stress relaxation in plastics
[PB94-124849] 08 p3318 N94-28841

SHROUDED BODIES
U SHROUDS

SHROUDED PROPELLERS
Noise levels from a model turbofan engine with simulated noise control measures applied
[NASA-TM-106318] 02 p0518 N94-14036
Flow analysis for the nacelle of an advanced ducted propeller at high angle-of-attack and at cruise with boundary layer control
[NASA-TM-106371] 03 p0858 N94-16571
Flying on the ground
[NASA-TM-109825] 10 p4132 N94-33579
Subsonic aerodynamic characteristic of semispan commercial transport model with wing-mounted advanced ducted propeller operating in reverse thrust --- conducted in the Langley 14 by 22 foot subsonic wind tunnel
[NASA-TP-3427] 12 p4384 N94-37505

SHROUDED TURBINES
Bulk-Flow Analysis, part A
[NASA-CR-193911-PT-A] 07 p2796 N94-27377
Influence of impeller shroud forces on turbopump rotor dynamics 07 p2796 N94-27378

Compressibility effects on rotor forces in the leakage path between a shrouded pump impeller and its housing
07 p2796 N94-27379

SHROUDS
Cammatic: An approach to improve DSS 13 antenna gravity-loading performance 02 p0608 N94-14374
Inverse design of radial flow impellers with prescribed velocity at hub and shroud 10 p4002 N94-34448
The electrical conductivities of candidate beam-waveguide antenna shroud materials
11 p4252 N94-35546

SHUNTS
U BYPASSES
U CIRCUITS

SHUTDOWNS
Impact of shutting down en route primary radars within CONUS interior
[DOT-VNTSC-FAA-93-1] 01 p0023 N94-11626
Aircraft turbine engine reliability and inspection investigations
[AD-A274860] 07 p2673 N94-26176
Startup and shutdown of the PULSAR Tokamak Reactor
[DE94-013128] 12 p4528 N94-37292

SHUTTLE BOOSTERS
U SPACE SHUTTLE BOOSTERS

SHUTTLE DERIVED VEHICLES
Shuttle-C, the future is now
[NASA-TM-109355] 04 p1332 N94-18954

SHUTTLE ENGINEERING SIMULATOR
STS-32 LDEF approach in SES
[NASA-TM-109474] 03 p0880 N94-15379
Status report of RMS active damping augmentation
07 p2684 N94-26285

SHUTTLE GLOW
U SPACECRAFT GLOW

SHUTTLE IMAGING RADAR
Spaceborne Imaging Radar-C instrument
03 p0990 N94-15890
X-SAR: The X-band synthetic aperture radar on board the Space Shuttle 03 p0990 N94-15891
Spaceborne radar for geoscientific applications in North China 03 p0993 N94-15915
Mission planning for Shuttle Imaging Radar-C (SIR-C) with a real-time interactive planning software
06 p2305 N94-23842
Precipitation measurement using SIR-C: A feasibility study
[NASA-CR-195104] 06 p2409 N94-24048
Precipitation measurement using SIR-C: A feasibility study. Investigation at nadir
[NASA-CR-195103] 06 p2410 N94-24126
Pointing mechanisms for the Shuttle Radar Laboratory
08 p3162 N94-29638
Optimal geological data extraction from SPOT-radar synergism with samples from Djebel Amour (Algeria), Red Sea Hills (Sudan), Sirte Basin (Libya), and Magdalena Valley (Colombia) 09 p3752 N94-32548

SHUTTLE MISSION SIMULATOR
Analysis of differences between seating positions in simulators and orbiters
[NASA-TM-104776] 02 p0737 N94-13399

SHUTTLE ORBITERS
U SPACE SHUTTLE ORBITERS

SI
U INTERNATIONAL SYSTEM OF UNITS

SIALON
Compositions and chemical bonding in ceramics by quantitative electron energy-loss spectrometry
[DE94-007208] 09 p3659 N94-32640

SIBERIA
Assimilation of solids during ascent of magmas from the Bartoy Field of the Baikal Region, Siberia
03 p1103 N94-16214
Primary differentiation in the early Earth: Nd and Sr isotopic evidence from diamondiferous eclogites for both old depleted and old enriched mantle, Yakutia, Siberia
05 p1862 N94-20776

SICKNESSES
NT ALTITUDE SICKNESS
NT DECOMPRESSION SICKNESS
Self-Motion Perception and Motion Sickness
[NASA-CR-194276] 05 p1885 N94-21897
Chronic obstructive pulmonary disease
06 p2425 N94-23324

SID (IONOSPHERIC DISTURBANCES)
U SUDDEN IONOSPHERIC DISTURBANCES

SIDE-LOOKING RADAR
Artificial oil pollution detection and wave observation in the sea adjacent to Japan by ERS-1 SAR
01 p0253 N94-12520
A comparative evaluation of SAR and SLAR
[DE94-002922] 07 p2848 N94-26277
Evaluation of synthetic aperture radar for oil-spill response
[AD-A278796] 11 p4284 N94-35674

SIDEBANDS
Numerical simulation of sidebands in free electron laser oscillators
[DE93-612675] 01 p0173 N94-10483
Experiments in sideband suppression on the Los Alamos National Laboratory Free-Electron Laser
[DE93-014466] 04 p1435 N94-17724
Direct digital RF synthesis and modulation for MSAT mobile applications 06 p2285 N94-22804

SIDELOBE REDUCTION
Improvements on the design of optimum SAW filters with the Remez Exchange Algorithm
05 p1773 N94-22123
MTI compatible coherent sidelobe canceller
[AD-D016300] 12 p4435 N94-37771

SIDELOBES
Adaptive beamforming with imperfect arrays: Pattern effects and their partial correction
[AD-A267079] 03 p0987 N94-15541
Frequency resolution of an acousto-optical spectrometer
[AD-A267822] 03 p1035 N94-17401
Nontraditional windows in spectral analysis
[AD-A271336] 04 p1553 N94-19583
Analyzing adaptive beamformer performance in a stable multipath environment
[AD-A274029] 07 p2766 N94-25766
A new guided wave lens structure and its application
[AD-A275541] 08 p3499 N94-28813
Low sidelobe reflector antenna design for communications
[AD-A276079] 09 p3673 N94-31463

SIDEREAL TIME
A method to determine asteroid poles
01 p0431 N94-12205

SIDERITE METEORITES
U IRON METEORITES

SIDERITES
More shock recovery experiments on mesosiderite analogs 11 p4351 N94-35455

SIDESLIP
Experimental study of vortex and aerodynamic characteristics of stack wings with sideslip
[AD-A267722] 03 p0860 N94-17274
Utilization of lasers for air data measurements
05 p1640 N94-22603
Pressure distributions on a 0.02-scale Space Shuttle orbiter nose at Mach 21.5 in helium
[NASA-TM-4495] 07 p2646 N94-26592
Contribution of body-mounted fins and tailplanes to lateral derivatives due to sideslip at subsonic speeds for general body width to height ratio
[ESDU-93007] 07 p2648 N94-28057
Wind tunnel measurements on a full-scale F/A-18 with a tangentially blowing slot — conducted in the Ames 80 by 120 foot wind tunnel 11 p4191 N94-35965

SIDEWINDER MISSILES
Parametric study of a finite element model of the Sidewinder missile
[AD-A267245] 03 p0865 N94-14976

SIEVES
Methane challenge of high performance molecular sieve oxygen concentrator
[AD-A275155] 08 p3337 N94-29033
Be3(AsO4)2.2H2O, a new berylloarsenate phase containing bridged tetrahedral 3-rings
[AD-A278826] 11 p4340 N94-35677

SIGHT
U VISUAL PERCEPTION

SIGNAL ANALYSIS
NT CEPSTRAL ANALYSIS
Signal feature analysis using neural networks and psychoacoustics
[AD-A266048] 01 p0340 N94-12398
A new formulation of longitudinal coherent instabilities
[DE93-014288] 02 p0789 N94-13220
The DREO Elint Browser Utility (DEBU) reference manual
[DSIS-92-03900] 02 p0603 N94-13837
Advanced Communications ESM System (ACES) testbed: Integration study
[DSIS-93-00345] 02 p0604 N94-13939
Envelope and instantaneous frequency estimation of narrowband modulated signals
[DREO-TN-92-3] 02 p0605 N94-14033
Deconvolution for positive signals
[DE93-013044] 02 p0773 N94-14314
Utilization of boundary element method for extraction of frequency dependent conductivity parameters of lossy intra-chip transmission lines
[ETN-93-94385] 02 p0771 N94-14807
Optimization of a subband coding for high definition television with motion controlled three dimensional frequency band decomposition
[ETN-93-94396] 02 p0617 N94-14817
Develop advanced nonlinear signal analysis topographical mapping system
[NASA-CR-194577] 03 p1082 N94-15646
Automatic suppression of anomalous propagation clutter for noncoherent weather radars
[KNMI-WR-92-06] 03 p1004 N94-17407
A non-homogeneous, spatio-temporal, wavelet multiresolution analysis and its application to the analysis of motion
[AD-A270621] 04 p1538 N94-19534
Use of switched capacitor filters to implement the discrete wavelet transform 05 p1755 N94-21097
Estimation of AR signal patterns using competitive neural networks 05 p1744 N94-22102
Signal classification and noise filtering using artificial neural networks 05 p1744 N94-22103
Segmentation and frequency domain ML pitch estimation of speech signals 05 p1747 N94-22212
Experiments with recursive estimation in astronomical image processing 05 p2047 N94-22457
Verification of the PROS timing analysis package
05 p1926 N94-22508
Automatic modulation recognition based on spatial pattern classification using artificial neural networks
[CTN-94-60897] 06 p2296 N94-24115
Detection and analysis of unbalanced QPSK in Gaussian noise, version 1.0
[DREO-12-020.1] 06 p2296 N94-24131
On the analysis of clear air radar echoes severely contaminated by clutter 06 p2306 N94-24423
Develop advanced nonlinear signal analysis topographical mapping system
[NASA-CR-195128] 06 p2388 N94-24827
Develop advanced nonlinear signal analysis topographical mapping system
[NASA-CR-194785] 06 p2389 N94-24856
Parametric time-scale methods in signal analysis
[AD-A274212] 07 p2773 N94-27068
Trace organic chemical detection using an ultraviolet excitation molecular beam fluorometer
[DE94-002649] 07 p2704 N94-27708
MUSIC for localization of thunderstorm cells
[DE94-004985] 07 p2897 N94-28146
SPC toolbox: An interactive MATLAB (tm) package for signal modeling, analysis, and communications
[AD-A275617] 08 p3241 N94-28634
The Stroemberg wavelet on the interval and the Franklin system
[TELECOM-93-C-002] 08 p3462 N94-30971
Automatic modulation recognition
09 p3686 N94-33153
Dyadic wavelet features for isolated word speaker dependent speech recognition
[AD-A278492] 10 p4034 N94-33756

SIGNAL ANALYZERS
Adaptive Signal Processing Testbed
[DSIS-93-00258] 02 p0604 N94-13869
Coherent transient systems evaluation
[AD-A268808] 04 p1576 N94-18204
Widget: A data acquisition system for a balloon borne Si particle calorimeter
[DE93-624668] 04 p1630 N94-18762
Dimensional analysis of acoustically propagated signals 06 p2528 N94-24217
Some subjects in digital audio, noise shaping, sample rate conversion, dynamic range compression and testing
[ISBN-9-09-005162-7] 06 p2530 N94-25220
Rapid prototyping of application specific signal processors (RASSP)
[AD-A274324] 07 p2772 N94-26884
Surface forward-scattered acoustic measurements and analysis
[AD-A276998] 09 p3788 N94-32000
Design of free space interconnected signal processor
[AD-A278129] 09 p3683 N94-33093

SIGNAL DETECTION
NT CORRELATION DETECTION
The theory for, and demonstration of, information theory applied to radar target identification
[DE93-006393] 01 p0132 N94-10315
Signal detection theory and methods for evaluating human performance in decision tasks
01 p0314 N94-11531
Comparison of multiresolution techniques for digital signal processing
[AD-A265364] 01 p0138 N94-12406
Signal design for data communication through rapidly varying linear channels
[ITN-93-85195] 02 p0601 N94-13567
A review of robust detection
[DSIS-93-00400] 02 p0603 N94-13829
Trellis coding with Continuous Phase Modulation (CPM) for satellite-based land-mobile communications
[NASA-CR-191325] 02 p0604 N94-13909

Advanced Communications ESM System (ACES) testbed: Integration study
[DSIS-93-00345] 02 p0604 N94-13939
Determining neural network connectivity using evolutionary programming
[AD-A266853] 02 p0766 N94-14882
New methods of generation of ultrashort laser pulses for ranging 03 p0913 N94-15565
Develop advanced nonlinear signal analysis topographical mapping system
[NASA-CR-194577] 03 p1082 N94-15646
Signal processing in impulsive electromagnetic interference
[AD-A266425] 03 p0998 N94-16557
Search for Extraterrestrial Intelligence (SETI) 03 p1125 N94-16620
Efficient computational methods to study new and innovative signal detection techniques in SETI
[NASA-CR-193602] 03 p0998 N94-16649
States of awareness 1: Subliminal perception relationship to situational awareness
[AD-A267249] 03 p1132 N94-16942
Signal detection in correlated Gaussian and non-Gaussian radar clutter
[AD-A267453] 03 p1001 N94-17033
A RFI measurement system for field sites
[AD-A269340] 04 p1385 N94-18301
Wavelet transform for time-frequency analysis of the vibrational signature and its application
[AD-A269928] 04 p1454 N94-18661
Generalized multichannel signal detection
[AD-A271385] 04 p1391 N94-19587
State-space models for multichannel detection
[AD-A270608] 05 p1715 N94-19816
Statistical fluctuations in lasers
[DE94-000710] 05 p1817 N94-20939
Evaluation of a nonlinear method for the enhancement of tonal signal detection
[NASA-CR-191562] 05 p1968 N94-21741
Asynchronous detection of SSB-SC data signals 05 p1747 N94-22217
Detection and analysis of unbalanced QPSK in Gaussian noise, version 1.0
[DREO-12-020.1] 06 p2296 N94-24131
Effects of atmospheric variations on acoustic system performance 06 p2527 N94-24211
Auditory spectro-temporal pattern analysis
[AD-A273554] 06 p2427 N94-24865
Evolving neural network connectivity
[AD-A273134] 06 p2490 N94-24921
Choice of filters for the detection of gravitational waves from coalescing binaries. 2: Detection in coloured noise
[DE93-616844] 06 p2604 N94-25211
A parallel algorithm for filtering gravitational waves from coalescing binaries
[DE93-616845] 06 p2604 N94-25212
Detection of transient vector-fields in additive noise
[FFI-93/7028] 07 p2768 N94-26232
Prewhitening of colored noise fields for detection of threshold sources
[AD-A274346] 07 p3010 N94-26923
Short-block data detection techniques employing channel estimation for fading time-dispersive channels
[ISBN-0-315-58970-1] 07 p2777 N94-27806
Acquisition time analysis of noncoherent PN sequence acquisition schemes
[AD-A275017] 08 p3244 N94-29094
Detection methods for stealth radio signals: A literature survey
[PB94-137452] 08 p3244 N94-29176
A review of signal detection using the bispectrum with applications in underwater acoustics
[AD-A275227] 08 p3478 N94-29388
Partially coherent detection of PSK signals in Rician channels
[ISBN-0-315-85799-4] 08 p3254 N94-30031
Sampling behaviour in a four instrument monitoring task: Effects of signal bandwidth and number of events per signal
[AD-B179613] 08 p3402 N94-30422
Some applications of GPS timing information 08 p3145 N94-30661
Optimal detector strategies for the phase contrast imaging for scanning transmission electron microscopes
[ETN-94-95747] 09 p3866 N94-31613
Auditory perception
[AD-A277414] 09 p3800 N94-32419
Mechanisms of temporal pattern discrimination by human observers
[AD-A277407] 09 p3801 N94-32577
Nonlocal methods for signal detection and estimation in the dependent nonstationary environment
[AD-A278472] 10 p4033 N94-33594
Multiparameter bifurcations and applications
[AD-A278365] 10 p4133 N94-33858
Detection of possible burst transmissions in a dense signal environment
[PB94-149259] 10 p4036 N94-34109
Spacecraft-spacecraft radio-metric tracking: Signal acquisition requirements and application to Mars approach navigation 11 p4254 N94-35557
Attention and signal detection. A study of attention divided between visual and auditory signals
[PB94-170594] 11 p4298 N94-36215
Distributed detection theory and data fusion
[AD-A280410] 12 p4434 N94-37183

SIGNAL DETECTORS
Observations of optical counterparts of Gamma-Ray bursts
[NASA-CR-193573] 01 p0485 N94-12589
Portable acoustic wave sensor systems for real-time monitoring of volatile organic compounds
[DE93-013753] 02 p0582 N94-14511
Two wavelength satellite laser ranging using SPAD 03 p0916 N94-15584
Development and analysis of ARMA parameter estimation schemes in the presence of noise
[AD-A267184] 03 p0989 N94-15786
High resolution radar profiling using higher-order statistics
[AD-D015891] 03 p1000 N94-16918
Signal detection in correlated Gaussian and non-Gaussian radar clutter
[AD-A267453] 03 p1001 N94-17033
Monolithic low noise preamplifier for piezoelectric sensors
[AD-D015860] 04 p1563 N94-18734
Mathematical model and analysis of the Tactical Unmanned Ground Vehicle (TUGV) using computer simulation
[AD-A272258] 05 p1824 N94-20576
Surface acoustic wave sensing of VOC's in harsh chemical environments
[DE93-040721] 05 p1968 N94-21751
The detection performance of a long-term spectral integrator using normalized and quantized data
[DREP-TM-93-11] 06 p2455 N94-24130
Signal amplifier-shapers for multiwire detectors
[DE93-634171] 07 p2783 N94-26438
High temperature sensor/microphone development for active noise control
[NASA-CR-195214] 07 p2812 N94-27214
A magnetically coupled quench detector for superconducting magnets
[DE94-006040] 08 p3268 N94-30904

SIGNAL DISCRIMINATORS
U SIGNAL DETECTORS

SIGNAL DISTORTION
NRL review for 1993
[AD-A265666] 01 p0497 N94-12334
Use of switched capacitor filters to implement the discrete wavelet transform 05 p1755 N94-21097
Night vision devices and characteristics 06 p2432 N94-23982
Three dimensional transient analysis of microstrip circuits in multilayered anisotropic media
[AD-A274995] 08 p3263 N94-28995
Kalman filtering approach to blind equalization
[AD-A276320] 09 p3671 N94-31299
Measurements of spatial and frequency coherence of an equatorial hf path during spread-F
[DE93-016615] 11 p4257 N94-36316

SIGNAL ENCODING
NT AMPLITUDE MODULATION
NT BINARY PHASE SHIFT KEYING
NT DELTA MODULATION
NT DIFFERENTIAL PULSE CODE MODULATION
NT FM/PM (MODULATION)
NT FREQUENCY MODULATION
NT FREQUENCY SHIFT KEYING
NT PHASE MODULATION
NT PHASE SHIFT KEYING
NT PULSE CODE MODULATION
NT PULSE DURATION MODULATION
NT PULSE MODULATION
NT PULSE POSITION MODULATION
NT QUADRATURE AMPLITUDE MODULATION
NT QUADRATURE PHASE SHIFT KEYING
NT TRELLIS CODING
Necessary conditions for the optimality of variable rate residual vector quantizers
[NASA-CR-193730] 01 p0326 N94-11197
Flexible high-speed CODEC
[NASA-CR-191169] 01 p0146 N94-12433
Recursive time-varying filter banks for subband image coding
[NASA-CR-193726] 02 p0598 N94-12920
Digital sound: The selection of critical programme material and preparation of recordings for CCIR tests on low bit-rate codecs
[BBC-RD-1993/1] 02 p0598 N94-12925
Digital sound: Subjective tests on commentary-quality codecs
[BBC-RD-1993/2] 02 p0598 N94-12926
Exact reconstruction analysis/synthesis filter banks with time-varying filters
[NASA-CR-193725] 02 p0600 N94-13466
Speaker independent recognition of isolated words using vector quantization and neural networks
[ETN-93-94390] 02 p0616 N94-14724
Optimization of a subband coding for high definition television with motion controlled three dimensional frequency band decomposition
[ETN-93-94396] 02 p0617 N94-14817
Friction drive position transducer
[AD-D015851] 04 p1424 N94-17717
Design of a new squaring function for the Viterbi algorithm 05 p1764 N94-21699
Schematic driven layout of Reed Solomon encoders 05 p1766 N94-21722
Encoding and decoding quasi-spherical signal sets 05 p1747 N94-22233
Algorithms for speech coding systems based on linear prediction
[EUT-92-E-260] 06 p2447 N94-22731
Encoders for space applications 06 p2363 N94-24046
Speech coding at low to medium bit rates
[ISBN-0-315-84012-9] 07 p2770 N94-26630
Coded communications with nonideal interleaving
[ITN-94-85235] 07 p2774 N94-27242
Non-orthogonal subband/transform coder
[NASA-CASE-LEW-15310-1] 08 p3246 N94-29589
A simple, low overhead data compression algorithm for converting lossy compression processes to lossless
[AD-A277905] 10 p4104 N94-33602
Studies on image compression and image reconstruction
[NASA-CR-196304] 12 p4433 N94-36810

SIGNAL FADEOUT
U SIGNAL FADING

SIGNAL FADING
NT SELECTIVE FADING
Long duration measurements of fading on a low elevation angle, 11-GHz satellite path 02 p0613 N94-14661
Large-scale rainfall diversity for ACTS 02 p0613 N94-14662
Rain rate duration statistics derived from the Mid-Atlantic coast rain gauge network 02 p0614 N94-14663
Contribution towards a draft revision of recommendations 681: Propagation data required for the design of Earth-space land mobile telecommunications systems 02 p0614 N94-14666
Characterisation of the LMS propagation channel at L- and S-bands: Narrowband experimental data and channel modelling 02 p0615 N94-14669
Results of multiband (L, S, Ku band) propagation measurements and model for high elevation angle land mobile satellite channel 02 p0615 N94-14670
Tree attenuation at 20 GHz: Foliage effects 02 p0615 N94-14672
Expansions of cumulative distribution functions directly from characteristic functions
[AD-A267727] 03 p1173 N94-17372
Radio wave propagation in structured ionization for satellite and radar applications
[AD-A268457] 04 p1382 N94-17844
The influence of lowpass filtering and the effects of fading on the group demodulation of QPSK signals 05 p1746 N94-22170
ARQ on fading channels 05 p1747 N94-22242
Performance of RS codes in lognormally shadowed Rician channels 05 p1792 N94-22244
Power attenuation characteristics as switch-over criterion in personal satellite mobile communications 06 p2277 N94-22756
ROCSAT-1 telecommunication experiments 06 p2279 N94-22770
Land mobile satellite propagation measurements in Japan using ETS-V satellite 06 p2282 N94-22790
K-band mobile propagation measurements using ACTS 06 p2283 N94-22792
Electromagnetic field strength prediction in an urban environment: A useful tool for the planning of LMSS 06 p2283 N94-22795
Systems implications of L-band fade data statistics for LEO mobile systems 06 p2284 N94-22799
Asynchronous timing and Doppler recovery in DSP based DPSK modems for fixed and mobile satellite applications 06 p2285 N94-22805
Separable concatenated codes with iterative map decoding for Rician fading channels 06 p2286 N94-22815
Diversity reception for advanced multi-satellite networks: A CDMA approach 06 p2286 N94-22816
Adaptive power control as a fade countermeasure on satellite links 08 p3253 N94-29897

Measurements of spatial and frequency coherence of an equatorial hf path during spread-F
[DE93-016615] 11 p4257 N94-36316

SIGNAL FLOW GRAPHS
SPROC: A multiple-processor DSP IC
04 p1398 N94-18347
A real-time convolution algorithm and architecture with applications in SAR processing
[AD-A273817] 07 p2959 N94-25963

SIGNAL GENERATORS
NT FREQUENCY SYNTHESIZERS
NT FUNCTION GENERATORS
Dielectric resonator
[US-PATENT-4,580,116] 01 p0141 N94-10668
Performance results of a digital test signal generator
02 p0609 N94-14382
The flight performance of the Galileo orbiter USO
02 p0611 N94-14398
Synchronous sampling phase and amplitude detection method and apparatus
[NASA-CASE-LAR-14725-1] 03 p1050 N94-15870
Improvements to pulsed phase locked loop strain monitor
[NASA-CASE-LAR-14887-1] 03 p1033 N94-15877
SATCOM simulator speeds MSS deployment and lowers costs 06 p2287 N94-22822
Digital test signal generation: An accurate SNR calibration approach for the DSN
06 p2305 N94-23912
System for producing synchronized signals
[AD-D016003] 06 p2302 N94-25057
Periodic and chaotic signal generation in a recursive artificial neural network 09 p3686 N94-33155
Arbitrary waveform generator
[AD-D016123] 10 p4041 N94-34149

SIGNAL MEASUREMENT
A new method of time difference measurement: The time difference method by dual phase coincidence points detection 01 p0357 N94-11002
Building penetration loss measurements for DAB signals at 211 MHz
[BBC-RD-1992/14] 01 p0133 N94-11024
Measurement of wave propagation for VHF/UHF and a comparison between measured and predicted values
[FFI/RAPPORT-92/7024] 02 p0605 N94-13968
Variable wide band fiber optic delay line
[AD-D015848] 04 p1576 N94-17716
The detection performance of a long-term spectral integrator using normalized and quantized data
[DREP-TM-93-11] 06 p2455 N94-24130

SIGNAL MIXING
Multi-channel spatialization systems for audio signals
[NASA-CASE-ARC-12013-1-CU]
08 p3245 N94-29364

SIGNAL PROCESSING
Variable rate transfer of optical information
[AD-D015758] 01 p0418 N94-10374
Wideband beamforming for a sparse nonuniform spaced sensor array
[AD-A265909] 01 p0133 N94-10660
Basic experiment on an ultrasonic method of localization
[DE93-754295] 01 p0358 N94-11042
Generalization of Dyson criterion for the amplitude-phase fluctuations case and for the system of interferometers 01 p0135 N94-11067
Necessary conditions for the optimality of variable rate residual vector quantizers
[NASA-CR-193730] 01 p0326 N94-11197
Chaotic time series analysis 01 p0031 N94-11490
Limited bandwidth microwave filter
[AD-D015744] 01 p0145 N94-12322
Comparison of multiresolution techniques for digital signal processing
[AD-A265364] 01 p0138 N94-12406
Ocean acoustic processing: A model-based approach
[DE93-011902] 02 p0725 N94-12876
Digital sound: The selection of critical programme material and preparation of recordings for CCIR tests on low bit-rate codecs
[BBC-RD-1993/1] 02 p0598 N94-12925
Digital sound: Subjective tests on commentary-quality codecs
[BBC-RD-1993/2] 02 p0598 N94-12926
An experimental study of tether reel system: A laboratory model
[NAL-TR-1176T] 02 p0539 N94-12943
HYMOSS signal processing for pushbroom spectral imaging
[NASA-CR-191341] 02 p0620 N94-13125
Exact reconstruction analysis/synthesis filter banks with time-varying filters
[NASA-CR-193725] 02 p0600 N94-13466
Signal design for data communication through rapidly varying linear channels
[ITN-93-85195] 02 p0601 N94-13567
Kalman filter based architectures for interference excision
[DSIS-93-00034] 02 p0603 N94-13818
Acousto-optical post-processor time-integrating correlator updates
[DSIS-93-00314] 02 p0777 N94-13831
Digital quadrature demodulation for radar ESM applications
[DREO-TN-92-10] 02 p0603 N94-13838
VMEC30 programming library: Reference manual
[DSIS-93-00350] 02 p0750 N94-13858
Adaptive Signal Processing Testbed
[DSIS-93-00258] 02 p0604 N94-13869
Adaptive Signal Processing Testbed: Software design specification
[DSIS-93-00259] 02 p0604 N94-13870
Advanced Communications ESM System (ACES) testbed: Integration study
[DSIS-93-00345] 02 p0604 N94-13939
VMEC30 software development: Tutorial manual
[DSIS-93-00351] 02 p0750 N94-13944
A rocket-borne lidar for studies of the middle atmosphere
[FFI/RAPPORT-92/7034] 02 p0715 N94-13949
Demonstration and acceptance test plan for real-time excision software on the Adaptive Signal Processing Testbed
[DSIS-93-00275] 02 p0751 N94-13990
ASPT software source code: SUN driver package
[DSIS-93-00262] 02 p0751 N94-14014
Adaptive Signal Processing Testbed: VME-based DSP board market survey
[DSIS-93-00274] 02 p0605 N94-14015
ASPT software source code: Development system package, VME-C30 component
[DSIS-93-00276] 02 p0751 N94-14016
Adaptive Signal Processing Testbed signal excision software: User's manual
[DSIS-93-00260] 02 p0606 N94-14037
Adaptive Signal Processing Testbed application software: User's manual
[DSIS-93-00261] 02 p0606 N94-14038
VMEC30 SUN software development utilities: User's manual
[DSIS-93-00348] 02 p0752 N94-14051
VMEC30 SUN device drivers: User's manual
[DSIS-93-00349] 02 p0752 N94-14052
Testing various time-frequency distribution techniques
[DREO-TN-92-17] 02 p0606 N94-14062
I/Q demodulation of radar signals with calibration and filtering
[DREO-RN-1119] 02 p0606 N94-14064
EWTEST signal excision testbed: System evaluation
[DSIS-93-00346] 02 p0607 N94-14065
DSP software development environments for the Adaptive Signal Processing Testbed
[DSIS-93-00347] 02 p0607 N94-14066
ASPT software source code: Host development system package
[DSIS-93-00277] 02 p0753 N94-14197
An exact processing algorithm for wide beam spaceborne SAR data 02 p0689 N94-14213
Deconvolution for positive signals
[DE93-013044] 02 p0773 N94-14314
FLATDAN beamformer enhancements and testing
[DSIS-93-00287] 02 p0777 N94-14360
Stability measurements of the radio science system at the 34-m high-efficiency antennas
02 p0609 N94-14381
Preliminary design and implementation of the baseline digital baseband architecture for advanced deep space transponders 02 p0611 N94-14393
Determining neural network connectivity using evolutionary programming
[AD-A266853] 02 p0766 N94-14882
VLSI for high-speed digital signal processing
[AD-A267709] 03 p1007 N94-14936
Optical residue processing module
[AD-A267721] 03 p1188 N94-14940
Compact disk error measurements
03 p1227 N94-14988
Broadband conventional beamforming incorporating adaptive equalization
[AD-A267090] 03 p0987 N94-15544
New methods of generation of ultrashort laser pulses for ranging 03 p0913 N94-15565
Test results from LAGEOS-2 optical characterization using pulsed lasers 03 p0915 N94-15577
Exploitation of cyclostationarity for signal-parameter estimation and system identification
[AD-A267137] 03 p0988 N94-15690
Higher order statistics in signal processing
[FFI-92/2008] 03 p0989 N94-15714
Simultaneous measurement of temperature and strain using four connecting wires
[NASA-TM-104271] 03 p1032 N94-15754
The bootstrapped algorithm: Fast algorithm for blind signal separation
[AD-A266671] 03 p1147 N94-15772
Development and analysis of ARMA parameter estimation schemes in the presence of noise
[AD-A267184] 03 p0989 N94-15786
Synthetic aperture radar signal processing: Trends and technologies 03 p0992 N94-15908
Windshear detection radar signal processing studies
[NASA-CR-194615] 03 p0994 N94-16022
Passive tracking of a target using an array of sensors
[DE93-015870] 03 p0997 N94-16169
Signal processing in impulsive electromagnetic interference
[AD-A266425] 03 p0998 N94-16557
Search for Extraterrestrial Intelligence (SETI)
03 p1125 N94-16620
Efficient computational methods to study new and innovative signal detection techniques in SETI
[NASA-CR-193602] 03 p0998 N94-16649
Reducing data dimension to lower signal processing computational requirements and maximize performance
[AD-A266606] 03 p0999 N94-16728
Analysis of temporal symmetry in non-gaussian random fields
[AD-A266496] 03 p0999 N94-16794
High resolution radar profiling using higher-order statistics
[AD-D015891] 03 p1000 N94-16918
Digital reverberation time measurement system
[AD-D015892] 03 p1177 N94-16919
Reference frames in vision
[AD-A266174] 03 p1132 N94-16925
Natural convection above a horizontal heat source
[AD-A267212] 03 p1026 N94-16965
Intelligent use of CFAR algorithms
[AD-A267755] 03 p1003 N94-17206
Method and apparatus for spur-reduced digital sinusoid synthesis
[NASA-CASE-NPO-18789-1-CU]
03 p1154 N94-17326
Asymmetric three-beam binary optic grating
03 p1195 N94-17340
Theory of dispersive microlenses
03 p1198 N94-17361
Expansions of cumulative distribution functions directly from characteristic functions
[AD-A267727] 03 p1173 N94-17372
High order nonlinear estimation with signal processing applications
[AD-A268407] 03 p1005 N94-17463
Fabrication of a NAVMAP, a deep-sea mapping system
[AD-A268630] 03 p1085 N94-17467
Femtosecond carrier processes in compound semiconductors and real time signal processing
[AD-A268122] 03 p1005 N94-17519
Activities of the Research Laboratory of Electronics
[AD-A266730] 03 p1304 N94-17651
Design of a general purpose and autonomous transmitter and receiver system for underwater acoustic experiments at sea
[AD-A269268] 04 p1495 N94-17822
Development and test of readout electronics for optical quadrature signals
[DLR-MITT-92-11] 04 p1395 N94-17920
Neural networks to classify speaker independent isolated words recorded in radio car environments
[REPT-93-013] 04 p1383 N94-17935
Analysis, representation and processing of the instrumental gesture: Application to keyboard instruments
[ETN-93-94402] 04 p1519 N94-17977
Coherent transient systems evaluation
[AD-A268808] 04 p1576 N94-18704
Magnetostatic waves-based integrated optic bragg cell modules with applications to RF signal processing
[AD-A269115] 04 p1577 N94-18295
Single phase dynamic CMOS PLA using charge sharing technique 04 p1397 N94-18341
SPROC: A multiple-processor DSP IC
04 p1398 N94-18347
An improved distributed arithmetic architecture
04 p1398 N94-18349
Low power signal processing research at Stanford
04 p1393 N94-18351
High accuracy switched-current circuits using an improved dynamic mirror 04 p1401 N94-18368
A verification logic representation of indeterministic signal states 04 p1401 N94-18372
On timing faults in digital logic circuits
[AD-A268714] 04 p1402 N94-18400
The identification of the computational significance of key neurobiological characteristics found in a number of telencephalic brain regions
[AD-A269374] 04 p1505 N94-18407

Development of parallel architectures for sensor array processing, volume 1
[AD-A270426] 04 p1534 N94-18507
Development of parallel architectures for sensor array processing. Volume 2: A parallel architecture for broad-band direction-of-arrival estimation
[AD-A270427] 04 p1534 N94-18508
Data acquisition in aerodynamic research 04 p1431 N94-18644
A general theory of signal integration for fault-tolerant dynamic distributed sensor networks
[AD-A270316] 04 p1534 N94-18699
VLSI for high-speed digital signal processing
[AD-A270406] 04 p1404 N94-18706
Programmable linear phase digital filters
[AD-A270413] 04 p1404 N94-18709
Monolithic low noise preamplifier for piezoelectric sensors
[AD-D015860] 04 p1563 N94-18734
Widget: A data acquisition system for a balloon borne Si particle calorimeter
[DE93-624668] 04 p1630 N94-18762
Neutral networks: An NRL perspective
[AD-A269122] 04 p1541 N94-18773
Spectral analysis on the canonical autoregressive decomposition
[AD-A270083] 04 p1549 N94-18798
Analytic approximations of an integral in remote sensing
[AD-A270085] 04 p1463 N94-18800
Introduction to wavelets
[AD-A268465] 04 p1389 N94-18801
Numerical and symbolic signal representation and processing
[AD-A270271] 04 p1389 N94-18811
A parallel and pipelined architecture for estimation of direction of arrival using a bilinear transformation method, volume 3
[AD-A270137] 04 p1389 N94-18897
Solution of the Poisson equation with application to radar imaging
[PB93-195865] 04 p1389 N94-18950
MIMD massively parallel methods for engineering and science problems
[DE93-019409] 04 p1531 N94-19562
Generalized multichannel signal detection
[AD-A271385] 04 p1391 N94-19587
A multi-level data-flow architecture for signal and data processing applications
[DE93-041272] 04 p1539 N94-19588
Systolic design with asynchronous controls for digital-signal processing
[AD-A270976] 04 p1392 N94-19680
Signal processing algorithms for heterogeneous architectures
[AD-A271248] 04 p1392 N94-19724
Algorithms and architectures for high speed signal processing
[AD-A271000] 04 p1392 N94-19736
Transcutaneous Analyte Measuring Methods (TAMM)
[AD-A271387] 04 p1408 N94-19756
A pipelined superconducting digital processor
[DE93-040852] 05 p1898 N94-19886
Literature review of the errors-in-variables approach to the problem of system identification
[AD-A271098] 05 p1949 N94-19907
Optical signal processing
[AD-A271036] 05 p1983 N94-20013
Proceedings of the 15th Annual Seismic Research Symposium
[AD-A271458] 05 p1855 N94-20090
Application of change detection to dynamic contact sensing
[AD-A270523] 05 p1939 N94-20105
Center for neural engineering
[AD-A271164] 05 p1890 N94-20185
High resolution signal processing
[AD-A271181] 05 p1717 N94-20215
Topographic slope from the SAR interferometric phase gradient 05 p1731 N94-20459
Signal processing in the linear statistical model
[AD-A272114] 05 p1736 N94-20570
An inverse DWT for nonorthogonal wavelets
[AD-A272064] 05 p1737 N94-20582
The Fifth NASA Symposium on VLSI Design
[NASA-CR-194644] 05 p1753 N94-21079
Adaptive analog video signal conditioner 05 p1744 N94-21099
VLSI mixed signal processing system 05 p1744 N94-21100
Using crosscorrelation techniques to determine the impulse response of linear systems 05 p1759 N94-21122
NAVSPASUR sensor system digital signal processing receiver. Volume 1: Hardware and software overview
[AD-A272899] 05 p1738 N94-21198
Use of the Weiss-Weinstein bound to compare the direction-finding performance of sparse arrays
[AD-A272582] 05 p1738 N94-21210
NAVSPASUR sensor system digital signal processing receiver. Volume 2: Function and capabilities of hardware and software components
[AD-A272900] 05 p1739 N94-21218
Polar processing project
[AD-A271583] 05 p1739 N94-21235
Comparison of higher order moment spectrum estimation techniques
[AD-A272967] 05 p1967 N94-21260
QPPM receiver for free-space laser communications
[NASA-TM-106424] 05 p1741 N94-21567
Applications of correlator chips in radio science 05 p1763 N94-21695
A real time correlator architecture using distributed arithmetic principles 05 p1768 N94-21734
A comparative robustness evaluation of feedforward neurofilters
[NASA-TM-106440] 05 p1650 N94-21742
Surface acoustic wave sensing of VOC's in harsh chemical environments
[DE93-040721] 05 p1968 N94-21751
Canadian Conference on Electrical and Computer Engineering, volumes 1 and 2
[ISBN-0-9694170-2-0] 05 p1770 N94-22101
Estimation of AR signal patterns using competitive neural networks 05 p1744 N94-22102
Signal classification and noise filtering using artificial neural networks 05 p1744 N94-22103
VLSI architectures for the new (T,L) algorithm 05 p1745 N94-22110
Design of a floating point convolution processor 05 p1775 N94-22133
CFAR processing for airborne pulse-Doppler radars 05 p1745 N94-22142
Space-based radar for moving target detection 05 p1745 N94-22143
A digital demodulation scheme for use in a high dynamic range radar system 05 p1745 N94-22144
An overview of synthetic aperture radar signal processing techniques 05 p1745 N94-22159
Timing recovery in the channel processor of a digital group demodulator 05 p1780 N94-22169
Interference reduction using neural networks 05 p1783 N94-22186
Acceleration of backpropagation learning using a parallel DSP machine 05 p1786 N94-22206
Speaker-independent isolated-digit recognition using neural networks and hidden Markov model 05 p1747 N94-22213
Asynchronous detection of SSB-SC data signals 05 p1747 N94-22217
Encoding and decoding quasi-spherical signal sets 05 p1747 N94-22233
The application of sample vector selection to adaptive nulling: Performance comparison for techniques combining Gram-Schmidt orthogonalization with averaging 05 p1747 N94-22234
A four-band infrared data acquisition facility for signal processing development 05 p1791 N94-22235
An adaptive method for group delay compensation using switched capacitor filters 05 p1793 N94-22248
Wideband source location in two-dimensional array processing 05 p1747 N94-22250
On coefficient quantization and computational roundoff effects in frequency interpolation filter banks 05 p1793 N94-22251
A feasibility study of a parallax-based passive missile approach warning system
[ISBN-0-315-60640-1] 05 p1743 N94-22410
A multiresolution wavelet representation in two or more dimensions 05 p1925 N94-22456
CCD data acquisition systems at Lick and Keck Observatories 05 p2047 N94-22495
The VLBA correlator: Real-time in the distributed era 05 p2049 N94-22547
Algorithms for speech coding systems based on linear prediction
[EUT-92-E-260] 06 p2447 N94-22731
Cockpit weather graphics using mobile satellite communications 06 p2280 N94-22775
Odyssey personal communications satellite system 06 p2282 N94-22787
Asynchronous timing and Doppler recovery in DSP based DPSK modems for fixed and mobile satellite applications 06 p2285 N94-22805
Performance of the unique-word-reverse-modulation type demodulator for mobile satellite communications 06 p2286 N94-22813
Progress on the design of a data push architecture for an array of optimized time tagging pixels
[DE93-041011] 06 p2307 N94-22955
A dataflow analysis tool for parallel processing of algorithms
[NASA-TM-109054] 06 p2448 N94-23086
Spur-reduced digital sinusoid synthesis 06 p2291 N94-23264
System identification using a wavelet-based approach
[DE94-002191] 06 p2293 N94-23473
Fault tolerant onboard packet switch architecture for communication satellites: Shared memory per beam approach
[NASA-TM-106397] 06 p2201 N94-23567
The HDTV digital audio matrix
[BBC-RD-1993/9] 06 p2295 N94-24085
Automatic modulation recognition based on spatial pattern classification using artificial neural networks
[CTN-94-60897] 06 p2296 N94-24115
ASPT software source code: ASPT signal excision software package
[CTN-94-60904] 06 p2296 N94-24133
ASPT software source code: Development system package, library component
[CTN-94-60905] 06 p2455 N94-24134
ASPT software source code: ASPT application software package, VME-C30 component
[CTN-94-60906] 06 p2455 N94-24135
Dimensional analysis of acoustically propagated signals 06 p2528 N94-24217
PROPWR: A versatile tool for 1/3 octave processing and narrowband line tracking
[DREA-TC-93-303] 06 p2297 N94-24298
Device for the selective detection of objects
[CA-PATENT-1-308-179] 06 p2544 N94-24489
Nondestructive evaluations
[DE94-003020] 06 p2373 N94-24613
Heterodyne array for measurement of target velocity
[AD-D016025] 06 p2545 N94-24722
Crosstie random access memory element having associated read/write circuitry
[AD-D016027] 06 p2446 N94-24724
Conveying digital data in noisy, unstable, multipath environments
[AD-D015980] 06 p2301 N94-25038
Bridge type optoelectronic sample and hold circuit
[AD-D015986] 06 p2312 N94-25042
Preprocessor and adaptive beamformer for linear-frequency modulation active signals
[AD-D016008] 06 p2302 N94-25048
System for cancelling phase noise in an interferometric fiber optic sensor arrangement
[AD-D015994] 06 p2345 N94-25053
Method and apparatus of generating sum or difference signals corresponding to an apparent beam in a monopulse radar system
[AD-D015998] 06 p2302 N94-25056
Method and apparatus for determining target elevation angle, altitude and range, and the like in a monopulse radar system with reduced multipath errors
[AD-D016005] 06 p2302 N94-25058
Psychophysical and signal-processing aspects of speech representation
[ETN-94-95292] 06 p2302 N94-25077
Wide bandwidth differential amplifier
[AD-D015985] 06 p2303 N94-25217
Some subjects in digital audio, noise shaping, sample rate conversion, dynamic range compression and testing
[ISBN-9-09-005162-7] 06 p2530 N94-25220
On the quality of synthetic speech evaluation and improvements
[ETN-94-95298] 06 p2304 N94-25234
Linear and nonlinear adaptive filtering and their application to speech intelligibility enhancement
[ISBN-9-09-005342-5] 06 p2304 N94-25292
Adaptive noise cancellation using recurrent radial basis function networks
[RR-472] 06 p2313 N94-25319
Digital data, composite video multiplexer and demultiplexer boards for an IBM PC/AT compatible computer 06 p2447 N94-25377
Modeling of the ground-to-SSFMB link networking features using SPW 06 p2306 N94-25381
Digital input module
[DIGEL-1993-6] 07 p2779 N94-25620
Analysis and simulation of a GPS receiver design using combined delay-lock and modified tanlock loops
[AD-A274037] 07 p2664 N94-25810
A real-time convolution algorithm and architecture with applications in SAR processing
[AD-A273817] 07 p2959 N94-25963
Developing a graphical user interface to support a real-time digital signal processing system
[AD-A274032] 07 p2960 N94-26018
Emerging technologies
[DE94-003022] 07 p3102 N94-26023

Code division multiple access local area network communications employing fiber optic signal processing techniques
[AD-A274897] 07 p3096 N94-26180
Direct-conversion-to-baseband for a nonlinear FM signal
[AD-A274861] 07 p2768 N94-26189
Machine intelligent gust front algorithm
[AD-A273695] 07 p2680 N94-26196
The 12-channel flash-ADC FASTBUS module
[DE93-634229] 07 p2783 N94-26380
Low threshold all-optical crossbar switch on GaAs-GaAlAs channel waveguide arrays
[AD-A274971] 07 p2783 N94-26536
An integrated delta-sigma based IIR filter
[ISBN-0-315-83593-1] 07 p2784 N94-26631
Design and implementation of a multiprocessor for DSP and communications systems algorithm evaluation
[ISBN-0-315-84128-1] 07 p2980 N94-26674
Development of GaAs charge-coupled devices
[ISBN-0-315-84116-8] 07 p3059 N94-26703
Combatting inherent vulnerabilities of CFAR algorithms and a new robust CFAR design
[AD-A274918] 07 p2770 N94-26751
Automated fabric inspection system
[AD-A274522] 07 p2835 N94-26833
A current evaluation of the digital beamforming testbed at Rome Laboratory
[AD-A274311] 07 p3032 N94-26881
Rapid prototyping of application specific signal processors (RASSP)
[AD-A274324] 07 p2772 N94-26884
Causal fir matrices with anticausal fir inverses, and application in characterization of biorthonormal filter banks
[AD-A274509] 07 p2998 N94-27035
Monaural and binaural processing of complex waveforms
[AD-A274209] 07 p3010 N94-27067
Parametric time-scale methods in signal analysis
[AD-A274212] 07 p2773 N94-27068
Enhanced adaptive statistical filter providing improved performance for target motion analysis noise discrimination statement of government interest
[AD-D016039] 07 p2786 N94-27109
CCD-Camera images of BEST-TWO and processing results
[AD-A274140] 07 p2811 N94-27134
Focal plane antenna array for millimeter waves
[AD-D016034] 07 p2774 N94-27202
Beamforming/null-steering adaptive array
[CA-PATENT-1325260] 07 p2775 N94-27270
Acousto-optical post-processor time-integrating correlator calibration updates
[DSIS-94-00053] 07 p2813 N94-27317
Development of digital resampling and pulse compression computer software
[DREP-92-32] 07 p2969 N94-27318
Fiber optic true time-delay array antenna feed system
[AD-D016063] 07 p2777 N94-27734
Thunderstorm Hypothesis Reasoner
[NASA-CR-195714] 07 p2897 N94-27884
The 1994 Space and Earth Science Data Compression Workshop
[NASA-CP-3255] 07 p2945 N94-28251
A space-based classification system for RF transients
[DE94-003933] 08 p3240 N94-28522
Data fusion and correlation techniques testbed development audio processing study
[SKD-1600-73-014] 08 p3241 N94-28532
Data fusion and correlation techniques testbed development. Phase 1: Interim report
[SKD-1600-73-015] 08 p3405 N94-28533
SPC toolbox: An interactive MATLAB (tm) package for signal modeling, analysis, and communications
[AD-A275617] 08 p3241 N94-28634
Advanced optical A/D converter
[AD-A275663] 08 p3498 N94-28656
Design of parallel systems for signal processing
[AD-A275490] 08 p3430 N94-28659
The bootstrapped algorithm: A fast algorithm for blind signal separation
[AD-A275759] 08 p3408 N94-28760
Modeling, analysis, and simulation of an optical time-division multiple-access network architecture
[AD-A275847] 08 p3498 N94-28780
Testing for a signal with unknown location and scale in a stationary Gaussian random field
[AD-A275320] 08 p3464 N94-28876
Spurs in digital radio frequency memory and applications of DRFM
[AD-A275013] 08 p3243 N94-28897
Removal of coherent Extremely Low Frequency (ELF) background noise by adaptivé noise cancellation
[AD-A275016] 08 p3243 N94-28898
Backscatter haze device for measurement of haze in aircraft transparencies
[AD-A275127] 08 p3146 N94-29042
Multi-channel spatialization systems for audio signals
[NASA-CASE-ARC-12013-1-CU] 08 p3245 N94-29364
Measurand transient signal suppressor
[NASA-CASE-MSC-22027-1] 08 p3435 N94-29466
Orbital debris radar instrumentation 08 p3248 N94-29626
A comparison of full-spectrum and complex-symbol combining techniques for the Galileo S-band mission 08 p3250 N94-29665
A complex symbol signal-to-noise ratio estimator and its performance 08 p3251 N94-29671
Method for ambiguity resolution in range-Doppler measurements
[NASA-CASE-GSC-13542-1] 08 p3252 N94-29739
High-resolution robot tracking and direction finding for space station environment 08 p3168 N94-29896
A novel approach to noise-filtering based on a gain-scheduling neural network architecture
[NASA-TM-106563] 08 p3155 N94-30204
An electromagnetic noncontacting sensor for thickness measurement in a dispersive medium
[AIAA PAPER 94-1200-CP] 08 p3443 N94-30551
Noise and drift analysis of non-equally spaced timing data 08 p3472 N94-30667
A bipolar analog front-end integrated circuit for the SDC silicon tracker
[DE94-005203] 08 p3267 N94-30711
The Stroemberg wavelet on the interval and the Franklin system
[TELECOM-93-C-002] 08 p3462 N94-30971
Noise reduction techniques for the restoration of musical recordings
[TELECOM-93-E-019] 08 p3291 N94-30979
The generalized multi delay adaptive filter: Structure and convergence analysis
[TELECOM-93-D-004] 09 p3808 N94-31094
Modulation and coding for the Gaussian channel, possibly affected by fluctuations
[TELECOM-93-E-009] 09 p3840 N94-31169
Fast autodidactic adaptive equalization algorithms
[TELECOM-93-E-018] 09 p3670 N94-31174
Scheduling techniques for multiple processor systems in real-time environments
[AD-A276149] 09 p3824 N94-31249
Algorithms and structures for real-time signal processing
[AD-A276101] 09 p3810 N94-31277
Kalman filtering approach to blind equalization
[AD-A276320] 09 p3671 N94-31299
Smart environmental monitor based on neural networks and multi-spectral pattern recognition
[AD-A276445] 09 p3829 N94-31301
Analysis using bi-spectral related technique
[AD-A276017] 09 p3672 N94-31386
Concurrent architectures for VLSI signal and image processing
[AD-A276124] 09 p3688 N94-31445
Analysis of the effect of routing strategies for parallel implementations of a selected avionics application
[AD-A276069] 09 p3581 N94-31458
Analysis of key performance parameters of phase sampling digital RF memories
[AD-A276019] 09 p3688 N94-31494
Linearly separable stack-like architecture for the design of weighted order statistic filters with application in image processing
[ISBN-0-315-87284-5] 09 p3675 N94-31731
Algorithms and parallel architectures for laser acoustic imaging
[ISBN-0-315-86466-4] 09 p3716 N94-31797
Analysis and design of a formal neural network for filtering a dynamic signal
[ISBN-0-315-86932-1] 09 p3832 N94-31873
Pulse-splitting and AM-FM conversion in a nonlinear dispersive medium
[AD-A277041] 09 p3861 N94-32262
Empirical modeling for intelligent, real-time manufacture control 09 p3839 N94-32424
A new high-speed IR camera system 09 p3713 N94-32459
Universal signal conditioning amplifier 09 p3699 N94-32460
The constant current loop: A new paradigm for resistance signal conditioning 09 p3685 N94-32461
Bounds on least-squares four-parameter sine-fit errors due to harmonic distortion and noise
[DE94-007859] 09 p3849 N94-32653
Arithmetic averaging: A versatile technique for smoothing and trend removal
[DE94-005274] 09 p3852 N94-32673
COVICS: A covert video communications system
[DE94-007568] 09 p3682 N94-32745
Noise cancellation for CELP voice encoders in an F/A-18 noise environment
[AD-A277652] 09 p3683 N94-33026
Design of free space interconnected signal processor
[AD-A278129] 09 p3683 N94-33093
High temperature superconducting Josephson junction array systems, phase 1
[AD-A277937] 09 p3908 N94-33246
Design, characterization and control of the Unique Mobility Corporation robot 09 p3603 N94-33296
Applied harmonic analysis
[AD-A278384] 09 p3685 N94-33353
A new tool for signal processing
[AD-A278385] 09 p3685 N94-33354
Nonlocal methods for signal detection and estimation in the dependent nonstationary environment
[AD-A278472] 10 p4033 N94-33594
Total hydrocarbon analysis by ion mobility spectrometry 10 p4101 N94-33642
Multiparameter bifurcations and applications
[AD-A278365] 10 p4133 N94-33858
Investigation and simulation of nonlinear processors for spread spectrum receivers. Volume 2: Users manual
[AD-A278026] 10 p4037 N94-34289
United States Air Force 1993 Summer Research Program. Volume 10: Wright Laboratory
[AD-A278512] 10 p4037 N94-34294
Three dimensional ICs intelligent sensors 10 p4057 N94-34354
A study on adaptive active noise control 10 p4122 N94-34372
A closed-loop time-alignment system for baseband combining 11 p4253 N94-35552
NAVSPACECOM space surveillance sensor system digital signal processing receiver. Volume 3: Operating system functions
[AD-A278839] 11 p4212 N94-35799
NAVSPACECOM space surveillance sensor system digital signal processing receiver. Volume 4: Hardware interfaces
[AD-A278845] 11 p4212 N94-35801
The CMU task parallel program suite
[AD-A278951] 11 p4311 N94-36015
Computational Mathematics Laboratory for multiscale analysis
[AD-A278597] 11 p4315 N94-36424
Chilbolton Advanced Meteorological Radar: A tool for multi-disciplinary atmospheric research
[PB94-167467] 12 p4432 N94-36567
Radar tracking in multipath: Techniques for improved performance 12 p4395 N94-36631
Multirate time-frequency distributions
[AD-A280595] 12 p4503 N94-36723
Signal processing for the 1992 Barents Sea tomography experiment
[AD-A278580] 12 p4476 N94-36971
VHF adaptive antenna development task
[AD-A280320] 12 p4434 N94-37127
Detection of the electrocardiogram P-wave using wavelet analysis
[DE94-010791] 12 p4481 N94-37197
KONRAD: Wide band digital HF receiver
[PB94-184686] 12 p4435 N94-37813
Wavefront simulator for evaluating RF communication array signal processors
[AD-D016281] 12 p4436 N94-37835
Phase shifter for directly sampled bandpass signals
[AD-D016320] 12 p4440 N94-37840

SIGNAL RECEPTION

NT SYLLABLES
NT SYMBOLS
Magnetic Earth Ionosphere Resonant Frequencies (MEIRF) project
[NASA-CR-193182] 01 p0276 N94-11355
Calibration of the receiver channel for the GOPEX precursor experiments 02 p0610 N94-14387
Photorefractive receiver study
[AD-A269352] 04 p1577 N94-18302
Layered parallel interface for an active antenna array
[AD-D016002] 06 p2301 N94-25045
Solid-state, active-phased arrays: Some aspects of receiver design
[AD-A275893] 08 p3527 N94-28779
A comparison of full-spectrum and complex-symbol combining techniques for the Galileo S-band mission 08 p3250 N94-29665
A combined electron beam/optical lithography process step for the fabrication of sub-half-micron-gate-length MMIC chips 08 p3240 N94-30445
Remote clocks linked by a fully calibrated two-way timing link 08 p3471 N94-30659
Some applications of GPS timing information 08 p3145 N94-30661
An evaluation of three GPS receivers for use in the GPS sounder
[AD-A278157] 09 p3577 N94-33253

SIGNAL REFLECTION
Binaural room simulation
[AD-A273823] 07 p3009 N94-25737
Three dimensional transient analysis of microstrip circuits in multilayered anisotropic media
[AD-A274995] 08 p3263 N94-28995
SIGNAL TO NOISE RATIOS
Lower bounds on time of arrival estimation of pulse compression waveforms
[ITN-93-85189] 02 p0599 N94-13196
Performance results of a digital test signal generator 02 p0609 N94-14382
Effects of window size and shape on accuracy of subpixel centroid estimation of target images
[NASA-TP-3331] 03 p1034 N94-15990
Spatial and frequency diversity in lidar systems
[AD-A266192] 03 p1039 N94-16124
The Clementine instrument complement 03 p1086 N94-16370
Simulation of ASTER data using AVIRIS images 03 p1071 N94-16693
Moving target indicator using higher order statistics
[AD-D015890] 03 p1000 N94-16917
High resolution radar profiling using higher-order statistics
[AD-D015891] 03 p1000 N94-16918
Performance of coded coherent FSK lightwave system with noncoherent detection
[AD-A267442] 03 p1193 N94-17028
SYDONI: An intensified system for night observation 03 p0891 N94-17153
The feasibility of tropospheric and total ozone determination using a Fabry-Perot interferometer as a satellite-based nadir-viewing atmospheric sensor
[NASA-TM-109342] 03 p1102 N94-17214
Optimisation and specification of Auger electron spectrometers for signal-to-noise ratio performance
[NPL-DMM(A)-101] 03 p1006 N94-17549
Laser imaging radar system
[AD-A270436] 04 p1387 N94-18510
A comparison of single-station backazimuth estimates with regional event locations in the Central Appalachians
[AD-A269897] 04 p1483 N94-18690
The use of velocity spectra for stacking receiver functions with application to IRIS/IDA stations OBNINSK (OBN) and ARTI (ARU), Russia
[AD-A269067] 04 p1483 N94-18717
Nontraditional windows in spectral analysis
[AD-A271336] 04 p1553 N94-19583
Transcutaneous Analyte Measuring Methods (TAMM)
[AD-A271387] 04 p1408 N94-19756
Feasibility study for a measuring system velocity projectile
[FEL-91-A368] 04 p1434 N94-19797
Determination of noise equivalent sigma(0) using highly correlated repeat-pass SAR images 05 p1720 N94-20411
Use of the Weiss-Weinstein bound to compare the direction-finding performance of sparse arrays
[AD-A272582] 05 p1738 N94-21210
A low cost alternative to high performance PCM bit synchronizers 05 p1813 N94-21347
Design of a new squaring function for the Viterbi algorithm 05 p1764 N94-21699
Evaluation of a nonlinear method for the enhancement of tonal signal detection
[NASA-CR-191562] 05 p1968 N94-21741
The application of sample vector selection to adaptive nulling: Performance comparison for techniques combining Gram-Schmidt orthogonalization with averaging 05 p1747 N94-22234
Estimation of frequency offset in mobile satellite modems 06 p2265 N94-22807
Theoretical and simulated performance for a novel frequency estimation technique 06 p2285 N94-22808
DS-SSMA capacity for a mobile satellite system 06 p2286 N94-22814
Beam-waveguide antenna servo design issues for tracking low earth-orbiting satellites 06 p2292 N94-23268
Digital test signal generation: An accurate SNR calibration approach for the DSN 06 p2305 N94-23912
Precipitation measurement using SIR-C: A feasibility study
[NASA-CR-195104] 06 p2409 N94-24048
Precipitation measurement using SIR-C: A feasibility study. Investigation at nadir
[NASA-CR-195103] 06 p2410 N94-24126
Detection and analysis of unbalanced QPSK in Gaussian noise, version 1.0
[DREO-12-020.1] 06 p2296 N94-24131
Mitigation of EMI/RFI produced by a 1.2 kW uninterruptible power supply
[AD-A273149] 06 p2299 N94-24670
Improvement of system properties of a pulsed laser Doppler anemometer with respect to an optical amplifier
[DLR-FB-93-19] 06 p2547 N94-25305
Hyperspectral analysis of space objects: Signal to noise evaluation
[AD-A273882] 07 p2765 N94-25728
Performance impacts for actuator misalignments and failures in large-aperture adaptive-optic telescopes
[AD-A273838] 07 p3034 N94-25742
Primary standards laboratory report 1st half 1993
[DE94-003138] 07 p2762 N94-26027
Decoder synchronization for deep space missions 08 p3250 N94-29664
A comparison of full-spectrum and complex-symbol combining techniques for the Galileo S-band mission 08 p3250 N94-29665
A complex symbol signal-to-noise ratio estimator and its performance 08 p3251 N94-29671
An analysis of carrier phase jitter in an MPSK receiver utilizing map estimation
[NASA-CR-195806] 08 p3164 N94-29880
The bases for the development of high-temperature integrated SQUID-systems
[DE94-607901] 08 p3267 N94-30073
Performance statistics bulletin. High latitude meteor scatter propagation February, March, April, May 1991
[AD-A276723] 09 p3678 N94-32158
Performance statistics bulletin. High latitude meteor scatter propagation October, November, December 1991, January 1992
[AD-A276724] 09 p3678 N94-32159
Performance statistics bulletin. High latitude meteor scatter propagation
[AD-A276695] 09 p3680 N94-32299
Performance statistics bulletin. High latitude meteor scatter propagation
[AD-A276696] 09 p3680 N94-32300
Performance statistics bulletin. High latitude meteor scatter propagation, June, July, August, September 1992
[AD-A277508] 09 p3685 N94-33347
Nonlocal methods for signal detection and estimation in the dependent nonstationary environment
[AD-A278472] 10 p4033 N94-33594
Solid state acoustics information time region separating methods for gear diagnosis of failures 10 p4068 N94-34351
Fluorescence detection of single molecules using pulsed near-field optical excitation and time correlated photon counting
[DE94-007553] 11 p4320 N94-35376
A closed-loop time-alignment system for baseband combining 11 p4253 N94-35552
Correlator data analysis for the array feed compensation system 11 p4253 N94-35553
Sensitivity and signal to noise ratio improvement of a one micron ladar system incorporating a neodymium doped optical fiber preamplifier. Laser radar testbed
[AD-A280235] 12 p4447 N94-37137
SIGNAL TRANSMISSION
NT ALOHA SYSTEM
NT CODE DIVISION MULTIPLE ACCESS
NT DATA TRANSMISSION
NT DOUBLE SIDEBAND TRANSMISSION
NT FREQUENCY DIVISION MULTIPLE ACCESS
NT IONOSPHERIC PROPAGATION
NT MICROWAVE ATTENUATION
NT MICROWAVE TRANSMISSION
NT MULTIPATH TRANSMISSION
NT MULTIPLE ACCESS
NT PACKET TRANSMISSION
NT RADAR TRANSMISSION
NT RADIO TELEMETRY
NT RADIO TRANSMISSION
NT SATELLITE TRANSMISSION
NT SHORT WAVE RADIO TRANSMISSION
NT SINGLE CHANNEL PER CARRIER TRANSMISSION
NT SINGLE SIDEBAND TRANSMISSION
NT TELEMETRY
NT TELEVISION TRANSMISSION
Underwater hydrophone location survey 01 p0290 N94-10975
Adaptive algorithms for use with digital filters in vibration control 01 p0071 N94-11338
NRL review for 1993
[AD-A265666] 01 p0497 N94-12334
Ocean acoustic processing: A model-based approach
[DE93-011902] 02 p0725 N94-12876
Digital sound: The selection of critical programme material and preparation of recordings for CCIR tests on low bit-rate codecs
[BBC-RD-1993/1] 02 p0598 N94-12925
Trellis coding with Continuous Phase Modulation (CPM) for satellite-based land-mobile communications
[NASA-CR-191325] 02 p0604 N94-13909
Calibration of the receiver channel for the GOPEX precursor experiments 02 p0610 N94-14387
GOPEX laser transmission and monitoring systems 02 p0611 N94-14391
VDM specification of the MD4 message digest algorithm
[NPL-DITC-204/92] 03 p1142 N94-14944
RAISE specification of the MD4 message digest algorithm
[NPL-DITC-206/92] 03 p1142 N94-15010
Improvements to pulsed phase locked loop strain monitor
[NASA-CASE-LAR-14887-1] 03 p1033 N94-15877
An electroacoustic transducer for purposes of photoacoustic spectroscopy
[IFTR-7/1992] 03 p1013 N94-17071
Wide angle, single screen, gridded square-loop frequency selective surface for diplexing two closely separated frequency bands
[NASA-CASE-NPO-18664-1-CU] 03 p1237 N94-17438
A virtual acoustic orientation instrument
[AD-A268181] 03 p1134 N94-17510
Optimisation and specification of Auger electron spectrometers for signal-to-noise ratio performance
[NPL-DMM(A)-101] 03 p1006 N94-17549
Design of a general purpose and autonomous transmitter and receiver system for underwater acoustic experiments at sea
[AD-A269268] 04 p1495 N94-17822
Swatch Pager 04 p1428 N94-18039
A method for eliminating skew introduced by non-uniform buffer delay and wire lengths in clock distribution trees
[AD-A270649] 04 p1544 N94-19530
Metrics for specifying and/or testing neural networks statement of government interest
[AD-D015946] 05 p1938 N94-19843
Trellis coded multi-orthogonal modulation 05 p1747 N94-22231
Quadrature biorthogonal modulation 05 p1747 N94-22232
Measurement of multipath delay profile in land mobile satellite channels 06 p2283 N94-22793
Wide band fiber-optic communications 06 p2304 N94-23231
Preliminary analysis of amplitude and phase fluctuations in the JAPE multiple tone data to distances of 500 meters 06 p2528 N94-24216
Layered parallel interface for an active antenna array
[AD-D016002] 06 p2301 N94-25045
Interference analysis of multichannel transmission lines: A system's analysis
[PB94-126505] 07 p2772 N94-26909
Monaural and binaural processing of complex waveforms
[AD-A274209] 07 p3010 N94-27067
Considerations in the modelling of seafloor acoustic backscatter
[AD-A275404] 08 p3478 N94-29206
The Rb 780-nanometer Faraday anomalous dispersion optical filter: Theory and experiment 08 p3250 N94-29659
Performance issues of signalling protocols for broadband ISDN
[PB94-150380] 08 p3255 N94-30374
The 25th Annual Precise Time and Time Interval (PTTI) Applications and Planning Meeting
[AD-A280955] 08 p3468 N94-30639
Optical techniques for time and frequency transfer 08 p3469 N94-30647
Some applications of GPS timing information 08 p3145 N94-30661
Channel equalization for block transmission systems
[TELECOM-93-D-002] 09 p3670 N94-31093
Multi-line passive fiber optic slipring
[AD-D016092] 09 p3883 N94-32738
Digital beamforming and filtering circuit
[AD-D016142] 09 p3697 N94-32976
Roll ring assemblies for the Space Station 09 p3603 N94-33294
International Space Station Alpha's bearing, motor, and roll ring module developmental testing and results 09 p3603 N94-33295
A self-organizing neural network architecture for auditory and speech perception with applications to acoustic and other temporal prediction problems
[AD-A277526] 10 p4095 N94-33708
Time-scale modification of complex acoustic signals in noise
[AD-A277535] 10 p4133 N94-34157
Signal processing for the 1992 Barents Sea tomography experiment
[AD-A278580] 12 p4476 N94-36971
SIGNATURE ANALYSIS
Satellite signatures in SLR observations 03 p0912 N94-15557

An analytical approach to error localization by using information derived from error signature
[REPT-93-023] 04 p1518 N94-17960
Wavelet transform for time-frequency analysis of the vibrational signature and its application
[AD-A269928] 04 p1454 N94-18661
Environmental characterization for target acquisition. Report 3: New concepts for evaluating low-grazing angle radar measurements
[AD-A269956] 04 p1388 N94-18777
Efficient chip signature checking for diagnosing boundary scan systems
[RR-901-I] 05 p1749 N94-20166
Progress in interpreting CO2 lidar signatures to obtain cirrus microphysical and optical properties
05 p1874 N94-22308
Vibration signature analysis of a faulted gear transmission system
[NASA-TM-106623] 12 p4450 N94-36953
NASA reload program
[NASA-CR-193972] 12 p4429 N94-37446

SIGNATURES
NT INFRARED SIGNATURES
NT MAGNETIC SIGNATURES
NT MICROWAVE SIGNATURES
NT MISSILE SIGNATURES
NT RADAR SIGNATURES
NT SPECTRAL SIGNATURES
Geophysical signature of the Pretoria saltpan impact structure and a possible satellite crater
01 p0282 N94-12103
Effects of typhoon on TOMS data
02 p0693 N94-14243
Surface and internal signatures of organized vortex motions in stratified fluid
[AD-A267015] 03 p1020 N94-15526
Satellite signatures in SLR observations
03 p0912 N94-15557
Work at Graz on satellite signatures
03 p0898 N94-15558
New perspectives for high accuracy SLR with second generation geodesic satellites 03 p0916 N94-15585
Rough surface scattering from moving ocean surfaces as an indicator of scattering mechanisms
05 p1726 N94-20439
Standard ML signatures for a protocol stack
[AD-A272060] 05 p1908 N94-20622
Development of a nondestructive vibration technique for bond assessment of Space Shuttle tiles
[NASA-CR-195163] 06 p2201 N94-24919
Special signature schemes
[ETN-94-95296] 06 p2446 N94-25081
The STAR experiment at the Relativistic Heavy Ion Collider
[DE94-003409] 07 p3017 N94-26083
Window least squares method applied to statistical noise smoothing of positron annihilation data
[DE93-634665] 07 p3003 N94-26385
Application of Space Shuttle Project Hercules imagery in the investigation of ship cloud tracks
[AD-A274923] 07 p2692 N94-26529
Signatures for hybrids
[DE94-004244] 07 p3020 N94-26574
Experimental studies of loudness and annoyance response to sonic booms 07 p2651 N94-28195
Variability of measured sonic boom signatures
07 p2651 N94-28197
Were all extinction events caused by impacts?
07 p2891 N94-28311
Energy distribution of the leptons in top decay to charged Higgs
[DE94-005231] 08 p3482 N94-28494
Digital camera with apparatus for authentication of images produced from an image file
[NASA-CASE-NPO-19108-1-CU]
08 p3287 N94-29373
The trustworthy digital camera: Restoring credibility to the photographic image 09 p3714 N94-32470
Overview of feasibility study on conducting overflight measurements of shaped sonic boom signatures using RPV's 10 p3973 N94-33475

SIGNIFICANCE
Example of statistical techniques applied to analysis of effects of small changes
[ESDU-93023] 07 p2670 N94-28094

SIGNS (SYMBOLS)
U SYMBOLS

SIGNS AND SYMPTOMS
NT ACQUIRED IMMUNODEFICIENCY SYNDROME
NT COUGH
NT EDEMA
NT HEADACHE
NT NAUSEA
NT VERTIGO
Effects of CSF hormones and ionic composition on salt/water metabolism
[NASA-CR-193232] 01 p0300 N94-11045
Monitoring cognitive function and need with the automated neuropsychological assessment metrics in Decompression Sickness (DCS) research
01 p0314 N94-11533
Risk of decompression sickness in the presence of circulating microbubbles 01 p0312 N94-11546
Promethazine and its use as a treatment for space motion sickness 01 p0312 N94-11550
Update on the incidence and treatment of space motion sickness 01 p0312 N94-11551
Autogenic feedback training experiment: A preventative method for space motion sickness
02 p0595 N94-13774
Flight simulator-induced sickness and visual displays evaluation
[AD-A267019] 03 p1122 N94-15845
Arsenic surveillance program
03 p1127 N94-16637
Predicting radiation induced performance decrements of AH-1 helicopter crews. Volume 1: Predicted veersus actual performance of AH-1 crews induced with symptoms simulating radiation sickness
[AD-A268376] 03 p1138 N94-17460
Using controlled daylight exposure and sleep timing in the prevention of shift lag during night operations
[AD-A269304] 04 p1504 N94-17824
Cerebral ischemia and reperfusion injury: A brief review
[AD-A270480] 04 p1507 N94-19675
Screening for asymptomatic coronary heart disease
06 p2423 N94-23315
Symptoms of hypoxia at simulated altitude of 25,000 feet 07 p2933 N94-27945
The Environmental Symptoms Questionnaire: Assessing reactions to environmental extremes in military operations 08 p3383 N94-28447
The effectiveness of ground level post-flight 100 percent oxygen breathing as therapy for pain-only altitude Decompression Sickness (DCS)
10 p4096 N94-33643
Cardiac pressure changes with venous gas embolism and decompression
[AD-A280412] 12 p4481 N94-37224
Profile analysis of after-effects experienced during exposure to several virtual reality environments
12 p4482 N94-37263
Some side-effects of immersion virtual reality
12 p4482 N94-37277

SIKORSKY AIRCRAFT
NT H-53 HELICOPTER
NT H-60 HELICOPTER
NT SH-3 HELICOPTER
NT UH-60A HELICOPTER
Wind tunnel test of a variable-diameter tiltrotor (VDTR) model
[NASA-CR-177629] 06 p2181 N94-24796
S-76 high intensity radiated fields, volume 1
[AD-A274571] 07 p2771 N94-26854
S-76 high intensity radiated fields, volume 3
[AD-A274416] 07 p2772 N94-26980

SIKORSKY HSS-2 HELICOPTER
U SH-3 HELICOPTER

SIKORSKY S-65 HELICOPTER
U H-53 HELICOPTER

SILANES
NT CHLOROSILANES
Toxicity study of dimethylethoxysilane (DMSES), the waterproofing agent for the Orbiter heat protective system 01 p0318 N94-11554
Adsorption and dissociation of disilane on Si(001) studied by STM
[AD-A265269] 01 p0402 N94-11684
Cathode sheath charge transfer effects
[AD-A268393] 03 p1186 N94-17536
NMR studies of enriched species at interfaces
[AD-A264703] 04 p1367 N94-17878
Adhesive electroless metallization of fluoropolymeric substrates
[AD-A271858] 05 p1703 N94-20526
Composite materials with improved properties in compression
[AD-A272837] 05 p1675 N94-21176
The importance of vibrationally excited nitrogen in silicon nitride deposition systems
[AD-A274874] 07 p2750 N94-26167
Silica scintillating materials prepared by sol-gel methods
[DE94-005123] 08 p3220 N94-30778
Spinnability of silica sols: The role of alkoxy group exchange
[DE94-010087] 11 p4244 N94-35702
Carborane-siloxane or silane-unsaturated hydrocarbon based polymers
[AD-D016220] 12 p4425 N94-37482
Carborane-(silane or siloxane)-unsaturated hydrocarbon based thermosetting polymers
[AD-D016311] 12 p4427 N94-37818

SILENCERS
Boundary layer control device for duct silencers
[NASA-CASE-ARC-12030-1] 08 p3478 N94-29362

SILICA
U SILICON DIOXIDE

SILICA GEL
Hydrolysis reaction and positronium decay in silica gels
[AD-A270028] 04 p1371 N94-18713
Surface chemistry and durability of borosilicate glass
[DE94-006734] 09 p3656 N94-32116
Time-resolved analytical methods for liquid/solid interfaces
[DE94-008352] 09 p3637 N94-32826
Multifunctional gel-silica optics
[AD-A278531] 10 p4141 N94-33670

SILICA GLASS
Material advances for lightweight TPS
01 p0062 N94-10049
Arcjet exploratory tests of ARC optical window design for the AFE vehicle
[NASA-CR-192655] 01 p0034 N94-10930
Thermal history effects on electrical relaxation and conductivity for potassium silicate glass with low alkali concentrations
[NASA-TM-106324] 02 p0583 N94-14845
Structural studies of sol-gel glasses
[AD-A266277] 03 p0967 N94-16472
Fabricating binary optics: An overview of binary optics process technology 03 p1195 N94-17343
Laser induced damage testing: Equipment and techniques
[DE93-017143] 04 p1437 N94-18060
Formation of colloidal Ag precipitates in fused silica by MeV ion implantation
[DE93-040268] 05 p2012 N94-19869
Inert strength of pristine silica glass fibers
[DE94-004685] 07 p2750 N94-26247
Nanoscale plasticity in silica glass
[DE94-004212] 07 p2751 N94-26554
The deposition of boron nitride and carbon films on silica glass fibers
[DE94-004684] 07 p2751 N94-26564
Mechanism of mechanical fatigue of silica glass
[DE94-003165] 07 p2753 N94-26783
Float polishing studies of fused silica
[AD-A275001] 08 p3213 N94-28886
Characterisation and processing of SiC/MAS-L glass ceramic matrix composite
[REPT-932-430-111] 08 p3179 N94-29412
Characterization of thermally annealed Sb implanted fused silica
[DE94-005464] 08 p3219 N94-30335
Oriented Si and Ge nanocrystals formed in Al2O3 by ion implantation and annealing
[DE94-005593] 09 p3901 N94-32172
Interface engineering in oxide fiber/oxide matrix composites
[AD-A277672] 09 p3627 N94-33029
Optical properties of doped sol-gel silica glasses
[AD-A278094] 09 p3884 N94-33267
Silica Fresnel lens for laser communications
[AD-A278329] 10 p4058 N94-33967
Multicomponent glass surfaces: Structure and adsorption
[DE94-010516] 11 p4246 N94-36283

SILICATES
NT ALUMINUM SILICATES
NT ANDESITE
NT ARAGONITE
NT CALCIUM SILICATES
NT ENSTATITE
NT FAYALITE
NT FELDSPARS
NT FLUOROSILICATES
NT FORSTERITE
NT GADOLINIUM-GALLIUM GARNET
NT GARNETS
NT MONTMORILLONITE
NT NEPHELINE
NT POTASSIUM SILICATES
NT PYROXENES
NT SODIUM SILICATES
NT TALC
NT YTTRIUM-ALUMINUM GARNET
NT YTTRIUM-IRON GARNET
NT ZEOLITES
The stability of hibonite and other aluminous phases in silicate melts: Implications for the origin of hibonite-bearing inclusions 01 p0080 N94-12052

Alkali-granitoids as fragments within the ordinary chondrite Adzhi-Bogdo: Evidence for highly fractionated, alkali-granitic liquids on asteroids
01 p0429 N94-12069
The solubility of gold in silicate melts: First results
01 p0087 N94-12086
Unequilibrated, equilibrated, and reduced aggregates in anhydrous interplanetary dust particles
01 p0429 N94-12098
The spectral effects of subsolidus reduction of olivine and pyroxene 01 p0081 N94-12110
Micro-zoning in minerals of a Landes silicate inclusion
01 p0432 N94-12231
In-situ crystallization of silicate glass films deposited on alpha- Al2O3
[DE93-012969] 01 p0095 N94-12596
Deposition of impact-generated vapors in the lunar regolith 02 p0843 N94-14302
NMR and theoretical investigation of cation binding with sol-gel silicates
[AD-A266999] 03 p0963 N94-15631
Trapping of water vapor from an atmosphere by condensed silicate matter formed by high-temperature pulse vaporization 03 p1248 N94-16180
Iron oxide bands in the visible and near-infrared reflectance spectra of primitive asteroids
03 p1242 N94-16274
An iridium-rich iron micrometeorite with silicate inclusions from the Moon 03 p1242 N94-16281
Partitioning of Nb, Mo, Ba, Ce, Pb, Th and U between immiscible carbonate and silicate liquids: Evaluating the effects of P2O5,F, and carbonate composition
03 p0953 N94-16283
Experimental partitioning of Zr, Ti, and Nb between silicate liquid and a complex noble metal alloy and the partitioning of Ti between perovskite and platinum metal
03 p0962 N94-16287
Complex radiation-thermal history of Kaidun meteorite on data of track study of silicate minerals
03 p1243 N94-16297
Catalytic crystallization of ices by small silicate smokes at temperatures less than 20K 03 p1219 N94-16420
Transformation toughening of composite ceramics
[AD-A267304] 03 p0971 N94-16980
Chemical tracer studies at IOSDL. 3: The measurement of silicate, nitrate and phosphate in seawater
[IOS-302-1992] 03 p1114 N94-17489
Cooperative formation of inorganic-organic interfaces in the synthesis of silicate mesostructures
[AD-A271196] 04 p1375 N94-19742
Neutron-scattering studies of Yb-bearing silicate glasses
[DE93-019768] 05 p1700 N94-20265
The Sm-Nd systematics of silicate inclusions in iron meteorites: Results from Caddo (IAB)
[CONTRIB-5241(804)] 05 p2084 N94-20795
Hydrothermal alteration experiments of olivine with varying Fe contents: An attempt to simulate aqueous alteration of the carbonaceous chondrites
05 p1686 N94-20810
The structure and spin dynamics of lanthanide-bearing silicate glasses
[DE94-001320] 06 p2252 N94-22992
Optimization of experimental conditions in IR reflectance determination of BPSG properties
[DE94-002742] 07 p2713 N94-25978
Ion implantation in silicate glasses
[DE94-003785] 07 p2757 N94-27726
Layered polysilicate: Properties and perspectives in applications 08 p3223 N94-29513
Advances and applications of dynamic-angle spinning nuclear magnetic resonance
[DE94-007031] 09 p3870 N94-32250
Displacive transformation in ceramics
[AD-A278442] 10 p4026 N94-33539
Materials for spectral hole burning research, phase 1
[AD-A278480] 10 p4146 N94-33753
Ultrastructure processing of advanced materials
[AD-A278285] 10 p4018 N94-33962
Grain rims on ilmenite in the lunar regolith: Comparison to vapor deposits on regolith silicates
11 p4359 N94-35418
Application of an alkylammonium method for characterization of phyllosilicates in CI chondrites
11 p4351 N94-35432
Inhomogeneous distribution of materials in Iodranites-acapulcoites and IAB irons and their common formation processes 11 p4364 N94-35463
Kinetics of phase transformations in glass forming systems
[NASA-CR-196082] 11 p4245 N94-35977
Textural constraints on the formation of alteration phases in CM chondrites 11 p4353 N94-36145
Preliminary results of sulfide melt/silicate wetting experiments in a partially melted ordinary chondrite
11 p4353 N94-36147
On the origin of porphyritic chondrules
[DE94-010464] 11 p4351 N94-36418
A possible origin of EL6 chondrites from a high temperature-high pressure solar gas
[DE94-010467] 12 p4548 N94-36759

SILICIDES
NT DISILICIDES
Fracture behavior of vanadium/vanadium silicide in-situ composites
[DE93-013422] 02 p0556 N94-13389
Schottky barrier focal plane arrays for SWIR and MWIR 03 p0903 N94-15050
Environmental embrittlement in ordered intermetallic alloys
[DE93-015307] 03 p0955 N94-15830
Recent advances in ordered intermetallics
[DE93-015308] 03 p0955 N94-15862
Thin Ni silicide formation by low temperature-induced metal atom reaction with ion implanted amorphous silicon
[DE93-015449] 03 p1209 N94-16066
UHV-stem studies on nucleation and growth of thin metal silicide films on silicon
[DE93-017604] 03 p1212 N94-16961
Plastic anisotropy in MoSi2 single crystals
[DE93-012650] 04 p1594 N94-17874
Bibliography on silicides
[AD-A270516] 04 p1374 N94-19532
Photo- and thermal-induced antiferromagnetic interlayer coupling in Fe/(Fe-Si) superlattices
[DE93-040822] 05 p2031 N94-21930
The effect of microstructural evolution on superplasticity in Ni3Si(V, Mo)
[DE93-041320] 05 p1694 N94-21943
Evaluation of A5Si3Z(x) intermetallics for use as high temperature structural materials
[DE93-041127] 06 p2227 N94-22977
Photo-induced antiferromagnetic interlayer coupling in Fe superlattices with iron silicide spacers
[DE94-001345] 06 p2559 N94-22995
Method of forming silicon structures with selectable optical characteristics
[NASA-CASE-NPO-18625-1-CU]
06 p2563 N94-23972
Binding of copper and nickel to cavities in silicon formed by helium ion implantation
[DE94-003769] 07 p3050 N94-25814
Dissolution of secondary phases during extrusion
[PB94-124583] 07 p2732 N94-25908
Stress relaxation in sputtered W films and W/GeSi/Si heterostructures
[DE94-004007] 07 p3055 N94-26239
Microstructures of Si surface layers implanted with Cu
[DE94-004690] 07 p3058 N94-26565
Fabrication and testing of plasma-spray formed MoSi2 and MoSi2 composite tubes
[DE94-004995] 08 p3175 N94-28581
Brittle composites modeling: Comparisons with MoSi2/ZrO2
[DE94-004978] 08 p3182 N94-29933
Microstructure and mechanical properties of nitrided molybdenum silicide coatings
[DE94-006249] 08 p3217 N94-30025
Creep behavior of MoSi2-SiC composites
[DE94-004980] 08 p3185 N94-30693
Magnetotransport measurements in magnetic fields up to 50T in SmB6 and FeSi
[DE94-006227] 08 p3520 N94-30848
Ion beam synthesis of IrSi3 by 1-MeV Ir ion implantation into Si(111)
[DE94-006556] 09 p3896 N94-31501
The effect of ductile phase (Nb) reinforcement morphology on the mechanical behavior of an intermetallic matrix (MoSi2) 09 p3615 N94-32500
Gettering of metal impurities by cavities in silicon
[DE94-005248] 09 p3645 N94-32672
The effects of in-situ processing methods on the microstructure and fracture toughness of V-V3Si composites
[DE94-009093] 10 p4019 N94-33681
High Temperature Silicides and Refractory Alloys Symposium, volume 322
[AD-A278373] 10 p4024 N94-33741
Infrared detectors based on Si/SiGe superlattices and silicide/SiGe Schotty barriers operating beyond 12 micrometers
[AD-A277900] 10 p4147 N94-34082
High temperature creep and oxidation resistant chromium silicide matrix alloy containing molybdenum
[NASA-CASE-LEW-15697-1] 11 p4241 N94-36275
Quadrupolar effects in PrCu2Si2
[DE94-011509] 12 p4534 N94-37054
Mechanical behavior of MoSi2 and MoSi2 composites
[DE94-013116] 12 p4405 N94-37289

SILICON
NT AMORPHOUS SILICON
NT SILICON ISOTOPES
Effect of gravity on the dissolution and liquid phase epitaxial growth processes in a horizontal sandwich system 01 p0118 N94-10208
Journal of Research of the National Institute of Standards and Technology, volume 98, number 2, March - April 1993
[PB93-196228] 01 p0485 N94-10850
Thermal-optical switching of a silicon based interference filter
[AD-A265152] 01 p0174 N94-11095
Characterization of the Si/SiO2 interfere morphology from quantum oscillations in Fowler-Nordheim tunneling currents
[AD-A265149] 01 p0143 N94-11160
Radiation hardness of Mo/Si multilayers designed for use in a soft x ray projection lithography system
[DE93-011879] 01 p0143 N94-11273
Production of electronic grade lunar silicon by disproportionation of silicon difluoride
01 p0435 N94-12017
The correlation of alkalis and aluminum during high-temperature volatilization of albite and nepheline
01 p0081 N94-12214
The adsorption and surface reaction of SiCl4 on Si(100)-(2x1)
[AD-A266124] 01 p0079 N94-12538
Synthesis and electronic properties of nanophase semiconductor materials
[AD-A265287] 01 p0146 N94-12584
Metal-semiconductor, composite radiation detectors
[DE93-013313] 02 p0619 N94-12994
Lattice site of helium implanted in Si and diamond
[DE93-015365] 02 p0805 N94-13012
Fracture behavior of vanadium/vanadium silicide in-situ composites
[DE93-013422] 02 p0556 N94-13389
Computational diagnostics for detecting phase transitions during nanoindentation
[DE93-016536] 02 p0813 N94-14439
Quantum state resolved desorption of CO from solid surfaces
[DE93-016876] 02 p0814 N94-14597
A high voltage dielectrically isolated smart power technology based on silicon direct bonding
[LAAS-92492] 02 p0626 N94-14698
Manufacturing and examination of integrated optical waveguide components in silicon
[ETN-93-94393] 02 p0793 N94-14704
Multicrystalline silicon solar cells: Gettering optimization and characterization
[DE93-015001] 02 p0705 N94-14861
BIB photodetectors based on antimony doped silicon
03 p0902 N94-15047
Gamma large area silicon telescope: Applying Si strip detector technology to the detection of gamma rays in space 03 p0904 N94-15061
CCD's on high resistivity bulk silicon for x ray spectroscopy on XMM 03 p0907 N94-15080
Silicon gallium doped photoconductor development for the AROME balloon borne instrument
03 p0908 N94-15087
Applications for large area silicon drift detectors on x ray and gamma ray astronomy 03 p0909 N94-15090
Silicon radiation sensor systems for gamma and x ray detection at SI 03 p0909 N94-15095
The epitaxial Si x ray bolometer an alternative to ion implanted devices 03 p0911 N94-15103
Structural investigation of electrochemically etched silicon
[DE93-015300] 03 p1207 N94-15827
Selective formation of porous silicon
[NASA-CASE-NPO-18735-1-CU]
03 p0966 N94-15960
Porous silicon for pumping solid-state lasers
[AD-A266293] 03 p1039 N94-16474
Thermal disorder in adsorbed Cl on Si(100)
[AD-A266295] 03 p1210 N94-16476
UHV-stem studies on nucleation and growth of thin metal silicide films on silicon
[DE93-017604] 03 p1212 N94-16961
Structural characterization of epitaxial layers for infrared detectors
[AD-A267875] 03 p0940 N94-17013
Buried porous silicon-germanium layers in monocrystalline silicon lattices and method of producing
[NASA-CASE-NPO-18836-1-CU]
03 p1215 N94-17327
Low voltage electron beam lithography
[AD-A267865] 03 p1215 N94-17389
Laser probing of the kinetics and dynamics of 3-5 semiconductor growth
[AD-A268388] 03 p1215 N94-17422

Characterization of Ni on Si wafers: Comparison of surface analysis techniques
[DE93-016501] 03 p0953 N94-17649
Selective electrochemical wafer thinning for silicon characterization
[DE93-015083] 04 p1592 N94-17742
Simplified processing for 23 percent-efficient silicon concentrator solar cells
[DE93-015018] 04 p1464 N94-17787
Pulsed LASER for testing silicon strip detectors
[DE93-017816] 04 p1436 N94-17883
Electron mobility in high resistivity silicon
[REPT-93-007] 04 p1565 N94-17933
High- and low-temperature bonding techniques for microstructures
[DE93-017173] 04 p1595 N94-17992
Electrostatic micrometers: Recent developments and perspectives of uses in clock and watch making
04 p1425 N94-18014
Silicon micro-actuator 04 p1408 N94-18017
High-efficiency silicon concentrator cell commercialization
[DE93-018491] 04 p1467 N94-18409
Research on stable, high-efficiency amorphous silicon multijunction modules
[DE93-010046] 04 p1467 N94-18518
Thermal stresses in the microchannel heatsink cooled by liquid nitrogen
[DE93-018660] 04 p1418 N94-18995
Binding of copper to nanocavity surfaces in silicon
[DE93-019073] 04 p1364 N94-19080
Silicon MCM substrates for integration of 3-5 photonic devices and CMOS IC's
[DE93-017894] 04 p1405 N94-19112
Studies of deep levels in high resistivity silicon detectors irradiated by high fluence fast neutrons using a thermally stimulated current spectrometer
[DE93-016133] 04 p1602 N94-19258
Picoindentation hardness measurements using atomic force microscopy
[AD-A270877] 04 p1604 N94-19579
Examination of charge carriers dynamics in silicon and silicon solar cells with photoinduced laser beam deflection
[ETN-93-95060] 04 p1470 N94-19654
Substrate recovery of Mo-Si multilayer coated optics
[DE93-019610] 05 p1698 N94-19810
Segregation of Si to the surface of Fe-29Ni-17Co alloy
[DE93-040053] 05 p1687 N94-19864
Photoconductive Semiconductor Switches for pulsed power applications
[DE93-019411] 05 p1750 N94-20294
Attenuation of epsilon(sub eff) of coplanar waveguide transmission lines on silicon substrates
05 p1733 N94-20504
Spectroscopic ellipsometry studies of HF treated Si (100) surfaces 05 p1734 N94-20508
Optical integrated structures and circuits on silicon
[VTT-PUBS-106] 05 p1988 N94-21594
A novel semiconductor process for optoelectronic applications on silicon substrate
05 p1988 N94-21595
Integrated optical coupling element on silicon substrate, appendix 2 05 p1988 N94-21596
Fibre pigtailed silicon based low cost passive optical components, appendix 5 05 p1989 N94-21599
Localization of pellicle-induced open contacts using charge-induced voltage alteration
[DE93-019407] 05 p1762 N94-21636
Micromachined actuator and sensor capabilities at the Microelectronics Development Laboratory
[DE93-019417] 05 p1769 N94-21918
Acoustic, fiber optic, and silicon microelectronic microsensors research and development activities at Sandia National Laboratories
[DE93-019075] 05 p1770 N94-22040
Silicon microelectronic field-emissive devices for advanced display technology
[DE94-000397] 05 p1794 N94-22380
Density functional studies: First principles and semi-emperical calculations of clusters and surfaces
[DE94-002836] 06 p2561 N94-23214
Magnetic resonance study of zinc-related defects in silicon with optimized EPR spectrometer
[PB93-224640] 06 p2561 N94-23223
Quantitative analysis in the Al-Mg-Si system with small amounts of Mg and Si
[PB93-201499] 06 p2241 N94-23446
Method of forming silicon structures with selectable optical characteristics
[NASA-CASE-NPO-18625-1-CU] 06 p2563 N94-23972
Photonic technology for implementation of generalizable neural networks: A synthetic approach
[AD-A273497] 06 p2474 N94-24622
Temperature dependent performance of Coplanar Waveguide (CPW) on substrates of various materials
[NASA-TM-106505] 06 p2313 N94-25170
Binding of copper and nickel to cavities in silicon formed by helium ion implantation
[DE94-003769] 07 p3050 N94-25814
Hydrogen uptake into silicon from an ECR plasma
[DE94-003771] 07 p3050 N94-25815
The structural, chemical, and electrical properties of He-implantation-induced nanocavities in silicon
[DE94-002681] 07 p3052 N94-25971
Determination of surface recombination velocity and bulk lifetime in detector grade silicon and germanium crystals
[DE94-003886] 07 p3053 N94-26094
Lithium drifted silicon detector fabrication on gettered floating-zone silicon
[DE94-003890] 07 p3054 N94-26095
Light emitting porous silicon
[AD-A274152] 07 p3038 N94-27137
Simulations of terrestrial in-situ cosmogenic-nuclide production
[DE94-004999] 07 p3117 N94-27826
Dry etching process development for submicron and nanometer semiconductor devices
[PB94-133196] 07 p2788 N94-28357
NSC 800, 8-bit CMOS microprocessor
[NASA-CR-195736] 08 p3405 N94-28845
Silicon germanium carbon heteroepitaxial growth on silicon
[AD-A275197] 08 p3512 N94-28889
Preparation and structure of amorphous hydrogenated carbon film deposited with RF plasma CVD
08 p3223 N94-29518
A sub-cm micromachined electron microscope
08 p3236 N94-29775
A broad-band microseismometer for planetary operations 08 p3237 N94-29778
Aggregation equilibria in arsenic doped silicon
[DE94-607269] 08 p3515 N94-30005
The role of plastic deformation in brittle and near-brittle cracking behavior 08 p3322 N94-30226
The influence of an in-situ electric field on H(+) and He(+) implantation induced defects insil icon
[DE94-006553] 08 p3518 N94-30249
Thin EFG octagons
[DE94-000257] 08 p3339 N94-30605
A high rate, low noise, x ray silicon strip detector system
[DE94-004557] 08 p3268 N94-30717
An extended approach to oxidations and nitridations of Si and Ge(x)Si(1-x) materials
[AD-A276056] 09 p3631 N94-31282
Ion beam synthesis of IrSi3 by 1-MeV Ir ion implantation into Si(111)
[DE94-006556] 09 p3896 N94-31501
A silicon condenser microphone: Modelling and electronic circuitry
[ISBN-9-09-005279-8] 09 p3688 N94-31517
A silicon condenser microphone: Materials and technology
[ISBN-9-09-005899-0] 09 p3688 N94-31518
Engineering of damage in ion implanted silicon
[ISBN-9-09-005097-3] 09 p3897 N94-31521
Electrochemical surface modification of silicon monocrystals: A surface analytic examination
[ETN-94-95733] 09 p3633 N94-31574
Ionizing radiation effects on silicon test structures
[DE94-006060] 09 p3865 N94-31607
Silicon-Film(tm) photovoltaic manufacturing technology
[DE94-000202] 09 p3760 N94-32143
Oriented Si and Ge nanocrystals formed in Al2O3 by ion implantation and annealing
[DE94-005593] 09 p3901 N94-32172
Novel optoelectronic devices based on combining GaAs and InP on Si
[AD-A277018] 09 p3693 N94-32301
Lowering the Schottky barrier at metal or silicide/Si interfaces to extend the range of infrared detectors
[AD-A277253] 09 p3903 N94-32322
Si/SiO2 interface studies by immersion ellipsometry
[AD-A277277] 09 p3881 N94-32324
Analytical solutions of minimum ionization particle induced current shapes of silicon detectors and simulation of charge collection properties
[DE94-007523] 09 p3870 N94-32355
Characterization of interface structure in multilayers using specular x ray reflectance
[DE94-007698] 09 p3657 N94-32358
Point defect production, geometry, and stability in silicon: A molecular dynamics simulation study
[DE94-008292] 09 p3903 N94-32411
A scanning defect mapping system for semiconductor characterization 09 p3885 N94-32446
Femtosecond probe-probe transmission studies of LT-grown GaAs near the band edge
[DE94-006660] 09 p3904 N94-32634
Gettering of metal impurities by cavities in silicon
[DE94-005248] 09 p3645 N94-32672
Ab initio study of the epitaxial growth of Ge on Si(100) surface
[DE94-007245] 09 p3904 N94-32724
Thin EFG octagons
[DE94-006855] 09 p3905 N94-32764
Silicon-Based Optoelectronic Materials Symposium and Materials Research Society Proceedings, volume 298
[AD-A277518] 09 p3662 N94-32952
Low energy ion beam assisted growth of homoepitaxial silicon films at low temperature
[AD-A278092] 09 p3908 N94-33039
Reconfigurable Array of Radiating Elements (RARE) controlled by light
[NASA-CR-195828] 09 p3884 N94-33073
Electrical characteristics of GaAs MESFET fabrication by ion implantation of Si or Se
[AD-A278416] 09 p3909 N94-33328
Characterization of defects in Si and SiO2-Si using positrons
[DE94-009044] 10 p4147 N94-33877
Relaxation of radiation damages in silicon planar detectors
[DE94-009084] 10 p4148 N94-34166
Three dimensional ICs intelligent sensors
10 p4057 N94-34354
A monolithic Si bolometer array for the Caltech Submillimeter Observatory
[NASA-TM-109402] 10 p4056 N94-34719
Laser drilling of vertical vias in silicon
[DE94-009250] 11 p4270 N94-35351
Large scale atomistic first principles study of adsorption and surface diffusion
[DE94-009450] 11 p4322 N94-35682
Chemical reactions of chlorine on a vicinal Si(100) surface studied by ESDIAD
[AD-A279059] 11 p4236 N94-35731
Electromagnetically levitated vibration isolation system for the manufacturing process of silicon monocrystals
11 p4223 N94-35906
Space-based crystal growth and thermocapillary flow
11 p4342 N94-35971
Determination of the Fermi level position for neutron irradiated high resistivity silicon detectors and materials using the Transient Charge Technique (TChT)
[DE94-009107] 11 p4260 N94-36221
Simulation of materials processing: Fantasy or reality?
11 p4230 N94-36404
B-lifetime measurements at the tevatron
[DE94-003617] 12 p4513 N94-36528
A possible origin of EL6 chondrites from a high temperature-high pressure solar gas
[DE94-010467] 12 p4548 N94-36759
Field emitter array RF amplifier development project. Cathode technology development. Phase 1
[AD-A280515] 12 p4437 N94-37108
Progress on the emitter wrap-through silicon solar cell
[DE94-010382] 12 p4462 N94-37189
Comparison of oxygen and silicon induced reactions at 14.6 A(GeV/C)
[DE94-011923] 12 p4518 N94-37364
A photoemission study of Au, Ge, and O2 deposition on NH4F etched Si(111)
[DE94-013352] 12 p4519 N94-37553

SILICON ALLOYS

Structure and properties of an RS Al-Si-Ni-Mn-Zr alloy for high temperature applications
01 p0064 N94-10063
EUSO-D2-experiment: Unidirectional solidification with quenching of an AlSi11 alloy 01 p0086 N94-10199
The 1.00 MeV proton radiation resistance studies of amorphous silicon-based alloy solar cells
02 p0703 N94-13639
The influence of a microgravity environment on the dendritic morphology during directional solidification of hypoeutectic Al-Si alloys
[NASA-CR-194139] 02 p0571 N94-13891
Evolving surface cusps during strained-layer epitaxy
[DE93-015430] 02 p0813 N94-14478
Research on stable, high-efficiency amorphous silicon multijunction modules
[DE93-010046] 04 p1467 N94-18518
Fundamental properties and device applications of Ge(x)Si(1-x)/Si superlattices (supplemental)
[AD-A269212] 04 p1600 N94-18884
Research on defects and transport in amorphous-silicon-based semiconductors
[DE93-017117] 05 p2013 N94-19939
Fundamental studies of defect generation in amorphous silicon alloys grown by remote plasma-enhanced chemical-vapor deposition
[DE93-017083] 05 p2029 N94-21615
Stable, high-efficiency amorphous-silicon solar cells with low hydrogen content
[DE93-018214] 05 p1848 N94-21826

Large-scale production of Si(0.8)Ge(0.2) thermoelectric alloys by mechanical alloying
[DE94-000695] 06 p2243 N94-23753
Study on production of materials with one direction solidification texture 07 p2727 N94-25572
Recombination and metastability in amorphous silicon and silicon germanium alloys
[DE94-000237] 07 p2736 N94-26481
Hot deformation behaviour of Si(p)/Al composites and their matrices and an Al-Mg-Si alloy
[ISBN-0-315-84699-2] 07 p2711 N94-27314
Continuous roll-to-roll a-Si photovoltaic manufacturing technology
[DE94-000260] 07 p2859 N94-27610
Production of an amorphous Fe(75)Si(10)B(15) sheet by a metallic mold casting method and its properties
07 p2746 N94-28170
Large-area triple-junction a-Si alloy production scale up
[DE94-000249] 08 p3339 N94-30604
In-situ characterization of growth and interfaces in a-Si:H devices
[DE94-000291] 09 p3760 N94-31812
Research on the stability, electronic properties, and structure of a-Si:H and its alloys
[DE94-000292] 09 p3899 N94-31813
Research on stable, high-efficiency amorphous silicon multijunction modules
[DE94-000298] 09 p3695 N94-32680
Large-area, triple-junction a-Si alloy production scale-up
[DE94-006856] 09 p3762 N94-32765

SILICON CARBIDES

Design concepts for load-carrying hot structures for reentry bodies 01 p0057 N94-10012
New processes for lightweight ceramic matrix composites 01 p0061 N94-10043
Study of the tribological behavior of SiC and Si3N4 ceramic couples in terms of temperature: The reality
01 p0064 N94-10061
High temperature composites in Aerospatiale activities
01 p0064 N94-10062
Damping mechanisms in chemically vapor deposited SiC fibers
[NASA-TM-106334] 01 p0066 N94-11135
The effects of an aggressive environment on the subcritical crack growth of a continuous-fiber ceramic composite
[DE93-011690] 01 p0073 N94-11612
Micromechanical modeling of laminated composites with interfaces and woven composites using the boundary element method
[NASA-TM-106280] 02 p0670 N94-13053
Processing and mechanical properties of silicon carbide platelet reinforced alumina composites
02 p0556 N94-13557
Problems and opportunities in microwave joining of ceramics
[DE93-014998] 02 p0579 N94-13888
Dynamic mechanical deformation of a SiC(sub p)/Al-Li (8090) composite
[DE93-014586] 02 p0558 N94-14121
Method of producing a silicon carbide fiber reinforced strontium aluminosilicate glass-ceramic matrix composite
[NASA-CASE-LEW-15263-2] 03 p0934 N94-15929
NEXTEL(trademark)/SiC composites using forced chemical vapor infiltration
[DE93-013532] 03 p0934 N94-16008
Environmental effects on elevated temperature subcritical crack growth of SiC/SiC composites
[DE93-015688] 03 p0934 N94-16158
Do SiC grains in Orgueil differ from those in Murchison? 03 p1242 N94-16260
The astrophysical interpretation of isotope anomalies in graphite and SiC grains of chondrites
03 p1244 N94-16343
Properties of thin films for high temperature flow sensors
[NASA-CR-191526] 03 p0967 N94-16541
Pseudomorphic semiconducting heterostructures from combinations of AlN, GaN and selected SiC polytypes: Theoretical advancement and its coordination with experimental studies of nucleation, growth, characterization and device deployment
[AD-A267561] 03 p1213 N94-17108
Diamond growth on carbide surfaces using a selective etching technique
[AD-A267989] 03 p0973 N94-17413
Interface chemistry in ceramic matrix composites
[AD-A268629] 03 p0973 N94-17466
Low temperature deposition and characterization of n- and p-type silicon carbide thin films and associated ohmic and Schottky contacts
[AD-A267966] 03 p0973 N94-17490
Carbon/carbon composites coated with SiC by chemical vapor deposition
[AD-A269934] 04 p1341 N94-18544
Shock compression properties of silicon carbide
[DE93-019927] 04 p1373 N94-19271
Analytical and experimental evaluation of joining silicon nitride to metal and silicon carbide to metal for advanced heat engine applications
[DE93-018128] 04 p1446 N94-19291
Hydrodynamic compressibility of high-strength ceramics
[DE93-019424] 05 p1698 N94-19903
Process for the homoepitaxial growth of single-crystal silicon carbide films on silicon carbide wafers
[NASA-CASE-LEW-15223-1] 05 p2017 N94-20381
Review of corrosion behavior of ceramic heat exchanger materals: Corrosion characteristics of silicon carbide and silicon nitride
[DE93-041307] 05 p1706 N94-21516
Fabrication of whisker-toughened alumina tubes
[DE94-001012] 05 p1677 N94-22022
Discontinuous phase formation and selective attack of SiC materials exposed to low oxygen partial pressure environments
[DE93-040161] 06 p2231 N94-22933
Theoretical considerations for Reaction-Formed Silicon Carbide (RFSC) formation by molten silicon infiltration into slurry-derived preforms
[NASA-TM-106414] 06 p2222 N94-23500
An overview on the main available ceramic composites and their processing routes 06 p2255 N94-24229
Ceramic matrix composites: Challenges and opportunities 06 p2255 N94-24230
An investigation of cavitation in a mechanically alloyed 15 volume percent SiCp/IN9021 aluminum composite
[DE94-003371] 07 p2748 N94-25959
Investigation of tension-compression fatigue behavior of a cross-ply metal matrix composite at room and elevated temperatures
[AD-A273731] 07 p2706 N94-25999
Effects of post-fabrication processing on the tensile properties of centrifugally cast SiC particulate reinforced aluminum composites
[AD-A274865] 07 p2707 N94-26190
Deposition of a-SiC:H using organosilanes in an argon/hydrogen plasma
[DE94-004428] 07 p2751 N94-26580
Electron microscopy of AlN-SiC interfaces and solid solutions
[DE94-002449] 07 p3059 N94-26765
Pseudomorphic semiconducting heterostructures from combinations of AlN, GaN and selected SiC polytypes: Theoretical advancement and its coordination with experimental studies of nucleation, growth, characterization and device development
[AD-A274247] 07 p3061 N94-26841
Atomic layer epitaxy of group 4 materials: Surface processes, thin films, devices and their characterization
[AD-A274325] 07 p3061 N94-26885
Low temperature deposition and characterization of N- and p-type silicon carbide thin films and associated ohmic and Schottky contacts
[AD-A274345] 07 p2754 N94-26974
Interface properties of wide bandgap semiconductor structures
[AD-A274356] 07 p3063 N94-27058
Technical report of ISSP. Ser. A, no. 2674: High-field cyclotron resonance and impurity transition in n- and p-3C-SiC at magnetic fields up to 175 T
[JTN-94-80560] 07 p3064 N94-27232
Hot deformation behaviour of Si(p)/Al composites and their matrices and an Al-Mg-Si alloy
[ISBN-0-315-84699-2] 07 p2711 N94-27314
Influence of lattice damage on retention and transport of deuterium in beta silicon carbide
[DE94-005206] 07 p3068 N94-27693
Experiment and research on materials irradiated by plasma radiation
[DE94-605011] 07 p2758 N94-27845
Low strain behaviour of a particulate reinforced aluminum alloy
[ISBN-0-315-84906-1] 07 p2744 N94-27961
Joining silicon carbide to austenitic stainless steel through diffusion welding
[PB94-126331] 08 p3297 N94-28399
Pull-test adhesion measurements of diamondlike carbon films on silicon carbide, silicon nitride, aluminum oxide, and zirconium oxide
[DE94-005469] 08 p3211 N94-28536
Characterization of structure and mechanical properties of MoSi2-SiC nanolayer composites
[DE94-004982] 08 p3175 N94-28579
MOCVD growth of GaN, AlN and AlGaN for UV photodetector applications
[AD-A275078] 08 p3512 N94-28871
A novel approach to the fabrication of SiC structures of arbitrary shape
[AD-A275475] 08 p3214 N94-29073
Thermal expansion and elastic anisotropy in single crystal Al2O3 and SiC reinforcements
[NASA-TM-106516] 08 p3214 N94-29105
Electrical conductivity measurements on a SiCp/Al alloy metal matrix composite
[PB94-138310] 08 p3263 N94-29120
Method of producing a ceramic fiber-reinforced glass-ceramic matrix composite
[NASA-CASE-LEW-15264-2] 08 p3180 N94-29508
Composite flexible blanket insulation
[NASA-CASE-ARC-11955-1-CU]
08 p3180 N94-29509
Effect of fiber coating on mechanical properties of Nicalon fibers and Nicalon-fiber/SiC matrix composites
[DE94-005477] 08 p3185 N94-30593
Creep behavior of MoSi2-SiC composites
[DE94-004980] 08 p3185 N94-30693
Synthesis of (SiC)3N4 thin films by ion implantation
[DE94-006311] 08 p3521 N94-30851
Processing of novel nanoparticle dispersion strengthened ceramics for improved mechanical performance
[AD-A275965] 09 p3649 N94-31276
Enhancement of oxidation resistance of silicon carbide by high-dose and multi-energy aluminum implantation
[DE94-006560] 09 p3640 N94-31314
The threshold energy for defect production in SiC: A molecular dynamic study
[DE94-007123] 09 p3896 N94-31499
The origin of neon-E: Neon-E in single interstellar silicon carbide and graphite grains 09 p3933 N94-31556
Interfacial behaviour: Wettability in SiC(sub p) metal matrix composites
[ISBN-0-315-87206-3] 09 p3621 N94-31835
Sodium sulfate corrosion of silicon carbide fiber-reinforced lithium aluminosilicate glass-ceramic matrix composites
[AD-A277224] 09 p3623 N94-32023
Pressureless sintering of ceramic composites
[AD-A277274] 09 p3657 N94-32404
Engineering scale development of the Vapor-Liquid-Solid (VLS) process for the production of silicon carbide fibrils
[DE94-007132] 09 p3659 N94-32618
Improved oxidation resistance of 3-D carbon/carbon composites
[AD-A277349] 09 p3625 N94-32624
Compositions and chemical bonding in ceramics by quantitative electron energy-loss spectrometry
[DE94-007208] 09 p3659 N94-32640
Conversion of polymers of methyl- and vinylsilane to Si-C ceramics
[NASA-TM-106554] 09 p3662 N94-32945
Novel precursor approached for CMC derived by polymer pyrolysis
[AD-A278383] 09 p3665 N94-33352
Laser processing of discontinuously reinforced aluminum composites
[AD-A277903] 10 p4018 N94-33593
Symposium on Inorganic and Organometallic Polymers
[AD-A277860] 10 p4027 N94-33772
Thermal cyclic oxidation behavior of the developed compositionally gradient graphite material of SiC and C in air environment
[DE94-727591] 10 p4027 N94-33872
Fabrication, phase transformation studies, and characterization of SiC-AlN-Al2OC ceramics
[DE94-009649] 10 p4028 N94-33919
Vertical and adiabatical ionization energies and electron affinities of new Si(n)C and Si(n)O (n=1-3) molecules
[AD-A278863] 11 p4324 N94-36050
Method of thermochemically treating silicon carbide fibers derived from polymers
[AD-D016218] 11 p4246 N94-36125
Properties of TMC processed by fibre coating and hiping 12 p4401 N94-36656
Fibre-matrix interface properties in Ti-matrix composites: Chemical compatibility and micromechanical behaviour
12 p4401 N94-36657
Prediction of thermal and mechanical stress-strain responses of TMC's subjected to complex TMF histories
12 p4402 N94-36666
Development of mechanical testing methods for titanium matrix composites (traction-ogligo-cyclic fatigue)
12 p4403 N94-36669
Development of nondestructive evaluation methods and prediction of effects of flaws on the fracture behavior of structural ceramics
[DE94-012466] 12 p4425 N94-37423
Theoretical studies of the transport properties in compound semiconductors
[NASA-CR-196109] 12 p4439 N94-37501

SILICON COMPOUNDS
NT ALEXANDRITE
NT ALUMINUM SILICATES
NT ANDESITE
NT ARAGONITE
NT CALCIUM SILICATES
NT CHLOROSILANES
NT DISILICIDES
NT ENSTATITE
NT FAYALITE
NT FELDSPARS
NT FLUOROSILICATES
NT FORSTERITE
NT GADOLINIUM-GALLIUM GARNET
NT GARNETS
NT MONTMORILLONITE
NT NEPHELINE
NT ORGANIC SILICON COMPOUNDS
NT POTASSIUM SILICATES
NT PYROXENES
NT QUARTZ
NT SILANES
NT SILICATES
NT SILICIDES
NT SILICON CARBIDES
NT SILICON DIOXIDE
NT SILICON NITRIDES
NT SILICON OXIDES
NT SODIUM SILICATES
NT STISHOVITE
NT TALC
NT YTTRIUM-ALUMINUM GARNET
NT YTTRIUM-IRON GARNET
NT ZEOLITES

Ellipsometric study of Si(0.5)Ge(0.5)/Si strained-layer superlattices 05 p1734 N94-20509

Spectroscopic ellipsometric characterization of Si/Si(1-x)Ge(x) strained-layer superlattices 05 p1734 N94-20510

Characteristics of shock-compressed configuration of Ti and Si powder mixtures
[DE93-018857] 05 p1713 N94-22033

Disilane LPCVD deposited silicon films: Deposition mechanisms, properties and capability of making transistors on thin films
[LAAS-93156] 06 p2252 N94-22910

Alkylene-bridged polygerm- and polygermsilsesqui-oxanes: New hybrid organic-inorganic materials
[DE94-005096] 08 p3174 N94-28557

X ray crystal structures of ((Me3SiCH2)2InCl)2 and ((Me3SiCH2)InCl2)
[AD-A275074] 08 p3513 N94-29155

Thermochemical data for CVD modeling from ab initio calculations
[DE94-005269] 08 p3222 N94-30909

Critical analysis by way of hole etching with a manufacturable RIE process using SiCl4 and BCl3 and Cl2 chemistries
[DE94-007736] 10 p4148 N94-35081

Measurement of the decay rate of the SiH feature as a function of temperature 11 p4318 N94-36171

Substituted silyl-terminated compounds and polymers thereof
[AD-D016310] 12 p4427 N94-37779

SILICON CONTROLLED RECTIFIERS

Design of power electronics for TVC EMA systems
[NASA-CR-193839] 04 p1407 N94-19642

SILICON DIOXIDE
NT QUARTZ
NT STISHOVITE

Thermal-optical switching of a silicon based interference filter
[AD-A265152] 01 p0174 N94-11095

Characterization of the Si/SiO2 interfere morphology from quantum oscillations in Fowler-Nordheim tunneling currents
[AD-A265149] 01 p0143 N94-11160

Radiation-induced aperiodicity in irradiated ceramics
[DE93-013335] 01 p0091 N94-11698

Development of a molecular beam technique to study early solar system silicon reactions 01 p0432 N94-12224

1/f noise and oxide traps in MOSFETs
[DE93-007581] 02 p0619 N94-12942

Linear and nonlinear spectroscopic probing of solute interactions with chemically modified silica surface
[DE93-014648] 02 p0562 N94-13001

Theory of the electronic and structural properties of solid state oxides
[DE93-016051] 02 p0811 N94-14296

Molecular simulator: A basic tool for submicron MOS processes development
[LAAS-92484] 02 p0814 N94-14697

Reactor studies of metal ions associated with chromatographic silica
[AD-A266675] 02 p0573 N94-14779

Fine-powder Al2O3 and SiO2 for preparation of multielement standards for rare-earth elements analysis
[DE93-625118] 02 p0567 N94-14884

NMR and theoretical investigation of cation binding with sol-gel silicates
[AD-A266999] 03 p0963 N94-15631

Optical and infrared spectra of thermally annealed Pb implanted SiO2 glasses
[DE93-015304] 03 p0965 N94-15828

Gas separations using ceramic membranes
[DE93-000278] 03 p0947 N94-15861

Removal of carbonaceous contaminants from silica aerogel 03 p0953 N94-16256

Silica-bearing objects in the Dengli H3.8 and Gorlovka H3-4 chondrites 03 p1242 N94-16265

An investigation of the hydrolytic resistance of sodium-calcium plate glass with a layer of silica deposited on its surface
[IFTR-34/1991] 03 p0971 N94-17120

Kinetics of silica-phase transitions
[DE93-016231] 03 p1217 N94-17659

Catalytic hydrocarbon reactions over supported metals
[DE93-018168] 04 p1345 N94-17808

Aerogels for microelectronic applications: Fast, inexpensive, and light as air
[DE93-017170] 04 p1395 N94-17882

Optical properties of oxide coatings prepared by ion-assisted deposition
[AD-A270024] 04 p1599 N94-18711

High resolution transmission electron microscopy of mesoporous MCM-41 type materials
[AD-A271271] 04 p1354 N94-19728

Quartz/fused silica chip carriers
[NASA-CR-194154] 05 p2016 N94-20340

Evaporation in equilibrium, in vacuum, and in hydrogen gas 05 p1684 N94-20638

Alumoxanes: Rationalization of black box materials
[AD-A272805] 05 p1704 N94-21170

Dynamics of adsorbed, swollen block copolymers
[AD-A272013] 05 p1706 N94-21460

Precision prism coupling setup applied to measure planar silica films on silicon, appendix 9 05 p1989 N94-21603

Glass-ceramic Li-Al-Si-O composition and process for its production
[CA-PATENT-APPL-SN-2043757] 06 p2254 N94-24129

Study on reactions between molten metal and oxide by magnetic flotation dissolution method 07 p2725 N94-25558

Study on synthesis and characteristics of intermetallic compound with strong electron correlation 07 p2726 N94-25563

The microstructural response of granular soil under uniaxial strain
[AD-A274808] 07 p2763 N94-26341

A space fiber-optic x ray burst detector
[DE94-002722] 07 p2696 N94-26808

Technical report of ISSP. Ser. A, no. 2671: Quasi-localization of light waves in Fibonacci dielectric multilayers
[JTN-94-80557] 07 p3064 N94-27231

Simulations of terrestrial in-situ cosmogenic-nuclide production
[DE94-004999] 07 p3117 N94-27826

Development of novel switchable protein surfaces
[AD-A275510] 08 p3384 N94-28667

Float polishing studies of fused silica
[AD-A275001] 08 p3213 N94-28886

Inorganic polymer-derived ceramic membranes
[DE94-000082] 08 p3216 N94-29830

Nanosize metal alloy particle formation in Ag and Cu sequentially implanted silica
[DE94-005592] 08 p3207 N94-30042

Kinetics of surface roughening and smoothing during ion sputtering
[DE94-006358] 08 p3219 N94-30263

Silica scintillating materials prepared by sol-gel methods
[DE94-005123] 08 p3220 N94-30778

Surface chemistry of boron-doped SiO2 CVD: Enhanced uptake of tetraethyl orthosilicate by hydroxyl groups bonded to boron
[DE94-005428] 08 p3221 N94-30896

Evidence for a correct SiO2 voltage acceleration model
[DE94-006578] 09 p3690 N94-31594

Hydrogen incorporation and radiation induced dynamics in metal-oxide-silicon structures: A study using nuclear reaction analysis
[ETN-94-95742] 09 p3898 N94-31610

Preparation of catalyst particles using methods of colloid chemistry. Part 1: Preparation of silica particles from alcohol solutions
[PB94-135597] 09 p3634 N94-31679

Electrical properties of double layer dielectric structures for space technology
[ISBN-0-315-86547-4] 09 p3610 N94-31910

Chemical vapor deposition of metal nitrides, phosphides, and arsenides
[DE94-008096] 09 p3654 N94-31976

Sol-gel coatings for high power laser optics: Past, present, and future
[DE94-007240] 09 p3718 N94-32252

Si/SiO2 interface studies by immersion ellipsometry
[AD-A277277] 09 p3881 N94-32324

Dynamics of block poly(styrene-co-vinylpyridine) (SVP) in solution and on silica
[AD-A277139] 09 p3657 N94-32364

Multiple size scale structures in silica/siloxane composites studied by small-angle scattering
[DE94-007300] 09 p3625 N94-32642

Enhanced thermal capacity aerogels summary report, FY 1993
[DE94-008888] 09 p3639 N94-33260

Purity and cleanness of aerogel as a cosmic dust capture medium 11 p4247 N94-35469

Cross-condensation reactions in an organically modified silica sol-gel
[DE94-010086] 11 p4244 N94-35701

Spinnability of silica sols: The role of alkoxy group exchange
[DE94-010087] 11 p4244 N94-35702

Kinetics of phase transformations in glass forming systems
[NASA-CR-196082] 11 p4245 N94-35977

Coatings for SiO2 optical fibers
[AD-D016197] 11 p4334 N94-36363

Mineralogy and metallurgical properties of iron ore sinter based on magnetite fines
[DE94-763309] 12 p4414 N94-36525

Low temperature atmospheric pressure chemical vapor deposition of group 14 oxide films
[DE94-013115] 12 p4425 N94-37317

SILICON FILMS

Workshop summary: New silicon cells 01 p0054 N94-11417

An ellipsometry investigation of nucleation and growth of electron cyclotron resonance plasma deposited silicon films
[AD-A265037] 01 p0401 N94-11651

Ion assisted sputter deposition of Mo-Si multilayers
[DE93-013830] 02 p0583 N94-14693

Thin Ni silicide formation by low temperature-induced metal atom reaction with ion implanted amorphous silicon
[DE93-015449] 03 p1209 N94-16066

Development of large-area monolithically integrated silicon-film photovoltaic modules
[DE93-010037] 04 p1464 N94-17731

Refractive index behaviour of phosphorus-doped planar silica waveguides, appendix 7 05 p1989 N94-21601

Precision prism coupling setup applied to measure planar silica films on silicon, appendix 9 05 p1989 N94-21603

Electron microscopy studies of undoped and phosphorus doped Si:H and Si,C:H films
[DE94-004738] 07 p3069 N94-27757

Silicon-Film (tm) photovoltaic manufacturing technology
[DE94-000258] 08 p3336 N94-28501

Energy losses of fast charged particles in thin silicon detectors
[DE94-606065] 08 p3483 N94-28552

Low energy ion beam assisted growth of homoepitaxial silicon films at low temperature
[AD-A278092] 09 p3908 N94-33039

SILICON ISOTOPES

Si-29 NMR spectroscopy of naturally-shocked quartz from Meteor Crater, Arizona: Correlation to Kieffer's classification scheme 01 p0080 N94-12087

NMR spectroscopy of experimentally shocked single crystal quartz: A reexamination of the NMR shock barometer 01 p0081 N94-12258

Office of Naval Research/DARPA publications: Composite materials with improved properties in compression
[AD-A265509] 02 p0560 N94-14794

Simulation studies for surfaces and materials strength
[NASA-CR-193387] 03 p1056 N94-15004

Do SiC grains in Orgueil differ from those in Murchison? 03 p1242 N94-16260

Direct images of thermal disorder in the Cl-Si and H-O-Si chemisorption bond on Si(100)
[AD-A272386] 05 p1680 N94-21145

Production of (phi) mesons in central Si + Au collisions at 14.6 AGeV/c
[DE94-003196] 07 p3012 N94-25795
On radiation defects in strip detectors
[DE93-616646] 07 p3015 N94-25916
The Cherenkov hadronic like-jets
[DE93-634525] 07 p3016 N94-26010
Sol-gel derived silica/siloxane composite materials: The effect of loading level and catalyst activity on silica domain formation
[DE94-002734] 07 p2712 N94-27710
Production of phi mesons in central Si+Au collisions at 14.6 A GeV/c
[DE94-011726] 12 p4516 N94-37152

SILICON JUNCTIONS
The influence of an in-situ electric field on H(+) and He(+) implantation induced defects insil icon
[DE94-006553] 08 p3518 N94-30249
Si/SiO2 interface studies by immersion ellipsometry
[AD-A277277] 09 p3881 N94-32324
Resistivity measurements on the neutron irradiated detector grade silicon materials
[DE94-009083] 09 p3906 N94-32822
A critical examination of charge funneling and its impact on single-event upset in Si devices
[DE94-007868] 11 p4261 N94-36373

SILICON NITRIDES
Study of the tribological behavior of SiC and Si3N4 ceramic couples in terms of temperature: The reality
01 p0064 N94-10061
Protective coatings for high-temperature polymer matrix composites
[NASA-TM-106276] 01 p0074 N94-12431
Quantitative mapping of pore fraction variations in silicon nitride using an ultrasonic contact scan technique
[NASA-TP-3377] 02 p0665 N94-13056
Processing and testing of high toughness silicon nitride ceramics
[NASA-CR-191190] 02 p0582 N94-14543
Laser assisted CVD growth of AlN and GaN
[AD-A267150] 03 p1206 N94-15764
The influence of microstructure on the mechanical behavior of silicon nitride ceramics
[DE93-015363] 03 p0966 N94-16018
Multiaxial deformation and life prediction model and experimental data for advanced silicon nitride ceramics
[DE93-015450] 03 p0967 N94-16067
Crystallization of grain boundary phases in silicon nitride with low additive contents by microwave annealing
[DE93-015801] 03 p1209 N94-16164
Detection of subsurface defects in machined silicon nitride ceramics by optical scattering methods
[DE93-015554] 03 p0968 N94-16658
Development of a constitutive model for creep and life prediction of advanced silicon nitride ceramics
[DE93-015894] 03 p0968 N94-16813
The Ceramic Technology Project: Ten years of progress
[DE93-015991] 03 p0968 N94-16843
Processing of complex sintered reaction bonded silicon nitride parts by microwave heating
[DE93-015811] 03 p0969 N94-16877
Equipment for investigation of cryogenic compaction of nanosize silicon nitride powders
[DE93-018740] 04 p1340 N94-18180
Analytical and experimental evaluation of joining silicon nitride to metal and silicon carbide to metal for advanced heat engine applications
[DE93-018128] 04 p1446 N94-19291
Atomic-scale friction and microfriction of graphite and diamond using friction force microscopy
[AD-A270952] 04 p1605 N94-19679
Sintering silicon nitride
[NASA-CASE-LEW-15489-1] 05 p1703 N94-20529
Microstructural modeling and toughening of Si3N4 ceramics for high temperature engine applications
[AD-A272897] 05 p1704 N94-21197
Review of corrosion behavior of ceramic heat exchanger materals: Corrosion characteristics of silicon carbide and silicon nitride
[DE93-041307] 05 p1706 N94-21516
A novel semiconductor process for optoelectronic applications on silicon substrate
05 p1988 N94-21595
Electron holography applied to the study of ceramic materials
[DE94-000329] 05 p1707 N94-21653
Surface and subsurface defect detection in Si3N4 components by laser scattering
[DE93-040829] 05 p1832 N94-21772
Effect of powder characteristics on gas-pressure sintering of Si3N4 with rare earth additives
[DE94-000330] 05 p1694 N94-21945
Particle formation in a laser-heated aerosol reactor. Application to silicon and silicon nitride synthesis
[PB93-217982] 06 p2347 N94-22982
Development of silicon nitride composites with continuous fiber reinforcement
[DE94-001996] 06 p2227 N94-23022
Wear reduction in ceramic bearings by surface generated pyrolytic carbon continuously replenished by ethylene gas
[AD-A278264] 06 p2364 N94-24090
Selection of polymer binders and fabrication of SiC fiber-reinforced reaction-bonded silicon nitride matrix composites
[NASA-CR-194874] 06 p2255 N94-24223
The mechanical properties of single crystal (alpha)-Si3N4
[DE94-002632] 06 p2563 N94-24517
The fracture behavior of a CVD crystalline Si3N4/amorphous Si3N4 composite
[DE94-002646] 07 p2750 N94-26124
The importance of vibrationally excited nitrogen in silicon nitride deposition systems
[AD-A274874] 07 p2750 N94-26167
Pull-test adhesion measurements of diamondlike carbon films on silicon carbide, silicon nitride, aluminum oxide, and zirconium oxide
[DE94-005469] 08 p3211 N94-28536
ECR plasma synthesis of silicon nitride films on GaAs and InSb
[DE94-005575] 08 p3515 N94-30006
Sliding friction and wear between titanium nitride, M50 steel and silicon nitride (round 3 of VAMAS wear test program)
[IMR-TM-TR-003] 08 p3303 N94-30019
Direct measurement of the reactivity of NH and OH on a silicon nitride surface
[DE94-005286] 08 p3199 N94-30260
Synthesis of (SiC)3N4 thin films by ion implantation
[DE94-006311] 08 p3521 N94-30851
Effects of oxidation and creep damage mechanisms on creep behavior in HIPed silicon nitrides
[DE94-006559] 09 p3618 N94-31313
Reliability analysis of structural ceramics subjected to biaxial flexure 09 p3650 N94-31454
Electrical properties of double layer dielectric structures for space technology
[ISBN-0-315-86547-4] 09 p3610 N94-31910
Chemical vapor deposition of metal nitrides, phosphides, and arsenides
[DE94-008096] 09 p3654 N94-31976
Joining of silicon nitrides using oxynitride glasses
[DE94-008517] 09 p3658 N94-32517
Novel precursor approached for CMC derived by polymer pyrolysis
[AD-A278383] 09 p3665 N94-33352
Symposium on Inorganic and Organometallic Polymers
[AD-A277860] 10 p4027 N94-33772
Tensile strength of dried gelcast green bodies
[DE94-009453] 10 p4028 N94-33930
Damage mechanisms and controlled crack propagation in a hot pressed silicon nitride ceramic
[NASA-TM-106595] 10 p4029 N94-34234
A combined experimental and theoretical study of the neutral, cationic and anionic Si3N cluster molecule
[AD-A278834] 11 p4323 N94-35792
The growth of silicon nitride crystalline films using microwave plasma enhanced chemical vapor deposition
[AD-A278862] 11 p4340 N94-35828

SILICON OXIDES
NT QUARTZ
NT SILICON DIOXIDE
NT STISHOVITE
Development of a molecular beam technique to study early solar system silicon reactions
01 p0432 N94-12224
Multicrystalline silicon solar cells: Gettering optimization and characterization
[DE93-015001] 02 p0705 N94-14861
Electrochemical planarization for microelectronic circuits
[DE93-017214] 02 p0627 N94-14870
SONOS technology for commercial and military nonvolatile memory applications
[DE93-015647] 03 p1011 N94-16661
Kinetics of silica-phase transitions
[DE93-016231] 03 p1217 N94-17659
Neutron-scattering studies of Yb-bearing silicate glasses
[DE93-019768] 05 p1700 N94-20265
Light scattering studies of an electrorheological fluid
[DE93-019419] 05 p1700 N94-20315
Properties of E-beam interactive oxide films for nanometer scale structures
[AD-A272848] 05 p1675 N94-21191
Shock compression of low-density foams
[DE93-040545] 05 p1707 N94-21546
Refractive index behaviour of phosphorus-doped planar silica waveguides, appendix 7 05 p1989 N94-21601
Sol-gel derived silica/siloxane composite materials: The effect of loading level and catalyst activity on silica domain formation
[DE94-002734] 07 p2712 N94-27710
Selection of the Space Station Freedom (SSF) Flat Collector Circuit (FCC) insulation material
08 p3165 N94-28701
Charge trapping and breakdown in N2O oxides
[DE94-003775] 08 p3266 N94-30040
Characterization of defects in Si and SiO2-Si using positrons
[DE94-009044] 10 p4147 N94-33877
Vertical and adiabatical ionization energies and electron affinities of new Si(n)C and Si(n)O (n=1-3) molecules
[AD-A278863] 11 p4324 N94-36050
Enhanced charge trapping in bipolar spacer oxides during low-dose-rate irradiation
[DE94-007863] 11 p4260 N94-36268

SILICON POLYMERS
NT METHYL POLYSILOXANES
NT SILICONES
NT SILOXANES
Optical diagnostic instrument for monitoring etch uniformity during plasma etching of polysilicon in a chlorine-helium plasma
[DE93-019582] 05 p1993 N94-20261
Particle behavior in an ECR plasma etch tool
[DE93-040343] 05 p1996 N94-21769
Color head down display program
[AD-A274807] 07 p2672 N94-26340
Layered polysilicate: Properties and perspectives in applications 08 p3223 N94-29513
Inorganic polymer-derived ceramic membranes
[DE94-000082] 08 p3216 N94-29830

SILICON RADIATION DETECTORS
Silicon-based elementary particle tracking system: Materials science and mechanical engineering design
[DE93-012630] 01 p0065 N94-10740
Fast trigger algorithm for B-events selection
[DE93-621452] 01 p0365 N94-11089
Relativistic heavy ion research
[DE93-013127] 01 p0367 N94-11373
Theory of elementary particles and accelerator theory. Task C: Experimental high energy physics
[DE93-013139] 01 p0368 N94-11696
Experimental particle physics at the University of Pittsburgh
[DE93-013326] 01 p0369 N94-12546
Metal-semiconductor, composite radiation detectors
[DE93-013313] 02 p0619 N94-12994
Proceedings of the Workshop on Applications of Synchrotron Radiation to Trace Impurity Analysis for Advanced Silicon Processing
[DE93-013389] 02 p0805 N94-13020
Gamma large area silicon telescope: Applying Si strip detector technology to the detection of gamma rays in space 03 p0904 N94-15061
Experimental research in high energy physics
[DE93-011912] 04 p1574 N94-18916
The GEM Silicon Tracking System
[DE93-040133] 05 p2016 N94-20322
Examination of the response capacity of a silicon pixel detector for ions and molecules in the energy area 100 to 300 keV
[MPE-241] 06 p2346 N94-25415
Lithium drifted silicon detector fabrication on gettered floating-zone silicon
[DE94-003890] 07 p3054 N94-26095
Gamma Large Area Silicon Telescope (GLAST): Applying silicon strip detector technology to the detection of gamma rays in space
[DE94-003451] 07 p3116 N94-27740
Energy losses of fast charged particles in thin silicon detectors
[DE94-606065] 08 p3483 N94-28552
Pulse height response of Si surface barrier detectors
08 p3497 N94-30221
A low noise silicon detector preamplifier system for room temperature x ray spectroscopy
[REPT-93-058] 08 p3291 N94-30930
Gamma Large Area Silicon Telescope (GLAST)
[DE94-006439] 09 p3925 N94-31786
Resistivity measurements on the neutron irradiated detector grade silicon materials
[DE94-009083] 09 p3906 N94-32822

SILICON SOLAR CELLS
U SOLAR CELLS

SILICON TRANSISTORS
NT SOS (SEMICONDUCTORS)
Technology transfers and reliable oxides
[AD-A266948] 03 p1175 N94-15758
Disilane LPCVD deposited silicon films: Deposition mechanisms, properties and capability of making transistors on thin films
[LAAS-93156] 06 p2252 N94-22910

Silicon device performance measurements to support temperature range enhancement
[NASA-CR-195265] 07 p2844 N94-27824
SILICON-ON-INSULATOR SEMICONDUCTORS
U SOI (SEMICONDUCTORS)
SILICON-ON-SAPPHIRE JUNCTIONS
U SOS (SEMICONDUCTORS)
SILICON-ON-SAPPHIRE SEMICONDUCTORS
U SOS (SEMICONDUCTORS)
SILICON-ON-SAPPHIRE TRANSISTORS
U SOS (SEMICONDUCTORS)
SILICONE RUBBER
Effects of orbital exposure on RTV during the LDEF mission 09 p3597 N94-31043
SILICONES
NT METHYL POLYSILOXANES
NT SILOXANES
Qualification test of the Ross Double Planetary Mixer
[NASA-CR-192600] 02 p0652 N94-14497
Laser driven hydrodynamic instability experiments
[DE93-040550] 05 p1818 N94-21547
Viscous rotary damper 06 p2361 N94-24031
Low Earth orbit durability evaluation of protected silicone for advanced refractive photovoltaic concentrator arrays
[NASA-TM-106543] 08 p3172 N94-28999
Silicone grease as a precursor to a pseudo crown-ether ligand: Crystal structure of (K(+)K(Me2SiO)7(+))(HIn(CH2CMe3)3(-))4)
[AD-A276343] 09 p3895 N94-31327
Syntheses and studies of acetylenic polymers
[DE94-011201] 11 p4245 N94-36057
Replacement of silicone polymer A with silicone polymer B and the subsequent characterization of the new cellular silicone materials
[DE94-010105] 12 p4421 N94-36474
SILK
Materials Research Society Symposium Proceedings, Volume 292: Biomolecular Materials
[AD-A265776] 03 p1116 N94-15138
SILOXANES
A non-halogenated, flame retarded polycarbonate 01 p0019 N94-10781
Unexpectedly rapid hydrosilation polymerization of the diallyl derivative of bisphenol A and 2,6-diallylphenol
[AD-A265832] 02 p0577 N94-12986
Intramolecular versus intermolecular condensation rates in the acidic polymerization of octaethoxytrisiloxane
[AD-A266982] 03 p0963 N94-15490
Sol-gel derived silica/siloxane composite materials: The effect of loading level and catalyst activity on silica domain formation
[DE94-002734] 07 p2712 N94-27710
Polyimides containing pendent siloxane groups
[NASA-CASE-LAR-14638-1] 08 p3215 N94-29555
Multiple size scale structures in silica/siloxane composites studied by small-angle scattering
[DE94-007300] 09 p3625 N94-32642
Organosilicon polymeric nonlinear optical materials for optical switching and modulation
[AD-A278245] 10 p4140 N94-33381
Carborane-siloxane or silane-unsaturated hydrocarbon based polymers
[AD-D016220] 12 p4425 N94-37482
SILTS
U SEDIMENTS
SILVER
The effects of organic adsorbates on the underpotential deposition of silver on Pt(111) electrodes
[AD-A265623] 01 p0404 N94-12376
Nonlinear optical spectroscopy of Ag(111) in electrolyte and in vacuum
[AD-A265622] 01 p0079 N94-12534
Performance of silvered Teflon thermal control blankets on spacecraft
[AD-A266284] 03 p0887 N94-16909
Growth of dielectric thin films by irradiation of condensed molecular precursors with synchrotron radiation
[DE93-016161] 03 p0974 N94-17676
Surface second harmonic generation studies of stepped Ag(111) electrode surfaces
[AD-A265205] 04 p1594 N94-17876
Optical frequency doubling at adsorbates of silver(110) surface
[ETN-93-94837] 04 p1603 N94-19355
The proximity effect in ultrathin granular Pb films
[AD-A271094] 05 p2012 N94-19848
Formation of colloidal Ag precipitates in fused silica by MeV ion implantation
[DE93-040268] 05 p2012 N94-19869
Silver lined ceramic vessel
[AD-D015917] 05 p1700 N94-20057
Some results of the oxidation investigation of copper and silver samples flown on LDEF 05 p1660 N94-21375
Thermomechanical processing of Ag-clad Bi2Sr2CaCu2O(x) superconductors
[DE94-002347] 06 p2563 N94-24624
Sweep rate and concentration effects on metastable structures formed in the underpotential deposition of silver on Pt(111)
[AD-A275369] 08 p3189 N94-29010
Crystallization of silver chromate from ethanol via salt metathesis reactions of solubilized precursors
[AD-A275178] 08 p3189 N94-29058
Halogen chemisorption on silver(111): Scanning tunneling microscopy of coadsorbed halogen atoms
[AD-A275219] 08 p3486 N94-29060
Nanosize metal alloy particle formation in Ag and Cu sequentially implanted silica
[DE94-005592] 08 p3207 N94-30042
High performance YBCO films
[AD-A276493] 09 p3897 N94-31531
On the formation of muon- and zeta-phases in Ag-Al system by mechanical alloying
[DE94-007125] 09 p3645 N94-32636
Effect of niobium interlayer on high-temperature sliding friction and wear of silver films on alumina
[DE94-010462] 11 p4275 N94-36232
SILVER ALLOYS
Liquid and solid solubility of Ag in Bi2Sr2CaCu2O8
[DE94-002829] 07 p2735 N94-26273
Giant magnetoresistance and microstructural characteristics of epitaxial Fe-Ag and Co-Ag granular thin films
[DE94-006287] 08 p3519 N94-30707
On the formation of muon- and zeta-phases in Ag-Al system by mechanical alloying
[DE94-007125] 09 p3645 N94-32636
Phase relationships and stability of the (mu)- and (zeta)-phases in the Ag-Al-X (X=Zn, Ga, Ge) systems
[DE94-009391] 09 p3648 N94-33270
SILVER BROMIDES
The Cherenkov hadronic like-jets
[DE93-634525] 07 p3016 N94-26010
SILVER COMPOUNDS
NT SILVER BROMIDES
NT SILVER OXIDES
SILVER HALIDES
NT SILVER BROMIDES
SILVER OXIDE ZINC BATTERIES
U SILVER ZINC BATTERIES
SILVER OXIDES
Silver oxide batteries: Recent improvements and developments 05 p1752 N94-20629
Atomic-scale chemistry of metal surfaces
[REPT-A-2657] 07 p3012 N94-25636
SILVER ZINC BATTERIES
Aerospace applications of batteries 06 p2390 N94-23346
Battery study for the Mars Environmental Survey (MESUR) Pathfinder 07 p2860 N94-28105
Bipolar Ag-Zn battery 07 p2864 N94-28135
Advanced silver zinc battery development for the SRB and ET range safety subsystems 07 p2865 N94-28136
Development of silver-zinc cells of improved cycle life and energy density
[AD-A277311] 09 p3693 N94-32329
SILVICULTURE
SIMA: A model for forest succession based on the carbon and nitrogen cycles with application to silvicultural management of the forest ecosystem
[SILVA-CARELICA-22] 07 p2848 N94-26258
SIM
STS-40 crew during spacelab Sim
[NASA-TM-109493] 03 p0876 N94-15452
SIMD (COMPUTERS)
Layering techniques for development of parallel systems: An algebraic approach
[MEMO-INF-92-62] 01 p0335 N94-10277
Efficient, massively parallel eigenvalue computation
[NASA-CR-194289] 02 p0760 N94-13921
An overview of parallel scientific visualization
[DE93-017105] 02 p0755 N94-14521
Identification of continuous-time dynamical systems: Neural network based algorithms and parallel implementation
[DE93-014427] 02 p0766 N94-14737
Parallel optimization algorithms and their implementation in VLSI design 04 p1401 N94-18374
Distributed memory parallel computers and computational fluid dynamics 04 p1413 N94-18568
Conception and analysis of numerical parallel algorithms: Realization on the Connection Machine
[ETN-93-95005] 04 p1531 N94-19517
Fast data parallel polygon rendering
[DE93-040157] 05 p1929 N94-20279
Application of multigrid methods to the solution of liquid crystal equations on a SIMD computer 06 p2484 N94-23686
An efficient three-dimensional Poisson solver for SIMD high-performance-computing architectures 09 p3823 N94-31120
Three-dimensional radiative transfer calculations on an SIMD machine applied to accretion disks 09 p3932 N94-31141
Proof of concept for the rewrite rule machine: Interensemble studies
[AD-A276506] 09 p3809 N94-31263
Methods of implementing the Viterbi algorithm on a massively parallel computer of the SIMD (single instruction multiple data) type
[ISBN-0-315-86783-3] 09 p3814 N94-31752
An analysis of instruction-cached SIMD computer architecture
[AD-A276519] 09 p3806 N94-31934
Transformational derivation of (parallel) programs using skeletons
[TR-93-20] 09 p3825 N94-32196
SIMICOR (IMAGE CORRELATOR)
U IMAGE CORRELATORS
SIMILARITIES
U ANALOGIES
SIMILARITY NUMBERS
Design of scaled down structural models 12 p4457 N94-37797
SIMILARITY THEOREM
Similarity solutions for gravity-dominated spreading of a lens of organic contaminant
[REPT-93-24] 04 p1420 N94-19139
Structural similitude and design of scaled down laminated models
[NASA-CR-194687] 05 p1673 N94-20172
SIMILITUDE LAW
Workshop on Scaling Effects in Composite Materials and Structures
[NASA-CP-3271] 12 p4457 N94-37796
Design of scaled down structural models 12 p4457 N94-37797
On nature's scaling effects 12 p4459 N94-37803
SIMPLE HARMONIC MOTION
An asymptotic expansion of an electromagnetic field in the velocity of a caustic in the form of simple waves
[IFTR-14/1991] 03 p1002 N94-17048
SIMPLEX METHOD
Design of a continuous resistively loaded monopole antenna
[AD-A265852] 01 p0138 N94-12281
Parallel optimization algorithms and their implementation in VLSI design 04 p1401 N94-18374
A teaching tool for linear programming
[AD-A270240] 04 p1523 N94-18905
A simplicial approach to integer programming, part 2
[REPT-93-47-PT-2] 07 p2958 N94-25764
SIMPLIFICATION
Simplification-driven automated partial evaluation
[DE93-012890] 02 p0768 N94-13391
Time dependent turbulence modeling and analytical theories of turbulence
[NASA-TM-106379] 03 p1029 N94-17385
SIMS (SPECTROMETRY)
U SECONDARY ION MASS SPECTROMETRY
SIMULATED ALTITUDE
U ALTITUDE SIMULATION
SIMULATED ANNEALING
Simulated annealing for the problem of multiresource location on graph
[REPT-93-033] 02 p0770 N94-13809
Data fusion through simulated annealing of registered range and reflectance images
[DE93-015910] 04 p1612 N94-17858
The application of simulated annealing to stochastic systems
[AD-A273850] 07 p3001 N94-25807
Use of snakes to link edge points to create left ventricular boundaries in echocardiographic images
[TELECOM-93-D-016] 08 p3395 N94-30970
An investigation of simulated annealing applied to structural optimization problems
[AD-A278461] 10 p4068 N94-33541
SIMULATION
NT ACOUSTIC SIMULATION
NT ALTITUDE SIMULATION
NT ANALOG SIMULATION
NT ATMOSPHERIC ENTRY SIMULATION
NT COMPUTER SYSTEMS SIMULATION
NT COMPUTERIZED SIMULATION
NT CONTROL SIMULATION
NT DIGITAL SIMULATION
NT ENVIRONMENT SIMULATION
NT FLIGHT SIMULATION
NT LANDING SIMULATION
NT MOTION SIMULATION
NT NEUTRAL BUOYANCY SIMULATION
NT SPACE ENVIRONMENT SIMULATION

NT SYSTEMS SIMULATION
NT THERMAL SIMULATION
NT WEIGHTLESSNESS SIMULATION
Functional reasoning, explanation, and analysis
[DE92-526832] 01 p0313 N94-10251
Photostimulated attenuation of hypersound in superlattice
[DE93-611231] 01 p0357 N94-10408
The development of an interactive synthesis tool for intelligent controllers of modular, reconfigurable robots
01 p0339 N94-10898
Simulation of images of water vapor channel and infrared split channel 01 p0190 N94-11081
Gas-Grain Simulation Facility (GGSF). Volume 2: Conceptual design definition
[NASA-CR-177613] 01 p0423 N94-11229
Large eddy simulations of the atmospheric boundary layer east of the Colorado Rockies
01 p0277 N94-11465
Discrete Kalman filtering equations of second-order form for control-structure interaction simulations
[NASA-CR-193723] 01 p0331 N94-11522
Simulation studies for surfaces and materials strength
[NASA-CR-193305] 02 p0671 N94-13179
Lightning simulation and determination of expected striking points
[ITN-93-85202] 02 p0719 N94-13188
Event-driven simulation in SELMON: An overview of EDSE
[NASA-CR-194505] 02 p0749 N94-13784
Development of test techniques to simulate high-frequency mechanical shock on weapon components
[KCP-613-4998] 02 p0675 N94-13907
Laboratory simulations of lunar darkening processes
02 p0843 N94-14301
Modeling surface area to volume effects on borosilicate glass dissolution
[DE93-011891] 02 p0581 N94-14432
Computational diagnostics for detecting phase transitions during nanoindentation
[DE93-016536] 02 p0813 N94-14439
Fuzzy control and fuzzy kinematic mapping for a redundant space robot
[AD-A266866] 03 p1163 N94-14950
STS-26 generic integrated IUS deploy simulation
[NASA-TM-109562] 03 p0875 N94-15332
STS-32 LDEF approach in SES
[NASA-TM-109474] 03 p0880 N94-15379
STS-31 HST deploy sim in SMS and MOCR
[NASA-TM-109482] 03 p0876 N94-15449
STS-26 long duration simulation: Crew entering SMS
[NASA-TM-109560] 03 p0876 N94-15474
A measurement station for study of Earth moving tools and ground cutting processes
[IFTR-10/1991] 03 p0985 N94-17068
Efficient simulation of DEDS by means of standard clock techniques: Queueing and integrated radio network examples
[AD-A269878] 04 p1432 N94-18681
Efficiency and biofidelity of occupant simulations
04 p1459 N94-19473
Evaluation of a scanning Hartmann device for single point turning applications
[DE93-019204] 05 p1821 N94-19891
Study of regional climate change
[DE93-018926] 05 p1850 N94-19941
A comparative study of an ABC and an artificial absorber for truncating finite element meshes
[NASA-CR-194275] 05 p1716 N94-20160
SPH modelling of energy partitioning during impacts on Venus 05 p2124 N94-20809
Atmospheric breakup of a small comet in the Earth's atmosphere 05 p2084 N94-20824
Synoptic observations of near surface processes of an insolated ice-dust body under space conditions: The case of KOSI 9 and 10 05 p2084 N94-20827
Application of a back-propagation neural network to isolated-word speech recognition
[AD-A272495] 05 p1945 N94-21430
New welding and finishing procedures
[DE94-602022] 06 p2352 N94-23025
Robust stability of second-order systems
[NASA-CR-195175] 06 p2488 N94-24564
Solid rocket combustion simulator technology using the hybrid rocket for simulation
[NASA-CR-195142] 06 p2265 N94-24578
Admittance model for the shuttle remote manipulator system in four configurations
[NASA-CR-4555] 06 p2474 N94-24635
Numerical simulation of cylindrical, self-field MPD thrusters with multiple propellants
[NASA-CR-194458] 06 p2220 N94-24714
BEM solution for the simulation of axisymmetric viscous sintering
[PB93-237717] 06 p2336 N94-24761
Simulation of the vortex motion in the high T(c) superconductors
[DE93-617138] 06 p2567 N94-25403
Zr-rich corner of the Zr-Sn-O diagram
[DE93-633764] 07 p2734 N94-26161
Fire simulation based on convection calculation
[VTT-TIED-1411] 07 p2762 N94-26259
Numerical simulation of plasma vertical position stabilization in ITER
[DE93-634588] 07 p3044 N94-26510
Feasibility study on introduction of transportation-use petroleum substitution energy
[DE94-725205] 07 p2759 N94-26905
Modal logic, transition systems and processes
[CWI-CS-R9321] 07 p2970 N94-27549
Forward and backward simulations. Part 1: Untimed systems
[CWI-CS-R9313-PT-1] 07 p2972 N94-27580
Forward and backward simulations. Part 2: Timing-based systems
[CWI-CS-R9314-PT-2] 07 p2972 N94-27581
Simulations of terrestrial in-situ cosmogenic-nuclide production
[DE94-004999] 07 p3117 N94-27826
Transient model applications. 1: Compressor heat soak/clearance effects modeling
07 p2828 N94-28048
CBSD: The celestial background scene descriptor
[AD-A275521] 08 p3538 N94-28671
Simulator for multistatic radar
[PB94-135506] 08 p3245 N94-29311
A coupled approach to spatially derived parameters necessary for ecosystem modeling on the North Slope of Alaska: Appendix A
[DE94-005853] 08 p3349 N94-30046
Logic of transition systems
[CT-93-03] 08 p3424 N94-30371
Three metric domains of processes for bisimulation
[CWI-CS-R9335] 08 p3459 N94-30427
A structural co-induction theorem
[CWI-CS-R9346] 08 p3461 N94-30753
A laboratory simulation of urban heat-island-induced circulation in a stratified environment
08 p3367 N94-30921
Plasma confinement theory and transport simulation
[DE94-006065] 09 p3888 N94-31619
Modular Simulator System (MSS) management guide
[AD-A277098] 09 p3588 N94-32014
Basic principles approach for studying nonlinear Alfven wave-alpha particle dynamics
[DE94-007112] 09 p3891 N94-32664
Purity and cleanness of aerogel as a cosmic dust capture medium 11 p4247 N94-35469
Bit-wise arithmetic coding for data compression
11 p4254 N94-35556
Determination of grain boundary volume expansion by HREM
[DE94-010452] 11 p4241 N94-36231
Introduction to the heavy quark effective theory, part 1
[DE94-618512] 12 p4514 N94-36749
Controlled atmospheric breakdown: Applications and research opportunities
[AD-A278584] 12 p4464 N94-36973
VHF adaptive antenna development task
[AD-A280320] 12 p4434 N94-37127
Simulation of three-dimensional multi-phase flow characteristics in the deswirl section of the CDIF MHD power train
[DE94-012644] 12 p4443 N94-37176

SIMULATOR TRAINING
U TRAINING SIMULATORS

SIMULATORS
NT COCKPIT SIMULATORS
NT ENVIRONMENT SIMULATORS
NT FLIGHT SIMULATORS
NT MOTION SIMULATORS
NT SHUTTLE ENGINEERING SIMULATOR
NT SHUTTLE MISSION SIMULATOR
NT SOLAR SIMULATORS
NT SPACE SIMULATORS
NT TRAINING SIMULATORS
NT VERTICAL MOTION SIMULATORS
NT VIBRATION SIMULATORS
TOLS (Telescience On-Line Simulator): An essential instrument for micro-gravity interactive experiment
01 p0039 N94-10134
A flexible modelling software for data acquisition
[DE93-612915] 01 p0322 N94-10484
Telerobot control system
[NASA-CASE-NPO-18116-1-CU]
01 p0179 N94-10670
Propulsion simulator for magnetically-suspended wind tunnel models
[NASA-CR-189560] 02 p0527 N94-13127
Event-driven simulation in SELMON: An overview of EDSE
[NASA-CR-194505] 02 p0749 N94-13784
Simulator for heterogeneous dataflow architectures
[NASA-CR-191545] 02 p0622 N94-13797
STS-40 crew during spacelab Sim
[NASA-TM-109493] 03 p0876 N94-15452
Liquid hydrogen and liquid oxygen feedline passive recirculation analysis
[TABES PAPER 93-620] 03 p1031 N94-16145
The Spacelab IPS Star Simulator
[TABES PAPER 93-650] 03 p0877 N94-16150
An overview of the SAFSIM computer program
[DE93-017657] 04 p1519 N94-18002
New applications for high average power beams
[DE93-018845] 04 p1439 N94-18522
Improved HF data network simulator, volume 1
[AD-A270953] 04 p1393 N94-19752
Improved HF data network simulator, software user's manual, volume 2
[AD-A270954] 04 p1393 N94-19753
A breakdown model for the bipolar transistor to be used with circuit simulators
[DE93-019422] 05 p1750 N94-20218
Physical modeling and dynamic simulation of planet vehicles: Application to the motion prediction
06 p2371 N94-23426
Micro SIL-1 simulator
[PB94-110889] 06 p2454 N94-23750
SIMSAT: An object oriented architecture for real-time satellite simulation 06 p2197 N94-23940
CF-18 AN/ALQ-126B-MG 13 IIP interface to the DREO Electronic Warfare Engagement Simulation Facility
[DREO-TN-93-4] 06 p2296 N94-24118
A study of the core module simulator floor capability
06 p2380 N94-24418
Integration and evaluation of a simulator designed to be used within a dynamic prototyping environment
06 p2198 N94-24436
A two-dimensional dispersion module for the TOUGH2 simulator
[DE94-002262] 06 p2335 N94-24655
X ray simulator theory support
[AD-A273613] 06 p2553 N94-24949
Knowledge organization in intelligent tutoring systems for diagnostic problem solving in complex dynamic domains
[AD-A273986] 07 p2984 N94-25899
Rocket engine numerical simulation
07 p2688 N94-27375
The design of a counter rotating ultra-high-bypass fan simulator for windtunnel investigation
[DLR-FB-93-20] 07 p2675 N94-27739
Simulating high-frequency wind for long durations
[DE94-002739] 07 p2682 N94-27997
Experimental studies of loudness and annoyance response to sonic booms 07 p2651 N94-28195
Fiscal 1990 geothermal development promotion survey
[DE94-732333] 08 p3337 N94-28628
Simulator for multistatic radar
[PB94-135506] 08 p3245 N94-29311
Simulation of fully automated air traffic control concepts 08 p3139 N94-29569
The Common Modular Simulator (CMS): An architecture test bed for future advanced ATM systems
08 p3141 N94-29582
A simulator for multi-radar analysis for realistic traffic
[AD-B179099] 08 p3142 N94-30439
Modular Simulator System (MSS) management guide
[AD-A277098] 09 p3588 N94-32014
Georgia Tech sonic boom simulator
10 p3977 N94-33501
Smart IR-camera: Description of a simulator
[PB94-149010] 10 p4143 N94-34127
Partial gravity simulation using a pneumatic actuator with closed loop mechanical amplification
[NASA-TM-104798] 10 p4012 N94-34395
Calibration and initial testing of a new hydraulic simulator
[AD-A280632] 12 p4390 N94-37163
SACS: A cache simulator incorporating timing analysis with buffer and memory management
[AD-A280472] 12 p4494 N94-37230
Immersive virtual environments as trainer: System design from a cognitive stance
12 p4484 N94-37267
Wavefront simulator for evaluating RF communication array signal processors
[AD-D016281] 12 p4436 N94-37835

SIMULTANEOUS IMAGE CORRELATOR
U IMAGE CORRELATORS

SINE SERIES
Operational equations for the five-point rectangle
[DE94-000366] 05 p1959 N94-21655

Some remarkable sine and cosine functions
[PB94-137759] 08 p3453 N94-29439

SINE WAVES

Vortex-induced forces on oscillating bluff cylinders
[AD-A265056] 01 p0154 N94-11865

Method and apparatus for spur-reduced digital sinusoid synthesis
[NASA-CASE-NPO-18789-1-CU] 03 p1154 N94-17326

Active control of periodic noise with time-varying frequency
[REPT-93-012] 04 p1562 N94-17934

Spectral analysis on the canonical autoregressive decomposition
[AD-A270083] 04 p1549 N94-18798

Spur-reduced digital sinusoid synthesis 06 p2291 N94-23264

Multiple model adaptive control of a large flexible space structure with purposeful dither for enhanced identifiability
[AD-A274132] 07 p2987 N94-27122

Multi-speed multi-phase resolver converter
[NASA-CASE-MFS-28855-1] 08 p3264 N94-29372

Polynomial modeling of analog-to-digital converters
[DE94-005579] 08 p3406 N94-30008

Visual evaluation of computer-generated textures
[AD-A277201] 09 p3816 N94-32093

Cooling and trapping of neutral atoms
[AD-A276957] 09 p3870 N94-32360

Bounds on least-squares four-parameter sine-fit errors due to harmonic distortion and noise
[DE94-007859] 09 p3849 N94-32653

Generation of the ambiguity function for ultra wideband radar waveforms
[AD-A277913] 09 p3684 N94-33261

A new robust adaptive algorithm based on intelligent integrators 10 p4122 N94-34371

SINGAPORE

Sun-synchronous and geo-synchronous satellite data utilization for environmental studies 01 p0037 N94-10689

SINGLE CHANNEL PER CARRIER TRANSMISSION

Improved frame synchronization schemes for INMARSAT-B/M SCPC and TDM channels 06 p2285 N94-22806

The two-way time synchronization system via a satellite voice channel 08 p3471 N94-30658

SINGLE CRYSTALS

Use of inert immiscible liquid for crystal separation out of its feeding solution in weightlessness 01 p0124 N94-10242

Recent developments in piezoelectric and electrostrictive sensors and actuators for smart structures 01 p0070 N94-11332

Investigation of ZnSe-coated silicon substrates for GaAs solar cells 01 p0052 N94-11405

Low energy electron diffraction and cyclic voltammetry studies of flame-annealed platinum single crystals
[AD-A263566] 01 p0401 N94-11518

Polaronic charge separation in mixed-halide MX solids
[AD-A266073] 01 p0403 N94-12345

The effects of organic adsorbates on the underpotential deposition of silver on Pt(111) electrodes
[AD-A265623] 01 p0404 N94-12376

Low voltage electron beam lithography
[AD-A265358] 01 p0145 N94-12405

Fatigue in single crystal nickel superalloys
[AD-A266116] 01 p0085 N94-12418

Deformation mechanisms in tungsten single crystals in ballistic impact experiments
[AD-A265701] 01 p0405 N94-12563

Tin whiskers in electronic circuits
[AD-A265917] 01 p0146 N94-12565

Determination of channeling perspectives for complex crystal structures
[DE93-012872] 02 p0805 N94-13009

Lattice site of helium implanted in Si and diamond
[DE93-015365] 02 p0805 N94-13012

Spacelab J experiment descriptions
[NASA-TM-4517] 02 p0586 N94-13732

Growth experiment of narrow band-gap semiconductor PbSnTe single crystals in space (M-1) 02 p0586 N94-13733

Growth of PbSnTe single crystal by traveling-zone method in low gravity (M-2) 02 p0586 N94-13734

Growth of semiconductor compound single crystal InSb by floating zone method (M-3) 02 p0586 N94-13735

Growth of Si spherical crystals and the surface oxidation (M-9) 02 p0587 N94-13741

Growth of samarskite crystal under microgravity conditions (M-20) 02 p0590 N94-13752

Growth experiment of organic metal crystal in low gravity (M-21) 02 p0590 N94-13753

Crystal growth of enzymes in low gravity (L-5) 02 p0592 N94-13762

Emitter Wrap-Through solar cell
[DE93-014996] 02 p0703 N94-13886

Measurement of penetration depth lambda(T) in YBa2Cu3O(7-delta) thin film
[DE93-014587] 02 p0810 N94-14122

Prism-film coupling in anisotropic planar waveguides of epitaxial (101) rutile thin films
[DE93-012912] 02 p0811 N94-14304

Small polaron conduction in Y2Ti2O7
[ITN-93-85221] 02 p0814 N94-14557

Magneto-optic superlattice thin films: Fabrication, structural and magnetic characterization 03 p0974 N94-14982

Growth of new materials for solid state laser applications. The growth of ZnGeP2 by the vertical Bridgman method
[NASA-CR-194571] 03 p1038 N94-15530

Laboratory for x ray optics
[AD-A267149] 03 p1189 N94-15735

Study of protein-H2O interactions by multidimensional NMR spectroscopy
[AD-A266955] 03 p0946 N94-15760

Passive oxide films on well-defined nickel surfaces: An examination of film growth on Ni(100) with ex situ scanning tunneling microscopy
[DE93-014056] 03 p1207 N94-15923

Optical properties and surface morphology studies of palladium contacts on mercuric iodide single crystals
[DE93-012510] 03 p1207 N94-15973

Thermal spray forming of refractory sample ampoule cartridges for single crystal growth space furnaces
[TABES PAPER 93-605] 03 p1051 N94-16141

Orientation of Planar Deformation Features (PDFs) in quartz 03 p1219 N94-16341

Growth of single crystals of mercuric iodide on the ground and in space
[DE93-015523] 03 p1209 N94-16442

Porous silicon for pumping solid-state lasers
[AD-A266293] 03 p1039 N94-16474

Thermal disorder in adsorbed Cl on Si(100)
[AD-A266295] 03 p1210 N94-16476

Tritium diffusion and desorption in single crystal LiAlO2
[DE93-015140] 03 p1211 N94-16805

High temperature materials technology research for advanced thermionic systems
[DE93-018302] 03 p0960 N94-16964

Growth and doping of Al(x)Ga(1-x)N films by electron cyclotron resonance assisted molecular beam epitaxy
[AD-A267305] 03 p1212 N94-16992

An alternative approach to the growth of single crystal gallium nitride
[AD-A267876] 03 p1213 N94-17037

Nitride semiconductors for ultraviolet detection
[AD-A267877] 03 p1012 N94-17040

Pseudomorphic semiconducting heterostructures from combinations of AlN, GaN and selected SiC polytypes: Theoretical advancement and its coordination with experimental studies of nucleation, growth, characterization and device deployment
[AD-A267561] 03 p1213 N94-17108

Single crystal diamond thin films
[AD-A266457] 03 p1214 N94-17216

Investigation of the origin of hot spots in deformed crystals: Ammonium perchlorate studies
[AD-A267692] 03 p1214 N94-17270

Synthesis, characterization, and polymerization of new ferrocene-fluorene complexes. A novel high-molecular weight conjugated polymer with pendant ferrocene groups
[AD-A267717] 03 p0972 N94-17273

Buried porous silicon-germanium layers in monocrystalline silicon lattices and method of producing
[NASA-CASE-NPO-18836-1-CU] 03 p1215 N94-17327

Low voltage electron beam lithography
[AD-A267865] 03 p1215 N94-17389

Laser probing of the kinetics and dynamics of 3-5 semiconductor growth
[AD-A268388] 03 p1215 N94-17422

Investigations of YBaCuO materials with near-room-temperature resistivity transitions
[AD-A268016] 03 p1216 N94-17477

Low temperature deposition and characterization of n- and p-type silicon carbide thin films and associated ohmic and Schottky contacts
[AD-A267966] 03 p0973 N94-17490

Growth, characterization and device development in monocrystalline diamond films
[AD-A268206] 03 p1216 N94-17553

Advanced thin-film deposition and physical properties of high-temperature and other novel superconducting materials
[AD-A268199] 03 p1216 N94-17561

Magnetic properties of single-crystalline UCu3Al2
[DE93-016607] 04 p1593 N94-17744

Plastic anisotropy in MoSi2 single crystals
[DE93-012650] 04 p1594 N94-17874

Recent studies of short-range order in alloys: The Cowley theory revisited
[DE93-016416] 04 p1358 N94-18111

Nitridation of GaAs(100) by laser-induced decomposition of HN3
[AD-A269147] 04 p1438 N94-18258

Photorefractive tungsten bronze crystals for optical computing
[AD-A268859] 04 p1596 N94-18320

The effect of crystallographic orientation on the performance of single crystal tungsten subscale penetrators
[AD-A268988] 04 p1597 N94-18468

Ionic and molecular environments in heterogeneous electrocatalysis: Studies by radioactive labeling and LEED/AUGER spectroscopy
[AD-A268850] 04 p1567 N94-18766

Experimental investigation of wave and fracture phenomena in impacted ceramics: Experiments on sapphire
[AD-A270040] 04 p1372 N94-18792

Growth, characterization and device development in monocrystalline diamond films
[AD-A270074] 04 p1599 N94-18797

Modeling of single-crystal laser-weld microstructures
[DE93-017853] 04 p1445 N94-18976

Surface phases and their influence on metal-oxide interfaces
[DE93-019931] 04 p1601 N94-19020

The electromechanical properties of tetragonal BaTiO3 and PbTiO3 single crystals
[DE93-019008] 04 p1603 N94-19550

Final report on subcontract B076260 --- borate synthesis
[DE93-019501] 04 p1604 N94-19565

Oxidation-reduction induced roughening of platinum (111) surface
[DE93-017408] 05 p1687 N94-19922

The multicomponent lineshape of the anharmonic A(1)(TO) phonon in PbTiO3
[DE93-018995] 05 p1970 N94-19971

Growth of zinc selenide single crystals by physical vapor transport in microgravity
[NASA-CR-194679] 05 p2017 N94-20346

Monocrystalline germanium film on sapphire
[AD-D015925] 05 p2017 N94-20348

Process for the homoepitaxial growth of single-crystal silicon carbide films on silicon carbide wafers
[NASA-CASE-LEW-15223-1] 05 p2017 N94-20381

Growth, characterization and device development in monocrystalline diamond films
[AD-A272715] 05 p2026 N94-21190

Techniques for the flux growth of optical materials: Growth of beta-barium borate
[AD-A272717] 05 p2028 N94-21505

Growth, characterization and device development in monocrystalline diamond films
[AD-A273097] 05 p2028 N94-21506

Single crystal diamond films
[AD-A266759] 05 p2028 N94-21517

Relaxation of hysteresis loop in a single crystal of YBa2Cu4O8
[DE93-019519] 05 p2029 N94-21649

Semiconductor isotope engineering
[DE93-040119] 05 p2030 N94-21744

Techniques for producing free-standing thin films on frames
[DE93-041144] 05 p1708 N94-21954

Temperature dependence of magnetic order in single-crystalline UPdSn
[DE93-040153] 05 p2033 N94-21991

The effect of correlated and point defects on the vortex lattice melting transition in single crystal YBa2Cu3O(7-delta)
[DE93-040277] 05 p2033 N94-21997

Temperature-dependent ion beam mixing
[DE93-040281] 05 p2033 N94-21999

Quantitative analysis of scanning tunneling microscopy images for surface structure determination: Sulfur on Re(0001)
[DE93-019235] 05 p2034 N94-22041

Inelastic neutron scattering of (gamma)-iron, and the determination of the elastic constants by lattice dynamics
[DE94-000694] 05 p1978 N94-22573

The elastic and electromechanical properties of BaTiO3 single crystal through the ferroelectric transition
[DE94-001437] 06 p2557 N94-22927

Anomalous magnetoresistance behavior of superconducting Nd(2-x)Ce(x)CuO(4-y) single crystal
[DE94-000806] 06 p2558 N94-22941

Application of maximum entropy and irreducible cluster integrals to joint probability distributions for x ray structure determination
[PB93-224152] 06 p2559 N94-23109
Proposed additions to the SHADOW ray-tracing code for general-asymmetric perfect-crystal optics
[DE94-001291] 06 p2560 N94-23188
Reduction of nitric oxide over platinum, rhodium and platinum-rhodium single crystal surfaces
[PB93-230092] 06 p2232 N94-23482
Inertial confinement fusion
[DE94-002602] 06 p2551 N94-23703
Polymer morphologh 06 p2226 N94-24353
The mechanical properties of single crystal (alpha)-Si3N4
[DE94-002632] 06 p2563 N94-24517
Ge-Au eutectic bonding of Ge (100) single crystals
[DE94-002281] 06 p2564 N94-24657
Two micron stimulated emission of activated insulating crystals
[REPT-94-002] 06 p2565 N94-25025
Study on synthesis and characteristics of intermetallic compound with strong electron correlation
07 p2726 N94-25563
Study on computerized experiment of amorphous transformation process by solid phase reaction
07 p2726 N94-25564
Ion implantation of diamond: Damage, doping, and lift-off
[DE94-001133] 07 p3054 N94-26137
Window least squares method applied to statistical noise smoothing of positron annihilation data
[DE93-634665] 07 p3003 N94-26385
Growth, characterization and device development in monocrystalline diamond films
[AD-A274245] 07 p3060 N94-26839
Atomic layer epitaxy of group 4 materials: Surface processes, thin films, devices and their characterization
[AD-A274325] 07 p3061 N94-26885
Indium donor complexes with cation vacancies in CdTe and ZnSe
[DE94-002731] 07 p3063 N94-26958
Deformation, constitutive behavior, and damage of advanced structural materials under multiaxial loading
[AD-A274165] 07 p2709 N94-27142
Float zone crystal growth using laser radiation
[DLR-FB-93-10] 07 p3066 N94-27590
Effect of temperature and recoil-energy spectra on irradiation-induced amorphization in Ca2La8(SiO4)6O2
[DE94-004371] 07 p3067 N94-27602
Interstitially stabilized phases in the zirconium-nickel system
[DE94-005561] 08 p3201 N94-28525
Hysteresis phenomena at spin-flop transition induced by the pulsed magnetic field
[DE94-606851] 08 p3511 N94-28626
Sputtering of single crystals: Experimental evidence of the ejection process
[AD-A275819] 08 p3512 N94-28775
Ion channeling peculiarities in YBa2Cu3 O7 monocrystal
[DE94-606885] 08 p3512 N94-28787
Synthesis and neutron diffraction study of Na3WN3 and Na3MoN3
[AD-A275158] 08 p3203 N94-29043
Thermal expansion and elastic anisotropy in single crystal Al2O3 and SiC reinforcements
[NASA-TM-106516] 08 p3214 N94-29105
X ray standing wave studies of underpotentially deposited metal monolayers
[AD-A275409] 08 p3513 N94-29215
Anode for rechargeable ambient temperature lithium cells
[NASA-CASE-NPO-18580-1-CU]
08 p3265 N94-29505
Dislocation loops in spinel crystals irradiated successively with deep and shallow ion implants
[DE94-005083] 08 p3517 N94-30201
Incommensurate magnetic order in UNi2Al3
[DE94-005449] 08 p3209 N94-30246
Studies of high temperature ternary phases in mixed-metal-rich early transition metal sulfide and phosphide systems
[DE94-006034] 08 p3209 N94-30336
Butterfly and scaling law in YBa2Cu4O8
[DE94-006037] 08 p3519 N94-30338
Magnetotransport measurements in magnetic fields up to 50T in SmB6 and FeSi
[DE94-006227] 08 p3520 N94-30848
Ion-beam-driven amorphization of Ca2La8(Si4)6O2 single crystals
[DE94-006219] 09 p3895 N94-31307
Electrooptic crystal growth and properties
[AD-A276023] 09 p3896 N94-31439
GaAs/GaN strained layer superlattice materials for high temperature transistors, phase 1
[AD-A276115] 09 p3897 N94-31528
Characterization of the rare earth orthophosphates and Ce-doped LaPO4 by x ray absorption spectroscopy
[DE94-006313] 09 p3898 N94-31630
The 4f heavy fermion photoelectron spectra do not exhibit the Kondo scale
[DE94-006252] 09 p3898 N94-31631
In-situ TEM crystallization of anorthite-glass films on (alpha)-Al2O3
[DE94-006317] 09 p3652 N94-31780
Thermocapillary convection in evaporating sessile drops
[NASA-TM-109758] 09 p3705 N94-31886
Group 12 thiolates: Syntheses, characterization and decomposition pathways
[AD-A277055] 09 p3900 N94-32011
Fatigue in single crystal nickel superalloys
[AD-A276662] 09 p3643 N94-32047
Effect of twin boundary density on the vortex melting transition in YBa2Cu3O(7-delta) single crystals
[DE94-007684] 09 p3904 N94-32601
SUNY beamline facilities at the National Synchrotron Light Source
[DE94-006343] 09 p3905 N94-32770
Hyperon polarization, crystal channeling, and E781 at Fermilab
[DE94-008224] 09 p3877 N94-32802
High temperature materials technology research for advanced thermionic systems
[DE94-008341] 09 p3646 N94-32825
Novel polydiacetylenes as materials for second and third order nonlinear optics
[AD-A277512] 09 p3664 N94-33082
Display projector technology by way of single crystal faceplate technology
[AD-A277800] 10 p4038 N94-33398
Single crystal faceplate evaluation
[AD-A277922] 10 p4038 N94-33399
High definition TV projection via single crystal faceplate technology
[AD-A277850] 10 p4034 N94-33768
Growth, characterization, and device development in monocrystalline diamond films
[AD-A277863] 10 p4146 N94-33774
Solidification microstructures in single-crystal stainless steel melt pools
[DE94-009839] 10 p4024 N94-33880
Redetermination of piperidinium hydrogen sulfide structure
[NASA-TM-106527] 10 p4022 N94-33959
Ultrastructure processing of advanced materials
[AD-A278285] 10 p4018 N94-33962
Hot section materials for small turbines
10 p4004 N94-34465
Be3(AsO4)2.2H2O, a new beryllioarsenate phase containing bridged tetrahedral 3-rings
[AD-A278826] 11 p4340 N94-35677
Electromagnetically levitated vibration isolation system for the manufacturing process of silicon monocrystals
11 p4223 N94-35906
Space-based crystal growth and thermocapillary flow
11 p4342 N94-35971
Twin spacing versus size of a monocrystal for the nonstoichiometric 1:2:3 superconductors
[DE94-615511] 11 p4340 N94-36029
Application of GaSe and AgGaSe2 crystal growth to non-linear optics
[PB94-170552] 11 p4341 N94-36212
Formation and stability of Fe-rich precipitates in dilute Zr(Fe) single-crystal alloys
[DE94-619027] 11 p4242 N94-36288
Substrate effects on the structure and optical properties of epitaxial PbTiO3 thin films prepared by metal-organic chemical vapor deposition
[DE94-010432] 12 p4535 N94-37192
Applications of high transition temperature superconductors at the Savannah River Site
[DE94-012938] 12 p4536 N94-37311
Perfluorodiethoxymethane on nickel and nickel oxide surfaces
[DE94-011200] 12 p4426 N94-37712

SINGLE ENGINE AIRCRAFT
NT F-16 AIRCRAFT
NT F-104 AIRCRAFT
NT F-106 AIRCRAFT

SINGLE EVENT UPSETS
Relationship between IBICC imaging and SEU in CMOS ICs
[DE93-009854] 01 p0143 N94-11285
Single event effects and laser simulation studies
[NASA-CR-194506] 02 p0657 N94-13812
Single Event Upset (SEU) testing of semiconductor components at the McMaster Accelerator Laboratory
[DSIS-93-00071] 02 p0623 N94-13834
Test report for single event effects of the 80386DX microprocessor
[NASA-CR-194509] 02 p0741 N94-13943
Experience with custom processors in space flight applications 04 p1336 N94-18338
An SEU immune logic family
04 p1398 N94-18342
Technology, design, simulation, and evaluation for SEP-hardened circuits 04 p1399 N94-18352
The LET spectrum and its uncertainty during the CRRES mission
[AD-A269977] 04 p1630 N94-18676
Static Computer Memory Integrity Testing (SCMIT): An experiment flown on STS-40 as part of GAS payload G-616 04 p1325 N94-19169
Single-event upset testing of the performance semiconductor 1750A CMOS/SOS chip set
[AD-A271158] 05 p2015 N94-20184
Comparison of single event upset rates for microelectronic memory devices during interplanetary solar particle events 05 p1754 N94-21085
STRV RADMON: An integrated high-energy particle detector 05 p1666 N94-21086
Test results for SEU and SEL immune memory circuits
05 p1754 N94-21087
Complementary heterojunction FET technology for space application 05 p1755 N94-21094
Design methods for fault-tolerant finite state machines
05 p1758 N94-21120
Single event phenomena: Testing and prediction
05 p1763 N94-21696
Defect-sensitivity analysis of an SEU immune CMOS logic family 05 p1765 N94-21711
Modeling and experimental verification of single event upsets 07 p2684 N94-26287
Advantages of the LBL 88-inch cyclotron ion beam for SEP studies
[AD-A275142] 08 p3494 N94-29065
Proceedings of the 1991 Single Event Upset Symposium
[DSIS-92-00652] 08 p3495 N94-30211
Single event upset and latchup measurements at Brookhaven National Laboratory
08 p3495 N94-30212
Single event upset susceptibilities of latchup immune CMOS process programmable gate arrays
08 p3495 N94-30214
Multiple single event upsets in CMOS static rams
08 p3496 N94-30215
McMaster accelerator facility
08 p3496 N94-30217
Advanced development of the Spectrum Sciences Model 5005-TF, single event test fixture
08 p3291 N94-30218
Using Cf-252 for single event upset testing
08 p3496 N94-30219
Charge collection spectroscopy applied to MOS RAM's 08 p3201 N94-30220
Radiation tolerant, high speed, low power, gallium arsenide logic
[AD-A277293] 09 p3694 N94-32509
Temperature dependence of single-event burnout in n-channel power MOSFET's
[AD-A277921] 09 p3698 N94-33177
The impact of ASIC devices on the SEU vulnerability of space-borne computers
[AD-A278134] 09 p3808 N94-33252
Spacecraft environmental anomalies expert system
[AD-A277962] 09 p3612 N94-33262
A critical examination of charge funneling and its impact on single-event upset in Si devices
[DE94-007868] 11 p4261 N94-36373
Single event mirroring and sense amplifier designs for enhanced SE tolerance of DRAMs
[DE94-010397] 12 p4438 N94-37190
A proposed SEU tolerant DRAM cell
[DE94-010758] 12 p4438 N94-37196

SINGLE INPUT SINGLE OUTPUT SYSTEMS
U SISO (CONTROL SYSTEMS)

SINGLE INSTRUCTION MULTIPLE DATASTREAM
U SIMD (COMPUTERS)

SINGLE SIDEBAND MODULATION
U SINGLE SIDEBAND TRANSMISSION

SINGLE SIDEBAND TRANSMISSION
Envelope and instantaneous frequency estimation of narrowband modulated signals
[DREO-TN-92-3] 02 p0605 N94-14033
Asynchronous detection of SSB-SC data signals
05 p1747 N94-22217

SINGLE STAGE ROCKET VEHICLES
NT BLACK BRANT SOUNDING ROCKETS
Single STAGE Rocket Technology (SSRT) DC-X test program environmental assessment
[AD-A265940] 04 p1337 N94-17879

SINGLE STAGE TO ORBIT VEHICLES
Hypersonic aerodynamic characteristics of SSTO-type aerospace planes. Part 1: The NAL 0-th configuration
[NAL-TR-1186] 02 p0514 N94-13459
Multidisciplinary design techniques applied to conceptual aerospace vehicle design
[NASA-CR-194409] 02 p0515 N94-13618
Spaceplane program at NAL: System concept and related technology issues 02 p0537 N94-14281
Space Propulsion Synergy Group ETO technology assessments
[TABES PAPER 93-641] 03 p0929 N94-16149
Access to space studies 06 p2199 N94-24434
Configuration development study of the OSU 1 hypersonic research vehicle
[NASA-CR-195522] 06 p2181 N94-24591
A conceptual design of an unmanned test vehicle using an airbreathing propulsion system
[NASA-CR-195550] 06 p2189 N94-25085
Hypersonic vehicle control law development using H(infinity) and micron-synthesis 06 p2163 N94-25104
Access to space study
[NASA-TM-109693] 07 p2685 N94-27151
A parametric sensitivity study for single-stage-to-orbit hypersonic vehicles using trajectory optimization
[NASA-CR-195703] 07 p2697 N94-27789
The National Aerospace Plane (NASP): Development issues for the follow-on vehicle
[AD-A278417] 09 p3581 N94-33329

SINGULAR INTEGRAL EQUATIONS
Integral equation methods for mixed boundary problem of fracture mechanics 01 p0188 N94-11617
Numerically solving a transient heat conduction problem with convection and radiation
[AD-A268521] 03 p1220 N94-17540
Hypersingular integrals at a corner
[DE94-000340] 05 p1961 N94-22379
The effects of anisotropy on the nonlinear behavior of bridged cracks in long strips
[NASA-CR-194453] 06 p2377 N94-24604

SINGULARITY (MATHEMATICS)
Numerical method of singular problems on singular integrals
[DE93-613654] 01 p0343 N94-10546
Finite-dimensional singletons of the quantum anti de Sitter algebra
[DE93-624771] 04 p1546 N94-17810
Some remarks on integrable Hamiltonian systems with two degrees of freedom
[DE93-624766] 04 p1546 N94-17815
Singularities and symmetries of nonlinear ordinary and partial differential equations
[DE93-040083] 04 p1550 N94-19190
Bits and relative order from residues, space efficiently
[TR-464] 04 p1530 N94-19482
Classical and generalized solutions of time-dependent linear differential algebraic equations
[AD-A272834] 05 p1954 N94-21173
Normal forms of kinematic singularities of 3R robot manipulators
[MEMO-1124] 06 p2469 N94-22712
Coordinate-free interpretations of the optimal costs for Lq problems subject to implicit systems
[PB94-118700] 06 p2473 N94-23760
Non-trivial examples of real isolated singularity at the origin
[PB94-110939] 06 p2487 N94-23787
Towards a theory of growing surfaces: Mapping two-dimensional Laplacian growth onto Hamiltonian dynamics and statistics
[DE94-002636] 07 p2991 N94-26079
Numerical solution of singularity-perturbed two-point boundary-value problems
[DE94-601542] 07 p2993 N94-26410
Finite-part integrals and the Euler-Maclaurin expansion
[DE94-006539] 09 p3844 N94-31665
Self-similar regimes of subsonic Langmuir wave collapse
[DE94-611466] 11 p4335 N94-35750
On a generalized bootstrap principle
[DE94-727517] 11 p4314 N94-35774
Local instabilities and the transition to chaos of non-linear waves
[PB94-170578] 11 p4341 N94-36213

SINKHOLES
Application of remote sensing and GIS techniques for environmental geologic investigation, Northeast Iowa 10 p4075 N94-33420

SINKS
NT HEAT SINKS
A method of influence regions in the theory of vacancy swelling of metals
[DE93-620579] 01 p0083 N94-11363
Simulation of the carbon cycle in the oceans
[DE94-000780] 07 p2898 N94-25791
Defect-solute interactions near irradiation grain boundaries
[DE94-006215] 09 p3641 N94-31627

SINKS (GEOLOGY)
U STRUCTURAL BASINS

SINTERING
NT LIQUID PHASE SINTERING
Ostwald ripening of solid cobalt particles in liquid copper 01 p0087 N94-10202
Production of reactive sintered nickel aluminide
[DE93-014434] 01 p0083 N94-11127
Creep deformation and mechanical properties of sintered glass and polycrystalline matrix composites 01 p0067 N94-11315
Effect of powder processing on slip casting parameters and sintering of Si3N4-Y2O3-SiO2
[AD-A264474] 01 p0083 N94-11445
Cold press sintering of simulated lunar basalt 01 p0131 N94-12026
General overview of an integrated lunar oxygen production/brickmaking system 01 p0131 N94-12027
Microwave hybrid heating of alumina filaments
[DE93-012642] 02 p0581 N94-14327
Microwave sintering of large alumina bodies
[DE93-012752] 02 p0581 N94-14340
How to read a phase equilibrium diagram for high-temperature ceramics material as main object
[DE93-512333] 02 p0582 N94-14513
Processing and testing of high toughness silicon nitride ceramics
[NASA-CR-191190] 02 p0582 N94-14543
Finite element analytical techniques for ceramic production in microgravity: A hypoelastic model 03 p0981 N94-16099
Chemical interactions between interconnect and electrode materials during sintering in solid oxide fuel cells
[DE93-015696] 03 p1092 N94-16160
Processing of complex sintered reaction bonded silicon nitride parts by microwave heating
[DE93-015811] 03 p0969 N94-16877
Low-temperature sintering and phase changes in chromite interconnect materials
[DE93-015676] 03 p0961 N94-17234
Pressureless densification of ceramic matrix composites
[AD-A269137] 04 p1371 N94-18691
Manufacturing technology
[DE93-019580] 04 p1381 N94-19480
Sol-spray preparation, particulate characteristics, and sintering of alumina powders
[DE93-018577] 05 p1690 N94-20183
Sintering silicon nitride
[NASA-CASE-LEW-15489-1] 05 p1703 N94-20529
An assessment of the cost of microwave sintering ceramic tiles for armor applications
[DE94-000978] 05 p1693 N94-21850
Effect of powder characteristics on gas-pressure sintering of Si3N4 with rare earth additives
[DE94-000330] 05 p1694 N94-21945
Fabrication of whisker-toughened alumina tubes
[DE94-001012] 05 p1677 N94-22022
Influence of sintering atmospheres on the aluminum sintering characteristics
[DE93-632412] 06 p2239 N94-22965
Particle formation in a laser-heated aerosol reactor. Application to silicon and silicon nitride synthesis
[PB93-217982] 06 p2347 N94-22982
Composite fiber structures for catalysts and electrodes 06 p2393 N94-23364
Combustion synthesis and engineering of nanoparticles for electronic, structural and superconductor applications
[DE94-001865] 06 p2254 N94-23720
Modelling the ignition of boron/titanium particles 06 p2159 N94-24273
Characteristics of products generated by selective sintering and stereolithography rapid prototyping processes 06 p2264 N94-24412
Thermomechanical processing of Ag-clad Bi2Sr2CaCu2O(x) superconductors
[DE94-002347] 06 p2563 N94-24624
BEM solution for the simulation of axisymmetric viscous sintering
[PB93-237717] 06 p2336 N94-24761
Solid state synthesis of Fe-B-Si alloys
[VTT-PUBS-118] 06 p2250 N94-25316
Study on high temperature damage control and life improvement 07 p2729 N94-25580
Grain boundary degradation of YBCO superconductors sintered in CO2-containing atmospheres
[DE94-003206] 07 p3053 N94-26029
Alternative materials for solid oxide fuel cells: Processing and interactions of materials
[DE94-000016] 07 p2855 N94-26114
Processing of LaCrO3 for solid oxide fuel cell applications
[DE94-002981] 07 p2857 N94-26747
Examination of hardness, fracture toughness and microstructure in Al2O3-B4C binary ceramics
[PB94-124237] 07 p2755 N94-27158
Transparent polycrystalline body with high ultraviolet transmittance, process for making and applications thereof
[CA-PATENT-1325511] 07 p3066 N94-27276
Analysis of pressureless densification of ceramic matrix composites 08 p3216 N94-29766
Pressureless sintering of ceramic composites
[AD-A277274] 09 p3657 N94-32404
Isothermal sintering, microstructure, and superconducting properties of Y1Ba2Cu3O(7-x) compound
[DE94-008132] 09 p3905 N94-32779
Enhanced thermal capacity aerogels summary report, FY 1993
[DE94-008888] 09 p3639 N94-33260
Digital control programmer for temperature control
[DE94-615584] 11 p4309 N94-36382
Advances in rapid prototyping
[DE94-010075] 12 p4430 N94-36447
Sintering of dioxide pellets in an oxidizing atmosphere (CO2)
[DE94-613046] 12 p4414 N94-36517
Mineralogy and metallurgical properties of iron ore sinter based on magnetite fines
[DE94-763309] 12 p4414 N94-36525
Characterization and processing of sintered products from nano-crystalline powders generated by the RTDS method
[DE94-004765] 12 p4415 N94-36553

SINUSOIDS
U SINE WAVES

SIR-A
U SHUTTLE IMAGING RADAR

SIR-B
U SHUTTLE IMAGING RADAR

SIRTF
U SPACE INFRARED TELESCOPE FACILITY

SIS (SEMICONDUCTORS)
Layered thin-edged field-emitter device
[AD-D015932] 05 p1751 N94-20350

SIS (SUPERCONDUCTORS)
Submillimeter wave observation experiment of Earth atmosphere with SIS mixer 01 p0130 N94-11837
Utilization of superconductivity in the area of space 01 p0131 N94-11843
Measurements on two-dimensional arrays of mesoscopic Josephson junctions
[AD-A265129] 02 p0807 N94-13359
Theoretical SIS mixer research
[AD-A266323] 02 p0807 N94-13580
Submillimeterwave SIS mixer developments 03 p0903 N94-15054
Preparation and properties of Nb/Al SIS and SIN junctions for millimeter and submillimeter radioastronomical receivers 03 p0907 N94-15078
Infrared detection with high-(Tc bolometers and response of Nb tunnel junctions to picosecond voltage pulses
[DE93-016963] 04 p1595 N94-17989
Quantum noise studies with superconducting tunnel junction mixers
[AD-A270897] 05 p2012 N94-19897
Layered thin-edged field-emitter device
[AD-D015932] 05 p1751 N94-20350
A low noise 665 GHz SIS quasi-particle waveguide receiver
[NASA-CR-194735] 06 p2296 N94-24105
A compact 150 GHz SIS receiver cooled by 4 K GM refrigerator
[REPT-36] 07 p2776 N94-27340
Picosecond response of the quasiparticle current in superconducting tunnel junctions
[DE94-006300] 08 p3515 N94-30009
High T(sub c) superconductor tunnel junctions for photon detectors
[DE94-007686] 09 p3904 N94-32602

SISO (CONTROL SYSTEMS)
Kalman filter input estimation
[NAL-TR-1182] 02 p0649 N94-13456
Flight controller design using mixed H2/H infinity optimization with a singular H infinity constraint
[AD-A273831] 06 p2191 N94-25525
A neural network-based technique for structural identification of SISO systems
[REPT-93-076] 08 p3449 N94-30941
Parameterised controller design for dominant multivariable systems 10 p4114 N94-34309
An accelerated gradient method for adaptive control using only input and output measurements 10 p4115 N94-34319

Implementation of a decoupled controller for a magnetic suspension system using electromagnets mounted in a planar array 11 p4216 N94-35853
Adaptive model reduction for continuous systems via recursive rational interpolation 11 p4219 N94-35876
Mixed H2/H-infinity optimization with multiple H infinity constraints
| AD-A280572 | 12 p4388 N94-36733

SITE SELECTION
Mars Analog Site Study (MASS) 03 p1252 N94-16200
Mars exobiology landing sites for future exploration 03 p1278 N94-16339
An electromagnetic interference study of potential transmitter sites for the HF Active Auroral Research Program (HAARP)
| AD-A267743 | 03 p1004 N94-17373
Ground wave emergency network. Final operational capability. Environmental assessment for south central Montana relay node, site no. RN8C925MT
| AD-A267795 | 05 p1716 N94-19964
Site comparison for optical visibility statistics in southern California 08 p3247 N94-29617
National facilities study. Volume 2A: Facility Study Office on the National Wind Tunnel Complex
| NASA-TM-109856 | 10 p4009 N94-34634
Fluvial processes in Ma'adim Vallis and the potential of Gusev crater as a high priority site 11 p4358 N94-35414
Autonomous hazard detection and avoidance
| NASA-CR-188331 | 11 p4309 N94-36439

SITES
NT LANDING SITES
NT LAUNCHING PADS
NT LAUNCHING SITES
NT LUNAR LANDING SITES
Facilities maintenance handbook
| NHB-8831.2 | 03 p1224 N94-15934

SITTING POSITION
Clinical physiology of bed rest
| NASA-TM-104010 | 02 p0727 N94-13447

SIZE (DIMENSIONS)
NT GRAIN SIZE

SIZE DETERMINATION
NT PRECIPITATION PARTICLE MEASUREMENT
Atomization characteristics of a prefilming airblast atomizer
| NAL-TM-644 | 01 p0148 N94-10727
Adaptively resizing populations: Algorithm, analysis, and first results
| NASA-CR-194277 | 02 p0742 N94-12808
Emission line variability in active galactic nuclei
| ITN-93-85209 | 02 p0849 N94-14553
Maximum likelihood techniques applied to quasi-elastic light scattering
| NASA-CR-193550 | 03 p1192 N94-16718
Properly synchronized measurements of droplet sizes for high-pressure intermittent coal-water slurry fuel sprays
| DE94-008960 | 10 p4059 N94-33694

SIZE DISTRIBUTION
NT PARTICLE SIZE DISTRIBUTION
The development of phytoplankton sensing system with optical fiber 01 p0203 N94-11967
Venus small volcano classification and description 01 p0438 N94-12037
Deviations from the straight line: Bumps (and grinds) in the collisionally evolved size distribution of asteroids 01 p0431 N94-12201
Laboratory studies on the velocity of fragments from impact disruptions 01 p0189 N94-12359
The seasonal change of phytoplankton size distribution using optical fiber sensor 01 p0210 N94-12656
Experimental determination of droplets local mean diameter of a sprag from impinging jets
| INPE-5469-TDI/500 | 02 p0631 N94-13365
Pore-size-distribution of cationic polyacrylamide hydrogels
| DE93-015218 | 02 p0581 N94-14400
Dispersion effects on millimeter wavelength attenuation efficiencies for a variety of fibers
| AD-A268992 | 04 p1386 N94-18454
Hydrolysis reaction and positronium decay in silica gels
| AD-A270028 | 04 p1371 N94-18713
Development of the microstructure based stochastic life prediction models
| AD-A270453 | 04 p1455 N94-18714
Intensity and polarization of light scattered by size distributions of randomly oriented nonspherical particles 05 p1721 N94-20416
Determination of cosmic bodies size-velocity distribution by observation of current impacts on Mars 05 p2082 N94-20648
Distribution of small volcanic cones on the surface of Venus by size and elevation: Implications for differential deposition of volcanic features 05 p2110 N94-20731
Size distributions and aerodynamic equivalence of metal chondrules and silicate chondrules in Acfer 059 05 p2084 N94-20773
Triton's cratering record and its time of capture 05 p2122 N94-20802
Particle size measurement for the control of industrial crystallizers
| PB94-119104 | 06 p2562 N94-23766
Infrared sensors and systems for enhanced vision/autonomous landing applications 06 p2439 N94-25491
Study of precipitation and recrystallization in Al alloy 2519 by backscattered electron imaging methods
| AD-A274919 | 07 p2736 N94-26533
Size distribution of retrogradely labeled dorsal root ganglion cells: Test of normality 07 p2906 N94-27500
Effect of precipitate structure on hot deformation of Al-Mg-Mn alloys
| DE94-004596 | 07 p2741 N94-27622
Large-scale velocity fields and small-scale magnetic fields during the maximum of solar cycle 22
| AD-A278378 | 10 p4165 N94-33743
Computer image analysis of wear debris with its applications to machine wear diagnosis 10 p4067 N94-34366
Anthropogenic sulfate and organic aerosols, CCN, and cloud project concentration at a marine site
| DE94-004210 | 11 p4286 N94-36025
Validation and implementation of optical diagnostics for particle sizing in rocket motors
| AD-A278581 | 12 p4428 N94-36972

SIZE SEPARATION
The carbon isotopic composition of Novo Urei diamonds 01 p0433 N94-12255

SIZING (SEPARATION)
U SIZE SEPARATION

SKELETON
U MUSCULOSKELETAL SYSTEM

SKEWNESS
Evolution of the shock front and turbulence structures in the shock/turbulence interaction 02 p0645 N94-14761
The theory of linear programming: Skew symmetric self-dual problems and the central path
| REPT-93-15 | 04 p1524 N94-19089
Static performance investigation of a skewed-throat multiaxis thrust-vectoring nozzle concept
| NASA-TP-3411 | 10 p3983 N94-34172
Short-tower sigma(theta) measurements in the Colorado Plateaus region
| DE94-007478 | 12 p4463 N94-36478

SKID LANDINGS
Aircraft accident/incident summary report: In-flight loss of control, leading to forced landing and runway overrun, Continental Express, Inc., N24706 Embraer EMB-120 RT, Pine Bluff, Arkansas, 29 April 1993
| PB94-910404 | 08 p3135 N94-29402

SKIDDING
Tests of highly loaded skids on a concrete runway
| NASA-TP-3435 | 07 p2669 N94-26608

SKILLS
U ABILITIES

SKIN (ANATOMY)
NT EPIDERMIS
Wound healing after laser injury to skin: The effect of occlusion and vitamin E
| AD-A266473 | 03 p1128 N94-16779
Physiologically based pharmacokinetic modelling of percutaneously absorbed dibromomethane utilizing multiple dermal sub-compartments
| AD-A271106 | 05 p1889 N94-19981
Enhancement of wound healing by biosynthetic growth factor
| AD-A272517 | 05 p1892 N94-21415
Thyroid hormone action in cultured human skin fibroblasts: Evaluation using spheroid culture 07 p2919 N94-27478
Changes in pain sensation induced by repetitive application of noxious heat pulses to the human skin 07 p2924 N94-27501
Hyperalgesia to cold in patients with Subacute Myelo-Optico-Neuropathy (SMON) 07 p2928 N94-27521
Effect of prostaglandin E1 on the relationship between skin sympathetic nerve activity and reduction in skin blood flow 07 p2929 N94-27524
Difference in skin blood flow reduction depending on activating maneuver of skin sympathetic nerve activity 07 p2929 N94-27525
An attempt of intraneural stimulation by microelectrode inserted in skin sympathetic nerve fascicle 07 p2930 N94-27529
Effects of make-up on the heat transfer from the head in hyperthermic conditions 08 p3394 N94-29864
Development of a video fluorescence system for assessing burn depth
| AD-A278127 | 09 p3798 N94-33092
Modeling heat exchange characteristics of long term space operations: Role of skin wettedness and exercise 10 p4101 N94-33650

SKIN (STRUCTURAL MEMBER)
Remelting of Fe-C-Si-alloy in a ceramic mold skin 03 p0945 N94-15169
Impact tests on fibre metal laminates under a tensile load
| PB94-126570 | 07 p2710 N94-27201
Investigation of the bond strength of a discrete skin-stiffener interface
| NLR-TP-92183-U | 07 p2670 N94-27796

SKIN FRICTION
NT AERODYNAMIC DRAG
NT FRICTION DRAG
NT SUPERSONIC DRAG
NT VISCOUS DRAG
Experimental and computational comparisons of Mach 6 high Reynolds number heat transfer and skin friction 01 p0006 N94-10443
Real gas and surface transpiration effects upon swept leading edge high speed flow including transition 01 p0008 N94-10452
A technique for direct measurement of skin friction in supersonic combustion flow 02 p0503 N94-13555
High freestream turbulence effects on the transport of heat and momentum 02 p0633 N94-13559
The turbulent wall jet
| AD-A267675 | 03 p0855 N94-14963
Active turbulence control in wall bounded flows using direct numerical simulation
| AD-A267261 | 03 p1028 N94-17286
In-flight pressure distributions and skin-friction measurements on a subsonic transport high-lift wing section 04 p1308 N94-18435
Principles and applications of oil film interferometry for measuring wall friction fields in air flows
| ETN-93-95062 | 05 p1798 N94-20147
The use of near-wall hot-wire probes for time-resolved skin-friction measurements 06 p2316 N94-22857
Skin friction measurement in complex flows using thin oil film techniques
| NASA-CR-194872 | 06 p2327 N94-24098
Analytical skin friction and heat transfer formula for compressible internal flows
| NASA-CR-191185 | 06 p2170 N94-25173
Computational prediction of isolated performance of an axisymmetric nozzle at Mach number 0.90
| NASA-TM-4506 | 07 p2646 N94-26547
An actively cooled floating element skin friction balance for direct measurement in high enthalpy supersonic flows 08 p3289 N94-29824
Flight test results of riblets at supersonic speeds
| NASA-TM-4387 | 09 p3572 N94-32880
Active thermal isolation for temperature responsive sensors
| NASA-CASE-LAR-14612-1 | 10 p4054 N94-35074

SKIN RESISTANCE
Transient skin effect in a massive cylinder by eccentric location of exciting conduction bands
| ETN-93-95048 | 04 p1391 N94-19646

SKIN TEMPERATURE (BIOLOGY)
Effects of a high-energy food supplement on cold-induced thermogenesis
| AD-A269301 | 04 p1504 N94-17823
Synchronisation of cold induced vasodilation at various locations of one hand
| IZF-1992-B3 | 04 p1504 N94-17966
Physiological efficacy of a lightweight ambient air cooling unit for various applications
| AD-A272952 | 05 p1896 N94-21247
Simulation of the effect of wind on clothing by measurements and calculations
| PB94-132289 | 08 p3399 N94-28406
A comparison of four methods of rewarming individuals cooled by immersion in cold water 08 p3382 N94-28442
Thermal strain generated by an enhanced anti-G protection system in a hot climate 08 p3383 N94-28445
Physiological responses during shipboard firefighting
| AD-A275104 | 08 p3391 N94-28912
Effects of make-up on the heat transfer from the head in hyperthermic conditions 08 p3394 N94-29864
Errors associated with the use of heat flow transducers 09 p3796 N94-31742

SKIN TEMPERATURE (NON-BIOLOGICAL)
The development and implementation of an interactive retrieval/analysis/forecast algorithm 02 p0692 N94-14234

SKIRTS
Stress relaxation forming of Ariane 5 front skirt outer skin panels 01 p0062 N94-10046
SRB thermal curtain design support
[NASA-CR-193857] 03 p0927 N94-17123
SRB thermal curtain design support
[NASA-CR-193858] 03 p0928 N94-17124
Heave dynamics of an air cushion vehicle bag and finger skirt
[ISBN-0-315-87053-2] 09 p3568 N94-31734
Use of photostress to analyze behavior of an aft skirt test specimen
[NASA-CR-195850] 10 p4069 N94-34075
SKULL
NT CRANIUM
SKY
NT NIGHT SKY
SKY RADIATION
NT AIRGLOW
NT DAYGLOW
NT GEOCORONAL EMISSIONS
NT NIGHTGLOW
NT TWILIGHT GLOW
Determination of sunshine duration from radiation intensity pyranometric measurements of global and sky radiation
[BER-181] 03 p1105 N94-15302
SKY SURVEYS (ASTRONOMY)
Preparing for the initial observations of the Targeted Search and the Sky Survey systems
[NASA-CR-193644] 01 p0318 N94-10865
First results of the seven-color asteroid survey 01 p0430 N94-12162
Archiving of HEAO-1 data products and the creation of a general user's guide to the archive
[NASA-CR-193415] 02 p0822 N94-13062
Search for extraterrestrial intelligence/high resolution microwave survey team member
[NASA-CR-194177] 02 p0739 N94-13086
ROSAT guest investigator program (AO-1). On a search for coronal x ray emissions from white dwarfs
[NASA-CR-193654] 02 p0835 N94-13171
A survey of compact planetary nebulae at radio wavelengths
[ISBN-0-315-61950-3] 02 p0829 N94-13371
A near-infrared faint galaxy survey: Evolution and the cosmological geometry from K band photometry 02 p0830 N94-13591
Sites of fine-scale electron density turbulence in the interstellar medium
[NASA-CR-193708] 02 p0839 N94-13864
X ray observations of late-type stars using the ROSAT all-sky survey
[NASA-CR-193716] 02 p0832 N94-14146
HRMS sky survey wideband feed system design for DSS 24 beam waveguide antenna 02 p0611 N94-14397
EUVE observations of the Moon 03 p1250 N94-16185
Search for Extraterrestrial Intelligence (SETI) 03 p1125 N94-16620
Participation in the north ecliptic pole sky survey
[NASA-CR-191933] 03 p1059 N94-16815
A deep x ray survey in the Lockman hole and the soft x ray log N - log S
[NASA-CR-194698] 05 p2054 N94-20174
Optical and Gamma Ray Space Observations
[NASA-TM-109389] 05 p2149 N94-20602
Second Annual Conference on Astronomical Data Analysis Software and Systems. Abstracts
[NASA-TM-108245] 05 p2057 N94-22438
Deep near-infrared survey of the Southern Sky (DENIS) 05 p2062 N94-22467
The extreme ultraviolet explorer archive 05 p2047 N94-22468
Visualizing the universe, part 2 05 p2063 N94-22472
Visualizing the universe, part 1 05 p2064 N94-22476
Data indexing techniques for the EUVE all-sky survey 05 p2048 N94-22503
Guide star catalogue data retrieval software 2 05 p1927 N94-22533
SkICAT: A cataloging and analysis tool for wide field imaging surveys 05 p2049 N94-22546
Miyun 232 MHz survey 1: Fields centered at: alpha:00(h)41(m), delta:41 deg 12 min and alpha: 07(h)00(m),delta:35 deg 00 min 05 p2080 N94-22554
ROSAT data analysis with EXSAS 05 p2080 N94-22555
Results from ROSAT 05 p2000 N94-22630
Compton Gamma Ray Observatory highlights of the sky survey 05 p2002 N94-22642
BATSE burst location accuracy and constraints on the fraction of repeating GRB sources
[DE94-004981] 07 p3116 N94-27714
Sloan Digital Sky Survey
[DE94-004662] 07 p3103 N94-27750
In search of Nemesis 07 p2888 N94-28297
X ray studies of the Hyades cluster
[NASA-CR-189325] 08 p3538 N94-29001
A study of recycled pulsars in globular clusters 08 p3539 N94-29825
A near-infrared survey of the star forming region NGC 2264 08 p3540 N94-29971
Multiwavelength search for protoplanetary disks 09 p3599 N94-31430
Near infrared surveys of high mass star forming regions 09 p3925 N94-31898
A multi-frequency study of an x ray selected sample of active galactic nuclei 09 p3937 N94-31987
Catalog and atlas from a sensitive 1.5 GHz radio survey around the North Ecliptic Pole
[AD-A277705] 10 p4085 N94-33440
Data acquisition systems for the Sloan Digital Sky Survey
[DE94-008992] 10 p4161 N94-33695
A search for pre- and post-burst emission from well-localized gamma-ray burst locations
[NASA-CR-195825] 10 p4167 N94-34990
The distributed development environment for SDSS software
[DE94-013238] 12 p4547 N94-37555
Sloan Digital Sky Survey
[DE94-011749] 12 p4547 N94-37667
SKY WAVES
NT WHISTLERS
Morphology and characteristics of disturbed HF skywave channels
[AD-A269755] 04 p1388 N94-18722
Northern Exposure 1992: An investigation of transauroral HF radio skywave propagation
[AD-A273363] 06 p2303 N94-25089
A physical optics model for scattering of HF radiation by irregular terrain
[DE94-006187] 08 p3255 N94-30106
Atmospheric effects assessment program: Ionospheric sounding
[AD-A276447] 09 p3770 N94-31303
SLABS
An analytic model for calculating pump-induced wavefront distortions in laser slabs
[DE93-011953] 01 p0174 N94-11126
Time-laplace-transform-domain analysis of wave propagation in planar waveguides
[PB93-215226] 05 p1960 N94-22096
A vibrating wire parallel to a type 2 superconducting slab of arbitrary thickness
[DE93-617134] 06 p2525 N94-25389
The effect of a transport current on the surface barrier of a uniaxial anisotropic superconducting slab
[DE93-617135] 06 p2566 N94-25390
Effects of a vibrating wire carrying DC current on a moving type 2 superconducting slab of arbitrary thickness
[DE93-617136] 06 p2566 N94-25391
Optical characterization and guided wave loss measurements for end-capped 6F-polybenzoxazole
[AD-A274586] 07 p3036 N94-26982
The 250 watt average power electro-quality Q-switched diode pumped power oscillator
[DE94-011644] 12 p4449 N94-37737
SLAGS
Detection of velocity in high temperature liquid metals 06 p2247 N94-25127
Study on reactions between molten metal and oxide by magnetic flotation dissolution method 07 p2725 N94-25558
Mineralogy and metallurgical properties of iron ore sinter based on magnetite fines
[DE94-763309] 12 p4414 N94-36525
SLANT
U SLOPES
SLANT PERCEPTION
U SPACE PERCEPTION
SLASHES
U CLEARINGS (OPENINGS)
SLEDS
The development of a horizontal impact sled facility and subsequent crashworthiness experiments
[NIAR-93-15] 07 p2680 N94-26200
Portable Linear Sled (PLS) for biomedical research 08 p3163 N94-29648
SLEEP
Noise levels and their effects on Shuttle crewmembers' performance: Operational concerns 01 p0314 N94-11538
Work/rest schedules and performance of S-3 aviators during fleet exercise
[AD-A265807] 02 p0734 N94-12975
Work/rest schedules and performance of F/A-18 aviators during Fleet Exercise 1992
[AD-A265826] 02 p0735 N94-12982
Sleep management user's guide for special operations personnel
[AD-A267746] 03 p1119 N94-14943
Using controlled daylight exposure and sleep timing in the prevention of shift lag during night operations
[AD-A269304] 04 p1504 N94-17824
A comparison of polygraphic and actigraphic monitoring of sleep using a 5-channel programmable-sensitivity actigraph
[AD-A270731] 04 p1507 N94-19608
Physiological correlates of stress-induced decrements in human perceptual performance
[DOT/FAA/AM-93/19] 05 p1893 N94-20081
A comparison of sleep scored from electroencephalography to sleep scored by wrist actigraphy
[AD-A273739] 07 p2910 N94-26748
Workload transition: Implications for individual and team performance
[AD-A274538] 07 p2941 N94-26964
Unit specific crew rest strategies: Phase 1 evaluation of the 1/212th Aviation Battalion during shiftwork transitions
[AD-A277122] 09 p3804 N94-32379
Proceedings of the 6th International Congress on Noise as a Public Health Problem, volume 1
[AD-A278259] 10 p4133 N94-33961
SLEEP DEPRIVATION
Work/rest schedules and performance of S-3 aviators during fleet exercise
[AD-A265807] 02 p0734 N94-12975
Work/rest schedules and performance of F/A-18 aviators during Fleet Exercise 1992
[AD-A265826] 02 p0735 N94-12982
Sleep management user's guide for special operations personnel
[AD-A267746] 03 p1119 N94-14943
Activity/rest patterns of instructor and rates student pilots during rapid transitions from daytime to nighttime duty hours at the Eastern Army Aviation Training site
[AD-A267038] 03 p1131 N94-15659
Effects of methamphetamine on vigilance and tracking during extended wakefulness
[AD-A274896] 07 p2909 N94-26179
Performance assessment in sustained operations using a computer-based synthetic work task
[AD-A274707] 07 p2937 N94-26430
Effects of methamphetamine and fatigue on long- and short-term memory
[AD-A276452] 09 p3799 N94-32187
Some solutions to reduce the human effects of extended operation times 11 p4196 N94-36339
SLENDER BODIES
NT SLENDER CONES
Stability of hypersonic flow over a blunt body 01 p0007 N94-10450
Vibrations in engineering structures: A review of model and full-scale test of a cable-stayed bridge and a traffic sign gantry
[NLR-TP-92321-U] 07 p2843 N94-27553
An improvement of the slender body theory for oscillating ships with finite forward speed 08 p3234 N94-29705
A new method for calculating wing along aerodynamics to angle of attack 180 deg
[AD-A277965] 09 p3574 N94-33263
SLENDER CONES
Pneumatic management of blunted-forebody flow asymmetry for high-angle-of-attack directional control 07 p2679 N94-28028
SLENDER WINGS
A grid generation package for high aspect ratio wings 02 p0510 N94-14608
SLEWING
General theory and algorithms for the non-casual inversion, slewing and control of space-based articulated structures
[AD-A275118] 08 p3167 N94-29002
A combined algorithm for minimum time slewing of flexible spacecraft 11 p4220 N94-35881
Input shaping for three-dimensional slew maneuvers of a precision pointing flexible spacecraft
[DE94-008937] 11 p4226 N94-36001
Modeling and control of intelligent flexible structures
[AD-A280478] 12 p4396 N94-37349
SLICING
Integrating interface slicing into software engineering processes
[NASA-CR-192761] 02 p0754 N94-14368
SLICKS
U OIL SLICKS
SLIDES
U CHUTES

SLIDING
Properties of interfacial tribo-films
[AD-A265591] 01 p0182 N94-12374
Wear-mechanism modelling
[DE93-012311] 02 p0579 N94-13974
The processing and mechanical properties of high temperature/high performance composites. Book 1: Coonstituent properties of composites
[AD-A266394] 03 p0935 N94-16483
Heterogeneous slip and rupture models of the San Andreas fault zone based upon three-dimensional earthquake tomography
[DE93-015037] 04 p1480 N94-17898
Fatigue resistant Ti3Al composites
[AD-A270305] 04 p1341 N94-18692
Study on variation of damage generation mechanism by fatigue on TiAl compounds due to different slip systems 07 p2729 N94-25579
SLIDING CONTACT
Tribological characteristics of sputtered Au/Cr films on alumina substrates at elevated temperatures
[NASA-TM-106078] 01 p0055 N94-11362
SLIDING FRICTION
Effect of surface cleanliness of bearing steel on adhesive strength and tribological properties of sputter-deposited gold films
[DE93-767974] 01 p0082 N94-10732
JPRS report: Science and technology. Central Eurasia: Materials science
[JPRS-UMS-93-005] 02 p0559 N94-14575
Integrated fundamental research on current collection
[AD-A266987] 03 p1008 N94-15494
The friction and wear of ceramic/ceramic and ceramic/metal combinations in sliding contact
[NASA-TM-106348] 03 p0930 N94-15769
Continuing research on friction and wear of materials
[AD-A268291] 03 p1049 N94-17566
Interdisciplinary research on wear of materials
[AD-A268190] 04 p1443 N94-17730
Atomic-scale friction and microfriction of graphite and diamond using friction force microscopy
[AD-A270952] 04 p1605 N94-19679
Tribological studies of silicon for magnetic recording applications (Invited)
[AD-A270878] 04 p1447 N94-19784
Microscopic modeling of tribological and interfacial phenomena
[AD-A271864] 05 p1823 N94-20464
In-vacuo slip testing of materials for SSRMS friction brakes 05 p1661 N94-21381
Detailed study of oxidation/wear mechanism in lox turbopump bearings
[NASA-TM-108434] 05 p1825 N94-21580
Wear characteristics of technical dry rolling/sliding systems with relations to corrugation problems 06 p2269 N94-23586
Surface observations of stick-slip oscillations in tightly conformal wheel/rail contacts 06 p2270 N94-23588
Development of a theory of the wear of ceramics
[DE94-002773] 06 p2254 N94-23783
Development of gears for space use 06 p2360 N94-24021
Wear reduction in ceramic bearings by surface generated pyrolytic carbon continuously replenished by ethylene gas
[AD-A278264] 06 p2364 N94-24090
Crystal chemistry and self-lubricating properties of monochalcogenides gallium selenide and tin selenide
[DE93-041177] 07 p2751 N94-26422
Guidelines for unlubricated sliding wear tests. Part 1: General approach
[PB94-119666] 07 p2825 N94-27322
Guidelines for unlubricated sliding wear tests. Part 2: Procedures for pin-on-disc testing
[PB94-123270] 07 p2825 N94-27324
Atomic-scale friction measurements using friction force microscopy. Part 2: Application to magnetic media
[AD-A275202] 08 p3298 N94-29290
Sliding friction and wear between titanium nitride, M50 steel and silicon nitride (round 3 of VAMAS wear test program)
[IMR-TM-TR-003] 08 p3303 N94-30019
XPS analysis of 440C steel surfaces lubricated with perfluoropolyethers under sliding conditions in high vacuum
[NASA-TM-106548] 08 p3218 N94-30177
Mechanics of failure of high temperature metal matrix composites
[AD-A277397] 09 p3624 N94-32342
Continuing research on friction and wear of materials
[AD-A277690] 10 p4059 N94-33437
Effect of niobium interlayer on high-temperature sliding friction and wear of silver films on alumina
[DE94-010462] 11 p4275 N94-36232
Wear-resisting oxide films for 900 C
[DE94-010093] 11 p4246 N94-36306

SLIP BANDS
U EDGE DISLOCATIONS
SLIP CASTING
Effect of powder processing on slip casting parameters and sintering of Si3N4-Y2O3-SiO2
[AD-A264474] 01 p0083 N94-11445
Nonaqueous slip casting of high temperature ceramic superconductors using an investment casting technique
[NASA-CASE-LAR-14918-1] 03 p0983 N94-15881
Finite element analytical techniques for ceramic production in microgravity: A hypoelastic model 03 p0981 N94-16099
Fabrication of advanced design (grooved) cermet anodes
[DE93-014590] 03 p1012 N94-16765
Improved ceramic slip casting technique --- application to aircraft model fabrication
[NASA-CASE-LAR-14471-1] 05 p1702 N94-20377
Fabrication of whisker-toughened alumina tubes
[DE94-001012] 05 p1677 N94-22022
Nonaqueous slip casting of YBa2Cu3O(7-x) superconductive ceramics
[NASA-CR-4575] 08 p3512 N94-29101
Pressureless sintering of ceramic composites
[AD-A277274] 09 p3657 N94-32404
SLIPSTREAMS
NT PROPELLER SLIPSTREAMS
Prediction of transonic potential flow with slipstreams around configurations
[FFA-TN-1992-15] 09 p3568 N94-31220
SLITS
Numerical simulation of the edge tone phenomenon
[NASA-CR-4581] 10 p3982 N94-33898
SLOPES
NT GLIDE PATHS
Evolution of steep Martian slopes 01 p0434 N94-11184
Power-law confusion: You say incremental, I say differential 01 p0347 N94-12175
Mapping bathymetric slopes from bathymetry data
[AD-A265923] 01 p0290 N94-12350
Emplacement of multiple flow units on very shallow slopes, east Kawelu Planitia flow field, Venus 03 p1260 N94-16235
Resonantly pumped, erbium-doped, GSGG, 2.8 micron, solid state laser with energy recycling and high slope efficiency
[AD-D015920] 05 p1815 N94-20060
Topographic slope from the SAR interferometric phase gradient 05 p1731 N94-20459
Comparison of flank modification on Ascraeus and Arsia Montes volcanoes, Mars 05 p2140 N94-20903
Seasonal snow of arctic Alaska R4D investigations
[DE93-040082] 07 p2892 N94-25939
Improved measurement accuracy in a Long Trace Profiler: Compensation for laser pointing instability
[DE94-003408] 07 p2816 N94-26130
Wing lift increment at zero angle of attack due to deployment of single-slotted flaps at low speeds
[ESDU-93019] 07 p2649 N94-28140
Influence of clearance and rake angles on the cutting force of rock 08 p3368 N94-29520
A coupled approach to spatially derived parameters necessary for ecosystem modeling on the North Slope of Alaska: Appendix A
[DE94-005853] 08 p3349 N94-30046
SLOSHING
U LIQUID SLOSHING
SLOT ANTENNAS
Recent activities in printed Antennas at LeRC 05 p1722 N94-20422
Linearly tapered slot antenna with dielectric superstrate 05 p1734 N94-20505
Slot-coupled patch antenna with coplanar waveguide feed 05 p1734 N94-20506
Linearly tapered slot antenna circular array for mobile communications
[NASA-TM-106441] 05 p1769 N94-21808
Radar signature related radome techniques for flush-mounted HF-, VHF- and, UHF communication antennas
[PB93-204618] 06 p2294 N94-23742
Spatial frequency multiplier with active linearly tapered slot antenna array
[NASA-TM-106494] 06 p2310 N94-24308
Printed circuit elements with applications to antennas, scattering, and circuits
[AD-A275512] 08 p3262 N94-28669
Radial microstrip slotline feed network for circular mobile communications array
[NASA-TM-106540] 08 p3267 N94-30198
Analysis of a slot coupled coplanar waveguide fed patch antenna
[NASA-TM-106567] 09 p3698 N94-33116
SLOTS
NT WING SLOTS
Wall interference and boundary simulation in a transonic wind tunnel with a discretely slotted test section
[NASA-TP-3334] 03 p0872 N94-15794
Manufacturing tolerance requirements for frequency selective surfaces
[AD-A266541] 03 p0999 N94-16797
High-Lift System Aerodynamics
[AGARD-CP-515] 04 p1305 N94-18415
Analysis of microstrip dipoles and slots transversely coupled to a microstrip line using the FDTD method 05 p1718 N94-20405
An analysis of pressure driven cross-flow through a long slot connecting two parallel channels
[DE93-040181] 05 p1804 N94-21765
Effects of slot on rock surface for percussive rock excavation: Water jet assisted percussive rock excavation 07 p2871 N94-28155
Applied Computational Electromagnetics Society Journal, volume 9, number 1, March 1994
[AD-A276753] 09 p3679 N94-32183
Mechanisms of flow control with the unsteady bleed technique 10 p3986 N94-34987
SLOTTED ANTENNAS
U SLOT ANTENNAS
SLOTTED WIND TUNNELS
Evaluation of the buoyancy drag on automobile models in low speed wind tunnels 07 p2658 N94-28352
Experimental studies of transonic flow field near a longitudinally slotted wind tunnel wall
[NASA-TP-3392] 08 p3130 N94-29545
SLOW NEUTRONS
U THERMAL NEUTRONS
SLUMPING
A review and evaluation of the ADAM 2.1 dispersion model
[AD-A269896] 04 p1474 N94-18688
SLURRIES
Coprocessing of fossil fuels and biomass for CO2 emission reduction in the transportation sector
[PB93-194165] 01 p0267 N94-11845
Reverse micelle synthesis of nanoscale metal containing catalysts
[DE93-012869] 02 p0572 N94-14184
Method of producing a silicon carbide fiber reinforced strontium aluminosilicate glass-ceramic matrix composite
[NASA-CASE-LEW-15263-2] 03 p0934 N94-15929
Advanced in macrostatistical hydrodynamics
[DE93-018479] 04 p1410 N94-18270
Metal slurry droplet and spray combustion
[AD-A269648] 04 p1349 N94-18736
Fabrication of porous ceramics by freeze-casting/freeze-drying
[PB93-202513] 05 p1705 N94-21425
Preparing polymeric matrix composites using an aqueous slurry technique
[NASA-CASE-LAR-14771-1] 06 p2252 N94-23076
Composite fiber structures for catalysts and electrodes 06 p2393 N94-23364
Theoretical considerations for Reaction-Formed Silicon Carbide (RFSC) formation by molten silicon infiltration into slurry-derived preforms
[NASA-TM-106414] 06 p2222 N94-23500
Dewatering of contaminated river sediments 08 p3354 N94-30472
Development of a catalytic system for gasification of wet biomass
[DE94-006216] 09 p3759 N94-31762
Effect of surface forces on the rheology of particle-liquid systems and the consolidation of ceramic powders
[AD-A277092] 09 p3657 N94-32391
Technology development for iron Fischer-Tropsch catalysts
[DE94-008723] 09 p3638 N94-32889
Coal-water slurry spray characteristics of an electronically-controlled accumulator fuel injection system
[DE94-008977] 10 p4060 N94-33946
Coal-water slurry sprays from an electronically controlled accumulator fuel injection system: Break-up distances and times
[DE94-008979] 10 p4061 N94-33981
Synchronized droplet size measurements for Coal-Water-Slurry (CWS) diesel sprays of an electronically-controlled fuel injection system
[DE94-008978] 10 p4061 N94-34017
Determination of extensional viscosity from capillary rheometer entrance pressure drop measurements using a numerical simulation of contraction flow
[PB94-171154] 11 p4263 N94-35603
Coal-fueled diesels for modular power generation
[DE94-002960] 11 p4275 N94-36348
SLURRY PROPELLANTS
NT SLUSH HYDROGEN
Electro-rheology fluids and liquid fuel flow
[AD-A273640] 06 p2337 N94-25032

SLUSH HYDROGEN
Experimental results of hydrogen slosh in a 62 cubic foot (1750 liter) tank
[NASA-TM-106625] 11 p4263 N94-35250
SM-65 MISSILE
U ATLAS LAUNCH VEHICLES
SMALL ASTRONOMY SATELLITES
U SAS
SMALL PERTURBATION FLOW
The velocity field created by a shallow bump in a boundary layer
[AD-A281064] 11 p4266 N94-35975
SMALL SCIENTIFIC SATELLITES
Estimation of the attitude motion of the small satellite ORIZURU
[NAL-TR-1145] 01 p0042 N94-10366
In-orbit performance tests and tele-command systems of the umbrella test satellite (DEBUT)
[NAL-TR-1165] 01 p0043 N94-10859
The 1971 highlights --- NASA programs and research
[NASA-TM-109629] 03 p1302 N94-15417
Small Satellites Systems and Services
[ISBN-2-85-428327-9] 03 p0888 N94-17131
Small satellite constellation system: Optimization criteria 03 p0888 N94-17132
AMIGAU: A prototype tool aimed at mission analysis for satellites and satellite constellations 03 p0888 N94-17133
Small launchers (current and future projects in the world) 03 p0878 N94-17137
Small satellite constellation deployment strategies 03 p0878 N94-17138
Delta launch vehicle: Accommodations for small satellites 03 p0878 N94-17139
ARIANE 5 light derivatives 03 p0878 N94-17140
NEXT launch system 03 p0878 N94-17141
Small missions for space science 03 p0874 N94-17142
Strategy for a small satellite program and a proposal for a first mission 03 p0874 N94-17143
Small satellite missions to long-period comets 03 p0874 N94-17144
BRIDGE: A small scientific satellite for geodesy 03 p0890 N94-17146
Cosmic dust and space debris measurements on board the small satellites HITEN and BREM-SAT 03 p0890 N94-17147
SYNMOD: A low-resource, low-cost means of monitoring the near-Earth space debris environment 03 p0891 N94-17148
Role and development of small satellite missions in space plasma physics 03 p0891 N94-17149
Earth observation from small satellites 03 p0891 N94-17150
Small imaging satellite for Earth observing system adjunct 03 p0891 N94-17151
Adequation of mini satellites to oceanic altimetry missions 03 p0891 N94-17152
SYDONI: An intensified system for night observation 03 p0891 N94-17153
A proposed ground segment design for small satellites 03 p0878 N94-17154
Ground segment definition for the Spanish small satellite program (MINISAT) 03 p0878 N94-17155
OREMUS: Prototype of an orbit determination center dedicated to mini-satellite control 03 p0878 N94-17156
Data processing system for ARSENE ground station: A tool for small satellite control and development 03 p0878 N94-17157
Satellite control: A comprehensive approach 03 p0878 N94-17158
Regulation of low Earth orbit satellites 03 p0892 N94-17159
A study on an experimental communication system using microsatellites 03 p0892 N94-17160
LEOCOM-SPES: Low cost message communications 03 p0892 N94-17161
TAOS (S80): A (LEO-MSS) system for position reporting and telemanagement services 03 p0893 N94-17162
The ORBCOMM system 03 p0893 N94-17163
MAGSS-14: Medium Altitude Global Mobile Satellite System with enhanced regional coverage 03 p0893 N94-17164
S 80/T: A micro satellite system combining high performances and limited resources 03 p0893 N94-17166
The ELLIPSO (tm) system: Elliptical low orbits for mobile communications 03 p0893 N94-17167
UoSAT: A decade of experience pioneering microsatellites 03 p0894 N94-17169
CERISE microsatellite system 03 p0894 N94-17170
Impact of advances in technology on future spacecraft design 03 p0894 N94-17171
S-80: A satellite for less than 50 MF 03 p0894 N94-17172
Small satellite modular design and application prospect 03 p0894 N94-17173
Arsene GaAs solar array 03 p0894 N94-17174
Small satellite nickel-hydrogen and nickel-metal hydride power applications 03 p0895 N94-17175
A power system for a microsatellite 03 p0895 N94-17176
Data handling strategy for the Spanish small satellite program (MINISAT) 03 p0895 N94-17177
The STRV On Board Data Handling (OBDH) system: An introduction 03 p0895 N94-17178
A mini satellite called Arsene: The way to make it at a minimum cost 03 p0895 N94-17179
TUBSAT: Low cost access to space technology 03 p0895 N94-17180
Standard platforms for small satellites 03 p0895 N94-17181
MINISAT programme 03 p0896 N94-17182
The space technology research vehicle: Development status 03 p0896 N94-17183
On-board spatial scientific experiment project on small satellites 03 p0896 N94-17184
ALEXIS and HETE: Two small, low cost, scientific satellite systems 03 p0896 N94-17185
TITUS: A micro-satellite for technology demonstration 03 p0896 N94-17186
Big results with small space systems: What small systems are doing today 03 p0896 N94-17187
Small satellite product assurance 03 p0896 N94-17188
Environment tests for mini satellites 03 p0896 N94-17189
Cost drivers: Why do conventional satellites cost so much? 03 p0897 N94-17190
Key trends of the small satellite market 03 p0897 N94-17191
WISPER: Wirless Space Power Experiment
[NASA-CR-195538] 06 p2396 N94-24701
Copernicus: Lunar surface mapper 07 p3081 N94-25702
Norwegian ionospheric satellite experiment: High latitude, low Earth orbit plasma measurements
[FFI-93/7025] 07 p2876 N94-25807
A simple satellite system to locate gamma ray bursters using scintillating fiber technology
[DE94-601287] 07 p3117 N94-27996
The ALEXIS mission recovery
[DE94-007549] 09 p3611 N94-32813
Technology for small spacecraft
[NASA-CR-196041] 10 p4015 N94-34411
Controller for the Electronically Scanned Thinned Array Radiometer (ESTAR) instrument
[NASA-TM-104608] 11 p4259 N94-36049
Characterization of spacecraft and environmental disturbances on a SmallSat
[NASA-CR-194915] 12 p4396 N94-36990
SMART STRUCTURES
Smart Structures for Aircraft and Spacecraft
[AGARD-CP-531] 01 p0068 N94-11317
Smart structures: A technology for next generation aircraft 01 p0027 N94-11318
Dynamic tests on the NASA Langley CSI evolutionary model 01 p0045 N94-11320
Smart materials for helicopter rotor active control 01 p0027 N94-11321
Intelligent structures: A technology overview and assessment 01 p0068 N94-11322
The Satellite Attack Warning and Assessment Flight Experiment (SAWAFE) 01 p0045 N94-11323
Optical fibre techniques for structural monitoring in composites 01 p0069 N94-11324
Smart processing of composite materials for enhanced performance and properties 01 p0069 N94-11325
Smart structures at Aastra Corporation 01 p0069 N94-11326
Fiber optic sensing for composite smart structures 01 p0069 N94-11327
On the stability of shape memory materials and their properties in static and dynamic applications 01 p0069 N94-11329
Smart polymeric system for electromechanical transduction 01 p0070 N94-11330
Recent developments in piezoelectric and electrostrictive sensors and actuators for smart structures 01 p0070 N94-11332
In-flight aircraft structure health monitoring based on smart structures technology 01 p0022 N94-11333
Structural health monitoring using embedded fibre optic sensors 01 p0022 N94-11334
Fault location in structures using neural networks 01 p0070 N94-11335
Factors affecting the embedding of optical fibre sensors in advanced composite structures 01 p0070 N94-11336
Fiber-optic sensor systems for measuring strain and the detection of acoustic emissions in smart structures 01 p0071 N94-11337
Structural analysis and optimization of adaptive structures by use of the finite element method 01 p0071 N94-11339
Fiber-optic interferometric strain gauge for smart structures applications: First flight tests 01 p0071 N94-11340
On possible applications of smart structures to control of space systems 01 p0045 N94-11342
Aircraft smart structures research in the USAF Wright Laboratory 01 p0072 N94-11343
Advances in adaptive structures at Jet Propulsion Laboratory 01 p0072 N94-11344
Multidimensional intelligent control for superlight air vehicles 01 p0027 N94-11347
Active vibration control of adaptive flexible structures using piezoelectric smart sensors and actuators 01 p0189 N94-11823
Feasibility study of an orbiting laboratory for testing CSI technology
[NASA-CR-191524] 02 p0540 N94-13016
Smart skin technology development for measuring ice accretion, stall, and high AOA aircraft performance. Part 1: Capacitive ice detector development
[NASA-CR-194252] 02 p0511 N94-13424
Smart materials/structures technical analysis
[AD-A266771] 02 p0766 N94-14785
Aeroelastic airfoil smart spar 03 p0868 N94-16865
The 6th Japan-U.S. conference on composite materials
[AD-A268535] 04 p1341 N94-18630
Use of shape memory alloys in the robust control of smart structures
[AD-A270827] 04 p1366 N94-19594
Quantification of uncertainties in the performance of smart composite structures
[NASA-TM-106335] 05 p1830 N94-20171
Intelligent Material Systems and Structures (IMSS). Part 5: Fiber optic registration of deformation in carbon laminates 91/92
[PB93-204600] 06 p2544 N94-23723
Probabilistic assessment of smart composite structures
[NASA-TM-106358] 06 p2378 N94-25188
Influence of embedded optical fibers on compressive strength of advanced composites
[AD-A273775] 07 p2705 N94-25859
Proceedings of Damping 1993, volume 3
[AD-A274228] 07 p2840 N94-27008
Smart structures, an overview
[AD-A274147] 07 p2987 N94-27093
Intelligent material systems and structures. Part 6: Measurements of adhesion between optical fibres and composite materials
[PB94-123577] 07 p2756 N94-27215
Collocated tunable wavenumber sensor/actuators for smart structures
[AD-A275872] 08 p3241 N94-28755
Report on smart materials
[PB94-137528] 08 p3203 N94-29015
Assessment of the fibre volume distribution around optical fibres
[FFA-TN-1993-12] 08 p3179 N94-29425
Intelligent material systems and structures. Part 7: Debonding and pull-out of two optical fibers from two epoxies
[PB94-137767] 08 p3180 N94-29475
Active control of delaminations in smart composite structures 08 p3181 N94-29593
Control and stabilization of distributed parameter systems; theoretical and computational aspects
[AD-A277239] 09 p3738 N94-32275
Structural integrity of intelligent materials and structures
[AD-A278397] 09 p3630 N94-33165
Coupled electromechanical response of composite beams with embedded piezoelectric sensors and actuators
[NASA-CR-195313] 10 p4019 N94-33899
Smart IR-camera: Description of a simulator
[PB94-149010] 10 p4143 N94-34127
A PDE-based methodology for modeling, parameter estimation and feedback control in structural and structural acoustic systems
[NASA-CR-194928] 12 p4500 N94-36924
Vibration suppression with approximate finite dimensional compensators for distributed systems: Computational methods and experimental results
[NASA-CR-194927] 12 p4500 N94-36928
Modeling and control of intelligent flexible structures
[AD-A280478] 12 p4396 N94-37349

SMELTING
Fabrication of advanced design (grooved) cermet anodes
[DE93-014590] 03 p1012 N94-16765
SMITH CHART
Manual design technique for broadband passive thin-film attenuators using the Smith chart
05 p1782 N94-22178
SMOG
Energy efficiency and the environment: Innovative ways to improve air quality in the Los Angeles Basin
[DE93-016964] 04 p1473 N94-18050
SMOKE
New thermoplastic laminating adhesives for the aircraft industry with low heat release and low smoke emission
01 p0017 N94-10767
A new low smoke, low heat release structural foam
01 p0017 N94-10768
A four-dimensional, mesoscale, non-gaussian multispectral smoke model. Phase 1: Feasibility study
[AD-A264805] 01 p0152 N94-11519
Information capability of NOAA-AVHRR data for monitoring oceanographic and atmospheric pollution
01 p0214 N94-12677
Estimation of the concentration versus the time profile of zinc chloride particles in smoke clouds generated by the Raufoss A/S instantaneous smoke RA-90 and DM-45 HC smoke generator
[FFI-93/6001] 02 p0708 N94-13821
Flight validation of a pulsed smoke flow visualization system
[NASA-CR-186026] 02 p0516 N94-14106
The MADONA experiments (Meteorology and Diffusion Over Non-uniform Areas): High-resolution in-plume concentration fluctuations measurements using lidar remote sensing technique
[AD-A267711] 03 p1105 N94-14938
Secondary smoke 03 p0924 N94-15220
Zinc and titanium smoke: Chemical composition and physical characteristics
[FOA-C-40277-4.9] 05 p1680 N94-20552
Chronic obstructive pulmonary disease
06 p2425 N94-23324
Field models: Their present and future application in fire safety engineering
[PB93-201622] 06 p2269 N94-23506
Zone fire modeling with natural building flows and a zero order shaft model
[PB94-112166] 06 p2270 N94-23735
The effects of zinc borate addition on the flammability characteristics of polyester, vinyl ester, and epoxy glass reinforced plastics
[AD-A273164] 06 p2262 N94-25136
Engineering Technical Letter (ETL) 93-5: Fire protection engineering criteria, electronic equipment installations
[AD-A274835] 07 p2762 N94-26084
SP industry calorimeter for rate of heat release measurements up to 10MW
[PB94-124211] 07 p2811 N94-27044
Flowfield prediction of NO(x) and smoke production in aircraft engines 08 p3191 N94-29252
The influence of air distribution on homogeneity and pollutant formation in the primary zone of a tubular combustor 08 p3194 N94-29274
NATO SOCMET trials 08 p3258 N94-30503
The effects of man-made smokes and battlefield-induced smokes on the propagation of electromagnetic radiation 08 p3258 N94-30505
SMOKE DETECTORS
Army aircraft fire-detection systems operation and reliability
[AD-A271327] 05 p1641 N94-20912
Design and development of experimental facilities for short duration, low-gravity combustion and fire experiments
[NASA-CR-196107] 12 p4389 N94-36967
Aircraft command in emergency situations prototype development users manual
[DOT/FAA/CT-94/24] 12 p4385 N94-37706
SMOKE TRAILS
Simulated wake characteristics of tapered annular wings by a discrete vortex method
[NAL-TR-1156] 01 p0013 N94-10855
SMOOTHING
NT DATA SMOOTHING
Improvement of the flow quality in the ARA transonic tunnel by means of a long cell honeycomb
[ARA-MEMO-375] 01 p0034 N94-10894
FFTSCAN: A program for spectral smoothing using Fourier transforms
[AD-A264921] 01 p0278 N94-11852
Shock-free acceleration of laser driven targets
[DE93-008050] 02 p0655 N94-13387
A time-frequency smoothing algorithm for cyclic spectral analysis
[DE93-016634] 04 p1519 N94-18097
Numerical study of a multigrid method with four smoothing methods for the incompressible Navier-Stokes equations in general coordinates
05 p1806 N94-21487
A lower bound on wait-free counting
[CWI-CS-R9307] 05 p1915 N94-21537
Nonlinear smoothing for random fields
[PB94-149531] 06 p2493 N94-22728
POISs3: A 3D poisson smoother of structured grids
[PB93-226231] 06 p2318 N94-23115
A nonconforming multigrid method using conforming subspaces 06 p2485 N94-23695
Time-step enlargement and optimal smoothing in Runge-Kutta time-integration algorithms by implicit and explicit smoothing
[NLR-TP-92221-U] 07 p2798 N94-27799
Output statistics of the SALFAS FM normalizer Smoothing/Prediction function
[AD-A275758] 08 p3463 N94-28759
The use of the AOA TTR-4P GPS receiver in operation at the BIPM for real-time restitution of GPS time
08 p3144 N94-30651
Filtering of satellite altimetry data with optimal smoothing cubic splines to compute geoid heights, along-tract geoid and gravity gradients in the Indonesian waters and its surroundings
[PB94-147527] 09 p3741 N94-31074
SMS (SHUTTLE)
U SHUTTLE MISSION SIMULATOR
SNATCHING
U SPACECRAFT RECOVERY
SNOW
Optical properties of CO2 ice and CO2 snow in the ultraviolet, visible, and infrared
[NASA-CR-194110] 02 p0686 N94-14081
Bibliography on snow and ice friction
[AD-A266868] 03 p1045 N94-14920
Atmospheric ionization by solar particles detected by nitrate measurement in antarctic snow
[AD-A267583] 03 p1299 N94-17208
Condensed gases under winter conditions: A study for the rescue services
[FOA-C-40305-4.5] 04 p1473 N94-18139
Studies of Greenland using the SEASAT scatterometer 05 p1725 N94-20433
Radar backscattering from snow facies of the Greenland ice sheet: Results from the AIRSAR 1991 campaign
05 p1725 N94-20434
The evolution of the early Martian climate and the initial emplacement of crustal H2O 05 p2143 N94-21665
The Martian valley networks: Origin by niveo-fluvial processes 05 p2146 N94-21682
Observations of multi-layered clouds using K-band radar 05 p1874 N94-22311
Close-up analysis of inflight ice accretion
[NASA-TM-106457] 06 p2172 N94-23523
Synthesis of passive microwave and radar altimeter data for estimating accumulation rates of polar snow
[NASA-CR-194864] 06 p2382 N94-23573
Snow modeling, water resources, climate change
[PB93-201770] 06 p2399 N94-24633
Seasonal snow of arctic Alaska R4D investigations
[DE93-040082] 07 p2892 N94-25939
Development of a method for predicting snowfall intensity and compacted snow on roads
07 p2853 N94-27990
Conception of snow information network system in Yamagata Prefecture 07 p2853 N94-27991
On the temperature distribution near a cold surface
[AD-A275162] 08 p3332 N94-29288
Satellite radar altimetry over the continental ice sheets
09 p3742 N94-31570
The evolution of jet features during the 1993 east coast white hurricane: A case study using the global spectral model
[AD-A277217] 09 p3783 N94-32021
Simulation of a precipitation event in the western United States
[DE94-004835] 09 p3786 N94-32791
Snowmelt forecasting: Further cold regions development of operational hydrological forecasting, volume 1
[AD-A278050] 10 p4074 N94-33410
SNOW AERIAL APPLICATOR AIRCRAFT S-2B
U S-2 AIRCRAFT
SNOW AIRCRAFT
NT S-2 AIRCRAFT
SNOW COVER
Signatures of Antarctic firn by means of ERS-1 AMI and by field measurements 01 p0237 N94-11737
Snow and glacier investigations by ERS-1 SAR: First results 01 p0247 N94-12481
Monitoring of snowcover in high mountain terrain with ERS-1 SAR 01 p0247 N94-12482
Application of ERS-1 SAR data to snow mapping
01 p0247 N94-12483
Disintegrating ice front of Shirase Glacier, East Antarctica 01 p0210 N94-12654
Snow cover models in operational watershed forecasting
[DE93-778332] 02 p0718 N94-12837
A snow wetness retrieval algorithm for SAR
03 p1075 N94-16732
Monitoring environmental state of Alaskan forests with AIRSAR 03 p1075 N94-16734
Snow cover measurements and areal assessment of precipitation and soil moisture
[WMO-749] 05 p1841 N94-21068
Application of ERS-1 active microwave instrumentation data to remote sensing of snow
[PB93-224756] 06 p2382 N94-23224
Remote sensing of global snowpack energy and mass balance: In-situ measurements on the snow of interior and Arctic Alaska
[NASA-CR-195704] 07 p2851 N94-27787
Report of the National Research Institute for Earth Science and Disaster Prevention, No. 51
[JTN-94-80509] 07 p2886 N94-27985
Development of a method for predicting snowfall intensity and compacted snow on roads
07 p2853 N94-27990
Conception of snow information network system in Yamagata Prefecture 07 p2853 N94-27991
Physical processes in snowpacks during rain or melt events
[AD-A275445] 08 p3325 N94-28881
On the temperature distribution near a cold surface
[AD-A275162] 08 p3332 N94-29288
Attenuation of outdoor sound propagation levels by a snow cover
[AD-A275387] 08 p3478 N94-29314
A newly developed snow vehicle (SM100S) for Antarctica. Part 5: Result of general performance tests
08 p3314 N94-29985
The role of sea ice dynamics in global climate change
08 p3350 N94-30620
Snowmelt forecasting. Further cold regions development of operational hydrological forecasting, volume 2
[AD-A278123] 09 p3757 N94-33269
The multiple scattering contributions in the strong fluctuation theory to the microwave brightness temperature
[AD-A277721] 10 p4075 N94-33442
Remote sensing of hydrologic variables in boreal areas, phase 1
[NASA-CR-189354] 10 p4077 N94-34134
SNOW S-2 AIRCRAFT
U S-2 AIRCRAFT
SNOWPLOW EFFECT
U PLASMA DYNAMICS
SOAPS
Guanidine based vehicle/binders for use with oxides, metals, and ceramics
[NASA-CASE-LEW-15314-1] 05 p1700 N94-20195
SOBOLEV SPACE
On the Sobolev systems with ellipsoid cavities
[DE92-641290] 01 p0148 N94-10530
Adaptive wavelet collocation methods for initial value boundary problems of nonlinear PDE's
[NASA-CR-191507] 03 p1169 N94-15833
On polynomials orthogonal with respect to an inner product involving differences (the general case)
[REPT-93-32] 04 p1551 N94-19285
Orthogonal pairs and zeros of Sobolev-type orthogonal polynomials
[REPT-92-46] 05 p1953 N94-21059
Polynomials orthogonal with respect to an inner product involving differences
[PB94-110731] 06 p2489 N94-24572
SOCIAL FACTORS
Predicted and real development in the aviation in the period 1961-1991 03 p0853 N94-15122
The clocks and the perception of time in the 18th century society 04 p1424 N94-18007
Soviet society informatization: The USSR state program 05 p2046 N94-22058
Microdynamic model of reproduction: Taxation and currency issue as regulators of economy
05 p2053 N94-22084
Proceedings of Technology and Governance in the 1990's
[PB93-192904] 06 p2597 N94-24312
HDGEC activity in Asia Pacific region
07 p2874 N94-28286
Using the National Information Infrastructure for social science, education, and informed decision making
[DE94-005442] 09 p3920 N94-32676
Math and science illiteracy: Social and economic impacts
[DE94-010801] 12 p4540 N94-37092

SOCIAL ISOLATION
A study of psychological factors affecting an extremely isolated environment 07 p2927 N94-27517
La Chalupa-30: Lessons learned from a 30-day subsea mission analogue 10 p4098 N94-33654
SOCIOLOGY
NT SOCIAL FACTORS
Female security as a general mobility condition [ISBN-3-79-831536-1] 05 p2039 N94-20153
The evolution of the laser: A systems perspective on science, technology and society [ETN-94-95319] 06 p2351 N94-25218
The contribution of aeronautics and astronautics to the quality of life on Earth [ILR-MITT-283(1993)] 09 p3764 N94-31611
Using the National Information Infrastructure for social science, education, and informed decision making [DE94-005442] 09 p3920 N94-32676
NASA/DOD Aerospace Knowledge Diffusion Research Project. Paper 42: An analysis of the transfer of Scientific and Technical Information (STI) in the US aerospace industry [NASA-TM-109863] 10 p4159 N94-34730
Space and the American imagination [NASA-CR-196131] 11 p4376 N94-35356
SOCKS
Comparative performance of a modified Space Shuttle Reentry Anti-G Suit (REAGS) with and without pressure socks 10 p4101 N94-33655
SODIUM
NT LIQUID SODIUM
NT SODIUM ISOTOPES
NT SODIUM VAPOR
Laser system design for the generation of a sodium-layer laser guide star [DE93-014127] 01 p0176 N94-12784
Multiplicity spectrometry on neutron filtered beams [DE93-617529] 02 p0790 N94-14843
Design of pulse stretching cell for a sodium guide star optical system [DE93-016436] 03 p1236 N94-14929
Contained liquids in microgravity, part 2 03 p0979 N94-16085
Sodium-mercury excimer laser, phase 1 [AD-A267728] 03 p1042 N94-17230
First on-sun test of NaK pool-boiler solar receiver [DE93-015003] 04 p1466 N94-18208
Developmental testing of a prototype all-reflection Michelson interferometer [AD-A269064] 04 p1430 N94-18406
Laser guide star adaptive optics: Present and future [DE93-018642] 05 p1989 N94-21619
Convergent close-coupling calculation of electron-sodium scattering [DE94-601815] 07 p3014 N94-25842
Zinc(2) oxide stability in alkaline sodium phosphate solutions at elevated temperatures [DE94-003316] 07 p2715 N94-26320
Calculation of total cross sections for electron and positron scattering on sodium and potassium [DE94-601814] 07 p3023 N94-26944
Fast and slow onsets of Na channel blocking actions due to lidocaine and disopyramide using concentration-clamp method 07 p2907 N94-27504
A study on tissue excitation of cardiac muscle under electrical field stimulation 07 p2907 N94-27510
Block of cardiac sodium channels by Ro 22-9194 (R), a new antiarrhythmic agent: Effects on the maximum upstroke velocity (Vmax) of single guinea pig ventricular myocytes 07 p2907 N94-27511
Electrophysiological effects of an antiarrhythmic drug, moricizine on isolated guinea pig ventricular muscles 07 p2907 N94-27512
Convective flow effects on protein crystal growth [NASA-CR-195785] 08 p3515 N94-30015
Near resonant absorption by atoms in intense fluctuating laser fields [DE94-005873] 09 p3714 N94-31200
Orthostatic responses to dietary sodium restriction during heat acclimation 10 p4096 N94-33640
X ray and gamma ray spectroscopy of solids under pressure [DE94-011207] 11 p4238 N94-36203
The determination of hydrogen in sodium by vacuum extraction [DE94-620278] 12 p4412 N94-37533
SODIUM ALLOYS
Bench-scale screening tests for a boiling sodium-potassium alloy solar receiver [DE93-018512] 04 p1469 N94-19040
SODIUM CHLORIDES
Pressures of supercritical salt solutions 03 p0945 N94-15166
Swelling equilibria for cationic 2-hydroxyethyl methacrylate (HEMA)-based hydrogels [DE94-000728] 05 p1707 N94-21856
Stress corrosion cracking properties of 15-5PH steel 06 p2251 N94-23244
SODIUM COMPOUNDS
NT NEPHELINE
NT SODIUM CHLORIDES
NT SODIUM FLUORIDES
NT SODIUM HYDRIDES
NT SODIUM HYDROXIDES
NT SODIUM IODIDES
NT SODIUM SILICATES
NT SODIUM SULFATES
NT TALC
Vaporization by shock loading of albite, jadeite, and pyrex glass: Experimental study 01 p0097 N94-12039
Neutron-scattering studies of Yb-bearing silicate glasses [DE93-019768] 05 p1700 N94-20265
Evaporation of a sodium tellurite melt in the jamic low gravity drop shaft 05 p1713 N94-20605
A new family of superconducting fullerides, Na(NH3)(x)C60(x = 2-8) [DE94-011480] 11 p4341 N94-36272
SODIUM FLUORIDES
Production of electronic grade lunar silicon by disproportionation of silicon difluoride 01 p0435 N94-12017
SODIUM HYDRIDES
Vacancy formation energy of Li(H, D) and Na(H, D) systems [DE93-633452] 06 p2558 N94-22978
SODIUM HYDROXIDES
A simple chemical procedure for extending the conductive state of polypyrrole to more negative potentials [AD-A266235] 03 p0969 N94-16928
Improvement of the stability of the process for synthesizing chemically prepared varistor powder [DE94-000345] 05 p1763 N94-21654
Aqueous alkaline cleaners: An alternative to organic solvents [AD-A273510] 06 p2260 N94-24848
SODIUM IODIDES
Monte Carlo calculations of low background detector response [DE94-004593] 07 p3116 N94-27621
SODIUM ISOTOPES
Sodium-23 NMR and complex impedance studies of gel electrolytes based on poly(acrylonitrile) [AD-A280330] 12 p4408 N94-37031
SODIUM SILICATES
NT TALC
Thermochemistry of silicate speciation in aqueous sodium silicate solutions: Ionization and polymerization of small silicate ion [AD-A266825] 03 p0964 N94-15683
SODIUM SULFATES
Sodium sulfate corrosion of silicon carbide fiber-reinforced lithium aluminosilicate glass-ceramic matrix composites [AD-A277224] 09 p3623 N94-32023
SODIUM SULFUR BATTERIES
Conceptual design of a sodium sulfur cell for US electric van batteries [DE93-018683] 04 p1405 N94-19035
Advanced batteries for electric vehicle applications: Nontechnical summary [DE93-019007] 05 p1748 N94-19885
Overview of Sandia's electric vehicle battery program [DE94-008944] 09 p3696 N94-32806
SODIUM VAPOR
Studies for the loss of atomic and molecular species from Io [NASA-CR-195702] 07 p3108 N94-27941
SOFIA (AIRBORNE OBSERVATORY)
Computation of the Fluid and Optical Fields About the Stratospheric Observatory for Infrared Astronomy (SOFIA) and the Coupling of Fluids, Dynamics, and Control Laws on Parallel Computers [NASA-CR-193168] 03 p0858 N94-16510
Selected computations of transonic cavity flows 03 p0858 N94-16511
Unsteady fluid and optical simulation of transonic aero-windows [AIAA PAPER 93-3017] 03 p0858 N94-16512
Aircraft system aft telescope cavity configuration study for Stratospheric Observatory for Infrared Astronomy (SOFIA), phase 2 [NASA-CR-194266] 08 p3147 N94-29685
SOFIA: Aircraft system, aft telescope cavity configuration, phase 2. Volume 1: Executive summary [NASA-CR-196362] 12 p4546 N94-36642
SOFT LANDING
Further development and flight test of an autonomous precision landing system using a parafoil [NASA-TM-4599] 10 p3983 N94-33995
SOFT LANDING SPACECRAFT
NT AEROSPACE PLANES
NT APOLLO LUNAR EXPERIMENT MODULE
NT BURAN SPACE SHUTTLE
NT FRIENDSHIP 7
NT LANDING MODULES
NT LUNAR LANDING MODULES
NT MERCURY SPACECRAFT
NT X-30 VEHICLE
SOFT RECOVERY
U SOFT LANDING
SOFTENING
Investigation of the reason for the softening behaviour of filled polymers 01 p0063 N94-10058
On the hardening and softening of nanocrystalline materials [DE93-012901] 02 p0810 N94-14185
Mean stress models for low cycle fatigue of a nickel-base superalloy 06 p2159 N94-24276
SOFTWARE (COMPUTERS)
U COMPUTER PROGRAMS
U COMPUTER SYSTEMS PROGRAMS
SOFTWARE ENGINEERING
System engineering concept demonstration, technology assessments, volume 5 [AD-A265471] 01 p0323 N94-10494
System engineering concept demonstration, trade studies, volume 6 [AD-A265472] 01 p0323 N94-10495
The Zipcode message-passing system [DE93-011958] 01 p0336 N94-11027
Development of generic field classes for finite element and finite difference problems [DE93-011678] 01 p0345 N94-11225
Computational mechanics needs study [NASA-CR-193712] 01 p0327 N94-11279
Proceedings of the Seventeenth Annual Software Engineering Workshop [NASA-CR-189349] 01 p0328 N94-11422
Experimental software engineering: Seventeen years of lessons in the SEL 01 p0328 N94-11423
The experience factory: Can it make you a 5? or what is its relationship to other quality and improvement concepts? 01 p0328 N94-11424
Impacts of object-oriented technologies: Seven years of SEL studies 01 p0329 N94-11425
The MERMAID project 01 p0329 N94-11426
Software process assessments 01 p0329 N94-11427
The role of metrics and measurements in a software intensive total quality management environment 01 p0329 N94-11428
Maximizing reuse: Applying common sense and discipline 01 p0329 N94-11429
Reuse: A knowledge-based approach 01 p0329 N94-11430
Large project experiences with object-oriented methods and reuse 01 p0329 N94-11431
Development and application of an acceptance testing model 01 p0330 N94-11432
A recent Cleanroom success story: The Redwing project 01 p0039 N94-11433
Insights into software development in Japan 01 p0330 N94-11435
Myths and realities: Defining re-engineering for a large organization 01 p0330 N94-11436
Development and implementation of a general purpose x-windows display program [AD-A265306] 01 p0332 N94-11860
The instrumentation of the multimodel and multilingual user interface [AD-A265444] 01 p0333 N94-12332
Generic software architecture based redesign 02 p0745 N94-13290
Software synthesis using generic architectures [NASA-CR-194201] 02 p0745 N94-13355
Architecture-driven reuse of code in KASE [NASA-CR-194200] 02 p0745 N94-13356
The KASE approach to domain-specific software systems 02 p0745 N94-13357
Creating a strategic plan for configuration management using computer aided software engineering (CASE) tools [DE93-013663] 02 p0746 N94-13394
A measurement and evaluation process model applied to software engineering environments [INPE-5345-PUD/048] 02 p0746 N94-13428
Software design by reusing architectures [NASA-CR-194151] 02 p0747 N94-13443
Mass market computers for software development [ERB-1035] 02 p0741 N94-13547
Space and Earth sciences, computer systems, and scientific data analysis support, volume 1 [NASA-CR-189319] 02 p0741 N94-13788
Parameter identification of a model of the process of software development [REPT-93-008] 02 p0750 N94-13807

Hypertext Compiling Tools (HCT): Developing model based applications with standard hypertext systems
[REPT-92-049] 02 p0750 N94-13822
Activities of Institute for Information Technology
[CNR-35024] 02 p0824 N94-14069
Guide to the software architectural design phase
[ESA-PSS-05-04-ISSUE-1] 02 p0753 N94-14190
Guide to the software detailed design and production phase
[ESA-PSS-05-05-ISSUE-1] 02 p0753 N94-14191
PC viruses: How do they do that?
[DE93-012581] 02 p0753 N94-14289
AXAF FITS standard for ray trace interchange
[NASA-CR-194025] 02 p0832 N94-14305
Integrating interface slicing into software engineering processes
[NASA-CR-192761] 02 p0754 N94-14368
Formal functional test designs with a test representation language 02 p0609 N94-14383
PC4CAST: A tool for DSN load forecasting and capacity planning 02 p0610 N94-14384
Visualization techniques to aid in the analysis of multi-spectral astrophysical data sets
[NASA-CR-194489] 02 p0840 N94-14482
A database for propagation models 02 p0614 N94-14665
Verification of critical software by statistical testing
[LAAS-93006] 02 p0756 N94-14714
Determining neural network connectivity using evolutionary programming
[AD-A266853] 02 p0766 N94-14882
Army Software Test and Evaluation Panel (STEP) software metrics initiatives report
[AD-A266889] 03 p1142 N94-14924
Lecture notes on engineering measurement for software engineers
[AD-A266959] 03 p1142 N94-14967
The value of reference implementations and prototyping in a formal design and testing methodology
[NPL-DITC-208/92] 03 p1142 N94-15011
The application of programming languages to the production of reference implementations
[NPL-DITC-209/92] 03 p1143 N94-15012
Testability of data security standards
[NPL-DITC-217/93] 03 p1143 N94-15022
SIMS: Single Interface to Multiple Systems
[AD-A266934] 03 p1143 N94-15175
Safety-critical software: Status report and annotated bibliography
[AD-A266993] 03 p1144 N94-15214
Concepts on measuring the benefits of software process improvements
[AD-A266994] 03 p1144 N94-15215
Software architecture for shared information systems
[AD-A266995] 03 p1144 N94-15216
Open environments to support systems engineering tool integration: A study using the Portable Common Tool Environment (PCTE)
[NASA-TM-4489] 03 p1144 N94-15486
An analysis of SEI software process assessment results: 1987-1991
[AD-A266996] 03 p1145 N94-15629
Process-centered development environments: An exploration of issues
[AD-A266997] 03 p1145 N94-15630
Dependable software technology exchange
[AD-A267103] 03 p1146 N94-15638
Reengineering: An engineering problem
[AD-A267117] 03 p1146 N94-15653
Flight instrument software for the F/A-18 research simulator
[AD-A267170] 03 p0872 N94-15856
Database for propagation models 03 p0996 N94-16049
Software Engineering Guidebook
[NASA-CR-177625] 03 p1150 N94-16656
Software for the derivation of scaled surface reflectances from AVIRIS data 03 p1072 N94-16700
KBSA concept demo
[AD-A267054] 03 p1166 N94-16770
Conflict Resolution (CORE) for software quality factors
[AD-A267248] 03 p1151 N94-16941
Development of dynamic, contex-driven help systems
[AD-A267409] 03 p1152 N94-16974
Design and implementation of an object-oriented interface for the multi-model/multi-lingual database system
[AD-A267413] 03 p1232 N94-16977
Sequential functions on indexed domains and full abstraction for a sub-language of PCF
[AD-A267838] 03 p1152 N94-17009
A proposed research program in strategic computing
[AD-A267516] 03 p1153 N94-17078
CALS test network handbook
[AD-A267567] 03 p1160 N94-17209
An object-oriented dynamic software process model
[AD-A267726] 03 p1154 N94-17371
Establishing a software measurement process
[AD-A267896] 03 p1154 N94-17396
An introduction to structural models
[AD-A268151] 03 p1155 N94-17429
A software process framework for the SEI capability maturity model: Repeatable level
[AD-A268059] 03 p1157 N94-17588
The development of flexible software for the Italian/Dutch satellite SAX: Advantages and disadvantages of the use of CASE tools
[NLR-TP-91288-U] 03 p1157 N94-17626
The design of the MAD Design Program
[DE93-013343] 04 p1539 N94-17696
The First International Conference on PCTE
[FEL-92-A134] 04 p1518 N94-17965
Format.m: A usage manual. Towards an efficient symbolic-numeric environment: Extending Mathematica's format rules
[MATHS-REPT-A-185] 04 p1547 N94-17969
Reference model for project support environments, version 1.0
[AD-A269110] 04 p1520 N94-18251
Teaching a computer simulation course with Ada
[AD-A267901] 04 p1521 N94-18308
Why are human-computer interfaces difficult to design and implement?
[AD-A268843] 04 p1514 N94-18317
VLSI synthesis of digital application specific neural networks 04 p1399 N94-18355
The CMU masters in software engineering core curriculum
[AD-A268983] 04 p1521 N94-18453
The evolution of the PVM concurrent computing system
[DE93-017764] 04 p1534 N94-18482
UUGM code development
[AD-A269945] 04 p1416 N94-18671
The development of a course sequence in real-time systems design
[AD-A269459] 04 p1522 N94-18726
Case studies of software development tools for parallel architectures
[AD-A269193] 04 p1535 N94-18866
ControlShell: A real-time software framework
[AD-A269172] 04 p1523 N94-18879
Modelling software for structure metrics
[MEMO-INF-93-13] 04 p1526 N94-19200
How to apply the IEEE standards to software testing
[DE93-018514] 04 p1527 N94-19245
Advanced software development workstation: Object-oriented methodologies and applications for flight planning and mission operations
[NASA-CR-193706] 04 p1513 N94-19349
A multi-level data-flow architecture for signal and data processing applications
[DE93-041272] 04 p1539 N94-19588
Technical development of a theory of programs
[ETN-93-95058] 04 p1532 N94-19652
Report of the Second CLICOM Experts Meeting
[WCDMP-19] 04 p1495 N94-19705
Software reuse: Major issues need to be resolved before benefits can be achieved. Report to the Chairman, Subcommittee on Defense, Committee on Appropriations, House of Representatives
[GAO/IMTEC-93-16] 04 p1532 N94-19716
Technology benefits model user manual, version 01.00.04
[AD-A270637] 04 p1620 N94-19777
Qualifying codes under software quality assurance: Two examples as guidelines for codes that are existing or under development
[DE93-040452] 05 p1904 N94-20097
Data and Analysis Center for Software
[AD-A270571] 05 p2041 N94-20106
A comprehensive software engineering educational experience
[AD-A270563] 05 p1905 N94-20109
A proposed research program in information processing
[NASA-CR-194271] 05 p2041 N94-20134
A proposal for reverse engineering CASE tools to support new software development
[DE93-040207] 05 p1906 N94-20281
Probability of detection calculations using MATLAB
[AD-A271958] 05 p1736 N94-20578
Advanced software development workstation: Knowledge base methodology: Methodology for first Engineering Script Language (ESL) knowledge base
[NASA-CR-193643] 05 p1930 N94-21065
Design of a computer assisted tool for object oriented acquisition, modeling and simulation of knowledge structure
[ETN-93-94183] 05 p1910 N94-21152
A practical software engineering curriculum: A pilot study
[AD-A272781] 05 p1911 N94-21183
An investigation into the state of the practice of CASE tool integration
[AD-A272441] 05 p1912 N94-21205
Development and operations of the Astrophysics Data System
[NASA-CR-194691] 05 p2043 N94-21270
The NCC project: A quality management perspective 05 p1828 N94-21324
Let your fingers do the walking: The projects most invaluable tool 05 p1922 N94-21325
Software metrics: The key to quality software on the NCC project 05 p1922 N94-21326
Network command processing system overview 05 p1935 N94-21351
MAYGEN: A symbolic debugger generation system
[AD-A272512] 05 p1913 N94-21413
Conversion and maintenance of Co-oP for Windows
[AD-A272513] 05 p1914 N94-21414
An evaluation of integration of the trace assertion method with the box structure method for coding in C++
[DE93-040480] 05 p1918 N94-21924
The Soviet software market: Current state and aspects of development 05 p1923 N94-22066
Application development in a PC/LAN environment 05 p1923 N94-22067
Industry standards: Key to distributed computing 05 p1938 N94-22070
Developing software to RTCA DO-178A 05 p1645 N94-22155
The why, what, and how of Ada software development 05 p1779 N94-22157
A software environment for the exploitation of the MAR image sensor 05 p1785 N94-22200
Trends in software reliability modeling 05 p1788 N94-22214
Second Annual Conference on Astronomical Data Analysis Software and Systems. Abstracts
[NASA-TM-108245] 05 p2057 N94-22438
Scientific computing in the 1990ies: An astronomical perspective 05 p2057 N94-22440
Fortran for the nineties 05 p1926 N94-22481
Programmability in AIPS++ 05 p1926 N94-22482
GammaCore: The Compton Observatory research environment 05 p2048 N94-22509
XPI: The Xanadu Parameter Interface 05 p1927 N94-22513
The ISO SWS on-line system 05 p1927 N94-22522
Khoros software specification format and interoperability 05 p1927 N94-22523
The evolution of the FIGARO data reduction system 05 p2048 N94-22528
An information retrieval logical model applied to the formalism of conceptual graphs: The ELEN prototype and its experimentation on a corpus of software components
[ETN-94-95162] 06 p2588 N94-22879
A general model for dynamic and complex information management: The ELEN prototype object manager for software engineering
[ETN-94-95163] 06 p2588 N94-22880
Definition and realization of a formal verification tool of LUSTRE programs: The LESAR system
[ETN-94-95164] 06 p2447 N94-22882
Software for scientific visualization: State of the art and experiences
[PB93-225183] 06 p2449 N94-23111
Guide to software configuration management
[ESA-PSS-05-09-ISSUE-1] 06 p2450 N94-23229
Cost benefits of advanced software: A review of methodology used at Kennedy Space Center 06 p2464 N94-23240
Formal methods and digital systems validation for airborne systems
[NASA-CR-4551] 06 p2466 N94-23293
ATOS-1: Designing the infrastructure for an advanced spacecraft operations system 06 p2197 N94-23849
SPOT4 Operational Control Center (CMP) 06 p2197 N94-23856
The Ulysses spacecraft control and monitoring concepts and realities 06 p2502 N94-23862
The Mars mapper science and mission planning tool 06 p2503 N94-23867
VMPLOT: A versatile analysis tool for mission operations 06 p2507 N94-23891
The Advanced Technology Operations System: ATOS 06 p2508 N94-23897
Making tomorrow's mistakes today: Evolutionary prototyping for risk reduction and shorter development time 06 p2197 N94-23902

SAO mission support software and data standards, version 1.0
[NASA-CR-193906] 06 p2454 N94-24050
Update of GRASP/Ada reverse engineering tools for Ada
[NASA-CR-193890] 06 p2455 N94-24111
Designers' models of the human-computer interface 06 p2433 N94-24188
New computing systems, future computing environment, and their implications on structural analysis and design 06 p2177 N94-24314
Integration and evaluation of a simulator designed to be used within a dynamic prototyping environment 06 p2198 N94-24436
Evaluation of the efficiency and fault density of software generated by code generators 06 p2465 N94-24445
Hydro-elastic analysis using a selection of commercial analysis programs
[PB94-118734] 06 p2376 N94-24478
High-performance computing and communications
[DE94-002215] 06 p2457 N94-24566
An investigation of requirements traceability to support systems development
[AD-A273167] 06 p2458 N94-24684
A type-theoretic approach to higher-order modules with sharing
[AD-A273566] 06 p2458 N94-24693
A methodology for software cost estimation using machine learning techniques
[AD-A273158] 06 p2459 N94-24775
Intelligent systems and advanced user interfaces for design, operation, and maintenance of command management systems
[NASA-CR-195172] 06 p2459 N94-24797
The use of design automation software by government-contracted architect/engineer firms: A status report
[AD-A273181] 06 p2459 N94-24812
Reengineering real-time software systems
[AD-A273408] 06 p2461 N94-25074
Future directions in flight simulation: A user perspective 06 p2162 N94-25101
An implementation of the REpresentation and MAintenance of Process knowledge (REMAP) model in the knowledge-based software assistant concept demonstration system
[AD-A273207] 06 p2461 N94-25138
Reuse-Driven Software Processes Guidebook, version 02.00.03
[AD-A273644] 06 p2461 N94-25148
Reuse Adoption Guidebook, version 02.00.05
[AD-A273652] 06 p2461 N94-25149
Computerized testing system software conversion and development: Identifying software and hardware portability issues and solutions
[AD-A273489] 06 p2462 N94-25287
A prototype to automate the video subsystem routing for the video distribution subsystem of Space Station Freedom 06 p2306 N94-25353
Software engineering methodologies and tools 06 p2465 N94-25382
A multimedia adult literacy program: Combining NASA technology, instructional design theory, and authentic literacy concepts 06 p2585 N94-25384
CADBIT 2: Computer-aided design for built-in test, volume 1
[AD-A273702] 06 p2463 N94-25455
CADBIT 2: Computer-aided design for built-in test, volume 2
[AD-A273703] 06 p2463 N94-25456
System software and tools for high performance computing environments: A report on the findings of the Pasadena Workshop
[DE94-003918] 07 p2956 N94-25602
IGES 4.0 to LCAD translator for CSG models
[AD-A274013] 07 p2957 N94-25753
Abstraction in, specification and proof of software for a 1D heat-transfer problem
[REPT-93-45] 07 p2790 N94-25763
ObjectSim: A reusable object oriented DIS visual simulation
[AD-A274030] 07 p2958 N94-25767
Design of dynamically reconfigurable real-time software using port-based objects
[NASA-CR-195178] 07 p2958 N94-25777
Domain analysis and modeling of a model-based software executive
[AD-A274087] 07 p2958 N94-25783
Parallel Assessment Window System (PAWS) enhancements
[AD-A274094] 07 p2979 N94-25786
A method for populating the knowledge base of APTAS, a domain-oriented application composition system
[AD-A274034] 07 p2766 N94-25797
The television as robot servant
[AD-A273985] 07 p2984 N94-25898
Object interaction in a parallel object-oriented discrete-event simulation
[AD-A274084] 07 p2959 N94-25942
Developing a graphical user interface to support a real-time digital signal processing system
[AD-A274032] 07 p2960 N94-26018
Using database technology to support domain-oriented application composition systems
[AD-A274091] 07 p3096 N94-26024
Software redesign for usability: A case study
[DE94-003704] 07 p2960 N94-26048
Multimedia in Views
[CWI-CS-R9263] 07 p2961 N94-26218
The MUSA design methodology
[CWI-CS-R9265] 07 p3097 N94-26220
Development and analysis of secure embedded software
[VTT-TIED-1430] 07 p2961 N94-26254
Deductive computer programming
[AD-A274966] 07 p2962 N94-26303
Software Error Estimation Program (SWEEP), version 02.00.00 user manual
[AD-A274697] 07 p2962 N94-26373
Information systems criteria for applying software reengineering: Guidelines for identifying information systems for software reengineering
[AD-A274699] 07 p3097 N94-26375
Programming in Fortran M
[DE94-002756] 07 p2963 N94-26407
Bathymetric data set extraction program. Users guide
[AD-A274761] 07 p2899 N94-26567
Institute for Information Technology
[NRC-37061] 07 p3118 N94-26709
Fault tolerant real-time processing system for space use 07 p2949 N94-26720
On-board software for the JET-X telescope on the Spectrum-X mission 07 p2951 N94-26727
Tool for performance analysis and off-line prediction of timing behaviour 07 p2952 N94-26732
Developing with Ada using HOOD design methodology 07 p2953 N94-26741
Use of HOOD coupled to real time monitors 07 p2953 N94-26742
Ada reusable software for satellite on-board data handling 07 p2953 N94-26743
The CODE-TOP (COncurrent system DEvelopment using Transformations Of Predicate-transition nets) method: Examples of using it for system architecture specification, software specification, and code generation 07 p2953 N94-26744
Parallel mathematical software
[DE94-001587] 07 p2967 N94-27020
Static task allocation for parallel processing systems during software development
[AD-A274204] 07 p2981 N94-27100
A method for populating the knowledge base of AFIT's domain-oriented application composition system
[AD-A274128] 07 p3099 N94-27118
Alternative architectures for domain-oriented application composition and generation systems
[AD-A274180] 07 p2968 N94-27128
Research in improved assessment of software reliability
[AD-A274161] 07 p2968 N94-27140
Sculpting in cyberspace: Parallel processing the development of new software 07 p2686 N94-27365
Human computer interface guide, revision A
[NASA-TM-109708] 07 p2955 N94-27769
A proposed software engineering environment for systems life cycle management
[ISBN-0-315-60634-7] 07 p2974 N94-27869
A formal approach to the comparison of object-oriented analysis and design methodologies 07 p2975 N94-27937
CASE tools for the support of object-oriented analysis and design methods 07 p2975 N94-27939
Software assurance standard
[NASA-TM-109705] 07 p2975 N94-27992
Advanced End-to-end Simulation for On-board Processing (AESOP) 07 p2945 N94-28255
Using formal specification in the Guidance and Control Software (GCS) experiment. Formal design and verification technology for life critical systems
[NASA-CR-194884] 07 p2956 N94-28267
Technology transition push. Part 1: A case study of rate monotonic analysis
[AD-A275616] 08 p3407 N94-28633
A conceptual framework for software technology transition
[AD-A275637] 08 p3407 N94-28639
Software Technology for Adaptable, Reliable Systems (STARS) program
[AD-A275675] 08 p3407 N94-28664
Software systems reengineering process model, version 1.0
[AD-A275711] 08 p3407 N94-28691
Demonstration of improved software support labor estimation for Air Force operational flight programs through functional orientation
[AD-A275789] 08 p3121 N94-28743
Cleanroom engineering handbook. Volume 3: Project execution in the cleanroom environment
[AD-A275860] 08 p3156 N94-28752
Cleanroom engineering handbook. Volume 4: Specification team practices
[AD-A275861] 08 p3156 N94-28753
Construction of a connectionist network supercomputer
[AD-A275765] 08 p3405 N94-28764
Cleanroom engineering handbook. Volume 2: Organization and project formation in the cleanroom environment
[AD-A275809] 08 p3156 N94-28772
Guide to the Environmental-Language
[AD-A275849] 08 p3408 N94-28784
Automated interface for retrieving reusable software components
[AD-A275004] 08 p3409 N94-28896
Advanced languages for systems software
[AD-A275272] 08 p3410 N94-29007
Investigation into formalization of domain-oriented parallel software development
[AD-A275177] 08 p3430 N94-29050
Reference model for project support environments, version 2.0
[AD-A275191] 08 p3410 N94-29068
A concurrent, object-based implementation for the tactical level of the rational behavior model
[AD-A275024] 08 p3410 N94-29115
Towards an information model and mechanisms for design rationale capture and use
[AD-A275060] 08 p3530 N94-29138
Ada, object-oriented techniques, and concurrency in teaching data structures and file management
[AD-A275385] 08 p3411 N94-29201
Aerospace Software Engineering for Advanced Systems Architectures
[AD-A277101] 08 p3412 N94-29315
Object versus functional oriented design 08 p3413 N94-29321
Experiences with the HOOD design method on avionics software development 08 p3414 N94-29325
Software engineering methods in the Hermes on-board software 08 p3414 N94-29326
Rome Laboratory software engineering technology program 08 p3414 N94-29330
A common Ada run-time system for avionics software 08 p3150 N94-29331
Software testing practices and their evolution for the 1990's 08 p3415 N94-29335
Validation and test of complex weapon systems 08 p3150 N94-29336
Testing Operational Flight Programs (OFPs) 08 p3415 N94-29337
Integrated formal verification and validation of safety critical software 08 p3416 N94-29338
A disciplined approach to software test and evaluation 08 p3416 N94-29339
The UNICON approach to through-life support and evolution of software-intensive systems 08 p3416 N94-29340
Application of information management methodologies for project quality improvement in a changing environment 08 p3416 N94-29342
The discipline of defining the software product 08 p3416 N94-29343
SDE's for the year 2000 and beyond: An EF perspective 08 p3417 N94-29344
A common approach for an aerospace software environment 08 p3417 N94-29346
DSSA-ADAGE: An environment for architecture-based avionics development 08 p3150 N94-29348
Entreprise 2: A PCTE integrated project support environment 08 p3417 N94-29349
Information engineering implementation and acceptance 08 p3530 N94-29533
Software Management Environment (SME) concepts and architecture, revision 1
[NASA-CR-189293] 08 p3419 N94-29727
Engineering specification editing tools
[AD-A275116] 08 p3419 N94-29746
Using RDD-100 with CoRE. Version 01.00.03
[AD-A275336] 08 p3419 N94-29797
Research and technology, 1992
[NASA-TM-103996] 08 p3555 N94-29891
Progress report for the PTUF Project-93 Q1 and Q2
[PB94-138591] 08 p3431 N94-29995
Software engineering and software management in a distributed UNIX environment
[NLR-TP-92233-U] 08 p3422 N94-30314

The ergonomics of computer interfaces: Designing a system for human use
[CWI-CS-R9258] 08 p3402 N94-30320
Graphics in the Views system
[CWI-CS-R9260] 08 p3422 N94-30322
The Views application environment
[CWI-CS-R9257] 08 p3423 N94-30341
The real-world navigator
[AIAA PAPER 94-1204-CP] 08 p3443 N94-30555
Design patterns mixing genericity and inheritance in the development of reusable components
[REPT-93-021] 09 p3808 N94-31178
Guide to software quality assurance
[ESA-PSS-05-11-ISSUE-1] 09 p3809 N94-31223
Cleanroom engineering handbook. Volume 6: Certification team practices
[AD-A275951] 09 p3587 N94-31346
Cleanroom engineering handbook. Volume 1: Cleanroom engineering process introduction and overview
[AD-A275949] 09 p3587 N94-31356
E-L user's manual
[AD-A276378] 09 p3810 N94-31370
The development and use of an evaluation mechanism for the assessment of software configuration management tools
[AD-A275961] 09 p3810 N94-31383
A model and algorithms for a software evolution control system
[AD-A276431] 09 p3811 N94-31449
Software reuse case study: TRILLIUM
[AD-A276108] 09 p3811 N94-31465
Overview of megaprogramming course: Lectures and exercises
[AD-A276169] 09 p3814 N94-31810
Getting a handle on designing for avionics software supportability and maintainability
[AD-A276362] 09 p3581 N94-32055
The advent of failure analysis software technology
[DE94-006593] 09 p3692 N94-32111
Integrated Trusted System Development Environment Process
[AD-A276414] 09 p3816 N94-32131
Modular Simulator System (MSS). Engineering design guide
[AD-A276967] 09 p3589 N94-32394
Modular Simulator System (MSS): Interface design document for the generic MSS
[AD-A277270] 09 p3590 N94-32403
Evolving software reengineering technology for the emerging innovative-competitive era
09 p3823 N94-32439
Emacs Lisp in Edwin scheme
[AD-A276721] 09 p3818 N94-32504
Case studies of software process improvement methods
[AD-A277289] 09 p3818 N94-32508
OPT++: An object-oriented class library for nonlinear optimization
[DE94-008890] 09 p3818 N94-32584
The role of guideline-based design tools
[DE94-007482] 09 p3804 N94-32596
A framework for developing and managing reusable avionics software
[AD-A276846] 09 p3582 N94-32909
Machine assisted implementation of complex algorithms and labor intensive software, closing report
[AD-A277662] 09 p3821 N94-33027
Implementing software safety in the NASA environment
[NASA-TM-106597] 09 p3731 N94-33032
Increasing the practical impact of formal methods for computer-aided software development: Software slicing, merging and integration
[AD-A277929] 09 p3822 N94-33179
Faultless software project
[AD-A278161] 09 p3822 N94-33188
Structuring Z specifications with views
[AD-A277618] 09 p3822 N94-33279
Ada support for the mathematical foundations of software engineering
[AD-A278031] 09 p3822 N94-33284
MODIS. Volume 1: MODIS level 1A software baseline requirements
[NASA-TM-104594-VOL-1] 09 p3823 N94-33287
A problem-solving approach to knowledge acquisition
09 p3854 N94-33344
A Fortran based learning system using multilayer back-propagation neural network techniques
[AD-A278463] 10 p4112 N94-33542
Program composition
[AD-A278377] 10 p4105 N94-33742
Formal connectors
[AD-A277611] 10 p4103 N94-33852
Reuse strategy model: Planning aid for reuse-based projects
[AD-A277641] 10 p4106 N94-33891
Framework for modelling evolving requirements
[PB94-148855] 10 p4107 N94-33979
C++ optimization and excluding middle-level code
[DE94-008743] 10 p4107 N94-34010
Software Management Environment (SME): Components and algorithms
[NASA-CR-189346] 10 p4109 N94-34996
C++ Planning and Resource Reasoning (PARR) shell
10 p4124 N94-35054
Engineering large-scale agent-based systems with consensus
10 p4127 N94-35071
Annotated bibliography of Software Engineering Laboratory literature
[NASA-CR-189350] 11 p4300 N94-35238
Cost and schedule estimation study report
[NASA-CR-189344] 11 p4300 N94-35256
Collected software engineering papers, volume 11
[NASA-CR-189347] 11 p4301 N94-35434
Modeling and managing risk early in software development
11 p4301 N94-35436
An information model for use in software management estimation and prediction
11 p4301 N94-35437
Measuring and assessing maintainability at the end of high level design
11 p4301 N94-35438
Impacts of object-oriented technologies: Seven years of SEL studies
11 p4301 N94-35439
Software architecture standard for simulation virtual machine, version 2.0
[NASA-CR-188291] 11 p4301 N94-35443
Developing software for ease of change: Metrics from later in the TRALAB system life cycle
[AD-A278759] 11 p4302 N94-35490
A software architecture for adding new interaction techniques to a command and control based testbed
[AD-A278760] 11 p4302 N94-35491
Exploring hypermedia information services for disseminating software engineering information
[AD-A278765] 11 p4302 N94-35495
Robust requirements specifications for safety-critical systems
[PB94-167806] 11 p4250 N94-35532
Proceedings of the 4th Workshop on the Next Generation of CASE Tools
[PB94-150372] 11 p4302 N94-35538
The development and application of composite complexity models and a relative complexity metric in a software maintenance environment
11 p4255 N94-35559
Overview of the MSTI 2 processor-in-the-loop simulator
11 p4207 N94-35631
Environment/tool integrator for software development, version 1.2
[AD-A278965] 11 p4303 N94-35660
Model engineering concepts for air quality models in an integrated environmental modeling system
[PB94-158623] 11 p4298 N94-35688
A taxonomy of coordination mechanisms used in real-time software based on domain analysis
[AD-A279014] 11 p4304 N94-35794
An object-oriented implementation of a graphical-programming system
[DE94-009298] 11 p4304 N94-35808
Experience with Ada on the F-18 High Alpha Research Vehicle flight test program
11 p4310 N94-35968
Object-oriented simulation pictures (OOSPic) for design and testing
[AD-A278798] 11 p4305 N94-36013
Certification of computational results
11 p4306 N94-36064
Certification trails and software design for testability
11 p4306 N94-36066
Using certification trails to achieve software fault tolerance
11 p4307 N94-36068
The EASE Visualization Community Club
[PB94-170529] 11 p4308 N94-36211
An environment for visualization, reliability, and knowledge acquisition in equational programming
[AD-A278639] 11 p4308 N94-36258
A practical guide to the technology and adoption of software process automation
[AD-A278719] 11 p4308 N94-36294
Software use control
[DE94-008429] 12 p4489 N94-36480
Proceedings of the Eighteenth Annual Software Engineering Workshop
[NASA-CR-189348] 12 p4489 N94-36484
The maturing of the quality improvement paradigm in the SEL
12 p4489 N94-36485
Process improvement as an investment: Measuring its worth
12 p4489 N94-36486
Recent SEL experiments and studies
12 p4490 N94-36487
Specification-based software sizing: An empirical investigation of function metrics
12 p4490 N94-36488
Software forecasting as it is really done: A study of JPL software engineers
12 p4490 N94-36489
Assessing efficiency of software production for NASA-SEL data
12 p4490 N94-36490
The (mis)use of subjective process measures in software engineering
12 p4490 N94-36491
Lessons learned applying CASE methods/tools to Ada software development projects
12 p4491 N94-36493
Software engineering with application-specific languages
12 p4491 N94-36494
Integrating end-to-end threads of control into object-oriented analysis and design
12 p4491 N94-36496
Fusing modeling techniques to support domain analysis for reuse opportunities identification
12 p4491 N94-36497
An empirical comparison of a dynamic software testability metric to static cyclomatic complexity
12 p4491 N94-36498
Software quality: Process or people
12 p4492 N94-36499
Profile of NASA software engineering: Lessons learned from building the baseline
12 p4492 N94-36500
Impact of Ada in the Flight Dynamics Division: Excitement and frustration
12 p4492 N94-36501
Software engineering technology transfer: Understanding the process
12 p4492 N94-36502
Earth Observing System/Advanced Microwave Sounding Unit-A (EOS/AMSU-A) software management plan
[NASA-CR-189362] 12 p4461 N94-36919
A survey of commonly applied methods for software process improvement
[AD-A278595] 12 p4493 N94-36974
Proto code generation techniques
[AD-A280275] 12 p4494 N94-37123
Advanced information processing system: Hosting of advanced guidance, navigation and control algorithms on AIPS using ASTER
[NASA-CR-194960] 12 p4499 N94-37583
Techniques for real-time parallel processing: Sensor processing case studies
[AD-A280633] 12 p4499 N94-37760

SOFTWARE ENGINEERING ENVIRONMENTS
U PROGRAMMING ENVIRONMENTS

SOFTWARE RELIABILITY
NT COMPUTER PROGRAM INTEGRITY
Techniques, processes, and measures for software safety and reliability
[DE93-012379] 01 p0322 N94-10347
The experience factory: Can it make you a 5? or what is its relationship to other quality and improvement concepts?
01 p0328 N94-11424
Software process assessments
01 p0329 N94-11427
A recent Cleanroom success story: The Redwing project
01 p0039 N94-11433
Applying reliability models to the maintenance of Space Shuttle software
01 p0330 N94-11434
Diskless supercomputers: Scalable, reliable I/O for the Tera-Op technology base
[NASA-CR-194089] 02 p0740 N94-13363
Switchover software reliability estimate for Paducah freezer/sublimer computer systems
[DE93-013844] 02 p0756 N94-14696
Verification of critical software by statistical testing
[LAAS-93006] 02 p0756 N94-14714
Army Software Test and Evaluation Panel (STEP) software metrics initiatives report
[AD-A266889] 03 p1142 N94-14924
Software reliability through fault-avoidance and fault-tolerance
[NASA-CR-194353] 03 p1143 N94-15114
Safety-critical software: Status report and annotated bibliography
[AD-A266993] 03 p1144 N94-15214
Concepts on measuring the benefits of software process improvements
[AD-A266994] 03 p1144 N94-15215
RAMCAD design methodology
[AD-A267010] 03 p1145 N94-15525
Process-centered development environments: An exploration of issues
[AD-A266997] 03 p1145 N94-15630
Dependable software technology exchange
[AD-A267103] 03 p1146 N94-15638
Software reliability management through metrics
[AD-A267129] 03 p1146 N94-15687
The design of self-checking reduced instruction set computers
[AD-A267012] 03 p1140 N94-15763

NASA trend analysis procedures
[NASA-RP-1290] 03 p1223 N94-15782
Performance Information Management System (PIMS) communication
[AD-A267040] 03 p1231 N94-16458
Consistent failure reporting in reliable communication systems
[AD-A266298] 03 p0997 N94-16477
Software Engineering Guidebook
[NASA-CR-177625] 03 p1150 N94-16656
Conflict Resolution (CORE) for software quality factors
[AD-A267248] 03 p1151 N94-16941
Fault-tolerant architectures for multiprocessor and VLSI-based systems
[AD-A267370] 03 p1140 N94-17005
Effects of inspection error on optimal inspection policies and software fault detection models
[AD-A267511] 03 p1153 N94-17075
The development of flexible software for the Italian/Dutch satellite SAX: Advantages and disadvantages of the use of CASE tools
[NLR-TP-91288-U] 03 p1157 N94-17626
An efficient implementation of error-valued semantics on imperative machines
[DE93-014658] 04 p1516 N94-17740
Software reliability: Estimation and prediction
[AD-A268895] 04 p1521 N94-18458
Software quality in test and measurment equipment
[PB93-197846] 04 p1528 N94-19333
Qualifying codes under software quality assurance: Two examples as guidelines for codes that are existing or under development
[DE93-040452] 05 p1904 N94-20097
Test and evaluation: DOD has been slow in improving testing of software-intensive systems
[AD-A271541] 05 p1908 N94-20917
An assessment of the statistical and editorial output of text analysis programs
[AD-A272185] 05 p2042 N94-20924
Fault tolerant real-time systems
[AD-A272878] 05 p1899 N94-21195
Real-time fault tolerant computer systems
[AD-A272909] 05 p1899 N94-21230
Using stream interleaving to eliminate the need for interlocks in deeply pipelined processors
05 p1781 N94-22175
Trends in software reliability modeling
05 p1788 N94-22214
Evaluation of the efficiency and fault density of software generated by code generators 06 p2465 N94-24445
A type-theoretic approach to higher-order modules with sharing
[AD-A273566] 06 p2458 N94-24693
Domain analysis and modeling of a model-based software executive
[AD-A274087] 07 p2958 N94-25783
Software Error Estimation Program (SWEEP), version 02.00.00 user manual
[AD-A274697] 07 p2962 N94-26373
Developing with Ada using HOOD design methodology
07 p2953 N94-26741
Specification performance optimization and executive generation for onboard multiprocessor real time application with SynDEx 07 p2954 N94-26745
Modeling systems by probabilistic process algebra: An event structures approach
[PB94-125259] 07 p3004 N94-26867
Research in improved assessment of software reliability
[AD-A274161] 07 p2968 N94-27140
Validation tests of TOPSIM 4
[ESA-STM-249] 07 p2972 N94-27582
Hardware and software reliability estimation using simulations
[NASA-CR-187588] 07 p2973 N94-27663
Software assurance standard
[NASA-TM-109705] 07 p2975 N94-27992
Engine simulation systems 07 p2829 N94-28054
Demonstration of improved software support labor estimation for Air Force operational flight programs through functional orientation
[AD-A275789] 08 p3121 N94-28743
Advanced languages for systems software
[AD-A275272] 08 p3410 N94-29007
Fault tolerant testbed evaluation, phase 1
[NASA-CR-188275] 08 p3171 N94-29035
Microcomputer-based protective functions in industrial production systems: Assessment method
[PB94-137817] 08 p3411 N94-29159
Statistical Modeling and Estimation of Reliability Functions for Software (SMERFS) user's guide, revision 3
[AD-A275390] 08 p3411 N94-29202
Statistical Modeling and Estimation of Reliability Functions for Software (SMERFS) library access guide, revision 3
[AD-A275405] 08 p3411 N94-29207
Object versus functional oriented design
08 p3413 N94-29321
The development procedures and tools applied for the attitude control software of the Italian satellite SAX
08 p3170 N94-29324
Potential software failures methodology analysis
08 p3414 N94-29329
A user's guide to the Software Testpilot
[CWI-CS-R9343] 08 p3426 N94-30435
Guide to software quality assurance
[ESA-PSS-05-11-ISSUE-1] 09 p3809 N94-31223
Cleanroom engineering handbook. Volume 6: Certification team practices
[AD-A275951] 09 p3587 N94-31346
Consistency checks for SCR-style requirements specifications
[AD-A276077] 09 p3811 N94-31461
Getting a handle on designing for avionics software supportability and maintainability
[AD-A276362] 09 p3581 N94-32055
A framework for developing and managing reusable avionics software
[AD-A276846] 09 p3582 N94-32909
Increasing the practical impact of formal methods for computer-aided software development: Software slicing, merging and integration
[AD-A277929] 09 p3822 N94-33179
Topological properties of typical interconnection networks: Fault tolerance, communication delay and connection cost
[PB94-148822] 10 p4111 N94-33976
Software fault tolerance: Dynamic combination of dependability and efficiency
[PB94-148830] 10 p4106 N94-33977
Design and implementation of Voltan fault-tolerant nodes for distributed systems
[PB94-148863] 10 p4107 N94-33980
Object-oriented construction of fault-tolerant software
[PB94-148806] 10 p4108 N94-34122
Building fault-tolerant distributed computing systems using standard components
[PB94-148889] 10 p4112 N94-34125
Modeling and managing risk early in software development 11 p4301 N94-35436
Certification trails for data structures
11 p4307 N94-36069
An environment for visualization, reliability, and knowledge acquisition in equational programming
[AD-A278639] 11 p4308 N94-36258
Analysis of a successful inspection program
12 p4490 N94-36492
Applying formal methods and object-oriented analysis to existing flight software 12 p4491 N94-36495
Software quality: Process or people
12 p4492 N94-36499
Impact of Ada in the Flight Dynamics Division: Excitement and frustration 12 p4492 N94-36501
United States Air Force Summer Research Program, 1993. Volume 9: Rome Laboratory
[AD-A278699] 12 p4551 N94-36984

SOFTWARE REUSE

Effective software reuse in an embedded realtime system
[AD-A264993] 01 p0326 N94-11220
The role of metrics and measurements in a software intensive total quality management environment
01 p0329 N94-11428
Maximizing reuse: Applying common sense and discipline 01 p0329 N94-11429
Reuse: A knowledge-based approach
01 p0329 N94-11430
Large project experiences with object-oriented methods and reuse 01 p0329 N94-11431
Analysis and guidelines for reusable Ada software
[AD-A264918] 01 p0332 N94-11850
Software synthesis using generic architectures
[NASA-CR-194201] 02 p0745 N94-13355
Architecture-driven reuse of code in KASE
[NASA-CR-194200] 02 p0745 N94-13356
Software design by reusing architectures
[NASA-CR-194151] 02 p0747 N94-13443
Integrating interface slicing into software engineering processes
[NASA-CR-192761] 02 p0754 N94-14368
Open environments to support systems engineering tool integration: A study using the Portable Common Tool Environment (PCTE)
[NASA-TM-4489] 03 p1144 N94-15486
Intel NX to PVM 3.2 message passing conversion library
[NASA-TM-109038] 03 p1152 N94-17060
An environment for requirement reuse
[REPT-92-082] 04 p1613 N94-17939
High performance Fortran: An overview
[DE93-017181] 04 p1519 N94-18072
Software reuse: Major issues need to be resolved before benefits can be achieved. Report to the Chairman, Subcommittee on Defense, Committee on Appropriations, House of Representatives
[GAO/IMTEC-93-16] 04 p1532 N94-19716
Advanced software development workstation: Knowledge base methodology: Methodology for first Engineering Script Language (ESL) knowledge base
[NASA-CR-193643] 05 p1930 N94-21065
Software reuse in spacecraft planning and scheduling systems 06 p2520 N94-23966
RITL: An information system for application reuse-in-the-large
[PB94-119088] 06 p2592 N94-24646
Intelligent systems and advanced user interfaces for design, operation, and maintenance of command management systems
[NASA-CR-195172] 06 p2459 N94-24797
Analyzing the properties of user interface software
[AD-A273601] 06 p2460 N94-24933
Reengineering real-time software systems
[AD-A273408] 06 p2461 N94-25074
Reuse-Driven Software Processes Guidebook, version 02.00.03
[AD-A273644] 06 p2461 N94-25148
Reuse Adoption Guidebook, version 02.00.05
[AD-A273652] 06 p2461 N94-25149
ObjectSim: A reusable object oriented DIS visual simulation
[AD-A274030] 07 p2958 N94-25767
Domain analysis and modeling of a model-based software executive
[AD-A274087] 07 p2958 N94-25783
Using database technology to support domain-oriented application composition systems
[AD-A274091] 07 p3096 N94-26024
The ergonomics of software porting: Automatically configuring software to the runtime environment or everything you wanted to know about your C compiler but didn't know who to ask
[CWI-CS-R9266] 07 p2961 N94-26221
Ada reusable software for satellite on-board data handling 07 p2953 N94-26743
Automated interface for retrieving reusable software components
[AD-A275004] 08 p3409 N94-28896
Advanced languages for systems software
[AD-A275272] 08 p3410 N94-29007
Program derivation by proof transformation
[AD-A275260] 08 p3453 N94-29304
A common Ada run-time system for avionics software
08 p3150 N94-29331
DSSA-ADAGE: An environment for architecture-based avionics development 08 p3150 N94-29348
Aid to Ada component reuse at Aerospatiale Cannes (France)
[REPT-932-440-102] 08 p3418 N94-29418
Design reuse experience of space and hazardous operations robots
[AIAA PAPER 94-1220-CP] 08 p3445 N94-30568
Design patterns mixing genericity and inheritance in the development of reusable components
[REPT-93-021] 09 p3808 N94-31178
Software reuse case study: TRILLIUM
[AD-A276108] 09 p3811 N94-31465
Evolving software reengineering technology for the emerging innovative-competitive era
09 p3823 N94-32439
A framework for developing and managing reusable avionics software
[AD-A276846] 09 p3582 N94-32909
Translation between representation languages
10 p4110 N94-34054
A toolbox and a record for scientific model development 10 p4110 N94-34062
Ada developers' supplement to the recommended approach
[NASA-CR-189345] 10 p4109 N94-34921
A taxonomy of coordination mechanisms used in real-time software based on domain analysis
[AD-A279014] 11 p4304 N94-35794
Fusing modeling techniques to support domain analysis for reuse opportunities identification
12 p4491 N94-36497
Porting industrial codes and developing sparse linear solvers on parallel computers
[PB94-170503] 12 p4497 N94-36547

SOFTWARE TOOLS

Propellant management in surface tension tanks
01 p0106 N94-10110

TOLS (Telescience On-Line Simulator): An essential instrument for micro-gravity interactive experiment
01 p0039 N94-10134
The super vectorfield package for REDUCE. Version 1.0
[MEMO-1099] 01 p0321 N94-10265
The INTEGRATOR package for REDUCE, version 1.0
[MEMO-1100] 01 p0322 N94-10418
System engineering concept demonstration, technology assessments, volume 5
[AD-A265471] 01 p0323 N94-10494
A toolkit for building Earth system models
[DE93-012147] 01 p0276 N94-11138
A tool for generation of expert system shells
[INPE-5493-TDI/510] 01 p0325 N94-11181
The MERMAID project 01 p0329 N94-11426
Large project experiences with object-oriented methods and reuse 01 p0329 N94-11431
System engineering concept demonstration, process model, volume 3
[AD-A265469] 01 p0333 N94-12008
Radarmap of Germany: First mosaic and classification
01 p0246 N94-12477
Use of SAR-wave, altimeter, and wind-scatterometer data in an operational swell forecasting system
01 p0250 N94-12503
Problem specific environments for parallel systems
[AD-A266129] 01 p0337 N94-12540
Artificial intelligence support for scientific model-building
[NASA-TM-109252] 02 p0761 N94-12890
Parachute system design, analysis, and simulation tool
[DE93-013755] 02 p0501 N94-13260
Architecture-driven reuse of code in KASE
[NASA-CR-194200] 02 p0745 N94-13356
The KASE approach to domain-specific software systems 02 p0745 N94-13357
Creating a strategic plan for configuration management using computer aided software engineering (CASE) tools
[DE93-013663] 02 p0746 N94-13394
Designing and generating a GUI module using GUI
02 p0747 N94-13437
Software design by reusing architectures
[NASA-CR-194151] 02 p0747 N94-13443
Rapid intelligent inspection process definition for dimensional measurement in advanced manufacturing
[DE93-011271] 02 p0748 N94-13480
Some computational tools for the analysis of through cracks in stiffened fuselage shells
[LR-701] 02 p0673 N94-13726
Hypertext Compiling Tools (HCT): Developing model based applications with standard hypertext systems
[REPT-92-049] 02 p0750 N94-13822
VMEC30 programming library: Reference manual
[DSIS-93-00350] 02 p0750 N94-13858
VMEC30 software development: Tutorial manual
[DSIS-93-00351] 02 p0750 N94-13944
A widget based operations simulator for a planetary camera: A model for the high resolution stereo camera on Mars 94
[DLR-FB-92-30] 02 p0651 N94-14044
VMEC30 SUN software development utilities: User's manual
[DSIS-93-00348] 02 p0752 N94-14051
DSP software development environments for the Adaptive Signal Processing Testbed
[DSIS-93-00347] 02 p0607 N94-14066
EVES: An overview
[DSIS-93-00238] 02 p0752 N94-14088
Guide to the software architectural design phase
[ESA-PSS-05-04-ISSUE-1] 02 p0753 N94-14190
Guide to the software detailed design and production phase
[ESA-PSS-05-05-ISSUE-1] 02 p0753 N94-14191
PC4CAST: A tool for DSN load forecasting and capacity planning 02 p0610 N94-14384
Computational Controls Workstation: Algorithms and hardware 02 p0678 N94-14626
Caesy: A software tool for computer-aided engineering
02 p0678 N94-14627
ASTEC and MODEL: Controls software development at Goddard Space Flight Center 02 p0678 N94-14628
An application of the IMC software to controller design for the JPL LSCL Experiment Facility
02 p0681 N94-14645
Safety-critical software: Status report and annotated bibliography
[AD-A266993] 03 p1144 N94-15214
Open environments to support systems engineering tool integration: A study using the Portable Common Tool Environment (PCTE)
[NASA-TM-4489] 03 p1144 N94-15486
A software interface for the ARL wind tunnel data acquisition system
[AD-A267114] 03 p1146 N94-15650
Software Engineering Guidebook
[NASA-CR-177625] 03 p1150 N94-16656
The Spectral Image Processing System (SIPS): Software for integrated analysis of AVIRIS data
03 p1067 N94-16674
Detailed example of using ACEC release 3.0 with the DEC VAX Ada compiler
[AD-A267880] 03 p1152 N94-17014
Theoretical crystallography with the Advanced Visualization System
[DE93-015692] 03 p1215 N94-17319
ACE: Lessons learned, volume 1
[AD-A267979] 03 p1155 N94-17411
Orpheus: A synthesis framework for regular architectures
[REPT-93-016] 03 p1156 N94-17504
Language-based document processing
[INRIA-RR-1731] 03 p1234 N94-17529
A protocol validator for the SCM and CFSM models
[AD-A268523] 03 p1156 N94-17541
The development of flexible software for the Italian/Dutch satellite SAX: Advantages and disadvantages of the use of CASE tools
[NLR-TP-91288-U] 03 p1157 N94-17626
A structured approach for modeling, analyzing and simulating real-time control systems
[REPT-93-044] 04 p1539 N94-17916
An environment for requirement reuse
[REPT-92-082] 04 p1613 N94-17939
The First International Conference on PCTE
[FEL-92-A134] 04 p1518 N94-17965
Software Toolkit for Analysis Research (STAR)
[DE93-017368] 04 p1519 N94-18086
Cut and paste based modeling with boundary features
[PB93-187250] 04 p1520 N94-18117
Dialog-Based Learning (DBL) for adaptive interface agents and programming-by-demonstrations systems
[AD-A269154] 04 p1540 N94-18261
A special purpose silicon compiler for designing supercomputing VLSI systems 04 p1402 N94-18379
VHDL simulation with access to transistor models
04 p1402 N94-18381
CONTACT: An Air Force technical report on military satellite control technology
[AD-A269375] 04 p1334 N94-18408
Embedded Computer Performance Measurement (ECPM). Advanced avionics subsystems and technology multiprocessor ECPM software documentation
[AD-A269921] 04 p1320 N94-18658
A case study in software maintenance
[AD-A269923] 04 p1521 N94-18659
NASA Electronic Library System (NELS) optimization
[NASA-CR-193688] 04 p1617 N94-18839
3D composite grids using Bezier curves and surfaces in component adaptive methods
[AD-A269188] 04 p1549 N94-18863
Case studies of software development tools for parallel architectures
[AD-A269193] 04 p1535 N94-18866
Early experiences with the IBM SP-1
[DE93-018398] 04 p1535 N94-19010
A least-squares computational tool kit
[DE93-018400] 04 p1557 N94-19011
A programming paradigm for distributed-memory computers
[DE93-018336] 04 p1524 N94-19024
CAVEMAN: Configuration and version management
[DE93-018066] 04 p1524 N94-19048
An ORACLE CASE history: Experiences with ORACLE CASE tools
[DE93-010827] 04 p1617 N94-19057
Computer codes for checking, plotting and processing of neutron cross-section covariance data and their application
[DE93-018459] 04 p1570 N94-19129
A multi-thread approach to coalescing small transfers generated by portable tool sets
[DE93-012128] 04 p1525 N94-19186
Vectorized presentation-level services for scientific distributed applications
[DE93-018091] 04 p1537 N94-19253
European network for the numerical simulation of space plasmas 04 p1331 N94-19641
Report of the Second CLICOM Experts Meeting
[WCDMP-19] 04 p1495 N94-19705
Data-Machine Independence (DMI)
[DE93-018008] 04 p1539 N94-19734
Technology benefits model user manual, version 01.00.04
[AD-A270637] 04 p1620 N94-19777
SISSY: An example of a multi-threaded, networked, object-oriented databased application
[DE93-019742] 05 p2041 N94-19811
Reference manual for a Requirements Specification Language (RSL), version 2.0
[NASA-CR-191460] 05 p1898 N94-20039
PREVAIL-DM: A framework-based environment for formal hardware verification
[RR-899] 05 p1905 N94-20164
Advanced software development workstation: Knowledge base methodology: Methodology for first Engineering Script Language (ESL) knowledge base
[NASA-CR-193643] 05 p1930 N94-21065
Experiments on technology mapping using different cell libraries 05 p1758 N94-21118
Design of a computer assisted tool for object oriented acquisition, modeling and simulation of knowledge structure
[ETN-93-94183] 05 p1910 N94-21152
An investigation into the state of the practice of CASE tool integration
[AD-A272441] 05 p1912 N94-21205
Integration opportunities for computer models, methods, and GIS used in Corps planning studies
[AD-A271714] 05 p2044 N94-21354
Combination of on ground experiments and analysis software for the evaluation of material degradation in space (SILEX project) 05 p1662 N94-21389
Security evaluation of Unix networks
[AD-A273076] 05 p1945 N94-21520
Computer-Aided Test Equipment Graphics System (CATEGS)
[DE94-000383] 05 p1915 N94-21561
Analog/digital pH meter system I.C.
05 p1764 N94-21701
Heuristic-based scheduling algorithm for high level synthesis 05 p1764 N94-21704
Model-based reasoning for power system management using KATE and the SSM/PMAD
[NASA-CR-193942] 05 p1671 N94-21882
Automated analysis tools for reducing spacecraft telemetry data
[DE94-000400] 05 p1657 N94-21981
Three original programmes for managers
05 p1923 N94-22083
Method and software for decision making in public problems 05 p1923 N94-22087
Formal hardware verification in Maple
05 p1771 N94-22112
Software systems used for unstructured grid generation at NASA Langley 05 p1918 N94-22351
NASA-Ames Research Center unstructured technology development 05 p1919 N94-22352
New IRAF stellar photometry software
05 p1925 N94-22464
SPPTOOLS: Programming tools for the IRAF SPP language 05 p1925 N94-22474
FITS data conversion efforts at the Compton Observatory Science Support Center
05 p1926 N94-22488
The IDL astronomy user's library
05 p2048 N94-22500
GRO/EGRET data analysis software: An integrated system of custom and commercial software using standard interfaces 05 p1926 N94-22501
XPI: The Xanadu Parameter Interface
05 p1927 N94-22513
Development of the FITS tools package for multiple software environments 05 p1927 N94-22516
Managing an archive of weather satellite images
05 p2048 N94-22525
Tools for the IDL widget set within the X-windows environment 05 p1927 N94-22538
DECONV-TOOL: An IDL based deconvolution software package 05 p1927 N94-22542
The STARLINK software collection
05 p1927 N94-22545
A general model for dynamic and complex information management: The ELEN prototype object manager for software engineering
[ETN-94-95163] 06 p2588 N94-22880
Definition and realization of a formal verification tool of LUSTRE programs: The LESAR system
[ETN-94-95164] 06 p2447 N94-22882
Verification of synchronous sequential numerical material systems: Application of the LUSTRE language and of the LESAR verification tool
[ETN-94-95181] 06 p2447 N94-22899
Users manual for the Chameleon parallel programming tools
[DE94-001934] 06 p2465 N94-22973
A dataflow analysis tool for parallel processing of algorithms
[NASA-TM-109054] 06 p2448 N94-23086
Tools reference manual for a Requirements Specification Language (RSL), version 2.0
[NASA-CR-191461] 06 p2445 N94-23125
The TOPSIM 4 graphic user interface
[ESA-STM-247] 06 p2450 N94-23228
A framework for SFC/DC system data analysis
06 p2523 N94-23234

The Automated Instrumentation and Monitoring System (AIMS) reference manual
[NASA-TM-108795] 06 p2452 N94-23510
Activity Catalog Tool (ACT) user manual, version 2.0
[NASA-CR-177634] 06 p2430 N94-23527
Simultaneous simulation and visualization using DGL
[PB93-201341] 06 p2453 N94-23534
Mean-value of product-form stochastic Petri net models of slotted-ring systems
[PB94-110871] 06 p2494 N94-23749
Magellan spacecraft and memory state tracking: Lessons learned, future thoughts
06 p2207 N94-23865
Integrating payload design, planning, and control in the Dutch Utilisation Centre 06 p2207 N94-23869
Making adaptable systems work for mission operations: A case study 06 p2506 N94-23883
The FOT tool kit concept 06 p2507 N94-23889
VMPLOT: A versatile analysis tool for mission operations 06 p2507 N94-23891
The mission events graphic generator software: A small tool with big results 06 p2464 N94-23893
Using SFOC to fly the Magellan Venus mapping mission 06 p2516 N94-23941
Expert diagnostics system as a part of analysis software for power mission operations 06 p2516 N94-23944
GenSAA: A tool for advancing satellite monitoring with graphical expert systems 06 p2516 N94-23945
From requirements to acceptance tests
06 p2464 N94-23962
Software reuse in spacecraft planning and scheduling systems 06 p2520 N94-23966
Integration and evaluation of a simulator designed to be used within a dynamic prototyping environment
06 p2198 N94-24436
Evaluation of the efficiency and fault density of software generated by code generators 06 p2465 N94-24445
Fact-based enterprise information management using NIAM
[DE93-041135] 06 p2591 N94-24501
MERILL: An equational reasoning system in standard ML: A user guide (prerelease version 0.4)
[PB93-204501] 06 p2456 N94-24534
An automated tool to facilitate code translation for software fault tree analysis
[AD-A273205] 06 p2457 N94-24556
High-performance computing and communications
[DE94-002215] 06 p2457 N94-24566
Timed coloured Petri nets and their application to logistics
[ETN-94-95310] 06 p2522 N94-25293
Genetic algorithms in control systems engineering
[RR-470] 06 p2463 N94-25315
Software engineering methodologies and tools
06 p2465 N94-25382
CADBIT 2: Computer-aided design for built-in test, volume 1
[AD-A273702] 06 p2463 N94-25455
CADBIT 2: Computer-aided design for built-in test, volume 2
[AD-A273703] 06 p2463 N94-25456
Parallel Assessment Window System (PAWS) enhancements
[AD-A274094] 07 p2979 N94-25786
Analysis and computer tools for separation processes involving nonideal mixtures
[DE94-004162] 07 p2960 N94-25986
The National Center for Advanced Information Components Manufacturing: Program update
[DE94-002647] 07 p2960 N94-26118
Survey of visualization and analysis tools
[NASA-TM-108436] 07 p2809 N94-26150
Implementing a multiple criteria model base in co-op with a graphical user interface generator
[AD-A274901] 07 p3093 N94-26181
Parallel grid generation algorithm for distributed memory computers
[NASA-TP-3429] 07 p2963 N94-26466
Verification and validation of the on-board software real time requirements 07 p2953 N94-26739
Asynchronous and packetized systems engineering tools 07 p2954 N94-26746
Diagnostics and microelectronics
[DE94-003016] 07 p2784 N94-26777
DUSOL: Improved software for analysis of ultrasonic velocity data on anisotropic materials
[NPL-DMM(A)-104] 07 p2965 N94-26816
Rapid prototyping of application specific signal processors (RASSP)
[AD-A274324] 07 p2772 N94-26884
Design of an online help facility for ExSpect
[PB94-126687] 07 p2966 N94-26955
Thirteen ways to say nothing with scientific visualization
[NASA-CR-195280] 07 p2970 N94-27542
A theory for simulator tools
[CWI-CS-R9302] 07 p2972 N94-27578
Smalltalk: A tool for development of an Ada implementation of EWCAC
[SKL-1600-46-003-01-0] 07 p2974 N94-27823
Visualization techniques to aid in the analysis of multispectral astrophysical data sets
[NASA-CR-195268] 07 p3105 N94-27932
Comparison of Object-Oriented Analysis and Design Methods: A Collection of Papers
[MEMO-INF-92-69] 07 p2975 N94-27936
CASE tools for the support of object-oriented analysis and design methods 07 p2975 N94-27939
Work-oriented development of interactive software tools: Understanding the work of software maintainers and making an interactive software tool for them
[PB94-132032] 08 p3406 N94-28401
Transferable Output ASCII Data (TOAD) editor version 1.0 user's guide
[NASA-CR-187507] 08 p3408 N94-28818
Business planning model user's guide
[AD-A274978] 08 p3409 N94-28895
Fault tolerant testbed evaluation, phase 1
[NASA-CR-188275] 08 p3171 N94-29035
HYPER-NPSNET: Embedded multimedia in a 3D virtual world
[AD-A275063] 08 p3410 N94-29152
The development procedures and tools applied for the attitude control software of the Italian satellite SAX
08 p3170 N94-29324
Rome Laboratory software engineering technology program 08 p3414 N94-29330
Design of a thinwire real-time multiprocessor operating system 08 p3415 N94-29333
The UNICON approach to through-life support and evolution of software-intensive systems
08 p3416 N94-29340
SDE's for the year 2000 and beyond: An EF perspective 08 p3417 N94-29344
DSSA-ADAGE: An environment for architecture-based avionics development 08 p3150 N94-29348
Entreprise 2: A PCTE integrated project support environment 08 p3417 N94-29349
Microvibrations on a GEO telecommunication satellite
[REPT-932-440-101] 08 p3168 N94-29415
Aid to Ada component reuse at Aerospatiale Cannes (France)
[REPT-932-440-102] 08 p3418 N94-29418
ASSIST internals reference manual
[NASA-TM-109102] 08 p3431 N94-29494
Application of FLUIDNET-G software to the preliminary thermal and hydraulic design of Hermes spaceplane
[REPT-932-440-107] 08 p3168 N94-29543
A study of the relationship between the performance and dependability of a fault-tolerant computer
[NASA-CR-195758] 08 p3406 N94-29695
Extending the X Window System
[DE94-006496] 08 p3420 N94-29844
Addendum to the final report for the investigation of proof techniques within the EVES verification technology
[TR-93-5451-03] 08 p3421 N94-30155
GNU debugger internal architecture
[DE94-006665] 08 p3422 N94-30251
Software engineering and software management in a distributed UNIX environment
[NLR-TP-92233-U] 08 p3422 N94-30314
Modelling interaction tools in the Views architecture
[CWI-CS-R9261] 08 p3423 N94-30323
A user's guide to the Software Testpilot
[CWI-CS-R9343] 08 p3426 N94-30435
A simulator for multi-radar analysis for realistic traffic
[AD-B179099] 08 p3142 N94-30439
A streamlined software environment for situated skills
[AIAA PAPER 94-1205-CP] 08 p3444 N94-30556
Engineering of systems for application of scientific computing in industry WP project management ISNaS 9209099
[PB94-126232] 08 p3428 N94-30739
Discovery systems for manufacturing
[AD-A276216] 09 p3828 N94-31061
A comparison of product realization frameworks
[AD-A275992] 09 p3810 N94-31357
The development and use of an evaluation mechanism for the assessment of software configuration management tools
[AD-A275961] 09 p3810 N94-31383
Consistency checks for SCR-style requirements specifications
[AD-A276077] 09 p3811 N94-31461
A hierarchical approach to test generation for CMOS VLSI circuits
[ISBN-9-09-005449-9] 09 p3689 N94-31535
DOME: Dynamic optimization on multiprocessor engines, a statistical approach 09 p3807 N94-31972
Incremental recompilation for Standard ML of New Jersey
[AD-A276522] 09 p3815 N94-32080
Experiences with EDO: An Evolutionary Database Optimizer
[TR-93-23] 09 p3918 N94-32105
The advent of failure analysis software technology
[DE94-006593] 09 p3692 N94-32111
Analytical Design Package (ADP2): A computer aided engineering tool for aircraft transparency design
09 p3823 N94-32430
CONFIG: Integrated engineering of systems and their operation 09 p3823 N94-32432
Spacecraft On-Board Information Extraction Computer (SOBIEC) 09 p3808 N94-32433
Emacs Lisp in Edwin scheme
[AD-A276721] 09 p3818 N94-32504
Production of terrain data: Optical radar complementarity 09 p3750 N94-32540
MADE: A Multiple Application Development Environment
[CWI-CS-R9360] 09 p3822 N94-33097
Selection criteria and facilitation training for the study of groupware
[NASA-CR-195906] 09 p3822 N94-33114
The hypermedia technology as front end to knowledge processing systems 09 p3854 N94-33343
Parallel programming methodologies for non-uniform structured problems in materials science
[AD-A277868] 10 p4111 N94-33777
Development of the static analyzer ANALYSIS/EX for FORTRAN programs
[DE94-727537] 10 p4105 N94-33868
Analyzing PICL trace data with MEDEA
[DE94-009173] 10 p4111 N94-33987
Agent oriented programming
10 p4110 N94-34059
A toolbox and a record for scientific model development 10 p4110 N94-34062
Equational reasoning support for Orwell
[PB94-149614] 10 p4107 N94-34110
Software Management Environment (SME): Components and algorithms
[NASA-CR-189346] 10 p4109 N94-34996
Space educators' handbook
[NASA-TM-109779] 11 p4343 N94-35339
A compile time model for composing parallel programs
[AD-A278896] 11 p4310 N94-35597
Environment/tool integrator for software development, version 1.2
[AD-A278965] 11 p4303 N94-35660
A collection of tools in support of automatic differentiation
[DE94-010104] 11 p4314 N94-35704
An object-oriented implementation of a graphical-programming system
[DE94-009298] 11 p4304 N94-35808
CABPRO: An expert system for process planning multiwire cables
[DE94-010213] 11 p4312 N94-35810
Software quality: Process or people
12 p4492 N94-36499
Interchangeable spline reference guide
[DE94-012368] 12 p4495 N94-37245

SOHO MISSION
The grazing incidence detectors for the SOHO coronal diagnostic spectrometer 03 p0905 N94-15063
Data processing system for flight spectrometer
03 p0908 N94-15086
Ultra-clean high-precision mechanisms for the SUMER EUV spectrometer on SOHO 06 p2356 N94-23999
Width modulator mechanism for spectrometer entrance slits 06 p2357 N94-24002
GOLF mechanisms 06 p2357 N94-24003
The development of the SOHO SUMER mechanisms
06 p2361 N94-24028
Examination of the response capacity of a silicon pixel detector for ions and molecules in the energy area 100 to 300 keV
[MPE-241] 06 p2346 N94-25415
Mounting of SSM's
[VTT-TIED-1442] 07 p2695 N94-26250
Three high duty cycle, space-qualified mechanisms
08 p3162 N94-29642

SOI (SEMICONDUCTORS)
Technology transfers and reliable oxides
[AD-A266948] 03 p1175 N94-15758
DLTS and dynamic transconductance analysis of deep-submicron fully-depleted SOI MOSFET's
[AD-A267291] 03 p1214 N94-17243
Fully-depleted silicon-on-sapphire and its application to advanced VLSI design 05 p1765 N94-21709
An investigation of distributed coupling in a nonlinear semiconductor waveguide 08 p3246 N94-29529
Advanced silicon technology for microwave circuits
[AD-A278039] 09 p3698 N94-33091

SOIL EROSION
Soil erosion rates caused by wind and saltating sand stresses in a wind tunnel
[DE93-009154] 02 p0706 N94-12905
Soil erosion mapping using remote sensing and GIS techniques 02 p0692 N94-14240
Three-dimensional high-resolution seismic profiling on the New Jersey outer continental shelf
[AD-A269835] 04 p1498 N94-18600
Gravity and the geoid in the Nepal Himalaya
[NASA-CR-194166] 04 p1463 N94-19430
Arid regions and wind erosion 09 p3780 N94-31005

SOIL MAPPING
Spectral reflectance of soils from Sao Paulo State
[INPE-5424-PRP/172] 02 p0684 N94-13377
Soil erosion mapping using remote sensing and GIS techniques 02 p0692 N94-14240
Land evaluation for agricultural productivity in North-East Thailand using LANDSAT TM data and geographic information 02 p0693 N94-14242
Analysis of hyper-spectral AVIRIS image data over a mixed-conifer forest in Maine 05 p1838 N94-20959
Mapping of soil humidity using C-band radar images
[ISBN-0-315-85076-0] 07 p2852 N94-27878
Possible complementarity of SPOT/ERS in mapping land use: Study on agricultural land in Brittany (France) 09 p3755 N94-32563

SOIL MECHANICS
Dynamic soil pressures on rigid cylindrical vaults
[DE93-013930] 02 p0676 N94-14585
A measurement station for study of Earth moving tools and ground cutting processes
[IFTR-10/1991] 03 p0985 N94-17068
Centrifuge modeling of explosion-induced craters in unsaturated sand
[AD-A270194] 04 p1417 N94-18780
Numerical analysis of pressure meter tests: Application of parameter identification of soils behavior
[ECL-92-52] 04 p1487 N94-19380
Proceedings: International Symposium on Thermal Engineering and Science for Cold Regions
[AD-A270636] 04 p1487 N94-19529
The microstructural response of granular soil under uniaxial strain
[AD-A274808] 07 p2763 N94-26341
Toward a molecular scale understanding of frost heaving, phase 1
[AD-A275446] 08 p3356 N94-28882
The undrained shear strength characteristics of undisturbed soil from fishing port areas 08 p3234 N94-29704
Microwave dielectric behavior of soils. Report 3: Measurement and modeling
[AD-A276060] 09 p3771 N94-31457
Contingency airfield construction: Mechanical stabilization using monofilament and fibrillated fibers
[AD-A277732] 10 p4008 N94-33444

SOIL MOISTURE
Design of a global soil moisture initialization procedure for the simple biosphere model
[NASA-TM-104590] 01 p0284 N94-10940
The impact of vegetation on the atmospheric boundary layer and convective storms 01 p0277 N94-11480
The use of ERS-1 SAR data to study surface states 01 p0247 N94-12480
Geoecological monitoring of an agricultural area 01 p0248 N94-12489
Extraction of plant and soil parameters from multitemporal ERS-1 SLC data of the Freiburg test site 01 p0248 N94-12491
Assessment of ERS-1 SAR data for soil moisture estimation 01 p0249 N94-12492
Temporal monitoring of soil moisture using ERS-1 SAR data 01 p0249 N94-12493
Measuring surface fluxes in CAPE
[NASA-CR-193664] 02 p0711 N94-12788
Phase aligner for the Electronically Scanned Thinned Array Radiometer (ESTAR) instrument
[NASA-TM-4518] 02 p0623 N94-13878
Circulation and rainfall climatology of a 10-year (1979 - 1988) integration with the Goddard Laboratory for atmospheres general circulation model
[NASA-TM-104591] 02 p0723 N94-14074
Mathematical model of frost heave and thaw settlement in pavements
[AD-A267037] 03 p0983 N94-15676
On hydrologic similarity: A dimensionless flood frequency model using a generalized geomorphologic unit hydrograph and partial area runoff generation
[PAPER-89WR01579] 03 p1083 N94-16027
Evapotranspiration and runoff from large land areas: Land surface hydrology for atmospheric general circulation models 03 p1083 N94-16029
Heterogeneity and scaling land-atmospheric water and energy fluxes in climate systems 03 p1083 N94-16030
Evaluation of a distributed catchment scale water balance model
[PAPER-93WR00398] 03 p1083 N94-16031
A detailed model for simulation of catchment scale subsurface hydrologic processes
[PAPER-92WR02333] 03 p1084 N94-16032
Scaling, soil moisture and evapotranspiration in runoff models 03 p1084 N94-16034
Bright soil units on Mars determined from ISM imaging spectrometer data 03 p1295 N94-16430
Processing of polarimetric SAR data for soil moisture estimation over Mahantango watershed area 03 p1079 N94-16754
Evaluation of polarimetric SAR parameters for soil moisture retrieval 03 p1079 N94-16755
Protocol for computation of surface boundary layer parameters used to determine soil moisture flux from meteorological data collected at LLNL, 1992-1993
[DE93-018906] 04 p1463 N94-19003
Synergism of active and passive microwave data for estimating bare surface soil moisture 05 p1727 N94-20444
Application of neural network to remote sensing of soil moisture using theoretical polarimetric backscattering coefficients 05 p1730 N94-20455
Measurement of evapotranspiration with combined reflective and thermal infrared radiance observations
[NASA-CR-194802] 05 p1837 N94-20951
Snow cover measurements and areal assessment of precipitation and soil moisture
[WMO-749] 05 p1841 N94-21068
Areally averaged estimates of surface heat flux from ARM field studies
[DE93-018569] 05 p1859 N94-22036
Estimates of monthly mean soil moisture for 1979-1989
[NASA-TM-104571] 06 p2407 N94-23132
Spatial and temporal variability of soil temperature, moisture and surface soil properties
[NASA-CR-194109] 06 p2401 N94-23337
Methodology for the assessment of surface resistance and soil water storage variability at mesoscale based on remote sensing measurements. A case study with HAPEX-EFEDA data. UNESCO-International Hydrological Program 4
[PB94-111721] 06 p2386 N94-23734
Groundtruth collection for the JPL-SAR and ERS-1 campaign in Flevoland and Veluwe, Netherlands, 1991
[BCRS-92-26] 06 p2386 N94-23755
Session on coupled land surface/hydrological/atmospheric models 06 p2414 N94-24395
Mapping of soil humidity using C-band radar images
[ISBN-0-315-85076-0] 07 p2852 N94-27878
Sensitivity and feedbacks associated with vegetation-related land surface parameters in a general circulation model 08 p3348 N94-29800
Microwave dielectric behavior of soils. Report 1: Summary of related research and applications
[AD-A275980] 09 p3771 N94-31351
Microwave dielectric behavior of soils. Report 2: A unique coaxial measurement apparatus
[AD-A275982] 09 p3771 N94-31353
Application of ERS-1 SAR data for hydrological studies 09 p3754 N94-32558
A long-term simulation of surface fluxes and soil moisture
[DE94-006661] 09 p3774 N94-32772
Remote sensing of hydrologic variables in boreal areas, phase 1
[NASA-CR-189354] 10 p4077 N94-34134
A model of the CO2 exchanges between biosphere and atmosphere in the tundra
[NASA-CR-196008] 11 p4289 N94-35389

SOIL SCIENCE
Sulfate reduction and other sedimentary biogeochemistry in a northern New England salt marsh 01 p0268 N94-12453
Sulfur transformations in the sediments of a New Hampshire salt marsh 01 p0270 N94-12463
Applications of the Advanced Light Source to problems in the earth, soil, and environmental sciences
[DE93-015258] 02 p0710 N94-14477
Soil temperatures
[KNMI-WR-92-05] 05 p1865 N94-20309
Visible-infrared properties of controlled laboratory soils 05 p1685 N94-20689
Spatial and temporal variability of soil temperature, moisture and surface soil properties
[NASA-CR-194109] 06 p2401 N94-23337
Time domain reflectometry for measuring bulk soil electrical conductivity and comparison with the Em38 instrument
[PB94-125432] 07 p2881 N94-27052
Speciation in Water and Soil: A literature review
[PB94-132388] 08 p3341 N94-28412
A toy model for estimating N2O emissions from natural soils 08 p3351 N94-30627
Development of simplified ecosystem models for applications in Earth system studies: The Century experience 08 p3352 N94-30629
A toy terrestrial carbon flow model 08 p3352 N94-30630
Microwave dielectric behavior of soils. Report 1: Summary of related research and applications
[AD-A275980] 09 p3771 N94-31351
Microwave dielectric behavior of soils. Report 2: A unique coaxial measurement apparatus
[AD-A275982] 09 p3771 N94-31353

SOILS
NT ALLUVIUM
NT GRAVELS
NT LUNAR DUST
NT LUNAR SOIL
NT MUD
NT PERMAFROST
NT SANDS
Immediate response to free product discovery
[PB93-182970] 01 p0265 N94-11015
In situ secondary ion mass spectrometry analysis
[DE93-012185] 01 p0076 N94-11140
Catalytic oxidation of organics in vapor streams at remediation sites
[PB93-182962] 01 p0266 N94-11472
Reflectance spectra of sulfate-and carbonate-bearing Fe(3+)-doped montmorillonites as Mars soil analogs 01 p0445 N94-12070
The effects of atmospheric pressure on infrared reflectance spectra of Martian analogs 01 p0445 N94-12071
A comparison of the visible and near infrared reflectance of hydrovolcanic palagonite tuffs and Martian weathered soils 01 p0477 N94-12245
Elevated acetate concentrations in the rhizosphere of Spartina alterniflora and potential influences on sulfate reduction 01 p0271 N94-12468
Evaluating the spread of red soil with LANDSAT TM data in coral reefs of Okinawa main island, southwestern Japan 01 p0212 N94-12668
Measuring surface fluxes in CAPE
[NASA-CR-193664] 02 p0711 N94-12788
Spectral reflectance of soils from Sao Paulo State
[INPE-5424-PRP/172] 02 p0684 N94-13377
Land evaluation for agricultural productivity in North-East Thailand using LANDSAT TM data and geographic information 02 p0693 N94-14242
Survey of subsurface geophysical exploration technologies adaptable to an airborne platform
[DE93-015080] 02 p0717 N94-14294
Dynamic soil pressures on rigid cylindrical vaults
[DE93-013930] 02 p0676 N94-14585
Coastal scour problems and methods for prediction of maximum scour
[AD-A266658] 02 p0726 N94-14775
HyperVentilate: Decision-support software for soil vapor extraction technology application
[PB93-134880] 03 p1094 N94-15136
X-SAR: The X-band synthetic aperture radar on board the Space Shuttle 03 p0990 N94-15891
Radar response of vegetation: An overview 03 p0991 N94-15898
Mars Analog Site Study (MASS) 03 p1252 N94-16200
A Moessbauer spectrometer for the mineralogical analysis of the Mars surface: First temperature dependent tests of the detector and drive system 03 p1259 N94-16233
Suggestion for extended Viking magnetic properties experiment on future Mars missions 03 p1285 N94-16375
Deucalionis Regio, Mars: Evidence for a unique mineralogic endmember and a crusted surface 03 p1291 N94-16406
Bright soil units on Mars determined from ISM imaging spectrometer data 03 p1295 N94-16430
Variations in the Fe mineralogy of bright Martian soil 03 p1295 N94-16431
Experimental study of nonassociated flow and instability of frictional materials
[AD-A266421] 03 p1024 N94-16555
Mapping the spectral variability in photosynthetic and non-photosynthetic vegetation, soils, and shade using AVIRIS 03 p1068 N94-16679
Soil conservation applications with C-band SAR 03 p1080 N94-16760

Rapid geophysical surveyor
[DE93-016637] 04 p1461 N94-17851
Applications of Quaternary stratigraphic, soil-geomorphic, and quantitative geomorphic analyses to the evaluation of tectonic activity and landscape evolution in the Upper Coastal Plain, South Carolina
[DE93-016269] 04 p1484 N94-18725
A general rough-surface inversion algorithm: Theory and application to SAR data 05 p1719 N94-20407
Visible-infrared properties of controlled laboratory soils 05 p1685 N94-20689
Thermal infrared remote sensing and Kirchhoff's law: 1. Laboratory measurements 05 p1685 N94-20733
Determination of Martian soil mineralogy and water content using the Thermal Analyzer for Planetary Soils (TAPS) 05 p1812 N94-22433
Mass spectrometer-pyrolysis experiment for atmospheric and soil sample analysis on the surface of Mars 05 p1812 N94-22435
Machines for moving in soil 06 p2369 N94-23411
Effect of land use change on the carbon cycle in Amazon soils
[NASA-CR-195168] 06 p2399 N94-24853
Human impacts on soil carbon dynamics of deep-rooted Amazonian forests
[NASA-CR-195127] 06 p2399 N94-24861
The microstructural response of granular soil under uniaxial strain
[AD-A274808] 07 p2763 N94-26341
Time domain reflectometry for measuring bulk soil electrical conductivity and comparison with the Em38 instrument
[PB94-125432] 07 p2881 N94-27052
Speciation in Water and Soil: A literature review
[PB94-132388] 08 p3341 N94-28412
Growth condition of an ice layer in freezing soils under applied loads. Part 1: Experiment
[AD-A275215] 08 p3357 N94-29070
Collecting cometary soil samples? Development of the ROSETTA sample acquisition system 08 p3160 N94-29628
The undrained shear strength characteristics of undisturbed soil from fishing port areas 08 p3234 N94-29704
A toy model for estimating N2O emissions from natural soils 08 p3351 N94-30627
Development of simplified ecosystem models for applications in Earth system studies: The Century experience 08 p3352 N94-30629
Fiber optic chemical sensors on Mars
[DE94-005251] 09 p3941 N94-31145
Microwave dielectric behavior of soils. Report 1: Summary of related research and applications
[AD-A275980] 09 p3771 N94-31351
Microwave dielectric behavior of soils. Report 2: A unique coaxial measurement apparatus
[AD-A275982] 09 p3771 N94-31353
Microwave dielectric behavior of soils. Report 3: Measurement and modeling
[AD-A276060] 09 p3771 N94-31457
Analysis of GER imaging spectrometry data for the identification of soil and vegetation parameters in land degradation studies 09 p3744 N94-31857
Possibilities of GER data for soil surface characteristics in the Almaden area 09 p3744 N94-31859
The effects of vegetation on the ability to map soils using GERIS data 09 p3744 N94-31860
Procedures for computing site seismicity
[AD-A277666] 09 p3775 N94-33028
Mars: Past, Present, and Future. Results from the MSATT Program, part 1
[NASA-CR-194279] 09 p3943 N94-33190
Thermal emission measurements (5-25 microns) of Hawaiian palagonitic soils with implications for Mars 09 p3944 N94-33193
The importance of environmental conditions in reflectance spectroscopy of laboratory analogs for Mars surface materials 09 p3944 N94-33195
Ferric sulfate montmorillonites as Mars soil analogs 09 p3944 N94-33196
Magmatic volatiles and the weathering of Mars 09 p3946 N94-33201
Martian spectral units derived from ISM imaging spectrometer data 09 p3949 N94-33220
Completing below-ground carbon budgets for pastures, recovering forests, and mature forests of Amazonia
[NASA-CR-195959] 10 p4076 N94-33948
Thermal emission measurements (5-25 microns) of palagonite/Fe-substituted montmorillonite intimate mixtures: Applications to Mars 11 p4292 N94-35453
Vapor-fortified QA/QC samples for the analysis of volatile organic compounds
[AD-A278712] 11 p4229 N94-35776

SOL-GEL PROCESSES

Fibre reinforced structures with glass matrix 01 p0064 N94-10064
Low temperature synthesis of monolithic transparent Ta2O5 gels from hydrolysis of metal alkoxide
[NASA-TM-106246] 01 p0089 N94-11204
Synthesis and thermal evolution of structure in alkoxide-derived niobium pentoxide gels
[NASA-TM-106259] 01 p0090 N94-11257
Structural development in ceramic precursor sols and gels
[AD-A264354] 01 p0090 N94-11281
Amorphous sol-gel insulating films
[DE93-012859] 02 p0576 N94-12866
Solution chemistry optimization of sol-gel processed PZT thin films
[DE93-013776] 02 p0814 N94-14695
Charge storage and switching phenomena with molecular assemblies of metal complexes
[AD-A266673] 02 p0787 N94-14778
Preparation of homogeneous aluminosilicate gels by sol/gel techniques
[AD-A266823] 03 p0962 N94-14914
Multinuclear NMR study of aluminosilicate sol-gel synthesis reasons for the homogeneous gelation using the prehydrolysis method
[AD-A266877] 03 p0962 N94-14921
Self-diffusion coefficients of sol-gel intermediates
[AD-A266957] 03 p0963 N94-15179
Intramolecular versus intermolecular condensation rates in the acidic polymerization of octaethoxytrisiloxane
[AD-A266982] 03 p0963 N94-15490
NMR and theoretical investigation of cation binding with sol-gel silicates
[AD-A266999] 03 p0963 N94-15631
Design, synthesis and characterization of novel nonlinear optical polymers
[AD-A267035] 03 p0964 N94-15675
Effects of aging time on V205 sol-gel coatings
[AD-A266824] 03 p0965 N94-15843
Use of microgravity in the synthesis of ceramics using sol gel techniques 03 p0979 N94-16088
Structural studies of sol-gel glasses
[AD-A266277] 03 p0967 N94-16472
Ceramic fiber coatings development and demonstration
[AD-A267286] 03 p0972 N94-17242
Electrical properties of sol-gel PZT thin films for decoupling capacitor applications
[DE93-016491] 03 p1015 N94-17648
Finite element modeling of evaporation and condensation during sol-gel film and fiber formation
[DE93-017655] 04 p1345 N94-17820
Novel electrochemical materials prepared by sol-gel chemistry
[AD-A269060] 04 p1578 N94-18405
Photo-induced and electrooptic properties of (Pb,La)(Zr,Ti)O3 films
[DE93-017496] 04 p1371 N94-18519
Hydrolysis reaction and positronium decay in silica gels
[AD-A270028] 04 p1371 N94-18713
Preparation and properties of sol-gel derived PZT thin films for decoupling capacitor applications
[DE93-018853] 05 p2013 N94-19961
Photonics and nonlinear optics with molecular materials and polymers
[AD-A271747] 05 p1988 N94-21457
Photo-induced and electrooptic properties of (Pb,La)(Zr,Ti)O3 films for optical memories
[DE93-019820] 06 p2542 N94-23202
Glass-ceramic Li-Al-Si-O composition and process for its production
[CA-PATENT-APPL-SN-2043757] 06 p2254 N94-24129
Conformal method of fabricating and optical waveguide on a semiconductor substrate
[AD-D015988] 06 p2546 N94-25043
Sol-gel derived silica/siloxane composite materials: The effect of loading level and catalyst activity on silica domain formation
[DE94-002734] 07 p2712 N94-27710
Densification and crystallization of zirconia thin films prepared by sol-gel processing
[DE94-005573] 08 p3518 N94-30315
Synthesis and characterization of advanced materials for Navy applications 08 p3223 N94-30474
Silica scintillating materials prepared by sol-gel methods
[DE94-005123] 08 p3220 N94-30778
Sol-gel metal oxide and metal oxide/polymer multilayers applied by meniscus coating
[DE94-005813] 09 p3649 N94-31199
Passive vibration damping materials: Piezoelectric ceramic composites for vibration damping applications
[AD-A276550] 09 p3653 N94-31935
The sol-gel-xerogel transition
[AD-A276647] 09 p3616 N94-32038
Ion-irradiation-induced densification of zirconia sol-gel thin films
[DE94-006248] 09 p3656 N94-32103
Sol-gel coatings for high power laser optics: Past, present, and future
[DE94-007240] 09 p3718 N94-32252
Nonlinear optical polymers derived from organic/inorganic composites
[AD-A277408] 09 p3659 N94-32610
Structure-property relationships of carbon aerogels
[DE94-007120] 09 p3660 N94-32687
Low loss second-order nonlinear optical polymers based on all organic sol-gel materials
[AD-A277482] 09 p3663 N94-32985
Optical properties of doped sol-gel silica glasses
[AD-A278094] 09 p3884 N94-33267
Novel sol-gel deposition for repair of conducting paths in polyceramic systems
[AD-A278381] 09 p3664 N94-33350
Multifunctional gel-silica optics
[AD-A278531] 10 p4141 N94-33670
Ultrastructure processing of advanced materials
[AD-A278285] 10 p4018 N94-33962
Silica Fresnel lens for laser communications
[AD-A278329] 10 p4058 N94-33967
Cross-condensation reactions in an organically modified silica sol-gel
[DE94-010086] 11 p4244 N94-35701
Spinnability of silica sols: The role of alkoxy group exchange
[DE94-010087] 11 p4244 N94-35702

SOLAR ACTIVITY

NT SOLAR FLARES
NT SOLAR PROMINENCES
NT SUNSPOTS
Effects of energetic particle events on VLF/LF propagation parameters/1989
[AD-A265266] 01 p0275 N94-11013
Disturbance Impact Assessment System (DIAS), version 2.0. System design document
[AD-A265251] 01 p0138 N94-11883
Yohkoh Bragg Crystal Spectrometer light curves for Ca XIX (3.1631-3.1912A): 1 October 1991 - 30 September 1992
[AD-A266090] 01 p0483 N94-12414
Variations common to the interplanetary magnetic field, the zonal atmospheric circulation and the Earth's rotation
[COMMUNICATIONS-SER-B-157] 02 p0837 N94-13504
Orbiting solar operations
[NASA-TM-109583] 03 p0884 N94-15267
FNAS/solar flare energetics
[NASA-CR-193574] 03 p1299 N94-17089
Solar Electro-Optical Network (SEON) upgrade/replacement program. Phase 1: Qualification operational test and evaluation plan
[AD-A266364] 03 p1237 N94-17225
Origins of solar activity. First year report, AASERT grant
[AD-A268848] 04 p1629 N94-18222
Solar proton events from a 180 year depth profile of nitrate concentrations from the central Greenland ice sheet
[AD-A272888] 05 p2147 N94-21196
High resolution studies of the structure of the solar atmosphere
[AD-A273084] 05 p2147 N94-21522
Determination of coronal magnetic fields from vector magnetograms
[NASA-CR-194744] 05 p2147 N94-21877
Solar-geophysical data number 584, April 1993. Part 1: (Prompt reports). Data for February, March, 1993, and late data
[PB93-198323] 06 p2626 N94-23738
Solar-geophysical data number 584, April 1993. Part 2: (Comprehensive reports). Data for October 1992, and miscellaneous
[PB93-198331] 06 p2627 N94-23739
Solar-geophysical data number 589, September 1993. Part 1: (Prompt reports). Data for August, July 1993, and late data
[PB94-117082] 06 p2628 N94-24993
Photospheric origins of chromospheric and coronal activity
[NASA-CR-195215] 07 p3110 N94-26590
Chaotic dynamics of the solar cycle
[AD-A274315] 07 p3110 N94-26883
Solar-geophysical data number 590, October 1993. Part 1: (Prompt reports). Data for September, August 1993, and late data
[PB94-125903] 07 p3110 N94-27053
Solar-geophysical data number 590, October 1993. Part 2: (Comprehensive reports). Data for April 1993, and miscellaneous
[PB94-125911] 07 p3110 N94-27054

Environmental conditions responsible for solar activity
[AD-A274191] 07 p3111 N94-27099
The effects of magnetic storm phases on F-layer irregularities from auroral to equatorial latitudes
[AD-A275203] 08 p3356 N94-28691
Solar-geophysical data number 591, November 1993. Part 1: Prompt reports. Data for September, October 1993 and late data
[PB94-140548] 08 p3550 N94-29122
Solar-geophysical data number 592, December 1993. Part 1: Prompt reports. Data for October, November 1993 and late data
[PB94-142130] 08 p3550 N94-29123
Solar-geophysical data number 592, December 1993. Part 2: Comprehensive reports. Data for June 1993 and miscellaneous
[PB94-142148] 08 p3550 N94-29124
Solar measurements from the Airglow-Solar Spectrometer Instrument (ASSI) on the San Marco 5 satellite
[NASA-CR-193815] 08 p3551 N94-30948
Proceedings of the International Workshop on Artificial Intelligence Applications in Solar-Terrestrial Physics
[PB94-142064] 09 p3832 N94-31808
Steps toward understanding the solar dynamo
[AD-A277398] 09 p3953 N94-32343
Solar activities at Sandia National Laboratories
[DE94-007737] 09 p3761 N94-32648
Diurnal, seasonal and solar activity variations of F-region parameters
[AD-A278106] 09 p3776 N94-33285
Large-scale velocity fields and small-scale magnetic fields during the maximum of solar cycle 22
[AD-A278378] 10 p4165 N94-33743
Solar-geophysical data number 593, January 1994. Part 1: (Prompt reports). Data for December, November 1993, and late data
[PB94-151578] 10 p4165 N94-34163
Solar-geophysical data number 593, January 1994. Part 2: (Comprehensive reports). Data for July 1993 and miscellaneous
[PB94-151586] 10 p4165 N94-34164
Space environment laboratory in review, 1993
[PB94-153004] 10 p4187 N94-34946
United States Air Force Summer Research Program, 1993. Volume 3: Phillips Laboratory
[AD-A278694] 12 p4550 N94-36979

SOLAR ACTIVITY EFFECTS
Radiation considerations for interplanetary missions
01 p0045 N94-11559
Results from a year-long auroral-E measurement campaign
[AD-A265059] 01 p0278 N94-11871
Determining the solar-flare photospheric scale height from SMM gamma-ray measurements
[NASA-CR-194084] 02 p0844 N94-13671
Tests of a simple data merging algorithm for the GONG project 05 p1927 N94-22549
Comparative investigation of high-latitude ionospheric structure and effects near solar maximum
[AD-A273799] 07 p2877 N94-25877
The Sixteenth Symposium on Coordinated Observations of the Ionosphere and the Magnetosphere in the Polar Regions: Program and abstracts
[JTN-94-80601] 07 p2882 N94-27300
Antarctic Record, Vol. 36, No. 2
[REPT-107] 07 p2883 N94-27963
Characteristics of 30-MHz interference noises observed by riometers 07 p2884 N94-27965
Solar-geophysical data number 591, November 1993. Part 1: Prompt reports. Data for September, October 1993 and late data
[PB94-140548] 08 p3550 N94-29122
ULF waves and magnetic field characteristics in the polar cusp observed at Godhavn 08 p3361 N94-29244
Evidence of solar oscillations in Rayleigh-scattered light 09 p3952 N94-31214
Automated maneuver planning using a fuzzy logic algorithm 11 p4203 N94-35610
Solar-Terrestrial Predictions, 4: Proceedings of a workshop. Volume 1: Workshop overview papers; working group reports; User community reports; Regional Warning Center Reports
[PB94-173176] 12 p4471 N94-37780
Solar-Terrestrial Predictions, 4: Proceedings of a workshop. Volume 2: Solar papers; magnetospheric papers
[PB94-173184] 12 p4471 N94-37781

SOLAR AND HELIOSPHERIC OBSERVATORY
U SOHO MISSION

SOLAR ARRAYS
NT SOLAR BLANKETS
Proceedings of the 12th Space Photovoltaic Research and Technology Conference (SPRAT 12)
[NASA-CP-3210] 01 p0048 N94-11380
Results of some initial space qualification testing on triple junction a-Si and CuInSe2 thin film solar cells
01 p0050 N94-11392
The efficiency of photovoltaic cells exposed to pulsed laser light 01 p0050 N94-11395
EOL performance comparison of GaAs/Ge and Si BSF/R solar arrays 01 p0051 N94-11398
A high specific power solar array for low to mid-power spacecraft 01 p0051 N94-11399
Results of thermal vacuum tests for the PASP+ flight modules 01 p0053 N94-11410
Computation of photovoltaic parameters under lunar temperature variation 01 p0053 N94-11411
Workshop on Solar Electric Propulsion
01 p0054 N94-11416
Workshop summary: Receivers for laser power beaming 01 p0054 N94-11419
Property changes induced by the space environment in composite materials on LDEF: Solar array materials passive LDEF experiment A0171 (SAMPLE)
[NASA-CR-192572] 01 p0073 N94-11484
Screening of solar cells
[NASA-TM-106298] 02 p0620 N94-13134
A photovoltaic catenary-tent array for the Martian surface
[NASA-TM-106306] 02 p0621 N94-13194
Solar radiation on Mars: Stationary photovoltaic array
[NASA-TM-106321] 02 p0626 N94-14730
ERS-1: 18 months in orbit 03 p0990 N94-15888
Recent advances in outdoor performance evaluation of PV systems
[DE93-015031] 03 p1091 N94-15994
Arsene GaAs solar array 03 p0894 N94-17174
A power system for a microsatellite
03 p0895 N94-17176
Space systems environmental interaction studies
[AD-A267280] 03 p0897 N94-17240
High voltage conductors in spacecraft
[AD-A267268] 03 p0897 N94-17266
Fabrication of stable large-area thin-film CdTe photovoltaic modules
[DE93-018204] 05 p1845 N94-20095
Self-deploying photovoltaic power system
[NASA-CASE-LEW-15308-1] 05 p1846 N94-20196
The Fifth European Space Mechanisms and Tribology Symposium
[ESA-SP-334] 06 p2355 N94-23985
The Columbus solar array mechanisms
06 p2356 N94-23994
Primary deployment mechanism for the European Polar Platform 06 p2207 N94-23995
The Submillimeter Wave Astronomy Satellite (SWAS) solar array system 06 p2361 N94-24029
Design of a new high-performance pointing controller for the Hubble Space Telescope
[NASA-CR-193891] 06 p2364 N94-24088
Optimal Space Station solar array gimbal angle determination via radial basis function neural networks
[NASA-TM-106482] 06 p2195 N94-24482
Thermal control system for Space Station Freedom photovoltaic power module
[NASA-TM-105650] 06 p2205 N94-24825
Low-cost photovoltaic inverters incorporating application-specific integrated circuits
[DE94-003270] 07 p2856 N94-26463
Charge efficiency of Ni/H2 cells during transfer orbit of Telstar 4 satellites 07 p2862 N94-28117
Battery charge control: Which approach is best?
07 p2863 N94-28124
Selection of the Space Station Freedom (SSF) Flat Collector Circuit (FCC) insulation material
08 p3165 N94-28701
Hypervelocity impact induced arcing and Kapton pyrolization in a plasma environment
[NASA-TM-106528] 08 p3167 N94-28814
Low Earth orbit durability evaluation of protected silicone for advanced refractive photovoltaic concentrator arrays
[NASA-TM-106543] 08 p3172 N94-28999
Hypervelocity impact testing of Space Station Freedom solar cells
[NASA-TM-106509] 08 p3167 N94-29383
The Solar Anomalous and Magnetospheric Particle Explorer (SAMPEX) yo-yo despin and solar array deployment mechanism 08 p3163 N94-29645
Modal analysis of solar panels using boundary integral equations
[NLT-TP-92218-U] 08 p3338 N94-30328
Atomic oxygen erosion considerations for spacecraft materials selection 09 p3593 N94-31022
Impact of LDEF photovoltaic experiment findings upon spacecraft solar array design and development requirements 09 p3594 N94-31026
Solar lunar power 09 p3599 N94-31427
A solar array module fabrication process for HALE solar electric UAVs
[DE94-006212] 09 p3760 N94-32174
Arcing in space structures in low Earth orbit
[NASA-CR-194223] 09 p3694 N94-32478
INSAT-2A and 2B development mechanisms
09 p3603 N94-33293
Space Station Freedom Solar Array tension mechanism development 09 p3604 N94-33300
Lessons learned from selecting and testing spaceflight potentiometers 09 p3607 N94-33318
Implementation of heaters on thermally actuated spacecraft mechanisms 09 p3607 N94-33320
The SAMPIE flight experimental final technical requirements document
[NASA-TM-106224] 10 p4015 N94-34729
Microprocessor control of multiple peak power tracking DC/DC converters for use with solar cell arrays
[NASA-CASE-GSC-13450-2] 11 p4282 N94-35540
Improved performance of degraded solar arrays at non-zero sun incidence angles
[AD-A278905] 11 p4282 N94-35804
Software for continuum modeling of controls-structures interactions 11 p4223 N94-35898
Neural network for positioning Space Station solar arrays
[NASA-TM-106656] 12 p4431 N94-36943

SOLAR ATMOSPHERE
ATLAS-2 and UARS correlative measurement opportunities during Space Shuttle mission on April 8-17, 1993
[NASA-TM-109020] 03 p1105 N94-15480
The solar optical telescope
[NASA-TM-109240] 04 p1621 N94-18850
High resolution studies of the structure of the solar atmosphere
[AD-A273084] 05 p2147 N94-21522
Solar imaging vector magnetograph
[NASA-CR-194729] 05 p1810 N94-21876
Some challenging problems of the structured and dynamical solar atmosphere 06 p2624 N94-22838
Goals of ground-based solar observations
06 p2624 N94-22840
Why put visible solar telescopes in space?
06 p2600 N94-22850
The calculation of theoretical chromospheric models and the interpretation of solar spectra from rockets and spacecraft
[NASA-CR-195083] 06 p2626 N94-23569
The resonance lines of MG2 as diagnostics of the upper solar chromosphere
[NASA-CR-195084] 06 p2627 N94-24300
On the physics of waves in the solar atmosphere: Wave heating and wind acceleration
[NASA-CR-195197] 06 p2628 N94-25264
High resolution studies of sunspots and flux tubes
[NASA-CR-195216] 07 p3111 N94-27321
The structure of solar magnetic fields and their associated electric currents 08 p3544 N94-29723
Theoretical studies of the solar atmosphere and interstellar pickup ions
[NASA-CR-195846] 10 p4166 N94-34716
SPARTAN high resolution solar studies
[NASA-CR-189340] 10 p4166 N94-34944
On the physics of waves in the solar atmosphere: Wave heating and wind acceleration
[NASA-CR-194119] 11 p4375 N94-36395

SOLAR AZIMUTH
U AZIMUTH
U SOLAR POSITION

SOLAR BLANKETS
Self-deploying photovoltaic power system
[NASA-CASE-LEW-15308-1] 05 p1846 N94-20196
Space Station Freedom solar array containment box mechanisms 09 p3603 N94-33292

SOLAR CELLS
Japan's Sunshine Project
[DE93-767980] 01 p0262 N94-10498
Proceedings of the 12th Space Photovoltaic Research and Technology Conference (SPRAT 12)
[NASA-CP-3210] 01 p0048 N94-11380
A detailed study of the photo-injection annealing of thermally diffused InP solar cells
01 p0048 N94-11381
High temperature annealing of minority carrier traps in irradiated MOCVD n(+)p InP solar cell junctions
01 p0048 N94-11382
Radiation effects in heteroepitaxial InP solar cells
01 p0048 N94-11383
Progress in p(+)n InP solar cells fabricated by thermal diffusion 01 p0048 N94-11384
Effects of solar cell environment on contact integrity
01 p0049 N94-11387
Surface passivation of InP solar cells with InAlAs layers 01 p0049 N94-11389
Polyimide based amorphous silicon solar modules
01 p0049 N94-11390

Investigation of the radiation resistance of triple-junction a-Si:H alloy solar cells irradiated with 1.00 MeV protons
01 p0050 N94-11391
Results of some initial space qualification testing on triple junction a-Si and CuInSe2 thin film solar cells
01 p0050 N94-11392
InGaAs concentrator cells for laser power converters and tandem cells 01 p0050 N94-11394
Response of silicon solar cell to pulsed laser illumination 01 p0051 N94-11396
Approaches to solar cell design for pulsed laser power receivers 01 p0051 N94-11397
A high specific power solar array for low to mid-power spacecraft 01 p0051 N94-11399
TAB interconnects for space concentrator solar cell arrays 01 p0051 N94-11400
New experimental techniques for solar cells
01 p0052 N94-11403
Radiation effects in Ga(0.47)In(0.53)As solar cells
01 p0052 N94-11404
Investigation of ZnSe-coated silicon substrates for GaAs solar cells 01 p0052 N94-11405
Heteroepitaxial InP, and ultrathin, directly glassed, GaAs 3-5 solar cells 01 p0052 N94-11406
UV testing of solar cells: Effects of antireflective coating, prior irradiation, and UV source
01 p0053 N94-11408
The UoSAT-5 solar cell experiment: First year in orbit
01 p0053 N94-11409
Results of thermal vacuum tests for the PASP+ flight modules 01 p0053 N94-11410
An overview of the Defence Research Agency photovoltaic programme 01 p0053 N94-11412
NASDA activities in space solar power system research, development and applications 01 p0054 N94-11413
Workshop on Heteroepitaxial InP Solar Cells
01 p0054 N94-11414
Thin film solar cell workshop
01 p0054 N94-11415
Workshop summary: New silicon cells
01 p0054 N94-11417
Multi-band gap and new solar cell options workshop
01 p0054 N94-11418
Measurement and modeling of the stability of hydrogenated amorphous silicon solar cells and films after intense illumination 01 p0263 N94-11638
The 1992 JSEE/JWEA Joint Conference
[DE93-793955] 02 p0700 N94-12822
Photovoltaic Subcontract Program
[DE93-000092] 02 p0700 N94-12868
Photovoltaics: Contract lists, fiscal year 1992
[DE93-000093] 02 p0701 N94-12902
Photovoltaics: Program overview, fiscal year 1992
[DE93-000055] 02 p0701 N94-12914
Screening of solar cells
[NASA-TM-106298] 02 p0620 N94-13134
Low temperature metal-organic chemical vapor deposition growth processes for high efficiency solar cells
[DE92-010562] 02 p0702 N94-13386
The 1.00 MeV proton radiation resistance studies of amorphous silicon-based alloy solar cells
02 p0703 N94-13639
Emitter Wrap-Through solar cell
[DE93-014996] 02 p0703 N94-13886
The Large Area Pulsed Solar Simulator (LAPSS)
[NASA-CR-194507] 02 p0703 N94-13940
Numerical simulation and analysis of electrical and optical properties of Al(x)Ga(1-x)As / GaAs
[ETN-93-94387] 02 p0703 N94-13997
Structural and electronic studies of a-SiGe:H alloys
[DE93-010021] 02 p0809 N94-14085
Continuous roll-to-roll a-Si photovoltaic manufacturing technology
[DE93-010006] 02 p0704 N94-14109
Optimization of transparent and reflecting electrodes for amorphous silicon solar cells
[DE93-010009] 02 p0704 N94-14110
Study of novel conductive paints for solar cell electromagnetic fields
[DE93-015088] 02 p0581 N94-14337
Photovoltaic advanced research and development project: Solar radiation research
[DE92-016430] 02 p0704 N94-14350
Activities of the Basic Sciences Branch
[DE93-010012] 02 p0851 N94-14455
Solar radiation on Mars: Stationary photovoltaic array
[NASA-TM-106321] 02 p0626 N94-14730
Multicrystalline silicon solar cells: Gettering optimization and characterization
[DE93-015001] 02 p0705 N94-14861
Solar absorptance of optical surfaces contaminated with spacecraft material outgassing products
[AD-A267202] 03 p0886 N94-15857
Progress in the concentrator initiative program
[DE93-015006] 03 p1091 N94-15984
Monolithic, two-terminal InP/Ga(0.47)In(0.53)As tandem solar cells
[DE93-014037] 03 p1093 N94-16824
Lattice-mismatched In(0.40)Al(0.60)As window layers for indium phosphide solar cells
[NASA-TM-106255] 03 p1013 N94-17113
A ten year review of performance of photovoltaic systems
[DE93-015649] 03 p1093 N94-17217
High voltage conductors in spacecraft
[AD-A267268] 03 p0897 N94-17266
Development of large-area monolithically integrated silicon-film photovoltaic modules
[DE93-010037] 04 p1464 N94-17731
Simplified processing for 23 percent-efficient silicon concentrator solar cells
[DE93-015018] 04 p1464 N94-17787
Photovoltaic concentrator initiative: Concentrator cell development
[DE93-018505] 04 p1466 N94-18335
High-efficiency silicon concentrator cell commercialization
[DE93-018491] 04 p1467 N94-18409
Gallium arsenide-based ternary compounds and multi-band-gap solar cell research
[DE93-010049] 04 p1467 N94-18483
Research on stable, high-efficiency amorphous silicon multijunction modules
[DE93-010046] 04 p1467 N94-18518
Polycrystalline thin-film cadmium telluride solar cells fabricated by electrodeposition
[DE93-018201] 04 p1468 N94-18944
Silicon concentrator solar cell research
[DE93-018489] 04 p1468 N94-19015
Defect behavior of polycrystalline solar cell silicon
[DE93-018490] 04 p1468 N94-19016
A Sandia Technology Bulletin: Testing technology, July 1993
[DE93-040197] 04 p1633 N94-19537
Examination of charge carriers dynamics in silicon and silicon solar cells with photoinduced laser beam deflection
[ETN-93-95060] 04 p1470 N94-19654
Amorphous silicon batch process cost analysis
[DE93-018203] 04 p1470 N94-19760
High efficiency epitaxial optical reflector solar cells
[DE93-017115] 05 p1845 N94-19805
Development of high-efficiency CdTe solar cells
[DE93-018206] 05 p1845 N94-19925
Development of a numerical simulation model for a-Si:H solar cells and application to the analysis of experimentally obtained spectral characteristics
[ETN-93-95061] 05 p1846 N94-20151
Advanced processing technology for high-efficiency thin-film CuInSe2 solar cells
[DE93-010045] 05 p1847 N94-21614
Fundamental studies of defect generation in amorphous silicon alloys grown by remote plasma-enhanced chemical-vapor deposition
[DE93-017083] 05 p2029 N94-21615
Research on polycrystalline thin-film submodules based on CuInSe2 materials
[DE93-018223] 05 p2029 N94-21617
Stable, high-efficiency amorphous-silicon solar cells with low hydrogen content
[DE93-018214] 05 p1848 N94-21826
Thin-film CdTe and CuInSe2 photovoltaic technologies
[DE93-018217] 05 p1848 N94-21827
Annual Report, Materials Science Branch, FY 1992
[DE94-000204] 05 p1849 N94-22015
Surveys on specific patterns of facility intallation of photovoltaic power generating technologies for international cooperation
[DE94-714901] 05 p1850 N94-22092
Research on stable, high-efficiency amorphous silicon multijunction modules
[DE93-018220] 05 p1850 N94-22257
Polycrystalline thin film materials and devices
[DE93-018213] 06 p2389 N94-22862
Feasibility study on a CO2 global recycling system using natural energy
[DE94-714889] 06 p2397 N94-23026
Research on polycrystalline thin-film CuInGaSe2 solar cells
[DE94-000203] 06 p2560 N94-23205
Amorphous silicon PVMaT, phase 2A
[DE93-018221] 06 p2390 N94-23295
Novel two-stage selenization methods for fabrication of thin-film CIS cells and submodules
[DE94-000220] 06 p2390 N94-23296
Transparent conducting thin films for spacecraft applications
[NASA-TM-106466] 06 p2218 N94-23370
JOVE NASA-FIT program: Microgravity and aeronomy projects
[NASA-CR-195121] 06 p2631 N94-24493
Thin film cadmium telluride photovoltaic cells
[DE94-000201] 06 p2395 N94-24509
Results of the 1993 NASA/JPL balloon flight solar cell calibration program
[NASA-CR-195158] 06 p2395 N94-24563
Electrical properties of p-type GaInP2
[AD-A273771] 07 p3051 N94-25856
The state of the art of thin-film photovoltaics
[DE94-000224] 07 p2855 N94-26115
Recombination and metastability in amorphous silicon and silicon germanium alloys
[DE94-000237] 07 p2736 N94-26481
Simplified high-efficiency silicon cell processing
[DE94-002683] 07 p2857 N94-26617
A direct current rectification scheme for microwave space power conversion using traveling wave electron acceleration 07 p2687 N94-27371
Research on high-efficiency, large-area, CuInSe2 based thin-film modules
[DE94-000259] 07 p3067 N94-27609
Continuous roll-to-roll a-Si photovoltaic manufacturing technology
[DE94-000260] 07 p2859 N94-27610
High-efficiency, thin-film solar cells
[DE94-000250] 07 p2860 N94-27625
Charge efficiency of Ni/H2 cells during transfer orbit of Telstar 4 satellites 07 p2862 N94-28117
Advanced development of PV encapsulents
[DE94-000219] 08 p3336 N94-28500
Silicon-Film (tm) photovoltaic manufacturing technology
[DE94-000258] 08 p3336 N94-28501
Hypervelocity impact testing of Space Station Freedom solar cells
[NASA-TM-106509] 08 p3167 N94-29383
Fiber optical solar simulator 08 p3341 N94-30486
Photovoltaic performance and reliability workshop
[DE94-000236] 08 p3339 N94-30601
PV Cz silicon manufacturing technology improvements
[DE94-000248] 08 p3339 N94-30603
Thin EFG octagons
[DE94-000257] 08 p3339 N94-30605
Crystalline-silicon solar cell development sponsored by the US Department of Energy
[DE94-003783] 08 p3340 N94-30609
NREL Photovoltaic Program FY 1993 bibliography
[DE94-000272] 08 p3340 N94-30820
Impact of LDEF photovoltaic experiment findings upon spacecraft solar array design and development requirements 09 p3594 N94-31028
Role of polycrystallinity in CdTe and CuInSe2 photovoltaic cells
[DE94-000293] 09 p3758 N94-31236
Automated solar cell assembly teamed process research
[DE94-000295] 09 p3759 N94-31279
Solar lunar power 09 p3599 N94-31427
In-situ characterization of growth and interfaces in a-Si:H devices
[DE94-000291] 09 p3760 N94-31812
Research on the stability, electronic properties, and structure of a-Si:H and its alloys
[DE94-000292] 09 p3899 N94-31813
Silicon-Film(tm) photovoltaic manufacturing technology
[DE94-000202] 09 p3760 N94-32143
A solar array module fabrication process for HALE solar electric UAVs
[DE94-006212] 09 p3760 N94-32174
A scanning defect mapping system for semiconductor characterization 09 p3885 N94-32446
Arcing in space structures in low Earth orbit
[NASA-CR-194223] 09 p3694 N94-32478
Research on stable, high-efficiency amorphous silicon multijunction modules
[DE94-000298] 09 p3695 N94-32680
Development of a computer model for polycrystalline thin-film CuInSe2 and CdTe solar cells
[DE94-006853] 09 p3762 N94-32763
Thin EFG octagons
[DE94-006855] 09 p3905 N94-32764
Large-area, triple-junction a-Si alloy production scale-up
[DE94-006856] 09 p3762 N94-32765
Combined contamination and space environmental effects on solar cells and thermal control surfaces
[NASA-TM-106592] 09 p3617 N94-33022
Space Station Freedom solar array containment box mechanisms 09 p3603 N94-33292
Space Station Freedom Solar Array tension mechanism development 09 p3604 N94-33300
High efficiency InP solar cells from low toxicity tertiarybutylphosphine
[NASA-TM-106598] 10 p4039 N94-33611
NREL preprints for the 23rd IEEE Photovoltaic Specialists Conference
[DE93-010027] 10 p4078 N94-33724

Status of photovoltaic concentrator modules and systems
[DE94-009281] 10 p4079 N94-34070
The SAMPIE flight experimental final technical requirements document
[NASA-TM-106224] 10 p4015 N94-34729
InP solar cell with windcw layer
[NASA-CASE-LEW-15606-1] 11 p4281 N94-35230
Microprocessor control of multiple peak power tracking DC/DC converters for use with solar cell arrays
[NASA-CASE-GSC-13450-2] 11 p4282 N94-35540
Development of novel II-VI solar cells
[PB94-159415] 11 p4282 N94-35739
Improved performance of degraded solar arrays at non-zero sun incidence angles
[AD-A278905] 11 p4282 N94-35804
Progress on the emitter wrap-through silicon solar cell
[DE94-010382] 12 p4462 N94-37189
Investigation of polycrystalline thin-film CuInSe2 solar cells based on ZnSe windows
[DE94-006936] 12 p4462 N94-37381
1993 JSES (Japan Solar Energy Society)/JWEA (Japa n Wind Energy Association) Joint Conference and 1993 Japan-Korea Joint Conference on Solar Energy
[DE94-767725] 12 p4462 N94-37418

SOLAR COLLECTORS
Department of Energy solar process heat program: FY 1991 solar process heat prefeasibility studies activity
[DE93-010010] 01 p0262 N94-10258
Renewable energy sources 1991, part 2
[DE93-605634] 01 p0263 N94-11506
The 1992 JSEE/JWEA Joint Conference
[DE93-793955] 02 p0700 N94-12822
High-flux testing of heat pipes for point-focus solar collector systems
[DE93-011581] 02 p0628 N94-12884
Reflective coatings for solar applications
[DE93-010026] 02 p0702 N94-13381
Field of solar collectors: Effect of shadowing on the optimal field design
[ITN-93-85197] 02 p0702 N94-13570
Colorado State University program for developing, testing, evaluating, and optimizing solar heating and cooling systems
[DE93-016018] 02 p0705 N94-14504
Progress in the concentrator initiative program
[DE93-015006] 03 p1091 N94-15984
Revisiting the BCS, a measurement system for characterizing the optics of solar collectors
[DE93-015030] 03 p1091 N94-15993
Recent advances in outdoor performance evaluation of PV systems
[DE93-015031] 03 p1091 N94-15994
Proposed guidelines for reporting performance of a solar dish/Stirling electric generation system
[DE93-016493] 03 p1092 N94-16112
High heat flux engineering in solar energy applications
[DE93-016500] 03 p1093 N94-16954
Overview of the solar dynamic ground test demonstration program
[NASA-TM-106296] 03 p0928 N94-17256
Development of a selective volumetric receiver for central receiver systems: Investigation of parameters and exergetic evaluation
[DLR-FB-93-05] 04 p1465 N94-18089
First on-sun test of NaK pool-boiler solar receiver
[DE93-015003] 04 p1466 N94-18208
Photovoltaic concentrator initiative: Concentrator cell development
[DE93-018505] 04 p1466 N94-18335
High-efficiency silicon concentrator cell commercialization
[DE93-018491] 04 p1467 N94-18409
Testing and evaluation of large-area heliostats for solar thermal applications
[DE93-018509] 04 p1467 N94-18520
Tehachapi solar thermal system
[DE93-018443] 04 p1468 N94-19014
Bench-scale screening tests for a boiling sodium-potassium alloy solar receiver
[DE93-018512] 04 p1469 N94-19040
The CAESAR project: Experimental and modeling investigations of methane reforming in a catalytically enhanced solar absorption receiver on a parabolic dish
[DE93-040203] 04 p1469 N94-19109
Fluid absorption solar energy receiver
[NASA-CR-194688] 05 p1846 N94-20229
Preliminary study concerning development of petroleum-substitution energy integration technology
[DE94-714902] 06 p2264 N94-23027
The hexagonal compound parabolic concentrator design and construction
[DLR-MITT-93-03] 06 p2396 N94-25464
The pressure loaded volumetric ceramic receiver 500 kW version design and construction
[DLR-MITT-93-02] 06 p2396 N94-25479
Solar energy in Israel: Utilization and research
07 p2853 N94-26051
Solar energy utilization in the USSR
07 p2853 N94-26052
The PLVCR 500 and HCPC, tests and results
[DLR-MITT-93-04] 07 p2858 N94-26813
Solar collector manufacturing activity, 1992
[DE94-003401] 07 p2859 N94-27048
Isothermal corrosion testing of steels in molten nitrate salts
[DE94-004695] 07 p2742 N94-27755
Quality and efficiency of solar collectors in Sweden
[PB94-137486] 08 p3337 N94-28909
Low Earth orbit durability evaluation of protected silicone for advanced refractive photovoltaic concentrator arrays
[NASA-TM-106543] 08 p3172 N94-28999
Performance of the Southern California Edison Company Stirling dish
[DE94-004676] 08 p3337 N94-29018
Crystalline-silicon solar cell development sponsored by the US Department of Energy
[DE94-003783] 08 p3340 N94-30609
Databases and demands for solar heating materials
[PB94-137494] 09 p3758 N94-31070
Solar energy in China
[PB94-137502] 09 p3758 N94-31071
Concentration system performance degradation in the aftermath of Mount Pinatubo
[DE94-001879] 09 p3764 N94-31602
Operational experience and evaluation of a dual-element stretched-membrane heliostat
[DE94-008827] 09 p3763 N94-32965
Status of photovoltaic concentrator modules and systems
[DE94-009281] 10 p4079 N94-34070
Detail design of a 10.4-m stretched-membrane dish
[DE94-009462] 10 p4079 N94-34167
1993 JSES (Japan Solar Energy Society)/JWEA (Japa n Wind Energy Association) Joint Conference and 1993 Japan-Korea Joint Conference on Solar Energy
[DE94-767725] 12 p4462 N94-37418

SOLAR CONVECTION (ASTRONOMY)
On the physics of waves in the solar atmosphere: Wave heating and wind acceleration
[NASA-CR-195197] 06 p2628 N94-25264
Observation of impulsive acoustic events and the excitation of solar oscillations
[AD-A274159] 07 p3111 N94-27096

SOLAR CONVERTERS
U SOLAR GENERATORS

SOLAR COOLING
Colorado State University program for developing, testing, evaluating, and optimizing solar heating and cooling systems
[DE93-016018] 02 p0705 N94-14504
Absorption technology for solar and waste heat utilization 07 p2854 N94-26053

SOLAR CORONA
NT CORONAL HOLES
NT CORONAL LOOPS
Why convective heat transport in the solar nebula was inefficient 01 p0458 N94-12143
Are cosmic rays effective for ionization of the solar nebula? 01 p0472 N94-12220
Basic research in solar physics
[NASA-CR-193632] 02 p0844 N94-13234
Evolution of the interplanetary magnetic field
[DE93-012631] 02 p0836 N94-13262
Measurements of the spatial structure and directivity of 100 KeV photon sources in solar flares using PVO and ISEE-3 spacecraft
[NASA-CR-194080] 02 p0845 N94-14492
The grazing incidence detectors for the SOHO coronal diagnostic spectrometer 03 p0905 N94-15063
The Solar Flare Myth in solar-terrestrial physics
[DE93-016487] 03 p1299 N94-16895
High resolution studies of the structure of the solar atmosphere
[AD-A273084] 05 p2147 N94-21522
Determination of coronal magnetic fields from vector magnetograms
[NASA-CR-194744] 05 p2147 N94-21877
Highlights of Yohkoh results 05 p2001 N94-22632
X ray jets in the solar corona: Observations with Yohkoh Soft X Ray Telescope 05 p2004 N94-22655
Large-scale structure of the solar plasma corona: An analysis of Yohkoh SXT images
05 p2004 N94-22657
MHD relaxation in magnetic loops
05 p2004 N94-22658
Scientific Requirements for Future Solar-Physics Space Missions
[ESA-SP-1157] 06 p2623 N94-22837
Keys to understanding the corona
06 p2624 N94-22839
Prospects for future solar-wind missions
06 p2624 N94-22841
The next Japanese solar satellite
06 p2625 N94-22846
Solar physics and the Coronas project
06 p2625 N94-22847
Requirements for future solar-physics missions with x ray instrumentation 06 p2625 N94-22849
Coronal abundances and their variation
[NASA-CR-194811] 06 p2626 N94-23276
Model development for Ulysses and SOHO
[NASA-CR-193884] 06 p2627 N94-24484
Photospheric origins of chromospheric and coronal activity
[NASA-CR-195215] 07 p3110 N94-26590
Coronal heating via nanoflares
[DE94-000773] 07 p3110 N94-26696
Remote sensing of inner heliospheric plasmas
[AD-A275021] 08 p3550 N94-29132
Correlative analysis of hard and soft x ray observations of solar flares
[NASA-CR-189329] 08 p3551 N94-29453
Coronal abundances and their variation
[NASA-CR-195767] 08 p3551 N94-29858
Working group 1: Coronal streamers
[DE94-009313] 10 p4165 N94-34091
A study of physical mechanisms for filament eruption and coronal mass ejection via numerical simulation
[NASA-CR-196087] 12 p4549 N94-36469
United States Air Force Summer Research Program, 1993. Volume 3: Phillips Laboratory
[AD-A278694] 12 p4550 N94-36979

SOLAR CORPUSCULAR RADIATION
NT SOLAR ELECTRONS
NT SOLAR NEUTRINOS
NT SOLAR NEUTRONS
NT SOLAR PROTONS
Solar flares and magnetospheric particles: Investigations based upon the ONR-602 and ONR-604 experiments
[AD-A269495] 04 p1629 N94-18705
A long-term change of the AR/KR/XE fractionation in the solar corpuscular radiation 05 p2136 N94-20875
Comparison of single event upset rates for microelectronic memory devices during interplanetary solar particle events 05 p1754 N94-21085
Mean elemental composition and He-3 enrichments in solar energetic particles 05 p2006 N94-22670

SOLAR COSMIC RAYS
Measurements of cosmogenic nuclides in lunar rock 64455 01 p0437 N94-12033
The SCR Ne-21 and Ar-38 in lunar rock 68815: The solar proton energy spectrum over the past 2 MYR
03 p1248 N94-16177
JPRS report: Science and technology. Central Eurasia: Space
[JPRS-USP-94-001] 11 p4201 N94-35518

SOLAR CYCLES
NT SUNSPOT CYCLE
Radiation considerations for interplanetary missions
01 p0045 N94-11559
Comments on possible causes of recent global warming
[DE93-010501] 01 p0272 N94-12592
A correlative comparison of geomagnetic storms and auroral substorms using geomagnetic indeces
[AD-A268081] 03 p1102 N94-17512
Solar magnetic cycle
[NASA-CR-195202] 06 p2628 N94-25275
Chaotic dynamics of the solar cycle
[AD-A274315] 07 p3110 N94-26883
Experimental investigation of possible geomagnetic feedback from energetic (0.1 to 16 keV) terrestrial O(+) ions in the magnetotail current sheet
[PAPER-93JA01991] 08 p3507 N94-30128
Large-scale velocity fields and small-scale magnetic fields during the maximum of solar cycle 22
[AD-A278378] 10 p4165 N94-33743
ATLAS solar pointing operations
11 p4201 N94-35626
Global changes of radiation situation at heights less than 1000 km
[DE94-610504] 11 p4290 N94-35780

SOLAR DISK
U SUN

SOLAR DYNAMIC POWER SYSTEMS
Solar dynamic power system development for Space Station Freedom
[NASA-RP-1310] 02 p0548 N94-12807
Futurepath 1 --- power systems
[NASA-TM-109431] 03 p0925 N94-15503
Proposed guidelines for reporting performance of a solar dish/Stirling electric generation system
[DE93-016493] 03 p1092 N94-16112
Overview of the solar dynamic ground test demonstration program
[NASA-TM-106296] 03 p0928 N94-17256

Performance mapping of the STM4-120 kinematic Stirling engine using a statistical design of experiments method
[DE93-015132] 04 p1464 N94-17798
Fluid absorption solar energy receiver
[NASA-CR-194688] 05 p1846 N94-20229
Structural evaluation of concepts for a solar energy concentrator for Space Station advanced development program
[NASA-TP-3375] 07 p2695 N94-26609
Performance and durability of high emittance heat receiver surfaces for solar dynamic power systems
[NASA-TM-106549] 08 p3172 N94-28834

SOLAR DYNAMICS
U HELIOSEISMOLOGY

SOLAR ECLIPSES
The 1970 highlights --- NASA programs and research
[NASA-TM-109628] 03 p1302 N94-15415
Total solar eclipse of 3 November 1994
[NASA-RP-1318] 03 p1236 N94-15481
C 141 KAO solar eclipse mission
[NASA-TM-109676] 03 p1298 N94-15522

SOLAR ELECTRIC PROPULSION
Workshop on Solar Electric Propulsion
01 p0054 N94-11416
TROPIX: A solar electric propulsion flight experiment
[NASA-TM-106297] 02 p0534 N94-13028

SOLAR ELECTRONS
Measurements of the spatial structure and directivity of 100 KeV photon sources in solar flares using PVO and ISEE-3 spacecraft
[NASA-CR-194080] 02 p0845 N94-14492
Correlative analysis of hard and soft x ray observations of solar flares
[NASA-CR-189329] 08 p3551 N94-29453
Solar-geophysical data number 594, February 1994. Part 2: (Comprehensive reports). Data for August 1993, and miscellaneous
[PB94-164001] 11 p4374 N94-36009

SOLAR ENERGY
Department of Energy solar process heat program: FY 1991 solar process heat prefeasibility studies activity
[DE93-010010] 01 p0262 N94-10258
Japan's Sunshine Project
[DE93-767980] 01 p0262 N94-10498
Space Solar Power Program
[DE93-011750] 01 p0055 N94-11675
Solar dynamic power system development for Space Station Freedom
[NASA-RP-1310] 02 p0548 N94-12807
Photovoltaic Subcontract Program
[DE93-000092] 02 p0700 N94-12868
Reflective coatings for solar applications
[DE93-010026] 02 p0702 N94-13381
Nimbus-7 Earth radiation budget calibration history. Part 1: The solar channels
[NASA-RP-1316] 02 p0844 N94-13963
Solar radiation on Mars: Stationary photovoltaic array
[NASA-TM-106321] 02 p0626 N94-14730
High heat flux engineering in solar energy applications
[DE93-016500] 03 p1093 N94-16954
Numerical modelling of an active direct nonpotable hot water heating system making use of the energy of solar radiation
[IFTR-38/1991] 03 p1093 N94-17070
Energy from the sun: Evolution of federal support for solar energy
[AD-A267944] 03 p1093 N94-17382
Solar radiation in Saudi Arabia
[AD-A269970] 04 p1493 N94-18781
Effects of the Mount Pinatubo eruption on solar insolation: Four case studies
[DE93-018454] 04 p1475 N94-18817
EIA publications directory, 1992
[DE93-016833] 04 p1617 N94-18983
Investigation on the chemically fixing technique of carbon dioxide utilizing solar energy
[DE94-714886] 05 p1849 N94-22043
Feasibility study on a CO2 global recycling system using natural energy
[DE94-714889] 06 p2397 N94-23026
Preliminary study concerning development of petroleum-substitution energy integration technology
[DE94-714902] 06 p2264 N94-23027
Power generation technology options for a Mars mission
[NASA-TM-106451] 06 p2220 N94-24681
Renewable energy systems in Mexico: Installation of a hybrid system
[DE93-013716] 07 p2853 N94-25946
The First Energy Conference: Israel and the Former USSR
[ISBN-965-229-098-X] 07 p2853 N94-26050
Solar energy in Israel: Utilization and research
07 p2853 N94-26051
Solar energy utilization in the USSR
07 p2853 N94-26052
Absorption technology for solar and waste heat utilization
07 p2854 N94-26053
NEMO 2: New energy systems and technologies
[DE94-702060] 07 p2855 N94-26240
Solar resource-utility load matching assessment: NREL photovoltaic project summary
[DE94-000232] 07 p2856 N94-26480
Cosmic energy equipment 08 p3229 N94-28945
Analysis and modeling of environmental and economic impacts of the solar hydrogen energy system
08 p3348 N94-29901
Interagency advanced power group: Solar working group
[DE94-004953] 08 p3340 N94-30833
Solar resource: Utility load-matching assessment
[DE94-000297] 09 p3758 N94-31264
Solar lunar power 09 p3599 N94-31427
NEMO: Advanced energy systems and technologies
[DE94-721996] 09 p3760 N94-31767
Renewable energy technology development at Sandia National Laboratories
[DE94-007734] 09 p3761 N94-32383
Solar activities at Sandia National Laboratories
[DE94-007737] 09 p3761 N94-32648
Model documentation: Renewable Fuels Module of the National Energy Modeling System
[DE94-009962] 11 p4282 N94-35672
1993 JSES (Japan Solar Energy Society)/JWEA (Japan Wind Energy Association) Joint Conference and 1993 Japan-Korea Joint Conference on Solar Energy
[DE94-767725] 12 p4462 N94-37418

SOLAR ENERGY ABSORBERS
Solar absorptance of optical surfaces contaminated with spacecraft material outgassing products
[AD-A267202] 03 p0886 N94-15857

SOLAR ENERGY CONVERSION
NT PHOTOTHERMAL CONVERSION
NT PHOTOVOLTAIC CONVERSION
The 1992 JSEE/JWEA Joint Conference
[DE93-793955] 02 p0700 N94-12822
Field of solar collectors: Effect of shadowing on the optimal field design
[ITN-93-85197] 02 p0702 N94-13570
Colorado State University program for developing, testing, evaluating, and optimizing solar heating and cooling systems
[DE93-016018] 02 p0705 N94-14504
Space Station thermal storage/refrigeration system research and development
[NASA-CR-193841] 03 p0879 N94-15191
Proposed guidelines for reporting performance of a solar dish/Stirling electric generation system
[DE93-016493] 03 p1092 N94-16112
High heat flux engineering in solar energy applications
[DE93-016500] 03 p1093 N94-16954
Numerical modelling of an active direct nonpotable hot water heating system making use of the energy of solar radiation
[IFTR-38/1991] 03 p1093 N94-17070
Energy from the sun: Evolution of federal support for solar energy
[AD-A267944] 03 p1093 N94-17382
Pulse radiolytic studies of electron transfer processes and applications to solar photochemistry
[DE93-018715] 04 p1464 N94-17781
S/EV 1992: Solar and Electric Vehicles. Volume 1: Proceedings
[DE93-015762] 04 p1445 N94-18307
Research on stable, high-efficiency amorphous silicon multijunction modules
[DE93-010046] 04 p1467 N94-18518
Silicon concentrator solar cell research
[DE93-018489] 04 p1468 N94-19015
Development of high-efficiency CdTe solar cells
[DE93-018206] 05 p1845 N94-19925
Fluid absorption solar energy receiver
[NASA-CR-194688] 05 p1846 N94-20229
Proceedings of the 1993 DOE/NREL Hydrogen Program Review
[DE93-018207] 05 p1847 N94-21616
Solar energy in Israel: Utilization and research
07 p2853 N94-26051
Solar energy utilization in the USSR
07 p2853 N94-26052
Performance of the Southern California Edison Company Stirling dish
[DE94-004676] 08 p3337 N94-29018
Solar energy in China
[PB94-137502] 09 p3758 N94-31071
Proceedings of the Seventeenth DOE Solar Photochemistry Research Conference
[DE94-005552] 09 p3759 N94-31648
NEMO: Advanced energy systems and technologies
[DE94-721996] 09 p3760 N94-31767
1993 JSES (Japan Solar Energy Society)/JWEA (Japan Wind Energy Association) Joint Conference and 1993 Japan-Korea Joint Conference on Solar Energy
[DE94-767725] 12 p4462 N94-37418

SOLAR FLARES
Proton transport methods for satellite shield modeling
[DE93-013602] 01 p0042 N94-10520
SMM x ray polychromator
[NASA-CR-193282] 01 p0483 N94-11048
Results from a year-long auroral-E measurement campaign
[AD-A265059] 01 p0278 N94-11871
Disturbance Impact Assessment System (DIAS), version 2.0. System design document
[AD-A265251] 01 p0138 N94-11883
Using solar flare track densities to determine the origin of interplanetary dust particles 01 p0429 N94-12078
Data analysis tasks: BATSE
[NASA-CR-192598] 01 p0483 N94-12427
Determining the solar-flare photospheric scale height from SMM gamma-ray measurements
[NASA-CR-194084] 02 p0844 N94-13671
Hard x ray/microwave spectroscopy of solar flares
[NASA-CR-194399] 02 p0844 N94-13958
Measurements of the spatial structure and directivity of 100 KeV photon sources in solar flares using PVO and ISEE-3 spacecraft
[NASA-CR-194080] 02 p0845 N94-14492
Solar-geophysical data number 584, April 1993. Part 1: (Prompt reports). Data for March, February 1993, and late data
[PB93-198323] 02 p0845 N94-14560
Comparative study of x ray and microwave emissions during solar flares
[NASA-CR-194532] 02 p0845 N94-14577
The Solar Flare Myth in solar-terrestrial physics
[DE93-016487] 03 p1299 N94-16895
Solar vector magnetic field research
[AD-A267367] 03 p1299 N94-17004
FNAS/solar flare energetics
[NASA-CR-193574] 03 p1299 N94-17089
Solar flares and magnetospheric particles: Investigations based upon the ONR-602 and ONR-604 experiments
[AD-A269495] 04 p1629 N94-18705
The solar optical telescope
[NASA-TM-109240] 04 p1621 N94-18850
EGRET Mission and Data Analysis
[MPE-PREPRINT-223] 04 p1622 N94-19462
Detection of a long-duration solar gamma-ray flare on Jun. 11, 1991 with EGRET on Compton-GRO
04 p1623 N94-19463
Comparison of single event upset rates for microelectronic memory devices during interplanetary solar particle events 05 p1754 N94-21085
Berne (Switzerland) solar observations: Data for April 1991 - August 1992
[REPT-59] 05 p2147 N94-21150
Development, refinement, and testing of a short term solar flare prediction algorithm
[NASA-CR-194726] 05 p2147 N94-21815
Development, refinement, and testing of a short term solar flare prediction algorithm
[NASA-CR-194727] 05 p2147 N94-21832
Solar imaging vector magnetograph
[NASA-CR-194729] 05 p1810 N94-21876
Highlights of Yohkoh results 05 p2001 N94-22632
Preliminary results of observations of solar flares with Nobeyama Radioheliograph 05 p2001 N94-22633
Radiation from solar flares 05 p2001 N94-22634
Energy release at Alfvenic fronts in solar flares
05 p2003 N94-22652
Non-equilibrium ionization in an M class solar flare
05 p2004 N94-22653
Numerical simulation of magnetic reconnection associated with emerging flux in the solar atmosphere
05 p2004 N94-22654
Yohkoh Gamma ray Spectral Observations (YGSO)
05 p2004 N94-22656
Large-scale structure of the solar plasma corona: An analysis of Yohkoh SXT images
05 p2004 N94-22657
MHD relaxation in magnetic loops
05 p2004 N94-22658
Current loop coalescence studied by 3-D electromagnetic particle code 05 p2005 N94-22660
Formation of fast magnetosonic shock waves during two current loops collision in solar flare
05 p2005 N94-22662
Acceleration of solar-flare particles as viewed from their chemical composition 05 p2006 N94-22672
Some challenging problems of the structured and dynamical solar atmosphere 06 p2624 N94-22838
The next Japanese solar satellite
06 p2625 N94-22846
Excitation of XUV radiation in solar flares
[NASA-CR-193703] 06 p2627 N94-24094

Magnetic shielding of interplanetary spacecraft against solar flare radiation
[NASA-CR-195539] 06 p2204 N94-24334
Solar-geophysical data number 587, July 1993. Part 1: (Prompt reports). Data for June, May 1993, and late data
[PB93-232874] 06 p2628 N94-24989
Solar-geophysical data number 587, July 1993. Part 2: (Comprehensive reports). Data for January 1993, and miscellaneous
[PB93-232882] 06 p2628 N94-24990
Solar-geophysical data number 588, August 1993. Part 1: (Prompt reports). Data for July, June 1993, and late data
[PB94-109089] 06 p2628 N94-24991
Solar-geophysical data number 588, August 1993. Part 2: (Comprehensive reports). Data for February 1993, and miscellaneous
[PB94-109105] 06 p2628 N94-24992
Solar-geophysical data number 589, September 1993. Part 1: (Prompt reports). Data for August, July 1993, and late data
[PB94-117082] 06 p2628 N94-24993
Solar-geophysical data number 589, September 1993. Part 2: (Comprehensive reports). Data for March 1993, and miscellaneous
[PB94-117405] 06 p2628 N94-24994
Solar flares and magnetospheric particles: Investigations based upon the ONR-602 and ONR-604 experiments
[AD-A273639] 06 p2628 N94-25031
Coronal heating via nanoflares
[DE94-000773] 07 p3110 N94-26696
Region 5395 of March 1989 — solar activity, geomagnetic disturbances, and terrestrial effects
[PB94-120714] 07 p3110 N94-26755
Solar-geophysical data number 590, October 1993. Part 1: (Prompt reports). Data for September, August 1993, and late data
[PB94-125903] 07 p3110 N94-27053
Acceleration of electrons and ions by strong lower-hybrid turbulence in solar flares
[NASA-TM-109723] 07 p3111 N94-27953
Solar-geophysical data number 591, November 1993. Part 2: (Comprehensive reports). Data for May 1993 and miscellaneous
[PB94-134830] 07 p3111 N94-28360
Identification of an unexpected space radiation hazard
[AD-A275170] 08 p3552 N94-29046
Remote sensing of inner heliospheric plasmas
[AD-A275021] 08 p3550 N94-29132
Correlative analysis of hard and soft x ray observations of solar flares
[NASA-CR-189329] 08 p3551 N94-29453
Collective acceleration in solar flares
[DE94-006288] 09 p3953 N94-31632
Steps toward understanding the solar dynamo
[AD-A277398] 09 p3953 N94-32343
BATSE data analysis
[NASA-CR-193959] 09 p3927 N94-32942
Spatial correlation of ionospheric variability
[AD-A278105] 09 p3776 N94-33041
Solar-geophysical data number 593, January 1994. Part 1: (Prompt reports). Data for December, November 1993, and late data
[PB94-151578] 10 p4165 N94-34163
Solar-geophysical data number 593, January 1994. Part 2: (Comprehensive reports). Data for July 1993 and miscellaneous
[PB94-151586] 10 p4165 N94-34164
A search for energetic ion directivity in large solar flares
[NASA-CR-196036] 11 p4374 N94-35993
Solar-geophysical data number 594, February 1994. Part 1: (Prompt reports). Data for December 1993, January 1994, and late data
[PB94-163995] 11 p4375 N94-36020
A study of physical mechanisms for filament eruption and coronal mass ejection via numerical simulation
[NASA-CR-196087] 12 p4549 N94-36469

SOLAR FLUX
The evaluation of radiative process in the atmosphere-ground system by Monte Carlo method 01 p0205 N94-11980
Present status of SAGE
[DE93-014350] 02 p0781 N94-13205
Revisiting the BCS, a measurement system for characterizing the optics of solar collectors
[DE93-015030] 03 p1091 N94-15993
The Sudbury Neutrino Observatory and the solar neutrino problem
[DE93-018528] 04 p1629 N94-19260
Berne (Switzerland) solar observations: Data for April 1991 - August 1992
[REPT-59] 05 p2147 N94-21150
Requirements for the early atmosphere of Mars from nitrogen isotope ratios 05 p2144 N94-21669
Mars and the early Sun 05 p2146 N94-21683
Comparisons of downwelling radiation to model predictions based on groundbased measurements during FIRE 1991 05 p1876 N94-22320
An analysis of Solar Mesospheric Explorer temperatures for the upper stratosphere and mesosphere
[NASA-CR-194861] 06 p2626 N94-23626
Numerical simulation of Ulysses nutation 06 p2207 N94-24017
Kamiokande results on solar neutrinos and a supernova search
[ICRR-REPT-294-93-6] 06 p2627 N94-24961
Solar neutrinos: Real-time experiments
[ICRR-REPT-293-93-5] 06 p2627 N94-24962
The status of the solar neutrino problem
[DE94-003934] 07 p3111 N94-27742
The effects of magnetic storm phases on F-layer irregularities from auroral to equatorial latitudes
[AD-A275203] 08 p3356 N94-28891
Production of fullerenes with concentrated solar flux
[DE94-000266] 08 p3514 N94-29801
Radiative flux calculations at UV and visible wavelengths
[DE94-004278] 08 p3350 N94-30613
Recent results from SAGE
[DE94-006229] 08 p3551 N94-30845
An evaluation of RAMS radiation schemes by field measurements
[DE94-008053] 09 p3767 N94-32750
Collective plasma corrections to the solar opacity
[PB94-170511] 11 p4375 N94-36210

SOLAR FLUX DENSITY
Accurate modeling of F-region electron densities
[NASA-CR-195781] 08 p3364 N94-30014

SOLAR FURNACES
Production of fullerenes with concentrated solar flux
[DE94-000266] 08 p3514 N94-29801
CATARACT: Computer code for improving power calculations at NREL's high-flux solar furnace
[DE94-000267] 10 p4078 N94-33727
Minipilot solar system: Design/operation of system and results of non-solar testing at MRI
[PB94-152238] 10 p4079 N94-34165

SOLAR GENERATORS
NT SOLAR CELLS
NT SOLAR DYNAMIC POWER SYSTEMS
Japan's Sunshine Project
[DE93-767980] 01 p0262 N94-10498
Field of solar collectors: Effect of shadowing on the optimal field design
[ITN-93-85197] 02 p0702 N94-13570
High heat flux engineering in solar energy applications
[DE93-016500] 03 p1093 N94-16954
First on-sun test of NaK pool-boiler solar receiver
[DE93-015003] 04 p1466 N94-18208
Investigation on the chemically fixing technique of carbon dioxide utilizing solar energy
[DE94-714886] 05 p1849 N94-22043
Surveys on specific patterns of facility intallation of photovoltaic power generating technologies for international cooperation
[DE94-714901] 05 p1850 N94-22092
Handbook of photovoltaic power generating design for introduction
[DE94-725199] 07 p2858 N94-26913
Metal hydrides in hydrogen energy systems
[VTT-TIED-1407] 09 p3759 N94-31655
Optimal planning of residential photovoltaic systems under various rate structure
[DE94-757272] 09 p3762 N94-32919

SOLAR GRANULATION
Photospheric origins of chromospheric and coronal activity
[NASA-CR-195215] 07 p3110 N94-26590

SOLAR GRAVITATION
New tests of the equivalence principle using non-metric couplings of electromagnetism and gravitation 01 p0413 N94-11821

SOLAR HEATING
Department of Energy solar process heat program: FY 1991 solar process heat prefeasibility studies activity
[DE93-010010] 01 p0262 N94-10258
Colorado State University program for developing, testing, evaluating, and optimizing solar heating and cooling systems
[DE93-016018] 02 p0705 N94-14504
Heliocentric zoning of the asteroid belt by aluminum-26 heating 03 p1241 N94-16205
Tehachapi solar thermal system
[DE93-018443] 04 p1468 N94-19014
Solar energy utilization in the USSR 07 p2853 N94-26052
Martian atmospheric radiation budget 07 p3107 N94-27887
Databases and demands for solar heating materials
[PB94-137494] 09 p3758 N94-31070
Solar energy in China
[PB94-137502] 09 p3758 N94-31071

SOLAR INSTRUMENTS
NT SPECTROHELIOGRAPHS
Continued development of an ultra-narrow bandpass filter for solar research
[NASA-CR-194169] 01 p0381 N94-10735
NASA Marshall Space Flight Center solar observatory report, January - June 1993
[NASA-TM-108417] 01 p0423 N94-10866
Vacuum ultraviolet instrumentation for solar irradiance and thermospheric airglow
[NASA-CR-194525] 02 p0652 N94-14684
Solar vector magnetic field research
[AD-A267367] 03 p1299 N94-17004
Concept report: Experimental vector magnetograph (EXVM) operational configuration balloon flight assembly
[NASA-CR-194702] 05 p1638 N94-21776
Solar imaging vector magnetograph
[NASA-CR-194729] 05 p1810 N94-21876
Polarization analysis of a balloon-borne solar magnetograph
[NASA-CR-193908] 06 p2345 N94-24852
NASA Marshall Space Flight Center Solar Observatory report, July - October 1993
[NASA-TM-108448] 08 p3160 N94-29470
Solar neutrino experiments: An update
[DE94-006061] 08 p3551 N94-30884
Evidence of solar oscillations in Rayleigh-scattered light 09 p3952 N94-31214
ATLAS solar pointing operations 11 p4201 N94-35626

SOLAR INTERIOR
Possible dust contamination of the early solar system 03 p1244 N94-16352

SOLAR LASERS
U SOLAR-PUMPED LASERS

SOLAR MAGNETIC FIELD
Basic research in solar physics
[NASA-CR-193632] 02 p0844 N94-13234
Solar-geophysical data number 584, April 1993. Part 1: (Prompt reports). Data for March, February 1993, and late data
[PB93-198323] 02 p0845 N94-14560
Comparative study of x ray and microwave emissions during solar flares
[NASA-CR-194532] 02 p0845 N94-14577
Solar vector magnetic field research
[AD-A267367] 03 p1299 N94-17004
Concept report: Experimental vector magnetograph (EXVM) operational configuration balloon flight assembly
[NASA-CR-194702] 05 p1638 N94-21776
Development, refinement, and testing of a short term solar flare prediction algorithm
[NASA-CR-194726] 05 p2147 N94-21815
Solar imaging vector magnetograph
[NASA-CR-194729] 05 p1810 N94-21876
Determination of coronal magnetic fields from vector magnetograms
[NASA-CR-194744] 05 p2147 N94-21877
Solar full-disk magnetic field image receiving system and observation software 05 p2079 N94-22552
Solar-geophysical data number 584, April 1993. Part 1: (Prompt reports). Data for February, March, 1993, and late data
[PB93-198323] 06 p2626 N94-23738
Solar-geophysical data number 587, July 1993. Part 1: (Prompt reports). Data for June, May 1993, and late data
[PB93-232874] 06 p2628 N94-24989
Solar-geophysical data number 588, August 1993. Part 1: (Prompt reports). Data for July, June 1993, and late data
[PB94-109089] 06 p2628 N94-24991
Solar-geophysical data number 589, September 1993. Part 1: (Prompt reports). Data for August, July 1993, and late data
[PB94-117082] 06 p2628 N94-24993
Solar magnetic cycle
[NASA-CR-195202] 06 p2628 N94-25275
Solar-geophysical data number 590, October 1993. Part 1: (Prompt reports). Data for September, August 1993, and late data
[PB94-125903] 07 p3110 N94-27053
Environmental conditions responsible for solar activity
[AD-A274191] 07 p3111 N94-27099
Direct evidence of the interplanetary magnetic field effect on the cosmic-ray shadow by the sun
[ICRR-296-93-8] 07 p3116 N94-27607
Solar-geophysical data number 591, November 1993. Part 1: Prompt reports. Data for September, October 1993 and late data
[PB94-140548] 08 p3550 N94-29122
The structure of solar magnetic fields and their associated electric currents 08 p3544 N94-29723

Solar measurements from the Airglow-Solar Spectrometer Instrument (ASSI) on the San Marco 5 satellite
[NASA-CR-193815] 08 p3551 N94-30948
Theoretical studies of magnetohydrodynamic equilibria and dynamics of a solar coronal loop
09 p3953 N94-31792
Steps toward understanding the solar dynamo
[AD-A277398] 09 p3953 N94-32343
Large-scale velocity fields and small-scale magnetic fields during the maximum of solar cycle 22
[AD-A278378] 10 p4165 N94-33743
Solar-geophysical data number 593, January 1994. Part 1: (Prompt reports). Data for December, November 1993, and late data
[PB94-151578] 10 p4165 N94-34163
Observations of loops and prominences
[NASA-CR-195942] 10 p4166 N94-34298
Solar-geophysical data number 594, February 1994. Part 2: (Comprehensive reports). Data for August 1993, and miscellaneous
[PB94-164001] 11 p4374 N94-36009
Solar-geophysical data number 594, February 1994. Part 1: (Prompt reports). Data for December 1993, January 1994, and late data
[PB94-163995] 11 p4375 N94-36020

SOLAR MAXIMUM MISSION
Ultraviolet Spectrometer and Polarimeter (UVSP) catalog of observations. Volume 3: Experiments 63058-99771 (February 1988 - November 1989)
[NASA-CR-4529] 02 p0844 N94-13146
Determining the solar-flare photospheric scale height from SMM gamma-ray measurements
[NASA-CR-194084] 02 p0844 N94-13671
Ultraviolet spectrometer and polarimeter (UVSP) catalog of observations. Volume 1: Experiments 1-30719, February 1980 - April 1985
[NASA-CR-4529-VOL-1] 03 p1298 N94-15023
Ultraviolet spectrometer and polarimeter (UVSP) catalog of observations. Volume 2: Experiments 30720-63057, April 1985 - February 1988
[NASA-CR-4529-VOL-2] 03 p1298 N94-15024
The 1980 highlights
[NASA-TM-109672] 03 p1303 N94-15509
Coronal abundances and their variation
[NASA-CR-194811] 06 p2626 N94-23276

SOLAR NEBULA
U SOLAR CORONA

SOLAR NEUTRINOS
Solar neutrinos with three flavor mixings
[DE93-011006] 01 p0483 N94-11619
Present status of SAGE
[DE93-014350] 02 p0781 N94-13205
Neutrino mass and mixing: Summary of the neutrino sessions
[DE93-014342] 03 p1183 N94-16801
Neutral-current detection in the Sudbury Neutrino Observatory
[DE93-014481] 03 p1185 N94-16951
Neutrino mass
[DE93-018467] 04 p1567 N94-18269
The Sudbury Neutrino Observatory and the solar neutrino problem
[DE93-018528] 04 p1629 N94-19260
Recent results from the Soviet-American Gallium Experiment
[DE94-000677] 06 p2626 N94-23020
Accelerator-based neutrino oscillation searches
[DE94-000818] 06 p2626 N94-23515
Solar neutrinos: Real-time experiments
[ICRR-REPT-293-93-5] 06 p2627 N94-24962
The status of the solar neutrino problem
[DE94-003934] 07 p3111 N94-27742
Recent results from SAGE
[DE94-006229] 08 p3551 N94-30845
Solar neutrino experiments: An update
[DE94-006061] 08 p3551 N94-30884
Nuclear physics and astrophysics
[DE94-007168] 09 p3939 N94-33147
Solar neutrino oscillations
[DE94-007265] 10 p4165 N94-33687

SOLAR NEUTRONS
Cosmic and solar gamma ray and neutron experiments
[NASA-CR-193359] 02 p0849 N94-13965

SOLAR NOISE
U SOLAR RADIO EMISSION

SOLAR OBSERVATORIES
NT OSO
NASA Marshall Space Flight Center solar observatory report, January - June 1993
[NASA-TM-108417] 01 p0423 N94-10866
Orbiting solar operations
[NASA-TM-109583] 03 p0884 N94-15267
Solar Electro-Optical Network (SEON) upgrade/replacement program. Phase 1: Qualification operational test and evaluation plan
[AD-A266364] 03 p1237 N94-17225
Tests of a simple data merging algorithm for the GONG project 05 p1927 N94-22549
Highlights of Yohkoh results 05 p2001 N94-22632
Yohkoh Gamma ray Spectral Observations (YGSO)
05 p2004 N94-22656
NASA Marshall Space Flight Center Solar Observatory report, July - October 1993
[NASA-TM-108448] 08 p3160 N94-29470

SOLAR OPTICAL TELESCOPE
The solar optical telescope
[NASA-TM-109240] 04 p1621 N94-18850
Width modulator mechanism for spectrometer entrance slits 06 p2357 N94-24002

SOLAR ORBITS
Using solar flare track densities to determine the origin of interplanetary dust particles 01 p0429 N94-12078
Ulysses: A solar odyssey
[NASA-TM-109820] 10 p4010 N94-33574
Catalog of Helios 90 deg photometer events
[PL-TR-94-2040] 11 p4375 N94-36264

SOLAR OSCILLATIONS
Interactions among convection, magnetic fields and p-mode oscillations in the sun
[NASA-CR-194477] 02 p0845 N94-14479
Generation of artificial helioseismic time-series
[NASA-CR-194612] 03 p1299 N94-15968
The Sudbury Neutrino Observatory and the solar neutrino problem
[DE93-018528] 04 p1629 N94-19260
Tests of a simple data merging algorithm for the GONG project 05 p1927 N94-22549
Some challenging problems of the structured and dynamical solar atmosphere 06 p2624 N94-22838
Observation of impulsive acoustic events and the excitation of solar oscillations
[AD-A274159] 07 p3111 N94-27096
Evidence of solar oscillations in Rayleigh-scattered light 09 p3952 N94-31214

SOLAR PHYSICS
Solar neutrinos with three flavor mixings
[DE93-011006] 01 p0483 N94-11619
Present status of SAGE
[DE93-014350] 02 p0781 N94-13205
Basic research in solar physics
[NASA-CR-193632] 02 p0844 N94-13234
Solar-geophysical data number 584, April 1993. Part 1: (Prompt reports). Data for March, February 1993, and late data
[PB93-198323] 02 p0845 N94-14560
Solar-geophysical data number 584, April 1993. Part 2: (Comprehensive reports). Data for October 1992 and miscellaneous
[PB93-198331] 02 p0845 N94-14561
Unmasking the Sun
[NASA-TM-109595] 03 p1298 N94-15287
Possible dust contamination of the early solar system
03 p1244 N94-16352
Origins of solar activity. First year report, AASERT grant
[AD-A268848] 04 p1629 N94-18222
The solar optical telescope
[NASA-TM-109240] 04 p1621 N94-18850
The Sudbury Neutrino Observatory and the solar neutrino problem
[DE93-018528] 04 p1629 N94-19260
Development, refinement, and testing of a short term solar flare prediction algorithm
[NASA-CR-194727] 05 p2147 N94-21832
Determination of coronal magnetic fields from vector magnetograms
[NASA-CR-194744] 05 p2147 N94-21877
Scientific Requirements for Future Solar-Physics Space Missions
[ESA-SP-1157] 06 p2623 N94-22837
Some challenging problems of the structured and dynamical solar atmosphere 06 p2624 N94-22838
Keys to understanding the corona
06 p2624 N94-22839
Goals of ground-based solar observations
06 p2624 N94-22840
Prospects for future ground-based solar observations
06 p2624 N94-22842
Prospects for improved instrumentation on future solar space missions 06 p2624 N94-22843
Solar physics within ESA's planning
06 p2624 N94-22844
Solar physics within NASA's planning
06 p2625 N94-22845
The next Japanese solar satellite
06 p2625 N94-22846
Solar physics and the Coronas project
06 p2625 N94-22847
Prospects for very-high-resolution solar physics with the Simuris inteferometric mission 06 p2625 N94-22848
Requirements for future solar-physics missions with x ray instrumentation 06 p2625 N94-22849
Why put visible solar telescopes in space?
06 p2600 N94-22850
Requirements for future solar-physics missions that include UV instrumentation 06 p2625 N94-22851
The calculation of theoretical chromospheric models and the interpretation of solar spectra from rockets and spacecraft
[NASA-CR-195083] 06 p2626 N94-23569
Solar-geophysical data number 584, April 1993. Part 1: (Prompt reports). Data for February, March, 1993, and late data
[PB93-198323] 06 p2626 N94-23738
Solar-geophysical data number 584, April 1993. Part 2: (Comprehensive reports). Data for October 1992, and miscellaneous
[PB93-198331] 06 p2627 N94-23739
Model development for Ulysses and SOHO
[NASA-CR-193884] 06 p2627 N94-24484
Solar-geophysical data number 587, July 1993. Part 1: (Prompt reports). Data for June, May 1993, and late data
[PB93-232874] 06 p2628 N94-24989
Solar-geophysical data number 587, July 1993. Part 2: (Comprehensive reports). Data for January 1993, and miscellaneous
[PB93-232882] 06 p2628 N94-24990
Solar-geophysical data number 588, August 1993. Part 1: (Prompt reports). Data for July, June 1993, and late data
[PB94-109089] 06 p2628 N94-24991
Solar-geophysical data number 588, August 1993. Part 2: (Comprehensive reports). Data for February 1993, and miscellaneous
[PB94-109105] 06 p2628 N94-24992
Solar-geophysical data number 589, September 1993. Part 1: (Prompt reports). Data for August, July 1993, and late data
[PB94-117082] 06 p2628 N94-24993
Solar-geophysical data number 589, September 1993. Part 2: (Comprehensive reports). Data for March 1993, and miscellaneous
[PB94-117405] 06 p2628 N94-24994
On the physics of waves in the solar atmosphere: Wave heating and wind acceleration
[NASA-CR-195197] 06 p2628 N94-25264
Solar-geophysical data number 590, October 1993. Part 1: (Prompt reports). Data for September, August 1993, and late data
[PB94-125903] 07 p3110 N94-27053
Solar-geophysical data number 590, October 1993. Part 2: (Comprehensive reports). Data for April 1993, and miscellaneous
[PB94-125911] 07 p3110 N94-27054
Observation of impulsive acoustic events and the excitation of solar oscillations
[AD-A274159] 07 p3111 N94-27096
Environmental conditions responsible for solar activity
[AD-A274191] 07 p3111 N94-27099
High resolution studies of sunspots and flux tubes
[NASA-CR-195216] 07 p3111 N94-27321
Solar-geophysical data number 591, November 1993. Part 1: Prompt reports. Data for September, October 1993 and late data
[PB94-140548] 08 p3550 N94-29122
Solar-geophysical data number 592, December 1993. Part 1: Prompt reports. Data for October, November 1993 and late data
[PB94-142130] 08 p3550 N94-29123
Solar-geophysical data number 592, December 1993. Part 2: Comprehensive reports. Data for June 1993 and miscellaneous
[PB94-142148] 08 p3550 N94-29124
Solar physics and terrestrial effects. A curriculum guide for teachers, grade 7-12
[PB94-142247] 09 p3953 N94-31595
Theoretical studies of magnetohydrodynamic equilibria and dynamics of a solar coronal loop
09 p3953 N94-31792
Proceedings of the International Workshop on Artificial Intelligence Applications in Solar-Terrestrial Physics
[PB94-142064] 09 p3832 N94-31808
High sensitivity and resolution decimetric spectroscope: Preliminary analysis of solar bursts
[INPE-5537-TDI/525] 09 p3954 N94-33080
Large-scale velocity fields and small-scale magnetic fields during the maximum of solar cycle 22
[AD-A278378] 10 p4165 N94-33743
Working group 1: Coronal streamers
[DE94-009313] 10 p4165 N94-34091
Solar-geophysical data number 593, January 1994. Part 1: (Prompt reports). Data for December, November 1993, and late data
[PB94-151578] 10 p4165 N94-34163

Solar-geophysical data number 593, January 1994. Part 2: (Comprehensive reports). Data for July 1993 and miscellaneous
[PB94-151586] 10 p4165 N94-34164
Theoretical studies of the solar atmosphere and interstellar pickup ions
[NASA-CR-195846] 10 p4166 N94-34716
Space environment laboratory in review, 1993
[PB94-153004] 10 p4187 N94-34946
ATLAS solar pointing operations 11 p4201 N94-35626
Solar-geophysical data number 594, February 1994. Part 2: (Comprehensive reports). Data for August 1993, and miscellaneous
[PB94-164001] 11 p4374 N94-36009
Solar-geophysical data number 594, February 1994. Part 1: (Prompt reports). Data for December 1993, January 1994, and late data
[PB94-163995] 11 p4375 N94-36020
Collective plasma corrections to the solar opacity
[PB94-170511] 11 p4375 N94-36210
A study of physical mechanisms for filament eruption and coronal mass ejection via numerical simulation
[NASA-CR-196087] 12 p4549 N94-36469

SOLAR PLANETARY INTERACTIONS
NT SOLAR TERRESTRIAL INTERACTIONS
Magnetic effects in Venus/solar wind interaction
[NASA-CR-194666] 03 p1299 N94-17281
Mars and the early Sun 05 p2146 N94-21683
The Sixteenth Symposium on Coordinated Observations of the Ionosphere and the Magnetosphere in the Polar Regions: Program and abstracts
[JTN-94-80601] 07 p2882 N94-27300
ULF waves and magnetic field characteristics in the polar cusp observed at Godhavn 08 p3361 N94-29244
Plasma waves in the nightside ionosphere of Venus 10 p4164 N94-33431
An investigation of solar wind effects on the evolution of the Martian atmosphere
[NASA-CR-193424] 12 p4549 N94-37012

SOLAR PLASMA (RADIATION)
U SOLAR WIND

SOLAR PONDS (HEAT STORAGE)
Solar energy in Israel: Utilization and research 07 p2853 N94-26051

SOLAR POSITION
Iron oxide bands in the visible and near-infrared reflectance spectra of primitive asteroids 03 p1242 N94-16274
Initial ultraviolet-B intensity data at Lawrence Livermore National Laboratory
[DE94-004279] 07 p2869 N94-27267

SOLAR POWER GENERATION
U SOLAR GENERATORS

SOLAR POWER SATELLITES
Space transportation alternatives for large space programs: The International Space University Summer Session, 1992
[NASA-TM-106271] 01 p0040 N94-10811
Construction and testing of a space ready rectenna
[NASA-CR-193310] 01 p0137 N94-11357
Large space structures and systems in the space station era: A bibliography with indexes (supplement 05)
[NASA-SP-7085(05)] 02 p0543 N94-14411

SOLAR POWER SOURCES
U SOLAR GENERATORS

SOLAR POWERED AIRCRAFT
Regenerative fuel cells for High Altitude Long Endurance Solar Powered Aircraft
[DE93-016991] 04 p1465 N94-17853
Effect of power system technology and mission requirements on high altitude long endurance aircraft
[NASA-CR-194455] 06 p2189 N94-25200
Solar powered multipurpose remotely powered aircraft 07 p2671 N94-25719
A solar array module fabrication process for HALE solar electric UAVs
[DE94-006212] 09 p3760 N94-32174

SOLAR PROBES
NT HELIOS A

SOLAR PROMINENCES
Solar-geophysical data number 589, September 1993. Part 2: (Comprehensive reports). Data for March 1993, and miscellaneous
[PB94-117405] 06 p2628 N94-24994
Solar-geophysical data number 590, October 1993. Part 2: (Comprehensive reports). Data for April 1993, and miscellaneous
[PB94-125911] 07 p3110 N94-27054
Solar-geophysical data number 591, November 1993. Part 2: (Comprehensive reports). Data for May 1993 and miscellaneous
[PB94-134830] 07 p3111 N94-28360
Solar-geophysical data number 593, January 1994. Part 2: (Comprehensive reports). Data for July 1993 and miscellaneous
[PB94-151586] 10 p4165 N94-34164
Observations of loops and prominences
[NASA-CR-195942] 10 p4166 N94-34298
A study of physical mechanisms for filament eruption and coronal mass ejection via numerical simulation
[NASA-CR-196087] 12 p4549 N94-36469

SOLAR PROPULSION
NT SOLAR ELECTRIC PROPULSION
S/EV 1992: Solar and Electric Vehicles. Volume 1: Proceedings
[DE93-015762] 04 p1445 N94-18307
One fantastic ride
[NASA-TM-109828] 10 p4016 N94-33582

SOLAR PROTONS
Proton transport methods for satellite shield modeling
[DE93-013602] 01 p0042 N94-10520
A comparison of solar wind parameters measured by IMP 8, Voyager 1 and Voyager 2
[AD-A266728] 03 p1298 N94-15821
The SCR Ne-21 and Ar-38 in lunar rock 68815: The solar proton energy spectrum over the past 2 MYR 03 p1248 N94-16177
Atmospheric ionization by solar particles detected by nitrate measurement in antarctic snow
[AD-A267583] 03 p1299 N94-17208
Solar proton events from a 180 year depth profile of nitrate concentrations from the central Greenland ice sheet
[AD-A272888] 05 p2147 N94-21196
Acceleration of solar-flare particles as viewed from their chemical composition 05 p2006 N94-22672
Magnetic shielding of interplanetary spacecraft against solar flare radiation
[NASA-CR-195539] 06 p2204 N94-24334
Solar-geophysical data number 591, November 1993. Part 2: (Comprehensive reports). Data for May 1993 and miscellaneous
[PB94-134830] 07 p3111 N94-28360
Solar proton produced neon in shergottite meteorites 11 p4351 N94-35428
Solar-geophysical data number 594, February 1994. Part 2: (Comprehensive reports). Data for August 1993, and miscellaneous
[PB94-164001] 11 p4374 N94-36009

SOLAR RADIATION
NT SOLAR CORPUSCULAR RADIATION
NT SOLAR COSMIC RAYS
NT SOLAR ELECTRONS
NT SOLAR NEUTRINOS
NT SOLAR NEUTRONS
NT SOLAR PROTONS
NT SOLAR RADIO BURSTS
NT SOLAR RADIO EMISSION
NT SOLAR WIND
NT SOLAR X-RAYS
NT SUNLIGHT
Estimating Photosynthetically Available Radiation (PAR) at the Earth's surface from satellite observations 01 p0230 N94-10955
A modeling perspective on cloud radiative forcing
[DE93-012383] 01 p0276 N94-11241
Estimation of solar radiation at the sea surface with geostationary meteorological satellite data 01 p0196 N94-11926
The evaluation of radiative process in the atmosphere-ground system by Monte Carlo method 01 p0205 N94-11980
Oxidation state of the Earth's upper mantle during the last 3800 million years: Implications for the origin of life 01 p0283 N94-12210
Comments on possible causes of recent global warming
[DE93-010501] 01 p0272 N94-12592
Photocatalysis for the treatment of waste water: Applications involving the removal of metals
[DE93-011669] 02 p0561 N94-12841
Basic research in solar physics
[NASA-CR-193632] 02 p0844 N94-13234
Net radiation mapping of mountainous terrain using Landsat-5 thematic mapper imagery and digital terrain data
[ISBN-0-315-57755-X] 02 p0685 N94-13475
Nimbus-7 Earth radiation budget calibration history. Part 1: The solar channels
[NASA-RP-1316] 02 p0844 N94-13963
Photovoltaic advanced research and development project: Solar radiation research
[DE92-016430] 02 p0704 N94-14350
NREL solar radiation resource assessment project: Status and outlook
[DE93-010034] 02 p0704 N94-14422
Vacuum ultraviolet instrumentation for solar irradiance and thermospheric airglow
[NASA-CR-194525] 02 p0652 N94-14684
Absolute Radiometric Measurements in Space: ARMS 03 p0908 N94-15085
Determination of sunshine duration from radiation intensity pyranometric measurements of global and sky radiation
[BER-181] 03 p1105 N94-15302
Analysis of leading edge and trailing edge cover glass samples before and after treatment with advanced satellite contamination removal techniques
[AD-A267055] 03 p0885 N94-15666
Absolute, Extreme-Ultraviolet Solar Spectral Irradiance Monitor (AESSIM)
[AD-A267045] 03 p1299 N94-15836
Dust grain resonant capture: A statistical study 03 p1245 N94-16384
Numerical modelling of an active direct nonpotable hot water heating system making use of the energy of solar radiation
[IFTR-38/1991] 03 p1093 N94-17070
Investigations into the recovery of waste sulfuric acid with concentrated solar radiation
[DLR-FB-93-11] 03 p0952 N94-17594
Pulse radiolytic studies of electron transfer processes and applications to solar photochemistry
[DE93-018715] 04 p1464 N94-17781
Global zones of particle precipitation as observed EXOS-C
[AD-A268758] 04 p1481 N94-18467
Solar radiation in Saudi Arabia
[AD-A269970] 04 p1493 N94-18781
Effects of the Mount Pinatubo eruption on solar insolation: Four case studies
[DE93-018454] 04 p1475 N94-18817
Marine-modified LOWTRAN: The contribution of sun glint
[AD-A269547] 04 p1500 N94-19762
SCR neon and argon in Kapoeta feldspar: Evidence for an active ancient Sun 05 p2106 N94-20712
The simulation of action of some space environment factors on Teflon and on rubber materials 05 p1661 N94-21380
The energy performance of prototype holographic glazings
[DE93-040451] 05 p1809 N94-21545
The young Sun and photochemistry of the primitive Martian atmosphere 05 p2145 N94-21679
Evolution of the Martian atmosphere 05 p2146 N94-21680
Surveys on specific patterns of facility intallation of photovoltaic power generating technologies for international cooperation
[DE94-714901] 05 p1850 N94-22092
The use of ERBE data for climate studies 05 p1860 N94-22286
Flight solar calibrations using the Mirror Attenuator Mosaic (MAM): Low scattering mirror 06 p2384 N94-23602
Solar-geophysical data number 589, September 1993. Part 2: (Comprehensive reports). Data for March 1993, and miscellaneous
[PB94-117405] 06 p2628 N94-24994
The hexagonal compound parabolic concentrator design and construction
[DLR-MITT-93-03] 06 p2396 N94-25464
Seasonal snow of arctic Alaska R4D investigations
[DE93-040082] 07 p2892 N94-25939
Initial ultraviolet-B intensity data at Lawrence Livermore National Laboratory
[DE94-004279] 07 p2869 N94-27267
Solar and airglow measurements aboard the two suborbital flights NASA 36.098 and 36.107
[NASA-CR-195279] 07 p2882 N94-27380
The automated rotating shadowband spectroradiometer
[DE94-001878] 08 p3269 N94-28464
Solar measurements from the Airglow-Solar Spectrometer Instrument (ASSI) on the San Marco 5 satellite
[NASA-CR-193815] 08 p3551 N94-30948
Model of spacecraft atomic oxygen and solar exposure microenvironments 09 p3593 N94-31021
Fluorescence observations of LDEF exposed materials as an indicator of induced material reactions 09 p3593 N94-31025
Laser-induced fluorescence of space-exposed polyurethane 09 p3593 N94-31026
Evidence of solar oscillations in Rayleigh-scattered light 09 p3952 N94-31214
Users manual for SERI QC software assessing the quality of solar radiation data
[DE93-018210] 09 p3953 N94-31491

Recommendations for meteorological data collection during physiological field studies
[AD-A276834] 09 p3901 N94-32153
Steps toward understanding the solar dynamo
[AD-A277398] 09 p3953 N94-32343
Solar-geophysical data number 593, January 1994. Part 2: (Comprehensive reports). Data for July 1993 and miscellaneous
[PB94-151586] 10 p4165 N94-34164
Solar radiation effects on glasses
[NASA-CR-195900] 10 p4029 N94-34232
The modelling of the ocean surface image in optical remote sensing 10 p4078 N94-34369
A statistical inference approach for the retrieval of the atmospheric ozone profile from simulated satellite measurements of solar backscattered ultraviolet radiation 10 p4083 N94-35060
Pseudogoldstone boson decay induced by light and search for the solar axion radiation
[DE94-616907] 11 p4326 N94-36133
Absolute, Extreme Ultraviolet Solar Spectral Irradiance Monitor (AESSIM)
[AD-A278709] 11 p4227 N94-36189

SOLAR RADIATION SHIELDING
Lunar surface operations. Volume 1: Lunar surface emergency shelter
[NASA-CR-195551] 08 p3299 N94-29354

SOLAR RADIO BURSTS
Solar-geophysical data number 584, April 1993. Part 2: (Comprehensive reports). Data for October 1992 and miscellaneous
[PB93-198331] 02 p0845 N94-14561
Solar-geophysical data number 584, April 1993. Part 2: (Comprehensive reports). Data for October 1992, and miscellaneous
[PB93-198331] 06 p2627 N94-23739
Solar-geophysical data number 587, July 1993. Part 2: (Comprehensive reports). Data for January 1993, and miscellaneous
[PB93-232882] 06 p2628 N94-24990
Solar-geophysical data number 588, August 1993. Part 2: (Comprehensive reports). Data for February 1993, and miscellaneous
[PB94-109105] 06 p2628 N94-24992
Solar-geophysical data number 589, September 1993. Part 1: (Prompt reports). Data for August, July 1993, and late data
[PB94-117082] 06 p2628 N94-24993
Solar-geophysical data number 589, September 1993. Part 2: (Comprehensive reports). Data for March 1993, and miscellaneous
[PB94-117405] 06 p2628 N94-24994
Solar-geophysical data number 591, November 1993. Part 2: (Comprehensive reports). Data for May 1993 and miscellaneous
[PB94-134830] 07 p3111 N94-28360
High sensitivity and resolution decimetric spectroscope: Preliminary analysis of solar bursts
[INPE-5537-TDI/525] 09 p3954 N94-33080
Solar-geophysical data number 593, January 1994. Part 2: (Comprehensive reports). Data for July 1993 and miscellaneous
[PB94-151586] 10 p4165 N94-34164
Studies of impulsive solar bursts observed with high spectral resolution in the range of 18 to 23 GHz
[INPE-5538-TDI/526] 10 p4165 N94-34219

SOLAR RADIO EMISSION
NT SOLAR RADIO BURSTS
Solar-geophysical data number 584, April 1993. Part 1: (Prompt reports). Data for March, February 1993, and late data
[PB93-198323] 02 p0845 N94-14560
Oceanic in situ Fraunhofer-line characteristics: Fraunhofer-line underwater experiment (FLUX)
[AD-A270659] 05 p1881 N94-19952
Solar-geophysical data number 584, April 1993. Part 1: (Prompt reports). Data for February, March, 1993, and late data
[PB93-198323] 06 p2626 N94-23738
Solar-geophysical data number 587, July 1993. Part 1: (Prompt reports). Data for June, May 1993, and late data
[PB93-232874] 06 p2628 N94-24989
Solar-geophysical data number 588, August 1993. Part 1: (Prompt reports). Data for July, June 1993, and late data
[PB94-109089] 06 p2628 N94-24991
Solar-geophysical data number 589, September 1993. Part 1: (Prompt reports). Data for August, July 1993, and late data
[PB94-117082] 06 p2628 N94-24993
Region 5395 of March 1989 --- solar activity, geomagnetic disturbances, and terrestrial effects
[PB94-120714] 07 p3110 N94-26755
Solar-geophysical data number 590, October 1993. Part 1: (Prompt reports). Data for September, August 1993, and late data
[PB94-125903] 07 p3110 N94-27053
The Rb 780-nanometer Faraday anomalous dispersion optical filter: Theory and experiment 08 p3250 N94-29659
Solar-geophysical data number 593, January 1994. Part 1: (Prompt reports). Data for December, November 1993, and late data
[PB94-151578] 10 p4165 N94-34163
Solar-geophysical data number 594, February 1994. Part 1: (Prompt reports). Data for December 1993, January 1994, and late data
[PB94-163995] 11 p4375 N94-36020

SOLAR RADIO WAVES
U SOLAR RADIO EMISSION

SOLAR RECEIVERS
U SOLAR COLLECTORS

SOLAR REFLECTORS
NT SOLAR COLLECTORS
Continuous roll-to-roll a-Si photovoltaic manufacturing technology
[DE93-010006] 02 p0704 N94-14109
Development of a selective volumetric receiver for central receiver systems: Investigation of parameters and exergetic evaluation
[DLR-FB-93-05] 04 p1465 N94-18089
High efficiency epitaxial optical reflector solar cells
[DE93-017115] 05 p1845 N94-19805
Mounting of SSM's
[VTT-TIED-1442] 07 p2695 N94-26250
Charge efficiency of Ni/H2 cells during transfer orbit of Telstar 4 satellites 07 p2862 N94-28117
An outdoor exposure testing program for optical materials used in solar thermal electric technologies
[DE94-000265] 08 p3500 N94-29799

SOLAR SEISMOLOGY
U HELIOSEISMOLOGY

SOLAR SELECTIVE COATINGS
U SELECTIVE SURFACES

SOLAR SENSORS
Estimation of the attitude motion of the small satellite ORIZURU
[NAL-TR-1145] 01 p0042 N94-10366
Space systems environmental interaction studies
[AD-A267280] 03 p0897 N94-17240
Multisensor pinhole yawsonde
[AD-A271715] 05 p1808 N94-20930
An Earth albedo model: A mathematical model for the radiant energy input to an orbiting spacecraft due to the diffuse reflectance of solar radiation from the Earth below
[NASA-TM-104596] 06 p2195 N94-24497
Operational support for Upper Atmosphere Research Satellite (UARS) attitude sensors 11 p4204 N94-35617
Spacecraft attitude determination accuracy from mission experience 11 p4204 N94-35618
ATLAS solar pointing operations 11 p4201 N94-35626
Overview of the Miniature Sensor Technology Integration (MSTI) spacecraft attitude control system 11 p4206 N94-35627
A geometric model of a V-slit Sun sensor correcting for spacecraft wobble 11 p4206 N94-35628
Overview of the MSTI 2 on-orbit alignment 11 p4206 N94-35629

SOLAR SIMULATORS
The Large Area Pulsed Solar Simulator (LAPSS)
[NASA-CR-194507] 02 p0703 N94-13940
Solar absorptance of optical surfaces contaminated with spacecraft material outgassing products
[AD-A267202] 03 p0886 N94-15857
Solar simulator for solar dynamic space power system testing
[NASA-TM-106393] 05 p1984 N94-20140
Fiber optical solar simulator 08 p3341 N94-30486

SOLAR SPECTRA
Solar neutrinos with three flavor mixings
[DE93-011006] 01 p0483 N94-11619
Remote sensing x ray fluorescence spectrometry for future lunar exploration missions 01 p0462 N94-12165
Near-infrared spectra of the Martian surface: Reading between the lines 01 p0465 N94-12184
The infrared solar spectrum
[COMMUNICATIONS-SER-B-159] 02 p0844 N94-13502
Vacuum ultraviolet instrumentation for solar irradiance and thermospheric airglow
[NASA-CR-194525] 02 p0652 N94-14684
Tunable ytterbium-doped solid state laser
[AD-D015878] 04 p1440 N94-18747
Berne (Switzerland) solar observations: Data for April 1991 - August 1992
[REPT-59] 05 p2147 N94-21150
The calculation of theoretical chromospheric models and the interpretation of solar spectra from rockets and spacecraft
[NASA-CR-195083] 06 p2626 N94-23569
The resonance lines of MG2 as diagnostics of the upper solar chromosphere
[NASA-CR-195084] 06 p2627 N94-24300
The solar spectral irradiances from x ray to radio wavelengths
[NASA-CR-195203] 06 p2629 N94-25260
Solar and airglow measurements aboard the two suborbital flights NASA 36.098 and 36.107
[NASA-CR-195279] 07 p2882 N94-27380
Fiber optical solar simulator 08 p3341 N94-30486
Solar measurements from the Airglow-Solar Spectrometer Instrument (ASSI) on the San Marco 5 satellite
[NASA-CR-193815] 08 p3551 N94-30948

SOLAR SPECTROMETERS
SMM x ray polychromator
[NASA-CR-193282] 01 p0483 N94-11048
The grazing incidence detectors for the SOHO coronal diagnostic spectrometer 03 p0905 N94-15063
Data processing system for flight spectrometer 03 p0908 N94-15086
Prospects for improved instrumentation on future solar space missions 06 p2624 N94-22843
Prospects for very-high-resolution solar physics with the Simuris inteferometric mission 06 p2625 N94-22848
Ultra-clean high-precision mechanisms for the SUMER EUV spectrometer on SOHO 06 p2356 N94-23999
Periscope mechanism for SWAN instrument 06 p2357 N94-24000
Width modulator mechanism for spectrometer entrance slits 06 p2357 N94-24002
The development of the SOHO SUMER mechanisms 06 p2361 N94-24028
High energy collimating fine grids for HESP program
[NASA-CR-189317] 06 p2209 N94-24767
Solar measurements from the Airglow-Solar Spectrometer Instrument (ASSI) on the San Marco 5 satellite
[NASA-CR-193815] 08 p3551 N94-30948

SOLAR STREAMS
U SOLAR CORPUSCULAR RADIATION

SOLAR SYSTEM
Development of a molecular beam technique to study early solar system silicon reactions 01 p0432 N94-12224
Discovery management workshop
[NASA-TM-108244] 02 p0531 N94-14080
The problem of traveling in outer space: The rocket motor
[NASA-TT-10002] 02 p0552 N94-14463
Do SiC grains in Orgueil differ from those in Murchison? 03 p1242 N94-16260
Chemical and isotopic compositions in acid residues from various meteorites 03 p1243 N94-16291
Tensor-scalar cosmological models and their relaxation toward general relativity
[PB93-220796] 06 p2601 N94-23099
Spiral Survey Expedition: A proposal to organize for the Survey, exploration and eventual colonization of the Milky Way Galaxy 07 p2686 N94-27366
Imaging spectrometry of the Earth and other solar system bodies 08 p3237 N94-29779
Non-equilibrium chemistry of the early solar system
[NASA-CR-195691] 10 p4163 N94-33603
Application of an alkylammonium method for characterization of phyllosilicates in CI chondrites 11 p4351 N94-35432
First observation of a mass independent isotopic fractionation in a condensation reaction 11 p4239 N94-35464
A quick look method of detecting water of hydration in small solar system bodies 11 p4352 N94-35470

SOLAR SYSTEM EVOLUTION
Origins of Solar Systems Workshop: The Origin, Evolution, and Detectability of Short Period Comets
[NASA-CR-194255] 01 p0427 N94-11628
The long-term dynamical behavior of short-period comets 01 p0427 N94-11629
Midplane temperatures in the solar nebula 01 p0448 N94-12088
Chondrule formation by clumpy accretion onto the solar nebula 01 p0448 N94-12089
Initiating solar system formation through stellar shock waves 01 p0448 N94-12090
Studies of the release of radiogenic Xe-129 from Bjurboele: Evidence against simple diffusion models 01 p0430 N94-12125
The giant impact produced a precipitated Moon 01 p0430 N94-12135

Recondensation of chondritic material in the early solar system: Results of thermodynamic simulation
01 p0432 N94-12226
Pioneer-Venus press clip --- Solar System formation and extraterrestrial life
[NASA-TM-109425] 03 p1239 N94-15495
FE-60 and the evolution of eucrites
05 p2083 N94-20768
Variety in planetary systems 05 p2086 N94-20871
Correlated petrographic, electron microprobe, and ion microprobe studies of selected primitive and processed phase assemblages in meteorites
[NASA-CR-194827] 06 p2601 N94-23499
A brief history of the universe
[DE93-616843] 06 p2604 N94-25210
Non-equilibrium chemistry of the early solar system
[NASA-CR-195691] 10 p4163 N94-33603

SOLAR TERRESTRIAL INTERACTIONS
The interplanetary origins and the main-phase development of moderate geomagnetic storms (1978 - 1979)
[INPE-5445-TDI/491] 02 p0835 N94-13174
Solar-geophysical data number 584, April 1993. Part 1: (Prompt reports). Data for March, February 1993, and late data
[PB93-198323] 02 p0845 N94-14560
The Solar Flare Myth in solar-terrestrial physics
[DE93-016487] 03 p1299 N94-16895
FNAS/solar flare energetics
[NASA-CR-193574] 03 p1299 N94-17089
Optimization of satellite coverage in observing cause and effect changes in the ionosphere, magnetosphere, and solar wind
[AD-A267956] 03 p1102 N94-17493
ISTP Global Geospace Science. Energy transfer in geospace
[NASA-TM-109239] 04 p1620 N94-18851
The Wave Experiment Consortium
04 p1328 N94-19623
Solar-terrestrial environmental laboratory
06 p2630 N94-23336
Solar-geophysical data number 584, April 1993. Part 1: (Prompt reports). Data for February, March, 1993, and late data
[PB93-198323] 06 p2626 N94-23738
Scientific study in solar and plasma physics relative to rocket and balloon projects
[NASA-CR-193885] 06 p2627 N94-24461
Solar-geophysical data number 587, July 1993. Part 1: (Prompt reports). Data for June, May 1993, and late data
[PB93-232874] 06 p2628 N94-24989
Solar-geophysical data number 588, August 1993. Part 1: (Prompt reports). Data for July, June 1993, and late data
[PB94-109089] 06 p2628 N94-24991
Region 5395 of March 1989 --- solar activity, geomagnetic disturbances, and terrestrial effects
[PB94-120714] 07 p3110 N94-26755
Solar-geophysical data number 590, October 1993. Part 1: (Prompt reports). Data for September, August 1993, and late data
[PB94-125903] 07 p3110 N94-27053
Solar-geophysical data number 590, October 1993. Part 2: (Comprehensive reports). Data for April 1993, and miscellaneous
[PB94-125911] 07 p3110 N94-27054
Direct evidence of the interplanetary magnetic field effect on the cosmic-ray shadow by the sun
[ICRR-296-93-8] 07 p3116 N94-27607
Solar-geophysical data number 591, November 1993. Part 1: Prompt reports. Data for September, October 1993 and late data
[PB94-140548] 08 p3550 N94-29122
A study of the formation and dynamics of the Earth's plasma sheet using ion composition data
[NASA-CR-195119] 08 p3507 N94-30126
Experimental investigation of possible geomagnetic feedback from energetic (0.1 to 16 keV) terrestrial O(+) ions in the magnetotail current sheet
[PAPER-93JA01991] 08 p3507 N94-30128
Solar physics and terrestrial effects. A curriculum guide for teachers, grade 7-12
[PB94-142247] 09 p3953 N94-31595
Proceedings of the International Workshop on Artificial Intelligence Applications in Solar-Terrestrial Physics
[PB94-142064] 09 p3832 N94-31808
Analysis of data from the plasma composition experiment on the International Sun-Earth Explorer (ISEE 1)
[NASA-CR-189353] 09 p3893 N94-33074
Solar-geophysical data number 593, January 1994. Part 1: (Prompt reports). Data for December, November 1993, and late data
[PB94-151578] 10 p4165 N94-34163
Space environment laboratory in review, 1993
[PB94-153004] 10 p4187 N94-34946
Solar-geophysical data number 594, February 1994. Part 1: (Prompt reports). Data for December 1993, January 1994, and late data
[PB94-163995] 11 p4375 N94-36020
A study of physical mechanisms for filament eruption and coronal mass ejection via numerical simulation
[NASA-CR-196087] 12 p4549 N94-36469
Analysis of plasma measurements for the Geotail mission
[NASA-CR-196274] 12 p4470 N94-37470
Solar-Terrestrial Predictions, 4: Proceedings of aworkshop. Volume 3: Geomagnetic papers; ionospheric papers
[PB94-173192] 12 p4470 N94-37530
Random and periodic substorms and their origins in the solar wind
[DE94-011693] 12 p4549 N94-37668
Solar-Terrestrial Predictions, 4: Proceedings of a workshop. Volume 1: Workshop overview papers; working group reports; User community reports; Regional Warning Center Reports
[PB94-173176] 12 p4471 N94-37780
Solar-Terrestrial Predictions, 4: Proceedings of a workshop. Volume 2: Solar papers; magnetospheric papers
[PB94-173184] 12 p4471 N94-37781

SOLAR THERMAL ELECTRIC POWER PLANTS
Solar energy in Israel: Utilization and research
07 p2853 N94-26051
Solar energy utilization in the USSR
07 p2853 N94-26052
An outdoor exposure testing program for optical materials used in solar thermal electric technologies
[DE94-000265] 08 p3500 N94-29799
Renewable energy technology development at Sandia National Laboratories
[DE94-007734] 09 p3761 N94-32383

SOLAR WIND
Solar wind channels for MeV particles
[DE93-012648] 01 p0482 N94-10741
SMM x ray polychromator
[NASA-CR-193282] 01 p0483 N94-11048
ICE/ISEE plasma wave data analysis
[NASA-CR-194375] 02 p0796 N94-13081
The interplanetary origins and the main-phase development of moderate geomagnetic storms (1978 - 1979)
[INPE-5445-TDI/491] 02 p0835 N94-13174
Basic research in solar physics
[NASA-CR-193632] 02 p0844 N94-13234
Evolution of the interplanetary magnetic field
[DE93-012631] 02 p0836 N94-13262
A comparison of solar wind parameters measured by IMP 8, Voyager 1 and Voyager 2
[AD-A266728] 03 p1298 N94-15821
Helium-3 inventory of lunar samples: A potential future energy resource for mankind? 03 p1295 N94-16428
Solar noble gases revealed by closed system stepped etching of a metal separate from Fayetteville
03 p0954 N94-16432
Nitrogen and light noble gases in Parsa enstatite chondrite 03 p1246 N94-16435
Magnetic effects in Venus/solar wind interaction
[NASA-CR-194666] 03 p1299 N94-17281
ISTP Global Geospace Science. Energy transfer in geospace
[NASA-TM-109239] 04 p1620 N94-18851
Radial evolution of the solar wind turbulence with application to charged particle transport
[NASA-CR-194081] 04 p1629 N94-19427
Modeling of the coupled magnetospheric and neutral wind dynamos
[NASA-CR-194728] 05 p1856 N94-20537
A long-term change of the AR/KR/XE fractionation in the solar corpuscular radiation 05 p2136 N94-20875
High resolution studies of the structure of the solar atmosphere
[AD-A273084] 05 p2147 N94-21522
Implications of Viking dayside auroral measurements
[ISBN-0-315-83273-8] 05 p1861 N94-22575
Laboratory relations between the solar wind dynamic pressure and the magnetospheric structures of the Earth and comets 05 p2003 N94-22647
Laboratory structure of the heliopause
05 p2003 N94-22648
Compressible MHD turbulence in the interplanetary medium 05 p2003 N94-22650
Tangential stress due to Kelvin-Helmholtz instability at the magnetospheric boundary 05 p2003 N94-22651
Solar wind-magnetosphere interaction as simulated by a 3D, EM particle code 05 p2007 N94-22674
Scientific Requirements for Future Solar-Physics Space Missions
[ESA-SP-1157] 06 p2623 N94-22837
Some challenging problems of the structured and dynamical solar atmosphere 06 p2624 N94-22838
Prospects for future solar-wind missions
06 p2624 N94-22841
Evolution of large-scale plasma structures in comets: Kinematics and physics
[NASA-CR-194777] 06 p2601 N94-23251
Scientific study in solar and plasma physics relative to rocket and balloon projects
[NASA-CR-193885] 06 p2627 N94-24461
Solar-geophysical data number 589, September 1993. Part 2: (Comprehensive reports). Data for March 1993, and miscellaneous
[PB94-117405] 06 p2628 N94-24994
On the physics of waves in the solar atmosphere: Wave heating and wind acceleration
[NASA-CR-195197] 06 p2628 N94-25264
High latitude cusp signature observations for southward IMF B sub Z
[AD-A273801] 06 p2406 N94-25536
Identification of an unexpected space radiation hazard
[AD-A275170] 08 p3552 N94-29046
Remote sensing of inner heliospheric plasmas
[AD-A275021] 08 p3550 N94-29132
Proceedings of the NIPR Symposium on Upper Atmosphere Physics, no. 6
[JTN-94-80593] 08 p3359 N94-29233
Signatures of dayside solar wind/magnetosphere/ionosphere coupling as revealed by the pace HF radars and associated experiments
08 p3359 N94-29236
A theory of current generator in the magnetosphere-ionosphere coupling
08 p3360 N94-29240
A study of the formation and dynamics of the Earth's plasma sheet using ion composition data
[NASA-CR-195119] 08 p3507 N94-30126
Analysis of data from the plasma composition experiment on the International Sun-Earth Explorer (ISEE 1)
[NASA-CR-189353] 09 p3893 N94-33074
Development of a preliminary solar wind transport magnetosheath forecast model
[AD-A278560] 10 p4165 N94-33785
Working group 1: Coronal streamers
[DE94-009313] 10 p4165 N94-34091
Utility of interplanetary scintillation maps in forecasting geomagnetic activity: A study based on single-station data from Cambridge, United Kingdom
[PB94-156775] 10 p4087 N94-34600
Theoretical studies of the solar atmosphere and interstellar pickup ions
[NASA-CR-195846] 10 p4166 N94-34716
Flank solar wind interaction
[NASA-CR-189327] 10 p4166 N94-35225
An investigation of solar wind effects on the evolution of the Martian atmosphere
[NASA-CR-193424] 12 p4549 N94-37012
Analysis of plasma measurements for the Geotail mission
[NASA-CR-196274] 12 p4470 N94-37470
Random and periodic substorms and their origins in the solar wind
[DE94-011693] 12 p4549 N94-37668

SOLAR WIND VELOCITY
A comparison of solar wind parameters measured by IMP 8, Voyager 1 and Voyager 2
[AD-A266728] 03 p1298 N94-15821

SOLAR X-RAYS
Remote sensing x ray fluorescence spectrometry for future lunar exploration missions
01 p0462 N94-12165
Measurements of the spatial structure and directivity of 100 KeV photon sources in solar flares using PVO and ISEE-3 spacecraft
[NASA-CR-194080] 02 p0845 N94-14492
Solar-geophysical data number 584, April 1993. Part 2: (Comprehensive reports). Data for October 1992 and miscellaneous
[PB93-198331] 02 p0845 N94-14561
FNAS/solar flare energetics
[NASA-CR-193574] 03 p1299 N94-17089
Solar-geophysical data number 584, April 1993. Part 2: (Comprehensive reports). Data for October 1992, and miscellaneous
[PB93-198331] 06 p2627 N94-23739
Solar-geophysical data number 589, September 1993. Part 2: (Comprehensive reports). Data for March 1993, and miscellaneous
[PB94-117405] 06 p2628 N94-24994
Region 5395 of March 1989 --- solar activity, geomagnetic disturbances, and terrestrial effects
[PB94-120714] 07 p3110 N94-26755
Solar-geophysical data number 590, October 1993. Part 2: (Comprehensive reports). Data for April 1993, and miscellaneous
[PB94-125911] 07 p3110 N94-27054

Solar-geophysical data number 591, November 1993. Part 2: (Comprehensive reports). Data for May 1993 and miscellaneous
[PB94-134830] 07 p3111 N94-28360
Solar-geophysical data number 592, December 1993. Part 2: Comprehensive reports. Data for June 1993 and miscellaneous
[PB94-142148] 08 p3550 N94-29124
Coronal abundances and their variation
[NASA-CR-195767] 08 p3551 N94-29858
Solar-geophysical data number 593, January 1994. Part 2: (Comprehensive reports). Data for July 1993 and miscellaneous
[PB94-151586] 10 p4165 N94-34164

SOLAR-PUMPED LASERS
Direct solar pumping of semiconductor lasers: A feasibility study
[NASA-CR-193760] 04 p1440 N94-18834

SOLDERED JOINTS
ENSAFE fireset flex circuit analysis
[DE93-013106] 01 p0144 N94-11478
Microstructural influences on the mechanical properties of solder
[DE93-015044] 02 p0573 N94-14474
Reliability analysis of Surface Mount Technology (SMT)
[AD-A267598] 03 p1055 N94-17194
Microstructurally based thermomechanical fatigue lifetime model of solder joints for electronic applications
[DE93-016508] 04 p1452 N94-17995
Embrittlement of surface mount solder joints by hot solder-dipped, gold-plated leads
[DE93-017659] 04 p1358 N94-18003
Wetting behavior of alternative solder alloys
[DE93-016730] 04 p1359 N94-18127
Reducing inadvertent alloying of metal/ceramic brazes
[DE93-009842] 04 p1373 N94-19308
Finite element mesh generation and analysis of solder joints for fatigue life predictions
[AD-A271329] 05 p1829 N94-19937
Process characterization and control of hand-soldered printed wiring assemblies
[DE93-041290] 05 p1763 N94-21652
Laser soldering of Sn plated brass integrator assembly housings
[DE94-001149] 06 p2270 N94-23790
Surface tension of tin and its alloys with particular reference to solders
[PB94-138302] 08 p3204 N94-29119
Microstructural development and mechanical behavior of eutectic bismuth-tin and eutectic indium-tin in response to high temperature deformation
[DE94-005202] 08 p3210 N94-30710

SOLDERING
Advanced soldering processes
[DE93-009856] 01 p0129 N94-11606
Solderability of surface mount devices
[AD-A265751] 02 p0620 N94-13040
Development of alternatives to lead-bearing solders
[DE93-016509] 04 p1357 N94-17862
Automatic soldering for watch circuit components 04 p1428 N94-18037
Solderability perservative coatings: Electroless tin versus organic azoles
[DE93-017634] 04 p1370 N94-18477
Solder technology in the manufacturing of electronic products
[DE93-018842] 05 p1699 N94-19960
Process characterization and control of hand-soldered printed wiring assemblies
[DE93-041290] 05 p1763 N94-21652
Laser soldering of Sn plated brass integrator assembly housings
[DE94-001149] 06 p2270 N94-23790
Experimental determination of the CU-IN-PB ternary phase diagram
[DE94-003765] 07 p2735 N94-26349
Joining of fibre reinforced metal matrix composite materials
[PB94-132453] 07 p2712 N94-28376
Intermetallic growth at the interface between copper and bismuth-tin solder
[AD-A275716] 08 p3202 N94-28643
Logistics for the implementation of lead-free solders on electronic assemblies
[DE94-004800] 08 p3206 N94-29936
Automated solar cell assembly teamed process research
[DE94-000295] 09 p3759 N94-31279
The 18th annual electronics manufacturing seminar
[AD-A276038] 09 p3687 N94-31281
Aging effects on the microstructure, surface characteristics and wettability of Cu pretinned with Sn-Pb solders
[DE94-007033] 09 p3641 N94-31638
Automated fiber pigtailing technology
[DE94-007072] 09 p3695 N94-32688
Space flight printed wiring board measling investigation
[NASA-TM-104602] 09 p3732 N94-33101
A comparison of paper and computer procedures in a Shuttle flight environment 10 p4101 N94-33634
SpaceHab 1 maintenance experiment 10 p4015 N94-33669
Manufacturing feasibility of several lead-free solders for electronic assembly
[DE94-007732] 11 p4258 N94-35564
Capillary flow solderability test for printed wiring boards
[DE94-010321] 11 p4259 N94-36094
Integrated environmentally compatible soldering technologies
[DE94-013456] 12 p4464 N94-37071

SOLDERS
Advanced soldering processes
[DE93-009856] 01 p0129 N94-11606
Development of alternatives to lead-bearing solders
[DE93-016509] 04 p1357 N94-17862
Wetting behavior of alternative solder alloys
[DE93-016730] 04 p1359 N94-18127
Solderability perservative coatings: Electroless tin versus organic azoles
[DE93-017634] 04 p1370 N94-18477
Finite element mesh generation and analysis of solder joints for fatigue life predictions
[AD-A271329] 05 p1829 N94-19937
Solder technology in the manufacturing of electronic products
[DE93-018842] 05 p1699 N94-19960
Laser soldering of Sn plated brass integrator assembly housings
[DE94-001149] 06 p2270 N94-23790
Experimental determination of the CU-IN-PB ternary phase diagram
[DE94-003765] 07 p2735 N94-26349
Research into the microstructure and mechanical behavior of eutectic Bi-Sn and In-Sn
[DE94-004558] 07 p2741 N94-27619
Intermetallic growth at the interface between copper and bismuth-tin solder
[AD-A275716] 08 p3202 N94-28643
Surface tension of tin and its alloys with particular reference to solders
[PB94-138302] 08 p3204 N94-29119
Logistics for the implementation of lead-free solders on electronic assemblies
[DE94-004800] 08 p3206 N94-29936
Microstructural development and mechanical behavior of eutectic bismuth-tin and eutectic indium-tin in response to high temperature deformation
[DE94-005202] 08 p3210 N94-30710
Aging effects on the microstructure, surface characteristics and wettability of Cu pretinned with Sn-Pb solders
[DE94-007033] 09 p3641 N94-31638
Manufacturing feasibility of several lead-free solders for electronic assembly
[DE94-007732] 11 p4258 N94-35564
Capillary flow solderability test for printed wiring boards
[DE94-010321] 11 p4259 N94-36094

SOLENOIDS
High-field conductor testing at the FENIX facility
[DE93-012318] 01 p0387 N94-10737
Spin characteristics of ion beams during the motion of electromagnetic elements
[DE93-617448] 01 p0364 N94-10848
Toroidal solenoids in the electromagnetic field and Aharonov-Casher effect
[DE93-629861] 04 p1566 N94-18152
Generalized energy principle for flute perturbations in axisymmetric mirror machines
[DE93-019399] 04 p1589 N94-19037
Performance of the high brightness linac for the Advanced Free Electron Laser Initiative at Los Alamos
[DE93-040141] 05 p1816 N94-20277
Structural analysis of a superconducting central solenoid for the Tokamak Physics Experiment
[DE94-001536] 06 p2549 N94-23014
Electromagnetic properties of a toroidal solenoid
[DE93-613032] 07 p2766 N94-25866
The static and nonstatic electrical solenoids
[DE94-606326] 08 p3261 N94-28585
Estimating the cost of large superconducting thin solenoid magnets
[DE94-006289] 08 p3468 N94-30026
Third-order beam optics of real solenoid magnetic lens
[DE94-608014] 08 p3500 N94-30084
Time-delay control of a magnetic levitated linear positioning system 11 p4217 N94-35862

SOLID ARGON
U SOLIDIFIED GASES

SOLID CRYOGENS
NT SOLID NITROGEN
Experiments with energetic (mu)d and (mu)t emitted from solid hydrogen
[DE93-010252] 01 p0373 N94-12542
Energy storage and conversion in solid hydrogen
[AD-A271439] 05 p1845 N94-20086
Trapped electrons in solid hydrogen
[DE93-018628] 07 p3052 N94-25947
Spectroscopy and dynamics of molecular and ionic impurities embedded in solid hydrogen
[AD-A274149] 07 p3064 N94-27095
Studies of the thermal and optical responses of H atoms in solid H2
[NASA-CR-196114] 12 p4514 N94-36964

SOLID ELECTRODES
Surface electrochemistry of metals
[AD-A272913] 05 p1691 N94-21245

SOLID ELECTROLYTES
Technical Update: Johnson Space Center system using a solid electrolytic cell in a remote location to measure oxygen fugacities in CO/CO2 controlled-atmosphere furnaces
[NASA-TM-104774] 01 p0423 N94-11183
Polymer electrolyte fuel cells: Potential transportation and stationary applications
[DE93-010734] 01 p0264 N94-11666
Study of multicomponent diffusion and transport phenomena
[DE93-015095] 02 p0804 N94-13005
Electrocatalysis issues in polymer electrolyte fuel cells
[DE93-014450] 02 p0702 N94-13402
Combustion synthesis and engineering of nanoparticles for electronic, structural, and superconductor applications
[DE93-016286] 02 p0809 N94-13981
Status of SOFC development in USA
[DE93-015568] 02 p0704 N94-14355
Chemical interactions between interconnect and electrode materials during sintering in solid oxide fuel cells
[DE93-015696] 03 p1092 N94-16160
Thin composite solid electrolyte film for lithium batteries
[NASA-CASE-NPO-18694-1-CU] 03 p1014 N94-17325
Mixed polymer electrolyte and mixed polymer electrolyte battery
[AD-D015856] 04 p1394 N94-17718
Oxygen reduction at a stabilized zirconia interface with Y(1-x)Ca(x)MnO3 or La(1-x)Sr(x)MnO3 cathode materials
[DE93-015681] 04 p1593 N94-17747
Fuel cell systems program plan, fiscal year 1993
[DE93-017828] 04 p1466 N94-18103
Novel electrochemical materials prepared by sol-gel chemistry
[AD-A269060] 04 p1578 N94-18405
Modeling of polymer electrolyte fuel cell systems
[DE93-041187] 05 p1847 N94-21774
The electrochemical performance of thin-electrolyte solid oxide fuel cells
[DE93-041184] 05 p1848 N94-21942
Survey on chemical engineering technologies for the global environmental protection
[DE94-714887] 05 p1852 N94-22044
Modelling of solid polymer and direct methanol fuel cells: Phenomenological equations and analytical solutions
[PB93-224897] 06 p2390 N94-23102
High power density proton exchange membrane fuel cells 06 p2393 N94-23359
The electrolyte challenge for a direct methanol air polymer electrolyte fuel cell operating at temperatures up to 200 C 06 p2393 N94-23360
Advances in direct oxidation methanol fuel cells 06 p2393 N94-23361
Development of SO(x) and NO(x) solid electrolyte sensors 07 p2725 N94-25562
Reference electrodes for solid polymer electrolytes
[DE94-004583] 07 p2780 N94-25806
Alternative materials for solid oxide fuel cells: Processing and interactions of materials
[DE94-000016] 07 p2855 N94-26114
Oxygen reduction at a YSZ interface with cathode materials La(1-x)(Ca or Sr)(x)MnO3(1-x)CaMnO3
[DE94-002954] 07 p3054 N94-26147
Processing of LaCrO3 for solid oxide fuel cell applications
[DE94-002981] 07 p2857 N94-26747
Low cost, radial flow, solid oxide fuel cell
[DE94-002982] 07 p2858 N94-26785
MSOFC development status
[DE94-003192] 07 p2858 N94-26792

High temperature solid oxide fuel cell: Customer test units
[DE94-002961] 07 p2858 N94-26869
High temperature solid oxide fuel development activities
[DE94-002973] 07 p2858 N94-26871
Perovskite solid electrolytes for SOFC
[DE94-001923] 07 p2859 N94-27005
Fuel Cell Seminar, 1992: Program and abstracts
[DE94-003882] 08 p3336 N94-28472
Enhanced ion dissociation of LiCF3SO3 by new carbonate plasticizers: Raman and IR studies
[DE94-005448] 08 p3485 N94-28741
Method for forming thin composite solid electrolyte film for lithium batteries
[NASA-CASE-NPO-18877-1-CU] 08 p3264 N94-29357
Novel electroactive polymers and block copolymers
[AD-A276119] 09 p3650 N94-31509
Conductivity measurements of ceria-based solid electrolytes using AC impedance
[DE94-007380] 09 p3694 N94-32593
A solid oxide fuel cell power system: 1992-1993 field operation
[DE94-010383] 11 p4283 N94-36109

SOLID LUBRICANTS
Study of the tribological behavior of SiC and Si3N4 ceramic couples in terms of temperature: The reality 01 p0064 N94-10061
Advanced model of gradual wear of viscoelastic surface film
[AD-A265130] 01 p0090 N94-11222
Properties of interfacial tribo-films
[AD-A265591] 01 p0182 N94-12374
Dry film lubricant evaluation
[DE93-013114] 02 p0578 N94-13118
Applications of surface science to solid lubricants
[SMC-TR-93-24] 02 p0579 N94-13903
Solid lubricants for space structures, phase 2
[AD-A266653] 03 p0968 N94-16767
Titanium carbon-hydrogen layers on decorative surfaces 04 p1375 N94-18010
Physico chemical and mechanic approach of lubricating properties of graphite + additive powders
[ECL-93-02] 04 p1373 N94-19405
New tribocoating combination for vacuum operation 06 p2355 N94-23990
Tribological characteristics of ball bearings lubricated with a sputtered molybdenum disulphide film in a vacuum under a high thrust load 06 p2355 N94-23992
The tribology of some MoS2-lubricated engineering ceramics 06 p2356 N94-23993
Development of gears for space use 06 p2360 N94-24021
An analytical ultra-high vacuum tribometer for solid lubricant studies 06 p2361 N94-24033
An assessment of solid lubricant films for use in high temperature space applications 06 p2363 N94-24044
The development of dry-lubricated ceramic cages 06 p2363 N94-24045
XPS analysis of 440C steel surfaces lubricated with perfluoropolyethers under sliding conditions in high vacuum
[NASA-TM-106548] 08 p3218 N94-30177
Soft x ray photoelectron spectroscopy study of the interaction of Cr with MoS2(0001)
[AD-A276916] 09 p3635 N94-32233
The effect of prolonged exposure to 750 C air on the tribological performance of PM212
[NASA-TM-106472] 09 p3617 N94-32941
Torque characteristics of solid lubricated precision bearings during oscillatory motion
[AD-A278133] 09 p3728 N94-33061
Development of long-life, low-noise linear bearings for atmospheric interferometry 09 p3606 N94-33312
Wear-resisting oxide films for 900 C
[DE94-010093] 11 p4246 N94-36306

SOLID MECHANICS
Thermal gradient-induced deflection of a thick-walled cylinder with bending residual stresses
[AD-A266347] 02 p0673 N94-13777
Variational approach to probabilistic finite elements
[NASA-CR-187179] 02 p0674 N94-13873
Elastic-plastic mixed-iterative finite element analysis: Implementation and performance assessment
[NASA-TM-106164] 02 p0675 N94-13919
JPRS report: Science and technology. Central Eurasia: Engineering and equipment
[JPRS-UEQ-93-006] 02 p0776 N94-14431
HEMP 3D: A finite difference program for calculating elastic-plastic flow, appendix B
[AD-A269171] 04 p1418 N94-18878
The program system for the diagnostics of strains and fracture prediction of solids 05 p1836 N94-22065
Computational mechanics
[DE94-003015] 07 p2965 N94-26775

SOLID NITROGEN
A Pluto thermal model 03 p1256 N94-16216
The temperature of nitrogen on Pluto 11 p4365 N94-35468

SOLID PHASES
Crystallographic phase identification in the scanning electron microscope: Backscattered electron Kikuchi patterns
[DE93-011574] 02 p0804 N94-12813
Multiphase equation of state for iron
[DE93-013956] 02 p0568 N94-12977
Automated crack identification for cement paste
[AD-A265753] 02 p0665 N94-13042
Thermodiffusion in heterogeneous elastic solids and homogenization
[REPT-14/1993] 02 p0578 N94-13468
Process of shaping an electrorheological solid
[AD-D015885] 03 p1012 N94-16914
Slip, twinning and transformation in Laves phases
[DE93-018164] 03 p0960 N94-16972
A new multiphase equation of state for iron
[DE93-017629] 04 p1357 N94-17819
Deformation mechanisms in a Laves phase
[DE93-018331] 04 p1361 N94-18806
Morphology, deformation, and defect structures of TiCr2 in Ti-Cr alloys
[DE93-018332] 04 p1361 N94-18807
Cooling apparatus and couplings therefor
[NASA-CASE-ARC-11921-1] 05 p1800 N94-20371
Some experiments on using backscattered electron and energy dispersive x ray imaging in determination of portland cement clinker phase composition 05 p1708 N94-21893
Predictive modeling of particle-laden, turbulent flows
[DE94-003298] 07 p2792 N94-26319
Interstitially stabilized phases in the zirconium-nickel system
[DE94-005561] 08 p3201 N94-28525
Directional solidification studies in Ni-Al alloys
[DE94-005562] 08 p3201 N94-28527
Experimental and theoretical studies of molecular solids
[AD-A275511] 08 p3485 N94-28668
Strongly coupled ionic mixtures and the H/He EOS
[DE94-006391] 09 p3934 N94-31782
Stability and precipitation kinetics in Si(1-y)C(y)/Si and Si(1-x-y)Ge(x)C(y)/Si heterostructures prepared by solid phase epitaxy
[DE94-006589] 09 p3902 N94-32296

SOLID PROPELLANT COMBUSTION
NT SOLID PROPELLANT IGNITION
Combustion-induced crack propagation process in a solid-propellant crack cavity 01 p0098 N94-10901
Combustion-induced crack/debond propagation in solid propellants 02 p0584 N94-13560
Numerical simulation of velocity-coupled combustion response of solid rocket propellants 02 p0585 N94-14490
Spectral studies of solid propellant combustion 4: Absorption and burn rate results for M43, XM39, and M10 propellants
[AD-A267119] 03 p0946 N94-15685
Detailed structure study of an H2/N2O/Ar flame employing molecular beam mass spectrometry, laser spectroscopy, and modeling
[AD-A270720] 05 p1679 N94-20111
Design considerations of hybrid rockets 06 p2156 N94-24254
Modelling the ignition of boron/titanium particles 06 p2159 N94-24273
Condensed-phase processes during solid propellant combustion. 3: Preliminary depth-profiling studies on XM39, JA2, M9, M30, and HMX2
[AD-A276595] 09 p3635 N94-32124
AFOSR Contractors Propulsion Meeting
[AD-A279028] 11 p4198 N94-35746
Processing solid propellants for recycling
[DE94-011433] 12 p4428 N94-37202
Effects of two-phase flow on the deflagration of porous energetic materials
[DE94-011423] 12 p4411 N94-37412

SOLID PROPELLANT IGNITION
Laser ignition of solid propellants: 1. Ignition delays
[AD-A268454] 03 p0976 N94-17538
Modelling the ignition of boron/titanium particles 06 p2159 N94-24273
Development of a new generation solid rocket motor ignition computer code
[NASA-CR-195734] 08 p3171 N94-28800
A study of solid propellants using a microprobe mass spectrometer system
[AD-A275325] 08 p3224 N94-28879
Correlation of cookoff behavior of rocket propellants with thermomechanical and thermochemical properties
[AD-A274983] 08 p3224 N94-29092
Shock tube ignition and combustion of aluminum/magnesium alloy particles in oxygen at high pressure 09 p3631 N94-31286
The 30th JANNAF Combustion Subcommittee Meeting, volume 1
[AD-A278793] 11 p4247 N94-35655

SOLID PROPELLANT ROCKET ENGINES
NT ADVANCED SOLID ROCKET MOTOR (STS)
NT SPACE SHUTTLE BOOSTERS
Combustion-induced crack propagation process in a solid-propellant crack cavity 01 p0098 N94-10901
Combustion-induced crack/debond propagation in solid propellants 02 p0584 N94-13560
Test/analysis correlation and model updating of the STARS 1 and 2 missile systems
[DE93-013774] 02 p0748 N94-13578
Numerical simulation of velocity-coupled combustion response of solid rocket propellants 02 p0585 N94-14490
Qualification test of the Ross Double Planetary Mixer
[NASA-CR-192600] 02 p0652 N94-14497
Technical Evaluation Motor No. 10 (TEM-10)
[NASA-CR-193846] 02 p0554 N94-14907
Advanced Solid Rocket Motor
[NASA-TM-109658] 03 p0924 N94-15229
Ultrasonic wave propagation model for nondestructive evaluation of solid rocker motor propellant
[AD-A267653] 03 p0976 N94-17248
Postflight hardware evaluation 360T026 (RSRM-26, STS-47)
[NASA-CR-192559] 03 p0882 N94-17656
Investigation of flame driving and flow turning in axial solid rocket instabilities
[AD-A271066] 05 p1667 N94-20015
Final postflight hardware evaluation report RSRM-28 (STS-53)
[NASA-CR-193902] 06 p2200 N94-24112
Impact damage in filament wound composite bottles 06 p2231 N94-24421
Micromechanical simulation of damage progression in carbon phenolic composites 06 p2231 N94-24446
An ultrasonic testing technique for monitoring the cure and mechanical properties of polymeric materials
[AD-A274536] 07 p2753 N94-26842
Development and application of contamination technology for MSFC managed space systems
[NASA-CR-193934] 07 p2697 N94-27421
Research and development of ramjets/ramrockets. Part 1: Integral solid propellant ramrockets 08 p3151 N94-29294
A variable selection heuristic for solid rocket motor design 08 p3173 N94-29544
The prediction of convective transfer on the thermal insulation of a solid-propellant rocket motor
[ONERA-NT-1993-15] 09 p3614 N94-31423
Combustor and nozzle effects on particulate behavior in solid rocket motors
[AD-A277304] 09 p3614 N94-32071
AFOSR Contractors Propulsion Meeting
[AD-A279028] 11 p4198 N94-35746
Energy partitioning in high speed impact of analog solid rocket motors
[AD-A278771] 11 p4228 N94-35825
Propellant stress relief groove for the Titan 4 SRMU
[AD-A278628] 11 p4228 N94-36254
An efficient, intelligent solution for viscous flows inside solid rocket motors
[AD-A278629] 11 p4228 N94-36255
Validation and implementation of optical diagnostics for particle sizing in rocket motors
[AD-A278581] 12 p4428 N94-36972
Processing solid propellants for recycling
[DE94-011433] 12 p4428 N94-37202
NASA reload program
[NASA-CR-193972] 12 p4429 N94-37446

SOLID PROPELLANTS
NT COMPOSITE PROPELLANTS
NT DOUBLE BASE ROCKET PROPELLANTS
NT HMX
NT HTPB PROPELLANTS
NT METAL PROPELLANTS
NT NITRAMINE PROPELLANTS
NT SOLID ROCKET PROPELLANTS
Polymeric nitrogen
[DE93-012600] 01 p0089 N94-11151
Distributed combustion in solid propellants
[AD-A265727] 01 p0099 N94-12564
Flamespreading in granular solid propellant: Design of an experiment
[AD-A266009] 02 p0583 N94-12987
Closed-chamber analysis of M5 propellant lot RAD-64597
[AD-A266321] 02 p0585 N94-14145

Ultrasonic wave propagation model for nondestructive evaluation of solid rocker motor propellant
[AD-A267653] 03 p0976 N94-17248
Damage evolution in filled elastomers
[AD-A268067] 03 p1062 N94-17507
Laser ignition of solid propellants: 1. Ignition delays
[AD-A268454] 03 p0976 N94-17538
Burning rate of double-base propellant in the presence of plasma 06 p2155 N94-24252
Modelling the ignition of boron/titanium particles 06 p2159 N94-24273
Experimental investigation of ignition of boron/titanium composite particles 06 p2159 N94-24275
Propellants and explosives in ballistic missiles
[UCRL-LR-113578] 07 p2760 N94-28222
A study of solid propellants using a microprobe mass spectrometer system
[AD-A275325] 08 p3224 N94-28879
A model of concurrent flow flame spread over a thin solid fuel 09 p3634 N94-31795
NATO Advanced Study Institute on Unsteady Combustion. Volume 2: Research papers, September 6-17, 1993
[AD-A276572] 09 p3634 N94-32033
The 30th JANNAF Combustion Subcommittee Meeting, volume 1
[AD-A278793] 11 p4247 N94-35655
DDT modeling and shock compression experiments of porous or damaged energetic materials
[DE94-011419] 12 p4428 N94-37052
Processing solid propellants for recycling
[DE94-011433] 12 p4428 N94-37202

SOLID ROCKET BOOSTERS (SPACE SHUTTLE)
U SPACE SHUTTLE BOOSTERS

SOLID ROCKET PROPELLANTS
NT DOUBLE BASE ROCKET PROPELLANTS
NT HMX
NT HTPB PROPELLANTS
NT METAL PROPELLANTS
Numerical simulation of velocity-coupled combustion response of solid rocket propellants 02 p0585 N94-14490
Fundamental studies of rocket combustion chemistry and combustion instability
[AD-A266248] 03 p0925 N94-16482
Space Shuttle solid rocket motor exposure monitoring 03 p0976 N94-16624
Adaptations to micropep and rocket to allow performance evaluation of multiple grain and/or airbreathing motors
[AD-A268798] 04 p1337 N94-18202
Materials characterization of propellants using ultrasonics
[NASA-CR-193877] 04 p1378 N94-19494
Chemistry of the burning surface
[AD-A272725] 05 p1681 N94-21181
Cryogenic size reduction of solid propellant
[AD-A274844] 07 p2759 N94-26800
An ultrasonic testing technique for monitoring the cure and mechanical properties of polymeric materials
[AD-A274536] 07 p2753 N94-26842
Uncertainties in the characterization of the thermal environment of a solid rocket propellant fire
[DE94-002023] 07 p2760 N94-27719
Introduction and overview of research and development of solid propellant ramrockets, liquid fuel ramjets and experimental hydrogen ram combustors 08 p3151 N94-29292
Research and development of ramjets/ramrockets. Part 1: Integral solid propellant ramrockets 08 p3151 N94-29294
Propellant stress relief groove for the Titan 4 SRMU
[AD-A278628] 11 p4228 N94-36254
Validation and implementation of optical diagnostics for particle sizing in rocket motors
[AD-A278581] 12 p4428 N94-36972
NASA reload program
[NASA-CR-193972] 12 p4429 N94-37446

SOLID ROTATION
U ROTATING BODIES

SOLID SOLUTIONS
Symmetry lowering in crystalline solid solutions: A study of cinnamamide-thienylacrylamide by x ray and neutron diffraction and solid-state photochemistry
[DE93-010871] 01 p0394 N94-10301
Materials for adaptive structural acoustic control, volume 3
[AD-A264621] 01 p0358 N94-11262
Effect of microstructure on passive film formation and breakdown on Al alloys
[AD-A265339] 02 p0569 N94-13050
First-principles studies of phase stability and the structural and dynamical properties of hydrogen-metal systems
[DE93-016129] 02 p0570 N94-13374
Ionic conductivity of alkali halides and their mixtures near liquid-solid phase transition
[ITN-93-85222] 02 p0566 N94-14558
Statics and kinetics of phase transformations in bcc Fe-Cr
[DE93-013839] 02 p0574 N94-14793
Ternary alloying effects in polycrystalline (beta)-NiAl
[DE93-012675] 03 p0955 N94-15885
Roles of oxygen defects in copper-oxide superconductors
[DE93-014875] 03 p1208 N94-15982
Chemical interactions between interconnect and electrode materials during sintering in solid oxide fuel cells
[DE93-015696] 03 p1092 N94-16160
Chemical and displacement atomic pair correlations in crystalline solid solutions recovered by anomalous x ray scattering in Fe-Ni alloys
[DE93-015906] 03 p1209 N94-16171
Rheology of water and ammonia-water ices 03 p0953 N94-16188
Pulsed laser deposition of metastable Ca(1-x)Sr(x)CuO2 thin films
[DE93-015804] 03 p1040 N94-16663
Pseudomorphic semiconducting heterostructures from combinations of AlN, GaN and selected SiC polytypes: Theoretical advancement and its coordination with experimental studies of nucleation, growth, characterization and device deployment
[AD-A267561] 03 p1213 N94-17108
Effects of shock loading on a solid-solution strengthened superalloy
[DE93-018345] 04 p1362 N94-18809
Metastable bcc phase formation in the Nb-Cr system
[DE93-018376] 05 p2012 N94-19926
An atom probe investigation of the influence of trace impurities on the mechanical behavior of NiAl
[DE94-002797] 07 p2734 N94-26272
Electron microscopy of AlN-SiC interfaces and solid solutions
[DE94-002449] 07 p3059 N94-26765
Experimental measurement of local displacement and chemical pair correlations in crystalline solid solutions
[DE94-001124] 07 p3065 N94-27251
On the formation of muon- and zeta-phases in Ag-Al system by mechanical alloying
[DE94-007125] 09 p3645 N94-32636
Phase relationships and stability of the (mu)- and (zeta)-phases in the Ag-Al-X (X=Zn, Ga, Ge) systems
[DE94-009391] 09 p3648 N94-33270
Pair correlations in crystalline solid solutions
[DE94-012319] 12 p4535 N94-37212

SOLID STATE
Solid state ionics 3. Materials Research Society Symposium Proceedings, volume 293
[AD-A265675] 01 p0395 N94-10416
Solid-state structures of guanidinium methane, ethane, and trifluoromethanesulfonate
[AD-A265293] 01 p0402 N94-11654
Hydrogen-bond polymorphs of guanidinium 4-biphenylsulfonate
[AD-A265294] 01 p0402 N94-11827
The 13C and 15N solid-state NMR of copolymers of nylon 6 and 7: Observation of a stable pseudohexagonal phase
[AD-A265799] 01 p0094 N94-12381
Engineering solid-state materials. Strategies for modeling and packing control of molecular assemblies into 3-D networks
[AD-A265291] 01 p0404 N94-12438
Characterization of 1:1 random copolymers obtained from 6-, 7-, 11-, and 12-carbon amino acids
[AD-A265827] 02 p0577 N94-12985
Theory of the electronic and structural properties of solid state oxides
[DE93-016051] 02 p0811 N94-14296
Design, synthesis and characterization of novel nonlinear optical polymers
[AD-A267035] 03 p0964 N94-15675
Detection and dosimetry of chemical contaminants in polymeric materials
[AD-A266605] 03 p0968 N94-16727
Polaron tunneling in high-temperature superconductors
[DE93-016880] 04 p1593 N94-17754
Microstructural analysis of solid-state resistance welds
[DE93-017295] 04 p1443 N94-17761
Solid State Sciences Committee Forum
[AD-A270454] 04 p1342 N94-18715
Solid-state dynamics in novel semiconductor nanostructures
[AD-A271249] 04 p1605 N94-19725
Shock wave interactions with exothermic mixtures
[AD-A271149] 05 p1829 N94-19836
An equation of state for shock in homogeneous materials and comparison to shock data
[AD-A271436] 05 p1829 N94-19881
Solid State Technology Branch of NASA Lewis Research Center: Fifth Annual Digest
[NASA-TM-106303] 05 p1732 N94-20497
High power, electron-beam induced switching in diamond
[DE93-040535] 05 p1768 N94-21770
In situ and ex situ spectroelectrochemical and x ray absorption studies on rechargeable, chemically-modified and other MnO2 materials
[DE94-001387] 06 p2234 N94-24545
Thermomechanical processing of Ag-clad Bi2Sr2CaCu2O(x) superconductors
[DE94-002347] 06 p2563 N94-24624
Solid state Time Base Corrector (TBC)
[AD-D015981] 06 p2312 N94-25039
Structure and properties of intermetallic composites synthesized in situ using solid state displacement reactions
[DE94-004312] 07 p2705 N94-25805
Powder synthesis, fabrication, and transport properties of long-length Ag clad Bi-2223 conductors
[DE94-002376] 07 p2740 N94-26957
Phase stability in the Cd-Mg system
[DE94-004976] 07 p2743 N94-27792
Summary of the 1993 Winter ACP Workshop on Collective Dynamics in Disordered System
[AD-A276355] 09 p3864 N94-31402
Solid-state resistance upset welding: A process with unique advantages for advanced materials
[DE94-005941] 09 p3723 N94-31524
Isothermal sintering, microstructure, and superconducting properties of Y1Ba2Cu3O(7-x) compound
[DE94-008132] 09 p3905 N94-32779
Solid state acoustics information time region separating methods for gear diagnosis of failures 10 p4068 N94-34351
NMR imaging of components and materials for DOE application
[DE94-010664] 11 p4238 N94-36084
Solid state research
[AD-A280573] 12 p4533 N94-36734

SOLID STATE DEVICES
NT ALUMINUM GALLIUM ARSENIDE LASERS
NT AVALANCHE DIODES
NT BIPOLAR TRANSISTORS
NT CHARGE COUPLED DEVICES
NT CHARGE FLOW DEVICES
NT CHARGE TRANSFER DEVICES
NT CMOS
NT FIELD EFFECT TRANSISTORS
NT GALLIUM ARSENIDE LASERS
NT HETEROJUNCTION DEVICES
NT HIGH ELECTRON MOBILITY TRANSISTORS
NT JFET
NT JUNCTION DIODES
NT JUNCTION TRANSISTORS
NT LIGHT EMITTING DIODES
NT METAL OXIDE SEMICONDUCTORS
NT MIS (SEMICONDUCTORS)
NT MODFETS
NT MSM (SEMICONDUCTORS)
NT PHOTODIODES
NT PHOTOTRANSISTORS
NT PHOTOVOLTAIC CELLS
NT QUANTUM WELL LASERS
NT RUBY LASERS
NT SCHOTTKY DIODES
NT SEMICONDUCTOR DEVICES
NT SEMICONDUCTOR LASERS
NT SILICON CONTROLLED RECTIFIERS
NT SILICON TRANSISTORS
NT SIS (SEMICONDUCTORS)
NT SIS (SUPERCONDUCTORS)
NT SOI (SEMICONDUCTORS)
NT SOLAR CELLS
NT SOLID STATE LASERS
NT SOS (SEMICONDUCTORS)
NT THERMISTORS
NT THYRISTORS
NT TRANSISTOR AMPLIFIERS
NT TRANSISTORS
NT VARACTOR DIODES
NT VARISTORS
NT YAG LASERS
Solid state ionics 3. Materials Research Society Symposium Proceedings, volume 293
[AD-A265675] 01 p0395 N94-10416
Metal-semiconductor, composite radiation detectors
[DE93-013313] 02 p0619 N94-12994
CdTe array detectors for high energy astronomy 03 p0899 N94-15029

The solid state detector technology for picosecond laser ranging 03 p0914 N94-15572
Portable, solid state, fiber optic coupled Doppler interferometer system for detonation and shock diagnostics
[DE93-013917] 04 p1423 N94-17700
Solid-state, resistive hydrogen sensors for safety monitoring
[DE93-017769] 04 p1424 N94-17778
New room temperature high resolution solid-state detector (CdZnTe) for hard x rays and gamma rays 04 p1324 N94-19165
Multiport solid-state imager characterization at variable pixel rates
[DE93-018366] 05 p1808 N94-20287
Compositional diversity of the lunar North Pole: Preliminary analyses of Galileo SSI data 05 p2101 N94-20686
Compact lightweight CO2 laser for SDIO application
[AD-A273010] 05 p1817 N94-21284
Non-volatile, solid state bistable electrical switch
[NASA-CASE-NPO-17621-1-CU] 06 p2309 N94-23820
Mesoscopic phenomena in metallic point contacts
[ETN-94-95371] 06 p2313 N94-25286
Solid state research
[AD-A274063] 07 p3049 N94-25645
Exploration of GaAs structures for solid-state detectors
[DE93-634191] 07 p3056 N94-26379
Center for space microelectronics technology
[NASA-CR-195282] 07 p2786 N94-27574
Solid-state, active-phased arrays: Some aspects of receiver design
[AD-A275893] 08 p3527 N94-28779
Fabrication of electronic materials in space 08 p3228 N94-28942
The 100 kA, 5000 V solid-state opening switch for inductive energy storage
[AD-A274993] 08 p3263 N94-28994
Miniaturization in x ray and gamma ray spectroscopy 08 p3236 N94-29773
Proceedings of the International Workshop on Computational Electronics
[AD-A277020] 09 p3692 N94-32259
Space electronics video: Research for today and tomorrow
[NASA-TM-109829] 10 p4039 N94-33583
Three dimensional ICs intelligent sensors 10 p4057 N94-34354
Electron and Proton Wide-Angle Spectrometer (EPAS) on the CRRES spacecraft
[AD-A278630] 11 p4227 N94-35362
A 32-GHz solid-state power amplifier for deep space communications 11 p4255 N94-35562
Solid state research
[AD-A280573] 12 p4533 N94-36734
Solid state fluorometer: Prototype development
[AD-A280321] 12 p4534 N94-37027
Stopping power of charged particles from 10 eV/amu to 10 GeV/amu
[DE94-719024] 12 p4518 N94-37387

SOLID STATE LASERS
NT ALUMINUM GALLIUM ARSENIDE LASERS
NT GALLIUM ARSENIDE LASERS
NT QUANTUM WELL LASERS
NT RUBY LASERS
NT YAG LASERS
NT YLF LASERS
Limitations to the quality of optical phase conjugation by stimulated Brillouin scattering
[AD-A266006] 01 p0383 N94-12389
Novel Co:MgF2 lidar for aerosol profiler
[NASA-CR-191525] 02 p0654 N94-13091
Solid state laser systems for space application
[NASA-CR-194133] 02 p0656 N94-13420
Design and performance of the terawatt Cr:LiSrAlF6 laser system
[DE93-014678] 02 p0657 N94-13882
Impact of shorter wavelengths on optical quality for laws
[NASA-CR-193433] 02 p0792 N94-14473
Independent adjustment of the higher order frequency dependent phase in chirped pulse amplification systems
[DE93-017106] 02 p0625 N94-14522
The solid state detector technology for picosecond laser ranging 03 p0914 N94-15572
Bench checkout equipment for spaceborne laser altimeter systems 03 p0921 N94-15618
Multi-beam laser altimeter 03 p0921 N94-15620
Full-wave simulation of the thumbtack laser
[DE93-015110] 03 p1039 N94-16054
Porous silicon for pumping solid-state lasers
[AD-A266293] 03 p1039 N94-16474
Integrated photonics research volume 10. Conference edition
[AD-A269298] 04 p1577 N94-18298
Quantum Optoelectronics. Organization of the 1993 photonics science topical meetings. Technical digest series, volume 8
[AD-A269026] 04 p1578 N94-18488
Advanced Solid-State Lasers/Compact Blue-Green Lasers. 1993 technical digest series. Volume 2: Organization of the 1993 photonics science topical meetings
[AD-A269058] 04 p1438 N94-18492
Photonics in Switching: Organization of the 1993 photonics science topical meetings. Technical digest
[AD-A269024] 04 p1578 N94-18528
Tunable ytterbium-doped solid state laser
[AD-D015878] 04 p1440 N94-18747
Impact of shorter wavelengths on optical quality for laws
[NASA-CR-193873] 04 p1579 N94-18858
Proof of the feasibility of coherent and incoherent schemes for pumping a gamma ray laser
[AD-A269173] 04 p1440 N94-18880
Tetravalent chromium (Cr(4+)) as laser-active ion for tunable solid-state lasers
[NASA-CR-194529] 04 p1441 N94-19369
Tetravalent chromium (Cr(4+)) as laser-active ion for tunable solid-state lasers
[NASA-CR-194528] 04 p1441 N94-19394
Center-of-Excellence: Microlaser microscope
[DE93-040688] 04 p1442 N94-19658
Suppression of relaxation oscillations in flashpumped, two-micron tunable solid state lasers
[AD-D015928] 05 p1814 N94-19800
Resonantly pumped, erbium-doped, GSGG, 2.8 micron, solid state laser with energy recycling and high slope efficiency
[AD-D015920] 05 p1815 N94-20060
Simulations of spectral broadening by cross-phase modulation (XPM) with chaotic light pulses
[DE93-019623] 05 p1819 N94-21872
Micro pulse laser radar
[NASA-CASE-GSC-13493-1] 06 p2294 N94-23827
Computer modeling of nonlinearities 06 p2458 N94-24661
Temporal model of an optically pumped co-doped solid state laser
[NASA-TM-109680] 06 p2350 N94-24851
Nonlinear dynamical control of lasers
[AD-A273359] 06 p2350 N94-24938
Laser energized high voltage direct current power supply
[AD-D015977] 06 p2312 N94-25036
Compact, solid-state femtosecond source
[AD-A273932] 07 p2817 N94-26271
Phase conjugation and pulse compression of high energy lasers: From nanoseconds to microseconds
[DE94-001061] 07 p2818 N94-26699
Phase conjugated lasers applied to commercial x ray lithography
[DE94-001529] 07 p2819 N94-27018
Kinoform/lens system for injecting a high power laser beam into an optical fiber
[DE94-003226] 07 p2819 N94-27262
Technical report of ISSP. Ser. A, no. 2686: High-order harmonic generation and ionization using ultrashort KrF and Ti:Sapphire lasers
[JTN-94-80572] 07 p2820 N94-27605
Optical parametric oscillator modeling with diffraction, depletion, and double refraction
[DE94-001504] 07 p3040 N94-27999
Dynamics of a coupled solid state laser array 08 p3294 N94-29551
Solid state laser systems for space application
[NASA-CR-195777] 08 p3294 N94-29914
Remote pumping of solid state lasers with nuclear driven fluorescers
[DE94-004846] 08 p3296 N94-30614
Diode-pumped solid-state-laser drivers and the competitiveness of inertial fusion energy
[DE94-006654] 08 p3296 N94-30830
Transient radiation-induced absorption in the materials for a GSGG laser
[DE94-005316] 09 p3714 N94-31148
High-power CW diode-laser-array-pumped solid-state lasers and efficient nonlinear optical frequency conversion
[AD-A276126] 09 p3714 N94-31278
Scenarios for multi-unit inertial fusion energy plants producing hydrogen fuel
[DE94-006614] 09 p3666 N94-32114
High conversion efficiency pumped-cavity second harmonic generation of a diode laser
[DE94-006805] 09 p3717 N94-32134
Ti:sapphire based ultrafast pump-probe laser source in the violet and ultraviolet
[DE94-007542] 09 p3718 N94-32270
Repetitively pulsed Cr:LiSAF laser for lidar applications
[DE94-007546] 09 p3720 N94-32761
Multifrequency, rapidly sequenced or simultaneous tunable laser
[AD-D016169] 09 p3721 N94-32968
Improved performance of high average power semiconductor arrays for applications in diode pumped solid state lasers
[DE94-009516] 11 p4271 N94-35665
System for end-pumping a solid state laser using a large aperture laser diode bar
[AD-D016213] 11 p4273 N94-36370
Diode array alternative to paint removal solid-state cw laser
[DE94-011482] 12 p4448 N94-37203
Diode-pumped, continuously tunable, 2.3 micron CW laser specification
[AD-D016312] 12 p4450 N94-37838

SOLID STATE PHYSICS
Activities of Institute for Microstructural Sciences
[NRC-32815] 02 p0810 N94-14198
Activities of Institute for Microstructural Sciences
[CNR-32815] 02 p0810 N94-14199
Solid State Sciences Committee Forum
[AD-A270454] 04 p1342 N94-18715
Spin-polaron theory of high-T(c) superconductivity. 3: Gap function and critical temperature
[DE93-019198] 05 p2030 N94-21831
Activities of the Laboratory of Physics, Helsinki University of Technology
[PB94-175247] 12 p4509 N94-37301

SOLID SURFACES
NT CRYSTAL SURFACES
Application of spin-sensitive electron spectroscopies to investigations of electronic and magnetic properties of solid surfaces and epitaxial systems
[DE93-015079] 01 p0076 N94-10854
Low energy neutral atom imaging techniques
[DE93-012744] 02 p0779 N94-12950
Thermodynamic status of static and dynamic contact angles
[ISBN-0-315-73844-8] 02 p0817 N94-13554
Construction and test of a facility for photon-stimulated field description using excimer laser and time of flight
[ETN-93-94386] 02 p0657 N94-13996
Quantum state resolved desorption of CO from solid surfaces
[DE93-016876] 02 p0814 N94-14597
NMR studies of enriched species at interfaces
[AD-A264703] 04 p1367 N94-17878
Surface physics with cold and thermal neutron reflectometry
[DE94-001447] 07 p2733 N94-26070
Solid surface
[NASA-TM-109746] 09 p3634 N94-31883
Innovative instrumentation for mineralogical and elemental analyses of solid extraterrestrial surfaces: The Backscatter Moessbauer Spectrometer/X Ray Fluorescence analyzer (BaMS/XRF) 11 p4239 N94-35459

SOLID SUSPENSIONS
Remote sensing of the suspended matter distribution with high concentration in China Sea 01 p0192 N94-11901
Analysis of the characteristic and mechanism of suspended matter transportation in Huanghe delta sea area using remote sensing techniques 01 p0197 N94-11930
Development of shipboard ocean lidar 01 p0140 N94-11965
A development on estimation method of undersea light 01 p0204 N94-11974
Proceedings of the PORSEC 1992 in Okinawa: Conference for Pacific Ocean Environments and Probing, volume 2
[JTN-93-80419] 01 p0207 N94-12635
Advanced in macrostatistical hydrodynamics
[DE93-018479] 04 p1410 N94-18270

SOLID WASTES
Integrated, flexible, and rapid geophysical surveying
[DE93-009989] 02 p0712 N94-12906
Vendor information system for innovative treatment technologies. User manual (VISITT version 2.0). Number 2
[PB93-196640] 02 p0821 N94-12936
Environmental awareness
[DE93-014192] 02 p0707 N94-13218
Environmental protection using social costing
[DE94-000492] 05 p1853 N94-22569
Investigating pyrolysis/incineration as a method of resource recovery from solid waste 06 p2444 N94-25375

Oil production from buckwheat stillage by thermochemical liquefaction 07 p2871 N94-28154
Model documentation: Renewable Fuels Module of the National Energy Modeling System
[DE94-009962] 11 p4282 N94-35672
Structural composite construction materials manufactured from municipal solid waste
[AD-A280635] 12 p4403 N94-36730
Estimates of US biomass energy consumption 1992
[DE94-011458] 12 p4463 N94-37567

SOLID-SOLID INTERFACES
Effect of experimental procedure on pattern formation and array disorder in cellular solidification 01 p0117 N94-10203
Surfaces and interfaces of ceramics and metals
[DE93-014959] 02 p0578 N94-13408
Laboratory for x ray optics
[AD-A267149] 03 p1189 N94-15735
Weibull analysis applied to the pull adhesion test and fracture of a metal-ceramic interface
[DE93-012913] 03 p1059 N94-15997
Low temperature deposition and characterization of n- and p-type silicon carbide thin films and associated ohmic and Schottky contacts
[AD-A267966] 03 p0973 N94-17490
Experimental contribution to the contact between two bodies and the effect of roughness
[ECL-91-41] 04 p1451 N94-17918
Micromechanics of interfaces in metal matrix composites
[AD-A271012] 04 p1345 N94-19776
Surface treatment of InP and contribution to the optimization of the InP(p)/InP(p) regrown interfaces grown by GSMBE
[ECL-92-48] 05 p2018 N94-20598
Contribution to the interface micromechanical study and to the damage fundamental phenomena in glass fiber epoxy resin model composites
[ISAL-93-0027] 06 p2227 N94-23133
Interface evaluation in ceramic composites 06 p2255 N94-24231
Chemically sensitive interfacial force microscopy: Contact potential measurements of self-assembling monolayer films
[AD-A273135] 06 p2234 N94-24772
Electron microscopy of AlN-SiC interfaces and solid solutions
[DE94-002449] 07 p3059 N94-26765
A transmission electron microscope study of Ni4W precipitates in a Ni-37 wt. percent W alloy
[ISBN-0-315-59932-4] 07 p2743 N94-27803
Effect of microstructure on the strength and fracture energy of bimaterial interfaces
[AD-A274987] 08 p3178 N94-29126
Interface engineering in alumina fiber/glass composites 08 p3182 N94-29852
A solid-on-solid invasion percolation model for self-affine interfaces
[DE94-608102] 08 p3521 N94-30888
Adsorption of water to the metal/polymer interface studied by neutron and x ray reflectivity
[DE94-005578] 09 p3651 N94-31649
New micro- and macroscopic models of contact and friction
[AD-A277240] 09 p3726 N94-32320
Effects of fiber, matrix, and interphase on carbon fiber composite compression strength
[NASA-CR-4601] 10 p4020 N94-34237

SOLIDIFICATION
NT DIRECTIONAL SOLIDIFICATION (CRYSTALS)
NT MELT SPINNING
Structure and properties of an RS Al-Si-Ni-Mn-Zr alloy for high temperature applications 01 p0064 N94-10063
Convection related radial segregation in an idealized horizontal Bridgman configuration 01 p0115 N94-10185
Wetting effects on nylon spheres engulfment in ice 01 p0115 N94-10189
Thermophysical properties of undercooled liquid metals 01 p0086 N94-10190
Solidification of undercooled Ni-32.5 wt percent Sn eutectic alloy 01 p0086 N94-10194
Undercooled W-Re and Mo-Re drops in an ultra high vacuum drop tube 01 p0086 N94-10195
Non-equilibrium solidification in undercooled Ni-B alloys 01 p0086 N94-10196
Ground results of the Mephisto program: Benefits and space experiments orientation 01 p0086 N94-10197
Solidification and metastable phase formation of highly undercooled Fe-Cr-Ni alloy melts 01 p0087 N94-10204
Thermosolutal convection and macrosegregation in dendritic alloys
[NASA-CR-194039] 02 p0567 N94-12825
Formation of deoxidization products in iron ingot by the addition of Al, Si, and/or Mn (M-5) 02 p0587 N94-13737
Diffusion in liquid state and solidification of binary system (M-7) 02 p0587 N94-13739
Study on solidification of immisible alloys (M-10) 02 p0588 N94-13742
Study on the mechanism of liquid phase sintering (M-12) 02 p0588 N94-13744
Solidification of eutectic system alloys in space (M-19) 02 p0589 N94-13751
Crystal growth of compound semiconductors in a low-gravity environment (InGaAs crystals) (M-22) 02 p0590 N94-13754
Containerless processing of undercooled melts
[NASA-CR-194350] 02 p0572 N94-14123
Measurements of crystal growth kinetics at extreme deviations from equilibrium
[DE93-014526] 02 p0815 N94-14798
Partial melting experiment of Y-Ba-Cu oxide 03 p0945 N94-15168
Remelting of Fe-C-Si-alloy in a ceramic mold skin 03 p0945 N94-15169
Separation behaviour of monotectic alloys 03 p0945 N94-15170
Mechanical properties of magnesium ammonium phosphate cements and their zeolite composites
[DE93-015155] 03 p0934 N94-16057
Particle Engulfment and Pushing by Solidifying Interfaces (PEPSI)
[NASA-CR-193856] 03 p0960 N94-17079
Prediction of non-equilibrium solidification modes in austenitic stainless steel laser welds
[DE93-018457] 04 p1364 N94-19203
Recent advances in high density tungsten composite processing
[AD-A270764] 04 p1344 N94-19576
Microstructure evolution in the presence of constraints and implications on the properties of Mg-Li and Nb-Al constraints
[AD-A272088] 05 p1674 N94-20623
The incongruent melting and melt textured solidification process of Bi2Sr2CaCu3O8
[DE93-041123] 05 p2032 N94-21936
Three-dimensional solidification and melting using magnetic field control 06 p2325 N94-23664
Workshop on the Thermophysical Properties of Molten Materials
[NASA-CP-10121] 06 p2246 N94-25120
Thermophysical property sensitivity effects in steel solidification 06 p2246 N94-25122
A thermodynamic approach to obtain materials properties for engineering applications 06 p2248 N94-25131
Study on the mechanism of titanium alloy toughness and the improvement of properties 07 p2726 N94-25566
Study on solidification of non-homogeneous melting/solidification materials 07 p2728 N94-25573
Solidification modeling of a spiral casting to determine material fluidity
[DE94-002212] 07 p2739 N94-26935
Morphology transitions during non-equilibrium growth processes
[ITN-94-85236] 07 p3065 N94-27243
Differential scanning calorimetric study of solid state amorphization and crystallization in Zr/Co and Zr/Ni multilayers 07 p2745 N94-28161
The corrosion behavior of sputter-deposited magnesium-valve metal alloys 07 p2745 N94-28164
Production of an amorphous Fe(75)Si(10)B(15) sheet by a metallic mold casting method and its properties 07 p2746 N94-28170
Formation and high mechanical strength of Al-based alloys containing a nanoscale icosahedral phase as a main constituent 07 p2746 N94-28171
Melt flow during alloy solidification: Dimensional analysis and model problems
[PB94-138625] 08 p3206 N94-29997
Volume averaged model for the mechanics of alloys solidification
[PB94-138617] 08 p3208 N94-30113
Near-net-shape manufacturing: Spray-formed metal matrix composites and tooling 08 p3186 N94-30447
Terfenol: A study of the phase equilibrium diagram and the solidification process
[DE94-004883] 08 p3209 N94-30690
Survey report of JSUP Space Environment Utilization Research Committee in fiscal year 1992: Metallic Materials Session
[JTN-94-80583] 08 p3159 N94-30794
Solidification structure synthesis in undercooled liquids
[AD-A276166] 09 p3910 N94-31054
Microstructures and mechanical properties of Al3Ti-based alloys: Analysis in single phase and multiphase systems
[ONERA-NT-1993-6] 09 p3640 N94-31420
Solidification microstructures in single-crystal stainless steel melt pools
[DE94-009839] 10 p4024 N94-33880
Ion beam surface treatment: A new capability for rapid melt and resolidification of surfaces
[DE94-008955] 10 p4025 N94-34014
Interface shape and convection during solidification and melting of succinonitrile
[NASA-TM-106487] 11 p4262 N94-35248
Computation of dendrites using a phase field model
[PB94-160744] 11 p4236 N94-35736

SOLIDIFIED GASES
NT SOLID CRYOGENS
NT SOLID NITROGEN
Modeling the reflectance of CO2 frost with new optical constants: Application to Martian south polar cap spectra 03 p1256 N94-16217
Stability of the face-centered-cubic phase of heavy rare gas solids
[DE93-019949] 05 p1679 N94-20319
Theoretical phase diagrams for solid H(sub 2)
[DE94-001049] 05 p1684 N94-22395
Studies of the thermal and optical responses of H atoms in solid H2
[NASA-CR-196114] 12 p4514 N94-36984

SOLIDS
NT SOLID CRYOGENS
NT SOLID NITROGEN
NT SOLIDIFIED GASES
X ray and gamma ray spectroscopy of solids under pressure
[DE93-014847] 01 p0076 N94-10653
Characterization of an excimer laser-ablated plasma and applications 01 p0392 N94-11450
Corrosion control by vitreous films on aluminum and high T(sub c) superconductors
[AD-A266016] 01 p0085 N94-12393
Micromechanical strength effects in shock compression of solids
[DE93-014425] 02 p0670 N94-12887
Assimilation of solids during ascent of magmas from the Bartoy Field of the Baikal Region, Siberia 03 p1103 N94-16214
Process of shaping an electrorheological solid
[AD-D015885] 03 p1012 N94-16914
Interaction of intense lasers and relativistic electron beams with solids, gases and plasmas
[AD-A269655] 04 p1439 N94-18737
Stress pulse phenomena
[DE93-019064] 04 p1456 N94-19078
Predictive modeling of particle-laden, turbulent flows
[DE94-003298] 07 p2792 N94-26319
The free vibration of plates, shallow shells and solids
[ISBN-0-315-83931-7] 07 p2838 N94-26622
Lisp interface to geometric modelling operations
[PB94-133121] 07 p3001 N94-28398
Laser-material interactions: A study of laser energy coupling with solids
[DE94-005212] 08 p3292 N94-28478
Two-phase power-law modeling of pipe flows displaying shear-thinning phenomena
[DE94-005115] 08 p3279 N94-30020
Calculation of inelastic mean free path and stopping power for electrons in solids from an optical-data model
[USIP-92-06] 08 p3494 N94-30980
Empirical and semi-empirical relationships of liquid-vapor, solid-vapor, and solid-liquid surface energies
[AD-A276480] 09 p3631 N94-31248
The Sixth Symposium on Unconventional Photoactive Solids. Abstracts
[AD-A277198] 09 p3655 N94-32016
The 10th International Conference on Internal Friction and Ultrasonic Attenuation in Solids (ICIFUAS)
[AD-A276849] 09 p3902 N94-32209
Advances and applications of dynamic-angle spinning nuclear magnetic resonance
[DE94-007031] 09 p3870 N94-32250
X ray and gamma ray spectroscopy of solids under pressure
[DE94-011207] 11 p4238 N94-36203
Determination of density of mass standards: Requirement and method
[PB94-163078] 12 p4508 N94-36718
Electronic balance and some gravimetric applications (the density of solids and liquids, pycnometry and mass)
[PB94-163052] 12 p4446 N94-36719

SOLIDS FLOW
Stability analysis for the flow of granular materials down an inclined plane using kinetic model
[DE93-016852] 03 p1026 N94-16958

Numerical study of the flow of granular materials down an inclined plane
[DE94-010729] 12 p4444 N94-37544

SOLIDUS

Partial melting of the St. Severin (LL) and Lost City (H) ordinary chondrites: One step backwards and two steps forward 11 p4353 N94-36146

SOLITARY WAVES

Marangoni-driven solitary waves 01 p0119 N94-10214
Quantum solitons with cylindrical symmetry
[DE93-617659] 01 p0344 N94-10881
Nonlinear excitation in quasi-one-dimensional Peierls dielectrics with charge density waves
[DE93-613827] 01 p0398 N94-11025
Creation and annihilation of solitons in nonlinear integrable systems
[DE93-621379] 01 p0365 N94-11078
Negative viscosity and generation of dissipative solitons and zonal dissipative structures by drift waves
[DE93-621656] 01 p0392 N94-11212
Femtosecond dynamics, photoexcitation, and ESR spectra of MX chain solids
[AD-A264689] 01 p0399 N94-11263
Solitons and 1/f noise in molecular chains
[DE93-622898] 02 p0778 N94-12879
Soliton equations and self-dual gauge fields
[DE93-626620] 02 p0818 N94-14887
Dynamics of douple stimulated Brillouin scattering 03 p1200 N94-15206
Soliton-like structures in double stimulated Brillouin scattering 03 p1200 N94-15207
The quantum mass shift of the soliton in Skyrme model
[ITN-93-85219] 03 p1180 N94-15283
Search for far infrared radiation from optically pumped defect modes
[AD-A266744] 03 p1206 N94-15822
Pulse propagation in inhomogeneous optical waveguides
[DE93-013378] 03 p1191 N94-16007
Lattice relaxation theory of localized excitations in quasi-one-dimensional systems
[DE93-624947] 03 p1215 N94-17437
A method for solving the KDV equation and some numerical experiments
[DE93-624726] 04 p1550 N94-19246
Investigations in gauge theories, topological solitons, and string theories
[DE93-015029] 04 p1609 N94-19250
Multidimensional solitons in fiber arrays
[DE93-019923] 05 p1983 N94-19862
Spatial patterns in semiconductor lasers
[DE93-040056] 05 p1814 N94-19865
Two-dimensional nonlinear Schrodinger equations and their properties
[AD-A272184] 05 p1952 N94-20923
The onset and spectra of a magnetized Langmuir turbulence 05 p2006 N94-22673
Coherent state approach for the (Phi)(sup 6)-lattice model and phase transitions
[DE93-613053] 07 p3050 N94-25825
Chaotic dynamics of the solar cycle
[AD-A274315] 07 p3110 N94-26883
Papers in meteorology and geophysics, vol. 44, no.1
[JTN-94-80585] 08 p3324 N94-28693
On the linear stability of Verkley's modons 08 p3324 N94-28695
A note on the Poisson brackets associated with Lax operators
[MATHS-REPT-A-195] 08 p3464 N94-29482
Forced generation of solitary waves in a rotating fluid and their stability 08 p3274 N94-29689
A relativistic solitary wave in electron positron plasma
[DE94-608107] 08 p3507 N94-30071
Langmuir waves in the electron-positron plasma
[DE94-608330] 08 p3508 N94-30191
Future directions of nonlinear dynamics in physical and biological systems. (Physica D nonlinear, volume 68, number 1)
[AD-A278085] 09 p3794 N94-33250
Theoretical studies of ultrashort phenomena
[AD-A278938] 11 p4332 N94-35664
Solitary waves and homoclinic orbits
[DE94-009428] 11 p4264 N94-35681
The 2+1-dimensional integrable generalization of the Sine-Gordon equation
[DE94-611074] 11 p4315 N94-36100
The nucleon-nucleon potential in the chromodielectric soliton model
[DE94-004646] 11 p4329 N94-36305
Nonlinearity with disorder: Spatio-temporal complex behavior arising from length scales competition
[DE94-000675] 12 p4502 N94-36685
Variational discrete symmetries
[DE94-618485] 12 p4507 N94-37062
Unstable solitary-wave solutions of the generalized Benjamin-Bona-Mahony equation
[DE94-013302] 12 p4496 N94-37549
Langmuir waves in the electron-positron plasma
[DE94-618779] 12 p4531 N94-37728

SOLITONS

U SOLITARY WAVES

SOLUBILITY

Determination of concentration profiles at interfaces and surfaces of partially miscible polymer blends
[DE93-013140] 01 p0089 N94-11007
Measurement of viscosity, density and gas solubility of refrigerant blends
[DE93-014772] 01 p0089 N94-11145
Joint pain and Doppler-detectable bubbles in altitude (Hypobaric) decompression 01 p0312 N94-11542
The solubility of epsilon-CL-20 in selected materials
[DE93-009304] 01 p0077 N94-11602
Polymer-polymer interactions
[AD-A265304] 01 p0091 N94-11830
The solubility of gold in silicate melts: First results 01 p0087 N94-12086
Graphite solubility and co-vesiculation in basalt-like melts at one-ATM 01 p0463 N94-12173
Breadboard activities for advanced protein crystal growth
[NASA-CR-193559] 02 p0803 N94-12796
Miscibility of lubricants with refrigerants, phase 1
[DE93-014766-PHASE-1] 02 p0596 N94-13407
Destruction of waste energetic materials using base hydrolysis
[DE93-012738] 02 p0584 N94-13491
Study on solidification of immisible alloys (M-10) 02 p0588 N94-13742
The Lindemann criterion of melting for pure and mixed ionic crystals
[ITN-93-85210] 02 p0814 N94-14554
Efficacy of flocculating and other emergency water purification tablets
[AD-A266695] 03 p1148 N94-15840
Siderophile elements in the upper mantle of the Earth: New clues from metal-silicate partition coefficients 03 p1103 N94-16250
Partitioning of Nb, Mo, Ba, Ce, Pb, Th and U between immiscible carbonate and silicate liquids: Evaluating the effects of P2O5,F, and carbonate composition 03 p0953 N94-16283
Soluble precursor route to polyanilines
[AD-A268015] 03 p0973 N94-17494
Molecular composites from liquid crystalline polymers and liquid crystalline thermosets
[DE93-016608] 04 p1368 N94-18096
Measurement of viscosity, density, and gas solubility of refrigerant blends in selected synthetic lubricants
[DE93-040221] 04 p1350 N94-18977
High performance heavy alloys by alloying and process control
[AD-A271129] 05 p1689 N94-20019
The use of x ray techniques in the in situ study of corrosion
[DE93-019845] 05 p1690 N94-20301
Cathode materials for the molten carbonate fuel cell
[DE93-019515] 05 p1848 N94-21870
Water-enhanced solvation of organics
[DE93-040297] 05 p1683 N94-21947
Di(hydroxyphenyl)- benzimidazole monomers
[NASA-CASE-LAR-14643-2] 06 p2253 N94-23305
Humidity effects on soluble core mechanical and thermal properties (polyvinyl alcohol/microballoon composite) type CG extendospheres, volume 2
[NASA-CR-193893] 06 p2229 N94-24224
Temperature dependence of protein solubility-determination, application to crystallization, and growth kinetics studies 06 p2224 N94-24344
Ultrastructure processing of macromolecular materials
[AD-A273413] 06 p2258 N94-24782
Center for advanced electrical and structural polymers
[AD-A273415] 06 p2259 N94-24783
Measurement of viscosity, density, and gas solubility of refrigerant blends in selected synthetic lubricants
[DE94-003609] 07 p2713 N94-25934
A Shuttle mechanism for molten-electrolyte lithium batteries
[DE94-002914] 07 p2781 N94-26144
Liquid and solid solubility of Ag in Bi2Sr2CaCu2O8
[DE94-002829] 07 p2735 N94-26273
Influence of lattice damage on retention and transport of deuterium in beta silicon carbide
[DE94-005206] 07 p3068 N94-27693
Solubility, viscosity, and density of refrigerant/lubricant mixtures
[DE94-004237] 07 p2721 N94-28069
Solubility of Nd in brine
[DE94-005099] 08 p3187 N94-28567
Crystallization of silver chromate from ethanol via salt metathesis reactions of solubilized precursors
[AD-A275178] 08 p3189 N94-29058
Cloud studies seen from a physical chemist's perspective
[DE94-006059] 09 p3771 N94-31527
Inorganic materials for anomalous-dispersion phase-matched second harmonic generation: Rubidium titanyl arsenate isomorphs, Rb(Ti(1-2x)Ln(x)Nb(x))OAsO4
[DE94-006141] 09 p3899 N94-31847
Measurement of viscosity, density, and gas solubility of refrigerant blends in selected synthetic lubricants
[DE94-007723] 09 p3653 N94-31917
Phase relationships and stability of the (mu)- and (zeta)-phases in the Ag-Al-X (X=Zn, Ga, Ge) systems
[DE94-009391] 09 p3648 N94-33270
Flooded cell permeation testing of elastomers
[AD-A277698] 10 p4026 N94-33438
Measurement of viscosity, density, and gas solubility of refrigerant blends in selected synthetic lubricants
[DE94-010426] 11 p4244 N94-35687
Solubility, viscosity and density of refrigerant/lubricant mixtures
[DE94-009996] 11 p4245 N94-35771
A classical model for closed-loop diagrams of binary liquid mixtures
[DE94-011011] 11 p4237 N94-36033
Methyl chloride via oxyhydrochlorination of methane
[DE94-010691] 12 p4406 N94-36450

SOLUTES

The effect of gravity modulation on thermosolutal convection 01 p0105 N94-10103
The effect of gravitational modulation on convection in vertical Bridgman growth 01 p0113 N94-10178
Experimental studies of the structure of grain boundaries
[DE93-013979] 01 p0402 N94-11700
The importance of hard core repulsion in models of activity coefficients in aqueous electrolyte solutions: Illustration in the case of hydration theory
[DE93-012476] 02 p0561 N94-12881
Linear and nonlinear spectroscopic probing of solute interactions with chemically modified silica surface
[DE93-014648] 02 p0562 N94-13001
Direct probing of chromatography columns by laser-induced fluorescence
[DE93-015208] 02 p0654 N94-13022
Pore-size-distribution of cationic polyacrylamide hydrogels
[DE93-015218] 02 p0581 N94-14400
Reactor studies of metal ions associated with chromatographic silica
[AD-A266675] 02 p0573 N94-14779
Measurements of crystal growth kinetics at extreme deviations from equilibrium
[DE93-014526] 02 p0815 N94-14798
The effect of composition on the mechanism of continuous recrystallization and superplastic response of aluminum-scandium alloys
[DE93-018594] 04 p1365 N94-19280
Melt spinning study
[NASA-CR-193823] 04 p1380 N94-19423
Water-enhanced solvation of organics
[DE93-040297] 05 p1683 N94-21947
Influence of grain structure and solute composition on the work hardening behavior of aluminium at cryogenic temperatures
[DE94-003415] 07 p2733 N94-26087
Defect-solute interactions near irradiation grain boundaries
[DE94-006215] 09 p3641 N94-31627
Solvent acidity and basicity in polar media and their role in solvation
[AD-A278604] 11 p4239 N94-36426
Elemental mapping of segregation in stainless steels with an imaging filter
[DE94-012659] 12 p4417 N94-37304

SOLUTIONS

NT AIR
NT AQUEOUS SOLUTIONS
NT COMPRESSED AIR
NT DETONABLE GAS MIXTURES
NT GAS MIXTURES
NT HIGH TEMPERATURE AIR
NT LIQUID AIR
NT NUCLEAR EMULSIONS
NT PHOTOGRAPHIC EMULSIONS
NT SOLID SOLUTIONS

Synthesis of molecular sieves from clear solution 01 p0124 N94-10245
Solution chemistry optimization of sol-gel processed PZT thin films
[DE93-013776] 02 p0814 N94-14695

Computer simulation of molecular interactions in supercritical solvents
[AD-A274977] 08 p3486 N94-29087
Solvent diffusion coefficient concentration dependence in polymer solutions
[AD-A277023] 09 p3655 N94-32005
Influence of trace components on the viscoelastic properties of a polymer solution
[AD-A277171] 09 p3656 N94-32253
Dynamics of block poly(styrene-co-vinylpyridine) (SVP) in solution and on silica
[AD-A277139] 09 p3657 N94-32364
Method of determining the concentration of a chemical of interest in a solution
[AD-D016165] 10 p4021 N94-33765

SOLVATION
Polar solvation and electron transfer
[DE93-013328] 01 p0365 N94-11010
Ultrafast photoinduced electron transfer reactions in supramolecular arrays: Studies of electronic coupling and solvation
[DE93-012910] 02 p0782 N94-13484
Removal of carbonaceous contaminants from silica aerogel 03 p0953 N94-16256
Supercritical thermodynamics of sulfur and nitrogen species
[DE93-017727] 03 p1220 N94-16997
Solvational barriers to interfacial electron transfer: Minimization by way of valence delocalization
[AD-A267371] 03 p0950 N94-17006
Continuum solvent models for computational chemistry
[DE93-016329] 03 p0953 N94-17660
Femtosecond Fourier-transform spectroscopy of low-frequency intermolecular motions in weakly interacting liquids
[DE93-017312] 04 p1566 N94-18085
Water-enhanced solvation of organics
[DE93-040297] 05 p1683 N94-21947
Structures of Cl(-)(H2O)(n) and F(-)(H2O)(n) (n equal to 2,3...15) clusters: Molecular dynamics computer simulations
[AD-A273474] 06 p2537 N94-24940
The electrochemistry of the solvated electron: A study of its properties and of its applications
[ETN-94-95313] 06 p2236 N94-25296
Radiation and photochemistry section
[DE94-008880] 09 p3873 N94-32757
The kinetics of heterogeneous electron transfer reactions in polar solvents
[AD-A278459] 10 p4136 N94-33540
United States Air Force Summer Research Program, 1993. Volume 6: Arnold Engineering Development Center, Frank J. Seiler Research Laboratory and Wilford Hall Medical Center
[AD-A278697] 12 p4551 N94-36982

SOLVENT EXTRACTION
Synthesis of organic ligands for f-element separations
[DE93-012915] 02 p0554 N94-14290
Theory, modeling, and simulation
[DE93-015607] 02 p0755 N94-14571
Summary report for supercritical carbon dioxide extraction and carbonization of Resorcinol-Formaldehyde (RF) foams
[DE93-016924] 04 p1346 N94-17987
Molecular structure of coal studied by solvent extraction 08 p3187 N94-28676
Methanol-mediated continuous extraction of phenolic compounds from coal liquid 08 p3188 N94-28679
Recovery of carboxylic acids at pH greater than pKa
[DE94-007030] 09 p3636 N94-32376
A spreadsheet algorithm for stagewise solvent extraction
[DE94-009735] 10 p4106 N94-33878
Study on extraction behavior of TRPO with different composition
[DE94-620287] 12 p4412 N94-37534

SOLVENTS
NT TETRAHYDROFURAN
Polar solvation and electron transfer
[DE93-013328] 01 p0365 N94-11010
Dynamics of charge-transfer excited states relevant to photochemical energy conversion
[DE93-013981] 01 p0263 N94-11116
Joint pain and Doppler-detectable bubbles in altitude (Hypobaric) decompression 01 p0312 N94-11542
Solvent dynamical effects in electron transfer: Molecular dynamics simulations of reactions in methanol
[AD-A266061] 01 p0369 N94-12420
Molecular solvent-dynamical effects on activated electron-transfer kinetics: How important is solvent friction?
[AD-A265886] 02 p0779 N94-12894
Experimental and theoretical study of inhomogeneous electron transfer in betaine: Comparisons of measured and predicted spectral dynamics
[AD-A265703] 02 p0780 N94-13051
Computer simulations for the adsorption of polymers onto surfaces
[DE93-016667] 02 p0577 N94-13070
Synthesis and properties of novel cluster phases
[DE93-017056] 02 p0577 N94-13072
Destruction of waste energetic materials using base hydrolysis
[DE93-012738] 02 p0584 N94-13491
Synthesis of organic ligands for f-element separations
[DE93-012915] 02 p0554 N94-14290
Workshop on Formation of Supermolecular Structures in Composite Fluid: Phase Rule and Dynamics
[DE93-782887] 02 p0581 N94-14421
Solution chemistry optimization of sol-gel processed PZT thin films
[DE93-013776] 02 p0814 N94-14695
The photophysics of poly(methylphenylphosphazene)
[AD-A267321] 03 p0970 N94-16949
Supercritical thermodynamics of sulfur and nitrogen species
[DE93-017727] 03 p1220 N94-16997
Pulsed laser kinetic studies of liquids under high pressure
[DE93-017826] 03 p1041 N94-16998
Continuum solvent models for computational chemistry
[DE93-016329] 03 p0953 N94-17660
Densities and viscosities of ternary ammonia/water fluids
[DE93-015966] 04 p1351 N94-19118
Femtosecond Raman-induced Kerr effect study of polar solvent dynamics: Amides
[DE93-017563] 05 p1678 N94-19924
Chain propagation/step propagation polymerization chemistry. The preparation of solvent resistant well phase-separated thermoplastic elastomers
[AD-A271128] 05 p1699 N94-20016
Integral equation calculation of solvent activation free energies for electron and proton transfer reactions
[AD-A272665] 05 p1681 N94-21216
Dynamics of adsorbed, swollen block copolymers
[AD-A272013] 05 p1706 N94-21460
Techniques for the flux growth of optical materials: Growth of beta-barium borate
[AD-A272717] 05 p2028 N94-21505
Femtosecond dynamics in hydrogen-bonded solvents
[DE93-019937] 05 p1683 N94-21842
Water-enhanced solvation of organics
[DE93-040297] 05 p1683 N94-21947
FTIR quantification of industrial hydraulic fluids in perchloroethylene 06 p2264 N94-23243
Phenylethynl-terminated poly(arylene ethers)
[NASA-CASE-LAR-14797-1] 06 p2253 N94-23307
Selection of polymer binders and fabrication of SiC fiber-reinforced reaction-bonded silicon nitride matrix composites
[NASA-CR-194874] 06 p2255 N94-24223
Ozone depletion, paradigms, and politics
[DE94-001600] 06 p2398 N94-24506
Aqueous alkaline cleaners: An alternative to organic solvents
[AD-A273510] 06 p2260 N94-24848
Potent solvents for C60 and their utility for the rapid acquisition of 13CNMR data for fullerenes
[AD-A273349] 06 p2235 N94-24925
The reactivity of lithium toward non-aqueous solvents of relevance to energy storage applications as studied by surface analytical techniques
[DE94-003483] 07 p2856 N94-26464
Effects of plastic media blasting on aircraft skin
[AD-A274817] 07 p2668 N94-26488
Evaluating non-chlorinated solvents for welding applications
[DE94-003332] 07 p2824 N94-27181
Solubility of Nd in brine
[DE94-005099] 08 p3187 N94-28567
Computer simulation of molecular interactions in supercritical solvents
[AD-A274977] 08 p3486 N94-29087
Poly(arylene ether-co-imidazole)s as toughness modifiers for epoxy resins
[NASA-CASE-LAR-15229-1-CU] 08 p3215 N94-29451
Non-aqueous cleaning solvent substitution
[DE94-005339] 08 p3219 N94-30245
Non-aqueous cleaning solvent substitution 08 p3354 N94-30466
Supersonic gas-liquid cleaning system 08 p3240 N94-30467
Regenerating using aqueous cleaners with ozone and electrolysis 08 p3240 N94-30468
Theory for electron-transfer reactions involving two Marcus surfaces with a different force constant
[DE94-005925] 08 p3493 N94-30874
Solvent diffusion coefficient concentration dependence in polymer solutions
[AD-A277023] 09 p3655 N94-32005
Dynamics of block poly(styrene-co-vinylpyridine) (SVP) in solution and on silica
[AD-A277139] 09 p3657 N94-32364
Radiation and photochemistry section
[DE94-008880] 09 p3873 N94-32757
The kinetics of heterogeneous electron transfer reactions in polar solvents
[AD-A278459] 10 p4136 N94-33540
Automated cleaning of electronic components
[DE94-008742] 10 p4082 N94-34009
Cleaning up our act: Alternatives for hazardous solvents used in cleaning
[DE94-006624] 11 p4285 N94-35943
Some perspectives on solution-phase electron-transfer processes
[AD-A278616] 11 p4238 N94-36252
Solvent acidity and basicity in polar media and their role in solvation
[AD-A278604] 11 p4239 N94-36426
Solvent effects on the energetics and dynamics of ultrafast electron transfer in chlorophyll-porphyrin-acceptor triads
[DE94-009693] 12 p4477 N94-36554
Integrated environmentally compatible soldering technologies
[DE94-013456] 12 p4464 N94-37071

SOMALIA
Human dimensions research team, operation restore hope
[AD-A274340] 07 p2939 N94-27056

SONAR
NT SONOBUOYS
Acoustic characteristics of side scan sonar and sub-bottom profiler for 10,000 m class ROV 01 p0172 N94-11916
Mapping bathymetric slopes from bathymetry data
[AD-A265923] 01 p0290 N94-12350
Signal feature analysis using neural networks and psychoacoustics
[AD-A266048] 01 p0340 N94-12398
Signal processing in impulsive electromagnetic interference
[AD-A266425] 03 p0998 N94-16557
Synthesis and evaluation of polymeric materials
[AD-A267809] 03 p0973 N94-17408
Fabrication of a NAVMAP, a deep-sea mapping system
[AD-A268630] 03 p1085 N94-17467
Processing and analysis of SeaMARC 2 data: Fieberling guyot; raw phase experiment in Norwegian-Greenland Sea
[AD-A269930] 04 p1498 N94-18662
A register of underwater acoustic test facilities in the US, Canada, and the United Kingdom
[AD-A270884] 04 p1500 N94-19785
A tracking sonar sensor for vehicle guidance
[OUEL-1956/92] 06 p2472 N94-23179
Improved magnetostrictive transducer drive elements achieved by reduction of crystalline defects and improved crystalline orientation
[AD-A273391] 06 p2313 N94-25276
Enhanced adaptive statistical filter providing improved performance for target motion analysis noise discrimination statement of government interest
[AD-D016039] 07 p2786 N94-27109
Seafloor characterization using texture
[AD-A275399] 08 p3377 N94-29204
Design of the biosonar simulator for dolphin's clicks waveform reproduction 08 p3234 N94-29707
Sonar sensing and obstable detection 08 p3309 N94-30301
Iterative removal of boundary minima of harmonic potential function for mobile robot navigation
[REPT-93-059] 08 p3449 N94-30962
Analysis using bi-spectral related technique
[AD-A276017] 09 p3672 N94-31386
Multi-scale studies of seafloor topography
[AD-A277008] 09 p3789 N94-32400
A predictive parametric model for volume scattering strength in the deep ocean with an application to nighttime near-surface scattering in the North Sargasso Sea below 16 kHz
[AD-A277902] 10 p4091 N94-33592

SONDES
NT IONOSONDES
NT RADIOSONDES
NT RAWINSONDES

Water vapor from sunradiometry in comparison with microwave and balloon-sonde measurements at the Southern Great Plains ARM Site
[DE94-007479] 09 p3786 N94-32759

SONIC ANEMOMETERS

Determination of momentum flux using a bivane and cup anemometer
[AD-A265414] 03 p1105 N94-15137
Comparison between 1-minute and 15-minute averages of turbulence parameters 06 p2528 N94-24218

SONIC BOOMS

The problem of the sonic boom for future high-speed transport aircraft
[ESA-TT-1286] 02 p0776 N94-13692
Variability of measured sonic boom signatures. Volume 1: Technical report
[NASA-CR-191483-VOL-1] 06 p2526 N94-24172
Variability of measured sonic boom signatures. Volume 2: Data report
[NASA-CR-191483-VOL-2] 06 p2526 N94-24173
Preliminary design of nine high speed civil transports 07 p2671 N94-25710
High-Speed Research: Sonic Boom, Volume 1
[NASA-CP-10132] 07 p2649 N94-28188
Progress in modeling atmospheric propagation of sonic booms 07 p2650 N94-28189
Implications for high speed research: The relationship between sonic boom signature distortion and atmospheric turbulence 07 p2650 N94-28190
Interaction of the sonic boom with atmospheric turbulence 07 p2650 N94-28191
Sonic boom propagation through turbulence: A ray theory approach 07 p2650 N94-28192
The propagation of spark-produced N waves through turbulence 07 p2650 N94-28193
On the aging of sonic booms 07 p2650 N94-28194
Experimental studies of loudness and annoyance response to sonic booms 07 p2651 N94-28195
Comparison of methods of predicting community response to impulsive and nonimpulsive noise 07 p2651 N94-28196
Variability of measured sonic boom signatures 07 p2651 N94-28197
Sonic booms and marine mammals: Informational status and recommendations 07 p2651 N94-28198
Numerical analysis of sonic boom in the near field 08 p3125 N94-28962
Subjective response to sonic booms having different shapes, rise times, and durations
[NASA-TM-109090] 08 p3479 N94-29464
Investigation of sonic boom for the Space Shuttle: High cross-range orbiter
[NASA-TM-108238] 09 p3860 N94-31336
Investigation of sonic boom for the Space Shuttle: Low cross-range orbiter
[NASA-TM-108237] 09 p3860 N94-31337
First Annual High-Speed Research Workshop, part 1
[NASA-CP-10087-PT-1] 10 p3970 N94-33447
Update on Douglas' high-speed civil transport studies 10 p3970 N94-33450
Headquarters summary reports 10 p3970 N94-33452
Airframe systems studies review 10 p3970 N94-33453
High-speed research program systems analysis activities at Ames Research Center 10 p3971 N94-33455
Overview of Langley systems studies 10 p3971 N94-33456
First Annual High-Speed Research Workshop, part 2
[NASA-CP-10087-PT-2] 10 p3972 N94-33462
Design and analysis of low boom concepts at Langley Research Center 10 p3973 N94-33470
HSCT design for reduced sonic boom 10 p3973 N94-33471
Sonic boom prediction and minimization using computational fluid dynamics 10 p3973 N94-33472
Sonic boom configuration minimization 10 p3973 N94-33473
Sonic boom predictions using a modified Euler code 10 p3973 N94-33474
Overview of feasibility study on conducting overflight measurements of shaped sonic boom signatures using RPV's 10 p3973 N94-33475
Aeroacoustics analysis and community noise overview 10 p3975 N94-33488
Atmospheric effects on sonic boom: A program review 10 p3976 N94-33495
Relaxation and turbulence effects on sonic boom signatures 10 p3976 N94-33496
The effect of turbulence and molecular relaxation on sonic boom signatures 10 p3976 N94-33497
Statistical and numerical study of the relation between weather and sonic boom characteristics 10 p3976 N94-33498
Overview of NASA human response to sonic boom program 10 p3976 N94-33499
Sonic boom acceptability studies 10 p3977 N94-33500
Georgia Tech sonic boom simulator 10 p3977 N94-33501
Sonic boom (human response and atmospheric effects) outdoor-to-indoor response to minimized sonic booms 10 p3977 N94-33502
Transonic airframe propulsion integration 10 p3978 N94-33507
A laboratory study of subjective annoyance response to sonic booms and aircraft flyovers
[NASA-TM-109113] 10 p4132 N94-33610

SONIC FATIGUE

U ACOUSTIC FATIGUE

SONIC FLOW

U TRANSONIC FLOW

SONIC NOZZLES

Control jets in interaction with hypersonic rarefied flow 07 p2698 N94-28020
Static performance investigation of a skewed-throat multiaxis thrust-vectoring nozzle concept
[NASA-TP-3411] 10 p3983 N94-34172

SONIC SPEED

U ACOUSTIC VELOCITY

SONOLUMINESCENCE

Sonoluminescence from flow over a hydrofoil in a cavitation tunnel
[ISVR-TR-223] 10 p4047 N94-34067

SOOT

Dust production in the envelopes of carbon stars: R Coronae Borealis
[ETN-93-94389] 02 p0839 N94-14075
Modeling study to evaluate the ionic mechanism of soot formation in flames
[AD-A266242] 03 p0950 N94-16930
Mechanistic models of soot formation
[AD-A267806] 03 p0950 N94-17008
Surface reactivity of combustion generated soot particles
[AD-A268017] 03 p0952 N94-17532
Novel catalysts for methane activation
[DE93-040630] 04 p1349 N94-18532
Dual-beam multiple wavelength light transmittance measurement for particle sizing in rocket motor plumes
[AD-A272491] 05 p1670 N94-21208
Numerical prediction of turbulent sooting diffusion flames 08 p3191 N94-29253
Measurements and predictions of the combustion characteristics of enclosed swirl-stabilized propane flames
[IECE-CFE-TR-001] 08 p3198 N94-30017
Soot and liquid-phase fuel distributions in a newly designed optically accessible DI diesel engine
[DE94-005648] 09 p3723 N94-31651
Photothermal laser deflection, an innovative technique to measure particles in exhausts
[AD-A277151] 09 p3718 N94-32366
Development of predictive reaction models of soot formation
[AD-A278366] 10 p4021 N94-33701
Detailed studies of soot formation in laminar diffusion flames for application to modeling studies
[AD-A278941] 11 p4235 N94-35604
Laser-saturated fluorescence measurements in laminar sooting diffusion flames
[NASA-CR-191025] 12 p4508 N94-36643

SORBENTS

NT ABSORBENTS
NT ADSORBENTS
A calcium oxide sorbent process for bulk separation of carbon dioxide
[DE93-019288] 05 p1847 N94-21540
Recovery of carboxylic acids at pH greater than pKa
[DE94-007030] 09 p3636 N94-32376
High temperature sorbents for oxygen
[NASA-CASE-NPO-18409-1-CU] 11 p4235 N94-35255

SORET COEFFICIENT

On the role of Soret effect in concentration distribution in crystals growing from the melt 01 p0112 N94-10173
Marangoni Benard instabilities in liquid mixtures with Soret effect 01 p0119 N94-10215

SORPTION

NT ADSORPTION
NT CHEMISORPTION
Ocean uptake of carbon dioxide
[DE93-012967] 02 p0707 N94-13384
Portable acoustic wave sensor systems for real-time monitoring of volatile organic compounds
[DE93-013753] 02 p0582 N94-14511
Fibers and materials of medical application 03 p0938 N94-16855
Application of the Positron Annihilation Technique to the study of vapor absorption process in polyethylene (LDPE) and in imide polymer (6FDA-TMPD PI)
[DE94-602737] 07 p2720 N94-27998
Diffusion and sorption of 1,4-dioxane into polychloroprene
[AD-A277743] 10 p4026 N94-33446
High temperature sorbents for oxygen
[NASA-CASE-NPO-18409-1-CU] 11 p4235 N94-35255
Diffusion and sorption of 1,4-dioxane into polychloroprene
[ARL-TR-338] 11 p4229 N94-35361
New materials and multidimensional cluster analysis for SAW chemical sensor arrays
[DE94-012066] 12 p4409 N94-37161

SORTING

U CLASSIFYING

SOS (SEMICONDUCTORS)

Porous silicon for pumping solid-state lasers
[AD-A266293] 03 p1039 N94-16474
Radiation hardened microprocessor for small payloads 04 p1327 N94-19184
Single-event upset testing of the performance semiconductor 1750A CMOS/SOS chip set
[AD-A271158] 05 p2015 N94-20184
Fully-depleted silicon-on-sapphire and its application to advanced VLSI design 05 p1765 N94-21709
Laser energized high voltage direct current power supply
[AD-D015977] 06 p2312 N94-25036

SOT

U SOLAR OPTICAL TELESCOPE

SOUND

U ACOUSTICS

SOUND ABSORPTION

U SOUND TRANSMISSION

SOUND AMPLIFICATION

Journal of rehabilitation research and development, volume 30, number 1, 1993
[AD-A272956] 05 p1893 N94-21613

SOUND BARRIER

U ACOUSTIC VELOCITY

SOUND DETECTING AND RANGING

Mathematical model and analysis of the Tactical Unmanned Ground Vehicle (TUGV) using computer simulation
[AD-A272258] 05 p1824 N94-20576
Ground characterization for JAPE 06 p2527 N94-24213
JAPE 91: Influence of terrain masking of the acoustic propagation of helicopter noise 06 p2528 N94-24214
Acoustic target detection and classification using neural networks 06 p2529 N94-24221
Preliminary analysis of the JAPE ground vehicle test data with an artificial neural network classifier 06 p2529 N94-24222
Prewhitening of colored noise fields for detection of threshold sources
[AD-A274346] 07 p3010 N94-26923
Enhanced adaptive statistical filter providing improved performance for target motion analysis noise discrimination statement of government interest
[AD-D016039] 07 p2786 N94-27109
A review of signal detection using the bispectrum with applications in underwater acoustics
[AD-A275227] 08 p3478 N94-29388
Nonlocal methods for signal detection and estimation in the dependent nonstationary environment
[AD-A278472] 10 p4033 N94-33594
Multiparameter bifurcations and applications
[AD-A278365] 10 p4133 N94-33858
Real-time SAW measurements of NVR in cleanroom and in microenvironment
[DE94-011937] 12 p4389 N94-37159

SOUND DETECTORS

U SOUND TRANSDUCERS

SOUND FIELDS

Determination of the viscous acoustic field for liquid drop positioning/forcing in an acoustic levitation chamber in microgravity 01 p0110 N94-10131
Underwater hearing: A review
[ISVR-TR-212] 02 p0777 N94-14130
Acoustic intensity measurements in the presence of low Mach number flow
[AD-A269995] 04 p1562 N94-18664
Beamforming in an acoustic shadow 06 p2528 N94-24219
Characterization of structural vibration: Field descriptors based on energy density and intensity
[PB94-132230] 08 p3316 N94-28404

Scattering of a random acoustic field by an infinite cylinder: Application to the modelization of the acoustic environment of the 'Ariane 5' launcher scale-model using experimental data
[ONERA-NT-1993-11] 09 p3860 N94-31226
Computer implementation of Arnott's formulation of thermoacoustics using MATLAB
[AD-A276356] 09 p3860 N94-31257
Wavevector-frequency analysis with applications to acoustics
[AD-A276618] 09 p3861 N94-32125
A geoacoustic model for fine-grained, unconsolidated calcareous sediments (ARSRP natural laboratory)
[AD-A277830] 10 p4092 N94-33831

SOUND FREQUENCIES
U ACOUSTIC FREQUENCIES

SOUND GENERATORS
Direct numerical simulation of hot jets
01 p0156 N94-12295
Acoustic propagation modeling using MATLAB
[AD-A270905] 04 p1564 N94-19750
Acoustic monitoring of global ocean variability
[AD-A271998] 05 p1883 N94-21366
Joint Acoustic Propagation Experiment (JAPE-91) Workshop
[NASA-CP-3231] 06 p2526 N94-24207
Joint Acoustic Propagation Experiment (JAPE)
06 p2527 N94-24208
Some results gained from JAPE: An overview
06 p2527 N94-24209
Effects of atmospheric variations on acoustic system performance 06 p2527 N94-24211
Modern photoacoustic spectroscopy problems. Theory and experiment (a review)
[IFTR-41/1993] 07 p2716 N94-26823
Hydroacoustic wave-fields generated by different source types, a computational study
[PB94-123536] 07 p3010 N94-27037
Analysis of spark-induced bubble experiments using CALE
[DE94-003667] 08 p3270 N94-28476
Design of the biosonar simulator for dolphin's clicks waveform reproduction 08 p3234 N94-29707
Experiments on the aerodynamic generation of noise in centrifugal turbomachinery 08 p3480 N94-30804
Miniature thermoacoustic refrigerator
[AD-A280326] 12 p4431 N94-37029

SOUND INTENSITY
NT ZERO SOUND
Minutes. Accredited Standards Committee on Noise, S12. US tag for ISO/TC 43/SC1 noise and ISO/TC 94/SC12 hearing protection
[AD-A275622] 08 p3477 N94-28636
Subjective response to sonic booms having different shapes, rise times, and durations
[NASA-TM-109090] 08 p3479 N94-29464
Survey method for determining sound power levels under reverberant conditions in situ: A pilot study. Nordtest project 1064-92
[PB94-149143] 10 p4133 N94-34145

SOUND LOCALIZATION
Human-machine interfaces
[AD-A270730] 04 p1513 N94-19764
Call sign intelligibility improvement using a spatial auditory display 10 p4038 N94-33617
Pattern analysis based models of masking by spatially separated sound sources
[AD-A277882] 10 p4095 N94-33779
3D sound experimental approach: Methodology and preliminary results 12 p4486 N94-37280

SOUND MEASUREMENT
U ACOUSTIC MEASUREMENT

SOUND PERCEPTION
U AUDITORY PERCEPTION

SOUND PRESSURE
Active control of acoustic pressure fields using smart material technologies
[NASA-CR-191480] 02 p0768 N94-13354
Study on the possibilities to apply spectrumindex
[VTT-PUBS-109] 02 p0777 N94-14034
Vibro-acoustic analysis of an aircraft maintenance dock
[AD-A266778] 03 p0871 N94-14908
Free-field sensitivity calibration of laboratory standard microphones by the reciprocity technique: Measurements for the 1991 EEC intercomparison
[NPL-RSA(EXT)-0043] 03 p1176 N94-15019
Cruise noise measurements of a scale model advanced ducted propulsor
[NASA-TM-105808] 03 p1176 N94-15115
Transducers and method for making same
[AD-D015949] 04 p1408 N94-19759
Stability curves for a thermoacoustic prime mover
[AD-A272607] 05 p1968 N94-21422
Computation of the sound generated by isotropic turbulence
[NASA-CR-191543] 05 p1804 N94-21880
Variability of measured sonic boom signatures. Volume 1: Technical report
[NASA-CR-191483-VOL-1] 06 p2526 N94-24172
Variability of measured sonic boom signatures. Volume 2: Data report
[NASA-CR-191483-VOL-2] 06 p2526 N94-24173
JAPE 91: Influence of terrain masking of the acoustic propagation of helicopter noise
06 p2528 N94-24214
Quadruplet expansion of the acoustic pressure field in a wedge shaped ocean
[AD-A275121] 08 p3477 N94-29003
A comparison of two computer models of sound propagation for a wedge shaped ocean over a penetrable bottom
[AD-A275031] 08 p3477 N94-29117
Determination of sound power levels of air terminal units according to ISO 5135-Nordic inter-laboratory tests, Nordtest project no. 968-91
[PB94-137411] 08 p3477 N94-29175
Report of National Institute for Resources and Environment. No. 8: Research on blasting sound related to it's measurement, propagation prediction, control and evaluation
[JTN-94-80605] 08 p3479 N94-29597
Modal analysis of solar panels using boundary integral equations
[NLT-TP-92218-U] 08 p3338 N94-30328
Investigation of sonic boom for the Space Shuttle: High cross-range orbiter
[NASA-TM-108238] 09 p3860 N94-31336
Investigation of sonic boom for the Space Shuttle: Low cross-range orbiter
[NASA-TM-108237] 09 p3860 N94-31337
Sonic boom (human response and atmospheric effects) outdoor-to-indoor response to minimized sonic booms
10 p3977 N94-33502
Measurements of correlation coefficients of vibration on a car body shell
[ISVR-TR-220] 10 p4070 N94-34307
Scattering cross section of sound waves by the modal element method
[NASA-TM-106667] 12 p4510 N94-37308

SOUND PROPAGATION
NT VOICE
The problem of the sonic boom for future high-speed transport aircraft
[ESA-TT-1286] 02 p0776 N94-13692
Discrete models of the Boltzmann equation: Structure of the collision operator of sound propagation
[IFTR-2/1992] 03 p1178 N94-17051
Sound exposure level prediction for impulse sound sources above variable terrain
[AD-A267535] 03 p1178 N94-17119
Ultrasonic technique for inspection of GPHS capsule girth weld integrity
[DE93-040072] 04 p1448 N94-19189
Numerical simulation of acoustic waves propagation in turbulent media
[ECL-92-37] 04 p1563 N94-19413
Examinations of converging cylindrically symmetric second sound propagation in He2
[MPIS-9/1992] 04 p1564 N94-19715
Mathematical model and analysis of the Tactical Unmanned Ground Vehicle (TUGV) using computer simulation
[AD-A272258] 05 p1824 N94-20576
Some results gained from JAPE: An overview
06 p2527 N94-24209
Comparison of measured and predicted pure tone propagation levels from JAPE-1: An evaluation of the performance of ASOPRAT 06 p2527 N94-24212
Comparisons of calculated and measured helicopter noise near instrument hill 06 p2528 N94-24215
Preliminary analysis of amplitude and phase fluctuations in the JAPE multiple tone data to distances of 500 meters 06 p2528 N94-24216
Analysis of modal evolution caused by a weakly range-dependent seabed in shallow water and its application to inversion for geoacoustic properties
[AD-A273656] 06 p2419 N94-25435
Progress in modeling atmospheric propagation of sonic booms 07 p2650 N94-28189
A comparison of two computer models of sound propagation for a wedge shaped ocean over a penetrable bottom
[AD-A275031] 08 p3477 N94-29117
Attenuation of outdoor sound propagation levels by a snow cover
[AD-A275387] 08 p3478 N94-29314
A non-local computational boundary condition for duct acoustics
[NASA-TM-109091] 08 p3478 N94-29382
Report of National Institute for Resources and Environment. No. 8: Research on blasting sound related to it's measurement, propagation prediction, control and evaluation
[JTN-94-80605] 08 p3479 N94-29597
New broadband shock noise model and computer code for ANOPP 10 p3975 N94-33489

SOUND RANGING
Some results gained from JAPE: An overview
06 p2527 N94-24209
Sonar sensing and obstable detection
08 p3309 N94-30301
Multi-scale studies of seafloor topography
[AD-A277008] 09 p3789 N94-32400

SOUND TRANSDUCERS
NT ELECTROACOUSTIC TRANSDUCERS
NT HYDROPHONES
NT LOUDSPEAKERS
NT MICROPHONES
Acoustic characteristics of side scan sonar and sub-bottom profiler for 10,000 m class ROV
01 p0172 N94-11916
Design of the biosonar simulator for dolphin's clicks waveform reproduction 08 p3234 N94-29707
Sensing the gas metal arc welding process
08 p3314 N94-30444

SOUND TRANSMISSION
Ultrasound absorption in molten salts
03 p0944 N94-15161
Nonlinear acoustics: Periodic waveguide, scattering of sound by sound, three-layer fluid, finite amplitude sound in a medium having a distribution of relaxation processes, and production of an isolated negative pulse in water
[AD-A267145] 03 p1177 N94-15732
Acoustic monitoring of global ocean variability
[AD-A271998] 05 p1883 N94-21366
Global acoustic mapping of ocean temperatures (GAMOT)
[AD-A273387] 06 p2418 N94-24719
Measurements and modeling of multitone, low-frequency acoustic data from the Arraial do Cabo range
[AD-A273406] 06 p2530 N94-25073
Hydroacoustic wave-fields generated by different source types, a computational study
[PB94-123536] 07 p3010 N94-27037
Monaural and binaural processing of complex waveforms
[AD-A274209] 07 p3010 N94-27067
A comparison of two computer models of sound propagation for a wedge shaped ocean over a penetrable bottom
[AD-A275031] 08 p3477 N94-29117
Vibrations of a heavy truck diesel engine and gearbox unit: Examining structure-borne sound transmission with statistical energy analysis
[CTH-E-93-04] 09 p3722 N94-31194
Acoustic window
[AD-D016171] 09 p3862 N94-33017

SOUND VELOCITY
U ACOUSTIC VELOCITY

SOUND WAVES
NT AERODYNAMIC NOISE
NT AIRCRAFT NOISE
NT BLADE SLAP NOISE
NT ENGINE NOISE
NT ION ACOUSTIC WAVES
NT JET AIRCRAFT NOISE
NT LAMB WAVES
NT NOISE (SOUND)
NT PROPELLER NOISE
NT SONIC BOOMS
NT THERMAL NOISE
Virtual sound for virtual reality
[DE93-010519] 01 p0321 N94-10291
Sensing glass transitions in thin polymer films on acoustic wave microsensors
[DE93-010805] 01 p0087 N94-10295
Estimation of the direct acoustic radiation from turbulent spots using boundary layer velocity measurements
01 p0357 N94-10358
Photostimulated attenuation of hypersound in superlattice
[DE93-611231] 01 p0357 N94-10408
Confinement of acoustical modes due to the electron-phonon interaction within 2D-electron gas
[DE93-613910] 01 p0396 N94-10800
Acoustics of bubbly sediments
[AD-A263726] 01 p0288 N94-11299
Near surface ocean processes: Acoustical observations, ambient sound, and Langmuir circulation
01 p0288 N94-11447
Study on color video pictures transmission by digital acoustic signal 01 p0139 N94-11917
NRL review for 1993
[AD-A265666] 01 p0497 N94-12334

Preliminary analysis of the FLIP array data from the NOBS experiment
[AD-A265911] 01 p0289 N94-12349
Ocean acoustic processing: A model-based approach
[DE93-011902] 02 p0725 N94-12876
Study of bubble behavior in weightlessness (effects of thermal gradient and acoustic stationary wave) (M-16) 02 p0589 N94-13748
Liquid metal drop ejection
[NASA-CR-193718] 02 p0572 N94-14133
Portable acoustic wave sensor systems for real-time monitoring of volatile organic compounds
[DE93-013753] 02 p0582 N94-14511
Atmospheric acoustic modeling
[DE93-016727] 02 p0718 N94-14518
Investigation of the dilatational dissipation in compressible homogeneous shear flow 02 p0645 N94-14758
Ultrasound absorption in molten salts 03 p0944 N94-15161
Dynamics of douple stimulated Brillouin scattering 03 p1200 N94-15206
On the use of the noncentral chi-square density function for the distribution of helicopter spectral estimates
[NASA-CR-191546] 03 p1176 N94-15487
Sound radiation from infinite laminated composite shell with periodic rib stiffening
[DRA/TM(USGR)92326] 03 p0933 N94-15699
Acousto-optical confirmation of the localized wave phenomena
[DE93-016425] 03 p1177 N94-16448
Cortical adaptive filtering in bioacoustic signal classification
[AD-A266229] 03 p1177 N94-16939
The shock Hugoniot of 316 SS and sound velocity measurements
[DE93-016525] 03 p1178 N94-16955
Acoustic waves in complicated geometries and their interactions with liquid-propellant droplet combustion
[AD-A267260] 03 p1178 N94-16991
An electroacoustic transducer for purposes of photoacoustic spectroscopy
[IFTR-7/1992] 03 p1013 N94-17071
Sound exposure level prediction for impulse sound sources above variable terrain
[AD-A267535] 03 p1178 N94-17119
Two-dimensional, high flow, precisely controlled monodisperse drop source
[AD-A267660] 03 p1028 N94-17250
Boundary conditions and the simulation of low Mach number flows
[NASA-TM-106374] 03 p1029 N94-17448
A virtual acoustic orientation instrument
[AD-A268181] 03 p1134 N94-17510
Comments on computational underwater acoustics
[DE93-013789] 04 p1562 N94-17873
Low-noise oscillators for airborne radar applications, revision 1
[AD-A269372] 04 p1403 N94-18471
Acoustic intensity measurements in the presence of low Mach number flow
[AD-A269995] 04 p1562 N94-18664
Estimating the oceanic sound speed environmental for long-range acoustic propagation
[AD-A270231] 04 p1499 N94-18903
Elastic properties of amorphous thin films studied by Rayleigh waves
[DE93-018375] 04 p1372 N94-19202
Comments on computational underwater acoustics
[DE93-019880] 04 p1563 N94-19270
Low frequency acoustics of laminated composite axisymmetric structures
[DRA-TM(USGR)-93302] 04 p1344 N94-19391
Numerical simulation of acoustic waves propagation in turbulent media
[ECL-92-37] 04 p1563 N94-19413
The electromechanical properties of tetragonal BaTiO3 and PbTiO3 single crystals
[DE93-019008] 04 p1603 N94-19550
Acoustic travel time perturbations due to an internal tide and internal wave field in the Barents Sea
[AD-A270879] 04 p1499 N94-19580
Seismic studies of the geologic structure and physical properties of the seabed
[AD-A270895] 04 p1500 N94-19747
Acoustic propagation modeling using MATLAB
[AD-A270905] 04 p1564 N94-19750
Nonlinear acoustics: Periodic waveguide, finite-amplitude propagation in a medium having a distribution of relaxation processes, and production of an isolated negative pulse in water
[AD-A270530] 05 p1967 N94-19894
Acoustic radiation damping of flat rectangular plates subjected to subsonic flows
[NASA-TM-109382] 05 p1967 N94-20211
Mathematical model and analysis of the Tactical Unmanned Ground Vehicle (TUGV) using computer simulation
[AD-A272258] 05 p1824 N94-20576
A survey of the impact on acoustic propagation of warm core ocean eddys
[AD-A272188] 05 p1883 N94-20925
Comparison of higher order moment spectrum estimation techniques
[AD-A272967] 05 p1967 N94-21260
Approximation to sound radiation and scattering by simply supported layered cylinder
[AD-A272964] 05 p1967 N94-21306
Speed of sound data and related models for mixtures of natural gas constituents
[PB93-200822] 05 p1968 N94-21447
Surface acoustic wave sensing of VOC's in harsh chemical environments
[DE93-040721] 05 p1968 N94-21751
Three dimensional ultrasonic imaging
[DE93-040549] 05 p1968 N94-22003
Acoustic, fiber optic, and silicon microelectronic microsensors research and development activities at Sandia National Laboratories
[DE93-019075] 05 p1770 N94-22040
Interface reflection of spherical acoustic waves in the first- and second-order rational parabolic approximations and their artifacts
[PB93-215424] 05 p1969 N94-22261
Transient acoustic wave modeling: Higher-order WKBJ asymptotics and symbolical manipulation (revised)
[PB93-215432] 05 p1969 N94-22262
Enhanced absorption of p-modes on sunspot and plage regions 05 p2006 N94-22671
Classical scattering theory of waves from the view point of an eigenvalue problem and application to target identification
[DE94-000472] 06 p2525 N94-23206
Chemically sensitive interfaces on SAW devices
[DE94-001832] 06 p2526 N94-23718
Similarity in wave propagation under a global relaxation law
[PB94-111028] 06 p2524 N94-23730
Analysis of time-domain acoustic wavefields in horizontally continuously layered configurations based on the modified Cagniard method
[PB94-111044] 06 p2524 N94-23731
Preliminary analysis of amplitude and phase fluctuations in the JAPE multiple tone data to distances of 500 meters 06 p2528 N94-24216
Dimensional analysis of acoustically propagated signals 06 p2528 N94-24217
Unstructured adaptive mesh computations of rotorcraft high-speed impulsive noise
[NASA-CR-195090] 06 p2529 N94-24307
The acoustic and instability waves of jets confined inside an acoustically lined rectangular duct
[AD-A276347] 06 p2334 N94-24602
Responses of a finite baffled plate subject to turbulent and mean flow excitations
[NASA-CR-191570] 06 p2334 N94-24605
Global acoustic mapping of ocean temperatures (GAMOT)
[AD-A273387] 06 p2418 N94-24719
Preprocessor and adaptive beamformer for linear-frequency modulation active signals
[AD-D016008] 06 p2302 N94-25048
Binaural room simulation
[AD-A273823] 07 p3009 N94-25737
The effect of high frequency electric field on hypersound amplification in superlattice
[DE93-634326] 07 p3057 N94-26384
New variational techniques for acoustic radiation and scattering from elastic shell structures
[AD-A274599] 07 p3010 N94-26889
Problems in nonlinear acoustics: Rayleigh waves, pulsed sound beams, and waveguides
[AD-A274587] 07 p3010 N94-26983
Hydroacoustic wave-fields generated by different source types, a computational study
[PB94-123536] 07 p3010 N94-27037
Monaural and binaural processing of complex waveforms
[AD-A274209] 07 p3010 N94-27067
Observation of impulsive acoustic events and the excitation of solar oscillations
[AD-A274159] 07 p3111 N94-27096
On the use of feedback to control sound radiation from a plate excited by a turbulent boundary layer
[ISVR-TR-227] 07 p2807 N94-28175
Broad geoacoustic assessment of some regional areas
[AD-A275504] 08 p3356 N94-28791
Analysis of 3-D acoustic problems using boundary element method 08 p3127 N94-28974
Quadruplet expansion of the acoustic pressure field in a wedge shaped ocean
[AD-A275121] 08 p3477 N94-29003
Considerations in the modelling of seafloor acoustic backscatter
[AD-A275404] 08 p3478 N94-29206
Improved in-flow acoustic sensor
[NASA-CASE-ARC-12001-1] 08 p3478 N94-29363
A non-local computational boundary condition for duct acoustics
[NASA-TM-109091] 08 p3478 N94-29382
Report of National Institute for Resources and Environment. No. 8: Research on blasting sound related to it's measurement, propagation prediction, control and evaluation
[JTN-94-80605] 08 p3479 N94-29597
Design of the biosonar simulator for dolphin's clicks waveform reproduction 08 p3234 N94-29707
Convective turbulence and transport in stars 08 p3546 N94-29913
Ocean acoustic propagation measurements and wave propagation in random media
[AD-A276165] 09 p3787 N94-31053
Quality of sound in large rooms: Alteration of room impulse responses
[CTH-E-93-02] 09 p3859 N94-31077
A preliminary investigation of high amplitude standing waves with laser Doppler anemometry
[AD-A276463] 09 p3860 N94-31242
Aeroacoustic sources in internal flows
[ISBN-9-03-86-0282-0] 09 p3860 N94-31653
Fiber optic sensors for the detection of surface acoustic waves on metals
[ISBN-0-315-87055-9] 09 p3878 N94-31736
Experimental and computational studies on propeller noise due to inflow distortion 09 p3860 N94-31846
Boundary control of scattering 09 p3861 N94-31899
Wavevector-frequency analysis with applications to acoustics
[AD-A276618] 09 p3861 N94-32125
Pulse-splitting and AM-FM conversion in a nonlinear dispersive medium
[AD-A277041] 09 p3861 N94-32262
Auditory perception
[AD-A277414] 09 p3800 N94-32419
Advanced satellite communication system
[NASA-CR-194211] 09 p3681 N94-32477
Digital beamforming and filtering circuit
[AD-D016142] 09 p3697 N94-32976
Acoustic window
[AD-D016171] 09 p3862 N94-33017
Energy absorption apparatus
[AD-D016163] 10 p4133 N94-33699
A self-organizing neural network architecture for auditory and speech perception with applications to acoustic and other temporal prediction problems
[AD-A277526] 10 p4095 N94-33708
Acoustic receptivity of compressible boundary layers: Receptivity by way of surface-temperature variations
[NASA-CR-4599] 10 p4046 N94-33897
Time-scale modification of complex acoustic signals in noise
[AD-A277535] 10 p4133 N94-34157
JPRS report: Science and technology. Central Eurasia: Physics and mathematics
[JPRS-UPM-93-003] 10 p4132 N94-35118
An electromagnetic finite difference time domain analog treatment of small signal acoustic interactions
[DE94-009978] 11 p4319 N94-35770
First, second and fourth sound in relativistic superfluidity theory with account for dissipative effects
[DE94-617393] 11 p4267 N94-36314
On the physics of waves in the solar atmosphere: Wave heating and wind acceleration
[NASA-CR-194119] 11 p4375 N94-36395
Elimination of numerical dispersion in finite-difference modeling and migration by flux-corrected transport
[DE94-004159] 12 p4510 N94-36551
Josephson acoustic radiation in superfluid helium
[AD-A280208] 12 p4533 N94-36742
Signal processing for the 1992 Barents Sea tomography experiment
[AD-A278580] 12 p4476 N94-36971
Scattering cross section of sound waves by the modal element method
[NASA-TM-106667] 12 p4510 N94-37308

SOUND-SOUND INTERACTIONS

Nonlinear acoustics: Periodic waveguide, scattering of sound by sound, three-layer fluid, finite amplitude sound in a medium having a distribution of relaxation processes, and production of an isolated negative pulse in water
[AD-A267145] 03 p1177 N94-15732

SOUNDERS

U SOUNDING

SOUNDING
NT ACOUSTIC SOUNDING
NT ATMOSPHERIC SOUNDING
NT BALLOON SOUNDING
NT ECHO SOUNDING
NT IONOSPHERIC SOUNDING
NT MICROWAVE SOUNDING
NT ROCKET SOUNDING
NT SATELLITE SOUNDING
Mars subsurface sounding with a ground penetrating radar 06 p2608 N94-23393

SOUNDING ROCKETS
NT BLACK BRANT SOUNDING ROCKETS
MUZO: The programmable multi zone furnace for gas payloads and sounding rockets 01 p0110 N94-10132
Microgravity experiments using TR-1A rocket 01 p0112 N94-10142
TEXUS 28 experiment: Convections and crystal growth of Ge:Ga. Analysis of temperature measurements 01 p0114 N94-10184
AD100/ADSIM, ACSL, and MATLAB output comparisons using frequency-response analysis [DE93-009640] 01 p0047 N94-11122
Sounding Rocket Experiments in Fluid Science and Materials Sciences: TEXUS 25 to 27 and MASER 4, volume 3 [ESA-SP-1132-VOL-3] 03 p0943 N94-15157
Measurements of Interfacial Tension: MITE 03 p0943 N94-15158
Benard convection of magnetic colloids under microgravity 03 p0943 N94-15159
Pool boiling: Single bubble experiment 03 p0944 N94-15160
Ultrasound absorption in molten salts 03 p0944 N94-15161
Orientation of DNA during free-solution electrophoresis 03 p0944 N94-15162
Electrophoresis visualisation 03 p0944 N94-15163
Temperature propagation in near-critical fluids prior to and during separation 03 p0944 N94-15165
Separation behaviour of monotectic alloys 03 p0945 N94-15170
Heat storage module 03 p0946 N94-15172
The 1973 highlights --- Pioneer and Mariner space probes and other advancements [NASA-TM-109624] 03 p1302 N94-15410
The 1968 highlights --- NASA programs and research [NASA-TM-109627] 03 p1302 N94-15413
The 1971 highlights --- NASA programs and research [NASA-TM-109629] 03 p1302 N94-15417
MAXUS: The new sounding rocket program for long duration microgravity flight 03 p0978 N94-16079
UVPI imaging from the LACE satellite: The Nihka rocket plume [AD-A268456] 04 p1334 N94-18149
PULSAUR 2 [NASA-CR-194832] 06 p2209 N94-23484
Sulfur dioxide in the atmosphere of Venus 1 sounding rocket observations [NASA-CR-195224] 07 p3106 N94-26237
Cosmic x ray physics [NASA-CR-195225] 07 p3115 N94-27236
Cosmic x ray physics [NASA-CR-195218] 07 p3115 N94-27419
Cosmic x ray physics [NASA-CR-195219] 07 p3115 N94-27420
Time series comparisons of satellite and rocketsonde temperatures in 1978-1979 [NASA-TP-3409] 08 p3370 N94-29455
SPARTAN high resolution solar studies [NASA-CR-189340] 10 p4166 N94-34944
Three flights into thunderstorms with the revised Rocket Electric Field Sounding (REFS) payload [AD-A280424] 12 p4473 N94-37217

SOUNDS (TOPOGRAPHIC FEATURES)
NT MCMURDO SOUND
Orographic microbursts in a severe winter windstorm [AD-A267651] 03 p1108 N94-17247

SOURCE PROGRAMS
Reuse: A knowledge-based approach 01 p0329 N94-11430
ASPT software source code: SUN driver package [DSIS-93-00262] 02 p0751 N94-14014
ASPT software source code: Development system package, VME-C30 component [DSIS-93-00276] 02 p0751 N94-14016
ASPT software source code: Host development system package [DSIS-93-00277] 02 p0753 N94-14197
Reductions to sets of low information content [TR-417] 03 p1150 N94-16579
Estimating task execution delay in a real-time system via static source code analysis [AD-A267496] 03 p1161 N94-17367
A parallelizing compiler based on partial evaluation [AD-A270838] 05 p1898 N94-19832
Application guide for universal source encoding for space [NASA-TP-3441] 05 p1741 N94-21783
Source code for the OO1 benchmark and the AFIT simulation benchmark [AD-A274035] 07 p2958 N94-25799
Incremental recompilation for Standard ML of New Jersey [AD-A276522] 09 p3815 N94-32080
Algebraic approach to compiler design [PB94-149630] 10 p4129 N94-34112
Symbolic debugging of globally optimized code: Data value problems and their solutions [AD-A278898] 11 p4302 N94-35572

SOUTH AFRICA
U REPUBLIC OF SOUTH AFRICA

SOUTH AMERICA
Cyclogenesis and cyclone over South America [INPE-5400-TDI/479] 02 p0719 N94-13175

SOUTH CAROLINA
Workshop for coordinating South Carolina's pre-college systemic initiatives in science and mathematics [DE93-012263] 02 p0818 N94-13216
Applications of Quaternary stratigraphic, soil-geomorphic, and quantitative geomorphic analyses to the evaluation of tectonic activity and landscape evolution in the Upper Coastal Plain, South Carolina [DE93-016269] 04 p1484 N94-18725

SOUTH KOREA
Overview of KITSAT 01 p0036 N94-10683
Korea space program 01 p0036 N94-10684
Country report on global change research for the Republic of Korea 07 p2873 N94-28278

SOUTH VIETNAM
U VIETNAM

SOUTHERN HEMISPHERE
NT ANTARCTIC REGIONS
NT MCMURDO SOUND
NT ROSS ICE SHELF
Southern and Northern Hemisphere total ozone as seen by TOMS [NASA-TM-109591] 03 p1098 N94-15282
Northern hemisphere dust storms on Mars 06 p2619 N94-24885
Generation mechanisms of quasi-stationary waves in the Southern Hemisphere 08 p3365 N94-30789

SOUTHERN OSCILLATION
Updated forecast of Atlantic seasonal hurricane activity for 1993 01 p0285 N94-11194
Current structures in the western equatorial Pacific during JAPACS cruises 01 p0193 N94-11911
Principal oscillation pattern analysis of sea level variations in the tropical Pacific measured by the GEOSAT altimeter 01 p0209 N94-12646
IAI topic: El Nino. Southern oscillation and interannual climate variability [INPE-5410-PRE/1757] 03 p1111 N94-15186
A synoptic study on periods of deficiency over Rio Grande do Sul/Brazil [INPE-5456-TDI/498] 07 p2896 N94-27422
Interannual-decadal variability in tropical climate systems: Stable isotope records and general circulation model experiments 08 p3373 N94-29962
On interannual variability and climate change in the North Pacific 08 p3374 N94-29963
Satellite estimation of the global distribution and interannual variability of photosynthetically active radiation 08 p3334 N94-29970
Air-sea interaction patterns in the equatorial Pacific [AD-A277305] 09 p3788 N94-32072
ENSO forced variations of the sea surface temperature and adjusted sea level along the west coast of the United States [AD-A277306] 09 p3789 N94-32327
US streamflow patterns associated with the extreme phases of the Southern Oscillation 10 p4088 N94-33359

SOUTHERN SKY
Deep near-infrared survey of the Southern Sky (DENIS) 05 p2062 N94-22467

SOVIET SATELLITES
NT MOLNIYA SATELLITES
NT SPUTNIK SATELLITES
NT VENERA SATELLITES
Almaz 03 p0898 N94-15889

SOVIET SPACECRAFT
NT BURAN SPACE SHUTTLE
NT MARS 4 SPACECRAFT
NT MIR SPACE STATION
NT SOYUZ SPACECRAFT
NT SPUTNIK SATELLITES
NT VENERA SATELLITES
Russian space system for the Earth remote sensing 01 p0037 N94-10688
The fragmentation of Kosmos 2163 [NASA-CR-191643] 03 p0887 N94-16503

SOVIET UNION
U U.S.S.R.

SOYBEANS
Chemical characterization of some aerobic liquids in CELSS 06 p2422 N94-23241

SOYUZ SPACECRAFT
Soyuz/ACRV accommodation study [NASA-TM-107733] 03 p0888 N94-17072

SPACE ADAPTATION SYNDROME
Cardiovascular dynamics during space sickness and deconditioning 01 p0311 N94-12007
Space adaptation [NASA-TM-109601] 03 p1120 N94-15309
Transfer of perceptual adaptation to space sickness: What enhances an individual's ability to adapt? [NASA-CR-188256] 06 p2427 N94-24227
Japanese Journal of Aerospace and Environmental Medicine, volume 30, no. 1 [JTN-94-80598] 08 p3389 N94-28850
Space and vertigo: In relation to space motion sickness 08 p3390 N94-28857
The MERSS 5th Symposium on Space Medicine: Medical and Physiological Experiment Utilizing Parabolic Flight [JTN-94-80588] 08 p3392 N94-29709
Relation of motion sickness susceptibility to vestibular and behavioral measures of orientation [NASA-CR-196121] 12 p4480 N94-37005
Profile analysis of after-effects experienced during exposure to several virtual reality environments 12 p4482 N94-37263

SPACE BASED RADAR
Spaceborne SAR study: LDRD 1992 [DE93-011485] 01 p0232 N94-11623
ERS-1 SAR calibration strategy 01 p0235 N94-11726
ERS-1 preliminary antenna elevation pattern measured by ground-receivers 01 p0235 N94-11727
Preliminary results of the experiment I-7 01 p0235 N94-11728
The ERS-1/CV 580 SAR cross-calibration experiment: Sault Ste Marie, October 26 - November 2, 1991 01 p0236 N94-11729
Calibration of the ERS-1 SAR fast-delivery images 01 p0236 N94-11730
Calibration results for the ERS-1, AIRSAR, and PHARS 01 p0236 N94-11731
An experiment for the radiometric calibration of the ERS-1 SAR 01 p0236 N94-11733
Techniques and applications of SAR interferometry for ERS-1: Topographic mapping, change detection, and slope measurement 01 p0236 N94-11734
SAR interferometry experiments with ERS-1 01 p0237 N94-11735
SAR-interferometry applying ERS-1: Some preliminary test results 01 p0237 N94-11736
Utilisation of ERS-1 data for mapping of Antarctica 01 p0237 N94-11740
Observations of surface signatures in the north-west Pacific Ocean with the spaceborne SAR 01 p0226 N94-12746
Ionospheric effects on a wide-bandwidth, polarimetric, space-based, synthetic-aperture radar [DE93-015084] 02 p0612 N94-14512
Proceedings of the Third Spaceborne Imaging Radar Symposium [NASA-CR-194104] 03 p0989 N94-15886
SIR-C/X-SAR free flyer concept 03 p0898 N94-15903
EOS SAR: A new approach 03 p0992 N94-15904
Space-based radar for moving target detection 05 p1745 N94-22143
Experimental evaluation of battery cells for space-based radar application 07 p2860 N94-28104
Ground independent landing system 08 p3137 N94-29564
Pointing mechanisms for the Shuttle Radar Laboratory 08 p3162 N94-29638
Radar rainfall measurements from space 09 p3782 N94-31889
Alaska SAR Facility mass storage, current system 10 p4156 N94-33823

SPACE BASES
NT LUNAR BASES
NT SPACE COLONIES

SPACE BIOLOGY
U EXOBIOLOGY

SPACE CAPSULES
NT FRIENDSHIP 7
NT MERCURY SPACECRAFT

SPACE CHARGE
A parallel implementation of particle tracking with space charge effects on an Intel iPSC/860 [DE93-012307] 01 p0335 N94-10340

Nonlinear space charge effect of bunched beam in linac
[DE93-612176] 01 p0371 N94-10409
Effect of effective mass differences on the tunneling current-voltage behaviour of a resonant diode in the presence of space charge build-up
[DE93-613817] 01 p0142 N94-10799
Time-resolved optical studies of charge relaxation and charge transfer at electrode interfaces
[DE93-013985] 01 p0398 N94-11117
Beam halo formation from space-charge dominated beams in uniform focusing channels
[DE93-014458] 02 p0789 N94-13209
Beam halo in high-intensity beams
[DE93-014565] 02 p0789 N94-13328
Wake-field and space charge effects on high brightness beams calculations and measured results for the laser driven photoelectrons at BNL-ATF
[DE93-015787] 02 p0659 N94-14572
Nuclear fusion of protons with ions of boron
[DE93-015399] 03 p1202 N94-16019
Polar 2 model of the wake shield experiment
[AD-A266243] 03 p0882 N94-16468
Prototype instrumentation and design studies
[AD-A266402] 03 p0882 N94-16530
A review of some dynamics models in six-dimensional phase space and their suitable conditions of motion equation
[DE93-623741] 03 p1175 N94-17317
Emittance growth in displaced, space-charge-dominated beams with energy spread
[DE93-016514] 03 p1188 N94-17672
Nonlinear Thomson scattering of intense laser pulse from beams and plasmas
[AD-A269556] 04 p1438 N94-18460
Halo formation in mismatched, space-charge-dominated beams
[DE93-018581] 04 p1574 N94-18934
Correction of longitudinal errors in accelerators for heavy-ion fusion
[DE93-018656] 04 p1575 N94-19106
Induction accelerator development for heavy ion fusion
[DE93-019228] 04 p1591 N94-19479
Space-charge dominated beam transport in magnetic quadrupoles with large aperture ratios
[DE93-040443] 05 p1992 N94-20004
Simulation studies of space-charge-dominated beam transport in large aperture ratio quadrupoles
[DE93-019238] 05 p1981 N94-21440
Evaluation of externally heated pulsed MPD thruster cathodes
[NASA-CR-191090] 05 p1670 N94-21565
Inverse free electron laser beat-wave accelerator research
[DE94-002597] 06 p2349 N94-23702
First principle calculation for magneto-crystalline anisotropy
[DE93-634653] 07 p3052 N94-26012
Development of a 3D numerical code to calculate the trajectories of the blow off electrons emitted by a vacuum surface discharge: Application to the study of the electromagnetic interference induced on a spacecraft
[ONERA-NT-1993-12] 09 p3863 N94-31227
Resistivity measurements on the neutron irradiated detector grade silicon materials
[DE94-009083] 09 p3906 N94-32822

SPACE COLONIES
Exploration planning in the context of human exploration and development of the Moon 01 p0474 N94-12229
Vision 21: Interdisciplinary Science and Engineering in the Era of Cyberspace
[NASA-CP-10129] 07 p2685 N94-27358
The Fermi paradox: An approach based on percolation theory 07 p2687 N94-27370
Marsville: The cosmic village
[NASA-TM-109752] 09 p3913 N94-31806

SPACE COMMERCIALIZATION
Potential markets for advanced satellite communications
[NASA-CR-191145] 01 p0041 N94-10512
Landsat as a commercial enterprise
[INPE-5477-TAE/019] 01 p0232 N94-11524
The guide to Design For On-orbit Spacecraft Servicing (DFOSS) manual: Producing a consensus document 01 p0421 N94-11575
Special investigation report: Commercial space launch incident, launch procedure anomaly orbital sciences corporation PEGASUS/SCD-1, 80 nautical miles east of Cape Canaveral, Florida, February 9, 1993
[PB93-917003] 01 p0040 N94-11893
Technology Applications Team: Applications of aerospace technology
[NASA-CR-194362] 02 p0828 N94-13104
Large space structures and systems in the space station era: A bibliography with indexes (supplement 05)
[NASA-SP-7085(05)] 02 p0543 N94-14411
TABES 1993: 9th Annual Technical and Business Exhibition and Symposium 03 p1050 N94-16129
Commercial space opportunities advanced concepts and technology overview
[TABES PAPER 93-240] 03 p1050 N94-16132
The closing window of opportunity: Addressing the US space launch vehicle crisis
[TABES PAPER 93-640] 03 p0878 N94-16148
Space commerce in a global economy: Comparison of US and Australian approaches
[NASA-TM-109341] 03 p1235 N94-17290
The impact of industry/university consortia programs on space education
[NASA-TM-109340] 03 p1222 N94-17441
An evolutionary approach to space launch commercialization
[AD-A269861] 04 p1331 N94-18411
Future energy source --- Mining Helium-3 on the moon
[NASA-TM-109363] 04 p1628 N94-18959
Space tourism: A flight of fantasy or the next major space product? Paper session 3: Products
[NASA-TM-109385] 06 p2194 N94-23710
National Institute of Standards and Technology Conference on Reducing the Cost of Space Infrastructure and Operations. Part 2: Topical papers
[PB94-113487] 06 p2194 N94-23819
Access to space studies 06 p2199 N94-24434
NASA technology applications team: Applications of aerospace technology
[NASA-CR-194775] 06 p2597 N94-24494
Design of a lunar propellant processing facility. NASA/USRA advanced program
[NASA-CR-195502] 06 p2266 N94-24618
MINOTAUR (Maryland's innovative orbital technologically advanced University rocket) 07 p2703 N94-25685
Future of aerospace
[PB94-120185] 07 p2669 N94-26906
Access to space study
[NASA-TM-109693] 07 p2685 N94-27151
The MERSS 5th Symposium on Space Medicine: Medical and Physiological Experiment Utilizing Parabolic Flight
[JTN-94-80588] 08 p3392 N94-29709
Start of space tourism 08 p3164 N94-29714
Access to space: The Space Shuttle's evolving rolee
[AD-A276785] 09 p3608 N94-32190
The second giant leap
[NASA-TM-109827] 10 p4149 N94-33581
Geostationary space launch vehicles and the US dilemma 11 p4210 N94-35377

SPACE COMMUNICATION
NT INTERPLANETARY COMMUNICATION
NT LUNAR COMMUNICATION
NT SATELLITE COMMUNICATION
NT SPACECRAFT COMMUNICATION
Use of low orbital satellite communications systems for humanitarian programs 01 p0308 N94-11808
Environmental projects. Volume 15: Environmental assessment: Proposed 1-megawatt radar transmitter at the Mars site
[NASA-CR-194098] 02 p0598 N94-13090
A millimeter-wave tunneladder TWT
[NASA-CR-182183] 02 p0620 N94-13106
The Telecommunications and Data Acquisition Report
[NASA-CR-194388] 02 p0607 N94-14369
Layout and cabling considerations for a large communications antenna array 02 p0611 N94-14395
ACTS propagation experiment discussion: Ka-band propagation measurements using the ACTS propagation terminal and the CSU-CHILL and Space Communications Technology Center Florida propagation program 02 p0616 N94-14678
STS-29 mission highlights resource tape
[NASA-TM-109542] 03 p0880 N94-15373
STS-26 missions highlight resource tape
[NASA-TM-109559] 03 p0881 N94-15407
Low-Complexity, High-Performance Bandwidth Efficient Coding and Coded Modulation Techniques for Satellite and Space Communications
[NASA-CR-194623] 03 p0997 N94-16506
Search for optimal distance spectrum convolutional codes 03 p0998 N94-16509
A compact, portable EHF/SHF antenna for advanced SCAMP
[AD-A272614] 05 p1739 N94-21211
Mission Operations Support Area (MOSA) for ground network support 05 p1932 N94-21331
Using manufacturing message specification for monitor and control at Venus 05 p1932 N94-21333
Predicting scheduling success 05 p1932 N94-21334
Generating and evaluating alternate schedules 05 p1933 N94-21336
The Test Analysis Retrieval System (TARS): Meeting the challenges of the network's test processes 05 p1933 N94-21337
The Telecommunications and Data Acquisition Report
[NASA-CR-194766] 06 p2290 N94-23256
Optical subnet concepts for the deep space network 06 p2292 N94-23269
Future trends in NASA space operations 06 p2498 N94-23836
A reference model for space data system interconnection services 06 p2305 N94-23847
Reliable transfer of data from ground to space 06 p2305 N94-23908
Verification of technical elements of the advanced spacecraft based upon the CCSDS recommendation 06 p2207 N94-23910
Digital test signal generation: An accurate SNR calibration approach for the DSN 06 p2305 N94-23912
A method for interference mitigation in space communications scheduling 06 p2305 N94-23918
New mission requirements methodologies for services provided by the Office of Space Communications 06 p2519 N94-23961
Resource allocation planning with international components 06 p2520 N94-23963
Scheduling the future NASA Space Network: Experiences with a flexible scheduling prototype 06 p2520 N94-23965
Failure detection and recovery in the assembly/contingency subsystem 06 p2306 N94-25360
Lasercom system architecture with reduced complexity
[NASA-CASE-NPO-19069-1-CU] 08 p3293 N94-29493
The Telecommunications and Data Acquisition Report
[NASA-CR-195694] 08 p3246 N94-29613
Design and analysis of a low-loss linear analog phase modulator for deep space spacecraft X-band transponder applications 08 p3248 N94-29625
The Rb 780-nanometer Faraday anomalous dispersion optical filter: Theory and experiment 08 p3250 N94-29659
Optimizing the Galileo space communication link 08 p3250 N94-29663
Decoder synchronization for deep space missions 08 p3250 N94-29664
The Telecommunications and Data Acquisition Report
[NASA-CR-196117] 11 p4252 N94-35542
A 32-GHz solid-state power amplifier for deep space communications 11 p4255 N94-35562
Error control techniques for satellite and space communications
[NASA-CR-196302] 12 p4433 N94-36931
Baseline antenna design for space exploration initiative
[NASA-CR-196298] 12 p4435 N94-37255

SPACE COOLING (BUILDINGS)
Transition of building energy consumption using multi-input, single-output dynamic model
[VTT-PUBS-116] 02 p0597 N94-14055

SPACE DEBRIS
Satellite situation report, volume 32, no. 1
[NASA-TM-109233] 01 p0042 N94-10562
Satellite situation report, volume 32, no. 2
[NASA-TM-109234] 01 p0042 N94-10563
Satellite situation report, volume 31, no. 4
[NASA-TM-109232] 01 p0039 N94-10659
The magnitude of impact damage on LDEF materials
[NASA-CR-188258] 01 p0043 N94-10666
Modelling hypervelocity impacts into aluminum structures based on LDEF data 01 p0190 N94-12178
Model of optical scatter from microimpacts on the Hubble Telescope 01 p0384 N94-12189
Procedures for analysis of debris relative to Space Shuttle systems
[NASA-TM-109190] 02 p0534 N94-12900
Experimental technique to simulate orbital-debris impact on space shields at impact velocities over 10 km/s
[DE93-011619] 02 p0539 N94-12909
Comparison of analytic Whipple bumper shield ballistic limits with CTH simulations
[DE93-015126] 02 p0539 N94-13006
Simulation of orbital debris impacts on bumper shields
[DE93-013773] 02 p0540 N94-13398
High velocity gas gun
[NASA-TM-109296] 02 p0541 N94-13637
Interactions between spacecraft and their environments
[NASA-TM-106115] 02 p0541 N94-13917

BALLIST: A computer program to empirically predict the bumper thickness required to prevent perforation of the Space Station by orbital debris
[NASA-CR-193825] 02 p0543 N94-14120
Secondary impact hazard assessment
[NASA-CR-188261] 02 p0543 N94-14483
Satellite situation report, volume 33, no. 3
[NASA-TM-109278] 03 p0885 N94-15712
Long Duration Exposure Facility experiment M0003 deintegration/findings and impacts
[AD-A267140] 03 p0885 N94-15749
An analysis of the dynamic response of the Space Station Freedom due to a module perforation by an orbital debris particle impact
[TABES PAPER 93-653] 03 p0899 N94-16154
Impact penetration experiments in teflon targets of variable thickness 03 p1063 N94-16253
The effect of an on-orbit near encounter on the number flux density of micron sized particles 03 p0899 N94-16374
Resolving LDEF's flux distribution: Orbital (debris?) and natural meteoroid populations 03 p1245 N94-16391
History of on-orbit satellite fragmentations
[NASA-CR-191644] 03 p0887 N94-16502
Cosmic dust and space debris measurements on board the small satellites HITEN and BREM-SAT 03 p0890 N94-17147
SYNMOD: A low-resource, low-cost means of monitoring the near-Earth space debris environment 03 p0891 N94-17148
Detecting small debris using a ground-based photon counting detector
[DE93-012623] 03 p0898 N94-17669
Space debris detection
[AD-A269254] 04 p1334 N94-18264
Proceedings of the 11th Space Surveillance Workshop
[AD-A269477] 04 p1462 N94-18729
Space Station trash removal system
[NASA-CASE-MSC-21723-1] 05 p1657 N94-20367
Numerical simulations of hypervelocity impact experiments involving single Whipple bumper shields
[AD-A272123] 05 p1831 N94-20572
Determination of parameters for hypervelocity dust grains encountered in near-Earth space 05 p2084 N94-20817
A fresh look at crater scaling laws for normal and oblique hypervelocity impacts 05 p1666 N94-20864
Orbital debris and micrometeoroids: LDEF and Mir data 05 p1659 N94-21368
The implications of the LDEF results on Space Station Freedom power system materials 05 p1660 N94-21377
Meteoroids and debris impact risk assessment on Columbus and Hermes using a realistic geometrical analysis tool 05 p1662 N94-21388
Power beaming to space using a nuclear reactor-pumped laser
[DE94-001208] 06 p2348 N94-23185
The possible effects of the natural and induced space environment on the optical and thermal properties of EOS surfaces 06 p2207 N94-23596
Debris/ice/TPS assessment and integrated photographic analysis for Shuttle mission STS-58
[NASA-TM-109194] 06 p2200 N94-24577
Orbital debris and near-Earth environmental management: A chronology
[NASA-RP-1320] 06 p2598 N94-24644
Satellite situation report, volume 33, number 4
[NASA-TM-109677] 06 p2205 N94-24824
Design of orbital debris shields for oblique hypervelocity impact
[NASA-CR-195152] 06 p2205 N94-24828
Autonomous space processor for orbital debris advanced design project in support of solar system exploration 07 p2697 N94-25667
Orbital debris radar instrumentation 08 p3248 N94-29626
Vulnerability of manned spacecraft to crew loss from orbital debris penetration
[NASA-TM-108452] 08 p3169 N94-30161
Space debris removal using a high-power ground-based laser
[DE94-006363] 08 p3169 N94-30264
Space environment durability of beta cloth in LDEF thermal blankets 09 p3591 N94-31015
Morphology correlation of craters formed by hypervelocity impacts 09 p3594 N94-31031
Micrometeoroid/space debris effects on materials 09 p3595 N94-31032
Mechanical failure probability of glasses in Earth orbit
[NASA-CR-195912] 10 p4031 N94-34947
Morphology of meteoroid and space debris craters on LDEF metal targets 11 p4353 N94-36159
Natural orbital environment definition guidelines for use in aerospace vehicle development
[NASA-TM-4527] 11 p4291 N94-36175

SPACE DIVERSITY
U RECEPTION DIVERSITY
SPACE ENVIRONMENT
U AEROSPACE ENVIRONMENTS
SPACE ENVIRONMENT SIMULATION
NT NEUTRAL BUOYANCY SIMULATION
NT WEIGHTLESSNESS SIMULATION
Novel oxygen atom source for material degradation studies
[NASA-CR-191323] 02 p0562 N94-13115
Laboratory simulation of spacecraft charging in the plasma wake region
[FFI-93-7007] 02 p0542 N94-14107
Atomic research
[NASA-CR-193843] 02 p0788 N94-14905
The 61-M long duration sim video highlights resource tape
[NASA-TM-109569] 03 p0875 N94-15299
Richards, Dick: Training clip
[NASA-TM-109503] 03 p0876 N94-15467
Apparatus for simulating an exoatmospheric structure
[NASA-CASE-MSC-21975-1] 05 p1653 N94-20339
New technique for oil backstreaming contamination measurements 05 p1652 N94-20511
Fifth International Symposium on Materials in a Space Environment
[ISBN-2-85-428293-0] 05 p1659 N94-21367
Flight and laboratory testing of materials in low Earth orbit 05 p1659 N94-21369
Complex-2: Low Earth orbital environment simulation facility for materials durability evaluation 05 p1653 N94-21370
The simulation of action of some space environment factors on Teflon and on rubber materials 05 p1661 N94-21380
Effect of geostationary environment constituents on secondary electron emission rates 05 p1661 N94-21382
Simulated space environmental effects on some experimental high performance polymers 05 p1662 N94-21385
Durability of thermal control and environmental protective materials for the SSRMS in simulated LEO environment 05 p1663 N94-21392
Atomic oxygen interaction with spacecraft materials: Relationship between orbital and ground-based testing for materials certification 05 p1663 N94-21393
Fast oxygen atom studies related to low Earth orbit activities 05 p1663 N94-21395
Altitude simulation facility for testing large space motors 06 p2156 N94-24255
A large high vacuum, high pumping speed space simulation chamber for electric propulsion
[NASA-TM-106453] 07 p2690 N94-26142
Telescience testbedding for physiological experiments under hypobaric hypoxic conditions 07 p2913 N94-27449
Telescience testbedding under hypobaric hypoxic conditions: Evaluation by operation ability and recognition ability 07 p2913 N94-27450
Telescience testbedding for physiological experiments under hypobaric hypoxic conditions: Development and evaluation in CNV measuring 07 p2913 N94-27451
Technology for robotic surface inspection in space
[AIAA PAPER 94-1193-CP] 08 p3442 N94-30544
Ground-based simulation of LEO environment: Investigations of a select LDEF material: FEP Teflon (trademark) 09 p3596 N94-31039
What LDEF means for development and testing of materials 09 p3598 N94-31050
Aerospace test facilities at NASA LERC Plumbrook
[NASA-TM-109755] 09 p3602 N94-31814
Virtual reality as a human factors design analysis tool: Macro-ergonomic application validation and assessment of the Space Station Freedom payload control area 10 p4100 N94-33620
A rapid algorithm for realistic human reaching and its use in a virtual reality system 10 p4101 N94-33621
Shared virtual environments for aerospace training 10 p4098 N94-34024
Partial gravity simulation using a pneumatic actuator with closed loop mechanical amplification
[NASA-TM-104798] 10 p4012 N94-34395
Design and simulation of EVA tools for first servicing mission of HST
[NASA-CR-196030] 11 p4298 N94-35266
Theoretical and experimental studies relevant to interpretation of auroral emissions
[NASA-CR-196032] 11 p4376 N94-36421
SPACE ENVIRONMENTAL LUBRICATION
U SPACECRAFT LUBRICATION
SPACE ERECTABLE STRUCTURES
NT BEACON SATELLITES
Advances in adaptive structures at Jet Propulsion Laboratory 01 p0072 N94-11344
On-orbit servicing for USAF space missions: A phased development approach 01 p0348 N94-11571
Definition of spacecraft standard interfaces by the NASA Space Assembly and Servicing Working Group (SASWG) 01 p0348 N94-11574
The Second Workshop on Deployment and Assembly Experiment of Large Space Structure on Orbit
[NASDA-CON-930003] 02 p0529 N94-13268
Structural design of hexa-link truss deployable antenna 02 p0529 N94-13269
Thermal distortion measurement of TETRUS type thermal test model of large deployable antenna for mobile communications satellite 02 p0529 N94-13270
Development of modular cable mesh deployable antenna 02 p0530 N94-13274
Research on inflatable structure for space use 02 p0530 N94-13275
Helical truss beam development for large space structure 02 p0530 N94-13276
Trial manufacture model and in-space verification method of deployable antenna 02 p0530 N94-13278
A concept on on-orbit experiments of deployable structures utilizing JEM/HOPE 02 p0531 N94-13279
Movement of deployable truss 02 p0531 N94-13280
Development and application of one dimensional deployable truss 02 p0531 N94-13281
Study of a one-dimensional deployable structure employing telescopic members 02 p0531 N94-13282
The study on large space structure assembly technology: The study on deployable truss structure, part 1
[NASDA-TMR-930002] 02 p0541 N94-13658
The study on large space structure assembly technology: The study on deployable truss structure, part 2 and 3
[NASDA-TMR-930003-PT-2-3] 02 p0541 N94-13659
Reliable redundant device for mechanisms 06 p2361 N94-24030
Space Habitat, assembly and repair facility 07 p2691 N94-25696
Selected topics in robotics for space exploration
[NASA-CP-10131] 07 p2682 N94-26278
Deployable reflector structure
[NASA-CASE-LAR-14513-1-SB] 08 p3245 N94-29360
A module concept for a cable-mesh deployable antenna 08 p3161 N94-29631
Low melting temperature alloy deployment mechanism and recent experiments 08 p3163 N94-29644
MSAT boom joint testing and load absorber design 09 p3606 N94-33315
Configurational evolution dynamics and stability during in-situ development of large orbiting spacecraft
[AD-A280482] 12 p4397 N94-37351
SPACE EXPER WITH PARTICLE ACCELERATORS
U SEPAC (PAYLOAD)
SPACE EXPLORATION
NT MARS EXPLORATION
ESA/ESOC: 25 years
[ESA-BR-90] 01 p0485 N94-11379
Sixth Annual Workshop on Space Operations Applications and Research (SOAR 1992), volume 2
[NASA-CP-3187-VOL-2] 01 p0486 N94-11527
In-space operations for lunar and Mars space transfer vehicles 01 p0348 N94-11568
Terrestrial case studies of ilmenite exploration and lunar implications 01 p0478 N94-12247
Conceptual studies report on lunar and planetary exploration
[NASDA-TK-SS0438] 01 p0481 N94-12323
Mars exploration missions 01 p0482 N94-12327
Technical problems on lunar an planetary exploration mission 01 p0482 N94-12328
Where no flag has gone before: Political and technical aspects of placing a flag on the Moon
[NASA-CR-188251] 02 p0827 N94-12800
Effects of radiobiological uncertainty on vehicle and habitat shield design for missions to the moon and Mars
[NASA-TP-3312] 02 p0846 N94-12875
MARS Mission research center
[NASA-CR-194034] 02 p0841 N94-13088
A modular gas-cooled cermet reactor system for planetary base power
[DE93-013672] 02 p0550 N94-13351
NASA images 11
[NASA-TM-109287] 02 p0842 N94-13626
Discovery management workshop
[NASA-TM-108244] 02 p0531 N94-14080
Asia-Pacific ISY conference, volume 1
[NASDA-CM-199-1] 02 p0532 N94-14096
Space transportation systems and space activities in the 21st century 02 p0537 N94-14274
Robotics in space
[NASA-TM-109584] 03 p1045 N94-15268
NASA: The 25th year
[NASA-TM-109457] 03 p1302 N94-15352

First US Mars landing
[NASA-TM-109669] 03 p0885 N94-15436
Mars laser altimeter based on a single photon ranging technique 03 p0921 N94-15619
Workshop on advanced technologies for planetary instruments
[NASA-CR-194585] 03 p1032 N94-15797
Space transfer concepts and analyses for exploration missions, phase 4
[NASA-CR-193849] 03 p0882 N94-15831
Twenty-Fourth Lunar and Planetary Science Conference. Part 2: G-M
[NASA-CR-193174] 03 p1247 N94-16173
Rover mounted ground penetrating radar as a tool for investigating the near-surface of Mars and beyong 03 p1007 N94-16197
Mars Analog Site Study (MASS) 03 p1252 N94-16200
Gamma ray spectrometer for Lunar Scout 2 03 p1037 N94-16426
Chairmanship of the Neptune/Pluto outer planets science working group
[NASA-CR-194625] 03 p1297 N94-16832
Small spacecraft for planetary exploration 03 p0874 N94-17145
Space transfer concepts and analyses for exploration missions
[NASA-CR-193876] 04 p1332 N94-18820
Shuttle-C, the future is now
[NASA-TM-109355] 04 p1332 N94-18954
Magellan, Galileo, and Ulysses
[NASA-TM-109362] 04 p1628 N94-18958
Spacework 17: O'Leary's Mars
[NASA-TM-109374] 04 p1629 N94-18966
Space exploration initiative
[NASA-TM-109366] 04 p1323 N94-18981
Low energy CMOS for space applications 05 p1768 N94-21735
Mars exploration study workshop 2
[NASA-CP-3243] 05 p2146 N94-21883
Robotic concepts for operation in barren terrain
[DE93-040539] 05 p1946 N94-21925
Advanced nuclear thermal propulsion concepts 06 p2217 N94-23068
Rover requirements for the planet surface segment of the space exploration initiative 06 p2369 N94-23377
Science strategy for Mars exploration 06 p2606 N94-23380
Prospects for using mobile vehicles in missions to Mars and other planets 06 p2607 N94-23384
The robotic Mars rover 06 p2608 N94-23390
Mission and system concepts for Mars robotic precursor missions 06 p2608 N94-23391
Mission and system design of a long range rover mission 06 p2608 N94-23392
Mars 96 rover: Science, instrumentation, and control 06 p2369 N94-23395
Balloon experiments at Mars 96 project 06 p2608 N94-23396
Feasibility study of an automatic vehicle for planetary exploration 06 p2369 N94-23399
Electrical power technology for robotic planetary rovers 06 p2314 N94-23401
Walking machines for space 06 p2369 N94-23406
The mass of massive rover software 06 p2464 N94-23410
Dual rover concept for Mars exploration 06 p2370 N94-23415
Results of the Mojave tests of the Mars 96 rover 06 p2370 N94-23416
The Jet Propulsion Laboratory space exploration: Past, present and future 06 p2153 N94-24242
NASA high performance computing and communications program
[NASA-TM-4554] 06 p2591 N94-24337
The 1993 NASA/ASEE Summer Faculty Fellowship Program
[NASA-CR-193862] 06 p2574 N94-24405
Demonstration of the feasibility of an integrated x ray laboratory for planetary exploration
[NASA-CR-177631] 06 p2598 N94-24832
The Ninth National Space Symposium
[ISBN-0-9616962-7-3] 06 p2598 N94-25006
The future of manned spaceflight 06 p2195 N94-25067
Proceedings of the 8th Annual Summer Conference: NASA/USRA Advanced Design Program
[NASA-CR-195118] 07 p3075 N94-25665
Planetary surface exploration MESUR/autonomous lunar rover 07 p2833 N94-25683
Project APEX: Advanced manned exploration of the Martian moon Phobos 07 p3079 N94-25688
Mars transportation system 07 p2833 N94-25689
Asteroid exploration and utilization 07 p3080 N94-25697
Selected topics in robotics for space exploration
[NASA-CP-10131] 07 p2682 N94-26278
Early lunar rover mission studies 07 p2684 N94-26290
Vision 21: Interdisciplinary Science and Engineering in the Era of Cyberspace
[NASA-CP-10129] 07 p2685 N94-27358
Telepresence in the human exploration of Mars: Field studies in analog environments 07 p2685 N94-27360
Spiral Survey Expedition: A proposal to organize for the Survey, exploration and eventual colonization of the Milky Way Galaxy 07 p2686 N94-27366
A direct current rectification scheme for microwave space power conversion using traveling wave electron acceleration 07 p2687 N94-27371
Comparison of the lossy image data compressions for the MESUR Pathfinder and for the Huygens Titan Probe 07 p2945 N94-28254
MUADEE: Mars Upper Atmosphere Dynamics, Energetics, and Evolution discovery mission. Executive summary volume
[NASA-CR-195732] 08 p3549 N94-28418
The Pluto fast flyby mission: Completing the reconnaissance of the solar system 08 p3235 N94-29768
Smart focal-plane technology for micro-instruments and micro-rovers 08 p3237 N94-29780
Evaluating success levels of mega-projects 09 p3599 N94-31432
NASA report to education, volume 9
[NASA-TM-109760] 09 p3913 N94-31817
NASA strategic plan
[NASA-TM-109780] 09 p3915 N94-32222
NASA report to education, volume 6
[NASA-TM-109818] 10 p4167 N94-33573
Ulysses: A solar odyssey
[NASA-TM-109820] 10 p4010 N94-33574
Microrover research at JPL 10 p4066 N94-34020
Design of the MESUR/pathfinder microrover 10 p4066 N94-34021
Vehicle development of Lunar/Mars exploration 10 p4067 N94-34030
Exobiology and solar system exploration
[NASA-TM-109850] 10 p4164 N94-34092
Johnson Space Center (JSC) research and technology
[NASA-TM-104788] 10 p4187 N94-34677
An automatic planetary vehicle for exploring Mars 11 p4354 N94-35336
Space educators' handbook
[NASA-TM-109779] 11 p4343 N94-35339
Space and the American imagination
[NASA-CR-196131] 11 p4376 N94-35356
Remote geochemical experiment package for Discovery class missions 11 p4350 N94-35420
Galileo: The Jovian laboratory
[NASA-CR-196043] 11 p4367 N94-35504
Voyager: National Air and Space Museum
[NASA-CR-195905] 11 p4367 N94-35505
Voyager last picture show
[NASA-CR-195796] 11 p4367 N94-35506
Magellan to Venus
[NASA-CR-195779] 11 p4201 N94-35510
Voyager science summary tape
[NASA-CR-195909] 11 p4367 N94-35513
Partners in space. International cooperation in space: Strategies for the new century
[ISBN-0-9629930-2-6] 11 p4348 N94-35901
The history of space exploration
[NASA-TM-109888] 11 p4201 N94-36440
Baseline antenna design for space exploration initiative
[NASA-CR-196298] 12 p4435 N94-37255

SPACE FLIGHT
NT APOLLO FLIGHTS
NT APOLLO 11 FLIGHT
NT APOLLO 15 FLIGHT
NT APOLLO 16 FLIGHT
NT APOLLO 17 FLIGHT
NT INTERPLANETARY FLIGHT
NT INTERSTELLAR TRAVEL
NT LONG DURATION SPACE FLIGHT
NT MANNED REENTRY
NT MANNED SPACE FLIGHT
NT MERCURY MA-6 FLIGHT
NT RETURN TO EARTH SPACE FLIGHT
NT SPACE SHUTTLE MISSION 51-F
NT SPACE SHUTTLE MISSION 51-L
NT SPACE SHUTTLE MISSION 61-A
NT SPACE SHUTTLE MISSIONS
Countermeasure for reducing post-flight orthostatic intolerance: Lower Body Negative Pressure (LBNP) experiment E140 02 p0594 N94-13772
Psychophysiological investigations of the biomedical problems of manned spaceflight
[NASA-CR-194107] 02 p0732 N94-13782
An improved approach for flight readiness certification: Methodology for failure risk assessment and application examples, volume 1
[NASA-CR-194498] 02 p0542 N94-14076
An improved approach for flight readiness certification: Methodology for failure risk assessment and application examples. Volume 2: Software documentation
[NASA-CR-194499] 02 p0542 N94-14077
An improved approach for flight readiness certification: Methodology for failure risk assessment and application examples. Volume 3: Structure and listing of programs
[NASA-CR-194500] 02 p0542 N94-14078
Laboratory simulation of spacecraft charging in the plasma wake region
[FFI-93-7007] 02 p0542 N94-14107
Cosmos 2229
[NASA-CR-194734] 05 p1895 N94-20338
Mission engineering 06 p2505 N94-23881
Transfer of perceptual adaptation to space sickness: What enhances an individual's ability to adapt?
[NASA-CR-188256] 06 p2427 N94-24227
NASA's spacecraft data system 07 p2950 N94-26723
Future of aerospace
[PB94-120185] 07 p2669 N94-26906
Nasa Langley Research Center seventy-fifth anniversary publications, 1992
[NASA-TM-109691] 07 p3118 N94-27431
NASA space and Earth science data on CD-ROM
[NASA-TM-109709] 08 p3528 N94-28414

SPACE FLIGHT FEEDING
Japanese Journal of Aerospace and Environmental Medicine, vol. 30, no. 3
[JTN-94-80606] 08 p3387 N94-28495
Some issues on Japan's space food development and relating preliminary experimental study 08 p3388 N94-28498

SPACE FLIGHT STRESS
Selection of behavioral tasks and development of software for evaluation of rhesus monkey behavior during spaceflight
[NASA-CR-194176] 02 p0728 N94-13865
Transfer of perceptual adaptation to space sickness: What enhances an individual's ability to adapt?
[NASA-CR-188256] 06 p2427 N94-24227
Artificial gravity in space flight
[AD-A273420] 06 p2427 N94-24928
Workshop on Countering Space Adaptation with Exercise: Current Issues
[NASA-CP-3252] 07 p2934 N94-28361
Muscular activity and its relationship to biomechanics and human performance 07 p2934 N94-28362
Response to graded Lower Body Negative Pressure (LBNP) after space flight 10 p4096 N94-33637

SPACE FLIGHT TRAINING
STS-33 Carter and Thorton during WETF activities
[NASA-TM-109471] 03 p1136 N94-15402
STS-36 crew EVA prep and post-training, bailout exercises, final bench review
[NASA-TM-109498] 03 p1137 N94-15462
STS-35 payload specialists Durrance and Parise: 70mm photo training and cabin familiarization
[NASA-TM-109499] 03 p1032 N94-15463

SPACE GLIDERS
U LIFTING REENTRY VEHICLES

SPACE HABITATS
Effects of radiobiological uncertainty on vehicle and habitat shield design for missions to the moon and Mars
[NASA-TP-3312] 02 p0846 N94-12875
Life support and habitability manual, volume 1
[ESA-PSS-03-406-ISSUE-1-VOL-1] 02 p0737 N94-13901
Life support and habitability manual, volume 2
[ESA-PSS-03-406-ISSUE-1-VOL-2] 02 p0738 N94-13902
Living well in space: Monitoring environment
[NASA-TM-109537] 03 p1120 N94-15368
STS-38 crew training: Habitation equipment procedures, bailout in CCT, 70mm photo class, EVA prep and post, and firefighting
[NASA-TM-109494] 03 p1136 N94-15453
An analysis of the dynamic response of the Space Station Freedom due to a module perforation by an orbital debris particle impact
[TABES PAPER 93-653] 03 p0899 N94-16154
Space transfer concepts and analyses for exploration missions
[NASA-CR-193876] 04 p1332 N94-18820
Proceedings of the NIST Conference on Reducing the Cost of Space Infrastructure and Operations: Part 1: Oral presentations and discussion
[PB94-111374] 06 p2194 N94-23770
National Institute of Standards and Technology Conference on Reducing the Cost of Space Infrastructure and Operations. Part 2: Topical papers
[PB94-113487] 06 p2194 N94-23819

Crew interface analysis: Selected articles on space human factors research, 1987 - 1991
[NASA-TM-104756] 06 p2433 N94-24185
Preliminary design of a universal Martian lander
[NASA-CR-195529] 06 p2206 N94-25007
Automation of closed environments in space for human comfort and safety 07 p2943 N94-25684
A widely adaptable habitat construction system utilizing space resources 07 p2688 N94-27374
Designing for human presence in space: An introduction to environmental control and life support systems
[NASA-RP-1324] 07 p2942 N94-27437
Summary report of mission acceleration measurements for Spacehab-01, STS-57 launched 21 June 1993
[NASA-TM-106514] 08 p3168 N94-29757

SPACE HEATING (BUILDINGS)
Transition of building energy consumption using multi-input, single-output dynamic model
[VTT-PUBS-116] 02 p0597 N94-14055
Maintaining acceptable thermal comfort with a low air temperature by means of local heating
[PB94-138526] 08 p3401 N94-29950
Control of heating, ventilation and air conditioning (HVAC) systems
[PB94-138807] 08 p3401 N94-30000
Thermal performance of residential duct systems in basements
[LBL-33962] 11 p4250 N94-35364

SPACE INDUSTRIALIZATION
NT SPACE MANUFACTURING
NT SPACE PROCESSING
Consortium for materials development in space
[NASA-CR-194411] 04 p1379 N94-18840
Space industrialization: A guide to government information
[RELEASE-1.3] 09 p3916 N94-31338
DOD space based requirements: Increasing DOD access to space
[AD-A276874] 09 p3601 N94-32211

SPACE INFRARED TELESCOPE FACILITY
The four great observatories
[NASA-TM-109311] 02 p0830 N94-13605

SPACE LABORATORIES
NT LONG DURATION EXPOSURE FACILITY
NT MANNED ORBITAL LABORATORIES
NT SPACELAB
Advanced protein, crystallization facility and associated new developments 01 p0039 N94-10119
The International Microgravity Laboratory, a Spacelab for materials and life sciences 01 p0125 N94-10249
The critical facility on IML-1 01 p0044 N94-10250
Effect of double density caging during Space Shuttle transport of laboratory rats
[NASA-CR-193228] 01 p0300 N94-11180
Present status of JEM utilization projects 02 p0530 N94-13273
Study on improvement of flammability, odor and offgassing tests for materials
[NASDA-CNT-930009] 02 p0563 N94-13471
Commitment to challenge
[NASA-TM-109523] 03 p0876 N94-15473
Scientific use of Space Station Freedom 03 p0977 N94-16072
Consortium for materials development in space
[NASA-CR-194411] 04 p1379 N94-18840
Opportunities and questions for the fundamental biological sciences in space 04 p1502 N94-19212
Manned Space-laboratories Control Center (MSCC) operations concept 06 p2505 N94-23882
RoboLab and virtual environments 10 p4015 N94-34027
A study of low mass x-ray binaries
[NASA-CR-195813] 10 p4162 N94-34119
Space environment laboratory in review, 1993
[PB94-153004] 10 p4187 N94-34946
Design and development of experimental facilities for short duration, low-gravity combustion and fire experiments
[NASA-CR-196107] 12 p4389 N94-36967
Technology demonstration of space intravehicular automation and robotics
[NASA-TM-109138] 12 p4501 N94-37589

SPACE LAW
Where no flag has gone before: Political and technical aspects of placing a flag on the Moon
[NASA-CR-188251] 02 p0827 N94-12800
Contributions to CD Space Committee 1992
[PB94-124401] 07 p3101 N94-27218
Legal regime of human activities in outer space law 09 p3599 N94-31431
Space history, space policy, and executive leadership
[NASA-TM-109787] 09 p3924 N94-33067
JPRS Report: Science and Technology. Central Eurasia: Space. Russian federation law on space
[JPRS-USP-94-002] 11 p4348 N94-35519
JPRS report: Science and technology. Central Eurasia: Space 12 p4391 N94-37003

SPACE LOGISTICS
Definition of spacecraft standard interfaces by the NASA Space Assembly and Servicing Working Group (SASWG) 01 p0348 N94-11574
Strategy for the reduction of total integrated fluid logistics to the Space Station Freedom
[NASA-TM-107744] 03 p1138 N94-17452
Space Station technology testbed: 2010 deep space transport 07 p2687 N94-27368
Advanced transportation system study: Manned launch vehicle concepts for two way transportation system payloads to LEO
[NASA-CR-193951] 09 p3608 N94-33100

SPACE MAINTENANCE
On-orbit refueling 01 p0038 N94-11566
Preliminary analysis of the benefits derived to US Air Force spacecraft from on-orbit refueling 01 p0038 N94-11567
Forecasting the impact of virtual environment technology on maintenance training 01 p0314 N94-11570
On-orbit servicing for USAF space missions: A phased development approach 01 p0348 N94-11571
More sense for less cents: Cost effective servicing of remote sensing satellites 01 p0348 N94-11572
Space Station maintenance studies using plaid graphics 01 p0335 N94-11578
Robotic servicing on Earth orbiting satellites 01 p0045 N94-11579
Space Shuttle Mission STS-61: Hubble Space Telescope servicing mission-01
[NASA-TM-109344] 05 p1653 N94-20192
EVA tools and equipment reference book
[NASA-TM-109350] 05 p1897 N94-21812
An intelligent planning and scheduling system for the HST servicing missions 06 p2520 N94-23964
A simulation system for Space Station extravehicular activity 06 p2434 N94-24192
Design and simulation of EVA tools for first servicing mission of HST
[NASA-CR-194784] 06 p2439 N94-24857
Space Habitat, assembly and repair facility 07 p2691 N94-25696
System for the installation and replacement of components in hostile environments
[NASA-CASE-LEW-14906-1-SB] 08 p3300 N94-29427
Extra-vehicular activity translation tool
[NASA-CASE-MSC-21955-1] 08 p3300 N94-29428
Use of a pitch adjustable foot restraint system: Operator strength capability and load requirements
[NASA-TP-3477] 09 p3805 N94-33050
Diagnosing anomalies of spacecraft for space maintenance and servicing 10 p4015 N94-33667
The SCRAM tool-kit 10 p4066 N94-33668
SpaceHab 1 maintenance experiment 10 p4015 N94-33669
Seventh Annual Workshop on Space Operations Applications and Research (SOAR 1993), volume 1
[NASA-CP-3240-VOL-1] 10 p4179 N94-34019
Design and simulation of EVA tools for first servicing mission of HST
[NASA-CR-196030] 11 p4298 N94-35266

SPACE MANUFACTURING
Solidification in immiscible systems: The influence of processing conditions on resulting microstructures 01 p0112 N94-10174
Space Solar Power Program
[DE93-011750] 01 p0055 N94-11675
The studies on lunar and planetary exploration and utilization: The study on lunar resources utilization
[NASDA-CNT-930014] 02 p0842 N94-13655
Asia-Pacific ISY conference, volume 1
[NASDA-CM-199-1] 02 p0532 N94-14098
China's devotion to space science and applications 02 p0532 N94-14273
TABES 1993: 9th Annual Technical and Business Exhibition and Symposium 03 p1050 N94-16129
Study of the National Science Foundation's South Pole Station as an analogous data base for the logistical support of a Moon laboratory
[NASA-TM-108429] 03 p1174 N94-17469
Activities of the Center for Space Construction
[NASA-CR-193717] 04 p1335 N94-19371
Study on melted solution stirring under microgravity 07 p2730 N94-25585
Prototype space fabrication platform
[AD-A273904] 07 p2694 N94-25659
Space Station technology testbed: 2010 deep space transport 07 p2687 N94-27368
A widely adaptable habitat construction system utilizing space resources 07 p2688 N94-27374
Prometheus in space: Research Committee on Functional New Material
[JTN-94-80580] 07 p2761 N94-28002
Overview of space environment utilization science
[JTN-94-80581] 08 p3227 N94-28938
Fluid and transportation phenomena under microgravity 08 p3227 N94-28939
Combustion studies under microgravity 08 p3228 N94-28940
Glass studies under microgravity 08 p3228 N94-28941
Fabrication of electronic materials in space 08 p3228 N94-28942
Protein crystal growth in microgravity 08 p3228 N94-28943
Cell culture in space 08 p3228 N94-28944
Cosmic energy equipment 08 p3229 N94-28945
Laser beam welding of AISI 316 stainless steel in microgravity environment: Experiments aboard a KC-135 flight
[ISBN-0-315-86095-2] 08 p3229 N94-30145
Survey report of JSUP Space Environment Utilization Research Committee in fiscal year 1992: Functional New Materials Session
[JTN-94-80582] 08 p3159 N94-30162
Survey report of JSUP Space Environment Utilization Research Committee in fiscal year 1992: Metallic Materials Session
[JTN-94-80583] 08 p3159 N94-30794
A large motion zero-gravity suspension system for experimental simulation of orbital construction and deployment
[NASA-CR-195881] 09 p3668 N94-33037
Design, characterization, and control of the NASA three degree of freedom reaction compensation platform 09 p3605 N94-33304

SPACE MECHANICS
NT ASTRODYNAMICS
NT CELESTIAL MECHANICS
NT ORBITAL MECHANICS

SPACE MEDICINE
U AEROSPACE MEDICINE

SPACE MISSIONS
NT ASTEROID MISSIONS
NT CASSINI MISSION
NT CLUSTER MISSION
NT COMET RENDEZVOUS ASTEROID FLYBY MISSION
NT FLYBY MISSIONS
NT GIOTTO MISSION
NT GRAND TOURS
NT MANNED MARS MISSIONS
NT MARINER-MERCURY 1973
NT MARS SAMPLE RETURN MISSIONS
NT SOHO MISSION
NT SOLAR MAXIMUM MISSION
NT ULYSSES MISSION
An analysis of the modes and states for generic avionics
[NASA-CR-188253] 01 p0027 N94-10664
The 1987 RIACS annual report
[NASA-CR-193220] 01 p0324 N94-11046
Analyzing human errors in flight mission operations 01 p0314 N94-11534
On-orbit servicing for USAF space missions: A phased development approach 01 p0348 N94-11571
Supervised autonomous control, shared control, and teleoperation for space servicing 01 p0183 N94-11577
Summary of the pre-AO of the JEM onboard scientific and engineering experiments for refrigerator utilization 01 p0129 N94-11832
Moessbauer spectrometer for mineralogical analysis of the Mars surface: Moessbauer source considerations 01 p0476 N94-12242
Conceptual studies report on lunar and planetary exploration
[NASDA-TK-SS0438] 01 p0481 N94-12323
Significance and scenarios of lunar and planetary exploration missions 01 p0482 N94-12324
Technical problems on lunar an planetary exploration mission 01 p0482 N94-12328
Interdisciplinary scientist participation in the Phobos mission
[NASA-CR-193715] 01 p0482 N94-12446
Present status of JEM utilization projects 02 p0530 N94-13273
Gas core nuclear thermal rocket engine research and development in the former USSR
[DE93-012165] 02 p0552 N94-14013
Asia-Pacific ISY conference, volume 1
[NASDA-CM-199-1] 02 p0532 N94-14098
Design and application of electromechanical actuators for deep space missions
[NASA-CR-194145] 02 p0663 N94-14134
China's devotion to space science and applications 02 p0532 N94-14273
Space transportation systems and space activities in the 21st century 02 p0537 N94-14274

The 1969 highlights
[NASA-TM-109630] 03 p1301 N94-15241
The 1972 highlights
[NASA-TM-109631] 03 p1301 N94-15242
The 1965 highlights --- NASA programs
[NASA-TM-109632] 03 p1301 N94-15243
The 1967 highlights
[NASA-TM-109633] 03 p1301 N94-15244
Return to Space Mission: The STS-26 crew report
[NASA-TM-109568] 03 p0880 N94-15317
Apollo presentation for Astrodome
[NASA-TM-109535] 03 p1302 N94-15366
Mars laser altimeter based on a single photon ranging technique 03 p0921 N94-15619
Approaching the new reality
[TABES PAPER 93-230] 03 p1050 N94-16131
Commercial space opportunities advanced concepts and technology overview
[TABES PAPER 93-240] 03 p1050 N94-16132
Role and development of small satellite missions in space plasma physics 03 p0891 N94-17149
MINISAT programme 03 p0896 N94-17182
Mission needs and system commonality for space nuclear power and propulsion
[DE93-016557] 04 p1337 N94-17863
Human Transportation System (HTS) study: Executive summary
[NASA-TM-104780] 04 p1332 N94-18669
Human Transportation System (HTS) study, volume 1
[NASA-TM-104779] 04 p1332 N94-18670
Report on the activities of Space Science Department, 1990 - mid 1992
[ESA-SP-1161] 04 p1633 N94-19404
Space Shuttle Mission STS-61: Hubble Space Telescope servicing mission-01
[NASA-TM-109344] 05 p1653 N94-20192
NEP Early Flight program: System performance and development considerations
[NASA-TM-106415] 05 p1654 N94-21570
A generic archive protocol and an implementation 05 p2047 N94-22493
Prospects for improved instrumentation on future solar space missions 06 p2624 N94-22843
Solar physics within NASA's planning 06 p2625 N94-22845
The next Japanese solar satellite 06 p2625 N94-22846
Prospects for very-high-resolution solar physics with the Simuris inteferometric mission 06 p2625 N94-22848
Requirements for future solar-physics missions with x ray instrumentation 06 p2625 N94-22849
Requirements for future solar-physics missions that include UV instrumentation 06 p2625 N94-22851
Mission and system concepts for Mars robotic precursor missions 06 p2608 N94-23391
Mission and system design of a long range rover mission 06 p2608 N94-23392
Electronic payloads for Martian missions: A preliminary assessment of technologies 06 p2610 N94-23408
OASIS-CC presentation 06 p2385 N94-23613
Commonality of flight control systems for support of European telecommunications missions 06 p2304 N94-23834
NASDA's view of ground control in mission operations 06 p2305 N94-23835
Future trends in NASA space operations 06 p2498 N94-23836
The space operations at CNES 06 p2498 N94-23837
Common front end systems for Space Shuttle and Space Station control centers at Johnson Space Center 06 p2305 N94-23838
Distributed science operations for JPL planetary missions 06 p2500 N94-23850
SCOS2: ESA's new generation of mission control systems 06 p2197 N94-23851
NASDA satellite mission operation system and operations 06 p2501 N94-23854
Mission activities planning for a Hermes mission by means of AI-technology 06 p2502 N94-23858
A review of mission planning systems 06 p2503 N94-23866
Techniques and software for optimum and efficient mission science sequence development 06 p2504 N94-23872
A packet-based concept for spacecraft command planning 06 p2504 N94-23873
Connecting science and operations: The operations coordinator 06 p2504 N94-23874
The instant sequencing task: Toward constraint-checking a complex spacecraft command sequence interactively 06 p2504 N94-23875
Generic mission planning concepts for space astronomy missions 06 p2505 N94-23878
A MOS for all seasons 06 p2505 N94-23879
An operations concept methodology to achieve low-cost mission operations 06 p2505 N94-23880
The Advanced Technology Operations System: ATOS 06 p2508 N94-23897
The application of total quality management principles to spacecraft mission operations 06 p2374 N94-23931
Mission operations and command assurance: Instilling quality into flight operations 06 p2374 N94-23932
Security aspects of space operations data 06 p2515 N94-23937
Mission and science activity scheduling language 06 p2515 N94-23938
Expert diagnostics system as a part of analysis software for power mission operations 06 p2516 N94-23944
Planning: Management of predictability and uncertainty and keeping abreast of developments 06 p2520 N94-23967
Estimating the Deep Space Network modification costs to prepare for future space missions by using major cost drivers 06 p2520 N94-23968
Space operations: Archiving space science data needs further management improvements. Report to the Chairman, Subcommittee on Investigations and Oversight, Committee on Science, Space, and Technology, House of Representatives
[GAO/NSIAD-94-25] 06 p2591 N94-24092
Use of infrared telemetry as part of a nonintrusive inflight data collection system to collect human factors data 06 p2434 N94-24193
A mission to Mercury and a mission to the moons of Mars
[NASA-CR-195530] 06 p2195 N94-24619
Ultraviolet, visible, and gravity astrophysics: A plan for the 1990's
[NASA-NP-152] 06 p2603 N94-24973
Access to space study
[NASA-TM-109693] 07 p2685 N94-27151
STS-57 Space Shuttle mission report
[NASA-CR-195739] 07 p2693 N94-28220
STS-56 Space Shuttle mission report
[NASA-CR-195740] 07 p2693 N94-28221
Comparison of the lossy image data compressions for the MESUR Pathfinder and for the Huygens Titan Probe 07 p2945 N94-28254
MUADEE: Mars Upper Atmosphere Dynamics, Energetics, and Evolution discovery mission. Executive summary volume
[NASA-CR-195732] 08 p3549 N94-28418
Decoder synchronization for deep space missions 08 p3250 N94-29664
The double probe electric field experiment on Freja: Description and first results
[TRITA-ALP-1993-02] 09 p3885 N94-31089
Participation in the scientific activities of the Waves in Space Plasma (WISP) project
[NASA-CR-195903] 09 p3894 N94-33113
The PLAID graphics analysis impact on the space program 10 p4110 N94-33632
Vista goes online: Decision-analytic systems for real-time decision-making in mission control 10 p4125 N94-35063
STS-58 Space Shuttle Mission Report
[NASA-TM-109867] 11 p4211 N94-35251
STS-51 Space Shuttle Mission Report
[NASA-TM-109866] 11 p4211 N94-35252
X-ray remote sensing and in-situ spectroscopy for planetary exploration missions and gamma-ray remote sensing and in-situ spectroscopy for planetary exploration missions
[NASA-CR-189352] 11 p4375 N94-35381
A 32-GHz solid-state power amplifier for deep space communications 11 p4255 N94-35562
NAVSPACECOM space surveillance sensor system digital signal processing receiver. Volume 3: Operating system functions
[AD-A278839] 11 p4212 N94-35799
NAVSPACECOM space surveillance sensor system digital signal processing receiver. Volume 4: Hardware interfaces
[AD-A278845] 11 p4212 N94-35801

SPACE NAVIGATION
NT INTERPLANETARY NAVIGATION
NASA's first in-space optical gyroscope: A technology experiment on the X ray Timing Explorer spacecraft
[NASA-TM-109242] 01 p0170 N94-10667
Lunar Scout Two spacecraft gravity experiment 01 p0459 N94-12152
Proceedings of the 11th Space Surveillance Workshop, volume 1
[AD-A265120] 02 p0531 N94-13358
The development and flight test of a deployable precision landing system for spacecraft recovery
[NASA-TM-4525] 02 p0537 N94-14853
Space flight: The application of orbital mechanics
[NASA-TM-109424] 03 p0874 N94-15493
A guidance and navigation system for two spacecraft rendezvous in translunar halo orbit
[AD-A267498] 03 p0898 N94-17368
Radiation induced darkening of the optical elements in the Startracker camera
[DE93-018907] 04 p1433 N94-19004
Pointing control design for autonomous space vehicle applications
[DE93-019943] 05 p1657 N94-19863
Real-time on-board orbit determination with DORIS 06 p2196 N94-23919
TOPEX/Poseidon precision orbit determination production and expert system 06 p2196 N94-23920
A real-time navigation monitoring expert system for the Space Shuttle Mission Control Center 06 p2202 N94-23921
XRTD: An X-Windows based, real-time radiometric display and analysis system 06 p2305 N94-23922
Navigation of space VLBI missions: Radioastron and VSOP 06 p2513 N94-23926
Satellite autonomous navigation and orbit determination using magnetometers 06 p2156 N94-24258
Fault tolerant testbed evaluation, phase 1
[NASA-CR-188275] 08 p3171 N94-29035
Enhanced orbit determination filter sensitivity analysis: Error budget development 08 p3159 N94-29655
Miniature wide field-of-view star trackers for spacecraft attitude sensing and navigation 08 p3144 N94-29794
A guidance and navigation system for two spacecraft rendezvous in translunar halo orbit 08 p3142 N94-29837
The contribution of aeronautics and astronautics to the quality of life on Earth
[ILR-MITT-283(1993)] 09 p3764 N94-31611
Spacecraft-spacecraft radio-metric tracking: Signal acquisition requirements and application to Mars approach navigation 11 p4254 N94-35557
Improved solution accuracy for TDRSS-based TOPEX/Poseidon orbit determination 11 p4205 N94-35620
TDRSS Onboard Navigation System (TONS) flight qualification experiment 11 p4206 N94-35625
Evaluation of GPS position and attitude determination for automated rendezvous and docking missions
[NASA-CR-4614] 12 p4397 N94-37506

SPACE OBSERVATIONS (FROM EARTH)
The 1.2 to 3.5 microns observations of asteroid 4179 Toutatis 01 p0430 N94-12111
Optical propagation through atmospheric turbulence. Model analysis of anisoplanatism and application to adaptive optics
[ONERA-P-1992-4] 02 p0716 N94-14192
Hubble Space Telescope
[NASA-TM-109359] 04 p1621 N94-19072
Co-ordination of ground-based observations with Cluster 04 p1331 N94-19640
Scientific Requirements for Future Solar-Physics Space Missions
[ESA-SP-1157] 06 p2623 N94-22837
Goals of ground-based solar observations 06 p2624 N94-22840
Prospects for future ground-based solar observations 06 p2624 N94-22842
Kamiokande results on solar neutrinos and a supernova search
[ICRR-REPT-294-93-6] 06 p2627 N94-24961
Solar neutrinos: Real-time experiments
[ICRR-REPT-293-93-5] 06 p2627 N94-24962
CO-to-H2 conversion factor in dwarf irregular galaxies
[REPT-333] 06 p2603 N94-24985
High spatial resolution observations of CO in CRL 618
[REPT-334] 06 p2604 N94-24986
Contributions to the 23rd ICRC from emulsion chamber experiments at Mt. Chacaltaya and Pamirs
[ICRR-REPT-295-93-7] 07 p3112 N94-25624
A study of very high energy hadron interactions through observation of cosmic-ray families with visible energy not less than 500 TeV, 3 07 p3112 N94-25627
Observation of characteristics of cosmic-ray hadron interactions in uniform-type thick lead chambers at Pamir, 1 07 p3112 N94-25628
Observation of characteristics of cosmic-ray hadron interactions in uniform-type thick lead chambers at Pamir, 2 07 p3113 N94-25629
Observation of characteristics of cosmic-ray hadron interactions in uniform-type thick lead chambers at Pamir, 3 07 p3113 N94-25630
Violation of Feynman scaling law in the forward region 07 p3113 N94-25633
Simultaneous observation of families and air showers at Mt. Chacaltaya 07 p3114 N94-25634

Correlation studies of Pioneer Venus imagery obtained from PV experiments with near IR imagery obtained from ground-based observations during Venus inferior conjunction
[NASA-CR-195772] 08 p3550 N94-29892

SPACE PERCEPTION
Characteristics of aimed arm movements in humans under low gravity 03 p0980 N94-16093
Neural basis of motion perception
[AD-A267267] 03 p1133 N94-17265
A virtual acoustic orientation instrument
[AD-A268181] 03 p1134 N94-17510
Psychophysical analyses of perceptual representations
[AD-A268711] 04 p1508 N94-18313
Modeling of driver behavior: Information perception, rule and control strategies in experiments and simulations
[ETN-93-95053] 04 p1510 N94-19649
Why stereo vision is not always about 3D reconstruction
[AD-A270522] 05 p1939 N94-19893
Perception and 3D environment modeling for mobile robot autonomous navigation
[LAAS-93117] 06 p2471 N94-22908
Perception in flight: Shape and motion perception, space perception, spatial orientation, and visual vestibular interaction 06 p2429 N94-23979
Extracting heading and temporal range from optic flow: Human performance issues 06 p2442 N94-25510
The effect of body orientation on the perception of vertical and horizontal distance in an outdoor setting 07 p2915 N94-27461
An investigation of methods for determining depth from focus
[ISBN-0-315-64015-4] 07 p2988 N94-27645
Disturbance of equilibrium on JAL flight crew 08 p3390 N94-28856
An investigation of stereopsis with AN/AVS-6 night vision goggles at varying levels of illuminance and contrast
[AD-A275332] 08 p3400 N94-28918
Extended occupancy grid method for modelling unknown dynamic environments 08 p3144 N94-30281
Using stereoscopic imaging for visualization applications
[DE94-006247] 08 p3536 N94-30706
A neural network model for the visual perception of the depth of a scene from stereoscopy and shading
[ISBN-0-315-86753-1] 09 p3831 N94-31750
Sensory sensitivities and discriminations and their roles in aviation
[AD-A277312] 09 p3800 N94-32276
Neural models of spatial orientation in novel environments
[AD-A277383] 09 p3835 N94-32340
Visual neural development and chromatic aberration
[AD-A277402] 09 p3800 N94-32345
Human factors for flight deck certification personnel
[AD-A280477] 12 p4487 N94-37347
Synthetic vision display evaluation studies
[NASA-CR-194963] 12 p4387 N94-37658

SPACE PHOTOGRAPHY
U SPACEBORNE PHOTOGRAPHY

SPACE PLASMAS
NT SOLAR WIND
NT STELLAR WINDS
Solar wind channels for MeV particles
[DE93-012648] 01 p0482 N94-10741
Imaging of magnetospheric dynamics using low energy neutral atom detection
[DE93-012656] 01 p0275 N94-10742
The influence of the propagation medium on the sensitivity and resolution of meter wavelength aperture synthesis systems 01 p0134 N94-11062
The International Colloquium on Atomic Spectra and Oscillator Strengths for Astrophysical and Laboratory Plasmas
[NASA-TM-109255] 02 p0849 N94-13376
The propagation characteristics and instability properties of low-frequency electromagnetic waves in the Io plasma torus 02 p0601 N94-13650
The role of ionospheric plasma in the magnetosphere
[NASA-CR-194404] 02 p0716 N94-13967
Terrestrial magnetospheric imaging: Numerical modeling of low energy neutral atoms
[DE93-014561] 02 p0717 N94-14328
Global auroral imaging: Dynamics of Explorer Miss ion
[NASA-CR-194284] 03 p1097 N94-15003
Polar 2 model of the wake shield experiment
[AD-A266243] 03 p0882 N94-16468
Prototype instrumentation and design studies
[AD-A266402] 03 p0882 N94-16530
Role and development of small satellite missions in space plasma physics 03 p0891 N94-17149
Space systems environmental interaction studies
[AD-A267280] 03 p0897 N94-17240
High voltage conductors in spacecraft
[AD-A267268] 03 p0897 N94-17266
Correlated charge-changing ion-atom collisions
[DE93-018717] 04 p1564 N94-17775
Detailed analysis of low energy plasma data under the Voyager Uranus data analysis program
[NASA-CR-193668] 04 p1628 N94-17842
Plasma properties research: Task 3
[DE93-017087] 04 p1583 N94-17854
An investigation of methods for updating ionospheric scintillation models using topside in-situ plasma density measurements
[AD-A269872] 04 p1483 N94-18655
Plasma contactor development for Space Station
[NASA-TM-106425] 04 p1587 N94-18861
Convection algorithms for magnetospheric particles
[AD-A270103] 04 p1493 N94-18871
Cluster: Mission, Payload, and Supporting Activities
[ESA-SP-1159] 04 p1328 N94-19622
The Cluster Ion Spectroscopy experiment 04 p1329 N94-19631
PEACE: A Plasma Electron and Current Experiment 04 p1329 N94-19632
European network for the numerical simulation of space plasmas 04 p1331 N94-19641
A study of Saturn's E-ring particles using the Voyager 1 plasma wave instrument
[NASA-CR-194694] 05 p2088 N94-20048
Ionospheric photoelectrons measured at geosynchronous orbit
[AD-A272431] 05 p1857 N94-21202
A new innovative instrument for space plasma instrumentation
[NASA-CR-194736] 05 p1666 N94-21780
Circumstellar environments of Be stars at infra-red and radio wavelengths
[ISBN-0-315-83135-9] 05 p2081 N94-22426
Consequences of chaotic particle motion for the stability of space plasma current sheets 05 p2001 N94-22636
Physical properties of dense astrophysical plasmas 05 p2001 N94-22637
Thermal properties and radiation processes in astrophysical plasmas 05 p2002 N94-22640
Pair plasmas in the galactic center region and in Nova Muscae 05 p2009 N94-22691
Prospects for very-high-resolution solar physics with the Simuris inteferometric mission 06 p2625 N94-22848
Evolution of large-scale plasma structures in comets: Kinematics and physics
[NASA-CR-194777] 06 p2601 N94-23251
Development of a power electronics unit for the Space Station plasma contactor
[NASA-TM-106486] 06 p2222 N94-25201
Norwegian ionospheric satellite experiment: High latitude, low Earth orbit plasma measurements
[FFI-93/7025] 07 p2876 N94-25807
Investigation of plasma instabilities in the polar cusp
[NASA-CR-195212] 07 p2879 N94-26599
Spectroscopy and dynamics of molecular and ionic impurities embedded in solid hydrogen
[AD-A274149] 07 p3064 N94-27095
Studies for Io's extended atmosphere and neutral clouds and their impact on the local satellite atmosphere and on the planetary magnetosphere
[NASA-CR-195255] 07 p3106 N94-27406
Collisionless shock structures of Earth and other planets
[NASA-CR-195257] 07 p3104 N94-27407
Configuration of the near-Earth plasma sheet
[NASA-CR-195271] 07 p2883 N94-27438
Acceleration of electrons and ions by strong lower-hybrid turbulence in solar flares
[NASA-TM-109723] 07 p3111 N94-27953
Equation of state of stellar plasmas
[DE94-004186] 08 p3542 N94-28526
Electron beams at geosynchronous orbit
[AD-A275471] 08 p3355 N94-28684
Active electron and ion beam experiments in space
[AD-A275570] 08 p3504 N94-28828
Computer simulations on development of the fast reconnection mechanism 08 p3360 N94-29241
Waves in space plasma dipole antenna subsystem 08 p3161 N94-29632
Coronal temperatures of unusually active K-dwarf binary systems
[NASA-CR-189335] 08 p3545 N94-29861
Simulation of space-energy distributions of hot plasma on a geostationary orbit
[DE94-607324] 08 p3365 N94-30107
A single-fluid, self-consistent formulation of particle transport and fluid dynamics 08 p3280 N94-30352
Laboratory and space experiments as a key to the plasma universe
[TRITA-ALP-1993-01] 09 p3885 N94-31088
Dispersion relations for a plasma-filled helix-loaded-waveguide
[DE94-006333] 09 p3675 N94-31781
Computer modeling of active experiments in space plasmas 09 p3890 N94-31927
Planetary magnetotails: Magnetic configuration and nonthermal plasma 09 p3942 N94-32326
Ionospheric plasma outflow in response to transverse ion heating: Self-consistent macroscopic treatment
[NASA-CR-195820] 09 p3893 N94-33048
Characteristics of ion flow in the quiet state of the inner plasma sheet
[AD-A277451] 09 p3894 N94-33106
The spatial development of the magnetospheric low-latitude boundary layer
[ISBN-0-315-77418-5] 09 p3776 N94-33111
Participation in the scientific activities of the Waves in Space Plasma (WISP) project
[NASA-CR-195903] 09 p3894 N94-33113
Multiple hollow cathode wear testing
[NASA-CR-195335] 10 p4016 N94-33975
The fine structure of Langmuir waves observed upstream of the bow shock at Venus
[NASA-CR-196123] 11 p4354 N94-35378
Spatial fluctuations of particle fluxes within the auroral zone inferred from the Intercosmos-Bulgaria-1300 satellite data
[DE94-615858] 11 p4350 N94-36128
Origins of energetic ions in the Earth's magnetosheath
[NASA-CR-189359] 12 p4471 N94-37703

SPACE PLATFORMS
NT COLUMBUS SPACE STATION
NT EURECA (ESA)
NT LONG DURATION EXPOSURE FACILITY
NT MAN TENDED FREE FLYERS
NT SYNCHRONOUS PLATFORMS
Robotic servicing on Earth orbiting satellites 01 p0045 N94-11579
Spaceborne SAR study: LDRD 1992
[DE93-011485] 01 p0232 N94-11623
ERS-1: 18 months in orbit 03 p0990 N94-15888
Ground integrated ET-derived space platforms for onorbit applications
[TABES PAPER 93-652] 03 p0899 N94-16152
Ground segment definition for the Spanish small satellite program (MINISAT) 03 p0878 N94-17155
TAOS (S80): A (LEO-MSS) system for position reporting and telemanagement services 03 p0893 N94-17162
TUBSAT: Low cost access to space technology 03 p0895 N94-17180
Standard platforms for small satellites 03 p0895 N94-17181
MINISAT programme 03 p0896 N94-17182
ALEXIS and HETE: Two small, low cost, scientific satellite systems 03 p0896 N94-17185
Military satellite communications: Opportunity to save billions of dollars. Report to the Chairman, Legislation, and National Security Subcommittee, Committee on Government Operations, House of Representatives
[AD-A267627] 03 p1002 N94-17199
ISOBUS: A new versatile spacecraft platform using Shuttle small payloads 04 p1327 N94-19183
Activities of the Center for Space Construction
[NASA-CR-193717] 04 p1335 N94-19371
Obtaining surface optical properties from space-based lidar systems
[AD-A272831] 05 p1987 N94-21172
Ground data system for Space Flyer Unit (SFU) 06 p2207 N94-23860
Prototype space fabrication platform
[AD-A273904] 07 p2694 N94-25659
NASA's space platform technology program and planning 09 p3597 N94-31044
Theoretical and experimental studies relevant to interpretation of auroral emissions
[NASA-CR-196032] 11 p4376 N94-36421

SPACE POWER REACTORS
The 40 kWe S-PRIME Thermionic Design and Technology Demonstration Program
[DE93-004738] 01 p0040 N94-10147
A critical assembly designed to measure neutronic benchmarks in support of the Space Nuclear Thermal Propulsion program
[DE92-040974] 01 p0371 N94-10529
Fully coupled neutronic and hydrodynamic analysis of space nuclear reactor reentry accidents
[DE93-005459] 01 p0372 N94-10890
A facility for testing 10- to 100-kWe space power reactors
[DE92-040420] 01 p0372 N94-11296
Proceedings of the 12th Space Photovoltaic Research and Technology Conference (SPRAT 12)
[NASA-CP-3210] 01 p0048 N94-11380
TFE verification program
[DE93-009609] 01 p0373 N94-11694

A modular gas-cooled cermet reactor system for planetary base power
[DE93-013672] 02 p0550 N94-13351
Preliminary nuclear safety assessment of the NEPST (Topaz 2) space reactor program
[DE93-012853] 02 p0551 N94-13514
Space reactor fuel element testing in upgraded TREAT
[DE93-012524] 02 p0554 N94-14806
Mission needs and system commonality for space nuclear power and propulsion
[DE93-016557] 04 p1337 N94-17863
Total hemispherical emittance of Niobium-1 percent zirconium fuel cladding for the SP-100 space reactor
[AD-A270456] 04 p1576 N94-19589
Preliminary SP-100/Stirling heat exchanger designs
[NASA-TM-106444] 05 p1670 N94-21809
SPACE-R Thermionic Space Nuclear Power System: Design and Technology Demonstration Program
[DE93-013969] 05 p1670 N94-21824
Temperature and Doppler coefficients of various space nuclear reactors
[DE94-001388] 05 p1671 N94-21979
An F2D analysis of the Flow Instability Test (FIT) experiment
[DE94-001420] 06 p2217 N94-23193
Assessment of an SP-100 bi-modal propulsion and power system
[DE94-000889] 06 p2218 N94-23433
SP-100 heat transport technology development
[DE94-000769] 06 p2218 N94-23452
Preliminary reentry safety assessment of the General Purpose Heat Source module for the Cassini mission: Aerospace Nuclear Safety Program
[DE94-001646] 07 p2699 N94-25926
Space-R thermionic space nuclear power system: Design and technology demonstration
[DE94-001890] 07 p2699 N94-25929
Space-R thermionic space nuclear power system design and technology demonstration
[DE94-002017] 07 p2700 N94-25930
Risk perspectives for Topaz 2 flight mission
[DE94-003229] 07 p2700 N94-25956
Pre-orbital criticality safety for the NEPSTP mission
[DE94-002600] 07 p3005 N94-26802
SP-100 control drive assembly development
08 p3163 N94-29651
Performance of CVD and CVR coated carbon-carbon in high temperature hydrogen
[DE94-005451] 08 p3487 N94-29841
Small low mass advanced PBR's for propulsion
[DE94-005142] 08 p3497 N94-30588
TOPAZ 2 system description
[DE94-006230] 08 p3498 N94-30846
The TOPAZ 2 space reactor response under accident conditions
[DE94-004998] 08 p3498 N94-30847
Utilizing a Russian space nuclear reactor for a United States space mission: Flight qualification issues
[DE94-004674] 09 p3613 N94-31265
Draft minutes of IAPG Mechanical Working Group meeting
[DE94-004954] 09 p3759 N94-31266
The development of CVR coatings for PBR fuels
[DE94-004233] 09 p3875 N94-31480
Development of lightweight radiators for lunar based power systems
[NASA-TM-106604] 09 p3726 N94-32272
A 1050 K Stirling space engine design
[NASA-CR-182149] 09 p3616 N94-32866
Independent safety assessment of the Topaz-2 space nuclear reactor power system
[DE94-008653] 09 p3877 N94-32879
Utilizing a Russian space nuclear reactor for a US space mission: Systems integration issues
[DE94-005585] 10 p4017 N94-34137
Conceptual design: TFE verification program
[DE94-012469] 12 p4398 N94-37433
TFE verification program
[DE94-009870] 12 p4398 N94-37514

SPACE PROBES

NT GALILEO PROBE
NT GALILEO SPACECRAFT
NT GIOTTO MISSION
NT HELIOS A
NT LUNAR PROBES
NT MAGELLAN SPACECRAFT (NASA)
NT MARINER SPACECRAFT
NT MARINER 6 SPACE PROBE
NT MARINER 7 SPACE PROBE
NT MARINER 9 SPACE PROBE
NT MARINER 10 SPACE PROBE
NT MARS OBSERVER
NT MARS PROBES
NT MARS 4 SPACECRAFT
NT PIONEER SPACE PROBES
NT VENERA SATELLITES
NT VIKING LANDER SPACECRAFT
NT VIKING SPACECRAFT
NT VOYAGER 1 SPACECRAFT
NT VOYAGER 2 SPACECRAFT
Estimation of the attitude motion of the small satellite ORIZURU
[NAL-TR-1145] 01 p0042 N94-10366
Real-time dynamics simulation of the Cassini spacecraft using DARTS. Part 1: Functional capabilities and the spatial algebra algorithm 02 p0680 N94-14638
Search for optimal distance spectrum convolutional codes 03 p0998 N94-16509
Predicted structural response of the lightweight-interceptor technology demonstration vehicle
[DE93-014676] 04 p1333 N94-17782
Comparison of the lossy image data compressions for the MESUR Pathfinder and for the Huygens Titan Probe 07 p2945 N94-28254
The double probe electric field experiment on Freja: Description and first results
[TRITA-ALP-1993-02] 09 p3885 N94-31089

SPACE PROCESSING

Proceedings of the 8th European Symposium on Materials and Fluid Sciences in Microgravity, volume 1
[ESA-SP-333-VOL-1] 01 p0099 N94-10070
Gas film levitator for containerless processing of glasses in microgravity conditions: Early concept and technology demonstration 01 p0108 N94-10122
TEMPUS: An electromagnetic levitation facility for containerless processing under micro-g in Spacelab 01 p0109 N94-10125
Microgravity Applications Furnace Facility (MAFF) for parabolic flights 01 p0109 N94-10128
High temperature processing and diagnostic technologies for microgravity applications 01 p0110 N94-10130
Determination of the viscous acoustic field for liquid drop positioning/forcing in an acoustic levitation chamber in microgravity 01 p0110 N94-10131
Laser beam deflection: A diagnostic tool for vapour growth experiments in microgravity 01 p0111 N94-10135
Mission support for crystal growth experiments in Russian unmanned carriers 01 p0111 N94-10139
AGF (Automatic Gradient Furnace): A proposed microgravity facility 01 p0112 N94-10141
Microgravity experiments using TR-1A rocket 01 p0112 N94-10142
Proceedings of the 8th European Symposium on Materials and Fluid Sciences in Microgravity, volume 2
[ESA-SP-333-VOL-2] 01 p0112 N94-10171
Scientific specifications for an automated facility for growing large semiconducting crystals from the melt in space 01 p0114 N94-10180
Variations of the temperature profile in the gradient furnace GFQ within a cylindrical sample used for directional solidification 01 p0114 N94-10181
Numerical simulation of multi-droplet hydrodynamic interactions in liquid dispersions 01 p0114 N94-10182
Convection related radial segregation in an idealized horizontal Bridgman configuration 01 p0115 N94-10185
TEM study of a space processed Al-Al2O3 metallic composite 01 p0075 N94-10186
In situ observation of temperature dependence of concentration field during growth of KB5 crystals by holographic interferometry 01 p0115 N94-10187
Crystal growth from low temperature vapour phase 01 p0115 N94-10191
Results of crystal growth experiments by FZM on Zona facilities in microgravity 01 p0116 N94-10193
Undercooled W-Re and Mo-Re drops in an ultra high vacuum drop tube 01 p0086 N94-10195
Effects of a microgravity environment on the crystallization of biological macromolecules 01 p0117 N94-10198
EUSO-D2-experiment: Unidirectional solidification with quenching of an AlSi11 alloy 01 p0086 N94-10199
Liquid phase sintering of tungsten composites under microgravity. Effect of matrix composition 01 p0118 N94-10207
Crystallization of zeolites in the microgravity environment of space 01 p0119 N94-10210
Crystal growth in the Zone Melting Facility (ZMF) 01 p0119 N94-10213
Memory effects in the organometallic chemical beam epitaxy of compound semiconductors
[NASA-CR-193106] 01 p0399 N94-11439
Cold press sintering of simulated lunar basalt 01 p0131 N94-12026
General overview of an integrated lunar oxygen production/brickmaking system 01 p0131 N94-12027
Thermodynamics of lunar ilmenite reduction 01 p0415 N94-12028
Reduce fluid experiment system flight data from IML-1
[NASA-CR-193835] 02 p0804 N94-12873
Marangoni effect induced convection in material processing under microgravity (M-18) 02 p0589 N94-13750
Solidification of eutectic system alloys in space (M-19) 02 p0589 N94-13751
Growth of samarskite crystal under microgravity conditions (M-20) 02 p0590 N94-13752
Growth experiment of organic metal crystal in low gravity (M-21) 02 p0590 N94-13753
Containerless processing of undercooled melts
[NASA-CR-194350] 02 p0572 N94-14123
Two color holographic interferometry for microgravity application
[NASA-CR-194424] 02 p0651 N94-14447
Visualization of solidification front phenomena
[NASA-CR-193838] 03 p0976 N94-15006
STS-26 protein growth (PCG) experiment
[NASA-TM-109533] 03 p0976 N94-15395
Payloads for the processing of high temperature materials 03 p0979 N94-16083
Materials processing in space: Issues for the third decade
[TABES PAPER 93-260] 03 p0983 N94-16133
Growth of single crystals of mercuric iodide on the ground and in space
[DE93-015523] 03 p1209 N94-16442
The first flight of the QUESTS GAS payload G-521 04 p1325 N94-19170
Space Applications Industrial Laser System (SAILS) 04 p1325 N94-19173
Melt-spin processing of high (Tc) oxide superconductors
[DE94-000696] 05 p2036 N94-22582
Processing of semicrystalline polymers 06 p2226 N94-24351
Design for producing fiberglass fabric in a lunar environment 07 p2765 N94-25676
Lunar preform manufacturing 07 p2765 N94-25677
Modelling of the MEA float zone using accelerometer data
[NASA-CR-193933] 07 p2761 N94-27220
Prometheus in space: Research Committee on Functional New Material
[JTN-94-80580] 07 p2761 N94-28002
Survey report of JSUP Space Environment Utilization Research Committee in fiscal year 1992: Protein Crystal Growth Session
[JTN-94-80584] 08 p3158 N94-28583
Overview of space environment utilization science
[JTN-94-80581] 08 p3227 N94-28938
Fluid and transportation phenomena under microgravity 08 p3227 N94-28939
Combustion studies under microgravity 08 p3228 N94-28940
Glass studies under microgravity 08 p3228 N94-28941
Fabrication of electronic materials in space 08 p3228 N94-28942
Protein crystal growth in microgravity 08 p3228 N94-28943
Cell culture in space 08 p3228 N94-28944
Cosmic energy equipment 08 p3229 N94-28945
Plasma heating for containerless and microgravity materials processing
[NASA-CASE-NPO-18819-1-CU] 08 p3229 N94-29371
The 1992-1993 advanced design program. Part 1: The Mars methane engine project. Part 2: The Mars oxygen processor new furnace
[NASA-CR-195513] 08 p3299 N94-29409
Thermal enclosure system functional simulation user's manual
[NASA-TM-109094] 08 p3466 N94-29489
Directional solidification characteristics of hyper-eutectic Al-Cu alloys under varying gravity conditions
[ISBN-0-315-86108-8] 08 p3209 N94-30146
Survey report of JSUP Space Environment Utilization Research Committee in fiscal year 1992: Functional New Materials Session
[JTN-94-80582] 08 p3159 N94-30162
Survey report of JSUP Space Environment Utilization Research Committee in fiscal year 1992: Metallic Materials Session
[JTN-94-80583] 08 p3159 N94-30794
Design, characterization, and control of the NASA three degree of freedom reaction compensation platform 09 p3605 N94-33304
Materials processing in space tasks. WBS task 5.4: Generic tasks
[NASA-CR-193979] 11 p4249 N94-35485

1993 Technical Paper Contest for Women. Gear Up 2000: Women in Motion
[NASA-CP-10134] 11 p4377 N94-35961
Ampoule failure sensor time response testing: Experiments 2 and 3
[NASA-TM-108458] 12 p4446 N94-36822
Technology demonstration of space intravehicular automation and robotics
[NASA-TM-109138] 12 p4501 N94-37589
Project JOVE --- microgravity experiments and applications
[NASA-CR-196292] 12 p4445 N94-37635

SPACE PROGRAMS
NT APOLLO PROJECT
NT AUSTRALIAN SPACE PROGRAM
NT CANADIAN SPACE PROGRAM
NT CHINESE SPACE PROGRAM
NT EUROPEAN SPACE PROGRAMS
NT FRENCH SPACE PROGRAM
NT GALILEO PROJECT
NT GERMAN SPACE PROGRAM
NT INDIAN SPACE PROGRAM
NT INDONESIAN SPACE PROGRAM
NT ITALIAN SPACE PROGRAM
NT JAPANESE SPACE PROGRAM
NT MAGELLAN PROJECT (NASA)
NT MARINER-MERCURY 1973
NT MERCURY PROJECT
NT NASA SPACE PROGRAMS
NT NATIONAL LAUNCH VEHICLE PROGRAM
NT NETHERLANDS SPACE PROGRAM
NT PAKISTAN SPACE PROGRAM
NT PIONEER PROJECT
NT PROJECT SETI
NT RUSSIAN SPACE PROGRAM
NT SCOUT PROJECT
NT SPANISH SPACE PROGRAM
NT SURVEYOR PROJECT
NT SWEDISH SPACE PROGRAM
NT U.S.S.R. SPACE PROGRAM
NT VIKING MARS PROGRAM
NT VOYAGER PROJECT

Analysis of the cost evaluation of ESA programmes and comparable national and international programmes
[GTS-92063] 01 p0416 N94-10145
Space Activities in the Asia Pacific Region
[JTN-93-80421] 01 p0035 N94-10676
Current status of space activities in Asia Pacific region 01 p0035 N94-10677
Considerations for future regional space cooperation 01 p0035 N94-10678
Space research and remote sensing programmes in Bangladesh 01 p0035 N94-10679
Overview of KITSAT 01 p0036 N94-10683
Korea space program 01 p0036 N94-10684
Space programme in Malaysia 01 p0036 N94-10685
National space programmes and application of the remote sensing data in Mongolia 01 p0036 N94-10686
Thailand ISY activities 01 p0037 N94-10690
Panel discussion: Role of space program in the Asia Pacific Region 01 p0037 N94-10694
Space Solar Power Program
[DE93-011750] 01 p0055 N94-11675
Medical care delivery in the US space program 01 p0307 N94-11806
Asia-Pacific ISY conference, volume 1
[NASDA-CM-199-1] 02 p0532 N94-14098
My experiences in manned space flight 02 p0698 N94-14276
Military space programs in the press: An analysis for change
[AD-A267799] 03 p0874 N94-17306
The impact of industry/university consortia programs on space education
[NASA-TM-109340] 03 p1222 N94-17441
Aerospace: Facts and figures, 1992-1993
[AD-A272571] 05 p1635 N94-21419
Solar physics and the Coronas project 06 p2625 N94-22847
National Institute of Standards and Technology Conference on Reducing the Cost of Space Infrastructure and Operations. Part 2: Topical papers
[PB94-113487] 06 p2194 N94-23819
Project Columbiad: Reestablishment of human presence on the Moon 07 p2689 N94-25687
Aeronautics and space report of the President: Fiscal year 1993 activities 09 p3966 N94-32854
Partners in space. International cooperation in space: Strategies for the new century
[ISBN-0-9629930-2-6] 11 p4348 N94-35901
JPRS report: Central Eurasia. Aviation and cosmonautics, No. 4, April 1993
[JPRS-UAC-94-003] 12 p4391 N94-36999
Space Station: Impact of the expanded Russian role on funding and research. Report to the Ranking Minority Member, Subcommittee on Oversight of Government Management, Committee on Governmental Affairs, US Senate
[GAO/NSIAD-94-220] 12 p4396 N94-37257

SPACE PSYCHOLOGY
La Chalupa-30: Lessons learned from a 30-day subsea mission analogue 10 p4098 N94-33654
Aerospace medicine and biology: A continuing bibliography with indexes (supplement 390)
[NASA-SP-7011(390)] 10 p4095 N94-34602

SPACE RADIATION
U EXTRATERRESTRIAL RADIATION

SPACE RADIATORS
U SPACECRAFT RADIATORS

SPACE RENDEZVOUS
NT EARTH ORBITAL RENDEZVOUS
NT ORBITAL RENDEZVOUS
A guidance and navigation system for two spacecraft rendezvous in translunar halo orbit
[AD-A267498] 03 p0898 N94-17368
Automated rendezvous and capture demonstration study
[NASA-CR-192587] 04 p1331 N94-19366
Manned Mars mission on-orbit operations FTS capabilities assessment
[NASA-CR-189328] 06 p2430 N94-23080
A guidance and navigation system for two spacecraft rendezvous in translunar halo orbit 08 p3142 N94-29837
Fuzzy logic application for modeling man-in-the-loop space shuttle proximity operations
[NASA-CR-188283] 09 p3835 N94-32359
A six degree of freedom, plume-fuel optimal trajectory planner for spacecraft proximity operations using an A* node search
[NASA-CR-188285] 09 p3601 N94-32388
Progress in navigation filter estimate fusion and its application to spacecraft rendezvous
[NASA-TM-104794] 12 p4392 N94-37386

SPACE SCIENCES
U AEROSPACE SCIENCES

SPACE SHUTTLE ASCENT STAGE
Results of wind tunnel tests of an ASRM configured 0.03 scale Space Shuttle integrated vehicle model (47-OTS) in the AEDC 16-foot transonic wind tunnel, volume 2
[NASA-CR-185697] 02 p0534 N94-12965
Results of wind tunnel tests of an ASRM configured 0.03 scale Space Shuttle integrated vehicle model (47-OTS) in the AEDC 16-foot Transonic wind tunnel (IA613A), volume 1
[NASA-CR-185696] 02 p0534 N94-13191

SPACE SHUTTLE BOOSTERS
NT ADVANCED SOLID ROCKET MOTOR (STS)
Space Shuttle solid rocket motor exposure monitoring 03 p0976 N94-16624
RSRM nozzle actuator bracket/lug fracture mechanics qualification test
[NASA-CR-193859] 03 p0927 N94-17080
SRB thermal curtain design support
[NASA-CR-193857] 03 p0927 N94-17123
SRB thermal curtain design support
[NASA-CR-193858] 03 p0928 N94-17124
Effect of temperature and O-ring gland finish on sealing ability of Viton V747-75
[NASA-TP-3391] 04 p1368 N94-18075
Parameters affecting hydrogen chloride measurements
[AD-A271326] 05 p1851 N94-20025
Debris/Ice/TPS assessment and integrated photographic analysis for Shuttle Mission STS-61
[NASA-TM-109195] 06 p2199 N94-24059
Final postflight hardware evaluation report RSRM-32 (STS-57)
[NASA-CR-193903] 06 p2200 N94-24065
Lightning tests and analyses of tunnel bond straps and shielded cables on the Space Shuttle solid rocket booster
[NASA-CR-193921] 06 p2200 N94-24801
Postflight hardware evaluation (RSRM-29, STS-54)
[NASA-CR-193895] 06 p2201 N94-24802
Structural analysis of a frangible nut used on the NASA Space Shuttle
[DE94-003672] 07 p2821 N94-25811
STS-56, RSRM-031, 360L031 KSC processing configuration and data report
[NASA-CR-193922] 07 p2691 N94-26135
STS-51, RSRM-033, 360T033 KSC processing configuration and data report
[NASA-CR-193923] 07 p2691 N94-26153
Advanced silver zinc battery development for the SRB and ET range safety subsystems 07 p2865 N94-28136
STS-55 Space Shuttle mission report
[NASA-CR-195741] 07 p2692 N94-28199
Development of a new generation solid rocket motor ignition computer code
[NASA-CR-195734] 08 p3171 N94-28800
Development of a unique polyurethane primer/topcoat 08 p3223 N94-30476
Debris/ice/TPS assessment and integrated photographic analysis for Shuttle Mission STS-62
[NASA-TM-109201] 10 p4012 N94-33423
Use of photostress to analyze behavior of an aft skirt test specimen
[NASA-CR-195850] 10 p4069 N94-34075

SPACE SHUTTLE MAIN ENGINE
Probabilistic evaluation of uncertainties and risks in aerospace components
[NASA-TM-105603] 01 p0185 N94-10361
Application of powder metallurgy techniques to produce improved bearing elements for liquid rocket engines
[NASA-CR-193731] 01 p0082 N94-10804
Enhancements to the Engine Data Interpretation System (EDIS)
[NASA-CR-192593] 01 p0180 N94-10815
A study of strength evaluations of EDNi/EDCu/NARloy-Z bonded joints
[NASA-TM-108418] 01 p0188 N94-11275
STS-55 pad abort: Engine 2011 oxidizer preburner augmented spark igniter check valve leak
[NASA-CR-193830] 02 p0533 N94-12806
SSME testing at Stennis Space Center
[NASA-TM-109310] 02 p0552 N94-13617
Identification and interpretation of patterns in rocket engine data
[NASA-CR-194534] 02 p0552 N94-14309
An integrated knowledge system for the Space Shuttle hazardous gas detection system
[NASA-CR-194533] 02 p0536 N94-14310
Investigation of the feasibility of optical diagnostic measurements at the exit of the SSME
[NASA-CR-193832] 02 p0553 N94-14682
Simulation of preburner sprays, volume 1
[NASA-CR-193844] 02 p0647 N94-14906
An assessment of finite-element modeling techniques for thick-solid/thin-shell joints analysis
[NASA-TM-108426] 03 p1058 N94-15534
Develop advanced nonlinear signal analysis topographical mapping system
[NASA-CR-194577] 03 p1082 N94-15646
Plasma arc welding repair of space flight hardware
[TABES PAPER 93-603] 03 p1049 N94-16139
Space Shuttle main engine. NASA has not evaluated the alternate fuel turbopump costs and benefits. Report to the Administrator of the National Aeronautics and Space Administration
[GAO/NSIAD-94-54] 03 p0926 N94-16834
Advanced transportation system studies technical area 3: Alternate propulsion subsystem concepts, volume 3
[NASA-CR-193864] 03 p0927 N94-17097
Advanced transportation system studies technical area 3: Alternate propulsion system concepts. SSME upper stage use
[NASA-CR-193865] 03 p0927 N94-17098
Technology test bed
[NASA-TM-109354] 04 p1322 N94-18953
FNAS/summer faculty fellowship research continuation program. Task 6: Integrated model development for liquid fueled rocket propulsion systems. Task 9: Aspects of model-based rocket engine condition monitoring and control
[NASA-CR-194574] 04 p1338 N94-19706
Space Shuttle Main Engine. Overview 05 p1667 N94-20070
Rocketdyne turbomachinery 05 p1667 N94-20071
Future technical directions 05 p1668 N94-20072
Entry velocities at Mars and Earth for short transit times
[AD-A272591] 05 p1665 N94-21420
Detailed study of oxidation/wear mechanism in lox turbopump bearings
[NASA-TM-108434] 05 p1825 N94-21580
SSME fuel preburner injector characterization 06 p2211 N94-23037
Flame trench analysis of NLS vehicles 06 p2199 N94-23249
Development of an analytical-numerical model to predict radiant emission or absorption
[NASA-CR-194860] 06 p2453 N94-23624
System for Anomaly and Failure Detection (SAFD) system development
[NASA-CR-193907] 06 p2372 N94-24174
CFD simulation of coaxial injectors 06 p2342 N94-24430
Space Shuttle Main Engine performance analysis 06 p2222 N94-24444
Using neural networks to assist in OPAD data analysis 06 p2477 N94-24452

Develop advanced nonlinear signal analysis topographical mapping system
[NASA-CR-195128] 06 p2388 N94-24827
STS-51 pad abort. OV103-engine 2033 (ME-2) fuel flowmeter sensor open circuit
[NASA-CR-193924] 07 p2701 N94-26230
Space Shuttle main engine turbopump bearing assessment program
[NASA-TM-108447] 07 p2833 N94-28265
Mechanical flexible joint design document
[NASA-CR-193941] 08 p3297 N94-28419
Composite load spectra for select space propulsion structural components
[NASA-CR-194476] 08 p3316 N94-28508
Specialized data analysis of SSME and advanced propulsion system vibration measurements
[NASA-CR-193940] 08 p3174 N94-29868
Design of a cold-flow test facility for the high pressure fuel turbopump turbine of the Space Shuttle main engine
[AD-A276743] 09 p3615 N94-32182
Real-time sensor data validation
[NASA-CR-195295] 09 p3616 N94-33099
Application of an improved Nelson-Nguyen analysis to eccentric, arbitrary profile liquid annular seals
10 p4062 N94-34182
Hotfire testing of a SSME HPOTP with an annular hydrostatic bearing 10 p4065 N94-34196
Instrumentation for in-flight SSME rocket engine plume spectroscopy
[NASA-TM-106596] 11 p4268 N94-35268
Experimental measurements and analytical analysis related to gas turbine heat transfer. Part 1: Time-averaged heat-flux and surface-pressure measurements on the vanes and blades of the SSME fuel-side turbine and comparison with prediction. Part 2: Phase-resolved surface-pressure and heat-flux measurements on the first blade of the SSME fuel-side turbine
[NASA-CR-196296] 12 p4442 N94-36969

SPACE SHUTTLE MISSION 51-F
Gearing up for 1988
[NASA-TM-109617] 03 p0880 N94-15346
Sights and sounds of space
[NASA-TM-109610] 03 p1302 N94-15424

SPACE SHUTTLE MISSION 51-L
Shuttle 51L: Challenger
[NASA-TM-109835] 10 p4012 N94-33788

SPACE SHUTTLE MISSION 61-A
STS-30 Magellan IUS/EVA training in WETF
[NASA-TM-109300] 02 p0737 N94-13601
STS-29 post-insertion/deorbit prep and crew bailout
[NASA-TM-109299] 02 p0535 N94-13641

SPACE SHUTTLE MISSIONS
NT SPACE SHUTTLE MISSION 51-F
NT SPACE SHUTTLE MISSION 51-L
NT SPACE SHUTTLE MISSION 61-A
Echocardiography in the flight program
01 p0309 N94-11993
STS-55 pad abort: Engine 2011 oxidizer preburner augmented spark igniter check valve leak
[NASA-CR-193830] 02 p0533 N94-12806
STS-32 mission highlights resource tape
[NASA-TM-109291] 02 p0531 N94-13631
Launch, entry, and landing resource clip
[NASA-TM-109297] 02 p0535 N94-13638
STS-26 Post-Flight Press Conference
[NASA-TM-109557] 03 p0879 N94-15261
STS-26 onboard 16mm photography quick release
[NASA-TM-109558] 03 p0879 N94-15262
STS-30 Post-Flight Press Conference --- Space Shuttle Launch, Magellan/IUS deploy, Crew Activites, and Landing
[NASA-TM-109580] 03 p0879 N94-15264
STS-30 suited ascent training in fixed base SMS
[NASA-TM-109581] 03 p0875 N94-15265
STS-30 mission tape --- Space Shuttle Launch, Crew Activities, Landing, and Air-to-Ground Transmission
[NASA-TM-109582] 03 p0879 N94-15266
STS-26 SSIP briefing --- Titanium Grain Formation Experiment and Crystal Membrane Experiment
[NASA-TM-109556] 03 p0976 N94-15280
The 61-M long duration sim video highlights resource tape
[NASA-TM-109569] 03 p0875 N94-15299
Text and graphics systems
[NASA-TM-109570] 03 p1229 N94-15300
STS-30 Magellan deploy Sim in SMS and MOCR
[NASA-TM-109571] 03 p0875 N94-15301
STS-30 EVA prep in CCT: Grabe, Lee, and Thagard
[NASA-TM-109572] 03 p1135 N94-15303
STS-29 Post-Flight Press Conference --- Shuttle Launch, TDRS-D/IUS Deployment, Crew Activites, and Shuttle Landing
[NASA-TM-109575] 03 p0880 N94-15306
STS-29 onboard 16mm photography quick release
[NASA-TM-109576] 03 p0880 N94-15307
STS-26 through STS-34, deploy activities
[NASA-TM-109566] 03 p1301 N94-15315
STS-32 IMAX camera training
[NASA-TM-109567] 03 p1031 N94-15316
STS-26 generic integrated IUS deploy simulation
[NASA-TM-109562] 03 p0875 N94-15332
STS-26 EVA rescue training
[NASA-TM-109563] 03 p0875 N94-15333
STS-26 Shuttle Earth views, April 1990, part 1 and part 2
[NASA-TM-109564] 03 p1082 N94-15334
STS-34 post-flight press conference
[NASA-TM-109459] 03 p0880 N94-15354
STS-34 onboard 16mm photography quick release
[NASA-TM-109460] 03 p0880 N94-15355
STS-34 mission highlights resource tape, part 1
[NASA-TM-109461] 03 p0880 N94-15356
STS-34 Galileo integrated deploy sim
[NASA-TM-109463] 03 p0880 N94-15358
STS-34 crew bailout exercise in CCT
[NASA-TM-109465] 03 p1135 N94-15360
STS-29 mission highlights resource tape
[NASA-TM-109542] 03 p0880 N94-15373
STS-29 IMAX camera audio class FFT
[NASA-TM-109543] 03 p1031 N94-15374
STS-29 EVA prep in FFT
[NASA-TM-109544] 03 p1135 N94-15375
STS-32 onboard 16mm photography quick release
[NASA-TM-109472] 03 p0880 N94-15376
STS-31 Post-Flight Conference
[NASA-TM-109477] 03 p0881 N94-15384
STS-33 crew post flight film
[NASA-TM-109470] 03 p0881 N94-15400
STS-27 crew presentation clip
[NASA-TM-109551] 03 p0881 N94-15403
STS-27 crew post-insertion deorbit-prep in CCT
[NASA-TM-109552] 03 p1136 N94-15404
STS-26 missions highlight resource tape
[NASA-TM-109559] 03 p0881 N94-15407
NASA report to education, volume 7
[NASA-TM-109435] 03 p1247 N94-15419
STS-31 onboard 16mm photography quick release --- Onboard Activities
[NASA-TM-109478] 03 p0881 N94-15438
STS-31 mission highlights resource tape
[NASA-TM-109479] 03 p0881 N94-15440
STS-31 Hubble space telescope deploy: Training at MDF with Hawley
[NASA-TM-109481] 03 p0876 N94-15442
STS-31 crew training inflight maintenance and bailout exercises in CCT and WFTF
[NASA-TM-109483] 03 p0876 N94-15450
STS-40 crew during spacelab Sim
[NASA-TM-109493] 03 p0876 N94-15452
STS-36 crew presentation clip
[NASA-TM-109497] 03 p0881 N94-15461
STS-36 crew EVA prep and post-training, bailout exercises, final bench review
[NASA-TM-109498] 03 p1137 N94-15462
STS-35 payload specialists Durrance and Parise: 70mm photo training and cabin familiarization
[NASA-TM-109499] 03 p1032 N94-15463
STS-35 onboard photography quick release
[NASA-TM-109500] 03 p0881 N94-15464
STS-35 mission highlights resource tape
[NASA-TM-109501] 03 p0881 N94-15465
Return to space
[NASA-TM-109356] 04 p1332 N94-18955
Your GAS experiment and the media or why does that other can get all of the publicity?
04 p1327 N94-19182
Mission planning for Shuttle Imaging Radar-C (SIR-C) with a real-time interactive planning software
06 p2305 N94-23842
Final postflight hardware evaluation report RSRM-32 (STS-57)
[NASA-CR-193903] 06 p2200 N94-24065
Prototype space fabrication platform
[AD-A273904] 07 p2694 N94-25659
STS-55 Space Shuttle mission report
[NASA-CR-195741] 07 p2692 N94-28199
Summary report of mission acceleration measurements for Spacehab-01, STS-57 launched 21 June 1993
[NASA-TM-106514] 08 p3168 N94-29757
OARE flight maneuvers and calibration measurements on STS-58
[NASA-TM-109093] 09 p3613 N94-32924
Chronology of KSC and KSC related events for 1993
[NASA-TM-109196] 09 p3966 N94-33072
STS-59/SRL-1
[NASA-TM-109837] 10 p4012 N94-33571
STS-57 post flight press conference
[NASA-TM-109838] 10 p4012 N94-33599
Flight controller alertness and performance during MOD shiftwork operations 10 p4098 N94-33624
An overview of Space Shuttle anthropometry and biomechanics research with emphasis on STS/Mir recumbent seat system design
10 p4101 N94-33629
A comparison of paper and computer procedures in a Shuttle flight environment 10 p4101 N94-33634
Response to graded Lower Body Negative Pressure (LBNP) after space flight 10 p4096 N94-33637
Exercise with prebreathe appears to increase protection from decompression sickness: Preliminary findings
10 p4096 N94-33639
Mission Evaluation Room Intelligent Diagnostic and Analysis System (MIDAS) 10 p4125 N94-35064
Debris/ice/TPS assessment and integrated photographic analysis for Shuttle Mission STS-59
[NASA-TM-109203] 11 p4211 N94-35523

SPACE SHUTTLE ORBITAL FLIGHT TEST 3
U SPACE TRANSPORTATION SYSTEM 3 FLIGHT

SPACE SHUTTLE ORBITAL FLIGHT TEST 4
U SPACE TRANSPORTATION SYSTEM 4 FLIGHT

SPACE SHUTTLE ORBITAL FLIGHT TESTS
U SPACE TRANSPORTATION SYSTEM FLIGHTS

SPACE SHUTTLE ORBITAL FLIGHTS
U SPACE TRANSPORTATION SYSTEM FLIGHTS

SPACE SHUTTLE ORBITER 099
U CHALLENGER (ORBITER)

SPACE SHUTTLE ORBITER 102
U COLUMBIA (ORBITER)

SPACE SHUTTLE ORBITER 103
U DISCOVERY (ORBITER)

SPACE SHUTTLE ORBITERS
NT CHALLENGER (ORBITER)
NT COLUMBIA (ORBITER)
NT DISCOVERY (ORBITER)
Extraction of stability and control derivatives from orbiter flight data
[NASA-TM-4500] 01 p0013 N94-10707
Space Shuttle hypersonic aerodynamic and aerothermodynamic flight research and the comparison to ground test results
[NASA-TM-4499] 01 p0013 N94-10820
Investigation of alternate power source for Space Shuttle Orbiter hydraulic system
[NASA-CR-193229] 01 p0046 N94-10911
Vigilance problems in orbiter processing
01 p0314 N94-11536
Results of wind tunnel tests of an ASRM configured 0.03 scale Space Shuttle integrated vehicle model (47-OTS) in the AEDC 16-foot transonic wind tunnel, volume 2
[NASA-CR-185697] 02 p0534 N94-12965
Results of wind tunnel tests of an ASRM configured 0.03 scale Space Shuttle integrated vehicle model (47-OTS) in the AEDC 16-foot Transonic wind tunnel (IA613A), volume 1
[NASA-CR-185696] 02 p0534 N94-13191
Analysis of differences between seating positions in simulators and orbiters
[NASA-TM-104776] 02 p0737 N94-13399
Six degree of freedom
[NASA-TM-109295] 02 p0749 N94-13636
Microgravity acceleration measurement environment characterization 02 p0590 N94-13755
Strategic avionics technology definition studies. Subtask 3-1A: Electrical Actuation (ELA) systems
[NASA-CR-194393] 02 p0536 N94-14323
Vertical-tail aerodynamic configuration of space shuttle orbiter
[AD-A267723] 03 p0879 N94-14941
Views from space
[NASA-TM-109634] 03 p1081 N94-15245
STS-30 Post-Flight Press Conference --- Space Shuttle Launch, Magellan/IUS deploy, Crew Activites, and Landing
[NASA-TM-109580] 03 p0879 N94-15264
STS-30 crew photo in building 4
[NASA-TM-109573] 03 p1031 N94-15304
STS-29 Post-Flight Press Conference --- Shuttle Launch, TDRS-D/IUS Deployment, Crew Activites, and Shuttle Landing
[NASA-TM-109575] 03 p0880 N94-15306
STS-34 Space Shuttle Portable Onboard Computer (SPOC) briefing
[NASA-TM-109458] 03 p0880 N94-15353
STS-34 final bench review
[NASA-TM-109464] 03 p1135 N94-15359
Crew escape certification test
[NASA-TM-109530] 03 p1136 N94-15392
STS-30 onboard 16mm photography quick release
[NASA-TM-109579] 03 p0881 N94-15423
Space Station/Orbiter berthing dynamics during an assembly flight
[NASA-TM-109049] 03 p1062 N94-17451
Pathfinder: Shuttle exhibit
[NASA-TM-109357] 04 p1333 N94-19071

A high resolution ultraviolet Shuttle glow spectrograph
04 p1325 N94-19174
Kennedy Space Center processing of Shuttle small payloads 04 p1326 N94-19177
Utilization of Shuttle small payload accommodations in the DOD Space Test Program 04 p1326 N94-19180
Compilation of reinforced carbon-carbon transatlantic abort landing arc jet test results
[NASA-TM-104778] 05 p1676 N94-21834
A real-time navigation monitoring expert system for the Space Shuttle Mission Control Center
06 p2202 N94-23921
Debris/Ice/TPS assessment and integrated photographic analysis for Shuttle Mission STS-61
[NASA-TM-109195] 06 p2199 N94-24059
Studies of Shuttle orbiter arrestment system
[NASA-TP-3370] 06 p2177 N94-24304
Orbital docking system centerline color television camera system test
[NASA-TM-104783] 06 p2205 N94-24625
Development of a nondestructive vibration technique for bond assessment of Space Shuttle tiles
[NASA-CR-195163] 06 p2201 N94-24919
Berthing of Space Station Freedom using the shuttle remote manipulator system 07 p2684 N94-26284
Pressure distributions on a 0.02-scale Space Shuttle orbiter nose at Mach 21.5 in helium
[NASA-TM-4495] 07 p2646 N94-26592
Report of the Shuttle Processing Review Team
[NASA-TM-109728] 07 p2692 N94-28178
Extra-vehicular activity translation tool
[NASA-CASE-MSC-21955-1] 08 p3300 N94-29428
Waves in space plasma dipole antenna subsystem
08 p3161 N94-29632
Investigation of sonic boom for the Space Shuttle: High cross-range orbiter
[NASA-TM-108238] 09 p3860 N94-31336
Investigation of sonic boom for the Space Shuttle: Low cross-range orbiter
[NASA-TM-108237] 09 p3860 N94-31337
Computational methods for frictional contact with applications to the Space Shuttle orbiter nose-gear tire
09 p3608 N94-32295
Analysis of the Shuttle Orbiter reinforced carbon-carbon oxidation protection system
[NASA-TM-104792] 11 p4262 N94-35245

SPACE SHUTTLE PAYLOADS
NT ASTRO MISSIONS (STS)
NT ATMOSPHERIC GENERAL CIRCULATION EXPERIMENT
NT EARTH RADIATION BUDGET EXPERIMENT
NT GET AWAY SPECIALS (STS)
NT PLASMA INTERACTION EXPERIMENT
NT SPACELAB
NT X RAY ASTROPHYSICS FACILITY
Compatibility tests for biological specimens to on-board experiments in the Space Shuttle flight
[NASDA-CNT-930003] 01 p0301 N94-12278
STS-30 Magellan IUS/EVA training in WETF
[NASA-TM-109300] 02 p0737 N94-13601
Mid-deck experiments, STS-26
[NASA-TM-109308] 02 p0570 N94-13616
Serpentine manipulator planning and control for NASA Space-Shuttle payload servicing
[AD-A266961] 03 p0879 N94-14969
STS-29 mission highlights resource tape
[NASA-TM-109542] 03 p0880 N94-15373
STS-32 onboard 16mm photography quick release
[NASA-TM-109472] 03 p0880 N94-15376
STS-35 onboard photography quick release
[NASA-TM-109500] 03 p0881 N94-15464
Science operation in space: Lessons
[NASA-TM-109502] 03 p0881 N94-15466
Long Duration Exposure Facility
[NASA-TM-109427] 03 p0885 N94-15497
The Canadian Space Station user development program. Where do we go from here? 03 p0898 N94-16084
Cost-effective test methods for Shuttle payloads
[TABES PAPER 93-651] 03 p0883 N94-16151
Looking at science on board Eureca
[ESA-BR-80] 03 p0874 N94-16584
LDEF update
[NASA-TM-109352] 04 p1334 N94-18921
The 1993 Shuttle Small Payloads Symposium
[NASA-CP-3233] 04 p1323 N94-19162
VPU(tm) demonstration mission vicinity processor unit(tm) overview 04 p1325 N94-19171
Space Applications Industrial Laser System (SAILS)
04 p1325 N94-19173
Kennedy Space Center processing of Shuttle small payloads 04 p1326 N94-19177
Utilization of Shuttle small payload accommodations in the DOD Space Test Program 04 p1326 N94-19180
ISOBUS: A new versatile spacecraft platform using Shuttle small payloads 04 p1327 N94-19183
Radiation hardened microprocessor for small payloads
04 p1327 N94-19184
Superfluid Helium On-Orbit Transfer (SHOOT) flight demonstration 04 p1327 N94-19185
Space Shuttle Mission STS-61: Hubble Space Telescope servicing mission-01
[NASA-TM-109344] 05 p1653 N94-20192
Mission planning for Shuttle Imaging Radar-C (SIR-C) with a real-time interactive planning software
06 p2305 N94-23842
The EURECA telecommanding chain: Experience with packet telecommand and telemetry systems
06 p2305 N94-23909
An approach to studying the reliability of microgravity experiments
[NASA-TM-106489] 07 p2834 N94-26199
STS-55 Space Shuttle mission report
[NASA-CR-195741] 07 p2692 N94-28199
Retention latch mechanism for the Wake Shield Facility 08 p3161 N94-29635
Pointing mechanisms for the Shuttle Radar Laboratory
08 p3162 N94-29638
Summary report of mission acceleration measurements for Spacehab-01, STS-57 launched 21 June 1993
[NASA-TM-106514] 08 p3168 N94-29757
End effector monitoring system: An illustrated case of operational prototyping 10 p4109 N94-33631
A comparison of paper and computer procedures in a Shuttle flight environment 10 p4101 N94-33634
The servicing aid tool: A teleoperated robotics system for space applications 10 p4067 N94-34039
Automated documentation generator for advanced protein crystal growth
[NASA-CR-193955] 10 p4147 N94-34072
A study of low mass x-ray binaries
[NASA-CR-195813] 10 p4162 N94-34119
Cargo systems manual: Heat Pipe Performance (HPP) STS-66
[NASA-TM-109784] 10 p4131 N94-34720
STS-58 Space Shuttle Mission Report
[NASA-TM-109867] 11 p4211 N94-35251
STS-51 Space Shuttle Mission Report
[NASA-TM-109866] 11 p4211 N94-35252
Structural assembly demonstration experiment, phase 1
[NASA-CR-193967] 11 p4212 N94-35484

SPACE SHUTTLE SOLID ROCKET MOTORS
U SPACE SHUTTLE BOOSTERS

SPACE SHUTTLES
NT BURAN SPACE SHUTTLE
NT HERMES MANNED SPACEPLANE
Space Shuttle hypersonic aerodynamic and aerothermodynamic flight research and the comparison to ground test results
[NASA-TM-4499] 01 p0013 N94-10820
Applying reliability models to the maintenance of Space Shuttle software 01 p0330 N94-11434
Microgravity vibration isolation technology: Development to demonstration
[NASA-TM-106320] 01 p0001 N94-11703
Results of experimental investigations to determine external tank protuberance loads using a 0.03-scale model of the Space Shuttle launch configuration (model 47-OTS) in the NASA/ARC unitary plan wind tunnel, volume 1
[NASA-CR-167690] 02 p0534 N94-12810
Procedures for analysis of debris relative to Space Shuttle systems
[NASA-TM-109190] 02 p0534 N94-12900
Results of wind tunnel tests of an ASRM configured 0.03 scale Space Shuttle integrated vehicle model (47-OTS) in the AEDC 16-foot Transonic wind tunnel (IA613A), volume 1
[NASA-CR-185696] 02 p0534 N94-13191
Analysis of differences between seating positions in simulators and orbiters
[NASA-TM-104776] 02 p0737 N94-13399
STS-53 Space Shuttle mission report
[NASA-CR-193101] 02 p0535 N94-13934
STS-54 Space Shuttle mission report
[NASA-CR-194116] 02 p0535 N94-13935
Results of experimental investigations to determine external tank protuberance loads using a 0.03-scale model of the Space Shuttle launch configuration (Model 47-OTS) in the NASA/ARC unitary plan wind tunnel, volume 2
[NASA-CR-167691] 02 p0536 N94-14047
STS-33 launch and landing clip
[NASA-TM-109468] 02 p0536 N94-14734
Vertical-tail aerodynamic configuration of space shuttle orbiter
[AD-A267723] 03 p0879 N94-14941
STS-29 pre-launch and post-landing egress
[NASA-TM-109574] 03 p1135 N94-15305
GAS highlights, 1988 --- Get Away Specials
[NASA-TM-109600] 03 p0873 N94-15308
Space Shuttle highlights
[NASA-TM-109606] 03 p0880 N94-15314
The 1979 highlights
[NASA-TM-109443] 03 p1247 N94-15342
STS-34 Space Shuttle Portable Onboard Computer (SPOC) briefing
[NASA-TM-109458] 03 p0880 N94-15353
STS-34 McCully and Baker during IFM training
[NASA-TM-109462] 03 p0880 N94-15357
STS-29 crew IMAX camera training
[NASA-TM-109546] 03 p1031 N94-15380
The 1978 highlights
[NASA-TM-109625] 03 p1302 N94-15411
The 1977 highlights
[NASA-TM-109626] 03 p1302 N94-15412
Spacework 16 --- Simulated Space Shuttle Program
[NASA-TM-109436] 03 p1221 N94-15420
The 1980 highlights
[NASA-TM-109672] 03 p1303 N94-15509
The Marshall Automated Weld System (MAWS)
[TABES PAPER 93-602] 03 p1049 N94-16138
Plasma arc welding repair of space flight hardware
[TABES PAPER 93-603] 03 p1049 N94-16139
Ground integrated ET-derived space platforms for onorbit applications
[TABES PAPER 93-652] 03 p0899 N94-16152
Power Reactant Storage Assembly (PRSA) (Space Shuttle). PRSA hydrogen and oxygen DVT tank refurbishment
[NASA-CR-188262] 03 p0926 N94-16922
Optical properties of water released in low Earth orbit
[AD-A266197] 03 p1192 N94-16936
Robotics
[NASA-TM-109351] 04 p1332 N94-18920
Langley's 50th year
[NASA-TM-109365] 04 p1632 N94-18980
A stereoscopic vision system with applications to automated docking and tracking
[AD-A270754] 04 p1333 N94-19765
Future technical directions 05 p1668 N94-20072
Space Shuttle Mission STS-61: Hubble Space Telescope servicing mission-01
[NASA-TM-109344] 05 p1653 N94-20192
Hurricane risk assessment: Rollback or ride out
06 p2416 N94-23248
Implementing the space shuttle data processing system with the space generic open avionics architecture
[NASA-CR-188254] 06 p2199 N94-23571
Common front end systems for Space Shuttle and Space Station control centers at Johnson Space Center
06 p2305 N94-23838
Ground data system for Space Flyer Unit (SFU)
06 p2207 N94-23860
Constraint-based scheduling 06 p2510 N94-23904
Liquid rocket propulsion: Retrospective and prospects
06 p2154 N94-24243
A compilation of technology spinoffs from the US Space Shuttle Program 06 p2578 N94-24424
Debris/ice/TPS assessment and integrated photographic analysis for Shuttle mission STS-58
[NASA-TM-109194] 06 p2200 N94-24577
Supersonic aerodynamic characteristics of a circular body Earth-to-Orbit vehicle
[NASA-TM-4533] 06 p2170 N94-24716
Parallel processing methods for space based power systems 06 p2222 N94-25352
Application of Space Shuttle Project Hercules imagery in the investigation of ship cloud tracks
[AD-A274923] 07 p2692 N94-26529
Access to space study
[NASA-TM-109693] 07 p2685 N94-27151
STS-55 Space Shuttle mission report
[NASA-CR-195741] 07 p2692 N94-28199
STS-57 Space Shuttle mission report
[NASA-CR-195739] 07 p2693 N94-28220
STS-56 Space Shuttle mission report
[NASA-CR-195740] 07 p2693 N94-28221
SOCRATES simulation of the emission at wavelength 6300 A generated by the interaction between the atmosphere and the Space Shuttle exhaust
[AD-A275567] 08 p3164 N94-28827
Wind tunnel testing and research
[NASA-CR-188273] 08 p3156 N94-29052
Wave generation by contaminant ions near a large spacecraft
[NASA-CR-195797] 08 p3169 N94-29917
Local interaction control for space construction
08 p3170 N94-30960
Theoretical basis for state vector comparison, relative position display, and relative position/rendezvous prediction
[AD-A277216] 09 p3608 N94-32020
Access to space: The Space Shuttle's evolving roles
[AD-A276785] 09 p3608 N94-32190
Fuzzy logic application for modeling man-in-the-loop space shuttle proximity operations
[NASA-CR-188283] 09 p3835 N94-32359

Limiting vibration in systems with constant amplitude actuators through command preshaping
[NASA-CR-188284] 09 p3739 N94-32907
Pip pin reliability and design 09 p3605 N94-33305
Application of statistical process control and process capability analysis procedures in orbiter processing activities at the Kennedy Space Center 10 p4068 N94-33626
An overview of Space Shuttle anthropometry and biomechanics research with emphasis on STS/Mir recumbent seat system design 10 p4101 N94-33629
Graphical programming: A systems approach for telerobotic servicing of space assets 10 p4066 N94-33666
Real-time RMS active damping augmentation: Heavy and very light payload evaluations
[NASA-TM-109134] 10 p4015 N94-34386
STS-58 Space Shuttle Mission Report
[NASA-TM-109867] 11 p4211 N94-35251
STS-51 Space Shuttle Mission Report
[NASA-TM-109866] 11 p4211 N94-35252
Aerospace Safety Advisory Panel
[NASA-TM-109840] 11 p4201 N94-35390
Space Shuttle orbit determination using empirical force modeling of attitude maneuvers for the German MOMS-02/D2 mission 11 p4207 N94-35634
A shadowgraph study of Space Transportation System (STS): The Space Shuttle Launch Vehicle (SSLV)
[NASA-RP-1341] 12 p4382 N94-36741
JPRS report: Central Eurasia. Aviation and cosmonautics, No. 4, April 1993
[JPRS-UAC-94-003] 12 p4391 N94-36999
Space Shuttle: Incomplete data and funding approach increase cost risk for upgrade program. Report to Congressional Requesters
[GAO/NSIAD-94-23] 12 p4392 N94-37026
Optimal control theory determination of feasible return-to-launch-site aborts for the HL-20 Personnel Launch System vehicle
[NASA-TP-3449] 12 p4396 N94-37260

SPACE SIMULATORS

Measurements of the dielectric properties of simulated comet material as part of the KOSI 10 experiment 05 p2085 N94-20841
Overview of the MSTI 2 processor-in-the-loop simulator 11 p4207 N94-35631

SPACE STATION FREEDOM

Microbiological test results using three urine pretreatment regimes with 316L stainless steel
[NASA-CR-192568] 01 p0299 N94-10360
Achievements and challenges of Space Station Freedom's safety review process
[NASA-TM-106199] 01 p0040 N94-10640
Space Station Redesign Team: Final report to the Advisory Committee on the Redesign of the Space Station
[NASA-TM-109241] 01 p0042 N94-10663
Space Station redesign option A: Modular buildup concept
[NASA-TM-108415] 01 p0043 N94-10808
Transportation systems analyses: Volume 1: Executive Summary
[NASA-CR-192583] 01 p0041 N94-10826
Transportation systems analyses. Volume 2: Technical/programmatics
[NASA-CR-192582] 01 p0041 N94-10827
Large project experiences with object-oriented methods and reuse 01 p0329 N94-11431
Sixth Annual Workshop on Space Operations Applications and Research (SOAR 1992), volume 2
[NASA-CP-3187-VOL-2] 01 p0486 N94-11527
Space Station maintenance studies using plaid graphics 01 p0335 N94-11578
Microgravity vibration isolation technology: Development to demonstration
[NASA-TM-106320] 01 p0001 N94-11703
Solar dynamic power system development for Space Station Freedom
[NASA-RP-1310] 02 p0548 N94-12807
Advancing automation and robotics technology for the Space Station Freedom and for the U.S. economy
[NASA-TM-104024] 02 p0739 N94-12838
System identification for Space Station Freedom using observer/Kalman filter Markov parameters
[NASA-CR-191521] 02 p0539 N94-12976
In-flight demonstration of the Space Station Freedom Health Maintenance Facility fluid therapy system (E300/E05) 02 p0595 N94-13775
Space Station Common Berthing Mechanism, a multi-body simulation application 02 p0544 N94-14640
Plasma contactor technology for Space Station Freedom
[NASA-TM-106291] 02 p0553 N94-14725
Space Station Freedom
[NASA-TM-109636] 03 p1031 N94-15247
Robotics for Space Station, tape 1
[NASA-TM-109588] 03 p1045 N94-15272
Space Station: The link to America's future
[NASA-TM-109653] 03 p0884 N94-15274
Futurepath 1
[NASA-TM-109439] 03 p0869 N94-15338
Dare to dream --- The Space Station Freedom development
[NASA-TM-109512] 03 p0885 N94-15458
Space Station Facility government estimating
[NASA-TM-109324] 03 p1223 N94-15545
Estimating and bidding for the Space Station Processing Facility
[NASA-TM-109323] 03 p1223 N94-15546
Preliminary analysis and design optimization of the short spacer truss of Space Station Freedom
[NASA-TM-4470] 03 p1058 N94-15709
A feasibility study of a microgravity enhancement system for Space Station Freedom
[NASA-CR-191550] 03 p0886 N94-15864
Scientific use of Space Station Freedom 03 p0977 N94-16072
The Canadian Space Station user development program. Where do we go from here? 03 p0898 N94-16084
An analysis of the dynamic response of the Space Station Freedom due to a module perforation by an orbital debris particle impact
[TABES PAPER 93-653] 03 p0899 N94-16154
Soyuz/ACRV accommodation study
[NASA-TM-107733] 03 p0888 N94-17072
Space Station/Orbiter berthing dynamics during an assembly flight
[NASA-TM-109049] 03 p1062 N94-17451
Strategy for the reduction of total integrated fluid logistics to the Space Station Freedom
[NASA-TM-107744] 03 p1138 N94-17452
Space Station Freedom electrical performance model
[NASA-TM-106395] 03 p0929 N94-17483
Designing Space Station
[NASA-TM-109353] 04 p1334 N94-18922
Space exploration initiative
[NASA-TM-109366] 04 p1323 N94-18981
Space Applications Industrial Laser System (SAILS) 04 p1325 N94-19173
Space research with intact organisms: The role of Space Station Freedom 04 p1502 N94-19213
Strategic plan, 1991: A strategy for leadership in space through excellence in space science and applications
[NASA-TM-109256] 04 p1611 N94-19434
System performance predictions for Space Station Freedom's electric power system
[NASA-TM-106396] 05 p1667 N94-20062
The International Telecommunications Satellite (INTELSAT) Solar Array Coupon (ISAC) atomic oxygen flight experiment: Techniques, results and summary 05 p1662 N94-21391
Space Station Freedom (SSF) Data Management System (DMS) performance model data base
[NASA-CR-188270] 06 p2590 N94-23289
Thermal control system for SSF sensor/electronics
[SAND-92-0652C] 06 p2321 N94-23640
Ground operation of robotics on Space Station Freedom 06 p2371 N94-23841
Space Station Freedom ground data system: Design and operations 06 p2518 N94-23957
Connector mechanisms in compliance with extreme space conditions 06 p2360 N94-24025
Spacecraft crew procedures from paper to computers 06 p2433 N94-24186
Using computer graphics to design Space Station Freedom viewing 06 p2434 N94-24191
A simulation system for Space Station extravehicular activity 06 p2434 N94-24192
Space Station Freedom coupling tasks: An evaluation of their telerobotic and EVA compatibility 06 p2436 N94-24200
Simulation of the human-telerobot interface on the Space Station 06 p2436 N94-24202
Weld joint concepts for on-orbit repair of Space Station Freedom fluid system tube assemblies 06 p2371 N94-24427
Optimal Space Station solar array gimbal angle determination via radial basis function neural networks
[NASA-TM-106482] 06 p2195 N94-24482
Thermal control system for Space Station Freedom photovoltaic power module
[NASA-TM-105650] 06 p2205 N94-24825
Preliminary design of a satellite observation system for Space Station Freedom
[NASA-CR-195514] 06 p2209 N94-24840
Design of a resistojet for Space Station Freedom
[NASA-CR-195506] 06 p2221 N94-24979
A prototype to automate the video subsystem routing for the video distribution subsystem of Space Station Freedom 06 p2306 N94-25353
Modelling early failures in Space Station Freedom 06 p2374 N94-25372
Modeling and analysis of selected space station communications and tracking subsystems 06 p2306 N94-25374
Space Station flexible dynamics under plume impingement 06 p2208 N94-25383
Assured crew return vehicle post landing configuration design and test 07 p2697 N94-25671
Automation of closed environments in space for human comfort and safety 07 p2943 N94-25684
Berthing of Space Station Freedom using the shuttle remote manipulator system 07 p2684 N94-26284
Autonomous rendezvous and docking for Space Station Freedom 07 p2684 N94-26286
Structural evaluation of concepts for a solar energy concentrator for Space Station advanced development program
[NASA-TP-3375] 07 p2695 N94-26609
Space Station evolution study oxygen loop closure
[NASA-CR-193938] 07 p2941 N94-26788
Designing for human presence in space: An introduction to environmental control and life support systems
[NASA-RP-1324] 07 p2942 N94-27437
Selection of the Space Station Freedom (SSF) Flat Collector Circuit (FCC) insulation material 08 p3165 N94-28701
Hypervelocity impact testing of Space Station Freedom solar cells
[NASA-TM-106509] 08 p3167 N94-29383
Electric power system test and verification program
[NASA-TM-106405] 08 p3169 N94-30123
A Space Station robot walker and its shared control software
[AIAA PAPER 94-1192-CP] 08 p3442 N94-30543
A study of the Space Station Freedom response to the disturbance environment 09 p3600 N94-31434
Solar connection
[NASA-TM-109761] 09 p3614 N94-31818
A hypertext system that learns from user feedback 09 p3923 N94-32428
Catalytic methods using molecular oxygen for treatment of PMMS and ECLSS waste streams, volume 2
[NASA-CR-190299] 09 p3804 N94-32697
Space Station evolution study
[NASA-CR-193937] 09 p3611 N94-32898
An investigation of acoustic noise requirements for the Space Station centrifuge facility
[NASA-TM-108811] 09 p3805 N94-32936
Space Station Freedom solar array containment box mechanisms 09 p3603 N94-33292
Roll ring assemblies for the Space Station 09 p3603 N94-33294
Space Station Freedom Solar Array tension mechanism development 09 p3604 N94-33300
Energy absorber for the CETA 09 p3604 N94-33303
John C. Stennis Space Center overview
[NASA-TM-109816] 10 p4011 N94-33567
Dynamic analysis for Space Station Freedom
[NASA-TM-109826] 10 p4014 N94-33580
Virtual reality as a human factors design analysis tool: Macro-ergonomic application validation and assessment of the Space Station Freedom payload control area 10 p4100 N94-33620
Continuous monitoring of bacterial attachment 10 p4094 N94-33658
Safety concerns for first entry operations of orbiting spacecraft 10 p4102 N94-33662
Electrical characterization of a Space Station Freedom alpha utility transfer assembly
[NASA-CR-191108] 10 p4017 N94-34235
Conceptual design and analysis of a dynamic scale model of the Space Station Freedom
[NASA-CR-4598] 10 p4070 N94-34236
Aerospace Safety Advisory Panel
[NASA-TM-109840] 11 p4201 N94-35390
Dynamic analysis of Space Shuttle/RMS configuration using continuum approach 11 p4221 N94-35887

SPACE STATION PAYLOADS

Columbus system support for telescience operations 06 p2505 N94-23877
Space Station evolution study
[NASA-CR-193937] 09 p3611 N94-32898
SpaceHab 1 maintenance experiment 10 p4015 N94-33669
Materials processing in space tasks. WBS task 5.4: Generic tasks
[NASA-CR-193979] 11 p4249 N94-35485

SPACE STATION POWER SUPPLIES

Space Station Freedom advanced photovoltaics and battery technology development planning 01 p0052 N94-11401

Futurepath 1
[NASA-TM-109439] 03 p0869 N94-15338
Futurepath 1 — power systems
[NASA-TM-109431] 03 p0925 N94-15503
Space Station Freedom electrical performance model
[NASA-TM-106395] 03 p0929 N94-17483
Plasma contactor development for Space Station
[NASA-TM-106425] 04 p1587 N94-18861
The implications of the LDEF results on Space Station Freedom power system materials
05 p1660 N94-21377
Thermal control system for Space Station Freedom photovoltaic power module
[NASA-TM-105650] 06 p2205 N94-24825
Structural evaluation of concepts for a solar energy concentrator for Space Station advanced development program
[NASA-TP-3375] 07 p2695 N94-26609
Space Station Freedom NiH2 cell testing program
07 p2861 N94-28108
Advanced nickel-hydrogen spacecraft battery development 07 p2863 N94-28129
Hypervelocity impact induced arcing and Kapton pyrolization in a plasma environment
[NASA-TM-106528] 08 p3167 N94-28814
Electric power system test and verification program
[NASA-TM-106405] 08 p3169 N94-30123
Solar lunar power 09 p3599 N94-31427
Solar connection
[NASA-TM-109761] 09 p3614 N94-31818
Electrical characterization of a Space Station Freedom alpha utility transfer assembly
[NASA-CR-191108] 10 p4017 N94-34235
Neural network for positioning Space Station solar arrays
[NASA-TM-106656] 12 p4431 N94-36943

SPACE STATION STRUCTURES
Space Station maintenance studies using plaid graphics 01 p0335 N94-11578
Secondary impact hazard assessment
[NASA-CR-188261] 02 p0543 N94-14483
STS-37 CETA evaluation with Ross
[NASA-TM-109495] 03 p1135 N94-15330
STS-37 astronauts Ross and Apt during CETA hardware checkout
[NASA-TM-109496] 03 p1137 N94-15460
Preliminary analysis and design optimization of the short spacer truss of Space Station Freedom
[NASA-TM-4470] 03 p1058 N94-15709
Spline screw payload fastening system
[NASA-CASE-GSC-13454-1] 05 p1821 N94-20126
Space Station flexible dynamics under plume impingement 06 p2208 N94-25383
Structural design feasibility study of Space Station long spacer truss
[NASA-TM-106346] 07 p2843 N94-27559
A study of the Space Station Freedom response to the disturbance environment 09 p3600 N94-31434

SPACE STATIONS
NT COLUMBUS SPACE STATION
NT MAN TENDED FREE FLYERS
NT MIR SPACE STATION
NT SPACE STATION FREEDOM
Transmission zeros of spacecraft attitude control system
[NAL-TR-1166] 02 p0540 N94-13339
Asia-Pacific ISY conference, volume 1
[NASDA-CM-199-1] 02 p0532 N94-14098
BALLIST: A computer program to empirically predict the bumper thickness required to prevent perforation of the Space Station by orbital debris
[NASA-CR-193825] 02 p0543 N94-14120
Large space structures and systems in the space station era: A bibliography with indexes (supplement 05)
[NASA-SP-7085(05)] 02 p0543 N94-14411
Computational Controls Workstation: Algorithms and hardware 02 p0678 N94-14626
Space Station thermal storage/refrigeration system research and development
[NASA-CR-193841] 03 p0879 N94-15191
Robotics for Space Station tape 2
[NASA-TM-109578] 03 p1045 N94-15263
Living well in space: Clinical care challenge
[NASA-TM-109539] 03 p1120 N94-15370
Answering the space medicine challenge
[NASA-TM-109511] 03 p1120 N94-15457
Space Station resource reel
[NASA-TM-109673] 03 p0885 N94-15510
The Japanese Space Station utilization plan
03 p0977 N94-16074
ALEXIS and HETE: Two small, low cost, scientific satellite systems 03 p0896 N94-17185
The 1994 NASA authorization, volume 2
[GPO-71-510] 04 p1620 N94-18842
Plasma contactor development for Space Station
[NASA-TM-106425] 04 p1587 N94-18861
Shuttle-C, the future is now
[NASA-TM-109355] 04 p1332 N94-18954
Space Station trash removal system
[NASA-CASE-MSC-21723-1] 05 p1657 N94-20367
Numerical simulations of hypervelocity impact experiments involving single Whipple bumper shields
[AD-A272123] 05 p1831 N94-20572
Rewetting of monogroove heat pipe in Space Station radiators
[NASA-CR-194781] 05 p1804 N94-21820
Proceedings of the NIST Conference on Reducing the Cost of Space Infrastructure and Operations: Part 1: Oral presentations and discussion
[PB94-111374] 06 p2194 N94-23770
Common front end systems for Space Shuttle and Space Station control centers at Johnson Space Center
06 p2305 N94-23838
Torque equilibrium attitudes for the Space Station
06 p2208 N94-24449
Embodiment design for a multipropellant resistojet
[NASA-CR-195505] 06 p2221 N94-24834
Development of a power electronics unit for the Space Station plasma contactor
[NASA-TM-106486] 06 p2222 N94-25201
Failure detection and recovery in the assembly/contingency subsystem
06 p2306 N94-25360
Space Station technology testbed: 2010 deep space transport 07 p2687 N94-27368
Risks and issues in fire safety on the Space Station
[NASA-TM-106430] 07 p2692 N94-27436
An analysis of the loads applied to a heavy Space Station rack during translation and rotation tasks
[NASA-TM-104790] 07 p2697 N94-28183
Heavy-lift vehicle-launched Space Station method and apparatus
[NASA-CASE-MSC-21760-1] 08 p3160 N94-29369
Technology transfer and evaluation for Space Station telerobotics
[AIAA PAPER 94-1190-CP] 08 p3441 N94-30541
Local interaction control for space construction
08 p3170 N94-30960
Space Station WP-2 application of LDEF MLI results
09 p3592 N94-31016
The Second Annual International Space University Alumni Conference
[NASA-CP-3253] 09 p3598 N94-31425
Access to space: The Space Shuttle's evolving rolee
[AD-A276785] 09 p3608 N94-32190
Fuzzy logic application for modeling man-in-the-loop space shuttle proximity operations
[NASA-CR-188283] 09 p3835 N94-32359
Research and technology, 1993
[NASA-TM-106376] 09 p3567 N94-33046
United States/Russia space cooperation documentary
[NASA-TM-109809] 10 p4014 N94-33561
A comparison of paper and computer procedures in a Shuttle flight environment 10 p4101 N94-33634
A volatile organic analyzer for Space Station: Description and evaluation of a gas chromatography/ ion mobility
10 p4102 N94-33661
Unique methods for on-orbit structural repair, maintenance, and assembly 10 p4102 N94-33663
RoboLab and virtual environments
10 p4015 N94-34027
Hardware interface for isolation of vibrations in flexible manipulators: Development and applications
10 p4067 N94-34036
International Space Station alpha remote manipulator system workstation controls test report
[NASA-TM-104796] 11 p4274 N94-35481
Materials processing in space tasks. WBS task 5.4: Generic tasks
[NASA-CR-193979] 11 p4249 N94-35485
Field demonstration of X-band photonic antenna remoting in the Deep Space Network
11 p4252 N94-35545
Self-rescue strategies for EVA crewmembers equipped with the SAFER backpack 11 p4207 N94-35633
Space Station: Impact of the expanded Russian role on funding and research. Report to the Ranking Minority Member, Subcommittee on Oversight of Government Management, Committee on Governmental Affairs, US Senate
[GAO/NSIAD-94-220] 12 p4396 N94-37257

SPACE STORAGE
Small rocket research and technology
06 p2211 N94-23038
Handbook for handling and storage of nickel-cadmium batteries: Lessons learned
[NASA-RP-1326] 07 p2702 N94-26613
Large scale cryogenic fluid systems testing
[NASA-TM-109735] 08 p3157 N94-29904
Cryogenic fluid management technologies for space transportation. Zero G thermodynamic vent system
[NASA-CR-193981] 12 p4430 N94-36806

SPACE SUITS
NT EXTRAVEHICULAR MOBILITY UNITS
Crew chief 01 p0335 N94-11564
Ancient skills: Modern use
[NASA-TM-109594] 03 p1135 N94-15286
STS-30 EVA prep in CCT: Grabe, Lee, and Thagard
[NASA-TM-109572] 03 p1135 N94-15303
STS-27 crew fire training and glove molding
[NASA-TM-109554] 03 p1136 N94-15406
STS-31 Hubble space telescope contingency training in WETF with McCandless and Sullivan
[NASA-TM-109480] 03 p1136 N94-15441
STS-36 crew EVA prep and post-training, bailout exercises, final bench review
[NASA-TM-109498] 03 p1137 N94-15462
STS-26 crew clothing, glove molding, and personal hygiene
[NASA-TM-109520] 03 p1137 N94-15470
Space suit design
[NASA-TM-109670] 03 p1137 N94-15507
Mark 111 suit test evaluation in WETF with Jerry Ross
[NASA-TM-109504] 03 p1137 N94-15514
Reach performance while wearing the Space Shuttle launch and entry suit during exposure to launch accelerations 06 p2436 N94-24204
Extra-Vehicular Activity (EVA) glove evaluation test protocol
[NASA-TM-108442] 07 p2943 N94-27952

SPACE SURVEILLANCE (GROUND BASED)
Super-resolution of multi-pixel and sub-pixel images for the SDI
[AD-A268537] 04 p1462 N94-18631
Proceedings of the 11th Space Surveillance Workshop
[AD-A269477] 04 p1462 N94-18729
NAVSPASUR sensor system digital signal processing receiver. Volume 1: Hardware and software overview
[AD-A272899] 05 p1738 N94-21198
NAVSPASUR sensor system digital signal processing receiver. Volume 2: Function and capabilities of hardware and software components
[AD-A272900] 05 p1739 N94-21218
Hyperspectral analysis of space objects: Signal to noise evaluation
[AD-A273882] 07 p2765 N94-25728

SPACE SURVEILLANCE (SPACEBORNE)
Space countersurveillance: A requisite for theater defense planning
[AD-A266871] 03 p0884 N94-15147
UVPI imaging from the LACE satellite: The Nihka rocket plume
[AD-A268456] 04 p1334 N94-18149
Proceedings of the 11th Space Surveillance Workshop
[AD-A269477] 04 p1462 N94-18729
Reduction procedures for accurate analysis of MSX surveillance experiment data 11 p4203 N94-35611

SPACE SYSTEMS ENGINEERING
U AEROSPACE ENGINEERING

SPACE TECHNOLOGY EXPERIMENTS
The Second Workshop on Refrigerating System Utilization Onboard the JEM
[NASDA-CON-930001] 01 p0129 N94-11831
Summary of the pre-AO of the JEM onboard scientific and engineering experiments for refrigerator utilization
01 p0129 N94-11832
Submillimeter wave observation experiment of Earth atmosphere with SIS mixer 01 p0130 N94-11837
Utilization of superconductivity in the area of space
01 p0131 N94-11843
The Third Workshop on Two Phase Fluid Experiment in the Space Environment
[NASDA-CON-930002] 01 p0161 N94-12547
Summary of studies on JEM utilization experiment projects 01 p0161 N94-12548
Compilation of proposals for boiling and evaporation experiments in space environments and proposals concerning experiment projects
01 p0161 N94-12549
Condensation phenomena 01 p0162 N94-12550
Developmental research of thermal control system in space environment 01 p0162 N94-12551
Two phase flow and isopycnic liquid-liquid two phase fluid in reduced gravity field 01 p0162 N94-12552
Research on two phase flow in microgravity
01 p0162 N94-12554
Organization and management policy for two phase fluid experiment in space environment
01 p0162 N94-12556
Present status of JEM utilization projects
02 p0530 N94-13273
Trial manufacture model and in-space verification method of deployable antenna 02 p0530 N94-13278
Study on superconducting basic technology for space application, part 1
[NASDA-CNT-930015-PT-1] 02 p0622 N94-13425
STS-37 CETA evaluation with Ross
[NASA-TM-109495] 03 p1135 N94-15330

STS-37 astronauts Ross and Apt during CETA hardware checkout
[NASA-TM-109496] 03 p1137 N94-15460
The Clementine instrument complement 03 p1086 N94-16370
The space technology research vehicle: Development status 03 p0896 N94-17183

SPACE TEMPERATURE
Determining noise temperatures in beam waveguide systems 08 p3249 N94-29657

SPACE TOOLS
STS-37 CETA evaluation with Ross
[NASA-TM-109495] 03 p1135 N94-15330
STS-37 astronauts Ross and Apt during CETA hardware checkout
[NASA-TM-109496] 03 p1137 N94-15460
EVA tools and equipment reference book
[NASA-TM-109350] 05 p1897 N94-21812
Design and simulation of EVA tools for first servicing mission of HST
[NASA-CR-194784] 06 p2439 N94-24857
Extra-vehicular activity translation tool
[NASA-CASE-MSC-21955-1] 08 p3300 N94-29428
Design and simulation of EVA tools for first servicing mission of HST
[NASA-CR-196030] 11 p4298 N94-35266

SPACE TRANSPORTATION
NT ADVANCED LAUNCH SYSTEM (STS)
NT SPACE TRANSPORTATION SYSTEM
Space transportation alternatives for large space programs: The International Space University Summer Session, 1992
[NASA-TM-106271] 01 p0040 N94-10811
Transportation systems analyses: Volume 1: Executive Summary
[NASA-CR-192583] 01 p0041 N94-10826
Transportation systems analyses. Volume 2: Technical/programmatics
[NASA-CR-192582] 01 p0041 N94-10827
Space Solar Power Program
[DE93-011750] 01 p0055 N94-11675
Space transportation systems within ESA programmes: Current status and perspectives 02 p0537 N94-14275
Space transfer concepts and analyses for exploration missions, phase 4
[NASA-CR-193849] 03 p0882 N94-15831
Comparisons of selected laser beam power missions to conventionally powered missions
[NASA-TM-106110] 03 p1040 N94-16522
Advanced transportation system studies technical area 3: Alternate propulsion subsystem concepts, volume 2
[NASA-CR-193863] 03 p0927 N94-17096
Advanced transportation system studies technical area 3: Alternate propulsion subsystem concepts, volume 3
[NASA-CR-193864] 03 p0927 N94-17097
Human Transportation System (HTS) study, volume 2
[NASA-TM-104779-VOL-2] 03 p0882 N94-17320
Human Transportation System (HTS) study: Executive summary
[NASA-TM-104780] 04 p1332 N94-18669
Human Transportation System (HTS) study, volume 1
[NASA-TM-104779] 04 p1332 N94-18670
NASA Propulsion Engineering Research Center, volume 1
[NASA-CR-194721-VOL-1] 05 p1671 N94-22428
Flame trench analysis of NLS vehicles 06 p2199 N94-23249
Proceedings of the NIST Conference on Reducing the Cost of Space Infrastructure and Operations: Part 1: Oral presentations and discussion
[PB94-111374] 06 p2194 N94-23770
National Institute of Standards and Technology Conference on Reducing the Cost of Space Infrastructure and Operations. Part 2: Topical papers
[PB94-113487] 06 p2194 N94-23819
The 1993 NASA/ASEE Summer Faculty Fellowship Program
[NASA-CR-193862] 06 p2574 N94-24405
Access to space studies 06 p2199 N94-24434
Lunar transportation system
[NASA-CR-195540] 06 p2365 N94-24805
Space transfer vehicle concepts and requirements. Volume 4: Summary of special studies
[NASA-CR-193918] 06 p2201 N94-24970
The Ninth National Space Symposium
[ISBN-0-9616962-7-3] 06 p2598 N94-25006
A comparison of users' and providers' perceptions of critical spacelift vehicle characteristics and capabilities
[AD-A273907] 07 p2691 N94-26017
Access to space study
[NASA-TM-109693] 07 p2685 N94-27151
Space Station technology testbed: 2010 deep space transport 07 p2687 N94-27368
Space transportation vehicle design evaluation using saturated designs 07 p2693 N94-27928
Lunar Transportation Facilities and Operations Study, option 1
[NASA-CR-195700] 07 p3109 N94-27982
Lunar Transportation Facilities and Operations Study, option 2
[NASA-CR-195701] 07 p3109 N94-27983
A transportronic solution to the problem of interorbital transportation
[NASA-CR-191152] 08 p3164 N94-29355
Design of a logistics model for building and supporting a lunar station
[ILR-MITT-282(1993)] 09 p3803 N94-31852
Access to space: The Space Shuttle's evolving rolee
[AD-A276785] 09 p3608 N94-32190
Geostationary space launch vehicles and the US dilemma 11 p4210 N94-35377
Space and transatmospheric propulsion technology 11 p4229 N94-36047

SPACE TRANSPORTATION SYSTEM
NT ADVANCED LAUNCH SYSTEM (STS)
Transportation systems analyses: Volume 1: Executive Summary
[NASA-CR-192583] 01 p0041 N94-10826
Transportation systems analyses. Volume 2: Technical/programmatics
[NASA-CR-192582] 01 p0041 N94-10827
Visual Earth observation performance in the space environment. Human performance measurement 4: Flight experiments 01 p0314 N94-11539
Toxicity study of dimethylethoxysilane (DMSES), the waterproofing agent for the Orbiter heat protective system 01 p0318 N94-11554
STS-55 pad abort: Engine 2011 oxidizer preburner augmented spark igniter check valve leak
[NASA-CR-193830] 02 p0533 N94-12806
STS-32 post-flight press conference
[NASA-TM-109294] 02 p0541 N94-13634
Asia-Pacific ISY Conference, volume 2
[NASDA-CM-199-VOL-2] 02 p0688 N94-14209
Space transportation systems and space activities in the 21st century 02 p0537 N94-14274
Research and development of space transportation systems in ISAS 02 p0537 N94-14277
Contributions of winged re-entry vehicle to space activities 02 p0537 N94-14278
Mission scenario of HOPE 02 p0537 N94-14279
The status of the HOPE concept study 02 p0537 N94-14280
Spaceplane program at NAL: System concept and related technology issues 02 p0537 N94-14281
STS-33 launch and landing clip
[NASA-TM-109468] 02 p0536 N94-14734
STS-35 post-flight press conference
[NASA-TM-109490] 02 p0537 N94-14736
STS-35 integrated sim in SMS and MOCR
[NASA-TM-109491] 02 p0533 N94-14787
The 1982 highlights
[NASA-TM-109671] 03 p1303 N94-15508
Advanced transportation system studies technical area 3: Alternate propulsion system concepts. SSME upper stage use
[NASA-CR-193865] 03 p0927 N94-17098
Flight 20 (STS-45) polysulfide gas path investigation
[NASA-CR-193861] 03 p0928 N94-17213
The 1994 NASA authorization, volume 2
[GPO-71-510] 04 p1620 N94-18842
A simulation model for probabilistic analysis of Space Shuttle abort modes
[NASA-TM-108432] 05 p1656 N94-21859
Johnson Space Center CFD grid generation requirements 05 p1919 N94-22355
A minimum cost tolerance allocation method for rocket engines and robust rocket engine design 06 p2222 N94-24419
Validation of a nonintrusive optical technique for the measurement of liquid mass distribution in a two-phase spray 06 p2548 N94-24420
Future space transportation system architecture avionics requirements 06 p2162 N94-25098
Access to space: The Space Shuttle's evolving rolee
[AD-A276785] 09 p3608 N94-32190
Pen-based computers: Computers without keys 09 p3808 N94-32434
Advanced transportation system study: Manned launch vehicle concepts for two way transportation system payloads to LEO
[NASA-CR-193951] 09 p3608 N94-33100
STS-57 post flight press conference
[NASA-TM-109838] 10 p4012 N94-33599
Flight controller alertness and performance during MOD shiftwork operations 10 p4098 N94-33624
Advanced transportation system study: Manned launch vehicle concepts for two way transportation system payloads to LEO. Work breakdown structure and work breakdown structure dictionary
[NASA-CR-193952] 10 p4012 N94-34911
Advanced transportation system study: Manned launch vehicle concepts for two way transportation system payloads to LEO. Program cost estimates document
[NASA-CR-193953] 10 p4013 N94-34912
A shadowgraph study of Space Transportation System (STS): The Space Shuttle Launch Vehicle (SSLV)
[NASA-RP-1341] 12 p4382 N94-36741
Operations and support cost modeling of conceptual space vehicles
[NASA-CR-196299] 12 p4397 N94-37580

SPACE TRANSPORTATION SYSTEM FLIGHTS
NT SPACE TRANSPORTATION SYSTEM 3 FLIGHT
NT SPACE TRANSPORTATION SYSTEM 4 FLIGHT
Debris/ice/TPS assessment and integrated photographic analysis for Shuttle Mission STS-57
[NASA-TM-107562] 01 p0040 N94-10805
Echocardiography in the flight program 01 p0309 N94-11993
STS-32 mission highlights resource tape
[NASA-TM-109291] 02 p0531 N94-13631
STS-32 post-flight press conference
[NASA-TM-109294] 02 p0541 N94-13634
STS-28 crew presentation clip
[NASA-TM-109298] 02 p0531 N94-13640
STS-53 Space Shuttle mission report
[NASA-CR-193101] 02 p0535 N94-13934
STS-54 Space Shuttle mission report
[NASA-CR-194116] 02 p0535 N94-13935
STS-35 post-flight press conference
[NASA-TM-109490] 02 p0537 N94-14736
STS-35 integrated sim in SMS and MOCR
[NASA-TM-109491] 02 p0533 N94-14787
Space Shuttle highlights
[NASA-TM-109606] 03 p0880 N94-15314
Return to Space Mission: The STS-26 crew report
[NASA-TM-109568] 03 p0880 N94-15317
STS-29 mission highlights resource tape
[NASA-TM-109542] 03 p0880 N94-15373
STS-29 EVA prep in FFT
[NASA-TM-109544] 03 p1135 N94-15375
STS-27 crew presentation clip
[NASA-TM-109551] 03 p0881 N94-15403
STS-27 crew post-insertion deorbit-prep in CCT
[NASA-TM-109552] 03 p1136 N94-15404
STS-40 crew during spacelab Sim
[NASA-TM-109493] 03 p0876 N94-15452
STS-36 crew presentation clip
[NASA-TM-109497] 03 p0881 N94-15461
STS-36 crew EVA prep and post-training, bailout exercises, final bench review
[NASA-TM-109498] 03 p1137 N94-15462
STS-35 payload specialists Durrance and Parise: 70mm photo training and cabin familiarization
[NASA-TM-109499] 03 p1032 N94-15463
STS-35 mission highlights resource tape
[NASA-TM-109501] 03 p0881 N94-15465
Science operation in space: Lessons
[NASA-TM-109502] 03 p0881 N94-15466
STS-27 crew deorbit prep in SMS with Gibson, Shepard, Mullane, Ross, and G. Gardner
[NASA-TM-109518] 03 p0882 N94-15468
STS-26 crew participation in meetings
[NASA-TM-109519] 03 p0873 N94-15469
STS-26 crew clothing, glove molding, and personal hygiene
[NASA-TM-109520] 03 p1137 N94-15470
STS-41 post-flight press presentation
[NASA-TM-109514] 03 p0882 N94-15516
STS-41 crew training bailout in CCT, 16mm camera class EVA prep, habitation equipment procedures, and food tasting
[NASA-TM-109517] 03 p0876 N94-15517
STS-41 onboard 16mm photography quick release
[NASA-TM-109515] 03 p0882 N94-15518
STS-41 mission highlights resource tape
[NASA-TM-109516] 03 p0882 N94-15521
Return to space
[NASA-TM-109356] 04 p1332 N94-18955
Space Shuttle Mission STS-61: Hubble Space Telescope servicing mission-01
[NASA-TM-109344] 05 p1653 N94-20192
Debris/ice/TPS assessment and integrated photographic analysis for Shuttle Mission STS-51
[NASA-TM-109189] 05 p1656 N94-21884
Common front end systems for Space Shuttle and Space Station control centers at Johnson Space Center 06 p2305 N94-23838
Debris/Ice/TPS assessment and integrated photographic analysis for Shuttle Mission STS-61
[NASA-TM-109195] 06 p2199 N94-24059
Debris/ice/TPS assessment and integrated photographic analysis for Shuttle mission STS-58
[NASA-TM-109194] 06 p2200 N94-24577
Postflight hardware evaluation (RSRM-29, STS-54)
[NASA-CR-193895] 06 p2201 N94-24802

Debris/ice/TPS assessment and integrated photographic analysis for Shuttle mission STS-60
[NASA-TM-109193] 07 p2692 N94-27956
STS-55 Space Shuttle mission report
[NASA-CR-195741] 07 p2692 N94-28199
JSC almanac
[NASA-TM-109702] 07 p3119 N94-28204
STS-57 Space Shuttle mission report
[NASA-CR-195739] 07 p2693 N94-28220
STS-56 Space Shuttle mission report
[NASA-CR-195740] 07 p2693 N94-28221
Physiological Anatomical Rodent Experiment (PARE) .04 feasibility test 2
[NASA-CR-195210] 08 p3385 N94-29968
Fuzzy logic application for modeling man-in-the-loop space shuttle proximity operations
[NASA-CR-188283] 09 p3835 N94-32359
Debris/ice/TPS assessment and integrated photographic analysis for Shuttle Mission STS-62
[NASA-TM-109201] 10 p4012 N94-33423
A comparison of paper and computer procedures in a Shuttle flight environment 10 p4101 N94-33634
STS-58 Space Shuttle Mission Report
[NASA-TM-109867] 11 p4211 N94-35251
STS-51 Space Shuttle Mission Report
[NASA-TM-109866] 11 p4211 N94-35252

SPACE TRANSPORTATION SYSTEM 3 FLIGHT
The 1982 highlights
[NASA-TM-109671] 03 p1303 N94-15508

SPACE TRANSPORTATION SYSTEM 4 FLIGHT
The 1982 highlights
[NASA-TM-109671] 03 p1303 N94-15508

SPACE TUGS
Hardware design of a grappling/docking device accommodating large lateral and angular misalignments 07 p2833 N94-25668

SPACE VEHICLE CHECKOUT PROGRAM
STS-31 crew training: firefighting, food tasting, EVA prep and post
[NASA-TM-109484] 03 p0876 N94-15451
Galileo probe spacecraft mission to Jupiter
[NASA-TM-109646] 03 p1247 N94-16070
The MACS-TSA applied in the ISO and SAX spacecraft projects
[PB94-126257] 08 p3170 N94-30857

SPACE VEHICLE CONTROL
U SPACECRAFT CONTROL

SPACE VEHICLES
U SPACECRAFT

SPACE WEAPONS
Not ready for the first space war. What about the second?
[AD-A266557] 03 p1174 N94-16665
A qualified radiation hardened nonvolatile memory for space and tactical weapons applications
[DE94-001211] 06 p2559 N94-23186
Vulnerability assessment of a space based weapon platform electronic system exposed to a thermonuclear weapon detonation
[DE94-007229] 09 p3611 N94-32667

SPACE-TIME CONTINUUM
U RELATIVITY

SPACE-TIME FUNCTIONS
Discrete space-time symmetries
[DE93-010199] 01 p0341 N94-10259
On the generalized Jordan-Brans-Dicke theory
[DE93-613051] 01 p0409 N94-10499
From the Weyl theory to a theory of locally anisotropic space-time
[DE92-644734] 01 p0410 N94-10535
Wavelets and spacetime squeeze 01 p0379 N94-10604
Dimensional transition of the space-time at the minimum action near the planck scale
[DE93-754192] 01 p0410 N94-10718
New developments in the method of space-time conservation element and solution element: Applications to the Euler and Navier-Stokes equations
[NASA-TM-106226] 01 p0150 N94-10939
A version of superstring with four space-time dimensions
[DE93-608196] 01 p0412 N94-11163
Aspects of symmetry violation
[DE93-011003] 02 p0779 N94-12997
The space-time and energy parameters of deuterium braking by the central collision with atoms
[DE93-624144] 02 p0788 N94-14881
Space and time as outcome of decoherence in an expanding universe
[DE93-016199] 04 p1624 N94-18047
Impulsive moving mirror model in a Schroedinger picture with impulse effect in a Banach space
[DE93-629864] 04 p1561 N94-18155
Space and time from quantum mechanics
[DE93-015263] 04 p1609 N94-18629
Interface reflection of spherical acoustic waves in the first- and second-order rational parabolic approximations and their artifacts
[PB93-215424] 05 p1969 N94-22261
Non commutative geometry and physics
[PB93-215499] 05 p1961 N94-22264
Canonically covariant formulation of Landau's Newtonian superfluid dynamics
[PB93-221034] 05 p1805 N94-22272
Introduction to a behavioral approach for continuous time systems
[ETN-94-95301] 06 p2492 N94-25277
The scattering and collision of gravitational waves in Friedmann-Robertson-Walker open universes
[MATHS-REPT-A-193] 06 p2406 N94-25430
The Dirac equation in Kerr spacetime, spheroidal coordinates and the M.I.T. bag model of hadrons
[DE94-601566] 07 p3006 N94-25886
Dimensional crossover from non-renormalizability to renormalizability
[DE93-613052] 07 p3006 N94-26193
Vortices in curved spacetime
[DE94-601559] 07 p3072 N94-26417
The extensions of space-time. Physics in the 8-dimensional homogeneous space D is equal to SU(2,2)/K
[DE93-634336] 07 p3072 N94-26551
Stochastic space-time, confinement potential and particle propagator
[DE94-606415] 07 p3074 N94-27680
Numerical analysis and computation of nonlinear partial differential equations from applied mathematics
[AD-A275582] 08 p3451 N94-28723
Three forms of relativity
[DE94-606338] 08 p3523 N94-28782
Anomalous algebraic structures in quantum field theories 08 p3524 N94-29911
On dyonic black holes and cosmic censorship 08 p3546 N94-29912
Physics, astronomy, and astrophysics: A numerical study of the black hole plus Brill wave spacetime 08 p3540 N94-29990
Theory of fundamental interactions
[DE94-608126] 08 p3525 N94-30169
Research in theoretical high-energy physics
[DE94-008388] 09 p3876 N94-32407
Localizability and the Planck mass
[DE94-009183] 10 p4149 N94-33988

SPACE-TIME METRIC
U SPACE-TIME FUNCTIONS

SPACEBORNE ASTRONOMY
Propagation Effects in Space VLBI 01 p0134 N94-11060
Yohkoh Bragg Crystal Spectrometer light curves for Ca XIX (3.1631-3.1912A): 1 October 1991 - 30 September 1992
[AD-A266090] 01 p0483 N94-12414
Planetary system detection by POINTS
[NASA-CR-194361] 02 p0545 N94-13067
Measurements of the spatial structure and directivity of 100 KeV photon sources in solar flares using PVO and ISEE-3 spacecraft
[NASA-CR-194080] 02 p0845 N94-14492
Analysis of the IUE spectra of the strongly interacting binary beta Lyrae
[NASA-CR-194118] 02 p0833 N94-14493
Proceedings of an ESA Symposium on Photon Detectors for Space Instrumentation
[ESA-SP-356] 03 p0899 N94-15025
Background suppression techniques in germanium detectors 03 p0899 N94-15026
X ray microcalorimeters: Principles and performance 03 p0899 N94-15027
A new approach to optical photon detection 03 p0899 N94-15028
Development of x ray CCDs 03 p0900 N94-15033
The development of back-illuminated CCD's for XMM 03 p0900 N94-15035
Microchannel plate detectors for space astronomy 03 p0901 N94-15038
Infrared detectors and coolers for space instrumentation: Summary and concluding remarks 03 p0904 N94-15059
The Einstein Observatory catalog of IPC x ray sources. Volume 4E: Right ascension range 08h 00m to 11h 59m
[NASA-TM-108401-VOL-4E] 04 p1625 N94-18612
The Einstein Observatory catalog of IPC x ray sources. Volume 5E: Right ascension range 12h 00m to 15h 59m
[NASA-TM-108401-VOL-5E] 04 p1625 N94-18613
The Einstein Observatory catalog of IPC x ray sources. Volume 6E: Right ascension range 16h 00m to 19h 59m
[NASA-TM-108401-VOL-6E] 04 p1625 N94-18615
The Einstein Observatory catalog of IPC x ray sources. Volume 7E: Right ascension range 20h 00m to 23h 59m
[NASA-TM-108401-VOL-7E] 04 p1625 N94-18618
The Einstein Observatory catalog of IPC x ray sources. Volume 1E: Documentation
[NASA-TM-108401-VOL-1E] 04 p1626 N94-18619
The Einstein Observatory catalog of IPC x ray sources. Volume 2E: Right ascension range 00h 00m to 03h 59m
[NASA-TM-108401-VOL-2E] 04 p1626 N94-18620
The Einstein Observatory catalog of IPC x ray sources. Volume 3E: Right ascension range 04h 00m to 07h 59m
[NASA-TM-108401-VOL-3E] 04 p1626 N94-18621
ASTRO-1 to explore invisible universe
[NASA-TM-109360] 04 p1336 N94-18956
The star identification, pointing and tracking system of UVSTAR, an attached payload instrument system for the Shuttle Hitchhiker-M platform 04 p1326 N94-19179
Particle induced background by Roentgen satellites
[MPE-242] 04 p1631 N94-19714
ASpect: A new spectrum and line analysis package for IRAF 05 p1926 N94-22485
SPIKE: Application for ASTRO-D mission planning 05 p1926 N94-22486
Quality control of EUVE databases 05 p2047 N94-22490
The application of artificial intelligence to astronomical scheduling problems 05 p1949 N94-22492
Scientific Requirements for Future Solar-Physics Space Missions
[ESA-SP-1157] 06 p2623 N94-22837
Prospects for future ground-based solar observations 06 p2624 N94-22842
Interferometric astronomy on the Moon 06 p2601 N94-23378
Generic mission planning concepts for space astronomy missions 06 p2505 N94-23878
Hubble Space Telescope high speed photometer orbital verification
[NASA-CR-189333] 06 p2204 N94-24226
Structure in gamma ray burst time profiles: Correlations with other observables 06 p2579 N94-24431
LOLA: Lunar Optical Long-baseline Array. 1992-1993 space design
[NASA-CR-195533] 06 p2298 N94-24582
LOITA: Lunar Optical/Infrared Telescope Array
[NASA-CR-195532] 06 p2546 N94-24816
Investigation relative to the Roentgen Satellite (ROSAT)
[NASA-CR-195192] 06 p2600 N94-25269
Cosmic Background Radiation Explorer (COBE)
[NASA-TM-109801] 10 p4014 N94-33559
Constraint-based integration of planning and scheduling for space-based observatory management 10 p4150 N94-34046
A study of low mass x-ray binaries
[NASA-CR-195813] 10 p4162 N94-34119
Hubble Space Telescope cycle 5 call for proposals
[NASA-CR-189363] 11 p4349 N94-36279
Hubble Space Telescope faint object spectrograph instrument handbook, version 5.0
[NASA-CR-189367] 12 p4546 N94-36794
Hubble Space Telescope cycle 5. Phase 1: Proposal instructions, version 4.0
[NASA-CR-189364] 12 p4547 N94-36963

SPACEBORNE EXPERIMENTS
NT PLASMA INTERACTION EXPERIMENT
Proceedings of the 8th European Symposium on Materials and Fluid Sciences in Microgravity, volume 1
[ESA-SP-333-VOL-1] 01 p0099 N94-10070
The formation and breakage of liquid bridges under microgravity 01 p0100 N94-10071
Towards real time numerical stimulation of Marangoni convection: A help for telescience microgravity experiments 01 p0102 N94-10087
Marangoni instability induced convection in an evaporating liquid droplet 01 p0104 N94-10094
Bubbles and drops behaviour under low-gravity: A space experiment for the IML-2 mission 01 p0104 N94-10098
Description of the liquid structure facility architecture and experimental demonstration of the diagnostic capabilities 01 p0039 N94-10118
Advanced protein, crystallization facility and associated new developments 01 p0039 N94-10119
MUZO: The programmable multi zone furnace for gas payloads and sounding rockets 01 p0110 N94-10132
The surface plasmon spectroscopy as diagnostic technique in microgravity experiments 01 p0110 N94-10133
TOLS (Telescience On-Line Simulator): An essential instrument for micro-gravity interactive experiment 01 p0039 N94-10134
Laser beam deflection: A diagnostic tool for vapour growth experiments in microgravity 01 p0111 N94-10135
The advanced fluid physics module: How to achieve scientific goals for Spacelab D2 01 p0039 N94-10138

Results of mission preparation support to microgravity experiments on board of Eureca 1
01 p0111 N94-10138
Mission support for crystal growth experiments in Russian unmanned carriers 01 p0111 N94-10139
Analysis of the alignment of a Schlieren system for tele-operation 01 p0111 N94-10140
AGF (Automatic Gradient Furnace): A proposed microgravity facility 01 p0112 N94-10141
Microgravity experiments using TR-1A rocket
01 p0112 N94-10142
Experimental approach to non-contact calorimetry in space 01 p0112 N94-10143
Proceedings of the 8th European Symposium on Materials and Fluid Sciences in Microgravity, volume 2 [ESA-SP-333-VOL-2] 01 p0112 N94-10171
Numerical calculation of the growth of InP by the travelling heater method in the first mission of the Space Flyer Unit 01 p0114 N94-10179
Results of crystal growth experiments by FZM on Zona facilities in microgravity 01 p0116 N94-10193
EUSO-D2-experiment: Unidirectional solidification with quenching of an AlSi11 alloy 01 p0086 N94-10199
Ripening of immiscible liquid droplets in microgravity with constrained Marangoni drift 01 p0117 N94-10200
Liquid phase sintering of tungsten composites under microgravity. Effect of matrix composition
01 p0118 N94-10207
A study of the quasibinary Al-W-Mo system. Part 1: Preliminary investigations and preparation for microgravity experiments 01 p0119 N94-10211
Transport of heat and mass in near-critical fluids
01 p0122 N94-10230
Measurements of heat capacity in undercooled metals
01 p0087 N94-10231
Columbus proto-planetesimal dust aggregation experiment 01 p0123 N94-10236
Use of inert immiscible liquid for crystal separation out of its feeding solution in weightlessness
01 p0124 N94-10242
Single bubble experiments in pool boiling: Results from TEXUS 26 01 p0124 N94-10243
The International Microgravity Laboratory, a Spacelab for materials and life sciences 01 p0125 N94-10249
The critical facility on IML-1 01 p0044 N94-10250
Space Activities in the Asia Pacific Region [JTN-93-80421] 01 p0035 N94-10676
Space environmental effects on the integrity of chromic acid anodized coatings [NASA-CR-191468] 01 p0055 N94-10947
Gas-Grain Simulation Facility (GGSF). Volume 2: Conceptual design definition [NASA-CR-177613] 01 p0423 N94-11229
An overview of the Defence Research Agency photovoltaic programme 01 p0053 N94-11412
Microgravity vibration isolation technology: Development to demonstration [NASA-TM-106320] 01 p0001 N94-11703
Summary of the pre-AO of the JEM onboard scientific and engineering experiments for refrigerator utilization
01 p0129 N94-11832
Submillimeter wave observation experiment of Earth atmosphere with SIS mixer 01 p0130 N94-11837
Utilization of superconductivity in the area of space
01 p0131 N94-11843
Lunar Scout Two spacecraft gravity experiment
01 p0459 N94-12152
The Third Workshop on Two Phase Fluid Experiment in the Space Environment [NASDA-CON-930002] 01 p0161 N94-12547
Summary of studies on JEM utilization experiment projects 01 p0161 N94-12548
Compilation of proposals for boiling and evaporation experiments in space environments and proposals concerning experiment projects
01 p0161 N94-12549
Condensation phenomena 01 p0162 N94-12550
Developmental research of thermal control system in space environment 01 p0162 N94-12551
Two phase flow and isopycnic liquid-liquid two phase fluid in reduced gravity field 01 p0162 N94-12552
Research on two phase flow in microgravity
01 p0162 N94-12554
Organization and management policy for two phase fluid experiment in space environment
01 p0162 N94-12556
Reduce fluid experiment system flight data from IML-1 [NASA-CR-193835] 02 p0804 N94-12873
Present status of JEM utilization projects
02 p0530 N94-13273
Trial manufacture model and in-space verification method of deployable antenna 02 p0530 N94-13278
A concept on on-orbit experiments of deployable structures utilizing JEM/HOPE 02 p0531 N94-13279
Study on superconducting basic technology for space application, part 1 [NASDA-CNT-930015-PT-1] 02 p0622 N94-13425
Mid-deck experiments, STS-26 [NASA-TM-109308] 02 p0570 N94-13616
Preparation of particle-dispersion alloys (M-6)
02 p0587 N94-13738
Study on solidification of immisible alloys (M-10)
02 p0588 N94-13742
Microgravity acceleration measurement environment characterization 02 p0590 N94-13755
Neurophysiological study on visuo-vestibular control of posture and movement in fish during adaptation to weightlessness 02 p0591 N94-13759
Crystal growth of enzymes in low gravity (L-5)
02 p0592 N94-13762
Studies on the effects of microgravity on the ultrastructure and functions of cultured mammalian cells (L-6) 02 p0592 N94-13763
Effect of low gravity on calcium metabolism and bone formation (L-7) 02 p0593 N94-13765
A circadian rhythm of conidiation in Neurospora crassa (L-12) 02 p0593 N94-13769
Partial analysis of LDEF experiment A-0114 [NASA-CR-193826] 02 p0564 N94-14025
Ethology in space, a unique opportunity for behavioural science [ESA-STM-246] 02 p0731 N94-14862
Sounding Rocket Experiments in Fluid Science and Materials Sciences: TEXUS 25 to 27 and MASER 4, volume 3 [ESA-SP-1132-VOL-3] 03 p0943 N94-15157
Electrophoresis visualisation 03 p0944 N94-15163
Remelting of Fe-C-Si-alloy in a ceramic mold skin
03 p0945 N94-15169
Heat storage module 03 p0946 N94-15172
Long Duration Exposure Facility is coming home [NASA-TM-109656] 03 p0884 N94-15227
STS-26 SSIP briefing --- Titanium Grain Formation Experiment and Crystal Membrane Experiment [NASA-TM-109556] 03 p0976 N94-15280
GAS highlights, 1988 --- Get Away Specials [NASA-TM-109600] 03 p0873 N94-15308
STS-29 crew with student experiment [NASA-TM-109545] 03 p1116 N94-15378
STS-26 protein growth (PCG) experiment [NASA-TM-109533] 03 p0976 N94-15395
STS-31 onboard 16mm photography quick release --- Onboard Activities [NASA-TM-109478] 03 p0881 N94-15438
STS-40 crew during spacelab Sim [NASA-TM-109493] 03 p0876 N94-15452
Science operation in space: Lessons [NASA-TM-109502] 03 p0881 N94-15466
Long Duration Exposure Facility experiment M0003 deintegration/findings and impacts [AD-A267140] 03 p0885 N94-15749
Explosive boiling at very low heat fluxes: A microgravity phenomenon [NASA-TM-106325] 03 p1046 N94-15817
Proceedings of the Second Workshop on Microgravity Experimentation [DSS-NR15-43-1990] 03 p0977 N94-16071
Scientific use of Space Station Freedom
03 p0977 N94-16072
The ESA telescience program
03 p0977 N94-16073
Canadian microgravity experiments flown in 1989-1990 03 p0977 N94-16075
MAXUS: The new sounding rocket program for long duration microgravity flight 03 p0978 N94-16079
QUESTS: A microgravity research facility for materials science experiments 03 p0978 N94-16082
The Canadian Space Station user development program. Where do we go from here? 03 p0898 N94-16084
Study of fractal aggregates 03 p0979 N94-16086
Polar 2 model of the wake shield experiment [AD-A266243] 03 p0882 N94-16468
Third LDEF Post-Retrieval Symposium Abstracts [NASA-CP-10120] 03 p1303 N94-16495
Looking at science on board Eureca [ESA-BR-80] 03 p0874 N94-16584
Design of an experiment hardware for the ESA space facility BIOPAN [DLR-FB-93-06] 03 p0876 N94-17548
Consortium for materials development in space [NASA-CR-194411] 04 p1379 N94-18840
Spacelab 3 [NASA-TM-108750] 04 p1323 N94-18849
California Student Get Away Special Payload GAS-450
04 p1324 N94-19164
MUZO flight experience with the programmable multizone furnace 04 p1324 N94-19167
Static Computer Memory Integrity Testing (SCMIT): An experiment flown on STS-40 as part of GAS payload G-616 04 p1325 N94-19169
The first flight of the QUESTS GAS payload G-521
04 p1325 N94-19170
VPU(tm) demonstration mission vicinity processor unit(tm) overview 04 p1325 N94-19171
Materials flight experiment carrier capability and future flight experiments on Hitchhiker-M carrier program
04 p1326 N94-19175
Limited Duration of Candidate Materials Exposure Experiment (LDCE): A Complex Autonomous Payload (CAP) using a Get Away Special (GAS) canister
04 p1326 N94-19176
Utilization of Shuttle small payload accommodations in the DOD Space Test Program 04 p1326 N94-19180
Your GAS experiment and the media or why does that other can get all of the publicity?
04 p1327 N94-19182
Space Life Sciences Research: The Importance of Long-Term Space Experiments [NASA-TM-4502] 04 p1502 N94-19210
Stability limits and dynamics of nonaxisymmetric liquid bridges [NASA-CR-194706] 05 p1797 N94-20037
Conversion of LDEF experiment M0003 sample observation database to MS-DOS formats [AD-A272945] 05 p1681 N94-21226
Flight and laboratory testing of materials in low Earth orbit 05 p1659 N94-21369
German space experiments on Spacelab D-2 and Eureca-1 to investigate atomic oxygen interaction with materials 05 p1662 N94-21390
The International Telecommunications Satellite (INTELSAT) Solar Array Coupon (ISAC) atomic oxgyen flight experiment: Techniques, results and summary
05 p1662 N94-21391
Design of a surface deformation measuring instrument for the Surface Tension Driven Convection Experiment (STDCE-2) [NASA-CR-194758] 06 p2343 N94-23285
PULSAUR 2 [NASA-CR-194832] 06 p2209 N94-23484
Columbus system support for telescience operations
06 p2505 N94-23877
Spacecraft vibrations due to mechanisms; measurements from Olympus on-station
06 p2207 N94-24018
Modeling of PCG fluid dynamics: Salient results
06 p2224 N94-24345
Progress toward ultra-stable lasers for use in space [NASA-TM-109678] 06 p2349 N94-24488
Proceedings of the 8th Annual Summer Conference: NASA/USRA Advanced Design Program [NASA-CR-195118] 07 p3075 N94-25665
Autonomous support for microorganism research in space 07 p2903 N94-25672
Microgravity ignition experiment
07 p2761 N94-25707
An approach to studying the reliability of microgravity experiments [NASA-TM-106489] 07 p2834 N94-26199
Long Duration Exposure Facility space optics handbook [AD-A274831] 07 p3035 N94-26572
Spacelab life sciences 2 post mission report [NASA-CR-188279] 07 p2942 N94-27410
Study on posture control and adaptation mechanism under weightlessness: Summary report of ground operations performed for carp experiment (FMPT/L-2) in Space Shuttle mission 07 p2912 N94-27447
Study on posture control and adaption mechanism under weightlessness: Differences in weight and shape of utricular otolith of carp 07 p2912 N94-27448
Gamma Large Area Silicon Telescope (GLAST): Applying silicon strip detector technology to the detection of gamma rays in space [DE94-003451] 07 p3116 N94-27740
Construction and test of experiment hardware for a space experiment on Spacelab mission IML-2 [DLR-FB-93-23] 07 p2903 N94-27743
Overview of space environment utilization science [JTN-94-80581] 08 p3227 N94-28938
Cryogenic on-orbit liquid depot storage acquisition and transfer (COLD-SAT) experiment subsystem instrumentation and wire harness design report [NASA-CR-189172] 08 p3168 N94-29405
GOME: Global Ozone Monitoring Experiment [ESA-SP-1151] 08 p3347 N94-29452
Analysis of selected materials flown on interior locations of the Long Duration Exposure Facility [NASA-CR-4586] 08 p3175 N94-29458
Thermal enclosure system functional simulation user's manual [NASA-TM-109094] 08 p3466 N94-29489
Retention latch mechanism for the Wake Shield Facility 08 p3161 N94-29635

Study of activation data of metal samples from LDEF-1 and Spacelab-2
[NASA-CR-193973] 08 p3205 N94-29736
Summary report of mission acceleration measurements for Spacehab-01, STS-57 launched 21 June 1993
[NASA-TM-106514] 08 p3168 N94-29757
Microgravity fluid science research in Europe
[AD-B179178] 08 p3229 N94-30409
Microencapsulation of anti-tumor, antibiotic and thrombolytic drugs in microgravity
08 p3397 N94-30453
A Modular Artificial Intelligence Inference Engine System (MAIS) for support of on orbit experiments
[AIAA PAPER 94-1237-CP] 08 p3448 N94-30584
Spacecraft contamination issues from LDEF: Issues for design 09 p3592 N94-31020
Impact of LDEF photovoltaic experiment findings upon spacecraft solar array design and development requirements 09 p3594 N94-31028
Space environmental effects on polymer composites: Research needs and opportunities
09 p3595 N94-31035
Spacecraft materials: Comparison between flight results obtained on LDEF and MIR 09 p3597 N94-31045
Design application and development of spacecraft in LEO utilizing LDEF results 09 p3597 N94-31047
What LDEF means for development and testing of materials 09 p3598 N94-31050
Laboratory and space experiments as a key to the plasma universe
[TRITA-ALP-1993-01] 09 p3885 N94-31088
Development concept for Dutch user support
[PB94-125523] 09 p3598 N94-31208
Various magnet options for Delta launched version of ASTROMAG
[DE94-006292] 09 p3955 N94-31635
Space acceleration measurement system
[NASA-TM-109754] 09 p3913 N94-31807
Steady thermal convection in multiple liquid layers
09 p3705 N94-31844
Computer modeling of active experiments in space plasmas 09 p3890 N94-31927
Pre-flight testing of Thermoelectric Quartz Crystal Microbalances (TQCM) for midcourse space experiment (MSX) spacecraft
[AD-A277054] 09 p3610 N94-32010
Implementation of heaters on thermally actuated spacecraft mechanisms 09 p3607 N94-33320
IMIS: An intelligence microscope imaging system
10 p4127 N94-33646
PI in the sky: The astronaut science advisor on SLS-2
10 p4110 N94-34060
Receiver design, performance analysis, and evaluation for space-borne laser altimeters and space-to-space laser ranging systems
[NASA-CR-195847] 10 p4058 N94-34066
Automated documentation generator for advanced protein crystal growth
[NASA-CR-193955] 10 p4147 N94-34072
US experiment flown on the Soviet biosatellite Cosmos 1667
[NASA-TM-108803] 10 p4102 N94-34951
Effect of microgravity on plant growth
[NASA-CR-196004] 11 p4296 N94-35257
Results from LDEF experiment A0114: The interaction of atomic oxygen with materials surfaces at orbital altitudes
[NASA-CR-196016] 11 p4235 N94-35388
Purity and cleanness of aerogel as a cosmic dust capture medium 11 p4247 N94-35469
Participation in the definition, conduct, and analysis of particle accelerator experiments for the first Spacelab Mission
[NASA-CR-193974] 11 p4330 N94-35483
Structural assembly demonstration experiment, phase 1
[NASA-CR-193967] 11 p4212 N94-35484
Materials processing in space tasks. WBS task 5.4: Generic tasks
[NASA-CR-193979] 11 p4249 N94-35485
Reduction procedures for accurate analysis of MSX surveillance experiment data 11 p4203 N94-35611
The control of satellites with microgravity constraints: The COMET Control System 11 p4207 N94-35632
Evaluation of Oxygen Interactions with Materials 3: Mission and induced environments
[NASA-TM-109349] 11 p4236 N94-35680
Microgravity isolation system design: A modern control synthesis framework 11 p4215 N94-35851
Design and development of experimental facilities for short duration, low-gravity combustion and fire experiments
[NASA-CR-196107] 12 p4389 N94-36967
Ground and space flight experiments of the effects of light, sound and/or temperature on animals
[NASA-CR-196102] 12 p4478 N94-36986

SPACEBORNE LASERS
Enhanced Damage-Resistant Optics for Spaceflight Laser Systems: Workshop findings and recommendations
[NASA-TM-109243] 01 p0381 N94-11054
Nd:YLF laser for airborne/spaceborne laser ranging
03 p0913 N94-15563
GLRS-R 2-colour retroreflector target design and predicted performance 03 p0921 N94-15615
Bench checkout equipment for spaceborne laser altimeter systems 03 p0921 N94-15618
Multi-beam laser altimeter 03 p0921 N94-15620
Satellite laser station Helwan status 1992
03 p0877 N94-15621
Direct solar pumping of semiconductor lasers: A feasibility study
[NASA-CR-193760] 04 p1440 N94-18834
SPNDL: A concept for a small satellite Doppler lidar wind sounder 04 p1327 N94-19181
Progress toward ultra-stable lasers for use in space
[NASA-TM-109678] 06 p2349 N94-24488
Lasercom system architecture with reduced complexity
[NASA-CASE-NPO-19069-1-CU] 08 p3293 N94-29493
GLRS-R 2-colour retroreflector target design and predicted performance
[REPT-932-440-106] 08 p3246 N94-29542
The Rb 780-nanometer Faraday anomalous dispersion optical filter: Theory and experiment
08 p3250 N94-29659
Solid state laser systems for space application
[NASA-CR-195777] 08 p3294 N94-29914
Receiver design, performance analysis, and evaluation for space-borne laser altimeters and space-to-space laser ranging systems
[NASA-CR-194747] 12 p4397 N94-36988

SPACEBORNE PHOTOGRAPHY
NT SATELLITE-BORNE PHOTOGRAPHY
Preliminary report of lunar observations by the Near-Infrared Mapping Spectrometer (NIMS) during the second Galileo Earth-Moon encounter
01 p0425 N94-12140
STS-30 crew photo in building 4
[NASA-TM-109573] 03 p1031 N94-15304
STS-34 Arriflex and IMAX camera training
[NASA-TM-109467] 03 p1031 N94-15397
STS-35 onboard photography quick release
[NASA-TM-109500] 03 p0881 N94-15464
The application of spaceborne synthetic aperture radar in the maritime environment
[DRA-TM(AWE)-91013] 05 p1737 N94-20596
An intelligent interactive visual database management system for Space Shuttle closeout image management
09 p3923 N94-32469
Hubble Space Telescope faint object camera instrument handbook (Post-COSTAR), version 5.0
[NASA-CR-189365] 12 p4546 N94-36795

SPACEBORNE TELESCOPES
NT HUBBLE SPACE TELESCOPE
NT INFRARED SPACE OBSERVATORY (ISO)
NT SOLAR OPTICAL TELESCOPE
NT SPACE INFRARED TELESCOPE FACILITY
NT X RAY ASTROPHYSICS FACILITY
An approach to high precision antenna structures by a CFRP core sandwich concept 01 p0057 N94-10008
Zerodur polishing process for high surface quality and high efficiency
[DE93-012596] 01 p0087 N94-10271
The four great observatories
[NASA-TM-109311] 02 p0830 N94-13605
An overview of the Galileo Optical Experiment (GOPEX) 02 p0610 N94-14386
Galileo Optical Experiment (GOPEX) optical train: Design and validation at the Table Mountain Facility
02 p0610 N94-14390
Fabrication 02 p0546 N94-14834
Laser power beaming system analyses
[NASA-CR-193840] 02 p0660 N94-14904
Gamma large area silicon telescope: Applying Si strip detector technology to the detection of gamma rays in space 03 p0904 N94-15061
The STIS MAMA status: Current detector performance
03 p0905 N94-15069
ASTRO-1 to explore invisible universe
[NASA-TM-109360] 04 p1336 N94-18956
UVSTAR: An imaging spectrograph with telescope for the Shuttle Hitchhiker-M platform
04 p1326 N94-19178
The star identification, pointing and tracking system of UVSTAR, an attached payload instrument system for the Shuttle Hitchhiker-M platform 04 p1326 N94-19179
UIT support observations archive
05 p2048 N94-22534
Scientific Requirements for Future Solar-Physics Space Missions
[ESA-SP-1157] 06 p2623 N94-22837
Prospects for improved instrumentation on future solar space missions 06 p2624 N94-22843
The next Japanese solar satellite
06 p2625 N94-22846
Why put visible solar telescopes in space?
06 p2600 N94-22850
Radioastron flight operations
06 p2502 N94-23861
An Earth observation telescope refocusing mechanism
06 p2359 N94-24014
Precision Displacement Mechanism (PDM)
06 p2360 N94-24026
LOLA: Lunar Optical Long-baseline Array. 1992-1993 space design
[NASA-CR-195533] 06 p2298 N94-24582
LOITA: Lunar Optical/Infrared Telescope Array
[NASA-CR-195532] 06 p2546 N94-24816
Feasibility study of a multiaperture telescope for deep-space Earth surveillance
[AD-A273903] 07 p3102 N94-25658
Project PARAS: Phased array radio astronomy from space 07 p3081 N94-25703
The PROTEL contamination code
[RXR-93071] 07 p3040 N94-28202
An Earth observation telescope refocusing mechanism
[REPT-932-440-103] 08 p3332 N94-29417
Providing hydrogen maser timing stability to orbiting VLBI radio telescope observations by post-measurement compensation of linked frequency standard imperfections 08 p3297 N94-30670
Lunar Ultraviolet Telescope Experiment (LUTE), phase A
[NASA-TM-4594] 10 p4162 N94-34920

SPACECRAFT
The 1972 highlights
[NASA-TM-109631] 03 p1301 N94-15242
The 1965 highlights --- NASA programs
[NASA-TM-109632] 03 p1301 N94-15243
The 1967 highlights
[NASA-TM-109633] 03 p1301 N94-15244

SPACECRAFT ANTENNAS
Layout and cabling considerations for a large communications antenna array
02 p0611 N94-14395
Missile antenna pattern coordinate system and data formats
[AD-A269153] 04 p1385 N94-18260
Magellan vertical polarization radar observations
05 p1744 N94-20691
Electrical performance of wire mesh for spacecraft deployable reflector antennas 06 p2275 N94-22744
Precision Displacement Mechanism (PDM)
06 p2360 N94-24026
Effective conductivity of wire mesh reflectors for space deployable antenna systems
[NASA-CR-191605] 07 p2788 N94-27770
A comparison of full-spectrum and complex-symbol combining techniques for the Galileo S-band mission
08 p3250 N94-29665
The 20 GHz circularly polarized, high temperature superconducting microstrip antenna array
[NASA-CR-195097] 09 p3683 N94-33083
The Galileo high gain antenna deployment anomaly
09 p3607 N94-33319
The Mars Observer Ka-band link experiment
11 p4255 N94-35563
Baseline antenna design for space exploration initiative
[NASA-CR-196298] 12 p4435 N94-37255

SPACECRAFT BREAKUP
History of on-orbit satellite fragmentations
[NASA-CR-191644] 03 p0887 N94-16500
The fragmentation of Kosmos 2163
[NASA-CR-191643] 03 p0887 N94-16503
The fragmentation of the Nimbus 6 rocket body
[NASA-CR-191645] 03 p0926 N94-16504
Orbital debris and near-Earth environmental management: A chronology
[NASA-RP-1320] 06 p2598 N94-24644

SPACECRAFT CABIN ATMOSPHERES
Atmosphere quality standards in manned space vehicles
[ESA-PSS-03-401-ISSUE-1] 09 p3802 N94-31224
Technical assessment of Mir-1 life support hardware for the international space station
[NASA-TM-108441] 09 p3803 N94-31380
Total hydrocarbon analysis by ion mobility spectrometry 10 p4101 N94-33642
A users' guide to the trace contaminant control simulation computer program
[NASA-TM-108456] 10 p4080 N94-33696

SPACECRAFT CABINS
First lunar outpost 07 p2943 N94-25694

Risks and issues in fire safety on the Space Station
[NASA-TM-106430] 07 p2692 N94-27436

SPACECRAFT CHARGING

Experimental measurement of the plasma conductivity of Z93 and Z93P thermal control paint
[NASA-TM-106284] 01 p0043 N94-10756
Analysis of geophysical measurements and spacecraft interactions
[AD-A266064] 01 p0043 N94-10944
NASCAP programmer's reference manual
[NASA-CR-191044] 01 p0278 N94-11702
Interactions between spacecraft and their environments
[NASA-TM-106115] 02 p0541 N94-13917
Laboratory simulation of spacecraft charging in the plasma wake region
[FFI-93-7007] 02 p0542 N94-14107
Polar 2 model of the wake shield experiment
[AD-A266243] 03 p0882 N94-16468
Prototype instrumentation and design studies
[AD-A266402] 03 p0882 N94-16530
Broadband RF spectrum from electrostatic discharges on spacecraft
[AD-A269543] 04 p1385 N94-18287
Active spacecraft potential control: An ion emitter experiment for Cluster 04 p1330 N94-19634
Effect of geostationary environment constituents on secondary electron emission rates
05 p1661 N94-21382
Electrostatic charging and secondary effects in materials submitted to radiation in space
05 p1661 N94-21383
TROPIX plasma interactions group report
[NASA-CR-191149] 05 p1666 N94-21864
IRMA: A program for three-dimensional color display of data
[AD-A273811] 07 p2959 N94-25879
Active electron and ion beam experiments in space
[AD-A275570] 08 p3504 N94-28828
Development of a 3D numerical code to calculate the trajectories of the blow off electrons emitted by a vacuum surface discharge: Application to the study of the electromagnetic interference induced on a spacecraft
[ONERA-NT-1993-12] 09 p3863 N94-31227
Arcing in space structures in low Earth orbit
[NASA-CR-194223] 09 p3694 N94-32478
Spacecraft environmental anomalies expert system
[AD-A277962] 09 p3612 N94-33262

SPACECRAFT COMMUNICATION

NT SATELLITE COMMUNICATION
Sensor operation of Advanced Earth Observing Satellite (ADEOS) 02 p0689 N94-14215
Transform coding for space applications
[NASA-TM-106362] 02 p0612 N94-14542
STS-35 mission highlights resource tape
[NASA-TM-109501] 03 p0881 N94-15465
Computer networking at SLR stations
03 p0917 N94-15594
Bandwidth characteristics of multimedia data traffic on a local area network
[NASA-TM-104026] 03 p0883 N94-15648
Future trends in NASA space operations
06 p2498 N94-23836
A user view of the EURECA ground segment
06 p2499 N94-23844
The EURECA telecommanding chain: Experience with packet telecommand and telemetry systems
06 p2305 N94-23909
Representing operations procedures using temporal dependency networks 06 p2305 N94-23914
Situation management in the Link Monitor and Control Operator Assistant (LMCOA) 06 p2305 N94-23915
Using Mach threads to control DSN operational sequences 06 p2477 N94-23916
Modeling and analysis of selected space station communications and tracking subsystems
06 p2306 N94-25374
Low-cost unmanned lunar lander
07 p2697 N94-25699
The Telecommunications and Data Acquisition Report
[NASA-CR-195689] 08 p3249 N94-29652
High-resolution robot tracking and direction finding for space station environment 08 p3168 N94-29896
Communications networks in stressed environments
[AD-A275967] 09 p3672 N94-31384
Apollo 11: The Goddard connection
[NASA-TM-109815] 10 p4010 N94-33566
Using task analysis to understand the Data System Operations Team 10 p4159 N94-33614
Field demonstration of X-band photonic antenna remoting in the Deep Space Network
11 p4252 N94-35545
Spacecraft-spacecraft radio-metric tracking: Signal acquisition requirements and application to Mars approach navigation 11 p4254 N94-35557
The Mars Observer Ka-band link experiment
11 p4255 N94-35563

SPACECRAFT COMPONENTS

NT APOLLO LUNAR EXPERIMENT MODULE
NT COMMAND MODULES
NT LANDING MODULES
NT LUNAR LANDING MODULES
NT SIM
NT SPACECRAFT CABINS
NT SPACECRAFT DOCKING MODULES
NT SPACECRAFT MODULES
Spinforming characteristics of a net shape forming process 01 p0056 N94-10004
Development tests for a high stability optical bench
01 p0062 N94-10047
Introducing SMaSE: An aide memoire on structural materials and space engineering
01 p0063 N94-10053
The properties of perfluoropolyethers used for space applications
[NASA-TM-106275] 01 p0088 N94-10864
The trial manufacture and test of critical components in docking mechanism
[NASDA-TMR-930005] 01 p0044 N94-12280
Conceptual studies report on lunar and planetary exploration
[NASDA-TK-SS0438] 01 p0481 N94-12323
Manned lunar exploration missions
01 p0482 N94-12326
Mars exploration missions 01 p0482 N94-12327
The Second Workshop on Deployment and Assembly Experiment of Large Space Structure on Orbit
[NASDA-CON-930003] 02 p0529 N94-13268
Research on inflatable structure for space use
02 p0530 N94-13275
Helical truss beam development for large space structure 02 p0530 N94-13276
Application of intelligently adaptable structure and robot to large space structure 02 p0530 N94-13277
Trial manufacture model and in-space verification method of deployable antenna 02 p0530 N94-13278
A concept on on-orbit experiments of deployable structures utilizing JEM/HOPE 02 p0531 N94-13279
Movement of deployable truss
02 p0531 N94-13280
Development and application of one dimensional deployable truss 02 p0531 N94-13281
Study of a one-dimensional deployable structure employing telescopic members
02 p0531 N94-13282
Study on improvement of flammability, odor and offgassing tests for materials
[NASDA-CNT-930009] 02 p0563 N94-13471
The study on large space structure assembly technology: The study on deployable truss structure, part 1
[NASDA-TMR-930002] 02 p0541 N94-13658
The study on large space structure assembly technology: The study on deployable truss structure, part 2 and 3
[NASDA-TMR-930003-PT-2-3] 02 p0541 N94-13659
The study on test of docking mechanism system, part 1 and 2
[NASDA-TMR-930004-PT-1-2] 02 p0541 N94-13660
Development of Japanese Earth Resources Satellite-1 (JERS-1; FUYO-1) and it's operational results
[NASDA-SPP-930001] 03 p0884 N94-15001
Galileo probe ready to go
[NASA-TM-109648] 03 p1247 N94-15432
High voltage conductors in spacecraft
[AD-A267268] 03 p0897 N94-17266
Clementine: An inexpensive mission to the Moon and Geographos 05 p1652 N94-20765
Process and apparatus for the release of a prestress initially applied to a mechanism such as a bearing on board a space vehicle
[CA-PATENT-APPL-SN-2,020,909]
05 p1824 N94-21142
Metal band drives in spacecraft mechanisms
06 p2355 N94-23987
Development of gears for space use
06 p2360 N94-24021
Second NASA Workshop on Wiring for Space Applications
[NASA-CP-3244] 08 p3165 N94-28697
ESTEC wiring test programme materials related properties 08 p3165 N94-28698
Robust 300 C wire insulation system
08 p3165 N94-28699
NASA wiring program: Survey of NASA experiences in wiring system safety 08 p3165 N94-28700
Metal band drives in spacecraft mechanisms
08 p3162 N94-29637
The use of screening tests in spacecraft lubricant evaluation 08 p3162 N94-29641
Advanced microfabrication technologies for microspacecraft 08 p3171 N94-29782
The 28th Aerospace Mechanisms Symposium
[NASA-CP-3260] 09 p3603 N94-33291
Aerospace applications of magnetic bearings
11 p4213 N94-35837

SPACECRAFT COMPUTERS

U AIRBORNE/SPACEBORNE COMPUTERS

SPACECRAFT CONFIGURATIONS

NT SATELLITE CONFIGURATIONS
NT SPACE SHUTTLE ASCENT STAGE
Space Station Redesign Team: Final report to the Advisory Committee on the Redesign of the Space Station
[NASA-TM-109241] 01 p0042 N94-10663
Small spacecraft for planetary exploration
03 p0874 N94-17145
A conceptual design study for a two-dimensional, electronically scanned thinned array radiometer
[NASA-TM-109051] 03 p1085 N94-17665
ISOBUS: A new versatile spacecraft platform using Shuttle small payloads 04 p1327 N94-19183
Supersonic aerodynamic characteristics of a circular body Earth-to-Orbit vehicle
[NASA-TM-4533] 06 p2170 N94-24716
Near Earth asteroid rendezvous
[NASA-CR-195518] 06 p2195 N94-24808
Dynamics and control of orbiting flexible systems: A formulation with applications
[ISBN-0-315-75390-0] 09 p3611 N94-32502
A rapid algorithm for realistic human reaching and its use in a virtual reality system 10 p4101 N94-33621
Configurational evolution dynamics and stability during in-situ development of large orbiting spacecraft
[AD-A280482] 12 p4397 N94-37351

SPACECRAFT CONSTRUCTION MATERIALS

Advanced Materials for Lightweight Structures
[ESA-SP-336] 01 p0056 N94-10001
The EUREKA project portfolio in new materials
01 p0056 N94-10002
Spinforming characteristics of a net shape forming process 01 p0056 N94-10004
Design and development of a CFRP central cylinder for satellites 01 p0056 N94-10007
Design and manufacturing of filament wound thrust cylinder 01 p0057 N94-10010
Design concepts for load-carrying hot structures for reentry bodies 01 p0057 N94-10012
Hybrid materials for use at elevated temperatures
01 p0057 N94-10013
Analytical prediction and test verification of the multiaxial behaviour of high-strength steel for lightweight structures
01 p0058 N94-10016
Aluminium-lithium forgings: Properties and potential satellite applications 01 p0058 N94-10021
Mechanical and fatigue properties of fibre reinforced aluminium-lithium alloy and aluminium-lithium MMC based laminates 01 p0058 N94-10022
Investigations on aluminium-lithium alloys for damage tolerant application 01 p0059 N94-10023
Design and manufacturing of CFRP rings by RTM
01 p0059 N94-10025
Aluminum-beryllium alloys for aerospace applications
01 p0060 N94-10029
Ceramic matrix composites: High performance materials for space application 01 p0062 N94-10044
Stress relaxation forming of Ariane 5 front skirt outer skin panels 01 p0062 N94-10046
Vectra insulative support structures within spacecraft
01 p0062 N94-10050
Introducing SMaSE: An aide memoire on structural materials and space engineering
01 p0063 N94-10053
Structural material, manufacture, and design requirements for high-temperature fasteners for space plane technologies 01 p0063 N94-10055
High temperature composites in Aerospatiale activities
01 p0064 N94-10062
Structure and properties of an RS Al-Si-Ni-Mn-Zr alloy for high temperature applications
01 p0064 N94-10063
Material characterization and modeling with shear ography
[NASA-CR-192576] 01 p0185 N94-10342
Fractography handbook of spaceflight metals
[NASA-RP-1291] 01 p0081 N94-10504
Failure prediction of thin beryllium sheets used in spacecraft structures
[NASA-CR-194164] 01 p0187 N94-11190
Vacuum stability requirements of polymeric material for spacecraft application
[NASA-TM-109216] 01 p0091 N94-11350
The Second Workshop on Deployment and Assembly Experiment of Large Space Structure on Orbit
[NASDA-CON-930003] 02 p0529 N94-13268
Research on radiation resistance properties of structural materials for space use 02 p0529 N94-13271

Measuring methods for CFRP laminates' bending and torsion rigidities characteristics
02 p0529 N94-13272
Arc-heating tests of thermal protection system materials for the H-2 rocket fairing
[NAL-TR-1181] 02 p0551 N94-13455
Tensile properties of LE-7 engine material with welded joint
[NAL-TR-1188] 02 p0570 N94-13460
The study on large space structure assembly technology: The study on deployable truss structure, part 1
[NASDA-TMR-930002] 02 p0541 N94-13658
The study on large space structure assembly technology: The study on deployable truss structure, part 2 and 3
[NASDA-TMR-930003-PT-2-3] 02 p0541 N94-13659
Materials/structures testing 02 p0506 N94-14164
Processing and protection of high temperature structural materials
[AD-A267292] 03 p0954 N94-14961
Aluminum-lithium technology
[TABES PAPER 93-601] 03 p0962 N94-16137
Third LDEF Post-Retrieval Symposium Abstracts
[NASA-CP-10120] 03 p1303 N94-16495
Performance of silvered Teflon thermal control blankets on spacecraft
[AD-A266284] 03 p0887 N94-16909
Low power arcjet system spacecraft impacts
[NASA-TM-106307] 04 p1336 N94-17856
Consortium for materials development in space
[NASA-CR-194411] 04 p1379 N94-18840
Materials flight experiment carrier capability and future flight experiments on Hitchhiker-M carrier program
04 p1326 N94-19175
Limited Duration of Candidate Materials Exposure Experiment (LDCE): A Complex Autonomous Payload (CAP) using a Get Away Special (GAS) canister
04 p1326 N94-19176
Fifth International Symposium on Materials in a Space Environment
[ISBN-2-85-428293-0] 05 p1659 N94-21367
Flight and laboratory testing of materials in low Earth orbit 05 p1659 N94-21369
Complex-2: Low Earth orbital environment simulation facility for materials durability evaluation
05 p1653 N94-21370
Results of the post flight analyses on system materials for the LDEF-FRECOPA experiment
05 p1659 N94-21371
Integrity and testing concerns of thermostructural materials 05 p1661 N94-21384
Materials evaluation at ESA/ESTEC
05 p1662 N94-21386
Columbus: Materials for 30 years habitability in space
05 p1662 N94-21387
The International Telecommunications Satellite (INTELSAT) Solar Array Coupon (ISAC) atomic oxgyen flight experiment: Techniques, results and summary
05 p1662 N94-21391
Durability of thermal control and environmental protective materials for the SSRMS in simulated LEO environment 05 p1663 N94-21392
Atomic oxygen interaction with spacecraft materials: Relationship between orbital and ground-based testing for materials certification 05 p1663 N94-21393
Evaluation of plasma-deposited protective coatings for spacecraft applications 05 p1663 N94-21394
Fast oxygen atom studies related to low Earth orbit activities 05 p1663 N94-21395
Thermostructural material composites for space applications 05 p1664 N94-21398
Thermal control coatings 05 p1664 N94-21400
Study of space factors effect on materials for spacecraft external surfaces in NPO Energia programs
05 p1664 N94-21401
Columbus PMP Critical Technologies Program: Approach for materials life time prediction
05 p1664 N94-21402
R and D to HOPE airframe 05 p1665 N94-21406
Material properties and behavior during simulated atmospheric reentry 05 p1665 N94-21408
Outgassing data for selecting spacecraft materials
[NASA-RP-1124-REV-3] 05 p1676 N94-21889
Diffuse panel studies: Conclusions
06 p2384 N94-23606
Establishment of computerized numerical databases on thermophysical and other properties of molten as well as solid materials and data evaluation and validation for generating recommended reliable reference data
06 p2246 N94-25123
X ray computed tomography for emerging aerospace materials and processes development
[AD-A273721] 07 p2705 N94-25779
NASA Lewis Research Center lean-, rich-burn materials test burner rig
[NASA-CR-194437] 07 p2680 N94-26141
Development and application of contamination technology for MSFC managed space systems
[NASA-CR-193934] 07 p2697 N94-27421
Proton irradiation on materials
07 p3030 N94-27898
Development of methodologies for the estimation of thermal properties associated with aerospace vehicles
07 p2846 N94-27920
NASA Parts Project Office: Basic goals
08 p3166 N94-28703
Electrical and mechanical testing of wire insulation for space applications 08 p3166 N94-28710
Evaluation of pyrolysis and arc tracking on candidate wire insulation designs for space applications
08 p3166 N94-28711
Wire insulation degradation and flammability in low gravity 08 p3166 N94-28712
Advanced microfabrication technologies for microspacecraft 08 p3171 N94-29782
Survey report of JSUP Space Environment Utilization Research Committee in fiscal year 1992: Functional New Materials Session
[JTN-94-80582] 08 p3159 N94-30162
Composite hot drape forming
08 p3240 N94-30448
Casting of weldable graphite/magnesium metal matrix composites with built-in metallic inserts
08 p3186 N94-30482
LDEF Materials Results for Spacecraft Applications
[NASA-CP-3257] 09 p3591 N94-31012
Model of spacecraft atomic oxygen and solar exposure microenvironments 09 p3593 N94-31021
Atomic oxygen erosion considerations for spacecraft materials selection 09 p3593 N94-31022
Performance of selected polymeric materials on LDEF
09 p3593 N94-31023
Fluorescence observations of LDEF exposed materials as an indicator of induced material reactions
09 p3593 N94-31025
On the linearity of fast atomic oxygen effects
09 p3594 N94-31027
Summary of materials and hardware performance on LDEF 09 p3595 N94-31037
LDEF materials special investigation group's data bases 09 p3596 N94-31038
An overview of the Evaluation of Oxygen Interaction with Materials-third phase (EOIM-3) experiment: Space Shuttle Mission 46 09 p3596 N94-31040
Analysis of leading edge and trailing edge cover glass samples before and after treatment with advanced satellite contamination removal techniques
09 p3596 N94-31041
Preliminary results from the CONCAP-2-01 and EIOM-3 experiments on STS-46 09 p3596 N94-31042
Design application and development of spacecraft in LEO utilizing LDEF results 09 p3597 N94-31047
What LDEF means for development and testing of materials 09 p3598 N94-31050
Computer modelling of cyclic deformation of high-temperature materials
[AD-A277056] 09 p3623 N94-32012
National aerospace plane
[NASA-TM-109843] 10 p4019 N94-33750
Mechanical failure probability of glasses in Earth orbit
[NASA-CR-195912] 10 p4031 N94-34947
Results from LDEF experiment A0114: The interaction of atomic oxygen with materials surfaces at orbital altitudes
[NASA-CR-196016] 11 p4235 N94-35388
Experimental impacts into Teflon targets and LDEF thermal blankets 11 p4352 N94-36141
Flame resistant fibrous structures development
[NASA-CR-185700] 12 p4421 N94-36641
Possibilities and pitfalls in aerospace applications of titanium matrix composites 12 p4400 N94-36650
Applications of Titanium Matrix Composite to large airframe structure 12 p4400 N94-36651
Composites based on titanium with external and internal reinforcement 12 p4401 N94-36654
Methodologies for thermal and mechanical testing of TMC materials 12 p4401 N94-36659
NASA-UVA Light Aerospace Alloy and Structures Technology Program (LA2ST)
[NASA-CR-196290] 12 p4415 N94-36809
JPRS report: Science and technology. Central Eurasia: Materials science
[JPRS-UMS-93-008] 12 p4404 N94-37010
Development of processing techniques for advanced thermal protection materials
[NASA-CR-196261] 12 p4426 N94-37510
Evaluation of seals and lubricants used on the Long Duration Exposure Facility
[NASA-CR-4604] 12 p4399 N94-37614
Effects of ply thickness on thermal cycle induced damage and thermal strain 12 p4459 N94-37806

SPACECRAFT CONTAMINATION

Analysis of geophysical measurements and spacecraft interactions
[AD-A266064] 01 p0043 N94-10944
Spacelab J air filter debris analysis
[NASA-CR-192569] 01 p0301 N94-11201
Atomic research
[NASA-CR-193843] 02 p0788 N94-14905
Analysis of leading edge and trailing edge cover glass samples before and after treatment with advanced satellite contamination removal techniques
[AD-A267055] 03 p0885 N94-15666
Solar absorptance of optical surfaces contaminated with spacecraft material outgassing products
[AD-A267202] 03 p0886 N94-15857
Long duration exposure facility experiment m0003 deintegration observation database
[AD-A267579] 03 p0951 N94-17207
Low power arcjet system spacecraft impacts
[NASA-TM-106307] 04 p1336 N94-17856
The application of jet spray and ion beam contamination removal techniques to samples from the LDEF spacecraft
[AD-A270973] 04 p1354 N94-19755
Measured space environmental effects to LDEF during retrieval 05 p1659 N94-21372
Residual atmosphere in the FRECOPA experiment and degassing of materials 05 p1660 N94-21374
Contamination control and plume assessment of low-energy thrusters
[NASA-TM-104585] 06 p2218 N94-23343
Microbiological analysis of debris from Space Transportation System (STS)-55 Spacelab D-2
[NASA-CR-193883] 06 p2421 N94-24310
Preliminary far-field plume sputtering characterization of the Stationary Plasma Thruster (SPT-100)
[NASA-TM-106464] 06 p2221 N94-24766
Spacecraft contamination issues from LDEF: Issues for design 09 p3592 N94-31020
Analysis of leading edge and trailing edge cover glass samples before and after treatment with advanced satellite contamination removal techniques
09 p3596 N94-31041
Preliminary results from the CONCAP-2-01 and EIOM-3 experiments on STS-46 09 p3596 N94-31042
An overview of the on-orbit contamination of the Long Duration Exposure Facility (LDEF)
09 p3598 N94-31049
Pre-flight testing of Thermoelectric Quartz Crystal Microbalances (TQCM) for midcourse space experiment (MSX) spacecraft
[AD-A277054] 09 p3610 N94-32010
Combined contamination and space environmental effects on solar cells and thermal control surfaces
[NASA-TM-106592] 09 p3617 N94-33022
Design and performance of the telescope and detector covers on the Extreme Ultraviolet Explorer satellite
09 p3605 N94-33309
A users' guide to the trace contaminant control simulation computer program
[NASA-TM-108456] 10 p4080 N94-33696
Trace contaminant control simulation computer program, version 8.1
[NASA-TM-108457] 10 p4100 N94-33973

SPACECRAFT CONTROL

NT SATELLITE ATTITUDE CONTROL
NT SATELLITE CONTROL
An analysis of the modes and states for generic avionics
[NASA-CR-188253] 01 p0027 N94-10664
Stability analysis and aerospace vehicle dynamics
01 p0031 N94-11491
Technical problems on lunar an planetary exploration mission 01 p0482 N94-12328
Low cost attitude control system reaction wheel development
[NASA-CR-191332] 02 p0540 N94-13140
A superconducting large-angle magnetic suspension
[NASA-CR-189735] 02 p0596 N94-13141
Application of intelligently adaptable structure and robot to large space structure 02 p0530 N94-13277
Electrical Actuation Technology Bridging
[NASA-CP-3213] 02 p0551 N94-13417
HOPE real time flight operations analyses for return to earth phase, part B
[NASDA-CNT-930011] 02 p0535 N94-13599
HOPE real time flight operations analyses for return to earth phase, part A
[NASDA-CNT-930010-PT-A] 02 p0535 N94-13645
Manual control in space research on perceptual-motor functions under zero gravity conditions (L-10)
02 p0593 N94-13767
Mongoose ASIC microcontroller programming guide
[NASA-RP-1319] 02 p0623 N94-13871

Strategic avionics technology definition studies. Subtask 3-1A: Electrical Actuation (ELA) systems
[NASA-CR-194393] 02 p0536 N94-14323
Large space structures and systems in the space station era: A bibliography with indexes (supplement 05)
[NASA-SP-7085(05)] 02 p0543 N94-14411
Real-time dynamics simulation of the Cassini spacecraft using DARTS. Part 1: Functional capabilities and the spatial algebra algorithm 02 p0680 N94-14638
An application of the IMC software to controller design for the JPL LSCL Experiment Facility 02 p0681 N94-14645
Control structural interaction testbed: A model for multiple flexible body verification 02 p0544 N94-14649
Pulse response based control for minimum time maneuver of flexible spacecraft
[AD-A266186] 03 p0886 N94-16455
Neighboring extremal guidance for systems with piecewise linear control using time as the reference variable
[AD-A267942] 03 p0874 N94-17010
A guidance and navigation system for two spacecraft rendezvous in translunar halo orbit
[AD-A267498] 03 p0898 N94-17368
Cooperative control of multiple space manipulators
[AD-A270291] 04 p1445 N94-18813
Phasing strategies of the Hermes type space shuttle: Its optimization considering the thrust failures
[LAAS-93242] 04 p1544 N94-19361
Automated rendezvous and capture demonstration study
[NASA-CR-192587] 04 p1331 N94-19366
Activities of the Center for Space Construction
[NASA-CR-193717] 04 p1335 N94-19371
Pointing control design for autonomous space vehicle applications
[DE93-019943] 05 p1657 N94-19863
Network command processing system overview 05 p1935 N94-21351
A user view of the EURECA ground segment 06 p2499 N94-23844
SCOS2: ESA's new generation of mission control systems 06 p2197 N94-23851
Operations concepts for Mars missions with multiple mobile spacecraft 06 p2501 N94-23852
NASA/Goddard Space Flight Center's testbed for CCSDS compatible systems 06 p2197 N94-23855
The Ulysses spacecraft control and monitoring concepts and realities 06 p2502 N94-23862
The instant sequencing task: Toward constraint-checking a complex spacecraft command sequence interactively 06 p2504 N94-23875
AGENDA: A task organizer and scheduler 06 p2504 N94-23876
A MOS for all seasons 06 p2505 N94-23879
AMFESYS: Modelling and diagnosis functions for operations support 06 p2506 N94-23887
ESSOPE: Towards S/C operations with reactive schedule planning 06 p2508 N94-23896
Customizing graphical user interface technology for spacecraft control centers 06 p2510 N94-23905
Automatic tools for system testing 06 p2197 N94-23913
XRTD: An X-Windows based, real-time radiometric display and analysis system 06 p2305 N94-23922
The application of total quality management principles to spacecraft mission operations 06 p2374 N94-23931
Space Station Freedom ground data system: Design and operations 06 p2518 N94-23957
The 33rd Israel Annual Conference on Aviation and Astronautics
[ITN-94-85227] 06 p2153 N94-24241
Weld joint concepts for on-orbit repair of Space Station Freedom fluid system tube assemblies 06 p2371 N94-24427
An Earth albedo model: A mathematical model for the radiant energy input to an orbiting spacecraft due to the diffuse reflectance of solar radiation from the Earth below
[NASA-TM-104596] 06 p2195 N94-24497
High performance flight computer developed for deep space applications 07 p2949 N94-26718
Implementing hard real-time systems: A case study 07 p2951 N94-26731
Test of onboard real time applications (LICE (tm)) 07 p2952 N94-26737
Dynamics and robust control for uncertain flexible space systems
[INPE-5510-TAE/020] 07 p2696 N94-27357
Superfluid helium sloshing dynamics induced oscillations and fluctuations of angular momentum, force and moment actuated on spacecraft driven by gravity gradient or jitter acceleration associated with slew motion
[NASA-CR-193928] 07 p2799 N94-27931
First experimental assessment of RCS plume-flow field interaction on Hermes leading edge thruster configuration 07 p2703 N94-28032
Using formal specification in the Guidance and Control Software (GCS) experiment. Formal design and verification technology for life critical systems
[NASA-CR-194884] 07 p2956 N94-28267
General theory and algorithms for the non-casual inversion, slewing and control of space-based articulated structures
[AD-A275118] 08 p3167 N94-29002
Software engineering methods in the Hermes on-board software 08 p3414 N94-29326
Micro guidance and control technology overview 08 p3144 N94-29772
Miniature wide field-of-view star trackers for spacecraft attitude sensing and navigation 08 p3144 N94-29794
Activities of Ishikawajima-Harima Heavy Industries Co. Ltd.
[PB94-137981] 08 p3555 N94-29798
Local interaction control for space construction 08 p3170 N94-30960
Phase-lock roll control of inertially pointing spacecraft 09 p3609 N94-31470
Adaptive nonlinear control of spacecraft 09 p3609 N94-31564
Dynamics and control of orbiting flexible systems: A formulation with applications
[ISBN-0-315-75390-0] 09 p3611 N94-32502
The Virtual Mission Operations Center 10 p4150 N94-33615
On-board emergent scheduling of autonomous spacecraft payload operations 10 p4123 N94-35047
A linguistic geometry for space applications 10 p4123 N94-35050
Vista goes online: Decision-analytic systems for real-time decision-making in mission control 10 p4125 N94-35063
Space/ground systems as cooperating agents 10 p4127 N94-35072
Automated maneuver planning using a fuzzy logic algorithm 11 p4203 N94-35610
Overview of the Miniature Sensor Technology Integration (MSTI) spacecraft attitude control system 11 p4206 N94-35627
A geometric model of a V-slit Sun sensor correcting for spacecraft wobble 11 p4206 N94-35628
Distributed parameter modelling of flexible spacecraft: Where's the beef? 11 p4217 N94-35866
Parameter estimation of the vibrational model for the SCOLE experimental facility 11 p4219 N94-35878
A case study in nonlinear dynamics and control of articulated spacecraft: The Space Station Freedom with a mobile remote manipulator system 11 p4220 N94-35879
A combined algorithm for minimum time slewing of flexible spacecraft 11 p4220 N94-35881
Control of the SCOLE configuration using distributed parameter models 11 p4221 N94-35885
An optimization-based approach for integrated controls-structures design of flexible spacecraft 11 p4221 N94-35889
Rational positive real approximations for LQG optimal compensators arising in active stabilization of flexible structures 11 p4222 N94-35892
Software for continuum modeling of controls-structures interactions 11 p4223 N94-35898
Input shaping for three-dimensional slew maneuvers of a precision pointing flexible spacecraft
[DE94-008937] 11 p4226 N94-36001
Neural network for positioning Space Station solar arrays
[NASA-TM-106656] 12 p4431 N94-36943

SPACECRAFT DEFENSE
An engineering code to analyze hypersonic thermal management systems 06 p2320 N94-23636

SPACECRAFT DESIGN
NT SATELLITE DESIGN
High temperature materials for hypersonic transport 01 p0056 N94-10003
Design and manufacturing of filament wound thrust cylinder 01 p0057 N94-10010
Aluminium-lithium forgings: Properties and potential satellite applications 01 p0058 N94-10021
Structural material, manufacture, and design requirements for high-temperature fasteners for space plane technologies 01 p0063 N94-10055
Planetary entry vehicle design for planned and potential ESA missions to Titan, Mars, and Earth return (FGE TN 51/92) 01 p0004 N94-10428
A CFD validation roadmap for hypersonic flows 01 p0005 N94-10439
Space Station Redesign Team: Final report to the Advisory Committee on the Redesign of the Space Station
[NASA-TM-109241] 01 p0042 N94-10663
An analysis of the modes and states for generic avionics
[NASA-CR-188253] 01 p0027 N94-10664
Space Station redesign option A: Modular buildup concept
[NASA-TM-108415] 01 p0043 N94-10808
Progress in multidisciplinary design optimization at NASA Langley
[NASA-TM-107754] 01 p0318 N94-10814
The guide to Design For On-orbit Spacecraft Servicing (DFOSS) manual: Producing a consensus document 01 p0421 N94-11575
The trial manufacture and test of critical components in docking mechanism
[NASDA-TMR-930005] 01 p0044 N94-12280
Conceptual studies report on lunar and planetary exploration
[NASDA-TK-SS0438] 01 p0481 N94-12323
Unmanned lunar exploration mission 01 p0482 N94-12325
Manned lunar exploration missions 01 p0482 N94-12326
Mars exploration missions 01 p0482 N94-12327
Dynamics of adaptive structures: Design through simulations
[NASA-CR-193724] 02 p0540 N94-13112
Spacecraft COst REduction Team (SCORE): TQM/CI on a massive scale 02 p0667 N94-13160
Study of a one-dimensional deployable structure employing telescopic members 02 p0531 N94-13282
HOPE conceptual design in FY 1991
[NASDA-CNT-930017] 02 p0535 N94-13600
Exploring Mars
[NASA-TM-109306] 02 p0842 N94-13613
Conceptual design on H-2 Orbiting Plane (HOPE)
[NASDA-CNT-930018] 02 p0535 N94-13656
The study on large space structure assembly technology: The study on deployable truss structure, part 1
[NASDA-TMR-930002] 02 p0541 N94-13658
The study on large space structure assembly technology: The study on deployable truss structure, part 2 and 3
[NASDA-TMR-930003-PT-2-3] 02 p0541 N94-13659
The study on test of docking mechanism system, part 1 and 2
[NASDA-TMR-930004-PT-1-2] 02 p0541 N94-13660
An improved approach for flight readiness certification: Methodology for failure risk assessment and application examples, volume 1
[NASA-CR-194498] 02 p0542 N94-14076
An improved approach for flight readiness certification: Methodology for failure risk assessment and application examples. Volume 2: Software documentation
[NASA-CR-194499] 02 p0542 N94-14077
An improved approach for flight readiness certification: Methodology for failure risk assessment and application examples. Volume 3: Structure and listing of programs
[NASA-CR-194500] 02 p0542 N94-14078
The concept study of the space transportation system HOPE in FY 1991
[NASDA-CNT-930016] 02 p0536 N94-14100
Research and development of space transportation systems in ISAS 02 p0537 N94-14277
The status of the HOPE concept study 02 p0537 N94-14280
Spaceplane program at NAL: System concept and related technology issues 02 p0537 N94-14281
An improved approach for flight readiness certification: Probabilistic models for flaw propagation and turbine blade failure. Volume 1: Methodology and applications
[NASA-CR-194496] 02 p0519 N94-14841
An improved approach for flight readiness certification: Probabilistic models for flaw propagation and turbine blade failure. Volume 2: Software documentation
[NASA-CR-194497] 02 p0519 N94-14842
The development and flight test of a deployable precision landing system for spacecraft recovery
[NASA-TM-4525] 02 p0537 N94-14853
Vertical-tail aerodynamic configuration of space shuttle orbiter
[AD-A267723] 03 p0879 N94-14941
Space Station resource reel
[NASA-TM-109673] 03 p0885 N94-15510
New perspectives for high accuracy SLR with second generation geodesic satellites 03 p0916 N94-15585
Flight testing of airbreathing hypersonic vehicles
[NASA-TM-4524] 03 p0886 N94-15753
Space transfer concepts and analyses for exploration missions, phase 4
[NASA-CR-193849] 03 p0882 N94-15831

Apparatus and method for producing an artificial gravitational field
[NASA-CASE-MSC-22021-1] 03 p0886 N94-15935
Lunar lander and return propulsion system trade study
[NASA-TP-3388] 03 p0925 N94-16496
ALS engine propellant effector system
[NASA-CR-194650] 03 p0926 N94-16590
Small spacecraft for planetary exploration 03 p0874 N94-17145
Feasibility study of a personal communications system IRIDIUM-like 03 p0893 N94-17165
Impact of advances in technology on future spacecraft design 03 p0894 N94-17171
Small satellite modular design and application prospect 03 p0894 N94-17173
Designing Space Station
[NASA-TM-109353] 04 p1334 N94-18922
Shuttle-C, the future is now
[NASA-TM-109355] 04 p1332 N94-18954
ISOBUS: A new versatile spacecraft platform using Shuttle small payloads 04 p1327 N94-19183
Activities of the Center for Space Construction
[NASA-CR-193717] 04 p1335 N94-19371
Cluster: Mission, Payload, and Supporting Activities
[ESA-SP-1159] 04 p1328 N94-19622
The Cluster spacecraft 04 p1330 N94-19635
Power conditioning system modelling for nuclear electric propulsion
[NASA-CR-191136] 05 p1846 N94-21179
TROPIX plasma interactions group report
[NASA-CR-191149] 05 p1666 N94-21864
Life cycle cost modeling of conceptual space vehicles
[NASA-CR-194813] 06 p2203 N94-23329
Soviet developments of planet rovers in period of 1964 - 1990 06 p2369 N94-23374
Past US studies and developments for planetary rovers 06 p2369 N94-23375
Integrating payload design, planning, and control in the Dutch Utilisation Centre 06 p2207 N94-23869
A packet-based concept for spacecraft command planning 06 p2504 N94-23873
Long term trending of engineering data for the Hubble Space Telescope 06 p2516 N94-23942
An opening mechanism for the scientific airlock outer hatch 06 p2360 N94-24027
Crew interface analysis: Selected articles on space human factors research, 1987 - 1991
[NASA-TM-104756] 06 p2433 N94-24185
Conceptual design of a two stage to orbit spacecraft
[NASA-CR-195536] 06 p2204 N94-24620
WISPER: Wirless Space Power Experiment
[NASA-CR-195538] 06 p2396 N94-24701
Supersonic aerodynamic characteristics of a circular body Earth-to-Orbit vehicle
[NASA-TM-4533] 06 p2170 N94-24716
Lunar transportation system
[NASA-CR-195540] 06 p2365 N94-24805
Near Earth asteroid rendezvous
[NASA-CR-195518] 06 p2195 N94-24808
Extended duration lunar lander
[NASA-CR-195527] 06 p2206 N94-24916
PERCIVAL mission to Mars
[NASA-CR-195541] 06 p2195 N94-24995
Preliminary design of a universal Martian lander
[NASA-CR-195529] 06 p2206 N94-25007
GRYPHON: Air launched space booster
[NASA-CR-195497] 06 p2199 N94-25022
MINOTAUR (Maryland's innovative orbital technologically advanced University rocket) 07 p2703 N94-25685
Asteroid exploration and utilization 07 p3080 N94-25697
Low-cost unmanned lunar lander 07 p2697 N94-25699
Low Earth orbit communications satellite 07 p2698 N94-25701
Project PARAS: Phased array radio astronomy from space 07 p3081 N94-25703
Project Minerva: A low-cost manned Mars mission based on indigenous propellant production 07 p2760 N94-25705
Project Ares 3 07 p2671 N94-25712
Minimum accommodation for aerobrake assembly, phase 2
[NASA-TM-107608] 07 p2692 N94-27774
Space transportation vehicle design evaluation using saturated designs 07 p2693 N94-27928
A pressure based charge control system for the DSPSE NiH2 CPV battery 07 p2863 N94-28127
Artemis common lunar lander. Phase 2: Study results for external review
[NASA-TM-109699] 07 p2692 N94-28205
ESTEC wiring test programme materials related properties 08 p3165 N94-28698
Code development for hypersonic real-gas flow simulations toward the design of space vehicles, part 2 08 p3125 N94-28966
The Solar Anomalous and Magnetospheric Particle Explorer (SAMPEX) yo-yo despin and solar array deployment mechanism 08 p3163 N94-29645
Analysis of EDP performance
[NASA-CR-195726] 08 p3420 N94-29945
The MACS-TSA applied in the ISO and SAX spacecraft projects
[PB94-126257] 08 p3170 N94-30857
LDEF Materials Results for Spacecraft Applications
[NASA-CP-3257] 09 p3591 N94-31012
Spacecraft contamination issues from LDEF: Issues for design 09 p3592 N94-31020
Model of spacecraft atomic oxygen and solar exposure microenvironments 09 p3593 N94-31021
The Second Annual International Space University Alumni Conference
[NASA-CP-3253] 09 p3598 N94-31425
Honeycomb sandwich structures: Vented versus unvented designs for space systems
[AD-A276713] 09 p3624 N94-32122
Virtual reality as a human factors design analysis tool: Macro-ergonomic application validation and assessment of the Space Station Freedom payload control area 10 p4100 N94-33620
An overview of Space Shuttle anthropometry and biomechanics research with emphasis on STS/Mir recumbent seat system design 10 p4101 N94-33629
Conceptual design and analysis of a dynamic scale model of the Space Station Freedom
[NASA-CR-4598] 10 p4070 N94-34236
Technology for small spacecraft
[NASA-CR-196041] 10 p4015 N94-34411
Space/ground systems as cooperating agents 10 p4127 N94-35072
Materials processing in space tasks. WBS task 5.4: Generic tasks
[NASA-CR-193979] 11 p4249 N94-35485
The control of satellites with microgravity constraints: The COMET Control System 11 p4207 N94-35632
GPHS-RTGs in support of the Cassini mission
[DE94-009994] 11 p4212 N94-35648
An optimization-based approach for integrated controls-structures design of flexible spacecraft 11 p4221 N94-35889
Approximate analysis for repeated eigenvalue problems with applications to controls-structure integrated design
[NASA-TP-3439] 12 p4397 N94-37502

SPACECRAFT DOCKING

Definition of spacecraft standard interfaces by the NASA Space Assembly and Servicing Working Group (SASWG) 01 p0048 N94-11574
Robotic servicing on Earth orbiting satellites 01 p0045 N94-11579
The trial manufacture and test of critical components in docking mechanism
[NASDA-TMR-930005] 01 p0044 N94-12280
Six degree of freedom
[NASA-TM-109295] 02 p0749 N94-13636
The study on test of docking mechanism system, part 1 and 2
[NASDA-TMR-930004-PT-1-2] 02 p0541 N94-13660
Space Station Common Berthing Mechanism, a multi-body simulation application 02 p0544 N94-14640
A mission concept of Phobos/Deimos exploration 03 p1287 N94-16387
Space Station/Orbiter berthing dynamics during an assembly flight
[NASA-TM-109049] 03 p1062 N94-17451
Automated rendezvous and capture demonstration study
[NASA-CR-192587] 04 p1331 N94-19366
A stereoscopic vision system with applications to automated docking and tracking
[AD-A270754] 04 p1333 N94-19765
Manned Mars mission on-orbit operations FTS capabilities assessment
[NASA-CR-189328] 06 p2430 N94-23080
Telerobotic rendezvous and docking vision system architecture
[NASA-CR-191329] 06 p2204 N94-23828
Docking mechanisms: An overview of different systems 06 p2357 N94-24004
Orbital docking system centerline color television camera system test
[NASA-TM-104783] 06 p2205 N94-24625
Hardware design of a grappling/docking device accommodating large lateral and angular misalignments 07 p2833 N94-25668
Autonomous rendezvous and docking for Space Station Freedom 07 p2684 N94-26286
Development and testing of the Automated Fluid Interface System 08 p3161 N94-29636
Local interaction control for space construction 08 p3170 N94-30960
Fuzzy logic application for modeling man-in-the-loop space shuttle proximity operations
[NASA-CR-188283] 09 p3835 N94-32359
A six degree of freedom, plume-fuel optimal trajectory planner for spacecraft proximity operations using an A* node search
[NASA-CR-188285] 09 p3601 N94-32388
Global Positioning System Synchronized Active Light Autonomous Docking System
[NASA-CASE-MFS-28853-1] 12 p4395 N94-36825
Evaluation of GPS position and attitude determination for automated rendezvous and docking missions
[NASA-CR-4614] 12 p4397 N94-37506
Permanent superconducting magnets for space applications
[NASA-CR-196293] 12 p4439 N94-37634

SPACECRAFT DOCKING MODULES

Hardware design of a grappling/docking device accommodating large lateral and angular misalignments 07 p2833 N94-25668

SPACECRAFT ELECTRONIC EQUIPMENT

Multiplexed and distributed optical fibre sensors 01 p0064 N94-10065
Satellite observations of red tide events: Plans for EESI 01 p0191 N94-11899
METEOSAT second generation programme SEVIRI: An enhanced visible and IR radiometer for meteorology 01 p0212 N94-12667
Study of the intermateability of Cannon and Souriau subminiature connectors
[CNES-NT-132] 02 p0624 N94-13951
Mongoose: Creation of a Rad-Hard MIPS R3000 05 p1754 N94-21090
Advanced mobile satellite communications using COMETS satellite in MM-wave and Ka-band 06 p2288 N94-22829
Aspects of the circuit board thermal design
[VTT-PUBS-132] 07 p2779 N94-25644
Time maintenance system for the BMDO MSX spacecraft 08 p3171 N94-30672
Characteristics of III-V semiconductor devices at high temperature
[NASA-TM-106574] 09 p3697 N94-33052
Effects of combined stressing on the electrical properties of film and ceramic capacitors
[NASA-TM-106605] 11 p4257 N94-35249
Space Generic Open Avionics Architecture (SGOAA) standard specification
[NASA-CR-188290] 12 p4387 N94-36933

SPACECRAFT ENVIRONMENTS

Living well in space: Monitoring environment
[NASA-TM-109537] 03 p1120 N94-15368
Precise measurement and utilization of acceleration data 03 p0923 N94-16100
Environmental control and life support
[ESA-PSS-03-40-ISSUE-1] 04 p1513 N94-19442
Cosmos 2229
[NASA-CR-194734] 05 p1895 N94-20338
Toxicity of thermal degradation in a manned space environment 05 p1664 N94-21403
Connector mechanisms in compliance with extreme space conditions 06 p2360 N94-24025
The radiation design handbook
[ESA-PSS-01-609-ISSUE-1] 07 p2696 N94-27397
Annals of the Research Inst. of Environmental Medicine, Nagoya Univ., volume 44
[REPT-44-VOL-44] 07 p2911 N94-27442
Comparative measurement of visual stability in cosmic space: Onboard experiment and pre-flight activities 07 p2916 N94-27463
Analysis of selected materials flown on interior locations of the Long Duration Exposure Facility
[NASA-CR-4586] 08 p3175 N94-29458
Modeling of LDEF contamination environment 09 p3592 N94-31019
Atmosphere quality standards in manned space vehicles
[ESA-PSS-03-401-ISSUE-1] 09 p3802 N94-31224
Technical assessment of Mir-1 life support hardware for the international space station
[NASA-TM-108441] 09 p3803 N94-31380
Spacecraft environmental anomalies expert system
[AD-A277962] 09 p3612 N94-33262
Safety concerns for first entry operations of orbiting spacecraft 10 p4102 N94-33662
Characterization of spacecraft and environmental disturbances on a SmallSat
[NASA-CR-194915] 12 p4396 N94-36990

SPACECRAFT EQUIPMENT

NT SPACECRAFT ELECTRONIC EQUIPMENT

Design of multisample, multistep phase partitioning apparatus for use on Space Shuttle Spacelab, and Spacelab missions 01 p0108 N94-10120
The Second Workshop on Refrigerating System Utilization Onboard the JEM
[NASDA-CON-930001] 01 p0129 N94-11831
Development of space refrigerator 01 p0129 N94-11833
Studies on refrigerator sensors and cooling section interface 01 p0129 N94-11834
Trend of miniature refrigerator utilization in earth observation area 01 p0130 N94-11835
Satellite observation of atmospheric tracer components: JEM/POP 01 p0130 N94-11836
Submillimeter wave observation experiment of Earth atmosphere with SIS mixer 01 p0130 N94-11837
Refrigerator utilization in infrared astronomy 01 p0130 N94-11838
Study on various cryogenic refrigeration cycles using all purpose refrigerators 01 p0130 N94-11839
Development test on 2 K cooling systems 01 p0130 N94-11840
Generation of superfluid He by G-M cycle cryogenic refrigerator 01 p0130 N94-11841
Development of 4 K refrigerator using highly efficient heat accumulating reservoir 01 p0130 N94-11842
Utilization of superconductivity in the area of space 01 p0131 N94-11843
Flight data analysis of Japanese Earth Resources Satellite-1 (JERS-1)
[NASDA-CNT-930004] 01 p0245 N94-12279
The trial manufacture and test of critical components in docking mechanism
[NASDA-TMR-930005] 01 p0044 N94-12280
Conceptual studies report on lunar and planetary exploration
[NASDA-TK-SS0438] 01 p0481 N94-12323
Unmanned lunar exploration mission 01 p0482 N94-12325
Manned lunar exploration missions 01 p0482 N94-12326
Mars exploration missions 01 p0482 N94-12327
The Third Workshop on Two Phase Fluid Experiment in the Space Environment
[NASDA-CON-930002] 01 p0161 N94-12547
Summary of studies on JEM utilization experiment projects 01 p0161 N94-12548
Devices related for thermal control systems used in microgravity 01 p0162 N94-12553
Research and development of cold plate for two phase fluid loop thermal control system 01 p0162 N94-12555
An experimental study of tether reel system: A laboratory model
[NAL-TR-1176T] 02 p0539 N94-12943
Structural design of hexa-link truss deployable antenna 02 p0529 N94-13269
Thermal distortion measurement of TETRUS type thermal test model of large deployable antenna for mobile communications satellite 02 p0529 N94-13270
Development of modular cable mesh deployable antenna 02 p0530 N94-13274
Trial manufacture model and in-space verification method of deployable antenna 02 p0530 N94-13278
Survey and study on Environmental Control and Life Support (ECLS) technologies, part 2
[NASDA-CNT-930012-PT-2] 02 p0737 N94-13472
The study on test of docking mechanism system, part 1 and 2
[NASDA-TMR-930004-PT-1-2] 02 p0541 N94-13660
Future TRMM follow-on mission 02 p0691 N94-14228
Pre-phase a study report of lunar polar orbiter
[NASDA-TK-SS0440] 03 p0873 N94-15000
Development of Japanese Earth Resources Satellite-1 (JERS-1; FUYO-1) and it's operational results
[NASDA-SPP-930001] 03 p0884 N94-15001
STS-36 crew EVA prep and post-training, bailout exercises, final bench review
[NASA-TM-109498] 03 p1137 N94-15462
Observations by ERS-1 start 08 p3327 N94-28933
Outline of JERS-1 system 08 p3330 N94-29220
Observatory system of Earth Resources Satellite-1 08 p3330 N94-29221
Pyrotechnic shock: Devices in pyrotechnic environment qualification logic
[REPT-932-430-108] 08 p3225 N94-29429
Development status of the Communications and Broadcasting Engineering Test Satellite (COMETS)
[JTN-94-80545] 08 p3169 N94-30811
Development status of COMETS missions
[JTN-94-80544] 08 p3170 N94-30932
Implementation of heaters on thermally actuated spacecraft mechanisms 09 p3607 N94-33320
Payload holddown and release mechanism 09 p3607 N94-33321
Advanced release technologies program 09 p3607 N94-33322
Preliminary design for a reverse Brayton cycle cryogenic cooler
[NASA-CR-189341] 12 p4461 N94-36805

SPACECRAFT GLOW
A high resolution ultraviolet Shuttle glow spectrograph 04 p1325 N94-19174

SPACECRAFT GUIDANCE
NT SATELLITE GUIDANCE
HOPE real time flight operations analyses for return to earth phase, part B
[NASDA-CNT-930011] 02 p0535 N94-13599
HOPE real time flight operations analyses for return to earth phase, part A
[NASDA-CNT-930010-PT-A] 02 p0535 N94-13645
Guidance law development for aeroassisted transfer vehicles using matched asymptotic expansions
[NASA-CR-194523] 02 p0508 N94-14538
Neighboring extremal guidance for systems with piecewise linear control using time as the reference variable
[AD-A267942] 03 p0874 N94-17010
A guidance and navigation system for two spacecraft rendezvous in translunar halo orbit
[AD-A267498] 03 p0898 N94-17368
A real-time navigation monitoring expert system for the Space Shuttle Mission Control Center 06 p2202 N94-23921
Space Station Freedom ground data system: Design and operations 06 p2518 N94-23957
Satellite autonomous navigation and orbit determination using magnetometers 06 p2156 N94-24258
Intelligent systems and advanced user interfaces for design, operation, and maintenance of command management systems
[NASA-CR-195172] 06 p2459 N94-24797
Hardware design of a grappling/docking device accommodating large lateral and angular misalignments 07 p2833 N94-25668
High performance flight computer developed for deep space applications 07 p2949 N94-26718
Using formal specification in the Guidance and Control Software (GCS) experiment. Formal design and verification technology for life critical systems
[NASA-CR-194884] 07 p2956 N94-28267
Fault tolerant testbed evaluation, phase 1
[NASA-CR-188275] 08 p3171 N94-29035
Micro guidance and control technology overview 08 p3144 N94-29772
Miniature wide field-of-view star trackers for spacecraft attitude sensing and navigation 08 p3144 N94-29794
A guidance and navigation system for two spacecraft rendezvous in translunar halo orbit 08 p3142 N94-29837
Global Positioning System Synchronized Active Light Autonomous Docking System
[NASA-CASE-MFS-28853-1] 12 p4395 N94-36825
Progress in navigation filter estimate fusion and its application to spacecraft rendezvous
[NASA-TM-104794] 12 p4392 N94-37386
Evaluation of GPS position and attitude determination for automated rendezvous and docking missions
[NASA-CR-4614] 12 p4397 N94-37506
Advanced information processing system: Hosting of advanced guidance, navigation and control algorithms on AIPS using ASTER
[NASA-CR-194960] 12 p4499 N94-37583

SPACECRAFT INSTRUMENTS
NT SATELLITE INSTRUMENTS
NT SPACECRAFT POSITION INDICATORS
The advanced fluid physics module: How to achieve scientific goals for Spacelab D2 01 p0039 N94-10136
Data processing units for eight magnetospheric particle and field sensors
[AD-A264403] 01 p0276 N94-11463
The Los Alamos neutron spectrometer for the Lunar Scout-1 mission 01 p0172 N94-12038
Flight data analysis of Japanese Earth Resources Satellite-1 (JERS-1)
[NASDA-CNT-930004] 01 p0245 N94-12279
Conceptual studies report on lunar and planetary exploration
[NASDA-TK-SS0438] 01 p0481 N94-12323
Unmanned lunar exploration mission 01 p0482 N94-12325
Manned lunar exploration missions 01 p0482 N94-12326
Mars exploration missions 01 p0482 N94-12327
Perspective on the National Aero-Space Plane Program instrumentation development
[NASA-TM-4505] 02 p0516 N94-13256
Phase aligner for the Electronically Scanned Thinned Array Radiometer (ESTAR) instrument
[NASA-TM-4518] 02 p0623 N94-13878
Development of an advanced spacecraft tandem mass spectrometer
[NASA-CR-194195] 02 p0545 N94-13953
Future TRMM follow-on mission 02 p0691 N94-14228
Pre-phase a study report of lunar polar orbiter
[NASDA-TK-SS0440] 03 p0873 N94-15000
Proceedings of an ESA Symposium on Photon Detectors for Space Instrumentation
[ESA-SP-356] 03 p0899 N94-15025
Background suppression techniques in germanium detectors 03 p0899 N94-15026
Discrete CMT infrared detectors for space application, from ISSR to second generation Meteosat and MIPAS 03 p0905 N94-15065
An adiabatic demagnetisation refrigerator with a mechanical pre-cooler for space applications 03 p0906 N94-15070
Extrinsic photoconductor detectors for the wavelength range 2 microns to 240 microns 03 p0906 N94-15073
The detector assemblies of ISOPHOT and the spectrometers ISO-SWS and ISO-LWS 03 p0906 N94-15074
Ionising radiation-induced effects in doped germanium FIR photoconductors 03 p0907 N94-15077
In orbit adiabatic demagnetization refrigeration for bolometric and microcalorimetric detectors 03 p0907 N94-15079
CCD's on high resistivity bulk silicon for x ray spectroscopy on XMM 03 p0907 N94-15080
Characterization of detectors and calibration of the ISOPHOT experiment 03 p0907 N94-15082
Characteristics of the ISO short wavelength spectrometer detectors 03 p0908 N94-15084
Absolute Radiometric Measurements in Space: ARMS 03 p0908 N94-15085
IR detectors and subsystems for space applications 03 p0909 N94-15091
Infrared detector annealing and calibration with IR-laser diodes 03 p0909 N94-15092
Performance of the position-sensitive proportional counters of the Yohkoh Bragg crystal spectrometer 03 p0909 N94-15094
Workshop on advanced technologies for planetary instruments
[NASA-CR-194585] 03 p1032 N94-15797
Precise measurement and utilization of acceleration data 03 p0923 N94-16100
The Clementine instrument complement 03 p1086 N94-16370
Principal investigators data package for Project Initiation Conference (PIC): EUVS sounding rocket no. 36.117CL. Target: Venus
[NASA-CR-194663] 03 p0923 N94-17126
Pioneer Venus data analysis for the retarding potential analyzer
[NASA-CR-194673] 03 p1297 N94-17292
A packet switched communications system for GRO 05 p1744 N94-21345
Database of proposed payloads and instruments for SEI missions 05 p1811 N94-22432
Distributed science operations for JPL planetary missions 06 p2500 N94-23850
A packet-based concept for spacecraft command planning 06 p2504 N94-23873
An Earth albedo model: A mathematical model for the radiant energy input to an orbiting spacecraft due to the diffuse reflectance of solar radiation from the Earth below
[NASA-TM-104596] 06 p2195 N94-24497
Technology development in space projects
[VTT-TIED-1438] 07 p2682 N94-26249
The radiation design handbook
[ESA-PSS-01-609-ISSUE-1] 07 p2696 N94-27397
Outline of JERS-1 system 08 p3330 N94-29220
Future manned systems advanced avionics study
[NASA-CR-188277] 08 p3150 N94-29377
Three high duty cycle, space-qualified mechanisms 08 p3162 N94-29642
Miniature wide field-of-view star trackers for spacecraft attitude sensing and navigation 08 p3144 N94-29794
Ground control system for the midcourse space experiment UTC clock 08 p3474 N94-30674
Space acceleration measurement system
[NASA-TM-109754] 09 p3913 N94-31807
Hubble Space Telescope faint object spectrograph instrument handbook, version 5.0
[NASA-CR-189367] 12 p4546 N94-36794
Hubble Space Telescope faint object camera instrument handbook (Post-COSTAR), version 5.0
[NASA-CR-189365] 12 p4546 N94-36795

A high precision gamma ray spectrometer for the Mars 1994 mission
[DE94-013133] 12 p4550 N94-37293

SPACECRAFT LANDING
NT LUNAR LANDING
NT MARS LANDING
NT PLANETARY LANDING
Launch, entry, and landing resource clip
[NASA-TM-109297] 02 p0535 N94-13638
STS-33 launch and landing clip
[NASA-TM-109468] 02 p0536 N94-14734
Return to Space Mission: The STS-26 crew report
[NASA-TM-109568] 03 p0880 N94-15317
STS-27 crew presentation clip
[NASA-TM-109551] 03 p0881 N94-15403
STS-26 missions highlight resource tape
[NASA-TM-109559] 03 p0881 N94-15407
STS-35 mission highlights resource tape
[NASA-TM-109501] 03 p0881 N94-15465
A mission concept of Phobos/Deimos exploration
03 p1287 N94-16387
Single STAGE Rocket Technology (SSRT) DC-X test program environmental assessment
[AD-A265940] 04 p1337 N94-17879
Tetrahedral lander
[NASA-CASE-MSC-22082-1] 05 p1658 N94-20590
BAG: A code for predicting the performance of a gas bag impact attenuation system for the Pathfinder lander
[DE94-003688] 08 p3165 N94-28477
Landing gear energy absorption system
[NASA-CASE-MSC-22277-1] 08 p3300 N94-29448
Further development and flight test of an autonomous precision landing system using a parafoil
[NASA-TM-4599] 10 p3983 N94-33995

SPACECRAFT LAUNCHING
Exergy decrease in shock waves and boundary layers of space launch vehicles
[AD-A265272] 01 p0042 N94-10493
Parametric analysis of atmospheric processes
[NASA-CR-192523] 01 p0347 N94-10757
Preliminary analysis of the benefits derived to US Air Force spacecraft from on-orbit refueling
01 p0038 N94-11567
The National Launch System Advanced Development Program: A brief overview 01 p0040 N94-11576
Special investigation report: Commercial space launch incident, launch procedure anomaly orbital sciences corporation PEGASUS/SCD-1, 80 nautical miles east of Cape Canaveral, Florida, February 9, 1993
[PB93-917003] 01 p0040 N94-11893
Flight data analysis of Japanese Earth Resources Satellite-1 (JERS-1)
[NASDA-CNT-930004] 01 p0245 N94-12279
Proceedings of the 11th Space Surveillance Workshop, volume 1
[AD-A265120] 02 p0531 N94-13358
Preliminary nuclear safety assessment of the NEPST (Topaz 2) space reactor program
[DE93-012853] 02 p0551 N94-13514
STS-32 mission highlights resource tape
[NASA-TM-109291] 02 p0531 N94-13631
HL-20 personnel launch system
[NASA-TM-109292] 02 p0504 N94-13632
Launch, entry, and landing resource clip
[NASA-TM-109297] 02 p0535 N94-13638
STS-28 crew presentation clip
[NASA-TM-109298] 02 p0531 N94-13640
STS-33 launch and landing clip
[NASA-TM-109468] 02 p0536 N94-14734
COBE video news
[NASA-TM-109598] 03 p0987 N94-15292
Return to Space Mission: The STS-26 crew report
[NASA-TM-109568] 03 p0880 N94-15317
Mission San Marco
[NASA-TM-109442] 03 p0878 N94-15341
STS-29 mission highlights resource tape
[NASA-TM-109542] 03 p0880 N94-15373
STS-27 crew presentation clip
[NASA-TM-109551] 03 p0881 N94-15403
STS-26 missions highlight resource tape
[NASA-TM-109559] 03 p0881 N94-15407
Long Duration Exposure Facility
[NASA-TM-109427] 03 p0885 N94-15497
RADARSAT program 03 p0898 N94-15893
Liquid hydrogen and liquid oxygen feedline passive recirculation analysis
[TABES PAPER 93-620] 03 p1031 N94-16145
The closing window of opportunity: Addressing the US space launch vehicle crisis
[TABES PAPER 93-640] 03 p0878 N94-16148
Space Propulsion Synergy Group ETO technology assessments
[TABES PAPER 93-641] 03 p0929 N94-16149
Prototype instrumentation and design studies
[AD-A266402] 03 p0882 N94-16530
Small Satellites Systems and Services
[ISBN-2-85-428327-9] 03 p0888 N94-17131
Impact of launching uncertainties on the visibility of communication satellite constellations without orbit control 03 p0889 N94-17135
Small launchers (current and future projects in the world) 03 p0878 N94-17137
Small satellite constellation deployment strategies
03 p0878 N94-17138
NEXT launch system 03 p0878 N94-17141
Role and development of small satellite missions in space plasma physics 03 p0891 N94-17149
Satellite situation report, volume 31, number 1
[NASA-TM-105088] 03 p0898 N94-17584
Single STAGE Rocket Technology (SSRT) DC-X test program environmental assessment
[AD-A265940] 04 p1337 N94-17879
An evolutionary approach to space launch commercialization
[AD-A269861] 04 p1331 N94-18411
Process and apparatus for the release of a prestress initially applied to a mechanism such as a bearing on board a space vehicle
[CA-PATENT-APPL-SN-2,020,909] 05 p1824 N94-21142
Specialized data analysis for the Space Shuttle Main Engine and diagnostic evaluation of advanced propulsion system components
[NASA-CR-194720] 05 p1656 N94-21813
Debris/ice/TPS assessment and integrated photographic analysis for Shuttle Mission STS-51
[NASA-TM-109189] 05 p1656 N94-21884
Spaceplane flight simulation: Project definition
[PB93-211399] 05 p1651 N94-22094
Channel and terminal description of the ACTS mobile terminal 06 p2284 N94-22802
Hurricane risk assessment: Rollback or ride out
06 p2416 N94-23248
GPHS-RTG's in support of the Cassini mission
[DE94-001445] 06 p2218 N94-23459
Galileo spacecraft anomaly and safing recovery
06 p2207 N94-23864
A MOS for all seasons 06 p2505 N94-23879
HISPASAT launch and early operations phases: Computation and monitoring of geostationary satellite positioning 06 p2514 N94-23928
Preloaded launch locking devices for SILEX
06 p2358 N94-24008
Reach performance while wearing the Space Shuttle launch and entry suit during exposure to launch accelerations 06 p2436 N94-24204
Design of an airborne launch vehicle for an air launched space booster
[NASA-CR-195534] 06 p2198 N94-24860
Project Columbiad: Reestablishment of human presence on the Moon 07 p2689 N94-25687
Comet nucleus and asteroid sample return missions
07 p2689 N94-25692
Access to space study
[NASA-TM-109693] 07 p2685 N94-27151
Debris/ice/TPS assessment and integrated photographic analysis for Shuttle mission STS-60
[NASA-TM-109193] 07 p2692 N94-27956
Lunar Transportation Facilities and Operations Study, option 2
[NASA-CR-195701] 07 p3109 N94-27983
Heavy-lift vehicle-launched Space Station method and apparatus
[NASA-CASE-MSC-21760-1] 08 p3160 N94-29369
Advanced microfabrication technologies for microspacecraft 08 p3171 N94-29782
Neural network application to Particle Impact Noise Detection 08 p3437 N94-29840
Fission-activated laser as primary power for CW laser propulsion
[DE94-006138] 08 p3295 N94-30367
Measurement of the frequency stability of responders in aircraft 08 p3261 N94-30673
The TOPAZ 2 space reactor response under accident conditions
[DE94-004998] 08 p3498 N94-30847
Scattering of a random acoustic field by an infinite cylinder: Application to the modelization of the acoustic environment of the 'Ariane 5' launcher scale-model using experimental data
[ONERA-NT-1993-11] 09 p3860 N94-31226
DOD space based requirements: Increasing DOD access to space
[AD-A276874] 09 p3601 N94-32211
Independent safety assessment of the Topaz-2 space nuclear reactor power system
[DE94-008653] 09 p3877 N94-32879
Chronology of KSC and KSC related events for 1993
[NASA-TM-109196] 09 p3966 N94-33072
Advanced transportation system study: Manned launch vehicle concepts for two way transportation system payloads to LEO
[NASA-CR-193951] 09 p3608 N94-33100
Design, development, and testing of a lightweight optical sensor cover system 09 p3604 N94-33302
Flight controller alertness and performance during MOD shiftwork operations 10 p4098 N94-33624
Application of statistical process control and process capability analysis procedures in orbiter processing activities at the Kennedy Space Center
10 p4068 N94-33626
Emergency medical services
10 p4096 N94-33644
KSC wildlife show
[NASA-TM-109808] 10 p4094 N94-33770
Shuttle 51L: Challenger
[NASA-TM-109835] 10 p4012 N94-33788
Launch-pad abort capabilities of the HL-20 lifting body
[NASA-TM-4550] 10 p4007 N94-34687
Advanced transportation system study: Manned launch vehicle concepts for two way transportation system payloads to LEO. Program cost estimates document
[NASA-CR-193953] 10 p4013 N94-34912
Geostationary space launch vehicles and the US dilemma 11 p4210 N94-35377
A shadowgraph study of Space Transportation System (STS): The Space Shuttle Launch Vehicle (SSLV)
[NASA-RP-1341] 12 p4382 N94-36741
Optimal control theory determination of feasible return-to-launch-site aborts for the HL-20 Personnel Launch System vehicle
[NASA-TP-3449] 12 p4396 N94-37260

SPACECRAFT LUBRICATION
Soft x ray photoelectron spectroscopy study of the interaction of Cr with MoS2(0001)
[AD-A276916] 09 p3635 N94-32233
A comparison of the performance of solid and liquid lubricants in oscillating spacecraft ball bearings
09 p3606 N94-33311
Development of long-life, low-noise linear bearings for atmospheric interferometry 09 p3606 N94-33312
The preliminary evaluation of liquid lubricants for space applications by vacuum tribometry
09 p3606 N94-33313
Properties of perfluoropolyethers for space applications
[NASA-TM-106616] 12 p4426 N94-37520
Evaluation of seals and lubricants used on the Long Duration Exposure Facility
[NASA-CR-4604] 12 p4399 N94-37614

SPACECRAFT MAINTENANCE
Definition of spacecraft standard interfaces by the NASA Space Assembly and Servicing Working Group (SASWG) 01 p0348 N94-11574
STS-31 crew training: firefighting, food tasting, EVA prep and post
[NASA-TM-109484] 03 p0876 N94-15451
Plasma arc welding repair of space flight hardware
[TABES PAPER 93-603] 03 p1049 N94-16139
Robotics
[NASA-TM-109351] 04 p1332 N94-18920
Graphical programming: A systems approach for telerobotic servicing of space assets
[DE93-019016] 06 p2472 N94-23201
Life cycle cost modeling of conceptual space vehicles
[NASA-CR-194813] 06 p2203 N94-23329
Ground operation of robotics on Space Station Freedom 06 p2371 N94-23841
A simulation system for Space Station extravehicular activity 06 p2434 N94-24192
Illumination requirements for operating a space remote manipulator 06 p2435 N94-24195
Weld joint concepts for on-orbit repair of Space Station Freedom fluid system tube assemblies
06 p2371 N94-24427
A comparative evaluation plan for the Maintenance, Inventory, and Logistics Planning (MILP) System Human-Computer Interface (HCI)
06 p2588 N94-25373
Space Habitat, assembly and repair facility
07 p2691 N94-25696
Orbit transfer rocket engine technology program
[AD-A277021] 07 p2702 N94-26542
On-orbit spacecraft servicing: An element in the evolution of space robotics applications
[AIAA PAPER 94-1236-CP] 08 p3448 N94-30583
Development of an interchangeable end effector mechanism for the Ranger telerobotic vehicle
09 p3604 N94-33297
Task network models in the prediction of workload imposed by extravehicular activities during the Hubble Space Telescope servicing mission
10 p4101 N94-33627
A comparison of paper and computer procedures in a Shuttle flight environment 10 p4101 N94-33634

On-orbit NDE: A novel approach to tube weld inspection 10 p4066 N94-33664
Graphical programming: A systems approach for telerobotic servicing of space assets 10 p4066 N94-33666
Diagnosing anomalies of spacecraft for space maintenance and servicing 10 p4015 N94-33667
The SCRAM tool-kit 10 p4066 N94-33668
SpaceHab 1 maintenance experiment 10 p4015 N94-33669
Robotic technologies of the Flight Telerobotic Servicer (FTS) including fault tolerance 10 p4067 N94-34034
EVA-SCRAM operations 10 p4102 N94-34035
Design and simulation of EVA tools for first servicing mission of HST
[NASA-CR-196030] 11 p4298 N94-35266
Space Shuttle: Incomplete data and funding approach increase cost risk for upgrade program. Report to Congressional Requesters
[GAO/NSIAD-94-23] 12 p4392 N94-37026
Operations and support cost modeling of conceptual space vehicles
[NASA-CR-196299] 12 p4397 N94-37580

SPACECRAFT MANEUVERS
NT ORBITAL MANEUVERS
Optimizing interplanetary trajectories with deep space maneuvers
[NASA-CR-4546] 02 p0532 N94-14851
Constant-thrust orbit-raising transfer charts
[AD-A269088] 04 p1334 N94-18718
XRTD: An X-Windows based, real-time radiometric display and analysis system 06 p2305 N94-23922
Kalman filtering applied to real-time monitoring of apogee maneuvers 06 p2196 N94-23923
OARE flight maneuvers and calibration measurements on STS-58
[NASA-TM-109093] 09 p3613 N94-32924

SPACECRAFT MODELS
Results of wind tunnel tests of an ASRM configured 0.03 scale Space Shuttle integrated vehicle model (47-OTS) in the AEDC 16-foot transonic wind tunnel, volume 2
[NASA-CR-185697] 02 p0534 N94-12965
Results of wind tunnel tests of an ASRM configured 0.03 scale Space Shuttle integrated vehicle model (47-OTS) in the AEDC 16-foot Transonic wind tunnel (IA613A), volume 1
[NASA-CR-185696] 02 p0534 N94-13191
HL-20 personnel launch system
[NASA-TM-109292] 02 p0504 N94-13632
Failure modes of reduced-order orbit determination filters and their remedies 02 p0532 N94-14373
Real-time dynamics simulation of the Cassini spacecraft using DARTS. Part 1: Functional capabilities and the spatial algebra algorithm 02 p0680 N94-14638
Space Station Freedom
[NASA-TM-109636] 03 p1031 N94-15247
Cost-effective test methods for Shuttle payloads
[TABES PAPER 93-651] 03 p0883 N94-16151
A virtual environment for satellite modeling and orbital analysis in a distributed interactive simulation
[AD-A274114] 07 p2694 N94-25904
Wind tunnel testing and research
[NASA-CR-188273] 08 p3156 N94-29052
Attitude dynamics of spinning rockets in space with internal mass motion 09 p3601 N94-31802
Configurational evolution dynamics and stability during in-situ development of large orbiting spacecraft
[AD-A280482] 12 p4397 N94-37351

SPACECRAFT MODULES
NT COMMAND MODULES
NT LANDING MODULES
NT LUNAR LANDING MODULES
NT SIM
The advanced fluid physics module: How to achieve scientific goals for Spacelab D2 01 p0039 N94-10136
The Japanese Space Station utilization plan 03 p0977 N94-16074
An analysis of the dynamic response of the Space Station Freedom due to a module perforation by an orbital debris particle impact
[TABES PAPER 93-653] 03 p0899 N94-16154
Small satellite modular design and application prospect 03 p0894 N94-17173
Assured crew return vehicle post landing configuration design and test 07 p2697 N94-25671
First lunar outpost 07 p2943 N94-25694
Calibration and initial testing of a new hydraulic simulator
[AD-A280632] 12 p4390 N94-37163

SPACECRAFT MOTION
Lunar Scout Two spacecraft gravity experiment 01 p0459 N94-12152
Sloshing dynamics on rotating helium dewar tank
[NASA-CR-194403] 02 p0637 N94-13959
Dynamic characterization of a lightweight, highly maneuverable spacecraft using modal and finite element analyses
[DE93-018095] 04 p1335 N94-18942
Superfluid helium sloshing dynamics induced oscillations and fluctuations of angular momentum, force and moment actuated on spacecraft driven by gravity gradient or jitter acceleration associated with slew motion
[NASA-CR-193928] 07 p2799 N94-27931

SPACECRAFT ORBITAL ASSEMBLY
U ORBITAL ASSEMBLY

SPACECRAFT ORBITS
NT GEOSYNCHRONOUS ORBITS
NT INTERPLANETARY TRANSFER ORBITS
NT PARKING ORBITS
NT POLAR ORBITS
NT SATELLITE ORBITS
NT TRANSFER ORBITS
On-orbit servicing for USAF space missions: A phased development approach 01 p0348 N94-11571
Lunar Scout Two spacecraft gravity experiment 01 p0459 N94-12152
Exploration planning in the context of human exploration and development of the Moon 01 p0474 N94-12229
The Cluster orbit and mission scenario 04 p1330 N94-19637
Combined contamination and space environmental effects on solar cells and thermal control surfaces
[NASA-TM-106592] 09 p3617 N94-33022
High Earth orbit design for lunar assisted small Explorer class missions 11 p4202 N94-35608
Automated maneuver planning using a fuzzy logic algorithm 11 p4203 N94-35610
Space Shuttle orbit determination using empirical force modeling of attitude maneuvers for the German MOMS-02/D2 mission 11 p4207 N94-35634

SPACECRAFT PERFORMANCE
Progress in multidisciplinary design optimization at NASA Langley
[NASA-TM-107754] 01 p0318 N94-10814
Flight data analysis of Japanese Earth Resources Satellite-1 (JERS-1)
[NASDA-CNT-930004] 01 p0245 N94-12279
ECS: Eighth year in orbit
[ESA-BR-82] 02 p0543 N94-14352
The flight performance of the Galileo orbiter USO 02 p0611 N94-14398
International testing of a Mars rover prototype 03 p1273 N94-16312
Orbital Signature Analyzer (OSA): A spacecraft health/safety monitoring and analysis tool 06 p2203 N94-23947
Nickel cadmium battery operations on-orbit: Trials, tribulations, and success on the Upper Atmosphere Research Satellite 07 p2862 N94-28120
Spacecraft contamination issues from LDEF: Issues for design 09 p3592 N94-31020
Space flight risk data collection and analysis project: Risk and reliability database
[NASA-CR-195879] 09 p3603 N94-32494

SPACECRAFT POSITION INDICATORS
Satellite autonomous navigation and orbit determination using magnetometers 06 p2156 N94-24258

SPACECRAFT POWER SUPPLIES
Fully coupled neutronic and hydrodynamic analysis of space nuclear reactor reentry accidents
[DE93-005459] 01 p0372 N94-10890
Investigation of alternate power source for Space Shuttle Orbiter hydraulic system
[NASA-CR-193229] 01 p0046 N94-10911
A facility for testing 10- to 100-kWe space power reactors
[DE92-040420] 01 p0372 N94-11296
Experimental and theoretical investigations of Cs-Ba vapor tacitron inverter for power conditioning in space power systems
[DE93-012971] 01 p0048 N94-11372
Polyimide based amorphous silicon solar modules 01 p0049 N94-11390
Flexible polycrystalline thin-film photovoltaics for space applications 01 p0050 N94-11393
Recent developments in refractive concentrators for space photovoltaic power systems 01 p0052 N94-11402
NASDA activities in space solar power system research, development and applications 01 p0054 N94-11413
An experimental study of tether reel system: A laboratory model
[NAL-TR-1176T] 02 p0539 N94-12943
Spacecraft COst REduction Team (SCORE): TQM/CI on a massive scale 02 p0667 N94-13160
A photovoltaic catenary-tent array for the Martian surface
[NASA-TM-106306] 02 p0621 N94-13194
NASA handbook for nickel-hydrogen batteries
[NASA-RP-1314] 02 p0550 N94-13265
Power converters for the 120 V bus supply control
[CNES-NT-134] 02 p0622 N94-13552
Futurepath 2
[NASA-TM-109285] 02 p0518 N94-13623
The Large Area Pulsed Solar Simulator (LAPSS)
[NASA-CR-194507] 02 p0703 N94-13940
Large space structures and systems in the space station era: A bibliography with indexes (supplement 05)
[NASA-SP-7085(05)] 02 p0543 N94-14411
Small scale adaptive optics experiment systems engineering
[NASA-CR-194419] 02 p0793 N94-14548
Primary and secondary electrical space power based on advanced PEM systems
[DE93-012643] 02 p0553 N94-14689
Results of an electrical power system fault study (CDDF)
[NASA-TP-3413] 03 p0884 N94-15007
SPDE/SPRE final summary report
[NASA-CR-187086] 03 p0924 N94-15482
The 1987 Goddard Space Flight Center Battery Workshop
[NASA-CP-3236] 03 p1012 N94-17062
Lattice-mismatched In(0.40)Al(0.60)As window layers for indium phosphide solar cells
[NASA-TM-106255] 03 p1013 N94-17113
Arsene GaAs solar array 03 p0894 N94-17174
Small satellite nickel-hydrogen and nickel-metal hydride power applications 03 p0895 N94-17175
A power system for a microsatellite 03 p0895 N94-17176
The space technology research vehicle: Development status 03 p0896 N94-17183
Overview of the solar dynamic ground test demonstration program
[NASA-TM-106296] 03 p0928 N94-17256
High voltage conductors in spacecraft
[AD-A267268] 03 p0897 N94-17266
Mission needs and system commonality for space nuclear power and propulsion
[DE93-016557] 04 p1337 N94-17863
Ultrasonic technique for inspection of GPHS capsule girth weld integrity
[DE93-040072] 04 p1448 N94-19189
Rationale for the power standard
[ESA-PSS-02-10-VOL-2-ISSUE-1] 04 p1338 N94-19516
Solar simulator for solar dynamic space power system testing
[NASA-TM-106393] 05 p1984 N94-20140
Power standard
[ESA-PSS-02-10-VOL-1-ISSUE-1] 05 p1669 N94-20241
Model-based reasoning for power system management using KATE and the SSM/PMAD
[NASA-CR-193942] 05 p1671 N94-21882
Power beaming to space using a nuclear reactor-pumped laser
[DE94-001208] 06 p2348 N94-23185
Aerospace applications of batteries 06 p2390 N94-23346
Review of super Ni/Cd cell designs and performance 06 p2391 N94-23348
Impedance measurements on a spiral-wound nickel/metal hydride cell cycled in a simulated Leo orbit 06 p2392 N94-23355
NASA Lewis advanced IPV nickel-hydrogen technology 06 p2392 N94-23356
Primary and secondary electrical space power based on advanced PEM systems 06 p2392 N94-23357
A high performance H2-Cl2 fuel cell for space power applications 06 p2394 N94-23366
The mass of massive rover software 06 p2464 N94-23410
Assessment of an SP-100 bi-modal propulsion and power system
[DE94-000889] 06 p2218 N94-23433
GPHS-RTG's in support of the Cassini mission
[DE94-001445] 06 p2218 N94-23459
Low power ground-based laser illumination for electric propulsion applications
[NASA-CR-194444] 06 p2219 N94-23555
A review of wiring system safety in space power systems
[NASA-CR-194439] 06 p2203 N94-23632
The Submillimeter Wave Astronomy Satellite (SWAS) solar array system 06 p2361 N94-24029
Near Earth asteroid rendezvous
[NASA-CR-195518] 06 p2195 N94-24808
Extended duration lunar lander
[NASA-CR-195527] 06 p2206 N94-24916
Parallel processing methods for space based power systems 06 p2222 N94-25352
Manned mission to Mars with periodic refueling from electrically propelled tankers 07 p2689 N94-25670

Low-cost unmanned lunar lander
07 p2697 N94-25699
Small low mass advanced PBR's for bi-modal operation
[DE94-003201] 07 p2699 N94-25798
Parametric analysis of the space power plants on the base of criterion of specific mass in generalized design variants
[DE93-634153] 07 p2701 N94-26166
NSWC Crane Aerospace Cell Test History Database
07 p2860 N94-28102
Advanced energy storage for space applications: A follow-up 07 p2860 N94-28103
Battery study for the Mars Environmental Survey (MESUR) Pathfinder 07 p2860 N94-28105
Ni-H2 cell characterization for INTELSAT programs
07 p2861 N94-28109
Cycle life versus depth of discharge update on modeling studies --- Nickel-Hydrogen Batteries
07 p2862 N94-28115
Charge efficiency of Ni/H2 cells during transfer orbit of Telstar 4 satellites 07 p2862 N94-28117
Orbital management and design considerations for NiCd satellite power systems 07 p2862 N94-28118
TOPEX/Poseidon battery performance during the first year of operation 07 p2862 N94-28119
Nickel cadmium battery operations on-orbit: Trials, tribulations, and success on the Upper Atmosphere Research Satellite 07 p2862 N94-28120
Performance test results of ETS-6 Ni-Cd cells
07 p2863 N94-28121
Discriminating performance parameters for 50 amp-hour and 60 amp-hour nickel-cadmium plates and battery cells 07 p2863 N94-28123
Some observations on battery charge control
07 p2863 N94-28125
Construction of temperature compensated constant voltage (VT) curves for super Ni-Cd (tm) cells
07 p2863 N94-28126
A pressure based charge control system for the DSPSE NiH2 CPV battery 07 p2863 N94-28127
Advanced nickel-hydrogen spacecraft battery development 07 p2863 N94-28129
Development of nickel-metal hydride cell: An update
07 p2864 N94-28130
Determination of thermal properties of commercial Ni-MH cells 07 p2864 N94-28132
Selection of the Space Station Freedom (SSF) Flat Collector Circuit (FCC) insulation material
08 p3165 N94-28701
TOPAZ 2 system description
[DE94-006230] 08 p3498 N94-30846
The TOPAZ 2 space reactor response under accident conditions
[DE94-004998] 08 p3498 N94-30847
Room temperature molten salts for advanced energy conversion and storage
[AD-A277777] 09 p3763 N94-33015
The 28th Aerospace Mechanisms Symposium
[NASA-CP-3260] 09 p3603 N94-33291
Roll ring assemblies for the Space Station
09 p3603 N94-33294
International Space Station Alpha's bearing, motor, and roll ring module developmental testing and results
09 p3603 N94-33295
The SAMPIE flight experimental final technical requirements document
[NASA-TM-106224] 10 p4015 N94-34729
GPHS-RTGs in support of the Cassini mission
[DE94-009994] 11 p4212 N94-35648
Mars vertical axis wind machines: The design of a tornado vortex machine for use on Mars
[NASA-CR-196144] 12 p4462 N94-36823
Conceptual design: TFE verification program
[DE94-012469] 12 p4398 N94-37433

SPACECRAFT PRELAUNCH TESTS
U SPACE VEHICLE CHECKOUT PROGRAM

SPACECRAFT PROPULSION
NT ELECTROMAGNETIC PROPULSION
NT ION PROPULSION
NT MATTER-ANTIMATTER PROPULSION
NT PLASMA PROPULSION
NT SOLAR ELECTRIC PROPULSION
NT SOLAR PROPULSION
Arcjet space thrusters
[NASA-CR-193191] 01 p0046 N94-10700
Space transportation alternatives for large space programs: The International Space University Summer Session, 1992
[NASA-TM-106271] 01 p0040 N94-10811
Applying design principles to fusion reactor configurations for propulsion in space
[NASA-TM-108247] 01 p0047 N94-11053
The National Launch System Advanced Development Program: A brief overview 01 p0040 N94-11576
Nuclear propulsion systems engineering
[DE93-010791] 02 p0548 N94-12870
MCNP benchmark analyses of critical experiments for the Space Nuclear Thermal Propulsion program
[DE93-014046] 02 p0548 N94-12981
Design, qualification and operation of nuclear rockets for safe Mars missions
[DE93-010792] 02 p0549 N94-12996
Generation of neutronic thermal data in support of space nuclear propulsion
[DE93-013148] 02 p0549 N94-13034
Two temperature modeling and experimental measurements of laser sustained hydrogen plasmas
[AD-A265750] 02 p0796 N94-13039
Mirror fusion propulsion system: A performance comparison with alternate propulsion systems for the manned Mars Mission
[NASA-TM-109248] 02 p0550 N94-13147
Electrical Actuation Technology Bridging
[NASA-CP-3213] 02 p0551 N94-13417
Low thrust space propulsion
[NASA-TM-109286] 02 p0552 N94-13625
The Large Area Pulsed Solar Simulator (LAPSS)
[NASA-CR-194507] 02 p0703 N94-13940
Gas core nuclear thermal rocket engine research and development in the former USSR
[DE93-012165] 02 p0552 N94-14013
Aeropropulsion facilities 02 p0506 N94-14161
Large space structures and systems in the space station era: A bibliography with indexes (supplement 05)
[NASA-SP-7085(05)] 02 p0543 N94-14411
Space reactor fuel element testing in upgraded TREAT
[DE93-012524] 02 p0554 N94-14806
Space transfer concepts and analyses for exploration missions, phase 4
[NASA-CR-193849] 03 p0882 N94-15831
Proteus three-dimensional Navier-Stokes computer code, version 1.0. Volume 3: Programmer's reference
[NASA-TM-106341] 03 p1022 N94-15865
Proteus two-dimensional Navier-Stokes computer code, version 2.0. Volume 3: Programmer's reference
[NASA-TM-106339] 03 p1022 N94-15867
Liquid hydrogen and liquid oxygen feedline passive recirculation analysis
[TABES PAPER 93-620] 03 p1031 N94-16145
Liquid Oxygen (LO2) propellant conditioning concept testing
[TABES PAPER 93-621] 03 p0976 N94-16146
Space Propulsion Synergy Group ETO technology assessments
[TABES PAPER 93-641] 03 p0929 N94-16149
Comparisons of selected laser beam power missions to conventionally powered missions
[NASA-TM-106110] 03 p1040 N94-16522
Power Reactant Storage Assembly (PRSA) (Space Shuttle). PRSA hydrogen and oxygen DVT tank refurbishment
[NASA-CR-188262] 03 p0926 N94-16922
Advanced transportation system studies technical area 3: Alternate propulsion subsystem concepts, volume 2
[NASA-CR-193863] 03 p0927 N94-17096
Advanced transportation system studies technical area 3: Alternate propulsion subsystem concepts, volume 3
[NASA-CR-193864] 03 p0927 N94-17097
Application of a NEPTUNE propulsion concept to a manned Mars excursion
[AD-A268053] 03 p0929 N94-17587
Mission needs and system commonality for space nuclear power and propulsion
[DE93-016557] 04 p1337 N94-17863
Critical technologies for reactors used in nuclear electric propulsion
[DE93-017685] 04 p1337 N94-17908
Technology test bed
[NASA-TM-109354] 04 p1322 N94-18953
Spacecraft Propulsion
[VKI-LS-1993-01] 05 p1667 N94-20068
Space Shuttle Main Engine. Overview
05 p1667 N94-20070
Rocketdyne turbomachinery 05 p1667 N94-20071
Turbine design 05 p1668 N94-20075
Cryogenic propellant rocket engine problems
05 p1668 N94-20076
Advanced transportation system studies, technical area 3. Alternate propulsion subsystem concepts: J-2S restart study
[NASA-CR-193874] 05 p1670 N94-21271
NEP Early Flight program: System performance and development considerations
[NASA-TM-106415] 05 p1654 N94-21570
Specialized data analysis for the Space Shuttle Main Engine and diagnostic evaluation of advanced propulsion system components
[NASA-CR-194720] 05 p1656 N94-21813
Advanced space propulsion concepts
06 p2216 N94-23067
Advanced nuclear thermal propulsion concepts
06 p2217 N94-23068
An antiproton driver for ICF propulsion
06 p2217 N94-23069
Lewis Research Center R and D Facilities
[NASA-TM-109400] 06 p2630 N94-23135
Ovonic nickel metal hydride batteries for space applications 06 p2391 N94-23352
Assessment of an SP-100 bi-modal propulsion and power system
[DE94-000889] 06 p2218 N94-23433
The 33rd Israel Annual Conference on Aviation and Astronautics
[ITN-94-85227] 06 p2153 N94-24241
NPS alternate techsat satellite, design project for AE-4871
[NASA-CR-195512] 06 p2204 N94-24590
Numerical simulation of cylindrical, self-field MPD thrusters with multiple propellants
[NASA-CR-194458] 06 p2220 N94-24714
Near Earth asteroid rendezvous
[NASA-CR-195518] 06 p2195 N94-24808
Embodiment design for a multipropellant resistojet
[NASA-CR-195505] 06 p2221 N94-24834
Systematic Propulsion Optimization Tools (SPOT)
07 p2976 N94-25666
Small low mass advanced PBR's for bi-modal operation
[DE94-003201] 07 p2699 N94-25798
Parametric analysis of the space power plants on the base of criterion of specific mass in generalized design variants
[DE93-634153] 07 p2701 N94-26166
Space Station technology testbed: 2010 deep space transport 07 p2687 N94-27368
Inertial electrostatic confinement as a power source for electric propulsion 07 p2688 N94-27373
Rocket engine numerical simulation
07 p2688 N94-27375
Nuclear electric propulsion: A better, safer, cheaper transportation system for human exploration of Mars
[NASA-TM-106406] 08 p3171 N94-28833
Some problems of scramjet propulsion for aerospace planes. Part 1: Scramjet: Aims and features
08 p3151 N94-29295
Research and development of ramjets/ramrockets. Part 2: Integral liquid fuel ramjets 08 p3152 N94-29297
Research and development of ramjets/ramrockets. Part 3: The study of gaseous hydrogen ram combustors
08 p3152 N94-29298
Some problems of scramjet propulsion for aerospace planes. Part 2: Scramjet: Development and test problems 08 p3152 N94-29301
A transportronic solution to the problem of interorbital transportation
[NASA-CR-191152] 08 p3164 N94-29355
Determination of pressure response times for gaseous flow in a tube
[AD-A275274] 08 p3272 N94-29435
Specialized data analysis of SSME and advanced propulsion system vibration measurements
[NASA-CR-193940] 08 p3174 N94-29868
Small low mass advanced PBR's for propulsion
[DE94-005142] 08 p3497 N94-30588
The 7.5K lbf thrust engine preliminary design for Orbit Transfer Vehicle
[AD-A277519] 09 p3614 N94-31618
Aerospace test facilities at NASA LERC Plumbrook
[NASA-TM-109755] 09 p3602 N94-31814
Performance evaluation and operating characteristics of a waveguide microwave applicator for space propulsion applications 09 p3614 N94-31908
Summary of particle bed reactor designs for the Space Nuclear Thermal Propulsion Program
[DE94-007434] 09 p3615 N94-32266
One fantastic ride
[NASA-TM-109828] 10 p4016 N94-33582
Possibilities and pitfalls in aerospace applications of titanium matrix composites 12 p4400 N94-36650
Characteristics of ions emitted from high-current hollow cathodes
[NASA-CR-195372] 12 p4398 N94-37764

SPACECRAFT RADIATORS
An analytical investigation of transient effects on rewetting of heated thin flat plates
[NASA-TM-106120] 02 p0628 N94-12968
Geometrical vapor blocker for parallel condensation tubes requiring cooling
[NASA-CASE-MSC-22090-1] 03 p1022 N94-15962
Rewetting of monogroove heat pipe in Space Station radiators
[NASA-CR-194781] 05 p1804 N94-21820

Heat pipe cooled heat rejection subsystem modelling for nuclear electric propulsion
[NASA-CR-191132] 06 p2219 N94-24061
Numerical simulation of a condenser in two-phase heat transport systems: A feasibility study
[AD-B173650] 08 p3282 N94-30855
Thermocapillary convection in evaporating sessile drops
[NASA-TM-109758] 09 p3705 N94-31886
Development of lightweight radiators for lunar based power systems
[NASA-TM-106604] 09 p3726 N94-32272
Investigation of moving belt radiator technology issues
[NASA-CR-195340] 10 p4032 N94-33950
Review of advanced radiator technologies for spacecraft power systems and space thermal control
[NASA-TM-4555] 12 p4398 N94-36821
Carbon-carbon heat pipe testing and evaluation
[NASA-TM-106630] 12 p4405 N94-37318
Reference manual for the Thermal Analyst's Help Desk Expert System
[NASA-CR-194941] 12 p4397 N94-37504

SPACECRAFT RECOVERY
Preliminary system design of a Three Arm Capture Mechanism (TACM) flight demonstration article
[NASA-CR-192573] 01 p0177 N94-10341
STS-32 mission highlights resource tape
[NASA-TM-109291] 02 p0531 N94-13631
The development and flight test of a deployable precision landing system for spacecraft recovery
[NASA-TM-4525] 02 p0537 N94-14853
Long Duration Exposure Facility retrieval animation
[NASA-TM-109426] 03 p0885 N94-15496
Long Duration Exposure Facility
[NASA-TM-109427] 03 p0885 N94-15497
LDEF update
[NASA-TM-109352] 04 p1334 N94-18921
Further development and flight test of an autonomous precision landing system using a parafoil
[NASA-TM-4599] 10 p3983 N94-33995
Attitude stability of a spinning spacecraft during appendage deployment/retraction 11 p4208 N94-35639

SPACECRAFT REENTRY
NT UNCONTROLLED REENTRY (SPACECRAFT)
New hypersonic test methods developed at ONERA: The R5 and F4 wind tunnels 01 p0004 N94-10429
Local measurement of temperatures and concentrations: A review for hypersonic flows 01 p0004 N94-10434
Fully coupled neutronic and hydrodynamic analysis of space nuclear reactor reentry accidents
[DE93-005459] 01 p0372 N94-10890
HOPE real time flight operations analyses for return to earth phase, part B
[NASDA-CNT-930011] 02 p0535 N94-13599
Launch, entry, and landing resource clip
[NASA-TM-109297] 02 p0535 N94-13638
HOPE real time flight operations analyses for return to earth phase, part A
[NASDA-CNT-930010-PT-A] 02 p0535 N94-13645
Development and application of an empirical probability distribution for the prediction error of re-entry body maximum dynamic pressure 06 p2207 N94-23653
Numerical simulation of aerothermodynamic heating of hypersonic space transportation vehicles 08 p3124 N94-28955
The influence of the deorbit-burn manoeuvre on the footprint of a re-entry capsule
[LR-727] 09 p3609 N94-31705
Implementation of a vibrationally linked chemical reaction model for DSMC
[NASA-TM-109109] 09 p3710 N94-33020

SPACECRAFT RELIABILITY
Gearing up for 1988
[NASA-TM-109617] 03 p0880 N94-15346
Lunar lander and return propulsion system trade study
[NASA-TP-3388] 03 p0925 N94-16496
The development of the SOHO SUMER mechanisms 06 p2361 N94-24028
Reliable redundant device for mechanisms 06 p2361 N94-24030
Develop advanced nonlinear signal analysis topographical mapping system
[NASA-CR-195128] 06 p2388 N94-24827
Possibilities and pitfalls in aerospace applications of titanium matrix composites 12 p4400 N94-36650
Probabilistic assessment of space nuclear propulsion system nozzle
[NASA-TM-106539] 12 p4457 N94-37704

SPACECRAFT RENDEZVOUS
U SPACE RENDEZVOUS

SPACECRAFT SENSORS
U SPACECRAFT INSTRUMENTS

SPACECRAFT SHIELDING
Debris/ice/TPS assessment and integrated photographic analysis for Shuttle Mission STS-57
[NASA-TM-107562] 01 p0040 N94-10805
Development of deterministic transport methods for low energy neutrons for shielding in space
[NASA-CR-194172] 01 p0366 N94-11199
Simulation of orbital debris impacts on bumper shields
[DE93-013773] 02 p0540 N94-13398
High temperature electromagnetic characterization of thermal protection system tile materials
[NASA-CR-189687] 02 p0578 N94-13431
CRRES to blaze new trails in orbit
[NASA-TM-109314] 02 p0713 N94-13620
Exposure fluctuations of astronauts due to orientation
[NASA-TP-3364] 03 p1300 N94-15816
Calculations of cosmic-ray helium transport in shielding materials
[NASA-TP-3354] 03 p1301 N94-17666
Thermally activated retainer means utilizing shape memory alloy
[NASA-CASE-MSC-21793-1] 05 p1654 N94-20304
Numerical simulations of hypervelocity impact experiments involving single Whipple bumper shields
[AD-A272123] 05 p1831 N94-20572
Hypervelocity impact
[AD-A272957] 05 p1831 N94-21249
Meteoroids and debris impact risk assessment on Columbus and Hermes using a realistic geometrical analysis tool 05 p1662 N94-21388
Magnetic shielding of interplanetary spacecraft against solar flare radiation
[NASA-CR-195539] 06 p2204 N94-24334
Design of orbital debris shields for oblique hypervelocity impact
[NASA-CR-195152] 06 p2205 N94-24828
Mounting of SSM's
[VTT-TIED-1442] 07 p2695 N94-26250
Physics of debris clouds from hypervelocity impacts
[NASA-CR-193932] 07 p2696 N94-26791
Electrical properties of double layer dielectric structures for space technology
[ISBN-0-315-86547-4] 09 p3610 N94-31910
High-temperature behavior of advanced spacecraft TPS
[NASA-CR-195832] 10 p4014 N94-34063
Estimates of cellular mutagenesis from cosmic rays
[NASA-TP-3453] 12 p4481 N94-37282

SPACECRAFT STABILITY
Stability analysis and aerospace vehicle dynamics 01 p0031 N94-11491
Numerical simulation of Ulysses nutation 06 p2207 N94-24017
Spacecraft vibrations due to mechanisms; measurements from Olympus on-station 06 p2207 N94-24018
An approximate solution for the spinup dynamics of near axisymmetric axial gyrostats using the method of multiple scales
[AD-A273723] 07 p2698 N94-26223
Superfluid helium sloshing dynamics induced oscillations and fluctuations of angular momentum, force and moment actuated on spacecraft driven by gravity gradient or jitter acceleration associated with slew motion
[NASA-CR-193928] 07 p2799 N94-27931
A gimbaled low noise momentum wheel 08 p3162 N94-29640
A geometric model of a V-slit Sun sensor correcting for spacecraft wobble 11 p4206 N94-35628
Attitude stability of a spinning spacecraft during appendage deployment/retraction 11 p4208 N94-35639

SPACECRAFT STERILIZATION
Analysis of leading edge and trailing edge cover glass samples before and after treatment with advanced satellite contamination removal techniques 09 p3596 N94-31041

SPACECRAFT STRUCTURES
The EUREKA project portfolio in new materials 01 p0056 N94-10002
Design and development of a CFRP central cylinder for satellites 01 p0056 N94-10007
Design and manufacturing of filament wound thrust cylinder 01 p0057 N94-10010
Special problems of 3-D ultrasonic QNDI techniques and applications to composites aerospace structures 01 p0061 N94-10036
Stress relaxation forming of Ariane 5 front skirt outer skin panels 01 p0062 N94-10046
Failure prediction of thin beryllium sheets used in spacecraft structures
[NASA-CR-194164] 01 p0187 N94-11190
Smart Structures for Aircraft and Spacecraft
[AGARD-CP-531] 01 p0068 N94-11317
Modelling hypervelocity impacts into aluminum structures based on LDEF data 01 p0190 N94-12178
Space truss zero gravity dynamics
[AD-A266130] 01 p0044 N94-12541
Experimental technique to simulate orbital-debris impact on space shields at impact velocities over 10 km/s
[DE93-011619] 02 p0539 N94-12909
Methods for evaluating the predictive accuracy of structural dynamic models
[NASA-CR-191337] 02 p0671 N94-13124
The Second Workshop on Deployment and Assembly Experiment of Large Space Structure on Orbit
[NASDA-CON-930003] 02 p0529 N94-13268
Research on inflatable structure for space use 02 p0530 N94-13275
Application of intelligently adaptable structure and robot to large space structure 02 p0530 N94-13277
Movement of deployable truss 02 p0531 N94-13280
Study of a one-dimensional deployable structure employing telescopic members 02 p0531 N94-13282
The study on test of docking mechanism system, part 1 and 2
[NASDA-TMR-930004-PT-1-2] 02 p0541 N94-13660
Characterization of composite materials for aerospace structures
[ESA-TT-1260] 02 p0557 N94-13804
Control structural interaction testbed: A model for multiple flexible body verification 02 p0544 N94-14649
An analysis of the dynamic response of the Space Station Freedom due to a module perforation by an orbital debris particle impact
[TABES PAPER 93-653] 03 p0899 N94-16154
Solid lubricants for space structures, phase 2
[AD-A266653] 03 p0968 N94-16767
Principal investigators data package for Project Initiation Conference (PIC): EUVS sounding rocket no. 36.117CL. Target: Venus
[NASA-CR-194663] 03 p0923 N94-17126
A mechanical system damping measurement technique using a one-degree-of-freedom (1DOF) cylindrical gas bearing
[AD-A268402] 03 p1048 N94-17462
Structural mechanics division research and technology accomplishments for CY 1992 and plans for CY 1993
[NASA-TM-107752] 03 p1062 N94-17479
Design considerations for remotely operated welding in space: Task definition and visual weld monitoring experiment
[AD-A268752] 04 p1445 N94-18634
Activities of the Center for Space Construction
[NASA-CR-193717] 04 p1335 N94-19371
Apparatus for simulating an exoatmospheric structure
[NASA-CASE-MSC-21975-1] 05 p1653 N94-20339
The Submillimeter Wave Astronomy Satellite (SWAS) solar array system 06 p2361 N94-24029
Reliable redundant device for mechanisms 06 p2361 N94-24030
Extended duration lunar lander
[NASA-CR-195527] 06 p2206 N94-24916
Project PARAS: Phased array radio astronomy from space 07 p3081 N94-25703
Proceedings of Damping 1993, volume 2
[AD-A274227] 07 p2840 N94-26953
Proceedings of Damping 1993, volume 3
[AD-A274228] 07 p2840 N94-27008
Reliability of composite material structures. Application: High pressure spherical coded tanks
[REPT-932-430-103] 08 p3180 N94-29478
Composite hot drape forming 08 p3240 N94-30448
Anodized aluminum on LDEF 09 p3592 N94-31017
Trajectory planning for space manipulators
[AD-A277229] 09 p3611 N94-32369
Arcing in space structures in low Earth orbit
[NASA-CR-194223] 09 p3694 N94-32478
On-orbit NDE: A novel approach to tube weld inspection 10 p4066 N94-33664
Advances in parameter estimation techniques applied to flexible structures 11 p4219 N94-35877
Software for continuum modeling of controls-structures interactions 11 p4223 N94-35898
Approximate analysis for repeated eigenvalue problems with applications to controls-structure integrated design
[NASA-TP-3439] 12 p4397 N94-37502

SPACECRAFT SURVIVABILITY
Development and application of an empirical probability distribution for the prediction error of re-entry body maximum dynamic pressure 06 p2207 N94-23653
Vulnerability of manned spacecraft to crew loss from orbital debris penetration
[NASA-TM-108452] 08 p3169 N94-30161

NASA report to education, volume 9
[NASA-TM-109760] 09 p3913 N94-31817
SPACECRAFT TELEVISION
NT DIGITAL SPACECRAFT TELEVISION
SPACECRAFT TEMPERATURE
Gravity dependent condensation pressure drop and heat transfer in ammonia two-phase heat transport systems
[NLR-TP-92121-U] 03 p1031 N94-17615
A comparison of TSS and TRASYS in form factor calculation 06 p2321 N94-23638
User's guide for the thermal analyst's help desk expert system
[NASA-CR-194885] 07 p2695 N94-26103
Physics of heat pipe rewetting
[NASA-CR-195902] 09 p3913 N94-33148
Reference manual for the Thermal Analyst's Help Desk Expert System
[NASA-CR-194941] 12 p4397 N94-37504
SPACECRAFT TRACKING
NT SATELLITE TRACKING
NT SATELLITE-TO-SATELLITE TRACKING
Sequential ranging: How it works
[NASA-CR-194508] 02 p0532 N94-13796
The Telecommunications and Data Acquisition Report
[NASA-CR-194388] 02 p0607 N94-14369
NAVSPASUR sensor system digital signal processing receiver. Volume 1: Hardware and software overview
[AD-A272899] 05 p1738 N94-21198
NAVSPASUR sensor system digital signal processing receiver. Volume 2: Function and capabilities of hardware and software components
[AD-A272900] 05 p1739 N94-21218
SpaceOps 1992: Proceedings of the Second International Symposium on Ground Data Systems for Space Mission Operations
[NASA-CR-194486] 06 p2497 N94-23832
Future trends in NASA space operations 06 p2498 N94-23836
Magellan spacecraft and memory state tracking: Lessons learned, future thoughts 06 p2207 N94-23865
GSMS and space views: Advanced spacecraft monitoring tools 06 p2507 N94-23890
VMPLOT: A versatile analysis tool for mission operations 06 p2507 N94-23891
Combining real-time monitoring and knowledge-based analysis in MARVEL 06 p2477 N94-23900
Resource allocation planning with international components 06 p2520 N94-23963
Scheduling the future NASA Space Network: Experiences with a flexible scheduling prototype 06 p2520 N94-23965
Modeling and analysis of selected space station communications and tracking subsystems 06 p2306 N94-25374
Radio science ground data system for the Voyager-Neptune encounter, part 1 08 p3248 N94-29623
The Telecommunications and Data Acquisition Report
[NASA-CR-195689] 08 p3249 N94-29652
Toward astrometric tracking with the infrared spatial interferometer 08 p3249 N94-29653
Line-of-sight tropospheric calibration from measurements in arbitrary directions 08 p3249 N94-29654
Enhanced orbit determination filter sensitivity analysis: Error budget development 08 p3159 N94-29655
Enhanced orbit determination filter: Inclusion of ground system errors as filter parameters 08 p3159 N94-29656
A dual-cavity ruby maser for the Ka-band link experiment 08 p3250 N94-29658
Status of frequency and time support for NASA systems 08 p3468 N94-30640
Apollo 11: The Goddard connection
[NASA-TM-109815] 10 p4010 N94-33566
The Mars Observer differential one-way range demonstration 11 p4210 N94-35543
Spacecraft-spacecraft radio-metric tracking: Signal acquisition requirements and application to Mars approach navigation 11 p4254 N94-35557
Improved solution accuracy for Landsat-4 (TDRSS-user) orbit determination 11 p4205 N94-35623
SPACECRAFT TRACKING AND DATA NETWORK
U STDN (NETWORK)
SPACECRAFT TRAJECTORIES
NT EARTH-MARS TRAJECTORIES
NT EARTH-MOON TRAJECTORIES
NT INTERPLANETARY TRAJECTORIES
NT LUNAR TRAJECTORIES
Neptune encounter highlights
[NASA-TM-109421] 03 p1246 N94-15240
Neighboring extremal guidance for systems with piecewise linear control using time as the reference variable
[AD-A267942] 03 p0874 N94-17010
Soyuz/ACRV accommodation study
[NASA-TM-107733] 03 p0888 N94-17072
Parallelization of the Air Force Space Command (AFSPACECOM) satellite motion models
[AD-A269327] 04 p1334 N94-18470
Constant-thrust orbit-raising transfer charts
[AD-A269088] 04 p1334 N94-18718
START user manual version 2.1
[LR-726] 04 p1335 N94-19614
Nearly uniform deployment/retrieval strategy for space tether systems 06 p2156 N94-24256
Manned mission to Mars with periodic refueling from electrically propelled tankers 07 p2689 N94-25670
An approximate solution for the spinup dynamics of near axisymmetric axial gyrostats using the method of multiple scales
[AD-A273723] 07 p2698 N94-26223
Arithmetic performances of onboard computers 07 p2952 N94-26738
A survey of uncontrolled satellite reentry and impact prediction
[AD-A274903] 07 p2695 N94-26750
Software engineering methods in the Hermes on-board software 08 p3414 N94-29326
Trajectory planning for space manipulators
[AD-A277229] 09 p3611 N94-32369
A six degree of freedom, plume-fuel optimal trajectory planner for spacecraft proximity operations using an A* node search
[NASA-CR-188285] 09 p3601 N94-32388
Spacecraft-spacecraft radio-metric tracking: Signal acquisition requirements and application to Mars approach navigation 11 p4254 N94-35557
Modal decomposition of Hamiltonian variational equations 11 p4202 N94-35606
Compatibility of TOPEX/Poseidon trajectory propagation with JPL and GSFC/FDF operational software 11 p4204 N94-35619
Improved solution accuracy for TDRSS-based TOPEX/Poseidon orbit determination 11 p4205 N94-35620
SPACECREWS
Noise levels and their effects on Shuttle crewmembers' performance: Operational concerns 01 p0314 N94-11538
Promethazine and its use as a treatment for space motion sickness 01 p0312 N94-11550
Update on the incidence and treatment of space motion sickness 01 p0312 N94-11551
Baseline characteristics of different strata of astronaut corps 01 p0312 N94-11552
Potential health effects of space radiation 01 p0312 N94-11558
Operational radiological support for the US manned space program 01 p0318 N94-11561
Crew chief 01 p0335 N94-11564
Medical care delivery in the US space program 01 p0307 N94-11806
STS-29 post-insertion/deorbit prep and crew bailout
[NASA-TM-109299] 02 p0535 N94-13641
STS-35 crew trash compactor briefing
[NASA-TM-109487] 02 p0533 N94-14735
STS-35 EVA payload training in WETF
[NASA-TM-109492] 02 p0739 N94-14790
Astro smile
[NASA-TM-109506] 03 p0879 N94-15225
STS-29 Post-Flight Press Conference --- Shuttle Launch, TDRS-D/IUS Deployment, Crew Activites, and Shuttle Landing
[NASA-TM-109575] 03 p0880 N94-15306
STS-26 IUS and latch contingency training
[NASA-TM-109561] 03 p0875 N94-15331
STS-26 generic integrated IUS deploy simulation
[NASA-TM-109562] 03 p0875 N94-15332
STS-34 post-flight press conference
[NASA-TM-109459] 03 p0880 N94-15354
STS-34 mission highlights resource tape, part 1
[NASA-TM-109461] 03 p0880 N94-15356
STS-34 McCully and Baker during IFM training
[NASA-TM-109462] 03 p0880 N94-15357
STS-34 final bench review
[NASA-TM-109464] 03 p1135 N94-15359
STS-29 mission highlights resource tape
[NASA-TM-109542] 03 p0880 N94-15373
STS-32 LDEF EVA training in WETF with Low and Dunbar
[NASA-TM-109473] 03 p1135 N94-15377
STS-29 crew IMAX camera training
[NASA-TM-109546] 03 p1031 N94-15380
STS-32 crew training for lower body negative pressure unit and AFE
[NASA-TM-109475] 03 p1120 N94-15381
STS-29 crew food tasting in building 45
[NASA-TM-109547] 03 p1136 N94-15382
STS-29 crew bailout in WETF
[NASA-TM-109548] 03 p1136 N94-15385
STS-28 Adamson and Brown EMU walk through
[NASA-TM-109549] 03 p1136 N94-15387
STS-34 Arriflex and IMAX camera training
[NASA-TM-109467] 03 p1031 N94-15397
STS-33 EVA prep and post with Gregory, Blaha, Carter, Thorton, and Musgrave in FFT
[NASA-TM-109469] 03 p0881 N94-15398
ASTP 15th anniversary clip-media release
[NASA-TM-109534] 03 p1302 N94-15399
STS-33 crew post flight film
[NASA-TM-109470] 03 p0881 N94-15400
STS-27 EMU and RMS contingency training
[NASA-TM-109550] 03 p1136 N94-15401
STS-33 Carter and Thorton during WETF activities
[NASA-TM-109471] 03 p1136 N94-15402
STS-27 crew post-insertion deorbit-prep in CCT
[NASA-TM-109552] 03 p1136 N94-15404
STS-27 crew fire training and glove molding
[NASA-TM-109554] 03 p1136 N94-15406
STS-26 missions highlight resource tape
[NASA-TM-109559] 03 p0881 N94-15407
STS-38 crew training: Habitation equipment procedures, bailout in CCT, 70mm photo class, EVA prep and post, and firefighting
[NASA-TM-109494] 03 p1136 N94-15453
Answering the space medicine challenge
[NASA-TM-109511] 03 p1120 N94-15457
STS-36 crew presentation clip
[NASA-TM-109497] 03 p0881 N94-15461
STS-36 crew EVA prep and post-training, bailout exercises, final bench review
[NASA-TM-109498] 03 p1137 N94-15462
STS-27 crew deorbit prep in SMS with Gibson, Shepard, Mullane, Ross, and G. Gardner
[NASA-TM-109518] 03 p0882 N94-15468
STS-26 crew participation in meetings
[NASA-TM-109519] 03 p0873 N94-15469
STS-26 crew clothing, glove molding, and personal hygiene
[NASA-TM-109520] 03 p1137 N94-15470
STS-41 onboard 16mm photography quick release
[NASA-TM-109515] 03 p0882 N94-15518
STS-41 mission highlights resource tape
[NASA-TM-109516] 03 p0882 N94-15521
Spaceflight Radiation Health program at the Lyndon B. Johnson Space Center
[NASA-TM-104782] 05 p1893 N94-21863
Mission activities planning for a Hermes mission by means of AI-technology 06 p2502 N94-23858
Crew interface analysis: Selected articles on space human factors research, 1987 - 1991
[NASA-TM-104756] 06 p2433 N94-24185
Use of infrared telemetry as part of a nonintrusive inflight data collection system to collect human factors data 06 p2434 N94-24193
Illumination requirements for operating a space remote manipulator 06 p2435 N94-24195
Reach performance while wearing the Space Shuttle launch and entry suit during exposure to launch accelerations 06 p2436 N94-24204
Development of biomechanical models for human factors evaluations 06 p2437 N94-24205
Design and development of the second generation Mars Habitat 07 p2943 N94-25693
First lunar outpost 07 p2943 N94-25694
Psychophysiology in microgravity and the role of exercise 07 p2936 N94-28374
Legal regime of human activities in outer space law 09 p3599 N94-31431
Task network models in the prediction of workload imposed by extravehicular activities during the Hubble Space Telescope servicing mission 10 p4101 N94-33627
An overview of Space Shuttle anthropometry and biomechanics research with emphasis on STS/Mir recumbent seat system design 10 p4101 N94-33629
Continuous monitoring of bacterial attachment 10 p4094 N94-33658
Characterization of spacecraft humidity condensate 10 p4102 N94-33659
Safety concerns for first entry operations of orbiting spacecraft 10 p4102 N94-33662
Self-rescue strategies for EVA crewmembers equipped with the SAFER backpack 11 p4207 N94-35633
SPACELAB
Comprehensive analysis of airborne contaminants from recent Spacelab missions 01 p0318 N94-11553
Reduce fluid experiment system flight data from IML-1
[NASA-CR-193835] 02 p0804 N94-12873
Spacelab J experiment descriptions
[NASA-TM-4517] 02 p0586 N94-13732
Study on the biological effect of cosmic radiation and the development of radiation protection technology (L-11) 02 p0593 N94-13768

The 1977 highlights
[NASA-TM-109626] 03 p1302 N94-15412
STS-40 crew during spacelab Sim
[NASA-TM-109493] 03 p0876 N94-15452
The Japanese Space Station utilization plan
03 p0977 N94-16074
The Spacelab IPS Star Simulator
[TABES PAPER 93-650] 03 p0877 N94-16150
Spacelab 3
[NASA-TM-108750] 04 p1323 N94-18849
German space experiments on Spacelab D-2 and Eureca-1 to investigate atomic oxygen interaction with materials 05 p1662 N94-21390
Microbiological analysis of debris from Space Transportation System (STS)-55 Spacelab D-2
[NASA-CR-193883] 06 p2421 N94-24310
Spacelab life sciences 2 post mission report
[NASA-CR-188279] 07 p2942 N94-27410
Construction and test of experiment hardware for a space experiment on Spacelab mission IML-2
[DLR-FB-93-23] 07 p2903 N94-27743
Study of activation data of metal samples from LDEF-1 and Spacelab-2
[NASA-CR-193973] 08 p3205 N94-29736
ATLAS solar pointing operations
11 p4201 N94-35626

SPACELAB PAYLOADS
NT ATMOSPHERIC GENERAL CIRCULATION EXPERIMENT
Bubbles and drops behaviour under low-gravity: A space experiment for the IML-2 mission
01 p0104 N94-10098
Benard and Marangoni convection in multiple liquid layers 01 p0105 N94-10100
Advanced protein, crystallization facility and associated new developments 01 p0039 N94-10119
TEMPUS: An electromagnetic levitation facility for containerless processing under micro-g in Spacelab
01 p0109 N94-10125
The advanced fluid physics module: How to achieve scientific goals for Spacelab D2
01 p0039 N94-10136
Marangoni motion during melting of a hypermonotectic alloy: Numerical simulations for the D2 experiment IHF04 01 p0113 N94-10177
EUSO-D2-experiment: Unidirectional solidification with quenching of an AlSi11 alloy 01 p0086 N94-10199
The International Microgravity Laboratory, a Spacelab for materials and life sciences 01 p0125 N94-10249
The critical facility on IML-1 01 p0044 N94-10250
Analysis and interpretation of high energy cosmic rays measured on Spacelab-2
[NASA-CR-193586] 01 p0485 N94-12771
STS-40 crew during spacelab Sim
[NASA-TM-109493] 03 p0876 N94-15452
Participation in the definition, conduct, and analysis of particle accelerator experiments for the first Spacelab Mission
[NASA-CR-193974] 11 p4330 N94-35483

SPACERS
Preliminary analysis and design optimization of the short spacer truss of Space Station Freedom
[NASA-TM-4470] 03 p1058 N94-15709
Structural design feasibility study of Space Station long spacer truss
[NASA-TM-106346] 07 p2843 N94-27559
On optimal placement of spacers in bundled conductors 11 p4258 N94-35354

SPACING
NT AIRCRAFT APPROACH SPACING
On optimal placement of spacers in bundled conductors 11 p4258 N94-35354

SPALLATION
Possibility of a crossed-beam experiment involving slow-neutron capture by unstable nuclei rapid-process-tron
[DE93-754288] 01 p0363 N94-10720
Separation of spallation and terrestrial C-14 in chondrites 01 p0431 N94-12183
A calibration of the production rate ratio P-21/P-26 by low energy secondry neutrons: Identification of Ne spallation components at the 10(exp 6) atoms/g level in terrestrial samples 03 p1187 N94-16194
Mechanical-property changes of structural composite materials after low-temperature proton irradiation: Implications for use in SSC magnet systems
[DE93-016735] 04 p1343 N94-18763
Optical model analyses of galactic cosmic ray fragmentation in hydrogen targets
[NASA-TP-3404] 06 p2540 N94-23509
Simulations of terrestrial in-situ cosmogenic-nuclide production
[DE94-004999] 07 p3117 N94-27826
H(-) injection simulation for a 5 MW spallation neutron source
[DE94-009003] 10 p4140 N94-33983
Time-of-flight diffraction at pulsed neutron sources: An introduction to the symposium
[DE94-010442] 11 p4327 N94-36225

SPALLING
Micrometeoroid/space debris effects on materials
09 p3595 N94-31032

SPANISH SPACE PROGRAM
Spain: Success story in space
[ESA-BR-81] 01 p0038 N94-11461
Ground segment definition for the Spanish small satellite program (MINISAT) 03 p0878 N94-17155
Data handling strategy for the Spanish small satellite program (MINISAT) 03 p0895 N94-17177

SPANWISE BLOWING
Navier-Stokes flowfield computation of wing/rotor interaction for a tilt rotor aircraft in hover
[NASA-CR-4532] 01 p0013 N94-10758
Turbulent boundary layer interacting with spanwise periodic longitudinal vortex arrays
01 p0165 N94-12626
Effects, limits, and limitations of spanwise blowing
07 p2659 N94-28027
Numerical study of the trailing vortex of a wing with wing-tip blowing
[NASA-CR-195803] 08 p3130 N94-29760

SPARE PARTS
Spare parts analysis of the MK.32B-751 AAR pod
[DSIS-93-00737] 02 p0774 N94-13549

SPARK DISCHARGES
U ELECTRIC SPARKS

SPARK GAPS
Evolution of high-repetition-rate induction accelerators through advancements in switching
[DE93-012599] 02 p0654 N94-12963
Development of UHF spark-switched L-C Oscillators
[DE93-015019] 02 p0623 N94-13892
High-power gas switch with hydride electrodes
[AD-D015956] 05 p1751 N94-20354
Comparative study of INPIStron and spark gap
05 p1995 N94-21293

SPARK IGNITION
Dynamic behavior of an electric arc gas discharge
[DE93-630197] 03 p1205 N94-17635
Evaluation of aftermarket LPG conversion kits in light-duty vehicle applications
[DE93-010035] 04 p1377 N94-18617
A comparison between direct spark ignition and prechamber ignition in an internal combustion engine
[DE94-008218] 11 p4275 N94-36206
Potential benefits of oxygen-enriched intake air in a vehicle powered by a spark-ignition engine
[DE94-013452] 12 p4451 N94-37070

SPARK SHADOWGRAPH PHOTOGRAPHY
U SHADOWGRAPH PHOTOGRAPHY

SPARKS
NT ELECTRIC SPARKS
An electronic imaging system for the Aeroballistic Research Facility
[AD-A267157] 03 p1033 N94-15826
Analysis of spark-induced bubble experiments using CALE
[DE94-003667] 08 p3270 N94-28476

SPARTAN SATELLITES
SPARTAN high resolution solar studies
[NASA-CR-189340] 10 p4166 N94-34944

SPATIAL DEPENDENCIES
Some practicable applications of quadtree data structures/representation in astronomy
05 p1927 N94-22515
Representing spatial information in a computational model for network management
[NASA-CR-191669] 11 p4306 N94-36040

SPATIAL DISTRIBUTION
NT HORIZONTAL DISTRIBUTION
NT STAR DISTRIBUTION
NT VERTICAL DISTRIBUTION
Monte Carlo algorithms in simulation of 2beta-decay and penetration of electrons through matter
[DE93-617741] 01 p0364 N94-10837
Experimental study of multiple droplet evaporative cooling
[PB93-198463] 01 p0149 N94-10851
Visual encoding of spatial relations
[AD-A266049] 01 p0313 N94-10909
Evaluation of ECMWF latent heat flux in TOGA CD-ROM 01 p0195 N94-11921
Sea surface heat flux in the beginning of the Kuroshio
01 p0195 N94-11923
Appearance, behavior, and oceanic structures of warm streamers in the Kuroshio Oyashio frontal region
01 p0198 N94-11937
The development of phytoplankton sensing system with optical fiber 01 p0203 N94-11967
Distribution of mineral aerosols over the North Pacific
01 p0204 N94-11976
Implications of aerosol retrieval and atmospheric correction in remote sensing 01 p0205 N94-11978
Overwater atmospheric dispersion of volcanic smokes from Mt. Sakurajima observed in NOAA-AVHRR data
01 p0205 N94-11979
SOFAR float tracking in the Shikoku basin
01 p0206 N94-11986
Spatial variation in the seasonal south polar cap of Mars as observed by Mariner 7 01 p0456 N94-12134
Mass and spatial distribution of carbonaceous component in Comet Halley 01 p0433 N94-12263
Sea surface temperature difference between NOAA/AVHRR and in-situ observation
01 p0215 N94-12680
Variability of spectral reflectance in coastal waters near the river plumes 01 p0226 N94-12744
Trajectory curving in underwater propagation of light
01 p0226 N94-12748
Mixing of drifter ensemble by mesoscale currents
01 p0228 N94-12760
Spatial and temporal variability of precipitation and chemistry: Case studies from the frontal boundary study
[DE93-007883] 02 p0708 N94-13910
Chemistry and transport in a multi-dimensional model
[NASA-CR-194425] 02 p0716 N94-13969
Potential evapotranspiration in Belgium: Spatial and temporal variability
[PUBL-SER-A-130] 02 p0686 N94-13994
The role of the dynamics for the deviation of the total ozone from the long-term mean at the edge of the polar vortex 02 p0694 N94-14250
The European Arctic ozone experiment: An investigation of Northern Hemisphere ozone depletion
02 p0694 N94-14251
Space-based activities: SAM 2 and SAGE 2
02 p0694 N94-14252
New evidences supported the Wei hypothesis about the formation of the Antarctic ozone hole
02 p0694 N94-14253
Measurements of the spatial structure and directivity of 100 KeV photon sources in solar flares using PVO and ISEE-3 spacecraft
[NASA-CR-194080] 02 p0845 N94-14 92
Quantitative luminescence imaging system
[DE93-015691] 02 p0793 N94-14702
Broadband conventional beamforming incorporating adaptive equalization
[AD-A267090] 03 p0987 N94-15544
Characterization of spatial and temporal variability of phytoplankton blooms in coastal waters
[AD-A267102] 03 p1116 N94-15633
Tessera terrain on Venus: Implications of tessera flooding models and boundary characteristics for global distribution and mode of formation
03 p1258 N94-16226
Reference frames in vision
[AD-A266174] 03 p1132 N94-16925
Biofilm structure and diversity
[AD-A267254] 03 p1118 N94-16989
Arctic and Antarctic sea ice, 1978-1987: Satellite passive-microwave observations and analysis
[NASA-SP-511] 03 p1114 N94-17439
Measurement of the velocity field and void fraction in a planar plunging jet
[AD-A268183] 03 p1030 N94-17511
Observations of comets with the IUE
[NASA-CR-193652] 04 p1624 N94-17843
A Bayesian approach to contaminant plume delineation
[DE93-012909] 04 p1472 N94-17890
Efficiency of fiber dispersion
[AD-A269740] 04 p1342 N94-18757
Spatiotemporal variability of non-urban ozone concentrations over the eastern United States and its potential replication by satellite data
[PB93-191328] 04 p1476 N94-19065
Spatial patterns in semiconductor lasers
[DE93-040056] 05 p1814 N94-19865
Spatial and temporal variations of satellite microwave measurements of latent heat release in tropic cyclones due to environmental forcing obtained from a numerical model
[AD-A267947] 05 p1865 N94-20482
Optical climatology of the Northeast Pacific Ocean
[AD-A271671] 05 p1866 N94-20559
Seafloor characterization/Galapagos propagating rift
[AD-A272001] 05 p1882 N94-20581
Lightning studies using LDAR and LLP data
06 p2416 N94-23238
Spatial and temporal variability of soil temperature, moisture and surface soil properties
[NASA-CR-194109] 06 p2401 N94-23337
Tools for visualizing landscape pattern for large geographic areas
[DE94-001121] 06 p2388 N94-24757

Dynamics of the atmosphere of Mars: Review of some outstanding problems 06 p2620 N94-24888
Seafloor characterization/Galapagos propagating rift [AD-A273586] 06 p2419 N94-25165
Spatial symmetry, local integrability and tetrahedron equations in the Baxter-Bazhanov model [DE93-634348] 07 p3002 N94-26038
Characterization of the energy deposition produced by the primary electron beam on the EXCEDE 3 program [AD-A274453] 07 p3033 N94-27084
Effect of precipitate structure on hot deformation of Al-Mg-Mn alloys [DE94-004596] 07 p2741 N94-27622
U-statistics of random-size samples and limit theorems for systems of Markovian particles with non-Poisson initial distributions [AD-A275018] 08 p3464 N94-29129
Multi-channel spatialization systems for audio signals [NASA-CASE-ARC-12013-1-CU] 08 p3245 N94-29364
Use of satellite data to improve parameterization of spatial and temporal variations of gaseous dry deposition in regional-scale models [DE94-005110] 08 p3334 N94-30022
A comparison between two Monte Carlo codes on determination of transient chemical yields [DE94-007224] 09 p3636 N94-32251
A study of the neutral hydrogen distribution of the Milky Way through 21 cm emission and Lyman alpha absorption 09 p3938 N94-32309
Visual encoding of spatial relations [AD-A277400] 09 p3800 N94-32344
A scanning defect mapping system for semiconductor characterization 09 p3885 N94-32446
Spatial correlation of ionospheric variability [AD-A278105] 09 p3776 N94-33041
Martian spectral units derived from ISM imaging spectrometer data 09 p3949 N94-33220
Martian deltas: Morphology and distribution 09 p3950 N94-33230
Snowmelt forecasting: Further cold regions development of operational hydrological forecasting, volume 1 [AD-A278050] 10 p4074 N94-33410
Environmental modeling with GIS: A strategy for dealing with spatial continuity 10 p4080 N94-33421
Spatio-temporal complexity and large-scale structures in problems of continuum mechanic [AD-A278473] 10 p4044 N94-33702
Global changes of radiation situation at heights less than 1000 km [DE94-610504] 11 p4290 N94-35780
Rescaled box counting for the topological analysis of spatial data [DE94-009820] 12 p4461 N94-36464

SPATIAL FILTERING
Presort processor --- optical filtering [AD-A263872] 01 p0382 N94-11300
Per-field filtering and classification of multitemporal ERS-1 SAR imagery 01 p0247 N94-12485
Estimation of the vortex length scale and intensity from two-dimensional samples 02 p0645 N94-14756
Optimization of a subband coding for high definition television with motion controlled three dimensional frequency band decomposition [ETN-93-94396] 02 p0617 N94-14817
Exploitation of cyclostationarity for signal-parameter estimation and system identification [AD-A267137] 03 p0988 N94-15690
Spatial filters for optical correlation [AD-A267199] 03 p1189 N94-15791
Neural-network-directed alignment of optical systems using the laser-beam spatial filter as an example [NASA-TP-3372] 03 p1034 N94-15961
Evaluation of a liquid crystal spatial light modulator capable of amplitude- and phase-modulating modes [AD-A269252] 04 p1577 N94-18262
Interferometer stations at the Air Force Aeroballistic Research Facility [AD-A268776] 04 p1322 N94-18330
A non-homogeneous, spatio-temporal, wavelet multiresolution analysis and its application to the analysis of motion [AD-A270621] 04 p1538 N94-19534
Optical signal processing [AD-A271036] 05 p1983 N94-20013
Phased array antenna with couplers in spatial filter arrangement [CA-PATENT-1,296,098] 05 p1737 N94-21031
Scale-space filtering and threshold hierarchy for image segmentation 05 p1777 N94-22149
Spatial region filtering in IRAF/PROS 05 p1927 N94-22524
Electromagnetic field strength prediction in an urban environment: A useful tool for the planning of LMSS 06 p2283 N94-22795
Characterization of germanium stripe x ray lasers [DE93-019629] 06 p2347 N94-22867
Enhanced coherence x ray laser experiments and simulations [DE94-005367] 08 p3295 N94-30060
Phase-only 128x128 spatial light modulator based on LASLM technology [AD-A277901] 10 p4141 N94-33591

SPATIAL ISOTROPY
U ISOTROPY
U SPATIAL DISTRIBUTION

SPATIAL ORIENTATION
U ATTITUDE (INCLINATION)

SPATIAL RESOLUTION
Interferometric and optical tests of water window imaging x ray microscopes [NASA-CR-193866] 01 p0375 N94-10506
Characterization of a scannerless LADAR system [DE93-011582] 01 p0174 N94-10959
Numerical simulations of thermal convection in rapidly rotating spherical fluid shells 01 p0153 N94-11635
Confocal profilometer with nanometric vertical resolution [DE93-622698] 02 p0653 N94-12857
High spatial resolution x ray microanalysis: Comparison of experiment and incoherent scattering calculations [DE93-011685] 02 p0648 N94-13044
Optical propagation through atmospheric turbulence. Model analysis of anisoplanatism and application to adaptive optics [ONERA-P-1992-4] 02 p0716 N94-14192
Imaging Fourier transform spectrometer [DE93-017193] 02 p0651 N94-14416
Streak camera based SLR receiver for two color atmospheric measurements 03 p0914 N94-15573
High resolution SAR applications and instrument design 03 p0993 N94-15913
Morphometric comparison of Icelandic lava shield volcanoes versus selected Venusian edifices 03 p1248 N94-16178
Multi-resolution processing for fractal analysis of airborne remotely sensed data 03 p1065 N94-16604
Spatial resolution and cloud optical thickness retrievals 03 p1066 N94-16671
Tip-tilt compensation: Resolution limits for ground-based telescopes using laser guide star adaptive optics [DE93-016426] 03 p1237 N94-16872
Effect of spatial resolution on the simulation of regional precipitation in China in a global climate model [DE93-013433] 04 p1489 N94-18053
The land component of the global climate system with adequate spatial resolution [DE93-018951] 04 p1474 N94-18183
High spatial resolution, range gated, underwater imaging method and apparatus [AD-D015882] 04 p1430 N94-18530
Description of an infrared zoomcollimator [FEL-93-A034] 04 p1580 N94-19424
Earth Penetration Radar Imaging System (EPRIS) [DE93-019890] 04 p1391 N94-19542
Uncertainty limited atomic position measurement using optical fields [AD-A271013] 05 p1970 N94-19822
Near atomic resolution microanalysis of interfaces by analytical electron microscopy [DE93-019437] 05 p1687 N94-19904
Ultrafast scanning microscopy [DE93-040121] 05 p1985 N94-20320
Transport in microstructures in the microwave and millimeter-wave regime [AD-A271875] 05 p2017 N94-20470
GMM-1: A 50 degree and order gravitational field model for Mars 05 p2117 N94-20774
Earth-based measurement of lunar topography using delayed radar interferometry 05 p2119 N94-20787
Linear mixing model applied to AVHRR LAC data 05 p1838 N94-20958
Breaking Kelvin-Helmholtz waves and cloud-top entrainment as revealed by K-band Doppler radar 05 p1874 N94-22310
Prospects for future ground-based solar observations 06 p2624 N94-22842
ASTER, a multinational Earth observing concept 06 p2382 N94-23840
Evaluation of image quality 06 p2443 N94-25514
Unsegmented electromagnetic calorimeter prototype. Energy and coordinate resolution [DE93-634185] 07 p2810 N94-26396
The OPAL vertex detector [ISBN-0-315-51152-4] 07 p2812 N94-27257
Simulation of the Indian and East-Asian summer monsoon in the ECMWF model: Sensitivity to horizontal resolution [DE94-004276] 07 p2897 N94-27571
Satellite estimation of the global distribution and interannual variability of photosynthetically active radiation 08 p3334 N94-29970
Ultrafast readout of scintillating fibers using upgraded position-sensitive photomultipliers [DE94-010419] 11 p4269 N94-36095
Submicrometer fiber-optic chemical sensors: Measuring pH inside single cells [DE94-004160] 12 p4525 N94-37532
Comparison of gaseous and semiconductor detectors for medical imaging [DE94-621344] 12 p4482 N94-37729

SPECIFIC GRAVITY
U DENSITY (MASS/VOLUME)

SPECIFIC HEAT
A new method for hysteresis measurements developed for C(sub v) measurements at the critical point during the D2-mission 01 p0107 N94-10114
The High Precision Thermostat HPT-HYDRA 01 p0109 N94-10124
Thermophysical properties of undercooled liquid metals 01 p0086 N94-10190
Measurements of heat capacity in undercooled metals 01 p0087 N94-10231
Thermodynamic model of air in chemical equilibrium 01 p0007 N94-10448
Gas atomized Er3Ni powder for cryocooler applications [DE93-011564] 02 p0568 N94-13000
Optical and physical properties of the LiSrAlF6:Cr laser crystal [DE93-014657] 02 p0808 N94-13881
Measurement of the specific heat capacity of the electron-beam graphite calorimeter [NPL-RSA(EXT)-40] 03 p1031 N94-15018
The specific heat of titanium disilicide [AD-A267543] 03 p0960 N94-17100
Convection effects on radial segregation and crystal melt interface in vertical Bridgman growth [NASA-CR-191541] 03 p1029 N94-17387
The low-temperature specific heat of CeCu2Ge2 at 0 and 9.5 kbar [DE93-014914] 04 p1360 N94-18398
Specific heat of La(1.875-x)Nd(x)Sr(0.125)CuO4: Magnetic and structural transitions [DE93-016978] 04 p1600 N94-18968
Thermophysical properties [DE93-040219] 04 p1351 N94-19134
Realistic theories of heavy electron and other strongly correlated materials [DE93-010350] 04 p1571 N94-19204
Shock induced condensation in fluids of high molar specific heat: Shock structure and relaxation [MPIS-106/1993] 05 p1798 N94-20145
Non-Fermi-liquid and multichannel Kondo phenomena in Y(1-x)U(x)Pd3 and related alloys [DE93-040135] 05 p2015 N94-20275
Non-fermi liquid and spin-glass behavior of the Sc(1-x)U(x)Pd3 system [DE93-040134] 05 p2016 N94-20335
Specific heat of YBa2Cu3O7 [DE93-040640] 05 p2031 N94-21926
Magnetism in CeRu2Ge2 and CeRh2Ge2 and its pressure dependence [DE93-040061] 05 p2032 N94-21987
Magnetic phases in UNiGe [DE94-000793] 06 p2239 N94-22939
Dynamic measurements of thermophysical properties of metals and alloys at high temperatures by subsecond pulse heating techniques 06 p2247 N94-25124
A thermodynamic approach to obtain materials properties for engineering applications 06 p2248 N94-25131
Microwave techniques for physical property measurements 06 p2238 N94-25134
Bulletin of the Institute for Chemical Reaction Science, Tohoku University, volume 2 [JTN-94-80602] 07 p2717 N94-27385
High-temperature and high-pressure flow calorimeter 07 p2718 N94-27390
Endothermic fuels for hypersonic aviation 08 p3197 N94-29285
Centrifugal atomization of lanthanide materials for cryogenic coolers [DE94-006035] 08 p3219 N94-30337
Scaling in heavy-fermion systems [DE94-005002] 08 p3492 N94-30775

SPECIFIC IMPULSE
In-reactor testing of the closed cycle gas core reactor: The Nuclear Light Bulb concept [DE93-004053] 01 p0370 N94-10149
Electromagnetic propulsion for spacecraft [NASA-CR-191186] 02 p0551 N94-13416
Energy storage and conversion in solid hydrogen [AD-A271439] 05 p1845 N94-20086

Optimization and performance analysis of a supersonic conical-flow waverider for a deck-launched intercept mission
[AD-A272498] 05 p1648 N94-21433
Powdered aluminum and oxygen rocket propellants: Subscale combustion experiments
[NASA-TM-106439] 05 p1713 N94-21760
Performance assessment of low pressure nuclear thermal propulsion
[NASA-TM-108433] 05 p1671 N94-21860
Analysis and experiments of a whistler-wave plasma thruster
[DE94-001533] 06 p2209 N94-23012
CFD modeling of microwave electrothermal thrusters 06 p2216 N94-23066
Design considerations of hybrid rockets 06 p2156 N94-24254
Inertial electrostatic confinement as a power source for electric propulsion 07 p2688 N94-27373
Operating characteristics of the Russian D-55 thruster with anode layer
[NASA-TM-106610] 10 p4016 N94-33606
Characteristics of ions emitted from high-current hollow cathodes
[NASA-CR-195372] 12 p4398 N94-37764

SPECIFICATIONS
NT AIRCRAFT SPECIFICATIONS
NT EQUIPMENT SPECIFICATIONS
NT FUNCTIONAL DESIGN SPECIFICATIONS
Test specifications, specimen design and instrumentation test data interpretation
[DE93-012338] 01 p0188 N94-11367
METEOSAT second generation programme SEVIRI: An enhanced visible and IR radiometer for meteorology 01 p0212 N94-12667
Design, qualification and operation of nuclear rockets for safe Mars missions
[DE93-010792] 02 p0549 N94-12996
The design of chain links and slings
[NPL-DMM(A)-94] 02 p0662 N94-13808
Security clauses in the writing and analysis of standards
[NPL-DITC-216-93] 02 p0824 N94-13879
VDM specification of the MD4 message digest algorithm
[NPL-DITC-204/92] 03 p1142 N94-14944
RAISE specification of the MD4 message digest algorithm
[NPL-DITC-206/92] 03 p1142 N94-15010
TITUS: A micro-satellite for technology demonstration 03 p0896 N94-17186
CALS test network handbook
[AD-A267587] 03 p1160 N94-17209
PostScript: A study in conformity
[NPL-DITC-214/93] 04 p1517 N94-17917
The TM manual version 1.3 working document
[MEMO-INF-93-06] 04 p1527 N94-19229
Reference manual for a Requirements Specification Language (RSL), version 2.0
[NASA-CR-191460] 05 p1898 N94-20039
Specification and generation of Markov reward models
[MEMO-INF-92-60] 05 p1963 N94-21058
A simplified token bus protocol specified using LOTOS
[TR-92-15] 05 p1910 N94-21062
Application of the structures query language of APROS for specification of industrial processes 05 p1923 N94-22078
Space Generic Open Avionics Architecture (SGOAA) standard specification
[NASA-CR-188269] 05 p1666 N94-22275
Setting test limits under prescribed consumer loss
[MEMO-1107] 06 p2478 N94-22725
Tools reference manual for a Requirements Specification Language (RSL), version 2.0
[NASA-CR-191461] 06 p2445 N94-23125
Specifications of ETS, the Enhanced Transport Service
[RR-907-I] 06 p2589 N94-23150
Towards the formal specification of the requirements and design of a processor interface unit: HOL listings
[NASA-CR-191465] 06 p2466 N94-23252
Towards the formal verification of the requirements and design of a processor interface unit
[NASA-CR-4522] 06 p2467 N94-24075
Design and specification of a centralized manufacturing data management and scheduling system 06 p2577 N94-24416
Primary standards laboratory report 1st half 1993
[DE94-003138] 07 p2762 N94-26027
The CODE-TOP (COncurrent system DEvelopment using Transformations Of Predicate-transition nets) method: Examples of using it for system architecture specification, software specification, and code generation 07 p2953 N94-26744
Specification performance optimization and executive generation for onboard multiprocessor real time application with SynDEx 07 p2954 N94-26745
Semantics of MANIFOLD: Specification in ASF+SDF and extension
[CWI-CS-R9269] 07 p2971 N94-27575
Telecommand decoder specification
[ESA-PSS-04-151-ISSUE-1] 07 p2693 N94-27583
ARM: Abstract Rewriting Machine
[CWI-CS-R9330] 07 p2974 N94-27794
Using formal specification in the Guidance and Control Software (GCS) experiment. Formal design and verification technology for life critical systems
[NASA-CR-194884] 07 p2956 N94-28267
Impact study on the use of biomass-derived fuels in gas turbines for power generation
[DE94-000261] 08 p3224 N94-28502
Cleanroom engineering handbook. Volume 4. Specification team practices
[AD-A275861] 08 p3156 N94-28753
Invariants, frames and postconditions: A comparison of two formal specification notations
[PB94-138153] 08 p3405 N94-29110
Engineering specification editing tools
[AD-A275116] 08 p3419 N94-29746
Using RDD-100 with CoRE. Version 01.00.03
[AD-A275336] 08 p3419 N94-29797
Second-order algebraic specification of state semantics
[CWI-CS-R9254] 08 p3453 N94-29889
Homomorphism preserving algebraic specifications require hidden sorts
[CWI-CS-R9344] 08 p3459 N94-30436
Service independent building blocks-1: Concepts, examples and formal specifications
[CWI-CS-R9326] 08 p3448 N94-30731
Robust requirements specifications for safety-critical systems
[PB94-167806] 11 p4250 N94-35532
Specification-based software sizing: An empirical investigation of function metrics 12 p4490 N94-36488
Software engineering with application-specific languages 12 p4491 N94-36494
Advanced distributed simulation technology advanced rotary wing aircraft. System/segment specification. Volume 4: Simulation system module RAH-66 Kit
[AD-A280261] 12 p4391 N94-37756

SPECIMEN GEOMETRY
Interfacial cracks in plates: A three-dimensional numerical investigation 04 p1456 N94-19116
Non-linear numerical analysis of the losipescu specimen for composite materials
[NASA-CR-195934] 10 p4020 N94-34306

SPECKLE INTERFEROMETRY
Material characterization and modeling with shear ography
[NASA-CR-192576] 01 p0185 N94-10342
Strain sensing technology for high temperature applications
[NASA-TM-4498] 02 p0648 N94-12874
Speckles statistics and decorrelation effects in complex ABCD optical systems
[AD-A267843] 03 p1193 N94-17012
Properties of the near-axis bispectrum applied to high-resolution astronomical imaging
[ISBN-0-315-85247-X] 07 p3103 N94-27302

SPECKLE PATTERNS
Study of speckle reduction when using a CO2 waveguide laser close to its threshold state
[DSIS-93-00250] 02 p0657 N94-14067
Spatial and frequency diversity in lidar systems
[AD-A266192] 03 p1039 N94-16124
Response of an airborne synthetic aperture radar to sea ice in the marginal ice zone
[ISBN-0-315-84243-1] 07 p2849 N94-26668
Theoretical and experimental analysis of the spatial and temporal behaviour of the intensity of an electro-magnetic wave reflected from a diffuse target after passing through a turbulent atmosphere
[ITN-94-85230] 07 p2774 N94-27234
Elastic modulus measurements of LDEF glasses and glass-ceramics using a speckle technique
[NASA-CR-195911] 09 p3653 N94-31851
Restoration of interferometric, polarimetric, radiometric, and textural information in SAR images 09 p3750 N94-32535

SPECTRA
NT ABSORPTION SPECTRA
NT ATOMIC SPECTRA
NT BALMER SERIES
NT CONTINUOUS SPECTRA
NT D LINES
NT ELECTROMAGNETIC SPECTRA
NT ELECTRONIC SPECTRA
NT EMISSION SPECTRA
NT ENERGY SPECTRA
NT FRAUNHOFER LINES
NT GAMMA RAY SPECTRA
NT H ALPHA LINE
NT H LINES
NT INFRARED SPECTRA
NT K LINES
NT LINE SPECTRA
NT LYMAN SPECTRA
NT MASS SPECTRA
NT MICROWAVE SPECTRA
NT MOLECULAR SPECTRA
NT NEUTRON SPECTRA
NT NOISE SPECTRA
NT OXYGEN SPECTRA
NT PLASMA SPECTRA
NT POWER SPECTRA
NT RADIATION SPECTRA
NT RADIO SPECTRA
NT RAMAN SPECTRA
NT ROTATIONAL SPECTRA
NT RYDBERG SERIES
NT SCHUMANN-RUNGE BANDS
NT SHOCK SPECTRA
NT SOLAR SPECTRA
NT SPECTRAL BANDS
NT STELLAR SPECTRA
NT UBV SPECTRA
NT ULTRAVIOLET SPECTRA
NT VEGARD-KAPLAN BANDS
NT VIBRATIONAL SPECTRA
NT VISIBLE SPECTRUM
NT X RAY SPECTRA
Stationary spectra in a magnetized current-carrying plasma
[DE93-617847] 01 p0386 N94-10397
Coherence effects in radiometry and in spectroscopy
[DE93-013437] 01 p0075 N94-10519
Stationary spectra in a sheared plasma (linear limit)
[DE93-617850] 01 p0387 N94-10540
Polar mesospheric waves and structure
[AD-A265360] 01 p0279 N94-12561
Inclusive single muons at DO
[DE93-012779] 02 p0783 N94-13494
A sum-rule of luminescence spectrum
[ITN-93-85223] 02 p0814 N94-14559
A posteriori error estimation for hierarchic models of elliptic boundary value problems on thin domains
[AD-A267714] 03 p1168 N94-14939
Why is the Moon dark? 03 p1256 N94-16219
Field observations of infragravity, sea and swell directional spectra
[AD-A266439] 03 p1113 N94-16561
Efficient computational methods to study new and innovative signal detection techniques in SETI
[NASA-CR-193602] 03 p0998 N94-16649
In-flight calibration of the spectral and radiometric characteristics of AVIRIS in 1991 03 p1037 N94-16667
A time-frequency smoothing algorithm for cyclic spectral analysis
[DE93-016634] 04 p1519 N94-18097
UVPI imaging from the LACE satellite: The Nihka rocket plume
[AD-A268456] 04 p1334 N94-18149
The LET spectrum and its uncertainty during the CRRES mission
[AD-A269977] 04 p1630 N94-18676
The optical constants and spectral specular reflectivity of Highly Oriented Pyrolytic Graphite (HOPG)
[DE93-040546] 05 p1709 N94-21970
Factors affecting the identification of phytoplankton groups by means of remote sensing
[NASA-TM-108799] 06 p2387 N94-24403
Multivariate spectral analysis to extract materials from multispectral data
[AD-A274142] 07 p2709 N94-27135
A comparison of spectral decorrelation techniques and performance evaluation metrics for a wavelet-based, multispectral data compression algorithm 07 p2946 N94-28258
Quantum dynamics in dual spaces
[DE94-008303] 09 p3913 N94-32824
Storm evolution of directional seas in shallow water
[AD-A278541] 10 p4089 N94-33404
Growth, characterization, and device development in monocrystalline diamond films
[AD-A277863] 10 p4146 N94-33774
The modelling of the ocean surface image in optical remote sensing 10 p4078 N94-34369
The crack severity index of monitored load spectra 10 p4071 N94-34585
High Resolution Transmission Electron Microscopy (HRTEM) of nanophase ferric oxides 11 p4239 N94-35433

Analysis spectral shapes from California and central United States ground motion
[DE94-010041] 12 p4469 N94-36758

SPECTRAL ABSORPTION
U ABSORPTION SPECTRA

SPECTRAL ANALYSIS
U SPECTRUM ANALYSIS

SPECTRAL BANDS
NT ABSORPTION SPECTRA
NT FRAUNHOFER LINES
NT SCHUMANN-RUNGE BANDS
NT VEGARD-KAPLAN BANDS

Review of SHARC 2.0 O3 kinetics and spectroscopy
[AD-A265481] 01 p0274 N94-10496
Thermographic properties of eight blue-emitting phosphors
[DE93-011459] 01 p0078 N94-11622
A comparison of telescopic and Phobos-2 ISM spectra of Mars in the short-wave near-infrared (0.76-1.02 microns) 01 p0424 N94-12053
Near-infrared spectra of the Martian surface: Reading between the lines 01 p0465 N94-12184
Computational methods for problems in aerodynamics using parallel and vector architectures
[AD-A265626] 01 p0016 N94-12377
New challenges in propagation research in the US 02 p0612 N94-14656
BIB photodetectors based on antimony doped silicon 03 p0902 N94-15047
Atmospheric transmittance between 1.0 and 2.0 micrometers
[AD-A267076] 03 p1098 N94-15539
Seasonal and spatial variations in phytoplanktonic chlorophyll in eutrophic Mono Lake, California, measured with the Airborne Visible and Infrared Imaging Spectrometer (AVIRIS) 03 p1069 N94-16684
Use of AVIRIS data to the definition of optimised specifications for land applications with future spaceborne imaging spectrometers 03 p1071 N94-16694
Spectroscopic investigations of nonambient systems with millimeter and submillimeter probes
[AD-A266537] 03 p0968 N94-16796
Earth observational research using multistage EOS-like data
[NASA-CR-194626] 03 p1084 N94-16831
The feasibility of tropospheric and total ozone determination using a Fabry-Perot interferometer as a satellite-based nadir-viewing atmospheric sensor
[NASA-TM-109342] 03 p1102 N94-17214
ASTER, a multinational Earth observing concept 06 p2389 N94-23840
Excitation mechanisms for XUV and x ray lasers
[DE93-617006] 06 p2351 N94-25482
Zodiacal light data investigation. Interim results for the Earthlimb Clutter Experiment
[AD-A274461] 07 p3104 N94-27265
Cooling the Martian atmosphere: The spectral overlap of the C02 15 micrometers band and dust 07 p3107 N94-27886
Wavelet compression techniques for hyperspectral data 07 p2947 N94-28263
Temperature depencence of the far infrared optical constants of polyethylene
[PB94-124336] 08 p3213 N94-28795
Imaging spectrometry of the Earth and other solar system bodies 08 p3237 N94-29779
Evolution of miniature detectors and focal plane arrays for infrared sensors 08 p3237 N94-29781
Characterization of the rare earth orthophosphates and Ce-doped LaPO4 by x ray absorption spectroscopy
[DE94-006313] 09 p3898 N94-31630

SPECTRAL CORRELATION
Nonlinear damping model for flexible structures
[NASA-CR-193711] 02 p0539 N94-12790
A time-frequency smoothing algorithm for cyclic spectral analysis
[DE93-016634] 04 p1519 N94-18097
A comparison of spectral decorrelation techniques and performance evaluation metrics for a wavelet-based, multispectral data compression algorithm 07 p2946 N94-28258

SPECTRAL EMISSION
Characterization of dissolved organic matter in the ocean by using the fluorescence excitation-emission matrix 01 p0211 N94-12659
Measurements of optical properties of waveshifting optical fiber for liquid scintillator hadron calorimetry
[DE93-012606] 02 p0791 N94-13482
A calibration procedure for radiation budget radiometers and its influence on interpretation of measured values
[MITT-82] 02 p0651 N94-14149
Plume radiation 03 p0924 N94-15223
Preliminary analysis of thermal-infrared multispectral scanner data of the Iron Hill, Colorado carbonatite-alkalic rock complex 03 p1065 N94-16605
Thermal infrared remote sensing and Kirchhoff's law: 1. Laboratory measurements 05 p1685 N94-20733
Spectral emissivity of cirrus clouds 05 p1876 N94-22322
Voyager planetary radio astronomy studies
[NASA-CR-194776] 06 p2614 N94-24328
Using contour maps to search for red-shifted 511 keV features in BATSE GRB spectra 06 p2585 N94-24455
Liquidus temperature and optical properties measurement by containerless techniques 06 p2247 N94-25126
Optical properties and emissivities of liquid metals and alloys 06 p2248 N94-25129
A numerical solution to the one and two dimensional line radiative transfer equation
[ISBN-0-315-84258-X] 07 p2994 N94-26640
Computational radiative heat transfer in homogeneous and nonhomogeneous nonscattering media 09 p3702 N94-31563
SeaWiFS technical report series. Volume 16: The second SeaWiFS Intercalibration Round-Robin Experiment, SIRREX-2, June 1993
[NASA-TM-104566-VOL-16] 10 p4093 N94-34412

SPECTRAL ENERGY DISTRIBUTION
Comparison of multiresolution techniques for digital signal processing
[AD-A265364] 01 p0138 N94-12406
The 1 to 5 micron imaging of deeply embedded young stellar objects 02 p0831 N94-13657
A long-term space astrophysics research program: The evolution of the quasar continuum
[NASA-CR-193714] 02 p0839 N94-14404
Acoustic intensity measurements in the presence of low Mach number flow
[AD-A269995] 04 p1562 N94-18664
Relation between the fluctuating wall pressure and the turbulent structure of a boundary layer on a cylinder in axial flow
[AD-A270242] 04 p1418 N94-18906
EXANA: A program for analysing extended energy loss fine structures, EXELFS spectra
[USIP-92-01] 04 p1525 N94-19145
Structuration processes in protoplanetary accretion disks
[MPE-243] 04 p1628 N94-19519
Comparison of higher order moment spectrum estimation techniques
[AD-A272967] 05 p1967 N94-21260
Energy concentration in high energy hadron-gamma families 07 p3113 N94-25632
Catalog of absolutely calibrated, range normalized, wideband, electric field waveforms from triggered lightning flashes in Florida
[AD-A273793] 07 p2892 N94-25873
Characterization of the energy deposition produced by the primary electron beam on the EXCEDE 3 program
[AD-A274453] 07 p3033 N94-27084
Investigations of the dynamical evolution of protoplanetary nebulae
[NASA-CR-195278] 07 p3105 N94-27428
Parameter identification of the rotordynamic coefficients of high-Reynolds-number hydrostatic bearings 08 p3311 N94-30792
Multiwavelength search for protoplanetary disks 09 p3599 N94-31430
Radio emission from pre-main-sequence stars 09 p3955 N94-31890
Near and far infrared observations of protostars and dark clouds 09 p3926 N94-31969
Note on the variance of autospectral density processed using Welch's method
[DE94-005352] 09 p3849 N94-32675
Adaptive estimation and approximation of continuously varying spectral density functions to airborne radar
[AD-A277532] 10 p4033 N94-33710

SPECTRAL LINE WIDTH
Selenium x ray laser line profile measurements
[DE93-012580] 02 p0658 N94-14175
Experimental measurements of selenium x-ray laser spectral line profiles
[DE93-016543] 02 p0659 N94-14595
Effect of exciton localization and delocalization on magnetic-field-dependent photoluminescence linewidths in semiconductors
[DE93-018860] 05 p1748 N94-19884
Investigation of the solid-solid surface adsorption of Eu2O3 on amorphous Al2O3
[DE93-613824] 06 p2566 N94-25332
Impact of observed hyperfine splitting on X-ray laser gain
[DE94-005822] 09 p3717 N94-32128
Final report on spectral broadening by cross-phase modulation in linearly birefringent optical fibers
[DE94-010406] 12 p4524 N94-37191

SPECTRAL LINES
U LINE SPECTRA

SPECTRAL METHODS
A spectral nodal method for the solution of the Sn equations in x, y geometry for highly absorbing deep penetration problems
[DE93-613520] 01 p0349 N94-10636
New developments in the method of space-time conservation element and solution element: Applications to the Euler and Navier-Stokes equations
[NASA-TM-106226] 01 p0150 N94-10939
Computational methods for problems in aerodynamics using parallel and vector architectures
[AD-A265626] 01 p0016 N94-12377
DNS on control of laminar-turbulent transition in channel flow with suction and blowing 01 p0163 N94-12613
Boundary conditions and bifurcations in plane Poiseuille flow 01 p0166 N94-12634
The Chebyshev-Legendre method: Implementing Legendre methods on Chebyshev points
[NASA-CR-191497] 02 p0769 N94-13725
On the geometry of external spectral factors and the Riccati inequality
[CWI-BS-R9227] 02 p0770 N94-14002
The spectral viscosity method applied to simulation of waves in a stratified atmosphere
[FFI-92/7047] 02 p0637 N94-14040
Numerical simulation of three-dimensional self-gravitating flow
[NASA-TM-109021] 03 p1021 N94-15768
Computational Fluid Dynamics
[VKI-LS-1993-04] 04 p1412 N94-18557
Introduction to spectral methods: Application to the Stokes problem 04 p1413 N94-18566
Introduction to spectral methods for hyperbolic system of conservation laws 04 p1413 N94-18567
On the numerical analysis of nonlinear Galerkin methods: Spectral approximation and finite elements
[ETN-93-94900] 04 p1552 N94-19407
Stability measurements of Rayleigh-Benard convection near the critical state using a spectral model
[MPIS-15/1992] 04 p1422 N94-19520
On the relationship between spectral domain approach and method of lines 05 p1794 N94-22254
Rigorous analysis of thick microstrip antennas and wire antennas embedded in a substrate
[EUT-92-E-263] 06 p2290 N94-22876
Relaxation schemes for Chebyshev spectral multigrid methods 06 p2484 N94-23688
Multi-grid domain decomposition approach for solution of Navier-Stokes equations in primitive variable form 06 p2341 N94-23693
On the dynamics of approximating schemes for dissipative nonlinear equations 06 p2332 N94-24168
Triangular spectral elements for incompressible fluid flow
[AD-A276838] 06 p2490 N94-24914
Rendering of three-dimensional data sets derived from finite-difference and spectral methods
[AD-A273724] 07 p3096 N94-25997
Recent advances in the spectral element method 07 p2657 N94-28348
A global forecast model comparison study - year 1
[AD-A275674] 08 p3369 N94-28663
Spectral analysis of wave propagation in connected waveguides 08 p3277 N94-29944
A spectral boundary integral equation method for the 2-D Helmholtz equation
[AD-A279021] 08 p3454 N94-30207
Process modelling for materials preparation experiments
[NASA-CR-195782] 08 p3175 N94-30242
An experimental study of nonlinear wave coupling and energy transfer characterizing the transition of a planar jet shear layer 08 p3282 N94-30953
Transition to turbulence in confined compressible mixing layers 08 p3283 N94-30958
Spectral analysis method and sample generation for real time visualization of speech
[ETN-94-95732] 09 p3674 N94-31573
A stability estimate based on numerical ranges with application to a spectral discretization of a convection-diffusion equation
[TW-93-12] 09 p3847 N94-32200
Analysis of a slot coupled coplanar waveguide fed patch antenna
[NASA-TM-106567] 09 p3698 N94-33116
A locally analytic method for the Euler equations 10 p4042 N94-33363
Pseudospectral collocation methods for fourth order differential equations
[AD-A281653] 10 p4129 N94-34260

On the Gibbs phenomenon 4: Recovering exponential accuracy in a sub-interval from a Gegenbauer partial sum of a piecewise analytic function
[AD-A281638] 10 p4129 N94-34261
A fast numerical solution of scattering by a cylinder: Spectral method for the boundary integral equations
[AD-A281617] 10 p4050 N94-34949
Periodized wavelets
[DE94-010365] 11 p4316 N94-36432

SPECTRAL NOISE
U WHITE NOISE

SPECTRAL RECONNAISSANCE
Remote sensing for hurricane Andrew impact assessment 09 p3758 N94-32464
Developments in ERS-1 SAR interferometry: Use of the spectral shift 09 p3756 N94-32569

SPECTRAL REFLECTANCE
High-reflectance water mass in Off-Sanriku area observed by CZCS 01 p0200 N94-11951
A comparison of telescopic and Phobos-2 ISM spectra of Mars in the short-wave near-infrared (0.76-1.02 microns) 01 p0424 N94-12053
Reflectance spectra of sulfate-and carbonate-bearing Fe(3+)-doped montmorillonites as Mars soil analogs 01 p0445 N94-12070
The effects of atmospheric pressure on infrared reflectance spectra of Martian analogs 01 p0445 N94-12071
Spectral and multispectral imaging studies of lunar mantled mare deposits 01 p0446 N94-12079
Compositional and textural information from the dual inversion of visible, near and thermal infrared remotely sensed data 01 p0258 N94-12097
How diverse is the asteroid belt? 01 p0430 N94-12124
Simulation of possible regolith optical alteration effects on carbonaceous chondrite meteorites 01 p0430 N94-12163
Spectral mixing models of S-Type asteroids 01 p0431 N94-12164
Olivine-rich asteroids, pallasitic olivine and olivine-metal mixtures: Comparisons of reflectance spectra 01 p0431 N94-12171
Chondrites, S asteroids, and space weathering: Thumping noises from the coffin? 01 p0433 N94-12244
A comparison of the visible and near infrared reflectance of hydrovolcanic palagonite tuffs and Martian weathered soils 01 p0477 N94-12245
Properties of spectral reflectance of crown and crown structure of mangrove species in Okinawa 01 p0218 N94-12700
Variability of spectral reflectance in coastal waters near the river plumes 01 p0226 N94-12744
Planetary astronomy of Mars. Mars data reduction
[NASA-CR-193515] 01 p0424 N94-12768
The optical constants and spectral specular reflectivity of Highly Oriented Pyrolytic Graphite (HOPG)
[DE93-011894] 02 p0790 N94-12865
Quantitative mapping of pore fraction variations in silicon nitride using an ultrasonic contact scan technique
[NASA-TP-3377] 02 p0665 N94-13056
Spectral reflectance of soils from Sao Paulo State
[INPE-5424-PRP/172] 02 p0684 N94-13377
Analytical framework for modeling scale-related variabilities in remote sensing 02 p0685 N94-13592
Operational test of the airborne data acquisition system: SADA, the Bara Bonita experiment
[INPE-5451-NTC/305] 02 p0685 N94-13610
The state of Fe in the lunar regolith and its relationship to the spectral reflectance properties of the moon 02 p0843 N94-14303
Fullerene superconductors
[AD-A266749] 03 p1010 N94-15954
Spectral evidence of size dependent space weathering processes on asteroid surfaces 03 p1241 N94-16174
Comparison of reflectance spectra of C asteroids and unique C chondrites Y86720, Y82162, and B7904 03 p1242 N94-16246
Iron oxide bands in the visible and near-infrared reflectance spectra of primitive asteroids 03 p1242 N94-16274
Mixing model analysis of telescopic lunar spectra 03 p1284 N94-16371
Galileo SSI lunar observations: Copernican craters and soils 03 p1288 N94-16395
Analysis of pyroxene absorptions observed in Martian dark regions 03 p1292 N94-16411
Optical effects of regolith processes on S asteroids as simulated by laser impulse alteration of ordinary chondrite 03 p1246 N94-16422
Terrestrial impact melts as analogues for the hematization of Martian surface materials 03 p1104 N94-16424
The spectrum of Phobos from Phobos 2 observations at 0.3-2.6 microns: Comparison to previous data and meteorite analogs 03 p1295 N94-16429
Variations in the Fe mineralogy of bright Martian soil 03 p1295 N94-16431
Composition of weakly altered Martian crust 03 p1296 N94-16436
From minerals to rocks: Toward modeling lithologies with remote sensing 03 p1086 N94-16437
The 1991 AVIRIS/POLDER experiment in Camargue, France 03 p1070 N94-16691
Tracking photosynthetic efficiency with narrow-band spectroradiometry
[CIW-PUBL-1133] 03 p1072 N94-16698
Oregon transect: Comparison of leaf-level reflectance with canopy-level and modelled reflectance 03 p1073 N94-16702
Discussion of band selection and methodologies for the estimation of precipitable water vapour from AVIRIS data 03 p1074 N94-16707
Comparison of remote sensing measurements with a two-scale polarimetric emission and scattering model for sea surfaces 05 p1721 N94-20415
Spectral reflectance studies of the Humorum Basin region 05 p2101 N94-20682
Optical effects of space weathering on lunar soils and the role of the finest fraction 05 p2101 N94-20687
Comparison of visible and near-infrared reflectance spectra of CM2 carbonaceous chondrites and primitive asteroids 05 p2085 N94-20848
Multispectral studies of selected crater- and basin-filling lunar Maria from Galileo Earth-Moon encounter 1 05 p2136 N94-20876
Optical component MAC Europe ground truth report: Flevoland 1991 (Netherlands)
[BCRS-92-27] 06 p2382 N94-23177
The measurement and analysis of leaf spectral reflectance of two stands of loblolly pine populations 06 p2389 N94-24442
In situ x ray reflectivity measurements of thin film structural evolution
[DE94-002289] 07 p3051 N94-25944
The optical properties of high-T(c) superconductors grown by pulsed laser deposition
[ISBN-0-315-84917-7] 07 p3039 N94-27962
Radiation/remote sensing: Review of the principal definitions 09 p3757 N94-30996
Modeling the interaction between solar radiation and terrestrial surfaces 09 p3779 N94-30999
Estimation of visible and near-infrared reflectivity for Peyto Glacier Basin using satellite data
[ISBN-0-315-87039-7] 09 p3743 N94-31733
Feasibility evaluation of new data interpretation approaches for vegetation analysis from airborne imaging spectroscopy 09 p3745 N94-31862
Monitoring fertilizer application by imaging spectrometry (Somerset Levels test site) 09 p3745 N94-31863
High resolution spectroscopy in agriculture: Results of the EISAC 1989 campaign 09 p3745 N94-31864
Evaluation of Fluorescence Line Imager (FLI) airborne imaging spectrometer data for roadside tree damage assessment 09 p3745 N94-31866
Parameterizing atmosphere-land surface exchange for climate models with satellite data: A case study for the Southern Great Plains CART site
[DE94-005109] 09 p3775 N94-32874
The importance of environmental conditions in reflectance spectroscopy of laboratory analogs for Mars surface materials 09 p3944 N94-33195
Ferric sulfate montmorillonites as Mars soil analogs 09 p3944 N94-33196
Mineralogical diversity (spectral reflectance and Moessbauer data) in compositionally similar impact melt rocks from Manicouagan Crater, Canada 09 p3948 N94-33219
Martian spectral units derived from ISM imaging spectrometer data 09 p3949 N94-33220
VEG: An intelligent workbench for analysing spectral reflectance data 10 p4125 N94-35059
Absolute calibration and atmospheric versus mineralogic origin of absorption features in 2.0 to 2.5 micron Mars spectra obtained during 1993 11 p4356 N94-35404
Wavelength calibration techniques and subtle surface and atmospheric absorption features in the Mariner 6, 7 IRS reflectance data 11 p4356 N94-35405
Possible spinel absorption bands in S-asteroid visible reflectance spectra 11 p4368 N94-36139
Hematite formed from pyroxene on Mars by meteoritic impact 11 p4372 N94-36165
Moessbauer mineralogy of calcined Murchison meteorite 11 p4353 N94-36166

SPECTRAL RESOLUTION
Effects of satellite spectral resolution and atmospheric water vapor on retrieval of near-ground temperatures
[AD-A264920] 01 p0245 N94-11851
Using high spectral resolution spectrophotometry to study broad mineral absorption features on Mars 01 p0446 N94-12077
Near-infrared spectra of the Martian surface: Reading between the lines 01 p0465 N94-12184
Spatial resolution and cloud optical thickness retrievals 03 p1066 N94-16671
Primary studies of trace quantities of green vegetation in Mono Lake area using 1990 AVIRIS data 03 p1071 N94-16695
AVIRIS as a tool for carbonatite exploration: Comparison of SPAM and Mbandmap data analysis methods 03 p1073 N94-16703
Earth observational research using multistage EOS-like data
[NASA-CR-194626] 03 p1084 N94-16831
The feasibility of tropospheric and total ozone determination using a Fabry-Perot interferometer as a satellite-based nadir-viewing atmospheric sensor
[NASA-TM-109342] 03 p1102 N94-17214
Monitoring the response of the upper troposphere/lower stratosphere to a greenhouse gas scenario
[DE93-014509] 04 p1470 N94-17710
Detailed analysis of low energy plasma data under the Voyager Uranus data analysis program
[NASA-CR-193668] 04 p1628 N94-17842
New room temperature high resolution solid-state detector (CdZnTe) for hard x rays and gamma rays 04 p1324 N94-19165
A high resolution ultraviolet Shuttle glow spectrograph 04 p1325 N94-19174
MinMap: An imaging spectrometer for high resolution compositional mapping of the Moon 05 p1813 N94-20688
Analysis of hyper-spectral AVIRIS image data over a mixed-conifer forest in Maine 05 p1838 N94-20959
Michelson Interferometer (MINT) 05 p1813 N94-21646
Multiorder etalon sounder (MOES) development and test for balloon experiment
[NASA-CR-194730] 05 p1859 N94-22026
Cirrus cloud retrievals from HIS observations during FIRE 2 05 p1875 N94-22315
Adaptive filtering of Echelle spectra of distant Quasars 05 p2072 N94-22520
How well was total ozone abundance inferred with Mariner 9? 07 p3108 N94-27891
Evolution of miniature detectors and focal plane arrays for infrared sensors 08 p3237 N94-29781
Evaluation of GER- and FLI-data with reference to forest 09 p3746 N94-31868
Studies of impulsive solar bursts observed with high spectral resolution in the range of 18 to 23 GHz
[INPE-5538-TDI/526] 10 p4165 N94-34219
A spectral atlas of the nu(sub 12) fundamental of (13)C(12)CH6 in the 12 micron region
[NASA-TM-104601] 10 p4138 N94-34945

SPECTRAL SENSITIVITY
Imaging Fourier transform spectrometer
[DE93-017193] 02 p0651 N94-14416
On coefficient quantization and computational roundoff effects in frequency interpolation filter banks 05 p1793 N94-22251
High degree gravitational sensitivity from Mars orbiters for the GMM-1 gravity model
[NASA-TM-104604] 10 p4088 N94-34992

SPECTRAL SIGNATURES
NT MICROWAVE SIGNATURES
Chondrites, S asteroids, and space weathering: Thumping noises from the coffin? 01 p0433 N94-12244
Spectral evidence of size dependent space weathering processes on asteroid surfaces 03 p1241 N94-16174
Terrestrial impact melts as analogues for the hematization of Martian surface materials 03 p1104 N94-16424
Mapping vegetation types with the multiple spectral feature mapping algorithm in both emission and absorption 03 p1069 N94-16686
Atmospheric correction of AVIRIS data in ocean waters 03 p1070 N94-16690
Use of AVIRIS data to the definition of optimised specifications for land applications with future spaceborne imaging spectrometers 03 p1071 N94-16694
Materials processing and manufacturing technologies for diamond substrates multichip modules
[AD-A268989] 04 p1599 N94-18764
A study of carbonates, sulfates, and phosphates using thermal emission spectroscopy 05 p1686 N94-20868
Predicting LANDSAT MSS endmember signatures from corresponding higher resolution TM fraction images 05 p1839 N94-20962

Mapping coastal habitats using an imaging spectrometer
[ISBN-0-315-84362-4] 07 p2848 N94-26664
Convection and electrodynamic signatures in the vicinity of a Sun-aligned arc: Results from the Polar Acceleration Regions and Convection Study (Polar ARCS) 09 p3954 N94-31102
Smart environmental monitor based on neural networks and multi-spectral pattern recognition
[AD-A276445] 09 p3829 N94-31301
European Imaging Spectroscopy Aircraft Campaign
[ESA-SP-360] 09 p3743 N94-31853
Inflight calibration, preprocessing, and data evaluation of GER 2 imaging spectrometry data 09 p3744 N94-31858
Extraction of agricultural parameters from imaging-spectrometry data and simulated MERIS data through red edge analysis 09 p3745 N94-31865
Near and far infrared observations of protostars and dark clouds 09 p3926 N94-31969
Mineralogical diversity (spectral reflectance and Moessbauer data) in compositionally similar impact melt rocks from Manicouagan Crater, Canada 09 p3948 N94-33219
The effects of cloud inhomogeneities upon radiative fluxes, and the supply of a cloud truth validation dataset
[NASA-CR-196080] 11 p4293 N94-35391
Thermal emission measurements (5-25 microns) of Hawaiian palagonitic soils with implications for Mars 11 p4292 N94-35452

SPECTRAL THEORY
HEAO-1 analysis of Low Energy Detectors (LED)
[NASA-CR-194087] 01 p0424 N94-12574
Phillips Laboratory global spectral numerical weather prediction model
[AD-A267293] 03 p1107 N94-17244
Full Boltzmann discrete spectral wave model, implementation and nondimensional tests
[AD-A269885] 04 p1498 N94-18685
Short-range cloud amount forecasting with model output statistics
[AD-A274769] 07 p2895 N94-26798
An enhanced global spectral model
[PL-TR-92-2011] 07 p2898 N94-28223
The evolution of jet features during the 1993 east coast white hurricane: A case study using the global spectral model
[AD-A277217] 09 p3783 N94-32021
Determination of extensional viscosity from capillary rheometer entrance pressure drop measurements using a numerical simulation of contraction flow
[PB94-171154] 11 p4263 N94-35603

SPECTROGRAMS
Comparison of higher order moment spectrum estimation techniques
[AD-A272967] 05 p1967 N94-21260
The cool-star spectral catalog: A uniform collection of IUE SWP-LOs 05 p2046 N94-22446

SPECTROGRAPHS
NT HIGH DISPERSION SPECTROGRAPHS
Vacuum ultraviolet instrumentation for solar irradiance and thermospheric airglow
[NASA-CR-194525] 02 p0652 N94-14684
UVSTAR: An imaging spectrograph with telescope for the Shuttle Hitchhiker-M platform 04 p1326 N94-19178
The star identification, pointing and tracking system of UVSTAR, an attached payload instrument system for the Shuttle Hitchhiker-M platform 04 p1326 N94-19179
Fiber optic Raman spectrograph for in situ environmental monitoring
[DE93-019466] 04 p1478 N94-19305
Writing instrument interfaces with xf/tktcl 05 p1925 N94-22480
SPECFOCUS: An IRAF task for focusing spectrographs 05 p1965 N94-22540
Hubble Space Telescope Goddard High Resolution Spectrograph (GHRS) Instrument Handbook (for the Post-COSTAR Observatory), version 5.0
[NASA-CR-189369] 11 p4349 N94-36282
Hubble Space Telescope faint object spectrograph instrument handbook, version 5.0
[NASA-CR-189367] 12 p4546 N94-36794
Guaranteed time observations support for Faint Object Spectrograph (FOS) on HST
[NASA-CR-196305] 12 p4547 N94-37037

SPECTROHELIOGRAPHS
Berne (Switzerland) solar observations: Data for April 1991 - August 1992
[REPT-59] 05 p2147 N94-21150
Preliminary results of observations of solar flares with Nobeyama Radioheliograph 05 p2001 N94-22633
Solar-geophysical data number 593, January 1994. Part 1: (Prompt reports). Data for December, November 1993, and late data
[PB94-151578] 10 p4165 N94-34163

SPECTROHELIOSCOPES
U SPECTROHELIOGRAPHS

SPECTROMETERS
NT EBERT SPECTROMETERS
NT FABRY-PEROT SPECTROMETERS
NT GAMMA RAY SPECTROMETERS
NT HIGH DISPERSION SPECTROGRAPHS
NT IMAGING SPECTROMETERS
NT INFRARED SPECTROMETERS
NT LASER SPECTROMETERS
NT MASS SPECTROMETERS
NT MICROWAVE SPECTROMETERS
NT NEUTRON SPECTROMETERS
NT SOLAR SPECTROMETERS
NT SPECTROHELIOGRAPHS
NT TIME OF FLIGHT SPECTROMETERS
NT TOTAL OZONE MAPPING SPECTROMETER
NT ULTRAVIOLET SPECTROMETERS
A new matrix for the ageless 21.6-keV Eu-151 nuclear gamma ray Moessbauer source
[DE93-009795] 01 p0075 N94-10338
Strange meson spectroscopy in K(omega) and K(phi) at 11 GeV/c and Cherenkov ring imaging at SLD
[DE93-013593] 01 p0363 N94-10748
Implications of aerosol retrieval and atmospheric correction in remote sensing 01 p0205 N94-11978
Remote sensing x ray fluorescence spectrometry for future lunar exploration missions 01 p0462 N94-12165
Moessbauer spectrometer for mineralogical analysis of the Mars surface: Moessbauer source considerations 01 p0476 N94-12242
Modis-N airborne simulator
[NASA-CR-189303] 02 p0792 N94-13719
E789 and P865: High-rate fixed-target studies of charm and beauty
[DE93-017223] 02 p0788 N94-14898
CdTe array detectors for high energy astronomy 03 p0899 N94-15029
The development of back-illuminated CCD's for XMM 03 p0900 N94-15035
Optimisation of FIR photoconductors for atmospheric spectroscopy 03 p0902 N94-15048
Applications for large area silicon drift detectors on x ray and gamma ray astronomy 03 p0909 N94-15090
Performance of the position-sensitive proportional counters of the Yohkoh Bragg crystal spectrometer 03 p0909 N94-15094
Preliminary results from bubble detector measurements aboard Biocosmos-2044 03 p0981 N94-16097
A Moessbauer spectrometer for the mineralogical analysis of the Mars surface: First temperature dependent tests of the detector and drive system 03 p1259 N94-16233
Frequency resolution of an acousto-optical spectrometer
[AD-A267822] 03 p1035 N94-17401
Optimisation and specification of Auger electron spectrometers for signal-to-noise ratio performance
[NPL-DMM(A)-101] 03 p1006 N94-17549
Comparison of computer predictions and magnetic field measurements for an iron spectrometer magnet
[DE93-016164] 03 p1176 N94-17658
Designs for optical components related to the Los Alamos free-electron laser
[DE93-016617] 04 p1436 N94-17865
Proceedings of the 3rd Workshop on Balloon-Borne Experiments with Superconducting Magnet Spectrometers
[DE93-788362] 04 p1630 N94-18219
Fiber optic Raman spectrograph for in situ environmental monitoring
[DE93-019466] 04 p1478 N94-19305
Legacy of the X Ray Laser Program
[DE93-019550] 04 p1442 N94-19554
Analysis of Ku-band cross section at low incidence angles 05 p1720 N94-20414
Rotational spectrum of a dark state in 2-fluoroethanol using microwave/radiofrequency-infrared multiple resonance
[AD-A272101] 05 p1817 N94-20583
Wavelength dispersive analysis with the synchrotron x ray fluorescence microprobe 05 p1685 N94-20717
Combined backscatter Moessbauer spectrometer/x ray fluorescence analyzer (BaMS/XRF) for extraterrestrial surfaces 05 p1686 N94-20761
Mirror velocity sampling errors in a Michelson interferometer
[AD-A273105] 05 p1809 N94-21508
Applications of correlator chips in radio science 05 p1763 N94-21695
A 1 GHz sample rate, 256-channel, 1-bit quantization, CMOS, digital correlator chip 05 p1768 N94-21732
Low power, CMOS digital autocorrelator spectrometer for spaceborne applications 05 p1666 N94-21733
A Backscatter Moessbauer Spectrometer (BaMS) for use on Mars 05 p1811 N94-22431
Magnetic resonance study of zinc-related defects in silicon with optimized EPR spectrometer
[PB93-224640] 06 p2561 N94-23223
Measurement of HO2 and other trace gases in the stratosphere using a high resolution far-infrared spectrometer
[NASA-CR-195173] 06 p2404 N94-24738
Performance of inverse photoemission spectrometer with a new bandpass photon detector of narrow bandwidth and high sensitivity
[REPT-A-2659] 06 p2345 N94-24977
Experimental characterization of the AFIT Neutron Facility
[AD-A273822] 06 p2539 N94-25519
Study on neutron activation analysis
[DE93-632191] 07 p3017 N94-26116
Inter-comparison of Wildfire and High-resolution Interferometer Sounder (HIS) data from STORM-FEST: An investigation of wildfire spectral channel discrepancies
[NASA-TM-108439] 08 p3333 N94-29553
Developing a diode array spectrometer for tropospheric chemistry studies 08 p3362 N94-29752
Backscatter Mossbauer Spectrometer (BaMS) for extraterrestrial applications 08 p3236 N94-29774
A Tevatron collider beauty factory
[DE94-004879] 08 p3488 N94-29930
Algorithm and program ORANGE for magnetic field simulation of magnetic system spectrometer STORS
[DE94-608013] 08 p3421 N94-30083
Instrumentation for EXELFS measurements using convergent beam diffraction coupling to the electron energy loss spectrometer
[USIP-93-07] 09 p3858 N94-31084
Odin aeronomy science: A phase-A report by the Aeronomy Science Working Group for the Odin satellite
[AP-31] 09 p3770 N94-31222
Elementary particle physics
[DE94-006071] 09 p3866 N94-31620
Various magnet options for Delta launched version of ASTROMAG
[DE94-006292] 09 p3955 N94-31635
Time domain spectroscopy for studying a monopole antenna immersed in a plasma
[ISBN-0-315-86526-1] 09 p3888 N94-31727
The Los Alamos National Laboratory precision double crystal spectrometer
[DE94-008075] 09 p3713 N94-32706
Ultraviolet Absorption Spectrometry (UVAS) and Liquid Atomic Emission Spectrometry (LAES) for oceanographic analysis systems
[AD-A278263] 10 p4091 N94-33413
Total hydrocarbon analysis by ion mobility spectrometry 10 p4101 N94-33642
Detection of the 267 GHz J = 1-0 rotational transition of PH3 in Saturn with a new Fourier transform spectrometer
[NASA-CR-194364] 10 p4162 N94-34718
Instrumentation for in-flight SSME rocket engine plume spectroscopy
[NASA-TM-106596] 11 p4268 N94-35268
Innovative instrumentation for mineralogical and elemental analyses of solid extraterrestrial surfaces: The Backscatter Moessbauer Spectrometer/X Ray Fluorescence analyzer (BaMS/XRF) 11 p4239 N94-35459
An indigenously developed photoacoustic spectrometer for study of actinide spectroscopy
[DE94-616508] 11 p4235 N94-35592
Airborne ROWS data report for the high resolution experiment, June 1993
[NASA-TM-104609] 12 p4477 N94-37397

SPECTROMETRY
U SPECTROSCOPY

SPECTROPHOTOMETERS
NT INFRARED SPECTROPHOTOMETERS
Vacuum ultraviolet instrumentation for solar irradiance and thermospheric airglow
[NASA-CR-194525] 02 p0652 N94-14684
Reflectometer employing an integrating sphere and lens-mirror concentrator
[AD-D016061] 07 p3039 N94-27676
Ultraviolet Absorption Spectrometry (UVAS) and Liquid Atomic Emission Spectrometry (LAES) for oceanographic analysis systems
[AD-A278263] 10 p4091 N94-33413
Determining the refractive index of a lambda/4 thin film on a thick substrate from a transmittance measurement
[DE93-019584] 12 p4523 N94-36693
Hubble Space Telescope Wide Field and Planetary Camera 2 Instrument handbook, version 2.0
[NASA-CR-189368] 12 p4547 N94-36918

SPECTROPHOTOMETRY
NT STELLAR SPECTROPHOTOMETRY

Using high spectral resolution spectrophotometry to study broad mineral absorption features on Mars
01 p0446 N94-12077
The 1.2 to 3.5 microns observations of asteroid 4179 Toutatis 01 p0430 N94-12111
Disk-resolved spectral characteristics of Saturn's medium-sized satellites 01 p0471 N94-12213
Properties of spectral reflectance of crown and crown structure of mangrove species in Okinawa
01 p0218 N94-12700
Laser fluorescent monitoring of dissolved organic matter in natural water 01 p0177 N94-12755
Heliocentric zoning of the asteroid belt by aluminum-26 heating 03 p1241 N94-16205
Evaluation of hemoglobin-oxygen equilibrium binding by rapid-scanning spectrophotometry and singular-value decomposition
[AD-A266453] 03 p1123 N94-16564
Comparison of visible and near-infrared reflectance spectra of CM2 carbonaceous chondrites and primitive asteroids 05 p2085 N94-20848
Digital image profilers for detecting faint sources which have bright companions
[NASA-CR-191348] 09 p3927 N94-32695
A quick look method of detecting water of hydration in small solar system bodies 11 p4352 N94-35470
Determination of copper in tap water using solid-phase spectrophotometry
[NASA-TM-106480] 12 p4408 N94-36537
Guaranteed time observations support for Faint Object Spectrograph (FOS) on HST
[NASA-CR-196305] 12 p4547 N94-37037

SPECTROPOLARIMETERS
U POLARIMETERS

SPECTRORADIOMETERS
Global monitoring of atmospheric properties by the EOS MODIS
[NASA-TM-109237] 01 p0231 N94-11485
Colorimetric qualification of shear sensitive liquid crystal coatings
[NASA-CR-194126] 02 p0806 N94-13291
Spectral reflectance of soils from Sao Paulo State
[INPE-5424-PRP/172] 02 p0684 N94-13377
Operational test of the airborne data acquisition system: SADA, the Bara Bonita experiment
[INPE-5451-NTC/305] 02 p0685 N94-13610
Advanced solid-state array spectroradiometer data collection during HAPEX-2 Sahel
[NASA-CR-194144] 02 p0808 N94-13875
Almaz 03 p0898 N94-15889
Intercomparison of MAS, AVIRIS, and HIS data from FIRE cirrus 2 05 p1872 N94-22298
Concept of ASTER calibration requirement
06 p2384 N94-23609
The measurement and analysis of leaf spectral reflectance of two stands of loblolly pine populations
06 p2389 N94-24442
Radiometric, spectral, and effectiveness equipment
[AD-A274208] 07 p3037 N94-27066
The automated rotating shadowband spectroradiometer
[DE94-001878] 08 p3269 N94-28464
Chamber optics for testing passive remote sensing vapor detectors
[AD-A275909] 09 p3878 N94-31340
MODIS. Volume 1: MODIS level 1A software baseline requirements
[NASA-TM-104594-VOL-1] 09 p3823 N94-33287

SPECTROSCOPES
U SPECTROMETERS

SPECTROSCOPIC ANALYSIS
Laser spectroscopy
[DE93-009403] 01 p0173 N94-10255
Review of SHARC 2.0 O3 kinetics and spectroscopy
[AD-A265481] 01 p0274 N94-10496
The multiplicity spectra of the (169)Tm(n, gamma) reaction
[DE93-617733] 01 p0364 N94-10835
Radiation effects in Ga(0.47)In(0.53)As solar cells
01 p0052 N94-11404
Characterization of an excimer laser-ablated plasma and applications 01 p0392 N94-11450
Moessbauer spectroscopy of the SNC meteorite Zagami 01 p0428 N94-12016
Measurements of cosmogenic nuclides in lunar rock 64455 01 p0437 N94-12033
Mineralogy of chondritic interplanetary dust particle impact residues from LDEF 01 p0080 N94-12045
Disk-resolved spectral characteristics of Saturn's medium-sized satellites 01 p0471 N94-12213
Atmospheric and spectroscopic research in the far infrared
[NASA-CR-193551] 01 p0280 N94-12582
Ecological application of Surface Enhanced Raman Spectroscopy 01 p0227 N94-12756
Procedures for analysis of debris relative to Space Shuttle systems
[NASA-TM-109190] 02 p0534 N94-12900
The evidence for clumpy accretion in the Herbig Ae star HR 5999
[NASA-CR-189314] 02 p0828 N94-12915
Determination of trace elements in triglycine sulfate solutions
[NASA-CR-193481] 02 p0562 N94-13048
Quantitative mapping of pore fraction variations in silicon nitride using an ultrasonic contact scan technique
[NASA-TP-3377] 02 p0665 N94-13056
Determination of spectroscopic properties of atmospheric molecules from high resolution vacuum ultraviolet cross section and wavelength measurements
[NASA-CR-194024] 02 p0712 N94-13092
Scanning tunneling microscopy studies of diamond films and optoelectronic materials
[NASA-CR-194363] 02 p0578 N94-13246
Colorimetric qualification of shear sensitive liquid crystal coatings
[NASA-CR-194126] 02 p0806 N94-13291
The International Colloquium on Atomic Spectra and Oscillator Strengths for Astrophysical and Laboratory Plasmas
[NASA-TM-109255] 02 p0849 N94-13376
Hard x ray/microwave spectroscopy of solar flares
[NASA-CR-194399] 02 p0844 N94-13958
E789 and P865: High-rate fixed-target studies of charm and beauty
[DE93-017223] 02 p0788 N94-14898
Effects of aging time on V205 sol-gel coatings
[AD-A266824] 03 p0965 N94-15843
A high flux radical beam diamond growth
[AD-A266754] 03 p1207 N94-15955
Application of Z-contrast imaging to obtain column-by-column spectroscopic analysis of materials
[DE93-015333] 03 p0947 N94-16014
Space Shuttle solid rocket motor exposure monitoring
03 p0976 N94-16624
Electron spectroscopy analysis
[NASA-CR-193591] 03 p0951 N94-17039
DLTS and dynamic transconductance analysis of deep-submicron fully-depleted SOI MOSFET's
[AD-A267291] 03 p1214 N94-17243
Analysis of neon soft x ray spectra from short-pulse laser-produced plasmas
[DE93-014420] 04 p1582 N94-17708
Flame structure studies of a lean 20-torr H2/N2O/Ar flame employing molecular beam mass spectrometry
[AD-A268889] 04 p1349 N94-18456
Nondestructive inspection of graphite-epoxy laminates for heat damage using DRIFT and LPF spectroscopies
[DE93-017228] 04 p1343 N94-18761
The minimum detection limits of RDX and TNT deposited on various surfaces as determined by ion mobility spectroscopy
[DE93-018521] 04 p1378 N94-19042
Examination of charge carriers dynamics in silicon and silicon solar cells with photoinduced laser beam deflection
[ETN-93-95060] 04 p1470 N94-19654
The application of jet spray and ion beam contamination removal techniques to samples from the LDEF spacecraft
[AD-A270973] 04 p1354 N94-19755
Micromechanics of interfaces in metal matrix composites
[AD-A271012] 04 p1345 N94-19776
Femtosecond Raman-induced Kerr effect study of polar solvent dynamics: Amides
[DE93-017563] 05 p1678 N94-19924
Microscopic origins of metastable effects in a-Si:H and deep defect characterization in a-Si,Ge:H alloys
[DE93-018205] 05 p1688 N94-19985
Magnetic properties and Moessbauer analyses of glass from the K-T boundary, Beloc, Haiti
05 p1685 N94-20753
Multielement analysis of interplanetary dust particles using TOF-SIMS 05 p2084 N94-20790
Asbestos characterization using scanning electron microscopy/light element x ray spectrometry
[AD-A271611] 05 p1681 N94-21241
Shock compression of low-density foams
[DE93-040545] 05 p1707 N94-21546
An attempt to comprehend Martian weathering conditions through the analysis of terrestrial palagonite samples 05 p2143 N94-21668
Local structure in oxygen-doped La2CuO(4+delta)
[DE93-040248] 05 p2030 N94-21768
Gamma ray spectrometry of LDEF samples: Results of 1992 analyses
[DE94-001177] 05 p1684 N94-22046
Low temperature absorption spectra and ground state electronic structure of tetrakis(2,6-di-tert-butylphenoxide)uranium(IV)
[DE94-000774] 05 p2035 N94-22387
Spectroscopic IR ellipsometry of 100 and 001 oriented YBa2Cu3O(7-delta) films
[PB93-201481] 06 p2561 N94-23445
Ultrastructure processing of macromolecular materials
[AD-A273413] 06 p2258 N94-24782
Electrochemical behavior of ion-plated TiN and Cu-Cr coatings
[AD-A273411] 06 p2235 N94-24784
Investigation of the solid-solid surface adsorption of Eu2O3 on amorphous Al2O3
[DE93-613824] 06 p2566 N94-25332
Study on analyzing method establishment for metallic material development 07 p2729 N94-25578
Hook spectroscopy as an atomic number density diagnostic applied to laser-ablated copper plasmas
[DE94-002645] 07 p3042 N94-26081
Gordon Research Conference on the Physics and Chemistry of Laser Diagnostics in Combustion
[AD-A274609] 07 p2716 N94-26893
Determination of lead isotope ratios in seawater by purge and trap GC/MS after ethylation
07 p2870 N94-28152
Measurement of tropospheric OH by laser long-path absorption spectroscopy 08 p3343 N94-28596
On the possibility of measuring atmospheric OH using intracavity laser spectroscopy 08 p3344 N94-28597
An improved method of measuring tropospheric NO2, NO3, HO2, and RO2 by Matrix Isolation and Electronic Spin Resonance (MIESR) 08 p3345 N94-28605
A novel spectroscopic measurement method of RF plasma for temperature and electron density diagnoses
08 p3188 N94-28682
Issues in light hadron spectroscopy
[PB94-138229] 08 p3486 N94-29112
Knowledge based system for identification of gamma sources
[PB94-137742] 08 p3487 N94-29683
Nanosize metal alloy particle formation in Ag and Cu sequentially implanted silica
[DE94-005592] 08 p3207 N94-30042
Crosslinking and surface reactions in macromolecules: Spectroscopic FT-IR studies 08 p3221 N94-30812
Summary of some data processing routines in the molecular physics group of Stockholm University
[USIP-93-05] 09 p3808 N94-31087
Infrared spectroelectrochemical study of cyanide adsorption and reactions at platinum electrodes in aqueous perchlorate electrolyte
[AD-A276402] 09 p3631 N94-31238
Compositions and chemical bonding in ceramics by quantitative electron energy-loss spectrometry
[DE94-007208] 09 p3659 N94-32640
Ionization probes of molecular structure and chemistry
[DE94-007605] 09 p3872 N94-32643
Gettering of metal impurities by cavities in silicon
[DE94-005248] 09 p3645 N94-32672
Characterization of thermally stable dye-doped polyimide based electrooptic materials
[DE94-005309] 09 p3882 N94-32674
Ferric sulfate montmorillonites as Mars soil analogs
09 p3944 N94-33196
Aerosols scattering and near-infrared observations of the Martian surface 09 p3946 N94-33204
Material engineering of the novel semiconductor structures
[AD-A278386] 09 p3910 N94-33355
Total hydrocarbon analysis by ion mobility spectrometry 10 p4101 N94-33642
Studies of ion acoustic decay
[DE94-009470] 10 p4138 N94-34168
A spectral atlas of the nu(sub 12) fundamental of (13)C(12)CH6 in the 12 micron region
[NASA-TM-104601] 10 p4138 N94-34945
Instrumentation for in-flight SSME rocket engine plume spectroscopy
[NASA-TM-106596] 11 p4268 N94-35268
Chemical and structural characterization of nitroaromatic adducts with hemoglobins
[AD-A280533] 12 p4480 N94-37089

SPECTROSCOPIC TELESCOPES
NT MULTISPECTRAL TRACKING TELESCOPES

SPECTROSCOPY
NT ABSORPTION SPECTROSCOPY
NT ASTRONOMICAL SPECTROSCOPY
NT AUGER SPECTROSCOPY
NT AURORAL SPECTROSCOPY
NT ELECTRON SPECTROSCOPY
NT FLAME SPECTROSCOPY
NT GAS SPECTROSCOPY
NT INFRARED SPECTROSCOPY
NT LASER SPECTROSCOPY
NT MAGNETIC SPECTROSCOPY

NT MASS SPECTROSCOPY
NT MOLECULAR SPECTROSCOPY
NT NUCLEAR RADIATION SPECTROSCOPY
NT OPTICAL EMISSION SPECTROSCOPY
NT PHOTOACOUSTIC SPECTROSCOPY
NT PHOTOELECTRON SPECTROSCOPY
NT RADIO SPECTROSCOPY
NT RAMAN SPECTROSCOPY
NT SECONDARY ION MASS SPECTROMETRY
NT SPECTROPHOTOMETRY
NT SPECTROSCOPIC ANALYSIS
NT STELLAR SPECTROPHOTOMETRY
NT ULTRASONIC SPECTROSCOPY
NT ULTRAVIOLET SPECTROSCOPY
NT VACUUM SPECTROSCOPY
NT X RAY SPECTROSCOPY

The surface plasmon spectroscopy as diagnostic technique in microgravity experiments
01 p0110 N94-10133

Photodetachment studies on few-electron atomic negative ions
|DE93-008474| 01 p0358 N94-10154

A new matrix for the ageless 21.6-keV Eu-151 nuclear gamma ray Moessbauer source
|DE93-009795| 01 p0075 N94-10338

Coherence effects in radiometry and in spectroscopy
|DE93-013437| 01 p0075 N94-10519

Strange meson spectroscopy in K(omega) and K(phi) at 11 GeV/c and Cherenkov ring imaging at SLD
|DE93-013593| 01 p0363 N94-10748

Ellipsometry studies of semiconductors surface cleaning
|AD-A265150| 01 p0142 N94-11094

Applications of spectroscopic ellipsometry to microelectronics
|AD-A265148| 01 p0143 N94-11159

FFTSCAN: A program for spectral smoothing using Fourier transforms
|AD-A264921| 01 p0278 N94-11852

Applications of in-situ ellipsometry to microwave electron cyclotron resonance plasma processes
|AD-A265197| 01 p0373 N94-11880

Moessbauer spectroscopy of the SNC meteorite Zagami 01 p0428 N94-12016

Reflectance spectra of sulfate-and carbonate-bearing Fe(3+)-doped montmorillonites as Mars soil analogs
01 p0445 N94-12070

Si-29 NMR spectroscopy of naturally-shocked quartz from Meteor Crater, Arizona: Correlation to Kieffer's classification scheme 01 p0080 N94-12087

Nonlinear optical spectroscopy of Ag(111) in electrolyte and in vacuum
|AD-A265622| 01 p0079 N94-12534

Development of nondestructive evaluation methods and prediction of effects of flaws on the fracture behavior of structural ceramics
|DE93-012942| 02 p0577 N94-13032

Fifteenth Combustion Research Conference
|DE93-015758| 02 p0562 N94-13045

A search for strong-field direct two electron ionization using coincidence spectroscopy
|DE93-013435| 02 p0781 N94-13241

Early baryon and meson spectroscopy culminating in the discovery of the Omega minus SU(3) and quarks
|DE93-014321| 02 p0787 N94-14580

Multiplicity spectrometry on neutron filtered beams
|DE93-617529| 02 p0790 N94-14843

Theoretical studies relating to the interaction of radiation with matter
|AD-A266894| 03 p1179 N94-14949

BIB photodetectors based on antimony doped silicon
03 p0902 N94-15047

Study of protein-H2O interactions by multidimensional NMR spectroscopy
|AD-A266955| 03 p0946 N94-15760

First results from a laboratory facility for measurement of emission spectra under simulated planetary conditions
03 p0954 N94-16372

Methods of tunneling spectroscopy with the STM
|AD-A266507| 03 p0948 N94-16787

Spectroscopic investigations of nonambient systems with millimeter and submillimeter probes
|AD-A266537| 03 p0968 N94-16796

Suppression of charge scattering in Moessbauer experiments using synchrotron radiation
|DE93-015406| 03 p1212 N94-16887

DLTS and dynamic transconductance analysis of deep-submicron fully-depleted SOI MOSFET's
|AD-A267291| 03 p1214 N94-17243

Analysis of HgI2 and PbI2 crystals and detectors by Particle-Induced X Ray Emission (PIXE) and Ion Backscattering Spectroscopy (IBS)
|DE93-017168| 04 p1594 N94-17896

Tunneling spectroscopy of ultrasmall clusters and grains
|AD-A268840| 04 p1598 N94-18539

Photodissociation studies of polyatomic free radicals
|AD-A270084| 04 p1350 N94-18799

High pressure metallization of Mott Insulators: Magnetic, structural and electronic properties
|DE93-018295| 04 p1404 N94-18805

Nontraditional windows in spectral analysis
|AD-A271336| 04 p1553 N94-19583

The Cluster Ion Spectroscopy experiment
04 p1329 N94-19631

Photoluminescence spectroscopy of zinc germanium diphosphide (ZnGeP2)
|AD-A270705| 05 p1678 N94-19953

Development of a numerical simulation model for a-Si:H solar cells and application to the analysis of experimentally obtained spectral characteristics
|ETN-93-95061| 05 p1846 N94-20151

Time-of-flight heavy ion backscattering spectrometry
|DE93-019067| 05 p1973 N94-20306

Characterization of amorphous material in shocked quartz by NMR spectroscopy
|DE93-019069| 05 p1679 N94-20307

Spectroscopic ellipsometry studies of HF treated Si (100) surfaces 05 p1734 N94-20508

Spectroscopic ellipsometric characterization of Si/Si(1-x)Ge(x) strained-layer superlattices
05 p1734 N94-20510

Validation of the design of a high resolution all-reflection Michelson interferometer for atmospheric spectroscopy
|AD-A272505| 05 p1987 N94-21410

Electronically metastable molecules of high symmetry
|AD-A272015| 05 p1974 N94-21461

Optical luminescence spectroscopy as a probe of the surface mineralogy of Mars 05 p1813 N94-22437

The spectral world coordinate systems in IRAF/NOAO
05 p2049 N94-22539

Inelastic electron scattering from surfaces
|DE94-001368| 06 p2531 N94-22733

Flue gas cleaning by pulse corona streamer
|EUT-93-E-272| 06 p2268 N94-23174

Evaluation of inorganic zinc-rich primers using Electrochemical Impedance Spectroscopy (EIS)
06 p2237 N94-23233

Strong interactions studies with medium energy probes
|DE94-001446| 06 p2540 N94-23791

On the mechanism of action of 3',5'-cyclic adenosine monophosphate: A study of four- and five-coordinated phosphorus compounds, modelling the activated state of cAMP
|ISBN-9-03-860222-7| 06 p2226 N94-25238

CsI(Tl)-photodiode detectors for spectroscopy at low radiation levels
|MPI-PHE/92-22| 06 p2314 N94-25457

Spectroscopic and vibrational energy transfer studies in molecular bromine
|AD-A273795| 07 p3014 N94-25875

Heavy quark production and spectroscopy
|DE94-003619| 07 p3015 N94-25935

Optimization of experimental conditions in IR reflectance determination of BPSG properties
|DE94-002742| 07 p2713 N94-25978

Multivariate calibration applied to near-infrared spectroscopy for the quantitative analysis of dilute aqueous solutions
|DE94-003231| 07 p2716 N94-26794

Meson spectroscopy and particle astrophysics
|DE94-001799| 07 p3115 N94-27003

Charmonium physics at a tau-charm factory
|PB94-124344| 07 p3024 N94-27199

Issues in light hadron spectroscopy
|PB94-138229| 08 p3486 N94-29112

Knowledge based system for identification of gamma sources
|PB94-137742| 08 p3487 N94-29683

Backscatter Mossbauer Spectrometer (BaMS) for extraterrestrial applications 08 p3236 N94-29774

Non-invasive temperature measurements using electron paramagnetic resonance spectroscopy
08 p3198 N94-29881

Charge collection spectroscopy applied to MOS RAM's 08 p3201 N94-30220

Time domain spectroscopy for studying a monopole antenna immersed in a plasma
|ISBN-0-315-86526-1| 09 p3888 N94-31727

Photopyroelectric spectroscopy as a non-intrusive technique for the determination of the optical absorption spectra of multiple quantum well samples
|ISBN-0-315-87164-4| 09 p3833 N94-31875

Workshop on Models for Plasma Spectroscopy
|AD-A276565| 09 p3890 N94-32031

Cooling and trapping of neutral atoms
|AD-A276957| 09 p3870 N94-32360

Theoretical studies of electron transfer and optical spectroscopy
|DE94-006985| 09 p3871 N94-32375

A miniaturized ASIC-based multichannel scaler instrument
|DE94-007222| 09 p3807 N94-32783

Technology development for iron Fischer-Tropsch catalysts
|DE94-008723| 09 p3638 N94-32889

Electron cyclotron resonance plasma oxidation studies of InP
|AD-A277431| 09 p3893 N94-33007

Characterization of defects in Si and SiO2-Si using positrons
|DE94-009044| 10 p4147 N94-33877

Study on contaminants on flight and other critical surfaces
|NASA-CR-193975| 11 p4235 N94-35447

Mercury: Mid-infrared (7.3 - 13.5 microns) spectroscopic observations showing features characteristic of plagioclase 11 p4370 N94-36150

X ray and gamma ray spectroscopy of solids under pressure
|DE94-011207| 11 p4238 N94-36203

Older muons are wiser: Using time information in (mu)LCR spectroscopy
|DE93-018556| 12 p4511 N94-36457

Activities of the Tandem Accelerator Center, University of Tsukuba
|DE94-748687| 12 p4522 N94-37237

Time-of-flight pulsed ion beam surface analysis as a means of in situ, real-time characterization of the growth of ferro-electric and conductive oxide heterostructures
|DE94-012628| 12 p4517 N94-37249

A high precision gamma ray spectrometer for the Mars 1994 mission
|DE94-013133| 12 p4550 N94-37293

A fast spectroscopic diagnostic for the measurement of plasma impurity ion dynamics
|DE94-012985| 12 p4529 N94-37354

SPECTRUM ANALYSIS
NT CEPSTRAL ANALYSIS
NT FLAME SPECTROSCOPY
NT MAXIMUM ENTROPY METHOD

The multiplicity spectra of the (169)Tm(n, gamma) reaction
|DE93-617733| 01 p0364 N94-10835

Measurement methods and algorithms for comparison of local and remote clocks 01 p0354 N94-10987

Study of the surface circulation to the North of Bransfield Strait, Antarctica
|INPE-5472-TDI/503| 01 p0288 N94-11200

The IR properties of ringed galaxies and the IRAS database
|NASA-CR-194286| 01 p0426 N94-11590

The morphologies of distant radio galaxies
01 p0426 N94-11597

Implementation and use of a computational ray-tracing program for the design and analysis of complex optical systems
|AD-A265075| 01 p0382 N94-11653

The Grand Banks ERS-1 SAR wave spectra validation experiment 01 p0232 N94-11708

The optical/computer hybrid processing of extracting ocean wave directional spectrum by airborne photograph
01 p0197 N94-11934

Spectral analysis of resting cardiovascular variables and responses to oscillatory LBNP before and after 6 degree head dowm bedrest 01 p0309 N94-11997

Cardiovascular dynamics during space sickness and deconditioning 01 p0311 N94-12007

Effects of microscopic iron metal on the reflectance spectra of glass and minerals 01 p0436 N94-12024

Fourier domain target transformation analysis in the thermal infrared 01 p0258 N94-12030

A comparison of telescopic and Phobos-2 ISM spectra of Mars in the short-wave near-infrared (0.76-1.02 microns) 01 p0424 N94-12053

Spectral analysis of the gravity and topography of Mars 01 p0444 N94-12085

The spectral effects of subsolidus reduction of olivine and pyroxene 01 p0081 N94-12110

Spectral mixing models of S-Type asteroids
01 p0431 N94-12164

Olivine-rich asteroids, pallasitic olivine and olivine-metal mixtures: Comparisons of reflectance spectra
01 p0431 N94-12171

Composition of the Martian aerosols through near-IR spectroscopy 01 p0475 N94-12235

Chondrites, S asteroids, and space weathering: Thumping noises from the coffin?
01 p0433 N94-12244

Cronstedtite and iron sulfide mineralogy of CM-type carbonaceous chondrites from cryogenic Moessbauer spectra 01 p0433 N94-12257

Comparison of multiresolution techniques for digital signal processing
|AD-A265364| 01 p0138 N94-12406

Spectrum analysis in beam diagnostics
[DE93-013401] 01 p0373 N94-12601
Characterization of dissolved organic matter in the ocean by using the fluorescence excitation-emission matrix
01 p0211 N94-12659
Field research of wind wave spectrum variability
01 p0223 N94-12727
Observations of film slicks and internal waves with Ka-band scatterometer 01 p0225 N94-12741
Wind-wave and foam dynamics from optical and radar airborne observations 01 p0226 N94-12745
Laser fluorescent monitoring of dissolved organic matter in natural water 01 p0177 N94-12755
Ecological application of Surface Enhanced Raman Spectroscopy 01 p0227 N94-12756
The algorithm of primary production determination
01 p0228 N94-12761
Non-image visible polarization remote sensing of the ocean 01 p0229 N94-12762
Spectral analysis for automated exploration and sample acquisition
[NASA-CR-194095] 02 p0545 N94-13189
Basic research in solar physics
[NASA-CR-193632] 02 p0844 N94-13234
Dendrometric variables estimation in homogeneous forests using LANDSAT TM data
[INPE-5455-TDI/497] 02 p0684 N94-13331
The onset of galactic winds in early-type galaxies
[NASA-CR-193640] 02 p0836 N94-13446
Bounds on time delay estimation given unknown signal spectral parameters
[ITN-93-85194] 02 p0601 N94-13566
Spectra of late type dwarf stars of known abundance for stellar population models
[NASA-CR-194301] 02 p0831 N94-13681
Maximum entropy spectral analysis of the geological time series of the oxygen isotope record from deep-sea cores
[INPE-5465-PRE/1773] 02 p0725 N94-13728
Analysis of microstrip patch antennas with nonzero surface resistance
[NASA-TP-3362] 02 p0604 N94-13916
Testing various time-frequency distribution techniques
[DREO-TN-92-17] 02 p0606 N94-14062
An exact processing algorithm for wide beam spaceborne SAR data 02 p0689 N94-14213
Spectroscopic method and data reduction algorithm for laser long-path absorption measurements using RIS
02 p0689 N94-14218
Analysis of the IUE spectra of the strongly interacting binary beta Lyrae
[NASA-CR-194118] 02 p0833 N94-14493
H2S data reduction
[NASA-CR-193389] 02 p0617 N94-14743
On the use of the noncentral chi-square density function for the distribution of helicopter spectral estimates
[NASA-CR-191546] 03 p1176 N94-15487
Spectral studies of solid propellant combustion 4: Absorption and burn rate results for M43, XM39, and M10 propellants
[AD-A267119] 03 p0946 N94-15685
Higher order statistics in signal processing
[FFI-92/2008] 03 p0989 N94-15714
Why is the Moon dark? 03 p1256 N94-16219
Remote sensing studies of the northeastern portion of the lunar nearside 03 p1258 N94-16225
Spectral study of Venus global topography and geoid from Magellan and PVO data 03 p1276 N94-16332
Lunar phase function effects on spectral ratios used for resource assessment 03 p1278 N94-16342
Mixing model analysis of telescopic lunar spectra
03 p1284 N94-16371
Optical effects of regolith processes on S asteroids as simulated by laser impulse alteration of ordinary chondrite 03 p1246 N94-16422
Search for Extraterrestrial Intelligence (SETI)
03 p1125 N94-16620
A field measure of the shade fraction
03 p1068 N94-16677
Mapping the spectral variability in photosynthetic and non-photosynthetic vegetation, soils, and shade using AVIRIS 03 p1068 N94-16679
Using endmembers in AVIRIS images to estimate changes in vegetative biomass
03 p1070 N94-16689
Separation of cirrus cloud from clear surface from AVIRIS data using the 1.38 micron water vapor band
03 p1072 N94-16699
Expert system-based mineral mapping using AVIRIS
03 p1073 N94-16704
Multitemporal diurnal AVIRIS images of a forested ecosystem 03 p1074 N94-16709
A comparison of LOWTRAN-7 corrected Airborne Visible/Infrared Imaging Spectrometer (AVIRIS) data with ground spectral measurements
03 p1074 N94-16710
Femtosecond growth dynamics of an underdense ionization front measured by spectral blueshifting
[DE93-013582] 03 p1183 N94-16818
Evaluation of site effects on a high frequency direction finding single site location system
[AD-A267465] 03 p1001 N94-17035
Chemical tracer studies at IOSDL. 3: The measurement of silicate, nitrate and phosphate in seawater
[IOS-302-1992] 03 p1114 N94-17489
Optimisation and specification of Auger electron spectrometers for signal-to-noise ratio performance
[NPL-DMM(A)-101] 03 p1006 N94-17549
Rapid analysis of mixed waste samples via the optical emission from laser initiated microplasmas
[DE93-014563] 04 p1582 N94-17727
A time-frequency smoothing algorithm for cyclic spectral analysis
[DE93-016634] 04 p1519 N94-18097
Spectral analysis of synoptic time scale disturbances over the tropical eastern Pacific during summer 1989, 1990 and 1991
[AD-A268821] 04 p1490 N94-18206
Full Boltzmann discrete spectral wave model, implementation and nondimensional tests
[AD-A269885] 04 p1498 N94-18685
The use of velocity spectra for stacking receiver functions with application to IRIS/IDA stations OBNINSK (OBN) and ARTI (ARU), Russia
[AD-A269087] 04 p1483 N94-18717
Spectral analysis on the canonical autoregressive decomposition
[AD-A270083] 04 p1549 N94-18798
Advanced fusion diagnostics
[DE93-040085] 04 p1589 N94-19133
EXANA: A program for analysing extended energy loss fine structures, EXELFS spectra
[USIP-92-01] 04 p1525 N94-19145
New room temperature high resolution solid-state detector (CdZnTe) for hard x rays and gamma rays
04 p1324 N94-19165
Detection of a long-duration solar gamma-ray flare on Jun. 11, 1991 with EGRET on Compton-GRO
04 p1623 N94-19463
EGRET observations of 3 C 273
04 p1623 N94-19464
Nontraditional windows in spectral analysis
[AD-A271336] 04 p1553 N94-19583
STAFF (Spatio-Temporal Analysis of Field Fluctuations) experiment for the Cluster mission
04 p1328 N94-19625
A study of Saturn's E-ring particles using the Voyager 1 plasma wave instrument
[NASA-CR-194694] 05 p2088 N94-20048
High resolution signal processing
[AD-A271181] 05 p1717 N94-20215
Temperature dependence of 4f PES features and hole occupancy in ytterbium heavy fermions
[DE93-040131] 05 p1691 N94-20321
Characterization of electromagnetic fields in an extended chamber at the Short Pulse Experimental Electron Device (SPEED) simulator
[AD-A265955] 05 p1717 N94-20329
Analysis of Ku-band cross section at low incidence angles 05 p1720 N94-20414
Rotational spectrum of a dark state in 2-fluoroethanol using microwave/radiofrequency-infrared multiple resonance
[AD-A272101] 05 p1817 N94-20583
Spectral reflectance studies of the Humorum Basin region 05 p2101 N94-20682
Visible-infrared properties of controlled laboratory soils
05 p1685 N94-20689
Detectability of crystalline ferric and ferrous minerals on Mars 05 p2110 N94-20730
The stability of oxyamphiboles: Existence of Ferric-bearing minerals under the reducing conditions on the surface of Venus 05 p2122 N94-20800
Determining the composition of olivine on asteroidal surfaces 05 p1686 N94-20805
Objective determination of image end-members in spectral mixture analysis 05 p1686 N94-20831
Multispectral studies of selected crater- and basin-filling lunar Maria from Galileo Earth-Moon encounter 1
05 p2136 N94-20876
Spectral analysis of chemisorbed CO2 on Mars analog materials 05 p2140 N94-20900
Comparative study of INPIStron and spark gap
05 p1995 N94-21293
RADCAL: A narrow-band model for radiation calculations in a combustion environment
[PB93-200889] 05 p1682 N94-21448
Defect motion as the origin of the 1/f conductance noise in solids
[EUT-92-E-259] 05 p2029 N94-21552
Radiation driven winds of hot stars: Some remarks on stationary models and spectrum synthesis in time-dependent simulations
[NASA-CR-194691] 05 p2081 N94-21578
Evaluation of a nonlinear method for the enhancement of tonal signal detection
[NASA-CR-191562] 05 p1968 N94-21741
On Plasma Edge Spectroscopy and Spectroscopic Studies of Impurity Densities and Impurity Transport
[IPF-92-2] 05 p1996 N94-21802
Plasma edge spectroscopy 05 p1996 N94-21803
Spectroscopic studies of impurity densities and impurity transport 05 p1997 N94-21804
Modal combination in response spectrum modal dynamic analysis
[DE94-000339] 05 p1833 N94-21956
Spectral variation of scattering and absorption by cirrus 05 p1876 N94-22321
ASpect: A new spectrum and line analysis package for IRAF 05 p1926 N94-22485
Interactive Spectral Analysis and Computation (ISAAC)
05 p1926 N94-22505
An x ray archive on your desk: The Einstein CD-ROM's 05 p2048 N94-22519
SPECFOCUS: An IRAF task for focusing spectrographs 05 p1965 N94-22540
What is normal among the A-type stars?
[ISBN-0-315-83947-3] 05 p2081 N94-22592
Laser linewidth measurement in the presence of RIN and using the recirculating self heterodyne method
[EUT-92-E-262] 06 p2347 N94-22874
Electron spectroscopic studies of the neutralization of slow multicharged ions during interactions with a metal surface
[DE93-041046] 06 p2532 N94-22956
The soft x ray halo of the spiral galaxy NGC4631
[NASA-CR-194820] 06 p2601 N94-23537
A rail joint: The possible initiator of corrugation?
06 p2269 N94-23583
Data analysis and theoretical studies of the upper mesosphere and lower thermosphere
[NASA-CR-195108] 06 p2402 N94-24089
An investigation into acceleration determination for airborne gravimetry using the global positioning system
[ISBN-0-315-59470-5] 06 p2175 N94-24176
ACES spectral display software: Software description
[SK-1600-99-003] 06 p2455 N94-24297
On the analysis of clear air radar echoes severely contaminated by clutter 06 p2306 N94-24423
The measurement and analysis of leaf spectral reflectance of two stands of loblolly pine populations
06 p2389 N94-24442
Optical wavelet transform processor
[AD-A273625] 06 p2546 N94-24731
Method for selection of wavelength bands for multispectral classification
[PB93-204378] 06 p2388 N94-24741
Laboratory detection of C5S by pulsed-discharge-nozzle Fourier-transform microwave spectroscopy
[JTN-94-80519] 06 p2235 N94-24984
Radar target discrimination by spectrum analysis
[AD-D015982] 06 p2301 N94-25040
On the hadron formation time in pion-nucleus interaction
[DE93-616879] 06 p2539 N94-25476
High latitude cusp signature observations for southward IMF B sub Z
[AD-A273801] 06 p2406 N94-25536
Hyperspectral analysis of space objects: Signal to noise evaluation
[AD-A273882] 07 p2765 N94-25728
The Latin American conference on the applications of the Moessbaer effect
[DE93-615942] 07 p3051 N94-25912
Buckyball microwave plasmas: Fragmentation and diamond-film growth
[DE94-003209] 07 p3053 N94-26031
BATSE Data Analysis
[NASA-CR-193930] 07 p3114 N94-26685
The continuum spectral characteristics of gamma ray bursts observed by BATSE 07 p3114 N94-26686
ARM Fourier transform spectrometer data analysis tools
[DE94-000865] 07 p2895 N94-26697
A current evaluation of the digital beamforming testbed at Rome Laboratory
[AD-A274311] 07 p3032 N94-26881
Multivariate spectral analysis to extract materials from multispectral data
[AD-A274142] 07 p2709 N94-27135
Spectral and temporal correlations of multifrequency waves in the turbulent atmosphere
[ITN-94-85229] 07 p2774 N94-27233
Trace organic chemical detection using an ultraviolet excitation molecular beam fluorometer
[DE94-002649] 07 p2704 N94-27708

SPECTRUM analysis of multispectral imagery in conjunction with wavelet/KLT data compression
[DE94-003961] 07 p2851 N94-27727
ACES spectral display software: User manual
[SKL-1600-99-002] 07 p2973 N94-27762
Multispectral and textural classifications of a SPOT HRV-1 image, region of Sherbrooke, Quebec, Canada
[ISBN-0-315-84978-9] 07 p2851 N94-27863
Cooling the Martian atmosphere: The spectral overlap of the C02 15 micrometers band and dust
07 p3107 N94-27886
Investigation of spectral analysis techniques for randomly sampled velocimetry data
07 p3009 N94-27924
NMR study of quasicrystal Al(70)Pd(20)T(M10) alloy (T(M):Cr, Mn, Fe, and Co) 07 p2745 N94-28162
Journal of NIRE, Vol. 2, No. 2
[JTN-94-80552] 08 p3187 N94-28675
A novel spectroscopic measurement method of RF plasma for temperature and electron density diagnoses
08 p3188 N94-28682
Principles and application tendency of remote sensing: Its principle, function and utilization
08 p3328 N94-29037
Investigation of intense XUV emission of nitrogen-puff Z-pinch with small energy input
[PH-23] 08 p3505 N94-29075
Multichannel x ray spectral measurement of hot plasma evolution in nitrogen-puff Z-pinch
[PH-24] 08 p3505 N94-29076
Spectral and polarimetric analysis of hyperspectral data collected by an acousto-optic tunable filter system
[AD-A275076] 08 p3329 N94-29095
Double-crystal analyser system for the PRISMA spectrometer: Test of a prototype
[PB94-138245] 08 p3286 N94-29113
A review of signal detection using the bispectrum with applications in underwater acoustics
[AD-A275227] 08 p3478 N94-29388
High redshift QSOs and the x ray background
[NASA-CR-195112] 08 p3540 N94-29957
Computational balance in real-time cyclic spectral analysis
[DE94-005091] 08 p3432 N94-30100
Theory and observations of horizontal and vertical structure of gravity wave perturbations in the middle atmosphere 08 p3366 N94-30802
Spectral analysis of heart rate and psychological state: A review of its validity as a workload index
[AD-B179387] 08 p3399 N94-30969
Noise reduction techniques for the restoration of musical recordings
[TELECOM-93-E-019] 08 p3291 N94-30979
Noninvasive spectral analysis and beam mapping of focused ultrasound, part 1
[AD-A276211] 09 p3859 N94-31060
Analysis using bi-spectral related technique
[AD-A276017] 09 p3672 N94-31386
Influence of long-range correlations on the spectral functions and response of 48Ca and 90Zr
[ETN-94-96017] 09 p3865 N94-31537
Impurities and conductivity in a D-wave superconductor
[DE94-006222] 09 p3898 N94-31628
Fractal and spectral analysis
[ISBN-0-315-86460-5] 09 p3676 N94-31796
Inflight calibration, preprocessing, and data evaluation of GER 2 imaging spectrometry data
09 p3744 N94-31858
Noninvasive spectral analysis and beam mapping of focused ultrasound, part 2
[AD-A276629] 09 p3861 N94-32059
Atmospheric structure simulation: An autoregressive model for smooth geophysical power spectra with known autocorrelation function
[AD-A276691] 09 p3773 N94-32118
Development, characterization, and applications of high temperature superconductor nanobridge Josephson junctions
[DE94-008113] 09 p3903 N94-32409
Noninvasive spectroscopic diagnosis of superficial ocular lesions and corneal infections
[DE94-006231] 09 p3797 N94-32732
Index and bulk parameters for frequency-direction spectra measured at CERC Field Research Facility
[AD-A277759] 09 p3791 N94-33085
Distribution and nature of UV absorbers on Triton's surface
[NASA-CR-195886] 09 p3943 N94-33104
Ultraviolet Absorption Spectrometry (UVAS) and Liquid Atomic Emission Spectrometry (LAES) for oceanographic analysis systems
[AD-A278263] 10 p4091 N94-33413
Comparison of standard multispectral and map-assisted classification methods with a new layered approach
10 p4075 N94-33422
Three-parameter characterization of shallow-water directional wind wave spectra
[AD-A278532] 10 p4091 N94-33671
The crack severity index of monitored load spectra
10 p4071 N94-34585
A combined approach to buffet response analyses and fatigue life prediction 10 p4072 N94-34587
Absolute calibration and atmospheric versus mineralogic origin of absorption features in 2.0 to 2.5 micron Mars spectra obtained during 1993 11 p4356 N94-35404
Wavelength calibration techniques and subtle surface and atmospheric absorption features in the Mariner 6, 7 IRS reflectance data 11 p4356 N94-35405
The temperature of nitrogen on Pluto
11 p4365 N94-35468
ROSAT/XRT-PSPC observations and the ionizing continuum of Seyfert 1 galaxy Mkn 478
[PB94-167053] 11 p4350 N94-35530
Ferromagnetic resonance spectra of H2-reduced minerals and glasses 11 p4240 N94-36164
Studies of the dayside boundary layer processes based on ground observations in the Svalbard area
[AD-A280715] 11 p4292 N94-36265
SYNTH: A spectrum synthesizer
[DE94-004719] 11 p4331 N94-36317
Index and bulk parameters for frequency-direction spectra measured at CERC Field Research Facility, September 1992 to August 1993
[AD-A280233] 12 p4476 N94-37135
Index and bulk parameters for frequency-direction spectra measured at CERC Field Research Facility, September 1990 to August 1991
[AD-A280423] 12 p4476 N94-37216
Index and bulk parameters for frequency-direction spectra measured at CERC Field Research Facility, September 1991 to August 1992
[AD-A280455] 12 p4477 N94-37229
Fatigue case study and loading spectra for wind turbines
[DE94-010798] 12 p4457 N94-37622

SPECULAR REFLECTION
Radome depolarization effects on monopulse receiver tracking performance
[AD-A267446] 03 p1001 N94-17031
Hazard calculations of diffuse reflected laser radiation for the SELENE program
[NASA-TM-4520] 03 p1042 N94-17285
Electro-optic beam steering using non-linear organic materials
[AD-A270809] 04 p1374 N94-19577
Marine-modified LOWTRAN: The contribution of sun glint
[AD-A269547] 04 p1500 N94-19762
Illumination in diverse codimensions
[AD-A277602] 07 p2971 N94-27572
Characterization of interface structure in multilayers using specular x ray reflectance
[DE94-007698] 09 p3657 N94-32358

SPEECH
NT ARTICULATION (SPEECH)
NT CONVERSATION
NT PHONEMES
NT PHONETICS
NT SYLLABLES
NT TALKING
NT WORDS (LANGUAGE)
Analysis of fundamental frequency pattern in speech
02 p0618 N94-13440
Segmentation and frequency domain ML pitch estimation of speech signals 05 p1747 N94-22212
Algorithms for speech coding systems based on linear prediction
[EUT-92-E-260] 06 p2447 N94-22731
Researches of the Electrotechnical Laboratory. No. 955: Speech recognition by description of acoustic characteristic variations
[JTN-94-80604] 07 p2775 N94-27249
Automatic translation among spoken languages
09 p3685 N94-32437
A self-organizing neural network architecture for auditory and speech perception with applications to acoustic and other temporal prediction problems
[AD-A277526] 10 p4095 N94-33708
Psychophysics of complex auditory and speech stimuli
[AD-A277605] 10 p4035 N94-33848
Learning new words from spontaneous speech: A project summary
[AD-A277612] 10 p4035 N94-33853

SPEECH DISCRIMINATION
U SPEECH RECOGNITION

SPEECH RECOGNITION
A new HMM learning algorithm for continuous speech recognition
[NHK-SERIAL-413] 01 p0132 N94-10560
A real-time spoken-language system for interactive problem solving
[AD-A266046] 01 p0324 N94-11104
Speaker independent recognition of isolated words using vector quantization and neural networks
[ETN-93-94390] 02 p0616 N94-14724
Call sign intelligibility improvement using a spatial auditory display
[NASA-TM-104014] 03 p1177 N94-15549
Segment-based acoustic models for continuous speech recognition
[AD-A267138] 03 p0988 N94-15691
A multilevel-multiresolution method for image processing. A Bayesian framework for reconstructing and representing shapes
[AD-A266772] 03 p1082 N94-15842
The influence of the level formants on the perception of synthetic vowel sounds
[IFTR-41/1991] 03 p1002 N94-17064
Neural networks to classify speaker independent isolated words recorded in radio car environments
[REPT-93-013] 04 p1383 N94-17935
Feasibility study in linguistically motivated object-oriented conceptual design of information systems
[PB93-197754] 04 p1618 N94-19331
A real-time spoken-language system for interactive problem-solving, combining linguistic and statistical technology for improved spoken language understanding
[AD-A270901] 04 p1392 N94-19749
Representation of spoken words in a self-organizing neural net 05 p1940 N94-20243
Modeling the human mental lexicon with self-organizing feature maps 05 p1743 N94-20244
Segment-based acoustic models for continuous speech recognition
[AD-A271483] 05 p1736 N94-20547
Application of a back-propagation neural network to isolated-word speech recognition
[AD-A272495] 05 p1945 N94-21430
Recognizing hesitation phenomena in continuous, spontaneous speech 05 p1746 N94-22210
A framework of connectionist network toward speech waveform coding 05 p1746 N94-22211
Segmentation and frequency domain ML pitch estimation of speech signals 05 p1747 N94-22212
Speaker-independent isolated-digit recognition using neural networks and hidden Markov model
05 p1747 N94-22213
On coefficient quantization and computational roundoff effects in frequency interpolation filter banks
05 p1793 N94-22251
Performing speech recognition research with hypercard 06 p2306 N94-24194
Psychophysical and signal-processing aspects of speech representation
[ETN-94-95292] 06 p2302 N94-25077
On the quality of synthetic speech evaluation and improvements
[ETN-94-95298] 06 p2304 N94-25234
Linear and nonlinear adaptive filtering and their application to speech intelligibility enhancement
[ISBN-9-09-005342-5] 06 p2304 N94-25292
A rough set approach to speech recognition
[ISBN-0-315-83894-9] 07 p2769 N94-26619
Signal- and listener-based factors in complex auditory pattern perception
[AD-A274148] 07 p2939 N94-27094
Researches of the Electrotechnical Laboratory. No. 955: Speech recognition by description of acoustic characteristic variations
[JTN-94-80604] 07 p2775 N94-27249
Subphonetic acoustic modeling for speaker-independent continuous speech recognition
[AD-A275217] 08 p3244 N94-29303
Application of the wavelet transform for speech processing 09 p3600 N94-31435
Segment-based acoustic models for continuous speech recognition
[AD-A276109] 09 p3673 N94-31466
Spectral analysis method and sample generation for real time visualization of speech
[ETN-94-95732] 09 p3674 N94-31573
High-performance speech recognition using consistency modeling
[AD-A276775] 09 p3679 N94-32185
Automatic translation among spoken languages
09 p3685 N94-32437
Neural networks applied to the phonemic segmentation of speech 09 p3686 N94-33152
Modular neural network architectures
09 p3838 N94-33156
Dialog structure and plan recognition in spontaneous spoken dialog
[AD-A277566] 10 p4032 N94-33393

Dyadic wavelet features for isolated word speaker dependent speech recognition
[AD-A278492] 10 p4034 N94-33756
Learning new words from spontaneous speech: A project summary
[AD-A277612] 10 p4035 N94-33853
Clustering techniques in speaker recognition
[AD-A278676] 11 p4255 N94-35689
Segment-based acoustic models for continuous speech recognition
[AD-A280332] 12 p4434 N94-37032
Noise reduction for speech enhancement using non-linear wavelet processing
[AD-A280469] 12 p4434 N94-37141

SPEECHES
U LECTURES

SPEED
U VELOCITY

SPEED CONTROL
Gas turbine and operating method of the same
[CA-PATENT-APPL-SN-2043039] 06 p2188 N94-24490
Variable speed controller 07 p2943 N94-25678

SPEED INDICATORS
Position error determination for the speedometer and altimeter of the NAL QSTOL experimental aircraft ASKA
[NAL-TR-1144] 02 p0517 N94-13451

SPEED REGULATION
U SPEED CONTROL

SPEEDOMETERS
U SPEED INDICATORS

SPENT FUELS
Development and application of the automated Monte Carlo biasing procedure in SAS4
[DE93-015205] 02 p0774 N94-14334
Development and characterization of adiabatic shear prone tungsten heavy alloys
[AD-A270477] 04 p1366 N94-19673

SPF (MATERIALS)
U SUPERPLASTIC FORMING

SPHALERITE
U ZINCBLENDE

SPHERES
NT ROTATING SPHERES
Wetting effects on nylon spheres engulfment in ice 01 p0115 N94-10189
Force-free magnetic fields, curl eigenfunctions, and the sphere in transform space, with applications to fluid dynamics and electromagnetic theory
[AD-A265805] 02 p0834 N94-12971
Theoretical investigation of scattering by homogeneous or coated dielectric spheres illuminated with a steady state or pulsed laser beam 02 p0657 N94-13624
Metastable superconductors as photon detectors 03 p0900 N94-15032
Use of microgravity in the synthesis of ceramics using sol gel techniques 03 p0979 N94-16088
Three dimensional hydrodynamic calculations with adaptive mesh refinement of the evolution of Rayleigh Taylor and Richtmyer Meshkov instabilities in converging geometry: Multi-mode perturbations
[DE93-017155] 03 p1025 N94-16903
Stability analysis for the flow of granular materials down an inclined plane using kinetic model
[DE93-016852] 03 p1026 N94-16958
Geometrical pattern learning
[DE93-017641] 04 p1542 N94-19007
Intensity and polarization of light scattered by size distributions of randomly oriented nonspherical particles 05 p1721 N94-20416
Static image method for computing the electric potential due to sources in a layered sphere
[PB93-224970] 06 p2308 N94-23105
Polarizability of gyrotropic sphere
[PB93-225019] 06 p2524 N94-23131
Fingered bola body, bola with same, and methods of use
[NASA-CASE-MSC-21967-1] 06 p2354 N94-23822
BEM solution for the simulation of axisymmetric viscous sintering
[PB93-237717] 06 p2336 N94-24761
Experimental characterization of the AFIT Neutron Facility
[AD-A273822] 06 p2539 N94-25519
Hardware design of a spherical mini-rover 07 p2833 N94-25669
Design and development of the second generation Mars Habitat 07 p2943 N94-25693
Dielectric polarizability of sphere with arbitrary anisotropy
[PB94-133113] 07 p2779 N94-28397
A study of the convergence of spherical harmonic expansions of gravity using distributed point-mass Earth models 08 p3362 N94-29909
Strictly positive definite functions on spheres
[AD-A276471] 09 p3855 N94-31244
Custom uniform source system
[NASA-CR-189332] 09 p3711 N94-31492
Quantum homogeneous spaces, duality, and quantum 2-spheres
[CWI-AM-R9309] 09 p3857 N94-32192
Simulation of rotary-drum and repose tests for frictional spheres and rigid sphere clusters
[DE94-008094] 10 p4044 N94-33841

SPHERICAL COORDINATES
A review of some dynamics models in six-dimensional phase space and their suitable conditions of motion equation
[DE93-623741] 03 p1175 N94-17317
Note on the use of spherical vectorfields in Clifford analysis
[PB93-237667] 06 p2480 N94-23437
Analytic rendering of curvilinear volume data
[DE94-004934] 08 p3407 N94-28506
Exact spherical wave solutions to Maxwell's equations with applications 08 p3252 N94-29733
Contact level fusion of radar and IRST contacts on almost electromagnetically silent platform 12 p4395 N94-36634

SPHERICAL HARMONICS
Project proposal for partial computational physics support for Survivability of Coatings program
[DE93-013788] 02 p0576 N94-12939
Spherical anharmonic oscillator in self-similar approximation
[DE93-626622] 02 p0772 N94-14890
Asymptotic derivation of the modified time-dependent SP2 equations and numerical calculations
[DE93-016466] 04 p1551 N94-19342
Geoid-to-topography ratios on Venus: A global perspective 09 p3940 N94-31110
High degree gravitational sensitivity from Mars orbiters for the GMM-1 gravity model
[NASA-TM-104604] 10 p4088 N94-34992

SPHERICAL SHELLS
Microgravity combustion of dust suspension in a spherical chamber 01 p0080 N94-10248
The fractional quantum Hall effect and the spherical shell model
[DE93-014553] 02 p0818 N94-14740
Symmetry-dictated trucation: Solutions of the spherical shell model for heavy nuclei
[DE94-000482] 05 p1976 N94-21961
Double diffusion convection in a rotating spherical shell 05 p2006 N94-22666

SPHERICAL TANKS
Pressurization and expulsion of a flightweight liquid hydrogen tank
[NASA-TM-106427] 05 p1799 N94-20177
Experimental results of hydrogen slosh in a 62 cubic foot (1750 liter) tank
[NASA-TM-106625] 11 p4263 N94-35250

SPHERICAL WAVES
Initiation and modification of reaction by energy addition: Kinetic and transport phenomena
[AD-A271315] 05 p1797 N94-19936
Interface reflection of spherical acoustic waves in the first- and second-order rational parabolic approximations and their artifacts
[PB93-215424] 05 p1969 N94-22261
Mach reflection of spherical detonation waves
[DE93-016604] 07 p2797 N94-27705
Exact spherical wave solutions to Maxwell's equations with applications 08 p3252 N94-29733
Development and implementation of a full-potential ASW method
[ETN-94-95757] 09 p3858 N94-31560

SPHEROIDS
NT OBLATE SPHEROIDS
NT PROLATE SPHEROIDS
The Navy tessellated spheroid map projection system: A comprehensive definition
[AD-A269989] 04 p1462 N94-18677
Color palette considerations for digital map displays
[AD-A269991] 04 p1462 N94-18679
Stable Ni isotopes and Be-10 and Al-26 in metallic spheroids from Meteor Crater, Arizona 05 p1863 N94-20889
Monoclonal antibodies directed against surface molecules of multicell spheroids
[NASA-CR-195102] 06 p2420 N94-23633
Single scattering of light by ensembles of particles with various shapes
[ETN-94-96016] 09 p3878 N94-31550

SPHEROMAKS
A spheromak ignition experiment reusing Mirror Fusion Test Facility (MFTF) equipment
[DE94-001856] 05 p2034 N94-22050
Power balance and characterization of impurities in the Maryland Spheromak, part 2
[DE94-009603] 11 p4335 N94-35670

SPHERULES
The stability of hibonite and other aluminous phases in silicate melts: Implications for the origin of hibonite-bearing inclusions 01 p0080 N94-12052
Arroyo el Mimbral, Mexico, K/T unit: Origin as debris flow/turbidite, not a tsunami deposit 01 p0281 N94-12084
K/T spherules from Haiti and Wyoming: Origin, diagenesis, and similarity to some microtektites 01 p0281 N94-12085
Microtektite-like glass spherules in Late Devonian (367 MA) shales 01 p0461 N94-12160
KT boundary impact glasses from the Gulf of Mexico region 01 p0282 N94-12161
Iron and nickel isotopic mass fractionation in deep-sea spherules 01 p0282 N94-12199
Modelling of dispersal and deposition of impact glass spherules from the Cretaceous-Tertiary boundary deposit 01 p0432 N94-12238
Cretaceous-tertiary boundary spherules and Cenozoic microtektites: Similarities and differences 03 p1241 N94-16186
Size distribution of interplanetary iron and stony particles related with deep-sea spherules 03 p1245 N94-16388
Siderophile element fractionation in meteor crater impact glasses and metallic spherules 03 p1246 N94-16414
Optical properties of water released in low Earth orbit
[AD-A266197] 03 p1192 N94-16936
First discovery of the organic materials in deep-sea iron cosmic spherule 05 p1685 N94-20677
Elemental depletions in Antarctic micrometeorites and Arctic cosmic spherules: Comparison and relationships 05 p2082 N94-20704
Research program on the Manson impact structure, Iowa 05 p1862 N94-20766

SPIKE ANTENNAS
U MONOPOLE ANTENNAS

SPIKING
Suppression of relaxation oscillations in flashpumped, two-micron tunable solid state lasers
[AD-D015928] 05 p1814 N94-19800

SPILLING
Condensed gases under winter conditions: A study for the rescue services
[FOA-C-40305-4.5] 04 p1473 N94-18139

SPIN
NT ELECTRON CAPTURE
NT ELECTRON SPIN
NT ISOTOPIC SPIN
NT METAL SPINNING
NT NUCLEAR SPIN
NT PARTICLE SPIN
NT SPIN-ORBIT INTERACTIONS
Systematology for elastic-plastic material equations by large deformations on the basis of the Cosserat-continuum model
[SCHRIFTENR-PHYSIKAL-ING-BD-23] 03 p1058 N94-15642
Phase space representations and quantum probability theory
[DE93-629863] 04 p1556 N94-18154
Nonlinear dynamics and instabilities in ferromagnetic resonance experiments: Examinations of spheres from yttrium iron garnet in coincidence area of the first Suhl instabilities
[ETN-93-95072] 04 p1604 N94-19612
Spin-polarized atomic hydrogen: Devices and phenomena
[ETN-94-95342] 07 p3016 N94-26002
Hysteresis phenomena at spin-flop transition induced by the pulsed magnetic field
[DE94-606851] 08 p3511 N94-28626
Spin-structure function of the neutron He-3: SLAC results
[DE94-008927] 09 p3875 N94-33189
Medium energy measurements of N-N parameters
[DE94-008340] 10 p4137 N94-33923
Resonance capture in unbalanced dual-spin spacecraft
[AD-A278501] 10 p4015 N94-34292
Spin effects in high energy quark-quark scattering
[DE94-616800] 11 p4330 N94-36080

SPIN DECOUPLING
The de Haas-van Alphen studies and Fermi surface properties of organic superconductors (ET)2X
[DE93-015157] 02 p0623 N94-13975

SPIN DYNAMICS
Crossing-odd spin effects in the dipole model of hadron scattering
[DE93-617692] 01 p0362 N94-10551
Squeezed spin states: Squeezing the spin uncertainty relations 01 p0377 N94-10585
Relativistic dynamics of spin in strong external fields
[NIKHEF-H/93-06] 03 p1240 N94-17604

T violating neutron spin rotation asymmetry
[DE93-018470] 04 p1570 N94-19126
Spin dynamics and implications for superconductivity: Some problems with the d-wave scenario
[DE94-001183] 05 p2032 N94-21972
The structure and spin dynamics of lanthanide-bearing silicate glasses
[DE94-001320] 06 p2252 N94-22992
Spin fluctuations in an ordered Heisenberg ferromagnet with dipolar interactions
[PB93-204493] 06 p2524 N94-24533
Optical conductivity and resistivity in the two-band Emery model
[DE94-601943] 07 p3051 N94-25945
Crossover between BCS and performed-Boson theories with increasing interactions
[DE93-019018] 07 p3017 N94-26078
Extended nonabelian symmetries for free fermionic model
[DE94-601554] 08 p3481 N94-28470
Spin dynamics in storage rings and linear accelerators
[DE94-010320] 11 p4330 N94-36106

SPIN EXCHANGE
Measurements of atomic interactions and frequency stability with a cryogenic hydrogen maser
[AD-A271132] 05 p1814 N94-19853
Encounters of H and D atoms with O2 in water: Relative diffusion and reaction rates
[DE93-018587] 05 p1970 N94-19956
Derivation of the macroscopic rate equations for the driven diffusive Ising model at pair level of approximation
[DE93-616839] 06 p2524 N94-25208

SPIN FORGING
U METAL SPINNING

SPIN GLASS
The peculiarities of the spin glass state in Fe(x)Mn(1-x)TiO3
[DE93-617882] 01 p0395 N94-10525
Retrieval properties of neural networks with infinitely many marked patterns
[PREPRINT-729] 02 p0766 N94-14718
Magnetic interactions and disorder - phase transitions in dilute spin-glasses and high temperature superconductors
[ITN-93-85217] 02 p0815 N94-14825
Study of (+-)J Ising spin glasses via multicanonical ensemble
[DE93-018269] 05 p2016 N94-20285
Non-fermi liquid and spin-glass behavior of the Sc(1-x)U(x)Pd3 system
[DE93-040134] 05 p2016 N94-20335
Technical report of ISSP. Ser. A, no. 2673: Two successive spin glass transitions in non-diluted Heisenberg-like spin glass Ni(0.42)Mn(0.58) TiO3
[JTN-94-80559] 07 p2756 N94-27241

SPIN REDUCTION
Aspects of the calibration and processing of the CRRES fluxgate magnetometer data
[AD-A270127] 04 p1432 N94-18875
One-loop QCD mass effects in the production of polarized bottom and top quarks
[PB94-138104] 08 p3487 N94-29145
The Solar Anomalous and Magnetospheric Particle Explorer (SAMPEX) yo-yo despin and solar array deployment mechanism 08 p3163 N94-29645
Overview of the Miniature Sensor Technology Integration (MSTI) spacecraft attitude control system 11 p4206 N94-35627

SPIN RESONANCE
The evolution of tensor polarization
[DE93-017209] 02 p0790 N94-14897
Polarized structure functions of the nucleon in the resonance region
[CEBAF-PR-94-001] 06 p2540 N94-24663

SPIN STABILIZATION
Apparatus for simulating an exoatmospheric structure
[NASA-CASE-MSC-21975-1] 05 p1653 N94-20339
A geometric model of a V-slit Sun sensor correcting for spacecraft wobble 11 p4206 N94-35628

SPIN TESTS
Reliability of autonomic responses and malaise across multiple motion sickness stimulation tests
[NASA-TM-108787] 03 p1121 N94-15711
The experimental behavior of spinning pretwisted laminated composite plates
[NASA-CR-195220] 07 p2711 N94-27352

SPIN WAVES
U MAGNONS

SPIN-LATTICE RELAXATION
Synthesis and magnetic properties of novel La*2-x*M*x*CuO*4 equals y* compositions (La equals La, Pr, Nd, Sm, Eu, Cd; M equals Ca, Sr, Ba; O (less than or equal) x 0.2; -0.5 (less than or equal) y (less than or equal) 0.5)
[DE93-011359] 01 p0403 N94-12363
NMR studies of oxygen-doped La2CuO(4+delta)
[DE93-040756] 05 p2034 N94-22007
Interplay of magnetic and superconducting heavy fermion ground states
[DE94-000680] 06 p2240 N94-23003
Relaxation of the density matrix for an arbitrary spin in random external fields
[DE94-618457] 12 p4509 N94-37078

SPIN-ORBIT INTERACTIONS
NT ELECTRON CAPTURE
Effects of spin-orbit coupling on disordered mesoscopic systems
[ITN-93-85220] 03 p1180 N94-15288
Spin-integrated and spin-dependent photoelectron diffraction
[DE93-016546] 04 p1565 N94-17850
Electron impact polarization and correlation properties of the inert gases
[DE93-018358] 04 p1570 N94-19125

SPINDLES
Design, construction, and testing of a five active axes magnetic bearing system 11 p4214 N94-35846

SPINE
Multimodal image correlation applied to computer aided pedicular screwing
[ETN-93-95018] 04 p1528 N94-19363
Image technology and information analysis of bone change with gravitational exposure 08 p3389 N94-28851

SPINEL
The stability of hibonite and other aluminous phases in silicate melts: Implications for the origin of hibonite-bearing inclusions 01 p0080 N94-12052
Limited subsolidus diffusion in type B1 CAI: Evidence from Ti distribution in spinel 03 p0954 N94-16401
Trace element compositions of spinel-rich refractory inclusions from the Murchison meteorite 05 p2086 N94-20897
Transparent polycrystalline body with high ultraviolet transmittance, process for making and applications thereof
[CA-PATENT-1325511] 07 p3066 N94-27276
Damage growth in MgAl2O4 crystals by Xe ion irradiations
[DE94-005009] 07 p3069 N94-27828
Dislocation loops in spinel crystals irradiated successively with deep and shallow ion implants
[DE94-005083] 08 p3517 N94-30201
Characterization and growth mechanisms of the MgAl2O4 phase in Al2O3-reinforced Al-Mg composites
[ISBN-0-315-86531-8] 09 p3620 N94-31706
Possible spinel absorption bands in S-asteroid visible reflectance spectra 11 p4368 N94-36139
Microstructure and chemistry of MgO- and CoO-doped nickel-titanate spinels
[DE94-012741] 12 p4537 N94-37382

SPINNING (METALLURGY)
U METAL SPINNING

SPINOR GROUPS
On the relativistic invariant representation of arbitrary bilinear combinations of Dirac spinors
[DE93-634343] 07 p3019 N94-26456
Relativistic two-body system in 1+1-dimensional QED. 1: On the circle S1
[DE94-603716] 07 p3067 N94-27647

SPIRAL ANTENNAS
A hybrid finite element-boundary integral for the analysis of cavity-backed antennas of arbitrary shape
[NASA-CR-193719] 02 p0599 N94-13236
Earth Penetration Radar Imaging System (EPRIS)
[DE93-019890] 04 p1391 N94-19542
Low cost antennas for MSAT vehicular applications 06 p2289 N94-22830
Predicting antenna parameters from antenna physical dimensions
[AD-A276442] 09 p3672 N94-31300

SPIRAL GALAXIES
NT ANDROMEDA GALAXY
NT BARRED GALAXIES
NT MILKY WAY GALAXY
Abundance markers in H II regions of late spiral galaxies
[ISBN-0-315-62457-4] 02 p0836 N94-13372
Ultraviolet observations of NGC 4395, the least luminous and nearest known Seyfert 1 nucleus
[NASA-CR-194304] 02 p0831 N94-13679
Visualizing the universe, part 2 05 p2063 N94-22472
Generation and maintenance of bisymmetric spiral magnetic fields in disk galaxies in differential rotation 05 p2010 N94-22695
Magnetic fields in spiral galaxies 05 p2010 N94-22697
The soft x ray halo of the spiral galaxy NGC4631
[NASA-CR-194820] 06 p2601 N94-23537
Multicolor photometry of barred spiral galaxies 08 p3541 N94-30270
The dynamical settling of warped disks and angular momentum transport in galaxies 09 p3928 N94-31121

SPIRALS (CONCENTRATORS)
Spiral fluid separator
[NASA-CASE-MFS-28658-1] 05 p1800 N94-20361

SPLASHING
Improvement of helicopter attitude stability by active control of the conventional swash plate
[NASA-CR-194786] 05 p1650 N94-20524

SPLINE FUNCTIONS
Spline approximation for system of n-th order nonlinear ordinary differential equations
[DE93-608188] 01 p0346 N94-11507
On convexity and Schoenberg's variation diminishing splines
[DE93-619673] 01 p0346 N94-11632
Growth curve analysis for plasma profiles using smoothing splines
[DE93-015741] 02 p0795 N94-12984
Evaluation of beta-spline interpolation in digital terrain models
[INPE-5475-TDI/506] 02 p0684 N94-13364
Adaptive wavelet collocation methods for initial value boundary problems of nonlinear PDE's
[NASA-CR-191507] 03 p1169 N94-15833
Three-dimensional analysis of anisotropic spatially reinforced structures 03 p0939 N94-16863
Aeroelastic airfoil smart spar 03 p0868 N94-16865
Multivariate wavelet representations and approximations
[AD-A269350] 04 p1546 N94-17825
Development and operation of the F/A-18 model control surface actuators
[AD-A271330] 05 p1645 N94-19914
Affine and non-affine blossoms
[RR-913-M] 05 p1950 N94-20200
A geometrical process for three dimensional osteotomy planning
[ETN-93-93602] 05 p1892 N94-21134
Higher order Bezier circles
[NASA-CR-177633] 05 p1897 N94-21784
Achieving high data reduction with integral cubic B-splines
[NASA-CR-177628] 05 p1966 N94-21881
The quantum structure of matter grand challenge project: Large-scale 3-D solutions in relativistic quantum dynamics
[DE94-000328] 05 p1960 N94-21955
Relativistic configuration interaction calculation of the correlation energies of highly-charged ions
[DE94-001055] 06 p2532 N94-22988
Approximate solution of the fourth order initial value problem using deficient spline polynomials
[DE93-613023] 07 p2991 N94-25880
On a spline-approximation method for solving ordinary differential equations
[DE93-634290] 07 p2994 N94-26471
Unified approach for direct and inverse boundary layer prediction using cubic spline collocation 07 p2653 N94-28326
Analysis of crustal structure of Venus utilizing residual Line-of-Sight (LOS) gravity acceleration and surface topography data. A trial of global modeling of Venus gravity field using harmonic spline method
[NASA-CR-195799] 08 p3549 N94-29737
Splines and ocean wave modelling
[PB94-139409] 08 p3378 N94-30002
Filtering of satellite altimetry data with optimal smoothing cubic splines to compute geoid heights, along-tract geoid and gravity gradients in the Indonesian waters and its surroundings
[PB94-147527] 09 p3741 N94-31074
Multivariate spline approximation
[AD-A276034] 09 p3842 N94-31441
Application of an improved Nelson-Nguyen analysis to eccentric, arbitrary profile liquid annular seals 10 p4062 N94-34182
High accuracy approximation of offset curves with rational geometric splines 10 p4110 N94-34352
TransFit: Finite element analysis data fitting software
[NASA-CR-193988] 11 p4307 N94-36118

SPLINES
Splines, contours and SVD subroutines
[DE93-016088] 02 p0757 N94-14866
On the spline-based wavelet differentiation matrix
[NASA-CR-191557] 05 p1950 N94-20087
Spline screw payload fastening system
[NASA-CASE-GSC-13454-1] 05 p1821 N94-20126
An extended UTD analysis for the scattering and diffraction from cubic polynomial strips
[NASA-CR-194581] 05 p1716 N94-20139

Unstructured surface grid generation
05 p1920 N94-22366
Spline screw multiple rotations mechanism
[NASA-CASE-GSC-13452-1] 06 p2352 N94-23078
Split spline screw
[NASA-CASE-GSC-13434-1] 06 p2352 N94-23082
Radial basis function approximation: From gridded centers to scattered centers
[AD-A274184] 07 p2998 N94-27103
The 2nd International Conference on Curves and Surfaces: Abstracts
[AD-A276805] 10 p4128 N94-33406
Interchangeable spline reference guide
[DE94-012368] 12 p4495 N94-37245

SPLITS (GEOLOGY)
U GEOLOGICAL FAULTS

SPLITTING
A flux splitting scheme with high-resolution and robustness for discontinuities
[NASA-TM-106452] 12 p4441 N94-36646

SPOILERS
A determination of the external forces required to move the benchmark active controls testing model in pure plunge and pure pitch
[NASA-TM-107743] 01 p0016 N94-12421
High Reynolds number configuration development of a high-lift airfoil 04 p1306 N94-18424
Numerical investigation of the incompressible flow around a wing with a fixed spoiler
[ISL-R-109/91] 04 p1313 N94-19524

SPONTANEOUS EMISSION
Improved super luminescent light source specification
[AD-D015746] 01 p0176 N94-12329
Coherence and linewidth studies of a 4-nm high power FEL
[DE93-018533] 04 p1441 N94-19030
Novel nonlinear laser diagnostic techniques
[AD-A270968] 04 p1442 N94-19788
Enhancement of the rate of radiative processes in the field of a magnetic monopole
[DE94-603717] 07 p3074 N94-27696
Fluorescence detection of single molecules using pulsed near-field optical excitation and time correlated photon counting
[DE94-007553] 11 p4320 N94-35376

SPOOLS
Electrostatic fiber spreader including a corona discharge device
[AD-D015793] 03 p0936 N94-16537

SPORADIC E LAYER
Results from a year-long auroral-E measurement campaign
[AD-A265059] 01 p0278 N94-11871
Sporadic-E observations during LoVHF transionospheric direction finder measurements
[AD-A270619] 05 p1716 N94-19951
High Frequency (HF) and meteor burst communications in a polar environment
[AD-A271604] 05 p1737 N94-20949

SPORES
Studies on bacterial spore ultraviolet light resistance and regulation of the activity of a spore protease
[AD-A275448] 08 p3384 N94-28884
Backscatter and transmission of aerosol at UV through middle IR wavelengths
[AD-A277127] 09 p3718 N94-32305

SPORTS MEDICINE
Postural strategies for the continuous control of static and dynamic balance in man
[PB94-184678] 12 p4487 N94-37812

SPOT (FRENCH SATELLITE)
Combined analysis of ERS-1 SAR and visible/infrared remote sensing data for land cover/land use mapping in a tropical zone: A case study in Guinea
01 p0246 N94-12478
Example of SPOT/ERS-1 complementarity
01 p0247 N94-12479
TREES project: A case study on the use of multi-temporal ERS-1 SAR data and SPOT data for monitoring tropical ecosystems 01 p0249 N94-12497
The space operations at CNES
06 p2498 N94-23837
SPOT satellite family: Past, present, and future of the operations in the mission and control center
06 p2500 N94-23846
SPOT4 Operational Control Center (CMP)
06 p2197 N94-23856
AGENDA: A task organizer and scheduler
06 p2504 N94-23876
Real-time on-board orbit determination with DORIS
06 p2196 N94-23919
Design principles of onboard management of a Sun synchronous satellite 07 p2950 N94-26722
From Optics to Radar, SPOT and ERS Applications
[ISBN-2-85428-345-7] 09 p3747 N94-32523
The complementary nature of the SPOT and ERS-1 systems and their place in major international programmes 09 p3748 N94-32524
From optics to radar: Environmental problems and the SPOT/ERS systems 09 p3748 N94-32525
Optics and radar: Cohabitation, rivality or happy marriage. Towards new planning tools
09 p3748 N94-32529
Assessment of region-based methods for automated SAR/optical registration, attribute extraction, and classification 09 p3750 N94-32536
Robust multisource classification method using the Markov random field methods 09 p3750 N94-32537
Technique of ERS-1 image processing in association with SPOT data 09 p3750 N94-32538
Airborne SAR as a complement to SPOT HRV in land-cover classification: The use of normalization and principal components analysis 09 p3750 N94-32539
Production of terrain data: Optical radar complementarity 09 p3750 N94-32540
Fusion of multispectral (XS) and Panchromatic (P) SPOT images and radar images 09 p3750 N94-32541
The use of SPOT and ERS-1 images to map the eruption of Nevado Sabancaya (Province of Arequipa, South Peru) and evaluate associated risks 09 p3751 N94-32546
Comparison of SPOT, ERS-1, SEASAT, LANDSAT TM, and merged imagery for geological investigations
09 p3752 N94-32547
Optimal geological data extraction from SPOT-radar synergism with samples from Djebel Amour (Algeria), Red Sea Hills (Sudan), Sirte Basin (Libya), and Magdalena Valley (Colombia) 09 p3752 N94-32548
Use of SPOT and ERS-1 SAR data to study the tectonic and climatic history of arid regions
09 p3752 N94-32550
Study of subpolar glaciers of Spitzbergen using SPOT, ERS-1, and hypsometric data: Results and perspectives
09 p3753 N94-32553
Use of SPOT and ERS-1 to map tropical vegetation and mangrove dynamics in Guiana 09 p3753 N94-32555
A case study comparing multi-temporal ERS-1 SAR data and SPOT data for tropical forest mapping
09 p3753 N94-32556
Rapid estimates of crop acreage and production at European scale using high resolution imagery
09 p3754 N94-32557
Monitoring landsurface characteristics in Niger using complementary SPOT and ERS-1 SAR data
09 p3754 N94-32560
European MARS project: The potential integration of SPOT and air- and satellite-borne radar data over two pilot areas for agricultural statistics. PROSPER programme and ERS-1 pilot project
[BRGM-93035] 09 p3754 N94-32561
Comparing SPOT and SIR A for mapping superficial formations in tropical forest regions: Example of the Yaoundy Region (Cameroon) 09 p3755 N94-32562
Possible complementarity of SPOT/ERS in mapping land use: Study on agricultural land in Brittany (France)
09 p3755 N94-32563
Land cover change detection with ERS-1 data and data from other remote sensing satellites. Example: The delta of the River Ebro (Spain) 09 p3755 N94-32564
ERS-1 SAR and optical data for land use/land cover mapping: A case study in a savannah zone of Guinea
09 p3755 N94-32565
Quantitative analysis of woody vegetation in Soudano-Sahalian region. Textural approach (application to a Burkina Faso region) 09 p3757 N94-32574
Statistical analysis and mapping of cotton and food crop cultivation surfaces in the west of Burkina Faso: Contribution of combined SPOT P and XS data
09 p3757 N94-32575
JPRS report: Central Eurasia. Aviation and cosmonautics, No. 6, June 1993
[JPRS-UAC-94-005] 12 p4391 N94-37001

SPOT WELDS
Study on interfacial reaction analysis at interfacial joining 07 p2728 N94-25574

SPRAY CHARACTERISTICS
Simulation of preburner sprays, volume 1
[NASA-CR-193844] 02 p0647 N94-14906
Cryogenic spray vaporization in high-velocity helium, argon and nitrogen gasflows
[NASA-TM-106363] 03 p1035 N94-17446
Droplet turbulence interactions under subcritical and supercritical conditions 06 p2211 N94-23036
Development of a droplet breakup model considering aerodynamic and droplet collision effects
06 p2213 N94-23045
Shear coaxial injector instability mechanisms
06 p2213 N94-23047
Experimental studies on effervescent atomizers with wide spray angles 08 p3196 N94-29280
Apparatus for testing high pressure injector elements
[NASA-CASE-MFS-28773-1] 08 p3299 N94-29365
Coal-water slurry spray characteristics of an electronically-controlled accumulator fuel injection system
[DE94-008977] 10 p4060 N94-33946
Analysis of a High Velocity Oxygen-Fuel (HVOF) thermal spray torch. Part 1: Numerical formulation
[DE94-005590] 11 p4267 N94-35996
Application of higher-order multipoint statistics to the ideal spray
[DE94-005104] 11 p4268 N94-36318

SPRAY NOZZLES
Atomization characteristics of a prefilming airblast atomizer
[NAL-TM-644] 01 p0148 N94-10727
Performance aspects of de Laval spray-forming nozzles
[DE93-013671] 01 p0163 N94-12604
Widebody cabin water spray optimization tests
[DOT/FAA/CT-TN93/29] 02 p0511 N94-14186
Simulation of preburner sprays, volume 1
[NASA-CR-193844] 02 p0647 N94-14906
Coaxial airblast atomizers
[NASA-CR-193845] 03 p1016 N94-15109
Two-dimensional, high flow, precisely controlled monodisperse drop source
[AD-A267660] 03 p1028 N94-17250
Extinguishment of enclosed gas fires with water sprays
[PB93-201663] 06 p2268 N94-23430

SPRAYED COATINGS
Performance aspects of de Laval spray-forming nozzles
[DE93-013671] 01 p0163 N94-12604
Application of thermal spray and ceramic coatings and reinforced epoxy for cavitation damage repair of hydroelectric turbines and pumps
[AD-A267624] 03 p0971 N94-17198
Thermal analysis of coatings and substrate materials during a disruption in fusion reactors
[DE93-017688] 04 p1588 N94-18971
Characterization and durability testing of plasma-sprayed zirconia-yttria and hafnia-yttria thermal barrier coatings. Part 2: Effect of spray parameters on the performance of several hafnia-yttria and zirconia-yttria coatings
[NASA-TP-3296] 06 p2242 N94-23467
Plasma sprayed thermal barrier coatings: Production, characterization and testing
[ISBN-9-03-860082-8] 06 p2555 N94-25439
Study on film generation phenomena by particle deposition 07 p2728 N94-25575
Attachment techniques for high temperature strain
[AD-A274766] 07 p2811 N94-26568
Plasma sprayed ceramic thermal barrier coating for NiAl-based intermetallic alloys
[NASA-CASE-LEW-15535-1] 08 p3205 N94-29507
Dual cure low-VOC coating process, phase 3
[DE94-003202] 08 p3221 N94-30826
Porosity in plasma sprayed alumina coatings
[DE94-008874] 10 p4028 N94-34011
Proceedings of the 57th National Congress of Japan Thermal Spraying Society
[DE94-731734] 10 p4029 N94-34133
Defect detection in multi-layered, plasma sprayed zirconia by time resolved infrared radiometry: A comparison between analytical and experimental methods
[DE94-009803] 11 p4245 N94-35779

SPRAYED PROTECTIVE COATINGS
U PROTECTIVE COATINGS
U SPRAYED COATINGS

SPRAYERS
Atomization characteristics of a prefilming airblast atomizer
[NAL-TM-644] 01 p0148 N94-10727
Combustion chamber analysis code
[NASA-CR-192585] 01 p0046 N94-10934
On the combustion of a laminar spray
[NASA-TM-106210] 01 p0028 N94-11238
KIVA-3: A KIVA program with block-structured mesh for complex geometries
[DE93-011986] 01 p0077 N94-11249
Performance aspects of de Laval spray-forming nozzles
[DE93-013671] 01 p0163 N94-12604
A computer model for liquid jet atomization in rocket thrust chambers
[NASA-CR-194194] 02 p0627 N94-12803
Widebody cabin water spray optimization tests
[DOT/FAA/CT-TN93/29] 02 p0511 N94-14186
Simulation of preburner sprays, volume 1
[NASA-CR-193844] 02 p0647 N94-14906
Thermal spray forming of refractory sample ampoule cartridges for single crystal growth space furnaces
[TABES PAPER 93-605] 03 p1051 N94-16141
Metal slurry droplet and spray combustion
[AD-A269648] 04 p1349 N94-18736

The application of jet spray and ion beam contamination removal techniques to samples from the LDEF spacecraft
[AD-A270973] 04 p1354 N94-19755
Particle dispersion in turbulent sprays
[AD-A271314] 05 p1796 N94-19913
Aircraft cabin water spray disbenefits study
[NASA-CR-194750] 05 p1642 N94-21818
Development of a droplet breakup model considering aerodynamic and droplet collision effects
06 p2213 N94-23045
Extinguishment of enclosed gas fires with water sprays
[PB93-201663] 06 p2268 N94-23430
Validation of a nonintrusive optical technique for the measurement of liquid mass distribution in a two-phase spray 06 p2548 N94-24420
Impact of improved materials and cabin water spray on commuter aircraft postcrash fire survivability
[AD-A274421] 07 p2660 N94-27081
Ducted kerosene spray flames
08 p3195 N94-29276
Spray combustion experiments and numerical predictions 08 p3195 N94-29277
Experimental studies on effervescent atomizers with wide spray angles 08 p3196 N94-29280
Aircraft evacuations: The effect of a cabin water spray system upon evacuation rates and behaviour
[CAA-PAPER-93008] 08 p3148 N94-29887
Near-net-shape manufacturing: Spray-formed metal matrix composites and tooling 08 p3186 N94-30447
Thermocapillary convection in evaporating sessile drops
[NASA-TM-109758] 09 p3705 N94-31886
Coal-water slurry spray characteristics of an electronically-controlled accumulator fuel injection system
[DE94-008977] 10 p4060 N94-33946
Coal-water slurry sprays from an electronically controlled accumulator fuel injection system: Break-up distances and times
[DE94-008979] 10 p4061 N94-33981
The effects of cold exposure on wet aircraft passengers: A review
[AD-280253] 10 p4100 N94-34389
Fundamental studies in blow-down and cryogenic cooling
[AD-A278967] 11 p4250 N94-35524
Analysis of a High Velocity Oxygen-Fuel (HVOF) thermal spray torch. Part 1: Numerical formulation
[DE94-005590] 11 p4267 N94-35996

SPRAYING
NT ARC SPRAYING
NT FLAME SPRAYING
NT METAL SPRAYING
NT PLASMA SPRAYING
Droplet turbulence interactions under subcritical and supercritical conditions 06 p2211 N94-23036
Numerical parametric studies of spray combustion instability 06 p2212 N94-23041
Cryogenic insulation studies
[NASA-CR-193950] 07 p2756 N94-27429
Modeling of the phase liquidates in combustion chambers 08 p3195 N94-29278
Experimental studies on effervescent atomizers with wide spray angles 08 p3196 N94-29280
Investigation of the two-phase flow in a research combustor under reacting and non-reacting conditions
08 p3196 N94-29282
Analysis of strong acoustic excitation on the breakup and dispersion of a liquid jet
[ONERA-NT-1993-9] 09 p3701 N94-31422
Proceedings of the 57th National Congress of Japan Thermal Spraying Society
[DE94-731734] 10 p4029 N94-34133

SPRAYING APPARATUS
U SPRAYERS

SPRAYS
U SPRAYERS

SPREAD F
Measurements of spatial and frequency coherence of an equatorial hf path during spread-F
[DE93-016615] 11 p4257 N94-36316
Channel probe measurements for the American Sector Clutter Experiment, January 1994
[DE94-013086] 12 p4469 N94-37314

SPREAD REFLECTION
Index and bulk parameters for frequency-direction spectra measured at CERC Field Research Facility, September 1990 to August 1991
[AD-A280423] 12 p4476 N94-37216
Index and bulk parameters for frequency-direction spectra measured at CERC Field Research Facility, September 1991 to August 1992
[AD-A280455] 12 p4477 N94-37229

SPREAD SPECTRUM TRANSMISSION
A fiber optic network system with low crosstalk using code-division multiplexing
[AD-D015763] 01 p0374 N94-10376
Fine time uplink synchronization for frequency-hopped spread spectrum satellite communication system
[ISBN-0-315-54370-1] 02 p0600 N94-13488
Kalman filter based architectures for interference excision
[DSIS-93-00034] 02 p0603 N94-13818
Adaptive Signal Processing Testbed
[DSIS-93-00258] 02 p0604 N94-13869
Adaptive Signal Processing Testbed: Software design specification
[DSIS-93-00259] 02 p0604 N94-13870
Simulation of downlink synchronization for a frequency-hopped satellite communication system
[DSIS-93-00477] 02 p0605 N94-13941
Adaptive Signal Processing Testbed signal excision software: User's manual
[DSIS-93-00260] 02 p0606 N94-14037
A comparison of recursive least squares and Kalman filtering excisors for swept tone interference
[DSIS-93-00362] 02 p0606 N94-14054
Four Frequency-Shift Keying (4-FSK) spread spectrum modulator and demodulator
[AD-A267433] 03 p1000 N94-16979
Military applications of high-accuracy frequency standards and clocks
[AD-A269303] 04 p1430 N94-18299
Application of wavelet transform techniques to spread spectrum demodulation and jamming
[AD-A267389] 04 p1389 N94-19009
Spread spectrum random access networks
[AD-A272280] 05 p1737 N94-20585
Capacity comparison between direct sequence PSK and MFSK spread spectrum systems in CDMA applications
05 p1747 N94-22224
ACTS advanced system concepts and experimentation 06 p2280 N94-22780
Odyssey personal communications satellite system
06 p2282 N94-22787
DS-SSMA capacity for a mobile satellite system
06 p2286 N94-22814
Coding for frequency hopped spread spectrum satellite communications
[ECE-91-1] 06 p2296 N94-24132
Analysis of time-diversity combining methods for frequency-hopped signals
[CU-DOE-92-09] 06 p2300 N94-24694
Composite sequences for rapid acquisition of direct-sequence spread spectrum signals
[CTN-94-60901] 06 p2300 N94-24696
Coding for frequency hopped spread spectrum satellite communications
[ECE-92-1] 06 p2300 N94-24697
Evaluation of an Acoustic Charge Transport (ACT) device for adaptive interference suppression in spread spectrum communications systems
[AD-A274073] 07 p2765 N94-25647
Analysis and simulation of a GPS receiver design using combined delay-lock and modified tanlock loops
[AD-A274037] 07 p2664 N94-25810
Code division multiple access local area network communications employing fiber optic signal processing techniques
[AD-A274897] 07 p3096 N94-26180
Kalman filtering of narrowband interference from direct sequence spread spectrum communications systems
[ISBN-0-315-84011-0] 07 p2784 N94-26627
The performance of nonorthogonal noncoherent frequency hopped M-ary FSK in additive white Gaussian noise, fading and jamming
[ISBN-0-315-85243-7] 07 p2775 N94-27301
Communications subsystem for the Petite Amateur Navy Satellite (PANSAT)
[AD-A275532] 08 p3242 N94-28812
Evaluation of wireless Local Area Networks
[AD-A275133] 08 p3243 N94-29064
Acquisition time analysis of noncoherent PN sequence acquisition schemes
[AD-A275017] 08 p3244 N94-29094
High-resolution robot tracking and direction finding for space station environment 08 p3168 N94-29896
Spread-spectrum radio systems and networks
[AD-A276449] 09 p3671 N94-31260
Communications networks in stressed environments
[AD-A275967] 09 p3672 N94-31384
Direct-sequence spread-spectrum performance in a multipath fading environment
[AD-A276080] 09 p3673 N94-31464
Applied harmonic analysis
[AD-A278384] 09 p3685 N94-33353
A new tool for signal processing
[AD-A278385] 09 p3685 N94-33354
Investigation and simulation of nonlinear processors for spread spectrum receivers, volume 1
[AD-A278025] 10 p4037 N94-34288
Investigation and simulation of nonlinear processors for spread spectrum receivers. Volume 2: Users manual
[AD-A278026] 10 p4037 N94-34289

SPREADING
Spreading of Bimodulated Ultra-relativistic Electron Beam (BUEB) in Atmospheric Plasma Channel (APCh)
[DE93-621658] 01 p0392 N94-11213
Electrostatic fiber spreader including a corona discharge device
[AD-D015793] 03 p0936 N94-16537
Oil spreading in surface waters with an ice cover
[PB93-190767] 04 p1476 N94-19064
Similarity solutions for gravity-dominated spreading of a lens of organic contaminant
[REPT-93-24] 04 p1420 N94-19139

SPRING (SEASON)
Surface-layer response over shrub-steppe canopy during springtime
[DE94-011235] 12 p4468 N94-37624

SPRINGS (ELASTIC)
Miniature mechanism assembly
[DE93-015595] 02 p0624 N94-13928
Mechanical energy absorber
[NASA-CASE-MSC-22111-1] 03 p1047 N94-15966
Shape memory metals
[DE94-001373] 05 p1695 N94-21976
Manufacturing methods for machining spring ends parallel at loaded length
[NASA-CASE-MFS-28767-1] 08 p3231 N94-29379
Transmissibility of nickel-titanium shape memory alloy springs
[AD-A276055] 09 p3640 N94-31456
Nonlinear analysis of springs using helical finite elements 09 p3859 N94-31906
Variable stiffness torsion springs
[NASA-CASE-MFS-28930-1] 12 p4509 N94-36782

SPRINGS (WATER)
Promotion of geothermal energy development in 1991
[DE93-799058] 02 p0701 N94-13215
Fronts at the confluences of spring-fed streams with Joekulsa a Fjoellum: Possibly thermal bars?
[MATHS-REPT-A-198] 08 p3333 N94-29528

SPUTNIK SATELLITES
The birth of NASA: The diary of T. Keith Glennan
[NASA-SP-4105] 06 p2630 N94-23333

SPUTTERING
NT MAGNETRON SPUTTERING
Effect of surface cleanliness of bearing steel on adhesive strength and tribological properties of sputter-deposited gold films
[DE93-767974] 01 p0082 N94-10732
Sources of Na for the Io atmosphere
01 p0455 N94-12127
Solar wind-induced secondary ions and their relation to lunar surface composition 01 p0474 N94-12232
Damage threshold study of ion beam sputtered coatings for a visible high-repetition laser at LLNL
[DE93-013430] 01 p0095 N94-12602
Metastability of yttrium-oxides
[DE93-016548] 02 p0813 N94-14440
Multicrystalline silicon solar cells: Gettering optimization and characterization
[DE93-015001] 02 p0705 N94-14861
Laboratory for x ray optics
[AD-A267149] 03 p1189 N94-15735
Interfacial structure of lattice mismatched bcc(110)/bcc(110) transition metal superlattices
[DE93-015162] 03 p1208 N94-16058
Sputtered ferroelectric thin films of KTN for electro-optic devices
[AD-A266573] 03 p0968 N94-16723
Epitaxial iron films
[AD-A268286] 03 p1217 N94-17579
Mechanical properties of interfaces and superlattices
[AD-A268591] 03 p1217 N94-17606
Sputtered TiN coatings in plastic
04 p1367 N94-18011
RF vacuum microelectronics
[AD-A270003] 04 p1403 N94-18667
The deposition of electro-optic films on semiconductors
[AD-A270823] 04 p1605 N94-19664
Neutral copper cluster sputtering yields: Ne(+), Ar(+) and Xe(+) bombardment
[DE93-019010] 05 p1690 N94-20288
Embedded microclusters in zeolites and cluster beam sputtering: Simulation on parallel computers
[DE94-000741] 05 p1701 N94-20352
Fabrication and evaluation of superconducting and semiconducting materials
[AD-A271645] 05 p2018 N94-20558

Properties of E-beam interactive oxide films for nanometer scale structures
[AD-A272848] 05 p1675 N94-21191
Advanced processing technology for high-efficiency thin-film CuInSe2 solar cells
[DE93-010045] 05 p1847 N94-21614
Research on polycrystalline thin-film submodules based on CuInSe2 materials
[DE93-018223] 05 p2029 N94-21617
Mars atmosphere loss and isotopic fractionation by solar-wind-induced sputtering and photochemical escape 05 p2144 N94-21672
Observation of x ray absorption magnetic circular dichroism in well-characterized iron-cobalt-platinum multilayers
[DE94-000303] 05 p1694 N94-21944
Direct detection of atomic ions from molecular photofragmentation during nonresonant multiphoton ionization of sputtered species
[DE93-040886] 05 p1976 N94-21951
Transmission electron microscopy study of thick copper-304 stainless steel multilayers
[DE94-001045] 05 p1696 N94-22394
Research on polycrystalline thin-film CuInGaSe2 solar cells
[DE94-000203] 06 p2560 N94-23205
Novel two-stage selenization methods for fabrication of thin-film CIS cells and submodules
[DE94-000220] 06 p2390 N94-23296
Selective hydrogen separation by palladium-based composite membranes
[PB93-201671] 06 p2254 N94-23431
The statistics of sputtering
[DE94-001128] 06 p2243 N94-23715
Thin film cadmium telluride photovoltaic cells
[DE94-000201] 06 p2395 N94-24509
Preliminary far-field plume sputtering characterization of the Stationary Plasma Thruster (SPT-100)
[NASA-TM-106464] 06 p2221 N94-24766
Investigation and application of microwave electron cyclotron resonance plasma physical vapour deposition
[DE93-613909] 06 p2555 N94-25333
Aluminum-ion sputtering from Al surfaces with very-low-energy ions
[REPT-A-2668] 07 p2733 N94-26073
Studies of thin-film growth, adsorption, and oxidation by in situ, real-time, and ex situ ion beam analysis
[DE94-002907] 07 p3055 N94-26275
The ZnO thin films with C-axis orientation prepared on the room temperature substrate by the ECR multipolar plasma sputtering method
[DE94-605039] 07 p2758 N94-27857
Sputtering of single crystals: Experimental evidence of the ejection process
[AD-A275819] 08 p3512 N94-28775
Kinetics of surface roughening and smoothing during ion sputtering
[DE94-006358] 08 p3219 N94-30263
Process parameter-growth environment-film property relationships for reactive sputter deposited metal (V, Nb, Zr, Y, Au) oxide, nitride, and oxynitride films
[AD-A276382] 09 p3640 N94-31258
Energy and angular distributions of secondary ions during electronic sputtering of nonconducting surfaces
[ETN-94-95756] 09 p3865 N94-31516
Amorphous/crystalline structure and phase transformations in metastable semiconducting Ge(1-x)Sn(x)
[DE94-006659] 09 p3901 N94-32115
Formation mechanism and yield of molecules ejected from ZnS, CdS, and FeS2 during ion bombardment
[DE94-008487] 09 p3871 N94-32515
Dependence of x ray absorption magnetic circular dichroism on layer periodicity in iron-platinum multilayers
[DE94-008786] 09 p3647 N94-32892
Mars atmospheric loss and isotopic fractionation by solar-wind-induced sputtering and photochemical escape 09 p3947 N94-33208
Processing of titanium matrix composites 12 p4401 N94-36653

SQUALLS
The cloud radiative feedback of a midlatitude squall line system and implication for climate study
[DE93-010511] 01 p0283 N94-10290
Opposing mesoscale flows in a broken midlatitude squall line
[AD-A268011] 03 p1109 N94-17492
Tropical squall lines 09 p3778 N94-30992
Effects of mesoscale convective organization and vertical wind shear on the cumulus-environment interaction 10 p4090 N94-34910

SQUARE WAVES
Multiple model adaptive control of a large flexible space structure with purposeful dither for enhanced identifiability
[AD-A274132] 07 p2987 N94-27122

SQUARE WELLS
P-matrix description of the two-particle interaction
[DE93-617690] 01 p0361 N94-10549
Acoustic propagation modeling using MATLAB
[AD-A270905] 04 p1564 N94-19750

SQUARES (MATHEMATICS)
Catalogue of simple perfect squared squares of orders 21 through 25
[PB93-191971] 04 p1550 N94-18991

SQUEEZE CASTING
Squeeze casting: A literature review
[PB94-124575] 07 p2741 N94-27326

SQUEEZE FILMS
Squeeze film dampers with oil hole feed 10 p4065 N94-34195

SQUEEZED STATES (QUANTUM THEORY)
The Second International Workshop on Squeezed States and Uncertainty Relations
[NASA-CP-3219] 01 p0375 N94-10564
Smoothly deformed light 01 p0375 N94-10566
Nonclassical states of the second optical harmonic in the presence of self-action 01 p0375 N94-10567
Quantum noise and squeezing in optical parametric oscillator with arbitrary output coupling 01 p0375 N94-10568
One dimensional representations in quantum optics 01 p0375 N94-10570
Harmonic oscillator interaction with squeezed radiation 01 p0376 N94-10571
Photon number amplification/duplication through parametric conversion 01 p0376 N94-10572
An exactly solvable model of an oscillator with nonlinear coupling and zeros of Bessel functions 01 p0349 N94-10573
Non classical effects in planar waveguides 01 p0376 N94-10574
Nonperturbative methods in the problem of multiphoton excitation of atom by squeezed light 01 p0376 N94-10575
Generalised squeezing and information theory approach to quantum entanglement 01 p0377 N94-10580
Completeness properties of the minimum uncertainty states 01 p0349 N94-10581
Dissipation in a squeezed-state environment 01 p0370 N94-10584
Squeezed spin states: Squeezing the spin uncertainty relations 01 p0377 N94-10585
Quantum entropy and uncertainty for two-mode squeezed, coherent and intelligent spin states 01 p0377 N94-10586
The uncertainty principle in resonant gravitational wave antennae and quantum non-demolition measurement schemes 01 p0378 N94-10587
Uncertainty relations, zero point energy and the linear canonical group 01 p0378 N94-10590
Supersqueezed states from squeezed states 01 p0378 N94-10591
Squeezed states of electrons and transitions of the density of states 01 p0370 N94-10593
Quantum mechanical effects of topological origin 01 p0378 N94-10594
Nonunitary and unitary approach to Eigenvalue problem of Boson operators and squeezed coherent states 01 p0350 N94-10595
Collision-induced squeezing in a harmonic oscillator 01 p0379 N94-10597
Squeezed colour states in gluon jet 01 p0379 N94-10599
New squeezed landau states 01 p0379 N94-10601
Wigner functions for nonclassical states of a collection of two-level atoms 01 p0379 N94-10603
Wavelets and spacetime squeeze 01 p0379 N94-10604
Non-stationary and non-linear dispersive medium as external field which generates the squeezed states 01 p0380 N94-10605
Relation of squeezed states between damped harmonic and simple harmonic oscillators 01 p0380 N94-10606
Wave and pseudo-diffusion equations from squeezed states 01 p0347 N94-10607
Infinite-mode squeezed coherent states and non-equilibrium statistical mechanics (phase-space-picture approach)
[LBL-32695] 01 p0380 N94-10608
Coherent states and uncertainty relations for the damped harmonic oscillator with time-dependent frequency 01 p0380 N94-10611
Quantum processes in resonators with moving walls 01 p0380 N94-10612
Generalized squeezed states from generalized coherent states
[DE94-002689] 12 p4512 N94-36515

SQUEEZING
U COMPRESSING

SQUIBS
Effects of repeating resistance testing on firing ability of igniter EP360-3
[AD-A274814] 07 p2759 N94-26486

SQUID (DETECTORS)
Large array SQUID magnetometer for NDE
[AD-A264799] 01 p0304 N94-11449
Superconducting SQUID amplifiers for IR detectors and other applications, phase 2
[AD-A265447] 01 p0145 N94-12333
Future development in cryogenic techniques for space 03 p0901 N94-15042
High resolution SQUID magnetometry for non-destructive evaluation
[AD-A268884] 04 p1447 N94-18225
Demonstration of monolithic co-fabrication of Y1Ba2Cu3O7-Sigma and CMOS devices on the same sapphire substrate
[AD-A274757] 07 p3059 N94-26566
Fabrication issues in optimizing YBa(2)Cu(3)O(7-x) flux transformers for low I/f noise
[DE94-005209] 08 p3261 N94-28546
The computer-aided system for the high resolution SQUID-magnetometer
[DE94-606138] 08 p3286 N94-28553
The bases for the development of high-temperature integrated SQUID-systems
[DE94-607901] 08 p3267 N94-30073
The bases for the development of high-temperature integrated SQUID-systems
[DE94-608462] 08 p3517 N94-30082
Report on a SQUID made from high temperature superconductor
[PB94-169307] 11 p4339 N94-35598
Magnetic properties of nanosize iron clusters
[DE94-011329] 11 p4318 N94-36204
Applications of high transition temperature superconductors at the Savannah River Site
[DE94-012938] 12 p4536 N94-37311

SR-71 AIRCRAFT
JPRS report: Central Eurasia. Aviation and cosmonautics, No. 6, June 1993
[JPRS-UAC-94-005] 12 p4391 N94-37001

SRB (SOLID ROCKET BOOSTERS)
U SPACE SHUTTLE BOOSTERS

STABILITY
NT ACOUSTIC INSTABILITY
NT AERODYNAMIC STABILITY
NT AIRCRAFT STABILITY
NT ATTITUDE STABILITY
NT BAROCLINIC INSTABILITY
NT BOUNDARY LAYER STABILITY
NT COMBUSTION STABILITY
NT CONTROL STABILITY
NT DIMENSIONAL STABILITY
NT DIRECTIONAL STABILITY
NT DYNAMIC STABILITY
NT FLAME STABILITY
NT FLOW STABILITY
NT FREQUENCY STABILITY
NT GOERTLER INSTABILITY
NT GYROSCOPIC STABILITY
NT HOVERING STABILITY
NT LATERAL STABILITY
NT LONGITUDINAL STABILITY
NT LOW SPEED STABILITY
NT MAGNETOHYDRODYNAMIC STABILITY
NT MAGNETOSPHERIC INSTABILITY
NT MOTION STABILITY
NT PHASE STABILITY (MATERIALS)
NT ROTARY STABILITY
NT SHELL STABILITY
NT SPACECRAFT STABILITY
NT STATIC STABILITY
NT STORAGE STABILITY
NT STRUCTURAL STABILITY
NT SURFACE STABILITY
NT SYSTEMS STABILITY
NT THERMAL STABILITY
Granular instability in fluidized beds: A small-over-large instability 01 p0122 N94-10235
Enhanced stability of magic clusters: A case study of icosahedric Al(sub 12)X, X=B, Al, Ga, C, Si, Ge, Ti, As
[DE93-613644] 01 p0395 N94-10386
Stability by linear processes
[NASA-CR-194131] 01 p0323 N94-10862
Vacuum stability requirements of polymeric material for spacecraft application
[NASA-TM-109216] 01 p0091 N94-11350
Analytical details of the instability threshold of the laser-Lorenz model
[DE93-619707] 01 p0175 N94-11634
Resist materials design: Base-catalyzed chemical amplification
[AD-A265286] 01 p0145 N94-11819

Preparation of stable photopatternable polymeric materials for non-linear optics
[AD-A265359] 01 p0095 N94-12577
Effect of pressure on order and stability in alloys: The case of Al-Ge
[DE93-013842] 02 p0567 N94-12899
A new formulation of longitudinal coherent instabilities
[DE93-014288] 02 p0789 N94-13220
Stability of reference masses 1: Evidence for posiible variations in the mass of reference kilograms arising from mercury contamination
[NPL-DMM(A)-86] 02 p0708 N94-13667
Exploiting structure: Introduction and motivation
[NASA-CR-194199] 02 p0750 N94-13828
Finding stable orientations of assemblies with linear programming
[AD-A266990] 03 p1143 N94-15212
Reliability of autonomic responses and malaise across multiple motion sickness stimulation tests
[NASA-TM-108787] 03 p1121 N94-15711
On the stability analysis of approximate factorization methods for 3D Euler and Navier-Stokes equations
[NASA-TM-106314] 03 p1169 N94-15818
Confinement and stability of a Crystal Beam
[DE93-015400] 03 p1181 N94-16020
Dynamics, stability, and control of maglev systems
[DE93-015163] 03 p1047 N94-16806
The stability of ions in a storage ring in the presence of small gap insertion devices
[DE93-015387] 03 p1184 N94-16828
Reference frames in vision
[AD-A266174] 03 p1132 N94-16925
Advanced transport systems for electron beams in high brightness accelerators and FELs
[AD-A267322] 03 p1041 N94-17001
Lectures of Fermi liquid theory
[DE93-016630] 04 p1592 N94-17714
Impulsive moving mirror model and the stability of linear homogeneous differential equations with impulse effect in a Banach space
[DE93-629906] 04 p1549 N94-18200
The microstructural mechanism of electromigration failure in narrow interconnects of Al alloys
[DE93-018598] 04 p1365 N94-19282
Electrocatalysts for oxygen electrodes
[DE93-040446] 04 p1354 N94-19653
A summary of studies of particle stability at RHIC
[DE93-040173] 05 p1970 N94-19868
Study of transverse coupled bunch instabilities by using non-linear Taylor maps for the Advanced Light Source (ALS)
[DE93-040287] 05 p1979 N94-19989
The stability of oxyamphiboles: Existence of Ferric-bearing minerals under the reducing conditions on the surface of Venus 05 p2122 N94-20800
Numerical ranges and stability estimates
[TW-92-10] 05 p1953 N94-21060
Stability analysis of unsteady ablation fronts
[DE93-019689] 05 p1819 N94-21839
Proof of stability of the hydrogen molecule
[PB93-221026] 05 p1977 N94-22271
Stable non-Gaussian diffusive profiles
[PB93-238053] 06 p2489 N94-24610
Numerical analysis of the motion of a rigid body with an attached spring-mass-damper
[AD-A273825] 06 p2379 N94-25520
Zinc(2) oxide stability in alkaline sodium phosphate solutions at elevated temperatures
[DE94-003316] 07 p2715 N94-26320
On the (Phi)(sub 0)-stability of functional differential equations
[DE94-601507] 07 p3006 N94-26460
A characterization of stable models using a non-monotonic operator
[CWI-CS-R9315] 07 p2970 N94-27543
Unsteady aspects of hot gas reingestion and statistical analysis 07 p2676 N94-28019
Stability properties of inclusive connectivity for graphs
[AD-A275360] 08 p3452 N94-29016
Improved QCD sum rule estimates of the higher twist contributions to polarised and unpolarised nucleon structure functions
[PB94-138112] 08 p3487 N94-29161
The stability of perfect elliptic disks
08 p3545 N94-29834
Russian national time scale long-term stability
08 p3475 N94-30679
The performance of thermal control coatings on LDEF and implications to future spacecraft
09 p3591 N94-31013
Nonlinear calculations of the time evolution of black hole accretion disks 09 p3929 N94-31127
Gravitational instabilities in protostellar disks
09 p3932 N94-31140
Multidimensional WAF-type schemes for model conservation laws
[CRANFIELD-AERO-9312] 09 p3843 N94-31541
Design of new polymers to improve radiation stability of plastic scintillators
[DE94-008220] 09 p3652 N94-31764
Modal analysis of multiterminal high voltage direct current transmission
[DE94-006426] 09 p3691 N94-31785
Stability and precipitation kinetics in Si(1-y)C(y)/Si and Si(1-x-y)Ge(x)C(y)/Si heterostructures prepared by solid phase epitaxy
[DE94-006589] 09 p3902 N94-32296
Research on stable, high-efficiency amorphous silicon multijunction modules
[DE94-000298] 09 p3695 N94-32680
Stability of tearing modes in tokamak plasmas
[DE94-009205] 09 p3892 N94-32911
Theoretical study of novel bonding in molecules: Metastable molecular fuels
[AD-A277807] 10 p4031 N94-33895
A note on high order schemes for one dimensional wave equation
[PB94-171006] 11 p4315 N94-35821
Numerical method to study the stability of periodic solutions of particle motion in nonlinear magnetic fields
[DE94-610740] 11 p4325 N94-36088
Local instabilities and the transition to chaos of non-linear waves
[PB94-170578] 11 p4341 N94-36213
Non-linear interaction of gravity waves with average jet flows, instabilities, and turbulence
[PB94-170586] 11 p4291 N94-36214
Formation and stability of Fe-rich precipitates in dilute Zr(Fe) single-crystal alloys
[DE94-619027] 11 p4242 N94-36288
Impedance and instability threshold estimates in the main injector 1
[DE94-010332] 11 p4332 N94-36431
Methyl chloride via oxyhydrochlorination of methane
[DE94-010691] 12 p4406 N94-36450
Experimental characterisation of gas microstrip detectors. Part 1: Gain characteristics
[PB94-167087] 12 p4445 N94-36531
New hollow-cathode electrode for high-power copper lasers
[DE94-011637] 12 p4448 N94-37244
Stability and dynamics of spatio-temporal structures
[DE94-013035] 12 p4412 N94-37491

STABILITY AUGMENTATION
Design, fabrication and test of a vertical attitude takeoff and landing unmanned air vehicle
[AD-A273003] 05 p1646 N94-21283
The decoupling design of aircraft lateral flight control systems with eigenstructure assignment
10 p4007 N94-34329
YAV-8B reaction control system bleed and control power usage in hover and transition
[NASA-TM-104021] 10 p4007 N94-34994

STABILITY DERIVATIVES
NT PITCHING MOMENTS
NT ROLLING MOMENTS
NT YAWING MOMENTS
Extraction of stability and control derivatives from orbiter flight data
[NASA-TM-4500] 01 p0013 N94-10707
Nonlinear aspects of transonic aeroelasticity
[UTIAS-345] 01 p0015 N94-11857
LinAir: A multi-element discrete vortex Weissinger aerodynamic prediction method
[NASA-TM-108786] 06 p2167 N94-23557
Linear modeling of rotorcraft for stability analysis and preliminary design
[AD-A274869] 07 p2677 N94-26192
A finite wake theory for two-dimensional rotary wing unsteady aerodynamics
[AD-A274921] 07 p2645 N94-26535
Trim calculation of tandem rotor helicopter using simplified rotor system mathematical model
10 p4008 N94-34337

STABILITY TESTS
NT FLIGHT STABILITY TESTS
NT WIND TUNNEL STABILITY TESTS
Marangoni instability in a liquid layer with two free surfaces
[NASA-TM-106166] 01 p0152 N94-11376
Stability analysis and aerospace vehicle dynamics
01 p0031 N94-11491
Stability model of the atmosphere
01 p0032 N94-11500
Functional differential equations with piecewise continuous argument
[AD-A266660] 02 p0772 N94-14840
Stability of flows in fluidized beds
[DE93-000245] 03 p1024 N94-16763
Stability analysis for the flow of granular materials down an inclined plane using kinetic model
[DE93-016852] 03 p1026 N94-16958
A one dimensional numerical model, with an application to the vertical distribution of dissolved oxygen in the ocean
[DE93-018481] 04 p1495 N94-17779
Competitive dynamics and self-organization in photorefractive systems
[AD-A269663] 04 p1430 N94-18569
Stability analysis of unsteady ablation fronts
[DE93-019689] 05 p1819 N94-21839
Stability analysis of anisotropic conical shells
[PB94-119054] 06 p2377 N94-24645
Stability of premixed laminar flames in a stagnation point flow to general disturbances
[AD-A273429] 06 p2234 N94-24673
Numerical experiment on finite element method for matching data
[DE94-701208] 07 p3000 N94-27731
Multidisciplinary aeroelastic analysis of a generic hypersonic vehicle
[NASA-TM-4544] 07 p2691 N94-27868
A simplified Von Neumann method for linear stability analysis
[CRANFIELD-AERO-9310] 09 p3843 N94-31540
Attitude dynamics of spinning rockets in space with internal mass motion 09 p3601 N94-31802
Stability analysis of an F/A-18 E/F cable mount m odel
[NASA-TM-108989] 12 p4386 N94-37636

STABILIZATION
NT SPIN STABILIZATION
NT THREE AXIS STABILIZATION
Magnetohydrodynamic computation of feedback stabilization of resistive-shell instabilities in the reversed field pinch
[DE93-013466] 01 p0388 N94-10852
Densifying and stabilizing ingredient
[AD-D015751] 03 p0975 N94-16934
TITUS: A micro-satellite for technology demonstration
03 p0896 N94-17186
Stabilization of time-delay systems: An overview of the algebraic approach
[PB93-191989] 04 p1553 N94-19556
Median stabilization degree of a median algebra
[PB93-220010] 06 p2479 N94-23093
Stabilization of the external kink and other MHD issues
[DE94-001541] 06 p2552 N94-24502
Genericity of stabilizability for time-delay systems
[PB93-237725] 06 p2475 N94-24762
Preliminary results on time-varying feedback stabilization of a nonholonomic car-like mobile robot
[INRIA-RR-1512] 06 p2475 N94-24963
Numerical simulation of plasma vertical position stabilization in ITER
[DE93-634588] 07 p3044 N94-26510
The addition of molecular oxygen to hydroperoxy-propyl radicals
[DE94-003662] 07 p2760 N94-27725
Passive stabilization of MHD instabilities at high (beta)n in the HBT-EP tokamak
[DE94-003317] 07 p3047 N94-27735
Stabilization of polyaniline solutions
[DE94-003958] 07 p2704 N94-27745
Automatic resonator alignment and power stabilization of high power C02 lasers
[ISBN-0-315-77217-4] 09 p3714 N94-31472
Stabilization method of A.C. arc plasma
[DE94-757268] 09 p3893 N94-32916
Contingency airfield construction: Mechanical stabilization using monofilament and fibrillated fibers
[AD-A277732] 10 p4008 N94-33444
Adaptive stabilization of linear and nonlinear systems
[AD-A278270] 10 p4113 N94-33855
Stabilization of flexible systems under a certain class of nonlinear feedback controls 10 p4114 N94-34314
Feedback stabilization of matrix second-order systems by solving Riccati equation 10 p4115 N94-34315
Robust stabilization of nonlinear systems with a class of unmatched uncertainties 10 p4115 N94-34322
Nominal H(exp 2)-optimization and strong stabilization: A practical example of U-parameterization design
10 p4122 N94-34370
Concurrent stabilization and imaging of a novel polymer for second harmonic generation via in situ photopolymerization
[AD-A278912] 11 p4243 N94-35588
Estimation with multisensor/multiscan detection fusion
[AD-A278753] 11 p4256 N94-36092

STABILIZED PLATFORMS
Development of a balloon-borne stabilized platform for measuring radiative flux profiles in the atmospheric boundary layer
[DE93-013186] 01 p0274 N94-10323

Inertial pseudo star reference unit
12 p4394 N94-36625

STABILIZERS (AGENTS)
Oxide pigments in water: The colloid-chemical point of view
[PB94-148616] 09 p3633 N94-31591

STABILIZERS (FLUID DYNAMICS)
NT HORIZONTAL TAIL SURFACES
Vertical-tail aerodynamic configuration of space shuttle orbiter
[AD-A267723] 03 p0879 N94-14941
Procedures and design data for the formulation of aircraft configurations
[AD-A270150] 04 p1318 N94-18779
Apparatus and method for improving spin recovery on aircraft
[NASA-CASE-LAR-14747-1] 05 p1650 N94-20556
Active control for fin buffet alleviation
[AD-A276844] 09 p3586 N94-32224

STABLE OSCILLATIONS
Regrouping of the beam in the IHEP PS for the UNK p-p programs
[DE93-634021] 07 p3032 N94-26164

STACKING FAULTS
U CRYSTAL DEFECTS

STACKS
Detailed design of the 2MW Demonstration Plant
[DE94-000042] 09 p3762 N94-32823

STADAN (SATELLITE TRACKING NETWORK)
U STDN (NETWORK)

STAGE SEPARATION
Estimation of the attitude motion of the small satellite ORIZURU
[NAL-TR-1145] 01 p0042 N94-10366

STAGGERING
FAS multigrid calculations of three dimensional flow using non-staggered grids 06 p2341 N94-23675

STAGING (ROCKETS)
U STAGE SEPARATION

STAGNATION FLOW
A model of elementary chemistry and fluid mechanics in the combustion of hydrogen on platinum surfaces
[DE93-012767] 01 p0077 N94-11370

STAGNATION POINT
Evolution of disturbances in stagnation point flow
[NASA-CR-191516] 02 p0636 N94-13724
Stability of hypersonic flow of a detonable gas mixture in the stagnation region of a blunt body and a forward facing step 06 p2154 N94-24248
Stagnation region heat transfer: The influence of turbulence parameters, Reynolds number and body shape
[NASA-TM-106504] 06 p2334 N94-24481
Stability of premixed laminar flames in a stagnation point flow to general disturbances
[AD-A273429] 06 p2234 N94-24673
Measurements of the influence of integral length scale on stagnation region heat transfer
[NASA-TM-106503] 06 p2338 N94-25183
Experimental studies of hypersonic transitional and turbulent boundary layers in hypersonic flow
[AD-A278441] 10 p4044 N94-33556

STAGNATION PRESSURE
Probe shapes that measure time-averaged streamwise momentum and cross-stream turbulence intensity
[NASA-CASE-ARC-11934-1] 06 p2317 N94-23077
Pressure-gain combustion
[DE94-002975] 07 p2719 N94-27712

STAGNATION REGION
U STAGNATION POINT

STAGNATION TEMPERATURE
A comparative study of turbulence models in predicting hypersonic inlet flows 04 p1314 N94-18553

STAINLESS STEELS
NT AUSTENITIC STAINLESS STEELS
NT FERRITIC STAINLESS STEELS
NT MARTENSITIC STAINLESS STEELS
Microbiological test results using three urine pretreatment regimes with 316L stainless steel
[NASA-CR-192568] 01 p0299 N94-10360
Welding tritium aged stainless steel
[DE93-011782] 01 p0181 N94-11228
BAKEOUT: A computer program for predicting diffusive outgassing from stainless steel
[DE93-012613] 02 p0573 N94-14364
Welding technologies as applied to nuclear manufacturing
[DE93-010924] 02 p0664 N94-14565
The effect of aging at 343 C on the mechanical properties and microstructure of type 308 stainless steel weldments
[DE93-015454] 03 p0957 N94-16103
Application of hard coatings to substrates at low temperatures
[NASA-CR-193867] 03 p0971 N94-17122
Stress corrosion cracking of 316 SS and Incoloy-800 in high temperature aqueous containing sulfate and chloride
[DE93-623325] 03 p0952 N94-17302
Assessment of an improved multiaxial strength theory based on creep-rupture data for Inconel 600
[DE93-015929] 04 p1356 N94-17791
Summary of work on coatings and claddings for fossil energy applications
[DE93-017005] 04 p1367 N94-17881
Development and application of specially-focused ultrasonic transducers to location and sizing of defects in 75 mm- to 127 mm-thick austenitic stainless steel weld metals
[DE93-015975] 04 p1453 N94-18108
A probability method of fracture mechanics analysis for HFIR vessel
[DE93-015510] 04 p1453 N94-18246
Aerosol filtration with steel fiber filters
[DE93-016990] 04 p1380 N94-18710
Foil support structure for large electron guns
[DE93-018478] 04 p1322 N94-18890
Finite difference program for calculating hydride bed wall temperature profiles
[DE93-019272] 04 p1523 N94-19005
The effects of radiolysis on the corrosion and stress corrosion behavior of 316 stainless steels
[DE93-019933] 04 p1363 N94-19021
Overlay welding irradiated stainless steel
[DE93-018767] 04 p1446 N94-19334
Thermocapillary and arc phenomena in stainless steel welds
[DE94-000518] 05 p1821 N94-19859
Microscopic evaluation of low-temperature embrittlement in type 308 stainless steel welds
[DE93-040266] 05 p1690 N94-20282
Transmission electron microscopy study of thick copper-304 stainless steel multilayers
[DE94-001045] 05 p1696 N94-22394
Tensile properties of 21-6-9 stainless steel at elevated temperatures
[DE94-001852] 06 p2240 N94-23017
Stress corrosion cracking properties of 15-5PH steel
06 p2251 N94-23244
Grain-boundary microchemistry and intergranular cracking of irradiated austenitic stainless steel
[DE94-000466] 06 p2242 N94-23457
JBK-75 stainless steel machinability study
[DE94-002268] 06 p2242 N94-23475
Weld joint concepts for on-orbit repair of Space Station Freedom fluid system tube assemblies
06 p2371 N94-24427
Welding of niobium to stainless
[DE94-003365] 06 p2365 N94-24614
Preceedings of the 12th International Congress: Corrosion Control for Low-Cost Reliability. Volume 3A: Corrosion: Specific issues
[AD-A273663] 06 p2251 N94-25450
Proceedings of the 12th International Congress: Corrosion Control for Low-Cost Reliability. Volume 3B: Corrosion: Specific issues
[AD-A273664] 06 p2251 N94-25451
R and D for creation, measurement, application of ultra-high vacuum 07 p2723 N94-25549
Study on high temperature damage control and life improvement 07 p2729 N94-25580
Study on evaluation of crack generation and crack growth behaviors under static loading at high temperature and under combined loading 07 p2730 N94-25583
Reference electrodes for solid polymer electrolytes
[DE94-004583] 07 p2780 N94-25806
New equation of state for stainless steel 347
[DE94-004189] 07 p2732 N94-25974
Effect of loading mode on the fracture toughness of a reduced activation ferritic/martensitic stainless steel
[DE94-004290] 07 p2732 N94-25987
Guidelines for controlling stress corrosion cracking and corrosion fatigue of stainless steels: A literature review
[VTT-TIED-1420] 07 p2837 N94-26262
Stability of reference masses 2: The effect of environment and cleaning methods on the surfaces of stainless steel and allied materials
[NPL-DMM(A)-95] 07 p2738 N94-26653
Vapor deposition of copper on stainless steel 304L
[DE94-001945] 07 p2740 N94-27006
Modification of a model for fatigue life predictions based on level-crossing
[PB94-123395] 07 p2842 N94-27198
Isothermal corrosion testing of steels in molten nitrate salts
[DE94-004695] 07 p2742 N94-27755
Upset welding process for 21-6-9 spherical vessels
[DE93-018194] 07 p2832 N94-28229
Fundamental studies on the corrosion behavior of weldments in marine microbial environments
[AD-A275247] 08 p3203 N94-28900
Insulative properties of two thermo-metal neoprenes
[AD-A275209] 08 p3401 N94-29302
The organometallic chemical vapor deposition of transition metal carbides: The use of homoleptic alkyls
[DE94-005577] 08 p3206 N94-30007
Laser beam welding of AISI 316 stainless steel in microgravity environment: Experiments aboard a KC-135 flight
[ISBN-0-315-86095-2] 08 p3229 N94-30145
Effect of vibratory stress relief during welding of thick stainless steel plate
[DE94-006557] 09 p3733 N94-31312
Solid-state resistance upset welding: A process with unique advantages for advanced materials
[DE94-005941] 09 p3723 N94-31524
Irradiation-assisted stress corrosion cracking of materials from commercial BWRs: Role of grain-boundary microchemistry
[DE94-006542] 09 p3643 N94-32109
Stage 1 behavior in a stress corrosion study of Type 304 stainless steel
[DE94-008054] 09 p3645 N94-32614
Modeling of residual stress mitigation in austenitic stainless steel pipe girth weldment
[DE94-007184] 09 p3738 N94-32639
Stainless steel surface treatment
[AD-D016135] 10 p4024 N94-33758
Solidification microstructures in single-crystal stainless steel melt pools
[DE94-009839] 10 p4024 N94-33880
Plane shock generator explosive lens: Shock characterization of 4340 and PH13-8Mo steels, C360 brass and PZT 65/35 ferro-electric ceramic
[DE94-009254] 11 p4266 N94-35979
Ability of the total strain version of strainrange partitioning to characterize thermomechanical fatigue behavior
[NASA-TM-4556] 12 p4455 N94-37102
AEM and AES of radiation-induced segregation in proton-irradiated stainless steels
[DE94-012734] 12 p4418 N94-37398

STANDARD DEVIATION
Moments of ambient Doppler spectra
[DE93-017948] 04 p1390 N94-19114
Performance evaluation of the JPL TOPSAR system: An across-track interferometric SAR system for topographic mapping 05 p1732 N94-20461
DECONV-TOOL: An IDL based deconvolution software package 05 p1927 N94-22542
Estimates of monthly mean soil moisture for 1979-1989
[NASA-TM-104571] 06 p2407 N94-23132
Example of statistical techniques applied to analysis of effects of small changes
[ESDU-93023] 07 p2670 N94-28094
Probabilistic material strength degradation model for Inconel 718 components subjected to high temperature, mechanical fatigue, creep and thermal fatigue effects
[NASA-CR-195284] 08 p3318 N94-28840
Development of a statistical method for estimating the downward longwave radiation at the surface from satellite observations 09 p3742 N94-31553
Process capability determination of new and existing equipment 11 p4230 N94-36406
Short-tower sigma(theta) measurements in the Colorado Plateaus region
[DE94-007478] 12 p4463 N94-36478

STANDARD ELECTROWEAK MODEL
U ELECTROWEAK MODEL

STANDARD MODEL (PARTICLE PHYSICS)
Standard model status (in search of new physics)
[DE93-013288] 01 p0410 N94-10528
Future high precision experiments and new physics beyond Standard Model
[DE93-011004] 01 p0373 N94-11618
Top quark polarization and T-odd spin correlations as tools for testing (non) Standard Model predictions
[DE93-622956] 02 p0778 N94-12847
Finding the missing pieces of the standard model
[ISBN-0-315-57174-8] 07 p3024 N94-27259
QCD corrections to inclusive B - S processes in the standard model
[ISBN-0-315-54572-0] 07 p3073 N94-27263
Report of the subgroup on the top quark
[DE94-004624] 08 p3481 N94-28462
Search for the top quark in the electron-electron and electron-muon channels at D0
[DE94-006174] 08 p3492 N94-30779
Spin and precision electroweak physics
[DE94-009074] 10 p4137 N94-33936
Top quark search at CDF
[DE94-003643] 12 p4511 N94-36459
Radiative and rare mu and pi decays
[DE94-618549] 12 p4515 N94-37066
Particle physics
[DE94-012944] 12 p4518 N94-37312

STANDARDIZATION
Progress on GPS standardization
01 p0024 N94-10965
MIL-STDS and PTTI: What's available and what needs to be done 01 p0352 N94-10973
Abbreviations, acronyms, and initialisms frequently used by Martin Marietta Energy Systems, Incorporated
[DE93-012509] 01 p0420 N94-11369
Longitudinal study of astronaut health: Mortality in the years 1959-1991 01 p0312 N94-11560
The guide to Design For On-orbit Spacecraft Servicing (DFOSS) manual: Producing a consensus document
01 p0421 N94-11575
The development of flexible software for the Italian/Dutch satellite SAX: Advantages and disadvantages of the use of CASE tools
[NLR-TP-91288-U] 03 p1157 N94-17626
PostScript: A study in conformity
[NPL-DITC-214/93] 04 p1517 N94-17917
Secure open systems: An investigation of current standardisation efforts for security in open systems
[FEL-92-B225] 04 p1618 N94-19450
The manager's guide to NASA graphics standards
[NHB-1430.2] 05 p2042 N94-20308
The electronics technology policy of the NLR Informatics Division: The NLR electronics CAE infrastructure
[NLR-TP-91001-U] 05 p1753 N94-21067
Government Open Systems Interconnection Profile (GOSIP) transition strategy
[AD-A273005] 05 p1740 N94-21308
Data format standards for civilian remote sensing satellites
[PB93-192920] 05 p1841 N94-21446
Operational test and evaluation of electronic combat systems
[AD-A273093] 05 p1647 N94-21500
Surveys on specific patterns of facility intallation of photovoltaic power generating technologies for international cooperation
[DE94-714901] 05 p1850 N94-22092
High-rate data link general specification for the NOAA-OPQ polar orbiting environmental satellites and EUMETSAT satellite systems
[NASA-TM-109384] 06 p2208 N94-23481
Definitions in use by the visible and near-infrared, and thermal working groups 06 p2383 N94-23598
Activities of NIST (National Inst. of Standards and Technology) 06 p2384 N94-23605
NASA/Goddard Space Flight Center's testbed for CCSDS compatible systems 06 p2197 N94-23855
Interoperability through standardization: Electronic mail, and X Window systems 06 p2575 N94-24406
A simulation and evaluation of NATO Standardization Agreement (STANAG) 4214
[AD-A273195] 06 p2297 N94-24554
Solid state Time Base Corrector (TBC)
[AD-D015981] 06 p2312 N94-25039
The question of standards for digital interactive television
[AD-A273872] 07 p2765 N94-25725
Standardizing exchange formats
[DE93-616798] 07 p3095 N94-25751
Development of the Air Force contingency contracting course framework
[AD-A273921] 07 p3093 N94-25895
International energy: Research organizations, 1988-1992
[DE93-017267] 07 p3098 N94-26398
Standardize Ada hard real-time services?
07 p2951 N94-26729
MILCOM 92 and standardization for HF-communication. A study tour to the USA in October 1992
[PB94-124427] 07 p2774 N94-27219
Software assurance standard
[NASA-TM-109705] 07 p2975 N94-27992
Air Force standards for nickel hydrogen battery
07 p2862 N94-28116
Open communication in manufacturing automation
[PB94-132479] 07 p2976 N94-28377
NASA Parts Program Office responsibilities
08 p3165 N94-28702
NASA Parts Project Office: Basic goals
08 p3166 N94-28703
NAVAIR aircraft wiring standardization and qualification program 08 p3166 N94-28704
Organized wiring systems 08 p3166 N94-28705
SI (Metric) handbook
[NASA-TM-109197] 08 p3231 N94-29376
A normative frame of reference for the metrology function
[REPT-932-430-102] 08 p3231 N94-29477
Neural network application to Particle Impact Noise Detection 08 p3437 N94-29840
Standardisation requirements for ultrasonic C-scanning of polymer matrix composites: An initial assessment
[PB94-139318] 08 p3184 N94-30438
Cascaded clocks measurement and simulation findings 08 p3469 N94-30649
Standardization and intellectual property control: A reflection on the informatics case
[TELECOM-93-E-016] 09 p3915 N94-31172
Untying the gordian data knot. A paper on Information Engineering (IE) and Corporate Information Management (CIM)
[AD-A276862] 09 p3918 N94-32210
International Energy: Subject Thesaurus, revision 1
[DE94-002590] 10 p4151 N94-33730
ATM technology and beyond
10 p4156 N94-33820
Building fault-tolerant distributed computing systems using standard components
[PB94-148889] 10 p4112 N94-34125
Standards in the architectural effort
12 p4541 N94-36852
Standards for data and document interchange
12 p4543 N94-37337

STANDARDS
NT FREQUENCY STANDARDS
An intercomparison of the radium mass standards of the UK and the USSR: 2
[NPL-RSA(EXT)-34] 01 p0359 N94-10266
The 17th Transducer Workshop
[AD-A265526] 01 p0141 N94-10509
Correspondence standards
[NHB-1450.10B] 01 p0420 N94-11589
Analysis and guidelines for reusable Ada software
[AD-A264918] 01 p0332 N94-11850
VIEWCACHE: An incremental pointer-base access method for distributed databases. Part 1: The universal index system design document. Part 2: The universal index system low-level design document. Part 3: User's guide. Part 4: Reference manual. Part 5: UIMS test suite
[NASA-CR-191788] 02 p0822 N94-13126
Specimen files in VAMAS standard data transfer format (EXAMPLE 1.TXT to EXAMPLE 4.TXT)
[NPL-DMM(A)-90] 02 p0749 N94-13688
The design of chain links and slings
[NPL-DMM(A)-94] 02 p0662 N94-13808
The use of formal methods in data security standards
[NPL-DITC-205/92] 03 p1142 N94-15008
The value of reference implementations and prototyping in a formal design and testing methodology
[NPL-DITC-208/92] 03 p1142 N94-15011
The application of programming languages to the production of reference implementations
[NPL-DITC-209/92] 03 p1143 N94-15012
Standards and conformance testing in data security: Results of initial programme of investigation
[NPL-DITC-218/92] 03 p1143 N94-15014
Testability of data security standards
[NPL-DITC-217/93] 03 p1143 N94-15022
Development of a proposed international standard for certification of aircraft to High Intensity Radiated Fields (HIRF)
[NASA-TM-106357] 03 p0863 N94-16520
CALS test network handbook
[AD-A267587] 03 p1160 N94-17209
Radar transmitter procedures
[AD-A268274] 03 p1005 N94-17523
PostScript: A study in conformity
[NPL-DITC-214/93] 04 p1517 N94-17917
The stability and utility of the ESPRIT project, MUSiC, performance-based indicators of usability and tools: An evaluation of the usability of the NPL iSDX telephone system
[NPL-DITC-213/92] 04 p1613 N94-17925
About time 04 p1426 N94-18024
Rationale for the power standard
[ESA-PSS-02-10-VOL-2-ISSUE-1] 04 p1338 N94-19516
Power standard
[ESA-PSS-02-10-VOL-1-ISSUE-1] 05 p1669 N94-20241
Goniospectrometric properties of a white standard
05 p1684 N94-20664
Named Venusian craters 05 p2109 N94-20725
U.S. Tag for ISO/TC 43, acoustics, IEC/TC 29 electroacoustics, and ISO/TC 108/SC4 human exposure to mechanical vibration and shock: Minutes of the accredited standards committee on bioacoustics, S3
[AD-A273014] 05 p1897 N94-21309
Space Generic Open Avionics Architecture (SGOAA) standard specification
[NASA-CR-188269] 05 p1666 N94-22275
NASA data exchange standards for computational fluid dynamics 05 p1920 N94-22371
Electronic publishing and intelligent information retrieval 05 p2047 N94-22479
Fortran for the nineties 05 p1926 N94-22481
Guide to software configuration management
[ESA-PSS-05-09-ISSUE-1] 06 p2450 N94-23229
Impacts: NIST Building and Fire Research Laboratory (technical and societal)
[PB94-113420] 06 p2270 N94-23737
US tag for ISO/TC 108 mechanical vibration and shock: Minutes of the accredited Standards Committee on Mechanical Vibration and Shock, S2
[AD-A273015] 06 p2376 N94-23789
Primary standards laboratory report 1st half 1993
[DE94-003138] 07 p2762 N94-26027
CEN-VAMAS round robin on grain size measurement for advanced technical ceramics
[VAMAS-TR-12] 07 p2752 N94-26654
Standardize Ada hard real-time services?
07 p2951 N94-26729
Guidelines for unlubricated sliding wear tests. Part 1: General approach
[PB94-119666] 07 p2825 N94-27322
Technical Report of National Research Institute of Fisheries Engineering: Fishing Boat and Instrument, No. 12
[JTN-94-80595] 07 p2764 N94-27976
Software assurance standard
[NASA-TM-109705] 07 p2975 N94-27992
Controls, monitoring and performance measurements
07 p2831 N94-28086
Air Force standards for nickel hydrogen battery
07 p2862 N94-28116
Air traffic administration enroute to Europe
07 p2661 N94-28238
Comparison of the lossy image data compressions for the MESUR Pathfinder and for the Huygens Titan Probe
07 p2945 N94-28254
NAVAIR aircraft wiring standardization and qualification program 08 p3166 N94-28704
Unscreened low tension cables scrape abrasion testing. Part 1: An interlaboratory study on scrape abrasion testing according to ISO DP 6722-1
[PB94-135605] 08 p3264 N94-29191
A normative frame of reference for the metrology function
[REPT-932-430-102] 08 p3231 N94-29477
A survey of NASA and military standards on fault tolerance and reliability applied to robotics
[AIAA PAPER 94-1211-CP] 08 p3445 N94-30562
The 25th Annual Precise Time and Time Interval (PTTI) Applications and Planning Meeting
[AD-A280955] 08 p3468 N94-30639
Time and frequency technology at NIST
08 p3468 N94-30641
European PTTI report 08 p3468 N94-30642
Report on NATO PTTI 08 p3469 N94-30645
Guidance notes for use with NPL low permeability reference materials
[NPL-DES-121] 08 p3476 N94-30780
Guide to software quality assurance
[ESA-PSS-05-11-ISSUE-1] 09 p3809 N94-31223
Minutes: Accredited Standards Committee on Bioacoustics, S3. US TAG for ISO/TC 43, acoustics, IEC/TC 29 electroacoustics, and ISO/TC 108/SC4 human exposure to mechanical vibration and shock
[AD-A276201] 09 p3795 N94-31490
Evaluation for the development of taxiway lighting intensity standards
[AD-A276706] 09 p3588 N94-32120
ATM technology and beyond
10 p4156 N94-33820
Minimum performance standards: Airborne low-range radar altimeters
[RTCA-DO-155] 11 p4198 N94-35344
Software architecture standard for simulation virtual machine, version 2.0
[NASA-CR-188291] 11 p4301 N94-35443
NASA STI Program Coordinating Council Eleventh Meeting: NASA STI Modernization Plan
[NASA-TM-109415] 12 p4540 N94-36841
Standards in the architectural effort
12 p4541 N94-36852
NASA STI Program Coordinating Council Twelfth Meeting: Standards
[NASA-TM-109925] 12 p4541 N94-36853
STI Architectural Framework Working Group
12 p4542 N94-36854
OSI and TCP/IP 12 p4542 N94-36855
A concise introduction to MARC
12 p4542 N94-36856
Open system environments 12 p4542 N94-36857
Open system environment procurement
12 p4542 N94-36858
Z39.50 and GILS model --- Government Information Locator Service 12 p4542 N94-36859
Government Information Locator Service (GILS). Draft report to the Information Infrastructure Task Force
12 p4542 N94-36860
Space Generic Open Avionics Architecture (SGOAA) standard specification
[NASA-CR-188290] 12 p4387 N94-36933

Standards for data and document interchange
12 p4543 N94-37337
Advanced distributed simulation technology. SIMWORLD data base
[AD-A280262] 12 p4545 N94-37757

STANDING WAVE RATIOS
Phase linearity of the 914H coupled-cavity traveling wave tube
[NASA-CR-191056] 06 p2290 N94-23087
ADC test support program
[AD-A274819] 07 p2783 N94-26491

STANDING WAVES
The x ray standing waves on surfaces
[AD-A265265] 01 p0402 N94-11682
Multi-bunch beam-break-up studies for a SWFEL/TBA
[DE93-016973] 02 p0658 N94-14414
The standing wave FEL/TBA: Realistic cavity geometry and energy extraction
[DE93-016972] 02 p0659 N94-14520
Three-dimensional simulation analysis of the first sections of a standing-wave free-electron laser two-beam accelerator
[DE93-016977] 04 p1436 N94-17869
X ray standing wave studies of underpotentially deposited metal monolayers
[AD-A275409] 08 p3513 N94-29215
A preliminary investigation of high amplitude standing waves with laser Doppler anemometry
[AD-A276463] 09 p3860 N94-31242
Observation of the traveling component of an x ray standing wave field
[DE94-007671] 09 p3672 N94-31317
Cooling and trapping of neutral atoms
[AD-A276957] 09 p3870 N94-32360
Fundamentals studies of radial wave thermoacoustic engines
[AD-A280534] 12 p4431 N94-37090
Suppression of beam-break-up in a standing wave free electron laser two-beam accelerator
[DE94-011348] 12 p4521 N94-37200

STANDS
U SUPPORTS

STANTON NUMBER
Experimental measurements and analytical analysis related to gas turbine heat transfer. Part 1: Time-averaged heat-flux and surface-pressure measurements on the vanes and blades of the SSME fuel-side turbine and comparison with prediction. Part 2: Phase-resolved surface-pressure and heat-flux measurements on the first blade of the SSME fuel-side turbine
[NASA-CR-196296] 12 p4442 N94-36969

STAR CATALOGS
U ASTRONOMICAL CATALOGS

STAR CLUSTERS
NT GLOBULAR CLUSTERS
NT OPEN CLUSTERS
Statistical analysis of trigonometric parallaxes
[NASA-CR-194558] 03 p1172 N94-15641
Ultraviolet observations of clusters of Wolf-Rayet stars in the SBm3 galaxy NGC 4214 and Ultraviolet and optical observations of LINER's
[NASA-CR-194307] 04 p1622 N94-19431
The distribution of dark matter in the A2256 cluster
[NASA-CR-194699] 05 p2055 N94-21579
X ray studies of the Hyades cluster
[NASA-CR-189325] 08 p3538 N94-29001
Circumstellar material around young stars in Orion
09 p3930 N94-31133
Near infrared surveys of high mass star forming regions
09 p3925 N94-31898

STAR DISTRIBUTION
The star identification, pointing and tracking system of UVSTAR, an attached payload instrument system for the Shuttle Hitchhiker-M platform 04 p1326 N94-19179
The distribution of dark matter in the A2256 cluster
[NASA-CR-194699] 05 p2055 N94-21579
Extracting galactic structure parameters from multivariated density estimation
05 p1964 N94-22458
Nonthermal accretion disk models around neutron stars 09 p3931 N94-31139

STAR FIELDS
U STAR DISTRIBUTION

STAR FORMATION
Detection of accreting circumstellar gas around weak emission-line Herbig Ae/Be stars
[NASA-TM-108256] 01 p0424 N94-11306
Analysis of interstellar fragmentation structure based on IRAS images
[NASA-CR-193518] 01 p0428 N94-12767
Analysis of interstellar cloud structure based on IRAS images
[NASA-CR-194341] 02 p0836 N94-13332
Search for x ray emitting young stars outside of massive molecular clouds
[NASA-CR-193609] 02 p0830 N94-13462
Millimeter and infrared studies of young stellar objects in dark cloud L1641 02 p0838 N94-13648
The origin of the far-infrared emission from galactic molecular clouds 02 p0848 N94-13654
ROSAT-IUE observations of symbiotic stars. The x ray morphology of high latitude associations
[NASA-CR-194616] 03 p1236 N94-16492
Collisional dynamics of perturbed particle disks in the solar system
[NASA-CR-193584] 03 p1239 N94-16648
Formation of the low-mass solar nebula
05 p2109 N94-20728
The formation of massive stars: A 30 Mo case study
[ISBN-0-315-83944-9] 05 p2081 N94-22593
Magnetohydrodynamic phenomena in star-forming processes and their environment
05 p2010 N94-22701
ROSAT observations of the x ray binary HD 154791
[NASA-CR-195189] 06 p2600 N94-25198
Investigations of the dynamical evolution of protoplanetary nebulae
[NASA-CR-195278] 07 p3105 N94-27428
The role of cloud collisions in N-body simulations of disk galaxies 08 p3545 N94-29755
A multi wavelength observational study of the Cartwheel ring galaxy 08 p3539 N94-29821
Multicolor photometry of barred spiral galaxies
08 p3541 N94-30270
Stellar and gas dynamics of interacting ring galaxies
08 p3548 N94-30340
Circumstellar material around young stars in Orion
09 p3930 N94-31133
Gravitational instabilities in protostellar disks
09 p3932 N94-31140
The stellar and gaseous content of massive low surface brightness disk galaxies 09 p3933 N94-31495
Double-lined pre-main-sequence binaries: A test of pre-main-sequence evolutionary theory
09 p3933 N94-31497
Evolution of stars and winds in the starburst galaxy M82 09 p3934 N94-31758
Near infrared surveys of high mass star forming regions 09 p3925 N94-31898
Near and far infrared observations of protostars and dark clouds 09 p3926 N94-31969

STAR FORMATION RATE
Evolution of stars and winds in the starburst galaxy M82 09 p3934 N94-31758
Ionized gas in the halos of edge-on infrared-bright galaxies: Evidence for starburst-driven superwinds
09 p3936 N94-31948

STAR TRACKERS
NT CCD STAR TRACKER
Time series photometry of faint cataclysmic variables with a CCD 02 p0831 N94-13646
The Spacelab IPS Star Simulator
[TABES PAPER 93-650] 03 p0877 N94-16150
Clementine: Anticipated scientific datasets from the Moon and Geographos 03 p1288 N94-16392
The star identification, pointing and tracking system of UVSTAR, an attached payload instrument system for the Shuttle Hitchhiker-M platform 04 p1326 N94-19179
Charge integrating optical position sensor
05 p1778 N94-22152
Miniature wide field-of-view star trackers for spacecraft attitude sensing and navigation
08 p3144 N94-29794
Design and early results of the sodium-layer laser guide star adaptive optics experiment at the Lawrence Livermore National Laboratory
[DE94-006653] 09 p3926 N94-32189
Fixed-head star tracker attitude updates on the Hubble Space Telescope 11 p4203 N94-35612
In-flight scale/distortion calibration of the Hubble Space Telescope fixed-head star trackers
11 p4203 N94-35613
Operational support for Upper Atmosphere Research Satellite (UARS) attitude sensors
11 p4204 N94-35617
Spacecraft attitude determination accuracy from mission experience 11 p4204 N94-35618
Application of star identification using pattern matching to space ground systems at GSFC
11 p4209 N94-35640
Color/magnitude calibration for National Aeronautics and Space Administration (NASA) standard Fixed-Head Star Trackers (FHST) 11 p4209 N94-35641

STAR TRACKING
U STAR TRACKERS

STARBURST GALAXIES
ROSAT and IRAS observations
[MPE-PREPRINT-231] 04 p1623 N94-19526
ROSAT X ray observation of the 30 Dor giant HII region 04 p1623 N94-19527
Weak bump quasars
[NASA-CR-195267] 07 p3103 N94-27933
The kinematics of molecular gas and dust in the nearby galaxies Centaurus A and M82
08 p3544 N94-29738
A multi wavelength observational study of the Cartwheel ring galaxy 08 p3539 N94-29821
Evolution of stars and winds in the starburst galaxy M82 09 p3934 N94-31758
Ionized gas in the halos of edge-on infrared-bright galaxies: Evidence for starburst-driven superwinds
09 p3936 N94-31948

STARCHES
Paint removal using wheat starch blast media
01 p0128 N94-10627

STARFIGHTER AIRCRAFT
U F-104 AIRCRAFT

STARK EFFECT
Equilibrium reconstruction of the q-profile in tokamaks from motional Stark effect data
[DE93-015815] 02 p0796 N94-13046
Stark broadening of the 2S state of hydrogen and deuterium in arc plasmas of low density
[ETN-94-95731] 09 p3888 N94-31572
High beta and second stability region transport and stability analysis
[DE94-009654] 10 p4145 N94-33920
Motional Stark effect upgrades on D3-D
[DE94-013146] 12 p4528 N94-37297

STARLIFTER AIRCRAFT
U C-141 AIRCRAFT

STARS
NT A STARS
NT ASYMPTOTIC GIANT BRANCH STARS
NT B STARS
NT BINARY STARS
NT BLACK HOLES (ASTRONOMY)
NT BLUE STARS
NT BROWN DWARF STARS
NT CARBON STARS
NT CATACLYSMIC VARIABLES
NT CEPHEID VARIABLES
NT COMPANION STARS
NT COOL STARS
NT DWARF STARS
NT EARLY STARS
NT ECLIPSING BINARY STARS
NT F STARS
NT FLARE STARS
NT G STARS
NT GIANT STARS
NT HOT STARS
NT INFRARED STARS
NT IRREGULAR VARIABLE STARS
NT K STARS
NT LATE STARS
NT M STARS
NT MAGNETIC STARS
NT MAIN SEQUENCE STARS
NT MASSIVE STARS
NT METALLIC STARS
NT MIRA VARIABLES
NT NEUTRON STARS
NT NOVAE
NT PECULIAR STARS
NT PRE-MAIN SEQUENCE STARS
NT PROTOSTARS
NT PULSARS
NT R CORONAE BOREALIS STARS
NT RED DWARF STARS
NT RED GIANT STARS
NT REFERENCE STARS
NT SHELL STARS
NT SUBDWARF STARS
NT SUN
NT SUPERGIANT STARS
NT SUPERNOVA 1987A
NT SUPERNOVAE
NT SYMBIOTIC STARS
NT T TAURI STARS
NT VARIABLE STARS
NT WHITE DWARF STARS
NT WHITE HOLES (ASTRONOMY)
NT WOLF-RAYET STARS
NT X RAY BINARIES
NT X RAY STARS

STARSPOTS
NT SUNSPOTS

STARTERS
NT ENGINE STARTERS

STARTING
Engine starting and stopping
07 p2828 N94-28047
Startup and shutdown of the PULSAR Tokamak Reactor
[DE94-013128] 12 p4528 N94-37292

STATE EQUATIONS
U EQUATIONS OF STATE

STATE ESTIMATION
Estimation with multisensor/multiscan detection fusion
[AD-A265673] 01 p0138 N94-12338
Calculation of the required sensor accuracy to obtain a specified state estimation accuracy
[NAL-TR-1173] 02 p0649 N94-13343
Attitude determination of stratospheric balloons using Kalman filters
[INPE-5498-TDI/513] 02 p0649 N94-13366
Comparison of a distributed Kalman filter versus a centralized Kalman filter with fault detection considerations
[AD-A270713] 05 p1903 N94-19969
A mixed map/variable structure observer for target tracking 06 p2157 N94-24263
Iterative methods for the WLS state estimation on RISC, vector, and parallel computers
[DE94-004260] 07 p3000 N94-27569
Systematic error estimation in multisensor fusion systems
[AD-B179298] 08 p3428 N94-30764
Robust control of robots via linear estimated state-feedback
[MEMO-1153] 08 p3449 N94-30963
Representation, prediction and identification of cyclostationary processes: A state-space approach
[REPT-93-041] 09 p3850 N94-31191
H-infinity estimation 10 p4114 N94-34313
Comparison of Kalman filter and optimal smoother estimates of spacecraft attitude
11 p4208 N94-35638
Advantages of estimating rate corrections during dynamic propagation of spacecraft rates: Applications to real-time attitude determination of SAMPEX
11 p4209 N94-35642
MME-based attitude dynamics identification and estimation for SAMPEX 11 p4209 N94-35643
Motion models in attitude estimation
11 p4210 N94-35646

STATE VECTORS
Nonlinear and dynamic analysis of flight
01 p0032 N94-11496
A rational interpolation method to compute frequency response 02 p0681 N94-14644
An extension of Wolovich's definition of equivalence of linear systems
[MATHS-REPT-A-183] 04 p1547 N94-18069
Space and time from quantum mechanics
[DE93-015263] 04 p1609 N94-18629
Symbolic model checking for sequential circuit verification
[AD-A274375] 07 p2786 N94-27061
Observations of the notion of minimality in the generalized state space
[MATHS-REPT-A-207] 09 p3840 N94-31162
A separation technique for asymptotic-numeric solution for general shells of revolution 09 p3736 N94-31961
Theoretical basis for state vector comparison, relative position display, and relative position/rendezvous prediction
[AD-A277216] 09 p3608 N94-32020
Compression of a radar track of a near Earth satellite into an Earth centered inertial state vector using least squares differential correction
[AD-A278498] 10 p4037 N94-34302
The study of optimal control with neural networks
10 p4115 N94-34316
Overview of the MST! 2 on-orbit alignment
11 p4206 N94-35629
Advantages of estimating rate corrections during dynamic propagation of spacecraft rates: Applications to real-time attitude determination of SAMPEX
11 p4209 N94-35642
Contact level fusion of radar and IRST contacts on almost electromagnetically silent platform
12 p4395 N94-36634
Progress in navigation filter estimate fusion and its application to spacecraft rendezvous
[NASA-TM-104794] 12 p4392 N94-37386

STATIC CHARACTERISTICS
Static and dynamic investigations of brittle elasto-optical material
[IFTR-3/1992] 03 p1061 N94-17086
Static characteristics of a conduction and radiation dominated electric arc in nitrogen
[DE93-627106] 03 p1204 N94-17311
Study and modeling of compressible flows of flapper nozzle type potentiometric systems
[ETN-93-95012] 04 p1421 N94-19495
Extending substructure based iterative solvers to multiple load and repeated analyses
[NASA-CR-194822] 06 p2466 N94-23504
METCAN demonstration manual, version 1.0
[NASA-TM-105607] 09 p3626 N94-32858
An experimental study on the static and dynamic characteristics of pump annular seals with two phase flow 10 p4062 N94-34179

STATIC ELECTRICITY
The response of an electron in a biased double well to a strong laser: Delocalization and low frequency generation
[AD-A265169] 01 p0366 N94-11100

STATIC LOADS
Nonlinear response of a clamped-clamped beam with internal resonance under sinusoidal excitation
01 p0186 N94-10897
Implementation of mixed formulation elements in PC/NASTRAN 04 p1449 N94-17828
Spectrum fatigue testing of T-shaped tension clips
[FFA-TN-1992-22] 04 p1452 N94-17970
Time-dependent reliability analysis of ceramic engine components 05 p1828 N94-22619
Foil bearings 06 p2371 N94-24415
Nonlinear equations of motion for a panel subject to external loads
[AD-A273142] 06 p2170 N94-24773
Investigation of compressive behavior for metal matrix composites with a circular hole
[AD-A273835] 07 p2705 N94-25739
Root-sum-square structural strength verification approach
[NASA-TM-108453] 08 p3322 N94-30206
Hydrodynamically induced loads on components submerged in high-level waste-storage tanks
[DE94-009663] 11 p4264 N94-35756

STATIC PRESSURE
NT HYDROSTATIC PRESSURE
Dynamic tester for rotor seals and bearings
[NASA-CASE-MFS-28493-1] 01 p0033 N94-10669
A wall interference assessment/correction system
[NASA-CR-194174] 02 p0500 N94-13076
Exploratory study of in-plane streamline curvature effects on a turbulent boundary layer at a Mach number of 3
[NASA-CR-193673] 02 p0501 N94-13292
Wind tunnel investigation of three axisymmetric cowls of different lengths at Mach numbers from 0.60 to 0.92
[NASA-TM-4488] 03 p0856 N94-15681
Static pressure measurements for near isentropic flows using laser induced iodine fluorescence
04 p1431 N94-18646
New test method to determine modulus of elasticity of rocket grain material
[AD-A269758] 04 p1377 N94-18758
Bridgman's concern
[DE93-040900] 06 p2558 N94-22953
Probe systems for measuring static pressure and turbulence intensity in fluid streams
[NASA-CASE-ARC-11935-1] 06 p2319 N94-23306
Experimental cavity pressure measurements at subsonic and transonic speeds. Static-pressure results
[NASA-TP-3358] 06 p2169 N94-24464
Computation of static pressure downstream of a normal shock for hypersonic flight (ambient temperature known)
[ESDU-93020] 07 p2649 N94-28091
Blast overpressure studies with animals and man
[AD-A275038] 08 p3391 N94-29150
Analysis of fluctuating static pressure measurements in a large high Reynolds number transonic cryogenic wind tunnel 08 p3158 N94-30788
Development of a cascade simulation of fan-passage flow
[AD-A277234] 09 p3584 N94-32026

STATIC STABILITY
NT DIMENSIONAL STABILITY
NT SHELL STABILITY
NT STRUCTURAL STABILITY
X-29: Longitudinal instability at high angle-of-attack
01 p0033 N94-11504
Test and evaluation methods
02 p0506 N94-14163
Development of a prototype kinestatic platform for application to space and ground servicing tasks. Phase 1: Concept Modeling
[NASA-CR-194036] 03 p0887 N94-16905
An experimental and theoretical study of the aerodynamic characteristics of some generic missile concepts at Mach numbers from 2 to 6.8
[NASA-TM-109110] 08 p3130 N94-29473
Robot grasping: Stability and optimization issues
09 p3724 N94-31724
X-29 flight control system: Lessons learned
[NASA-TM-4598] 10 p3984 N94-34384
An aerodynamic and static-stability analysis of the Hypersonic Applied Research Technology (HART) missile
[AD-A280631] 12 p4382 N94-36729
Aerodynamic characteristics of the National Launch System (NLS) 1 1/2 stage launch vehicle
[NASA-TP-3488] 12 p4384 N94-37577

STATIC TESTS
Technical Evaluation Motor No. 10 (TEM-10)
[NASA-CR-193846] 02 p0554 N94-14907
Aerodynamic control of NASP-type vehicles through Vortex manipulation. Volume 2: Static wind tunnel tests
[NASA-CR-177626-VOL-2] 03 p0856 N94-15677
Effects of internal yaw-vectoring devices on the static performance of a pitch-vectoring nonaxisymmetric convergent-divergent nozzle
[NASA-TP-3369] 03 p0858 N94-16572
Static Computer Memory Integrity Testing (SCMIT): An experiment flown on STS-40 as part of GAS payload G-616 04 p1325 N94-19169
Optimization of laminate orientation to enhance failure properties
[ISBN-0-315-83539-7] 06 p2227 N94-22892
Summary of lift and lift/cruise fan powered lift concept technology
[NASA-CR-177619] 06 p2176 N94-23489
Effect of longitudinal vibration on the capillary limit of a wrapped screen wick copper/water heat pipe
[AD-A273830] 06 p2571 N94-25524
Estimation of Weibull modulus from dynamic and static fatigue experiments
[PB94-138641] 08 p3322 N94-30114
Analysis and design of inflatable aerospace structures
08 p3403 N94-30799
Probabilistic assessment of uncertain adaptive hybrid composites
[NASA-TM-106515] 10 p4069 N94-33951
Static performance investigation of a skewed-throat multiaxis thrust-vectoring nozzle concept
[NASA-TP-3411] 10 p3983 N94-34172
Residual strength and life prediction techniques for Ti MMC 12 p4402 N94-36662

STATIC THRUST
Internal performance of a nonaxisymmetric nozzle with a rotating upper flap and a center-pivoted lower flap
[NASA-TP-3385] 05 p1637 N94-21569

STATICS
NT ELECTROSTATICS
NT HYDROSTATICS
Statics and kinetics of phase transformations in bcc Fe-Cr
[DE93-013839] 02 p0574 N94-14793
Mass properties measurement system: Dynamics and statics measurements 06 p2368 N94-23236

STATIONKEEPING
CNES organization for station positioning of geostationary satellites 06 p2501 N94-23857
The geo-control system for station keeping and colocation of geostationary satellites
06 p2464 N94-23927
Nearly uniform deployment/retrieval strategy for space tether systems 06 p2156 N94-24256

STATIONS
NT AUTOMATIC WEATHER STATIONS
NT COLUMBUS SPACE STATION
NT CREW WORKSTATIONS
NT EARTH TERMINALS
NT GLOBAL TRACKING NETWORK
NT GROUND STATIONS
NT HYDROELECTRIC POWER STATIONS
NT INTEGRATED MISSION CONTROL CENTER
NT MAN TENDED FREE FLYERS
NT MIR SPACE STATION
NT PAYLOAD STATIONS
NT SPACE STATION FREEDOM
NT SPACE STATIONS
NT STDN (NETWORK)
NT TRACKING STATIONS
NT WEATHER STATIONS
NT WORKSTATIONS

STATISTICAL ANALYSIS
NT AMPLITUDE DISTRIBUTION ANALYSIS
NT ANALYSIS OF VARIANCE
NT BIVARIATE ANALYSIS
NT CORRELATION COEFFICIENTS
NT COVARIANCE
NT DISCRIMINANT ANALYSIS (STATISTICS)
NT FACTOR ANALYSIS
NT GOODNESS OF FIT
NT KOLMOGOROV-SMIRNOV TEST
NT LIKELIHOOD RATIO
NT MAXWELL-BOLTZMANN DENSITY FUNCTION
NT MULTIVARIATE STATISTICAL ANALYSIS
NT NONPARAMETRIC STATISTICS
NT NORMAL DENSITY FUNCTIONS
NT ORTHOGONALITY
NT PEARSON DISTRIBUTIONS
NT POISSON DENSITY FUNCTIONS
NT PROBABILITY DENSITY FUNCTIONS
NT PROBABILITY DISTRIBUTION FUNCTIONS
NT QUANTILES
NT RANK TESTS
NT RAYLEIGH DISTRIBUTION

NT REGRESSION ANALYSIS
NT REGRESSION COEFFICIENTS
NT SEQUENTIAL ANALYSIS
NT STANDARD DEVIATION
NT STATISTICAL CORRELATION
NT STATISTICAL DECISION THEORY
NT STATISTICAL TESTS
NT VARIANCE (STATISTICS)
NT WEIBULL DENSITY FUNCTIONS

General renormalized statistical approach with finite cross-field correlations
[DE93-617846] 01 p0386 N94-10396

Stationary spectra in a plasma with a shear (renormalized statistical approach with non-zero eigenfrequencies)
[DE93-617851] 01 p0386 N94-10523

A window least squares algorithm for statistical noise smoothing of 2D-ACAR data
[DE93-613828] 01 p0395 N94-10537

The Langevin's approach to the statistical theory of bounded plasma
[DE93-617842] 01 p0388 N94-10839

Stationary spectra of short-wave convective and magnetostatic fluctuations in a finite-pressure plasma and anomalous heat conductivity
[DE93-617852] 01 p0388 N94-10840

Advanced statistical methods for improved data analysis of NASA astrophysics missions
[NASA-CR-193514] 01 p0425 N94-10943

Statistical analysis of environmental variability within the CELSS breadboard project's biomass production chamber
[NASA-TM-109188] 01 p0315 N94-11258

Three-dimensional object recognition using an unsupervised BCM network: The usefulness of distinguishing features
[AD-A264576] 01 p0304 N94-11261

Statistical and optimization methods to expedite neural network training for transient identification
[DE93-009985] 01 p0340 N94-11644

General aviation aircraft-normal acceleration data analysis and collection project
[AD-A265055] 01 p0026 N94-11858

Computing science and statistics, Volume 24: Graphics and visualization
[AD-A265181] 01 p0332 N94-11878

Statistical process control in the hybrid microelectronics manufacturing industry: A Navy view point
[AD-A265164] 01 p0145 N94-11884

A statistical method to determine aerosol path radiance and its application to atmospheric correction for CZCS imagery 01 p0191 N94-11897

Remote sensing of the suspended matter distribution with high concentration in China Sea 01 p0192 N94-11901

Statistical study of HF ocean radar echo 01 p0139 N94-11905

A new expression for the production rate of sea water droplets on the sea surface 01 p0195 N94-11920

Estimation of solar radiation at the sea surface with geostationary meteorological satellite data 01 p0196 N94-11926

Incident shortwave and longwave radiations over the western North Pacific and the Sea of Okhotsk derived from GMS-WEFAX images 01 p0205 N94-11982

A statistical analysis of sea state surface ERS-1 SAR-wave mode imagettes 01 p0251 N94-12507

Further study of the Non-Regression-Coefficient SST retrieval method 01 p0213 N94-12674

Aspects of applying a relaxation method to computing sea surface velocities from sea surface temperature images 01 p0214 N94-12679

Sea surface temperature difference between NOAA/AVHRR and in-situ observation 01 p0215 N94-12680

Coastal upwelling monitored by satellite data: Methodologies and results 01 p0220 N94-12712

Advective surface velocity in the north west Pacific derived from NOAA AVHRR images 01 p0222 N94-12721

Problem of climate change predictability and satellite radiation budget observations 01 p0229 N94-12766

Feature extraction and classification algorithms for high dimensional data
[NASA-CR-194298] 02 p0743 N94-13023

Degradation of the visible and near-infrared channels of the advanced very high resolution radiometer on the NOAA-9 spacecraft: Assessment and recommendations for corrections
[NOAA-TR-NESDIS-70] 02 p0544 N94-13029

Object-oriented productivity metrics 02 p0667 N94-13161

Spatial variability of throughfall chemistry in a tropical rainforest (Central Amazonia, Brazil)
[INPE-5431-PRE/1765] 02 p0720 N94-13429

Trellis coding with Continuous Phase Modulation (CPM) for satellite-based land-mobile communications
[NASA-CR-191325] 02 p0604 N94-13909

Stochastic performance modeling and evaluation of obstacle detectability with imaging range sensors
[NASA-CR-194510] 02 p0605 N94-13946

Generic results of the space physics community survey
[NASA-CR-194538] 02 p0818 N94-13984

An improved approach for flight readiness certification: Methodology for failure risk assessment and application examples, volume 1
[NASA-CR-194498] 02 p0542 N94-14076

An improved approach for flight readiness certification: Methodology for failure risk assessment and application examples. Volume 2: Software documentation
[NASA-CR-194499] 02 p0542 N94-14077

An improved approach for flight readiness certification: Methodology for failure risk assessment and application examples. Volume 3: Structure and listing of programs
[NASA-CR-194500] 02 p0542 N94-14078

A method for estimation of partial cloud cover within a pixel and its effect 02 p0697 N94-14269

Atmospheric correction for sea surface temperature by application of microwave dual-channel technique to VTIR data 02 p0697 N94-14271

Statistical results from the Virginia Tech propagation experiment using the Olympus 12, 20, and 30 GHz satellite beacons 02 p0613 N94-14658

Results of multiband (L, S, Ku band) propagation measurements and model for high elevation angle land mobile satellite channel 02 p0615 N94-14670

An improved approach for flight readiness certification: Probabilistic models for flaw propagation and turbine blade failure. Volume 1: Methodology and applications
[NASA-CR-194496] 02 p0519 N94-14841

An improved approach for flight readiness certification: Probabilistic models for flaw propagation and turbine blade failure. Volume 2: Software documentation
[NASA-CR-194497] 02 p0519 N94-14842

On the statistical theory of the even-even nucleons levels' density
[DE93-623990] 02 p0788 N94-14875

A posteriori error estimation for hierarchic models of elliptic boundary value problems on thin domains
[AD-A267714] 03 p1168 N94-14939

US civil airmen statistics: Calendar year 1992
[AD-A267708] 03 p0853 N94-14965

Statistical computation of tolerance limits
[NASA-TM-108424] 03 p1172 N94-15535

Poisson filtering of laser ranging data 03 p0917 N94-15593

Statistical analysis of trigonometric parallaxes
[NASA-CR-194558] 03 p1172 N94-15641

A simplistic look at limit stresses from random loading
[NASA-TM-108427] 03 p1058 N94-15710

Higher order statistics in signal processing
[FFI-92/2008] 03 p0989 N94-15714

Brightness temperature and attenuation statistics at 20.6 and 31.65 GHz 03 p0996 N94-16045

Statistical techniques for study design of microgravity life sciences experiments 03 p0980 N94-16094

Dust grain resonant capture: A statistical study 03 p1245 N94-16384

Moving target indicator using higher order statistics
[AD-D015890] 03 p1000 N94-16917

The use of the Air Force Academy high wind alert system in forecasting moderate intensity wind events for military bases in the Colorado Springs area
[AD-A267648] 03 p1107 N94-17245

A Geographic Information System approach to modeling nutrient and sediment transport
[DE93-013747] 03 p1097 N94-17426

Statistics and physical oceanography
[AD-A268565] 03 p1115 N94-17598

Planning under uncertainty solving large-scale stochastic linear programs
[DE93-013920] 04 p1516 N94-17701

Statistical intercomparison of global climate models: A common principal component approach with application to GCM data
[DE93-017951] 04 p1473 N94-18005

Putting knowledge to use: The acquisition and transfer of knowledge in situated problem solving environments
[AD-A269746] 04 p1509 N94-18744

Spectral analysis on the canonical autoregressive decomposition
[AD-A270083] 04 p1549 N94-18798

Statistical learning theory and algorithms
[AD-A270209] 04 p1523 N94-18901

Stochastic grammars: Theory and applications
[PB94-149556] 04 p1528 N94-19262

Mathematical communications, volume 27, numbers 1 and 2, 1992. List and abstracts of memoranda published in the period July - December 1991
[PB93-191997] 04 p1553 N94-19557

A real-time spoken-language system for interactive problem-solving, combining linguistic and statistical technology for improved spoken language understanding
[AD-A270901] 04 p1392 N94-19749

Stochastic optimization by simulation: Convergence proofs for the G1/G/1 queue in steady-state
[AD-A271141] 05 p1962 N94-19999

VLSI design for reliability-current density
[AD-A270719] 05 p1749 N94-20110

Statistical object recognition
[AD-A270887] 05 p1962 N94-20113

Neural data oriented parsing 05 p1940 N94-20248

Retrieval of ice thickness from polarimetric SAR data 05 p1724 N94-20432

Signal processing in the linear statistical model
[AD-A272114] 05 p1736 N94-20570

Functional statistical data analysis and modeling
[AD-A271520] 05 p1963 N94-20913

Performance management systems: A statistical analysis
[AD-A272989] 05 p2043 N94-21266

Some evidence on determinants of fuel economy as a function of driving cycle and test type
[DE93-019511] 05 p1825 N94-21637

Mars: Noachian hydrology by its statistics and topology 05 p2143 N94-21664

A statistical-based scheduling algorithm in automated data path synthesis 05 p1764 N94-21706

Applications of a two-dimensional nonlinear filters to image restoration 05 p1789 N94-22225

GRO/EGRET data analysis software: An integrated system of custom and commercial software using standard interfaces 05 p1926 N94-22501

Detector noise statistics in the non-linear regime 05 p1748 N94-22526

Application of maximum entropy and irreducible cluster integrals to joint probability distributions for x ray structure determination
[PB93-224152] 06 p2559 N94-23109

Maximal type test statistics based on conditional processes
[PB94-111614] 06 p2494 N94-23771

Decision making with imprecise probabilities
[PB94-111622] 06 p2494 N94-23772

Asymptotic confidence intervals for the length of the shortt under random censoring
[PB93-237816] 06 p2494 N94-23774

Some generalized subset selection procedures
[PB94-111655] 06 p2487 N94-23799

Specifying design conservatism: Worst case versus probabilistic analysis 06 p2374 N94-23939

Computation of large-scale statistics in decaying isotropic turbulence 06 p2332 N94-24167

Attachment methods in composite joints - analysis of test results by controlled experiments method 06 p2158 N94-24269

Verification and validation of models
[PB94-110566] 06 p2456 N94-24507

Tail processes under heavy random censorship with applications
[PB94-110632] 06 p2495 N94-24508

A comparison of approximate interval estimators for the Bernoulli parameter
[AD-A276322] 06 p2458 N94-24680

Annual review of aircraft accident data. US general aviation calendar year 1990
[PB94-126869] 06 p2173 N94-24841

Statistical methods in physical oceanography
[AD-A273612] 06 p2419 N94-24948

A statistical analysis of recent Naval Experimental Diving Unit (NEDU) single-depth human exposures to 100 percent oxygen at pressure
[AD-A273488] 06 p2427 N94-24950

Correlation function estimator performance in non-Gaussian spherically invariant random processes
[AD-A273498] 06 p2496 N94-24951

Neutron star mergers and gamma-ray bursts
[NASA-CR-195176] 06 p2629 N94-25091

NASA STI program database: Journal coverage (1990-1992)
[NASA-TM-109720] 06 p2593 N94-25168

Designs with a small number of runs for factorial experiments
[ISBN-9-03-860162-X] 06 p2462 N94-25237

Solving the ranking and selection indifference-zone formulation for normal distributions using computer software
[AD-A273821] 06 p2496 N94-25518

A nighttime structure model of atmospheric optical turbulence, c2(n), derived from thermosonde and high resolution rawinsonde measurements
[AD-A273803] 06 p2406 N94-25537

Study on knowledge extraction and systematization for material design 07 p2727 N94-25568

Vulnerability assessment using a fuzzy logic based method
[AD-A274075] 07 p2957 N94-25649
Improved quality of reconstructed images through sifting of data in statistical image reconstruction
[AD-A273884] 07 p3034 N94-25730
Developing prediction regions for a time series model for hurricane forecasting
[AD-A273777] 07 p2892 N94-25861
Surfaces allowing for fractional statistics
[DE93-614526] 07 p3002 N94-25910
An evaluation of the utility of ground-based high resolution interferometer (GB-HIS) soundings of the planetary boundary layer
[DE94-000960] 07 p3106 N94-25981
Statistical quality management
[MEMO-COSOR-92-43] 07 p2834 N94-26008
Towards a theory of growing surfaces: Mapping two-dimensional Laplacian growth onto Hamiltonian dynamics and statistics
[DE94-002636] 07 p2991 N94-26079
Quantum statistical inference for density estimation
[DE94-002625] 07 p3073 N94-26805
The use of EEG as a workload assessment tool in flight test
[AD-A274568] 07 p2910 N94-26847
Some contributions to the theory of monotone dependence
[PB94-124922] 07 p3004 N94-27051
Enhanced tracking of airborne targets using forward looking infrared and laser return measurements
[AD-A274181] 07 p3037 N94-27102
Limit theorems for functionals of Markov processes and renormalizable stable fields
[AD-A274645] 07 p3004 N94-27106
Research in improved assessment of software reliability
[AD-A274161] 07 p2968 N94-27140
Is probability of frequency too narrow?
[DE94-000687] 07 p3004 N94-27612
Analysis of S-wave seismogram envelope of deep earthquakes and estimation of random inhomogeneities in the Kanto-Tokai area 07 p2886 N94-27988
Unsteady aspects of hot gas reingestion and statistical analysis 07 p2676 N94-28019
Weak coupling in statistical energy analysis ion Research, Univ. of Southampton, Southampton SO9 5NH, England)
[ISVR-TR-228] 07 p2832 N94-28174
Equation of state of stellar plasmas
[DE94-004186] 08 p3542 N94-28526
Probabilistic material strength degradation model for Inconel 718 components subjected to high temperature, mechanical fatigue, creep and thermal fatigue effects
[NASA-CR-195264] 08 p3318 N94-28840
U-statistics of random-size samples and limit theorems for systems of Markovian particles with non-Poisson initial distributions
[AD-A275018] 08 p3464 N94-29129
Statistical Modeling and Estimation of Reliability Functions for Software (SMERFS) user's guide, revision 3
[AD-A275390] 08 p3411 N94-29202
Statistical Modeling and Estimation of Reliability Functions for Software (SMERFS) library access guide, revision 3
[AD-A275405] 08 p3411 N94-29207
Statistical characterization of rugged propagation paths with application to Rg scattering study
[AD-A275237] 08 p3361 N94-29393
Simulation of interference between Earth stations and Earth-orbiting satellites 08 p3252 N94-29673
Evolution of the large-scale vortices in turbulent mixing-layers 08 p3273 N94-29686
Yield and variability optimization of integrated circuits: Principles and practical solutions 08 p3266 N94-29805
Comparison of Savannah River Site's meteorological databases
[DE94-001751] 08 p3373 N94-29817
Acceptance sampling methods for sample results verification
[DE94-002882] 08 p3465 N94-29925
Comparison of 14 MeV isomer production of Hf-178m1 and Hf-179m2 using Feshbach-Kerman-Koonin and exciton preequilibrium models
[DE94-002640] 08 p3488 N94-30039
Statistical description of hot and dense clustering matter
[DE94-608155] 08 p3490 N94-30112
Prediction and standard error estimation for a finite universe total when a stratum is not sampled
[DE94-004929] 08 p3465 N94-30696
Statistical analysis of a satellite imagery time series: Implications for the study of coastal and estuarine circulation 08 p3335 N94-30919
Substructure, dynamics and evolution in clusters of galaxies 08 p3548 N94-30951
Vibrations of a heavy truck diesel engine and gearbox unit: Examining structure-borne sound transmission with statistical energy analysis
[CTH-E-93-04] 09 p3722 N94-31194
Development of a statistical method for estimating the downward longwave radiation at the surface from satellite observations 09 p3742 N94-31553
DOME: Dynamic optimization on multiprocessor engines, a statistical approach 09 p3807 N94-31972
Development of phase-only filters for sensor imagery
[AD-A276722] 09 p3880 N94-32151
Area-interaction point processes
[CWI-BS-R9318] 09 p3847 N94-32197
European MARS project: The potential integration of SPOT and air- and satellite-borne radar data over two pilot areas for agricultural statistics. PROSPER programme and ERS-1 pilot project
[BRGM-93035] 09 p3754 N94-32561
Arithmetic averaging: A versatile technique for smoothing and trend removal
[DE94-005274] 09 p3852 N94-32673
Using the National Information Infrastructure for social science, education, and informed decision making
[DE94-005442] 09 p3920 N94-32676
Faultless software project
[AD-A278161] 09 p3822 N94-33188
Formal design and evaluation of a variety of medical diagnostic programs
[PB94-149622] 10 p4095 N94-34111
Compression of a radar track of a near Earth satellite into an Earth centered inertial state vector using least squares differential correction
[AD-A278498] 10 p4037 N94-34302
Zero-time-delay video processor circuit
[AD-D016191] 10 p4042 N94-34404
Automated analysis of complex data 10 p4124 N94-35056
A statistical inference approach for the retrieval of the atmospheric ozone profile from simulated satellite measurements of solar backscattered ultraviolet radiation 10 p4083 N94-35060
Point and interval estimation of series system reliability using small data sets
[AD-A278647] 11 p4316 N94-35575
Improved solution accuracy for TDRSS-based TOPEX/Poseidon orbit determination 11 p4205 N94-35620
Environmental Monitoring and Assessment Program assessment framework
[PB94-158862] 11 p4285 N94-35741
Activity report 1990-1992 and proceedings, volume 1
[DE94-610480] 11 p4290 N94-35830
The development of a statistical report software for computer system usages
[DE94-611061] 11 p4346 N94-35832
A comparison of artificial neural networks and statistical analyses
[DE94-010846] 11 p4312 N94-36195
Application of higher-order multipoint statistics to the ideal spray
[DE94-005104] 11 p4268 N94-36318
Recovering depth from focus using iterative image estimation techniques
[DE94-010994] 12 p4524 N94-37165
Statistical characterization of rare events 12 p4454 N94-37327
Predicting defect behaviour 12 p4455 N94-37331
Fatigue case study and loading spectra for wind turbines
[DE94-010798] 12 p4457 N94-37622

STATISTICAL COMMUNICATION THEORY
U COMMUNICATION THEORY

STATISTICAL CORRELATION
Chaos, entropy, and reversibility: A simple example 01 p0031 N94-11495
Analysis of gravity, magnetic, and seismic reflection data from Tibet and neighboring regions of China
[NASA-CR-193405] 01 p0278 N94-11886
The extraction of bottom characteristics and mapping in Kin Bay, Okinawa Main Island, Japan, using LANDSAT-5/TM and SPOT-1/HRV data 01 p0197 N94-11931
Statistical analysis of the m rankings problem: Kendall's prototype and the grouping estimate method based on normal scores
[DSIS-93-00139] 02 p0773 N94-13848
Speckles statistics and decorrelation effects in complex ABCD optical systems
[AD-A267843] 03 p1193 N94-17012
Correlations in the actions of periodic orbits derived from quantum chaos
[DE93-616866] 06 p2571 N94-25340
Aspects of goodness-of-fit
[AD-A274826] 07 p3003 N94-26495
Correlation between electrical activity and the size of single sinoatrial node cells 07 p2907 N94-27513
Analysis of ionospheric parameters in Europe and creation of the prediction algorithm
[AD-A276342] 09 p3771 N94-31326
Selection of climate station data using clustering and triangulated irregular network techniques
[AD-A276658] 09 p3784 N94-32046
Spatio-temporal complexity and large-scale structures in problems of continuum mechanic
[AD-A278473] 10 p4044 N94-33702
Measurements of correlation coefficients of vibration on a car body shell
[ISVR-TR-220] 10 p4070 N94-34307

STATISTICAL DECISION THEORY
Examination of metrics and assumptions used in correlation filter design
[DE93-017636] 04 p1576 N94-18000
Bounds for expected loss in Bayesian decision theory with imprecise prior probabilities
[PB93-197507] 04 p1558 N94-19327
Problems in probability, statistics and reliability
[AD-A270830] 04 p1559 N94-19595
Bayesian decision theory with imprecise prior probabilities applied to replacement problems
[PB93-237634] 06 p2481 N94-23456

STATISTICAL DISTRIBUTIONS
NT BRIGHTNESS DISTRIBUTION
NT PEARSON DISTRIBUTIONS
NT PROBABILITY DISTRIBUTION FUNCTIONS
NT RAYLEIGH DISTRIBUTION
Imprecise highest density regions related to intervals of measures
[MEMO-COSOR-92-54] 01 p0347 N94-10876
A CM chondrite cluster and CM streams 01 p0432 N94-12215
An analog clustering network from a biological model
[AD-A265637] 02 p0762 N94-12969
The MADONA experiments (Meteorology and Diffusion Over Non-uniform Areas): High-resolution in-plume concentration fluctuations measurements using lidar remote sensing technique
[AD-A267711] 03 p1105 N94-14938
Moments in statistics: Approximations to densities and goodness-of-fit
[AD-A266600] 03 p1173 N94-16726
Mean strain effects on the strain life fatigue curve
[AD-A267211] 03 p0960 N94-16984
JSEP fellowship: Fractal noise processes
[AD-A268841] 04 p1557 N94-18540
Statistical description of the bistatic radar cross section distributions for a right circular cylinder
[AD-A270001] 04 p1387 N94-18666
Bahadur-Kiefer theorem beyond the largest observation
[PB93-197473] 04 p1558 N94-19325
High resolution signal processing
[AD-A271181] 05 p1717 N94-20215
A formulation of quantum statistical mechanics based on the Feynman path centroid density 1: Equilibrium properties
[AD-A272809] 05 p2037 N94-21171
Data compression by using wavelet transforms and vector quantization
[AD-A272763] 05 p1738 N94-21182
Paired comparison models with time-varying parameters
[AD-A272016] 05 p1964 N94-21442
Stochastic simulation for imaging spatial uncertainty: Comparison and evaluation of available algorithms
[DE93-040058] 05 p1916 N94-21761
Experiments with recursive estimation in astronomical image processing 05 p2047 N94-22457
Limiting distribution of fractional parts of extreme order statistics
[PB93-237733] 06 p2494 N94-23440
Maximal type test statistics based on conditional processes
[PB94-111614] 06 p2494 N94-23771
Infinite divisible and stable distributions modulo 1
[PB94-110640] 06 p2495 N94-23815
A comparison of approximate interval estimators for the Bernoulli parameter
[AD-A276322] 06 p2458 N94-24680
Infinitely divisible processes and their nonlinear functionals; a study of their structural, statistical and sample path properties and their prediction problems
[AD-A273468] 06 p2496 N94-25147
Bisexual branching diffusions
[AD-A274698] 07 p3008 N94-26374
Fuzzy robust statistics for application to the fuzzy c-means clustering algorithm
[AD-A274719] 07 p3003 N94-26436
Statistical mechanical properties of Z(N)(sup n-1) broken model
[DE93-634344] 07 p2993 N94-26457

Some contributions to the theory of monotone dependence
[PB94-124922] 07 p3004 N94-27051
Variability of measured sonic boom signatures 07 p2651 N94-28197
A random distribution reacting mixing layer model
[NASA-TM-106517] 08 p3150 N94-28923
Conditional dependence in probabilistic networks
[RUU-CS-92-34] 08 p3464 N94-29450
Machinery monitoring and diagnostics using pseudo Wigner-Ville distribution and backpropagation neural network
[AD-A276219] 09 p3828 N94-31064
On the minimum of independent geometrically distributed random variables
[AD-A279629] 09 p3821 N94-33075
Growth and nonlinearity
[DE94-007366] 10 p4021 N94-33689
Application of a Monte Carlo accuracy assessment tool to TDRS and GPS 11 p4207 N94-35635
Statistical characterization of rare events 12 p4454 N94-37327

STATISTICAL MECHANICS
Lattice gas hydrodynamics: Theory and simulations
[DE93-013297] 01 p0147 N94-10320
Infinite-mode squeezed coherent states and non-equilibrium statistical mechanics (phase-space-picture approach)
[LBL-32695] 01 p0380 N94-10608
Discussion of stress tensor nonuniqueness with application to nonuniform, particulate systems
[DE93-014352] 02 p0816 N94-13206
Statistical mechanical theory of liquid entropy
[DE93-016524] 02 p0817 N94-14593
Retrieval properties of neural networks with infinitely many marked patterns
[PREPRINT-729] 02 p0766 N94-14718
Advanced in macrostatistical hydrodynamics
[DE93-018479] 04 p1410 N94-18270
A formulation of quantum statistical mechanics based on the Feynman path centroid density 2 dynamical properties
[AD-A272698] 05 p2037 N94-21166
A formulation of quantum statistical mechanics based on the Feynman path centroid density 1: Equilibrium properties
[AD-A272809] 05 p2037 N94-21171
One- and multi-component theories of mixtures
[DE93-040543] 05 p1966 N94-21511
Fracture simulations via massively parallel molecular dynamics
[DE93-040159] 06 p2374 N94-22871
Quantum statistical inference for density estimation
[DE94-002625] 07 p3073 N94-26805
Refractive and dielectric properties of helium, argon and nitrogen gases
[PB94-123783] 07 p3008 N94-26851
Thermodynamics of computation and information distance
[CWI-CS-R9341] 08 p3526 N94-30433
The Boltzmann entropy and randomness tests
[CWI-CS-R9342] 08 p3426 N94-30434
A cross-disciplinary report on the mathematical sciences applied to materials science, part 1
[AD-A276116] 09 p3843 N94-31529
The 14th Annual West Coast Theoretical Chemistry/Statistical Mechanics Conference
[AD-A276942] 09 p3656 N94-32239

STATISTICAL MOMENTS
U DISTRIBUTION MOMENTS

STATISTICAL PROBABILITY
U PROBABILITY THEORY

STATISTICAL TESTS
NT KOLMOGOROV-SMIRNOV TEST
NT RANK TESTS
Object recognition in industrial environment by means of tactile sensor
[ITN-93-85200] 01 p0178 N94-10393
Robust estimators and tests in one-sample location problem with particular consideration on modified maximum likelihood process
[ETN-93-94391] 02 p0774 N94-14703
Formation of on-site normal points 03 p0917 N94-15592
Bounds on inconsistent inferences for sequences of trials with varying probabilities
[AD-A267146] 03 p1172 N94-15733
Moments in statistics: Approximations to densities and goodness-of-fit
[AD-A266600] 03 p1173 N94-16726
The European Southern Observatory-MIDAS table file system 05 p2048 N94-22518
Aspects of goodness-of-fit
[AD-A274826] 07 p3003 N94-26495
Estimation and tests-of-fit for the three parameter Weibull distribution
[AD-A274827] 07 p3004 N94-26496
Wieand's theorem
[PB94-126711] 07 p3004 N94-27223
Example of statistical techniques applied to analysis of effects of small changes
[ESDU-93023] 07 p2670 N94-28094
A moment plotting method for characterizing aircraft fatigue data population distributions
[AD-A275500] 08 p3145 N94-28660
Comparison of Savannah River Site's meteorological databases
[DE94-001751] 08 p3373 N94-29817
The Boltzmann entropy and randomness tests
[CWI-CS-R9342] 08 p3426 N94-30434
Nonlinear model validation using correlation tests
[RR-463] 09 p3842 N94-31394
Statistical inference for coherent systems from partial information and in resampling techniques in survival analysis
[AD-A277382] 09 p3852 N94-32339
Multidimensional scaling of user information satisfaction
[AD-A277230] 09 p3920 N94-32633
Fault detection and isolation for the Bluebird test bed aircraft
[AD-A277979] 09 p3586 N94-33086
Statistical characteristics of bistatic surface scatter and mean bistatic surface scattering strengths
[AD-A278155] 09 p3862 N94-33096
Several modified goodness-of-fit tests for the cauchy distribution with unknown scale and location parameters
[AD-A278496] 10 p4130 N94-34301

STATISTICAL WEATHER FORECASTING
Developing prediction regions for a time series model for hurricane forecasting
[AD-A273777] 07 p2892 N94-25861

STATISTICS
Selected data on academic science and engineering R and D expenditures: Fiscal Year 1991
[NSF-92-329] 02 p0819 N94-13982
Monograph of the Aviation Epidemiology Data Register for CY 1992
[AD-A274400] 07 p2911 N94-27130

STATOR BLADES
Viscous analysis of three-dimensional rotor flows using a multigrid method
[NASA-TM-106266] 01 p0152 N94-11481
Simulation of unsteady flows through stator and rotor blades of a gas turbine using the Chimera method 06 p2323 N94-23652

STATORS
Laser anemometer measurements and computations for transonic flow conditions in an annular cascade of high turning core turbine vanes
[NASA-TP-3383] 01 p0015 N94-11133
Rotor stator CGI
[NASA-TM-109313] 02 p0518 N94-13608
Circle diagram approach for self excited induction generators
[DE93-010031] 03 p1010 N94-15971
Operation of a test bed axial-gap brushless dc rotor with a superconducting stator
[DE93-019167] 05 p1769 N94-21830
Experimental contribution to the study of secondary flows in centrifugal turbopump stator components
[ECL-92-35] 07 p2789 N94-25654
Wake passage effects on the losses in a linear turbine cascade
[AD-A273794] 07 p2790 N94-25874
Laser Doppler velocimetry in a low speed multistage compressor
[AD-A274836] 07 p2818 N94-26498
Numerical study on internal flows of centrifugal compressors 08 p3127 N94-28977
Rotary blood pump
[NASA-CASE-MSC-22424-1] 08 p3299 N94-29370
Rotordynamic analysis of annular honeycomb-stator turbulent gas seals using a new friction-factor model based on flat plate tests 08 p3302 N94-29916
Theoretical principles for designing long stator/linear motors with iron
[ETN-94-95741] 09 p3688 N94-31374
Hotwire measurements of the turbulent flow into a cascade of controlled-diffusion compressor blades
[AD-A277297] 09 p3706 N94-32042
Design of a low aspect ratio transonic compressor stage using CFD techniques
[NASA-TM-106636] 10 p3998 N94-33971
Experimental investigation of turbine blade-tip excitation forces 10 p4062 N94-34177
Test results for rotordynamic coefficients of anti-swirl self-injection seals 10 p4062 N94-34180

STDN (NETWORK)
Developing a space network interface simulator: The NTS approach 05 p1933 N94-21343

STEADY FLOW
NT COUETTE FLOW
Averaging techniques for steady and unsteady calculations of a transonic fan stage
[NASA-TM-106231] 02 p0499 N94-13108
Canonical forms of multidimensional steady inviscid flows
[NASA-CR-191488] 02 p0769 N94-13722
The structure of laminar flow in a three-dimensional driven cavity 02 p0640 N94-14601
A new Lagrangian method for three-dimensional steady supersonic flows
[NASA-TM-106068] 02 p0510 N94-14847
Study into the limits of an Euler equation method applied to leading-edge vortex flow
[NLR-TP-91350-U] 03 p1031 N94-17627
Cell vertex methods for steady inviscid flow 04 p1413 N94-18563
Two-dimensional boundary surfaces for axi-symmetric external transonic flows
[AD-A269678] 04 p1312 N94-18571
Numerical solutions for a flow with mixed convection in a vertical geometry
[DE93-011592] 04 p1419 N94-19058
Detailed description of two calculation programs for incompressible, steady state boundary layer flows, applied to determine the aerodynamic characteristics of NACA12 and OA312 foils at low Reynolds numbers
[ISL-N-604/92] 06 p2171 N94-25461
Evaluation of a concentration probe for application in a supersonic flow field
[AD-A273915] 07 p2643 N94-25592
Steady pressure measurements on an Aeroelastic Research Wing (ARW-2)
[NASA-TM-109046] 08 p3122 N94-28658
Nominally two-dimensional flow about a normal flat plate 08 p3275 N94-29838
Numerical solution of the two-dimensional time-dependent incompressible Euler equations
[NASA-CR-195775] 08 p3277 N94-29859
Aeroacoustic sensitivity analysis and optimal aeroacoustic design of turbomachinery blades
[NASA-CR-195786] 08 p3153 N94-30013
Numerical comparison of convective heat transfer augmentation devices used in cooling channels of hypersonic vehicles
[NASA-TM-106546] 08 p3279 N94-30147
Canonical-variables multigrid method for steady-state Euler equations
[AD-A279020] 08 p3454 N94-30208
A new orthogonal decomposition method for turbulent flows 08 p3281 N94-30494
Numerical simulation of leading-edge vortex flow
[AD-B175154] 08 p3134 N94-30871
CFD-based drag prediction: State-of-the-art, theory, prospects
[AD-B179297] 09 p3567 N94-31180
Additional capabilities of the unified waves model
[AD-A276114] 09 p3702 N94-31467
JPRS report: Science and technology. Central Eurasia: Physics and mathematics
[JPRS-UPM-93-003] 10 p4132 N94-35118

STEADY STATE
Material removal processes: Engineering mechanics consideration
[DE93-010733] 01 p0126 N94-10293
A model for the subduction mechanics of flexible lithosphere and its viscous coupling to the mantle using power-law rheologies 01 p0277 N94-11585
Preconditioning and the limit to the incompressible flow equations
[NASA-CR-191500] 02 p0769 N94-13717
Logarithmic asymptotics for steady-state tail probabilities in a single-server queue
[AD-A266746] 03 p1165 N94-15775
Fast simulation of steady-state availability in non-Markovian highly dependable systems
[AD-A266747] 03 p1174 N94-15823
Evolutionary implications of a steady-state water abundance on Venus 03 p1254 N94-16206
High power steady state MPD thrusters
[AD-A267277] 03 p0928 N94-17308
Static characteristics of a conduction and radiation dominated electric arc in nitrogen
[DE93-627106] 03 p1204 N94-17311
An overview of the SAFSIM computer program
[DE93-017657] 04 p1519 N94-18002
Decomposition invariance of generalized steady-state of a 1-D diffusion system
[REPT-93-26] 04 p1550 N94-19141
Excited atomic bromine energy transfer and quenching mechanisms
[AD-A270672] 04 p1572 N94-19607

Control of catalytic hydrotreating selectivity with ammonia
[DE93-041223] 04 p1354 N94-19660
Stochastic optimization by simulation: Numerical experiments with M/M/1 queue in steady-state
[AD-A271143] 05 p1949 N94-19854
Some topics in regenerative steady-state simulation
[AD-A271145] 05 p1902 N94-19855
Design of a controllable pitch underwater thruster system
[AD-A271140] 05 p1821 N94-20021
Stability curves for a thermoacoustic prime mover
[AD-A272607] 05 p1968 N94-21422
Stability of an uncooled segment of a high-temperature superconductor
[DE94-000476] 05 p2032 N94-21932
The TST: A small steady-state tokamak for integrated divertor testing
[DE94-001016] 05 p1998 N94-22045
On the estimation of the correlation dimension and its application to radar reflector discrimination
[NASA-CR-4564] 06 p2309 N94-23304
A direct approach to finding unknown boundary conditions in steady heat conduction 06 p2322 N94-23645
A theorem regarding roots of the zero-order Bessel function of the first kind 06 p2325 N94-23667
Numerical solution of flame sheet problems with and without multigrid methods 06 p2237 N94-23683
Enhanced absorption cycle computer model
[DE94-001997] 06 p2271 N94-23793
Space Shuttle Main Engine performance analysis 06 p2222 N94-24444
Decay of non-equilibrium polariton condensate in semiconductors
[DE94-604016] 07 p3068 N94-27678
Ion-driven permeation of deuterium in metals
[DE94-701104] 07 p2744 N94-27876
Gas-turbine engine steady-state behavior 07 p2828 N94-28044
Transient performance 07 p2828 N94-28045
Frequency-domain analysis of nonlinear microwave circuits
[PB94-132024] 08 p3261 N94-28400
Non-isolated 30 kW class arcjet PCU
[NASA-CR-189148] 08 p3173 N94-29444
Numerical simulations of cluster cooling flows 08 p3544 N94-29725
Two-phase power-law modeling of pipe flows displaying shear-thinning phenomena
[DE94-005115] 08 p3279 N94-30020
Advanced steady-state operating scenarios
[DE94-004810] 08 p3509 N94-30768
Invariance of the generalized steady-state for 1-D distributed parameter systems
[REPT-93-66] 09 p3825 N94-31662
Generalized steady-state method for solving 2-D diffusion systems
[REPT-93-83] 09 p3825 N94-31700
Analysis of rig test data for an axial/centrifugal compressor in the 12 kg/sec 10 p4000 N94-34437
Three-photon micromasers
[DE94-611106] 11 p4272 N94-35782
Uniqueness of a solution of a steady state photochemical problem: Applications to Mars 11 p4370 N94-36151
Preconditioned implicit solvers for the Navier-Stokes equations on distributed-memory machines
[NASA-TM-106449] 12 p4502 N94-36647

STEADY STATE CREEP
Creep properties of vanadium-base alloys
[DE94-006541] 09 p3641 N94-31486
Modeling of thermal barrier coatings
[NASA-CR-195365] 12 p4421 N94-36637

STEADY STATE FLOW
U EQUILIBRIUM FLOW

STEALTH BOMBER
U B-2 AIRCRAFT

STEAM
Nuclear thermal propulsion engine based on particle bed reactor using light water steam as a propellant
[DE93-014336] 02 p0552 N94-14111
Second law analysis of a conventional steam power plant 06 p2322 N94-23646
Evaluation of reducing gas turbine emissions through hydrogen-enhanced steam-injected combustion
[PB94-109873] 06 p2187 N94-23709
Configuration and performance of the indirect-fired fuel cell bottomed turbine cycle
[DE94-005961] 08 p3338 N94-30313
Non-polluting gas turbine as a result of self-heating working fluid in a closed circuit 10 p4000 N94-34436
Combined SO(x)/NO(x) control via SOXAL (tm) process: An electrodialytic regenerative wet scrubbing process
[DE94-009053] 11 p4284 N94-35346

STEAM FLOW
Simulation: A tool for steam plant dynamic analysis 07 p2831 N94-28084
Steam plant: Steam turbines for combined cycles 07 p2831 N94-28085

STEAM GENERATORS
U BOILERS

STEAM TURBINES
Knowledge organization in intelligent tutoring systems for diagnostic problem solving in complex dynamic domains
[AD-A273986] 07 p2984 N94-25899
Combined Cycles for Power Plants
[VKI-LS-1993-08] 07 p2830 N94-29077
Introduction to combined cycles 07 p2789 N94-28078
Thermodynamics of combined cycle plant 07 p2831 N94-28079
Steam plant for combined cycles: Heat recovery steam generators, design principles, and construction details 07 p2831 N94-28083
Simulation: A tool for steam plant dynamic analysis 07 p2831 N94-28084
Steam plant: Steam turbines for combined cycles 07 p2831 N94-28085
Application of microcomputer governed speed rise and loadcontrol appliance in the 200MW steam turbine 10 p4118 N94-34342
The influence of fin height and wall conductivity on integral-fin tubes during steam condensation
[AD-A280597] 12 p4539 N94-36725
Integrated gasification combined cycle and steam injection gas turbine powered by biomass joint-venture evaluation
[DE94-006905] 12 p4461 N94-36740

STEATITE
U TALC

STEEL STRUCTURES
Microstructure-based fatigue life prediction methods for naval steel structures
[AD-A265429] 01 p0085 N94-12426
The fire resistance of profiled thin steel sheet structures
[VTT-TIED-1320] 04 p1380 N94-19373
Fire safety engineering research in Norway
[PB93-201630] 06 p2268 N94-23429
Study on fatigue crack propagation characteristics around welded joint interface in complexed conditions 07 p2730 N94-25584
The structural behaviour of the steel or composite concrete and steel frames and the connections of frame members during the fire: A literature review
[VTT-TIED-1437] 07 p2837 N94-26307
Geometry changes in the elastic-plastic analysis of steel spatial skeletal structures
[IFTR-37/1993] 07 p2839 N94-26825
Modification of a model for fatigue life predictions based on level-crossing
[PB94-123395] 07 p2842 N94-27198
Photovoltaic power without batteries for continuous cathodic protection 08 p3341 N94-30465
Evaluation of corrosion protective organic coatings for steel structures in fresh water
[PB94-138484] 09 p3649 N94-31072

STEELS
NT AUSTENITIC STAINLESS STEELS
NT CARBON STEELS
NT CHROMIUM STEELS
NT FERRITIC STAINLESS STEELS
NT HIGH STRENGTH STEELS
NT LOW CARBON STEELS
NT MARAGING STEELS
NT MARTENSITIC STAINLESS STEELS
NT NICKEL STEELS
NT STAINLESS STEELS
Spinforming characteristics of a net shape forming process 01 p0056 N94-10004
Heavy-section steel technology program
[DE93-009222] 01 p0184 N94-10155
Effect of surface cleanliness of bearing steel on adhesive strength and tribological properties of sputter-deposited gold films
[DE93-767974] 01 p0082 N94-10732
Advanced zinc phosphate conversion and pre-ceramic polymetallosiloxane coatings for corrosion protection of steel and aluminum, and characteristics of polyphenylethereetherketone-based materials
[DE93-008717] 01 p0088 N94-10891
Immediate response to free product discovery
[PB93-182970] 01 p0265 N94-11015
Applications of surface science to solid lubricants
[SMC-TR-93-24] 02 p0579 N94-13903
Heavy section steel irradiation experiment
[DE93-015517] 02 p0573 N94-14537
A study of hydrogen effects on fracture behavior of radioactive waste storage tanks
[DE93-018171] 02 p0574 N94-14873
The corrosion protection of metals by ion vapor deposited aluminum
[NASA-TM-108425] 03 p0955 N94-15832
Measurement and theory of the dependence of hardness on residual stress
[AD-A267553] 03 p1061 N94-17105
Influence of grain size on the energy storing ability during uniaxial stretching of austenite steel
[IFTR-22/1992] 03 p0961 N94-17121
The effect of electric discharge machined notches on the fracture toughness of several structural alloys
[AD-A268605] 03 p0962 N94-17464
Evaluation of hybrid reinforcement (fiber-reinforced-plastic rod with steel core)
[AD-A268009] 03 p0941 N94-17473
Environment enhanced fatigue crack propagation in metals: Inputs to fracture mechanics life prediction models
[NASA-CR-191538] 03 p0942 N94-17638
Inelastic deformation and damage at high temperature
[DE93-018155] 04 p1448 N94-17814
Effects of irradiation temperature on embrittlement of nuclear pressure vessel steels
[DE93-015428] 04 p1359 N94-18245
The effect of crystallographic orientation on the performance of single crystal tungsten subscale penetrators
[AD-A268988] 04 p1597 N94-18468
Effects of irradiation temperature on Charpy and tensile properties of high-copper, low upper-shelf, submerged-arc welds
[DE93-017858] 04 p1445 N94-19047
PVDF gauge characterization of hypervelocity-impact-generated debris clouds
[DE93-018831] 05 p1829 N94-19943
Atom probe field ion microscopy characterizations of VVER steels
[DE93-017864] 05 p1689 N94-20180
Lubricated wear of steel-ceramic and ceramic-ceramic systems
[PB93-202356] 05 p1825 N94-21450
Thermal fatigue: A literature review
[PB93-226306] 06 p2375 N94-23120
Weld cladding of hard surfaces
[PB93-201598] 06 p2353 N94-23448
Impacts: NIST Building and Fire Research Laboratory (technical and societal)
[PB94-113420] 06 p2270 N94-23737
Wear reduction in ceramic bearings by surface generated pyrolytic carbon continuously replenished by ethylene gas
[AD-A278264] 06 p2364 N94-24090
Thermophysical property sensitivity effects in steel solidification 06 p2246 N94-25122
Proceedings of the 12th International Congress: Corrosion Control for Low-Cost Reliability. Volume 1: Coatings
[AD-A273661] 06 p2251 N94-25448
Interactions between corrosion fatigue and stress corrosion crack on steel for light water reactors 07 p2722 N94-25547
Preparation of creep data sheet: Material strength data sheet 07 p2723 N94-25548
Knowledge base systems for chemical compounds designing support 07 p2723 N94-25550
Fundamental study on monitoring technology on local surface damages 07 p2724 N94-25555
Microstructural development in low activation ferritic alloys irradiated to 200 dpa at 420 C
[DE94-004269] 07 p2731 N94-25803
General Motors Corporation and Pacific Northwest Laboratory staff exchange: Inspection of case hardened steels and metal-matrix composites
[DE94-003470] 07 p2706 N94-25982
Cracking of textured zinc coating during forming process
[DE94-003414] 07 p2750 N94-26085
An experimental study on the effects of compressive stress on the fatigue crack growth of low-alloy steel
[DE94-004447] 07 p2737 N94-26582
The influence of weld metal alloying additions to extend the heat input range for the submerged arc welding of high strength steels
[AD-A274284] 07 p2738 N94-26679
Evaluation of crack arrest fracture toughness of parent plate, weld metal and heat affected zone of BIS 812 EMA ship plate steel
[AD-A274871] 07 p2839 N94-26859
The role of point defect clusters in reactor pressure vessel embrittlement
[DE94-001122] 07 p2739 N94-26931

Development and application of contamination technology for MSFC managed space systems
[NASA-CR-193934] 07 p2697 N94-27421
Fatigue propagation behaviour of short cracks (1-2 mm) in steels
[ESDU-93033] 07 p2845 N94-28145
Method of bonding molybdenum to steel
[AD-D016079] 07 p2747 N94-28187
Analysis of data by long-time mechanical properties of 08KH18N10T steel irradiated by neutrons
[DE94-605337] 08 p3202 N94-28551
Corrosion inhibition by electrodeposited conductive-polymer film
[AD-A275456] 08 p3213 N94-28806
Low temperature behavior of virgin martensite
[PB94-132925] 08 p3204 N94-29142
Effect of non-metallic inclusions on the machinability of steel
[PB93-230233] 08 p3204 N94-29387
Sliding friction and wear between titanium nitride, M50 steel and silicon nitride (round 3 of VAMAS wear test program)
[IMR-TM-TR-003] 08 p3303 N94-30019
Development of evaluated data bank of physical properties of perspective nuclear engineering steels and alloys
[DE94-607999] 08 p3207 N94-30076
XPS analysis of 440C steel surfaces lubricated with perfluoropolyethers under sliding conditions in high vacuum
[NASA-TM-106548] 08 p3218 N94-30177
Metafusion: A breakthrough in metallurgy 08 p3211 N94-30446
Photovoltaic power without batteries for continuous cathodic protection 08 p3341 N94-30465
Experimental and analytical comparison of constraint effects due to biaxial loading and shallow-flaws
[DE94-004794] 08 p3323 N94-30689
Design of a variable-conductance vacuum insulation
[DE94-000270] 08 p3268 N94-30819
Correlation of flux composition and inclusion characteristics with submerged arc weld metal properties in HY-100 steel
[AD-A277040] 09 p3726 N94-32261
Reactor pressure vessel structural integrity research in the US Nuclear Regulatory Commission HSST and HSSI Programs
[DE94-006550] 09 p3739 N94-32771
Method and apparatus for inhibiting the disbonding of a paint from metal surfaces
[AD-D016106] 09 p3663 N94-32960
Robotic weld overlay coatings for erosion control
[DE94-009703] 10 p4060 N94-33902
Testing of the fracture resistance of rails 11 p4279 N94-35353
The electrical conductivities of candidate beam-waveguide antenna shroud materials 11 p4252 N94-35546
Evaluation of flame-sprayed polymer coatings for civil works navigation structures
[AD-A280507] 12 p4422 N94-37104
The development of short, high surface area activated carbon fibers
[AD-A280509] 12 p4404 N94-37105
Interfaces of high-protection performance polyaryls-coated zinc phosphated steels
[DE94-011732] 12 p4417 N94-37153
Alternate melting and refining routes 12 p4421 N94-37323
Exploratory study on H13 steel dies
[DE94-012118] 12 p4420 N94-37678
Numerical simulation of dynamic fracture and failure in solids
[DE94-010379] 12 p4457 N94-37705

STEEP GRADIENT AIRCRAFT
U V/STOL AIRCRAFT

STEEPEST ASCENT METHOD
U STEEPEST DESCENT METHOD

STEEPEST DESCENT METHOD
Steepest descent approximations for accretive operator equations
[DE93-628586] 03 p1171 N94-17667
Steepest descent method for set-valued locally accretive mappings
[DE93-628592] 04 p1548 N94-18106

STEEPNESS
U SLOPES

STEERABLE ANTENNAS
Adaptive array antenna for satellite cellular and direct broadcast communications 06 p2275 N94-22745
Flight testing of GPS and GPS-aided systems
[NLR-TP-92151-U] 07 p2666 N94-27831
Switched-beam radiometer front-end network analysis
[NASA-CR-194922] 11 p4252 N94-35247

STEERING
Laser beam steering device 03 p1045 N94-17357
Electro-optic beam steering using non-linear organic materials
[AD-A270809] 04 p1374 N94-19577
Proceedings of the Twentieth Annual Technologyfest 05 p1645 N94-20188
Aeronautical satellite antenna steering using magnetic field sensors 06 p2289 N94-22836
Cockpit control system conceptual design
[NASA-CR-195543] 06 p2190 N94-24551
Studies of non-linear optical effects for agile beam steering
[AD-A273998] 07 p3034 N94-25902
Theoretical aspects of the agile mirror
[AD-A274890] 07 p2767 N94-26177
Characterization of a diffraction grating as a simulant of a selective frequency antenna for radiometric applications
[AD-A275793] 08 p3241 N94-28745
Optical processing of MMW for agile beamsteering and beamforming
[AD-A277161] 09 p3880 N94-32068
Immersive virtual environments as trainer: System design from a cognitive stance 12 p4484 N94-37267

STEFAN-BOLTZMANN LAW
Total hemispherical emittance of Niobium-1 percent zirconium fuel cladding for the SP-100 space reactor
[AD-A270456] 04 p1576 N94-19589
Examination for optimization of synchrotron radiation spectrum for the x ray depth lithography
[BONN-IR-92-32] 05 p1987 N94-21148

STELLAR (STAR TRACKER)
U CCD STAR TRACKER

STELLAR ACTIVITY
NT SOLAR ACTIVITY
NT SOLAR FLARES
NT SOLAR PROMINENCES
NT SUNSPOTS
Ultraviolet observations of NGC 4395, the least luminous and nearest known Seyfert 1 nucleus
[NASA-CR-194304] 02 p0831 N94-13679
Surface differential rotation in a sample of cool dwarf stars 08 p3545 N94-29827

STELLAR ATMOSPHERES
NT CHROMOSPHERE
NT SOLAR ATMOSPHERE
Unified NLTE model atmospheres including spherical extension and stellar winds, 4: Improved line transfer and wind contamination of H, He profiles
[MPA-905] 04 p1624 N94-17736
Molecular equilibria and condensation sequences in carbon rich gases 05 p2083 N94-20756
Molecular abundances in the envelopes around evolved stars
[PB94-104916] 06 p2602 N94-23812
Model atmosphere analysis of selected luminous B stars
[NASA-CR-195098] 06 p2599 N94-24051
The solar spectral irradiances from x ray to radio wavelengths
[NASA-CR-195203] 06 p2629 N94-25260
Abundance patterns in red-giant CH stars 08 p3539 N94-29820
A critical examination of stellar atmosphere theory for metal-poor K-giant stars 09 p3927 N94-32308

STELLAR COLOR
The controlling parameters of the integrated flux of a stellar population 01 p0426 N94-11187
Polarization and variability of active galaxies and quasars 02 p0837 N94-13550
Near infrared surveys of high mass star forming regions 09 p3925 N94-31898
Color/magnitude calibration for National Aeronautics and Space Administration (NASA) standard Fixed-Head Star Trackers (FHST) 11 p4209 N94-35641

STELLAR COMPOSITION
The abundances of the elements in sharp-lined early type stars
[NASA-CR-194055] 01 p0424 N94-12573
Abundance markers in H II regions of late spiral galaxies
[ISBN-0-315-62457-4] 02 p0836 N94-13372
Determination of nitrogen to carbon abundance ratios from transition layer emission lines
[NASA-CR-191921] 04 p1622 N94-19421
What is normal among the A-type stars?
[ISBN-0-315-83947-3] 05 p2081 N94-22592
Abundance patterns in red-giant CH stars 08 p3539 N94-29820
Coronal abundances and their variation
[NASA-CR-195767] 08 p3551 N94-29858
Study of the stellar populations of the Fornax dwarf spheroidal galaxy
[ISBN-0-315-85526-6] 08 p3541 N94-30231
Line-strength gradients and kinematic profiles in elliptical galaxies 09 p3934 N94-31788
A critical examination of stellar atmosphere theory for metal-poor K-giant stars 09 p3927 N94-32308
Stellar alchemy: The origin of the chemical elements
[DE94-011903] 11 p4350 N94-36229

STELLAR CONVECTION
NT SOLAR CONVECTION (ASTRONOMY)

STELLAR CORES
Millimeter and infrared studies of young stellar objects in dark cloud L1641 02 p0838 N94-13648

STELLAR CORONAS
NT CORONAL HOLES
NT CORONAL LOOPS
NT SOLAR CORONA
Studies of gas in cooling flow clusters
[NASA-CR-193597] 02 p0628 N94-12959
ROSAT guest investigator program (AO-1). On a search for coronal x ray emissions from white dwarfs
[NASA-CR-193654] 02 p0835 N94-13171
Stellar coronae at the end of the main sequence: A Rosat survey of the late M dwarfs
[NASA-CR-194700] 04 p1628 N94-19794
Coronal temperatures of unusually active K-dwarf binary systems
[NASA-CR-189335] 08 p3545 N94-29861

STELLAR DOPPLER SHIFT
U DOPPLER EFFECT

STELLAR ENVELOPES
Detection of accreting circumstellar gas around weak emission-line Herbig Ae/Be stars
[NASA-TM-108256] 01 p0424 N94-11306
Why convective heat transport in the solar nebula was inefficient 01 p0458 N94-12143
X ray emission from Wolf-Rayet stars with recurrent dust formation
[NASA-CR-189321] 03 p1300 N94-15533
The chromosphere of VV cephei and the distribution of circumstellar dust around red giants and supergiants
[NASA-CR-193594] 03 p1297 N94-16866
Detection of accreting gas toward HD 45677: A newly recognized, Herbig Be proto-planetary system
[NASA-CR-189312] 04 p1621 N94-19288
The molecular environment of S106 IR
[MPE-PREPRINT-241] 04 p1622 N94-19417
The circumstellar environments of intermediate mass main sequence stars
[NASA-CR-189311] 05 p2055 N94-21498
Circumstellar environments of Be stars at infra-red and radio wavelengths
[ISBN-0-315-83135-9] 05 p2081 N94-22426
Molecular abundances in the envelopes around evolved stars
[PB94-104916] 06 p2602 N94-23812
X ray enhancement of SN 1987A due to interaction with its ring-like nebula
[NIFS-265] 06 p2602 N94-24867
Observational studies of the clearing phase in proto-planetary disk systems
[NASA-CR-195182] 06 p2604 N94-25265
Investigations of the dynamical evolution of protoplanetary nebulae
[NASA-CR-195278] 07 p3105 N94-27428
Observations of accretion and angular momentum regulation in young circumstellar disks and the implications for planetary formation 09 p3928 N94-31122
Circumstellar material around young stars in Orion 09 p3930 N94-31133
Multiwavelength search for protoplanetary disks 09 p3599 N94-31430

STELLAR EVOLUTION
NT STAR FORMATION
NT STELLAR MASS ACCRETION
The controlling parameters of the integrated flux of a stellar population 01 p0426 N94-11187
Carbon and nitrogen in Type 2 supernova diamonds 01 p0431 N94-12166
Analysis of interstellar cloud structure based on IRAS images
[NASA-CR-194341] 02 p0836 N94-13332
The physical and chemical evolution of protostellar disks. The growth of protostellar disks: Progress to date
[NASA-CR-194111] 02 p0836 N94-13423
The spectroscopic evolution of novae in the bulge of M31 and a search for their possible origin in the M31 globular cluster system 02 p0831 N94-13668
Charge-exchange reactions and weak interaction rates for Type 2 supernovae
[DE93-015104] 02 p0783 N94-13893
Wind mass and energy deposition
[DE93-013345] 02 p0839 N94-14341
ROSAT observations of clusters with wide-angle tailed radio sources
[NASA-CR-193784] 02 p0833 N94-14405
ROSAT-IUE observations of symbiotic stars. The x ray morphology of high latitude associations
[NASA-CR-194616] 03 p1236 N94-16492

A new approach to the study of the turbulence layer
[NASA-CR-194546] 04 p1487 N94-19397
Structuration processes in protoplanetary accretion disks
[MPE-243] 04 p1628 N94-19519
Formation of the low-mass solar nebula
05 p2109 N94-20728
Variety in planetary systems 05 p2086 N94-20871
The circumstellar environments of intermediate mass main sequence stars
[NASA-CR-189311] 05 p2055 N94-21498
New production mechanisms for unstable nuclei in stars, supernovae, and the big bang
[DE93-018627] 05 p2081 N94-21618
Physical properties of dense astrophysical plasmas
05 p2001 N94-22637
Neutrino emission processes in dense high-temperature plasmas 05 p2001 N94-22638
Molecular abundances in the envelopes around evolved stars
[PB94-104916] 06 p2602 N94-23812
Binary-single star scattering: An investigation of a realistic chaotic scattering system
08 p3543 N94-29719
Convective turbulence and transport in stars
08 p3546 N94-29913
Theoretical asteroseismology of white dwarf stars: The encyclopedia Seismologica 08 p3547 N94-30011
Observations of accretion and angular momentum regulation in young circumstellar disks and the implications for planetary formation 09 p3928 N94-31122
Binary-binary collisions involving main-sequence stars, white dwarfs and neutron stars in globular clusters
[DE94-005086] 10 p4163 N94-33415
Non-equilibrium chemistry of the early solar system
[NASA-CR-195691] 10 p4163 N94-33603
Ferromagnetic resonance spectra of H2-reduced minerals and glasses 11 p4240 N94-36164
Stellar alchemy: The origin of the chemical elements
[DE94-011903] 11 p4350 N94-36229

STELLAR FIELDS
U STAR DISTRIBUTION

STELLAR FLARES
NT SOLAR FLARES

STELLAR GRAVITATION
NT SOLAR GRAVITATION
Structuration processes in protoplanetary accretion disks
[MPE-243] 04 p1628 N94-19519

STELLAR INTERIORS
NT SOLAR INTERIOR
NT STELLAR CORES

STELLAR LUMINOSITY
Time series photometry of faint cataclysmic variables with a CCD 02 p0831 N94-13646
Pre-main sequence stars in the Chamaeleon cloud and pre-main sequence stars in the Rho Ophiuchi cloud core
[NASA-CR-194713] 05 p2080 N94-20337
Model atmosphere analysis of selected luminous B stars
[NASA-CR-195098] 06 p2599 N94-24051
Globular cluster photometry near the turnoff: Blue stragglers, relative ages, and the horizontal branch
08 p3538 N94-29732
Spatially resolved spectroscopy of AG Carinae, and direct evidence for stellar evolution: The central star of NGC 2392
[NASA-CR-189291] 08 p3545 N94-29871
A near-infrared survey of the star forming region NGC 2264 08 p3540 N94-29971
Near-critical spherically symmetric accretion by neutron stars 08 p3546 N94-29991
Spectral and temporal behavior of low mass x ray binaries observed with the Einstein SSS and MPC, and the Broad Band X Ray Telescope
08 p3542 N94-30862
Near infrared surveys of high mass star forming regions 09 p3925 N94-31898

STELLAR MAGNETIC FIELDS
NT SOLAR MAGNETIC FIELD
Shock formation in magnetohydrodynamical accretion onto a black hole 05 p2010 N94-22699
Magnetohydrodynamic phenomena in star-forming processes and their environment
05 p2010 N94-22701
Protoplanetary disks: Theory and observation by millimeter and sub-millimeter arrays
[REPT-331] 06 p2603 N94-24983
Dynamics of flux tubes in accretion disks
09 p3932 N94-31142
Hydrodynamics of neutron star interiors and laboratory superfluids 09 p3936 N94-31949

STELLAR MAGNETOSPHERES
NT PULSAR MAGNETOSPHERES
General relativistic winds in a black hole magnetosphere 05 p2002 N94-22644
Two populations and models of gamma ray bursts
[NASA-CR-194762] 06 p2629 N94-22947

STELLAR MAGNITUDE
Search for x ray emitting young stars outside of massive molecular clouds
[NASA-CR-193609] 02 p0830 N94-13462
Photometry and spectroscopy in the open cluster Alpha Persei, 2
[NASA-CR-193397] 02 p0833 N94-14358
Globular cluster photometry near the turnoff: Blue stragglers, relative ages, and the horizontal branch
08 p3538 N94-29732
Near infrared surveys of high mass star forming regions 09 p3925 N94-31898
Color/magnitude calibration for National Aeronautics and Space Administration (NASA) standard Fixed-Head Star Trackers (FHST) 11 p4209 N94-35641

STELLAR MASS
Carbon and nitrogen in Type 2 supernova diamonds
01 p0431 N94-12166
Formation of the low-mass solar nebula
05 p2109 N94-20728
AGB stars as a source of short-lived radioactive nuclei in the solar nebula 05 p2133 N94-20859
The distribution of dark matter in the A2256 cluster
[NASA-CR-194699] 05 p2055 N94-21579
Mars and the early Sun 05 p2146 N94-21683
Observational studies of the clearing phase in proto-planetary disk systems
[NASA-CR-195182] 06 p2604 N94-25265
A study of recycled pulsars in globular clusters
08 p3539 N94-29825
Theoretical asteroseismology of white dwarf stars: The encyclopedia Seismologica 08 p3547 N94-30011
Near infrared surveys of high mass star forming regions 09 p3925 N94-31898
A chemical analysis of solar neighborhood dwarfs
09 p3926 N94-31951
Absolute limit on rotation of gravitationally bound stars
[DE94-011367] 12 p4548 N94-37049

STELLAR MASS ACCRETION
Detection of accreting circumstellar gas around weak emission-line Herbig Ae/Be stars
[NASA-TM-108256] 01 p0424 N94-11306
ROSAT-IUE observations of symbiotic stars. The x ray morphology of high latitude associations
[NASA-CR-194616] 03 p1236 N94-16492
Variability of the Seyfert galaxy MKN 766 in the Rosat all sky survey
[MPE-PREPRINT-221] 03 p1240 N94-17591
Detection of accreting gas toward HD 45677: A newly recognized, Herbig Be proto-planetary system
[NASA-CR-189312] 04 p1621 N94-19288
VVNRS: Variable phenomena in VV Cephei
[NASA-CR-194731] 05 p2056 N94-21835
The formation of massive stars: A 30 Mo case study
[ISBN-0-315-83944-9] 05 p2081 N94-22593
Time variation of MHD accretion onto a black hole
05 p2009 N94-22692
Accretion of a hot plasma onto the central black hole: Fokker-Planck formulation 05 p2009 N94-22693
Shock formation in magnetohydrodynamical accretion onto a black hole 05 p2010 N94-22699
UV spectral variability in the Herbig Ae star HR 5999. 11: The accretion interpretation
[NASA-CR-189313] 06 p2599 N94-23334
Protoplanetary disks: Theory and observation by millimeter and sub-millimeter arrays
[REPT-331] 06 p2603 N94-24983
A study of white dwarf radiative accretion shocks
08 p3544 N94-29731
Near-critical spherically symmetric accretion by neutron stars 08 p3546 N94-29991
Reactive flows in compact objects
09 p3934 N94-31567
Structure and stability of spherical accretion flows onto compact objects 09 p3935 N94-31946
IUE observations of new A star candidate proto-planetary systems
[NASA-CR-189355] 10 p4162 N94-34267

STELLAR MASS EJECTION
Nuclear astrophysics
[DE93-010569] 01 p0425 N94-10292
MHD shocks in coronal mass ejections
[NASA-CR-193418] 02 p0828 N94-12970
ICE/ISEE plasma wave data analysis
[NASA-CR-194375] 02 p0796 N94-13081
The interplanetary origins and the main-phase development of moderate geomagnetic storms (1978 - 1979)
[INPE-5445-TDI/491] 02 p0835 N94-13174
Evolution of the interplanetary magnetic field
[DE93-012631] 02 p0836 N94-13262
Solar-geophysical data number 584, April 1993. Part 2: (Comprehensive reports). Data for October 1992 and miscellaneous
[PB93-198331] 02 p0845 N94-14561
Helical kink instability of jets from young stellar objects 05 p2008 N94-22686
Solar-geophysical data number 584, April 1993. Part 2: (Comprehensive reports). Data for October 1992, and miscellaneous
[PB93-198331] 06 p2627 N94-23739
Molecular abundances in the envelopes around evolved stars
[PB94-104916] 06 p2602 N94-23812
Solar-geophysical data number 587, July 1993. Part 2: (Comprehensive reports). Data for January 1993, and miscellaneous
[PB93-232882] 06 p2628 N94-24990
Solar-geophysical data number 589, September 1993. Part 2: (Comprehensive reports). Data for March 1993, and miscellaneous
[PB94-117405] 06 p2628 N94-24994
Solar-geophysical data number 590, October 1993. Part 2: (Comprehensive reports). Data for April 1993, and miscellaneous
[PB94-125911] 07 p3110 N94-27054
Solar-geophysical data number 591, November 1993. Part 2: (Comprehensive reports). Data for May 1993 and miscellaneous
[PB94-134830] 07 p3111 N94-28360
Remote sensing of inner heliospheric plasmas
[AD-A275021] 08 p3550 N94-29132
Theoretical studies of the solar atmosphere and interstellar pickup ions
[NASA-CR-195846] 10 p4166 N94-34716
Catalog of Helios 90 deg photometer events
[PL-TR-94-2040] 11 p4375 N94-36264
A study of physical mechanisms for filament eruption and coronal mass ejection via numerical simulation
[NASA-CR-196087] 12 p4549 N94-36469
The winds of cataclysmic variables
[DE94-010897] 12 p4548 N94-37164

STELLAR MODELS
Analysis of interstellar cloud structure based on IRAS images
[NASA-CR-194341] 02 p0836 N94-13332
Spectra of late type dwarf stars of known abundance for stellar population models
[NASA-CR-194301] 02 p0831 N94-13681
Computational astrophysics: Pulsating stars
[DE93-018369] 04 p1627 N94-18857
Structuration processes in protoplanetary accretion disks
[MPE-243] 04 p1628 N94-19519
High-energy astrophysics: A theoretical analysis of thermal radiation from neutron stars
[NASA-CR-194808] 05 p2055 N94-20952
Mars and the early Sun 05 p2146 N94-21683
The cool-star spectral catalog: A uniform collection of IUE SWP-LOs 05 p2046 N94-22446
The formation of massive stars: A 30 Mo case study
[ISBN-0-315-83944-9] 05 p2081 N94-22593
Magnetohydrodynamic phenomena in star-forming processes and their environment
05 p2010 N94-22701
The calculation of theoretical chromospheric models and the interpretation of solar spectra from rockets and spacecraft
[NASA-CR-195083] 06 p2626 N94-23569
Model atmosphere analysis of selected luminous B stars
[NASA-CR-195098] 06 p2599 N94-24051
Model development for Ulysses and SOHO
[NASA-CR-193884] 06 p2627 N94-24484
Chaotic dynamics of the solar cycle
[AD-A274315] 07 p3110 N94-26883
Investigations of the dynamical evolution of protoplanetary nebulae
[NASA-CR-195278] 07 p3105 N94-27428
Equation of state of neutron star matter, limiting rotational periods of fast pulsars, and the properties of strange stars
[DE94-005214] 08 p3542 N94-28480
Equation of state of stellar plasmas
[DE94-004186] 08 p3542 N94-28526
CBSD: The celestial background scene descriptor
[AD-A275521] 08 p3538 N94-28671
Abundance patterns in red-giant CH stars
08 p3539 N94-29820
Near-critical spherically symmetric accretion by neutron stars 08 p3546 N94-29991
Theoretical asteroseismology of white dwarf stars: The encyclopedia Seismologica 08 p3547 N94-30011
Evolution of vaporizing pulsars
09 p3929 N94-31128

Double-lined pre-main-sequence binaries: A test of pre-main-sequence evolutionary theory
09 p3933 N94-31497
Theoretical studies of magnetohydrodynamic equilibria and dynamics of a solar coronal loop
09 p3953 N94-31792
Structure and stability of spherical accretion flows onto compact objects 09 p3935 N94-31946
A critical examination of stellar atmosphere theory for metal-poor K-giant stars 09 p3927 N94-32308
Convection in Type 2 supernovae
[DE94-009373] 09 p3938 N94-32914
Working group 1: Coronal streamers
[DE94-009313] 10 p4165 N94-34091

STELLAR MOTIONS
NT SOLAR OSCILLATIONS
NT STELLAR ORBITS
NT STELLAR OSCILLATIONS
NT STELLAR ROTATION

STELLAR OCCULTATION
Wave structure in planetary rings
01 p0434 N94-11185
Submission of Earth-based ring occultation observations to the NASA planetary data system rings discipline node
[NASA-CR-193469] 01 p0427 N94-12557
Cloud, dust, and ozone vertical profiles from solar occultation measurements: Implications for dynamics
06 p2617 N94-24877

STELLAR ORBITS
A study of recycled pulsars in globular clusters
08 p3539 N94-29825

STELLAR OSCILLATIONS
NT SOLAR OSCILLATIONS
On observing neutron star oscillations
08 p3538 N94-29795
Near-critical spherically symmetric accretion by neutron stars 08 p3546 N94-29991
Theoretical asteroseismology of white dwarf stars: The encyclopedia Seismologica 08 p3547 N94-30011

STELLAR PARALLAX
Statistical analysis of trigonometric parallaxes
[NASA-CR-194558] 03 p1172 N94-15641

STELLAR PHYSICS
NT SOLAR PHYSICS
New production mechanisms for unstable nuclei in stars, supernovae, and the big bang
[DE93-018627] 05 p2081 N94-21618
VVNRS: Variable phenomena in VV Cephei
[NASA-CR-194731] 05 p2056 N94-21835
The formation of massive stars: A 30 Mo case study
[ISBN-0-315-83944-9] 05 p2081 N94-22593
Stellar alchemy: The origin of the chemical elements
[DE94-011903] 11 p4350 N94-36229
Absolute limit on rotation of gravitationally bound stars
[DE94-011367] 12 p4548 N94-37049

STELLAR RADIATION
NT STELLAR WINDS
Search for ultra-high energy emission from Geminga and five unidentified EGRET sources
[DE93-012717] 02 p0846 N94-12816
The soft x ray transient Cen X-4 in quiescence
[NASA-CR-194033] 02 p0833 N94-14406
A comparison of calculated and observed monochromatic type Ia supernova light curves
[MPA-709] 03 p1237 N94-17629
Computational astrophysics: Pulsating stars
[DE93-018369] 04 p1627 N94-18857
Factor analysis as a tool for spectral line component separation 21cm emission in the direction of L1780
05 p1965 N94-22536
Properties of x ray emission from x ray novae
05 p2007 N94-22676
Time variations of x rays from black hole candidates: Canonical time variations in high and low intensity states
05 p2009 N94-22690
Nonequilibria in thermal emission from supernova remnants
[NIFS-264] 06 p2602 N94-24866
X ray enhancement of SN 1987A due to interaction with its ring-like nebula
[NIFS-265] 06 p2602 N94-24867
An April 1991 outburst from 4U0115+63 observed by BATSE
[DE94-007093] 07 p3116 N94-27440
A study of white dwarf radiative accretion shocks
08 p3544 N94-29731
On observing neutron star oscillations
08 p3538 N94-29795
A study of ultra high-energy radiation associated with Hercules X-1 08 p3552 N94-29823
Coronal temperatures of unusually active K-dwarf binary systems
[NASA-CR-189335] 08 p3545 N94-29861
Spatially resolved spectroscopy of AG Carinae, and direct evidence for stellar evolution: The central star of NGC 2392
[NASA-CR-189291] 08 p3545 N94-29871
A search for 100 TeV gamma ray emission from the x ray binary pulsar 4U 0115+63 using the CYGNUS extensive air-shower array 09 p3955 N94-31900

STELLAR ROTATION
Photometry and spectroscopy in the open cluster Alpha Persei, 2
[NASA-CR-193397] 02 p0833 N94-14358
Plasma properties research: Task 3
[DE93-017087] 04 p1583 N94-17854
Pulse-timing studies of x ray pulsars
[NASA-CR-193778] 04 p1621 N94-18611
Dynamo driven by weak plasma turbulence: The effect of differential rotation 05 p2005 N94-22665
Particle acceleration on the Alfven surface of a plasma ejecting axisymmetric rotator 05 p2008 N94-22681
Shock formation in magnetohydrodynamical accretion onto a black hole 05 p2010 N94-22699
Chaotic dynamics of the solar cycle
[AD-A274315] 07 p3110 N94-26883
Equation of state of neutron star matter, limiting rotational periods of fast pulsars, and the properties of strange stars
[DE94-005214] 08 p3542 N94-28480
Surface differential rotation in a sample of cool dwarf stars 08 p3545 N94-29827
Convective turbulence and transport in stars
08 p3546 N94-29913
The evolutionary status of PSR 1259-63
[DE94-007094] 09 p3938 N94-32503
Absolute limit on rotation of gravitationally bound stars
[DE94-011367] 12 p4548 N94-37049

STELLAR SPECTRA
NT SOLAR SPECTRA
Physical properties of gas disks around shell stars with and without dust
[NASA-CR-193655] 02 p0835 N94-13239
The spectroscopic evolution of novae in the bulge of M31 and a search for their possible origin in the M31 globular cluster system 02 p0831 N94-13668
Spectra of late type dwarf stars of known abundance for stellar population models
[NASA-CR-194301] 02 p0831 N94-13681
A long-term space astrophysics research program: The evolution of the quasar continuum
[NASA-CR-193714] 02 p0839 N94-14404
Analysis of the IUE spectra of the strongly interacting binary beta Lyrae
[NASA-CR-194118] 02 p0833 N94-14493
Solar-geophysical data number 584, April 1993. Part 1: (Prompt reports). Data for March, February 1993, and late data
[PB93-198323] 02 p0845 N94-14560
Determination of nitrogen to carbon abundance ratios from transition layer emission lines
[NASA-CR-191921] 04 p1622 N94-19421
The circumstellar environments of intermediate mass main sequence stars
[NASA-CR-189311] 05 p2055 N94-21498
Circumstellar environments of Be stars at infra-red and radio wavelengths
[ISBN-0-315-83135-9] 05 p2081 N94-22426
The cool-star spectral catalog: A uniform collection of IUE SWP-LOs 05 p2046 N94-22446
ASpect: A new spectrum and line analysis package for IRAF 05 p1926 N94-22485
What is normal among the A-type stars?
[ISBN-0-315-83947-3] 05 p2081 N94-22592
Voyager observations of globular clusters
[NASA-CR-194806] 06 p2598 N94-23330
Molecular abundances in the envelopes around evolved stars
[PB94-104916] 06 p2602 N94-23812
Infrared and SiO maser observations of OH/IR stars
[PB94-104890] 06 p2599 N94-24780
BATSE Data Analysis
[NASA-CR-193930] 07 p3114 N94-26685
Solar-geophysical data number 590, October 1993. Part 1: (Prompt reports). Data for September, August 1993, and late data
[PB94-125903] 07 p3110 N94-27053
The role of cloud collisions in N-body simulations of disk galaxies 08 p3545 N94-29755
Surface differential rotation in a sample of cool dwarf stars 08 p3545 N94-29827
Coronal temperatures of unusually active K-dwarf binary systems
[NASA-CR-189335] 08 p3545 N94-29861
Inhomogeneities in the wind from Wolf-Rayet stars
[ISBN-0-315-85893-1] 08 p3548 N94-30058
Reconstruction of stellar images from correlations
[ISBN-0-315-85382-4] 08 p3541 N94-30133
Spectral and temporal behavior of low mass x ray binaries observed with the Einstein SSS and MPC, and the Broad Band X Ray Telescope
08 p3542 N94-30862
Extreme ultraviolet opacity sources in the DA white dwarf G191-B2B 09 p3924 N94-31210
A chemical analysis of solar neighborhood dwarfs
09 p3926 N94-31951
UV spectroscopy of low-redshift active galaxies
[NASA-CR-189323] 10 p4161 N94-33904
Ferromagnetic resonance spectra of H2-reduced minerals and glasses 11 p4240 N94-36164
Ultraviolet spectropolarimetry of high redshift quasars with the Hubble Space Telescope
[NASA-CR-196014] 12 p4546 N94-36690

STELLAR SPECTROPHOTOMETRY
Abundance markers in H II regions of late spiral galaxies
[ISBN-0-315-62457-4] 02 p0836 N94-13372
Time series photometry of faint cataclysmic variables with a CCD 02 p0831 N94-13646
The spectroscopic evolution of novae in the bulge of M31 and a search for their possible origin in the M31 globular cluster system 02 p0831 N94-13668
New IRAF stellar photometry software
05 p1925 N94-22464
In search of Nemesis 07 p2888 N94-28297

STELLAR STRUCTURE
A new approach to the study of the turbulence layer
[NASA-CR-194546] 04 p1487 N94-19397
Physical properties of dense astrophysical plasmas
05 p2001 N94-22637
Model development for Ulysses and SOHO
[NASA-CR-193884] 06 p2627 N94-24484

STELLAR SYSTEMS
ROSAT-IUE observations of symbiotic stars. The x ray morphology of high latitude associations
[NASA-CR-194616] 03 p1236 N94-16492
Study of the stellar populations of the Fornax dwarf spheroidal galaxy
[ISBN-0-315-85526-6] 08 p3541 N94-30231
Study of stellar associations located in the region contained between the Magellanic Clouds
[ISBN-0-315-86692-6] 09 p3935 N94-31913

STELLAR TEMPERATURE
Spectrophotometry of emission-line stars in the magellanic clouds
[NASA-CR-194082] 04 p1628 N94-19425
Model atmosphere analysis of selected luminous B stars
[NASA-CR-195098] 06 p2599 N94-24051
UV extinction and IR emission in diffuse H2 regions
[NASA-CR-195194] 06 p2600 N94-25270
Coronal temperatures of unusually active K-dwarf binary systems
[NASA-CR-189335] 08 p3545 N94-29861

STELLAR WINDS
The onset of galactic winds in early-type galaxies
[NASA-CR-193640] 02 p0836 N94-13446
Wind mass and energy deposition
[DE93-013345] 02 p0839 N94-14341
The astrophysical interpretation of isotope anomalies in graphite and SiC grains of chondrites
03 p1244 N94-16343
Unified NLTE model atmospheres including spherical extension and stellar winds, 4: Improved line transfer and wind contamination of H, He profiles
[MPA-905] 04 p1624 N94-17736
Spectrophotometry of emission-line stars in the magellanic clouds
[NASA-CR-194082] 04 p1628 N94-19425
Radiation driven winds of hot stars: Some remarks on stationary models and spectrum synthesis in time-dependent simulations
[NASA-CR-194691] 05 p2081 N94-21578
Asymptotic structure of magnetically driven MHD wind
05 p2008 N94-22682
Hydrodynamical winds from an accretion disk
05 p2008 N94-22683
MHD flows from compact objects: Effects on magnetic field configurations 05 p2008 N94-22684
Magnetic fields in spiral galaxies
05 p2010 N94-22697
X ray enhancement of SN 1987A due to interaction with its ring-like nebula
[NIFS-265] 06 p2602 N94-24867
Inhomogeneities in the wind from Wolf-Rayet stars
[ISBN-0-315-85893-1] 08 p3548 N94-30058
Evolution of stars and winds in the starburst galaxy M82 09 p3934 N94-31758
Winds from disks in compact binaries
[DE94-007452] 09 p3938 N94-32137
The evolutionary status of PSR 1259-63
[DE94-007094] 09 p3938 N94-32503
The winds of cataclysmic variables
[DE94-010897] 12 p4548 N94-37164

STELLARATORS
Transport mechanisms acting in toroidal devices: A theoretician's view
[DE93-013463] 01 p0385 N94-10310
Characterization of high-power RF structures using time-domain field codes
[DE93-013416] 01 p0132 N94-10518
Looking beyond ITER: Toroidal concept improvement
[DE93-012762] 01 p0388 N94-10744
Calculation of Mercier stability criterium in stellarators
[DE93-621599] 01 p0389 N94-11091
Possibilities of magnetic diagnostics in stellarators
[DE93-621608] 01 p0389 N94-11092
Charged particle motion in torsatrons, part 1
[DE93-621639] 01 p0389 N94-11119
Particle transport analysis in torsatron configurations
[DE93-621640] 01 p0390 N94-11120
Probability of particle trapping/detrapping in torsatrons
[DE93-621641] 01 p0390 N94-11121
Analytical description of the torsatron Uragan-2M magnetic configuration with account of plasma pressure and external correcting magnetic field
[DE93-620983] 01 p0391 N94-11174
Characteristics of ICR-produced peripheral plasma in the Uragan-3M torsatron
[DE93-621666] 01 p0392 N94-11214
Magnetic island suppression in torsatron configurations
[DE93-621681] 01 p0392 N94-11215
Ion cyclotron heating experiments and plans for the Advanced Toroidal Facility (ATF)
[DE93-012965] 02 p0795 N94-13033
Interferometric investigation methods of plasma spatial characteristics on stellarators and tokamaks in submillimeter region
[DE93-621606] 02 p0798 N94-13507
Nonlinear gyrofluid models of shear Alfven instabilities in ignited and beam heated toroidal plasmas
[DE93-016235] 03 p1203 N94-16869
Fast ion behavior during neutral beam injection in ATF
[DE93-040267] 05 p1992 N94-20058
Effects of magnetic field perturbations in the ATF torsatron
[DE94-000474] 05 p1999 N94-22568
Assessment of stellarators as reactors
[DE93-017775] 06 p2548 N94-22916
Overview of the ATF stellarator program
[DE94-000371] 06 p2550 N94-23462
Some theoretical problems of magnetic diagnostics in tokamaks and stellarators
[NIFS-262] 06 p2551 N94-24306
Pellet ablation in the large helical device
[NIFS-260] 06 p2551 N94-24358
Proposal of Modular Heliotron: Advanced modular helical system compatible with closed helical divertor
[NIFS-261] 06 p2552 N94-24458
Fusion reactor systems studies
[DE94-003162] 07 p3046 N94-27686
A 6MeV heavy ion beam probe for the Large Helical Device
[AD-B183695L] 08 p3505 N94-29397
The effect of magnetic field configuration on particle pinch velocity in Compact Helical System (CHS)
[AD-B183299L] 08 p3505 N94-29398
Efficiencies of the ICRF minority heating in the CHS and LHD plasmas
[AD-B183300L] 08 p3506 N94-29499
Overview of the US stellarator reactor study
[DE94-006042] 08 p3508 N94-30339
L-H confinement mode dynamics in three-dimensional state space
[DE94-007113] 09 p3887 N94-31396
Collisional and chaotic transport of energetic particles in toroidal plasma
[DE94-006504] 09 p3889 N94-31787
Stability of bootstrap current driven magnetic islands in stellarators
[DE94-009207] 09 p3893 N94-32912
Particle orbit analysis for LHD helical axis configurations
[DE94-718995] 11 p4336 N94-35773
Neoclassical current and related MHD stability, gap modes, and radial electric field effects in heliotron and torsatron plasmas
[DE94-718987] 11 p4337 N94-35938
Improved models of beta-limit, anomalous transport and radial electric field with loss cone loss in heliotron/torsatron
[DE94-718976] 11 p4324 N94-35984
Design study of LHD helical divertor and high temperature divertor plasma operation
[DE94-718975] 11 p4338 N94-36352
MHD and confinement characteristics in the high-beta regime on the CHS low-aspect-ratio heliotron/torsatron
[DE94-718981] 11 p4339 N94-36357
Confinement improvement in H-mode-like plasmas in helical systems
[DE94-727619] 12 p4528 N94-37231
STEP FAULTS
U GEOLOGICAL FAULTS
STEPPES
Evolution of the lower planetary boundary layer over strongly contrasting surfaces
[DE93-010667] 02 p0717 N94-14424
Parameterizing atmosphere-land surface exchange for climate models with satellite data: A case study for the Southern Great Plains CART site
[DE94-005109] 09 p3775 N94-32874
An experimental and numerical study of boundary layer structure over areas of inhomogeneous sensible heat fluxes
[DE94-011441] 12 p4474 N94-37565
Surface-layer response over shrub-steppe canopy during springtime
[DE94-011235] 12 p4468 N94-37624
STEPPING MOTORS
Tilt mechanism
[AD-D015780] 03 p1047 N94-16548
Control of torque in stepping motors of quartz watches and clocks 04 p1408 N94-18023
The One-Day Workshop on Batteries, Stepping Motors, and Electronic Clock Displays
[ETN-93-94632] 05 p1752 N94-20628
Lavet type stepping motors and associated controls 05 p1752 N94-20632
Test device for Lavet motors 05 p1752 N94-20633
The development of the SOHO SUMER mechanisms 06 p2361 N94-24028
Development of a Low-Temperature Gear Motor (LOG) 06 p2361 N94-24032
Magnetically suspended stepping motors for clean room and vacuum environments 11 p4225 N94-35915
STEREOCHEMISTRY
Microbial degradation of poly-b-esters: A mechanistic study, cellulose acetate biodegradability
[AD-A271368] 04 p1374 N94-19586
STEREOGRAPHY
U STEREOPHOTOGRAPHY
STEREOLITHOGRAPHY
U LITHOGRAPHY
STEREOPHONICS
Head related transfer function pseudo-stereophony
[NASA-CASE-ARC-11919-1-NP] 06 p2525 N94-23312
3D sound experimental approach: Methodology and preliminary results 12 p4486 N94-37280
STEREOPHOTOGRAPHY
On resolution of underwater stereo photogrammetry 01 p0172 N94-11966
A widget based operations simulator for a planetary camera: A model for the high resolution stereo camera on Mars 94
[DLR-FB-92-30] 02 p0651 N94-14044
Robust photo-topography by fusing shape-from-shading and stereo
[NASA-CR-194697] 05 p1806 N94-19920
The High Resolution Stereo Camera (HRSC) for the Lunar Scout 1 Mission 05 p1813 N94-20650
On line quantification of crystal surfaces by stereo imaging
[NASA-CR-195277] 07 p3066 N94-27561
The use of digital stereo photogrammetric methods in historical photo analysis
[AD-A275287] 08 p3288 N94-29437
STEREOSCOPIC PHOTOGRAPHY
U STEREOPHOTOGRAPHY
STEREOSCOPIC VISION
Close range 3-D position sensing using stereo vision and point-of-correspondance through mathematical morphology
[ISBN-0-315-61012-3] 02 p0763 N94-13515
Stochastic performance modeling and evaluation of obstacle detectability with imaging range sensors
[NASA-CR-194510] 02 p0605 N94-13946
Depths from focusing and defocusing
[AD-A266644] 02 p0735 N94-14797
ARPA unmanned ground vehicle stereo vision program at Teleos Research
[AD-A267632] 03 p1167 N94-17202
Neural basis of motion perception
[AD-A267267] 03 p1133 N94-17265
A stereoscopic vision system with applications to automated docking and tracking
[AD-A270754] 04 p1333 N94-19765
Why stereo vision is not always about 3D reconstruction
[AD-A270522] 05 p1939 N94-19893
Robust photo-topography by fusing shape-from-shading and stereo
[NASA-CR-194697] 05 p1806 N94-19920
A pyramid neural network architecture for stereo fusion 05 p1785 N94-22201
Stereo for gazing and converging cameras. Part 1: Basic geometry
[OUEL-1915/92] 06 p2343 N94-23162
Towards real-time stereovision systems for planetary missions 06 p2370 N94-23422
Parallel algorithm for dominant points correspondences in robot binocular stereo vision 07 p2686 N94-27364
An algorithm for stereo correspondence problems on the analogy of human vision
[NAL-TR-1185] 07 p2940 N94-27584
Visual surface perception: Surface reconstruction from shading and stereo
[ISBN-0-315-60974-5] 07 p2975 N94-27872
An investigation of stereopsis with AN/AVS-6 night vision goggles at varying levels of illuminance and contrast
[AD-A275332] 08 p3400 N94-28918
Automating geographically referenced digital mosaics from aerial videography with area-based feature matching 08 p3333 N94-29540
Stereo imaging based particle velocimeter
[NASA-CR-195800] 08 p3289 N94-29742
Navigation of military and space unmanned ground vehicles in unstructured terrains 08 p3144 N94-30282
Variable-resolution stereo matching 08 p3308 N94-30298
Obstacle detection for an autonomous vehicle 08 p3309 N94-30302
Stereoscopic correspondence based on the structure of shading
[ISBN-0-315-86418-4] 09 p3814 N94-31718
A neural network model for the visual perception of the depth of a scene from stereoscopy and shading
[ISBN-0-315-86753-1] 09 p3831 N94-31750
Effective declutter of complex flight displays using stereoptic 3-D cueing
[AD-A279764] 10 p3989 N94-33536
Low cost software-based rendering and stereoscopic interfaces for teleoperation and virtual reality 12 p4486 N94-37279
STEREOSCOPY
NT STEREOPHOTOGRAPHY
Preliminary studies on the application of ERS-1 data to topographic mapping 01 p0246 N94-12476
EOS workstation
[NASA-CR-191326] 02 p0736 N94-13132
Measurements of the spatial structure and directivity of 100 KeV photon sources in solar flares using PVO and ISEE-3 spacecraft
[NASA-CR-194080] 02 p0845 N94-14492
The 3-D Moons: The Voyager stereo atlas of the outer solar system 05 p2111 N94-20740
Multiple-camera/motion stereoscopy for range estimation in helicopter flight 06 p2441 N94-25505
Aurora stereo observation in Iceland 08 p3359 N94-29234
Using stereoscopic imaging for visualization applications
[DE94-006247] 08 p3536 N94-30706
Alternatives to hierarchical techniques in stereo correlation
[AD-A276570] 09 p3746 N94-31938
STERILIZATION
NT SPACECRAFT STERILIZATION
Comparison of numerical simulation and experimental data for steam-in-place sterilization 06 p2326 N94-23669
STERNS
U AFTERBODIES
STEROIDS
NT CHOLESTEROL
NT PROSTAGLANDINS
Phase-shifting effect of light and exercise on the human circadian clock
[AD-A265732] 02 p0732 N94-13038
Changes in plasma vasopressin during motion sickness in cats 05 p1885 N94-21898
STIELTJES INTEGRAL
On the asymptotically uniform distribution modulo 1 of extreme order statistics
[MEMO-COSOR-91-38-REV] 06 p2493 N94-23142
Two-point PADE approximants for Stieltjes series 06 p2490 N94-24768
STIFF STRUCTURES
U RIGID STRUCTURES
STIFFENING
Geometric stiffening in multibody dynamics formulations 02 p0677 N94-14619
Compression strength of composite primary structural components
[NASA-CR-194562] 04 p1457 N94-19350

Improvements to a method for the geometrically nonlinear analysis of compressively loaded stiffened composite panels
[NASA-CR-194715] 05 p1832 N94-21814
Post buckling behaviour of stiffened composite panels loaded in cyclic compression and shear
06 p2157 N94-24260
Stiffening of deployable space booms: Automated Protein Crystal Growth Facility
[NASA-CR-195547] 06 p2196 N94-24820
Investigation of the bond strength of a discrete skin-stiffener interface
[NLR-TP-92183-U] 07 p2670 N94-27796
Test and analysis results for composite transport fuselage and wing structures 09 p3628 N94-33129
Influence of an asymmetric ring on the modeling of an orthogonally stiffened cylindrical shell
[NASA-CR-195953] 10 p4070 N94-34262
Fatigue and residual strength behaviour of ARALL3 panels with bonded-on doublers
[AD-B181062] 11 p4279 N94-36226

STIFFNESS
Analytical models for describing the mechanical behavior of fiber reinforced composites
[AD-A265906] 01 p0074 N94-12347
Measuring methods for CFRP laminates' bending and torsion rigidities characteristics
02 p0529 N94-13272
Some frequency and damping measurements of laminated beryllium beams
[DE93-015909] 02 p0676 N94-14530
Packaging, deployment, and panel design concepts for a truss-stiffened 7-panel precision deployable reflector with feed boom
[NASA-TM-109000] 04 p1333 N94-17765
Analysis of high contact resistances associated with hermetic and lightning arrestor connectors
[DE93-014850] 04 p1395 N94-17783
Joint stiffness estimation based on force sensor measurements in industrial manipulators
[REPT-92-053] 04 p1443 N94-17937
Elastic properties of a polyimide film determined by Brillouin scattering and mechanical techniques
[DE93-017404] 04 p1368 N94-18098
A constitutive theory for rigid polyurethane foam
[DE93-011596] 04 p1372 N94-19059
Frequency and temperature dependence of high damping elastomers
[DE93-019539] 05 p1697 N94-19809
Compression strength of composite primary structural components
[NASA-CR-194561] 05 p1830 N94-20159
Graphite/polyurethane flexible composites: Mechanical and vibration damping properties
[AD-A271608] 05 p1674 N94-20950
A vibration model for centrifugal contactors
[DE93-040645] 05 p1833 N94-21927
Ceramic matrix composite parts design
06 p2256 N94-24237
Ultrasonic nondestructive evaluation as a tool for the development of aerospace structural ceramic composites 06 p2257 N94-24240
Post buckling behaviour of stiffened composite panels loaded in cyclic compression and shear
06 p2157 N94-24260
Attachment methods in composite joints - analysis of test results by controlled experiments method
06 p2158 N94-24269
Precision drive and speed reduction device
[AD-D016004] 06 p2367 N94-25046
Experimental and numerical vibration analyses of a stiffened panel
[VTT-PUBS-129] 07 p2836 N94-25650
Formulae for the buckling of simply-supported corrugated panels of orthotropic material under shear load
[PB94-126547] 07 p2840 N94-26911
Performance of a higher-order triangular finite element for composite laminated structures
08 p3181 N94-29810
Transient thermal fatigue of ceramic composites
08 p3216 N94-29874
Effect of elevated temperature and cyclic loading on properties and damage modes in ceramic composites
[DE94-008736] 09 p3662 N94-32891
Modeling the impact behavior of high strength ceramics
[AD-A277744] 10 p4028 N94-33894
An investigation of angular stiffness and damping coefficients of an axial spline coupling in high-speed rotating machinery 10 p4064 N94-34192
A test apparatus and facility to identify the rotordynamic coefficients of high-speed hydrostatic bearings
10 p4065 N94-34199
A waved journal bearing concept with improved steady-state and dynamic performance
10 p4065 N94-34200
Analysis of woven and braided fabric reinforced composites
[NASA-CR-194930] 10 p4020 N94-34399
Variable stiffness torsion springs
[NASA-CASE-MFS-28930-1] 12 p4509 N94-36782

STIFFNESS MATRIX
Approximation to sound radiation and scattering by simply supported layered cylinder
[AD-A272964] 05 p1967 N94-21306
Response statistics of shell structures with geometrical and material nonlinearities, volume 1
[ISBN-0-315-84006-4] 05 p1833 N94-22590
A multigrid solver for the semiconductor equations
06 p2482 N94-23674
Wavelet multiresolution analyses adapted for the fast solution of boundary value ordinary differential equations
06 p2485 N94-23691
Vibrations of variable cross section Timoshenko beams 06 p2160 N94-24279
On the error committed by stopping the Newton iteration in implicit Runge-Kutta methods
[TW-93-02] 07 p2992 N94-26229
Stiffness-generated rigid-body mode shapes for Lanczos eigensolution with SUPORT DOF by way of a MSC/NASTRAN DMAP alter
[NASA-TM-106537] 08 p3319 N94-29406
Experimental determination of orthotropic elastic constants
[FFA-TN-1991-35] 08 p3215 N94-29424
Closed form expressions for a consistent stress material nonlinear finite element 08 p3322 N94-30258
Minimization of computational requirements in the hybrid stress finite element method
[AD-A277120] 09 p3846 N94-32048
Distributed parameter modeling of repeated truss structures 11 p4218 N94-35868

STILBENE
Preparation of stable photopatternable polymeric materials for non-linear optics
[AD-A265359] 01 p0095 N94-12577

STIMULANTS
NT ATROPINE
NT CAFFEINE
NT CENTRAL NERVOUS SYSTEM STIMULANTS
NT NOREPINEPHRINE
Effects of methamphetamine and fatigue on long- and short-term memory
[AD-A276452] 09 p3799 N94-32187

STIMULATED EMISSION
Problems related to stimulated electromagnetic emissions, strong turbulence and ionospheric modification
[IRF-SR-212] 04 p1480 N94-17720
Experimental and theoretical features of strong suppression and shifting phenomena in odd-photon resonant excitations and stimulated emissions
[DE94-000341] 06 p2535 N94-24510
Computer modeling of nonlinearities
06 p2458 N94-24661
Two micron stimulated emission of activated insulating crystals
[REPT-94-002] 06 p2565 N94-25025
Numerical simulation and analysis of experimental results on stimulated Raman scattering in laser-plasma Hohlraum targets
[DE93-613719] 06 p2554 N94-25330
Light emitting porous silicon
[AD-A274152] 07 p3038 N94-27137
Observation of stimulated emission from an MBE grown GaN film on sapphire
[DE94-003638] 07 p3068 N94-27724
Spectroscopic and dynamical studies of highly energized small polyatomic molecules
[DE94-006509] 08 p3489 N94-30061
Basic study of the pumping of a gamma ray laser
[AD-A278537] 10 p4057 N94-33673

STIMULATED EMISSION DEVICES
NT AIRBORNE LASERS
NT ALUMINUM GALLIUM ARSENIDE LASERS
NT ARGON LASERS
NT ATMOSPHERIC LASERS
NT CARBON DIOXIDE LASERS
NT CARBON LASERS
NT CARBON MONOXIDE LASERS
NT CHEMICAL LASERS
NT CONTINUOUS WAVE LASERS
NT DISTRIBUTED FEEDBACK LASERS
NT DYE LASERS
NT EXCIMER LASERS
NT FREE ELECTRON LASERS
NT GALLIUM ARSENIDE LASERS
NT GAMMA RAY LASERS
NT GAS LASERS
NT GASDYNAMIC LASERS
NT GLASS LASERS
NT HELIUM-NEON LASERS
NT HF LASERS
NT HIGH POWER LASERS
NT HYDROGEN MASERS
NT INFRARED LASERS
NT INTERSTELLAR MASERS
NT IODINE LASERS
NT KRYPTON FLUORIDE LASERS
NT LASERS
NT LIQUID LASERS
NT MASERS
NT METAL VAPOR LASERS
NT NEODYMIUM LASERS
NT NITROGEN LASERS
NT NOVA LASER SYSTEM
NT NUCLEAR PUMPED LASERS
NT PULSED LASERS
NT Q SWITCHED LASERS
NT QUANTUM WELL LASERS
NT RAMAN LASERS
NT RING LASERS
NT RUBY LASERS
NT SEMICONDUCTOR LASERS
NT SOLAR-PUMPED LASERS
NT SOLID STATE LASERS
NT SPACEBORNE LASERS
NT SURFACE EMITTING LASERS
NT TEA LASERS
NT TUNABLE LASERS
NT TWO-WAVELENGTH LASERS
NT ULTRASHORT PULSED LASERS
NT ULTRAVIOLET LASERS
NT WATER MASERS
NT WAVEGUIDE LASERS
NT X RAY LASERS
NT XENON CHLORIDE LASERS
NT YAG LASERS
NT YLF LASERS

STIMULATION
NT AUDITORY STIMULI
NT SENSORY STIMULATION
Recovery of the vomiting reflex following area postrema ablation in squirrel monkeys 05 p1886 N94-21904
Motion sickness elicited by passive rotation in squirrel monkeys 05 p1887 N94-21905
Immunocytochemical localization of glutamic acid decarboxylase (GAD) and substance P in neural areas mediating motion-induced emesis: Effects of vagal stimulation on GAD immunoreactivity
05 p1887 N94-21909
Experimental studies of gastric dysfunction in motion sickness: The effect of gastric and vestibular stimulation on the vagal and splanchnic gastric efferents
05 p1888 N94-21911
Radar stimulator interface protocol, preliminary interface design and Doppler Beam Sharpening implementation
[DE94-002567] 06 p2453 N94-23701
Convective instabilities in traveling fronts of addition polymerization 06 p2226 N94-24352
Endogeneous and exogenous control of visual selection: A review of the literature
[AD-A273761] 07 p2908 N94-25871
Development of stimulus-seeking scale for expecting individual differences against confinement stress
07 p2915 N94-27460
Effect of PGE2 receptor agonists butaprost, M and B 28767 and an antagonist AH 6809 on the BK response of visceral polymodal receptors
07 p2906 N94-27494
Analysis of the Electrically Evoked Response (EER) of the cat 07 p2908 N94-27519
Electrical stimulation in exercise training
07 p2935 N94-28371
The value of electrical stimulation as an exercise training modality 07 p2936 N94-28372

STIRLING CYCLE
The superfluid Stirling refrigerator, a new method for cooling below 0.5 K
[DE93-012672] 01 p0128 N94-11161
Three-stage linear, split-Stirling cryocooler for 1 to 2K magnetic cold stage
[NASA-CR-4538] 02 p0776 N94-13897
A recuperative superfluid Stirling refrigerator
[DE93-016521] 02 p0597 N94-14592
Proposed guidelines for reporting performance of a solar dish/Stirling electric generation system
[DE93-016493] 03 p1092 N94-16112
Performance mapping of the STM4-120 kinematic Stirling engine using a statistical design of experiments method
[DE93-015132] 04 p1464 N94-17798
The 7th International Cryocooler Conference
[AD-A268451] 04 p1379 N94-18147

Regenerator optimization for Stirling cycle refrigeration
[DE93-018468] 04 p1380 N94-18818
Preliminary SP-100/Stirling heat exchanger designs
[NASA-TM-106444] 05 p1670 N94-21809
Controllability of free-piston Stirling engine/linear alternator driving a dynamic load
[NASA-TM-106497] 06 p2521 N94-24302
Performance of the Southern California Edison Company Stirling dish
[DE94-004676] 08 p3337 N94-29018
The 4 K Stirling cryocooler demonstration
[NASA-CR-191792] 09 p3669 N94-32484
Detail design of a 10.4-m stretched-membrane dish
[DE94-009462] 10 p4079 N94-34167
A precise passive narrow-beam filter infrared radiometer and its use with LIDAR in the ARM program
[DE94-004167] 11 p4269 N94-36085

STIRLING ENGINES

Establishing baseline data for an experimental appratus that measures heat transfer under conditions of oscillating pressure and flow
[NASA-CR-193772] 01 p0413 N94-12343
Futurepath 2
[NASA-TM-109285] 02 p0518 N94-13623
Insoluble coatings for Stirling engine heat pipe condenser surfaces
[NASA-CR-191188] 02 p0554 N94-14771
SPDE/SPRE final summary report
[NASA-CR-187086] 03 p0924 N94-15482
Proposed guidelines for reporting performance of a solar dish/Stirling electric generation system
[DE93-016493] 03 p1092 N94-16112
Performance mapping of the STM4-120 kinematic Stirling engine using a statistical design of experiments method
[DE93-015132] 04 p1464 N94-17798
The FY1992 survey on commercialization of Stirling engine utilization equipment
[DE94-707416] 05 p1849 N94-22029
Performance of the Southern California Edison Company Stirling dish
[DE94-004676] 08 p3337 N94-29018
Oscillating-flow loss test results in rectangular heat exchanger passages
[NASA-CR-185297] 09 p3615 N94-32792
A 1050 K Stirling space engine design
[NASA-CR-182149] 09 p3616 N94-32866
The Stirling engine
[NASA-TM-109832] 10 p4059 N94-33586
Detail design of a 10.4-m stretched-membrane dish
[DE94-009462] 10 p4079 N94-34167

STIRRING

Hydrodynamics of stirred gas-liquid dispersions
[ETN-94-95368] 06 p2339 N94-25254
Study on melted solution stirring under microgravity
07 p2730 N94-25585

STISHOVITE

Shock induced reaction in Chicxulub target materials (CaSO4 and SiO2) and their relation to extinctions
01 p0282 N94-12149

STOCHASTIC PROCESSES

NT MARKOV CHAINS
NT MARKOV PROCESSES
NT RANDOM PROCESSES
NT RANDOM WALK

Canonical operator formulation of nonequilibrium thermodynamics
[DE93-613028] 01 p0409 N94-10388
A multi-variance analysis in the time domain
01 p0146 N94-10999
Kinetic effects in stochastic topologically nontrivial field
[DE93-621642] 01 p0391 N94-11207
Simple kinetic model for plasma in stochastic helical field
[DE93-621643] 01 p0391 N94-11208
Experimental investigation of wake field excitation in plasma by a periodic succession of relativistic particle clots
[DE93-621655] 01 p0391 N94-11211
Further studies using matched filter theory and stochastic simulation for gust loads prediction
[NASA-TM-109010] 01 p0026 N94-11587
A stochastic-deterministic approach as an alternative to classical cross-over techniques in small ocean basins
01 p0242 N94-11767
Nonlinear resonance: Noise-assisted information processing in physical and neurophysiological systems
[AD-A265161] 01 p0313 N94-11890
Mapping closures for turbulent combustion
[AD-A265671] 01 p0079 N94-12378
Ocean acoustic processing: A model-based approach
[DE93-011902] 02 p0725 N94-12876
Stochastic dynamics: Crossover from 1/f(sup 3) to flicker noise
[DE93-622862] 02 p0772 N94-12896
Investigation for improving Global Positioning System (GPS) orbits using a discrete sequential estimator and stochastic models of selected physical processes
[NASA-CR-194167] 02 p0512 N94-13082
A stochastic model for behavior analysis of fiber-reinforced quasi-brittle materials
02 p0672 N94-13594
Robust synthesis of discrete-time multivariable control systems with induced delays 02 p0662 N94-13642
Stochastic realization of finite-valued processes and primes in the positive matrices
[CWI-BS-R9222] 02 p0773 N94-13677
Observation of the coalescing of beam into an asymmetric RF bucket by stochastic cooling
[DE93-015133] 02 p0783 N94-13895
Stochastic performance modeling and evaluation of obstacle detectability with imaging range sensors
[NASA-CR-194510] 02 p0605 N94-13946
On the geometry of external spectral factors and the Riccati inequality
[CWI-BS-R9227] 02 p0770 N94-14002
Stochastic scheduling games with Markov decision arrival processes
[CWI-BS-R9231] 02 p0773 N94-14005
Tuning of Gaussian stochastic control systems
[CWI-BS-R9223] 02 p0765 N94-14018
Hybrid S(sub N)/Monte Carlo research and results
[DE93-012677] 02 p0773 N94-14178
Stochastic bounds for a polling system
[CWI-BS-R9230] 02 p0765 N94-14361
Inflow characteristics associated with high-blade-loading events in a wind farm
[DE93-010042] 02 p0704 N94-14423
Investigations of transitions from order to chaos in dynamical systems
[DE93-014438] 02 p0818 N94-14738
Stochastic modeling of turbulent reacting flows
02 p0647 N94-14768
Functional differential equations with piecewise continuous argument
[AD-A266660] 02 p0772 N94-14840
Determining neural network connectivity using evolutionary programming
[AD-A266853] 02 p0766 N94-14882
Looking at Fokker-Planck dynamics with a noisy instrument
[AD-A267049] 03 p1117 N94-15662
Theoretical studies relating to the interaction of radiation with matter
[AD-A267134] 03 p1180 N94-15689
Segment-based acoustic models for continuous speech recognition
[AD-A267138] 03 p0988 N94-15691
Stochastic scheduling in in-forest networks
[INRIA-RR-1719] 03 p1164 N94-15695
Efficient algorithmic techniques for combinatorial problems
[AD-A267151] 03 p1172 N94-15777
Generation of artificial helioseismic time-series
[NASA-CR-194612] 03 p1299 N94-15968
A novel approach for structural mechanics problems with stochasticity
[AD-A266189] 03 p1059 N94-16123
Interferometric GPS attitude: A stochastic error model, DREO report
[AD-A266411] 03 p0864 N94-16457
Stochastic damage evolution in textile laminates
03 p0939 N94-16861
Nonlinear analysis of mechanical systems under combined harmonic and stochastic excitation
[AD-A266217] 03 p1173 N94-16937
Stochastic chaos: An analog of quantum chaos
[DE93-016619] 03 p1220 N94-16956
A handbook of cost risk analysis methods
[AD-A267253] 03 p1235 N94-16988
An approximation for computing reduction in bandwidth requirements using intelligent multiplexers
[AD-A267434] 03 p1001 N94-17026
Energy deposition fluctuations induced by ions in microvolumes and nanovolumes: An analytic approach. 1: Theory
[AD-A267959] 03 p1173 N94-17495
Stochastic scheduling in a multiclass G/G/1 queue
[INRIA-RR-1746] 03 p1162 N94-17537
State space partitioning methods for solving a class of stochastic network problems
[AD-A267494] 03 p1173 N94-17585
Planning under uncertainty solving large-scale stochastic linear programs
[DE93-013920] 04 p1516 N94-17701
Data fusion through simulated annealing of registered range and reflectance images
[DE93-015910] 04 p1612 N94-17858
Stochastic models of attention and search
[AD-A268622] 04 p1508 N94-18292
JSEP fellowship: Fractal noise processes
[AD-A268841] 04 p1557 N94-18540
Development of the microstructure based stochastic life prediction models
[AD-A269880] 04 p1454 N94-18683
Development of the microstructure based stochastic life prediction model
[AD-A269742] 04 p1361 N94-18742
Coupled neural-dendritic processes: Cooperative stochastic effects and the analysis of spike trains
[AD-A270041] 04 p1506 N94-18793
Statistical learning theory and algorithms
[AD-A270209] 04 p1523 N94-18901
Adaptive path planning: Algorithm and analysis
[DE93-008348] 04 p1523 N94-18926
A numerical study of hybrid optimization methods for the molecular conformation problems
[DE93-017898] 04 p1569 N94-18985
A simple calculus of finite probabilistic processes
[MEMO-INF-93-08] 04 p1558 N94-19195
Stochastic grammars: Theory and applications
[PB94-149556] 04 p1528 N94-19262
Excursions of stochastic processes, Cox-point processes, entrance behavior and resolvents
[PB93-197291] 04 p1558 N94-19323
The brain electrical activity in different G situations
[AERONAUTICA-ACTA-A-372-1993] 04 p1507 N94-19523
Equivalence and reduction of hidden Markov models
[AD-A270762] 04 p1560 N94-19768
Stochastic optimization by simulation: Numerical experiments with M/M/1 queue in steady-state
[AD-A271143] 05 p1949 N94-19854
Robust, high-speed network design for large-scale multiprocessing
[AD-A271003] 05 p1716 N94-19977
SIMBAT theoretical manual
[AD-A271063] 05 p1882 N94-19979
Stochastic optimization by simulation: Convergence proofs for the G1/G/1 queue in steady-state
[AD-A271141] 05 p1962 N94-19999
Stochastic differential equations and numerical simulation for pedestrians
[DE93-040651] 05 p1949 N94-20006
Asymptotics of the GLRT for the disorder problem in diffusion processes
[INRIA-RR-1735] 05 p1951 N94-20227
A general rough-surface inversion algorithm: Theory and application to SAR data 05 p1719 N94-20407
Closure properties of stochastic languages
[TR-441] 05 p1907 N94-20521
Segment-based acoustic models for continuous speech recognition
[AD-A271483] 05 p1736 N94-20547
The Seventh International Symposium on Methodologies for Intelligent Systems (Poster Session)
[AD-A272125] 05 p1942 N94-20573
Space-efficient deterministic simulation of probabilistic automata
[TR-463] 05 p1900 N94-21281
Dependability and performability analysis
[NASA-CR-191565] 05 p1965 N94-21463
Simulated behaviour of large scale SCI rings and tori
[DE93-040149] 05 p1935 N94-21745
Stochastic simulation for imaging spatial uncertainty: Comparison and evaluation of available algorithms
[DE93-040058] 05 p1916 N94-21761
Algorithmic advances in stochastic programming
[DE94-001160] 05 p1921 N94-22406
Experiments with recursive estimation in astronomical image processing 05 p2047 N94-22457
Nonlinear smoothing for random fields
[PB94-149531] 06 p2493 N94-22728
Mean-value of product-form stochastic Petri net models of slotted-ring systems
[PB94-110871] 06 p2494 N94-23749
A mixed map/variable structure observer for target tracking 06 p2157 N94-24263
Maximum likelihood modal parameter identification and realization of stochastic systems
06 p2157 N94-24265
Uniform limit theorems for marked point processes
[PB94-118726] 06 p2488 N94-24526
Probabilistic methods in problems of applied analysis
[PB94-110681] 06 p2495 N94-24571
Evolving neural network connectivity
[AD-A273134] 06 p2490 N94-24921
Change-point detection and adaptive control of time-varying systems
[AD-A273509] 06 p2475 N94-24943
Statistical methods in physical oceanography
[AD-A273612] 06 p2419 N94-24948
Determining neural network hidden layer size using evolutionary programming
[AD-A273242] 06 p2475 N94-25139

An exploratory stochastic model for toxic effects on cells
[AD-A273438] 06 p2422 N94-25146
An attempt at a macrorealistic quantum worldview
[DE93-616821] 06 p2570 N94-25206
Approximation to nonlinear equations using nonlinear rational models
[RR-448] 06 p2492 N94-25306
The anomalous transport caused by particles transverse drift
[DE93-613685] 06 p2554 N94-25329
The application of simulated annealing to stochastic systems
[AD-A273850] 07 p3001 N94-25607
Stochastic resonance in a periodic potential system under a constant force
[DE93-616817] 07 p3008 N94-25831
Modeling defect production in high energy collision cascades
[DE94-003810] 07 p3017 N94-26049
Towards a theory of growing surfaces: Mapping two-dimensional Laplacian growth onto Hamiltonian dynamics and statistics
[DE94-002636] 07 p2991 N94-26079
Eleventh Symposium on Energy Engineering Sciences: Proceedings
[DE93-019930] 07 p2763 N94-26429
Cone-valued Lyapunov functions and the stability of stochastic differential equations
[DE94-601504] 07 p2994 N94-26458
About stochastization of motion of charged particles in geomagnetic field and in the field of a wave packet
[DE93-634309] 07 p2879 N94-26502
Stochastic solution to quantum dynamics
[NASA-TP-3408] 07 p3114 N94-26550
Modeling systems by probabilistic process algebra: An event structures approach
[PB94-125259] 07 p3004 N94-26867
Recursive bundle event structures
[PB94-125275] 07 p3004 N94-26870
Single-server queues with spatially distributed arrivals
[PB94-126638] 07 p2986 N94-26916
A superprocess with a disappearing self-interaction
[AD-A274647] 07 p3009 N94-27108
White noise theory of robust nonlinear filtering with correlated state and observation noises
[PB94-126661] 07 p3004 N94-27211
Stochastic space-time, confinement potential and particle propagator
[DE94-606415] 07 p3074 N94-27680
Temporal stochasticity leads to nondeterministic chaos in a model for blood cell production
[DE94-003943] 07 p2933 N94-27744
Modulating terrestrial impacts from Oort cloud comets by the adiabatically changing galactic tides
07 p2890 N94-28305
Research activities of Martin C. Casdagli at SFI September 1989--May 1991
[DE94-005655] 08 p3463 N94-28548
Derivation of a Fokker-Planck equation for bunched beams
[DE94-004950] 08 p3483 N94-28565
The lectures in complex systems, volume 5
[AD-A275458] 08 p3466 N94-28807
The modified Cramer-von mises goodness-of-fit criterion for time series
[AD-A275377] 08 p3464 N94-29014
Stability of dynamical systems in the presence of noise
[AD-A275383] 08 p3243 N94-29072
Hierarchical structures and asymmetric stochastic processes on p-adics and adeles
[PB94-138203] 08 p3464 N94-29178
On-line search for optimal controller parameters using interconnected learning automata
[MATHS-REPT-A-196] 08 p3436 N94-29526
Effects of diffusion and inertia on chaotic mixing: A computational and experimental study
08 p3488 N94-29903
Stochastic stability and nonlinear control in mechanical systems 08 p3303 N94-29966
Exclusive many-particle diffusion in disordered media and correlation functions for random vertex models
[DE94-608134] 08 p3525 N94-30121
Langmuir waves in the electron-positron plasma
[DE94-608330] 08 p3508 N94-30191
A stochastic control approach to flight path monitoring
[AD-B174630] 08 p3143 N94-30853
Theory for electron-transfer reactions involving two Marcus surfaces with a different force constant
[DE94-005925] 08 p3493 N94-30874
Theory for electron-transfer reactions in a three-component system: The degenerate regime
[DE94-005919] 08 p3493 N94-30903
The ant system: An autocatalytic optimizing process
[REPT-91-016-REV] 09 p3824 N94-31177
Representation, prediction and identification of cyclostationary processes: A state-space approach
[REPT-93-041] 09 p3850 N94-31191
Near resonant absorption by atoms in intense fluctuating laser fields
[DE94-005873] 09 p3714 N94-31200
Towards simplicity: Noise and cooperation in the perfect integrator
[AD-A276256] 09 p3799 N94-31291
Identification of polynomial and rational NARMAX models
[RR-483] 09 p3842 N94-31413
Light-traffic analysis for queues with spatially distributed arrivals
[MEMO-1150] 09 p3832 N94-31826
On the convergence of stochastic iterative dynamic programming
[AD-A276517] 09 p3815 N94-31933
Utility-based planning
[NASA-CR-195878] 09 p3816 N94-32086
Modeling and control of nonlinear systems
[AD-A277377] 09 p3834 N94-32095
Kaplan-Meier estimators of interpoint distance distributions for spatial point processes
[CWI-BS-R9315] 09 p3846 N94-32107
Atmospheric structure simulation: An autoregressive model for smooth geophysical power spectra with known autocorrelation function
[AD-A276691] 09 p3773 N94-32118
Multiserver queues with impatient customers
[CWI-BS-R9319] 09 p3835 N94-32198
Stochastic realization of a Gaussian stochastic control system
[CWI-BS-R9320] 09 p3852 N94-32350
Notes on the Langevin model for turbulent diffusion of marked particles
[DE94-007847] 09 p3708 N94-32652
State-space self-tuner for on-line adaptive control
[NASA-CR-195836] 09 p3835 N94-32943
Stochastic models in reliability theory
[AD-A277529] 09 p3731 N94-32953
SynRGen: An extensible file reference generator
[AD-A277678] 09 p3821 N94-33030
On the minimum of independent geometrically distributed random variables
[AD-A279629] 09 p3821 N94-33075
Adaptive control of nonlinear and stochastic systems
[AD-A278411] 09 p3839 N94-33325
An investigation of simulated annealing applied to structural optimization problems
[AD-A278461] 10 p4068 N94-33541
Stochastic models of attention and search
[AD-A278538] 10 p4097 N94-33674
On stochastic approximation algorithms for classes of PAC learning problems
[DE94-007417] 10 p4113 N94-33690
Analysis of stochastic particle behavior in a magnetic island due to electrostatic drift waves
[DE94-727553] 10 p4137 N94-33869
Enhanced algorithms for stochastic programming
[DE94-009423] 10 p4106 N94-33912
Reinforcement learning in scheduling
10 p4099 N94-34045
Differential GPS positioning: DGPS modelling using pseudo range observations
[PB94-149697] 10 p3988 N94-34113
Time delay measurement correlator and its application
10 p4042 N94-34350
Developing interpretable models with optimized set reduction for identifying high risk software components
11 p4301 N94-35435
Stopping rules for a class of sampling-based stochastic programming algorithms
[AD-A278654] 11 p4303 N94-35577
Cramer-von Mises variance estimators for simulations
[AD-A278799] 11 p4316 N94-35675
Effects of noise variance model on optimal feedback design and actuator placement
11 p4220 N94-35883
Design and evaluation of a Stochastic Optimal Feed-forward and Feedback Technology (SOFFT) flight control architecture
[NASA-TP-3419] 12 p4388 N94-37014
Segment-based acoustic models for continuous speech recognition
[AD-A280332] 12 p4434 N94-37032

STOCKPILING
Replacement of silicone polymer A with silicone polymer B and the subsequent characterization of the new cellular silicone materials
[DE94-010105] 12 p4421 N94-36474

STOICHIOMETRY
Synthesis and magnetic properties of novel La*2-x*M*x*CuO*4 equals y* compositions (La equals La, Pr, Nd, Sm, Eu, Cd; M equals Ca, Sr, Ba; O (less than or equal) x 0.2; -0.5 (less than or equal) y (less than or equal) 0.5)
[DE93-011359] 01 p0403 N94-12363
Unexpectedly rapid hydrosilation polymerization of the diallyl derivative of bisphenol A and 2,6-diallylphenol
[AD-A265832] 02 p0577 N94-12986
Gas atomized Er3Ni powder for cryocooler applications
[DE93-011564] 02 p0568 N94-13000
MeV ion-beam analysis of optical data storage films
03 p1226 N94-14984
Scintillation mechanism in stoichiometric cerium compounds
[DE93-015499] 03 p0948 N94-16771
Transient phenomena following precipitation and re-solution anneals in a NiTi alloy
[AD-A267557] 03 p0961 N94-17106
Laser-deposited biocompatible films and methods and apparatuses for producing same
[AD-D016017] 06 p2350 N94-24952
Ferroelectric thin film microstructure development and related property enhancement
[DE94-002741] 07 p3061 N94-26856
Numerical simulation of the reignition of detonation by reflected shocks
[AD-A274755] 07 p2795 N94-27252
Terfenol: A study of the phase equilibrium diagram and the solidification process
[DE94-004883] 08 p3209 N94-30690
Influence of surface defects and local structure on oxygenate reaction pathways over metal oxide surfaces
[DE94-005680] 08 p3522 N94-30901
Properties of doped and undoped (Ca,Sr)CuO2 thin films
[DE94-007230] 09 p3905 N94-32785

STOKES FLOW
Surface path lines in plane Stokes flow driven by capillarity
[DE93-041277] 05 p1803 N94-21651
Mixed finite element and finite volume methods
[ISBN-0-315-63035-3] 05 p1805 N94-22417
Mathematical addenda to Hopper's model of plane stokes flow driven by capillarity on a free surface
[PB93-237691] 06 p2480 N94-23438
BEM solution for the simulation of axisymmetric viscous sintering
[PB93-237717] 06 p2336 N94-24761
A thermodynamically consistent constitutive theory for a rigid solid-stokesian fluid mixture
[DE93-633202] 07 p2792 N94-26401

STOKES LAW (FLUID MECHANICS)
Numerical simulation of multi-droplet hydrodynamic interactions in liquid dispersions
01 p0114 N94-10182

STOKES THEOREM (VECTOR CALCULUS)
Geoid determination: With help of the alternative scattering method
[ETN-94-95375] 07 p2847 N94-25746

STOL AIRCRAFT
U SHORT TAKEOFF AIRCRAFT

STOMACH
Detection of emetic activity in the cat by monitoring venous pressure and audio signals
05 p1886 N94-21903
The effects of area postrema lesions and selective vagotomy on motion-induced conditioned taste aversion
05 p1888 N94-21910
The electrogastrogram during parabolic flight
07 p2913 N94-27452

STONES (ROCKS)
U ROCKS

STONY METEORITES
NT ACHONDRITES
NT ALLENDE METEORITE
NT AUSTRALITES
NT BONDOC METEORITE
NT BRUDERHEIM METEORITE
NT CARBONACEOUS CHONDRITES
NT CARBONACEOUS METEORITES
NT CHASSIGNITES
NT CHONDRITES
NT COLD BOKKEVELD METEORITE
NT KAPOETA ACHONDRITE
NT MURCHISON METEORITE
NT MURRAY METEORITE
NT NAKHLITES
NT ORGUEIL METEORITE
NT SHERGOTTITES
NT TEKTITES
NT UREILITES

Size distribution of interplanetary iron and stony particles related with deep-sea spherules
03 p1245 N94-16388

STONY-IRON METEORITES
Metal-rich meteorites from the aubrite parent body
01 p0430 N94-12142
Experimental segregation of iron-nickel metal, iron-sulfide, and olivine in a thermal gradient: Preliminary results
03 p1243 N94-16288
A new Antarctic meteorite with chromite, orthopyroxene and metal with reference to a formation model of S asteroids
05 p2084 N94-20813
Chemical zoning and diffusion of Ca, Al, Mn, and Cr in olivine of springwater pallasite 05 p2086 N94-20902
More shock recovery experiments on mesosiderite analogs
11 p4351 N94-35455

STOPPING
General optimal stopping theorems for semi-Markov processes
[PB93-214989] 06 p2496 N94-24744
Modular termination proofs for logic and pure PROLOG programs
[CWI-CS-R9316] 07 p2970 N94-27544
An analysis of stopping criteria in artificial neural networks
[AD-A278491] 10 p4113 N94-33755

STOPPING POWER
Experimental efforts and results in finding new heavy scintillators
[DE93-010406] 01 p0371 N94-10156
Stopping powers and cross sections due to two-photon processes in relativistic nucleus-nucleus collisions
[NASA-CR-4574] 07 p3033 N94-27646
Calculation of inelastic mean free path and stopping power for electrons in solids from an optical-data model
[USIP-92-06] 08 p3494 N94-30980
Comment on observation of the striking departure from velocity proportionality in low-energy electronic stopping
[DE94-009821] 10 p4138 N94-34242
Stopping power of charged particles from 10 eV/amu to 10 GeV/amu
[DE94-719024] 12 p4518 N94-37387

STORABLE PROPELLANTS
Ageing studies on a composite propellant containing a new organo-copper burn rate catalyst
[AD-A271060] 05 p1711 N94-19906
Small rocket research and technology
06 p2211 N94-23038

STORAGE BATTERIES
NT LEAD ACID BATTERIES
NT NICKEL CADMIUM BATTERIES
NT NICKEL HYDROGEN BATTERIES
NT NICKEL ZINC BATTERIES
NT SILVER ZINC BATTERIES
NT ZINC-BROMIDE BATTERIES
Primary and secondary electrical space power based on advanced PEM systems
[DE93-012643] 02 p0553 N94-14689
In situ Raman spectroscopy of lithium electrode surface in ambient temperature lithium secondary battery
[DE93-015238] 03 p1010 N94-16061
Field investigation of the relationship between battery size and PV system performance
[DE93-016503] 03 p1016 N94-17671
Mechanically refuelable zinc/air electric vehicle cells
[DE93-016446] 04 p1394 N94-17770
Surveys on specific patterns of facility intallation of photovoltaic power generating technologies for international cooperation
[DE94-714901] 05 p1850 N94-22092
Space Electrochemical Research and Technology
[NASA-CP-3228] 06 p2390 N94-23345
Primary and secondary electrical space power based on advanced PEM systems 06 p2392 N94-23357
High energy density aluminum-oxygen cell
06 p2393 N94-23363
Overcharge and overdischarge protection of ambient temperature secondary lithium cells
[NASA-CASE-NPO-18343-1-CU]
06 p2310 N94-23823
Method of optimizing the charging of a battery of storage cells, and apparatus for performing the method
[AD-D016066] 07 p2781 N94-26102
Development of nickel-metal hydride cell: An update
07 p2864 N94-28130
Ni-MH storage test and cycle life test
07 p2864 N94-28131
Determination of thermal properties of commercial Ni-MH cells 07 p2864 N94-28132
Method for forming thin composite solid electrolyte film for lithium batteries
[NASA-CASE-NPO-18877-1-CU]
08 p3264 N94-29357
Dendrite preventing separator for secondary lithium batteries
[NASA-CASE-NPO-18585-1-CU]
08 p3265 N94-29411
NEMO: Advanced energy systems and technologies
[DE94-721996] 09 p3760 N94-31767
Performance of the Sony lithium-ion rechargeable battery
[AD-A277076] 09 p3693 N94-32303
Development of nickel and metal hydride secondary battery
[DE94-757270] 09 p3697 N94-32917
Field operation test of utility interactive load conditioner with photovoltaic cells at a demonstration house
[DE94-757271] 09 p3762 N94-32918
Optimal planning of residential photovoltaic systems under various rate structure
[DE94-757272] 09 p3762 N94-32919
Sodium/nickel-chloride battery development
[DE94-011481] 12 p4437 N94-37053

STORAGE RINGS (PARTICLE ACCELERATORS)
Radiation hardness of Mo/Si multilayers designed for use in a soft x ray projection lithography system
[DE93-011879] 01 p0143 N94-11273
Recent study of beam stability in the PSR
[DE93-014473] 02 p0780 N94-13173
Construction of the Courant-Snyder invariants for the non-linear equations of motion under presence of the linear coupling
[DE93-017565] 02 p0788 N94-14872
Fundamental-mode RF design in e(+)e(-) storage ring factories
[DE93-015249] 03 p1183 N94-16809
The stability of ions in a storage ring in the presence of small gap insertion devices
[DE93-015387] 03 p1184 N94-16828
Simulation of emittance dilution in electron storage ring from Compton backscattering
[DE93-017611] 04 p1386 N94-18503
Effects of transverse coupling on transverse beam size, simulation and measurements
[DE93-017804] 04 p1574 N94-18972
Simulation of the ALS longitudinal multibunch feedback system
[DE93-019227] 04 p1575 N94-19152
Study of coupled-bunch collective effects in the ALS
[DE93-019236] 04 p1575 N94-19558
Control and readout of the extraction septum of AmPS
[DIGEL-1993-2] 05 p1979 N94-20117
New preamplifiers for the SEM scanner
[DIGEL-1993-3] 05 p1979 N94-20118
Bundle profile monitor for AmPS
[DIGEL-1992-8] 05 p1979 N94-20123
Study of coupled-bunch collective effects in the PEP-2 B-Factory
[DE93-040117] 05 p1979 N94-20274
Measurement and computation of the higher order modes of the ALS 500 MHz accelerating cavities
[DE93-019256] 05 p1980 N94-20292
Energy and luminosity limits of hadron supercolliders
[DE93-019248] 05 p1980 N94-20300
Power supply and controller for the Sextupole magnet of AmPS
[DIGEL-1992-3] 05 p1753 N94-21064
Survey and alignment analysis for the ALS storage ring using computer spreadsheets
[DE93-019254] 05 p1917 N94-21917
Studies of the deuteron at high energy and momentum transfer
[DE93-041162] 05 p1976 N94-21941
Proceedings of the Fifth Users Meeting for the Advanced Photon Source
[DE93-040692] 06 p2531 N94-22948
RF-station control crate
[DIGEL-1992-9] 07 p2779 N94-25618
Alignment of the Amsterdam Pulse Stretcher (AmPS)
[MTG-93-02] 07 p2809 N94-25637
Technical report of ISSP. Ser. A, no. 2688: Suppression of higher-order modes in an RF cavity by resistive material
[JTN-94-80574] 07 p2787 N94-27606
Physics at HERA
[DE94-005117] 08 p3483 N94-28569
Tuning of AmPS
[NIKHEF-K-AMPS-93-01] 08 p3494 N94-29422
BPM901N monitor electronics for the determination of the bundle profile in the extraction line of AmPS
[DIGEL-1993-9] 08 p3495 N94-29467
Activity report of Synchrotron Radiation Laboratory 1992
[JTN-94-80600] 08 p3495 N94-29596
Stripline monitor electronics for the bundle position determination in AmPS
[DIGEL-1993-8] 08 p3495 N94-29888
The measurement of the hadronic energy flow and jet production with the ZEUS calorimeter in deep inelastic scattering events at HERA
[ETN-94-96021] 09 p3865 N94-31534
Results from the H1 experiment at HERA
[PB94-145174] 09 p3868 N94-32008
Spin dynamics in storage rings and linear accelerators
[DE94-010320] 11 p4330 N94-36106
Dynamic aperture and transverse proton diffusion in HERA
[DE94-010309] 11 p4331 N94-36224
Direct photoproduction of jets in the k(T)-factorisation prescription
[PB94-171139] 12 p4513 N94-36549
High Energy Physics Division of research activities
[DE93-019681] 12 p4521 N94-36694
Determination of the upsilon(1s) leptonic width
[DE94-618534] 12 p4516 N94-37096
Activities of the Photon Factory
[DE94-748682] 12 p4522 N94-37236
Laser cooling of 24Mg+ in the ASTRID storage ring
[DE94-010445] 12 p4523 N94-37619

STORAGE STABILITY
Space Storable Rocket Technology program (SSRT). Option 1 program
[NASA-CR-191171] 01 p0046 N94-10938
A study of hydrogen effects on fracture behavior of radioactive waste storage tanks
[DE93-018171] 02 p0574 N94-14873
Efficacy of flocculating and other emergency water purification tablets
[AD-A266695] 03 p1148 N94-15840
Lithium D-cell study
[NASA-CR-192705] 03 p1011 N94-16505
Practical reporting times for environmental samples
[DE93-013461] 04 p1472 N94-17910
Ageing studies on a composite propellant containing a new organo-copper burn rate catalyst
[AD-A271060] 05 p1711 N94-19906
Evaluation of pre-extraction analytical holding times for nitroaromatic and nitramine explosives in water
[AD-A271547] 05 p1712 N94-20927
NASA Lewis advanced IPV nickel-hydrogen technology 06 p2392 N94-23356
Ni-MH storage test and cycle life test
07 p2864 N94-28131
An investigation of the radiolytic stability of a resorcinol-formaldehyde ion exchange resin
[DE94-007971] 09 p3660 N94-32698
Unleaded AVGAS program
[AD-A278650] 11 p4247 N94-35795

STORAGE TANKS
Immediate response to free product discovery
[PB93-182970] 01 p0265 N94-11015
The feasibility of producing aluminum-lithium structures for cryogenic tankage applications by laser beam welding
[NASA-CR-191527] 02 p0595 N94-14026
A study of hydrogen effects on fracture behavior of radioactive waste storage tanks
[DE93-018171] 02 p0574 N94-14873
Ground testing for the no-vent fill of cryogenic tanks: Results of tests for a 71 cubic foot tank
[NASA-TM-106293] 03 p1030 N94-17486
Environmental use of a Laser Range Finder and the Advanced Visualization System
[DE93-016163] 03 p1043 N94-17677
Pressurization and expulsion of a flightweight liquid hydrogen tank
[NASA-TM-106427] 05 p1799 N94-20177
On demand, non-halon, fire extinguishing systems
[AD-D015957] 05 p1714 N94-20355
Analysis and test of low profile aluminum aerospace tank dome
[NASA-TP-3442] 06 p2375 N94-23294
Flow and temperature distribution in a naturally stratified thermal storage tank
[AD-A273511] 06 p2336 N94-24821
Thermodynamic models for bounding pressurant mass requirements of cryogenic tanks
[NASA-TM-106476] 06 p2346 N94-25202
Metal hydride storage
[VTT-JULK-769] 06 p2396 N94-25417
Automated in-situ inspection systems for underground storage tanks
[AD-A274644] 07 p2764 N94-27144
Large scale cryogenic fluid systems testing
[NASA-TM-109735] 08 p3157 N94-29904
Experimental investigation of jet-induced mixing of a large liquid hydrogen storage tank
[NASA-TM-106629] 10 p4044 N94-33607
Decision and systems analysis for underground storage tank waste retrieval systems and tank waste remediation system
[SAND94-0065] 11 p4286 N94-35957

STORE RELEASE
U EXTERNAL STORE SEPARATION
STORM DAMAGE
Examination of micro- and macro-physical structures and processes in hailstorms with respect to their modification
[DLR-FB-93-25] 07 p2897 N94-27751
Remote sensing for hurricane Andrew impact assessment 09 p3758 N94-32464
STORM SURGES
The performance of drag relations in the WAQUA storm surge model
[KNMI-TR-149] 04 p1496 N94-17923
Wind products for use in coastal wave and surge models
[AD-A269753] 04 p1497 N94-18414
STORMS
NT CYCLONES
NT DUST STORMS
NT HAILSTORMS
NT HURRICANES
NT MAGNETIC STORMS
NT MICROBURSTS (METEOROLOGY)
NT POLAR SUBSTORMS
NT RAINSTORMS
NT STORMS (METEOROLOGY)
NT SUDDEN IONOSPHERIC DISTURBANCES
NT THUNDERSTORMS
NT TORNADOES
NT TROPICAL STORMS
NT TYPHOONS
Orographic microbursts in a severe winter windstorm
[AD-A267651] 03 p1108 N94-17247
Propagation characteristics of mesoscale convective systems
[AD-A268130] 03 p1109 N94-17522
United States Weather Research Program (USWRP)
06 p2411 N94-24375
Thunderstorm Hypothesis Reasoner
[NASA-CR-195714] 07 p2897 N94-27884
Remote sensor observations during WISP91: The use of microwave radiometers, RASS, and lidar ceilometers for detection of aircraft icing conditions
[PB94-142106] 08 p3136 N94-30890
The evolution of jet features during the 1993 east coast white hurricane: A case study using the global spectral model
[AD-A277217] 09 p3783 N94-32021
Storm evolution of directional seas in shallow water
[AD-A278541] 10 p4089 N94-33404
Multiparameter radar and aircraft based studies of microphysical, kinematic, and electrical structure of convective clouds during CaPE
[AD-A278544] 10 p4085 N94-33677
Three flights into thunderstorms with the revised Rocket Electric Field Sounding (REFS) payload
[AD-A280424] 12 p4473 N94-37217
STORMS (METEOROLOGY)
NT CYCLONES
NT DUST STORMS
NT HAILSTORMS
NT HURRICANES
NT MICROBURSTS (METEOROLOGY)
NT RAINSTORMS
NT THUNDERSTORMS
NT TORNADOES
NT TROPICAL STORMS
NT TYPHOONS
The impact of vegetation on the atmospheric boundary layer and convective storms 01 p0277 N94-11480
Rainfall-runoff estimation using digital radar
[AD-A265390] 01 p0286 N94-12408
A study of the Merritt Island, Florida sea breeze flow regimes and their effect on surface heat and moisture fluxes
[NASA-CR-4537] 01 p0286 N94-12580
Storm prediction through barometric field analysis
[PUBL-SER-A-129] 02 p0720 N94-13587
Diabatic forcing and initialization with assimilation of cloud and rain water in a forecast model: Methodology
04 p1491 N94-18603
Tropical squall lines 09 p3778 N94-30992
Extrapolating storm location using the Integrated Terminal Weather System (ITWS) storm motion algorithm
[AD-A278611] 11 p4295 N94-36249
STOSS-AND-LEE TOPOGRAPHY
U GLACIAL DRIFT
STOVL AIRCRAFT
Criteria for design of integrated flight/propulsion control systems for STOVL fighter aircraft
[NASA-TP-3356] 01 p0030 N94-11134
Application of controller partitioning optimization procedure to integrated flight/propulsion control design for a STOVL aircraft
[NASA-TM-106265] 01 p0030 N94-11251
Moving-base simulation evaluation of thrust margins for vertical landing for the NASA YAV-8B Harrier aircraft
[NASA-TM-104008] 01 p0030 N94-11259
Design criteria for integrated flight/propulsion control systems for STOVL fighter aircraft
02 p0521 N94-13297
The lift-fan powered-lift aircraft concept: Lessons learned
[NASA-CR-177616] 03 p0866 N94-15718
Lift-fan aircraft: Lessons learned-the pilot's perspective
[NASA-CR-177620] 03 p0867 N94-15950
Lift and pitching moment induced on jet STOVL aircraft hovering in ground effect
[AD-A269700] 04 p1317 N94-18577
Lift and pitching moment induced on jet STOVL aircraft by the ground vortex
[AD-A269816] 04 p1318 N94-18733
Overview of STOVL aircraft propulsion research offtakes and vertical lift systems
[NASA-TM-106387] 04 p1321 N94-19353
Survey of lift-fan aerodynamic technology
[NASA-CR-177615] 05 p1646 N94-21592
Experiments into the scaling parameters required for exhaust gas ingestion testing of vertical landing aircraft
07 p2671 N94-28017
Transitional flight characteristics of a geometrically simplified STOVL model 07 p2672 N94-28035
Antiwindup analysis and design approaches for MIMO systems
[NASA-CR-195304] 09 p3584 N94-32075
Powered lift facility at NASA Lewis Research Center's Aeroacoustic Propulsion Laboratory
[NASA-TM-106577] 10 p4009 N94-33604
STOVL
[NASA-TM-109845] 10 p3989 N94-33790
A direct application of the non-linear inverse transformation flight control system design on a STOVL aircraft
[NASA-TM-108808] 10 p3969 N94-33942
YAV-8B reaction control system bleed and control power usage in hover and transition
[NASA-TM-104021] 10 p4007 N94-34994
STRAIGHT WINGS
U RECTANGULAR WINGS
STRAIN AGING
U PRECIPITATION HARDENING
STRAIN DISTRIBUTION
Estimation of strain in 1-kW primary containment vessels by microstructural examination
[DE93-013053] 02 p0573 N94-14316
J-integral and HRR field associated with stable crack growth in thin aluminum SEN specimen
[AD-A267879] 03 p0960 N94-17041
Damage evolution in filled elastomers
[AD-A268067] 03 p1062 N94-17507
Spectrum fatigue testing of T-shaped tension clips
[FFA-TN-1992-22] 04 p1452 N94-17970
Analysis of regional deformation and strain accumulation data adjacent to the San Andreas fault
[NASA-CR-194072] 04 p1487 N94-19428
Characteristics of 0.8- and 0.2-microns gate length In(x)Ga(1-x) As/In(0.52)Al(0.48)As/InP (0.53 less than or equal to x less than or equal to 0.70) modulation-doped field-effect transistors at cryogenic temperatures
05 p1733 N94-20499
Wrinkle ridges, reverse faulting, and the depth penetration of lithospheric stress in lunae planum, Mars
05 p2141 N94-20910
Ceramic matrix composites: Challenges and opportunities 06 p2255 N94-24230
Use of photostress to characterize the mechanical behavior of weldments
[NASA-CR-195201] 06 p2378 N94-25267
Study on elucidation of damage generation process by electron beam lithography 07 p2729 N94-25581
Plane stress stable crack growth and J-integral/HRR field
[AD-A275761] 08 p3317 N94-28761
Analyses of stationary and growing crack tip deformation by digital image processing 08 p3320 N94-29690
Field methods to measure surface displacement and strain with the Video Image Correlation method
[NASA-CR-193968] 08 p3316 N94-29724
Isolating strain parameters correlated to skeletal adaptation 09 p3797 N94-31960
Near tip stress and strain fields for short elastic cracks 10 p4068 N94-33418
Use of photostress to analyze behavior of an aft skirt test specimen
[NASA-CR-195850] 10 p4069 N94-34075
Notch fatigue assessment of aircraft components using a fracture mechanics based parameter
10 p4072 N94-34588
STRAIN ENERGY METHODS
Geometric stiffening in multibody dynamics formulations 02 p0677 N94-14619
Integrated active and passive control design methodology for the LaRC CSI evolutionary model
[NASA-CR-4580] 08 p3164 N94-28417
An analysis of isothermal, bithermal, and thermomechanical fatigue data of Haynes 188 and B1900+Hf by energy considerations
[NASA-TM-106359] 08 p3317 N94-28819
Development of thermoplastic composite aircraft structures
[NASA-CR-189593] 09 p3626 N94-32860
STRAIN ENERGY RELEASE RATE
Understanding cracking failures of coatings: A fracture mechanics approach 01 p0187 N94-11218
J-integral and HRR field associated with stable crack growth in thin aluminum SEN specimen
[AD-A267879] 03 p0960 N94-17041
Analysis of local delaminations caused by angle ply matrix cracks
[NASA-TM-109052] 06 p2228 N94-24083
Plane stress stable crack growth and J-integral/HRR field
[AD-A275761] 08 p3317 N94-28761
Transient thermal fatigue of ceramic composites
08 p3216 N94-29874
Computational simulation of composite structures with and without damage
[NASA-CR-194433] 08 p3183 N94-30190
Acoustic emission from crack growth in 7050 aluminum and 7075 aluminum as a function of temperature and heat treatment
[DREP-CRS-93-15] 09 p3642 N94-31871
STRAIN FATIGUE
U FATIGUE (MATERIALS)
STRAIN GAGE BALANCES
Monopiece strain gauge sting mounted wind tunnel balance
[CA-PATENT-1-311-626] 03 p1032 N94-15697
STRAIN GAGES
Design and development of a miniature column-based interface (MCBI) stress gage
[AD-A266054] 01 p0170 N94-10873
Fiber-optic interferometric strain gauge for smart structures applications: First flight tests
01 p0071 N94-11340
Localized and distributed fiber-optic strain sensors embedded in composite materials
[UTIAS-346] 01 p0073 N94-12013
Strain sensing technology for high temperature applications
[NASA-TM-4498] 02 p0648 N94-12874
The ASCOR test: A simple automated method for stress corrosion testing of aluminium alloys
[NLR-TP-91438-U] 02 p0570 N94-13532
A technique for direct measurement of skin friction in supersonic combustion flow 02 p0503 N94-13555
Use of photostress and strain gages to analyze behavior of weldments and use of photostress and strain gages to analyze behavior of an aft skirt test specimen
[NASA-CR-194575] 03 p1058 N94-15716
Simultaneous measurement of temperature and strain using four connecting wires
[NASA-TM-104271] 03 p1032 N94-15754
Automated strain gauge plethysmograph
[AD-A267323] 03 p1035 N94-17002
Characteristics and pulsed radiation response of non-ideal quartz shock stress gauges
[DE93-017628] 04 p1424 N94-17999
Residual strain measurement on the production-grade class 4 flextensional transducer shell
[AD-A268828] 04 p1430 N94-18537
A comparative evaluation of in-plane shear test methods for laminated graphite-epoxy composites
[NASA-CR-193808] 04 p1456 N94-19095
Experiments and analysis of lateral piezoresistance gauges
[DE93-017874] 04 p1433 N94-19111
High temperature strain measurement with a resistance strain gage
[NASA-CR-194441] 04 p1434 N94-19314
PVDF gauge characterization of hypervelocity-impact-generated debris clouds
[DE93-018831] 05 p1829 N94-19943
Apparatus and method for measuring subject work rate on an exercise device
[NASA-CASE-MSC-21752-1] 05 p1895 N94-20194
High accuracy die mechanical stress measurement with the ATC04 Assembly Test Chip
[DE93-019435] 05 p1830 N94-20477
OTDR strain gauge for smart skins
[DE93-041043] 05 p1810 N94-21953
Demodulation of a fiber Fabry-Perot strain rosette using white light interferometry
[ISBN-0-315-83427-7] 05 p1990 N94-22579

Phase demodulation of interferometric fiber-optic sensors
[ISBN-0-315-83425-0] 05 p1991 N94-22581
Strain gage measurement errors in the transient heating of structural components
[NASA-TM-104274] 06 p2376 N94-23487
Attachment techniques for high temperature strain
[AD-A274766] 07 p2811 N94-26568
Damage identification in composites using built-in piezoelectrics 08 p3184 N94-30355
A laboratory study of multiple site damage in fuselage lap splices
[PB94-151230] 09 p3578 N94-31078
Strain sensing using optical fibers
[NASA-CR-195807] 09 p3740 N94-32940

STRAIN HARDENING

A modeling investigation of thermal and strain induced recovery and nonlinear hardening in potential based viscoplasticity
[NASA-TM-106122] 01 p0188 N94-11482
The effect of oxygen, grain size, and strain rate on the mechanical behavior of forged P/M tantalum
[DE93-011251] 03 p0959 N94-16764
Fatigue life program using strain-life methods
[AD-A267310] 03 p1060 N94-16943
A review of the stages of work hardening
[DE93-016456] 04 p1359 N94-18114
Effects of shock loading on a solid-solution strengthened superalloy
[DE93-018345] 04 p1362 N94-18809
Two-dimensional finite element analysis of porous media at multikilobar stress levels
[AD-A271540] 05 p1831 N94-20916
Use of photostress to characterize the mechanical behavior of weldments
[NASA-CR-195201] 06 p2378 N94-25267
Influence of grain structure and solute composition on the work hardening behavior of aluminium at cryogenic temperatures
[DE94-003415] 07 p2733 N94-26087
Low strain behaviour of a particulate reinforced aluminum alloy
[ISBN-0-315-84906-1] 07 p2744 N94-27961
Mechanical properties and microstructure of thermomechanically processed, high manganese steel
[ARL-TR-146] 07 p2747 N94-28212
A modeling study of the effect of stress state on void linking during ductile fracture
[AD-A275505] 08 p3317 N94-28811
Experimental and finite-element simulation results for a plane-strain punch-test using isotropic and anisotropic materials
[DE94-011711] 12 p4457 N94-37670
Mechanical performance of austempered ductile iron
[AD-A280452] 12 p4420 N94-37758

STRAIN MEASUREMENT

An electro-optical system for the measurement of strains 01 p0186 N94-10900
Smart structures at Aastra Corporation 01 p0069 N94-11326
Fiber optic sensing for composite smart structures 01 p0069 N94-11327
Strain measurement of carbon/epoxy composite with fibre optics white light quasi distributed polarimetric sensor 01 p0069 N94-11328
Structural health monitoring using embedded fibre optic sensors 01 p0022 N94-11334
Factors affecting the embedding of optical fibre sensors in advanced composite structures 01 p0070 N94-11336
Fiber-optic sensor systems for measuring strain and the detection of acoustic emissions in smart structures 01 p0071 N94-11337
Fiber-optic interferometric strain gauge for smart structures applications: First flight tests 01 p0071 N94-11340
Localized and distributed fiber-optic strain sensors embedded in composite materials
[UTIAS-346] 01 p0073 N94-12013
Strain sensing technology for high temperature applications
[NASA-TM-4498] 02 p0648 N94-12874
Correlations of the growth, structure, and stress with the adhesion of diamond films on tungsten
[DE93-012855] 02 p0576 N94-12912
Measurement of residual strain in composites by means of time-of-flight neutron diffraction
[DE93-012939] 02 p0555 N94-13248
Measurement of strain in individual phases of composites before, during, and after mechanical loading
[DE93-014585] 02 p0558 N94-14119
Cammatic: An approach to improve DSS 13 antenna gravity-loading performance 02 p0608 N94-14374
Report of the International Center for Earth Tides for the period 1985-1989 03 p1099 N94-15801
Cooperative projects in geodynamical instrumentation between the State Seismological Bureau (China) and the Royal Observatory of Belgium 03 p1037 N94-15806
Earth tides results obtained with gravimeters, clinometers, and strainmeters in Belgium and in Grand Duchy of Luxembourg 03 p1100 N94-15809
Damage evolution in filled elastomers
[AD-A268067] 03 p1062 N94-17507
The photonical, pure grid method
[NLR-TP-91478-U] 03 p1062 N94-17600
Instrumented experiments aboard the frigate WOLF. Wolf 2: Measurement results of the 5.5 kg TNT in the crew aft sleeping compartment
[PML-1992-12] 04 p1451 N94-17931
Residual strain measurement on the production-grade class 4 flextensional transducer shell
[AD-A268828] 04 p1430 N94-18537
High temperature strain measurement with a resistance strain gage
[NASA-CR-194441] 04 p1434 N94-19314
Delamination in composite materials as observed using an optical fiber strain gage
[AD-A270803] 04 p1344 N94-19662
OTDR strain gauge for smart skins
[DE93-041043] 05 p1810 N94-21953
Phase demodulation of interferometric fiber-optic sensors
[ISBN-0-315-83425-0] 05 p1991 N94-22581
Strain gage measurement errors in the transient heating of structural components
[NASA-TM-104274] 06 p2376 N94-23487
Intelligent Material Systems and Structures (IMSS). Part 5: Fiber optic registration of deformation in carbon laminates 91/92
[PB93-204600] 06 p2544 N94-23723
Dual-purpose RTOF diffractometer facility at the ET-RR-1 reactor
[VTT-TIED-1425] 06 p2566 N94-25347
Studies on the measurement of subsurface fractures and geostress using acoustic emission technique for deep coalbed development
[REPT-7] 07 p2879 N94-26475
Attachment techniques for high temperature strain
[AD-A274766] 07 p2811 N94-26568
Aircraft wheel life assessment
[AD-A274378] 07 p2823 N94-26976
High intensity x ray instrumentation for residual strain measurements in composites and textured materials
[ISBN-0-315-85169-4] 07 p2842 N94-27278
A laboratory test on construction of ice domes and their load-carrying capacity 07 p2884 N94-27966
The estimation of pre-stress by deformation rate analysis and suggestion of a mechanism from the elast-plastical theory 07 p2871 N94-28156
Experimental determination of orthotropic elastic constants
[FFA-TN-1991-35] 08 p3215 N94-29424
Fiber optic sensors for the detection of surface acoustic waves on metals
[ISBN-0-315-87055-9] 09 p3878 N94-31736
Strain sensing using optical fibers
[NASA-CR-195807] 09 p3740 N94-32940
Improvements in spiral-bevel gears to reduce noise and increase strength
[NASA-TM-106613] 10 p4059 N94-33609
Mapping of residual strains of a ceramic-to-metal joint using x ray diffraction
[DE94-007421] 10 p4069 N94-33691
The use of pulsed neutron diffraction to measure strain in composites
[DE94-007536] 10 p4019 N94-33693
Notch fatigue assessment of aircraft components using a fracture mechanics based parameter 10 p4072 N94-34588

STRAIN RATE

Material removal processes: Engineering mechanics consideration
[DE93-010733] 01 p0126 N94-10293
Facility for stress corrosion cracking test of irradiated material in high temperature water
[DE93-753189] 01 p0084 N94-11593
Parameterization of subgrid-scale stress by the velocity gradient tensor 01 p0155 N94-12286
A stochastic model for behavior analysis of fiber-reinforced quasi-brittle materials 02 p0672 N94-13594
Non-uniqueness in dynamic rate-independent non-associated plasticity
[AD-A266342] 02 p0769 N94-13731
Dynamic mechanical deformation of a SiC(sub p)/Al-Li (8090) composite
[DE93-014586] 02 p0558 N94-14121
Machining and grinding: High rate deformation in practice
[DE93-010718] 02 p0664 N94-14457
Search for subgrid scale parameterization by projection pursuit regression 02 p0643 N94-14749
Yield properties of tungsten and tungsten heavy alloys
[AD-A266833] 02 p0575 N94-14878
Rheology of water and ammonia-water ices 03 p0953 N94-16188
Experimental study of nonassociated flow and instability of frictional materials
[AD-A266421] 03 p1024 N94-16555
The effect of oxygen, grain size, and strain rate on the mechanical behavior of forged P/M tantalum
[DE93-011251] 03 p0959 N94-16764
Creep ductility of iron at very low strain rates: The effects of sulfur
[DE93-015490] 03 p0959 N94-16890
Time dependent turbulence modeling and analytical theories of turbulence
[NASA-TM-106379] 03 p1029 N94-17385
Tensile and stress-rupture behavior of hafnium carbide dispersed molybdenum and tungsten base alloy wires
[NASA-TM-106350] 03 p0962 N94-17652
Shear wave measurements in shock-induced, high-pressure phases
[DE93-016461] 03 p1062 N94-17664
Modeling microstructural evolution and the mechanical response of superplastic materials
[DE93-014417] 04 p1355 N94-17711
Atlas of formability: Ultimet
[AD-A268352] 04 p1355 N94-17767
Atlas of formability: HAYNES 556
[AD-A268354] 04 p1356 N94-17768
Atlas of formability: HAYNES 188
[AD-A268355] 04 p1356 N94-17769
Atlas of formability: NICKELVAC K-500
[AD-A268351] 04 p1356 N94-17772
Atlas of formability: INCONEL 718
[AD-A268350] 04 p1356 N94-17789
Atlas of formability: Hastelloy C-22
[AD-A268324] 04 p1356 N94-17796
Atlas of formability: Permalloy - 80 flow stress curves
[AD-A268263] 04 p1356 N94-17801
Atlas of formability: Nickelvac C-276
[AD-A268264] 04 p1357 N94-17802
Atlas of formability: Ti-6Al-4V ELI
[AD-A268300] 04 p1357 N94-17803
Atlas of formability: ALLVAC 718
[AD-A268304] 04 p1357 N94-17804
Atlas of formability: Waspaloy
[AD-A268323] 04 p1593 N94-17805
A review of the stages of work hardening
[DE93-016456] 04 p1359 N94-18114
Several fundamental issues in the mechanics of inelastic behavior
[AD-A269455] 04 p1453 N94-18285
Implementation of a nonisothermal unified inelastic-strain theory into ADINA6.0 for a titanium alloy: User guide
[AD-A269927] 04 p1360 N94-18660
Dislocation-drag contribution to high-rate plastic deformation in shock-loaded tantalum
[DE93-018286] 04 p1361 N94-18802
Effects of shock loading on a solid-solution strengthened superalloy
[DE93-018345] 04 p1362 N94-18809
Three-dimensional shock wave physics simulations with MIMD PAGOSA on massively parallel computers
[DE93-011682] 04 p1455 N94-18829
Effect of internal heating during hot compression testing on the stress-strain behavior and hot working characteristics of alloy 304L
[DE93-012701] 04 p1362 N94-18917
The effect of composition on the mechanism of continuous recrystallization and superplastic response of aluminum-scandium alloys
[DE93-018594] 04 p1365 N94-19280
Impact strength and indentation hardness of high-strength ceramics
[DE93-018833] 04 p1373 N94-19338
Dynamical behavior of octahedrite from the Henbury meteorite
[DE93-018834] 04 p1627 N94-19339
Mechanical response comparison of gun propellants evaluated under equivalent time-temperature conditions
[AD-A270479] 04 p1378 N94-19674
Coupling of smooth particle hydrodynamics with PRONTO
[DE93-019080] 05 p1915 N94-21539
The effect of microstructural evolution on superplasticity in Ni3Si(V, Mo)
[DE93-041320] 05 p1694 N94-21943
Tensile properties of 21-6-9 stainless steel at elevated temperatures
[DE94-001852] 06 p2240 N94-23017
Stress corrosion cracking properties of 15-5PH steel 06 p2251 N94-23244

Theory of extrusion: Advances and challenges
[PB93-201572] 06 p2241 N94-23447
Dynamic localization and second-order subgrid-scale models in large eddy simulations of channel flow
06 p2329 N94-24149
On the deformation kinetics constitutive law of plastic deformation: The rate equation
06 p2161 N94-24289
Procedures for determining MATMOD-4V material constants
[DE94-002638] 06 p2245 N94-24520
High strain rate superplasticity in metals and composites
[DE94-001521] 06 p2229 N94-24547
Three-dimensional, inelastic response of single-edge notch bend specimens subjected to impact loading
[AD-A273302] 06 p2378 N94-25143
Deviatoric stresses and plastic strain rates in strong shock waves for six metals
[DE94-002964] 07 p2733 N94-26022
Deformation twinning: Influence of strain rate
[DE94-002693] 07 p2738 N94-26621
The high strain rate behaviour of tantalum
[ISBN-0-315-84472-8] 07 p2740 N94-27305
Research into the microstructure and mechanical behavior of eutectic Bi-Sn and In-Sn
[DE94-004558] 07 p2741 N94-27619
Failures to model the development of a cube texture during the high temperature compression of Al-Mg alloys
[DE94-005013] 08 p3201 N94-28544
Numerical analysis of dynamic direct tension and direct compression tests
[AD-A275255] 08 p3319 N94-29433
The effect of various metallurgical parameters on the flow and fracture behavior of polycrystalline NiAl near the brittle-to-ductile transition
[NASA-TM-106534] 08 p3205 N94-29758
Mechanisms and effects of heat generation at the tips of dynamic cracks and notches in metals
08 p3321 N94-29808
Nanodislocation structures generated in shocked crystals 08 p3514 N94-29915
Fatigue of carbon and low-alloy steels in LWR environments
[DE94-005116] 08 p3207 N94-30021
Influence of tungsten alloying additions on the mechanical properties and texture of tantalum
[DE94-004994] 08 p3210 N94-30774
Tensile properties of commercially pure vanadium from room temperature to 1200 C
[DE94-006622] 09 p3641 N94-31581
Isolating strain parameters correlated to skeletal adaptation 09 p3797 N94-31960
Modeling the impact behavior of high strength ceramics
[AD-A277744] 10 p4028 N94-33894
Ability of the total strain version of strainrange partitioning to characterize thermomechanical fatigue behavior
[NASA-TM-4556] 12 p4455 N94-37102
Experimental and finite-element simulation results for a plane-strain punch-test using isotropic and anisotropic materials
[DE94-011711] 12 p4457 N94-37670

STRAIN SOFTENING
U PLASTIC DEFORMATION

STRAITS
Tide-generated nonlinear internal wave packets in the Strait of Gibraltar observed by the synthetic aperture radar aboard the ERS-1 satellite 01 p0252 N94-12510

STRAKES
Lift enhancement of a wing/strake using pneumatic blowing
[AD-A265074] 01 p0026 N94-11872
Measurements of wing and fin buffeting on the standard dynamics model
[IAR-AN-76] 02 p0526 N94-13859
Wind tunnel investigations of forebody strakes for yaw control on F/A-18 model at subsonic and transonic speeds
[NASA-TP-3360] 03 p0859 N94-16573
An experimental investigation of the effect of leading edge extensions on directional stability and the effectiveness of forebody nose strakes
08 p3155 N94-29728
F/A-18 forebody vortex control. Volume 2: Rotary-balance tests
[NASA-CR-4582-VOL-2] 10 p3984 N94-34430
F/A-18 forebody vortex control. Volume 1: Static tests
[NASA-CR-4582-VOL-1] 11 p4190 N94-35991

STRANGE ATTRACTORS
Detecting non-linearities in stationary time series
[W-9223] 01 p0344 N94-10906
Stability of subharmonics and escape phenomena in the twin-well potential duffing system
02 p0775 N94-13235
Homoclinic crises in a model for the CO2 laser
[DE93-624900] 04 p1436 N94-17954
The brain electrical activity in different G situations
[AERONAUTICA-ACTA-A-372-1993]
04 p1507 N94-19523
On the estimation of the correlation dimension and its application to radar reflector discrimination
[NASA-CR-4564] 06 p2309 N94-23304
Controlling chaos in plasma filled diodes
[AD-A275525] 08 p3504 N94-28686
Boundary layer coherent structures
[AD-A275007] 08 p3272 N94-29195
Heteroclinic attractors: Time averages and moduli of topological conjugacy
[W-9318] 09 p3844 N94-31690
Deterministic chaos 09 p3912 N94-31896
Theoretical investigations of chaotic dynamics
[AD-A280325] 12 p4507 N94-37028

STRANGENESS
Production of strange clusters in relativistic heavy ion collisions
[DE93-010876] 01 p0359 N94-10303
Strangeness production with protons and pions
[DE93-010879] 01 p0359 N94-10304
A generalized Bethe-Weizsaecker mass formula for strange hadronic matter
[DE93-011010] 01 p0368 N94-11620
Neutral strange particle production at the AGS
[DE93-014044] 02 p0780 N94-13098
Measuring strangeness in the nucleon
[DE93-014861] 02 p0785 N94-14471
Fast pulsars, compact stars, and the strange matter hypothesis
[DE93-015039] 03 p1239 N94-16052
Institute for Nuclear Theory
[DE93-017369] 04 p1568 N94-18824
Measurement of the strange quark distribution function in W(+) charm quark events
[DE93-018267] 05 p1973 N94-20474
Strange Dibaryons
[DE94-003005] 07 p3022 N94-26769
Equation of state of neutron star matter, limiting rotational periods of fast pulsars, and the properties of strange stars
[DE94-005214] 08 p3542 N94-28480
Weak decays of charged K-mesons and charm particles
[PB94-138062] 08 p3486 N94-29143
A quark model of bar Lambda production in bar Rho interactions
[DE94-008071] 11 p4324 N94-35824
Strangeness and the quark-gluon plasma: An experimenter's perspective
[DE94-011377] 12 p4519 N94-37558
Hadron production in S+nucleus collisions at 200 GeV/nucleon
[DE94-011344] 12 p4520 N94-37715

STRAPDOWN INERTIAL GUIDANCE
Analysis of the accuracy of strapdown inertial surveying systems
[SER-C-391] 03 p1081 N94-15156

STRAPS
Lightning tests and analyses of tunnel bond straps and shielded cables on the Space Shuttle solid rocket booster
[NASA-CR-193921] 06 p2200 N94-24801

STRATA
NT SUBSTRATES
The nonlinear evolution of modes on unstable stratified shear layers
[NASA-CR-191492] 01 p0149 N94-10810
Post-impact alteration of the Manson impact structure
01 p0282 N94-12188
Dynamic soil pressures on rigid cylindrical vaults
[DE93-013930] 02 p0676 N94-14585
On the sources of North Atlantic deep water
[AD-A270854] 05 p1881 N94-19895
The biostratigraphy and paleogeography of Maastrichtian inoceramids 07 p2889 N94-28303

STRATEGY
A method for cognitive task analysis
[IZF-1992-B5] 04 p1508 N94-17967
Powerful selling and sales strategy
07 p2662 N94-28245

STRATIFICATION
NT ATMOSPHERIC STRATIFICATION
NT INTERCALATION
Turbulent diffusion in homogeneous shear flow with stable density stratification
[DLR-FB-92-26] 02 p0639 N94-14443
Subwavelength structured surfaces and their applications 03 p1194 N94-17337
Modeling deep equatorial circulation
08 p3378 N94-29815
Steady thermal convection in multiple liquid layers
09 p3705 N94-31844
Stratification of deforested areas by vegetation types in Amazonia, using geographic information systems: Study of case at SB20 Purus map
[INPE-5541-TDI/529] 10 p4077 N94-34230

STRATIFIED FLOW
Similarity states of homogeneous stably-stratified turbulence at infinite Froude number
01 p0156 N94-12292
Mixing in a stratified shear flow: Energetics and sampling 01 p0159 N94-12311
Effects of surface thermal forcing on stratified flow past an isolated obstacle 02 p0633 N94-13553
Surface and internal signatures of organized vortex motions in stratified fluid
[AD-A267015] 03 p1020 N94-15526
Numerical simulations of turbulent buoyant flows by finite element method: Application to the study of strongly heated or cooled stratified flow
[ECL-92-28] 04 p1421 N94-19399
Meso-Beta scale numerical simulation studies of terrain-induced jet streak mass/momentum perturbations
[NASA-CR-194627] 05 p1864 N94-20138
Laser-induced fluorescence/particle tracking system for stratified flow research
[AD-A275917] 09 p3701 N94-31341
Effects of buoyancy on fluid flows and turbulence
[AD-A276586] 09 p3706 N94-32123
JPRS report: Science and technology. Central Eurasia
[JPRS-UST-94-006] 11 p4249 N94-35226

STRATIFIED LAYERS
U STRATA

STRATIGRAPHY
The Lathrop Wells Volcanic Center: Status of field and geochronology studies
[DE93-008917] 01 p0273 N94-10285
Twenty-fourth Lunar and Planetary Science Conference. Part 1: A-F
[NASA-CR-193095] 01 p0435 N94-12015
Estimation of age of Dali-Ganis rifting and associated volcanic activity, Venus 01 p0440 N94-12046
Apollo 16 core 60013/14 as a product of path 1 and path 2 regolith evolution processes
01 p0440 N94-12050
The great 8 MA event and the structure of the H-chondrite parent body 01 p0429 N94-12058
Stratigraphy and sedimentology of the K/T boundary deposit in Haiti 01 p0282 N94-12138
Differential scaling: Implications for central structures in large lunar craters 01 p0461 N94-12158
Geomorphology of Triton's polar materials
01 p0466 N94-12185
Rover mounted ground penetrating radar as a tool for investigating the near-surface of Mars and beyong
03 p1007 N94-16197
Remote sensing studies of the northeastern portion of the lunar nearside 03 p1258 N94-16225
Geochemical evidences for two chondritic-like cometary or asteroidal impacts before and at the K/T boundary
03 p1244 N94-16359
Three-dimensional high-resolution seismic profiling on the New Jersey outer continental shelf
[AD-A269835] 04 p1498 N94-18600
Applications of Quaternary stratigraphic, soil-geomorphic, and quantitative geomorphic analyses to the evaluation of tectonic activity and landscape evolution in the Upper Coastal Plain, South Carolina
[DE93-016269] 04 p1484 N94-18725
Stratigraphy of the Martian northern plains
05 p2091 N94-20398
The Koshak section: Evidence for element fractionation and an oxidation event at the K/T boundary
05 p1862 N94-20641
Modelling the gravity and magnetic field anomalies of the Chicxulub crater 05 p1862 N94-20668
Diapirs and cantaloupes: Layering and overturn of Triton's crust 05 p2111 N94-20738
Geology of the southern hemisphere of Triton: No polar cap 05 p2111 N94-20739
Iridium in sediments containing large abundances of Australasian microtektites from DSDP hole 758B in the Eastern Indian Ocean and from DSDP hole 769A in the Sulu Sea 05 p2083 N94-20741
Research program on the Manson impact structure, Iowa 05 p1862 N94-20766
Field guide to Cretaceous-tertiary boundary sections in northeastern Mexico
[NASA-CR-195719] 08 p3354 N94-28416
Analysis of deep seismic reflection and other data from the southern Washington Cascades
[DE94-005958] 09 p3771 N94-31525
Environmental process tomography in the United States
[DE94-006402] 10 p4081 N94-33718

STRATOCUMULUS CLOUDS
Linkage of anthropogenic aerosol to clouds and climate
[DE93-016434] 02 p0719 N94-13080
Remote sensing of low level cloud optical characteristics 02 p0691 N94-14229
Clouds: Their prediction and simulation
[AD-A271161] 05 p1864 N94-19900
The analysis of global cloud and radiation data for the study of cloud-climate interactions
[NASA-CR-193388] 05 p1865 N94-20535
The FIRE Cirrus Science Results 1993
[NASA-CP-3238] 05 p1871 N94-22292
A regional analysis of cloudy mean spherical albedo over the marine stratocumulus region and the tropical Atlantic Ocean
[NASA-CR-194771] 06 p2409 N94-24049
The numerical simulation of marine boundary layer clouds
[AD-A273669] 07 p2894 N94-26195
An integrated cloud observation and modeling investigation in support of the ARM program
[DE94-003160] 09 p3785 N94-32716
Development of a radiative cloud parameterization scheme of stratocumulus and stratus clouds which includes the impact of CCN on cloud albedo
[DE94-005476] 10 p4081 N94-33714
STRATOFORTRESS AIRCRAFT
U B-52 AIRCRAFT
STRATOSPHERE
NT OZONOSPHERE
Implications of aerosol retrieval and atmospheric correction in remote sensing 01 p0205 N94-11978
Identification of cometary and asteroidal particles in stratospheric IDP collections 01 p0430 N94-12115
Studies of dynamical processes affecting the distribution of stratospheric ozone
[NASA-CR-193477] 01 p0279 N94-12560
Stratospheric aircraft exhaust plume and wake chemistry
[NASA-CR-191495] 01 p0279 N94-12572
Project AIRSTREAM: Trace gas
[DE93-008849] 02 p0706 N94-12904
Airborne Arctic stratospheric expedition: Ozone
[NASA-TM-109312] 02 p0515 N94-13606
Weather forecasting support for AASE-2
[NASA-CR-194342] 02 p0721 N94-13675
Modeling of the partitioning of reactive odd nitrogen in the lower stratosphere using aircraft measurements of NOy, NO, and other trace species
[NASA-CR-194305] 02 p0714 N94-13707
Measurement of HO2 and other trace gases in the stratosphere using a high resolution far-infrared spectrometer at 28 km
[NASA-CR-194175] 02 p0714 N94-13816
Space-based activities: SAM 2 and SAGE 2 02 p0694 N94-14252
New evidences supported the Wei hypothesis about the formation of the Antarctic ozone hole 02 p0694 N94-14253
Middle atmospheric electric fields over thunderstorms
[NASA-CR-194619] 03 p1106 N94-16493
Monitoring the response of the upper troposphere/lower stratosphere to a greenhouse gas scenario
[DE93-014509] 04 p1470 N94-17710
Screening analysis for chlorine-free alternative refrigerants to replace R-22 in air conditioning applications
[DE93-015920] 04 p1367 N94-17847
Ozone hole
[NASA-TM-109368] 04 p1476 N94-18960
Intrusion of stratospheric ozone in the troposphere through tropopause folding and cold air droplets
[REPT-87] 05 p1851 N94-20154
Stratospheric Aerosol and Gas Experiment (SAGE 3) 05 p1869 N94-21644
The 5-6 December 1991 FIRE IFO 2 jet stream cirrus case study: The influence of volcanic aerosols 05 p1877 N94-22326
The atmospheric effects of stratospheric aircraft: A third program report
[NASA-RP-1313] 06 p2398 N94-24104
Measurement of HO2 and other trace gases in the stratosphere using a high resolution far-infrared spectrometer
[NASA-CR-195173] 06 p2404 N94-24738
Carbon and hydrogen isotope composition and C-14 concentration in methane from sources and from the atmosphere: Implications for a global methane budget
[NASA-CR-195166] 06 p2399 N94-25092
Collection and evaluation of numerical models with the aim to investigate the impact of aircraft emissions
[DLR-MITT-93-06] 06 p2400 N94-25414
Isotopically labeled CO2 from stratosphere: A tracer of carbon biogeochemistry
[DE94-002777] 07 p2877 N94-26015
Auroral Tomography Workshop Proceedings
[PB94-123718] 07 p2881 N94-27040
In situ Mars ozone detector 07 p3108 N94-27892
Observation of the upper atmosphere physics at Asuka Station by the 30th Japanese Antarctic Research Expedition in 1989 07 p2885 N94-27972
Harvard ER-2 OH laser-induced fluorescence instrument 08 p3343 N94-28592
Time series comparisons of satellite and rocketsonde temperatures in 1978-1979
[NASA-TP-3409] 08 p3370 N94-29455
Laboratory studies of chemical and photochemical processes relevant to stratospheric ozone
[NASA-CR-189351] 08 p3347 N94-29549
Radar estimations of atmospheric winds in the troposphere and lower stratosphere 08 p3370 N94-29697
Odin aeronomy science: A phase-A report by the Aeronomy Science Working Group for the Odin satellite
[AP-31] 09 p3770 N94-31222
One: Microphysics of frost metamorphism: Applications to Triton and Mars. Two: A global analysis of the ozone deficit in the upper stratosphere and lower mesosphere. Three: The diabatic circulation in the stratosphere as diagnosed from Microwave Limb Sounder data 09 p3942 N94-31975
Quantified estimates of total GWPs for greenhouse gases taking into account tropospheric chemistry
[DE94-007846] 09 p3768 N94-32817
Counting particles emitted by stratospheric aircraft and measuring size of particles emitted by stratospheric aircraft
[NASA-CR-195908] 09 p3769 N94-33170
Stratospheric models and measurements: A critical comparison 10 p3971 N94-33457
Previous model comparisons 10 p3971 N94-33458
Model capabilities, 2-D 10 p3971 N94-33459
Comparison of the impact of volcanic eruptions and aircraft emissions on the aerosol mass loading and sulfur budget in the stratosphere 10 p3971 N94-33460
High resolution infrared datasets useful for validating stratospheric models 10 p3971 N94-33461
Ozone hole airborne Arctic stratospheric expedition (pre-flight)
[NASA-TM-109800] 10 p4080 N94-33551
Project report: Aircraft --- atmospheric effects of stratospheric aircraft
[DE94-011759] 12 p4465 N94-37155
Jet aircraft engine exhaust emissions database development: Year 1990 and 2015 scenarios
[NASA-CR-4613] 12 p4466 N94-37252
Stratospheric emissions effects database development
[NASA-CR-4592] 12 p4467 N94-37607
STRATOSPHERIC AEROSOL & GAS EXPERIMENT
U SAGE SATELLITE
STRATOSPHERIC OBSERVATORY FOR IR ASTRONOMY
U SOFIA (AIRBORNE OBSERVATORY)
STRATOSPHERIC WARMING
Investigate wave-mean flow interaction and transport in the extratropical winter stratosphere
[NASA-CR-194555] 03 p1098 N94-15639
STRATOTANKER AIRCRAFT
U C-135 AIRCRAFT
STRATUS CLOUDS
Three-dimensional cloud visualization based on satellite imagery
[AD-A269318] 04 p1490 N94-18300
A documentation of icing relevant cloud physical parameters on horizontal soundings of stratiform clouds (continuation)
[DLR-MITT-92-10] 05 p1871 N94-22280
Breaking Kelvin-Helmholtz waves and cloud-top entrainment as revealed by K-band Doppler radar 05 p1874 N94-22310
The numerical simulation of marine boundary layer clouds
[AD-A273669] 07 p2894 N94-26195
The appearance of the Sun and Moon seen through clouds
[AD-A275338] 08 p3551 N94-29212
Development of a radiative cloud parameterization scheme of stratocumulus and stratus clouds which includes the impact of CCN on cloud albedo
[DE94-005476] 10 p4081 N94-33714
Sensitivity of cloud forcing to the cloud cover parameterization in a GCM
[DE94-000678] 10 p4089 N94-33728
Detection and analysis of fog at night using GOES multispectral infrared imagery
[NOAA-TR-NESDIS-75] 10 p4143 N94-34913
A stratiform cloud parameterization for general circulation models
[DE94-011442] 12 p4474 N94-37568
STREAK CAMERAS
Plans to improve the experimental limit in the comparison of the east-west and west-east one-way light propagation times on the rotating earth 01 p0351 N94-10971
Image motion photography
[DE93-013962] 02 p0653 N94-14858
Streak camera based SLR receiver for two color atmospheric measurements 03 p0914 N94-15573
The first satellite laser echoes recorded on the streak camera 03 p0914 N94-15574
Test results from LAGEOS-2 optical characterization using pulsed lasers 03 p0915 N94-15577
Two color satellite laser ranging upgrades at Goddard's 1.2m telescope facility 03 p0915 N94-15581
Two wavelength satellite laser ranging using SPAD 03 p0916 N94-15584
New perspectives for high accuracy SLR with second generation geodesic satellites 03 p0916 N94-15585
Station report on the Goddard Space Flight Center (GSFC) 1.2 meter telescope facility 03 p0922 N94-15625
Development and characterization of a time-, position- and energy-resolved x ray diagnostic for PBFA 2 target experiments
[DE93-019429] 05 p1808 N94-20297
Neutron detectors for fusion reaction-rate measurements
[DE94-010407] 11 p4330 N94-36114
Streak tube photocathode development program
[DE94-009905] 11 p4270 N94-36350
STREAM FUNCTIONS (FLUIDS)
Contributions to numerical solution of Navier-Stokes equations in two and three dimensional flows
[ETN-93-94395] 02 p0647 N94-14816
Numerical investigation of the incompressible flow around a wing with a fixed spoiler
[ISL-R-109/91] 04 p1313 N94-19524
Transition to turbulence in an elliptic vortex 06 p2331 N94-24161
Finite element vorticity-based methods for the solution of the incompressible and compressible Navier-Stokes equations
[ISBN-0-315-87265-9] 09 p3703 N94-31730
STREAMLINE FLOW
U LAMINAR FLOW
STREAMLINED BODIES
NT FAIRINGS
STREAMLINING
Exploratory study of in-plane streamline curvature effects on a turbulent boundary layer at a Mach number of 3
[NASA-CR-193673] 02 p0501 N94-13292
STREAMS
NT GAS STREAMS
An application of reduced gravity model to mesoscale eddies 01 p0199 N94-11945
SOFAR float tracking in the Shikoku basin 01 p0206 N94-11986
On an upwelling front, propagation of upwelling and vertical velocity in the eastern Arabian Sea during monsoon, 1987 01 p0206 N94-11987
A numerical study of deep convection at high latitudes 01 p0210 N94-12652
Study on diffusion phenomena of river effluents issued into sea around Japan with satellite remote sensing data 01 p0212 N94-12664
Sedimentation rates and particulate fluxes in the slope and deep sea areas off eastern Taiwan 01 p0220 N94-12709
A detailed investigation of the benthic regime in the Clarion-Clipperton province of the Pacific and a forecast of consequences of manganese nodule mining 01 p0224 N94-12733
Bottom currents and possibilities for near bottom layer environmental investigations in the Pacific by means of self contained bottom stations 01 p0224 N94-12734
Convective and dynamic instability in meridional trenches 01 p0225 N94-12739
Coupled numerical model for altimetric data assimilation and velocity field analysis 01 p0227 N94-12752
Complex (hydrodynamic, satellite) monitoring of dynamic structures in the western Pacific with the aim of forecasting the marine ecosystems behaviour 01 p0227 N94-12753
Mesoscale dynamic structures of the Subarctic Frontal Zone in the Pacific Ocean 01 p0227 N94-12754
Mixing of drifter ensemble by mesoscale currents 01 p0228 N94-12760
Generation of internal waves near the shelf boundary 01 p0229 N94-12763
Experimental and theoretical investigation of undular bore formation upstream the bank 01 p0229 N94-12764
Model of Kuroshio region circulation 01 p0229 N94-12765

Tracking of change of a warm-core ring structure
02 p0696 N94-14267
Warm streamers extended from Warm Core Rings (WCR's) and their role on fish migration and fishing ground formation
02 p0697 N94-14270
Measuring variation in ecosystem sensitivity to stress
[AD-A274232] 07 p2868 N94-26817
Development and application of a thermistor current meter
[AD-A275816] 08 p3286 N94-28831
Fronts at the confluences of spring-fed streams with Joekulsa a Fjoellum: Possibly thermal bars?
[MATHS-REPT-A-198] 08 p3333 N94-29528

STRENGTH OF MATERIALS
U MECHANICAL PROPERTIES

STRESS (BIOLOGY)
Programs and resources for control of job stress in the Federal workplace
03 p1124 N94-16617

STRESS (PHYSIOLOGY)
NT ACCELERATION STRESSES (PHYSIOLOGY)
NT CENTRIFUGING STRESS
Motion and spatial disorientation systems: Special research capabilities
[AD-A265155] 01 p0303 N94-11097
P2NBC2 Heat Strain Decision Aid. User's guide, version 2.1
[AD-A266072] 01 p0304 N94-11224
Central circulatory hemodynamics as a function of gravitational stress
01 p0309 N94-11995
Cellular mechanism of turnover of the stress induced protein HSP 70
[AD-A265723] 02 p0732 N94-13061
Physiological Anatomical Rodent Experiment (PARE) .04 Feasibility Test 1
[NASA-CR-194423] 02 p0728 N94-13473
Variability of prediction of maximal oxygen concumption on the cycle ergometer using standard equations
[NASA-TP-3412] 02 p0729 N94-14032
Sleep management user's guide for special operations personnel
[AD-A267746] 03 p1119 N94-14943
Activity/rest patterns of instructor and rates student pilots during rapid transitions from daytime to nighttime duty hours at the Eastern Army Aviation Training site
[AD-A267038] 03 p1131 N94-15659
Programs and resources for control of job stress in the Federal workplace
03 p1124 N94-16617
Effects of a high-energy food supplement on cold-induced thermogenesis
[AD-A269301] 04 p1504 N94-17823
Road march performance of special operations soldiers carrying various loads and load distributions
[AD-A269198] 04 p1512 N94-18882
Physiological correlates of stress-induced decrements in human perceptual performance
[DOT/FAA/AM-93/19] 05 p1893 N94-20081
Studies of neural and cognitive function in subjects exposed to the marine-air interface, phases 1 and 2
[AD-A272282] 05 p1891 N94-20624
Human responses to exercise-heat stress
[AD-A272581] 05 p1892 N94-21209
Changes in fluid and electrolyte metabolism during water immersion at high or thermoneutral temperature
07 p2912 N94-27445
Implications of climatic extremes in aircrew NBC operations
08 p3383 N94-28446
Physiological responses during shipboard firefighting
[AD-A275104] 08 p3391 N94-28912
Stress and ergonomic design and evaluation of person-machine systems
[AD-A275156] 08 p3400 N94-29034
Effects of endurance training on heat-exercise tolerance in men wearing NBC protective clothing
[AD-A275176] 08 p3391 N94-29049
Muscle disuse through tail-suspension: Etiology and therapeutics
09 p3796 N94-31746
Stress and brain protein synthesis
[PB94-170750] 11 p4296 N94-35601
Cardiac pressure changes with venous gas embolism and decompression
[AD-A280412] 12 p4481 N94-37224
Cerebral neurochemical mechanisms in stress and anxiety
[AD-A280473] 12 p4482 N94-37233

STRESS (PSYCHOLOGY)
Aviators, air combat, and combat stress: An Air F orce commander's primer
[AD-A265083] 01 p0313 N94-11867
Scuba-diving, anxiety and task performance
03 p1132 N94-15938
Programs and resources for control of job stress in the Federal workplace
03 p1124 N94-16617
Performance assessment in sustained operations using a computer-based synthetic work task
[AD-A274707] 07 p2937 N94-26430
Human dimensions research team, operation restore hope
[AD-A274340] 07 p2939 N94-27056
Task demand, workload, and performance
[PB94-123627] 07 p2942 N94-27155
Development of stimulus-seeking scale for expecting individual differences against confinement stress
07 p2915 N94-27460
Strategies to sustain and enhance performance in stressful environments
[AD-A275223] 08 p3398 N94-29027
Stress and ergonomic design and evaluation of person-machine systems
[AD-A275156] 08 p3400 N94-29034
Spectral analysis of heart rate and psychological state: A review of its validity as a workload index
[AD-B179387] 08 p3399 N94-30969
Development and enhancement of a model of performance and decision making under stress in a real life setting
[AD-A276029] 09 p3799 N94-31440
Stress-induced enhancement of the startle reflex
[AD-A278414] 09 p3802 N94-33327
Crisis and disaster research: A review
[PB94-149234] 10 p4097 N94-34108
Cerebral neurochemical mechanisms in stress and anxiety
[AD-A280473] 12 p4482 N94-37233

STRESS ANALYSIS
NT BOUNDARY ELEMENT METHOD
Design and development of a miniature column-based interface (MCBI) stress gage
[AD-A266054] 01 p0170 N94-10873
Imperfection sensitivity of the Brazier effect for orthotropic cylindrical shells
[LR-687] 01 p0186 N94-10879
An electro-optical system for the measurement of strains
01 p0186 N94-10900
Computational gearing mechanics
[NASA-CR-193666] 01 p0181 N94-11157
Fatigue life prediction for wind turbines: A case study on loading spectra and parameter sensitivity
[DE93-011597] 01 p0263 N94-11173
A study of strength evaluations of EDNi/EDCu/NARloy-Z bonded joints
[NASA-TM-108418] 01 p0188 N94-11275
An analysis of fiber-matrix interface failure stresses for a range of ply stress states
[NASA-TM-108999] 01 p0067 N94-11276
RAMCAD (reliability, availability, and maintainability in computer-aided design)
[AD-A265143] 01 p0331 N94-11679
Horizontal stresses induced by vertical processes in planetary lithospheres
01 p0281 N94-12042
A normal stress subgrid-scale eddy viscosity model in large eddy simulation
01 p0155 N94-12288
Application of a Reynolds stress model to separating boundary layers
01 p0157 N94-12299
Analytical models for describing the mechanical behavior of fiber reinforced composites
[AD-A265906] 01 p0074 N94-12347
Advances in low carbon, high strength ferrous alloys
[AD-A265264] 01 p0085 N94-12532
Body/cushion contact stress analysis during sitting
[ITN-93-85204] 02 p0736 N94-13229
LUTE telescope structural design
[NASA-CR-192594] 02 p0830 N94-13448
Autofrettage: Stress distribution under load and retained stresses after depressurization. A modified plane-strain case
[AD-A266320] 02 p0671 N94-13579
Finite element analysis of composite plates by use of modified complementary energy principle
02 p0672 N94-13596
Computational methods for reliable fatigue and damage tolerance dimensioning of aircraft structures
[FFA-TN-1993-05] 02 p0515 N94-13690
Some computational tools for the analysis of through cracks in stiffened fuselage shells
[LR-701] 02 p0673 N94-13726
Thermal gradient-induced deflection of a thick-walled cylinder with bending residual stresses
[AD-A266347] 02 p0673 N94-13777
Contribution to comparison of methods for determining welding procedures for the avoidance of hydrogen cracking
[VTT-PUBS-107] 02 p0674 N94-13887
Compressive buckling of curved, anisotropic panels stiffened in two directions. Part 1: Derivation of the governing equations
[LR-694] 02 p0675 N94-13931
Stress stiffening and approximate equations in flexible multibody dynamics
02 p0677 N94-14620
The effect of initial imperfections on shell stability: An updated review
[LR-695] 02 p0682 N94-14692
Construction and calculation
03 p0931 N94-15256
High temperature advanced structural composites. Volume 3: Mechanics
[AD-A267024] 03 p0933 N94-15626
A simplistic look at limit stresses from random loading
[NASA-TM-108427] 03 p1058 N94-15710
Continuous fabrication of SiC fiber tows by chemical vapor deposition
[AD-A266460] 03 p0936 N94-16569
Programs and resources for control of job stress in the Federal workplace
03 p1124 N94-16617
Elastooptical brittle materials in experimental studies of the state of stress and deformation
[IFTR-22/1991] 03 p1059 N94-16651
Stress analysis of laminated composites with preformed holes. Part 1: Single plies with embedded material discontinuities
[AD-A266524] 03 p0936 N94-16795
Creep ductility of iron at very low strain rates: The effects of sulfur
[DE93-015490] 03 p0959 N94-16890
Static analysis of beams on an elastic base as stated by generalized functions
[IFTR-27/1991] 03 p1060 N94-16923
Mean strain effects on the strain life fatigue curve
[AD-A267211] 03 p0960 N94-16984
Surface waves in an inhomogeneous, isotropic, elastic half-space
[IFTR-18/1991] 03 p1060 N94-17047
Analysis of the strengthening of aluminum alloy undergoing plastic deformation under conditions of a compound state of stress
[IFTR-21/1991] 03 p0960 N94-17093
A review of Australian and New Zealand investigations on aeronautical fatigue during the period April 1991 to March 1993
[AD-A267532] 03 p0868 N94-17117
Elastic-plastic finite-difference analysis of unidirectional composites subjected to thermomechanical cyclic loading
[AD-A267666] 03 p1061 N94-17269
Solution of elastic-plastic stress analysis problems by the p-version of the finite element method
[NASA-CR-194267] 03 p1062 N94-17445
PVDF measurement of soft x ray induced shock and filter debris impulse
[DE93-017633] 04 p1382 N94-17806
Generalized seismic analysis
04 p1449 N94-17832
Current development in selected stress and thermal analysis software interfaces with PRO-ENGINEER
[DE93-014935] 04 p1518 N94-17943
Characteristics and pulsed radiation response of non-ideal quartz shock stress gauges
[DE93-017628] 04 p1424 N94-17999
Numerical integration of structural elements in NIKE3D and DYNA3D
[DE93-016325] 04 p1452 N94-18049
Steep geometric grating for use in moire interferometry
[AD-A268759] 04 p1453 N94-18328
The 6th Japan-U.S. conference on composite materials
[AD-A268535] 04 p1341 N94-18630
Fatigue technology assessment and strategies for fatigue avoidance in marine structures. Appendices
[AD-A269053] 04 p1455 N94-18716
A constitutive theory for rigid polyurethane foam
[DE93-011596] 04 p1372 N94-19059
Plastic mechanism analysis of T-joints in RHS subject to combined bending and concentrated force
[PB93-195774] 04 p1456 N94-19061
A comparative evaluation of in-plane shear test methods for laminated graphite-epoxy composites
[NASA-CR-193808] 04 p1456 N94-19095
Interfacial cracks in plates: A three-dimensional numerical investigation
04 p1456 N94-19116
The interpretation of optical caustics in the presence of dynamic non-uniform crack-tip motion histories: A study based on a higher order transient crack-tip expansion
[SM91-12] 04 p1456 N94-19130
Modeling and characterization of mechanoelectric conversion piezoelectric generators through dynamical or quasi static uniaxial stress
[ISAL-92-0097] 04 p1406 N94-19490
Finite element mesh generation and analysis of solder joints for fatigue life predictions
[AD-A271329] 05 p1829 N94-19937
Audit report. Navy's aircraft structural life surveillance program data recorders
[AD-A270391] 05 p1645 N94-20040
A design optimization procedure for epicyclic gears
[MATHS-REPT-A-188] 05 p1822 N94-20146
Biaxial flexural testing of a carbon fiber reinforced epoxy composite
[AD-A271956] 05 p1674 N94-20577

Preliminary SP-100/Stirling heat exchanger designs
[NASA-TM-106444] 05 p1670 N94-21809
A finite element formulation and adaptive solution approach for large-scale thermomechanical problems with complex contact conditions
[DE93-019605] 05 p1960 N94-21996
Modeling of failure and response to laminated composites subjected to in-plane loads
05 p1834 N94-22612
Life prediction systems for critical rotating components
05 p1835 N94-22615
Computation of flows in a turn-around duct and a turbine cascade using advanced turbulence models
06 p2216 N94-23062
Control of the internal stresses in plane elasticity
[PB93-225514] 06 p2374 N94-23112
Internal friction associated with dislocation relaxations in virgin martensite
[PB93-226280] 06 p2240 N94-23119
A numerical analysis of crack propagation in microcracking ceramic and ceramic composites
[DE94-001192] 06 p2253 N94-23183
Fully coupled nonlinear thermomechanical analysis including general contact in PALM2D
[DE94-001661] 06 p2568 N94-23216
Determination of fiber-matrix interface failure parameters from off-axis tests
[NASA-TM-109043] 06 p2241 N94-23274
Out of plane gradients in laminated composites
[NASA-CR-194875] 06 p2228 N94-23566
Contact analysis of rough rail surfaces
06 p2270 N94-23589
Dynamic localization and second-order subgrid-scale models in large eddy simulations of channel flow
06 p2329 N94-24149
Integrated stress and strength analysis of airplane structures using the data processing tool ISSY
06 p2178 N94-24320
Buckling of circular cylindrical shells subjected to combined loads (axial compression, normal pressure, bending and transverse shear loading)
[PB93-215358] 06 p2378 N94-24745
FRANC2D: A two-dimensional crack propagation simulator. Version 2.7: User's guide
[NASA-CR-4572] 06 p2246 N94-25118
The complete stress field due to a dislocation located anywhere in two bonded quarter planes
[OUEL-1990/93] 06 p2379 N94-25478
Determination of fracture stress and effective crack tip radius from toughness (Klc) and yield strength (Y)
[AD-A274014] 07 p2836 N94-25754
A nonlinear three-dimensional micromechanics model for fiber-reinforced laminated composites
[AD-A273772] 07 p2705 N94-25857
Evaluation of helium cooling for fusion divertors
[DE94-002680] 07 p3042 N94-25976
Deviatoric stresses and plastic strain rates in strong shock waves for six metals
[DE94-002964] 07 p2733 N94-26022
Development of detection technique for fatigue crack due to thermal stratification phenomena in RCS piping
[DE93-632968] 07 p2838 N94-26400
Studies on the measurement of subsurface fractures and geostress using acoustic emission technique for deep coalbed development
[REPT-7] 07 p2879 N94-26475
Stress analysis of a secondary-bending specimen
[AD-A274842] 07 p2838 N94-26501
User's guide for the frequency domain algorithms in the LIFE2 fatigue analysis code
[DE94-004678] 07 p2838 N94-26563
Nonlinear hysteresis in an endochronic solid
[AD-A274594] 07 p2880 N94-26855
Refined triangular plate and shell elements
[PB94-126356] 07 p2839 N94-26875
Computation of stress intensity factors by the mode enrichment technique with applications to geometrically nonlinear problems
[PB94-126513] 07 p2840 N94-26910
Formulae for the buckling of simply-supported corrugated panels of orthotropic material under shear load
[PB94-126547] 07 p2840 N94-26911
Baseline for a Nordtest method. Reliability stress screening of components. A guide for component users
[PB94-123775] 07 p2835 N94-27042
Series solution for a cylindrical composite shell subject to axisymmetric loadings
[ISBN-0-315-60559-6] 07 p2844 N94-27810
Mechanically fastened composite laminates subjected to combined bearing-bypass and shear loading
07 p2712 N94-27914
Development of methodologies for the estimation of thermal properties associated with aerospace vehicles
07 p2846 N94-27920
On the Lagrangian and updated Lagrangian nonlinear finite element formulations
[ISBN-0-315-61111-1] 07 p3001 N94-27948
Contact stress in disc cams with roller followers
[ESDU-93001] 07 p2829 N94-28055
Flat rectangular orthotropic plates under uniformly distributed normal pressure. Elastic stresses and deflections for various forms of edge restraint
[ESDU-93011] 07 p2845 N94-28061
Three-dimensional elastic stress concentration factors: Plain or countersunk hole in a wide plate subjected to tension, bending, or pin loading
[ESDU-93030] 07 p2845 N94-28143
Journal of NIRE, volume 2, number 4
[JTN-94-80554] 07 p2869 N94-28147
The estimation of pre-stress by deformation rate analysis and suggestion of a mechanism from the elast-plastical theory 07 p2871 N94-28156
Viscous and elastic-plastic material model in the ABAQUS
[PB94-132347] 08 p3316 N94-28409
A modeling study of the effect of stress state on void linking during ductile fracture
[AD-A275505] 08 p3317 N94-28811
An anisotropic extension of Bodner's model of viscoplasticity: Model development
[NASA-CR-195289] 08 p3318 N94-28821
Modelling and analysis of creep deformation and fracture in a 1 Cr 1/2 Mo ferritic steel
[PB94-138328] 08 p3319 N94-29121
Low temperature behavior of virgin martensite
[PB94-132925] 08 p3204 N94-29142
Numerical analysis of dynamic direct tension and direct compression tests
[AD-A275255] 08 p3319 N94-29433
Stress transfer mechanics for multiple perfectly bonded concentric cylinder models of unidirectional composites
[PB94-138633] 08 p3181 N94-29524
Free edge and size effects on failure initiation and ultimate strength of laminates containing a center hole
08 p3181 N94-29735
Performance of a higher-order triangular finite element for composite laminated structures
08 p3181 N94-29810
Higher order asymptotic crack tip fields in a power-law hardening material 08 p3321 N94-29829
Estimation of Weibull modulus from dynamic and static fatigue experiments
[PB94-138641] 08 p3322 N94-30114
Multiple Concentric Cylinder Model (MCCM) user's guide
[NASA-CR-195299] 08 p3183 N94-30125
Micromechanical analysis of thermo-inelastic multiphase short-fiber composites
[NASA-CR-195290] 08 p3183 N94-30178
Potential capabilities of Reynolds stress turbulence model in the COMMIX-RSM code
08 p3285 N94-30450
Approximate estimation of the effects of asymmetry on the testing of tensile specimens
[NPL-DMM(A)-117] 08 p3322 N94-30523
An investigation of fatigue crack propagation under mode 1 and mixed mode 1/2 loadings
08 p3323 N94-30814
Fatigue management and verification of airframes
[FFA-TN-1993-55] 08 p3149 N94-30947
Numerical modeling and prediction of the thermomechanical behavior of fiber-reinforced composites 08 p3186 N94-30956
Aspects of modelling the tectonics of large volcanoes on the terrestrial planets 09 p3940 N94-31107
State of stress, faulting, and eruption characteristics of large volcanoes on Mars 09 p3940 N94-31108
On the mechanics of stress analysis of fiber-reinforced composites 09 p3619 N94-31481
Contribution to the study of multiaxial fatigue under periodic or random stresses
[ISAL-92-0004] 09 p3734 N94-31544
A novel CFD/structural analysis of a cross parachute
[DE94-005271] 09 p3568 N94-31578
An approximate solution for interlaminar stresses in laminated composites 09 p3621 N94-31901
Finite element analysis of damage in fibrous composites using a micromechanical model
[AD-A277226] 09 p3623 N94-32024
Bond stress-slip characteristics of FRP rebars
[AD-A277191] 09 p3623 N94-32070
Mechanics of the single fiber pullout problem with several interface conditions 09 p3623 N94-32078
Finite element analysis of MB326H Macchi wing lower spar cap fatigue cracks
[AD-A277062] 09 p3580 N94-32264
A critical evaluation of the Reynolds stress turbulence closure for the flow of a turbulent free-stream over a turbulent boundary layer
[ISBN-0-315-75792-2] 09 p3707 N94-32497
Development of an advanced continuum theory for composite laminates, volume 1
[AD-A277275] 09 p3625 N94-32591
Development of an advanced continuum theory for composite laminates, volume 2
[AD-A277276] 09 p3625 N94-32592
A thermal viscoelastic analysis for thick-walled composite cylinders
[AD-A274143] 09 p3625 N94-32604
Design and evaluation of coils for a 50 mm diameter induction coilgun launcher
[DE94-005244] 09 p3603 N94-32671
METCAN demonstration manual, version 1.0
[NASA-TM-105607] 09 p3626 N94-32858
A procedure for 3-D contact stress analysis of spiral bevel gears
[NASA-CR-194472] 09 p3728 N94-32929
Personal cooling systems: Possibilities and limitations
10 p4101 N94-33649
Use of photostress to analyze behavior of an aft skirt test specimen
[NASA-CR-195850] 10 p4069 N94-34075
Micromechanical characterization of nonlinear behavior of advanced polymer matrix composites
[NASA-TM-109129] 10 p4025 N94-34397
Engine static structures behaviour under impact load using 3D modelling 10 p4004 N94-34464
An Assessment of Fatigue Damage and Crack Growth Prediction Techniques
[AD-280273] 10 p4071 N94-34581
Miner's rule revisited 10 p4071 N94-34582
The crack severity index of monitored load spectra
10 p4071 N94-34585
Fatigue management and verification of airframes
10 p3996 N94-34591
Can the compressive response of fiber-reinforced composites be modelled by means of layered arrays?
[AD-A278864] 11 p4233 N94-35944
Propellant stress relief groove for the Titan 4 SRMU
[AD-A278628] 11 p4228 N94-36254
Metal matrix composites: Analysis of simple specimens and model components under creep and fatigue loading
12 p4402 N94-36661
Jumper connector analysis
[DE94-010373] 12 p4451 N94-37188
Some considerations for modeling the creep behavior of composite materials
[DE94-012112] 12 p4404 N94-37205
Strength evaluation of socket joints
[NASA-CR-4608] 12 p4389 N94-37259
Transient thermal and dynamic stresses in strongback-design blankets
[DE94-012639] 12 p4530 N94-37441
Fatigue case study and loading spectra for wind turbines
[DE94-010798] 12 p4457 N94-37622
A simple evaluation of thermally-induced stresses in the vicinity of the stitch in a through-thickness reinforced cross-ply laminate
[NASA-CR-196317] 12 p4406 N94-37653
Scaling, elasticity, and CLPT
12 p4458 N94-37800

STRESS CALCULATIONS

U STRESS ANALYSIS

STRESS CONCENTRATION

Analytical models for describing the mechanical behavior of fiber reinforced composites
[AD-A265906] 01 p0074 N94-12347
Evolving surface cusps during strained-layer epitaxy
[DE93-015430] 02 p0813 N94-14478
ITER-HARD Toroidal Field coil structural analysis
[DE93-014834] 03 p1201 N94-15981
Fatigue life program using strain-life methods
[AD-A267310] 03 p1060 N94-16943
Fatigue technology assessment and strategies for fatigue avoidance in marine structures. Appendices
[AD-A269053] 04 p1455 N94-18716
Mechanically fastened composite laminates subjected to combined bearing-bypass and shear loading
07 p2712 N94-27914
Three-dimensional elastic stress concentration factors: Plain or countersunk hole in a wide plate subjected to tension, bending, or pin loading
[ESDU-93030] 07 p2845 N94-28143
Physical properties of glasses exposed to Earth-facing and trailing-side environments on LDEF
09 p3594 N94-31030
Micromechanical analysis of the interface and basic damage modes in glass fiber/epoxy resin model composites
[ONERA-NT-1993-4] 09 p3618 N94-31225
Reliability analysis of structural ceramics subjected to biaxial flexure 09 p3650 N94-31454
Tension fracture of laminates for transport fuselage. Part 1: Material screening 09 p3629 N94-33130

Structural integrity of intelligent materials and structures
[AD-A278397] 09 p3630 N94-33165
Fundamental studies in crack initiation
[AD-A278387] 09 p3741 N94-33356
Variations of a global constraint factor in cracked bodies under tension and bending loads
[NASA-TM-109119] 10 p4071 N94-34385
Fatigue life and crack growth prediction methodology 10 p4071 N94-34583
Graphing techniques for materials laboratory using Excel 11 p4232 N94-36414
Modeling of thermal barrier coatings
[NASA-CR-195365] 12 p4421 N94-36637

STRESS CORROSION
NT STRESS CORROSION CRACKING
Corrosion behavior of metal matrix composites
[AD-A265352] 01 p0085 N94-12404
The ASCOR test: A simple automated method for stress corrosion testing of aluminium alloys
[NLR-TP-91438-U] 02 p0570 N94-13532
Environmentally assisted cracking of nickel anode substrates in Li/SOCl2 cells: An engineering approach
[DE93-015130] 04 p1405 N94-18928
The effects of radiolysis on the corrosion and stress corrosion behavior of 316 stainless steels
[DE93-019933] 04 p1363 N94-19021
Benefits of thread rolling process to the stress corrosion cracking and fatigue resistance of high strength fasteners
[DE93-040438] 05 p1833 N94-22001
Analysis of Alloy 600 and X-750 stress corrosion cracks
[DE94-001578] 06 p2238 N94-22936
Fracture kinetics analysis of empirical and semi-empirical corrosion fatigue relations 06 p2159 N94-24277
Preceedings of the 12th International Congress: Corrosion Control for Low-Cost Reliability. Volume 2: Process Industries Plant Operations
[AD-A273662] 06 p2251 N94-25449
Preceedings of the 12th International Congress: Corrosion Control for Low-Cost Reliability. Volume 3A: Corrosion: Specific issues
[AD-A273663] 06 p2251 N94-25450
Inner fiber observation for metal matrix composites under the stress load condition utilizing Synchrotron Orbital Radiation (SR) by X-ray CT 07 p2724 N94-25553
Study on improvements in fretting fatigue characteristics of high strength structural member 07 p2726 N94-25567
Radiation hardening effects on localized deformation and stress corrosion cracking of stainless steels
[DE94-004308] 07 p2731 N94-25804

STRESS CORROSION CRACKING
Facility for stress corrosion cracking test of irradiated material in high temperature water
[DE93-753189] 01 p0084 N94-11593
Corrosion behavior of metal matrix composites
[AD-A265352] 01 p0085 N94-12404
Interfacial precipitation, segregation and deformation in alloy 600: Implications on primary-side IGSCC
[DE93-013161] 02 p0568 N94-13035
Radiation hardening and radiation-induced chromium depletion effects on intergranular stress corrosion cracking of austenitic stainless steels
[DE93-011602] 02 p0572 N94-14058
JPRS report: Science and technology. Central Eurasia: Materials science
[JPRS-UMS-93-005] 02 p0559 N94-14575
Environmental effects on elevated temperature subcritical crack growth of SiC/SiC composites
[DE93-015688] 03 p0934 N94-16158
Stress corrosion cracking of 316 SS and Incoloy-800 in high temperature aqueous containing sulfate and chloride
[DE93-623325] 03 p0952 N94-17302
Environment enhanced fatigue crack propagation in metals: Inputs to fracture mechanics life prediction models
[NASA-CR-191538] 03 p0942 N94-17638
Environmental degradation of Alloy 600 and welded filler metal EN82 in an elevated temperature aqueous environment
[DE93-018049] 04 p1363 N94-18940
Benefits of thread rolling process to the stress corrosion cracking and fatigue resistance of high strength fasteners
[DE93-040438] 05 p1833 N94-22001
Analysis of Alloy 600 and X-750 stress corrosion cracks
[DE94-001578] 06 p2238 N94-22936
Thermally activated low temperature creep and primary water stress corrosion cracking of NiCrFe alloys
[DE94-001756] 06 p2241 N94-23219
NASA/ASEE Summer Faculty Fellowship Program
[NASA-CR-194678] 06 p2571 N94-23230
Stress corrosion cracking properties of 15-5PH steel 06 p2251 N94-23244
Grain-boundary microchemistry and intergranular cracking of irradiated austenitic stainless steel
[DE94-000466] 06 p2242 N94-23457
Effect of irradiation on the stress corrosion cracking behavior of Alloy X-750 and Alloy 625
[DE94-001759] 06 p2244 N94-23792
Feasibility study of shot-peening modeling
[CTN-94-60926] 06 p2244 N94-24170
Microstructure and micromechanical behaviour of CMCs 06 p2256 N94-24236
Bulletin of National Research Institute for Metals in Fiscal Year 1993, no. 14
[REPT-14] 07 p2722 N94-25544
Interactions between corrosion fatigue and stress corrosion crack on steel for light water reactors 07 p2722 N94-25547
Study on performance evaluation of pressure vessel steel in corrosion environments with sulfide 07 p2730 N94-25582
Radiation hardening effects on localized deformation and stress corrosion cracking of stainless steels
[DE94-004308] 07 p2731 N94-25804
Grain by grain study of the mechanisms of crack propagation during iodine SCC of Zry-4
[DE93-633765] 07 p2734 N94-26162
Guidelines for controlling stress corrosion cracking and corrosion fatigue of stainless steels: A literature review
[VTT-TIED-1420] 07 p2837 N94-26262
Stress corrosion cracking and dealloying of copper-gold alloy in iodine vapor
[DE93-633790] 07 p2734 N94-26264
Development of non-destructive testing technology for the crack of steam generator tubes
[DE93-632953] 07 p2835 N94-26399
Early stages in the development of stress corrosion cracks
[DE94-003867] 07 p2838 N94-26524
Grain boundary chromium concentration effects on the IGSCC and IASCC of austenitic stainless steels
[DE94-004268] 07 p2741 N94-27570
An anodic dissolution-based mechanism for the rapid cracking, pre-exposure phenomenon demonstrated by Al-Li-Cu alloys
[DE94-004798] 07 p2742 N94-27788
The transition from stress corrosion cracking to corrosion fatigue in AA-7075 and AA-8090
[ISBN-0-315-59526-4] 07 p2744 N94-27950
Irradiation-assisted stress corrosion cracking of materials from commercial BWRs: Role of grain-boundary microchemistry
[DE94-006542] 09 p3643 N94-32109
Stage 1 behavior in a stress corrosion study of Type 304 stainless steel
[DE94-008054] 09 p3645 N94-32614
Modeling of residual stress mitigation in austenitic stainless steel pipe girth weldment
[DE94-007184] 09 p3738 N94-32639
Susceptibility of grade 8 fasteners to stress corrosion cracking
[AD-A277883] 10 p4069 N94-33552
Theoretical study of reactions at the electrode-electrolyte interface
[DE94-009658] 10 p4138 N94-34100
Irradiation assisted stress corrosion cracking of HTH Alloy X-750 and Alloy 625
[DE94-012667] 12 p4416 N94-37080

STRESS CYCLES
Defining the normal turbine inflow within a wind park environment
[DE93-010032] 04 p1489 N94-18046
Fundamentals of fatigue analysis
[PB93-226264] 06 p2374 N94-23118
Review of super Ni/Cd cell designs and performance 06 p2391 N94-23348

STRESS DISTRIBUTION
NT STRESS CONCENTRATION
Elastic plastic fracture mechanics methodology for surface cracks
[NASA-CR-194129] 01 p0185 N94-10712
Parameterization of subgrid-scale stress by the velocity gradient tensor 01 p0155 N94-12286
Body/cushion contact stress analysis during sitting
[ITN-93-85204] 02 p0736 N94-13229
Numerical simulations and experiments on physics of high Mach number shockwave: Turbulent flow interactions
[DE93-013424] 02 p0631 N94-13249
Autofrettage: Stress distribution under load and retained stresses after depressurization. A modified plane-strain case
[AD-A266320] 02 p0671 N94-13579
A process for evaluation of mechanical behavior of surface films
[W-1/92] 02 p0579 N94-14007
Machining and grinding: High rate deformation in practice
[DE93-010718] 02 p0664 N94-14457
Thermal stresses of a trimaterial medium in a nonuniform temperature field
[AD-A267243] 03 p0930 N94-14975
Spatially extensive uniform stress fields on Venus inferred from radial dike swarm geometries: The Aphrodite Terra example 03 p1254 N94-16207
Highly transient elastodynamic crack growth in a bimaterial interface: Higher order asymptotic analysis and optical experiments
[AD-A266465] 03 p1059 N94-16587
Static analysis of beams on an elastic base as stated by generalized functions
[IFTR-27/1991] 03 p1060 N94-16923
High temperature materials technology research for advanced thermionic systems
[DE93-018302] 03 p0960 N94-16964
Measurement and theory of the dependence of hardness on residual stress
[AD-A267553] 03 p1061 N94-17105
Elastic-plastic finite-difference analysis of unidirectional composites subjected to thermomechanical cyclic loading
[AD-A267666] 03 p1061 N94-17269
Implementation of mixed formulation elements in PC/NASTRAN 04 p1449 N94-17828
Impact response of composite laminates: A guide to closed form solutions
[FFA-TN-1992-33] 04 p1339 N94-17971
Numerical integration of structural elements in NIKE3D and DYNA3D
[DE93-016325] 04 p1452 N94-18049
New test method to determine modulus of elasticity of rocket grain material
[AD-A269758] 04 p1377 N94-18758
A numerical analysis of crack growth in brittle microcracking composites
[DE93-011562] 04 p1343 N94-18914
Fundamental studies of stress distributions and stress relaxation in oxide scales on high temperature alloys
[DE94-001444] 05 p1693 N94-21854
Post-Palbozoic crustal responses to the contemporary stress field in the eastern United States
[DE93-040604] 05 p1859 N94-22006
A numerical analysis of crack propagation in microcracking ceramic and ceramic composites
[DE94-001192] 06 p2253 N94-23183
Development of a theory of the wear of ceramics
[DE94-002773] 06 p2254 N94-23783
Ceramic matrix composites: Challenges and opportunities 06 p2255 N94-24230
Interface evaluation in ceramic composites 06 p2255 N94-24231
Fracture kinetics analysis of empirical and semi-empirical corrosion fatigue relations 06 p2159 N94-24277
The complete stress field due to a dislocation located anywhere in two bonded quarter planes
[OUEL-1990/93] 06 p2379 N94-25478
Development of detection technique for fatigue crack due to thermal stratification phenomena in RCS piping
[DE93-632968] 07 p2838 N94-26400
An experimental study on the effects of compressive stress on the fatigue crack growth of low-alloy steel
[DE94-004447] 07 p2737 N94-26582
Deformation, constitutive behavior, and damage of advanced structural materials under multiaxial loading
[AD-A274165] 07 p2709 N94-27142
Behaviour modification of space trusses
[ISBN-0-315-84701-8] 07 p2842 N94-27315
Flat rectangular orthotropic plates under uniformly distributed normal pressure. Elastic stresses and deflections for various forms of edge restraint
[ESDU-93011] 07 p2845 N94-28061
Damage meso-modeling of 3D evolutive composites
[REPT-932-430-106] 08 p3179 N94-29442
Stress transfer mechanics for multiple perfectly bonded concentric cylinder models of unidirectional composites
[PB94-138633] 08 p3181 N94-29524
Higher order asymptotic crack tip fields in a power-law hardening material 08 p3321 N94-29829
Delamination of woven E-glass fabric composites
[DE94-003227] 08 p3185 N94-30827
State of stress, faulting, and eruption characteristics of large volcanoes on Mars 09 p3940 N94-31108
Influences of pressure-sensitive yielding and non-singular stress on plane-stress elastic-plastic crack-tip fields 09 p3737 N94-31965
Minimization of computational requirements in the hybrid stress finite element method
[AD-A277120] 09 p3846 N94-32048
Mechanics of the single fiber pullout problem with several interface conditions 09 p3623 N94-32078
Analysis of new composite architectures
[NASA-CR-195303] 09 p3626 N94-32904

A procedure for 3-D contact stress analysis of spiral bevel gears
[NASA-CR-194472] 09 p3728 N94-32929
Tension fracture of laminates for transport fuselage. Part 1: Material screening 09 p3629 N94-33130
Near tip stress and strain fields for short elastic cracks 10 p4068 N94-33418
Effects of assumed tow architecture on the predicted moduli and stresses in woven composites
[NASA-CR-195310] 10 p4020 N94-34258
Studies of the effect of microstructure on the dynamic behavior of granular and particulate media
[AD-A279012] 12 p4455 N94-36520
Size effect in composite materials and structures: Basic concepts and design considerations
12 p4460 N94-37808

STRESS FIELDS
U STRESS DISTRIBUTION

STRESS FUNCTIONS
Elastic-plastic mixed-iterative finite element analysis: Implementation and performance assessment
[NASA-TM-106164] 02 p0675 N94-13919
Stability analysis of anisotropic conical shells
[PB94-119054] 06 p2377 N94-24645

STRESS INTENSITY FACTORS
The effects of an aggressive environment on the subcritical crack growth of a continuous-fiber ceramic composite
[DE93-011690] 01 p0073 N94-11612
Finite element calculation of stress-intensity factors for thumb-nail cracks in DEN specimens
[LTR-ST-1929] 02 p0850 N94-13548
Finite element calculation of stress-intensity factors for thru-thickness cracks in DEN specimens
[LTR-ST-1905] 02 p0675 N94-14035
Environmental effects on elevated temperature subcritical crack growth of SiC/SiC composites
[DE93-015688] 03 p0934 N94-16158
Environment enhanced fatigue crack propagation in metals: Inputs to fracture mechanics life prediction models
[NASA-CR-191538] 03 p0942 N94-17638
Interfacial cracks in plates: A three-dimensional numerical investigation 04 p1456 N94-19116
The interpretation of optical caustics in the presence of dynamic non-uniform crack-tip motion histories: A study based on a higher order transient crack-tip expansion
[SM91-12] 04 p1456 N94-19130
Subcritical crack growth in continuous-fiber reinforced ceramic composites
[DE93-018784] 04 p1343 N94-19335
Residual strength predictions for fibre metal laminates: The R-curves approach
[LR-717] 04 p1344 N94-19666
Fatigue life and crack growth prediction methodology
[NASA-TM-109044] 06 p2228 N94-23279
Effect of irradiation on the stress corrosion cracking behavior of Alloy X-750 and Alloy 625
[DE94-001759] 06 p2244 N94-23792
FRANC2D: A two-dimensional crack propagation simulator. Version 2.7: User's guide
[NASA-CR-4572] 06 p2246 N94-25118
Computation of stress intensity factors by the mode enrichment technique with applications to geometrically nonlinear problems
[PB94-126513] 07 p2840 N94-26910
Method for calculating stress intensity factors for surface cracks (appendix 2/1) 07 p2841 N94-27188
Implementation of thermal residual stresses in the analysis of fiber bridged matrix crack growth in titanium matrix composites
[NASA-TM-109082] 07 p2711 N94-27658
The development of stress intensity factors
[DRA-TR-93057] 07 p2845 N94-27954
Fatigue propagation behaviour of short cracks (1-2 mm) in steels
[ESDU-93033] 07 p2845 N94-28145
Estimation of Weibull modulus from dynamic and static fatigue experiments
[PB94-138641] 08 p3322 N94-30114
A fracture mechanics methodology for characterizing the performance of flawed polymeric dielectric materials
09 p3654 N94-31956
Effects of interphases on the mechanical, thermal and hygromechanical response of fiber-reinforced composites 09 p3624 N94-32496
Stage 1 behavior in a stress corrosion study of Type 304 stainless steel
[DE94-008054] 09 p3645 N94-32614
Compliance measurements of chevron notched four point bend specimen
[NASA-TM-106538] 09 p3740 N94-32932
Composite repairs of cracked metallic airframe structures
[AD-A277680] 10 p3969 N94-33590
Small-crack effects in high-strength aluminum alloys
[NASA-RP-1309] 10 p4070 N94-34299
Fatigue life and crack growth prediction methodology
10 p4071 N94-34583
Frequency domain analysis of the random loading of cracked panels
[NASA-CR-196021] 11 p4279 N94-35974
Irradiation assisted stress corrosion cracking of HTH Alloy X-750 and Alloy 625
[DE94-012667] 12 p4416 N94-37080
A methodology to predict damage initiation, damage growth and residual strength in titanium matrix composites
[NASA-TM-109135] 12 p4405 N94-37320
Defects and their effects on the integrity of nickel based aeroengine discs 12 p4421 N94-37328
Strength characteristics and crack growth behavior of a composite with well aligned fibers
12 p4459 N94-37804

STRESS MEASUREMENT
Design and development of a miniature column-based interface (MCBI) stress gage
[AD-A266054] 01 p0170 N94-10873
Residual contact restraints in cryogenics
[ETN-93-94375] 02 p0671 N94-13501
Thermal stress effects in intermetallic matrix composites
[NASA-CR-191191] 03 p1054 N94-16518
The processing and mechanical properties of high temperature/high performance composites. Book 5: Processing and miscellaneous properties
[AD-A266398] 03 p0935 N94-16529
Shear wave measurements in shock-induced, high-pressure phases
[DE93-016461] 03 p1062 N94-17664
PVDF measurement of soft x ray induced shock and filter debris impulse
[DE93-017633] 04 p1382 N94-17806
Application of piezoelectric stress gauges to the measurement of fast-rise-time multimegampere electric currents
[DE93-017625] 04 p1429 N94-18102
A comparative evaluation of in-plane shear test methods for laminated graphite-epoxy composites
[NASA-CR-193808] 04 p1456 N94-19095
Time-resolved shock compression of porous rutile: Wave dispersion in porous solids
[DE93-018848] 05 p1829 N94-19927
High accuracy die mechanical stress measurement with the ATC04 Assembly Test Chip
[DE93-019435] 05 p1830 N94-20477
Method of determining shear stress employing a monomer-polymer laminate structure
[NASA-CASE-LAR-14654-2] 06 p2375 N94-23308
Skin friction measurement in complex flows using thin oil film techniques
[NASA-CR-194872] 06 p2327 N94-24098
Feasibility study of shot-peening modeling
[CTN-94-60926] 06 p2244 N94-24170
Alternatives for reinforcement: Fiber composites
[VTT-TIED-1412] 06 p2230 N94-25386
Dynamic response of S-2 glass reinforced plastic structural armor
[AD-A273868] 07 p2747 N94-25596
Studies on the measurement of subsurface fractures and geostress using acoustic emission technique for deep coalbed development
[REPT-7] 07 p2879 N94-26475
Stress analysis of a secondary-bending specimen
[AD-A274842] 07 p2838 N94-26501
The renewing of the test section of the NAL transonic wind tunnel. Part 1: Reconstruction of the 1st corner turning vanes and aerodynamic stress measurement
[NAL-TM-651] 07 p2681 N94-27247
High intensity x ray instrumentation for residual strain measurements in composites and textured materials
[ISBN-0-315-85169-4] 07 p2842 N94-27278
A hydrostatic stress-dependent anisotropic model of viscoplasticity
[NASA-TM-106525] 07 p2711 N94-27640
AF Ni-Cd cell qualification program
07 p2863 N94-28122
Vacuum chamber and adaptors for shearography and holography
[NASA-CR-192467] 08 p3157 N94-29956
Shearographic inspection of a DeHavilland DHC-7
[AD-A276716] 09 p3566 N94-32157
Compilation of diamond-like carbon properties for barriers and hard coatings
[DE94-008231] 09 p3661 N94-32803
Bottom boundary layer stress measurements with BASS tripods: Data report STRESS 1988-1989
[AD-A277864] 10 p4092 N94-33775

STRESS PROPAGATION
Bulletin of National Research Institute for Metals in Fiscal Year 1993, no. 14
[REPT-14] 07 p2722 N94-25544
Interactions between corrosion fatigue and stress corrosion crack on steel for light water reactors
07 p2722 N94-25547

STRESS RATIO
Fatigue-life behavior and matrix fatigue crack spacing in unnotched SCS-6/Timetal 21S metal matrix composites
[NASA-CR-191467] 01 p0185 N94-10715
Fatigue propagation behaviour of short cracks (1-2 mm) in steels
[ESDU-93033] 07 p2845 N94-28145

STRESS RELAXATION
Stress relaxation forming of Ariane 5 front skirt outer skin panels 01 p0062 N94-10046
Investigation of the reason for the softening behaviour of filled polymers 01 p0063 N94-10058
Time-temperature shift factors for gun propellants
[AD-A264979] 01 p0097 N94-10489
Crack suppression in GaInSb buffer layers initially under tensile stress
[DE93-012839] 01 p0396 N94-10745
Lifetime prediction of materials exposed to the natural space environment
[NASA-CR-193833] 02 p0561 N94-12830
Evolving surface cusps during strained-layer epitaxy
[DE93-015430] 02 p0813 N94-14478
On the design of structural components using materials with time-dependent properties
[NASA-TM-108428] 03 p1059 N94-16519
Mechanical response comparison of gun propellants evaluated under equivalent time-temperature conditions
[AD-A270479] 04 p1378 N94-19674
Synthesis and properties of mismatched heterojunction/substrate interfaces
[AD-A272904] 05 p1760 N94-21229
Fundamental studies of stress distributions and stress relaxation in oxide scales on high temperature alloys
[DE94-001444] 05 p1693 N94-21854
Thermally activated low temperature creep and primary water stress corrosion cracking of NiCrFe alloys
[DE94-001756] 06 p2241 N94-23219
On the deformation kinetics constitutive law of plastic deformation: The rate equation
06 p2161 N94-24289
Stress relaxation in dough moulding compounds
[PB94-124872] 07 p2748 N94-25894
Stress relaxation in sputtered W films and W/GeSi/Si heterostructures
[DE94-004007] 07 p3055 N94-26239
Mechanical behavior of amorphous alloys at elevated temperatures 07 p2746 N94-28167
Measurement and modelling of bolted joint stress relaxation in plastics
[PB94-124849] 08 p3318 N94-28841
Processing of novel nanoparticle dispersion strengthened ceramics for improved mechanical performance
[AD-A275965] 09 p3649 N94-31276
Effect of vibratory stress relief during welding of thick stainless steel plate
[DE94-006557] 09 p3733 N94-31312
Replacement of silicone polymer A with silicone polymer B and the subsequent characterization of the new cellular silicone materials
[DE94-010105] 12 p4421 N94-36474
Residual stresses in a multi-pass weld in an austenitic stainless steel plate before and after thermal stress relief
[DE94-013278] 12 p4420 N94-37548

STRESS RELIEVING
Process and apparatus for the release of a prestress initially applied to a mechanism such as a bearing on board a space vehicle
[CA-PATENT-APPL-SN-2,020,909]
05 p1824 N94-21142

STRESS RUPTURE STRENGTH
U CREEP RUPTURE STRENGTH

STRESS TENSORS
A local dynamic model for large eddy simulation
01 p0155 N94-12285
Discussion of stress tensor nonuniqueness with application to nonuniform, particulate systems
[DE93-014352] 02 p0816 N94-13206
Systematology for elastic-plastic material equations by large deformations on the basis of the Cosserat-continuum model
[SCHRIFTENR-PHYSIKAL-ING-BD-23]
03 p1058 N94-15642
On a conformal perfect fluid in the classical vacuum
[DE93-624797] 04 p1480 N94-17682

Assessment of an improved multiaxial strength theory based on creep-rupture data for Inconel 600
[DE93-015929] 04 p1356 N94-17791
On the large eddy simulation of turbulent flows in complex geometry 06 p2329 N94-24148
Super Beltrami differentials and N equal to 4 superconformal anomalies
[DE93-613047] 06 p2491 N94-25166
The nonlinear Galerkin method: A multi-scale method applied to the simulation of homogeneous turbulent flows
[AD-A277432] 07 p2792 N94-26499

STRESS WAVES
Time-resolved shock compression of porous rutile: Wave dispersion in porous solids
[DE93-018848] 05 p1829 N94-19927
Asteroid collisions: Target size effects and resultant velocity distributions 05 p2083 N94-20729
Bibliographic Retrieval System (BARS), Sandia Shock Compression (SSC) database Shock Physics Index
[DE94-001679] 06 p2589 N94-23126
Bibliographic Retrieval System (BARS). Sandia Shock Compression (SSC) database Shock Physics Index (SPHINX) database. Volume 1: UNIX version query guide customized application for INGRES
[DE94-001703] 06 p2589 N94-23127
Dynamic response of ceramics
[AD-A275396] 08 p3214 N94-29203

STRESS-STRAIN DIAGRAMS
Development of bioelastic material for aspects of wound repair
[AD-A267832] 05 p1673 N94-20208
Constitutive modelling of fiber-reinforced concrete under uniaxial tensile loading
[VTT-JULK-774] 06 p2379 N94-25385

STRESS-STRAIN RELATIONSHIPS
A modeling investigation of thermal and strain induced recovery and nonlinear hardening in potential based viscoplasticity
[NASA-TM-106122] 01 p0188 N94-11482
Autofrettage: Stress distribution under load and retained stresses after depressurization. A modified plane-strain case
[AD-A266320] 02 p0671 N94-13579
Micromechanical damage theories for brittle solids with interacting microcracks
[AD-A266348] 02 p0673 N94-13778
Measurement of strain in individual phases of composites before, during, and after mechanical loading
[DE93-014585] 02 p0558 N94-14119
Elastic-plastic finite element analyses of an unidirectional, 9 vol percent tungsten fiber reinforced copper matrix composite
[NASA-TM-106304] 02 p0559 N94-14719
Forced harmonic vibration of the generally orthotropic cylindrical shell with inner and outer fluid loading
[AD-A266985] 03 p1057 N94-15150
Systematology for elastic-plastic material equations by large deformations on the basis of the Cosserat-continuum model
[SCHRIFTENR-PHYSIKAL-ING-BD-23] 03 p1058 N94-15642
Experimental study of nonassociated flow and instability of frictional materials
[AD-A266421] 03 p1024 N94-16555
Effect of tow alignment on the mechanical performance of 3D woven textile composites 03 p0937 N94-16851
Fatigue life program using strain-life methods
[AD-A267310] 03 p1060 N94-16943
Mean strain effects on the strain life fatigue curve
[AD-A267211] 03 p0960 N94-16984
Quantitative assessment of the accuracy of constitutive laws for plasticity with an emphasis on cyclic deformation
[AD-A267562] 03 p0961 N94-17109
Aspects of high temperature damage in fiber reinforced titanium metal matrix composites
[AD-A267907] 03 p0941 N94-17379
The effect of electric discharge machined notches on the fracture toughness of several structural alloys
[AD-A268605] 03 p0962 N94-17464
Damage evolution in filled elastomers
[AD-A268067] 03 p1062 N94-17507
Modeling microstructural evolution and the mechanical response of superplastic materials
[DE93-014417] 04 p1355 N94-17711
Atlas of formability: Ultimet
[AD-A268352] 04 p1355 N94-17767
Atlas of formability: HAYNES 556
[AD-A268354] 04 p1356 N94-17768
Atlas of formability: HAYNES 188
[AD-A268355] 04 p1356 N94-17769
Atlas of formability: Nickelvac C-276
[AD-A268264] 04 p1357 N94-17802
Ceramic films and interfaces: Chemical and mechanical properties
[DE93-018416] 04 p1369 N94-18163
Evaluation of the production-grade class 4 flextensional transducer shell
[AD-A268796] 04 p1340 N94-18201
A finite strain ring dynamical model for pneumatic tires
[AD-A269286] 04 p1444 N94-18266
Residual strain measurement on the production-grade class 4 flextensional transducer shell
[AD-A268828] 04 p1430 N94-18537
Implementation of a nonisothermal unified inelastic-strain theory into ADINA6.0 for a titanium alloy: User guide
[AD-A269927] 04 p1360 N94-18660
Dislocation-drag contribution to high-rate plastic deformation in shock-loaded tantalum
[DE93-018286] 04 p1361 N94-18802
Wave propagation near explosive sources
[AD-A270102] 04 p1418 N94-18870
Effect of internal heating during hot compression testing on the stress-strain behavior and hot working characteristics of alloy 304L
[DE93-012701] 04 p1362 N94-18917
Experiments and analysis of lateral piezoresistance gauges
[DE93-017874] 04 p1433 N94-19111
Shock compression properties of silicon carbide
[DE93-019927] 04 p1373 N94-19271
A review of aeronautical fatigue investigations in Sweden during the period May 1991 to April 1993
[FFA-TN-1993-22] 04 p1457 N94-19358
Current capabilities for simulating the extreme distortion of thin structures subjected to severe impacts 04 p1459 N94-19474
Development of engineering models for calculation of failure loads and defect states of steel concrete beams and plates
[ETN-93-95052] 04 p1460 N94-19648
Residual strength predictions for fibre metal laminates: The R-curves approach
[LR-717] 04 p1344 N94-19666
Two-dimensional finite element analysis of porous media at multikilobar stress levels
[AD-A271540] 05 p1831 N94-20916
Dynamic response of multiphase porous media
[AD-A272915] 05 p1831 N94-21219
Coupling of smooth particle hydrodynamics with the finite element method
[DE93-019081] 05 p1805 N94-22556
Life assessment of structural components using inelastic finite element analyses 05 p1834 N94-22614
The effects of texture and strain on the r-va lue of heavy gauge tantalum plate
[DE94-000690] 06 p2242 N94-23541
Material data representation of hysteresis loops for Hastelloy X using artificial neural networks
[NASA-TM-105990] 06 p2376 N94-23551
Microstructure and micromechanical behaviour of CMCs 06 p2256 N94-24236
Mean stress models for low cycle fatigue of a nickel-base superalloy 06 p2159 N94-24276
Evaluation of advanced materials through experimental mechanics and modelling 06 p2374 N94-24454
Test methods for composites: A status report. Volume 3: Shear test methods
[AD-A273561] 06 p2230 N94-25163
Inner fiber observation for metal matrix composites under the stress load condition utilizing Synchrotron Orbital Radiation (SR) by X-ray CT 07 p2724 N94-25553
A study of graphite peek composite with central elliptical holes under tension
[AD-A273779] 07 p2705 N94-25863
Investigation of tension-compression fatigue behavior of a cross-ply metal matrix composite at room and elevated temperatures
[AD-A273731] 07 p2706 N94-25999
The microstructural response of granular soil under uniaxial strain
[AD-A274808] 07 p2763 N94-26341
Studies on the measurement of subsurface fractures and geostress using acoustic emission technique for deep coalbed development
[REPT-7] 07 p2879 N94-26475
Aircraft wheel life assessment
[AD-A274378] 07 p2823 N94-26976
Interface phenomena in metal-ceramic composites
[AD-A274167] 07 p2709 N94-27125
The high strain rate behaviour of tantalum
[ISBN-0-315-84472-8] 07 p2740 N94-27305
Research into the microstructure and mechanical behavior of eutectic Bi-Sn and In-Sn
[DE94-004558] 07 p2741 N94-27619
The deformation of copper-tungsten composites
[ISBN-0-315-84939-8] 07 p2712 N94-27688
Use of photostress and strain gages to analyze behavior of weldments
[NASA-CR-195269] 07 p2843 N94-27765
The Science Reports of the Research Institutes, Tohoku University. Series A: Physics, Chemistry, and Metallurgy. Volume 38, No. 1: Amorphous Materials 14
[JTN-94-80610] 07 p2744 N94-28158
Viscous and elastic-plastic material model in the ABAQUS
[PB94-132347] 08 p3316 N94-28409
Prediction of stress-strain response of SCS-6/Timetal-21S subjected to a hypersonic flight profile
[NASA-TM-109026] 08 p3177 N94-28823
Granular bases for heavily loaded pavements
[AD-A275171] 08 p3156 N94-29047
Fatigue of carbon and low-alloy steels in LWR environments
[DE94-005116] 08 p3207 N94-30021
Boron and hydrogen in Ni3Al. Part 2: Mechanical testing of bicrystals
[DE94-007441] 09 p3904 N94-32606
On the mechanics of microballoon-reinforced metal matrix composites
[AD-A277928] 09 p3630 N94-33178
A fully associative, non-linear kinematic, unified viscoplastic model for titanium based matrices
[NASA-TM-106609] 10 p4069 N94-33958
A real-time 2-D composite damage monitoring system employing neural network 10 p4074 N94-34355
Graphing techniques for materials laboratory using Excel 11 p4232 N94-36414
Micromechanical modeling of damage growth in titanium based metal-matrix composites 12 p4402 N94-36664
Prediction of thermal and mechanical stress-strain responses of TMC's subjected to complex TMF histories 12 p4402 N94-36666
A fully coupled thermal, chemical, mechanical cookoff model
[DE94-011432] 12 p4428 N94-37201
A comparison of graphite/epoxy tape laminates and 2-D braided composites mechanical properties
[NASA-CR-4610] 12 p4420 N94-37582

STRESS-STRAIN-TIME RELATIONS
Brief summary of the evolution of high-temperature creep-fatigue life prediction models for crack initiation 05 p1834 N94-22613

STRESSES
NT AXIAL STRESS
NT COMBINED STRESS
NT CRITICAL LOADING
NT INTERLAMINAR STRESS
NT PHOTOSTRESSES
NT PLANE STRESS
NT RESIDUAL STRESS
NT REYNOLDS STRESS
NT SHEAR STRESS
NT TENSILE STRESS
NT THERMAL STRESSES
NT TORSIONAL STRESS
NT TRIAXIAL STRESSES
NT VIBRATIONAL STRESS
Protective coatings for high-temperature polymer matrix composites
[NASA-TM-106276] 01 p0074 N94-12431
A model for non-linear creep and physical ageing in PVC
[NPL-DMM(A)-91] 03 p1057 N94-15016
Stress sensitivity of dielectric resonators
[AD-A266767] 03 p1009 N94-15825
The respectiveness of response in a bar under static and transient loads
[VTT-TIED-1377] 04 p1452 N94-17959
Drying deformable media: Kinetics, shrinkage and stresses
[ETN-94-95314] 06 p2236 N94-25302
A laboratory test on construction of ice domes and their load-carrying capacity 07 p2884 N94-27966

STRETCHING
JPRS report: Science and technology. Central Eurasia: Materials science
[JPRS-UMS-93-005] 02 p0559 N94-14575
Investigation of the dilatational dissipation in compressible homogeneous shear flow 02 p0645 N94-14758
Response of a supersonic boundary layer to a compression corner 02 p0645 N94-14759
Vortex-induced disturbance field in a compressible shear layer 02 p0645 N94-14760
Influence of grain size on the energy storing ability during uniaxial stretching of austenite steel
[IFTR-22/1992] 03 p0961 N94-17121

Intelligent Material Systems and Structures (IMSS). Part 5: Fiber optic registration of deformation in carbon laminates 91/92
[PB93-204600] 06 p2544 N94-23723
On some general properties of parabolic conservation equations
[DE94-006101] 08 p3461 N94-30758

STRIATION
Electron runaway in RF discharges
[DE93-771407] 01 p0363 N94-10661
Temperature dependence of protein solubility-determination, application to crystallization, and growth kinetics studies 06 p2224 N94-24344
On the nature of striae in strontium barium niobate
[DE94-006486] 09 p3901 N94-32176

STRING THEORY
Some new/old approaches to QCD
[DE93-010451] 01 p0408 N94-10261
On renormalization group flow in matrix model
[DE93-613050] 01 p0409 N94-10413
Green-Schwarz superstrings in the generalized harmonical Newmann-Penrose formalism
[DE93-621422] 01 p0412 N94-11088
A version of superstring with four space-time dimensions
[DE93-608196] 01 p0412 N94-11163
The solutions of cosmic string loop equation in expanding universe
[DE93-619717] 01 p0427 N94-11692
Divergences in the moduli space integral and accumulating handles in the infinite-genus limit
[DE93-619722] 01 p0346 N94-11693
On the symmetry algebra of the discrete states in d less than 2 closed string theory
[DE93-622903] 02 p0769 N94-13536
A classical instability for black strings and p-branes
[DE93-014577] 02 p0839 N94-14116
Mathematics and string theory
[DE93-017903] 02 p0817 N94-14417
Theoretical high energy physics research at the University of Chicago
[DE93-016863] 03 p1187 N94-16116
Particle physics and cosmology, Task C
[DE93-016865] 03 p1239 N94-16118
Gauge coupling unification in superstring derived standard-like models
[DE93-624801] 04 p1607 N94-17950
Neutrino masses in superstring derived standard-like models
[DE93-624802] 04 p1565 N94-17951
Cabibbo mixing in superstring derived standard-like models
[DE93-624814] 04 p1607 N94-17953
Investigations in gauge theories, topological solitons, and string theories
[DE93-015029] 04 p1609 N94-19250
Flavor changing strings and domain walls
[DE93-633217] 06 p2532 N94-22970
The current status of observational constraints on cosmic strings
[DE94-001505] 06 p2601 N94-23010
The Casimir energy of the rigid string with massive ends
[DE93-616851] 06 p2492 N94-25338
Superconducting cosmic strings near the electroweak scale and cosmic-ray propagation
[MPI-PHE/93-05] 06 p2629 N94-25459
On the hadron formation time in pion-nucleus interaction
[DE93-616879] 06 p2539 N94-25476
Topological amplitudes in string theory
[DE94-601561] 07 p3071 N94-25882
On string theory interacting with two-dimensional gravity
[DE94-601562] 07 p3071 N94-25883
Aspects of nonrenormalizable terms in a superstring standard-like models
[DE93-614530] 07 p3071 N94-25911
A research program in experimental and theoretical high energy physics
[DE94-002156] 07 p3031 N94-25931
Dynamical group of relativistic straight-line string
[DE93-634347] 07 p3072 N94-26037
Affine algebras on the torus
[DE94-601556] 07 p3006 N94-26414
Higher spin extensions of the Virasoro algebra, area-preserving algebras and the matrix algebra a-bar(sub (infinity))
[DE94-601557] 07 p3006 N94-26415
Gauging of Chern-Simons p-Barnes
[DE94-601553] 07 p2993 N94-26425
Statistical mechanical properties of Z(N)(sup n-1) broken model
[DE93-634344] 07 p2993 N94-26457
String hypothesis and characters of coset CFTs
[DE93-634337] 07 p3007 N94-26552
Stochastic space-time, confinement potential and particle propagator
[DE94-606415] 07 p3074 N94-27680
Twistor-like type 2 superstring and bosonic string
[DE94-606339] 08 p3523 N94-28802
Problems in particle theory
[DE94-003665] 08 p3491 N94-30685
Gravitational effects of cosmic strings
[ISBN-0-315-75484-2] 09 p3934 N94-31789
New QCD results from string theory
[DE94-005226] 09 p3911 N94-31823
The Kaluza-Klein approach and gauge supersymmetry
[ISBN-0-315-86553-9] 09 p3912 N94-31911
Tensor gauge potentials in loop space formulation of Yang-Mills fields
[PB94-147147] 09 p3912 N94-31924
String-parton model description of relativistic heavy-ion collisions
[DE94-009164] 09 p3874 N94-32850
Is it possible to assign physical meaning to field theory with higher derivatives?
[DE94-618468] 12 p4539 N94-37172

STRINGERS
CORSS: Cylinder Optimization of Rings, Skin, and Stringers
[NASA-TP-3457] 06 p2490 N94-24727

STRINGS
On the relativistic string size at finite temperature
[DE93-617658] 01 p0409 N94-10394
Classical gravity coupled to Liouville theory
[DE93-613049] 01 p0275 N94-10798
A classical instability for black strings and p-branes
[DE93-014577] 02 p0839 N94-14116
Testing string superprimitivity in parallel
[AD-A267814] 03 p1155 N94-17399
Tight comparison bounds for the string prefix-matching problem
[CWI-CS-R9250] 05 p1952 N94-21029
Quantizable configurations of the relativistic string
[DE93-634346] 07 p3072 N94-26036
Dynamical group of relativistic straight-line string
[DE93-634347] 07 p3072 N94-26037
Controlling the material properties of in vitro collagen through directed orientation and cross-linking of fibrils 08 p3221 N94-30797

STRIP MINING
Manned Mars mission on-orbit operations FTS capabilities assessment
[NASA-CR-189328] 06 p2430 N94-23080

STRIP TRANSMISSION LINES
NT MICROSTRIP TRANSMISSION LINES
Determination of equivalent circuit for PVDF shock-pressure gauges
[DE93-016492] 03 p1034 N94-16452

STRIPPING
Environmentally Safe and Effective Processes for Paint Removal
[AGARD-R-791] 01 p0126 N94-10613
Paint removal activities in the US Navy 01 p0126 N94-10614
Paint removal activities in Canada 01 p0126 N94-10615
Procedures without danger to the environment and efficiency (PSDEE) for the removal of paint. Point on the French activities concerning the removal of paint 01 p0126 N94-10616
Paint removal activities in Germany 01 p0126 N94-10617
The development of alternative paint removal techniques in the RAF 01 p0126 N94-10618
Operational aspects of F.16 plastic media blasting, as carried out by Fokker Aircraft Services 01 p0126 N94-10619
Use of robots for aircraft dry stripping via plastic media blasting 01 p0127 N94-10620
German Air Forces experiences with plastic media blasting and future requirements 01 p0127 N94-10621
Plastic media blasting activities at Hill Air Force Base 01 p0127 N94-10622
Large Aircraft Robotic Paint Stripping (LARPS) system and the high pressure water process 01 p0127 N94-10623
Automated Laser Paint Stripping (ALPS) update 01 p0127 N94-10624
Aquastrip (tm): An innovative paint removal technology 01 p0127 N94-10625
Paint removal and surface cleaning using ice particles 01 p0128 N94-10626
Paint removal using wheat starch blast media 01 p0128 N94-10627
IATA taskforce: Paintstripping 01 p0128 N94-10628
Selectively strippable paint schemes 01 p0128 N94-10629

STROBOSCOPES
Channel of the system for pulse charged particle beam diagnostics
[DE93-623867] 03 p1179 N94-14931

STROKE VOLUME
Echocardiography in the flight program 01 p0309 N94-11993
Characterization of fluid physics effects on cardiovascular response to microgravity (G-572) 04 p1323 N94-19163
Evaluation of bioimpedance for the measurement of physiologic variables as related to hemodynamic studies in space flight 06 p2427 N94-25378
Response to graded Lower Body Negative Pressure (LBNP) after space flight 10 p4096 N94-33637

STRONG INTERACTIONS (FIELD THEORY)
Top quark polarization and T-odd spin correlations as tools for testing (non) Standard Model predictions
[DE93-622956] 02 p0778 N94-12847
The quantum mass shift of the soliton in Skyrme model
[ITN-93-85219] 03 p1180 N94-15283
QCD corrections to inclusive B - S processes in the standard model
[ISBN-0-315-54572-0] 07 p3073 N94-27263
A jet calculus approach including coherence effects and the associated problem of moment inversion
[ISBN-0-315-51715-8] 07 p3025 N94-27266
The D0 upgrade
[DE94-006953] 09 p3867 N94-31671
Baryogenesis from a primordial lepton asymmetry
[PB94-145166] 09 p3868 N94-31921
Chromogravity explains strong gravity
[DE94-009184] 10 p4149 N94-33989

STRONGLY COUPLED PLASMAS
Conceptual study of moderately coupled plasmas and experimental comparison of laboratory x ray sources
[DE94-005828] 08 p3506 N94-30045
Analytic formulation for the ac electrical conductivity in two-temperature, strongly coupled, overdense plasma: FORTRAN subroutine
[DE94-009466] 09 p3893 N94-32915

STRONTIUM
NT STRONTIUM ISOTOPES
Column chromatographic separation of Y(3+) from Sr(2+) by polymeric ionizable crown ether resins
[DE94-000935] 05 p1683 N94-22021

STRONTIUM COMPOUNDS
NT STRONTIUM OXIDES
NT STRONTIUM TITANATES
An improved light source for laser ranging 03 p0913 N94-15567
Technical report of ISSP. Ser. A, no. 2669: Relations between oxygen deficiency and structures in the La-Sr-Cu-O system. 3: Oxygen contents and structure of (La, Sr)8Cu8O(16+delta) phase
[JTN-94-80555] 07 p3066 N94-27353
High T(sub c) copper-oxide superconductors comprising Tl-Sr-Ca-Cu-O
[AD-D016307] 12 p4538 N94-37776

STRONTIUM ISOTOPES
Strontium and oxygen isotope study of M-1, M-3 and M-4 drill core samples from the Manson impact structure, Iowa: Comparison with Haitian K-T impact glasses 01 p0281 N94-12080
Elevated initial Sr-87/Sr-86 in ordinary chondrite metal 05 p1685 N94-20695

STRONTIUM OXIDES
Method of producing a silicon carbide fiber reinforced strontium aluminosilicate glass-ceramic matrix composite
[NASA-CASE-LEW-15263-2] 03 p0934 N94-15929
Specific heat of La(1.875-x)Nd(x)Sr(0.125)CuO4: Magnetic and structural transitions
[DE93-016978] 04 p1600 N94-18968
Preparation and characterization of high temperature superconductor film surfaces
[AD-A274293] 07 p3059 N94-26681
Influence of doping on the electronic structure of (La, Sr)2CuO4
[DE94-006383] 08 p3516 N94-30054
Investigation of the phase equilibria and phase transformations associated with the Bi2Sr2CaCu2O(y) superconductor
[DE94-004889] 08 p3519 N94-30691
On the nature of striae in strontium barium niobate
[DE94-006486] 09 p3901 N94-32176
Determination of interface structure and bonding at atomic resolution in the stem
[DE94-011466] 12 p4517 N94-37238

STRONTIUM TITANATES
Phase transitions and neutron scattering
[DE93-016748] 04 p1594 N94-17866
Investigation of the effect of various oxide and fluoride additives on the microstructure, electronic properties, and phase shifting ability of Ba(1-x)Sr(x)TiO3
[AD-A271756] 05 p2027 N94-21303

Defect structure of semiconducting and insulating epitaxial oxides
[DE94-009650] 10 p4146 N94-33845
Dielectric measurements of selected ceramics at microwave frequencies 11 p4232 N94-36412
Atomic resolution characterization of a SrTiO3 grain boundary in the STEM
[DE94-011469] 12 p4538 N94-37545
The MBE growth and optical quality of BaTiO3 and SrTiO3 thin films on MgO
[DE94-011468] 12 p4538 N94-37570
STROUHAL NUMBER
Computational fluid mechanics
[NASA-CR-194765] 06 p2337 N94-24859
STRUCTURAL ANALYSIS
NT DYNAMIC STRUCTURAL ANALYSIS
NT ENERGY METHODS
NT EQUILIBRIUM METHODS
NT FLUTTER ANALYSIS
NT MATRIX METHODS
NT STRAIN ENERGY METHODS
Computational procedures for determining parameters in Ramberg-Osgood elastoplastic model based on modulus and damping versus strain
[DE93-013309] 01 p0185 N94-10306
Probabilistic evaluation of uncertainties and risks in aerospace components
[NASA-TM-105603] 01 p0185 N94-10361
NASTRAN modeling of flight test components for UH-60A airloads program test configuration
[NASA-CR-193614] 01 p0186 N94-10937
Functional approximation using artificial neural networks in structural mechanics
[NASA-TM-105820] 01 p0188 N94-11254
Computational mechanics needs study
[NASA-CR-193712] 01 p0327 N94-11279
Structural analysis and optimization of adaptive structures by use of the finite element method
01 p0071 N94-11339
A high specific power solar array for low to mid-power spacecraft 01 p0051 N94-11399
A structural and petrographic investigation of the pretoria saltpan impact structure 01 p0282 N94-12102
Structural design/margin assessment
[NASA-TP-3410] 02 p0669 N94-12831
A general contact detection algorithm for finite element analysis
[DE93-012646] 02 p0742 N94-12956
Relegation for decentralized control
[AD-A265720] 02 p0819 N94-13059
Test/analysis correlation and model updating of the STARS 1 and 2 missile systems
[DE93-013774] 02 p0748 N94-13578
Finite element analysis of composite plates by use of modified complementary energy principle
02 p0672 N94-13596
Boundary formulations for nonlinear design sensitivity analysis 02 p0672 N94-13669
Some computational tools for the analysis of through cracks in stiffened fuselage shells
[LR-701] 02 p0673 N94-13726
The development of inspection and repair methods for the C-17 aft cargo door
[LR-704] 02 p0499 N94-13904
Hierarchical nonlinear behavior of hot composite structures
[NASA-TM-106229] 02 p0676 N94-14041
Materials/structures testing 02 p0506 N94-14164
Control system design for flexible structures using data models 02 p0527 N94-14646
An assessment of finite-element modeling techniques for thick-solid/thin-shell joints analysis
[NASA-TM-108426] 03 p1058 N94-15534
Structural investigation of electrochemically etched silicon
[DE93-015300] 03 p1207 N94-15827
Parallel processing and scientific applications
[AD-A267179] 03 p1159 N94-15849
ITER-HARD Toroidal Field coil structural analysis
[DE93-014834] 03 p1201 N94-15981
The design and analysis of a modular microgravity test platform for use aboard the NASA KC-135 aircraft
03 p0899 N94-16101
A novel approach for structural mechanics problems with stochasticity
[AD-A266189] 03 p1059 N94-16123
On the design of structural components using materials with time-dependent properties
[NASA-TM-108428] 03 p1059 N94-16519
Evaluation of hemoglobin-oxygen equilibrium binding by rapid-scanning spectrophotometry and singular-value decomposition
[AD-A266453] 03 p1123 N94-16564
ASTROS enhancements. Volume 1: ASTRO user's manual
[AD-A266818] 03 p1151 N94-16768
ASTROS enhancements. Volume 2: ASTRO programmer's manual
[AD-A266819] 03 p1151 N94-16769
Quantification of processing artifacts in textile composites 03 p0939 N94-16860
Three-dimensional analysis of anisotropic spatially reinforced structures 03 p0939 N94-16863
Finite element analysis of structural engineering problems using a viscoplastic model incorporating two back stresses
[NASA-TM-106046] 03 p1060 N94-16881
Static analysis of beams on an elastic base as stated by generalized functions
[IFTR-27/1991] 03 p1060 N94-16923
Superconducting ceramics: Selected properties and methods of production
[IFTR-23/1991] 03 p0969 N94-16924
Modeling, estimation and control of distributed parameter systems
[AD-A267325] 03 p1026 N94-17003
Structure of high Reynolds number turbulent boundary layer
[AD-A267476] 03 p0860 N94-17099
Design of a fluid elastic actuator with application to structure control
[AD-A267649] 03 p0897 N94-17246
Structural mechanics division research and technology accomplishments for CY 1992 and plans for CY 1993
[NASA-TM-107752] 03 p1062 N94-17479
The Twenty-First NASTRAN (R) Users' Colloquium
[NASA-CP-3203] 04 p1449 N94-17827
Implementation of mixed formulation elements in PC/NASTRAN 04 p1449 N94-17828
The respectiveness of response in a bar under static and transient loads
[VTT-TIED-1377] 04 p1452 N94-17959
Numerical integration of structural elements in NIKE3D and DYNA3D
[DE93-016325] 04 p1452 N94-18049
Computational strategies for composite structures
[PB93-195097] 04 p1452 N94-18079
Preliminary structural design: Defining the design space
[AD-A268898] 04 p1317 N94-18227
The 6th Japan-U.S. conference on composite materials
[AD-A268535] 04 p1341 N94-18630
Potential dependent structural changes of underpotentially deposited copper on an iodine treated platinum surface determined in situ by surface EXAFS and its polarization dependence
[AD-A269890] 04 p1360 N94-18687
Research activities, Faculty of Civil Engineering, Delft University of Technology, 1990 - 1991
[PB93-195022] 04 p1380 N94-19254
Preparation and characterisation of the compound Tl(0.65) Bi(0.35) Ca(0.8) Sr(1.7) Cu2 O(y) using oxalate coprecipitation and analytical CBED and an initial preparation of Bi2Ca(n-1) Sr2Cu(n) O(4+2n) for n=5
[DE93-625470] 04 p1602 N94-19277
Design for cyclic loading endurance of composites
[NASA-TM-106407] 04 p1457 N94-19351
Time dependent identification of nonlinear structures
[ECL-92-64] 04 p1457 N94-19403
Refinement of unit cell parameters by least-squares: Comments on an old technique and the development of a new computer program
[AD-A270610] 04 p1531 N94-19590
Femtosecond Raman-induced Kerr effect study of polar solvent dynamics: Amides
[DE93-017563] 05 p1678 N94-19924
The p-version of the finite element method in incremental elasto-plastic analysis
[NASA-CR-194707] 05 p1830 N94-20036
Total systems design analysis of high performance structures
[NASA-TP-3432] 05 p1653 N94-20141
Compression strength of composite primary structural components
[NASA-CR-194561] 05 p1830 N94-20159
Quantification of uncertainties in the performance of smart composite structures
[NASA-TM-106335] 05 p1830 N94-20171
Aviation safety research at the National Institute for Aviation Research, Wichita State University
[NIAR-93-4] 05 p1641 N94-20189
Complex structure of the Thaumasia region of Mars
05 p2125 N94-20815
The 1992 USAF structural integrity program conference
[AD-A272876] 05 p1635 N94-21194
Adhesive bonded joint with improved cyclic fatigue life for alumina-ceramic cylinders and hemispheres: Fourth generation housings
[AD-A273061] 05 p1831 N94-21310
Modeling of outgassing and matrix decomposition in carbon-phenolic composites
[NASA-CR-194741] 05 p1676 N94-21743
Probabilistic assessment of composite structures
[NASA-TM-106368] 05 p1832 N94-21757
Development of BEM for ceramic composites
[NASA-CR-194718] 05 p1676 N94-21777
Nonlinear aerodynamics and the design of wing tips
[NASA-CR-194732] 05 p1638 N94-21833
Symposium on Microscopy and Image Analysis of Building Materials
[VTT-SYMP-136] 05 p1707 N94-21890
Microstructure in mortar: A summary of a new project of research 05 p1708 N94-21896
The program system for the diagnostics of strains and fracture prediction of solids 05 p1836 N94-22065
Life assessment of structural components using inelastic finite element analyses 05 p1834 N94-22614
Recent advances in computational structural reliability analysis methods 05 p1828 N94-22616
An overview of computational simulation methods for composite structures failure and life analysis
05 p1835 N94-22617
Probabilistic analysis of mechanical systems
[DE93-041145] 06 p2371 N94-22918
Structural analysis of a superconducting central solenoid for the Tokamak Physics Experiment
[DE94-001536] 06 p2549 N94-23014
Review of the probabilistic failure analysis methodology and other probabilistic approaches for application in aerospace structural design
[NASA-TP-3434] 06 p2376 N94-23342
A structural design decomposition method utilizing substructuring
[NASA-TM-107750] 06 p2376 N94-23368
A review of the Workshop on Fatigue Life Methodologies for Wind Turbines
[DE94-002039] 06 p2394 N94-23472
A prediction method for the compressive strength of impact damaged composite laminates
[CTN-94-60925] 06 p2229 N94-24137
New computing systems, future computing environment, and their implications on structural analysis and design
06 p2177 N94-24314
Integrated stress and strength analysis of airplane structures using the data processing tool ISSY
06 p2178 N94-24320
Structural design criteria for filament-wound composite shells
[NASA-CR-195125] 06 p2229 N94-24402
A study of the core module simulator floor capability
06 p2380 N94-24418
Hydro-elastic analysis using a selection of commercial analysis programs
[PB94-118734] 06 p2376 N94-24478
Stability analysis of anisotropic conical shells
[PB94-119054] 06 p2377 N94-24645
CORSS: Cylinder Optimization of Rings, Skin, and Stringers
[NASA-TP-3457] 06 p2490 N94-24727
Pre-design study of a general purpose vehicle simulator platform
[PB93-215366] 06 p2193 N94-24739
Conceptual design proposal: HUGO global range/mobility transport aircraft
[NASA-CR-195501] 06 p2181 N94-24787
Aircraft empennage structural detail design
[NASA-CR-195486] 06 p2183 N94-24969
Probabilistic assessment of smart composite structures
[NASA-TM-106358] 06 p2378 N94-25188
Structural analysis of a frangible nut used on the NASA Space Shuttle
[DE94-003672] 07 p2821 N94-25811
The Latin American conference on the applications of the Moessbaer effect
[DE93-615942] 07 p3051 N94-25912
Polar and chemical domain structures of lead scandium tantalate (PST)
[DE94-600760] 07 p3056 N94-26363
Regrowth zones in laser annealed radiation damaged diamond
[DE94-600821] 07 p3056 N94-26364
User's guide for the frequency domain algorithms in the LIFE2 fatigue analysis code
[DE94-004678] 07 p2838 N94-26563
Geometry changes in the elastic-plastic analysis of steel spatial skeletal structures
[IFTR-37/1993] 07 p2839 N94-26825
An automatic contact algorithm in DYNA3D for impact problems
[DE94-002856] 07 p2965 N94-26862
Refined triangular plate and shell elements
[PB94-126356] 07 p2839 N94-26875
Proceedings of Damping 1993, volume 2
[AD-A274227] 07 p2840 N94-26953

Proceedings of Damping 1993, volume 3
[AD-A274228] 07 p2840 N94-27008
Modification of a model for fatigue life predictions based on level-crossing
[PB94-123395] 07 p2842 N94-27198
Behaviour modification of space trusses
[ISBN-0-315-84701-8] 07 p2842 N94-27315
Structural design feasibility study of Space Station long spacer truss
[NASA-TM-106346] 07 p2843 N94-27559
Thermal/Structural Tailoring of Engine Blades (T/STAEBL): User's manual
[NASA-CR-194461] 07 p2843 N94-27776
Wing design for a civil tiltrotor transport aircraft: A preliminary study 07 p2671 N94-27917
Viscous and elastic-plastic material model in the ABAQUS
[PB94-132347] 08 p3316 N94-28409
Composite load spectra for select space propulsion structural components
[NASA-CR-194476] 08 p3316 N94-28508
Effects of repair on structural integrity
[PB94-143336] 08 p3145 N94-28647
Service life prediction of composite structures through fiber testing
[AD-A275661] 08 p3176 N94-28654
Thermal/structural tailoring of engine blades (T/SEAEBL). Theoretical manual
[NASA-CR-194462] 08 p3317 N94-28815
Structural/aerodynamic blade analyzer (SAB) user's guide, version 1.0
[NASA-CR-194460] 08 p3151 N94-29103
Study of bridge design and technology
[PB94-137916] 08 p3121 N94-29160
Performing specifications for complex systems' software 08 p3155 N94-29317
A method for the probabilistic design assessment of composite structures
[NASA-TM-106384] 08 p3319 N94-29384
Large-scale computations in analysis of structures
[DE94-004022] 08 p3321 N94-29951
Root-sum-square structural strength verification approach
[NASA-TM-108453] 08 p3322 N94-30206
Sensitivity analysis of the static aeroelastic response of a wing 08 p3134 N94-30525
Fullerenes as precursors for diamond film growth without hydrogen or oxygen additions
[DE94-004582] 08 p3519 N94-30718
Structural analysis of amorphous phosphates using high performance liquid chromatography
[DE94-004791] 08 p3199 N94-30723
Thin-walled orthotropic laminated beam theory 08 p3324 N94-30920
A novel CFD/structural analysis of a cross parachute
[DE94-005271] 09 p3568 N94-31578
Nonlinear analysis of springs using helical finite elements 09 p3859 N94-31906
Theory of thick, laminated composite shallow shells 09 p3622 N94-31953
Prediction of hydrogen entry and permeation in metals and alloys
[AD-A276637] 09 p3642 N94-31995
Finite element analysis of damage in fibrous composites using a micromechanical model
[AD-A277226] 09 p3623 N94-32024
QUAD4 seminar
[AD-A277366] 09 p3818 N94-32330
Structural study in an alteritic region: Contribution of ERS-1 SAR data of the Mauges Plateau (Loire Atlantique, France)
[BRGM-93032] 09 p3752 N94-32551
Molecular Science Research Center
[DE94-007464] 09 p3871 N94-32605
Innovative fabrication processing of advanced composite materials concepts for primary aircraft structures
[NASA-CR-189558] 09 p3626 N94-32877
A case study of analysis methods for large deflections of a cantilever beam
[NASA-TM-108454] 09 p3739 N94-32903
Institute for Computational Mechanics in Propulsion (ICOMP)
[NASA-TM-106542] 09 p3710 N94-32969
HSCT airframe materials: The Boeing perspective 10 p3979 N94-33515
HSCT materials and structures: An MDC perspective 10 p3979 N94-33516
Composite repairs of cracked metallic airframe structures
[AD-A277680] 10 p3969 N94-33590
A new automatic contact formulation in DYNA3D
[DE94-008299] 10 p4105 N94-33843
Coupled electromechanical response of composite beams with embedded piezoelectric sensors and actuators
[NASA-CR-195313] 10 p4019 N94-33899
Probabilistic assessment of uncertain adaptive hybrid composites
[NASA-TM-106515] 10 p4069 N94-33951
Influence of an asymmetric ring on the modeling of an orthogonally stiffened cylindrical shell
[NASA-CR-195953] 10 p4070 N94-34262
Structural controllability of a class of composite systems composed of subsystems with identical structure 10 p4115 N94-34318
A distributed optical fiber strain sensor for monitoring structural deformations 10 p4057 N94-34361
Notch fatigue assessment of aircraft components using a fracture mechanics based parameter 10 p4072 N94-34588
Analysis of wavelet technology for NASA applications
[NASA-CR-195929] 10 p3985 N94-34704
Design oriented structural analysis
[NASA-TM-109124] 10 p4073 N94-34722
Aspects of robust computational modeling for plain and reinforced concrete
[PB94-169240] 11 p4251 N94-35820
Integrated design of structures, controls, and materials 11 p4218 N94-35869
Neutron diffraction study of aluminum chloride imidazolium chloride molten salts
[DE94-009679] 11 p4239 N94-36349
ALCHEMI formulated for delocalization and anti-site defects
[DE94-012740] 12 p4537 N94-37400
JPRS report: Science and technology. Central Eurasia: Engineering and equipment
[JPRS-UEQ-93-005] 12 p4432 N94-37538
Hierarchically parallelized constrained nonlinear solvers with automated substructuring
[NASA-CR-194474] 12 p4456 N94-37554
Probabilistic assessment of space nuclear propulsion system nozzle
[NASA-TM-106539] 12 p4457 N94-37704
Workshop on Scaling Effects in Composite Materials and Structures
[NASA-CP-3271] 12 p4457 N94-37796
Effects of scale in predicting global structural response 12 p4458 N94-37799

STRUCTURAL BASINS
NT RIVER BASINS
NT SINKHOLES
NT WATERSHEDS
Sandia ocean modeling system programmer's guide and user's manual
[DE93-007427] 01 p0287 N94-10153
SOFAR float tracking in the Shikoku basin 01 p0206 N94-11986
Morphology of large impact craters and basins on Venus: Implications for ring formation 01 p0436 N94-12023
Viscous relaxation of the Moho under large lunar basins 01 p0452 N94-12113
Do large impact basins in the southern hemisphere of Mars control the distribution of polar structures and deposits? 01 p0481 N94-12266
Similarity and scale in catchment storm response
[PAPER-89RG01615] 03 p1083 N94-16028
Evaluation of a distributed catchment scale water balance model
[PAPER-93WR00398] 03 p1083 N94-16031
Martian crater degradation by eolian processes: Analogy with the Rio Cuarto Crater Field, Argentina 03 p1251 N94-16196
Lunar impact basins: New data for the nearside northern high latitudes and eastern limb from the second Galileo flyby 03 p1258 N94-16228
Modes of formation of lunar light plains and the detection of cryptomaria deposits 03 p1259 N94-16231
Hellas basin, Mars: Formation by oblique impact 03 p1280 N94-16350
Evidence for an ice sheet/frozen lake in Utopia Planitia, Mars 05 p2089 N94-20388
Possible occurrence and origin of massive ice in Utopia Planitia 05 p2090 N94-20390
Ice in the northern plains: Relic of a frozen ocean? 05 p2090 N94-20391
A marine sedimentary model for the evolution of the northern plains 05 p2091 N94-20395
Seismic-triggering history of the catastrophic outflows in the Chryse region of Mars 05 p2091 N94-20399
Spectral reflectance studies of the Humorum Basin region 05 p2101 N94-20682
Geologic mapping of Harmakhis and Reull Valles region, Mars: Evidence for multiple resurfacing and drainage events 05 p1844 N94-20705
Chicxulub impact basin: Gravity characteristics and implications for basin morphology and deep structure 05 p1862 N94-20757
Impact basins on Venus and some interplanetary comparisons 05 p2119 N94-20785
Geology and deposits of the Serenitatis basin 05 p2119 N94-20786
Origin of the Vredefort structure, South Africa: Impact model 05 p1863 N94-20826
Multispectral studies of selected crater- and basin-filling lunar Maria from Galileo Earth-Moon encounter 1 05 p2136 N94-20876
Morphologic classes of impact basins on Venus 05 p2137 N94-20883
Role of remote sensing in energy, water, and carbon cycle studies over the Amazon
[INPE-5486-PRE/1786] 07 p2852 N94-27957
Some implications of large impact craters and basins on Venus for terrestrial ringed craters and planetary evolution 07 p2890 N94-28306
Thermal studies of Martian channels and valleys using Termoskan data: New results 09 p3944 N94-33194
Apron heights around stepped massifs in the Cydonia Mensae region: Do they record the local paleobathymetry of Oceanus Borealis? 09 p3949 N94-33224
Typhoon monitoring using passive satellite observations
[AD-A277859] 10 p4089 N94-33769
Impact basins in Southern Daedalia, Mars: Evidence for clustered impactors? 11 p4360 N94-35426
Effects due to overlapping large impact basins on Mars 11 p4360 N94-35427
Noachian and Hesperian modification of the original Chryse impact basin topography 11 p4364 N94-35462
Analysis of deep seismic reflection and other data from the Southern Washington Cascades
[DE94-004075] 12 p4470 N94-37489

STRUCTURAL BEAMS
U BEAMS (SUPPORTS)

STRUCTURAL DESIGN
NT PRESSURE VESSEL DESIGN
NASTRAN modeling of flight test components for UH-60A airloads program test configuration
[NASA-CR-193614] 01 p0186 N94-10937
A study of strength evaluations of EDNi/EDCu/NARloy-Z bonded joints
[NASA-TM-108418] 01 p0188 N94-11275
RAMCAD (reliability, availability, and maintainability in computer-aided design)
[AD-A265143] 01 p0331 N94-11679
The trial manufacture and test of critical components in docking mechanism
[NASDA-TMR-930005] 01 p0044 N94-12280
Fracture behavior of ionomers and ionomeric blends
[AD-A265379] 01 p0094 N94-12407
Structural design/margin assessment
[NASA-TP-3410] 02 p0669 N94-12831
Advanced Turbine Technology Applications Project (ATTAP)
[NASA-CR-195366] 02 p0828 N94-12931
A photovoltaic catenary-tent array for the Martian surface
[NASA-TM-106306] 02 p0621 N94-13194
The Second Workshop on Deployment and Assembly Experiment of Large Space Structure on Orbit
[NASDA-CON-930003] 02 p0529 N94-13268
Structural design of hexa-link truss deployable antenna 02 p0529 N94-13269
Thermal distortion measurement of TETRUS type thermal test model of large deployable antenna for mobile communications satellite 02 p0529 N94-13270
Development of modular cable mesh deployable antenna 02 p0530 N94-13274
Research on inflatable structure for space use 02 p0530 N94-13275
Helical truss beam development for large space structure 02 p0530 N94-13276
A concept on on-orbit experiments of deployable structures utilizing JEM/HOPE 02 p0531 N94-13279
Movement of deployable truss 02 p0531 N94-13280
Development and application of one dimensional deployable truss 02 p0531 N94-13281
Study of a one-dimensional deployable structure employing telescopic members 02 p0531 N94-13282
LUTE telescope structural design
[NASA-CR-192594] 02 p0830 N94-13448
Poling of thin polymer films in electro optic applications
[AD-A266562] 02 p0579 N94-13584
The study on large space structure assembly technology: The study on deployable truss structure, part 1
[NASDA-TMR-930002] 02 p0541 N94-13658
The study on large space structure assembly technology: The study on deployable truss structure, part 2 and 3
[NASDA-TMR-930003-PT-2-3] 02 p0541 N94-13659

The study on test of docking mechanism system, part 1 and 2
[NASDA-TMR-930004-PT-1-2] 02 p0541 N94-13660
Mathematical optimization: A tool for aircraft design
[MBB-LME-251-S-PUB-0492] 02 p0751 N94-14006
Large space structures and systems in the space station era: A bibliography with indexes (supplement 05)
[NASA-SP-7085(05)] 02 p0543 N94-14411
Animation of multi-flexible body systems and its use in control system design 02 p0678 N94-14629
Flexibility and costs in the design process: A decision support model
[ISBN-9-06-814522-3] 02 p0597 N94-14808
Processing and protection of high temperature structural materials
[AD-A267292] 03 p0954 N94-14961
Minimum accommodation for aerobrake assembly. Phase 2: Structural concepts for a lunar transfer vehicle aerobrake which can be assembled on orbit
[NASA-TM-107610] 03 p0885 N94-15446
Helicopter structures: A review of loads, fatigue design techniques, and usage monitoring
[AD-A267115] 03 p0866 N94-15651
Recent advances in ordered intermetallics
[DE93-015308] 03 p0955 N94-15862
Hoph bifurcation in viscous, low speed flows about an airfoil with structural coupling
[AD-A266542] 03 p0859 N94-16798
Optimal tuning of heavy equipment motion controllers
[AD-A267873] 03 p1167 N94-17392
The effect of electric discharge machined notches on the fracture toughness of several structural alloys
[AD-A268605] 03 p0962 N94-17464
Structural mechanics division research and technology accomplishments for CY 1992 and plans for CY 1993
[NASA-TM-107752] 03 p1062 N94-17479
X ray computed tomography for casting demonstration
[AD-A268084] 03 p1056 N94-17596
Nonlinear random response prediction using MSC/NASTRAN
[NASA-TM-109029] 03 p1179 N94-17650
Design optimization studies using COSMIC NASTRAN 04 p1450 N94-17834
Preliminary structural design: Defining the design space
[AD-A268898] 04 p1317 N94-18227
Centrifuge modeling of explosion-induced craters in unsaturated sand
[AD-A270194] 04 p1417 N94-18780
Optimizing wind turbine control system parameters
[DE93-018861] 04 p1469 N94-19036
Numerical simulation of vehicle crashworthiness and occupant protection 04 p1459 N94-19471
Total systems design analysis of high performance structures
[NASA-TP-3432] 05 p1653 N94-20141
Structural similitude and design of scaled down laminated models
[NASA-CR-194687] 05 p1673 N94-20172
Design, fabrication and test of a vertical attitude takeoff and landing unmanned air vehicle
[AD-A273003] 05 p1646 N94-21283
Life assessment of structural components using inelastic finite element analyses 05 p1834 N94-22614
Recent advances in computational structural reliability analysis methods 05 p1828 N94-22616
The history of development of molybdenum alloys for structural applications
[DE94-000389] 06 p2239 N94-22958
Control of the internal stresses in plane elasticity
[PB93-225514] 06 p2374 N94-23112
Review of the probabilistic failure analysis methodology and other probabilistic approaches for application in aerospace structural design
[NASA-TP-3434] 06 p2376 N94-23342
A structural design decomposition method utilizing substructuring
[NASA-TM-107750] 06 p2376 N94-23368
Strain gage measurement errors in the transient heating of structural components
[NASA-TM-104274] 06 p2376 N94-23487
A structural design methodology for large angle articulated trusses considering realistic joint modeling 06 p2376 N94-23560
An Earth observation telescope refocusing mechanism 06 p2359 N94-24014
The Submillimeter Wave Astronomy Satellite (SWAS) solar array system 06 p2361 N94-24029
CMC design consequences 06 p2256 N94-24238
Integrated approach in modelling, testing, and design of gradient-CVI derived CMC components 06 p2256 N94-24239
Aeroelastic, aeromechanical and vibration problems in helicopters 06 p2154 N94-24244
Application of concurrent engineering principles to aircraft structural design 06 p2178 N94-24321
Some practical problems in multidisciplinary design and optimisation 06 p2178 N94-24322
Current and future design methods for large transport aircraft 06 p2179 N94-24324
Impact damage in filament wound composite bottles 06 p2231 N94-24421
Active control of buildings during earthquakes
[NASA-TM-109033] 06 p2271 N94-24473
Pre-design study of a general purpose vehicle simulator platform
[PB93-215366] 06 p2193 N94-24739
Design of a recumbent seating system
[NASA-CR-195503] 06 p2438 N94-24786
Merits and limitations of optimality criteria method for structural optimization
[NASA-TP-3373] 06 p2378 N94-24845
Aircraft empennage structural detail design
[NASA-CR-195486] 06 p2183 N94-24969
Aircraft wing structural detail design (wing, aileron, flaps, and subsystems)
[NASA-CR-195487] 06 p2183 N94-24974
Project WISH: The Emerald City 07 p2703 N94-25690
Low-cost unmanned lunar lander 07 p2697 N94-25699
The identification of inflow fluid dynamics parameters that can be used to scale fatigue loading spectra of wind turbine structural components
[DE94-000231] 07 p2791 N94-26117
Design and life-time of polymer matrix composite structures: Summary
[VTT-TIED-1415] 07 p2707 N94-26260
The structural behaviour of the steel or composite concrete and steel frames and the connections of frame members during the fire: A literature review
[VTT-TIED-1437] 07 p2837 N94-26307
Thermoplastic or thermosetting composites in aircrafts
[PB94-123809] 07 p2710 N94-27253
Structural design feasibility study of Space Station long spacer truss
[NASA-TM-106346] 07 p2843 N94-27559
Reliability-based structural optimization: A proposed analytical-experimental study
[NASA-TM-109055] 07 p2844 N94-27830
Study of bridge design and technology
[PB94-137916] 08 p3121 N94-29160
Review of sonic fatigue technology
[NASA-CR-4587] 08 p3479 N94-29407
Field methods to measure surface displacement and strain with the Video Image Correlation method
[NASA-CR-193968] 08 p3316 N94-29724
Dynamic fracture mechanics analysis for an edge delamination crack
[NASA-TM-109106] 08 p3479 N94-29856
Rotorcraft airframe structural optimization for vibration and dynamic stress reduction including damping treatment 08 p3147 N94-29878
Improved ground-penetrating radar, bridge decks
[DE94-004863] 08 p3254 N94-29929
Hopf bifurcation in viscous, low-speed flows about an airfoil with structural coupling 08 p3134 N94-30865
Integrated structure/control design of nonrigid robot arms for high-speed manipulation 08 p3312 N94-30866
Structural design of the superconducting Poloidal Field coils for the Tokamak Physics Experiment
[DE94-007078] 09 p3887 N94-31406
Multidisciplinary optimization of high-speed civil transport configurations using variable-complexity modeling 09 p3578 N94-31881
Fracture and fatigue strength evaluation of multiple site damaged aircraft fuselages - curved panel testing and analysis
[PB94-152808] 09 p3579 N94-32015
Inorganic polymer engineering materials
[DE94-008519] 09 p3659 N94-32655
Structural probability concepts adapted to electrical engineering
[NASA-TM-106499] 09 p3739 N94-32735
Local design optimization for composite transport fuselage crown panels 09 p3629 N94-33132
Leveraging metal matrix composites to reduce costs in space mechanisms 09 p3604 N94-33301
Multilevel decomposition approach to integrated aerodynamic/dynamic/structural optimization of helicopter rotor blades
[NASA-TM-109084] 10 p3989 N94-33900
An Assessment of Fatigue Damage and Crack Growth Prediction Techniques
[AD-280273] 10 p4071 N94-34581
Harrier 2: A comparison of US and UK approaches to fatigue clearance 10 p3996 N94-34596
Fatigue design, test and in-service experience of the BAe Hawk 10 p3996 N94-34597
Integrated design of structures, controls, and materials 11 p4218 N94-35869
An optimization-based approach for integrated controls-structures design of flexible spacecraft 11 p4221 N94-35889
Application of sequential quadratic programming to large-scale structural design problems
[AD-A278574] 11 p4307 N94-36185
High Altitude Long Endurance aircraft design studies 11 p4193 N94-36322
Applications of Titanium Matrix Composite to large airframe structure 12 p4400 N94-36651
Optimization for minimum sensitivity to uncertain parameters
[NASA-TM-109139] 12 p4386 N94-37256
Statistical characterization of rare events 12 p4454 N94-37327
Examination of weldability of Ni-Cr-W superalloys
[DE94-719014] 12 p4418 N94-37385
Approximate analysis for repeated eigenvalue problems with applications to controls-structure integrated design
[NASA-TP-3439] 12 p4397 N94-37502

STRUCTURAL DESIGN CRITERIA

Development and application of a comprehensive, design-sensitive weight prediction method for wing structures of transport category aircraft
[LR-693] 02 p0515 N94-13687
The effect of initial imperfections on shell stability: An updated review
[LR-695] 02 p0682 N94-14692
ADAS implementation of a panel method for the prediction of aerodynamic loads
[LR-723] 04 p1313 N94-19667
The Columbus solar array mechanisms 06 p2356 N94-23994
Primary deployment mechanism for the European Polar Platform 06 p2207 N94-23995
HERA (Hermes robot arm) overview 06 p2357 N94-24005
Preloaded launch locking devices for SILEX 06 p2358 N94-24008
The development of the HERA Test Facility (HTF) 06 p2197 N94-24020
The low noise momentum wheel MW-X: EM design and predicted properties 06 p2360 N94-24024
The Submillimeter Wave Astronomy Satellite (SWAS) solar array system 06 p2361 N94-24029
Multipurpose clamping device with electrical connector for in orbit attachment of payloads 06 p2361 N94-24035
Continuous gust response and sensitivity derivatives using state-space models 06 p2161 N94-24287
Structural design criteria for filament-wound composite shells
[NASA-CR-195125] 06 p2229 N94-24402
Merits and limitations of optimality criteria method for structural optimization
[NASA-TP-3373] 06 p2378 N94-24845
Design of cold-formed HSS channels for bending and eccentric compression: Bending in the plane of symmetry
[VTT-TIED-1403] 07 p2762 N94-25622
Applications of the weight function method (appendix 4/1) 07 p2842 N94-27190
A method for the probabilistic design assessment of composite structures
[NASA-TM-106384] 08 p3319 N94-29384

STRUCTURAL DYNAMICS

U DYNAMIC STRUCTURAL ANALYSIS

STRUCTURAL ENGINEERING

Smart Structures for Aircraft and Spacecraft
[AGARD-CP-531] 01 p0068 N94-11317
An improved approach for flight readiness certification: Methodology for failure risk assessment and application examples, volume 1
[NASA-CR-194498] 02 p0542 N94-14076
An improved approach for flight readiness certification: Methodology for failure risk assessment and application examples. Volume 2: Software documentation
[NASA-CR-194499] 02 p0542 N94-14077
An improved approach for flight readiness certification: Methodology for failure risk assessment and application examples. Volume 3: Structure and listing of programs
[NASA-CR-194500] 02 p0542 N94-14078
Design Quality Task Force survey comments
[AD-A266283] 03 p1225 N94-16473
Finite element analysis of structural engineering problems using a viscoplastic model incorporating two back stresses
[NASA-TM-106046] 03 p1060 N94-16881
Scaling laws for diffraction loading by air blast
[PML-1991-54] 04 p1452 N94-17941
The ecological and environmental impacts of manmade marshes
[AD-A269213] 04 p1475 N94-18885
Research activities, Faculty of Civil Engineering, Delft University of Technology, 1990 - 1991
[PB93-195022] 04 p1380 N94-19254

Impacts: NIST Building and Fire Research Laboratory (technical and societal)
[PB94-113420] 06 p2270 N94-23737
LSS systems planning and performance program
[NASA-CR-193882] 06 p2196 N94-24309
Frameworks for integrated airframe design 06 p2178 N94-24318
Earthquake Engineering Research Center: 25th anniversary edition
[PB94-160645] 11 p4291 N94-36019

STRUCTURAL FAILURE
Failure prediction of thin beryllium sheets used in spacecraft structures
[NASA-CR-194164] 01 p0187 N94-11190
Fiber optic sensing for composite smart structures 01 p0069 N94-11327
Strain concentration assessment of laminates subjected to low velocity impact
[AD-A264497] 01 p0073 N94-11446
Microstructure-based fatigue life prediction methods for naval steel structures
[AD-A265429] 01 p0085 N94-12426
Resistivity and radar void detectors for tunneling machines 01 p0140 N94-12706
Comparison of analytic Whipple bumper shield ballistic limits with CTH simulations
[DE93-015126] 02 p0539 N94-13006
The numerical simulation of the collapse process of axially compressed cylindrical shells with measured imperfections
[LR-705] 02 p0674 N94-13905
MSD in fuselage lap joints: Requirements for inspection intervals for typical fuselage lap joint panels with Multiple Site Damage
[LR-697] 02 p0675 N94-13986
The effect of initial imperfections on shell stability: An updated review
[LR-695] 02 p0682 N94-14692
An improved approach for flight readiness certification: Probabilistic models for flaw propagation and turbine blade failure. Volume 1: Methodology and applications
[NASA-CR-194496] 02 p0519 N94-14841
An improved approach for flight readiness certification: Probabilistic models for flaw propagation and turbine blade failure. Volume 2: Software documentation
[NASA-CR-194497] 02 p0519 N94-14842
Influence of the loading rate on the endurance and deformability of cement matrix composites
[IFTR-1/1992] 03 p1060 N94-17052
Computational strategies for composite structures
[PB93-195097] 04 p1452 N94-18079
Fluid-structure-interaction analyses of reactor vessel using improved hybrid Lagrangian Eulerian code ALICE-II
[DE93-015536] 04 p1409 N94-18248
Fundamental research in nonlinear random vibration for aerospace applications
[AD-A268929] 04 p1454 N94-18487
Impact analysis of composite aircraft structures 04 p1458 N94-19468
Delamination in composite materials as observed using an optical fiber strain gage
[AD-A270803] 04 p1344 N94-19662
Structural crashworthiness and failure
[AD-A270429] 05 p1828 N94-19815
Delamination, durability, and damage tolerance of laminated composite materials 05 p1678 N94-22622
Probabilistic analysis of mechanical systems
[DE93-041145] 06 p2371 N94-22918
A study of the core module simulator floor capability 06 p2380 N94-24418
Impact damage in filament wound composite bottles 06 p2231 N94-24421
J-integral patch for finite element analysis of dynamic fracture due to impact of pressure vessels 06 p2381 N94-24429
Mechanically fastened composite laminates subjected to combined bearing-bypass and shear loading 07 p2712 N94-27914
The development of stress intensity factors
[DRA-TR-93057] 07 p2845 N94-27954
Effects of repair on structural integrity
[PB94-143336] 08 p3145 N94-28647
Numerical and experimental investigation of the bending response of thin-walled composite cylinders
[NASA-CR-195730] 08 p3317 N94-28801
Test and analysis of a stitched RFI graphite-epoxy panel with a fuel access door
[NASA-TM-108992] 08 p3178 N94-29100
Deformation and rupture of cylindrical shells under dynamic loading 09 p3733 N94-31288
Reactor pressure vessel structural integrity research in the US Nuclear Regulatory Commission HSST and HSSI Programs
[DE94-006550] 09 p3739 N94-32771
Structural integrity of intelligent materials and structures
[AD-A278397] 09 p3630 N94-33165
Design, development, and testing of a lightweight optical sensor cover system 09 p3604 N94-33302
On-orbit NDE: A novel approach to tube weld inspection 10 p4066 N94-33664
Assessment of in-service aircraft fatigue monitoring process 10 p3996 N94-34593
Mechanical failure probability of glasses in Earth orbit
[NASA-CR-195912] 10 p4031 N94-34947
History and prognosis of material discontinuity effects on engine components structural integrity 12 p4453 N94-37322
Turbine disks: Lifing against defects and materials development 12 p4454 N94-37329

STRUCTURAL FATIGUE
U FATIGUE (MATERIALS)

STRUCTURAL FOUNDATIONS
U FOUNDATIONS

STRUCTURAL MATERIALS
U CONSTRUCTION MATERIALS

STRUCTURAL MEMBERS
NT ANISOTROPIC PLATES
NT ANNULAR PLATES
NT BEAMS (SUPPORTS)
NT BOX BEAMS
NT CANTILEVER BEAMS
NT CIRCULAR PLATES
NT COLUMNS (SUPPORTS)
NT CORRUGATED PLATES
NT CURVED BEAMS
NT ELASTIC PLATES
NT FLAT PLATES
NT GIRDERS
NT I BEAMS
NT MEMBRANE STRUCTURES
NT METAL PLATES
NT ORTHOTROPIC PLATES
NT PERFORATED PLATES
NT PLATES (STRUCTURAL MEMBERS)
NT POROUS PLATES
NT RECTANGULAR BEAMS
NT RECTANGULAR PLATES
NT REINFORCED PLATES
NT SKIN (STRUCTURAL MEMBER)
NT STRAKES
NT STRINGERS
NT STRUTS
NT TIMOSHENKO BEAMS
NT TRUSSES
NT WING PANELS
Method of recertifying a loaded bearing member using a phase point
[NASA-CASE-LAR-14741-1] 01 p0185 N94-10671
Dynamic response analysis of composite structural members during missile launch
[AD-A270023] 04 p1332 N94-18760
Inverse dynamics of a rigid rod system as a simplified model of flexible beam 06 p2160 N94-24281
Reduction of structural loads using maneuver load control on the Advanced Fighter Technology Integration (AFTI)/F-111 mission adaptive wing
[NASA-TM-4526] 06 p2168 N94-24295
Wing design for a civil tiltrotor transport aircraft: A preliminary study 07 p2671 N94-27917
Advanced microfabrication technologies for microspacecraft 08 p3171 N94-29782
EVA-SCRAM operations 10 p4102 N94-34035

STRUCTURAL PROPERTIES (GEOLOGY)
On the mechanical development of the Flexible External Insulation (FEI) for Hermes spaceplane 01 p0062 N94-10048
Twenty-fourth Lunar and Planetary Science Conference. Part 1: A-F
[NASA-CR-193095] 01 p0435 N94-12015
Lineament analysis and tectonic interpretation for the Tharsis region 01 p0437 N94-12031
Horizontal stresses induced by vertical processes in planetary lithospheres 01 p0281 N94-12042
A structural origin for the cantaloupe terrain of Triton 01 p0449 N94-12095
Sources of Na for the Io atmosphere 01 p0455 N94-12127
Volcanism in southern Guinevere Planitia, Venus: Regional volcanic history and morphology of volcanic domes 01 p0467 N94-12190
Large volcanoes on Venus: Examples of geologic and structural characteristics from different classes 01 p0467 N94-12195
Characteristics of arachnoids from Magellan data 01 p0469 N94-12204
Classification of Martian deltas 01 p0470 N94-12207
Giant radiating dyke swarms on Earth and Venus 01 p0263 N94-12236
Morphotectonics of Venus 01 p0478 N94-12248
The nature and origin of periodically spaced tectonic features on Mars
[NASA-CR-193821] 02 p0842 N94-13199
Importance of expansion and contraction in the formation of tectonic features on the Moon 03 p1250 N94-16189
Structural mapping of Maxwell Montes 03 p1271 N94-16304
Was Martian mantle wet? A possible consequence of rapid core formation 03 p1277 N94-16335
Seismic studies of the geologic structure and physical properties of the seabed
[AD-A270895] 04 p1500 N94-19747
Evidence for an ice sheet/frozen lake in Utopia Planitia, Mars 05 p2089 N94-20388
Geologic mapping of Northern Atla Regio on Venus: Preliminary data 05 p2095 N94-20654
Gravity investigation of the Manson impact structure, Iowa 05 p2082 N94-20694
Studying Venus using a GIS database 05 p2105 N94-20707
Diapirs and cantaloupes: Layering and overturn of Triton's crust 05 p2111 N94-20738
Geology of the southern hemisphere of Triton: No polar cap 05 p2111 N94-20739
The 3-D Moons: The Voyager stereo atlas of the outer solar system 05 p2111 N94-20740
Large, ancient, compressional structures on Mars 05 p2125 N94-20816
Original size of the Vredefort structure, South Africa 05 p1863 N94-20825
Origin of the Vredefort structure, South Africa: Impact model 05 p1863 N94-20826
Distribution and geologic history of materials excavated by the lunar crater Bullialdus 05 p2128 N94-20832
Geology of Galileo Regio quadrangle, Ganymede 05 p2130 N94-20842
Studies on the measurement of subsurface fractures and geostress using acoustic emission technique for deep coalbed development
[REPT-7] 07 p2879 N94-26475
Report of the National Research Institute for Earth Science and Disaster Prevention, No. 51
[JTN-94-80509] 07 p2886 N94-27985
Underground structure in the eastern part of Kanagawa Prefecture inferred from explosion seismic observations 07 p2886 N94-27987
Analysis of S-wave seismogram envelope of deep earthquakes and estimation of random inhomogeneities in the Kanto-Tokai area 07 p2886 N94-27988
Application of remote sensing techniques for the seismo-tectonic study of Nahanni earthquake area
[ISBN-0-315-85942-3] 08 p3334 N94-30037
Analysis of deep seismic reflection and other data from the southern Washington Cascades
[DE94-005915] 08 p3367 N94-30883
The basement fracture pattern of southern Ontario: A tectonic interpretation based on Landsat TM imagery, airphotos and field data
[ISBN-0-315-87086-9] 09 p3772 N94-31834
Procedures for computing site seismicity
[AD-A277666] 09 p3775 N94-33028

STRUCTURAL RELIABILITY
Elastic plastic fracture mechanics methodology for surface cracks
[NASA-CR-194129] 01 p0185 N94-10712
The Ceramic Technology Project: Ten years of progress
[DE93-015991] 03 p0968 N94-16843
Overview of the FAA/DCA/NLR programs related to ageing aircraft
[NLR-TR-92119-U] 03 p0854 N94-17614
FAROW: A tool for fatigue and reliability of wind turbines
[DE93-017639] 04 p1465 N94-18001
The 1992 USAF structural integrity program conference
[AD-A272876] 05 p1635 N94-21194
Recent advances in computational structural reliability analysis methods 05 p1828 N94-22616
Impacts: NIST Building and Fire Research Laboratory (technical and societal)
[PB94-113420] 06 p2270 N94-23737
Reliability-based structural optimization: A proposed analytical-experimental study
[NASA-TM-109055] 07 p2844 N94-27830
A method for the probabilistic design assessment of composite structures
[NASA-TM-106384] 08 p3319 N94-29384
Structural probability concepts adapted to electrical engineering
[NASA-TM-106499] 09 p3739 N94-32735
Structural integrity of intelligent materials and structures
[AD-A278397] 09 p3630 N94-33165

An Assessment of Fatigue Damage and Crack Growth Prediction Techniques
[AD-280273] 10 p4071 N94-34581
Rotorcraft fatigue life-prediction: Past, present, and future 10 p4072 N94-34590
Collection, processing, and reporting of damage tolerant design data for non-aerospace structural materials
[NASA-CR-196046] 11 p4347 N94-36435
Probability techniques for reliability analysis of composite materials
[NASA-CR-195294] 12 p4406 N94-37633

STRUCTURAL RIGIDITY
U STRUCTURAL STABILITY

STRUCTURAL STABILITY
NT SHELL STABILITY
The impact of active controls technology on the structural integrity of aeronautical vehicles 01 p0027 N94-11341
Measuring methods for CFRP laminates' bending and torsion rigidities characteristics 02 p0529 N94-13272
Boundary stability under nonequilibrium conditions
[DE93-016259] 02 p0809 N94-13980
The stability and dynamics of elastic structures and fluid flows
[AD-A267990] 03 p1029 N94-17414
Structural stability of 1100 C heated Pd/k during absorption cycling in protium
[DE93-016270] 04 p1346 N94-18048
About structurally stable generating mechanism for invariant hyperbolic sets
[DE93-629858] 04 p1561 N94-18150
A study of the structural stability of an unbalanced sandwich composite configuration
[AD-A272496] 05 p1675 N94-21431
Electron emission from nanometer-size metallic clusters: Electronic states and structural stability of supported Au clusters
[DE93-040184] 05 p1975 N94-21766
Study of bridge design and technology
[PB94-137916] 08 p3121 N94-29160
Modelling soft impacts for vibrational excitation of civil engineering structures
[PB94-137619] 08 p3320 N94-29681
Structural stability and bifurcations 09 p3911 N94-31895
Alleviation of whirl-flutter on a joined-wing tilt-rotor aircraft configuration using active controls
[NASA-CR-196103] 11 p4200 N94-36436
Correlation of analytical and experimental hot structure vibration results
[NASA-TM-104269] 12 p4386 N94-36644

STRUCTURAL STRAIN
Strain concentration assessment of laminates subjected to low velocity impact
[AD-A264497] 01 p0073 N94-11446
JPRS report: Science and technology. Central Eurasia: Materials science
[JPRS-UMS-93-004] 02 p0559 N94-14574
A review of Australian and New Zealand investigations on aeronautical fatigue during the period April 1991 to March 1993
[AD-A267532] 03 p0868 N94-17117
Structural similitude and design of scaled down laminated models
[NASA-CR-194687] 05 p1673 N94-20172
Mean stress models for low cycle fatigue of a nickel-base superalloy 06 p2159 N94-24276
Deformation and rupture of cylindrical shells under dynamic loading 09 p3733 N94-31288
Structurally compliant rocket engine combustion chamber: Experimental and analytical validation
[NASA-TP-3431] 10 p4017 N94-34392

STRUCTURAL VIBRATION
NT BENDING VIBRATION
NT FLUTTER
NT LINEAR VIBRATION
NT MISSILE VIBRATION
NT SELF INDUCED VIBRATION
NT SUBSONIC FLUTTER
NT SUPERSONIC FLUTTER
NT TORSIONAL VIBRATION
NT TRANSONIC FLUTTER
Computational gearing mechanics
[NASA-CR-193666] 01 p0181 N94-11157
Active landing gear control for improved ride quality during ground roll 01 p0027 N94-11345
Active vibration control of adaptive flexible structures using piezoelectric smart sensors and actuators 01 p0189 N94-11823
On curve veering and flutter of rotating blades
[NASA-TM-106282] 02 p0670 N94-12872
System identification for Space Station Freedom using observer/Kalman filter Markov parameters
[NASA-CR-191521] 02 p0539 N94-12976
Active control of acoustic pressure fields using smart material technologies
[NASA-CR-191480] 02 p0768 N94-13354
Nonlinear vibrations of thick composite plates: Higher-order shear deformation plate theory 02 p0556 N94-13558
Some frequency and damping measurements of laminated beryllium beams
[DE93-015909] 02 p0676 N94-14530
Vibro-acoustic analysis of an aircraft maintenance dock
[AD-A266778] 03 p0871 N94-14908
Forced harmonic vibration of the generally orthotropic cylindrical shell with inner and outer fluid loading
[AD-A266985] 03 p1057 N94-15150
In-flight investigation of a rotating cylinder-based structural excitation system for flutter testing
[NASA-TM-4512] 03 p0867 N94-15783
Hoph bifurcation in viscous, low speed flows about an airfoil with structural coupling
[AD-A266542] 03 p0859 N94-16798
A comparative study of analog and digital control laws for the UMCSL truss
[AD-A267980] 03 p0871 N94-17412
A mechanical system damping measurement technique using a one-degree-of-freedom (1DOF) cylindrical gas bearing
[AD-A268402] 03 p1048 N94-17462
Modelling chaotic vibrations using NASTRAN 04 p1449 N94-17830
Generalization of optimal control theory: Linear and nonlinear structures
[PB93-188621] 04 p1540 N94-18125
The effects of initial conditions and control time on optimal actuator placement by way of a max-min genetic algorithm
[DE93-017640] 04 p1525 N94-19124
Adaptation of model parameters of a rail model at measured rail compliances
[ILR-MITT-274(1992)] 05 p1831 N94-21153
The modern rotor aerodynamic limits survey: A report and data survey
[NASA-TM-4446] 05 p1635 N94-21490
Probabilistic assessment of composite structures
[NASA-TM-106368] 05 p1832 N94-21757
Aircraft noise effects on cultural resources: Recommendation and rationale for further research
[PB93-205326] 05 p1968 N94-22053
Aircraft noise effects on cultural resources: Annotated bibliography
[PB93-205334] 05 p1969 N94-22054
System identification of the Daisy large space structure emulator
[ISBN-0-315-83533-8] 05 p1653 N94-22588
Adaptive nonlinear polynomial neural networks for control of boundary layer/structural interaction
[NASA-CR-189645] 06 p2525 N94-23698
Control algorithms for effective operation of variable-speed wind turbines
[DE94-002607] 06 p2394 N94-23704
Microwelding due to random vibration 06 p2359 N94-24019
Vibrational power transmission analysis of machinery installations in ships with the objective of noise reduction
[ISVR-TR-216] 06 p2363 N94-24076
Responses of a finite baffled plate subject to turbulent and mean flow excitations
[NASA-CR-191570] 06 p2334 N94-24605
Influence of backup bearings and support structure dynamics on the behavior of rotors with active supports
[NASA-CR-195106] 06 p2365 N94-24751
Space Station flexible dynamics under plume impingement 06 p2208 N94-25383
Modeling of a large undamped space structure using time domain techniques
[AD-A273828] 06 p2206 N94-25523
Identification and H(infinity)/(mu)-synthesis control of the Sandia truss
[DE94-002735] 07 p2839 N94-26810
New variational techniques for acoustic radiation and scattering from elastic shell structures
[AD-A274599] 07 p3010 N94-26889
Proceedings of Damping 1993, volume 1
[AD-A274226] 07 p2840 N94-26922
Report of three microgravity experiments by the drop shaft
[JTN-94-80579] 07 p2761 N94-27341
Vibrations in engineering structures: A review of model and full-scale test of a cable-stayed bridge and a traffic sign gantry
[NLR-TP-92321-U] 07 p2843 N94-27553
Methods of testing for endurance of structural elements using simulated acoustic loading
[ESDU-93027] 07 p3011 N94-28141
Weak coupling in statistical energy analysis ion Research, Univ. of Southampton, Southampton SO9 5NH, England)
[ISVR-TR-228] 07 p2832 N94-28174
Characterization of structural vibration: Field descriptors based on energy density and intensity
[PB94-132230] 08 p3316 N94-28404
Study of bridge design and technology
[PB94-137916] 08 p3121 N94-29160
Experimental validation of finite element and boundary element methods for predicting structural vibration and radiated noise
[NASA-CR-4561] 08 p3301 N94-29552
Modelling soft impacts for vibrational excitation of civil engineering structures
[PB94-137619] 08 p3320 N94-29681
Rotorcraft airframe structural optimization for vibration and dynamic stress reduction including damping treatment 08 p3147 N94-29878
Spectral analysis of wave propagation in connected waveguides 08 p3277 N94-29944
Analysis and design of inflatable aerospace structures 08 p3403 N94-30799
Vibrations of a heavy truck diesel engine and gearbox unit: Examining structure-borne sound transmission with statistical energy analysis
[CTH-E-93-04] 09 p3722 N94-31194
Effect of vibratory stress relief during welding of thick stainless steel plate
[DE94-006557] 09 p3733 N94-31312
Rotordynamic effects driven by fluid forces from a geometrically imperfect labyrinth
[AD-A276424] 09 p3722 N94-31333
Study of wave propagation and dynamic response of laminated composite structures
[AD-A276123] 09 p3619 N94-31444
Random vibrations of composite beams and plates 09 p3735 N94-31777
Vibrational and acoustic response of ribbed plates 09 p3736 N94-31955
Nonlinear vibration analysis of laminated plates on linear and nonlinear elastic foundations 09 p3737 N94-32079
Feed-forward control of gear mesh vibration using piezoelectric actuators
[NASA-TM-106366] 09 p3728 N94-32902
An analytical study of the vibration of beams fitted with neutralizers. Part 2: Assessment of the effects of mounting configurations
[ISVR-TR-225-PT-2] 09 p3740 N94-32982
Reciprocity-based experimental determination of dynamic forces and moments: A feasibility study
[NASA-CR-194905] 09 p3862 N94-33023
Vibration Isolation Technology (VIT) ATD project
[NASA-TM-106496] 09 p3567 N94-33064
Response of a cantilevered plate in supersonic flow
[AD-A277487] 09 p3580 N94-33107
Structural damping studies at cryogenic temperatures
[NASA-TM-109073] 09 p3740 N94-33118
Improvements in spiral-bevel gears to reduce noise and increase strength
[NASA-TM-106613] 10 p4059 N94-33609
Parameter identification of a rotor supported in a pressurized bearing lubricated with water 10 p4065 N94-34197
An analytical study of the vibration of beams fitted with neutralizers. Part 1: Assessment of the effects of neutralizer design parameters
[ISVR-TR-224-PT-1] 10 p4070 N94-34304
Measurements of correlation coefficients of vibration on a car body shell
[ISVR-TR-220] 10 p4070 N94-34307
Adaptive automatic balancing of magnetic bearing systems 10 p4067 N94-34338
Solid state acoustics information time region separating methods for gear diagnosis of failures 10 p4068 N94-34351
Vibrations of structures with cyclic symmetry: Application to the case of turbine engines 10 p4004 N94-34463
Optimal disturbance rejecting control of hyperbolic systems 11 p4220 N94-35882
Transfer function modeling of damping mechanisms in distributed parameter models 11 p4222 N94-35895
Software for continuum modeling of controls-structures interactions 11 p4223 N94-35898
Frequency domain analysis of the random loading of cracked panels
[NASA-CR-196021] 11 p4279 N94-35974
Correlation of analytical and experimental hot structure vibration results
[NASA-TM-104269] 12 p4386 N94-36644
A Galerkin method for linear PDE systems in circular geometries with structural acoustic applications
[NASA-CR-194925] 12 p4503 N94-36923

A PDE-based methodology for modeling, parameter estimation and feedback control in structural and structural acoustic systems
[NASA-CR-194928] 12 p4500 N94-36924
Vibration suppression with approximate finite dimensional compensators for distributed systems: Computational methods and experimental results
[NASA-CR-194927] 12 p4500 N94-36928
Parameter estimation in a structural acoustic system with fully nonlinear coupling conditions
[NASA-CR-194926] 12 p4503 N94-36991
Laminated thin shell structures subjected to free vibration in a hygrothermal environment
[NASA-TM-106600] 12 p4456 N94-37456

STRUCTURAL WEIGHT
Regenerative fuel cells for High Altitude Long Endurance Solar Powered Aircraft
[DE93-016991] 04 p1465 N94-17853
Nonlinear aerodynamics and the design of wing tips
[NASA-CR-194732] 05 p1638 N94-21833
Wing design for a civil tiltrotor transport aircraft: A preliminary study 07 p2671 N94-27917
Aircraft weight prediction capability. Volume 1: Weight study and results
[AD-A277206] 09 p3579 N94-32062

STRUCTURED PROGRAMMING
Bundle event structures: A non-interleaving semantics for LOTOS
[MEMO-INF-92-73] 01 p0320 N94-10164
Guide to the software architectural design phase
[ESA-PSS-05-04-ISSUE-1] 02 p0753 N94-14190
Guide to the software detailed design and production phase
[ESA-PSS-05-05-ISSUE-1] 02 p0753 N94-14191
Implementation of a portable nested data-parallel language
[AD-A270524] 05 p1902 N94-19932
A conceptual database design and performance analysis of the MILSATCOM requirements database
[AD-A272672] 05 p1658 N94-21217
Structured multimedia authoring
[CWI-CS-R9304] 05 p2044 N94-21535
Editing tree structures
[CWI-CS-R9264] 07 p2961 N94-26219
CMSC-130 introductory computer science, lecture notes
[AD-A274369] 07 p2967 N94-27060
Object-based design of embedded software
[PB94-132073] 08 p3407 N94-28403
The ABC structure editor: Structure-based editing for the ABC programming environment
[CWI-CS-R9256] 08 p3418 N94-29487
Compositionality of application oriented structuring mechanisms for algebraic specification languages with initial semantics
[ETN-94-95736] 09 p3812 N94-31577

STRUCTURES
The making of the time capsule
[NASA-TM-109807] 10 p4011 N94-33560

STRUTS
Flow-field interference produced by an asymmetrical support strut
[IAR-AN-75] 02 p0504 N94-14031
Continuum representations of cellular solids
[DE94-001706] 06 p2375 N94-23217
Design of a recumbent seating system
[NASA-CR-195503] 06 p2438 N94-24786
Mars rover mechanisms designed for Rocky 4 08 p3161 N94-29630
The reduction of takeoff ground roll by the application of a nose gear jump strut
[NASA-TM-108822] 11 p4198 N94-36380

STS
U SPACE TRANSPORTATION SYSTEM

STS-3
U SPACE TRANSPORTATION SYSTEM 3 FLIGHT

STS-4
U SPACE TRANSPORTATION SYSTEM 4 FLIGHT

STUDENTS
A summer program in mathematics and computer science for academically oriented student
[AD-A263467] 01 p0415 N94-11517
Career Information in the Mathematical Sciences (CIMS)
[DE93-013780] 01 p0318 N94-11817
Lecture notes on software process improvement
[AD-A265200] 02 p0744 N94-13049
Workshop for coordinating South Carolina's pre-college systemic initiatives in science and mathematics
[DE93-012263] 02 p0818 N94-13216
Characteristics of the amateur radio means of the Arsene satellite
[CNES-NT-131] 02 p0605 N94-13950
Center of excellence in rotary wing technology
[AD-A266655] 02 p0510 N94-14799
US civil airmen statistics: Calendar year 1992
[AD-A267708] 03 p0853 N94-14965
Developments in the Higher Technical Aerospace Education 03 p0854 N94-15130
Student researchers
[NASA-TM-109441] 03 p1221 N94-15340
STS-29 crew with student experiment
[NASA-TM-109545] 03 p1116 N94-15378
Questioning mechanisms during tutoring, conversation, and human-computer interaction
[AD-A266199] 03 p1137 N94-16108
Spaceship Earth: A partnership in curriculum writing 03 p1222 N94-16356
From the Moons of Jupiter to the Milky Way
[NASA-CR-194649] 03 p1240 N94-17059
Magnetic Fusion Energy Technology Fellowship: Report on survey of institutional coordinators
[DE93-014646] 04 p1583 N94-17739
Joint services electronics program
[AD-A269383] 04 p1403 N94-18638
National Boy Scout Jamboree
[NASA-TM-109367] 04 p1610 N94-18982
California Student Get Away Special Payload GAS-450 04 p1324 N94-19164
Undergraduate origins of recent science and engineering doctorate recipients
[NSF-92-332] 04 p1610 N94-19389
Undergraduate course and curriculum development program and calculus and the bridge to calculus program: 1992 awards
[NSF-93-24] 04 p1610 N94-19446
A comprehensive software engineering educational experience
[AD-A270583] 05 p1905 N94-20109
A description of psychological type at the Defense Systems Management College, 1993 edition
[AD-A271612] 05 p1894 N94-21237
Design of an airborne launch vehicle for an air launched space booster
[NASA-CR-195534] 06 p2198 N94-24860
The Triton: Design concepts and methods
[NASA-CR-195542] 06 p2184 N94-25004
Magnetic Earth Ionosphere Resonant Frequencies
[NASA-CR-195131] 06 p2303 N94-25191
Predoctoral training grant in the area of physical sciences
[DE94-004406] 07 p3039 N94-27603
Summer intern program
[AD-A275194] 08 p3466 N94-28888
Application of digital video to hypermedia training systems
[AD-A274989] 08 p3409 N94-28910
An interactive, design and educational tool for supersonic external-compression inlets
[NASA-TM-106581] 08 p3421 N94-30174
An interactive educational tool for compressible aerodynamics
[NASA-TM-106568] 08 p3422 N94-30175
Ada support for the mathematical foundations of software engineering
[AD-A278031] 09 p3822 N94-33284
Summer High School Apprenticeship Research Program (SHARP)
[NASA-CR-195956] 10 p4149 N94-34717
NASA/DOD Aerospace Knowledge Diffusion Research Project. Paper 40: Technical communications in aerospace education: A study of AIAA student members
[NASA-TM-109868] 11 p4344 N94-35254

STUDS (STRUCTURAL MEMBERS)
Instability around an isolated roughness element 01 p0165 N94-12629

STYPHNATES
Energy transfer dynamics and impact sensitivity
[DE93-009551] 01 p0098 N94-11269

STYRENES
NT POLYSTYRENE
Dynamics of adsorbed, swollen block copolymers
[AD-A272013] 05 p1706 N94-21460
Microstructure of styrene methyl methacrylate copolymers grafted onto polybutadiene seeds
[ETN-94-95360] 06 p2262 N94-25225
Ballistic performance of polycarbonate/polyester and polycarbonate/styrene- acrylonitrile microlayer sheets
[AD-A275462] 08 p3177 N94-28735
Design of new polymers to improve radiation stability of plastic scintillators
[DE94-008220] 09 p3652 N94-31764
Dynamics of block poly(styrene-co-vinylpyridine) (SVP) in solution and on silica
[AD-A277139] 09 p3657 N94-32364
Iron hydrous titanium oxide catalysts for the dehydrogenation of ethylbenzene to styrene
[DE94-010381] 12 p4412 N94-37542

SUBARCTIC REGIONS
The marine light-mixed layer experiment cruise and data report: R/V endeavor cruise EN-224, mooring deployment, 27 April-1 May 1991: Cruise EN-227, mooring recovery, 5-23 September 1991
[AD-A271175] 05 p1864 N94-20186

SUBASSEMBLIES
MODIL cryocooler producibility demonstration project results
[DE93-019213] 12 p4430 N94-36444

SUBCARRIER WAVES
U CARRIER WAVES

SUBCIRCUITS
U CIRCUITS
U SUBASSEMBLIES

SUBCRITICAL FLOW
A numerical experiment of boundary layer transition at subcritical Reynolds numbers 01 p0165 N94-12625

SUBDUCTION (GEOLOGY)
A model for the subduction mechanics of flexible lithosphere and its viscous coupling to the mantle using power-law rheologies 01 p0277 N94-11585
The subduction experiment. Cruise report, R/V Oceanus, cruise number 250 legs 1 and 2. Subduction 2 mooring deployment and recovery cruise, 25 January-26 February 1992
[AD-A264922] 01 p0289 N94-11853
Flexure and the role of inplane force around coronae on Venus 01 p0452 N94-12112
Buoyant subduction on Venus: Implications for subduction around coronae 01 p0455 N94-12130
Convective and dynamic instability in meridional trenches 01 p0225 N94-12739
Chemical differentiation, thermal evolution, and catastrophic overturn on Venus: Predictions and geologic observations 03 p1259 N94-16232
Estimates of lithospheric thickness on Venus 03 p1267 N94-16277
Models of thermal/chemical boundary layer convection: Potential application to Venus 03 p1279 N94-16348
Subduction on the margins of coronae on Venus: Evidence from radiothermal emissivity measurements 05 p2107 N94-20718
Parga and Hecate Chasmata, Venus: Structure, volcanism and models of formation 05 p2121 N94-20796
Photogeological analysis of Europan tectonic features 05 p2129 N94-20838
Reactive trace metals as indicators of subduction and ventilation processes in the ocean
[AD-A273585] 06 p2419 N94-25164
The rupture process of large earthquakes along convergent margins: Cast studies from Alaska and Armenia 08 p3363 N94-29969
The tectonic and volcanic evolution of Venus: Catastrophic or gradual? 09 p3940 N94-31111
Cruise report: Oceanus 250 leg 4 high resolution profiler survey for the North Atlantic Tracer Release Experiment, 25 March - 24 April, 1992
[AD-A277935] 09 p3791 N94-33245
Mantle melting and crustal recycling in subduction zones 10 p4084 N94-33368

SUBDWARF STARS
UV-bright stars in globular clusters
[NASA-CR-189324] 06 p2599 N94-24666

SUBGRAVITY
U MICROGRAVITY

SUBGROUPS
Simple currents versus orbifolds with discrete torsion: A complete classification
[NIKHEF-H/93-13] 07 p2995 N94-26812
Quantum subgroups and quantum co-set spaces and differential calculi on them
[DE94-602520] 07 p3073 N94-26876
A note on cocycles in a semidirect product
[REPT-93-65] 09 p3851 N94-31661
Quantum homogeneous spaces, duality, and quantum 2-spheres
[CWI-AM-R9309] 09 p3857 N94-32192

SUBHARMONIC GENERATORS
Stability of subharmonics and escape phenomena in the twin-well potential duffing system 02 p0775 N94-13235

SUBJECTS
Catalog of Air Force weather technical publications 1992-1993
[AD-A275635] 08 p3368 N94-28638

SUBLATTICES
U LATTICES (MATHEMATICS)
U SUBGROUPS

SUBLAYERS
U SUBSTRATES

SUBLETHAL DOSAGE
The relationship of metallothionein induction to the heat shock response
[AD-A266634] 03 p1122 N94-15741

SUBLIMATION
Thermal inertia and radar reflectivity of the Martian north polar ERG: Low-density aggregates
03 p1260 N94-16238
Equatorial ground ice on Mars: Steady-state stability
03 p1290 N94-16403
The distribution of ground ice on Mars
05 p2090 N94-20394
On the stability of the process of formation of combustion generated particles by coagulation and simultaneous shrinkage due to particle oxidation
06 p2159 N94-24274
Why is the north polar cap on Mars different than the south polar cap?
07 p3107 N94-27889
Obliquity variation in a Mars climate evolution model
09 p3951 N94-33236
SUBLIMINAL STIMULI
States of awareness 1: Subliminal perception relationship to situational awareness
[AD-A267249] 03 p1132 N94-16942
SUBMARINES
Submarine internal waves
[MRL-GD-0049] 01 p0098 N94-11303
Evaluation of crack arrest fracture toughness of parent plate, weld metal and heat affected zone of BIS 812 EMA ship plate steel
[AD-A274871] 07 p2839 N94-26859
Propellants and explosives in ballistic missiles
[UCRL-LR-113578] 07 p2760 N94-28222
SUBMERGED BODIES
NT DIVING (UNDERWATER)
NT UNDERWATER RESEARCH LABORATORIES
Surface and internal signatures of organized vortex motions in stratified fluid
[AD-A267015] 03 p1020 N94-15526
SUBMERGING
A model for predicting central nervous system toxicity from hyperbaric oxygen exposure in man: Effects of immersion, exercise, and old and new data
[AD-A278348] 10 p4095 N94-34005
Piggyback balance experiment: An illustration of Archimedes' principles and Newton's third law
[PB94-163060] 11 p4265 N94-35942
SUBMILLIMETER WAVES
Investigation of passive atmospheric sounding using millimeter and submillimeter wavelength channels
[NASA-CR-193627] 01 p0274 N94-10726
Submillimeter wave observation experiment of Earth atmosphere with SIS mixer
01 p0130 N94-11837
Interferometric investigation methods of plasma spatial characteristics on stellarators and tokamaks in submillimeter region
[DE93-621606] 02 p0798 N94-13507
Instability heating of the HDZP
[DE93-012641] 02 p0798 N94-13513
Theoretical SIS mixer research
[AD-A266323] 02 p0807 N94-13580
Submillimeter, millimeter, and microwave spectral line catalogue, revision 3
[NASA-CR-194501] 02 p0602 N94-13813
Direct submillimeter absorptivity measurements on epitaxial Ba(1-x)K(x)BiO3 films at 2K
[DE93-013904] 02 p0815 N94-14699
Submillimeterwave SIS mixer developments
03 p0903 N94-15054
Hot electron mixers, the potential competition
03 p0903 N94-15055
Submm/FIR bolometers 03 p0904 N94-15056
Optically-switched submillimeter-wave oscillator and radiator
[NASA-CASE-NPO-18547-1-CU]
03 p1014 N94-17324
Millimeter wave imaging technology
[AD-A271257] 05 p1715 N94-19912
Investigation of passive atmospheric sounding using millimeter and submillimeter wavelength channels
[NASA-CR-194858] 06 p2404 N94-24843
Submillimeter residual losses in high-(Tc) superconductors
[DE94-003241] 07 p3058 N94-26516
Optically switched submillimeter-wave oscillator
[AD-A278014] 09 p3698 N94-33249
High precision moving magnet chopper for variable operation conditions
09 p3605 N94-33307
Detection of the 267 GHz J = 1-0 rotational transition of PH3 in Saturn with a new Fourier transform spectrometer
[NASA-CR-194364] 10 p4162 N94-34718
A monolithic Si bolometer array for the Caltech Submillimeter Observatory
[NASA-TM-109402] 10 p4056 N94-34719
Submillimeter quasioptical Josephson junction oscillator with integrated tuning elements
[AD-A280380] 12 p4534 N94-37036
SUBORBITAL FLIGHT
Astronauts number 2
[NASA-TM-109429] 03 p0873 N94-15500
SUBREFLECTORS
Multi-band reflector antenna with double-ring element frequency selective subreflector
05 p1728 N94-20447
Beam scanning offset Cassegrain reflector antennas by subreflector movement
[NASA-CR-191604] 08 p3160 N94-28836
High precision moving magnet chopper for variable operation conditions
09 p3605 N94-33307
SUBROUTINE LIBRARIES (COMPUTERS)
Intel NX to PVM 3.2 message passing conversion library
[NASA-TM-109038] 03 p1152 N94-17060
Cesar user library
[FFI-93/7021] 04 p1529 N94-19378
An object-oriented data reduction system in Fortran
05 p2046 N94-22447
The IDL astronomy user's library
05 p2048 N94-22500
The Keck Task Library (KTL)
05 p2048 N94-22504
Development of the FITS tools package for multiple software environments
05 p1927 N94-22516
The STARLINK software collection
05 p1927 N94-22545
Users manual for the Chameleon parallel programming tools
[DE94-001934] 06 p2465 N94-22973
ASPT software source code: Development system package, library component
[CTN-94-60905] 06 p2455 N94-24134
Horatio: Libraries for vision applications, release 2.0
[OUEL-1967/92] 06 p2593 N94-25326
Ma42: A new frontal code for solving sparse unsymmetric systems
[PB94-124302] 07 p2998 N94-27115
Development of Calcomp compatible interface library 'pflib' on X Window System
[DE94-701190] 07 p2973 N94-27702
Program derivation by proof transformation
[AD-A275260] 08 p3453 N94-29304
Object-oriented particle simulation on parallel computers
[DE94-009353] 10 p4111 N94-33908
Analyzing PICL trace data with MEDEA
[DE94-009173] 10 p4111 N94-33987
Review of Mathematical Function Library for Microsoft-FORTRAN, John Wiley and Sons, 1989
[PB94-160793] 11 p4305 N94-36010
ZLIB++: Object-oriented numerical library for differential algebra
[DE94-010839] 12 p4495 N94-37453
SUBROUTINES
Subroutine functions for generating animation data
[DE93-767973] 01 p0313 N94-10731
FORTRAN graphics routines for the Macintosh
[DE93-013092] 02 p0742 N94-12864
Splines, contours and SVD subroutines
[DE93-016088] 02 p0757 N94-14866
Mobile and replicated alignment of arrays in data-parallel programs
[NASA-CR-194294] 03 p1158 N94-15113
Mechanistic models of soot formation
[AD-A267806] 03 p0950 N94-17008
Intel NX to PVM 3.2 message passing conversion library
[NASA-TM-109038] 03 p1152 N94-17060
Radio wave propagation in structured ionization for satellite and radar applications
[AD-A268457] 04 p1382 N94-17844
Power conditioning system modelling for nuclear electric propulsion
[NASA-CR-191136] 05 p1846 N94-21179
NAVSPASUR sensor system digital signal processing receiver. Volume 2: Function and capabilities of hardware and software components
[AD-A272900] 05 p1739 N94-21218
The three-dimensional Event-Driven Graphics Environment (3D-EDGE) 05 p1922 N94-21342
Documentation for PCDIST, a FORTRAN subroutine to calculate Pollack-Cuzzi scattering
[AD-A273070] 05 p1988 N94-21491
An object-oriented data reduction system in Fortran
05 p2046 N94-22447
Implementation of the Baldwin-Barth turbulence model into the ZETA code and its diagnosis
[NASA-CR-194795] 06 p2335 N94-24640
Review and analysis of dense linear system solver package for distributed memory machines
07 p2978 N94-27916
Lisp interface to geometric modelling operations
[PB94-133121] 07 p3001 N94-28398
Arnoldi code for computing selected eigenvalues of sparse real unsymmetric matrices
[PB94-145182] 09 p3813 N94-31682
Analytic formulation for the ac electrical conductivity in two-temperature, strongly coupled, overdense plasma: FORTRAN subroutine
[DE94-009466] 09 p3893 N94-32915
Description and use of LSODE, the Livermore Solver for Ordinary Differential Equations
[NASA-RP-1327] 11 p4313 N94-35259
SUBSETS (MATHEMATICS)
U SET THEORY
SUBSIDENCE
Ground movements associated with gas hydrate production
[DE93-019887] 04 p1486 N94-19018
SUBSONIC AIRCRAFT
Strain sensing technology for high temperature applications
[NASA-TM-4498] 02 p0648 N94-12874
Subsonic aerodynamic characteristics of the HL-20 lifting-body configuration
[NASA-TM-4515] 03 p0861 N94-17284
Nonlinear and progressive failure aspects of transport composite fuselage damage tolerance
05 p1834 N94-22609
Examples of excrescence drag prediction for typical wing components of a subsonic transport aircraft at the cruise condition
[ESDU-93032] 07 p2649 N94-28144
SUBSONIC FLOW
High order accurate solutions of viscous problems
[NASA-TM-106267] 01 p0151 N94-11253
Study of possible mechanisms of instability due to heat transfer
[INPE-5448-TDI/494] 02 p0628 N94-12966
Transition prediction and control in subsonic flow over a hump
[NASA-CR-4543] 02 p0629 N94-13066
Development of a general purpose multigrid accelerated Navier-Stokes solver
02 p0641 N94-14613
Effect of wind tunnel acoustic modes on linear oscillating cascade aerodynamics
[NASA-TM-106367] 03 p0869 N94-15866
On solving the compressible Navier-Stokes equations for unsteady flows at very low Mach numbers
[NASA-TM-106380] 03 p1027 N94-17128
Study into the limits of an Euler equation method applied to leading-edge vortex flow
[NLR-TP-91350-U] 03 p1031 N94-17627
A fast computing method for the flow over high-lift wings
04 p1308 N94-18437
Fluid dynamic mechanisms and interactions within separated flows
[AD-A271037] 05 p1797 N94-19978
Acoustic radiation damping of flat rectangular plates subjected to subsonic flows
[NASA-TM-109382] 05 p1967 N94-20211
A study of the compressible flow through a diffusing S-duct
[NASA-TM-106411] 05 p1638 N94-21591
An experimental study of the flow field surrounding a subsonic jet in a cross flow
[NASA-CR-194770] 06 p2317 N94-23072
Two-dimensional Navier-Stokes computations of subsonic and supersonic flows through turbine cascades
[PB93-226223] 06 p2317 N94-23114
Computational study of GA(W)-1: Airfoil near stall
[PB93-226249] 06 p2165 N94-23116
Refraction of high frequency noise in an arbitrary jet flow
[NASA-TM-106465] 06 p2525 N94-23464
Unsteady jet flow computation towards noise prediction
[NASA-CR-194449] 06 p2153 N94-23553
Three dimensional study of an airplane wing and its wake in the subsonic regime
[ISBN-0-315-58963-9] 06 p2168 N94-24178
Development and validation of RNG methodology for compressible turbulence
[AD-A273469] 06 p2337 N94-24929
Sub-sonic flow about a slender profile in a tunnel having perforated walls
[AD-A273184] 06 p2170 N94-25137
A numerical investigation of the artificial compressibility method for the solution of the Navier-Stokes equations
[CRANFIELD-AERO-9213] 06 p2340 N94-25486
Off-design performance of crenulated blades in a linear compressor cascade
[AD-A273744] 06 p2340 N94-25534
A numerical determination of bifurcation points for low Reynolds number conical flows
[AD-A273984] 07 p2791 N94-25991
Influence of the transonic doublet in the farfield of a lifting airfoil
[IAR-AN-78] 07 p2647 N94-26702

A comprehensive comparison of turbulence models in the far wake 07 p2808 N94-27899
Separated flow generated by a vectored jet in a crossflow 07 p2800 N94-28007
Scalar mixing in the subsonic jet in crossflow 07 p2800 N94-28008
Experimental investigation of the interaction of a thrust reverser jet with an external subsonic flow 07 p2801 N94-28011
A numerical investigation of a subsonic jet in a crossflow 07 p2803 N94-28023
Navier-Stokes simulation of two and three dimensional jets in crossflow, effects of grid, and boundary conditions 07 p2804 N94-28026
Measurements of steady and dynamic pressure on an F/A-18 wind tunnel model at high angles of attack 07 p2653 N94-28323
The 3-D LDV measurements on a 30-degree swept wing with a simulated ice accretion [NASA-CR-195327] 08 p3132 N94-30124
Canonical-variables multigrid method for steady-state Euler equations [AD-A279020] 08 p3454 N94-30208
Numerical investigation into high-angle-of-attack leading-edge vortex flow [PB94-125564] 08 p3133 N94-30388
Aspects of the modeling and numerical simulation of leading-edge vortex flow [AD-B179108] 08 p3133 N94-30492
A residual correction method applied to 2D multi-point airfoil design and 3D single-point wing design [NLR-TP-92524-U] 08 p3134 N94-30493
An experimental study of the flowfield on a semispan rectangular wing with a simulated glaze ice accretion [NASA-CR-195301] 09 p3571 N94-32475
Shear flow control of cold and heated rectangular jets by mechanical tabs. Volume 1: Results and discussion [NASA-CR-182296-VOL-1] 09 p3708 N94-32867
Shear flow control of cold and heated rectangular jets by mechanical tabs. Volume 2: Tabulated data [NASA-CR-182296-VOL-2] 09 p3709 N94-32869
Automatic computation of Euler-marching and subsonic grids for wing-fuselage configurations [NASA-TM-4573] 12 p4383 N94-36950

SUBSONIC FLUTTER

Laser velocimeter measurements of the flow field generated by a forward-swept propfan during flutter [NASA-TM-106195] 01 p0014 N94-10892
Aeroelastic vibrations of lifting surfaces [ECL-91-01] 09 p3585 N94-31677
Alleviation of whirl-flutter on a joined-wing tilt-rotor aircraft configuration using active controls [NASA-CR-196103] 11 p4200 N94-36436

SUBSONIC SPEED

Performance seeking control: Program overview and future directions [NASA-TM-4531] 02 p0519 N94-14855
Wind tunnel investigation of three axisymmetric cowls of different lengths at Mach numbers from 0.60 to 0.92 [NASA-TM-4488] 03 p0856 N94-15681
Flow analysis for the nacelle of an advanced ducted propeller at high angle-of-attack and at cruise with boundary layer control [NASA-TM-106371] 03 p0858 N94-16571
Wind tunnel investigations of forebody strakes for yaw control on F/A-18 model at subsonic and transonic speeds [NASA-TP-3360] 03 p0859 N94-16573
Wind-tunnel investigation of aerodynamic efficiency of three planar elliptical wings with curvature of quarter-chord line [NASA-TP-3359] 03 p0859 N94-16574
Experimental cavity pressure measurements at subsonic and transonic speeds. Static-pressure results [NASA-TP-3358] 06 p2169 N94-24464
Nonlinear aerodynamic modeling using multivariate orthogonal functions 06 p2164 N94-25110
Normal force of low aspect ratio cropped-delta wings at pre-stall angles of attack and subsonic speeds [ESDU-93034] 07 p2648 N94-27955
Program for calculation of maximum lift coefficient of plain aerofoils and wings at subsonic speeds [ESDU-93015] 07 p2649 N94-28076
Examples of flight path optimisation using a multivariate gradient-search method [ESDU-93021] 07 p2670 N94-28092
Installed F/A-18 inlet flow calculations at 30 degrees angle-of-attack: A comparative study [NASA-CR-195297] 09 p3573 N94-33119
HSCT high-lift technology requirements 10 p3980 N94-33523
Wind tunnel measurements on a full-scale F/A-18 with a tangentially blowing slot --- conducted in the Ames 80 by 120 foot wind tunnel 11 p4191 N94-35965
Subsonic aerodynamic characteristic of semispan commercial transport model with wing-mounted advanced ducted propeller operating in reverse thrust --- conducted in the Langley 14 by 22 foot subsonic wind tunnel [NASA-TP-3427] 12 p4384 N94-37505

SUBSONIC WIND TUNNELS

Wall interference correction based on interface measurements in subsonic wind tunnel testing 01 p0015 N94-11154
Determining the effect of endwall boundary layer suction in a large scale subsonic compressor cascade [AD-A267208] 03 p0859 N94-16913
User's manual for the Langley Research Center 14- by 22- foot subsonic tunnel static data acquisition system [NASA-TM-109027] 03 p0861 N94-17639
Fiber-optic-based laser vapor screen flow visualization system for aerodynamic research in larger scale subsonic and transonic wind tunnels [NASA-TM-4514] 07 p2647 N94-26706
Experimental investigation of the flow quality in the GLT20 subsonic-transonic boundary layer wind tunnel [PB94-126539] 07 p2681 N94-26815
The nozzle acoustic test rig: An acoustic and aerodynamic free-jet facility [NASA-TM-106495] 08 p3156 N94-28749
User's manual for the model interface and plugboard cabinets in the 14- by 22-foot subsonic tunnel [NASA-TM-109062] 08 p3133 N94-30176
Hotwire measurements of the turbulent flow into a cascade of controlled-diffusion compressor blades [AD-A277297] 09 p3706 N94-32042
National facilities study. Volume 2: Task group on aeronautical research and development facilities report [NASA-TM-109855] 10 p4009 N94-34633
Flow quality studies of the NASA Lewis Research Center Icing Research Tunnel [NASA-TM-106545] 10 p4010 N94-34919
Langley 14- by 22-foot subsonic tunnel test engineer's data acquisition and reduction manual [NASA-TM-4563] 11 p4189 N94-35246

SUBSTANCES

U MATERIALS

SUBSTITUTES

Prioritization methodology for chemical replacement [NASA-TP-3421] 03 p0976 N94-15723
Development of alternatives to lead-bearing solders [DE93-016509] 04 p1357 N94-17862
US Department of Energy phaseout of CFC-refrigerants [DE94-001668] 06 p2397 N94-23016
Ozone depletion, paradigms, and politics [DE94-001600] 06 p2398 N94-24506
Alternative fuel vehicles for the state fleets: Results of the 5-year planning process [DE94-004709] 08 p3224 N94-28577
Practical applications of plasma surface modification [DE94-004892] 08 p3349 N94-29932
Logistics for the implementation of lead-free solders on electronic assemblies [DE94-004800] 08 p3206 N94-29936
Non-aqueous cleaning solvent substitution [DE94-005339] 08 p3219 N94-30245
Non-aqueous cleaning solvent substitution 08 p3354 N94-30466
Proceedings of the 1993 Windsor Workshop on Alternative Fuels [DE94-003908] 08 p3226 N94-30612
Materials Compatibility and Lubricant Research on CFC-refrigerant substitutes [DE94-012352] 12 p4425 N94-37373

SUBSTITUTION

U SUBSTITUTES

SUBSTRATES

Zerodur polishing process for high surface quality and high efficiency [DE93-012596] 01 p0087 N94-10271
Rapid thermal processing for strained-layer semiconductor devices [DE93-013754] 01 p0396 N94-10809
Needs for super-smooth surfaces [DE93-012482] 01 p0382 N94-11242
Carbon analyses of IDP's sectioned in sulfur and supported on beryllium films 01 p0081 N94-12099
Analysis of the economics of DC arc CVD diamond [AD-A265688] 01 p0403 N94-12339
Dynamic high-pressure shock compaction of diamond powders [AD-A266004] 01 p0093 N94-12354
Development of ultra-low noise, high sensitivity planar metal grating coupled 3 to 5 multiquantum well infrared detectors for focal plane array staring IR sensor systems [AD-A265599] 01 p0404 N94-12375
Corrosion and passivation of high temperature superconductors [AD-A265402] 01 p0405 N94-12586
Electrophoretic and electrolytic deposition of ceramic particles on porous substrates [AD-A265141] 02 p0575 N94-12812
Project proposal for partial computational physics support for Survivability of Coatings program [DE93-013788] 02 p0576 N94-12939
The study of structure-processing-property relations in copper oxide based high (Tc) superconductors [DE93-015066] 02 p0804 N94-13003
Effects of growth conditions and substrate orientation on the properties of InSb [DE93-013766] 02 p0812 N94-14344
Kinetics of photodeposition of superconducting films [DE93-015511] 02 p0812 N94-14348
Metastability of yttrium-oxides [DE93-016548] 02 p0813 N94-14440
Ion assisted sputter deposition of Mo-Si multilayers [DE93-013830] 02 p0583 N94-14693
Solution chemistry optimization of sol-gel processed PZT thin films [DE93-013776] 02 p0814 N94-14695
Characterization of diamond film growth in a combustion flame [AD-A266659] 02 p0816 N94-14839
Substrate effects in superconducting tunnel junction detectors 03 p0908 N94-15083
Selective formation of porous silicon [NASA-CASE-NPO-18735-1-CU] 03 p0966 N94-15960
Polished substrate surface and cleaning study for coated optic quality [DE93-014116] 03 p1190 N94-15975
Ablation, surface activation, and electroless metallization of insulating materials by pulsed excimer laser irradiation [DE93-015808] 03 p1040 N94-16664
Materials processing and manufacturing technologies for diamond substrate multichip modules (DSMCM) [AD-A267316] 03 p0969 N94-16946
Single crystal diamond thin films [AD-A266457] 03 p1214 N94-17216
Growth, characterization and device development in monocrystalline diamond films [AD-A268206] 03 p1216 N94-17553
Metal-nanocluster composites made by ion implantation: A novel third-order nonlinear material [DE93-015908] 04 p1339 N94-17846
Characterization of diamond film nucleation and growth surface [AD-A269400] 04 p1597 N94-18459
Kinetic aspects of lattice mismatch in molecular beam epitaxial growth on planar and patterned substrates [AD-A270424] 04 p1597 N94-18506
Diamond brazed to a metal [AD-D015877] 04 p1371 N94-18746
Growth, characterization and device development in monocrystalline diamond films [AD-A270074] 04 p1599 N94-18797
Thermal analysis of coatings and substrate materials during a disruption in fusion reactors [DE93-017688] 04 p1588 N94-18971
The minimum detection limits of RDX and TNT deposited on various surfaces as determined by ion mobility spectroscopy [DE93-018521] 04 p1378 N94-19042
Silicon MCM substrates for integration of 3-5 photonic devices and CMOS IC's [DE93-017894] 04 p1405 N94-19112
The microstructural mechanism of electromigration failure in narrow interconnects of Al alloys [DE93-018598] 04 p1365 N94-19282
Study of GaAs substrates by ambient temperature photoluminescence imagery [ECL-92-61] 04 p1603 N94-19357
Testing of protective coatings in hydrogen [DE93-040326] 04 p1375 N94-19651
Substrate recovery of Mo-Si multilayer coated optics [DE93-019610] 05 p1698 N94-19810
Quartz/fused silica chip carriers [NASA-CR-194154] 05 p2016 N94-20340
Adhesive electroless metallization of fluoropolymeric substrates [AD-A271858] 05 p1703 N94-20526
Growth, characterization and device development in monocrystalline diamond films [AD-A272715] 05 p2026 N94-21190
Analysis of semi-insulating bulk GaAs using glow discharge mass spectrometry [AD-A273032] 05 p1682 N94-21435
Growth, characterization and device development in monocrystalline diamond films [AD-A273097] 05 p2028 N94-21506
The n-p(p(+))-n Al(yGa)(1-y) As-GaAs-In(x)Ga(1-x) as quantum well laser with p(+)-n(+)GaAs-InGaAs tunnel contact on n GaAs [AD-A271292] 05 p2030 N94-21805

MOCVD growth and structure of PbTiO3 thin films
[DE93-040230] 05 p2033 N94-21994
Shock temperature measurements of iron to 350 GPa
[DE94-001058] 05 p1695 N94-22024
Theoretical studies of wave propagation in multilayered piezoelectric media
[DE93-040273] 06 p2371 N94-22872
Novel two-stage selenization methods for fabrication of thin-film CIS cells and submodules
[DE94-000220] 06 p2390 N94-23296
Method of determining shear stress employing a monomer-polymer laminate structure
[NASA-CASE-LAR-14654-2] 06 p2375 N94-23308
Hairy carbon electrodes studied by cyclic voltammetry and battery discharge testing 06 p2394 N94-23367
Infrared analysis of vapor phase deposited tricresylphosphate (TCP)
[NASA-TM-106423] 06 p2253 N94-23371
Method of forming silicon structures with selectable optical characteristics
[NASA-CASE-NPO-18625-1-CU] 06 p2563 N94-23972
Chemically sensitive interfacial force microscopy: Contact potential measurements of self-assembling monolayer films
[AD-A273135] 06 p2234 N94-24772
Laser-deposited biocompatible films and methods and apparatuses for producing same
[AD-D016017] 06 p2350 N94-24952
Field emitter array
[AD-D016023] 06 p2303 N94-25150
Study of the homogeneity of InP wafers
[AD-A273658] 07 p3055 N94-26194
Comparison of technology for high-power laser mirrors and synchrotron radiation mirrors
[DE94-002913] 07 p3035 N94-26276
Demonstration of monolithic co-fabrication of Y1Ba2Cu3O7-Sigma and CMOS devices on the same sapphire substrate
[AD-A274757] 07 p3059 N94-26566
Growth, characterization and device development in monocrystalline diamond films
[AD-A274245] 07 p3060 N94-26839
The growth and characterization of GaN as a photodetector
[AD-A274570] 07 p3063 N94-26965
Electro-optic materials by solid source MOCVD
[DE94-005120] 07 p2757 N94-27716
Bipolar lead-acid batteries for electrical actuation applications 07 p2864 N94-28134
Pull-test adhesion measurements of diamondlike carbon films on silicon carbide, silicon nitride, aluminum oxide, and zirconium oxide
[DE94-005469] 08 p3211 N94-28536
Development of large area RF induction plasma for cost effective diamond
[AD-A275888] 08 p3504 N94-28776
MOCVD growth of GaN, AlN and AlGaN for UV photodetector applications
[AD-A275078] 08 p3512 N94-28871
Silicon germanium carbon heteroepitaxial growth on silicon
[AD-A275197] 08 p3512 N94-28889
Dual-use applications of infrared sensitive materials
[AD-A275140] 08 p3499 N94-29694
Ionic conduction mechanisms in CaF2 and CaF2-Al2O3 nanocomposite films on Al2O3 substrates
[DE94-004792] 08 p3520 N94-30773
Surface chemistry of boron-doped SiO2 CVD: Enhanced uptake of tetraethyl orthosilicate by hydroxyl groups bonded to boron
[DE94-005428] 08 p3221 N94-30896
A new mechanism for surface diffusion: Motion of a substrate-adsorbate complex
[AD-A276072] 09 p3632 N94-31459
In-situ TEM crystallization of anorthite-glass films on (alpha)-Al2O3
[DE94-006317] 09 p3652 N94-31780
Epitaxial liftoff technology onto processed silicon foundry wafers
[AD-A277116] 09 p3900 N94-31985
Materials processing and manufacturing technologies for diamond substrates multichip modules
[AD-A276904] 09 p3692 N94-32215
Stability and precipitation kinetics in Si(1-y)C(y)/Si and Si(1-x-y)Ge(x)C(y)/Si heterostructures prepared by solid phase epitaxy
[DE94-006589] 09 p3902 N94-32296
An electrical test system for conductor formation process analysis
[DE94-007291] 09 p3696 N94-32786
Conductive paints
[DE94-008508] 09 p3661 N94-32788
Ultrahigh-current-density metal-ion implantation and diamondlike-hydrocarbon films for tribological applications
[DE94-008958] 09 p3906 N94-32843
High definition TV projection via single crystal faceplate technology
[AD-A277850] 10 p4034 N94-33768
Adhesion of phospholipid monolayers to planar supports deposited with the Langmuir-Blodgett technique
[PB94-148699] 10 p4029 N94-34102
Efficient chemistry for selective modification and metallization of substrates
[AD-D016162] 10 p4023 N94-34287
Three dimensional ICs intelligent sensors 10 p4057 N94-34354
Morphological aspects of surface reactions
[DE94-010184] 11 p4236 N94-35685
Thick film fabrication of aluminum nitride microcircuits
[DE94-010107] 11 p4259 N94-35706
Study and fabrication of GaSb-based laser heterostructures
[PB94-170677] 11 p4273 N94-36218
Effect of niobium interlayer on high-temperature sliding friction and wear of silver films on alumina
[DE94-010462] 11 p4275 N94-36232
Demonstration of a high heat removal CVD diamond substrate edge-cooled multichip module
[DE94-010748] 11 p4260 N94-36245
Determining the refractive index of a lambda/4 thin film on a thick substrate from a transmittance measurement
[DE93-019584] 12 p4523 N94-36693
Substrate effects on the structure and optical properties of epitaxial PbTiO3 thin films prepared by metal-organic chemical vapor deposition
[DE94-010432] 12 p4535 N94-37192
X-ray diffraction studies of evaporated gold thin films deposited on aluminum nitride substates
[AD-A280454] 12 p4536 N94-37228
Development of low dielectric constant alumina-based ceramics for microelectronic substrates
[DE94-011360] 12 p4439 N94-37302
Morphological aspects of surface reactions
[DE94-011208] 12 p4413 N94-37713
Gas microstrip detectors on resistive plastic substrates
[DE94-011336] 12 p4426 N94-37714

SUBSTRUCTURES
Multilevel computer-aided optimum design of structural systems using multiple basis vectors 01 p0187 N94-11055
Extending substructure based iterative solvers to multiple load and repeated analyses
[NASA-CR-194822] 06 p2466 N94-23504
Substructure synthesis methods for viscoelastic structures
[UTIAS-349] 07 p2695 N94-26712
Transport phenomena in the Earth's plasma sheet 09 p3772 N94-31970

SUBTROPICAL REGIONS
U TEMPERATE REGIONS
U TROPICAL REGIONS

SUBURBAN AREAS
Spatiotemporal variability of non-urban ozone concentrations over the eastern United States and its potential replication by satellite data
[PB93-191328] 04 p1476 N94-19065

SUCROSE
Contained liquids in microgravity, part 2 03 p0979 N94-16085

SUCTION
DNS on control of laminar-turbulent transition in channel flow with suction and blowing 01 p0163 N94-12613
The transient behavior of a boundary layer exposed to uniform suction
[ITN-93-85205] 02 p0630 N94-13197
Determining the effect of endwall boundary layer suction in a large scale subsonic compressor cascade
[AD-A267208] 03 p0859 N94-16913
Vortex generation and wave-vortex interaction over a concave plate with roughness and suction
[AD-A276839] 06 p2337 N94-24869
Numerical simulation of receptivity and transition in a boundary layer on a flat plate with a suction hole
[NASA-CR-195708] 07 p2798 N94-27782
Localized and distributed boundary-layer receptivity to convected unsteady wake in free stream
[NASA-CR-4578] 07 p2808 N94-28180
Results for the hybrid laminar flow control experiment conducted in the NASA Langley 8-foot transonic pressure tunnel on a 7-foot chord model
[NASA-TM-107582] 09 p3601 N94-32870
Acoustic receptivity of compressible boundary layers: Receptivity by way of surface-temperature variations
[NASA-CR-4599] 10 p4046 N94-33897
Inverse design of radial flow impellers with prescribed velocity at hub and shroud 10 p4002 N94-34448
Dynamic tests to demonstrate lateral control using forebody suction on large scale models in the DRA 24 foot wind tunnel 10 p3991 N94-34613
The unsteady pressure field and vorticity productiion at the suction surface of a pitching airfoil 10 p3986 N94-34972
Toward the optimization of control of unsteady separation 10 p4053 N94-34985
An algorithm for the automatic control of boundary layer flow
[ISVR-TR-233] 12 p4442 N94-36817
Experimental measurements and analytical analysis related to gas turbine heat transfer. Part 1: Time-averaged heat-flux and surface-pressure measurements on the vanes and blades of the SSME fuel-side turbine and comparison with prediction. Part 2: Phase-resolved surface-pressure and heat-flux measurements on the first blade of the SSME fuel-side turbine
[NASA-CR-196296] 12 p4442 N94-36969
Unsteady flow field of large-amplitude pitching airfoils
[AD-A280444] 12 p4383 N94-37219

SUD AVIATION AIRCRAFT
Remote vibration measurements at a sud aviation alouette 3 helicopter with a CW CO2-laser system
[AD-A273818] 06 p2190 N94-25516

SUDAN
Assessment of tropical forests using satellite data
[SILVA-CARELICA-21] 07 p2850 N94-27182
Woody biomass density in the Tendelti area of the central Sudan 07 p2850 N94-27185

SUDDEN IONOSPHERIC DISTURBANCES
Solar-geophysical data number 584, April 1993. Part 1: (Prompt reports). Data for March, February 1993, and late data
[PB93-198323] 02 p0845 N94-14560
Solar-geophysical data number 584, April 1993. Part 1: (Prompt reports). Data for February, March, 1993, and late data
[PB93-198323] 06 p2626 N94-23738
Solar-geophysical data number 587, July 1993. Part 1: (Prompt reports). Data for June, May 1993, and late data
[PB93-232874] 06 p2628 N94-24989
Solar-geophysical data number 590, October 1993. Part 1: (Prompt reports). Data for September, August 1993, and late data
[PB94-125903] 07 p3110 N94-27053
Solar-geophysical data number 591, November 1993. Part 1: Prompt reports. Data for September, October 1993 and late data
[PB94-140548] 08 p3550 N94-29122
Solar-geophysical data number 593, January 1994. Part 1: (Prompt reports). Data for December, November 1993, and late data
[PB94-151578] 10 p4165 N94-34163

SUGARS
NT DEXTRANS
NT GLUCOSE
NT SUCROSE
Instrumental development of novel detection and separation methods for capillary electrophoresis
[DE94-005554] 08 p3187 N94-28519

SUHL EFFECT
Nonlinear dynamics and instabilities in ferromagnetic resonance experiments: Examinations of spheres from yttrium iron garnet in coincidence area of the first Suhl instabilities
[ETN-93-95072] 04 p1604 N94-19612

SUITS
NT EXTRAVEHICULAR MOBILITY UNITS
NT PRESSURE SUITS
NT SPACE SUITS
Cool suit
[NASA-TM-109639] 03 p1120 N94-15250
Insulative properties of two thermo-metal neoprenes
[AD-A275209] 08 p3401 N94-29302

SULFATES
NT MAGNESIUM SULFATES
NT SODIUM SULFATES
Second and third order nonlinear optical properties of crystalline inorganic/organic complexes
[DE93-011883] 01 p0173 N94-10755
Sulfate reduction and other sedimentary biogeochemistry in a northern New England salt marsh 01 p0268 N94-12453
Acetate concentrations and oxidation in salt marsh sediments 01 p0269 N94-12459
The effects of acid deposition on sulfate reduction and methane production in peatlands 01 p0270 N94-12465
Determination of trace elements in triglycine sulfate solutions
[NASA-CR-193481] 02 p0562 N94-13048
Stress corrosion cracking of 316 SS and Incoloy-800 in high temperature aqueous containing sulfate and chloride
[DE93-623325] 03 p0952 N94-17302

The global atmospheric sulfur cycle: An evaluation of model predictions and observations
[CM-81] 04 p1479 N94-19379
Impact-induced devolatilization of CaSO4 anhydrite and implications for K-T extinctions: Preliminary results 05 p2085 N94-20840
Effect of copper sulphate on the rate of afferent discharge in the gastric branch of the vagus nerve in the rat 05 p1887 N94-21907
Experimental studies of gastric dysfunction in motion sickness: The effect of gastric and vestibular stimulation on the vagal and splanchnic gastric efferents 05 p1888 N94-21911
Integrated hydrometallurgical jarosite treatment
[PB93-217990] 06 p2232 N94-22983
Cloud-free aerosol optical depth determination over oceans from satellite radiometry
[DE94-001897] 06 p2386 N94-23779
Development of SO(x) and NO(x) solid electrolyte sensors 07 p2725 N94-25562
Journal of NIRE, volume 2, number 4
[JTN-94-80554] 07 p2869 N94-28147
Effects of p-chlorophenol on sulfate reduction in marine sediments 07 p2870 N94-28150
The adsorption of sulfate on gold(111) in acidic aqueous media: Adlayer structural inferences from infrared spectroscopy and scanning tunneling microscopy
[AD-A276643] 09 p3642 N94-31997
Evaluation of sulfate aerosol optical depths over the North Atlantic and comparison with satellite observations
[DE94-005457] 09 p3746 N94-32100
Fine resolution atmospheric sulfate model driven by operational meteorological data: Comparison with observations
[DE94-002994] 09 p3766 N94-32691
Climate effects of anthropogenic sulfate: Simulations from a coupled chemistry/climate model
[DE94-004352] 09 p3767 N94-32789
Ferric sulfate montmorillonites as Mars soil analogs 09 p3944 N94-33196
Modeling the atmospheric input of nutrients, heavy metals, and pesticides to the Great Lakes
[DE94-005481] 11 p4286 N94-36007
Anthropogenic sulfate and organic aerosols, CCN, and cloud project concentration at a marine site
[DE94-004210] 11 p4286 N94-36025
Isolated SO4-2 and PO4-3 anions do not exist
[AD-A278831] 12 p4512 N94-36521
Indicators for sulfate-reducing bacteria in microbiologically influenced corrosion
[AD-A278914] 12 p4477 N94-36522

SULFATION

Superacid catalysis of light hydrocarbon conversion
[DE94-011132] 12 p4411 N94-37431

SULFIDATION

Development and commercialization status of Fe3Al-based intermetallic alloys
[DE93-015802] 03 p0957 N94-16165
Vanadium corrosion studies
[AD-A266489] 03 p0959 N94-16781
Surface modification for corrosion resistance
[DE93-017419] 05 p1693 N94-21825
Ultraviolet photosulfidation of III-V compound semiconductors for electronic passivation
[DE94-001417] 06 p2555 N94-22717

SULFIDES

NT CADMIUM SULFIDES
NT CARBON DISULFIDE
NT COPPER SULFIDES
NT DISULFIDES
NT HYDROGEN SULFIDE
NT MOLYBDENUM DISULFIDES
NT MOLYBDENUM SULFIDES
NT POLYSULFIDES
NT PYRITES
NT TROILITE
NT WURTZITE
NT ZINC SULFIDES
NT ZINCBLENDE

Thermal stability of sealants for military aircraft: Modification of polysulfide prepolymers with ether and thioether monomers
[AD-A264079] 01 p0089 N94-11107
Biogeochemical factors which regulate the formation and fate of sulfide in wetlands 01 p0270 N94-12464
An investigation of the role of second phase particles in the design of ultra high strength steels of improved toughness
[AD-A266774] 02 p0573 N94-14786
The global atmospheric sulfur cycle: An evaluation of model predictions and observations
[CM-81] 04 p1479 N94-19379
The role of CO2 in weathering reactions and the presence of S2 on Venus: Implications for the pyrite stability field 05 p2122 N94-20799
Lewis Cliff 87057: A new metal-rich E3 chondrite with similarities to Mt. Egerton, Shallowater and Happy Canyon 05 p2086 N94-20901
High-resolution soft x ray photoionization studies of selected molecules
[DE94-000568] 06 p2532 N94-23002
Spin fluctuations in an ordered Heisenberg ferromagnet with dipolar interactions
[PB93-204493] 06 p2524 N94-24533
Laboratory detection of C5S by pulsed-discharge-nozzle Fourier-transform microwave spectroscopy
[JTN-94-80519] 06 p2235 N94-24984
Voltammetric studies of poly(carbon disulfide)
[DE94-001385] 07 p2717 N94-26951
Interstitially stabilized phases in the zirconium-nickel system
[DE94-005561] 08 p3201 N94-28525
Studies of high temperature ternary phases in mixed-metal-rich early transition metal sulfide and phosphide systems
[DE94-006034] 08 p3209 N94-30336
New molecular-based routes to binary main group metal sulfides
[AD-A277005] 09 p3900 N94-32003
Processable, chemical routes to binary metal sulfides
[AD-A277006] 09 p3642 N94-32004
Group 12 thiolates: Syntheses, characterization and decomposition pathways
[AD-A277055] 09 p3900 N94-32011
The relative performance of FeS2 and CoS in long-life thermal-battery applications
[DE94-006145] 09 p3695 N94-32663
Gasoline from natural gas by sulfur processing
[DE94-011130] 11 p4248 N94-36035
Preliminary results of sulfide melt/silicate wetting experiments in a partially melted ordinary chondrite 11 p4353 N94-36147

SULFONATES

Solid-state structures of guanidinium methane, ethane, and trifluoromethanesulfonate
[AD-A265293] 01 p0402 N94-11654
Hydrogen-bond polymorphs of guanidinium 4-biphenylsulfonate
[AD-A265294] 01 p0402 N94-11827

SULFONES

New aromatic activated dihalides and bisphenol monomers for the preparation of novel poly(arylene ethers)
[NASA-CR-193190] 01 p0055 N94-10513
Poly(arylene ether-co-imidazole)s as toughness modifiers for epoxy resins
[NASA-CASE-LAR-15229-1-CU] 08 p3215 N94-29451

SULFONIC ACID

Metal ion complexation by ionizable crown ethers
[DE94-008301] 09 p3661 N94-32847

SULFUR

Hydrogen partitioning and transport in titanium aluminides
[NASA-CR-194117] 01 p0076 N94-10713
Carbon analyses of IDP's sectioned in sulfur and supported on beryllium films 01 p0081 N94-12099
Sulfur transformations in the sediments of a New Hampshire salt marsh 01 p0270 N94-12463
Emissions of biogenic sulfur gases from northern bogs and fens 01 p0271 N94-12467
Sulfur gas exchange in Sphagnum-dominated wetlands 01 p0271 N94-12470
Creep ductility of iron at very low strain rates: The effects of sulfur
[DE93-015490] 03 p0959 N94-16890
Synthesis, reactivity, and characterization of (-hexacarbocyclic) manganese dicarbonyl complexes with sulfur and phosphorus ligands
[AD-A267592] 03 p0930 N94-17192
The d(exp 3)delta-a(exp 3)delta and b(exp 3)phi-a(exp 3)delta systems of ZrS, Part 2: Appendix, list of wavenumbers
[USIP-92-05] 04 p1602 N94-19293
Sulfur-bonded thiophenes in organometallic rhenium complexes and adsorption of isocyanides on gold
[DE93-041126] 05 p1694 N94-21937
Electrochemical sulfur passivation of visible (approximately 670nm) AlGaInP lasers
[DE94-002293] 06 p2350 N94-24659
The intramolecular cyclization of bis-2,5-dimethylene-2,5-dihydrofurans and bis-2,5-dimethylene-2,5-dihydrothiophenes: An approach to macrocycles
[DE94-007060] 09 p3657 N94-32377
Fine resolution atmospheric sulfate model driven by operational meteorological data: Comparison with observations
[DE94-002994] 09 p3766 N94-32691
Comparison of the impact of volcanic eruptions and aircraft emissions on the aerosol mass loading and sulfur budget in the stratosphere 10 p3971 N94-33460
Antarctic weathering of the CK chondrites EET90004, 90007, and 90022: Nickel and sulfur mobility 11 p4351 N94-35451

SULFUR COMPOUNDS

NT CADMIUM SULFIDES
NT CARBON DISULFIDE
NT COPPER SULFIDES
NT CYSTEINE
NT DISULFIDES
NT HYDROGEN SULFIDE
NT MAGNESIUM SULFATES
NT MOLYBDENUM DISULFIDES
NT MOLYBDENUM SULFIDES
NT ORGANIC SULFUR COMPOUNDS
NT POLYSULFIDES
NT PYRITES
NT SODIUM SULFATES
NT SULFATES
NT SULFIDES
NT SULFONATES
NT SULFONES
NT SULFUR DIOXIDES
NT SULFUR FLUORIDES
NT SULFUR HEXAFLUORIDE
NT SULFUR OXIDES
NT SULFURIC ACID
NT THIOLS
NT TROILITE
NT WURTZITE
NT ZINC SULFIDES
NT ZINCBLENDE

Terminal Decomposition and Gaseous Sulfur Release from Tidal Wetlands
[NASA-CR-193466] 01 p0267 N94-12451
A preliminary study of the variability and magnitude of the flux of biogenic sulfur gases from a New Hampshire salt marsh 01 p0267 N94-12452
Emissions of biogenic sulfur gases from Alaskan tundra 01 p0268 N94-12455
Factors controlling fluxes of volatile sulfur compounds in Sphagnum peatlands 01 p0268 N94-12456
Emissions of sulfur gases from marine and freshwater wetlands of the Florida Everglades: Rates and extrapolation using remote sensing 01 p0269 N94-12457
Emissions of sulfur gases from wetlands 01 p0269 N94-12458
Application of static and dynamic enclosures in determining DMS and OCS fluxes in Sphagnum peatlands 01 p0269 N94-12460
Effects of inorganic sulfur addition on fluxes of volatile sulfur compounds in Sphagnum peatlands 01 p0270 N94-12461
Environmental factors controlling fluxes of dimethyl sulfide in a New Hampshire fen 01 p0270 N94-12462
Factors controlling sulfur gas exchange in Sphagnum-dominated wetlands 01 p0271 N94-12469
Performance effects of coal-derived contaminants on the carbonate fuel cell
[DE93-013801] 02 p0703 N94-13693
Importance of sprays for long range transport of harmful substances in the troposphere
[MITT-81] 02 p0711 N94-14723
Supercritical thermodynamics of sulfur and nitrogen species
[DE93-041221] 04 p1610 N94-19670
Reactivity of nitrate radical (NO3) toward organic compounds 07 p2704 N94-27387
Polyimides containing the penta fluoro sulfanyl benzene moiety
[NASA-CASE-LAR-15082-1] 08 p3175 N94-29554
Processable, chemical routes to binary metal sulfides
[AD-A277006] 09 p3642 N94-32004
Laser spectroscopy and dynamics of transient species
[DE94-009318] 10 p4058 N94-33905

SULFUR DIOXIDES

Study of climatic effects of cloud-aerosol interaction 01 p0204 N94-11977
An examination of utility emissions contributions to elevated ozone concentrations in the Chicago area
[DE93-012852] 02 p0708 N94-13495
Summary of conclusions and recommendations from a visibility science workshop
[DE93-012770] 02 p0710 N94-14523
Promotion of geothermal energy development in 1991
[DE93-799061] 02 p0705 N94-14679
Signal and reference wavelengths for the elimination of SO2 cross sensitivity in remote measurements of tropospheric ozone with lidar
[GKSS/92/E/24] 02 p0617 N94-14819

The mobile lidar system ARGOS for spatial resolution remote measuring of gaseous air pollutants
[GKSS/92/E/26] 02 p0617 N94-14820
The use of TIMS data to estimate the SO2 concentrations of volcanic plumes: A case study at Mount Etna, Sicily 03 p1065 N94-16608
Condensed gases under winter conditions: A study for the rescue services
[FOA-C-40305-4.5] 04 p1473 N94-18139
Photodissociation studies of polyatomic free radicals
[AD-A270084] 04 p1350 N94-18799
Effects of the Mount Pinatubo eruption on solar insolation: Four case studies
[DE93-018454] 04 p1475 N94-18817
The global atmospheric sulfur cycle: An evaluation of model predictions and observations
[CM-81] 04 p1479 N94-19379
SO2 on Venus: IUE, HST and ground-based measurements, and the active volcanism connection 05 p2092 N94-20637
Participation in TOMS missions
[NASA-CR-195110] 06 p2398 N94-24078
Nimbus-7 Total Ozone Mapping Spectrometer (TOMS) data products user's guide
[NASA-RP-1323] 06 p2410 N94-24355
SO2 on Venus: A final cross-calibration with Pioneer Venus
[NASA-CR-195162] 06 p2599 N94-24988
Sulfur dioxide in the atmosphere of Venus 1 sounding rocket observations
[NASA-CR-195224] 07 p3106 N94-26237
Cloud studies seen from a physical chemist's perspective
[DE94-006059] 09 p3771 N94-31527
Time-dependent behavior of Mount Pinatubo aerosol
[DE94-001877] 09 p3764 N94-31601
Concentration system performance degradation in the aftermath of Mount Pinatubo
[DE94-001879] 09 p3764 N94-31602
Volcanic gas emissions and their effect on ambient air character
[DE94-005675] 10 p4081 N94-33715
Combined SO(x)/NO(x) control via SOXAL (tm) process: An electrodialytic regenerative wet scrubbing process
[DE94-009053] 11 p4284 N94-35346
State-to-state dynamics of molecular energy transfer
[DE94-009651] 11 p4324 N94-35816
Air quality implications associated with the selection of power plants in the Pacific Northwest
[DE94-004783] 11 p4287 N94-36027
Treatment of toxic gases SO2 and NO(x) by electron beam irradiation
[DE94-615424] 11 p4330 N94-36028
SIHTI: Energy and environmental technology
[DE94-763290] 12 p4464 N94-37007

SULFUR FLUORIDES
NT SULFUR HEXAFLUORIDE
Studies of critical point phenomena of fluids: Bulk fluids, fluids in pores, and at interfaces 01 p0080 N94-10228
Application of an atmospheric dispersion model to simulated pollutant releases in the Colorado Front range
[DE93-017118] 04 p1480 N94-19732
Radiative forcing calculations for SF6 and CH4 using a correlated k-distribution transmission model
[DE94-001855] 06 p2397 N94-23700
Research for electric energy systems
[DE94-001839] 06 p2293 N94-23719

SULFUR HEXAFLUORIDE
Transport of heat and mass in near-critical fluids 01 p0122 N94-10230
Field-emitter arrays for RF vacuum microelectronics
[AD-A268397] 03 p1015 N94-17526
High-resolution soft x ray photoionization studies of selected molecules
[DE94-000568] 06 p2532 N94-23002

SULFUR OXIDES
NT SULFUR DIOXIDES
User's manual for the plume visibility model PLUVUE 2 (revised)
[PB93-188233] 01 p0265 N94-11016
Photodissociation studies of polyatomic free radicals
[AD-A270084] 04 p1350 N94-18799
Development of SO(x) and NO(x) solid electrolyte sensors 07 p2725 N94-25562
Study on performance evaluation of pressure vessel steel in corrosion environments with sulfide 07 p2730 N94-25582
Identification of research relating to the critical loads concept and its potential application to the regulation of acidic deposition
[DE94-008234] 09 p3767 N94-32752

SULFURIC ACID
Reduction and analysis of seasons 15 and 16 (1991 - 1992) Pioneer Venus radio occultation data and correlative studies with observations of the near-infrared emission of Venus
[NASA-CR-194128] 02 p0841 N94-13083
Investigations into the recovery of waste sulfuric acid with concentrated solar radiation
[DLR-FB-93-11] 03 p0952 N94-17594
A comparison of sulfuric acid/boric acid anodize and chromic acid anodize processes
[AD-A271933] 05 p1703 N94-20614
Global blackout following the K/T Chicxulub impact: Results of impact and atmospheric modeling 05 p1854 N94-20698
Examination of the observed synoptic scale cirrus cloud environment: The December 3-6 FIRE cirrus case study 05 p1877 N94-22325
Measuring variation in ecosystem sensitivity to stress
[AD-A274232] 07 p2868 N94-26817
Ion-assisted tropospheric OH measurement technique 08 p3344 N94-28601
Anodized aluminum on LDEF 09 p3592 N94-31017
Climate effects of anthropogenic sulfate: Simulations from a coupled chemistry/climate model
[DE94-004352] 09 p3767 N94-32789
H2O-H2SO4 system in Venus' clouds and OCS, CO, and H2SO4 profiles in Venus' troposphere 11 p4370 N94-36152
The corrosion protection of several aluminum alloys by chromic acid and sulfuric acid anodizing
[NASA-TP-3490] 12 p4420 N94-37578

SUM RULES
The off shell (rho)-(omega) mixing in the QCD sum rules
[DE93-014845] 02 p0786 N94-14527
Nucleon-nucleon scattering lengths in QCD sum rules
[DE93-520239] 07 p3015 N94-25922
Nuclear Theory Group, University of Washington recent and planned research
[DE94-002729] 07 p3022 N94-26809
Improved QCD sum rule estimates of the higher twist contributions to polarised and unpolarised nucleon structure functions
[PB94-138112] 08 p3487 N94-29161
Theoretical studies in hadronic and nuclear physics
[DE94-003524] 08 p3492 N94-30838
Spin-structure function of the neutron He-3: SLAC results
[DE94-006927] 09 p3875 N94-33189
Leptonic decay constants of heavy quarkonia in effective QCD sum rules
[DE94-611160] 11 p4322 N94-35784
Sum rules for 1/m corrections to the form factors of semileptonic B decays
[DE94-618548] 12 p4514 N94-37065

SUMMARIES
NT ABSTRACTS
NT PRELAUNCH SUMMARIES
Summaries of FY 1993 research in the chemical sciences
[DE93-011855] 04 p1632 N94-18915

SUMMER
A summer program in mathematics and computer science for academically oriented student
[AD-A263467] 01 p0415 N94-11517
Spectral analysis of synoptic time scale disturbances over the tropical eastern Pacific during summer 1989, 1990 and 1991
[AD-A268821] 04 p1490 N94-18206
Summer intern program
[AD-A275194] 08 p3466 N94-28888

SUMS
Summation by parts, projections, and stability
[NASA-CR-194290] 01 p0346 N94-12776

SUN
Orbital simulations of satellite escape/capture and the origin of satellites such as Triton 01 p0429 N94-12057
Unmasking the Sun
[NASA-TM-109595] 03 p1298 N94-15287
Mars and the early Sun 05 p2146 N94-21683
The calculation of theoretical chromospheric models and the interpretation of solar spectra from rockets and spacecraft
[NASA-CR-195083] 06 p2626 N94-23569
Direct evidence of the interplanetary magnetic field effect on the cosmic-ray shadow by the sun
[ICRR-296-93-8] 07 p3116 N94-27607
The appearance of the Sun and Moon seen through clouds
[AD-A275338] 08 p3551 N94-29212
Ulysses: A solar odyssey
[NASA-TM-109820] 10 p4010 N94-33574
Observations of loops and prominences
[NASA-CR-195942] 10 p4166 N94-34298
SPARTAN high resolution solar studies
[NASA-CR-189340] 10 p4166 N94-34944
Formation of iron metal and grain coagulation in the solar nebula 11 p4373 N94-36170
On the physics of waves in the solar atmosphere: Wave heating and wind acceleration
[NASA-CR-194119] 11 p4375 N94-36395

SUN SENSORS
U SOLAR SENSORS

SUNLIGHT
A development on estimation method of undersea light 01 p0204 .N94-11974
The evaluation of radiative process in the atmosphere-ground system by Monte Carlo method 01 p0205 N94-11980
Incident shortwave and longwave radiations over the western North Pacific and the Sea of Okhotsk derived from GMS-WEFAX images 01 p0205 N94-11982
Effects of levitated dust on astronomical observations from the lunar surface 03 p1239 N94-16433
Spectral inhomogeneity of the bacterial light-harvesting antennae: Causes and consequences
[ETN-94-96020] 09 p3792 N94-31533
The properties of sunflecks in a flexible plant canopy, and their relationship to turbulence 09 p3782 N94-31775

SUNSPOT CYCLE
Surface differential rotation in a sample of cool dwarf stars 08 p3545 N94-29827

SUNSPOTS
Mars and the early Sun 05 p2146 N94-21683
Large-scale structure of the solar plasma corona: An analysis of Yohkoh SXT images 05 p2004 N94-22657
Enhanced absorption of p-modes on sunspot and plage regions 05 p2006 N94-22671
Region 5395 of March 1989 --- solar activity, geomagnetic disturbances, and terrestrial effects
[PB94-120714] 07 p3110 N94-26755
High resolution studies of sunspots and flux tubes
[NASA-CR-195216] 07 p3111 N94-27321
Characteristics of 30-MHz interference noises observed by riometers 07 p2884 N94-27965

SUPER FORTRESS AIRCRAFT
U B-50 AIRCRAFT

SUPERALLOYS
U HEAT RESISTANT ALLOYS

SUPERCHARGERS
Experimental evaluation of oxygen-enriched air and emulsified fuels in a six-cylinder diesel engine
[DE94-000907] 05 p1811 N94-22391
Development of advanced high temperature in-cylinder components and tribological systems for low heat rejection diesel engines, phase 1
[NASA-CR-187158] 07 p2827 N94-27984
Nozzle guide vane flow in radial inflow turbines 10 p4004 N94-34460

SUPERCHARGING
U SUPERCHARGERS

SUPERCOMPUTERS
NT CONNECTION MACHINE
NT CRAY COMPUTERS
An account of Sandia's research booth at Supercomputing 1992: A collaborative effort in high-performance computing and networking
[DE93-012397] 01 p0319 N94-10268
Numerical wind tunnel project and computational fluid dynamics at National Aerospace Laboratory, Japan
[NAL-TM-648T] 01 p0149 N94-10861
The DOE Program in High-Performance Computing and Communications (HPCC)
[DE93-013813] 01 p0334 N94-12606
The NAS parallel benchmarks
[NASA-TM-103863] 02 p0740 N94-13200
Advanced computers and simulation
[DE93-014354] 02 p0740 N94-13286
Diskless supercomputers: Scalable, reliable I/O for the Tera-Op technology base
[NASA-CR-194089] 02 p0740 N94-13363
Analysis and effects of the number of nests of DO loops during vector supercomputing
[NAL-TR-1146] 02 p0748 N94-13453
Computational mechanics and supercomputing at LLNL
[DE93-016453] 02 p0754 N94-14435
An overview of parallel scientific visualization
[DE93-017105] 02 p0755 N94-14521
Parallel processing and scientific applications
[AD-A267179] 03 p1159 N94-15849
Requirements for supercomputing in energy research: The transition to massively parallel computing
[DE93-012376] 03 p1160 N94-16774

ONRASIA scientific information bulletin, volume 18, number 2
[AD-A267798] 03 p1304 N94-17305
Benchmarking massively parallel architectures
[DE93-016486] 03 p1162 N94-17646
Introductory user's guide to the ARL supercomputer facility at Aberdeen Proving Ground
[AD-A265204] 04 p1514 N94-17877
An evolving infrastructure for scientific computing and the integration of new graphics technology
[DE93-017164] 04 p1520 N94-18133
A special purpose silicon compiler for designing supercomputing VLSI systems 04 p1402 N94-18379
Visualization for applications in shock physics
[DE93-012849] 04 p1418 N94-18918
The world's most powerful computer
[NASA-TM-109369] 04 p1514 N94-18961
Particle image velocimetry
[DE93-040657] 05 p1804 N94-21748
The transition to massively parallel computing within a production environment at a DOE access center
[DE93-019155] 05 p1936 N94-21828
Introduction to the LaRC central scientific computing complex
[NASA-TM-104092-REV-1] 05 p1900 N94-22100
Seeing the forest for the trees: Networked workstations as a parallel processing computer
05 p1938 N94-22454
Supercomputer networking for space science applications
[NASA-CR-194876] 06 p2465 N94-23085
Applications of CFD codes and supercomputers to aircraft design activities 06 p2177 N94-24316
High-performance computing and communications
[DE94-002215] 06 p2457 N94-24566
Achieving high performance on the Intel Paragon
[DE94-003108] 07 p2979 N94-25953
High performance computing in chemistry and massively parallel computers: A simple transition?
[DE94-004318] 07 p2982 N94-27600
Communication on the Paragon
[DE94-003103] 07 p2983 N94-27713
The High Performance Storage System
[DE94-004350] 08 p3404 N94-28505
Construction of a connectionist network supercomputer
[AD-A275765] 08 p3405 N94-28764
Parallel Fortran programming for NWT
08 p3129 N94-28991
A method of user interface for NWT
08 p3129 N94-28993
A porting methodology for parallel database systems
[AD-A275256] 08 p3529 N94-29053
Progress report for the PTUF Project-93 Q1 and Q2
[PB94-138591] 08 p3431 N94-29995
Engineering of systems for application of scientific computing in industry WP project management ISNaS 9209099
[PB94-126232] 08 p3428 N94-30739
Information system for flow simulation based on the Navier-Stokes equations vectorization
[AD-B179293] 08 p3281 N94-30763
Modeling data throughput on communication networks
[DE94-005077] 08 p3260 N94-30772
Computing at the leading edge: Research in the energy sciences
[DE94-006121] 08 p3563 N94-30844
Supercomputing has to be part of an organization-wide automation concept
[AD-B174654] 08 p3433 N94-30913
Sandia's research network for Supercomputing 1993: A demonstration of advanced technologies for building high-performance networks
[DE94-005319] 09 p3823 N94-31149
Parallel supercomputing: Advanced methods, algorithms, and software for large-scale linear and nonlinear problems
[DE94-008446] 09 p3836 N94-32992
HIPPI, Fibre Channel, and ATM as gigabit/s LAN's
[DE94-005089] 10 p4103 N94-34373
Hardware implementation of a desktop supercomputer for high performance image processing
[AD-A280550] 12 p4489 N94-36731
A scalable high-performance I/O system
[DE94-011513] 12 p4498 N94-37519

SUPERCONDUCTING CAVITY RESONATORS
Fabrication and test of a superconducting RFQ
[DE93-010860] 01 p0140 N94-10300
Nonlinear effects in ferrite tuned cavities
[DE93-014136] 01 p0374 N94-12785
Space applications of superconducting microwave electronics at NASA Lewis Research Center
05 p1671 N94-20513
Ten GHz YBa2Cu3O(7-delta) superconducting ring resonators on NdGaO3 substrates
05 p1735 N94-20515
Welding of niobium to stainless
[DE94-003365] 06 p2365 N94-24614

SUPERCONDUCTING DEVICES
NT SIS (SUPERCONDUCTORS)
NT SQUID (DETECTORS)
NT SUPERCONDUCTING CAVITY RESONATORS
NT SUPERCONDUCTING MAGNETS
Fabrication and test of a superconducting RFQ
[DE93-010860] 01 p0140 N94-10300
Improvement of azimuthal homogeneity in permanent-magnet bearing rotors
[DE93-009954] 01 p0144 N94-11607
Utilization of superconductivity in the area of space
01 p0131 N94-11843
Substrate effects in superconducting tunnel junction detectors 03 p0908 N94-15083
A multilayered approach to superconducting tunnel junction x ray detectors 03 p0908 N94-15089
Nontidal gravity changes observed with a superconducting gravimeter 03 p1100 N94-15808
Superconducting flux flow devices, digital circuits and memories
[DE93-019072] 04 p1405 N94-19079
A pipelined superconducting digital processor
[DE93-040852] 05 p1898 N94-19886
Quantum noise studies with superconducting tunnel junction mixers
[AD-A270897] 05 p2012 N94-19897
Prospects for utilization of superconductors in the power industry 07 p2854 N94-26057
Demonstration of monolithic co-fabrication of Y1Ba2Cu3O7-Sigma and CMOS devices on the same sapphire substrate
[AD-A274757] 07 p3059 N94-26566
Epitaxial heterojunctions of oxide semiconductors and metals on high temperature superconductors
[NASA-CASE-NPO-18483-1-CU] 08 p3513 N94-29501
Future directions of nonlinear dynamics in physical and biological systems. (Physica D nonlinear, volume 68, number 1)
[AD-A278085] 09 p3794 N94-33250
Microstructures and epitaxy in oxide superconductor thin films and devices
[AD-A278427] 09 p3910 N94-33332
Fiber optic transceiver for interfacing digital superconducting electronics
[DE94-006284] 10 p4040 N94-33842
High temperature superconducting digital circuits and subsystems
[DE94-001207] 12 p4436 N94-36557
Microwave detection of a superconducting infrared sensor
[AD-D016297] 12 p4440 N94-37769

SUPERCONDUCTING FILMS
Processing and transport properties of high J(sub c) silver clad Bi-2223 tapes and coils
[DE93-010674] 01 p0398 N94-11073
Multicomponent and multilayered thin films for advanced microtechnologies: Techniques, fundamentals, and devices
[AD-A265685] 01 p0405 N94-12442
Non-linear effects in vortex viscous flow in superconductors-role of finite heat removal velocity
[DE93-621785] 02 p0618 N94-12856
High-resolution Z-contrast imaging and hole concentration mapping of YBCO thin films
[DE93-015803] 02 p0808 N94-13930
Measurement of penetration depth lambda(T) in YBa2Cu3O(7-delta) thin film
[DE93-014587] 02 p0810 N94-14122
Formation of textured YBCO films by laser ablation
[DE93-013131] 02 p0581 N94-14319
Superconductivity devices: Commercial use of space
[NASA-CR-194163] 02 p0625 N94-14324
Kinetics of photodeposition of superconducting films
[DE93-015511] 02 p0812 N94-14348
Effects of depositon rate on Bi2Sr2CaCu2O(8+x) and Bi2Sr(1.6)La(0.4)CuO(6+x) epitaxial thin film growth by pulsed-laser ablation
[DE93-015797] 02 p0812 N94-14362
High temperature superconductivity
[AD-A267006] 03 p1008 N94-15635
Local environment about O atoms in Pr-Y-Ba-Cu-O films studied by O K-edge XAFS
[DE93-016218] 03 p1209 N94-16447
Advanced thin-film deposition and physical properties of high-temperature and other novel superconducting materials
[AD-A268199] 03 p1216 N94-17561
Synthesis and study of high-T(sub c) superconducting electronic materials
[AD-A268851] 04 p1402 N94-18390
Fabrication and microstructural development of Ag-clad TlBa2Ca2Cu3O(x) tapes
[DE93-017407] 04 p1597 N94-18500
High performance YBCO films
[AD-A269090] 04 p1599 N94-18719
Fabrication and characterization of high-T(sub c) tapes and coils made from Ag-clad Bi-2223 superconductors
[DE93-018615] 04 p1601 N94-18993
LLE Review
[DE93-017618] 04 p1602 N94-19123
Particles on surfaces of laser ablated Y1Ba2Cu3O(7-delta) films
[DE93-040269] 05 p2013 N94-19929
Superconducting property measurements in tape geometry
[DE93-018943] 05 p2014 N94-19970
Ten GHz YBa2Cu3O(7-delta) superconducting ring resonators on NdGaO3 substrates
05 p1735 N94-20515
A 10 GHz Y-Ba-Cu-O/GaAs hybrid oscillator proximity coupled to a circular microstrip patch antenna
05 p1736 N94-20517
Microwave properties and characterization of co-evaporated BSCCO thin films
05 p1709 N94-20518
The effect of fluctuations on the electrical transport behavior in YBa2Cu3O(7-x) 05 p1736 N94-20519
Thin-film fabrication of Pb-doped BiSrCaCuO superconductor 05 p1781 N94-22176
Spectroscopic IR ellipsometry of 100 and 001 oriented YBa2Cu3O(7-delta) films
[PB93-201481] 06 p2561 N94-23445
Investigation and application of microwave electron cyclotron resonance plasma physical vapour deposition
[DE93-613909] 06 p2555 N94-25333
Flux flow, pinning, and resistive behavior in superconducting networks
[DE94-003400] 07 p3050 N94-25848
Submillimeter residual losses in high-(Tc) superconductors
[DE94-003241] 07 p3058 N94-26516
Processing and properties of Ag-clad Bi-2223 tapes
[DE94-004603] 07 p2783 N94-26589
Preparation and characterization of high temperature superconductor film surfaces
[AD-A274293] 07 p3059 N94-26681
Fabrication issues in optimizing YBa(2)Cu(3)O(7-x) flux transformers for low I/f noise
[DE94-005209] 08 p3261 N94-28546
Exploratory research for a high temperature superconducting integrated circuit
[AD-A275798] 08 p3262 N94-28767
Ion channeling peculiarities in YBa2Cu3 O7 monocrystal
[DE94-606885] 08 p3512 N94-28787
High Tc superconducting bolometric and nonbolometric infrared (IR) detectors
[NASA-CR-195728] 08 p3262 N94-28846
The bases for the development of high-temperature integrated SQUID-systems
[DE94-607901] 08 p3267 N94-30073
The bases for the development of high-temperature integrated SQUID-systems
[DE94-608462] 08 p3517 N94-30082
Research on the atomic layer-by-layer growth of high-temperature superconductor thin films at the Institute of Scientific and Industrial Research, Japan
[DE94-003739] 08 p3519 N94-30611
Preliminary results from the CONCAP-2-01 and EIOM-3 experiments on STS-46 09 p3596 N94-31042
High performance YBCO films
[AD-A276493] 09 p3897 N94-31531
The charging effect in high-Tc superconducting thin films
[AD-A277265] 09 p3900 N94-32040
Microanalytical study of defect formation in thin bismuth strontium calcium copper oxide films
[DE94-008217] 09 p3661 N94-32751
Microstructures and epitaxy in oxide superconductor thin films and devices
[AD-A278427] 09 p3910 N94-33332
Report on a SQUID made from high temperature superconductor
[PB94-169307] 11 p4329 N94-35598
Flux-pinning related defects in YBa2Cu3O(7-x) thin films grown on miscut LaAlO3 (001) substrates
[DE94-011463] 11 p4342 N94-36377
Electrically conductive, thermally insulating cryogenic current leads
[NASA-CASE-LAR-14964-1-CU] 12 p4437 N94-36781
Development of high Tc (greater than 100 K) Bi, Tl and Y-based materials as superconducting circuit elements
[NASA-CR-196276] 12 p4534 N94-37103
Critical-state flux-density profiles in type-2 superconducting thin-film strips and disks
[DE94-011199] 12 p4535 N94-37166
Superconducting TlCa2Ba2Cu3O9 thick films
[DE94-010436] 12 p4535 N94-37193

Activities of the Tandem Accelerator Center, University of Tsukuba
[DE94-748687] 12 p4522 N94-37237
The MBE growth and optical quality of BaTiO3 and SrTiO3 thin films on MgO
[DE94-011468] 12 p4538 N94-37570

SUPERCONDUCTING MAGNETS
High-field conductor testing at the FENIX facility
[DE93-012318] 01 p0387 N94-10737
Technology assessments of advanced energy storage systems for electric and hybrid vehicles
[DE93-014395] 02 p0701 N94-12913
Heat and seed recovery technology project
[DE93-009203] 02 p0800 N94-13913
Engineering design of a high-temperature superconductor current lead
[DE93-015156] 03 p1013 N94-17226
The inverse problem to the evaluation of magnetic fields
[DE93-015239] 03 p1175 N94-17288
Corroboration of magnetic forces in US Maglev design
[DE93-014918] 04 p1443 N94-17785
A superconducting short period undulator for a harmonic generation FEL experiment
[DE93-017581] 04 p1436 N94-17998
Development and application of specially-focused ultrasonic transducers to location and sizing of defects in 75 mm- to 127 mm-thick austenitic stainless steel weld metals
[DE93-015975] 04 p1453 N94-18108
Proceedings of the 3rd Workshop on Balloon-Borne Experiments with Superconducting Magnet Spectrometers
[DE93-788362] 04 p1630 N94-18219
Analysis of superconducting magnetic energy storage applications at a proposed wind farm site near Browning, Montana
[DE93-018793] 04 p1466 N94-18276
Magnetic field measurements of a superconducting undulator for a Harmonic Generation FEL experiment at the NSLS
[DE93-017621] 04 p1438 N94-18504
Fabrication and characterization of high-T(sub c) tapes and coils made from Ag-clad Bi-2223 superconductors
[DE93-018615] 04 p1601 N94-18993
Thermo-hydraulic analysis of superconducting toroidal-field magnets for the Tokamak Physics Experiment
[DE93-018096] 04 p1590 N94-19269
Incology 908 database report: On process-structure-property relationship
[DE93-017616] 04 p1366 N94-19546
Tensile and shear fracture behavior of fiber reinforced plastics at 77K irradiated by various radiation sources
[DE93-040280] 05 p1706 N94-21542
The 13th International Conference on Magnetically Levitated Systems and Linear Drives MAGLEV 1993
[DE93-040381] 05 p1825 N94-21544
Operation of a test bed axial-gap brushless dc rotor with a superconducting stator
[DE93-019167] 05 p1769 N94-21830
Stability of an uncooled segment of a high-temperature superconductor
[DE94-000476] 05 p2032 N94-21932
Tensile strength of fiber reinforced plastics at 77K irradiated by various radiation sources
[DE93-040826] 05 p1709 N94-22008
Assessment of stellarators as reactors
[DE93-017775] 06 p2548 N94-22916
Design of microchannels for cryostabilization of high temperature superconducting magnets
[DE94-001324] 06 p2559 N94-22993
Superconducting magnet system for the TPX Tokamak
[DE94-001535] 06 p2549 N94-23013
Structural analysis of a superconducting central solenoid for the Tokamak Physics Experiment
[DE94-001536] 06 p2549 N94-23014
Simple estimate of stored energy and conductor insulation voltage-withstand requirements for advanced solenoid magnet designs
[DE93-041048] 06 p2307 N94-23019
A system for managing information at ATLAS
[DE94-001337] 06 p2590 N94-23190
Normal zone propagation and thermal hydraulic quenchback in a cable-in-conduit superconductor
[DE94-002457] 06 p2271 N94-24568
Prospects for utilization of superconductors in the power industry 07 p2854 N94-26057
A study on the development of high T(sub c) superconducting materials
[DE93-633529] 07 p3057 N94-26404
Evaluation of APC NbTi superconductor in a model dipole magnet
[DE94-003258] 07 p3060 N94-26795
The TPX Cryostat Conceptual Design
[DE94-002857] 07 p3045 N94-26863
Calculation of the electromagnetic critical state response of high T(sub c) superconductor tape
[DE94-002894] 07 p3061 N94-26868
Battery energy and superconducting magnetic energy storage for utility applications: A qualitative analysis
[DE94-005382] 08 p3336 N94-28489
Estimating the cost of large superconducting thin solenoid magnets
[DE94-006289] 08 p3468 N94-30026
Algorithm and program ORANGE for magnetic field simulation of magnetic system spectrometer STORS
[DE94-608013] 08 p3421 N94-30083
A magnetically coupled quench detector for superconducting magnets
[DE94-006040] 08 p3268 N94-30904
AC losses for the self field of an AC transport current with a DC transport current offset in high T(c) superconducting magnet coils for MagLev application
[DE94-005187] 08 p3268 N94-30907
Structural design of the superconducting Poloidal Field coils for the Tokamak Physics Experiment
[DE94-007078] 09 p3887 N94-31406
Various magnet options for Delta launched version of ASTROMAG
[DE94-006292] 09 p3955 N94-31635
Quench detection and instrumentation for the Tokamak Physics Experiment magnets
[DE94-006656] 09 p3888 N94-31667
On the unsteady-motion theory of magnetic forces for maglev
[DE94-007765] 09 p3727 N94-32778
RHIC chromatic correction system
[DE94-008532] 09 p3883 N94-32994
Second International Symposium on Magnetic Suspension Technology, part 1
[NASA-CP-3247-PT-1] 11 p4212 N94-35836
System concept definition of the Grumman superconducting Electromagnetic Suspension (EMS) Maglev design 11 p4213 N94-35840
Measurement and characterization of force dynamics in high T(sub c) superconductors 11 p4214 N94-35844
Superconducting Electromagnetic Suspension (EMS) system for Grumman Maglev concept 11 p4215 N94-35849
Second International Symposium on Magnetic Suspension Technology, part 2
[NASA-CP-3247-PT-2] 11 p4223 N94-35902
Concepts of flywheels for energy storage using autostable high-T(sub c) superconducting magnetic bearings 11 p4224 N94-35909
Models for interpreting interstrand resistance measurements in Rutherford cables
[DE94-010844] 11 p4259 N94-36194
Pulsed field magnets at the United States National High Magnetic Field Laboratory
[DE94-002624] 12 p4436 N94-36514
Fabrication and properties of Ag-clad Bi-2223 conductors and magnets
[DE94-011502] 12 p4438 N94-37111
Melt-processing of Y-Ba-Cu-O superconductors for improved levitation
[DE94-011503] 12 p4537 N94-37377
Permanent superconducting magnets for space applications
[NASA-CR-196293] 12 p4439 N94-37634

SUPERCONDUCTING POWER TRANSMISSION
The effect of Ti conduit on the critical current in (Nb, Ti)3Sn cable-in-conduit conductors
[DE94-701204] 07 p2788 N94-27817

SUPERCONDUCTING QUANTUM INTERFEROMETERS
U SQUID (DETECTORS)

SUPERCONDUCTING SUPER COLLIDER
Database computing in HEP
[DE93-011765] 01 p0419 N94-11105
Nonlinear effects in ferrite tuned cavities
[DE93-014136] 01 p0374 N94-12785
Building the repositories to serve --- Superconducting Super Collider information system
[DE93-014100] 02 p0821 N94-12983
Integrating PAW, a graphical analysis interface to Sybase
[DE93-014172] 02 p0755 N94-14581
Proton-proton scattering contribution to emittance growth
[DE93-016090] 02 p0787 N94-14588
The (delta)f algorithm for beam dynamics
[DE93-015632] 03 p1187 N94-16660
Statistics of the half-integer stopband
[DE93-016101] 03 p1173 N94-17236
Mechanical-property changes of structural composite materials after low-temperature proton irradiation: Implications for use in SSC magnet systems
[DE93-016735] 04 p1343 N94-18763
Experimental research in high energy physics
[DE93-011912] 04 p1574 N94-18916
Investigation of physical structures and interactions at high energy
[DE93-014444] 04 p1574 N94-18927
Longitudinal beam dynamics with RF noise
[DE93-018649] 04 p1574 N94-18994
SSC detector muon sub-system beam tests
[DE93-018415] 04 p1569 N94-19013
High energy physics program. Task A: Experiment and theory. Task B: Numerical simulation
[DE93-018140] 04 p1575 N94-19050
Extraction of Z(prime) coupling data from Z(prime) (yields) jj at the LHC and SSC
[DE93-018576] 04 p1570 N94-19096
Design verification and acceptance tests of the ASST-A helium refrigeration system
[DE93-019746] 04 p1381 N94-19540
High rate resistive plate chambers: An inexpensive, fast, large area detector of energetic charged particles for accelerator and non-accelerator applications
[DE93-018664] 04 p1572 N94-19545
Energy and luminosity limits of hadron supercolliders
[DE93-019248] 05 p1980 N94-20300
B-quark production at hadron colliders
[DE94-001459] 06 p2534 N94-23806
The use of harmonics in 3-D magnetic fields
[DE94-002274] 06 p2299 N94-24656
Secondary particle in background levels and effects on detectors at future hadron colliders
[DE94-003378] 07 p3011 N94-25598
Temperature dependence of the radiation induced change of depletion voltage in silicon PIN detectors
[DE94-002705] 07 p3052 N94-25972
Indiana University high energy physics, task A
[DE94-000961] 07 p3033 N94-27614
Using neural networks as an event trigger in elementary particle physics experiments
[DE94-006316] 10 p4136 N94-33716
Models for interpreting interstrand resistance measurements in Rutherford cables
[DE94-010844] 11 p4259 N94-36194
The 24/36/48 Cathode Strip Chamber layout for SSC GEM detector muon subsystem
[DE94-012676] 12 p4439 N94-37306

SUPERCONDUCTIVITY
NT KONDO EFFECT
Orbital glass in HTSC
[DE93-613988] 01 p0395 N94-10415
Power losses of a type 2 superconducting slab of arbitrary thickness in the presence of alternating current conductors
[DE93-617892] 01 p0396 N94-10716
Development and testing of a superconducting link for an IR detector
[NASA-CR-193674] 01 p0170 N94-10948
Assessment of the impact of HTSC's on superconducting fault-current limiters
[DE93-009986] 01 p0143 N94-11454
Fullerene superconductors: Phase stability and anomalously low T(sub c)'s in some ternary compounds
[DE93-010687] 01 p0400 N94-11457
Synthesis and magnetic properties of novel La*2-x*M*x*CuO*4 equals y* compositions (La equals La, Pr, Nd, Sm, Eu, Cd; M equals Ca, Sr, Ba; O (less than or equal) x 0.2; -0.5 (less than or equal) y (less than or equal) 0.5)
[DE93-011359] 01 p0403 N94-12363
Quark and lepton masses
[DE93-012308] 01 p0370 N94-12787
To the theory of triplet pairing in Fermi-liquid model
[DE93-621770] 02 p0816 N94-12855
A superconducting large-angle magnetic suspension
[NASA-CR-189735] 02 p0596 N94-13141
Study on superconducting basic technology for space application, part 1
[NASDA-CNT-930015-PT-1] 02 p0622 N94-13425
Theoretical SIS mixer research
[AD-A266323] 02 p0807 N94-13580
Direct submillimeter absorptivity measurements on epitaxial Ba(1-x)K(x)BiO3 films at 2K
[DE93-013904] 02 p0815 N94-14699
Muon spin relaxation studies of heavy fermion superconductors
[DE93-014576] 02 p0815 N94-14773
Experimental investigations of superconductivity in quasi-two-dimensional epitaxial copper oxide superlattices and trilayers
[DE93-015306] 03 p1207 N94-15829
Fullerene superconductors
[AD-A266749] 03 p1010 N94-15954
Theoretical high energy physics
[DE93-015884] 03 p1187 N94-16170
Structural phase transition and superconductivity in La(2-x)Ba(x)CuO4
[DE93-015812] 03 p1212 N94-16868

Superconducting ceramics: Selected properties and methods of production
[IFTR-23/1991] 03 p0969 N94-16924
A modified two-fluid model of conductivity for superconducting surface resistance calculation
[AD-A267549] 03 p1013 N94-17104
Basic optical studies of high T(c) oxide superconductors
[AD-A268148] 03 p1014 N94-17428
High temperature deformation behavior of YBa2Cu3O(6+x) superconducting ceramic materials
[AD-A268164] 03 p0973 N94-17430
Phase separation and superconductivity in La2CuO(4 + delta): Effects of oxygen diffusion
[DE93-016610] 04 p1594 N94-17907
Report of the 1991 Workshop on Particle-Material Interactions for Fusion Research
[DE93-788393] 04 p1573 N94-18156
Superconducting/semiconducting hybrids and advance memory concepts for superconducting electronics
[AD-A268679] 04 p1397 N94-18312
High energy resolution ARPES measurements of the normal and superconducting states of Bi2Sr2CaCu2O(8 + delta)
[DE93-018294] 04 p1599 N94-18804
Specific heat of La(1.875-x)Nd(x)Sr(0.125)CuO4: Magnetic and structural transitions
[DE93-016978] 04 p1600 N94-18968
Superconductivity and magnetism in niobium doped YBa2Cu3O7 related high-(Tc) ceramics
[DE93-018086] 04 p1601 N94-19049
Fabrication, properties, and microstructures of high (Tc) tapes and coils made from Ag-clad Bi-2223 superconductor
[DE93-017405] 04 p1602 N94-19122
Crossover from BCS to Bose superconductivity: A functional integral approach
[DE93-019503] 04 p1604 N94-19566
Numerical experiments on the Ginzburg-Landau equations
[DE93-019504] 04 p1604 N94-19567
Dynamics of vortices in superconductors
[DE93-019535] 05 p2011 N94-19808
Spin-polaron theory of high-(Tc) superconductivity. 1: Spin polarons and high (Tc) pairing
[DE93-019196] 05 p2014 N94-20002
Machinable oxide ceramic
[AD-D015927] 05 p1699 N94-20017
Solid State Technology Branch of NASA Lewis Research Center: Fifth Annual Digest
[NASA-TM-106303] 05 p1732 N94-20497
Space applications of superconducting microwave electronics at NASA Lewis Research Center
05 p1671 N94-20513
Fabrication and evaluation of superconducting and semiconducting materials
[AD-A271645] 05 p2018 N94-20558
Local structure and superconductivity in La(2-x)Ba(x)CuO4 for x=0.125 and x=0.15
[DE93-040193] 05 p2029 N94-21555
Local structure in oxygen-doped La2CuO(4+delta)
[DE93-040248] 05 p2030 N94-21768
Spin-polaron theory of high-T(c) superconductivity. 3: Gap function and critical temperature
[DE93-019198] 05 p2030 N94-21831
Fullerene derivatives and fullerene superconductors
[DE93-019568] 05 p2031 N94-21871
Specific heat of YBa2Cu3O7
[DE93-040640] 05 p2031 N94-21926
Spin dynamics and implications for superconductivity: Some problems with the d-wave scenario
[DE94-001183] 05 p2032 N94-21972
NMR studies of oxygen-doped La2CuO(4+delta)
[DE93-040756] 05 p2034 N94-22007
Anomalous magnetoresistance behavior of superconducting Nd(2-x)Ce(x)CuO(4-y) single crystal
[DE94-000806] 06 p2558 N94-22941
A valence-fluctuation theory of cuprate superconductivity
[DE94-000887] 06 p2558 N94-22942
Interplay of magnetic and superconducting heavy fermion ground states
[DE94-000680] 06 p2240 N94-23003
Muon spin relaxation studies of the interplay between magnetism and superconductivity in heavy fermion systems
[DE94-000700] 06 p2559 N94-23006
Structural analysis of a superconducting central solenoid for the Tokamak Physics Experiment
[DE94-001536] 06 p2549 N94-23014
Exact transformation of the anisotropic Ginzburg-Landau model and its consequences
[DE94-002208] 06 p2562 N94-23795
Reduction of hydrocarbon impurities in 200 l/h helium liquefier-refrigerator system
[NIFS-259] 06 p2271 N94-24459
Superconducting energy storage
[DE94-002248] 06 p2395 N94-24654
On superconductivity of alpha-(BEDT-TTF)2KHg(SCN)4
[REPT-A-2660] 06 p2564 N94-24978
Tunnelling in metallic contacts on high-T(c) superconductors: A story of charge carriers in YBa2Cu3O(7-delta) and Bi2CaSr2Cu2O(8+delta)
[ISBN-9-03-860142-5] 06 p2565 N94-25280
Lattice dynamics of Ba(1-x)K(x)BiO3 as studied by neutron scattering and computer simulation
[DE93-617053] 06 p2567 N94-25424
Superconducting cosmic strings near the electroweak scale and cosmic-ray propagation
[MPI-PHE/93-05] 06 p2629 N94-25459
Study on measurement and evaluation methods for superconductive characteristics
07 p2725 N94-25560
Growth of small fatigue cracks in Incoloy-908
[DE94-003406] 07 p2836 N94-26129
Strongly interacting fermion systems
[DE94-002674] 07 p3021 N94-2[illegible]
A mechanism for resistive dissipation in Ag sh[illegible] Bi2Sr2CaCu2O8 and Bi2Sr2Ca2Cu3O10
[DE94-003009] 07 p3060 N94-26771
Powder synthesis, fabrication, and transport properties of long-length Ag clad Bi-2223 conductors
[DE94-002376] 07 p2740 N94-26957
Tokamak Physics Experiment poloidal field design
[DE94-001542] 07 p3045 N94-27019
Excited Landau levels, orbital angular momentum and axial anomaly
[DE94-606407] 07 p3068 N94-27679
Axial anomaly in e(+)e(-) yields gamma gamma and anyon superconductivity
[DE94-606406] 07 p3070 N94-27859
Normal state resistivity of MBa2Cu3O(7-x) ceramics
[DE94-608456] 08 p3220 N94-30745
On some general properties of parabolic conservation equations
[DE94-006101] 08 p3461 N94-30758
Synthesis, characterization, phase diagrams and superconducting, and normal state magnetic properties of La(2-x)Sr(x)CuO4 (0 is less than or equal to x which is less than or equal to 0.08) and electrochemically oxidized La(2-x)Sr(x)CuO(4 + delta) (0 is less than or equal to x which is less than or equal to 0.33, 0 is less than or equal to delta which is less than or equal to 0.12)
[DE94-005260] 09 p3895 N94-31067
Experimental evidence for lattice effects in high temperature superconductors
[DE94-006250] 09 p3899 N94-31633
Finite element analysis of time-independent superconductivity 09 p3691 N94-31905
Isothermal sintering, microstructure, and superconducting properties of Y1Ba2Cu3O(7-x) compound
[DE94-008132] 09 p3905 N94-32779
Investigation of superconductivity and magnetism in d and f-electron materials
[DE94-008535] 09 p3907 N94-32933
Superconducting and semiconducting hybrids and advance memory concepts for superconducting electronics
[AD-A277766] 09 p3907 N94-32988
A quest for a new superconducting state
[DE94-008439] 09 p3908 N94-32991
Superconducting Meissner effect bearings for cryogenic turbomachines, phase 2
[AD-A277865] 10 p4059 N94-33776
Superconducting rebalance acceleration and rate sensor 11 p4223 N94-35904
Feasibility study of superconducting LSM rocket launcher system 11 p4225 N94-35914
Distance dependent fractional statistics in a P, T-invariant model
[DE94-617360] 11 p4325 N94-36083
Superconducting transistors
[PB94-170743] 11 p4260 N94-36260
A new family of superconducting fullerides, Na(NH3)(x)C60(x = 2-8)
[DE94-011480] 11 p4341 N94-36272
Temperature dependence of superconduction bands in HTSC
[DE94-617361] 11 p4341 N94-36312
Pairing and low temperature properties of 2D Fermi-systems with attraction between particles
[DE94-615510] 11 p4329 N94-36434
High temperature superconducting digital circuits and subsystems
[DE94-001207] 12 p4436 N94-36557
Critical-state flux-density profiles in type-2 superconducting thin-film strips and disks
[DE94-011199] 12 p4535 N94-37166
ORNL superconducting technology program for electric power systems
[DE94-011471] 12 p4438 N94-37239
Midwest Superconductivity Consortium
[DE94-012716] 12 p4536 N94-37285

SUPERCONDUCTOR INSULATOR
SUPERCONDUCTORS
U SIS (SUPERCONDUCTORS)

SUPERCONDUCTORS (MATERIALS)
NT BSCCO SUPERCONDUCTORS
NT HIGH TEMPERATURE SUPERCONDUCTORS
NT ORGANIC SUPERCONDUCTORS
NT YBCO SUPERCONDUCTORS

High-energy density physics at Los Alamos
[DE93-010271] 01 p0371 N94-10260
Development of passive superconducting bearings. Phase 3
[AD-A266050] 01 p0180 N94-10706
Power losses of a type 2 superconducting slab of arbitrary thickness in the presence of alternating current conductors
[DE93-617892] 01 p0396 N94-10716
High-field conductor testing at the FENIX facility
[DE93-012318] 01 p0387 N94-10737
Similarity of the leading contributions to the self-energy and the thermodynamics in two- and three-dimensional Fermi Liquids
[DE93-012673] 01 p0412 N94-11162
Fullerene superconductors: Phase stability and anomalously low T(sub c)'s in some ternary compounds
[DE93-010687] 01 p0400 N94-11457
Study on superconducting basic technology for space application, part 1
[NASDA-CNT-930015-PT-1] 02 p0622 N94-13425
Empirical tight-binding parameters for solid C(sub 60)
[DE93-623061] 02 p0807 N94-13510
Casting of superconducting composite materials (M-4)
02 p0586 N94-13736
Combustion synthesis and engineering of nanoparticles for electronic, structural, and superconductor applications
[DE93-016286] 02 p0809 N94-13981
Superconductivity devices: Commercial use of space
[NASA-CR-194163] 02 p0625 N94-14324
Theoretical studies of breakdown in random media
[DE93-018107] 02 p0558 N94-14418
Is K3C60 a line phase?
[DE93-016700] 02 p0813 N94-14517
Muon spin relaxation studies of heavy fermion superconductors
[DE93-014576] 02 p0815 N94-14773
A new approach to optical photon detection
03 p0899 N94-15028
Superconductive x ray photon detectors
03 p0900 N94-15031
Metastable superconductors as photon detectors
03 p0900 N94-15032
Hot electron mixers, the potential competition
03 p0903 N94-15055
Quasiparticle trapping in distributed superconducting three-terminal tunnel junction devices
03 p0910 N94-15101
Fullerene superconductors
[AD-A266749] 03 p1010 N94-15954
Density of states and tunneling characteristics of layered superconductors
[DE93-015898] 03 p1211 N94-16839
Superconducting/semiconducting hybrids and advance memory concepts for superconducting electronics
[AD-A268679] 04 p1397 N94-18312
The low-temperature specific heat of CeCu2Ge2 at 0 and 9.5 kbar
[DE93-014914] 04 p1360 N94-18398
Thin film studies of the proximity Josephson effect
[AD-A270129] 04 p1600 N94-18876
Ultrafast Electronics and Optoelectronics: Summaries of papers. Technical digest conference edition
[AD-A269233] 04 p1405 N94-18909
Dimensional crossover in the torque in a layered superconductor
[DE93-019544] 04 p1407 N94-19553
Dynamics of vortices in superconductors
[DE93-019535] 05 p2011 N94-19808
The proximity effect in ultrathin granular Pb films
[AD-A271094] 05 p2012 N94-19848
Fullerene derivatives and fullerene superconductors
[DE93-019568] 05 p2031 N94-21871
A nonlinear degenerating parabolic problem from the theory of type 2 superconductors
[PB94-150299] 06 p2555 N94-22730
Interplay of magnetic and superconducting heavy fermion ground states
[DE94-000680] 06 p2240 N94-23003

Muon spin relaxation studies of the interplay between magnetism and superconductivity in heavy fermion systems
[DE94-000700] 06 p2559 N94-23006
Normal zone propagation and thermal hydraulic quenchback in a cable-in-conduit superconductor
[DE94-002457] 06 p2271 N94-24568
Thermomechanical processing of Ag-clad Bi2Sr2CaCu2O(x) superconductors
[DE94-002347] 06 p2563 N94-24624
Superconducting energy storage
[DE94-002248] 06 p2395 N94-24654
On superconductivity of alpha-(BEDT-TTF)2KHg(SCN)4
[REPT-A-2660] 06 p2564 N94-24978
A vibrating wire parallel to a type 2 superconducting slab of arbitrary thickness
[DE93-617134] 06 p2525 N94-25389
Effects of a vibrating wire carrying DC current on a moving type 2 superconducting slab of arbitrary thickness
[DE93-617136] 06 p2566 N94-25391
Bulletin of National Research Institute for Metals in Fiscal Year 1993, no. 14
[REPT-14] 07 p2722 N94-25544
Study on characteristics and electronic structures of materials with strong electronic correlations by ferromagnetic fields 07 p2724 N94-25557
Study on measurement and evaluation methods for superconductive characteristics 07 p2725 N94-25560
Prospects for utilization of superconductors in the power industry 07 p2854 N94-26057
Growth of small fatigue cracks in Incoloy-908
[DE94-003406] 07 p2836 N94-26129
Multi-channel Kondo necklace
[DE93-634754] 07 p3057 N94-26389
The influence of energy losses with time in NbTi superconductors in pulsed magnetic fields
[DE93-634761] 07 p3058 N94-26512
Evaluation of APC NbTi superconductor in a model dipole magnet
[DE94-003258] 07 p3060 N94-26795
List of papers published by the members of Institute for Materials Research, Tohoku University 1992
[JTN-94-80608] 07 p3118 N94-27355
Experimental results of 40-kA Nb3Al conductor
[DE94-701207] 07 p2788 N94-27821
Computing at the leading edge: Research in the energy sciences
[DE94-006121] 08 p3563 N94-30844
Calculating the J(c), B, T surface for commercial niobium tin conductors using a reduced state model
[DE94-006296] 08 p3520 N94-30850
Mathematical models of hysteresis
[DE94-005681] 08 p3260 N94-30902
Various magnet options for Delta launched version of ASTROMAG
[DE94-006292] 09 p3955 N94-31635
Finite element analysis of time-independent superconductivity 09 p3691 N94-31905
The 10th International Conference on Internal Friction and Ultrasonic Attenuation in Solids (ICIFUAS)
[AD-A276849] 09 p3902 N94-32209
Strongly anisotropic s-wave versus d-wave gap in cuprate superconductors: Evidence and theory
[DE94-007579] 09 p3904 N94-32746
Superconducting and semiconducting hybrids and advance memory concepts for superconducting electronics
[AD-A277766] 09 p3907 N94-32988
Growth and nonlinearity
[DE94-007366] 10 p4021 N94-33689
Multifilamentary superconducting cable and a method of manufacturing it
[AD-D016146] 10 p4040 N94-33837
Data reduction, analysis and results of LACV-30-07 air cushion vehicle tests, Fort Story, VA, August - September 1993
[AD-A278859] 11 p4190 N94-35826
Continuum fluorescence of Cu in NbTi/Cu composite wires
[DE94-008940] 11 p4241 N94-36242
A new family of superconducting fullerides, Na(NH3)(x)C60(x = 2-8)
[DE94-011480] 11 p4341 N94-36272
Critical-state flux-density profiles in type-2 superconducting thin-film strips and disks
[DE94-011199] 12 p4535 N94-37166

SUPERCOOLING
NT CRYOGENIC COOLING
Solidification from supercooled melt under microgravity 01 p0113 N94-10176
Numerical calculation of the growth of InP by the travelling heater method in the first mission of the Space Flyer Unit 01 p0114 N94-10179
Thermophysical properties of undercooled liquid metals 01 p0086 N94-10190
Solidification of undercooled Ni-32.5 wt percent Sn eutectic alloy 01 p0086 N94-10194
Undercooled W-Re and Mo-Re drops in an ultra high vacuum drop tube 01 p0086 N94-10195
Non-equilibrium solidification in undercooled Ni-B alloys 01 p0086 N94-10196
Solidification and metastable phase formation of highly undercooled Fe-Cr-Ni alloy melts 01 p0087 N94-10204
Study on the production of flaky amorphous alloy powders by impact flattening of atomized liquid droplets on a rapidly rotating wheel 07 p2746 N94-28169
Solidification structure synthesis in undercooled liquids
[AD-A276166] 09 p3910 N94-31054

SUPERCRITICAL AIRFOILS
NT SUPERCRITICAL WINGS
Navier-Stokes simulation of flow field around a blown-flap high-lift system 04 p1307 N94-18429
JB-300: An advanced medium size transport for 2005
[NASA-CR-195499] 06 p2179 N94-24401
Calculation of viscous drag of two low angle of attack supercritical profiles
[FFA-TN-1984-22] 07 p2644 N94-26104
Computational investigation of the compressible dynamic stall characteristics of the Sikorsky SSC-A09 airfoil
[AD-A274867] 07 p2644 N94-26191
Experimental investigations into the wall interference and sidewall boundary layer effects in the National Research Council/Inst. for Aerospace Research High Reynolds Number 2-D Test Facility 07 p2658 N94-28350
Steady pressure measurements on an Aeroelastic Research Wing (ARW-2)
[NASA-TM-109046] 08 p3122 N94-28658

SUPERCRITICAL FLOW
Droplet-turbulence interactions in sprays exposed to supercritical environmental conditions
[NASA-CR-194408] 02 p0638 N94-14308

SUPERCRITICAL FLUIDS
Polymer-polymer interactions
[AD-A265304] 01 p0091 N94-11830
Extraction and isotopic analysis of medium molecular weight hydrocarbons from Murchison using supercritical carbon dioxide 03 p1241 N94-16184
Removal of carbonaceous contaminants from silica aerogel 03 p0953 N94-16256
Supercritical thermodynamics of sulfur and nitrogen species
[DE93-017727] 03 p1220 N94-16997
Supercritical thermodynamics of sulfur and nitrogen species
[DE93-041221] 04 p1610 N94-19670
Integral equations for the microstructures of supercritical fluids
[DE94-002460] 06 p2535 N94-24569
Computer simulation of molecular interactions in supercritical solvents
[AD-A274977] 08 p3486 N94-29087
Biocatalytic processing polymers in supercritical fluids
[AD-A276120] 09 p3651 N94-31510
Improved oxidation resistance of 3-D carbon/carbon composites
[AD-A277349] 09 p3625 N94-32624
Dynamic structural effects and ultrafast biomolecular kinetics in photoinduced charge transfer reactions
[DE94-010421] 11 p4329 N94-36390

SUPERCRITICAL PRESSURES
Removal of carbonaceous contaminants from silica aerogel 03 p0953 N94-16256

SUPERCRITICAL WINGS
X-29: Longitudinal instability at high angle-of-attack 01 p0033 N94-11504
Physical properties of the benchmark models program supercritical wing
[NASA-TM-4457] 03 p0866 N94-15722
High lift and the forward swept wing 04 p1308 N94-18436
Reduction of structural loads using maneuver load control on the Advanced Fighter Technology Integration (AFTI)/F-111 mission adaptive wing
[NASA-TM-4526] 06 p2168 N94-24295
Wind tunnel investigation of propfan slipstream/wing interactions on a De Havilland air motor powered semispan model at Mach numbers 0.6 and 0.7 07 p2651 N94-28316

SUPERFLUID FLOW
U SUPERFLUIDITY

SUPERFLUIDITY
On the doubling of hydrodynamic theorems in relativistic theory of superfluidity
[DE93-617895] 01 p0148 N94-10717
Quantum dynamics of helium clusters
[AD-A266060] 01 p0411 N94-10874
The superfluid Stirling refrigerator, a new method for cooling below 0.5 K
[DE93-012672] 01 p0128 N94-11161
Superfluid turbulence 01 p0158 N94-12307
To the theory of triplet pairing in Fermi-liquid model
[DE93-621770] 02 p0816 N94-12855
Sidewall thermometry perturbations to nonlinear heat transport near the (lambda) transition in He-4
[DE93-014990] 02 p0817 N94-14453
On the statistical theory of the even-even nucleons levels' density
[DE93-623990] 02 p0788 N94-14875
The 7th International Cryocooler Conference
[AD-A268451] 04 p1379 N94-18147
Superfluid Helium On-Orbit Transfer (SHOOT) flight demonstration 04 p1327 N94-19185
Two-dimensional turbulent nonstationary superfluid counterflows: Numerical simulations, qualitative effects
[MPIS-23/1992] 04 p1422 N94-19510
Examinations of converging cylindrically symmetric second sound propagation in He2
[MPIS-9/1992] 04 p1564 N94-19715
Acoustic microscopy and nonlinear effects in pressurized superfluid helium
[AD-A270598] 05 p1967 N94-19949
Canonically covariant formulation of Landau's Newtonian superfluid dynamics
[PB93-221034] 05 p1805 N94-22272
Acoustic and optical investigations of superfluid He-3
[PB93-224889] 06 p2523 N94-23101
Crossover between BCS and performed-Boson theories with increasing interactions
[DE93-019018] 07 p3017 N94-26078
A numerical study of quantized vortices in Hell
[ISBN-9-03-860232-4] 07 p2792 N94-26479
Superfluid helium sloshing dynamics induced oscillations and fluctuations of angular momentum, force and moment actuated on spacecraft driven by gravity gradient or jitter acceleration associated with slew motion
[NASA-CR-193928] 07 p2799 N94-27931
Acoustic and optical investigations of superfluid (3)He
[PB94-135415] 08 p3477 N94-29186
Hydrodynamics of neutron star interiors and laboratory superfluids 09 p3936 N94-31949
Spatio-temporal properties of centrifugal instabilities: Abstracts of 8th Couette-Taylor Meeting
[PB94-150240] 11 p4266 N94-35981
On possible types of vortexes in relativistic superfluid system
[DE94-617392] 11 p4267 N94-36098
Taking into account dissipative processes in relativistic superfluid systems
[DE94-617391] 11 p4267 N94-36313
First, second and fourth sound in relativistic superfluidity theory with account for dissipative effects
[DE94-617393] 11 p4267 N94-36314
Josephson acoustic radiation in superfluid helium
[AD-A280208] 12 p4533 N94-36742

SUPERGIANT STARS
NT R CORONAE BOREALIS STARS
The chromosphere of VV cephei and the distribution of circumstellar dust around red giants and supergiants
[NASA-CR-193594] 03 p1297 N94-16866
Determination of nitrogen to carbon abundance ratios from transition layer emission lines
[NASA-CR-191921] 04 p1622 N94-19421
VVNRS: Variable phenomena in VV Cephei
[NASA-CR-194731] 05 p2056 N94-21835

SUPERGRAVITY
The 2D supergravity and integrable systems
[DE93-616848] 06 p2570 N94-25336
Topological amplitudes in string theory
[DE94-601561] 07 p3071 N94-25882
Anomaly candidates and invariants of D 4, N 1 supergravity theories
[NIKHEF-H/93-12] 07 p3072 N94-26541
The super Weierstrass (zeta)-function and operator product expansions in 2D-induced supergravity on the supertorus
[DE94-603664] 07 p3074 N94-27627

SUPERHEATING
Explosive boiling at very low heat fluxes: A microgravity phenomenon
[NASA-TM-106325] 03 p1046 N94-15817
Surface barrier of a uniaxial anisotropic type 2 superconducting cylinder
[DE93-617137] 06 p2566 N94-25392
An experimental investigation of flow patterns and liquid entrainment in a horizontal-tube evaporator 08 p3277 N94-29899

SUPERHETERODYNE RECEIVERS
FM interference in radio navigation receivers 05 p1645 N94-22219

SUPERHIGH FREQUENCIES
Wide band 140 GHz TWTA 01 p0132 N94-10514

Nonlinear analysis of a magnicon output cavity
[AD-A265342] 01 p0145 N94-12424
Fundamental studies of radar scattering from water surfaces: The Lake Washington experiment
[NASA-CR-194030] 01 p0139 N94-12778
Rain rate duration statistics derived from the Mid-Atlantic coast rain gauge network 02 p0614 N94-14663
Tree attenuation at 20 GHz: Foliage effects 02 p0615 N94-14672
Johnson-Gierhart program predictions of excess propagation loss for super-high frequency air-to-ground paths. Volume 1: Theory and numerical results
[AD-A267105] 03 p0988 N94-15649
X-SAR: The X-band synthetic aperture radar on board the Space Shuttle 03 p0990 N94-15891
High resolution SAR applications and instrument design 03 p0993 N94-15913
Data acquisition, preprocessing and analysis for the Virginia Tech OLYMPUS experiment 03 p0995 N94-16038
The ACTS propagation program 03 p0995 N94-16039
Numerical modelling of fringing fields and their use for complex permittivity measurements at high frequencies
[AD-A270198] 04 p1388 N94-18782
Some superhigh-frequency and magnetic properties of chemically precipitated films
[AD-A266195] 04 p1351 N94-19110
Ku-band ocean radar backscatter observations during SWADE 05 p1720 N94-20413
Analysis of Ku-band cross section at low incidence angles 05 p1720 N94-20414
Studies of Greenland using the SEASAT scatterometer 05 p1725 N94-20433
Mobile antenna development at JPL 05 p1731 N94-20457
An in-depth analysis and modelling of the Shuttle to MILA S-band telemetry link 05 p1657 N94-21340
Heterojunction bipolar transistor technology for data acquisition and communication 05 p1763 N94-21697
Radio wave propagation studies along an Earth-space satellite link
[ISBN-0-315-60627-4] 05 p1742 N94-22408
The provision of spectrum for feeder links of non-geostationary mobile satellites 06 p2276 N94-22751
Measurements on the satellite-mobile channel at L and S bands 06 p2282 N94-22791
K-band mobile propagation measurements using ACTS 06 p2283 N94-22792
Performance of the X-/Ka/KABLE-band dichroic plate in the DSS-13 beam waveguide antenna 06 p2291 N94-23261
Precipitation measurement using SIR-C: A feasibility study. Investigation at nadir
[NASA-CR-195103] 06 p2410 N94-24126
A small satellite design for deep space network testing and training
[NASA-CR-195526] 06 p2205 N94-24702
Analyzing adaptive beamformer performance in a stable multipath environment
[AD-A274029] 07 p2766 N94-25766
Annex report FEL-92-A163: Description of the LInk and BER Test Analysis System (LIBERTAS) for the frequency band V (14.5 - 15.3 GHz)
[FEL-92-A442] 07 p2770 N94-26650
X-/Ka-band dichroic plate design and grating lobe study 08 p3247 N94-29616
A portable X-band front-end test package for beam-waveguide antenna performance evaluation. Part 2: Tests on the antenna 08 p3247 N94-29620
Design and analysis of a low-loss linear analog phase modulator for deep space spacecraft X-band transponder applications 08 p3248 N94-29625
Optimizing the Galileo space communication link 08 p3250 N94-29663
X-band ultralow-noise maser amplifier performance 08 p3251 N94-29672
Adaptive power control as a fade countermeasure on satellite links 08 p3253 N94-29897
Measurement basis of near fields in spherical coordinates in the 100 MHz to 6 GHz band
[REPT-932-430-107] 08 p3255 N94-30153
Design of a high power x-band magnicon amplifier
[AD-A277001] 09 p3692 N94-32199
YBCO Josephson Junction arrays
[AD-A277426] 09 p3908 N94-33005
The 20 GHz circularly polarized, high temperature superconducting microstrip antenna array
[NASA-CR-195097] 09 p3683 N94-33083
Field demonstration of X-band photonic antenna remoting in the Deep Space Network 11 p4252 N94-35545
DSS-13 S-/X-band microwave feed system 11 p4253 N94-35550
The Mars Observer Ka-band link experiment 11 p4255 N94-35563
Analysis of recent agile mirror data
[AD-A278758] 11 p4318 N94-36427

SUPERHYBRID MATERIALS

NT GRAPHITE-EPOXY COMPOSITES

SUPERLATTICES

Photostimulated attenuation of hypersound in superlattice
[DE93-611231] 01 p0357 N94-10408
Rapid thermal processing for strained-layer semiconductor devices
[DE93-013754] 01 p0396 N94-10809
Organometallic chemical vapor deposition and characterization of ZnGe(1-x)Si(x)P2-Ge alloys on GaP substrates 01 p0400 N94-11443
The additional contribution caused by Coulomb interaction to the exciton dispersion in multiple quantum wells and superlattices for direct band gap cubic semiconductors
[DE93-613538] 01 p0402 N94-11659
Electronic and total energy properties of ternary and quaternary semiconductor compounds, alloys and superlattices
[NASA-CR-192905] 01 p0405 N94-12570
Surfaces and interfaces of ceramics and metals
[DE93-014959] 02 p0578 N94-13408
Electronic states in systems of reduced dimensionality
[DE93-014440] 02 p0815 N94-14739
Magneto-optic superlattice thin films: Fabrication, structural and magnetic characterization 03 p0974 N94-14982
A multilayered approach to superconducting tunnel junction x ray detectors 03 p0908 N94-15089
Design, synthesis and characterization of novel nonlinear optical polymers
[AD-A267035] 03 p0964 N94-15675
Experimental investigations of superconductivity in quasi-two-dimensional epitaxial copper oxide superlattices and trilayers
[DE93-015306] 03 p1207 N94-15829
The growth of InAs(1-x)Sb(x)/InAs strained-layer superlattices by metal-organic chemical vapor deposition
[DE93-015028] 03 p1208 N94-16012
Interfacial structure of lattice mismatched bcc(110)/bcc(110) transition metal superlattices
[DE93-015162] 03 p1208 N94-16058
Rational design, construction, and processing of high-performance nonlinear optical materials
[AD-A266185] 03 p1191 N94-16454
Microstructure of Zr3Al after 2 MeV proton bombardment
[DE93-015331] 03 p1211 N94-16814
Neutron and x ray scattering studies of (FeF2)(sub m)(CoF2)(sub n) multilayers
[DE93-015809] 03 p1184 N94-16838
Pseudomorphic semiconducting heterostructures from combinations of AlN, GaN and selected SiC polytypes: Theoretical advancement and its coordination with experimental studies of nucleation, growth, characterization and device deployment
[AD-A267561] 03 p1213 N94-17108
Characterization of metallic multilayers using x ray diffraction analysis
[NIAR-93-13] 03 p0961 N94-17282
Precise flux control for lattice matched superlattice materials
[AD-A268254] 03 p1215 N94-17417
Mechanical properties of interfaces and superlattices
[AD-A268591] 03 p1217 N94-17606
Superhardness effect in Au/Ni multilayers
[DE93-016444] 04 p1357 N94-17860
Phenomenological explanation of elastic anomalies in superlattices
[DE93-017475] 04 p1594 N94-17871
Fundamental properties and device applications of Ge(x)Si(1-x)/Si superlattices (supplemental)
[AD-A269212] 04 p1600 N94-18884
Neutron-induced collision cascade mixing in Nb/V superlattices
[DE93-018575] 04 p1600 N94-18933
Growth of epitaxial semiconductor alloys and superlattices with continuously variable composition by pulsed-laser ablation
[DE93-018726] 04 p1601 N94-18998
Suppressed electron-phonon scattering in superlattices
[AD-A270834] 04 p1604 N94-19597
Investigation of quantum effects in heterostructures
[AD-A270938] 05 p2011 N94-19817
Theory of energy-assisted epitaxy; theory of ordered semiconductor alloys: In(1-x)Tl(x)Sb as a long-wave infrared material
[AD-A271007] 05 p2012 N94-19835
Ellipsometric study of Si(0.5)Ge(0.5)/Si strained-layer superlattices 05 p1734 N94-20509
Spectroscopic ellipsometric characterization of Si/Si(1-x)Ge(x) strained-layer superlattices 05 p1734 N94-20510
Semiconductor isotope engineering
[DE93-040119] 05 p2030 N94-21744
Photo- and thermal-induced antiferromagnetic interlayer coupling in Fe/(Fe-Si) superlattices
[DE93-040822] 05 p2031 N94-21930
Orientationally independent antiferromagnetic coupling in epitaxial Fe/Cr (211) and (100) superlattices
[DE94-001270] 05 p2035 N94-22564
High-T(c) superconducting superlattices
[DE93-019200] 06 p2556 N94-22864
Report of the Joint Seminar on Solid State Physics, Atomic and Molecular Physics, and Materials Science in the Energy Region of Tandem Accelerators
[DE93-508268] 06 p2548 N94-22924
Photo-induced antiferromagnetic interlayer coupling in Fe superlattices with iron silicide spacers
[DE94-001345] 06 p2559 N94-22995
Quantum tunneling transport of electrons in double-barrier heterostructures: Theory and modeling
[ETN-94-95332] 06 p2565 N94-25059
Effect of high frequency field on the transport properties of superlattice
[DE93-617047] 06 p2568 N94-25447
MBE grown 3 to 5 strain relaxed buffer layers and superlattices characterized by atomic force microscopy
[DE94-002931] 07 p3056 N94-26308
The effect of high frequency electric field on hypersound amplification in superlattice
[DE93-634326] 07 p3057 N94-26384
Modulation wavelength dependence of ion mixing in metallic superlattices
[DE94-004608] 07 p3059 N94-26591
AB-Initio calculation of the valence-band offset at strained GaAs/InAs (001) heterojunction
[DE94-602538] 07 p3061 N94-26878
Carrier collection and scattering in quantum well and superlattice devices
[AD-A275443] 08 p3512 N94-28880
Band structure of superlattice with (delta)-like potential
[DE94-608108] 08 p3516 N94-30072
Interband optical absorption in the Wannier-Stark ladder under the electron-LO-phonon resonance condition
[DE94-608097] 08 p3267 N94-30092
The growth of InAsSb/inGaAs strained-layer superlattices by metal-organic chemical vapor deposition
[DE94-005576] 08 p3518 N94-30316
Experimental and theoretical studies of hydrogenated amorphous semiconductor alloys and superlattices
[AD-A276159] 09 p3686 N94-31079
A 1-picosecond InGaAs photodetector for operation at 1300-1600 nm
[AD-A275959] 09 p3895 N94-31350
The relationship of the electronic structures of semiconductor surfaces and heterostructures to crystal growth
[AD-A276465] 09 p3896 N94-31473
Ion beam synthesis of IrSi3 by 1-MeV Ir ion implantation into Si(111)
[DE94-006556] 09 p3896 N94-31501
GaAs/GaN strained layer superlattice materials for high temperature transistors, phase 1
[AD-A276115] 09 p3897 N94-31528
Energetics, bonding mechanism, and electronic structure of ceramic/ceramic and metal/ceramic interfaces
[DE94-008551] 09 p3659 N94-32656
Microanalytical study of defect formation in thin bismuth strontium calcium copper oxide films
[DE94-008217] 09 p3661 N94-32751
Interface controlled amorphization of crystalline Ni/Ti multilayers
[DE94-008685] 09 p3906 N94-32884
The use of selective area growth for the reduction of threading dislocation densities in heteroepitaxy
[AD-A278282] 10 p4147 N94-33856
Infrared detectors based on Si/SiGe superlattices and silicide/SiGe Schotty barriers operating beyond 12 micrometers
[AD-A277900] 10 p4147 N94-34082
Dynamics of supermatrix semiconductor growth
[AD-A278380] 10 p4147 N94-34085
The optimization of interfaces in InAsSb/InGaAs strained-layer superlattices grown by metal-organic chemical vapor deposition
[DE94-010070] 11 p4340 N94-35698
Activities of the optoelectronics laboratory
[PB94-171196] 11 p4334 N94-36190
Forward scattering of neutrons from polymeric and magnetic multilayers
[DE93-041158] 12 p4513 N94-36696

SUPERMAGNETS

U HIGH FIELD MAGNETS

SUPERNOVA REMNANTS
Acceleration of positrons in supernova shocks
[NASA-CR-193713] 01 p0425 N94-10511
VLBI and the detection of interstellar magnetohydrodynamic waves 01 p0135 N94-11066
A comparison of calculated and observed monochromatic type Ia supernova light curves
[MPA-709] 03 p1237 N94-17629
Nonequilibria in thermal emission from supernova remnants
[NIFS-264] 06 p2602 N94-24866
X ray enhancement of SN 1987A due to interaction with its ring-like nebula
[NIFS-265] 06 p2602 N94-24867
Shocked clouds in the Cygnus Loop
[NASA-CR-195190] 06 p2600 N94-25178
Investigation relative to the Roentgen Satellite (ROSAT)
[NASA-CR-195192] 06 p2600 N94-25269
Supernovae and mass extinctions 07 p2891 N94-28314
A multiwavelength study of two prototypical supernova remnants 08 p3540 N94-29833
Structure and stability of spherical accretion flows onto compact objects 09 p3935 N94-31946
SUPERNOVA 1987A
Carbon and nitrogen in Type 2 supernova diamonds 01 p0431 N94-12166
Electron acceleration in and radio emission from SN1987A 05 p2007 N94-22677
X ray enhancement of SN 1987A due to interaction with its ring-like nebula
[NIFS-265] 06 p2602 N94-24867
Balloon-borne measurements of the SN1987A hard x ray continuum 07 p3115 N94-26689
SUPERNOVAE
NT SUPERNOVA 1987A
Nuclear astrophysics
[DE93-010569] 01 p0425 N94-10292
Acceleration of positrons in supernova shocks
[NASA-CR-193713] 01 p0425 N94-10511
Search for effects of a supernova explosion 30 to 40 thousand years ago in chondrites 01 p0428 N94-12022
Cosmic physics data analysis program
[NASA-CR-194357] 02 p0846 N94-12826
A program of correlated observations using the EGRET instrument on GRO and the IMB neutrino detector
[NASA-CR-194367] 02 p0783 N94-13856
Charge-exchange reactions and weak interaction rates for Type 2 supernovae
[DE93-015104] 02 p0783 N94-13893
A comparison of calculated and observed monochromatic type Ia supernova light curves
[MPA-709] 03 p1237 N94-17629
Evolution of r-process elements in the hot supernova bubble
[DE93-017169] 04 p1624 N94-17897
Weak neutral currents and collapse initiated supernova
[DE93-018652] 04 p1627 N94-19284
New production mechanisms for unstable nuclei in stars, supernovae, and the big bang
[DE93-018627] 05 p2081 N94-21618
Kamiokande results on solar neutrinos and a supernova search
[ICRR-REPT-294-93-6] 06 p2627 N94-24961
Supernovae and mass extinctions 07 p2891 N94-28314
Reactive flows in compact objects 09 p3934 N94-31567
Evolution of stars and winds in the starburst galaxy M82 09 p3934 N94-31758
Convection in Type 2 supernovae
[DE94-009373] 09 p3938 N94-32914
A search for radiative neutrino decay from supernovae
[NASA-CR-196011] 11 p4376 N94-35515
SUPERPLASTIC FORMING
Numerical simulation of industrial workpiece superplastic forming
[REPT-932-600-102] 08 p3418 N94-29479
Numerical simulation of industrial workpiece superplastic forming
[REPT-932-600-102] 08 p3418 N94-29479
SUPERPLASTICITY
SPF/DB: A manufacturing technique for lightweight structures 01 p0059 N94-10026
Effect of thermal processing practices on the properties of superplastic Al-Li alloys
[NASA-CR-4548] 02 p0574 N94-14850
High temperature deformation behavior of YBa2Cu3O(6+x) superconducting ceramic materials
[AD-A268164] 03 p0973 N94-17430
Modeling microstructural evolution and the mechanical response of superplastic materials
[DE93-014417] 04 p1355 N94-17711
Ceramic films and interfaces: Chemical and mechanical properties
[DE93-018416] 04 p1369 N94-18163
The effect of composition on the mechanism of continuous recrystallization and superplastic response of aluminum-scandium alloys
[DE93-018594] 04 p1365 N94-19280
The use of backscattered electron imaging mode to assess the effect of fine dispersions on development of superplastic microstructure in Al-Mg alloys
[AD-A272426] 05 p1691 N94-21258
Materials Science and Engineering
[DE93-040497] 05 p1675 N94-21530
The effect of microstructural evolution on superplasticity in Ni3Si(V, Mo)
[DE93-041320] 05 p1694 N94-21943
Gas-pressure forming of superplastic ceramic sheet
[DE94-001520] 06 p2252 N94-22930
Materials Science and Engineering
[DE94-003018] 06 p2228 N94-23493
High strain rate superplasticity in metals and composites
[DE94-001521] 06 p2229 N94-24547
The nanometer-scale mechanics of gold films
[AD-A273307] 06 p2565 N94-25086
An investigation of cavitation in a mechanically alloyed 15 volume percent SiCp/IN9021 aluminum composite
[DE94-003371] 07 p2748 N94-25959
Study of precipitation and recrystallization in Al alloy 2519 by backscattered electron imaging methods
[AD-A274919] 07 p2736 N94-26533
Superplasticity in fine-grained ceramics
[AD-A275461] 08 p3212 N94-28733
Numerical simulation of industrial workpiece superplastic forming
[REPT-932-600-102] 08 p3418 N94-29479
A state variable material model for superplastic titanium-6 percent Al-4 percent V 09 p3644 N94-32498
SUPERPRESSURE BALLOONS
Electrodynamics of the middle atmosphere: Superpressure balloon program
[NASA-CR-193671] 02 p0712 N94-13293
SUPERSATURATION
Study of vapor bubble growth in a supersaturated liquid 01 p0122 N94-10232
Film condensation in a shock wave
[MPIS-22/1992] 04 p1422 N94-19509
Hypobaric decompression sickness model development. Part 1: Diffusion of inert gas from a viscoelastic fluid (blood) into an expanding gas phase
[AD-A280298] 12 p4481 N94-37124
SUPERSONIC AIRCRAFT
NT B-70 AIRCRAFT
NT F-5 AIRCRAFT
NT F-15 AIRCRAFT
NT F-16 AIRCRAFT
NT F-22 AIRCRAFT
NT F-104 AIRCRAFT
NT F-106 AIRCRAFT
NT F-111 AIRCRAFT
NT FIREBEE 2 TARGET DRONE AIRCRAFT
NT SR-71 AIRCRAFT
NT SUPERSONIC COMMERCIAL AIR TRANSPORT
NT SUPERSONIC TRANSPORTS
NT T-38 AIRCRAFT
NT X-15 AIRCRAFT
Turbulence modeling of free shear layers for high-performance aircraft
[NASA-CR-193659] 02 p0520 N94-12799
High flux heat exchanger
[AD-A266341] 02 p0636 N94-13730
Sabot high speed interceptor AE 4273 aircraft design
[NASA-CR-195495] 06 p2183 N94-24971
Report of the defense science board task force on aircraft assessment
[AD-A274531] 07 p2669 N94-26835
Advanced fuel properties: A computer program for estimating property values
[AD-A275248] 08 p3224 N94-28901
Numerical analysis of supersonic transport wings 08 p3124 N94-28959
Development of a cascade simulation of fan-passage flow
[AD-A277234] 09 p3584 N94-32026
HSR combustion analytical research 10 p3974 N94-33483
High performance jet-engine flight test data base for HSR 10 p3976 N94-33493
Overview of NASA HSR high-lift program 10 p3979 N94-33518
HSR high lift research program: Status and plans 10 p3980 N94-33521
HSCT high lift system aerodynamic requirements 10 p3980 N94-33522
A direct application of the non-linear inverse transformation flight control system design on a STOVL aircraft
[NASA-TM-108808] 10 p3969 N94-33942
SUPERSONIC AIRFOILS
Estimation of critical values and vibration characteristics on supersonic delta wings. Part 2: Locally-stationary time series analysis of nonstationary random responses
[NAL-TR-1179] 02 p0502 N94-13345
SUPERSONIC BOUNDARY LAYERS
The effects of successive distortions on a turbulent boundary layer in a supersonic flow 01 p0014 N94-11058
Exploratory study of in-plane streamline curvature effects on a turbulent boundary layer at a Mach number of 3
[NASA-CR-193673] 02 p0501 N94-13292
A three-dimensional supersonic turbulent boundary layer generated by an isentropic compression 02 p0503 N94-13556
Investigation of the dilatational dissipation in compressible homogeneous shear flow 02 p0645 N94-14758
Response of a supersonic boundary layer to a compression corner 02 p0645 N94-14759
Incorporation of boundary layer heating predictive methodology into NSWCDD aeroprediction code
[AD-A267000] 03 p1020 N94-15632
The structure of turbulent boundary layers and shock wave boundary layer interactions
[AD-A266240] 03 p1026 N94-16929
Studies on high pressure and unsteady flame phenomena: Revision
[AD-A269138] 04 p1348 N94-18257
Relationship between transition and modes of instability in supersonic boundary layers
[NASA-CR-4562] 06 p2336 N94-24725
Theoretical and experimental investigation of converging cylindrical shock waves propagating in narrow cylindrical chambers
[ISBN-0-315-84694-1] 07 p2795 N94-27313
Effect of pressure gradient on first mode of instability in high-speed boundary layers
[AD-280579] 10 p4048 N94-34130
Expansion effects on supersonic turbulent boundary layers
[AD-A278989] 11 p4190 N94-35950
Supersonic laminar flow control research
[NASA-CR-196260] 12 p4384 N94-37511
SUPERSONIC COMBUSTION
Direct simulation of compressible wall-bounded turbulence 01 p0156 N94-12294
Theories of turbulent combustion in high speed flows
[AD-A265735] 01 p0079 N94-12403
Chemical reactions in scramjet engines: Reduced kinetic models for ignition, combustion and nozzle flow
[NAL-TR-1184] 02 p0563 N94-13458
A technique for direct measurement of skin friction in supersonic combustion flow 02 p0503 N94-13555
Modeling and simulation of transport and combustion phenomena in a supersonic mixing layer
[ONERA-NT-1992-11] 02 p0565 N94-14194
Supersonic Combustion Research Laboratory. Volume 1: Design and fabrication
[AD-A267667] 03 p0943 N94-14962
Studies on nonequilibrium phenomena in supersonic chemically reacting flows
[NASA-CR-194662] 03 p1027 N94-17215
Chemical reactions in turbulent mixing flows
[AD-A268287] 03 p0861 N94-17580
Studies on high pressure and unsteady flame phenomena: Revision
[AD-A269138] 04 p1348 N94-18257
Numerical simulation of fluid dynamics and combustion for ram accelerator projectile/obturator interaction
[AD-A269715] 04 p1320 N94-18748
Instantaneous velocity field imaging instrument for supersonic reacting flows
[NASA-CR-191162] 05 p1809 N94-21607
Proceedings of Workshop on Laser Diagnostics in Fluid Mechanics and Combustion
[AD-A272808] 06 p2347 N94-22914
A numerical study of mixing and combustion in hypervelocity flows through a scramjet combustor model 07 p2808 N94-27911
Scramjet CFD methods and analysis. Part 2: Scramjet CFD analysis. Numerical simulation of supersonic mixing and combustion applied to scramjet combustor 08 p3152 N94-29300
Fuel-rich catalytic combustion of a high density fuel
[NASA-TP-3281] 08 p3197 N94-29356
Ignition delays, heats of combustion, and reaction rates of aluminum alkyl derivatives used as ignition and combustion enhancers for supersonic combustion
[NASA-CR-189581] 09 p3638 N94-32668

Turbulent reacting flows and supersonic combustion
[AD-A277462] 09 p3639 N94-33242
Low emissions combustor technology for high-speed civil transport engines 10 p3974 N94-33481
LeRC in-house experimental research 10 p3975 N94-33484
Rich burn combustor technology at Pratt and Whitney 10 p3975 N94-33486
AFOSR Contractors Propulsion Meeting
[AD-A279028] 11 p4198 N94-35746

SUPERSONIC COMBUSTION RAMJET ENGINES

Studies on scramjet nozzles. Part 1: Performance of two dimensional nozzles
[NAL-TR-1149] 01 p0027 N94-10367
Numerical calculation of scramjet inlet flow
[NAL-TR-1174T] 01 p0027 N94-10370
Numerical simulation of the flow through a scramjet engine 01 p0003 N94-10425
Schlieren photographs and internal pressure distributions for three-dimensional sidewall-compression scramjet inlets at a Mach number of 6 in CF4
[NASA-TM-4479] 01 p0148 N94-10644
An environmental study of the National Aerospace Plane
[AD-A266071] 01 p0025 N94-10945
Preprints of the 13th Hydrogen Energy System Symposium
[DE93-781115] 01 p0099 N94-11444
An experimental investigation of mixing enhancement in a simulated scramjet combustor by use of swirling jets
[NASA-TM-109246] 02 p0518 N94-13190
Chemical reactions in scramjet engines: Reduced kinetic models for ignition, combustion and nozzle flow
[NAL-TR-1184] 02 p0563 N94-13458
A technique for direct measurement of skin friction in supersonic combustion flow 02 p0503 N94-13555
Flight testing of airbreathing hypersonic vehicles
[NASA-TM-4524] 03 p0886 N94-15753
Analysis of supersonic flows using k-epsilon model and the RPLUS code: Progress towards high speed combustor analysis 04 p1411 N94-18551
Optimization and performance analysis of a supersonic conical-flow waverider for a deck-launched intercept mission
[AD-A272498] 05 p1648 N94-21433
Experimental investigation of generic three-dimensional sidewall-compression scramjet inlets at Mach 6 in tetrafluoromethane
[NASA-TM-4497] 06 p2319 N94-23339
Shock tunnel studies of scramjet phenomena, supplement 7
[NASA-CR-191572] 06 p2319 N94-23513
Shock tunnel studies of scramjet phenomena, supplement 8
[NASA-CR-191573] 06 p2320 N94-23532
NASA/USRA advanced design program
[NASA-CR-195548] 06 p2180 N94-24492
HYPULSE combustor analysis
[NASA-CR-191579] 06 p2336 N94-24771
Effect of aeroelastic-propulsive interactions on flight dynamics of a hypersonic vehicle 06 p2164 N94-25113
Development and implementation of a scramjet cycle analysis code with a finite-rate-chemistry combustion model for use on a personal computer
[AD-A273834] 07 p2673 N94-25617
A study on heat transfer in a scramjet leading edge model
[NAL-TR-1187T] 07 p2675 N94-27608
A numerical study of mixing and combustion in hypervelocity flows through a scramjet combustor model 07 p2808 N94-27911
Numerical study on the interaction between scramjet engine modules caused by thermal choke 08 p3125 N94-28960
Research and Development of Ram/Scramjets and Turboramjets in Russia
[AD-A275588] 08 p3151 N94-29291
Introduction and overview of research and development of solid propellant ramrockets, liquid fuel ramjets and experimental hydrogen ram combustors 08 p3151 N94-29292
Some problems of scramjet propulsion for aerospace planes. Part 1: Scramjet: Aims and features 08 p3151 N94-29295
Scramjet CFD methods and analysis. Part 1: Scramjet CFD methods. Numerical simulation of the flow in scramjet duct 08 p3152 N94-29296
Scramjet CFD methods and analysis. Part 2: Scramjet CFD analysis. Numerical simulation of supersonic mixing and combustion applied to scramjet combustor 08 p3152 N94-29300
Some problems of scramjet propulsion for aerospace planes. Part 2: Scramjet: Development and test problems 08 p3152 N94-29301
Liquid atomization in supersonic flows 08 p3276 N94-29839
A numerical method for mixing/chemically reacting compressible flow with finite rate chemistry 09 p3634 N94-31824
Computational study of generic hypersonic vehicle flow fields
[NASA-CR-195938] 10 p3984 N94-34277
Experimental investigation of nozzle/plume aerodynamics at hypersonic speeds
[NASA-CR-195829] 12 p4382 N94-36687

SUPERSONIC COMMERCIAL AIR TRANSPORT

The evolution of the high-speed civil transport
[NASA-TM-109089] 07 p3117 N94-26155

SUPERSONIC CRUISE AIRCRAFT RESEARCH

Status of the variable diameter centerbody inlet program 10 p3978 N94-33509

SUPERSONIC DRAG

Aerodynamics of a sphere and an oblate spheroid for Mach numbers from 0.6 to 10.5 including some effects of test conditions
[NASA-TM-109016] 02 p0500 N94-13172
Overview of NASA HSR high-lift program 10 p3979 N94-33518

SUPERSONIC FLIGHT

Preliminary supersonic flight test evaluation of performance seeking control
[NASA-TM-4494] 01 p0028 N94-11205
The problem of the sonic boom for future high-speed transport aircraft
[ESA-TT-1286] 02 p0776 N94-13692
Performance seeking control: Program overview and future directions
[NASA-TM-4531] 02 p0519 N94-14855
An experimental investigation of a Mach 3.0 high-speed civil transport at supersonic speeds
[NASA-TP-3365] 06 p2169 N94-24311
Experimental investigation of three-dimensional vortex-airfoil interaction in a supersonic stream
[AD-A275107] 08 p3122 N94-28899
Design and analysis of low boom concepts at Langley Research Center 10 p3973 N94-33470
Sonic boom prediction and minimization using computational fluid dynamics 10 p3973 N94-33472
Overview of feasibility study on conducting overflight measurements of shaped sonic boom signatures using RPV's 10 p3973 N94-33475
Overview of NASA human response to sonic boom program 10 p3976 N94-33499

SUPERSONIC FLOW

Estimation of critical values and vibration characteristics on supersonic delta wings. Part 1: On-line time series analysis of stationary random response
[NAL-TR-1153] 01 p0002 N94-10363
Studies on scramjet nozzles. Part 1: Performance of two dimensional nozzles
[NAL-TR-1149] 01 p0027 N94-10367
Exergy decrease in shock waves and boundary layers of space launch vehicles
[AD-A265272] 01 p0042 N94-10493
Examination of wall functions for a parabolized Navier-Stokes code for supersonic flow
[DE93-011590] 01 p0014 N94-11111
An experimental investigation of mixing enhancement in a simulated scramjet combustor by use of swirling jets
[NASA-TM-109246] 02 p0518 N94-13190
High speed transition prediction
[NASA-CR-194125] 02 p0502 N94-13422
An experimental investigation of shock wave/vortex interaction 02 p0634 N94-13574
Development of a general purpose multigrid accelerated Navier-Stokes solver 02 p0641 N94-14613
Response of a supersonic boundary layer to a compression corner 02 p0645 N94-14759
A new Lagrangian method for three-dimensional steady supersonic flows
[NASA-TM-106068] 02 p0510 N94-14847
Advanced methods for cascade testing
[AGARD-AG-328] 03 p1016 N94-15119
Special course on Shock-Wave/Boundary-Layer Interactions in Supersonic and Hypersonic Flows
[AGARD-R-792] 03 p1017 N94-15196
Swept shock wave/laminar boundary layer interactions, experimental, and numerical results 03 p1017 N94-15198
Unsteady phenomena in shock wave/boundary layer interaction 03 p1017 N94-15200
Contribution of laser Doppler velocimetry to the physical description of shock wave/turbulent boundary layer interactions with incidence on turbulence modelling 03 p1018 N94-15201
On the interaction between the shock wave attached to a wedge and freestream disturbances
[NASA-CR-191528] 03 p1019 N94-15478
Numerical investigations in three-dimensional internal flows
[NASA-CR-194594] 03 p1020 N94-15551
Numerical solution of SUPG finite-element method for supersonic viscous flow
[AD-A267762] 03 p0860 N94-17222
Supersonic flow visualization of a nacelle in close proximity to a simulated wing
[NASA-CR-194675] 03 p0860 N94-17260
Single block three-dimensional volume grids about complex aerodynamic vehicles
[NASA-TM-108986] 03 p1030 N94-17476
Thin-layer and full Navier-Stokes calculations for turbulent supersonic flow over a cone at an angle of attack
[NASA-CR-189103] 03 p0861 N94-17558
An investigation of oblique shock/boundary layer interaction control
[AD-A268106] 03 p0861 N94-17574
Laser velocimetry measurements of vortex flows on a delta wing at Mach 1.9
[AD-A268596] 03 p0861 N94-17609
Analysis of supersonic flows using k-epsilon model and the RPLUS code: Progress towards high speed combustor analysis 04 p1411 N94-18551
Fluid dynamic mechanisms and interactions within separated flows
[AD-A271037] 05 p1797 N94-19978
Instantaneous velocity field imaging instrument for supersonic reacting flows
[NASA-CR-191162] 05 p1809 N94-21607
Three-dimensional simulations of cosmic jets employing the smoothed particle hydrodynamics technique 05 p2008 N94-22685
Two-dimensional Navier-Stokes computations of subsonic and supersonic flows through turbine cascades
[PB93-226223] 06 p2317 N94-23114
Direct simulation of isothermal-wall supersonic channel flow 06 p2172 N94-24164
Effects of shock strength on shock turbulence interaction 06 p2332 N94-24165
Numerical solutions of the complete Navier-Stokes equations
[NASA-CR-194780] 06 p2337 N94-24858
Development and validation of RNG methodology for compressible turbulence
[AD-A273469] 06 p2337 N94-24929
Turbulence models and Reynolds analogy for two-dimensional supersonic compression ramp flow
[NASA-TM-106474] 06 p2337 N94-25119
Evaluation of a concentration probe for application in a supersonic flow field
[AD-A273915] 07 p2643 N94-25592
A numerical determination of bifurcation points for low Reynolds number conical flows
[AD-A273984] 07 p2791 N94-25991
A sensitivity equation approach to shape optimization in fluid flows
[AD-A278423] 07 p2999 N94-27415
Experimental study on the interactions between a transverse heated supersonic jet and an external supersonic flow 07 p2659 N94-28039
Solution of the Euler equations using unstructured grids 07 p2656 N94-28338
Experimental investigation of three-dimensional vortex-airfoil interaction in a supersonic stream
[AD-A275107] 08 p3122 N94-28899
Higher-order accurate numerical simulation of 3D supersonic mixing layers 08 p3124 N94-28954
Numerical simulation of supersonic flow around space plane with engine installed 08 p3125 N94-28961
Study on mixing and injection of hydrogen into a supersonic flow 08 p3127 N94-28975
Scramjet CFD methods and analysis. Part 2: Scramjet CFD analysis. Numerical simulation of supersonic mixing and combustion applied to scramjet combustor 08 p3152 N94-29300
An actively cooled floating element skin friction balance for direct measurement in high enthalpy supersonic flows 08 p3289 N94-29824
Liquid atomization in supersonic flows 08 p3276 N94-29839
An interactive educational tool for compressible aerodynamics
[NASA-TM-106568] 08 p3422 N94-30175
The enhancement of compressible turbulent mixing via streamwise vorticity 08 p3280 N94-30487
Shock-dependent, optimum thrust wings in supersonic flow 09 p3570 N94-32027
Shear flow control of cold and heated rectangular jets by mechanical tabs. Volume 1: Results and discussion
[NASA-CR-182296-VOL-1] 09 p3708 N94-32867
Shear flow control of cold and heated rectangular jets by mechanical tabs. Volume 2: Tabulated data
[NASA-CR-182296-VOL-2] 09 p3709 N94-32869

Flutter analysis of a supersonic cascade in time domain using an ADI Euler solver
[NASA-TM-105625] 09 p3739 N94-32883
An analysis of supersonic flows with low-Reynolds number compressible two-equation turbulence models using LU finite volume implicit numerical techniques
[NASA-CR-195302] 09 p3572 N94-32926
A mathematical model for simulating noise suppression of lined ejectors
[NASA-TP-3425] 09 p3861 N94-32930
Response of a cantilevered plate in supersonic flow
[AD-A277487] 09 p3580 N94-33107
Turbulent reacting flows and supersonic combustion
[AD-A277462] 09 p3639 N94-33242
New broadband shock noise model and computer code for ANOPP 10 p3975 N94-33489
First Annual High-Speed Research Workshop, part 4
[NASA-CP-10087-PT-4] 10 p3979 N94-33517
NASA F-16XL supersonic laminar flow control program overview 10 p3980 N94-33525
Supersonic LFC: Challenges and opportunities 10 p3981 N94-33526
Status of F16XL SSLFC numerical design validation 10 p3981 N94-33527
Code validation for the simulation of supersonic viscous flow about the F-16XL 10 p3981 N94-33528
Inviscid and viscous flow calculations for the F16XL configuration 10 p3981 N94-33529
Supersonic HLFC: Potential benefits and technology development requirements 10 p3982 N94-33531
A shock tube study of aerodynamic heating of gaps in a cylinder subjected to supersonic cross flow
[AD-A278550] 10 p3982 N94-33782
Magnetic field waves at Uranus
[NASA-CR-194807] 10 p4164 N94-34000
A review and development of correlations for base pressure and base heating in supersonic flow
[SAND93-0280] 11 p4189 N94-35360
A supersonic tunnel for laser and flow-seeding techniques
[NASA-TM-106588] 11 p4265 N94-35945
Recovery of frozen flow losses in arcjets
[AD-A278739] 11 p4228 N94-36089
Supersonic laminar flow control research
[NASA-CR-196260] 12 p4384 N94-37511

SUPERSONIC FLOW INLETS
U SUPERSONIC INLETS

SUPERSONIC FLUTTER
Development of a high-speed mechanical drive system for oscillating an annular blade row in the bending mode
[NAL-TR-1170] 02 p0502 N94-13342
Aerothermoelastic analysis of a NASP demonstrator model
[NASA-TM-109007] 03 p0867 N94-17055
Aeroelastic vibrations of lifting surfaces
[ECL-91-01] 09 p3585 N94-31677

SUPERSONIC HEAT TRANSFER
Numerical simulation of aerothermodynamic heating of hypersonic space transportation vehicles 08 p3124 N94-28955

SUPERSONIC INLETS
Numerical investigations in three-dimensional internal flows
[NASA-CR-194594] 03 p1020 N94-15551
An interactive, design and educational tool for supersonic external-compression inlets
[NASA-TM-106581] 08 p3421 N94-30174
Results of a preliminary investigation of inlet unstart on a high-speed civil transport airplane concept 10 p3978 N94-33508
Computational methods for HSCT-inlet controls/CFD interdisciplinary research
[NASA-TM-106618] 11 p4198 N94-35352

SUPERSONIC JET FLOW
Control of jet noise
[NASA-CR-193612] 01 p0358 N94-11176
High order accurate solutions of viscous problems
[NASA-TM-106267] 01 p0151 N94-11253
Mixing noise reduction for rectangular supersonic jets by nozzle shaping and induced screech mixing
[NASA-TM-106364] 02 p0508 N94-14208
Computational aero-acoustics as a branch of turbulence research 04 p1411 N94-18552
Unimolecular photodissociation dynamics of ketene (CH2CO): The singlet/triplet branching ratio and experimental observation of the vibrational level thresholds of the transition-state
[DE93-019252] 04 p1352 N94-19304
Supersonic jets from bevelled rectangular nozzles
[NASA-TM-106403] 04 p1313 N94-19484
Instability modes excited by natural screech tones in a supersonic rectangular jet
[NASA-TM-106409] 05 p1638 N94-22274
Refraction of high frequency noise in an arbitrary jet flow
[NASA-TM-106465] 06 p2525 N94-23464
The acoustic and instability waves of jets confined inside an acoustically lined rectangular duct
[AD-A276347] 06 p2334 N94-24602
The effects of profiles on supersonic jet noise
[NASA-CR-195184] 06 p2530 N94-25177
The growth and characterization of GaN as a photodetector
[AD-A274570] 07 p3063 N94-26965
Transient flow features of a supersonic jet in a low speed cross flow 07 p2800 N94-28005
Experimental study on the interactions between a transverse heated supersonic jet and an external supersonic flow 07 p2659 N94-28039
Liquid atomization in supersonic flows 08 p3276 N94-29839
Theoretical aspects of supersonic jet noise 10 p3972 N94-33469
Partial spreading of a laser beam into a light sheet by shock waves and its use as a shock detection technique
[NASA-CR-195329] 10 p4144 N94-34923
Boundary conditions for jet flow computations
[NASA-TM-106648] 11 p4266 N94-35976
An experimental investigation of active control of thrust vectoring nozzle flow fields
[AD-A278702] 11 p4229 N94-36291
Mixing and noise benefit versus thrust penalty in supersonic jets using impingement tones
[NASA-TM-106583] 12 p4382 N94-36686

SUPERSONIC NOZZLES
Control of jet noise
[NASA-CR-193612] 01 p0358 N94-11176
Chemical reactions in scramjet engines: Reduced kinetic models for ignition, combustion and nozzle flow
[NAL-TR-1184] 02 p0563 N94-13458
Mixing noise reduction for rectangular supersonic jets by nozzle shaping and induced screech mixing
[NASA-TM-106364] 02 p0508 N94-14208
Shock-free supersonic elliptic nozzles and method of forming same
[NASA-CASE-LAR-14054-1] 03 p0925 N94-15947
Studies on nonequilibrium phenomena in supersonic chemically reacting flows
[NASA-CR-194662] 03 p1027 N94-17215
Electrically excited CO-lasers with gas dynamic cooling
[DLR-FB-93-08] 04 p1437 N94-18061
MHD integrated topping cycle project
[DE93-040520] 04 p1588 N94-18978
MHD Integrated Topping Cycle Project
[DE93-040521] 04 p1589 N94-19055
Supersonic minimum length nozzle design for dense gases 06 p2171 N94-23656
Supersonic gas-liquid cleaning system 08 p3240 N94-30467
NASA HSR phase 1 low noise nozzle technology program overview 10 p3972 N94-33463
HSCT nozzle source noise programs at Pratt and Whitney 10 p3972 N94-33465
HSCT noise reduction technology development at GE Aircraft Engines 10 p3972 N94-33466
A supersonic tunnel for laser and flow-seeding techniques
[NASA-TM-106588] 11 p4265 N94-35945

SUPERSONIC SPEED
A comparison of computational and experimental data for a subscale high speed propulsive nozzle at low mach numbers
[AD-A266543] 02 p0504 N94-13705
A computational study of the base region flow field for the M865 projectile
[ARL-TR-109] 02 p0504 N94-13795
Development of a quiet supersonic wind tunnel with a cryogenic adaptive nozzle
[NASA-CR-194548] 03 p0871 N94-15117
Numerical prediction of transition of the F-16 wing at supersonic speeds
[NASA-CR-194407] 04 p1312 N94-19433
Options for thrust augmentation for the Beta 2 two-stage-to-orbit launch vehicle
[NASA-TM-106418] 05 p1649 N94-21759
A numerical study of high-speed missile configurations using a block-structured parallel algorithm
[AD-A273776] 07 p2979 N94-25860
Investigation of sonic boom for the Space Shuttle: High cross-range orbiter
[NASA-TM-108238] 09 p3860 N94-31336
Flight test results of riblets at supersonic speeds
[NASA-TM-4387] 09 p3572 N94-32880
New broadband shock noise model and computer code for ANOPP 10 p3975 N94-33489
Status of an inlet configuration trade study for the Douglas HSCT 10 p3977 N94-33506
HSCT high-lift technology requirements 10 p3980 N94-33523
Expansion effects on supersonic turbulent boundary layers
[AD-A278989] 11 p4190 N94-35950
An experimental investigation of active control of thrust vectoring nozzle flow fields
[AD-A278702] 11 p4229 N94-36291
An aerodynamic and static-stability analysis of the Hypersonic Applied Research Technology (HART) missile
[AD-A280631] 12 p4382 N94-36729

SUPERSONIC TRANSPORTS
NT SUPERSONIC COMMERCIAL AIR TRANSPORT
Supersonic airplane study and design
[NASA-CR-193219] 01 p0025 N94-11150
Stratospheric aircraft exhaust plume and wake chemistry
[NASA-CR-191495] 01 p0279 N94-12572
Proceedings of the Twentieth Annual Technologyfest 05 p1645 N94-20188
Simplified, inverse, ejector design tool
[NASA-CR-194438] 06 p2166 N94-23511
The atmospheric effects of stratospheric aircraft: A third program report
[NASA-RP-1313] 06 p2398 N94-24104
Discrete sensitivity derivatives of the Navier-Stokes equations with a parallel Krylov solver
[NASA-TM-106481] 06 p2265 N94-24301
An experimental investigation of a Mach 3.0 high-speed civil transport at supersonic speeds
[NASA-TP-3365] 06 p2169 N94-24311
Integrated design and manufacturing for the high speed civil transport
[NASA-CR-195511] 06 p2182 N94-24968
High-order technology: Applying technical excellence to new airplane development 06 p2185 N94-25069
Preliminary design of nine high speed civil transports 07 p2671 N94-25710
Supercruiser Arrow HS-8 07 p2671 N94-25711
Tesseract supersonic business transport 07 p2671 N94-25713
Combustion for future supersonic transport propulsion 08 p3190 N94-29249
A study of low emissions gas turbine combustions
[NASA-CR-195763] 08 p3152 N94-29860
Multidisciplinary optimization of high-speed civil transport configurations using variable-complexity modeling 09 p3578 N94-31881
Use of Navier-Stokes methods for the calculation of high-speed nozzle flow fields
[NASA-TM-106551] 09 p3573 N94-32984
First Annual High-Speed Research Workshop, part 1
[NASA-CP-10087-PT-1] 10 p3970 N94-33447
First Annual HSR Program Workshop: Headquarters perspective 10 p3970 N94-33448
NASA Annual HSR Workshop: Boeing HSCT program summary 10 p3970 N94-33449
Update on Douglas' high-speed civil transport studies 10 p3970 N94-33450
General Electric/Pratt and Whitney summary report 10 p3970 N94-33451
Headquarters summary reports 10 p3970 N94-33452
Airframe systems studies review 10 p3970 N94-33453
Douglas Aircraft HSCT status and future research needs 10 p3970 N94-33454
High-speed research program systems analysis activities at Ames Research Center 10 p3971 N94-33455
Overview of Langley systems studies 10 p3971 N94-33456
Comparison of the impact of volcanic eruptions and aircraft emissions on the aerosol mass loading and sulfur budget in the stratosphere 10 p3971 N94-33460
First Annual High-Speed Research Workshop, part 2
[NASA-CP-10087-PT-2] 10 p3972 N94-33462
NASA HSR phase 1 low noise nozzle technology program overview 10 p3972 N94-33463
HSCT nozzle source noise programs at Pratt and Whitney 10 p3972 N94-33465
HSCT noise reduction technology development at GE Aircraft Engines 10 p3972 N94-33466
Design and analysis of low boom concepts at Langley Research Center 10 p3973 N94-33470
HSCT design for reduced sonic boom 10 p3973 N94-33471
Sonic boom configuration minimization 10 p3973 N94-33473
The NASA sponsored HSCT propulsion studies 10 p3974 N94-33476
A NASA Lewis comparative propulsion system assessment for the High-Speed Civil Transport 10 p3974 N94-33477
P and W/GE propulsion systems studies introduction 10 p3974 N94-33478

Results of GEAE HSCT propulsion system studies
10 p3974 N94-33479
P and W propulsion systems studies results/status
10 p3974 N94-33480
Low emissions combustor technology for high-speed civil transport engines 10 p3974 N94-33481
Theoretical study of thermodynamic properties and reaction rates of importance in the high-speed research program 10 p3974 N94-33482
Lean burn combustor technology at GE Aircraft Engines 10 p3975 N94-33485
Rich burn combustor technology at Pratt and Whitney
10 p3975 N94-33486
Results of a preliminary investigation of inlet unstart on a high-speed civil transport airplane concept
10 p3978 N94-33508
Status of the variable diameter centerbody inlet program 10 p3978 N94-33509
HSCT integrated propulsion control issues
10 p3978 N94-33510
Combustor materials requirements and status of ceramic matrix composites 10 p3978 N94-33512
Airframe materials for HSR 10 p3979 N94-33514
HSCT airframe materials: The Boeing perspective
10 p3979 N94-33515
HSCT materials and structures: An MDC perspective
10 p3979 N94-33516
Computational methods for HSCT-inlet controls/CFD interdisciplinary research
[NASA-TM-106618] 11 p4198 N94-35352
Future supersonic commercial transport aircraft: A technological challenge for long haul traffic
11 p4193 N94-36324
Project report: Aircraft --- atmospheric effects of stratospheric aircraft
[DE94-011759] 12 p4465 N94-37155
Jet aircraft engine exhaust emissions database development: Year 1990 and 2015 scenarios
[NASA-CR-4613] 12 p4466 N94-37252
Synthetic vision display evaluation studies
[NASA-CR-194963] 12 p4387 N94-37658

SUPERSONIC TURBINES

Computation of flows in a turn-around duct and a turbine cascade using advanced turbulence models
06 p2216 N94-23062
Two-dimensional Navier-Stokes computations of subsonic and supersonic flows through turbine cascades
[PB93-226223] 06 p2317 N94-23114
Development of a HP-turbine for a small helicopter engine 10 p4003 N94-34456

SUPERSONIC WAKES

Numerical study on internal flows of centrifugal compressors 08 p3127 N94-28977

SUPERSONIC WIND TUNNELS

CNSFV code development, virtual zone Navier-Stokes computations of oscillating control surfaces and computational support of the laminar flow supersonic wind tunnel
[NASA-CR-194259] 02 p0504 N94-14030
Supersonic Combustion Research Laboratory. Volume 1: Design and fabrication
[AD-A267667] 03 p0943 N94-14962
Development of a quiet supersonic wind tunnel with a cryogenic adaptive nozzle
[NASA-CR-194548] 03 p0871 N94-15117
Error propagation equations and tables for estimating the uncertainty in high-speed wind tunnel test results
[DE93-018685] 04 p1311 N94-18275
Lewis Research Center R and D Facilities
[NASA-TM-109400] 06 p2630 N94-23135
Improved pressure measurement system for calibration of the NASA LeRC 10x10 supersonic wind tunnel
[NASA-TM-106470] 06 p2344 N94-24362
Laminar Flow Supersonic Wind Tunnel primary air injector 08 p3158 N94-29649
A supersonic tunnel for laser and flow-seeding techniques
[NASA-TM-106588] 11 p4265 N94-35945

SUPERSONICS

Integrated design and manufacturing for the high speed civil transport
[NASA-CR-195511] 06 p2182 N94-24968

SUPERSTRING THEORY

U STRING THEORY

SUPERSYMMETRY

The super vectorfield package for REDUCE. Version 1.0
[MEMO-1099] 01 p0321 N94-10265
The INTEGRATOR package for REDUCE, version 1.0
[MEMO-1100] 01 p0322 N94-10418
The ring structure of chiral operators for minimal models coupled to 2D gravity
[DE93-613119] 01 p0409 N94-10500
Supersqueezed states from squeezed states
01 p0378 N94-10591
Superfield description of N = 2 extended one-dimensional supersymmetric quantum mechanics
[DE93-621420] 01 p0412 N94-11087
Green-Schwarz superstrings in the generalized harmonical Newmann-Penrose formalism
[DE93-621422] 01 p0412 N94-11088
A version of superstring with four space-time dimensions
[DE93-608196] 01 p0412 N94-11163
Three-dimensional N = 4 extended supersymmetrical quantum mechanics
[DE93-621421] 01 p0412 N94-11164
Supersymmetry of gauge equations and geometric nonadiabatic phases
[DE93-626671] 03 p1219 N94-14935
Theoretical high energy physics research at the University of Chicago
[DE93-016863] 03 p1187 N94-16116
Existence of a new instanton in constrained Yang-Mills-Higgs theory
[NIKHEF-H/93-02] 03 p1186 N94-17601
The universality of the shift of the Chern-Simons parameter for a general class of BRS invariant regularizations
[NIKHEF-H/93-03] 03 p1220 N94-17602
SUSY in the sky
[NIKHEF-H/93-04] 03 p1240 N94-17603
Derivation of the Verlinde formula from Chern-Simons theory and the G/G model
[DE93-628620] 03 p1221 N94-17632
Tensorial structure of a q-deformed sp(4,R) superalgebra
[DE93-624808] 04 p1545 N94-17685
Renormalizations in supersymmetric and nonsupersymmetric non-abelian Chern-Simons field theories with matter
[DE93-626646] 04 p1593 N94-17748
Paragrassmann analysis and quantum groups
[DE93-628593] 04 p1561 N94-18168
Experimental consequences of supersymmetry
[DE93-018270] 04 p1569 N94-18945
Simulating supersymmetry with ISAJET 7.0/ISASUSY 1.0
[DE93-018266] 05 p1969 N94-19804
On the twisted N=2 superconformal structure in 2d gravity coupled to matter
[DE93-628627] 05 p2037 N94-20178
Theoretical particle physics
[DE94-000538] 05 p1973 N94-20938
Stitching the Yukawa quilt
[PB93-204477] 06 p2569 N94-24532
Super Beltrami differentials and N equal to 4 superconformal anomalies
[DE93-613047] 06 p2491 N94-25166
Applications of supersymmetric quantum mechanics
[ETN-94-95385] 06 p2570 N94-25257
The 2D supergravity and integrable systems
[DE93-616848] 06 p2570 N94-25336
(2,0) superconformal anomaly
[DE93-613046] 07 p2991 N94-25867
Aspects of nonrenormalizable terms in a superstring standard-like models
[DE93-614530] 07 p3071 N94-25911
Higher spin extensions of the Virasoro algebra, area-preserving algebras and the matrix algebra a-bar(sub (infinity))
[DE94-601557] 07 p3006 N94-26415
The Hamiltonian structures of the super KP hierarchy associated with an even parity superlax operator
[DE94-601506] 07 p2994 N94-26459
Construction of a new electroweak sphaleron
[NIKHEF-H/93-09] 07 p3020 N94-26540
Anomaly candidates and invariants of D 4, N 1 supergravity theories
[NIKHEF-H/93-12] 07 p3072 N94-26541
Progress in SSC Higgs physics: Report of the Higgs working group
[DE94-003224] 07 p3022 N94-26793
Thermodynamics and form factors of supersymmetric integrable field theories
[DE94-602557] 07 p3073 N94-26896
Excited Landau levels, orbital angular momentum and axial anomaly
[DE94-606407] 07 p3068 N94-27679
Emission of supersymmetric neutron pair by charged lepton in magnetic field
[DE93-634365] 08 p3481 N94-28468
Model of polylinear Bose- and Fermi-like oscillator
[DE94-606303] 08 p3485 N94-28718
Twistor-like type 2 superstring and bosonic string
[DE94-606339] 08 p3523 N94-28802
Operator analysis for quark and lepton masses in SO(10)
[DE94-005201] 08 p3491 N94-30709
Graded Froelicher-Nijenhuis brackets and the theory of recursion operators for super differential equations
[MEMO-1147] 08 p3460 N94-30736
High energy physics studies
[DE94-005970] 09 p3876 N94-31505
Some calculations on supersymmetric graphs as communication networks
[REPT-93-72] 09 p3824 N94-31641
Conformal field theory and geometry of strings
[PB94-148442] 09 p3857 N94-31770
Production of charginos and neutralinos for the reaction positron electron yields Z' boson yields chargino(+) (sub i) chargino(-) (sub j) or neutralino (sub i) neutralino (sub j) in SU(2) (sub L) x SU(2) (sub R) x U(1) (sub B-L)
[ISBN-0-315-87316-7] 09 p3867 N94-31832
The Kaluza-Klein approach and gauge supersymmetry
[ISBN-0-315-86553-9] 09 p3912 N94-31911
Baryogenesis from a primordial lepton asymmetry
[PB94-145166] 09 p3868 N94-31921
Tensor gauge potentials in loop space formulation of Yang-Mills fields
[PB94-147147] 09 p3912 N94-31924
Proceedings of 2nd Working meeting: Physics at VLEPP, volume 1
[DE94-616200] 11 p4320 N94-35569
Universal SU(2/1) and the Higgs and fermion masses
[DE94-009182] 11 p4323 N94-35814
Exact multiplicities in the three-anion spectrum
[DE94-616768] 11 p4325 N94-36075
Proceedings of 2nd Working Meeting on Physics at VLEPP, volume 2
[DE94-616167] 11 p4326 N94-36182
N = 4 supersymmetry from the quantum affine algebra U(sub q)(A-circumflex(sup 1)(sub 3))
[DE94-611145] 11 p4317 N94-36307

SUPINE POSITION

Pulmonary function in microgravity: KC-135 experience
01 p0309 N94-11994
Exercise with prebreathe appears to increase protection from decompression sickness: Preliminary findings
10 p4096 N94-33639

SUPPORT INTERFERENCE

Flow-field interference produced by an asymmetrical support strut
[IAR-AN-75] 02 p0504 N94-14031

SUPPORT SYSTEMS

NT CLOSED ECOLOGICAL SYSTEMS
NT EMERGENCY LIFE SUSTAINING SYSTEMS
NT GROUND OPERATIONAL SUPPORT SYSTEM
NT GROUND SUPPORT SYSTEMS
NT LIFE SUPPORT SYSTEMS
NT PORTABLE LIFE SUPPORT SYSTEMS
Building the repositories to serve --- Superconducting Super Collider information system
[DE93-014100] 02 p0821 N94-12983
An evaluation of ZIM and entity-relational models in managing databases for decision support systems
[ERB-1034] 02 p0824 N94-14202
NASA Lewis 9- by 15-foot low-speed wind tunnel user manual
[NASA-TM-106247] 03 p0872 N94-15819
Reference model for project support environments, version 1.0
[AD-A269110] 04 p1520 N94-18251
Lunar base Controlled Ecological Life Support System (LCELSS): Preliminary conceptual design study
[NASA-CR-188479] 04 p1511 N94-18484
Military satellite communications decision support system requirements analysis and user interface design
[AD-A273047] 05 p1740 N94-21436
A comparison of IDEF1X and NIAM ISDM
[DE93-040899] 05 p1921 N94-22383
Hypermedia support for engineering design system
[PB93-226256] 06 p2449 N94-23117
Object oriented simulation implementation in support of robust system design
[DE93-011687] 06 p2452 N94-23488
ATOS-1: Designing the infrastructure for an advanced spacecraft operations system 06 p2197 N94-23849
Influence of a new generation of operations support systems on current spacecraft operations philosophy: The users feedback 06 p2507 N94-23894
PILOT: An intelligent distributed operations support system 06 p2508 N94-23895
The Advanced Technology Operations System: ATOS
06 p2508 N94-23897
Telemetry ground system development via the component approach 06 p2203 N94-23949
Multi-sensoral approach to night flight: Perceptive and Cognitive limitations 06 p2432 N94-23981
Towards the formal specification of the requirements and design of a processor interface unit
[NASA-CR-4521] 06 p2467 N94-24463
An investigation of requirements traceability to support systems development
[AD-A273167] 06 p2458 N94-24684

Space Station technology testbed: 2010 deep space transport 07 p2687 N94-27368
Flight command software development: RAFALE studies 08 p3413 N94-29320
A Modular Artificial Intelligence Inference Engine System (MAIS) for support of on orbit experiments [AIAA PAPER 94-1237-CP] 08 p3448 N94-30584
New approaches for real time decision support systems 09 p3915 N94-32426
Knowledge-based commodity distribution planning 09 p3915 N94-32427
Selection criteria and facilitation training for the study of groupware [NASA-CR-195906] 09 p3822 N94-33114
A decision support system for electronic warfare analysts 09 p3853 N94-33336
Human factors involvement in bringing the power of AI to a heterogeneous user population 10 p4110 N94-33633
Johnson Space Center (JSC) research and technology [NASA-TM-104788] 10 p4187 N94-34677
Training and operations support system (TOPS) 12 p4545 N94-37344
NASA commercial technology. Agenda for change [NASA-TM-109898] 12 p4546 N94-37765

SUPPORTS
NT PYLONS
NT TRIPODS
Vibration isolation mount with locking means [AD-D015769] 01 p0178 N94-10381
Reliability analysis of Surface Mount Technology (SMT) [AD-A267598] 03 p1055 N94-17194
Shaft mount for data coupler system [NASA-CASE-LAR-13805-1] 05 p1822 N94-20365
Landing gear with swivelling beam [CA-PATENT-1323020] 06 p2176 N94-24181
SAG compensated vibration isolation mount [AD-D016040] 07 p2841 N94-27110
Installation of models in the 2 m x 3 m low speed wind tunnel [LTR-LA-286] 07 p2681 N94-27594
Rotor instability induced by dead band clearance in bearing supports 08 p3312 N94-30809
Method and means for isolating equipment from shock loads [AD-D016161] 10 p4070 N94-34286
The electrical conductivities of candidate beam-waveguide antenna shroud materials 11 p4252 N94-35546
Selectively lockable knee brace [NASA-CASE-MFS-28991-1] 12 p4486 N94-36838
Stability analysis of an F/A-18 E/F cable mount m odel [NASA-TM-109989] 12 p4386 N94-37636

SUPPRESSION
U RETARDING

SUPPRESSORS
NT ECHO SUPPRESSORS
Corner vortex suppressor [AD-D015772] 01 p0147 N94-10383
Measurand transient signal suppressor [NASA-CASE-MSC-22027-1] 08 p3435 N94-29466
An adaptive Kalman filter excisor for suppressing narrowband interference [AD-A276286] 09 p3671 N94-31253
High speed jet noise research at NASA Lewis 10 p3972 N94-33464
Turn-on transient overcurrent response suppressor [AD-D016151] 10 p4039 N94-33759

SURFACE ACOUSTIC WAVE DEVICES
Integrated optics technology transfer [DSIS-93-00179] 02 p0792 N94-13868
Portable acoustic wave sensor systems for real-time monitoring of volatile organic compounds [DE93-013753] 02 p0582 N94-14511
Improvements on the design of optimum SAW filters with the Remez Exchange Algorithm 05 p1773 N94-22123
SAW based systems for mobile communications satellites 06 p2275 N94-22746
Chemically sensitive interfaces on SAW devices [DE94-001832] 06 p2526 N94-23718
Ultralinear wideband integrated circuit design [ISBN-0-315-84130-3] 07 p2784 N94-26675
Real-time SAW measurements of NVR in cleanroom and in microenvironment [DE94-011937] 12 p4389 N94-37159
New materials and multidimensional cluster analysis for SAW chemical sensor arrays [DE94-012066] 12 p4409 N94-37161
SAW chemical sensor arrays using new thin-film materials [DE94-011940] 12 p4411 N94-37365

SURFACE COOLING
A structural origin for the cantaloupe terrain of Triton 01 p0449 N94-12095
Lava flows on Venus: Analysis of motion and cooling 01 p0457 N94-12137
Boiling heat-transfer processes and their application in the cooling of high heat flux devices [AD-A266086] 01 p0413 N94-12535
Excimer laser surface processing of titanium [DE93-012633] 02 p0570 N94-13512
Modelling of the temperature distribution in a copper roll for the design of a system of cooled rolls adapted to vertical strip casting [IMI-93RT-21200-1436-G] 02 p0557 N94-13866
The thermal consequences of giant impacts in the early solar system 08 p3543 N94-29698

SURFACE CRACKS
Elastic plastic fracture mechanics methodology for surface cracks [NASA-CR-194129] 01 p0185 N94-10712
Matrix fatigue cracking mechanisms of alpha(2) TMC for hypersonic applications [NASA-TM-106506] 06 p2230 N94-25186
Fundamental study on monitoring technology on local surface damages 07 p2724 N94-25555
Study on high temperature damage control and life improvement 07 p2729 N94-25580
Optical surface contouring for non-destructive inspection of turbomachinery [NASA-CR-195245] 07 p2835 N94-26691
Temperature-humidity-bias aging technique to identify defective surface mount capacitors [DE94-005354] 09 p3660 N94-32727
Fundamental studies in crack initiation [AD-A278387] 09 p3741 N94-33356
Composite repairs of cracked metallic airframe structures [AD-A277680] 10 p3969 N94-33590
Exploratory study on H13 steel dies [DE94-012118] 12 p4420 N94-37678

SURFACE DEFECTS
Invariance of the mobility edge in anodic titanium oxides [DE92-642136] 01 p0394 N94-10281
Potential change in flaw geometry during pressurized-thermal-shock transients [DE93-009709] 01 p0184 N94-10288
Absorption and damage thresholds of low defect density hafnia deposited with activated oxygen [DE93-013853] 02 p0655 N94-13243
Optical properties and surface morphology studies of palladium contacts on mercuric iodide single crystals [DE93-012510] 03 p1207 N94-15973
Defects in GaAs bulk crystals and multi-layers caused by In diffusion [DE93-016968] 04 p1595 N94-18054
Surface modification of sapphire for IR window application [DE93-019168] 04 p1602 N94-19075
Surface and subsurface defect detection in Si3N4 components by laser scattering [DE93-040829] 05 p1832 N94-21772
Surface modification of sapphire for enhanced infrared window performance [DE94-000333] 06 p2543 N94-23458
Design of novel catalysts for the partial oxidation of methane to methanol [PB94-114212] 06 p2235 N94-24920
Simulation studies for surfaces and materials strength [NASA-CR-195185] 06 p2565 N94-25093
Effect of nitrocarburizing on shape of titanium alloy parts [DE94-004040] 07 p2 2 N94-25822
Optical surface contouring for non-des ctive inspection of turbomachinery [NASA-CR-195245] 07 p2835 N94-26691
Influence of surface defects and local structure on oxygenate reaction pathways over metal oxide surfaces [DE94-005680] 08 p3522 N94-30901
Reliability analysis of structural ceramics subjected to biaxial flexure 09 p3650 N94-31454
Intra-cascade surface recombination of point defects during ion bombardment of Ge(001) [DE94-007740] 09 p3903 N94-32384
Reactor pressure vessel structural integrity research in the US Nuclear Regulatory Commission HSST and HSSI Programs [DE94-006550] 09 p3739 N94-32771

SURFACE DIFFUSION
Surface reactivity of combustion generated soot particles [AD-A268017] 03 p0952 N94-17532
Tunneling microscopy of semiconductors [AD-A270232] 04 p1600 N94-18904
Diffusion on Cu surfaces 06 p2251 N94-24428
Influence of lattice damage on retention and transport of deuterium in beta silicon carbide [DE94-005206] 07 p3068 N94-27693
Synthesis, characterization, phase diagrams and superconducting, and normal state magnetic properties of La(2-x)Sr(x)CuO4 (0 is less than or equal to x which is less than or equal to 0.08) and electrochemically oxidized La(2-x)Sr(x)CuO(4 + delta) (0 is less than or equal to x which is less than or equal to 0.33, 0 is less than or equal to delta which is less than or equal to 0.12) [DE94-005260] 09 p3895 N94-31067
A new mechanism for surface diffusion: Motion of a substrate-adsorbate complex [AD-A276072] 09 p3632 N94-31459
Large scale atomistic first principles study of adsorption and surface diffusion [DE94-009450] 11 p4322 N94-35682

SURFACE DISTORTION
An analytic model for calculating pump-induced wavefront distortions in laser slabs [DE93-011953] 01 p0174 N94-11126
PO/PTD diffraction synthesis of array-fed reflector antennas for satellite and radar applications 01 p0137 N94-11636
A benchmark bending test of a thick specimen, Part 1: Experiments [ARL-RR-6-PT-1] 02 p0670 N94-12927
A benchmark bending test of a thick specimen. Part 2: Surface displacement measurements [ARL-RR-6-PT-2] 02 p0670 N94-12928
Measuring machines for digitalizing and measuring complex surfaces, models and matrices [CRIF-MC-97] 04 p1444 N94-17963
A benchmark bending test of a thick specimen. Part 1: Experiments [AD-A268730] 04 p1360 N94-18325
Principles and applications of oil film interferometry for measuring wall friction fields in air flows [ETN-93-95062] 05 p1798 N94-20147
Feasibility study of a synthesis procedure for array feeds to improve radiation performance of large distorted reflector antennas [NASA-CR-195167] 06 p2301 N94-25005
TransFit: Finite element analysis data fitting software [NASA-CR-193988] 11 p4307 N94-36118

SURFACE EMITTING LASERS
Preliminary surface-emitting laser logic device evaluation [AD-A266111] 01 p0383 N94-12416
Horizontal-cavity surface-emitting lasers, superluminescent LEDs, and amplifiers, and parabolic gain unstable resonator semiconductor lasers 02 p0656 N94-13573
JSEP fellowship [AD-A266568] 03 p1211 N94-16800
Curved grating fabrication techniques for concentric-circle grating, surface-emitting semiconductor lasers 03 p1045 N94-17349
Spectrally and temporally resolved laser emission from vertical cavity surface emitting lasers [DE93-019410] 04 p1442 N94-19563
Spatial patterns in semiconductor lasers [DE93-040056] 05 p1814 N94-19865
InGaAsP/InP based 1.3/1.55 micron vertical cavity surface emitting lasers for wavelength division multiplexed high speed distributed computing, phase 1 [AD-A271081] 06 p2348 N94-23123
The effects of optical feedback on polarization of vertical cavity surface emitting lasers [AD-A273728] 06 p2351 N94-25445
Characterization of nonlinear effects in optically pumped vertical cavity surface emitting lasers [AD-A273840] 07 p2815 N94-25744
Ultra-high aggregate bandwidth two-dimensional multiple-wavelength diode laser arrays [AD-A274018] 07 p2815 N94-25756
Bulletin of Precision and Intelligence Laboratory, No. 68 [JTN-94-80609] 07 p3010 N94-27282
Visible vertical cavity surface emitting lasers [AD-A275334] 08 p3293 N94-28919
Passivation of III-V compound semiconductor based devices [AD-A276178] 09 p3894 N94-31056
Large-diameter InGaAs/AlGaAs vertical-cavity surface-emitting lasers with low threshold current density fabricated using a simple chemical etch process [AD-A277733] 09 p3721 N94-33003
Phase-locked arrays of vertical-cavity surface-emitting lasers [DE94-009279] 11 p4272 N94-36178

SURFACE ENERGY
Measuring surface fluxes in CAPE [NASA-CR-193664] 02 p0711 N94-12788
Simulation studies for surfaces and materials strength [NASA-CR-193387] 03 p1056 N94-15004

Two-dimensional, high flow, precisely controlled monodisperse drop source
[AD-A267660] 03 p1028 N94-17250
Regulation of attached bacterial growth by adsorbed proteins
[AD-A267756] 03 p1118 N94-17275
A surface energy budget model modifying heat flow by foliage effects
[AD-A268598] 03 p1085 N94-17610
Surface energy balance modeling at mesoscale: The contribution of the future Earth observing system
[BCRS-91-04] 03 p1085 N94-17616
Measurement of evapotranspiration with combined reflective and thermal infrared radiance observations
[NASA-CR-194802] 05 p1837 N94-20951
Role of surface characteristics in urban meteorology and air quality
[DE93-040929] 05 p1851 N94-21740
Multilayer relaxation and surface structure of ordered alloys
[NASA-TM-106433] 06 p2243 N94-23578
An investigation of current and future satellite and in-situ data for the remote sensing of the land surface energy balance
[NASA-CR-195138] 06 p2387 N94-24596
Simulation studies for surfaces and materials strength
[NASA-CR-195185] 06 p2565 N94-25093
Structure and energetics of high index Fe, Al, Cu and Ni surfaces using equivalent crystal theory
[NASA-TM-106408] 06 p2249 N94-25171
Se EXAFS study of the elevated wurtzite to rock salt structural phase transition in CdSe nanocrystals
[DE94-003247] 07 p3054 N94-26125
Differentiating the role of land surface variability and cloudiness variability on global energy transport within the atmosphere and oceans
[NASA-CR-195229] 07 p2847 N94-26222
Surface roughness lengths
[AD-A274550] 07 p2895 N94-26846
Surface energy changes produced by ultraviolet-ozone irradiation of poly(methylmethacrylate), polycarbone and polytetrafluoroethylene
[NASA-TM-106460] 08 p3213 N94-28922
Empirical and semi-empirical relationships of liquid-vapor, solid-vapor, and solid-liquid surface energies
[AD-A276480] 09 p3631 N94-31248
Modelling of surfaces. Part 1: Monatomic metallic surfaces using equivalent crystal theory
[NASA-TM-106680] 12 p4419 N94-37459

SURFACE FINISHING

Protective coatings for high-temperature polymer matrix composites
[NASA-TM-106276] 01 p0074 N94-12431
Impedance-power effects on plasma polymer surface finish using a helical resonator discharge
[DE93-016454] 02 p0803 N94-14590
Electrochemical planarization for microelectronic circuits
[DE93-017214] 02 p0627 N94-14870
Assessment of chromate and non-chromate conversion coatings for Al alloys using electrochemical impedance spectroscopy
[AD-A267205] 03 p0965 N94-15859
The effect of process parameters on the surface finish of plasma polymers
[DE93-014112] 03 p0966 N94-15924
The role of carbon and temperature in determining electrical conductivity of basins, crust and mantle
[DE93-015936] 03 p1101 N94-16840
Application of hard coatings to substrates at low temperatures
[NASA-CR-193867] 03 p0971 N94-17122
Titanium carbon-hydrogen layers on decorative surfaces 04 p1375 N94-18010
Effect of temperature and O-ring gland finish on sealing ability of Viton V747-75
[NASA-TP-3391] 04 p1368 N94-18075
Soft X Ray Projection Lithography. Organization of the 1993 photonics science optical meetings
[AD-A269159] 04 p1579 N94-18693
Synchrotron/crystal sample preparation
[NASA-CR-193837] 04 p1603 N94-19513
Precision machining and polishing of scintillating crystals for large calorimeters and hodoscopes
[DE93-018663] 04 p1381 N94-19544
Oxidation resistant protective coating system for gas turbine components and process for penetration thereof
[CA-PATENT-1,294,155] 05 p1704 N94-21143
Laser driven hydrodynamic instability experiments
[DE93-040550] 05 p1818 N94-21547
Experiments with a fluid deicing system for cleaning laminar wings 05 p1640 N94-22601
Weld cladding of hard surfaces
[PB93-201598] 06 p2353 N94-23448
JBK-75 stainless steel machinability study
[DE94-002268] 06 p2242 N94-23475
Corrosion resistance at welded zones of nuclear fuel reprocessing system 07 p2722 N94-25546
R and D for creation, measurement, application of ultra-high vacuum 07 p2723 N94-25549
Modelling the inhibition cure behaviour of unsaturated polyester moulding materials
[PB94-124864] 07 p2748 N94-25893
Calculations of material removal, removal rate, and Preston coefficient in continuous lapping/polishing machines
[DE94-002619] 07 p2763 N94-26804
Laser surface modification of intermetallic compounds
[DREA-CR-92-416] 07 p2820 N94-27668
Effect of surface finish on turbine airfoil cascade losses 07 p2652 N94-28320
Analysis of cost: CVD diamond deposition and finishing --- Quarterly report
[AD-A275586] 08 p3212 N94-28725
Float polishing studies of fused silica
[AD-A275001] 08 p3213 N94-28886
Practical applications of plasma surface modification
[DE94-004892] 08 p3349 N94-29932
Logistics for the implementation of lead-free solders on electronic assemblies
[DE94-004800] 08 p3206 N94-29936
Evaluation of corrosion protecting properties of modern aircraft paint systems
[AD-B179388] 08 p3220 N94-30420
Analysis of leading edge and trailing edge cover glass samples before and after treatment with advanced satellite contamination removal techniques 09 p3596 N94-31041
Neutral ion sources in precision manufacturing 09 p3875 N94-32447
Polyurethane self-priming topcoats
[AD-D016131] 10 p4027 N94-33697
Strategic choices in surface treatments
[PB94-170669] 12 p4414 N94-36534
Robotic weld overlay coatings for erosion control
[DE94-013477] 12 p4417 N94-37116

SURFACE GEOMETRY

Multigrid solution of internal flows using unstructured solution adaptive meshes
[NASA-CR-194233] 02 p0638 N94-14356
Morphology of polymerized membranes on an amorphous substrate at molecular resolution by AFM
[AD-A268760] 04 p1370 N94-18403
Automatic procedures for computing complete configuration geometry from individual component descriptions
[NASA-TM-4607] 12 p4382 N94-36942

SURFACE INTERACTIONS

U SURFACE REACTIONS

SURFACE IONIZATION

Solar wind-induced secondary ions and their relation to lunar surface composition 01 p0474 N94-12232
Characterization of Ni on Si wafers: Comparison of surface analysis techniques
[DE93-016501] 03 p0953 N94-17649
SALI chemical analysis of provided samples
[NASA-CR-194138] 06 p2232 N94-23524

SURFACE LAYERS

Marangoni flows in open cavities with differentially heated end walls 01 p0104 N94-10097
The surface plasmon spectroscopy as diagnostic technique in microgravity experiments 01 p0110 N94-10133
Remote sensing x ray fluorescence spectrometry for future lunar exploration missions 01 p0462 N94-12165
Incomplete melting of the Au(100) surface
[DE93-623192] 02 p0569 N94-13227
About the influence of inert gas ion implantation on metal corrosion stability
[DE93-620574] 02 p0569 N94-13360
In situ Raman spectroscopy of lithium electrode surface in ambient temperature lithium secondary battery
[DE93-015238] 03 p1010 N94-16061
Spectral evidence of size dependent space weathering processes on asteroid surfaces 03 p1241 N94-16174
Kinetics of silica-phase transitions
[DE93-016231] 03 p1217 N94-17659
Mechanical properties of excimer laser modified titanium surfaces
[DE93-012663] 04 p1358 N94-17875
Time-resolved probing of electron thermal conduction in femtosecond-laser-pulse-produced plasmas
[DE93-016996] 04 p1585 N94-18129
Polarimetric thermal emission from periodic water surfaces 05 p1728 N94-20445
A theoretical investigation of unsteady separation phenomena related to dynamic stall
[AD-A271865] 05 p1636 N94-20465
Spectroscopic ellipsometric characterization of Si/Si(1-x)Ge(x) strained-layer superlattices 05 p1734 N94-20510
Laser Raman and x ray scattering studies of corrosion films on metals
[DE93-040243] 05 p1692 N94-21558
Free energy profiles for Li(+) and I(-) ions approaching Pt(100) surface: A molecular dynamics study
[AD-A273455] 06 p2536 N94-24675
Surface compositional variations of Mo-47Re alloy as a function of temperature
[NASA-TP-3402] 06 p2245 N94-25117
Metallic multilayers: Experimental investigation of magnetic anisotropy and magnetic interlayer coupling
[ETN-94-95364] 06 p2250 N94-25242
Tunnelling in metallic contacts on high-T(c) superconductors: A story of charge carriers in YBa2Cu3O(7-delta) and Bi2CaSr2Cu2O(8+delta)
[ISBN-9-03-860142-5] 06 p2565 N94-25280
Effect of nitrocarburizing on shape of titanium alloy parts
[DE94-004040] 07 p2732 N94-25822
Neutron reflection interferometry
[DE94-601876] 07 p2714 N94-26170
Studies of thin-film growth, adsorption, and oxidation by in situ, real-time, and ex situ ion beam analysis
[DE94-002907] 07 p3055 N94-26275
Radar detection of low-altitude targets in a maritime environment. Volume 2: Meteorological and radar data
[AD-A274658] 07 p2768 N94-26335
Microstructures of Si surface layers implanted with Cu
[DE94-004690] 07 p3058 N94-26565
Failure behaviour of high density polyethylene with an embrittled surface layer due to weathering
[PB94-126406] 07 p2840 N94-26960
The Martian atmospheric planetary boundary layer stability, fluxes, spectra, and similarity
[NASA-CR-195711] 07 p3108 N94-27935
Large eddy simulation of the upper atmospheric surface layer
[ISBN-0-315-85393-X] 08 p3365 N94-30134
Adsorption of water to the metal/polymer interface studied by neutron and x ray reflectivity
[DE94-005578] 09 p3651 N94-31649
High-resolution synthetic aperture radar observations of the Moon 09 p3676 N94-31952
Dielectric properties of Mars' surface: Proposed measurement on a Mars lander 09 p3951 N94-33237
Surface-layer response over shrub-steppe canopy during springtime
[DE94-011235] 12 p4468 N94-37624

SURFACE NAVIGATION

Real-time tomography mooring
[AD-A264923] 01 p0289 N94-11854
Passive recovery of scene geometry for an unmanned ground vehicle
[AD-A266670] 02 p0766 N94-14777
Perception for outdoor navigation
[AD-A266867] 03 p0863 N94-14919
Survey of collision avoidance and ranging sensors for mobile robots, revision 1
[AD-A269846] 04 p1541 N94-18474
Robotic concepts for operation in barren terrain
[DE93-040539] 05 p1946 N94-21925
Lunar rover navigation concepts 06 p2607 N94-23386
Mars 96 rover: Science, instrumentation, and control 06 p2369 N94-23395
Mars 96 rover: Technical vision and navigation 06 p2370 N94-23417
Marsohkod movement control 06 p2370 N94-23418
Experiments with a small behaviour controlled planetary rover 06 p2371 N94-23427
Mars 1994/1996: The French navigation tasks 06 p2195 N94-23924
Worldwide vessel locating and tracking system, volume 1
[PB93-193217] 06 p2175 N94-24474
Design of a wheeled articulating land rover
[NASA-CR-195520] 06 p2365 N94-24806
Automatic control steps for aircraft taxi guidance 08 p3141 N94-29584
Navigation of military and space unmanned ground vehicles in unstructured terrains 08 p3144 N94-30282
A probabilistic approach to motion planning for car-like robots
[RUU-CS-93-18] 08 p3438 N94-30410

SURFACE PRESSURE

U PRESSURE

SURFACE PROPERTIES

NT ADHESION
NT ADSORPTIVITY
NT COEFFICIENT OF FRICTION

NT INTERFACIAL TENSION
NT SKIN TEMPERATURE (NON-BIOLOGICAL)
NT SPECTRAL REFLECTANCE
NT SURFACE CRACKS
NT SURFACE DEFECTS
NT SURFACE ENERGY
NT SURFACE ROUGHNESS
NT SURFACE STABILITY
NT SURFACE TEMPERATURE
NT WALL TEMPERATURE

Wetting effects on nylon spheres engulfment in ice
01 p0115 N94-10189

Hydrogen partitioning and transport in titanium aluminides
[NASA-CR-194117] 01 p0076 N94-10713

Evolution of steep Martian slopes
01 p0434 N94-11184

Characterization of gas-aerosol interaction kinetics using morphology dependent stimulated Raman scattering
[DE93-012324] 01 p0077 N94-11359

Organometallic chemical vapor deposition and characterization of ZnGeP2/GaP multiple heterostructures on GaP substrates 01 p0400 N94-11442

Property changes induced by the space environment in composite materials on LDEF: Solar array materials passive LDEF experiment A0171 (SAMPLE)
[NASA-CR-192572] 01 p0073 N94-11484

The x ray standing waves on surfaces
[AD-A265265] 01 p0402 N94-11682

Wind and surface features in SAR images: The Canadian program 01 p0234 N94-11718

A comparison of telescopic and Phobos-2 ISM spectra of Mars in the short-wave near-infrared (0.76-1.02 microns) 01 p0424 N94-12053

Thermal-infrared emission spectroscopy of natural surfaces: Application to coated surfaces
01 p0081 N94-12156

Near-infrared spectra of the Martian surface: Reading between the lines 01 p0465 N94-12184

Examination of the surface second harmonic response at infrared wavelengths
[AD-A265206] 01 p0403 N94-12371

Interdisciplinary scientist participation in the Phobos mission
[NASA-CR-193715] 01 p0482 N94-12446

Theoretical treatment of the bulk and surface properties of fluids containing long, flexible molecules
[DE93-015560] 02 p0575 N94-12861

Procedures for analysis of debris relative to Space Shuttle systems
[NASA-TM-109190] 02 p0534 N94-12900

Computer simulations for the adsorption of polymers onto surfaces
[DE93-016667] 02 p0577 N94-13070

Surface analysis of bearings
[AD-A266800] 02 p0661 N94-13122

Computer code for scattering from impedance bodies of revolution. Part 3: Surface impedance with s and phi variation. Analytical and numerical results
[NASA-CR-193396] 02 p0599 N94-13264

High resolution electron energy loss studies of surface vibrations
[DE93-014441] 02 p0781 N94-13283

Barium fluoride research and development at Lawrence Livermore National Laboratory
[DE93-014682] 02 p0807 N94-13405

Surfaces and interfaces of ceramics and metals
[DE93-014959] 02 p0578 N94-13408

Surface science instrumentation for the study of important catalytic and electrochemical interfaces
[DE93-015068] 02 p0563 N94-13413

Excimer laser surface processing of titanium
[DE93-012633] 02 p0570 N94-13512

Applications of surface science to solid lubricants
[SMC-TR-93-24] 02 p0579 N94-13903

Analysis of microstrip patch antennas with nonzero surface resistance
[NASA-TP-3362] 02 p0604 N94-13916

The de Haas-van Alphen studies and Fermi surface properties of organic superconductors (ET)2X
[DE93-015157] 02 p0623 N94-13925

Kinetics of photodeposition of superconducting films
[DE93-015511] 02 p0812 N94-14348

Ploughing on gold using a Scanning Tunneling Microscope
[DE93-012632] 02 p0812 N94-14365

Determination of the surface cleanliness of metals by FT-IR spectroscopy
[DE93-013252] 02 p0565 N94-14525

Ultra-soft x ray absorption spectroscopy: A bulk and surface probe of materials
[DE93-014325] 02 p0566 N94-14582

Surface characterization of LDEF materials
[NASA-CR-194519] 02 p0543 N94-14683

Engineering design of sub-micron topographies for simultaneously adherent and reflective metal-polymer interfaces
[NASA-CR-194573] 03 p0964 N94-15700

Analytical and experimental investigation of the feasibility of accelerated lifetime testing of materials exposed to an atomic oxygen beam
[NASA-CR-193851] 03 p0946 N94-15766

Passive oxide films on well-defined nickel surfaces: An examination of film growth on Ni(100) with ex situ scanning tunneling microscopy
[DE93-014056] 03 p1207 N94-15923

Spectral evidence of size dependent space weathering processes on asteroid surfaces
03 p1241 N94-16174

Discussion of band selection and methodologies for the estimation of precipitable water vapour from AVIRIS data 03 p1074 N94-16707

Electron spectroscopy analysis
[NASA-CR-193591] 03 p0951 N94-17039

A modified two-fluid model of conductivity for superconducting surface resistance calculation
[AD-A267549] 03 p1013 N94-17104

Automated image analysis method for the detection of cracks on wood surface
[VTT-JULK-755] 03 p1056 N94-17542

Guide to Magellan image interpretation
[NASA-CR-194340] 03 p1298 N94-17654

Friction drive position transducer
[AD-D015851] 04 p1424 N94-17717

A radial transmission line material measurement apparatus
[DE93-018508] 04 p1394 N94-17780

Mechanical properties of excimer laser modified titanium surfaces
[DE93-012663] 04 p1358 N94-17875

Surface second harmonic generation studies of stepped Ag(111) electrode surfaces
[AD-A265205] 04 p1594 N94-17876

Accelerated tests on the tarnish resistance of gold alloys 04 p1367 N94-18008

Energy efficiency and the environment: Innovative ways to improve air quality in the Los Angeles Basin
[DE93-016964] 04 p1473 N94-18050

Working group for planetary system nomenclature
[NASA-CR-194406] 04 p1626 N94-18841

Surface modification of sapphire for IR window application
[DE93-019168] 04 p1602 N94-19075

Surface science at the solid liquid interface
[AD-A271422] 05 p1678 N94-19839

Formation of colloidal Ag precipitates in fused silica by MeV ion implantation
[DE93-040268] 05 p2012 N94-19869

Particles on surfaces of laser ablated Y1Ba2Cu3O(7-delta) films
[DE93-040269] 05 p2013 N94-19929

The metallic bond for monolayer transition metal layers on transition metal surfaces
[DE93-019060] 05 p1691 N94-20313

Direct imaging of the surface microstructure of dielectric materials using an atomic force microscope
[AD-A272251] 05 p2018 N94-20575

Distribution of small volcanic cones on the surface of Venus by size and elevation: Implications for differential deposition of volcanic features 05 p2110 N94-20731

Obtaining surface optical properties from space-based lidar systems
[AD-A272831] 05 p1987 N94-21172

An analysis of pool surface deformation due to a plunging liquid jet
[AD-A272970] 05 p1802 N94-21261

A method of measuring the thermoradiative properties of ceramic materials in a space environment
05 p1665 N94-21405

The early Martian environment: Clues from the cratered highlands and the Precambrian Earth
05 p2143 N94-21667

Role of surface characteristics in urban meteorology and air quality
[DE93-040929] 05 p1851 N94-21740

Surface and subsurface defect detection in Si3N4 components by laser scattering
[DE93-040829] 05 p1832 N94-21772

Spin dynamics and implications for superconductivity: Some problems with the d-wave scenario
[DE94-001183] 05 p2032 N94-21972

Dynamics of surface thermal expansion and diffusivity using two-color reflection transient gratings
[DE93-040547] 05 p1990 N94-22002

Areally averaged estimates of surface heat flux from ARM field studies
[DE93-018569] 05 p1859 N94-22036

Quantitative analysis of scanning tunneling microscopy images for surface structure determination: Sulfur on Re(0001)
[DE93-019235] 05 p2034 N94-22041

Surface-induced brightness temperature variations and their effects on detecting thin cirrus clouds using IR emission channels in the 8-12 micrometer region
05 p1880 N94-22341

Atomic probes of surface structure and dynamics
[DE94-001651] 06 p2530 N94-22720

Influence of sintering atmospheres on the aluminum sintering characteristics
[DE93-632412] 06 p2239 N94-22965

SALI chemical analysis of provided samples
[NASA-CR-194138] 06 p2232 N94-23524

Surface and interfacial properties of polymer blends. A literature survey
[PB93-230191] 06 p2254 N94-23561

Chemically sensitive interfaces on SAW devices
[DE94-001832] 06 p2526 N94-23718

Coupled land surface/hydrologic/atmospheric models
06 p2413 N94-24387

Thermal phase behavior of metal surfaces: X-ray scattering studies of Pt(001)
[DE94-002991] 06 p2245 N94-24612

Martian mesoscale circulations induced by variations in surface optical and thermal characteristics: A numerical study 06 p2622 N94-24899

A thermodynamic approach to obtain materials properties for engineering applications
06 p2248 N94-25131

Scanning probe surface modification
[AD-A273178] 06 p2346 N94-25151

Selected bibliography 2: Diamond surface chemistry
[AD-A273518] 06 p2565 N94-25160

Use of scanning tunneling microscope in corrosion studies
[VTT-TIED-1416] 06 p2250 N94-25346

Observation on metal surface in aqueous solution using an electrochemical Scanning Tunneling Microscope (STM) 07 p2724 N94-25554

Study on substance diffusion in thin films with controlled structures 07 p2727 N94-25570

Study on production of materials with one direction solidification texture 07 p2727 N94-25572

Study on interfacial reaction analysis at interfacial joining 07 p2728 N94-25574

Hydrogen uptake into silicon from an ECR plasma
[DE94-003771] 07 p3050 N94-25815

Determination of surface recombination velocity and bulk lifetime in detector grade silicon and germanium crystals
[DE94-003886] 07 p3053 N94-26094

Studies of thin-film growth, adsorption, and oxidation by in situ, real-time, and ex situ ion beam analysis
[DE94-002907] 07 p3055 N94-26275

Eleventh Symposium on Energy Engineering Sciences: Proceedings
[DE93-019930] 07 p2763 N94-26429

Interfacial area and interfacial transfer in two-phase flow
[DE93-041226] 07 p2792 N94-26468

Translational-energy-resolved studies of photogenerated carrier-induced reactions on UHV semiconductor surfaces
[DE94-004169] 07 p3058 N94-26526

Calculating the surface properties for the liquid-vapour interface: Illustrating the thermodynamic stability of the spherical microstructures
[DE94-601992] 07 p3073 N94-26837

Interface properties of wide bandgap semiconductor structures
[AD-A274356] 07 p3063 N94-27058

Laser surface modification of intermetallic compounds
[DREA-CR-92-416] 07 p2820 N94-27668

Geometric structures of thin film: Pt on Pd(110) and NiO on Ni(100)
[DE94-005564] 08 p3211 N94-28530

Density reduction: A mechanism for amorphization at high ion doses
[DE94-004793] 08 p3483 N94-28559

Surface structure and stereochemical properties of self-assembled monolayer materials
[DE94-004960] 08 p3484 N94-28578

Lead detection and mapping with reference to relationships between scale, sensor characteristics, surface conditions and atmospheric properties
[AD-A275321] 08 p3377 N94-28877

Near-ultraviolet laser photoemission: Scanning microscopy, buried interfaces and image-potential states
08 p3294 N94-29531

The performance of gloss meters on curving surfaces
[NPL-DMM(A)-111] 08 p3501 N94-30522

Nuclear magnetic relaxation studies of semiconductor nanocrystals and solids
[DE94-006301] 08 p3520 N94-30842

Influence of surface defects and local structure on oxygenate reaction pathways over metal oxide surfaces
[DE94-005680] 08 p3522 N94-30901
The surface parameters: Remote sensing observations and climatology applications 09 p3779 N94-31001
Modification of semiconductor surface properties with chemically bound molecular films
[AD-A276162] 09 p3895 N94-31081
Molecular dynamics computer simulations of charged metal electrode-aqueous electrolyte interfaces
[AD-A276401] 09 p3863 N94-31237
Electromagnetic scattering through loaded aperture panels with nonzero contact impedance
[ONERA-NT-1993-2] 09 p3673 N94-31418
A new mechanism for surface diffusion: Motion of a substrate-adsorbate complex
[AD-A276072] 09 p3632 N94-31459
The relationship of the electronic structures of semiconductor surfaces and heterostructures to crystal growth
[AD-A276465] 09 p3896 N94-31473
Satellite radar altimetry over the continental ice sheets 09 p3742 N94-31570
Prediction of hydrogen entry and permeation in metals and alloys
[AD-A276637] 09 p3642 N94-31995
Metal clusters: Dynamics and structure
[AD-A276842] 09 p3643 N94-32091
Visual neural development and chromatic aberration
[AD-A277402] 09 p3800 N94-32345
SUNY beamline facilities at the National Synchrotron Light Source
[DE94-006343] 09 p3905 N94-32770
Parameterizing atmosphere-land surface exchange for climate models with satellite data: A case study for the Southern Great Plains CART site
[DE94-005109] 09 p3775 N94-32874
Imaging of surface structure with energy-dependent photoelectron diffraction
[DE94-009096] 09 p3907 N94-32934
Surface conforming flexible eddy current probe for scanning varying surface contours
[AD-D016173] 09 p3627 N94-33018
Distribution and nature of UV absorbers on Triton's surface
[NASA-CR-195886] 09 p3943 N94-33104
The importance of environmental conditions in reflectance spectroscopy of laboratory analogs for Mars surface materials 09 p3944 N94-33195
Martian spectral units derived from ISM imaging spectrometer data 09 p3949 N94-33220
Atomic force microscopy
[AD-A277589] 10 p4026 N94-33429
Symposium on Inorganic and Organometallic Polymers
[AD-A277860] 10 p4027 N94-33772
Block distributions on the lunar surface: A comparison between measurements obtained from surface and orbital photography 11 p4359 N94-35419
Exopaleontology and the search for a fossil record on Mars 11 p4360 N94-35425
Innovative instrumentation for mineralogical and elemental analyses of solid extraterrestrial surfaces: The Backscatter Moessbauer Spectrometer/X Ray Fluorescence analyzer (BaMS/XRF) 11 p4239 N94-35459
First results from the Los Alamos plasma source ion implantation experiment
[DE94-003931] 12 p4414 N94-36461
EM-ANIMATE: A computer program for displaying and animating electromagnetic near-field and surface-current solutions: Video supplement to NASA Technical Memorandum 4539
[NASA-TM-4539-VIDEO-SUPPL] 12 p4492 N94-36518
Production of amorphous metal layers using ion implantation and investigation of the related modification of some surface properties
[DE94-617509] 12 p4414 N94-36541
Nonlinear optical spectroscopy for surface studies
[DE94-011623] 12 p4408 N94-37056
Atomic and electronic structure of metals and alloys: Rare earths, ultrathin films and surface alloys
[DE94-011581] 12 p4516 N94-37113
Laser probing of interfaces
[DE94-011300] 12 p4449 N94-37628

SURFACE REACTIONS

CRESLAF. Version 4.0: A Fortran program for modeling laminar, chemically reacting, boundary-layer flow in cylindrical or planar channels
[DE93-012835] 01 p0152 N94-11371
Wide Band-Gap Semiconductors. 1991 Materials Research Society Symposium proceedings
[AD-A263418] 01 p0401 N94-11515
Real-space formation and dissipation dynamics of hexagonal reconstruction on Au(100) in aqueous media as explored by potentiodynamic scanning tunneling microscopy
[AD-A266138] 01 p0368 N94-11658
The adsorption and surface reaction of SiCl4 on Si(100)-(2x1)
[AD-A266124] 01 p0079 N94-12538
Applications of surface science to solid lubricants
[SMC-TR-93-24] 02 p0579 N94-13903
Machining and grinding: High rate deformation in practice
[DE93-010718] 02 p0664 N94-14457
Quantum state resolved desorption of CO from solid surfaces
[DE93-016876] 02 p0814 N94-14597
The thermal dissociation of NH2CHO(ND2CHO) on Si(100)-2x1
[AD-A266903] 03 p0942 N94-14956
The role of interfacial chemistry in surface nucleation and growth of calcium oxalate
[DE93-015689] 03 p1209 N94-16159
An investigation of the hydrolytic resistance of sodium-calcium plate glass with a layer of silica deposited on its surface
[IFTR-34/1991] 03 p0971 N94-17120
Laser probing of the kinetics and dynamics of 3-5 semiconductor growth
[AD-A268388] 03 p1215 N94-17422
Surface reactivity of combustion generated soot particles
[AD-A268017] 03 p0952 N94-17532
Interdisciplinary research on wear of materials
[AD-A268190] 04 p1443 N94-17730
Kinetic growth of random-like and ballistic-like deposition models
[DE93-624946] 04 p1595 N94-17956
Accelerated tests on the tarnish resistance of gold alloys 04 p1367 N94-18008
Report of the 1991 Workshop on Particle-Material Interactions for Fusion Research
[DE93-788393] 04 p1573 N94-18156
The land component of the global climate system with adequate spatial resolution
[DE93-018951] 04 p1474 N94-18183
Experimental and theoretical investigation of surface chemistry induced by direct and indirect electronic excitation
[AD-A268846] 04 p1348 N94-18221
Hydrolysis reaction and positronium decay in silica gels
[AD-A270028] 04 p1371 N94-18713
Scaling laws for diamond chemical vapor deposition. Diamond surface chemistry
[AD-A269874] 04 p1599 N94-18745
Ionic and molecular environments in heterogeneous electrocatalysis: Studies by radioactive labeling and LEED/AUGER spectroscopy
[AD-A268850] 04 p1567 N94-18766
Surface species in tribology
[AD-A270970] 04 p1446 N94-19754
Materials processing and manufacturing technologies for Diamond Substrate MultiChip Modules (DSMCM)
[AD-A271011] 05 p2011 N94-19821
Segregation of Si to the surface of Fe-29Ni-17Co alloy
[DE93-040053] 05 p1687 N94-19864
Oxidation-reduction induced roughening of platinum (111) surface
[DE93-017408] 05 p1687 N94-19922
The modification of polymer surfaces and the fabrication of submicron-scale functionalized structures by deep-UV and electron beam lithography
[AD-A265956] 05 p1700 N94-20328
In-situ electrochemical surface science
[AD-A265942] 05 p1680 N94-20330
Surface science and modeling studies of endothermic fuels catalysis
[AD-A272850] 05 p1712 N94-21192
Model for liquid boron oxide droplet gasification in H/O/C/F combustion environments
[AD-A272911] 05 p1682 N94-21243
Fast oxygen atom studies related to low Earth orbit activities 05 p1663 N94-21395
Vapor-delivered lubrication of steel-steel and steel-ceramic systems
[PB93-202364] 05 p1825 N94-21451
Sulfur-bonded thiophenes in organometallic rhenium complexes and adsorption of isocyanides on gold
[DE93-041126] 05 p1694 N94-21937
SALI chemical analysis of provided samples
[NASA-CR-194138] 06 p2232 N94-23524
Chemically sensitive interfaces on SAW devices
[DE94-001832] 06 p2526 N94-23718
Fundamental and experimental studies on the catalytic combustion of methane
[PB94-112661] 06 p2233 N94-23736
Selection of polymer binders and fabrication of SiC fiber-reinforced reaction-bonded silicon nitride matrix composites
[NASA-CR-194874] 06 p2255 N94-24223
Synthesis and characterization of two-dimensional molecular recognition interfaces
[AD-A273177] 06 p2536 N94-24729
Chemically sensitive interfacial force microscopy: Contact potential measurements of self-assembling monolayer films
[AD-A273135] 06 p2234 N94-24772
Adsorption, desorption, and decomposition of HCl and HBr on Ge(100): Competitive pairingand near-first-order desorption kinetics
[AD-A273504] 06 p2235 N94-24790
Surface chemistry of liquid metals 06 p2249 N94-25133
Selected bibliography 2: Diamond surface chemistry
[AD-A273518] 06 p2565 N94-25160
Observation on metal surface in aqueous solution using an electrochemical Scanning Tunneling Microscope (STM) 07 p2724 N94-25554
Study on interfacial reaction analysis at interfacial joining 07 p2728 N94-25574
Atomic-scale chemistry of metal surfaces
[REPT-A-2657] 07 p3012 N94-25636
The reactivity of lithium toward non-aqueous solvents of relevance to energy storage applications as studied by surface analytical techniques
[DE94-003483] 07 p2856 N94-26464
A mimic model of Pt-Rh catalyst prepared by electrochemical deposition of Rh on Pt (100) surface
[REPT-A-2664] 07 p2715 N94-26476
Mechanistic studies of opto-electronic materials and syntheses using multiple laser and surface diagnostics
[AD-A274528] 07 p3036 N94-26834
Atomic layer epitaxy of group 4 materials: Surface processes, thin films, devices and their characterization
[AD-A274325] 07 p3061 N94-26885
International bulletin on atomic and molecular data for fusion. No. 42-45, Mar. 1991 - Dec. 1992
[DE94-601817] 07 p3045 N94-26946
International bulletin on atomic and molecular data for fusion. No. 46
[DE94-601818] 07 p3023 N94-26947
Development of novel switchable protein surfaces
[AD-A275510] 08 p3384 N94-28667
The effects of molecular orientation geometry and surface anisotropy upon etching
[AD-A275154] 08 p3486 N94-29032
Electrochemical behavior and surface chemistry of nonequilibrium aluminum alloys: Passivity mechanism and fabrication methods
[AD-A275401] 08 p3204 N94-29196
Theoretical investigation of gas-surface interactions
[NASA-CR-195755] 08 p3272 N94-29378
Effect of non-metallic inclusions on the machinability of steel
[PB93-230233] 08 p3204 N94-29387
Computer simulation of the interaction of fast hydrogen atoms with a molybdenum containing sorbed hydrogen
[DE94-608419] 08 p3209 N94-30253
Direct measurement of the reactivity of NH and OH on a silicon nitride surface
[DE94-005286] 08 p3199 N94-30260
An investigation of the corrosion properties of aluminum-tantalum alloys using electrochemical impedance spectroscopy and local electrochemical impedance spectroscopy 08 p3209 N94-30521
Modelling erosion damage from low-energy plasma gun simulations of disruptions
[DE94-005196] 08 p3509 N94-30697
Crosslinking and surface reactions in macromolecules: Spectroscopic FT-IR studies 08 p3221 N94-30812
Surface chemistry of boron-doped SiO2 CVD: Enhanced uptake of tetraethyl orthosilicate by hydroxyl groups bonded to boron
[DE94-005428] 08 p3221 N94-30896
Ground-based simulation of LEO environment: Investigations of a select LDEF material: FEP Teflon (trademark) 09 p3596 N94-31039
An overview of the Evaluation of Oxygen Interaction with Materials-third phase (EOIM-3) experiment: Space Shuttle Mission 46 09 p3596 N94-31040
Effects of orbital exposure on RTV during the LDEF mission 09 p3597 N94-31043
Solidification structure synthesis in undercooled liquids
[AD-A276166] 09 p3910 N94-31054
Mechanisms of laser induced reactions in opaque heterogeneous environments
[AD-A276642] 09 p3717 N94-31996
A new-type of long-range restructuring of ordered metal surfaces induced by lateral adsorbate interactions: Iodide on AU(110) electrodes
[AD-A276633] 09 p3643 N94-32060

Surface chemistry and durability of borosilicate glass
|DE94-006734| 09 p3656 N94-32116
Soft x ray photoelectron spectroscopy study of the interaction of Cr with MoS2(0001)
|AD-A276916| 09 p3635 N94-32233
Chemical structure and kinetics at liquid/solid interfaces
|AD-A277112| 09 p3636 N94-32304
Chemisorbed-molecule potential-energy surfaces and electronically-stimulated processes
|DE94-007932| 09 p3719 N94-32603
Surface probes of porous toluene/water ices: Adsorption kinetics and annealing spectra measured by second harmonic generation
|DE94-007564| 09 p3637 N94-32743
Time-resolved analytical methods for liquid/solid interfaces
|DE94-008352| 09 p3637 N94-32826
Induced adsorption of chloride and bromide by submonolayer amounts of copper underpotentially deposited on Pt(111)
|AD-A278023| 09 p3648 N94-33182
Slow collisions of multicharged ions with metal surfaces
|DE94-009449| 10 p4136 N94-33684
Adhesion of phospholipid monolayers to planar supports deposited with the Langmuir-Blodgett technique
|PB94-148699| 10 p4029 N94-34102
Morphological aspects of surface reactions
|DE94-010184| 11 p4236 N94-35685
Chemical reactions of chlorine on a vicinal Si(100) surface studied by ESDIAD
|AD-A279059| 11 p4236 N94-35731
Heterogeneous reaction mechanisms and kinetics relevant to the CVD of semiconductor materials
|DE94-011001| 11 p4340 N94-36032
Gas-Phase and Surface Chemistry in Electronic Materials Processing. Materials Research Society Symposium proceedings, volume 334
|AD-A280586| 12 p4408 N94-36735
A photoemission study of Au, Ge, and O2 deposition on NH4F etched Si(111)
|DE94-013352| 12 p4519 N94-37553
Morphological aspects of surface reactions
|DE94-011208| 12 p4413 N94-37713
Diosmacycloalkanes as models for the formation of hydrocarbons from surface methylenes
|DE94-011211| 12 p4413 N94-37754

SURFACE ROUGHNESS

Ultrasonic inspection, material noise and surface roughness
|DE93-011560| 01 p0183 N94-11110
Needs for super-smooth surfaces
|DE93-012482| 01 p0382 N94-11242
Plating under reduced pressure
|DE93-011896| 01 p0084 N94-11668
The physics of pattern formation of liquid interfaces
|DE93-013333| 01 p0154 N94-11814
Interpretation of lunar and planetary electromagnetic scattering using the full wave solutions
01 p0440 N94-12049
Coherent structure in near wall turbulence with riblets
01 p0165 N94-12628
Instability around an isolated roughness element
01 p0165 N94-12629
Transition prediction and control in subsonic flow over a hump
|NASA-CR-4543| 02 p0629 N94-13066
Processing and mechanical properties of silicon carbide platelet reinforced alumina composites
02 p0556 N94-13557
Experimental measurement of local heat transfer coefficients over discrete roughened plates using infrared thermography 02 p0635 N94-13652
Impedance-power effects on plasma polymer surface finish using a helical resonator discharge
|DE93-016454| 02 p0803 N94-14590
Investigation of Zerodur material processing
|NASA-CR-193842| 02 p0793 N94-14903
On the receptivity problem for 0(1) wavelength Goertler vortices
|NASA-CR-191519| 03 p1016 N94-15005
Johnson-Gierhart program predictions of excess propagation loss for super-high frequency air-to-ground paths. Volume 1: Theory and numerical results
|AD-A267105| 03 p0988 N94-15649
Method and apparatus for non-destructive evaluation of composite materials with cloth surface impressions
|NASA-CASE-LAR-14535-1| 03 p0933 N94-15878
The effect of process parameters on the surface finish of plasma polymers
|DE93-014112| 03 p0966 N94-15924
Polished substrate surface and cleaning study for coated optic quality
|DE93-014116| 03 p1190 N94-15975
The processing and mechanical properties of high temperature/high performance composites. Book 1: Coonstituent properties of composites
|AD-A266394| 03 p0935 N94-16483
Scattering from binary optics
03 p1195 N94-17341
Guide to Magellan image interpretation
|NASA-CR-194340| 03 p1298 N94-17654
Experimental contribution to the contact between two bodies and the effect of roughness
|ECL-91-41| 04 p1451 N94-17918
Turbulence modeling in aircraft icing
04 p1412 N94-18555
Multigrid methods for flow transition in three-dimensional boundary layers with surface roughness
|NASA-CR-4540| 04 p1417 N94-18843
Synchrotron/crystal sample preparation
|NASA-CR-193837| 04 p1603 N94-19513
Precision machining and polishing of scintillating crystals for large calorimeters and hodoscopes
|DE93-018663| 04 p1381 N94-19544
Comparative evaluation of Kirchhoff, perturbation, and full wave methods for rough surface scattering
|AD-A271198| 04 p1392 N94-19718
Atomic-scale friction measurements using friction force microscopy. Part 2: Application to magnetic media
|AD-A270759| 04 p1447 N94-19767
Substrate recovery of Mo-Si multilayer coated optics
|DE93-019610| 05 p1698 N94-19810
Radar backscatter measurements from simulated sea ice during CRRELEX 1990
|AD-A271034| 05 p1715 N94-19823
Oxidation-reduction induced roughening of platinum (111) surface
|DE93-017408| 05 p1687 N94-19922
Study of electromagnetic wave scattering from characterized rough surfaces
|AD-A270931| 05 p1716 N94-19934
Growth mechanisms and characterization of hydrogenated amorphous-silicon-alloy films
|DE93-018202| 05 p1699 N94-20047
Measuring liquid properties with smooth and textured-surface resonators
|DE93-019433| 05 p1749 N94-20054
Analysis of Ku-band cross section at low incidence angles 05 p1720 N94-20414
Rough surface scattering from moving ocean surfaces as an indicator of scattering mechanisms
05 p1726 N94-20439
Synergism of active and passive microwave data for estimating bare surface soil moisture
05 p1727 N94-20444
Wavelength dependence of limb-darkening of Mars from visible and near-IR telescopic spectral imaging
05 p2101 N94-20685
The roughness of the Martian surface: A scale dependent model 05 p2115 N94-20762
Flow transition with 2-D roughness elements in a 3-D channel 05 p1806 N94-21466
Role of surface characteristics in urban meteorology and air quality
|DE93-040929| 05 p1851 N94-21740
Experiments with a fluid deicing system for cleaning laminar wings 05 p1640 N94-22601
Characteristics of surface roughness associated with leading edge ice accretion
|NASA-TM-106459| 06 p2166 N94-23522
A rail joint: The possible initiator of corrugation?
06 p2269 N94-23583
Surface analysis of corrugated rail treads
06 p2270 N94-23587
Contact analysis of rough rail surfaces
06 p2270 N94-23589
Groundtruth collection for the JPL-SAR and ERS-1 campaign in Flevoland and Veluwe, Netherlands, 1991
|BCRS-92-26| 06 p2386 N94-23755
Interface evaluation in ceramic composites
06 p2255 N94-24231
Vortex generation and wave-vortex interaction over a concave plate with roughness and suction
|AD-A276839| 06 p2337 N94-24869
Examination of the physical, electrical, and microwave evolution of water into young sea ice
|AD-A273559| 06 p2418 N94-24918
The measurement of the film thickness and the roughness deformation of lubricated elastomers
|ETN-94-95293| 06 p2261 N94-25078
Surface-induced static undulations in multilayer films of liquid-crystalline polymers
|AD-A273517| 06 p2262 N94-25159
Analytical skin friction and heat transfer formula for compressible internal flows
|NASA-CR-191185| 06 p2170 N94-25173
The determination of surface roughness from reflected step edges
|AD-A273987| 07 p2984 N94-25900
In situ x ray reflectivity measurements of thin film structural evolution
|DE94-002289| 07 p3051 N94-25944
MBE grown 3 to 5 strain relaxed buffer layers and superlattices characterized by atomic force microscopy
|DE94-002931| 07 p3056 N94-26308
Validated heat-transfer and pressure-drop prediction methods based on the discrete-element method. Phase 2: Two-dimensional rib roughness
|DE94-002379| 07 p2794 N94-26763
Surface roughness lengths
|AD-A274550| 07 p2895 N94-26846
Equivalent performance in different helical resonator plasma polymerization coater platforms
|DE94-001517| 07 p2753 N94-26933
Turbulent boundary layer inner-outer interactions
|AD-A274357| 07 p2794 N94-27059
Mapping of soil humidity using C-band radar images
|ISBN-0-315-85076-0| 07 p2852 N94-27878
Localized and distributed boundary-layer receptivity to convected unsteady wake in free stream
|NASA-CR-4578| 07 p2808 N94-28180
Considerations in the modelling of seafloor acoustic backscatter
|AD-A275404| 08 p3478 N94-29206
Sensitivity and feedbacks associated with vegetation-related land surface parameters in a general circulation model 08 p3348 N94-29800
Radar returns from a low-flying target over a rough sea surface under multipath and clutter conditions
08 p3253 N94-29882
Observation of the phase shift of the wave function of the neutron under total reflection
|DE94-608244| 08 p3489 N94-30096
An experimental study of the aerodynamics of a swept and unswept semispan wing with a simulated glaze ice accretion
|NASA-CR-195330| 08 p3133 N94-30152
Kinetics of surface roughening and smoothing during ion sputtering
|DE94-006358| 08 p3219 N94-30263
Experiments and theoretical considerations regarding the allowable roughness height in laminar flow
|PB94-125556| 08 p3133 N94-30389
Strain relaxation and surface roughness as a function of growth temperature in linearly graded In(x)Al(1-x)As (x = 0.05 to 0.25) buffers
|DE94-005430| 08 p3519 N94-30592
An asymptotic analysis for compressible gas lubrication of rough surfaces 08 p3222 N94-30922
New micro- and macroscopic models of contact and friction
|AD-A277240| 09 p3726 N94-32320
Almaz marine applications 09 p3751 N94-32544
Metal cluster-rare gas van der Waals complexes: Microscopic models of physisorption
|DE94-008134| 09 p3873 N94-32797
Interface engineering in oxide fiber/oxide matrix composites
|AD-A277672| 09 p3627 N94-33029
Ocean surface roughness from infrared measurements: A failure of shape from reflection
|AD-A278008| 10 p4091 N94-33435
Growth and nonlinearity
|DE94-007366| 10 p4021 N94-33689
Stainless steel surface treatment
|AD-D016135| 10 p4024 N94-33758
Bistatic clutter RCS simulation using scale model surfaces with two scale roughness
|AD-A277604| 10 p4035 N94-33847
The microstructure and morphology of carbon black: A study using small angle neutron scattering and contrast variation
|DE94-009315| 10 p4022 N94-34098
Mesoscale roughness of Venus
11 p4361 N94-35430
Rescaled box counting for the topological analysis of spatial data
|DE94-009820| 12 p4461 N94-36464
X-ray diffraction studies of evaporated gold thin films deposited on aluminum nitride substates
|AD-A280454| 12 p4536 N94-37228
Angle interferometer cross axis errors
|DE94-006190| 12 p4446 N94-37388

SURFACE ROUGHNESS EFFECTS

Ultrasonic inspection, material noise and surface roughness
|DE93-011560| 01 p0183 N94-11110
Coherent structure in near wall turbulence with riblets
01 p0165 N94-12628
Instability around an isolated roughness element
01 p0165 N94-12629
Two-dimensional Navier-Stokes heat transfer analysis for rough turbine blades
|NASA-TM-106008| 02 p0629 N94-13027

Transition prediction and control in subsonic flow over a hump
| NASA-CR-4543 | 02 p0629 N94-13066
Preliminary results of polarization signatures for glacial moraines in the Mono Basin, Eastern Sierra Nevada
03 p1078 N94-16746
Detecting surface roughness effects on the atmospheric boundary layer via AIRSAR data: A field experiment in Death Valley, California 03 p1078 N94-16747
Polarimetric thermal emission from rough surfaces
05 p1727 N94-20441
Symmetry in polarimetric remote sensing
05 p1729 N94-20449
A comparison of rough surface parabolic equation models
| AD-A278090 | 09 p3791 N94-33185
An approximate model for vertical polarization and surface roughness using the parabolic equation
| AD-A278091 | 09 p3684 N94-33186

SURFACE STABILITY
Evaporation under microgravity conditions
01 p0102 N94-10086
Fermi surface instability at 0.4 K in a heavy-fermion YbBiPt: SDW?
| DE94-006224 | 09 p3899 N94-31916

SURFACE TEMPERATURE
NT SKIN TEMPERATURE (NON-BIOLOGICAL)
NT WALL TEMPERATURE
Design and production of insulated wind tunnel models of the Hermes shuttle for heat transfer measurements at hypersonic speeds 01 p0004 N94-10431
Experimental study of multiple droplet evaporative cooling
| PB93-198463 | 01 p0149 N94-10851
Central Equatorial Pacific Experiment (CEPEX)
| DE93-011656 | 01 p0190 N94-11674
Effects of satellite spectral resolution and atmospheric water vapor on retrieval of near-ground temperatures
| AD-A264920 | 01 p0245 N94-11851
Rates of fluvio-thermal erosion on Mars
01 p0435 N94-12018
Comments on possible causes of recent global warming
| DE93-010501 | 01 p0272 N94-12592
Measuring surface fluxes in CAPE
| NASA-CR-193664 | 02 p0711 N94-12788
Coupled thermal response of objects and participating media in fires and large combustion systems
| DE93-012848 | 02 p0561 N94-12819
Effects of surface thermal forcing on stratified flow past an isolated obstacle 02 p0633 N94-13553
Experimental investigation of the effects of blowing ratio parameter on heat transfer to a film-cooled flat plate
| AD-A266599 | 02 p0636 N94-13780
Wear-mechanism modelling
| DE93-012311 | 02 p0579 N94-13974
The accuracy of approximating radiative heat transfer using a temperature dependent thermal conductivity
| DE93-013105 | 02 p0638 N94-14318
Testing the waters from space --- Thermal mapping
| NASA-TM-109623 | 03 p1082 N94-15409
Particle kinetic simulation of high altitude hypervelocity flight
| NASA-CR-194599 | 03 p0856 N94-15678
In situ Raman spectroscopy of lithium electrode surface in ambient temperature lithium secondary battery
| DE93-015238 | 03 p1010 N94-16061
Effective elastic thickness of the Venusian lithosphere with lateral viscosity variations in the mantle
03 p1293 N94-16421
Numerically solving a transient heat conduction problem with convection and radiation
| AD-A268521 | 03 p1220 N94-17540
Development of a multi-point two-color pyrometer for tube and wall temperature and emissivity measurement at the CFFF
| DE93-014716 | 04 p1429 N94-18207
The application of liquid crystal techniques to determine heat transfer rates 04 p1432 N94-18654
Soil temperatures
| KNMI-WR-92-05 | 05 p1865 N94-20309
Measurement of evapotranspiration with combined reflective and thermal infrared radiance observations
| NASA-CR-194802 | 05 p1837 N94-20951
High-energy astrophysics: A theoretical analysis of thermal radiation from neutron stars
| NASA-CR-194808 | 05 p2055 N94-20952
A carbon dioxide/methane greenhouse atmosphere on early Mars 05 p2142 N94-21662
A model for the evolution of CO2 on Mars
05 p2144 N94-21671
Early Mars: The inextricable link between internal and external influences on valley network formation
05 p2146 N94-21681
Fluorescent microthermographic imaging
| DE93-040332 | 05 p1810 N94-22000
Dynamics of surface thermal expansion and diffusivity using two-color reflection transient gratings
| DE93-040547 | 05 p1990 N94-22002
Evaporation and combustion of LOX under supercritical and subcritical conditions 06 p2211 N94-23035
Spatial and temporal variability of soil temperature, moisture and surface soil properties
| NASA-CR-194109 | 06 p2401 N94-23337
Lightning, atmospheric electricity, and climate change
| DE94-002003 | 06 p2408 N94-23471
Synthesis of passive microwave and radar altimeter data for estimating accumulation rates of polar snow
| NASA-CR-194864 | 06 p2382 N94-23573
An investigation of current and future satellite and in-situ data for the remote sensing of the land surface energy balance
| NASA-CR-195138 | 06 p2387 N94-24596
Heat transfer and flow structure in end-wall boundary layers
| AD-A273470 | 06 p2335 N94-24689
Investigation of the heat handling capabilities of DIII-D neutral beamline internal components
| DE94-001107 | 06 p2553 N94-24756
Examination of the physical, electrical, and microwave evolution of water into young sea ice
| AD-A273559 | 06 p2418 N94-24918
An extended laser flash technique for thermal diffusivity measurement of high-temperature materials
06 p2238 N94-25132
The IRGen infrared data base modeler
06 p2440 N94-25496
Aerodynamic heating in hypersonic flows
07 p2658 N94-27919
Adsorption and desorption studies of cesium on sapphire surfaces
| DE94-003798 | 07 p3070 N94-28067
Prediction of survival times on land in a cold climate
08 p3379 N94-28423
Objective analysis of a coastal ocean eddy using satellite AVHRR and in situ hydrographic data
| AD-A275715 | 08 p3376 N94-28642
Thermal variation in vegetated or snow-covered background scenes and its effect on passive infrared systems
| AD-A275174 | 08 p3325 N94-28849
The effects of molecular orientation geometry and surface anisotropy upon etching
| AD-A275154 | 08 p3486 N94-29032
On the temperature distribution near a cold surface
| AD-A275162 | 08 p3332 N94-29288
Dual-Band Infrared (DBIR) imaging inspections of Boeing 737 and KC-135 aircraft panels
| DE94-005700 | 08 p3122 N94-29842
Nonlinear absorption in high reflector multilayers
| DE94-005818 | 08 p3295 N94-30598
Dual-band infrared imaging for quantitative corrosion detection in aging aircraft
| DE94-004187 | 08 p3149 N94-30687
RHEED studies of the nucleation, growth, and mobility of Ag atoms on the Si(111)7 x 7 surface
| DE94-005551 | 08 p3521 N94-30899
Heat transfer studies on a rectangular channel with offset plate fins
| AD-A277300 | 09 p3912 N94-32043
Sensitivity analysis of the AVHRR infrared cirrus model
| AD-A276690 | 09 p3784 N94-32117
Synergy of thermal infrared and microwave remote sensing for evaporation estimation
09 p3754 N94-32559
Dual-band infrared imaging to detect corrosion damage within airframes and concrete structures
| DE94-006047 | 09 p3580 N94-32658
Development of lightweight ceramic ablators and arc-jet test results
| NASA-TM-108798 | 09 p3617 N94-33117
Acoustic receptivity of compressible boundary layers: Receptivity by way of surface-temperature variations
| NASA-CR-4599 | 10 p4046 N94-33897
Multiwavelength pyrometer for gray and non-gray surfaces in the presence of interfering radiation
| NASA-CASE-LEW-15250-1 | 11 p4269 N94-35383
The temperature of nitrogen on Pluto
11 p4365 N94-35468
Measurement of a surface heat flux and temperature
11 p4231 N94-36407
Correlation of analytical and experimental hot structure vibration results
| NASA-TM-104269 | 12 p4386 N94-36644
Reference manual for the Thermal Analyst's Help Desk Expert System
| NASA-CR-194941 | 12 p4397 N94-37504

SURFACE TENSION
U INTERFACIAL TENSION

SURFACE TO SURFACE MISSILES
NT CRUISE MISSILES
NT FLEET BALLISTIC MISSILES
NT INTERCONTINENTAL BALLISTIC MISSILES
NT MINUTEMAN ICBM

SURFACE TREATMENT
NT SURFACE FINISHING
Fracture behavior of surface-modified ceramics
| DE93-013707 | 01 p0088 N94-10710
Ellipsometry studies of semiconductors surface cleaning
| AD-A265150 | 01 p0142 N94-11094
Excimer laser surface processing of titanium
| DE93-012633 | 02 p0570 N94-13512
Free-exciton recombination in GaAs
| DE93-009843 | 02 p0809 N94-14079
Studies of changes in the energy stored in metals as a result of subjecting them to a surface type technological process
| IFTR-25/1991 | 03 p0960 N94-17063
Atomic layer epitaxy group IV materials: Surface processes, thin films, devices and their characterization
| AD-A267527 | 03 p1213 N94-17116
Dry stripping as a surface treatment method
| VTT-TIED-1348 | 03 p0985 N94-17544
Influence of the granular surface on the oxygen uptake in YBa2Cu3O(6+delta) ceramics
| DE93-629162 | 03 p0974 N94-17634
The effect of surface treatment and gaseous rust protection paper on the atmospheric corrosion stability of aluminium alloy
| DE93-623326 | 04 p1355 N94-17679
Cutting and drilling studies using high power visible lasers
| DE93-019149 | 04 p1441 N94-19294
Substrate recovery of Mo-Si multilayer coated optics
| DE93-019610 | 05 p1698 N94-19810
The modification of polymer surfaces and the fabrication of submicron-scale functionalized structures by deep-UV and electron beam lithography
| AD-A265956 | 05 p1700 N94-20328
Surface treatment of InP and contribution to the optimization of the InP(p)/InP(p) regrown interfaces grown by GSMBE
| ECL-92-48 | 05 p2018 N94-20598
A comparison of sulfuric acid/boric acid anodize and chromic acid anodize processes
| AD-A271933 | 05 p1703 N94-20614
Surface modification for corrosion resistance
| DE93-017419 | 05 p1693 N94-21825
Diffusion of hydrogen in iron oxides
| DE93-632430 | 06 p2239 N94-22966
Surface modification of sapphire for enhanced infrared window performance
| DE94-000333 | 06 p2543 N94-23458
Repair of cracked aluminum aircraft structure with composite patches 06 p2156 N94-24259
Low-gravity electrodeposition and growth of polymer thin films with large third-order optical nonlinearities by electrochemical processes for devices: Thiophene-based polymers 06 p2225 N94-24346
Ge-Au eutectic bonding of Ge (100) single crystals
| DE94-002281 | 06 p2564 N94-24657
Investigation and application of microwave electron cyclotron resonance plasma physical vapour deposition
| DE93-613909 | 06 p2555 N94-25333
Proceedings of the 12th International Congress: Corrosion Control for Low-Cost Reliability. Volume 1: Coatings
| AD-A273661 | 06 p2251 N94-25448
Effect of nitrocarburizing on shape of titanium alloy parts
| DE94-004040 | 07 p2732 N94-25822
Plasma surface cleaning using microwave plasmas
| DE94-002754 | 07 p2713 N94-26014
Determination of surface recombination velocity and bulk lifetime in detector grade silicon and germanium crystals
| DE94-003886 | 07 p3053 N94-26094
Stability of reference masses 2: The effect of environment and cleaning methods on the surfaces of stainless steel and allied materials
| NPL-DMM(A)-95 | 07 p2738 N94-26653
Low temperature deposition and characterization of N- and p-type silicon carbide thin films and associated ohmic and Schottky contacts
| AD-A274345 | 07 p2754 N94-26974
Evaluating non-chlorinated solvents for welding applications
| DE94-003332 | 07 p2824 N94-27181
Fuel injector design for high temperature aircraft engine 08 p3154 N94-29263
The effect of mechanical paint stripping on the fatigue and fracture of thin aluminum airplane skin
08 p3205 N94-29900
Practical applications of plasma surface modification
| DE94-004892 | 08 p3349 N94-29932

Ablation of polymers by ultraviolet pulsed laser
[DE94-608100] 08 p3218 N94-30066
Plasma treatment of polymer dielectric films to improve capacitive energy storage 08 p3223 N94-30479
Operation of D3-D with all-graphite walls
[DE94-004858] 09 p3886 N94-31304
Large-area conditioning of optics for high-power laser systems
[DE94-007028] 09 p3716 N94-31636
Fatigue testing of 2024-T3 material after four cycles of PMB stripping
[AD-A276926] 09 p3644 N94-32237
Evaluation of the Hughes conversion coating touch-up pen
[AD-A278398] 09 p3664 N94-33166
Stainless steel surface treatment
[AD-D016135] 10 p4024 N94-33758
Thermal cyclic oxidation behavior of the developed compositionally gradient graphite material of SiC and C in air environment
[DE94-727591] 10 p4027 N94-33872
Ion beam surface treatment: A new capability for rapid melt and resolidification of surfaces
[DE94-008955] 10 p4025 N94-34014
Microporous structure with layered interstitial surface treatment, and method and apparatus for preparation thereof
[NASA-CASE-MSC-21487-3] 11 p4235 N94-35229
The electrical conductivities of candidate beam-waveguide antenna shroud materials 11 p4252 N94-35546
Processing and properties of high temperature metal/fiber-reinforced-thermoplastic laminates
[AD-A278791] 11 p4232 N94-35654
Strategic choices in surface treatments
[PB94-170669] 12 p4414 N94-36534
The cyclic fatigue behaviour of adhesive joints
[AD-A280453] 12 p4456 N94-37186

SURFACE VEHICLES
NT AIRCRAFT CARRIERS
NT AUTOMATED GUIDEWAY TRANSIT VEHICLES
NT AUTOMATED TRANSIT VEHICLES
NT AUTOMOBILES
NT CRAWLER TRACTORS
NT ELECTRIC AUTOMOBILES
NT ELECTRIC HYBRID VEHICLES
NT ELECTRIC MOTOR VEHICLES
NT LUNAR MOBILE LABORATORIES
NT LUNAR ROVING VEHICLES
NT LUNAR SURFACE VEHICLES
NT LUNOKHOD LUNAR ROVING VEHICLES
NT MAGNETIC LEVITATION VEHICLES
NT MANNED LUNAR SURFACE VEHICLES
NT MOTOR VEHICLES
NT ROVING VEHICLES
NT SLEDS
NT SURFACE EFFECT SHIPS
NT TANKS (COMBAT VEHICLES)
NT TRACKED VEHICLES
NT TRANSPORTER
NT TRUCKS
NT WALKING MACHINES
Safety of high speed ground transportation systems: X2000 US demonstration vehicle dynamics trials, preliminary test report, October 1992 - January 1993
[PB93-194645] 01 p0422 N94-10736
EUTELTRACS: The European experience on mobile satellite services 06 p2281 N94-22781
Perception and 3D environment modeling for mobile robot autonomous navigation
[LAAS-93117] 06 p2471 N94-22908
Mars 1994/1996: The French navigation tasks 06 p2195 N94-23924
Test Operations Procedure (TOP) 2-2-800 wheeled vehicle center of gravity
[AD-A273937] 07 p2821 N94-25794
Three dimensional simulation of compressible flow induced by a high-speed train moving into a tunnel 08 p3126 N94-28967
A generic semi-autonomous ground vehicle control system 08 p3306 N94-30283
Encoding technique for automated guided vehicle POSE recovery in a structured environment 08 p3144 N94-30286
Navy Omni-Directional Vehicle (ODV) development program 09 p3729 N94-32451

SURFACE WATER
Sandia ocean modeling system programmer's guide and user's manual
[DE93-007427] 01 p0287 N94-10153
Remote surface water monitoring radio based telemetry system
[DE93-009643] 01 p0041 N94-11282
Mars: The initial emplacement of ground ice in response to the thermal evolution of its early crust 01 p0462 N94-12168
The thermodynamic case for a water-rich Mars 01 p0463 N94-12170
Educational module for the Higher Agricultural Education. Part 2: Eutrophication observed by remote sensing: An educational approach to water quality monitoring
[BCRS-92-11B] 02 p0818 N94-14462
Heterogeneity and scaling land-atmospheric water and energy fluxes in climate systems 03 p1083 N94-16030
Oil spreading in surface waters with an ice cover
[PB93-190767] 04 p1476 N94-19064
Mathematical modeling of the free surface hydrodynamic and of transport in suspensions of non cohesive sediments: Aid to the interpretation of spatial images
[ETN-93-95011] 04 p1421 N94-19502
Ice in the northern plains: Relic of a frozen ocean? 05 p2090 N94-20391
Evolution of the global water cycle on Mars: The geological evidence 05 p2142 N94-21660
The evolution of the early Martian climate and the initial emplacement of crustal H2O 05 p2143 N94-21665
Performance of prefabricated geocomposite subdrainage system in an airport runway
[DOT/FAA/RD-93/23] 06 p2192 N94-23303
Free energy profiles for Li(+) and I(-) ions approaching Pt(100) surface: A molecular dynamics study
[AD-A273455] 06 p2536 N94-24675
Detection of water on road surface by the polarized light 07 p2886 N94-27989
Fluvial processes in Ma'adim Vallis and the potential of Gusev crater as a high priority site 11 p4358 N94-35414
Exopaleontology and the search for a fossil record on Mars 11 p4360 N94-35425
Atmospheric gas
[DE94-007439] 12 p4465 N94-37187

SURFACE WAVES
NT BAROCLINIC WAVES
NT CAPILLARY WAVES
NT GRAVITY WAVES
NT RIPPLES
Uni-directional waves over slowly varying bottom. Part 1: Derivation of a KdV-type of equation
[MEMO-1098] 01 p0147 N94-10275
Wave propagation characteristics of short-period crustal phases near ARCESS and NORESS
[AD-A265959] 01 p0275 N94-11102
Near surface ocean processes: Acoustical observations, ambient sound, and Langmuir circulation 01 p0288 N94-11447
Decay interaction of bulk and surface Langmuir waves
[DE93-617843] 01 p0393 N94-11477
Air-sea fluxes and universal constants in weak-turbulence theory of surface gravity waves 01 p0195 N94-11922
Topics in pattern formation and chaotic systems
[AD-A265922] 01 p0161 N94-12342
Excitation of coupled waves in plasma periodic structures by relativistic electron beam and acceleration of charged particles
[DE93-621657] 02 p0794 N94-12853
Fine scale measurements of microwave backscatter from the ocean surface
[AD-A264516] 03 p1111 N94-15134
Determination of the electromagnetic fields radiated from the ARES EMP simulator
[AD-A267069] 03 p0988 N94-15668
Observations and modelling of winds and waves during the Surface Wave Dynamics Experiment. Report 1: Intensive observation period IOP-1, 20-31 October 1990
[AD-A266384] 03 p1113 N94-16517
Surface waves in an inhomogeneous, isotropic, elastic half-space
[IFTR-18/1991] 03 p1060 N94-17047
The phase mixing of shear Alfven waves
[DE93-624920] 04 p1581 N94-17688
Resonant absorption of Alfven waves near a neutral point
[DE93-628761] 04 p1586 N94-18172
High resolution geological site characterization utilizing ground motion data
[AD-A268926] 04 p1481 N94-18485
Constraints on crustal structure from long period pressure and displacement measurements on the deep seafloor
[AD-A269931] 04 p1498 N94-18663
Surface wave group velocity tomography of East Asia, part 1
[AD-A270100] 04 p1484 N94-18868
Inverse scattering of surface waves: A new look at surface consistency
[REPT-93-25] 04 p1486 N94-19140
An iterative inverse scattering method for the removal of scattered surface waves
[REPT-93-18] 04 p1488 N94-19644
Ku-band ocean radar backscatter observations during SWADE 05 p1720 N94-20413
Ocean wave height transformation model using surface roller theory
[AD-A272610] 05 p1883 N94-21423
Theory and simulation of plasma sheath waves
[DE94-001305] 05 p1999 N94-22567
Global ocean modeling on the Connection Machine
[DE94-000888] 06 p2417 N94-23517
Hydro-elastic analysis using a selection of commercial analysis programs
[PB94-118734] 06 p2376 N94-24478
The rupture process of large earthquakes along convergent margins: Cast studies from Alaska and Armenia 08 p3363 N94-29969
On the nonlinear dynamics of ocean wave systems 08 p3378 N94-30790
Observations and modelling of winds and waves during the surface wave dynamics experiment. Report 2: Intensive observation period IOP-3
[AD-A278368] 10 p4093 N94-34375
Investigation of ultrasonic surface wave interaction with porous saturated rocks
[DE94-013378] 12 p4469 N94-37177

SURFACE-ACTIVE AGENTS
U SURFACTANTS

SURFACES
Calculating intersections of surfaces in screen space
[NASA-CR-191498] 02 p0745 N94-13185
Response surface design comparisons
[AD-A274690] 07 p2838 N94-26448
An automatic contact algorithm in DYNA3D for impact problems
[DE94-002856] 07 p2965 N94-26862
Aeroelastic vibrations of lifting surfaces
[ECL-91-01] 09 p3585 N94-31677

SURFACTANTS
Computer simulations for the adsorption of polymers onto surfaces
[DE93-016667] 02 p0577 N94-13070
Surfactant studies for bench-scale operation
[NASA-CR-194097] 02 p0701 N94-13187
Surfactant studies for bench-scale operation
[NASA-CR-194511] 02 p0564 N94-13947
Cooperative formation of inorganic-organic interfaces in the synthesis of silicate mesostructures
[AD-A271196] 04 p1375 N94-19742
Thrust expansion engine
[AD-D015896] 05 p1669 N94-20121
Non-ionic surfactants in the treatment of third degree burns
[AD-A271582] 05 p1891 N94-21035
Synthesis and catalytic properties of metal and semiconductor nanoclusters
[DE93-019418] 05 p2028 N94-21541
Measurement of interfacial tension by use of pendant drop video techniques
[DE93-000168] 06 p2345 N94-24831
The epitaxial growth of Ge on Si(100) using Te as a surfactant
[DE94-003437] 07 p3056 N94-26326
Regenerating using aqueous cleaners with ozone and electrolysis 08 p3240 N94-30468
Generalized syntheses of periodic surfactant and inorganic composite materials
[AD-A278001] 10 p4019 N94-34160
Chemiluminescent microemulsions
[AD-D016292] 12 p4413 N94-37761

SURGEONS
NT FLIGHT SURGEONS
Quantitative 3-D imaging topogrammetry for telemedicine applications 10 p4096 N94-33645

SURGERY
Laser artery repair
[NASA-TM-109604] 03 p1120 N94-15312
Multimodal image correlation applied to computer aided pedicular screwing
[ETN-93-95018] 04 p1528 N94-19363
A geometrical process for three dimensional osteotomy planning
[ETN-93-93602] 05 p1892 N94-21134
Development of surgical CW Nd:YAG laser with optical fiber delivery system
[DE93-632902] 07 p2817 N94-26185
Digital tracking and control of retinal images
[AD-A275469] 08 p3389 N94-28810
A force-controllable macro-micro manipulator and its application to medical robots 08 p3314 N94-30441
Dual use of image based tracking techniques: Laser eye surgery and low vision prosthesis 08 p3397 N94-30455
Dexterity enhancement in microsurgery using telemicro-robotics
[AIAA PAPER 94-1230-CP] 08 p3447 N94-30579
Telemedicine, virtual reality, and surgery 10 p4096 N94-33641

Surgery applications of virtual reality
10 p4096 N94-34025
Channel in hip implant stem
[NASA-CASE-MFS-28987-1] 12 p4486 N94-36840
Task-specific usability requirements for virtual information environments: Interface design and data representation for human operators of complex medical systems 12 p4483 N94-37262
On the feasibility of virtual environments in medicine
12 p4483 N94-37264

SURGES
Potential transients, transmission and electrochemical corrosion detection
[DE93-014055] 03 p0956 N94-15922
OSA proceedings on Ultrafast Electronics and Optoelectronics, volume 14
[AD-A267972] 03 p1014 N94-17410
The Central American cold surge: An observational analysis of the deep southward penetration of North American cold fronts
[AD-A268592] 03 p1110 N94-17607
Properties of the Central American cold surge
[NASA-CR-194849] 07 p2893 N94-26138
Detection of transient vector-fields in additive noise
[FFI-93/7028] 07 p2768 N94-26232
An investigation of the surge behavior of a high-speed ten-stage axial flow compressor
[AD-A274910] 07 p2674 N94-26345
Hot gas ingestion effects on fuel control surge recovery and AH-1 rotor drive train torque spikes
[NASA-CR-191047] 10 p4005 N94-34993

SURGICAL INSTRUMENTS
Quantitative 3-D imaging topogrammetry for telemedicine applications 10 p4096 N94-33645

SURVEILLANCE
NT SPACE SURVEILLANCE (GROUND BASED)
NT SPACE SURVEILLANCE (SPACEBORNE)
Estimation with multisensor/multiscan detection fusion
[AD-A265673] 01 p0138 N94-12338
Alternative optical architectures for multichannel adaptive optical processing
[AD-A267052] 03 p1189 N94-15664
Decomposition of large sparse symmetric systems for parallel computation. Part 1: Theoretical foundations
[AD-A267144] 03 p1159 N94-15750
Military applications of high-accuracy frequency standards and clocks
[AD-A269303] 04 p1430 N94-18299
Feasibility study of a multiaperture telescope for deep-space Earth surveillance
[AD-A273903] 07 p3102 N94-25658
Design analysis of a combined optical/LADAR deep-space surveillance satellite
[AD-A274040] 07 p2694 N94-25832
Emerging technologies
[DE94-003022] 07 p3102 N94-26023
An unavailability model for errors made during surveillance testing
[DE94-000816] 07 p2835 N94-27613
Cockpit video: A low cost BDA source
[AD-A275228] 08 p3150 N94-29389
ACCS Surveillance Exploratory Prototype (ASEP)
08 p3138 N94-29566
Airside ground movements surveillance
08 p3141 N94-29585
TacSats for NATO
[AD-A277710] 08 p3169 N94-30350
Millimeter wave, high-resolution, holographic surveillance system
[DE94-004289] 09 p3712 N94-31831
An investigation of methods for improving models of ionospheric plasma-density irregularities and radio-frequency scintillation
[AD-A278568] 10 p4033 N94-33703
Aerial robotic data acquisition system
[DE94-009114] 10 p4076 N94-33938

SURVEILLANCE RADAR
NT AIRBORNE SURVEILLANCE RADAR
NT MULTISTATIC RADAR
Military applications of high-accuracy frequency standards and clocks
[AD-A269303] 04 p1430 N94-18299
State-space models for multichannel detection
[AD-A270608] 05 p1715 N94-19816
The application of spaceborne synthetic aperture radar in the maritime environment
[DRA-TM(AWE)-91013] 05 p1737 N94-20596
Analysis and surveillance performance at Chicago O'Hare Airport
[DOT/FAA/RD-92/29] 06 p2175 N94-24127
Machine intelligent gust front algorithm
[AD-A273695] 07 p2680 N94-26196
GPS/GNSS for ATM 08 p3138 N94-29565
Development of precision runway monitor system for increasing capacity of parallel runway operations
08 p3142 N94-29587

SURVEYING
U SURVEYS

SURVEYOR PROJECT
The 1968 highlights --- NASA programs and research
[NASA-TM-109627] 03 p1302 N94-15413

SURVEYS
NT GEODETIC SURVEYS
NT GEOLOGICAL SURVEYS
NT SKY SURVEYS (ASTRONOMY)
Survey to determine the value of DYNA
[DE93-012390] 01 p0321 N94-10267
Aerosol sampling models survey
[AD-A265903] 01 p0075 N94-10337
Computer models used to support cleanup decision-making at hazardous and radioactive waste sites
[PB93-183333] 01 p0274 N94-10698
National patterns of R and D resources, 1992
[NSF-92-330] 01 p0422 N94-11186
A survey of techniques for corrosion monitoring
[DE93-012131] 01 p0083 N94-11250
NASA/DOD Aerospace Knowledge Diffusion Research Project. Report 17: A comparison of the technical communication practices of Dutch and US aerospace engineers and scientists
[NASA-TM-108987] 01 p0419 N94-11352
Pattern of federal procurement from minority and women-owned small business
[PB93-189355] 01 p0417 N94-11844
Aviators, air combat, and combat stress: An Air F orce commander's primer
[AD-A265083] 01 p0313 N94-11867
NASA/DOD Aerospace Knowledge Diffusion Research Project. Report 18: A comparison of the technical communication practices of aerospace engineers and scientists in India and the United States
[NASA-TM-109006] 02 p0821 N94-13057
Defining the performance gap: Conducting a self-assessment 02 p0666 N94-13155
User observations on information sharing (corporate knowledge and lessons learned)
[NASA-TM-104781] 02 p0819 N94-13400
Magic mirror on the wall, who's the fastest database of them all? A survey of database benchmarks
[AD-A266437] 02 p0823 N94-13701
A review of robust detection
[DSIS-93-00400] 02 p0603 N94-13829
Selected data on academic science and engineering R and D expenditures: Fiscal Year 1991
[NSF-92-329] 02 p0819 N94-13982
Generic results of the space physics community survey
[NASA-CR-194538] 02 p0818 N94-13984
Design Quality Task Force survey comments
[AD-A266283] 03 p1225 N94-16473
Identifying and responding to customer needs at the Kennedy Space Center 03 p1056 N94-16626
What is the radar tracking Glint problem and can it be solved?
[AD-A266509] 03 p0999 N94-16789
Maximizing participation of women in collegiate aviation education
[NIAR-93-14] 03 p1222 N94-17261
Magnetic Fusion Energy Technology Fellowship: Report on survey of institutional coordinators
[DE93-014646] 04 p1583 N94-17739
Rapid geophysical surveyor
[DE93-016637] 04 p1461 N94-17851
A survey on technical problems in designing high-speed rotors with developing materials
[DE93-788519] 04 p1444 N94-18159
Aircrew life support, AFSC 122X0(1T1X1)
[AD-A268998] 04 p1511 N94-18394
Survey of collision avoidance and ranging sensors for mobile robots, revision 1
[AD-A269846] 04 p1541 N94-18474
Commercialization effort in support of electroslag-casting technology
[DE93-017988] 04 p1366 N94-19733
Relating ground truth collection to model sensitivity
05 p1719 N94-20409
Performance management systems: A statistical analysis
[AD-A272989] 05 p2043 N94-21266
Implementing Electronic Data Interchange (EDI) with small business suppliers in the pre-award acquisition process
[AD-A271767] 05 p1945 N94-21305
Survey and alignment analysis for the ALS storage ring using computer spreadsheets
[DE93-019254] 05 p1917 N94-21917
Current situation in developing petroleum substituting energy (the United Kingdom)
[DE94-714897] 05 p1713 N94-22091
Surveys on specific patterns of facility intallation of photovoltaic power generating technologies for international cooperation
[DE94-714901] 05 p1850 N94-22092
Space technology: A study of the significance of recognition for innovators of spinoff technologies. Commercial Space Expo-USA, 1993
[NASA-CR-194833] 06 p2596 N94-23528
Prototype Space Technology Hall of Fame exhibit at Technology 2003: Analysis of data from computer-based questionaire
[NASA-CR-194834] 06 p2596 N94-23540
Cross-calibration survey (VISNIR)
06 p2383 N94-23599
Verification and validation of models
[PB94-110566] 06 p2456 N94-24507
Hydraulics and morphology of mountain rivers: A literature survey. Communications on hydraulic and geotechnical engineering
[PB94-110772] 06 p2388 N94-24636
NASA/DOD Aerospace Knowledge Diffusion Research Project. Report number 20: The use of selected information products and services by US aerospace engineers and scientists: Results of two surveys
[AD-A276068] 06 p2592 N94-24649
A biological survey for the nation
[LC-93-85920] 06 p2421 N94-24704
Evaluation of the UH-1N instrument panel
[AD-A273145] 06 p2186 N94-24774
General aviation activity survey
[AD-A273284] 06 p2162 N94-24923
Perceptions of organizational support and affectivity as predictors of job satisfaction
[DOT/FAA/AM-94/2] 06 p2429 N94-25442
A comparison of users' and providers' perceptions of critical spacelift vehicle characteristics and capabilities
[AD-A273907] 07 p2691 N94-26017
Hydrographic and Acoustic Doppler Current Profiler (ADCP) data from the ONR eastern boundary current accelerated research initiative, 9-16 June 1992
[AD-A274115] 07 p2898 N94-26076
Survey of visualization and analysis tools
[NASA-TM-108436] 07 p2809 N94-26150
HPm-tubes: Literature survey comprising 1992
[PB94-123643] 07 p2785 N94-27038
Solar collector manufacturing activity, 1992
[DE94-003401] 07 p2859 N94-27048
Microbiology research at some research institutes in the former Soviet Union: A survey of scientific publications
[PB94-123320] 07 p2902 N94-27171
Macrobenthic fauna in the dutch sector of the north sea in 1991
[PB94-126414] 07 p2868 N94-27200
COMPETENCE 2000: Study on training requirements of the Norwegian metallurgical industry
[PB94-124609] 07 p2741 N94-27328
Spiral Survey Expedition: A proposal to organize for the Survey, exploration and eventual colonization of the Milky Way Galaxy 07 p2686 N94-27366
Advanced development of PV encapsulents
[DE94-000219] 08 p3336 N94-28500
NASA wiring program: Survey of NASA experiences in wiring system safety 08 p3165 N94-28700
An evaluation of techniques for ranking academic information systems journals
[AD-A275179] 08 p3529 N94-29066
Statistical Modeling and Estimation of Reliability Functions for Software (SMERFS) library access guide, revision 3
[AD-A275405] 08 p3411 N94-29207
A survey of NASA and military standards on fault tolerance and reliability applied to robotics
[AIAA PAPER 94-1211-CP] 08 p3445 N94-30562
Results of real-time testing and demonstration of the US Army Corps of Engineers real-time on-the-fly positioning system
[AD-A276160] 09 p3576 N94-31080
Active matrix liquid crystal display. Industry survey results
[AD-A276415] 09 p3895 N94-31329
Hydrographic service Royal Australian Navy
[AD-A277134] 09 p3788 N94-32066
Aircraft communication and navigation systems and communication and navigation systems
[AD-A277309] 09 p3582 N94-32328
The relationship between integrative task design for information systems professionals and perceived information systems effectiveness
09 p3919 N94-32487
Relationships between access and use in information systems: Remote access to and browsing of online catalogs 09 p3919 N94-32488
Multidimensional scaling of user information satisfaction
[AD-A277230] 09 p3920 N94-32633

A review of an updated synthesis of noise/annoyance relationships
[NASA-CR-194950] 10 p4134 N94-34303
NASA/DOD Aerospace Knowledge Diffusion Research Project. Paper 35: The US government technical report and aerospace knowledge diffusion: Results of an on-going investigation
[NASA-TM-109861] 10 p4159 N94-34603
NASA/DOD Aerospace Knowledge Diffusion Research Project. Paper 41: Technical communication practices of Dutch and US aerospace engineers and scientists: International perspective on aerospace
[NASA-TM-109862] 10 p4159 N94-34604
A 1- to 10-GHz downconverter for high-resolution microwave survey 11 p4253 N94-35551
Good applications for crummy machine translation
[AD-A278689] 11 p4345 N94-35651
California residential indoor air quality study. Volume 1: Methodology and descriptive statistics. Appendix
[PB94-166055] 12 p4464 N94-36995
Toward a new National Weather Service: National Weather Service employee feedback 12 p4474 N94-37467

SURVIVAL
Evaluation of medical treatments to increase survival of ebullism in guinea pigs 01 p0302 N94-11548
STS-29 crew bailout in WETF
[NASA-TM-109548] 03 p1136 N94-15385
1990 ASCAN land survival training
[NASA-TM-109527] 03 p1136 N94-15390
On predicting the person-in-water drift for search and rescue
[AD-A268083] 03 p1055 N94-17514
Survival suit for submarine personnel: Summary of evaluation studies
[PB93-204634] 06 p2430 N94-23743
Aircraft evacuation testing: Research and technology issues
[PB94-107620] 06 p2173 N94-24750
Prediction of survival times on land in a cold climate 08 p3379 N94-28423
Effectiveness of protection clothing for cold weather conditions after ejection over sea: A case report 08 p3381 N94-28435
Advanced integrated cold protection for aircrew 08 p3381 N94-28436
Thermoregulation in the extreme cold environment 08 p3381 N94-28438
NASA report to education, volume 9
[NASA-TM-109760] 09 p3913 N94-31817

SUSCEPTIBILITY (MAGNETISM)
U MAGNETIC PERMEABILITY

SUSPENDING (HANGING)
NT MAGNETIC SUSPENSION
A large motion zero-gravity suspension system for experimental simulation of orbital construction and deployment
[NASA-CR-195881] 09 p3668 N94-33037

SUSPENDING (MIXING)
Separation of gravitational effects on the flow of suspension in tubes by measurements in weightlessness 01 p0105 N94-10105

SUSPENSION SYSTEMS (VEHICLES)
Electrodynamic forces of the cross-connected figure-eight null-flux coil suspension system
[DE93-015139] 03 p1048 N94-16969
Vehicle/guideway interaction and ride comfort in maglev systems
[DE94-001319] 06 p2352 N94-22991
Vibration isolating engine mount
[CA-PATENT-1-320-710] 06 p2353 N94-23215
The Enabler: A concept for a lunar work vehicle 07 p2833 N94-25675
Identification of the damping ratio relationship of an autovehicle suspension
[REPT-93-063] 08 p3313 N94-30937
System concept definition of the Grumman superconducting Electromagnetic Suspension (EMS) Maglev design 11 p4213 N94-35840
Transrapid (the first high-speed Maglev train system certified ready for application): Development status and prospects for deployment 11 p4213 N94-35841
Control of maglev vehicles with aerodynamic and guideway disturbances 11 p4213 N94-35842
Fault tolerant computer control for a Maglev transportation system 11 p4215 N94-35848
Superconducting Electromagnetic Suspension (EMS) system for Grumman Maglev concept 11 p4215 N94-35849
Study of Japanese electrodynamic-suspension maglev systems
[DE94-011486] 12 p4452 N94-37515

SUSPENSIONS
The solubility of epsilon-CL-20 in selected materials
[DE93-009304] 01 p0077 N94-11602
Electrokinetic transport of heterogeneous particles in suspensions
[NASA-CR-194478] 04 p1353 N94-19367
Micromechanics and effective properties of particulate composites and fluid suspensions 09 p3703 N94-31744

SWAMPS
U MARSHLANDS

SWASH
U SPLASHING

SWEAT
Modifications to an interactive model of the human body during exercise: With special emphasis on thermoregulation 01 p0317 N94-12368
Cool suit
[NASA-TM-109639] 03 p1120 N94-15250
Modeling heat exchange characteristics of long term space operations: Role of skin wettedness and exercise 10 p4101 N94-33650
Prediction modeling of physiological responses and human performance in the heat with application to space operations 10 p4098 N94-33652

SWEAT COOLING
Modeling heat exchange characteristics of long term space operations: Role of skin wettedness and exercise 10 p4101 N94-33650
The prediction of nozzle performance and heat transfer in hydrogen/oxygen rocket engines with transpiration cooling, film cooling, and high area ratios
[NASA-TM-106617] 10 p4017 N94-34924
Experimental studies of transpiration cooling with shock interaction in hypersonic flow, part B
[NASA-CR-195958] 10 p3985 N94-34965
Modeling of outgassing and matrix decomposition in carbon-phenolic composites
[NASA-CR-196319] 12 p4405 N94-37471

SWEATING
U PERSPIRATION

SWEDEN
Experiences from the Swedish sea ice programme during BEERS-1992 01 p0239 N94-11751
The Swedish ISY contribution 02 p0695 N94-14256

SWEEP ANGLE
NT LEADING EDGE SWEEP

SWEEP EFFECT
Wing lift increment at zero angle of attack due to deployment of single-slotted flaps at low speeds
[ESDU-93019] 07 p2649 N94-28140

SWEEP FREQUENCY
Parameter identification of a rotor supported in a pressurized bearing lubricated with water 10 p4065 N94-34197

SWEEPBACK
NT LEADING EDGE SWEEP

SWELLING
A method of influence regions in the theory of vacancy swelling of metals
[DE93-620579] 01 p0083 N94-11363
An experimental study on the effect of die geometry on swell and sag in the parison extrusion stage
[IMI-93RT-42400-1476-G] 02 p0597 N94-14070
Swelling equilibria for temperature-sensitive ampholytic hydrogels
[DE93-015264] 03 p0966 N94-15996
Swelling equilibria for cationic 2-hydroxyethyl methacrylate (HEMA)-based hydrogels
[DE94-000728] 05 p1707 N94-21856
High specific energy, high capacity nickel-hydrogen cell design 06 p2391 N94-23350
Conceptual design of a device to measure hand swelling in a micro-gravity environment
[NASA-CR-195509] 06 p2437 N94-24330
Microstructural development in irradiated vanadium alloys
[DE94-004307] 07 p2737 N94-26556
He(+) and H(+) microbeam damage, swelling and annealing in diamonds
[DE94-601912] 07 p3063 N94-26987
Relationship between swelling and irradiation creep in cold-worked PCA stainless steel irradiated to approximately 178 dpa at approximately 400 C
[DE94-004368] 08 p3201 N94-28456
Molecular aspects of transport in thin films of controlled architecture
[DE94-004552] 08 p3211 N94-28457
Radiation effects in beryllium used for plasma protection
[DE94-004599] 08 p3201 N94-28460
The influence of transmutation, void swelling, and flux/spectra uncertainties on the electrical properties of copper and copper alloys
[DE94-006213] 09 p3641 N94-31626
Effect of irradiation damage and helium on the swelling and structure of vanadium-base alloys
[DE94-006540] 09 p3641 N94-31666

SWEPT FORWARD WINGS
X-29: Longitudinal instability at high angle-of-attack 01 p0033 N94-11504
X-29: Experiment in flight
[NASA-TM-109454] 03 p0865 N94-15327
High lift and the forward swept wing 04 p1308 N94-18436
X-29: Research aircraft
[NASA-TM-109370] 04 p1318 N94-18962
Experimental study on interference aerodynamics of close-coupled canard configuration
[AD-A267760] 05 p1636 N94-19963
Forward sweep, low noise rotor blade
[NASA-CASE-LAR-14569-1] 12 p4386 N94-36767

SWEPT WINGS
NT DELTA WINGS
NT SWEPT FORWARD WINGS
NT SWEPTBACK WINGS
Physics of forebody flow control
[NASA-CR-193626] 01 p0015 N94-11195
Modeling nonlinear aerodynamic loads for aircraft stability and control analysis 01 p0032 N94-11499
Three-Dimensional Boundary-Layer program (BL3D) for swept subsonic or supersonic wings with application to laminar flow control
[NASA-CR-4531] 02 p0629 N94-13073
Special course on Shock-Wave/Boundary-Layer Interactions in Supersonic and Hypersonic Flows
[AGARD-R-792] 03 p1017 N94-15196
Aerodynamic control of NASP-type vehicles through vortex manipulation. Volume 3: Wing rock experiments
[NASA-CR-177626] 03 p0857 N94-15780
Comparison between swept and delta canards on a model of a combat aircraft
[AD-A269561] 04 p1317 N94-17826
Viscous-inviscid calculation of high-lift separated compressible flows over airfoils and wings 04 p1309 N94-18440
Numerical prediction of transition of the F-16 wing at supersonic speeds
[NASA-CR-194407] 04 p1312 N94-19433
Surface hot film measurements at ATTAS laminar glove 05 p1639 N94-22598
Reduction of structural loads using maneuver load control on the Advanced Fighter Technology Integration (AFTI)/F-111 mission adaptive wing
[NASA-TM-4526] 06 p2168 N94-24295
Prediction of leading-edge transition and relaminarization phenomena on a subsonic multi-element high-lift system 07 p2659 N94-27929
Steady pressure measurements on an Aeroelastic Research Wing (ARW-2)
[NASA-TM-109046] 08 p3122 N94-28658
The 3-D LDV measurements on a 30-degree swept wing with a simulated ice accretion
[NASA-CR-195327] 08 p3132 N94-30124
An experimental study of the aerodynamics of a swept and unswept semispan wing with a simulated glaze ice accretion
[NASA-CR-195330] 08 p3133 N94-30152
Numerical analysis of transonic wing buffet 09 p3586 N94-32713
NASA F-16XL supersonic laminar flow control program overview 10 p3980 N94-33525
Supersonic LFC: Challenges and opportunities 10 p3981 N94-33526
Status of F16XL SSLFC numerical design validation 10 p3981 N94-33527
Code validation for the simulation of supersonic viscous flow about the F-16XL 10 p3981 N94-33528
Will the real dynamic instability mechanism please be recognized! 10 p4052 N94-34976
The reduction of takeoff ground roll by the application of a nose gear jump strut
[NASA-TM-108822] 11 p4198 N94-36380

SWEPTBACK WINGS
NT DELTA WINGS
An experimental investigation of the optimum slat setting on a combat aircraft model 04 p1308 N94-18431
An experimental investigation of attachment-line transition on the slat of a combat aircraft model 04 p1308 N94-18432
Design and fabrication of forward-swept counterrotation blade configuration for wind tunnel testing
[NASA-CR-191193] 08 p3155 N94-28510

SWINE
Increased vascular resistance with hemoglobin-based oxygen carriers
[AD-A266454] 03 p1123 N94-16565
Skeletal development and ossification of the swine fetuses 07 p2905 N94-27491

SWING WINGS
Supercruiser Arrow HS-8 07 p2671 N94-25711

SWINGBY TECHNIQUE
Project APEX: Advanced manned exploration of the Martian moon Phobos 07 p3079 N94-25688

SWIRLING
SWIRL as a means of liquid management in low gravity
[NASA-CR-4545] 01 p0412 N94-11523
An experimental investigation of mixing enhancement in a simulated scramjet combustor by use of swirling jets
[NASA-TM-109246] 02 p0518 N94-13190
Collaborative research on combustion diagnostics and modeling between Rolls-Royce, Inc. and the United States Air Force Wright Laboratory
[AD-A270660] 04 p1354 N94-19778
Decay of swirl in turbulent pipe flows
[ETN-94-95353] 06 p2339 N94-25248
Navier-Stokes analysis of a swirling jet in crossflow 07 p2806 N94-28038
Modeling turbulence in flows with a strong rotational component
[DE94-003577] 08 p3270 N94-28475
Hydrodynamic stability analysis of swirling jets 08 p3278 N94-29974
The effect of inlet swirl on the dynamics of long annular seals in centrifugal pumps 10 p4063 N94-34184

SWIRLING WAKES
U TURBULENT WAKES

SWITCHES
NT CAPACITANCE SWITCHES
NT ELECTRIC RELAYS
NT ELECTRIC SWITCHES
NT SWITCHING CIRCUITS
NT THERMOSTATS
NT VACUUM ARC SWITCHES
A picosecond high pressure gas switch
[DE93-011897] 01 p0142 N94-11050
Experimental and theoretical investigations of Cs-Ba vapor tacitron inverter for power conditioning in space power systems
[DE93-012971] 01 p0048 N94-11372
GaAs PCSS: High gain switching and device reliability
[DE93-009851] 01 p0401 N94-11605
A thermal ionization model for the sustaining phase of lock-on in GaAs
[DE93-011558] 01 p0144 N94-11624
Development of UHF spark-switched L-C Oscillators
[DE93-015019] 02 p0623 N94-13892
Plasma flow switch and foil implosion experiments on Pegasus 2
[DE93-016464] 03 p1013 N94-17318
Isochronets: A high-speed network switching architecture
[AD-A267811] 03 p1161 N94-17409
Fabrication process for cantilever beam micromechanical switches
[AD-A269716] 04 p1404 N94-18749
Improved optical pseudospark switch
[AD-D015821] 04 p1580 N94-18947
Photoconductive Semiconductor Switches for pulsed power applications
[DE93-019411] 05 p1750 N94-20294
Optically controlled current filamentation in GaAs photoconductive semiconductor switches
[DE93-019427] 05 p2016 N94-20296
High current density contacts for photoconductive semiconductor switches
[DE93-018837] 05 p1750 N94-20312
High-power gas switch with hydride electrodes
[AD-D015956] 05 p1751 N94-20354
Two dimensional simulation of the electric arc behavior in a cut-off device
[ECL-92-41] 05 p1751 N94-20595
Results from long conduction time plasma opening switch experiments at Sandia National Laboratories
[DE93-019063] 05 p1762 N94-21632
Ultrafast gas switching experiments
[DE93-019071] 05 p1762 N94-21634
Picosecond High Pressure Gas Switch experiment
[DE93-040853] 06 p2307 N94-22950
Switch configuration for migration to optical fiber network 06 p2447 N94-23250
Viewing hybrid systems as products of control systems and automata
[NASA-CR-194792] 06 p2472 N94-23300
Non-volatile, solid state bistable electrical switch
[NASA-CASE-NPO-17621-1-CU] 06 p2309 N94-23820
Computer modeling of plasma flow switches-high current switching on Procyon
[DE93-040189] 06 p2311 N94-24500
X ray simulator theory support
[AD-A273613] 06 p2553 N94-24949
Control panel dimensions for gloved operation study 2: Toggle switches minimum spacing required between toggle
[AD-A274518] 07 p2942 N94-27089
A tri-state optical switch for local area network communications 07 p2789 N94-27922
The 100 kA, 5000 V solid-state opening switch for inductive energy storage
[AD-A274993] 08 p3263 N94-28994
Proton switches
[AD-A275150] 08 p3167 N94-29022
Electron-beam controlled semiconductor switches
[AD-A276198] 09 p3686 N94-31057
Studies of the plasma triggering mechanism of inverse pinch switch
[AD-A276117] 09 p3887 N94-31530
The named-state register file
[AD-A276796] 09 p3825 N94-32165
Reconfigurable optical switches with monolithic electrical-to-optical interfaces
[DE94-007745] 09 p3881 N94-32385
High power switch design for the Nova upgrade laser (Project HERCULES: High Energy Research Concerning the Ultimate Lifetime of Experimental Switches)
[DE94-007921] 09 p3719 N94-32654
Optically switched submillimeter-wave oscillator
[AD-A278014] 09 p3698 N94-33249
Experimental and theoretical studies of a high temperature cesium-barium tacitron, with application to low voltage-high current inversion
[DE94-008182] 11 p4228 N94-35349
Molecular systems for ultrafast optical switching: Controlling electron transfer reactions with femtosecond laser pulses
[DE94-009695] 11 p4332 N94-35671

SWITCHING
NT MAGNETIC SWITCHING
NT MICROWAVE SWITCHING
NT OPTICAL SWITCHING
NT PACKET SWITCHING
A picosecond high pressure gas switch
[DE93-011897] 01 p0142 N94-11050
Experimental and theoretical investigations of Cs-Ba vapor tacitron inverter for power conditioning in space power systems
[DE93-012971] 01 p0048 N94-11372
Assessment of the impact of HTSC's on superconducting fault-current limiters
[DE93-009986] 01 p0143 N94-11454
GaAs PCSS: High gain switching and device reliability
[DE93-009851] 01 p0401 N94-11605
Ceramic actuators for smart materials
[AD-A265664] 01 p0093 N94-12331
Charge storage and switching phenomena with molecular assemblies of metal complexes
[AD-A266673] 02 p0787 N94-14778
Plasma-puff initiation of high Coulomb transfer switches
[NASA-CR-193186] 04 p1591 N94-19441
Delivery of very high bandwidth with ATM switches and SONET
[DE93-019432] 05 p1899 N94-20476
An application of the Cerebellar Model Articulation Controller for a switched reluctance rotor position estimator
[AD-A271769] 05 p1943 N94-20926
Low-latency digital frequency synthesizer using the residue number system 05 p1759 N94-21121
Optimization of fixed time polling schemes
[CWI-BS-R9237] 05 p1945 N94-21233
Research on plasma-puff initiation of high Coulomb transfer switches
[NASA-CR-194371] 05 p1994 N94-21289
Plasma-puff initiation of high Coulomb transfer switches 05 p1994 N94-21290
Characteristics of plasma-puff trigger for a inverse-pinch plasma switch 05 p1995 N94-21291
Characteristics of switching plasma in an inverse-pinch switch 05 p1995 N94-21292
Comparative study of INPIStron and spark gap 05 p1995 N94-21293
INPIStron switched pulsed power for dense plasma pinches 05 p1995 N94-21294
Ultrafast gas switching experiments
[DE93-019071] 05 p1762 N94-21634
Evaluation of DEC's GIGAswitch for distributed parallel computing
[DE94-001356] 05 p1936 N94-21853
Picosecond High Pressure Gas Switch experiment
[DE93-040853] 06 p2307 N94-22950
Viewing hybrid systems as products of control systems and automata
[NASA-CR-194792] 06 p2472 N94-23300
A prototype to automate the video subsystem routing for the video distribution subsystem of Space Station Freedom 06 p2306 N94-25353
Quantum interference phenomena and novel switching in split gate high electron mobility transistors 08 p3266 N94-29734
Studies of the plasma triggering mechanism of inverse pinch switch
[AD-A276117] 09 p3887 N94-31530
High power switch design for the Nova upgrade laser (Project HERCULES: High Energy Research Concerning the Ultimate Lifetime of Experimental Switches)
[DE94-007921] 09 p3719 N94-32654
Adaptive stabilization of linear and nonlinear systems
[AD-A278270] 10 p4113 N94-33855
Experimental and theoretical studies of a high temperature cesium-barium tacitron, with application to low voltage-high current inversion
[DE94-008182] 11 p4228 N94-35349
Determining the refractive index of a lambda/4 thin film on a thick substrate from a transmittance measurement
[DE93-019584] 12 p4523 N94-36693

SWITCHING CIRCUITS
Evolution of high-repetition-rate induction accelerators through advancements in switching
[DE93-012599] 02 p0654 N94-12963
Stray insensitive switched capacitor composite operational amplifiers
[AD-A267412] 03 p1012 N94-16976
Design of broadband wire antennas for frequency hopping applications
[AD-A267405] 03 p1001 N94-17025
Non-blocking crossbar permutation engine with constant routing latency
[NASA-CASE-NPO-18864-1-CU] 03 p1161 N94-17328
A scalable wrap-around shuffle exchange network with deflection routing
[NASA-CASE-NPO-18983-1-CU] 03 p1161 N94-17330
Pulsed LASER for testing silicon strip detectors
[DE93-017816] 04 p1436 N94-17883
Training product unit neural networks with genetic algorithms 04 p1399 N94-18354
Asynchronous sequential circuit design using pass transistor iterative logic arrays 04 p1402 N94-18376
Pulse mode VLSI asynchronous circuits 04 p1402 N94-18377
Improved self arbitrated VLSI asynchronous circuits 04 p1402 N94-18378
Compensation approach for three or more dimensional random walks
[PB93-197499] 04 p1543 N94-19326
Evaluation of laser diode based optical switches for optical processors
[AD-A270949] 04 p1581 N94-19602
SPICE macromodel for a 1-megawatt power MOSFET switch
[DE93-019415] 05 p1748 N94-19844
Computational model of a magnetic modulator for copper lasers
[DE93-019603] 05 p1815 N94-20223
Photoconductive Semiconductor Switches for pulsed power applications
[DE93-019411] 05 p1750 N94-20294
Novel N x N integrated channel waveguide optical crossbars for large scale high speed non-blocking data switching
[AD-A272065] 05 p1986 N94-20922
High power, electron-beam induced switching in diamond
[DE93-040535] 05 p1768 N94-21770
A FET-switched induction accelerator cell
[DE93-019604] 05 p1769 N94-21838
A shared buffer memory switch with maximum queue and minimum allocation 05 p1773 N94-22119
An adaptive method for group delay compensation using switched capacitor filters 05 p1793 N94-22248
Mobilesat (tm): A world first 06 p2281 N94-22783
Exciplex laser study: Discharge and magnetic switching systems
[PB93-199768] 06 p2349 N94-24629
Contribution to the study of HF converters radiated disturbances
[ECL-92-34] 06 p2313 N94-25421
Study of a system for producing a pulsed magnetic field (B 2T) with a frequency of 50 Hz
[ISL-N-601/92] 06 p2314 N94-25460
Low threshold all-optical crossbar switch on GaAs-GaAlAs channel waveguide arrays
[AD-A274971] 07 p2783 N94-26536
An electronic switch based on quantum interference
[ISBN-0-315-84609-7] 07 p2787 N94-27650
Photoconductive switching for high power microwave generation
[PB94-137460] 08 p3244 N94-29177
Electron-beam controlled semiconductor switches
[AD-A276198] 09 p3686 N94-31057
Examination of fast semiconductor diodes (recovery) with respect to switching valves in PWM and resonance devices
[ETN-94-95740] 09 p3690 N94-31609
The named-state register file
[AD-A276796] 09 p3825 N94-32165

Characterization of thermally stable dye-doped polyimide based electrooptic materials
[DE94-005309] 09 p3882 N94-32674
Fiber optic continuous true time-delay modulator
[AD-D016098] 09 p3883 N94-32720
Buffered feedthrough crossbar switch
[AD-D016145] 09 p3697 N94-32967
Efficiency consideration of DC link soft-switching inverters for motor drive applications
[DE94-003604] 10 p4039 N94-33732
Integral testing of relays and circuit breakers
[DE94-009075] 10 p4041 N94-33937
Switched-beam radiometer front-end network analysis
[NASA-CR-194922] 11 p4252 N94-35247
Time-dependent simulations of filament propagation in photoconducting switches
[DE94-012146] 12 p4438 N94-37213
Neurocontrol of a broadband (ATM) Clos' switching network
[PB94-179389] 12 p4441 N94-37851

SWITCHING ELEMENTS
U SWITCHING CIRCUITS

SWITCHING THEORY
Throughput and blocking in circuit-switched interconnection networks 05 p1784 N94-22189
Buffer allocation in an ATM switch with output buffer and speed constraints 05 p1746 N94-22203

SWIVELS
Parachute Swivel Mechanism for planetary entry 08 p3162 N94-29643

SYLLABLES
Generalization performance of backpropagation learning on a syllabification task 05 p1940 N94-20246

SYMBIOSIS
Biofilm structure and diversity
[AD-A267254] 03 p1118 N94-16989
Symbiosis in marine luminous bacteria
[AD-A273540] 06 p2422 N94-24791

SYMBIOTIC STARS
ROSAT-IUE observations of symbiotic stars. The x ray morphology of high latitude associations
[NASA-CR-194616] 03 p1236 N94-16492

SYMBOLIC PROGRAMMING
Visual parallel programming with determinacy: A language specification, an analysis technique, and a programming tool
[AD-A267560] 03 p1153 N94-17107
ATOS-1: Designing the infrastructure for an advanced spacecraft operations system 06 p2197 N94-23849
Efficient implementation of high-level parallel symbolic languages 07 p2955 N94-27196
Combining symbolic computation and theorem proving: Some problems of Ramanujan
[AD-A278899] 11 p4303 N94-35573
Computationally efficient multibody simulations 11 p4222 N94-35896

SYMBOLS
Symbolic dynamics and description of complexity
[DE93-613030] 01 p0418 N94-10485
Application of symbolic and algebraic manipulation software in solving applied mechanics problems
[NASA-CR-4544] 02 p0596 N94-13798
SeaWiFS technical report series. Volume 12, SeaWiFS technical report series cumulative index: Volumes 1-11
[NASA-TM-104566-VOL-12] 03 p1111 N94-15529
Testing string superprimitivity in parallel
[AD-A267814] 03 p1155 N94-17399
Links between N-modular redundancy and the theory of error-correcting codes 05 p1765 N94-21713
Conveying digital data in noisy, unstable, multipath environments
[AD-D015980] 06 p2301 N94-25038
Saving comparisons in the Crochemore-Perrin string matching algorithm
[CWI-CS-R9322] 07 p2971 N94-27550
A comparison of three aircraft attitude display symbology structures
[AD-A275172] 08 p3150 N94-29048
Beginning the 21st century with advanced Automatic Parts Identification (API) 09 p3923 N94-32444

SYMMETRICAL BODIES
NT AXISYMMETRIC BODIES
NT BODIES OF REVOLUTION
NT CONICAL BODIES
NT CYLINDRICAL BODIES
NT ELLIPSOIDS
NT FAIRINGS
NT LENTICULAR BODIES
NT ROTATING CYLINDERS
NT ROTATING SPHERES
NT SLENDER CONES
NT SPHERES
NT TORUSES
On the effect of the damping coefficients on the trajectories of symmetric and non-symmetric stores 06 p2155 N94-24250

SYMMETRY
NT BROKEN SYMMETRY
NT CHIRALITY
NT SUPERSYMMETRY
Symmetry lowering in crystalline solid solutions: A study of cinnamamide-thienylacrylamide by x ray and neutron diffraction and solid-state photochemistry
[DE93-010871] 01 p0394 N94-10301
Exact solutions of a many-anyon problem
[DE93-617646] 01 p0411 N94-10832
Quantum solitons with cylindrical symmetry
[DE93-617659] 01 p0344 N94-10881
Quenched chiral logarithms
[DE93-010195] 01 p0346 N94-11663
Engineering solid-state materials. Strategies for modeling and packing control of molecular assemblies into 3-D networks
[AD-A265291] 01 p0404 N94-12438
Aspects of symmetry violation
[DE93-011003] 02 p0779 N94-12997
Determination of channeling perspectives for complex crystal structures
[DE93-012872] 02 p0805 N94-13009
Resonant x ray Raman scattering from atoms and molecules
[DE93-015158] 02 p0784 N94-13896
Application of symmetry properties to polarimetric remote sensing with JPL AIRSAR data 03 p1079 N94-16752
Analysis of temporal symmetry in non-gaussian random fields
[AD-A266496] 03 p0999 N94-16794
On the difference caused by CP violation in the energy spectra of pions in K(sup (+-))(yields)(pi)(+-)(pi)(+-)(pi)-+ decays
[DE93-624828] 04 p1564 N94-17687
Beauty without charm in B-meson decays
[PREPRINT-732] 04 p1565 N94-17972
Deformed traces and covariant quantum algebras for quantum groups GL(sub qp)(2) and GL(sub qp)(1/1)
[DE93-629862] 04 p1561 N94-18153
About symmetry of the gravitational action
[DE93-629955] 04 p1608 N94-18252
The theory of linear programming: Skew symmetric self-dual problems and the central path
[REPT-93-15] 04 p1524 N94-19089
Symmetry in polarimetric remote sensing 05 p1729 N94-20449
High resolution infrared spectroscopy of cyclobutane: A study of vibrational mode coupling involving large amplitude, low frequency modes
[AD-A271987] 05 p1973 N94-20619
Symmetries and conservation laws of the system: u(x) = vw(x), v(y) = uw(y), uv + w(xx) + w(yy) = 0
[MEMO-1084] 05 p1953 N94-21046
Electronically metastable molecules of high symmetry
[AD-A272015] 05 p1974 N94-21461
Lattice gauge theory: Present status
[DE93-041154] 05 p2038 N94-21692
Symmetry-dictated trucation: Solutions of the spherical shell model for heavy nuclei
[DE94-000482] 05 p1976 N94-21961
Transient analysis of conducting half-plane problem with noncausal scattering image
[PB93-225027] 06 p2524 N94-23110
Observation of non-centrosymmetry and determination of polarity in III-V semiconductors
[PB93-201416] 06 p2561 N94-23503
A working algorithm to isolate integrable surfaces in E cubed
[SSCL-PREPRINT-761] 06 p2452 N94-23518
On BRST quantization of constrained systems
[ETN-94-95386] 06 p2570 N94-25258
Weak interactions in a bilocal chiral theory
[DE93-616887] 06 p2539 N94-25477
Experimental study of the near threshold pi(sup +)p yields (pi(sup +))(pi(sup +))(n) cross section and chiral symmetry
[DE94-601671] 07 p3014 N94-25840
The algebra of non-local charges in non-linear sigma models
[DE94-601563] 07 p2991 N94-25884
Principles of gauge theory of real hadrons
[DE93-616857] 07 p3015 N94-25920
Spatial symmetry, local integrability and tetrahedron equations in the Baxter-Bazhanov model
[DE93-634348] 07 p3002 N94-26038
Simple currents versus orbifolds with discrete torsion: A complete classification
[NIKHEF-H/93-13] 07 p2995 N94-26812
Normal forms for perturbations of the euler top
[PB94-125390] 07 p3009 N94-26968
Some remarks on the symmetry of self-conjugate minimal surfaces in R3
[DE94-603670] 07 p3007 N94-27633
Surface modes and chiral symmetry (Wilson fermions in a box)
[DE94-004946] 07 p3029 N94-27814
Polarizability matrix of layered chiral sphere
[PB94-132834] 07 p2778 N94-28355
Plane wave propagation and polarization properties in transversely bianisotropic uniaxial medium
[PB94-132883] 07 p2778 N94-28380
Electromagnetic modeling of bi-isotropic media
[PB94-132909] 07 p2778 N94-28382
Some constraints and solutions of the Kadomtsev-Petviashvili equation
[DE93-634355] 08 p3466 N94-28467
Extended nonabelian symmetries for free fermionic model
[DE94-601554] 08 p3481 N94-28470
Remarks on Galois symmetry in RCFT
[PB94-138179] 08 p3467 N94-29147
A numerical study of gravitational collapse 08 p3548 N94-30271
N(exp n(n-1)/2)-state R-matrix related with U(sub q)(sl(n)) algebra at q(exp 2N) = 1
[DE94-608140] 09 p3902 N94-32247
Fabrication, phase transformation studies and characterization of SiC-AlN-Al2OC ceramics
[DE94-008587] 09 p3659 N94-32657
Vibrations of structures with cyclic symmetry: Application to the case of turbine engines 10 p4004 N94-34463
CP violation outside the standard model phenomenology for pedestrians
[DE94-002216] 12 p4511 N94-36512
Variational discrete symmetries
[DE94-618485] 12 p4507 N94-37062

SYMMETRY BREAKING
U BROKEN SYMMETRY

SYMPATHETIC NERVOUS SYSTEM
Valsalva maneuver: Insights into baroreflex modulation of human sympathetic activity 01 p0310 N94-12000
Hormonal regulation of fluid and electrolyte metabolism in zero-g and bedrest 01 p0311 N94-12004
Melatonin, the pineal gland, and circadian rhythms
[AD-A268200] 03 p1129 N94-17478
Excitation of cutaneous polymodal receptor induced by sympathetic stimulation in adjuvant-induced arthritis rats 07 p2906 N94-27495
Effect of prostaglandin E1 on the relationship between skin sympathetic nerve activity and reduction in skin blood flow 07 p2929 N94-27524
Difference in skin blood flow reduction depending on activating maneuver of skin sympathetic nerve activity 07 p2929 N94-27525
Sympathetic nerve activity during dynamic leg exercise 07 p2929 N94-27527
An attempt of intraneural stimulation by microelectrode inserted in skin sympathetic nerve fascicle 07 p2930 N94-27529
Muscle sympathetic nerve activity in patients with hyper-and hypothyroidism: A microneurographic study 07 p2930 N94-27531
Enhancement of skin sympathetic nerve activity in amyotrophic lateral sclerosis 07 p2930 N94-27532
Mechanism for regulation of myocardial contractility by autonomic drugs: Pathophysiological relevance in congestive heart failure 07 p2931 N94-27536
Muscle sympathetic nerve activity in humans 07 p2932 N94-27538
The role of beta-adrenoceptor stimulation in the progression of chronic heart failure 07 p2932 N94-27541
Japanese Journal of Aerospace and Environmental Medicine, vol. 30, no. 2
[JTN-94-80599] 08 p3394 N94-29863
Effect of water immersion on muscle sympathetic nerve response during static muscle contraction 08 p3394 N94-29865

SYMPATHOMIMETICS
U ADRENERGICS

SYMPOSIA
U CONFERENCES

SYMPTOMOLOGY
Flight simulator-induced sickness and visual displays evaluation
[AD-A267019] 03 p1122 N94-15845
The Environmental Symptoms Questionnaire: Assessing reactions to environmental extremes in military operations 08 p3383 N94-28447

SYMPTOMS
U SIGNS AND SYMPTOMS

SYNAPSES
Determining neural network connectivity using evolutionary programming
[AD-A266853] 02 p0766 N94-14882
Theoretical and experimental research into biological mechanisms underlying learning and memory
[AD-A267441] 03 p1133 N94-17022

Synaptic plasticity and memory formation
| AD-A267988 | 03 p1133 N94-17453
The identification of the computational significance of key neurobiological characteristics found in a number of telencephalic brain regions
| AD-A269374 | 04 p1505 N94-18407
Customizable VLSI artificial neural network chips based on a novel technology
| DE94-001418 | 06 p2307 N94-23008
Electrophysiology of the rat nucleus accumbens: Local circuitry, neuromodulation and synaptic plasticity
| PB93-232254 | 06 p2420 N94-23454
Synaptogenesis, selective stabilization, and free association
| AD-A275250 | 08 p3392 N94-29431

SYNCHROCYCLOTRONS
On modelling nuclear reactions in meteorites 05 p2085 N94-20844
On the (mu)SR activity at LNP JINR phasotron
| DE94-608385 | 08 p3517 N94-30195

SYNCHRONISM
NT BIT SYNCHRONIZATION
An object-oriented model for extensible concurrent systems: The composition-filters approach
| MEMO-INF-92-87 | 01 p0320 N94-10166
LASSO observations at McDonald and OCA/CERGA: A preliminary analysis 01 p0352 N94-10972
PTTI-aided ephemeris calculation and rapid data link acquisition for manned space flight 01 p0042 N94-10974
Timing in private digital telecommunication networks 01 p0139 N94-10991
SONET synchronization: What's happening 01 p0355 N94-10992
Solving integer programs from dependence and synchronization problems
| AD-A265702 | 02 p0767 N94-13284
A hardware implementation of a provably correct design of a fault-tolerant clock synchronization circuit
| NASA-TM-109001 | 02 p0759 N94-13450
Fine time uplink synchronization for frequency-hopped spread spectrum satellite communication system
| ISBN-0-315-54370-1 | 02 p0600 N94-13488
Simulation of downlink synchronization for a frequency-hopped satellite communication system
| DSIS-93-00477 | 02 p0605 N94-13941
Complexity analysis of real-time reinforcement learning applied to finding shortest paths in deterministic domains
| AD-A266636 | 03 p1131 N94-15742
Digital laser range finder emulator
| AD-D015811 | 03 p1040 N94-16540
Hydraulic pump with integral electric motor
| AD-D015782 | 03 p1011 N94-16549
Asynchronous design for parallel processing architectures
| AD-A266523 | 03 p1160 N94-16791
Verification of fault-tolerant clock synchronization systems
| NASA-TP-3349 | 03 p1161 N94-17449
On asynchronous testing
| MEMO-INF-93-03 | 04 p1543 N94-19226
Systolic design with asynchronous controls for digital-signal processing
| AD-A270976 | 04 p1392 N94-19680
Structural modeling: An application framework and development process for flight simulators
| AD-A271348 | 05 p1650 N94-19880
Time warp operating system version 2.7 internals manual
| NASA-CR-194798 | 05 p1899 N94-20549
Avoiding and tolerating latency in large-scale next-generation shared-memory multiprocessors 05 p1753 N94-21081
Reliable interface design for combining asynchronous and synchronous circuits 05 p1758 N94-21119
Partition algebraic design of asynchronous sequential circuits 05 p1759 N94-21125
Structured multimedia authoring
| CWI-CS-R9304 | 05 p2044 N94-21535
The Amsterdam hypermedia model: Extending hypertext to support real multimedia
| CWI-CS-R9306 | 05 p2045 N94-21536
A mechanized process algebra for verification of device synchronization protocols 05 p1766 N94-21716
Asynchronous timing and Doppler recovery in DSP based DPSK modems for fixed and mobile satellite applications 06 p2285 N94-22805
A CDMA synchronisation scheme 06 p2285 N94-22810
DS-SSMA capacity for a mobile satellite system 06 p2286 N94-22814
Incomplete corrections in nonlinear problems
| PB93-225746 | 06 p2479 N94-23106
Modeling parallelism and synchronization
| ETN-94-95179 | 06 p2465 N94-23134
Solid state Time Base Corrector (TBC)
| AD-D015981 | 06 p2312 N94-25039
System for producing synchronized signals
| AD-D016003 | 06 p2302 N94-25057
Modulation and synchronization technique for MF-TDMA system
| NASA-CR-194448 | 06 p2304 N94-25266
Specification performance optimization and executive generation for onboard multiprocessor real time application with SynDEx 07 p2954 N94-26745
Asynchronous and packetized systems engineering tools 07 p2954 N94-26746
Design of a parallel discrete event simulation coprocessor
| AD-A274135 | 07 p2982 N94-27123
Synchronization in multistatic radar
| PB94-136975 | 08 p3242 N94-28885
Acquisition time analysis of noncoherent PN sequence acquisition schemes
| AD-A275017 | 08 p3244 N94-29094
Synchronization of microwave oscillators by direct optical injection
| ISBN-0-315-85546-0 | 08 p3500 N94-30233
On blocks: Locality and asynchronous communication (extended abstract)
| RUU-CS-92-44 | 08 p3424 N94-30347
The 25th Annual Precise Time and Time Interval (PTTI) Applications and Planning Meeting
| AD-A280955 | 08 p3468 N94-30639
Loran-C time management 08 p3144 N94-30644
Optical techniques for time and frequency transfer 08 p3469 N94-30647
Relativistic theory for picosecond time transfer in the vicinity of Earth 08 p3470 N94-30653
The two-way time synchronization system via a satellite voice channel 08 p3471 N94-30658
LASSO experiment: Intercalibrations of the LASSO ranging stations 08 p3297 N94-30666
Time synchronized video systems 08 p3261 N94-30675
Using GLONASS signal for clock synchronization 08 p3475 N94-30680
Extension of the LUSTRE language and application to circuit design: The LUSTRE V4 language and the POLLUX system
| ETN-94-95918 | 09 p3812 N94-31543
ATM technology and beyond 10 p4156 N94-33820
Synchronized droplet size measurements for Coal-Water-Slurry (CWS) diesel sprays of an electronically-controlled fuel injection system
| DE94-008978 | 10 p4061 N94-34017
Analysis of optimistic window-based synchronization
| AD-280468 | 10 p4102 N94-34918
Runtime support for data parallel tasks
| AD-A280899 | 11 p4300 N94-35240
The weakest failure detector for solving Consensus
| NASA-CR-190545 | 11 p4300 N94-35365
Mathematical theory of synchronous communication
| PB94-169224 | 11 p4252 N94-35537
Obtaining coincident image observations for Mission to Planet Earth science data return 11 p4202 N94-35609
Synthesis of asynchronous systems from data flow specifications
| AD-A278687 | 11 p4303 N94-35662

SYNCHRONIZATION
U SYNCHRONISM

SYNCHRONOUS DETECTORS
U CORRELATORS

SYNCHRONOUS MOTORS
Design and application of electromechanical actuators for deep space missions
| NASA-CR-194145 | 02 p0663 N94-14134
Circuits and control processes for combining direct converters and inverter motors
| ETN-93-94399 | 03 p1008 N94-15448
Flow and heat transfer model for a rotating cryogenic motor
| DE94-001151 | 05 p1794 N94-22405
Design and application of electromechanical actuators for deep space missions
| NASA-CR-195134 | 06 p2365 N94-24842
Theoretical principles for designing long stator/linear motors with iron
| ETN-94-95741 | 09 p3688 N94-31374
Applicable dimensioning and measure and technological examination of long stator-linear motors for magnetic high-speed railways
| ETN-94-95734 | 09 p3689 N94-31575
Feasibility study of superconducting LSM rocket launcher system 11 p4225 N94-35914

SYNCHRONOUS PLATFORMS
Progress in multidisciplinary design optimization at NASA Langley
| NASA-TM-107754 | 01 p0318 N94-10814
Geostationary payload concepts for personal satellite communications 06 p2278 N94-22765
Global coverage Mobile Satellite Systems: System availability versus channel propagation impairments 06 p2284 N94-22798
A practical system for regional mobile satellite services 06 p2288 N94-22828
Advanced mobile satellite communications using COMETS satellite in MM-wave and Ka-band 06 p2288 N94-22829
CNES organization for station positioning of geostationary satellites 06 p2501 N94-23857
Time transfer using geostationary satellites: Implementation of a Kalman filter 08 p3471 N94-30657
Geostationary space launch vehicles and the US dilemma 11 p4210 N94-35377

SYNCHRONOUS SATELLITES
NT GOES SATELLITES
NT GOES 4
NT GOES 7
NT TD-1 SATELLITE
Sun-synchronous and geo-synchronous satellite data utilization for environmental studies 01 p0037 N94-10689
AMIGAU: A prototype tool aimed at mission analysis for satellites and satellite constellations 03 p0888 N94-17133
ARIANE 5 light derivatives 03 p0878 N94-17140
Small imaging satellite for Earth observing system adjunct 03 p0891 N94-17151
Adequation of mini satellites to oceanic altimetry missions 03 p0891 N94-17152
A study on an experimental communication system using microsatellites 03 p0892 N94-17160
The provision of spectrum for feeder links of non-geostationary mobile satellites 06 p2276 N94-22751
Multi-access laser communications terminal
| NASA-CR-191251 | 06 p2295 N94-23830
Commonality of flight control systems for support of European telecommunications missions 06 p2304 N94-23834
The geo-control system for station keeping and colocation of geostationary satellites 06 p2464 N94-23927
HISPASAT launch and early operations phases: Computation and monitoring of geostationary satellite positioning 06 p2514 N94-23928
Microvibrations on a GEO telecommunication satellite
| REPT-932-440-101 | 08 p3168 N94-29415

SYNCHROPHASOTRONS
Experimental setups and methods to obtain new nuclear data at intermediate and high energies
| DE94-607850 | 08 p3489 N94-30052

SYNCHROTRON RADIATION
Laser Synchrotron Source (LSS)
| AD-D015755 | 01 p0173 N94-10371
Cosmological gamma-ray burst model
| NASA-CR-193368 | 01 p0484 N94-10507
Proceedings of the Workshop on Applications of Synchrotron Radiation to Trace Impurity Analysis for Advanced Silicon Processing
| DE93-013389 | 02 p0805 N94-13020
Measurement of the spin of a particle using undulator radiation
| DE93-014334 | 02 p0780 N94-13149
Application of synchrotron radiation in chemical dynamics
| DE93-015040 | 02 p0563 N94-13411
Applications of surface science to solid lubricants
| SMC-TR-93-24 | 02 p0579 N94-13903
Comparative study of x ray and microwave emissions during solar flares
| NASA-CR-194532 | 02 p0845 N94-14577
Powder diffraction studies using anomalous dispersion
| DE93-012531 | 03 p1210 N94-16775
Application of cylindrical distribution functions to anisotropic scattering from amorphous films
| DE93-015256 | 03 p1183 N94-16811
Suppression of charge scattering in Moessbauer experiments using synchrotron radiation
| DE93-015406 | 03 p1212 N94-16887
Growth of dielectric thin films by irradiation of condensed molecular precursors with synchrotron radiation
| DE93-016161 | 03 p0974 N94-17676
Conical geometry for sagittal focusing as applied to x rays from synchrotrons
| DE93-017238 | 04 p1593 N94-17760
Nonlinear Thomson scattering of intense laser pulse from beams and plasmas
| AD-A269556 | 04 p1438 N94-18460
A tunable compact high power far-infrared grating free-electron laser
| AD-A269875 | 04 p1440 N94-18771

Simulation of the ALS longitudinal multibunch feedback system
[DE93-019227] 04 p1575 N94-19152
Study of coupled-bunch collective effects in the ALS
[DE93-019236] 04 p1575 N94-19558
Synchrotron x ray diffraction analysis of photorefractive crystals and their gratings
[AD-A271176] 05 p2015 N94-20213
Examination for optimization of synchrotron radiation spectrum for the x ray depth lithography
[BONN-IR-92-32] 05 p1987 N94-21148
Radio and optical emission: Spectral shapes and breaks in GRB
[NASA-CR-194763] 05 p2150 N94-21781
Monte Carlo calculation of multi-electron effects on synchrotron radiation
[DE94-001259] 05 p1982 N94-21974
Proceedings of the Fifth Users Meeting for the Advanced Photon Source
[DE93-040692] 06 p2531 N94-22948
Activities of Academia Sinica
[DE93-614529] 06 p2541 N94-25335
Fast photoconductor CdTe detectors for synchrotron x ray studies
[DE94-001334] 07 p3054 N94-26139
Comparison of technology for high-power laser mirrors and synchrotron radiation mirrors
[DE94-002913] 07 p3035 N94-26276
Activity report of Synchrotron Radiation Laboratory 1992
[JTN-94-80600] 08 p3495 N94-29596
Photoelectron diffraction and holography: Some new directions
[DE94-006297] 08 p3289 N94-30027
A high rate, low noise, x ray silicon strip detector system
[DE94-004557] 08 p3268 N94-30717
Characterization of the rare earth orthophosphates and Ce-doped LaPO4 by x ray absorption spectroscopy
[DE94-006313] 09 p3898 N94-31630
Double photoionization of helium with synchrotron x rays: Proceedings
[DE94-006737] 09 p3866 N94-31668
Near edge x ray spectroscopy theory
[DE94-008179] 09 p3905 N94-32799
Integral characteristics of the magnetic bremsstrahlung
[DE94-616788] 11 p4256 N94-36078
X ray and gamma ray spectroscopy of solids under pressure
[DE94-011207] 11 p4238 N94-36203
In situ studies of zeolite syntheses using powder diffraction methods: Crystallization of instant zeolite A powder and CoAPO-5
[DE94-006570] 11 p4341 N94-36358
Physics Division annual review, 1 April 1992 - 31 March 1993
[DE94-002497] 12 p4512 N94-36513
Activities of the Photon Factory
[DE94-748682] 12 p4522 N94-37236
Guiding hard x rays with glass polycapillary fiber
[DE94-004949] 12 p4525 N94-37258
Arterial cross-section measurements from dual energy transvenous coronary angiography images
[DE94-011193] 12 p4482 N94-37444

SYNCHROTRONS
NT STORAGE RINGS (PARTICLE ACCELERATORS)
Upgraded D(O) calorimeter electronics for short Tevatron bunch space and the effect of pile-up on the W mass measurement
[DE93-013566] 01 p0146 N94-12603
Proceedings of the Workshop on Applications of Synchrotron Radiation to Trace Impurity Analysis for Advanced Silicon Processing
[DE93-013389] 02 p0805 N94-13020
A new formulation of longitudinal coherent instabilities
[DE93-014288] 02 p0789 N94-13220
The evolution of tensor polarization
[DE93-017209] 02 p0790 N94-14897
Study of the rare decays K(sub L)(sup 0) yields (mu)e, K(sub L)(sup 0) yields ee, and K(sub L)(sup 0) yields (mu)(mu) at KEK
[DE93-753247] 03 p1180 N94-15135
The (delta)f algorithm for beam dynamics
[DE93-015632] 03 p1187 N94-16660
Fundamental-mode RF design in e(+)e(-) storage ring factories
[DE93-015249] 03 p1183 N94-16809
ARIES tokamak reactor study
[DE93-017059] 03 p1203 N94-16901
Synchrotron beam-loading stability with a higher RF harmonic
[DE93-014549] 04 p1573 N94-17726
Conical geometry for sagittal focusing as applied to x rays from synchrotrons
[DE93-017238] 04 p1593 N94-17760
Magnetic field measurements of a superconducting undulator for a Harmonic Generation FEL experiment at the NSLS
[DE93-017621] 04 p1438 N94-18504
Laser powered beam conditioner for free-electron lasers and synchrotrons
[DE93-017821] 04 p1441 N94-18974
The 1982 to 1992 decade of research on the vacuum ultraviolet ring at National Synchrotron Light Source
[DE93-019469] 04 p1603 N94-19564
A summary of studies of particle stability at RHIC
[DE93-040173] 05 p1970 N94-19868
ALE project
[AD-A271080] 05 p2014 N94-19980
Synchrotron x ray diffraction analysis of photorefractive crystals and their gratings
[AD-A271176] 05 p2015 N94-20213
Jet shapes in hadron and electron colliders
[DE93-019386] 05 p1979 N94-20216
The cross section for the production of b(bar-b) pairs in p(bar p) collisions at the square root of s equals 1.8 TeV
[DE93-019900] 05 p1972 N94-20225
National Synchrotron Light Source user's manual: Guide to the VUV and x ray beamlines
[DE93-019564] 05 p2015 N94-20260
Energy and luminosity limits of hadron supercolliders
[DE93-019248] 05 p1980 N94-20300
Wavelength dispersive analysis with the synchrotron x ray fluorescence microprobe 05 p1685 N94-20717
Infrared FEL photochemistry: Multiple-photon dissociation of freon gas
[DE94-000817] 05 p1820 N94-22585
Inverse free electron laser beat-wave accelerator research
[DE94-002597] 06 p2349 N94-23702
Low mass muon pair production in 450 GeV p-Be collisions
[PB94-110699] 06 p2533 N94-23746
Fast photoconductor CdTe detectors for synchrotron x ray studies
[DE94-001334] 07 p3054 N94-26139
Regrouping of the beam in the IHEP PS for the UNK p-p programs
[DE93-634021] 07 p3032 N94-26164
Longitudinal diffusion of a proton bunch under external noise
[DE93-634022] 07 p3032 N94-26165
Comparison of technology for high-power laser mirrors and synchrotron radiation mirrors
[DE94-002913] 07 p3035 N94-26276
Experimental measurement of local displacement and chemical pair correlations in crystalline solid solutions
[DE94-001124] 07 p3065 N94-27251
Measurement of the W mass in the D0 detector
[DE94-006002] 08 p3490 N94-30103
Search for the top quark in the electron-electron and electron-muon channels at D0
[DE94-006174] 08 p3492 N94-30779
Time-dependent behavior of active galactic nuclei with pair production 09 p3929 N94-31125
Particle diffusion from the beam-beam interaction in synchrotron colliders
[DE94-007111] 09 p3876 N94-32685
H(-) injection simulation for a 5 MW spallation neutron source
[DE94-009003] 10 p4140 N94-33983
Measurements of the SIS: Magnets and SIS control system 10 p4067 N94-34359
Activities of the optoelectronics laboratory
[PB94-171196] 11 p4334 N94-36190
X ray and gamma ray spectroscopy of solids under pressure
[DE94-011207] 11 p4238 N94-36203
Electroweak physics at the Tevatron collider
[DE93-040927] 12 p4513 N94-36695
Physics with primary beams of the KEK-PS
[DE94-748635] 12 p4522 N94-37234

SYNCOM SATELLITES
NT SYNCOM 4 SATELLITE

SYNCOM 4 SATELLITE
STS-32 mission highlights resource tape
[NASA-TM-109291] 02 p0531 N94-13631
STS-32 onboard 16mm photography quick release
[NASA-TM-109472] 03 p0880 N94-15376

SYNCOPE
NT BLACKOUT (PHYSIOLOGY)
Pulse waveform and transcranial Doppler analysis during lower body negative pressure
[AD-A274516] 07 p2911 N94-27088
Orthostatic responses to dietary sodium restriction during heat acclimation 10 p4096 N94-33640

SYNDROMES
U SIGNS AND SYMPTOMS

SYNOPTIC METEOROLOGY
TOVS soundings: Impact on the synoptic analysis over the south and southeast regions of Brazil from March 18 to March 19, 1991
[INPE-5497-TDI/512] 01 p0230 N94-11179
Storm prediction through barometric field analysis
[PUBL-SER-A-129] 02 p0720 N94-13587
AMIP: Diagnostic subproject on the variability in the tropics: Synoptic to intraseasonal time scales
[DE93-009287] 02 p0721 N94-13914
Spectral analysis of synoptic time scale disturbances over the tropical eastern Pacific during summer 1989, 1990 and 1991
[AD-A268821] 04 p1490 N94-18206
Reports of the 1992 Synoptic Symposium
[KNMI-TR-151] 04 p1494 N94-19698
The life cycles of intense cyclonic and anticyclonic circulation systems observed over oceans
[NASA-CR-194760] 05 p1865 N94-20353
A synoptic-scale overview of the TOGA COARE intensive observing period November 1992 to February 1993 based on analyses from US operational global data assimilation systems
[NASA-TM-104593] 05 p1868 N94-21605
A documentation of icing relevant cloud physical parameters on horizontal soundings of stratiform clouds (continuation)
[DLR-MITT-92-10] 05 p1871 N94-22280
Examination of the observed synoptic scale cirrus cloud environment: The December 3-6 FIRE cirrus case study 05 p1877 N94-22325
Cirrus cloud development in a mobile upper tropospheric trough: The November 26th FIRE cirrus case study 05 p1878 N94-22329
Modelling TOVS radiances of synoptic systems
[NASA-CR-194847] 06 p2408 N94-23620
Mesospheric and lower thermospheric winds, temperatures densities, and volume emission rates
[NASA-CR-195147] 06 p2403 N94-24486
Analyzing Martian winds and tracer concentrations using Mars Observer data 06 p2619 N94-24883
Observed and Navy operational global model climatologies of synoptic disturbances over the tropical western Pacific during winter 1991-1992
[AD-A273400] 06 p2416 N94-25071
The evaluation of ASOS for the Kennedy Space Center's Shuttle Landing Facility
[NASA-CR-195685] 06 p2416 N94-25271
Propagation of cold air masses in East Asia and its associated planetary-scale function
[AD-A274304] 07 p2895 N94-26850
A synoptic study on periods of deficiency over Rio Grande do Sul/Brazil
[INPE-5456-TDI/498] 07 p2896 N94-27422
Dynamics in the tropics and synoptic disturbances 09 p3778 N94-30990

SYNTAX
NT SENTENCES
NT SYLLABLES
NT WORDS (LANGUAGE)
Processing proper nouns in machine translation for English news
[NHK-SERIAL-414] 01 p0418 N94-10559
Proposal for a numerical array library
[DE93-015017] 04 p1516 N94-17786
Better termination analysis for active databases
[REPT-93-026] 04 p1614 N94-18144
Attribute evaluation during generalized parsing
[MEMO-INF-92-85] 04 p1526 N94-19224
Feasibility study in linguistically motivated object-oriented conceptual design of information systems
[PB93-197754] 04 p1618 N94-19331
Representation of idioms in connectionist models 05 p1940 N94-20247
Hopfield models as neural-network acceptors 05 p1941 N94-20250
Syntactic neural networks for natural language processing 05 p1941 N94-20254
COCOLOG: A conditional observer and controller logic for finite machines
[INRIA-RR-1714] 05 p1910 N94-21063
Recognizing hesitation phenomena in continuous, spontaneous speech 05 p1746 N94-22210
Fortran for the nineties 05 p1926 N94-22481
Design and specification of a generic task model for solving boolean constraint satisfaction problems
[PB94-118841] 06 p2486 N94-23762
Models of the untyped lambda-calculus in semi Cartesian closed categories
[ML-93-05] 08 p3456 N94-30381
The Vanilla meta-interpreter for definite logic programs and ambivalent syntax
[CT-93-01] 08 p3424 N94-30386

The conjoinability relation in Lambek calculus in linear logic
| ML-93-03 | 08 p3457 N94-30397
Comparative semantics for linear arrays of communicating processes
| CWI-CS-R9336 | 08 p3426 N94-30491
Federal grammars and modular compilers
| REPT-93-054 | 08 p3429 N94-30928
Correspondence theory for extended modal logics, version 3.0
| ML-93-16 | 09 p3856 N94-31417
Compositionality of application oriented structuring mechanisms for algebraic specification languages with initial semantics
| ETN-94-95736 | 09 p3812 N94-31577
Informal introduction to the extended affix grammar formalism and its compiler
| TR-93-19 | 09 p3817 N94-32287
An epistemic proof system for parallel processes
| TR-93-17 | 09 p3826 N94-32291
Probabilities and priorities in timed CSP
| PB94-169216 | 11 p4316 N94-35536
Mathematical theory of synchronous communication
| PB94-169224 | 11 p4252 N94-35537
Refinement types ML
| AD-A278937 | 11 p4304 N94-35709

SYNTHESIS (CHEMISTRY)
NT COPOLYMERIZATION
NT DIMERIZATION
NT POLYMERIZATION
Synthesis of molecular sieves from clear solution
01 p0124 N94-10245
New aromatic activated dihalides and bisphenol monomers for the preparation of novel poly(arylene ethers)
| NASA-CR-193190 | 01 p0055 N94-10513
Primaset (tm): A safer material for aircraft interior applications 01 p0018 N94-10772
Low temperature synthesis of monolithic transparent Ta2O5 gels from hydrolysis of metal alkoxide
| NASA-TM-106246 | 01 p0089 N94-11204
Synthesis and thermal evolution of structure in alkoxide-derived niobium pentoxide gels
| NASA-TM-106259 | 01 p0090 N94-11257
Synthesis and electronic properties of nanophase semiconductor materials
| AD-A265287 | 01 p0146 N94-12584
Photogenerated base in polymer imaging. Synthesis and photopatterning of poly(2-cyano-2-(p-vinylphenyl) butanoic acid)
| AD-A265288 | 01 p0095 N94-12585
Correlations of the growth, structure, and stress with the adhesion of diamond films on tungsten
| DE93-012855 | 02 p0576 N94-12912
Synthesis inversion of atmospheric CO2 using the GISS tracer transport model
| CSIRO-TP-29 | 02 p0709 N94-14095
Catalytic arene hydrogenation using early transition metal hydride compounds
| DE93-015500 | 02 p0573 N94-14402
Synthesis and chemistry of novel cyclic fluorocarbons
| AD-A267148 | 03 p0929 N94-15734
High temperature advanced structural composites. Volume 1: Executive summary and intermetallic compounds
| AD-A267022 | 03 p0933 N94-15835
Ion doped quantum well lasers
| AD-A267198 | 03 p1038 N94-15853
Synthesis of ceramic oxide powders in a microwave plasma device
| DE93-012741 | 03 p0965 N94-15920
Use of microgravity in the synthesis of ceramics using sol gel techniques 03 p0979 N94-16088
High octane ethers from synthesis gas-derived alcohols
| DE93-016861 | 03 p0975 N94-16898
Amide and tetrazene complexes of transition and main group elements as precursors for the low temperature synthesis of elemental nitrides
| AD-A266246 | 03 p0950 N94-16931
Photodegradation of MDI based polyurethane/urea elastomers
| AD-A267308 | 03 p0971 N94-16994
Theoretical studies of nonlinear optical properties of conjugated polymers
| AD-A267390 | 03 p1193 N94-17024
Synthesis of potential high-energy fuels
| AD-A267508 | 03 p0975 N94-17073
Synthesis, reactivity, and characterization of (-hexacarbocyclic) manganese dicarbonyl complexes with sulfur and phosphorus ligands
| AD-A267592 | 03 p0930 N94-17192
Synthesis, characterization, and polymerization of new ferrocene-fluorene complexes. A novel high-molecular weight conjugated polymer with pendant ferrocene groups
| AD-A267717 | 03 p0972 N94-17273
Synthesis and characterization of new low-dimensional metal complex conductors
| AD-A268251 | 03 p0952 N94-17416
Modified aequorin shows increased bioluminescence activity
| AD-A268774 | 04 p1347 N94-18185
Conversion of ethane and of propane to higher olefin hydrocarbons
| DE93-015282 | 04 p1347 N94-18194
Synthesis of higher alcohols from carbon monoxide and hydrogen in a slurry reactor
| DE93-015086 | 04 p1347 N94-18209
Nanostructured materials: Mind over matter
| DE93-017690 | 04 p1597 N94-18480
Royal Society of Chemistry, Heterocyclic Chemistry Group, Lakeland Heterocyclic Symposium
| AD-A270374 | 04 p1338 N94-18703
Temperature lowering in cryogenic chemical-synthesis techniques and system
| DE93-018348 | 04 p1562 N94-18810
Molecular and polymeric ceramic precursors
| DE93-040364 | 04 p1372 N94-18891
Final report on subcontract B076260 --- borate synthesis
| DE93-019501 | 04 p1604 N94-19565
Isolation mechanisms in III-V devices
| AD-A271197 | 04 p1605 N94-19717
Synthesis and structural characterization of new light molecular weight inorganic oxidizers and relative derivatives, volume 1
| AD-A271437 | 05 p2012 N94-19842
Electrochemical synthesis of ultrathin film composite membranes
| AD-A272721 | 05 p1681 N94-21168
Development of bioelastic material for aspects of wound repair
| AD-A272000 | 05 p1892 N94-21503
Synthesis and catalytic properties of metal and semiconductor nanoclusters
| DE93-019418 | 05 p2028 N94-21541
Particle formation in a laser-heated aerosol reactor. Application to silicon and silicon nitride synthesis
| PB93-217982 | 06 p2347 N94-22982
Di(hydroxyphenyl)- 1,2,4-triazole monomers
| NASA-CASE-LAR-14440-2 | 06 p2252 N94-23075
Reaction of isocyanates with carboxylic acids and its application to polymer synthesis
| PB94-118858 | 06 p2254 N94-23763
Synthesis and in-vivo detection of boronated compounds for use in BNCT
| DE94-001899 | 06 p2233 N94-23780
New methane chemistry synthesis of materials for reversible uptake and useful functionalization of methane
| PB94-112786 | 06 p2233 N94-23801
Synthesis of soluble halogenated polyphenylenes: Mechanism for the coupling halogenated lithiobenzenes
| AD-A273547 | 06 p2257 N94-24558
Metal-catalyzed alkynylation of (Bromophenyl)Oligophenylenes: A rapid route to thermoset precursors of high density monolithic glass-like carbon
| AD-A273219 | 06 p2260 N94-24863
Development of SO(x) and NO(x) solid electrolyte sensors 07 p2725 N94-25562
Fundamental study on new synthetic technology by phthalocyanine complexes 07 p2721 N94-25569
Template synthesis of metal microtubule ensembles utilizing chemical, electrochemical, and vacuum deposition techniques
| AD-A274676 | 07 p2715 N94-26444
Structure and properties of composites synthesized in situ using solid state displacement reactions
| DE94-004589 | 07 p2737 N94-26585
Molecular surface electrostatic potentials in the analysis of non-hydrogen-bonding noncovalent interactions
| AD-A274612 | 07 p3022 N94-26894
Synthesis, rheology, and forming of Y-Ba-Cu-O ceramics
| DE94-005558 | 07 p2757 N94-27695
Preparation, characterization, and thermal behaviour study of lanthanides (3) and yttrium (3) 4-methoxy benzylidene pyruvate in solid state
| DE94-604079 | 07 p3068 N94-27697
Synthesis and characterization of novel ternary and quaternary reduced molybdenum oxides
| DE94-005563 | 08 p3510 N94-28529
Preparation, characterization, and facile thermolysis of (X2GaP(SiMe3)2) (X = Br, I) and (Cl3Ga2P)n; new precursors to nanocrystalline gallium phosphide
| AD-A275019 | 08 p3513 N94-29130
Synthesis and molecular structures of R(Me3CCH2)2In-E(SiMe3) (R = Me3CCH2, E = P or As; R = Me, E = P)
| AD-A275020 | 08 p3486 N94-29131
Tris(trimethylsily)arsine and lithium bis(trimethylsily)arsenide
| AD-A275075 | 08 p3189 N94-29140
The synthesis and structural characterization of Na3WO3N
| AD-A275243 | 08 p3204 N94-29395
Preparation of monodispersed fine particles containing rare metals and rare earths 08 p3201 N94-29514
Study on the formation of ultrafine particles of Sm-Co intermetallic compounds using RF thermal plasma 08 p3211 N94-29516
Preparation of graphite fibers from polyimide 08 p3223 N94-29517
Production of fullerenes with concentrated solar flux
| DE94-000266 | 08 p3514 N94-29801
Bench-scale synthesis of nanoscale materials 08 p3240 N94-30473
Synthesis and characterization of advanced materials for Navy applications 08 p3223 N94-30474
Feasibility study to evaluate plasma quench process for natural gas conversion applications
| DE94-000086 | 09 p3758 N94-31234
Novel electroactive polymers and block copolymers
| AD-A276119 | 09 p3650 N94-31509
Biocatalytic processing polymers in supercritical fluids
| AD-A276120 | 09 p3651 N94-31510
Inorganic materials for anomalous-dispersion phase-matched second harmonic generation: Rubidium titanyl arsenate isomorphs, Rb(Ti(1-2x)Ln(x)Nb(x))OAsO4
| DE94-006141 | 09 p3899 N94-31847
Tetraalkyldiarsines as potential precursors for electronic materials: Synthesis and characterization of various iso-propyl arsenic compounds
| AD-A277003 | 09 p3900 N94-32001
Processable, chemical routes to binary metal sulfides
| AD-A277006 | 09 p3642 N94-32004
Group 12 thiolates: Syntheses, characterization and decomposition pathways
| AD-A277055 | 09 p3900 N94-32011
High octane ethers from synthesis gas-derived alcohols
| DE94-006774 | 09 p3667 N94-32133
Towards a detailed understanding of the structural variability in lignins: A new approach
| DE94-007449 | 09 p3793 N94-32267
Development of a catalyst for conversion of syngas-derived materials to isobutylene
| DE94-009698 | 10 p4021 N94-33901
Generalized syntheses of periodic surfactant and inorganic composite materials
| AD-A278001 | 10 p4019 N94-34160
Be3(AsO4)2.2H2O, a new berylloarsenate phase containing bridged tetrahedral 3-rings
| AD-A278826 | 11 p4340 N94-35677
Third European Technical Symposium on Polyimides and High Performance Polymers: STEPI 3
| PB94-148491 | 11 p4246 N94-36177
Tert-butylalumoxanes: Synthetic analogs for methylalumoxane (MAO) and new catalytic routes to polyolefins and polyketones
| AD-A280511 | 12 p4399 N94-37106
Cyclization of bis-urethanes as a new method for the synthesis of 5-substituted, 6-membered cyclic ureas
| AD-A280232 | 12 p4399 N94-37134
Midwest Superconductivity Consortium
| DE94-012716 | 12 p4536 N94-37285
Theoretical and experimental investigations of fullerene derivatives: C60H2, C60H4, C70H2 and C60CH22
| DE94-012727 | 12 p4536 N94-37287
Copper-containing ceramic precursor synthesis: Solid-state transformations and materials technology
| NASA-TM-106556 | 12 p4399 N94-37315
Iron hydrous titanium oxide catalysts for the dehydrogenation of ethylbenzene to styrene
| DE94-010381 | 12 p4412 N94-37542
High T(sub c) copper-oxide superconductors comprising Tl-Sr-Ca-Cu-O
| AD-D016307 | 12 p4538 N94-37776
Substituted silyl-terminated compounds and polymers thereof
| AD-D016310 | 12 p4427 N94-37779
Carborane-(silane or siloxane)-unsaturated hydrocarbon based thermosetting polymers
| AD-D016311 | 12 p4427 N94-37818
Double network elastomers and method of making same
| AD-D016323 | 12 p4427 N94-37831

SYNTHESIZERS
Modelling the late part of room impulse responses using adaptive filtering: On the recreation of reality
| CTH-E-93-01 | 09 p3859 N94-31076

High-speed digital project, HSD test capability
[DE94-010885] 11 p4260 N94-36197
SYNTH: A spectrum synthesizer
[DE94-004719] 11 p4331 N94-36317
SYNTHETIC APERTURE RADAR
NT SIDE-LOOKING RADAR
Spaceborne SAR study: LDRD 1992
[DE93-011485] 01 p0232 N94-11623
Proceedings of First ERS-1 Symposium on Space at the Service of Our Environment, volume 1
[ESA-SP-359-VOL-1] 01 p0232 N94-11704
Validation of directional wave spectra from the ERS-1 during the ESA CAL/VAL campaign
01 p0232 N94-11707
The Grand Banks ERS-1 SAR wave spectra validation experiment 01 p0232 N94-11708
Use of ERS-1 data at Saclant Undersea Research Centre 01 p0233 N94-11714
Mapping of the East Australian current with the ERS-1 SAR and shipborne studies 01 p0234 N94-11717
Wind and surface features in SAR images: The Canadian program 01 p0234 N94-11718
Coastal ocean studies with ERS-1 SAR during NORCSEX 1991 01 p0234 N94-11720
SAR imaging of dynamical features in the English Channel 01 p0234 N94-11721
SAR ocean imaging in the Gulf of Alaska
01 p0235 N94-11723
ERS-1 SAR calibration strategy
01 p0235 N94-11726
ERS-1 preliminary antenna elevation pattern measured by ground-receivers 01 p0235 N94-11727
Preliminary results of the experiment I-7
01 p0235 N94-11728
The ERS-1/CV 580 SAR cross-calibration experiment: Sault Ste Marie, October 26 - November 2, 1991
01 p0236 N94-11729
Calibration of the ERS-1 SAR fast-delivery images
01 p0236 N94-11730
Calibration results for the ERS-1, AIRSAR, and PHARS 01 p0236 N94-11731
The use of active devices in the ERS-1 radiometric calibration 01 p0236 N94-11732
An experiment for the radiometric calibration of the ERS-1 SAR 01 p0236 N94-11733
Techniques and applications of SAR interferometry for ERS-1: Topographic mapping, change detection, and slope measurement 01 p0236 N94-11734
SAR interferometry experiments with ERS-1
01 p0237 N94-11735
SAR-interferometry applying ERS-1: Some preliminary test results 01 p0237 N94-11736
Monitoring of the Greenland Ice Sheet using ERS-1 synthetic aperture radar imagery
01 p0237 N94-11741
Investigations of Arctic ice-sheets and glaciers using ERS-1 SAR 01 p0238 N94-11743
Spatial patterns in backscatter strength across the Greenland Ice Sheet 01 p0238 N94-11744
Ice studies in the Barents Sea by ERS-1 SAR during SIZEX 92 01 p0238 N94-11745
Validation of ERS-1 SAR measurements of sea ice during ARCTIC-1991 01 p0238 N94-11747
Waves and mesoscale features in the marginal ice zone 01 p0240 N94-11757
Ocean circulation revealed by ice floe tracking
01 p0240 N94-11759
Preliminary evaluation of ERS-1 SAR data for operational use in the Canadian sea ice monitoring program
01 p0241 N94-11760
Summer Arctic ice concentrations and characteristics from SAR and SSM/I data 01 p0241 N94-11762
Ocean wave detection by SAR
01 p0197 N94-11932
On the determination of the SAR ocean surface scattering patch size 01 p0197 N94-11933
Ocean-ice interaction study of waves and mesoscale features 01 p0197 N94-11935
Characteristics of arachnoids from Magellan data
01 p0469 N94-12204
ISAR motion compensation using the burst derivative measure as a focal quality indicator
[AD-A265647] 01 p0138 N94-12440
Proceedings of 1st ERS-1 Symposium on Space at the Service of Our Environment, Volume 2
[ESA-SP-359-VOL-2] 01 p0245 N94-12471
Segmented land use classification of multitemporal ERS-1 SAR data using a majority filter
01 p0245 N94-12472
Land cover monitoring with multi-temporal ERS-1 SAR observations in the Netherlands
01 p0246 N94-12473
Mapping a dynamic playa surface using multitemporal ERS-1 SAR data: First results 01 p0246 N94-12474
Preliminary studies on the application of ERS-1 data to topographic mapping 01 p0246 N94-12476
Radarmap of Germany: First mosaic and classification
01 p0246 N94-12477
Combined analysis of ERS-1 SAR and visible/infrared remote sensing data for land cover/land use mapping in a tropical zone: A case study in Guinea
01 p0246 N94-12478
Example of SPOT/ERS-1 complementarity
01 p0247 N94-12479
The use of ERS-1 SAR data to study surface states
01 p0247 N94-12480
Snow and glacier investigations by ERS-1 SAR: First results 01 p0247 N94-12481
Monitoring of snowcover in high mountain terrain with ERS-1 SAR 01 p0247 N94-12482
Application of ERS-1 SAR data to snow mapping
01 p0247 N94-12483
Per-field filtering and classification of multitemporal ERS-1 SAR imagery 01 p0247 N94-12485
Preliminary ERS-1 assessment for Canadian agriculture and forestry applications 01 p0248 N94-12486
Segmentation and change detection in ERS-1 images over East Anglia 01 p0248 N94-12487
ERS-1 SAR crop monitoring experiment in East Anglia, UK 01 p0248 N94-12488
Geoecological monitoring of an agricultural area
01 p0248 N94-12489
Assessment of ERS-1 SAR data for soil moisture estimation 01 p0249 N94-12492
Temporal monitoring of soil moisture using ERS-1 SAR data 01 p0249 N94-12493
Observations of ERS-1 SAR sensitivities to changes in aboveground biomass in young loblolly pine forests
01 p0249 N94-12494
Seeing the Black Forest by ERS-1 and AIRSAR: A comparison 01 p0249 N94-12495
The TREES project: Pre-processing and generation of terrain data for inclusion in an ERS-1 SAR classification scheme 01 p0249 N94-12496
TREES project: A case study on the use of multi-temporal ERS-1 SAR data and SPOT data for monitoring tropical ecosystems 01 p0249 N94-12497
TREES project: A suite of tools for information extraction from ERS-1 SAR data 01 p0250 N94-12498
TREES project: Overview and status of the ERS-1 SAR contribution 01 p0250 N94-12499
A statistical analysis of sea state surface ERS-1 SAR-wave mode imagettes 01 p0251 N94-12507
A new model for Synthetic Aperture Radar (SAR) images from ocean scatter 01 p0251 N94-12508
On the extraction of ocean wave spectra from ERS-1 SAR wave mode image spectra
01 p0251 N94-12509
Tide-generated nonlinear internal wave packets in the Strait of Gibraltar observed by the synthetic aperture radar aboard the ERS-1 satellite 01 p0252 N94-12510
Artificial oil pollution detection and wave observation in the sea adjacent to Japan by ERS-1 SAR
01 p0253 N94-12520
Ship traffic monitoring using the ERS-1 SAR
01 p0253 N94-12521
Oil spill detection using satellite-based SAR: Experience from a field experiment 01 p0253 N94-12522
Pilot project PPF12. Coastal and fluvial environment in French Guiana: First results of ERS-1 SAR data analysis
01 p0254 N94-12523
Coastal morphodynamics and energetic characteristics of swell studied with ERS-1 SAR
01 p0254 N94-12524
Mapping of sea bottom topography with ERS-1 C-band SAR 01 p0254 N94-12525
ERS-1 imaging radar over the Waddensea-North Netherlands 01 p0254 N94-12526
SAR imaging of geology and bathymetry: Kent coastal area - southern North Sea 01 p0254 N94-12527
Applications of ERS-1 SAR data for analyzing riverine and coastal processes and geomorphology
01 p0254 N94-12528
Comparison of ERS-1 SAR images of the Western Mediterranean to in situ oceanographic data: PRIM-1 Cruise (May 1992) 01 p0255 N94-12529
Ice studies in the Barents Sea by ERS-1 during SIZEX 1992 01 p0210 N94-12653
Observations of surface signatures in the north-west Pacific Ocean with the spaceborne SAR
01 p0226 N94-12746
Preparations for and first results of the calibration and interpretation of ERS-1 SAR imagery over land
[BCRS-92-13] 02 p0684 N94-13123
A combined analogue and digital pulse compression system using large time bandwidth product signals for use in synthetic aperture radar
[ISBN-0-315-54373-6] 02 p0600 N94-13489
Phase aligner for the Electronically Scanned Thinned Array Radiometer (ESTAR) instrument
[NASA-TM-4518] 02 p0623 N94-13878
Feature discovery on segmented objects in SAR imagery using self-organizing neural networks
[DE93-010685] 02 p0686 N94-14056
Testing various time-frequency distribution techniques
[DREO-TN-92-17] 02 p0606 N94-14062
Earth Observation Center Annual Report on Research and Development, Fiscal Year 1992
[EOC-92-01-0007] 02 p0687 N94-14091
Calibration and in-house validation results of JERS-1 data 02 p0687 N94-14092
Results from ERS-1 and JERS-1 SAR calibration experiments and data analysis 02 p0688 N94-14210
Geologic application of JERS-1 SAR data
02 p0688 N94-14211
Artificial oil pollution detection and wave observation in the sea adjacent to Japan by ERS-1 SAR
02 p0688 N94-14212
An exact processing algorithm for wide beam spaceborne SAR data 02 p0689 N94-14213
Survey of subsurface geophysical exploration technologies adaptable to an airborne platform
[DE93-015080] 02 p0717 N94-14294
Ionospheric effects on a wide-bandwidth, polarimetric, space-based, synthetic-aperture radar
[DE93-015084] 02 p0612 N94-14512
Microwave interconnection
[DE93-016580] 02 p0625 N94-14533
Overview of Enhanced Data Stream Array Processor (EDSAP)
[AD-A266986] 03 p1158 N94-15492
Proceedings of the Third Spaceborne Imaging Radar Symposium
[NASA-CR-194104] 03 p0989 N94-15886
Almaz 03 p0898 N94-15889
X-SAR: The X-band synthetic aperture radar on board the Space Shuttle 03 p0990 N94-15891
ENVISAT ASAR 03 p0898 N94-15892
RADARSAT program 03 p0898 N94-15893
Recent scientific advances in the use of radar in scientific hydrology 03 p0991 N94-15895
Recent advances in radar remote sensing of forest
03 p0991 N94-15897
Multifrequency observations 03 p0992 N94-15902
SIR-C/X-SAR free flyer concept
03 p0898 N94-15903
EOS SAR: A new approach 03 p0992 N94-15904
TOPSAT: Global space topographic mission
03 p0992 N94-15905
Calibration: Practical experience with ERS-1
03 p0992 N94-15907
Synthetic aperture radar signal processing: Trends and technologies 03 p0992 N94-15908
Recent advances and plans in processing and geocoding of SAR data at the DFD
03 p0992 N94-15909
Data distribution 03 p0993 N94-15910
SAR sensor electronics: T/R modules
03 p0993 N94-15911
Advanced antennas for SAR spacecraft
03 p0993 N94-15912
High resolution SAR applications and instrument design 03 p0993 N94-15913
Primary studies of Chinese spaceborne SAR
03 p0993 N94-15916
International collaboration in SAR ground data systems 03 p0993 N94-15917
AIRSAR South American deployment: Operation plan, version 3.0 03 p0994 N94-15919
Summaries of the Third Annual JPL Airborne Geoscience Workshop. Volume 1: AVIRIS Workshop
[NASA-CR-194540] 03 p1066 N94-16666
MAC Europe 1991: Evaluation of AVIRIS, GER imaging spectrometry data for the land application testsite Oberpfaffenhofen 03 p1070 N94-16688
Summaries of the Third Annual JPL Airborne Geoscience Workshop. Volume 3: AIRSAR Workshop
[NASA-CR-194542] 03 p1075 N94-16731
A snow wetness retrieval algorithm for SAR
03 p1075 N94-16732
Comparison of JPL-AIRSAR and DLR E-SAR images from the MAC Europe 1991 campaign over testsite Oberpfaffenhofen: Frequency and polarization dependent backscatter variations from agricultural fields
03 p1075 N94-16733
Monitoring environmental state of Alaskan forests with AIRSAR 03 p1075 N94-16734
Comparison of modeled backscatter with SAR data at P-band 03 p1076 N94-16735
SAR backscatter from coniferous forest gaps
03 p1076 N94-16736
Retrieval of pine forest biomass using JPL AIRSAR data 03 p1076 N94-16737
Characterization of wetland, forest, and agricultural ecosystems in Belize with airborne radar (AIRSAR)
03 p1076 N94-16738

Strategies for detection of floodplain inundation with multi-frequency polarimetric SAR
03 p1076 N94-16739
Supervised fully polarimetric classification of the Black Forest test site: From MAESTROI to MAC Europe
03 p1076 N94-16740
Relating multifrequency radar backscattering to forest biomass: Modeling and AIRSAR measurement
03 p1077 N94-16741
SAR observations in the Gulf of Mexico
03 p1077 N94-16742
Investigation of AIRSAR signatures of the Gulf Stream
03 p1077 N94-16743
Mapping of sea bottom topography
03 p1077 N94-16744
Sea bottom topography imaging with SAR
03 p1077 N94-16745
Preliminary results of polarization signatures for glacial moraines in the Mono Basin, Eastern Sierra Nevada
03 p1078 N94-16746
Extraction of quantitative surface characteristics from AIRSAR data for Death Valley, California
03 p1078 N94-16748
The TOPSAR interferometric radar topographic mapping instrument 03 p1078 N94-16749
Evaluation of the TOPSAR performance by using passive and active calibrators 03 p1078 N94-16750
Fitting a three-component scattering model to polarimetric SAR data 03 p1079 N94-16751
Application of symmetry properties to polarimetric remote sensing with JPL AIRSAR data
03 p1079 N94-16752
External calibration of polarimetric radar images using distributed targets 03 p1079 N94-16753
Processing of polarimetric SAR data for soil moisture estimation over Mahantango watershed area
03 p1079 N94-16754
Evaluation of polarimetric SAR parameters for soil moisture retrieval 03 p1079 N94-16755
Interaction types and their like-polarization phase-angle difference signatures 03 p1079 N94-16756
Application of modified VICAR/IBIS GIS to analysis of July 1991 Flevoland AIRSAR data
03 p1080 N94-16757
Radar Analysis and Visualization Environment (RAVEN): Software for polarimetric radar analysis
03 p1080 N94-16758
Measuring ocean coherence time with dual-baseline interferometry 03 p1080 N94-16759
Soil conservation applications with C-band SAR
03 p1080 N94-16760
Comparison of edges detected at different polarisations in MAESTRO data 03 p1080 N94-16761
Lithological and textural controls on radar and diurnal thermal signatures of weathered volcanic deposits, Lunar Crater region, Nevada 03 p1080 N94-16762
Measurements of the radar cross section and Inverse Synthetic Aperture Radar (ISAR) images of a Piper Navajo at 9.5 GHz and 49 GHz
[AD-A267570] 03 p1002 N94-17110
Arctic cyclones and Marginal Ice Zone (MIZ) variability
[AD-A268610] 03 p1108 N94-17465
Flight demonstration of image fix-taking with SAR
[DE93-016499] 04 p1382 N94-17861
Tomographic mathematical ideas applied to radar detection
[AD-A268789] 04 p1384 N94-18186
AN/APS-137 Forward Looking Airborne Radar (FLAR) evaluation Spring 1992 experiment
[AD-A268899] 04 p1384 N94-18228
The spatial variance of ionospherically-induced phase errors in SAR imagery
[DE93-015643] 04 p1385 N94-18232
Arctic ice studies
[AD-A268608] 04 p1497 N94-18277
Application of Fourier-based features for classification of synthetic aperture radar imagery
[AD-A270450] 04 p1387 N94-18513
Resolution in radar mapping
[AD-A269730] 04 p1462 N94-18753
Modeling of current features in Gulf Stream SAR imagery
[AD-A270734] 04 p1499 N94-19609
Theoretical and experimental research on coherent microwave backscatter from the ocean
[AD-A271276] 04 p1500 N94-19743
Modifications to the three-component classification algorithm for SAR data 05 p1719 N94-20410
Determination of noise equivalent sigma(0) using highly correlated repeat-pass SAR images
05 p1720 N94-20411
Topographic mapping using a monopulse SAR system
05 p1721 N94-20417
Classification of simple vegetation types using POLSAR image data 05 p1722 N94-20420
Two microstrip arrays for interferometric SAR applications 05 p1722 N94-20421
Observation of pressure ridges in SAR images of sea ice: Scattering theory and comparison with observations
05 p1723 N94-20427
On evaluating the accuracy of SAR sea-ice classification using multifrequency polarimetric AIRSAR data
05 p1724 N94-20428
Direction angle sensitivity of agricultural field backscatter with AIRSAR data 05 p1724 N94-20430
Retrieval of ice thickness from polarimetric SAR data
05 p1724 N94-20432
Radar backscattering from snow facies of the Greenland ice sheet: Results from the AIRSAR 1991 campaign
05 p1725 N94-20434
C-band radar backscatter of sea ice in the Weddell Sea, Antarctica during the austral winter of 1992
05 p1725 N94-20435
Mapping of taiga forest units using AIRSAR data and/or optical data, and retrieval of forest parameters
05 p1729 N94-20452
The Brewster angle effect in SAR polarimetry
05 p1731 N94-20456
Topographic slope from the SAR interferometric phase gradient 05 p1731 N94-20459
Interferometric detection of freeze-thaw displacements of Alaskan permafrost using ERS-1 data
05 p1732 N94-20460
Performance evaluation of the JPL TOPSAR system: An across-track interferometric SAR system for topographic mapping 05 p1732 N94-20461
Use of microwave polarimetry to enhance SAR images of the ocean surface
[AD-A271911] 05 p1882 N94-20489
The application of spaceborne synthetic aperture radar in the maritime environment
[DRA-TM(AWE)-91013] 05 p1737 N94-20596
Beta Regio rift system on Venus: Geologic interpretation of Magellan images 05 p2095 N94-20655
Beta Regio - Phoebe Regio on Venus: Geologic mapping with the Magellan data 05 p2096 N94-20656
Magellan vertical polarization radar observations
05 p1744 N94-20691
Magellan Mission 05 p1652 N94-20829
Massachusetts Institute of Technology Lincoln Laboratory Journal volume 6, number 1, Spring 1993
[AD-A272273] 05 p1737 N94-20944
Neural network studies
[AD-A271593] 05 p1943 N94-20947
The 7th Brazilian Remote Sensing Symposium, volume 3 05 p1839 N94-20960
Evaluation of C-band SAR data from SAREX 1992: Tapajos study site 05 p1839 N94-20964
An overview of synthetic aperture radar signal processing techniques 05 p1745 N94-22159
Target angular motion and its effects on simulated SSAR ship images 05 p1745 N94-22161
A motion extraction method for synthetic aperture radars
[DLR-FB-92-31] 05 p1742 N94-22279
STAR-1 SAR road extraction using texture analysis and mathematical morphology
[ISBN-0-315-83255-X] 05 p1843 N94-22429
Optical component MAC Europe ground truth report: Flevoland 1991 (Netherlands)
[BCRS-92-27] 06 p2382 N94-23177
Application of ERS-1 active microwave instrumentation data to remote sensing of snow
[PB93-224756] 06 p2382 N94-23224
Mission planning for Shuttle Imaging Radar-C (SIR-C) with a real-time interactive planning software
06 p2305 N94-23842
The down, release, and deployment of the RADARSAT SAR antenna 06 p2305 N94-23986
Investigations into deployment complications of the ERS-1 SAR antenna 06 p2305 N94-23996
Precipitation measurement using SIR-C: A feasibility study. Investigation at nadir
[NASA-CR-195103] 06 p2410 N94-24126
Free-surface/vorticity interaction
[AD-A273263] 06 p2335 N94-24686
Use of microwave polarimetry to enhance SAR images of the ocean surface
[AD-A273568] 06 p2419 N94-24944
Edge detection using a complex wavelet
[AD-A273699] 06 p2493 N94-25452
The Radar Image Generation (RIG) model
06 p2306 N94-25497
A real-time convolution algorithm and architecture with applications in SAR processing
[AD-A273817] 07 p2959 N94-25963
Weapon system sensor integration for a DIS-compatible virtual cockpit
[AD-A274088] 07 p2672 N94-26021
A comparative evaluation of SAR and SLAR
[DE94-002922] 07 p2848 N94-26277
Response of an airborne synthetic aperture radar to sea ice in the marginal ice zone
[ISBN-0-315-84243-1] 07 p2849 N94-26668
Leadex environmental phenomena and effects observed by DMSP, NOAA, and ERS-1 satellites
[AD-A274596] 07 p2868 N94-26888
Processing of wide-angle synthetic aperture radar signals for target detection
[AD-A274225] 07 p2773 N94-27073
Method of correcting rotational motion error in SAR and ISAR imagery
[AD-D016033] 07 p2773 N94-27146
Image quality analysis of compressed synthetic aperture radar imagery
[AD-A273399] 07 p2774 N94-27170
Non-adaptive robust filters for speckle noise reduction
[INPE-5519-PRE/1794] 07 p2776 N94-27335
Calibration of SAR systems
[DLR-FB-93-18] 07 p2777 N94-27738
Mapping of soil humidity using C-band radar images
[ISBN-0-315-85076-0] 07 p2852 N94-27878
A comparative study of SAR data compression schemes 07 p2946 N94-28259
Perceptual compression of magnitude-detected synthetic aperture radar imagery
07 p2946 N94-28260
Proceedings of the International Symposium on Remote Sensing
[JTN-94-80578] 08 p3325 N94-28925
Keynote address --- Japanese Earth Resources Satellite 1 (JERS-1) and future remote sensing projects
08 p3326 N94-28926
Synthetic aperture radar applications: Now and in the future 08 p3260 N94-28927
Observations by ERS-1 start
08 p3327 N94-28933
Sea ice and oceans applications of SAR
08 p3327 N94-28934
Observatory system of Earth Resources Satellite-1
08 p3330 N94-29221
Application of JERS-1 data to geologic analyses
08 p3330 N94-29222
SAR-related stress variability in the Marine Atmospheric Boundary Layer (MABL)
[AD-A275275] 08 p3377 N94-29436
Automatic focus and registration of synthetic aperture radar images 08 p3246 N94-29536
Pointing mechanisms for the Shuttle Radar Laboratory
08 p3162 N94-29638
Analysis and an image recovery algorithm for ultrasonic tomography system 08 p3397 N94-30456
Phase unwrapping problems in ISAR images
[TELECOM-93-D-008] 09 p3670 N94-31097
High-resolution synthetic aperture radar observations of the Moon 09 p3676 N94-31952
Validation support of the ERIM ocean model
[AD-A277364] 09 p3788 N94-32284
From Optics to Radar, SPOT and ERS Applications
[ISBN-2-85428-345-7] 09 p3747 N94-32523
Contribution of SAR ERS1 data to study the French Guiana tropical coast environment
[BRGM-93034] 09 p3748 N94-32527
Monitoring land cover and crop types in Denmark using ERS-1 SAR and optical satellite images
09 p3748 N94-32528
The use of ERS images for mapping
09 p3749 N94-32531
Example of SPOT/ERS-1 complementarity
09 p3749 N94-32533
Restoration of interferometric, polarimetric, radiometric, and textural information in SAR images
09 p3750 N94-32535
Assessment of region-based methods for automated SAR/optical registration, attribute extraction, and classification 09 p3750 N94-32536
Airborne SAR as a complement to SPOT HRV in land-cover classification: The use of normalization and principal components analysis 09 p3750 N94-32539
Ship traffic monitoring and oil spill detection using the ERS-1 SAR 09 p3751 N94-32542
SAR image feature extraction system: A pre-operational application of ERS-1 SAR 09 p3751 N94-32543
Almaz marine applications 09 p3751 N94-32544
The use of ERS-1 within an operational ice monitoring program 09 p3751 N94-32545
The use of SPOT and ERS-1 images to map the eruption of Nevado Sabancaya (Province of Arequipa, South Peru) and evaluate associated risks 09 p3751 N94-32546
Respective contributions of VIS-PIR, SAR-ERS 1, and airborne radar data for morphostructural and morphoneotectonic analysis: Practical examples
09 p3752 N94-32549
Use of SPOT and ERS-1 SAR data to study the tectonic and climatic history of arid regions
09 p3752 N94-32550

Structural study in an alteritic region: Contribution of ERS-1 SAR data of the Mauges Plateau (Loire Atlantique, France)
[BRGM-93032] 09 p3752 N94-32551
Evaluation of the potential of SAR data for mapping of landslide risks
[BRGM-93033] 09 p3753 N94-32552
Use of SPOT and ERS-1 to map tropical vegetation and mangrove dynamics in Guiana 09 p3753 N94-32555
A case study comparing multi-temporal ERS-1 SAR data and SPOT data for tropical forest mapping 09 p3753 N94-32556
Application of ERS-1 SAR data for hydrological studies 09 p3754 N94-32558
Synergy of thermal infrared and microwave remote sensing for evaporation estimation 09 p3754 N94-32559
Monitoring landsurface characteristics in Niger using complementary SPOT and ERS-1 SAR data 09 p3754 N94-32560
Possible complementarity of SPOT/ERS in mapping land use: Study on agricultural land in Brittany (France) 09 p3755 N94-32563
ERS-1 SAR and optical data for land use/land cover mapping: A case study in a savannah zone of Guinea 09 p3755 N94-32565
SAR interferometry with ERS-1 09 p3755 N94-32566
Techniques and applications of SAR interferometry for ERS-1 09 p3756 N94-32568
Developments in ERS-1 SAR interferometry: Use of the spectral shift 09 p3756 N94-32569
Fields of experiments in ERS-1 SAR interferometry in Bonn and Naples 09 p3756 N94-32572
The processing technology and some applications of Almaz-1 data 09 p3756 N94-32573
Ultra wide band radar holographic imaging of subsurface targets
[DE94-004271] 09 p3713 N94-32681
Alaska SAR Facility mass storage, current system 10 p4156 N94-33823
A SAR image-formation algorithm that compensates for the spatially-variant effects of antenna motion
[DE94-008456] 10 p4078 N94-34382
Quantifying shapes of volcanoes on Venus 11 p4361 N94-35429
Insight to global change: EOS/SAR mission
[NASA-CR-196133] 11 p4284 N94-35503
Evaluation of synthetic aperture radar for oil-spill response
[AD-A278796] 11 p4284 N94-35674
Controller for the Electronically Scanned Thinned Array Radiometer (ESTAR) instrument
[NASA-TM-104608] 11 p4259 N94-36049
Radially combined 30 W, 14-16 GHz amplifier
[DE94-010078] 12 p4432 N94-36471
Imaging targets embedded in a lossy half space with Synthetic Aperture Radar
[DE94-010807] 12 p4435 N94-37391

SYNTHETIC APERTURES
Sampling and position effects in the Electronically Steered Thinned Array Radiometer (ESTAR)
[NASA-TM-108998] 01 p0245 N94-12432
Spaceborne Imaging Radar-C instrument 03 p0990 N94-15890
A conceptual design study for a two-dimensional, electronically scanned thinned array radiometer
[NASA-TM-109051] 03 p1085 N94-17665
Ultra wide band radar holographic imaging of subsurface targets
[DE94-004271] 09 p3713 N94-32681

SYNTHETIC FIBERS
NT ARAMID FIBERS
NT CERAMIC FIBERS
NT GLASS FIBERS
NT NYLON (TRADEMARK)
NT RAYON
NT VYCOR
Mechanical interaction between synthetic fiber and cement base matrix in FRC composites
[AD-A265310] 01 p0073 N94-11686
Preparation of graphite fibers from polyimide 08 p3223 N94-29517
The flow field near the body surface with thin filaments 08 p3234 N94-29706

SYNTHETIC FUELS
NT GASOHOL (FUEL)
Status and future opportunities for conversion of synthesis gas to liquid energy fuels
[DE93-010025] 02 p0584 N94-14089
Fifteenth Symposium on Biotechnology for Fuels and Chemicals: Program and Abstracts
[DE93-010005] 04 p1376 N94-18045
Data collection plan for phase 2 Alternative Fuels Bus Data Collection Program
[DE93-010047] 04 p1378 N94-18913
Proceedings of the 1993 Windsor Workshop on Alternative Fuels
[DE94-003908] 08 p3226 N94-30612
Proceedings of the low cost materials of construction for biological processes workshop
[DE94-000218] 08 p3226 N94-30761
Heterogeneous catalytic process for alcohol fuels from syngas
[DE94-008729] 09 p3667 N94-32583
Development of a catalyst for conversion of syngas-derived materials to isobutylene
[DE94-009698] 10 p4021 N94-33901
Heterogeneous catalytic process for alcohol fuels from syngas
[DE94-010263] 11 p4248 N94-36299

SYNTHETIC RESINS
NT ACRYLIC RESINS
NT ADDITION RESINS
NT EPOXY RESINS
NT KEVLAR (TRADEMARK)
NT NYLON (TRADEMARK)
NT PEEK
NT PHENOLIC RESINS
NT POLYAMIDE RESINS
NT POLYESTER RESINS
NT POLYETHER RESINS
NT POLYMETHYL METHACRYLATE
NT THERMOPLASTIC FILMS
NT THERMOPLASTIC RESINS
NT THERMOSETTING RESINS
NT VINYL COPOLYMERS

SYNTHETIC RUBBERS
NT ADIPRENE (TRADEMARK)
NT CHLOROPRENE RESINS
NT ELASTOMERS
NT VITON RUBBER (TRADEMARK)
Thermal stability of sealants for military aircraft: Modification of polysulfide prepolymers with ether and thioether monomers
[AD-A264079] 01 p0089 N94-11107

SYSTEM EFFECTIVENESS
Denver TMA assessment
[NASA-CR-4554] 04 p1315 N94-18844
Molten carbonate fuel cell networks: Principles, analysis, and performance
[DE93-000281] 04 p1468 N94-18925
Automatic tools for system testing 06 p2197 N94-23913
Aircraft wheel life assessment
[AD-A274378] 07 p2823 N94-26976
The relationship between integrative task design for information systems professionals and perceived information systems effectiveness 09 p3919 N94-32487
Multidimensional scaling of user information satisfaction
[AD-A277230] 09 p3920 N94-32633
Operational agility
[AGARD-AR-314] 10 p3989 N94-33875
The Federal Aviation Administration plan for research, engineering and development 11 p4376 N94-35262
An analysis of operational suitability for test and evaluation of highly reliable systems
[AD-A278573] 11 p4192 N94-36184

SYSTEM FAILURES
STS-55 pad abort: Engine 2011 oxidizer preburner augmented spark igniter check valve leak
[NASA-CR-193830] 02 p0533 N94-12806
Computational problems with the binomial failure rate model and incomplete common cause failure reliability data
[DE93-014346] 02 p0669 N94-14143
Concurrent garbage collection of persistent heaps
[AD-A266831] 03 p1141 N94-14915
The distributed database dynamic reconfiguration project
[AD-A267116] 03 p1229 N94-15652
Reliability characterization of digital microcircuits: Investigation of an in-process oxide reliability screening method
[AD-A267053] 03 p1008 N94-15665
Fast simulation of steady-state availability in non-Markovian highly dependable systems
[AD-A266747] 03 p1174 N94-15823
Consistent failure reporting in reliable communication systems
[AD-A266298] 03 p0997 N94-16477
Disconnected operation in a distributed file system
[AD-A266461] 03 p1231 N94-16570
Understanding partitions and the no partition assumption
[AD-A266296] 03 p1000 N94-16911
Workshop on multifactor aging mechanisms and models
[AD-A268668] 04 p1397 N94-18311
On timing faults in digital logic circuits
[AD-A268714] 04 p1402 N94-18400
Development and testing of a reliability performance index for modular robotic systems
[AD-A271901] 05 p1942 N94-20488
Real-time fault tolerant computer systems
[AD-A272909] 05 p1899 N94-21230
Reducing the cognitive workload: Trouble managing power systems
[NASA-TM-106413] 05 p1714 N94-21564
A review of wiring system safety in space power systems
[NASA-CR-194439] 06 p2203 N94-23632
A cross-disciplinary response to improve test activities: The corporate memory capitalization in Ariane4 test domain 06 p2508 N94-23899
System for Anomaly and Failure Detection (SAFD) system development
[NASA-CR-193907] 06 p2372 N94-24174
Diagnosing process faults using neural network models
[DE94-002633] 06 p2473 N94-24518
Develop advanced nonlinear signal analysis topographical mapping system
[NASA-CR-195128] 06 p2388 N94-24827
Reliability analysis of a repairable dependent parallel system
[ETN-94-95312] 06 p2373 N94-25295
Fast incremental compiler transformations for multiple instruction retry
[NASA-CR-195209] 07 p2964 N94-26680
Hardware and software reliability estimation using simulations
[NASA-CR-187588] 07 p2973 N94-27663
Simulating fail-stop in asynchronous distributed systems
[AD-A278101] 07 p2974 N94-27767
Algorithms for treating redundancy in repairable and non-repairable systems
[DE94-005289] 08 p3315 N94-29020
Potential software failures methodology analysis 08 p3414 N94-29329
Distributed applications and failure tolerance programs using a reconfigurable parallel architecture 08 p3417 N94-29345
TOTAL user manual
[NASA-TM-109101] 08 p3432 N94-30160
Flight simulator evaluation of advanced MLS procedures
[AD-B174270] 08 p3143 N94-30915
Spacecraft contamination issues from LDEF: Issues for design 09 p3592 N94-31020
Principles of ultradependability in chaotic routing
[AD-A277422] 09 p3827 N94-32995
Discovering operating modes in telemetry data from the Shuttle Reaction Control System 10 p4013 N94-34051
An intelligent control system for failure detection and controller reconfiguration 10 p4126 N94-35066
Flight testing a propulsion-controlled aircraft emergency flight control system on an F-15 airplane
[NASA-TM-4590] 11 p4199 N94-35258
Asynchronous optimistic rollback recovery using secure distributed time
[AD-A278978] 11 p4344 N94-35526
Network survivability performance
[AD-A278746] 12 p4433 N94-36756
Network survivability performance (computer diskette)
[AD-M000332] 12 p4433 N94-36757

SYSTEM GENERATED ELECTROMAGNETIC PULSES
Safety guidelines for the operation of the DREO 10 m EMP simulator DREMPS
[DREO-TN-93-5] 06 p2193 N94-24117
TEM cell safety report
[DREO-TN-93-9] 06 p2193 N94-24123

SYSTEM IDENTIFICATION
System identification for Space Station Freedom using observer/Kalman filter Markov parameters
[NASA-CR-191521] 02 p0539 N94-12976
Feasibility study of an orbiting laboratory for testing CSI technology
[NASA-CR-191524] 02 p0540 N94-13016
An analytic modeling and system identification study of rotor/fuselage dynamics at hover 02 p0524 N94-13312
Flight testing and frequency domain analysis for rotorcraft handling qualities characteristics 02 p0526 N94-13324
Test/analysis correlation and model updating of the STARS 1 and 2 missile systems
[DE93-013774] 02 p0748 N94-13578
Identification of continuous-time dynamical systems: Neural network based algorithms and parallel implementation
[DE93-014427] 02 p0766 N94-14737

Exploitation of cyclostationarity for signal-parameter estimation and system identification
[AD-A267137] 03 p0988 N94-15690
The design and analysis of robust feedback systems
[AD-A267152] 03 p1165 N94-15778
Development and analysis of ARMA parameter estimation schemes in the presence of noise
[AD-A267184] 03 p0989 N94-15786
Heat transfer parametric system identification
[AD-A268525] 03 p0929 N94-17543
Advances in the identification of transfer function models using Prony analysis
[DE93-017980] 04 p1548 N94-18094
Literature review of the errors-in-variables approach to the problem of system identification
[AD-A271098] 05 p1949 N94-19907
Experimental modification and identification of the DSS-13 antenna control system model
06 p2291 N94-23260
System identification using a wavelet-based approach
[DE94-002191] 06 p2293 N94-23473
Asymptotically stable neural networks for identification of nonlinear dynamic systems
[ISBN-0-315-84328-4] 07 p2985 N94-26629
Grey-box modelling and identification topics
[PB94-126380] 07 p2986 N94-27029
Control oriented system identification
[AD-A274162] 07 p2987 N94-27124
Improved modeling of GPS selective availability
07 p2642 N94-27290
On modeling and controlling intelligent systems
[DE94-002446] 07 p2988 N94-27706
System identification of the Large-Angle Magnetic Suspension Test Facility (LAMSTF)
07 p2682 N94-27908
A neural network-based technique for structural identification of SISO systems
[REPT-93-076] 08 p3449 N94-30941
A new methodology of system parameter estimation
[MATHS-REPT-A-208] 09 p3808 N94-31163
Optimal adaptive estimation algorithm for harmonic current reduction using power limited active line conditioners
[AD-A277354] 09 p3693 N94-32336
Stochastic realization of a Gaussian stochastic control system
[CWI-BS-R9320] 09 p3852 N94-32350
Parametric robust control and system identification: Unified approach
[NASA-CR-195826] 09 p3836 N94-32980
Revisiting the connection problem of identification and control 10 p4114 N94-34311
NTT crosscorrelation recursive least squares procedure for on-line identification of process parameters
10 p4116 N94-34325
X-31A system identification applied to post-stall flight: Aerodynamics and thrust vectoring
10 p3992 N94-34619
Defense RDT and E online system (DROLS) retrieval reference guide
[AD-A278972] 11 p4344 N94-35525
Advances in parameter estimation techniques applied to flexible structures 11 p4219 N94-35877
An overview of recent advances in system identification 11 p4220 N94-35880

SYSTEMS ANALYSIS
NT SYSTEM IDENTIFICATION
Transportation systems analyses. Volume 2: Technical/programmatics
[NASA-CR-192582] 01 p0041 N94-10827
Design for testability and diagnosis at the system-level
01 p0184 N94-11563
Space Life Support Engineering Program
[NASA-CR-193474] 01 p0316 N94-12365
Systems analysis of a closed loop ECLSS using the ASPEN simulation tool. Thermodynamic efficiency analysis of ECLSS components 01 p0316 N94-12366
Analysis of the Army's installation support modules with the private sector's open information systems
[AD-A265667] 01 p0421 N94-12579
Nuclear propulsion systems engineering
[DE93-010791] 02 p0548 N94-12870
Analysis and effects of the number of nests of DO loops during vector supercomputing
[NAL-TR-1146] 02 p0748 N94-13453
The OOA technique in information systems
[REPT-72-92] 02 p0823 N94-13863
Heat and seed recovery technology project
[DE93-009203] 02 p0800 N94-13913
Transformation and composition of refusal graphs: Testability analysis
[LAAS-92435] 02 p0751 N94-13995
Optical systems integrated modeling
02 p0547 N94-14837
Laser power beaming system analyses
[NASA-CR-193840] 02 p0660 N94-14904
Integrated trusted systems development environment
[AD-A267029] 03 p1146 N94-15674
A handbook of cost risk analysis methods
[AD-A267253] 03 p1235 N94-16988
Soyuz/ACRV accommodation study
[NASA-TM-107733] 03 p0888 N94-17072
Small Satellites Systems and Services
[ISBN-2-85-428327-9] 03 p0888 N94-17131
TANGO: A notation for describing advanced transaction models
[REPT-93-014] 04 p1613 N94-17936
An overview of the SAFSIM computer program
[DE93-017657] 04 p1519 N94-18002
Specification and analysis of a high speed transport protocol
[AD-A268941] 04 p1386 N94-18449
Deadbeat control by measurement feedback: A two sided approach
[REPT-93-20] 04 p1542 N94-19091
Scale sensitivity in the multiplicative AHP and SMART
[REPT-93-37] 04 p1611 N94-19157
Context-related scaling of human judgement in the multiplicative AHP, SMART and ELECTRE
[REPT-93-38] 04 p1611 N94-19158
Goal-driven LOTOS execution
[MEMO-INF-93-04] 04 p1527 N94-19227
A unified performability evaluation framework for computer and communication systems
[PB94-149549] 04 p1537 N94-19264
Optimal safety system design using fault tree analysis
[MATHS-REPT-A-187] 04 p1529 N94-19382
SISSY: An example of a multi-threaded, networked, object-oriented databased application
[DE93-019742] 05 p2041 N94-19811
Interval timed coloured petri nets and their analysis
[PB93-191732] 05 p1903 N94-19992
System performance predictions for Space Station Freedom's electric power system
[NASA-TM-106396] 05 p1667 N94-20062
Multi-disciplinary coupling effects for integrated design of propulsion systems
[NASA-TM-106349] 05 p1830 N94-20170
Test and evaluation: DOD has been slow in improving testing of software-intensive systems
[AD-A271541] 05 p1908 N94-20917
Specification and generation of Markov reward models
[MEMO-INF-92-60] 05 p1963 N94-21058
N parallel queueing systems with server breakdown and repair
[CWI-BS-R9236] 05 p1944 N94-21232
Building integrated photovoltaic systems analysis
[DE93-018208] 05 p1846 N94-21298
Physics Detector Simulation Facility (PDSF) architecture/utilization
[DE93-019744] 05 p1936 N94-21919
Mathematical modelling of economic systems
05 p2050 N94-22060
Macromodel of centrally planned economy
05 p2050 N94-22062
Mesoscale simulations of the November 25-26 and December 5-6 cirrus cases using the RAMS model
05 p1878 N94-22331
APLAC: An object-oriented analog circuit simulator and design tool. 6.1 system simulations manual
[PB93-224871] 06 p2450 N94-23226
A framework for SFC/DC system data analysis
06 p2523 N94-23234
Phased-mission system analysis using Boolean algebraic methods
[NASA-CR-191564] 06 p2451 N94-23340
Systems engineering: A formal approach. Part 1: System concepts
[PB93-225308] 06 p2268 N94-23476
GenSAA: A tool for advancing satellite monitoring with graphical expert systems 06 p2516 N94-23945
Operational characterisation of requirements and early validation environment for high demanding space systems 06 p2519 N94-23959
A review of ISEAS design 06 p2465 N94-24410
Systems engineering: A formal approach. Part 4: Analysis methods
[PB94-101417] 06 p2271 N94-24475
Systems engineering: A formal approach. Part 3: Modeling methods
[PB94-101409] 06 p2456 N94-24513
Analyzing the properties of user interface software
[AD-A273601] 06 p2460 N94-24933
Expert system rule-base evaluation using real-time parallel processing
[AD-A273701] 06 p2469 N94-25454
Vulnerability assessment using a fuzzy logic based method
[AD-A274075] 07 p2957 N94-25649
Performance measurement of three commercial object-oriented database management systems
[AD-A274028] 07 p3096 N94-25765
Technical description of the Vulcano software library
[FFI-93/7024] 07 p2767 N94-26105
A linear description of the discrete lot-sizing and scheduling problem
[MEMO-COSOR-92-47] 07 p2992 N94-26227
On the phi(sub 0)-stability of perturbed nonlinear differential systems
[DE93-634304] 07 p2993 N94-26441
Tool for performance analysis and off-line prediction of timing behaviour 07 p2952 N94-26732
Formal methods for dependable real-time systems
07 p2953 N94-26740
Asynchronous and packetized systems engineering tools 07 p2954 N94-26746
Interference analysis of multichannel transmission lines: A system's analysis
[PB94-126505] 07 p2772 N94-26909
Freeness analysis for logic programs-and correctness
[PB94-126703] 07 p2966 N94-26956
DALIA: A language for the description and analysis of digital systems 07 p2954 N94-27192
Parallel discrete event simulation
07 p2955 N94-27194
On modeling and controlling intelligent systems
[DE94-002446] 07 p2988 N94-27706
Object-oriented development methods
07 p2975 N94-27938
Artificial Intelligence Research Branch future plans
[NASA-TM-109733] 07 p2989 N94-28065
SAFSIM theory manual: A computer program for the engineering simulation of flow systems
[DE94-005381] 08 p3270 N94-28488
Identification of components to optimize improvement in system reliability
[DE94-001601] 08 p3315 N94-28503
Rome Laboratory software engineering technology program 08 p3414 N94-29330
Dependability analysis of parallel systems using a simulation-based approach
[NASA-CR-195762] 08 p3431 N94-29846
Modelling the evolution of information systems
[TR-92-36] 08 p3535 N94-30329
Evolving information systems: Meeting the ever-changing environment
[TR-92-24] 08 p3535 N94-30359
A new methodology of system parameter estimation
[MATHS-REPT-A-208] 09 p3808 N94-31163
Covert channel analysis of trusted systems. A guide to understanding
[AD-A276418] 09 p3916 N94-31331
On a formal approach to the methodology of information planning
[MEMO-INF-93-42] 09 p3917 N94-31415
Modal analysis of multiterminal high voltage direct current transmission
[DE94-006426] 09 p3691 N94-31785
System analysis of ultra-wideband instrumentation radars: Impulse versus stepped-chirp approaches
[AD-A276624] 09 p3677 N94-32087
World height system definition and implementation
[AD-A276725] 09 p3747 N94-32160
A polling system with a dormant server
[CWI-BS-R9313] 09 p3835 N94-32193
Hierarchical modeling for reliability analysis using Markov models
[NASA-CR-188288] 09 p3731 N94-32862
Workshop on Self-Determination in Developing and Evolving systems
[AD-A278367] 10 p4097 N94-33737
Discovering operating modes in telemetry data from the Shuttle Reaction Control System
10 p4013 N94-34051
Management issues in automated audit analysis
[DE94-007571] 10 p4112 N94-34297
Techniques for aerodynamic characterization and performance evaluation at high angle of attack
10 p3991 N94-34614
Developing software for ease of change: Metrics from later in the TRALAB system life cycle
[AD-A278759] 11 p4302 N94-35490
Decision and systems analysis for underground storage tank waste retrieval systems and tank waste remediation system
[SAND94-0065] 11 p4286 N94-35957
An automated method for Low Level Windshear Alert System (LLWAS) data quality analysis
[AD-A280313] 12 p4472 N94-37126

SYSTEMS COMPATIBILITY
The conformance testing methodology to CTRON (communication and central TRON) extended OS
05 p1772 N94-22118
Low earth orbit satellite/terrestrial mobile service compatibility 06 p2288 N94-22827
Utilizing a Russian space nuclear reactor for a US space mission: Systems integration issues
[DE94-005585] 10 p4017 N94-34137

SYSTEMS DESIGN
U SYSTEMS ENGINEERING
SYSTEMS ENGINEERING
NT COMPUTER SYSTEMS DESIGN
NT CONTROL SYSTEMS DESIGN
System engineering concept demonstration, technology assessments, volume 5
[AD-A265471] 01 p0323 N94-10494
System engineering concept demonstration, trade studies, volume 6
[AD-A265472] 01 p0323 N94-10495
System monitoring and diagnosis with qualitative models
[NASA-CR-193812] 01 p0323 N94-10711
Space Station redesign option A: Modular buildup concept
[NASA-TM-108415] 01 p0043 N94-10808
Progress in multidisciplinary design optimization at NASA Langley
[NASA-TM-107754] 01 p0318 N94-10814
Transportation systems analyses: Volume 1: Executive Summary
[NASA-CR-192583] 01 p0041 N94-10826
Transportation systems analyses. Volume 2: Technical/programmatics
[NASA-CR-192582] 01 p0041 N94-10827
National Airspace System operational concept
[DOT/FAA/SE-93/1] 01 p0023 N94-10933
MIL-STDS and PTTI: What's available and what needs to be done 01 p0352 N94-10973
The guide to Design For On-orbit Spacecraft Servicing (DFOSS) manual: Producing a consensus document 01 p0421 N94-11575
The National Launch System Advanced Development Program: A brief overview 01 p0040 N94-11576
System engineering concept demonstration, process model, volume 3
[AD-A265469] 01 p0333 N94-12008
Integrating the services' imagery architectures
[AD-A265487] 01 p0171 N94-12335
Machine translation technology: A potential key to the information age
[PB93-134336] 01 p0421 N94-12385
Solar dynamic power system development for Space Station Freedom
[NASA-RP-1310] 02 p0548 N94-12807
Nuclear propulsion systems engineering
[DE93-010791] 02 p0548 N94-12870
Design, qualification and operation of nuclear rockets for safe Mars missions
[DE93-010792] 02 p0549 N94-12996
Glossary of SSDC terms and acronyms
[DE93-013697] 02 p0823 N94-13352
Electrical Actuation Technology Bridging
[NASA-CP-3213] 02 p0551 N94-13417
Space and Earth sciences, computer systems, and scientific data analysis support, volume 1
[NASA-CR-189319] 02 p0741 N94-13788
Hypersonic overview 02 p0505 N94-14154
Integrating interface slicing into software engineering processes
[NASA-CR-192761] 02 p0754 N94-14368
Formal functional test designs with a test representation language 02 p0609 N94-14383
The further development and refinement of an expert-systems approach to the creative design of mechanisms and mechanical systems
[AD-A266812] 02 p0665 N94-14901
The detector assemblies of ISOPHOT and the spectrometers ISO-SWS and ISO-LWS 03 p0906 N94-15074
RAMCAD design methodology
[AD-A267010] 03 p1145 N94-15525
ECS: Ninth year in orbit
[ESA-BR-91] 03 p0987 N94-15644
Integrated trusted systems development environment
[AD-A267029] 03 p1146 N94-15674
Department of Defense technical architecture framework for information management. Volume 3: Architecture concepts and design guidance, version 2.0
[AD-A267195] 03 p1230 N94-15789
Remote diagnosis as used for mechanized parking systems 03 p0984 N94-16004
Center of Excellence in Laser Medicine
[DE93-016541] 03 p1122 N94-16113
Microwave reflectometer ionization sensor
[NASA-CR-191464] 03 p0922 N94-17083
Human Transportation System (HTS) study, volume 2
[NASA-TM-104779-VOL-2] 03 p0882 N94-17320
Design and diagnosis problem solving with multifunctional technical knowledge bases
[AD-A268375] 03 p1234 N94-17419
Gravity dependent condensation pressure drop and heat transfer in ammonia two-phase heat transport systems
[NLR-TP-92121-U] 03 p1031 N94-17615
Reference model for project support environments, version 1.0
[AD-A269110] 04 p1520 N94-18251
VHDL simulation with access to transistor models 04 p1402 N94-18381
Lunar base Controlled Ecological Life Support System (LCELSS): Preliminary conceptual design study
[NASA-CR-188479] 04 p1511 N94-18484
Integrated Terminal Weather System (ITWS)
[AD-A269884] 04 p1492 N94-18684
Operator performance in pattern matching as a function of reference material structure
[AD-A269889] 04 p1509 N94-18686
The development of a course sequence in real-time systems design
[AD-A269459] 04 p1522 N94-18726
MHD Integrated Topping Cycle Project
[DE93-040521] 04 p1589 N94-19055
Pegasus: Operating system support for distributed multimedia systems
[MEMO-INF-92-76] 04 p1536 N94-19160
The Cluster spacecraft 04 p1330 N94-19635
Systems engineering for Air Force C3I systems
[AD-A270482] 04 p1391 N94-19676
Model checking, abstraction, and compositional verification
[AD-A270552] 05 p1902 N94-19919
Total systems design analysis of high performance structures
[NASA-TP-3432] 05 p1653 N94-20141
Design considerations for a fiber optic communications network for power systems
[DE93-018404] 05 p1984 N94-20179
Design structuring and allocation optimization (Destination) prototype level 1 user's manual
[AD-A272115] 05 p1929 N94-20571
Let your fingers do the walking: The projects most invaluable tool 05 p1922 N94-21325
Canadian Conference on Electrical and Computer Engineering, volumes 1 and 2
[ISBN-0-9694170-2-0] 05 p1770 N94-22101
ScaRaB and its subsystems 05 p1860 N94-22285
SATCOM simulator speeds MSS deployment and lowers costs 06 p2287 N94-22822
Prospects for very-high-resolution solar physics with the Simuris inteferometric mission 06 p2625 N94-22848
Flexible framework for contingent information systems modelling
[PB93-220549] 06 p2589 N94-23095
How much integral action can a control system tolerate?
[OUEL-1923/92] 06 p2471 N94-23147
The design of a turbine vane cooling system used in the topping cycle
[OUEL-1963/92] 06 p2353 N94-23164
Missions, Technologies, and Design of Planetary Mobile Vehicles
[ISBN-2-85428-331-7] 06 p2605 N94-23373
The study of the mobile lunar explorer 06 p2607 N94-23389
The robotic Mars rover 06 p2608 N94-23390
Mission and system concepts for Mars robotic precursor missions 06 p2608 N94-23391
The new family of JPL planetary surface vehicles 06 p2369 N94-23398
Electronic payloads for Martian missions: A preliminary assessment of technologies 06 p2610 N94-23408
The Mars 96 balloon guiderope: An autonomous system in extreme environment conditions 06 p2369 N94-23412
Dual rover concept for Mars exploration 06 p2370 N94-23415
Bond graph modeling, simulation, and reflex control of the Mars planetary automatic vehicle 06 p2370 N94-23424
Systems engineering: A formal approach. Part 1: System concepts
[PB93-225308] 06 p2268 N94-23476
A review of wiring system safety in space power systems
[NASA-CR-194439] 06 p2203 N94-23632
Advanced design concepts for open distributed systems development
[PB94-110897] 06 p2454 N94-23751
Design and specification of a generic task model for solving boolean constraint satisfaction problems
[PB94-118841] 06 p2486 N94-23762
Automatic tools for system testing 06 p2197 N94-23913
Using Mach threads to control DSN operational sequences 06 p2477 N94-23916
Deep Space Network (DSN), Network Operations Control Center (NOCC) computer-human interfaces 06 p2447 N94-23917
A real-time navigation monitoring expert system for the Space Shuttle Mission Control Center 06 p2202 N94-23921
XRTD: An X-Windows based, real-time radiometric display and analysis system 06 p2305 N94-23922
Operability engineering in the Deep Space Network 06 p2514 N94-23930
Training: Plugging the information gaps 06 p2429 N94-23934
An overview of a generic multi-sensor integrated navigation system design
[CTN-94-60916] 06 p2174 N94-24120
Technology utilization office data base analysis and design 06 p2577 N94-24417
A minimum cost tolerance allocation method for rocket engines and robust rocket engine design 06 p2222 N94-24419
Systems engineering: A formal approach. Part 4: Analysis methods
[PB94-101417] 06 p2271 N94-24475
Systems engineering: A formal approach. Part 3: Modeling methods
[PB94-101409] 06 p2456 N94-24513
An automated tool to facilitate code translation for software fault tree analysis
[AD-A273205] 06 p2457 N94-24556
Systems engineering: A formal approach. Part 2: Frameworks
[PB94-101391] 06 p2489 N94-24615
RITL: An information system for application reuse-in-the-large
[PB94-119088] 06 p2592 N94-24646
What makes industries believe in formal methods
[PB94-110848] 06 p2272 N94-24648
An investigation of requirements traceability to support systems development
[AD-A273167] 06 p2458 N94-24684
Advanced avionics architecture and technology review. Executive summary and volume 1: Avionics tech nology. Volume 2: Avionics systems engineering
[AD-A273630] 06 p2186 N94-24733
Intelligent systems and advanced user interfaces for design, operation, and maintenance of command management systems
[NASA-CR-195172] 06 p2459 N94-24797
Integrated design and manufacturing for the high speed civil transport
[NASA-CR-195511] 06 p2182 N94-24968
Reuse-Driven Software Processes Guidebook, version 02.00.03
[AD-A273644] 06 p2461 N94-25148
New Technologies for Space Avionics, 1993
[NASA-CR-188272] 06 p2272 N94-25193
Appendix A: Proposed statement of work, 1994 06 p2272 N94-25194
Appendix B: Rapid development approaches for system engineering and design 06 p2272 N94-25195
Appendix C: Rapid development approaches for system engineering and design 06 p2272 N94-25196
Design of gas bearing systems for precision applications
[ISBN-9-03-860112-3] 06 p2367 N94-25249
A soft robot interface
[OUEL-1948/92] 06 p2463 N94-25468
Stability questions in predictive control
[OUEL-1970/93] 06 p2477 N94-25469
Safety analysis in conceptual design of process control
[VTT-PUBS-117] 07 p2762 N94-25641
Copernicus: Lunar surface mapper 07 p3081 N94-25702
Technology drivers for flight telerobotic system software 07 p2684 N94-26289
Information systems criteria for applying software reengineering: Guidelines for identifying information systems for software reengineering
[AD-A274699] 07 p3097 N94-26375
Merging photovoltaic hardware development with hybrid applications in the USA
[DE94-002682] 07 p2857 N94-26612
Asynchronous and packetized systems engineering tools 07 p2954 N94-26746
Automated information management for designers: Functional requirements for computer based associates that support access and use of technical information in design
[AD-A274603] 07 p3099 N94-26891
Interdisciplinary technology 07 p2686 N94-27363
Space Station technology testbed: 2010 deep space transport 07 p2687 N94-27368
The radiation design handbook
[ESA-PSS-01-609-ISSUE-1] 07 p2696 N94-27397
Test and evaluation of the Litton (Canada) Canadian strapdown gyroscope (CSG-2) Performance Evaluation Unit (PEU)
[DREO-1010] 07 p2813 N94-27597

Compressor stability 07 p2828 N94-28046
Transient model applications. 1: Compressor heat soak/clearance effects modeling 07 p2828 N94-28048
Combined Cycles for Power Plants [VKI-LS-1993-08] 07 p2830 N94-28077
Development of the gas turbine. Part 1: Design philosophy and performance 07 p2831 N94-28080
Development of the gas turbine. Part 2: Manufacturing, commissioning, and operation 07 p2831 N94-28081
Steam plant for combined cycles: Heat recovery steam generators, design principles, and construction details 07 p2831 N94-28083
Simulation: A tool for steam plant dynamic analysis 07 p2831 N94-28084
Steam plant: Steam turbines for combined cycles 07 p2831 N94-28085
Controls, monitoring and performance measurements 07 p2831 N94-28086
Advanced End-to-end Simulation for On-board Processing (AESOP) 07 p2945 N94-28255
Design of parallel systems for signal processing [AD-A275490] 08 p3430 N94-28659
NASA wiring program: Survey of NASA experiences in wiring system safety 08 p3165 N94-28700
Cleanroom engineering handbook. Volume 3: Project execution in the cleanroom environment [AD-A275860] 08 p3156 N94-28752
Designing for performance: A cognitive systems engineering approach to modifying an AWACS human computer interface [AD-A275187] 08 p3399 N94-28861
Towards an information model and mechanisms for design rationale capture and use [AD-A275060] 08 p3530 N94-29138
Artificial intelligence technology program at Rome Laboratory 08 p3414 N94-29328
Rome Laboratory software engineering technology program 08 p3414 N94-29330
On ground system integration and testing: A modern approach 08 p3150 N94-29334
A disciplined approach to software test and evaluation 08 p3416 N94-29339
A generalization of the software engineering maturity model 08 p3416 N94-29341
A common approach for an aerospace software environment 08 p3417 N94-29346
ISO overview: General presentation of the satellite, cryogenic aspects [REPT-932-440-102] 08 p3231 N94-29416
The Common Modular Simulator (CMS): An architecture test bed for future advanced ATM systems 08 p3141 N94-29582
Advanced Design of Ventilation Systems [VKI-LS-1993-07] 08 p3231 N94-29598
Introduction to the design of ventilation systems 08 p3231 N94-29599
Industrial ventilation 08 p3232 N94-29604
Advanced vehicle concepts systems and design analysis studies [NASA-CR-195115] 08 p3147 N94-29721
A performance analysis method for distributed real-time robotic systems: A case study of remote teleoperation [AIAA PAPER 94-1212-CP] 08 p3445 N94-30563
Engineering of systems for application of scientific computing in industry WP project management ISNaS 9209099 [PB94-126232] 08 p3428 N94-30739
Solar photovoltaics for development applications [DE94-006116] 08 p3340 N94-30843
A review of the status and capabilities of Navstar GPS [AD-B174629] 08 p3143 N94-30854
Validation experiments with an Ethernet model using the simulation tool 'PROMISE' [AD-B174795] 08 p3429 N94-30912
A new methodology of system parameter estimation [MATHS-REPT-A-208] 09 p3808 N94-31163
A neural network methodology for engineering applications: The learning control of robotic systems [RR-480] 09 p3830 N94-31500
Effective information modelling support [PB94-148236] 09 p3917 N94-31586
Modular Simulator System (MSS). System/segment specification for the generic modular simulator system-flight station module, volume 2 [AD-A276969] 09 p3588 N94-32313
A PC program to optimize system configuration for desired reliability at minimum cost 09 p3823 N94-32438
Research and technology, 1993 [NASA-TM-106376] 09 p3567 N94-33046
Real-time centimeter positioning with GPS: A system developed by the US Army Corps of Engineers [AD-A278152] 09 p3577 N94-33095
Task allocation and scheduling for high level synthesis [AD-A277570] 10 p4110 N94-33395
Systems design factors: The essential ingredients of system design, version 0.4 [AD-A277702] 10 p4031 N94-33439
A handling qualities investigation of conventional, rate command and attitude hold, and attitude command and attitude hold response types in the probe and drogue air refueling task [AD-A278464] 10 p4006 N94-33543
Mission operations and command assurance: Flight operations quality improvements 10 p4150 N94-33616
End effector monitoring system: An illustrated case of operational prototyping 10 p4109 N94-33631
On-orbit NDE: A novel approach to tube weld inspection 10 p4066 N94-33664
Workshop on Self-Determination in Developing and Evolving systems [AD-A278367] 10 p4097 N94-33737
The importance of robust error control in data compression applications 10 p4157 N94-33829
A systems engineering approach to AIS accreditation [DE94-009354] 10 p4158 N94-33909
Engineering design knowledge recycling in near-real-time 10 p4160 N94-34061
Materials processing in space tasks. WBS task 5.4: Generic tasks [NASA-CR-193979] 11 p4249 N94-35485
ORDIT: A new methodology to assist in the process of eliciting and modelling organisational requirements [PB94-167814] 11 p4345 N94-35533
DSS-13 S-/X-band microwave feed system 11 p4253 N94-35550
SOFIA: Aircraft system, aft telescope cavity configuration, phase 2. Volume 1: Executive summary [NASA-CR-196362] 12 p4546 N94-36642
The Engineering Review Board 12 p4540 N94-36843
H infinity control for nonlinear and linear systems [AD-A280450] 12 p4494 N94-37226
Virtual Interfaces: Research and Applications [AGARD-CP-541] 12 p4482 N94-37261
Immersive virtual environments as trainer: System design from a cognitive stance 12 p4484 N94-37267
On the use of fuzzy logic assessment for high consequence implementation risk analysis [DE94-011417] 12 p4507 N94-37564
Ordering design tasks based on coupling strengths [NASA-TM-109137] 12 p4387 N94-37762

SYSTEMS INTEGRATION

STGT program: Ada coding and architecture lessons learned 01 p0330 N94-11437
System integration and demonstration of adhesive bonded high temperature aluminum alloys for aerospace structure, phase 2 [NASA-CR-191459] 02 p0575 N94-12792
Electric propulsion system technology [NASA-CR-194100] 02 p0549 N94-13055
Integration between geographic information systems and environmental simulation models [REPT-93-004] 02 p0823 N94-13806
Advanced Communications ESM System (ACES) testbed: Integration study [DSIS-93-00345] 02 p0804 N94-13939
Activities of Institute for Information Technology [CNR-35024] 02 p0824 N94-14069
Experimental instrumentation system for the Phased Array Mirror Extendible Large Aperture (PAMELA) test program [NASA-CR-194421] 02 p0705 N94-14430
Small scale adaptive optics experiment systems engineering [NASA-CR-194419] 02 p0793 N94-14548
Optical systems integrated modeling 02 p0547 N94-14837
SIMS: Single Interface to Multiple Systems [AD-A266934] 03 p1143 N94-15175
Software architecture for shared information systems [AD-A266995] 03 p1144 N94-15216
Integration ToolKit and Methods (ITKM) manufacturing methods and prototype toolkit. A combined modeling method using IDEFO, IDEF1x and XSpec [AD-A266176] 03 p0984 N94-16981
Soyuz/ACRV accommodation study [NASA-TM-107733] 03 p0888 N94-17072
Integration of several computer systems within a heterogeneous environment [AD-A267978] 03 p1155 N94-17500
On the use of differential GPS for automatic approach and landing of space and aircraft [DLR-MITT-93-05] 04 p1316 N94-17921
Coordination of software-development activities among sites that are geographically separated [DE93-019201] 04 p1524 N94-19076
Problem of control in an integral vision system: Use of a multi-agent system [ETN-93-95007] 04 p1530 N94-19488
SISSY: An example of a multi-threaded, networked, object-oriented databased application [DE93-019742] 05 p2041 N94-19811
A modular design for connectionist parsing 05 p1941 N94-20252
Space Generic Open Avionics Architecture (SGOAA) standard specification [NASA-CR-188269] 05 p1666 N94-22275
Channel and terminal description of the ACTS mobile terminal 06 p2284 N94-22802
Low earth orbit satellite/terrestrial mobile service compatibility 06 p2288 N94-22827
Resource allocation planning with international components 06 p2520 N94-23963
Cockpit/NVG visual integration issues 06 p2432 N94-23983
Integration and test of high-speed transmitter electronics for free-space laser communications [NASA-TM-106295] 06 p2295 N94-24101
Integrated Airframe Design Technology [AGARD-R-794] 06 p2177 N94-24313
Multi-disciplinary coupling for integrated design of propulsion systems 06 p2179 N94-24326
Declarative Object Manipulation Environment (DOME): Alpha version [AD-A273233] 06 p2460 N94-24935
Passive millimeter-wave imaging 06 p2306 N94-25494
Weapon system integration for the AFIT virtual cockpit [AD-A274058] 07 p2667 N94-25772
Microwave and pulsed power [DE94-003019] 07 p2782 N94-26312
Merging photovoltaic hardware development with hybrid applications in the USA [DE94-002682] 07 p2857 N94-26612
Institute for Information Technology [NRC-37061] 07 p3118 N94-26709
Test of onboard real time applications (LICE (tm)) 07 p2952 N94-26737
Interdisciplinary technology 07 p2686 N94-27363
Minimum accommodation for aerobrake assembly, phase 2 [NASA-TM-107608] 07 p2692 N94-27774
Integrated coal gasification combined cycle 07 p2832 N94-28090
Arcjet system integration development [NASA-CR-187147] 08 p3171 N94-28736
On ground system integration and testing: A modern approach 08 p3150 N94-29334
Future manned systems advanced avionics study [NASA-CR-188277] 08 p3150 N94-29377
Automation of the NDT diagnostic using neural nets. Application: Inspection of Airbus longitudinal joints during maintenance [REPT-932-600-104] 08 p3315 N94-29474
Air-ground integration of the ATM system in PHARE 08 p3141 N94-29579
Integration of pyrotechnics into aerospace systems 08 p3161 N94-29634
Programmable Automated Welding System (PAWS) [AIAA PAPER 94-1221-CP] 08 p3446 N94-30570
Robotic NDE inspection of advanced solid rocket motor casings [AIAA PAPER 94-1222-CP] 08 p3446 N94-30571
The Automated Aircraft Rework System (AARS): A system integration approach [AIAA PAPER 94-1225-CP] 08 p3446 N94-30574
View integration: A survey of current developments [REPT-93-053] 08 p3536 N94-30927
Channel and terminal description of the ACTS mobile terminal 09 p3599 N94-31428
An information system organized as stratified hypermedia [TR-93-12] 09 p3918 N94-32289
Modular Simulator System (MSS). System/segment specification for the generic MSS-system integration, volume 1 [AD-A276968] 09 p3588 N94-32312
Modular Simulator System (MSS): Interface design document for the generic MSS [AD-A277270] 09 p3590 N94-32403
Overview of Langley systems studies 10 p3971 N94-33456
Propulsion airframe integration session overview and review of Lewis PAI efforts 10 p3977 N94-33503
HSCT inlet development issues 10 p3977 N94-33505
Transonic airframe propulsion integration 10 p3978 N94-33507
HSCT integrated propulsion control issues 10 p3978 N94-33510

Integration of the Molecular Sieve Oxygen Generating System (MSOGS) into the UH-60Q MEDEVAC Blackhawk
[AD-A277668] 10 p4099 N94-33589
Intelligent vehicle control: Opportunities for terrestrial-space system integration 10 p4127 N94-34038
The servicing aid tool: A teleoperated robotics system for space applications 10 p4067 N94-34039
Utilizing a Russian space nuclear reactor for a US space mission: Systems integration issues
[DE94-005585] 10 p4017 N94-34137
Specifications of auxiliary power units for conformity with helicopter turboshaft engines 10 p4001 N94-34441
Terminal Doppler Weather Radar (TDWR) Low Level Wind Shear Alert System 3 (LLWAS 3) integration studies at Orlando International Airport
[AD-A278957] 11 p4294 N94-35807
North American ISDN Users' Forum agreements on Integrated Services Digital Network
[PB94-162559] 11 p4305 N94-35940
Fuel Cell Handbook update
[DE94-002958] 11 p4282 N94-36021
Multidisciplinary studies of integrated neural network systems
[AD-A278774] 11 p4312 N94-36309
The use of a tactile interface to convey position and motion perceptions 12 p4486 N94-37281

SYSTEMS MANAGEMENT
Analysis of the Army's installation support modules with the private sector's open information systems
[AD-A265667] 01 p0421 N94-12579
The organizational preparation of existing relational databases for the integration of expert systems
[AD-A268823] 04 p1614 N94-18191
Report of the Second CLICOM Experts Meeting
[WCDMP-19] 04 p1495 N94-19705
Distributed Virtual System (DIVIRS) project
[NASA-CR-194360] 05 p1905 N94-20228
Government Open Systems Interconnection Profile (GOSIP) transition strategy
[AD-A273005] 05 p1740 N94-21308
Intervention strategies for the management of human error
[NASA-CR-4547] 05 p1642 N94-22373
A framework for SFC/DC system data analysis 06 p2523 N94-23234
Link monitor and control operator assistant: A prototype demonstrating semiautomated monitor and control 06 p2292 N94-23267
Planning for the future of the DREnet: The way ahead
[NRNS-002-00-001-01] 07 p2983 N94-28042
Publications of the NASA Controlled Ecological Life Support System (CELSS) program 1989-1992
[NASA-CR-4603] 08 p3401 N94-30122
DoD information systems capacity management function
[AD-A275987] 09 p3916 N94-31355
Distributed VIRtual System (DIVIRS) project
[NASA-CR-196262] 12 p4495 N94-37509

SYSTEMS SIMULATION
System monitoring and diagnosis with qualitative models
[NASA-CR-193812] 01 p0323 N94-10711
Real-time dynamic simulation of the Cassini spacecraft using DARTS. Part 2: Parallel/vectorized real-time implementation 02 p0680 N94-14639
Space Station Common Berthing Mechanism, a multi-body simulation application 02 p0544 N94-14640
Fast simulation of steady-state availability in non-Markovian highly dependable systems
[AD-A266747] 03 p1174 N94-15823
Space Station Freedom electrical performance model
[NASA-TM-106395] 03 p0929 N94-17483
Goal-driven LOTOS execution
[MEMO-INF-93-04] 04 p1527 N94-19227
Sensitivity and uncertainty analysis of Markov reward models
[MEMO-INF-92-89] 04 p1559 N94-19386
Automated qualitative modeling of dynamic physical systems
[AD-A270835] 04 p1422 N94-19598
Model checking, abstraction, and compositional verification
[AD-A270552] 05 p1902 N94-19919
Back and forth bisimulations on prime event structures
[RR-888-I-IMAG-124-LIFIA] 05 p1929 N94-20124
Multi-disciplinary coupling effects for integrated design of propulsion systems
[NASA-TM-106349] 05 p1830 N94-20170
SATCOM simulator speeds MSS deployment and lowers costs 06 p2287 N94-22822
Causal labeled transition systems: A new approach for describing the behavior of concurrent systems
[LAAS-93179] 06 p2447 N94-22911
Mathematical modeling of MCFC cells/stacks and networks
[DE94-001914] 06 p2390 N94-23212
A simulation system for Space Station extravehicular activity 06 p2434 N94-24192
From circuit to signal: Development of a piecewise linear simulator
[ISBN-9-09-005713-7] 06 p2462 N94-25263
Asynchronous and packetized systems engineering tools 07 p2954 N94-26746
Thermal enclosure system functional simulation user's manual
[NASA-TM-109094] 08 p3466 N94-29489
The Common Modular Simulator (CMS): An architecture test bed for future advanced ATM systems 08 p3141 N94-29582
The use of task network simulation in workload prediction
[DCIEM-92-32] 08 p3402 N94-30132
A finite state machine model for object oriented systems
[REPT-93-040] 09 p3809 N94-31212
Self-calibrating models for dynamic monitoring and diagnosis 10 p4127 N94-34052
Computer aided design of robotic control systems 10 p4110 N94-34336
Real-time RMS active damping augmentation: Heavy and very light payload evaluations
[NASA-TM-109134] 10 p4015 N94-34386

SYSTEMS STABILITY
On the stability of stationary regimes in a distributed autovibration system with external feedback
[DE93-620979] 01 p0141 N94-10543
Nonlinear analysis of mechanical systems under combined harmonic and stochastic excitation
[AD-A266217] 03 p1173 N94-16937
Control of nonlinear systems
[AD-A270141] 04 p1542 N94-18898
Limit theorems for functionals of Markov processes and renormalizable stable fields
[AD-A274645] 07 p3004 N94-27106
Stability of dynamical systems in the presence of noise
[AD-A275383] 08 p3243 N94-29072
Self-stabilizing l-exclusion algorithms
[RUU-CS-93-01] 08 p3424 N94-30379
Dynamics and control of tethered satellite systems 08 p3170 N94-30864
Local interaction control for space construction 08 p3170 N94-30960
Structural stability and bifurcations 09 p3911 N94-31895
Decentralized control of flexible, multibody systems 10 p4058 N94-33366
Adaptive stabilization of linear and nonlinear systems
[AD-A278270] 10 p4113 N94-33855
Stability and stability degree of a cracked flexible rotor supported on journal bearings 10 p4064 N94-34193
Parameterised controller design for dominant multivariable systems 10 p4114 N94-34309
Stabilization of flexible systems under a certain class of nonlinear feedback controls 10 p4114 N94-34314
Feedback stabilization of matrix second-order systems by solving Riccati equation 10 p4115 N94-34315
Robust stabilization of nonlinear systems with a class of unmatched uncertainties 10 p4115 N94-34322
Robust stabilization of marginally stable positive-real systems
[NASA-TM-109136] 12 p4500 N94-37058

SYSTOLE
Strategies and methodologies to develop techniques for computer-assisted analysis of gas phase formation during altitude decompression 01 p0312 N94-11547
Mechanism for regulation of myocardial contractility by autonomic drugs: Pathophysiological relevance in congestive heart failure 07 p2931 N94-27536

SYSTOLIC ARRAYS
Systolic array IC for genetic computation 04 p1400 N94-18361
A bit serial first level calorimeter trigger for an LHC detector
[USIP-92-08] 04 p1574 N94-18845
A programmable systolic trigger processor for FERA-bus data
[USIP-92-04] 04 p1405 N94-19292
Systolic design with asynchronous controls for digital-signal processing
[AD-A270976] 04 p1392 N94-19680
The Fifth NASA Symposium on VLSI Design
[NASA-CR-194644] 05 p1753 N94-21079
Practical issues in implementing roving spares in VLSI systolic arrays 05 p1758 N94-21114
Bit-systolic arithmetic arrays using dynamic differential gallium arsenide circuits 05 p1767 N94-21724
A 1 GHz sample rate, 256-channel, 1-bit quantization, CMOS, digital correlator chip 05 p1768 N94-21732
Design of a floating point convolution processor 05 p1775 N94-22133
Systolic matrix inversion using a Monte Carlo method
[PB94-148798] 10 p4130 N94-34257

SYSTOLIC PRESSURE
Autogenic-feedback training: A potential treatment for post-flight orthostatic intolerance in aerospace crews
[NASA-TM-108785] 06 p2426 N94-24102

T

T TAIL SURFACES
Experimental and theoretical studies of T-tail configurations for commuter aircraft applications 07 p2653 N94-28322

T TAURI STARS
Why convective heat transport in the solar nebula was inefficient 01 p0458 N94-12143
Search for x ray emitting young stars outside of massive molecular clouds
[NASA-CR-193609] 02 p0830 N94-13462
Pre-main sequence stars in the Chamaeleon cloud and pre-main sequence stars in the Rho Ophiuchi cloud core
[NASA-CR-194713] 05 p2080 N94-20337
The Nobeyama millimeter array survey for protoplanetary disks around protostar candidates and T Tauri stars in Taurus
[REPT-336] 06 p2604 N94-24987
ROSAT observations of the x ray binary HD 154791
[NASA-CR-195189] 06 p2600 N94-25198
Observational studies of the clearing phase in proto-planetary disk systems
[NASA-CR-195182] 06 p2604 N94-25265
Investigations of the dynamical evolution of protoplanetary nebulae
[NASA-CR-195278] 07 p3105 N94-27428
Observations of accretion and angular momentum regulation in young circumstellar disks and the implications for planetary formation 09 p3928 N94-31122
Evolution of dynamo-generated magnetic fields in accretion disks around compact and young stars 09 p3931 N94-31138
Multiwavelength search for protoplanetary disks 09 p3599 N94-31430

T-38 AIRCRAFT
Static aeroelastic response of an aircraft with asymmetric wing planforms representative of combat damage
[AD-A266890] 03 p0865 N94-14951
Adamson, Jim --- ASCAN training programs
[NASA-TM-109507] 03 p1137 N94-15454

T-39 AIRCRAFT
Installation of an FTIR spectrometer in the TP86 Sabreliner
[PB94-149036] 10 p3990 N94-34128

T-53 ENGINE
Hot gas ingestion effects on fuel control surge recovery and AH-1 rotor drive train torque spikes
[NASA-CR-191047] 10 p4005 N94-34993

TABLES (DATA)
A benchmark bending test of a thick specimen. Part 2: Surface displacement measurements
[ARL-RR-6-PT-2] 02 p0670 N94-12928
Royal Belgium observatory calendar: 156th year
[ETN-93-94221] 02 p0833 N94-14811
Module interconnection frameworks for a real-time spreadsheet
[AD-A267317] 03 p1153 N94-17220
Human central nervous system oxygen toxicity data from 1945 to 1986
[AD-A268225] 03 p1130 N94-17556
Satellite situation report, volume 31, number 1
[NASA-TM-105088] 03 p0898 N94-17584
Station climatic summaries, North America. Volume 2: Alaska, Canada and Greenland
[AD-A269793] 04 p1493 N94-18732
Solar radiation in Saudi Arabia
[AD-A269970] 04 p1493 N94-18781
Evaluation of RDBMS packages for use in astronomy 05 p2048 N94-22514
The European Southern Observatory-MIDAS table file system 05 p2048 N94-22518
NASA STI program database: Journal coverage (1990-1992)
[NASA-TM-109720] 06 p2593 N94-25168
Module interconnection frameworks for a real-time spreadsheet
[AD-A273853] 07 p2956 N94-25588
Kiruna geophysical data. Data summary 93/4-6, April-June 1993
[PB94-123700] 07 p2881 N94-27039
Kiruna geophysical data. Data summary 93/1-3, January-March, 1993
[PB94-123791] 07 p2881 N94-27043

JARE data reports. No. 186: Upper atmosphere physics data. Syowa and Asuka Stations, 1990
[JTN-94-80594] 07 p2881 N94-27299
Transferable Output ASCII Data (TOAD) editor version 1.0 user's guide
[NASA-CR-187507] 08 p3408 N94-28818

TABLETS
Efficacy of flocculating and other emergency water purification tablets
[AD-A266695] 03 p1148 N94-15840

TABS (CONTROL SURFACES)
Compilation of 1992 annual reports of the navy ELF communications system ecological monitoring program. Volume 3: Tabs G - I
[AD-A269727] 04 p1388 N94-18741
Effect of delta tabs on mixing and axis switching in jets from asymmetric nozzles
[NASA-TM-106450] 06 p2167 N94-23592
Shear flow control of cold and heated rectangular jets by mechanical tabs. Volume 1: Results and discussion
[NASA-CR-182296-VOL-1] 09 p3708 N94-32867
Shear flow control of cold and heated rectangular jets by mechanical tabs. Volume 2: Tabulated data
[NASA-CR-182296-VOL-2] 09 p3709 N94-32869
Enhancement of mixing in a rectangular jet by mechanical tabs
[NASA-CR-185207] 09 p3709 N94-32872
Numerical investigation of multi-element airfoils
[NASA-CR-194592] 11 p4191 N94-36394

TABULATING
U TABULATION PROCESSES

TABULATION PROCESSES
FEEST: A method for tabulating equation of state and opacity tables
[DE93-017965] 04 p1347 N94-18092

TACHYONS
The Casimir energy of the rigid string with massive ends
[DE93-616851] 06 p2492 N94-25338

TACTICS
Optimal tactics for agile aircraft technology: A differential game methodology 10 p3994 N94-34631

TACTILE DISCRIMINATION
Application of change detection to dynamic contact sensing
[AD-A270523] 05 p1939 N94-20105
Investigation of hand capabilities under a variety of performance conditions and an attempt to explain performance differences 06 p2444 N94-25354
Tactility as a function of grasp force: Effects of glove, orientation, pressure, load, and handle
[NASA-TP-3474] 08 p3402 N94-30210

TACTILE SENSATION
U TOUCH

TACTILE SENSORS (ROBOTICS)
Object recognition in industrial environment by means of tactile sensor
[ITN-93-85200] 01 p0178 N94-10393
Development of a tactile and vision integrated system, and object identification techniques for SPDM applications
[DSIS-93-00153] 02 p0764 N94-13842
Development of a computer vision system to supplement the active tactile sensing capability in a structured environment
[DSIS-93-00072] 02 p0764 N94-13844
Tactile sensing and control in humans and robotic/teleoperated systems
[AD-A267710] 03 p1163 N94-14937
Application of change detection to dynamic contact sensing
[AD-A270523] 05 p1939 N94-20105

TAGGING
U MARKING

TAGN
Molecular structure of low temperature form of triaminoguanidinium nitrate (TAGN)
[AD-A270409] 04 p1377 N94-18708

TAIL ASSEMBLIES
Low-speed wind tunnel tests on four types of joined-wing aircraft models
[NAL-TR-1167] 02 p0501 N94-13340
Vertical-tail aerodynamic configuration of space shuttle orbiter
[AD-A267723] 03 p0879 N94-14941
Apparatus and method for improving spin recovery on aircraft
[NASA-CASE-LAR-14747-1] 05 p1650 N94-20556
Aircraft empennage structural detail design
[NASA-CR-195496] 06 p2179 N94-24332
Aircraft empennage structural detail design
[NASA-CR-195486] 06 p2183 N94-24969
Experimental and theoretical studies of T-tail configurations for commuter aircraft applications 07 p2653 N94-28322
A combined approach to buffet response analyses and fatigue life prediction 10 p4072 N94-34587
Damage tolerance management of the X-29 vertical tail 10 p3996 N94-34595
Aerodynamic design of super maneuverable aircraft 10 p3992 N94-34617

TAIL MOUNTINGS
U TAIL ASSEMBLIES

TAIL PLANES
U HORIZONTAL TAIL SURFACES

TAIL ROTORS
Acquisition, design modification, assembly, and ground test of NPS Hummingbird remotely piloted helicopter
[AD-A275546] 08 p3146 N94-28837

TAIL SURFACES
NT HORIZONTAL TAIL SURFACES
NT T TAIL SURFACES

TAILLESS AIRCRAFT
NT F-106 AIRCRAFT
NASA advanced design program. Design and analysis of a radio-controlled flying wing aircraft
[NASA-CR-195515] 06 p2180 N94-24589

TAILS (ASSEMBLIES)
U TAIL ASSEMBLIES

TAIWAN
Sedimentation rates and particulate fluxes in the slope and deep sea areas off eastern Taiwan 01 p0220 N94-12709

TAKEOFF
NT VERTICAL TAKEOFF
Wake structure and aerodynamic behavior of high lift aircraft configurations during unsteady maneuvers in ground effect 04 p1309 N94-18439
Procedures and design data for the formulation of aircraft configurations
[AD-A270150] 04 p1318 N94-18779
Influence of headwind on hot gas reingestion and consideration of pressure ratio scaling 07 p2675 N94-28018
Scattering of a random acoustic field by an infinite cylinder: Application to the modelization of the acoustic environment of the 'Ariane 5' launcher scale-model using experimental data
[ONERA-NT-1993-11] 09 p3860 N94-31226
Overview of NASA HSR high-lift program 10 p3979 N94-33518
Direct reduced order mixed H2/H infinity control for the Short Take-Off and Landing/Maneuver Technology Demonstrator (STOL/MTD)
[AD-A278675] 11 p4199 N94-35796
The reduction of takeoff ground roll by the application of a nose gear jump strut
[NASA-TM-108822] 11 p4198 N94-36380

TAKEOFF RUNS
Take-off performance monitoring system algorithm and display development
[NLR-TP-91395-U] 04 p1317 N94-17734
System for generating, aboard an aircraft, during takeoff, of a signal capable of producing an alert or an alarm, in case of malfunction
[CA-PATENT-APPL-SN-2,018,940] 07 p2659 N94-26293

TALC
Chromate-free talc chemical conversion coatings for aluminum alloys
[DE94-001567] 06 p2238 N94-22932
Non-chromate talc conversion coatings for aluminum
[DE94-005281] 08 p3207 N94-30053

TALKING
NT SYLLABLES
NT WORDS (LANGUAGE)
Recognizing hesitation phenomena in continuous, spontaneous speech 05 p1746 N94-22210
Spectral analysis method and sample generation for real time visualization of speech
[ETN-94-95732] 09 p3674 N94-31573
Dialog structure and plan recognition in spontaneous spoken dialog
[AD-A277566] 10 p4032 N94-33393

TALON AIRCRAFT
U T-38 AIRCRAFT

TANDEM MIRRORS
Applying design principles to fusion reactor configurations for propulsion in space
[NASA-TM-108247] 01 p0047 N94-11053
Potential formation and transport in open field line systems
[DE94-718910] 11 p4337 N94-35983

TANDEM ROTOR HELICOPTERS
Trim calculation of tandem rotor helicopter using simplified rotor system mathematical model 10 p4008 N94-34337

TANKER AIRCRAFT
Spare parts analysis of the MK.32B-751 AAR pod
[DSIS-93-00737] 02 p0774 N94-13549
Effectiveness of protection clothing for cold weather conditions after ejection over sea: A case report 08 p3381 N94-28435
Future tanker considerations and requirements 11 p4197 N94-36342
Tanker system and technology requirements definition: A tanker technology road map 11 p4197 N94-36344
Hose-drogue versus boom receptacle air refueling 11 p4197 N94-36345
The KDC-10 programme of the Royal Netherlands Air Force 11 p4197 N94-36346
CC-130H(T) tactical aerial refuelling tanker development flight test programme 11 p4198 N94-36347

TANKS (COMBAT VEHICLES)
Preliminary analysis of the JAPE ground vehicle test data with an artificial neural network classifier 06 p2529 N94-24222

TANKS (CONTAINERS)
NT CYLINDRICAL TANKS
NT EXTERNAL TANKS
NT FUEL TANKS
NT PROPELLANT TANKS
NT SPHERICAL TANKS
NT STORAGE TANKS
NT WING TANKS

TANTALUM
Shock compression and quasielastic release in tantalum
[DE93-014566] 02 p0811 N94-14329
The effect of oxygen, grain size, and strain rate on the mechanical behavior of forged P/M tantalum
[DE93-011251] 03 p0959 N94-16764
Laser weld repair of tantalum sheet
[DE93-016417] 03 p1041 N94-16871
Dislocation-drag contribution to high-rate plastic deformation in shock-loaded tantalum
[DE93-018286] 04 p1361 N94-18802
Dynamical behavior of tantalum
[DE93-017877] 04 p1362 N94-18919
Influence of peak pressure and temperature on the shock-loading response of tantalum
[DE93-018561] 04 p1457 N94-19279
The metallic bond for monolayer transition metal layers on transition metal surfaces
[DE93-019060] 05 p1691 N94-20313
Gamma ray spectrometry of LDEF samples: Results of 1992 analyses
[DE94-001177] 05 p1684 N94-22046
Texture gradient effects in tantalum
[DE94-000689] 06 p2240 N94-23021
The effects of texture and strain on the r-va lue of heavy gauge tantalum plate
[DE94-000690] 06 p2242 N94-23541
X ray diffraction analysis of electrodeposited beta-tantalum
[AD-A273254] 06 p2249 N94-25142
Deviatoric stresses and plastic strain rates in strong shock waves for six metals
[DE94-002964] 07 p2733 N94-26022
The high strain rate behaviour of tantalum
[ISBN-0-315-84472-8] 07 p2740 N94-27305
Influence of tungsten alloying additions on the mechanical properties and texture of tantalum
[DE94-004994] 08 p3210 N94-30774

TANTALUM ALLOYS
Metastability of yttrium-oxides
[DE93-016548] 02 p0813 N94-14440
Processing and protection of high temperature structural materials
[AD-A267292] 03 p0954 N94-14961
The high strain rate behaviour of tantalum
[ISBN-0-315-84472-8] 07 p2740 N94-27305
The corrosion behavior of sputter-deposited magnesium-valve metal alloys 07 p2745 N94-28164
CO2 methanation catalysts prepared from amorphous Ni-valve metal alloys containing platinum group elements 07 p2745 N94-28166
An investigation of the corrosion properties of aluminum-tantalum alloys using electrochemical impedance spectroscopy and local electrochemical impedance spectroscopy 08 p3209 N94-30521
Influence of tungsten alloying additions on the mechanical properties and texture of tantalum
[DE94-004994] 08 p3210 N94-30774
Nature of dissolution of binary tantalum-titanium alloys by molten plutonium
[DE94-005090] 08 p3210 N94-30776
Electrooptic crystal growth and properties
[AD-A276023] 09 p3896 N94-31439

TANTALUM CARBIDES
Performance of carbon-based hot frit substrates
[DE94-000509] 05 p1676 N94-21754
Deposition of tantalum carbide coatings on graphite by laser interactions 08 p3223 N94-30475

TANTALUM COMPOUNDS
NT TANTALUM CARBIDES
NT TANTALUM OXIDES
NNN-Ising model simulation of nanodomain textures in relaxor-type lead scandium tantalate
[DE94-601884] 07 p2748 N94-25844
Polar and chemical domain structures of lead scandium tantalate (PST)
[DE94-600760] 07 p3056 N94-26363
Vertical electron detachment energies for octahedral closed-shell multiply charged anions
[AD-A278835] 11 p4322 N94-35753
TANTALUM OXIDES
Low temperature synthesis of monolithic transparent Ta2O5 gels from hydrolysis of metal alkoxide
[NASA-TM-106246] 01 p0089 N94-11204
The effect of oxygen, grain size, and strain rate on the mechanical behavior of forged P/M tantalum
[DE93-011251] 03 p0959 N94-16764
A quantitative model for interpreting nanometer scale hardness measurements of thin films
[DE93-040601] 05 p2034 N94-22005
TAPE RECORDERS
NT VIDEO TAPE RECORDERS
Laser weld repair of tantalum sheet
[DE93-016417] 03 p1041 N94-16871
Recording system using multiplexed inputs to a multichannel recorder
[AD-D015971] 05 p1808 N94-21278
Architectural constructs of Ampex DST 10 p4153 N94-33805
Volume server: A scalable high speed and high capacity magnetic tape archive architecture with concurrent multi-host access 10 p4154 N94-33807
TAPER
U TAPERING
TAPERED WINGS
U SWEPT WINGS
TAPERING
A study of two dimensional tapered periodic edge treatments to reduce wideband edge diffraction
[AD-A274054] 07 p2766 N94-25824
TARE (DATA REDUCTION)
U DATA REDUCTION
TARGET ACQUISITION
Fuzzification of ASAT's rule based aimpoint selection
[AD-A266068] 01 p0043 N94-11223
Aircraft windscreens enhance visual search disruption produced by laser glare
[AD-A265167] 01 p0026 N94-11892
Estimation with multisensor/multiscan detection fusion
[AD-A265673] 01 p0138 N94-12338
Infrared transmission and path radiance through dust and fog
[AD-A265825] 02 p0791 N94-12979
A piloted simulation investigation of the normal load factor and longitudinal thrust required for air-to-air acquisition and tracking 02 p0522 N94-13301
EVA retriever demonstration
[NASA-TM-109510] 03 p1046 N94-15456
Airborne 2 color ranging experiment 03 p0920 N94-15614
Pixel-level fusion using interest images
[AD-A266640] 03 p1164 N94-15746
Environmental characterization for target acquisition. Report 1: Site descriptions and measurements
[AD-A267192] 03 p1106 N94-15851
Exploiting world structure to efficiently search for objects
[TR-434] 03 p1231 N94-16576
Enhanced down-range profiles of complex targets using wideband radar echo returns
[AD-A266508] 03 p0999 N94-16788
Target detection by way of Kalman filtering
[AD-A267314] 03 p1000 N94-16945
Signal detection in correlated Gaussian and non-Gaussian radar clutter
[AD-A267453] 03 p1001 N94-17033
A virtual acoustic orientation instrument
[AD-A266181] 03 p1134 N94-17510
AN/APS-137 Forward Looking Airborne Radar (FLAR) evaluation Spring 1992 experiment
[AD-A268899] 04 p1384 N94-18228
Environmental characterization for target acquisition. Report 3: New concepts for evaluating low-grazing angle radar measurements
[AD-A269956] 04 p1388 N94-18777
The star identification, pointing and tracking system of UVSTAR, an attached payload instrument system for the Shuttle Hitchhiker-M platform 04 p1326 N94-19179
Target motion detecting impulse Doppler radar system
[AD-D015898] 05 p1717 N94-20198
Probability of detection calculations using MATLAB
[AD-A271958] 05 p1736 N94-20578
Development of a lidar for integration with the Naval Postgraduate School Infrared Search and Target Designation (NPS-IRSTD) system
[AD-A271847] 05 p1817 N94-20611
Current directions in the vulnerability/lethality process structure
[AD-A272836] 05 p1964 N94-21175
NAVSPASUR sensor system digital signal processing receiver. Volume 2: Function and capabilities of hardware and software components
[AD-A272900] 05 p1739 N94-21218
Experimental evaluation of camouflage effectiveness in the thermal infrared
[FEL-93-A043] 06 p2381 N94-22896
Analysis of passive acoustic ranging of helicopters from the joint acoustic propagation experiment 06 p2529 N94-24220
Acoustic target detection and classification using neural networks 06 p2529 N94-24221
Mitsubishi 3-5 micrometers IR imager for machine-vision/ATA applications
[AD-A273812] 07 p3034 N94-25940
Radar detection of low-altitude targets in a maritime environment. Volume 2: Meteorological and radar data
[AD-A274658] 07 p2768 N94-26335
Capture and location of blobs in digital images
[ISBN-0-315-84382-9] 07 p3036 N94-26666
Processing of wide-angle synthetic aperture radar signals for target detection
[AD-A274225] 07 p2773 N94-27073
Using multiple searchers to locate a randomly moving target
[AD-A275602] 08 p3463 N94-28768
Environmental characterization for target acquisition. Analysis of thermal and visible imagery
[AD-A275414] 08 p3242 N94-28862
GLRS-R 2-colour retroreflector target design and predicted performance
[REPT-932-440-106] 08 p3246 N94-29542
ACCS Surveillance Exploratory Prototype (ASEP) 08 p3138 N94-29566
Radar returns from a low-flying target over a rough sea surface under multipath and clutter conditions 08 p3253 N94-29882
Infrared polarization signatures 08 p3258 N94-30506
Model for the simulation of atmospheric effects on targets to background passive signatures 08 p3258 N94-30507
The effect of enhanced backscattering on target detection 08 p3258 N94-30508
A hybrid electromagnetic-statistical approach for characterizing MMW scattering by terrain 08 p3259 N94-30510
Radar cross sections of ground clutter at 95 GHz for summer and fall conditions 08 p3259 N94-30512
Peak detection of Swerling type targets. Part 1: Detection probabilities in white noise
[AD-A276217] 09 p3670 N94-31062
Analysis using bi-spectral related technique
[AD-A276017] 09 p3672 N94-31386
Waveform generation for ultra-wideband radar system
[AD-A276352] 09 p3673 N94-31401
Detection of a chi-square fluctuating target in Gaussian noise
[AD-A276078] 09 p3850 N94-31462
Visual processing of object velocity and acceleration
[AD-A277425] 09 p3801 N94-32998
The application of a radial basis function neural network for radar tracking over the sea 09 p3686 N94-33150
Some neural computing approaches to target tracking 09 p3837 N94-33151
Multi-sensor data fusion for target acquisition 09 p3837 N94-33154
Effective declutter of complex flight displays using stereoptic 3-D cueing
[AD-A279764] 10 p3989 N94-33536
Laboratory and in-flight experiments to evaluate 3-D audio display technology 10 p4038 N94-33618
Radar detection of low-altitude targets in a maritime environment. Volume 1: Final analysis
[AD-A278493] 10 p4037 N94-34376
Pointing and Tracking Systems
[AGARD-CP-539] 12 p4392 N94-36616
Laser designation pods optimized concept for day/night operations 12 p4393 N94-36620
Infrared search and track demonstrator programme 12 p4393 N94-36622
Multiple target track-while-scan in the airborne EO environment 12 p4394 N94-36629
Efficient contact determination between geometric models
[AD-A280244] 12 p4494 N94-37120
Distributed detection theory and data fusion
[AD-A280410] 12 p4434 N94-37183

TARGET DRONE AIRCRAFT
NT FIREBEE 2 TARGET DRONE AIRCRAFT
AIAA Techfest 29 proceedings
[NIAR-93-1] 05 p1635 N94-20191
TARGET PENETRATION
U TERMINAL BALLISTICS
TARGET RECOGNITION
The theory for, and demonstration of, information theory applied to radar target identification
[DE93-006393] 01 p0132 N94-10315
Spatial light rebroadcaster architecture study
[AD-A266102] 01 p0382 N94-11421
Airborne optical tracking control system design study
[DE93-009515] 01 p0382 N94-11662
A hybrid neural network and feature extraction technique for target recognition
[AD-D015732] 01 p0333 N94-12386
ISAR motion compensation using the burst derivative measure as a focal quality indicator
[AD-A265647] 01 p0138 N94-12440
Pixel-level fusion using interest images
[AD-A266640] 03 p1164 N94-15746
Development and analysis of ARMA parameter estimation schemes in the presence of noise
[AD-A267184] 03 p0989 N94-15786
Environmental characterization for target acquisition. Report 1: Site descriptions and measurements
[AD-A267192] 03 p1106 N94-15851
Enhanced down-range profiles of complex targets using wideband radar echo returns
[AD-A266508] 03 p0999 N94-16788
An analog retina model for detecting dim moving objects against a bright moving background 04 p1399 N94-18350
Operator performance in pattern matching as a function of reference material structure
[AD-A269889] 04 p1509 N94-18686
Environmental characterization for target acquisition. Report 3: New concepts for evaluating low-grazing angle radar measurements
[AD-A269956] 04 p1388 N94-18777
Applications of motion estimation in image processing
[FEL-92-B356] 04 p1580 N94-19455
A non-homogeneous, spatio-temporal, wavelet multiresolution analysis and its application to the analysis of motion
[AD-A270621] 04 p1538 N94-19534
Tracking with time-delayed data in multisensor systems
[AD-A271334] 04 p1391 N94-19582
Recognition by prototypes
[AD-A271687] 05 p1943 N94-20921
Massachusetts Institute of Technology Lincoln Laboratory Journal volume 6, number 1, Spring 1993
[AD-A272273] 05 p1737 N94-20944
Improvement in invariant pattern recognition with neural networks and Fourier-Mellin filters 05 p1780 N94-22164
A modified moment invariants technique for classification of noisy objects 05 p1780 N94-22165
Signal processing and target discrimination algorithms for a rosette scan tracker 05 p1747 N94-22237
Radar imaging of moving targets 05 p1747 N94-22238
Imaging System (INEL) T805 prototype
[DE94-002807] 06 p2382 N94-23492
UAV current technology and future trends 06 p2154 N94-24245
Object recognition through image understanding for an autonomous mobile robot
[AD-A273206] 06 p2475 N94-24862
Radar target discrimination by spectrum analysis
[AD-D015982] 06 p2301 N94-25040
Hyperspectral analysis of space objects: Signal to noise evaluation
[AD-A273882] 07 p2765 N94-25728
Color image segmentation
[AD-A274027] 07 p2984 N94-25759
Zernike moments and rotation invariant object recognition. A neural network oriented case study
[AD-A273749] 07 p2767 N94-26011
New binary integration strategies and corresponding R90 calculations
[AD-A274786] 07 p2769 N94-26359
Combatting inherent vulnerabilities of CFAR algorithms and a new robust CFAR design
[AD-A274918] 07 p2770 N94-26751
The morphological processing of binary images
[AD-A274310] 07 p2996 N94-26972
Joint services electronics program
[AD-A274643] 07 p2785 N94-27027
Processing of wide-angle synthetic aperture radar signals for target detection
[AD-A274225] 07 p2773 N94-27073

Image quality analysis of compressed synthetic aperture radar imagery
[AD-A273399] 07 p2774 N94-27170
Environmental characterization for target acquisition. Analysis of thermal and visible imagery
[AD-A275414] 08 p3242 N94-28862
Spectral and polarimetric analysis of hyperspectral data collected by an acousto-optic tunable filter system
[AD-A275076] 08 p3329 N94-29095
ACCS Surveillance Exploratory Prototype (ASEP) 08 p3138 N94-29566
Psychophysiological study on the effects of co-existence of lines for detecting dot target 08 p3394 N94-29867
Knowledge combination and data fusion with application to recognition systems 08 p3259 N94-30513
Correlation filter synthesis using neural networks
[AD-A278124] 09 p3836 N94-33043
A novel optoelectronic system for distortion-invariant ATR
[AD-A277985] 09 p3884 N94-33087
Multi-sensor data fusion for target acquisition 09 p3837 N94-33154
Forward-looking infrared: Capabilities for search and rescue
[AD-A277895] 10 p4141 N94-33548
Color-coded radar plan position indicator
[AD-D016200] 11 p4257 N94-36364
Efficient contact determination between geometric models
[AD-A280244] 12 p4494 N94-37120

TARGET THICKNESS
An electromagnetic noncontacting sensor for thickness measurement in a dispersive medium
[AIAA PAPER 94-1200-CP] 08 p3443 N94-30551

TARGET TRACKING
U TRACKING (POSITION)

TARGETS
NT LASER TARGETS
NT PARTICLE ACCELERATOR TARGETS
NT RADAR TARGETS
GRAFTED (GRAphical Fault Tree EDitor): A fault tree description program for target vulnerability/survivability analysis
[AD-A264078] 01 p0328 N94-11301
Projectile-target mixing in melted ejecta formed during a hypervelocity impact cratering event 01 p0432 N94-12241
Effects of window size and shape on accuracy of subpixel centroid estimation of target images
[NASA-TP-3331] 03 p1034 N94-15990
Passive tracking of a target using an array of sensors
[DE93-015870] 03 p0997 N94-16169
An algorithm for the estimation of bounds on the emissivity and temperatures from thermal multispectral airborne remotely sensed data 03 p1064 N94-16603
Hydrodynamic instability modeling for ICF
[DE93-018634] 04 p1587 N94-18274
A program for passively tracking a target using an array of sensors
[DE93-019554] 04 p1390 N94-19306
Effects of location cuing on redundant target processing
[IZF-1993-B-1] 04 p1510 N94-19443
Facilities for in situ ion beam studies in transmission electron microscopes
[DE93-019567] 05 p1979 N94-20222
Geometrical analysis of the microcraters found on LDEF samples 05 p1666 N94-20890
Antipodal fragment velocities for porous and weak targets at catastrophic impacts 05 p1836 N94-20891
A mixed map/variable structure observer for target tracking 06 p2157 N94-24263
An algorithm to find the intersection of two convex polygons
[AD-A274722] 07 p2961 N94-26148
Psychophysiological study on the effects of co-existence of lines for detecting dot target 08 p3394 N94-29867
Experimental evaluation of camouflage effectiveness in the thermal infrared 08 p3257 N94-30502
Inertial confinement fusion target component fabrication and technology development report
[DE94-009973] 11 p4335 N94-35673

TASK COMPLEXITY
Vigilance problems in orbiter processing 01 p0314 N94-11536
Development and evaluation of a predictive algorithm for telerobotic task complexity 01 p0341 N94-11562
NASA/DOD Aerospace Knowledge Diffusion Research Project. Report 15: Technical uncertainty and project complexity as correlates of information use by US industry-affiliated aerospace engineers and scientists: Results of an exploratory investigation
[NASA-TM-107693] 03 p1233 N94-17291
Theoretical implications and empirical findings on instructional control and part-whole-task training
[AD-A267826] 03 p0872 N94-17403
Pilot evaluation system 06 p2158 N94-24266
The central executive component of working memory
[AD-A274295] 07 p2938 N94-26683
Attention and signal detection. A study of attention divided between visual and auditory signals
[PB94-170594] 11 p4298 N94-36215

TASK PLANNING (ROBOTICS)
Task planning with uncertainty for robotic systems
[NASA-CR-193253] 01 p0338 N94-10638
Development and evaluation of a predictive algorithm for telerobotic task complexity 01 p0341 N94-11562
Robot programming, natural computation and conceptual graphs
[ITN-93-85193] 02 p0748 N94-13539
Robot-task compliance: The energy criterion
[ITN-93-85196] 02 p0763 N94-13568
Efficient domain-independent experimentation
[AD-A269530] 04 p1557 N94-18640
An architecture for teleprogramming autonomous mobile robots at task level
[LAAS-93107] 06 p2470 N94-22906
A system for the challenging task of collecting samples from a comet surface 06 p2358 N94-24007
Admittance model for the shuttle remote manipulator system in four configurations
[NASA-CR-4555] 06 p2474 N94-24635
Graphical programming at Sandia National Laboratories
[DE94-003803] 07 p2958 N94-25818
A multitasking behavioral control system for the Robotic All-Terrain Lunar Exploration Rover (RATLER) 07 p2685 N94-26292
A Space Station robot walker and its shared control software
[AIAA PAPER 94-1192-CP] 08 p3442 N94-30543
Task-level control for autonomous robots
[AIAA PAPER 94-1210-CP] 08 p3444 N94-30561
Using generic tool kits to build intelligent systems
[AIAA PAPER 94-1214-CP] 08 p3445 N94-30565
A reactive system for open terrain navigation: Performance and limitations
[AIAA PAPER 94-1218-CP] 08 p3445 N94-30566
The road plan model: Information model for planning road building activities
[AIAA PAPER 94-1219-CP] 08 p3445 N94-30567
A high-performance multi-arm environment: Theoretical aspects and practical implementation
[RR-479] 09 p3722 N94-31379
Contingency-tolerant robot motion planning and control 09 p3830 N94-31482
Advanced teleoperation: Technology innovations and applications 09 p3806 N94-32453

TASKS
NT VISUAL TASKS
Crew chief 01 p0335 N94-11564
Career Information in the Mathematical Sciences (CIMS)
[DE93-013780] 01 p0318 N94-11817
Locus coeruleus, vigilance, and stress: Brain mechanisms of adaptive behavioral responsiveness
[AD-A265657] 01 p0302 N94-12441
Work/rest schedules and performance of F/A-18 aviators during Fleet Exercise 1992
[AD-A265826] 02 p0735 N94-12982
Preliminary validation of the task analysis/workload methodology
[AD-A267514] 03 p1138 N94-17077
Building a joint-service classification research roadmap: Criterion-related issues
[AD-A269735] 04 p1512 N94-18754
Development of the UTC-PAB normative database
[AD-A271319] 05 p1893 N94-20023
Multilist scheduling: A new parallel programming model
[AD-A270549] 05 p1929 N94-20084
The role of visual context in manual target localization 06 p2429 N94-25351
Long term learning: Integration of knowledge acquisition and knowledge compilation
[AD-A274775] 07 p3098 N94-26570
Scheduling tasks with unpredictable timing parameters in hard real-time systems 07 p2951 N94-26728
Fault-tolerant scheduling in distributed critical real-time systems 07 p2952 N94-26735
Simulation Networking/Training Requirements Relational Database: User's guide
[AD-A275634] 08 p3528 N94-28637
Toward a model of expert knowledge structure and their role in cognitive task performance
[AD-A275641] 08 p3529 N94-28645
Cognitive approach to specifications on air traffic controllers' decision assistance systems 08 p3139 N94-29571
Considerations on graphical user interfaces for intelligent ATM support systems 08 p3139 N94-29572
The use of task network simulation in workload prediction
[DCIEM-92-32] 08 p3402 N94-30132
Robotic vehicle mobility and task performance: A flexible control modality for manned systems 10 p4067 N94-34040
Refinement types ML
[AD-A278937] 11 p4304 N94-35709

TASTE
STS-29 crew food tasting in building 45
[NASA-TM-109547] 03 p1136 N94-15382
Reassessment of area postrema's role in motion sickness and conditioned taste aversion 05 p1886 N94-21901
Recovery of the vomiting reflex following area postrema ablation in squirrel monkeys 05 p1886 N94-21904
Conditioned taste aversion induced by motion is prevented by selective vagotomy in the rat 05 p1887 N94-21908
The effects of area postrema lesions and selective vagotomy on motion-induced conditioned taste aversion 05 p1888 N94-21910
Role of the area postrema in three putative measures of motion sickness in the rat 05 p1888 N94-21912
Investigating motion sickness using the conditioned taste aversion paradigm 05 p1888 N94-21913
Conditioned taste aversion and motion sickness in cats and squirrel monkeys 05 p1888 N94-21914
Some issues on Japan's space food development and relating preliminary experimental study 08 p3388 N94-28498

TATB
Temperature effects on failure thickness and deflagration-to-detonation transition in PBX 9502 and TATB
[DE93-010742] 01 p0097 N94-10294
The use of post detonation analysis of stable isotope ratios to determine the type and production process of the explosive involved
[DE93-018497] 04 p1378 N94-19242
Condensed-phase thermal decomposition of TATB investigated by Atomic Force Microscopy (AFM) and Simultaneous Thermogravimetric Modulated Beam Mass Spectrometry (STMBMS)
[DE94-000396] 06 p2232 N94-23298

TAURUS CONSTELLATION
ROSAT observations of the x ray binary HD 154791
[NASA-CR-195189] 06 p2600 N94-25198

TAXIING
A study of parallel pier finger airport terminal configuration
[ISBN-0-315-83128-6] 05 p1652 N94-22425
System for automatic transportation of aircraft on the ground
[CA-PATENT-1-322-361] 06 p2193 N94-24785
Automatic control steps for aircraft taxi guidance 08 p3141 N94-29584
Airside ground movements surveillance 08 p3141 N94-29585
A novel near-range radar network for airport surface control 08 p3142 N94-29586
Evaluation for the development of taxiway lighting intensity standards
[AD-A276706] 09 p3588 N94-32120
Improved taxiway exit identification system
[AD-A277892] 10 p4008 N94-33538

TAXONOMY
How diverse is the asteroid belt? 01 p0430 N94-12124
First results of the seven-color asteroid survey 01 p0430 N94-12162
The biostratigraphy and paleogeography of Maastrichtian inoceramids 07 p2889 N94-28303
A taxonomy of coordination mechanisms used in real-time software based on domain analysis
[AD-A279014] 11 p4304 N94-35794

TAYLOR INSTABILITY
Mechanism of intermittent atomization
[AD-A266625] 03 p1021 N94-15770
Dynamic response of ceramics
[AD-A275396] 08 p3214 N94-29203
A review of the ablative stabilization of the Rayleigh-Taylor instability in regimes relevant to ICF
[DE94-005809] 08 p3509 N94-30597
Design of an electromagnetic accelerator for turbulent hydrodynamic mix studies
[DE94-005821] 08 p3281 N94-30600
LLE review, volume 57
[DE94-009186] 10 p4145 N94-33990
A review of the ablative stabilization of the Rayleigh-Taylor instability in regimes relevant to inertial confinement region
[DE94-008300] 10 p4145 N94-35080

Spatio-temporal properties of centrifugal instabilities: Abstracts of 8th Couette-Taylor Meeting
[PB94-150240] 11 p4266 N94-35981

TAYLOR SERIES
Automatic differentiation of limit functions
[DE93-016376] 03 p1168 N94-14928
A handbook of cost risk analysis methods
[AD-A267253] 03 p1235 N94-16988
A finite strain ring dynamical model for pneumatic tires
[AD-A269286] 04 p1444 N94-18266
Error propagation equations and tables for estimating the uncertainty in high-speed wind tunnel test results
[DE93-018685] 04 p1311 N94-18275
Application of body fitted-coordinates in heat conduction problems
[ETN-94-95338] 06 p2340 N94-25484
Probability distributions with given marginals and given correlation that have maximal entropy
[REPT-93-81] 09 p3851 N94-31698
Light-traffic analysis for queues with spatially distributed arrivals
[MEMO-1150] 09 p3832 N94-31826
Compression of a radar track of a near Earth satellite into an Earth centered inertial state vector using least squares differential correction
[AD-A278498] 10 p4037 N94-34302

TAYLOR THEOREM
U TAYLOR SERIES

TAYLOR-GOERTLER INSTABILITY
U GOERTLER INSTABILITY

TD SATELLITES
NT TD-1 SATELLITE

TDMA
U TIME DIVISION MULTIPLE ACCESS

TDR SATELLITES
STGT program: Ada coding and architecture lessons learned 01 p0330 N94-11437
STS-26 Post-Flight Press Conference
[NASA-TM-109557] 03 p0879 N94-15261
STS-26 onboard 16mm photography quick release
[NASA-TM-109558] 03 p0879 N94-15262
TDRS video clip
[NASA-TM-109585] 03 p0884 N94-15269
STS-26 through STS-34, deploy activities
[NASA-TM-109566] 03 p1301 N94-15315
STS-26 generic integrated IUS deploy simulation
[NASA-TM-109562] 03 p0875 N94-15332
STS-29 mission highlights resource tape
[NASA-TM-109542] 03 p0880 N94-15373
STS-26 missions highlight resource tape
[NASA-TM-109559] 03 p0881 N94-15407
TDRS press release
[NASA-TM-109373] 04 p1335 N94-18965
The NCC project: A quality management perspective 05 p1828 N94-21324
Software metrics: The key to quality software on the NCC project 05 p1922 N94-21326
Problem reporting management system performance simulation 05 p1931 N94-21328
Enhanced networks operations using the X Window System 05 p1932 N94-21329
Space network scheduling benchmark: A proof-of-concept process for technology transfer 05 p1932 N94-21332
Analysis of the TDRS multiple access system for possible use as an attitude control system sensor 05 p1666 N94-21338
The Automated Conflict Resolution System (ACRS) 05 p1744 N94-21341
Satellite Communication Hardware Emulation System (SCHES) 05 p1744 N94-21344
Using the USCCS for sub microsecond spacecraft clock calibration 05 p1813 N94-21346
Advanced coding and modulation schemes for TDRSS 05 p1744 N94-21350
Utilizing a TDRS satellite for direct broadcast satellite-radio propagation experiments and demonstrations 06 p2274 N94-22740
A review of GPS-based tracking techniques for TDRS orbit determination 06 p2196 N94-23257
A method for interference mitigation in space communications scheduling 06 p2305 N94-23918
Modeling and analysis of selected space station communications and tracking subsystems 06 p2306 N94-25374
Improved solution accuracy for TDRSS-based TOPEX/Poseidon orbit determination 11 p4205 N94-35620
Improved solution accuracy for Landsat-4 (TDRSS-user) orbit determination 11 p4205 N94-35623
Optimum satellite relay positions with application to a TDRS-1 Indian Ocean relay 11 p4205 N94-35624
TDRSS Onboard Navigation System (TONS) flight qualification experiment 11 p4206 N94-35625
Application of a Monte Carlo accuracy assessment tool to TDRS and GPS 11 p4207 N94-35635

TEA LASERS
Development of an industrial CO2 laser for mask marking
[DE93-632901] 07 p2816 N94-26184

TEACHERS
U INSTRUCTORS

TEACHING
U EDUCATION

TEACHING MACHINES
Computer-assisted instruction and natural language systems
[MEMO-INF-92-86] 04 p1527 N94-19225
Reinforcement learning for robots using neural networks 08 p3437 N94-29853
Use of bad training data for better predictions
[DE94-006233] 08 p3427 N94-30705

TEAMS
Cognitive limitations in coordination in hierarchical information processing structures
[AD-A268825] 04 p1616 N94-18535
Factors associated with continuance commitment to FAA matrix teams
[DOT/FAA/AM-93/18] 05 p2040 N94-21626
Workload transition: Implications for individual and team performance
[AD-A274538] 07 p2941 N94-26964
An investigation of integrated product development implementation issues: A case study of Bosma Machine and Tool Corp.
[AD-A273917] 07 p2942 N94-27320

TEARING
Crack-tip-opening angle measurements and crack tunneling under stable tearing in thin sheet 2024-T3 aluminum alloy
[NASA-CR-191523] 03 p0931 N94-15184
Prediction of stable tearing of 2024-T3 aluminum alloy using the crack-tip opening angle approach
[NASA-TM-109023] 03 p0955 N94-15708
Measurement and analysis of critical CTOA for an aluminum alloy sheet
[NASA-TM-109024] 03 p0956 N94-15948
Tearing resistance of a thin shell against projectile penetration: Material property effects
[DE94-007466] 09 p3733 N94-31316

TEARING MODES (PLASMAS)
Reversed-field pinch studies in the Madison Symmetric Torus
[DE93-013464] 01 p0388 N94-10747
Simulation study of dynamo structure in reversed field pinch
[DE93-771406] 01 p0390 N94-11128
Macroscopic behaviour and discrete dynamo of RFP plasma in high theta discharge
[DE93-771408] 01 p0392 N94-11239
Nonlinear evolution of tearing modes in inhomogeneous plasmas
[PPL-133] 02 p0798 N94-13564
Resonant absorption of Alfven waves near a neutral point
[DE93-628761] 04 p1586 N94-18172
Effects of magnetic field perturbations in the ATF torsatron
[DE94-000474] 05 p1999 N94-22568
Effect of LHCD (low hybrid current drive) on tearing mode instability
[DE93-613700] 06 p2555 N94-25344
Nonlinear growth of strongly unstable tearing modes
[DE94-003366] 07 p3042 N94-25958
TFTR experimental data analysis collaboration
[DE94-004166] 07 p3047 N94-27690
Numerical experiment on finite element method for matching data
[DE94-701208] 07 p3000 N94-27731
Stability of tearing modes in tokamak plasmas
[DE94-009205] 09 p3892 N94-32911
High beta and second stability region transport and stability analysis
[DE94-009654] 10 p4145 N94-33920
Collisonless dynamics of the magnetosphere
[AD-A278886] 11 p4290 N94-35708

TECHNETIUM COMPOUNDS
The potential for large critical currents in the high T(sub c) oxides 07 p2854 N94-26058

TECHNICAL WRITING
The impact of report of investigation writing style on the assessment times, impressions, perceptions and preferences of adjudicators
[AD-A265748] 03 p1223 N94-15682
An assessment of the statistical and editorial output of text analysis programs
[AD-A272185] 05 p2042 N94-20924
The MUSA design methodology
[CWI-CS-R9265] 07 p3097 N94-26220
Using International English to prepare technical text for translation
[DE94-002628] 11 p4347 N94-36102

TECHNOLOGICAL FORECASTING
NT PATTERN METHOD (FORECASTING)
Space Station Freedom advanced photovoltaics and battery technology development planning 01 p0052 N94-11401
Aviation and the KLM: Past and future 03 p0853 N94-15126
Expectations for the future of Fokker 03 p0854 N94-15127
Expectations for the future of military aviation 03 p0854 N94-15128
Expectations for the future of the National Aerospace Laboratory 03 p0854 N94-15129
Expectations for the future of the Faculty of Aeronautics and Astronautics of the Technical University of Delft 03 p0854 N94-15131
Emerging technologies planning guide, 1993 edition --- information systems technology
[DE93-017196] 04 p1616 N94-18689

TECHNOLOGIES
NT BIOTECHNOLOGY
NT ENERGY TECHNOLOGY
NT GEOTHERMAL TECHNOLOGY
NT MARINE TECHNOLOGY
NT MILITARY TECHNOLOGY
NT REACTOR TECHNOLOGY
JPRS report: Science and technology. Central Eurasia: Space
[JPRS-USP-93-003] 02 p0828 N94-13182
Heidegger's thinking 02 p0736 N94-13442
Science, technology, and the federal government: National goals for a new era 02 p0827 N94-14115
Solid State Sciences Committee Forum
[AD-A270454] 04 p1342 N94-18715
Program descriptions
[NSF-92-123] 04 p1531 N94-19619
Prototype Space Technology Hall of Fame exhibit at Technology 2003: Analysis of data from computer-based questionaire
[NASA-CR-194834] 06 p2596 N94-23540
Emerging technologies
[DE94-003022] 07 p3102 N94-26023
Vision 21: Interdisciplinary Science and Engineering in the Era of Cyberspace
[NASA-CP-10129] 07 p2685 N94-27358
Proceedings: SISAL 1993
[DE94-006641] 08 p3420 N94-30056
OPTIONS for systemic change in mathematics, science, and technology education: Scientist/teacher partnerships
[DE94-007472] 09 p3914 N94-32910
Science and engineering indicators, 1993
[NSB-93-1] 10 p4149 N94-34169
JPRS report: Science and technology. Central Eurasia
[JPRS-UST-94-006] 11 p4249 N94-35226
JPRS report: Science and technology. Central Eurasia
[JPRS-UST-94-001] 11 p4229 N94-35340
JPRS report: Science and technology. Central Eurasia
[JPRS-UST-94-004] 11 p4249 N94-35341
JPRS report: Science and technology. Central Eurasia
[JPRS-UST-94-005] 11 p4249 N94-35342
JPRS report: Science and technology. Central Eurasia
[JPRS-UST-94-010] 11 p4250 N94-35385
JPRS report: Science and technology. Central Eurasia
[JPRS-UST-94-011] 11 p4250 N94-35386
JPRS report: Science and technology. Central Eurasia
[JPRS-UST-94-012] 11 p4250 N94-35387
JPRS report: Science and technology. Central Eurasia: Space
[JPRS-USP-93-005] 11 p4201 N94-36011
National Educators' Workshop: Update 1993. Standard Experiments in Engineering Materials Science and Technology
[NASA-CP-3259] 11 p4229 N94-36398
JPRS report: Science and technology. Central Eurasia: Space
[JPRS-USP-94-004] 12 p4391 N94-37002
JPRS report: Science and technology. Central Eurasia: Space 12 p4391 N94-37003
JPRS report: Science and technology. Central Eurasia
[JPRS-UST-94-013] 12 p4509 N94-37006
JPRS report: Science and technology. Central Eurasia: Materials science
[JPRS-UMS-93-008] 12 p4404 N94-37010

TECHNOLOGY ASSESSMENT
Protein, glass, aerosol research, containerless processing and diagnostics technology for microgravity application 01 p0106 N94-10112
High temperature processing and diagnostic technologies for microgravity applications 01 p0110 N94-10130
The 40 kWe S-PRIME Thermionic Design and Technology Demonstration Program
[DE93-004738] 01 p0040 N94-10147

Department of Energy solar process heat program: FY 1991 solar process heat prefeasibility studies activity
[DE93-010010] 01 p0262 N94-10258
System engineering concept demonstration, technology assessments, volume 5
[AD-A265471] 01 p0323 N94-10494
Intelligent structures: A technology overview and assessment 01 p0068 N94-11322
Workshop summary: New silicon cells 01 p0054 N94-11417
Software process assessments 01 p0329 N94-11427
TFE verification program
[DE93-009609] 01 p0373 N94-11694
Where no flag has gone before: Political and technical aspects of placing a flag on the Moon
[NASA-CR-188251] 02 p0827 N94-12800
Technology assessments of advanced energy storage systems for electric and hybrid vehicles
[DE93-014395] 02 p0701 N94-12913
Compendium of executive summaries from the maglev system concept definition
[PB93-154938/GAR] 02 p0661 N94-13285
Status and future opportunities for conversion of synthesis gas to liquid energy fuels
[DE93-010025] 02 p0584 N94-14089
Optical systems integrated modeling 02 p0547 N94-14837
Advanced optical instruments technology 02 p0547 N94-14838
X ray microcalorimeters: Principles and performance 03 p0899 N94-15027
Superconductive x ray photon detectors 03 p0900 N94-15031
Metastable superconductors as photon detectors 03 p0900 N94-15032
Development of x ray CCDs 03 p0900 N94-15033
Large scientific 2-D arrays for the 1-5 micron region 03 p0902 N94-15044
Submm/FIR bolometers 03 p0904 N94-15056
NASA's Ultraviolet Astrophysics Branch: Present and future detector program 03 p0910 N94-15102
Expectations for the future of the National Aerospace Laboratory 03 p0854 N94-15129
Information Technology Resources Assessment
[DE93-013899] 03 p1230 N94-16010
Space Propulsion Synergy Group ETO technology assessments
[TABES PAPER 93-641] 03 p0929 N94-16149
Space Nuclear Facility test capability at the Baikal-1 and IGR sites Semipalatinsk-21, Kazakhstan
[DE93-011662] 03 p0926 N94-16773
An overview of the NASA textile composites program 03 p0937 N94-16846
Plasma Science Committee (PLSC) and the Panel on Opportunities in Plasma Science and Technology (OPST)
[DE93-018142] 03 p1204 N94-16995
Key trends of the small satellite market 03 p0897 N94-17191
Binary optics: Trends and limitations 03 p1194 N94-17333
Satellite communications systems and technology. Executive summary
[NASA-TM-109346] 03 p1006 N94-17661
Metals 2000
[DE93-016761] 04 p1355 N94-17752
Cost effective energy strategies for the reduction of CO2 emissions in the United States: Country report for ETSAP Annex 4
[DE93-016842] 04 p1472 N94-17852
Information technology resources assessment
[DE93-015276] 04 p1613 N94-17894
Critical technologies for reactors used in nuclear electric propulsion
[DE93-017685] 04 p1337 N94-17908
Laboratory microfusion capability study
[DE93-014373] 04 p1583 N94-17912
The stability and utility of the ESPRIT project, MUSiC, performance-based indicators of usability and tools: An evaluation of the usability of the NPL iSDX telephone system
[NPL-DITC-213/92] 04 p1613 N94-17925
The perspectives in application of hot casting technology for ceramic parts of timekeeping devices 04 p1375 N94-18013
Safeguarding our energy future
[DE93-016001] 04 p1466 N94-18109
Workshop on Innovation in Materials Processing and Manufacture: Exploratory Concepts for Energy Applications
[DE93-017674] 04 p1467 N94-18478
Fatigue technology assessment and strategies for fatigue avoidance in marine structures. Appendices
[AD-A269053] 04 p1455 N94-18716
Survey of ceramic machining in Japan
[DE93-018277] 04 p1372 N94-18946
Statement of David E. Baldwin, Associate Director for Energy, Lawrence Livermore National Laboratory and John C. Crawford, Vice President, Sandia National Laboratories, California, to the Subcommittee on Research and Development of the Committee on Environment and Public Works, US Senate, Washington, DC, 22 March 1993
[DE93-017991] 05 p1844 N94-19803
Data format standards for civilian remote sensing satellites
[PB93-192920] 05 p1841 N94-21446
NEP Early Flight program: System performance and development considerations
[NASA-TM-106415] 05 p1654 N94-21570
Survey of lift-fan aerodynamic technology
[NASA-CR-177615] 05 p1646 N94-21592
Thin-film CdTe and CuInSe2 photovoltaic technologies
[DE93-018217] 05 p1848 N94-21827
Microtechnology: The key to the technical challenges of the 21st century
[DE94-000403] 05 p1769 N94-21959
Survey on evaluation of energy technology contributing to preservation of the global environment. 2
[DE94-714884] 05 p1853 N94-22051
Study on possibility of developing energy integration technology
[DE94-714903] 05 p1849 N94-22052
Manufacturing and information technology 05 p2046 N94-22082
Spaceplane flight simulation: Project definition
[PB93-211399] 05 p1651 N94-22094
Advanced display technologies in Russia, Ukraine, and Belarus. Viewgraphs 06 p2630 N94-22893
Making government work: Electronic delivery of Federal services
[OTA-TCT-578] 06 p2290 N94-23081
A review of European applications of artificial intelligence to space
[NASA-TM-108789] 06 p2453 N94-23568
Satellite communications systems and technology. Executive Summary
[NASA-TM-109388] 06 p2293 N94-23622
Satellite communications systems and technology. Volume 2: Site reports
[NASA-TM-109399] 06 p2293 N94-23628
Overview of molten carbonate fuel cell technology development
[DE94-001911] 06 p2394 N94-23781
A fifteen years lifetime mechanism for an infrared Earth sensor 06 p2362 N94-24040
Proceedings of Technology and Governance in the 1990's
[PB93-192904] 06 p2597 N94-24312
Overview of the status and progress in photovoltaics research in the United States
[DE94-000981] 06 p2395 N94-24512
Advanced avionics architecture and technology review. Executive summary and volume 1: Avionics tech nology. Volume 2: Avionics systems engineering
[AD-A273630] 06 p2186 N94-24733
The future of rotary-wing aircraft 06 p2185 N94-25070
US general aviation: The ingredients for a renaissance. A vision and technology strategy for US industry, NASA, FAA, universities 06 p2162 N94-25097
Nuclear electric propulsion for future NASA space science missions
[DE93-019086] 07 p2700 N94-25969
Prospects for utilization of superconductors in the power industry 07 p2854 N94-26057
The National Center for Advanced Information Components Manufacturing: Program update
[DE94-002647] 07 p2960 N94-26118
Scientific and Technical Information (STI)....what's the status?
[DE94-003731] 07 p3097 N94-26348
Computing in space: Issues and answers 07 p2948 N94-26714
Advanced nickel-hydrogen spacecraft battery development 07 p2863 N94-28129
A conceptual framework for software technology transition
[AD-A275637] 08 p3407 N94-28639
Technology base enhancement program. Metal matrix composites
[AD-A275531] 08 p3176 N94-28688
Report on smart materials
[PB94-137528] 08 p3203 N94-29015
Combustion technology needs for advanced high pressure cycle engines 08 p3190 N94-29248
Proceedings of the Workshop on Microtechnologies and Applications to Space Systems
[NASA-CR-195688] 08 p3235 N94-29767
Micro guidance and control technology overview 08 p3144 N94-29772
Technical analysis of alternative fueled vehicles
[DE94-744238] 08 p3304 N94-30269
A look into the crystal ball: The next 25 years 08 p3475 N94-30681
Frequency standards from government laboratories over the next 25 years 08 p3475 N94-30682
Frequency standards from industry over the next 25 years 08 p3475 N94-30683
The future of time and frequency dissemination 08 p3476 N94-30684
DOE New Technology: Sharing New Frontiers, April 1, 1993 - September 30, 1993
[DE93-041289] 08 p3535 N94-30699
DOE/KEURP site operator program
[DE94-005832] 08 p3267 N94-30701
Investigation of the technology development status of alternate fuel vehicles
[DE94-744237] 08 p3312 N94-30831
A review of the status and capabilities of Navstar GPS
[AD-B174629] 08 p3143 N94-30854
Compressed natural gas fueled vehicles: The Houston experience
[DE94-005804] 08 p3312 N94-30878
High-temperature superconducting transformer performance, cost, and market evaluation
[DE94-005494] 09 p3687 N94-31152
Active matrix liquid crystal display. Industry survey results
[AD-A276415] 09 p3895 N94-31329
Technical assessment of Mir-1 life support hardware for the international space station
[NASA-TM-108441] 09 p3803 N94-31380
Semiconductor microcavity lasers
[DE94-006143] 09 p3716 N94-31622
Benchmarking of the state-of-the-art in nondestructive testing/evaluation for applicability in the Composite Armored Vehicle (CAV) Advanced Technology Demonstrator (ATD) program, phase 1
[AD-A276660] 09 p3730 N94-32088
LLNL casting technology
[DE94-008282] 09 p3669 N94-32839
Application of a design-build-team approach to low cost and weight composite fuselage structure
[NASA-CR-4418] 09 p3626 N94-32863
Science and engineering indicators, 1993
[NSB-93-1] 10 p4149 N94-34169
Technology for small spacecraft
[NASA-CR-196041] 10 p4015 N94-34411
Combustor technology for small aircraft engines 10 p4003 N94-34453
State of the art in high-power microwaves: An overview
[DE94-007075] 11 p4272 N94-35978
JTEC/WTEC report and program summary 11 p4379 N94-36042
Information and communication technology 11 p4257 N94-36043
Advanced composites in Japan 11 p4234 N94-36045
Space robotics in Japan 11 p4278 N94-36046
Space and transatmospheric propulsion technology 11 p4229 N94-36047
Phase-locked arrays of vertical-cavity surface-emitting lasers
[DE94-009279] 11 p4272 N94-36178
Tanker system and technology requirements definition: A tanker technology road map 11 p4197 N94-36344
Activities of the Laser and Plasma Technology Division
[DE94-617113] 11 p4273 N94-36393
Feasibility study for a novel pulsed neutral beam diagnostics for tokamaks
[DE94-617129] 11 p4339 N94-36417
LNG vehicle technology, economics, and safety assessment
[PB94-165487] 12 p4450 N94-36721
Review of advanced radiator technologies for spacecraft power systems and space thermal control
[NASA-TM-4555] 12 p4398 N94-36821
Conceptual design: TFE verification program
[DE94-012469] 12 p4398 N94-37433
Refrigeration and Air-Conditioning Technology Workshop
[DE94-010813] 12 p4431 N94-37452
Remote use of distributed robotics resources to enhance technology development and insertion
[DE94-009285] 12 p4502 N94-37785

TECHNOLOGY TRANSFER

NT AEROSPACE TECHNOLOGY TRANSFER
Survey to determine the value of DYNA
[DE93-012390] 01 p0321 N94-10267
Technology transfer at Lawrence Berkeley Laboratory
[DE93-010460] 01 p0423 N94-11059
Tropical medicine: Telecommunications and technology transfer 01 p0305 N94-11793

Catalysis and biocatalysis program
[NASA-CR-194105] 02 p0727 N94-12793
Integrated optics technology transfer
[DSIS-93-00179] 02 p0792 N94-13868
Center of excellence in rotary wing technology
[AD-A266655] 02 p0510 N94-14799
From space to Earth
[NASA-TM-109638] 03 p1235 N94-15249
Medical imaging
[NASA-TM-109675] 03 p1229 N94-15520
NASA Space Engineering Research Center for VLSI System Design
[NASA-CR-194587] 03 p1008 N94-15547
Dependable software technology exchange
[AD-A267103] 03 p1146 N94-15638
Technology transfers and reliable oxides
[AD-A266948] 03 p1175 N94-15758
KBSA concept demo
[AD-A267054] 03 p1166 N94-16770
Earth observational research using multistage EOS-like data
[NASA-CR-194626] 03 p1084 N94-16831
Technology transfer. Determining industry needs: A guide for communities
[NASA-CR-194676] 03 p1235 N94-17293
Technology in action
[NASA-TM-109345] 03 p1235 N94-17294
Interactive Collaborative Environments (ICE) in the design to manufacturing process
[DE93-014994] 04 p1518 N94-17944
Lightweight materials for transportation: Program plan
[DE93-017381] 04 p1340 N94-18087
White House technology reinvestment project: Briefing and transcripts
[PB93-169829] 04 p1611 N94-18090
New applications for high average power beams
[DE93-018845] 04 p1439 N94-18522
Solid State Sciences Committee Forum
[AD-A270454] 04 p1342 N94-18715
MHD technology transfer, integration and review committee
[DE93-040519] 04 p1588 N94-18892
Silicon concentrator solar cell research
[DE93-018489] 04 p1468 N94-19015
The applications of modified metals in the construction industry
[VTT-TIED-1329] 04 p1365 N94-19374
Manufacturing technology
[DE93-019580] 04 p1381 N94-19480
The development of remote sensing in Brazil and Canada: Comparative case studies
05 p1840 N94-20968
Networks Technology Conference
[NASA-CP-3241] 05 p1931 N94-21323
First Biomass Conference of the Americas: Energy, Environment, Agriculture, and Industry, volume 2
[DE94-000435] 05 p1847 N94-21562
Index to 1992 NASA Tech Briefs, volume 16, numbers 1-12
[NASA-TM-109377] 05 p2053 N94-21736
Index to 1991 NASA Tech Briefs, volume 15, numbers 1-12
[NASA-TM-109376] 05 p2053 N94-21737
Cumulative index to NASA Tech Briefs, 1986-1990, volumes 10-14
[NASA-TM-109378] 05 p2054 N94-21738
Spinoff, 1992
[NASA-NP-201] 05 p2054 N94-21739
Microtechnology: The key to the technical challenges of the 21st century
[DE94-000403] 05 p1769 N94-21959
Space technology: A study of the significance of recognition for innovators of spinoff technologies. 1993 activities/1994, 1995 plans
[NASA-CR-194836] 06 p2596 N94-23526
Space technology: A study of the significance of recognition for innovators of spinoff technologies. Commercial Space Expo-USA, 1993
[NASA-CR-194833] 06 p2596 N94-23528
Contributions of DOE weapons labs and NIST to semicondutor technology
[OTA-ITE-585] 06 p2630 N94-23572
Proceedings of the NIST Conference on Reducing the Cost of Space Infrastructure and Operations: Part 1: Oral presentations and discussion
[PB94-111374] 06 p2194 N94-23770
The Electronics Quality/Reliability Center: Lessons learned from partnering with industry
[DE94-001501] 06 p2309 N94-23777
National Institute of Standards and Technology Conference on Reducing the Cost of Space Infrastructure and Operations. Part 2: Topical papers
[PB94-113487] 06 p2194 N94-23819
Object-oriented technologies in a multi-mission data system 06 p2506 N94-23885
Activities involving aeronautical, space science, and technology support for minority institutions
[NASA-CR-195095] 06 p2574 N94-24225
Technology utilization office data base analysis and design 06 p2577 N94-24417
A compilation of technology spinoffs from the US Space Shuttle Program 06 p2578 N94-24424
NASA tech brief evaluations
[NASA-CR-195150] 06 p2597 N94-24829
Collaborating with our customers: NIST building and fire research laboratory
[PB94-110194] 06 p2272 N94-24955
Spinoff 1993
[NASA-NP-211] 06 p2597 N94-25018
National Academy of Sciences-Academy of Sciences of the USSR Workshop on the Mechanics of Ice and its Applications
[AD-A273338] 06 p2419 N94-25088
Advanced Information Processing System (AIPS) 06 p2165 N94-25115
Reuse Adoption Guidebook, version 02.00.05
[AD-A273652] 06 p2461 N94-25149
Wind climate and urban geometry
[ISBN-9-03-860132-8] 06 p2416 N94-25261
National Aeronautics and Space Administration (NASA)/American Society for Engineering Education (ASEE) Summer Faculty Fellowship Program, 1993, volume 1
[NASA-CR-188271-VOL-1] 06 p2632 N94-25348
UV absorption technique for monitoring mobile source NO emissions
[AD-A273858] 07 p2713 N94-25964
General Motors Corporation and Pacific Northwest Laboratory staff exchange: Inspection of case hardened steels and metal-matrix composites
[DE94-003470] 07 p2706 N94-25982
The National Center for Advanced Information Components Manufacturing: Program update
[DE94-002647] 07 p2960 N94-26118
Overview of the Photovoltaic Manufacturing Technology (PVMaT) project
[DE93-018234] 07 p2856 N94-26426
Computing in space: Issues and answers 07 p2948 N94-26714
Computational mechanics
[DE94-003015] 07 p2965 N94-26775
Feasibility study on construction of a global environment research and development information network
[DE94-725198] 07 p2868 N94-26904
Retrieval using plausible inference
[AD-A274252] 07 p3099 N94-27013
Joint services electronics program
[AD-A274643] 07 p2785 N94-27027
Opportunities for High Aspect Ratio Micro-Electro-Magnetic-Mechanical Systems (HAR-MEMMS) at Lawrence Berkeley Laboratory
[DE94-003499] 07 p2827 N94-27722
Spin-off companies as agents of technology transfer: An empirical study of the spin-off companies of the Technical Research Centre of Finland
[PB94-132248] 08 p3537 N94-28405
Cleanroom engineering handbook. Volume 3: Project execution in the cleanroom environment
[AD-A275860] 08 p3156 N94-28752
Cleanroom engineering handbook. Volume 4. Specification team practices
[AD-A275861] 08 p3156 N94-28753
Technology transfer initiatives
[NASA-CR-195151] 08 p3537 N94-29410
Overview of microoptics: Past, present, and future 08 p3235 N94-29771
Technology 2003: The Fourth National Technology Transfer Conference and Exposition, volume 1
[NASA-CP-3249-VOL-1] 08 p3555 N94-30440
Precision and manufacturing at the Lawrence Livermore National Laboratory 08 p3240 N94-30449
Technology transfer and evaluation for Space Station telerobotics
[AIAA PAPER 94-1190-CP] 08 p3441 N94-30541
DOE New Technology: Sharing New Frontiers, April 1, 1993 - September 30, 1993
[DE93-041289] 08 p3535 N94-30699
Geothermal direct-heat utilization assistance
[DE94-005831] 08 p3340 N94-30700
Photovoltaics: Program overview, fiscal year 1993
[DE94-000246] 09 p3758 N94-31235
Cleanroom engineering handbook. Volume 1: Cleanroom engineering process introduction and overview
[AD-A275949] 09 p3587 N94-31356
Naval Surface Warfare Center Dahlgren Division Technical Digest: Advanced materials technology
[AD-A276448] 09 p3668 N94-31364
Renewable energy technology development at Sandia National Laboratories
[DE94-007734] 09 p3761 N94-32383
Technology 2003: The Fourth National Technology Transfer Conference and Exposition, volume 2
[NASA-CP-3249-VOL-2] 09 p3956 N94-32420
Information systems to enhance technology exchange
[DE94-007744] 09 p3920 N94-32808
Sandia's photonic program and its changing national role
[DE94-008616] 09 p3883 N94-32878
Research and technology, 1993
[NASA-TM-106376] 09 p3567 N94-33046
NDE activities and technology transfer at Sandia National Laboratories
[DE94-007294] 10 p4067 N94-33688
Environmental process tomography in the United States
[DE94-006402] 10 p4081 N94-33718
Economic espionage and information security
[DE94-003692] 10 p4161 N94-33733
Proceedings SAFECOMP 1993: The 12th International Conference on Computer Safety, Reliability and Security
[AD-A278165] 10 p4103 N94-34083
Computer Systems Laboratory
[PB94-162518] 11 p4333 N94-36002
Software engineering technology transfer: Understanding the process 12 p4492 N94-36502
ORNL superconducting technology program for electric power systems
[DE94-011471] 12 p4438 N94-37239

TECHNOLOGY UTILIZATION

Advanced Materials for Lightweight Structures
[ESA-SP-336] 01 p0056 N94-10001
New technology applied to telemedicine 01 p0306 N94-11796
Machine translation technology: A potential key to the information age
[PB93-134336] 01 p0421 N94-12385
Technology Applications Team: Applications of aerospace technology
[NASA-CR-194362] 02 p0828 N94-13104
Technology parks and the cooperation among universities and firms: The cases of Campinas, Sao Jose dos Campos e Sao Carlos
[INPE-5251-TAE/04] 02 p0818 N94-13427
Sequestering carbon dioxide in industrial polymers: Building materials for the 21st century
[DE93-016087] 02 p0580 N94-14297
NASA/DOD Aerospace Knowledge Diffusion Research Project. Paper 38: Computer Mediated Communication (CMC) and the communication of technical information in aerospace
[NASA-TM-109330] 02 p0826 N94-14489
Transform coding for space applications
[NASA-TM-106362] 02 p0612 N94-14542
Workshop Proceedings: Optical Systems Technology for Space Astrophysics in the 21st Century, volume 3
[NASA-CR-194102] 02 p0545 N94-14830
From space to Earth
[NASA-TM-109638] 03 p1235 N94-15249
Monitoring history
[NASA-TM-109640] 03 p1229 N94-15251
Saving Yellowstone
[NASA-TM-109596] 03 p1094 N94-15289
Finding fish from above --- remote sensing
[NASA-TM-109602] 03 p1081 N94-15310
NASA images 7
[NASA-TM-109438] 03 p1235 N94-15337
NASA images 16
[NASA-TM-109440] 03 p1235 N94-15339
Unistick vehicle controller
[NASA-TM-109618] 03 p1046 N94-15347
Improved mapping system
[NASA-TM-109643] 03 p1082 N94-15428
Workshop on advanced technologies for planetary instruments
[NASA-CR-194585] 03 p1032 N94-15797
The strategic environmental research and development program: A new paradigm for space, the environment, and national security
[AD-A266222] 03 p1174 N94-16109
Commercial space opportunities advanced concepts and technology overview
[TABES PAPER 93-240] 03 p1050 N94-16132
A Moessbauer spectrometer for the mineralogical analysis of the Mars surface: First temperature dependent tests of the detector and drive system
03 p1259 N94-16233
Techno-economic requirements for automotive composites 03 p0937 N94-16847
Technology in action
[NASA-TM-109345] 03 p1235 N94-17294
Micro-optics technology and sensor systems applications 03 p1197 N94-17350
Reliability and maintainability of modular robot systems: A roadmap for design
[AD-A268104] 03 p1168 N94-17517

Smart Power: New power integrated circuit technologies and their applications
[VTT-TIED-1358] 03 p1015 N94-17546
Current information technology resource requirements of the federal government: Fiscal year 1994 04 p1612 N94-17756
Lightweight materials for transportation: Program plan
[DE93-017381] 04 p1340 N94-18087
Safeguarding our energy future
[DE93-016001] 04 p1466 N94-18109
Engineering research, development and technology thrust area report, FY92
[DE93-016334] 04 p1632 N94-18856
Beryllium processing technology review for applications in plasma-facing components
[DE93-018396] 04 p1363 N94-19028
Application of new technologies in the virtual library: Seminars in Turkey, Portugal, and Spain
[NASA-TM-109718] 04 p1611 N94-19131
Space Applications Industrial Laser System (SAILS) 04 p1325 N94-19173
The applications of modified metals in the construction industry
[VTT-TIED-1329] 04 p1365 N94-19374
Legacy of the X Ray Laser Program
[DE93-019550] 04 p1442 N94-19554
Commercialization effort in support of electroslag-casting technology
[DE93-017988] 04 p1366 N94-19733
Space applications of superconducting microwave electronics at NASA Lewis Research Center 05 p1671 N94-20513
Lithium batteries: Future batteries 05 p1752 N94-20630
Rad-hard computer elements for space applications 05 p1753 N94-21082
Conversion of LDEF experiment M0003 sample observation database to MS-DOS formats
[AD-A272945] 05 p1681 N94-21226
Index to 1992 NASA Tech Briefs, volume 16, numbers 1-12
[NASA-TM-109377] 05 p2053 N94-21736
Index to 1991 NASA Tech Briefs, volume 15, numbers 1-12
[NASA-TM-109376] 05 p2053 N94-21737
Cumulative index to NASA Tech Briefs, 1986-1990, volumes 10-14
[NASA-TM-109378] 05 p2054 N94-21738
Spinoff, 1992
[NASA-NP-201] 05 p2054 N94-21739
Acoustic, fiber optic, and silicon microelectronic microsensors research and development activities at Sandia National Laboratories
[DE93-019075] 05 p1770 N94-22040
The history of development of molybdenum alloys for structural applications
[DE94-000389] 05 p2239 N94-22958
Power beaming to space using a nuclear reactor-pumped laser
[DE94-001208] 06 p2348 N94-23185
Pushing technology to satisfy world applications
[DE93-001365] 06 p2353 N94-23191
Influence of a new generation of operations support systems on current spacecraft operations philosophy: The users feedback 06 p2507 N94-23894
Technology utilization office data base analysis and design 06 p2577 N94-24417
NASA technology applications team: Applications of aerospace technology
[NASA-CR-194775] 06 p2597 N94-24494
Space Technology: A study of the significance of recognition for innovators of spinoff technologies. A case study on the impact of the space technology hall of fame award
[NASA-CR-194835] 06 p2597 N94-24496
Power generation technology options for a Mars mission
[NASA-TM-106451] 06 p2220 N94-24681
NASA tech brief evaluations
[NASA-CR-195150] 06 p2597 N94-24829
A white paper: NASA virtual environment research, applications, and technology
[NASA-TM-109682] 06 p2428 N94-24855
Spinoff 1993
[NASA-NP-211] 06 p2597 N94-25018
High-order technology: Applying technical excellence to new airplane development 06 p2185 N94-25069
The potential for the Department of Defense to use space-based remote sensing to support DOD and other government agencies' environmental programs
[AD-A273895] 07 p2847 N94-25656
Radiation applications of physical chemistry 07 p2854 N94-26054
Prospects for utilization of superconductors in the power industry 07 p2854 N94-26057
Frontiers of science and measurement: Report on a seminar jointly organized by the National Physical Laboratory and the Institute of Physics
[PB94-124310] 07 p3009 N94-27131
Robotics handbook. Version 1: For the interested party and professional
[NASA-TM-109690] 07 p2824 N94-27238
Research and Development Annual Report, 1992
[NASA-TM-104777] 07 p3119 N94-27993
Advanced energy storage for space applications: A follow-up 07 p2860 N94-28103
Spin-off companies as agents of technology transfer: An empirical study of the spin-off companies of the Technical Research Centre of Finland
[PB94-132248] 08 p3537 N94-28405
Current leads and magnetic bearings
[DE94-004607] 08 p3297 N94-28461
Survey report of JSUP Space Environment Utilization Research Committee in fiscal year 1992: Protein Crystal Growth Session
[JTN-94-80584] 08 p3158 N94-28583
Remote sensing and global management 08 p3328 N94-28937
Computational fluid dynamics in ventilation. 4: Commercial application of CFD in ventilation 08 p3233 N94-29609
A 32 GHz microstrip array antenna for microspacecraft application 08 p3251 N94-29668
Human and institutional factors in GIS implementation by local governments 08 p3532 N94-29804
Robotics and the battlefield of the future 08 p3304 N94-30277
Hybrid optics for space applications
[ESA-CP-1158] 08 p3501 N94-30418
Cubanes: Super explosives and potential pharmaceutical intermediates 08 p3227 N94-30454
Dual use of image based tracking techniques: Laser eye surgery and low vision prosthesis 08 p3397 N94-30455
Composite redesign of obstetrical forceps 08 p3397 N94-30457
Intelligent robotics can boost America's economic growth
[AIAA PAPER 94-1301-CP] 08 p3439 N94-30527
On-orbit spacecraft servicing: An element in the evolution of space robotics applications
[AIAA PAPER 94-1236-CP] 08 p3448 N94-30583
DOE New Technology: Sharing New Frontiers, April 1, 1993 - September 30, 1993
[DE93-041289] 08 p3535 N94-30699
High-temperature superconducting transformer performance, cost, and market evaluation
[DE94-005494] 09 p3687 N94-31152
Putting the information infrastructure to work: Report of the Information Infrastructure Task Force Committee on Applications and Technology
[NIST/SP-857] 09 p3916 N94-31228
AMS beyond 2000
[DE94-006666] 09 p3632 N94-31352
A study of theoretical models for managing technology change and a comparison to a radio frequency identification implementation
[AD-A276012] 09 p3672 N94-31385
The contribution of aeronautics and astronautics to the quality of life on Earth
[ILR-MITT-283(1993)] 09 p3764 N94-31611
Workshop on Commercialization of Pulsed Power Science and Technology Proceedings
[AD-A276987] 09 p3692 N94-32258
Advanced teleoperation: Technology innovations and applications 09 p3806 N94-32453
Research and technology, 1993
[NASA-TM-106376] 09 p3567 N94-33046
Spacecraft environmental anomalies expert system
[AD-A277962] 09 p3612 N94-33262
Advanced release technologies program 09 p3607 N94-33322
Knowledge based multi-level secure network technology
[AD-A278043] 10 p4111 N94-33400
Hurricane Andrew mission
[NASA-TM-109797] 10 p4089 N94-33550
Refocusing space technology
[NASA-TM-109833] 10 p4161 N94-33569
Hotfire testing of a SSME HPOTP with an annular hydrostatic bearing 10 p4065 N94-34196
Technology for small spacecraft
[NASA-CR-196041] 10 p4015 N94-34411
The 1994 Goddard Conference on Space Applications of Artificial Intelligence
[NASA-CP-3268] 10 p4122 N94-35043
Technology Reinvestment Project's Focus Area: Low Cost Electronic Packaging
[PB94-161155] 11 p4259 N94-35748
Knowledge-based systems in Japan 11 p4347 N94-36044
Abstracts of 2nd International Conference on Lasers and their Applications
[DE94-617409] 12 p4448 N94-37169
Advanced Turbine Technology Applications Project (ATTAP)
[NASA-CR-195367] 12 p4452 N94-37763
NASA commercial technology. Agenda for change
[NASA-TM-109898] 12 p4546 N94-37765

TECTONIC MOVEMENT

U TECTONICS

TECTONICS

Statistical description of tectonic motions
[NASA-CR-193701] 01 p0275 N94-10950
Analysis of gravity, magnetic, and seismic reflection data from Tibet and neighboring regions of China
[NASA-CR-193405] 01 p0278 N94-11886
Lineament analysis and tectonic interpretation for the Tharsis region 01 p0437 N94-12031
Horizontal stresses induced by vertical processes in planetary lithospheres 01 p0281 N94-12042
Estimation of age of Dali-Ganis rifting and associated volcanic activity, Venus 01 p0440 N94-12046
Global organization of tectonic deformation on Venus 01 p0444 N94-12066
Buoyant subduction on Venus: Implications for subduction around coronae 01 p0455 N94-12130
Stratigraphy and sedimentology of the K/T boundary deposit in Haiti 01 p0282 N94-12138
Porosity and the ecology of icy satellites 01 p0431 N94-12186
Tectonics on Triton 01 p0466 N94-12187
Regional mantle upwelling on Venus: The Beta-Atla-Themis anomaly and correlation with global tectonic patterns 01 p0467 N94-12196
Transmantle flux tectonics 01 p0283 N94-12249
Pseudo magnetic anomaly derived from satellite altimetry and its application to the tectonics in the North Fuji Basin 01 p0208 N94-12645
The nature and origin of periodically spaced tectonic features on Mars
[NASA-CR-193821] 02 p0842 N94-13199
The 1990 Western Pacific Geophysics meeting
[NASA-CR-193456] 02 p0712 N94-13334
The American Geophysical Union Chapman Conference on Tectonics and Topography
[NASA-CR-193454] 02 p0713 N94-13335
Regional tectonic analysis of Venus as part of the Pioneer Venus guest investigator project
[NASA-CR-194079] 02 p0842 N94-13561
Overview: Gas hydrate geology and geography
[DE93-014043] 02 p0688 N94-14151
Organic Geochemical and tectonic evolution of the Midcontinent Rift system
[DE93-015093] 02 p0717 N94-14338
Laser tracking for vertical control 03 p0911 N94-15553
Experience and results of the 1991 MTLRS-1 USSR campaign 03 p0914 N94-15575
Papers presented at the Eleventh International Symposium on Earth Tides
[COMMUNICATIONS-SER-B-158] 03 p1098 N94-15800
Tidal gravity anomalies and tectonics 03 p1101 N94-15814
Magellan: Principal Venus science findings 03 p0989 N94-15887
Tectonic deformation in southern California
[NASA-CR-194621] 03 p1101 N94-16021
Pargo Chasma and its relationship to global tectonics 03 p1249 N94-16181
The formation and evolution of Alpha and Tellus tesserae on Venus 03 p1249 N94-16183
Rheology of water and ammonia-water ices 03 p0953 N94-16188
Importance of expansion and contraction in the formation of tectonic features on the Moon 03 p1250 N94-16189
The Karakul depression in Pamirs: The first impact structure in Central Asia 03 p1241 N94-16212
Morphology and models for the evolution of eastern Hecate Chasma, Venus 03 p1256 N94-16215
The three ages of Venus: A hypothesis based on the cratering record 03 p1261 N94-16239
Tessera terrain on Venus: Global characterization from Magellan data 03 p1264 N94-16262
Density of impact craters on tessera, Venus 03 p1264 N94-16263
Estimates of lithospheric thickness on Venus 03 p1267 N94-16277
Tectonics of Neyterkob corona on Venus 03 p1270 N94-16299
On the relationship between tectonic plates and thermal mantle plume morphology 03 p1104 N94-16349
Tectonic resurfacing of Venus 03 p1285 N94-16380

Aspects of modelling the tectonics of large volcanoes on the terrestrial planets 03 p1104 N94-16396
Guide to Magellan image interpretation
[NASA-CR-194340] 03 p1298 N94-17654
Belgian Royal Observatory Communications, Series A, No. 104, Geophysics Series No. 175
[COMMUNICATIONS-SER-A-104]
04 p1482 N94-18622
Current (1985-1988) seismic activity in Belgium: Comparison with historical and instrumental seismic data
04 p1482 N94-18624
What can gravimetry contribute to recent and current tectonics in Belgium? 04 p1482 N94-18626
Applications of Quaternary stratigraphic, soil-geomorphic, and quantitative geomorphic analyses to the evaluation of tectonic activity and landscape evolution in the Upper Coastal Plain, South Carolina
[DE93-016269] 04 p1484 N94-18725
The interpretation of crustal dynamics data in terms of plate motions and regional deformation near plate boundaries
[NASA-CR-194302] 04 p1487 N94-19432
Beta Regio rift system on Venus: Geologic interpretation of Magellan images 05 p2095 N94-20655
Formation and evolution of radial fracture systems on Venus 05 p2099 N94-20672
Venus magmatic and tectonic evolution
05 p2101 N94-20683
Crater destruction on the Venusian highlands by tectonic processes 05 p2103 N94-20696
Strength and deformation properties of basaltic lava flows on planetary surfaces 05 p1862 N94-20747
Volcanic rises on Venus: Geology, formation, and sequence of evolution 05 p2113 N94-20755
Geoid, topography, and convection-driven crustal deformation on Venus 05 p2116 N94-20769
Response of the topography and gravity field on Venus to mantle upwelling beneath a chemical boundary layer
05 p2117 N94-20775
A tectonic resurfacing model for Venus
05 p2118 N94-20781
Delimitation of terrestrial impact craters by way of pseudotachylytic rock distribution
05 p1863 N94-20783
Parga and Hecate Chasmata, Venus: Structure, volcanism and models of formation
05 p2121 N94-20796
Extensional history of Mars' Tharsis Region
05 p2125 N94-20814
Complex structure of the Thaumasia region of Mars
05 p2125 N94-20815
Photogeological analysis of Europan tectonic features
05 p2129 N94-20838
Is there uniformitarian or catastrophic tectonics on Venus? 05 p2129 N94-20839
Wrinkle ridges, reverse faulting, and the depth penetration of lithospheric stress in lunae planum, Mars
05 p2141 N94-20910
On the origin and evolution of circular forms observed in remote sensing images of the Rio de Janeiro State, Brazil 05 p1839 N94-20963
Mobility of salt domes
[BCRS-92-08] 05 p1857 N94-21016
Post-Palbozoic crustal responses to the contemporary stress field in the eastern United States
[DE93-040604] 05 p1859 N94-22006
GPS survey of the western Tien Shan
[NASA-CR-195174] 06 p2175 N94-24826
Tectonic Evolution of Mars
[NASA-CR-194714] 06 p2623 N94-24996
The geophysical signal of the martian global dichotomy 06 p2623 N94-24997
Impacts, extinctions, volcanism, glaciations, and tectonics: Matches and mismatches
07 p2888 N94-28298
Studies in Jurassic and Cretaceous North American apparent polar wander 08 p3362 N94-29940
The rupture process of large earthquakes along convergent margins: Cast studies from Alaska and Armenia 08 p3363 N94-29969
Tectonic History of the Terrestrial Planets
[NASA-CR-195696] 09 p3939 N94-31105
Patterns of deformation and volcanic flows associated with lithospheric loading by large volcanoes on Venus
09 p3776 N94-31106
Aspects of modelling the tectonics of large volcanoes on the terrestrial planets 09 p3940 N94-31107
State of stress, faulting, and eruption characteristics of large volcanoes on Mars 09 p3940 N94-31108
Geoid-to-topography ratios on Venus: A global perspective 09 p3940 N94-31110
The tectonic and volcanic evolution of Venus: Catastrophic or gradual? 09 p3940 N94-31111
A tectonic resurfacing model for Venus
09 p3941 N94-31113
The resurfacing controversy for Venus: An overview and a mechanistic perspective 09 p3941 N94-31114
Plains tectonism on Venus: The deformation belts of Lavinia Planitia 09 p3941 N94-31115
Respective contributions of VIS-PIR, SAR-ERS 1, and airborne radar data for morphostructural and morphoneotectonic analysis: Practical examples
09 p3752 N94-32549
Use of SPOT and ERS-1 SAR data to study the tectonic and climatic history of arid regions
09 p3752 N94-32550
Permanent GPS Geodetic Array in Southern California (PGGA) and GPS observations in Indonesia
[NASA-CR-195897] 10 p3988 N94-33534
NASA Space Geodesy Program: GSFC data analysis, 1993. VLBI geodetic results 1979 - 1992
[NASA-TM-104605] 11 p4281 N94-35261
Rheology, tectonics, and the structure of the Venus lithosphere 11 p4367 N94-35479
Formation of fold and thrust belts on Venus due to horizontal shortening of a laterally heterogeneous lithosphere 11 p4367 N94-35480
Activity Report, 1990 - 1992 and proceedings, volume 2
[DE94-610481] 11 p4291 N94-36087
Patterns of brittle deformation under extension on Venus 11 p4373 N94-36168

TEDLAR (TRADEMARK)

U POLYVINYL FLUORIDE

TEFLON (TRADEMARK)

Dimensional scaling for impact cratering and perforation
[NASA-CR-188259] 01 p0042 N94-10665
Impact penetration experiments in teflon targets of variable thickness 03 p1063 N94-16253
Performance of silvered Teflon thermal control blankets on spacecraft
[AD-A266284] 03 p0887 N94-16909
Interleaved bismaleimide composites
[AD-A272233] 05 p1674 N94-20574
The simulation of action of some space environment factors on Teflon and on rubber materials
05 p1661 N94-21380
Characterization of physically vapor deposited AF2400 thin films
[DE94-004019] 07 p2749 N94-25985
High damage threshold anti-reflectors by physical vapor deposited amorphous fluoropolymer
[DE94-004865] 08 p3212 N94-28560
Performance of silvered Teflon (trademark) thermal control blankets on spacecraft 09 p3591 N94-31014
Follow-up on the effects of the space environment on UHCRE thermal blankets 09 p3592 N94-31018
Ground-based simulation of LEO environment: Investigations of a select LDEF material: FEP Teflon (trademark) 09 p3596 N94-31039
A comparison of atomic oxygen erosion yields of carbon and selected polymers exposed in ground based facilities and in low Earth orbit
[NASA-TM-106622] 11 p4243 N94-35243
Effects of combined stressing on the electrical properties of film and ceramic capacitors
[NASA-TM-106605] 11 p4257 N94-35249
Experimental impacts into Teflon targets and LDEF thermal blankets 11 p4352 N94-36141
An amorphous fluoropolymer: Next generation optical coating candidate
[DE94-012386] 12 p4425 N94-37422

TEKTITES

NT AUSTRALITES
Vaporization by shock loading of albite, jadeite, and pyrex glass: Experimental study 01 p0097 N94-12039
K/T spherules from Haiti and Wyoming: Origin, diagenesis, and similarity to some microtektites
01 p0281 N94-12085
Minor and trace element composition and age of Yukon probable-microtektites 01 p0429 N94-12094
Oxygen isotopes as tracers of tektite source rocks: An example from the Ivory Coast tektites and Lake Bosumtwi Crater 01 p0430 N94-12146
Microtektite-like glass spherules in Late Devonian (367 MA) shales 01 p0461 N94-12160
KT boundary impact glasses from the Gulf of Mexico region 01 p0282 N94-12161
Soret diffusion: A possible cause of compositional heterogeneity within tektites 01 p0432 N94-12211
Modelling of dispersal and deposition of impact glass spherules from the Cretaceous-Tertiary boundary deposit 01 p0432 N94-12238
Cretaceous-tertiary boundary spherules and Cenozoic microtektites: Similarities and differences
03 p1241 N94-16186
Trace-element composition of Chicxulub crater melt rock, K/T tektites and Yucatan basement
03 p1242 N94-16245
Osmium isotopes in Ivory Coast tektites: Confirmation of a meteoritic component and rhenium depletion
03 p1244 N94-16321
Modelling the gravity and magnetic field anomalies of the Chicxulub crater 05 p1862 N94-20668
Iridium in sediments containing large abundances of Australasian microtektites from DSDP hole 758B in the Eastern Indian Ocean and from DSDP hole 769A in the Sulu Sea 05 p2083 N94-20741
Further analyses of Rio Cuarto impact glass
05 p1685 N94-20745
Magnetic properties and Moessbauer analyses of glass from the K-T boundary, Beloc, Haiti
05 p1685 N94-20753
An extraterrestrial event at the tertiary-quaternary boundary 07 p2890 N94-28309

TELECHIRICS

U REMOTE HANDLING

TELECOMMUNICATION

NT AIRCRAFT COMMUNICATION
NT ALOHA SYSTEM
NT BROADCASTING
NT CLOSED CIRCUIT TELEVISION
NT CODE DIVISION MULTIPLE ACCESS
NT COLOR TELEVISION
NT COMMUNICATION
NT DATA LINKS
NT DEFENSE COMMUNICATIONS SYSTEM (DCS)
NT DEMAND ASSIGNMENT MULTIPLE ACCESS
NT DIGITAL SPACECRAFT TELEVISION
NT EDUCATIONAL TELEVISION
NT ELECTRONIC MAIL
NT FACSIMILE COMMUNICATION
NT FREQUENCY DIVISION MULTIPLE ACCESS
NT GROUND-AIR-GROUND COMMUNICATION
NT INTERPLANETARY COMMUNICATION
NT LINE OF SIGHT COMMUNICATION
NT LUNAR COMMUNICATION
NT MULTICHANNEL COMMUNICATION
NT MULTIPLE ACCESS
NT OPTICAL COMMUNICATION
NT PACKET TRANSMISSION
NT PULSE COMMUNICATION
NT RADIO COMMUNICATION
NT RADIO RELAY SYSTEMS
NT RADIO TELEMETRY
NT RADIOTELEPHONES
NT SATELLITE COMMUNICATION
NT SHIP TO SHORE COMMUNICATION
NT SINGLE CHANNEL PER CARRIER TRANSMISSION
NT SPACE COMMUNICATION
NT SPACECRAFT ANTENNAS
NT SPACECRAFT COMMUNICATION
NT TELEMETRY
NT TELEPHONY
NT TIME DIVISION MULTIPLE ACCESS
NT UNDERWATER COMMUNICATION
NT VIDEO COMMUNICATION
NT VOICE COMMUNICATION
NT WIDEBAND COMMUNICATION
NT WIRELESS COMMUNICATION
Potential markets for advanced satellite communications
[NASA-CR-191145] 01 p0041 N94-10512
The 24th Annual Precise Time and Time Interval (PTTI) Applications and Planning Meeting
[NASA-CP-3218] 01 p0350 N94-10963
Synopsis of timing measurement techniques used in telecommunications 01 p0139 N94-10990
Timing in private digital telecommunication networks
01 p0139 N94-10991
Telescience capability for the Sondre Stromfjord, Greenland, incoherent-scatter radar facility
[NASA-CR-193683] 01 p0136 N94-11206
Telemetering and telecommunications research
[NASA-CR-193235] 01 p0042 N94-11297
International Telemedicine/Disaster Medicine Conference: Papers and Presentations
[NASA-NP-207] 01 p0304 N94-11787
The Canadian experience: Using telemedicine for the support of medical care at remote sites
01 p0305 N94-11789
Global considerations for implementation of telemedicine 01 p0305 N94-11792
Tropical medicine: Telecommunications and technology transfer 01 p0305 N94-11793
Applications of the INTELSAT system to remote health care 01 p0306 N94-11794
Clinical aspects of telemedicine
01 p0306 N94-11795
Commercial applications of telemedicine
01 p0306 N94-11798
The use of communication technology in medicine
01 p0306 N94-11800

A telemedicine health care delivery system
01 p0307 N94-11803
Communications infrastructure requirements for telemedicine/telehealth in the context of planning for and responding to natural disasters: Considering the need for shared regional networks 01 p0307 N94-11804
International disaster research
01 p0307 N94-11805
Medical care delivery in the US space program
01 p0307 N94-11806
US-USSR telemedicine consultation spacebridge to Armenia and Ufa 01 p0308 N94-11809
The revitalization of health and education in Rural America Act of 1992 01 p0308 N94-11810
Asynchronous Transfer Mode (ATM) technology: An overview
[AD-A266087] 01 p0383 N94-12413
Adaptive Signal Processing Testbed
[DSIS-93-00258] 02 p0604 N94-13869
Computer Science and Telecommunications Board activities
[DE93-018141] 03 p1000 N94-17000
Nonlinear methods for communications
[AD-A267376] 03 p1001 N94-17019
An approximation for computing reduction in bandwidth requirements using intelligent multiplexers
[AD-A267434] 03 p1001 N94-17026
Feasibility study of a personal communications system IRIDIUM-like 03 p0893 N94-17165
TUBSAT: Low cost access to space technology
03 p0895 N94-17180
Big results with small space systems: What small systems are doing today 03 p0896 N94-17187
Ground wave emergency network final operational capability: Environmental assessment for central Utah relay node, site number RN 8C920UT
[AD-A267628] 03 p1003 N94-17211
Activities of the Research Laboratory of Electronics
[AD-A266730] 03 p1304 N94-17651
The stability and utility of the ESPRIT project, MUSiC, performance-based indicators of usability and tools: An evaluation of the usability of the NPL iSDX telephone system
[NPL-DITC-213/92] 04 p1613 N94-17925
Broadband RF spectrum from electrostatic discharges on spacecraft
[AD-A269543] 04 p1385 N94-18287
CONTACT: An Air Force technical report on military satellite control technology
[AD-A269375] 04 p1334 N94-18408
Morphology and characteristics of disturbed HF skywave channels
[AD-A269755] 04 p1388 N94-18722
Compilation of 1992 annual reports of the navy ELF communications system ecological monitoring program. Volume 3: Tabs G - I
[AD-A269727] 04 p1388 N94-18741
Optoelectronic packaging: A review
[DE93-040059] 04 p1515 N94-19535
Program descriptions
[NSF-92-123] 04 p1531 N94-19619
Optimization of fixed time polling schemes
[CWI-BS-R9237] 05 p1945 N94-21233
Networks Technology Conference
[NASA-CP-3241] 05 p1931 N94-21323
Telecommunications services for multimedia data exchange support
[AD-A271704] 05 p1740 N94-21352
IAS telecommunication infrastructure and value added network services provided by IASNET
05 p1744 N94-22069
Everything you might want to know about the Internet but are afraid to ask!
[DE93-041118] 05 p2046 N94-22413
Global coverage Mobile Satellite Systems: System availability versus channel propagation impairments
06 p2284 N94-22798
Channel and terminal description of the ACTS mobile terminal 06 p2284 N94-22802
Code generation for the attribute evaluator of the protocol engine grammar processor unit
[EUT-93-E-271] 06 p2450 N94-23173
The TOPSIM 4 graphic user interface
[ESA-STM-247] 06 p2450 N94-23228
Advanced design concepts for open distributed systems development
[PB94-110897] 06 p2454 N94-23751
A simulation and evaluation of NATO Standardization Agreement (STANAG) 4214
[AD-A273195] 06 p2297 N94-24554
Service description of communication systems supporting multi-media multi-user applications
[PB94-110855] 06 p2299 N94-24650
ELF communications system ecological monitoring program
[AD-A273456] 06 p2299 N94-24676
Analog communication transmitter and receiver test procedures
[AD-A273423] 06 p2300 N94-24687
Standardize Ada hard real-time services?
07 p2951 N94-26729
MILCOM 92 and standardization for HF-communication. A study tour to the USA in October 1992
[PB94-124427] 07 p2774 N94-27219
Coded communications with nonideal interleaving
[ITN-94-85235] 07 p2774 N94-27242
Emerging computer technologies and the news media of the future 07 p2688 N94-27372
Telescience testbedding for physiological experiments under hypobaric hypoxic conditions
07 p2913 N94-27449
Telescience testbedding under hypobaric hypoxic conditions: Evaluation by operation ability and recognition ability 07 p2913 N94-27450
Telescience testbedding for physiological experiments under hypobaric hypoxic conditions: Development and evaluation in CNV measuring 07 p2913 N94-27451
Single term off-line coins
[CWI-CS-R9318] 07 p2776 N94-27546
Validation tests of TOPSIM 4
[ESA-STM-249] 07 p2972 N94-27582
A comparative study of SAR data compression schemes 07 p2946 N94-28259
The Telecommunications and Data Acquisition Report
[NASA-CR-195694] 08 p3246 N94-29613
Hypra/TR: A tuple oriented recovery method for a continuously available distributed DBMS on a shared nothing multi-computer
[PB94-141264] 08 p3533 N94-29921
The Nomad Explorer assembly assist vehicle: An architecture for rapid global extraterrestrial base infrastructure establishment 09 p3599 N94-31429
Telecommunications issues of intelligent database management for ground processing systems in the EOS era 10 p4126 N94-35067
JPRS report: Science and technology. Central Eurasia
[JPRS-UST-94-001] 11 p4229 N94-35340
Trace-shortened Reed-Solomon codes
11 p4254 N94-35554
SandiaXTP, an object-oriented implementation of XTP 3.7
[DE94-011752] 11 p4257 N94-36354
Telecommuting (work-at-home) at NASA Lewis Research Center
[NASA-CR-195334] 11 p4347 N94-36396
Network survivability performance
[AD-A278746] 12 p4433 N94-36756
Network survivability performance (computer diskette)
[AD-M000332] 12 p4433 N94-36757

TELECONFERENCING
International Telemedicine/Disaster Medicine Conference: Papers and Presentations
[NASA-NP-207] 01 p0304 N94-11787
Telemedicine and international disaster response: Medical consultation to Armenia and Russia via a telemedicine spacebridge 01 p0305 N94-11790
Clinical aspects of telemedicine
01 p0306 N94-11795
Information technology resources assessment
[DE93-015276] 04 p1613 N94-17894
Performance evaluation of video on ethernet
[DE93-040696] 05 p1936 N94-21749
Deployable video conference table
[NASA-CASE-ARC-11950-1] 06 p2192 N94-23310
Security aspects of computer supported collaborative work
[AD-A275638] 08 p3528 N94-28640
The impact of scaling on a multimedia connection architecture
[AD-A278700] 11 p4300 N94-35652

TELECONNECTIONS (METEOROLOGY)
Short term teleconnections associated with an individual tropical cyclone
[AD-A277210] 09 p3783 N94-32019

TELEMETERS
U TELEMETRY

TELEMETRY
NT RADIO TELEMETRY
Telemetering and telecommunications research
[NASA-CR-193235] 01 p0042 N94-11297
A telemedicine health care delivery system
01 p0307 N94-11803
Real-time tomography mooring
[AD-A264923] 01 p0289 N94-11854
The structure of hydrophysical measuring systems of vertical sounding and self-contained stations
01 p0227 N94-12751
Evaluation of midband analog fiber optic telemetry links
[DE93-015128] 03 p0883 N94-16056
MAXUS: The new sounding rocket program for long duration microgravity flight 03 p0978 N94-16079
Principal investigators data package for Project Initiation Conference (PIC): EUVS sounding rocket no. 36.117CL. Target: Venus
[NASA-CR-194663] 03 p0923 N94-17126
Satellite control: A comprehensive approach
03 p0878 N94-17158
Missile antenna pattern coordinate system and data formats
[AD-A269153] 04 p1385 N94-18260
A rugged, low-cost advanced data acquisition system for field test projects
[DE93-010041] 04 p1615 N94-18334
The EXOSAT operational experience
[ESA-STM-248] 05 p1657 N94-20235
SIMA: An integrated environmental monitoring system
05 p1840 N94-20967
Mission Operations Support Area (MOSA) for ground network support 05 p1932 N94-21331
An in-depth analysis and modelling of the Shuttle to MILA S-band telemetry link 05 p1657 N94-21340
Developing a space network interface simulator: The NTS approach 05 p1933 N94-21343
Concept report: Experimental vector magnetograph (EXVM) operational configuration balloon flight assembly
[NASA-CR-194702] 05 p1638 N94-21776
Reentry vehicle adaptive telemetry
[DE94-001168] 05 p1656 N94-21852
A packet based, data driven telemetry system for autonomous experimental sub-orbital spacecraft
[DE94-000399] 05 p1657 N94-21980
Automated analysis tools for reducing spacecraft telemetry data
[DE94-000400] 05 p1657 N94-21981
Command/telemetry bus general specification for the NOAA-OPO polar orbiting environmental satellites and EUMETSAT polar satellite systems
[NASA-TM-109407] 06 p2208 N94-23479
SpaceOps 1992: Proceedings of the Second International Symposium on Ground Data Systems for Space Mission Operations
[NASA-CR-194486] 06 p2497 N94-23832
Common front end systems for Space Shuttle and Space Station control centers at Johnson Space Center
06 p2305 N94-23838
SAMPEX payload operation control center implementation 06 p2197 N94-23843
A reference model for space data system interconnection services 06 p2305 N94-23847
NASDA satellite mission operation system and operations 06 p2501 N94-23854
NASA/Goddard Space Flight Center's testbed for CCSDS compatible systems 06 p2197 N94-23855
The Ulysses spacecraft control and monitoring concepts and realities 06 p2502 N94-23862
Ulysses log 1992 06 p2502 N94-23863
Magellan spacecraft and memory state tracking: Lessons learned, future thoughts
06 p2207 N94-23865
A MOS for all seasons 06 p2505 N94-23879
AMFESYS: Modelling and diagnosis functions for operations support 06 p2506 N94-23887
GSMS and space views: Advanced spacecraft monitoring tools 06 p2507 N94-23890
ESSOPE: Towards S/C operations with reactive schedule planning 06 p2508 N94-23896
Combining real-time monitoring and knowledge-based analysis in MARVEL 06 p2477 N94-23900
Making tomorrow's mistakes today: Evolutionary prototyping for risk reduction and shorter development time 06 p2197 N94-23902
The EURECA telecommanding chain: Experience with packet telecommand and telemetry systems
06 p2305 N94-23909
Using SFOC to fly the Magellan Venus mapping mission 06 p2516 N94-23914
High performance, low cost, self-contained, multipurpose PC based ground systems
06 p2516 N94-23943
Expert diagnostics system as a part of analysis software for power mission operations 06 p2516 N94-23944
GenSAA: A tool for advancing satellite monitoring with graphical expert systems 06 p2516 N94-23945
The evolving trend in spacecraft health analysis
06 p2202 N94-23946
Orbital Signature Analyzer (OSA): A spacecraft health/safety monitoring and analysis tool
06 p2203 N94-23947
Telemetry ground system development via the component approach 06 p2203 N94-23949
The European Space Agency standard for space packet utilisation 06 p2203 N94-23954
Compression for an effective management of telemetry data 06 p2518 N94-23956
Use of infrared telemetry as part of a nonintrusive inflight data collection system to collect human factors data
06 p2434 N94-24193

Telecommand decoder specification
[ESA-PSS-04-151-ISSUE-1] 07 p2693 N94-27583
A space-based classification system for RF transients
[DE94-003933] 08 p3240 N94-28522
Phasing the Very Large Array on Galileo in the presence of Jupiter's strong radio emission
08 p3164 N94-29621
Design and analysis of a low-loss linear analog phase modulator for deep space spacecraft X-band transponder applications 08 p3248 N94-29625
A dual-cavity ruby maser for the Ka-band link experiment 08 p3250 N94-29658
A digital combining-weight estimation algorithm for broadband sources with the array feed compensation system 08 p3250 N94-29660
Data processing algorithms for on-board satellite event analysis
[AD-A278406] 09 p3838 N94-33168
The Virtual Mission Operations Center
10 p4150 N94-33615
Telemetry data word selector and processor
[AD-D016174] 10 p4013 N94-33722
A data distribution strategy for the 1990s (files are not enough) 10 p4156 N94-33822
Mission Evaluation Room Intelligent Diagnostic and Analysis System (MIDAS) 10 p4125 N94-35064
A distributed computing model for telemetry data processing 10 p4013 N94-35069
ISTAR: Intelligent System for Telemetry Analysis in Real-time 10 p4013 N94-35070
The Mars Observer differential one-way range demonstration 11 p4210 N94-35543
A closed-loop time-alignment system for baseband combining 11 p4253 N94-35552
Preliminary PANSAT ground station software design and use of an expert system to analyze telemetry
[AD-A280600] 12 p4392 N94-36726

TELEOPERATOR MANEUVERING SYSTEM
U TELEOPERATORS

TELEOPERATORS
TOLS (Telescience On-Line Simulator): An essential instrument for micro-gravity interactive experiment
01 p0039 N94-10134
Analysis of the alignment of a Schlieren system for tele-operation 01 p0111 N94-10140
Telerobot control system
[NASA-CASE-NPO-18116-1-CU]
01 p0179 N94-10670
A portable controller for unmanned ground vehicles
[AD-A264963] 01 p0181 N94-11290
Sixth Annual Workshop on Space Operations Applications and Research (SOAR 1992), volume 2
[NASA-CP-3187-VOL-2] 01 p0486 N94-11527
Supervised autonomous control, shared control, and teleoperation for space servicing
01 p0183 N94-11577
Force reflecting hand controller for manipulator teleoperation
[NASA-CR-191345] 02 p0661 N94-13129
Tactile sensing and control in humans and robotic/teleoperated systems
[AD-A267710] 03 p1163 N94-14937
The ESA telescience program
03 p0977 N94-16073
MAXUS: The new sounding rocket program for long duration microgravity flight 03 p0978 N94-16079
Contextually dependent control strategies for manipulation
[TR-416] 03 p1165 N94-16580
Magnetostrictive actuators for human sensory feedback
[AD-A269266] 04 p1511 N94-17841
Teleoperation with virtual force feedback
[DE93-019406] 05 p1942 N94-20293
Manned Mars mission on-orbit operations FTS capabilities assessment
[NASA-CR-189328] 06 p2430 N94-23080
Telerobotic rendezvous and docking vision system architecture
[NASA-CR-191329] 06 p2204 N94-23828
SAMPEX payload operation control center implementation 06 p2197 N94-23843
Columbus system support for telescience operations
06 p2505 N94-23877
Mars 1994/1996: The French navigation tasks
06 p2195 N94-23924
Connector mechanisms in compliance with extreme space conditions 06 p2360 N94-24025
Precision Displacement Mechanism (PDM)
06 p2360 N94-24026
Crew interface analysis: Selected articles on space human factors research, 1987 - 1991
[NASA-TM-104756] 06 p2433 N94-24185
Hand controller commonality evaluation process
06 p2435 N94-24197
Programmable display pushbuttons on the Space Station's telerobot control panel
06 p2435 N94-24198
Space Station Freedom coupling tasks: An evaluation of their telerobotic and EVA compatibility
06 p2436 N94-24200
The effects of spatially displaced visual feedback on remote manipulator performance
06 p2436 N94-24201
Development of a force feedback anthropomorphic teleoperation input device for control of robot hands
[NASA-CR-195109] 06 p2437 N94-24329
Graphical programming at Sandia National Laboratories
[DE94-003803] 07 p2958 N94-25818
Performance measures from the explorer platform berthing experiment 07 p2683 N94-26283
Early lunar rover mission studies
07 p2684 N94-26290
Telepresence in the human exploration of Mars: Field studies in analog environments
07 p2685 N94-27360
Telescience testbedding under hypobaric hypoxic conditions: Evaluation by operation ability and recognition ability 07 p2913 N94-27450
Telescience testbedding for physiological experiments under hypobaric hypoxic conditions: Development and evaluation in CNV measuring 07 p2913 N94-27451
Teleoperated systems for nuclear reactors: Inspection and maintenance
[AIAA PAPER 94-1176-CP] 08 p3439 N94-30528
Object-based task-level control: A hierarchical control architecture for remote operation of space robots
[AIAA PAPER 94-1209-CP] 08 p3444 N94-30560
A performance analysis method for distributed real-time robotic systems: A case study of remote teleoperation
[AIAA PAPER 94-1212-CP] 08 p3445 N94-30563
A control method for bilateral teleoperating systems
[ISBN-0-315-78705-8] 08 p3313 N94-30952
Adaptive control of telerobotic systems worn by humans
[AD-A276608] 09 p3834 N94-32036
Advanced teleoperation: Technology innovations and applications 09 p3806 N94-32453
Technology transfer of operator-in-the-loop simulation
09 p3802 N94-32472
Development of an interchangeable end effector mechanism for the Ranger telerobotic vehicle
09 p3604 N94-33297
End effector monitoring system: An illustrated case of operational prototyping 10 p4109 N94-33631
Telemedicine, virtual reality, and surgery
10 p4096 N94-33641
Quantitative 3-D imaging topogrammetry for telemedicine applications 10 p4096 N94-33645
Air Force construction automation/robotics
10 p4066 N94-34022
RoboLab and virtual environments
10 p4015 N94-34027
Development and demonstration of a telerobotic excavation system 10 p4066 N94-34028
A teleoperated system for remote site characterization
10 p4066 N94-34029
Controlling telerobots with video data and compensating for time-delayed video using Omniview
10 p4127 N94-34031
Robotic technologies of the Flight Telerobotic Servicer (FTS) including fault tolerance 10 p4067 N94-34034
EVA-SCRAM operations 10 p4102 N94-34035
Ground vehicle control at NIST: From teleoperation to autonomy 10 p4127 N94-34037
The servicing aid tool: A teleoperated robotics system for space applications 10 p4067 N94-34039
Bilateral control to coordinate operators with supporting systems by force sensed grips 10 p4067 N94-34335
Adjustable control station with movable monitors and cameras for viewing systems in robotics and teleoperations
[NASA-CASE-NPO-17837-1-CU]
11 p4332 N94-35384
Teleoperation and supervised autonomy for ORU exchange
[NASA-CR-196101] 11 p4274 N94-35512
Task-specific usability requirements for virtual information environments: Interface design and data representation for human operators of complex medical systems 12 p4483 N94-37262
Operator gaze position control interfaces: Investigation of psychophysical and operational parameters
12 p4485 N94-37273
Low cost software-based rendering and stereoscopic interfaces for teleoperation and virtual reality
12 p4486 N94-37279

TELEPHONES
NT RADIOTELEPHONES
Performances of a date dissemination code on telephone lines using commercial modems
01 p0139 N94-10984
Conversion of the proprietary ROLM (tm) inter-node link from multimode to singlemode operation
05 p1744 N94-21349
The Iridium (tm) system: Personal communications anytime, anyplace 06 p2281 N94-22785
The Globalstar mobile satellite system for worldwide personal communications 06 p2282 N94-22786
Odyssey personal communications satellite system
06 p2282 N94-22787
Remote sensing for urban planning
09 p3758 N94-32465
North American ISDN Users' Forum agreements on Integrated Services Digital Network
[PB94-162559] 11 p4305 N94-35940

TELEPHONY
Mobilesat (tm): A world first 06 p2281 N94-22783
INMARSAT's personal communicator system
06 p2282 N94-22788
A high quality voice coder with integrated echo canceller and voice activity detector for mobile satellite applications 06 p2286 N94-22812
Remote sensing for urban planning
09 p3758 N94-32465
Reliable communication in the presence of severe noise or jamming
[AD-A278410] 09 p3684 N94-33173

TELEROBOTICS
Telerobotic control of a mobile coordinated robotic server
[NASA-CR-193465] 01 p0338 N94-10345
Telerobot control system
[NASA-CASE-NPO-18116-1-CU]
01 p0179 N94-10670
Development and evaluation of a predictive algorithm for telerobotic task complexity 01 p0341 N94-11562
In-space operations for lunar and Mars space transfer vehicles 01 p0348 N94-11568
In-space assembly-servicing requirements
01 p0348 N94-11569
More sense for less cents: Cost effective servicing of remote sensing satellites 01 p0348 N94-11572
Supervised autonomous control, shared control, and teleoperation for space servicing
01 p0183 N94-11577
Force reflecting hand controller for manipulator teleoperation
[NASA-CR-191345] 02 p0661 N94-13129
Tactile sensing and control in humans and robotic/teleoperated systems
[AD-A267710] 03 p1163 N94-14937
Hidden Markov model approach to skill learning and its application to telerobotics
[AD-A266989] 03 p1164 N94-15502
Ground integrated ET-derived space platforms for onorbit applications
[TABES PAPER 93-652] 03 p0899 N94-16152
A computer-based training system combining virtual reality and multimedia
[DE93-013768] 03 p1132 N94-16819
Magnetostrictive actuators for human sensory feedback
[AD-A269266] 04 p1511 N94-17841
Telerobotic control of a mobile coordinated robotic server, executive summary
[NASA-CR-194685] 05 p1821 N94-20044
An architecture for teleprogramming autonomous mobile robots at task level
[LAAS-93107] 06 p2470 N94-22906
Manned Mars mission on-orbit operations FTS capabilities assessment
[NASA-CR-189328] 06 p2430 N94-23080
Graphical programming: A systems approach for telerobotic servicing of space assets
[DE93-019016] 06 p2472 N94-23201
The remote-operated autonomous-robot concept: From deep sea to outer space applications
06 p2370 N94-23413
Lunar exploration rover program developments
[DE93-040759] 06 p2613 N94-23469
Ground operation of robotics on Space Station Freedom 06 p2371 N94-23841
Hand controller commonality evaluation process
06 p2435 N94-24197
Programmable display pushbuttons on the Space Station's telerobot control panel
06 p2435 N94-24198
Speech versus manual control of camera functions during a telerobotic task 06 p2436 N94-24199
Space Station Freedom coupling tasks: An evaluation of their telerobotic and EVA compatibility
06 p2436 N94-24200

The effects of spatially displaced visual feedback on remote manipulator performance
06 p2436 N94-24201
Simulation of the human-telerobot interface on the Space Station 06 p2436 N94-24202
Selected topics in robotics for space exploration
[NASA-CP-10131] 07 p2682 N94-26278
Technology drivers for flight telerobotic system software 07 p2684 N94-26289
Utility fog: A universal physical substance
07 p2687 N94-27367
A new method for recognizing quadric surfaces from range data and its application to telerobotics and automation, final phase
[NASA-CR-195733] 08 p3408 N94-28825
Thermal enclosure system functional simulation user's manual
[NASA-TM-109094] 08 p3466 N94-29489
Aspects of the operator interface for military robotic applications in unstructured environments
08 p3309 N94-30304
A multiplexed two-way solid communications link for teleoperated robots 08 p3310 N94-30310
Task automation in a successful industrial telerobot
[AIAA PAPER 94-1189-CP] 08 p3441 N94-30539
Technology transfer and evaluation for Space Station telerobotics
[AIAA PAPER 94-1190-CP] 08 p3441 N94-30541
Space flight manipulator technologies and requirements for the NASA Flight Telerobotic Servicer (FTS)
[AIAA PAPER 94-1191-CP] 08 p3441 N94-30542
A Space Station robot walker and its shared control software
[AIAA PAPER 94-1192-CP] 08 p3442 N94-30543
Technology for robotic surface inspection in space
[AIAA PAPER 94-1193-CP] 08 p3442 N94-30544
Object-based task-level control: A hierarchical control architecture for remote operation of space robots
[AIAA PAPER 94-1209-CP] 08 p3444 N94-30560
A performance analysis method for distributed real-time robotic systems: A case study of remote teleoperation
[AIAA PAPER 94-1212-CP] 08 p3445 N94-30563
Dexterity enhancement in microsurgery using telemicro-robotics
[AIAA PAPER 94-1230-CP] 08 p3447 N94-30579
Terrestrial applications of NASA space telerobotics technologies
[AIAA PAPER 94-1235-CP] 08 p3448 N94-30582
A control method for bilateral teleoperating systems
[ISBN-0-315-78705-8] 08 p3313 N94-30952
Remote robot manipulator coupled with remote-controlled guide vehicle for soil sampling in hazardous waste sites 09 p3723 N94-31569
Applying robotics to HAZMAT
09 p3729 N94-32452
Advanced teleoperation: Technology innovations and applications 09 p3806 N94-32453
Technology transfer of operator-in-the-loop simulation
09 p3802 N94-32472
Development of an interchangeable end effector mechanism for the Ranger telerobotic vehicle
09 p3604 N94-33297
Quantitative 3-D imaging topogrammetry for telemedicine applications 10 p4096 N94-33645
Graphical programming: A systems approach for telerobotic servicing of space assets
10 p4066 N94-33666
Air Force construction automation/robotics
10 p4066 N94-34022
Lunar exploration rover program developments
10 p4066 N94-34023
RoboLab and virtual environments
10 p4015 N94-34027
Development and demonstration of a telerobotic excavation system 10 p4066 N94-34028
Controlling telerobots with video data and compensating for time-delayed video using Omniview
10 p4127 N94-34031
Undersea applications of dexterous robotics
10 p4067 N94-34033
Robotic technologies of the Flight Telerobotic Servicer (FTS) including fault tolerance 10 p4067 N94-34034
Robotics Demo Peer Group review
[NASA-TM-109849] 10 p4061 N94-34117
Bilateral control to coordinate operators with supporting systems by force sensed grips 10 p4067 N94-34335
Adjustable control station with movable monitors and cameras for viewing systems in robotics and teleoperations
[NASA-CASE-NPO-17837-1-CU]
11 p4332 N94-35384
Teleoperation and supervised autonomy for ORU exchange
[NASA-CR-196101] 11 p4274 N94-35512
Virtual Interfaces: Research and Applications
[AGARD-CP-541] 12 p4482 N94-37261

TELESCOPES
NT GAMMA RAY TELESCOPES
NT HUBBLE SPACE TELESCOPE
NT INFRARED SPACE OBSERVATORY (ISO)
NT INFRARED TELESCOPES
NT MULTISPECTRAL TRACKING TELESCOPES
NT PARTICLE TELESCOPES
NT RADIO TELESCOPES
NT REFLECTING TELESCOPES
NT SCHMIDT TELESCOPES
NT SOLAR OPTICAL TELESCOPE
NT SPACE INFRARED TELESCOPE FACILITY
NT SPACEBORNE TELESCOPES
NT SPECTROSCOPIC TELESCOPES
NT ULTRAVIOLET TELESCOPES
NT VERY LARGE ARRAY (VLA)
NT VERY LONG BASELINE ARRAY (VLBA)
NT X RAY ASTROPHYSICS FACILITY
NT X RAY TELESCOPES
Continued development of an ultra-narrow bandpass filter for solar research
[NASA-CR-194169] 01 p0381 N94-10735
Monochromator SP-017. The results of the first experiments
[DE93-617463] 01 p0372 N94-10849
NASA Marshall Space Flight Center solar observatory report, January - June 1993
[NASA-TM-108417] 01 p0423 N94-10866
Visual Earth observation performance in the space environment. Human performance measurement 4: Flight experiments 01 p0314 N94-11539
A comparison of telescopic and Phobos-2 ISM spectra of Mars in the short-wave near-infrared (0.76-1.02 microns) 01 p0424 N94-12053
Model of optical scatter from microimpacts on the Hubble Telescope 01 p0384 N94-12189
Galileo EM-2 contributions to the lunar control network 01 p0468 N94-12198
Laser system design for the generation of a sodium-layer laser guide star
[DE93-014127] 01 p0176 N94-12784
Some flow properties of telescope enclosures estimated from water channel tests: Application of the flow visualization techniques
[NAL-TR-1178T] 02 p0830 N94-13452
Rocket and laboratory studies in astronomy
[NASA-CR-194410] 02 p0832 N94-13966
Telescope pointing for GOPEX
02 p0610 N94-14389
Experimental instrumentation system for the Phased Array Mirror Extendible Large Aperture (PAMELA) test program
[NASA-CR-194421] 02 p0705 N94-14430
Small scale adaptive optics experiment systems engineering
[NASA-CR-194419] 02 p0793 N94-14548
Design of pulse stretching cell for a sodium guide star optical system
[DE93-016436] 03 p1236 N94-14929
Fault management for data systems
[NASA-TM-103953] 03 p1116 N94-15548
Two color satellite laser ranging upgrades at Goddard's 1.2m telescope facility 03 p0915 N94-15581
A computer-controlled x-y offset guiding stage for the MLRS 03 p0918 N94-15598
Matera Laser Ranging Observatory (MLRO): An overview 03 p0877 N94-15601
Performance of the upgraded Orroral laser ranging system 03 p0877 N94-15602
Transputer based control system for MTLRS
03 p0877 N94-15613
Station report on the Goddard Space Flight Center (GSFC) 1.2 meter telescope facility
03 p0922 N94-15625
Tip-tilt compensation: Resolution limits for ground-based telescopes using laser guide star adaptive optics
[DE93-016426] 03 p1237 N94-16872
Optical displays: A tutorial on images and image formation
[AD-A266230] 03 p1192 N94-16926
Diffractive optical elements for generating arbitrary line foci 03 p1195 N94-17338
Test methods for acceptance testing of telescopes
[AD-A268316] 03 p1237 N94-17568
Origins of solar activity. First year report, AASERT grant
[AD-A268848] 04 p1629 N94-18222
Calibration of a high frequency monostatic acoustic echosounder
[AD-A268901] 04 p1481 N94-18229
Space debris detection
[AD-A269254] 04 p1334 N94-18264
Laser guide star measurements at Lawrence Livermore National Laboratory
[DE93-018081] 04 p1441 N94-19251
Conically scanned holographic lidar telescope
[NASA-CASE-GSC-13462-1] 05 p1986 N94-20591
Advanced far infrared detectors
[DE93-040289] 05 p1988 N94-21528
Laser guide star adaptive optics: Present and future
[DE93-018642] 05 p1989 N94-21619
Archiving data from ground-based telescopes
05 p2046 N94-22442
Programmability in AIPS++
05 p1926 N94-22482
Telescope image modelling software in STSDAS
05 p1926 N94-22483
The University of Hawaii Institute for Astronomy CCD camera control system 05 p1828 N94-22489
The ADAM environment and transputers
05 p1926 N94-22494
The VLBA correlator: Real-time in the distributed era
05 p2049 N94-22547
Solar full-disk magnetic field image receiving system and observation software 05 p2079 N94-22552
Multi-access laser communications terminal
[NASA-CR-191251] 06 p2295 N94-23830
ASTER, a multinational Earth observing concept
06 p2389 N94-23840
Data analysis and interpretation of lunar dust exosphere 06 p2623 N94-25349
Distributing functionality in the drift scan camera system
[DE94-003640] 07 p2809 N94-25599
Performance impacts for actuator misalignments and failures in large-aperture adaptive-optic telescopes
[AD-A273838] 07 p3034 N94-25742
NASA Marshall Space Flight Center Solar Observatory report, July - October 1993
[NASA-TM-108448] 08 p3160 N94-29470
Aircraft system aft telescope cavity configuration study for Stratospheric Observatory for Infrared Astronomy (SOFIA), phase 2
[NASA-CR-194266] 08 p3147 N94-29685
Design and early results of the sodium-layer laser guide star adaptive optics experiment at the Lawrence Livermore National Laboratory
[DE94-006653] 09 p3926 N94-32189
Digital image profilers for detecting faint sources which have bright companions
[NASA-CR-191348] 09 p3927 N94-32695
Performance of adaptive optics at Lick Observatory
[DE94-009382] 10 p4142 N94-33911
Advanced technology lunar telescope
11 p4350 N94-35473
Predicted optical performance of the High-Altitude Balloon Experiment (HABE) telescope in an adverse thermal environment
[DE94-008949] 11 p4349 N94-35998

TELESCOPING STRUCTURES
U FOLDING STRUCTURES

TELEVISION CAMERAS
A compact, four-way image splitter
[AD-A266107] 01 p0382 N94-11656
Initial laboratory evaluation of color video cameras, phase 2
[DE93-040201] 05 p1809 N94-21556
Orbital docking system centerline color television camera system test
[NASA-TM-104783] 06 p2205 N94-24625
Development of a 2f optical performance measurement system
[DE94-003489] 07 p3039 N94-27721

TELEVISION EQUIPMENT
NT TELEVISION CAMERAS
Measurement of display transfer characteristics using test pictures
[BBC-RD-1992/13] 01 p0133 N94-11023

TELEVISION SYSTEMS
NT CLOSED CIRCUIT TELEVISION
NT COLOR TELEVISION
NT DIGITAL SPACECRAFT TELEVISION
NT EDUCATIONAL TELEVISION
NT HIGH DEFINITION TELEVISION
A compact, four-way image splitter
[AD-A266107] 01 p0382 N94-11656
International testing of a Mars rover prototype
03 p1273 N94-16312
Mars 96 rover: Technical vision and navigation
06 p2370 N94-23417
Reducing video frame rate increases remote optimal focus time
[NASA-TM-104018] 06 p2431 N94-23970
HORACE: Presentation-level protocol standard for digital transmission of monochrome television images
[AD-A273395] 06 p2197 N94-25064
The television as robot servant
[AD-A273985] 07 p2984 N94-25898
VENI, video, VICI: The merging of computer and video technologies 07 p2686 N94-27362

A space-based classification system for RF transients
[DE94-003933] 08 p3240 N94-28522
The development and testing of a backscatter absorption gas imaging (BAGI) system designed to image at a range of 300 m
[DE94-006192] 09 p3675 N94-31761
Welcome to the Ohio Aerospace Institute
[NASA-TM-109756] 09 p3913 N94-31815
Low cost software-based rendering and stereoscopic interfaces for teleoperation and virtual reality
12 p4486 N94-37279

TELEVISION TRANSMISSION
NHK Science and Technical Research Laboratories
05 p2151 N94-20342
HORACE: Presentation-level protocol standard for digital transmission of monochrome television images
[AD-A273395] 06 p2197 N94-25064
Equations for estimating the strength of TV signals scattered by wind turbines
[NASA-CR-194468] 10 p4049 N94-34916

TELLEGEN THEORY
U NETWORK ANALYSIS
U NETWORK SYNTHESIS

TELLURIC CURRENTS
The influence of orography on the transport of atmospheric constituents 06 p2619 N94-24886

TELLURIDES
NT CADMIUM TELLURIDES
NT INDIUM TELLURIDES
NT LEAD TELLURIDES
NT MERCURY TELLURIDES
NT TIN TELLURIDES
NT ZINC TELLURIDES
Evaporation of a sodium tellurite melt in the jamic low gravity drop shaft 05 p1713 N94-20605

TELLURIUM
The epitaxial growth of Ge on Si(100) using Te as a surfactant
[DE94-003437] 07 p3056 N94-26326
Thermodynamic behaviour of tellurium at high temperatures
[DE94-612823] 11 p4240 N94-35960

TELLURIUM ALLOYS
Thermodynamics of molten K-TE alloys
[DE94-608095] 08 p3208 N94-30090
Structural ordering in liquid K-Te alloys
[DE94-008477] 09 p3645 N94-32514

TELLURIUM COMPOUNDS
NT CADMIUM TELLURIDES
NT INDIUM TELLURIDES
NT LEAD TELLURIDES
NT MERCURY CADMIUM TELLURIDES
NT MERCURY TELLURIDES
NT TELLURIDES
NT TIN TELLURIDES
NT ZINC TELLURIDES

TELSTAR SATELLITES
Charge efficiency of Ni/H2 cells during transfer orbit of Telstar 4 satellites 07 p2862 N94-28117

TEM (MICROSCOPY)
U TRANSMISSION ELECTRON MICROSCOPY

TEMPERATE REGIONS
The cloud radiative feedback of a midlatitude squall line system and implication for climate study
[DE93-010511] 01 p0283 N94-10290
Nonlinear relationships between particulate absorption and chlorophyll: Detritus or pigment packaging?
[AD-A266806] 02 p0731 N94-14899
Are tropical cirrus brighter than mid-latitude cirrus?
05 p1881 N94-22343
Nonlinear dynamics applied to atmospheric prediction
[AD-A273437] 06 p2404 N94-24674
Short-range cloud amount forecasting with model output statistics
[AD-A274769] 07 p2895 N94-26798
US streamflow patterns associated with the extreme phases of the Southern Oscillation
10 p4088 N94-33359
Effects of mesoscale convective organization and vertical wind shear on the cumulus-environment interaction 10 p4090 N94-34910
Aerosol optical depth derived from solar radiometry observations at northern mid-latitude sites
[DE94-007476] 11 p4287 N94-36053
Ionospheric plasma drift and structure studies at high and mid-latitudes
[AD-A279415] 11 p4291 N94-36116

TEMPERATURE
NT AMBIENT TEMPERATURE
NT ATMOSPHERIC TEMPERATURE
NT BODY TEMPERATURE
NT BRIGHTNESS TEMPERATURE
NT COMBUSTION TEMPERATURE
NT CRITICAL TEMPERATURE
NT CRYOGENIC TEMPERATURE
NT CURIE TEMPERATURE
NT FLAME TEMPERATURE
NT GAS TEMPERATURE
NT GLASS TRANSITION TEMPERATURE
NT HIGH TEMPERATURE
NT IGNITION TEMPERATURE
NT INLET TEMPERATURE
NT ION TEMPERATURE
NT LAND SURFACE TEMPERATURE
NT LOW TEMPERATURE
NT LUNAR TEMPERATURE
NT NEEL TEMPERATURE
NT NOISE TEMPERATURE
NT OCEAN TEMPERATURE
NT OPERATING TEMPERATURE
NT PLANETARY TEMPERATURE
NT PLASMA TEMPERATURE
NT ROOM TEMPERATURE
NT SEA SURFACE TEMPERATURE
NT SKIN TEMPERATURE (BIOLOGY)
NT SKIN TEMPERATURE (NON-BIOLOGICAL)
NT SPACE TEMPERATURE
NT STAGNATION TEMPERATURE
NT STELLAR TEMPERATURE
NT SURFACE TEMPERATURE
NT TRANSITION TEMPERATURE
NT WALL TEMPERATURE
NT WATER TEMPERATURE
The temperature at the phase boundary during quasi-static motions of a two-phase thermoelastic bar
[AD-A268769] 04 p1596 N94-18388
Estimation of the net production of moss community at Langhovde, East Antarctica 08 p3358 N94-29081

TEMPERATURE COMPENSATION
Sea surface temperature difference between NOAA/AVHRR and in-situ observation
01 p0215 N94-12680
Precise flux control for lattice matched superlattice materials
[AD-A268254] 03 p1215 N94-17417

TEMPERATURE CONTROL
The Third Workshop on Two Phase Fluid Experiment in the Space Environment
[NASDA-CON-930002] 01 p0161 N94-12547
Summary of studies on JEM utilization experiment projects 01 p0161 N94-12548
Compilation of proposals for boiling and evaporation experiments in space environments and proposals concerning experiment projects
01 p0161 N94-12549
Condensation phenomena 01 p0162 N94-12550
Developmental research of thermal control system in space environment 01 p0162 N94-12551
Two phase flow and isopycnic liquid-liquid two phase fluid in reduced gravity field 01 p0162 N94-12552
Devices related for thermal control systems used in microgravity 01 p0162 N94-12553
Research and development of cold plate for two phase fluid loop thermal control system
01 p0162 N94-12555
Organization and management policy for two phase fluid experiment in space environment
01 p0162 N94-12556
Thermal Expert System (TEXSYS): Systems automony demonstration project, volume 1. Overview
[NASA-TM-102877-VOL-1] 02 p0538 N94-13201
Miscibility of lubricants with refrigerants, phase 1
[DE93-014766-PHASE-1] 02 p0596 N94-13407
Thermal Expert System (TEXSYS): Systems autonomy demonstration project, volume 2. Results
[NASA-TM-102877-VOL-2] 02 p0538 N94-13989
Propulsion integration 02 p0508 N94-14174
Microchannel cooled heatsinks for high average power laser diode arrays
[DE93-016533] 02 p0658 N94-14442
Thermal design of hybrid circuits: Tools and methodology
[LAAS-92515] 02 p0626 N94-14713
Analysis, approximation, and computation of a coupled solid/fluid temperature control problem
[NASA-TM-106351] 02 p0771 N94-14731
Development of Japanese Earth Resources Satellite-1 (JERS-1; FUYO-1) and it's operational results
[NASDA-SPP-930001] 03 p0884 N94-15001
Cool suit
[NASA-TM-109639] 03 p1120 N94-15250
Advanced cooling for high power electric actuators
[AD-A266984] 03 p0866 N94-15761
Solar absorptance of optical surfaces contaminated with spacecraft material outgassing products
[AD-A267202] 03 p0886 N94-15857
Performance of silvered Teflon thermal control blankets on spacecraft
[AD-A266284] 03 p0887 N94-16909
Variational principles of heat exchange and their applications in construction physics, part 2
[IFTR-19/1991] 03 p1061 N94-17069
Overview of the solar dynamic ground test demonstration program
[NASA-TM-106296] 03 p0928 N94-17256
Substrate temperature measurement and control during thermal plasma CVD
[DE93-040305] 04 p1433 N94-19135
Materials processing and manufacturing technologies for diamond substrate multichip modules
[AD-A271484] 05 p2027 N94-21319
SPACE-R Thermionic Space Nuclear Power System: Design and Technology Demonstration Program
[DE93-013969] 05 p1670 N94-21824
An engineering code to analyze hypersonic thermal management systems 06 p2320 N94-23636
Thermal control system for SSF sensor/electronics
[SAND-92-0652C] 06 p2321 N94-23640
Utilization of recently developed codes for high power Brayton and Rankine cycle power systems
06 p2222 N94-23641
Hubble Space Telescope high speed photometer orbital verification
[NASA-CR-189333] 06 p2204 N94-24226
Temperature dependence of protein solubility-determination, application to crystallization, and growth kinetics studies 06 p2224 N94-24344
Weld joint concepts for on-orbit repair of Space Station Freedom fluid system tube assemblies
06 p2371 N94-24427
Near Earth asteroid rendezvous
[NASA-CR-195518] 06 p2195 N94-24808
Thermal control system for Space Station Freedom photovoltaic power module
[NASA-TM-105650] 06 p2205 N94-24825
Thermistor controlled current source versatile temperature sensor
[AD-D015979] 06 p2345 N94-25037
Project WISH: The Emerald City
07 p2703 N94-25690
The 1991-1992 project summaries
07 p2943 N94-25698
Physical modelling and adaptive predictive control of diffusion/LPCVD reactors
[PB94-126398] 07 p2763 N94-26819
Variable temperature cold stage for microscope observation 07 p2718 N94-27389
Fuels combustion research
[AD-A275122] 08 p3189 N94-29004
An alternate method for achieving temperature control in the -160 to +90 C range
[NASA-CASE-NPO-18995-1-CU]
08 p3288 N94-29497
Maintaining acceptable thermal comfort with a low air temperature by means of local heating
[PB94-138526] 08 p3401 N94-29950
Numerical comparison of convective heat transfer augmentation devices used in cooling channels of hypersonic vehicles
[NASA-TM-106546] 08 p3279 N94-30147
Application of fuzzy logic to the control of wind tunnel settling chamber temperature
[NASA-TM-109105] 08 p3157 N94-30200
Process modelling for materials preparation experiments
[NASA-CR-195782] 08 p3175 N94-30242
Performance of silvered Teflon (trademark) thermal control blankets on spacecraft 09 p3591 N94-31014
Space environment durability of beta cloth in LDEF thermal blankets 09 p3591 N94-31015
Draft minutes of IAPG Mechanical Working Group meeting
[DE94-004954] 09 p3759 N94-31266
Metal hydride heat pump engineering demonstration and evaluation model
[NASA-CR-188286] 09 p3669 N94-32857
Combined contamination and space environmental effects on solar cells and thermal control surfaces
[NASA-TM-106592] 09 p3617 N94-33022
Airframe materials for HSR 10 p3979 N94-33514
Personal cooling systems: Possibilities and limitations
10 p4101 N94-33649
Evaluation of a liquid cooling garment as a component of the Launch and Entry Suit (LES)
10 p4101 N94-33653
Active thermal isolation for temperature responsive sensors
[NASA-CASE-LAR-14612-1] 10 p4054 N94-35074
Demonstration of a high heat removal CVD diamond substrate edge-cooled multichip module
[DE94-010748] 11 p4260 N94-36245
Digital control programmer for temperature control
[DE94-615584] 11 p4309 N94-36382
Review of advanced radiator technologies for spacecraft power systems and space thermal control
[NASA-TM-4555] 12 p4398 N94-36821

Microscopic image processing systems for measuring nonuniform film thickness profiles
[DE94-005336] 12 p4424 N94-37223

TEMPERATURE DEPENDENCE

On the relativistic string size at finite temperature
[DE93-617658] 01 p0409 N94-10394
Experiments in ultracold collisions
[DE93-012110] 01 p0365 N94-11029
Phase equilibria and volumetric properties for the system NaCl-CaCl2-H2O
[DE93-013590] 01 p0076 N94-11244
Computation of photovoltaic parameters under lunar temperature variation 01 p0053 N94-11411
Apical Cu-O bond in YBa2Cu3O(7-delta) superconductors by XAFS
[DE93-010861] 01 p0400 N94-11458
Thermographic properties of eight blue-emitting phosphors
[DE93-011459] 01 p0078 N94-11622
The role of the geothermal gradient in the emplacement and replenishment of ground ice on Mars
01 p0463 N94-12169
Environmental factors controlling fluxes of dimethyl sulfide in a New Hampshire fen
01 p0270 N94-12462
Breadboard activities for advanced protein crystal growth
[NASA-CR-193559] 02 p0803 N94-12796
Modeling ignition chemistry
[DE93-012340] 02 p0561 N94-12910
Temperature dependence of diffusivities, preliminary definition phase
[NASA-CR-192613] 02 p0648 N94-13326
High temperature electromagnetic characterization of thermal protection system tile materials
[NASA-CR-189687] 02 p0578 N94-13431
High temperature behavior of glass (M-8)
02 p0587 N94-13740
A circadian rhythm of conidiation in Neurospora crassa (L-12) 02 p0593 N94-13769
The accuracy of approximating radiative heat transfer using a temperature dependent thermal conductivity
[DE93-013105] 02 p0638 N94-14318
The pressure broadening of HDO by O2, N2, H2, and He between 100 K and 600 K
[AD-A267118] 03 p0946 N94-15684
Experimental investigations of superconductivity in quasi-two-dimensional epitaxial copper oxide superlattices and trilayers
[DE93-015306] 03 p1207 N94-15829
Density of states and tunneling characteristics of layered superconductors
[DE93-015898] 03 p1211 N94-16839
Chemical vapor deposition of Ta2O5 corrosion resistant coatings
[DE93-015488] 03 p0969 N94-16889
Transient studies of low temperature catalysts for methane conversion
[DE93-017710] 03 p0950 N94-16962
Mechanical properties of interfaces and superlattices
[AD-A268591] 03 p1217 N94-17606
Phase transitions and neutron scattering
[DE93-016748] 04 p1594 N94-17866
Pulsed LASER for testing silicon strip detectors
[DE93-017816] 04 p1436 N94-17883
Fin-efficiency calculation for condensation in the presence of noncondensable gases
[DE93-017684] 04 p1409 N94-18004
Effect of phase change in a debris cloud on a backwall structure
[DE93-017506] 04 p1358 N94-18100
Relaxation of polar orientational order in nonlinear optical polymers by second harmonic generation
[AD-A269059] 04 p1370 N94-18515
In-situ growth monitoring of molecular beam epitaxy processes
[AD-A269287] 04 p1598 N94-18616
In situ observation of radiation induced amorphization of crystals with apatite structure
[DE93-018450] 04 p1599 N94-18816
Densities and viscosities of ternary ammonia/water fluids
[DE93-015966] 04 p1351 N94-19118
Thermodynamic q-distributions that aren't
[DE93-017385] 04 p1609 N94-19121
Selective methane oxidation over promoted oxide catalysts
[DE93-040002] 04 p1351 N94-19132
Thermophysical properties
[DE93-040219] 04 p1351 N94-19134
Selective methane oxidation over promoted oxide catalysts
[DE93-040001] 04 p1351 N94-19150
A simple description of flow instability with application to a packed bed
[DE93-017492] 04 p1420 N94-19345
Ultraviolet absorption cross-sections of some carbonyl compounds and their temperature dependence
[AERONAUTICA-ACTA-A-368-1993] 04 p1353 N94-19456
Temperature of aircraft cargo flame exposure during accidents involving fuel spills
[DE93-019633] 04 p1381 N94-19539
Excited atomic bromine energy transfer and quenching mechanisms
[AD-A270672] 04 p1572 N94-19607
Testing of protective coatings in hydrogen
[DE93-040326] 04 p1375 N94-19651
Frequency and temperature dependence of high damping elastomers
[DE93-019539] 05 p1697 N94-19809
Temperature dependence of 4f PES features and hole occupancy in ytterbium heavy fermions
[DE93-040131] 05 p1691 N94-20321
High energy ionization in liquids: The free ion yield
[DE93-040329] 05 p1973 N94-20324
Ten GHz YBa2Cu3O(7-delta) superconducting ring resonators on NdGaO3 substrates
05 p1735 N94-20515
Stability of an uncooled segment of a high-temperature superconductor
[DE94-000476] 05 p2032 N94-21932
Investigation of moisture-induced embrittlement of iron aluminides
[DE93-040841] 05 p1695 N94-21949
Temperature dependence of magnetic order in single-crystalline UPdSn
[DE93-040153] 05 p2033 N94-21991
Temperature-dependent ion beam mixing
[DE93-040281] 05 p2033 N94-21999
Dynamics of surface thermal expansion and diffusivity using two-color reflection transient gratings
[DE93-040547] 05 p1990 N94-22002
Temperature dependence of CsI(Tl) gamma ray excited scintillation characteristics
[DE94-000836] 05 p2034 N94-22028
Microstructural evolution of neutron-irradiated Fe-Cr-Ni ternary alloys at high helium generation rates
[DE93-018786] 05 p1696 N94-22037
First-principles pressure-temperature phase diagrams in metals
[DE94-001056] 05 p1696 N94-22398
Test results of two high temperature superconducting sample coils
[DE94-000496] 05 p2035 N94-22570
Alloying studies in U(1-x)Th(x)Pd2Al3 (0 (le) x (le) 1)
[DE94-000807] 05 p2036 N94-22584
Electrical transport in La(2-x)Sr(x)CuO(4-y)
[DE93-040885] 06 p2556 N94-22912
Low temperature diffusion of hydrogenic species in oxide crystals: Radiation induced diffusion
[DE94-000374] 06 p2558 N94-22957
Effects of neutron irradiation and hydrogen on ductile-brittle transition temperatures of V-Cr-Ti alloys
[DE94-001466] 06 p2240 N94-23009
Tensile properties of 21-6-9 stainless steel at elevated temperatures
[DE94-001852] 06 p2240 N94-23017
Thermally activated low temperature creep and primary water stress corrosion cracking of NiCrFe alloys
[DE94-001756] 06 p2241 N94-23219
Conductors with small Fermi energies and small gap energies
[DE93-040887] 06 p2561 N94-23432
Physics of iron
[DE94-002002] 06 p2402 N94-23721
Disorder effects on small-polaron formation and hopping
[DE94-001205] 06 p2534 N94-23804
Temperature dependence of protein solubility-determination, application to crystallization, and growth kinetics studies 06 p2224 N94-24344
The mechanical properties of single crystal (alpha)-Si3N4
[DE94-002632] 06 p2563 N94-24517
Surface compositional variations of Mo-47Re alloy as a function of temperature
[NASA-TP-3402] 06 p2245 N94-25117
On the thermal ignition with variable pre-exponential factor
[DE93-616009] 07 p2713 N94-25913
Optical conductivity and resistivity in the two-band Emery model
[DE94-601943] 07 p3051 N94-25945
Debye-Waller factors of the light actinide metals
[DE94-000685] 07 p2733 N94-26069
The formation of conducting gold films by thermal decomposition and direct patterning using electron beam lithography of the gold cluster Au55P(C6H5)312C16
[AD-A273720] 07 p2749 N94-26074
Temperature dependence of static RAM volatility
[DE93-040345] 07 p2948 N94-26111
Toward insulating quasicrystalline alloy in Al-Pd-Re icosahedral phase
[REPT-A-2666] 07 p2736 N94-26477
Measurements of the p (mu)d-molecule formation rate at different hydrogen temperature
[DE93-634636] 07 p3020 N94-26511
Ion beam mixing of marker layers into amorphous aluminum oxide
[DE94-000901] 07 p2752 N94-26676
Electrical conductivity of perovskite-magnesiowuestite as a function of pressure and temperature
[DE94-002714] 07 p2880 N94-26806
Experimental and analytical studies of high heat flux components for fusion experimental reactor
[DE94-707671] 08 p3504 N94-28556
Atomic and magnetic structure of YBa2(Cu(1-x)Fe(x))3O(6+y) at 0.05 less than or equal to x less than or equal to 0.30, y is approximately equal to 1 and y is approximately equal to 0.5
[DE94-606852] 08 p3513 N94-29210
Creep and physical aging of PVC: Dependence on stress and temperature
[NPL-DMM(A)-115] 08 p3217 N94-29886
Particle kinetic simulation of high altitude hypervelocity flight
[NASA-CR-194535] 08 p3131 N94-29893
Global patterns of cloud optical thickness variation with temperature and the implications for climate change
08 p3374 N94-29972
Study of the ultraviolet absorption and photoconduction spectra of polyimide films fabricated at various curing temperatures
[ISBN-0-315-85923-7] 08 p3218 N94-30036
The bases for the development of high-temperature integrated SQUID-systems
[DE94-607901] 08 p3267 N94-30073
On the structure and atomic motions in liquid sodium
[DE94-608386] 08 p3490 N94-30182
Peculiarities of heat transfer in the experiments of beam injection heating of a plasma at the GOL-3 device
[DE94-608357] 08 p3508 N94-30194
Strain relaxation and surface roughness as a function of growth temperature in linearly graded In(x)Al(1-x)As (x = 0.05 to 0.25) buffers
[DE94-005430] 08 p3519 N94-30592
Terfenol: A study of the phase equilibrium diagram and the solidification process
[DE94-004883] 08 p3209 N94-30690
Scaling in heavy-fermion systems
[DE94-005002] 08 p3492 N94-30775
The 4f heavy fermion photoelectron spectra do not exhibit the Kondo scale
[DE94-006252] 09 p3898 N94-31631
Acoustic emission from crack growth in 7050 aluminum and 7075 aluminum as a function of temperature and heat treatment
[DREP-CRS-93-15] 09 p3642 N94-31871
Fermi surface instability at 0.4 K in a heavy-fermion YbBiPt: SDW?
[DE94-006224] 09 p3899 N94-31916
Creep-fatigue criteria and inelastic behavior of modified 9Cr-1Mo steel at elevated temperatures
[DE94-007915] 09 p3642 N94-31918
Temperature dependence of the exciton-exciton annihilation rate constant in poly(di-n-hexylsilane)
[DE94-005584] 09 p3655 N94-32102
Computerized Ultrasonic Testing System (CUTS) for in-process thickness determination
09 p3862 N94-32456
Computational modeling of convective heat transfer to liquid hydrogen coolant 09 p3707 N94-32485
Rate coefficient for the reaction H + O2 yields OH + O: Results from 2000 to 5300 K
[DE94-008105] 09 p3871 N94-32615
The relative performance of FeS2 and CoS in long-life thermal-battery applications
[DE94-006145] 09 p3695 N94-32663
Temperature dependence of single-event burnout in n-channel power MOSFET's
[AD-A277921] 09 p3898 N94-33177
Growth, characterization, and device development in monocrystalline diamond films
[AD-A277863] 10 p4146 N94-33774
Effects of catalytic mineral matter on CO and CO2 temperature and burning time for char combustion
[DE94-009130] 10 p4022 N94-33939
Experimental studies of equation of gases state for hydrogen and deuterium
[DE94-609877] 10 p4022 N94-34101
Methane production and consumption in grassland and boreal ecosystems
[NASA-CR-196085] 11 p4284 N94-35486
Alkali element constraints on Earth-Moon relations
11 p4354 N94-36169

Temperature dependence of superconduction bands in HTSC
[DE94-617361] 11 p4341 N94-36312
Portable high precision pressure transducer system
[DE94-010137] 11 p4270 N94-36389
A possible origin of EL6 chondrites from a high temperature-high pressure solar gas
[DE94-010467] 12 p4548 N94-36759
Effect of temperature on the electron attachment and detachment properties of c-C4F6
[DE94-012750] 12 p4518 N94-37383
Coupled Marangoni-Benard/Rayleigh-Benard instability with temperature dependent viscosity
[NASA-TM-106646] 12 p4444 N94-37507

TEMPERATURE DIFFERENCES
U TEMPERATURE GRADIENTS

TEMPERATURE DISTRIBUTION
Marangoni and buoyant convections in zone melting of GaAs with liquid encapsulation
01 p0101 N94-10081
Simulation of images of water vapor channel and infrared split channel 01 p0190 N94-11081
On temperature distribution in non-participating medium with radiation boundary condition
[DE93-619375] 01 p0153 N94-11604
Observations of the fractal properties of the Japan sea surface temperature patterns 01 p0205 N94-11984
On an upwelling front, propagation of upwelling and vertical velocity in the eastern Arabian Sea during monsoon, 1987 01 p0206 N94-11987
Roles of the NEC and MC in the formation and evolution of the Equatorial Pacific Warm Pool
01 p0206 N94-11990
Does the thermal wind exist near the Earth's core boundary? 01 p0283 N94-12217
Search for structures in the cosmic microwave background radiation
[INPE-5491-TDI/508] 01 p0484 N94-12357
Observation of cold coastal water with high turbidity around the southwestern tip of Korean Peninsula
01 p0216 N94-12689
The relationship between skin and bulk sea surface temperatures 01 p0221 N94-12716
Atmospheric correction for determination of average SST fields based on AVHRR data
01 p0227 N94-12750
Modelling of the temperature distribution in a copper roll for the design of a system of cooled rolls adapted to vertical strip casting
[IMI-93RT-21200-1436-G] 02 p0557 N94-13866
ROSAT observations of clusters with wide-angle tailed radio sources
[NASA-CR-193784] 02 p0833 N94-14405
Thermal stresses of a trimaterial medium in a nonuniform temperature field
[AD-A267243] 03 p0930 N94-14975
Near-surface temperature gradients and their effects on thermal-infrared emission spectra of particulate planetary surfaces 03 p1260 N94-16236
Volcanic thermal features observed by AVIRIS
03 p1068 N94-16680
Aerothermoelastic analysis of a NASP demonstrator model
[NASA-TM-109007] 03 p0867 N94-17055
Numerically solving a transient heat conduction problem with convection and radiation
[AD-A268521] 03 p1220 N94-17540
Mixture distributions in climatological research
[DE93-014125] 04 p1488 N94-17942
Development of a selective volumetric receiver for central receiver systems: Investigation of parameters and exergetic evaluation
[DLR-FB-93-05] 04 p1465 N94-18089
Spectral analysis of synoptic time scale disturbances over the tropical eastern Pacific during summer 1989, 1990 and 1991
[AD-A268821] 04 p1490 N94-18206
Application of infrared thermography in fluid mechanics 04 p1431 N94-18649
Liquid crystal heat transfer measurements
04 p1432 N94-18653
Three-dimensional dynamic thermal imaging of structural flaws by dual-band infrared computed tomography
[DE93-019575] 05 p1906 N94-20316
Comparison of mixing calculations for reacting and non-reacting flows in a cylindrical duct
[NASA-TM-106435] 05 p1649 N94-21758
A random distribution reacting mixing layer model
[NASA-CR-194445] 06 p2187 N94-23552
An analysis of Solar Mesospheric Explorer temperatures for the upper stratosphere and mesosphere
[NASA-CR-194861] 06 p2626 N94-23626
A direct approach to finding unknown boundary conditions in steady heat conduction
06 p2322 N94-23645
Convection equation modeling: A non-iterative direct matrix solution algorithm for use with SINDA
06 p2323 N94-23651
Experimental and analytical study of cryogenic propellant boiloff to develop and verify alternate pressurization concepts for Space Shuttle external tank using a scaled down tank 06 p2266 N94-23657
Unsteady three-dimensional thermal field prediction in turbine blades using nonlinear BEM
06 p2325 N94-23665
Flow and temperature distribution in a naturally stratified thermal storage tank
[AD-A273511] 06 p2336 N94-24821
Diagnostic calculations of the circulation in the Martian atmosphere 06 p2622 N94-24898
Two-dimensional modeling of thermal inversion layers in the middle atmosphere of Mars
06 p2622 N94-24900
Mars Observer: Applications to atmospheric transport
06 p2623 N94-24904
Thermophysical property sensitivity effects in steel solidification 06 p2246 N94-25122
Hydride thermodynamic machines
[VTT-JULK-768] 06 p2571 N94-25416
Ultra-high aggregate bandwidth two-dimensional multiple-wavelength diode laser arrays
[AD-A274018] 07 p2815 N94-25756
Verification of thermal analysis codes for modeling solid rocket nozzles
[NASA-CR-195248] 07 p2702 N94-27150
Ice surface temperature retrieval from AVHRR, ATSR, and passive microwave satellite data: Algorithm development and application
[NASA-CR-195276] 07 p2851 N94-27849
The validation of ATSR measurements with in situ sea temperatures
[DE94-003195] 07 p2852 N94-27875
Objective analysis of a coastal ocean eddy using satellite AVHRR and in situ hydrographic data
[AD-A275715] 08 p3376 N94-28642
A novel spectroscopic measurement method of RF plasma for temperature and electron density diagnoses
08 p3188 N94-28682
A random distribution reacting mixing layer model
[NASA-TM-106517] 08 p3150 N94-28923
The mixing process in the quenching zone of the rich-lean-combustion concept 08 p3196 N94-29281
On the temperature distribution near a cold surface
[AD-A275162] 08 p3332 N94-29288
Four-dimensional data assimilation using the adjoint method 08 p3455 N94-30353
Intra- versus interlayer pairing in the copper oxide superconductors: Response to a magnetic field
[DE94-005475] 08 p3521 N94-30898
Atomic oxygen interaction at defect sights in protective coatings on polymers flown on LDEF
09 p3593 N94-31024
CO observations in external galaxies and gas mass determination 09 p3925 N94-31790
Computational modeling of convective heat transfer to liquid hydrogen coolant 09 p3707 N94-32485
IRTM brightness temperature maps of the Martian south polar region during the polar night: The cold spots don't move 09 p3949 N94-33222
Induction heating model for high-frequency induction joining and repair of complex-shape graphite fiber/polymer matrix composites 10 p4018 N94-33362
EOF characterization of Atlantic SST fields using AVHRR data
[INPE-5535-TDI/523] 10 p4093 N94-34203
Reducing Temperature Distribution Factor (TDF) for advanced small gas turbine engines
10 p4003 N94-34455
An adaptive, unstructured, finite-element, multi-material, thermal analysis
[AD-A278632] 11 p4343 N94-36256

TEMPERATURE EFFECTS
In situ observation of temperature dependence of concentration field during growth of KB5 crystals by holographic interferometry 01 p0115 N94-10187
Temperature effects on failure thickness and deflagration-to-detonation transition in PBX 9502 and TATB
[DE93-010742] 01 p0097 N94-10294
Kinetics of high concentration arsenic deactivation at moderate to low temperatures
[DE93-013349] 01 p0395 N94-10516
Hydrogen partitioning and transport in titanium aluminides
[NASA-CR-194117] 01 p0076 N94-10713
Computational simulation of hot composite structures
[NASA-TM-106200] 01 p0186 N94-10762
Flammability parameters of materials: Ignition, combustion, and flame spread 01 p0020 N94-10788
Factors that affect OSU thermal performance of aircraft interior materials 01 p0020 N94-10789
The influence of irradiation conditions, type, and concentration of impurities on radiation defects characteristics in indium antimonide under electron irradiation
[DE93-617201] 01 p0397 N94-10843
Time-resolved optical studies of charge relaxation and charge transfer at electrode interfaces
[DE93-013985] 01 p0398 N94-11117
DBTT measurement by use of Small Punch (SP) test
[DE93-753188] 01 p0183 N94-11168
Thermal testing of aluminized Mylar
[NASA-TM-108414] 01 p0089 N94-11175
P2NBC2 Heat Strain Decision Aid. User's guide, version 2.1
[AD-A266072] 01 p0304 N94-11224
Thermographic properties of eight blue-emitting phosphors
[DE93-011459] 01 p0078 N94-11622
Changes in Hawaiian palagonite FE mineralogy associated with thermal alteration: Implications for Mars
01 p0281 N94-12055
Primordial lightning: Evidence preserved in chondrites
01 p0432 N94-12230
On the origin of (4)He and (40)Ar in natural gold
01 p0087 N94-12240
Thermal error compensation feasibility study using artificial intelligence
[AD-A266084] 01 p0340 N94-12411
NiAl alloys for structural uses
[NASA-CR-194113] 01 p0085 N94-12447
Molecular properties of polymeric materials for space applications
[NASA-CR-194370] 01 p0094 N94-12450
Non-linear effects in vortex viscous flow in superconductors-role of finite heat removal velocity
[DE93-621785] 02 p0618 N94-12856
Quantitative mapping of pore fraction variations in silicon nitride using an ultrasonic contact scan technique
[NASA-TP-3377] 02 p0665 N94-13056
Thermal gradient-induced deflection of a thick-walled cylinder with bending residual stresses
[AD-A266347] 02 p0673 N94-13777
Materials/structures testing 02 p0506 N94-14154
Multiwavelength observations of unidentified high energy gamma ray sources
[NASA-CR-194536] 02 p0840 N94-14688
Phases and phase transitions of polymeric liquid crystals: A high resolution x ray diffraction and light scattering study
[ITN-93-85218] 02 p0816 N94-14826
Thermal history effects on electrical relaxation and conductivity for potassium silicate glass with low alkali concentrations
[NASA-TM-106324] 02 p0583 N94-14845
Quenching and annealing effects on the specific heat of YBa2Cu3O(7-delta)
[DE93-016483] 02 p0816 N94-14868
Thyroid alterations in porcine after prolonged exposure to cold or heat
[AD-A266840] 02 p0733 N94-14879
Thermal stresses of a trimaterial medium in a nonuniform temperature field
[AD-A267243] 03 p0930 N94-14975
The influence of thermal aging on the microstructure and fatigue properties of modified 9Cr-1Mo steel
[DE93-015489] 03 p0957 N94-16106
Effects of alloying and temperature on the high-temperature oxidation of Cr-Cr2Nb
[DE93-015800] 03 p0957 N94-16163
Rheology of water and ammonia-water ices
03 p0953 N94-16188
Effective elastic thickness of the Venusian lithosphere with lateral viscosity variations in the mantle
03 p1293 N94-16421
A hydrogen isotope study of CO3 type carbonaceous chondrites; comparison with type 3 ordinary chondrites
03 p1246 N94-16425
Temperature and pressure effects on capacitance probe cryogenic liquid level measurement accuracy
[NASA-CR-190763] 03 p1034 N94-16521
Chemical vapor deposition of Ta2O5 corrosion resistant coatings
[DE93-015488] 03 p0969 N94-16889
Creep ductility of iron at very low strain rates: The effects of sulfur
[DE93-015490] 03 p0959 N94-16890
Studies on nonequilibrium phenomena in supersonic chemically reacting flows
[NASA-CR-194662] 03 p1027 N94-17215
Prediction of thermal cycling induced cracking in polymer matrix composites
[NASA-CR-194677] 03 p0941 N94-17295
Mesons at finite temperature in the NJL model with gluon condensate
[DE93-626697] 03 p1185 N94-17310

Precise flux control for lattice matched superlattice materials
[AD-A268254] 03 p1215 N94-17417
High temperature deformation behavior of YBa2Cu3O(6+x) superconducting ceramic materials
[AD-A268164] 03 p0973 N94-17430
Heat transfer parametric system identification
[AD-A268525] 03 p0929 N94-17543
Design, development and characterization studies of a large aperture high power Nd: Glass rod amplifier stage
[DE93-624944] 03 p1042 N94-17630
Modeling microstructural evolution and the mechanical response of superplastic materials
[DE93-014417] 04 p1355 N94-17711
Atlas of formability: Ultimet
[AD-A268352] 04 p1355 N94-17767
Atlas of formability: HAYNES 556
[AD-A268354] 04 p1356 N94-17768
Atlas of formability: HAYNES 188
[AD-A268355] 04 p1356 N94-17769
Atlas of formability: NICKELVAC K-500
[AD-A268351] 04 p1356 N94-17772
Atlas of formability: Haynes 230
[AD-A268325] 04 p1356 N94-17788
Atlas of formability: INCONEL 718
[AD-A268350] 04 p1356 N94-17789
Atlas of formability: Hastelloy C-22
[AD-A268324] 04 p1356 N94-17796
Atlas of formability: Permalloy - 80 flow stress curves
[AD-A268263] 04 p1356 N94-17801
Atlas of formability: Nickelvac C-276
[AD-A268264] 04 p1357 N94-17802
Atlas of formability: Ti-6Al-4V ELI
[AD-A268300] 04 p1357 N94-17803
Atlas of formability: ALLVAC 718
[AD-A268304] 04 p1357 N94-17804
Atlas of formability: Waspaloy
[AD-A268323] 04 p1593 N94-17805
Charpy impact toughness of martensitic steels irradiated in FFTF: Effect of heat treatment
[DE93-015960] 04 p1450 N94-17848
Synchronisation of cold induced vasodilation at various locations of one hand
[IZF-1992-B3] 04 p1504 N94-17966
Fin-efficiency calculation for condensation in the presence of noncondensable gases
[DE93-017684] 04 p1409 N94-18004
Effect of temperature and O-ring gland finish on sealing ability of Viton V747-75
[NASA-TP-3391] 04 p1368 N94-18075
Effect of phase change in a debris cloud on a backwall structure
[DE93-017506] 04 p1358 N94-18100
Evaluation of physiological and psychological impairment of human performance in cold stressed subjects
[AD-A268637] 04 p1506 N94-18632
Work plan for the Marine Aerosol Properties and the Thermal Imager Performance Trial (MAPTIP)
[AD-A270026] 04 p1483 N94-18712
Nondestructive inspection of graphite-epoxy laminates for heat damage using DRIFT and LPF spectroscopies
[DE93-017228] 04 p1343 N94-18761
LX-17 chemical kinetic material model for Chemical TOPAZ2D
[DE93-014363] 04 p1377 N94-18893
Effect of internal heating during hot compression testing on the stress-strain behavior and hot working characteristics of alloy 304L
[DE93-012701] 04 p1362 N94-18917
Environmental degradation of Alloy 600 and welded filler metal EN82 in an elevated temperature aqueous environment
[DE93-018049] 04 p1363 N94-18940
Thermal stresses in the microchannel heatsink cooled by liquid nitrogen
[DE93-018660] 04 p1418 N94-18995
Effects of irradiation temperature on Charpy and tensile properties of high-copper, low upper-shelf, submerged-arc welds
[DE93-017858] 04 p1445 N94-19047
Densities and viscosities of ternary ammonia/water fluids
[DE93-015966] 04 p1351 N94-19118
Thermodynamic q-distributions that aren't
[DE93-017385] 04 p1609 N94-19121
Shrinkage void formation and its effect on freeze and thaw processes of lithium and lithium-fluoride for space applications
[DE93-019303] 04 p1338 N94-19128
Influence of peak pressure and temperature on the shock-loading response of tantalum
[DE93-018561] 04 p1457 N94-19279
Suppressed electron-phonon scattering in superlattices
[AD-A270834] 04 p1604 N94-19597
Pressure and temperature effects on the kinetics and quality of diamond films
[AD-A270876] 04 p1606 N94-19771
Parametric variations of ion transport in TFTR
[DE93-012653] 05 p1991 N94-19883
Thermal behavior of natural zeolites
[DE93-040091] 05 p1699 N94-19975
Energy storage and conversion in solid hydrogen
[AD-A271439] 05 p1845 N94-20086
Strengthening of NiAl matrix composites
[AD-A271491] 05 p1674 N94-20550
Tambo Quemado: Extraordinary concentrations of REE and refractory trace elements caused by artificial heating 05 p1684 N94-20667
Further analyses of Rio Cuarto impact glass 05 p1685 N94-20745
A classification scheme for the morphology of lava flow fields 05 p1863 N94-20879
Chemical reaction fouling model for single-phase heat transfer
[DE93-019556] 05 p1802 N94-20942
Human responses to exercise-heat stress
[AD-A272581] 05 p1892 N94-21209
Description and assessment of a new Optical Pressure Measurement System (OPMS) demonstrated in the high speed wind tunnel in Goettingen (Germany)
[DLR-FB-92-24] 05 p1651 N94-21280
A quantitative S.E.M. image analysis of cement paste microstructure 05 p1708 N94-21894
Photo- and thermal-induced antiferromagnetic interlayer coupling in Fe/(Fe-Si) superlattices
[DE93-040822] 05 p2031 N94-21930
First-principles pressure-temperature phase diagrams in metals
[DE94-001056] 05 p1696 N94-22398
Projections on structures and material strength in the computational context 05 p1834 N94-22610
Discontinuous phase formation and selective attack of SiC materials exposed to low oxygen partial pressure environments
[DE93-040161] 06 p2231 N94-22933
Development of a computational testbed for numerical simulation of combustion instability 06 p2213 N94-23046
Shear coaxial injector instability mechanisms 06 p2213 N94-23047
Thermodynamics of nickel-cadmium and nickel-hydrogen batteries 06 p2391 N94-23349
A method to remove intercalates from bromine and iodine intercalated carbon fibers
[NASA-TM-106443] 06 p2222 N94-23591
Development of a theory of the wear of ceramics
[DE94-002773] 06 p2254 N94-23783
Laser soldering of Sn plated brass integrator assembly housings
[DE94-001149] 06 p2270 N94-23790
The mechanical properties of single crystal (alpha)-Si3N4
[DE94-002632] 06 p2563 N94-24517
Prediction of thermal cycling induced cracking in polmer matrix composites
[NASA-CR-195135] 06 p2229 N94-24579
Flex bearing UUEC, volume 2
[NASA-CR-193901] 06 p2365 N94-24588
Thermal phase behavior of metal surfaces: X-ray scattering studies of Pt(001)
[DE94-002991] 06 p2245 N94-24612
Crashworthiness analysis using advanced material models in DYNA3D
[DE94-002988] 06 p2229 N94-24632
Relationship between transition and modes of instability in supersonic boundary layers
[NASA-CR-4562] 06 p2336 N94-24725
Dipolar relaxation in a second-order nonlinear optical interpenetrating polymer network
[AD-A273626] 06 p2258 N94-24732
Measurement of electron temperature and density in the DIII-D neutral beam ion source arc chamber
[DE94-001099] 06 p2553 N94-24746
The role of atmospheric heat transport in the seasonal carbon dioxide cycle 06 p2621 N94-24896
On superconductivity of alpha-(BEDT-TTF)2KHg(SCN)4
[REPT-A-2660] 06 p2564 N94-24978
Lattice dynamics of Ba(1-x)K(x)BiO3 as studied by neutron scattering and computer simulation
[DE93-617053] 06 p2567 N94-25424
Bulletin of National Research Institute for Metals in Fiscal Year 1993, no. 14
[REPT-14] 07 p2722 N94-25544
Preparation of creep data sheet: Material strength data sheet 07 p2723 N94-25548
Study on variation of damage generation mechanism by fatigue on TiAl compounds due to different slip systems 07 p2729 N94-25579
Radiation hardening effects on localized deformation and stress corrosion cracking of stainless steels
[DE94-004308] 07 p2731 N94-25804
Microscopic study of local structure and charge distribution in metallic La2CuO(4+delta)
[DE94-003801] 07 p3050 N94-25817
Formation of three types of quasi-crystals in Al-Pd-Mg system
[REPT-A-2667] 07 p3053 N94-26071
Comparison of technology for high-power laser mirrors and synchrotron radiation mirrors
[DE94-002913] 07 p3035 N94-26278
MBE grown 3 to 5 strain relaxed buffer layers and superlattices characterized by atomic force microscopy
[DE94-002931] 07 p3056 N94-26308
On the electron mobility in slightly compensated heavily doped gallium arsenide at low temperatures
[DE93-634712] 07 p3057 N94-26387
Study of precipitation and recrystallization in Al alloy 2519 by backscattered electron imaging methods
[AD-A274919] 07 p2736 N94-26533
Methodology for first wall design
[DE94-002795] 07 p3045 N94-26861
Interface phenomena in metal-ceramic composites
[AD-A274167] 07 p2709 N94-27125
Process modelling of aluminium alloys. Modelling of the quench sensitivity of alloy AA6082
[PB94-124567] 07 p2741 N94-27325
Annals of the Research Inst. of Environmental Medicine, Nagoya Univ., volume 44
[REPT-44-VOL-44] 07 p2911 N94-27442
Changes in fluid and electrolyte metabolism during water immersion at high or thermoneutral temperature 07 p2912 N94-27445
The mechanism of caloric nystagmus under microgravity. 1: Changes of endolymphatic pressure in the semicircular canal of pigeon by caloric stimulation 07 p2914 N94-27457
Cardiovascular function during thermoneutral head-out water immersion in the elderly 07 p2915 N94-27458
Effects of 40 C hot water immersion for an hour on thermoregulatory functions in humans: Comparison with 34 C thermoneutral immersion 07 p2915 N94-27459
Effects of bathing at 40 C on cardiovascular system in humans: Comparison with 34 C thermoneutral bathing 07 p2918 N94-27473
Effects of 41 C bathing for 20 minutes on cardiovascular and thermoregulatory functions in humans 07 p2918 N94-27474
Monthly variation of physiological and psychological responses under unsteady thermal conditions 07 p2918 N94-27475
Man's ability to adapt himself for the seasonal climatic changes: From viewpoint of anticipation and seasonable behavior 07 p2919 N94-27476
Effect of temperature and recoil-energy spectra on irradiation-induced amorphization in Ca2La8(SiO4)6O2
[DE94-004371] 07 p3067 N94-27602
Creep rupture properties of a nickel-base heat-resistant alloy Hastelloy XR under varying temperature/stress condition
[DE94-701175] 07 p2743 N94-27807
Silicon device performance measurements to support temperature range enhancement
[NASA-CR-195265] 07 p2844 N94-27824
Damage growth in MgAl2O4 crystals by Xe ion irradiations
[DE94-005009] 07 p3069 N94-27828
NASA-UVA light aerospace alloy and structures technology program (LA2ST)
[NASA-CR-195275] 07 p2844 N94-27851
Kinetic parameters from thermogravimetric analysis 07 p2721 N94-27909
Evaluation of high temperature superconductive thermal bridges for space-borne cryogenic infrared detectors 07 p2815 N94-27921
Experimental study on the interactions between a transverse heated supersonic jet and an external supersonic flow 07 p2659 N94-28039
Orthobaric densities and molar volumes of liquids: Aliphatic and cyclic ketones
[ESDU-93010] 07 p2720 N94-28060
Viscosity of liquids: Halogenated ethanes
[ESDU-93012] 07 p2720 N94-28062
Thermal modeling of NiH2 batteries 07 p2862 N94-28113
Determination of thermal properties of commercial Ni-MH cells 07 p2864 N94-28132
Mechanical behavior of amorphous alloys at elevated temperatures 07 p2746 N94-28167
MODIS airborne simulator visible and near-infrared calibration, 1991 FIRE-Cirrus field experiment. Calibration version: FIRE King 1.1
[NASA-TM-104600] 07 p2897 N94-28182

Proposed law of nature linking impacts, plume volcanism, and Milankovitch cycles to terrestrial vertebrate mass extinctions via greenhouse-embryo death coupling
07 p2876 N94-28307

Measurement of volatile metal species at elevated temperatures
[PB94-132321] 08 p3186 N94-28407

Physiological investigations of the isolated rat's liver in hypothermia and hypoxia and their relevance in aircraft incidents above the sea 08 p3382 N94-28439

High temperature polymer dielectric film insulation
08 p3167 N94-28715

Probabilistic material strength degradation model for Inconel 718 components subjected to high temperature, mechanical fatigue, creep and thermal fatigue effects
[NASA-CR-195284] 08 p3318 N94-28840

Low temperature behavior of virgin martensite
[PB94-132925] 08 p3204 N94-29142

Pollutant emissions from and within a model gas turbine combustor at elevated pressures and temperatures
08 p3194 N94-29271

The influence of temperature on microelectronic device failure mechanisms, phase 2
[AD-A275029] 08 p3265 N94-29511

Finite element analysis of axisymmetric deformations of thick thermoviscoplastic targets
08 p3320 N94-29688

Mechanisms and effects of heat generation at the tips of dynamic cracks and notches in metals
08 p3321 N94-29808

An actively cooled floating element skin friction balance for direct measurement in high enthalpy supersonic flows 08 p3289 N94-29824

The effect of temperature on creep and physical ageing of PVC
[NPL-DMM(A)-93] 08 p3217 N94-29885

Antarctic Record, vol. 36, no. 3
[REPT-108] 08 p3363 N94-29978

Theory and application of a Radio-Acoustic Sounding System (RASS) 08 p3367 N94-30869

Computational study of single-expansion-ramp nozzles with external burning
[NASA-TM-106550] 09 p3700 N94-31229

Tensile properties of commercially pure vanadium from room temperature to 1200 C
[DE94-006622] 09 p3641 N94-31581

Experimental evidence for lattice effects in high temperature superconductors
[DE94-006250] 09 p3899 N94-31633

A model of the ion chemistry of electrified convection
09 p3868 N94-31993

Effects of interphases on the mechanical, thermal and hygromechanical response of fiber-reinforced composites 09 p3624 N94-32496

Temperature-humidity-bias aging technique to identify defective surface mount capacitors
[DE94-005354] 09 p3660 N94-32727

Deuterium absorption and material phase characteristics of SAES St198 Zr-Fe alloy
[DE94-008275] 09 p3646 N94-32781

Effect of elevated temperature and cyclic loading on properties and damage modes in ceramic composites
[DE94-008736] 09 p3662 N94-32891

Numerical model of the thermal behavior of an extremity in a cold environment including counter-current heat exchange between the blood vessels
[AD-A278099] 09 p3798 N94-33040

Advanced high frequency partial discharge measuring system
[NASA-CR-195240] 09 p3697 N94-33044

Space flight printed wiring board measling investigation
[NASA-TM-104602] 09 p3732 N94-33101

Development of lightweight ceramic ablators and arc-jet test results
[NASA-TM-108798] 09 p3617 N94-33117

Structural damping studies at cryogenic temperatures
[NASA-TM-109073] 09 p3740 N94-33118

Physics of heat pipe rewetting
[NASA-CR-195902] 09 p3913 N94-33148

Implementation of heaters on thermally actuated spacecraft mechanisms 09 p3607 N94-33320

Characteristics of vaporizing cryogenic sprays for rocket combustion modeling
[NASA-TM-106615] 10 p4055 N94-33605

Experimental observations of thermal spikes in microwave processing of ceramic oxide fibers
[DE94-009348] 10 p4027 N94-33683

Effects of heat acclimation on heat-exercise tolerance in untrained and endurance-trained men wearing NBC protective clothing
[AD-A277522] 10 p4099 N94-33707

Thermal cyclic oxidation behavior of the developed compositionally gradient graphite material of SiC and C in air environment
[DE94-727591] 10 p4027 N94-33872

Wafer-level pulsed-DC electromigration response at very high frequencies
[DE94-008455] 10 p4040 N94-33927

Creep rupture properties under varying load and temperature conditions on a nickel-base heat-resistant alloy strengthened by boron addition
[DE94-727594] 10 p4024 N94-33933

Theoretic study of Green's modes
[INPE-5536-TDI/524] 10 p4090 N94-34202

Analysis of the Shuttle Orbiter reinforced carbon-carbon oxidation protection system
[NASA-TM-104792] 11 p4262 N94-35245

Thermal performance of residential duct systems in basements
[LBL-33962] 11 p4250 N94-35364

Mineralogy of artificially heated carbonaceous chondrites 11 p4352 N94-35477

Improved performance of degraded solar arrays at non-zero sun incidence angles
[AD-A278905] 11 p4282 N94-35804

Properties and applications of powder-filled evacuated-panel superinsulations
[DE94-009169] 11 p4233 N94-35932

Thermodynamic behaviour of tellurium at high temperatures
[DE94-612823] 11 p4240 N94-35960

Predicted optical performance of the High-Altitude Balloon Experiment (HABE) telescope in an adverse thermal environment
[DE94-008949] 11 p4349 N94-35998

Twin spacing and the structural phase transitions in 1:2:3 high-Tc superconductors
[DE94-615647] 11 p4340 N94-36041

Moessbauer mineralogy of calcined Murchison meteorite 11 p4353 N94-36166

Measurement of the decay rate of the SiH feature as a function of temperature 11 p4318 N94-36171

Design and analysis of high-field quasi-continuous magnets
[DE94-000762] 12 p4508 N94-36556

Correlation of analytical and experimental hot structure vibration results
[NASA-TM-104269] 12 p4386 N94-36644

Hot dynamic test rig for measuring hypersonic engine seal flow and durability
[NASA-TM-106507] 12 p4450 N94-36645

Ground and space flight experiments of the effects of light, sound and/or temperature on animals
[NASA-CR-196102] 12 p4478 N94-36986

Some effects of heat release in premixed flames
[DE94-011346] 12 p4409 N94-37199

A fully coupled thermal, chemical, mechanical cookoff model
[DE94-011432] 12 p4428 N94-37201

Measurement uncertainty and feasibility study of a flush airdata system for a hypersonic flight experiment
[NASA-TM-4627] 12 p4383 N94-37378

Effect of temperature on the electron attachment and detachment properties of c-C4F6
[DE94-012750] 12 p4518 N94-37383

Material and design considerations for the carbon armored ITER divertor
[DE94-737854] 12 p4530 N94-37415

A method for thermal analysis of spiral bevel gears
[NASA-TM-106612] 12 p4451 N94-37451

Laminated thin shell structures subjected to free vibration in a hygrothermal environment
[NASA-TM-106600] 12 p4456 N94-37456

Mechanical performance of austempered ductile iron
[AD-A280452] 12 p4420 N94-37758

TEMPERATURE FIELDS
U TEMPERATURE DISTRIBUTION

TEMPERATURE GRADIENTS
NT THERMOCLINES

Coupled thermogravitational and thermocapillary convection in a two-layer fluid system
01 p0105 N94-10101

Boundary layers along horizontal free surfaces due to combined effects of temperature and concentration gradients 01 p0106 N94-10108

A study of the quasibinary Al-Mo-W system. Part 2: A physico-mechanical investigation of the system fabricated under the gravitylessness conditions
01 p0119 N94-10212

Crystal growth in the Zone Melting Facility (ZMF)
01 p0119 N94-10213

Numerical investigations on Marangoni-Benard instability in multi layer systems
01 p0120 N94-10217

Convective motion in a multi-layered system with a free surface 01 p0120 N94-10219

Appearance of convective instabilities caused by liquid-liquid phase separation under small buoyancy forces 01 p0120 N94-10221

A theoretical kinematical study of the gradient of any cosmic scalar field
[DE92-644731] 01 p0425 N94-11136

The role of the geothermal gradient in the emplacement and replenishment of ground ice on Mars
01 p0463 N94-12169

Does the thermal wind exist near the Earth's core boundary? 01 p0283 N94-12217

A user appraisal of ATSR near-real-time products
01 p0252 N94-12516

Investigation of meso-scale fronts, eddies and upwellings in China Seas with AVHRR data
01 p0220 N94-12711

Ceramic matrix composites by microwave assisted CVI
[DE93-012640] 02 p0576 N94-12916

Study of bubble behavior in weightlessness (effects of thermal gradient and acoustic stationary wave) (M-16)
02 p0589 N94-13748

Thermal gradient-induced deflection of a thick-walled cylinder with bending residual stresses
[AD-A266347] 02 p0673 N94-13777

The accuracy of approximating radiative heat transfer using a temperature dependent thermal conductivity
[DE93-013105] 02 p0638 N94-14318

Thermoelastic response of metal matrix composites with large-diameter fibers subjected to thermal gradients
[NASA-TM-106344] 02 p0560 N94-14823

Anomalous ion transport and feedback control
[DE93-018324] 02 p0803 N94-14874

Near-surface temperature gradients and their effects on thermal-infrared emission spectra of particulate planetary surfaces 03 p1260 N94-16236

Experimental segregation of iron-nickel metal, iron-sulfide, and olivine in a thermal gradient: Preliminary results 03 p1243 N94-16288

Implementation of an anisotropic turbulence model in the COMMIX-1C/ATM computer code
[DE93-015541] 03 p1023 N94-16444

Numerical modeling of the temperature gradients and spectra of the plasma armature on Thunderbolt
[AD-A266414] 03 p0878 N94-16552

A surface energy budget model modifying heat flow by foliage effects
[AD-A268598] 03 p1085 N94-17610

Transport in the self-organized relaxed state of ion temperature gradient instability
[DE93-016769] 04 p1584 N94-17983

Geothermal activity near Clearlake, California
[DE93-016627] 04 p1485 N94-18894

Finite difference program for calculating hydride bed wall temperature profiles
[DE93-019272] 04 p1523 N94-19005

A laboratory model of a cooled continental shelf
[AD-A270862] 04 p1500 N94-19792

The distribution of ground ice on Mars
05 p2090 N94-20394

Stability curves for a thermoacoustic prime mover
[AD-A272607] 05 p1968 N94-21422

Low Reynolds-number turbulent boundary layers
[AD-A272011] 05 p1803 N94-21459

Shock temperature measurements of iron to 350 GPa
[DE94-001058] 05 p1695 N94-22024

Kinetic resonance damping rate of the toroidal ion temperature gradient mode
[DE94-001234] 05 p1998 N94-22561

Fluid simulations of Delta T(sub e)-driven turbulence and transport in boundary plasmas
[DE94-001304] 05 p1999 N94-22566

Electron temperature gradient driven instability in the tokamak boundary plasma
[DE94-001307] 05 p1999 N94-22596

Experimental evaluation of camouflage effectiveness in the thermal infrared
[FEL-93-A043] 06 p2381 N94-22896

Nonlinear ion-mixing-mode particle transport in the dissipative trapped electron regime
[DE94-000989] 06 p2533 N94-23435

Modelling TOVS radiances of synoptic systems
[NASA-CR-194847] 06 p2408 N94-23620

A nighttime structure model of atmospheric optical turbulence, c2(n), derived from thermosonde and high resolution rawinsonde measurements
[AD-A273803] 06 p2406 N94-25537

Kinetic resonance damping rate of the toroidal ion temperature gradient mode
[DE94-003511] 07 p3041 N94-25823

A transient symmetrical method for the measurement of temperature dependent thermal diffusivity
[VTT-TIED-1452] 07 p3008 N94-26256

Development of detection technique for fatigue crack due to thermal stratification phenomena in RCS piping
[DE93-632968] 07 p2838 N94-26400

NASA-UVA light aerospace alloy and structures technology program (LA2ST)
[NASA-CR-195275] 07 p2844 N94-27851

Lock-up failure of a four-bar linkage deployment mechanism 08 p3163 N94-29646
Theory and application of a Radio-Acoustic Sounding System (RASS) 08 p3367 N94-30869
Nozzle material requirements and the status of intermetallic matrix composites 10 p3979 N94-33513
Rheology, tectonics, and the structure of the Venus lithosphere 11 p4367 N94-35479
Predicted optical performance of the High-Altitude Balloon Experiment (HABE) telescope in an adverse thermal environment
[DE94-008949] 11 p4349 N94-35998
Isotope scaling and eta(i) mode with impurities in tokamak plasmas
[DE94-012763] 12 p4529 N94-37361

TEMPERATURE INDICATORS
U INDICATING INSTRUMENTS
U TEMPERATURE MEASURING INSTRUMENTS

TEMPERATURE INSTRUMENTS
U TEMPERATURE MEASURING INSTRUMENTS

TEMPERATURE INVERSIONS
NT CENTRIFUGING STRESS
Two-dimensional modeling of thermal inversion layers in the middle atmosphere of Mars 06 p2622 N94-24900
Application of differential inversion to DMSP microwave sounder data
[AD-A278575] 11 p4294 N94-36186

TEMPERATURE MEASUREMENT
Low cost and thermally stable sandwich design for FIRST 01 p0057 N94-10009
Experimental analysis of Benard-convection by the combined application of liquid crystals and PIV 01 p0106 N94-10109
The pyrene laser induced fluorescence technique as a diagnostic tool for combustion thermometry in microgravity 01 p0107 N94-10113
A new method for hysteresis measurements developed for C(sub v) measurements at the critical point during the D2-mission 01 p0107 N94-10114
High temperature processing and diagnostic technologies for microgravity applications 01 p0110 N94-10130
TEXUS 28 experiment: Convections and crystal growth of Ge:Ga. Analysis of temperature measurements 01 p0114 N94-10184
Ground results of the Mephisto program: Benefits and space experiments orientation 01 p0086 N94-10197
Local measurement of temperatures and concentrations: A review for hypersonic flows 01 p0004 N94-10434
Experiments in ultracold collisions
[DE93-012110] 01 p0365 N94-11029
Electron temperature measurements of x ray laser plasmas
[DE93-011874] 01 p0389 N94-11074
A laboratory model of a hydrogen/oxygen engine for combustion and nozzle studies
[NASA-TM-106281] 01 p0047 N94-11252
Heat flux measurements on ceramics with thin film thermocouples
[NASA-TM-106305] 01 p0170 N94-11310
A detailed study of the photo-injection annealing of thermally diffused InP solar cells 01 p0048 N94-11381
The excitation of cyanogen and ionized carbon in interstellar and extragalactic gas clouds 01 p0426 N94-11582
Overview of the 1989 Wind Tunnel Calibration Workshop
[NASA-TP-3393] 01 p0034 N94-11869
Trouble areas in the IRT measurement of the Earth surface temperature 01 p0193 N94-11910
Ocean measuring experiments using optical fiber distributed temperature sensor 01 p0172 N94-11968
Remote sensing of subsurface water temperature profile and backscattering coefficient in the China Sea by Ocean Lidar (OLIDAR) 01 p0203 N94-11970
Calorimetric thermometry of meteoritic troilite: A feasibility study 01 p0428 N94-12025
Establishing baseline data for an experimental appratus that measures heat transfer under conditions of oscillating pressure and flow
[NASA-CR-193772] 01 p0413 N94-12343
Preliminary validation of ATSR sea surface temperatures near the Faeroes 01 p0253 N94-12519
Ohmic heating of composite candidate graphite-fiber/coating combinations
[NASA-TM-4491] 02 p0554 N94-12871
Two temperature modeling and experimental measurements of laser sustained hydrogen plasmas
[AD-A265750] 02 p0796 N94-13039
The corrosion behavior of 8001 Al under heat-transfer conditions in an aqueous loop system
[DE93-013450] 02 p0569 N94-13242
Adaptive control of interface by temperature and interface profile feedback in transparent multi-zone crystal growth furnace
[NASA-CR-194140] 02 p0762 N94-13253
An experimental investigation of the redistribution of gas stream total temperature in a high turning angle transonic planar cascade
[ISBN-0-315-60791-2] 02 p0502 N94-13369
Experimental measurement of local heat transfer coefficients over discrete roughened plates using infrared thermography 02 p0635 N94-13652
Recent flight-test results of optical airdata techniques
[NASA-TM-4504] 02 p0517 N94-13791
High frame rate thermal imager for hypersonic wind tunnel applications
[ONERA-NT-1992-12] 02 p0650 N94-14009
NASA metrology and calibration, 1993
[NASA-TM-109280] 02 p0597 N94-14410
Two color holographic interferometry for microgravity application
[NASA-CR-194424] 02 p0651 N94-14447
Investigation of the feasibility of optical diagnostic measurements at the exit of the SSME
[NASA-CR-193832] 02 p0553 N94-14682
Time resolved measurement of electron temperatures of exploding foil x ray laser plasmas
[DE93-017161] 02 p0803 N94-14894
Description of cooling water calorimetry and wall thermometry diagnostic at tokamak ASDEX-Upgrade
[IPP-5/46] 03 p1200 N94-14966
Measurement of the specific heat capacity of the electron-beam graphite calorimeter
[NPL-RSA(EXT)-40] 03 p1031 N94-15018
Temperature propagation in near-critical fluids prior to and during separation 03 p0944 N94-15165
Optical fiber spectroscopy: A study of the luminescent properties of the europium ion for thermal sensors
[NASA-CR-194576] 03 p1189 N94-15647
Simultaneous measurement of temperature and strain using four connecting wires
[NASA-TM-104271] 03 p1032 N94-15754
Temperature measurements 03 p1037 N94-15804
Pyroxene equilibration temperatures in metamorphosed ordinary chondrites 03 p1242 N94-16224
The cooling rates of pahoehoe flows: The importance of lava porosity 03 p1103 N94-16282
Analysis of TIMS performance subjected to simulated wind blast 03 p1063 N94-16598
Sensitivity of blackbody reference panels to wind blast 03 p1063 N94-16599
An algorithm for the estimation of bounds on the emissivity and temperatures from thermal multispectral airborne remotely sensed data 03 p1064 N94-16603
Considerations for the use of the modified line reversal technique for gas temperature measurement
[DE93-015752] 04 p1576 N94-17857
Mixture distributions in climatological research
[DE93-014125] 04 p1488 N94-17942
Boundary layer heat budgets from wind profiler/RASS data: A feasibility study
[DE93-013187] 04 p1489 N94-18052
Development of a multi-point two-color pyrometer for tube and wall temperature and emissivity measurement at the CFFF
[DE93-014716] 04 p1429 N94-18207
Flame structure studies of a lean 20-torr H2/N2O/Ar flame employing molecular beam mass spectrometry
[AD-A268889] 04 p1349 N94-18456
Fundamentals of infrared thermography 04 p1431 N94-18648
Heat transfer quantitative characterization: Passive and active methods 04 p1431 N94-18650
Liquid crystal heat transfer measurements 04 p1432 N94-18653
The application of liquid crystal techniques to determine heat transfer rates 04 p1432 N94-18654
Imaging and blackbody emission spectra of hot particulates generated during laser ablation
[DE93-015818] 04 p1439 N94-18724
Substrate temperature measurement and control during thermal plasma CVD
[DE93-040305] 04 p1433 N94-19135
Construction and evaluation of an environmental chamber for calibration of temperature and pressure sensors for laser interferometers
[PB93-197838] 04 p1322 N94-19332
Global and regional comparative performance of linear and nonlinear satellite multichannel sea surface temperature algorithms
[AD-A270475] 05 p1837 N94-20028
Acoustic monitoring of global ocean variability
[AD-A271998] 05 p1863 N94-21366
Fluorescent microthermographic imaging
[DE93-040332] 05 p1810 N94-22000
Shock temperature measurements of iron to 350 GPa
[DE94-001058] 05 p1695 N94-22024
Overview of microphysical and state parameter measurements from FIRE 2 05 p1871 N94-22293
Alloying studies in U(1-x)Th(x)Pd2Al3 (0 (le) x (le) 1)
[DE94-000807] 05 p2036 N94-22584
Measurement Technology for Flight Tests
[ILR-MITT-256(1991)] 05 p1639 N94-22597
Surface hot film measurements at ATTAS laminar glove 05 p1639 N94-22598
Testing of a multisensor hot film technique in wind tunnel and free flight 05 p1639 N94-22599
A field evaluation of remote sensor measurements of wind, temperature, and moisture for ARM integrated sounding system research
[DE94-000565] 06 p2381 N94-23001
Droplet turbulence interactions under subcritical and supercritical conditions 06 p2211 N94-23036
Fiber optic temperature sensor using a Y2O2S:Eu thermographic phosphor
[DE94-000331] 06 p2543 N94-23461
High temperature, oxidation resistant noble metal-Al alloy thermocouple
[NASA-CASE-LEW-15515-1] 06 p2343 N94-23826
Comparison between 1-minute and 15-minute averages of turbulence parameters 06 p2528 N94-24218
White-light, pressure, and temperature interferopolarimetric sensor featuring optical fibers
[PB93-199792] 06 p2545 N94-24631
Measurement of electron temperature and density in the DIII-D neutral beam ion source arc chamber
[DE94-001099] 06 p2553 N94-24746
Containerless measurements on liquids at high temperatures 06 p2238 N94-25125
Liquidus temperature and optical properties measurement by containerless techniques 06 p2247 N94-25126
Temperature measurement using infrared imaging systems during turbine engine altitude testing
[NASA-TM-105871] 06 p2193 N94-25184
Hydride thermodynamic machines
[VTT-JULK-768] 06 p2571 N94-25416
Analysis of the effects of wake passage on heat transfer in a linear turbine cascade
[AD-A273729] 06 p2339 N94-25446
Interpreting the implied meridional oceanic energy transport in AMIP
[DE94-001538] 07 p2898 N94-26072
Gordon Research Conference on the Physics and Chemistry of Laser Diagnostics in Combustion
[AD-A274609] 07 p2716 N94-26893
Shine through measurements with hydrogen beam in JT-60
[DE94-701113] 07 p3047 N94-27699
Uncertainties in the characterization of the thermal environment of a solid rocket propellant fire
[DE94-002023] 07 p2760 N94-27719
Ice surface temperature retrieval from AVHRR, ATSR, and passive microwave satellite data: Algorithm development and application
[NASA-CR-195276] 07 p2851 N94-27849
The validation of ATSR measurements with in situ sea temperatures
[DE94-003195] 07 p2852 N94-27875
Objective analysis of a coastal ocean eddy using satellite AVHRR and in situ hydrographic data
[AD-A275715] 08 p3376 N94-28642
Global Acoustic Mapping of Ocean Temperatures (GAMOT)
[AD-A275777] 08 p3376 N94-28740
Heat flux instrumentation for Hyflite thermal protection system
[NASA-CR-195731] 08 p3286 N94-28824
System for improving measurement accuracy of transducer by measuring transducer temperature and resistance change using thermoelectric voltages
[NASA-CASE-ARC-12014-1] 08 p3287 N94-29361
Determining noise temperatures in beam waveguide systems 08 p3249 N94-29657
Non-invasive temperature measurements using electron paramagnetic resonance spectroscopy 08 p3198 N94-29881
A low noise silicon detector preamplifier system for room temperature x ray spectroscopy
[REPT-93-058] 08 p3291 N94-30930
Profiling ALACE instruments
[AD-A277246] 09 p3789 N94-32321
Design of a two dimensional planer pressurized air labyrinth seal test rig
[AD-A277232] 09 p3726 N94-32370
Homogeneous global mean temperature time series
[DE94-002194] 09 p3766 N94-32690
Radiometry spot measurement system
[NASA-TM-106561] 09 p3883 N94-32777
High resolution molecular spectroscopy of atmospheric species
[AD-A278382] 09 p3776 N94-33351

Measurement of the coolant channel temperatures and pressures of a cooled radial-inflow turbine
[NASA-TM-106594] 10 p3997 N94-33706
A new type of temperature and humidity detection-control system 10 p4057 N94-34365
Correction-free pyrometry in radiant wall furnaces
[NASA-CASE-NPO-18655-1-CU] 10 p4056 N94-35114
Multiwavelength pyrometer for gray and non-gray surfaces in the presence of interfering radiation
[NASA-CASE-LEW-15250-1] 11 p4269 N94-35383
Measurement of a surface heat flux and temperature 11 p4231 N94-36407
Laser-saturated fluorescence measurements in laminar sooting diffusion flames
[NASA-CR-191025] 12 p4508 N94-36643
Methodologies for thermal and mechanical testing of TMC materials 12 p4401 N94-36659
Fiber optic (flight quality) sensors for advanced aircraft propulsion
[NASA-CR-191195] 12 p4387 N94-37401
Study on the measurement uncertainty of noise properties of a millimeter wave amplifier
[PB94-170917] 12 p4510 N94-37632

TEMPERATURE MEASURING INSTRUMENTS
NT BATHYTHERMOGRAPHS
NT OPTICAL PYROMETERS
NT PNEUMATIC PROBES
NT PYROMETERS
NT RADIATION PYROMETERS
NT TEMPERATURE PROBES
NT THERMOMETERS
The High Precision Thermostat HPT-HYDRA 01 p0109 N94-10124
A comparison of ATSR and shipboard radiometer SST measurements along transects between the UK and the Antarctic 01 p0253 N94-12518
Construction and evaluation of an environmental chamber for calibration of temperature and pressure sensors for laser interferometers
[PB93-197838] 04 p1322 N94-19332
Radiometry spot measurement system
[NASA-TM-106561] 09 p3883 N94-32777

TEMPERATURE PROBES
Ocean measuring experiments using optical fiber distributed temperature sensor 01 p0172 N94-11968

TEMPERATURE PROFILES
The electron beam furnace: A new facility for materials science research 01 p0109 N94-10126
Variations of the temperature profile in the gradient furnace GFQ within a cylindrical sample used for directional solidification 01 p0114 N94-10181
Effects of satellite spectral resolution and atmospheric water vapor on retrieval of near-ground temperatures
[AD-A264920] 01 p0245 N94-11651
Remote sensing of subsurface water temperature profile and backscattering coefficient in the China Sea by Ocean Lidar (OLIDAR) 01 p0203 N94-11970
Study of possible mechanisms of instability due to heat transfer
[INPE-5448-TDI/494] 02 p0628 N94-12966
Pool boiling: Single bubble experiment 03 p0944 N94-15160
Static characteristics of a conduction and radiation dominated electric arc in nitrogen
[DE93-627106] 03 p1204 N94-17311
An investigation of the Ground-Based High-Resolution Interferometer Sounder (GB-HIS) in a costal marine environment
[AD-A268052] 03 p1114 N94-17503
A surface energy budget model modifying heat flow by foliage effects
[AD-A268598] 03 p1085 N94-17610
Dynamic behavior of an electric arc gas discharge
[DE93-630197] 03 p1205 N94-17635
An atlas of bathy-thermograph temperature cross-sections for Coral and Tasman Sea transects from 1960 to 1987
[AD-A268775] 04 p1497 N94-18329
Flame structure studies of a lean 20-torr H2/N2O/Ar flame employing molecular beam mass spectrometry
[AD-A268889] 04 p1349 N94-18456
Finite difference program for calculating hydride bed wall temperature profiles
[DE93-019272] 04 p1523 N94-19005
Impact of copper vapour contamination on argon arcs 05 p1994 N94-21053
Low Reynolds-number turbulent boundary layers
[AD-A272011] 05 p1803 N94-21459
A pressurized thermogravimetric analyzer for use in studies of gas/solid systems
[DE94-001224] 06 p2342 N94-22989
Spatial and temporal variability of soil temperature, moisture and surface soil properties
[NASA-CR-194109] 06 p2401 N94-23337
An analysis of Solar Mesospheric Explorer temperatures for the upper stratosphere and mesosphere
[NASA-CR-194861] 06 p2626 N94-23626
Retrieval of temperature profiles from Martian infrared spectra 06 p2620 N94-24893
Examination of the physical, electrical, and microwave evolution of water into young sea ice
[AD-A273559] 06 p2418 N94-24918
Piecewise least squares fitting technique using finite interval method with Hermite polynomials
[VTT-PUBS-135] 07 p2990 N94-25733
Modelling the mass migration phenomena in partially frozen heat pipes
[DE94-002716] 07 p2797 N94-27709
Predictions of momentum and scalar fields in a jet in cross-flow using first and second order turbulence closures 07 p2803 N94-28025
On the temperature distribution near a cold surface
[AD-A275162] 08 p3332 N94-29288
Fronts at the confluences of spring-fed streams with Joekulsa a Fjoellum: Possibly thermal bars?
[MATHS-REPT-A-198] 08 p3333 N94-29528
Atmospheric moisture fields derived by satellite observations over the tropical Pacific Ocean 08 p3375 N94-30863
Effects of the deep tropical convection in the large scale atmospheric flow 09 p3778 N94-30994
Multiwavelength search for protoplanetary disks 09 p3599 N94-31430
Profiling ALACE instruments
[AD-A277246] 09 p3789 N94-32321
Mars atmospheric dust properties: A synthesis of Mariner 9, Viking, and Phobos observations 09 p3945 N94-33200
Degradation of radiant ceramic structures in combustion atmospheres
[PB94-157849] 10 p4030 N94-34601
Probing flame chemistry with MBMS, theory, and modeling
[DE94-011224] 12 p4413 N94-37623

TEMPERATURE RATIO
The effects of radiation transport on line ratios used as temperature and density diagnostic
[DE93-016424] 03 p1205 N94-17663

TEMPERATURE SENSORS
NT THERMISTORS
A laboratory model of a hydrogen/oxygen engine for combustion and nozzle studies
[NASA-TM-106281] 01 p0047 N94-11252
Arctic internal waves (CEAREX)
[AD-A265822] 03 p1111 N94-15139
Optical fiber spectroscopy: A study of the luminescent properties of the europium ion for thermal sensors
[NASA-CR-194576] 03 p1189 N94-15647
Properties of thin films for high temperature flow sensors
[NASA-CR-191526] 03 p0967 N94-16541
Synoptic ocean prediction experiment. EN216 CTD section data report
[AD-A268903] 04 p1497 N94-18230
Description of an infrared zoomcollimator
[FEL-93-A034] 04 p1580 N94-19424
The marine light-mixed layer experiment cruise and data report: R/V endeavor cruise EN-224, mooring deployment, 27 April-1 May 1991: Cruise EN-227, mooring recovery, 5-23 September 1991
[AD-A271175] 05 p1864 N94-20186
On demand, non-halon, fire extinguishing systems
[AD-D015957] 05 p1714 N94-20355
Army aircraft fire-detection systems operation and reliability
[AD-A271327] 05 p1641 N94-20912
Fiber optic temperature sensor using a Y2O2S:Eu thermographic phosphor
[DE94-000331] 06 p2543 N94-23461
White-light, pressure, and temperature interferopolarimetric sensor featuring optical fibers
[PB93-199792] 06 p2545 N94-24631
Thermistor controlled current source versatile temperature sensor
[AD-D015979] 06 p2345 N94-25037
Heat flux instrumentation for Hyflite thermal protection system
[NASA-CR-195731] 08 p3286 N94-28824
Active thermal isolation for temperature responsive sensors
[NASA-CASE-LAR-14612-1] 10 p4054 N94-35074
Fiber optic (flight quality) sensors for advanced aircraft propulsion
[NASA-CR-191195] 12 p4387 N94-37401

TEMPLATES
Developmental testing of a prototype all-reflection Michelson interferometer
[AD-A269064] 04 p1430 N94-18406
Template based low data rate speech encoder
[AD-A270900] 04 p1392 N94-19748
An insensitive algorithm for template matching with correlation 05 p1793 N94-22249
Template synthesis of metal microtubule ensembles utilizing chemical, electrochemical, and vacuum deposition techniques
[AD-A274676] 07 p2715 N94-26444
Three dimensional object recognition using a complex autoregressive model
[AD-A274388] 07 p2995 N94-26829
An algorithm for stereo correspondence problems on the analogy of human vision
[NAL-TR-1185] 07 p2940 N94-27584
Template synthesized nanoscopic gold particles: Optical spectra and the effects of particle size and shape
[AD-A275378] 08 p3197 N94-29312
A collection of tools in support of automatic differentiation
[DE94-010104] 11 p4314 N94-35704

TEMPORAL DISTRIBUTION
Distribution of mineral aerosols over the North Pacific 01 p0204 N94-11976
Spatial and temporal variability of precipitation and chemistry: Case studies from the frontal boundary study
[DE93-007883] 02 p0708 N94-13910
Chemistry and transport in a multi-dimensional model
[NASA-CR-194425] 02 p0716 N94-13969
Potential evapotranspiration in Belgium: Spatial and temporal variability
[PUBL-SER-A-130] 02 p0686 N94-13994
Characterization of spatial and temporal variability of phytoplankton blooms in coastal waters
[AD-A267102] 03 p1116 N94-15633
A decade's overview of Io's volcanic activity 03 p1245 N94-16386
Temporal variation in spectral detection thresholds of substrate and vegetation in AVIRIS images 03 p1073 N94-16706
Arctic and Antarctic sea ice, 1978-1987: Satellite passive-microwave observations and analysis
[NASA-SP-511] 03 p1114 N94-17439
Observations of comets with the IUE
[NASA-CR-193652] 04 p1624 N94-17843
Spatiotemporal variability of non-urban ozone concentrations over the eastern United States and its potential replication by satellite data
[PB93-191328] 04 p1476 N94-19065
Radial evolution of the solar wind turbulence with application to charged particle transport
[NASA-CR-194081] 04 p1629 N94-19427
Spatial and temporal variations of satellite microwave measurements of latent heat release in tropic cyclones due to environmental forcing obtained from a numerical model
[AD-A267947] 05 p1865 N94-20482
Spatial and temporal variability of soil temperature, moisture and surface soil properties
[NASA-CR-194109] 06 p2401 N94-23337
Dynamics of the atmosphere of Mars: Review of some outstanding problems 06 p2620 N94-24888
An analysis of gamma ray burst time histories
[NASA-CR-195191] 06 p2629 N94-25199
Use of satellite data to improve parameterization of spatial and temporal variations of gaseous dry deposition in regional-scale models
[DE94-005110] 08 p3334 N94-30022
Time and frequency technology at NIST 08 p3468 N94-30641
Spatio-temporal complexity and large-scale structures in problems of continuum mechanic
[AD-A278473] 10 p4044 N94-33702

TEMPORAL LOGIC
Negation by default for framing in temporal logic programming
[PB94-148848] 10 p4107 N94-33978
Projection in temporal logic programming
[PB94-148814] 10 p4108 N94-34123

TEMPORAL RESOLUTION
SAR interferometry experiments with ERS-1 01 p0237 N94-11735
Segmented land use classification of multitemporal ERS-1 SAR data using a majority filter 01 p0245 N94-12472
Mapping a dynamic playa surface using multitemporal ERS-1 SAR data: First results 01 p0246 N94-12474
Snow and glacier investigations by ERS-1 SAR: First results 01 p0247 N94-12481
Per-field filtering and classification of multitemporal ERS-1 SAR imagery 01 p0247 N94-12485
Extraction of plant and soil parameters from multitemporal ERS-1 SLC data of the Freiburg test site 01 p0248 N94-12491
Temporal monitoring of soil moisture using ERS-1 SAR data 01 p0249 N94-12493
TREES project: A case study on the use of multi-temporal ERS-1 SAR data and SPOT data for monitoring tropical ecosystems 01 p0249 N94-12497

High time resolution studies of binary x ray pulsars
[NASA-CR-194395] 02 p0832 N94-13894
Supervised classification of remotely sensed images
[DLR-FB-92-07] 02 p0700 N94-14428
How to squeeze high quantum efficiency and high time resolution out of a SPAD 03 p0914 N94-15571
An RS-170 to 700 frame per second CCD camera
[DE93-018367] 04 p1432 N94-18828
Spectrally and temporally resolved laser emission from vertical cavity surface emitting lasers
[DE93-019410] 04 p1442 N94-19563
Ultrafast scanning microscopy
[DE93-040121] 05 p1985 N94-20320
Measurement of thermal-hydraulic parameters in two-phase flow using flow visualization image analysis
[DE93-006255] 05 p1805 N94-22269
Dimensional analysis of acoustically propagated signals 06 p2528 N94-24217
Temporal behavior of the electron density profile during limiter biasing in the HYBTOK-2 tokamak
[NIFS-257] 06 p2552 N94-24456
Dynamic measurements of thermophysical properties of metals and alloys at high temperatures by subsecond pulse heating techniques 06 p2247 N94-25124
Evaluation of image quality 06 p2443 N94-25514
Morphodynamics of inter-tidal areas: The Wadden Sea
[NLR-TP-92356-U] 07 p2851 N94-27555
Evolution of miniature detectors and focal plane arrays for infrared sensors 08 p3237 N94-29781
Development of high time-resolution laser flash equipment for thermal diffusivity measurements using miniature-size specimens
[AD-B183270L] 08 p3295 N94-30186
Multitemporal analysis of a braiding river: The advanced study of 1992
[NLR-TP-93100-U] 08 p3335 N94-30942
A case study comparing multi-temporal ERS-1 SAR data and SPOT data for tropical forest mapping 09 p3753 N94-32556
A comparison of modeled and observed ocean mixed layer behavior in a sea breeze influenced coastal region
[AD-A277911] 10 p4092 N94-33922
Computation of dendrites using a phase field model
[PB94-160744] 11 p4236 N94-35736
Ultrafast readout of scintillating fibers using upgraded position-sensitive photomultipliers
[DE94-010419] 11 p4269 N94-36095

TENDONS

Minimization of carpal tunnel syndrome
[AD-A276409] 09 p3795 N94-31363

TENSILE CREEP

The effect of temperature on creep and physical ageing of PVC
[NPL-DMM(A)-93] 08 p3217 N94-29885
Toughening mechanisms in the high strain rate deformation of rubber-modified polymer glasses 09 p3653 N94-31942
High-temperature deformation and fracture toughness of duplex ceramic microstructures 09 p3653 N94-31945

TENSILE DEFORMATION

The effects of texture and strain on the r-va lue of heavy gauge tantalum plate
[DE94-000690] 06 p2242 N94-23541
An approximate solution for interlaminar stresses in laminated composites 09 p3621 N94-31901
Bond stress-slip characteristics of FRP rebars
[AD-A277191] 09 p3623 N94-32070

TENSILE PROPERTIES

NT TENSILE STRENGTH
Physical properties of injection molded liquid crystal polymers and high temperature engineering polymers
[AD-A264912] 01 p0087 N94-10508
The effect of processing on the microstructure and tensile properties of a (gamma)-TiAl based alloy
[DE93-013221] 01 p0084 N94-11488
Ceramic technology project database
[DE93-012432] 01 p0091 N94-11673
Tensile properties of LE-7 engine material with welded joint
[NAL-TR-1188] 02 p0570 N94-13460
UK interlaboratory tensile tests on Al alloy/SiC particulate metal matrix composites
[NPL-DMM(A)-77] 02 p0570 N94-13666
Effect of thermal processing practices on the properties of superplastic Al-Li alloys
[NASA-CR-4548] 02 p0574 N94-14850
A reexamination of grain boundary fracture in Ni3Al: Environmental and alloying effects
[DE93-015431] 03 p1208 N94-16063
The effect of long-term aging on the impact properties of modified 9Cr-1Mo steel
[DE93-015453] 03 p0957 N94-16068
The effect of irradiation on the mechanical properties of 6061-T651 aluminum
[DE93-015825] 03 p0958 N94-16168
The processing and mechanical properties of high temperature/high performance composites. Book 2: Coonstituent properties and macroscopic performance
[AD-A266395] 03 p0935 N94-16484
The Hall-Petch relationship and mechanisms of fracture in B2 compounds
[DE93-018887] 04 p1359 N94-18182
Effects of irradiation temperature on embrittlement of nuclear pressure vessel steels
[DE93-015428] 04 p1359 N94-18245
Continuum modeling of materials that can undergo martensitic phase transitions
[AD-A268767] 04 p1360 N94-18386
Development of ductile Fe3Al-based aluminides
[DE93-017865] 04 p1362 N94-18938
Tensile properties of as-cast iron-aluminide alloys
[DE93-017852] 04 p1363 N94-18975
Effects of irradiation temperature on Charpy and tensile properties of high-copper, low upper-shelf, submerged-arc welds
[DE93-017858] 04 p1445 N94-19047
Rapid heating tensile testing update: 304L stainless steel
[DE93-018770] 05 p1688 N94-19942
Investigation of cracking and erratic behavior of the uranium-titanium alloy
[DE93-018591] 05 p1688 N94-19957
Weldalite (tm) 049 (Al 2095-T8): Anisotropy effects at cryogenic conditions
[AD-A272658] 05 p1691 N94-21188
Applicability and performance benefits of XD (Tradename) titanium aluminides to expendable gas turbine engines
[AD-A272998] 05 p1648 N94-21268
Tensile and shear fracture behavior of fiber reinforced plastics at 77K irradiated by various radiation sources
[DE93-040280] 05 p1706 N94-21542
Tensile properties of 21-6-9 stainless steel at elevated temperatures
[DE94-001852] 06 p2240 N94-23017
Effect of neutron irradiation on tensile properties of V-Cr-Ti alloys
[DE94-001433] 06 p2240 N94-23194
The effects of texture and strain on the r-va lue of heavy gauge tantalum plate
[DE94-000690] 06 p2242 N94-23541
Ceramic matrix composites: Challenges and opportunities 06 p2255 N94-24230
Test methods for composites: A status report. Volume 3: Shear test methods
[AD-A273561] 06 p2230 N94-25163
Structural analysis of a frangible nut used on the NASA Space Shuttle
[DE94-003672] 07 p2821 N94-25811
Effects of post-fabrication processing on the tensile properties of centrifugally cast SiC particulate reinforced aluminum composites
[AD-A274865] 07 p2707 N94-26190
Titanium 1992: Science and Technology, volume 1
[AD-A274798-VOL-1] 07 p2739 N94-26799
Aluminum alloy 8090-T8771 thick plate material characterization
[AD-A274146] 07 p2987 N94-27077
Effects of thermomechanical processing on tensile and long-time creep behavior of Nb-1 percent Zr-0.1 percent C sheet
[NASA-TM-106319] 08 p3202 N94-28822
An analysis of the microstructure and reinforcement distribution of an extruded particle-reinforced Al 6061-10 volume percent Al2O3 metal matrix composite
[AD-A275050] 08 p3178 N94-29166
Low dielectric polyimide fibers
[NASA-CASE-LAR-14526-1] 08 p3214 N94-29359
Tensile properties of commercially pure vanadium from room temperature to 1200 C
[DE94-006622] 09 p3641 N94-31581
Evaluating in-plane elastic constants of damaged carbon-epoxy laminates using a quantitative ultrasonic technique 09 p3621 N94-31793
Boron and hydrogen in Ni3Al. Part 2: Mechanical testing of bicrystals
[DE94-007441] 09 p3904 N94-32606
Influence of volume fraction of component materials and interlayer bond strength on fracture toughness of multi-layer Al 6090-25 volume percent SiCp and Al 5182 laminates
[DE94-007141] 09 p3626 N94-32665
Properties of TMC processed by fibre coating and hiping 12 p4401 N94-36656
Metal matrix composites: Analysis of simple specimens and model components under creep and fatigue loading 12 p4402 N94-36661
Mechanical performance of austempered ductile iron
[AD-A280452] 12 p4420 N94-37758

TENSILE STRENGTH

Design with high strength steel: A case of failure and its implications 01 p0058 N94-10017
Mechanical properties of magnesium/carbon composites developed by hot pressing under medium pressure 01 p0059 N94-10024
High temperature stability, interface bonding, and mechanical behavior in (beta)-NiAl and Ni3Al matrix composites with reinforcements modified by ion beam enhanced deposition
[DE93-013977] 01 p0398 N94-11115
Thermal testing of aluminized Mylar
[NASA-TM-108414] 01 p0089 N94-11175
Interface considerations in Al2O3/NiAl composite
[NASA-CR-191167] 01 p0066 N94-11202
The processing and mechanical properties of high temperature/high performance composites. Book 3: Coonstituent properties and macroscopic performance
[AD-A266396] 03 p0935 N94-16485
The processing and mechanical properties of high temperature/high performance composites. Book 4: Coonstitutive laws and design
[AD-A266397] 03 p0935 N94-16528
Weaving multi-layer fabrics for reinforcement of engineering components 03 p0937 N94-16850
Effect of tow alignment on the mechanical performance of 3D woven textile composites 03 p0937 N94-16851
New textile composite materials development, production, application 03 p0938 N94-16853
Influence of the loading rate on the endurance and deformability of cement matrix composites
[IFTR-1/1992] 03 p1060 N94-17052
Fiber strength utilization in carbon/carbon composites
[AD-A267713] 03 p0940 N94-17271
Tensile and stress-rupture behavior of hafnium carbide dispersed molybdenum and tungsten base alloy wires
[NASA-TM-106350] 03 p0962 N94-17652
Strength and deformation properties of basaltic lava flows on planetary surfaces 05 p1862 N94-20747
Tensile strength of fiber reinforced plastics at 77K irradiated by various radiation sources
[DE93-040826] 05 p1709 N94-22008
Humidity effects on soluble core mechanical and thermal properties (polyvinyl alcohol/microballoon composite) type CG extendospheres, volume 2
[NASA-CR-193893] 06 p2229 N94-24224
Assessment of impact damage of composite rocket motor cases
[NASA-CR-195143] 06 p2220 N94-24595
The mechanical property data base from an Air Force/Industry Cooperative Test Program on advanced aluminum alloys (7064 and CW67)
[AD-A273741] 06 p2251 N94-25531
Study on ferromagnetic field magnet using strong and highly conductive material 07 p2725 N94-25559
Study on alloy films for hydrogen separation 07 p2726 N94-25565
Inert strength of pristine silica glass fibers
[DE94-004685] 07 p2750 N94-26247
Fatigue resistance under tension-compression of laminates IM6/5245C and AS4/3501-6
[IAR-CR-25] 07 p2708 N94-26711
Processing and mechanical properties of laminated metal composites of Al 6090-25 volume percent SiC(sub p) and Al 5182
[DE94-001070] 07 p2708 N94-26930
High temperature tension test equipment of heat resistant composite materials
[NAL-TM-652] 07 p2710 N94-27255
Formation and high mechanical strength of Al-based alloys containing a nanoscale icosahedral phase as a main constituent 07 p2746 N94-28171
Microstructure/property relationships for SCS6/Timetal 21-S composite
[AD-A275056] 08 p3178 N94-29135
Numerical analysis of dynamic direct tension and direct compression tests
[AD-A275255] 08 p3319 N94-29433
Preliminary evaluation of hybrid titanium composite laminates
[NASA-TM-109095] 08 p3180 N94-29472
Delamination growth in composites under cyclic loads 08 p3183 N94-30256
Controlling the material properties of in vitro collagen through directed orientation and cross-linking of fibrils 08 p3221 N94-30797
Ceramic Technology Project database
[DE94-008494] 09 p3659 N94-32632
Development of stitched/RTM composite primary structures 09 p3628 N94-33127
Tensile strength of dried gelcast green bodies
[DE94-009453] 10 p4028 N94-33930

The effect of thermomechanical processing on mechanical properties of a cast 6061 aluminum metal matrix composite
[AD-A277995] 10 p4019 N94-34220
Through-the-thickness tensile strength of textile composites
[NASA-TM-109115] 11 p4233 N94-35946
Method of thermochemically treating silicon carbide fibers derived from polymers
[AD-D016218] 11 p4246 N94-36125
Design and construction of a tensile tester for the testing of simple composites 11 p4230 N94-36401
Tensile strength of simulated and welded butt joints in W-Cu composite sheet
[NASA-TM-4584] 12 p4405 N94-37460
A comparison of graphite/epoxy tape laminates and 2-D braided composites mechanical properties
[NASA-CR-4610] 12 p4420 N94-37582
Size effect in composite materials and structures: Basic concepts and design considerations
12 p4460 N94-37808

TENSILE STRESS
Extensions of some guidelines for the mechanical design of coaxial compression pin seals
[DE93-012385] 01 p0177 N94-10348
Crack suppression in GaInSb buffer layers initially under tensile stress
[DE93-012839] 01 p0396 N94-10745
High temperature stability, interface bonding, and mechanical behavior in (beta)-NiAl and Ni3Al matrix composites with reinforcements modified by ion beam enhanced deposition
[DE93-013977] 01 p0398 N94-11115
Damage thresholds of fluoride multilayers at 355 nm
[DE93-009523] 01 p0090 N94-11230
Non-uniqueness in dynamic rate-independent non-associated plasticity
[AD-A266342] 02 p0769 N94-13731
Simulation studies for surfaces and materials strength
[NASA-CR-193387] 03 p1056 N94-15004
A model for non-linear creep and physical ageing in PVC
[NPL-DMM(A)-91] 03 p1057 N94-15016
J-integral and HRR field associated with stable crack growth in thin aluminum SEN specimen
[AD-A267879] 03 p0960 N94-17041
Interfacial shear behavior and its influence on fiber damage in sapphire-reinforced gamma titanium aluminide composites
[AD-A267943] 03 p1060 N94-17043
Influence of the loading rate on the endurance and deformability of cement matrix composites
[IFTR-1/1992] 03 p1060 N94-17052
Assessment of an improved multiaxial strength theory based on creep-rupture data for Inconel 600
[DE93-015929] 04 p1356 N94-17791
Construction of a tension-torsion anisotropic brittle damage elastic model
[ECL-91-27] 04 p1457 N94-19375
Delamination in composite materials as observed using an optical fiber strain gage
[AD-A270803] 04 p1344 N94-19662
Fracture simulations via massively parallel molecular dynamics
[DE93-040159] 06 p2374 N94-22871
Tensile properties of 21-6-9 stainless steel at elevated temperatures
[DE94-001852] 06 p2240 N94-23017
Determination of fracture stress and effective crack tip radius from toughness (KIc) and yield strength (Y)
[AD-A274014] 07 p2836 N94-25754
Investigation of tension-compression fatigue behavior of a cross-ply metal matrix composite at room and elevated temperatures
[AD-A273731] 07 p2706 N94-25999
Grain by grain study of the mechanisms of crack propagation during iodine SCC of Zry-4
[DE93-633765] 07 p2734 N94-26162
Micromechanics of the dynamic response of ceramics and ceramic composites 08 p3217 N94-29975
Torque-balanced extendable fiber optic cable
[AD-D016097] 09 p3882 N94-32719
Through-the-thickness tensile strength of textile composites
[NASA-TM-109115] 11 p4233 N94-35946

TENSILE TESTS
Mechanical and fatigue properties of fibre reinforced aluminium-lithium alloy and aluminium-lithium MMC based laminates 01 p0058 N94-10022
A method for determination of the elongational viscosity of viscoelastic fluids without body forces
01 p0124 N94-10247
UK interlaboratory tensile tests on Al alloy/SiC particulate metal matrix composites
[NPL-DMM(A)-77] 02 p0570 N94-13666
The feasibility of producing aluminum-lithium structures for cryogenic tankage applications by laser beam welding
[NASA-CR-191527] 02 p0595 N94-14026
Elastic-plastic finite element analyses of an unidirectional, 9 vol percent tungsten fiber reinforced copper matrix composite
[NASA-TM-106304] 02 p0559 N94-14719
The effect of aging at 343 C on the mechanical properties and microstructure of type 308 stainless steel weldments
[DE93-015454] 03 p0957 N94-16103
Development of test methods for textile composites
03 p0939 N94-16862
RSRM nozzle actuator bracket/lug fracture mechanics qualification test
[NASA-CR-193859] 03 p0927 N94-17080
Evaluation of hybrid reinforcement (fiber-reinforced-plastic rod with steel core)
[AD-A268009] 03 p0941 N94-17473
Effects of irradiation temperature on Charpy and tensile properties of high-copper, low upper-shelf, submerged-arc welds
[DE93-017858] 04 p1445 N94-19047
Rapid heating tensile testing update: 304L stainless steel
[DE93-018770] 05 p1688 N94-19942
Stress-induced cracking of fluorocarbon rubber MTL-0002 after exposure to DS-2
[AD-A271753] 05 p1705 N94-21302
Tensile and shear fracture behavior of fiber reinforced plastics at 77K irradiated by various radiation sources
[DE93-040280] 05 p1706 N94-21542
Results of the second Round Robin on opening-load measurement conducted by ASTM Task Group E24.04.04 on crack closure measurement and analysis
[NASA-TM-109032] 05 p1832 N94-21624
Tensile strength of fiber reinforced plastics at 77K irradiated by various radiation sources
[DE93-040826] 05 p1709 N94-22008
Nonlinear and progressive failure aspects of transport composite fuselage damage tolerance
05 p1834 N94-22609
Stress corrosion cracking properties of 15-5PH steel
06 p2251 N94-23244
Time dependent behavior of a graphite/thermoplastic composite and the effects of stress and physical aging
[NASA-TM-109047] 06 p2228 N94-23280
Grain-boundary microchemistry and intergranular cracking of irradiated austenitic stainless steel
[DE94-000466] 06 p2242 N94-23457
Effect of hydrogen exposure on a Cu-8 Cr-4 Nb alloy
[NASA-TM-106429] 06 p2243 N94-23556
Test methods for composites: A status report. Volume 1: Tension test methods
[AD-A273501] 06 p2230 N94-24942
Structural analysis of a frangible nut used on the NASA Space Shuttle
[DE94-003672] 07 p2821 N94-25811
A study of graphite peek composite with central elliptical holes under tension
[AD-A273779] 07 p2705 N94-25863
An investigation of cavitation in a mechanically alloyed 15 volume percent SiCp/IN9021 aluminum composite
[DE94-003371] 07 p2748 N94-25959
SP/MSP tests for the evaluation of FGM
[NAL-SP-17] 07 p2710 N94-27279
SP/MSP tests for the evaluation of FGM
07 p2710 N94-27280
Research on the development of fracture characteristics evaluation system for ceramics and metal composite materials 07 p2710 N94-27281
Development of a new seal for use on large openings of pressurized spacecraft
[NASA-TM-108444] 07 p2825 N94-27560
Use of photostress and strain gages to analyze behavior of weldments
[NASA-CR-195269] 07 p2843 N94-27765
Investigation of the bond strength of a discrete skin-stiffener interface
[NLR-TP-92183-U] 07 p2670 N94-27796
Mechanical properties and microstructure of thermomechanically processed, high manganese steel
[ARL-TR-146] 07 p2747 N94-28212
Fatigue behavior of a cross-ply ceramic matrix composite at elevated temperatures under tension-tension loading
[AD-A275466] 08 p3176 N94-28673
Fatigue behavior of a cross-ply ceramic matrix composite under strain controlled tension-tension and tension-compression loading
[AD-A275374] 08 p3177 N94-29012
Microstructure/property relationships for SCS6/Timetal 21-S composite
[AD-A275056] 08 p3178 N94-29135
The effect of temperature on creep and physical ageing of PVC
[NPL-DMM(A)-93] 08 p3217 N94-29885
Particulate metal matrix composites: Draft procedure for tensile tests at ambient temperature
[PB94-149721] 08 p3184 N94-30419
Approximate estimation of the effects of asymmetry on the testing of tensile specimens
[NPL-DMM(A)-117] 08 p3322 N94-30523
Tensile properties of commercially pure vanadium from room temperature to 1200 C
[DE94-006622] 09 p3641 N94-31581
Irradiation-assisted stress corrosion cracking of materials from commercial BWRs: Role of grain-boundary microchemistry
[DE94-006542] 09 p3643 N94-32109
Boron and hydrogen in Ni3Al. Part 2: Mechanical testing of bicrystals
[DE94-007441] 09 p3904 N94-32606
Investigation of moisture-induced embrittlement of iron aluminides
[DE94-010881] 11 p4241 N94-36196
Design and construction of a tensile tester for the testing of simple composites 11 p4230 N94-36401
Metal matrix composites: Analysis of simple specimens and model components under creep and fatigue loading
12 p4402 N94-36661
ASTM and VAMAS activities in titanium matrix composites test methods development
12 p4403 N94-36668
Methodologies for the thermomechanical characterization of continuous-fiber ceramic matrix composites: A review of test methods
[DE94-012111] 12 p4405 N94-37370

TENSION
Space Station Freedom Solar Array tension mechanism development 09 p3604 N94-33300
On nature's scaling effects 12 p4459 N94-37803

TENSOR ANALYSIS
The evolution of tensor polarization
[DE93-017209] 02 p0790 N94-14897
Tensoral for post-processing users and simulation authors 06 p2333 N94-24169

TENSOR FIELDS
U TENSORS

TENSORS
NT STRESS TENSORS
Regular tensor Green functions of the round waveguide
[DE93-621354] 01 p0345 N94-11036
Parameterization of subgrid-scale stress by the velocity gradient tensor 01 p0155 N94-12286
The evolution of tensor polarization
[DE93-017209] 02 p0790 N94-14897
Tensorial structure of a q-deformed sp(4,R) superalgebra
[DE93-624808] 04 p1545 N94-17685
Mass properties measurement system dynamics
06 p2368 N94-23235
Tensoral for post-processing users and simulation authors 06 p2333 N94-24169
A note on Riemannian 2-space
[DE94-602560] 07 p3073 N94-27024
The Einstein tensor characterizing some Riemann spaces
[DE94-603663] 07 p3074 N94-27626
Modeling turbulence in flows with a strong rotational component
[DE94-003577] 08 p3270 N94-28475
A note on the Poisson brackets associated with Lax operators
[MATHS-REPT-A-195] 08 p3464 N94-29482
Anomalous algebraic structures in quantum field theories 08 p3524 N94-29911
Homogeneous Poisson structures
[DE94-608112] 08 p3453 N94-30119
Tensor gauge potentials in loop space formulation of Yang-Mills fields
[PB94-147147] 09 p3912 N94-31924
Complex Kohn variational principle for two-nucleon bound-state and scattering with the tensor potential
[DE94-616651] 11 p4321 N94-35595
Tensor-GMRES method for large sparse systems of nonlinear equations
[NASA-CR-196379] 12 p4505 N94-37655

TERBIUM
Improved magnetostrictive transducer drive elements achieved by reduction of crystalline defects and improved crystalline orientation
[AD-A273391] 06 p2313 N94-25276

TERBIUM COMPOUNDS
Synthesis and characterization of charge-substituted garnets YCaLnGa5O12 (Ln = Ce, Pr, Tb)
[DE93-040227] 05 p2033 N94-21992

Spectroscopic studies of magnetic transitions in TbPO4
[DE94-001274] 05 p2035 N94-22565
Laser surface modification of intermetallic compounds
[DREA-CR-92-416] 07 p2820 N94-27668
Terfenol: A study of the phase equilibrium diagram and the solidification process
[DE94-004883] 08 p3209 N94-30690

TERCOM
Flight testing of GPS and GPS-aided systems
[NLR-TP-92151-U] 07 p2666 N94-27831

TEREPHTHALATE
NT POLYETHYLENE TEREPHTHALATE

TERMINAL BALLISTICS
Deformation mechanisms in tungsten single crystals in ballistic impact experiments
[AD-A265701] 01 p0405 N94-12563
The motion of a conical shaped liner driven by explosive load
[ITN-93-85215] 02 p0585 N94-14507
Impactor control of central peak and peak-ring formation 05 p1862 N94-20744
Hypervelocity impact
[AD-A272957] 05 p1831 N94-21249
Bibliographic Retrieval System (BARS), Sandia Shock Compression (SSC) database Shock Physics Index
[DE94-001679] 06 p2589 N94-23126
Dynamic response of S-2 glass reinforced plastic structural armor
[AD-A273868] 07 p2747 N94-25596
Design study of fiber-composite penetrator cases
[DE94-003203] 07 p2707 N94-26099
Trajectories of ballistic impact ejecta on a rotating Earth 07 p2887 N94-28295
Least-squares determination of burst-point coordinates
[AD-A275423] 08 p3452 N94-28864
Tearing resistance of a thin shell against projectile penetration: Material property effects
[DE94-007466] 09 p3733 N94-31316
Experimental measurement of dynamic failure and fragmentation properties of metals
[DE94-007377] 09 p3737 N94-32135
The surface and interior of Phobos 11 p4355 N94-35400
Energy partitioning in high speed impact of analog solid rocket motors
[AD-A278771] 11 p4228 N94-35825

TERMINAL FACILITIES
NT SHIP TERMINALS
Airport terminals: Optimum configurations and gate position requirement
[ISBN-0-315-61722-5] 02 p0528 N94-13544
MAGSS-14: Medium Altitude Global Mobile Satellite System with enhanced regional coverage 03 p0893 N94-17164
Terminal area forecasts, FY 1993-2005
[AD-A269855] 04 p1316 N94-18336
Passenger terminal level of service measurement: A utility theoretic approach
[ISBN-0-315-59037-8] 05 p1651 N94-22418
Passenger terminal simulation model
[ISBN-0-315-61113-8] 05 p1652 N94-22423
A study of parallel pier finger airport terminal configuration
[ISBN-0-315-83128-6] 05 p1652 N94-22425
The design of a long-range megatransport aircraft 07 p2671 N94-25718
Cockpit Electronic Display Workshop: A synopsis
[AD-A277728] 09 p3583 N94-33280

TERMINAL GUIDANCE
NT LASER GUIDANCE
Evaluation of the capacity and delay benefits of terminal air traffic control automation
[AD-A265323] 01 p0024 N94-11863
Hypervelocity orbital intercept guidance using certainty control
[AD-A267297] 03 p1174 N94-17219
Evaluation of GPS position and attitude determination for automated rendezvous and docking missions
[NASA-CR-4614] 12 p4397 N94-37506

TERMINAL VELOCITY
On the motion through a viscous fluid of a spherical particle touching a plane wall: Slip boundary conditions
[DE93-012540] 02 p0628 N94-12961

TERMINATING
U STOPPING

TERMINOLOGY
Abbreviations, acronyms, and initialisms frequently used by Martin Marietta Energy Systems, Incorporated
[DE93-012509] 01 p0420 N94-11369
Glossary of SSDC terms and acronyms
[DE93-013697] 02 p0823 N94-13352
NASA's online machine aided indexing system
[NASA-CR-4518] 03 p1228 N94-15009
Illustrated glossary of textile terms for composites
[NASA-CR-191539] 03 p0933 N94-15484
Definitions of terms relating to aircraft windscreens, canopies, and transparencies
[AD-A268403] 03 p0868 N94-17425
Technical development of a theory of programs
[ETN-93-95058] 04 p1532 N94-19652
Qualifying codes under software quality assurance: Two examples as guidelines for codes that are existing or under development
[DE93-040452] 05 p1904 N94-20097
Understanding Open Systems Interconnection (OSI)
[AD-A271877] 05 p1929 N94-20472
The Keck keyword layer 05 p1925 N94-22460
Glossary knowledge engineering
[NLR-TP-91435-U] 06 p2471 N94-23137
Definitions in use by the visible and near-infrared, and thermal working groups 06 p2383 N94-23598
Correspondence dictionary from free English term to INIS descriptors
[DE94-701173] 07 p3100 N94-27700
Total Quality Management implementation guidelines
[DE94-007232] 09 p3915 N94-32723
DTIC Thesaurus on diskette with dBase 4.1 runtime (computer diskette)
[AD-M000311] 10 p4159 N94-34213
Advanced transportation system study: Manned launch vehicle concepts for two way transportation system payloads to LEO. Work breakdown structure and work breakdown structure dictionary
[NASA-CR-193952] 10 p4012 N94-34911
Alternative fuel information: Glossary
[DE94-006889] 12 p4429 N94-37403
A graphic view of Geometric Dimensioning and Tolerancing
[DE94-011478] 12 p4435 N94-37736

TERMS
Glossary of SSDC terms and acronyms
[DE93-013697] 02 p0823 N94-13352
Definitions of terms relating to aircraft windscreens, canopies, and transparencies
[AD-A268403] 03 p0868 N94-17425
Defense Technical Information Center thesaurus
[AD-A268855] 04 p1615 N94-18319
Correspondence dictionary from free English term to INIS descriptors
[DE94-701173] 07 p3100 N94-27700
Index expression belief networks for information disclosure
[TR-92-23] 08 p3465 N94-30358
Total termination of term rewriting
[RUU-CS-92-42] 08 p3460 N94-30744
DTIC Thesaurus on diskette with dBase 4.1 runtime (computer diskette)
[AD-M000306] 09 p3922 N94-33256
DTIC Thesaurus on diskette (ASC2) (computer diskette)
[AD-M000309] 09 p3922 N94-33257
DTIC Thesaurus on diskette without runtime (computer diskette)
[AD-M000310] 09 p3923 N94-33258
DTIC Thesaurus on diskette without runtime (computer diskette)
[AD-M000312] 09 p3923 N94-33259
International Energy: Subject Thesaurus, revision 1
[DE94-002590] 10 p4151 N94-33730

TERNARY ALLOYS
NT ASTROLOY (TRADEMARK)
Lattice-matched heteroepitaxy of wide gap ternary compound semiconductors 01 p0400 N94-11441
Electronic and total energy properties of ternary and quaternary semiconductor compounds, alloys and superlattices
[NASA-CR-192905] 01 p0405 N94-12570
Electronic structure and phase stability properties in ternary substitutional alloys
[DE93-013848] 02 p0569 N94-13137
Crystal growth of ZnSe and related ternary compound semiconductors by physical vapor transport
[NASA-CR-193834] 02 p0807 N94-13444
Ternary alloying effects in polycrystalline (beta)-NiAl
[DE93-012675] 03 p0955 N94-15885
Powder diffraction studies using anomalous dispersion
[DE93-012531] 03 p1210 N94-16775
Slip, twinning and transformation in Laves phases
[DE93-018164] 03 p0960 N94-16972
Magnetic properties of single-crystalline UCu3Al2
[DE93-016607] 04 p1593 N94-17744
Magnetic and crystallographic structures in UTX intermetallic compounds
[DE93-018291] 04 p1605 N94-19735
Non-fermi liquid and spin-glass behavior of the Sc(1-x)U(x)Pd3 system
[DE93-040134] 05 p2016 N94-20335
Microstructural evolution of neutron-irradiated Fe-Cr-Ni ternary alloys at high helium generation rates
[DE93-018786] 05 p1696 N94-22037
Study on improvement in physical analysis method of metallic materials 07 p2728 N94-25577
Zr-rich corner of the Zr-Sn-O diagram
[DE93-633764] 07 p2734 N94-26161
A tri-junction diffusion couple analysis of the Nb-Cr-Ti system at 950 C
[DE94-002637] 07 p2737 N94-26607
NMR study of quasicrystal Al(70)Pd(20)T(M10) alloy (T(M):Cr, Mn, Fe, and Co) 07 p2745 N94-28162
Terfenol: A study of the phase equilibrium diagram and the solidification process
[DE94-004883] 08 p3209 N94-30690
Processing and mechanical properties of NiAl-based in-situ composites
[NASA-CR-195333] 12 p4416 N94-36954

TERNARY SYSTEMS
Rapid thermal processing for strained-layer semiconductor devices
[DE93-013754] 01 p0396 N94-10809
Fabrication of Si-As-Te ternary amorphous semiconductor in the microgravity environment (M-13) 02 p0588 N94-13745
Calculation of the LiF-CeF3-BeF2 and LiF-PuF3-BeF2 ternary phase diagrams
[DE93-017437] 04 p1360 N94-18501
Zr-rich corner of the Zr-Sn-O diagram
[DE93-633764] 07 p2734 N94-26161
The synthesis and structural characterization of Na3WO3N
[AD-A275243] 08 p3204 N94-29395
Studies of high temperature ternary phases in mixed-metal-rich early transition metal sulfide and phosphide systems
[DE94-006034] 08 p3209 N94-30336
Phase relationships and stability of the (mu)- and (zeta)-phases in the Ag-Al-X (X=Zn, Ga, Ge) systems
[DE94-009391] 09 p3648 N94-33270

TERNARY SYSTEMS (DIGITAL)
U DIGITAL SYSTEMS

TERPENES
NT AZULENE

TERRACES (LANDFORMS)
NT MESAS
NT PLATEAUS
Descriptions and preliminary interpretations of cores recovered from the Manson Impact Structure (Iowa) 01 p0281 N94-12032
Applications of Quaternary stratigraphic, soil-geomorphic, and quantitative geomorphic analyses to the evaluation of tectonic activity and landscape evolution in the Upper Coastal Plain, South Carolina
[DE93-016269] 04 p1484 N94-18725
Milankovitch insulation forcing and cyclic formation of large-scale glacial, fluvial, and eolian landforms in central Alaska 05 p2089 N94-20386
Cryoplanation terraces of interior and western Alaska 05 p2091 N94-20396

TERRAIN
Measures for simulator evaluation of a helicopter obstacle avoidance system 01 p0035 N94-11535
A structural origin for the cantaloupe terrain of Triton 01 p0449 N94-12095
Venus mountain-top mineralogy: Misconceptions about pyrite as the high radar-reflecting phase 01 p0455 N94-12129
Relation between ages and elevations of Martian channels 01 p0472 N94-12216
Do large impact basins in the southern hemisphere of Mars control the distribution of polar structures and deposits? 01 p0481 N94-12266
Free-air and Bouguer gravity anomalies and the Martian crustal dichotomy 01 p0481 N94-12267
Evaluation of beta-spline interpolation in digital terrain models
[INPE-5475-TDI/506] 02 p0684 N94-13364
Net radiation mapping of mountainous terrain using Landsat-5 thematic mapper imagery and digital terrain data
[ISBN-0-315-57755-X] 02 p0685 N94-13475
Improved mapping system
[NASA-TM-109643] 03 p1082 N94-15428
Johnson-Gierhart program predictions of excess propagation loss for super-high frequency air-to-ground paths. Volume 1: Theory and numerical results
[AD-A267105] 03 p0988 N94-15649
Environmental characterization for target acquisition. Report 1: Site descriptions and measurements
[AD-A267192] 03 p1106 N94-15851
Multifrequency observations 03 p0992 N94-15902
Fluvial erosion on Mars: Implications for paleoclimatic change 03 p1241 N94-16210
Tessera terrain on Venus: Global characterization from Magellan data 03 p1264 N94-16262
Density of impact craters on tessera, Venus 03 p1264 N94-16263

Complex terrain wind model evaluation
[AD-A266467] 03 p1096 N94-16589
Fitting a three-component scattering model to polarimetric SAR data 03 p1079 N94-16751
Sound exposure level prediction for impulse sound sources above variable terrain
[AD-A267535] 03 p1178 N94-17119
An automated approach for classifying generic terrain features using digital elevation data
[AD-A266385] 03 p1084 N94-17421
Environmental characterization for target acquisition. Report 3: New concepts for evaluating low-grazing angle radar measurements
[AD-A269956] 04 p1388 N94-18777
Robot navigation in unknown terrains: Introductory survey of non-heuristic algorithms
[DE93-019221] 04 p1316 N94-19300
Remote sensing of Earth terrain
[NASA-CR-194598] 04 p1464 N94-19681
Meso-Beta scale numerical simulation studies of terrain-induced jet streak mass/momentum perturbations
[NASA-CR-194627] 05 p1864 N94-20138
A wet-geology and cold-climate Mars model: Punctuation of a slow dynamic approach to equilibrium 05 p2090 N94-20389
Possible occurrence and origin of massive ice in Utopia Planitia 05 p2090 N94-20390
A model for the origin of Martian polygonal terrain 05 p2090 N94-20393
The thumbprint terrain: What will Mars Observer tell us? 05 p2091 N94-20397
A formational model for the polygonal terrains of Mars: Taking a crack at the genesis of the Martian polygons 05 p2091 N94-20400
Balloon exploration of the northern plains of Mars near and north of the Viking 2 landing site 05 p2092 N94-20401
Geomorphic evidence for an eolian contribution to the formation of the Martian northern plains 05 p2092 N94-20402
Topographic mapping using a monopulse SAR system 05 p1721 N94-20417
Diapirs and cantaloupes: Layering and overturn of Triton's crust 05 p2111 N94-20738
Geology of the southern hemisphere of Triton: No polar cap 05 p2111 N94-20739
Complex ridged terrain-related ridge belts on Venus: Global distribution and classification 05 p2129 N94-20835
Early Mars: A regional assessment of denudation chronology 05 p2145 N94-21676
Role of surface characteristics in urban meteorology and air quality
[DE93-040929] 05 p1851 N94-21740
K-band mobile propagation measurements using ACTS 06 p2283 N94-22792
Mobility analysis, simulation, and scale model testing for the design of wheeled planetary rovers 06 p2370 N94-23425
Joint Acoustic Propagation Experiment (JAPE) 06 p2527 N94-24208
Tools for visualizing landscape pattern for large geographic areas
[DE94-001121] 06 p2388 N94-24757
Recent ASCOT experiments in multi-layered flows
[DE94-002360] 07 p2880 N94-26762
Conifer tree influence on Digital Terrain Elevation Data (DTED): A case study at Dulles International Airport
[AD-A274213] 07 p2849 N94-27069
An overview of the ASCOT program
[DE94-004356] 07 p2869 N94-27601
Landscape dynamics of northeastern forests
[NASA-CR-195272] 07 p2852 N94-28070
Environmental characterization for target acquisition. Analysis of thermal and visible imagery
[AD-A275414] 08 p3242 N94-28862
Feature mapping in a photogrammetric GIS
[AD-A275418] 08 p3325 N94-28863
The uses and limitations of fractal geometry in digital terrain modelling 08 p3333 N94-29958
A physical optics model for scattering of HF radiation by irregular terrain
[DE94-006187] 08 p3255 N94-30106
A hybrid electromagnetic-statistical approach for characterizing MMW scattering by terrain 08 p3259 N94-30510
A paraperspective factorization method for shape and motion recovery
[AD-A276513] 09 p3712 N94-31929
Alternatives to hierarchical techniques in stereo correlation
[AD-A276570] 09 p3746 N94-31938
Monitoring landsurface characteristics in Niger using complementary SPOT and ERS-1 SAR data 09 p3754 N94-32560
A multitasking behavioral control system for the Robotic All Terrain Lunar Exploration Rover (RATLER)
[DE94-007293] 09 p3835 N94-32787
Numerical simulation of thermally induced near-surface flows over Martian terrain 09 p3949 N94-33223
An ethnographic object-oriented analysis of explorer presence in a volcanic terrain environment: Claims and evidence
[NASA-TM-108823] 10 p4099 N94-33608
A format for storing and managing multiple level of detail terrain for simulated environments
[AD-A278497] 10 p4159 N94-34377
The fretted terrain of the Nilosyrtis Mensae region of Mars: Clues to the timing of dichotomy formation and the emplacement of the northern plains 11 p4360 N94-35424
Space Shuttle orbit determination using empirical force modeling of attitude maneuvers for the German MOMS-02/D2 mission 11 p4207 N94-35634
Atmospheric and dispersion modeling in areas of highly complex terrain employing a four-dimensional data assimilation technique
[DE94-004041] 11 p4285 N94-35823

TERRAIN ANALYSIS
Sources of Na for the Io atmosphere 01 p0455 N94-12127
Terrestrial case studies of ilmenite exploration and lunar implications 01 p0478 N94-12247
Spectral reflectance of soils from Sao Paulo State
[INPE-5424-PRP/172] 02 p0684 N94-13377
Satellite imagery and exogenous data integration by neural network in automation land-cover classification
[INPE-5480-PRE/1778] 02 p0686 N94-13729
Nonlinear aspects of data integration for land-cover classification in a neural network environment
[INPE-5479-PRE/1778] 02 p0686 N94-13789
Application of Cloude's target decomposition theorem to polarimetric imaging radar data 05 p1724 N94-20429
Geology and radiophysical properties of the Venera and Vega landing sites 05 p2135 N94-20867
Detecting topographical regions in digital terrain maps
[AD-A272889] 05 p1841 N94-21453
Construction and applications of the two dimensional Delaunay triangulated irregular network and the three dimensional Delaunay tetrahedron model
[ETN-94-95034] 07 p2848 N94-26651
The uses and limitations of fractal geometry in digital terrain modelling 08 p3333 N94-29958
Applicability of digital terrain analyses to wind energy prospecting and siting
[DE94-004363] 08 p3374 N94-30587
Example of SPOT/ERS-1 complementarity 09 p3749 N94-32533
Production of terrain data: Optical radar complementarity 09 p3750 N94-32540
Evaluation of the potential of SAR data for mapping of landslide risks
[BRGM-93033] 09 p3753 N94-32552
Study of subpolar glaciers of Spitzbergen using SPOT, ERS-1, and hypsometric data: Results and perspectives 09 p3753 N94-32553
Comparing SPOT and SIR A for mapping superficial formations in tropical forest regions: Example of the Yaoundy Region (Cameroon) 09 p3755 N94-32562
Evaluation of surface phase change on large zones 09 p3755 N94-32567
Precision and level of artefacts in the computation of digital terrain models by interferometry 09 p3756 N94-32571
Fields of experiments in ERS-1 SAR interferometry in Bonn and Naples 09 p3756 N94-32572
Rescaled box counting for the topological analysis of spatial data
[DE94-009820] 12 p4461 N94-36464

TERRAIN CONTOUR MATCHING NAVIGATION SYSTEM
U TERCOM

TERRAIN FOLLOWING AIRCRAFT
Advanced information processing system: The Army Fault-Tolerant Architecture detailed design overview
[NASA-CR-194924] 12 p4497 N94-36962

TERRESTRIAL DUST BELT
The effect of an on-orbit near encounter on the number flux density of micron sized particles 03 p0899 N94-16374

TERRESTRIAL MAGNETISM
U GEOMAGNETISM

TERRESTRIAL PLANETS
NT EARTH (PLANET)
NT MARS (PLANET)
NT MERCURY (PLANET)
NT VENUS (PLANET)
Giant impact-induced atmospheric blow-off 01 p0435 N94-12019
Differential scaling: Implications for central structures in large lunar craters 01 p0461 N94-12158
Rover mounted ground penetrating radar as a tool for investigating the near-surface of Mars and beyond 03 p1007 N94-16197
Aspects of modelling the tectonics of large volcanoes on the terrestrial planets 03 p1104 N94-16396
Planetary plasma waves
[NASA-CR-194295] 04 p1629 N94-19094
Determination of cosmic bodies size-velocity distribution by observation of current impacts on Mars 05 p2082 N94-20648
Largest impact features on Venus: Non-preserved or non-recognizable? 05 p2096 N94-20657
Numerical simulation of lava flows: Applications to the terrestrial planets 05 p1863 N94-20904
Tectonic History of the Terrestrial Planets
[NASA-CR-195696] 09 p3939 N94-31105
Aspects of modelling the tectonics of large volcanoes on the terrestrial planets 09 p3940 N94-31107

TERRESTRIAL RADIATION
A comparison of the visible and near infrared reflectance of hydrovolcanic palagonite tuffs and Martian weathered soils 01 p0477 N94-12245
Sensitivity of cloud forcing to the cloud cover parameterization in a GCM
[DE94-000678] 10 p4089 N94-33728
Theoretical and experimental studies relevant to interpretation of auroral emissions
[NASA-CR-196032] 11 p4376 N94-36421

TERTIARY PERIOD
An extraterrestrial event at the tertiary-quaternary boundary 07 p2890 N94-28309

TESSERAL HARMONICS
Implementing a 50x50 gravity field model in an orbit determination system
[AD-A267548] 03 p0888 N94-17103

TEST BEDS
U TEST STANDS

TEST CHAMBERS
NT ANECHOIC CHAMBERS
NT HYPERBARIC CHAMBERS
NT PRESSURE CHAMBERS
NT VACUUM CHAMBERS
Unitary plan wind tunnel landmark dedication and revitalization
[NASA-TM-109649] 03 p1302 N94-15434
First results from a laboratory facility for measurement of emission spectra under simulated planetary conditions 03 p0954 N94-16372
Acoustic intensity measurements in the presence of low Mach number flow
[AD-A269995] 04 p1562 N94-18664
Measurement of thermal-hydraulic parameters in two-phase flow using flow visualization image analysis
[DE93-006255] 05 p1805 N94-22269
Dual-bell altitude compensating nozzles 06 p2215 N94-23057
Automatic pressure control system for the Wright Laboratory Compressor Research Facility
[AD-A273827] 06 p2194 N94-25522
Program for calculation of maximum lift coefficient of plain aerofoils and wings at subsonic speeds
[ESDU-93015] 07 p2649 N94-28076
Vacuum chamber and adaptors for shearography and holography
[NASA-CR-192467] 08 p3157 N94-29956
A modernised HST of NLR
[AD-B179220] 08 p3158 N94-30423
Design of a two dimensional planer pressurized air labyrinth seal test rig
[AD-A277232] 09 p3726 N94-32370

TEST EQUIPMENT
Dynamic tester for rotor seals and bearings
[NASA-CASE-MFS-28493-1] 01 p0033 N94-10669
Programmable logic devices
[DE93-013117] 01 p0144 N94-11479
Hot-gas-side heat transfer characteristics of subscale, plug-nozzle rocket calorimeter chamber
[NASA-TP-3380] 01 p0055 N94-12569
CFM technologies for space transportation: Multipurpose hydrogen testbed system definition and tank procurement
[NASA-CR-194355] 02 p0539 N94-12827
The Large Area Pulsed Solar Simulator (LAPSS)
[NASA-CR-194507] 02 p0703 N94-13940
Bench checkout equipment for spaceborne laser altimeter systems 03 p0921 N94-15618
The Spacelab IPS Star Simulator
[TABES PAPER 93-650] 03 p0877 N94-16150
Airport pavement test machine design and cost study
[DOT/FAA/CT-93/51] 06 p2192 N94-24072
An analysis of traditional operational testing to project how testing will be conducted in the future
[AD-A273189] 06 p2372 N94-24553
High temperature solid oxide fuel cell: Customer test units
[DE94-002961] 07 p2858 N94-26869

Modelling soft impacts for vibrational excitation of civil engineering structures
[PB94-137619] 08 p3320 N94-29681
Design of a two dimensional planer pressurized air labyrinth seal test rig
[AD-A277232] 09 p3726 N94-32370
Atomic oxygen reactor having at least one sidearm conduit
[NASA-CASE-MSC-21487-4] 11 p4250 N94-35445
High-speed digital project, HSD test capability
[DE94-010885] 11 p4260 N94-36197
Design and construction of a tensile tester for the testing of simple composites 11 p4230 N94-36401
Internally damped, self-arresting vertical drop-weight apparatus
[NASA-CASE-LAR-15003-1] 12 p4389 N94-36826

TEST FACILITIES
NT ANECHOIC CHAMBERS
NT BALLISTIC RANGES
NT BLOWDOWN WIND TUNNELS
NT CASCADE WIND TUNNELS
NT COMBUSTION WIND TUNNELS
NT CRYOGENIC WIND TUNNELS
NT ENGINE TESTING LABORATORIES
NT ENVIRONMENTAL LABORATORIES
NT HOTSHOT WIND TUNNELS
NT HYPERSONIC WIND TUNNELS
NT HYPERVELOCITY WIND TUNNELS
NT LOW SPEED WIND TUNNELS
NT MISSILE RANGES
NT ROCKET TEST FACILITIES
NT SHOCK TUNNELS
NT SLOTTED WIND TUNNELS
NT SUBSONIC WIND TUNNELS
NT SUPERSONIC WIND TUNNELS
NT TEST RANGES
NT TEST STANDS
NT TRANSONIC WIND TUNNELS
NT WIND TUNNELS

High-field conductor testing at the FENIX facility
[DE93-012318] 01 p0387 N94-10737
Aircraft material fire testing and the creation of an international working group 01 p0021 N94-10790
Experimental approach to the physics of the high density divertor
[DE93-009149] 01 p0391 N94-11170
A facility for testing 10- to 100-kWe space power reactors
[DE92-040420] 01 p0372 N94-11296
Development of a high specific 1.5 to 5 kW thermal arcjet
[NASA-CR-193133] 01 p0047 N94-11354
An overview of the capabilities of ARA for the measurement of nozzle discharge and thrust
[ARA-MEMO-378] 01 p0055 N94-12283
Molten carbonate fuel cell product development test environmental assessment/protection plan
[DE93-000288] 02 p0702 N94-13380
Miscibility of lubricants with refrigerants, phase 1
[DE93-014766-PHASE-1] 02 p0596 N94-13407
Development of test techniques to simulate high-frequency mechanical shock on weapon components
[KCP-613-4998] 02 p0675 N94-13907
Heat and seed recovery technology project
[DE93-009203] 02 p0800 N94-13913
Advanced Communications ESM System (ACES) testbed: Integration study
[DSIS-93-00345] 02 p0604 N94-13939
EWTEST signal excision testbed: System evaluation
[DSIS-93-00346] 02 p0607 N94-14065
A program for the investigation of the Multibody Modeling, Verification, and Control Laboratory 02 p0682 N94-14652
A guide to the DRA 13 ft x 9 ft Low Speed Wind Tunnel Facility
[AD-A267739] 02 p0528 N94-14876
Supersonic Combustion Research Laboratory. Volume 1: Design and fabrication
[AD-A267667] 03 p0943 N94-14962
A test facility to calibrate EUV detectors 03 p0873 N94-15062
GFSC-TV demo tape
[NASA-TM-109586] 03 p0875 N94-15270
Facilities maintenance handbook
[NHB-8831.2] 03 p1224 N94-15934
The ESA telescience program 03 p0977 N94-16073
Payloads for the processing of high temperature materials 03 p0979 N94-16083
The design and analysis of a modular microgravity test platform for use aboard the NASA KC-135 aircraft 03 p0899 N94-16101
Structured finite volume modeling of US Navy aircraft engine test cells task 2: Turboprop engine, volume 1
[AD-A267833] 03 p0872 N94-17405
Structured finite volume modeling of US Navy aircraft engine test cells. Task 2: Turboprop engine. Volume 2: Code documentation and listings
[AD-A268386] 03 p0873 N94-17569
High-efficiency silicon concentrator cell commercialization
[DE93-018491] 04 p1467 N94-18409
A register of underwater acoustic test facilities in the US, Canada, and the United Kingdom
[AD-A270884] 04 p1500 N94-19785
High temperature simulation chambers. Physico-chemical and thermal effect of atmospheric reentry on ceramic materials 05 p1653 N94-21404
Material properties and behavior during simulated atmospheric reentry 05 p1665 N94-21408
The development of the HERA Test Facility (HTF) 06 p2197 N94-24020
TEM cell safety report
[DREO-TN-93-9] 06 p2193 N94-24123
Altitude simulation facility for testing large space motors 06 p2156 N94-24255
LSS systems planning and performance program
[NASA-CR-193882] 06 p2196 N94-24309
An analysis of traditional operational testing to project how testing will be conducted in the future
[AD-A273189] 06 p2372 N94-24553
Collaborating with our customers: NIST building and fire research laboratory
[PB94-110194] 06 p2272 N94-24955
Primary standards laboratory report 1st half 1993
[DE94-003138] 07 p2762 N94-26027
NASA Lewis Research Center lean-, rich-burn materials test burner rig
[NASA-CR-194437] 07 p2680 N94-26141
The development of a horizontal impact sled facility and subsequent crashworthiness experiments
[NIAR-93-15] 07 p2680 N94-26200
A method for testing of HVAC automation equipment using the emulator and the application of the method
[VTT-TIED-1435] 07 p2822 N94-26306
Fusion Energy Advisory Committee: Advice and recommendations to the US Department of Energy in response to the charge letter of September 1, 1992
[DE93-019842] 07 p3043 N94-26428
An assessment of testing requirement impacts on nuclear thermal propulsion ground test facility design
[DE94-002933] 07 p2702 N94-26560
Research and test facilities
[NASA-TM-109685] 07 p2681 N94-26684
Calibrating/testing meters in hot water test bench VM7
[PB94-124294] 07 p2812 N94-27160
Description of the Experimental Avionics Systems Integration Laboratory (EASILY)
[NASA-TM-109072] 07 p2681 N94-27425
Design, implementation and experimental results of robotic environment input into the Robot Controller Test Station (RCTS)
[ISBN-0-315-85355-7] 07 p2826 N94-27596
Experimental data for CFD validation of impinging jets in crossflow with application to ASTOVL flow problems 07 p2801 N94-28010
Testing laboratories as notified bodies
[PB94-132396] 08 p3160 N94-28413
Data fusion and correlation techniques testbed development. Phase 1: Interim report
[SKD-1600-73-015] 08 p3405 N94-28533
Cryogenic probe station for use in automated microwave and noise figure measurements
[NASA-TM-106560] 08 p3286 N94-29000
CIAM experimental turboramjets 08 p3152 N94-29299
Development of electromagnetic compatibility tests
[REPT-932-430-110] 08 p3245 N94-29421
McMaster accelerator facility 08 p3496 N94-30217
Advanced development of the Spectrum Sciences Model 5005-TF, single event test fixture 08 p3291 N94-30218
Using Cf-252 for single event upset testing 08 p3496 N94-30219
A testbed for the development of ground-based control of space-based manipulators 08 p3309 N94-30306
Technology transfer and evaluation for Space Station telerobotics
[AIAA PAPER 94-1190-CP] 08 p3441 N94-30541
Free-floating dual-arm robots for space assembly
[AIAA PAPER 94-1195-CP] 08 p3442 N94-30546
The MACS-TSA applied in the ISO and SAX spacecraft projects
[PB94-126257] 08 p3170 N94-30857
Analysis of beam-on-target interaction in a neutron-source test facility
[DE94-005392] 09 p3863 N94-31151
Implementation of instruments and facilities at the SGP CART site
[DE94-006839] 09 p3781 N94-31322
Aerospace test facilities at NASA LERC Plumbrook
[NASA-TM-109755] 09 p3602 N94-31814
Real-time control and application to robotics: Hardware and software architectures
[ISBN-0-315-87192-X] 09 p3833 N94-31876
Design of a cold-flow test facility for the high pressure fuel turbopump turbine of the Space Shuttle main engine
[AD-A276743] 09 p3815 N94-32182
High power switch design for the Nova upgrade laser (Project HERCULES: High Energy Research Concerning the Ultimate Lifetime of Experimental Switches)
[DE94-007921] 09 p3719 N94-32654
The preliminary evaluation of liquid lubricants for space applications by vacuum tribometry 09 p3606 N94-33313
Stennis Space Center 1992
[NASA-TM-109796] 10 p4011 N94-33558
John C. Stennis Space Center overview
[NASA-TM-109816] 10 p4011 N94-33567
High Heat Flux Facility
[NASA-TM-109834] 10 p4009 N94-33570
Powered lift facility at NASA Lewis Research Center's Aeroacoustic Propulsion Laboratory
[NASA-TM-106577] 10 p4009 N94-33604
Way station to space: The history of Stennis Space Center
[NASA-TM-109819] 10 p4011 N94-33771
Measured channel parameters for the disturbed wide-bandwidth HF channel
[AD-A277877] 10 p4034 N94-33778
National Facilities study
[NASA-TM-109851] 10 p4009 N94-34071
A test apparatus and facility to identify the rotordynamic coefficients of high-speed hydrostatic bearings 10 p4065 N94-34199
National facilities study. Volume 1: Facilities inventory
[NASA-TM-109854] 10 p4009 N94-34632
National facilities study. Volume 2: Task group on aeronautical research and development facilities report
[NASA-TM-109855] 10 p4009 N94-34633
Data acquisition systems
[DE94-009848] 11 p4345 N94-35817
Engineering directorate technical facilities catalog
[NASA-TM-109895] 12 p4390 N94-37443

TEST FIRING
SSME testing at Stennis Space Center
[NASA-TM-109310] 02 p0552 N94-13617
A computational study of the base region flow field for the M865 projectile
[ARL-TR-109] 02 p0504 N94-13795
Technical Evaluation Motor No. 10 (TEM-10)
[NASA-CR-193846] 02 p0554 N94-14907
Technology test bed
[NASA-TM-109354] 04 p1322 N94-18953
ASRM testing at Stennis Space Center (proposed)
[NASA-TM-109795] 10 p4016 N94-33557

TEST PATTERN GENERATORS
Automatic test case generation using PROLOG
[NPL-DITC-215/93] 07 p2964 N94-26655
An UIO-based method for protocol conformance testing
[REPT-93-060] 08 p3429 N94-30931
A hierarchical approach to test generation for CMOS VLSI circuits
[ISBN-9-09-005449-9] 09 p3689 N94-31535

TEST PILOTS
Quantitative EEG patterns of differential in-flight workload 01 p0317 N94-11528

TEST RANGES
NT BALLISTIC RANGES
NT MISSILE RANGES

Hydrologic Database user's manual
[DE94-003950] 09 p3743 N94-31603

TEST STANDS
Operational characteristics of a 100-mA, 2-MeV radio-frequency quadrupole
[DE93-014474] 01 p0374 N94-12786
Advanced Turbine Technology Applications Project (ATTAP)
[NASA-CR-195366] 02 p0828 N94-12931
Test plan for the evaluation of the initial capability of the National Satellite Test Bed: Phase 1D
[DOT/FAA/RD-93/20] 03 p0876 N94-16025
Technology test bed
[NASA-TM-109354] 04 p1322 N94-18953
Optimization and control of a small angle ion source using an adaptive neural network controller
[DE93-040063] 05 p1946 N94-21845
A real-time infrared image processing testbed 05 p1790 N94-22227
NASA/Goddard Space Flight Center's testbed for CCSDS compatible systems 06 p2197 N94-23855

Design and application of electromechanical actuators for deep space missions
[NASA-CR-195134] 06 p2365 N94-24842
Performance measurements of the multimedia testbed on Mach 3.0: Experience writing real-time device drivers, servers, and applications
[AD-A273600] 06 p2460 N94-24932
The ISL rotor bench
[ISL-R-108/92] 06 p2185 N94-25301
Shake test results of the MDHC test stand in the 40-by 80-foot wind tunnel
[NASA-TM-108801] 07 p2641 N94-26596
Space Station technology testbed: 2010 deep space transport 07 p2687 N94-27368
Advanced development of particle beam probe diagnostic system
[DE94-002316] 07 p3047 N94-27720
Technology rigs: A tool for afterburner development 08 p3154 N94-29270
Implementation of instruments and facilities at the SGP CART site
[DE94-006839] 09 p3781 N94-31322
An experimental testbed for a free-floating manipulator
[AD-A277350] 09 p3726 N94-32334

TEST VEHICLES
NT FLIGHT TEST VEHICLES
High energy density aluminum-oxygen cell 06 p2393 N94-23363
Ferroelectric fluoride memory FET development
[AD-A274341] 07 p2785 N94-27057
Mars rover mechanisms designed for Rocky 4 08 p3161 N94-29630
DOE/KEURP site operator program
[DE94-005832] 08 p3267 N94-30701

TESTERS
U TEST EQUIPMENT

TESTING
U TESTS

TESTING MACHINES
U TEST EQUIPMENT

TESTING TIME
Validation and test of complex weapon systems 08 p3150 N94-29336

TESTS
Goddard Space Flight Center robotics demo
[NASA-TM-109302] 02 p0662 N94-13604
Optical testing 02 p0547 N94-14836
Automatic tools for system testing 06 p2197 N94-23913

TETHERED BALLOONS
Development of a balloon-borne stabilized platform for measuring radiative flux profiles in the atmospheric boundary layer
[DE93-013186] 01 p0274 N94-10323
Middle atmospheric electric fields over thunderstorms
[NASA-CR-194619] 03 p1106 N94-16493
Three flights into thunderstorms with the revised Rocket Electric Field Sounding (REFS) payload
[AD-A280424] 12 p4473 N94-37217

TETHERED SATELLITES
An experimental study of tether reel system: A laboratory model
[NAL-TR-1176T] 02 p0539 N94-12943
Prototype instrumentation and design studies
[AD-A266402] 03 p0882 N94-16530
Radiation of plasma wave wings through an electrodynamic tether satellite system with any sharp angle geometry
[REPT-85] 05 p1993 N94-20156
Data analysis support for the SPREE instruments on the TSS-1 shuttle flight
[AD-A272445] 05 p1654 N94-21429
Nearly uniform deployment/retrieval strategy for space tether systems 06 p2156 N94-24256
Dynamics and control of tethered satellite systems 08 p3170 N94-30864
Definition of ground test for verification of large space structure control
[NASA-CR-193945] 10 p4014 N94-34074

TETHERING
An experimental study of tether reel system: A laboratory model
[NAL-TR-1176T] 02 p0539 N94-12943
Data analysis support for the SPREE instruments on the TSS-1 shuttle flight
[AD-A272445] 05 p1654 N94-21429
Fingered bola body, bola with same, and methods of use
[NASA-CASE-MSC-21967-1] 06 p2354 N94-23822
An electronic interface for a fiber optic tethered unmanned underwater vehicle
[AD-A279046] 11 p4333 N94-35747
Permanent superconducting magnets for space applications
[NASA-CR-196293] 12 p4439 N94-37634

TETHERLINES
An experimental study of tether reel system: A laboratory model
[NAL-TR-1176T] 02 p0539 N94-12943
Prototype instrumentation and design studies
[AD-A266402] 03 p0882 N94-16530
Nearly uniform deployment/retrieval strategy for space tether systems 06 p2156 N94-24256
The 1991-1992 project summaries 07 p2943 N94-25698

TETRACHLORIDES
The adsorption and surface reaction of SiCl4 on Si(100)-(2x1)
[AD-A266124] 01 p0079 N94-12538

TETRACHLOROMETHANE
U CARBON TETRACHLORIDE

TETRAETHYL ORTHOSILICATE
Sol-gel derived silica/siloxane composite materials: The effect of loading level and catalyst activity on silica domain formation
[DE94-002734] 07 p2712 N94-27710
Surface chemistry of boron-doped SiO2 CVD: Enhanced uptake of tetraethyl orthosilicate by hydroxyl groups bonded to boron
[DE94-005428] 08 p3221 N94-30896
Preparation of catalyst particles using methods of colloid chemistry. Part 1: Preparation of silica particles from alcohol solutions
[PB94-135597] 09 p3634 N94-31679
Cross-condensation reactions in an organically modified silica sol-gel
[DE94-010086] 11 p4244 N94-35701

TETRAGONS
NT RECTANGLES
NT SQUARES (MATHEMATICS)
NT TRAPEZOIDS
Low-speed wind tunnel tests on four types of joined-wing aircraft models
[NAL-TR-1167] 02 p0501 N94-13340
Low-speed wind tunnel tests on a joined-wing aircraft model with various upper-fin
[NAL-TR-1169] 02 p0501 N94-13341
Eta percent-superconvergence in the interior of locally refined meshes of quadrilaterals: Superconvergence of the gradient in finite element solutions of Laplace's and Poisson's equations
[AD-A277242] 09 p3848 N94-32331

TETRAHEDRONS
Structural studies of sol-gel glasses
[AD-A266277] 03 p0967 N94-16472
Tetrahedral lander
[NASA-CASE-MSC-22082-1] 05 p1658 N94-20590
Dynamic mesh adaption for triangular and tetrahedral grids 05 p1920 N94-22363
Structures of tetrahedrization: A mathematical and algorithmical point of view
[ETN-94-95172] 06 p2480 N94-23166
Spatial symmetry, local integrability and tetrahedron equations in the Baxter-Bazhanov model
[DE93-634348] 07 p3002 N94-26038
Rotator phases in narrow-gap semiconductors
[DE94-005472] 08 p3521 N94-30897
Rare Earth Doped Semiconductors and Materials Research Society Symposium Proceedings, Volume 301
[AD-A277517] 09 p3908 N94-33055
Be3(AsO4)2.2H2O, a new beryllоarsenate phase containing bridged tetrahedral 3-rings
[AD-A278826] 11 p4340 N94-35677
Microstructure and chemistry of MgO- and CoO-doped nickel-titanate spinels
[DE94-012741] 12 p4537 N94-37382

TETRAHYDROFURAN
The reactivity of lithium toward non-aqueous solvents of relevance to energy storage applications as studied by surface analytical techniques
[DE94-003483] 07 p2856 N94-26464
Solution characterization of poly(isobornyl methacrylate) in tetrahydrofuran
[AD-A280497] 12 p4409 N94-37145

TETRANITROTETRAZACYCLOOCTANE
U HMX

TETROONS
U SUPERPRESSURE BALLOONS

TEXTBOOKS
Processes involved in the integration of pictures and discourse
[AD-A268150] 03 p1134 N94-17468
A teaching tool for linear programming
[AD-A270240] 04 p1523 N94-18905
Solar physics and terrestrial effects. A curriculum guide for teachers, grade 7-12
[PB94-142247] 09 p3953 N94-31595

TEXTILES
NT RAYON
New technology for effective control of flammability in polyolefin fiber/textiles 01 p0018 N94-10774
Resin transfer molding of textile composites
[NASA-CR-191505] 02 p0554 N94-12833
Flammability of clothing, volume 2
[DSIS-93-00036-VOL-2] 02 p0564 N94-13819
Graphite fiber textile preform/copper matrix composites
[NASA-CR-193797] 02 p0558 N94-14050
Processing, properties and applications of composites using powder-coated epoxy towpreg technology 03 p0933 N94-15277
Illustrated glossary of textile terms for composites
[NASA-CR-191539] 03 p0933 N94-15484
Verification of a two-dimensional infiltration model for the resin transfer molding process
[NASA-CR-194597] 03 p0964 N94-15656
FIBER-TEX 1992: The Sixth Conference on Advanced Engineering Fibers and Textile Structures for Composites
[NASA-CP-3211] 03 p0936 N94-16845
An overview of the NASA textile composites program 03 p0937 N94-16846
Research in textile composites at KU, Leuven 03 p0937 N94-16848
Effect of tow alignment on the mechanical performance of 3D woven textile composites 03 p0937 N94-16851
An engineering approach for the application of textile composites to a structural component 03 p0938 N94-16852
New textile composite materials development, production, application 03 p0938 N94-16853
Production and application of chemical fibers with special properties for manufacturing composite materials and goods of different usage 03 p0938 N94-16854
Textile composite processing science 03 p0938 N94-16856
Development of braided fiber seals for engine applications 03 p0939 N94-16859
Quantification of processing artifacts in textile composites 03 p0939 N94-16860
Stochastic damage evolution in textile laminates 03 p0939 N94-16861
Development of test methods for textile composites 03 p0939 N94-16862
Composites and textile reinforcement
[VTT-TIED-1424] 06 p2231 N94-25420
The potential of new textiles in improving survival prospects 08 p3380 N94-28430
Fire-resistant water vapour permeable buoyant insulation 08 p3380 N94-28431
Development of braided rope engine seals
[NASA-TM-105902] 08 p3298 N94-28838
Low dielectric polyimide fibers
[NASA-CASE-LAR-14526-1] 08 p3214 N94-29359
Physical interpretation and development of ultrasonic nondestructive evaluation techniques applied to the quantitative characterization of textile composite materials
[NASA-CR-195766] 08 p3183 N94-30016
Analysis of new composite architectures
[NASA-CR-195303] 09 p3626 N94-32904
Fracture micromechanics of continuous fiber and textile reinforced metal and ceramic matrix composites
[AD-A277434] 09 p3627 N94-33008
Second NASA Advanced Composites Technology Conference
[NASA-CP-3154] 09 p3627 N94-33121
Recent progress in NASA Langley Research Center textile reinforced composites program 09 p3629 N94-33134
Advanced textile applications for primary aircraft structures 09 p3629 N94-33135
Comparison of resin film infusion, resin transfer molding, and consolidation of textile preforms for primary aircraft structure 09 p3630 N94-33136
Characterization and manufacture of braided composites for large commercial aircraft structures 09 p3630 N94-33137
Through-the-thickness tensile strength of textile composites
[NASA-TM-109115] 11 p4233 N94-35946
ASTM test methods for composite characterization and evaluation 11 p4229 N94-36399

TEXTS
Abbreviations, acronyms, and initialisms frequently used by Martin Marietta Energy Systems, Incorporated
[DE93-012509] 01 p0420 N94-11369
Hypertext Compiling Tools (HCT): Developing model based applications with standard hypertext systems
[REPT-92-049] 02 p0750 N94-13822
Intelligent help facilities: Generating natural language descriptions with examples
[AD-A269555] 04 p1521 N94-18290
Automatic documentation generation: The interaction of text and examples
[AD-A269670] 04 p1616 N94-18570

Generating object descriptions: Intergrating examples with text
| AD-A269992 | 04 p1522 N94-18680
Speech synthesis with artificial neural networks
05 p1743 N94-20245
An assessment of the statistical and editorial output of text analysis programs
| AD-A272185 | 05 p2042 N94-20924
CMIFed: A presentation environment for porta ble hypermedia documents
| CWI-CS-R9305 | 05 p2044 N94-21494
The Amsterdam hypermedia model: Extending hypertext to support real multimedia
| CWI-CS-R9306 | 05 p2045 N94-21536
World processor: An interface for textual display and manipulation in virtual reality
| PB94-118643 | 06 p2592 N94-24642
Full-text information services at the desktop
| DE94-003728 | 07 p3096 N94-25813
Detecting the erosion of hierarchic information structures
| RUU-CS-93-10 | 09 p3916 N94-31365
High-speed data search 09 p3923 N94-32441
Emacs Lisp in Edwin scheme
| AD-A276721 | 09 p3818 N94-32504
Finding all periods and initial palindromes of a string in parallel
| AD-B175069 | 09 p3827 N94-33002
Report of the workshops: Automated generation of electronic technical manuals
| AD-A278046 | 10 p4150 N94-33401
A collection of tools in support of automatic differentiation
| DE94-010104 | 11 p4314 N94-35704

TEXTURES
Texture analysis of high Tc superconductors
01 p0399 N94-11314
Compositional and textural information from the dual inversion of visible, near and thermal infrared remotely sensed data 01 p0258 N94-12097
The EET87513 clast N: A CM2 fragment in an HED polymict breccia 01 p0453 N94-12117
Trace element distributions in primitive achondrites
01 p0431 N94-12200
Segmenting textured 3D surfaces using the space/frequency representation
| AD-A266960 | 03 p1163 N94-14968
Multiplicity of chondrule heating events and the coarsening of chondrule textures
05 p2085 N94-20860
Texture gradient effects in tantalum
| DE94-000689 | 06 p2240 N94-23021
The effects of texture and strain on the r-va lue of heavy gauge tantalum plate
| DE94-000690 | 06 p2242 N94-23541
Failures to model the development of a cube texture during the high temperature compression of Al-Mg alloys
| DE94-005013 | 08 p3201 N94-28544
Seafloor characterization using texture
| AD-A275399 | 08 p3377 N94-29204
Unsupervised texture image segmentation by improved neural network ART2
| AIAA PAPER 94-1199-CP | 08 p3442 N94-30549
Influence of tungsten alloying additions on the mechanical properties and texture of tantalum
| DE94-004994 | 08 p3210 N94-30774
A comparison of the evolution of cold and hot deformation microstructures and textures in fcc metals
| DE94-005103 | 08 p3210 N94-30777
Texture generation on irregular regions
| AD-A275999 | 09 p3841 N94-31359
Radar image classification by texture measurements
| ONERA-NT-1993-3 | 09 p3673 N94-31419
Visual evaluation of computer-generated textures
| AD-A277201 | 09 p3816 N94-32093
Quantitative analysis of woody vegetation in Soudano-Sahalian region. Textural approach (application to a Burkina Faso region) 09 p3757 N94-32574
Visual motion perception and visual information processing
| AD-A278370 | 10 p4097 N94-33738
Alteration and formation of rims on the CM parent body 11 p4357 N94-35411
On the possible role of elemental carbon in the formation of reduced chondrules 11 p4351 N94-35421
Textural constraints on the formation of alteration phases in CM chondrites 11 p4353 N94-36145

TFX AIRCRAFT
U F-111 AIRCRAFT

THAILAND
Thailand ISY activities 01 p0037 N94-10690
Detecting land cover changes in Chiang-Mai area in Thailand 02 p0693 N94-14241
Land evaluation for agricultural productivity in North-East Thailand using LANDSAT TM data and geographic information 02 p0693 N94-14242
The Environmental Research and Training Centre
07 p2873 N94-28280
Changes in phytoplankton population in the Chao Phraya estuary, Thailand, during the eutrophication mechanisms studies 07 p2875 N94-28287
Land use change in Thailand and its impact on environmental change: Joint Thai-Japanese research project (1993-1995) 07 p2875 N94-28288
Utilization of remote sensing data in Southeast Asia
08 p3327 N94-28936

THALAMUS
Cortical mechanisms of attention, discrimination, and motor response to somesthetic stimuli
| AD-A274163 | 07 p2940 N94-27141

THALLIUM
Characterization of InTlSb grown by low pressure metalorganic chemical vapor deposition on GaAs substrate
| AD-A266878 | 03 p1206 N94-14922
Fabrication and microstructural development of Ag-clad TlBa2Ca2Cu3O(x) tapes
| DE93-017407 | 04 p1597 N94-18500
Preparation and characterisation of the compound Tl(0.65) Bi(0.35) Ca(0.8) Sr(1.7) Cu2 O(y) using oxalate coprecipitation and analytical CBED and an initial preparation of Bi2Ca(n-1) Sr2Cu(n) O(4+2n) for n=5
| DE93-625470 | 04 p1602 N94-19277
Superconductivity Technology Program for Electric Power Systems: Proceedings
| DE93-040074 | 05 p2011 N94-19825
CsI(Tl)-photodiode detectors for spectroscopy at low radiation levels
| MPI-PHE/92-22 | 06 p2314 N94-25457

THALLIUM ALLOYS
Effect of experimental procedure on pattern formation and array disorder in cellular solidification
01 p0117 N94-10203

THALLIUM COMPOUNDS
Characterization of InTlSb grown by low pressure metalorganic chemical vapor deposition on GaAs substrate
| AD-A266878 | 03 p1206 N94-14922
Theory of energy-assisted epitaxy; theory of ordered semiconductor alloys: In(1-x)Tl(x)Sb as a long-wave infrared material
| AD-A271007 | 05 p2012 N94-19835
TlCaBaCuO high Tc superconducting microstrip ring resonators designed for 12 GHz
05 p1735 N94-20516
InTlSb for long-wavelength infrared photodetectors and arrays
| AD-A275079 | 08 p3512 N94-28872
The path for long range conduction in high J(sub c) TlBa2Ca2Cu3O(8+x) spray-pyrolyzed deposits
| DE94-007211 | 09 p3909 N94-33271
Vertical electron detachment energies for octahedral closed-shell multiply charged anions
| AD-A278835 | 11 p4322 N94-35753
Development of high Tc (greater than 100 K) Bi, Tl and Y-based materials as superconducting circuit elements
| NASA-CR-196276 | 12 p4534 N94-37103
InTlSb for long-wavelength infrared photodetectors and arrays
| AD-A280207 | 12 p4524 N94-37149
Effect of thermal annealing on grain boundary chemistry of polycrystalline TlBa2Ca2Cu3O(y) films
| DE94-011464 | 12 p4538 N94-37569
High T(sub c) copper-oxide superconductors comprising Tl-Sr-Ca-Cu-O
| AD-D016307 | 12 p4538 N94-37776

THAWING
U MELTING

THEMATIC MAPPERS (LANDSAT)
Combined analysis of ERS-1 SAR and visible/infrared remote sensing data for land cover/land use mapping in a tropical zone: A case study in Guinea
01 p0246 N94-12478
Dendrometric variables estimation in homogeneous forests using LANDSAT TM data
| INPE-5455-TDI/497 | 02 p0684 N94-13331
Volcanic thermal features observed by AVIRIS
03 p1068 N94-16680
Integrating remote sensing techniques at Cuprite, Nevada: AVIRIS, Thematic Mapper, and field spectroscopy 03 p1072 N94-16701
Linear mixing model applied to AVHRR LAC data
05 p1838 N94-20958
The 7th Brazilian Remote Sensing Symposium, volume 3 05 p1839 N94-20960
Evaluation of C-band SAR data from SAREX 1992: Tapajos study site 05 p1839 N94-20964
Information extraction for multispectral images using radiation interaction models
| BCRS-90-22 | 05 p1841 N94-21015
Chromaticity analysis of LANDSAT multispectral scanner and thematic mapper imagery of Chilko Lake, British Columbia, using a theoretical optical water quality model
| ISBN-0-315-63832-X | 05 p1843 N94-22422
Comparison of SPOT, ERS-1, SEASAT, LANDSAT TM, and merged imagery for geological investigations
09 p3752 N94-32547
Optimal geological data extraction from SPOT-radar synergism with samples from Djebel Amour (Algeria), Red Sea Hills (Sudan), Sirte Basin (Libya), and Magdalena Valley (Colombia) 09 p3752 N94-32548
Rapid estimates of crop acreage and production at European scale using high resolution imagery
09 p3754 N94-32557
ERS-1 SAR and optical data for land use/land cover mapping: A case study in a savannah zone of Guinea
09 p3755 N94-32565

THEMATIC MAPPING
Satellite inventory of Minnesota forest resources
| NASA-CR-193565 | 01 p0231 N94-11521
Basal scarp, paleoglacier, and fissure flows of Elysium Mons, Mars 01 p0459 N94-12148
Synthesis of global thematic mapping, Venus: Geologic correlations/questions for the Magellan gravity mission
01 p0467 N94-12194
Geoecological monitoring of an agricultural area
01 p0248 N94-12489
Dendrometric variables estimation in homogeneous forests using LANDSAT TM data
| INPE-5455-TDI/497 | 02 p0684 N94-13331
Net radiation mapping of mountainous terrain using Landsat-5 thematic mapper imagery and digital terrain data
| ISBN-0-315-57755-X | 02 p0685 N94-13475
Satellite imagery and exogenous data integration by neural network in automation land-cover classification
| INPE-5480-PRE/1778 | 02 p0686 N94-13729
Do it yourself remote sensing: Generating an inexpensive, high tech, real science lake mapping project for the classroom 03 p1086 N94-16407
Mapping vegetation types with the multiple spectral feature mapping algorithm in both emission and absorption 03 p1069 N94-16686
Classification of simple vegetation types using POLSAR image data 05 p1722 N94-20420
Geology and radiophysical properties of the Venera and Vega landing sites 05 p2135 N94-20867
Evaluation of simulated JERS-1 data for geologic mapping at Drum Mountains, Utah, Silver Bell, Arizona, and Wind River, Wyoming under the GEOSAT-ERSDAC/JAPEX/JGI/RESTEC joint studies
08 p3326 N94-28929
Extrapolation of point data for resource mapping
08 p3334 N94-29959
The effects of vegetation on the ability to map soils using GERIS data 09 p3744 N94-31860
A case study comparing multi-temporal ERS-1 SAR data and SPOT data for tropical forest mapping
09 p3753 N94-32556
Comparing SPOT and SIR A for mapping superficial formations in tropical forest regions: Example of the Yaoundy Region (Cameroon) 09 p3755 N94-32562
ERS-1 SAR and optical data for land use/land cover mapping: A case study in a savannah zone of Guinea
09 p3755 N94-32565
Stratification of deforested areas by vegetation types in Amazonia, using geographic information systems: Study of case at SB20 Purus map
| INPE-5541-TDI/529 | 10 p4077 N94-34230

THEODOLITES
NT CINETHEODOLITES

THEOREM PROVING
Operator substitution
| MEMO-COSOR-92-51 | 01 p0343 N94-10867
Wait-free linearization with an assertional proof
| CS-9208 | 01 p0323 N94-10878
EVES: An overview
| DSIS-93-00238 | 02 p0752 N94-14088
An elementary tutorial on formal specification and verification using PVS
| NASA-TM-108991 | 03 p1158 N94-15536
Global solutions to a system of strongly coupled reaction-diffusion equations
| DE93-628587 | 03 p1171 N94-17640
Distributively generated matrix near rings
| DE93-628588 | 03 p1175 N94-17641
Contribution to the analysis of tableaus based decision methods
| ETN-93-94355 | 04 p1560 N94-18067
Formal hardware verification of digital circuits
04 p1401 N94-18367
Updated Contributions to the Twente Workshop on Hamiltonian Graph Theory
| MEMO-1076 | 04 p1554 N94-19683

On Hamilton-connectedness of Cayley graphs
04 p1554 N94-19684
On Hamiltonian properties of 2-tough graphs
04 p1554 N94-19685
The complete closure of a graph
04 p1555 N94-19690
Twenty odd statements in Twente
04 p1555 N94-19691
Generalized closures of graphs
04 p1555 N94-19692
COCOLOG: A conditional observer and controller logic for finite machines
[INRIA-RR-1714] 05 p1910 N94-21063
Partition algebraic design of asynchronous sequential circuits 05 p1759 N94-21125
The Robinson-Schensted and Schuetzenberger algorithms. Part 1: New combinatorial proofs
[CWI-AM-R9208-PT-1] 05 p1911 N94-21156
On semisimple cocommutative bialgebras
[CWI-AM-R9210] 05 p1954 N94-21158
Hilbert 90 for polynomial matrices
[CWI-AM-R9211] 05 p1954 N94-21159
An NP set with no co-DP sparse subset
[TR-475] 05 p1954 N94-21199
A mechanized process algebra for verification of device synchronization protocols 05 p1766 N94-21716
HDL to verification logic translator
05 p1766 N94-21717
Semi-stability and heights of cycles
[PB93-215507] 05 p1961 N94-22377
Exploiting structure: Introduction and motivation
[NASA-CR-195136] 06 p2490 N94-24847
On the inversion of the n-dimensional Laplace transform
[RR-461] 06 p2492 N94-25310
Extension problem for generalized multi-monogenic functions in Clifford analysis
[DE93-616818] 06 p2493 N94-25433
A reachability test for systems over polynomial rings using Groebner bases
[MEMO-COSOR-92-38] 06 p2493 N94-25527
Partial support for the Second International Symposium on Artificial Intelligence and Mathematics
[AD-A275199] 08 p3434 N94-29026
Program derivation by proof transformation
[AD-A275260] 08 p3453 N94-29304
Addendum to the final report for the investigation of proof techniques within the EVES verification technology
[TR-93-5451-03] 08 p3421 N94-30155
A smart child of Peano's
[ML-92-10] 08 p3455 N94-30325
Only few graphs have bounded treewidth
[RUU-CS-92-35] 08 p3455 N94-30333
Two algorithms for finding rectangular duals of planar graphs
[RUU-CS-92-41] 08 p3423 N94-30345
Derivation lengths in term rewriting from interpretations in the naturals
[RUU-CS-92-43] 08 p3455 N94-30346
The transient period of a cyclic process: An horizon theorem
[MEMO-1149] 08 p3427 N94-30585
Bisimulations and predicate logic
[CWI-CS-R9333] 08 p3460 N94-30735
Formal verification of systolic multipliers with the Boyer-Moore theorem prover
[RR-897-M] 09 p3839 N94-31082
OTTER 3.0 reference manual and guide
[DE94-007457] 09 p3829 N94-31315
Proving theorems of the Lambek calculus of order 2 in polynomial time
[CT-93-05] 09 p3842 N94-31393
The p-q-r-medial axis algorithm requires only local operations
[CWI-BS-R9317] 09 p3849 N94-32507
Interpreter composition issues in the formal verification of a processor-memory module
[NASA-CR-4594] 09 p3820 N94-32775
New proof and extension of Sarkovskii's theorem
[AD-A278347] 10 p4129 N94-34004
Combining symbolic computation and theorem proving: Some problems of Ramanujan
[AD-A278899] 11 p4303 N94-35573
Priorities and nonmonotonic reasoning
[PB94-171170] 11 p4346 N94-35959

THEOREMS
NT BAYES THEOREM
NT BERNOULLI THEOREM
NT BINOMIAL THEOREM
NT DUALITY THEOREM
NT EXISTENCE THEOREMS
NT FLOQUET THEOREM
NT GAUSS-MARKOV THEOREM
NT LEBESGUE THEOREM
NT LIOUVILLE THEOREM
NT RECIPROCITY THEOREM
NT SIMILARITY THEOREM
NT STOKES THEOREM (VECTOR CALCULUS)
NT UNIQUENESS THEOREM
NT VIRIAL THEOREM
Convergence theorems for a class of nonlinear maps in uniformly smooth Banach spaces
[DE92-641347] 01 p0343 N94-10531
On the doubling of hydrodynamic theorems in relativistic theory of superfluidity
[DE93-617895] 01 p0148 N94-10717
No-lost theorem for parity violating nucleon-nucleon scattering experiments
[DE93-012737] 02 p0779 N94-12949
Fast parallel string prefix-matching
[AD-A267758] 02 p0760 N94-13924
Fixed point iterations for strictly hemi-contractive maps in uniformly smooth Banach spaces
[DE93-628591] 03 p1175 N94-17644
Polling systems: Moment stability of station times and central limit theorems
[PB93-191955] 04 p1560 N94-18990
Attribute evaluation during generalized parsing
[MEMO-INF-92-85] 04 p1526 N94-19224
Excursions of stochastic processes, Cox-point processes, entrance behavior and resolvents
[PB93-197291] 04 p1558 N94-19323
On Hamilton-connectedness of Cayley graphs
04 p1554 N94-19684
Symmetries and conservation laws of the system: u(x) = vw(x), v(y) = uw(y), uv + w(xx) + w(yy) = 0
[MEMO-1084] 05 p1953 N94-21046
Hilbert 90 for polynomial matrices
[CWI-AM-R9211] 05 p1954 N94-21159
Instruction set commutivity 05 p1766 N94-21719
On the numerical computation of invariant manifolds
[W-9306] 06 p2480 N94-23140
The cusp horseshoe and its bifurcations in the unfolding of an inclination-flip homoclinic orbit
[W-9307] 06 p2480 N94-23141
A theorem regarding roots of the zero-order Bessel function of the first kind 06 p2325 N94-23667
The Third Twente Workshop on Graphs and Combinatorial Optimization
[PB94-110947] 06 p2486 N94-23722
Egalitarian non-average contribution method for cooperative games
[PB94-111705] 06 p2497 N94-23800
Tail processes under heavy random censorship with applications
[PB94-110632] 06 p2495 N94-24508
Reduced game properties of egalitarian division rules for cooperative games
[PB94-111689] 06 p2521 N94-24523
Tool sharing, part 3
[PB94-111697] 06 p2467 N94-24524
Polynomials orthogonal with respect to an inner product involving differences
[PB94-110731] 06 p2489 N94-24572
Chebyshev-Markov rational functions over several intervals
[PB94-125333] 07 p2998 N94-27116
Wieand's theorem
[PB94-126711] 07 p3004 N94-27223
The Einstein tensor characterizing some Riemann spaces
[DE94-603663] 07 p3074 N94-27626
Dynamic generalized quantifiers and monotonicity
[LP-93-02] 08 p3454 N94-30319
Modal quantification over structured domains
[ML-93-02] 08 p3457 N94-30396
The transient period of a cyclic process: An horizon theorem
[MEMO-1149] 08 p3427 N94-30585
Perfect binary space partitions
[RUU-CS-93-23] 08 p3460 N94-30728
The structure of exponentials: Uncovering the dynamics of linear logic proofs
[ML-93-10] 08 p3430 N94-30973
Inventory of fragments and exact models in intuitionistic proportional logic
[ML-93-11] 08 p3463 N94-30974
Undecidability in diagonalizable algebras
[ML-93-13] 08 p3463 N94-30976
Remarks on a result of LAV Carvalho
[AD-A276404] 09 p3841 N94-31360
Generalization of a theorem of Kusmin
[REPT-93-74] 09 p3844 N94-31643
The Cameron-Martin theorem
[W-9315] 09 p3844 N94-31676
The p-q-r-medial axis algorithm requires only local operations
[CWI-BS-R9317] 09 p3849 N94-32507
Combining symbolic computation and theorem proving: Some problems of Ramanujan
[AD-A278899] 11 p4303 N94-35573
Some theorems on a class of harmonic manifolds
[DE94-611102] 11 p4315 N94-35934

THEORETICAL PHYSICS
NT NEWTON THEORY
NT QUANTUM THEORY
On parity conservation and the question of the missing, right-handed neutrino
[DE93-613092] 01 p0361 N94-10414
A version of superstring with four space-time dimensions
[DE93-608196] 01 p0412 N94-11163
Experimental and theoretical high energy physics program
[DE93-013336] 01 p0373 N94-12600
Quaternions and the heuristic role of mathematical structures in physics
[DE93-622865] 02 p0816 N94-12844
Research in theoretical nuclear physics
[DE93-015096] 02 p0839 N94-14330
Theoretical high energy physics research at the University of Chicago
[DE93-016863] 03 p1187 N94-16116
Experimental study of weak interactions by precision measurement by rare kaon decay
[DE93-016864] 03 p1182 N94-16117
Theoretical high energy physics
[DE93-015884] 03 p1187 N94-16170
Neutrino mass and mixing: Summary of the neutrino sessions
[DE93-014342] 03 p1183 N94-16801
Heavy ion physics research at Creighton University
[DE93-016809] 03 p1185 N94-16957
Derivation of the Verlinde formula from Chern-Simons theory and the G/G model
[DE93-628620] 03 p1221 N94-17632
On the difference caused by CP violation in the energy spectra of pions in K(sup (+-))(yields)(pi)(+-)(pi)(+-)(pi)-+ decays
[DE93-624828] 04 p1564 N94-17687
International Centre for Theoretical Physics, Trieste Scientific activities in 1991
[DE93-624757] 04 p1606 N94-17792
Center of Excellence in Theoretical Geoplasma Research
[AD-A270210] 04 p1588 N94-18902
Experimental research in high energy physics
[DE93-011912] 04 p1574 N94-18916
Extensions of 2D gravity
[DE93-018525] 04 p1485 N94-18929
Search for top quark with D0 detector
[DE93-040170] 04 p1572 N94-19536
Energy and luminosity limits of hadron supercolliders
[DE93-019248] 05 p1980 N94-20300
High energy physics program at Texas A/M University
[DE93-041089] 05 p1980 N94-20933
Theoretical particle physics
[DE94-000538] 05 p1973 N94-20938
Non commutative geometry and physics
[PB93-215499] 05 p1961 N94-22264
Towards a theory of quark and lepton masses
[DE94-001726] 06 p2533 N94-23218
Theoretical atomic physics for fusion
[DE94-000712] 06 p2533 N94-23543
Heavy flavour physics at LEP
[NIKHEF-H/92-19] 06 p2539 N94-25465
Orbit spaces over commutative rings and projectives as semi-isomorphisms
[DE93-616822] 06 p2493 N94-25473
Duality for multiparametric quantum GL(n) and for a Lorentz quantum group
[DE93-613048] 07 p3005 N94-25868
Theoretical and experimental studies of elementary physics
[DE94-002310] 07 p3008 N94-25988
Z(sub N)(sup n-1) broken model
[DE93-634357] 07 p3072 N94-26039
Lepton masses in an SU(3)(sub L) x U(1)(sub N) gauge model
[DE93-634366] 07 p3016 N94-26040
Dimensional crossover from non-renormalizability to renormalizability
[DE93-613052] 07 p3006 N94-26193
Stability of large scale interconnected dynamical systems
[DE94-601536] 07 p2993 N94-26408
Characterization of self-conjugate minimal surfaces in R(sup 3)
[DE94-601538] 07 p2993 N94-26409
Enumeration of n-fold tangent hyperplanes to a surface
[DE94-601544] 07 p2993 N94-26412
On the phi(sub 0)-stability of perturbed nonlinear differential systems
[DE93-634304] 07 p2993 N94-26441

Anomaly candidates and invariants of D 4, N 1 supergravity theories
[NIKHEF-H/93-12] 07 p3072 N94-26541
Strange Dibaryons
[DE94-003005] 07 p3022 N94-26769
Flavor changing neutral currents in SU(3) x U(1) models
[DE94-602576] 07 p3022 N94-26899
Specialized data base management system for data processing in the experiments at low energies
[DE94-606268] 08 p3485 N94-28621
Weak decays of charged K-mesons and charm particles
[PB94-138062] 08 p3486 N94-29143
Magnetic properties of a quantum transverse spin-1 Blume-Emery-Griffiths model
[DE94-608114] 08 p3517 N94-30109
Research laboratories annual report 1992
[DE94-608124] 08 p3555 N94-30168
Conformal field theory and geometry of strings
[PB94-148442] 09 p3857 N94-31770
New QCD results from string theory
[DE94-005226] 09 p3911 N94-31823
The 14th Annual West Coast Theoretical Chemistry/Statistical Mechanics Conference
[AD-A276942] 09 p3656 N94-32239
Research program in particle physics
[DE94-008449] 09 p3871 N94-32512
Experimental and theoretical high energy physics research
[DE94-008339] 10 p4139 N94-33844
Three-photon micromasers
[DE94-611106] 11 p4272 N94-35782
Physics Division annual review, 1 April 1992 - 31 March 1993
[DE94-002497] 12 p4512 N94-36513
High Energy Physics Division of research activities
[DE93-019681] 12 p4521 N94-36694
Quantum and quasi-classical analyses of high order emission processes
[DE93-041348] 12 p4513 N94-36697
Direct photoionization of excited helium
[DE94-618732] 12 p4516 N94-37097
Is it possible to assign physical meaning to field theory with higher derivatives?
[DE94-618468] 12 p4539 N94-37172
Activities of the Laboratory of Physics, Helsinki University of Technology
[PB94-175247] 12 p4509 N94-37301

THERAPY
NT CHEMOTHERAPY
NT RADIATION THERAPY
Center of Excellence in Laser Medicine
[DE93-016541] 03 p1122 N94-16113
Rewarming methodologies in the field
[AD-A274744] 07 p2909 N94-26173
Development of surgical CW Nd:YAG laser with optical fiber delivery system
[DE93-632902] 07 p2817 N94-26185
Bakteriella toxiner-morgondagens hot (bacterial toxins-the threat of tomorrow)
[PB94-124229] 07 p2902 N94-27045
The effectiveness of ground level post-flight 100 percent oxygen breathing as therapy for pain-only altitude Decompression Sickness (DCS)
10 p4096 N94-33643
On the feasibility of virtual environments in medicine
12 p4483 N94-37264

THERMAL ABSORPTION
NT POLAR CAP ABSORPTION
The annual pressure cycle on Mars: Results from the LMD Martian atmospheric general circulation model
06 p2619 N94-24884

THERMAL AGITATION
U THERMAL ENERGY

THERMAL ANALYSIS
Fire resistance and mechanical properties for phenolic prepregs 01 p0020 N94-10786
A high specific power solar array for low to mid-power spacecraft 01 p0051 N94-11399
Results of thermal vacuum tests for the PASP+ flight modules 01 p0053 N94-11410
Lifetime prediction of materials exposed to the natural space environment
[NASA-CR-193833] 02 p0561 N94-12830
Ohmic heating of composite candidate graphite-fiber/coating combinations
[NASA-TM-4491] 02 p0554 N94-12871
Boundary formulations for nonlinear design sensitivity analysis 02 p0672 N94-13669
Optimization of the processing parameters of high temperature superconducting glass-ceramics: Center Director's discretionary fund final report
[NASA-TM-108421] 02 p0808 N94-13938
Computer program for analysis of high speed, single row, angular contact, spherical roller bearing, SASHBEAN. Volume 1: User's guide
[NASA-CR-191183] 02 p0663 N94-14445
Computer program for analysis of high speed, single row, angular contact, spherical roller bearing, SASHBEAN. Volume 2: Mathematical formulation and analysis
[AD-A276235] 02 p0664 N94-14446
A novel solid-state optical temporal analyzer with picosecond resolution and picowatt sensitivity
[AD-A266804] 03 p0986 N94-14912
High temperature advanced structural composites. Volume 2: Ceramic matrix composites, fiber processiing and properties, and interfaces
[AD-A267023] 03 p0933 N94-15528
A Pluto thermal model 03 p1256 N94-16216
Comparative magnetic and thermoanalytical study of two enstatite chondrites: Adhi Kot and Atlanta
03 p1244 N94-16329
SRB thermal curtain design support
[NASA-CR-193857] 03 p0927 N94-17123
SRB thermal curtain design support
[NASA-CR-193858] 03 p0928 N94-17124
Overview of the solar dynamic ground test demonstration program
[NASA-TM-106296] 03 p0928 N94-17256
ASRM nozzle thermal analysis
[NASA-CR-194672] 03 p0928 N94-17277
Structural mechanics division research and technology accomplishments for CY 1992 and plans for CY 1993
[NASA-TM-107752] 03 p1062 N94-17479
FEM/SINDA: Combining the strengths of NASTRAN, SINDA, I-DEAS, and PATRAN for thermal and structural analysis 04 p1449 N94-17831
Heat load analysis on the cable-in-conduit with central core conductor for the TF coil Rebut layer design
[DE93-013783] 04 p1395 N94-17872
Current development in selected stress and thermal analysis software interfaces with PRO-ENGINEER
[DE93-014935] 04 p1518 N94-17943
Infrared detection with high-(Tc bolometers and response of Nb tunnel junctions to picosecond voltage pulses
[DE93-016963] 04 p1595 N94-17989
Knowledge sources for an intelligent MCM analyzer
[AD-A269224] 04 p1542 N94-18887
Thermal analysis of coatings and substrate materials during a disruption in fusion reactors
[DE93-017688] 04 p1588 N94-18971
Accelerated screening methods for determining chemical and thermal stability of refrigerant-lubricant mixtures. Part 1: Method assessment
[DE93-040215] 04 p1351 N94-19136
Thermo-hydraulic analysis of superconducting toroidal-field magnets for the Tokamak Physics Experiment
[DE93-018096] 04 p1590 N94-19269
Effects of pressure on the orientational ordering and phase transitions in solid C(60) and C(70)
[DE93-018858] 04 p1603 N94-19347
Proceedings: International Symposium on Thermal Engineering and Science for Cold Regions
[AD-A270636] 04 p1487 N94-19529
Transient thermal analysis of cryocondensation pump for JET
[DE93-040372] 05 p1992 N94-20003
Three-dimensional dynamic thermal imaging of structural flaws by dual-band infrared computed tomography
[DE93-019575] 05 p1906 N94-20316
Kinetics of phase transformations in glass forming systems
[NASA-CR-194270] 05 p1701 N94-20347
A study of the induction heating of organic composites
[AD-A272657] 05 p1675 N94-21187
Estimating the rotation rate of mesoscale ocean rings from satellite altimetry
[AD-A272922] 05 p1883 N94-21222
Thermal stress analysis of composites in the space environment 05 p1661 N94-21379
Concept report: Experimental vector magnetograph (EXVM) operational configuration balloon flight assembly
[NASA-CR-194702] 05 p1638 N94-21776
Development of BEM for ceramic composites
[NASA-CR-194718] 05 p1676 N94-21777
Preliminary SP-100/Stirling heat exchanger designs
[NASA-TM-106444] 05 p1670 N94-21809
A finite element formulation and adaptive solution approach for large-scale thermomechanical problems with complex contact conditions
[DE93-019605] 05 p1960 N94-21996
In situ identification of the Martian surface material and its interaction with the Martian atmosphere using DTA/GC 05 p1812 N94-22434
A pressurized thermogravimetric analyzer for use in studies of gas/solid systems
[DE94-001224] 06 p2342 N94-22989
Fully coupled nonlinear thermomechanical analysis including general contact in PALM2D
[DE94-001661] 06 p2568 N94-23216
Improved thermal force modeling for GPS satellites
06 p2207 N94-23259
Mechanical and thermal buckling analysis of sandwich panels under different edge conditions
[NASA-TM-4535] 06 p2228 N94-23514
The Fifth Annual Thermal and Fluids Analysis Workshop
[NASA-CP-10122] 06 p2320 N94-23634
Advanced X ray Astrophysics Facility-Imaging (AXAF-I) thermal analyses using Integrated Thermal Analysis System (ITAS) program 06 p2320 N94-23635
Uncertainty analysis of diffuse-gray radiation enclosure problems: A hypersensitive case study
06 p2320 N94-23637
A comparison of TSS and TRASYS in form factor calculation 06 p2321 N94-23638
Accuracy control in Monte Carlo radiative calculations
06 p2321 N94-23639
Some useful innovations with TRASYS and SINDA-85
06 p2322 N94-23647
Analysis of high vacuum systems using SINDA'85
06 p2322 N94-23648
Thermal analysis of combinatorial solid geometry models using SINDA 06 p2323 N94-23650
Unsteady three-dimensional thermal field prediction in turbine blades using nonlinear BEM
06 p2325 N94-23665
Response-coefficient method for heat-conduction transients with time-dependent inputs
06 p2326 N94-23671
Thermal-fluid analysis of the fill and drain operations of a cryrogenic fuel tank
[NASA-TM-104273] 06 p2334 N94-24495
Aspects of the circuit board thermal design
[VTT-PUBS-132] 07 p2779 N94-25644
Modelling the inhibition cure behaviour of unsaturated polyester moulding materials
[PB94-124864] 07 p2748 N94-25893
Evaluation of helium cooling for fusion divertors
[DE94-002680] 07 p3042 N94-25976
User's guide for the thermal analyst's help desk expert system
[NASA-CR-194885] 07 p2695 N94-26103
Design of gasifiers to optimize fuel cell systems
[DE94-000010] 07 p2856 N94-26581
Thermal/structural tailoring of engine blades (T/STAEBL). User's manual
[NASA-CR-194463] 07 p2839 N94-26692
Verification of thermal analysis codes for modeling solid rocket nozzles
[NASA-CR-195248] 07 p2702 N94-27150
Thermal/Structural Tailoring of Engine Blades (T/STAEBL): User's manual
[NASA-CR-194461] 07 p2843 N94-27776
Evaluation of high temperature superconductive thermal bridges for space-borne cryogenic infrared detectors
07 p2815 N94-27921
Thermal modeling of NiH2 batteries
07 p2862 N94-28113
Use of calorimetry for end of charge determination
07 p2863 N94-28128
Thermal/structural tailoring of engine blades (T/SEAEBL). Theoretical manual
[NASA-CR-194462] 08 p3317 N94-28815
Modelling and analysis of creep deformation and fracture in a 1 Cr 1/2 Mo ferritic steel
[PB94-138328] 08 p3319 N94-29121
Application of FLUIDNET-G software to the preliminary thermal and hydraulic design of Hermes spaceplane
[REPT-932-440-107] 08 p3168 N94-29543
Study of iron exchanged zeolites by Moessbauer effect and electron spin resonance spectroscopy
[DE94-605138] 08 p3514 N94-29691
Analysis of infrared radiation heating process considering chemical reaction of material to be heated
[DE94-744116] 08 p3199 N94-30267
Terfenol: A study of the phase equilibrium diagram and the solidification process
[DE94-004883] 08 p3209 N94-30690
A thermal viscoelastic analysis for thick-walled composite cylinders
[AD-A274143] 09 p3625 N94-32604
THERM3D: A boundary element computer program for transient heat conduction problems
[DE94-008112] 09 p3708 N94-32709
Novel precursor approached for CMC derived by polymer pyrolysis
[AD-A278383] 09 p3665 N94-33352
Induction heating model for high-frequency induction joining and repair of complex-shape graphite fiber/polymer matrix composites 10 p4018 N94-33362

Prediction modeling of physiological responses and human performance in the heat with application to space operations 10 p4098 N94-33652
A 32-GHz solid-state power amplifier for deep space communications 11 p4255 N94-35562
Demonstration of a high heat removal CVD diamond substrate edge-cooled multichip module
[DE94-010748] 11 p4260 N94-36245
An adaptive, unstructured, finite-element, multi-material, thermal analysis
[AD-A278632] 11 p4343 N94-36256
Preliminary analysis for a Mach 8 crossilow transition experiment on the Pegasus (R) space booster
[NASA-TM-104272] 12 p4381 N94-36648
Methodologies for thermal and mechanical testing of TMC materials 12 p4401 N94-36659
United States Air Force Summer Research Program, 1993. Volume 6: Arnold Engineering Development Center, Frank J. Seiler Research Laboratory and Wilford Hall Medical Center
[AD-A278697] 12 p4551 N94-36982
Transient thermal and dynamic stresses in strongback-design blankets
[DE94-012639] 12 p4530 N94-37441
A method for thermal analysis of spiral bevel gears
[NASA-TM-106612] 12 p4451 N94-37451
Reference manual for the Thermal Analyst's Help Desk Expert System
[NASA-CR-194941] 12 p4397 N94-37504

THERMAL BATTERIES

Effects of repeating resistance testing on firing ability of igniter EP360-3
[AD-A274814] 07 p2759 N94-26486
The relative performance of FeS2 and CoS in long-life thermal-battery applications
[DE94-006145] 09 p3695 N94-32663

THERMAL BLOOMING

Internally folded scalable laser
[AD-D015978] 06 p2350 N94-25216

THERMAL BOUNDARY LAYER

Boundary layers along horizontal free surfaces due to combined effects of temperature and concentration gradients 01 p0106 N94-10108
Models of thermal/chemical boundary layer convection: Potential application to Venus 03 p1279 N94-16348
On the relationship between tectonic plates and thermal mantle plume morphology 03 p1104 N94-16349
Experimental investigation of turbulent Prandtl number and Reynolds analogy in transitional and post-transitional boundary layers
[AD-A270092] 04 p1418 N94-18867
EHD enhancement of pool and in-tube boiling of alternate refrigerants
[DE94-000787] 05 p1798 N94-20101
Hydrodynamics of convection under winter polar leads
[AD-A275182] 08 p3369 N94-29067

THERMAL BUCKLING

Mechanical and thermal buckling analysis of sandwich panels under different edge conditions
[NASA-TM-4535] 06 p2228 N94-23514
Free vibration of thermally loaded panels including initial imperfections and post-buckling effects
[NASA-TM-109097] 08 p3479 N94-29461
Effective computational strategy for predicting the response of complex systems
[AD-A277452] 09 p3740 N94-33011
Mechanical and thermal buckling analysis of rectangular sandwich panels under different edge conditions
[NASA-TM-4585] 10 p4069 N94-33704
Analysis of high speed flow, thermal and structural interactions
[NASA-CR-196017] 11 p4268 N94-36420

THERMAL COMFORT

Thermal strain generated by an enhanced anti-G protection system in a hot climate 08 p3383 N94-28445
Recent Canadian advances in active thermal protection 08 p3384 N94-28451
Maintaining acceptable thermal comfort with a low air temperature by means of local heating
[PB94-138526] 08 p3401 N94-29950

THERMAL CONDUCTIVITY

Measurement of the thermal conductivity of molten InSb in a drop shaft 01 p0105 N94-10102
Thermophysical properties of undercooled liquid metals 01 p0086 N94-10190
Stationary spectra of short-wave convective and magnetostatic fluctuations in a finite-pressure plasma and anomalous heat conductivity
[DE93-617852] 01 p0388 N94-10840
Experimental study of multiple droplet evaporative cooling
[PB93-198463] 01 p0149 N94-10851
Low-expansion ceramics initiative
[DE93-011860] 01 p0089 N94-11106
Progress toward atomic layer epitaxy of diamond: Diamond films grown one layer at a time
[AD-A265530] 01 p0403 N94-12010
Martian particle size based on thermal inertia corrected for elevation-dependent atmospheric properties 01 p0430 N94-12107
Does the thermal wind exist near the Earth's core boundary? 01 p0283 N94-12217
Experimental investigation of the effects of blowing ratio parameter on heat transfer to a film-cooled flat plate
[AD-A266599] 02 p0636 N94-13780
Optical and physical properties of the LiSrAlF6:Cr laser crystal
[DE93-014657] 02 p0808 N94-13881
Thermal conductance of pressed metallic contacts augmented with Indium foil or Apiezon-N (tm) grease at liquid helium temperatures
[NASA-TM-108779] 02 p0776 N94-14027
Physical and structural properties of a sputtered zirconia-yttria layer used as a thermal resistance
[ONERA-NT-1992-10] 02 p0810 N94-14193
The accuracy of approximating radiative heat transfer using a temperature dependent thermal conductivity
[DE93-013105] 02 p0638 N94-14318
Anomalous ion transport and feedback control
[DE93-018324] 02 p0803 N94-14874
A posteriori error estimation for hierarchic models of elliptic boundary value problems on thin domains
[AD-A267714] 03 p1168 N94-14939
Modeling the thermal conductivity of fiber-reinforced ceramic composites
[DE93-015340] 03 p0934 N94-16017
SRB thermal curtain design support
[NASA-CR-193858] 03 p0928 N94-17124
Low dielectric constant insulators and gold metallization for GHz multi-chip modules, part 2
[AD-A268590] 03 p1176 N94-17605
Coefficients for calculating thermodynamic and transport properties of individual species
[NASA-TM-4513] 03 p1220 N94-17624
Coupled MHD and transport analysis of improved confinement D3-D discharges
[DE93-016985] 04 p1585 N94-18057
Development of a cryogenic heat pipe
[DE93-018448] 04 p1417 N94-18831
A database of selected transport coefficients for combustion studies
[DE93-041278] 05 p1678 N94-19889
A parametric study of heat transfer within a planar thermosyphon
[DE93-019546] 05 p1799 N94-20258
Thermal conductivity measurements of particulate materials under Martian conditions 05 p1685 N94-20703
Fully coupled nonlinear thermomechanical analysis including general contact in PALM2D
[DE94-001661] 06 p2568 N94-23216
Fire safety engineering research in Norway
[PB93-201630] 06 p2268 N94-23429
Uncertainty analysis of diffuse-gray radiation enclosure problems: A hypersensitive case study 06 p2320 N94-23637
Features of a SINDA/FLUINT model of a liquid oxygen supply line 06 p2322 N94-23649
Thermal conductivity of PAX 2A explosive by DSC
[AD-A274721] 07 p2759 N94-26437
Sound, speed, reflectivity, absorption, and thermal diffusivity measurements in Arctic ice in 1990
[AD-A274326] 07 p2899 N94-26886
Thermal conductivity of liquid aliphatic alcohols
[ESDU-93008] 07 p2720 N94-28058
Thermal conductivity of liquid carboxylic acids
[ESDU-93017] 07 p2721 N94-28138
Properties of graphite fiber reinforced copper matrix composites for space power applications
[NASA-CR-191026] 08 p3178 N94-29208
Insulative properties of two thermo-metal neoprenes
[AD-A275209] 08 p3401 N94-29302
Prediction of fluid flow and heat transfer in internally finned tubes 08 p3280 N94-30228
Irradiation-induced structure and property changes in tokamak plasma-facing, carbon-carbon composites
[DE94-006046] 08 p3508 N94-30365
Thermal conductivities, electrical resistivities, and Seebeck coefficients of YBa2Cu3O(7-x) superconductors from 80 to 300 K
[DE94-004796] 08 p3520 N94-30724
Design of a variable-conductance vacuum insulation
[DE94-000270] 08 p3268 N94-30819
Self-similar variables and the problem of nonlocal electron heat conductivity
[DE94-005826] 08 p3493 N94-30881
The impact of LDEF results on the space application of metal matrix composites 09 p3595 N94-31034
Materials processing and manufacturing technologies for diamond substrates multichip modules
[AD-A276904] 09 p3692 N94-32215
Ceramic Technology Project database
[DE94-008494] 09 p3659 N94-32632
Snowmelt forecasting. Further cold regions development of operational hydrological forecasting, volume 2
[AD-A278123] 09 p3757 N94-33269
Thermal conductivity and ultrasonic measurements in low-density solid He-4 10 p4146 N94-33367
Heat transfer device
[NASA-CASE-LEW-14162-4] 10 p4020 N94-35076
Analysis of current diffusive ballooning mode
[DE94-718992] 11 p4336 N94-35811
Theory of anomalous transport in H-mode plasmas
[DE94-727546] 12 p4531 N94-37485

THERMAL CONTROL COATINGS

Experimental measurement of the plasma conductivity of Z93 and Z93P thermal control paint
[NASA-TM-106284] 01 p0043 N94-10756
Vacuum stability requirements of polymeric material for spacecraft application
[NASA-TM-109216] 01 p0091 N94-11350
Combustion synthesis and engineering of nanoparticles for electronic, structural, and superconductor applications
[DE93-016286] 02 p0809 N94-13981
Robotics
[NASA-TM-109351] 04 p1332 N94-18920
Calibration of a calorimeter for measuring the performance of thermal control surfaces 05 p1660 N94-21378
Characterization and durability testing of plasma-sprayed zirconia-yttria and hafnia-yttria thermal barrier coatings. Part 2: Effect of spray parameters on the performance of several hafnia-yttria and zirconia-yttria coatings
[NASA-TP-3296] 06 p2242 N94-23467
Structural characterization and thermal cycling behaviour of EB-PVD thermal barrier coating systems
[ISBN-0-315-83365-3] 06 p2257 N94-24468
An x ray diffraction investigation of alpha-Al2O2 addition to Yttria Stabilized Zirconia (YSZ) thermal barrier coatings subject to destabilizing vanadium pentoxide (V2O5) exposure
[AD-A273403] 06 p2261 N94-25072
Thick thermal barrier coatings for diesel components
[NASA-CR-187111] 08 p3537 N94-29350
Plasma sprayed ceramic thermal barrier coating for NiAl-based intermetallic alloys
[NASA-CASE-LEW-15535-1] 08 p3205 N94-29507
The performance of thermal control coatings on LDEF and implications to future spacecraft 09 p3591 N94-31013
Anodized aluminum on LDEF 09 p3592 N94-31017
Fluorescence observations of LDEF exposed materials as an indicator of induced material reactions 09 p3593 N94-31025
High-temperature behavior of advanced spacecraft TPS
[NASA-CR-195832] 10 p4014 N94-34063
Proceedings of the 57th National Congress of Japan Thermal Spraying Society
[DE94-731734] 10 p4029 N94-34133
Modeling of thermal barrier coatings
[NASA-CR-195365] 12 p4421 N94-36637

THERMAL CONVECTION

U FREE CONVECTION

THERMAL CURRENTS

U CONVECTIVE FLOW

THERMAL CYCLING TESTS

Transport of heat and mass in near-critical fluids 01 p0122 N94-10230
TAB interconnects for space concentrator solar cell arrays 01 p0051 N94-11400
Density and temperature relaxation near the critical point of carbon dioxide under reduced gravity 03 p0944 N94-15164
Hollow cathode heater development for the Space Station plasma contactor
[NASA-CR-191131] 03 p0926 N94-16880
Reliability analysis of Surface Mount Technology (SMT)
[AD-A267598] 03 p1055 N94-17194
Elastic-plastic finite-difference analysis of unidirectional composites subjected to thermomechanical cyclic loading
[AD-A267666] 03 p1061 N94-17269
Prediction of thermal cycling induced cracking in polymer matrix composites
[NASA-CR-194677] 03 p0941 N94-17295
Microstructurally based thermomechanical fatigue lifetime model of solder joints for electronic applications
[DE93-016508] 04 p1452 N94-17995

Embrittlement of surface mount solder joints by hot solder-dipped, gold-plated leads
[DE93-017659] 04 p1358 N94-18003
Structural stability of 1100 C heated Pd/k during absorption cycling in protium
[DE93-016270] 04 p1346 N94-18048
Solderability perservative coatings: Electroless tin versus organic azoles
[DE93-017634] 04 p1370 N94-18477
Damage accumulation in advanced metal matrix composites under thermal cycling/creep loadings
[AD-A271207] 04 p1344 N94-19720
Investigation of austenitic alloys for advanced heat recovery and hot gas cleanup systems
[DE93-017863] 05 p1687 N94-19802
The implications of the LDEF results on Space Station Freedom power system materials
05 p1660 N94-21377
Materials evaluation at ESA/ESTEC
05 p1662 N94-21386
Durability of thermal control and environmental protective materials for the SSRMS in simulated LEO environment 05 p1663 N94-21392
A method of measuring the thermoradiative properties of ceramic materials in a space environment
05 p1665 N94-21405
Analysis of thermal mechanical fatigue in titanium matrix composites 05 p1835 N94-22618
Structural characterization and thermal cycling behaviour of EB-PVD thermal barrier coating systems
[ISBN-0-315-83365-3] 06 p2257 N94-24468
Prediction of thermal cycling induced cracking in polmer matrix composites
[NASA-CR-195135] 06 p2229 N94-24579
Synthesis of polyphenylenes via Bergman cyclization of enediyne monomers
[AD-A273298] 06 p2260 N94-24924
Electron beam irradiation experiments of monoblock divertor mock-up
[DE94-707497] 08 p3503 N94-28555
Performance and durability of high emittance heat receiver surfaces for solar dynamic power systems
[NASA-TM-106549] 08 p3172 N94-28834
Static fracture behavior of a ceramic matrix composite at elevated temperatures
[AD-A275363] 08 p3177 N94-29008
Evaluation of oxide-coated iridium-rhenium chambers
[NASA-TM-106442] 08 p3172 N94-29097
Performance of CVD and CVR coated carbon-carbon in high temperature hydrogen
[DE94-005451] 08 p3487 N94-29841
Laser-induced fluorescence of space-exposed polyurethane 09 p3593 N94-31026
Space environmental effects on polymer composites: Research needs and opportunities
09 p3595 N94-31035
Pre-flight testing of Thermoelectric Quartz Crystal Microbalances (TQCM) for midcourse space experiment (MSX) spacecraft
[AD-A277054] 09 p3610 N94-32010
Thermal cyclic oxidation behavior of the developed compositionally gradient graphite material of SiC and C in air environment
[DE94-727591] 10 p4027 N94-33872
Hot dynamic test rig for measuring hypersonic engine seal flow and durability
[NASA-TM-106507] 12 p4450 N94-36645
Prediction of thermal and mechanical stress-strain responses of TMC's subjected to complex TMF histories
12 p4402 N94-36666
Carbon-carbon heat pipe testing and evaluation
[NASA-TM-106630] 12 p4405 N94-37318
Effects of ply thickness on thermal cycle induced damage and thermal strain 12 p4459 N94-37806

THERMAL DECOMPOSITION
NT PYROLYSIS
Low temperature metal-organic chemical vapor deposition growth processes for high efficiency solar cells
[DE92-010562] 02 p0702 N94-13386
ALE project
[AD-A271080] 05 p2014 N94-19980
Chemistry of the burning surface
[AD-A272725] 05 p1681 N94-21181
Condensed-phase thermal decomposition of TATB investigated by Atomic Force Microscopy (AFM) and Simultaneous Thermogravimetric Modulated Beam Mass Spectrometry (STMBMS)
[DE94-000396] 06 p2232 N94-23298
The formation of conducting gold films by thermal decomposition and direct patterning using electron beam lithography of the gold cluster Au55P(C6H5)312C16
[AD-A273720] 07 p2749 N94-26074
Mechanistic studies of opto-electronic materials and syntheses using multiple laser and surface diagnostics
[AD-A274528] 07 p3036 N94-26834
Bench-scale synthesis of nanoscale materials
[DE94-004787] 07 p2742 N94-27786
Peroxy radical measurements with NCAR's chemical amplifier 08 p3345 N94-28603
Insensitive energetic materials: The importance of physical properties and molecular structure
[AD-A275393] 08 p3225 N94-29308
Bench-scale synthesis of nanoscale materials
08 p3240 N94-30473
Characterization and processing of sintered products from nano-crystalline powders generated by the RTDS method
[DE94-004765] 12 p4415 N94-36553
Thermal-oxidative pretreatment and evaluation of poly (hexafluoropropene oxide) fluids
[NASA-TM-106659] 12 p4424 N94-37300
Thermal decomposition reactions of HMX and RDX and their importance in predicting cookoff hazards
[DE94-011430] 12 p4429 N94-37413

THERMAL DEFOCUSING
U THERMAL BLOOMING

THERMAL DEGRADATION
Advanced diagnostics for in situ measurement of particle formation and deposition in thermally stressed jet fuels
[DE93-009798] 01 p0098 N94-11366
Advanced thermally stable coal-derived jet fuels: Compositional factors affecting thermal degradation of jet fuels
[AD-A265842] 01 p0099 N94-12282
Effect of stabilization on the recycling of polyolefins in blow moulding
[IMI-93RT-42400-1477-G] 02 p0596 N94-13684
Advanced thermally stable jet fuels
[DE93-017711] 03 p0975 N94-16996
Study on radiation-induced deterioration of grease at high temperature, 3
[DE93-788368] 04 p1369 N94-18220
Workshop on multifactor aging mechanisms and models
[AD-A268668] 04 p1397 N94-18311
Ageing studies on a composite propellant containing a new organo-copper burn rate catalyst
[AD-A271060] 05 p1711 N94-19906
Toxicity of thermal degradation in a manned space environment 05 p1664 N94-21403
Electrochemical sulfur passivation of visible (approximately 670nm) AlGaInP lasers
[DE94-002293] 06 p2350 N94-24659
Kinetic parameters from thermogravimetric analysis
07 p2721 N94-27909
Advanced development of PV encapsulents
[DE94-000219] 08 p3336 N94-28500
Fatigue in single crystal nickel superalloys
[AD-A276662] 09 p3643 N94-32047

THERMAL DIFFUSION
Marangoni Benard instabilities in liquid mixtures with Soret effect 01 p0119 N94-10215
Progress in p(+)n InP solar cells fabricated by thermal diffusion 01 p0048 N94-11384
Electrochemical characterization of p(+)n and n(+)p diffused InP structures 01 p0049 N94-11385
Micro-zoning in minerals of a Landes silicate inclusion
01 p0432 N94-12231
Thermodiffusion in heterogeneous elastic solids and homogenization
[REPT-14/1993] 02 p0578 N94-13468
Implementation of manufacturing techniques for planar, single mode waveguides on lithium niobate
[DSIS-93-00101] 02 p0792 N94-13845
The role of electric field shear stabilization of turbulence in the H-mode to VH-mode transition in D3-D
[DE93-015474] 02 p0802 N94-14583
LX-17 chemical kinetic material model for Chemical TOPAZ2D
[DE93-014363] 04 p1377 N94-18893
Hydrogen isotope separation experience at the Savannah River Site
[DE93-019832] 05 p1679 N94-20266
Eddy mixing coefficient upper limit derived from the photochemical balance of O2 06 p2621 N94-24897
Calculation of propulsive nozzle flowfields in multidiffusing chemically reacting environments
[NASA-TM-106532] 08 p3271 N94-28835
RHEED studies of the nucleation, growth, and mobility of Ag atoms on the Si(111)7 x 7 surface
[DE94-005551] 08 p3521 N94-30899
The prediction of nozzle performance and heat transfer in hydrogen/oxygen rocket engines with transpiration cooling, film cooling, and high area ratios
[NASA-TM-106617] 10 p4017 N94-34924

THERMAL DIFFUSIVITY
Small scale magnetic islands in collisionless plasmas
[PPL-131] 02 p0799 N94-13836
Collisional effects of trapped electrons on the anomalous particle and thermal pinches
[PPL-128] 02 p0800 N94-13853
Anomalous transport due to small scale electromagnetic and large scale electrostatic modes in tokamaks
[PPL-140] 02 p0801 N94-14206
Numerical simulations of turbulent premixed H2/O2/N2 flames with complex chemistry
02 p0567 N94-14765
Investigation of radiative interaction in laminar flows using Monte Carlo simulation
[NASA-CR-194604] 03 p1021 N94-15795
Dynamics of surface thermal expansion and diffusivity using two-color reflection transient gratings
[DE93-040547] 05 p1990 N94-22002
Characterization and durability testing of plasma-sprayed zirconia-yttria and hafnia-yttria thermal barrier coatings. Part 2: Effect of spray parameters on the performance of several hafnia-yttria and zirconia-yttria coatings
[NASA-TP-3296] 06 p2242 N94-23467
Containerless measurements on liquids at high temperatures 06 p2238 N94-25125
An extended laser flash technique for thermal diffusivity measurement of high-temperature materials
06 p2238 N94-25132
Microwave techniques for physical property measurements 06 p2238 N94-25134
Sound, speed, reflectivity, absorption, and thermal diffusivity measurements in Arctic ice in 1990
[AD-A274326] 07 p2899 N94-26886
TFTR experimental data analysis collaboration
[DE94-004166] 07 p3047 N94-27690
Beta enhancement of thermal diffusivity in tokamaks
[PPL-141] 08 p3508 N94-30159
Development of high time-resolution laser flash equipment for thermal diffusivity measurements using miniature-size specimens
[AD-B183270L] 08 p3295 N94-30186
Ceramic Technology Project database
[DE94-008494] 09 p3659 N94-32632
Dynamic and thermal turbulent time scale modelling for homogeneous shear flows
[NASA-TM-106635] 11 p4263 N94-35253
MHD and confinement characteristics in the high-beta regime on the CHS low-aspect-ratio heliotron/torsatron
[DE94-718981] 11 p4339 N94-36357
Self-sustained turbulence and L-mode confinement in toroidal plasmas
[DE94-748497] 12 p4532 N94-37734

THERMAL DISSOCIATION
Tribological characteristics of hot-pressed self-lubricating composites
[NAL-TR-1160] 01 p0066 N94-10858
The thermal dissociation of NH2CHO(ND2CHO) on Si(100)-2x1
[AD-A266903] 03 p0942 N94-14956
Atomic probes of surface structure and dynamics
[DE94-001651] 06 p2530 N94-22720
Preparation, characterization, and facile thermolysis of (X2GaP(SiMe3)2) (X = Br, I) and (Cl3Ga2P)n; new precursors to nanocrystalline gallium phosphide
[AD-A275019] 08 p3513 N94-29130

THERMAL EFFECTS
U TEMPERATURE EFFECTS

THERMAL EFFICIENCY
U THERMODYNAMIC EFFICIENCY

THERMAL EMISSION
NT THERMIONIC EMISSION
Galileo/NIMS near-infrared thermal imagery of the surface of Venus 01 p0457 N94-12139
Thermal-infrared emission spectroscopy of natural surfaces: Application to coated surfaces
01 p0081 N94-12156
Thermal inertia and radar reflectivity of the Martian north polar ERG: Low-density aggregates
03 p1260 N94-16238
A decade's overview of Io's volcanic activity
03 p1245 N94-16386
Comparison of preliminary results from Airborne Aster Simulator (AAS) with TIMS data
03 p1064 N94-16600
Ejecta patterns of Meteor Crater, Arizona derived from the linear un-mixing of TIMS data and laboratory thermal emission spectra 03 p1065 N94-16607
Simulation of ASTER data using AVIRIS images
03 p1071 N94-16693
Polarimetric thermal emission from rough surfaces
05 p1727 N94-20441
Polarimetric thermal emission from periodic water surfaces 05 p1728 N94-20445
A study of carbonates, sulfates, and phosphates using thermal emission spectroscopy
05 p1686 N94-20868
Michelson Interferometer (MINT)
05 p1813 N94-21646
Imaging XUV spectroscopy of a Z-pinch plasma in the former Soviet Union
[DE93-040849] 06 p2549 N94-22949

ASTER, a multinational Earth observing concept
06 p2389 N94-23840
Nonequilibria in thermal emission from supernova remnants
[NIFS-264] 06 p2602 N94-24866
Temporal and spatial mapping of surface albedo and atmospheric dust opacity on Mars
06 p2619 N94-24887
Retrieval of temperature profiles from Martian infrared spectra 06 p2620 N94-24893
Martian atmospheric radiation budget
07 p3107 N94-27887
Global approach towards the evaluation of thermal infrared countermeasures 08 p3258 N94-30504
Dual-band infrared imaging to detect corrosion damage within airframes and concrete structures
[DE94-006047] 09 p3580 N94-32658
Thermal emission measurements (5-25 microns) of Hawaiian palagonitic soils with implications for Mars
09 p3944 N94-33193
Thermal studies of Martian channels and valleys using Termoskan data: New results 09 p3944 N94-33194
Regional sedimentological variations among dark crater floor features: Toward a model for modern eolian sand distribution on Mars 09 p3946 N94-33203
Temporal and spatial mapping of atmospheric dust opacity and surface albedo on Mars
09 p3947 N94-33211
Thermal emission measurements (5-25 microns) of Hawaiian palagonitic soils with implications for Mars
11 p4292 N94-35452
Thermal emission measurements (5-25 microns) of palagonite/Fe-substituted montmorillonite intimate mixtures: Applications to Mars 11 p4292 N94-35453
Atmospheric effects on the mapping of Martian thermal inertia and thermally derived albedo
11 p4368 N94-36137

THERMAL ENERGY
Transition of building energy consumption using multi-input, single-output dynamic model
[VTT-PUBS-116] 02 p0597 N94-14055
Optical and infrared spectra of thermally annealed Pb implanted SiO2 glasses
[DE93-015304] 03 p0965 N94-15828
Synthesis of ceramic oxide powders in a microwave plasma device
[DE93-012741] 03 p0965 N94-15920
GAM-HEAT: A computer code to compute heat transfer in complex enclosures
[DE93-014724] 03 p1023 N94-15980
High heat flux engineering in solar energy applications
[DE93-016500] 03 p1093 N94-16954
Emittance growth in displaced, space-charge-dominated beams with energy spread
[DE93-016514] 03 p1188 N94-17672
Techniques for the estimation of Heats of Explosion (HEX) using thermochemical codes
[AD-A268584] 04 p1609 N94-18310
Melt spinning study
[NASA-CR-193823] 04 p1380 N94-19423
Effects of processing history on the creep strength of Nb-1Zr
[DE93-015905] 05 p1689 N94-20093
Modeling of the coupled magnetospheric and neutral wind dynamos
[NASA-CR-194726] 05 p1856 N94-20537
Second law analysis of a conventional steam power plant 06 p2322 N94-23646
Ulysses log 1992 06 p2502 N94-23863
Infrared sensors and systems for enhanced vision/autonomous landing applications
06 p2439 N94-25491
Development of global/chemistry model for jet-fuel thermal stability based on observations from static and flowing experiments 08 p3192 N94-29262
Thermal continua of AGN accretion disks
09 p3931 N94-31137
Stability and precipitation kinetics in Si(1-y)C(y)/Si and Si(1-x-y)Ge(x)C(y)/Si heterostructures prepared by solid phase epitaxy
[DE94-006589] 09 p3902 N94-32296

THERMAL ENERGY STORAGE
U HEAT STORAGE

THERMAL ENVIRONMENTS
The spectral effects of subsolidus reduction of olivine and pyroxene 01 p0081 N94-12110
Low altitude plume impingement handbook
[NASA-CR-194193] 02 p0643 N94-14741
First results from a laboratory facility for measurement of emission spectra under simulated planetary conditions
03 p0954 N94-16372
Diffractive optics in adverse environments
03 p1197 N94-17352
Development and experimental validation of computational methods to simulate abnormal thermal and structural environments
[DE94-000554] 06 p2268 N94-23000
Uncertainties in the characterization of the thermal environment of a solid rocket propellant fire
[DE94-002023] 07 p2760 N94-27719
Light in Thermal Environments (LITE) Workshop
[NASA-CR-195851] 09 p3790 N94-32981
Advanced integrated life support system update
10 p4102 N94-33657
Predicted optical performance of the High-Altitude Balloon Experiment (HABE) telescope in an adverse thermal environment
[DE94-008949] 11 p4349 N94-35998

THERMAL EXPANSION
Low cost and thermally stable sandwich design for FIRST 01 p0057 N94-10009
Sensing glass transitions in thin polymer films on acoustic wave microsensors
[DE93-010805] 01 p0087 N94-10295
Method for producing a hybridization of detector array and integrated circuit for readout
[NASA-CASE-NPO-18062-1-CU]
01 p0141 N94-10656
Ceramic technology project database
[DE93-012432] 01 p0091 N94-11673
An advanced test technique to quantify thermomechanical fatigue damage accumulation in composite materials
[NASA-CR-191147] 02 p0555 N94-13139
JPRS report: Science and technology. Central Eurasia: Materials science
[JPRS-UMS-93-006] 02 p0558 N94-14573
Thermal stresses of a trimaterial medium in a nonuniform temperature field
[AD-A267243] 03 p0930 N94-14975
High temperature advanced structural composites. Volume 3: Mechanics
[AD-A267024] 03 p0933 N94-15626
Carbon-carbon grid for ion engines
[NASA-CASE-NPO-19174-1-CU]
03 p0925 N94-15876
Structural stability of 1100 C heated Pd/k during absorption cycling in protium
[DE93-016270] 04 p1346 N94-18048
Thermal behavior of natural zeolites
[DE93-040091] 05 p1699 N94-19975
A process for preparing an assembly of an article and a soluble polyimide which resists dimensional change, delamination, and debonding when exposed to changes in temperature
[NASA-CASE-LAR-14763-1] 05 p1702 N94-20373
Thermal expansion of electronic highly correlated materials
[ETN-93-93605] 05 p2026 N94-21135
Space environmental effects on polymer matrix composites: The UTIAS/LDEF experiment
05 p1660 N94-21373
Integrity and testing concerns of thermostructural materials 05 p1661 N94-21384
High temperature size selective membranes
[DE93-019865] 05 p1709 N94-21982
Magnetism in CeRu2Ge2 and CeRh2Ge2 and its pressure dependence
[DE93-040061] 05 p2032 N94-21987
Dynamics of surface thermal expansion and diffusivity using two-color reflection transient gratings
[DE93-040547] 05 p1990 N94-22002
Developments in materials for high-field magnets
[DE94-000761] 06 p2307 N94-22987
Humidity effects on soluble core mechanical and thermal properties (polyvinyl alcohol/microballoon composite) type CG extendospheres, volume 2
[NASA-CR-193893] 06 p2229 N94-24224
Dynamic measurements of thermophysical properties of metals and alloys at high temperatures by subsecond pulse heating techniques 06 p2247 N94-25124
Thermal expansion and elastic anisotropy in single crystal Al2O3 and SiC reinforcements
[NASA-TM-106516] 08 p3214 N94-29105
Properties of graphite fiber reinforced copper matrix composites for space power applications
[NASA-CR-191026] 08 p3178 N94-29208
Controlled thermal expansion printed wiring boards based on liquid crystal polymer dielectrics
[NASA-CR-189338] 08 p3287 N94-29400
Scaling in heavy-fermion systems
[DE94-005002] 08 p3492 N94-30775
Thermal-vacuum response of polymer matrix composites in space 09 p3595 N94-31033
The impact of LDEF results on the space application of metal matrix composites 09 p3595 N94-31034
Chemical vapor deposition fluid flow simulation modelling tool
[NASA-CR-189648] 09 p3707 N94-32480
Mechanics of cracking for composite material
09 p3624 N94-32501
Inorganic polymer engineering materials
[DE94-008519] 09 p3659 N94-32655
Interface engineering in oxide fiber/oxide matrix composites
[AD-A277672] 09 p3627 N94-33029
Modeling of thermal barrier coatings
[NASA-CR-195365] 12 p4421 N94-36637
Effects of ply thickness on thermal cycle induced damage and thermal strain 12 p4459 N94-37806

THERMAL FATIGUE
Crystallization of grain boundary phases in silicon nitride with low additive contents by microwave annealing
[DE93-015801] 03 p1209 N94-16164
Hollow cathode heater development for the Space Station plasma contactor
[NASA-CR-191131] 03 p0926 N94-16880
Prediction of thermal cycling induced cracking in polymer matrix composites
[NASA-CR-194677] 03 p0941 N94-17295
Aspects of high temperature damage in fiber reinforced titanium metal matrix composites
[AD-A267907] 03 p0941 N94-17379
Finite difference program for calculating hydride bed wall temperature profiles
[DE93-019272] 04 p1523 N94-19005
Analysis of thermal mechanical fatigue in titanium matrix composites 05 p1835 N94-22618
Thermal fatigue: A literature review
[PB93-226306] 06 p2375 N94-23120
Elevated temperature crack propagation
[NASA-TM-106490] 06 p2377 N94-24715
Characterization of fatigue damage in a metal matrix composite (SCS-6/Ti-15-3) at elevated temperature
[AD-A273797] 07 p2706 N94-25876
Investigation of tension-compression fatigue behavior of a cross-ply metal matrix composite at room and elevated temperatures
[AD-A273731] 07 p2706 N94-25999
Development of detection technique for fatigue crack due to thermal stratification phenomena in RCS piping
[DE93-632968] 07 p2838 N94-26400
An analysis of isothermal, bithermal, and thermomechanical fatigue data of Haynes 188 and B1900+Hf by energy considerations
[NASA-TM-106359] 08 p3317 N94-28819
Probabilistic material strength degradation model for Inconel 718 components subjected to high temperature, mechanical fatigue, creep and thermal fatigue effects
[NASA-CR-195284] 08 p3318 N94-28840
Transient thermal fatigue of ceramic composites
08 p3216 N94-29874
The impact of LDEF results on the space application of metal matrix composites 09 p3595 N94-31034
Development and characterization of intermediary layers allowing the bond between a metal alloy and a plasma sprayed ceramic
[ECL-91-39] 09 p3619 N94-31377
Thermal-mechanical fatigue crack growth in aircraft engine materials
[ISBN-0-315-86543-1] 09 p3734 N94-31707
Fatigue in single crystal nickel superalloys
[AD-A276662] 09 p3643 N94-32047
Structurally compliant rocket engine combustion chamber: Experimental and analytical validation
[NASA-TP-3431] 10 p4017 N94-34392
Isothermal damage and fatigue behavior of SCS-6/Timetal 21S (0/90)s composite at 650 C
[NASA-CR-195345] 11 p4234 N94-35995
Prediction of thermal and mechanical stress-strain responses of TMC's subjected to complex TMF histories
12 p4402 N94-36666
Creep-fatigue interaction property of a nickel-base heat-resistant alloy Hastelloy XR in simulated HTGR helium gas environment
[DE94-737934] 12 p4418 N94-37416
Effects of ply thickness on thermal cycle induced damage and thermal strain 12 p4459 N94-37806

THERMAL GRAVIMETRY
U THERMOGRAVIMETRY

THERMAL INSTABILITY
Study of possible mechanisms of instability due to heat transfer
[INPE-5448-TDI/494] 02 p0628 N94-12966
Disk instability and the spectral evolution of the 1992 outburst of the intermediate polar GK Persei
09 p3928 N94-31123
Disk irradiation and light curves of x ray novae
09 p3929 N94-31124
Can a variable alpha induce limit cycle behavior and exponential luminosity decay in transient soft x ray sources?
09 p3929 N94-31129
The physics of black hole x ray novae
09 p3932 N94-31143

THERMAL INSULATION
Material advances for lightweight TPS
01 p0062 N94-10049
Vectra insulative support structures within spacecraft
01 p0062 N94-10050
Polyimide foam insulation systems: A major weight reduction and improvement in fire resistance of sidewall systems 01 p0017 N94-10769
A new FR water resistant acoustic insulation material for aircraft 01 p0018 N94-10773
Arc-heating tests of thermal protection system materials for the H-2 rocket fairing
[NAL-TR-1181] 02 p0551 N94-13455
Impact penetration experiments in teflon targets of variable thickness 03 p1063 N94-16253
SRB thermal curtain design support
[NASA-CR-193857] 03 p0927 N94-17123
SRB thermal curtain design support
[NASA-CR-193858] 03 p0928 N94-17124
Thermal insulation of wet shielded metal arc welds
[AD-A268697] 04 p1445 N94-18465
Features of a SINDA/FLUINT model of a liquid oxygen supply line 06 p2322 N94-23649
Micromechanical simulation of damage progression in carbon phenolic composites 06 p2231 N94-24446
Thermal-fluid analysis of the fill and drain operations of a cryrogenic fuel tank
[NASA-TM-104273] 06 p2334 N94-24495
Cryogenic insulation studies
[NASA-CR-193950] 07 p2756 N94-27429
Fire-resistant water vapour permeable buoyant insulation 08 p3380 N94-28431
Selection of the Space Station Freedom (SSF) Flat Collector Circuit (FCC) insulation material
08 p3165 N94-28701
High temperature arc-track resistant aerospace insulation 08 p3167 N94-28716
Quality and efficiency of solar collectors in Sweden
[PB94-137486] 08 p3337 N94-28909
Insulative properties of two thermo-metal neoprenes
[AD-A275209] 08 p3401 N94-29302
Composite flexible blanket insulation
[NASA-CASE-ARC-11955-1-CU]
08 p3180 N94-29509
Design of a variable-conductance vacuum insulation
[DE94-000270] 08 p3268 N94-30819
Space environment durability of beta cloth in LDEF thermal blankets 09 p3591 N94-31015
Follow-up on the effects of the space environment on UHCRE thermal blankets 09 p3592 N94-31018
The prediction of convective transfer on the thermal insulation of a solid-propellant rocket motor
[ONERA-NT-1993-15] 09 p3614 N94-31423
Proceedings of the DCIEM Diver Thermal Protection Workshop
[DCIEM-92-10] 09 p3795 N94-31738
Thermotropic liquid crystals: A variable Clo material
09 p3796 N94-31739
High-temperature behavior of advanced spacecraft TPS
[NASA-CR-195832] 10 p4014 N94-34063
Thermal performance of residential duct systems in basements
[LBL-33962] 11 p4250 N94-35364
Properties and applications of powder-filled evacuated-panel superinsulations
[DE94-009169] 11 p4233 N94-35932
Experimental impacts into Teflon targets and LDEF thermal blankets 11 p4352 N94-36141
Electrically conductive, thermally insulating cryogenic current leads
[NASA-CASE-LAR-14964-1-CU]
12 p4437 N94-36781
Development of processing techniques for advanced thermal protection materials
[NASA-CR-196261] 12 p4426 N94-37510

THERMAL MAPPING
Compositional and textural information from the dual inversion of visible, near and thermal infrared remotely sensed data 01 p0258 N94-12097
Martian particle size based on thermal inertia corrected for elevation-dependent atmospheric properties
01 p0430 N94-12107
Galileo/NIMS near-infrared thermal imagery of the surface of Venus 01 p0457 N94-12139
A simple model of clastic sediments on Mars
01 p0460 N94-12155
High frame rate thermal imager for hypersonic wind tunnel applications
[ONERA-NT-1992-12] 02 p0650 N94-14009
Ground truth spectrometry and imagery of eruption clouds to maximize utility of satellite imagery
[NASA-CR-194358] 03 p1081 N94-15181
Testing the waters from space --- Thermal mapping
[NASA-TM-109623] 03 p1082 N94-15409
Sand transport on Mars: Preliminary results from models 03 p1252 N94-16198
Clementine: Anticipated scientific datasets from the Moon and Geographos 03 p1288 N94-16392
Thermogeologic mapping of the Moon from lunar orbit
03 p1290 N94-16405
TIMS performance evaluation summary
03 p1063 N94-16596
Atmospheric propagation analysis program
[AD-A268231] 03 p1006 N94-17565
Infrared thermography 04 p1432 N94-18652
Degradation sequence of young lunar craters from orbital infrared survey 05 p2136 N94-20874
Fluorescent microthermographic imaging
[DE93-040332] 05 p1810 N94-22000
Temporal and spatial mapping of surface albedo and atmospheric dust opacity on Mars
06 p2619 N94-24887
Evidence for dust transport in Viking IR thermal mapper opacity data 06 p2620 N94-24892
Eddy mixing coefficient upper limit derived from the photochemical balance of O2 06 p2621 N94-24897
Diagnostic calculations of the circulation in the Martian atmosphere 06 p2622 N94-24898
An apparatus for measurement of ignition and burning characteristics of metallic particles
[AD-A274815] 07 p2716 N94-26487
Evolution of miniature detectors and focal plane arrays for infrared sensors 08 p3237 N94-29781
Thermal imaging for a mobile robot
08 p3308 N94-30300
Thermal studies of Martian channels and valleys using Termoskan data: New results 09 p3944 N94-33194
Regional sedimentological variations among dark crater floor features: Toward a model for modern eolian sand distribution on Mars 09 p3946 N94-33203
Temporal and spatial mapping of atmospheric dust opacity and surface albedo on Mars
09 p3947 N94-33211
Studies of atmospheric dust from Viking IR thermal mapper data 09 p3948 N94-33216
IRTM brightness temperature maps of the Martian south polar region during the polar night: The cold spots don't move 09 p3949 N94-33222
Atmospheric effects on the mapping of Martian thermal inertia and thermally derived albedo
11 p4368 N94-36137

THERMAL NEUTRONS
Possibility of a crossed-beam experiment involving slow-neutron capture by unstable nuclei rapid-process-tron
[DE93-754288] 01 p0363 N94-10720
The multiplicity spectra of the (169)Tm(n, gamma) reaction
[DE93-617733] 01 p0364 N94-10835
Analytic expression for epithermal neutron spectra amplitudes as a function of water content
01 p0473 N94-12227
Criticality benchmark comparisons leading to cross-section upgrades
[DE93-017184] 04 p1556 N94-18073
Thermal neutron multiplicity measurements using the pyrochemical multiplicity counter at Lawrence Livermore National Laboratory
[DE93-018538] 04 p1571 N94-19278
Surface physics with cold and thermal neutron reflectometry
[DE94-001447] 07 p2733 N94-26070
Neutron-neutron scattering: Possibility of in-beam experiment
[DE94-606459] 07 p3027 N94-27682

THERMAL NOISE
Using a focal-plane array to estimate antenna pointing errors
[NASA-CR-194502] 02 p0602 N94-13810
Cryogenic measurements of aerojet GaAs n-JFETs
[NASA-TM-103972] 03 p1009 N94-15765
Thermally-sustained structure in convectively unstable systems
[NASA-TM-106375] 03 p1027 N94-17112
Geometrical resonances in the nyquist noise spectrum for ballistic conductors
[DE94-603668] 07 p3027 N94-27631
Computer implementation of Arnott's formulation of thermoacoustics using MATLAB
[AD-A276356] 09 p3860 N94-31257

THERMAL PLASMAS
Momentum and heat frictions between fast ions and thermal plasma species
[DE93-771240] 01 p0390 N94-11149
An ellipsometry investigation of nucleation and growth of electron cyclotron resonance plasma deposited silicon films
[AD-A265037] 01 p0401 N94-11651
Advanced fusion diagnostics
[DE93-040085] 04 p1589 N94-19133
Substrate temperature measurement and control during thermal plasma CVD
[DE93-040305] 04 p1433 N94-19135
On one numerical approach to Stefan problem
[IPPCZ-330] 05 p1996 N94-21572
Analysis and experiments of a whistler-wave plasma thruster
[DE94-001533] 06 p2209 N94-23012
Modelling of thermal argon plasmas
[ETN-94-95363] 06 p2554 N94-25300
Theoretical aspects of the agile mirror
[AD-A274890] 07 p2767 N94-26177
Coulomb field effect on plasma focusing and wake field acceleration
[DE94-004937] 08 p3504 N94-28564
Study on the formation of ultrafine particles of Sm-Co intermetallic compounds using RF thermal plasma
08 p3211 N94-29516
Activities of the Laser and Plasma Technology Division
[DE94-617113] 11 p4273 N94-36393
D-D fusion experiments using fast z-pinches
[DE94-010090] 12 p4526 N94-36448
Time-resolved probing of electron thermal transport in plasma produced by femtosecond laser pulses
[DE94-012061] 12 p4530 N94-37392

THERMAL PROPERTIES
U THERMODYNAMIC PROPERTIES

THERMAL PROTECTION
On the mechanical development of the Flexible External Insulation (FEI) for Hermes spaceplane
01 p0062 N94-10048
Material advances for lightweight TPS
01 p0062 N94-10049
Debris/ice/TPS assessment and integrated photographic analysis for Shuttle Mission STS-57
[NASA-TM-107562] 01 p0040 N94-10805
Space Storable Rocket Technology program (SSRT). Option 1 program
[NASA-CR-191171] 01 p0046 N94-10938
High temperature electromagnetic characterization of thermal protection system tile materials
[NASA-CR-189687] 02 p0578 N94-13431
Arc-heating tests of thermal protection system materials for the H-2 rocket fairing
[NAL-TR-1181] 02 p0551 N94-13455
Flammability of clothing, volume 2
[DSIS-93-00036-VOL-2] 02 p0564 N94-13819
Review of test methods for material flammability
[DSIS-93-00480] 02 p0564 N94-13942
Processing and protection of high temperature structural materials
[AD-A267292] 03 p0954 N94-14961
LX-17 chemical kinetic material model for Chemical TOPAZ2D
[DE93-014363] 04 p1377 N94-18893
Materials evaluation at ESA/ESTEC
05 p1662 N94-21386
Durability of thermal control and environmental protective materials for the SSRMS in simulated LEO environment 05 p1663 N94-21392
Forecasting technique of variations of the optical absorptivity of thermal control coatings under different simultaneous radiations 05 p1664 N94-21399
Thermal control coatings 05 p1664 N94-21400
A method of measuring the thermoradiative properties of ceramic materials in a space environment
05 p1665 N94-21405
R and D to HOPE airframe 05 p1665 N94-21406
Material properties and behavior during simulated atmospheric reentry 05 p1665 N94-21408
Compilation of reinforced carbon-carbon transatlantic abort landing arc jet test results
[NASA-TM-104778] 05 p1676 N94-21834
NASA/USRA advanced design program
[NASA-CR-195548] 06 p2180 N94-24492
Debris/ice/TPS assessment and integrated photographic analysis for Shuttle mission STS-58
[NASA-TM-109194] 06 p2200 N94-24577
Configuration development study of the OSU 1 hypersonic research vehicle
[NASA-CR-195522] 06 p2181 N94-24591
Development of a nondestructive vibration technique for bond assessment of Space Shuttle tiles
[NASA-CR-195163] 06 p2201 N94-24919
Plasma sprayed thermal barrier coatings: Production, characterization and testing
[ISBN-9-03-860082-8] 06 p2555 N94-25439
Effect of longitudinal vibration on the capillary limit of a wrapped screen wick copper/water heat pipe
[AD-A273830] 06 p2571 N94-25524
Minimum accommodation for aerobrake assembly, phase 2
[NASA-TM-107608] 07 p2692 N94-27774

Debris/ice/TPS assessment and integrated photographic analysis for Shuttle mission STS-60
[NASA-TM-109193] 07 p2692 N94-27956
Alleviation of thermal strain in the CF: Keeping our cool during the Gulf conflict 08 p3383 N94-28449
Recent Canadian advances in active thermal protection 08 p3384 N94-28451
Test of a new protection suit in a climatic chamber 08 p3384 N94-28452
Heat flux instrumentation for Hyflite thermal protection system
[NASA-CR-195731] 08 p3286 N94-28824
Fuel injector design for high temperature aircraft engine 08 p3154 N94-29263
Numerical comparison of convective heat transfer augmentation devices used in cooling channels of hypersonic vehicles
[NASA-TM-106546] 08 p3279 N94-30147
Development and characterization of intermediary layers allowing the bond between a metal alloy and a plasma sprayed ceramic
[ECL-91-39] 09 p3619 N94-31377
Proceedings of the DCIEM Diver Thermal Protection Workshop
[DCIEM-92-10] 09 p3795 N94-31738
Thermotropic liquid crystals: A variable Clo material 09 p3796 N94-31739
Application of statistical process control and process capability analysis procedures in orbiter processing activities at the Kennedy Space Center 10 p4068 N94-33626
High-temperature behavior of advanced spacecraft TPS
[NASA-CR-195832] 10 p4014 N94-34063
Proceedings of the 57th National Congress of Japan Thermal Spraying Society
[DE94-731734] 10 p4029 N94-34133
Debris/ice/TPS assessment and integrated photographic analysis for Shuttle Mission STS-59
[NASA-TM-109203] 11 p4211 N94-35523
Development of processing techniques for advanced thermal protection materials
[NASA-CR-196261] 12 p4426 N94-37510
Active cooling from the sixties to NASP
[NASA-TM-109079] 12 p4456 N94-37541

THERMAL RADIATION
NT BLACK BODY RADIATION
In-reactor testing of the closed cycle gas core reactor: The Nuclear Light Bulb concept
[DE93-004053] 01 p0370 N94-10149
The heat transfer by radiation between two media
[DE93-617820] 01 p0149 N94-10838
The Langevin's approach to the statistical theory of bounded plasma
[DE93-617842] 01 p0388 N94-10839
Combustion chamber analysis code
[NASA-CR-192585] 01 p0046 N94-10934
Near-surface temperature gradients and their effects on thermal-infrared emission spectra of particulate planetary surfaces 03 p1260 N94-16236
A decade's overview of Io's volcanic activity 03 p1245 N94-16386
Altitude profile of aerosols on Mars from measurements of its thermal radiation on limb 03 p1294 N94-16423
Effects of hydrodynamics and thermal radiation in the atmosphere after comet impacts 05 p1862 N94-20649
Thermal infrared remote sensing and Kirchhoff's law: 1. Laboratory measurements 05 p1685 N94-20733
High-energy astrophysics: A theoretical analysis of thermal radiation from neutron stars
[NASA-CR-194808] 05 p2055 N94-20952
Improved thermal force modeling for GPS satellites 06 p2207 N94-23259
Uncertainty analysis of diffuse-gray radiation enclosure problems: A hypersensitive case study 06 p2320 N94-23637
The IRGen infrared data base modeler 06 p2440 N94-25496
User's guide for the thermal analyst's help desk expert system
[NASA-CR-194885] 07 p2695 N94-26103
Computer model for generation of infrared images
[PB94-123551] 07 p3005 N94-27172
Researches of the Electrotechnical Laboratory. No. 53: Spectral emission from combustion gas containing scattering media
[JTN-94-80603] 07 p2717 N94-27246
Thermal variation in vegetated or snow-covered background scenes and its effect on passive infrared systems
[AD-A275174] 08 p3325 N94-28849
Thermal continua of AGN accretion disks 09 p3931 N94-31137
Radiometry spot measurement system
[NASA-TM-106561] 09 p3883 N94-32777
Light in Thermal Environments (LITE) Workshop
[NASA-CR-195851] 09 p3790 N94-32981
Radiative signals from impact of Shoemaker-Levy on Jupiter 11 p4355 N94-35396

THERMAL REACTORS
A critical assembly designed to measure neutronic benchmarks in support of the Space Nuclear Thermal Propulsion program
[DE92-040974] 01 p0371 N94-10529
Review of nuclear thermal propulsion carbide reactor fuel corrosion and exhibit
[DE93-016605] 02 p0585 N94-14535
A review of carbide fuel corrosion for nuclear thermal propulsion applications
[DE94-003938] 07 p2699 N94-25613

THERMAL RESISTANCE
Advanced Materials for Lightweight Structures
[ESA-SP-336] 01 p0056 N94-10001
Protective coatings for high-temperature polymer matrix composites
[NASA-TM-106276] 01 p0074 N94-12431
Arc-heating tests of thermal protection system materials for the H-2 rocket fairing
[NAL-TR-1181] 02 p0551 N94-13455
JPRS report: Science and technology. Central Eurasia: Materials science
[JPRS-UMS-93-004] 02 p0559 N94-14574
Crystallization of grain boundary phases in silicon nitride with low additive contents by microwave annealing
[DE93-015801] 03 p1209 N94-16164
Development and commercialization status of Fe3Al-based intermetallic alloys
[DE93-015802] 03 p0957 N94-16165
Study on radiation-induced deterioration of grease at high temperature, 3
[DE93-788368] 04 p1369 N94-18220
The fire resistance of profiled thin steel sheet structures
[VTT-TIED-1320] 04 p1380 N94-19373
Advanced materials for radiation-cooled rockets 06 p2214 N94-23052
Study on high temperature damage control and life improvement 07 p2729 N94-25580
Method for improving electromagnetic shielding performance of composite materials by electropulsing
[AD-D016050] 07 p2709 N94-27076
Simulation of the effect of wind on clothing by measurements and calculations
[PB94-132289] 08 p3399 N94-28406
Evaluation of oxide-coated iridium-rhenium chambers
[NASA-TM-106442] 08 p3172 N94-29097
Insulative properties of two thermo-metal neoprenes
[AD-A275209] 08 p3401 N94-29302
Creep rupture properties under varying load and temperature conditions on a nickel-base heat-resistant alloy strengthened by boron addition
[DE94-727594] 10 p4024 N94-33933
JPRS report: Science and technology. Central Eurasia: Materials science
[JPRS-UMS-93-007] 11 p4240 N94-35517
Properties and applications of powder-filled evacuated-panel superinsulations
[DE94-009169] 11 p4233 N94-35932
Third European Technical Symposium on Polyimides and High Performance Polymers: STEPI 3
[PB94-148491] 11 p4246 N94-36177
Measurement of a surface heat flux and temperature 11 p4231 N94-36407
Characterisation of Fibre Reinforced Titanium Matrix Composites
[AGARD-R-796] 12 p4400 N94-36649
Creep-fatigue interaction property of a nickel-base heat-resistant alloy Hastelloy XR in simulated HTGR helium gas environment
[DE94-737934] 12 p4418 N94-37416

THERMAL RESOURCES
NT GEOTHERMAL RESOURCES
NT GEYSERS

THERMAL SHIELDING
U HEAT SHIELDING

THERMAL SHOCK
Potential change in flaw geometry during pressurized-thermal-shock transients
[DE93-009709] 01 p0184 N94-10288
Assessment of damage in ceramics and ceramic matrix composites using ultrasonic techniques
[NASA-TM-106121] 01 p0067 N94-11237
Cellular mechanism of turnover of the stress induced protein HSP 70
[AD-A265723] 02 p0732 N94-13061
Thermal shock resistance of ceramic matrix composites
[NASA-CR-189136] 02 p0557 N94-13920
The relationship of metallothionein induction to the heat shock response
[AD-A266634] 03 p1122 N94-15741
Design of a cruciform bend specimen for determination of out-of-plane biaxial tensile stress effects on fracture toughness for shallow cracks
[DE93-015455] 03 p1059 N94-16104
Heat shock protein induction in human cells by CO2 laser irradiation
[AD-A266430] 03 p1117 N94-16545
Euhedral metallic-Fe-Ni grains in extraterrestrial samples 05 p1697 N94-20724
Fabrication of whisker-toughened alumina tubes
[DE94-001012] 05 p1677 N94-22022
Plasma sprayed thermal barrier coatings: Production, characterization and testing
[ISBN-9-03-860082-8] 06 p2555 N94-25439
Collaborative research on ion implantation of ceramics
[DE93-019177] 07 p2749 N94-26080
Evaluation of oxide-coated iridium-rhenium chambers
[NASA-TM-106442] 08 p3172 N94-29097
Mechanical properties of vacuum-sintered yttria ceramics
[DE94-008138] 09 p3659 N94-32617
A versatile rocket engine hot gas facility
[NASA-CR-195339] 10 p4011 N94-34131

THERMAL SIMULATION
Venusian pancake domes: Insights from terrestrial voluminous silicic lavas and thermal modeling 03 p1286 N94-16381
High temperature simulation chambers. Physico-chemical and thermal effect of atmospheric reentry on ceramic materials 05 p1653 N94-21404

THERMAL SINKS
U HEAT SINKS

THERMAL STABILITY
An approach to high precision antenna structures by a CFRP core sandwich concept 01 p0057 N94-10008
A wide-band fiber optic frequency distribution system employing thermally controlled phase compensation 01 p0355 N94-10995
Thermal stability of sealants for military aircraft: Modification of polysulfide prepolymers with ether and thioether monomers
[AD-A264079] 01 p0089 N94-11107
High temperature stability, interface bonding, and mechanical behavior in (beta)-NiAl and Ni3Al matrix composites with reinforcements modified by ion beam enhanced deposition
[DE93-013977] 01 p0398 N94-11115
Thermal testing of aluminized Mylar
[NASA-TM-108414] 01 p0089 N94-11175
Vacuum stability requirements of polymeric material for spacecraft application
[NASA-TM-109216] 01 p0091 N94-11350
Processing and properties of coated HPZ fiber reinforced glass-ceramic matrix composites
[AD-A265177] 01 p0092 N94-11876
The stability of hibonite and other aluminous phases in silicate melts: Implications for the origin of hibonite-bearing inclusions 01 p0080 N94-12052
A novel test method for fuel thermal stability
[AD-A265853] 01 p0099 N94-12275
Advanced thermally stable coal-derived jet fuels: Compositional factors affecting thermal degradation of jet fuels
[AD-A265842] 01 p0099 N94-12282
Liquid Cooled Heat Sink with through Vias (LCHS)
[AD-A266008] 01 p0073 N94-12344
Photogenerated base in polymer imaging. Synthesis and photopatterning of poly(2-cyano-2-(p-vinylphenyl) butanoic acid)
[AD-A265288] 01 p0095 N94-12585
Structure stability and spectroscopy of metal clusters
[DE93-016142] 02 p0567 N94-12836
Cellular mechanism of turnover of the stress induced protein HSP 70
[AD-A265723] 02 p0732 N94-13061
Thermal design of hybrid circuits: Tools and methodology
[LAAS-92515] 02 p0626 N94-14713
Scholarly research program in fuel analysis and combustion research
[AD-A266789] 03 p0942 N94-14911
Compounds containing meta-biphenylenedioxy moieties and polymers therefrom
[NASA-CASE-LAR-14517-1] 03 p0965 N94-15879
Isolation of thermostable enzyme mutants by cloning and selection in thermophilic bacteria
[AD-A266378] 03 p1117 N94-16514
Electrical conductivity of ion implanted ladder and semi-ladder polymers
[AD-A267432] 03 p0970 N94-16978
Advanced thermally stable jet fuels
[DE93-017711] 03 p0975 N94-16996
Diffractive optics in adverse environments 03 p1197 N94-17352

Study on radiation-induced deterioration of grease at high temperature, 3
[DE93-788368] 04 p1369 N94-18220
Analysis of deposit precursors in jet fuels using Fourier transform infrared spectroscopy
[AD-A269035] 04 p1377 N94-18489
Strained ring energetic binders
[AD-A269056] 04 p1377 N94-18491
Accelerated screening methods for determining chemical and thermal stability of refrigerant-lubricant mixtures. Part 1: Method assessment
[DE93-040215] 04 p1351 N94-19136
Isolation mechanisms in III-V devices
[AD-A271197] 04 p1605 N94-19717
Further examinations on the thermodynamic stability of the Mie-Grueneisen equation of state
[AD-A270526] 05 p2037 N94-19831
Microstructural stability of wrought, laser and electron beam glazed NARloy-Z alloy at elevated temperatures
[NASA-TM-108431] 05 p1689 N94-20100
N,N'-bis(4,4,4-trinitro butyryl) hydrazine
[AD-D015897] 05 p1712 N94-20122
Polyimides containing amide and perfluoroisopropylidene connecting groups
[NASA-CASE-LAR-14608-1] 05 p1702 N94-20374
Stability curves for a thermoacoustic prime mover
[AD-A272607] 05 p1968 N94-21422
Thermal stability relationships between PMR-15 resin and its composites
[NASA-TM-106285] 05 p1675 N94-21488
Polyimide-based electrooptic materials
[DE93-019416] 05 p1706 N94-21526
Fullerene derivatives and fullerene superconductors
[DE93-019568] 05 p2031 N94-21871
Balanced arrow Mach-Zehnder interferometer
05 p1789 N94-22221
Non-linear thermal instability of optical thin molecular structures 05 p2006 N94-22667
On the nonlinear instability of thermal structures
05 p2006 N94-22668
Shear coaxial injector instability mechanisms
06 p2213 N94-23047
Condensed-phase thermal decomposition of TATB investigated by Atomic Force Microscopy (AFM) and Simultaneous Thermogravimetric Modulated Beam Mass Spectrometry (STMBMS)
[DE94-000396] 06 p2232 N94-23298
Ceramic silicon-boron-carbon fibers from organic silicon-boron-polymers
[NASA-CASE-ARC-11956-1-SB]
06 p2253 N94-23311
A method to remove intercalates from bromine and iodine intercalated carbon fibers
[NASA-TM-106443] 06 p2222 N94-23591
Hubble Space Telescope high speed photometer orbital verification
[NASA-CR-189333] 06 p2204 N94-24226
An overview on the main available ceramic composites and their processing routes 06 p2255 N94-24229
CMC design consequences 06 p2256 N94-24238
Preparation and properties of translucent gamma-aluminium oxynitride
[ETN-94-95305] 06 p2263 N94-25281
Accelerated screening methods for determining chemical and thermal stability of refrigerant-lubricant mixtures. Part 2: Experimental comparison and verification of methods
[DE94-003664] 07 p2749 N94-26007
The influence of weld metal alloying additions to extend the heat input range for the submerged arc welding of high strength steels
[AD-A274284] 07 p2738 N94-26679
Thermally stable oxygen and nitrogen implant isolation of C-doped Al(0.35)Ga(0.65)As
[DE94-004799] 07 p3069 N94-27790
Broad specification fuels combustion technology program, phase 2
[NASA-CR-191066] 07 p2719 N94-27854
New monomers for high performance polymers
07 p2758 N94-27904
Kinetic parameters from thermogravimetric analysis
07 p2721 N94-27909
Barley cell culture as a producer of heterologous protein
[PB94-132339] 08 p3379 N94-28408
Flammability, odor, offgassing, thermal vacuum stability, and compatibility with aerospace fluids of wire insulations 08 p3166 N94-28709
High temperature resistant jet fuels
08 p3192 N94-29260
Research and development of high thermal stability fuels 08 p3192 N94-29261
Development of global/chemistry model for jet-fuel thermal stability based on observations from static and flowing experiments 08 p3192 N94-29262
Insensitive energetic materials: The importance of physical properties and molecular structure
[AD-A275393] 08 p3225 N94-29308
Advanced thermally stable jet fuels
[DE94-006760] 09 p3667 N94-32150
Characterization of thermally stable dye-doped polyimide based electrooptic materials
[DE94-005309] 09 p3882 N94-32674
An investigation of the radiolytic stability of a resorcinol-formaldehyde ion exchange resin
[DE94-007971] 09 p3660 N94-32698
The development of precipitated iron catalysts with improved stability
[DE94-008711] 09 p3638 N94-32886
The effect of prolonged exposure to 750 C air on the tribological performance of PM212
[NASA-TM-106472] 09 p3617 N94-32941
Novel polydiacetylenes as materials for second and third order nonlinear optics
[AD-A277512] 09 p3664 N94-33082
Thermal stability studies of diamond-like carbon films
[DE94-009280] 10 p4028 N94-34069
Effects of combined stressing on the electrical properties of film and ceramic capacitors
[NASA-TM-106605] 11 p4257 N94-35249
Advanced thermally stable, coal-derived, jet fuels development program. Experiment system and model development
[AD-A278968] 12 p4428 N94-36505
Process simulation and modeling for advanced intermetallic alloys
[AD-A280327] 12 p4416 N94-37030
Thermodynamics of minerals stable near the Earth's surface
[DE94-012479] 12 p4539 N94-37094
Organic nonlinear optical (NLO) polymers. 4: Thermally stable NLO polymers
[AD-A280196] 12 p4423 N94-37148
Interferometric JFTOT tube deposit measuring device
[AD-D016295] 12 p4430 N94-37768

THERMAL STRESSES

Arcjet exploratory tests of ARC optical window design for the AFE vehicle
[NASA-CR-192655] 01 p0034 N94-10930
Advanced diagnostics for in situ measurement of particle formation and deposition in thermally stressed jet fuels
[DE93-009798] 01 p0098 N94-11366
Instantaneous engine frictional torque: Its components and piston assembly friction
[DE93-011639] 01 p0182 N94-11625
A novel test method for fuel thermal stability
[AD-A265853] 01 p0099 N94-12275
Analytical models for describing the mechanical behavior of fiber reinforced composites
[AD-A265906] 01 p0074 N94-12347
Thermal gradient-induced deflection of a thick-walled cylinder with bending residual stresses
[AD-A266347] 02 p0673 N94-13777
Thermal shock resistance of ceramic matrix composites
[NASA-CR-189136] 02 p0557 N94-13920
Computational strategies in the dynamic simulation of constrained flexible MBS 02 p0679 N94-14635
Scholarly research program in fuel analysis and combustion research
[AD-A266789] 03 p0942 N94-14911
XPS analysis of Al/EPDM bondlines from IUS SRM-1 polar bosses
[AD-A266851] 03 p1056 N94-14945
Thermal stresses of a trimaterial medium in a nonuniform temperature field
[AD-A267243] 03 p0930 N94-14975
High temperature advanced structural composites. Volume 3: Mechanics
[AD-A267024] 03 p0933 N94-15626
Thermal stress effects in intermetallic matrix composites
[NASA-CR-191191] 03 p1054 N94-16518
Elastic-plastic finite-difference analysis of unidirectional composites subjected to thermomechanical cyclic loading
[AD-A267666] 03 p1061 N94-17269
Fiber strength utilization in carbon/carbon composites
[AD-A267713] 03 p0940 N94-17271
Aspects of high temperature damage in fiber reinforced titanium metal matrix composites
[AD-A267907] 03 p0941 N94-17379
Workshop on multifactor aging mechanisms and models
[AD-A268668] 04 p1397 N94-18311
Effect of internal heating during hot compression testing on the stress-strain behavior and hot working characteristics of alloy 304L
[DE93-012701] 04 p1362 N94-18917
Thermal stresses in the microchannel heatsink cooled by liquid nitrogen
[DE93-018660] 04 p1418 N94-18995
Strengthening of NiAl matrix composites
[AD-A271491] 05 p1674 N94-20550
Thermal stress analysis of composites in the space environment 05 p1661 N94-21379
Improvements to a method for the geometrically nonlinear analysis of compressively loaded stiffened composite panels
[NASA-CR-194715] 05 p1832 N94-21814
A finite element formulation and adaptive solution approach for large-scale thermomechanical problems with complex contact conditions
[DE93-019605] 05 p1960 N94-21996
Analysis of thermal mechanical fatigue in titanium matrix composites 05 p1835 N94-22618
Thermal fatigue: A literature review
[PB93-226306] 06 p2375 N94-23120
Fully coupled nonlinear thermomechanical analysis including general contact in PALM2D
[DE94-001661] 06 p2568 N94-23216
Analysis of local delaminations caused by angle ply matrix cracks
[NASA-TM-109052] 06 p2228 N94-24083
Numerical modeling of physical vapor transport under microgravity conditions: Effect of thermal creep and stress 06 p2223 N94-24340
Strength and life of pressure vessels subjected to impacts and thermomechanical GFRP loading
[VTT-JULK-771] 06 p2379 N94-25418
A review of carbide fuel corrosion for nuclear thermal propulsion applications
[DE94-003938] 07 p2699 N94-25613
The fracture behavior of a CVD crystalline Si3N4/amorphous Si3N4 composite
[DE94-002646] 07 p2750 N94-26124
Electrical analysis of wideband and distributed windows using time-dependent field codes
[DE94-002987] 07 p2768 N94-26310
Baseline for a Nordtest method. Reliability stress screening of components. A guide for component users
[PB94-123775] 07 p2835 N94-27042
Implementation of thermal residual stresses in the analysis of fiber bridged matrix crack growth in titanium matrix composites
[NASA-TM-109082] 07 p2711 N94-27658
Development of methodologies for the estimation of thermal properties associated with aerospace vehicles
07 p2846 N94-27920
Thermal strain generated by an enhanced anti-G protection system in a hot climate
08 p3383 N94-28445
Composite load spectra for select space propulsion structural components
[NASA-CR-194476] 08 p3316 N94-28508
An analysis of isothermal, bithermal, and thermomechanical fatigue data of Haynes 188 and B1900+Hf by energy considerations
[NASA-TM-106359] 08 p3317 N94-28819
Prediction of stress-strain response of SCS-6/Timetal-21S subjected to a hypersonic flight profile
[NASA-TM-109026] 08 p3177 N94-28823
Research and development of high thermal stability fuels 08 p3192 N94-29261
The influence of temperature on microelectronic device failure mechanisms, phase 2
[AD-A275029] 08 p3265 N94-29511
Transient thermal fatigue of ceramic composites
08 p3216 N94-29874
Multiple Concentric Cylinder Model (MCCM) user's guide
[NASA-CR-195299] 08 p3183 N94-30125
Evolution of the interface properties with temperature in the T800H/ bismaleimide composites
[ONERA-NT-1993-14] 09 p3619 N94-31478
Validation and sensitivity analysis of Texas human thermal model predictions during cold water immersion
[AD-A275240] 09 p3797 N94-32156
Development of high temperature property database for Alloy 800H
[DE94-727589] 10 p4024 N94-33870
Effects of combined stressing on the electrical properties of film and ceramic capacitors
[NASA-TM-106605] 11 p4257 N94-35249
Advanced thermally stable, coal-derived, jet fuels development program. Experiment system and model development
[AD-A278968] 12 p4428 N94-36505
Correlation of analytical and experimental hot structure vibration results
[NASA-TM-104269] 12 p4386 N94-36644
Material and design considerations for the carbon armored ITER divertor
[DE94-737854] 12 p4530 N94-37415

Transient thermal and dynamic stresses in strongback-design blankets
[DE94-012639] 12 p4530 N94-37441
Residual stresses in a multi-pass weld in an austenitic stainless steel plate before and after thermal stress relief
[DE94-013278] 12 p4420 N94-37548
A simple evaluation of thermally-induced streses in the vicinity of the stitch in a through-thickness reinforced cross-ply laminate
[NASA-CR-196317] 12 p4406 N94-37653

THERMAL VACUUM TESTS
Results of thermal vacuum tests for the PASP+ flight modules 01 p0053 N94-11410
Calibration of a calorimeter for measuring the performance of thermal control surfaces 05 p1660 N94-21378
Thermal control system for SSF sensor/electronics
[SAND-92-0652C] 06 p2321 N94-23640
Arcjet system integration development
[NASA-CR-187147] 08 p3171 N94-28736
An alternate method for achieving temperature control in the -160 to +90 C range
[NASA-CASE-NPO-18995-1-CU] 08 p3288 N94-29497
Thermal-vacuum response of polymer matrix composites in space 09 p3595 N94-31033

THERMALIZATION (ENERGY ABSORPTION)
Positron implantation in solids
[DE94-013029] 12 p4537 N94-37499

THERMIONIC CONVERSION SYSTEMS
U THERMIONIC POWER GENERATION

THERMIONIC CONVERTERS
NT SOLAR BLANKETS
TFE verification program
[DE93-009609] 01 p0373 N94-11694
High temperature materials technology research for advanced thermionic systems
[DE93-018302] 03 p0960 N94-16964
TOPAZ 2 system description
[DE94-006230] 08 p3498 N94-30846
High temperature materials technology research for advanced thermionic systems
[DE94-008341] 09 p3646 N94-32825
TFE verification program
[DE94-009870] 12 p4398 N94-37514

THERMIONIC DIODES
Collective acceleration of ions in near-anode plasma of a strong-current relativistic diode
[DE93-620977] 01 p0387 N94-10541
Observation of reflected waves on the SABRE positive polarity inductive adder MITL
[DE93-019413] 05 p1980 N94-20295
Investigations of large area electron beam diodes for excimer lasers
[DE94-005670] 08 p3295 N94-30595

THERMIONIC EMISSION
Channel model for AC electric arc
[PB94-124591] 07 p2786 N94-27327

THERMIONIC EMITTERS
TFE verification program
[DE93-009609] 01 p0373 N94-11694
High temperature materials technology research for advanced thermionic systems
[DE93-018302] 03 p0960 N94-16964
TFE verification program
[DE94-009870] 12 p4398 N94-37514

THERMIONIC POWER GENERATION
The 40 kWe S-PRIME Thermionic Design and Technology Demonstration Program
[DE93-004738] 01 p0040 N94-10147
Space-R thermionic space nuclear power system design and technology demonstration
[DE94-002017] 07 p2700 N94-25930
TOPAZ 2 system description
[DE94-006230] 08 p3498 N94-30846
The TOPAZ 2 space reactor response under accident conditions
[DE94-004998] 08 p3498 N94-30847

THERMIONIC REACTORS
U ION ENGINES
U NUCLEAR ROCKET ENGINES

THERMISTORS
Analysis of TIMS performance subjected to simulated wind blast 03 p1063 N94-16598
Advanced far infrared detectors
[DE93-040289] 05 p1988 N94-21528
Thermistor controlled current source versatile temperature sensor
[AD-D015979] 06 p2345 N94-25037
Development and application of a thermistor current meter
[AD-A275816] 08 p3286 N94-28831
The use of thermistors in the NPL electron-beam calorimeter
[PB94-139334] 08 p3290 N94-30782
Automatic resonator alignment and power stabilization of high power C02 lasers
[ISBN-0-315-77217-4] 09 p3714 N94-31472
Bottom boundary layer stress measurements with BASS tripods: Data report STRESS 1988-1989
[AD-A277864] 10 p4092 N94-33775

THERMOCHEMICAL PROPERTIES
NT HEAT OF COMBUSTION
NT HEAT OF DISSOCIATION
NT HEAT OF FORMATION
NT HEAT OF FUSION
NT HEAT OF SOLUTION
NT LATENT HEAT
Closed-chamber analysis of M5 propellant lot RAD-64597
[AD-A266321] 02 p0585 N94-14145
Laser ignition of solid propellants: 1. Ignition delays
[AD-A268454] 03 p0976 N94-17538
Advanced fuel properties: A computer program for estimating property values
[AD-A275248] 08 p3224 N94-28901
Ignition delays, heats of combustion, and reaction rates of aluminum alkyl derivatives used as ignition and combustion enhancers for supersonic combustion
[NASA-CR-189581] 09 p3638 N94-32868

THERMOCHEMISTRY
NT AEROTHERMOCHEMISTRY
NT COMBUSTION CHEMISTRY
Technical Update: Johnson Space Center system using a solid electrolytic cell in a remote location to measure oxygen fugacities in CO/CO2 controlled-atmosphere furnaces
[NASA-TM-104774] 01 p0423 N94-11183
Chemical Vapor Deposition of Refractory Metals and Ceramics 2. Materials Research Society Symposium proceedings
[AD-A265072] 01 p0092 N94-11866
Crystal-chemistry and partitioning of REE in whitlockite 01 p0408 N94-12174
The rate of chemical weathering of pyrite on the surface of Venus 01 p0477 N94-12246
Conversion of light hydrocarbon gases to metal carbides for production of liquid fuels and chemicals
[DE93-014962] 02 p0583 N94-13002
Performance effects of coal-derived contaminants on the carbonate fuel cell
[DE93-013801] 02 p0703 N94-13693
Thermochemistry of transition metal clusters
[DE93-016201] 02 p0571 N94-13977
Processing and protection of high temperature structural materials
[AD-A267292] 03 p0954 N94-14961
Rocket motor plume flowfields: Phenomenology and simulation 03 p0924 N94-15221
Thermochemistry of silicate speciation in aqueous sodium silicate solutions: Ionization and polymerization of small silicate ion
[AD-A266825] 03 p0964 N94-15683
Particle simulation of hypersonic flow
[AD-A267185] 03 p0857 N94-15787
Ceramic fiber coatings development and demonstration
[AD-A267286] 03 p0972 N94-17242
Interface chemistry in ceramic matrix composites
[AD-A268629] 03 p0973 N94-17466
Techniques for the estimation of Heats of Explosion (HEX) using thermochemical codes
[AD-A268584] 04 p1609 N94-18310
Evaporation in equilibrium, in vacuum, and in hydrogen gas 05 p1684 N94-20638
Thermochemistry of the actinides
[DE94-000895] 06 p2231 N94-22943
The addition of molecular oxygen to hydroperoxy-propyl radicals
[DE94-003662] 07 p2760 N94-27725
Gas phase thermochemistry of organogermanium compounds
[DE94-004885] 08 p3187 N94-28561
Brief summary of accomplishments since our DOE-sponsored radon project commenced
[DE94-004643] 08 p3348 N94-29926
NEQPAK, the AEDC thermochemical nonequilibrium package: Theory and use
[AD-A279005] 11 p4266 N94-35951
CSTL technical activities, 1991
[PB94-160769] 11 p4318 N94-36003
Method of thermochemically treating silicon carbide fibers derived from polymers
[AD-D016218] 11 p4246 N94-36125
The thermochemistry and reaction mechanisms in the decomposition of energetic materials
[DE94-011420] 11 p4248 N94-36376
Thermodynamics of minerals stable near the Earth's surface
[DE94-012479] 12 p4539 N94-37094
CHEETAH: A fast thermochemical code for detonation
[DE94-012586] 12 p4429 N94-37427

THERMOCLINES
The subduction experiment. Cruise report, R/V Oceanus, cruise number 250 legs 1 and 2. Subduction 2 mooring deployment and recovery cruise, 25 January-26 February 1992
[AD-A264922] 01 p0289 N94-11853
On an upwelling front, propagation of upwelling and vertical velocity in the eastern Arabian Sea during monsoon, 1987 01 p0206 N94-11987
The Pacific Subarctic Frontal Zone: Structure and dynamics 01 p0223 N94-12731
Generation of internal waves near the shelf boundary 01 p0229 N94-12763
Vertical motion in the SYNOP central array
[AD-A273593] 06 p2418 N94-24795
Flow and temperature distribution in a naturally stratified thermal storage tank
[AD-A273511] 06 p2336 N94-24821

THERMOCOUPLES
NT THERMOPILES
High temperature processing and diagnostic technologies for microgravity applications 01 p0110 N94-10130
Widebody cabin water spray optimization tests
[DOT/FAA/CT-TN93/29] 02 p0511 N94-14186
Simultaneous measurement of temperature and strain using four connecting wires
[NASA-TM-104271] 03 p1032 N94-15754
Wind tunnel investigation with an operational turbojet engine
[TABES PAPER 93-662] 03 p0870 N94-16157
Flame structure studies of a lean 20-torr H2/N2O/Ar flame employing molecular beam mass spectrometry
[AD-A268889] 04 p1349 N94-18456
High temperature, oxidation resistant noble metal-Al alloy thermocouple
[NASA-CASE-LEW-15515-1] 06 p2343 N94-23826
Investigation of the heat handling capabilities of DIII-D neutral beamline internal components
[DE94-001107] 06 p2553 N94-24756
Verification of thermal analysis codes for modeling solid rocket nozzles
[NASA-CR-195248] 07 p2702 N94-27150
Effects of free-stream turbulence on a jet in a cross flow 07 p2805 N94-28036
System for improving measurement accuracy of transducer by measuring transducer temperature and resistance change using thermoelectric voltages
[NASA-CASE-ARC-12014-1] 08 p3287 N94-29361
Measurement of the coolant channel temperatures and pressures of a cooled radial-inflow turbine
[NASA-TM-106594] 10 p3997 N94-33706
A shock tube study of aerodynamic heating of gaps in a cylinder subjected to supersonic cross flow
[AD-A278550] 10 p3982 N94-33782
A method available for processing the signal of thermocouples by computer 10 p4057 N94-34360
Dual active surface, miniature, plug-type heat flux gauge
[NASA-CASE-LEW-15643-1] 10 p4056 N94-35078
Digital control programmer for temperature control
[DE94-615584] 11 p4309 N94-36382
Measurement of a surface heat flux and temperature 11 p4231 N94-36407
Initial report on calorimetry for the Tore Supra Outboard pump Limiter
[DE94-011244] 12 p4531 N94-37626

THERMODYNAMIC COUPLING
Homogeneous-hetergeneous combustion: Thermal and chemical coupling
[DE93-016050] 02 p0565 N94-14403

THERMODYNAMIC CYCLES
NT BRAYTON CYCLE
NT CARNOT CYCLE
NT RANKINE CYCLE
NT STIRLING CYCLE
Study on various cryogenic refrigeration cycles using all purpose refrigerators 01 p0130 N94-11839
Combustor technology for future small gas turbine aircraft
[NASA-TM-106312] 02 p0517 N94-13142
Some single-piston closed-cycle machines and Peter Tailer's thermal lag engine
[DE93-015983] 03 p1049 N94-17675
Thermodynamic theory of exergy analysis
[PB93-187847] 04 p1607 N94-18120
Adsorption analysis of ammonia in an aqueous solution
[DE93-019512] 04 p1353 N94-19552
Alternative refrigerants and refrigeration cycles for domestic refrigerators
[DE93-040481] 05 p1714 N94-20099

Hydrogen isotope separation experience at the Savannah River Site
[DE93-019832] 05 p1679 N94-20266
Advanced Turbine Systems (ATS). Phase 1: System scoping and feasibility studies
[DE93-041130] 05 p1826 N94-21938
Performance calculations and research direction for a water enhanced regenerative gas turbine cycle
[DE93-019866] 05 p1826 N94-21983
Enhanced absorption cycle computer model
[DE94-001997] 06 p2271 N94-23793
A technique for integrating engine cycle and aircraft configuration optimization
[NASA-CR-191602] 07 p2668 N94-26606
Gas fired advanced turbine system
[DE94-003193] 07 p2827 N94-27874
Combined Cycles for Power Plants
[VKI-LS-1993-08] 07 p2830 N94-28077
Chambers of turboreactors with variable geometry: A response to the matrix of pollution in cycles at high temperature, high pressure 08 p3194 N94-29273
Application of natural refrigerants: A rational solution to a pressing problem
[PB94-138781] 09 p3668 N94-31073

THERMODYNAMIC EFFICIENCY

Space Life Support Engineering Program
[NASA-CR-193474] 01 p0316 N94-12365
Systems analysis of a closed loop ECLSS using the ASPEN simulation tool. Thermodynamic efficiency analysis of ECLSS components 01 p0316 N94-12366
An estimate of the second law thermodynamic efficiency of the various units comprising an Environmental Control and Life Support System (ECLSS) 01 p0317 N94-12369
Two temperature modeling and experimental measurements of laser sustained hydrogen plasmas
[AD-A265750] 02 p0796 N94-13039
Jet engine performance enhancement through use of a wave-rotor topping cycle
[NASA-TM-4486] 03 p0870 N94-17470
Advanced Turbine Systems (ATS). Phase 1: System scoping and feasibility studies
[DE93-041130] 05 p1826 N94-21938
Performance calculations and research direction for a water enhanced regenerative gas turbine cycle
[DE93-019866] 05 p1826 N94-21983
Experimental evaluation of oxygen-enriched air and emulsified fuels in a six-cylinder diesel engine
[DE94-000907] 05 p1811 N94-22391
CFD modeling of microwave electrothermal thrusters 06 p2216 N94-23066
The effect of high altitude pressure on the power and efficiency of an airborne two-stroke engine 06 p2155 N94-24253
Pressure-gain combustion
[DE94-002975] 07 p2719 N94-27712
Gas fired advanced turbine system
[DE94-003193] 07 p2827 N94-27874
Feasibility study on introduction of a large methanol engine power generation plant
[DE94-732338] 08 p3224 N94-28629
Quality and efficiency of solar collectors in Sweden
[PB94-137486] 08 p3337 N94-28909

THERMODYNAMIC EQUILIBRIUM

Rapid thermal processing for strained-layer semiconductor devices
[DE93-013754] 01 p0396 N94-10809
Stability and dynamics of spatio-temporal structures
[DE93-011374] 01 p0401 N94-11610
Thermodynamics of lunar ilmenite reduction 01 p0415 N94-12028
Modeling study to evaluate the ionic mechanism of soot formation in flames
[AD-A266242] 03 p0950 N94-16930
Modeling the minimum energy state of the Earth's magnetotail
[AD-A267984] 05 p1856 N94-20485
Thermodynamic models for bounding pressurant mass requirements of cryogenic tanks
[NASA-TM-106476] 06 p2346 N94-25202
Antiproton studies in penning traps
[AD-A274250] 07 p3024 N94-27011
Phase stability in the Cd-Mg system
[DE94-004976] 07 p2743 N94-27792
Theoretical studies of solid-fluid phase equilibria
[DE94-006406] 08 p3226 N94-30708
Non-equilibrium electrodynamics in the large N expansion
[DE94-006156] 09 p3911 N94-31760
SOLGAS refined: A computerized thermodynamic equilibrium calculation tool
[DE94-009021] 09 p3913 N94-32846
Boson spectra and correlations in thermal locally equilibrium systems
[DE94-616799] 11 p4325 N94-36079
Stability and dynamics of spatio-temporal structures
[DE94-013035] 12 p4412 N94-37491

THERMODYNAMIC PROPERTIES

NT CRITICAL POINT
NT CRITICAL PRESSURE
NT CRITICAL TEMPERATURE
NT EMISSIVITY
NT ENTHALPY
NT ENTROPY
NT FREE ENERGY
NT GIBBS FREE ENERGY
NT HEAT OF COMBUSTION
NT HEAT OF DISSOCIATION
NT HEAT OF FORMATION
NT HEAT OF FUSION
NT HEAT OF SOLUTION
NT LATENT HEAT
NT MELTING POINTS
NT PYROELECTRICITY
NT SPECIFIC HEAT
NT SUPERCRITICAL PRESSURES
NT SURFACE ENERGY
NT THERMAL CONDUCTIVITY
NT THERMAL DIFFUSION
NT THERMAL DIFFUSIVITY
NT THERMAL EXPANSION
NT THERMAL INSTABILITY
NT THERMAL STABILITY
NT THERMOCHEMICAL PROPERTIES
NT THERMOPHYSICAL PROPERTIES
NT VAPOR PRESSURE
NT VOLATILITY

LAMINV: A computer code for creating laminates having prescribed properties 01 p0065 N94-10069
Experimental approach to non-contact calorimetry in space 01 p0112 N94-10143
On thermodynamic properties of heavy fermion systems in magnetic field
[DE93-613819] 01 p0409 N94-10403
Thermodynamic model of air in chemical equilibrium 01 p0007 N94-10448
Exergy decrease in shock waves and boundary layers of space launch vehicles
[AD-A265272] 01 p0042 N94-10493
The effect of pressure and quadrupolar interactions on the nematic-isotropic transition properties: Numerical results for a system of prolate ellipsoids including second and fourth rank orientational order parameters
[DE93-613540] 01 p0410 N94-10536
Primaset (tm): A safer material for aircraft interior applications 01 p0018 N94-10772
Level 3 material characterization of NARC HRPF, HRHU, HRHF, and HRPU
[NASA-CR-192579] 01 p0065 N94-10812
Variability of wind stress, and sensible and latent heat flux in the North Atlantic during SEASAT 01 p0194 N94-11918
Evaluation of ECMWF latent heat flux in TOGA CD-ROM 01 p0195 N94-11921
Thermodynamics of lunar ilmenite reduction 01 p0415 N94-12028
Variability of the mixed layer depth in the North Pacific Ocean as calculated by a 3-D semi-analytical mixed layer remote sensing model 01 p0221 N94-12718
Laser photoheterodyne interferometers for oceanographic investigations 01 p0177 N94-12732
Theoretical treatment of the bulk and surface properties of fluids containing long, flexible molecules
[DE93-015560] 02 p0575 N94-12861
A time-accurate numerical method for chemically reacting flows at all Mach numbers 02 p0500 N94-13198
Performance effects of coal-derived contaminants on the carbonate fuel cell
[DE93-013801] 02 p0703 N94-13693
Thermochemistry of transition metal clusters
[DE93-016201] 02 p0571 N94-13977
Lawrence Berkeley Laboratory Chemical Sciences Division
[DE93-015260] 02 p0851 N94-14401
Review of nuclear thermal propulsion carbide reactor fuel corrosion and exhibit
[DE93-016605] 02 p0585 N94-14535
Yield properties of tungsten and tungsten heavy alloys
[AD-A266833] 02 p0575 N94-14878
Processing and protection of high temperature structural materials
[AD-A267292] 03 p0954 N94-14961
PHENIX Conceptual Design Report
[DE93-015759] 03 p1182 N94-16161
The effect of irradiation on the mechanical properties of 6061-T651 aluminum
[DE93-015825] 03 p0958 N94-16168
Cation ordering in orthopyroxenes and cooling rates of meteorites: Low temperature cooling rates of Estherville, Bondoc and Shaw 03 p1241 N94-16176
Thermal disorder in adsorbed Cl on Si(100)
[AD-A266295] 03 p1210 N94-16476
On-line gas chromatographic studies of Rutherfordium (element 104), hahnium (element 105), and homologs
[DE93-013890] 03 p0948 N94-16821
Modeling study to evaluate the ionic mechanism of soot formation in flames
[AD-A266242] 03 p0950 N94-16930
Mechanistic models of soot formation
[AD-A267806] 03 p0950 N94-17008
Convection effects on radial segregation and crystal melt interface in vertical Bridgman growth
[NASA-CR-191541] 03 p1029 N94-17387
Flow instability tests for a particle bed reactor nuclear thermal rocket fuel element
[AD-A268012] 03 p0929 N94-17474
Soluble precursor route to polyanilines
[AD-A268015] 03 p0973 N94-17494
Numerically solving a transient heat conduction problem with convection and radiation
[AD-A268521] 03 p1220 N94-17540
A new multiphase equation of state for iron
[DE93-017629] 04 p1357 N94-17819
Diffusion in ordered alloys
[AD-A268232] 04 p1359 N94-18322
Carbon/carbon composites coated with SiC by chemical vapor deposition
[AD-A269934] 04 p1341 N94-18544
Wettability and reaction kinetics in metal matrix composites
[AD-A270377] 04 p1342 N94-18704
Structure-property relationships in radical-cation (electron-donor molecule) and anion-based (including fullerides) organic superconductors and their use in the design of new materials
[DE93-018617] 04 p1601 N94-19022
A free energy simulation method based study of interfacial segregation
[DE93-019462] 04 p1364 N94-19032
Thermophysical properties
[DE93-040219] 04 p1351 N94-19134
Proceedings: International Symposium on Thermal Engineering and Science for Cold Regions
[AD-A270636] 04 p1487 N94-19529
Adsorption analysis of ammonia in an aqueous solution
[DE93-019512] 04 p1353 N94-19552
Supercritical thermodynamics of sulfur and nitrogen species
[DE93-041221] 04 p1610 N94-19670
Damage accumulation in advanced metal matrix composites under thermal cycling/creep loadings
[AD-A271207] 04 p1344 N94-19720
Pressure and temperature effects on the kinetics and quality of diamond films
[AD-A270876] 04 p1606 N94-19771
Complex and stereoregular nonlinear optical materials
[AD-A271067] 05 p1983 N94-19846
Technology to prevent greenhouse effect gases
[DE94-707421] 05 p1850 N94-19976
Absorption heat pump for space applications
[NASA-CR-194693] 05 p1845 N94-20066
Catalytic hydrogenation of carbon monoxide
[DE94-000881] 05 p1678 N94-20103
The thermodynamic properties to 700 K of naphthalene and 2,7-dimethylnaphthalene
[DE93-000160] 05 p2037 N94-20473
Mathematical model and analysis of the Tactical Unmanned Ground Vehicle (TUGV) using computer simulation
[AD-A272258] 05 p1824 N94-20576
Analysis of cost: CVD diamond deposition
[AD-A271980] 05 p2018 N94-20616
Recondensation in the early solar system: Physical conditions and source material 05 p2085 N94-20849
Direct images of thermal disorder in the Cl-Si and H-O-Si chemisorption bond on Si(100)
[AD-A272386] 05 p1680 N94-21145
Chemistry of the burning surface
[AD-A272725] 05 p1681 N94-21181
Recent developments in aromatic azo polymers research
[AD-A272966] 05 p1705 N94-21259
Electron emission from nanometer-size metallic clusters: Electronic states and structural stability of supported Au clusters
[DE93-040184] 05 p1975 N94-21766
High power, electron-beam induced switching in diamond
[DE93-040535] 05 p1768 N94-21770
Particle formation in a laser-heated aerosol reactor. Application to silicon and silicon nitride synthesis
[PB93-217982] 06 p2347 N94-22982
Heat transfer in rocket combustion chambers 06 p2214 N94-23051

Thermodynamics of nickel-cadmium and nickel-hydrogen batteries 06 p2391 N94-23349
Instrument interface description for NOAA 2000 instruments with European morning spacecraft and/or NOAA-OPQ spacecraft
[NASA-TM-109406] 06 p2208 N94-23478
The possible effects of the natural and induced space environment on the optical and thermal properties of EOS surfaces 06 p2207 N94-23596
Enhanced absorption cycle computer model
[DE94-001997] 06 p2271 N94-23793
Humidity effects on soluble core mechanical and thermal properties (polyvinyl alcohol/microballoon composite) type CG extendospheres, volume 2
[NASA-CR-193893] 06 p2229 N94-24224
Coupled land surface/hydrologic/atmospheric models 06 p2413 N94-24387
A study of element interaction in thermoacoustic engines
[AD-A273228] 06 p2569 N94-24777
Flow and temperature distribution in a naturally stratified thermal storage tank
[AD-A273511] 06 p2336 N94-24821
Thermophysical properties of simple liquid metals: A brief review of theory 06 p2248 N94-25130
Zr-rich corner of the Zr-Sn-O diagram
[DE93-633764] 07 p2734 N94-26161
Microwave and pulsed power
[DE94-003019] 07 p2782 N94-26312
Titanium 1992: Volume 3: Science and technology
[AD-A274800] 07 p2735 N94-26337
How reliable is the HMSA integral equation for the pair structure of supercooled and amorphous mixtures?
[DE94-601543] 07 p3006 N94-26411
New rubber qualification for the igniter adapter
[NASA-CR-193936] 07 p2752 N94-26708
Thermophysical properties of HFC-143a and HFC-152a
[DE94-004236] 07 p2719 N94-27567
Phase stability in the Cd-Mg system
[DE94-004976] 07 p2743 N94-27792
Development of methodologies for the estimation of thermal properties associated with aerospace vehicles 07 p2846 N94-27920
Innovative processing of composites for ultra-high temperature applications, book 3
[AD-A275599] 08 p3177 N94-28731
WINDOW 4.0: Documentation of calculation procedures
[DE94-004935] 08 p3410 N94-29019
Surface tension of tin and its alloys with particular reference to soiders
[PB94-138302] 08 p3204 N94-29119
Mechanical alloying processing with application to structural materials: ASSERT supplement
[AD-A275400] 08 p3204 N94-29205
Thermomechanical properties of 3-D transition metals
[DE94-604015] 08 p3487 N94-29500
The influence of temperature on microelectronic device failure mechanisms, phase 2
[AD-A275029] 08 p3265 N94-29511
Aspects of model-based rocket engine condition monitoring and control
[NASA-CR-195116] 08 p3173 N94-29848
Transient thermal fatigue of ceramic composites 08 p3216 N94-29874
Particle kinetic simulation of high altitude hypervelocity flight
[NASA-CR-194535] 08 p3131 N94-29893
Thermodynamics of molten K-TE alloys
[DE94-608095] 08 p3208 N94-30090
Volume averaged model for the mechanics of alloys solidification
[PB94-138617] 08 p3208 N94-30113
The role of sea ice dynamics in global climate change 08 p3350 N94-30620
A numerical method for mixing/chemically reacting compressible flow with finite rate chemistry 09 p3634 N94-31824
Group 12 thiolates: Syntheses, characterization and decomposition pathways
[AD-A277055] 09 p3900 N94-32011
Isomeric poly(benzophenone)s: Synthesis of highly crystalline poly (4, 4 foot-benzophenone) and amorphous poly (2, 5-benzophenone), a soluble poly (p-phenylene) derivative
[AD-A277261] 09 p3655 N94-32017
Some perspectives on solution-phase electron-transfer processes
[AD-A276906] 09 p3635 N94-32216
Inorganic polymer engineering materials
[DE94-008519] 09 p3659 N94-32655
Investigation of superconductivity and magnetism in d and f-electron materials
[DE94-008535] 09 p3907 N94-32933
CET93 and CETPC: An interim updated version of the NASA Lewis computer program for calculating complex chemical equilibria with applications
[NASA-TM-4557] 09 p3638 N94-32948
Regional sedimentological variations among dark crater floor features: Toward a model for modern eolian sand distribution on Mars 09 p3946 N94-33203
Theoretical study of thermodynamic properties and reaction rates of importance in the high-speed research program 10 p3974 N94-33482
AFDM: An advanced fluid-dynamics model, volume 6
[DE94-009596] 11 p4264 N94-35669
Performance analysis of reciprocating regenerative magnetic heat pumping
[DE94-009488] 11 p4264 N94-35683
Chirped-pulse amplification with flashlamp-pumped Ti:Sapphire amplifiers
[DE94-010055] 11 p4272 N94-35695
Properties and bibliography of GaSe
[AD-A279064] 11 p4340 N94-35733
NEQPAK, the AEDC thermochemical nonequilibrium package: Theory and use
[AD-A279005] 11 p4266 N94-35951
Thermodynamic behaviour of tellurium at high temperatures
[DE94-612823] 11 p4240 N94-35960
Thermophysical properties of HFC-143a and HFC-152a
[DE94-009995] 11 p4251 N94-36008
A new association-model for binary VLE of alcohol/hydrocarbon and amine/hydrocarbon mixtures
[DE94-011012] 11 p4248 N94-36034
Quantum mechanics and thermodynamics of particles with distance dependent statistics
[DE94-616620] 11 p4343 N94-36072
NMR imaging of components and materials for DOE application
[DE94-010664] 11 p4238 N94-36084
On the origin of porphyritic chondrules
[DE94-010464] 11 p4351 N94-36418
A possible origin of EL6 chondrites from a high temperature-high pressure solar gas
[DE94-010467] 12 p4548 N94-36759
Ability of the total strain version of strainrange partitioning to characterize thermomechanical fatigue behavior
[NASA-TM-4556] 12 p4455 N94-37102
Solution characterization of poly(isobornyl methacrylate) in tetrahydrofuran
[AD-A280497] 12 p4409 N94-37145
Azobenzene-containing polymers: Some optoelectronic properties
[AD-A280448] 12 p4424 N94-37185
Development of durable high-temperature catalysts for natural gas combustion: Catalytic materials (CATMAT (trade name)) properties database
[PB94-171824] 12 p4412 N94-37462

THERMODYNAMICS
NT AEROTHERMODYNAMICS
NT COMBUSTION PHYSICS
NT NONEQUILIBRIUM THERMODYNAMICS
Coupled thermovibrational and thermocapillary convection in liquid bridge (floating zone system) 01 p0101 N94-10082
A lattice gas model for enzyme kinetics with next-nearest neighbor interactions
[DE93-613026] 01 p0410 N94-10631
Similarity of the leading contributions to the self-energy and the thermodynamics in two- and three-dimensional Fermi Liquids
[DE93-012673] 01 p0412 N94-11162
A modeling investigation of thermal and strain induced recovery and nonlinear hardening in potential based viscoplasticity
[NASA-TM-106122] 01 p0188 N94-11482
Chaos, entropy, and reversibility: A simple example 01 p0031 N94-11495
Proposed framework for thermomechanical life modeling of metal matrix composites
[NASA-TP-3320] 01 p0074 N94-12449
The thermodynamics of the nonlinear shear flows 01 p0169 N94-12728
Implementation of ADI: Schemes on MIMD parallel computers
[NASA-CR-193720] 02 p0759 N94-13204
Thermodynamic status of static and dynamic contact angles
[ISBN-0-315-73844-8] 02 p0817 N94-13554
Optical and physical properties of the LiSrAlF6:Cr laser crystal
[DE93-014657] 02 p0808 N94-13881
Selective excitation, relaxation, and energy channeling in molecular systems
[DE93-018819] 02 p0785 N94-14420
Statistical mechanical theory of liquid entropy
[DE93-016524] 02 p0817 N94-14593
Analysis, approximation, and computation of a coupled solid/fluid temperature control problem
[NASA-TM-106351] 02 p0771 N94-14731
Thermomechanical and isothermal fatigue behavior of a (90)sub 8 titanium matrix composite
[NASA-CR-191196] 02 p0560 N94-14822
On the statistical theory of the even-even nucleons levels' density
[DE93-623990] 02 p0788 N94-14875
Inelastic deformation of metal matrix composites
[NASA-CR-191522] 03 p0930 N94-15106
High temperature advanced structural composites. Volume 1: Executive summary and intermetallic compounds
[AD-A267022] 03 p0933 N94-15835
Implementation of an anisotropic turbulence model in the COMMIX-1C/ATM computer code
[DE93-015541] 03 p1023 N94-16444
Supercritical thermodynamics of sulfur and nitrogen species
[DE93-017727] 03 p1220 N94-16997
Thermo-mechanical analysis of oxidation protected carbon-carbon composites
[AD-A268191] 03 p0941 N94-17597
Lectures of Fermi liquid theory
[DE93-016630] 04 p1592 N94-17714
Thermodynamics of computation and information distance
[DE93-012730] 04 p1517 N94-17812
Thermodynamic theory of exergy analysis
[PB93-187847] 04 p1607 N94-18120
Structure, thermodynamics, and dynamical properties of supercooled liquids
[DE93-788387] 04 p1607 N94-18211
The temperature at the phase boundary during quasi-static motions of a two-phase thermoelastic bar
[AD-A268769] 04 p1596 N94-18388
Competitive dynamics and self-organization in photorefractive systems
[AD-A269663] 04 p1430 N94-18569
Molten carbonate fuel cell networks: Principles, analysis, and performance
[DE93-000281] 04 p1468 N94-18925
Ground movements associated with gas hydrate production
[DE93-019887] 04 p1486 N94-19018
Energy Conversion and Storage Program
[DE93-018602] 04 p1469 N94-19098
Thermodynamic q-distributions that aren't
[DE93-017385] 04 p1609 N94-19121
Supercritical thermodynamics of sulfur and nitrogen species
[DE93-041221] 04 p1610 N94-19670
Further examinations on the thermodynamic stability of the Mie-Grueneisen equation of state
[AD-A270526] 05 p2037 N94-19831
CTH: A software family for multi-dimensional shock physics analysis
[DE93-019428] 05 p1904 N94-20052
A parametric study of heat transfer within a planar thermosyphon
[DE93-019546] 05 p1799 N94-20258
Mathematical theory of thermodynamics of computation
[CWI-CS-R9251] 05 p2038 N94-21533
A thermodynamic theory of dynamic fragmentation
[DE93-019066] 05 p1833 N94-21916
Universality in blow-up for non linear heat equations
[PB93-215465] 05 p2038 N94-22095
A thermodynamic analysis of propagating subcritical cracks with cohesive zones 05 p1834 N94-22611
Study of improved methods for predicting chemical equilibria
[DE94-001647] 06 p2568 N94-22719
Computational fluid dynamic modelling of cavitation 06 p2215 N94-23060
Lewis Research Center R and D Facilities
[NASA-TM-109400] 06 p2630 N94-23135
Alloys for hydrogen storage in nickel/hydrogen and nickel/metal hydride batteries 06 p2391 N94-23353
Effect of hydrogen exposure on a Cu-8 Cr-4 Nb alloy
[NASA-TM-106429] 06 p2243 N94-23556
Second law analysis of a conventional steam power plant 06 p2322 N94-23646
Improved gas core propulsion model
[DE94-000929] 06 p2220 N94-24511
Integral equations for the microstructures of supercritical fluids
[DE94-002460] 06 p2535 N94-24569
Stable non-Gaussian diffusive profiles
[PB93-238053] 06 p2489 N94-24610
Thermodynamic models for bounding pressurant mass requirements of cryogenic tanks
[NASA-TM-106476] 06 p2346 N94-25202

Phase structure of the two-dimensional phi(4) field theory within thermo-field dynamics
[DE93-616850] 06 p2570 N94-25337
Hydride thermodynamic machines
[VTT-JULK-768] 06 p2571 N94-25416
A thermodynamically consistent constitutive theory for a rigid solid-stokesian fluid mixture
[DE93-633202] 07 p2792 N94-26401
Calculating the surface properties for the liquid-vapour interface: Illustrating the thermodynamic stability of the spherical microstructures
[DE94-601992] 07 p3073 N94-26837
Thermodynamics and form factors of supersymmetric integrable field theories
[DE94-602557] 07 p3073 N94-26896
Integrated model development for liquid fueled rocket propulsion systems
[NASA-CR-195253] 07 p2702 N94-27166
Process modelling of aluminium alloys. Modelling of the quench sensitivity of alloy AA6082
[PB94-124567] 07 p2741 N94-27325
Thermodynamics of combined cycle plant 07 p2831 N94-28079
Dynamic response of ceramics
[AD-A275396] 08 p3214 N94-29203
Thermodynamic analysis of chemical compatibility of several compounds with Fe-Cr-Al alloys
[NASA-CR-191166] 08 p3181 N94-29684
Statistical description of hot and dense clustering matter
[DE94-608155] 08 p3490 N94-30112
Thermodynamics of computation and information distance
[CWI-CS-R9341] 08 p3526 N94-30433
The Boltzmann entropy and randomness tests
[CWI-CS-R9342] 08 p3426 N94-30434
The role of sea ice dynamics in global climate change 08 p3350 N94-30620
Reactive flows in compact objects 09 p3934 N94-31567
Strongly coupled ionic mixtures and the H/He EOS
[DE94-006391] 09 p3934 N94-31782
Numerical simulations of monsoon rainfall with the NRL/NCSU regional nested grid model 09 p3782 N94-31791
SOLGAS refined: A computerized thermodynamic equilibrium calculation tool
[DE94-009021] 09 p3913 N94-32846
Modelling and optimal control of Pb-Sn continuous crystallization process 10 p4118 N94-34345
Degradation of radiant ceramic structures in combustion atmospheres
[PB94-157849] 10 p4030 N94-34601
CSTL technical activities, 1991
[PB94-160769] 11 p4318 N94-36003
Determination of grain boundary volume expansion by HREM
[DE94-010452] 11 p4241 N94-36231
A-TOUGH: A multimedia fluid-flow/energy-transport model for fully-coupled atmospheric-subsurface interactions
[DE94-004304] 12 p4472 N94-36739
United States Air Force Summer Research Program, 1993. Volume 5A: Wright Laboratory
[AD-A278696] 12 p4551 N94-36981
Thermodynamics of minerals stable near the Earth's surface
[DE94-012479] 12 p4539 N94-37094
Thermomechanical studies of tungsten heavy alloys
[AD-A280250] 12 p4417 N94-37122
Time-of-flight pulsed ion beam surface analysis as a means of in situ, real-time characterization of the growth of ferro-electric and conductive oxide heterostructures
[DE94-012628] 12 p4517 N94-37249
Modeling of outgassing and matrix decomposition in carbon-phenolic composites
[NASA-CR-196319] 12 p4405 N94-37471

THERMOELASTICITY
NT AEROTHERMOELASTICITY
Thermoelastic response of metal matrix composites with large-diameter fibers subjected to thermal gradients
[NASA-TM-106344] 02 p0560 N94-14823
Thermal stresses of a trimaterial medium in a nonuniform temperature field
[AD-A267243] 03 p0930 N94-14975
The temperature at the phase boundary during quasi-static motions of a two-phase thermoelastic bar
[AD-A268769] 04 p1596 N94-18388
Stress analysis of a secondary-bending specimen
[AD-A274842] 07 p2838 N94-26501

THERMOELECTRIC CONVERSION SYSTEMS
U THERMOELECTRIC POWER GENERATION

THERMOELECTRIC GENERATORS
Feasibility survey of thermoelectric conversion technology using semiconductors
[DE93-520882] 04 p1595 N94-18105
Ultrasonic technique for inspection of GPHS capsule girth weld integrity
[DE93-040072] 04 p1448 N94-19189
SP-100 heat transport technology development
[DE94-000769] 06 p2218 N94-23452
Development testing of the two-watt RTG heat source and Hastelloy-S/T-111 alloy compatibility studies
[DE94-002875] 06 p2243 N94-23784
Preliminary reentry safety assessment of the General Purpose Heat Source module for the Cassini mission: Aerospace Nuclear Safety Program
[DE94-001646] 07 p2699 N94-25926
Digital control and data acquisition for high-value GTA welding
[DE94-000885] 07 p2821 N94-25980
GPHS-RTGs in support of the Cassini mission
[DE94-009994] 11 p4212 N94-35648

THERMOELECTRIC MATERIALS
Feasibility survey of thermoelectric conversion technology using semiconductors
[DE93-520882] 04 p1595 N94-18105
Large-scale production of Si(0.8)Ge(0.2) thermoelectric alloys by mechanical alloying
[DE94-000695] 06 p2243 N94-23753

THERMOELECTRIC POWER GENERATION
High efficiency direct thermal to electric energy conversion from radioisotope decay using selective emitters and spectrally tuned solar cells
[NASA-TM-106227] 01 p0047 N94-11307
Feasibility survey of thermoelectric conversion technology using semiconductors
[DE93-520882] 04 p1595 N94-18105
Hybrid power system for remote communications stations
[AD-A274963] 07 p2782 N94-26301

THERMOELECTRICITY
Simultaneous measurement of temperature and strain using four connecting wires
[NASA-TM-104271] 03 p1032 N94-15754
Deep ion implantation into manganin to modify its pressure and electrothermocharacteristics
[DE93-630229] 04 p1359 N94-18218
Thermoelectric cooled, purge-and-trap device for enhancing the utility of fiber optic VOC sensors
[DE94-001772] 06 p2541 N94-22722
Large-scale production of Si(0.8)Ge(0.2) thermoelectric alloys by mechanical alloying
[DE94-000695] 06 p2243 N94-23753
Pre-flight testing of Thermoelectric Quartz Crystal Microbalances (TQCM) for midcourse space experiment (MSX) spacecraft
[AD-A277054] 09 p3610 N94-32010

THERMOGRAMS
U TEMPERATURE MEASURING INSTRUMENTS

THERMOGRAPHY
Thermal flux measurements in hypersonic flows: A review 01 p0005 N94-10438
Experimental study of multiple droplet evaporative cooling
[PB93-198463] 01 p0149 N94-10851
Thermographic properties of eight blue-emitting phosphors
[DE93-011459] 01 p0078 N94-11622
Experimental measurement of local heat transfer coefficients over discrete roughened plates using infrared thermography 02 p0635 N94-13652
High frame rate thermal imager for hypersonic wind tunnel applications
[ONERA-NT-1992-12] 02 p0650 N94-14009
Measurement Techniques
[VKI-LS-1993-05] 04 p1430 N94-18643
Fundamentals of infrared thermography 04 p1431 N94-18648
Application of infrared thermography in fluid mechanics 04 p1431 N94-18649
Heat transfer quantitative characterization: Passive and active methods 04 p1431 N94-18650
Perspective and future possibilities 04 p1431 N94-18651
Infrared thermography 04 p1432 N94-18652
Three-dimensional dynamic thermal imaging of structural flaws by dual-band infrared computed tomography
[DE93-019575] 05 p1906 N94-20316
Fluorescent microthermographic imaging
[DE93-040332] 05 p1810 N94-22000
Fiber optic temperature sensor using a Y2O2S:Eu thermographic phosphor
[DE94-000331] 06 p2543 N94-23461
Dual-Band Infrared (DBIR) imaging inspections of Boeing 737 and KC-135 aircraft panels
[DE94-005700] 08 p3122 N94-29842
Study of the problems of nonuniformity of heating in infrared vision applied to the inspection of materials having non-planar relief
[ISBN-0-315-85637-8] 08 p3316 N94-30235
Dual-band infrared imaging for quantitative corrosion detection in aging aircraft
[DE94-004187] 08 p3149 N94-30687

THERMOGRAVIMETRY
Analytical method for water vapor collection and analysis in aircraft cabin fires
[DOT/FAA/CT-TN93/33] 01 p0022 N94-12575
Direct catalytic decomposition of nitric oxide
[DE93-016689] 03 p0949 N94-16896
Ageing studies on a composite propellant containing a new organo-copper burn rate catalyst
[AD-A271060] 05 p1711 N94-19906
A pressurized thermogravimetric analyzer for use in studies of gas/solid systems
[DE94-001224] 06 p2342 N94-22989
Potent solvents for C60 and their utility for the rapid acquisition of 13CNMR data for fullerenes
[AD-A273349] 06 p2235 N94-24925
Thermogravimetric study of oxidation of a PdCr alloy used for high-temperature sensors
[NASA-TM-106473] 07 p2741 N94-27426
Kinetic parameters from thermogravimetric analysis 07 p2721 N94-27909
Study of iron exchanged zeolites by Moessbauer effect and electron spin resonance spectroscopy
[DE94-605138] 08 p3514 N94-29691
New molecular-based routes to binary main group metal sulfides
[AD-A277005] 09 p3900 N94-32003
Basic solutions to carbon/carbon oxidation: Science and technology
[AD-A280447] 12 p4404 N94-37232

THERMOLUMINESCENCE
Meteorites from recent amor-type orbits 01 p0429 N94-12059
Natural thermoluminescence profiles in lunar cores and implications for meteorites 01 p0443 N94-12060
Diamond thermoluminescence properties of different chondrites 01 p0433 N94-12252
Optical fiber spectroscopy: A study of the luminescent properties of the europium ion for thermal sensors
[NASA-CR-194576] 03 p1189 N94-15647
Induced thermoluminescence study of experimentally shock-loaded oligoclase 03 p0953 N94-16266
Shock-thermal history of Kapoeta howardite matter on data of thermoluminescence analysis of individual mineral grains 03 p0953 N94-16267
Temperature dependence of CsI(Tl) gamma ray excited scintillation characteristics
[DE94-000836] 05 p2034 N94-22028

THERMOMECHANICAL TREATMENT
NT HOT ISOSTATIC PRESSING
NT HOT PRESSING
Development and commercialization status of Fe3Al-based intermetallic alloys
[DE93-015802] 03 p0957 N94-16165
Elastic-plastic finite-difference analysis of unidirectional composites subjected to thermomechanical cyclic loading
[AD-A267666] 03 p1061 N94-17269
Development of ductile Fe3Al-based aluminides
[DE93-017865] 04 p1362 N94-18938
Effects of processing history on the creep strength of Nb-1Zr
[DE93-015905] 05 p1689 N94-20093
The use of backscattered electron imaging mode to assess the effect of fine dispersions on development of superplastic microstructure in Al-Mg alloys
[AD-A272426] 05 p1691 N94-21258
Examinations of composition and deformation behavior of intermetallic phases on the basis of Fe3(AlSi)
[GKSS-92/E/16] 05 p1692 N94-21311
Characterization of the microstructure of Nb-1wt.%Zr-0.1wt.%C tubes as affected by thermomechanical processing
[NASA-TM-106381] 06 p2242 N94-23550
Thermomechanical processing of Ag-clad Bi2Sr2CaCu2O(x) superconductors
[DE94-002347] 06 p2563 N94-24624
Effects of post-fabrication processing on the tensile properties of centrifugally cast SiC particulate reinforced aluminum composites
[AD-A274865] 07 p2707 N94-26190
Study of precipitation and recrystallization in Al alloy 2519 by backscattered electron imaging methods
[AD-A274919] 07 p2736 N94-26533
Mechanical properties and microstructure of thermomechanically processed, high manganese steel
[ARL-TR-146] 07 p2747 N94-28212
Effects of thermomechanical processing on tensile and long-time creep behavior of Nb-1 percent Zr-0.1 percent C sheet
[NASA-TM-106319] 08 p3202 N94-28822
A state variable material model for superplastic titanium-6 percent Al-4 percent V 09 p3644 N94-32498

Influence of volume fraction of component materials and interlayer bond strength on fracture toughness of multi-layer Al 6090-25 volume percent SiCp and Al 5182 laminates
[DE94-007141] 09 p3626 N94-32665
The effect of thermomechanical processing on mechanical properties of a cast 6061 aluminum metal matrix composite
[AD-A277995] 10 p4019 N94-34220
Process simulation and modeling for advanced intermetallic alloys
[AD-A280327] 12 p4416 N94-37030
Fabrication and properties of Ag-clad Bi-2223 conductors and magnets
[DE94-011502] 12 p4438 N94-37111
Maintaining constant standards during the forging process 12 p4421 N94-37326

THERMOMECHANICS
U THERMODYNAMICS

THERMOMETERS
Preliminary results of the comparison of ATSR measurements with in situ sea temperatures
[DE93-013399] 01 p0287 N94-10517
Trouble areas in the IRT measurement of the Earth surface temperature 01 p0193 N94-11910
Temperature measurements 03 p1037 N94-15804

THERMOMETRY
U TEMPERATURE MEASUREMENT

THERMONUCLEAR ENERGY
U THERMONUCLEAR POWER GENERATION

THERMONUCLEAR EXPLOSIONS
Vulnerability assessment of a space based weapon platform electronic system exposed to a thermonuclear weapon detonation
[DE94-007229] 09 p3611 N94-32667

THERMONUCLEAR POWER GENERATION
Methodology for first wall design
[DE94-002795] 07 p3045 N94-26861
Overview of the US stellarator reactor study
[DE94-006042] 08 p3508 N94-30339

THERMONUCLEAR PROPULSION
U NUCLEAR PROPULSION

THERMONUCLEAR REACTIONS
NT CONTROLLED FUSION
NT NUCLEAR FUSION
High heat flux components and plasma surface interactions
[DE93-008786] 01 p0385 N94-10253
Nuclear fusion of protons with ions of boron
[DE93-014284] 02 p0781 N94-13219
Charged-particle evaluation methodology at Lawrence Livermore National Laboratory
[DE93-013429] 02 p0781 N94-13251
The status of cold fusion
[DE93-012731] 02 p0802 N94-14567
Nuclear fusion of protons with ions of boron
[DE93-015399] 03 p1202 N94-16019
Generalized energy principle for flute perturbations in axisymmetric mirror machines
[DE93-019399] 04 p1589 N94-19037
Anomalous thermalization of fast ions .n magnetized plasma
[DE94-007109] 09 p3891 N94-32631

THERMOPHILES
Conversion of acetic acid to methane by thermophiles
[DE93-014433] 01 p0300 N94-10652
Isolation of thermostable enzyme mutants by cloning and selection in thermophilic bacteria
[AD-A266378] 03 p1117 N94-16514
Conversion of acetic acid to methane by thermophiles
[DE94-012478] 12 p4479 N94-37434

THERMOPHILIC PLANTS
NT BLUE GREEN ALGAE

THERMOPHORESIS
Transport phenomena and interfacial kinetics in multiphase combustion systems
[AD-A270202] 04 p1349 N94-18785

THERMOPHYSICAL PROPERTIES
NT CRITICAL POINT
NT CRITICAL PRESSURE
NT CRITICAL TEMPERATURE
NT EMISSIVITY
NT HEAT OF FUSION
NT HEAT OF SOLUTION
NT LATENT HEAT
NT MELTING POINTS
NT PYROELECTRICITY
NT SPECIFIC HEAT
NT SUPERCRITICAL PRESSURES
NT THERMAL CONDUCTIVITY
NT THERMAL DIFFUSION
NT THERMAL DIFFUSIVITY
NT THERMAL STABILITY
NT VAPOR PRESSURE
NT VOLATILITY
Multiphase equation of state for iron
[DE93-013956] 02 p0568 N94-12977
The specific heat of titanium disilicide
[AD-A267543] 03 p0960 N94-17100
Malone refrigeration
[DE93-014468] 04 p1379 N94-17725
Thermophysical properties
[DE93-040219] 04 p1351 N94-19134
Initial development of a high-pressure crystal growth facility: Center director's discretionary fund
[NASA-TM-108430] 05 p2030 N94-21807
Workshop on the Thermophysical Properties of Molten Materials
[NASA-CP-10121] 06 p2246 N94-25120
Thermophysical property sensitivity effects in steel solidification 06 p2246 N94-25122
Establishment of computerized numerical databases on thermophysical and other properties of molten as well as solid materials and data evaluation and validation for generating recommended reliable reference data 06 p2246 N94-25123
Dynamic measurements of thermophysical properties of metals and alloys at high temperatures by subsecond pulse heating techniques 06 p2247 N94-25124
An overview of the measurements of thermophysical properties and some results on molten superalloys and semiconductors 06 p2248 N94-25128
Thermophysical properties of simple liquid metals: A brief review of theory 06 p2248 N94-25130
Microwave techniques for physical property measurements 06 p2238 N94-25134
Electrostatic levitation technology for thermophysical properties of molten materials 06 p2238 N94-25135
Zr-rich corner of the Zr-Sn-O diagram
[DE93-633764] 07 p2734 N94-26161
Eleventh Symposium on Energy Engineering Sciences: Proceedings
[DE93-019930] 07 p2763 N94-26429
Thermophysical properties of HFC-143a and HFC-152a
[DE94-004236] 07 p2719 N94-27567
Thermophysical properties of refrigerant R-134a (1,1,1,2-tetrafluoroethane)
[ESDU-93001] 07 p2720 N94-27959
Thermal modeling of NiH2 batteries 07 p2862 N94-28113
Characterisation and processing of SiC/MAS-L glass ceramic matrix composite
[REPT-932-430-111] 08 p3179 N94-29412
Glass-ceramic matrix composites
[REPT-932-430-112] 08 p3179 N94-29413
Computational modeling of convective heat transfer to liquid hydrogen coolant 09 p3707 N94-32485
AFDM: An advanced fluid-dynamics model, volume 6
[DE94-009596] 11 p4264 N94-35669
Thermophysical properties of HFC-143a and HFC-152a
[DE94-009995] 11 p4251 N94-36008
Research update: Materials Compatibility and Lubricant Research (MCLR) program
[DE94-010001] 11 p4247 N94-36387

THERMOPHYSICS
U THERMODYNAMICS

THERMOPILES
Radiometry spot measurement system
[NASA-TM-106561] 09 p3883 N94-32777
Measurement of a surface heat flux and temperature 11 p4231 N94-36407

THERMOPLASTIC FILMS
Interfaces of high-protection performance polyaryls-coated zinc phosphated steels
[DE94-011732] 12 p4417 N94-37153

THERMOPLASTIC RESINS
NT PEEK
NT THERMOPLASTIC FILMS
Universal adjustable mould for antenna reflectors 01 p0059 N94-10027
Deformation mechanisms of continuous fibre-reinforced thermoplastic composites during manufacturing: A probabilistic approach 01 p0060 N94-10030
Heat analysis of thermoplastic components during the initial stages of manufacturing: A probabilistic approach 01 p0060 N94-10031
Cost effectiveness of structural applications of fibre reinforced thermoplastics 01 p0060 N94-10032
Application of advanced thermoplastics 01 p0060 N94-10033
Low cost thermoplastic composites for structural applications: Design concepts using new materials and processes 01 p0060 N94-10034
Tape winding of thermoplastic composites 01 p0060 N94-10035
Applications of continuous fiber reinforced thermoplastics in aircraft interiors 01 p0018 N94-10775
Uralane (tm) 5774-A/B: Ciba-Geigy's advanced urethane adhesive for the aircraft industry 01 p0018 N94-10777
Fire-resistant hydrolytically stable poly(arylene phosphine oxide) material systems 01 p0019 N94-10780
Dry in-line thermoplastic matrix impregnation, phase 1
[AD-A265016] 01 p0067 N94-11221
A new NASA LaRC Multi-Purpose Prepregging Unit 03 p0932 N94-15276
Process of shaping an electrorheological solid
[AD-D015885] 03 p1012 N94-16914
Analysis of pultrusion processing for long fiber reinforced thermoplastic composite system
[NASA-CR-194504] 04 p1339 N94-17766
Process for preparing thermoplastic composites
[AD-D015864] 04 p1339 N94-18074
Polymer technology publication. Series no. 14, 1993
[PB93-195964] 04 p1372 N94-19052
Chain propagation/step propagation polymerization chemistry. The preparation of solvent resistant well phase-separated thermoplastic elastomers
[AD-A271128] 05 p1699 N94-20016
Graphite/polyurethane flexible composites: Mechanical and vibration damping properties
[AD-A271608] 05 p1674 N94-20950
A study of the induction heating of organic composites
[AD-A272657] 05 p1675 N94-21187
Surface and interfacial properties of polymer blends. A literature survey
[PB93-230191] 06 p2254 N94-23561
Continuous fiber reinforced thermoplastic composites: Literature survey
[VTT-TIED-1422] 07 p2704 N94-25651
Design for producing fiberglass fabric in a lunar environment 07 p2765 N94-25676
Thermoplastic elastomers having alternate crystalline structure for us as high energy binders
[AD-D016035] 07 p2755 N94-27203
Thermoplastic or thermosetting composites in aircrafts
[PB94-123809] 07 p2710 N94-27253
Polymer infiltration studies
[NASA-CR-195729] 08 p3213 N94-28748
Composite redesign of obstetrical forceps 08 p3397 N94-30457
Improved construction materials for polar regions using microcellular thermoplastic foams 08 p3223 N94-30483
Empirical optimization of the consolidation of thermoplastic prepregs
[ISBN-0-315-86455-9] 09 p3652 N94-31722
Development of thermoplastic composite aircraft structures
[NASA-CR-189593] 09 p3626 N94-32860
Characterization and manufacture of braided composites for large commercial aircraft structures 09 p3630 N94-33137
Spirobislactone acrylate polymers
[AD-D016190] 10 p4030 N94-34403
Polymer from DIIMIDO-DI-PHTHALONITRILE
[AD-D016189] 10 p4030 N94-34682
Tough high performance composite matrix
[NASA-CASE-LAR-14239-2] 11 p4232 N94-35372
Processing and properties of high temperature metal/fiber-reinforced-thermoplastic laminates
[AD-A278791] 11 p4232 N94-35654
Design for manufacturability evaluation: Composite National Ignition Facility (NIF) pockel cell body
[DE94-010669] 11 p4338 N94-36284
Laminated thermoplastic composite material from recycled high density polyethylene 11 p4230 N94-36403
Structural composite construction materials manufactured from municipal solid waste
[AD-A280635] 12 p4403 N94-36730

THERMOPLASTICITY
New thermoplastic laminating adhesives for the aircraft industry with low heat release and low smoke emission 01 p0017 N94-10767
Crystallinity and dielectric properties of PEEK, a thermoplastic poly(ether ether ketone)
[AD-A266027] 01 p0091 N94-11487
Development of time-dependent orthotropic constitutive law of a thermoplastic composite material 02 p0556 N94-13595
Machine development 03 p0932 N94-15258
Analysis of pultrusion processing for long fiber reinforced thermoplastic composite system
[NASA-CR-194504] 04 p1339 N94-17766
Strained ring energetic binders
[AD-A269056] 04 p1377 N94-18491
Chain propagation/step propagation polymerization chemistry. The preparation of solvent resistant well phase-separated thermoplastic elastomers
[AD-A271128] 05 p1699 N94-20016

A study of the induction heating of organic composites
[AD-A272657] 05 p1675 N94-21187
Full-scale fire testing of seat component materials
[AD-A273499] 06 p2174 N94-24941
Lunar preform manufacturing
07 p2765 N94-25677
Impact tests on fibre metal laminates under a tensile load
[PB94-126570] 07 p2710 N94-27201
Thermoplastic or thermosetting composites in aircrafts
[PB94-123809] 07 p2710 N94-27253
Finite element analysis of axisymmetric deformations of thick thermoviscoplastic targets
08 p3320 N94-29688
Polymer from DIIMIDO-DI-PHTHALONITRILE
[AD-D016189] 10 p4030 N94-34682
Micromechanical modeling of damage growth in titanium based metal-matrix composites
12 p4402 N94-36664

THERMOREGULATION
Modifications to an interactive model of the human body during exercise: With special emphasis on thermoregulation 01 p0317 N94-12368
Melatonin, the pineal gland, and circadian rhythms
[AD-A268200] 03 p1129 N94-17478
Metabolic changes and hemodynamic dysfunction following hypothermic shock
[AD-A269780] 04 p1506 N94-18598
Human responses to exercise-heat stress
[AD-A272581] 05 p1892 N94-21209
Plasma volume shifts and exercise thermoregulation with water immersion and six-degree head-down tilt
[NASA-TM-108781] 07 p2901 N94-26093
Thermoregulatory effects of caffeine ingestion during rest and exercise in men
[NASA-TM-108783] 07 p2901 N94-26210
Effects of 40 C hot water immersion for an hour on thermoregulatory functions in humans: Comparison with 34 C thermoneutral immersion 07 p2915 N94-27459
Effects of 41 C bathing for 20 minutes on cardiovascular and thermoregulatory functions in humans
07 p2918 N94-27474
Prediction of survival times on land in a cold climate
08 p3379 N94-28423
Fuelling shivering in humans during cold water immersion 08 p3379 N94-28426
Biochemical enhancement of cold tolerance
08 p3380 N94-28427
Treatment of mild immersion hypothermia by body-to-body and forced-air warming
08 p3380 N94-28428
The potential of new textiles in improving survival prospects 08 p3380 N94-28430
Thermoregulation in the extreme cold environment
08 p3381 N94-28438
Thermal strain generated by an enhanced anti-G protection system in a hot climate
08 p3383 N94-28445
Alleviation of thermal strain in the CF: Keeping our cool during the Gulf conflict 08 p3383 N94-28449
Japanese Journal of Aerospace and Environmental Medicine, vol. 30, no. 2
[JTN-94-80599] 08 p3394 N94-29863
Effects of make-up on the heat transfer from the head in hyperthermic conditions 08 p3394 N94-29864
Hydration and blood volume effects on human thermoregulation in the heat: Space applications
10 p4096 N94-33651

THERMOSETTING RESINS
NT EPOXY RESINS
NT KEVLAR (TRADEMARK)
NT NYLON (TRADEMARK)
NT PHENOLIC RESINS
NT POLYAMIDE RESINS
Ceramics formed by pyrolysis of either linear or thermosetting carborane (siloxane or silane) acetylene based precursor polymers
[AD-D015747] 01 p0093 N94-12330
Synthesis and polymerization of oligomeric multiple aromatic ether-containing phthalonitriles
[AD-D015729] 01 p0094 N94-12399
A new NASA LaRC Multi-Purpose Prepregging Unit
03 p0932 N94-15276
Analysis of pultrusion processing for long fiber reinforced thermoplastic composite system
[NASA-CR-194504] 04 p1339 N94-17766
Molecular composites from liquid crystalline polymers and liquid crystalline thermosets
[DE93-016608] 04 p1368 N94-18096
Fiber reinforced thermosetting resin composition with coated fibers for improved toughness
[CA-PATENT-1,306,320] 05 p1674 N94-21040
Metal-catalyzed alkynylation of brominated polyphenylenes: Thermoset precursors of high density monolithic glassy carbon
[AD-A273232] 06 p2259 N94-24789
Metal-catalyzed alkynylation of (Bromophenyl)Oligophenylenes: A rapid route to thermoset precursors of high density monolithic glass-like carbon
[AD-A273219] 06 p2260 N94-24863
Ultrasonic measurement technique to determine the state of cure in thermosetting materials
[PB94-124328] 07 p2756 N94-27217
Thermoplastic or thermosetting composites in aircrafts
[PB94-123809] 07 p2710 N94-27253
Evolution of the interface properties with temperature in the T800H/ bismaleimide composites
[ONERA-NT-1993-14] 09 p3619 N94-31478
Polymer from DIIMIDO-DI-PHTHALONITRILE
[AD-D016189] 10 p4030 N94-34682
Phenylethynyl endcapping reagents and reactive diluents
[NASA-CASE-LAR-14796-1] 10 p4023 N94-35077
Tough high performance composite matrix
[NASA-CASE-LAR-14239-2] 11 p4232 N94-35372
Carborane-siloxane or silane-unsaturated hydrocarbon based polymers
[AD-D016220] 12 p4425 N94-37482
Synthesis of phthalonitrile resins containing ether and imide linkages with aromatic diamine curing agent
[AD-D016309] 12 p4427 N94-37778
Carborane-(silane or siloxane)-unsaturated hydrocarbon based thermosetting polymers
[AD-D016311] 12 p4427 N94-37818

THERMOSIPHONS
A parametric study of heat transfer within a planar thermosyphon
[DE93-019546] 05 p1799 N94-20258
Determination of the dispersion constant in a constrained vapor bubble thermosyphon
[NASA-CR-196124] 12 p4442 N94-36992

THERMOSPHERE
Atomic hydrogen and nitrogen distributions from atmosphere explorer measurements
[NASA-CR-194336] 02 p0714 N94-13825
A physical model for one-dimension and time-dependent ionosphere. Part 1: Description of the model
[DE93-627958] 04 p1486 N94-19255
Venus lower thermosphere studies
[NASA-CR-193546] 04 p1629 N94-19418
Validation of the design of a high resolution all-reflection Michelson interferometer for atmospheric spectroscopy
[AD-A272505] 05 p1987 N94-21410
Empirical wind model for the middle and lower atmosphere. Part 2: Local time variations
[NASA-TM-104592] 05 p1870 N94-21862
Data analysis and theoretical studies of the upper mesosphere and lower thermosphere
[NASA-CR-195108] 06 p2402 N94-24089
Mesospheric and lower thermospheric winds, temperatures densities, and volume emission rates
[NASA-CR-195147] 06 p2403 N94-24486
Upper atmosphere neutral and plasma density modeling
[AD-A274768] 07 p2879 N94-26569
Solar and airglow measurements aboard the two suborbital flights NASA 36.098 and 36.107
[NASA-CR-195279] 07 p2882 N94-27380
A study of the thermospheric dynamics of the high-latitude E region using a spectral thermospheric general circulation model 08 p3362 N94-29743
Thermospheric modeling accuracies using F10.7 and Ap
[AD-A277355] 09 p3773 N94-32337
Modeling of the magnetosphere-ionosphere-atmosphere system
[NASA-CR-195157] 11 p4288 N94-35244
Natural orbital environment definition guidelines for use in aerospace vehicle development
[NASA-TM-4527] 11 p4291 N94-36175

THERMOSTABILITY
U THERMAL STABILITY

THERMOSTATS
The High Precision Thermostat HPT-HYDRA
01 p0109 N94-10124
Stress relaxation in dough moulding compounds
[PB94-124872] 07 p2748 N94-25894

THERMOTROPISM
U ANISOTROPY
U TEMPERATURE EFFECTS

THESAURI
A browsing tool for the Internet Logical Library of the HPCC Software Exchange
[NASA-CR-194545] 03 p1143 N94-15189
Defense Technical Information Center thesaurus
[AD-A268855] 04 p1615 N94-18319
Correspondence dictionary from free English term to INIS descriptors
[DE94-701173] 07 p3100 N94-27700
Computer-based linking of thesauri
08 p3534 N94-29961
DTIC Thesaurus on diskette with dBase 4.1 runtime (computer diskette)
[AD-M000306] 09 p3922 N94-33256
DTIC Thesaurus on diskette (ASC2) (computer diskette)
[AD-M000309] 09 p3922 N94-33257
DTIC Thesaurus on diskette without runtime (computer diskette)
[AD-M000310] 09 p3923 N94-33258
DTIC Thesaurus on diskette without runtime (computer diskette)
[AD-M000312] 09 p3923 N94-33259
International Energy: Subject Thesaurus, revision 1
[DE94-002590] 10 p4151 N94-33730
DTIC Thesaurus on diskette with dBase 4.1 runtime (computer diskette)
[AD-M000311] 10 p4159 N94-34213
NASA Thesaurus. Volume 1: Hierarchical listing. Volume 2: Access vocabulary. Volume 3: Definitions
[NASA-SP-7096-VOL-1/2/3] 11 p4346 N94-36037

THESES
Numerical and symbolic signal representation and processing
[AD-A270271] 04 p1389 N94-18811
Influence of geoid model uncertainty on the determination of ocean circulation with satellite altimetry
[PB93-219301] 05 p1842 N94-22097
Automation of formation flight control
[AD-A274137] 07 p2678 N94-27132
Overview of Ph.D. theses and memoranda, 1992 (University of Twente, Department of Computer Science)
[PB94-149598] 10 p4103 N94-34129

THETA PINCH
Coaxial slow source
[DE94-008191] 09 p3892 N94-32800

THICK FILMS
Deposition of crystalline boron thick layers from gas phase
[DE93-620499] 02 p0576 N94-12867
Superconductivity devices: Commercial use of space
[NASA-CR-194163] 02 p0625 N94-14324
Solution chemistry optimization of sol-gel processed PZT thin films
[DE93-013776] 02 p0814 N94-14695
Mechanical properties and crystal growth studies of semiconductor alloys
[AD-A268144] 03 p1216 N94-17454
Electro-optic materials by solid source MOCVD
[DE94-005120] 07 p2757 N94-27716
New thick film feedthrough configurations
[DE94-008706] 09 p3694 N94-32582
Method for forming aligned superconducting BI-SR-CA-CU-O
[AD-D016192] 10 p4148 N94-34405
Thick film fabrication of aluminum nitride microcircuits
[DE94-010107] 11 p4259 N94-35706
Electrically conductive, thermally insulating cryogenic current leads
[NASA-CASE-LAR-14964-1-CU] 12 p4437 N94-36781
Superconducting TlCa2Ba2Cu3O9 thick films
[DE94-010436] 12 p4535 N94-37193

THICK PLATES
Nonlinear vibrations of thick composite plates: Higher-order shear deformation plate theory
02 p0556 N94-13558
Role of microstructure on fatigue durability of aluminum aircraft alloys
[AD-A266350] 02 p0571 N94-13697
Performance of the X-/Ka/KABLE-band dichroic plate in the DSS-13 beam waveguide antenna
06 p2291 N94-23261
Further investigation of curve veering phenomena
08 p3460 N94-30515
An efficient higher order theory for laminated composite plates and a finite element implementation
09 p3617 N94-31215
Residual stresses in a multi-pass weld in an austenitic stainless steel plate before and after thermal stress relief
[DE94-013278] 12 p4420 N94-37548

THICKNESS
Material removal processes: Engineering mechanics consideration
[DE93-010733] 01 p0126 N94-10293
Temperature effects on failure thickness and deflagration-to-detonation transition in PBX 9502 and TATB
[DE93-010742] 01 p0097 N94-10294
Radiation considerations for interplanetary missions
01 p0045 N94-11559
Dielectric breakdown and its influence on ignition
[AD-A264925] 01 p0078 N94-11855
The use of polarised neutron reflection for unique density profile determination in thin films
[PB93-187136] 02 p0579 N94-13783

BALLIST: A computer program to empirically predict the bumper thickness required to prevent perforation of the Space Station by orbital debris
[NASA-CR-193825] 02 p0543 N94-14120
Experimental investigations into the deflagration to detonation transition at TNO/PML
[AD-A266753] 03 p1021 N94-15755
The Acraman impact structure: Estimation of the diameter by the ejecta layer thickness
03 p1103 N94-16211
Estimates of lithospheric thickness on Venus
03 p1267 N94-16277
On the a-posteriori estimation of the modelling error for the heat conduction in a plate and its use for adaptive hierarchic modelling
[AD-A267965] 03 p1029 N94-17384
Development of the microstructure based stochastic life prediction model
[AD-A269742] 04 p1361 N94-18742
Foil support structure for large electron guns
[DE93-018478] 04 p1322 N94-18890
Quantitative evaluation of material composition of composites using x ray energy-dispersive NDE technique
[DE93-041157] 05 p1672 N94-19888
Retrieval of ice thickness from polarimetric SAR data
05 p1724 N94-20432
Differentiation of magma oceans and the thickness of the depleted layer on Venus 05 p2118 N94-20780
Enhanced software for the GT1022 automated gaging system
[DE94-001374] 05 p1918 N94-21977
Echocardiographic findings in trained aircrew: The effect of +Gz on cardiac structure (working group 18)
06 p2424 N94-23320
Left ventricular hypertrophy and athlete's heart
06 p2424 N94-23321
Examination of the physical, electrical, and microwave evolution of water into young sea ice
[AD-A273559] 06 p2418 N94-24918
Automated in-situ inspection systems for underground storage tanks
[AD-A274644] 07 p2764 N94-27144
Dual-Band Infrared (DBIR) imaging inspections of Boeing 737 and KC-135 aircraft panels
[DE94-005700] 08 p3122 N94-29842
Three-dimensional free vibration analysis of thick arbitrarily laminated, rectangular, cylindrical and spherical composite panels 08 p3184 N94-30257
An electromagnetic noncontacting sensor for thickness measurement in a dispersive medium
[AIAA PAPER 94-1200-CP] 08 p3443 N94-30551
Materials processing and manufacturing technologies for diamond substrates multichip modules
[AD-A276904] 09 p3692 N94-32215
Computerized Ultrasonic Testing System (CUTS) for in-process thickness determination
09 p3862 N94-32456
Effects of ply thickness on thermal cycle induced damage and thermal strain 12 p4459 N94-37806

THIN AIRFOILS
NT THIN WINGS
A new flux-conserving numerical scheme for the steady, incompressible Navier-Stokes equations
[NASA-TM-106520] 08 p3273 N94-29471
Robust control design techniques for active flutter suppression 11 p4200 N94-35875

THIN FILMS
NT DIAMOND FILMS
NT ENERGY ABSORPTION FILMS
NT FERROMAGNETIC FILMS
NT LANGMUIR-BLODGETT FILMS
NT MONOMOLECULAR FILMS
Invariance of the mobility edge in anodic titanium oxides
[DE92-642136] 01 p0394 N94-10281
Sensing glass transitions in thin polymer films on acoustic wave microsensors
[DE93-010805] 01 p0087 N94-10295
Thin-film edge field emitter device and method of manufacture therefore
[AD-D015764] 01 p0140 N94-10377
Crack suppression in GaInSb buffer layers initially under tensile stress
[DE93-012839] 01 p0396 N94-10745
Determination of concentration profiles at interfaces and surfaces of partially miscible polymer blends
[DE93-013140] 01 p0089 N94-11007
Characterization of the Si/SiO2 interfere morphology from quantum oscillations in Fowler-Nordheim tunneling currents
[AD-A265149] 01 p0143 N94-11160
Materials for adaptive structural acoustic control, volume 3
[AD-A264621] 01 p0358 N94-11262
Structural development in ceramic precursor sols and gels
[AD-A264354] 01 p0090 N94-11281
Thin film preparation and interfacial reaction study of solid oxide fuel cell materials 01 p0263 N94-11313
Tribological characteristics of sputtered Au/Cr films on alumina substrates at elevated temperatures
[NASA-TM-106078] 01 p0055 N94-11362
Investigation of the radiation resistance of triple-junction a-Si:H alloy solar cells irradiated with 1.00 MeV protons
01 p0050 N94-11391
Results of some initial space qualification testing on triple junction a-Si and CuInSe2 thin film solar cells
01 p0050 N94-11392
Flexible polycrystalline thin-film photovoltaics for space applications 01 p0050 N94-11393
Thin film solar cell workshop
01 p0054 N94-11415
Remote plasma enhanced chemical vapor deposition of GaP with in situ generation of phosphine precursors
01 p0399 N94-11440
In situ XANES studies of the passive film on Fe and Fe-26Cr
[DE93-010869] 01 p0084 N94-11459
Wide Band-Gap Semiconductors. 1991 Materials Research Society Symposium proceedings
[AD-A263418] 01 p0401 N94-11515
Chemical Vapor Deposition of Refractory Metals and Ceramics 2. Materials Research Society Symposium proceedings
[AD-A265072] 01 p0092 N94-11866
Applications of in-situ ellipsometry to microwave electron cyclotron resonance plasma processes
[AD-A265197] 01 p0373 N94-11880
NRL review for 1993
[AD-A265666] 01 p0497 N94-12334
Ballistic electron transport studies using BEEM
[AD-A266029] 01 p0369 N94-12395
Multicomponent and multilayered thin films for advanced microtechnologies: Techniques, fundamentals, and devices
[AD-A265685] 01 p0405 N94-12442
In-situ crystallization of silicate glass films deposited on alpha- Al2O3
[DE93-012969] 01 p0095 N94-12596
Amorphous sol-gel insulating films
[DE93-012859] 02 p0576 N94-12866
Photovoltaic Subcontract Program
[DE93-000092] 02 p0700 N94-12868
Recovery of materials impacted at high velocity
[DE93-014150] 02 p0576 N94-12885
Processing, fabrication and demonstration of HTS integrated microwave circuits
[AD-A265789] 02 p0619 N94-12892
Canted magnetic moments at the Gd(0001) surface
[DE93-014327] 02 p0805 N94-13102
Electrocatalysis issues in polymer electrolyte fuel cells
[DE93-014450] 02 p0702 N94-13402
Poling of thin polymer films in electro optic applications
[AD-A266562] 02 p0579 N94-13584
Studies of momentum and energy transfer across wavy gas-liquid interfaces
[AD-A266432] 02 p0635 N94-13699
High-resolution Z-contrast imaging and hole concentration mapping of YBCO thin films
[DE93-015803] 02 p0808 N94-13930
Boundary stability under nonequilibrium conditions
[DE93-016259] 02 p0809 N94-13980
Measurement of penetration depth lambda(T) in YBa2Cu3O(7-delta) thin film
[DE93-014587] 02 p0810 N94-14122
Spin polarized photoemission studies of interfacial and thin film magnetism
[DE93-014326] 02 p0580 N94-14142
A quartz crystal microbalance study of lithium insertion and removal into evaporated films MO(y) (M = Mo, Fe, and V)
[DSIS-93-00649] 02 p0810 N94-14203
Prism-film coupling in anisotropic planar waveguides of epitaxial (101) rutile thin films
[DE93-012912] 02 p0811 N94-14304
Formation of textured YBCO films by laser ablation
[DE93-013131] 02 p0581 N94-14319
Microstructural mechanisms that enhance electromigration resistance in Al-Cu thin films
[DE93-013770] 02 p0812 N94-14345
Effects of depositon rate on Bi2Sr2CaCu2O(8+x) and Bi2Sr(1.6)La(0.4)CuO(6+x) epitaxial thin film growth by pulsed-laser ablation
[DE93-015797] 02 p0812 N94-14362
Ion assisted sputter deposition of Mo-Si multilayers
[DE93-013830] 02 p0583 N94-14693
Solution chemistry optimization of sol-gel processed PZT thin films
[DE93-013776] 02 p0814 N94-14695
Molecular simulator: A basic tool for submicron MOS processes development
[LAAS-92484] 02 p0814 N94-14697
Direct submillimeter absorptivity measurements on epitaxial Ba(1-x)K(x)BiO3 films at 2K
[DE93-013904] 02 p0815 N94-14699
A study of thin liquid sheet flows
[NASA-TM-106323] 02 p0642 N94-14732
Ion mixing of thin ZrO2 films on sapphire
[DE93-015214] 03 p1206 N94-14925
Preparation and investigation of improved low voltage electron excitable phosphors
[AD-A266852] 03 p0963 N94-14948
Magneto-optic superlattice thin films: Fabrication, structural and magnetic characterization
03 p0974 N94-14982
A new NASA LaRC Multi-Purpose Prepregging Unit
03 p0932 N94-15276
Photochemistry in thin polymeric films
[AD-A266716] 03 p0964 N94-15729
Diamond epitaxy and diamondlike coatings
[AD-A266657] 03 p1206 N94-15747
Laser assisted CVD growth of AlN and GaN
[AD-A267150] 03 p1206 N94-15764
Experimental investigations of superconductivity in quasi-two-dimensional epitaxial copper oxide superlattices and trilayers
[DE93-015306] 03 p1207 N94-15829
Absolute, Extreme-Ultraviolet Solar Spectral Irradiance Monitor (AESSIM)
[AD-A267045] 03 p1299 N94-15836
Multilayer thin film design for far ultraviolet polarizers using an induced transmission and absorption technique
[NASA-CR-194631] 03 p1190 N94-15869
Cyanoresin, cyanoresin/cellulose triacetate blends for thin film, dielectric capacitors
[NASA-CASE-NPO-18913-1-CU]
03 p0966 N94-15930
Cellulose triacetate, thin film dielectric capacitor
[NASA-CASE-NPO-18935-1-CU]
03 p1010 N94-15952
Modification of fluoropolymer surfaces with electronically conductive polymers
[AD-A266294] 03 p0967 N94-16475
Apparatus for and a method of growing thin films of elemental semiconductors
[AD-D015813] 03 p1210 N94-16487
VUV thin films, chapter 7
[NASA-CR-194634] 03 p0967 N94-16494
Properties of thin films for high temperature flow sensors
[NASA-CR-191526] 03 p0967 N94-16541
Pulsed laser deposition of metastable Ca(1-x)Sr(x)CuO2 thin films
[DE93-015804] 03 p1040 N94-16663
Sputtered ferroelectric thin films of KTN for electro-optic devices
[AD-A266573] 03 p0968 N94-16723
Neutron and x ray scattering studies of (FeF2)(sub m)(CoF2)(sub n) multilayers
[DE93-015809] 03 p1184 N94-16838
Performance of silvered Teflon thermal control blankets on spacecraft
[AD-A266284] 03 p0887 N94-16909
A simple chemical procedure for extending the conductive state of polypyrrole to more negative potentials
[AD-A266235] 03 p0969 N94-16928
UHV-stem studies on nucleation and growth of thin metal silicide films on silicon
[DE93-017604] 03 p1212 N94-16961
Nitride semiconductors for ultraviolet detection
[AD-A267877] 03 p1012 N94-17040
Atomic layer epitaxy group IV materials: Surface processes, thin films, devices and their characterization
[AD-A267527] 03 p1213 N94-17116
Single crystal diamond thin films
[AD-A266457] 03 p1214 N94-17216
Characterization of metallic multilayers using x ray diffraction analysis
[NIAR-93-13] 03 p0961 N94-17282
Thin composite solid electrolyte film for lithium batteries
[NASA-CASE-NPO-18694-1-CU]
03 p1014 N94-17325
Low temperature deposition and characterization of n- and p-type silicon carbide thin films and associated ohmic and Schottky contacts
[AD-A267966] 03 p0973 N94-17490
Advanced thin-film deposition and physical properties of high-temperature and other novel superconducting materials
[AD-A268199] 03 p1216 N94-17561
Epitaxial iron films
[AD-A268286] 03 p1217 N94-17579

Mechanical properties of interfaces and superlattices
[AD-A268591] 03 p1217 N94-17606
A new method of designing multilayer optical thin film coatings
[DE93-624683] 03 p0974 N94-17611
Electrical properties of sol-gel PZT thin films for decoupling capacitor applications
[DE93-016491] 03 p1015 N94-17648
Growth of dielectric thin films by irradiation of condensed molecular precursors with synchrotron radiation
[DE93-016161] 03 p0974 N94-17676
Vibrational and electronic properties of clusters and ultrathin films
[DE93-012291] 04 p1367 N94-17678
Polarized thin films from dye-substituted polymers containing hydrophobically terminated stilbazolium radicals
[AD-D015873] 04 p1367 N94-17706
Finite element modeling of evaporation and condensation during sol-gel film and fiber formation
[DE93-017655] 04 p1345 N94-17820
Superhardness effect in Au/Ni multilayers
[DE93-016444] 04 p1357 N94-17860
Experimental contribution to the contact between two bodies and the effect of roughness
[ECL-91-41] 04 p1451 N94-17918
Titanium carbon-hydrogen layers on decorative surfaces 04 p1375 N94-18010
Studies of interactions between conducting polymer and organic vapors: Applications to chemical sensing
[DE93-015694] 04 p1369 N94-18233
Synthesis and study of high-T(sub c) superconducting electronic materials
[AD-A268851] 04 p1402 N94-18390
Solderability perservative coatings: Electroless tin versus organic azoles
[DE93-017634] 04 p1370 N94-18477
Mesoepitaxy: A universal route to oriented materials
[AD-A270437] 04 p1598 N94-18511
Growth of structures for integrated optoelectronic devices
[AD-A269014] 04 p1598 N94-18527
In-situ growth monitoring of molecular beam epitaxy processes
[AD-A269287] 04 p1598 N94-18616
Integration of ferroelectric/semiconductor thin films for SLM and photorefractive applications
[AD-A268645] 04 p1598 N94-18633
Scaling laws for diamond chemical vapor deposition. Diamond surface chemistry
[AD-A269874] 04 p1599 N94-18745
Thin film studies of the proximity Josephson effect
[AD-A270129] 04 p1600 N94-18876
Polycrystalline thin-film cadmium telluride solar cells fabricated by electrodeposition
[DE93-018201] 04 p1468 N94-18944
Growth of epitaxial semiconductor alloys and superlattices with continuously variable composition by pulsed-laser ablation
[DE93-018726] 04 p1601 N94-18998
Some superhigh-frequency and magnetic properties of chemically precipitated films
[AD-A266195] 04 p1351 N94-19110
Elastic properties of amorphous thin films studied by Rayleigh waves
[DE93-018375] 04 p1372 N94-19202
The microstructural mechanism of electromigration failure in narrow interconnects of Al alloys
[DE93-018598] 04 p1365 N94-19282
Picoindentation hardness measurements using atomic force microscopy
[AD-A270877] 04 p1604 N94-19579
Ionized-cluster beam/partially ionized beam deposition of electro-optical and nonlinear optical organic materials and device development
[AD-A270832] 04 p1604 N94-19596
The deposition of electro-optic films on semiconductors
[AD-A270823] 04 p1605 N94-19664
Single source precursors for the OMCVD of 3/5 compound semiconductors
[AD-A271147] 04 p1606 N94-19739
Nanofabrication by focused ion beam
[AD-A271290] 04 p1345 N94-19746
Magnetic Ultrathin Films: Multilayers and Surfaces, Interfaces, and Characterization, volume 313
[AD-A271402] 04 p1375 N94-19758
The proximity effect in ultrathin granular Pb films
[AD-A271094] 05 p2012 N94-19848
Development of high-efficiency CdTe solar cells
[DE93-018206] 05 p1845 N94-19925
Preparation and properties of sol-gel derived PZT thin films for decoupling capacitor applications
[DE93-018853] 05 p2013 N94-19961
A novel method for characterizing the electrical Priorities of lead Zirconate Titanate (PZT) ferroelectric films and memory devices
[AD-A270463] 05 p2013 N94-19966
Proceedings of the 8th International Symposium on Applications of Ferroelectrics
[AD-A270679] 05 p1749 N94-20012
Fabrication of stable large-area thin-film CdTe photovoltaic modules
[DE93-018204] 05 p1845 N94-20095
X ray, extreme and far ultraviolet optical thin films for space applications
[NASA-CR-194635] 05 p1984 N94-20128
Atom probe field ion microscopy characterizations of VVER steels
[DE93-017864] 05 p1689 N94-20180
Layered thin-edged field-emitter device
[AD-D015932] 05 p1751 N94-20350
Polyimides containing amide and perfluoroisopropylidene connecting groups
[NASA-CASE-LAR-14608-1] 05 p1702 N94-20374
Microwave properties and characterization of co-evaporated BSCCO thin films
05 p1709 N94-20518
The effect of fluctuations on the electrical transport behavior in YBa2Cu3O(7-x) 05 p1736 N94-20519
Development of fundamental understanding of friction and wear mechanisms by atomic-scale tribological studies of ceramic materials and multilayered thin films
[AD-A271485] 05 p1703 N94-20548
Study of the utilization of thin oxides in indium phosphides for the realisation of electron components
[ECL-92-38] 05 p2018 N94-20593
Electrochemical synthesis of ultrathin film composite membranes
[AD-A272721] 05 p1681 N94-21168
Alumoxanes: Rationalization of black box materials
[AD-A272805] 05 p1704 N94-21170
Efficiency of reversible optical storage in azo polymers
[AD-A272923] 05 p1705 N94-21223
Field emitter array RF amplifier development project, phase 1, option 1
[AD-A272567] 05 p1740 N94-21361
Intelligent processing of ferroelectric thin films
[AD-A272518] 05 p1705 N94-21416
Advanced processing technology for high-efficiency thin-film CuInSe2 solar cells
[DE93-010045] 05 p1847 N94-21614
Fundamental studies of defect generation in amorphous silicon alloys grown by remote plasma-enhanced chemical-vapor deposition
[DE93-017083] 05 p2029 N94-21615
Research on polycrystalline thin-film submodules based on CuInSe2 materials
[DE93-018223] 05 p2029 N94-21617
High power, electron-beam induced switching in diamond
[DE93-040535] 05 p1768 N94-21770
Stable, high-efficiency amorphous-silicon solar cells with low hydrogen content
[DE93-018214] 05 p1848 N94-21826
Thin-film CdTe and CuInSe2 photovoltaic technologies
[DE93-018217] 05 p1848 N94-21827
Observation of x ray absorption magnetic circular dichroism in well-characterized iron-cobalt-platinum multilayers
[DE94-000303] 05 p1694 N94-21944
Techniques for producing free-standing thin films on frames
[DE93-041144] 05 p1708 N94-21954
MOCVD growth and structure of PbTiO3 thin films
[DE93-040230] 05 p2033 N94-21994
Interactions of slow H, H2, and H3 with thin foils
[DE93-040263] 05 p1976 N94-21995
A quantitative model for interpreting nanometer scale hardness measurements of thin films
[DE93-040601] 05 p2034 N94-22005
Thin-film fabrication of Pb-doped BiSrCaCuO superconductor 05 p1781 N94-22176
Research on stable, high-efficiency amorphous silicon multijunction modules
[DE93-018220] 05 p1850 N94-22257
Silicon microelectronic field-emissive devices for advanced display technology
[DE94-000397] 05 p1794 N94-22380
Advanced research and technology development of MCFCs
[DE94-001918] 06 p2389 N94-22723
Polycrystalline thin film materials and devices
[DE93-018213] 06 p2389 N94-22862
Disilane LPCVD deposited silicon films: Deposition mechanisms, properties and capability of making transistors on thin films
[LAAS-93156] 06 p2252 N94-22910
A new automatic design method to develop multilayer thin film devices for high power laser applications
[DE93-632490] 06 p2347 N94-22967
Design refinement of multilayer optical thin film devices with two optimization techniques
[DE93-634228] 06 p2542 N94-22979
Customizable VLSI artificial neural network chips based on a novel technology
[DE94-001418] 06 p2307 N94-23008
A novel process monitoring and control system based on a neural manufacturing concept
[DE94-001516] 06 p2471 N94-23011
Generic microelectronic smart sensor platform for detection of toxic, hazardous, and flammable gases
[DE93-017626] 06 p2343 N94-23200
Research on polycrystalline thin-film CuInGaSe2 solar cells
[DE94-000203] 06 p2560 N94-23205
Amorphous silicon PVMaT, phase 2A
[DE93-018221] 06 p2390 N94-23295
Novel two-stage selenization methods for fabrication of thin-film CIS cells and submodules
[DE94-000220] 06 p2390 N94-23296
Transparent conducting thin films for spacecraft applications
[NASA-TM-106466] 06 p2218 N94-23370
Infrared analysis of vapor phase deposited tricresylphosphate (TCP)
[NASA-TM-106423] 06 p2253 N94-23371
Selective hydrogen separation by palladium-based composite membranes
[PB93-201671] 06 p2254 N94-23431
Pulsed Ion Beam Surface Analysis (PIBSA) as a means of in-situ real-time analysis of thin films during growth
[DE94-001276] 06 p2562 N94-23805
Skin friction measurement in complex flows using thin oil film techniques
[NASA-CR-194872] 06 p2327 N94-24098
Ordered organic thin films self-assembled from the vapor phase 06 p2223 N94-24339
Low-gravity electrodeposition and growth of polymer thin films with large third-order optical nonlinearities by electrochemical processes for devices: Thiophene-based polymers 06 p2225 N94-24346
Polydiacetylene thin films for nonlinear optical applications 06 p2225 N94-24347
Nonlinear optical thin films 06 p2225 N94-24349
Diffusion on Cu surfaces 06 p2251 N94-24428
Thin film cadmium telluride photovoltaic cells
[DE94-000201] 06 p2395 N94-24509
Ge-Au eutectic bonding of Ge (100) single crystals
[DE94-002281] 06 p2564 N94-24657
Electrochemically mediated polymerization of 2-pentadecylaniline confined to a planar liquid-liquid interface
[AD-A273541] 06 p2259 N94-24792
Ferroelectric thin films 3
[AD-A273394] 06 p2565 N94-25027
The nanometer-scale mechanics of gold films
[AD-A273307] 06 p2565 N94-25086
The nanostructure of multilayered films: A NMR study
[ETN-94-95347] 06 p2262 N94-25222
Metallic multilayers: Experimental investigation of magnetic anisotropy and magnetic interlayer coupling
[ETN-94-95364] 06 p2250 N94-25242
Laser ablation and deposition of metals
[ETN-94-95311] 06 p2351 N94-25294
Investigation and application of microwave electron cyclotron resonance plasma physical vapour deposition
[DE93-613909] 06 p2555 N94-25333
Template synthesis of electronically conductive polymers
[AD-A273673] 06 p2263 N94-25409
Development of intermetallic compounds for high performance luminescence elements
07 p2722 N94-25545
Hydrogen trapping with Pd coated alloy films
07 p2723 N94-25551
Study on synthesis and characteristics of intermetallic compound with strong electron correlation
07 p2726 N94-25563
Study on alloy films for hydrogen separation
07 p2726 N94-25565
Fundamental study on new synthetic technology by phthalocyanine complexes 07 p2721 N94-25569
Study on substance diffusion in thin films with controlled structures 07 p2727 N94-25570
Object imaging accomplished with an integrated circuit robotic tactile sensor incorporating a piezoelectric polyvinylidene fluoride thin film
[AD-A274038] 07 p2780 N94-25845
Crystallization and microstructural control of ferroelectric thin-films and glass-ceramics
[AD-A273767] 07 p2748 N94-25854

In situ x ray reflectivity measurements of thin film structural evolution
[DE94-002289] 07 p3051 N94-25944
Optimization of experimental conditions in IR reflectance determination of BPSG properties
[DE94-002742] 07 p2713 N94-25978
Characterization of physically vapor deposited AF2400 thin films
[DE94-004019] 07 p2749 N94-25985
Plasma surface cleaning using microwave plasmas
[DE94-002754] 07 p2713 N94-26014
Buckyball microwave plasmas: Fragmentation and diamond-film growth
[DE94-003209] 07 p3053 N94-26031
Micropyrolysis of polymer thin films for ceramics
[ECL-92-62] 07 p2750 N94-26088
The state of the art of thin-film photovoltaics
[DE94-000224] 07 p2855 N94-26115
Stress relaxation in sputtered W films and W/GeSi/Si heterostructures
[DE94-004007] 07 p3055 N94-26239
Studies of thin-film growth, adsorption, and oxidation by in situ, real-time, and ex situ ion beam analysis
[DE94-002907] 07 p3055 N94-26275
The epitaxial growth of Ge on Si(100) using Te as a surfactant
[DE94-003437] 07 p3056 N94-26326
The deposition of boron nitride and carbon films on silica glass fibers
[DE94-004684] 07 p2751 N94-26564
An x ray absorption fine structure study of ordering in polythiophene thin films
[AD-A274235] 07 p2753 N94-26822
Nitride semiconductors for ultraviolet detection
[AD-A274246] 07 p3060 N94-26840
Pseudomorphic semiconducting heterostructures from combinations of AlN, GaN and selected SiC polytypes: Theoretical advancement and its coordination with experimental studies of nucleation, growth, characterization and device development
[AD-A274247] 07 p3061 N94-26841
Ferroelectric thin film microstructure development and related property enhancement
[DE94-002741] 07 p3061 N94-26856
Atomic layer epitaxy of group 4 materials: Surface processes, thin films, devices and their characterization
[AD-A274325] 07 p3061 N94-26885
Processing, fabrication, and demonstration of HTS integrated microwave circuits, appendix A
[AD-A274600] 07 p2785 N94-26890
Ion implantation and dynamic recovery of tin-doped indium oxide films
[DE94-001126] 07 p3062 N94-26932
The growth and characterization of GaN as a photodetector
[AD-A274570] 07 p3063 N94-26965
Low temperature deposition and characterization of N- and p-type silicon carbide thin films and associated ohmic and Schottky contacts
[AD-A274345] 07 p2754 N94-26974
Ferroelectric fluoride memory FET development
[AD-A274341] 07 p2785 N94-27057
High intensity x ray instrumentation for residual strain measurements in composites and textured materials
[ISBN-0-315-85169-4] 07 p2842 N94-27278
Synthesis of diamond film assisted by an arcjet plasma source, part 2
[INPE-5527-PRP/178-PT-2] 07 p3066 N94-27329
List of papers published by the members of Institute for Materials Research, Tohoku University 1992
[JTN-94-80608] 07 p3118 N94-27355
Research on high-efficiency, large-area, CuInSe2 based thin-film modules
[DE94-000259] 07 p3067 N94-27609
High-efficiency, thin-film solar cells
[DE94-000250] 07 p2860 N94-27625
Electro-optic materials by solid source MOCVD
[DE94-005120] 07 p2757 N94-27716
The ZnO thin films with C-axis orientation prepared on the room temperature substrate by the ECR multipolar plasma sputtering method
[DE94-605039] 07 p2758 N94-27857
Aerodynamic heating in hypersonic flows
07 p2658 N94-27919
Prometheus in space: Research Committee on Functional New Material
[JTN-94-80580] 07 p2761 N94-28002
The Science Reports of the Research Institutes, Tohoku University. Series A: Physics, Chemistry, and Metallurgy. Volume 38, No. 1: Amorphous Materials 14
[JTN-94-80610] 07 p2744 N94-28158
Differential scanning calorimetric study of solid state amorphization and crystallization in Zr/Co and Zr/Ni multilayers 07 p2745 N94-28161
Molecular aspects of transport in thin films of controlled architecture
[DE94-004552] 08 p3211 N94-28457
Silicon-Film (tm) photovoltaic manufacturing technology
[DE94-000258] 08 p3336 N94-28501
Geometric structures of thin film: Pt on Pd(110) and NiO on Ni(100)
[DE94-005564] 08 p3211 N94-28530
A 3M high temperature dielectric film
08 p3167 N94-28717
Ion channeling peculiarities in YBa2Cu3 O7 monocrystal
[DE94-606885] 08 p3512 N94-28787
MOCVD growth of GaN, AlN and AlGaN for UV photodetector applications
[AD-A275078] 08 p3512 N94-28871
Method for forming thin composite solid electrolyte film for lithium batteries
[NASA-CASE-NPO-18877-1-CU] 08 p3264 N94-29357
Vacuum vapor deposition
[NASA-CASE-MFS-28652-1] 08 p3215 N94-29446
Preparation and structure of amorphous hydrogenated carbon film deposited with RF plasma CVD
08 p3223 N94-29518
Retention latch mechanism for the Wake Shield Facility 08 p3161 N94-29635
Optical properties of cadmium sulfide, zinc selenide, and zinc manganese selenide semiconductor films
08 p3500 N94-29759
Micro-opto-mechanical devices and systems using epitaxial lift off 08 p3239 N94-29793
Lubricant rheology at high shear rates
08 p3217 N94-29967
ECR plasma synthesis of silicon nitride films on GaAs and InSb
[DE94-005575] 08 p3515 N94-30006
The organometallic chemical vapor deposition of transition metal carbides: The use of homoleptic alkyls
[DE94-005577] 08 p3206 N94-30007
Study of the ultraviolet absorption and photoconduction spectra of polyimide films fabricated at various curing temperatures
[ISBN-0-315-85923-7] 08 p3218 N94-30036
The bases for the development of high-temperature integrated SQUID-systems
[DE94-608462] 08 p3517 N94-30082
Plasma enhanced chemical vapor deposition of ZrO2 thin films
[DE94-006031] 08 p3218 N94-30104
Distribution functions of electrons within aluminium oxide thin films
[DE94-608418] 08 p3490 N94-30184
Effects of hydrogen on the resistivity of thin Au and Cu films 08 p3218 N94-30225
Electrooptical and optical evaluation of Pb(Zr,Ti)O3 thin films using waveguide refractometry
[DE94-006374] 08 p3518 N94-30247
Densification and crystallization of zirconia thin films prepared by sol-gel processing
[DE94-005573] 08 p3518 N94-30315
Metafusion: A breakthrough in metallurgy
08 p3211 N94-30446
Research on the atomic layer-by-layer growth of high-temperature superconductor thin films at the Institute of Scientific and Industrial Research, Japan
[DE94-003739] 08 p3519 N94-30611
Ionic conduction mechanisms in CaF2 and CaF2-Al2O3 nanocomposite films on Al2O3 substrates
[DE94-004792] 08 p3520 N94-30773
Synthesis of (SiC)3N4 thin films by ion implantation
[DE94-006311] 08 p3521 N94-30851
RHEED studies of the nucleation, growth, and mobility of Ag atoms on the Si(111)7 x 7 surface
[DE94-005551] 08 p3521 N94-30899
Sol-gel metal oxide and metal oxide/polymer multilayers applied by meniscus coating
[DE94-005813] 09 p3649 N94-31199
Adsorption of water to the metal/polymer interface studied by neutron and x ray reflectivity
[DE94-005578] 09 p3651 N94-31649
Degenerate four-wave mixing as a diagnostic of plasma chemistry
[DE94-008588] 09 p3889 N94-31766
Electrical properties of double layer dielectric structures for space technology
[ISBN-0-315-86547-4] 09 p3610 N94-31910
RF vacuum microelectronics
[AD-A276512] 09 p3691 N94-31928
A fracture mechanics methodology for characterizing the performance of flawed polymeric dielectric materials
09 p3654 N94-31956
Chemical vapor deposition of metal nitrides, phosphides, and arsenides
[DE94-008096] 09 p3654 N94-31976
The charging effect in high-Tc superconducting thin films
[AD-A277265] 09 p3900 N94-32040
Processing boron and boron carbide thin films for protective coatings and device fabrication
[AD-A277266] 09 p3900 N94-32041
Anomalous small angle x ray scattering studies of amorphous metal-germanium alloys
[DE94-007258] 09 p3900 N94-32065
Metal clusters: Dynamics and structure
[AD-A276842] 09 p3643 N94-32091
Correlations between micromagnetic, microstructural and microchemical properties in ultrathin epitaxial magnetic structures
[AD-A277200] 09 p3901 N94-32092
Ion-irradiation-induced densification of zirconia sol-gel thin films
[DE94-006248] 09 p3656 N94-32103
Determination of BPSG thin-film properties using IR reflection spectroscopy of product wafers
[DE94-006591] 09 p3634 N94-32110
Materials processing and manufacturing technologies for diamond substrates multichip modules
[AD-A276904] 09 p3692 N94-32215
NMR studies of organic thin films
[AD-A276953] 09 p3656 N94-32221
Si/SiO2 interface studies by immersion ellipsometry
[AD-A277277] 09 p3881 N94-32324
Stable second-order nonlinear optical materials based on interpenetrating polymer networks
[AD-A277410] 09 p3658 N94-32579
Femtosecond probe-probe transmission studies of LT-grown GaAs near the band edge
[DE94-006660] 09 p3904 N94-32634
Thin-film decoupling capacitors for multi-chip modules
[DE94-007743] 09 p3695 N94-32650
Energetics, bonding mechanism, and electronic structure of ceramic/ceramic and metal/ceramic interfaces
[DE94-008551] 09 p3659 N94-32656
Microanalytical study of defect formation in thin bismuth strontium calcium copper oxide films
[DE94-008217] 09 p3661 N94-32751
Development of a computer model for polycrystalline thin-film CuInSe2 and CdTe solar cells
[DE94-006853] 09 p3762 N94-32763
Thin EFG octagons
[DE94-006855] 09 p3905 N94-32764
Properties of doped and undoped (Ca,Sr)CuO2 thin films
[DE94-007230] 09 p3905 N94-32785
Nucleation and growth of cubic boron nitride films produced by ion-assisted pulsed laser deposition
[DE94-007295] 09 p3661 N94-32796
Ultrahigh-current-density metal-ion implantation and diamondlike-hydrocarbon films for tribological applications
[DE94-008958] 09 p3906 N94-32843
X ray absorption study of pulsed laser deposited boron nitride films
[DE94-008295] 09 p3662 N94-32855
Frictional behavior and adhesion of Ag and Au films applied to aluminum oxide by oxygen-ion assisted Screen Cage Ion Plating (SCIP)
[NASA-TM-106522] 09 p3647 N94-32931
Low energy ion beam assisted growth of homoepitaxial silicon films at low temperature
[AD-A278092] 09 p3908 N94-33039
Rare Earth Doped Semiconductors and Materials Research Society Symposium Proceedings, Volume 301
[AD-A277517] 09 p3908 N94-33055
Ceramic and metal composite circuit-board-level technology for application specific electronic modules (ASEM)
[AD-A277961] 09 p3630 N94-33180
Microstructures and epitaxy in oxide superconductor thin films and devices
[AD-A278427] 09 p3910 N94-33332
Atomic force microscopy
[AD-A277589] 10 p4026 N94-33429
Growth and nonlinearity
[DE94-007366] 10 p4021 N94-33689
Ultrastructure processing of advanced materials
[AD-A278285] 10 p4018 N94-33962
Thermal stability studies of diamond-like carbon films
[DE94-009280] 10 p4028 N94-34069
Resonant photoemission and magnetic x-ray circular dichroism in the M shell of ultrathin films of Fe
[DE94-007453] 10 p4029 N94-34120
The growth of silicon nitride crystalline films using microwave plasma enhanced chemical vapor deposition
[AD-A278862] 11 p4340 N94-35828
Method for making a symmetrical layered thin film edge field-emitter-array
[AD-D016214] 11 p4246 N94-36121

Microstructural development in solution derived PZT thin films
[DE94-008744] 11 p4246 N94-36209
Ion modulated electroactivity in thin film metallopolymers
[AD-A278618] 11 p4246 N94-36253
Multicomponent glass surfaces: Structure and adsorption
[DE94-010516] 11 p4246 N94-36283
High temperature heterojunction bipolar transistors
[AD-A278605] 11 p4261 N94-36360
Flux-pinning related defects in YBa2Cu3O(7-x) thin films grown on miscut LaAlO3 (001) substrates
[DE94-011463] 11 p4342 N94-36377
Measurement of a surface heat flux and temperature 11 p4231 N94-36407
Mechanical properties of crosslinked polymer coatings 11 p4231 N94-36410
Irradiation effects in Fe-30 percent Ni alloy during Ar ion implantation
[DE94-619057] 12 p4415 N94-36564
Determining the refractive index of a lambda/4 thin film on a thick substrate from a transmittance measurement
[DE93-019584] 12 p4523 N94-36693
Diamond deposition and defect chemistry studied via solid state NMR
[AD-A280609] 12 p4533 N94-36727
Small-angle x ray scattering studies of microvoids in amorphous-silicon-based semiconductors
[DE94-006931] 12 p4533 N94-36745
Atomic and electronic structure of metals and alloys: Rare earths, ultrathin films and surface alloys
[DE94-011581] 12 p4516 N94-37113
Poly(p-phenylene) derivatives new high performance nonlinear optical polymers
[AD-A280248] 12 p4422 N94-37121
New materials and multidimensional cluster analysis for SAW chemical sensor arrays
[DE94-012066] 12 p4409 N94-37161
Critical-state flux-density profiles in type-2 superconducting thin-film strips and disks
[DE94-011199] 12 p4535 N94-37166
Substrate effects on the structure and optical properties of epitaxial PbTiO3 thin films prepared by metal-organic chemical vapor deposition
[DE94-010432] 12 p4535 N94-37192
Microscopic image processing systems for measuring nonuniform film thickness profiles
[DE94-005336] 12 p4424 N94-37223
X-ray diffraction studies of evaporated gold thin films deposited on aluminum nitride substates
[AD-A280454] 12 p4536 N94-37228
Time-of-flight pulsed ion beam surface analysis as a means of in situ, real-time characterization of the growth of ferro-electric and conductive oxide heterostructures
[DE94-012628] 12 p4517 N94-37249
SAW chemical sensor arrays using new thin-film materials
[DE94-011940] 12 p4411 N94-37365
Investigation of polycrystalline thin-film CuInSe2 solar cells based on ZnSe windows
[DE94-006936] 12 p4462 N94-37381
Scanning x-ray diffraction: A technique with high compositional resolution for studying phase formation in co-deposited thin films
[DE94-011496] 12 p4420 N94-37516
Residual stress and Raman spectra of laser deposited highly-tetrahedral-coordinated-amorphous-carbon films
[DE94-012067] 12 p4426 N94-37537
The MBE growth and optical quality of BaTiO3 and SrTiO3 thin films on MgO
[DE94-011468] 12 p4538 N94-37570

THIN PLATES
Boundary element method for eigenvalue problems of thin plates
[ITN-93-85199] 01 p0343 N94-10392
Experimental technique to simulate orbital-debris impact on space shields at impact velocities over 10 km/s
[DE93-011619] 02 p0539 N94-12909
Role of microstructure on fatigue durability of aluminum aircraft alloys
[AD-A266350] 02 p0571 N94-13697
Analysis of electromagnetic scattering from irregularly shaped, thin, metallic flat plates
[NASA-TP-3361] 03 p0998 N94-16655
Effect of phase change in a debris cloud on a backwall structure
[DE93-017506] 04 p1358 N94-18100
Toward a characterization of the debris cloud created in a hypervelocity impact on a thin plate
[AD-A269190] 04 p1455 N94-18864
Interfacial cracks in plates: A three-dimensional numerical investigation 04 p1456 N94-19116
Radial basis function approximation: From gridded centers to scattered centers
[AD-A274184] 07 p2998 N94-27103
A numerical approach to Stefan problem
[IPPCZ-334] 07 p2844 N94-27841
Performance of a higher-order triangular finite element for composite laminated structures 08 p3181 N94-29810
Nonlinear vibration analysis of laminated plates on linear and nonlinear elastic foundations 09 p3737 N94-32079
The dynamic flexibility method in structural dynamics: Application to nonuniform beams and plates and to cavity-backed plates 10 p4068 N94-33370

THIN WALLED SHELLS
Distortions and stresses in thin shells due to anisotropic thermal expansion 01 p0057 N94-10014
Buckling analysis of laminated thin shells in a hot environment
[NASA-TM-106302] 02 p0683 N94-14776
Current capabilities for simulating the extreme distortion of thin structures subjected to severe impacts 04 p1459 N94-19474
Energy estimates and asymptotic analysis in the theory of shells
[PB93-225738] 06 p2374 N94-23113
The plastic response of a cylindrical shell subjected to an internal blast wave with a finite width shock front 06 p2154 N94-24246
Tearing resistance of a thin shell against projectile penetration: Material property effects
[DE94-007466] 09 p3733 N94-31316
Laminated thin shell structures subjected to free vibration in a hygrothermal environment
[NASA-TM-106600] 12 p4456 N94-37456

THIN WALLS
Perforated plates for thin-walled structures 01 p0063 N94-10056
Study of possible mechanisms of instability due to heat transfer
[INPE-5448-TDI/494] 02 p0628 N94-12966
Growth of small fatigue cracks in Incoloy-908
[DE94-003406] 07 p2836 N94-26129
Numerical and experimental investigation of the bending response of thin-walled composite cylinders
[NASA-CR-195730] 08 p3317 N94-28801
Thin-walled orthotropic laminated beam theory 08 p3324 N94-30920

THIN WINGS
Simulated wake characteristics of tapered annular wings by a discrete vortex method
[NAL-TR-1156] 01 p0013 N94-10855
Simulated and experimental aerodynamic characteristics of tapered annular wings
[NAL-TR-1157] 01 p0013 N94-10856

THINNERS
U SOLVENTS

THIOLS
NT CYSTEINE
Interactions between organized, surface-confined monolayers and vapor-phase probe molecules. 7: Comparison of self-assemblying organomercaptan monolayers deposited on gold from liquid and vapor phases
[AD-A273196] 06 p2535 N94-24555
Synthesis and characterization of two-dimensional molecular recognition interfaces
[AD-A273177] 06 p2536 N94-24729
Chemically sensitive interfacial force microscopy: Contact potential measurements of self-assembling monolayer films
[AD-A273135] 06 p2234 N94-24772
Group 12 thiolates: Syntheses, characterization and decomposition pathways
[AD-A277055] 09 p3900 N94-32011
Bond selective chemistry beyond the adiabatic approximation
[DE94-012486] 12 p4408 N94-37095

THIOUREAS
Second and third order nonlinear optical properties of crystalline inorganic/organic complexes
[DE93-011883] 01 p0173 N94-10755

THIXOTROPIC PROPELLANTS
U GELLED ROCKET PROPELLANTS

THOMAS-FERMI MODEL
Radiative properties of strongly magnetized plasmas
[DE93-014098] 01 p0389 N94-11118

THOMAS-FERMI THEORY
U THOMAS-FERMI MODEL

THOMSON EFFECT
U THERMOELECTRICITY

THOMSON SCATTERING
Optimization of a CO2 laser Thomson scattering alpha particle diagnostic
[DE93-012782] 01 p0173 N94-10160
Bridging the gap between the Rayleigh and Thomson limits for various convex bodies
[DSIS-93-00613] 02 p0607 N94-14204
Nonlinear Thomson scattering of intense laser pulse from beams and plasmas
[AD-A269556] 04 p1438 N94-18460
1993 annual report for the Phaedrus-T RF current drive experiments
[DE94-001369] 06 p2550 N94-23192
Characterization of heat transport and radiation hydrodynamics in collisional laser plasmas using collective Thomson scattering
[DE94-001502] 06 p2349 N94-23209
New Thomson scattering laser control for D3-D
[DE94-002890] 07 p3043 N94-26274
Photon counting spectroscopy as done with a Thomson scattering diagnostic
[DE94-005543] 08 p3503 N94-28515
Studies of ion acoustic decay
[DE94-009470] 10 p4138 N94-34168
Design of the divertor Thomson scattering system on D3-D
[DE94-012672] 12 p4527 N94-37081

THORAX
Hormonal regulation of fluid and electrolyte metabolism during periods of headward fluid shifts 01 p0311 N94-12005

THORIUM
NT THORIUM ISOTOPES
Th-230 - U-238 series disequilibrium of the Olkaria rhyolites Gregory Rift Valley, Kenya: Residence times 01 p0281 N94-12076
Crystallographic phase transitions in actinide metals as a function of pressure
[DE93-040138] 05 p2011 N94-19827
K, U, and Th behavior in Martian environmental conditions 05 p2141 N94-20908

THORIUM COMPOUNDS
Muon spin relaxation studies of heavy fermion superconductors
[DE93-014576] 02 p0815 N94-14773
Digital control programmer for temperature control
[DE94-615584] 11 p4309 N94-36382

THORIUM ISOTOPES
LEW88516 and SNC meteorites 01 p0430 N94-12150
The Th and U abundances in chondritic meteorites 01 p0430 N94-12151

THORIUM 228
U THORIUM ISOTOPES

THORIUM 230
U THORIUM ISOTOPES

THORIUM 234
U THORIUM ISOTOPES

THORON
U RADON ISOTOPES

THREADS
Self locking set screw
[AD-D015969] 05 p1824 N94-21277
Benefits of thread rolling process to the stress corrosion cracking and fatigue resistance of high strength fasteners
[DE93-040438] 05 p1833 N94-22001
An experimental and analytical investigation of a threaded fastener
[VTT-JULK-786] 09 p3724 N94-31654

THREAT EVALUATION
NASA security handbook
[NHB-1620.3C] 03 p1224 N94-15937
Sensor data fusion for air to air situation awareness beyond visual range 12 p4395 N94-36633

THREE AXIS STABILIZATION
Standard platforms for small satellites 03 p0895 N94-17181
Decentralized autonomous attitude determination using an inertially stabilized payload 06 p2157 N94-24264

THREE BODY PROBLEM
Three-nucleon problem with phase equivalent potentials
[DE93-617731] 01 p0363 N94-10722
On the depletion in the outer asteroid belt and the structure of the 4 to 3 mean motion resonance 01 p0426 N94-11596
Orbital simulations of satellite escape/capture and the origin of satellites such as Triton 01 p0429 N94-12057
Energy potential analysis of zero velocity curves in the restricted three-body problem
[AD-A267512] 03 p1170 N94-17076
A guidance and navigation system for two spacecraft rendezvous in translunar halo orbit
[AD-A267498] 03 p0898 N94-17368
Muon transfer rates in collisions of hydrogen isotope mesic atoms on bare nuclei: Multichannel adiabatic approach
[DE94-606752] 07 p3030 N94-27861
A guidance and navigation system for two spacecraft rendezvous in translunar halo orbit 08 p3142 N94-29837

Optimal low-thrust, Earth-Moon trajectories
08 p3159 N94-30961
A three-body calculation of the O-16(d,p)O-17 reaction using a two-term separable potential for the s-wave nucleon-core interaction
[DE94-616652] 11 p4320 N94-35579
Relativistic three-particle dynamical equations. 2: Application to the trinucleon system
[DE94-616653] 11 p4320 N94-35580
Relativistic three-particle dynamical equations. 2: Theoretical development
[DE94-616654] 11 p4320 N94-35581
Exact multiplicities in the three-anion spectrum
[DE94-616768] 11 p4325 N94-36075
P-matrix approach and three-nucleon problem
[DE94-616887] 11 p4326 N94-36131

THREE DIMENSIONAL BODIES
Recognizing 3-D objects using 2-D images
[AD-A271005] 05 p1983 N94-19819
Robust and efficient 3D recognition by alignment
[AD-A270839] 05 p1904 N94-20041
Recognition by prototypes
[AD-A271687] 05 p1943 N94-20921
The local measurement and global interpretation of 3D motion field generated by several moving objects from range image sequences 05 p1777 N94-22146
Extracting projective information from single views of 3D point sets
[OUEL-1973/93] 06 p2464 N94-25471
Combining shape and color information for 3D object recognition
[AD-A274123] 07 p2967 N94-27064
Comparison of RCS prediction techniques, computations and measurements
[PB94-125515] 08 p3256 N94-30392
Visual perception of 3-dimensional structure from different types of optical deformation
[AD-A278272] 09 p3884 N94-33141
The measurement and three dimensional reconstruction for configuration of air vehicle using image processing techniques 10 p3996 N94-34356
The problems of the minimal surface and minimal lineal measure in three dimensions
[DE94-013002] 12 p4479 N94-37355

THREE DIMENSIONAL BOUNDARY LAYER
On nonlinear Tollmien-Schlichting/vortex interaction in three-dimensional boundary layers
[NASA-TM-106184] 01 p0152 N94-11377
Experiments on near-wall structure of three-dimensional boundary layers 01 p0159 N94-12309
Criteria for onset of boundary-layer transition on spinning bodies 01 p0164 N94-12620
Curvature effects in three-dimensional boundary layers 01 p0164 N94-12623
Numerical study of the effects of icing on viscous flow over wings
[NASA-CR-193306] 02 p0500 N94-13180
High speed transition prediction
[NASA-CR-194125] 02 p0502 N94-13422
A three-dimensional supersonic turbulent boundary layer generated by an isentropic compression 02 p0503 N94-13556
Three-dimensional turbulent boundary layer
[AD-A266261] 03 p1025 N94-16908
Structure of turbulence in three-dimensional boundary layers
[NASA-CR-194655] 03 p1027 N94-17130
Multigrid direct numerical simulation of the whole process of flow transition in 3-D boundary layers
[NASA-TM-106369] 03 p1030 N94-17557
Viscous-inviscid calculation of high-lift separated compressible flows over airfoils and wings 04 p1309 N94-18440
Multigrid methods for flow transition in three-dimensional boundary layers with surface roughness
[NASA-CR-4540] 04 p1417 N94-18843
The effect of fine surface riblets on the flow around an inclined axially symmetrical body
[MPIS-105/1993] 04 p1420 N94-19356
Numerical investigation of laminar-turbulent transition in two- and three-dimensional boundary layers
[DLR-FB-92-36] 05 p1800 N94-20533
Transition for three-dimensional, compressible boundary layers 07 p2653 N94-28327
Euler and Navier-Stokes wing/fuselage computations of the De Havilland Dash 8 aircraft 07 p2654 N94-28329
Long-wavelength asymptotics of unstable crossflow modes, including the effect of surface curvature
[NASA-CR-4579] 08 p3273 N94-29460
Computation of three-dimensional compressible boundary layers to fourth-order accuracy on wings and fuselages
[NASA-CR-4269] 09 p3709 N94-32871
Linear stability theory and three-dimensional boundary layer transition 10 p3981 N94-33530

THREE DIMENSIONAL COMPOSITES
JPRS report: Science and technology. Central Eurasia: Materials science
[JPRS-UMS-93-002] 04 p1339 N94-18833
Fatigue resistance of unnotched and post impact(+/-30 deg/0 deg) 3-D braided composites
[NASA-CR-191590] 07 p2711 N94-27433
On the dynamic mechanical behavior of 3-D integrated fabric reinforced composites
[AD-A275424] 08 p3177 N94-28865
A thermal viscoelastic analysis for thick-walled composite cylinders
[AD-A274143] 09 p3625 N94-32604
Can the compressive response of fiber-reinforced composites be modelled by means of layered arrays?
[AD-A278864] 11 p4233 N94-35944

THREE DIMENSIONAL FLOW
NT SECONDARY FLOW
Three-dimensional hypersonic rarefied flow calculations using direct simulation Monte Carlo method 01 p0007 N94-10449
Development of a Delaunay-based adaption scheme with applications to complex three-dimensional rotational flows 01 p0149 N94-10824
Theoretical investigation of 3-D shock wave turbulent boundary layer interactions
[AD-A265275] 01 p0150 N94-11014
KIVA-3: A KIVA program with block-structured mesh for complex geometries
[DE93-011986] 01 p0077 N94-11249
Viscous analysis of three-dimensional rotor flows using a multigrid method
[NASA-TM-106266] 01 p0152 N94-11481
The flow structure around a cylindrical pier for the flow of transcritical Reynolds number 01 p0169 N94-11944
Numerical simulation using vorticity-vector potential formulation 01 p0157 N94-12297
Reynolds stress closure modeling in wall-bounded flows 01 p0157 N94-12298
Experiments on near-wall structure of three-dimensional boundary layers 01 p0159 N94-12309
The three-dimensional evolution of a plane wake 01 p0159 N94-12310
Towards a cell-vertex Navier-Stokes algorithm for three-dimensional structured/unstructured meshes
[ARA-MEMO-366] 01 p0161 N94-12437
Simultaneous 3D turbulent large-scale structures in a flood flow by multi-channels measuring system 01 p0165 N94-12624
VIB3D: Method for calculating 3-D unsteady flow through turbomachinery blades
[CUED/A-TURBO/TR.128] 01 p0166 N94-12777
VIB2D: Quasi 3-D unsteady viscous flow method for blade flutter calculation
[CUED/A-TURBO/TR.129] 01 p0166 N94-12779
Three-Dimensional Boundary-Layer program (BL3D) for swept subsonic or supersonic wings with application to laminar flow control
[NASA-CR-4531] 02 p0629 N94-13073
The three-dimensional flow past a rapidly rotating circular cylinder
[NASA-CR-191512] 02 p0630 N94-13075
Three-dimensional structure of straight and curved plane wakes
[NASA-CR-194420] 02 p0501 N94-13266
Numerical simulation of steady three-dimensional flows in axial turbomachinery bladerows 02 p0634 N94-13630
A control volume finite element method for three-dimensional, incompressible, viscous fluid flow
[ISBN-0-315-72019-0] 02 p0635 N94-13683
Evolution of disturbances in stagnation point flow
[NASA-CR-191516] 02 p0636 N94-13724
Images constructed from computed flow fields
[NASA-CR-194397] 02 p0650 N94-13814
Numerical investigations in three-dimensional internal flows
[NASA-CR-194143] 02 p0637 N94-13827
Multigrid solution of internal flows using unstructured solution adaptive meshes
[NASA-CR-194233] 02 p0638 N94-14356
Least-squares finite element solutions for three-dimensional backward-facing step flow
[NASA-TM-106353] 02 p0770 N94-14407
An experimental study of a turbulent boundary layer in the trailing edge region of a curculation-control airfoil
[NASA-CR-194522] 02 p0508 N94-14541
Navier-Stokes simulation of transonic vortex flow over a delta wing 02 p0640 N94-14606
A finite volume method for computation of viscous flow in complex configurations 02 p0640 N94-14607
Behavior of streamwise rib vortices in a three-dimensional mixing layer 02 p0644 N94-14754
A new Lagrangian method for three-dimensional steady supersonic flows
[NASA-TM-106068] 02 p0510 N94-14847
The development of a scalable parallel 3-D CFD algorithm for turbomachinery
[NASA-CR-193604] 02 p0664 N94-14848
Numerical simulation of 3-D shock wave turbulent boundary layer interactions 03 p1017 N94-15199
Numerical investigations in three-dimensional internal flows
[NASA-CR-194594] 03 p1020 N94-15551
Numerical simulation of three-dimensional self-gravitating flow
[NASA-TM-109021] 03 p1021 N94-15768
On the stability analysis of approximate factorization methods for 3D Euler and Navier-Stokes equations
[NASA-TM-106314] 03 p1169 N94-15818
Inviscid instability of streamwise corner flow
[NASA-CR-191514] 03 p1021 N94-15834
Proteus three-dimensional Navier-Stokes computer code, version 1.0. Volume 1: Analysis description
[NASA-TM-106337] 03 p1024 N94-16527
Adaptive Cartesian grid methods for representing geometry in inviscid compressible flow
[DE93-016430] 03 p1025 N94-16894
Computational aerodynamics with icing effects
[AD-A267509] 03 p0860 N94-17074
Application of ARC/INFO to regional scale hydrogeologic modeling
[DE93-015673] 04 p1461 N94-18107
An algebraic turbulence model for turbomachinery 04 p1411 N94-18554
Several examples where turbulence models fail in inlet flow field analysis 04 p1412 N94-18556
Theoretical examination of the flow around a cylinder with a low dimensional Galerkin process
[MPIS-25/1992] 04 p1422 N94-19525
Visualization of turbulent flow with particles
[PB94-149671] 04 p1423 N94-19645
Three dimensional unsteady flow calculations in radial components 05 p1669 N94-20080
Some practical turbulence modeling options for Reynolds-averaged full Navier-Stokes calculations of three-dimensional flows
[NASA-TM-106399] 05 p1637 N94-20534
Finite element numerical simulation of three dimensional turbulent flows with dispersion: Eulerian and Lagrangian approaches
[ECL-92- 2] 05 p1801 N94-20597
An efficient numerical method for three-dimensional hypersonic flow
[AD-A272506] 05 p1637 N94-21411
Users manual for the NASA Lewis three-dimensional ice accretion code (LEWICE 3D)
[NASA-TM-105974] 05 p1642 N94-21590
Three-dimensional unstructured grid method applied to turbomachinery 05 p1919 N94-22360
The 3D Euler solutions using automated Cartesian grid generation 05 p1920 N94-22367
Efficiency and reliability enhancements in propulsion flowfield modeling 06 p2215 N94-23055
Development and application of new algorithms for the simulation of viscous compressible flows with moving bodies in three dimensions
[AD-A273514] 06 p2338 N94-25157
The high Reynolds number flow through an axial-flow pump
[AD-A273844] 07 p2789 N94-25604
Effects of crenulations on three dimensional losses in a linear compressor cascade
[AD-A273778] 07 p2790 N94-25862
The effects of three-dimensional imposed 3-d disturbances on bluff-body near wake flows
[AD-A274845] 07 p2791 N94-26187
Program to develop a performance and heat load prediction system for multistage turbines
[NASA-CR-195223] 07 p2674 N94-26588
Computational strategies for three-dimensional flow simulations on distributed computer systems
[NASA-CR-195249] 07 p2793 N94-26595
Research on bluff body vortex wakes
[AD-A273780] 07 p2796 N94-27319
Agglomeration multigrid for the three-dimensional Euler equations
[AD-A277557] 07 p2999 N94-27557
Navier-Stokes simulation of two and three dimensional jets in crossflow, effects of grid, and boundary conditions 07 p2804 N94-28026
An initial investigation into methods of computing transonic aerodynamic sensitivity coefficients
[NASA-CR-195705] 07 p2648 N94-28072
Boundary layers induced by three-dimensional vortex loops
[AD-A275678] 08 p3270 N94-28665

Proceedings of the 10th NAL Symposium on Aircraft Computational Aerodynamics
[NAL-SP-19] 08 p3123 N94-28946
On the numerical analysis of shear flows
08 p3126 N94-28972
Verification of a three-dimensional viscous flow analysis for a single stage compressor 08 p3127 N94-28976
Application of flow field simulation to turbine vane design 08 p3127 N94-28978
Three-dimensional external flow computations using prismatic grid 08 p3127 N94-28979
An elliptic-hyperbolic grid generation method and application to compressor flows
08 p3128 N94-28981
An implicit upwind scheme for the three-dimensional Euler equations using a pointwise relaxation method
08 p3128 N94-28983
A free-wake Euler and Navier-Stokes CFD method and its application to helicopter rotors including dynamic stall
[AD-A275416] 08 p3129 N94-29197
Numerical simulation of aerothermal characteristics in gas turbine combustors with complex geometries
08 p3154 N94-29255
Time-resolved measurements in a three dimensional model combustor 08 p3196 N94-29283
RNS optimization procedure for three-dimensional composite velocity multi-block applications
08 p3273 N94-29534
An improvement of the slender body theory for oscillating ships with finite forward speed 08 p3234 N94-29705
Direct and large-eddy simulations of turbulent flow in a square duct 08 p3275 N94-29809
Numerical solution of 3-D Navier-Stokes equations in vorticity-velocity form for incompressible flows
08 p3276 N94-29843
Unsteady transonic aerodynamics in frequency domain for flutter analysis 08 p3131 N94-29879
The 3-D LDV measurements on a 30-degree swept wing with a simulated ice accretion
[NASA-CR-195327] 08 p3132 N94-30124
Three-dimensional flow characteristics downstream of a blade endwall corner 08 p3280 N94-30229
The design of a system of codes for industrial calculations of flows around aircraft and other complex aerodynamic configurations
[PB94-125598] 08 p3133 N94-30387
Three dimensional compressible turbulent flow computations for a diffusing S-duct with/without vortex generators 08 p3281 N94-30519
A heterogeneous computing environment for simulating astrophysical fluid flows 09 p3928 N94-31119
Three-dimensional velocity measurements on a 6:1 prolate spheroid at 10 deg angle of attack
[AD-A276485] 09 p3702 N94-31476
A new inverse method for generating high-speed aerodynamic flows with application to waverider design
09 p3569 N94-31828
Solution of the average-passage equations for the incompressible flow through multiple-blade-row turbomachinery
[AD-A276515] 09 p3583 N94-31931
A study of the development and attenuation of wing-generated, vortical wakes
09 p3570 N94-31971
An experimental study of the flowfield on a semispan rectangular wing with a simulated glaze ice accretion
[NASA-CR-195301] 09 p3571 N94-32475
Boundary element analysis of three-dimensional nonlinear hydrodynamics in a reduced gravity environment 09 p3668 N94-32715
Inlet distortion in engines on VSTOL aircraft
[NASA-CR-195841] 09 p3584 N94-33035
Some aspects of unsteady separation
10 p3986 N94-34979
Experiments on an unsteady, three-dimensional separation 10 p4052 N94-34981
JPRS report: Science and technology. Central Eurasia: Physics and mathematics
[JPRS-UPM-93-003] 10 p4132 N94-35118
A three dimensional multigrid Reynolds-averaged Navier-Stokes solver for unstructured meshes
[AD-A280998] 11 p4191 N94-35994
Simulation of three-dimensional multi-phase flow characteristics in the deswirl section of the CDIF MHD power train
[DE94-012644] 12 p4443 N94-37176
Evaluation of parameterizations for pollutant transport and dispersion in an urban street canyon using a three-dimensional dynamic flow model
[DE94-012641] 12 p4467 N94-37429
Development of advanced Navier-Stokes solver
[NASA-CR-195094] 12 p4504 N94-37449
Unstructured grid methods for the simulation of 3D transient flows
[NASA-CR-196139] 12 p4444 N94-37525

THREE DIMENSIONAL MODELS

Transient three-dimensional numerical simulation of Marangoni flow in a liquid column under microgravity
01 p0101 N94-10079
Calculation of the effects of magnetic field damping in fluid flow: Comparison of magnetohydrodynamic models of different complexity 01 p0103 N94-10089
Venus resurfacing rates: Constraints provided by 3-D Monte Carlo simulations 01 p0453 N94-12119
Engineering solid-state materials. Strategies for modeling and packing control of molecular assemblies into 3-D networks
[AD-A265291] 01 p0404 N94-12438
The 3-D massively parallel impact simulations using PCTH
[DE93-011593] 02 p0670 N94-12908
Numerical simulation of hypersonic flow for the design of the H-2 orbiting plane (HOPE), part 3
[NAL-TR-1168-PT-3] 02 p0499 N94-12948
View generated database
[NASA-CR-191397] 02 p0822 N94-13116
Imaging microscopy with x ray lasers at Lawrence Livermore National Laboratory
[DE93-013419] 02 p0655 N94-13258
Micromechanical damage theories for brittle solids with interacting microcracks
[AD-A266348] 02 p0673 N94-13778
Eye-gaze and intent: Application in 3D interface control
[DE93-015210] 02 p0738 N94-14335
Three-dimensional modeling of diesel engine intake flow, combustion and emissions-2
[NASA-CR-191189] 02 p0519 N94-14448
Liquid and gas evanescent wave spectroscopy via tunable lasers and silver halide fibers
[ITN-93-85226] 02 p0565 N94-14465
Statics and kinetics of phase transformations in bcc Fe-Cr
[DE93-013839] 02 p0574 N94-14793
Nonlinear wave forces on large ocean structures
[AD-A266820] 02 p0683 N94-14902
Surface and internal signatures of organized vortex motions in stratified fluid
[AD-A267015] 03 p1020 N94-15526
Cooperativity and 3-D representation
[AD-A267180] 03 p1131 N94-15694
Display of dynamic, volume graphic images by holographic voxel projection: Initial investigation
[AD-A267622] 03 p1035 N94-17197
Strategic planning for aircraft noise route impact analysis: A three dimensional approach
[NASA-CR-191484] 03 p1178 N94-17278
Single block three-dimensional volume grids about complex aerodynamic vehicles
[NASA-TM-108986] 03 p1030 N94-17476
Three dimensional visualization of GOES cloud data using OCTRESS
[AD-A268102] 03 p1109 N94-17572
Three-dimensional simulation analysis of the first sections of a standing-wave free-electron laser two-beam accelerator
[DE93-016977] 04 p1436 N94-17869
Texture splats for 3D vector and scalar field visualization
[DE93-017104] 04 p1520 N94-18130
High-performance multiprocessor architecture for a 3-D lattice gas model 04 p1400 N94-18362
The GARTEUR high lift research programme
04 p1307 N94-18430
ADCIRC: An advanced three-dimensional circulation model for shelves, coasts, and estuaries. Report 3: Development of a tidal constituent database for the western North Atlantic and Gulf of Mexico
[AD-A268685] 04 p1497 N94-18455
3D composite grids using Bezier curves and surfaces in component adaptive methods
[AD-A269188] 04 p1549 N94-18863
Flow volumes for interactive vector field visualization
[DE93-017102] 04 p1418 N94-18888
Volume rendering of 3D scalar and vector fields at Lawrence Livermore National Laboratory
[DE93-018000] 04 p1528 N94-19276
Crossover from BCS to Bose superconductivity: A functional integral approach
[DE93-019503] 04 p1604 N94-19566
Three dimensional modeling of cirrus during the 1991 FIRE IFO 2: Detailed process study
05 p1877 N94-22327
Robust unstructured grid generation with VGRID
05 p1919 N94-22359
Current loop coalescence studied by 3-D electromagnetic particle code 05 p2005 N94-22660
Solar wind-magnetosphere interaction as simulated by a 3D, EM particle code 05 p2007 N94-22674
Mobility analysis, simulation, and scale model testing for the design of wheeled planetary rovers
06 p2370 N94-23425
A structural design methodology for large angle articulated trusses considering realistic joint modeling
06 p2376 N94-23560
Unsteady three-dimensional thermal field prediction in turbine blades using nonlinear BEM
06 p2325 N94-23665
Analysis of time-domain acoustic wavefields in horizontally continuously layered configurations based on the modified Cagniard method
[PB94-111044] 06 p2524 N94-23731
Generalized three-dimensional simulation of ferruled coupled-cavity traveling-wave-tube dispersion and impedance characteristics
[NASA-TP-3389] 06 p2310 N94-24056
Conceptual design of a device to measure hand swelling in a micro-gravity environment
[NASA-CR-195509] 06 p2437 N94-24330
Recent developments in the mathematical modelling and physical understanding of transport and dispersion in aquatic systems, with special reference to tidal waters
[PB94-111135] 06 p2418 N94-24600
Multiannual simulations with the Mars climate model
06 p2618 N94-24881
Three-dimensional numerical simulation of near-surface flows over the Martian north polar cap
06 p2621 N94-24895
Image analysis technology applied to problems in crystallography
[AD-A273516] 06 p2566 N94-25288
Calculation of a 3-D pose of a known object in a single perspective view
[VTT-PUBS-122] 07 p2957 N94-25642
A nonlinear three-dimensional micromechanics model for fiber-reinforced laminated composites
[AD-A273772] 07 p2705 N94-25857
Satellite attitude determination using linear combination of models
[AD-A274082] 07 p2694 N94-25996
Correlation of experimental data and three-dimensional finite element modeling of a spinning quadrupole
[DE93-041173] 07 p3008 N94-26421
Extracting complete 3-dimensional boundary representation from multiple range images
[ISBN-0-315-63776-4] 07 p2963 N94-26615
A preliminary shear velocity model for Central Asia
[AD-A274972] 07 p2880 N94-26752
Building 3-D models from unregistered range images
[AD-A274126] 07 p2986 N94-27032
Dynamic and kinematic P wave tracing for a three-dimensional elastic inhomogeneous media by the asymptotic ray theory and application
[ITN-94-85239] 07 p2775 N94-27244
The three-dimensional hydrogen atom in crossed magnetic and electric fields
[DE94-606301] 07 p3029 N94-27847
Lisp interface to geometric modelling operations
[PB94-133121] 07 p3001 N94-28398
Three-dimensional finite element modeling of a magnet array spinning above a conductor
[DE94-004573] 08 p3468 N94-28459
Exploitation of stereophotogrammetrically derived 3-D wireframe models to produce urban simulations
[AD-A275459] 08 p3325 N94-28808
Active electron and ion beam experiments in space
[AD-A275570] 08 p3504 N94-28828
Higher-order accurate numerical simulation of 3D supersonic mixing layers 08 p3124 N94-28954
Three dimensional simulation of compressible flow induced by a high-speed train moving into a tunnel
08 p3126 N94-28967
Some efficient procedures for correcting triangulated models
[PB94-136926] 08 p3452 N94-29171
Damage meso-modeling of 3D evolutive composites
[REPT-932-430-106] 08 p3179 N94-29442
Computational fluid dynamics in ventilation. 3: The IEA annex 20 work 08 p3233 N94-29608
Effects and implications of fault zone heterogeneity and anisotropy on earthquake strong ground motion
08 p3363 N94-29941
Three-dimensional effects for radio frequency antenna modeling
[DE94-006102] 08 p3255 N94-30105
Magnetic properties of the three dimensional Ising model with interface single-ion anisotropy
[DE94-608116] 08 p3525 N94-30164
Magnetic properties of a transverse spin-1 Ising model with longitudinal crystal field interactions
[DE94-608118] 08 p3517 N94-30165
A deterministic algorithm for the three-dimensional diameter problem
[RUU-CS-92-45] 08 p3424 N94-30348

Three dimensional compressible turbulent flow computations for a diffusing S-duct with/without vortex generators
08 p3281 N94-30519
Sensitivity analysis of the static aeroelastic response of a wing
08 p3134 N94-30525
A laboratory simulation of urban heat-island-induced circulation in a stratified environment
08 p3367 N94-30921
The dynamical settling of warped disks and angular momentum transport in galaxies
09 p3928 N94-31121
An investigation of the spin-coating process and a model for three-dimensional regular foams
09 p3649 N94-31206
Development of a 3D numerical code to calculate the trajectories of the blow off electrons emitted by a vacuum surface discharge: Application to the study of the electromagnetic interference induced on a spacecraft
[ONERA-NT-1993-12] 09 p3863 N94-31227
Development of a three-dimensional icing model for predicting ice accretion on aircraft
[ONERA-NT-1993-5] 09 p3574 N94-31230
ADCIRC: An advanced three-dimensional circulation model for shelves, coasts, and estuaries. User's manual for ADCIRC-2DDI
[AD-A276150] 09 p3787 N94-31250
Multidimensional WAF-type schemes for model conservation laws
[CRANFIELD-AERO-9312] 09 p3843 N94-31541
Finite element analysis of damage in fibrous composites using a micromechanical model
[AD-A277226] 09 p3623 N94-32024
Complete model description of an electron beam using ACCEPT Monte Carlo simulation code
[DE94-007063] 09 p3872 N94-32628
Climate effects of anthropogenic sulfate: Simulations from a coupled chemistry/climate model
[DE94-004352] 09 p3767 N94-32789
Fast nonsupervised 3D registration of PET and MR images of the brain
[TELECOM-93-C-006] 09 p3798 N94-33069
Flow through three-dimensional arrangements of cylinders with alternating streamwise planar tilt
[DE94-008968] 10 p4047 N94-34015
C.A.D. representation of ternary and quaternary phase diagrams
[NASA-CR-195845] 10 p4025 N94-34170
Engine static structures behaviour under impact load using 3D modelling
10 p4004 N94-34464
Space Shuttle orbit determination using empirical force modeling of attitude maneuvers for the German MOMS-02/D2 mission
11 p4207 N94-35634
Distributed parameter modeling of repeated truss structures
11 p4218 N94-35868
Three-dimensional force data acquisition and boundary corrections for the Walter H. Beech Memorial 7 x 10 foot low speed wind tunnel
[AR93-2] 11 p4200 N94-36437
Finite-rate chemistry and transient effects in Direct Numerical Simulations of turbulent non-premixed flames
[DE94-005250] 12 p4410 N94-37222
Evaluation of parameterizations for pollutant transport and dispersion in an urban street canyon using a three-dimensional dynamic flow model
[DE94-012641] 12 p4467 N94-37429
A computational model for three-dimensional jointed media with a single joint set
[DE94-007582] 12 p4470 N94-37527
Three-dimensional gyrokinetic particle-in-cell simulation of plasmas on a massively parallel computer: LDRD Core Competency Project
[DE94-013367] 12 p4532 N94-37732

THREE DIMENSIONAL MOTION
NT SECONDARY FLOW
NT THREE DIMENSIONAL FLOW
Visual tracking
[AD-A271686] 05 p1943 N94-20920
A study of the compressible flow through a diffusing S-duct
[NASA-TM-106411] 05 p1638 N94-21591
The local measurement and global interpretation of 3D motion field generated by several moving objects from range image sequences
05 p1777 N94-22146
Quantitative assessment of human motion using video motion analysis
06 p2436 N94-24203
Heat transfer and flow structure in end-wall boundary layers
[AD-A273470] 06 p2335 N94-24689
Nominally two-dimensional flow about a normal flat plate
08 p3275 N94-29838
Dynamic modeling of multibody flexible structures
08 p3323 N94-30813
Identification and control of structures in space
[NASA-CR-195910] 09 p3612 N94-33115
Research in image understanding
[AD-A278540] 10 p4104 N94-33675
Input shaping for three-dimensional slew maneuvers of a precision pointing flexible spacecraft
[DE94-008937] 11 p4226 N94-36001

THRESHOLD CURRENTS
AlGaAs diode laser blue shift resulting from fast neutron irradiation
[AD-A266642] 02 p0659 N94-14681
First results on InGaAsP separate confinement heterostructure diode lasers
[AD-A270849] 05 p1815 N94-19878
Optical amplification and threshold behavior on InGaAs/InGaAsP multiquantum well structures
[ETN-93-94181] 05 p2026 N94-21151
Large-diameter InGaAs/AlGaAs vertical-cavity surface-emitting lasers with low threshold current density fabricated using a simple chemical etch process
[AD-A277733] 09 p3721 N94-33003
Study and fabrication of GaSb-based laser heterostructures
[PB94-170677] 11 p4273 N94-36218

THRESHOLD LOGIC
Threshold computation and cryptographic security
[TR-443] 05 p1907 N94-20536

THRESHOLD VOLTAGE
Evaluation of radiation effects in re-oxidized nitrided oxide devices by hot carrier stressing at 77 K
05 p1754 N94-21084
Low energy CMOS for space applications
05 p1768 N94-21735
Generic microelectronic smart sensor platform for detection of toxic, hazardous, and flammable gases
[DE93-017626] 06 p2343 N94-23200
The role of emitter states in magnetotunneling through double-barrier resonant-tunneling diodes at high magnetic fields
[REPT-A-2658] 06 p2564 N94-24959
Estimating low-dose rate irradiation response of MOSFETs
[DE94-007292] 11 p4342 N94-36367

THRESHOLDS (PERCEPTION)
Computer software and hardware to determine contrast sensitivity using three methods: Tracking, limits, and constant stimuli
[AD-A265168] 01 p0324 N94-11099
Underwater hearing: A review
[ISVR-TR-212] 02 p0777 N94-14130
The effects of reverberant impulse noise (blast waves) on hearing: Parametric studies
[AD-A269242] 04 p1506 N94-18911

THROATS
Experimental studies on a gas dynamic laser with narrow throat and high area-ratio grid nozzles
[AD-A267818] 03 p1042 N94-17400
Static performance investigation of a skewed-throat multiaxis thrust-vectoring nozzle concept
[NASA-TP-3411] 10 p3983 N94-34172

THROTTLING
Electric propulsion system technology
[NASA-CR-194100] 02 p0549 N94-13055
Method of reducing hydraulic instability
[NASA-CASE-LEW-15463-1] 08 p3273 N94-29539
Flight testing a propulsion-controlled aircraft emergency flight control system on an F-15 airplane
[NASA-TM-4590] 11 p4199 N94-35258

THRUST
NT JET THRUST
NT LEADING EDGE THRUST
NT LOW THRUST
NT ROCKET THRUST
NT STATIC THRUST
NT VARIABLE THRUST
Constant-thrust orbit-raising transfer charts
[AD-A269088] 04 p1334 N94-18718
Shock-dependent, optimum thrust wings in supersonic flow
09 p3570 N94-32027
Guide to the measurement of the transient performance of aircraft turbine engines and components
[AD-280272] 10 p3997 N94-33874
Evaluating the dynamic response of in-flight thrust calculation techniques during throttle transients
[NASA-TM-4591] 11 p4193 N94-35241

THRUST AUGMENTATION
Thrust augmentation options for the Beta 2 two-stage-to-orbit vehicle
[NASA-TM-106448] 05 p1648 N94-21563
Options for thrust augmentation for the Beta 2 two-stage-to-orbit launch vehicle
[NASA-TM-106418] 05 p1649 N94-21759

THRUST BEARINGS
Improvement of azimuthal homogeneity in permanent-magnet bearing rotors
[DE93-009954] 01 p0144 N94-11607
Spline screw multiple rotations mechanism
[NASA-CASE-GSC-13452-1] 06 p2352 N94-23078
Parachute Swivel Mechanism for planetary entry
08 p3162 N94-29643
An air bearing system for small high speed gas turbines
10 p4004 N94-34466

THRUST CHAMBERS
Space Storable Rocket Technology program (SSRT). Option 1 program
[NASA-CR-191171] 01 p0046 N94-10938
Small rocket flowfield diagnostic chambers
06 p2210 N94-23030
An experimental study of characteristic combustion-driven flows for CFD validation
06 p2212 N94-23040
Numerical investigation of two- and three-dimensional heat transfer in expander cycle engines
06 p2213 N94-23048
Advanced materials for radiation-cooled rockets
06 p2214 N94-23052
Effect of hydrogen exposure on a Cu-8 Cr-4 Nb alloy
[NASA-TM-106429] 06 p2243 N94-23556
STE thrust chamber technology: Main injector technology program and nozzle Advanced Development Program (ADP)
[NASA-CR-193919] 06 p2221 N94-25019
Evaluation of oxide-coated iridium-rhenium chambers
[NASA-TM-106442] 08 p3172 N94-29097

THRUST CONTROL
NT THRUST VECTOR CONTROL
Preliminary flight results of a fly-by-throttle emergency flight control system on an F-15 airplane
[NASA-TM-4503] 02 p0520 N94-13254
Design criteria for integrated flight/propulsion control systems for STOVL fighter aircraft
02 p0521 N94-13297
A piloted simulation investigation of the normal load factor and longitudinal thrust required for air-to-air acquisition and tracking
02 p0522 N94-13301
A four-axis hand controller for helicopter flight control
02 p0522 N94-13305
Phasing strategies of the Hermes type space shuttle: Its optimization considering the thrust failures
[LAAS-93242] 04 p1544 N94-19361
A six degree of freedom, plume-fuel optimal trajectory planner for spacecraft proximity operations using an A* node search
[NASA-CR-188285] 09 p3601 N94-3...388
Powered lift facility at NASA Lewis Research Center's Aeroacoustic Propulsion Laboratory
[NASA-TM-106577] 10 p4009 N94-33604
Integrated flight/thrust control systems with constant angle-of-attack
10 p4007 N94-34326

THRUST FAULTS
U GEOLOGICAL FAULTS

THRUST MEASUREMENT
Characterization of in-flight performance of ion propulsion systems
[NASA-TM-106283] 01 p0046 N94-10761
An overview of the capabilities of ARA for the measurement of nozzle discharge and thrust
[ARA-MEMO-378] 01 p0055 N94-12283
Simulating indirect thrust measurement methods as used on modern high-bypass turbofans
[ISBN-0-315-84123-0] 07 p2674 N94-26673
Operating characteristics of the Russian D-55 thruster with anode layer
[NASA-TM-106610] 10 p4016 N94-33606

THRUST POWER
U THRUST

THRUST REVERSAL
Turbulence modeling for thrust reverser flow field prediction methods
[AD-A266139] 01 p0154 N94-11641
Experimental investigation of the interaction of a thrust reverser jet with an external subsonic flow
07 p2801 N94-28011
A study of jet effect and ground effect interference on a STOL fighter
07 p2671 N94-28034
Subsonic aerodynamic characteristic of semispan commercial transport model with wing-mounted advanced ducted propeller operating in reverse thrust --- conducted in the Langley 14 by 22 foot subsonic wind tunnel
[NASA-TP-3427] 12 p4384 N94-37505

THRUST VECTOR CONTROL
Static internal performance of a single expansion ramp nozzle with multiaxis thrust vectoring capability
[NASA-TM-4450] 01 p0012 N94-10675
AD100/ADSIM, ACSL, and MATLAB output comparisons using frequency-response analysis
[DE93-009640] 01 p0047 N94-11122
Adaptive reconfigurable flight controls for high angle of attack aircraft agility
01 p0032 N94-11502
Evaluation of dual flow thrust vector nozzles with exhaust stream impingement
[NASA-CR-193392] 02 p0630 N94-13078
Advanced electric motor technology flux mapping
[NASA-CR-193824] 02 p0621 N94-13186
Electrical Actuation Technology Bridging
[NASA-CP-3213] 02 p0551 N94-13417

Design and evaluation of single and dual flow thrust vector nozzles with post exit vanes
[NASA-CR-193393] 02 p0638 N94-14086
Design and application of electromechanical actuators for deep space missions
[NASA-CR-194145] 02 p0663 N94-14134
Effects of internal yaw-vectoring devices on the static performance of a pitch-vectoring nonaxisymmetric convergent-divergent nozzle
[NASA-TP-3369] 03 p0858 N94-16572
Equations of motion of a hinged body over a spherical earth
[AD-A268408] 03 p0868 N94-17435
Heat transfer parametric system identification
[AD-A268525] 03 p0929 N94-17543
Effects of thrust vector control on the performance of the aerobang orbital plane change maneuver
[AD-A272532] 05 p1646 N94-21418
Internal performance of a nonaxisymmetric nozzle with a rotating upper flap and a center-pivoted lower flap
[NASA-TP-3385] 05 p1637 N94-21569
Thrust vectoring theory, laboratory and flight tests
06 p2155 N94-24251
Development of high-angle-of-attack nose-down pitch control margin design guidelines for combat aircraft
06 p2164 N94-25107
Evaluation of moderate angle of attack roll of a dual engine, thrust vectoring aircraft using quantitative feedback theory
[AD-A274118] 07 p2667 N94-25905
Vectored jets-induced interference on aircraft, prediction and verification 07 p2801 N94-28012
Numerical investigation of thrust vectoring by injection of secondary air into nozzle flows
07 p2801 N94-28013
A study of jet effect and ground effect interference on a STOL fighter 07 p2671 N94-28034
Design and test of electromechanical actuators for thrust vector control 08 p3163 N94-29650
Static performance investigation of a skewed-throat multiaxis thrust-vectoring nozzle concept
[NASA-TP-3411] 10 p3983 N94-34172
Thrust vector aided maneuvering of the YF-22 Advanced Tactical Fighter prototype 10 p3991 N94-34610
Results from the STOL and Maneuver Technology Demonstration program 10 p3991 N94-34611
Aerodynamic design of super maneuverable aircraft
10 p3992 N94-34617
X-31A control law design 10 p3992 N94-34618
X-31A system identification applied to post-stall flight: Aerodynamics and thrust vectoring
10 p3992 N94-34619
X-31 tactical utility: Initial results
10 p3992 N94-34620
Direct reduced order mixed H2/H infinity control for the Short Take-Off and Landing/Maneuver Technology Demonstrator (STOL/MTD)
[AD-A278675] 11 p4199 N94-35796
Experience with Ada on the F-18 High Alpha Research Vehicle flight test program 11 p4310 N94-35968
An experimental investigation of active control of thrust vectoring nozzle flow fields
[AD-A278702] 11 p4229 N94-36291

THRUST-WEIGHT RATIO
Static internal performance of a single expansion ramp nozzle with multiaxis thrust vectoring capability
[NASA-TM-4450] 01 p0012 N94-10675
Small low mass advanced PBR's for propulsion
[DE94-005142] 08 p3497 N94-30588
The reduction of takeoff ground roll by the application of a nose gear jump strut
[NASA-TM-108822] 11 p4198 N94-36380

THRUSTORS
Arcjet space thrusters
[NASA-CR-193191] 01 p0046 N94-10700
A laboratory model of a hydrogen/oxygen engine for combustion and nozzle studies
[NASA-TM-106281] 01 p0047 N94-11252
Segmented ion thruster
[NASA-CASE-NPO-18192-1-CU]
05 p1669 N94-20496
Optimization of energy transfer in microwave electrothermal thrusters 06 p2216 N94-23065
CFD modeling of microwave electrothermal thrusters
06 p2216 N94-23066
Advanced space propulsion concepts
06 p2216 N94-23067
Stationary plasma thruster plume characteristics
[NASA-CR-194454] 06 p2219 N94-24361
Characteristics of ions emitted from high-current hollow cathodes
[NASA-CR-195372] 12 p4398 N94-37764

THULIUM
NT THULIUM ISOTOPES
Growth of new materials for solid state laser applications. The growth of ZnGeP2 by the vertical Bridgman method
[NASA-CR-194571] 03 p1038 N94-15530
Investigation of the optical and laser properties of Tm and Ho in YAG anf YLF
[REPT-94-001] 06 p2563 N94-24404
Excited state dynamics of thulium ions in yttrium aluminum garnets
[NASA-CR-195159] 06 p2564 N94-25024
The development of Cr, Tm, Ho:YAG lasers for airborne lidar
[AD-A274895] 07 p2816 N94-26178

THULIUM ISOTOPES
The multiplicity spectra of the (169)Tm(n, gamma) reaction
[DE93-617733] 01 p0364 N94-10835

THULIUM 171
U THULIUM ISOTOPES

THUNDERSTORMS
The application of VAS satellite imagery to thunderstorm forecasting at Cape Canaveral
[NASA-CR-193563] 02 p0718 N94-12839
Sensitivity testing of a single-Doppler temperature retrieval and forecast system
[AD-A267278] 03 p1105 N94-14958
Venus lightning
[NASA-TM-109644] 03 p1105 N94-15430
Radar diagnostic parameters as indicators of severe weather in central Florida
[PB93-183507] 03 p1106 N94-16465
Middle atmospheric electric fields over thunderstorms
[NASA-CR-194619] 03 p1106 N94-16493
Remote sensing of precipitation and electrification with a dual-polarization, coherent, wideband radar system
[AD-A267479] 03 p1004 N94-17364
Station climatic summaries: North America. Volume 1: The contiguous United States
[AD-A269567] 04 p1490 N94-18303
Station climatic summaries, North America. Volume 2: Alaska, Canada and Greenland
[AD-A269793] 04 p1493 N94-18732
Multiple scattering effects on the Linear Depolarization Ratio (LDR) measured during CaPE by a Ka-band air-borne radar 05 p1728 N94-20446
Localization from near-source quasi-static electromagnetic fields
[DE93-040390] 05 p1732 N94-20479
A parametric representation of a thunderstorm cell
[AD-A271983] 05 p1866 N94-20579
Lightning studies using LDAR and LLP data
06 p2416 N94-23238
A modeling study of the mesocyclone
[AD-A274889] 07 p2893 N94-26168
Examination of micro- and macro-physical structures and processes in hailstorms with respect to their modification
[DLR-FB-93-25] 07 p2897 N94-27751
Thunderstorm Hypothesis Reasoner
[NASA-CR-195714] 07 p2897 N94-27884
MUSIC for localization of thunderstorm cells
[DE94-004985] 07 p2897 N94-28146
Numerical simulations of a mountain thunderstorm. A comparison with Doppler radar observations
[AD-A275296] 08 p3369 N94-28873
A numerical study of thunderstorm electrification
[AD-A277531] 10 p4089 N94-33709
Kinetic theory of runaway air breakdown and the implications for lightning initiation
[DE94-001683] 11 p4295 N94-36240
Three flights into thunderstorms with the revised Rocket Electric Field Sounding (REFS) payload
[AD-A280424] 12 p4473 N94-37217

THYRATRONS
Computational model of a magnetic modulator for copper lasers
[DE93-019603] 05 p1815 N94-20223

THYRISTORS
NT SILICON CONTROLLED RECTIFIERS
Some experiences of solving 1-D semiconductor device equations on a matrix coprocessor by a domain decomposition method
[CWI-NM-R9304] 05 p1935 N94-21492
A study of DC-DC converters with MCT's for arcjet power supplies
[NASA-CR-191204] 07 p2703 N94-27662
Silicon device performance measurements to support temperature range enhancement
[NASA-CR-195265] 07 p2844 N94-27824

THYROID GLAND
Calcitonin control of calcium metabolism during weightlessness
[NASA-CR-193622] 02 p0731 N94-12960
Thyroid alterations in porcine after prolonged exposure to cold or heat
[AD-A266840] 02 p0733 N94-14879
Muscle sympathetic nerve activity in patients with hyper-and hypothyroidism: A microneurographic study
07 p2930 N94-27531

THYROXINE
Expression analysis of Thyroxine-Binding Globulin Complete Deficiency in Japanese (TBG-CDJ)
07 p2905 N94-27482

TIBET
Analysis of gravity, magnetic, and seismic reflection data from Tibet and neighboring regions of China
[NASA-CR-193405] 01 p0278 N94-11886

TID
U TRAVELING IONOSPHERIC DISTURBANCES

TIDAL FLATS
Morphodynamics of inter-tidal areas: The Wadden Sea
[NLR-TP-92356-U] 07 p2851 N94-27555

TIDAL OSCILLATION
U TIDES

TIDAL WAVES
Generation of internal waves near the shelf boundary
01 p0229 N94-12763
Experimental and theoretical investigation of undular bore formation upstream the bank
01 p0229 N94-12764
Artificial oil pollution detection and wave observation in the sea adjacent to Japan by ERS-1 SAR
02 p0688 N94-14212

TIDES
NT ATMOSPHERIC TIDES
NT EARTH TIDES
A stochastic-deterministic approach as an alternative to classical cross-over techniques in small ocean basins
01 p0242 N94-11767
Experimental and theoretical investigation of undular bore formation upstream the bank
01 p0229 N94-12764
Cold dark matter halos 02 p0838 N94-13649
Characterization of spatial and temporal variability of phytoplankton blooms in coastal waters
[AD-A267102] 03 p1116 N94-15633
Tidal interaction: A possible explanation for geysers and other fluid phenomena in the Neptune-Triton system
03 p1272 N94-16311
ADCIRC: An advanced three-dimensional circulation model for shelves, coasts, and estuaries. Report 3: Development of a tidal constituent database for the western North Atlantic and Gulf of Mexico
[AD-A268685] 04 p1497 N94-18455
Method for extracting tidal and inertial motion from ARGOS ice buoys applied to the Barents Sea during CEAREX
[PB93-190213] 04 p1499 N94-19063
Dynamics of the atmosphere of Mars: Review of some outstanding problems 06 p2620 N94-24888
Upper atmosphere neutral and plasma density modeling
[AD-A274768] 07 p2879 N94-26569
Macrobenthic fauna in the dutch sector of the north sea in 1991
[PB94-126414] 07 p2868 N94-27200
Modulating terrestrial impacts from Oort cloud comets by the adiabatically changing galactic tides
07 p2890 N94-28305
Tidal atlas software development
[AD-A275251] 08 p3377 N94-29432
Some aspects of simultaneously flying Topex Follow-On in a Topex orbit with Geosat Follow-On in a Geosat orbit
[NASA-CR-196075] 10 p4077 N94-34214

TIG WELDING
U GAS TUNGSTEN ARC WELDING

TILES
Toxicity study of dimethylethoxysilane (DMSES), the waterproofing agent for the Orbiter heat protective system 01 p0318 N94-11554
High temperature electromagnetic characterization of thermal protection system tile materials
[NASA-CR-189687] 02 p0578 N94-13431
Thermally activated retainer means utilizing shape memory alloy
[NASA-CASE-MSC-21793-1] 05 p1654 N94-20304
An assessment of the cost of microwave sintering ceramic tiles for armor applications
[DE94-000978] 05 p1693 N94-21850
Development of a nondestructive vibration technique for bond assessment of Space Shuttle tiles
[NASA-CR-195163] 06 p2201 N94-24919
Design and evaluation of an electromagnetic beam waveguide for measuring electrical properties of materials
[NASA-TP-3418] 07 p2769 N94-26611

TILT
U ATTITUDE (INCLINATION)

TILT ROTOR AIRCRAFT
NT V-22 AIRCRAFT
NT XV-15 AIRCRAFT

Navier-Stokes flowfield computation of wing/rotor interaction for a tilt rotor aircraft in hover
[NASA-CR-4532] 01 p0013 N94-10758
Piloting considerations for terminal area operations of civil tiltwing and tiltrotor aircraft
02 p0525 N94-13320
Evaluation of two cockpit display concepts for civil tiltrotor instrument operations on steep approaches
02 p0517 N94-13323
XV-15: Tiltrotor
[NASA-TM-109455] 03 p0865 N94-15328
Wind tunnel test of a variable-diameter tiltrotor (VDTR) model
[NASA-CR-177629] 06 p2181 N94-24796
Aeroelastic response and stability of tiltrotors with elastically-coupled composite rotor blades
[NASA-TM-108758] 06 p2182 N94-24953
Design optimization of high-speed proprotor aircraft
[NASA-TM-103988] 07 p2667 N94-26151
Wing design for a civil tiltrotor transport aircraft: A preliminary study 07 p2671 N94-27917
Civil tiltrotor market penetration: Effects on Northeast corridor airport delay
[AD-A277534] 09 p3576 N94-32955
An experimental study of pilot/vehicle dynamics using a tilt rotor flying machine
[AD-A277516] 09 p3805 N94-33349
The convertible (helicopter/airplane) EUROFAR: General considerations on the technical progress and on future advances 11 p4195 N94-36331
Alleviation of whirl-flutter on a joined-wing tilt-rotor aircraft configuration using active controls
[NASA-CR-196103] 11 p4200 N94-36436
Analysis of vertiport studies funded by the Airport Improvement Program (AIP)
[SCT-93RR-21] 12 p4390 N94-37424

TILT ROTOR RESEARCH AIRCRAFT PROGRAM
XV-15: Tiltrotor
[NASA-TM-109455] 03 p0865 N94-15328

TILT WING AIRCRAFT
Piloting considerations for terminal area operations of civil tiltwing and tiltrotor aircraft
02 p0525 N94-13320
Design optimization of high-speed proprotor aircraft
[NASA-TM-103988] 07 p2667 N94-26151
Piloted simulation study of two tilt-wing flap control concepts, phase 2
[NASA-TM-108817] 10 p4006 N94-33998
1993 Technical Paper Contest for Women. Gear Up 2000: Women in Motion
[NASA-CP-10134] 11 p4377 N94-35961
Piloted simulation study of two tilt-wing control concepts 11 p4200 N94-35962

TILTING
U ATTITUDE (INCLINATION)

TILTING ROTORS
Navier-Stokes flowfield computation of wing/rotor interaction for a tilt rotor aircraft in hover
[NASA-CR-4532] 01 p0013 N94-10758
XV-15: Tiltrotor
[NASA-TM-109455] 03 p0865 N94-15328
Aeroelastic response and stability of tiltrotors with elastically-coupled composite rotor blades
[NASA-TM-108758] 06 p2182 N94-24953
Design optimization of high-speed proprotor aircraft
[NASA-TM-103988] 07 p2667 N94-26151

TILTMETERS
Long baseline watertubes 03 p1037 N94-15803
Cooperative projects in geodynamical instrumentation between the State Seismological Bureau (China) and the Royal Observatory of Belgium 03 p1037 N94-15806
Earth tides results obtained with gravimeters, clinometers, and strainmeters in Belgium and in Grand Duchy of Luxembourg 03 p1100 N94-15809
Instrumentation developed at the Royal Observatory of Belgium for measuring slow displacements of the Earth
04 p1483 N94-18628
Evaluation of the prototype dual-axis wall attitude measurement sensor
[NASA-TM-109056] 07 p2811 N94-26707
Observation with STS seismometer at Nakaizu, central Japan: Observation system and comparison with tiltmeter 07 p2886 N94-27986

TIMBER IDENTIFICATION
Properties of spectral reflectance of crown and crown structure of mangrove species in Okinawa
01 p0218 N94-12700
Mangrove afforestation monitoring using remote sensing 02 p0695 N94-14260
The extraction and representation of forest inventory information using continuous density surfaces
[ISBN-0-315-85658-0] 08 p3334 N94-30236

TIMBER INVENTORY
Dendrometric variables estimation in homogeneous forests using LANDSAT TM data
[INPE-5455-TDI/497] 02 p0684 N94-13331
The extraction and representation of forest inventory information using continuous density surfaces
[ISBN-0-315-85658-0] 08 p3334 N94-30236
The forest inventory project at the Tapajos National Forest, volume 1
[INPE-5423-PRP/171] 10 p4033 N94-33434

TIME
NT ACCESS TIME
NT BURNING TIME
NT DOWNTIME
NT EPHEMERIS TIME
NT FLIGHT TIME
NT MTBF
NT REACTION TIME
NT RELAXATION TIME
NT RESPONSE TIME (COMPUTERS)
NT SIDEREAL TIME
NT TESTING TIME
NT TRANSIT TIME
NT UNIVERSAL TIME
The 24th Annual Precise Time and Time Interval (PTTI) Applications and Planning Meeting
[NASA-CP-3218] 01 p0350 N94-10963
About time 04 p1426 N94-18024
Space and time from quantum mechanics
[DE93-015263] 04 p1609 N94-18629
Paired comparison models with time-varying parameters
[AD-A272016] 05 p1964 N94-21442
Tandem queues with deterministic service times
[CWI-BS-R9238] 05 p1946 N94-21577
A time reasoning system based on the event calculus for scheduling in aeronautic maintenance
[REPT-932-710-101] 08 p3122 N94-29463

TIME CONSTANT
NT PERCEPTUAL TIME CONSTANT
Rime-, mixed- and glaze-ice evaluations of three scaling laws
[NASA-TM-106461] 06 p2173 N94-24047
Automation of formation flight control
[AD-A274137] 07 p2678 N94-27132
Electron beam irradiation experiments of monoblock divertor mock-up
[DE94-707497] 08 p3503 N94-28555

TIME DELAY
U TIME LAG

TIME DEPENDENCE
Coherent states and uncertainty relations for the damped harmonic oscillator with time-dependent frequency
01 p0380 N94-10611
The angular structure of second harmonic emission from laser-produced plasmas irradiated at moderate intensity
[DE93-013102] 01 p0389 N94-11114
The effects of an aggressive environment on the subcritical crack growth of a continuous-fiber ceramic composite
[DE93-011690] 01 p0073 N94-11612
Parametric study of diffusion-enhancement networks for spatiotemporal grouping in real-time artificial vision
[AD-A265065] 01 p0331 N94-11652
Large eddy simulations of time-dependent and buoyancy-driven channel flows
01 p0155 N94-12287
Three dimensional time-dependent hydrodynamic and propagation modeling of x ray laser emission
[DE93-012575] 02 p0654 N94-12962
Development of time-dependent orthotropic constitutive law of a thermoplastic composite material
02 p0556 N94-13595
Deconvolution for positive signals
[DE93-013044] 02 p0773 N94-14314
Selective excitation, relaxation, and energy channeling in molecular systems
[DE93-018819] 02 p0785 N94-14420
An adaptive projection method for the incompressible Euler equations
[DE93-016428] 02 p0639 N94-14434
A conduction model for the vacuum arc remelting process
[NPL-DMM(A)-98] 02 p0639 N94-14464
Multiplicative noise: Applications in cosmology and field theory
[DE93-016624] 02 p0840 N94-14536
Time resolved measurement of electron temperatures of exploding foil x ray laser plasmas
[DE93-017161] 02 p0803 N94-14894
Timebias corrections to predictions
03 p0875 N94-15591
Formation of on-site normal points
03 p0917 N94-15592
Reliability characterization of digital microcircuits: Investigation of an in-process oxide reliability screening method
[AD-A267053] 03 p1008 N94-15665
On the design of structural components using materials with time-dependent properties
[NASA-TM-108428] 03 p1059 N94-16519
The use of General Circulation Models in detecting climate change induced by greenhouse gases
[DE93-014369] 03 p1096 N94-16802
Finite difference time domain analysis of chirped dielectric gratings 03 p1195 N94-17339
Time dependent turbulence modeling and analytical theories of turbulence
[NASA-TM-106379] 03 p1029 N94-17385
On the stability of a time dependent boundary layer
[NASA-CR-191542] 03 p1030 N94-17450
A physical model for one-dimension and time-dependent ionosphere. Part 2: Results and discussions
[DE93-627959] 03 p1103 N94-17631
Exact solution of the generalized time-dependent Jaynes-Cummings Hamiltonian
[DE93-624773] 04 p1546 N94-17811
Three-dimensional simulation analysis of the first sections of a standing-wave free-electron laser two-beam accelerator
[DE93-016977] 04 p1436 N94-17869
Variable time-step integration for intense field effects
[DE93-013296] 04 p1382 N94-17909
Practical reporting times for environmental samples
[DE93-013461] 04 p1472 N94-17910
The effects of initial conditions and control time on optimal actuator placement by way of a max-min genetic algorithm
[DE93-017640] 04 p1525 N94-19124
Asymptotic derivation of the modified time-dependent SP2 equations and numerical calculations
[DE93-016466] 04 p1551 N94-19342
Time dependent identification of nonlinear structures
[ECL-92-64] 04 p1457 N94-19403
Neural network for processing both spatial and temporal data with time based back-propagation
[NASA-CASE-MSC-21874-1] 05 p1942 N94-20366
Classical and generalized solutions of time-dependent linear differential algebraic equations
[AD-A272834] 05 p1954 N94-21173
Finite difference methods for time-dependent, linear differential algebraic equations
[AD-A272835] 05 p1954 N94-21174
Characteristic based methods for the time-domain Maxwell equations
[AD-A272973] 05 p1802 N94-21263
Time-accurate Navier-Stokes calculations with multigrid acceleration 05 p1956 N94-21469
Surface path lines in plane Stokes flow driven by capillarity
[DE93-041277] 05 p1803 N94-21651
Monte Carlo calculation of multi-electron effects on synchrotron radiation
[DE94-001259] 05 p1982 N94-21974
Time-dependent reliability analysis of ceramic engine components 05 p1828 N94-22619
Feedback linearization of parametrized nonlinear time-varying systems
[MEMO-1126] 06 p2470 N94-22714
The theoretical accuracy of Runge-Kutta time discretizations for the initial boundary value problem: A careful study of the boundary error
[NASA-CR-191561] 06 p2480 N94-23272
Time dependent behavior of a graphite/thermoplastic composite and the effects of stress and physical aging
[NASA-TM-109047] 06 p2228 N94-23280
Response-coefficient method for heat-conduction transients with time-dependent inputs
06 p2326 N94-23671
Computation of large-scale statistics in decaying isotropic turbulence 06 p2332 N94-24167
A statistical analysis of recent Naval Experimental Diving Unit (NEDU) single-depth human exposures to 100 percent oxygen at pressure
[AD-A273488] 06 p2427 N94-24950
Preliminary results on time-varying feedback stabilization of a nonholonomic car-like mobile robot
[INRIA-RR-1512] 06 p2475 N94-24963
The effect of the time restrictions on information search and information integration in a dynamic task environment
[AD-A273759] 07 p3095 N94-25723
Theoretical determination of chemical rate constants using novel time-dependent methods
[NASA-CR-195221] 07 p2714 N94-26205
Electrical analysis of wideband and distributed windows using time-dependent field codes
[DE94-002987] 07 p2768 N94-26310
Analytical solution of Mori's equation with secant hyperbolic memory
[DE94-601541] 07 p3006 N94-26368
Local uniform grid refinement and systems of coupled partial differential equations
[CWI-NM-R9307] 07 p2995 N94-26773

Mechanism of mechanical fatigue of silica glass
[DE94-003165] 07 p2753 N94-26783
Experiments and numerical simulations of electromagnetic wave propagation in plasma varying rapidly in space and time
[AD-A274376] 07 p2772 N94-26975
The effect of naloxone on sleeping time in adjuvant arthritic rats 07 p2906 N94-27498
Forward and backward simulations. Part 2: Timing-based systems
[CWI-CS-R9314-PT-2] 07 p2972 N94-27581
Feasibility study on introduction of a large methanol engine power generation plant
[DE94-732338] 08 p3224 N94-28629
The h-p adaptive methods for incompressible viscous flow problems 08 p3275 N94-29836
Numerical solution of the two-dimensional time-dependent incompressible Euler equations
[NASA-CR-195775] 08 p3277 N94-29859
Large-scale 3-D solutions of the time-dependent Dirac equation
[DE94-005591] 08 p3454 N94-30317
Time-dependent behavior of active galactic nuclei with pair production 09 p3929 N94-31125
The physics of black hole x ray novae 09 p3932 N94-31143
A theory of distributed time
[AD-A276631] 09 p3815 N94-31994
Prediction of the plane wave beamformed acoustic arrival structure for the 1992 Barents Sea coastal tomography test
[AD-A276741] 09 p3788 N94-32181
Arithmetic averaging: A versatile technique for smoothing and trend removal
[DE94-005274] 09 p3852 N94-32673
Deuterium absorption and material phase characteristics of SAES St198 Zr-Fe alloy
[DE94-008275] 09 p3646 N94-32781
Space flight printed wiring board measling investigation
[NASA-TM-104602] 09 p3732 N94-33101
The design and realization of a real-time multitasking control system by using AMX multitasking executive 10 p4118 N94-34343
A search for pre- and post-burst emission from well-localized gamma-ray burst locations
[NASA-CR-195825] 10 p4167 N94-34990
Magnetoresistance of films and strips with the diffuse surface scattering
[DE94-611100] 11 p4340 N94-35933
Classical time machine
[DE94-616616] 11 p4342 N94-36070
On quantization of time-dependent systems with constraints
[DE94-611114] 11 p4343 N94-36351

TIME DISCRIMINATION

Mechanisms of temporal pattern discrimination by human observers
[AD-A277407] 09 p3801 N94-32577

TIME DIVISION MULTIPLE ACCESS

Destination-directed, packet-switched architecture for a geostationary communications satellite network
[NASA-TP-3379] 02 p0538 N94-13111
User needs for propagation data 02 p0613 N94-14657
A laboratory system for the investigation of rain fade compensation techniques for Ka-band satellites
[NASA-CR-191200] 05 p1762 N94-21566
TDMA satellite communication systems for ISDN services 05 p1746 N94-22171
Adaptive data rate control TDMA systems as a rain attenuation compensation technique 06 p2287 N94-22821
Modulation and synchronization technique for MF-TDMA system
[NASA-CR-194448] 06 p2304 N94-25266
Analysis of a multiaccess/switching technique for multibeam satellites in a prioritized ISDN environment
[ISBN-0-315-84632-1] 07 p2776 N94-27345
Modeling, analysis, and simulation of an optical time-division multiple-access network architecture
[AD-A275847] 08 p3498 N94-28780
M-interference queue analysis by decomposition method
[ISBN-0-315-85795-1] 08 p3453 N94-30139
Reliable communication in the presence of severe noise or jamming
[AD-A278410] 09 p3684 N94-33173

TIME DIVISION MULTIPLEXING

Technical support for digital systems technology development. Task order 1: ISP contention analysis and control
[NASA-CR-190758] 02 p0537 N94-12809
Destination-directed, packet-switched architecture for a geostationary communications satellite network
[NASA-TP-3379] 02 p0538 N94-13111
VHF air/ground communications for air traffic control. Volume 1: A decision tree approach to system innovations
[AD-A268485] 04 p1316 N94-18384
Improved frame synchronization schemes for INMARSAT-B/M SCPC and TDM channels 06 p2285 N94-22806
Design of a shared coherent cache for a multiple channel architecture
[AD-A274026] 07 p3034 N94-25758
Improved performance of hybrid error control techniques for real-time digital communications over noisy channels
[ISBN-0-315-84281-4] 07 p2770 N94-26625
Design and test of a regenerative satellite transmultiplexer
[ISBN-0-315-85280-1] 07 p2786 N94-27303

TIME FUNCTIONS

A formulation of quantum statistical mechanics based on the Feynman path centroid density 2 dynamical properties
[AD-A272698] 05 p2037 N94-21166
The Stroemberg wavelet on the interval and the Franklin system
[TELECOM-93-C-002] 08 p3462 N94-30971

TIME LAG

Plans to improve the experimental limit in the comparison of the east-west and west-east one-way light propagation times on the rotating earth 01 p0351 N94-10971
Performances of a date dissemination code on telephone lines using commercial modems 01 p0139 N94-10984
Time signal distribution in communication networks based on synchronous digital hierarchy 01 p0139 N94-10989
Comments on possible causes of recent global warming
[DE93-010501] 01 p0272 N94-12592
Investigation of the effects of bandwidth and time delay on helicopter roll-axis handling qualities 02 p0522 N94-13300
Handling qualities effects of display latency 02 p0517 N94-13316
Primary display latency criteria based on flying qualities and performance data 02 p0525 N94-13318
Bounds on time delay estimation given unknown signal spectral parameters
[ITN-93-85194] 02 p0601 N94-13566
Assessment of TDI operation of a frame transfer CCD for high resolution imaging from a fast spinning spacecraft 03 p0910 N94-15097
System architecture of optically controlled phased array radar
[AD-A267056] 03 p0988 N94-15667
Passive tracking of a target using an array of sensors
[DE93-015870] 03 p0997 N94-16169
Pulse response based control for minimum time maneuver of flexible spacecraft
[AD-A266186] 03 p0886 N94-16455
Measuring ocean coherence time with dual-baseline interferometry 03 p1080 N94-16759
True time delay optically controlled dual band transmitter
[AD-A267663] 03 p1003 N94-17228
Shop problems with two machines and time lags
[REPT-93-020] 04 p1518 N94-17927
A method for eliminating skew introduced by non-uniform buffer delay and wire lengths in clock distribution trees
[AD-A270649] 04 p1544 N94-19530
Stabilization of time-delay systems: An overview of the algebraic approach
[PB93-191989] 04 p1553 N94-19556
Tracking with time-delayed data in multisensor systems
[AD-A271334] 04 p1391 N94-19582
Measurement of multipath delay profile in land mobile satellite channels 06 p2283 N94-22793
Linear time algorithm to schedule trees with communication delays optimally on two machines
[PB93-237782] 06 p2451 N94-23441
Genericity of stabilizability for time-delay systems
[PB93-237725] 06 p2475 N94-24762
Develop advanced nonlinear signal analysis topographical mapping system
[NASA-CR-194785] 06 p2389 N94-24856
Predicting nonlinear time series
[AD-A274051] 07 p2990 N94-25834
Hook spectroscopy as an atomic number density diagnostic applied to laser-ablated copper plasmas
[DE94-002645] 07 p3042 N94-26081
Fiber optic true time-delay array antenna feed system
[AD-D016063] 07 p2777 N94-27734
Development of a method to predict transonic limit cycle oscillation characteristics of fighter aircraft (continued)
[NLR-TP-92156-U] 08 p3148 N94-30342
End-to-end delay reduction in narrow bandwidth real-time multimedia tele-education applications
[AD-B179614] 08 p3260 N94-30518
Tropospheric corrections to GPS measurements using locally measured meteorological parameters compared with general tropospheric corrections 08 p3144 N94-30655
A comparison of several GPS data reduction methods 08 p3145 N94-30662
Ionospheric corrections to precise time transfer using GPS 08 p3145 N94-30677
A theory of distributed time
[AD-A276631] 09 p3815 N94-31994
Fiber optic continuous true time-delay modulator
[AD-D016098] 09 p3883 N94-32720
Time delay measurement correlator and its application 10 p4042 N94-34350
Time-delay control of a magnetic levitated linear positioning system 11 p4217 N94-35862

TIME MARCHING

Multigrid time-accurate integration of Navier-Stokes equations
[NASA-TM-106373] 03 p1028 N94-17258
An algebraic turbulence model for turbomachinery 04 p1411 N94-18554
Time-domain analysis of planar microstrip devices using a generalized Yee-algorithm based on unstructured grids 05 p1724 N94-20431
Approximate methods for N-component solute transport and ion-exchange
[CWI-NM-R9223] 05 p1910 N94-21078
Time-marching aeroelastic and spatial adaptation procedures on triangular and tetrahedral meshes using an unstructured-grid Euler method 08 p3131 N94-29877
Three dimensional compressible turbulent flow computations for a diffusing S-duct with/without vortex generators 08 p3281 N94-30519
Preconditioned time-difference methods for advection-diffusion-reaction equations
[DE94-006472] 09 p3638 N94-32840

TIME MEASUREMENT

The 24th Annual Precise Time and Time Interval (PTTI) Applications and Planning Meeting
[NASA-CP-3218] 01 p0350 N94-10963
The time keeping system for GPS block IIR 01 p0024 N94-10964
Progress on GPS standardization 01 p0024 N94-10965
Comparison of GPS and GLONASS common-view time transfers 01 p0024 N94-10967
Pulsar astrometry by using VLBI (PSR0329 between Kashima 26mPhi and Usuda 64mPhi) 01 p0351 N94-10968
An ensemble pulsar time 01 p0351 N94-10969
Experimental comparison of time synchronization techniques by means of light signals and clock transport on the rotating earth 01 p0351 N94-10970
LASSO observations at McDonald and OCA/CERGA: A preliminary analysis 01 p0352 N94-10972
MIL-STDS and PTTI: What's available and what needs to be done 01 p0352 N94-10973
Possible applications of atomic frequency standards with an internal high resolution digital synthesizer 01 p0353 N94-10979
Development of a cryogenic hydrogen maser at the NPL 01 p0176 N94-10982
Performances of a date dissemination code on telephone lines using commercial modems 01 p0139 N94-10984
TimeSet: A computer program that accesses five atomic time services on two continents 01 p0334 N94-10985
RighTime: A real time clock correcting program for MS-DOS-based computer systems 01 p0334 N94-10986
Measurement methods and algorithms for comparison of local and remote clocks 01 p0354 N94-10987
Advances in time-scale algorithms 01 p0334 N94-10988
Time signal distribution in communication networks based on synchronous digital hierarchy 01 p0139 N94-10989
Synopsis of timing measurement techniques used in telecommunications 01 p0139 N94-10990
Analysis of the eastern range multiplexed fiber optic IRIG B120 distribution system 01 p0139 N94-10996
A new method of time difference measurement: The time difference method by dual phase coincidence points detection 01 p0357 N94-11002
Confidence of the three-point estimator of frequency drift 01 p0357 N94-11003
Rhenium-osmium isotope systematics of Group 2A and Group 4A iron meteorites 01 p0431 N94-12182
An optoelectronic graphics display processor
[AD-A266011] 01 p0171 N94-12391

Activities report of the National Electrotechnical Institute Galileo Ferraris
[ETN-93-94224] 02 p0627 N94-14812
Time resolved measurement of electron temperatures of exploding foil x ray laser plasmas
[DE93-017161] 02 p0803 N94-14894
Adaptive median filtering for preprocessing of time series measurements 03 p0912 N94-15561
Measuring ocean coherence time with dual-baseline interferometry 03 p1080 N94-16759
Digital reverberation time measurement system
[AD-D015892] 03 p1177 N94-16919
Target detection by way of Kalman filtering
[AD-A267314] 03 p1000 N94-16945
Quartz crystal resonators and oscillators for frequency control and timing applications: A tutorial, revision 6.1
[AD-A268205] 03 p1216 N94-17480
Proceedings of the 4th European Congress on Chronometry
[ETN-93-94633] 04 p1424 N94-18006
The clocks and the perception of time in the 18th century society 04 p1424 N94-18007
About time 04 p1426 N94-18024
Marine chronometry in the Neuchatel mountains (Switzerland) 04 p1427 N94-18025
Restoration of an 18th century English clock 04 p1427 N94-18026
Techniques for low consumption circuits 04 p1428 N94-18032
Evaluation of the consumption of electronic clocks 04 p1408 N94-18033
Development of atomic standards at the Neuchatel Observatory 04 p1428 N94-18038
Multifunction chronograph movement using a modular structure multimotor 04 p1429 N94-18044
Using the USCCS for sub microsecond spacecraft clock calibration 05 p1813 N94-21346
Verification of the PROS timing analysis package 05 p1926 N94-22508
An x ray archive on your desk: The Einstein CD-ROM's 05 p2048 N94-22519
Solid state Time Base Corrector (TBC)
[AD-D015981] 06 p2312 N94-25039
Tool for performance analysis and off-line prediction of timing behaviour 07 p2952 N94-26732
A real-time executive implementing priority inheritance protocols 07 p2952 N94-26733
Fault-tolerant scheduling in distributed critical real-time systems 07 p2952 N94-26735
Geological Dating by Ar-40 - Ar-39 method
[DE94-601975] 07 p2880 N94-26874
Coherence and satisfiability of waveform timing specifications
[ISBN-0-315-57769-X] 07 p3009 N94-27268
Cosmogenic C-14 in Antarctic and non-Antarctic meteorites and lunar samples
[NASA-CR-195795] 08 p3546 N94-29905
The MSRC ab initio methods benchmark suite: A measurement of hardware and software performance in the area of electronic structure methods
[DE94-006428] 08 p3514 N94-30001
The 25th Annual Precise Time and Time Interval (PTTI) Applications and Planning Meeting
[AD-A280955] 08 p3468 N94-30639
Status of frequency and time support for NASA systems 08 p3468 N94-30640
Time and frequency technology at NIST 08 p3468 N94-30641
European PTTI report 08 p3468 N94-30642
Loran-C time management 08 p3144 N94-30644
Report on NATO PTTI 08 p3469 N94-30645
GPS common-view time transfer 08 p3144 N94-30648
Cascaded clocks measurement and simulation findings 08 p3469 N94-30649
Time and position accuracy using codeless GPS 08 p3144 N94-30650
Relativistic theory for picosecond time transfer in the vicinity of Earth 08 p3470 N94-30653
Tropospheric corrections to GPS measurements using locally measured meteorological parameters compared with general tropospheric corrections 08 p3144 N94-30655
The two-way time synchronization system via a satellite voice channel 08 p3471 N94-30658
Remote clocks linked by a fully calibrated two-way timing link 08 p3471 N94-30659
Some applications of GPS timing information 08 p3145 N94-30661
A comparison of several GPS data reduction methods 08 p3145 N94-30662
Cesium and rubidium frequency standards status and performance on the GPS program 08 p3145 N94-30663
Comparison of LASSO and GPS time transfers 08 p3145 N94-30665
Noise and drift analysis of non-equally spaced timing data 08 p3472 N94-30667
An algorithm for the Italian atomic time scale 08 p3473 N94-30668
A comparative study of clock rate and drift estimation 08 p3473 N94-30669
Time maintenance system for the BMDO MSX spacecraft 08 p3171 N94-30672
Hydrogen maser clocks in space for solid-Earth research and time-transfer applications: Experiment overview and evaluation of Russian miniature sapphire loaded cavity 08 p3474 N94-30676
Russian national time scale long-term stability 08 p3475 N94-30679
Using GLONASS signal for clock synchronization 08 p3475 N94-30680
A look into the crystal ball: The next 25 years 08 p3475 N94-30681
The future of time and frequency dissemination 08 p3476 N94-30684
VME rollback hardware for time warp multiprocessor systems
[NASA-CR-191796] 09 p3826 N94-32483
Time resolved measurements of light produced by onset of plasma formation on electrodes of fast pulsed high voltage diodes
[AD-A277974] 09 p3894 N94-33264
Time delay measurement correlator and its application 10 p4042 N94-34350
Electronics for the SND scintillation counter system
[DE94-616453] 11 p4259 N94-36104
X ray radiographic imaging of hydrodynamic phenomena in radiation driven materials: Shock propagation and shear flow
[DE94-010891] 11 p4318 N94-36201
SACS: A cache simulator incorporating timing analysis with buffer and memory management
[AD-A280472] 12 p4494 N94-37230
Chemical recognition software
[DE94-012918] 12 p4495 N94-37496
Techniques for real-time parallel processing: Sensor processing case studies
[AD-A280633] 12 p4499 N94-37760

TIME MEASURING INSTRUMENTS
NT ATOMIC CLOCKS
NT AUTONOMOUS SPACECRAFT CLOCKS
NT CHRONOMETERS
NT CLOCKS
NT TIMING DEVICES
A new method of time difference measurement: The time difference method by dual phase coincidence points detection 01 p0357 N94-11002

TIME OF FLIGHT SPECTROMETERS
Measurement of polycyclic aromatic hydrocarbon (PAHs) in interplanetary dust particles 01 p0431 N94-12167
Construction and test of a facility for photon-stimulated field description using excimer laser and time of flight
[ETN-93-94386] 02 p0657 N94-13996
Laser photoionization time-of-flight mass spectrometry of nitrated polycyclic aromatic hydrocarbons and nitrated heterocyclic compounds
[AD-A268126] 03 p0952 N94-17520
Detonation reaction steps frozen by free expansion and analyzed by mass spectrometry
[DE93-012734] 04 p1376 N94-17813
Matrix- and substrate-assisted laser desorption for fast DNA sequencing
[DE93-015332] 04 p1501 N94-18242
The study of the phase structure of hadronic matter by searching for the deconfined quark-gluon phase transition using 2 TeV (bar-p)-p collisions, and by searching for critical phenomena in an exclusive study of multifragmentation using 1 GeV/nucleon heavy ion collisions
[DE93-018925] 04 p1570 N94-19103
Time-of-flight heavy ion backscattering spectrometry
[DE93-019067] 05 p1973 N94-20306
Multielement analysis of interplanetary dust particles using TOF-SIMS 05 p2084 N94-20790
Dual-purpose RTOF diffractometer facility at the ET-RR-1 reactor
[VTT-TIED-1425] 06 p2566 N94-25347
A double arm time-of-flight spectrometer based on position-sensitive parallel-grid avalanche counters
[DE93-616665] 07 p3012 N94-25750
Experimental setup for study of hadron and hard photon production in nucleus-nucleus collisions
[DE94-607849] 08 p3489 N94-30051
Production and detection of metastable atomic oxygen
[ISBN-0-315-87364-7] 09 p3868 N94-31915
Time-of-flight diffraction at pulsed neutron sources: An introduction to the symposium
[DE94-010442] 11 p4327 N94-36225

TIME OPTIMAL CONTROL
The effects of initial conditions and control time on optimal actuator placement by way of a max-min genetic algorithm
[DE93-017640] 04 p1525 N94-19124
Throughput time control and due date reliability in tool and die shops
[ISBN-9-03-860182-4] 06 p2587 N94-25283
Pulse response based minimum time control of flexible structures 08 p3436 N94-29720
Nearly time-optimal feedback control of a magnetically levitated photolithography positioning system
[DE94-005288] 08 p3266 N94-30055
Neural network based time-optimal control of a magnetically levitated precision positioning system
[DE94-006573] 08 p3437 N94-30250
Infinite dimensional generalized time optimal control problem 10 p4115 N94-34321

TIME RESPONSE
Target detection by way of Kalman filtering
[AD-A267314] 03 p1000 N94-16945
The two-way time synchronization system via a satellite voice channel 08 p3471 N94-30658
The Second International Workshop on Discrete Time Domain Modelling of Electromagnetic Fields and Networks. Program and information
[AD-A277136] 09 p3677 N94-32067

TIME SERIES ANALYSIS
Estimation of critical values and vibration characteristics on supersonic delta wings. Part 1: On-line time series analysis of stationary random response
[NAL-TR-1153] 01 p0002 N94-10363
Detecting non-linearities in stationary time series
[W-9223] 01 p0344 N94-10906
Chaotic time series analysis 01 p0031 N94-11490
Advective surface velocity in the north west Pacific derived from NOAA AVHRR images 01 p0222 N94-12721
Study of the admixture diffusion in the sea using remote techniques 01 p0228 N94-12759
Adaptive Transfer Function Networks
[DE93-014344] 02 p0745 N94-13151
Estimation of critical values and vibration characteristics on supersonic delta wings. Part 2: Locally-stationary time series analysis of nonstationary random responses
[NAL-TR-1179] 02 p0502 N94-13345
Time series photometry of faint cataclysmic variables with a CCD 02 p0831 N94-13646
Maximum entropy spectral analysis of the geological time series of the oxygen isotope record from deep-sea cores
[INPE-5465-PRE/1773] 02 p0725 N94-13728
Arctic internal waves (CEAREX)
[AD-A265822] 03 p1111 N94-15139
Adaptive median filtering for preprocessing of time series measurements 03 p0912 N94-15561
Generation of artificial helioseismic time-series
[NASA-CR-194612] 03 p1299 N94-15968
Linear parameter identification methods for ARMA models with periodic coefficients
[REPT-92-070] 04 p1556 N94-17938
Fast-training algorithm for hidden-layer forward-feed neural networks
[AD-A269253] 04 p1540 N94-18263
Spectral analysis on the canonical autoregressive decomposition
[AD-A270083] 04 p1549 N94-18798
A survey of current approaches to modelling of hydrological time-series with respect to climate variability and change
[WMO/TD-534] 04 p1463 N94-19435
Methods for description and control of dynamical systems and their application
[MPIS-17/1992] 04 p1553 N94-19522
Generalized multichannel signal detection
[AD-A271385] 04 p1391 N94-19587
State-space models for multichannel detection
[AD-A270608] 05 p1715 N94-19816
SIMBAT theoretical manual
[AD-A271063] 05 p1882 N94-19979
Partial empirical autocorrelation of a vectorial chronological series
[RR-896-M] 05 p1963 N94-20162
Studies of Greenland using the SEASAT scatterometer 05 p1725 N94-20433
Signal processing in the linear statistical model
[AD-A272114] 05 p1736 N94-20570
Functional statistical data analysis and modeling
[AD-A271520] 05 p1963 N94-20913
Direct simulation of shock-induced mixing layer
[DE93-040498] 05 p1803 N94-21531
Registering and resampling images in STSDAS 05 p1927 N94-22550
A review of the Workshop on Fatigue Life Methodologies for Wind Turbines
[DE94-002039] 06 p2394 N94-23472

First order conditions for the maximum likelihood estimation of an exact ARMA model
[PB94-110533] 06 p2495 N94-23814
Dimensional analysis of acoustically propagated signals 06 p2528 N94-24217
Predicting nonlinear time series
[AD-A274051] 07 p2990 N94-25834
Developing prediction regions for a time series model for hurricane forecasting
[AD-A273777] 07 p2892 N94-25861
MIMO recursive least squares control algorithm for the AN/FPN-44A Loran-C transmitter
[AD-A274820] 07 p2664 N94-26493
Feasibility study on introduction of transportation-use petroleum substitution energy
[DE94-725205] 07 p2759 N94-26905
Limit theorems for functionals of Markov processes and renormalizable stable fields
[AD-A274645] 07 p3004 N94-27106
Research activities of Martin C. Casdagli at SFI September 1989--May 1991
[DE94-005655] 08 p3463 N94-28548
A fractal analysis of near-field atmospheric concentration data
[AD-A275460] 08 p3355 N94-28728
The modified Cramer-von mises goodness-of-fit criterion for time series
[AD-A275377] 08 p3464 N94-29014
Time series comparisons of satellite and rocketsonde temperatures in 1978-1979
[NASA-TP-3409] 08 p3370 N94-29455
Surface differential rotation in a sample of cool dwarf stars 08 p3545 N94-29827
Statistical analysis of a satellite imagery time series: Implications for the study of coastal and estuarine circulation 08 p3335 N94-30919
A radial basis function approach to financial time series analysis
[AD-A276408] 09 p3924 N94-31361
Exploring phase space concepts in the forecasting of time series with artificial neural networks
[DE94-005810] 09 p3834 N94-32127
Arithmetic averaging: A versatile technique for smoothing and trend removal
[DE94-005274] 09 p3852 N94-32673
Homogeneous global mean temperature time series
[DE94-002194] 09 p3766 N94-32690
SEASOAR and CTD observations during a COARE surveys cruise, W9211C, 22 January - 22 February, 1993
[AD-A277925] 09 p3791 N94-33244
Growth and nonlinearity
[DE94-007366] 10 p4021 N94-33689
Iterative regression analysis of periodicities in Be-10 and C-14 atmospheric cosmonuclides variations
[INPE-5547-TDI/533] 10 p4087 N94-34228
Analysis of DE-1 PWI electric field data
[NASA-CR-195950] 10 p4036 N94-34280
A combined approach to buffet response analyses and fatigue life prediction 10 p4072 N94-34587
Workshop on the Martian Northern Plains: Sedimentological, periglacial, and paleoclimatic evolution
[NASA-CR-196134] 11 p4354 N94-35359
A new presentation of complex voltage data for Goldstone radar astronomy 11 p4255 N94-35561
Cramer-von Mises variance estimators for simulations
[AD-A278799] 11 p4316 N94-35675
A comparison of artificial neural networks and statistical analyses
[DE94-010846] 11 p4312 N94-36195
Embedded chaotic time series: Applications in prediction and spatio-temporal classification
[AD-A280690] 12 p4508 N94-37130
Index and bulk parameters for frequency-direction spectra measured at CERC Field Research Facility, September 1990 to August 1991
[AD-A280423] 12 p4476 N94-37216
Index and bulk parameters for frequency-direction spectra measured at CERC Field Research Facility, September 1991 to August 1992
[AD-A280455] 12 p4477 N94-37229

TIME SHARING

Processor capacity reserves for multimedia operating systems
[AD-A266639] 03 p1158 N94-15745
Scheduling tasks with unpredictable timing parameters in hard real-time systems 07 p2951 N94-26728
Ada multiple-programming for hard real time applications in space systems 07 p2951 N94-26730

TIME SIGNALS

A precise GPS-based time and frequency system 01 p0353 N94-10978
TimeSet: A computer program that accesses five atomic time services on two continents 01 p0334 N94-10985
Time signal distribution in communication networks based on synchronous digital hierarchy 01 p0139 N94-10989
Synopsis of timing measurement techniques used in telecommunications 01 p0139 N94-10990
Performance of low-cost commercial fiber-optic transceivers for reference frequency distribution 01 p0355 N94-10993
Analysis of the eastern range multiplexed fiber optic IRIG B120 distribution system 01 p0139 N94-10996
Estimating the instabilities of N clocks by means of comparison measurements 01 p0356 N94-10997
Neighboring extremal guidance for systems with piecewise linear control using time as the reference variable
[AD-A267942] 03 p0874 N94-17010
Femtosecond carrier processes in compound semiconductors and real time signal processing
[AD-A268122] 03 p1005 N94-17519
Recording system using multiplexed inputs to a multichannel recorder
[AD-D015971] 05 p1808 N94-21278
Using the USCCS for sub microsecond spacecraft clock calibration 05 p1813 N94-21346
Progress on the design of a data push architecture for an array of optimized time tagging pixels
[DE93-041011] 06 p2307 N94-22955
The 25th Annual Precise Time and Time Interval (PTTI) Applications and Planning Meeting
[AD-A280955] 08 p3468 N94-30639
Two-way satellite time transfer: Overview and recent developments 08 p3469 N94-30646
Optical techniques for time and frequency transfer 08 p3469 N94-30647
Time transfer using geostationary satellites: Implementation of a Kalman filter 08 p3471 N94-30657
Comparison of LASSO and GPS time transfers 08 p3145 N94-30665
Time maintenance system for the BMDO MSX spacecraft 08 p3171 N94-30672
Time synchronized video systems 08 p3261 N94-30675
Ionospheric corrections to precise time transfer using GPS 08 p3145 N94-30677
The NIST Internet time service 08 p3475 N94-30678
Using GLONASS signal for clock synchronization 08 p3475 N94-30680
Machinery monitoring and diagnostics using pseudo Wigner-Ville distribution and backpropagation neural network
[AD-A276219] 09 p3828 N94-31064
IRIG J asynchronous ASCII time code formats
[AD-A277244] 09 p3681 N94-32332

TIME TEMPERATURE PARAMETER

Time-temperature shift factors for gun propellants
[AD-A264979] 01 p0097 N94-10489
Advanced diagnostics for in situ measurement of particle formation and deposition in thermally stressed jet fuels
[DE93-009798] 01 p0098 N94-11366
FEM/SINDA: Combining the strengths of NASTRAN, SINDA, I-DEAS, and PATRAN for thermal and structural analysis 04 p1449 N94-17831
Mechanical response comparison of gun propellants evaluated under equivalent time-temperature conditions
[AD-A270479] 04 p1378 N94-19674
Performance of CVD and CVR coated carbon-carbon in high temperature hydrogen
[DE94-005451] 08 p3487 N94-29841
XCHEM-1D: A heat transfer/chemical kinetics computer program for multilayered reactive materials
[DE94-005072] 08 p3226 N94-30615
Deuterium absorption and material phase characteristics of SAES St198 Zr-Fe alloy
[DE94-008275] 09 p3646 N94-32781

TIMERS

U TIMING DEVICES

TIMING

U TIME MEASUREMENT

TIMING DEVICES

Experimental comparison of time synchronization techniques by means of light signals and clock transport on the rotating earth 01 p0351 N94-10970
Disciplined rubidium oscillator with GPS selective availability 01 p0353 N94-10977
Development of the OMPAT neuropsychological/psychomotor performance evaluation and OMPAT data and timing support programs
[AD-A266954] 03 p1122 N94-15759
Proceedings of the 4th European Congress on Chronometry
[ETN-93-94633] 04 p1424 N94-18006
The clocks and the perception of time in the 18th century society 04 p1424 N94-18007
The perspectives in application of hot casting technology for ceramic parts of timekeeping devices 04 p1375 N94-18013
The optimal numerical algorithm for processing of phase coded time signals for radio-clocks 04 p1426 N94-18018
Marine chronometry in the Neuchatel mountains (Switzerland) 04 p1427 N94-18025
Restoration of an 18th century English clock 04 p1427 N94-18026
The mystery of the perpetual motion clock of Geiser and Son 04 p1427 N94-18027
Gear train behavior analyzer using laser beam scanning for watch movement 04 p1427 N94-18028
Universal measurement device for electronic watches and small clocks 04 p1427 N94-18029
Reliability control for wrist watches and their casements 04 p1427 N94-18030
Mutrometre: Construction for fast water proof measurements under low pressure and air suppression 04 p1427 N94-18031
Multifunction chronograph movement using a modular structure multimotor 04 p1429 N94-18044
Military applications of high-accuracy frequency standards and clocks
[AD-A269303] 04 p1430 N94-18299
The One-Day Workshop on Batteries, Stepping Motors, and Electronic Clock Displays
[ETN-93-94632] 05 p1752 N94-20628
Verification of the PROS timing analysis package 05 p1926 N94-22508
Modulation and synchronization technique for MF-TDMA system
[NASA-CR-194448] 06 p2304 N94-25266
Status of frequency and time support for NASA systems 08 p3468 N94-30640
Time and frequency technology at NIST 08 p3468 N94-30641
European PTTI report 08 p3468 N94-30642
Report on NATO PTTI 08 p3469 N94-30645
LASSO experiment: Intercalibrations of the LASSO ranging stations 08 p3297 N94-30666

TIMOSHENKO BEAMS

Control of large space structures with varying configuration
[AD-A265764] 01 p0044 N94-12387
Vibrations of variable cross section Timoshenko beams 06 p2160 N94-24279

TIN

Reference electrodes for solid polymer electrolytes
[DE94-004583] 07 p2780 N94-25806
Crystal chemistry and self-lubricating properties of monochalcogenides gallium selenide and tin selenide
[DE93-041177] 07 p2751 N94-26422
Intermetallic growth at the interface between copper and bismuth-tin solder
[AD-A275716] 08 p3202 N94-28643
Pit initiation on passivated metal surfaces: Crystallographic orientation and environmental effects
[ISBN-0-315-85433-2] 08 p3208 N94-30138
Calculating the J(c), B, T surface for commercial niobium tin conductors using a reduced state model
[DE94-006296] 08 p3520 N94-30850
Lowering the Schottky barrier at metal or silicide/Si interfaces to extend the range of infrared detectors
[AD-A277253] 09 p3903 N94-32322
Interface engineering in oxide fiber/oxide matrix composites
[AD-A277672] 09 p3627 N94-33029
Modelling and optimal control of Pb-Sn continuous crystallization process 10 p4118 N94-34345

TIN ALLOYS

Solidification of undercooled Ni-32.5 wt percent Sn eutectic alloy 01 p0086 N94-10194
Thermosolutal convection and macrosegregation in dendritic alloys
[NASA-CR-194039] 02 p0567 N94-12825
Magnetic instability of Kondo insulators
[DE93-040064] 05 p1768 N94-21762
Temperature dependence of magnetic order in single-crystalline UPdSn
[DE93-040153] 05 p2033 N94-21991
Structure of the modulated magnetic phase of Mn3Sn
[DE94-002788] 07 p2733 N94-26092
Grain by grain study of the mechanisms of crack propagation during iodine SCC of Zry-4
[DE93-633765] 07 p2734 N94-26162
Zr-Sn-Nb alloys: Preliminary studies
[DE93-633767] 07 p2734 N94-26263
Research into the microstructure and mechanical behavior of eutectic Bi-Sn and In-Sn
[DE94-004558] 07 p2741 N94-27619
Study of the hyperfine magnetic field at Ta-181 site in the Heusler Co2ScSn, Co2ScGa, and Co2HfSn alloys
[DE94-603989] 07 p3067 N94-27623

The effect of Ti conduit on the critical current in (Nb, Ti)3Sn cable-in-conduit conductors
[DE94-701204] 07 p2788 N94-27817
Surface tension of tin and its alloys with particular reference to solders
[PB94-138302] 08 p3204 N94-29119
Logistics for the implementation of lead-free solders on electronic assemblies
[DE94-004800] 08 p3206 N94-29936
Microstructural development and mechanical behavior of eutectic bismuth-tin and eutectic indium-tin in response to high temperature deformation
[DE94-005202] 08 p3210 N94-30710
Calculating the J(c), B, T surface for commercial niobium tin conductors using a reduced state model
[DE94-006296] 08 p3520 N94-30850
Aging effects on the microstructure, surface characteristics and wettability of Cu pretinned with Sn-Pb solders
[DE94-007033] 09 p3641 N94-31638
A dynamic model of the vacuum furnace for separating Pb from Sn-Pb alloy 10 p4026 N94-34346
Manufacturing feasibility of several lead-free solders for electronic assembly
[DE94-007732] 11 p4258 N94-35564
Use of rotation to suppress thermosolutal convection in directionally solidified binary alloys
[NASA-CR-196372] 12 p4415 N94-36811

TIN COMPOUNDS
NT TIN OXIDES
NT TIN TELLURIDES
The polymerization of epsilon-caprolactone with stannous catalyst and lactide/epsilon-caprolactone (LA/epsilon-CL) and lactide/glycolide (LA/GA) copolymers. Polymer technology publication series no. 15
[PB94-137551] 08 p3220 N94-30713
Amorphous/crystalline structure and phase transformations in metastable semiconducting Ge(1-x)Sn(x)
[DE94-006659] 09 p3901 N94-32115

TIN OXIDES
Solderability perservative coatings: Electroless tin versus organic azoles
[DE93-017634] 04 p1370 N94-18477
Corrosion inhibition in high temperature environment
[AD-D015910] 05 p1698 N94-19830
Structure and morphology of Pd overlayers on epitaxial SnO2 films studies with the atomic force microscope
[AD-A271827] 05 p2028 N94-21458
Surface chemistry of liquid metals
06 p2249 N94-25133
Reference electrodes for solid polymer electrolytes
[DE94-004583] 07 p2780 N94-25806
Zr-rich corner of the Zr-Sn-O diagram
[DE93-633764] 07 p2734 N94-26161
Interface engineering in alumina fiber/glass composites 08 p3182 N94-29852
Chemical vapor deposition of metal nitrides, phosphides, and arsenides
[DE94-008096] 09 p3654 N94-31976
Low temperature atmospheric pressure chemical vapor deposition of group 14 oxide films
[DE94-013115] 12 p4425 N94-37317

TIN TELLURIDES
Growth of PbSnTe single crystal by traveling-zone method in low gravity (M-2) 02 p0586 N94-13734
Thermodynamic behaviour of tellurium at high temperatures
[DE94-612823] 11 p4240 N94-35960

TIP SPEED
Near wake measurements on a rotor model with Mie-vanes in the Delft open jet tunnel
[PB93-215382] 05 p1638 N94-22260
An overview of a model rotor icing test in the NASA Lewis Icing Research Tunnel
[NASA-TM-106471] 06 p2166 N94-23299
Tipjet 80-inch model rotor hover test: Test no. 1198
[AD-A279680] 11 p4191 N94-36261

TIP VANES
The design of a turbine vane cooling system used in the topping cycle
[OUEL-1963/92] 06 p2353 N94-23164

TIPS
NT BLADE TIPS
NT CRACK TIPS
NT NOSE TIPS
NT WING TIPS

TIRES
NT AIRCRAFT TIRES
Remote tire pressure sensing technique
[NASA-CASE-LAR-14160-1] 03 p1033 N94-15884
A finite strain ring dynamical model for pneumatic tires
[AD-A269286] 04 p1444 N94-18266
Measuring methods for evaluation of dynamic tyre properties
[ETN-93-95054] 04 p1381 N94-19650
Asphaltic concrete performance under heavy fighter aircraft loading
[AD-A275046] 08 p3157 N94-29151
Analysis of ambient monitoring data in the vicinity of open tire fires
[PB94-156197] 10 p4083 N94-34402

TIROS N SERIES SATELLITES
TOVS soundings: Impact on the synoptic analysis over the south and southeast regions of Brazil from March 18 to March 19, 1991
[INPE-5497-TDI/512] 01 p0230 N94-11179

TIROS SATELLITES
NT TIROS N SERIES SATELLITES
TOVS Pathfinder product validation and intercomparison 06 p2384 N94-23603

TISSUES (BIOLOGY)
NT ADIPOSE TISSUES
Research on acoustic coupling to electromagnetic pulses in tissue
[AD-A264764] 01 p0301 N94-11583
Momentum induced by laser-tissue interaction
[DE93-010737] 01 p0301 N94-11667
Monoclonal antibodies directed against surface molecules of multicell spheroids
[NASA-CR-193560] 02 p0727 N94-12795
An apparatus for measuring the biological oxidation of hydrogen gas under hyperbaric conditions
[AD-A266834] 03 p1119 N94-14916
Cultured normal mammalian tissue and process
[NASA-CASE-MSC-21984-1] 03 p1117 N94-15969
Cellular and tissue injury during nonfreezing cold injury and frostbite
[AD-A270883] 06 p2423 N94-22732
Autonomous support for microorganism research in space 07 p2903 N94-25672
Multi-cellular, three-dimensional living mammalian tissue
[NASA-CASE-MSC-21560-2] 11 p4296 N94-35232
High density cell culture system
[NASA-CASE-MSC-22060-1] 11 p4296 N94-35366
Three dimensional optic tissue culture and process
[NASA-CASE-MSC-22368-1] 12 p4478 N94-36765
Chemical and structural characterization of nitroaromatic adducts with hemoglobins
[AD-A280533] 12 p4480 N94-37089

TITAN
Laboratory studies of low temperature rate coefficients: The atmospheric chemistry of the outer planets
[NASA-CR-193485] 05 p1972 N94-20130
Science planning and sequencing for Cassini
06 p2504 N94-23871
Infrared spectroscopy of Jupiter and Saturn
[NASA-CR-196294] 12 p4549 N94-36961

TITAN LAUNCH VEHICLES
NT TITAN 4 LAUNCH VEHICLE
Liquid rocket propulsion: Retrospective and prospects
06 p2154 N94-24243

TITAN 4 LAUNCH VEHICLE
Real time radiography of Titan 4 booster
[DE93-012450] 02 p0548 N94-12911
Propellant stress relief groove for the Titan 4 SRMU
[AD-A278628] 11 p4228 N94-36254

TITANATES
NT BARIUM TITANATES
NT ILMENITE
NT LEAD TITANATES
NT LEAD ZIRCONATE TITANATES
NT PEROVSKITES
NT PIEZOELECTRIC CERAMICS
NT STRONTIUM TITANATES
NT ZIRCONIUM TITANATES
Grain boundaries in complex oxides
[DE93-013986] 01 p0398 N94-11012
Small polaron conduction in Y2Ti2O7
[ITN-93-85221] 02 p0814 N94-14557
The electromechanical properties of tetragonal BaTiO3 and PbTiO3 single crystals
[DE93-019008] 04 p1603 N94-19550
MOCVD growth and structure of PbTiO3 thin films
[DE93-040230] 05 p2033 N94-21994
The elastic and electromechanical properties of BaTiO3 single crystal through the ferroelectric transition
[DE94-001437] 06 p2557 N94-22927

TITANIA
Transport phenomena and interfacial kinetics in multiphase combustion systems
[AD-A270202] 04 p1349 N94-18785
Morphological aspects of surface reactions
[DE94-011208] 12 p4413 N94-37713

TITANIUM
An advanced test technique to quantify thermomechanical fatigue damage accumulation in composite materials
[NASA-CR-191147] 02 p0555 N94-13139
The structure and mechanical properties of Ru-Cu and Ru-Ti nanolayer composites
[DE93-014453] 02 p0558 N94-14469
Thermomechanical and isothermal fatigue behavior of a (90)sub 8 titanium matrix composite
[NASA-CR-191196] 02 p0560 N94-14822
STS-26 SSIP briefing --- Titanium Grain Formation Experiment and Crystal Membrane Experiment
[NASA-TM-109556] 03 p0976 N94-15280
Limited subsolidus diffusion in type B1 CAI: Evidence from Ti distribution in spinel 03 p0954 N94-16401
Interfacial shear behavior and its influence on fiber damage in sapphire-reinforced gamma titanium aluminide composites
[AD-A267943] 03 p1060 N94-17043
The specific heat of titanium disilicide
[AD-A267543] 03 p0960 N94-17100
Aspects of high temperature damage in fiber reinforced titanium metal matrix composites
[AD-A267907] 03 p0941 N94-17379
The efficiency of continuous output of some titanium-doped gem-crystal lasers has exceeded 1 W
[AD-A269953] 04 p1439 N94-18674
Multi-terrawatt, 100 fsec laser system using flashlamp-pumped, dye-converted Ti:sapphire as an amplifier
[DE93-017190] 04 p1440 N94-18889
Origin of the Apollo 15 very low Ti green glass. A perspective from the compositional diversity in the very low Ti glasses 05 p1685 N94-20759
Shattering the myth of the resonantly photo-pumped neon-like titanium laser
[DE93-019624] 05 p1819 N94-21873
Analysis of thermal mechanical fatigue in titanium matrix composites 05 p1835 N94-22618
Combustion synthesis method
07 p2721 N94-25561
Characterization of fatigue damage in a metal matrix composite (SCS-6/Ti-15-3) at elevated temperature
[AD-A273797] 07 p2706 N94-25876
Investigation of tension-compression fatigue behavior of a cross-ply metal matrix composite at room and elevated temperatures
[AD-A273731] 07 p2706 N94-25999
Diffusion of substitutional elements in Ti in its hcp phase
[DE93-633762] 07 p2733 N94-26160
Titanium 1992: Volume 3: Science and technology
[AD-A274800] 07 p2735 N94-26337
Titanium 1992: Science and technology, volume 2 rence (7th) in san diego, california on june 29-july 2, 1992. Volume 2
[AD-A274799] 07 p2736 N94-26362
X ray absorption studies of Ti/polymer and Cr/polymer interfaces
[DE94-003008] 07 p2753 N94-26770
The coordination and atom transfer chemistry of titanium porphyrin complexes
[DE94-003091] 07 p2704 N94-26779
Technical report of ISSP. Ser. A, no. 2685: ASE-free terawatt KrF/Ti : sapphire hybrid laser system
[JTN-94-80571] 07 p2820 N94-27339
The effect of Ti conduit on the critical current in (Nb, Ti)3Sn cable-in-conduit conductors
[DE94-701204] 07 p2788 N94-27817
Corrosion inhibition by electrodeposited conductive-polymer film
[AD-A275456] 08 p3213 N94-28806
Insulative properties of two thermo-metal neoprenes
[AD-A275209] 08 p3401 N94-29302
Preliminary evaluation of hybrid titanium composite laminates
[NASA-TM-109095] 08 p3180 N94-29472
A low cost igniter utilizing an SCB and titanium sub-hydride potassium perchlorate pyrotechnic
[DE94-006467] 09 p3666 N94-31827
Interface controlled amorphization of crystalline Ni/Ti multilayers
[DE94-008685] 09 p3906 N94-32884
A fully associative, non-linear kinematic, unified viscoplastic model for titanium based matrices
[NASA-TM-106609] 10 p4069 N94-33958
Isothermal damage and fatigue behavior of SCS-6/Timetal 21S (0/90)s composite at 650 C
[NASA-CR-195345] 11 p4234 N94-35995
Partition coefficients for Al, Ca, Ti, Cr, and Ni in olivine obtained by melting experiment on an LL6 chondrite
11 p4353 N94-36163
Characterisation of Fibre Reinforced Titanium Matrix Composites
[AGARD-R-796] 12 p4400 N94-36649

Possibilities and pitfalls in aerospace applications of titanium matrix composites 12 p4400 N94-36650
Applications of Titanium Matrix Composite to large airframe structure 12 p4400 N94-36651
SCS-6 (tm) fiber reinforced titanium 12 p4400 N94-36652
Processing of titanium matrix composites 12 p4401 N94-36653
Composites based on titanium with external and internal reinforcement 12 p4401 N94-36654
Manufacture and properties of sigma fibre reinforced titanium 12 p4401 N94-36655
Methodologies for thermal and mechanical testing of TMC materials 12 p4401 N94-36659
Ultrasonic nondestructive characterization methods for the development and life prediction of titanium matrix composites 12 p4401 N94-36660
Metal matrix composites: Analysis of simple specimens and model components under creep and fatigue loading 12 p4402 N94-36661
Residual strength and life prediction techniques for Ti MMC 12 p4402 N94-36662
Micromechanical modeling of damage growth in titanium based metal-matrix composites 12 p4402 N94-36664
Crack growth under cycle loading in fibre reinforced titanium metal matrix composites 12 p4402 N94-36665
Pre-standardisation work on fatigue and fracture testing of titanium matrix composites 12 p4402 N94-36667
ASTM and VAMAS activities in titanium matrix composites test methods development 12 p4403 N94-36668
A methodology to predict damage initiation, damage growth and residual strength in titanium matrix composites
[NASA-TM-109135] 12 p4405 N94-37320

TITANIUM ALLOYS

NT NITINOL ALLOYS
Hydrogen partitioning and transport in titanium aluminides
[NASA-CR-194117] 01 p0076 N94-10713
Titanium alloys milling assistance by high pressure lubricoolant jet
[DE93-013302] 01 p0082 N94-11008
Electronic structure and phase stability properties in ternary substitutional alloys
[DE93-013848] 02 p0569 N94-13137
NDE of titanium alloy MMC rings for gas turbine engines
[NASA-TM-106188] 02 p0555 N94-13138
Excimer laser surface processing of titanium
[DE93-012633] 02 p0570 N94-13512
The microstructural response of near gamma-TiAl+W to heat treatment
[DSIS-93-00237] 02 p0571 N94-13840
The corrosion protection of metals by ion vapor deposited aluminum
[NASA-TM-108425] 03 p0955 N94-15832
Bulk and defect properties of ordered intermetallics: A first-principles total-energy investigation
[DE93-015492] 03 p0959 N94-16873
Transient phenomena following precipitation and re-solution anneals in a NiTi alloy
[AD-A267557] 03 p0961 N94-17106
Characterization of metallic multilayers using x ray diffraction analysis
[NIAR-93-13] 03 p0961 N94-17282
Atlas of formability: Ti-6Al-4V ELI
[AD-A268300] 04 p1357 N94-17803
Mechanical properties of excimer laser modified titanium surfaces
[DE93-012663] 04 p1358 N94-17875
Implementation of a nonisothermal unified inelastic-strain theory into ADINA6.0 for a titanium alloy: User guide
[AD-A269927] 04 p1360 N94-18660
Fatigue resistant Ti3Al composites
[AD-A270305] 04 p1341 N94-18692
Intelligent materials systems and structures. Part 4: The influence of thermomechanical loading on the life of shape memory alloys
[PB93-195923] 04 p1363 N94-18952
Bibliography on silicides
[AD-A270516] 04 p1374 N94-19532
Microstructure and texture control of fatigue in hydrogen and marine environments
[AD-A271277] 04 p1344 N94-19744
On the experimental determination of low order structure factors in TiAl by energy filtered convergent beam electron diffraction
[DE93-019521] 05 p1687 N94-19806
Investigation of cracking and erratic behavior of the uranium-titanium alloy
[DE93-018591] 05 p1688 N94-19957
Production of NiAl and TiAl intermetallics by mechanical alloying
[VTT-JULK-760] 05 p1691 N94-20530
First principles calculations for analysis martensitic transformations
[DE94-000666] 05 p1695 N94-21964
Shape memory metals
[DE94-001373] 05 p1695 N94-21976
Interfacial reactions between titanium and borate glass
[DE93-012847] 05 p1683 N94-22031
Surface modification of Ti3Al for improved oxidation resistance
[DE93-018297] 05 p1696 N94-22034
Miniaturized disk-bend testing, nano-indentation, and the microstructure of ion-irradiated titanium aluminides
[DE93-040600] 05 p1697 N94-22559
Relationship of microstructure and mechanical properties for V-Cr-Ti alloys
[DE94-001431] 06 p2238 N94-22718
Evaluation of A5Si3Z(x) intermetallics for use as high temperature structural materials
[DE93-041127] 06 p2227 N94-22977
New extensions in the development of deformation processed metal-metal matrix composites
[DE94-000692] 06 p2227 N94-23004
Effect of neutron irradiation on tensile properties of V-Cr-Ti alloys
[DE94-001433] 06 p2240 N94-23194
Environmentally assisted cracking of high strength beta titanium alloys
[AD-A273598] 06 p2245 N94-24823
Matrix fatigue cracking mechanisms of alpha(2) TMC for hypersonic applications
[NASA-TM-106506] 06 p2230 N94-25186
Study on the mechanism of titanium alloy toughness and the improvement of properties 07 p2726 N94-25566
Study on improvements in fretting fatigue characteristics of high strength structural member 07 p2726 N94-25567
Study on knowledge extraction and systematization for material design 07 p2727 N94-25568
Study on improvement in physical analysis method of metallic materials 07 p2728 N94-25577
Effect of nitrocarburizing on shape of titanium alloy parts
[DE94-004040] 07 p2732 N94-25822
Titanium 1992: Volume 3: Science and technology
[AD-A274800] 07 p2735 N94-26337
Titanium 1992: Science and technology, volume 2 rence (7th) in san diego, california on june 29-july 2, 1992. Volume 2
[AD-A274799] 07 p2736 N94-26362
The influence of energy losses with time in NbTi superconductors in pulsed magnetic fields
[DE93-634761] 07 p3058 N94-26512
Deformation twinning: Influence of strain rate
[DE94-002693] 07 p2738 N94-26621
The processing of powder metallurgically produced near gamma-titanium aluminide
[ISBN-0-315-84018-8] 07 p2738 N94-26633
Evaluation of APC NbTi superconductor in a model dipole magnet
[DE94-003258] 07 p3060 N94-26795
Titanium 1992: Science and Technology, volume 1
[AD-A274798-VOL-1] 07 p2739 N94-26799
Material optimization and manufacturing development of reduced cost powder metal titanium alloy components for gas turbine engine application, phase 2
[AD-A274410] 07 p2709 N94-26978
Formation and crystallization of hydrogen-induced amorphous Ti3InH(4.5) alloy 07 p2745 N94-28163
The corrosion behavior of sputter-deposited magnesium-valve metal alloys 07 p2745 N94-28164
CO2 methanation catalysts prepared from amorphous Ni-valve metal alloys containing platinum group elements 07 p2745 N94-28166
Effect of surface condition on strength and fatigue behavior of alumina ceramic
[AD-A275053] 08 p3214 N94-29133
Nature of dissolution of binary tantalum-titanium alloys by molten plutonium
[DE94-005090] 08 p3210 N94-30776
Fractographic and microstructural analysis of fatigue crack growth in Ti-6Al-4V fan disc forgings
[AD-B174765] 08 p3153 N94-30914
High temperature ductility loss in titanium alloys: A review
[DE94-006606] 09 p3640 N94-31345
Microstructures and mechanical properties of Al3Ti-based alloys: Analysis in single phase and multiphase systems
[ONERA-NT-1993-6] 09 p3640 N94-31420
Transmissibility of nickel-titanium shape memory alloy springs
[AD-A276055] 09 p3640 N94-31456
Creep properties of vanadium-base alloys
[DE94-006541] 09 p3641 N94-31486
Thermal-mechanical fatigue crack growth in aircraft engine materials
[ISBN-0-315-86543-1] 09 p3734 N94-31707
A state variable material model for superplastic titanium-6 percent Al-4 percent V 09 p3644 N94-32498
Structure, stability, and mechanical properties of intermetallic phases
[DE94-009178] 09 p3647 N94-32852
Fatigue life and crack growth prediction methodology 10 p4071 N94-34583
Continuum fluorescence of Cu in NbTi/Cu composite wires
[DE94-008940] 11 p4241 N94-36242
Characterisation of Fibre Reinforced Titanium Matrix Composites
[AGARD-R-796] 12 p4400 N94-36649
Composites based on titanium with external and internal reinforcement 12 p4401 N94-36654
Properties of TMC processed by fibre coating and hiping 12 p4401 N94-36656
Fibre-matrix interface properties in Ti-matrix composites: Chemical compatibility and micromechanical behaviour 12 p4401 N94-36657
Oxidation behavior of titanium aluminide matrix materials 12 p4401 N94-36658
Process/composite concurrent tailoring of SiC/Ti composites 12 p4402 N94-36663
Prediction of thermal and mechanical stress-strain responses of TMC's subjected to complex TMF histories 12 p4402 N94-36666
Development of mechanical testing methods for titanium matrix composites (traction-ogligo-cyclic fatigue) 12 p4403 N94-36669
Modelling and testing fibre reinforced titanium for design purposes 12 p4403 N94-36670
Process simulation and modeling for advanced intermetallic alloys
[AD-A280327] 12 p4416 N94-37030
Feasibility of (IMC)(sub d)-reinforced metal matrix composites
[AD-A280626] 12 p4404 N94-37044
Alternate melting and refining routes 12 p4421 N94-37323
Maintaining constant standards during the forging process 12 p4421 N94-37326

TITANIUM BORIDES

Production and evaluation of dense ceramic compounds by combustion synthesis and dynamic compaction
[AD-A266742] 03 p0965 N94-15773
Dynamic testing and characterization of pre-fractured ceramic
[DE93-016457] 03 p0972 N94-17238
Hydrodynamic compressibility of high-strength ceramics
[DE93-019424] 05 p1698 N94-19903
Interfacial reactions between titanium and borate glass
[DE93-012847] 05 p1683 N94-22031
Experimental investigation of ignition of boron/titanium composite particles 06 p2159 N94-24275
Feasibility of (IMC)(sub d)-reinforced metal matrix composites
[AD-A280626] 12 p4404 N94-37044

TITANIUM CARBIDES

The reaction between titanium carbide and aluminium carbide in liquid aluminium; a microgravity study 01 p0123 N94-10238
Wear resistant titanium material development
[AD-A266474] 03 p0959 N94-16780
In-vacuum performance of Fomblin Z25-lubricated, 52100 steel bearings with TiC-coated balls 06 p2358 N94-24011
Experiment and research on materials irradiated by plasma radiation
[DE94-605011] 07 p2758 N94-27845
Photoelectron spectroscopic studies of the electronic structure and bonding in TiC and TiN
[ATR-93(8361)-2] 07 p2746 N94-28185
The organometallic chemical vapor deposition of transition metal carbides: The use of homoleptic alkyls
[DE94-005577] 08 p3206 N94-30007
Metafusion: A breakthrough in metallurgy 08 p3211 N94-30446

TITANIUM CHLORIDES

Zinc and titanium smoke: Chemical composition and physical characteristics
[FOA-C-40277-4.9] 05 p1680 N94-20552

TITANIUM COMPOUNDS
NT ANATASE
NT BARIUM TITANATES
NT ILMENITE
NT LEAD TITANATES
NT LEAD ZIRCONATE TITANATES
NT PEROVSKITES
NT PIEZOELECTRIC CERAMICS
NT RUTILE
NT STRONTIUM TITANATES
NT TITANATES
NT TITANIUM BORIDES
NT TITANIUM CARBIDES
NT TITANIUM CHLORIDES
NT TITANIUM NITRIDES
NT TITANIUM OXIDES
NT ZIRCONIUM TITANATES
Hydrogen partitioning and transport in titanium aluminides
[NASA-CR-194117] 01 p0076 N94-10713
Inelastic deformation mechanisms in SCS-6/Ti 15-3 MMC lamina under compression
[NASA-CR-191170] 02 p0555 N94-13378
Structural studies of sol-gel glasses
[AD-A266277] 03 p0967 N94-16472
Titanium carbon-hydrogen layers on decorative surfaces 04 p1375 N94-18010
Applicability and performance benefits of XD (Tradename) titanium aluminides to expendable gas turbine engines
[AD-A272998] 05 p1648 N94-21268
Characteristics of shock-compressed configuration of Ti and Si powder mixtures
[DE93-018857] 05 p1713 N94-22033
Status of the development of rechargeable lithium cells 06 p2392 N94-23354
Study on variation of damage generation mechanism by fatigue on TiAl compounds due to different slip systems 07 p2729 N94-25579
Development of K(1-x)Na(x)TiOPO4 crystals for nonlinear applications
[AD-A274336] 07 p3063 N94-27055
Technical report of ISSP. Ser. A, no. 2673: Two successive spin glass transitions in non-diluted Heisenberg-like spin glass Ni(0.42)Mn(0.58) TiO3
[JTN-94-80559] 07 p2756 N94-27241
Microstructure and mechanical behaviour of L1(2) titanium trialuminides
[ISBN-0-315-84488-4] 07 p2740 N94-27306
Inorganic materials for anomalous-dispersion phase-matched second harmonic generation: Rubidium titanyl arsenate isomorphs, Rb(Ti(1-2x)Ln(x)Nb(x))OAsO4
[DE94-006141] 09 p3899 N94-31847
Metal cluster alloys and oxides: Elucidating structural and electronic effects in governing the reactivity and catalytic role of matter in finite dimensions
[DE94-010224] 11 p4328 N94-36298
TITANIUM DIOXIDE
U TITANIUM OXIDES
TITANIUM NITRIDES
Sputtered TiN coatings in plastic
04 p1367 N94-18011
Electrochemical behavior of ion-plated TiN and Cu-Cr coatings
[AD-A273411] 06 p2235 N94-24784
Combustion synthesis method
07 p2721 N94-25561
Photoelectron spectroscopic studies of the electronic structure and bonding in TiC and TiN
[ATR-93(8361)-2] 07 p2746 N94-28185
Sliding friction and wear between titanium nitride, M50 steel and silicon nitride (round 3 of VAMAS wear test program)
[IMR-TM-TR-003] 08 p3303 N94-30019
TITANIUM OXIDES
NT ANATASE
NT ILMENITE
NT RUTILE
Grain boundaries in complex oxides
[DE93-013986] 01 p0398 N94-11012
Photocatalysis for the treatment of waste water: Applications involving the removal of metals
[DE93-011669] 02 p0561 N94-12841
Searching for neuKREEP: An EMP study of Apollo 11 Group A basalts 03 p1266 N94-16275
Lunar phase function effects on spectral ratios used for resource assessment 03 p1278 N94-16342
Nanostructured materials: Mind over matter
[DE93-017690] 04 p1597 N94-18480
Optical properties of oxide coatings prepared by ion-assisted deposition
[AD-A270024] 04 p1599 N94-18711
Ti-bearing oxide minerals in lunar meteorite Y793169 with the VLT affinity 05 p2084 N94-20812
Petrology and geochemistry of VLT glasses from double drive tube 79001/2 05 p1687 N94-20870
Investigation of the effect of various oxide and fluoride additives on the microstructure, electronic properties, and phase shifting ability of Ba(1-x)Sr(x)TiO3
[AD-A271756] 05 p2027 N94-21303
Electronic structure of a single oxygen vacancy in rutile TiO2
[DE94-602717] 07 p3062 N94-26901
Technical report of ISSP. Ser. A, no. 2671: Quasi-localization of light waves in Fibonacci dielectric multilayers
[JTN-94-80557] 07 p3064 N94-27231
Technical report of ISSP. Ser. A, no. 2670: Electronic structure of light transition metal compounds studied by photoemission
[JTN-94-80556] 07 p3065 N94-27239
Pitting corrosion of titanium
[AD-A274980] 08 p3203 N94-29089
Induced crystallization in CW laser-irradiated sol-gel deposited titania films
[DE94-006527] 08 p3207 N94-30062
Oxide pigments in water: The colloid-chemical point of view
[PB94-148616] 09 p3633 N94-31591
Processing and characterization of functionally gradient ceramic materials
[AD-A277154] 09 p3657 N94-32367
Polyurethane self-priming topcoats
[AD-D016160] 10 p4030 N94-34285
Substrate effects on the structure and optical properties of epitaxial PbTiO3 thin films prepared by metal-organic chemical vapor deposition
[DE94-010432] 12 p4535 N94-37192
Determination of interface structure and bonding at atomic resolution in the stem
[DE94-011466] 12 p4517 N94-37238
Numerical analysis of an impinging jet reactor for the CVD and gas-phase nucleation of titania
[NASA-TM-106619] 12 p4431 N94-37254
Bibliography of work on the photocatalytic removal of hazardous compounds from water and air
[DE94-006906] 12 p4467 N94-37405
Iron hydrous titanium oxide catalysts for the dehydrogenation of ethylbenzene to styrene
[DE94-010381] 12 p4412 N94-37542
TITRATION
Measurement of atmospheric OH by titration of near-IR fluorescent dyes 08 p3344 N94-28599
The active titration method for measuring local hydroxyl radical concentration 08 p3345 N94-28602
A fuzzy classifier system for process control
09 p3839 N94-32422
Isothermal sintering, microstructure, and superconducting properties of Y1Ba2Cu3O(7-x) compound
[DE94-008132] 09 p3905 N94-32779
TNT (TRINITROTOLUENE)
U TRINITROTOLUENE
TOBACCO
Chronic obstructive pulmonary disease
06 p2425 N94-23324
TOCOPHEROL
Wound healing after laser injury to skin: The effect of occlusion and vitamin E
[AD-A266473] 03 p1128 N94-16779
TOKAMAK DEVICES
NT JOINT EUROPEAN TORUS
Efficiency of fast wave current drive for a weakly relativistic plasma
[DE93-012775] 01 p0385 N94-10159
Optimization of a CO2 laser Thomson scattering alpha particle diagnostic
[DE93-012782] 01 p0173 N94-10160
Physics and modelling of scrape-off layer transport
[DE93-010510] 01 p0385 N94-10289
Transport mechanisms acting in toroidal devices: A theoretician's view
[DE93-013463] 01 p0385 N94-10310
Texas experimental tokamak
[DE93-013377] 01 p0386 N94-10321
A flexible modelling software for data acquisition
[DE93-612915] 01 p0322 N94-10484
Characterization of high-power RF structures using time-domain field codes
[DE93-013416] 01 p0132 N94-10518
Optimization of break-down conditions in tokamak TOTUS
[DE93-617863] 01 p0386 N94-10524
Looking beyond ITER: Toroidal concept improvement
[DE93-012762] 01 p0388 N94-10744
Reversed-field pinch studies in the Madison Symmetric Torus
[DE93-013464] 01 p0388 N94-10747
Kinetic approach to long wave length modes in rotating plasmas
[DE93-771286] 01 p0388 N94-10807
Possibilities of magnetic diagnostics in stellarators
[DE93-621608] 01 p0389 N94-11092
Physics of tokamak scrape-off layer confinement
[DE93-011949] 01 p0390 N94-11125
Gyrosheath near the tokamak edge
[DE93-012191] 01 p0390 N94-11142
Studies on the parametric decay of waves in fusion plasmas
[DE93-621659] 01 p0390 N94-11148
Intense neutron sources for fusion materials studies
[DE93-009782] 01 p0391 N94-11171
The role of plasma rotation on MHD instabilities in tokamaks
[DE93-013486] 01 p0393 N94-11512
Helium transport scaling law studies
[DE93-013487] 01 p0393 N94-11513
Results from the D3-D advanced divertor program
[DE93-015472] 01 p0393 N94-11514
Initial assessment of lower hybrid current drive in D3-D
[DE93-013310] 01 p0394 N94-12370
An emerging understanding of H-mode discharges in tokamaks
[DE93-012829] 01 p0394 N94-12544
Statistical approach to LHCD modeling using the wave kinetic equation
[DE93-012831] 01 p0394 N94-12545
A 3D gyrokinetic particle-in-cell simulation of fusion plasma microturbulence on parallel computers
[DE93-012503] 02 p0794 N94-12846
Test apparatus for ITER blanket cooling water distribution design
[DE93-753157] 02 p0795 N94-12944
Dimensionally similar discharges with central RF heating on the D3-D tokamak
[DE93-012776] 02 p0795 N94-12953
Growth curve analysis for plasma profiles using smoothing splines
[DE93-015741] 02 p0795 N94-12984
Equilibrium reconstruction of the q-profile in tokamaks from motional Stark effect data
[DE93-015815] 02 p0796 N94-13046
Effect on antenna structure of high power RF during plasma operation
[DE93-013278] 02 p0797 N94-13144
Interferometric investigation methods of plasma spatial characteristics on stellarators and tokamaks in submillimeter region
[DE93-621606] 02 p0798 N94-13507
Activities of the University of Saskatchewan, Plasma Physics Laboratory
[CTN-93-60831] 02 p0798 N94-13518
Nonlinear evolution of tearing modes in inhomogeneous plasmas
[PPL-133] 02 p0798 N94-13564
Folded waveguide designs for tokamaks
[DE93-013274] 02 p0798 N94-13577
Studies of non-inductive current drive in the CDX-U tokamak 02 p0799 N94-13680
Scattering of reflectometer signals from rippled surfaces
[PPL-138] 02 p0602 N94-13802
Experiments on the current rampdown phase in the STOR-M tokamak for AC operation
[PPL-132] 02 p0799 N94-13835
Plasma auto-biasing during Ohmic H-mode in the STOR-M tokamak
[PPL-136] 02 p0799 N94-13849
Semi-local kinetic analysis of the toroidal ion temperature gradient mode
[PPL-130] 02 p0800 N94-13851
Anomalous transport due to the ion acoustic instability in tokamaks
[PPL-129] 02 p0800 N94-13852
Dependence of beta(tau) on plasma shape in D3-D
[DE93-015473] 02 p0800 N94-13900
Stability and confinement properties of small-aspect-ratio tokamak
[INPE-5463-PRE/1771] 02 p0801 N94-14024
Anomalous transport due to small scale electromagnetic and large scale electrostatic modes in tokamaks
[PPL-140] 02 p0801 N94-14206
Electrical characterization of the JET A(sub 2) antenna: Comparison of model with measurements Wade, T.
[DE93-012964] 02 p0607 N94-14291
Direct electron heating and current drive with fast waves in D3-D
[DE93-013028] 02 p0801 N94-14293
Variation of divertor plasma parameters with divertor depth for H-mode discharges in D3-D
[DE93-015475] 02 p0801 N94-14347
D3-D research operations
[DE93-016729] 02 p0802 N94-14519

Measurements of edge fluctuations by phase contrast imaging on DIII-D
[DE93-014018] 02 p0802 N94-14579
Design of the ion cyclotron system for TPX
[DE93-012961] 02 p0803 N94-14770
Anomalous ion transport and feedback control
[DE93-018324] 02 p0803 N94-14874
Description of cooling water calorimetry and wall thermometry diagnostic at tokamak ASDEX-Upgrade
[IPP-5/46] 03 p1200 N94-14966
Studies on the parametric decay of waves in fusion plasmas
[VTT-PUBS-110] 03 p1200 N94-15204
Current drive with free electron lasers in high and low temperature tokamaks 03 p1201 N94-15209
ITER-HARD Toroidal Field coil structural analysis
[DE93-014834] 03 p1201 N94-15981
High beta and confinement studies of TFTR
[DE93-016204] 03 p1202 N94-16446
Inductive effects during second harmonic current drive experiments on T-10
[DE93-014411] 03 p1202 N94-16803
Recent results from the 60 GHz inside launch ECH system on the D3-D tokamak
[DE93-013027] 03 p1203 N94-16816
Simulation of enhanced tokamak performance on D3-D using fast wave current drive
[DE93-014009] 03 p1203 N94-16823
Nonlinear gyrofluid models of shear Alfven instabilities in ignited and beam heated toroidal plasmas
[DE93-016235] 03 p1203 N94-16869
ARIES tokamak reactor study
[DE93-017059] 03 p1203 N94-16901
Power compensators for phased operation of antenna arrays on JET and D3-D
[DE93-013208] 04 p1581 N94-17694
Arc detection and protection in high-power antenna systems
[DE93-013272] 04 p1382 N94-17695
ITER EDA design confinement capability
[DE93-013729] 04 p1582 N94-17697
Limits on m = 2, n = 1 error field induced locked mode instability in TPX with typical sources of poloidal field coil error field and a proto type correction coil, C-coil
[DE93-014408] 04 p1582 N94-17702
Using the Tritium Plasma Experiment to evaluate ITER PFC safety
[DE93-016614] 04 p1582 N94-17713
Plasma properties research: Task 3
[DE93-017087] 04 p1583 N94-17854
Heat load analysis on the cable-in-conduit with central core conductor for the TF coil Rebut layer design
[DE93-013783] 04 p1395 N94-17872
Filamentation, current profiles and transport in a tokamak
[DE93-016768] 04 p1584 N94-17948
Transport in the self-organized relaxed state of ion temperature gradient instability
[DE93-016769] 04 p1584 N94-17983
Analysis of the ITER H-mode confinement database
[DE93-016984] 04 p1585 N94-18056
Dependence of helium transport on plasma current and ELM frequency in H-mode discharges in D3-D
[DE93-016986] 04 p1585 N94-18058
AEOLUS-IT MHD simulation code based on a toroidally incompressible plasma model
[DE93-788461] 04 p1586 N94-18157
User's manual of Tokamak Simulation Code
[DE93-788388] 04 p1586 N94-18212
Active neutral particle diagnostics for high temperature plasma
[DE93-788457] 04 p1586 N94-18214
Ion mobility and transport barriers in the tokamak plasmas
[DE93-040320] 04 p1587 N94-18524
Parametric analysis of the ARIES-3D-He-3 tokamak reactor
[DE93-018293] 04 p1587 N94-18803
Thermal analysis of coatings and substrate materials during a disruption in fusion reactors
[DE93-017688] 04 p1588 N94-18971
Viscosity in the edge of tokamak plasmas
[DE93-018039] 04 p1588 N94-18988
Review Committee report on the conceptual design of the tokamak physics experiment
[DE93-018408] 04 p1588 N94-19012
The effects of radiolysis on the corrosion and stress corrosion behavior of 316 stainless steels
[DE93-019933] 04 p1363 N94-19021
Lower hybrid counter current drive for edge current density modification in D3-D
[DE93-019157] 04 p1589 N94-19073
Experiments on nonlinear absorption of ECH waves in MTX and a comparison with theory
[DE93-019158] 04 p1589 N94-19074
Thermo-hydraulic analysis of superconducting toroidal-field magnets for the Tokamak Physics Experiment
[DE93-018096] 04 p1590 N94-19269
ICRF direct electron heating experiments in TFTR
[DE93-017857] 04 p1590 N94-19273
Electron cyclotron resonance heating in the microwave tokamak experiment
[DE93-018083] 04 p1590 N94-19289
Radiative divertor modeling studies
[DE93-018092] 04 p1590 N94-19290
Behavior of the particle transport coefficients near the density limit in MTX
[DE93-019108] 04 p1591 N94-19311
Modelization, numerical simulation and optimal control of NET tokamak plasma configuration evolution for the future generation of fusion reactors
[ETN-93-95019] 04 p1591 N94-19364
Theoretical studies of turbulence and anomalous transport in toroidal confinement devices
[DE93-040684] 04 p1592 N94-19656
Transient thermal analysis of cryocondensation pump for JET
[DE93-040372] 05 p1992 N94-20003
Theoretical and numerical studies in magnetic fusion
[DE94-000536] 05 p1993 N94-20937
Fusion plasma theory grant. Task 3: Auxiliary radiofrequency heating of tokamaks
[DE94-000779] 05 p1994 N94-20940
Shear flow generation by Reynolds stress and suppression of resistive g-modes
[DE93-040911] 05 p1995 N94-21514
On effects of a local plasma density growth due to ponderomotive forces at fast wave launching in tokamaks
[IPPCZ-328] 05 p1996 N94-21571
On the stability of shear-Alfven vortices
[DE93-040912] 05 p1996 N94-21752
Edge plasma experiments on CASTOR tokamak
[IPPCZ-332] 05 p1997 N94-21816
A moving finite element model of the tokamak scrapeoff layer
[DE94-000673] 05 p1997 N94-21965
Fusion Plasma Theory. Task 1: Magnetic confinement fusion plasma theory
[DE94-000778] 05 p1998 N94-22019
Enhanced confinement regimes and control technology in the DIII-D tokamak
[DE93-019004] 05 p1998 N94-22039
The TST: A small steady-state tokamak for integrated divertor testing
[DE94-001016] 05 p1998 N94-22045
Use of open systems for control, analysis, and data acquisition of the DIII-D tokamak
[DE94-001101] 05 p1998 N94-22089
Continuum damping of ideal toroidal Alfven eigenmodes
[DE94-001233] 05 p1998 N94-22560
A two-dimensional kinetic model of the scrape-off layer
[DE94-001235] 05 p1999 N94-22562
Fluid simulations of Delta T(sub e)-driven turbulence and transport in boundary plasmas
[DE94-001304] 05 p1999 N94-22566
Effects of magnetic field perturbations in the ATF torsatron
[DE94-000474] 05 p1999 N94-22568
Electron temperature gradient driven instability in the tokamak boundary plasma
[DE94-001307] 05 p1999 N94-22596
MHD instabilities of fusion oriented plasmas 05 p2000 N94-22627
Massachusetts Institute of Technology Plasma Fusion Center 1992-1993 report to the President
[DE94-001725] 06 p2548 N94-22721
Active probing of plasma edge turbulence and feedback studies on the Texas Experimental Tokamak (TEXT)
[DE94-001017] 06 p2548 N94-22945
Superconducting magnet system for the TPX Tokamak
[DE94-001535] 06 p2549 N94-23013
Structural analysis of a superconducting central solenoid for the Tokamak Physics Experiment
[DE94-001536] 06 p2549 N94-23014
CAMAC throughput of a new RISC-based data acquisition computer at the DIII-D tokamak
[DE94-001113] 06 p2550 N94-23182
1993 annual report for the Phaedrus-T RF current drive experiments
[DE94-001369] 06 p2550 N94-23192
Chaos and simple determinism in reversed field pinch plasmas: Nonlinear analysis of numerical simulation and experimental data
[DE94-001575] 06 p2550 N94-23211
Nonlinear ion-mixing-mode particle transport in the dissipative trapped electron regime
[DE94-000989] 06 p2533 N94-23435
Computational model of surface ablation from tokamak disruptions
[DE94-002204] 06 p2550 N94-23474
The role of the radial electric field in confinement and transport in H-mode and VH-mode discharges in the DIII-D tokamak
[DE94-002746] 06 p2551 N94-23782
Performance characteristics of the DIII-D advanced divertor cryopump
[DE94-002745] 06 p2354 N94-23797
Fusion plasma theory project summaries
[DE94-001712] 06 p2551 N94-23808
IPP Prague Contributions to the IAEA Technical Committee Meeting on Research Using Small Tokamaks
[IPPCZ-329] 06 p2551 N94-24293
Some theoretical problems of magnetic diagnostics in tokamaks and stellarators
[NIFS-262] 06 p2551 N94-24306
Pellet ablation in the large helical device
[NIFS-260] 06 p2551 N94-24358
Temporal behavior of the electron density profile during limiter biasing in the HYBTOK-2 tokamak
[NIFS-257] 06 p2552 N94-24456
Stabilization of the external kink and other MHD issues
[DE94-001541] 06 p2552 N94-24502
Plasma initiation in a tokamak with conducting superstructure: First results from Alcator C-MOD
[DE94-001565] 06 p2552 N94-24504
Start-up simulations of the PULSAR pulsed tokamak reactor
[DE94-002634] 06 p2552 N94-24519
Tokamak Physics Experiment (TPX) cost and performance trade studies using supercode
[DE94-002720] 06 p2553 N94-24628
Investigation of the heat handling capabilities of DIII-D neutral beamline internal components
[DE94-001107] 06 p2553 N94-24756
Fluid velocity and electromagnetic forces measured by a rotating Langmuir probe in the scrape off layer of JFT-2M
[OUEL-1968/92] 06 p2554 N94-25327
LHCD (low hybrid current drive) experiment on the HT-6B tokamak
[DE93-613720] 06 p2555 N94-25331
Effect of LHCD (low hybrid current drive) on tearing mode instability
[DE93-613700] 06 p2555 N94-25344
Review of tokamak experiments on direct electron heating and current drive with fast waves
[DE94-004185] 07 p3041 N94-25801
Heavy neutral beam probe for edge plasma analysis in tokamaks
[DE94-003391] 07 p3041 N94-25846
Design of folded waveguide antenna for Alcator C-Mod
[DE94-003584] 07 p2767 N94-25924
RF modeling and design of a folded waveguide launcher for the Alcator C-Mod tokamak
[DE94-003588] 07 p3041 N94-25933
Evaluation of helium cooling for fusion divertors
[DE94-002680] 07 p3042 N94-25976
High-speed repetitive pellet injector for plasma fueling of magnetic confinement fusion devices
[DE94-002792] 07 p3042 N94-26140
Development of fusion technology
[DE93-633444] 07 p3042 N94-26159
Limitations of power conversion systems under transient loads and impact on the pulsed tokamak power reactor
[DE94-003404] 07 p3043 N94-26324
Fusion Energy Advisory Committee: Advice and recommendations to the US Department of Energy in response to the charge letter of September 1, 1992
[DE93-019842] 07 p3043 N94-26428
Numerical simulation of plasma vertical position stabilization in ITER
[DE93-634588] 07 p3044 N94-26510
Maryland controlled fusion research program
[DE94-003533] 07 p3044 N94-26523
The dynamics of interacting nonlinearities governing long wavelength driftwave turbulence
[DE94-001785] 07 p2793 N94-26558
Probability of accessing the multiple saturated states in the resistive interchange instability
[DE94-000478] 07 p3044 N94-26694
Conceptual design of the tokamak radiation shielding for the Tokamak Physics Experiment (TPX)
[DE94-002791] 07 p3044 N94-26858
Potential of commercial tokamak reactors with improved physics
[DE94-002794] 07 p3044 N94-26860
Methodology for first wall design
[DE94-002795] 07 p3045 N94-26861

The TPX Cryostat Conceptual Design
[DE94-002857] 07 p3045 N94-26863
New conditioning procedure derived from operating experience with the Common Long-Pulse Ion Source
[DE94-002891] 07 p3045 N94-26865
Role of core toroidal rotation shear on turbulence and transport in the improved confinement regimes of the D3-D tokamak
[DE94-001215] 07 p3045 N94-26950
Tokamak Physics Experiment poloidal field design
[DE94-001542] 07 p3045 N94-27019
Design and control of phased ICRF antenna arrays
[DE94-002796] 07 p3046 N94-27261
High gas-efficiency hydrogen negative ion sources
[PB93-232163] 07 p3025 N94-27348
Fast wave current drive technology development at ORNL
[DE94-004243] 07 p3046 N94-27568
Fusion reactor systems studies
[DE94-003162] 07 p3046 N94-27686
Cryogenic fracture behavior of 316LN in magnetic fields up to 14.6 T
[DE94-005215] 07 p2742 N94-27694
Shine through measurements with hydrogen beam in JT-60
[DE94-701113] 07 p3047 N94-27699
Passive stabilization of MHD instabilities at high (beta)n in the HBT-EP tokamak
[DE94-003317] 07 p3047 N94-27735
Helium transport and exhaust studies of H-mode discharges in the D3-D tokamak
[DE94-004744] 07 p3048 N94-27785
Fuel ion rotation measurement and its implications on H-mode theories
[DE94-004860] 07 p3048 N94-27791
Performance of a 14-MeV neutron generator as an in situ calibration source for TFTR
[DE94-004993] 07 p3048 N94-27825
Preliminary considerations on the diffraction (quasi-optical) grill in CASTOR tokamak
[IPPCZ-335] 07 p3048 N94-27842
Determination of the plasma column shape in the Tokamak Novillo cross section by magnetic probes
[DE94-604986] 07 p3048 N94-27844
Modelling and control of plasma position in the STOR-M tokamak
[ISBN-0-315-58891-8] 07 p3049 N94-27949
Theoretical reversed field pinch and tokamak studies
[DE94-005409] 08 p3503 N94-28490
Proceedings of Japan-US Workshop P-196 on High Heat Flux Components and Plasma Surface Interactions for Next Devices
[DE94-701164] 08 p3503 N94-28513
Electron beam irradiation experiments of monoblock divertor mock-up
[DE94-707497] 08 p3503 N94-28555
TFTR Ion Cyclotron Range of Frequencies (ICRF) experimental data analysis collaboration
[DE94-004699] 08 p3504 N94-28575
Argon frost continuous cryopump for fusion applications
[DE94-004478] 08 p3230 N94-29017
Liquid metal MHD and heat transfer in a tokamak blanket slotted coolant channel
[DE94-004622] 08 p3506 N94-29510
Higher order collisionless ballooning mode in tokamaks
[PPL-143] 08 p3507 N94-30156
Eigenmode analysis of the destabilized ion acoustic mode in tokamaks
[PPL-142] 08 p3507 N94-30158
Beta enhancement of thermal diffusivity in tokamaks
[PPL-141] 08 p3508 N94-30159
The impact of improved physics on commercial tokamak reactors
[DE94-006103] 08 p3509 N94-30760
Advanced steady-state operating scenarios
[DE94-004810] 08 p3509 N94-30768
Application of divertor cryopumping to H-mode density control in DIII-D
[DE94-004859] 08 p3510 N94-30832
Superdiffusion
[DE94-002333] 08 p3492 N94-30834
Magnetic flux reconstruction methods for shaped tokamaks
[DE94-005827] 08 p3510 N94-30882
Operation of D3-D with all-graphite walls
[DE94-004858] 09 p3886 N94-31304
Noninductive current drive experiments on D3-D, and future plans
[DE94-007373] 09 p3886 N94-31324
L-H confinement mode dynamics in three-dimensional state space
[DE94-007113] 09 p3887 N94-31396
Structural design of the superconducting Poloidal Field coils for the Tokamak Physics Experiment
[DE94-007078] 09 p3887 N94-31406
Spectroscopy and atomic physics in EBIT and SuperEBIT
[DE94-006050] 09 p3864 N94-31508
Two-gigawatt burst-mode operation of the Intense Microwave Prototype (IMP) Free-Electron Laser (FEL) for the Microwave Tokamak Experiment (MTX)
[DE94-006613] 09 p3715 N94-31580
Plasma confinement theory and transport simulation
[DE94-006065] 09 p3888 N94-31619
High beta tokamak research
[DE94-006513] 09 p3888 N94-31664
Quench detection and instrumentation for the Tokamak Physics Experiment magnets
[DE94-006656] 09 p3888 N94-31667
First-wall heat-flux measurements during ELMing H-mode plasma
[DE94-008310] 09 p3888 N94-31765
Collisional and chaotic transport of energetic particles in toroidal plasma
[DE94-006504] 09 p3889 N94-31787
FWCD and ECCD experiments on D3-D
[DE94-007371] 09 p3890 N94-32201
Fusion applications of high power millimeter wave sources
[DE94-007374] 09 p3718 N94-32202
An edge density fluctuation diagnostic for D3-D using lithium beams
[DE94-008554] 09 p3890 N94-32519
Experimental survey of the L-H transition conditions in the D3-D tokamak
[DE94-007428] 09 p3891 N94-32595
Recent VH-mode results on D3-D
[DE94-007429] 09 p3891 N94-32611
Overview of H-mode studies in D3-D
[DE94-007430] 09 p3891 N94-32612
Characterization of atomic and molecular impurity sources and transport at the tokamak edge
[DE94-007212] 09 p3891 N94-32619
Basic principles approach for studying nonlinear Alfven wave-alpha particle dynamics
[DE94-007112] 09 p3891 N94-32664
Cooperative program on D3-D (FY 1993)
[DE94-008343] 09 p3892 N94-32820
The Numerical Tokamak Project (NTP) simulation of turbulent transport in the core plasma: A grand challenge in plasma physics
[DE94-008279] 09 p3892 N94-32838
Stability of tearing modes in tokamak plasmas
[DE94-009205] 09 p3892 N94-32911
Analysis of stochastic particle behavior in a magnetic island due to electrostatic drift waves
[DE94-727553] 10 p4137 N94-33869
Development of a VME and CAMAC based data acquisition and transfer system for JT-60 control
[DE94-727590] 10 p4158 N94-33871
Beat wave current drive experiment on the Davis Diverted Tokamak (DDT)
[DE94-009770] 10 p4144 N94-33879
Summary of experimental progress and suggestions for future work
[DE94-008893] 10 p4145 N94-34012
Transport properties of interacting magnetic islands in tokamak plasmas
[DE94-009208] 10 p4145 N94-34140
Magnetic island effects, interactions in tokamaks
[DE94-009209] 10 p4145 N94-34221
A triggering mechanism of fast crash in sawtooth oscillation
[DE94-718974] 11 p4336 N94-35772
NIFS Symposium: Toward the research of fusion burning plasmas, present status and future strategy
[DE94-727618] 11 p4336 N94-35775
Optimization of turn position of tokamak inductor
[DE94-612627] 11 p4336 N94-35791
Analysis of current diffusive ballooning mode
[DE94-718992] 11 p4336 N94-35811
Thickness of the layer of strong radial electric field in JFT-2M H-mode plasmas
[DE94-718993] 11 p4336 N94-35812
Applications of non-resonant RF forces for improvement of tokamak reactor performances. Part 1: Application of ponderomotive force
[DE94-718994] 11 p4336 N94-35813
Atomic physics and radiation processes in plasmas
[DE94-727617] 11 p4337 N94-35939
A survey of reflectometry techniques with applications to TFTR
[DE94-010202] 11 p4338 N94-36093
Scaling laws for TEXT plasma profiles
[DE94-010832] 11 p4338 N94-36200
The new features of Ion Bernstein Wave Heating in JIPP T-2U tokamak
[DE94-718978] 11 p4338 N94-36247
Feasibility study for a novel pulsed neutral beam diagnostics for tokamaks
[DE94-617129] 11 p4339 N94-36417
Design of the divertor Thomson scattering system on D3-D
[DE94-012672] 12 p4527 N94-37081
The role of heating and current drive in ITER
[DE94-012679] 12 p4527 N94-37082
Initial studies of reflectometer for ITER
[DE94-012476] 12 p4528 N94-37167
Towards nuclear fusion reactors
[DE94-748680] 12 p4528 N94-37235
Startup and shutdown of the PULSAR Tokamak Reactor
[DE94-013128] 12 p4528 N94-37292
Motional Stark effect upgrades on D3-D
[DE94-013146] 12 p4528 N94-37297
MARFE's in tokamak edge plasma: Pattern formation under nonlocal constraints
[DE94-012766] 12 p4529 N94-37309
ELMy-H mode as limit cycle and transient responses of H-modes in tokamaks
[DE94-727510] 12 p4529 N94-37358
Isotope scaling and eta(i) mode with impurities in tokamak plasmas
[DE94-012763] 12 p4529 N94-37361
A role of neutral hydrogen in CHS plasmas with reheat and collapse and comparison with JIPPT-IIU tokamak plasmas
[DE94-718985] 12 p4530 N94-37384
Material and design considerations for the carbon armored ITER divertor
[DE94-737854] 12 p4530 N94-37415
Recent DIII-D high power heating and current drive experiments
[DE94-012509] 12 p4530 N94-37436
Two-dimensional over-all neutronics analysis of the ITER device
[DE94-718963] 12 p4530 N94-37464
Improvement study of the divertor configuration of the Steady State Tokamak Reactor (SSTR)
[DE94-718961] 12 p4531 N94-37484
Research using small tokamaks
[DE94-621827] 12 p4531 N94-37493
Initial report on calorimetry for the Tore Supra Outboard pump Limiter
[DE94-011244] 12 p4531 N94-37626

TOLERANCES (MECHANICS)
NT IMPACT TOLERANCES
Geometric tolerance assessment
[NPL-DITC-210/92] 03 p1049 N94-15013
A review of Australian and New Zealand investigations on aeronautical fatigue during the period April 1991 to March 1993
[AD-A267532] 03 p0868 N94-17117
Feature-based tolerancing for intelligent inspection process definition
[DE93-017984] 05 p1906 N94-20311
Mold bolt and means for achieving close tolerances between bolts and bolt holes
[NASA-CASE-MFS-28720-1] 05 p1823 N94-20379
Damage tolerance of pressurized graphite/epoxy tape cylinders under uniaxial and biaxial loading
[NASA-CR-195101] 06 p2377 N94-24587
Damage tolerance assessment handbook. Volume 1: Introduction fracture mechanics fatigue crack propagation
[AD-A274777] 07 p2836 N94-26186
Damage tolerance assessment handbook. Volume 2: Aircraft damage tolerance evaluation
[AD-A274778] 07 p2837 N94-26357
Thermoplastic or thermosetting composites in aircrafts
[PB94-123809] 07 p2710 N94-27253
NASA-UVA light aerospace alloy and structures technology program (LA2ST)
[NASA-CR-195275] 07 p2844 N94-27851
Assessment of impact damage in composite structures
[AD-A277063] 09 p3624 N94-32265
Tension fracture of laminates for transport fuselage. Part 1: Material screening 09 p3629 N94-33130
The crack severity index of monitored load spectra 10 p4071 N94-34585
Damage tolerance management of the X-29 vertical tail 10 p3996 N94-34595
Tough, processable semi-interpenetrating polymer networks from monomer reactants
[NASA-CASE-LAR-14838-1] 11 p4242 N94-35233
Turbine disks: Lifing against defects and materials development 12 p4454 N94-37329

TOLERANCES (PHYSIOLOGY)
NT ACCELERATION TOLERANCE
NT ALTITUDE TOLERANCE
NT COLD TOLERANCE

NT HEAT TOLERANCE
NT HUMAN TOLERANCES
NT RADIATION TOLERANCE

TOLLMIEN-SCHLICHTING WAVES
On nonlinear Tollmien-Schlichting/vortex interaction in three-dimensional boundary layers
[NASA-TM-106184] 01 p0152 N94-11377
Tollmien-Schlichting/vortex interactions in compressible boundary layer flows
[NASA-CR-191515] 03 p1017 N94-15183
Receptivity of boundary layers to convected gusts
[AD-A267206] 03 p1022 N94-15860
Higher-order accurate Osher schemes with application to compressible boundary layer stability
[NASA-TM-106355] 03 p1026 N94-17056
On the stability of a time dependent boundary layer
[NASA-CR-191542] 03 p1030 N94-17450
Computational fluid mechanics
[NASA-CR-194765] 06 p2337 N94-24859
A phase equation approach to boundary layer instability theory: Tollmien Schlichting waves
[AD-280580] 10 p4049 N94-34394

TOLUENE
Reactivity of nitrate radical (NO3) toward organic compounds 07 p2704 N94-27387
Fuels combustion research
[AD-A275122] 08 p3189 N94-29004
Energy transfer properties and mechanisms
[DE94-007403] 09 p3636 N94-32594
Surface probes of porous toluene/water ices: Adsorption kinetics and annealing spectra measured by second harmonic generation
[DE94-007564] 09 p3637 N94-32743
Minipilot solar system: Design/operation of system and results of non-solar testing at MRI
[PB94-152238] 10 p4079 N94-34165
California residential indoor air quality study. Volume 1: Methodology and descriptive statistics
[PB94-166048] 12 p4464 N94-36994

TOMBOLOS
U BARS (LANDFORMS)

TOMOGRAPHY
NT COMPUTER AIDED TOMOGRAPHY
Real-time tomography mooring
[AD-A264923] 01 p0289 N94-11854
Mathematical algorithms for multidimensional inverse scattering problems in inhomogeneous medium
[AD-A266440] 02 p0749 N94-13702
Current distribution tomography for determination of internal current density distributions
[DE93-015463] 02 p0604 N94-13899
Electronic schematics for the Donner 600 Crystal Tomograph
[DE93-015277] 02 p0625 N94-14336
Requirements on CCD-detectors for ground-based auroral imaging 03 p0909 N94-15093
Tomographic mathematical ideas applied to radar detection
[AD-A268789] 04 p1384 N94-18186
Surface wave group velocity tomography of East Asia, part 1
[AD-A270100] 04 p1484 N94-18868
Single sided tomography of extremely large dense objects
[DE93-017993] 04 p1580 N94-19268
Ionospheric tomography using the FORTE satellite
[DE93-018545] 05 p1854 N94-19955
Variable-permittivity linear inverse problem for the H(sub z)-polarized case 05 p1719 N94-20408
High resolution, three dimensional soft x ray imaging
[DE93-018667] 05 p1989 N94-21630
Reconstruction of multiple cracks from experimental electrostatic boundary measurements
[AD-A277433] 07 p2994 N94-26601
Auroral Tomography Workshop Proceedings
[PB94-123718] 07 p2881 N94-27040
Experimental verification of tomographic reconstruction of turbulent air flow structure using optical wavefront measurements
[AD-A274392] 07 p2795 N94-27129
Atomic processes in Inertial Electrostatic Confinement (IEC) devices
[DE94-005015] 07 p3047 N94-27715
Dual-Band Infrared (DBIR) imaging inspections of Boeing 737 and KC-135 aircraft panels
[DE94-005700] 08 p3122 N94-29842
Analysis and an image recovery algorithm for ultrasonic tomography system 08 p3397 N94-30456
Ultrasonic tomography in fiber-reinforced composite materials 09 p3620 N94-31565
Prediction of the plane wave beamformed acoustic arrival structure for the 1992 Barents Sea coastal tomography test
[AD-A276741] 09 p3788 N94-32181
Ocean optics, ocean imaging and optical tomography
[AD-A277010] 09 p3789 N94-32402
Tomographic imaging of internal Earth structure: The core-mantle boundary and the trade-off between volumetric and topographic structure 10 p4083 N94-33358
Environmental process tomography in the United States
[DE94-006402] 10 p4081 N94-33718
Resolution of iterative inverses in seismic tomography
[DE94-008079] 10 p4087 N94-34132
Recursive recovery of Markov transition probabilities from boundary value data
[DE94-011914] 11 p4317 N94-36235
Signal processing for the 1992 Barents Sea tomography experiment
[AD-A278580] 12 p4476 N94-36971
Density and composition analysis using focused MeV ion microbeam techniques
[DE94-012241] 12 p4517 N94-37210
The effects of proton-beam quality on the production of gamma rays for nuclear resonance absorption in nitrogen
[DE94-011609] 12 p4523 N94-37629
A note on analytic recovery of transition probabilities in three dimensional diffuse tomography
[DE94-011378] 12 p4506 N94-37719

TOMS
U TOTAL OZONE MAPPING SPECTROMETER

TONE
U PITCH

TONGUE
NCVS, volume 5
[AD-A274975] 07 p2902 N94-27165

TONOMETRY
U PRESSURE MEASUREMENT

TONUS
U MUSCULAR TONUS

TOOLING
Material optimization and manufacturing development of reduced cost powder metal titanium alloy components for gas turbine engine application, phase 2
[AD-A274410] 07 p2709 N94-26978
Near-net-shape manufacturing: Spray-formed metal matrix composites and tooling 08 p3186 N94-30447
Analytical Design Package (ADP2): A computer aided engineering tool for aircraft transparency design 09 p3823 N94-32430
Innovative fabrication processing of advanced composite materials concepts for primary aircraft structures
[NASA-CR-189558] 09 p3626 N94-32877

TOOLS
NT BORING MACHINES
NT GRINDING MACHINES
NT MACHINE TOOLS
NT MILLING MACHINES
NT SPACE TOOLS
NT WRENCHES
Loads produced by a suited subject performing tool tasks without the use of foot restraints
[NASA-TP-3424] 05 p1896 N94-20606
Strength capabilities and load requirements while performing torquing tasks in zero gravity
[NASA-TP-3433] 05 p1897 N94-21627
A system for the challenging task of collecting samples from a comet surface 06 p2358 N94-24007
The SCRAM tool-kit 10 p4066 N94-33668

TOPEX
Topex orbit determination using GPS tracking system 01 p0038 N94-10359
Topex/Poseidon: A United States/France mission. Oceanography from space: The oceans and climate
[NASA-TM-108253] 01 p0043 N94-10699
Analysis of TOPEX laser retroreflector array characteristics 03 p0915 N94-15578
TOPEX/Poseidon precision orbit determination production and expert system 06 p2196 N94-23920
TOPEX/Poseidon battery performance during the first year of operation 07 p2862 N94-28119
TOPEX/POSEIDON operational orbit determination results using global positioning satellites 08 p3160 N94-29666
Lessons learned from selecting and testing spaceflight potentiometers 09 p3607 N94-33318
Some aspects of simultaneously flying Topex Follow-On in a Topex orbit with Geosat Follow-On in a Geosat orbit
[NASA-CR-196075] 10 p4077 N94-34214
Compatibility of TOPEX/Poseidon trajectory propagation with JPL and GSFC/FDF operational software 11 p4204 N94-35619
Improved solution accuracy for TDRSS-based TOPEX/Poseidon orbit determination 11 p4205 N94-35620
Tracking system options for future altimeter satellite missions 11 p4205 N94-35622

TOPOGRAPHY
NT LUNAR TOPOGRAPHY
NT TERRAIN
New x ray scanning topographic approaches to nondestructive evaluation of composites 01 p0061 N94-10039
First results for the simultaneous estimation of the geoid and the sea surface topography by ERS-1 altimeter data 01 p0241 N94-11765
A stochastic-deterministic approach as an alternative to classical cross-over techniques in small ocean basins 01 p0242 N94-11767
Analysis of gravity, magnetic, and seismic reflection data from Tibet and neighboring regions of China
[NASA-CR-193405] 01 p0278 N94-11886
Lineament analysis and tectonic interpretation for the Tharsis region 01 p0437 N94-12031
Spectral analysis of the gravity and topography of Mars 01 p0444 N94-12065
Venus' center of mass - center of figure displacement and implications 01 p0444 N94-12067
A structural and petrographic investigation of the pretoria saltpan impact structure 01 p0282 N94-12102
Flexure and the role of inplane force around coronae on Venus 01 p0452 N94-12112
Can weak crust explain the correlation of geoid and topography on Venus? 01 p0453 N94-12118
Landscape and geomorphic survey of Zhamanshin area, Northern Kazakhstan: Preliminary report on 1992 field trip data 01 p0282 N94-12123
An ancient inner lake in Maadim Vallis 01 p0456 N94-12133
Geology and surface characteristics of Bell Regio, Venus 01 p0457 N94-12136
Differential scaling: Implications for central structures in large lunar craters 01 p0461 N94-12158
Using lunar sounder imagery to distinguish surface from subsurface reflectors in lunar highlands areas 01 p0464 N94-12179
Morphotectonics of Venus 01 p0478 N94-12248
Transmantle flux tectonics 01 p0283 N94-12249
New Mars free-air and Bouguer gravity: Correlation with topography, geology and large impact basins 01 p0481 N94-12268
Interdisciplinary scientist participation in the Phobos mission
[NASA-CR-193715] 01 p0482 N94-12446
ERS-1 altimetry of inland water and land 01 p0246 N94-12475
Preliminary studies on the application of ERS-1 data to topographic mapping 01 p0246 N94-12476
The TREES project: Pre-processing and generation of terrain data for inclusion in an ERS-1 SAR classification scheme 01 p0249 N94-12496
Topography of the Western Mediterranean from the ERS-1 altimeter 01 p0255 N94-12531
Venus gravity
[NASA-CR-194077] 02 p0841 N94-12823
Cyclogenesis and cyclone over South America
[INPE-5400-TDI/479] 02 p0719 N94-13175
Error analysis of real time and post processed or bit determination of GFO using GPS tracking
[NASA-CR-193646] 02 p0512 N94-13238
The American Geophysical Union Chapman Conference on Tectonics and Topography
[NASA-CR-193454] 02 p0713 N94-13335
Improved mapping system
[NASA-TM-109643] 03 p1082 N94-15428
Multi-beam laser altimeter 03 p0921 N94-15620
Engineering design of sub-micron topographies for simultaneously adherent and reflective metal-polymer interfaces
[NASA-CR-194573] 03 p0964 N94-15700
A multilevel-multiresolution method for image processing. A Bayesian framework for reconstructing and representing shapes
[AD-A266772] 03 p1082 N94-15842
Ray tracing on topographic Rossby waves
[AD-A267014] 03 p1112 N94-15844
Magellan: Principal Venus science findings 03 p0989 N94-15887
TOPSAT: Global space topographic mission 03 p0992 N94-15905
Research into the influence of spatial variability and scale on the parameterization of hydrological processes
[NASA-CR-194610] 03 p1082 N94-16026
Similarity and scale in catchment storm response
[PAPER-89RG01615] 03 p1083 N94-16028
Evapotranspiration and runoff from large land areas: Land surface hydrology for atmospheric general circulation models 03 p1083 N94-16029
Heterogeneity and scaling land-atmospheric water and energy fluxes in climate systems 03 p1083 N94-16030

A detailed model for simulation of catchment scale subsurface hydrologic processes
[PAPER-92WR02333] 03 p1084 N94-16032
Morphology and models for the evolution of eastern Hecate Chasma, Venus 03 p1256 N94-16215
Ishtar deformed belts: Evidence for deformation from below? 03 p1256 N94-16218
Confirmation of saturation equilibrium conditions in crater populations 03 p1103 N94-16222
Megaplumes on Venus 03 p1271 N94-16301
An inversion of geoid and topography for mantle and crustal structure on Mars 03 p1273 N94-16315
Separation of topographic and intrinsic backscatter variations in biscopic radar images: A magic airbrush 03 p1086 N94-16318
The cartography of Venus with Magellan data 03 p1274 N94-16320
Meander properties of Venusian channels 03 p1275 N94-16324
Spectral study of Venus global topography and geoid from Magellan and PVO data 03 p1276 N94-16332
Resolving topographic detail on Venus by modeling complex Magellan altimetry echoes 03 p1283 N94-16368
Sedimentation, volcanism, and ancestral lakes in the Valles Marineris: Clues from topography 03 p1283 N94-16369
Effective elastic thickness of the Venusian lithosphere with lateral viscosity variations in the mantle 03 p1293 N94-16421
Dust-dynamic feedbacks in the Martian atmosphere: Surface dust lifting 03 p1296 N94-16434
Mapping of sea bottom topography 03 p1077 N94-16744
Sea bottom topography imaging with SAR 03 p1077 N94-16745
Detecting surface roughness effects on the atmospheric boundary layer via AIRSAR data: A field experiment in Death Valley, California 03 p1078 N94-16747
The TOPSAR interferometric radar topographic mapping instrument 03 p1078 N94-16749
A geological and geophysical information system for Eurasia
[AD-A267841] 03 p1232 N94-17036
Three-dimensional high-resolution seismic profiling on the New Jersey outer continental shelf
[AD-A269835] 04 p1498 N94-18600
JPRS report: Central Eurasia. Aviation and cosmonautics, no. 1, January 1993
[JPRS-UAC-93-007] 04 p1632 N94-19147
Measurements of ocean surface and bottom backscattering strengths in the northwestern Atlantic Ocean
[AD-A270893] 04 p1500 N94-19786
Robust photo-topography by fusing shape-from-shading and stereo
[NASA-CR-194697] 05 p1806 N94-19920
Topographic mapping using a monopulse SAR system 05 p1721 N94-20417
Polarimetric backscattering from sea ice 05 p1723 N94-20426
Topographic slope from the SAR interferometric phase gradient 05 p1731 N94-20459
Interferometric detection of freeze-thaw displacements of Alaskan permafrost using ERS-1 data 05 p1732 N94-20460
Performance evaluation of the JPL TOPSAR system: An across-track interferometric SAR system for topographic mapping 05 p1732 N94-20461
Seafloor characterization/Galapagos propagating rift
[AD-A272001] 05 p1882 N94-20581
Beta Regio rift system on Venus: Geologic interpretation of Magellan images 05 p2095 N94-20655
Some deformation trends and topographic characteristics of tesserae on Venus 05 p2105 N94-20706
Chronology, eruption duration, and atmospheric contribution of Apollinaris Patera, Mars 05 p2108 N94-20720
Comparative hypsometric analysis of both Earth and Venus topographic distributions 05 p2108 N94-20722
Distribution of small volcanic cones on the surface of Venus by size and elevation: Implications for differential deposition of volcanic features 05 p2110 N94-20731
Local topography of Mars and its relationship to surface weathering processes 05 p2111 N94-20737
The 3-D Moons: The Voyager stereo atlas of the outer solar system 05 p2111 N94-20740
Geoid, topography, and convection-driven crustal deformation on Venus 05 p2116 N94-20769
Response of the topography and gravity field on Venus to mantle upwelling beneath a chemical boundary layer 05 p2117 N94-20775
Contributions of the Clementine mission to our understanding of the processes and history of the Moon 05 p2119 N94-20784
Magellan Mission 05 p1652 N94-20829
Is there uniformitarian or catastrophic tectonics on Venus? 05 p2129 N94-20839
Possible flexural signatures around Olympus and Ascraeus Montes, Mars 05 p2142 N94-20911
Ocean mapping using satellite radar altimetry
[ETN-93-93470] 05 p1841 N94-21017
Detecting topographical regions in digital terrain maps
[AD-A272889] 05 p1841 N94-21453
Role of surface characteristics in urban meteorology and air quality
[DE93-040929] 05 p1851 N94-21740
A DTM-based path planning method for planetary rovers 06 p2370 N94-23423
Nonlinear dynamics applied to atmospheric prediction
[AD-A273437] 06 p2404 N94-24674
Tools for visualizing landscape pattern for large geographic areas
[DE94-001121] 06 p2388 N94-24757
Seafloor characterization/Galapagos propagating rift
[AD-A273586] 06 p2419 N94-25165
Correlation between the gravity field and the bathymetry in the North Atlantic Ocean
[ETN-94-95036] 07 p2899 N94-26108
A preliminary analysis of the US west climatology
[DE94-003028] 07 p2894 N94-26313
Conifer tree influence on Digital Terrain Elevation Data (DTED): A case study at Dulles International Airport
[AD-A274213] 07 p2849 N94-27069
Landscape dynamics of northeastern forests
[NASA-CR-195272] 07 p2852 N94-28070
Objective analysis of a coastal ocean eddy using satellite AVHRR and in situ hydrographic data
[AD-A275715] 08 p3376 N94-28642
Exploitation of stereophotogrammetrically derived 3-D wireframe models to produce urban simulations
[AD-A275459] 08 p3325 N94-28808
Feature mapping in a photogrammetric GIS
[AD-A275418] 08 p3325 N94-28863
Statistical characterization of rugged propagation paths with application to Rg scattering study
[AD-A275237] 08 p3361 N94-29393
Applicability of digital terrain analyses to wind energy prospecting and siting
[DE94-004363] 08 p3374 N94-30587
Patterns of deformation and volcanic flows associated with lithospheric loading by large volcanoes on Venus 09 p3776 N94-31106
Geoid-to-topography ratios on Venus: A global perspective 09 p3940 N94-31110
Three dimensional vorticity field in the California current system
[AD-A276951] 09 p3788 N94-32220
Modular Simulator System (MSS). System/segment specification for the generic modular simulator system-environment module, volume 13
[AD-A276980] 09 p3589 N94-32319
Multi-scale studies of seafloor topography
[AD-A277008] 09 p3789 N94-32400
The use of ERS images for mapping 09 p3749 N94-32531
Use of SPOT and ERS-1 SAR data to study the tectonic and climatic history of arid regions 09 p3752 N94-32550
Monitoring landsurface characteristics in Niger using complementary SPOT and ERS-1 SAR data 09 p3754 N94-32560
Comparing SPOT and SIR A for mapping superficial formations in tropical forest regions: Example of the Yaoundy Region (Cameroon) 09 p3755 N94-32562
SAR interferometry with ERS-1 09 p3755 N94-32566
Techniques and applications of SAR interferometry for ERS-1 09 p3756 N94-32568
Developments in ERS-1 SAR interferometry: Use of the spectral shift 09 p3756 N94-32569
Differential interferometry study of an earthquake 09 p3756 N94-32570
Simulation of a precipitation event in the western United States
[DE94-004835] 09 p3786 N94-32791
Quantitative modeling of bottom morphology and subbottom properties
[AD-A278142] 09 p3790 N94-33062
Fine and microstructure observations at Fieberlin g Guyot R/V new horizon cruise report
[AD-A277917] 09 p3791 N94-33109
Modelling topographic effects on digital remotely sensed data 10 p4074 N94-33360
A foundation for fusion
[AD-A277521] 10 p4074 N94-33372
Mesoscale roughness of Venus 11 p4361 N94-35430
The Twenty-Fifth Lunar and Planetary Science Conference. Part 3: P-Z
[NASA-CR-195745] 11 p4362 N94-35448
The topography of Mars: A re-evaluation of current data 11 p4364 N94-35460
Noachian and Hesperian modification of the original Chryse impact basin topography 11 p4364 N94-35462
Formation of fold and thrust belts on Venus due to horizontal shortening of a laterally heterogeneous lithosphere 11 p4367 N94-35480
Tracking system options for future altimeter satellite missions 11 p4205 N94-35622
Preliminary solutions for the lunar gravity field from analysis of lunar orbiter tracking data 11 p4371 N94-36156
Four beam interferometer manual: Operating instructions for the INEL diffraction Moire interferometer
[DE94-010772] 12 p4453 N94-36452
Representing the influence of subgrid topography on hydrology
[DE94-004595] 12 p4474 N94-37379

TOPOLOGY
NT FIXED POINTS (MATHEMATICS)
NT HOMOTOPY THEORY
NT METRIC SPACE
On local frame fields and fermion dynamics in space with nontrivial topologies
[DE93-617657] 01 p0349 N94-10548
Quantum mechanical effects of topological origin 01 p0378 N94-10594
On the possible unobservability of the Wu-Yang phase factor in curved space
[DE93-617645] 01 p0411 N94-10831
The Lip microbundle representation theorem
[DE93-619671] 01 p0346 N94-11348
Evolution of the interplanetary magnetic field
[DE93-012631] 02 p0836 N94-13262
Heat flows and harmonic maps with a free boundary
[DE93-622856] 02 p0632 N94-13509
Nonrecursive formulations of multibody dynamics and concurrent multiprocessing 02 p0679 N94-14632
WBNGRID, a program for generation of C-H and C-O topology grids around wing/body/nacelle configurations: User's guide
[FFA-TN-1992-09] 04 p1311 N94-17721
Working visit to the University of L'Aquila, Italy
[FEL-93-B020] 04 p1618 N94-19452
The effects of initial conditions on the 3-D topology of temporally evolving wakes (ARI on 3-D bluff body wakes)
[AD-A271008] 04 p1423 N94-19774
On the topological size of p-m-complete degrees
[TR-459] 05 p1965 N94-21286
Superpatch
[NASA-CR-177627] 05 p1914 N94-21489
Mars: Noachian hydrology by its statistics and topology 05 p2143 N94-21664
IAS telecommunication infrastructure and value added network services provided by IASNET 05 p1744 N94-22069
Vanishing theorem on arithmetic surfaces
[PB93-215481] 05 p1961 N94-22263
Non commutative geometry and physics
[PB93-215499] 05 p1961 N94-22264
Semi-stability and heights of cycles
[PB93-215507] 05 p1961 N94-22377
Supercomputer networking for space science applications
[NASA-CR-194876] 06 p2465 N94-23085
Structures of tetrahedrization: A mathematical and algorithmical point of view
[ETN-94-95172] 06 p2480 N94-23166
Lacunary series as quadratic differentials in conformal dynamics
[PB93-238061] 06 p2481 N94-23547
When an infinitely-renormalizable endomorphism of the interval can be smoothed
[PB93-238087] 06 p2481 N94-23548
Non-trivial examples of real isolated singularity at the origin
[PB94-110939] 06 p2487 N94-23787
Tools for visualizing landscape pattern for large geographic areas
[DE94-001121] 06 p2388 N94-24757
Quantum optical aspects of topological phases, such as Berry's phase
[AD-A273632] 06 p2570 N94-25028
Radar target discrimination systems using artificial neural network topology
[AD-D015984] 06 p2301 N94-25041
The fundamental group of the complement of complexified real arrangements
[DE93-616847] 06 p2491 N94-25214
Surfaces allowing for fractional statistics
[DE93-614526] 07 p3002 N94-25910

Characterization of self-conjugate minimal surfaces in R(sup 3)
[DE94-601538] 07 p2993 N94-26409
Topological conditions for the existence of invariant measures for unimodal maps
[PB94-123296] 07 p2849 N94-26866
Graphs satisfying a local ore-type condition
[PB94-126679] 07 p3007 N94-27222
Reidemeister numbers of equivariant maps
[PB94-138286] 08 p3452 N94-29118
High throughput network for multiprocessor interconnections
[VTT-PUBS-147] 08 p3245 N94-29468
Symplectic topology of integrable Hamiltonian systems
[DE94-608120] 08 p3467 N94-30166
Topological models for higher order control flow
[CWI-CS-R9340] 08 p3425 N94-30432
A monotonicity conjecture for real cubic maps
[DE94-003969] 08 p3335 N94-30610
Non-commutative geometry
[PB94-139342] 08 p3462 N94-30889
The small-scale topology of a 2:1 aspect-ratio elliptic jet 09 p3699 N94-31184
Strictly positive definite functions on spheres
[AD-A276471] 09 p3855 N94-31244
SU(2) WZNW model at higher genera from gauge field functional integral
[PB94-148467] 09 p3857 N94-31589
Heteroclinic attractors: Time averages and moduli of topological conjugacy
[W-9318] 09 p3844 N94-31690
The 2nd International Conference on Curves and Surfaces: Abstracts
[AD-A276805] 10 p4128 N94-33406
Topological properties of typical interconnection networks: Fault tolerance, communication delay and connection cost
[PB94-148822] 10 p4111 N94-33976
Rescaled box counting for the topological analysis of spatial data
[DE94-009820] 12 p4461 N94-36464
Note on certain rigid subshifts
[PB94-179058] 12 p4506 N94-37833
Localization of topological Pontryagin classes by propagation with finite speed
[PB94-180866] 12 p4506 N94-37852

TOPPING CYCLE ENGINES
The design of a turbine vane cooling system used in the topping cycle
[OUEL-1963/92] 06 p2353 N94-23164

TORCHES
Hydrogen-oxygen torch ignitor
[NASA-TM-106493] 07 p2691 N94-27424
Vacuum vapor deposition
[NASA-CASE-MFS-28652-1] 08 p3215 N94-29446
Plasma arc welding weld imaging
[NASA-CASE-MFS-28797-1] 11 p4273 N94-35367
Analysis of a High Velocity Oxygen-Fuel (HVOF) thermal spray torch. Part 1: Numerical formulation
[DE94-005590] 11 p4267 N94-35996

TORNADOES
Radar diagnostic parameters as indicators of severe weather in central Florida
[PB93-183507] 03 p1106 N94-16465
Effectiveness of protection clothing for cold weather conditions after ejection over sea: A case report 08 p3381 N94-28435
On the origins of low-level tornadic circulations within the remnants of hurricane Andrews
[AD-A275373] 08 p3369 N94-29011
Dynamics of tornado-like vortices 08 p3371 N94-29753

TOROIDAL PLASMAS
Reversed-field pinch studies in the Madison Symmetric Torus
[DE93-013464] 01 p0388 N94-10747
Macroscopic behaviour and discrete dynamo of RFP plasma in high theta discharge
[DE93-771408] 01 p0392 N94-11239
Conversion of the four-strap array in D3-D to a tunable traveling wave antenna
[DE93-012085] 01 p0137 N94-11453
Dimensionally similar discharges with central RF heating on the D3-D tokamak
[DE93-012776] 02 p0795 N94-12953
Nonlinear evolution of tearing modes in inhomogeneous plasmas
[PPL-133] 02 p0798 N94-13564
The propagation characteristics and instability properties of low-frequency electromagnetic waves in the Io plasma torus 02 p0601 N94-13650
Studies of non-inductive current drive in the CDX-U tokamak 02 p0799 N94-13680
Plasma auto-biasing during Ohmic H-mode in the STOR-M tokamak
[PPL-136] 02 p0799 N94-13849
On MHD mode equations in toroidal plasmas
[PPL-139] 02 p0800 N94-13877
Dependence of beta(tau) on plasma shape in D3-D
[DE93-015473] 02 p0800 N94-13900
D3-D research operations
[DE93-016729] 02 p0802 N94-14519
ITER-HARD Toroidal Field coil structural analysis
[DE93-014834] 03 p1201 N94-15981
Structure and damping of toroidal drift waves (and their implications for anomalous transport)
[DE93-014005] 03 p1203 N94-16822
Nonlinear gyrofluid models of shear Alfven instabilities in ignited and beam heated toroidal plasmas
[DE93-016235] 03 p1203 N94-16869
Limits on m = 2, n = 1 error field induced locked mode instability in TPX with typical sources of poloidal field coil error field and a proto type correction coil, C-coil
[DE93-014408] 04 p1582 N94-17702
Self-regulated shear flow turbulence in confined plasmas
[DE93-015823] 04 p1583 N94-17743
Transport in the self-organized relaxed state of ion temperature gradient instability
[DE93-016769] 04 p1584 N94-17983
Toroidal solenoids in the electromagnetic field and Aharonov-Casher effect
[DE93-629861] 04 p1566 N94-18152
User's manual of Tokamak Simulation Code
[DE93-788388] 04 p1586 N94-18212
Ion mobility and transport barriers in the tokamak plasmas
[DE93-040320] 04 p1587 N94-18524
Lower hybrid counter current drive for edge current density modification in D3-D
[DE93-019157] 04 p1589 N94-19073
Finite beta plasma equilibrium in toroidally linked mirrors
[DE93-040318] 04 p1590 N94-19193
Modelization, numerical simulation and optimal control of NET tokamak plasma configuration evolution for the future generation of fusion reactors
[ETN-93-95019] 04 p1591 N94-19364
Theoretical studies of turbulence and anomalous transport in toroidal confinement devices
[DE93-040684] 04 p1592 N94-19656
Transient thermal analysis of cryocondensation pump for JET
[DE93-040372] 05 p1992 N94-20003
Continuum damping of ideal toroidal Alfven eigenmodes
[DE94-001233] 05 p1998 N94-22560
Kinetic resonance damping rate of the toroidal ion temperature gradient mode
[DE94-001234] 05 p1998 N94-22561
Effects of magnetic field perturbations in the ATF torsatron
[DE94-000474] 05 p1999 N94-22568
MHD instabilities of fusion oriented plasmas 05 p2000 N94-22627
Physics of transport phenomena in magnetic confinement plasmas 05 p2000 N94-22628
Dynamo driven by weak plasma turbulence: The effect of differential rotation 05 p2005 N94-22665
Chaos in plasma simulation and experiment
[DE94-001574] 06 p2549 N94-22963
Plasma research in the Madison Symmetric Torus (MST)
[DE94-002318] 06 p2549 N94-22976
Fluctuations and confinement in ATF
[DE94-000485] 06 p2549 N94-22998
Superconducting magnet system for the TPX Tokamak
[DE94-001535] 06 p2549 N94-23013
1993 annual report for the Phaedrus-T RF current drive experiments
[DE94-001369] 06 p2550 N94-23192
Fusion plasma theory project summaries
[DE94-001712] 06 p2551 N94-23808
Pellet ablation in the large helical device
[NIFS-260] 06 p2551 N94-24358
Stabilization of the external kink and other MHD issues
[DE94-001541] 06 p2552 N94-24502
Plasma initiation in a tokamak with conducting superstructure: First results from Alcator C-MOD
[DE94-001565] 06 p2552 N94-24504
Toroidal plasma beta-FLR limit in a toroidally linked mirror system
[DE94-003119] 07 p3041 N94-25792
Kinetic resonance damping rate of the toroidal ion temperature gradient mode
[DE94-003511] 07 p3041 N94-25923
Development of fusion technology
[DE93-633444] 07 p3042 N94-26159
Scaling of sustained ZT-40 M reversed field pinches
[DE94-003318] 07 p3043 N94-26321
The TPX Cryostat Conceptual Design
[DE94-002857] 07 p3045 N94-26863
Role of core toroidal rotation shear on turbulence and transport in the improved confinement regimes of the D3-D tokamak
[DE94-001215] 07 p3045 N94-26950
Tokamak Physics Experiment poloidal field design
[DE94-001542] 07 p3045 N94-27019
TFTR experimental data analysis collaboration
[DE94-004166] 07 p3047 N94-27690
Passive stabilization of MHD instabilities at high (beta)n in the HBT-EP tokamak
[DE94-003317] 07 p3047 N94-27735
Preliminary considerations on the diffraction (quasi-optical) grill in CASTOR tokamak
[IPPCZ-335] 07 p3048 N94-27842
Determination of the plasma column shape in the Tokamak Novillo cross section by magnetic probes
[DE94-604986] 07 p3048 N94-27844
Analysis of density limit and efficiency in lower hybrid current drive
[DE94-604995] 07 p3049 N94-27856
A 6MeV heavy ion beam probe for the Large Helical Device
[AD-B183695L] 08 p3505 N94-29397
Formation and self-healing of magnetic islands in finite-beta helias equilibria
[AD-B183271L] 08 p3505 N94-29483
Numerical method for the investigation of the magnetohydrodynamic stability of three dimensional plasma equilibria
[ETN-94-95752] 09 p3887 N94-31512
Toroidal pinch experiments
[DE94-005876] 09 p3887 N94-31558
First-wall heat-flux measurements during ELMing H-mode plasma
[DE94-008310] 09 p3888 N94-31765
Collisional and chaotic transport of energetic particles in toroidal plasma
[DE94-006504] 09 p3889 N94-31787
Experimental survey of the L-H transition conditions in the D3-D tokamak
[DE94-007428] 09 p3891 N94-32595
The Numerical Tokamak Project (NTP) simulation of turbulent transport in the core plasma: A grand challenge in plasma physics
[DE94-008279] 09 p3892 N94-32838
Stability of tearing modes in tokamak plasmas
[DE94-009205] 09 p3892 N94-32911
Anomalous transport equations in toroidal plasmas
[DE94-009206] 09 p3893 N94-32922
Beat wave current drive experiment on the Davis Diverted Tokamak (DDT)
[DE94-009770] 10 p4144 N94-33879
High beta and second stability region transport and stability analysis
[DE94-009654] 10 p4145 N94-33920
Magnetic island effects, interactions in tokamaks
[DE94-009209] 10 p4145 N94-34221
Power balance and characterization of impurities in the Maryland Spheromak, part 2
[DE94-009603] 11 p4335 N94-35670
Improved models of beta-limit, anomalous transport and radial electric field with loss cone loss in heliotron/torsatron
[DE94-718976] 11 p4324 N94-35984
Scaling laws for TEXT plasma profiles
[DE94-010832] 11 p4338 N94-36200
Confinement improvement in H-mode-like plasmas in helical systems
[DE94-727619] 12 p4528 N94-37231
Towards nuclear fusion reactors
[DE94-748680] 12 p4528 N94-37235
MARFE's in tokamak edge plasma: Pattern formation under nonlocal constraints
[DE94-012766] 12 p4529 N94-37309
Isotope scaling and eta(i) mode with impurities in tokamak plasmas
[DE94-012763] 12 p4529 N94-37361
A role of neutral hydrogen in CHS plasmas with reheat and collapse and comparison with JIPPT-IIU tokamak plasmas
[DE94-718985] 12 p4530 N94-37384
Recent DIII-D high power heating and current drive experiments
[DE94-012509] 12 p4530 N94-37436
Theory of anomalous transport in H-mode plasmas
[DE94-727546] 12 p4531 N94-37485
Fast electron generation and transport in a turbulent, magnetized plasma
[DE94-012986] 12 p4531 N94-37730
Self-sustained turbulence and L-mode confinement in toroidal plasmas
[DE94-748497] 12 p4532 N94-37734

TOROIDS
Mutual inductance between partially wound tori and a bifilar conductor
[ETN-93-94388] 02 p0624 N94-13998
Electromagnetic properties of a toroidal solenoid
[DE93-613032] 07 p2766 N94-25866
Experimental results of 40-kA Nb3Al conductor
[DE94-701207] 07 p2788 N94-27821
TORQUE
Instantaneous engine frictional torque: Its components and piston assembly friction
[DE93-011639] 01 p0182 N94-11625
On the motion through a viscous fluid of a spherical particle touching a plane wall: Slip boundary conditions
[DE93-012540] 02 p0628 N94-12961
Design and control of a macro-micro robot for precise force applications 02 p0682 N94-14651
Tooth form design supporting system in module design 04 p1428 N94-18036
Cooperative control of multiple space manipulators
[AD-A270291] 04 p1445 N94-18813
Dimensional crossover in the torque in a layered superconductor
[DE93-019544] 04 p1407 N94-19553
FSR based force torque transducer design
[AD-A271337] 05 p1650 N94-19879
Loads produced by a suited subject performing tool tasks without the use of foot restraints
[NASA-TP-3424] 05 p1896 N94-20606
Strength capabilities and load requirements while performing torquing tasks in zero gravity
[NASA-TP-3433] 05 p1897 N94-21627
Spline screw multiple rotations mechanism
[NASA-CASE-GSC-13452-1] 06 p2352 N94-23078
A novel rotary actuator for spacecraft 06 p2361 N94-24034
Establishing a relationship between maximum torque production of isolated joints to simulate EVA ratchet push-pull maneuver: A case study 06 p2437 N94-24206
The effect of high altitude pressure on the power and efficiency of an airborne two-stroke engine 06 p2155 N94-24253
Torque equilibrium attitudes for the Space Station 06 p2208 N94-24449
Bolt and nut evaluator
[NASA-CASE-GSC-13468-1] 08 p3288 N94-29538
The response of flexible manipulators to a new computed torque control strategy: Simulation results 08 p3308 N94-30295
Flexible drive shaft coupling
[AD-D016096] 09 p3727 N94-32718
Torque-balanced extendable fiber optic cable
[AD-D016097] 09 p3882 N94-32719
Torque characteristics of solid lubricated precision bearings during oscillatory motion
[AD-A278133] 09 p3728 N94-33061
A comparison of the performance of solid and liquid lubricants in oscillating spacecraft ball bearings 09 p3606 N94-33311
Dexterous end effector flight demonstration 10 p4067 N94-34032
Torque application technique and apparatus
[AD-D016124] 10 p4061 N94-34150
Hot gas ingestion effects on fuel control surge recovery and AH-1 rotor drive train torque spikes
[NASA-CR-191047] 10 p4005 N94-34993
The control of satellites with microgravity constraints: The COMET Control System 11 p4207 N94-35632
A dynamic method for magnetic torque measurement 11 p4216 N94-35856
Variable stiffness torsion springs
[NASA-CASE-MFS-28930-1] 12 p4509 N94-36782
Dynamics of a split torque helicopter transmission
[NASA-TM-106410] 12 p4452 N94-37457
TORQUE MEASURING APPARATUS
U TORQUEMETERS
TORQUE MOTORS
Low melting temperature alloy deployment mechanism 06 p2356 N94-23997
Development of a Low-Temperature Gear Motor (LOG) 06 p2361 N94-24032
High resolution encoder-motor used in the orbital spin scan radiometer, GOES VAS satellites 06 p2209 N94-24038
Reconfigurable aircraft stick control
[AD-D016043] 07 p2681 N94-27113
Suspension system for gimbal supported scanning payloads
[NASA-CASE-MFS-28817-1] 08 p3287 N94-29358
International Space Station Alpha's bearing, motor, and roll ring module developmental testing and results 09 p3603 N94-33295
Rotating unbalanced mass proof-of-concept
[NASA-TM-109814] 10 p4141 N94-33720
TORQUE SENSORS (NONROBOTICS)
U TORQUEMETERS
TORQUEMETERS
Control of torque in stepping motors of quartz watches and clocks 04 p1408 N94-18023
Bolt and nut evaluator
[NASA-CASE-GSC-13468-1] 08 p3288 N94-29538
Torque application technique and apparatus
[AD-D016124] 10 p4061 N94-34150
A dynamic method for magnetic torque measurement 11 p4216 N94-35856
TORSION
Damping measurements for ultra-high carbon steel/brass laminates
[DE93-011886] 01 p0082 N94-11076
Measuring methods for CFRP laminates' bending and torsion rigidities characteristics 02 p0529 N94-13272
Torsion spring powered missile wing deployment system
[CA-PATENT-1,306,384] 05 p1645 N94-21051
The torsion space nucleic acids molecular mechanics program DUPLEX: Surveying conformation space by potential energy minimization
[DE94-002441] 06 p2563 N94-24567
Simple currents versus orbifolds with discrete torsion: A complete classification
[NIKHEF-H/93-13] 07 p2995 N94-26812
Cyclic axial-torsional deformation behavior of a cobalt-base superalloy
[NASA-TM-106372] 08 p3203 N94-28921
Interlaminar fracture analysis for laminated composites under combined loading 08 p3182 N94-29964
Flexible drive shaft coupling
[AD-D016096] 09 p3727 N94-32718
Technology integration box beam failure study 09 p3628 N94-33126
An examination of the aerodynamic moment on rotor blade tips using flight test data and analysis
[NASA-TM-104006] 10 p3985 N94-34948
Variable stiffness torsion springs
[NASA-CASE-MFS-28930-1] 12 p4509 N94-36782
TORSIONAL STRESS
Construction of a tension-torsion anisotropic brittle damage elastic model
[ECL-91-27] 04 p1457 N94-19375
TORSIONAL VIBRATION
Payload sensitivity in coupled bending and torsional vibrations in flexible beams
[MEMO-1102] 01 p0184 N94-10161
Interactive simulation package for coupled bending and torsional vibrations in flexible robot arms
[MEMO-1089] 05 p1944 N94-21140
A new method for torsional critical speed calculation of practical industrial rotors
[IMR-T&M-TR-001] 07 p2828 N94-28041
Sensitivity of lag-damping correlations to structural and aerodynamic approximations of isolated experimental rotors in forward flight
[NASA-CR-195822] 10 p3983 N94-33991
A procedure for oscillatory parameter identification
[DE94-008047] 11 p4259 N94-36054
Vibration reduction in helicopter rotors using an actively controlled partial span trailing edge flap located on the blade
[NASA-CR-4611] 11 p4280 N94-36423
TORUSES
Contact 3-manifolds, integrable Hamiltonian systems and exotic symplectic structures in R(sup 4)
[DE93-624767] 04 p1551 N94-19248
Plasma research in the Madison Symmetric Torus (MST)
[DE94-002318] 06 p2549 N94-22976
Number of moduli of families of curves on toric surfaces
[PB93-230381] 06 p2479 N94-23121
Affine algebras on the torus
[DE94-601556] 07 p3006 N94-26414
Higher spin extensions of the Virasoro algebra, area-preserving algebras and the matrix algebra a-bar(sub (infinity))
[DE94-601557] 07 p3006 N94-26415
The super Weierstrass (zeta)-function and operator product expansions in 2D-induced supergravity on the supertorus
[DE94-603664] 07 p3074 N94-27627
Infrared properties of obscuring dust tori in active galactic nuclei 08 p3545 N94-29832
TOTAL ENERGY SYSTEMS
Diffusion on Cu surfaces 06 p2251 N94-24428
TOTAL OZONE MAPPING SPECTROMETER
Effects of typhoon on TOMS data 02 p0693 N94-14243
Southern and Northern Hemisphere total ozone as seen by TOMS
[NASA-TM-109591] 03 p1098 N94-15282
TOMS computer graphics
[NASA-TM-109597] 03 p1094 N94-15290
Atlas of TOMS ozone, 1978-1988
[NASA-TM-109456] 03 p1094 N94-15329
October 1979-1989 Southern Hemisphere total ozone as seen by TOMS
[NASA-TM-109375] 04 p1476 N94-18967
Participation in TOMS missions
[NASA-CR-195110] 06 p2398 N94-24078
Nimbus-7 Total Ozone Mapping Spectrometer (TOMS) data products user's guide
[NASA-RP-1323] 06 p2410 N94-24355
TOTAL QUALITY MANAGEMENT
The 17th Transducer Workshop
[AD-A265526] 01 p0141 N94-10509
Engineering performance metrics
[DE93-012084] 01 p0128 N94-11028
The role of metrics and measurements in a software intensive total quality management environment 01 p0329 N94-11428
Development and application of an acceptance testing model 01 p0330 N94-11432
Analyzing human errors in flight mission operations 01 p0314 N94-11534
Lecture notes on software process improvement
[AD-A265200] 02 p0744 N94-13049
Ninth Annual NASA/Contractors Conference on Quality and Productivity. World Class Excellence: The Journey Continues. Keynote presentations
[NASA-CR-194513] 02 p0665 N94-13148
Ninth Annual NASA/Contractors Conference on Quality and Productivity. World Class Excellence: The Journey Continues. Conference presentations
[NASA-CR-194514] 02 p0665 N94-13153
Measuring quality progress 02 p0666 N94-13154
Defining the performance gap: Conducting a self-assessment 02 p0666 N94-13155
What's the bottom line payback for TQM? 02 p0666 N94-13156
Partnership with the customer 02 p0666 N94-13157
Strategic planning as a focus for continuous improvement. A case study 02 p0666 N94-13158
The power of cross-functional teams in driving total quality 02 p0666 N94-13159
Spacecraft COst REduction Team (SCORE): TQM/CI on a massive scale 02 p0667 N94-13160
Object-oriented productivity metrics 02 p0667 N94-13161
Kennedy Space Center's NASA/Contractor Team-Centered Total Quality Management Seminar: Results, methods, and lessons learned 02 p0667 N94-13162
Here's the beef: A case study in organizational transformation 02 p0667 N94-13163
Building a quality culture in the Office of Space Flight: Approach, lessons learned and implications for the future 02 p0667 N94-13164
NASA Johnson Space Center: Total quality partnership 02 p0668 N94-13165
Teamwork for Oversight of Processes and Systems (TOPS). Implementation guide for TOPS version 2.0, 10 August 1992 02 p0668 N94-13167
NASA/contractor partnership on the second TDRSS ground terminal program: Breaking barriers 02 p0668 N94-13168
Government/contractor partnerships for continuous improvement. A Goddard Space Flight Center example 02 p0669 N94-13169
Pollution prevention through total quality
[DE93-013814] 02 p0707 N94-13390
George M. Low Trophy: NASA's quality and excellence award. 1992 recipients: Honeywell Clearwater, IBM Houston
[NASA-TM-109265] 02 p0669 N94-13396
The Eighth Annual NASA/Contractors Conference and 1991 National Symposium on Quality and Productivity: Extending the boundaries of total quality management
[NASA-TM-109276] 02 p0669 N94-14321
Army Software Test and Evaluation Panel (STEP) software metrics initiatives report
[AD-A266889] 03 p1142 N94-14924
Creating and maintaining a visionary quality program
[DE93-015122] 03 p1050 N94-16055
Impact of TQM concepts on inspection of aerospace systems
[TABES PAPER 93-350] 03 p1050 N94-16130
Total quality environmental management leadership through quality
[TABES PAPER 93-540] 03 p1050 N94-16135
Identifying and responding to customer needs at the Kennedy Space Center 03 p1056 N94-16626
Document control and conduct of operations
[DE93-016555] 04 p1613 N94-17880

Quality, management, and the interplay of self-assessment, process assessments, and performance-based observations
[DE93-018787] 04 p1448 N94-19336
The NCC project: A quality management perspective
05 p1828 N94-21324
NCCDS configuration management process improvement 05 p1931 N94-21327
Problem reporting management system performance simulation 05 p1931 N94-21328
The automated ground network system
05 p1932 N94-21330
The application of total quality management principles to spacecraft mission operations
06 p2374 N94-23931
Mission operations and command assurance: Instilling quality into flight operations 06 p2374 N94-23932
Statistical quality management
[MEMO-COSOR-92-43] 07 p2834 N94-26008
Qualified manufacturing and interoperability for space applications 07 p2949 N94-26719
The development and demonstration of the metric assessment tool
[AD-A275788] 08 p3230 N94-28742
An evaluation of techniques for ranking academic information systems journals
[AD-A275179] 08 p3529 N94-29066
Why TQM fails (and what you can do about it)
[DE93-018945] 08 p3527 N94-30698
Process mapping: A user-friendly tool for process improvement
[DE94-004357] 09 p3730 N94-31605
Application of Artificial Intelligence to the DoD Corporate Information Management (CIM) program
[AD-A276656] 09 p3834 N94-32061
CIM in space: Corporate Information Management (CIM) implications for space-based information systems
[AD-A276882] 09 p3600 N94-32126
Case studies of software process improvement methods
[AD-A277289] 09 p3818 N94-32508
Agile total quality guidelines for enhancing teamwork and success
[DE93-019972] 09 p3915 N94-32678
Total Quality Management implementation guidelines
[DE94-007232] 09 p3915 N94-32723
Mission operations and command assurance: Flight operations quality improvements
10 p4150 N94-33616
A survey of commonly appiied methods for software process improvement
[AD-A278595] 12 p4493 N94-36974

TOTAL VARIATION DIMINISHING SCHEMES
U TVD SCHEMES

TOUCH
NT TACTILE DISCRIMINATION
Cortical substrate of haptic representation
[AD-A269583] 04 p1508 N94-18304
Robot navigation in unknown terrains: Introductory survey of non-heuristic algorithms
[DE93-019221] 04 p1316 N94-19300
Mechanisms of eye-hand coordination
[AD-A273687] 06 p2428 N94-25437

TOUGHNESS
NT NOTCH SENSITIVITY
Damping measurements for ultra-high carbon steel/brass laminates
[DE93-011886] 01 p0082 N94-11076
Processing and properties of coated HPZ fiber reinforced glass-ceramic matrix composites
[AD-A265177] 01 p0092 N94-11876
Processing and testing of high toughness silicon nitride ceramics
[NASA-CR-191190] 02 p0582 N94-14543
An investigation of the role of second phase particles in the design of ultra high strength steels of improved toughness
[AD-A266774] 02 p0573 N94-14786
Transformation toughening of composite ceramics
[AD-A267304] 03 p0971 N94-16980
Micromechanisms of monotonic and cyclic subcritical crack growth in advanced high melting point low-ductility intermetallics
[AD-A267764] 03 p0961 N94-17223
Charpy impact toughness of martensitic steels irradiated in FFTF: Effect of heat treatment
[DE93-015960] 04 p1450 N94-17848
Mechanism-dependent fractal character of fracture surfaces in high strength and toughness ASTM A723 steels
[AD-A268956] 04 p1360 N94-18542
Properties and potential of high-temperature niobium beryllides
[DE93-019169] 05 p1690 N94-20233
Weldalite (tm) 049 (Al 2095-T8): Anisotropy effects at cryogenic conditions
[AD-A272658] 05 p1691 N94-21188
Determination of fracture stress and effective crack tip radius from toughness (Klc) and yield strength (Y)
[AD-A274014] 07 p2836 N94-25754
Numerical simulations of interfacial debonding in ductile-phase reinforced intermetallic matrix composites
[DE94-003639] 07 p2706 N94-25938
Interface phenomena in metal-ceramic composites
[AD-A274167] 07 p2709 N94-27125
Testing procedure for toughness characterisation of ceramic matrix composites
[REPT-932-430-101] 07 p2711 N94-27586
Toughening mechanisms in ultrahigh-strength steels
[AD-A275439] 08 p3202 N94-28867
Poly(arylene ether-co-imidazole)s as toughness modifiers for epoxy resins
[NASA-CASE-LAR-15229-1-CU]
08 p3215 N94-29451
Toughening mechanisms in the high strain rate deformation of rubber-modified polymer glasses
09 p3653 N94-31942
Toughening mechanisms in fiber-reinforced ceramic-matrix composites 09 p3622 N94-31943
Correlation of flux composition and inclusion characteristics with submerged arc weld metal properties in HY-100 steel
[AD-A277040] 09 p3726 N94-32261
The effect of ductile phase (Nb) reinforcement morphology on the mechanical behavior of an intermetallic matrix (MoSi2)
09 p3615 N94-32500
New mechanism for toughening ceramic materials
[AD-A278479] 10 p4027 N94-33747
Tough, processable semi-interpenetrating polymer networks from monomer reactants
[NASA-CASE-LAR-14838-1] 11 p4242 N94-35233

TOWED BODIES
A microprocessor controller for a towing tank drive and flow visualisation system
[AD-A267087] 03 p0872 N94-15543
Nominally two-dimensional flow about a normal flat plate 08 p3275 N94-29838
A handling qualities investigation of conventional, rate command and attitude hold, and attitude command and attitude hold response types in the probe and drogue air refueling task
[AD-A278464] 10 p4006 N94-33543
Hose-drogue versus boom receptacle air refueling
11 p4197 N94-36345

TOWED TARGETS
U TARGETS
U TOWED BODIES

TOWERS
NT AIRPORT TOWERS
Cooling towers for combined cycles: Design philosophy, performance testing, and operating problems
07 p2832 N94-28087
Study of bridge design and technology
[PB94-137916] 08 p3121 N94-29160

TOWING
Calibration of anemometers at low speed by means of towing carriage 01 p0164 N94-12619
A microprocessor controller for a towing tank drive and flow visualisation system
[AD-A267087] 03 p0872 N94-15543
Unscreened low tension cables scrape abrasion testing
[PB94-123767] 07 p2823 N94-26849

TOWNSEND DISCHARGE
NT GAS DISCHARGES
High counting rate resistive-plate chamber
[DE93-014928] 02 p0651 N94-14452

TOXIC DISEASES
NT LEAD POISONING
Fibers and materials of medical application
03 p0938 N94-16855

TOXIC HAZARDS
Estimation of the concentration versus the time profile of zinc chloride particles in smoke clouds generated by the Raufoss A/S instantaneous smoke RA-90 and DM-45 HC smoke generator
[FFI-93/6001] 02 p0708 N94-13821
Toxic Substances Control Act (TSCA) chemical substances inventory: Revised inventory synonym and preferred name file, Jan. 1993 documentation
[PB93-155166] 02 p0710 N94-14508
Toxic substances registry system: Index of material safety data sheets
[NASA-TM-109332] 03 p1121 N94-15658
Proceedings of the 1992 Annual Meeting NASA Occupational Health Program
[NASA-CR-193462] 03 p1123 N94-16609
Emergency preparedness and planning
03 p1124 N94-16613
Lead poisoning: An overview
03 p1124 N94-16614
Medical surveillance and biological monitoring of lead exposed employees 03 p1124 N94-16615
Education and training of professional industrial hygienists for 2020 03 p1125 N94-16618
Arsenic surveillance program
03 p1127 N94-16637
Lead Surveillance Program 03 p1127 N94-16640
Respiratory Protection Program medical clearance for respirator use 03 p1127 N94-16642
General Medical Surveillance Program
03 p1127 N94-16643
Environmental use of a Laser Range Finder and the Advanced Visualization System
[DE93-016163] 03 p1043 N94-17677
Review of short-term, high-level exposure to metals: Antimony, barium, and cadmium
[AD-A268896] 04 p1505 N94-18392
A review and evaluation of the ADAM 2.1 dispersion model
[AD-A269896] 04 p1474 N94-18688
Automated in-situ inspection systems for underground storage tanks
[AD-A274644] 07 p2764 N94-27144
Characterization of air emissions from the simulated open combustion of fiberglass materials
[PB94-136231] 08 p3347 N94-29192
Toxicity of carbon monoxide-hydrogen cyanide gas mixtures: Exposure concentration, time-to-incapacitation, carboxyhemoglobin, and blood cyanide parameters
[DOT/FAA/AM-94/7] 08 p3395 N94-29919
Applying robotics to HAZMAT
09 p3729 N94-32452
Controlling hazardous energy sources (lockout/tagout)
[NASA-TM-105290] 09 p3669 N94-32861
Air quality assessment and control
[DE94-000046] 10 p4081 N94-33725
Crystal growth furnace safety system validation
[NASA-CR-193964] 10 p4056 N94-34266
Solid state fluorometer: Prototype development
[AD-A280321] 12 p4534 N94-37027

TOXICITY
NT LEAD POISONING
Toxic chemical release inventory reporting Form R and instructions. Revised 1992 version. Section 313 of the Emergency Planning and Community Right-to-Know Act
[PB93-194140] 01 p0264 N94-10836
Toxicity study of dimethylethoxysilane (DMSES), the waterproofing agent for the Orbiter heat protective system 01 p0318 N94-11554
A combustion products analyzer for contingency use during thermodegradation events on spacecraft
01 p0318 N94-11555
Wind system documentation
[DE93-010381] 01 p0285 N94-11664
Biomass production chamber air analysis of wheat study (BWT931)
[NASA-TM-109192] 02 p0737 N94-13712
Synthetic lubricants and high-performance functional fluids: Phosphazenes
[ARL-TR-45] 02 p0580 N94-14126
Toxic Substances Control Act (TSCA) chemical substances inventory: Revised inventory synonym and preferred name file, Jan. 1993 documentation
[PB93-155166] 02 p0710 N94-14508
Toxic substances registry system: Index of material safety data sheets
[NASA-TM-109332] 03 p1121 N94-15658
Neurotoxicity of hemoglobin in cortical cell culture
[AD-A266506] 03 p1128 N94-16786
A review and evaluation of the ADAM 2.1 dispersion model
[AD-A269896] 04 p1474 N94-18688
The role of chemical inhibition of gap junctional intercellular communication in toxicology
[AD-A269251] 04 p1502 N94-18924
A study of the effect of hydrocarbon structure on the induction of male rat nephropathy and metabolic structure
[AD-A270969] 04 p1504 N94-19789
Manual of DRANC (release 1.1): A computer program for the Dutch risk assessment of new chemical substances
[PB93-194827] 05 p1851 N94-19998
Toxicity of thermal degradation in a manned space environment 05 p1664 N94-21403
Exploratory report nickel and nickel compounds
[PB93-223998] 06 p2242 N94-23496
Exploratory report antimony and antimony compounds
[PB93-224004] 06 p2397 N94-23497
In vitro system for studying metabolism of environmental chemicals in human cells
[AD-A273427] 06 p2421 N94-24688

A statistical analysis of recent Naval Experimental Diving Unit (NEDU) single-depth human exposures to 100 percent oxygen at pressure
[AD-A273488] 06 p2427 N94-24950
The effects of zinc borate addition on the flammability characteristics of polyester, vinyl ester, and epoxy glass reinforced plastics
[AD-A273164] 06 p2262 N94-25136
An exploratory stochastic model for toxic effects on cells
[AD-A273438] 06 p2422 N94-25146
Toxicity of carbon monoxide-hydrogen cyanide gas mixtures: Exposure concentration, time-to-incapacitation, carboxyhemoglobin, and blood cyanide parameters
[DOT/FAA/AM-94/7] 08 p3395 N94-29919
Intermedia transfer factors for fifteen toxic pollutants released to air basins in California
[DE94-005699] 08 p3349 N94-30044
Computerized in vitro test for chemical toxicity based on tetrahymena swimming patterns
08 p3354 N94-30463
Formation of gas-phase peroxides in a rural atmosphere: An interpretation of the recent SOS/SERON field results
[DE94-002995] 09 p3766 N94-32692
High efficiency InP solar cells from low toxicity tertiarybutylphosphine
[NASA-TM-106598] 10 p4039 N94-33611
A model for predicting central nervous system toxicity from hyperbaric oxygen exposure in man: Effects of immersion, exercise, and old and new data
[AD-A276348] 10 p4095 N94-34005
Toxic emissions from aircraft engines: A search of available literature
[PB94-156486] 10 p3999 N94-34400
Toxic emissions from aircraft firefighting training: A search of available literature
[PB94-156783] 10 p4083 N94-34409
CAirTOX: A compartment model for assessing the fate of and human exposure to toxic-chemical emissions to air
[DE94-010084] 11 p4284 N94-35700
Treatment of toxic gases SO2 and NO(x) by electron beam irradiation
[DE94-615424] 11 p4330 N94-36028

TOXICITY AND SAFETY HAZARD
Environmentally Safe and Effective Processes for Paint Removal
[AGARD-R-791] 01 p0126 N94-10613
Toxic Substances Control Act (TSCA) chemical substances inventory: Revised inventory synonym and preferred name file, Jan. 1993 documentation
[PB93-155166] 02 p0710 N94-14508
Emergency preparedness and planning
03 p1124 N94-16613
Medical surveillance and biological monitoring of lead exposed employees 03 p1124 N94-16615
Fire behavior of aeronautical materials
[REPT-932-600-105] 08 p3197 N94-29457
Toxic emissions from aircraft firefighting training: A search of available literature
[PB94-156783] 10 p4083 N94-34409

TOXICOLOGY
A combustion products analyzer for contingency use during thermodegradation events on spacecraft
01 p0318 N94-11555
Development of pattern recognition techniques for the evaluation of toxicant impacts to multispecies systems
[AD-A267197] 03 p1095 N94-15790
The behavioral toxicology of high-peak, low average power, pulsed microwave irradiation
[AD-A268392] 03 p1134 N94-17535
Review of short-term, high-level exposure to metals: Antimony, barium, and cadmium
[AD-A268896] 04 p1505 N94-18392
The role of chemical inhibition of gap junctional intercellular communication in toxicology
[AD-A269251] 04 p1502 N94-18924
Proceedings of the symposium on current concepts and approaches on animal test alternatives
[AD-A273926] 07 p2900 N94-25593
Bakteriella toxiner-morgondagens hot (bacterial toxins-the threat of tomorrow)
[PB94-124229] 07 p2902 N94-27045

TOXINS AND ANTITOXINS
An exploratory stochastic model for toxic effects on cells
[AD-A273438] 06 p2422 N94-25146
Bakteriella toxiner-morgondagens hot (bacterial toxins-the threat of tomorrow)
[PB94-124229] 07 p2902 N94-27045
Effects of pressure on membrane-associated receptors and effector elements
[AD-A275813] 08 p3384 N94-28829

TQM (QUALITY CONTROL)
U TOTAL QUALITY MANAGEMENT

TRACE CONTAMINANTS
Project AIRSTREAM: Trace gas
[DE93-008849] 02 p0706 N94-12904
Performance effects of coal-derived contaminants on the carbonate fuel cell
[DE93-013801] 02 p0703 N94-13693
Destruction of problematic airborne contaminants by hydrogen reduction using a Catalytically Active, Regenerable Sorbent (CARS)
[NASA-CR-194354] 02 p0709 N94-14103
Importance of sprays for long range transport of harmful substances in the troposphere
[MITT-81] 02 p0711 N94-14723
Gas separations using ceramic membranes
[DE93-000278] 03 p0947 N94-15861
Application of non-thermal plasmas to pollution control
[DE93-016432] 03 p1096 N94-16449
Trace analysis of chemical warfare agents in air: Sampling in porous polymers followed with thermal desorption analysis
[FOA-C-40302-4.6] 03 p1097 N94-17625
Characterization of Ni on Si wafers: Comparison of surface analysis techniques
[DE93-016501] 03 p0953 N94-17649
A technique for measuring winds in the lower atmosphere using incoherent Doppler lidar
[DE93-017163] 04 p1488 N94-17758
Analysis of HgI2 and PbI2 crystals and detectors by Particle-Induced X Ray Emission (PIXE) and Ion Backscattering Spectroscopy (IBS)
[DE93-017168] 04 p1594 N94-17896
A mobile remote sensing laboratory for water vapor, trace gas, aerosol, and wind speed measurements
[DE93-017158] 04 p1489 N94-18132
CDIAC catalog of numeric data and computer model packages
[DE93-017675] 04 p1475 N94-18832
Suitability of infrared spectroscopy for remote sensing of tropospheric trace gases
[KFK-5183] 04 p1479 N94-19507
Application of an atmospheric dispersion model to simulated pollutant releases in the Colorado Front range
[DE93-017118] 04 p1480 N94-19732
Ethylene trace-gas techniques for high-speed flows
[NASA-TM-106491] 06 p2169 N94-24335
Evaluation of a Canadian minitube air sampling system
[FOA-C-40307-4.6] 07 p2866 N94-25809
Assessing the climatic effect of carbon dioxide and other trace gases using an interactive two-dimensional climate-chemistry model
[DE94-001741] 07 p2866 N94-25927
Developing a diode array spectrometer for tropospheric chemistry studies 08 p3362 N94-29752
Using spacecraft trace contaminant control systems to cure sick building syndrome 08 p3354 N94-30470
A new material for removing heavy metals from water
08 p3354 N94-30471
Control and monitoring of heavy metal emissions
[VTT-TIED-1508] 09 p3765 N94-31657
Safety concerns for first entry operations of orbiting spacecraft 10 p4102 N94-33662
A users' guide to the trace contaminant control simulation computer program
[NASA-TM-108456] 10 p4080 N94-33696
Trace contaminant control simulation computer program, version 8.1
[NASA-TM-108457] 10 p4100 N94-33973
Global tropospheric chemistry models for radiatively important trace species: Design and research recommendations
[DE94-007089] 11 p4288 N94-36359

TRACE ELEMENTS
Minor and trace element composition and age of Yukon probable-microtektites 01 p0429 N94-12094
Trace-element abundances in several new ureilites
01 p0080 N94-12096
SXRF determination of trace elements in chondrule rims in the unequilibrated CO3 chondrite, ALH A77307
01 p0429 N94-12106
Trace element distributions in primitive achondrites
01 p0431 N94-12200
Isotopic and trace element characteristics of an unusual refractory inclusion from Essebi
01 p0471 N94-12212
Trace element content of chondritic cosmic dust: Volatile enrichments, thermal alterations, and the possibility of contamination 01 p0433 N94-12260
New low-Ni (igneous?) particles among the C and C? types of cosmic dust 01 p0433 N94-12262
Project AIRSTREAM: Trace gas
[DE93-008849] 02 p0706 N94-12904
Determination of trace elements in triglycine sulfate solutions
[NASA-CR-193481] 02 p0562 N94-13048
Modeling of the partitioning of reactive odd nitrogen in the lower stratosphere using aircraft measurements of NOy, NO, and other trace species
[NASA-CR-194305] 02 p0714 N94-13707
Measurement of HO2 and other trace gases in the stratosphere using a high resolution far-infrared spectrometer at 28 km
[NASA-CR-194175] 02 p0714 N94-13816
A proposed mechanism for the pyrolysis of diborane
[DE93-014275] 03 p0947 N94-15977
Assimilation of solids during ascent of magmas from the Bartoy Field of the Baikal Region, Siberia
03 p1103 N94-16214
Trace-element composition of Chicxulub crater melt rock, K/T tektites and Yucatan basement
03 p1242 N94-16245
Searching for neuKREEP: An EMP study of Apollo 11 Group A basalts 03 p1266 N94-16275
On the composition of neuKREEP: QMD contamination at Apollo 11? 03 p1266 N94-16276
Partitioning of Nb, Mo, Ba, Ce, Pb, Th and U between immiscible carbonate and silicate liquids: Evaluating the effects of P2O5,F, and carbonate composition
03 p0953 N94-16283
Explosive volcanism and the compositions of the cores of differentiated asteroids 03 p1243 N94-16306
An experimental study of trace element partitioning between perovskite, hibonite and melt: Equilibrium values 03 p0954 N94-16313
Noble gases in twenty Yamato H-chondrites: Comparison with Allan Hills chondrites and modern falls
03 p1244 N94-16361
Sensitive detection of gas-phase nitro-containing energetic materials employing 226-nm radiation
[AD-A267633] 03 p0951 N94-17203
Electron reversal ionizer for detection of trace species using a spherical cathode
[NASA-CASE-NPO-18870-1-CU]
03 p1185 N94-17329
Chemical tracer studies at IOSDL. 3: The measurement of silicate, nitrate and phosphate in seawater
[IOS-302-1992] 03 p1114 N94-17489
Carbon Dioxide Information Analysis Center: FY 1992 activities
[DE93-013845] 04 p1471 N94-17774
Analysis of HgI2 and PbI2 crystals and detectors by Particle-Induced X Ray Emission (PIXE) and Ion Backscattering Spectroscopy (IBS)
[DE93-017168] 04 p1594 N94-17896
CDIAC catalog of numeric data and computer model packages
[DE93-017675] 04 p1475 N94-18832
Global three dimensional model of tropospheric trace gases chemistry and transport
[AERONAUTICA-ACTA-A-370-1993]
04 p1479 N94-19518
Remote sounding of tropospheric minor constituents
[NASA-CR-194265] 05 p1855 N94-20132
Volatility in the lunar crust: Trace element analyses of lunar minerals by PIXE proton microprobe
05 p2097 N94-20661
Tambo Quemado: Extraordinary concentrations of REE and refractory trace elements caused by artificial heating
05 p1684 N94-20667
Orthopyroxenes as recorders of diogenite petrogenesis: Major and minor element systematics
05 p1684 N94-20670
Origin of the Apollo 15 very low Ti green glass. A perspective from the compositional diversity in the very low Ti glasses 05 p1685 N94-20759
Orthopyroxenes as recorders of diogenite petrogenesis: Trace element systematics 05 p1686 N94-20760
The formation of FeO-rich pyroxene and enstatite in unequilibrated enstatite chondrites: A petrologic-trace element (SIMS) study 05 p2086 N94-20866
Trace element compositions of spinel-rich refractory inclusions from the Murchison meteorite
05 p2086 N94-20897
Global emissions and models of photochemically active compounds
[DE93-040490] 05 p1852 N94-21969
Ethylene trace-gas techniques for high-speed flows
[NASA-TM-106491] 06 p2169 N94-24335
A dynamic melting model for the origin of Apollo 15 olivine-normative and quartz-normative mare basalts
06 p2615 N94-24371
Measurement of HO2 and other trace gases in the stratosphere using a high resolution far-infrared spectrometer
[NASA-CR-195173] 06 p2404 N94-24738
Rice cultivation and methane emission: Documentation of distributed geographic data sets
[NASA-TM-104595] 06 p2381 N94-24800
Reactive trace metals as indicators of subduction and ventilation processes in the ocean
[AD-A273585] 06 p2419 N94-25164

Study on neutron activation analysis
[DE93-632191] 07 p3017 N94-26116
JPL Fourier transform ultraviolet spectrometer
08 p3343 N94-28593
Absolute determination of local tropospheric OH concentrations 08 p3343 N94-28594
Developing a diode array spectrometer for tropospheric chemistry studies 08 p3362 N94-29752
Use of satellite data to improve parameterization of spatial and temporal variations of gaseous dry deposition in regional-scale models
[DE94-005110] 08 p3334 N94-30022
Evaluating models of climate and forest vegetation
08 p3353 N94-30637
The development and evaluation of a tunable diode laser trace gas sensor for the measurement of N2O and CH4 fluxes using micrometeorological techniques
[ISBN-0-315-78975-1] 08 p3296 N94-30801
Geochemical and fluid dynamic investigations into the nature of chemical variability in the Earth's mantle
08 p3367 N94-30917
Control and monitoring of heavy metal emissions
[VTT-TIED-1508] 09 p3765 N94-31657
Surface fluxes of trace gases derived from convective-layer profiles 09 p3704 N94-31774
Development of sample charge compensation for characterization of impurities in semiconductor materials
[AD-A277113] 09 p3899 N94-31983
Air quality assessment and control
[DE94-000046] 10 p4081 N94-33725
Global changes in biogeochemical cycles in response to human activities
[NASA-CR-191896] 10 p4083 N94-34685
Ar-39-Ar-40 ages of four ureilites
11 p4357 N94-35410
Distribution of siderophile and other trace elements in melt rock at the Chicxulub impact structure
11 p4352 N94-35456
Anatomy of a cluster IDP. Part 2: Noble gas abundances, trace element geochemistry, isotopic abundances, and trace organic chemistry of several fragments from L2008#5 11 p4352 N94-35465
The anatomy of a cluster IDP. Part 1: Carbon abundance, bulk chemistry, and mineralogy of fragments from L2008#5 11 p4352 N94-35466
Synthetic and natural Nakhla pyroxenes: Parent melt composition and REE partition coefficients
11 p4353 N94-36161
Integrated science model for assessment of climate change
[DE94-011758] 11 p4288 N94-36286
Accelerated line-by-line calculations for the radiative transfer of trace gases related to climate studies
[DE94-004404] 12 p4464 N94-36552

TRACERS
Cruise report: Oceanus 250 leg 4 high resolution profiler survey for the North Atlantic Tracer Release Experiment, 25 March - 24 April, 1992
[AD-A277935] 09 p3791 N94-33245

TRACHYTE
Stable isotope analyses of the peralkaline volcanics Gregory Rift Valley, Kenya 01 p0281 N94-12072

TRACKED VEHICLES
A newly developed snow vehicle (SM100S) for Antarctica. Part 1: Necessity and process of the development 08 p3314 N94-29981
A newly developed snow vehicle (SM100S) for Antarctica. Part 2: Design of the system
08 p3314 N94-29982
A newly developed snow vehicle (SM100S) for Antarctica. Part 3: Low temperature toughness of the welded joints of the structural steel
08 p3364 N94-29983
A newly developed snow vehicle (SM100S) for Antarctica. Part 4: Low temperature properties of crawler belt 08 p3314 N94-29984
A newly developed snow vehicle (SM100S) for Antarctica. Part 5: Result of general performance tests
08 p3314 N94-29985

TRACKING (POSITION)
NT CCD STAR TRACKER
NT COMPENSATORY TRACKING
NT INFRARED TRACKING
NT MISSILE TRACKING
NT MULTIPLE TARGET TRACKING
NT OPTICAL TRACKING
NT PHOTOGRAPHIC TRACKING
NT PURSUIT TRACKING
NT RADAR TRACKING
NT RADIO TRACKING
NT RANGE AND RANGE RATE TRACKING
NT SATELLITE TRACKING
NT SATELLITE-TO-SATELLITE TRACKING
NT SPACECRAFT TRACKING
NT STAR TRACKERS
NT VIDEO LANDMARK ACQUISITION AND TRACKING
Underwater hydrophone location survey
01 p0290 N94-10975
Quantitative EEG patterns of differential in-flight workload 01 p0317 N94-11528
Programmable Remapper project
[NASA-TM-109508] 03 p1164 N94-15515
Effects of window size and shape on accuracy of subpixel centroid estimation of target images
[NASA-TP-3331] 03 p1034 N94-15990
Visually guided touching and manual tracking
[TR-412] 03 p1166 N94-16581
Tracking with time-delayed data in multisensor systems
[AD-A271334] 04 p1391 N94-19582
A stereoscopic vision system with applications to automated docking and tracking
[AD-A270754] 04 p1333 N94-19765
A summary of studies of particle stability at RHIC
[DE93-040173] 05 p1970 N94-19868
Aviation safety research at the National Institute for Aviation Research, Wichita State University
[NIAR-93-4] 05 p1641 N94-20189
A flight test system design for the microwave landing system 05 p1645 N94-22156
A tracking sonar sensor for vehicle guidance
[OUEL-1956/92] 06 p2472 N94-23179
An adaptive multigrid model for hurricane track prediction 06 p2416 N94-23687
A mixed map/variable structure observer for target tracking 06 p2157 N94-24263
Predictive head movement tracking using innovations generated by Kalman filters
[ISBN-0-315-83371-8] 06 p2427 N94-24467
Digital tracking and control of retinal images
[AD-A275469] 08 p3389 N94-28810
Non-intrusive gaze tracking using artificial neural networks
[AD-A275186] 08 p3397 N94-28860
General theory and algorithms for the non-casual inversion, slewing and control of space-based articulated structures
[AD-A275118] 08 p3167 N94-29002
ACCS Surveillance Exploratory Prototype (ASEP)
08 p3138 N94-29566
An improved conscan algorithm based on a Kalman filter 08 p3251 N94-29670
Tracking roads in an aerial image by Kalman filtering
[TELECOM-93-D-007] 09 p3711 N94-31096
Study of a path planning and tracking system for an articulated mobile robot
[ISBN-0-315-86502-4] 09 p3831 N94-31800
A paraperspective factorization method for shape and motion recovery
[AD-A276513] 09 p3712 N94-31929
Automated detection of ship tracks in multispectral satellite data
[AD-A276697] 09 p3746 N94-32119
Fuzzy-neural control of an aircraft tracking camera platform 09 p3839 N94-32423
Effective declutter of complex flight displays using stereoptic 3-D cueing
[AD-A279764] 10 p3989 N94-33536
Tracking system options for future altimeter satellite missions 11 p4205 N94-35622
Estimation with multisensor/multiscan detection fusion
[AD-A278753] 11 p4256 N94-36092
Pointing and Tracking Systems
[AGARD-CP-539] 12 p4392 N94-36616
Landing of an unmanned helicopter on a moving platform. High accuracy navigation and tracking
12 p4387 N94-36618
Advanced helmet tracking technology developments for Naval aviation 12 p4393 N94-36623
Advances in helmet trackers
12 p4394 N94-36624
High accuracy control algorithm application to a tracking turret 12 p4394 N94-36626
Aeroservoelastic stabilization considerations for pointing and tracking systems 12 p4394 N94-36627
Studies and simulations on sensor fusion and cueing for fighter application 12 p4395 N94-36632
Sensor data fusion for air to air situation awareness beyond visual range 12 p4395 N94-36633
Global Positioning System Synchronized Active Light Autonomous Docking System
[NASA-CASE-MFS-28853-1] 12 p4395 N94-36825
Signal processing for the 1992 Barents Sea tomography experiment
[AD-A278580] 12 p4476 N94-36971
Manual tracking performance using a virtual hand controller: A comparison study 12 p4484 N94-37271
A comparison of two examples of magnetic tracker systems 12 p4485 N94-37275

TRACKING AND DATA RELAY SATELLITES
U TDR SATELLITES

TRACKING ANTENNAS
U DIRECTIONAL ANTENNAS

TRACKING FILTERS
Tracking with time-delayed data in multisensor systems
[AD-A271334] 04 p1391 N94-19582
Predictive head movement tracking using innovations generated by Kalman filters
[ISBN-0-315-83371-8] 06 p2427 N94-24467
Some neural computing approaches to target tracking
09 p3837 N94-33151

TRACKING NETWORKS
NT DEEP SPACE NETWORK
NT GLOBAL TRACKING NETWORK
NT MANNED SPACE FLIGHT NETWORK
NT RADAR NETWORKS
NT STDN (NETWORK)
Analysis of the eastern range multiplexed fiber optic IRIG B120 distribution system 01 p0139 N94-10996
On the accuracy of ERS-1 orbit predictions
03 p0874 N94-15589
Resource allocation planning with international components 06 p2520 N94-23963
Scheduling the future NASA Space Network: Experiences with a flexible scheduling prototype
06 p2520 N94-23965
Real-time tracking with a 3D-flow processor array
[DE94-003981] 07 p2980 N94-25984
The 25th Annual Precise Time and Time Interval (PTTI) Applications and Planning Meeting
[AD-A280955] 08 p3468 N94-30639

TRACKING PROBLEM
Derivation of three closed loop kinematic velocity models using normalized quaternion feedback for an autonomous redundant manipulator with application to inverse kinematics
[DE93-012823] 01 p0340 N94-12543
What is the radar tracking Glint problem and can it be solved?
[AD-A266509] 03 p0999 N94-16789
Feasibility and stability results for constrained stable generalized predictive control
[MATHS-REPT-A-203] 09 p3828 N94-31158
Strategy for tracking and grabbing a moving object with the aid of a decouplable manipulator with six degrees of freedom general architecture, guided by a vision system
[ISBN-0-315-86864-3] 09 p3831 N94-31757
The application of a radial basis function neural network for radar tracking over the sea 09 p3686 N94-33150
Some neural computing approaches to target tracking
09 p3837 N94-33151
The tracking control of nonlinear uncertain systems
10 p4008 N94-34331

TRACKING RADAR
Cancellation of multipath for monopulse radars
[ITN-93-85191] 02 p0600 N94-13538
Infrared spot tracker
[AD-D015778] 03 p1191 N94-16547

TRACKING STATIONS
NT GLOBAL TRACKING NETWORK
NT STDN (NETWORK)
Pre-operation analysis of ERS-1 tracking and operation, part 2-F
[NASDA-CNT-930002-PT-2-F] 01 p0230 N94-11130
Use of global positioning system measurements to determine geocentric coordinates and variations in Earth orientation 02 p0514 N94-14372
New perspectives for high accuracy SLR with second generation geodesic satellites 03 p0916 N94-15585
Computer networking at SLR stations
03 p0917 N94-15594
LLR: Activities in Wettzell 03 p0876 N94-15600
Upgrading of the Borowiec laser station
03 p0877 N94-15604
WLRS — Wettzell Laser Ranging System (WLRS)
03 p0877 N94-15606
Ground based laser ranging for satellite location
03 p0919 N94-15607
The third generation SLR station Potsdam no. 7836
03 p0877 N94-15623
Station report on the Goddard Space Flight Center (GSFC) 1.2 meter telescope facility
03 p0922 N94-15625
Enhanced networks operations using the X Window System 05 p1932 N94-21329
The automated ground network system
05 p1932 N94-21330
An in-depth analysis and modelling of the Shuttle to MILA S-band telemetry link 05 p1657 N94-21340
NASDA satellite mission operation system and operations 06 p2501 N94-23854

Radioastron flight operations
06 p2502 N94-23861
Automating satellite range scheduling
[AD-A273829] 07 p2694 N94-25738
Radio science ground data system for the Voyager-Neptune encounter, part 1
08 p3248 N94-29623
A genetic algorithm approach to automating satellite range scheduling
[AD-A278577] 11 p4226 N94-36188

TRACKING STUDIES
U TRACKING (POSITION)

TRACTION
Continuum modeling of materials that can undergo martensitic phase transitions
[AD-A268767] 04 p1360 N94-18386
The longitudinal free vibrations of a fixed-free two-phase elastic bar
[AD-A268768] 04 p1453 N94-18387
The temperature at the phase boundary during quasi-static motions of a two-phase thermoelastic bar
[AD-A268769] 04 p1596 N94-18388

TRACTORS
NT CRAWLER TRACTORS
NT TRACKED VEHICLES

TRACTS
U SITES

TRADEOFFS
Lunar lander and return propulsion system trade study
[NASA-TP-3388] 03 p0925 N94-16496
Squaring-down and the problems of almost-zeros for continuous-time systems
[PB93-237758] 06 p2489 N94-24608
Tokamak Physics Experiment (TPX) cost and performance trade studies using supercode
[DE94-002720] 06 p2553 N94-24628
Lunar base habitat designs: Characterizing the environment, and selecting habitat designs for future trade-offs
[NASA-CR-195687] 07 p2943 N94-27934
On the use of fuzzy logic assessment for high consequence implementation risk analysis
[DE94-011417] 12 p4507 N94-37564

TRAFFIC
NT AIR TRAFFIC
Traffic noise in a roundabout way
05 p1966 N94-21799
Estimation of delays and emissions at four-way junctions with different forms of regulation, principally four-way mandatory stop
[PB94-105236] 06 p2398 N94-23813
SIHTI: Energy and environmental technology
[DE94-763290] 12 p4464 N94-37007

TRAFFIC CONTROL
NT AIR TRAFFIC CONTROL
NT RADAR APPROACH CONTROL
Routing of freeway traffic: A discrete-time state space model and routing problems
[CWI-BS-R9232] 05 p1944 N94-21033
Emerging technologies
[DE94-003022] 07 p3102 N94-26023
Conception of snow information network system in Yamagata Prefecture 07 p2853 N94-27991

TRAILERS
Pressurized Lunar Rover (PLR)
07 p2833 N94-25704
Lunar surface operations. Volume 4: Lunar rover trailer
[NASA-CR-195554] 08 p3299 N94-29386
Implementation of instruments and facilities at the SGP CART site
[DE94-006839] 09 p3781 N94-31322

TRAILING EDGE FLAPS
Control effectiveness at hypersonic speeds
01 p0003 N94-10426
Calculation of maximum and high lift characteristics of multi element aerofoils 04 p1305 N94-18419
Efficient simulation of incompressible viscous flow over multi-element airfoils 04 p1306 N94-18421
Navier-Stokes calculations on multi-element airfoils using a chimera-based solver 04 p1306 N94-18422
Numerical solution of the Navier-Stokes equations for high-lift configurations on structured composite grids
04 p1306 N94-18423
High Reynolds number configuration development of a high-lift airfoil 04 p1306 N94-18424
A viscous-inviscid solver for high-lift incompressible flows over multi-element airfoils at deep separation conditions 04 p1306 N94-18425
Prediction of the high-lift performance of multi-element aerofoils using an unstructured Navier-Stokes solver
04 p1307 N94-18427
Navier-Stokes simulation of flow field around a blown-flap high-lift system 04 p1307 N94-18429
An experimental investigation of the optimum slat setting on a combat aircraft model 04 p1308 N94-18431
An experimental investigation of attachment-line transition on the slat of a combat aircraft model
04 p1308 N94-18432
Viscous phenomena affecting high-lift systems and suggestions for future CFD development
04 p1308 N94-18433
In-flight pressure distributions and skin-friction measurements on a subsonic transport high-lift wing section 04 p1308 N94-18435
High lift and the forward swept wing
04 p1308 N94-18436
A fast computing method for the flow over high-lift wings 04 p1308 N94-18437
Calculation of multielement airfoils and wings at high lift 04 p1309 N94-18438
Forty years of high-lift R/D: An aircraft manufacturer's experience 04 p1309 N94-18441
High-lift research: Application to the design of the ATR72 flap 04 p1309 N94-18442
The aero-mechanical design of a novel Fowler flap mechanism 04 p1309 N94-18443
High-lift design for large civil aircraft
04 p1310 N94-18445
High lift systems for transport aircraft with advanced airfoils 04 p1310 N94-18446
Choice and optimization of a high-lift system for an advanced amphibious aircraft 04 p1310 N94-18447
Reduction of structural loads using maneuver load control on the Advanced Fighter Technology Integration (AFTI)/F-111 mission adaptive wing
[NASA-TM-4526] 06 p2168 N94-24295
Selected topics on the active control of helicopter aeromechanical and vibration problems
11 p4200 N94-35874
Vibration reduction in helicopter rotors using an actively controlled partial span trailing edge flap located on the blade
[NASA-CR-4611] 11 p4280 N94-36423

TRAILING EDGES
NT BLUNT TRAILING EDGES
New aerodynamic information obtained from the solution of the inverse problem for aerofoils
[NAL-TR-1172] 01 p0014 N94-10860
An experimental study of a turbulent boundary layer in the trailing edge region of a curculation-control airfoil
[NASA-CR-194522] 02 p0508 N94-14541
The effect of the nose shape and wing location toward the wing vortex breakdown
[AD-A267724] 03 p0855 N94-14942
Lift enhancement device
[AD-D015868] 04 p1317 N94-17704
A design procedure for slotted flaps
04 p1305 N94-18418
Off-design performance of crenulated blades in a linear compressor cascade
[AD-A273744] 06 p2340 N94-25534
Effects of crenulations on three dimensional losses in a linear compressor cascade
[AD-A273778] 07 p2790 N94-25862
Control jets in interaction with hypersonic rarefied flow
07 p2698 N94-28020
Program for calculation of maximum lift coefficient of plain aerofoils and wings at subsonic speeds
[ESDU-93015] 07 p2649 N94-28076
Wing lift increment at zero angle of attack due to deployment of single-slotted flaps at low speeds
[ESDU-93019] 07 p2649 N94-28140
Potential flow modelling of airfoil stall
07 p2654 N94-28332
Attached and separated trailing edge flow measurements with a triple-split hot-film probe
07 p2656 N94-28339
Numerical analysis of airfoil for helicopter blade at high angle of attack using Navier-Stokes code
08 p3124 N94-28958
Numerical investigation of multi-element airfoils
[NASA-CR-194592] 11 p4191 N94-36394

TRAINEES
U STUDENTS

TRAINERS
U TRAINING DEVICES

TRAINING
U EDUCATION

TRAINING AIRCRAFT
NT T-38 AIRCRAFT
NT T-39 AIRCRAFT
STS-26 STA training (Hauck)
[NASA-TM-109555] 03 p0870 N94-15279
Aircraft wing structure detail design
[NASA-CR-195485] 06 p2180 N94-24498
Cockpit control system
[NASA-CR-195488] 06 p2190 N94-24957
Aircraft wing structural detail design (wing, aileron, flaps, and subsystems)
[NASA-CR-195487] 06 p2183 N94-24974
Design project: Viper
[NASA-CR-195484] 06 p2184 N94-25021
Fatigue design, test and in-service experience of the BAe Hawk 10 p3996 N94-34597

TRAINING ANALYSIS
Teaching high-performance skills using above-real-time training
[NASA-CR-4528] 01 p0315 N94-11627
SATORI: Situation Assessment Through the Re-creation of Incidents
[DOT/FAA/AM-93/12] 01 p0038 N94-12567
An information processing classification of beyond-visual-range air intercepts
[AD-A266927] 03 p1131 N94-15108
Aircrew life support, AFSC 122X0(1T1X1)
[AD-A268998] 04 p1511 N94-18394
Modelling decision-making by pilots
[NASA-CR-194767] 05 p2040 N94-21821
The effects of Above Real-Time Training (ARTT) in an F-16 simulator 09 p3591 N94-32474

TRAINING DEVICES
NT TEACHING MACHINES
Quantitative EEG patterns of differential in-flight workload 01 p0317 N94-11528
Defense RDT&E online system (DROLS) handbook
[AD-A267546] 03 p1232 N94-17101
Weather tutor 1: Stability basics
[AD-A270758] 05 p1866 N94-20565
Sparking young minds with Moon rocks and meteorites 05 p2039 N94-20819
Intelligent tutoring and aiding in satellite ground control 06 p2443 N94-23929
Aircraft empennage structural detail design
[NASA-CR-195496] 06 p2179 N94-24332
Cockpit control system conceptual design
[NASA-CR-195543] 06 p2190 N94-24551
A cognitive model of decision making: Chunking and the radar detection device
[AD-A275185] 08 p3242 N94-28859
Modular Simulator System (MSS) management guide
[AD-A277098] 09 p3588 N94-32014
Modular Simulator System (MSS). Executive report
[AD-A276966] 09 p3588 N94-32241
Modular Simulator System (MSS). System/segment specification for the generic MSS-system integration, volume 1
[AD-A276968] 09 p3588 N94-32312
Modular Simulator System (MSS). System/segment specification for the generic modular simulator system-flight station module, volume 2
[AD-A276969] 09 p3588 N94-32313
Modular Simulator System (MSS). System/segment specification for the generic modular simulator system-radar module, volume 8
[AD-A276975] 09 p3589 N94-32314
Modular Simulator System (MSS). System/segment specification for the generic modular simulator system-electronic warfare module, volume 9
[AD-A276976] 09 p3589 N94-32315
Modular Simulator System (MSS). System/segment specification for the generic modular simulator system-physical cues module, volume 10
[AD-A276977] 09 p3589 N94-32316
Modular Simulator System (MSS). System/segment specification for the generic modular simulator system-visual module, volume 11
[AD-A276978] 09 p3589 N94-32317
Modular Simulator System (MSS). System/segment specification for the generic modular simulator system-instructor/operator station module, volume 12
[AD-A276979] 09 p3589 N94-32318
Modular Simulator System (MSS). System/segment specification for the generic modular simulator system-environment module, volume 13
[AD-A276980] 09 p3589 N94-32319
Modular Simulator System (MSS). System/segment specification for the generic modular simulator system-flight controls module, volume 3
[AD-A276970] 09 p3590 N94-32395
Modular Simulator System (MSS). System/segment specification for the generic modular simulator system-flight dynamics module, volume 4
[AD-A276971] 09 p3590 N94-32396
Modular Simulator System (MSS). System/segment specification for the generic modular simulator system-propulsion module propulsion module, volume 5
[AD-A276972] 09 p3590 N94-32397
Modular Simulator System (MSS). System/segment specification for the generic modular simulator system-navigation/communication module, volume 6
[AD-A276973] 09 p3590 N94-32398
Modular Simulator System (MSS). System/segment specification for the generic modular simulator system-weapons module, volume 7
[AD-A276974] 09 p3590 N94-32399

Modular Simulator System (MSS): Interface design document for the generic MSS
[AD-A277270] 09 p3590 N94-32403
A systems approach to computer-based training 09 p3823 N94-32436
An evaluation framework for designing a night vision, computer-based trainer
[AD-A278005] 09 p3590 N94-33139
Telemedicine, virtual reality, and surgery 10 p4096 N94-33641
Using experimental design modules for process characterization in manufacturing/materials processes laboratories 11 p4230 N94-36405
Graphing techniques for materials laboratory using Excel 11 p4232 N94-36414
Evaluation of a tool for producing and presenting interactive videodisc job aids
[AD-A278599] 12 p4432 N94-36473
Assistance in instruction and training of air traffic controllers 12 p4483 N94-37265
Immersive virtual environments as trainer: System design from a cognitive stance 12 p4484 N94-37267

TRAINING EVALUATION
Teaching high-performance skills using above-real-time training
[NASA-CR-4528] 01 p0315 N94-11627
Mathematics B for the study direction VWO: A reconnaissance
[REPT-92-80] 05 p1950 N94-20032
KSC management training system project 06 p2574 N94-23246
Benefits estimation for simulation systems used for aircrew training in a multiship environment
[AD-A274313] 07 p2938 N94-26882
Aircraft simulation and pilot proficiency: From surrogate flying towards effective training
[AD-B179300] 09 p3587 N94-31179

TRAINING SIMULATORS
NT COCKPIT SIMULATORS
NT FLIGHT SIMULATORS
Teaching high-performance skills using above-real-time training
[NASA-CR-4528] 01 p0315 N94-11627
Space adaptation
[NASA-TM-109601] 03 p1120 N94-15309
Richards, Dick: Training clip
[NASA-TM-109503] 03 p0876 N94-15467
Infrared spot tracker
[AD-D015778] 03 p1191 N94-16547
An introduction to structural models
[AD-A268151] 03 p1155 N94-17429
Benefits estimation for simulation systems used for aircrew training in a multiship environment
[AD-A274313] 07 p2938 N94-26882
Data fusion and correlation techniques testbed development. Phase 1: Interim report
[SKD-1600-73-015] 08 p3405 N94-28533
Simulation Networking/Training Requirements Relational Database: User's guide
[AD-A275634] 08 p3528 N94-28637
Aircraft simulation and pilot proficiency: From surrogate flying towards effective training
[AD-B179300] 09 p3587 N94-31179
Virtual reality as a human factors design analysis tool: Macro-ergonomic application validation and assessment of the Space Station Freedom payload control area 10 p4100 N94-33620
Shared virtual environments for aerospace training 10 p4098 N94-34024
The application of fuzzy logic to SAFOR in SIMNET
[AD-A279058] 11 p4312 N94-35730
Immersive virtual environments as trainer: System design from a cognitive stance 12 p4484 N94-37267

TRAJECTORIES
NT ABORT TRAJECTORIES
NT ASCENT TRAJECTORIES
NT BALLISTIC TRAJECTORIES
NT DESCENT TRAJECTORIES
NT EARTH-MARS TRAJECTORIES
NT EARTH-MOON TRAJECTORIES
NT ELECTRON TRAJECTORIES
NT INTERORBITAL TRAJECTORIES
NT INTERPLANETARY TRAJECTORIES
NT LUNAR TRAJECTORIES
NT MISSILE TRAJECTORIES
NT MOLECULAR TRAJECTORIES
NT PARTICLE TRAJECTORIES
NT REENTRY TRAJECTORIES
NT RENDEZVOUS TRAJECTORIES
NT SPACECRAFT TRAJECTORIES
Feature association without a motion estimate
[AD-A265162] 01 p0138 N94-11891
Parachute system design, analysis, and simulation tool
[DE93-013755] 02 p0501 N94-13260
Inverse dynamics: Simultaneous trajectory tracking and vibration reduction with distributed actuators 02 p0678 N94-14624
Application of the A* algorithm to aircraft trajectory generation
[AD-A268728] 04 p1317 N94-18315
Cooperative control of multiple space manipulators
[AD-A270291] 04 p1445 N94-18813
Development and testing of a reliability performance index for modular robotic systems
[AD-A271901] 05 p1942 N94-20488
Decoupling problems around a trajectory: From linearity to nonlinearity
[MEMO-1115] 06 p2469 N94-22703
On the first integrals of geodesics
[DE93-612974] 07 p3007 N94-25603
Breakwire technique for hypervelocity measurement
[AD-A274779] 07 p2809 N94-26358
Iterative procedure as equation of motion
[DE94-608008] 08 p3453 N94-30078
Fast precise algorithm for simulation of ionization energy losses
[DE94-608010] 08 p3421 N94-30080
Visual processing of object velocity and acceleration
[AD-A277425] 09 p3801 N94-32998
Low encounter speed comet COMA sample return missions 11 p4202 N94-35607
Self-rescue strategies for EVA crewmembers equipped with the SAFER backpack 11 p4207 N94-35633

TRAJECTORY ANALYSIS
On renormalization group flow in matrix model
[DE93-613050] 01 p0409 N94-10413
Study of the surface circulation to the North of Bransfield Strait, Antarctica
[INPE-5472-TDI/503] 01 p0288 N94-11200
Modelling of dispersal and deposition of impact glass spherules from the Cretaceous-Tertiary boundary deposit 01 p0432 N94-12238
Simulation reduction using the Taguchi method
[NASA-CR-4542] 03 p1055 N94-17082
Flexible integration of path-planning capabilities
[AD-A269594] 04 p1541 N94-18463
Constant-thrust orbit-raising transfer charts
[AD-A269088] 04 p1334 N94-18718
Electrokinetic transport of heterogeneous particles in suspensions
[NASA-CR-194478] 04 p1353 N94-19367
Trajectory computations for an improved cinetheodolite tracking system 05 p1791 N94-22236
Path planning by querying persistent stores of trajectory segments
[NASA-CR-194789] 06 p2451 N94-23301
On the effect of the damping coefficients on the trajectories of symmetric and non-symmetric stores 06 p2155 N94-24250
Comparison of c.t.s. based prediction of store trajectory with flight test data 06 p2158 N94-24268
NASA/USRA advanced design program
[NASA-CR-195548] 06 p2180 N94-24492
NASA LaRC Workshop on Guidance, Navigation, Controls, and Dynamics for Atmospheric Flight, 1993
[NASA-CP-10127] 06 p2162 N94-25096
A survey of uncontrolled satellite reentry and impact prediction
[AD-A274903] 07 p2695 N94-26750
General theory and algorithms for the non-casual inversion, slewing and control of space-based articulated structures
[AD-A275118] 08 p3167 N94-29002
Advanced air traffic control and flight management system concepts 08 p3140 N94-29576
Experimental flight management system 08 p3141 N94-29580
Optimal low-thrust, Earth-Moon trajectories 08 p3159 N94-30961
Using Monte Carlo techniques and parallel processing for debris hazard analysis of rocket systems
[DE94-007250] 09 p3609 N94-31382
A paraperspective factorization method for shape and motion recovery
[AD-A276513] 09 p3712 N94-31929
Self-consistent effects of magnetospheric hydromagnetic waves on ring current ions
[AD-A277406] 09 p3774 N94-32346
Compatibility of TOPEX/Poseidon trajectory propagation with JPL and GSFC/FDF operational software 11 p4204 N94-35619
Improved solution accuracy for TDRSS-based TOPEX/Poseidon orbit determination 11 p4205 N94-35620
Angular momentum in the Local Group
[DE94-009322] 11 p4350 N94-35980

TRAJECTORY CONTROL
NT TRAJECTORY OPTIMIZATION
Neighboring extremal guidance for systems with piecewise linear control using time as the reference variable
[AD-A267942] 03 p0874 N94-17010
An application of parameter estimation to the stability and control of the BQM-147 unmanned aerial vehicle
[AD-A268741] 04 p1321 N94-18401
ControlShell: A real-time software framework
[AD-A269172] 04 p1523 N94-18879
Marsohkod movement control 06 p2370 N94-23418
A 6MeV heavy ion beam probe for the Large Helical Device
[AD-B183695L] 08 p3505 N94-29397
Profile negotiation: An air/ground automation integration concept for managing arrival traffic 08 p3140 N94-29578
Optimal low-thrust, Earth-Moon trajectories 08 p3159 N94-30961
ControlShell: A real-time software framework
[AD-A276481] 09 p3811 N94-31475
Trajectory learning with a direct drive robotic manipulator 09 p3831 N94-31794
Adaptive control of a robot in Cartesian coordinates: Analysis and implementation
[ISBN-0-315-86493-1] 09 p3831 N94-31798
On-line physical parameter identification and adaptive control of a launch vehicle 09 p3602 N94-31891
High-speed path constrained manipulator operation using optimal-feedback combined controller 09 p3833 N94-31962
Trajectory planning for space manipulators
[AD-A277229] 09 p3611 N94-32369
The tracking control of nonlinear uncertain systems 10 p4008 N94-34331
Yaw control by tangential forebody blowing 10 p3992 N94-34615
A linguistic geometry for space applications 10 p4123 N94-35050
A genetic technique for planning a control sequence to navigate the state space with a quasi-minimum-cost output trajectory for a non-linear multi-dimnensional system 10 p4123 N94-35052
Advanced information processing system: Hosting of advanced guidance, navigation and control algorithms on AIPS using ASTER
[NASA-CR-194960] 12 p4499 N94-37583

TRAJECTORY MEASUREMENT
Photogrammetric methods for trajectory measurements
[NLR-TP-91166-U] 02 p0650 N94-13527
About the accuracy of an image-based navigation system during the runway approach
[DLR-MITT-93-01] 04 p1316 N94-18146
Missile antenna pattern coordinate system and data formats
[AD-A269153] 04 p1385 N94-18260
Comparison of c.t.s. based prediction of store trajectory with flight test data 06 p2158 N94-24268
A simulator for multi-radar analysis for realistic traffic
[AD-B179099] 08 p3142 N94-30439

TRAJECTORY OPTIMIZATION
Progress in multidisciplinary design optimization at NASA Langley
[NASA-TM-107754] 01 p0318 N94-10814
Trajectory optimization for the national aerospace plane
[NASA-CR-194146] 02 p0516 N94-14104
Optimizing interplanetary trajectories with deep space maneuvers
[NASA-CR-4546] 02 p0532 N94-14851
Trajectory optimization for the National Aerospace Plane
[NASA-CR-194618] 03 p0867 N94-16498
Application of the A* algorithm to aircraft trajectory generation
[AD-A268728] 04 p1317 N94-18315
Flexible integration of path-planning capabilities
[AD-A269594] 04 p1541 N94-18463
Perspective of creation of means for collecting information concerning transport situation 06 p2370 N94-23420
A DTM-based path planning method for planetary rovers 06 p2370 N94-23423
Approximate optimal guidance for the advanced launch system
[NASA-CR-4568] 06 p2198 N94-24752
Optimal RTLS abort trajectories for an HL-20 personnel launch vehicle 06 p2165 N94-25114
Optimal nonlinear estimation for aircraft flight control in wind shear 07 p2643 N94-27296
Local performance optimization for a class of redundant eight-degree-of-freedom manipulators
[NASA-TP-3417] 07 p2989 N94-27773

A parametric sensitivity study for single-stage-to-orbit hypersonic vehicles using trajectory optimization
[NASA-CR-195703] 07 p2697 N94-27789
Profile negotiation: An air/ground automation integration concept for managing arrival traffic
08 p3140 N94-29578
Optimal low-thrust, Earth-Moon trajectories
08 p3159 N94-30961
Optimal control theory determination of feasible return-to-launch-site aborts for the HL-20 Personnel Launch System vehicle
[NASA-TP-3449] 12 p4396 N94-37260

TRAJECTORY PLANNING
Trajectory pattern inverse dynamics and control of nonlinear dynamics systems with application to flexible structures 01 p0181 N94-11219
Experiments in mobile robot navigation and range imaging
[DE93-013280] 01 p0341 N94-12598
Implementation and experimentation with a motion planning system
[ITN-93-85213] 02 p0755 N94-14505
An object-oriented program specification for a mobile robot motion control language
[AD-A267213] 03 p1166 N94-16986
Path planning for robotic truss assembly
[NASA-CR-194652] 03 p0897 N94-17280
Environmental use of a Laser Range Finder and the Advanced Visualization System
[DE93-016163] 03 p1043 N94-17677
Flexible integration of path-planning capabilities
[AD-A269594] 04 p1541 N94-18463
Adaptive path planning: Algorithm and analysis
[DE93-008348] 04 p1523 N94-18926
Robot skill learning and the effects of basis function choice
[TR-437] 05 p1939 N94-20135
Development and evaluation of a profile negotiation process for integrating aircraft and air traffic control automation
[NASA-TM-4360] 05 p1643 N94-21606
An adaptive control to enable a robot to follow Cartesian trajectories 05 p1790 N94-22229
An algorithm for the interference detection among polygonal surfaces 05 p1791 N94-22239
Strategy for motion of a moving body of quasi-polygonal form within a polygonal space 05 p1792 N94-22240
Analytical representation of working articulation space of a plane manipulator in an encumbered environment
05 p1792 N94-22241
Motion planning for a non-holonomic mobile in a dynamic workspace
[ETN-94-95180] 06 p2470 N94-22898
Path planning by querying persistent stores of trajectory segments
[NASA-CR-194789] 06 p2451 N94-23301
Perspective of creation of means for collecting information concerning transport situation
06 p2370 N94-23420
A DTM-based path planning method for planetary rovers 06 p2370 N94-23423
Physical modeling and dynamic simulation of planet vehicles: Application to the motion prediction
06 p2371 N94-23426
Conflict-free trajectory planning for air traffic control automation
[NASA-TM-108790] 06 p2174 N94-25272
A global approach to kinematic path planning to robots with holonomic and nonholonomic constraints
07 p2683 N94-26279
Application of the CIRSSE cooperating robot path planner to the NASA Langley truss assembly problem
07 p2683 N94-26280
Adaptive path planning in changing environments
[DE94-003269] 07 p2985 N94-26462
Dynamic control of kinematically redundant manipulators
[ISBN-0-315-84627-5] 07 p2825 N94-27344
Local performance optimization for a class of redundant eight-degree-of-freedom manipulators
[NASA-TP-3417] 07 p2989 N94-27773
A parametric sensitivity study for single-stage-to-orbit hypersonic vehicles using trajectory optimization
[NASA-CR-195703] 07 p2697 N94-27789
Integration of a path generation algorithm into off-line programming of airbus panels
[REPT-932-600-103] 08 p3435 N94-29480
Air-ground integration of the ATM system in PHARE
08 p3141 N94-29579
Experimental flight management system
08 p3141 N94-29580
The PHARE advanced tools 08 p3141 N94-29581
Collision avoidance and control of multiple revolute manipulators 08 p3302 N94-29684
The NRC mobile robot project
08 p3305 N94-30280
An optimal obstacle avoidance path planning algorithm for the Excalibur robot 08 p3306 N94-30287
Motion control of mobile robots
08 p3310 N94-30309
Unmanned vehicle mobility: Limits of autonomous navigation 08 p3310 N94-30311
A probabilistic approach to motion planning for car-like robots
[RUU-CS-93-18] 08 p3438 N94-30410
Fuzzy logic based robotic controller
[AIAA PAPER 94-1202-CP] 08 p3443 N94-30553
Aspects of vision and planning in a dynamic, uncertain environment 08 p3448 N94-30803
The experimental flight management system: An air traffic management research tool
[NLR-TP-92253-U] 08 p3143 N94-30943
ControlShell: A real-time software framework
[AD-A276481] 09 p3811 N94-31475
Abstracts of the Workshop on Computational Geometry (CG 1992)
[PB94-147022] 09 p3844 N94-31684
Penetration distances and their applications to path planning 09 p3858 N94-31725
Strategy for tracking and grabbing a moving object with the aid of a decouplable manipulator with six degrees of freedom general architecture, guided by a vision system
[ISBN-0-315-86864-3] 09 p3831 N94-31757
Study of a path planning and tracking system for an articulated mobile robot
[ISBN-0-315-86502-4] 09 p3831 N94-31800
Trajectory planning for space manipulators
[AD-A277229] 09 p3611 N94-32369
A six degree of freedom, plume-fuel optimal trajectory planner for spacecraft proximity operations using an A* node search
[NASA-CR-188285] 09 p3601 N94-32388
A test system of pose repeatability precision of multi-path robot 10 p4067 N94-34341
A genetic technique for planning a control sequence to navigate the state space with a quasi-minimum-cost output trajectory for a non-linear multi-dimnensional system 10 p4123 N94-35052
Robot trajectory planning via dynamic programming
[DE94-008424] 12 p4501 N94-37529

TRANSATMOSPHERIC VEHICLES
Hypersonic, nonequilibrium flow over a cylindrically blunted 6 deg wedge
[NASA-TM-108994] 01 p0162 N94-12571
Numerical study on the interaction between scramjet engine modules caused by thermal choke
08 p3125 N94-28960
The National Aerospace Plane (NASP): Development issues for the follow-on vehicle
[AD-A278417] 09 p3581 N94-33329

TRANSCEIVERS
U TRANSMITTER RECEIVERS

TRANSCENDENTAL FUNCTIONS
NT COSINE SERIES
NT EXPONENTIAL FUNCTIONS
NT LOGARITHMS
NT PERIODIC FUNCTIONS
NT SINE SERIES
NT TRIGONOMETRIC FUNCTIONS
Applications of computer algebra to distributed parameter systems 02 p0677 N94-14623
Variations in the modal characteristics of a telescopically deploying beam 11 p4218 N94-35872
Review of Mathematical Function Library for Microsoft-FORTRAN, John Wiley and Sons, 1989
[PB94-160793] 11 p4305 N94-36010

TRANSCONDUCTANCE
DLTS and dynamic transconductance analysis of deep-submicron fully-depleted SOI MOSFET's
[AD-A267291] 03 p1214 N94-17243
Field emitter array RF amplifier development project, phase 1, option 1
[AD-A268687] 04 p1396 N94-18293
DC and small-signal physical models for the AlGaAs/GaAs high electron mobility transistor
04 p1401 N94-18370

TRANSDUCERS
NT DIGITAL TRANSDUCERS
NT ELECTROACOUSTIC TRANSDUCERS
NT ELECTRONIC TRANSDUCERS
NT HYDROPHONES
NT LOUDSPEAKERS
NT MICROPHONES
NT PIEZOELECTRIC GAGES
NT PIEZOELECTRIC TRANSDUCERS
NT PIEZORESISTIVE TRANSDUCERS
NT PRESSURE SENSORS
NT SOUND TRANSDUCERS
NT THERMOPILES
NT TORQUERS
NT ULTRASONIC WAVE TRANSDUCERS
The 17th Transducer Workshop
[AD-A265526] 01 p0141 N94-10509
Direct current transducer
[DE92-644548] 01 p0141 N94-10533
Design of a matching network for dipole antennas
[AD-A265115] 01 p0136 N94-11158
Strategies and methodologies to develop techniques for computer-assisted analysis of gas phase formation during altitude decompression 01 p0312 N94-11547
Ceramic actuators for smart materials
[AD-A265664] 01 p0093 N94-12331
Liquid metal drop ejection
[NASA-CR-193718] 02 p0572 N94-14133
A description of the computer program CALDK38 which controls instrumentation set-up and data acquisition during deadweight calibration using an HBM DK 38 S6 digital measuring unit
[LTR-ST-1935] 02 p0754 N94-14496
Long baseline watertubes 03 p1037 N94-15803
Cooperative projects in geodynamical instrumentation between the State Seismological Bureau (China) and the Royal Observatory of Belgium 03 p1037 N94-15806
Evaluation of the production-grade class 4 flextensional transducer shell
[AD-A268796] 04 p1340 N94-18201
Residual strain measurement on the production-grade class 4 flextensional transducer shell
[AD-A268828] 04 p1430 N94-18537
Transducers and method for making same
[AD-D015949] 04 p1408 N94-19759
FSR based force torque transducer design
[AD-A271337] 05 p1650 N94-19879
Three dimensional ultrasonic imaging
[DE93-040549] 05 p1968 N94-22003
Improved magnetostrictive transducer drive elements achieved by reduction of crystalline defects and improved crystalline orientation
[AD-A273391] 06 p2313 N94-25276
Characterization of structural vibration: Field descriptors based on energy density and intensity
[PB94-132230] 08 p3316 N94-28404
System for improving measurement accuracy of transducer by measuring transducer temperature and resistance change using thermoelectric voltages
[NASA-CASE-ARC-12014-1] 08 p3287 N94-29361
Method and apparatus for indicating disbonds in joint regions
[NASA-CASE-LAR-14626-1] 08 p3315 N94-29548
Errors associated with the use of heat flow transducers 09 p3796 N94-31742
Universal signal conditioning amplifier
09 p3699 N94-32460
The constant current loop: A new paradigm for resistance signal conditioning 09 p3685 N94-32461
Acoustic window
[AD-D016171] 09 p3862 N94-33017
A microcomputer measuring-controlling system for the performance test of fogging nozzles
10 p4032 N94-34362
Smart accelerometer --- vibration damage detection
[NASA-CASE-MSC-21951-1] 11 p4268 N94-35235
Analysis of achievable disturbance attenuation in a precision magnetically-suspended motion control system
11 p4225 N94-35917

TRANSFER
U TRANSFERRING

TRANSFER FUNCTIONS
NT LOOP TRANSFER FUNCTIONS
NT MODULATION TRANSFER FUNCTION
NT OPTICAL TRANSFER FUNCTION
ERS-1 scatterometer data characteristics and wind retrieval skill 01 p0233 N94-11709
The ideal Kolmogorov inertial range and constant
01 p0158 N94-12305
The helical decomposition and the instability assumption 01 p0158 N94-12306
Adaptive Transfer Function Networks
[DE93-014344] 02 p0745 N94-13151
Exploiting structure: Introduction and motivation
[NASA-CR-194199] 02 p0750 N94-13828
Water-vapour, total water and rainrate from passive microwave satellite data over ocean
[DLR-FB-92-37] 02 p0723 N94-14189
Selective excitation, relaxation, and energy channeling in molecular systems
[DE93-018819] 02 p0785 N94-14420
Report of the working group on theoretical tidal model
03 p1101 N94-15815
Fast-training algorithm for hidden-layer forward-feed neural networks
[AD-A269253] 04 p1540 N94-18263
Acoustic propagation modeling using MATLAB
[AD-A270905] 04 p1564 N94-19750
A theory for optical wavelength control in short pulse free electron laser oscillators
[AD-A271706] 05 p1817 N94-21353

Stochastic simulation for imaging spatial uncertainty: Comparison and evaluation of available algorithms
[DE93-040058] 05 p1916 N94-21761
Head related transfer function pseudo-stereophony
[NASA-CASE-ARC-11919-1-NP] 06 p2525 N94-23312
Squaring-down and the problems of almost-zeros for continuous-time systems
[PB93-237758] 06 p2489 N94-24608
Exploiting structure: Introduction and motivation
[NASA-CR-195136] 06 p2490 N94-24847
Human visual system enhancement of reconstructed satellite images
[AD-A273867] 07 p2693 N94-25595
Binaural room simulation
[AD-A273823] 07 p3009 N94-25737
Using a transfer function to describe the load-balancing problem
[DE94-004218] 07 p2979 N94-25802
Frequency-domain transfer-function identification using Chebyshev polynomials
[DE94-004777] 08 p3451 N94-28739
Polynomial modeling of analog-to-digital converters
[DE94-005579] 08 p3406 N94-30008
Structural properties of inverse linear systems
[MATHS-REPT-A-200] 09 p3840 N94-31156
Observations of the notion of minimality in the generalized state space
[MATHS-REPT-A-207] 09 p3840 N94-31162
Analysis and synthesis of MOS translinear circuits
[ISBN-9-09-005495-2] 09 p3690 N94-31616
Performance statistics bulletin. High latitude meteor scatter propagation October, November, December 1991, January 1992
[AD-A276724] 09 p3678 N94-32159
Performance statistics bulletin. High latitude meteor scatter propagation, June, July, August, September 1992
[AD-A277508] 09 p3685 N94-33347
Identification of mechanical systems using probabilistic neural networks
[DE94-007555] 10 p4114 N94-34296
A new robust adaptive algorithm based on intelligent integrators 10 p4122 N94-34371
Adaptive model reduction for continuous systems via recursive rational interpolation 11 p4219 N94-35876
LQG optimal compensator transfer function for the NASA LaRC CSI Evolutionary Model
11 p4221 N94-35891
Transfer function modeling of damping mechanisms in distributed parameter models 11 p4222 N94-35895

TRANSFER OF TRAINING

Transfer of training for aerospace operations: How to measure, validate, and improve it
01 p0314 N94-11530
Summer High School Apprenticeship Research Program (SHARP)
[NASA-CR-195956] 10 p4149 N94-34717

TRANSFER ORBITS

NT INTERPLANETARY TRANSFER ORBITS
In-space operations for lunar and Mars space transfer vehicles 01 p0348 N94-11568
In-space assembly-servicing requirements
01 p0348 N94-11569
Two temperature modeling and experimental measurements of laser sustained hydrogen plasmas
[AD-A265750] 02 p0796 N94-13039
Theory and computation of optimal low- and medium-thrust transfers
[NASA-CR-194812] 06 p2217 N94-23275
Assessment of an SP-100 bi-modal propulsion and power system
[DE94-000889] 06 p2218 N94-23433
HISPASAT launch and early operations phases: Computation and monitoring of geostationary satellite positioning 06 p2514 N94-23928
Charge efficiency of Ni/H2 cells during transfer orbit of Telstar 4 satellites 07 p2862 N94-28117
Theory and computation of optimal low- and medium-thrust transfers
[NASA-CR-196077] 11 p4202 N94-35487
A geometric model of a V-slit Sun sensor correcting for spacecraft wobble 11 p4206 N94-35628

TRANSFERRING

Attention and signal detection. A study of attention divided between visual and auditory signals
[PB94-170594] 11 p4298 N94-36215

TRANSFORM INTEGRALS

U INTEGRAL TRANSFORMATIONS

TRANSFORMATION TENSORS

U TENSORS

TRANSFORMATIONS (MATHEMATICS)

NT COORDINATE TRANSFORMATIONS
NT DISCRETE COSINE TRANSFORM
NT FAST FOURIER TRANSFORMATIONS
NT FOURIER TRANSFORMATION
NT FOURIER-BESSEL TRANSFORMATIONS
NT HILBERT TRANSFORMATION
NT INTEGRAL TRANSFORMATIONS
NT LAPLACE TRANSFORMATION
NT LINEAR TRANSFORMATIONS
Subband/transform functions for image processing
[NASA-TM-106183] 01 p0323 N94-10639
Analytical framework for modeling scale-related variabilities in remote sensing 02 p0685 N94-13592
Transform coding for space applications
[NASA-TM-106362] 02 p0612 N94-14542
On the nature of mirror particles
[DE93-626670] 03 p1179 N94-14934
Groups on transformations in Finslerian spaces
[DE93-624765] 04 p1606 N94-17794
A noniterative improvement of Guyan reduction
04 p1449 N94-17833
Avoiding degenerate coframes in an affine gauge approach to quantum gravity
[DE93-013146] 04 p1607 N94-17892
Deformed traces and covariant quantum algebras for quantum groups GL(sub qp)(2) and GL(sub qp)(1/1)
[DE93-629862] 04 p1561 N94-18153
On paragrassmann differential calculus
[DE93-628594] 04 p1548 N94-18169
A general solution of the BV-master equation and BRST field theories
[DE93-628622] 04 p1561 N94-18171
EDF tests for normality in linear models after a Box-Cox transformation
[AD-A269068] 04 p1557 N94-18517
Speech synthesis with artificial neural networks
05 p1743 N94-20245
Causal reconstruction
[AD-A271692] 05 p1908 N94-20929
Use of switched capacitor filters to implement the discrete wavelet transform 05 p1755 N94-21097
Classical and generalized solutions of time-dependent linear differential algebraic equations
[AD-A272834] 05 p1954 N94-21173
Data compression by using wavelet transforms and vector quantization
[AD-A272763] 05 p1738 N94-21182
Model-based automatic generation of grasping regions
[NASA-TM-104785] 05 p1946 N94-21550
Reduction of blocking effects for the JPEG baseline image compression standard 05 p1765 N94-21714
An in-place and in-order algorithm for the discrete cosine transform 05 p1771 N94-22111
The 3-D unstructured mesh generation using local transformations 05 p1919 N94-22356
Efficient transfer of images over networks
05 p1748 N94-22517
Implementation and parallelization of fast matrix multiplication for a fast Legendre transform
[DE94-002184] 06 p2478 N94-22975
Integer cosine transform compression for Galileo at Jupiter: A preliminary look 06 p2292 N94-23266
System identification using a wavelet-based approach
[DE94-002191] 06 p2293 N94-23473
Relational algebra and equational proofs
[PB94-110822] 06 p2486 N94-23724
Exact transformation of the anisotropic Ginzburg-Landau model and its consequences
[DE94-002208] 06 p2562 N94-23795
Quasiconformal mappings, operators on Hilbert space, and local formulae for characteristic classes
[PB93-238079] 06 p2488 N94-24536
Optical wavelet transform processor
[AD-A273625] 06 p2546 N94-24731
Deviation equations of Synge and Schild in spaces with affine connection and metric, and equations for gravitational waves detectors
[DE93-616852] 06 p2571 N94-25339
DCT quantization matrices visually optimized for individual images 06 p2442 N94-25509
Filtering, coding, and compression with Malvar wavelets
[AD-A274055] 07 p2780 N94-25770
Satellite attitude determination using linear combination of models
[AD-A274082] 07 p2694 N94-25996
The modal solution to the Moon's orbit using canonical Floquet perturbation theory
[AD-A273732] 07 p2690 N94-26001
Semantics, orderings and recursion in the weakest precondition calculus
[CWI-CS-R9267] 07 p2995 N94-26776
The Hough transform algorithm for sea ice lead analysis: An evaluation
[AD-A274535] 07 p2899 N94-26853
Topological conditions for the existence of invariant measures for unimodal maps
[PB94-123296] 07 p2849 N94-26866
The morphological processing of binary images
[AD-A274310] 07 p2996 N94-26972
Reidemeister numbers of equivariant maps
[PB94-138286] 08 p3452 N94-29118
Trace formulas and dynamical zeta functions in the Nielsen theory
[PB94-138195] 08 p3467 N94-29163
Integer cosine transform for image compression
08 p3247 N94-29619
Parsing in ISBES
[TR-92-32] 08 p3432 N94-30363
Isomorphisms between predicate and state transformers
[RUU-CS-93-09] 08 p3458 N94-30403
Termination of term rewriting by semantic labelling
[RUU-CS-93-24] 08 p3459 N94-30424
Isomorphisms between predicate and state transformers
[CWI-CS-R9338] 08 p3459 N94-30430
Relating state transformation semantics and predicate transformer semantics for parallel programs
[CWI-CS-R9339] 08 p3433 N94-30431
Application of radon transformation for improved analysis of sparsely sampled data: A feasibility study
[PB94-147535] 09 p3741 N94-31075
Structural properties of inverse linear systems
[MATHS-REPT-A-200] 09 p3840 N94-31156
An algebraic view on Rosetta
[CL-93-02] 09 p3841 N94-31391
Minimization of computational requirements in the hybrid stress finite element method
[AD-A277120] 09 p3846 N94-32048
Modeling and control of nonlinear systems
[AD-A277377] 09 p3834 N94-32095
Transformational derivation of (parallel) programs using skeletons
[TR-93-20] 09 p3825 N94-32196
Steepest descent paths for integrals defining the modified Bessel functions of imaginary order
[CWI-AM-R9303] 09 p3848 N94-32227
On gauge transformations in constrained theories
[DE94-614440] 10 p4148 N94-33865
Evaluation of the IHS transformation use on the integration of geophysical (aeromagnetometry) and remote sensing (TM-Landsat) data for the geological investigation in the Pojuca area (Serra dos Carajas, PA)
[INPE-5532-TDI/521] 10 p4077 N94-34223
Entropy of graphs, semigroups and groups
[PB94-167749] 11 p4314 N94-35763
Executable transformational rules from Core ELLA to the Kernel
[DRA-MEMO-4629] 11 p4307 N94-36113
Multitarget track initiation using a modified Hough transform 12 p4395 N94-36630
Variational discrete symmetries
[DE94-618485] 12 p4507 N94-37062
The canonical symmetry for integral systems
[DE94-618486] 12 p4504 N94-37375
Parallel tridiagnoalization through two-step band reduction
[DE94-011512] 12 p4505 N94-37518

TRANSFORMERS

NT VOLTAGE CONVERTERS (AC TO AC)
Design of a matching network for dipole antennas
[AD-A265115] 01 p0136 N94-11158
Characterization of the pulse transformer
[AD-A263414] 01 p0143 N94-11298
Forback DC-to-DC converter
[NASA-CASE-GSC-13404-1] 03 p1010 N94-15874
A 27 channels, 1 MHz fibre-optic measuring system
[AD-A266943] 03 p1003 N94-17307
Solid-state, resistive hydrogen sensors for safety monitoring
[DE93-017769] 04 p1424 N94-17778
Computational model of a magnetic modulator for copper lasers
[DE93-019603] 05 p1815 N94-20223
Development of fusion technology
[DE93-633444] 07 p3042 N94-26159
Fiber optic Faraday flux transformer specification
[AD-D016058] 07 p3039 N94-27674
Plane wave propagation and polarization properties in transversely bianisotropic uniaxial medium
[PB94-132883] 07 p2778 N94-28380
Eigenwaves in the general uniaxial bianisotropic medium with symmetric parameter dyadics
[PB94-132891] 07 p2778 N94-28381
Plane wave propagation in an anisotropic chiral medium with isotropic permittivity and permeability
[PB94-133097] 07 p2778 N94-28384
Fabrication issues in optimizing YBa(2)Cu(3)O(7-x) flux transformers for low I/f noise
[DE94-005209] 08 p3261 N94-28546
High-temperature superconducting transformer performance, cost, and market evaluation
[DE94-005494] 09 p3687 N94-31152

Experimental measurement and calculation of losses in planar radial magnetic bearings
11 p4214 N94-35847

TRANSFORMS
U TRANSFORMATIONS (MATHEMATICS)

TRANSFUSION
Evaluation of dried storage of platelets for transfusion: Physiologic integrity and hemostatic functionality
[AD-A270756] 04 p1507 N94-19593

TRANSGRANULAR CORROSION
Stress corrosion cracking of 316 SS and Incoloy-800 in high temperature aqueous containing sulfate and chloride
[DE93-623325] 03 p0952 N94-17302

TRANSIENT HEATING
NT PULSE HEATING
NT SHOCK HEATING
Primordial lightning: Evidence preserved in chondrites
01 p0432 N94-12230
Gas-grain energy transfer in solar nebula shock waves: Implications for the origin of chondrules
03 p1262 N94-16251
Liquid crystal heat transfer measurements
04 p1432 N94-18653
A simple description of flow instability with application to a packed bed
[DE93-017492] 04 p1420 N94-19345
Strain gage measurement errors in the transient heating of structural components
[NASA-TM-104274] 06 p2376 N94-23487
Advanced X ray Astrophysics Facility-Imaging (AXAF-I) thermal analyses using Integrated Thermal Analysis System (ITAS) program 06 p2320 N94-23635
Response-coefficient method for heat-conduction transients with time-dependent inputs
06 p2326 N94-23671
Performance analysis of reciprocating regenerative magnetic heat pumping
[DE94-009488] 11 p4264 N94-35683

TRANSIENT LOADS
NT BLAST LOADS
NT GUST LOADS
NT IMPACT LOADS
NT LANDING LOADS
NT SHOCK LOADS
Response of composite laminates to dynamic surface loads 01 p0066 N94-10902
Development and comparison of advanced reduced-basis methods for the transient structural analysis of unconstrained structures
[NASA-TM-109015] 03 p1061 N94-17259
Transient response of a viscous and anchored liquid bridge to an axial pulse
[LRT-WE-9-FB-7-1992] 04 p1379 N94-19492
Structural design feasibility study of Space Station long spacer truss
[NASA-TM-106346] 07 p2843 N94-27559
Stiffness-generated rigid-body mode shapes for Lanczos eigensolution with SUPORT DOF by way of a MSC/NASTRAN DMAP alter
[NASA-TM-106537] 08 p3319 N94-29406
Transient analysis mode participation for modal survey target mode selection using MSC/NASTRAN DMAP
[NASA-TM-106536] 08 p3319 N94-29469
Transient thermal fatigue of ceramic composites
08 p3216 N94-29874

TRANSIENT OSCILLATIONS
The soft x ray transient Cen X-4 in quiescence
[NASA-CR-194033] 02 p0833 N94-14406
Advanced CFD methodology for fast transients encountered in nonlinear combustion instability problems. Volume 1: Theory and validation
[NASA-CR-191351] 09 p3637 N94-32696
Modelling of ELMs and dynamic responses of the H-mode
[DE94-718977] 11 p4339 N94-36353

TRANSIENT PRESSURES
NASA metrology and calibration, 1993
[NASA-TM-109280] 02 p0597 N94-14410
Guide to the measurement of the transient performance of aircraft turbine engines and components
[AD-280272] 10 p3997 N94-33874

TRANSIENT RESPONSE
Transient effects in the Benard instabilities: Coupling between capillary and gravity effects
01 p0119 N94-10216
Statistical and optimization methods to expedite neural network training for transient identification
[DE93-009985] 01 p0340 N94-11644
The transient behavior of a boundary layer exposed to uniform suction
[ITN-93-85205] 02 p0630 N94-13197
Some aspects of sheet forming simulation using explicit finite element techniques
[DE93-012479] 02 p0663 N94-13975
Nonstationary behaviour of low background photon detectors 03 p0902 N94-15049
Dynamic behavior of fiber and particle reinforced composites
[AD-A266905] 03 p0930 N94-15143
Pulse response based control for minimum time maneuver of flexible spacecraft
[AD-A266186] 03 p0886 N94-16455
Development and comparison of advanced reduced-basis methods for the transient structural analysis of unconstrained structures
[NASA-TM-109015] 03 p1061 N94-17259
Precise flux control for lattice matched superlattice materials
[AD-A268254] 03 p1215 N94-17417
Heat transfer parametric system identification
[AD-A268525] 03 p0929 N94-17543
Transient response of a viscous and anchored liquid bridge to an axial pulse
[LRT-WE-9-FB-7-1992] 04 p1379 N94-19492
Methods for description and control of dynamical systems and their application
[MPIS-17/1992] 04 p1553 N94-19522
Simulation of the behavior of micro-electronic capacitive pressure sensors
[LAAS-93190] 04 p1434 N94-19659
Dynamic, multiaxial impact response of confined and unconfined ceramic rods
[DE93-040057] 05 p1829 N94-19824
Transient analysis of circuits including frequency-dependent components using transgyrator and convolution
[PB93-225001] 06 p2308 N94-23130
A transient symmetrical method for the measurement of temperature dependent thermal diffusivity
[VTT-TIED-1452] 07 p3008 N94-26256
Response of structures to impact loads using elastic and plastic analysis
[ISBN-0-315-84647-X] 07 p2842 N94-27309
Influence of impeller shroud forces on turbopump rotor dynamics 07 p2796 N94-27378
Gas Turbine Engine Transient Behaviour
[VKI-LS-1993-06] 07 p2828 N94-28043
Transient performance 07 p2828 N94-28045
Transient engine simulation 07 p2829 N94-28052
A space-based classification system for RF transients
[DE94-003933] 08 p3240 N94-28522
Performance evaluation of a 22.5/30 kW 270 volts direct current generator system
[AD-A275106] 08 p3263 N94-28913
Evaluation of the transient operation of advanced gas turbine combustors 08 p3154 N94-29269
Transient analysis mode participation for modal survey target mode selection using MSC/NASTRAN DMAP
[NASA-TM-106536] 08 p3319 N94-29469
Concurrent simulation and constraint stabilization for flexible multibody systems 08 p3154 N94-29532
Study of wave propagation and dynamic response of laminated composite structures
[AD-A276123] 09 p3619 N94-31444
Turn-on transient overcurrent response suppressor
[AD-D016151] 10 p4039 N94-33759
Modelling of ELMs and dynamic responses of the H-mode
[DE94-718977] 11 p4339 N94-36353
ELMy-H mode as limit cycle and transient responses of H-modes in tokamaks
[DE94-727510] 12 p4529 N94-37358

TRANSIENTS (SURGES)
U SURGES

TRANSISTOR AMPLIFIERS
A cryogenic seven-element HEMT front end for DSS 13 02 p0608 N94-14375
Field emitter array RF amplifier development project, phase 1, option 1
[AD-A272567] 05 p1740 N94-21361
Cryogenic, low-noise high electron mobility transistor amplifiers for the Deep Space Network
06 p2291 N94-23262
Signal amplifier-shapers for multiwire detectors
[DE93-634171] 07 p2783 N94-26438
NASA satellite communications application research, phase 2 addendum. Efficient high power, solid state amplifier for EHF communications
[NASA-CR-195712] 07 p2777 N94-27946

TRANSISTOR CIRCUITS
Delay analysis of combinations of pass transistors and classical logic gates 05 p1756 N94-21103
Design and implementation of GaAs HBT circuits with ACME 05 p1758 N94-21117
Fully-depleted silicon-on-sapphire and its application to advanced VLSI design 05 p1765 N94-21709
Interpolative modeling of GaAs FET S-parameter data bases for use in Monte Carlo simulations
05 p1767 N94-21723
A VLSI implementation of DCT using pass transistor technology 05 p1767 N94-21725
On fast carry select adders 05 p1767 N94-21728
Non-linear analysis of the electrical properties of the active circuits of high-frequency oscillators
05 p1785 N94-22195
A physics-based heterojunction bipolar transistor model for integrated circuit simulation
[AD-A274081] 07 p2781 N94-25995
Silicon device performance measurements to support temperature range enhancement
[NASA-CR-195265] 07 p2844 N94-27824
Analysis and synthesis of MOS translinear circuits
[ISBN-9-09-005495-2] 09 p3690 N94-31616

TRANSISTOR LOGIC
Asynchronous sequential circuit design using pass transistor iterative logic arrays 04 p1402 N94-18376
Pulse mode VLSI asynchronous circuits
04 p1402 N94-18377
Improved self arbitrated VLSI asynchronous circuits
04 p1402 N94-18378
VHDL simulation with access to transistor models
04 p1402 N94-18381
Power optimization in logic isomers
05 p1756 N94-21101
Delay analysis of combinations of pass transistors and classical logic gates 05 p1756 N94-21103
Novel failure analysis techniques using photon probing with a scanning optical microscope
[DE94-006594] 09 p3692 N94-32112

TRANSISTORS
NT BIPOLAR TRANSISTORS
NT CHARGE FLOW DEVICES
NT FIELD EFFECT TRANSISTORS
NT HIGH ELECTRON MOBILITY TRANSISTORS
NT JFET
NT JUNCTION TRANSISTORS
NT MODFETS
NT PHOTOTRANSISTORS
NT SILICON TRANSISTORS
NT SOS (SEMICONDUCTORS)
Effect of switched-bias bakes on the postirradiation electrical response of MOS devices
[DE93-009629] 01 p0143 N94-11271
Design and optimization of high voltage lateral DMOS devices using RESURF technology
[LAAS-92511] 02 p0626 N94-14711
Large signal characterization and modeling of heterojunction bipolar transistors
[AD-A266184] 03 p1012 N94-16935
VLSI for high-speed digital signal processing
[AD-A270406] 04 p1404 N94-18706
Superconducting flux flow devices, digital circuits and memories
[DE93-019072] 04 p1405 N94-19079
Localization of pellicle-induced open contacts using charge-induced voltage alteration
[DE93-019407] 05 p1762 N94-21636
HDL to verification logic translator
05 p1766 N94-21717
A VLSI implementation of DCT using pass transistor technology 05 p1767 N94-21725
A high speed CMOS A/D converter
05 p1767 N94-21726
On fast carry select adders 05 p1767 N94-21728
Low energy CMOS for space applications
05 p1768 N94-21735
Self assembly: An approach to terascale integration
[DE93-040104] 05 p1769 N94-21846
Simple method to estimate MOS oxide-trap, interface-trap, and border-trap densities
[DE93-041138] 05 p2032 N94-21939
Floating well based design methodology aimed to improve latch-up immunity in a CMOS/DMOS smart power technology
[LAAS-93093] 06 p2556 N94-22905
Fabrication of sub-40-nm p-n junctions for 0.18 micron MOS device applications using a cluster-tool-compatible, nanosecond thermal doping technique
[DE94-001608] 06 p2309 N94-23520
Advanced qualification techniques
[DE94-003709] 07 p2780 N94-25812
Demonstration of monolithic co-fabrication of Y1Ba2Cu3O7-Sigma and CMOS devices on the same sapphire substrate
[AD-A274757] 07 p3059 N94-26566
Processing, fabrication, and demonstration of HTS integrated microwave circuits, appendix A
[AD-A274600] 07 p2785 N94-26890
Tunnelling hot electron transfer amplifiers
[AD-A275529] 08 p3262 N94-28687
Nonvolatile programmable neural network synaptic array
[NASA-CASE-NPO-18578-1-CU] 08 p3265 N94-29426

Charge trapping and breakdown in N2O oxides
[DE94-003775] 08 p3266 N94-30040
GaAs/GaN strained layer superlattice materials for high temperature transistors, phase 1
[AD-A276115] 09 p3897 N94-31528
Analysis and synthesis of MOS translinear circuits
[ISBN-9-09-005495-2] 09 p3690 N94-31616
RF vacuum microelectronics
[AD-A276512] 09 p3691 N94-31928
Application of the modified voltage-dividing potentiometer to overlay metrology in a CMOS/bulk process
[DE94-007937] 09 p3695 N94-32700
Superconducting transistors
[PB94-170743] 11 p4260 N94-36260
Single event mirroring and sense amplifier designs for enhanced SE tolerance of DRAMs
[DE94-010397] 12 p4438 N94-37190
Role of burn-in during qualification testing
[DE94-007864] 12 p4439 N94-37513

TRANSIT TIME
Electron runaway in RF discharges
[DE93-771407] 01 p0363 N94-10661
Entry velocities at Mars and Earth for short transit times
[AD-A272591] 05 p1685 N94-21420

TRANSITION
Modal logic, transition systems and processes
[CWI-CS-R9321] 07 p2970 N94-27549

TRANSITION FLIGHT
Design criteria for integrated flight/propulsion control systems for STOVL fighter aircraft
02 p0521 N94-13297
Data link development for the archytas vertical takeoff and landing transitional flight unmanned aerial vehicle
[AD-A272499] 05 p1646 N94-21548
Transitional flight characteristics of a geometrically simplified STOVL model 07 p2672 N94-28035
YAV-8B reaction control system bleed and control power usage in hover and transition
[NASA-TM-104021] 10 p4007 N94-34994

TRANSITION FLOW
A research program for improving heat transfer prediction for the laminar to turbulent transition region of turbine vanes/blades
[NASA-TM-106278] 01 p0151 N94-11256
Boundary layer transition: Prediction and wind tunnel simulation 01 p0032 N94-11498
DNS on control of laminar-turbulent transition in channel flow with suction and blowing 01 p0163 N94-12613
Criteria for onset of boundary-layer transition on spinning bodies 01 p0164 N94-12620
Turbulent boundary layer interacting with spanwise periodic longitudinal vortex arrays
01 p0165 N94-12626
Large-eddy simulation of laminar-turbulent breakdown at high speeds with dynamic subgrid-scale modeling
[NASA-CR-4533] 02 p0629 N94-13064
Transition prediction and control in subsonic flow over a hump
[NASA-CR-4543] 02 p0629 N94-13066
High speed transition prediction
[NASA-CR-194125] 02 p0502 N94-13422
Effects of surface thermal forcing on stratified flow past an isolated obstacle 02 p0633 N94-13553
Parallel spatial direct numerical simulations on the Intel iPSC/860 hypercube
[NASA-CR-191513] 03 p1144 N94-15483
Inviscid instability of streamwise corner flow
[NASA-CR-191514] 03 p1021 N94-15834
Turbulence and transition modeling for high-speed flows
[AD-A266748] 03 p1022 N94-15953
Research activities at the Center for Modeling of Turbulence and Transition 04 p1410 N94-18546
Numerical investigation of complex, transitional, and chemically reacting flows 04 p1411 N94-18550
Numerical prediction of transition of the F-16 wing at supersonic speeds
[NASA-CR-194407] 04 p1312 N94-19433
Flow transition with 2-D roughness elements in a 3-D channel 05 p1806 N94-21466
Transition to turbulence in an elliptic vortex
06 p2331 N94-24161
Vortical structure in a forced plane mixing layer
06 p2331 N94-24162
Sound radiation due to boundary layer transition
06 p2332 N94-24163
Center for modeling of turbulence and transition: Research briefs, 1993
[NASA-TM-106383] 06 p2333 N94-24336
Workshop on Computational Turbulence Modeling
[NASA-CP-10130] 06 p2333 N94-24460
Relationship between transition and modes of instability in supersonic boundary layers
[NASA-CR-4562] 06 p2336 N94-24725
Computational fluid mechanics
[NASA-CR-194765] 06 p2337 N94-24859
Prediction of leading-edge transition and relaminarization phenomena on a subsonic multi-element high-lift system 07 p2659 N94-27929
Forced convection heat transfer in straight tubes. Part 2: Laminar and transitional flow
[ESDU-93018-PT-2] 07 p2807 N94-28139
Long-wavelength asymptotics of unstable crossflow modes, including the effect of surface curvature
[NASA-CR-4579] 08 p3273 N94-29460
An experimental study of nonlinear wave coupling and energy transfer characterizing the transition of a planar jet shear layer 08 p3282 N94-30953
Transition to turbulence in confined compressible mixing layers 08 p3283 N94-30958
Analysis of the photodiode boundary layer transition indicator
[DE94-005311] 09 p3701 N94-31268
Linear stability theory and three-dimensional boundary layer transition 10 p3981 N94-33530
Special Course on Progress in Transition Modelling
[AGARD-R-793] 10 p4045 N94-33884
Physical description of boundary-layer transition: Experimental evidence 10 p4045 N94-33885
Asymptotic approaches to transition modelling
10 p4045 N94-33887
Direct numerical simulation of transition: The spatial approach 10 p4046 N94-33889
Transition receptivity and control: Computations
[AD-A278339] 10 p4047 N94-33970

TRANSITION METALS
NT CADMIUM
NT CHROMIUM
NT COBALT
NT COBALT ISOTOPES
NT COBALT 60
NT COPPER
NT GOLD
NT GOLD ISOTOPES
NT HAFNIUM ISOTOPES
NT IRIDIUM
NT IRON
NT IRON ISOTOPES
NT IRON 57
NT MANGANESE
NT MANGANESE ISOTOPES
NT MERCURY (METAL)
NT MOLYBDENUM
NT NICKEL
NT NICKEL ISOTOPES
NT NIOBIUM
NT OSMIUM
NT OSMIUM ISOTOPES
NT PALLADIUM
NT PLATINUM
NT RHENIUM
NT RHENIUM ISOTOPES
NT RHODIUM
NT RUTHENIUM
NT SCANDIUM
NT SILVER
NT TANTALUM
NT TITANIUM
NT TUNGSTEN
NT VANADIUM
NT YTTRIUM
NT ZINC
NT ZIRCONIUM
NT ZIRCONIUM ISOTOPES
Non-empirical interatomic potentials for transition metals
[DE93-013705] 01 p0365 N94-11011
Interatomic interactions in BCC and FCC lattices of transition metals
[DE93-621541] 01 p0398 N94-11090
Polaronic charge separation in mixed-halide MX solids
[AD-A266073] 01 p0403 N94-12345
Determination of trace elements in triglycine sulfate solutions
[NASA-CR-193481] 02 p0562 N94-13048
Thermochemistry of transition metal clusters
[DE93-016201] 02 p0571 N94-13977
Reactor studies of metal ions associated with chromatographic silica
[AD-A266675] 02 p0573 N94-14779
Magneto-optic superlattice thin films: Fabrication, structural and magnetic characterization
03 p0974 N94-14982
Photochemistry in thin polymeric films
[AD-A266716] 03 p0964 N94-15729
Interfacial structure of lattice mismatched bcc(110)/bcc(110) transition metal superlattices
[DE93-015162] 03 p1208 N94-16058
Transition metals in superheat melts
03 p0962 N94-16273
Heat shock protein induction in human cells by CO2 laser irradiation
[AD-A266430] 03 p1117 N94-16545
Synthetic and mechanistic investigation of olefin polymerization catalyzed by early transition metal compounds
[DE93-018301] 03 p0970 N94-16963
Synthesis and characterization of new low-dimensional metal complex conductors
[AD-A268251] 03 p0952 N94-17416
Pressure induced metallization of the Mott Insulator 6(sub 2)
[DE93-018296] 04 p1600 N94-18969
Resonance Raman and photophysical studies of transition metal complexes in solution and entrapped in zeolites
[DE93-019892] 04 p1383 N94-19019
Electrocatalysts for oxygen electrodes
[DE93-040446] 04 p1354 N94-19653
Photochemically induced transformations of transition complexes
[AD-A271112] 05 p2014 N94-19982
The metallic bond for monolayer transition metal layers on transition metal surfaces
[DE93-019060] 05 p1691 N94-20313
Wavelength dispersive analysis with the synchrotron x ray fluorescence microprobe 05 p1685 N94-20717
Theoretical studies of structural phase transitions in actinide metals
[DE94-000796] 05 p1696 N94-22388
First-principles pressure-temperature phase diagrams in metals
[DE94-001056] 05 p1696 N94-22398
Vaporization behavior of non-stoichiometric refractory carbide materials and direct observations of the vapor phase using laser diagnostics
[DE93-040094] 06 p2348 N94-23203
Density functional studies: First principles and semi-emperical calculations of clusters and surfaces
[DE94-002836] 06 p2561 N94-23214
Magnetic resonance studies of 3d transition metal impurities in compound semiconductors
[PB93-232197] 06 p2243 N94-23714
New methane chemistry synthesis of materials for reversible uptake and useful functionalization of methane
[PB94-112786] 06 p2233 N94-23801
Transition metal activation and functionalization of carbon-hydrogen bonds
[DE94-003650] 07 p2715 N94-26369
Transition metals in highly correlated discotic phases: Designing metallomesogens with selected intermolecular organizations
[AD-A274695] 07 p2736 N94-26452
Polymer technology publication series no. 16
[PB94-135522] 08 p3214 N94-29157
Thermomechanical properties of 3-D transition metals
[DE94-604015] 08 p3487 N94-29500
The organometallic chemical vapor deposition of transition metal carbides: The use of homoleptic alkyls
[DE94-005577] 08 p3206 N94-30007
Studies of high temperature ternary phases in mixed-metal-rich early transition metal sulfide and phosphide systems
[DE94-006034] 08 p3209 N94-30336
A polynomial representation of the valence orbital ionization potentials
[USIP-93-06] 09 p3640 N94-31083
Combinatorial ion sensors
[AD-A276567] 09 p3825 N94-32032
Vibrational spectroscopy at metal-solution interfaces: Some perspectives and prospects for electrochemical surface science
[AD-A276781] 09 p3644 N94-32169
Experimental investigations and molecular dynamics simulations of radiation induced surface damage
[AD-A277323] 09 p3871 N94-32621
Optical properties of lanthanide-doped RbTiOAsO4 and transition metal-doped KTiOPO4
[DE94-008433] 09 p3907 N94-32963
Electronic structure and stability of simple and complex phases in transition metals
[DE94-009090] 10 p4024 N94-33679
Generalized syntheses of periodic surfactant and inorganic composite materials
[AD-A278001] 10 p4019 N94-34160
Consequences of competing hybridization for magnetic ordering in correlated-electron lattices
[DE94-011648] 12 p4534 N94-37057

TRANSITION POINTS
Transition prediction and control in subsonic flow over a hump
[NASA-CR-4543] 02 p0629 N94-13066
Dynamical behavior of octahedrite from the Henbury meteorite
[DE93-018834] 04 p1627 N94-19339

Ductile-brittle transition behavior of tungsten under shock loading conditions
[DE93-019945] 05 p1693 N94-21843
Effects of neutron irradiation and hydrogen on ductile-brittle transition temperatures of V-Cr-Ti alloys
[DE94-001466] 06 p2240 N94-23009
Transition for three-dimensional, compressible boundary layers 07 p2653 N94-28327
The silent phase transition in mesonic bags and lattice theory
[DE94-616852] 11 p4321 N94-35583
ILSE combiner study
[DE94-011009] 11 p4331 N94-36202

TRANSITION PRESSURE
Heavy-section steel technology program
[DE93-009222] 01 p0184 N94-10155

TRANSITION PROBABILITIES
Probability of particle trapping/detrapping in torsatrons
[DE93-621641] 01 p0390 N94-11121
Theoretical investigations of metastability and energy storage in molecular systems
[AD-A271849] 05 p1973 N94-20612
Recursive recovery of Markov transition probabilities from boundary value data
[DE94-011914] 11 p4317 N94-36235

TRANSITION TEMPERATURE
Apical Cu-O bond in YBa2Cu3O(7-delta) superconductors by XAFS
[DE93-010861] 01 p0400 N94-11458
X-ray and neutron scattering studies of magnetic critical fluctuations in holmium
[DE93-010873] 01 p0400 N94-11467
Room temperature degradation of YBa2Cu3O(7-x) superconductors in varying relative humidity environments
[NASA-TP-3368] 02 p0813 N94-14409
Muon spin relaxation studies of heavy fermion superconductors
[DE93-014576] 02 p0815 N94-14773
High temperature superconductivity
[AD-A267006] 03 p1008 N94-15635
Roles of oxygen defects in copper-oxide superconductors
[DE93-014875] 03 p1208 N94-15982
The effect of long-term aging on the impact properties of modified 9Cr-1Mo steel
[DE93-015453] 03 p0957 N94-16068
Density of states and tunneling characteristics of layered superconductors
[DE93-015898] 03 p1211 N94-16839
Structural phase transition and superconductivity in La(2-x)Ba(x)CuO4
[DE93-015812] 03 p1212 N94-16868
Phase separation and superconductivity in La2CuO(4 + delta): Effects of oxygen diffusion
[DE93-016610] 04 p1594 N94-17907
Role of pressure in the study of fullerenes
[DE93-018839] 04 p1602 N94-19340
Development of bioelastic material for aspects of wound repair
[AD-A267832] 05 p1673 N94-20208
Spin-polaron theory of high-T(c) superconductivity. 3: Gap function and critical temperature
[DE93-019198] 05 p2030 N94-21831
Spin dynamics and implications for superconductivity: Some problems with the d-wave scenario
[DE94-001183] 05 p2032 N94-21972
NMR studies of oxygen-doped La2CuO(4+delta)
[DE93-040756] 05 p2034 N94-22007
Thin-film fabrication of Pb-doped BiSrCaCuO superconductor 05 p1781 N94-22176
Anisotropic uniaxial pressure effects in YBa2Cu3O(7-delta)
[DE94-001456] 06 p2557 N94-22929
Anomalous magnetoresistance behavior of superconducting Nd(2-x)Ce(x)CuO(4-y) single crystal
[DE94-000806] 06 p2558 N94-22941
Irradiation damage behavior of low alloy steel wrought and weld materials
[DE94-000519] 06 p2239 N94-22999
Effects of neutron irradiation and hydrogen on ductile-brittle transition temperatures of V-Cr-Ti alloys
[DE94-001466] 06 p2240 N94-23009
Development of small punch testing technique and its application to evaluation of mechanical properties degradation
[DE94-001193] 06 p2375 N94-23184
Microscopic study of local structure and charge distribution in metallic La2CuO(4+delta)
[DE94-003601] 07 p3050 N94-25617
The effect of processing on the microstructure of Ag-sheathed Bi-2223 wires
[DE94-004627] 07 p3055 N94-26243
Strongly interacting fermion systems
[DE94-002674] 07 p3021 N94-26677
Atomic and magnetic structure of YBa2(Cu(1-x)Fe(x))3O(6+y) at 0.05 less than or equal to x less than or equal to 0.30, y is approximately equal to 1 and y is approximately equal to 0.5
[DE94-606852] 08 p3513 N94-29210
The effect of various metallurgical parameters on the flow and fracture behavior of polycrystalline NiAl near the brittle-to-ductile transition
[NASA-TM-106534] 08 p3205 N94-29758
Calculating the J(c), B, T surface for commercial niobium tin conductors using a reduced state model
[DE94-006296] 08 p3520 N94-30850
Fermi surface instability at 0.4 K in a heavy-fermion YbBiPt: SDW?
[DE94-006224] 09 p3899 N94-31916
Short coherence length superconductors: Intermediate regime between BCS and bosons
[DE94-007694] 09 p3904 N94-32645
A quest for a new superconducting state
[DE94-008439] 09 p3908 N94-32991
Polymer from DIIMIDO-DI-PHTHALONITRILE
[AD-D016189] 10 p4030 N94-34682
Calorimetric thermometry of meteoritic troilite: Preliminary thermometer relationships 11 p4355 N94-35399
A new family of superconducting fullerides, Na(NH3)(x)C60(x = 2-8)
[DE94-011480] 11 p4341 N94-36272

TRANSITS
NT CINETHEODOLITES

TRANSLATING
NT MACHINE TRANSLATION
On the motion through a viscous fluid of a spherical particle touching a plane wall: Slip boundary conditions
[DE93-012540] 02 p0628 N94-12961
Efficient and correct translation of strict applicative programming languages
[ETN-93-95056] 05 p1903 N94-20020
System level modelling using Petri nets and VHDL 05 p1772 N94-22113
Projectile transverse motion and stability in electromagnetic induction launchers
[DE94-001557] 06 p2198 N94-23210
An automated tool to facilitate code translation for software fault tree analysis
[AD-A273205] 06 p2457 N94-24556
Satellite attitude determination using linear combination of models
[AD-A274082] 07 p2694 N94-25996
A strategy for dynamic interpretation: A fragment and an implementation
[CWI-CS-R9317] 07 p2970 N94-27545
More problems on rewriting
[CWI-CS-R9332] 08 p3428 N94-30734
Combinatory reduction systems: Introduction and survey
[CWI-CS-R9362] 09 p3849 N94-32349
Automatic translation among spoken languages 09 p3685 N94-32437
Translating an AI application from Lisp to Ada: A case study
[NASA-TM-103845] 09 p3820 N94-32906
Energy absorber for the CETA 09 p3604 N94-33303
Priorities and nonmonotonic reasoning
[PB94-171170] 11 p4346 N94-35959
Using International English to prepare technical text for translation
[DE94-002628] 11 p4347 N94-36102
Determination of grain boundary volume expansion by HREM
[DE94-010452] 11 p4241 N94-36231

TRANSLATIONAL MOTION
NT SECONDARY FLOW
NT THREE DIMENSIONAL FLOW
NT THREE DIMENSIONAL MOTION
Implementation and experimentation with a motion planning system
[ITN-93-85213] 02 p0755 N94-14505
Linear encoding device
[NASA-CASE-GSC-13562-1] 03 p1147 N94-15703
Translation and rotation invariant pattern recognition
[PB94-123676] 07 p2968 N94-27157
A paraperspective factorization method for shape and motion recovery
[AD-A276513] 09 p3712 N94-31929
Vibration localization in dual-span axially moving elastic systems 09 p3736 N94-31964

TRANSLUNAR SPACE
U INTERPLANETARY SPACE

TRANSMISSION
NT ACOUSTIC PROPAGATION
NT AERODYNAMIC HEAT TRANSFER
NT ALOHA SYSTEM
NT CODE DIVISION MULTIPLE ACCESS
NT CODE DIVISION MULTIPLEXING
NT CONDUCTIVE HEAT TRANSFER
NT CONVECTIVE HEAT TRANSFER
NT DATA TRANSMISSION
NT DEMAND ASSIGNMENT MULTIPLE ACCESS
NT DEMULTIPLEXING
NT DIFFRACTION PROPAGATION
NT DOUBLE SIDEBAND TRANSMISSION
NT ELECTRIC POWER TRANSMISSION
NT ELECTROMAGNETIC WAVE TRANSMISSION
NT FREQUENCY DIVISION MULTIPLE ACCESS
NT FREQUENCY DIVISION MULTIPLEXING
NT GROUND WAVE PROPAGATION
NT HALOS
NT HEAT TRANSFER
NT HEAT TRANSMISSION
NT HYPERSONIC HEAT TRANSFER
NT IONOSPHERIC PROPAGATION
NT LAMINAR HEAT TRANSFER
NT LIGHT SCATTERING
NT LIGHT TRANSMISSION
NT MICROWAVE ATTENUATION
NT MICROWAVE TRANSMISSION
NT MULTIPATH TRANSMISSION
NT MULTIPLE ACCESS
NT MULTIPLEXING
NT PACKET TRANSMISSION
NT RADAR TRANSMISSION
NT RADIATIVE HEAT TRANSFER
NT RADIO TELEMETRY
NT RADIO TRANSMISSION
NT SATELLITE TRANSMISSION
NT SCATTER PROPAGATION
NT SHOCK WAVE PROPAGATION
NT SHORT WAVE RADIO TRANSMISSION
NT SIGNAL TRANSMISSION
NT SINGLE CHANNEL PER CARRIER TRANSMISSION
NT SINGLE SIDEBAND TRANSMISSION
NT SOUND TRANSMISSION
NT SPREAD SPECTRUM TRANSMISSION
NT STRESS PROPAGATION
NT SUPERSONIC HEAT TRANSFER
NT TELEMETRY
NT TELEPHONY
NT TELEVISION TRANSMISSION
NT TIME DIVISION MULTIPLE ACCESS
NT TIME DIVISION MULTIPLEXING
NT TURBULENT HEAT TRANSFER
NT WAVE PROPAGATION
NT WAVELENGTH DIVISION MULTIPLEXING
Laser CO2 beam transmission through hollow metallic waveguide coated by a thin internal dielectric layer
[ITN-93-85201] 02 p0656 N94-13571
Spread spectrum random access networks
[AD-A272280] 05 p1737 N94-20585
A combined electron beam/optical lithography process step for the fabrication of sub-half-micron-gate-length MMIC chips 08 p3240 N94-30445

TRANSMISSION EFFICIENCY
Optimisation and specification of Auger electron spectrometers for signal-to-noise ratio performance
[NPL-DMM(A)-101] 03 p1006 N94-17549
Tooth form design supporting system in module design 04 p1428 N94-18036
Specification and formal verification of the safety criterion in the alternating bit protocol 05 p1784 N94-22193
Efficient transfer of images over networks 05 p1748 N94-22517
End-to-end delay reduction in narrow bandwidth real-time multimedia tele-education applications
[AD-B179614] 08 p3260 N94-30518
Guiding hard x rays with glass polycapillary fiber
[DE94-004949] 12 p4525 N94-37258

TRANSMISSION ELECTRON MICROSCOPY
HRTEM in protein crystallography
[DE93-610322] 01 p0395 N94-10406
Test of a method for phase retrieval in HRTEM
[DE93-612641] 01 p0170 N94-10630
Mineralogy of chondritic interplanetary dust particle impact residues from LDEF 01 p0080 N94-12045
Flux-pinning related defect structures in melt-processed YBa2Cu3O(7-x)
[DE93-012759] 02 p0804 N94-12818
Changes in electrical device characteristics during the formation of dislocations in situ in the TEM
[DE93-013910] 02 p0808 N94-13694
The effect of crystal tilt on high resolution micrographs of small metal particles
[DE93-013915] 02 p0574 N94-14795
Application of Z-contrast imaging to obtain column-by-column spectroscopic analysis of materials
[DE93-015333] 03 p0947 N94-16014
Insights into semiconducting materials and growth phenomena through Z-contrast STEM
[DE93-015964] 03 p1212 N94-16841

UHV-stem studies on nucleation and growth of thin metal silicide films on silicon
[DE93-017604] 03 p1212 N94-16961
Characterization of vapor plume species and deposition residues resulting from pulsed laser ablation of a graphite/epoxy composite
[AD-A270101] 04 p1343 N94-18869
High resolution transmission electron microscopy of mesoporous MCM-41 type materials
[AD-A271271] 04 p1354 N94-19728
Facilities for in situ ion beam studies in transmission electron microscopes
[DE93-019567] 05 p1979 N94-20222
Growth, characterization and device development in monocrystalline diamond films
[AD-A273097] 05 p2028 N94-21506
Electron holography applied to the study of ceramic materials
[DE94-000329] 05 p1707 N94-21653
Transmission electron microscopy study of thick copper-304 stainless steel multilayers
[DE94-001045] 05 p1696 N94-22394
Magnetic properties and transmission electron microscopy investigations of Nd-Fe-B-Co-Al melt spun ribbons
[PB93-201531] 06 p2561 N94-23428
Ge-Au eutectic bonding of Ge (100) single crystals
[DE94-002281] 06 p2564 N94-24657
Crystal potential retrieval in HRTEM
[DE94-601883] 07 p3055 N94-26171
An atom probe investigation of the influence of trace impurities on the mechanical behavior of NiAl
[DE94-002797] 07 p2734 N94-26272
Electron microscopy studies of undoped and phosphorus doped Si:H and Si,C:H films
[DE94-004738] 07 p3069 N94-27757
Incoherent imaging by Z-contrast stem: Towards 1 Angstrom resolution
[DE94-006551] 09 p3896 N94-31489
Engineering of damage in ion implanted silicon
[ISBN-9-09-005097-3] 09 p3897 N94-31521
Optimal detector strategies for the phase contrast imaging for scanning transmission electron microscopes
[ETN-94-95747] 09 p3866 N94-31613
Gettering of metal impurities by cavities in silicon
[DE94-005248] 09 p3645 N94-32672
Nucleation and growth of cubic boron nitride films produced by ion-assisted pulsed laser deposition
[DE94-007295] 09 p3661 N94-32796
High Resolution Transmission Electron Microscopy (HRTEM) of nanophase ferric oxides
11 p4239 N94-35433
High-resolution imaging using Z-contrast Scanning Transmission Electron Microscopy
[DE94-008510] 11 p4333 N94-36055
Irradiation-related amorphization and crystallization: In situ transmission electron microscope studies
[DE94-009823] 11 p4241 N94-36222

TRANSMISSION LINES
NT COAXIAL CABLES
NT COMMUNICATION CABLES
NT FLUID TRANSMISSION LINES
NT MICROSTRIP TRANSMISSION LINES
NT POWER LINES
NT STRIP TRANSMISSION LINES
Locally non-uniform finite-difference time domain with application to stealth, crosstalk, and narrow apertures
[DE93-013958] 02 p0601 N94-13696
The developments of satellite communications of China 02 p0618 N94-14282
The current situation, trends, international cooperation of space communication technological development in the Republic of Korea 02 p0699 N94-14283
Joint experiments using ETS-5
02 p0618 N94-14284
Space communications technology research in CRL
02 p0618 N94-14285
NTT's activities in satellite communications technology development 02 p0618 N94-14286
Future outlook on international satellite communications in Asia Pacific region 02 p0618 N94-14287
Utilization of boundary element method for extraction of frequency dependent conductivity parameters of lossy intra-chip transmission lines
[ETN-93-94385] 02 p0771 N94-14807
Determination of the electromagnetic fields radiated from the ARES EMP simulator
[AD-A267069] 03 p0988 N94-15668
Design and test of a low jitter metal to metal contact solid dielectric switch
[DE93-016957] 04 p1394 N94-17755
A radial transmission line material measurement apparatus
[DE93-018508] 04 p1394 N94-17780
Robust, high-speed network design for large-scale multiprocessing
[AD-A271003] 05 p1716 N94-19977
Interinjection-locked quasioptical power combiners and phased arrays
[AD-A271178] 05 p2015 N94-20214
Observation of reflected waves on the SABRE positive polarity inductive adder MITL
[DE93-019413] 05 p1980 N94-20295
Analysis of microstrip dipoles and slots transversely coupled to a microstrip line using the FDTD method
05 p1718 N94-20405
Solid State Technology Branch of NASA Lewis Research Center: Fifth Annual Digest
[NASA-TM-106303] 05 p1732 N94-20497
Attenuation of epsilon(sub eff) of coplanar waveguide transmission lines on silicon substrates
05 p1733 N94-20504
High temperature superconducting planar circuit structure for high frequency applications
[AD-A273083] 05 p2028 N94-21521
Manual design technique for broadband passive thin-film attenuators using the Smith chart
05 p1782 N94-22178
Electromagnetic interference and shielding: An introduction (revised version of 1991-23)
[PB93-215275] 05 p1742 N94-22348
Layered parallel interface for an active antenna array
[AD-D016002] 06 p2301 N94-25045
Temperature dependent performance of Coplanar Waveguide (CPW) on substrates of various materials
[NASA-TM-106505] 06 p2313 N94-25170
Interference analysis of multichannel transmission lines: A system's analysis
[PB94-126505] 07 p2772 N94-26909
Preliminary analysis of Asynchronous Transfer Mode (ATM) over microwave channels
[AD-A275214] 08 p3243 N94-29069
Development of an accurate transmission line fault locator using the global positioning system satellites
08 p3144 N94-30652
Electric power lines: Questions and answers on research into health effects
[DE94-005637] 08 p3353 N94-30757
Studies of an optical multi-processor interconnect
[AD-A277093] 09 p3881 N94-32392
Torque-balanced extendable fiber optic cable
[AD-D016097] 09 p3882 N94-32719
A novel transition between rectangular waveguide and layered ridge dielectric waveguide
[NASA-TM-106661] 12 p4433 N94-36955

TRANSMISSION LOSS
Building penetration loss measurements for DAB signals at 211 MHz
[BBC-RD-1992/14] 01 p0133 N94-11024
Infrared transmission and path radiance through dust and fog
[AD-A265825] 02 p0791 N94-12979
Measurement of wave propagation for VHF/UHF and a comparison between measured and predicted values
[FFI/RAPPORT-92/7024] 02 p0605 N94-13968
Antenna gain loss and pattern degradation due to transmission through dielectric radomes
[AD-A267242] 03 p0986 N94-14974
Johnson-Gierhart program predictions of excess propagation loss for super-high frequency air-to-ground paths. Volume 2: Appendices
[AD-A267021] 03 p0987 N94-15527
Johnson-Gierhart program predictions of excess propagation loss for super-high frequency air-to-ground paths. Volume 1: Theory and numerical results
[AD-A267105] 03 p0988 N94-15649
OETC optical backplane bus testbed. IBM tasks: Receiver OEIC and link simulation tools and analysis
[AD-A266198] 03 p1191 N94-16128
Comparison of HF groundwave propagation models
[AD-A273146] 06 p2299 N94-24668
Design and testing of ubitron amplifier tubes
[AD-A273297] 06 p2311 N94-24818
Investigation on application of genetic algorithms to optimal reactive power dispatch of power systems
[MATHS-REPT-A-197] 08 p3266 N94-29527
A transmission-loss monitor using current transformers
[DE94-003974] 08 p3267 N94-30716
Optimal reactive power dispatch of power systems using nonlinear programming
[MATHS-REPT-A-209] 09 p3808 N94-31164
Low altitude near-the-horizon propagation: A comparison between RPO and M-layer
[AD-A277358] 09 p3679 N94-32282

TRANSMISSION RATE (COMMUNICATIONS)
Causality-preserving timestamps in distributed programs
[AD-A267534] 03 p1153 N94-17118
Protocol service decomposition for high-performance networking
[AD-A270613] 04 p1538 N94-19533
Adaptive data rate control TDMA systems as a rain attenuation compensation technique
06 p2287 N94-22821
Compression for an effective management of telemetry data 06 p2518 N94-23956
Reducing video frame rate increases remote optimal focus time
[NASA-TM-104018] 06 p2431 N94-23970
A small satellite design for deep space network testing and training
[NASA-CR-195526] 06 p2205 N94-24702
Delay-insensitive communication
[ETN-94-95315] 06 p2304 N94-25303

TRANSMISSION SPEED (COMMUNICATIONS)
U TRANSMISSION RATE (COMMUNICATIONS)

TRANSMISSIONS (MACHINE ELEMENTS)
Roller-gear drives for robotic manipulators design, fabrication and test
[NASA-CR-194248] 02 p0660 N94-12602
Mechanical Systems Technology Branch research summary, 1985 - 1992
[AD-A276450] 03 p1049 N94-17583
Metal band drives in spacecraft mechanisms
06 p2355 N94-23987
NASA/Army rotorcraft transmission research, a review of recent significant accomplishments
[NASA-TM-106508] 06 p2367 N94-25181
Study of the kinematic and dynamic characteristics of a wormgear transmission for helicopter applications
[NASA-CR-195287] 07 p2826 N94-27657
Experimental validation of finite element and boundary element methods for predicting structural vibration and radiated noise
[NASA-CR-4561] 08 p3301 N94-29552
Metal band drives in spacecraft mechanisms
08 p3162 N94-29637
Spur, helical, and spiral bevel transmission life modeling
[NASA-TM-106552] 09 p3728 N94-32979
Improvements in spiral-bevel gears to reduce noise and increase strength
[NASA-TM-106613] 10 p4059 N94-33609
Comparison of transmission error predictions with noise measurements for several spur and helical gears
[NASA-TM-106647] 10 p4060 N94-33954
Prediction of contact path and load sharing in spiral bevel gears
[NASA-CR-195305] 10 p4061 N94-34148
Vibration signature analysis of a faulted gear transmission system
[NASA-TM-106623] 12 p4450 N94-36953
Dynamics of a split torque helicopter transmission
[NASA-TM-106410] 12 p4452 N94-37457

TRANSMISSIVITY
Time-resolved probing of electron thermal conduction in femtosecond-laser-pulse-produced plasmas
[DE93-016996] 04 p1585 N94-18129
Development of a statistical method for estimating the downward longwave radiation at the surface from satellite observations 09 p3742 N94-31553

TRANSMISSOMETERS
Bottom boundary layer stress measurements with BASS tripods: Data report STRESS 1988-1989
[AD-A277864] 10 p4092 N94-33775

TRANSMITTANCE
A development on estimation method of undersea light 01 p0204 N94-11974
Propagation of light pulses through a three-layer medium (cloud, pure air, and ocean water)
01 p0222 N94-12725
Characterization of InTlSb grown by low pressure metalorganic chemical vapor deposition on GaAs substrate
[AD-A266878] 03 p1206 N94-14922
Atmospheric transmittance between 1.0 and 2.0 micrometers
[AD-A267076] 03 p1098 N94-15539
Filters for the International Solar Terrestrial Physics (ISTP) mission far ultraviolet imager
[NASA-CR-194633] 03 p1190 N94-15868
Multilayer thin film design for far ultraviolet polarizers using an induced transmission and absorption technique
[NASA-CR-194631] 03 p1190 N94-15869
VUV thin films, chapter 7
[NASA-CR-194634] 03 p0967 N94-16494
A comparison of LOWTRAN-7 corrected Airborne Visible/Infrared Imaging Spectrometer (AVIRIS) data with ground spectral measurements
03 p1074 N94-16710
Atmospheric propagation analysis program
[AD-A268231] 03 p1006 N94-17565

Dual-beam multiple wavelength light transmittance measurement for particle sizing in rocket motor plumes
[AD-A272491] 05 p1670 N94-21208
Transmittance fluctuations and non-linearity in random chains in the presence of applied electric fields
[DE94-603665] 07 p2787 N94-27628
SHARC, a model for calculating atmospheric and infrared radiation under non-equilibrium conditions
[AD-A275207] 08 p3357 N94-28893
Multispectral transmittance measurements through man-made water fogs 08 p3257 N94-30499
Estimation of transmittance from satellite imagery 08 p3257 N94-30500
Degradation of optical components in space 09 p3594 N94-31029
Fast acting optical deflection
[AD-A276630] 09 p3879 N94-32037
Materials processing apparatus development for fluoride glass
[NASA-CR-193963] 10 p4030 N94-34388
Transmission measurements (4000-400 cm(exp -1), 2.5-25 microns) of crystalline ferric oxides and ferric oxyhydroxides: Implications for Mars 11 p4292 N94-35454
Determining the refractive index of a lambda/4 thin film on a thick substrate from a transmittance measurement
[DE93-019584] 12 p4523 N94-36693
Three-stage attenuation using Glan-Thompson prisms
[AD-A280481] 12 p4525 N94-37350

TRANSMITTER RECEIVERS
Development of an on-board aircraft optical fiber data bus system
[NAL-TR-1163] 02 p0514 N94-13338
Infrared remote activity transceiver universal model
[AD-A266965] 03 p1188 N94-15144
SAR sensor electronics: T/R modules 03 p0993 N94-15911
Microwave reflectometer ionization sensor
[NASA-CR-191464] 03 p0922 N94-17083
Design of a general purpose and autonomous transmitter and receiver system for underwater acoustic experiments at sea
[AD-A269268] 04 p1495 N94-17822
Automated HMC assembly
[DE93-040641] 05 p1749 N94-20005
The Globalstar mobile satellite system for worldwide personal communications 06 p2282 N94-22786
Integration and test of high-speed transmitter electronics for free-space laser communications
[NASA-TM-106295] 06 p2295 N94-24101
Analog communication transmitter and receiver test procedures
[AD-A273423] 06 p2300 N94-24687
Layered parallel interface for an active antenna array
[AD-D016002] 06 p2301 N94-25045
Method and apparatus of generating sum or difference signals corresponding to an apparent beam in a monopulse radar system
[AD-D015998] 06 p2302 N94-25056
Optoelectronic technology consortium
[AD-A274595] 07 p3036 N94-26857
Microprocessor chip incorporating optical signal coupling transceiver
[AD-D016077] 07 p2788 N94-28186
Solid-state, active-phased arrays: Some aspects of receiver design
[AD-A275893] 08 p3527 N94-28779
Ground independent landing system 08 p3137 N94-29564
A commercialized, continuous flow fiber optic sensor for trichloroethylene and haloforms 08 p3502 N94-30462
Advanced optical fiber communication systems
[AD-A276416] 09 p3878 N94-31330
Analysis and design of a high speed, wide range stepwise tunable optical filter/amplifier
[PB94-149572] 09 p3698 N94-33169
High temperature superconducting Josephson junction array systems, phase 1
[AD-A277937] 09 p3908 N94-33246
Low level serial transceiver
[AD-D016166] 10 p4039 N94-33766
Fiber optic transceiver for interfacing digital superconducting electronics
[DE94-008264] 10 p4040 N94-33842
A 32-GHz solid-state power amplifier for deep space communications 11 p4255 N94-35562
Design and analysis of a mode B and mode JD satellite Earth station
[AD-A280417] 12 p4391 N94-37225

TRANSMITTERS
NT IONOSONDES
NT RADAR TRANSMITTERS
NT RADIO BEACONS
NT RADIO TRANSMITTERS
NT RADIOSONDES
NT RADIOTELEPHONES
NT RAWINSONDES
NT REPEATERS
NT SONOBUOYS
NT TRANSMITTER RECEIVERS
Galileo EM-2 contributions to the lunar control network 01 p0468 N94-12198
Development of UHF spark-switched L-C Oscillators
[DE93-015019] 02 p0623 N94-13892
Infrared remote activity transceiver universal model
[AD-A266965] 03 p1188 N94-15144
The new MTLRS transmitting system 03 p0877 N94-15612
Development of the Mars Observer Laser Altimeter (MOLA) 03 p0921 N94-15617
Multi-beam laser altimeter 03 p0921 N94-15620
OETC optical backplane bus testbed. IBM tasks: Receiver OEIC and link simulation tools and analysis
[AD-A266198] 03 p1191 N94-16128
Evaluation of site effects on a high frequency direction finding single site location system
[AD-A267465] 03 p1001 N94-17035
True time delay optically controlled dual band transmitter
[AD-A267663] 03 p1003 N94-17228
Extending bandwidth of optical emitters using active matching technique
[AD-D015875] 04 p1394 N94-17707
Intentionally Short Range Communications (ISRC)
[AD-A268788] 04 p1384 N94-18216
The asymptotic theory of the reflection and transmission of a pulsed electromagnetic beam field at a planar interface separating two dispersive media
[AD-A269033] 04 p1385 N94-18404
Photoconductive Semiconductor Switches for pulsed power applications
[DE93-019411] 05 p1750 N94-20294
Spread spectrum random access networks
[AD-A272280] 05 p1737 N94-20585
Conversion of the proprietary ROLM (tm) inter-node link from multimode to singlemode operation 05 p1744 N94-21349
Systems implications of L-band fade data statistics for LEO mobile systems 06 p2284 N94-22799
Performance of the unique-word-reverse-modulation type demodulator for mobile satellite communications 06 p2286 N94-22813
S-76 high intensity radiated fields, volume 2
[AD-A274572] 07 p2771 N94-26836
A tri-state optical switch for local area network communications 07 p2789 N94-27922
A space-based classification system for RF transients
[DE94-003933] 08 p3240 N94-28522
Multicast communication with guaranteed quality of service
[AD-A277650] 09 p3682 N94-33025

TRANSMUTATION
Semiconductor isotope engineering
[DE93-040119] 05 p2030 N94-21744
The influence of transmutation, void swelling, and flux/spectra uncertainties on the electrical properties of copper and copper alloys
[DE94-006213] 09 p3641 N94-31626
Characterization of nuclear transmutations in materials irradiated test facilities
[DE94-013309] 12 p4420 N94-37552

TRANSOCEANIC FLIGHT
Opportunities for integrating the aircraft FMS, aeronautical operational control centers, and future air traffic management systems in oceanic airspace 08 p3140 N94-29577

TRANSONIC AIRCRAFT
U SUPERSONIC AIRCRAFT

TRANSONIC COMPRESSORS
The 3D pneumatic and 2D dynamic probes: Their development and subsequent use in a transonic fan
[RAE-TM-AERO/PROP-22] 02 p0653 N94-14827
Analysis and characteristics of compressor stall precursor signals in forward and AFT swept high speed compressor
[AD-A273820] 06 p2171 N94-25517
Design of a low aspect ratio transonic compressor stage using CFD techniques
[NASA-TM-106636] 10 p3998 N94-33971
Compact diffusers for small transonic compressors 10 p4002 N94-34449
Design and analysis of a highly loaded transonic compressor cascade 10 p4002 N94-34451

TRANSONIC FLIGHT
The problem of the sonic boom for future high-speed transport aircraft
[ESA-TT-1286] 02 p0776 N94-13692
Numerical investigation of thrust vectoring by injection of secondary air into nozzle flows 07 p2801 N94-28013
Vortex generators for control of shock-induced separation. Part 3: Examples of applications of vortex generators to aircraft
[ESDU-93026-PT-3] 07 p2807 N94-28096

TRANSONIC FLOW
Nonlinear aspects of transonic aeroelasticity 01 p0002 N94-10357
Flow analysis around ONERA model M5 configuration
[PAPER-3D-2] 01 p0012 N94-10478
Flow analysis around ONERA model M5 configuration
[PAPER-3D-3] 01 p0012 N94-10479
Flow analysis around ONERA model M5 configuration
[PAPER-3D-4] 01 p0012 N94-10480
Laser anemometer measurements and computations for transonic flow conditions in an annular cascade of high turning core turbine vanes
[NASA-TP-3383] 01 p0015 N94-11133
Nonlinear aspects of transonic aeroelasticity
[UTIAS-345] 01 p0015 N94-11857
Fundamental study of shock wave/turbulent boundary layer interactions with passive control in transonic flows
[ESA-TT-1278] 02 p0630 N94-13117
An experimental investigation of the redistribution of gas stream total temperature in a high turning angle transonic planar cascade
[ISBN-0-315-80791-2] 02 p0502 N94-13369
Analysis of the Harrier forebody/inlet design using computational techniques
[NASA-CR-193616] 02 p0503 N94-13463
Clebsch variable model for unsteady, transonic flow; application to 2D airfoils
[NLR-TP-91387-U] 02 p0503 N94-13530
A robust quasi-simultaneous interaction method for a full potential flow with a boundary layer with application to wing/body configurations
[NLR-TP-91397-U] 02 p0503 N94-13531
Development of full-potential codes in the decade 1983-1993 02 p0639 N94-14600
Navier-Stokes simulation of transonic vortex flow over a delta wing 02 p0640 N94-14606
Development of a general purpose multigrid accelerated Navier-Stokes solver 02 p0641 N94-14613
Intra-blade quantitative transonic flow measurements at the DRA Pyestock Isentropic Light Piston Facility using PIV (Particle Image Velocimetry)
[RAE-TM-AERO/PROP-21] 02 p0509 N94-14706
Laser Doppler velocimetry measurements across a normal shock in transonic flow
[AD-A267240] 03 p0855 N94-14973
Advanced methods for cascade testing
[AGARD-AG-328] 03 p1016 N94-15119
Contribution of laser Doppler velocimetry to the physical description of shock wave/turbulent boundary layer interactions with incidence on turbulence modelling 03 p1018 N94-15201
Computation of the Fluid and Optical Fields About the Stratospheric Observatory for Infrared Astronomy (SOFIA) and the Coupling of Fluids, Dynamics, and Control Laws on Parallel Computers
[NASA-CR-193168] 03 p0858 N94-16510
Selected computations of transonic cavity flows 03 p0858 N94-16511
Unsteady fluid and optical simulation of transonic aero-windows
[AIAA PAPER 93-3017] 03 p0858 N94-16512
Two-dimensional boundary surfaces for axi-symmetric external transonic flows
[AD-A269678] 04 p1312 N94-18571
Navier-Stokes, dynamics and aeroelastic computations for vortical flows, buffet and flutter applications
[NASA-CR-194520] 04 p1313 N94-19621
Transonic flow calculations: Integral method
[ISBN-0-315-83538-9] 05 p1639 N94-22586
Experiments with a fluid deicing system for cleaning laminar wings 05 p1640 N94-22601
Issac, Jason Cherian ses in transonic flow
[NASA-CR-194837] 06 p2167 N94-24052
Evaluation of turbulence models in the PARC code for transonic diffuser flows
[NASA-TM-106391] 06 p2168 N94-24084
Experimental study of a turbulent boundary layer in presence of external manipulators of NACA 0009 profile in the transonic regime
[ISBN-0-315-57633-2] 06 p2333 N94-24177
An investigation of the effects of the high maximum-thickness-to-chord ratio on the performance of nozzle guide vanes in a transonic planar cascade
[ISBN-0-315-84107-9] 07 p2793 N94-26671
Influence of the transonic doublet in the farfield of a lifting airfoil
[IAR-AN-78] 07 p2647 N94-26702
Prediction of undsteady flows in turbomachinery using the linearized Euler equations on deforming grids
[NASA-CR-195285] 07 p2675 N94-27654
Computation of transonic viscous flow past the NTF 65-degree Delta Wing 07 p2659 N94-27930

An initial investigation into methods of computing transonic aerodynamic sensitivity coefficients
[NASA-CR-195705] 07 p2648 N94-28072
Interaction of the sonic boom with atmospheric turbulence 07 p2650 N94-28191
Measurements of steady and dynamic pressure on an F/A-18 wind tunnel model at high angles of attack 07 p2653 N94-28323
Solution-adaptive simulation of transonic cascade flows 07 p2657 N94-28344
Steady pressure measurements on an Aeroelastic Research Wing (ARW-2)
[NASA-TM-109046] 08 p3122 N94-28658
Numerical solution of inverse problem in aerodynamics 08 p3125 N94-28965
Verification of a three-dimensional viscous flow analysis for a single stage compressor 08 p3127 N94-28976
Investigation of advanced counterrotation blade configuration concepts for high speed turboprop systems. Task 2: Unsteady ducted propfan analysis computer program users manual
[NASA-CR-187105] 08 p3152 N94-29438
Experimental studies of transonic flow field near a longitudinally slotted wind tunnel wall
[NASA-TP-3392] 08 p3130 N94-29545
Unsteady transonic aerodynamics in frequency domain for flutter analysis 08 p3131 N94-29879
Development of a method to predict transonic limit cycle oscillation characteristics of fighter aircraft (continued)
[NLR-TP-92156-U] 08 p3148 N94-30342
A residual correction method applied to 2D multi-point airfoil design and 3D single-point wing design
[NLR-TP-92524-U] 08 p3134 N94-30493
Mixed Eulerian-Lagrangian finite element solutions of unsteady flow and flutter in transonic cascade 08 p3282 N94-30816
Prediction of transonic potential flow with slipstreams around configurations
[FFA-TN-1992-15] 09 p3568 N94-31220
Numerical simulation of combined external/internal transonic flow on the forebody/inlet of the AV-8B Harrier 2 09 p3569 N94-31759
An adaptive method for the exact resolution of shock waves and contact discontinuities
[ISBN-0-315-86498-2] 09 p3704 N94-31799
Numerical analysis of transonic wing buffet 09 p3586 N94-32713
A finite-difference approximate-factorization algorithm for solution of the unsteady transonic small-disturbance equation
[NASA-TP-3129] 09 p3572 N94-32865
Flow field analysis in a high pressure ratio centrifugal compressor 10 p4001 N94-34447

TRANSONIC FLUTTER

Understanding and development of a prediction method of transonic limit cycle oscillation characteristics of fighter aircraft
[NLR-TP-92210-U] 07 p2679 N94-27798
Prospects of time-linearized unsteady calculation methods for exponentially diverging motions in aeroelasticity
[PB94-126224] 08 p3134 N94-30740
Mixed Eulerian-Lagrangian finite element solutions of unsteady flow and flutter in transonic cascade 08 p3282 N94-30816
Numerical analysis of transonic wing buffet 09 p3586 N94-32713

TRANSONIC INLETS

U SUPERSONIC INLETS

TRANSONIC NOZZLES

Development of a code for wall contour design in the transonic region of axisymmetric and square nozzles
[NASA-CR-194857] 06 p2167 N94-23625

TRANSONIC SPEED

Aerodynamic characteristics analysis of Garabedian-Korn 75-06-12 airfoil
[PAPER-2D-2] 01 p0010 N94-10468
Results of wind tunnel tests of an ASRM configured 0.03 scale Space Shuttle integrated vehicle model (47-OTS) in the AEDC 16-foot Transonic wind tunnel (IA613A), volume 1
[NASA-CR-185696] 02 p0534 N94-13191
Wind tunnel investigations of forebody strakes for yaw control on F/A-18 model at subsonic and transonic speeds
[NASA-TP-3360] 03 p0859 N94-16573
Highly transient elastodynamic crack growth in a bimaterial interface: Higher order asymptotic analysis and optical experiments
[AD-A266465] 03 p1059 N94-16587
A study of the influence of a delta wing geometry on the induced drag at transonic speed (M=0.55) and high angles of attack
[FFA-TN-1992-14] 04 p1311 N94-17722
Options for thrust augmentation for the Beta 2 two-stage-to-orbit launch vehicle
[NASA-TM-106418] 05 p1649 N94-21759
Experimental cavity pressure measurements at subsonic and transonic speeds. Static-pressure results
[NASA-TP-3358] 06 p2169 N94-24464
Investigation of aerodynamic design issues with regions of separated flow 07 p2658 N94-27902
Statistical and numerical study of the relation between weather and sonic boom characteristics 10 p3976 N94-33498

TRANSONIC TURBINES

U SUPERSONIC TURBINES

TRANSONIC WIND TUNNELS

Improvement of the flow quality in the ARA transonic tunnel by means of a long cell honeycomb
[ARA-MEMO-375] 01 p0034 N94-10894
The evolution of whole field optical diagnostics for external transonic testing
[ARA-MEMO-379] 01 p0383 N94-11887
A software interface for the ARL wind tunnel data acquisition system
[AD-A267114] 03 p1146 N94-15650
Physical properties of the benchmark models program supercritical wing
[NASA-TM-4457] 03 p0866 N94-15722
Wall interference and boundary simulation in a transonic wind tunnel with a discretely slotted test section
[NASA-TP-3334] 03 p0872 N94-15794
Wind tunnel investigation with an operational turbojet engine
[TABES PAPER 93-662] 03 p0870 N94-16157
Error propagation equations and tables for estimating the uncertainty in high-speed wind tunnel test results
[DE93-018685] 04 p1311 N94-18275
Fiber-optic-based laser vapor screen flow visualization system for aerodynamic research in larger scale subsonic and transonic wind tunnels
[NASA-TM-4514] 07 p2647 N94-26706
Experimental investigation of the flow quality in the GLT20 subsonic-transonic boundary layer wind tunnel
[PB94-126539] 07 p2681 N94-26815
The renewing of the test section of the NAL transonic wind tunnel. Part 1: Reconstruction of the 1st corner turning vanes and aerodynamic stress measurement
[NAL-TM-651] 07 p2681 N94-27247
Experimental studies of transonic flow field near a longitudinally slotted wind tunnel wall
[NASA-TP-3392] 08 p3130 N94-29545
A modernised HST of NLR
[AD-B179220] 08 p3158 N94-30423
Analysis of fluctuating static pressure measurements in a large high Reynolds number transonic cryogenic wind tunnel 08 p3158 N94-30788
Results for the hybrid laminar flow control experiment conducted in the NASA Langley 8-foot transonic pressure tunnel on a 7-foot chord model
[NASA-TM-107582] 09 p3601 N94-32870
Semi-span model testing in the national transonic facility
[NASA-CR-195952] 10 p4048 N94-34300
National facilities study. Volume 2: Task group on aeronautical research and development facilities report
[NASA-TM-109855] 10 p4009 N94-34633
Experimental uncertainty and drag measurements in the national transonic facility
[NASA-CR-4600] 12 p4389 N94-36945

TRANSONICS

U TRANSONIC FLOW

TRANSPARENCE

Optimization of transparent and reflecting electrodes for amorphous silicon solar cells
[DE93-010009] 02 p0704 N94-14110
Aberration correction of unstable resonators
[NASA-CASE-NPO-18791-1-CU] 03 p1034 N94-15987
Time-resolved probing of electron thermal conduction in femtosecond-laser-pulse-produced plasmas
[DE93-016996] 04 p1585 N94-18129
Polyimide-based electrooptic materials
[DE93-019416] 05 p1706 N94-21526
Transparent conducting thin films for spacecraft applications
[NASA-TM-106466] 06 p2218 N94-23370
Backscatter haze device for measurement of haze in aircraft transparencies
[AD-A275127] 08 p3146 N94-29042
Proposal to produce novel, transparent radiation hard low refractive index
[AD-A278476] 10 p4029 N94-34087

TRANSPARENT MATERIALS

U TRANSPARENCE

TRANSPIRATION

Real gas and surface transpiration effects upon swept leading edge high speed flow including transition 01 p0008 N94-10452
Evapotranspiration and runoff from large land areas: Land surface hydrology for atmospheric general circulation models 03 p1083 N94-16029
Integrated use of hydrological modelling and remote sensing in the province of Drenthe (The Netherlands): Possibilities and restrictions
[REPT-61] 06 p2382 N94-23148
Calculation of propulsive nozzle flowfields in multidiffusing chemically reacting environments
[NASA-TM-106532] 08 p3271 N94-28835
A long-term simulation of surface fluxes and soil moisture
[DE94-006661] 09 p3774 N94-32772

TRANSPIRATION COOLING

U SWEAT COOLING

TRANSPONDERS

Performance of traffic-alert collision avoidance (TCAS) antennas in the presence of scatterers
[NASA-CR-193569] 01 p0023 N94-11525
Impact of shutting down en route primary radars within CONUS interior
[DOT-VNTSC-FAA-93-1] 01 p0023 N94-11626
Preliminary design and implementation of the baseline digital baseband architecture for advanced deep space transponders 02 p0611 N94-14393
Calibration: Practical experience with ERS-1 03 p0992 N94-15907
Planned LMSS propagation experiment using ACTS: Preliminary antenna pointing results during mobile operations 03 p0995 N94-16041
Range safety transponder catalog
[AD-A270882] 04 p1323 N94-19581
Quasi-optical transponder using FET's and patch antennas
[AD-A271339] 04 p1407 N94-19584
ROCSAT-1 telecommunication experiments 06 p2279 N94-22770
Odyssey personal communications satellite system 06 p2282 N94-22787
Design and analysis of a low-loss linear analog phase modulator for deep space spacecraft X-band transponder applications 08 p3248 N94-29625
Design and implementation of a hybrid digital phase-locked loop with a TMS320C25: An application to a transponder receiver breadboard 08 p3251 N94-29667
Measurement of the frequency stability of responders in aircraft 08 p3261 N94-30673
Performance evaluation of digital phase-locked loops for advanced deep space transponders 11 p4254 N94-35558

TRANSPORT AIRCRAFT

NT A-310 AIRCRAFT
NT BOEING 720 AIRCRAFT
NT BOEING 727 AIRCRAFT
NT BOEING 737 AIRCRAFT
NT BOEING 747 AIRCRAFT
NT BOEING 757 AIRCRAFT
NT BOEING 767 AIRCRAFT
NT C-130 AIRCRAFT
NT C-131 AIRCRAFT
NT C-135 AIRCRAFT
NT C-141 AIRCRAFT
NT CARGO AIRCRAFT
NT DC 8 AIRCRAFT
NT DC 10 AIRCRAFT
NT EUROPEAN AIRBUS
NT H-53 HELICOPTER
NT LIGHT TRANSPORT AIRCRAFT
NT MD 11 AIRCRAFT
NT MYSTERE 20 AIRCRAFT
NT SH-3 HELICOPTER
NT SHORT HAUL AIRCRAFT
NT TANKER AIRCRAFT
NT UH-60A HELICOPTER
NT YC-14 AIRCRAFT
High temperature materials for hypersonic transport 01 p0056 N94-10003
AGBT advanced counter-rotating gearbox detailed design report
[NASA-CR-180883] 01 p0179 N94-10400
Evaluation of two cockpit display concepts for civil tiltrotor instrument operations on steep approaches 02 p0517 N94-13323
Embedded computer systems: Status of C-17 software
[AD-A267307] 03 p1160 N94-16993
Metals 2000
[DE93-016761] 04 p1355 N94-17752
In-flight pressure distributions and skin-friction measurements on a subsonic transport high-lift wing section 04 p1308 N94-18435
High-lift design for large civil aircraft 04 p1310 N94-18445
High lift systems for transport aircraft with advanced airfoils 04 p1310 N94-18446

Procedures and design data for the formulation of aircraft configurations
[AD-A270150] 04 p1318 N94-18779
Pilot-vehicle interface
[DOT/FAA/CT-92/21] 06 p2430 N94-23083
Influence of active controls on the design process of a large transport aircraft 06 p2178 N94-24323
Current and future design methods for large transport aircraft 06 p2179 N94-24324
JB-300: An advanced medium size transport for 2005
[NASA-CR-195499] 06 p2179 N94-24401
NASA/USRA University Advanced Design Program, 1992-1993. The Diamondback: A simulated commercial air transportation study
[NASA-CR-195523] 06 p2180 N94-24462
The cetaceopteryx: A global range military transport aircraft
[NASA-CR-195519] 06 p2181 N94-24711
Conceptual design proposal: HUGO global range/mobility transport aircraft
[NASA-CR-195501] 06 p2181 N94-24787
Pilot-vehicle interface handbook, chapter 19. Volume 2: Digital systems validation
[DOT/FAA/CT-88/10-VOL-2] 06 p2438 N94-24830
Dumbo heavy lifter aircraft
[NASA-CR-195500] 06 p2182 N94-24915
The AC-120: The advanced commercial transport
[NASA-CR-195491] 06 p2182 N94-24966
A global range military transport: The ostrich
[NASA-CR-195494] 06 p2183 N94-24972
Weasel works SA-150: Design study of a 100 to 150 passenger transport aircraft
[NASA-CR-195489] 06 p2183 N94-24975
The RTL-46: A simulated commercial air transportation study
[NASA-CR-195524] 06 p2184 N94-25017
C-17 lot 3 production contract
[AD-A273180] 06 p2174 N94-25153
The application of a C(star) flight control law to large civil transport aircraft
[CRANFIELD-AERO-9303] 07 p2676 N94-25640
Supercruiser Arrow HS-8 07 p2671 N94-25711
The evolution of the high-speed civil transport
[NASA-TM-109089] 07 p3117 N94-26155
Optical communications for transport aircraft 07 p2643 N94-27298
Techniques to improve maneuver stability characteristics of a nonlinear wide-body transport airplane in cruise flight
[NASA-TM-4521] 07 p2679 N94-27660
Wing design for a civil tiltrotor transport aircraft: A preliminary study 07 p2671 N94-27917
Examples of flight path optimisation using a multivariate gradient-search method
[ESDU-93021] 07 p2670 N94-28092
Examples of excrescence drag prediction for typical wing components of a subsonic transport aircraft at the cruise condition
[ESDU-93032] 07 p2649 N94-28144
Numerical analysis of supersonic transport wings 08 p3124 N94-28959
Advanced vehicle concepts systems and design analysis studies
[NASA-CR-195115] 08 p3147 N94-29721
CFD-based drag prediction: State-of-the-art, theory, prospects
[AD-B179297] 09 p3567 N94-31180
Airborne Trailblazer: Two decades with NASA Langley's 737 flying laboratory
[NASA-SP-4216] 09 p3566 N94-32793
Application of a design-build-team approach to low cost and weight composite fuselage structure
[NASA-CR-4418] 09 p3626 N94-32663
Designer's unified cost model 09 p3627 N94-33122
COINS: A composites information database system 09 p3627 N94-33123
Composite fuselage shell structures research at NASA Langley Research Center 09 p3628 N94-33124
Structural testing of the technology integration box beam 09 p3628 N94-33125
Local design optimization for composite transport fuselage crown panels 09 p3629 N94-33132
Recent progress in NASA Langley Research Center textile reinforced composites program 09 p3629 N94-33134
First Annual HSR Program Workshop: Headquarters perspective 10 p3970 N94-33448
Update on Douglas' high-speed civil transport studies 10 p3970 N94-33450
Status of an inlet configuration trade study for the Douglas HSCT 10 p3977 N94-33506
The future of large capacity/long range multipurpose air cargo fleets 11 p4194 N94-36326
Tanker system and technology requirements definition: A tanker technology road map 11 p4197 N94-36344
Subsonic aerodynamic characteristic of semispan commercial transport model with wing-mounted advanced ducted propeller operating in reverse thrust --- conducted in the Langley 14 by 22 foot subsonic wind tunnel
[NASA-TP-3427] 12 p4384 N94-37505

TRANSPORT COEFFICIENTS
U TRANSPORT PROPERTIES

TRANSPORT PROPERTIES
NT CARRIER MOBILITY
NT DIFFUSION COEFFICIENT
NT EDDY VISCOSITY
NT ELECTRICAL RESISTIVITY
NT ELECTRON MOBILITY
NT GAS VISCOSITY
NT GASEOUS DIFFUSION
NT HOLE MOBILITY
NT IONIC MOBILITY
NT IONOSPHERIC CONDUCTIVITY
NT KONDO EFFECT
NT MAGNETORESISTIVITY
NT PHOTOCONDUCTIVITY
NT PLASMA CONDUCTIVITY
NT SORET COEFFICIENT
NT SUPERCONDUCTIVITY
NT THERMAL CONDUCTIVITY
NT THERMAL DIFFUSIVITY
NT VISCOSITY

Physics and modelling of scrape-off layer transport
[DE93-010510] 01 p0385 N94-10289
Transport mechanisms acting in toroidal devices: A theoretician's view
[DE93-013463] 01 p0385 N94-10310
Aerosol sampling models survey
[AD-A265903] 01 p0075 N94-10337
Arcjet space thrusters
[NASA-CR-193191] 01 p0046 N94-10700
Hydrogen partitioning and transport in titanium aluminides
[NASA-CR-194117] 01 p0076 N94-10713
Processing and transport properties of high J(sub c) silver clad Bi-2223 tapes and coils
[DE93-010674] 01 p0398 N94-11073
Process modelling for materials preparation experiments
[NASA-CR-193556] 01 p0056 N94-12588
Modeling ignition chemistry
[DE93-012340] 02 p0561 N94-12910
Equilibrium reconstruction of the q-profile in tokamaks from motional Stark effect data
[DE93-015815] 02 p0796 N94-13046
Research on chemical vapor deposition processes for advanced ceramic coatings
[NASA-CR-193613] 02 p0577 N94-13089
Transport properties of disordered porous media from the microstructure
[DE93-016065] 02 p0806 N94-13152
A time-accurate numerical method for chemically reacting flows at all Mach numbers 02 p0500 N94-13198
Measurements on two-dimensional arrays of mesoscopic Josephson junctions
[AD-A265129] 02 p0807 N94-13359
On energy transport equations for turbulent magnetized plasma
[PPL-135] 02 p0800 N94-13850
Direct determination of alpha particle transport coefficients
[DE93-013488] 02 p0787 N94-14691
Effects of spin-orbit coupling on disordered mesoscopic systems
[ITN-93-85220] 03 p1180 N94-15288
X ray laser program
[AD-A267075] 03 p1038 N94-15628
High temperature superconductivity
[AD-A267006] 03 p1008 N94-15635
Optoelectronics based on SiGe/Si heterostructures
[AD-A267178] 03 p1190 N94-15848
Gas bubble generation and transport in microgravity 03 p0980 N94-16089
General order characteristic methods for solving neutron transport problems
[DE93-015824] 03 p1170 N94-16167
Sand transport on Mars: Preliminary results from models 03 p1252 N94-16198
Pulsed laser deposition of metastable Ca(1-x)Sr(x)CuO2 thin films
[DE93-015804] 03 p1040 N94-16663
Factors determining the release of nitric oxide --- Calcium/cadmium transport by renal cortical collectin duct cells
[AD-A266232] 03 p1118 N94-17224
Plasma instabilities and transport in the MPD thruster
[AD-A268268] 03 p1204 N94-17575
Coefficients for calculating thermodynamic and transport properties of individual species
[NASA-TM-4513] 03 p1220 N94-17624
Granular fluctuations in plasma turbulence and their role in transport
[DE93-013465] 03 p1187 N94-17674
Electron mobility in high resistivity silicon
[REPT-93-007] 04 p1565 N94-17933
Dependence of helium transport on plasma current and ELM frequency in H-mode discharges in D3-D
[DE93-016986] 04 p1585 N94-18058
Assessment and development of second order turbulence models 04 p1411 N94-18548
Optical and transport properties of metallic and semiconductor nanostructures
[AD-A270009] 04 p1598 N94-18609
Scaling laws for diamond chemical vapor deposition. 2: Atomic hydrogen transport
[AD-A269842] 04 p1371 N94-18740
Transport phenomena and interfacial kinetics in multiphase combustion systems
[AD-A270202] 04 p1349 N94-18785
LAHET calculations for accelerator neutron production
[DE93-016518] 04 p1570 N94-19120
ICRF direct electron heating experiments in TFTR
[DE93-017857] 04 p1590 N94-19273
Behavior of the particle transport coefficients near the density limit in MTX
[DE93-019108] 04 p1591 N94-19311
Electrokinetic transport of heterogeneous particles in suspensions
[NASA-CR-194478] 04 p1353 N94-19367
Radial evolution of the solar wind turbulence with application to charged particle transport
[NASA-CR-194081] 04 p1629 N94-19427
Global three dimensional model of tropospheric trace gases chemistry and transport
[AERONAUTICA-ACTA-A-370-1993] 04 p1479 N94-19518
Boost-phase discrimination research
[NASA-TM-109347] 05 p1666 N94-19818
Parametric variations of ion transport in TFTR
[DE93-012653] 05 p1991 N94-19883
A database of selected transport coefficients for combustion studies
[DE93-041278] 05 p1678 N94-19889
Computed potential energy surfaces for chemical reactions
[NASA-CR-194600] 05 p1679 N94-20169
Growth of zinc selenide single crystals by physical vapor transport in microgravity
[NASA-CR-194679] 05 p2017 N94-20346
Optical and transport properties of metallic and semiconductor nanostructures
[AD-A271716] 05 p2018 N94-20554
Establishing the basis for validated predictions of highly non-equilibrium flows (with 9 attachments)
[AD-A272918] 05 p1802 N94-21220
IR materials producibility
[AD-A273031] 05 p1987 N94-21321
Dephasing processes in III-V semiconductors
[AD-A271677] 05 p2028 N94-21362
Local uniform grid refinement and brine transport in porous media with inhomogeneities
[CWI-NM-R9224] 05 p1803 N94-21609
Fundamental studies of defect generation in amorphous silicon alloys grown by remote plasma-enhanced chemical-vapor deposition
[DE93-017083] 05 p2029 N94-21615
Atomic-scale structure of grain boundaries: Correlations to grain boundary properties
[DE94-001289] 06 p2558 N94-22990
Modelling of solid polymer and direct methanol fuel cells: Phenomenological equations and analytical solutions
[PB93-224897] 06 p2390 N94-23102
Investigation of evolution-related aspects of bacterial rhodopsins
[NASA-CR-194826] 06 p2420 N94-23501
Comparison of numerical simulation and experimental data for steam-in-place sterilization 06 p2326 N94-23669
Two-point PADE approximants for Stieltjes series 06 p2490 N94-24768
Evidence for dust transport in Viking IR thermal mapper opacity data 06 p2620 N94-24892
Dust transport in the Martian atmosphere 06 p2621 N94-24894
Modelling of thermal argon plasmas
[ETN-94-95363] 06 p2554 N94-25300
Effect of high frequency field on the transport properties of superlattice
[DE93-617047] 06 p2568 N94-25447
Selfsimilar solutions of a nonlinear transport equation
[REPT-93-42] 07 p2865 N94-25760
A positive finite-difference advection scheme applied on locally refined grids
[CWI-NM-R9309] 07 p2867 N94-26216

Recombination and metastability in amorphous silicon and silicon germanium alloys
[DE94-000237] 07 p2736 N94-26481
A concurrent, multigroup, discrete ordinates model of neutron transport
[DE94-004334] 07 p3020 N94-26577
Powder synthesis, fabrication, and transport properties of long-length Ag clad Bi-2223 conductors
[DE94-002376] 07 p2740 N94-26957
Computer simulation and experiments on the quasi-static mechanics and transport properties of granular materials
[AD-A274192] 07 p2823 N94-27104
Gauge invariance and transport properties in superconductors above T(c)
[DE94-604013] 07 p3068 N94-27677
On radio frequency wave induced radial transport and wave helicity
[IPPCZ-326] 07 p2777 N94-27838
On helicon wave induced radial plasma transport
[IPPCZ-333] 07 p3048 N94-27840
Molecular aspects of transport in thin films of controlled architecture
[DE94-004552] 08 p3211 N94-28457
Transport properties of epitaxial lift off films
[NASA-TM-106156] 08 p3264 N94-29209
The effect of magnetic field configuration on particle pinch velocity in Compact Helical System (CHS)
[AD-B183299L] 08 p3505 N94-29398
Nonadiabatic effects in the quantum Hall regime
08 p3513 N94-29530
Conceptual study of moderately coupled plasmas and experimental comparison of laboratory x ray sources
[DE94-005828] 08 p3506 N94-30045
Volume averaged model for the mechanics of alloys solidification
[PB94-138617] 08 p3208 N94-30113
Process modelling for materials preparation experiments
[NASA-CR-195782] 08 p3175 N94-30242
The long-range transport of aerosol particles over the North Atlantic Ocean 08 p3366 N94-30867
Studying transient mobility and energy loss using scanning tunneling microscopy
[AD-A276292] 09 p3877 N94-31256
Transport properties of quark and gluon plasmas
[DE94-007043] 09 p3864 N94-31405
Compressible convection with ionization
09 p3911 N94-31498
Adjacent-cell Preconditioners for solving optically thick neutron transport problems
[DE94-007219] 09 p3872 N94-32666
Anomalous transport equations in toroidal plasmas
[DE94-009206] 09 p3893 N94-32922
CET93 and CETPC: An interim updated version of the NASA Lewis computer program for calculating complex chemical equilibria with applications
[NASA-TM-4557] 09 p3638 N94-32948
Computed potential energy surfaces for chemical reactions
[NASA-CR-195835] 09 p3639 N94-33036
Transport and diffusion in turbulent fields modeling and measurements techniques
[AD-A278114] 09 p3769 N94-33110
Diffusion at the magnetopause: A theoretical perspective
[DE94-009356] 10 p4086 N94-33910
Transport properties of interacting magnetic islands in tokamak plasmas
[DE94-009208] 10 p4145 N94-34140
Magnetic island effects, interactions in tokamaks
[DE94-009209] 10 p4145 N94-34221
Diffusion and sorption of 1,4-dioxane into polychloroprene
[ARL-TR-338] 11 p4229 N94-35361
Determination of extensional viscosity from capillary rheometer entrance pressure drop measurements using a numerical simulation of contraction flow
[PB94-171154] 11 p4263 N94-35603
On the various forms of the energy equation for a dilute, monatomic mixture of nonreacting gases
[NASA-CR-4612] 11 p4190 N94-35864
K-epsilon model of anomalous transport in resistive interchange turbulence
[DE94-718983] 11 p4337 N94-35937
NEQPAK, the AEDC thermochemical nonequilibrium package: Theory and use
[AD-A279005] 11 p4266 N94-35951
Improved models of beta-limit, anomalous transport and radial electric field with loss cone loss in heliotron/torsatron
[DE94-718976] 11 p4324 N94-35984
Thermophysical properties of HFC-143a and HFC-152a
[DE94-009995] 11 p4251 N94-36008
Beam transport
[DE94-010755] 11 p4331 N94-36199
Computational chemistry research
[NASA-CR-196120] 12 p4408 N94-36989
Confinement improvement in H-mode-like plasmas in helical systems
[DE94-727619] 12 p4528 N94-37231
Midwest Superconductivity Consortium
[DE94-012716] 12 p4536 N94-37285
Theoretical studies of the transport properties in compound semiconductors
[NASA-CR-196109] 12 p4439 N94-37501
Effects of molecular transport on turbulence-chemistry interactions in a hydrogen-argon-air jet diffusion flame
[DE94-005107] 12 p4413 N94-37711
Self-sustained turbulence and L-mode confinement in toroidal plasmas
[DE94-748497] 12 p4532 N94-37734
Flux creep: Its dependence on current denisty and relation to critical current densities from transport and magnetic measurements
[DE94-011701] 12 p4440 N94-37738

TRANSPORT THEORY
NT CHAPMAN-ENSKOG THEORY
NT MIXING LENGTH FLOW THEORY
A spectral nodal method for discrete ordinates problems in x,y geometry
[DE93-610128] 01 p0342 N94-10283
Physics and modelling of scrape-off layer transport
[DE93-010510] 01 p0385 N94-10289
A spectral nodal method for the solution of the Sn equations in x, y geometry for highly absorbing deep penetration problems
[DE93-613520] 01 p0349 N94-10636
The searchlight problem for neutrons in a semi-infinite medium
[DE93-010796] 01 p0365 N94-10952
Development of deterministic transport methods for low energy neutrons for shielding in space
[NASA-CR-194172] 01 p0366 N94-11199
Helium transport scaling law studies
[DE93-013487] 01 p0393 N94-11513
Grid optimization and multigrid techniques for fluid flow and transport problems 01 p0154 N94-11824
Study of multicomponent diffusion and transport phenomena
[DE93-015095] 02 p0804 N94-13005
Variance reduction unique to coupled electron/photon Monte Carlo transport
[DE93-014999] 02 p0782 N94-13409
Dynamical model for the distribution of geomagnetically trapped anomalous-component ions
[ATR-91(9558)-6] 02 p0784 N94-13936
A transport equation for eddy viscosity
02 p0646 N94-14762
Toward a quasi-linear closure for compressible turbulence
[DE93-017185] 02 p0647 N94-14895
Turbulence modelling for shock wave/boundary layer interactions specific issues and examples of applications
03 p1018 N94-15202
Shielding from space radiations
[NASA-CR-194578] 03 p1180 N94-15715
General order characteristic methods for solving neutron transport problems
[DE93-015824] 03 p1170 N94-16167
Shielding from space radiations
[NASA-CR-194664] 03 p1301 N94-17255
Linear characteristic spatial quadrature for discrete ordinates neutral particle transport on arbitrary triangles
[AD-A267485] 03 p1185 N94-17365
A preliminary model for crack-tip hydrogen transport
[NPL-DMM(A)-84] 04 p1451 N94-17899
Ratio of specimen thickness to detection area for reliable hydrogen permeation measurement
[NPL-DMM(A)-103] 04 p1451 N94-17929
Chemical reactions in turbulent mixing flows
[AD-A269377] 04 p1410 N94-18472
Asymptotic derivation of the modified time-dependent SP2 equations and numerical calculations
[DE93-016466] 04 p1551 N94-19342
Improved approximations applied to the S(sub N) even-parity equation
[DE93-016467] 04 p1551 N94-19343
Exponential characteristic spatial quadrature for discrete ordinates neutral particle transport in two-dimensional cartesian coordinates
[AD-A270458] 04 p1554 N94-19671
Shielding from space radiations
[NASA-CR-194683] 05 p1895 N94-20063
Neoclassical kinetic theory near an X-point: Plateau regime
[DE93-019825] 05 p1951 N94-20224
Numerical modeling of physical vapor transport under microgravity conditions: Effect of thermal creep and stress 06 p2223 N94-24340
Conservation equations for reacting gas flow
[PB94-111168] 06 p2334 N94-24574
The transition from diapirism to dike intrusion: Implications for planetary volcanism
[NASA-CR-195133] 06 p2403 N94-24580
The anomalous transport caused by particles transverse drift
[DE93-613685] 06 p2554 N94-25329
Collection and evaluation of numerical models with the aim to investigate the impact of aircraft emissions
[DLR-MITT-93-06] 06 p2400 N94-25414
Applications of the homogenization method to flow and transport in porous media
[BER-9110] 06 p2340 N94-25467
Shear flow generation from the interaction of neoclassical and drift wave transport processes
[DE94-003135] 07 p2791 N94-26096
Analytical solution of Mori's equation with secant hyperbolic memory
[DE94-601541] 07 p3006 N94-26368
Pre-orbital criticality safety for the NEPSTP mission
[DE94-002600] 07 p3005 N94-26802
Refractive and dielectric properties of helium, argon and nitrogen gases
[PB94-123783] 07 p3008 N94-26851
Solution of charged particle transport equation by Monte-Carlo method in the BRANDZ code system
[DE94-606270] 08 p3484 N94-28614
A vorticity transport closure method for turbulent reacting flows 08 p3274 N94-29761
Overview of the US stellarator reactor study
[DE94-006042] 08 p3508 N94-30339
Ten new checks to assess the statistical quality of Monte Carlo solutions in MCNP
[DE94-006137] 08 p3465 N94-30366
Theory of ultra dense matter and the dynamics of high energy interactions involving nuclei
[DE94-004178] 08 p3491 N94-30686
Superdiffusion
[DE94-002333] 08 p3492 N94-30834
Transport suppression by shear flow generation in multihelicity resistive-g turbulence
[DE94-007108] 09 p3886 N94-31366
Plasma confinement theory and transport simulation
[DE94-006065] 09 p3888 N94-31619
Non-equilibrium electrodynamics in the large N expansion
[DE94-006156] 09 p3911 N94-31760
Parallel Monte Carlo reactor neutronics
[DE94-007642] 09 p3826 N94-32357
Monoenergetic neutral particle transport in semi-infinite media
[AD-A277155] 09 p3870 N94-32368
Numerical transport theory
[DE94-009064] 09 p3857 N94-32589
Characterization of atomic and molecular impurity sources and transport at the tokamak edge
[DE94-007212] 09 p3891 N94-32619
Adjacent-cell Preconditioners for solving optically thick neutron transport problems
[DE94-007219] 09 p3872 N94-32666
Analytic formulation for the ac electrical conductivity in two-temperature, strongly coupled, overdense plasma: FORTRAN subroutine
[DE94-009466] 09 p3893 N94-32915
Anomalous transport equations in toroidal plasmas
[DE94-009206] 09 p3893 N94-32922
Dynamical nature of inviscid power law for two-dimensional turbulences and self-consistent spectrum and transport of plasma filaments
[DE94-009425] 10 p4144 N94-33913
Anomalous cross field flux in CHS
[DE94-727547] 12 p4529 N94-37359
Neutron transport methods on scalable shared memory multiprocessors
[DE94-012324] 12 p4498 N94-37419
Bounce resonance heating and transport in a magnetic mirror
[DE94-727545] 12 p4531 N94-37466
Theory of anomalous transport in H-mode plasmas
[DE94-727546] 12 p4531 N94-37485

TRANSPORTATION
NT ADVANCED LAUNCH SYSTEM (STS)
NT AIR TRANSPORTATION
NT RAIL TRANSPORTATION
NT RAPID TRANSIT SYSTEMS
NT SPACE TRANSPORTATION
NT SPACE TRANSPORTATION SYSTEM
NT URBAN TRANSPORTATION
Polymer electrolyte fuel cells: Potential transportation and stationary applications
[DE93-010734] 01 p0264 N94-11666
Activities of Bombardier, Inc.
[ISBN-2-921393-11-5] 02 p0499 N94-13520
A verification of the Euroguidance: A guidance forecast for transportation and tourism
[KNMI-TR-145] 02 p0722 N94-13993

Research activities, Faculty of Civil Engineering, Delft University of Technology, 1990 - 1991
[PB93-195022] 04 p1380 N94-19254
National Program Plan Fuel Cells in Transportation
[DE93-017557] 04 p1469 N94-19346
Multigrid approach to solving the long transportation problem on a regular grid in cost space
[AD-A272323] 05 p1909 N94-21038
The 13th International Conference on Magnetically Levitated Systems and Linear Drives MAGLEV 1993
[DE93-040381] 05 p1825 N94-21544
A multilevel cost-space approach to solving the balanced long transportation problem 06 p2483 N94-23678
The general pickup and delivery problem
[MEMO-COSOR-92-44] 07 p2992 N94-26226
Electrical engineering and industrial electronics education days: Control of asynchronous generators
[PB94-135514] 08 p3266 N94-29523
TCM exemptions to promote alternative-fuel vehicles: The good, the bad, and the ugly
[DE94-005924] 08 p3311 N94-30703
Fuel cycle evaluations of biomass-ethanol and reformulated gasoline
[DE94-000227] 08 p3226 N94-30818
Review and status of Maglev in the United States
[DE94-006832] 09 p3722 N94-31319
Sandia technology engineering and science accomplishments
[DE94-008312] 09 p3668 N94-32412
Future ultra-speed tube-flight
11 p4225 N94-35918
LNG vehicle technology, economics, and safety assessment
[PB94-165487] 12 p4450 N94-36721
The implementation of Electronic Data Interchange (EDI) with defense transportation operations
[AD-A280568] 12 p4493 N94-37040

TRANSPORTATION ENERGY
Low pressure storage of natural gas on activated carbon
[DE93-014053] 02 p0660 N94-12851
First Biomass Conference of the Americas: Energy, Environment, Agriculture, and Industry, volume 2
[DE94-000435] 05 p1847 N94-21562

TRANSPORTER
An update on Lab Rover: A hospital material transporter
[AIAA PAPER 94-1228-CP] 08 p3447 N94-30577

TRANSPUTERS
Application of parallel processing to a surface patch/wire junction EFIE code
[AD-A264965] 01 p0336 N94-10488
Data processing system for flight spectrometer
03 p0908 N94-15086
Reactive system verification case study: Fault-tolerant transputer communication
[NASA-TM-108784] 03 p1145 N94-15538
Transputer based control system for MTLRS
03 p0877 N94-15613
Comparative examinations of several field oriented position control structures for asynchronous servomotors with a multitransputer system
[ETN-93-95051] 04 p1406 N94-19390
Two-dimensional particle-in-cell simulation on transputer arrays
[DE93-017977] 05 p1972 N94-20181
The ADAM environment and transputers
05 p1926 N94-22494
A parallel PROLOG system for distributed memory multiprocessor
[ETN-94-95173] 06 p2465 N94-23167
High performance, low cost, self-contained, multipurpose PC based ground systems
06 p2516 N94-23943
Transputer benchmarks and performance comparisons with other computing machines
[RR-467] 06 p2446 N94-25312
Advanced control structures: A transputer-based multi-robot system
[RR-468] 06 p2446 N94-25313
Horatio: Libraries for vision applications, release 2.0
[OUEL-1967/92] 06 p2593 N94-25326
Parallel processing methods for space based power systems 06 p2222 N94-25352
The transputer
[AD-A273688] 06 p2446 N94-25438
A Multitransputer Parallel Processing System (MTPPS)
[DE94-604652] 07 p2981 N94-26903
Inverted pendulum control apparatus using transputers
[DE94-701224] 07 p2973 N94-27732
Design and implementation of Voltan fault-tolerant nodes for distributed systems
[PB94-148863] 10 p4107 N94-33980
Computer automation and artificial intelligence
[DE94-611058] 11 p4312 N94-35831

TRANSURANIUM ELEMENTS
NT AMERICIUM
NT CALIFORNIUM
NT CALIFORNIUM ISOTOPES
NT CURIUM
NT NEPTUNIUM
NT PLUTONIUM
NT PLUTONIUM 238
Studies of heavy-ion reactions and transuranic nuclei
[DE94-004642] 07 p3029 N94-27783

TRANSVERSE ACCELERATION
A comparison of in-bore projectile motion from an electromagnetic railgun versus that of a conventional cannon barrel
[AD-A273473] 06 p2198 N94-24690

TRANSVERSE LOADS
Development of engineering models for calculation of failure loads and defect states of steel concrete beams and plates
[ETN-93-95052] 04 p1460 N94-19648
Improvements to a method for the geometrically nonlinear analysis of compressively loaded stiffened composite panels
[NASA-CR-194715] 05 p1832 N94-21814
On the constitutive response of transversely loaded fiber composites with compliant interphases
09 p3619 N94-31555

TRANSVERSE OSCILLATION
NT H WAVES
Study of wave propagation and dynamic response of laminated composite structures
[AD-A276123] 09 p3619 N94-31444
Transverse mode analysis of hole-coupled free-electron lasers
[ETN-94-96019] 09 p3715 N94-31532
Vibration localization in dual-span axially moving elastic systems 09 p3736 N94-31964
Is it possible to assign physical meaning to field theory with higher derivatives?
[DE94-618468] 12 p4539 N94-37172

TRANSVERSE VIBRATION
U TRANSVERSE OSCILLATION

TRANSVERSE WAVES
NT H WAVES
Acoustic waves in complicated geometries and their interactions with liquid-propellant droplet combustion
[AD-A267260] 03 p1178 N94-16991
The electromechanical properties of tetragonal BaTiO3 and PbTiO3 single crystals
[DE93-019008] 04 p1603 N94-19550
An electromagnetic finite difference time domain analog treatment of small signal acoustic interactions
[DE94-009978] 11 p4319 N94-35770

TRANSVERSELY EXCITED ATMOSPHERIC LASERS
U TEA LASERS

TRAPATT DIODES
U AVALANCHE DIODES

TRAPEZOIDS
Trapezoid-oriented compression of run length coded map data
[PB94-123312] 07 p2849 N94-26848
Transformational derivation of (parallel) programs using skeletons
[TR-93-20] 09 p3825 N94-32196

TRAPPED PARTICLES
NT INNER RADIATION BELT
NT MAGNETICALLY TRAPPED PARTICLES
NT PROTON BELTS
NT RADIATION BELTS
Laser cooling and trapping of atoms in microgravity: Ultracold atoms collisions 01 p0124 N94-10241
Quantum non demolition measurement of cyclotron excitations in a Penning trap 01 p0376 N94-10578
Kinetic approach to long wave length modes in rotating plasmas
[DE93-771286] 01 p0388 N94-10807
Analysis of geophysical measurements and spacecraft interactions
[AD-A266064] 01 p0043 N94-10944
The 24th Annual Precise Time and Time Interval (PTTI) Applications and Planning Meeting
[NASA-CP-3218] 01 p0350 N94-10963
Particle transport analysis in torsatron configurations
[DE93-621640] 01 p0390 N94-11120
Probability of particle trapping/detrapping in torsatrons
[DE93-621641] 01 p0390 N94-11121
Energetic neutral atoms: Imaging the magnetospheric ring current
[NASA-CR-194339] 02 p0715 N94-13826
Collisional effects of trapped electrons on the anomalous particle and thermal pinches
[PPL-128] 02 p0800 N94-13853
Studies on equatorial shock formation during plasmaspheric refilling
[NASA-CR-194392] 02 p0715 N94-13954
Quasiparticle trapping in distributed superconducting three-terminal tunnel junction devices
03 p0910 N94-15101
Nitrogen and light noble gases in Parsa enstatite chondrite 03 p1246 N94-16435
Kinetic plasma processes occurring in the outer plasmasphere
[NASA-CR-193452] 03 p1300 N94-17524
Research on defects and transport in amorphous-silicon-based semiconductors
[DE93-017117] 05 p2013 N94-19939
Energy storage and conversion in solid hydrogen
[AD-A271439] 05 p1845 N94-20086
Ionospheric photoelectrons measured at geosynchronous orbit
[AD-A272431] 05 p1857 N94-21202
Detailed analysis case studies of trapped plasmas at the Earth's magnetic equator
[AD-A272497] 05 p1858 N94-21432
Radial diffusion of toroidally trapped particles induced by lower hybrid and fast waves
[IPPCZ-327] 05 p1996 N94-21593
Fluctuations and confinement in ATF
[DE94-000485] 06 p2549 N94-22998
Trapped electrons in solid hydrogen
[DE93-018628] 07 p3052 N94-25947
Antiproton studies in penning traps
[AD-A274250] 07 p3024 N94-27011
Charge trapping and breakdown in N2O oxides
[DE94-003775] 08 p3266 N94-30040
Langmuir waves in the electron-positron plasma
[DE94-608330] 08 p3508 N94-30191
Collisional and chaotic transport of energetic particles in toroidal plasma
[DE94-006504] 09 p3889 N94-31787
The PS 200 catching trap: A new tool for ultra-low energy antiproton physics
[DE94-009309] 10 p4137 N94-34089
LDEF satellite radiation study
[NASA-CR-193948] 10 p4015 N94-34147
Collisonless dynamics of the magnetosphere
[AD-A278886] 11 p4290 N94-35708
Particle orbit analysis for LHD helical axis configurations
[DE94-718995] 11 p4336 N94-35773
Spontaneous force optical traps
[AD-A280574] 12 p4514 N94-37041

TRAPPED VORTICES
Lift enhancement by trapped vortex
10 p3980 N94-33524

TRAPPING
Laser cooling and trapping of atoms in microgravity: Ultracold atoms collisions 01 p0124 N94-10241
Bond distortion and electron trapping in charged C60
[DE93-613642] 01 p0396 N94-10637
Probability of particle trapping/detrapping in torsatrons
[DE93-621641] 01 p0390 N94-11121
EBIT Trapping Program
[DE93-014422] 02 p0788 N94-13208
Trapping of water vapor from an atmosphere by condensed silicate matter formed by high-temperature pulse vaporization 03 p1248 N94-16180
Orbital evolution of dust from comet Schwassmann-Wachmann 1: A case of one-to-one resonance trapping 03 p1242 N94-16270
Evaluation of a diffusion/trapping model for hydrogen ingress in high-strength alloys
[AD-A271328] 05 p1689 N94-20027
Hydrogen trapping with Pd coated alloy films
07 p2723 N94-25551
Calculations of population transfer during intense laser pulses
[DE94-001060] 07 p2818 N94-26698
Charge trapping and breakdown in N2O oxides
[DE94-003775] 08 p3266 N94-30040
Langmuir waves in the electron-positron plasma
[DE94-608330] 08 p3508 N94-30191
Cooling and trapping of neutral atoms
[AD-A276957] 09 p3870 N94-32360
The PS 200 catching trap: A new tool for ultra-low energy antiproton physics
[DE94-009309] 10 p4137 N94-34089
Enhanced charge trapping in bipolar spacer oxides during low-dose-rate irradiation
[DE94-007863] 11 p4260 N94-36268

TRAPS
NT COLD TRAPS
NT ION TRAPS (INSTRUMENTATION)
NT VAPOR TRAPS
Simple method to estimate MOS oxide-trap, interface-trap, and border-trap densities
[DE93-041138] 05 p2032 N94-21939

TRAVELING IONOSPHERIC DISTURBANCES
Detection of traveling ionospheric disturbances induced by atmospheric gravity waves using the global positioning system 05 p1723 N94-20425

TRAVELING SALESMAN PROBLEM
Bibliographic notes on Voronoi diagrams
[PB93-189298] 01 p0343 N94-10825
Electronic neural network for solving traveling salesman and similar global optimization problems
[NASA-CASE-NPO-17807-2-CU] 05 p1942 N94-20360
On some approximately balanced combinatorial cooperative games
[MEMO-1113] 06 p2493 N94-22702
The ant system: An autocatalytic optimizing process
[REPT-91-016-REV] 09 p3824 N94-31177
A worst-case analysis of two approximate algorithms for the symmetric travelling salesman problem
[REPT-93-036] 09 p3840 N94-31187
Simple Patch: A new heuristic for the product traveling salesman problem
[REPT-93-85] 09 p3845 N94-31702
TRAVELING WAVE AMPLIFIERS
Wide band 140 GHz TWTA 01 p0132 N94-10514
A laboratory system for the investigation of rain fade compensation techniques for Ka-band satellites
[NASA-CR-191200] 05 p1762 N94-21566
Inverse free electron laser beat-wave accelerator research
[DE94-002597] 06 p2349 N94-23702
TRAVELING WAVE TUBES
NT BACKWARD WAVE TUBES
A millimeter-wave tunneladder TWT
[NASA-CR-182183] 02 p0620 N94-13106
Low-current traveling wave tube for use in the microwave power module
[NASA-TP-3344] 02 p0620 N94-13110
Phase linearity of the 914H coupled-cavity traveling wave tube
[NASA-CR-191056] 06 p2290 N94-23087
Generalized three-dimensional simulation of ferruled coupled-cavity traveling-wave-tube dispersion and impedance characteristics
[NASA-TP-3389] 06 p2310 N94-24056
A direct current rectification scheme for microwave space power conversion using traveling wave electron acceleration 07 p2687 N94-27371
Dielectric loaded broadband gyro-TWT system
[AD-A277889] 10 p4040 N94-33861
Theoretical, experimental, and computational evaluation of a tunnel ladder slow-wave structure
[NASA-TM-106642] 10 p4041 N94-33945
Evaluation of some slow-wave vane structures for aminiature traveling-wave tube at 30 GHz
[NASA-TM-106654] 12 p4437 N94-36819
TRAVELING WAVES
NT SOLITARY WAVES
Conversion of the four-strap array in D3-D to a tunable traveling wave antenna
[DE93-012085] 01 p0137 N94-11453
The x ray standing waves on surfaces
[AD-A265265] 01 p0402 N94-11682
Traveling disturbances appearing in yawed cylinder boundary layer transition 01 p0166 N94-12632
Velocity matched millimeterwave electro-optic modulator
[AD-A267264] 03 p1188 N94-14957
High Speed/High Frequency Optoelectronics
[AD-A271985] 05 p1751 N94-20580
Simulation of traveling-wave output structures for high power RF tubes
[DE93-041005] 05 p1763 N94-21685
The characterization of reaction-convection-diffusion processes by travelling waves
[PB94-150315] 06 p2273 N94-22729
Inverse free electron laser beat-wave accelerator research
[DE94-002597] 06 p2349 N94-23702
Annual summary of basic research thermoacoustic heat transport, 1993
[AD-A275751] 08 p3230 N94-28644
Langmuir waves in the electron-positron plasma
[DE94-608330] 08 p3508 N94-30191
Development of an accurate transmission line fault locator using the global positioning system satellites 08 p3144 N94-30652
On some general properties of parabolic conservation equations
[DE94-006101] 08 p3461 N94-30758
Observation of the traveling component of an x ray standing wave field
[DE94-007671] 09 p3672 N94-31317
Study on active control of waveguide with piezoceramic actuator 10 p4042 N94-34349
Solitary waves and homoclinic orbits
[DE94-009428] 11 p4264 N94-35681
Spatio-temporal properties of centrifugal instabilities: Abstracts of 8th Couette-Taylor Meeting
[PB94-150240] 11 p4266 N94-35981
TRAYS
Long duration exposure facility experiment m0003 deintegration observation database
[AD-A267579] 03 p0951 N94-17207
Long Duration Exposure Facility (LDEF) contamination study
[AD-A272419] 05 p1658 N94-21147
TREADMILLS
Apparatus and method for measuring subject work rate on an exercise device
[NASA-CASE-MSC-21752-1] 05 p1895 N94-20194
Dual-cycle ergometry as an exercise modality during prebreathe with 100 percent oxygen 10 p4096 N94-33638
TREADS
Rail Corrugations
[ILR-BER-59] 06 p2269 N94-23581
Surface analysis of corrugated rail treads 06 p2270 N94-23587
TREES
Seed viability detection using computerized false-color radiographic image enhancement 08 p3387 N94-30461
TREES (MATHEMATICS)
NT FAULT TREES
Marginal allocations in the core of minimal chain-games
[MEMO-1103] 01 p0348 N94-10162
Algorithms for the maximum clique problem
[MEMO-1101] 01 p0322 N94-10419
An introduction to chordal graphs and clique trees
[DE93-012508] 01 p0332 N94-11695
Tree reconstruction from partial orders
[DE93-009841] 02 p0743 N94-12991
Construction of d-dimensional hyperoctrees on a hypercube multiprocessor
[INRIA-RR-1752] 03 p1162 N94-17539
Contribution to the analysis of tableaus based decision methods
[ETN-93-94355] 04 p1560 N94-18067
A parallel hashed oct-tree N-body algorithm
[DE93-012654] 04 p1526 N94-19205
Compensation approach for three or more dimensional random walks
[PB93-197499] 04 p1543 N94-19326
The complexity of the optimal spanning hypertree problem
[TR-471] 04 p1561 N94-19481
Heap construction in the parallel comparison tree model
[TR-409] 04 p1538 N94-19512
Finding the strong components in a directed graph
[PB93-187342] 04 p1555 N94-19708
Generalized regression trees: Function estimation via recursive partitioning and maximum likelihood
[AD-A271259] 04 p1560 N94-19726
Totally strong and strong graphs
[RR-902-I] 05 p1951 N94-20237
Graph minors: Structure theory and algorithms
[AD-A271851] 05 p1952 N94-20613
The combinatorics of reconstructing evolutionary trees
[CWI-BS-R9233] 05 p1963 N94-21022
On the core-structure of minimum cost spanning tree games
[MEMO-1085] 05 p1953 N94-21047
Fourier calculus on evolutionary trees
[CWI-BS-R9234] 05 p1954 N94-21231
A neural M-ary tree method for data compression 05 p1780 N94-22166
Causal labeled transition systems: A new approach for describing the behavior of concurrent systems
[LAAS-93179] 06 p2447 N94-22911
The explicit computation of integration algorithms and first integrals for ordinary differential equations with polynomials coefficients using trees
[NASA-CR-194787] 06 p2448 N94-23074
Medians and steiner trees
[PB94-110616] 06 p2486 N94-23708
The Third Twente Workshop on Graphs and Combinatorial Optimization
[PB94-110947] 06 p2486 N94-23722
Irreducible core of a minimum cost spanning tree game
[PB94-110962] 06 p2489 N94-24653
Data structures and amortized complexity in a functional setting
[ETN-94-95307] 06 p2476 N94-25290
Detecting actin fibers in cell images using minimal spanning trees
[AD-A273914] 07 p2984 N94-25591
Editing tree structures
[CWI-CS-R9264] 07 p2961 N94-26219
Efficient rebalancing of tree-type main memory dictionaries
[PB94-133105] 07 p3100 N94-28396
Only few graphs have bounded treewidth
[RUU-CS-92-35] 08 p3455 N94-30333
Pearl's belief propagation: The proofs
[RUU-CS-92-47] 08 p3456 N94-30378
Treewidth of circle graphs
[RUU-CS-93-12] 08 p3458 N94-30405
A more compact visibility representation
[RUU-CS-93-26] 08 p3425 N94-30426
Efficient and constructive algorithms for the pathwidth and treewidth of graphs
[RUU-CS-93-27] 08 p3426 N94-30488
Symplectic Runge-Kutta schemes 3: Canonical elementary differentials
[MATHS-REPT-A-204] 09 p3840 N94-31159
Symbolic derivation of Runge-Kutta methods
[MATHS-REPT-A-205] 09 p3840 N94-31160
A worst-case analysis of two approximate algorithms for the symmetric travelling salesman problem
[REPT-93-036] 09 p3840 N94-31187
A worst-case analysis of an approximate algorithm for finding the minimum hamiltonian cycle on paths
[REPT-93-042] 09 p3809 N94-31192
Dynamic subtrees: A new data structure for manipulating trees
[DE94-009168] 10 p4128 N94-33985
TREES (PLANTS)
NT CONIFERS
NT DECIDUOUS TREES
Satellite inventory of Minnesota forest resources
[NASA-CR-193565] 01 p0231 N94-11521
The carbon dioxide emissions game: Playing the net
[DE93-017670] 04 p1471 N94-17821
Mapping of taiga forest units using AIRSAR data and/or optical data, and retrieval of forest parameters 05 p1729 N94-20452
SIMA: A model for forest succession based on the carbon and nitrogen cycles with application to silvicultural management of the forest ecosystem
[SILVA-CARELICA-22] 07 p2848 N94-26258
Caesium-137 in a boreal forest ecosystem: Aspects on the long-term behavior
[PB94-137809] 08 p3347 N94-29158
Fractal approach to computer-analytical modelling of tree crown
[DE94-608089] 08 p3467 N94-30088
TRELLIS CODING
Trellis coding with Continuous Phase Modulation (CPM) for satellite-based land-mobile communications
[NASA-CR-191325] 02 p0604 N94-13909
Low-Complexity, High-Performance Bandwidth Efficient Coding and Coded Modulation Techniques for Satellite and Space Communications
[NASA-CR-194623] 03 p0997 N94-16506
Advanced coding and modulation schemes for TDRSS 05 p1744 N94-21350
Design of a new squaring function for the Viterbi algorithm 05 p1764 N94-21699
Coded 64QAM using a binary convolutional code 05 p1747 N94-22223
Trellis coded multi-orthogonal modulation 05 p1747 N94-22231
TREND ANALYSIS
NASA trend analysis procedures
[NASA-RP-1290] 03 p1223 N94-15782
Long term trending of engineering data for the Hubble Space Telescope 06 p2516 N94-23942
TRENDS
Potential markets for advanced satellite communications
[NASA-CR-191145] 01 p0041 N94-10512
National patterns of R and D resources, 1992
[NSF-92-330] 01 p0422 N94-11186
Trends in Information Management at Department of Energy Headquarters
[DE93-017197] 04 p1615 N94-18496
Industry standards: Key to distributed computing 05 p1938 N94-22070
Current situation in developing petroleum substituting energy (the United Kingdom)
[DE94-714897] 05 p1713 N94-22091
Investigations on trends in global environment adaptive industrial technologies
[DE94-714888] 05 p1853 N94-22258
Interannual temperature variability and cyclone frequency over Eastern Canada and the New England States. A case study: Winter seasons 1931-1932 to 1984-1985
[ISBN-0-315-74841-9] 08 p3373 N94-29908
TRESCA FLOW
Assessment of an improved multiaxial strength theory based on creep-rupture data for Inconel 600
[DE93-015929] 04 p1358 N94-17791
TRIAMINOGUANIDINENITRATE
U TAGN
TRIAMINOTRINITROBENZENE
U TATB

TRIANGLES

Linear characteristic spatial quadrature for discrete ordinates neutral particle transport on arbitrary triangles
[AD-A267485] 03 p1185 N94-17365

Are bilinear quadrilaterals better than linear triangles?
[DE93-019223] 04 p1551 N94-19301

Toughness and triangle-free graphs
[MEMO-1127] 06 p2478 N94-22715

A survey of numerical cubature over triangles
[DE94-006810] 09 p3841 N94-31274

Hidden surface removal in a computer model for generation of infrared images
[PB94-149192] 10 p4143 N94-34095

TRIANGULAR WINGS

U DELTA WINGS

TRIANGULATION

Finding a covering triangulation whose maximum angle is provably small
[DE93-010691] 01 p0334 N94-12593

Approaches to high aspect ratio triangulations
[NASA-TM-107684] 02 p0739 N94-12886

Parallel implementation of an algorithm for Delaunay triangulation
[NASA-TM-103951] 02 p0740 N94-12973

The cartography of Venus with Magellan data
03 p1274 N94-16320

Refining a triangulation of a planar straight-line graph to eliminate large angles
[DE93-016510] 04 p1528 N94-19344

Numerical modelling of crystal growth
[AD-A271206] 04 p1605 N94-19719

Geometric optimization
[DE93-040152] 05 p1917 N94-21764

Hierarchical surface triangulation of range data
05 p1771 N94-22108

Unstructured surface grid generation
05 p1920 N94-22366

Computational geometry issues
05 p1920 N94-22370

Surface acquisition through virtual milling
05 p1920 N94-22372

Structures of tetrahedrization: A mathematical and algorithmical point of view
[ETN-94-95172] 06 p2480 N94-23166

Dynamic ray tracing and its application in triangulated media
[DE94-000875] 06 p2402 N94-23516

An implicit numerical scheme for the simulation of internal viscous flows on unstructured grids
[NASA-TM-106437] 06 p2481 N94-23554

Expansion-based passive ranging
06 p2176 N94-25504

Construction and applications of the two dimensional Delaunay triangulated irregular network and the three dimensional Delaunay tetrahedron model
[ETN-94-95034] 07 p2848 N94-26651

A parallel computational fluid dynamics unstructured grid generator
[AD-A274129] 07 p2795 N94-27119

Some efficient procedures for correcting triangulated models
[PB94-136926] 08 p3452 N94-29171

L(sub)p optimal d dimensional triangulations for piecewise linear interpolation: A new result on data dependent triangulations
[RUU-CS-93-13] 08 p3458 N94-30406

Optimal size finite element meshes without obtuse and small angles
[RUU-CS-92-39] 08 p3462 N94-30860

Abstracts of the Workshop on Computational Geometry (CG 1992)
[PB94-147022] 09 p3844 N94-31684

Selection of climate station data using clustering and triangulated irregular network techniques
[AD-A276658] 09 p3784 N94-32046

Incremental triangulation by way of edge swapping and local optimization
[NASA-TM-103979] 09 p3709 N94-32946

Three-dimensional unstructured grid refinement and optimization using edge-swapping
[NASA-TM-103966] 11 p4299 N94-35393

Linear-size nonobtuse triangulation of polygons
[DE94-010746] 12 p4505 N94-37620

TRIATOMIC MOLECULES

The global potential energy surfaces of the lowest two 1A' states of the ozone molecule: Theoretical determination and analysis 01 p0267 N94-12269

Electronically metastable molecules of high symmetry
[AD-A272015] 05 p1974 N94-21461

Energy transfer in solid explosives
[DE94-001523] 06 p2265 N94-23778

TRIAXIAL STRESSES

J-integral and HRR field associated with stable crack growth in thin aluminum SEN specimen
[AD-A267879] 03 p0960 N94-17041

Grain by grain study of the mechanisms of crack propagation during iodine SCC of Zry-4
[DE93-633765] 07 p2734 N94-26162

Computer simulation and experiments on the quasi-static mechanics and transport properties of granular materials
[AD-A274192] 07 p2823 N94-27104

A modeling study of the effect of stress state on void linking during ductile fracture
[AD-A275505] 08 p3317 N94-28811

Granular bases for heavily loaded pavements
[AD-A275171] 08 p3156 N94-29047

TRIAXIALITY

U TRIAXIAL STRESSES

TRIBOLOGY

Study of the tribological behavior of SiC and Si3N4 ceramic couples in terms of temperature: The reality
01 p0064 N94-10061

Durability of a carbon segmented circumferential seal for a liquid oxygen turbopump
[NAL-TR-1155] 01 p0178 N94-10369

Effect of surface cleanliness of bearing steel on adhesive strength and tribological properties of sputter-deposited gold films
[DE93-767974] 01 p0082 N94-10732

Tribological characteristics of hot-pressed self-lubricating composites
[NAL-TR-1160] 01 p0066 N94-10858

The properties of perfluoropolyethers used for space applications
[NASA-TM-106275] 01 p0088 N94-10864

Advanced model of gradual wear of viscoelastic surface film
[AD-A265130] 01 p0090 N94-11222

Tribological characteristics of sputtered Au/Cr films on alumina substrates at elevated temperatures
[NASA-TM-106078] 01 p0055 N94-11362

Ceramics technology project database
[DE93-012431] 01 p0091 N94-11672

Properties of interfacial tribo-films
[AD-A265591] 01 p0182 N94-12374

A vacuum four-ball tribometer to evaluate liquid lubricants for space applications
[NASA-TM-106264] 02 p0575 N94-12842

Applications of surface science to solid lubricants
[SMC-TR-93-24] 02 p0579 N94-13903

The friction and wear of ceramic/ceramic and ceramic/metal combinations in sliding contact
[NASA-TM-106348] 03 p0930 N94-15769

Atomic-scale friction measurements using friction force microscopy. Part 1: General principles and new measurement techniques
[AD-A268391] 03 p1048 N94-17533

Continuing research on friction and wear of materials
[AD-A268291] 03 p1049 N94-17566

Titanium carbon-hydrogen layers on decorative surfaces 04 p1375 N94-18010

Physico chemical and mechanic approach of lubricating properties of graphite + additive powders
[ECL-93-02] 04 p1373 N94-19405

Contribution to the tribological study of magnetic-tape head contact
[ECL-92-57] 04 p1434 N94-19414

Microtribology of magnetic media
[AD-A271209] 04 p1407 N94-19722

Surface species in tribology
[AD-A270970] 04 p1446 N94-19754

Atomic-scale friction measurements using friction force microscopy. Part 2: Application to magnetic media
[AD-A270759] 04 p1447 N94-19767

Tribological studies of silicon for magnetic recording applications (Invited)
[AD-A270878] 04 p1447 N94-19784

Microscopic modeling of tribological and interfacial phenomena
[AD-A271864] 05 p1823 N94-20464

Development of fundamental understanding of friction and wear mechanisms by atomic-scale tribological studies of ceramic materials and multilayered thin films
[AD-A271485] 05 p1703 N94-20548

Utilization of metals to improve the lubrication of ceramic load-bearing devices
[PB93-202448] 05 p1825 N94-21424

Integrity testing of brush seal in a T-700 engine
05 p1654 N94-21792

A rail corrugation theory which allows for contact patch size 06 p2269 N94-23582

A linear model for corrugation and its limit of validity
06 p2269 N94-23584

Lateral high frequency oscillations and stability of a wheel rolling on a flexible track
06 p2269 N94-23585

Surface analysis of corrugated rail treads
06 p2270 N94-23587

Surface observations of stick-slip oscillations in tightly conformal wheel/rail contacts 06 p2270 N94-23588

Contact analysis of rough rail surfaces
06 p2270 N94-23589

An application of small-gap equations in sealing devices 06 p2325 N94-23668

The Fifth European Space Mechanisms and Tribology Symposium
[ESA-SP-334] 06 p2355 N94-23985

New tribocoating combination for vacuum operation
06 p2355 N94-23990

Tribological behaviour of fluorinated resins and polyimide resins sliding over a metallic surface in liquid nitrogen
06 p2355 N94-23991

Tribological characteristics of ball bearings lubricated with a sputtered molybdenum disulphide film in a vacuum under a high thrust load 06 p2355 N94-23992

The tribology of some MoS2-lubricated engineering ceramics 06 p2356 N94-23993

HERA (Hermes robot arm) overview
06 p2357 N94-24005

Thermal vacuum performance of cycloid and harmonic gearboxes with solid (MoS2) and liquid (Braycote 601) lubrication 06 p2358 N94-24009

Tribological characterization of spatial wet lubricants under vacuum 06 p2264 N94-24010

In-vacuum performance of Fomblin Z25-lubricated, 52100 steel bearings with TiC-coated balls
06 p2358 N94-24011

Development of gears for space use
06 p2360 N94-24021

New pin-on-disk equipment for vacuum tribometry
06 p2360 N94-24023

An analytical ultra-high vacuum tribometer for solid lubricant studies 06 p2361 N94-24033

An assessment of solid lubricant films for use in high temperature space applications
06 p2363 N94-24044

The development of dry-lubricated ceramic cages
06 p2363 N94-24045

Investigation of the ultrafiltration technique using military greases
[AD-A273633] 06 p2261 N94-25029

Lubrication in cold rolling: Numerical simulation using multigrid techniques
[ISBN-9-09-005313-1] 06 p2262 N94-25030

Atomic-scale friction measurements using friction force microscopy. Part 2: Application to magnetic media
[AD-A275202] 08 p3298 N94-29290

Lubrication of space systems
[NASA-TM-106392] 08 p3214 N94-29399

The 27th Aerospace Mechanisms Symposium
[NASA-CP-3205] 08 p3160 N94-29627

Metal band drives in spacecraft mechanisms
08 p3162 N94-29637

The use of screening tests in spacecraft lubricant evaluation 08 p3162 N94-29641

An asymptotic analysis for compressible gas lubrication of rough surfaces 08 p3222 N94-30922

Cracking induced in small fretting: Application to the case of aeronautical aluminum alloys
[ECL-92-50] 09 p3735 N94-31870

New micro- and macroscopic models of contact and friction
[AD-A277240] 09 p3726 N94-32320

Lubrication with binary mixtures: Liquid-liquid emulsion in elastohydrodynamics and metal forming
09 p3658 N94-32490

Ultrahigh-current-density metal-ion implantation and diamondlike-hydrocarbon films for tribological applications
[DE94-008958] 09 p3906 N94-32843

The effect of prolonged exposure to 750 C air on the tribological performance of PM212
[NASA-TM-106472] 09 p3617 N94-32941

A comparison of the performance of solid and liquid lubricants in oscillating spacecraft ball bearings
09 p3606 N94-33311

Development of long-life, low-noise linear bearings for atmospheric interferometry 09 p3606 N94-33312

The preliminary evaluation of liquid lubricants for space applications by vacuum tribometry
09 p3606 N94-33313

Continuing research on friction and wear of materials
[AD-A277690] 10 p4059 N94-33437

The effect of alternative fuels on the stability and lubricity of crankcase lubricants
[DE94-010353] 11 p4245 N94-36108

Wear-resisting oxide films for 900 C
[DE94-010093] 11 p4246 N94-36306

Evaluation of the EHL film thickness and extreme pressure additives on gear surface fatigue life
[NASA-TM-106663] 12 p4451 N94-37319

Properties of perfluoropolyethers for space applications
[NASA-TM-106616] 12 p4426 N94-37520

TRIBUTARIES
DYNLET1 model formulation and user's guide
[AD-A269843] 04 p1498 N94-18723
Numerical simulation of nocturnal drainage flows in an idealized valley-tributary system
[DE94-011684] 12 p4472 N94-37115
The influence of tributaries on nocturnal valley flows
[DE94-011613] 12 p4473 N94-37242
TRICHLORIDES
U CHLORIDES
TRIGGER CIRCUITS
Upgraded D(O) calorimeter electronics for short Tevatron bunch space and the effect of pile-up on the W mass measurement
[DE93-013566] 01 p0146 N94-12603
Results from a water-Cerenkov array
[DE93-012715] 02 p0849 N94-14461
The 3D-Flow processor for a programmable level-1 trigger (feasibility study)
[DE93-016045] 03 p1159 N94-16172
Design and test of a low jitter metal to metal contact solid dielectric switch
[DE93-016957] 04 p1394 N94-17755
A bit serial first level calorimeter trigger for an LHC detector
[USIP-92-08] 04 p1574 N94-18845
Improved optical pseudospark switch
[AD-D015821] 04 p1580 N94-18947
A programmable systolic trigger processor for FERA-bus data
[USIP-92-04] 04 p1405 N94-19292
Results from long conduction time plasma opening switch experiments at Sandia National Laboratories
[DE93-019063] 05 p1762 N94-21632
VLSI-based video event triggering for image data compression
[NASA-TM-106500] 06 p2345 N94-25116
The data-acquisition and second level trigger system for ZEUS calorimeter
[ETN-94-95384] 06 p2541 N94-25256
Use of parallel counters for triggering
[DE93-616656] 07 p2979 N94-25918
Relativistic heavy ion physics
[DE94-003161] 07 p3031 N94-26097
Development of fusion technology
[DE93-633444] 07 p3042 N94-26159
Recent results from testing fast ADCs
[DE94-005565] 08 p3406 N94-30004
Using neural networks as an event trigger in elementary particle physics experiments
[DE94-006316] 10 p4136 N94-33716
Beam tests of a prototype level-1 calorimeter trigger for LHC experiments
[PB94-170495] 11 p4269 N94-35599
TRIGGERS
U ACTUATORS
TRIGONOMETRIC FUNCTIONS
NT COSINE SERIES
NT SINE SERIES
Mathematic methods and algorithms for real-time applications
[AD-A266776] 02 p0771 N94-14789
Statistical analysis of trigonometric parallaxes
[NASA-CR-194558] 03 p1172 N94-15641
Fast fourier transforms for nonequispaced data
[AD-A272687] 05 p1954 N94-21164
Rational trigonometric approximations using Fourier series partial sums
[NASA-CR-191535] 05 p1959 N94-21568
Systematic construction of trigonometric neural networks
[PB93-200228] 06 p2474 N94-24544
Some remarkable sine and cosine functions
[PB94-137759] 08 p3453 N94-29439
TRIM (BALANCE)
U AERODYNAMIC BALANCE
TRIMERS
The synthesis of photocrosslinkable chalcone-bearing polyphosphazenes
[AD-A264915] 01 p0092 N94-11849
Intramolecular versus intermolecular condensation rates in the acidic polymerization of octaethoxytrisiloxane
[AD-A266982] 03 p0963 N94-15490
Electrochemical and electronic properties of neural and oxidized soluble orthogonally-fused thiophene oligomers
[AD-A273283] 06 p2260 N94-24815
New anionic states of the lithium trimer
[AD-A278832] 11 p4323 N94-35797
TRIMETHYL COMPOUNDS
Tris(trimethylsily)arsine and lithium bis(trimethylsily)arsenide
[AD-A275075] 08 p3189 N94-29140
Surface chemistry of boron-doped SiO2 CVD: Enhanced uptake of tetraethyl orthosilicate by hydroxyl groups bonded to boron
[DE94-005428] 08 p3221 N94-30896
TRINITRO COMPOUNDS
N,N'-bis(4,4,4-trinitro butyryl) hydrazine
[AD-D015897] 05 p1712 N94-20122
TRINITROTOLUENE
Instrumented experiments aboard the frigate WOLF. Wolf 2: Measurement results of the 5.5 kg TNT in the crew aft sleeping compartment
[PML-1992-12] 04 p1451 N94-17931
The minimum detection limits of RDX and TNT deposited on various surfaces as determined by ion mobility spectroscopy
[DE93-018521] 04 p1378 N94-19042
Evaluation of pre-extraction analytical holding times for nitroaromatic and nitramine explosives in water
[AD-A271547] 05 p1712 N94-20927
TRINITROTRIAZOCYCLOHEXANE
U RDX
TRIODES
RF vacuum microelectronics
[AD-A268399] 03 p1014 N94-17423
Silicon microelectronic field-emissive devices for advanced display technology
[DE94-000397] 05 p1794 N94-22380
RF vacuum microelectronics
[AD-A276512] 09 p3691 N94-31928
TRIPLE AXIS SPECTROMETERS
U NEUTRON SPECTROMETERS
TRIPLET EXCITATION
U ATOMIC ENERGY LEVELS
TRIPLET STATE
U ATOMIC ENERGY LEVELS
TRIPODS
Simulation of tripod gaits for a hexapod underwater walking machine
[AD-A271719] 05 p1945 N94-21355
TRIPROPELLANTS
U LIQUID ROCKET PROPELLANTS
TRITIUM
High-energy density physics at Los Alamos
[DE93-010271] 01 p0371 N94-10260
The effect of a scalar boson coupled to neutrinos on the behavior of the tritium beta decay spectrum near the end point
[DE93-012655] 01 p0361 N94-10349
Three-nucleon problem with phase equivalent potentials
[DE93-617731] 01 p0363 N94-10722
Welding tritium aged stainless steel
[DE93-011782] 01 p0181 N94-11228
Charged-particle evaluation methodology at Lawrence Livermore National Laboratory
[DE93-013429] 02 p0781 N94-13251
Materials compatibility of hydride storage materials with austenitic stainless steels
[DE93-013688] 02 p0703 N94-13691
A study of hydrogen effects on fracture behavior of radioactive waste storage tanks
[DE93-018171] 02 p0574 N94-14873
An apparatus for measuring the biological oxidation of hydrogen gas under hyperbaric conditions
[AD-A266834] 03 p1119 N94-14916
Tritium diffusion and desorption in single crystal LiAlO2
[DE93-015140] 03 p1211 N94-16805
Using the Tritium Plasma Experiment to evaluate ITER PFC safety
[DE93-016614] 04 p1582 N94-17713
The rise of accuracy for the multichannel scattering problem solving
[DE93-630145] 04 p1608 N94-18253
Finite difference program for calculating hydride bed wall temperature profiles
[DE93-019272] 04 p1523 N94-19005
Hydrogen isotope separation experience at the Savannah River Site
[DE93-019832] 05 p1679 N94-20266
Spectroscopy and dynamics of molecular and ionic impurities embedded in solid hydrogen
[AD-A274149] 07 p3064 N94-27095
Argon frost continuous cryopump for fusion applications
[DE94-004478] 08 p3230 N94-29017
Search for neutrons from deuterated palladium subject to high electrical currents
[DE94-009342] 10 p4139 N94-33907
Tritiated ammonia formation
[DE94-011170] 11 p4237 N94-36056
TRITON
Orbital simulations of satellite escape/capture and the origin of satellites such as Triton
01 p0429 N94-12057
A structural origin for the cantaloupe terrain of Triton
01 p0449 N94-12095
Geomorphology of Triton's polar materials
01 p0466 N94-12185
Tectonics on Triton 01 p0466 N94-12187
On the unique structure of the magnetic fields of Uranus and Neptune 01 p0472 N94-12221
Neptune encounter highlights
[NASA-TM-109421] 03 p1246 N94-15240
Tidal interaction: A possible explanation for geysers and other fluid phenomena in the Neptune-Triton system
03 p1272 N94-16311
Evolution of Triton's volatile budget
03 p1284 N94-16373
Working group for planetary system nomenclature
[NASA-CR-194406] 04 p1626 N94-18841
Diapirs and cantaloupes: Layering and overturn of Triton's crust 05 p2111 N94-20738
Geology of the southern hemisphere of Triton: No polar cap 05 p2111 N94-20739
One: Microphysics of frost metamorphism: Applications to Triton and Mars. Two: A global analysis of the ozone deficit in the upper stratosphere and lower mesosphere. Three: The diabatic circulation in the stratosphere as diagnosed from Microwave Limb Sounder data
09 p3942 N94-31975
Distribution and nature of UV absorbers on Triton's surface
[NASA-CR-195886] 09 p3943 N94-33104
TRIVALENT IONS
Excited state dynamics of thulium ions in yttrium aluminum garnets
[NASA-CR-195159] 06 p2564 N94-25024
TROCHOIDS
U PIVOTS
TROILITE
Calorimetric thermometry of meteoritic troilite: A feasibility study 01 p0428 N94-12025
Calorimetric thermometry of meteoritic troilite: Preliminary thermometer relationships
11 p4355 N94-35399
TROPICAL METEOROLOGY
TRMM radar 03 p0990 N94-15894
Spatial and temporal variations of satellite microwave measurements of latent heat release in tropic cyclones due to environmental forcing obtained from a numerical model
[AD-A267947] 05 p1865 N94-20482
Diagnostic budgets of analyzed and modelled tropical plumes
[NASA-CR-194853] 06 p2409 N94-23621
Observational and modeling studies of heat, moisture, precipitation and global-scale circulation patterns
[NASA-CR-195148] 06 p2415 N94-24485
Observed and Navy operational global model climatologies of synoptic disturbances over the tropical western Pacific during winter 1991-1992
[AD-A273400] 06 p2416 N94-25071
Satellite estimation of the global distribution and interannual variability of photosynthetically active radiation 08 p3334 N94-29970
The use of meteorological satellite data for studying tropical atmospheric phenomena
09 p3779 N94-31000
Air-sea interaction patterns in the equatorial Pacific
[AD-A277305] 09 p3788 N94-32072
Tropical cyclone forecasters reference guide. 5: Numerical track forecast guidance
[AD-A277318] 09 p3785 N94-32278
TRMM-related research: Tropical rainfall and energy analysis experiment
[NASA-CR-195834] 09 p3787 N94-33288
TROPICAL REGIONS
NT AMAZON REGION (SOUTH AMERICA)
Technical Conference on Tropical Urban Climates: Extended Abstracts
[WMO/TD-538] 01 p0283 N94-10561
An overview of intertropical convergence and intertropical discontinuity
[DE93-619229] 01 p0277 N94-11603
Central Equatorial Pacific Experiment (CEPEX)
[DE93-011656] 01 p0190 N94-11674
Evaluation of ECMWF latent heat flux in TOGA CD-ROM 01 p0195 N94-11921
Methodological considerations for use of ERS-1 imagery for the delineation of river networks in tropical forest areas 01 p0247 N94-12484
TREES project: A case study on the use of multi-temporal ERS-1 SAR data and SPOT data for monitoring tropical ecosystems 01 p0249 N94-12497
TREES project: Overview and status of the ERS-1 SAR contribution 01 p0250 N94-12499
Principal oscillation pattern analysis of sea level variations in the tropical Pacific measured by the GEOSAT altimeter 01 p0209 N94-12646
Preliminary results from a satellite altimetric data assimilation using a Kalman filter and smoother
01 p0209 N94-12648
The application of VAS satellite imagery to thunderstorm forecasting at Cape Canaveral
[NASA-CR-193563] 02 p0718 N94-12839

Bibliography of urban climate in tropical/subtropical areas, 1981-1991
[WCASP-25] 02 p0718 N94-12918
Spectral reflectance of soils from Sao Paulo State
[INPE-5424-PRP/172] 02 p0684 N94-13377
Spatial variability of throughfall chemistry in a tropical rainforest (Central Amazonia, Brazil)
[INPE-5431-PRE/1765] 02 p0720 N94-13429
AMIP: Diagnostic subproject on the variability in the tropics: Synoptic to intraseasonal time scales
[DE93-009287] 02 p0721 N94-13914
TRMM system overview and status in the United States 02 p0690 N94-14221
TRMM Project in Japan: Overview and status 02 p0690 N94-14222
Clouds and the Earth's Radiant Energy System (CERES) on the Tropical Rainfall Measuring Mission (TRMM) 02 p0690 N94-14223
TRMM precipitation radar algorithm 02 p0690 N94-14224
Estimate of sampling errors of TRMM rainfall observation by using radar-AMeDAS composite data 02 p0690 N94-14225
Future TRMM follow-on mission 02 p0691 N94-14228
Nonlinear relationships between particulate absorption and chlorophyll: Detritus or pigment packaging?
[AD-A266806] 02 p0731 N94-14899
IAI topic: El Nino. Southern oscillation and interannual climate variability
[INPE-5410-PRE/1757] 03 p1111 N94-15186
Validation and analysis of microwave-derived rainfall over the tropics
[AD-A267785] 03 p1108 N94-17303
Meridional circulation in the tropical north atlantic
[AD-A268222] 03 p1114 N94-17555
An empirical study of tropical cloud clusters using special sensor microwave imager data
[AD-A268072] 03 p1110 N94-17595
Spectral analysis of synoptic time scale disturbances over the tropical eastern Pacific during summer 1989, 1990 and 1991
[AD-A268821] 04 p1490 N94-18206
Internal instability of nonparallel flow on an equatorial beta-plane
[AD-A268927] 04 p1490 N94-18486
Orbit and sampling requirements: TRMM experience 05 p1870 N94-21647
Are tropical cirrus brighter than mid-latitude cirrus? 05 p1881 N94-22343
Modal structure of variations in the tropical climate system. Part 2: Origins of the low-frequency mode
[MPIM-96] 06 p2407 N94-23199
Atmospheric moisture fields derived by satellite observations over the tropical Pacific Ocean
[NASA-CR-194852] 06 p2408 N94-23542
Convective organization in the Pacific ITCZ: Merging OLR, TOVS, and SSM/I information
[NASA-CR-194850] 06 p2408 N94-23619
A regional analysis of cloudy mean spherical albedo over the marine stratocumulus region and the tropical Atlantic Ocean
[NASA-CR-194771] 06 p2409 N94-24049
Worst case analysis: Earth sensor assembly for the tropical rainfall measuring mission observatory
[NASA-CR-189320] 06 p2311 N94-24754
Human impacts on soil carbon dynamics of deep-rooted Amazonian forests
[NASA-CR-195127] 06 p2399 N94-24861
Interactions between a tropical mixed boundary layer and cumulus convection in a radiative-convective model
[DE94-000848] 07 p2877 N94-25979
Short-range cloud amount forecasting with model output statistics
[AD-A274769] 07 p2895 N94-26798
Global barotropic response to a tropical forcing
[NASA-CR-195256] 07 p2896 N94-27408
The dynamics of tropical intraseasonal variability 08 p3371 N94-29741
On the annual cycle of the tropical Pacific atmosphere and ocean 08 p3371 N94-29763
Interannual-decadal variability in tropical climate systems: Stable isotope records and general circulation model experiments 08 p3373 N94-29962
FAME: A Forest Assessment and Monitoring Environment scenario
[AD-B179106] 08 p3335 N94-30759
Subtropical Climates and Their Evolution: From Space-Based Observation to Modelling
[ISBN-2-85-428333-3] 09 p3776 N94-30981
Dynamics in the tropics and synoptic disturbances 09 p3778 N94-30990
Low frequency variability observed in the tropical Atlantic Ocean 09 p3778 N94-30991
Tropical squall lines 09 p3778 N94-30992
Effects of the deep tropical convection in the large scale atmospheric flow 09 p3778 N94-30994
Behavior and dynamics of tropical forests and savannas 09 p3757 N94-31004
The ozone and the physico-chemical processes in tropical regions 09 p3770 N94-31010
The effect of westerly wind bursts on a tropical ocean general circulation model
[AD-A276423] 09 p3788 N94-31448
Use of SPOT and ERS-1 to map tropical vegetation and mangrove dynamics in Guiana 09 p3753 N94-32555
A case study comparing multi-temporal ERS-1 SAR data and SPOT data for tropical forest mapping 09 p3753 N94-32556
Comparing SPOT and SIR A for mapping superficial formations in tropical forest regions: Example of the Yaoundy Region (Cameroon) 09 p3755 N94-32562
EOF characterization of Atlantic SST fields using AVHRR data
[INPE-5535-TDI/523] 10 p4093 N94-34203
Effects of mesoscale convective organization and vertical wind shear on the cumulus-environment interaction 10 p4090 N94-34910
Contributions of the low-latitude boundary layer to the finite width magnetotail convection model
[NASA-CR-196116] 11 p4289 N94-35392
ULF waves in the low-latitude boundary layer and their relationship to magnetospheric pulsations: A multisatellite observation
[AD-A278906] 11 p4289 N94-35587

TROPICAL STORMS
NT HURRICANES
NT TYPHOONS
Updated forecast of Atlantic seasonal hurricane activity for 1993 01 p0285 N94-11194
Forecast model applications of retrieved three dimensional liquid water fields 04 p1492 N94-18606
Moist wind relationships 04 p1492 N94-18607
Spatial and temporal variations of satellite microwave measurements of latent heat release in tropic cyclones due to environmental forcing obtained from a numerical model
[AD-A267947] 05 p1865 N94-20482
Large-scale circulation regimes and tropical cyclone characteristics over the western pacific ocean
[AD-A273004] 05 p1867 N94-21307
Development and testing of the Coupled Ocean/Atmosphere Mesoscale Prediction System (COAMPS)
[AD-A273925] 07 p2892 N94-25793
Tropical cyclone report, 1992
[AD-A274464] 07 p2896 N94-27025
Short term teleconnections associated with an individual tropical cyclone
[AD-A277210] 09 p3783 N94-32019
Tropical cyclone forecasters reference guide. 5: Numerical track forecast guidance
[AD-A277318] 09 p3785 N94-32278
Forecasters handbook for the Philippine Islands and surrounding waters
[AD-A277993] 09 p3787 N94-33089
Typhoon monitoring using passive satellite observations
[AD-A277859] 10 p4089 N94-33769

TROPICS
U TROPICAL REGIONS

TROPISM
NT GRAVITROPISM
NT GYROTROPISM

TROPOPAUSE
Intrusion of stratospheric ozone in the troposphere through tropopause folding and cold air droplets
[REPT-87] 05 p1851 N94-20154

TROPOSPHERE
NT TROPOPAUSE
In situ detection of tropospheric OH, HO2, NO2, and NO by laser-induced fluorescence in detection chambers at reduced pressures
[NASA-CR-193189] 01 p0274 N94-10701
Preliminary validation of the low frequency variability of tropospheric temperature and circulation simulated for the AMIP by the ECMWF model
[DE93-012382] 01 p0284 N94-10739
An overview of intertropical convergence and intertropical discontinuity
[DE93-619229] 01 p0277 N94-11603
Project AIRSTREAM: Trace gas
[DE93-008849] 02 p0706 N94-12904
Description of the EURAD chemistry-transport model. Version 2 (CTM2)
[REPT-83] 02 p0720 N94-13589
AMIP: Diagnostic subproject on the variability in the tropics: Synoptic to intraseasonal time scales
[DE93-009287] 02 p0721 N94-13914
Radio metric errors due to mismatch and offset between a DSN antenna beam and the beam of a troposphere calibration instrument 02 p0607 N94-14370
Importance of sprays for long range transport of harmful substances in the troposphere
[MITT-81] 02 p0711 N94-14723
Signal and reference wavelengths for the elimination of SO2 cross sensitivity in remote measurements of tropospheric ozone with lidar
[GKSS/92/E/24] 02 p0617 N94-14819
Hyperspectral modeling for extracting aerosols from aircraft/satellite data 03 p1067 N94-16673
The feasibility of tropospheric and total ozone determination using a Fabry-Perot interferometer as a satellite-based nadir-viewing atmospheric sensor
[NASA-TM-109342] 03 p1102 N94-17214
An investigation of the Ground-Based High-Resolution Interferometer Sounder (GB-HIS) in a costal marine environment
[AD-A268052] 03 p1114 N94-17503
Kinetics programs for simulation of tropospheric photochemistry on the global scale
[DE93-019035] 04 p1476 N94-19104
Analysis of satellite-derived ozone and water vapor measurements
[NASA-CR-193610] 04 p1486 N94-19237
The split-step algorithm for microwave propagation modeling above a conducting surface
[FEL-92-A430] 04 p1390 N94-19447
Suitability of infrared spectroscopy for remote sensing of tropospheric trace gases
[KFK-5183] 04 p1479 N94-19507
Global three dimensional model of tropospheric trace gases chemistry and transport
[AERONAUTICA-ACTA-A-370-1993] 04 p1479 N94-19518
Tropospheric chemistry of natural hydrocarbons, aldehydes, and peroxy radicals: Their connections to sulfuric acid production and climate effects
[DE93-019525] 05 p1855 N94-20220
Spatial and temporal variations of satellite microwave measurements of latent heat release in tropic cyclones due to environmental forcing obtained from a numerical model
[AD-A267947] 05 p1865 N94-20482
Earth observing scanning polarimeter 05 p1844 N94-21645
Michelson Interferometer (MINT) 05 p1813 N94-21646
Global emissions and models of photochemically active compounds
[DE93-040490] 05 p1852 N94-21969
Breaking Kelvin-Helmholtz waves and cloud-top entrainment as revealed by K-band Doppler radar 05 p1874 N94-22310
Analysis of the GOES 6.7 micrometer channel observations during FIRE 2 05 p1875 N94-22316
Examination of the observed synoptic scale cirrus cloud environment: The December 3-6 FIRE cirrus case study 05 p1877 N94-22325
The 5-6 December 1991 FIRE IFO 2 jet stream cirrus case study: The influence of volcanic aerosols 05 p1877 N94-22326
A comparison of small and larger mesoscale latent heat and radiative fluxes: December 6 case study 05 p1879 N94-22335
In situ detection of tropospheric OH, HO2, NO2, and NO by laser-induced fluorescence in detection chambers at reduced pressures
[NASA-CR-194810] 06 p2397 N94-23277
Tropospheric Ozone Lidar Intercomparison Experiment, TROLIX 1991
[MPIM-102] 06 p2402 N94-24108
Implementation of a state of the art automated system for the production of cloud/water vapor motion winds from geostationary satellites
[NASA-CR-195087] 06 p2410 N94-24125
Northern hemisphere tropospheric mid-latitude circulation after violent volcanic eruptions
[MPIM-107] 06 p2403 N94-24491
The influence of orography on the transport of atmospheric constituents 06 p2619 N94-24886
Local Measurement of Tropospheric HO(x)
[NASA-CP-3245] 08 p3342 N94-28587
In situ detection of tropospheric OH and HO2 by laser-induced fluorescence in a detection chamber at low pressure 08 p3342 N94-28589
Tropospheric HO determination by FAGE 08 p3342 N94-28590
Detection of tropospheric OH and HO2 by laser-induced fluorescence at low pressure using the 308nm excitation of OH 08 p3343 N94-28591
Absolute determination of local tropospheric OH concentrations 08 p3343 N94-28594
UV laser long-path absorption spectroscopy 08 p3343 N94-28595

Measurement of tropospheric OH by laser long-path absorption spectroscopy 08 p3343 N94-28596
Ion-assisted tropospheric OH measurement technique 08 p3344 N94-28601
An improved method of measuring tropospheric NO2, NO3, HO2, and RO2 by Matrix Isolation and Electronic Spin Resonance (MIESR) 08 p3345 N94-28605
Tropospheric HO2 determination by FAGE 08 p3345 N94-28606
Near-IR diode laser absorption for measurement of tropospheric HO2 08 p3345 N94-28607
Line-of-sight tropospheric calibration from measurements in arbitrary directions 08 p3249 N94-29654
Radar estimations of atmospheric winds in the troposphere and lower stratosphere 08 p3370 N94-29697
Developing a diode array spectrometer for tropospheric chemistry studies 08 p3362 N94-29752
Radiative flux calculations at UV and visible wavelengths [DE94-004278] 08 p3350 N94-30613
Tropospheric corrections to GPS measurements using locally measured meteorological parameters compared with general tropospheric corrections 08 p3144 N94-30655
Modeling studies of frontogenesis in the upper and middle troposphere 08 p3375 N94-30868
Tropospheric radiative forcing of O3 for the 1994 IPCC report [DE94-005698] 08 p3367 N94-30876
The ozone and the physico-chemical processes in tropical regions 09 p3770 N94-31010
Quantified estimates of total GWPs for greenhouse gases taking into account tropospheric chemistry [DE94-007846] 09 p3768 N94-32817
Dry deposition of PAN to grassland vegetation [DE94-005111] 09 p3768 N94-32894
Model calculations of radiative transfer and tropospheric chemistry 10 p4084 N94-33361
Model capabilities, 2-D 10 p3971 N94-33459
Traineeship augmentation for aerosol optical properties study [AD-A278466] 10 p4085 N94-33544
H2O-H2SO4 system in Venus' clouds and OCS, CO, and H2SO4 profiles in Venus' troposphere 11 p4370 N94-36152
Global tropospheric chemistry models for radiatively important trace species: Design and research recommendations [DE94-007089] 11 p4288 N94-36359
Measurements and modeling of the effect of convective clouds on the upper tropospheric moisture budget [NASA-TM-109894] 12 p4473 N94-37371
Tropospheric radiative forcing of CH4 [DE94-011628] 12 p4468 N94-37631

TROPOSPHERIC SCATTERING
Results from a study of scintillation behavior at 12, 20, and 30 GHz using the results from the Virginia Tech Olympus receivers 02 p0613 N94-14659
Johnson-Gierhart program predictions of excess propagation loss for super-high frequency air-to-ground paths. Volume 1: Theory and numerical results [AD-A267105] 03 p0988 N94-15649

TROPOSPHERIC WAVES
NT PLANETARY WAVES

TROUBLESHOOTING
U MAINTENANCE

TROUGHS
Fault geometries and extension in the Valles Marineris, Mars 01 p0458 N94-12144
Shallow crustal discontinuities and graben and scarp formation in the Tharsis region of Mars 01 p0469 N94-12203
Ventilated oscillatory boundary layers [AD-A266226] 03 p1023 N94-16110
Morphology and models for the evolution of eastern Hecate Chasma, Venus 03 p1256 N94-16215
Sedimentation, volcanism, and ancestral lakes in the Valles Marineris: Clues from topography 03 p1283 N94-16369
Possible flexural signatures around Olympus and Ascraeus Montes, Mars 05 p2142 N94-20911

TRUCKS
Lightweight materials for transportation: Program plan [DE93-017381] 04 p1340 N94-18087
Conceptual design of a sodium sulfur cell for US electric van batteries [DE93-018683] 04 p1405 N94-19035
UV absorption technique for monitoring mobile source NO emissions [AD-A273858] 07 p2713 N94-25964
Processing of wide-angle synthetic aperture radar signals for target detection [AD-A274225] 07 p2773 N94-27073
Prediction and standard error estimation for a finite universe total when a stratum is not sampled [DE94-004929] 08 p3465 N94-30696
Compressed natural gas fueled vehicles: The Houston experience [DE94-005804] 08 p3312 N94-30878
Final regulatory impact analysis: Refueling emission regulations for light duty vehicles and trucks and heavy duty vehicles [PB94-164027] 11 p4285 N94-35754

TRUNCATION (MATHEMATICS)
U APPROXIMATION

TRUNCATION ERRORS
Finite difference schemes for long-time integration [NASA-CR-191471] 01 p0343 N94-10642

TRUNKS (LINES)
U TRANSMISSION LINES

TRUNNIONS
U SHAFTS (MACHINE ELEMENTS)

TRUSSES
Space truss zero gravity dynamics [AD-A266130] 01 p0044 N94-12541
Feasibility study of an orbiting laboratory for testing CSI technology [NASA-CR-191524] 02 p0540 N94-13016
The Second Workshop on Deployment and Assembly Experiment of Large Space Structure on Orbit [NASDA-CON-930003] 02 p0529 N94-13268
Helical truss beam development for large space structure 02 p0530 N94-13276
Movement of deployable truss 02 p0531 N94-13280
Development and application of one dimensional deployable truss 02 p0531 N94-13281
Study of a one-dimensional deployable structure employing telescopic members 02 p0531 N94-13282
Preliminary analysis and design optimization of the short spacer truss of Space Station Freedom [NASA-TM-4470] 03 p1058 N94-15709
End-effector: Joint conjugates for robotic assembly of large truss structures in space: Extended concepts [NASA-CR-193576] 03 p1048 N94-17088
A comparative study of analog and digital control laws for the UMCSL truss [AD-A267980] 03 p0871 N94-17412
A structural design methodology for large angle articulated trusses considering realistic joint modeling 06 p2376 N94-23560
Identification and H(infinity)/(mu)-synthesis control of the Sandia truss [DE94-002735] 07 p2839 N94-26810
Behaviour modification of space trusses [ISBN-0-315-84701-8] 07 p2842 N94-27315
Report of three microgravity experiments by the drop shaft [JTN-94-80579] 07 p2761 N94-27341
Structural design feasibility study of Space Station long spacer truss [NASA-TM-106346] 07 p2843 N94-27559
Reliability-based structural optimization: A proposed analytical-experimental study [NASA-TM-109055] 07 p2844 N94-27830
Real-time control of the Trussarm variable-geometry-truss manipulator utilizing machine vision [ISBN-0-315-87054-0] 09 p3830 N94-31735
A real-time computer control and trajectory generation environment for Trussarm [ISBN-0-315-87060-5] 09 p3832 N94-31833
Dynamic error compensation in robotic trusses 09 p3738 N94-32486
Unique methods for on-orbit structural repair, maintenance, and assembly 10 p4102 N94-33663
Robotic technologies of the Flight Telerobotic Servicer (FTS) including fault tolerance 10 p4067 N94-34034
Kinematic modeling of a double octahedral Variable Geometry Truss (VGT) as an extensible gimbal [NASA-TM-109127] 11 p4311 N94-35242
Distributed parameter modeling of repeated truss structures 11 p4218 N94-35868
Applying transfer matrix method to the estimation of the modal characteristics of the NASA Mini-Mass Truss 11 p4218 N94-35870

TRYPSIN
Quasi-elastic neutron scattering studies of protein dynamics [DE93-015074] 02 p0782 N94-13414

TRYPTAMINES
NT SEROTONIN

TRYPTOPHAN
Strategies for enhancing catecholamine-mediated neurotransmission [NASA-CR-193807] 04 p1506 N94-18862

TUBE CATHODES
NT COLD CATHODES
NT PHOTOCATHODES
Multiple hollow cathode wear testing [NASA-CR-195335] 10 p4016 N94-33975

TUBE HEAT EXCHANGERS
Study of possible mechanisms of instability due to heat transfer [INPE-5448-TDI/494] 02 p0628 N94-12966

TUBERCULOSIS
Tuberculosis: A case for increased screening 03 p1126 N94-16627
Summary of follow-up results from potential tuberculosis exposures 03 p1126 N94-16628
Rapid susceptibility testing of Mycobacterium avium complex and Mycobacterium tuberculosis isolated from AIDS patients [NASA-CR-196268] 12 p4478 N94-36996

TUBES
Spiral fluid separator [NASA-CASE-MFS-28658-1] 05 p1800 N94-20361
Porous vycor glass tube joined to borosilicate glass 07 p2718 N94-27392
Modeling of forced CVI for tube fabrication [DE94-012718] 12 p4410 N94-37286
First-principles determination of the polarizabilities of carbon tubules as a function of length [DE94-013015] 12 p4537 N94-37356

TUBING
U PIPES (TUBES)

TUMBLING MOTION
Predicting the vibrations of a spinning inflated membrane [DE93-010690] 02 p0676 N94-14456
Self-rescue strategies for EVA crewmembers equipped with the SAFER backpack 11 p4207 N94-35633

TUMORS
NT CANCER
NT NEOPLASMS
Quantitative method of measuring cancer cell urokinase and metastatic potential [NASA-CASE-MSC-21715-1] 03 p1117 N94-15967
The role of constitutive and inducible processes in the response of human squamous cell carcinoma cell lines to ionizing radiation [DE93-015150] 03 p1129 N94-16970
Calculation and optimization of electromagnetic fields in a patient by local hyperthermia utilization [ETN-93-95059] 05 p1889 N94-20024
Monoclonal antibodies directed against surface molecules of multicell spheroids [NASA-CR-195102] 06 p2420 N94-23633
Annual research progress report, fiscal year 1992. Volume 2: Department of Clinical Investigation [AD-A273584] 06 p2427 N94-24945

TUNABLE LASERS
Thermal-optical switching of a silicon based interference filter [AD-A265152] 01 p0174 N94-11095
Laser system design for the generation of a sodium-layer laser guide star [DE93-014127] 01 p0176 N94-12784
Gathering and exchange information on atmospheric chemistry and polluted atmospheres [DE93-009940] 02 p0705 N94-12869
Novel Co:MgF2 lidar for aerosol profiler [NASA-CR-191525] 02 p0654 N94-13091
Predicted performance of a dc beam driven FEM oscillator designed for fusion applications at 200-250 GHz [DE93-013414] 02 p0655 N94-13145
Tetravalent chromium (Cr(4+)) as laser-active ion for tunable solid-state lasers [NASA-CR-194527] 02 p0659 N94-14576
AlGaAs diode laser blue shift resulting from fast neutron irradiation [AD-A266642] 02 p0659 N94-14681
Variable wide band fiber optic delay line [AD-D015848] 04 p1576 N94-17716
The copper-pumped dye laser system at Lawrence Livermore National Laboratory [DE93-014429] 04 p1435 N94-17723
Design of a tunable 4-MW free electron maser for heating fusion plasmas [DE93-017172] 04 p1437 N94-18134
Tunable synchronously pumped intracavity two-stage optical frequency upconversion [AD-A269105] 04 p1438 N94-18250
Single-transverse-mode, narrow-bandwidth pulsed tunable dye laser with hollow circular intracavity dielectric waveguide [AD-A270022] 04 p1439 N94-18614
Tunable ytterbium-doped solid state laser [AD-D015878] 04 p1440 N94-18747

A tunable compact high power far-infrared grating free-electron laser
[AD-A269875] 04 p1440 N94-18771
Tetravalent chromium (Cr(4+)) as laser-active ion for tunable solid-state lasers
[NASA-CR-194529] 04 p1441 N94-19369
Tetravalent chromium (Cr(4+)) as laser-active ion for tunable solid-state lasers
[NASA-CR-194528] 04 p1441 N94-19394
Suppression of relaxation oscillations in flashpumped, two-micron tunable solid state lasers
[AD-D015928] 05 p1814 N94-19800
Initial performance of Los Alamos advanced free electron laser
[DE93-040158] 05 p1814 N94-19828
Evaluation of a single stage of the LADS filter
[AD-A271101] 05 p1814 N94-19851
Tunable laser frequency stabilizing system
[AD-D015904] 05 p1815 N94-20055
Rotational spectrum of a dark state in 2-fluoroethanol using microwave/radiofrequency-infrared multiple resonance
[AD-A272101] 05 p1817 N94-20583
Compact free electron lasers for medical applications
[AD-A273609] 06 p2350 N94-24934
Tunable lasers pumped by visible laser diodes
[AD-D016000] 06 p2350 N94-25044
Broad band tunable dye laser development
[DE93-632978] 07 p2816 N94-26157
Fiber laser amplifiers and oscillators
[AD-A274231] 07 p2820 N94-28068
Near-IR diode laser absorption for measurement of tropospheric HO2 08 p3345 N94-28607
HO2 detection by near infrared absorption using tunable diode lasers 08 p3346 N94-28608
Advances in tunable powerful lasers: The advanced free-electron laser
[DE94-004997] 08 p3294 N94-29934
Ionization probes of molecular structure and chemistry
[DE94-007605] 09 p3872 N94-32643
A reliable low-maintenance flashlamp-pumped Ti:sapphire laser operating at 120 PPS
[DE94-009030] 09 p3721 N94-32848
Multifrequency, rapidly sequenced or simultaneous tunable laser
[AD-D016169] 09 p3721 N94-32968
900-mW average power and tunability from a diode-pumped 2.94 micron Er:YAG oscillator
[DE94-009511] 11 p4271 N94-35679
Diode-pumped, continuously tunable, 2.3 micron CW laser specification
[AD-D016312] 12 p4450 N94-37838

TUNDRA
Energy flow in an Arctic aquatic ecosystem
[DE93-013178] 01 p0267 N94-11697
Emissions of biogenic sulfur gases from Alaskan tundra 01 p0268 N94-12455
Emissions of sulfur gases from wetlands 01 p0269 N94-12458
A model of the CO2 exchanges between biosphere and atmosphere in the tundra
[NASA-CR-196008] 11 p4289 N94-35389

TUNERS
Display system employing acousto-optic tunable filter
[NASA-CASE-NPO-18736-1-CU] 03 p1190 N94-15933

TUNGSTATES
NT CALCIUM TUNGSTATES

TUNGSTEN
Liquid phase sintering of tungsten composites under microgravity. Effect of matrix composition 01 p0118 N94-10207
Deformation mechanisms in tungsten single crystals in ballistic impact experiments
[AD-A265701] 01 p0405 N94-12563
Correlations of the growth, structure, and stress with the adhesion of diamond films on tungsten
[DE93-012855] 02 p0576 N94-12912
Liquid phase sintering of tungsten composites under microgravity. Effect of matrix composition 03 p0945 N94-15171
Photorefractive tungsten bronze crystals for optical computing
[AD-A268859] 04 p1596 N94-18320
The effect of crystallographic orientation on the performance of single crystal tungsten subscale penetrators
[AD-A268988] 04 p1597 N94-18468
Recent advances in high density tungsten composite processing
[AD-A270764] 04 p1344 N94-19576
Core formation in the Moon: The mystery of the excess depletion of Mo, W and P 05 p2095 N94-20651
Electron emission from nanometer-size metallic clusters: Electronic states and structural stability of supported Au clusters
[DE93-040184] 05 p1975 N94-21766
Ductile-brittle transition behavior of tungsten under shock loading conditions
[DE93-019945] 05 p1693 N94-21843
High energy collimating fine grids for HESP program
[NASA-CR-189317] 06 p2209 N94-24767
Stress relaxation in sputtered W films and W/GeSi/Si heterostructures
[DE94-004007] 07 p3055 N94-26239
The deformation of copper-tungsten composites
[ISBN-0-315-84939-8] 07 p2712 N94-27688
Influence of tungsten alloying additions on the mechanical properties and texture of tantalum
[DE94-004994] 08 p3210 N94-30774
Studies of supported molybdenum and tungsten
[DE94-006207] 08 p3210 N94-30839
Chemical vapour deposition of tungsten for the application in integrated circuits
[ISBN-9-09-005151-1] 09 p3641 N94-31519
High temperature materials technology research for advanced thermionic systems
[DE94-008444] 09 p3644 N94-32416
Non-alloyed, refractory metal contact optimization with shallow implantations of Zn and Mg
[DE94-010392] 11 p4240 N94-36110
X ray and gamma ray spectroscopy of solids under pressure
[DE94-011207] 11 p4238 N94-36203
Preradiation studies for non-thermal Z-pinch wire load experiments on Saturn
[DE94-013459] 12 p4527 N94-37072
Thermomechanical studies of tungsten heavy alloys
[AD-A280250] 12 p4417 N94-37122

TUNGSTEN ALLOYS
A history of tungsten- and molybdenum-base alloys
[DE93-010283] 01 p0082 N94-11108
Metastability of yttrium-oxides
[DE93-016548] 02 p0813 N94-14440
Yield properties of tungsten and tungsten heavy alloys
[AD-A266833] 02 p0575 N94-14878
Tensile and stress-rupture behavior of hafnium carbide dispersed molybdenum and tungsten base alloy wires
[NASA-TM-106350] 03 p0962 N94-17652
Atlas of formability: HAYNES 188
[AD-A268355] 04 p1356 N94-17769
Bibliography on silicides
[AD-A270516] 04 p1374 N94-19532
Recent advances in high density tungsten composite processing
[AD-A270764] 04 p1344 N94-19576
Development and characterization of adiabatic shear prone tungsten heavy alloys
[AD-A270477] 04 p1366 N94-19673
Strengthening and toughening in refractory metal alloys
[DE93-019942] 05 p1695 N94-21986
Chemical vapor deposition and characterization of tungsten boron alloy films
[DE94-002648] 07 p2738 N94-26610
A transmission electron microscope study of Ni4W precipitates in a Ni-37 wt. percent W alloy
[ISBN-0-315-59932-4] 07 p2743 N94-27803
Electrochemical behavior and surface chemistry of nonequilibrium aluminum alloys: Passivity mechanism and fabrication methods
[AD-A275401] 08 p3204 N94-29196
Influence of tungsten alloying additions on the mechanical properties and texture of tantalum
[DE94-004994] 08 p3210 N94-30774
Thermomechanical studies of tungsten heavy alloys
[AD-A280250] 12 p4417 N94-37122
Examination of weldability of Ni-Cr-W superalloys
[DE94-719014] 12 p4418 N94-37385

TUNGSTEN CARBIDES
Diamond growth on carbide surfaces using a selective etching technique
[AD-A267989] 03 p0973 N94-17413
Metafusion: A breakthrough in metallurgy 08 p3211 N94-30446

TUNGSTEN COMPOUNDS
NT CALCIUM TUNGSTATES
NT TUNGSTEN CARBIDES
NT TUNGSTEN FLUORIDES
NT TUNGSTEN OXIDES
Dry film lubricant evaluation
[DE93-013114] 02 p0578 N94-13118
Interstitially stabilized phases in the zirconium-nickel system
[DE94-005561] 08 p3201 N94-28525
Laser flash photolysis, EPR and Raman studies of liquids at elevated pressures
[DE94-008351] 09 p3718 N94-32413

TUNGSTEN FLUORIDES
Multiphoton ionization studies of WF6 and UF6
[DE93-016232] 03 p1181 N94-15863
The reaction mechanism of W-CVD in Si
[ETN-94-95329] 06 p2261 N94-25084

TUNGSTEN HALIDES
NT TUNGSTEN FLUORIDES

TUNGSTEN INERT GAS WELDING
U GAS TUNGSTEN ARC WELDING

TUNGSTEN OXIDES
A quartz crystal microbalance study of lithium insertion and removal into evaporated films MO(y) (M = Mo, Fe, and V)
[DSIS-93-00649] 02 p0810 N94-14203
Optical switch evaluation support
[AD-A270948] 04 p1581 N94-19601

TUNING
Lightweight linear alternators with and without capacitive tuning
[NASA-CR-185273] 01 p0140 N94-10505
Fine tuning of stretched-VISSR image mapping 01 p0190 N94-11080
The laser second threshold: Its exact analytical dependence on detuning and relaxation rates
[DE93-619706] 01 p0175 N94-11633
Nonlinear effects in ferrite tuned cavities
[DE93-014136] 01 p0374 N94-12785
Self tuning and adaptive control: Evaluations and improvements of algorithms
[ITN-93-85192] 02 p0762 N94-13329
Tuning of Gaussian stochastic control systems
[CWI-BS-R9223] 02 p0765 N94-14018
Computational issues in optimal tuning and placement of passive dampers 02 p0681 N94-14647
Fabrication and phase tuning of an optical waveguide device
[AD-D015815] 03 p1191 N94-16489
Design of broadband wire antennas for frequency hopping applications
[AD-A267405] 03 p1001 N94-17025
Optimal tuning of heavy equipment motion controllers
[AD-A267873] 03 p1167 N94-17392
Decoherence and recoherence of beam in phase space
[DE93-014885] 04 p1573 N94-17784
Automatic tuning of an integral fuzzy controller
[REPT-93-006] 04 p1383 N94-17932
Limitations on the fidelity of 100 fs pulses produced by chirped pulse amplification
[DE93-017167] 04 p1396 N94-17991
A tunable CMOS constant current source 04 p1401 N94-18369
The gyrotron backward-wave-oscillator experiment --- final progress report
[AD-A268982] 04 p1403 N94-18452
A summary of studies of particle stability at RHIC
[DE93-040173] 05 p1970 N94-19868
Novel N x N integrated channel waveguide optical crossbars for large scale high speed non-blocking data switching
[AD-A272065] 05 p1986 N94-20922
Multibunch beam break-up in detuned structures
[DE93-041056] 05 p1981 N94-21686
Compact free electron lasers for medical applications
[AD-A273609] 06 p2350 N94-24934
A theoretical investigation of electrically tunable birefringent optical filters as the special discriminator in hyperspectral imaging systems
[AD-A273743] 06 p2547 N94-25533
Sum frequency generation using an optical parametric oscillator
[DE94-001827] 07 p3040 N94-28000
Tuning of AmPS
[NIKHEF-K-AMPS-93-01] 08 p3494 N94-29422
Auto tuning of PID controllers 10 p4115 N94-34323
Filter parameter tuning analysis for operational orbit determination support 11 p4208 N94-35637
Fabrication and phase tuning of an optical waveguide device
[AD-D016215] 11 p4334 N94-36122
Tune modulation due to gradient ripple and the dynamic aperture
[DE94-011922] 12 p4524 N94-37157

TUNING FORK GYROSCOPES
Emerging technologies in microguidance and control 08 p3144 N94-29788

TUNISIA
The use of SPOT, and the contribution of ERS-1, in the assessment of urban pressure on agriculture land in Greater Tunis (Tunisia) 09 p3749 N94-32534

TUNNEL DIODES
Submillimeterwave SIS mixer developments 03 p0903 N94-15054
Substrate effects in superconducting tunnel junction detectors 03 p0908 N94-15083

A multilayered approach to superconducting tunnel junction x ray detectors 03 p0908 N94-15089
Quasiparticle trapping in distributed superconducting three-terminal tunnel junction devices 03 p0910 N94-15101
The role of emitter states in magnetotunneling through double-barrier resonant-tunneling diodes at high magnetic fields
[REPT-A-2658] 06 p2564 N94-24959
Investigation of ACC/CCI tunnel diodes
[AD-A274549] 07 p2785 N94-26845

TUNNEL JUNCTIONS
Theoretical SIS mixer research
[AD-A266323] 02 p0807 N94-13580
Monolithic, two-terminal InP/Ga(0.47)In(0.53)As tandem solar cells
[DE93-014037] 03 p1093 N94-16824
Synthesis and study of high-T(sub c) superconducting electronic materials
[AD-A268851] 04 p1402 N94-18390
Quantum noise studies with superconducting tunnel junction mixers
[AD-A270897] 05 p2012 N94-19897
The n-p(p(+))-n Al(yGa)(1-y) As-GaAs-In(x)Ga(1-x) as quantum well laser with p(+)-n(+)GaAs-InGaAs tunnel contact on n GaAs
[AD-A271292] 05 p2030 N94-21805
Energy-resolving x ray detectors with charge amplification due to multiple quasiparticle tunneling
[DE93-019506] 05 p2031 N94-21869
Research on stable, high-efficiency amorphous silicon multijunction modules
[DE93-018220] 05 p1850 N94-22257
Picosecond response of the quasiparticle current in superconducting tunnel junctions
[DE94-006300] 08 p3515 N94-30009
Strong overlap and transmission in triple barrier resonant structures
[DE94-608103] 08 p3516 N94-30067
High T(sub c) superconductor tunnel junctions for photon detectors
[DE94-007686] 09 p3904 N94-32602

TUNNEL RESISTORS
U ELECTRON TUNNELING
U RESISTORS

TUNNELING (EXCAVATION)
Resistivity and radar void detectors for tunneling machines 01 p0140 N94-12706

TUNNELS
Three dimensional simulation of compressible flow induced by a high-speed train moving into a tunnel 08 p3126 N94-28967
Proceedings of the 4th Tunnel Detection Symposium on Subsurface Exploration Technology
[AD-A276372] 09 p3771 N94-31369

TURBIDITY
Solar radiation in Saudi Arabia
[AD-A269970] 04 p1493 N94-18781
Distribution of turbidity in Australian tropical waters
[AD-A271059] 05 p1881 N94-19905
Statistical analysis of a satellite imagery time series: Implications for the study of coastal and estuarine circulation 08 p3335 N94-30919

TURBINE BLADES
Comprehensive dynamic analysis of a bladed disk-turborotor-bearing system
[ISBN-0-315-73646-1] 01 p0180 N94-11155
Fatigue life prediction for wind turbines: A case study on loading spectra and parameter sensitivity
[DE93-011597] 01 p0263 N94-11173
Blading models for TURBAN and CSPAN turbomachine design codes
[NASA-CR-191164] 01 p0015 N94-11203
Field evaluation of six protective coatings applied to T-56 turbine blades after 2500 hours of engine use
[ARL-TR-27] 01 p0090 N94-11311
VIB3D: Method for calculating 3-D unsteady flow through turbomachinery blades
[CUED/A-TURBO/TR.128] 01 p0166 N94-12777
VIB2D: Quasi 3-D unsteady viscous flow method for blade flutter calculation
[CUED/A-TURBO/TR.129] 01 p0166 N94-12779
Two-dimensional Navier-Stokes heat transfer analysis for rough turbine blades
[NASA-TM-106008] 02 p0629 N94-13027
Numerical simulations of unsteady flows in turbomachines 02 p0633 N94-13569
Numerical simulation of steady three-dimensional flows in axial turbomachinery bladerows 02 p0634 N94-13630
Multigrid solution of internal flows using unstructured solution adaptive meshes
[NASA-CR-194233] 02 p0638 N94-14356
Inflow characteristics associated with high-blade-loading events in a wind farm
[DE93-010042] 02 p0704 N94-14423
JPRS report: Science and technology. Central Eurasia: Materials science
[JPRS-UMS-93-006] 02 p0558 N94-14573
Turbine blade tip film cooling measurements
[AD-A267686] 03 p0868 N94-14964
Slidesurfaces with adaptive new definitions (SAND) for transient analysis
[DE93-014909] 03 p1059 N94-15983
Effects of rotation on coolant passage heat transfer. Volume 2: Coolant passages with trips normal and skewed to the flow
[NASA-CR-4396-VOL-2] 03 p1023 N94-15991
Defining the normal turbine inflow within a wind park environment
[DE93-010032] 04 p1489 N94-18046
SAND contact in DYNA3D
[DE93-016451] 04 p1340 N94-18113
The application of nondestructive techniques to the testing of a wind turbine blade
[DE93-016731] 04 p1447 N94-18128
Turbine design 05 p1668 N94-20075
Oxidation resistant protective coating system for gas turbine components and process for penetration thereof
[CA-PATENT-1,294,155] 05 p1704 N94-21143
Integrity testing of brush seal in a T-700 engine 05 p1654 N94-21792
Recent advances in computational structural reliability analysis methods 05 p1828 N94-22616
Two stage turbine for rockets 06 p2215 N94-23059
The use of transition region characteristics to improve the numerical simulation of heat transfer in bypass transitional flows
[NASA-TM-106445] 06 p2320 N94-23525
Unsteady three-dimensional thermal field prediction in turbine blades using nonlinear BEM 06 p2325 N94-23665
Nondestructive evaluations
[DE94-003020] 06 p2373 N94-24613
Wake passage effects on the losses in a linear turbine cascade
[AD-A273794] 07 p2790 N94-25874
An investigation of the effects of the high maximum-thickness-to-chord ratio on the performance of nozzle guide vanes in a transonic planar cascade
[ISBN-0-315-84107-9] 07 p2793 N94-26671
Thermal/structural tailoring of engine blades (T/STAEBL). User's manual
[NASA-CR-194463] 07 p2839 N94-26692
Thermal/Structural Tailoring of Engine Blades (T/STAEBL): User's manual
[NASA-CR-194461] 07 p2843 N94-27776
Analysis of cooling jets near the leading edge of turbine blades 07 p2676 N94-28037
Effect of surface finish on turbine airfoil cascade losses 07 p2652 N94-28320
The effect of axial velocity ratio, turbulence intensity, incidence, and leading edge geometry on the midspan performance of a turbine cascade 07 p2652 N94-28321
Design and fabrication of forward-swept counterrotation blade configuration for wind tunnel testing
[NASA-CR-191193] 08 p3155 N94-28510
Thermal/structural tailoring of engine blades (T/SEAEBL). Theoretical manual
[NASA-CR-194462] 08 p3317 N94-28815
Application of flow field simulation to turbine vane design 08 p3127 N94-28978
Automated inspection of turbine blades: Challenges and opportunities
[AIAA PAPER 94-1226-CP] 08 p3446 N94-30575
WISPER and WISPERX: Final definition of two standardised fatigue loading sequences for wind turbine blades
[AD-B175835] 08 p3324 N94-30872
Computational study of simultaneous heat and mass transfer in turbulent separated flows 09 p3704 N94-31843
Experimental investigation of turbine blade-tip excitation forces 10 p4062 N94-34177
Development of a HP-turbine for a small helicopter engine 10 p4003 N94-34456
Effect of tip clearance on the performance of a highly loaded turbine stage 10 p4003 N94-34458
Design and aerodynamic performance evaluation of a high-work mixed flow turbine stage 10 p4003 N94-34459
Nozzle guide vane flow in radial inflow turbines 10 p4004 N94-34460
Turbine blade dynamics and blade-vane interaction in a radial inflow turbine 10 p4004 N94-34461
Engine static structures behaviour under impact load using 3D modelling 10 p4004 N94-34464
Hot section materials for small turbines 10 p4004 N94-34465
Mars vertical axis wind machines. The design of a Darreus and a Giromill for use on Mars
[NASA-CR-196143] 12 p4462 N94-36807
A combined experiment/computational study of flow in turbine blade cooling passage
[NASA-CR-4584] 12 p4442 N94-36957
Process enhancements of superalloy material 12 p4421 N94-37324

TURBINE ENGINES
NT CF-700 ENGINE
NT DUCTED FAN ENGINES
NT GAS TURBINE ENGINES
NT J-85 ENGINE
NT JET ENGINES
NT RAMJET ENGINES
NT SUPERSONIC COMBUSTION RAMJET ENGINES
NT T-53 ENGINE
NT TURBOFAN ENGINES
NT TURBOJET ENGINES
NT TURBOPROP ENGINES
NT TURBORAMJET ENGINES
Laser anemometer measurements and computations for transonic flow conditions in an annular cascade of high turning core turbine vanes
[NASA-TP-3383] 01 p0015 N94-11133
A research program for improving heat transfer prediction for the laminar to turbulent transition region of turbine vanes/blades
[NASA-TM-106278] 01 p0151 N94-11256
Turbulent particle dispersion in confined swirling flows
[DLR-FB-92-32] 02 p0637 N94-14045
Integrity testing of brush seal in a T-700 engine 05 p1654 N94-21792
Modeling bristle lift-off in idealized brush seal configurations 05 p1655 N94-21797
Aircraft turbine engine reliability and inspection investigations
[AD-A274860] 07 p2673 N94-26176
Community noise sources and noise control issues 10 p3972 N94-33467
Engine seal technology requirements to meet NASA's advanced subsonic technology program goals
[NASA-TM-106582] 10 p4060 N94-33960
An experimental and theoretical study of structural damping in compliant foil bearings 10 p4064 N94-34194
Vibrations of structures with cyclic symmetry: Application to the case of turbine engines 10 p4004 N94-34463
Propulsion system selection for a High Altitude Long Endurance aircraft 11 p4195 N94-36333

TURBINE EXHAUST NOZZLES
Studies on scramjet nozzles. Part 1: Performance of two dimensional nozzles
[NAL-TR-1149] 01 p0027 N94-10367

TURBINE PUMPS
Durability of a carbon segmented circumferential seal for a liquid oxygen turbopump
[NAL-TR-1155] 01 p0178 N94-10369
Application of powder metallurgy techniques to produce improved bearing elements for liquid rocket engines
[NASA-CR-193731] 01 p0082 N94-10804
Liquid Oxygen (LO2) propellant conditioning concept testing
[TABES PAPER 93-621] 03 p0976 N94-16146
Space Shuttle main engine. NASA has not evaluated the alternate fuel turbopump costs and benefits. Report to the Administrator of the National Aeronautics and Space Administration
[GAO/NSIAD-94-54] 03 p0926 N94-16834
ALS liquid hydrogen turbopump
[NASA-CR-194646] 03 p0927 N94-17016
Rocketdyne turbomachinery 05 p1667 N94-20071
Turbine design 05 p1668 N94-20075
Distributed loss model: Application to a spatial turbopump inducer 05 p1668 N94-20078
Actively controlled shaft seals for aerospace applications
[NASA-CR-194759] 05 p1823 N94-20538
Detailed study of oxidation/wear mechanism in lox turbopump bearings
[NASA-TM-108434] 05 p1825 N94-21580
The 1992 Seals Flow Code Development Workshop
[NASA-CP-10124] 05 p1654 N94-21790
Dynamics of face seals for high speed turbomachinery 05 p1655 N94-21796
SSME fuel preburner injector characterization 06 p2211 N94-23037
Computational Fluid Dynamics (CFD) applications in rocket propulsion analysis and design 06 p2214 N94-23054
Two stage turbine for rockets 06 p2215 N94-23059
Brush seals for cryogenic applications 06 p2216 N94-23063
Foil bearings 06 p2371 N94-24415

Simulation of cryogenic turbopump annular seals
06 p2371 N94-24440
Advanced launch system. Advanced development oxidizer turbopump program
[NASA-CR-193920] 06 p2367 N94-25174
Experimental contribution to the study of secondary flows in centrifugal turbopump stator components
[ECL-92-35] 07 p2789 N94-25654
Test results of the RS-44 integrated component evaluator liquid oxygen/hydrogen rocket engine
[AD-A277085] 07 p2701 N94-26231
Pump CFD code validation tests
[NASA-CR-193939] 07 p2822 N94-26597
Orbital transfer vehicle engine technology high velocity ratio diffusing crossover
[AD-A277180] 07 p2703 N94-27212
Enhanced simulation software for rocket turbopump, turbulent, annular liquid seals
[NASA-CR-195239] 07 p2825 N94-27383
Space Shuttle main engine turbopump bearing assessment program
[NASA-TM-108447] 07 p2833 N94-28265
CFD analyses for advanced pump design
[NASA-CR-193969] 08 p3300 N94-29550
The 7.5K lbf thrust engine preliminary design for Orbit Transfer Vehicle
[AD-A277519] 09 p3614 N94-31618
Solution of the average-passage equations for the incompressible flow through multiple-blade-row turbomachinery
[AD-A276515] 09 p3583 N94-31931
Design of a cold-flow test facility for the high pressure fuel turbopump turbine of the Space Shuttle main engine
[AD-A276743] 09 p3615 N94-32182
An experimental study on the static and dynamic characteristics of pump annular seals with two phase flow 10 p4062 N94-34179
Application of an improved Nelson-Nguyen analysis to eccentric, arbitrary profile liquid annular seals
10 p4062 N94-34182
Occurrence of sub-synchronous vibration in a multistage turbine pump and its prevention
10 p4064 N94-34189
An investigation of angular stiffness and damping coefficients of an axial spline coupling in high-speed rotating machinery 10 p4064 N94-34192
Hotfire testing of a SSME HPOTP with an annular hydrostatic bearing 10 p4065 N94-34196
Inducer analysis/pump model development
[NASA-CR-196005] 10 p4066 N94-34963

TURBINE WHEELS
Comprehensive dynamic analysis of a bladed disk-turborotor-bearing system
[ISBN-0-315-73646-1] 01 p0180 N94-11155
JPRS report: Science and technology. Central Eurasia: Materials science
[JPRS-UMS-93-006] 02 p0558 N94-14573
Streamwise vorticity in a turbine rotor with conical endwalls
[DLR-FB-93-13] 07 p2826 N94-27591
Expendable gas turbine engine technology advances
10 p4000 N94-34438

TURBINES
NT AXIAL FLOW TURBINES
NT GAS TURBINES
NT SHROUDED TURBINES
NT STEAM TURBINES
NT SUPERSONIC TURBINES
NT TIP VANES
NT TWO STAGE TURBINES
NT WIND TURBINES
Method of reducing drag in aerodynamic systems
[NASA-CASE-LEW-14791-1] 01 p0012 N94-10672
Heat transfer and aerodynamics of a 3D design nozzle guide vane tested in the Pyestock isentropic light piston facility
[RAE-TM-AERO/PROP-19] 03 p0856 N94-15696
ALS liquid hydrogen turbopump
[NASA-CR-194646] 03 p0927 N94-17016
Application of thermal spray and ceramic coatings and reinforced epoxy for cavitation damage repair of hydroelectric turbines and pumps
[AD-A267624] 03 p0971 N94-17198
Potassium-Rankine power conversion subsystem modeling for nuclear electric propulsion
[NASA-CR-191134] 04 p1468 N94-18821
Turbine design 05 p1668 N94-20075
Measurement and prediction of the flow through an annular turbine cascade
[AD-A272530] 05 p1803 N94-21417
Computation of flows in a turn-around duct and a turbine cascade using advanced turbulence models
06 p2216 N94-23062
Wake passage effects on the losses in a linear turbine cascade
[AD-A273794] 07 p2790 N94-25874
Program to develop a performance and heat load prediction system for multistage turbines
[NASA-CR-195223] 07 p2674 N94-26588
Development of laser velocimetry for the measurements of turbulence intensity and flow velocity ahead of a NGV row in a full-stage rotating turbine
[AD-A275712] 08 p3270 N94-28692
Laser measurements and analysis of flow in a radial inflow turbine inlet guide vanes and rotor
10 p3997 N94-33365
Measurement of the coolant channel temperatures and pressures of a cooled radial-inflow turbine
[NASA-TM-106594] 10 p3997 N94-33706
Experimental investigation of turbine blade-tip excitation forces 10 p4062 N94-34177
University participation in the ATS program
[DE94-003191] 11 p4275 N94-36022
Tipjet 80-inch model rotor hover test: Test no. 1198
[AD-A279680] 11 p4191 N94-36261

TURBOCHARGERS
U SUPERCHARGERS
U TURBOCOMPRESSORS

TURBOCOMPRESSORS
Vane optimization for maximum efficiency using Design Of Experiments (DOX)
[AD-A270270] 04 p1320 N94-18907
Experimental evaluation of oxygen-enriched air and emulsified fuels in a six-cylinder diesel engine
[DE94-000907] 05 p1811 N94-22391
Turbine engine with induced pre-swirl at the compressor inlet
[CA-PATENT-1-317-467] 06 p2186 N94-23253
The 3-D numerical study of airflow in the compressor/combustor prediffuser and dump diffuser of an industrial gas turbine 06 p2324 N94-23660
Analysis and characteristics of compressor stall precursor signals in forward and AFT swept high speed compressor
[AD-A273820] 06 p2171 N94-25517
Off-design performance of crenulated blades in a linear compressor cascade
[AD-A273744] 06 p2340 N94-25534
Effects of crenulations on three dimensional losses in a linear compressor cascade
[AD-A273778] 07 p2790 N94-25862
An investigation of the surge behavior of a high-speed ten-stage axial flow compressor
[AD-A274910] 07 p2674 N94-26345
Laser Doppler velocimetry in a low speed multistage compressor
[AD-A274836] 07 p2818 N94-26498
Development of advanced high temperature in-cylinder components and tribological systems for low heat rejection diesel engines, phase 1
[NASA-CR-187158] 07 p2827 N94-27984
Gas-turbine engine steady-state behavior
07 p2828 N94-28044
Inlet distortion in engines on VSTOL aircraft
[NASA-CR-195841] 09 p3584 N94-33035
Analysis of rig test data for an axial/centrifugal compressor in the 12 kg/sec 10 p4000 N94-34437
Experimental investigation and performance analysis of the turbojet engine T117 10 p4000 N94-34439
Microturbo's experience in the field of APU for civil and military applications and our role in the face of the challenges of the future 10 p4000 N94-34440
Advanced concepts for next generation small gas turbine engine compressors 10 p4001 N94-34443
The centrifugal compressor, an essential component of small and medium power engines
10 p4001 N94-34445
Compact diffusers for small transonic compressors
10 p4002 N94-34449
Nozzle guide vane flow in radial inflow turbines
10 p4004 N94-34460
Prediction of unsteady airfoil flows at large angles of incidence 10 p3986 N94-34978

TURBOFAN AIRCRAFT
NT BOEING 720 AIRCRAFT
NT BOEING 727 AIRCRAFT
NT BOEING 737 AIRCRAFT
NT BOEING 757 AIRCRAFT
NT BOEING 767 AIRCRAFT
NT C-141 AIRCRAFT
NT DC 8 AIRCRAFT
NT F-5 AIRCRAFT
NT F-111 AIRCRAFT
NT MYSTERE 20 AIRCRAFT
Conceptual design proposal: HUGO global range/mobility transport aircraft
[NASA-CR-195501] 06 p2181 N94-24787
Design of the advanced regional aircraft, the DART-75
07 p2671 N94-25708
P and W propulsion systems studies results/status
10 p3974 N94-33480

TURBOFAN ENGINES
NT CF-700 ENGINE
Analysis of gas turbine engines using water and oxygen injection to achieve high Mach numbers and high thrust
[NASA-TM-106270] 02 p0518 N94-13143
Noise levels from a model turbofan engine with simulated noise control measures applied
[NASA-TM-106318] 02 p0518 N94-14036
New techniques for contrail forecasting
[AD-A269686] 04 p1490 N94-18573
On the estimation algorithm used in adaptive performance optimization of turbofan engines
[NASA-TM-4551] 05 p1649 N94-21879
Rolls-Royce in perspective: Past, present and future
[PNR-90882] 06 p2187 N94-23519
The RB211: The first 25 years
[PNR-90977] 06 p2187 N94-23570
A comparison of two multi-variable integrator windup protection schemes
[NASA-CR-194436] 06 p2190 N94-23590
JB-300: An advanced medium size transport for 2005
[NASA-CR-195499] 06 p2179 N94-24401
Fan noise research at NASA
[NASA-TM-106512] 06 p2530 N94-25172
The design of a long-range megatransport aircraft
07 p2671 N94-25718
Simulating indirect thrust measurement methods as used on modern high-bypass turbofans
[ISBN-0-315-84123-0] 07 p2674 N94-26673
Experimental and theoretical investigations of the influence of the jet on the flow around a bypass-engine
[DLR-FB-93-17] 07 p2675 N94-27593
Broad specification fuels combustion technology program, phase 2
[NASA-CR-191066] 07 p2719 N94-27854
Spray combustion experiments and numerical predictions 08 p3195 N94-29277
Integrated propulsion-airframe dynamics and control
08 p3147 N94-29854
Development of a cascade simulation of fan-passage flow
[AD-A277234] 09 p3584 N94-32026
Analysis of intermediate level maintenance following F404-GE-400 engine component life reductions
[AD-A277918] 09 p3585 N94-33283
Aircraft high bypass fan engine performance
[AD-A277722] 10 p3997 N94-33443
Community noise sources and noise control issues
10 p3972 N94-33467
P and W propulsion systems studies results/status
10 p3974 N94-33480
Technology Requirements for Small Gas Turbines
[AD-280274] 10 p3999 N94-34431

TURBOFANS
Vane optimization for maximum efficiency using Design Of Experiments (DOX)
[AD-A270270] 04 p1320 N94-18907
Fan noise research at NASA
[NASA-TM-106512] 06 p2530 N94-25172
Experimental and theoretical investigations of the influence of the jet on the flow around a bypass-engine
[DLR-FB-93-17] 07 p2675 N94-27593
Coupled 2-dimensional cascade theory for noise an d unsteady aerodynamics of blade row interaction in turbofans. Volume 2: Documentation for computer code CUP2D
[NASA-CR-4506-VOL-2] 07 p2675 N94-27778
Gas-turbine engine steady-state behavior
07 p2828 N94-28044
Aircraft high bypass fan engine performance
[AD-A277722] 10 p3997 N94-33443
Coupled 2-dimensional cascade theory for noise and unsteady aerodynamics of blade row interaction in turbofans. Volume 1: Theory development and parametric studies
[NASA-CR-4506-VOL-1] 10 p3998 N94-34146

TURBOJET AIRCRAFT
U JET AIRCRAFT

TURBOJET ENGINES
NT CF-700 ENGINE
NT DUCTED FAN ENGINES
NT J-85 ENGINE
NT T-53 ENGINE
NT TURBOFAN ENGINES
NT TURBOPROP ENGINES
NT TURBORAMJET ENGINES
Analysis of gas turbine engines using water and oxygen injection to achieve high Mach numbers and high thrust
[NASA-TM-106270] 02 p0518 N94-13143
Development of a high-speed mechanical drive system for oscillating an annular blade row in the bending mode
[NAL-TR-1170] 02 p0502 N94-13342
A hot dynamic seal rig for measuring hypersonic engine seal durability and flow performance
[NASA-TM-106294] 02 p0664 N94-14727

Wind tunnel investigation with an operational turbojet engine
[TABES PAPER 93-662] 03 p0870 N94-16157
Aerothermochemical calculations in afterburners
08 p3154 N94-29258
CIAM experimental turboramjets
08 p3152 N94-29299
Community noise sources and noise control issues
10 p3972 N94-33467
Experimental investigation and performance analysis of the turbojet engine T117 10 p4000 N94-34439
Compact diffusers for small transonic compressors
10 p4002 N94-34449
Aerodynamic design and investigation of a mixed flow compressor stage 10 p4002 N94-34450

TURBOMACHINE BLADES
NT COMPRESSOR BLADES
NT ROTOR BLADES (TURBOMACHINERY)
NT STATOR BLADES
NT TURBINE BLADES
Probabilistic evaluation of uncertainties and risks in aerospace components
[NASA-TM-105603] 01 p0185 N94-10361
Blade row interaction effects on flutter and forced response
[NASA-TM-106438] 05 p1649 N94-21586
Streamwise vorticity in a turbine rotor with conical endwalls
[DLR-FB-93-13] 07 p2826 N94-27591
Development of the gas turbine. Part 2: Manufacturing, commissioning, and operation 07 p2831 N94-28081
Structural/aerodynamic blade analyzer (SAB) user's guide, version 1.0
[NASA-CR-194460] 08 p3151 N94-29103
Turbomachinery forced response prediction system (FREPS): User's manual
[NASA-CR-194465] 08 p3319 N94-29104
Aeroacoustic sensitivity analysis and optimal aeroacoustic design of turbomachinery blades
[NASA-CR-195786] 08 p3153 N94-30013
Mixed Eulerian-Lagrangian finite element solutions of unsteady flow and flutter in transonic cascade
08 p3282 N94-30816
Computational prediction of stall flutter in spanwise-finite blade cascades 09 p3584 N94-31967
Hotwire measurements of the turbulent flow into a cascade of controlled-diffusion compressor blades
[AD-A277297] 09 p3706 N94-32042

TURBOMACHINERY
NT AXIAL FLOW TURBINES
NT CENTRIFUGAL COMPRESSORS
NT CENTRIFUGAL PUMPS
NT GAS TURBINES
NT SHROUDED TURBINES
NT STEAM TURBINES
NT SUPERSONIC TURBINES
NT TIP VANES
NT TURBINE PUMPS
NT TURBINES
NT TURBOCOMPRESSORS
NT TURBOFANS
NT TWO STAGE TURBINES
NT WIND TURBINES
VIB3D: Method for calculating 3-D unsteady flow through turbomachinery blades
[CUED/A-TURBO/TR.128] 01 p0166 N94-12777
VIB2D: Quasi 3-D unsteady viscous flow method for blade flutter calculation
[CUED/A-TURBO/TR.129] 01 p0166 N94-12779
Averaging techniques for steady and unsteady calculations of a transonic fan stage
[NASA-TM-106231] 02 p0499 N94-13108
Residual contact restraints in cryogenics
[ETN-93-94375] 02 p0671 N94-13501
Numerical simulations of unsteady flows in turbomachines 02 p0633 N94-13569
Passage-averaged approximation of turbomachinery flows using vorticity-potential method
[ISBN-0-315-72716-0] 02 p0634 N94-13598
The development of a scalable parallel 3-D CFD algorithm for turbomachinery
[NASA-CR-193604] 02 p0664 N94-14848
A mechanical system damping measurement technique using a one-degree-of-freedom (1DOF) cylindrical gas bearing
[AD-A268402] 03 p1048 N94-17462
Workshop on Computational Turbulence Modeling
[NASA-TM-109266] 04 p1410 N94-18545
An algebraic turbulence model for turbomachinery
04 p1411 N94-18554
Simulation of three dimensional unsteady viscous flows in turbomachines
[ECL-92-15] 04 p1420 N94-19398
Dynamics of face seals for high speed turbomachinery
05 p1655 N94-21796
Three-dimensional unstructured grid method applied to turbomachinery 05 p1919 N94-22360
Foil bearing research at Penn State
06 p2215 N94-23058
An analysis for high Reynolds number inviscid/viscid interactions in cascades
[NASA-CR-4519] 06 p2169 N94-24606
Optical surface contouring for non-destructive inspection of turbomachinery
[NASA-CR-195245] 07 p2835 N94-26691
Orbital transfer rocket engine technology 7.5K-LB thrust rocket engine preliminary design
[AD-A276954] 07 p2703 N94-27213
Prediction of undsteady flows in turbomachinery using the linearized Euler equations on deforming grids
[NASA-CR-195285] 07 p2675 N94-27654
A numerical method for confined unsteady flows related to fluid-structure interactions
[ISBN-0-315-74739-0] 08 p3277 N94-29902
A solution adaptive structured-unstructured grid procedure for unsteady flows 09 p3700 N94-31217
Solution of the average-passage equations for the incompressible flow through multiple-blade-row turbomachinery
[AD-A276515] 09 p3583 N94-31931
Incorporating radial mixing in axisymmetric streamline curvature through-flow analysis
[AD-A277325] 09 p3706 N94-32279
Superconducting Meissner effect bearings for cryogenic turbomachines, phase 2
[AD-A277865] 10 p4059 N94-33776
Design of a low aspect ratio transonic compressor stage using CFD techniques
[NASA-TM-106636] 10 p3998 N94-33971
TIGGERC: Turbomachinery interactive grid generator for 2-D grid applications and users guide
[NASA-TM-106586] 10 p3998 N94-33974
Rotordynamic Instability Problems in High-Performance Turbomachinery, 1993
[NASA-CP-3239] 10 p4061 N94-34176
Test results for rotordynamic coefficients of anti-swirl self-injection seals 10 p4062 N94-34180
Eccentricity effects upon the flow field inside a whirling annular seal 10 p4062 N94-34181
A 3D-CFD code for accurate prediction of fluid flows and fluid forces in seals 10 p4063 N94-34183
Whirl measurements on leakage flows in turbomachine models 10 p4054 N94-34185
Departure solutions of the unsteady thin-layer and full Navier-Stokes equations solved using streamline curvature based iteration techniques 10 p4052 N94-34980
Experiments on an unsteady, three-dimensional separation 10 p4052 N94-34981
Preliminary design for a reverse Brayton cycle cryogenic cooler
[NASA-CR-189341] 12 p4461 N94-36805

TURBOPROP AIRCRAFT
NT C-130 AIRCRAFT
Futurepath 1 --- power systems
[NASA-TM-109431] 03 p0925 N94-15503
Piloted simulation study of an ILS approach of a twin-pusher business/commuter turboprop aircraft configuration
[NASA-TM-4516] 07 p2646 N94-26602

TURBOPROP ENGINES
NT T-53 ENGINE
Futurepath 2
[NASA-TM-109285] 02 p0518 N94-13623
Futurepath 1
[NASA-TM-109439] 03 p0869 N94-15338
Structured finite volume modeling of US Navy aircraft engine test cells task 2: Turboprop engine, volume 1
[AD-A267833] 03 p0872 N94-17405
Structured finite volume modeling of US Navy aircraft engine test cells. Task 2: Turboprop engine. Volume 2: Code documentation and listings
[AD-A268386] 03 p0873 N94-17589
Wing mounted unducted fan engine
[CA-PATENT-1323353] 06 p2188 N94-24180
S-2E Tracker maritime patrol aircraft re-engine and system upgrade program 06 p2158 N94-24270
The AC-120: The advanced commercial transport
[NASA-CR-195491] 06 p2182 N94-24966
Eagle RTS: A design of a regional transport
07 p2671 N94-25709
Aerodynamic characteristics of a propeller-powered high-lift semispan wing
[NASA-TM-4541] 08 p3132 N94-29937

TURBOPUMPS
U TURBINE PUMPS

TURBORAMJET ENGINES
Hypersonic propulsion characterization
02 p0505 N94-14156
Research and Development of Ram/Scramjets and Turboramjets in Russia
[AD-A275588] 08 p3151 N94-29291
Introduction and overview of research and development of solid propellant ramrockets, liquid fuel ramjets and experimental hydrogen ram combustors
08 p3151 N94-29292
Turboramjet engines: Types and performances
08 p3151 N94-29293
Research and development of ramjets/ramrockets. Part 3: The study of gaseous hydrogen ram combustors
08 p3152 N94-29298

TURBOROTORS
U TURBINE WHEELS

TURBOSHAFTS
Structured finite volume modeling of US Navy aircraft engine test cells. Task 1: Turboshaft engine, volume 1
[AD-A268176] 03 p0873 N94-17432
Structured finite volume modeling of US Navy aircraft engine test cells. Task 1: Turboshaft engine-code documentation and listings, volume 2
[AD-A268177] 03 p0873 N94-17508
Technology Requirements for Small Gas Turbines
[AD-280274] 10 p3999 N94-34431
MTR390, the new generation turboshaft engine
10 p3999 N94-34434
Non-polluting gas turbine as a result of self-heating working fluid in a closed circuit
10 p4000 N94-34436
Analysis of rig test data for an axial/centrifugal compressor in the 12 kg/sec 10 p4000 N94-34437
The centrifugal compressor, an essential component of small and medium power engines
10 p4001 N94-34445

TURBULENCE
NT ATMOSPHERIC TURBULENCE
NT GUSTS
NT HOMOGENEOUS TURBULENCE
NT ISOTROPIC TURBULENCE
NT LANGMUIR TURBULENCE
NT MAGNETOHYDRODYNAMIC TURBULENCE
NT PLASMA TURBULENCE
An experimental investigation of the sources of propeller noise due to turbulence ingestion
01 p0358 N94-11057
The effects of successive distortions on a turbulent boundary layer in a supersonic flow
01 p0014 N94-11058
Examination of wall functions for a parabolized Navier-Stokes code for supersonic flow
[DE93-011590] 01 p0014 N94-11111
Control of jet noise
[NASA-CR-193612] 01 p0358 N94-11176
Turbulence modeling for thrust reverser flow field prediction methods
[AD-A266139] 01 p0154 N94-11641
The coherent structure in the oceanic turbulence around Japan Islands Chain forced by an air, sea, and solid Earth interaction 01 p0198 N94-11940
Annual Research Briefs, 1992
[NASA-CR-194389] 01 p0155 N94-12284
Local isotropy in high Reynolds number turbulent shear flows 01 p0157 N94-12302
The ideal Kolmogorov inertial range and constant
01 p0158 N94-12305
Plane mixing layer vortical structure kinematics
01 p0159 N94-12313
Numerical simulation of the non-Newtonian mixing layer 01 p0159 N94-12314
Mapping closures for turbulent combustion
[AD-A265671] 01 p0079 N94-12378
Fluctuations of longitudinal vortices along a concave wall 01 p0016 N94-12616
Coherent structure in near wall turbulence with riblets
01 p0165 N94-12628
Turbulence generation in the Pacific undercurrent by shear 01 p0223 N94-12730
Sites of fine-scale electron density turbulence in the interstellar medium
[NASA-CR-193708] 02 p0839 N94-13864
An experimental study of a turbulent boundary layer in the trailing edge region of a curculation-control airfoil
[NASA-CR-194522] 02 p0508 N94-14541
Studying Turbulence Using Numerical Simulation Databases. 4: Proceedings of the 1992 Summer Program
[NASA-CR-194556] 02 p0643 N94-14745
A small-scale turbulence model
02 p0643 N94-14746
Triad interactions in the dissipation range
02 p0644 N94-14750
Isotropy of small scale turbulence
02 p0644 N94-14752
Estimation of the vortex length scale and intensity from two-dimensional samples 02 p0645 N94-14756
Toward a quasi-linear closure for compressible turbulence
[DE93-017185] 02 p0647 N94-14895

Large eddy simulation and direct numerical simulation of high speed turbulent reacting flows
[NASA-CR-193131] 03 p1018 N94-15427
An experimental study of ASTOVL related jet flows to produce CFD code validation data. Phase 3: Results of experiments
[TT-9203] 03 p1020 N94-15645
Inviscid instability of streamwise corner flow
[NASA-CR-191514] 03 p1021 N94-15834
Detecting surface roughness effects on the atmospheric boundary layer via AIRSAR data: A field experiment in Death Valley, California 03 p1078 N94-16747
Three dimensional hydrodynamic calculations with adaptive mesh refinement of the evolution of Rayleigh Taylor and Richtmyer Meshkov instabilities in converging geometry: Multi-mode perturbations
[DE93-017155] 03 p1025 N94-16903
The structure of turbulent boundary layers and shock wave boundary layer interactions
[AD-A266240] 03 p1026 N94-16929
Studies in turbulence and turbulence control
[AD-A266318] 03 p1026 N94-16950
Structure of turbulence in three-dimensional boundary layers
[NASA-CR-194655] 03 p1027 N94-17130
Transition induced by fixed and freely convecting spherical particles in laminar boundary layers
[AD-A267757] 03 p1028 N94-17276
Active turbulence control in wall bounded flows using direct numerical simulation
[AD-A267261] 03 p1028 N94-17286
Lifted turbulent jet flames
[AD-A267911] 03 p0952 N94-17381
Measurement of the velocity field and void fraction in a planar plunging jet
[AD-A268183] 03 p1030 N94-17511
Vortex methods and statistics
[DE93-016974] 04 p1556 N94-17886
Defining the normal turbine inflow within a wind park environment
[DE93-010032] 04 p1489 N94-18046
Workshop on Computational Turbulence Modeling
[NASA-TM-109266] 04 p1410 N94-18545
Research activities at the Center for Modeling of Turbulence and Transition 04 p1410 N94-18546
Research on two equation models 04 p1411 N94-18547
Assessment and development of second order turbulence models 04 p1411 N94-18548
Computational aero-acoustics as a branch of turbulence research 04 p1411 N94-18552
Turbulence modeling in aircraft icing 04 p1412 N94-18555
Several examples where turbulence models fail in inlet flow field analysis 04 p1412 N94-18556
STREMR: Numerical model for depth-averaged incompressible flow
[AD-A269949] 04 p1417 N94-18672
Correlation of incoming boundary layer pitot pressure fluctuations with the unsteadiness of fin-induced shock wave turbulent boundary layer interactions
[AD-A270059] 04 p1417 N94-18796
Experimental investigation of turbulent Prandtl number and Reynolds analogy in transitional and post-transitional boundary layers
[AD-A270092] 04 p1418 N94-18867
Relation between the fluctuating wall pressure and the turbulent structure of a boundary layer on a cylinder in axial flow
[AD-A270242] 04 p1418 N94-18906
Numerical simulation of turbulent mixing and combustion near the inlet of a burner
[DE93-017960] 04 p1350 N94-18987
Particle dispersion in turbulent sprays
[AD-A271314] 05 p1796 N94-19913
Wavefront sensors for optical diagnostics in fluid mechanics: Application to heated flow, turbulence, and droplet evaporation
[DE93-040060] 05 p1797 N94-19974
Some practical turbulence modeling options for Reynolds-averaged full Navier-Stokes calculations of three-dimensional flows
[NASA-TM-106399] 05 p1637 N94-20534
Magnetically controlled solar nebula 05 p2120 N94-20791
Long-range laser imaging
[AD-A273020] 05 p1817 N94-21253
Direct simulation of shock-induced mixing layer
[DE93-040498] 05 p1803 N94-21531
Turbulization of free shear flows: 3D perturbations 05 p2000 N94-22626
Droplet turbulence interactions under subcritical and supercritical conditions 06 p2211 N94-23036
Computation of flows in a turn-around duct and a turbine cascade using advanced turbulence models 06 p2216 N94-23062
Probe shapes that measure time-averaged streamwise momentum and cross-stream turbulence intensity
[NASA-CASE-ARC-11934-1] 06 p2317 N94-23077
Computational study of GA(W)-1: Airfoil near stall
[PB93-226249] 06 p2165 N94-23116
Probe systems for measuring static pressure and turbulence intensity in fluid streams
[NASA-CASE-ARC-11935-1] 06 p2319 N94-23306
The use of transition region characteristics to improve the numerical simulation of heat transfer in bypass transitional flows
[NASA-TM-106445] 06 p2320 N94-23525
Aircraft accident report: In-flight engine separation. Japan Airlines, Inc., flight 46E, Boeing 747-121, N473EV, Anchorage, Alaska, 31 March 1993
[PB93-410407] 06 p2173 N94-24062
Annual research briefs, 1993 --- Center for Turbulence Research
[NASA-CR-194755] 06 p2327 N94-24138
Stretch-induced quenching in flame-vortex interactions 06 p2237 N94-24156
On streak spacing in wall-bounded turbulent flows 06 p2331 N94-24159
Transition to turbulence in an elliptic vortex 06 p2331 N94-24161
Vortical structure in a forced plane mixing layer 06 p2331 N94-24162
Sound radiation due to boundary layer transition 06 p2332 N94-24163
Direct simulation of isothermal-wall supersonic channel flow 06 p2172 N94-24164
Tensoral for post-processing users and simulation authors 06 p2333 N94-24169
Center for modeling of turbulence and transition: Research briefs, 1993
[NASA-TM-106383] 06 p2333 N94-24336
Workshop on Computational Turbulence Modeling
[NASA-CP-10130] 06 p2333 N94-24460
Development and validation of RNG methodology for compressible turbulence
[AD-A273469] 06 p2337 N94-24929
High lift aerodynamics
[NASA-CR-195183] 06 p2184 N94-25268
Numerical simulation of tomographic reconstruction for the study of turbulence using optical wavefront sensor measurements
[AD-A273851] 07 p2789 N94-25587
The identification of inflow fluid dynamics parameters that can be used to scale fatigue loading spectra of wind turbine structural components
[DE94-000231] 07 p2791 N94-26117
Feature isolation and quantification of evolving datasets
[NASA-CR-195230] 07 p2961 N94-26207
Predictive modeling of particle-laden, turbulent flows
[DE94-003298] 07 p2792 N94-26319
Potential capabilities of Reynolds stress turbulence model in the COMMIX-RSM code
[DE94-003716] 07 p2792 N94-26331
Experimental verification of tomographic reconstruction of turbulent air flow structure using optical wavefront measurements
[AD-A274392] 07 p2795 N94-27129
Orbital transfer vehicle engine technology high velocity ratio diffusing crossover
[AD-A277180] 07 p2703 N94-27212
Simulating high-frequency wind for long durations
[DE94-002739] 07 p2682 N94-27997
Unsteady aspects of hot gas reingestion and statistical analysis 07 p2676 N94-28019
Calculation of single and multiple jets in cross-flow with and without impingement using Reynolds-stress-transport closure 07 p2803 N94-28024
Predictions of momentum and scalar fields in a jet in cross-flow using first and second order turbulence closures 07 p2803 N94-28025
Effects of free-stream turbulence on a jet in a cross flow 07 p2805 N94-28036
Analysis of cooling jets near the leading edge of turbine blades 07 p2676 N94-28037
Lift-curve slope for structural response calculations
[ESDU-93013] 07 p2648 N94-28063
A modelling of the noise from simple coaxial jets. Part 3: With hot primary flow
[ISVR-TR-230-PT-3] 07 p2807 N94-28173
Sonic boom propagation through turbulence: A ray theory approach 07 p2650 N94-28192
Evolution of the large-scale vortices in turbulent mixing-layers 08 p3273 N94-29686
Dynamics of tornado-like vortices 08 p3371 N94-29753
Convective turbulence and transport in stars 08 p3546 N94-29913
Correction of X hot-wire measurements for gradients normal to the plane of the wires
[PB94-125473] 08 p3157 N94-30399
A laboratory simulation of urban heat-island-induced circulation in a stratified environment 08 p3367 N94-30921
Transition to turbulence in confined compressible mixing layers 08 p3283 N94-30958
Rotational effects in turbulence driven by convection 09 p3930 N94-31131
A priori tests of large eddy simulation of the compressible plane mixing layer
[MEMO-1152] 09 p3699 N94-31185
Response of wall turbulence to high frequency streamwise and spanwise oscillations 09 p3700 N94-31211
Turbulence structure of a premixed flame in a coaxial free air jet in the presence or absence of a base flow
[ISBN-0-315-78739-2] 09 p3633 N94-31471
Three-dimensional velocity measurements on a 6:1 prolate spheroid at 10 deg angle of attack
[AD-A276485] 09 p3702 N94-31476
Observations of turbulence, internal waves and background flows: An inquiry into the relationships between scales of motion 09 p3705 N94-31988
Hotwire measurements of the turbulent flow into a cascade of controlled-diffusion compressor blades
[AD-A277297] 09 p3706 N94-32042
A non-local model for prediction of the probability density function of turbulent fluctuations in boundary-layer flows 09 p3706 N94-32076
Effects of buoyancy on fluid flows and turbulence
[AD-A276586] 09 p3706 N94-32123
A critical evaluation of the Reynolds stress turbulence closure for the flow of a turbulent free-stream over a turbulent boundary layer
[ISBN-0-315-75792-2] 09 p3707 N94-32497
Transport and diffusion in turbulent fields modeling and measurements techniques
[AD-A278114] 09 p3769 N94-33110
The structure of high Reynolds number turbulent boundary layers, part A
[AD-A278392] 09 p3710 N94-33162
Scalar imaging velocimetry studies of turbulent flow structure and dynamics
[AD-A278395] 09 p3710 N94-33164
Laser measurements and analysis of flow in a radial inflow turbine inlet guide vanes and rotor 10 p3997 N94-33365
Theoretical study of thermodynamic properties and reaction rates of importance in the high-speed research program 10 p3974 N94-33482
Experimental studies of hypersonic transitional and turbulent boundary layers in hypersonic flow
[AD-A278441] 10 p4044 N94-33556
Growth and nonlinearity
[DE94-007366] 10 p4021 N94-33689
The structure of high Reynolds number turbulent boundary layers
[AD-A278489] 10 p4044 N94-33754
A comparison of modeled and observed ocean mixed layer behavior in a sea breeze influenced coastal region
[AD-A277911] 10 p4092 N94-33922
Turbulence compressibility corrections
[NASA-TM-108827] 10 p4047 N94-33999
New proof and extension of Sarkovskii's theorem
[AD-A278347] 10 p4129 N94-34004
A user's manual for the program TRES4: Random vibration analysis of vertical-axis wind turbines in turbulent winds
[DE94-009012] 10 p4079 N94-34078
Computational study of generic hypersonic vehicle flow fields
[NASA-CR-195938] 10 p3984 N94-34277
Direct simulation of a self-similar plane wake
[NASA-TM-108815] 10 p4050 N94-34917
Turbulence modelling for unsteady separated flows 10 p4053 N94-34984
Experimental studies of very-high Mach number hydrodynamics
[AD-A278761] 11 p4263 N94-35492
Expansion effects on supersonic turbulent boundary layers
[AD-A278989] 11 p4190 N94-35950
Non-linear interaction of gravity waves with average jet flows, instabilities, and turbulence
[PB94-170586] 11 p4291 N94-36214
On the physics of waves in the solar atmosphere: Wave heating and wind acceleration
[NASA-CR-194119] 11 p4375 N94-36395
The alternative faces of turbulent flow
[TM-5-94] 12 p4442 N94-36934
Finite-rate chemistry and transient effects in Direct Numerical Simulations of turbulent non-premixed flames
[DE94-005250] 12 p4410 N94-37222
Evolution of turbulent fields in explosions
[DE94-010405] 12 p4444 N94-37390

Effects of molecular transport on turbulence-chemistry interactions in a hydrogen-argon-air jet diffusion flame
[DE94-005107] 12 p4413 N94-37711
Fast electron generation and transport in a turbulent, magnetized plasma
[DE94-012986] 12 p4531 N94-37730
Self-sustained turbulence and L-mode confinement in toroidal plasmas
[DE94-748497] 12 p4532 N94-37734

TURBULENCE EFFECTS

Estimation of the direct acoustic radiation from turbulent spots using boundary layer velocity measurements
01 p0357 N94-10358
Direct simulation of compressible wall-bounded turbulence 01 p0156 N94-12294
High freestream turbulence effects on the transport of heat and momentum 02 p0633 N94-13559
Numerical studies of spray combustion in liquid-fueled engines 02 p0564 N94-13685
Effects of turbulence on the geodynamic laser ranging system 03 p0921 N94-15616
Plasma instabilities and transport in the MPD thruster
[AD-A268268] 03 p1204 N94-17575
Work plan for the Marine Aerosol Properties and the Thermal Imager Performance Trial (MAPTIP)
[AD-A270026] 04 p1483 N94-18712
Experimental investigation of turbulent Prandtl number and Reynolds analogy in transitional and post-transitional boundary layers
[AD-A270092] 04 p1418 N94-18867
Numerical simulation of acoustic waves propagation in turbulent media
[ECL-92-37] 04 p1563 N94-19413
Coherent lidar design and performance verification
[NASA-CR-193813] 05 p1816 N94-20341
Evaluation of turbulence models in the PARC code for transonic diffuser flows
[NASA-TM-106391] 06 p2168 N94-24084
Variability of measured sonic boom signatures. Volume 1: Technical report
[NASA-CR-191483-VOL-1] 06 p2526 N94-24172
Variability of measured sonic boom signatures. Volume 2: Data report
[NASA-CR-191483-VOL-2] 06 p2526 N94-24173
Effects of atmospheric variations on acoustic system performance 06 p2527 N94-24211
Stagnation region heat transfer: The influence of turbulence parameters, Reynolds number and body shape
[NASA-TM-106504] 06 p2334 N94-24481
Shear flow generation from the interaction of neoclassical and drift wave transport processes
[DE94-003135] 07 p2791 N94-26096
Topics in longshore currents
[AD-A274788] 07 p2899 N94-26361
Modelling atmospheric turbulence effects on ground-based telescope systems
[DE94-004211] 07 p3102 N94-26528
Experimental verification of tomographic reconstruction of turbulent air flow structure using optical wavefront measurements
[AD-A274392] 07 p2795 N94-27129
Effects of free-stream turbulence on a jet in a cross flow 07 p2805 N94-28036
Study of bridge design and technology
[PB94-137916] 08 p3121 N94-29160
Theory and application of a Radio-Acoustic Sounding System (RASS) 08 p3367 N94-30869
Phase-only correction of scintillated laser beams: Downrange experimental results
[AD-A277778] 09 p3722 N94-33282
Atmospheric effects on sonic boom: A program review
10 p3976 N94-33495
Relaxation and turbulence effects on sonic boom signatures 10 p3976 N94-33496
Statistical and numerical study of the relation between weather and sonic boom characteristics
10 p3976 N94-33498
Spatial fluctuations of particle fluxes within the auroral zone inferred from the Intercosmos-Bulgaria-1300 satellite data
[DE94-615858] 11 p4350 N94-36128

TURBULENCE METERS

Experimental Methods in Separated Flows
[ILR-MITT-260(1991)] 06 p2315 N94-22852
Turbulence sensors for separated flows: Current capabilities, future requirements
06 p2315 N94-22853

TURBULENCE MODELS

NT K-EPSILON TURBULENCE MODEL
Numerical calculation of scramjet inlet flow
[NAL-TR-1174T] 01 p0027 N94-10370
Problems in the validation of CFD codes through comparison with experiment 01 p0006 N94-10441
Experimental, analytical, and computational methods applied to hypersonic compression ramp flows
01 p0006 N94-10444
Aerodynamic characteristics analysis of Garabedian-Korn 75-06-12 airfoil: Computation using q-omega 2 equation turbulence model
[PAPER-2D-4] 01 p0010 N94-10470
Aerodynamic characteristics analysis of Garabedian-Korn 75-06-12 airfoils: Computation using Baldwin-Lomax turbulence model
[PAPER-2D-5] 01 p0011 N94-10471
Aerodynamic characteristics analysis of Garabedian-Korn 75-06-12 aircraft
[PAPER-2D-7] 01 p0011 N94-10472
Aerodynamic characteristics analysis of Garabedian-Korn 75-06-12 airfoil
[PAPER-2D-8] 01 p0011 N94-10473
Flow analysis around ONERA model M5 configuration
[PAPER-3D-1] 01 p0011 N94-10477
Examination of wall functions for a parabolized Navier-Stokes code for supersonic flow
[DE93-011590] 01 p0014 N94-11111
A research program for improving heat transfer prediction for the laminar to turbulent transition region of turbine vanes/blades
[NASA-TM-106278] 01 p0151 N94-11256
A four-dimensional, mesoscale, non-gaussian multispectral smoke model. Phase 1: Feasibility study
[AD-A264805] 01 p0152 N94-11519
Modelling quasi-two-dimensional turbulent shear flow
01 p0153 N94-11616
Turbulence modeling for thrust reverser flow field prediction methods
[AD-A266139] 01 p0154 N94-11641
Annual Research Briefs, 1992
[NASA-CR-194389] 01 p0155 N94-12284
Large eddy simulations of time-dependent and buoyancy-driven channel flows
01 p0155 N94-12287
A normal stress subgrid-scale eddy viscosity model in large eddy simulation 01 p0155 N94-12288
Large eddy simulation of shock turbulence interaction
01 p0155 N94-12289
Application of a dynamic subgrid-scale model to turbulent recirculating flows 01 p0156 N94-12290
Large-eddy simulation of turbulent flow with a surface-mounted two-dimensional obstacle
01 p0156 N94-12291
Similarity states of homogeneous stably-stratified turbulence at infinite Froude number
01 p0156 N94-12292
Application of incremental unknowns to the Burgers equation 01 p0156 N94-12293
Direct simulation of compressible wall-bounded turbulence 01 p0156 N94-12294
Application of a Reynolds stress model to separating boundary layers 01 p0157 N94-12299
The ideal Kolmogorov inertial range and constant
01 p0158 N94-12305
PDF approach for turbulent scalar field: Some recent developments 01 p0160 N94-12315
Proceedings of the 9th and 10th NAL Workshop on Investigation and Control of Boundary-Layer Transition
[NAL-SP-18] 01 p0163 N94-12611
Turbulence modeling and compressibility
01 p0163 N94-12614
Force-free magnetic fields, curl eigenfunctions, and the sphere in transform space, with applications to fluid dynamics and electromagnetic theory
[AD-A265805] 02 p0834 N94-12971
Two-dimensional Navier-Stokes heat transfer analysis for rough turbine blades
[NASA-TM-106008] 02 p0629 N94-13027
Averaging techniques for steady and unsteady calculations of a transonic fan stage
[NASA-TM-106231] 02 p0499 N94-13108
A multiple-scale turbulence model for incompressible flow
[NASA-TM-106113] 02 p0631 N94-13385
Numerical simulation of steady three-dimensional flows in axial turbomachinery bladerows
02 p0634 N94-13630
A control volume finite element method for three-dimensional, incompressible, viscous fluid flow
[ISBN-0-315-72019-0] 02 p0635 N94-13683
Development of a recursion RNG-based turbulence model
[NASA-CR-191511] 02 p0636 N94-13718
Analysis of reacting flowfields in low-thrust rocket engines and plumes 02 p0552 N94-14491
Studying Turbulence Using Numerical Simulation Databases. 4: Proceedings of the 1992 Summer Program
[NASA-CR-194556] 02 p0643 N94-14745
A small-scale turbulence model
02 p0643 N94-14746
On the local nature of the energy cascade
02 p0643 N94-14748
Search for subgrid scale parameterization by projection pursuit regression 02 p0643 N94-14749
Triad interactions in the dissipation range
02 p0644 N94-14750
Rapid distortion analysis and direct simulation of compressible homogeneous turbulence at finite Mach number 02 p0645 N94-14757
Investigation of the dilatational dissipation in compressible homogeneous shear flow
02 p0645 N94-14758
The evolution equation for the flame surface density in turbulent premixed combustion
02 p0567 N94-14764
Numerical simulations of turbulent premixed H2/O2/N2 flames with complex chemistry
02 p0567 N94-14765
Structure of turbulent non-premixed flames modeled with two-step chemistry 02 p0567 N94-14767
Mesoscale modeling of the atmosphere
[AD-A263236] 03 p1098 N94-15132
Numerical simulation of 3-D shock wave turbulent boundary layer interactions 03 p1017 N94-15199
Contribution of laser Doppler velocimetry to the physical description of shock wave/turbulent boundary layer interactions with incidence on turbulence modelling
03 p1018 N94-15201
Turbulence modelling for shock wave/boundary layer interactions specific issues and examples of applications
03 p1018 N94-15202
Proteus two-dimensional Navier-Stokes computer code, version 2.0. Volume 2: User's guide
[NASA-TM-106338-VOL-2] 03 p1019 N94-15475
Proteus two-dimensional Navier-Stokes computer code, version 2.0. Volume 1: Analysis description
[NASA-TM-106336-VOL-1] 03 p1019 N94-15485
Proteus three-dimensional Navier-Stokes computer code, version 1.0. Volume 2: User's guide
[NASA-TM-106340-VOL-2] 03 p1020 N94-15488
Turbulence and transition modeling for high-speed flows
[AD-A266748] 03 p1022 N94-15953
Selected computations of transonic cavity flows
03 p0858 N94-16511
Computation of confined coflow jets with three turbulence models
[NASA-TM-106378] 03 p1025 N94-16879
The structure of turbulent boundary layers and shock wave boundary layer interactions
[AD-A266240] 03 p1026 N94-16929
Investigation of high-speed free shear flows using improved pressure-strain correlated Reynolds stress turbulence model
[NASA-CR-194661] 03 p1027 N94-17127
Structure of turbulence in three-dimensional boundary layers
[NASA-CR-194655] 03 p1027 N94-17130
Time dependent turbulence modeling and analytical theories of turbulence
[NASA-TM-106379] 03 p1029 N94-17385
Navier-Stokes calculations on multi-element airfoils using a chimera-based solver 04 p1306 N94-18422
Workshop on Computational Turbulence Modeling
[NASA-TM-109266] 04 p1410 N94-18545
Research activities at the Center for Modeling of Turbulence and Transition 04 p1410 N94-18546
Assessment and development of second order turbulence models 04 p1411 N94-18548
Numerical investigation of complex, transitional, and chemically reacting flows 04 p1411 N94-18550
Computational aero-acoustics as a branch of turbulence research 04 p1411 N94-18552
A comparative study of turbulence models in predicting hypersonic inlet flows 04 p1314 N94-18553
An algebraic turbulence model for turbomachinery
04 p1411 N94-18554
Turbulence modeling in aircraft icing
04 p1412 N94-18555
Several examples where turbulence models fail in inlet flow field analysis 04 p1412 N94-18556
Introduction to the Modeling of Turbulence
[VKI-LS-1993-02] 04 p1414 N94-18578
An introduction to the modelling of turbulence
04 p1414 N94-18579
An introduction to second moment closure
04 p1414 N94-18580
Modelling force-field effects on turbulence
04 p1414 N94-18581
A new form of second-moment closure
04 p1414 N94-18582
An introduction to single-point closure methodology
04 p1414 N94-18583
Second-moment closure: Present... and future?
04 p1414 N94-18584

Contribution to the modelling of near-wall turbulence
04 p1414 N94-18585
Two-equation models for high-Reynolds-number flow
04 p1415 N94-18586
Application of second-moment closure in complex flows 04 p1415 N94-18590
Modelling engineering flows with Reynolds stress turbulence closure 04 p1415 N94-18591
Turbulence modelling challenges posed by complex flows 04 p1415 N94-18592
Turbulence modeling for compressible flows and implementation in Navier-Stokes solvers
04 p1416 N94-18597
Turbulence modeling for high speed compressible flows
[NASA-CR-194547] 05 p1799 N94-20210
Some practical turbulence modeling options for Reynolds-averaged full Navier-Stokes calculations of three-dimensional flows
[NASA-TM-106399] 05 p1637 N94-20534
Flow interaction experiment. Volume 1: Aerothermal modeling, phase 2
[NASA-CR-189192-VOL-1] 05 p1648 N94-21582
Flow interaction experiment. Volume 2: Aerothermal modeling, phase 2
[NASA-CR-189192-VOL-2] 05 p1648 N94-21583
New results on the realizability of Reynolds stress turbulence closures
[NASA-CR-191548] 05 p1804 N94-21875
Reliability in second moment turbulence closures revisited
[NASA-TM-106469] 06 p2326 N94-24063
Evaluation of turbulence models in the PARC code for transonic diffuser flows
[NASA-TM-106391] 06 p2168 N94-24084
Annual research briefs, 1993 --- Center for Turbulence Research
[NASA-CR-194755] 06 p2327 N94-24138
Toward modeling wingtip vortices
06 p2171 N94-24142
New concepts for Reynolds stress transport equation modeling of inhomogeneous flows
06 p2171 N94-24143
Turbulence modeling for non-equilibrium flows
06 p2328 N94-24144
Computation of turbulent flows over backward and forward-facing steps using a near-wall Reynolds stress model 06 p2172 N94-24145
Large eddy simulation of a boundary layer with concave streamwise curvature 06 p2328 N94-24146
Large-eddy simulation of flow in a plane, asymmetric diffuser 06 p2328 N94-24147
The combustion program at CTR
06 p2237 N94-24155
Computation of large-scale statistics in decaying isotropic turbulence 06 p2332 N94-24167
Center for modeling of turbulence and transition: Research briefs, 1993
[NASA-TM-106383] 06 p2333 N94-24336
Workshop on Computational Turbulence Modeling
[NASA-CP-10130] 06 p2333 N94-24460
Implementation of the Baldwin-Barth turbulence model into the ZETA code and its diagnosis
[NASA-CR-194795] 06 p2335 N94-24640
A vorticity dynamics based model for the turbulent dissipation: Model development and validation
[NASA-TM-106177] 06 p2336 N94-24713
Computational fluid mechanics
[NASA-CR-194765] 06 p2337 N94-24859
LES, DNS and RANS for the analysis of high-speed turbulent reacting flows
[NASA-CR-195196] 06 p2337 N94-25094
Development and application of new algorithms for the simulation of viscous compressible flows with moving bodies in three dimensions
[AD-A273514] 06 p2338 N94-25157
Decay of swirl in turbulent pipe flows
[ETN-94-95353] 06 p2339 N94-25248
Performance of renormalization group algebraic turbulence model on boundary layer transition simulation
[NASA-CR-194486] 07 p2644 N94-26131
Potential capabilities of Reynolds stress turbulence model in the COMMIX-RSM code
[DE94-003716] 07 p2792 N94-26331
The nonlinear Galerkin method: A multi-scale method applied to the simulation of homogeneous turbulent flows
[AD-A277432] 07 p2792 N94-26499
A rapid-pressure correlation representation consistent with the Taylor-Proudman theorem materially-frame-indifferent in the 2D limit
[AD-A277582] 07 p2796 N94-27435
A comprehensive comparison of turbulence models in the far wake 07 p2808 N94-27899
Computational and Experimental Assessment of Jets in Cross Flow
[AGARD-CP-534] 07 p2799 N94-28003
A numerical investigation of a subsonic jet in a crossflow 07 p2803 N94-28023
Theoretical and experimental investigation of a delta wing with turbulent leading-edge jets
07 p2659 N94-28029
Navier-Stokes analysis of a swirling jet in crossflow
07 p2806 N94-28038
Sonic boom propagation through turbulence: A ray theory approach 07 p2650 N94-28192
Study of modeling of turbulence of renormalization group analysis 08 p3126 N94-28970
An alternative assessment of second-order closure models in turbulent shear flows
[AD-A279072] 08 p3272 N94-29381
A vorticity transport closure method for turbulent reacting flows 08 p3274 N94-29761
Direct and large-eddy simulations of turbulent flow in a square duct 08 p3275 N94-29809
Potential capabilities of Reynolds stress turbulence model in the COMMIX-RSM code
08 p3285 N94-30450
Three dimensional compressible turbulent flow computations for a diffusing S-duct with/without vortex generators 08 p3281 N94-30519
Turbulence models and their application in implosion analyses with two-phase flow
[GKSS-92/E/98] 08 p3284 N94-30967
A critical evaluation of the Reynolds stress turbulence closure for the flow of a turbulent free-stream over a turbulent boundary layer
[ISBN-0-315-75792-2] 09 p3707 N94-32497
Additive turbulent decomposition of the incompressible and compressible Navier-Stokes equations
[AD-A277321] 09 p3708 N94-32511
Performance of a new wind updating system for a prognostic meteorological model in the environs of Mexico City
[DE94-006243] 09 p3786 N94-32937
Modification of the MML turbulence model for adverse pressure gradient flows
[NASA-TM-106544] 09 p3709 N94-32947
Use of Navier-Stokes methods for the calculation of high-speed nozzle flow fields
[NASA-TM-106551] 09 p3573 N94-32984
Renormalization group theory of Bolgiano scaling in Boussinesq turbulence
[NASA-TM-106602] 09 p3710 N94-33070
Turbulence compressibility corrections
[NASA-TM-108827] 10 p4047 N94-33999
Prediction of unsteady airfoil flows at large angles of incidence 10 p3986 N94-34978
Turbulence modelling for unsteady separated flows
10 p4053 N94-34984
Dynamic and thermal turbulent time scale modelling for homogeneous shear flows
[NASA-TM-106635] 11 p4263 N94-35253
Comparison of PDF and moment closure methods in the modeling of turbulent reacting flows
[NASA-TM-106614] 11 p4265 N94-35948
Evolution of turbulent fields in explosions
[DE94-010405] 12 p4444 N94-37390

TURBULENT BOUNDARY LAYER

Problems in the validation of CFD codes through comparison with experiment 01 p0006 N94-10441
Aerodynamic characteristics analysis of Garabedian-Korn 75-06-12 airfoil: Compendium of results 01 p0011 N94-10475
Flowfield structure of swept shock wave/turbulent boundary-layer interactions 01 p0149 N94-10899
Theoretical investigation of 3-D shock wave turbulent boundary layer interactions
[AD-A265275] 01 p0150 N94-11014
The effects of successive distortions on a turbulent boundary layer in a supersonic flow
01 p0014 N94-11058
Remote sensing and the air-sea boundary layers
01 p0191 N94-11896
Application of a Reynolds stress model to separating boundary layers 01 p0157 N94-12299
Progress in modeling hypersonic turbulent boundary layers 01 p0157 N94-12300
An investigation of small scales of turbulence in a boundary layer at high Reynolds numbers
01 p0157 N94-12303
Experiments on near-wall structure of three-dimensional boundary layers 01 p0159 N94-12309
Suppression of the near wall burst process of a fully developed turbulent pipe flow
[AD-A265995] 01 p0161 N94-12352
Experiment on a high Reynolds number turbulent boundary layer 01 p0164 N94-12617
Turbulent boundary layer interacting with spanwise periodic longitudinal vortex arrays
01 p0165 N94-12626
Coherent structure in near wall turbulence with riblets
01 p0165 N94-12628
The transient behavior of a boundary layer exposed to uniform suction
[ITN-93-85205] 02 p0630 N94-13197
Three-dimensional structure of straight and curved plane wakes
[NASA-CR-194420] 02 p0501 N94-13266
Exploratory study of in-plane streamline curvature effects on a turbulent boundary layer at a Mach number of 3
[NASA-CR-193673] 02 p0501 N94-13292
A technique for direct measurement of skin friction in supersonic combustion flow 02 p0503 N94-13555
A three-dimensional supersonic turbulent boundary layer generated by an isentropic compression
02 p0503 N94-13556
High freestream turbulence effects on the transport of heat and momentum 02 p0633 N94-13559
An experimental study of a turbulent boundary layer in the trailing edge region of a curculation-control airfoil
[NASA-CR-194522] 02 p0508 N94-14541
Direct simulation of polymer drag reduction in free shear flows and vortex dipoles 02 p0644 N94-14755
Response of a supersonic boundary layer to a compression corner 02 p0645 N94-14759
A transport equation for eddy viscosity
02 p0646 N94-14762
Interaction of two glancing, crossing shock waves with a turbulent boundary-layer at various Mach numbers
[NASA-TM-103740] 02 p0509 N94-14780
Numerical simulation of 3-D shock wave turbulent boundary layer interactions 03 p1017 N94-15199
Contribution of laser Doppler velocimetry to the physical description of shock wave/turbulent boundary layer interactions with incidence on turbulence modelling
03 p1018 N94-15201
Turbulence and transition modeling for high-speed flows
[AD-A266748] 03 p1022 N94-15953
Ventilated oscillatory boundary layers
[AD-A266226] 03 p1023 N94-16110
Three-dimensional turbulent boundary layer
[AD-A266261] 03 p1025 N94-16908
The structure of turbulent boundary layers and shock wave boundary layer interactions
[AD-A266240] 03 p1026 N94-16929
Studies in turbulence and turbulence control
[AD-A266318] 03 p1026 N94-16950
Structure of high Reynolds number turbulent boundary layer
[AD-A267476] 03 p0860 N94-17099
Structure of turbulence in three-dimensional boundary layers
[NASA-CR-194655] 03 p1027 N94-17130
An experimental investigation of the effects of leading edge geometry on the dynamics of blunt fin-induced shock wave turbulent boundary layer interaction
[AD-A267656] 03 p0860 N94-17221
Transmission of light through a turbulent mixing layer
[AD-A267266] 03 p1193 N94-17264
Transition induced by fixed and freely convecting spherical particles in laminar boundary layers
[AD-A267757] 03 p1028 N94-17276
Active turbulence control in wall bounded flows using direct numerical simulation
[AD-A267261] 03 p1028 N94-17286
An experimental study of fluctuating wall pressures in a highly swept, sharp fin-induced, Mach 5 shock wave/turbulent boundary layer interaction
[AD-A268394] 03 p0861 N94-17461
An investigation of oblique shock/boundary layer interaction control
[AD-A268106] 03 p0861 N94-17574
Research on two equation models
04 p1411 N94-18547
Calculation of turbulent boundary layer wall pressure spectra
[AD-A269549] 04 p1416 N94-18642
Correlation of incoming boundary layer pitot pressure fluctuations with the unsteadiness of fin-induced shock wave turbulent boundary layer interactions
[AD-A270059] 04 p1417 N94-18796
Relation between the fluctuating wall pressure and the turbulent structure of a boundary layer on a cylinder in axial flow
[AD-A270242] 04 p1418 N94-18906
A new approach to the study of the turbulence layer
[NASA-CR-194546] 04 p1487 N94-19397
The effect of transverse curvature on the fluctuating wall pressure and structure of boundary layer turbulence
[AD-A271868] 05 p1800 N94-20466

Some practical turbulence modeling options for Reynolds-averaged full Navier-Stokes calculations of three-dimensional flows
[NASA-TM-106399] 05 p1637 N94-20534
Investigation of the physics of the turbulent boundary layer focusing on vortex structures
[AD-A272879] 05 p1802 N94-21155
Computational and analytical methods in nonlinear fluid dynamics
[AD-A272722] 05 p1802 N94-21169
Low Reynolds-number turbulent boundary layers
[AD-A272011] 05 p1803 N94-21459
Measurements and modeling of flow structure in the wake of a low profile wishbone vortex generator
[NASA-TM-106468] 06 p2166 N94-23465
An analytic study of a two-phase laminar airfoil in simulated heavy rain 06 p2171 N94-23661
Adaptive nonlinear polynomial neural networks for control of boundary layer/structural interaction
[NASA-CR-189645] 06 p2525 N94-23698
Optimal feedback control of turbulent channel flow 06 p2327 N94-24139
Boundary layer receptivity and control 06 p2327 N94-24141
New concepts for Reynolds stress transport equation modeling of inhomogeneous flows 06 p2171 N94-24143
Local isotropy in distorted turbulent boundary layers at high Reynolds number 06 p2332 N94-24166
Experimental study of a turbulent boundary layer in presence of external manipulators of NACA 0009 profile in the transonic regime
[ISBN-0-315-57633-2] 06 p2333 N94-24177
Experimental cavity pressure measurements at subsonic and transonic speeds. Static-pressure results
[NASA-TP-3358] 06 p2169 N94-24464
Heat transfer and flow structure in end-wall boundary layers
[AD-A273470] 06 p2335 N94-24689
Interactive control in turbulent shear layers
[AD-A273544] 06 p2336 N94-24793
Coherent structures over grooved surfaces
[ETN-94-95308] 06 p2339 N94-25291
A study on structure of benthic boundary layer in coastal waters
[REPT-4] 07 p2898 N94-25635
Experimental investigation of the flow quality in the GLT20 subsonic-transonic boundary layer wind tunnel
[PB94-126539] 07 p2681 N94-26815
Turbulent boundary layer inner-outer interactions
[AD-A274357] 07 p2794 N94-27059
Flowfield dynamics in blunt fin-induced shock wave/turbulent boundary layer interactions
[NASA-CR-195170] 07 p2798 N94-27802
An experimental study of siphonal jets in a turbulent boundary layer crossflow 07 p2802 N94-28015
Pneumatic management of blunted-forebody flow asymmetry for high-angle-of-attack directional control 07 p2679 N94-28028
On the use of feedback to control sound radiation from a plate excited by a turbulent boundary layer
[ISVR-TR-227] 07 p2807 N94-28175
Wall pressure events from the direct numerical simulation of a turbulent wall-bounded flow
[AD-A275890] 08 p3271 N94-28778
A flow visualization study of acoustically enhanced hairpin vortices
[AD-A275467] 08 p3271 N94-28809
An alternative assessment of second-order closure models in turbulent shear flows
[AD-A279072] 08 p3272 N94-29381
The effect of pressure gradient on the structure of an equilibrium turbulent boundary layer 08 p3282 N94-30807
Shock impingement near mild hypersonic expansion corners 09 p3569 N94-31879
A non-local model for prediction of the probability density function of turbulent fluctuations in boundary-layer flows 09 p3706 N94-32076
A critical evaluation of the Reynolds stress turbulence closure for the flow of a turbulent free-stream over a turbulent boundary layer
[ISBN-0-315-75792-2] 09 p3707 N94-32497
Flight test results of riblets at supersonic speeds
[NASA-TM-4387] 09 p3572 N94-32880
An analysis of supersonic flows with low-Reynolds number compressible two-equation turbulence models using LU finite volume implicit numerical techniques
[NASA-CR-195302] 09 p3572 N94-32926
Modification of the MML turbulence model for adverse pressure gradient flows
[NASA-TM-106544] 09 p3709 N94-32947
The spatial development of the magnetospheric low-latitude boundary layer
[ISBN-0-315-77418-5] 09 p3776 N94-33111
The structure of high Reynolds number turbulent boundary layers, part A
[AD-A278392] 09 p3710 N94-33162
Experimental studies of hypersonic transitional and turbulent boundary layers in hypersonic flow
[AD-A278441] 10 p4044 N94-33556
The structure of high Reynolds number turbulent boundary layers
[AD-A278489] 10 p4044 N94-33754
Modeling the transition region 10 p4046 N94-33890
Forced unsteady deceleration of a turbulent boundary layer from a temporal perspective 10 p4053 N94-34983
A review and development of correlations for base pressure and base heating in supersonic flow
[SAND93-0280] 11 p4189 N94-35360
The aerodynamic and heat transfer effects of an endwall boundary layer fence in a 90 degree turning square duct
[AD-A278903] 11 p4265 N94-35803
Expansion effects on supersonic turbulent boundary layers
[AD-A278989] 11 p4190 N94-35950
Hypersonic shock/boundary-layer interaction database: New and corrected data
[NASA-CR-177638] 12 p4441 N94-36519

TURBULENT COMBUSTION

The evolution equation for the flame surface density in turbulent premixed combustion 01 p0081 N94-12316
Study and modeling of finite rate chemistry effects in turbulent non-premixed flames 01 p0081 N94-12317
Generation of two-dimensional vortices in a cross-flow 01 p0160 N94-12318
Why does preferential diffusion strongly affect premixed turbulent combustion? 01 p0081 N94-12319
Mapping closures for turbulent combustion
[AD-A265671] 01 p0079 N94-12378
Theories of turbulent combustion in high speed flows
[AD-A265735] 01 p0079 N94-12403
A coherent flame model of premixed turbulent combustion in a counterflow geometry
[CUED/A-THERMO/TR.60] 02 p0562 N94-13085
Analysis of reacting flowfields in low-thrust rocket engines and plumes 02 p0552 N94-14491
Studying Turbulence Using Numerical Simulation Databases. 4: Proceedings of the 1992 Summer Program
[NASA-CR-194556] 02 p0643 N94-14745
The evolution equation for the flame surface density in turbulent premixed combustion 02 p0567 N94-14764
Numerical simulations of turbulent premixed H2/O2/N2 flames with complex chemistry 02 p0567 N94-14765
Structure of turbulent non-premixed flames modeled with two-step chemistry 02 p0567 N94-14767
Reaction and diffusion in turbulent combustion
[DE93-017085] 03 p0943 N94-15146
Spectral radiance measurements on a bluff body stabilized flame: Characterization of the IR signature
[PB93-195899] 04 p1347 N94-18081
Research activity on particle spin systems and related problems
[AD-A269456] 04 p1562 N94-18286
A coupled implicit solution method for turbulent spray combustion in propulsion systems 04 p1411 N94-18549
Numerical simulation of turbulent mixing and combustion near the inlet of a burner
[DE93-017960] 04 p1350 N94-18987
Reaction zone models for vortex simulation of turbulent combustion
[AD-A272723] 05 p1681 N94-21213
Simulations of diffusion-reaction equations with implications to turbulent combustion modeling
[NASA-CR-191536] 05 p1804 N94-21861
A random distribution reacting mixing layer model
[NASA-CR-194445] 06 p2187 N94-23552
The combustion program at CTR 06 p2237 N94-24155
Stretch-induced quenching in flame-vortex interactions 06 p2237 N94-24156
A transport equation for the scalar dissipation in reacting flows with variable density: First results 06 p2331 N94-24157
Study of streamwise vorticity-stirred combustion
[NASA-CR-194450] 06 p2234 N94-24565
Numerical solutions of the complete Navier-Stokes equations
[NASA-CR-194780] 06 p2337 N94-24858
High resolution measurements of mixing and reaction processes in turbulent flows
[AD-A274970] 07 p2793 N94-26534
A random distribution reacting mixing layer model
[NASA-TM-106517] 08 p3150 N94-28923
Simulation of pollutant formation in turbulent combustors using an extended coherent flame model 08 p3190 N94-29251
Numerical prediction of turbulent sooting diffusion flames 08 p3191 N94-29253
Lifted turbulent jet flames 08 p3198 N94-29676
A vorticity transport closure method for turbulent reacting flows 08 p3274 N94-29761
An investigation of the reacting vortex structures associated with pulse combustion 08 p3200 N94-30911
AFOSR Contractors Propulsion Meeting
[AD-A279028] 11 p4198 N94-35746
Comparison of PDF and moment closure methods in the modeling of turbulent reacting flows
[NASA-TM-106614] 11 p4265 N94-35948
Some effects of heat release in premixed flames
[DE94-011346] 12 p4409 N94-37199

TURBULENT DIFFUSION

Aerosol sampling models survey
[AD-A265903] 01 p0075 N94-10337
A self-consistent model of non-linear parameterization of turbulent diffusion in atmospheric boundary layer
[DE93-011950] 01 p0275 N94-11052
Why does preferential diffusion strongly affect premixed turbulent combustion? 01 p0081 N94-12319
Theories of turbulent combustion in high speed flows
[AD-A265735] 01 p0079 N94-12403
Sub-grid scale modeling for large eddy simulations in analysis of shock-turbulence interactions
[DE93-013425] 02 p0631 N94-13250
Turbulent diffusion in homogeneous shear flow with stable density stratification
[DLR-FB-92-26] 02 p0639 N94-14443
Structure of turbulent non-premixed flames modeled with two-step chemistry 02 p0567 N94-14767
Simulations of diffusion-reaction equations with implications to turbulent combustion modeling
[NASA-CR-191536] 05 p1804 N94-21861
Eddy mixing coefficient values derived from simulations with the NASA Ames Mars GCM 06 p2617 N94-24875
Eddy mixing coefficient upper limit derived from the photochemical balance of O2 06 p2621 N94-24897
Similarity solutions and numerical modeling in buoyancy controlled turbulent diffusion flames
[AD-A275820] 08 p3188 N94-28777
Incorporating radial mixing in axisymmetric streamline curvature through-flow analysis
[AD-A277325] 09 p3706 N94-32279
Notes on the Langevin model for turbulent diffusion of marked particles
[DE94-007847] 09 p3708 N94-32652
Interference between parallel, convergent and divergent jet diffusion flames
[INPE-5542-TDI/530] 10 p4023 N94-34229
Short-tower sigma(theta) measurements in the Colorado Plateaus region
[DE94-007478] 12 p4463 N94-36478
Influences of flame-vortex interactions on formation of oxides of nitrogen in curved methane-air diffusion flamelets
[DE94-005105] 12 p4409 N94-37221
Spray combustion model improvement study, 1
[NASA-CR-196122] 12 p4410 N94-37250
Effects of molecular transport on turbulence-chemistry interactions in a hydrogen-argon-air jet diffusion flame
[DE94-005107] 12 p4413 N94-37711

TURBULENT FLOW

NT CAVITATION FLOW
Combustion chamber analysis code
[NASA-CR-192585] 01 p0046 N94-10934
Examination of wall functions for a parabolized Navier-Stokes code for supersonic flow
[DE93-011590] 01 p0014 N94-11111
Physics of tokamak scrape-off layer confinement
[DE93-011949] 01 p0390 N94-11125
Turbulent wall jet in blast wave precursor
[DE93-011955] 01 p0151 N94-11144
A Galilean and tensorial invariant k-epsilon model for near wall turbulence
[NASA-TM-106263] 01 p0151 N94-11192
KIVA-3: A KIVA program with block-structured mesh for complex geometries
[DE93-011986] 01 p0077 N94-11249
A research program for improving heat transfer prediction for the laminar to turbulent transition region of turbine vanes/blades
[NASA-TM-106278] 01 p0151 N94-11256
Dynamics and control of coherent structures in the turbulent wall layer: An overview 01 p0031 N94-11494
Modelling quasi-two-dimensional turbulent shear flow 01 p0153 N94-11616

A two-stage (turbulent-drainage) mechanism for the emplacement of impact crater outflows on Venus
01 p0458 N94-12145
Annual Briefs, 1992
[NASA-CR-194389] 01 p0155 N94-12284
A normal stress subgrid-scale eddy viscosity model in large eddy simulation 01 p0155 N94-12288
Large eddy simulation of shock turbulence interaction
01 p0155 N94-12289
Application of a dynamic subgrid-scale model to turbulent recirculating flows 01 p0156 N94-12290
Large-eddy simulation of turbulent flow with a surface-mounted two-dimensional obstacle
01 p0156 N94-12291
Similarity states of homogeneous stably-stratified turbulence at infinite Froude number
01 p0156 N94-12292
Application of incremental unknowns to the Burgers equation 01 p0156 N94-12293
Direct simulation of compressible wall-bounded turbulence 01 p0156 N94-12294
Direct numerical simulation of turbulent flow over a backward-facing step 01 p0156 N94-12296
Numerical simulation using vorticity-vector potential formulation 01 p0157 N94-12297
Local isotropy in high Reynolds number turbulent shear flows 01 p0157 N94-12302
An investigation of small scales of turbulence in a boundary layer at high Reynolds numbers
01 p0157 N94-12303
The helical decomposition and the instability assumption 01 p0158 N94-12306
Superfluid turbulence 01 p0158 N94-12307
Regeneration of near-wall turbulence structures
01 p0158 N94-12308
Mixing in a stratified shear flow: Energetics and sampling 01 p0159 N94-12311
LIF measurements of scalar mixing in turbulent shear layers 01 p0159 N94-12312
The evolution equation for the flame surface density in turbulent premixed combustion
01 p0081 N94-12316
Study and modeling of finite rate chemistry effects in turbulent non-premixed flames 01 p0081 N94-12317
Why does preferential diffusion strongly affect premixed turbulent combustion? 01 p0081 N94-12319
Tensoral: A system for post-processing turbulence simulation data 01 p0075 N94-12320
Topics in pattern formation and chaotic systems
[AD-A265922] 01 p0161 N94-12342
Suppression of the near wall burst process of a fully developed turbulent pipe flow
[AD-A265995] 01 p0161 N94-12352
Mapping closures for turbulent combustion
[AD-A265671] 01 p0079 N94-12378
Theories of turbulent combustion in high speed flows
[AD-A265735] 01 p0079 N94-12403
Development of the one-component diode-array velocimeter
[AD-A265552] 01 p0171 N94-12533
DNS on control of laminar-turbulent transition in channel flow with suction and blowing 01 p0163 N94-12613
Turbulence modeling and compressibility
01 p0163 N94-12614
Fluctuations of longitudinal vortices along a concave wall 01 p0016 N94-12616
Simultaneous 3D turbulent large-scale structures in a flood flow by multi-channels measuring system
01 p0165 N94-12624
Turbulent boundary layer interacting with spanwise periodic longitudinal vortex arrays
01 p0165 N94-12626
Coherent structure in near wall turbulence with riblets
01 p0165 N94-12628
Transition prediction and control in subsonic flow over a hump
[NASA-CR-4543] 02 p0629 N94-13066
Numerical simulations and experiments on physics of high Mach number shockwave: Turbulent flow interactions
[DE93-013424] 02 p0631 N94-13249
Sub-grid scale modeling for large eddy simulations in analysis of shock-turbulence interactions
[DE93-013425] 02 p0631 N94-13250
Fully developed turbulent flow in rectangular interrupted-plate ducts
[ISBN-0-315-63594-0] 02 p0632 N94-13474
An experimental investigation of shock wave/vortex interaction 02 p0634 N94-13574
Numerical simulation of steady three-dimensional flows in axial turbomachinery bladerows
02 p0634 N94-13630
A solution algorithm for the prediction of compressible laminar and turbulent shear flows
02 p0634 N94-13635
Studies of turbulent shear flows and their control
[NASA-CR-194114] 02 p0635 N94-13676
Numerical studies of spray combustion in liquid-fueled engines 02 p0564 N94-13685
Development of a recursion RNG-based turbulence model
[NASA-CR-191511] 02 p0636 N94-13718
Experimental investigation of the effects of blowing ratio parameter on heat transfer to a film-cooled flat plate
[AD-A266599] 02 p0636 N94-13780
Turbulent particle dispersion in confined swirling flows
[DLR-FB-92-32] 02 p0637 N94-14045
Droplet-turbulence interactions in sprays exposed to supercritical environmental conditions
[NASA-CR-194408] 02 p0638 N94-14308
Inflow characteristics associated with high-blade-loading events in a wind farm
[DE93-010042] 02 p0704 N94-14423
Interactions among convection, magnetic fields and p-mode oscillations in the sun
[NASA-CR-194477] 02 p0845 N94-14479
An implicit finite volume nodal point scheme for the solution of two-dimensional compressible Navier-Stokes equations 02 p0640 N94-14603
Development of an explicit multiblock/multigrid flow solver for viscous flows in complex geometries
[NASA-TM-106356] 02 p0642 N94-14728
Studying Turbulence Using Numerical Simulation Databases. 4: Proceedings of the 1992 Summer Program
[NASA-CR-194556] 02 p0643 N94-14745
A small-scale turbulence model
02 p0643 N94-14746
The structure of intense vorticity in homogeneous isotropic turbulence 02 p0643 N94-14747
On the local nature of the energy cascade
02 p0643 N94-14748
Search for subgrid scale parameterization by projection pursuit regression 02 p0643 N94-14749
Triad interactions in the dissipation range
02 p0644 N94-14750
A study of the fine scale motions of incompressible time-developing mixing layers 02 p0644 N94-14751
Isotropy of small scale turbulence
02 p0644 N94-14752
LES versus DNS: A comparative study
02 p0644 N94-14753
Behavior of streamwise rib vortices in a three-dimensional mixing layer 02 p0644 N94-14754
Direct simulation of polymer drag reduction in free shear flows and vortex dipoles 02 p0644 N94-14755
Estimation of the vortex length scale and intensity from two-dimensional samples 02 p0645 N94-14756
Investigation of the dilatational dissipation in compressible homogeneous shear flow
02 p0645 N94-14758
A transport equation for eddy viscosity
02 p0646 N94-14762
DNS and modeling of the interaction between turbulent premixed flames and walls 02 p0646 N94-14763
The evolution equation for the flame surface density in turbulent premixed combustion
02 p0567 N94-14764
Structure of turbulent non-premixed flames modeled with two-step chemistry 02 p0567 N94-14767
Stochastic modeling of turbulent reacting flows
02 p0647 N94-14768
Development of experimental demonstration processes for laminar-turbulent flow states at wing profiles in free flight
[ILR-MITT-280(1993)] 02 p0510 N94-14800
Toward a quasi-linear closure for compressible turbulence
[DE93-017185] 02 p0647 N94-14895
Large-Eddy Simulations (LES) of flows and turbulence distribution
[AD-A267182] 03 p1016 N94-15151
Turbulence modelling for shock wave/boundary layer interactions specific issues and examples of applications
03 p1018 N94-15202
Large eddy simulation and direct numerical simulation of high speed turbulent reacting flows
[NASA-CR-193131] 03 p1018 N94-15427
Inviscid instability of streamwise corner flow
[NASA-CR-191514] 03 p1021 N94-15834
Turbulence and transition modeling for high-speed flows
[AD-A266748] 03 p1022 N94-15953
Implementation of an anisotropic turbulence model in the COMMIX-1C/ATM computer code
[DE93-015541] 03 p1023 N94-16444
Search for chaos in free shear flows
[AD-A266245] 03 p1023 N94-16470
Selected computations of transonic cavity flows
03 p0858 N94-16511
Computation of confined coflow jets with three turbulence models
[NASA-TM-106378] 03 p1025 N94-16879
Three-dimensional turbulent boundary layer
[AD-A266261] 03 p1025 N94-16908
Studies in turbulence and turbulence control
[AD-A266318] 03 p1026 N94-16950
Adaptive Navier-Stokes calculations for vortical flow
[AD-A266236] 03 p1026 N94-16966
Natural convection above a horizontal heat source
[AD-A267212] 03 p1026 N94-16985
Structure of high Reynolds number turbulent boundary layer
[AD-A267476] 03 p0860 N94-17099
Active turbulence control in wall bounded flows using direct numerical simulation
[AD-A267261] 03 p1028 N94-17286
Lifted turbulent jet flames
[AD-A267911] 03 p0952 N94-17381
Time dependent turbulence modeling and analytical theories of turbulence
[NASA-TM-106379] 03 p1029 N94-17385
Thin-layer and full Navier-Stokes calculations for turbulent supersonic flow over a cone at an angle of attack
[NASA-CR-189103] 03 p0861 N94-17558
Laser velocimetry measurements of vortex flows on a delta wing at Mach 1.9
[AD-A268596] 03 p0861 N94-17609
Defining the normal turbine inflow within a wind park environment
[DE93-010032] 04 p1489 N94-18046
On memory effects in turbulence
[DLR-FB-93-03] 04 p1409 N94-18124
Research activity on particle spin systems and related problems
[AD-A269456] 04 p1562 N94-18286
Applications of the program UIFLOW-2D to the numerical simulation of axisymmetric flows
[AD-A268731] 04 p1410 N94-18326
Navier-Stokes computations of turbulent flow around high-lift configurations 04 p1306 N94-18420
Dispersion effects on millimeter wavelength attenuation efficiencies for a variety of fibers
[AD-A268992] 04 p1386 N94-18454
Chemical reactions in turbulent mixing flows
[AD-A269377] 04 p1410 N94-18472
Workshop on Computational Turbulence Modeling
[NASA-TM-109266] 04 p1410 N94-18545
Research activities at the Center for Modeling of Turbulence and Transition 04 p1410 N94-18546
Research on two equation models
04 p1411 N94-18547
Assessment and development of second order turbulence models 04 p1411 N94-18548
A coupled implicit solution method for turbulent spray combustion in propulsion systems
04 p1411 N94-18549
Numerical investigation of complex, transitional, and chemically reacting flows 04 p1411 N94-18550
Analysis of supersonic flows using k-epsilon model and the RPLUS code: Progress towards high speed combustor analysis 04 p1411 N94-18551
A comparative study of turbulence models in predicting hypersonic inlet flows 04 p1314 N94-18553
An algebraic turbulence model for turbomachinery
04 p1411 N94-18554
Introduction to the Modeling of Turbulence
[VKI-LS-1993-02] 04 p1414 N94-18578
An introduction to the modelling of turbulence
04 p1414 N94-18579
An introduction to single-point closure methodology
04 p1414 N94-18583
Inclusion of second-moment closures into finite-volume solvers 04 p1415 N94-18588
Application of second-moment closure in complex flows 04 p1415 N94-18590
Modelling engineering flows with Reynolds stress turbulence closure 04 p1415 N94-18591
Turbulence modelling challenges posed by complex flows 04 p1415 N94-18592
Examples of turbulence model applications
04 p1415 N94-18593
Large-eddy simulation of turbulent diffusion in stably stratified shear flow 04 p1416 N94-18595
Numerical simulation of turbulent convective flow over wavy terrain 04 p1416 N94-18596
STREMR: Numerical model for depth-averaged incompressible flow
[AD-A269949] 04 p1417 N94-18672
Computational Fluid Dynamics (CFD) research branch technical briefs
[AD-A269698] 04 p1417 N94-18739

Experimental investigation of turbulent Prandtl number and Reynolds analogy in transitional and post-transitional boundary layers
[AD-A270092] 04 p1418 N94-18867

Relation between the fluctuating wall pressure and the turbulent structure of a boundary layer on a cylinder in axial flow
[AD-A270242] 04 p1418 N94-18906

Numerical simulations of turbulent buoyant flows by finite element method: Application to the study of strongly heated or cooled stratified flow
[ECL-92-28] 04 p1421 N94-19399

Numerical prediction of transition of the F-16 wing at supersonic speeds
[NASA-CR-194407] 04 p1312 N94-19433

Two-dimensional turbulent nonstationary superfluid counterflows: Numerical simulations, qualitative effects
[MPIS-23/1992] 04 p1422 N94-19510

Visualization of turbulent flow with particles
[PB94-149671] 04 p1423 N94-19645

A review of hot-wire technique in compressible flows
[LR-724] 04 p1423 N94-19668

Forward scattering of a pulsed continuous wave signal through laminar and turbulent thermal plumes
[AD-A271210] 04 p1564 N94-19723

Collaborative research on combustion diagnostics and modeling between Rolls-Royce, Inc. and the United States Air Force Wright Laboratory
[AD-A270660] 04 p1354 N94-19778

Particle dispersion in turbulent sprays
[AD-A271314] 05 p1796 N94-19913

Wavefront sensors for optical diagnostics in fluid mechanics: Application to heated flow, turbulence, and droplet evaporation
[DE93-040060] 05 p1797 N94-19974

The effect of transverse curvature on the fluctuating wall pressure and structure of boundary layer turbulence
[AD-A271868] 05 p1800 N94-20466

Some practical turbulence modeling options for Reynolds-averaged full Navier-Stokes calculations of three-dimensional flows
[NASA-TM-106399] 05 p1637 N94-20534

Two-point laser Doppler velocimetry measurements of length-turbulent scales
[ECL-92-12] 05 p1801 N94-20542

Four-dimensional remote sensing of the marine boundary layer with a digital beamforming radar wind profiler
[AD-A270627] 05 p1882 N94-20564

Finite element numerical simulation of three dimensional turbulent flows with dispersion: Eulerian and Lagrangian approaches
[ECL-92-42] 05 p1801 N94-20597

Low Reynolds-number turbulent boundary layers
[AD-A272011] 05 p1803 N94-21459

Shear flow generation by Reynolds stress and suppression of resistive g-modes
[DE93-040911] 05 p1995 N94-21514

Consequences of plasma-maser in plasma astrophysics 05 p2006 N94-22669

A multigrid multiblock solver for compressible turbulent flow
[MEMO-1125] 06 p2315 N94-22713

Experimental Methods in Separated Flows
[ILR-MITT-260(1991)] 06 p2315 N94-22852

Turbulence sensors for separated flows: Current capabilities, future requirements 06 p2315 N94-22853

Measurement of kinematically unstationary separated flows 06 p2315 N94-22854

Pressure oscillation measurements in turbulent flows 06 p2316 N94-22855

SFOLDA: A semiconductor LDA for measurements in complex flows 06 p2316 N94-22856

The use of near-wall hot-wire probes for time-resolved skin-friction measurements 06 p2316 N94-22857

Turbulent separated flows above an obstacle in an open channel 06 p2316 N94-22859

A photogrammetric solution to a particular problem
[NASA-TP-3415] 06 p2381 N94-22961

Efficiency and reliability enhancements in propulsion flowfield modeling 06 p2215 N94-23055

Computation of flows in a turn-around duct and a turbine cascade using advanced turbulence models 06 p2216 N94-23062

Shock-induced turbulent flow in baffle systems
[DE94-001532] 06 p2319 N94-23470

The use of transition region characteristics to improve the numerical simulation of heat transfer in bypass transitional flows
[NASA-TM-106445] 06 p2320 N94-23525

The 3-D CFD modeling of gas turbine combustor-integral bleed flow interaction 06 p2189 N94-23658

A comparative study of computational solutions to flow over a backward-facing step 06 p2326 N94-23670

Compressible turbulent flow simulation with a multigrid multiblock method 06 p2342 N94-23694

Reliability in second moment turbulence closures revisited
[NASA-TM-106469] 06 p2326 N94-24063

Thermohydrodynamic analysis of cryogenic liquid turbulent flow fluid film bearings
[NASA-CR-194869] 06 p2363 N94-24081

Annual research briefs, 1993 --- Center for Turbulence Research
[NASA-CR-194755] 06 p2327 N94-24138

Optimal feedback control of turbulent channel flow 06 p2327 N94-24139

Drag reduction at a plane wall 06 p2327 N94-24140

Toward modeling wingtip vortices 06 p2171 N94-24142

Computation of turbulent flows over backward and forward-facing steps using a near-wall Reynolds stress model 06 p2172 N94-24145

On the large eddy simulation of turbulent flows in complex geometry 06 p2329 N94-24148

Toward large eddy simulation of turbulent flow over an airfoil 06 p2172 N94-24150

Unstructured grid large eddy simulation of wall bounded turbulent flows 06 p2329 N94-24151

Investigation of the asymptotic state of rotating turbulence using large-eddy simulation 06 p2330 N94-24152

Energy transfer and constrained simulations in isotropic turbulence 06 p2330 N94-24153

A large eddy simulation scheme for turbulent reacting flows 06 p2330 N94-24154

The combustion program at CTR 06 p2237 N94-24155

Stretch-induced quenching in flame-vortex interactions 06 p2237 N94-24156

A transport equation for the scalar dissipation in reacting flows with variable density: First results 06 p2331 N94-24157

The production of premixed flame surface area in turbulent shear flow 06 p2237 N94-24158

On streak spacing in wall-bounded turbulent flows 06 p2331 N94-24159

Direct simulation of isothermal-wall supersonic channel flow 06 p2172 N94-24164

Effects of shock strength on shock turbulence interaction 06 p2332 N94-24165

Local isotropy in distorted turbulent boundary layers at high Reynolds number 06 p2332 N94-24166

Computation of large-scale statistics in decaying isotropic turbulence 06 p2332 N94-24167

Joint Acoustic Propagation Experiment (JAPE-91) Workshop
[NASA-CP-3231] 06 p2526 N94-24207

Center for modeling of turbulence and transition: Research briefs, 1993
[NASA-TM-106383] 06 p2333 N94-24336

Workshop on Computational Turbulence Modeling
[NASA-CP-10130] 06 p2333 N94-24460

Responses of a finite baffled plate subject to turbulent and mean flow excitations
[NASA-CR-191570] 06 p2334 N94-24605

Implementation of the Baldwin-Barth turbulence model into the ZETA code and its diagnosis
[NASA-CR-194795] 06 p2335 N94-24640

Carrying the mass flux terms exactly in the first and second moment equations of compressible turbulence
[AD-A276346] 06 p2335 N94-24712

Interactive control in turbulent shear layers
[AD-A273544] 06 p2336 N94-24793

Numerical solutions of the complete Navier-Stokes equations
[NASA-CR-194780] 06 p2337 N94-24858

Development and validation of RNG methodology for compressible turbulence
[AD-A273469] 06 p2337 N94-24929

The influence of flow type, particle type and gravity on orthokinetic coagulation
[ETN-94-95333] 06 p2267 N94-25060

LES, DNS and RANS for the analysis of high-speed turbulent reacting flows
[NASA-CR-195196] 06 p2337 N94-25094

The effects of profiles on supersonic jet noise
[NASA-CR-195184] 06 p2530 N94-25177

Measurements of the influence of integral length scale on stagnation region heat transfer
[NASA-TM-106503] 06 p2338 N94-25183

Measurement of the volume mass by spontaneous Raman scattering. Study of turbulent fluctuations of mixing in a subsonic free jet. Measurements in supersonic wind tunnels
[ISL-R-102/92] 06 p2339 N94-25462

Direct measurement of turbulent dissipation rate using dual laser doppler velocimeters
[AD-A273740] 06 p2340 N94-25530

Numerical simulation of tomographic reconstruction for the study of turbulence using optical wavefront sensor measurements
[AD-A273851] 07 p2789 N94-25587

The high Reynolds number flow through an axial-flow pump
[AD-A273844] 07 p2789 N94-25604

The identification of inflow fluid dynamics parameters that can be used to scale fatigue loading spectra of wind turbine structural components
[DE94-000231] 07 p2791 N94-26117

Predictive modeling of particle-laden, turbulent flows
[DE94-003298] 07 p2792 N94-26319

Potential capabilities of Reynolds stress turbulence model in the COMMIX-RSM code
[DE94-003716] 07 p2792 N94-26331

On prediction of equilibrium states in homogeneous compressible turbulence
[NASA-CR-4570] 07 p2792 N94-26467

The nonlinear Galerkin method: A multi-scale method applied to the simulation of homogeneous turbulent flows
[AD-A277432] 07 p2792 N94-26499

High resolution measurements of mixing and reaction processes in turbulent flows
[AD-A274970] 07 p2793 N94-26534

Validated heat-transfer and pressure-drop prediction methods based on the discrete-element method. Phase 2: Two-dimensional rib roughness
[DE94-002379] 07 p2794 N94-26763

Numerical studies on the dynamics of bubble, turbulent, free shear flows: Effect of the inter-phase coupling on the global flow evolution
[AD-A274521] 07 p2794 N94-26832

Experimental verification of tomographic reconstruction of turbulent air flow structure using optical wavefront measurements
[AD-A274392] 07 p2795 N94-27129

A rapid-pressure correlation representation consistent with the Taylor-Proudman theorem materially-frame-indifferent in the 2D limit
[AD-A277582] 07 p2796 N94-27435

The numerical calculation of laminar and turbulent flows using penalty function finite volume methods
[ISBN-0-315-61377-7] 07 p2799 N94-27947

Predictions of momentum and scalar fields in a jet in cross-flow using first and second order turbulence closures 07 p2803 N94-28025

Recent developments in the simulation of steady and transient transverse jet interactions for missile, rotorcraft, and propulsive applications 07 p2804 N94-28030

Numerical assessment of aerodynamic interactions on missiles with transverse jets control 07 p2659 N94-28031

Analysis of cooling jets near the leading edge of turbine blades 07 p2676 N94-28037

Navier-Stokes analysis of a swirling jet in crossflow 07 p2806 N94-28038

Experimental study on the interactions between a transverse heated supersonic jet and an external supersonic flow 07 p2659 N94-28039

Calculation methods for steadily loaded axial groove hydrodynamic journal bearings (guide to use of computer program A9305)
[ESDU-93005] 07 p2830 N94-28074

Calculation methods for steadily loaded axial groove hydrodynamic journal bearings. Low viscosity process fluid lubrication (guide to use of computer program A9306)
[ESDU-93006] 07 p2830 N94-28075

Forced convection heat transfer in straight tubes. Part 2: Laminar and transitional flow
[ESDU-93018-PT-2] 07 p2807 N94-28139

Journal of NIRE, volume 2, number 4
[JTN-94-80554] 07 p2869 N94-28147

Numerical simulation of turbulent free jet by TFKE model 07 p2871 N94-28157

Attached and separated trailing edge flow measurements with a triple-split hot-film probe 07 p2656 N94-28339

A study of blunt trailing edge airfoils using the Navier Stokes code: ARC2D 07 p2656 N94-28340

Multigrid solutions of the 2D Euler/Navier-Stokes equations on unstructured meshes 07 p2658 N94-28349

New parameters for characterizing turbulence at a potential wind site
[DE94-004355] 08 p3368 N94-28455

Modeling turbulence in flows with a strong rotational component
[DE94-003577] 08 p3270 N94-28475

Development of laser velocimetry for the measurements of turbulence intensity and flow velocity ahead of a NGV row in a full-stage rotating turbine
[AD-A275712] 08 p3270 N94-28692

Papers in meteorology and geophysics, vol. 44, no.1
[JTN-94-80585] 08 p3324 N94-28693

Structure of neutrally stratified turbulent Ekman layer as predicted by closure models with prognostic equation for master length scale 08 p3325 N94-28696
Wall pressure events from the direct numerical simulation of a turbulent wall-bounded flow [AD-A275890] 08 p3271 N94-28778
Study of modeling of turbulence of renormalization group analysis 08 p3126 N94-28970
Similarity between turbulent flows through curved pipe and orthogonal rotating pipe 08 p3128 N94-28986
Hydrodynamics of convection under winter polar leads [AD-A275182] 08 p3369 N94-29067
Numerical modelling of turbine combustion chambers 08 p3154 N94-29254
Numerical simulation of aerothermal characteristics in gas turbine combustors with complex geometries 08 p3154 N94-29255
A new Eulerian model for turbulent evaporating sprays in recirculating flows 08 p3195 N94-29279
Time-resolved measurements in a three dimensional model combustor 08 p3196 N94-29283
An alternative assessment of second-order closure models in turbulent shear flows [AD-A279072] 08 p3272 N94-29381
Finite element method for numerical simulation of turbulent flows. The N3S code 08 p3233 N94-29612
Spherical model for turbulence 08 p3274 N94-29730
A vorticity transport closure method for turbulent reacting flows 08 p3274 N94-29761
Direct and large-eddy simulations of turbulent flow in a square duct 08 p3275 N94-29809
A numerical method for confined unsteady flows related to fluid-structure interactions [ISBN-0-315-74739-0] 08 p3277 N94-29902
Wall pressure fluctuations in the reattachment region of a supersonic free shear layer [NASA-CR-195790] 08 p3132 N94-29920
Electromagnetic effect on turbulent transport in liquid metals and electrolytes (bath) [PB94-138450] 08 p3206 N94-29946
Prediction of fluid flow and heat transfer in internally finned tubes 08 p3280 N94-30228
The effect of a wavy boundary on turbulent flow 08 p3280 N94-30272
Potential capabilities of Reynolds stress turbulence model in the COMMIX-RSM code 08 p3285 N94-30450
The enhancement of compressible turbulent mixing via streamwise vorticity 08 p3280 N94-30487
A new orthogonal decomposition method for turbulent flows 08 p3281 N94-30494
Three dimensional compressible turbulent flow computations for a diffusing S-duct with/without vortex generators 08 p3281 N94-30519
Development and application of particle image velocimetry in high-speed separated flow: Two-dimensional base cavities 08 p3282 N94-30791
The effect of pressure gradient on the structure of an equilibrium turbulent boundary layer 08 p3282 N94-30807
Hopf bifurcation in viscous, low-speed flows about an airfoil with structural coupling 08 p3134 N94-30865
Turbulence models and their application in implosion analyses with two-phase flow [GKSS-92/E/98] 08 p3284 N94-30967
Convective solar nebula 09 p3930 N94-31130
The small-scale topology of a 2:1 aspect-ratio elliptic jet 09 p3699 N94-31184
Response of wall turbulence to high frequency streamwise and spanwise oscillations 09 p3700 N94-31211
Research in marine boundary layer intermittency [AD-A276076] 09 p3701 N94-31460
Mixture model simulating reactive turbulent flows: Testing of Eulerian-Lagrangian probabilistic models [ONERA-NT-1993-13] 09 p3702 N94-31477
Finite volume discretization of the k-epsilon turbulence model in general coordinates [REPT-93-90] 09 p3703 N94-31703
Finite element numerical simulation of turbulent flows [ISBN-0-315-86416-8] 09 p3703 N94-31717
Numerical modelling of turbulence [ISBN-0-315-86439-7] 09 p3703 N94-31720
Computational study of simultaneous heat and mass transfer in turbulent separated flows 09 p3704 N94-31843
Multigrid diagonal implicit solutions for compressible turbulent flows and their evaluation 09 p3705 N94-31941
NATO Advanced Study Institute on Unsteady Combustion. Volume 2: Research papers, September 6-17, 1993 [AD-A276572] 09 p3634 N94-32033
Hotwire measurements of the turbulent flow into a cascade of controlled-diffusion compressor blades [AD-A277297] 09 p3706 N94-32042
A non-local model for prediction of the probability density function of turbulent fluctuations in boundary-layer flows 09 p3706 N94-32076
Effects of buoyancy on fluid flows and turbulence [AD-A276586] 09 p3706 N94-32123
Wavevector-frequency analysis with applications to acoustics [AD-A276618] 09 p3861 N94-32125
Aerodynamic drag of droplets in turbulent flow fields [ISBN-0-315-75827-9] 09 p3571 N94-32491
A critical evaluation of the Reynolds stress turbulence closure for the flow of a turbulent free-stream over a turbulent boundary layer [ISBN-0-315-75792-2] 09 p3707 N94-32497
Additive turbulent decomposition of the incompressible and compressible Navier-Stokes equations [AD-A277321] 09 p3708 N94-32511
Notes on the Langevin model for turbulent diffusion of marked particles [DE94-007847] 09 p3708 N94-32652
Numerical analysis of transonic wing buffet 09 p3586 N94-32713
An analysis of supersonic flows with low-Reynolds number compressible two-equation turbulence models using LU finite volume implicit numerical techniques [NASA-CR-195302] 09 p3572 N94-32926
Control of low-speed turbulent separated flow over a backward-facing ramp [NASA-TM-109740] 09 p3573 N94-33071
Scalar imaging velocimetry studies of turbulent flow structure and dynamics [AD-A278395] 09 p3710 N94-33164
Turbulent reacting flows and supersonic combustion [AD-A277462] 09 p3639 N94-33242
Control and management of unsteady and turbulent flows [AD-A278474] 10 p4043 N94-33396
Turbulence structure associated with intercomponent and interscale energy transfer and modification by forcing [AD-A278269] 10 p4043 N94-33414
Interaction of oblique instability waves with weak streamwise vortices [NASA-TM-106584] 10 p4043 N94-33432
A predictor-corrector scheme for vortex identification [AD-A279751] 10 p4043 N94-33433
Experimental studies of hypersonic transitional and turbulent boundary layers in hypersonic flow [AD-A278441] 10 p4044 N94-33556
Physical description of boundary-layer transition: Experimental evidence 10 p4045 N94-33885
Modeling the transition region 10 p4046 N94-33890
Visualization of secondary flow development in high aspect ratio channels with curvature [NASA-TM-106658] 10 p4046 N94-33941
Turbulence compressibility corrections [NASA-TM-108827] 10 p4047 N94-33999
Experimental studies of shock-wave/wall-jet interaction in hypersonic flow [NASA-CR-195844] 10 p4048 N94-34171
Calculation and measurement of the influence of flow parameters on rotordynamic coefficients in labyrinth seals 10 p4063 N94-34187
Dynamic force response of spherical hydrostatic journal bearing for cryogenic applications 10 p4065 N94-34198
Computational study of generic hypersonic vehicle flow fields [NASA-CR-195938] 10 p3984 N94-34277
Numerical simulation of airfoil film cooling: A jet in crossflow 10 p4004 N94-34462
Direct simulation of a self-similar plane wake [NASA-TM-108815] 10 p4050 N94-34917
Inducer analysis/pump model development [NASA-CR-196005] 10 p4066 N94-34963
Experimental studies of shock-wave/wall-jet interaction in hypersonic flow, part A [NASA-CR-195957] 10 p3985 N94-34964
Experimental studies of transpiration cooling with shock interaction in hypersonic flow, part B [NASA-CR-195958] 10 p3985 N94-34965
Turbulence modelling for unsteady separated flows 10 p4053 N94-34984
Active thermal isolation for temperature responsive sensors [NASA-CASE-LAR-14612-1] 10 p4054 N94-35074
Comparison of PDF and moment closure methods in the modeling of turbulent reacting flows [NASA-TM-106614] 11 p4265 N94-35948
Vortex tubes in turbulent flows: Identification, representation, reconstruction [AD-A280504] 11 p4267 N94-35992
A three dimensional multigrid Reynolds-averaged Navier-Stokes solver for unstructured meshes [AD-A280998] 11 p4191 N94-35994
Analysis of a High Velocity Oxygen-Fuel (HVOF) thermal spray torch. Part 1: Numerical formulation [DE94-005590] 11 p4267 N94-35996
Preliminary analysis for a Mach 8 crossflow transition experiment on the Pegasus (R) space booster [NASA-TM-104272] 12 p4381 N94-36648
The alternative faces of turbulent flow [TM-5-94] 12 p4442 N94-36934
Simulation of three-dimensional multi-phase flow characteristics in the deswirl section of the CDIF MHD power train [DE94-012644] 12 p4443 N94-37176
The stabilizing effect of compressibility in turbulent shear flow [NASA-CR-194932] 12 p4444 N94-37605

TURBULENT HEAT TRANSFER

Two-dimensional Navier-Stokes heat transfer analysis for rough turbine blades [NASA-TM-106008] 02 p0629 N94-13027
High freestream turbulence effects on the transport of heat and momentum 02 p0633 N94-13559
Investigation of two-phase flow and boiling heat transfer during quenching of a tube under microgravity 03 p0979 N94-16087
Turbulence models and Reynolds analogy for two-dimensional supersonic compression ramp flow [NASA-TM-106474] 06 p2337 N94-25119
A flow visualization study of acoustically enhanced hairpin vortices [AD-A275467] 08 p3271 N94-28809
Potential capabilities of Reynolds stress turbulence model in the COMMIX-RSM code 08 p3285 N94-30450
Mixture model simulating reactive turbulent flows: Testing of Eulerian-Lagrangian probabilistic models [ONERA-NT-1993-13] 09 p3702 N94-31477

TURBULENT JETS

Turbulent wall jet in blast wave precursor [DE93-011955] 01 p0151 N94-11144
The turbulent wall jet [AD-A267675] 03 p0855 N94-14963
Lifted turbulent jet flames [AD-A267911] 03 p0952 N94-17381
Combustion instability phenomena of importance to liquid propellant engines [AD-A268800] 04 p1348 N94-18389
Particle dispersion in turbulent sprays [AD-A271314] 05 p1796 N94-19913
Combustion in turbulent jets and buoyant flames [PB93-202372] 05 p1682 N94-21452
Flow interaction experiment. Volume 1: Aerothermal modeling, phase 2 [NASA-CR-189192-VOL-1] 05 p1648 N94-21582
Flow interaction experiment. Volume 2: Aerothermal modeling, phase 2 [NASA-CR-189192-VOL-2] 05 p1648 N94-21583
Spray formation processes of impinging jet injectors 06 p2212 N94-23042
Transient Ejector Analysis (TEA) code user's guide [NASA-TM-106310] 06 p2186 N94-23466
Theoretical and experimental investigation of a delta wing with turbulent leading-edge jets 07 p2659 N94-28029
Experimental study on the interactions between a transverse heated supersonic jet and an external supersonic flow 07 p2659 N94-28039
Lifted turbulent jet flames 08 p3198 N94-29676
The instantaneous concentration field in the self-similar region of a high Schmidt number round jet 08 p3278 N94-29976
Evolution of turbulent fields in explosions [DE94-010405] 12 p4444 N94-37390

TURBULENT MIXING

A normal stress subgrid-scale eddy viscosity model in large eddy simulation 01 p0155 N94-12288
LIF measurements of scalar mixing in turbulent shear layers 01 p0159 N94-12312
PDF approach for turbulent scalar field: Some recent developments 01 p0160 N94-12315
Radar imaging of sub-mesoscale ocean phenomena [AD-A266339] 02 p0725 N94-13581
Modeling and simulation of transport and combustion phenomena in a supersonic mixing layer [ONERA-NT-1992-11] 02 p0565 N94-14194
Turbulent diffusion in homogeneous shear flow with stable density stratification [DLR-FB-92-26] 02 p0639 N94-14443
Analysis of reacting flowfields in low-thrust rocket engines and plumes 02 p0552 N94-14491
Stochastic modeling of turbulent reacting flows 02 p0647 N94-14768

Surface and internal signatures of organized vortex motions in stratified fluid
[AD-A267015] 03 p1020 N94-15526
Three dimensional hydrodynamic calculations with adaptive mesh refinement of the evolution of Rayleigh Taylor and Richtmyer Meshkov instabilities in converging geometry: Multi-mode perturbations
[DE93-017155] 03 p1025 N94-16903
Transmission of light through a turbulent mixing layer
[AD-A267266] 03 p1193 N94-17264
Chemical reactions in turbulent mixing flows
[AD-A268287] 03 p0861 N94-17580
Chemical reactions in turbulent mixing flows
[AD-A269377] 04 p1410 N94-18472
Numerical investigation of complex, transitional, and chemically reacting flows 04 p1411 N94-18550
Numerical simulation of turbulent mixing and combustion near the inlet of a burner
[DE93-017960] 04 p1350 N94-18987
Turbulence modeling for high speed compressible flows
[NASA-CR-194547] 05 p1799 N94-20210
Simulations of diffusion-reaction equations with implications to turbulent combustion modeling
[NASA-CR-191536] 05 p1804 N94-21861
Shock-induced turbulent flow in baffle systems
[DE94-001532] 06 p2319 N94-23470
A random distribution reacting mixing layer model
[NASA-CR-194445] 06 p2187 N94-23552
Eddy mixing coefficient values derived from simulations with the NASA Ames Mars GCM
06 p2617 N94-24875
Topics in longshore currents
[AD-A274788] 07 p2899 N94-26361
High resolution measurements of mixing and reaction processes in turbulent flows
[AD-A274970] 07 p2793 N94-26534
Higher-order accurate numerical simulation of 3D supersonic mixing layers 08 p3124 N94-28954
Study on mixing and injection of hydrogen into a supersonic flow 08 p3127 N94-28975
Modeling of the phase liquidates in combustion chambers 08 p3195 N94-29278
A new Eulerian model for turbulent evaporating sprays in recirculating flows 08 p3195 N94-29279
Computational fluid dynamics in ventilation. 5: New developments in CFD with relevance to ventilation
08 p3233 N94-29610
Evolution of the large-scale vortices in turbulent mixing-layers 08 p3273 N94-29686
Effects of diffusion and inertia on chaotic mixing: A computational and experimental study
08 p3488 N94-29903
The enhancement of compressible turbulent mixing via streamwise vorticity 08 p3280 N94-30487
Design of an electromagnetic accelerator for turbulent hydrodynamic mix studies
[DE94-005821] 08 p3281 N94-30600
A priori tests of large eddy simulation of the compressible plane mixing layer
[MEMO-1152] 09 p3699 N94-31185
Laser-induced fluorescence/particle tracking system for stratified flow research
[AD-A275917] 09 p3701 N94-31341
Observations of turbulence, internal waves and background flows: An inquiry into the relationships between scales of motion 09 p3705 N94-31988
Use of Navier-Stokes methods for the calculation of high-speed nozzle flow fields
[NASA-TM-106551] 09 p3573 N94-32984
Turbulent reacting flows and supersonic combustion
[AD-A277462] 09 p3639 N94-33242
Cruise report: Oceanus 250 leg 4 high resolution profiler survey for the North Atlantic Tracer Release Experiment, 25 March - 24 April, 1992
[AD-A277935] 09 p3791 N94-33245
Theoretical aspects of supersonic jet noise
10 p3972 N94-33469
Forced unsteady deceleration of a turbulent boundary layer from a temporal perspective
10 p4053 N94-34983
Evolution of turbulent fields in explosions
[DE94-010405] 12 p4444 N94-37390

TURBULENT WAKES
NT PROPELLER SLIPSTREAMS
NT SLIPSTREAMS
The three-dimensional evolution of a plane wake
01 p0159 N94-12310
On the wake behind a high speed train
01 p0164 N94-12618
The 1970 highlights --- NASA programs and research
[NASA-TM-109628] 03 p1302 N94-15415
Applications of the program UIFLOW-2D to the numerical simulation of axisymmetric flows
[AD-A268731] 04 p1410 N94-18326
Theoretical examination of the flow around a cylinder with a low dimensional Galerkin process
[MPIS-25/1992] 04 p1422 N94-19525
Prediction and control of vortex-dominated and vortex-wake flows
[NASA-CR-194722] 05 p1637 N94-21054
LDA measurements of the unsteady near wake behind an airfoil undergoing transient and periodic pitching motions
[ISL-CO-215/92] 06 p2165 N94-23161
Decay of swirl in turbulent pipe flows
[ETN-94-95353] 06 p2339 N94-25248
High lift aerodynamics
[NASA-CR-195183] 06 p2184 N94-25268
A comprehensive comparison of turbulence models in the far wake 07 p2808 N94-27899
Direct simulation of a self-similar plane wake
[NASA-TM-108815] 10 p4050 N94-34917

TURING MACHINES
Finite state machine microarchitecture transformations described with relational algebra
[MEMO-INF-92-63] 01 p0319 N94-10278
FSM test: A functional test generation system for sequential circuits
[REPT-93-017] 03 p1014 N94-17505
Reducing extended transition systems
[MEMO-INF-93-09] 04 p1526 N94-19196
Threshold computation and cryptographic security
[TR-443] 05 p1907 N94-20536
COCOLOG: A conditional observer and controller logic for finite machines
[INRIA-RR-1714] 05 p1910 N94-21063
Design methods for fault-tolerant finite state machines
05 p1758 N94-21120
Advice from nonadaptive queries to NP
[TR-470] 05 p1911 N94-21200
Space-efficient deterministic simulation of probabilistic automata
[TR-463] 05 p1900 N94-21281
Threshold computation and cryptographic security
[TR-461] 05 p1912 N94-21285
Promises and fault-tolerant database access
[TR-447] 05 p2043 N94-21287
Beta(sub k)-complete problems and greediness
[TR-455] 05 p1913 N94-21318
On the closure properties of #P in the context of PF of #P
[TR-445] 05 p1955 N94-21456
Verification of synchronous sequential numerical material systems: Application of the LUSTRE language and of the LESAR verification tool
[ETN-94-95181] 06 p2447 N94-22899
A note on the complexity of local search problems
[CT-93-02] 08 p3456 N94-30370
A finite state machine model for object oriented systems
[REPT-93-040] 09 p3809 N94-31212
Models for asynchronous circuit behaviour with OR causality
[PB94-148897] 10 p4112 N94-34126

TURNING FLIGHT
VMC left turn curved approaches, test results --- (visual meteorological conditions)
[AD-A269476] 04 p1316 N94-18728

TURRET
High accuracy control algorithm application to a tracking turret 12 p4394 N94-36626

TVC (CONTROL)
U THRUST VECTOR CONTROL

TVD SCHEMES
Large time-step stability of explicit one-dimensional advection schemes
[NASA-TM-106203] 01 p0342 N94-10362
Numerical calculation of scramjet inlet flow
[NAL-TR-1174T] 01 p0027 N94-10370
Aerodynamic characteristics analysis of Garabedian-Korn 75-06-12 airfoil
[PAPER-2D-2] 01 p0010 N94-10468
Aerodynamic characteristics analysis of Garabedian-Korn 75-06-12 aircraft
[PAPER-2D-7] 01 p0011 N94-10472
Flow analysis around ONERA model M5 configuration
[PAPER-3D-2] 01 p0012 N94-10478
Flow analysis around ONERA model M5 configuration
[PAPER-3D-4] 01 p0012 N94-10480
Viscous flow simulation using an upwind method for hexahedral based adaptive meshes
[AD-A265901] 01 p0148 N94-10703
Numerical simulation of dynamic stall of NACA0012 airfoil oscillating near static stall angle using the Navier-Stokes equations
[DE93-767970] 02 p0505 N94-14061
Hypersonic viscous flow computations
02 p0510 N94-14612
Computational Fluid Dynamics
[VKI-LS-1993-04] 04 p1412 N94-18557
Multidimensional wave decompositions for the Euler equations 04 p1413 N94-18562
Unified approach for incompressible flows
06 p2342 N94-25356
Arbitrary-order high resolution schemes for model hyperbolic conservation laws
[CRANFIELD-AERO-9209] 07 p3005 N94-25823
TVD flux-difference split methods for high-speed thermochemical nonequilibrium flows with strong shocks
[UTIAS-350] 07 p2799 N94-27880
A design of third-generation airfoils for helicopter rotor blades using Navier-Stokes 08 p3124 N94-28957
Numerical analysis of sonic boom in the near field
08 p3125 N94-28962
Numerical analysis of two dimensional/axisymmetric non-equilibrium hypersonic flow
08 p3125 N94-28963
Role of computational fluid dynamics in aeronautical engineering. Part 10: Numerical analysis of flow around 2-D multi-element HLD 08 p3125 N94-28964
Viscous limiter functions for model convection-diffusion equations
[CRANFIELD-AERO-9103] 09 p3702 N94-31559

TWILIGHT GLOW
Aircraft windscreens enhance visual search disruption produced by laser glare
[AD-A265167] 01 p0026 N94-11892

TWINNING
NT MECHANICAL TWINNING
Deposition of crystalline boron thick layers from gas phase
[DE93-620499] 02 p0576 N94-12867
Atomic structure of the 310 twin in niobium: Theoretical predictions and comparison with experimental observation
[DE93-013421] 02 p0806 N94-13136
Radiation hardening effects on localized deformation and stress corrosion cracking of stainless steels
[DE94-004308] 07 p2731 N94-25804
Cracking of textured zinc coating during forming process
[DE94-003414] 07 p2750 N94-26085
Effect of twin boundary density on the vortex melting transition in YBa2Cu3O(7-delta) single crystals
[DE94-007684] 09 p3904 N94-32601
Substrate effects on the structure and optical properties of epitaxial PbTiO3 thin films prepared by metal-organic chemical vapor deposition
[DE94-010432] 12 p4535 N94-37192

TWO BODY ORBITS
U TWO BODY PROBLEM

TWO BODY PROBLEM
P-matrix description of the two-particle interaction
[DE93-617690] 01 p0361 N94-10549
Studies of P-matrix formalism on the basis of the potential description of two-particle interaction
[DE93-617691] 01 p0362 N94-10550
Exact solutions of a many-anyon problem
[DE93-617646] 01 p0411 N94-10832
Tidal regime of intact planetoid capture model for the Earth-Moon system: Does it relate to the archean sedimentary rock record? 03 p1245 N94-16378
Relativistic two-body system in 1+1-dimensional QED. 1: On the circle S1
[DE94-603716] 07 p3067 N94-27647
Quasipotential in the fourth order of perturbation theory
[DE94-606299] 08 p3484 N94-28584
The solving of the relativistic two-body problem with a nonlinear dependence upon a spectrum parameter
[DE94-606343] 08 p3451 N94-28783
Relativistic three-particle dynamical equations. 2: Theoretical development
[DE94-616654] 11 p4320 N94-35581
Logarithmic corrections of the two-body QED problem
[DE94-611157] 11 p4322 N94-35783
Quantum mechanics and thermodynamics of particles with distance dependent statistics
[DE94-616620] 11 p4343 N94-36072
Notes on possible S-wave resonances in relativistic two-particle systems
[DE94-616889] 11 p4329 N94-36392
Variational method in relativistic two-body problem
[DE94-612462] 11 p4315 N94-36416

TWO DIMENSIONAL BODIES
Two-dimensional boundary surfaces for axi-symmetric external transonic flows
[AD-A269678] 04 p1312 N94-18571
Surfaces allowing for fractional statistics
[DE93-614526] 07 p3002 N94-25910
Research on bluff body vortex wakes
[AD-A273780] 07 p2796 N94-27319

TWO DIMENSIONAL BOUNDARY LAYER
Numerical investigation of laminar-turbulent transition in two- and three-dimensional boundary layers
[DLR-FB-92-36] 05 p1800 N94-20533

Experiments on an unsteady, three-dimensional separation 10 p4052 N94-34981
TWO DIMENSIONAL FLOW
NT COUETTE FLOW
Thermocapillary instabilities in cylindrical liquid bridges: Mechanisms and transition boundaries 01 p0101 N94-10077
Solving the inverse problem for incompressible potential flow through two-dimensional cascades [NAL-TR-1162] 01 p0147 N94-10365
Modelling quasi-two-dimensional turbulent shear flow 01 p0153 N94-11616
Aerodynamic sound due to interaction between a two-dimensional free shear layer and the leading edge of a parallel flat plate 01 p0163 N94-12615
Boundary conditions and bifurcations in plane Poiseuille flow 01 p0166 N94-12634
Transition prediction and control in subsonic flow over a hump [NASA-CR-4543] 02 p0629 N94-13066
Clebsch variable model for unsteady, transonic flow; application to 2D airfoils [NLR-TP-91387-U] 02 p0503 N94-13530
Images constructed from computed flow fields [NASA-CR-194397] 02 p0650 N94-13814
Stability of spatially developing boundary layers 02 p0640 N94-14605
Development of a general purpose multigrid accelerated Navier-Stokes solver 02 p0641 N94-14613
A small-scale turbulence model 02 p0643 N94-14746
Modal element method for potential flow in non-uniform ducts: Combining closed form analysis with CFD [NASA-TM-106347] 03 p1169 N94-15799
Inviscid instability of streamwise corner flow [NASA-CR-191514] 03 p1021 N94-15834
A rapid computational model for estimating the performance of compliant airfoils in cascades [AD-A266275] 03 p0857 N94-16471
Determining the effect of endwall boundary layer suction in a large scale subsonic compressor cascade [AD-A267208] 03 p0859 N94-16913
An upwind multigrid method for solving viscous flows on unstructured triangular meshes [NASA-TM-109343] 03 p1027 N94-17061
Investigation of high-speed free shear flows using improved pressure-strain correlated Reynolds stress turbulence model [NASA-CR-194661] 03 p1027 N94-17127
Development of iterative techniques for the solution of unsteady compressible viscous flows [NASA-CR-194657] 03 p1027 N94-17129
Two-dimensional, high flow, precisely controlled monodisperse drop source [AD-A267660] 03 p1028 N94-17250
Calculation of multielement airfoils and wings at high lift 04 p1309 N94-18438
Numerical solutions for a flow with mixed convection in a vertical geometry [DE93-011592] 04 p1419 N94-19058
Multigrid for a groundwater flow problem [PB94-149655] 04 p1420 N94-19144
Two-dimensional turbulent nonstationary superfluid counterflows: Numerical simulations, qualitative effects [MPIS-23/1992] 04 p1422 N94-19510
Formulation of a next-generation interior ballistic code [AD-A271539] 05 p1801 N94-20915
F2D users manual: A two-dimensional compressible gas flow code [DE94-000653] 05 p1805 N94-22386
A theoretical evaluation of aluminum gel propellant two-phase flow losses on vehicle performance 06 p2210 N94-23031
Two-dimensional Navier-Stokes computations of subsonic and supersonic flows through turbine cascades [PB93-226223] 06 p2317 N94-23114
Upwind MacCormack Euler solver with non-equilibrium chemistry 06 p2326 N94-23672
Numerical simulation of non-Newtonian free shear flows 06 p2331 N94-24160
Transition to turbulence in an elliptic vortex 06 p2331 N94-24161
Turbulence models and Reynolds analogy for two-dimensional supersonic compression ramp flow [NASA-TM-106474] 06 p2337 N94-25119
Two-dimensional CFD modeling of wave rotor flow dynamics [NASA-TM-106261] 06 p2189 N94-25185
Nominally 2-dimensional flow about a normal flat plate [AD-A274472] 07 p2794 N94-27026
Parallel implicit unstructured grid Euler solvers [AD-A277581] 07 p2999 N94-27434
High-lift system analysis method using unstructured meshes [NLR-TP-92351-U] 07 p2647 N94-27554
A study on heat transfer in a scramjet leading edge model [NAL-TR-1187T] 07 p2675 N94-27608
A comprehensive comparison of turbulence models in the far wake 07 p2808 N94-27899
Comparison of the interactions of two and three dimensional transverse jets with a hypersonic free stream 07 p2659 N94-28021
Navier-Stokes simulation of two and three dimensional jets in crossflow, effects of grid, and boundary conditions 07 p2804 N94-28026
Experimental investigations into the wall interference and sidewall boundary layer effects in the National Research Council/Inst. for Aerospace Research High Reynolds Number 2-D Test Facility 07 p2658 N94-28350
Computation of wind-tunnel side-wall interference using 3D Navier-Stokes code 07 p2658 N94-28351
Nominally two-dimensional flow about a normal flat plate 08 p3275 N94-29838
Calculus of variations applied to 2D multi-point airfoil design [PB94-125457] 08 p3133 N94-30401
A solution adaptive structured-unstructured grid procedure for unsteady flows 09 p3700 N94-31217
A fully two-dimensional, non-oscillatory advection scheme for momentum and scalar transport equations [DM-66] 09 p3700 N94-31221
Multigrid diagonal implicit solutions for compressible turbulent flows and their evaluation 09 p3705 N94-31941
On an adaptation method for dense, 2D, C-type grids [W-9321] 09 p3706 N94-32045
Surface boundary conditions and related technical issues concerning Burnett equations for 2-D hypersonic flow [AD-A277322] 09 p3706 N94-32256
Lift enhancement by trapped vortex 10 p3980 N94-33524
Real-time adaptive control of mixing in a plane shear layer [AD-A278379] 10 p4113 N94-33744
Investigation of Burnett equations for two-dimensional hypersonic flow [AD-A278942] 11 p4190 N94-35717
A method for flow simulation about complex geometries using both structured and unstructured grids [NASA-TM-106633] 12 p4383 N94-37283
TWO DIMENSIONAL JETS
Direct numerical simulation of hot jets 01 p0156 N94-12295
TWO DIMENSIONAL MODELS
Numerical simulation of Marangoni convection around gas bubbles in a liquid matrix 01 p0106 N94-10107
Flow transitions in a 2D directional solidification model 01 p0114 N94-10183
Marangoni Benard instabilities in liquid mixtures with Soret effect 01 p0119 N94-10215
Simulations of D3-D divertor biasing with the LEDGE code [DE93-010500] 01 p0385 N94-10262
On a class of two-dimensional nearest neighboring random walks [CWI-BS-R9220] 01 p0347 N94-10353
Axisymmetric single shear element combustion instability experiment [NASA-TM-106327] 01 p0046 N94-10763
Classical gravity coupled to Liouville theory [DE93-613049] 01 p0275 N94-10798
Finite element simulation of the 2D collapse of a polyelectrolyte gel disk [DE93-010693] 01 p0091 N94-11665
Explorations in quantum gravity: From one loop effective actions to two-dimensional theories 01 p0413 N94-11822
Two-dimensional simulations of foil implosion experiments on the Los Alamos capacitor bank [DE93-012676] 02 p0794 N94-12814
Body/cushion contact stress analysis during sitting [ITN-93-85204] 02 p0736 N94-13229
Dilaton quantum cosmology in two dimensions [DE93-621377] 02 p0836 N94-13361
Chemistry and transport in a multi-dimensional model [NASA-CR-194425] 02 p0716 N94-13969
The motion of a conical shaped liner driven by explosive load [ITN-93-85215] 02 p0585 N94-14507
An implicit finite volume nodal point scheme for the solution of two-dimensional compressible Navier-Stokes equations 02 p0640 N94-14603
Time resolved measurement of electron temperatures of exploding foil x ray laser plasmas [DE93-017161] 02 p0803 N94-14894
A posteriori error estimation for hierarchic models of elliptic boundary value problems on thin domains [AD-A267714] 03 p1168 N94-14939
Crack-tip-opening angle measurements and crack tunneling under stable tearing in thin sheet 2024-T3 aluminum alloy [NASA-CR-191523] 03 p0931 N94-15184
Mechanical modeling of the growth of salt structures [DE93-015342] 04 p1596 N94-18243
The GARTEUR high lift research programme 04 p1307 N94-18430
ADCIRC: An advanced three-dimensional circulation model for shelves, coasts, and estuaries. Report 3: Development of a tidal constituent database for the western North Atlantic and Gulf of Mexico [AD-A268685] 04 p1497 N94-18455
STREMR: Numerical model for depth-averaged incompressible flow [AD-A269949] 04 p1417 N94-18672
Subcritical crack growth in continuous-fiber reinforced ceramic composites [DE93-018784] 04 p1343 N94-19335
The influence of the target strength model on computed perforation [DE93-018659] 04 p1460 N94-19543
Two-dimensional particle-in-cell simulation on transputer arrays [DE93-017977] 05 p1972 N94-20181
Investigation of the effects of the macrophysical and microphysical properties of cirrus clouds on the retrieval of optical properties: Results for FIRE 2 05 p1880 N94-22339
Robust unstructured grid generation with VGRID 05 p1919 N94-22359
A two-dimensional kinetic model of the scrape-off layer [DE94-001235] 05 p1999 N94-22562
Verification of frequency scaling laws for capacitive rf discharges using two-dimensional simulations [DE94-001306] 05 p1999 N94-22595
An F2D analysis of the Flow Instability Test (FIT) experiment [DE94-001420] 06 p2217 N94-23193
X ray simulator theory support [AD-A273613] 06 p2553 N94-24949
Modelling of premixed laminar flames [ETN-94-95317] 06 p2236 N94-25284
Modelling of thermal argon plasmas [ETN-94-95363] 06 p2554 N94-25300
Two-dimensional pattern analysis and classification using a complex orthogonal estimation algorithm [RR-475] 06 p2463 N94-25321
Assessing the climatic effect of carbon dioxide and other trace gases using an interactive two-dimensional climate-chemistry model [DE94-001741] 07 p2866 N94-25927
Two dimensional self-consistent fluid simulation of RF inductive sources [DE94-003635] 07 p2767 N94-25937
Crossover between BCS and performed-Boson theories with increasing interactions [DE93-019018] 07 p3017 N94-26078
Ising critical behaviour in the one-dimensional frustrated quantum XY model [DE93-634755] 07 p3057 N94-26390
Interacting cortical filters for object recognition [PB94-125374] 07 p2938 N94-26873
Orientation competition in cortical filters [PB94-125366] 07 p2939 N94-27001
A note on Riemannian 2-space [DE94-602560] 07 p3073 N94-27024
Active electron and ion beam experiments in space [AD-A275570] 08 p3504 N94-28828
Role of computational fluid dynamics in aeronautical engineering. Part 10: Numerical analysis of flow around 2-D multi-element HLD 08 p3125 N94-28964
Computational fluid dynamics in ventilation. 2: Theory and codes 08 p3233 N94-29607
Computational fluid dynamics in ventilation. 3: The IEA annex 20 work 08 p3233 N94-29608
A fully two-dimensional, non-oscillatory advection scheme for momentum and scalar transport equations [DM-66] 09 p3700 N94-31221
Multidimensional WAF-type schemes for model conservation laws [CRANFIELD-AERO-9312] 09 p3843 N94-31541
Qualitative properties of two-dimensional predator-prey systems [REPT-93-75] 09 p3844 N94-31644
A predator-prey model with Ivlev's functional response [REPT-93-79] 09 p3844 N94-31696
Perturbative aspects of lower-dimensional gauge theories [ISBN-0-315-86269-6] 09 p3911 N94-31712
On an adaptation method for 2-dimensional C-type grids [W-9322] 09 p3569 N94-31822

The 2D deterministic radiation transport with the discontinuous finite element method
[DE94-004687] 09 p3849 N94-32670
Model capabilities, 2-D 10 p3971 N94-33459
Local instabilities and the transition to chaos of non-linear waves
[PB94-170578] 11 p4341 N94-36213
Numerical investigation of multi-element airfoils
[NASA-CR-194592] 11 p4191 N94-36394
MARFE's in tokamak edge plasma: Pattern formation under nonlocal constraints
[DE94-012766] 12 p4529 N94-37309
Atmospheric structure simulation: An ARMA model for smooth isotropic two-dimensional geophysical power spectra
[AD-A280476] 12 p4470 N94-37649

TWO FLUID MODELS
On the coupling of electromagnetic radiation into cavities
[DE93-011406] 01 p0137 N94-11621
Boundary layer flow of air over water on a flat plate
[NASA-CR-191517] 03 p1019 N94-15479
A modified two-fluid model of conductivity for superconducting surface resistance calculation
[AD-A267549] 03 p1013 N94-17104
Measurement of thermal-hydraulic parameters in two-phase flow using flow visualization image analysis
[DE93-006255] 05 p1805 N94-22269
Mixing and unmixedness in plasma jets 1: Near-field analysis 06 p2323 N94-23655
Three-dimensional solidification and melting using magnetic field control 06 p2325 N94-23664
Predictive modeling of particle-laden, turbulent flows
[DE94-003298] 07 p2792 N94-26319
An experimental study of plunging liquid jet induced air carryunder and dispersion
[AD-A274414] 07 p2794 N94-26979
Numerical simulation of turbulent free jet by TFKE model 07 p2871 N94-28157
A single-fluid, self-consistent formulation of particle transport and fluid dynamics 08 p3280 N94-30352
Analysis of phase distribution phenomena in microgravity environments
[NASA-CR-196038] 11 p4249 N94-35237

TWO PHASE FLOW
Two-phase flow heat transfer and hydrodynamics in an electric field 01 p0103 N94-10093
Separation of gravitational effects on the flow of suspension in tubes by measurements in weightlessness 01 p0105 N94-10105
Laboratory study on the natural modes of a rotating two-phase fluid system subject to axial excitation 01 p0106 N94-10106
FORCE2: A state-of-the-art two-phase code for hydrodynamic calculations
[DE93-010661] 01 p0150 N94-11072
KIVA-3: A KIVA program with block-structured mesh for complex geometries
[DE93-011986] 01 p0077 N94-11249
The physics of pattern formation of liquid interfaces
[DE93-013333] 01 p0154 N94-11814
The Third Workshop on Two Phase Fluid Experiment in the Space Environment
[NASDA-CON-930002] 01 p0161 N94-12547
Summary of studies on JEM utilization experiment projects 01 p0161 N94-12548
Compilation of proposals for boiling and evaporation experiments in space environments and proposals concerning experiment projects 01 p0161 N94-12549
Condensation phenomena 01 p0162 N94-12550
Developmental research of thermal control system in space environment 01 p0162 N94-12551
Two phase flow and isopycnic liquid-liquid two phase fluid in reduced gravity field 01 p0162 N94-12552
Devices related for thermal control systems used in microgravity 01 p0162 N94-12553
Research on two phase flow in microgravity 01 p0162 N94-12554
Research and development of cold plate for two phase fluid loop thermal control system 01 p0162 N94-12555
Organization and management policy for two phase fluid experiment in space environment 01 p0162 N94-12556
Thermal gravitational modelling and scaling of two-phase heat transport systems: Similarity considerations and useful equations predictions versus experimental results
[NLR-TP-91477-U] 02 p0632 N94-13533
Studies of momentum and energy transfer across wavy gas-liquid interfaces
[AD-A266432] 02 p0635 N94-13699
Stability of oscillatory two phase Couette flow
[NASA-CR-191501] 02 p0636 N94-13817
Turbulent particle dispersion in confined swirling flows
[DLR-FB-92-32] 02 p0637 N94-14045
Review of mathematical and physical basis of two-phase flow modeling
[KFK-4759] 02 p0642 N94-14708
Investigation of two-phase flow and boiling heat transfer during quenching of a tube under microgravity 03 p0979 N94-16087
Cryogenic spray vaporization in high-velocity helium, argon and nitrogen gasflows
[NASA-TM-106363] 03 p1035 N94-17446
Gravity dependent condensation pressure drop and heat transfer in ammonia two-phase heat transport systems
[NLR-TP-92121-U] 03 p1031 N94-17615
Study of multi-phase flow characteristics in an MHD power train
[DE93-018570] 04 p1586 N94-18272
A coupled implicit solution method for turbulent spray combustion in propulsion systems 04 p1411 N94-18549
Formulation of a next-generation interior ballistic code
[AD-A271539] 05 p1801 N94-20915
Measurement of thermal-hydraulic parameters in two-phase flow using flow visualization image analysis
[DE93-006255] 05 p1805 N94-22269
A theoretical evaluation of aluminum gel propellant two-phase flow losses on vehicle performance 06 p2210 N94-23031
Numerical parametric studies of spray combustion instability 06 p2212 N94-23041
Performance assessment of low pressure nuclear thermal propulsion 06 p2217 N94-23070
Studies of two phase flow
[NASA-CR-195099] 06 p2267 N94-23594
An analytic study of a two-phase laminar airfoil in simulated heavy rain 06 p2171 N94-23661
Three-dimensional solidification and melting using magnetic field control 06 p2325 N94-23664
Dispersion of fire suppression agents discharged from high pressure vessels: Establishing initial/boundary conditions for the flow outside the vessel
[PB94-103660] 06 p2172 N94-23810
Validation of a nonintrusive optical technique for the measurement of liquid mass distribution in a two-phase spray 06 p2548 N94-24420
Ignition and combustion characteristics of metallized propellants, phase 2
[NASA-CR-195107] 06 p2266 N94-24700
Interfacial area and interfacial transfer in two-phase flow
[DE93-041226] 07 p2792 N94-26468
Gravity dependence or pressure drop and heat transfer in straight two-phase heat transport system condenser ducts
[NLR-TP-92167-U] 07 p2798 N94-27853
Numerical simulation of aerothermal characteristics in gas turbine combustors with complex geometries 08 p3154 N94-29255
Modeling of the phase liquidates in combustion chambers 08 p3195 N94-29278
A new Eulerian model for turbulent evaporating sprays in recirculating flows 08 p3195 N94-29279
Experimental studies on effervescent atomizers with wide spray angles 08 p3196 N94-29280
Investigation of the two-phase flow in a research combustor under reacting and non-reacting conditions 08 p3196 N94-29282
An experimental investigation of flow patterns and liquid entrainment in a horizontal-tube evaporator 08 p3277 N94-29899
Two-phase power-law modeling of pipe flows displaying shear-thinning phenomena
[DE94-005115] 08 p3279 N94-30020
Numerical simulation of a condenser in two-phase heat transport systems: A feasibility study
[AD-B173650] 08 p3282 N94-30855
Local two-phase flow simulations including interface tracking with mass transfer 08 p3283 N94-30954
Turbulence models and their application in implosion analyses with two-phase flow
[GKSS-92/E/98] 08 p3284 N94-30967
Numerical simulation and prediction of implosion phenomena
[GKSS-92/E/99] 08 p3284 N94-30968
An experimental study on the static and dynamic characteristics of pump annular seals with two phase flow 10 p4062 N94-34179
Time delay measurement correlator and its application 10 p4042 N94-34350
Analysis of phase distribution phenomena in microgravity environments
[NASA-CR-196038] 11 p4249 N94-35237
Analysis of a High Velocity Oxygen-Fuel (HVOF) thermal spray torch. Part 1: Numerical formulation
[DE94-005590] 11 p4267 N94-35996
Simulation of three-dimensional multi-phase flow characteristics in the deswirl section of the CDIF MHD power train
[DE94-012644] 12 p4443 N94-37176
Flow visualization for Lagrangian particle methods
[DE94-010757] 12 p4443 N94-37195
Effects of two-phase flow on the deflagration of porous energetic materials
[DE94-011423] 12 p4411 N94-37412

TWO PHASE SYSTEMS
U BINARY SYSTEMS (MATERIALS)

TWO PHOTON COHERENT STATES
U SQUEEZED STATES (QUANTUM THEORY)

TWO STAGE TURBINES
Two stage turbine for rockets 06 p2215 N94-23059
Design and experimental performance of a two stage partial admission turbine. Task B.1/B.4
[AD-A277095] 07 p2824 N94-27228
Experimental measurements and analytical analysis related to gas turbine heat transfer. Part 1: Time-averaged heat-flux and surface-pressure measurements on the vanes and blades of the SSME fuel-side turbine and comparison with prediction. Part 2: Phase-resolved surface-pressure and heat-flux measurements on the first blade of the SSME fuel-side turbine
[NASA-CR-196296] 12 p4442 N94-36969

TWO-WAVELENGTH LASERS
An improved light source for laser ranging 03 p0913 N94-15567
Investigations of large area electron beam diodes for excimer lasers
[DE94-005670] 08 p3295 N94-30595

TYPHOONS
Effects of typhoon on TOMS data 02 p0693 N94-14243
The activities of equatorial anticyclones of the Western Pacific and the South China Sea and their effects on the tracks of typhoon movement
[AD-A269954] 04 p1492 N94-18675
Recurvature dynamics of a typhoon
[AD-A276792] 09 p3784 N94-32164
Typhoon havens handbook for the western Pacific and Indian Oceans, change 3
[AD-A277030] 09 p3784 N94-32260
Forecasters handbook for the Philippine Islands and surrounding waters
[AD-A277993] 09 p3787 N94-33089
Typhoon monitoring using passive satellite observations
[AD-A277859] 10 p4089 N94-33769

TYROSINE
Theoretical prediction of the UV adsorption and fluorescence spectra of tyrosine and phenylalanine
[AD-A266970] 03 p0943 N94-15111
Strategies for enhancing catecholamine-mediated neurotransmission
[NASA-CR-193807] 04 p1506 N94-18862

T3J AIRCRAFT
U T-39 AIRCRAFT

U

U BENDS
Corrosion behavior of metal matrix composites
[AD-A265352] 01 p0085 N94-12404
Analysis of Alloy 600 and X-750 stress corrosion cracks
[DE94-001578] 06 p2238 N94-22936
Flow and heat transfer in a rotating square sectioned U-bend 08 p3128 N94-28984

U.S.S.R.
Gas core nuclear thermal rocket engine research and development in the former USSR
[DE93-012165] 02 p0552 N94-14013
NASA/DOD Aerospace Knowledge Diffusion Research Project. Paper 32: A new era in international technical communication: American-Russian collaboration
[NASA-TM-109336] 03 p1230 N94-15838
Soviet society informatization: The USSR state program 05 p2046 N94-22058
The Soviet software market: Current state and aspects of development 05 p1923 N94-22066
Models of transient processes in centrally planned economy 05 p2051 N94-22071
Microbiology research at some research institutes in the former Soviet Union: A survey of scientific publications
[PB94-123320] 07 p2902 N94-27171
Station climatic summaries: China, the former USSR, and Mongolia
[AD-A276548] 09 p3784 N94-32057
Information systems to enhance technology exchange
[DE94-007744] 09 p3920 N94-32808

U.S.S.R. SPACE PROGRAM
Russian space system for the Earth remote sensing
01 p0037 N94-10688
JPRS report: Science and technology. Central Eurasia: Space
[JPRS-USP-93-003] 02 p0828 N94-13182
Soviet developments of planet rovers in period of 1964 - 1990 06 p2369 N94-23374
Mars 96 small rover: Mission strategy
06 p2606 N94-23381
Radioastron flight operations
06 p2502 N94-23861
United States/Russia space cooperation documentary
[NASA-TM-109809] 10 p4014 N94-33561
JPRS report: Science and technology. Central Eurasia: Space
[JPRS-USP-94-004] 12 p4391 N94-37002

U-2 AIRCRAFT
Weather forecasting support for AASE-2
[NASA-CR-194342] 02 p0721 N94-13675
Modis-N airborne simulator
[NASA-CR-189303] 02 p0792 N94-13719
Bi-directional reflectance and other radiation parameters of cirrus from ER-2 observations
05 p1871 N94-22296

UARS (SATELLITE)
U UPPER ATMOSPHERE RESEARCH SATELLITE (UARS)

UBV SPECTRA
First results of the seven-color asteroid survey
01 p0430 N94-12162
Polarization and variability of active galaxies and quasars 02 p0837 N94-13550

UH-1 HELICOPTER
Aviation system safety risk management tool analysis. Volume 2: Appendices
[AD-A273502] 06 p2173 N94-24864

UH-60A HELICOPTER
A feasibility study regarding the addition of a fifth control to a rotorcraft in-flight simulator
[NASA-CR-193240] 01 p0030 N94-10895
Helicopter approach capability using the differential Global Positioning System
[NASA-CR-177618] 01 p0024 N94-12355
Preliminary design features of the RASCAL: A NASA /Army rotorcraft in-flight simulator
02 p0526 N94-13325
Fidelity assessment of a UH-60A simulation on the NASA Ames vertical motion simulator
[NASA-TM-104016] 03 p0870 N94-15793
Aerodynamic characteristics of a helicopter rotor airfoil as affected by simulated ballistic damage
[AD-A269206] 04 p1311 N94-18413
The modern rotor aerodynamic limits survey: A report and data survey
[NASA-TM-4446] 05 p1635 N94-21490
Aviation system safety risk management tool analysis. Volume 2: Appendices
[AD-A273502] 06 p2173 N94-24864
A critical assessment of UH-60 main rotor blade airfoil data
[NASA-TM-103985] 09 p3571 N94-32063

ULLAGE
On demand, non-halon, fire extinguishing systems
[AD-D015957] 05 p1714 N94-20355
Cryogenic fluid management technologies for space transportation. Zero G thermodynamic vent system
[NASA-CR-193981] 12 p4430 N94-36806

ULTRA SHORT WAVE RADIO EQUIPMENT
U VERY HIGH FREQUENCY RADIO EQUIPMENT

ULTRAHIGH FREQUENCIES
NT P BAND
Development of UHF spark-switched L-C Oscillators
[DE93-015019] 02 p0623 N94-13892
Effects of the equatorial ionosphere on L-band Earth-space transmissions 02 p0615 N94-14671
Tree attenuation at 20 GHz: Foliage effects
02 p0615 N94-14672
An overview of the text propagation effects for land-mobile-satellite systems: Experimental and modeling results 03 p0996 N94-16048
High efficiency low cost monolithic module for SARSAT distress beacons
[NASA-CR-194234] 04 p1315 N94-18852
Application of Cloude's target decomposition theorem to polarimetric imaging radar data
05 p1724 N94-20429
Mapping of taiga forest units using AIRSAR data and/or optical data, and retrieval of forest parameters
05 p1729 N94-20452
Mobile antenna development at JPL
05 p1731 N94-20457
Mobile terminal antennas for helicopters
05 p1731 N94-20458
An in-depth analysis and modelling of the Shuttle to MILA S-band telemetry link 05 p1657 N94-21340
The European Mobile System (EMS)
06 p2282 N94-22789
Measurements on the satellite-mobile channel at L and S bands 06 p2282 N94-22791
K-band mobile propagation measurements using ACTS 06 p2283 N94-22792
Systems implications of L-band fade data statistics for LEO mobile systems 06 p2284 N94-22799
Microstrip monopulse antenna for land mobile communications 06 p2289 N94-22833
L-band mobile terminal antennas for helicopters
06 p2289 N94-22835
Radar signature related radome techniques for flush-mounted HF-, VHF- and, UHF communication antennas
[PB93-204618] 06 p2294 N94-23742
Simulation of adjacent channel interference in a UHF satellite system
[AD-A273147] 06 p2299 N94-24669
Electromagnetic interference impact of the proposed emitters for the High Frequency Active Auroral Research Program (HAARP)
[AD-A273401] 06 p2301 N94-24926
Extension of On-Surface Radiation Condition (OSRC) theory to full-vector electromagnetic wave scattering by three-dimensional conducting, dielectric, and coated targets
[AD-A274023] 07 p2766 N94-25757
Comparative investigation of high-latitude ionospheric structure and effects near solar maximum
[AD-A273799] 07 p2877 N94-25877
VHF-UHF noise surveys at Gulkana, Elmensdorf AFB, Galena AFB, Kotzebue and Cape Lisburne, Alaska and NRL, Pomonkey, Maryland
[PL-TR-93-2136] 07 p2777 N94-28211
ULF waves and magnetic field characteristics in the polar cusp observed at Godhavn 08 p3361 N94-29244
Precision frequency synthesizing sources with excellent time/frequency performances 08 p3473 N94-30671
A multichannel architecture for Naval Task Force Communication
[AD-A276230] 09 p3673 N94-31446
System analysis of ultra-wideband instrumentation radars: Impulse versus stepped-chirp approaches
[AD-A276624] 09 p3677 N94-32087
Millstone Hill radar studies of plasma waves and turbulence
[AD-A278409] 09 p3684 N94-33172
Numerical computation and measurement of radar cross section for impulse radar
[PB94-149200] 10 p4036 N94-34096
DSS-13 S-/X-band microwave feed system
11 p4253 N94-35550
TIPC user manual
[DE94-004470] 12 p4432 N94-36443

ULTRAHIGH VACUUM
Scanning tunneling microscopy studies of diamond films and optoelectronic materials
[NASA-CR-194363] 02 p0578 N94-13246
UHV-stem studies on nucleation and growth of thin metal silicide films on silicon
[DE93-017604] 03 p1212 N94-16961
Thin film studies of the proximity Josephson effect
[AD-A270129] 04 p1600 N94-18876
Fabrication and evaluation of superconducting and semiconducting materials
[AD-A271645] 05 p2018 N94-20558
Interface science of controlled metal/metal and metal/ceramic interfaces prepared using ultrahigh vacuum diffusion bonding
[DE94-001066] 05 p1696 N94-22025
An analytical ultra-high vacuum tribometer for solid lubricant studies 06 p2361 N94-24033
Surface chemistry of liquid metals
06 p2249 N94-25133
R and D for creation, measurement, application of ultra-high vacuum 07 p2723 N94-25549
Study on utilization of super clean, high vacuum space
07 p2682 N94-25586
Inert strength of pristine silica glass fibers
[DE94-004685] 07 p2750 N94-26247
The reactivity of lithium toward non-aqueous solvents of relevance to energy storage applications as studied by surface analytical techniques
[DE94-003483] 07 p2856 N94-26464
Retention latch mechanism for the Wake Shield Facility 08 p3161 N94-29635
Heterogeneous reaction mechanisms and kinetics relevant to the CVD of semiconductor materials
[DE94-011001] 11 p4340 N94-36032

ULTRALOW FREQUENCIES
U EXTREMELY LOW RADIO FREQUENCIES

ULTRALOW TEMPERATURE
U CRYOGENIC TEMPERATURE

ULTRASHORT PULSED LASERS
Tetravalent chromium (Cr(4+)) as laser-active ion for tunable solid-state lasers
[NASA-CR-194527] 02 p0659 N94-14576
Study of the dynamics of a nonlinear coupled-cavity laser system
[ISBN-0-315-86717-5] 09 p3716 N94-31748

ULTRASONIC AGITATION
Novel ultrasonic method for food hydration
[AD-A277411] 09 p3804 N94-32580

ULTRASONIC FLAW DETECTION
Ultrasonic inspection, material noise and surface roughness
[DE93-011560] 01 p0183 N94-11110
Assessment of damage in ceramics and ceramic matrix composites using ultrasonic techniques
[NASA-TM-106121] 01 p0067 N94-11237
Resin transfer molding of textile composites
[NASA-CR-191505] 02 p0554 N94-12833
Quantitative mapping of pore fraction variations in silicon nitride using an ultrasonic contact scan technique
[NASA-TP-3377] 02 p0665 N94-13056
Enhanced NDE systems
[NASA-CR-192603] 02 p0669 N94-14101
Physical interpretation and development of ultrasonic nondestructive evaluation techniques applied to the quantitative characterization of textile composite materials
[NASA-CR-194549] 03 p0931 N94-15190
Component testing and quality assurance
03 p0932 N94-15259
Nondestructive inspection of graphite-epoxy laminates for heat damage using DRIFT and LPF spectroscopies
[DE93-017228] 04 p1343 N94-18761
Three dimensional ultrasonic imaging: An aging aircraft nondestructive inspection tool
[DE93-018088] 04 p1448 N94-19252
Nondestructive evaluations
[DE94-003020] 06 p2373 N94-24613
Demonstration of polyscann ultrasonic butt-fusion inspection system for polyethylene pipes
[AD-A273279] 06 p2373 N94-24814
Physical interpretation and development of ultrasonic nondestructive evaluation techniques applied to the quantitative characterization of textile composite materials
[NASA-CR-195766] 08 p3183 N94-30016
Standardisation requirements for ultrasonic C-scanning of polymer matrix composites: An initial assessment
[PB94-139318] 08 p3184 N94-30438
Sensing the gas metal arc welding process
08 p3314 N94-30444
Evaluating in-plane elastic constants of damaged carbon-epoxy laminates using a quantitative ultrasonic technique 09 p3621 N94-31793
Ultrasonic characterization of damage in a simulated CF-18 composite structure
[DREP-LN-93-26] 09 p3730 N94-31872
Ultrasonic nondestructive characterization methods for the development and life prediction of titanium matrix composites 12 p4401 N94-36660

ULTRASONIC RADIATION
Nonlinear excitation in quasi-one-dimensional Peierls dielectrics with charge density waves
[DE93-613827] 01 p0398 N94-11025
Inverting ultrasonic data on solid/fluid mixtures for Biot-Gassmann parameters
[DE93-011952] 01 p0150 N94-11026
Study of chemical reactions under the influence of ultrasound
[DE93-016458] 02 p0778 N94-14867
Method and apparatus to characterize ultrasonically reflective contrast agents
[NASA-CASE-LAR-14969-1] 03 p1129 N94-17085
An automated system for ultrasound measurements of liquids by the resonance (Eggers) method
[IFTR-17/1992] 03 p1178 N94-17087
Ultrasonic wave propagation model for nondestructive evaluation of solid rocker motor propellant
[AD-A267653] 03 p0976 N94-17248
Development of ultrasonic motor and application to silent alarm analog quartz watch 04 p1425 N94-18016
Ultrasonic process for destruction of chlorinated organic compounds in aqueous solution
[DE93-015551] 04 p1348 N94-18249
DUSOL: Improved software for analysis of ultrasonic velocity data on anisotropic materials
[NPL-DMM(A)-104] 07 p2965 N94-26816
Interaction of sound with sound by novel mechanisms: Ultrasonic four-wave mixing mediated by a suspension and ultrasonic three-wave mixing at a free surface
08 p3479 N94-29988
Analysis and an image recovery algorithm for ultrasonic tomography system 08 p3397 N94-30456

Noninvasive spectral analysis and beam mapping of focused ultrasound, part 2
[AD-A276629] 09 p3861 N94-32059
Absolute calibration technique for broadband ultrasonic transducers
[NASA-CASE-LAR-14672-1] 11 p4268 N94-35368
Investigation of ultrasonic surface wave interaction with porous saturated rocks
[DE94-013378] 12 p4469 N94-37177

ULTRASONIC SCANNERS

Basic experiment on an ultrasonic method of localization
[DE93-754295] 01 p0358 N94-11042
Quantitative mapping of pore fraction variations in silicon nitride using an ultrasonic contact scan technique
[NASA-TP-3377] 02 p0665 N94-13056
Method and apparatus to characterize ultrasonically reflective contrast agents
[NASA-CASE-LAR-14969-1] 03 p1129 N94-17085
Ultrasonic sensor vision in robotics 05 p1775 N94-22131
Conceptual design of a device to measure hand swelling in a micro-gravity environment
[NASA-CR-195509] 06 p2437 N94-24330
Conformal external radiotherapy of prostatic carcinoma: Requirements and preliminary results 08 p3395 N94-30029
Three methods to improve the accuracy of a PUMA 560 robot 08 p3307 N94-30290
Standardisation requirements for ultrasonic C-scanning of polymer matrix composites: An initial assessment
[PB94-139318] 08 p3184 N94-30438
Ultrasonic characterization of damage in a simulated CF-18 composite structure
[DREP-LN-93-26] 09 p3730 N94-31872
A versatile nondestructive evaluation imaging workstation 09 p3732 N94-32458

ULTRASONIC SPECTROSCOPY

Resonant ultrasound spectroscopy for elastic constant measurements
[DE94-005016] 08 p3480 N94-30098

ULTRASONIC TESTS

Special problems of 3-D ultrasonic QNDI techniques and applications to composites aerospace structures 01 p0061 N94-10036
High temperature processing and diagnostic technologies for microgravity applications 01 p0110 N94-10130
Method of recertifying a loaded bearing member using a phase point
[NASA-CASE-LAR-14741-1] 01 p0185 N94-10671
Ultrasonic inspection, material noise and surface roughness
[DE93-011560] 01 p0183 N94-11110
Project ARGO: Gas phase formation in simulated microgravity
[NASA-TM-104762] 01 p0125 N94-11235
Assessment of damage in ceramics and ceramic matrix composites using ultrasonic techniques
[NASA-TM-106121] 01 p0067 N94-11237
Characterization of the cyclic plasticity of polycrystalline aluminum in the 90-300K domain: Use of the ultrasonic wave coupling technique - low frequency restraint
[ISAL-92-0083] 03 p0954 N94-14930
Physical interpretation and development of ultrasonic nondestructive evaluation techniques applied to the quantitative characterization of textile composite materials
[NASA-CR-194549] 03 p0931 N94-15190
Transcranial Doppler ultrasound studies of cerebral blood-flow in microgravity 03 p0981 N94-16095
Development and application of specially-focused ultrasonic transducers to location and sizing of defects in 75 mm- to 127 mm-thick austenitic stainless steel weld metals
[DE93-015975] 04 p1453 N94-18108
Ultrasonic technique for inspection of GPHS capsule girth weld integrity
[DE93-040072] 04 p1448 N94-19189
Three dimensional ultrasonic imaging: An aging aircraft nondestructive inspection tool
[DE93-018088] 04 p1448 N94-19252
Materials characterization of propellants using ultrasonics
[NASA-CR-193877] 04 p1378 N94-19494
Three dimensional ultrasonic imaging
[DE93-040549] 05 p1968 N94-22003
Cold starting an alcohol-fueled engine with ultrasonic fuel atomization
[PB93-206597] 05 p1826 N94-22093
Strength, ultrasonic and metallurgical evaluation of diffusion bonds
[DE94-000665] 05 p1697 N94-22571
Fiber optic detection of laser generated ultrasound for materials characterization
[ISBN-0-315-83541-9] 06 p2541 N94-22891
Acoustic and optical investigations of superfluid He-3
[PB93-224889] 06 p2523 N94-23101
Strength, acoustic evaluation and metallurgy of diffusion bonds
[DE94-001804] 06 p2243 N94-23717
Ultrasonic nondestructive evaluation as a tool for the development of aerospace structural ceramic composites 06 p2257 N94-24240
Fiber optic detection of ultrasound and its application to cure monitoring
[ISBN-0-315-83424-2] 06 p2544 N94-24466
Non-contact ultrasonic inspection
[VTT-TIED-1454] 07 p2835 N94-26257
An ultrasonic testing technique for monitoring the cure and mechanical properties of polymeric materials
[AD-A274536] 07 p2753 N94-26842
Automated in-situ inspection systems for underground storage tanks
[AD-A274644] 07 p2764 N94-27144
Ultrasonic measurement technique to determine the state of cure in thermosetting materials
[PB94-124328] 07 p2756 N94-27217
Physical interpretation and development of ultrasonic nondestructive evaluation techniques applied to the quantitative characterization of textile composite materials
[NASA-CR-195766] 08 p3183 N94-30016
Resonant ultrasound spectroscopy for elastic constant measurements
[DE94-005016] 08 p3480 N94-30098
Computerized Ultrasonic Testing System (CUTS) for in-process thickness determination 09 p3862 N94-32456
Differential phase acoustic microscope for micro-NDE
[NASA-CR-189617] 09 p3731 N94-32481
PSIDD: A Post-Scan Interactive Data Display system for ultrasonic scans
[NASA-TM-4545] 09 p3732 N94-33038
Thermal conductivity and ultrasonic measurements in low-density solid He-4 10 p4146 N94-33367
Ultrasonic nondestructive characterization methods for the development and life prediction of titanium matrix composites 12 p4401 N94-36660

ULTRASONIC WAVE TRANSDUCERS

Development and application of specially-focused ultrasonic transducers to location and sizing of defects in 75 mm- to 127 mm-thick austenitic stainless steel weld metals
[DE93-015975] 04 p1453 N94-18108
Fiber optic detection of ultrasound and its application to cure monitoring
[ISBN-0-315-83424-2] 06 p2544 N94-24466
Fiber optic sensors for the detection of surface acoustic waves on metals
[ISBN-0-315-87055-9] 09 p3878 N94-31736
Absolute calibration technique for broadband ultrasonic transducers
[NASA-CASE-LAR-14672-1] 11 p4268 N94-35368

ULTRASONIC WAVES

U ULTRASONIC RADIATION

ULTRASONICS

Comparison of Al-Fe alloys produced by PFC and USGA techniques 01 p0058 N94-10019
Use of ultrasound in altitude decompression modeling 01 p0317 N94-11540
Transcranial Doppler ultrasound and the etiology of neurologic decompression sickness during altitude decompression 01 p0312 N94-11544
Study of chemical reactions under the influence of ultrasound
[DE93-016458] 02 p0778 N94-14867
Thermal stress effects in intermetallic matrix composites
[NASA-CR-191191] 03 p1054 N94-16518
Ultrasonic wave propagation model for nondestructive evaluation of solid rocker motor propellant
[AD-A267653] 03 p0976 N94-17248
Ultrasonic process for curing adhesives
[AD-A273175] 06 p2259 N94-24788
An ultrasonic testing technique for monitoring the cure and mechanical properties of polymeric materials
[AD-A274536] 07 p2753 N94-26842
Acoustic and optical investigations of superfluid (3)He
[PB94-135415] 08 p3477 N94-29186
Interaction of sound with sound by novel mechanisms: Ultrasonic four-wave mixing mediated by a suspension and ultrasonic three-wave mixing at a free surface 08 p3479 N94-29988
Noninvasive spectral analysis and beam mapping of focused ultrasound, part 1
[AD-A276211] 09 p3859 N94-31060
Ultrasonic tomography in fiber-reinforced composite materials 09 p3620 N94-31565
Noninvasive spectral analysis and beam mapping of focused ultrasound, part 2
[AD-A276629] 09 p3861 N94-32059
Novel ultrasonic method for food hydration
[AD-A277411] 09 p3804 N94-32580
Refocusing space technology
[NASA-TM-109833] 10 p4161 N94-33569

ULTRAVIOLET ABSORPTION

ADP study of the structure of the IUE halo
[NASA-CR-194374] 01 p0428 N94-12595
Gathering and exchange information on atmospheric chemistry and polluted atmospheres
[DE93-009940] 02 p0705 N94-12869
Detection of accreting gas toward HD 45677: A newly recognized, Herbig Be proto-planetary system
[NASA-CR-189312] 04 p1621 N94-19288
Ultraviolet absorption cross-sections of some carbonyl compounds and their temperature dependence
[AERONAUTICA-ACTA-A-368-1993] 04 p1353 N94-19456
Temperature dependence of ultraviolet absorption cross-sections of alternative hydrochlorofluorocarbons
[AERONAUTICA-ACTA-A-369-1993] 04 p1353 N94-19459
In situ and ex situ spectroelectrochemical and x ray absorption studies on rechargeable, chemically-modified and other MnO2 materials
[DE94-001387] 06 p2234 N94-24545
UV absorption technique for monitoring mobile source NO emissions
[AD-A273858] 07 p2713 N94-25964
In situ Mars ozone detector 07 p3108 N94-27892
Optical modeling of visibility and visibility instrumentation using stratified Mie theory 08 p3348 N94-29750
Study of the ultraviolet absorption and photoconduction spectra of polyimide films fabricated at various curing temperatures
[ISBN-0-315-85923-7] 08 p3218 N94-30036
Laser and Fourier transform spectroscopy of novel propellant molecules
[AD-A277506] 09 p3667 N94-33013
Distribution and nature of UV absorbers on Triton's surface
[NASA-CR-195886] 09 p3943 N94-33104
Ultraviolet Absorption Spectrometry (UVAS) and Liquid Atomic Emission Spectrometry (LAES) for oceanographic analysis systems
[AD-A278263] 10 p4091 N94-33413
Symposium on Inorganic and Organometallic Polymers
[AD-A277860] 10 p4027 N94-33772

ULTRAVIOLET ASTRONOMY

UV extinction properties of carina nebular dust
[NASA-CR-189308] 02 p0835 N94-13233
Physical properties of gas disks around shell stars with and without dust
[NASA-CR-193655] 02 p0835 N94-13239
Radiative transfer in the dynamic atmospheres of Mira-type variables
[NASA-CR-193324] 02 p0829 N94-13287
Analysis of the IUE spectra of the strongly interacting binary beta Lyrae
[NASA-CR-194118] 02 p0833 N94-14493
The next century astrophysics program 02 p0546 N94-14832
NASA's Ultraviolet Astrophysics Branch: Present and future detector program 03 p0910 N94-15102
The spectrum of Phobos from Phobos 2 observations at 0.3-2.6 microns: Comparison to previous data and meteorite analogs 03 p1295 N94-16429
Determination of nitrogen to carbon abundance ratios from transition layer emission lines
[NASA-CR-191921] 04 p1622 N94-19421
Ultraviolet observations of clusters of Wolf-Rayet stars in the SBm3 galaxy NGC 4214 and Ultraviolet and optical observations of LINER's
[NASA-CR-194307] 04 p1622 N94-19431
X ray, extreme and far ultraviolet optical thin films for space applications
[NASA-CR-194635] 05 p1984 N94-20128
VVNRS: Variable phenomena in VV Cephei
[NASA-CR-194731] 05 p2056 N94-21835
UIT support observations archive 05 p2048 N94-22534
Scientific Requirements for Future Solar-Physics Space Missions
[ESA-SP-1157] 06 p2623 N94-22837
Requirements for future solar-physics missions that include UV instrumentation 06 p2625 N94-22851
Voyager observations of globular clusters
[NASA-CR-194806] 06 p2598 N94-23330
UV spectral variability in the Herbig Ae star HR 5999. 11: The accretion interpretation
[NASA-CR-189313] 06 p2599 N94-23334
The resonance lines of MG2 as diagnostics of the upper solar chromosphere
[NASA-CR-195084] 06 p2627 N94-24300
UV-bright stars in globular clusters
[NASA-CR-189324] 06 p2599 N94-24666

Ultraviolet, visible, and gravity astrophysics: A plan for the 1990's
[NASA-NP-152] 06 p2603 N94-24973
Shocked clouds in the Cygnus Loop
[NASA-CR-195190] 06 p2600 N94-25178
Ultraviolet observations of astronomical sources
[NASA-CR-195232] 07 p3102 N94-26234
Observation of Jovian auroral Ly-alpha line profile and emission variability with a sounding rocket and the IUE archives 08 p3550 N94-30798
Extreme ultraviolet opacity sources in the DA white dwarf G191-B2B 09 p3924 N94-31210
IUE observations of new A star candidate proto-planetary systems
[NASA-CR-189355] 10 p4162 N94-34267
Lunar Ultraviolet Telescope Experiment (LUTE), phase A
[NASA-TM-4594] 10 p4162 N94-34920
SPARTAN high resolution solar studies
[NASA-CR-189340] 10 p4166 N94-34944
Ultraviolet spectropolarimetry of high redshift quasars with the Hubble Space Telescope
[NASA-CR-196014] 12 p4546 N94-36690

ULTRAVIOLET DETECTORS
NT TOTAL OZONE MAPPING SPECTROMETER
NT ULTRAVIOLET SPECTROMETERS
Ultraviolet plume instrument description and plume data reduction methodology
[AD-A266141] 01 p0054 N94-11643
A new approach to optical photon detection 03 p0899 N94-15028
Microchannel plate imaging detectors for the ultraviolet 03 p0901 N94-15037
Microchannel plate detectors for space astronomy 03 p0901 N94-15038
Development of an ultra violet auroral imager for the Freja project 03 p0904 N94-15060
A test facility to calibrate EUV detectors 03 p0873 N94-15062
The grazing incidence detectors for the SOHO coronal diagnostic spectrometer 03 p0905 N94-15063
The TAUVEX experiment 03 p0905 N94-15064
The Rutherford Appleton Laboratory photon counting detector 03 p0910 N94-15096
NASA's Ultraviolet Astrophysics Branch: Present and future detector program 03 p0910 N94-15102
Ultraviolet plume instrument calibration and sensor assessment
[AD-A269687] 04 p1337 N94-18574
UVPI imaging from the LACE satellite: The Strypi rocket plume
[AD-A270967] 04 p1335 N94-19787
UVPI imaging from the LACE satellite: The Starbird rocket plume
[AD-A271981] 05 p1658 N94-20617
Electrophoresis in open capillaries: Some fundamental aspects
[ETN-94-95290] 06 p2236 N94-25232
MOCVD growth of GaN, AlN and AlGaN for UV photodetector applications
[AD-A275078] 08 p3512 N94-28871

ULTRAVIOLET EMISSION
Weak bump quasars
[NASA-CR-195267] 07 p3103 N94-27933
A multiwavelength study of two prototypical supernova remnants 08 p3540 N94-29833
Observation of Jovian auroral Ly-alpha line profile and emission variability with a sounding rocket and the IUE archives 08 p3550 N94-30798
Laser and Fourier transform spectroscopy of novel propellant molecules
[AD-A277506] 09 p3667 N94-33013

ULTRAVIOLET FILTERS
Alkali metal for ultraviolet band-pass filter
[NASA-CASE-NPO-18433-1-CU] 01 p0381 N94-10657
Filters for the International Solar Terrestrial Physics (ISTP) mission far ultraviolet imager
[NASA-CR-194633] 03 p1190 N94-15868
X ray, extreme and far ultraviolet optical thin films for space applications
[NASA-CR-194635] 05 p1984 N94-20128
Discrete vacuum ultra violet reflective interference filter
[AD-D016059] 07 p2756 N94-27675

ULTRAVIOLET LASERS
UV and IR laser ablation for inductively coupled plasma mass spectrometry
[DE93-017124] 02 p0658 N94-14415
Modification of fluoropolymer surfaces with electronically conductive polymers
[AD-A266294] 03 p0967 N94-16475
Ultra-shallow box-like profiles fabricated by pulsed UV-laser doping process
[DE93-017221] 04 p1437 N94-18083
Ocular damage induced by ultrashort laser pulses
[AD-A271859] 05 p1890 N94-20462
Optical metrology of magnetically trapped hydrogen
[AD-A272110] 05 p1680 N94-20584
Demonstration of ultraviolet lasing with a low energy electron beam
[DE93-040192] 05 p1818 N94-21554
UV laser long-path absorption spectroscopy 08 p3343 N94-28595
On the possibility of measuring atmospheric OH using intracavity laser spectroscopy 08 p3344 N94-28597
Ablation of polymers by ultraviolet pulsed laser
[DE94-608100] 08 p3218 N94-30066
Investigations into ultraviolet matrix-assisted laser desorption
[DE94-005265] 08 p3296 N94-30908
Ti:sapphire based ultrafast pump-probe laser source in the violet and ultraviolet
[DE94-007542] 09 p3718 N94-32270
Single-shot intensity and phase measurements of detuning and saturation effects in an ultrashort XeCl amplifier
[DE94-007535] 10 p4058 N94-33860
Concepts for UV-FEL optics
[DE94-008996] 10 p4142 N94-33982

ULTRAVIOLET LIGHT
U ULTRAVIOLET RADIATION

ULTRAVIOLET MICROSCOPY
Near-ultraviolet laser photoemission: Scanning microscopy, buried interfaces and image-potential states 08 p3294 N94-29531

ULTRAVIOLET PHOTOGRAPHY
UVPI imaging from the LACE satellite: The Strypi rocket plume
[AD-A270967] 04 p1335 N94-19787
Far ultraviolet images of the nighttime ionosphere
[AD-A275083] 08 p3356 N94-28843

ULTRAVIOLET PHOTOMETRY
Characterization of the energy deposition produced by the primary electron beam on the EXCEDE 3 program
[AD-A274453] 07 p3033 N94-27084
In situ Mars ozone detector 07 p3108 N94-27892

ULTRAVIOLET RADIATION
NT EXTREME ULTRAVIOLET RADIATION
NT FAR ULTRAVIOLET RADIATION
NT LYMAN ALPHA RADIATION
NT NEAR ULTRAVIOLET RADIATION
NT ULTRAVIOLET EMISSION
UV testing of solar cells: Effects of antireflective coating, prior irradiation, and UV source 01 p0053 N94-11408
Oxidation state of the Earth's upper mantle during the last 3800 million years: Implications for the origin of life 01 p0283 N94-12210
UV extinction properties of carina nebular dust
[NASA-CR-189308] 02 p0835 N94-13233
Advances in low energy neutral atom imaging techniques
[DE93-012745] 02 p0782 N94-13492
Quantifying lifetime exposure to ultraviolet radiation in the epidemiology of cutaneous malignant melanoma: A pilot study
[DE93-015274] 03 p1128 N94-16812
The feasibility of tropospheric and total ozone determination using a Fabry-Perot interferometer as a satellite-based nadir-viewing atmospheric sensor
[NASA-TM-109342] 03 p1102 N94-17214
Air pollution effects field research facility. 3: UV-B exposure and monitoring system
[DE93-013098] 04 p1470 N94-17773
Photosynthetic responses to the environment, volume 8
[AD-A269584] 04 p1502 N94-18305
Ultraviolet plume instrument calibration and sensor assessment
[AD-A269687] 04 p1337 N94-18574
Improved optical pseudospark switch
[AD-D015821] 04 p1580 N94-18947
Scientific studies in association with the Shuttle Solar Backscatter Ultraviolet (SSBUV) project
[NASA-CR-193404] 04 p1630 N94-19437
The modification of polymer surfaces and the fabrication of submicron-scale functionalized structures by deep-UV and electron beam lithography
[AD-A265956] 05 p1700 N94-20328
The implications of the LDEF results on Space Station Freedom power system materials 05 p1660 N94-21377
The simulation of action of some space environment factors on Teflon and on rubber materials 05 p1661 N94-21380
Simulated space environmental effects on some experimental high performance polymers 05 p1662 N94-21385
A carbon dioxide/methane greenhouse atmosphere on early Mars 05 p2142 N94-21662
The possible effects of the natural and induced space environment on the optical and thermal properties of EOS surfaces 06 p2207 N94-23596
UV extinction and IR emission in diffuse H2 regions
[NASA-CR-195194] 06 p2600 N94-25270
Numerical analysis of the photo-dissociation/radical oxidation of formaldehyde by ultraviolet light in a photolytic reactor
[AD-A274539] 07 p2868 N94-26843
Initial ultraviolet-B intensity data at Lawrence Livermore National Laboratory
[DE94-004279] 07 p2869 N94-27267
Sum frequency generation using an optical parametric oscillator
[DE94-001827] 07 p3040 N94-28000
Studies on bacterial spore ultraviolet light resistance and regulation of the activity of a spore protease
[AD-A275448] 08 p3384 N94-28884
Radiative flux calculations at UV and visible wavelengths
[DE94-004278] 08 p3350 N94-30613
Radiation transport in cloudy and aerosol loaded atmospheres 08 p3366 N94-30805
Model of spacecraft atomic oxygen and solar exposure microenvironments 09 p3593 N94-31021
Fluorescence observations of LDEF exposed materials as an indicator of induced material reactions 09 p3593 N94-31025
Laser-induced fluorescence of space-exposed polyurethane 09 p3593 N94-31026
UV spectroscopy of low-redshift active galaxies
[NASA-CR-189323] 10 p4161 N94-33904
Absolute, Extreme Ultraviolet Solar Spectral Irradiance Monitor (AESSIM)
[AD-A278709] 11 p4227 N94-36189
Theoretical and experimental studies relevant to interpretation of auroral emissions
[NASA-CR-196032] 11 p4376 N94-36421

ULTRAVIOLET REFLECTION
Design and fabrication of a reflection far ultraviolet polarizer and retarder
[NASA-CR-194630] 03 p1191 N94-16023
Deformed ellipsoidal diffraction grating blank
[NASA-CR-189334] 08 p3289 N94-29872

ULTRAVIOLET SPECTRA
On renormalization group flow in matrix model
[DE93-613050] 01 p0409 N94-10413
The evidence for clumpy accretion in the Herbig Ae star HR 5999
[NASA-CR-189314] 02 p0828 N94-12915
UV extinction properties of carina nebular dust
[NASA-CR-189308] 02 p0835 N94-13233
Ultraviolet observations of NGC 4395, the least luminous and nearest known Seyfert 1 nucleus
[NASA-CR-194304] 02 p0831 N94-13679
Spectra of late type dwarf stars of known abundance for stellar population models
[NASA-CR-194301] 02 p0831 N94-13681
The distance to the high velocity clouds of neutral hydrogen
[NASA-CR-194343] 02 p0838 N94-13716
Optical properties of CO2 ice and CO2 snow in the ultraviolet, visible, and infrared
[NASA-CR-194110] 02 p0686 N94-14081
Analysis of the IUE spectra of the strongly interacting binary beta Lyrae
[NASA-CR-194118] 02 p0833 N94-14493
Theoretical prediction of the UV adsorption and fluorescence spectra of tyrosine and phenylalanine
[AD-A266970] 03 p0943 N94-15111
Air pollution effects field research facility. 3: UV-B exposure and monitoring system
[DE93-013098] 04 p1470 N94-17773
Determination of nitrogen to carbon abundance ratios from transition layer emission lines
[NASA-CR-191921] 04 p1622 N94-19421
Spectrophotometry of emission-line stars in the magellanic clouds
[NASA-CR-194082] 04 p1628 N94-19425
Ultraviolet observations of clusters of Wolf-Rayet stars in the SBm3 galaxy NGC 4214 and Ultraviolet and optical observations of LINER's
[NASA-CR-194307] 04 p1622 N94-19431
Voyager observations of globular clusters
[NASA-CR-194806] 06 p2598 N94-23330
UV spectral variability in the Herbig Ae star HR 5999. 11: The accretion interpretation
[NASA-CR-189313] 06 p2599 N94-23334
SO2 on Venus: A final cross-calibration with Pioneer Venus
[NASA-CR-195162] 06 p2599 N94-24988
Sulfur dioxide in the atmosphere of Venus 1 sounding rocket observations
[NASA-CR-195224] 07 p3106 N94-26237

Solar and airglow measurements aboard the two suborbital flights NASA 36.098 and 36.107
[NASA-CR-195279] 07 p2882 N94-27380
Analysis of EUV/FUV dayglow and auroral measurements
[NASA-CR-195237] 07 p2883 N94-27393
Probing the Martian atmosphere in the ultraviolet
07 p3108 N94-27890
How well was total ozone abundance inferred with Mariner 9?
07 p3108 N94-27891
Spatially resolved spectroscopy of AG Carinae, and direct evidence for stellar evolution: The central star of NGC 2392
[NASA-CR-189291] 08 p3545 N94-29871
Study of the ultraviolet absorption and photoconduction spectra of polyimide films fabricated at various curing temperatures
[ISBN-0-315-85923-7] 08 p3218 N94-30036
Disk instability and the spectral evolution of the 1992 outburst of the intermediate polar GK Persei
09 p3928 N94-31123
The 4f heavy fermion photoelectron spectra do not exhibit the Kondo scale
[DE94-006252] 09 p3898 N94-31631
An analysis of ionospheric dayglow from observations of the Naval Postgraduate School Middle Ultraviolet Spectrograph (MUSTANG)
[AD-A277351] 09 p3773 N94-32335
Distribution and nature of UV absorbers on Triton's surface
[NASA-CR-195886] 09 p3943 N94-33104
How well was total ozone abundance inferred with Mariner 9
09 p3947 N94-33212
UV spectroscopy of low-redshift active galaxies
[NASA-CR-189323] 10 p4161 N94-33904
Lunar Ultraviolet Telescope Experiment (LUTE), phase A
[NASA-TM-4594] 10 p4162 N94-34920
ROSAT/XRT-PSPC observations and the ionizing continuum of Seyfert 1 galaxy Mkn 478
[PB94-167053] 11 p4350 N94-35530

ULTRAVIOLET SPECTROGRAPHS
U ULTRAVIOLET SPECTROMETERS

ULTRAVIOLET SPECTROMETERS
NT HIGH DISPERSION SPECTROGRAPHS
NT TOTAL OZONE MAPPING SPECTROMETER
Ultraviolet spectrometer and polarimeter (UVSP) catalog of observations. Volume 1: Experiments 1-30719, February 1980 - April 1985
[NASA-CR-4529-VOL-1] 03 p1298 N94-15023
Ultraviolet spectrometer and polarimeter (UVSP) catalog of observations. Volume 2: Experiments 30720-63057, April 1985 - February 1988
[NASA-CR-4529-VOL-2] 03 p1298 N94-15024
The spectrum of Phobos from Phobos 2 observations at 0.3-2.6 microns: Comparison to previous data and meteorite analogs 03 p1295 N94-16429
Chemical dynamics in time and energy space
[DE93-018595] 04 p1350 N94-19097
A high resolution ultraviolet Shuttle glow spectrograph
04 p1325 N94-19174
The development of the SOHO SUMER mechanisms
06 p2361 N94-24028
Reanalysis of Mariner 9 UV Spectrometer Data for Ozone, Cloud, and Dust Abundances, and Their Interaction Over Climate Timescales
[NASA-CR-195244] 07 p3107 N94-27885
Probing the Martian atmosphere in the ultraviolet
07 p3108 N94-27890
How well was total ozone abundance inferred with Mariner 9?
07 p3108 N94-27891
Broadband EUV survey spectrometer for short-timescale experiments
[DE94-005459] 08 p3498 N94-28534
JPL Fourier transform ultraviolet spectrometer
08 p3343 N94-28593
A multiwavelength study of two prototypical supernova remnants 08 p3540 N94-29833
Deformed ellipsoidal diffraction grating blank
[NASA-CR-189334] 08 p3289 N94-29872
A sounding rocket program in extreme and far ultraviolet interferometry
[NASA-CR-195114] 08 p3289 N94-29907
Instrumentation on the RAIDS experiment 2: Extreme ultraviolet spectrometer, photometer, and near IR spectrometer
[AD-A278543] 10 p4085 N94-33676

ULTRAVIOLET SPECTROSCOPY
Detection of accreting circumstellar gas around weak emission-line Herbig Ae/Be stars
[NASA-TM-108256] 01 p0424 N94-11306
The STIS MAMA status: Current detector performance
03 p0905 N94-15069
Photodegradation of MDI based polyurethane/urea elastomers
[AD-A267308] 03 p0971 N94-16994
Principal investigators data package for Project Initiation Conference (PIC): EUVS sounding rocket no. 36.117CL. Target: Venus
[NASA-CR-194663] 03 p0923 N94-17126
IRAS high resolution studies and modeling of closely interacting galaxies. Galaxy collisions: Infrared observations and analysis of numerical models. UV spectroscopy of massive young stellar populations in interacting galaxies
[NASA-CR-194483] 04 p1627 N94-19218
Novel nonlinear laser diagnostic techniques
[AD-A270968] 04 p1442 N94-19788
Width modulator mechanism for spectrometer entrance slits 06 p2357 N94-24002
Reanalysis of Mariner 9 UV Spectrometer Data for Ozone, Cloud, and Dust Abundances, and Their Interaction Over Climate Timescales
[NASA-CR-195244] 07 p3107 N94-27885
Mars ozone: Mariner 9 revisited
07 p3107 N94-27888
Structure of ordinary ice I(sub h). Part 1: Ideal structure of ice
[AD-A275149] 08 p3486 N94-29021
An analysis of ionospheric dayglow from observations of the Naval Postgraduate School Middle Ultraviolet Spectrograph (MUSTANG)
[AD-A277351] 09 p3773 N94-32335
Fiber optic chemical sensors
[AD-A277128] 09 p3881 N94-32380
UV spectroscopy of low-redshift active galaxies
[NASA-CR-189323] 10 p4161 N94-33904
Poly(p-phenylene) derivatives new high performance nonlinear optical polymers
[AD-A280248] 12 p4422 N94-37121

ULTRAVIOLET TELESCOPES
Lunar-Ultraviolet Telescope Experiment (LUTE) integrated program plan
[NASA-CR-193267] 01 p0424 N94-11356
LUTE telescope structural design
[NASA-CR-192594] 02 p0830 N94-13448
The TAUVEX experiment 03 p0905 N94-15064
UV-bright stars in globular clusters
[NASA-CR-189324] 06 p2599 N94-24666
Lunar Ultraviolet Telescope Experiment (LUTE), phase A
[NASA-TM-4594] 10 p4162 N94-34920

ULYSSES MISSION
STS-41 post-flight press presentation
[NASA-TM-109514] 03 p0882 N94-15516
STS-41 onboard 16mm photography quick release
[NASA-TM-109515] 03 p0882 N94-15518
STS-41 mission highlights resource tape
[NASA-TM-109516] 03 p0882 N94-15521
Strategy for a small satellite program and a proposal for a first mission 03 p0874 N94-17143
Magellan, Galileo, and Ulysses
[NASA-TM-109362] 04 p1628 N94-18958
The Ulysses spacecraft control and monitoring concepts and realities 06 p2502 N94-23862
Ulysses log 1992 06 p2502 N94-23863
Numerical simulation of Ulysses nutation
06 p2207 N94-24017
Ulysses: A solar odyssey
[NASA-TM-109820] 10 p4010 N94-33574

UMBILICAL CONNECTORS
Microgravity isolation system design: A modern control synthesis framework 11 p4215 N94-35851

UMKLAPP PROCESS
Window least squares method applied to statistical noise smoothing of positron annihilation data
[DE93-634665] 07 p3003 N94-26385
Fermi surface ridge at second and third Umklapp positron annihilations in Y Ba2Cu3O(7-delta)
[DE93-634760] 07 p3070 N94-27995

UNCAMBERED WINGS
NT RING WINGS
Normal force of low aspect ratio cropped-delta wings at pre-stall angles of attack and subsonic speeds
[ESDU-93034] 07 p2648 N94-27955

UNCONSCIOUSNESS
NT BLACKOUT (PHYSIOLOGY)
Performance recovery in the baboon following (+)G sub z-induced loss of consciousness
[AD-A274411] 07 p2902 N94-26991

UNCONTROLLED REENTRY (SPACECRAFT)
A survey of uncontrolled satellite reentry and impact prediction
[AD-A274903] 07 p2695 N94-26750

UNDAMPED OSCILLATIONS
Flutter analysis using transversality theory
[NASA-TM-106382] 03 p1062 N94-17481
Transformation of energy and momentum due to Landau damping in space
[DE93-624921] 04 p1581 N94-17689

UNDERGROUND EXPLOSIONS
Sensitivities of calculated residual stress to separation distances of two simultaneous events
[DE92-019571] 01 p0098 N94-10751
Atmospheric acoustic modeling
[DE93-016727] 02 p0718 N94-14518
A comparison of single-station backazimuth estimates with regional event locations in the Central Appalachians
[AD-A269897] 04 p1483 N94-18690
Centrifuge modeling of explosion-induced craters in unsaturated sand
[AD-A270194] 04 p1417 N94-18780
Proceedings of the 15th Annual Seismic Research Symposium
[AD-A271458] 05 p1855 N94-20090
Parametric and nonparametric discriminants for regional earthquakes and explosions
[AD-A273807] 06 p2406 N94-25538
Processed seismic motion records from earthquakes, 1982-1993: Recorded at Scotty's Castle, California
[DE94-001371] 10 p4086 N94-33729
A comparison of artificial neural networks and statistical analyses
[DE94-010846] 11 p4312 N94-36195

UNDERGROUND STORAGE
Immediate response to free product discovery
[PB93-182970] 01 p0265 N94-11015
Catalytic oxidation of organics in vapor streams at remediation sites
[PB93-182962] 01 p0266 N94-11472
Environmental use of a Laser Range Finder and the Advanced Visualization System
[DE93-016163] 03 p1043 N94-17677
Automated in-situ inspection systems for underground storage tanks
[AD-A274644] 07 p2764 N94-27144
Hydrodynamically induced loads on components submerged in high-level waste-storage tanks
[DE94-009663] 11 p4264 N94-35756
Decision and systems analysis for underground storage tank waste retrieval systems and tank waste remediation system
[SAND94-0065] 11 p4286 N94-35957

UNDERGROUND STRUCTURES
Design and development of a miniature column-based interface (MCBI) stress gage
[AD-A266054] 01 p0170 N94-10873
Resistivity and radar void detectors for tunneling machines 01 p0140 N94-12706
Promotion of geothermal energy development in 1991
[DE93-799058] 02 p0701 N94-13215
Proceedings of the 4th Tunnel Detection Symposium on Subsurface Exploration Technology
[AD-A276372] 09 p3771 N94-31369

UNDERWATER ACOUSTICS
Underwater hydrophone location survey
01 p0290 N94-10975
Acoustics of bubbly sediments
[AD-A263726] 01 p0288 N94-11299
Use of ERS-1 data at Saclant Undersea Research Centre 01 p0233 N94-11714
Acoustic characteristics of side scan sonar and sub-bottom profiler for 10,000 m class ROV
01 p0172 N94-11916
Study on color video pictures transmission by digital acoustic signal 01 p0139 N94-11917
Signal feature analysis using neural networks and psychoacoustics
[AD-A266048] 01 p0340 N94-12398
Mathematical algorithms for multidimensional inverse scattering problems in inhomogeneous medium
[AD-A266440] 02 p0749 N94-13702
Underwater hearing: A review
[ISVR-TR-212] 02 p0777 N94-14130
FLATDAN beamformer enhancements and testing
[DSIS-93-00287] 02 p0777 N94-14360
Design of a general purpose and autonomous transmitter and receiver system for underwater acoustic experiments at sea
[AD-A269268] 04 p1495 N94-17822
Comments on computational underwater acoustics
[DE93-013789] 04 p1562 N94-17873
Parallel and vector adaptations of the underwater finite element parabolic equation model
[AD-A269990] 04 p1563 N94-18678
Estimating the oceanic sound speed environmental for long-range acoustic propagation
[AD-A270231] 04 p1499 N94-18903
BACKSCATTER.FOR: A program to calculate the backscattering strength of an inhomogeneous seabed
[AD-A269235] 04 p1499 N94-18910
Liquid sound speeds at pressure from the optical analyzer technique
[DE93-018362] 04 p1563 N94-19151
Comments on computational underwater acoustics
[DE93-019880] 04 p1563 N94-19270

Acoustic travel time perturbations due to an internal tide and internal wave field in the Barents Sea
[AD-A270879] 04 p1499 N94-19580
Analysis of data from Columbia Point Arena Ocean-Bottom Seismic Station (OBSS)
[AD-A271263] 04 p1500 N94-19727
Seismic studies of the geologic structure and physical properties of the seabed
[AD-A270895] 04 p1500 N94-19747
A register of underwater acoustic test facilities in the US, Canada, and the United Kingdom
[AD-A270884] 04 p1500 N94-19785
A survey of the impact on acoustic propagation of warm core ocean eddys
[AD-A272188] 05 p1883 N94-20925
Acoustic monitoring of global ocean variability
[AD-A271998] 05 p1883 N94-21366
Transient acoustic wave modeling: Higher-order WKBJ asymptotics and symbolical manipulation (revised)
[PB93-215432] 05 p1969 N94-22262
Diffraction analysis of transient acoustic waves: Half-plane in a layered medium
[PB94-110988] 06 p2526 N94-23726
Measurements and modeling of multitone, low-frequency acoustic data from the Arraial do Cabo range
[AD-A273406] 06 p2530 N94-25073
Analysis of modal evolution caused by a weakly range-dependent seabed in shallow water and its application to inversion for geoacoustic properties
[AD-A273656] 06 p2419 N94-25435
Problems in nonlinear acoustics: Rayleigh waves, pulsed sound beams, and waveguides
[AD-A274587] 07 p3010 N94-26983
Hydroacoustic wave-fields generated by different source types, a computational study
[PB94-123536] 07 p3010 N94-27037
Analysis of spark-induced bubble experiments using CALE
[DE94-003667] 08 p3270 N94-28476
Global Acoustic Mapping of Ocean Temperatures (GAMOT)
[AD-A275777] 08 p3376 N94-28740
Broad geoacoustic assessment of some regional areas
[AD-A275504] 08 p3356 N94-28791
Quadruplet expansion of the acoustic pressure field in a wedge shaped ocean
[AD-A275121] 08 p3477 N94-29003
A review of signal detection using the bispectrum with applications in underwater acoustics
[AD-A275227] 08 p3478 N94-29388
Bulletin of National Research Institute of Fisheries Engineering, No. 13
[JTN-94-80596] 08 p3233 N94-29701
Design of the biosonar simulator for dolphin's clicks waveform reproduction 08 p3234 N94-29707
Interaction of sound with sound by novel mechanisms: Ultrasonic four-wave mixing mediated by a suspension and ultrasonic three-wave mixing at a free surface 08 p3479 N94-29988
Ocean acoustic propagation measurements and wave propagation in random media
[AD-A276165] 09 p3787 N94-31053
Vibrational and acoustic response of ribbed plates 09 p3736 N94-31955
Surface forward-scattered acoustic measurements and analysis
[AD-A276998] 09 p3788 N94-32000
Sound scattering by cylinders of noncircular cross section
[AD-A276663] 09 p3861 N94-32089
Long transect seafloor seismic array: A component of SAMSON (Sources of Ambient Micro Seismic Ocean ic Noise)
[AD-A277009] 09 p3789 N94-32401
Acoustic window
[AD-D016171] 09 p3862 N94-33017
Statistical characteristics of bistatic surface scatter and mean bistatic surface scattering strengths
[AD-A278155] 09 p3862 N94-33096
A predictive parametric model for volume scattering strength in the deep ocean with an application to nighttime near-surface scattering in the North Sargasso Sea below 16 kHz
[AD-A277902] 10 p4091 N94-33592
Signal processing for the 1992 Barents Sea tomography experiment
[AD-A278580] 12 p4476 N94-36971

UNDERWATER BREATHING APPARATUS
Advanced seal delivery system life support parameters
[AD-A275304] 08 p3401 N94-29184

UNDERWATER COMMUNICATION
Study on color video pictures transmission by digital acoustic signal 01 p0139 N94-11917
Oceanic in situ Fraunhofer-line characteristics: Fraunhofer-line underwater experiment (FLUX)
[AD-A270659] 05 p1881 N94-19952
An electronic interface for a fiber optic tethered unmanned underwater vehicle
[AD-A279046] 11 p4333 N94-35747

UNDERWATER EXPLOSIONS
Dynamic loading in manufacturing and service: Australia's shock testing capability
[AD-A268334] 01 p0128 N94-11304
An improvement in the modified finite element procedure for underwater shock analysis
[DE94-004451] 07 p2797 N94-27617
Analysis of spark-induced bubble experiments using CALE
[DE94-003667] 08 p3270 N94-28476
A study of near-surface and underwater explosions by computer simulations
[DE94-009038] 09 p3708 N94-32849

UNDERWATER OPTICS
Trajectory curving in underwater propagation of light 01 p0226 N94-12748
Ocean optics, ocean imaging and optical tomography
[AD-A277010] 09 p3789 N94-32402
Comparison of numerical models for computing underwater light fields
[AD-A278256] 10 p4140 N94-33411

UNDERWATER PHOTOGRAPHY
On resolution of underwater stereo photogrammetry 01 p0172 N94-11966
High spatial resolution, range gated, underwater imaging method and apparatus
[AD-D015882] 04 p1430 N94-18530
Evaluation of lens distortion errors using an underwater camera system for video-based motion analysis
[NASA-TM-104795] 10 p4099 N94-33957

UNDERWATER PHYSIOLOGY
Proceedings of the DCIEM Diver Thermal Protection Workshop
[DCIEM-92-10] 09 p3795 N94-31738

UNDERWATER RESEARCH LABORATORIES
La Chalupa-30: Lessons learned from a 30-day subsea mission analogue 10 p4098 N94-33654

UNDERWATER RESOURCES
A detailed investigation of the benthic regime in the Clarion-Clipperton province of the Pacific and a forecast of consequences of manganese noduie mining 01 p0224 N94-12733
Journal of NIRE, Vol. 2, No. 2
[JTN-94-80552] 08 p3187 N94-28675
On United States-Japan Conference on Development and Utilization of Natural Resources: Report of the 14th Joint Meeting of U. S. and Japan Marine Mining Panel 08 p3188 N94-28683

UNDERWATER SOUND
U UNDERWATER ACOUSTICS

UNDERWATER STRUCTURES
Coastal processes due to nearshore current around an upheaving island 01 p0199 N94-11942
The flow structure around a cylindrical pier for the flow of transcritical Reynolds number 01 p0169 N94-11944
Idea of underground airplane 01 p0027 N94-12630
The acoustic arrangement for measuring vertical structure of sea current 01 p0223 N94-12729
Fatigue technology assessment and strategies for fatigue avoidance in marine structures. Appendices
[AD-A269053] 04 p1455 N94-18716
Development of the breakwater with submerged mound for interchanging sea water 08 p3234 N94-29703

UNDERWATER TESTS
NT NEUTRAL BUOYANCY SIMULATION
Underwater hydrophone location survey 01 p0290 N94-10975
Dynamic loading in manufacturing and service: Australia's shock testing capability
[AD-A268334] 01 p0128 N94-11304
Mutrometre: Construction for fast water proof measurements under low pressure and air suppression 04 p1427 N94-18031
A register of underwater acoustic test facilities in the US, Canada, and the United Kingdom
[AD-A270884] 04 p1500 N94-19785

UNDERWATER VEHICLES
NT SUBMARINES
NT UNDERWATER RESEARCH LABORATORIES
Development of a shuttle AUV for oceanographic measurement 01 p0217 N94-12692
Damping in ferrous shape memory alloys
[AD-A271009] 04 p1366 N94-19775
Design of a controllable pitch underwater thruster system
[AD-A271140] 05 p1821 N94-20021
A software architecture for a small autonomous underwater vehicle navigation system
[AD-A272322] 05 p1643 N94-21037
Simulation of tripod gaits for a hexapod underwater walking machine
[AD-A271719] 05 p1945 N94-21355
Telepresence in the human exploration of Mars: Field studies in analog environments 07 p2685 N94-27360
Alumina ceramic: A cost effective replacement for titanium in deep submergence pressure housings
[AD-A275640] 08 p3212 N94-28641
The state transition diagram with path priority and it's applications
[AD-A275524] 08 p3434 N94-28672
A concurrent, object-based implementation for the tactical level of the rational behavior model
[AD-A275024] 08 p3410 N94-29115
Effect of surface condition on strength and fatigue behavior of alumina ceramic
[AD-A275053] 08 p3214 N94-29133
Advanced seal delivery system life support parameters
[AD-A275304] 08 p3401 N94-29184
Undersea applications of dexterous robotics 10 p4067 N94-34033
An electronic interface for a fiber optic tethered unmanned underwater vehicle
[AD-A279046] 11 p4333 N94-35747

UNIAXIAL STRAIN
U AXIAL STRAIN

UNIFIED FIELD THEORY
NT ELECTROWEAK MODEL
NT STANDARD MODEL (PARTICLE PHYSICS)
The magnetic field of rotating bodies
[DE93-619769] 01 p0427 N94-11812
Quark and lepton masses
[DE93-012308] 01 p0370 N94-12787
Gauge coupling unification in superstring derived standard-like models
[DE93-624801] 04 p1607 N94-17950
Experimental and theoretical studies of molecular solids
[AD-A275511] 08 p3485 N94-28668

UNIFORM FLOW
NT BLASIUS FLOW
The three-dimensional flow past a rapidly rotating circular cylinder
[NASA-CR-191512] 02 p0630 N94-13075
Flow past a circular cylinder with a permeable wake splitter plate
[AD-A273765] 07 p2790 N94-25872
Flow past a circular cylinder with a permeable wake splitter plate 08 p3275 N94-29764
Hypervelocity Tunnel 9 Mach 10/14 Calibration
[AD-A275960] 09 p3587 N94-31318

UNIPOLAR TRANSISTORS
U FIELD EFFECT TRANSISTORS

UNIQUENESS
Non-uniqueness in dynamic rate-independent non-associated plasticity
[AD-A266342] 02 p0769 N94-13731
Multigrid methods for a semilinear PDE in the theory of pseudoplastic fluids 06 p2341 N94-23689
Approximate solution of the fourth order initial value problem using deficient spline polynomials
[DE93-613023] 07 p2991 N94-25880
Some results on the phase diagram of the antiferromagnetic Potts model in an external magnetic field
[DE94-608115] 08 p3468 N94-30110
Qualitative properties of two-dimensional predator-prey systems
[REPT-93-75] 09 p3844 N94-31644
Time-dependent, linear DAE's with discontinuous inputs
[AD-A277839] 10 p4128 N94-33834

UNIQUENESS THEOREM
A predator-prey model with Iviev's functional response
[REPT-93-79] 09 p3844 N94-31696

UNITED KINGDOM
Where is high-lift today? A review of past UK research programmes 04 p1305 N94-18416
Current situation in developing petroleum substituting energy (the United Kingdom)
[DE94-714897] 05 p1713 N94-22091
NASA/DOD Aerospace Knowledge Diffusion Research Project. Report 25: The technical communications practices of British aerospace engineers and scientists: Results of the phase 4 RAeS mail survey
[NASA-TM-109098] 09 p3922 N94-32836

UNITED NATIONS
Contributions to CD Space Committee 1992
[PB94-124401] 07 p3101 N94-27218

UNITED STATES
NT ALASKA
NT ARIZONA
NT ARKANSAS
NT CALIFORNIA
NT CONNECTICUT
NT HAWAII
NT IDAHO
NT INDIANA
NT IOWA
NT MARYLAND
NT MINNESOTA
NT MISSISSIPPI
NT SOUTH CAROLINA
NT WASHINGTON
National patterns of R and D resources, 1992
[NSF-92-330] 01 p0422 N94-11186
From red tape to results: Creating a government that works better and costs less 01 p0422 N94-11351
From red tape to results: Creating a government that works better and costs less. Executive summary 01 p0422 N94-11353
Insights into software development in Japan 01 p0330 N94-11435
Landsat as a commercial enterprise
[INPE-5477-TAE/019] 01 p0232 N94-11524
NASA/DOD Aerospace Knowledge Diffusion Research Project. Report 18: A comparison of the technical communication practices of aerospace engineers and scientists in India and the United States
[NASA-TM-109006] 02 p0821 N94-13057
Science, technology, and the federal government: National goals for a new era 02 p0827 N94-14115
NASA/DOD Aerospace Knowledge Diffusion Research Project. Paper 37: The impact of political control on technical communications: A comparative study of Russian and US aerospace engineers and scientists
[NASA-TM-109329] 02 p0826 N94-14488
The closing window of opportunity: Addressing the US space launch vehicle crisis
[TABES PAPER 93-640] 03 p0878 N94-16148
The standardized precipitation index and its use in the western contiguous United States
[AD-A267547] 03 p1107 N94-17102
Space commerce in a global economy: Comparison of US and Australian approaches
[NASA-TM-109341] 03 p1235 N94-17290
Current information technology resource requirements of the federal government: Fiscal year 1994 04 p1612 N94-17756
Terminal area forecasts, FY 1993-2005
[AD-A269855] 04 p1316 N94-18336
Trends in Information Management at Department of Energy Headquarters
[DE93-017197] 04 p1615 N94-18496
Seasonal variability of wind electric potential in the US
[DE93-018182] 04 p1493 N94-19051
Spatiotemporal variability of non-urban ozone concentrations over the eastern United States and its potential replication by satellite data
[PB93-191328] 04 p1476 N94-19065
Biofuels: Project summaries
[DE93-010003] 05 p1712 N94-19984
Post-Palbozoic crustal responses to the contemporary stress field in the eastern United States
[DE93-040604] 05 p1859 N94-22006
Making government work: Electronic delivery of Federal services
[OTA-TCT-578] 06 p2290 N94-23081
On United States-Japan Conference on Development and Utilization of Natural Resources: Report of the 14th Joint Meeting of U. S. and Japan Marine Mining Panel 08 p3188 N94-28683
The European community directive: An alternative environmental impact assessment procedure after Massey?
[AD-A275550] 08 p3347 N94-28844
National Transportation Safety Board annual review of aircraft accident data. US general aviation, 1990
[PB94-126869] 08 p3135 N94-29185
Prediction and standard error estimation for a finite universe total when a stratum is not sampled
[DE94-004929] 08 p3465 N94-30696
Review and status of Maglev in the United States
[DE94-006832] 09 p3722 N94-31319
Aeronautics and space report of the President: Fiscal year 1993 activities 09 p3966 N94-32854
Science and engineering indicators, 1993
[NSB-93-1] 10 p4149 N94-34169
Trends in working on the Framework Convention on Climate Change in industrialized countries in Europe and America
[DE94-757292] 10 p4082 N94-34222
Federal aviation regulations. Part 91: General operating and flight rules, change 3
[PB94-159910] 10 p3987 N94-34410
Proceedings of the Workshop on the Federal Criteria for Information Technology Security
[PB94-162583] 11 p4346 N94-36005
Math and science illiteracy: Social and economic impacts
[DE94-010801] 12 p4540 N94-37092
UNITS OF MEASUREMENT
NT INTERNATIONAL SYSTEM OF UNITS
SI (Metric) handbook
[NASA-TM-109197] 08 p3231 N94-29376
UNIVERSAL TIME
A precise GPS-based time and frequency system 01 p0353 N94-10978
Combining GPS and VLBI earth-rotation data for improved universal time 08 p3144 N94-29614
Loran-C time management 08 p3144 N94-30644
Report on NATO PTTI 08 p3469 N94-30645
A real-time prediction of UTC 08 p3470 N94-30654
UNIVERSE
Dimensional transition of the space-time at the minimum action near the planck scale
[DE93-754192] 01 p0410 N94-10718
A theoretical kinematical study of the gradient of any cosmic scalar field
[DE92-644731] 01 p0425 N94-11136
The solutions of cosmic string loop equation in expanding universe
[DE93-619717] 01 p0427 N94-11692
Rare attributes in finite universe: Hypotheses testing specification and exact randomized upper confidence bounds
[DE93-012783] 02 p0775 N94-12955
Redshift distortions of galaxy correlation functions
[DE93-014007] 02 p0834 N94-12980
Inflation after COBE: Lectures on inflationary cosmology
[DE93-014008] 02 p0834 N94-13096
Dilaton quantum cosmology in two dimensions
[DE93-621377] 02 p0836 N94-13361
Radiation perturbation theory in gravity and quantum universe as a hydrogen atom
[DE93-626621] 02 p0849 N94-14889
The universe at moderate redshift
[NASA-CR-193771] 04 p1627 N94-19093
Visualizing the universe, part 1 05 p2064 N94-22476
Tensor-scalar cosmological models and their relaxation toward general relativity
[PB93-220796] 06 p2601 N94-23099
A brief history of the universe
[DE93-616843] 06 p2604 N94-25210
The meaning of EROS/MACHO
[DE94-003003] 07 p3104 N94-26311
A cosmological field theory
[ISBN-0-315-84271-7] 07 p3104 N94-26638
Cosmological phase transitions
[DE94-003001] 07 p3104 N94-26786
Pigs in cyberspace 07 p2689 N94-27376
Cosmic no-hair in Brans-Dicke theory
[DE94-603673] 07 p3074 N94-27636
Energetic events in the early universe 08 p3547 N94-30012
A theory approach for creation of the matter of universe
[DE94-608109] 08 p3548 N94-30163
Testing for preferred-frame effects in gravity with artificial Earth satellites
[PB94-148459] 09 p3610 N94-31771
Primordial nucleosynthesis in conformal Weyl gravity
[DE94-003002] 11 p4327 N94-36241
UNIVERSITIES
Flight Dynamics Directorate (FDD) Historically Black Colleges and Universities (HBCU's) database managment system: A user's guide
[AD-A264947] 01 p0419 N94-11288
Technology parks and the cooperation among universities and firms: The cases of Campinas, Sao Jose dos Campos e Sao Carlos
[INPE-5251-TAE/04] 02 p0818 N94-13427
Selected data on academic science and engineering R and D expenditures: Fiscal Year 1991
[NSF-92-329] 02 p0819 N94-13982
Maximizing participation of women in collegiate aviation education
[NIAR-93-14] 03 p1222 N94-17261
The impact of industry/university consortia programs on space education
[NASA-TM-109340] 03 p1222 N94-17441
California Student Get Away Special Payload GAS-450 04 p1324 N94-19164
The GAMCIT gamma ray burst detector 04 p1324 N94-19168
Undergraduate origins of recent science and engineering doctorate recipients
[NSF-92-332] 04 p1610 N94-19389
Undergraduate course and curriculum development program and calculus and the bridge to calculus program: 1992 awards
[NSF-93-24] 04 p1610 N94-19446
A comprehensive software engineering educational experience
[AD-A270583] 05 p1905 N94-20109
Schools of the Pacific rainfall climate experiment 05 p1881 N94-20699
Magnetic Earth Ionosphere Resonant Frequencies
[NASA-CR-195131] 06 p2303 N94-25191
National Aeronautics and Space Administration (NASA)/American Society for Engineering Education (ASEE) Summer Faculty Fellowship Program, 1993, volume 1
[NASA-CR-188271-VOL-1] 06 p2632 N94-25348
Federal Information Exchange (FEDIX) user's guide: Fall 1993, Version 5.0/Release 1.0
[DE94-003826] 07 p3097 N94-26350
Selected data on Federal support to universities and colleges: FY 1991
[NSF-93-320] 07 p3101 N94-28201
ISU in an era of partial reconvergence --- International Space University 09 p3600 N94-31438
NASA/DOD Aerospace Knowledge Diffusion Research Project. Paper 6: Aerospace knowledge diffusion in the academic community: A report of phase 3 activities of the NASA/DOD Aerospace Knowledge Diffusion Research Project
[NASA-TM-109771] 09 p3921 N94-32830
Aviation human factors research in US universities: Potential contributions to national needs
[NASA-TM-108814] 09 p3575 N94-32927
Activities of the Laboratory of Physics, Helsinki University of Technology
[PB94-175247] 12 p4509 N94-37301
UNIVERSITY PROGRAM
Weather forecasting support for AASE-2
[NASA-CR-194342] 02 p0721 N94-13675
Symposium on the Future of Aeronautics in the Netherlands
[ETN-93-93780] 03 p0853 N94-15120
University Joint Venture: JOVE
[NASA-TM-109660] 03 p1229 N94-15231
The impact of industry/university consortia programs on space education
[NASA-TM-109340] 03 p1222 N94-17441
The first flight of the QUESTS GAS payload G-521 04 p1325 N94-19170
Roles, uses, and benefits of general aviation aircraft in aerospace engineering education
[NASA-TM-106463] 06 p2153 N94-24100
NPS alternate techsat satellite, design project for AE-4871
[NASA-CR-195512] 06 p2204 N94-24590
A mission to Mercury and a mission to the moons of Mars
[NASA-CR-195530] 06 p2195 N94-24619
VLCT-13: A commercial transport for the 21st Century
[NASA-CR-195492] 06 p2181 N94-24803
Stiffening of deployable space booms: Automated Protein Crystal Growth Facility
[NASA-CR-195547] 06 p2196 N94-24820
Design of an airborne launch vehicle for an air launched space booster
[NASA-CR-195534] 06 p2198 N94-24860
RIACS/USRA
[NASA-CR-195117] 06 p2631 N94-25003
The Triton: Design concepts and methods
[NASA-CR-195542] 06 p2184 N94-25004
Activities of Academia Sinica
[DE93-614529] 06 p2541 N94-25335
National Aeronautics and Space Administration (NASA)/American Society for Engineering Education (ASEE) Summer Faculty Fellowship Program, 1993, volume 1
[NASA-CR-188271-VOL-1] 06 p2632 N94-25348
Strategies for recruiting additional African Americans into the NASA JSC summer faculty fellows program 06 p2585 N94-25362
Image remapping strategies applied as protheses for the visually impaired 06 p2444 N94-25363
National Aeronautics and Space Administration (NASA)/American Society for Engineering Education (ASEE) Summer Faculty Fellowship Program, 1993, volume 2
[NASA-CR-188271-VOL-2] 06 p2636 N94-25367
MINOTAUR (Maryland's innovative orbital technologically advanced University rocket) 07 p2703 N94-25685
The 1991-1992 walking robot design 07 p2833 N94-25686
FAA/NASA Joint University Program for Air Transportation Research, 1992-1993
[NASA-CP-3246] 07 p2641 N94-27284

An investigation of air transportation technology at the Massachusetts Institute of Technology, 1992-1993
07 p2641 N94-27285
Investigation of air transportation technology at Ohio University, 1992-1993 07 p2642 N94-27288
Investigation of air transportation technology at Princeton University, 1992-1993
07 p2643 N94-27294
University program management information system, FY 1993
[NASA-TM-109719] 07 p3100 N94-27413
The 1993 NASA-ODU American Society for Engineering Education (ASEE) Summer Faculty Fellowship Program
[NASA-CR-191544] 07 p3085 N94-27893
Selected data on Federal support to universities and colleges: FY 1991
[NSF-93-320] 07 p3101 N94-28201
Welcome to the Ohio Aerospace Institute
[NASA-TM-109756] 09 p3913 N94-31815
Introduction to USRA
[NASA-CR-195980] 11 p4376 N94-35590
National Educators' Workshop: Update 1993. Standard Experiments in Engineering Materials Science and Technology
[NASA-CP-3259] 11 p4229 N94-36398
Beginning a dialogue on the changing environment for the physical and mathematical sciences
12 p4509 N94-36948
Design and development of experimental facilities for short duration, low-gravity combustion and fire experiments
[NASA-CR-196107] 12 p4389 N94-36967
United States Air Force Summer Research Program, 1993. Volume 7: Armstrong Laboratory
[AD-A278655] 12 p4550 N94-36975
United States Air Force Summer Research Program, 1993. Volume 14: Rome Laboratory
[AD-A278656] 12 p4550 N94-36976
United States Air Force Summer Research Program, 1993. Volume 13: Phillips Laboratory
[AD-A278657] 12 p4550 N94-36977
United States Air Force Summer Research Program, 1993. Volume 16: Arnold Engineering Development Center, Frank J. Seiler Research Laboratory and Wilford Hall Medical Center
[AD-A278658] 12 p4550 N94-36978
United States Air Force Summer Research Program, 1993. Volume 3: Phillips Laboratory
[AD-A278694] 12 p4550 N94-36979
United States Air Force Summer Research Program, 1993. Volume 4: Rome Laboratory
[AD-A278695] 12 p4551 N94-36980
United States Air Force Summer Research Program, 1993. Volume 5A: Wright Laboratory
[AD-A278696] 12 p4551 N94-36981
United States Air Force Summer Research Program, 1993. Volume 6: Arnold Engineering Development Center, Frank J. Seiler Research Laboratory and Wilford Hall Medical Center
[AD-A278697] 12 p4551 N94-36982
United States Air Force Summer Research Program, 1993. Volume 8: Phillips Laboratory
[AD-A278698] 12 p4551 N94-36983
United States Air Force Summer Research Program, 1993. Volume 9: Rome Laboratory
[AD-A278699] 12 p4551 N94-36984

UNIX (OPERATING SYSTEM)
A distributed version of the NASA Engine Performance Program
[NASA-TM-106208] 01 p0327 N94-11231
Kerberos: A UNIX-TCP/IP network authentication system
[DE93-011677] 02 p0760 N94-14011
Uniform user and group IDs on a large network
[DE93-013047] 02 p0760 N94-14315
Upgrading NASA/DOSE laser ranging system control computers 03 p0918 N94-15595
HP upgrade operational streamlining
03 p0918 N94-15596
Lunar laser ranging data processing in a Unix/X windows environment 03 p0918 N94-15599
User manual and program description of the data acquisition system of PML-pulse physics
[AD-A266752] 03 p1147 N94-15776
Department of Defense technical architecture framework for information management. Volume 2: Technical reference model and standards profile, version 2.0
[AD-A267194] 03 p1229 N94-15788
CAVEMAN: Configuration and version management
[DE93-018066] 04 p1524 N94-19048
Cesar user library
[FFI-93/7021] 04 p1529 N94-19378
Lightweight recoverable virtual memory
[AD-A270576] 05 p1898 N94-20107
Security evaluation of Unix networks
[AD-A273076] 05 p1945 N94-21520
Database activity in the Italian Astronet: DIRA 2
05 p2047 N94-22452
VETA x ray data acquisition and control system
05 p2047 N94-22455
Writing instrument interfaces with xf/tktcl
05 p1925 N94-22480
The University of Hawaii Institute for Astronomy CCD camera control system 05 p1828 N94-22489
The ADAM environment and transputers
05 p1926 N94-22494
CCD data acquisition systems at Lick and Keck Observatories 05 p2047 N94-22495
CADBIT 2: Computer-aided design for built-in test, volume 1
[AD-A273702] 06 p2463 N94-25455
CADBIT 2: Computer-aided design for built-in test, volume 2
[AD-A273703] 06 p2463 N94-25456
Summer intern program
[AD-A275194] 08 p3466 N94-28888
The MSRC ab initio methods benchmark suite: A measurement of hardware and software performance in the area of electronic structure methods
[DE94-006428] 08 p3514 N94-30001
Comparative semantics for linear arrays of communicating processes
[CWI-CS-R9336] 08 p3426 N94-30491
Mapping objects to files: A UNIX file system interface to an object management system
[RUU-CS-93-08] 08 p3428 N94-30746
Extender's guide for artifacts and drafts
[AD-A276344] 09 p3810 N94-31328
An MS-DOS file system for UNIX
[AD-A276523] 09 p3816 N94-32081
Moving BASISplus and TECHLIBplus from VAX/VMS to UNIX
[DE94-004696] 09 p3826 N94-32248
Use and administration of UNIX (tm) systems
09 p3821 N94-33051
Data visualization for ONEDANT and TWODANT discrete ordinates codes
[DE94-005087] 10 p4105 N94-33713
Introduction of the UNIX International Performance Management Work Group 10 p4154 N94-33810

UNLOADING
Efficiency and biofidelity of occupant simulations
04 p1459 N94-19473

UNMANNED AERIAL VEHICLES
U PILOTLESS AIRCRAFT

UNMANNED SPACECRAFT
NT GALILEO PROBE
NT GALILEO SPACECRAFT
NT GIOTTO MISSION
NT HEAO 1
NT HEAO 2
NT HELIOS A
NT LUNAR PROBES
NT MAGELLAN SPACECRAFT (NASA)
NT MARINER SPACECRAFT
NT MARINER 6 SPACE PROBE
NT MARINER 7 SPACE PROBE
NT MARINER 9 SPACE PROBE
NT MARINER 10 SPACE PROBE
NT MARS OBSERVER
NT MARS PROBES
NT MARS 4 SPACECRAFT
NT PIONEER SPACE PROBES
NT PIONEER VENUS SPACECRAFT
NT PIONEER VENUS 1 SPACECRAFT
NT SPACE PROBES
NT TECHNOLOGY FEASIBILITY SPACECRAFT
NT VENERA SATELLITES
NT VIKING LANDER SPACECRAFT
NT VIKING SPACECRAFT
NT VOYAGER 1 SPACECRAFT
NT VOYAGER 2 SPACECRAFT
NASA images 11
[NASA-TM-109287] 02 p0842 N94-13626
Contributions of winged re-entry vehicle to space activities 02 p0537 N94-14278
Mission scenario of HOPE 02 p0537 N94-14279
The status of the HOPE concept study
02 p0537 N94-14280
PERCIVAL mission to Mars
[NASA-CR-195541] 06 p2195 N94-24995
Low-cost unmanned lunar lander
07 p2697 N94-25699

UNSTEADY AERODYNAMICS
A method of predicting quasi-steady aerodynamics for flutter analysis of high speed vehicles using steady CFD calculations
[NASA-TM-109009] 02 p0514 N94-12850
Actuator and aerodynamic modeling for high-angle-of-attack aeroservoelasticity
[NASA-TM-4493] 02 p0520 N94-13255
Numerical simulation of dynamic stall of NACA0012 airfoil oscillating near static stall angle using the Navier-Stokes equations
[DE93-767970] 02 p0505 N94-14061
Domain connectivity among systems of overset grids
[NASA-CR-193390] 02 p0508 N94-14326
Effect of wind tunnel acoustic modes on linear oscillating cascade aerodynamics
[NASA-TM-106367] 03 p0869 N94-15866
Aerodynamic/dynamic/control interaction
[AD-A266187] 03 p0871 N94-16107
Aeroelastic airfoil smart spar
03 p0868 N94-16865
Progress in computational unsteady aerodynamics
[NASA-CR-177630] 03 p0860 N94-17081
Comparison between swept and delta canards on a model of a combat aircraft
[AD-A269561] 04 p1317 N94-17826
ISAC: A tool for aeroservoelastic modeling and analysis
[NASA-TM-109031] 04 p1321 N94-19316
Blade row interaction effects on flutter and forced response
[NASA-TM-106438] 05 p1649 N94-21586
Compressibility effects on dynamic stall of airfoils undergoing rapid transient pitching motion
[NASA-TM-109681] 06 p2167 N94-23975
Issac, Jason Cherian ses in transonic flow
[NASA-CR-194837] 06 p2167 N94-24052
An analysis for high Reynolds number inviscid/viscid interactions in cascades
[NASA-CR-4519] 06 p2169 N94-24606
Nonlinear equations of motion for a panel subject to external loads
[AD-A273142] 06 p2170 N94-24773
A finite wake theory for two-dimensional rotary wing unsteady aerodynamics
[AD-A274921] 07 p2645 N94-26535
Methods in unsteady aerodynamics
[DLR-FB-93-21] 07 p2648 N94-27741
Coupled 2-dimensional cascade theory for noise an d unsteady aerodynamics of blade row interaction in turbofans. Volume 2: Documentation for computer code CUP2D
[NASA-CR-4506-VOL-2] 07 p2675 N94-27778
Understanding and development of a prediction method of transonic limit cycle oscillation characteristics of fighter aircraft
[NLR-TP-92210-U] 07 p2679 N94-27798
Multidisciplinary aeroelastic analysis of a generic hypersonic vehicle
[NASA-TM-4544] 07 p2691 N94-27868
Interaction of the sonic boom with atmospheric turbulence 07 p2650 N94-28191
Numerical study on the interaction between scramjet engine modules caused by thermal choke
08 p3125 N94-28960
Unsteady aerodynamic computations around NACA0012 at high angles of attack
08 p3126 N94-28969
Unsteady transonic aerodynamics in frequency domain for flutter analysis 08 p3131 N94-29879
Algorithm and code development for unsteady three-dimensional Navier-Stokes equations
[NASA-CR-195774] 08 p3277 N94-29942
Aeroacoustic sensitivity analysis and optimal aeroacoustic design of turbomachinery blades
[NASA-CR-195786] 08 p3153 N94-30013
Computational analysis of high resolution unsteady airloads for rotor aeroacoustics
[NASA-CR-194894] 08 p3480 N94-30274
Development of a method to predict transonic limit cycle oscillation characteristics of fighter aircraft (continued)
[NLR-TP-92156-U] 08 p3148 N94-30342
An adaptive finite element method for unsteady compressible rotor airfoil aerodynamics
09 p3567 N94-31204
Aeroelastic vibrations of lifting surfaces
[ECL-91-01] 09 p3585 N94-31677
Experimental and computational studies on propeller noise due to inflow distortion 09 p3860 N94-31846
Computational prediction of stall flutter in spanwise-finite blade cascades 09 p3584 N94-31967
Numerical analysis of transonic wing buffet
09 p3586 N94-32713
Study of dynamic stall phenomenon and its control using vorticity, stream function and circulation form of the unsteady Navier-Stokes equations
09 p3572 N94-32714
In flight measurement of steady and unsteady blade surface pressure of a single rotation large scale advanced prop-fan installed on the PTA aircraft
[NASA-CR-187096] 09 p3584 N94-32859

A finite-difference approximate-factorization algorithm for solution of the unsteady transonic small-disturbance equation
[NASA-TP-3129] 09 p3572 N94-32865
Flutter analysis of a supersonic cascade in time domain using an ADI Euler solver
[NASA-TM-105625] 09 p3739 N94-32883
Modeling of aircraft unsteady aerodynamic characteristics. Part 1: Postulated models
[NASA-TM-109120] 09 p3586 N94-32951
The analysis of wake-induced unsteady aerodynamics related to higher harmonic control
[AD-A277914] 09 p3573 N94-33108
Similarity in separated flow fields producing large-scale vortices 10 p3969 N94-33382
Coupled 2-dimensional cascade theory for noise and unsteady aerodynamics of blade row interaction in turbofans. Volume 1: Theory development and parametric studies
[NASA-CR-4506-VOL-1] 10 p3998 N94-34146
Techniques for aerodynamic characterization and performance evaluation at high angle of attack 10 p3991 N94-34614
Unsteady separation process and vorticity balance on unsteady airfoils 10 p3986 N94-34970
Robust control design techniques for active flutter suppression 11 p4200 N94-35875

UNSTEADY FLOW
NT OSCILLATING FLOW
A dynamically adaptive mesh method for internal flows 01 p0149 N94-10896
Unsteady flow past a NACA 0012 airfoil pitching at constant rates
[AD-A265159] 01 p0016 N94-11889
VIB3D: Method for calculating 3-D unsteady flow through turbomachinery blades
[CUED/A-TURBO/TR.128] 01 p0166 N94-12777
VIB2D: Quasi 3-D unsteady viscous flow method for blade flutter calculation
[CUED/A-TURBO/TR.129] 01 p0166 N94-12779
Averaging techniques for steady and unsteady calculations of a transonic fan stage
[NASA-TM-106231] 02 p0499 N94-13108
Clebsch variable model for unsteady, transonic flow; application to 2D airfoils
[NLR-TP-91387-U] 02 p0503 N94-13530
Numerical simulations of unsteady flows in turbomachines 02 p0633 N94-13569
A comparison of computational and experimental data for a subscale high speed propulsive nozzle at low mach numbers
[AD-A266543] 02 p0504 N94-13705
Numerical simulation of a powered-lift landing, tracking flow features using overset grids, and simulation of high lift devices on a fighter-lift-and-control wing
[NASA-CR-194260] 02 p0527 N94-14322
A vortex method for viscous unsteady flows 02 p0640 N94-14602
An implicit finite volume nodal point scheme for the solution of two-dimensional compressible Navier-Stokes equations 02 p0640 N94-14603
Unsteady separated flows: Empirical model and control
[AD-A267282] 03 p0855 N94-14959
Computation of the Fluid and Optical Fields About the Stratospheric Observatory for Infrared Astronomy (SOFIA) and the Coupling of Fluids, Dynamics, and Control Laws on Parallel Computers
[NASA-CR-193168] 03 p0858 N94-16510
Proteus three-dimensional Navier-Stokes computer code, version 1.0. Volume 1: Analysis description
[NASA-TM-106337] 03 p1024 N94-16527
The structure of turbulent boundary layers and shock wave boundary layer interactions
[AD-A266240] 03 p1026 N94-16929
On solving the compressible Navier-Stokes equations for unsteady flows at very low Mach numbers
[NASA-TM-106380] 03 p1027 N94-17128
Development of iterative techniques for the solution of unsteady compressible viscous flows
[NASA-CR-194657] 03 p1027 N94-17129
Multigrid time-accurate integration of Navier-Stokes equations
[NASA-TM-106373] 03 p1028 N94-17258
On the stability of a time dependent boundary layer
[NASA-CR-191542] 03 p1030 N94-17450
An investigation of oblique shock/boundary layer interaction control
[AD-A268106] 03 p0861 N94-17574
Numerical investigation of complex, transitional, and chemically reacting flows 04 p1411 N94-18550
Computational Fluid Dynamics
[VKI-LS-1993-04] 04 p1412 N94-18557
Interferometric investigations of compressible dynamic stall over a transiently pitching airfoil
[NASA-TM-109380] 04 p1312 N94-19119
A simple description of flow instability with application to a packed bed
[DE93-017492] 04 p1420 N94-19345
Simulation of three dimensional unsteady viscous flows in turbomachines
[ECL-92-15] 04 p1420 N94-19398
Examinations of the friction behavior in nonstationary flow processes in pipes
[MITT-7] 04 p1423 N94-19730
Transient thermal analysis of cryocondensation pump for JET
[DE93-040372] 05 p1992 N94-20003
Three dimensional unsteady flow calculations in radial components 05 p1669 N94-20080
Rotorwash wind sensor evaluation
[AD-A268987] 05 p1807 N94-20203
System and method for cancelling expansion waves in a wave rotor
[NASA-CASE-LEW-15218-1] 05 p1801 N94-20588
Computational and analytical methods in nonlinear fluid dynamics
[AD-A272722] 05 p1802 N94-21169
An efficient numerical method for three-dimensional hypersonic flow
[AD-A272506] 05 p1637 N94-21411
Active control of wake/blade-row interaction noise through the use of blade surface actuators
[NASA-CR-4556] 05 p1968 N94-21608
Local uniform grid refinement and brine transport in porous media with inhomogeneities
[CWI-NM-R9224] 05 p1803 N94-21609
Time-dependent grid adaptation for meshes of triangles and tetrahedra 05 p1920 N94-22369
Measurement of kinematically unstationary separated flows 06 p2315 N94-22854
A new experimental apparatus for the study of the unsteady flowfield over an airfoil in pitching and heaving motions using laser Doppler anemometry
[ISL-CO-229/92] 06 p2165 N94-23149
Unsteady jet flow computation towards noise prediction
[NASA-CR-194449] 06 p2153 N94-23553
Simulation of unsteady flows through stator and rotor blades of a gas turbine using the Chimera method 06 p2323 N94-23652
Transient studies of capillary-induced flow 06 p2325 N94-23662
A multilevel adaptive projection method for unsteady incompressible flow 06 p2341 N94-23690
Compressibility effects on dynamic stall of airfoils undergoing rapid transient pitching motion
[NASA-TM-109681] 06 p2167 N94-23975
Sound radiation due to boundary layer transition 06 p2332 N94-24163
Free-surface/vorticity interaction
[AD-A273263] 06 p2335 N94-24686
Computational fluid mechanics
[NASA-CR-194765] 06 p2337 N94-24859
Two-dimensional CFD modeling of wave rotor flow dynamics
[NASA-TM-106261] 06 p2189 N94-25185
Dynamic response of a compressor research facility
[AD-A273836] 07 p2679 N94-25740
Laser Doppler velocimetry in a low speed multistage compressor
[AD-A274836] 07 p2818 N94-26498
Program to develop a performance and heat load prediction system for multistage turbines
[NASA-CR-195223] 07 p2674 N94-26588
Prediction of undsteady flows in turbomachinery using the linearized Euler equations on deforming grids
[NASA-CR-195285] 07 p2675 N94-27654
Flowfield dynamics in blunt fin-induced shock wave/turbulent boundary layer interactions
[NASA-CR-195170] 07 p2798 N94-27802
Unsteady wake structures in transverse jets 07 p2800 N94-28006
Localized and distributed boundary-layer receptivity to convected unsteady wake in free stream
[NASA-CR-4578] 07 p2808 N94-28180
Calculation of unsteady incompressible inviscid flow about wings and bodies using CANAERO-T panel model 07 p2655 N94-28334
Techniques for accurately solving unsteady shock waves and contact discontinuities 07 p2656 N94-28342
Unsteady three dimensional Euler solutions on moving grids 07 p2657 N94-28347
Recent advances in the spectral element method 07 p2657 N94-28348
Boundary layers induced by three-dimensional vortex loops
[AD-A275678] 08 p3270 N94-28665
An experimental study of wing tip vortex in the near wake of a rectangular wing
[AD-A275389] 08 p3129 N94-29306
Investigation of advanced counterrotation blade configuration concepts for high speed turboprop systems. Task 2: Unsteady ducted propfan analysis computer program users manual
[NASA-CR-187105] 08 p3152 N94-29438
Numerical solution of the two-dimensional time-dependent incompressible Euler equations
[NASA-CR-195775] 08 p3277 N94-29859
A numerical method for confined unsteady flows related to fluid-structure interactions
[ISBN-0-315-74739-0] 08 p3277 N94-29902
Effects of diffusion and inertia on chaotic mixing: A computational and experimental study 08 p3488 N94-29903
Aeroacoustic sensitivity analysis and optimal aeroacoustic design of turbomachinery blades
[NASA-CR-195786] 08 p3153 N94-30013
A new orthogonal decomposition method for turbulent flows 08 p3281 N94-30494
Prospects of time-linearized unsteady calculation methods for exponentially diverging motions in aeroelasticity
[PB94-126224] 08 p3134 N94-30740
Development and application of particle image velocimetry in high-speed separated flow: Two-dimensional base cavities 08 p3282 N94-30791
Experiments on the aerodynamic generation of noise in centrifugal turbomachinery 08 p3480 N94-30804
Mixed Eulerian-Lagrangian finite element solutions of unsteady flow and flutter in transonic cascade 08 p3282 N94-30816
An adaptive finite element method for unsteady compressible rotor airfoil aerodynamics 09 p3567 N94-31204
A solution adaptive structured-unstructured grid procedure for unsteady flows 09 p3700 N94-31217
Simulations of the creation and motion of vortex rings
[W-9319] 09 p3703 N94-31691
NATO Advanced Study Institute on Unsteady Combustion. Volume 2: Research papers, September 6-17, 1993
[AD-A276572] 09 p3634 N94-32033
Study of dynamic stall phenomenon and its control using vorticity, stream function and circulation form of the unsteady Navier-Stokes equations 09 p3572 N94-32714
A three-dimensional multigrid technique for unsteady incompressible viscous flows 10 p4042 N94-33364
Laser measurements and analysis of flow in a radial inflow turbine inlet guide vanes and rotor 10 p3997 N94-33365
Similarity in separated flow fields producing large-scale vortices 10 p3969 N94-33382
Control and management of unsteady and turbulent flows
[AD-A278474] 10 p4043 N94-33396
Numerical simulation of the edge tone phenomenon
[NASA-CR-4581] 10 p3982 N94-33898
Unsteady separation experiments on 2-D airfoils, 3-D wings, and model helicopter rotors 10 p3986 N94-34967
Comparison of pitch rate history effects on dynamic stall 10 p3996 N94-34968
Unsteady flow past an airfoil pitched at constant rate 10 p3986 N94-34969
Unsteady separation process and vorticity balance on unsteady airfoils 10 p3986 N94-34970
Control of leading-edge vortices on a delta wing 10 p3986 N94-34971
The unsteady pressure field and vorticity productiion at the suction surface of a pitching airfoil 10 p3986 N94-34972
Investigation of mechanisms for vorticity generation and flow separation on bodies in unsteady motion 10 p4051 N94-34973
Characterization of dynamic stall phenomenon using two-dimensional unsteady Navier-Stokes equations 10 p3986 N94-34974
Computed unsteady flows of airfoils at high incidence 10 p3986 N94-34975
Computation of unsteady flows over airfoils 10 p3986 N94-34977
Prediction of unsteady airfoil flows at large angles of incidence 10 p3986 N94-34978
Experiments on an unsteady, three-dimensional separation 10 p4052 N94-34981
Turbulence modelling for unsteady separated flows 10 p4053 N94-34984
Toward the optimization of control of unsteady separation 10 p4053 N94-34985
The quest for stall-free dynamic lift 10 p3986 N94-34986
Mechanisms of flow control with the unsteady bleed technique 10 p3986 N94-34987

Concepts and application of dynamic separation for agility and super-maneuverability of aircraft: An assessment 10 p3997 N94-34968
On the nonlinear stability of viscous modes within the Rayleigh problem on an infinite flat plate
[NASA-CR-194909] 11 p4263 N94-35497
Unsteady structure of leading-edge vortices on a delta wing
[AD-A278988] 11 p4190 N94-35529
A multilevel adaptive projection method for unsteady incompressible flow
[DE93-016418] 11 p4267 N94-36315
Experimental investigation of nozzle/plume aerodynamics at hypersonic speeds
[NASA-CR-195829] 12 p4382 N94-36687
On automating domain connectivity for overset grids
[NASA-CR-198113] 12 p4493 N94-36920
Unsteady flow field of large-amplitude pitching airfoils
[AD-A280444] 12 p4383 N94-37219
Development of advanced Navier-Stokes solver
[NASA-CR-195094] 12 p4504 N94-37449
Unstructured grid methods for the simulation of 3D transient flows
[NASA-CR-196139] 12 p4444 N94-37525

UNSTEADY STATE
Unsteady three-dimensional thermal field prediction in turbine blades using nonlinear BEM 06 p2325 N94-23665

UNSWEPT WINGS
NT RECTANGULAR WINGS
NT RING WINGS
An experimental study of the aerodynamics of a swept and unswept semispan wing with a simulated glaze ice accretion
[NASA-CR-195330] 08 p3133 N94-30152

UPDRAFTS
U VERTICAL AIR CURRENTS

UPGRADING
S-2E Tracker maritime patrol aircraft re-engine and system upgrade program 06 p2158 N94-24270

UPLINKING
Sequential ranging: How it works
[NASA-CR-194508] 02 p0532 N94-13796
Stability measurements of the radio science system at the 34-m high-efficiency antennas 02 p0609 N94-14381
An overview of the Galileo Optical Experiment (GOPEX) 02 p0610 N94-14386
Data analysis for GOPEX image frames 02 p0610 N94-14388
Galileo Optical Experiment (GOPEX) optical train: Design and validation at the Table Mountain Facility 02 p0610 N94-14390
GOPEX at the Starfire Optical Range 02 p0611 N94-14392
The provision of spectrum for feeder links of non-geostationary mobile satellites 06 p2276 N94-22751
A quick uplink, expandable executable for the NSSC-1 of the Hubble Space Telescope 06 p2305 N94-23859
Voyager uplink planning in the interstellar mission era 06 p2305 N94-23870
Reliable transfer of data from ground to space 06 p2305 N94-23908
The EURECA telecommanding chain: Experience with packet telecommand and telemetry systems 06 p2305 N94-23909
Adaptive power control as a fade countermeasure on satellite links 08 p3253 N94-29897
Providing hydrogen maser timing stability to orbiting VLBI radio telescope observations by post-measurement compensation of linked frequency standard imperfections 08 p3297 N94-30670
Time maintenance system for the BMDO MSX spacecraft 08 p3171 N94-30672

UPPER AIR
U UPPER ATMOSPHERE

UPPER ATMOSPHERE
NT D REGION
NT E REGION
NT EARTH IONOSPHERE
NT EXOSPHERE
NT F REGION
NT F 2 REGION
NT SPORADIC E LAYER
NT THERMOSPHERE
Pakistan Space and Upper Atmosphere Research Commission 01 p0037 N94-10693
Selected upper-air wind speed distributions
[AD-A264822] 01 p0284 N94-10871
The Air Force Interactive Meteorological System: A research tool for satellite meteorology
[AD-A265957] 01 p0284 N94-11113
The upwelling radiation at the top of the atmosphere in coastal region 01 p0205 N94-11981
Southern and Northern Hemisphere total ozone as seen by TOMS
[NASA-TM-109591] 03 p1098 N94-15282
Optical measurements of NASA/USAF CRRES high altitude rocket borne chemical release experiments in conjunction with the USAF airborne ionospheric observatory aircraft
[AD-A266404] 03 p1101 N94-16551
Opposing mesoscale flows in a broken midlatitude squall line
[AD-A268011] 03 p1109 N94-17492
Second flight of the Spacelab grille spectrometer during the Atlas-1 mission
[AERONAUTICA-ACTA-A-367-1992] 03 p0923 N94-17592
The Central American cold surge: An observational analysis of the deep southward penetration of North American cold fronts
[AD-A268592] 03 p1110 N94-17607
Prediction of three sigma maximum dispersed density for aerospace applications 06 p2207 N94-23654
Properties of the Central American cold surge
[NASA-CR-194849] 07 p2893 N94-26138
Upper atmosphere neutral and plasma density modeling
[AD-A274768] 07 p2879 N94-26569
Kiruna geophysical data. Data summary 93/4-6, April-June 1993
[PB94-123700] 07 p2881 N94-27039
Kiruna geophysical data. Data summary 93/1-3, January-March, 1993
[PB94-123791] 07 p2881 N94-27043
JARE data reports. No. 186: Upper atmosphere physics data. Syowa and Asuka Stations, 1990
[JTN-94-80594] 07 p2881 N94-27299
Predissociation in N2(C'4, 1 Sigma u +) and other N2 states and its importance in the atmospheres of Titan and Triton
[NASA-CR-195727] 08 p3549 N94-28816
Far ultraviolet images of the nighttime ionosphere
[AD-A275083] 08 p3356 N94-28843
US National Weather experiment STORM-FEST: Waves and turbulence in frontal zones
[AD-A275084] 08 p3369 N94-28847
Large eddy simulation of the upper atmospheric surface layer
[ISBN-0-315-85393-X] 08 p3365 N94-30134
Atmosphere, ocean, and land: Critical gaps in Earth system models 08 p3350 N94-30617
Theory, Image Simulation, and Data Analysis of Chemical Release Experiments
[NASA-CR-194865] 09 p3954 N94-31101
Upper-air quality control: A comparison study
[AD-A277884] 10 p4080 N94-33553
Study of gravity wave in the upper atmosphere by way of OH* (9-4) and O2(b 1 Sigma(+,g), 0-1) bands nightglow observations
[INPE-5539-TDI/527] 10 p4087 N94-34227

UPPER ATMOSPHERE RESEARCH SATELLITE (UARS)
ATLAS-2 and UARS correlative measurement opportunities during Space Shuttle mission on April 8-17, 1993
[NASA-TM-109020] 03 p1105 N94-15480
An overview of the UARS data validation effort 06 p2386 N94-23617
Nickel cadmium battery operations on-orbit: Trials, tribulations, and success on the Upper Atmosphere Research Satellite 07 p2862 N94-28120
In-flight estimation of gyro noise on the Upper Atmosphere Research Satellite (UARS) and Extreme Ultraviolet Explorer (EUVE) missions 11 p4204 N94-35616
Operational support for Upper Atmosphere Research Satellite (UARS) attitude sensors 11 p4204 N94-35617
Color/magnitude calibration for National Aeronautics and Space Administration (NASA) standard Fixed-Head Star Trackers (FHST) 11 p4209 N94-35641

UPPER IONOSPHERE
NT F REGION
NT F 2 REGION

UPPER STAGE ROCKET ENGINES
Two stage turbine for rockets 06 p2215 N94-23059

UPPER SURFACE BLOWING
Flight path control for the approach and landing of the quiet STOL experimental aircraft ASKA
[NAL-TR-1183] 02 p0513 N94-13457
Design, development, and flight evaluation of the Boeing YC-14 USB powered lift aircraft 04 p1310 N94-18444
An experimental investigation of the effect of upper surface blowing on dynamic stall
[NASA-CR-194863] 06 p2165 N94-22894
The reduction of takeoff ground roll by the application of a nose gear jump strut
[NASA-TM-108822] 11 p4198 N94-36380

UPSTREAM
Experimental and theoretical investigation of undular bore formation upstream the bank 01 p0229 N94-12764
Evolution of the shock front and turbulence structures in the shock/turbulence interaction 02 p0645 N94-14761
An experimental investigation of the effects of leading edge geometry on the dynamics of blunt fin-induced shock wave turbulent boundary layer interaction
[AD-A267656] 03 p0860 N94-17221
Wake passage effects on the losses in a linear turbine cascade
[AD-A273794] 07 p2790 N94-25874
Wall pressure events from the direct numerical simulation of a turbulent wall-bounded flow
[AD-A275890] 08 p3271 N94-28778
Experimental investigation of three-dimensional vortex-airfoil interaction in a supersonic stream
[AD-A275107] 08 p3122 N94-28899

UPWELLING
U UPWELLING WATER

UPWELLING WATER
Ocean-ice interaction study of waves and mesoscale features 01 p0197 N94-11935
On an upwelling front, propagation of upwelling and vertical velocity in the eastern Arabian Sea during monsoon, 1987 01 p0206 N94-11987
Variation of the photosynthetic products in the regional upwelling area around the Izu Islands, Japan 01 p0211 N94-12661
Swordfish (Xiphias gladius) catch distributions relative to environmental features observed from satellites off Coquimbo, Chile (30 deg S) 01 p0216 N94-12688
Investigation of meso-scale fronts, eddies and upwellings in China Seas with AVHRR data 01 p0220 N94-12711
Coastal upwelling monitored by satellite data: Methodologies and results 01 p0220 N94-12712
A possibility to define the location of epipelagic fish concentrations with assistance of satellite sensing 01 p0228 N94-12757
High biological production of the tidal mixing zones on Japan Sea shelf 01 p0228 N94-12758
Evolution of upwelling fronts off the coast of Portugal
[NASA-CR-195692] 09 p3790 N94-33045

UPWIND SCHEMES (MATHEMATICS)
Hypersonic viscous flow computations 02 p0510 N94-14612
Accurate upwind methods for the Euler equations
[NASA-TM-106388] 03 p1170 N94-16882
An upwind multigrid method for solving viscous flows on unstructured triangular meshes
[NASA-TM-109343] 03 p1027 N94-17061
Investigation of a matrix-model for the artificial dissipation in a cell vertex finite volume scheme for solving the Navier-Stokes equations
[DLR-FB-92-33] 04 p1409 N94-18076
Efficient simulation of incompressible viscous flow over multi-element airfoils 04 p1306 N94-18421
High-lift system analysis method using unstructured meshes 04 p1307 N94-18426
Three dimensional network generation and Euler calculation for a wing fuselage canard configuration
[MBB-LME-211-S-PUB-511-A] 04 p1319 N94-19500
Order of accuracy of QUICK and related convection-diffusion schemes
[NASA-TM-106402] 05 p1959 N94-21588
Locally modified Bott-scheme for highly convective flows
[MPIM-99] 06 p2400 N94-23157
Upwind MacCormack Euler solver with non-equilibrium chemistry 06 p2326 N94-23672
A continuing search for a near-perfect numerical flux scheme. Part 1: AUSM+
[NASA-TM-106524] 06 p2338 N94-25180
A robust upwind discretization method for advection, diffusion and source terms
[CWI-NM-R9306] 07 p2868 N94-26774
Code development for hypersonic real-gas flow simulations toward the design of space vehicles, part 2 08 p3125 N94-28966
On the numerical analysis of shear flows 08 p3126 N94-28972
Upwind method using local interpolation 08 p3128 N94-28982
An implicit upwind scheme for the three-dimensional Euler equations using a pointwise relaxation method 08 p3128 N94-28983
Time-marching aeroelastic and spatial adaptation procedures on triangular and tetrahedral meshes using an unstructured-grid Euler method 08 p3131 N94-29877

Multidimensional WAF-type schemes for model conservation laws
[CRANFIELD-AERO-9312] 09 p3843 N94-31541

URANIUM
NT URANIUM ISOTOPES
NT URANIUM 238
Th-230 - U-238 series disequilibrium of the Olkaria rhyolites Gregory Rift Valley, Kenya: Residence times 01 p0281 N94-12076
Crystallographic phase transitions in actinide metals as a function of pressure
[DE93-040138] 05 p2011 N94-19827
A weighted least-squares lump correction algorithm for transmission-corrected gamma ray nondestructive assay
[DE93-018474] 05 p1904 N94-20049
K, U, and Th behavior in Martian environmental conditions 05 p2141 N94-20908
Evaluation of uranium transitions for isotopically-selective laser induced fluorescence with diode lasers (technical report for ST064)
[DE94-002000] 06 p2347 N94-22974
Structure and phase transformations in uranium metal
[DE94-003892] 07 p2732 N94-26004
Deviatoric stresses and plastic strain rates in strong shock waves for six metals
[DE94-002964] 07 p2733 N94-26022
Unsegmented electromagnetic calorimeter prototype. Energy and coordinate resolution
[DE93-634185] 07 p2810 N94-26396
Spectroscopy and atomic physics in EBIT and SuperEBIT
[DE94-006050] 09 p3864 N94-31508
An indigenously developed photoacoustic spectrometer for study of actinide spectroscopy
[DE94-616508] 11 p4235 N94-35592

URANIUM ALLOYS
Magnetic properties of single-crystalline UCu3Al2
[DE93-016607] 04 p1593 N94-17744
Realistic theories of heavy electron and other strongly correlated materials
[DE93-010350] 04 p1571 N94-19204
Investigation of cracking and erratic behavior of the uranium-titanium alloy
[DE93-018591] 05 p1688 N94-19957
Non-Fermi-liquid and multichannel Kondo phenomena in Y(1-x)U(x)Pd3 and related alloys
[DE93-040135] 05 p2015 N94-20275
Non-fermi liquid and spin-glass behavior of the Sc(1-x)U(x)Pd3 system
[DE93-040134] 05 p2016 N94-20335
Temperature dependence of magnetic order in single-crystalline UPdSn
[DE93-040153] 05 p2033 N94-21991
Magnetic phases in UNiGe
[DE94-000793] 06 p2239 N94-22939
Interplay of magnetic and superconducting heavy fermion ground states
[DE94-000680] 06 p2240 N94-23003
Incommensurate magnetic order in UNi2Al3
[DE94-005449] 08 p3209 N94-30246
Investigation of superconductivity and magnetism in d and f-electron materials
[DE94-008535] 09 p3907 N94-32933

URANIUM CARBIDES
The development of CVR coatings for PBR fuels
[DE94-004233] 09 p3875 N94-31480
Digital control programmer for temperature control
[DE94-615584] 11 p4309 N94-36382

URANIUM COMPOUNDS
NT URANIUM CARBIDES
NT URANIUM FLUORIDES
NT URANIUM OXIDES
Muon spin relaxation studies of heavy fermion superconductors
[DE93-014576] 02 p0815 N94-14773
Magnetic and crystallographic structures in UTX intermetallic compounds
[DE93-018291] 04 p1605 N94-19735
Theoretical studies of the structures and electronic properties of U(NH2)(sub 3) and Np(NH2)(sub 3)
[DE94-000768] 05 p2031 N94-21857
Low temperature absorption spectra and ground state electronic structure of tetrakis(2,6-di-tert-butylphenoxide)uranium(IV)
[DE94-000774] 05 p2035 N94-22387
Study on synthesis and characteristics of intermetallic compound with strong electron correlation 07 p2726 N94-25563
Heavy-electron behavior in large coordination compounds CeZn11 and UZn12
[REPT-A-2663] 07 p3049 N94-25614
Technical report of ISSP. Ser. A, no. 2683: Itinerant character of 5f electrons in UNi2Ga
[JTN-94-80569] 07 p3025 N94-27337

URANIUM FLUORIDES
Multiphoton ionization studies of WF6 and UF6
[DE93-016232] 03 p1181 N94-15863

URANIUM ISOTOPES
NT URANIUM 238
Radiogenic age and isotopic studies
[DE93-610548] 01 p0274 N94-10407
Spin characteristics of ion beams during the motion of electromagnetic elements
[DE93-617448] 01 p0364 N94-10848
LEW88516 and SNC meteorites 01 p0430 N94-12150
The Th and U abundances in chondritic meteorites 01 p0430 N94-12151
Safety approaches for high power modular laser operation
[DE93-017213] 04 p1435 N94-17759
U-Pb isotopic ages and characteristics of ancient (greater than 4.0 Ga) lunar highland rocks 05 p2104 N94-20700
U-Pb provenance ages of shocked zircons from the K-T boundary, Raton Basin, Colorado 05 p1685 N94-20701
U-Pb isotopic systematics of ferroan anorthosite 60025 05 p1685 N94-20702
Evaluation of uranium transitions for isotopically-selective laser induced fluorescence with diode lasers (technical report for ST064)
[DE94-002000] 06 p2347 N94-22974

URANIUM OXIDES
Sintering of dioxide pellets in an oxidizing atmosphere (CO2)
[DE94-613046] 12 p4414 N94-36517

URANIUM 238
A high-intensity He-jet production source for radioactive beams
[DE93-040247] 05 p1981 N94-21767

URANUS (PLANET)
On the unique structure of the magnetic fields of Uranus and Neptune 01 p0472 N94-12221
Precession of Uranus and Neptune and their magnetic field 01 p0473 N94-12222
Voyager encounters Uranus
[NASA-TM-109619] 03 p1247 N94-15348
NASA images 12 --- Voyager encounters
[NASA-TM-109417] 03 p1247 N94-15511
NASA images 13
[NASA-TM-109418] 03 p1247 N94-15512
Mapping the stability region of the 3:2 Neptune-Pluto resonance 03 p1280 N94-16351
Detailed analysis of low energy plasma data under the Voyager Uranus data analysis program
[NASA-CR-193668] 04 p1628 N94-17842
Structural evidence for reorientation of Miranda about a paleo-pole 05 p2098 N94-20671
The Jet Propulsion Laboratory space exploration: Past, present and future 06 p2153 N94-24242
Radio science ground data system for the Voyager-Neptune encounter, part 1 08 p3248 N94-29623
Planetary magnetotails: Magnetic configuration and nonthermal plasma 09 p3942 N94-32326
Magnetic field waves at Uranus
[NASA-CR-194807] 10 p4164 N94-34000

URANUS SATELLITES
NT MIRANDA
NT TITANIA

URBAN AREAS
U CITIES

URBAN DEVELOPMENT
AVIRIS data and neural networks applied to an urban ecosystem 03 p1073 N94-16705
Urban applications of satellite remote sensing and GIS analysis
[PB93-202174] 05 p1842 N94-21855
Cities for tomorrow: Directions for change
[PB94-136850] 08 p3537 N94-29168
The use of SPOT, and the contribution of ERS-1, in the assessment of urban pressure on agriculture land in Greater Tunis (Tunisia) 09 p3749 N94-32534

URBAN PLANNING
Technical Conference on Tropical Urban Climates: Extended Abstracts
[WMO/TD-538] 01 p0283 N94-10561
Urban applications of satellite remote sensing and GIS analysis
[PB93-202174] 05 p1842 N94-21855
Wind climate and urban geometry
[ISBN-9-03-860132-8] 06 p2416 N94-25261
Cities for tomorrow: Directions for change
[PB94-136850] 08 p3537 N94-29168
Remote sensing for urban planning 09 p3758 N94-32465
The contribution of satellite data in communication infrastructure projects 09 p3749 N94-32530
Digital mapping, charting, and geodesy analysis program technical review of Urban Vector Smart Map (UV(sub Map)) prototype 1
[AD-A277831] 10 p4076 N94-33832

URBAN RESEARCH
Bibliography of urban climate in tropical/subtropical areas, 1981-1991
[WCASP-25] 02 p0718 N94-12918
The suitability of low-cost urban airshed modeling in the Chicago area
[DE94-005114] 08 p3349 N94-30023

URBAN TRANSPORTATION
Electromechanical battery research and development at the Lawrence Livermore National Laboratory
[DE93-019159] 05 p1762 N94-21620
Optimization techniques for a dial-a-ride transportation system in urban environment
[REPT-93-051] 08 p3537 N94-30926
Greenhouse gas emission impacts of electric vehicles under varying driving cycles in various countries and US cities
[DE94-007647] 09 p3765 N94-32600
Bus application of oxygen-enrichment technology and diesel-electric hybrid systems
[DE94-009835] 11 p4285 N94-35765

UREAS
NT THIOUREAS
Engineering solid-state materials. Strategies for modeling and packing control of molecular assemblies into 3-D networks
[AD-A265291] 01 p0404 N94-12438
Photodegradation of MDI based polyurethane/urea elastomers
[AD-A267308] 03 p0971 N94-16994
Cyclization of bis-urethanes as a new method for the synthesis of 5-substituted, 6-membered cyclic ureas
[AD-A280232] 12 p4399 N94-37134

UREILITES
Trace-element abundances in several new ureilites 01 p0080 N94-12096
Stalking the LREE-enriched component in ureilites 03 p1241 N94-16190
Euromet Ureilite Consortium: A preliminary report on carbon and nitrogen geochemistry 03 p1241 N94-16192
A carbon and nitrogen isotope study of carbonaceous vein material in ureilite meteorites 05 p2083 N94-20726
Ar-39-Ar-40 ages of four ureilites 11 p4357 N94-35410

URETHANES
Uralane (tm) 5774-A/B: Ciba-Geigy's advanced urethane adhesive for the aircraft industry 01 p0018 N94-10777
Dual cure low-VOC coating process
[DE94-000365] 07 p2756 N94-27611
Cyclization of bis-urethanes as a new method for the synthesis of 5-substituted, 6-membered cyclic ureas
[AD-A280232] 12 p4399 N94-37134

URINALYSIS
Changes in fluid and electrolyte metabolism during water immersion at high or thermoneutral temperature 07 p2912 N94-27445
Markov chains for random urinalysis 3: Daily model and drug kinetics
[AD-A275540] 08 p3389 N94-28797

URINE
Microbiological test results using three urine pretreatment regimes with 316L stainless steel
[NASA-CR-192568] 01 p0299 N94-10360
A prototype urine collection device for female aircrew 01 p0317 N94-11549
Strategy for the reduction of total integrated fluid logistics to the Space Station Freedom
[NASA-TM-107744] 03 p1138 N94-17452
Nuclear Medicine Program
[DE93-013896] 04 p1504 N94-17699
Changes in circadian variations of urine excretion in tail-suspended rats 07 p2911 N94-27443

US-2A AIRCRAFT
U S-2 AIRCRAFT

USA (UNITED STATES)
U UNITED STATES

USER MANUALS (COMPUTER PROGRAMS)
Sandia ocean modeling system programmer's guide and user's manual
[DE93-007427] 01 p0287 N94-10153
PANACEA user's manual for PANACEA version 2.0
[DE93-012502] 01 p0321 N94-10263
User's manual for the plume visibility model PLUVUE 2 (revised)
[PB93-188233] 01 p0265 N94-11016
Landing Craft Air Cushion (LCAC) crew selection system manual
[AD-A265158] 01 p0313 N94-11098

User's manual for the DAD-1 data acquisition daughter board for the SuperCard-2
[DE93-012153] 01 p0325 N94-11139
ACARA user's manual
[NASA-TM-106277] 01 p0183 N94-11167
P2NBC2 Heat Strain Decision Aid. User's guide, version 2.1
[AD-A266072] 01 p0304 N94-11224
Flight Dynamics Directorate (FDD) Historically Black Colleges and Universities (HBCU's) database managment system: A user's guide
[AD-A264947] 01 p0419 N94-11288
GRAFTED (GRAphical Fault Tree EDitor): A fault tree description program for target vulnerability/survivability analysis
[AD-A264078] 01 p0328 N94-11301
Software management guide
[DE93-012034] 01 p0330 N94-11452
NASCAP programmer's reference manual
[NASA-CR-191044] 01 p0278 N94-11702
The 1991 version of the plume impingement computer program. Volume 2: User's input guide
[NASA-CR-194191] 01 p0166 N94-12774
VIB3D: Method for calculating 3-D unsteady flow through turbomachinery blades
[CUED/A-TURBO/TR.128] 01 p0166 N94-12777
VIB2D: Quasi 3-D unsteady viscous flow method for blade flutter calculation
[CUED/A-TURBO/TR.129] 01 p0166 N94-12779
PACT user's guide
[DE93-013093] 02 p0742 N94-12840
Vendor information system for innovative treatment technologies. User manual (VISITT version 2.0). Number 2
[PB93-196640] 02 p0821 N94-12936
Archiving of HEAO-1 data products and the creation of a general user's guide to the archive
[NASA-CR-193415] 02 p0822 N94-13062
ULTRA 2 user's manual for ULTRA 2 revision 3.0
[DE93-015970] 02 p0744 N94-13120
SCORE user's manual
[DE93-015987] 02 p0822 N94-13121
VIEWCACHE: An incremental pointer-base access method for distributed databases. Part 1: The universal index system design document. Part 2: The universal index system low-level design document. Part 3: User's guide. Part 4: Reference manual. Part 5: UIMS test suite
[NASA-CR-191788] 02 p0822 N94-13126
The DREO Elint Browser Utility (DEBU) reference manual
[DSIS-92-03900] 02 p0603 N94-13837
VMEC30 programming library: Reference manual
[DSIS-93-00350] 02 p0750 N94-13858
HELSCAM V2.0: Development and application guide
[DSIS-93-00137] 02 p0515 N94-13867
VMEC30 software development: Tutorial manual
[DSIS-93-00351] 02 p0750 N94-13944
CMAPP user's manual, part 2
[DSIS-93-00858-PT-2] 02 p0751 N94-14017
Adaptive Signal Processing Testbed signal excision software: User's manual
[DSIS-93-00260] 02 p0606 N94-14037
Adaptive Signal Processing Testbed application software: User's manual
[DSIS-93-00261] 02 p0606 N94-14038
VMEC30 SUN software development utilities: User's manual
[DSIS-93-00348] 02 p0752 N94-14051
VMEC30 SUN device drivers: User's manual
[DSIS-93-00349] 02 p0752 N94-14052
Payload/GSE/data system interface: Users guide for the VPF (Vertical Processing Facility)
[NASA-CR-194385] 02 p0532 N94-14148
FLATDAN beamformer enhancements and testing
[DSIS-93-00287] 02 p0777 N94-14360
The CAML numbers reference manual
[INRIA-RT-141] 03 p1142 N94-14979
Proteus two-dimensional Navier-Stokes computer code, version 2.0. Volume 2: User's guide
[NASA-TM-106338-VOL-2] 03 p1019 N94-15475
Proteus three-dimensional Navier-Stokes computer code, version 1.0. Volume 2: User's guide
[NASA-TM-106340-VOL-2] 03 p1020 N94-15488
TAFVER 2 users manual
[AD-A266850] 03 p1106 N94-15757
User manual and program description of the data acquisition system of PML-pulse physics
[AD-A266752] 03 p1147 N94-15776
User's manual for the HYPGEN hyperbolic grid generator and the HGUI graphical user interface
[NASA-TM-108791] 03 p1148 N94-15784
ASTROS enhancements. Volume 1: ASTRO user's manual
[AD-A266818] 03 p1151 N94-16768
ASTROS enhancements. Volume 2: ASTRO programmer's manual
[AD-A266819] 03 p1151 N94-16769
Missile datcom user's manual
[AD-A267447] 03 p1152 N94-17032
Defense RDT&E online system (DROLS) handbook
[AD-A267546] 03 p1232 N94-17101
BACKSCAT lidar simulation version 3.0: Technical documentation and users guide
[AD-A267296] 03 p1003 N94-17268
User's manual for the Langley Research Center 14- by 22- foot subsonic tunnel static data acquisition system
[NASA-TM-109027] 03 p0861 N94-17639
WBNGRID, a program for generation of C-H and C-O topology grids around wing/body/nacelle configurations: User's guide
[FFA-TN-1992-09] 04 p1311 N94-17721
Introductory user's guide to the ARL supercomputer facility at Aberdeen Proving Ground
[AD-A265204] 04 p1514 N94-17877
Format.m: A usage manual. Towards an efficient symbolic-numeric environment: Extending Mathematica's format rules
[MATHS-REPT-A-185] 04 p1547 N94-17969
APLAC: An object-oriented analog circuit simulator and design tool. 6.1 reference manual
[PB93-187193] 04 p1396 N94-18091
User's manual of Tokamak Simulation Code
[DE93-788388] 04 p1586 N94-18212
Teaching a computer simulation course with Ada
[AD-A267901] 04 p1521 N94-18308
DYNLET1 model formulation and user's guide
[AD-A269843] 04 p1498 N94-18723
Department of Defense Gateway Information System (DGIS) users' guide
[AD-A270140] 04 p1617 N94-18752
CAVEMAN: Configuration and version management
[DE93-018066] 04 p1524 N94-19048
Cesar user library
[FFI-93/7021] 04 p1529 N94-19378
START user manual version 2.1
[LR-726] 04 p1335 N94-19614
Improved HF data network simulator, software user's manual, volume 2
[AD-A270954] 04 p1393 N94-19753
Technology benefits model user manual, version 01.00.04
[AD-A270637] 04 p1620 N94-19777
Planning process software: A user guide for the DMCA
[AD-A271252] 05 p1902 N94-19911
SIMBAT theoretical manual
[AD-A271063] 05 p1882 N94-19979
The best of GYMNOS: A users guide
[DE93-041275] 05 p1992 N94-19991
Manual of DRANC (release 1.1): A computer program for the Dutch risk assessment of new chemical substances
[PB93-194827] 05 p1851 N94-19998
Mint tutorial and user manual
[TR-452] 05 p1905 N94-20143
Time warp operating system version 2.7 internals manual
[NASA-CR-194798] 05 p1899 N94-20549
Design structuring and allocation optimization (Destination) prototype level 1 user's manual
[AD-A272115] 05 p1929 N94-20571
GWB: Manual for the Grammar WorkBench version 1.5
[TR-92-14] 05 p1909 N94-21061
The Mercury user's manual
[TR-465] 05 p1913 N94-21316
The term processor Kimwitu manual and cookbook
[MEMO-INF-92-67] 05 p1914 N94-21454
Development of BEM for ceramic composites
[NASA-CR-194718] 05 p1676 N94-21777
User manual for EXCALIBUR: A FE-BI numerical laboratory for cavity-backed antennas in a circular cylinder, version 1.2 05 p1741 N94-21888
Parallel runway requirement analysis study. Volume 2: Simulation manual
[NASA-CR-191549-VOL-2] 05 p1644 N94-22278
F2D users manual: A two-dimensional compressible gas flow code
[DE94-000653] 05 p1805 N94-22386
Users manual for the Chameleon parallel programming tools
[DE94-001934] 06 p2465 N94-22973
Programming in Fortran M
[DE94-000541] 06 p2450 N94-23207
GLview user's guide
[PB93-201366] 06 p2452 N94-23444
The Automated Instrumentation and Monitoring System (AIMS) reference manual
[NASA-TM-108795] 06 p2452 N94-23510
Activity Catalog Tool (ACT) user manual, version 2.0
[NASA-CR-177634] 06 p2430 N94-23527
SPDB (science processing database): Quick reference guide 06 p2383 N94-23597
Automatic modulation recognition based on spatial pattern classification using artificial neural networks
[CTN-94-60897] 06 p2296 N94-24115
MERILL: An equational reasoning system in standard ML: A user guide (prerelease version 0.4)
[PB93-204501] 06 p2456 N94-24534
DARPA DICE manufacturing optimization
[AD-A273345] 06 p2461 N94-25156
Naval Interactive Data Analysis System (NIDAS), software user's manual
[NASA-CR-195179] 07 p2956 N94-25606
INM, Integrated Noise Model. Version 4.11: User's guide, supplement
[AD-A273885] 07 p3009 N94-25731
EcarHeart2 version 1.0: Programmers documentation
[PB94-124633] 07 p2909 N94-25909
EGADS: A microcomputer program for estimating the aerodynamic performance of general aviation aircraft
[NASA-TM-104013] 07 p2667 N94-26091
Laser altimetry simulator. Version 3.0: User's guide
[NASA-TM-104588] 07 p2877 N94-26152
Red's natural editor: A program designed to edit FORTRAN programs
[DE94-003271] 07 p2962 N94-26318
OPM Scheme Editor 2: A graphical editor for specifying object-protocol structures
[DE94-003477] 07 p2962 N94-26327
Federal Information Exchange (FEDIX) user's guide: Fall 1993, Version 5.0/Release 1.0
[DE94-003826] 07 p3097 N94-26350
The Chaco user's guide
[DE94-003669] 07 p2962 N94-26370
Users manual for CATNIP: A Computer Analysis Tool for Normal Impact Penetration
[DE94-003671] 07 p2962 N94-26371
Software Error Estimation Program (SWEEP), version 02.00.00 user manual
[AD-A274697] 07 p2962 N94-26373
User's guide for the frequency domain algorithms in the LIFE2 fatigue analysis code
[DE94-004678] 07 p2838 N94-26563
Bathymetric data set extraction program. Users guide
[AD-A274761] 07 p2899 N94-26567
Thermal/structural tailoring of engine blades (T/STAEBL). User's manual
[NASA-CR-194463] 07 p2839 N94-26692
New FORTRAN computer programs to acquire and process isotopic mass spectrometric data: Operator's manual
[DE94-003174] 07 p2965 N94-26784
The NOGAPS ten year AMIP integration
[AD-A274332] 07 p2900 N94-26887
An XCP user's guide and reference manual
[AD-A274519] 07 p2900 N94-27090
Ma42: A new frontal code for solving sparse unsymmetric systems
[PB94-124302] 07 p2998 N94-27115
Radar cross section visualization using sample buffer progressive refinement volume rendering
[AD-A274179] 07 p2773 N94-27127
Users guide for GRIKURV: A code for drawing graphs
[PB94-123593] 07 p2968 N94-27154
Computer code for controller partitioning with IFPC application: A user's manual
[NASA-CR-195291] 07 p2678 N94-27414
Modulation Simulation Program: Programmer's manual, version 1.00
[DREO-16] 07 p2973 N94-27761
ACES spectral display software: User manual
[SKL-1600-99-002] 07 p2973 N94-27762
Thermal/Structural Tailoring of Engine Blades (T/STAEBL): User's manual
[NASA-CR-194461] 07 p2843 N94-27776
Coupled 2-dimensional cascade theory for noise an d unsteady aerodynamics of blade row interaction in turbofans. Volume 2: Documentation for computer code CUP2D
[NASA-CR-4506-VOL-2] 07 p2675 N94-27778
Modulation Simulation Program: Operator's manual, version 1.00
[DREO-16] 07 p2975 N94-27951
A program for rapid computation of multioffset vertical seismic profile synthetic seismograms for layered media
[AD-A275464] 08 p3355 N94-28737
Thermal/structural tailoring of engine blades (T/SEAEBL). Theoretical manual
[NASA-CR-194462] 08 p3317 N94-28815
Transferable Output ASCII Data (TOAD) editor version 1.0 user's guide
[NASA-CR-187507] 08 p3408 N94-28818

Laser velocimeter data acquisition system for the Langley 14- by 22-foot subsonic tunnel. Software reference guide version 3.3
[NASA-CR-191606] 08 p3293 N94-28839
Procedural guide for modelling and analyzing the flight characteristics of a helicopter design using flightlab
[AD-A275077] 08 p3146 N94-28870
Business planning model user's guide
[AD-A274978] 08 p3409 N94-28895
Learning about the Internet bibliography and beginners' guide
[AD-A275205] 08 p3430 N94-29051
Financial resource review model user's guide
[AD-A274979] 08 p3410 N94-29088
Structural/aerodynamic blade analyzer (SAB) user's guide, version 1.0
[NASA-CR-194460] 08 p3151 N94-29103
Turbomachinery forced response prediction system (FREPS): User's manual
[NASA-CR-194465] 08 p3319 N94-29104
EXTdesign. Version 1.0: Reference manual
[PB94-136827] 08 p3411 N94-29193
Statistical Modeling and Estimation of Reliability Functions for Software (SMERFS) user's guide, revision 3
[AD-A275390] 08 p3411 N94-29202
Animation techniques in BRL-CAD
[AD-A275232] 08 p3417 N94-29392
Thermal enclosure system functional simulation user's manual
[NASA-TM-109094] 08 p3466 N94-29489
ASSIST internals reference manual
[NASA-TM-109102] 08 p3431 N94-29494
RIPE integrity primitives, part 1 (RACE Integrity Primitives Evaluation)
[CWI-CS-R9324-PT-1] 08 p3252 N94-29692
RIPE integrity primitives, part 2 (RACE Integrity Primitives Evaluation)
[CWI-CS-R9325-PT-2] 08 p3252 N94-29693
AFGWC Dial-In Subsystem (AFDIS) software users manual, version 2.2
[AD-A275844] 08 p3371 N94-29747
Multiple Concentric Cylinder Model (MCCM) user's guide
[NASA-CR-195299] 08 p3183 N94-30125
TOTAL user manual
[NASA-TM-109101] 08 p3432 N94-30160
A user's guide to the Software Testpilot
[CWI-CS-R9343] 08 p3426 N94-30435
ADCIRC: An advanced three-dimensional circulation model for shelves, coasts, and estuaries. User's manual for ADCIRC-2DDI
[AD-A276150] 09 p3787 N94-31250
Predicting antenna parameters from antenna physical dimensions
[AD-A276442] 09 p3672 N94-31300
OTTER 3.0 reference manual and guide
[DE94-007457] 09 p3829 N94-31315
Extender's guide for artifacts and drafts
[AD-A276344] 09 p3810 N94-31328
Developing the Multimedia User Interface Component (MUSIC) for the Icarus Presentation System (IPS)
[AD-A276341] 09 p3810 N94-31335
E-L user's manual
[AD-A276378] 09 p3810 N94-31370
Users manual for SERI QC software assessing the quality of solar radiation data
[DE93-018210] 09 p3953 N94-31491
Hydrologic Database user's manual
[DE94-003950] 09 p3743 N94-31603
Arnoldi code for computing selected eigenvalues of sparse real unsymmetric matrices
[PB94-145182] 09 p3813 N94-31682
Noninvasive spectral analysis and beam mapping of focused ultrasound, part 2
[AD-A276629] 09 p3861 N94-32059
MICA, a facility to achieve portability for message-passing and dynamic memory management in FORTRAN
[DE94-006692] 09 p3807 N94-32147
The intelligent monitoring system: Generic Database Interface (GDI). Revised user manual
[AD-A277131] 09 p3919 N94-32382
GRAFTED - GRAphical fault tree EDitor: A fault tree description program for target vulnerability/survivability analysis. User manual
[AD-A277067] 09 p3818 N94-32390
Heliport Noise Model (HNM) version 2.2 (user's guide)
[AD-A277072] 09 p3861 N94-32418
THERM3D: A boundary element computer program for transient heat conduction problems
[DE94-008112] 09 p3708 N94-32709
METCAN demonstration manual, version 1.0
[NASA-TM-105607] 09 p3626 N94-32858
User's guide for a flat wake rotor inflow/wake velocity prediction code, DOWN
[NASA-TM-104139] 09 p3572 N94-32873
MOM3D method of moments code theory manual
[NASA-CR-189594] 09 p3682 N94-32897
BUCKY instruction manual, version 3.3
[NASA-TM-104793] 09 p3820 N94-32899
Incremental triangulation by way of edge swapping and local optimization
[NASA-TM-103979] 09 p3709 N94-32946
CET93 and CETPC: An interim updated version of the NASA Lewis computer program for calculating complex chemical equilibria with applications
[NASA-TM-4557] 09 p3638 N94-32948
Spur, helical, and spiral bevel transmission life modeling
[NASA-TM-106552] 09 p3728 N94-32979
Use and administration of UNIX (tm) systems 09 p3821 N94-33051
A computer program to obtain time-correlated gust loads for nonlinear aircraft using the matched-filter-based method
[NASA-TM-109768] 10 p4006 N94-33378
A users' guide to the trace contaminant control simulation computer program
[NASA-TM-108456] 10 p4080 N94-33696
Users guide for SENTRAN7, version 2.0
[AD-A278562] 10 p4105 N94-33787
Software user's manual for stability and transition analysis with the codes LSH and PSH
[AD-A277593] 10 p4045 N94-33846
GRACE manual
[DE94-727456] 10 p4105 N94-33867
A TRALINET guide to the Internet
[AD-A277651] 10 p4106 N94-33892
User's guide for ABCI version 8.8, azimuthal beam cavity interaction
[DE94-009638] 10 p4139 N94-33916
TIGGERC: Turbomachinery interactive grid generator for 2-D grid applications and users guide
[NASA-TM-106586] 10 p3998 N94-33974
Automated documentation generator for advanced protein crystal growth
[NASA-CR-193955] 10 p4147 N94-34072
A user's manual for the program TRES4: Random vibration analysis of vertical-axis wind turbines in turbulent winds
[DE94-009012] 10 p4079 N94-34078
Investigation and simulation of nonlinear processors for spread spectrum receivers. Volume 2: Users manual
[AD-A278026] 10 p4037 N94-34289
Optimization of residual stresses in MMC's using compensating/compliant interfacial layers. Part 2: OPTCOMP user's guide
[NASA-CR-195337] 11 p4278 N94-35239
Langley 14- by 22-foot subsonic tunnel test engineer's data acquisition and reduction manual
[NASA-TM-4563] 11 p4189 N94-35246
Description and use of LSODE, the Livermore Solver for Ordinary Differential Equations
[NASA-RP-1327] 11 p4313 N94-35259
Defense RDT and E online system (DROLS) retrieval reference guide
[AD-A278972] 11 p4344 N94-35525
Environment/tool integrator for software development, version 1.2
[AD-A278965] 11 p4303 N94-35660
Fire data management system, FDMS 2.0, technical documentation
[PB94-164019] 11 p4346 N94-35819
ONED90: 1-dimensional diffusion code
[DE94-611063] 11 p4305 N94-35834
User's guide for an interactive personal computer interface for the aeroprediction code
[NSWCDD/TR-94/107] 11 p4305 N94-35958
HST archive primer, version 4.1
[NASA-CR-189370] 11 p4349 N94-36280
SandiaXTP, an object-oriented implementation of XTP 3.7
[DE94-011752] 11 p4257 N94-36354
TIPC user manual
[DE94-004470] 12 p4432 N94-36443
Rotorwash analysis handbook. Volume 2: Appendixes
[SCT-93RR-17-VOL-2] 12 p4382 N94-36467
NIPER Lab WARDEN: Descriptive panels and diagrams for NIPER Lab WARDEN software, volume 2
[DE94-000126] 12 p4493 N94-36699
Eigensystem realization algorithm user's guide forVAX/VMS computers: Version 931216
[NASA-TM-109066] 12 p4493 N94-36818
An arbitrary grid CFD algorithm for configuration aerodynamics analysis. Volume 2: FEMNAS user guide
[NASA-CR-196135] 12 p4493 N94-36922
TRENDS: A flight test relational database user's guide and reference manual
[NASA-TM-108806] 12 p4381 N94-37332
Development of durable high-temperature catalysts for natural gas combustion: Catalytic materials (CATMAT (trade name)) properties database
[PB94-171824] 12 p4412 N94-37462
Reference manual for the Thermal Analyst's Help Desk Expert System
[NASA-CR-194941] 12 p4397 N94-37504
User's manual for SNL-SAND-2 code
[DE94-011744] 12 p4496 N94-37673

USER REQUIREMENTS

Studies on refrigerator sensors and cooling section interface 01 p0129 N94-11834
Data management strategy for the Tampa Bay National Estuary Program: Recommendations and implementation plan
[PB93-191633] 01 p0267 N94-11864
Devices related for thermal control systems used in microgravity 01 p0162 N94-12553
Advanced display object selection methods for enhancing user-computer productivity
[AD-A265806] 02 p0743 N94-12974
Information requirements of self-managing teams
[DE93-010319] 02 p0824 N94-14048
Computer-human interface issues: Theory and application
[AD-A268013] 03 p1138 N94-17475
The First International Conference on PCTE
[FEL-92-A134] 04 p1518 N94-17965
Computer/information security design approaches for Complex 21/Reconfiguration facilities
[DE93-018547] 04 p1535 N94-18930
Application of new technologies in the virtual library: Seminars in Turkey, Portugal, and Spain
[NASA-TM-109718] 04 p1611 N94-19131
Research in image management and access
[NASA-CR-194797] 05 p1907 N94-20376
PEGASUS, electronic bulletin board system user's guide
[AD-A271679] 05 p2044 N94-21363
Software systems used for unstructured grid generation at NASA Langley 05 p1918 N94-22351
Proceedings of the Third International Mobile Satellite Conference (IMSC 1993)
[NASA-CR-194516] 06 p2273 N94-22735
Canadian aeronautical mobile data trials 06 p2279 N94-22773
The Westinghouse Series 1000 Mobile Phone: Technology and applications 06 p2284 N94-22800
Software for scientific visualization: State of the art and experiences
[PB93-225183] 06 p2449 N94-23111
Training: Plugging the information gaps 06 p2429 N94-23934
From requirements to acceptance tests 06 p2464 N94-23962
The use of analytical models in human-computer interface design 06 p2434 N94-24190
Worldwide vessel locating and tracking system, volume 1
[PB93-193217] 06 p2175 N94-24474
A usage profile and evaluation of a wide-area distributed file system
[AD-A273590] 06 p2593 N94-24946
Human factors of mission planning systems: Applications and implementation 06 p2522 N94-25011
Factors influencing perceived usability and utility of LIBERTAS at Cranfield: Implications for system modification and user education
[CRANFIELD-AERO-9212] 06 p2594 N94-25485
A comparison of users' and providers' perceptions of critical spacelift vehicle characteristics and capabilities
[AD-A273907] 07 p2691 N94-26017
Design of an online help facility for ExSpect
[PB94-126687] 07 p2966 N94-26955
Interactive control of a parallel simulation from a remote graphics workstation
[AD-A274217] 07 p2981 N94-27070
Reinventing information services to increase customer satisfaction
[DE93-003718] 07 p3100 N94-27563
Human computer interface guide, revision A
[NASA-TM-109708] 07 p2955 N94-27769
User-centered guidelines for environmental management
[DE94-004313] 08 p3341 N94-28454
A survey of geographical information systems applications for the Earth Science and Applications Division, Space Sciences Laboratory, Marshall Space Flight Center
[NASA-TM-108438] 08 p3529 N94-28820
Aid to Ada component reuse at Aerospatiale Cannes (France)
[REPT-932-440-102] 08 p3418 N94-29418
Information engineering implementation and acceptance 08 p3530 N94-29533

Use of advanced technologies in ATM (air traffic management) domain 08 p3137 N94-29561
Information center assessment 08 p3533 N94-29855
Pausing behavior of end-users in online searching 08 p3533 N94-29960
Automatic generation of context-sensitive textual help [REPT-93-68] 09 p3812 N94-31646
A hypertext system that learns from user feedback 09 p3923 N94-32428
From optics to radar: Environmental problems and the SPOT/ERS systems 09 p3748 N94-32525
On the implementation of error handling in dynamic interfaces to scientific codes [DE94-008970] 09 p3818 N94-32585
Storage system architectures and their characteristics 10 p4155 N94-33815
The Command and Control Reference Model for modeling, simulations, and technology applications [AD-A278300] 10 p4035 N94-33964
Framework for modelling evolving requirements [PB94-148855] 10 p4107 N94-33979
C++ optimization and excluding middle-level code [DE94-008743] 10 p4107 N94-34010

USER-COMPUTER INTERFACE
U HUMAN-COMPUTER INTERFACE

UTILITIES
Intergovernmental decisionmaking for environmental protection and public works [PB93-176824] 01 p0266 N94-11584
An examination of utility emissions contributions to elevated ozone concentrations in the Chicago area [DE93-012852] 02 p0708 N94-13495
Utility emissions associated with electric and hybrid vehicle (EHV) charging [DE93-013734] 03 p1011 N94-16459
The value of windpower: An investigation using a qualified production cost model [DE93-010043] 04 p1465 N94-17888
Directory of Energy Information Administration Models 1993 [DE93-016987] 04 p1616 N94-18707
Wind energy: Program overview, FY 1992 [DE93-000056] 05 p1845 N94-19921
Statistical procedures for corrosion studies [PB93-199412] 06 p2244 N94-23802
Superconducting energy storage [DE94-002248] 06 p2395 N94-24654
Solar resource-utility load matching assessment: NREL photovoltaic project summary [DE94-000232] 07 p2856 N94-26480
High temperature solid oxide fuel cell: Customer test units [DE94-002961] 07 p2858 N94-26869
Nuclear energy related research [DE94-606286] 08 p3494 N94-28623
Solar resource: Utility load-matching assessment [DE94-000297] 09 p3758 N94-31264
Remote sensing for urban planning 09 p3758 N94-32465
The potential impact of externalities considerations on the market for biomass power technologies [DE94-000247] 10 p4078 N94-33726

UTILITY AIRCRAFT
NT S-2 AIRCRAFT
NT T-39 AIRCRAFT
NT U-2 AIRCRAFT
NT UH-1 HELICOPTER
NT UH-60A HELICOPTER
Idea of underground airplane 01 p0027 N94-12630

UTILIZATION
NT COAL UTILIZATION
NT GEOTHERMAL ENERGY UTILIZATION
NT LASER ABLATION
NT LASER ANNEALING
NT LASER APPLICATIONS
NT LASER CUTTING
NT LASER DEPOSITION
NT LASER DRILLING
NT LASER FUSION
NT LASER GUIDANCE
NT LASER HEATING
NT LASER INTERFEROMETRY
NT LASER MICROSCOPY
NT LASER POWER BEAMING
NT LASER PROPULSION
NT LASER SPECTROSCOPY
NT LASER WEAPONS
NT LASER WELDING
NT PULSED LASER DEPOSITION
NT REUSE
NT SOFTWARE REUSE
NT TECHNOLOGY UTILIZATION
NT WASTE ENERGY UTILIZATION
NT WASTE UTILIZATION
NT WINDPOWER UTILIZATION
Prospects for using mobile vehicles in missions to Mars and other planets 06 p2607 N94-23384
Unmanned lunar rovers: Utilization for exploration 06 p2607 N94-23387
Biomedical polyurethane networks [ETN-94-95391] 07 p2750 N94-26211
The universal applications of microtubes and microtube composites 08 p3186 N94-30452
Classification of advanced technical ceramics [REPT-15] 11 p4243 N94-35335

UV CETI STARS
U FLARE STARS

UV LASERS
U ULTRAVIOLET LASERS

V

V BAND
U EXTREMELY HIGH FREQUENCIES

V GROOVES
NT RIBLETS

V-5 AIRCRAFT
U XV-5 AIRCRAFT

V-22 AIRCRAFT
Handling qualities effects of display latency 02 p0517 N94-13316
Organized wiring systems 08 p3166 N94-28705
V-22: Dual-use technology or red herring? [AD-A276577] 09 p3579 N94-32058

V/STOL AIRCRAFT
NT AH-1G HELICOPTER
NT AH-64 HELICOPTER
NT FLYING PLATFORMS
NT H-53 HELICOPTER
NT H-60 HELICOPTER
NT HELICOPTERS
NT LIGHT HELICOPTERS
NT MILITARY HELICOPTERS
NT OH-6 HELICOPTER
NT QUESTOL AIRCRAFT
NT RIGID ROTOR HELICOPTERS
NT ROTARY WING AIRCRAFT
NT ROTOR SYSTEMS RESEARCH AIRCRAFT
NT SH-3 HELICOPTER
NT SHORT TAKEOFF AIRCRAFT
NT TANDEM ROTOR HELICOPTERS
NT TILT ROTOR AIRCRAFT
NT UH-1 HELICOPTER
NT UH-60A HELICOPTER
NT V-22 AIRCRAFT
NT VERTICAL TAKEOFF AIRCRAFT
NT X-14 AIRCRAFT
NT XV-5 AIRCRAFT
NT XV-15 AIRCRAFT
Moving-base simulation evaluation of thrust margins for vertical landing for the NASA YAV-8B Harrier aircraft [NASA-TM-104008] 01 p0030 N94-11259
Lift-fan aircraft: Lessons learned-the pilot's perspective [NASA-CR-177620] 03 p0867 N94-15950
Some VTOL head-up display drive-law problems and solutions [NASA-TM-104027] 05 p1635 N94-20035
Transient Ejector Analysis (TEA) code user's guide [NASA-TM-106310] 06 p2186 N94-23466
Optimal control of helicopters following power failure [NAL-TR-1190] 07 p2678 N94-27206
Vectored jets-induced interference on aircraft, prediction and verification 07 p2801 N94-28012
Influence of headwind on hot gas reingestion and consideration of pressure ratio scaling 07 p2675 N94-28018
Unsteady aspects of hot gas reingestion and statistical analysis 07 p2676 N94-28019
Computation of wind tunnel wall effects for complex models using a low-order panel method [NASA-TM-104019] 08 p3132 N94-30151
Inlet distortion in engines on VSTOL aircraft [NASA-CR-195841] 09 p3584 N94-33035

VACANCIES (CRYSTAL DEFECTS)
NT FRENKEL DEFECTS
Invariance of the mobility edge in anodic titanium oxides [DE92-642136] 01 p0394 N94-10281
Electronic characterization of defects in narrow gap semiconductors [NASA-CR-193568] 01 p0397 N94-10819
Adsorption and dissociation of disilane on Si(001) studied by STM [AD-A265269] 01 p0402 N94-11684
Vacancy condensation as the precursor to passivity breakdown [DE93-012925] 03 p0956 N94-15998
Crystal structure and short-range oxygen defects in La- and Nd-modified ZrO2 [DE93-040229] 05 p2033 N94-21993
The role of point defect clusters in reactor pressure vessel embrittlement [DE94-001122] 07 p2739 N94-26931
Indium-vacancy complexes in mercury cadmium telluride [AD-A276177] 09 p3894 N94-31055
Thermal conductivity and ultrasonic measurements in low-density solid He-4 10 p4146 N94-33367

VACCINES
Bakteriella toxiner-morgondagens hot (bacterial toxins-the threat of tomorrow) [PB94-124229] 07 p2902 N94-27045

VACUUM
NT HIGH VACUUM
NT ULTRAHIGH VACUUM
Vacuum stability requirements of polymeric material for spacecraft application [NASA-TM-109216] 01 p0091 N94-11350
Evaluation of medical treatments to increase survival of ebullism in guinea pigs 01 p0302 N94-11548
The 1991 version of the plume impingement computer program. Volume 1: Description [NASA-CR-194192] 01 p0166 N94-12775
Compatibility testing of vacuum seal materials [DE93-014366] 02 p0663 N94-14113
A study of thin liquid sheet flows [NASA-TM-106323] 02 p0642 N94-14732
On a conformal perfect fluid in the classical vacuum [DE93-624797] 04 p1480 N94-17682
Impulsive moving mirror model in a Schroedinger picture with impulse effect in a Banach space [DE93-629864] 04 p1561 N94-18155
Impulsive moving mirror model and the stability of Schroedinger equation with impulse effect in a Banach space [DE93-629866] 04 p1548 N94-18196
RF vacuum microelectronics [AD-A269454] 04 p1396 N94-18284
RF vacuum microelectronics [AD-A270003] 04 p1403 N94-18667
Evaporation in equilibrium, in vacuum, and in hydrogen gas 05 p1684 N94-20638
Outgassing data for selecting spacecraft materials [NASA-RP-1124-REV-3] 05 p1676 N94-21889
RF vacuum microelectronics [AD-A275221] 08 p3263 N94-28915
Fabrication of electronic materials in space 08 p3228 N94-28942
Collecting cometary soil samples? Development of the ROSETTA sample acquisition system 08 p3160 N94-29628
Periodic electromagnetic vacuum in the two-dimensional Yang-Mills theory with the Chern-Simons mass [DE94-608128] 08 p3525 N94-30170
Survey report of JSUP Space Environment Utilization Research Committee in fiscal year 1992: Metallic Materials Session [JTN-94-80583] 08 p3159 N94-30794
Design of a variable-conductance vacuum insulation [DE94-000270] 08 p3268 N94-30819
Space environment durability of beta cloth in LDEF thermal blankets 09 p3591 N94-31015
Vibrational spectroscopy at metal-solution interfaces: Some perspectives and prospects for electrochemical surface science [AD-A276781] 09 p3644 N94-32169
Pinched propagation of high-power, pulsed electron beams for welding and materials processing applications [AD-A276925] 09 p3726 N94-32236
On a complex vacuum structure in non-Abelian gauge theories and on the place of Majorana particles in these theories [DE94-611147] 10 p4136 N94-33864
On new theories of physical vacuum [DE94-616613] 11 p4318 N94-35955
Network analyzer calibration for cryogenic on-wafer measurements [DE94-010089] 11 p4262 N94-36430
A nonconservative scheme for isentropic gas dynamics [DE94-011488] 12 p4445 N94-37724

VACUUM APPARATUS
NT IONIZATION GAGES
NT VACUUM CHAMBERS
NT VACUUM FURNACES
NT VACUUM PUMPS
Investigation of onset of plasma formation at anode of fast-pulsed high-voltage vacuum diode [AD-A267214] 03 p1204 N94-16987

Field-emitter arrays for RF vacuum microelectronics
[AD-A268397] 03 p1015 N94-17526
Mechanical properties and impact damage resistance of composites fabricated by low cost, vacuum assisted, resin transfer molding
[AD-A270361] 04 p1342 N94-18702
Turntable mechanism
[NASA-CASE-MFS-28522-1] 05 p1823 N94-20380
Study on utilization of super clean, high vacuum space 07 p2682 N94-25586
Micro-electron deflector
[AD-D016055] 07 p2787 N94-27672
Composite hot drape forming 08 p3240 N94-30448
RF vacuum microelectronics
[AD-A276512] 09 p3691 N94-31928

VACUUM ARC SWITCHES
Theoretical studies on ionospheric irregularities and ion diode performance
[AD-A277115] 09 p3772 N94-31984

VACUUM CHAMBERS
Scanning tunneling microscopy studies of diamond films and optoelectronic materials
[NASA-CR-194363] 02 p0578 N94-13246
Detonation reaction steps frozen by free expansion and analyzed by mass spectrometry
[DE93-012734] 04 p1376 N94-17813
Process for preparing thermoplastic composites
[AD-D015864] 04 p1339 N94-18074
Characterization of electromagnetic fields in an extended chamber at the Short Pulse Experimental Electron Device (SPEED) simulator
[AD-A265955] 05 p1717 N94-20329
New technique for oil backstreaming contamination measurements 05 p1652 N94-20511
Initial operation of a large-scale plasma source ion implantation experiment
[DE94-000805] 05 p2036 N94-22583
New pin-on-disk equipment for vacuum tribometry 06 p2360 N94-24023
Study on utilization of super clean, high vacuum space 07 p2682 N94-25586
A large high vacuum, high pumping speed space simulation chamber for electric propulsion
[NASA-TM-106453] 07 p2690 N94-26142
Vacuum chamber and adaptors for shearography and holography
[NASA-CR-192467] 08 p3157 N94-29956

VACUUM DEPOSITION
Implementation of manufacturing techniques for planar, single mode waveguides on lithium niobate
[DSIS-93-00101] 02 p0792 N94-13845
Fabrication and evaluation of superconducting and semiconducting materials
[AD-A271645] 05 p2018 N94-20558
Template synthesis of metal microtubule ensembles utilizing chemical, electrochemical, and vacuum deposition techniques
[AD-A274676] 07 p2715 N94-26444
The optical properties of high-T(c) superconductors grown by pulsed laser deposition
[ISBN-0-315-84917-7] 07 p3039 N94-27962
Vacuum vapor deposition
[NASA-CASE-MFS-28652-1] 08 p3215 N94-29446
Research on the atomic layer-by-layer growth of high-temperature superconductor thin films at the Institute of Scientific and Industrial Research, Japan
[DE94-003739] 08 p3519 N94-30611
Comprehensive investigation of HgCdTe metalorganic chemical vapor deposition
[NASA-CR-195933] 10 p4030 N94-34278

VACUUM EFFECTS
Surface science at the solid liquid interface
[AD-A271422] 05 p1678 N94-19839
Static adhesion in preloaded contacts subjected to long-term vacuum exposure 06 p2363 N94-24043
Fabrication of electronic materials in space 08 p3228 N94-28942
The impact of electrically charged microspheres with planar surfaces under vacuum conditions 08 p3320 N94-29765
Dispersion relations for a plasma-filled helix-loaded-waveguide
[DE94-006333] 09 p3675 N94-31781

VACUUM FURNACES
A dynamic model of the vacuum furnace for separating Pb from Sn-Pb alloy 10 p4026 N94-34346
Digital control programmer for temperature control
[DE94-615584] 11 p4309 N94-36382

VACUUM GAGES
NT IONIZATION GAGES

VACUUM MELTING
A conduction model for the vacuum arc remelting process
[NPL-DMM(A)-98] 02 p0639 N94-14464
Investigation of materials processing technology
[AD-A277588] 10 p4031 N94-33428
The influence of VAR processes and parameters on white spot formation in Alloy 718
[DE94-012071] 12 p4417 N94-37367

VACUUM PUMPS
A survey on technical problems in designing high-speed rotors with developing materials
[DE93-788519] 04 p1444 N94-18159

VACUUM SPECTROSCOPY
Structural and dynamical aspects of electrodeposition
[AD-A266786] 03 p0942 N94-14909
Chemical dynamics in time and energy space
[DE93-018595] 04 p1350 N94-19097

VACUUM SYSTEMS
Compatibility testing of vacuum seal materials
[DE93-014366] 02 p0663 N94-14113
BAKEOUT: A computer program for predicting diffusive outgassing from stainless steel
[DE93-012613] 02 p0573 N94-14364
Temperature lowering in cryogenic chemical-synthesis techniques and system
[DE93-018348] 04 p1562 N94-18810
Analysis of high vacuum systems using SINDA'85 06 p2322 N94-23648
Development of fusion technology
[DE93-633444] 07 p3042 N94-26159
Electrical analysis of wideband and distributed windows using time-dependent field codes
[DE94-002987] 07 p2768 N94-26310
Outgas and vacuum seal characteristics of irradiated polyimide O-ring
[DE94-701200] 07 p2757 N94-27812
Argon frost continuous cryopump for fusion applications
[DE94-004478] 08 p3230 N94-29017

VACUUM TESTS
NT THERMAL VACUUM TESTS
An investigation of conducted and radiated emissions from a hollow-cathode plasma contactor
[NASA-CR-191172] 01 p0386 N94-10346
A vacuum four-ball tribometer to evaluate liquid lubricants for space applications
[NASA-TM-106264] 02 p0575 N94-12842
Ohmic heating of composite candidate graphite-fiber/coating combinations
[NASA-TM-4491] 02 p0554 N94-12871
Solar simulator for solar dynamic space power system testing
[NASA-TM-106393] 05 p1984 N94-20140
In-vacuo slip testing of materials for SSRMS friction brakes 05 p1661 N94-21381
Tribological characterization of spatial wet lubricants under vacuum 06 p2264 N94-24010
In-vacuum performance of Fomblin Z25-lubricated, 52100 steel bearings with TiC-coated balls 06 p2358 N94-24011
Flammability, odor, offgassing, thermal vacuum stability, and compatibility with aerospace fluids of wire insulations 08 p3166 N94-28709

VACUUM TUBE OSCILLATORS
Experimental and theoretical investigation of broadband high-power windows for millimeter waves
[KFK-5157] 04 p1391 N94-19617

VACUUM TUBES
NT BACKWARD WAVE TUBES
NT CATHODE RAY TUBES
NT CYCLOTRON RESONANCE DEVICES
NT KLYSTRONS
NT MAGNETRONS
NT MICROWAVE TUBES
NT TRAVELING WAVE TUBES
NT VACUUM TUBE OSCILLATORS
RF vacuum microelectronics
[AD-A268399] 03 p1014 N94-17423

VACUUM ULTRAVIOLET RADIATION
U FAR ULTRAVIOLET RADIATION

VALENCE
Enhanced stability of magic clusters: A case study of icosahedric Al(sub 12)X, X=B, Al, Ga, C, Si, Ge, Ti, As
[DE93-613644] 01 p0395 N94-10386
X ray and gamma ray spectroscopy of solids under pressure
[DE93-014847] 01 p0076 N94-10653
Novel electrochemical materials prepared by sol-gel chemistry
[AD-A269060] 04 p1578 N94-18405
Characterization of diamond film nucleation and growth surface
[AD-A269400] 04 p1597 N94-18459
High pressure metallization of Mott Insulators: Magnetic, structural and electronic properties
[DE93-018295] 04 p1404 N94-18805
The x ray microprobe determination of chromium oxidation state in olivine from lunar basalt and kimberlitic diamonds 05 p1686 N94-20807
Microanalysis of iron oxidation state in iron oxides using X Ray Absorption Near Edge Structure (XANES) 05 p1686 N94-20808
A valence-fluctuation theory of cuprate superconductivity
[DE94-000887] 06 p2558 N94-22942
AB-Initio calculation of the valence-band offset at strained GaAs/InAs (001) heterojunction
[DE94-602538] 07 p3061 N94-26878
Band structure of superlattice with (delta)-like potential
[DE94-608108] 08 p3516 N94-30072
A polynomial representation of the valence orbital ionization potentials
[USIP-93-06] 09 p3640 N94-31083
Characterization of the rare earth orthophosphates and Ce-doped LaPO4 by x ray absorption spectroscopy
[DE94-006313] 09 p3898 N94-31630
Periodicity and peculiarity in 120 first and second row diatomic molecules
[AD-A278836] 11 p4323 N94-35793
New anionic states of the lithium trimer
[AD-A278832] 11 p4323 N94-35797

VALIDATION
U PROVING

VALIDITY
Handbook. Volume 3: Digital systems validation book plan
[DOT/FAA/CT-93/16-VOL-3] 05 p1647 N94-20053
TOVS Pathfinder product validation and intercomparison 06 p2384 N94-23603
Validating a large geophysical data set: Experiences with satellite-derived cloud parameters 06 p2385 N94-23615
Experience of the JPL Exploratory Data Analysis Team at validating HIRS2/MSU cloud parameters 06 p2385 N94-23616
An overview of the UARS data validation effort 06 p2386 N94-23617

VALKYRIE AIRCRAFT
U B-70 AIRCRAFT

VALLEYS
NT DEATH VALLEY (CA)
Thermal studies of Martian channels and valleys using Termoskan data 01 p0443 N94-12064
Mars: The initial emplacement of ground ice in response to the thermal evolution of its early crust 01 p0462 N94-12168
Fluvial erosion on Mars: Implications for paleoclimatic change 03 p1241 N94-16210
Beta Regio rift system on Venus: Geologic interpretation of Magellan images 05 p2095 N94-20655
Evolution of the global water cycle on Mars: The geological evidence 05 p2142 N94-21660
Ancient Martian valley genesis and paleoclimatic inference: The present as a key to the past 05 p2142 N94-21661
Early Mars: The inextricable link between internal and external influences on valley network formation 05 p2146 N94-21681
The Martian valley networks: Origin by niveo-fluvial processes 05 p2146 N94-21682
Glacial landforms and late Cenozoic history of the western Soer-Rondane mountains 08 p3357 N94-29080
Geomorphological map of the region of the Paraiba Valley and the northern coastal zone of Sao Paulo State
[INPE-5531-PRP/179] 10 p4077 N94-34226
Numerical simulation of nocturnal drainage flows in an idealized valley-tributary system
[DE94-011684] 12 p4472 N94-37115
The influence of tributaries on nocturnal valley flows
[DE94-011613] 12 p4473 N94-37242

VALSALVA EXERCISE
Valsalva maneuver: Insights into baroreflex modulation of human sympathetic activity 01 p0310 N94-12000

VALSALVA MANEUVER
U VALSALVA EXERCISE

VALUE
NT Q VALUES
NASA/DOD Aerospace Knowledge Diffusion Research Project. Paper 24: A general approach to measuring the value of aerospace information products and services
[NASA-TM-109775] 10 p4150 N94-33371

VALUE ENGINEERING
Optimization of a satellite localization and message sending system
[ETN-93-94448] 05 p1737 N94-20592

VALVES
NT ARTIFICIAL HEART VALVES
NT CONTROL VALVES
NT DAMPERS (VALVES)
NT FUEL VALVES
NT GAS VALVES
NT HEART VALVES
NT PRESSURE REGULATORS
NT RELIEF VALVES

Check valve with poppet damping mechanism
[NASA-CASE-MSC-21903-1] 01 p0179 N94-10655
Check valve with poppet dashpot/frictional damping mechanism
[NASA-CASE-MSC-21950-1] 01 p0179 N94-10658
STS-55 pad abort: Engine 2011 oxidizer preburner augmented spark igniter check valve leak
[NASA-CR-193830] 02 p0533 N94-12806
Electrically controlled liquid-crystal heat valve
[AD-D015872] 04 p1443 N94-17705
Vapor-delivered lubrication of steel-steel and steel-ceramic systems
[PB93-202364] 05 p1825 N94-21451
Accelerated screening methods for determining chemical and thermal stability of refrigerant-lubricant mixtures. Part 2: Experimental comparison and verification of methods
[DE94-003664] 07 p2749 N94-26007
Rotary hydraulic servo or throttle valve
[AD-D016134] 10 p4059 N94-33757
A dynamic model of a linear actuator based on polymer hydrogel
[DE94-010800] 12 p4408 N94-37091

VAN ALLEN RADIATION BELTS
U RADIATION BELTS

VAN DE GRAAFF ACCELERATORS
Knowledge engineering for PACES, the particle accelerator control expert system
09 p3854 N94-33342

VAN DER WAALS FORCES
Electronic spectroscopy of the gas-phase OH-Kr van der Waals complex
[AD-A266891] 03 p0942 N94-14946
The roles of fluid motion and other transport phenomena in the morphology of materials
[NASA-CR-194665] 03 p1028 N94-17298
Investigation of heterojunctions and multiple quantum well structures using crystalline organic semiconductors
[AD-A272113] 05 p2018 N94-20569
One- and multi-component theories of mixtures
[DE93-040543] 05 p1966 N94-21511
Wave packet studies of the vibrational predissociation of three and four-atom van der Waals complexes
[DE94-007623] 09 p3871 N94-32598
Metal cluster-rare gas van der Waals complexes: Microscopic models of physisorption
[DE94-008134] 09 p3873 N94-32797

VANADIUM
Fracture behavior of vanadium/vanadium silicide in-situ composites
[DE93-013422] 02 p0556 N94-13389
The corrosion protection of metals by ion vapor deposited aluminum
[NASA-TM-108425] 03 p0955 N94-15832
Effects of aging time on V2O5 sol-gel coatings
[AD-A266824] 03 p0965 N94-15843
Development of vanadium-phosphate catalysts for methanol production by selective oxidation of methane
[DE93-016850] 03 p0949 N94-16897
Transient studies of low temperature catalysts for methane conversion
[DE93-041232] 05 p1680 N94-20934
Volume dependence of vanadium magnetism
[DE94-601838] 07 p3050 N94-25843
Tensile properties of commercially pure vanadium from room temperature to 1200 C
[DE94-006622] 09 p3641 N94-31581

VANADIUM ALLOYS
Electronic structure and phase stability properties in ternary substitutional alloys
[DE93-013848] 02 p0569 N94-13137
Fracture behavior of vanadium/vanadium silicide in-situ composites
[DE93-013422] 02 p0556 N94-13389
The corrosion protection of metals by ion vapor deposited aluminum
[NASA-TM-108425] 03 p0955 N94-15832
Effect of oxygen concentration and ordering on vanadium-oxygen alloy vibrational spectra
[DE93-627003] 04 p1355 N94-17692
Atlas of formability: Ti-6Al-4V ELI
[AD-A268300] 04 p1357 N94-17803
Bibliography on silicides
[AD-A270516] 04 p1374 N94-19532
Relationship of microstructure and mechanical properties for V-Cr-Ti alloys
[DE94-001431] 06 p2238 N94-22718
Effect of neutron irradiation on tensile properties of V-Cr-Ti alloys
[DE94-001433] 06 p2240 N94-23194
Hydrogen trapping with Pd coated alloy films
07 p2723 N94-25551
Study on alloy films for hydrogen separation
07 p2726 N94-25565
Microstructural development in irradiated vanadium alloys
[DE94-004307] 07 p2737 N94-26556
Deformation twinning: Influence of strain rate
[DE94-002693] 07 p2738 N94-26621
Creep properties of vanadium-base alloys
[DE94-006541] 09 p3641 N94-31486
Effect of irradiation damage and helium on the swelling and structure of vanadium-base alloys
[DE94-006540] 09 p3641 N94-31666
A state variable material model for superplastic titanium-6 percent Al-4 percent V
09 p3644 N94-32498
The effects of in-situ processing methods on the microstructure and fracture toughness of V-V3Si composites
[DE94-009093] 10 p4019 N94-33681
Transient thermal and dynamic stresses in strongback-design blankets
[DE94-012639] 12 p4530 N94-37441
Characterization of nuclear transmutations in materials irradiated test facilities
[DE94-013309] 12 p4420 N94-37552

VANADIUM COMPOUNDS
NT VANADIUM OXIDES
Molecular/polymeric magnetism
[DE94-005888] 09 p3649 N94-31201
Development of vanadium-phosphate catalysts for methanol production by selective oxidation of methane
[DE94-006759] 09 p3759 N94-31272
Metal cluster alloys and oxides: Elucidating structural and electronic effects in governing the reactivity and catalytic role of matter in finite dimensions
[DE94-010224] 11 p4328 N94-36298

VANADIUM OXIDES
A quartz crystal microbalance study of lithium insertion and removal into evaporated films MO(y) (M = Mo, Fe, and V)
[DSIS-93-00649] 02 p0810 N94-14203
Vanadium corrosion studies
[AD-A266489] 03 p0959 N94-16781
Effect of oxygen concentration and ordering on vanadium-oxygen alloy vibrational spectra
[DE93-627003] 04 p1355 N94-17692
Nanostructured materials: Mind over matter
[DE93-017690] 04 p1597 N94-18480
Technical report of ISSP. Ser. A, no. 2670: Electronic structure of light transition metal compounds studied by photoemission
[JTN-94-80556] 07 p3065 N94-27239

VANELESS DIFFUSERS
Experimental and computational investigation of the NASA low-speed centrifugal compressor flow field
[NASA-TM-4481] 03 p0869 N94-17386
Fluid dynamic noise in a centrifugal pump
[AD-A275264] 08 p3477 N94-28904
Active control of vaneless diffuser rotating stall
10 p4062 N94-34178
Experimental and computational results from a large low-speed centrifugal impeller 10 p4001 N94-34446

VANES
NT GUIDE VANES
NT JET VANES
NT WIND VANES
Laser anemometer measurements and computations for transonic flow conditions in an annular cascade of high turning core turbine vanes
[NASA-TP-3383] 01 p0015 N94-11133
A research program for improving heat transfer prediction for the laminar to turbulent transition region of turbine vanes/blades
[NASA-TM-106278] 01 p0151 N94-11256
Performance characteristics of the INS 25.5-MHz split coaxial RFQ
[DE93-753168] 01 p0144 N94-11508
Multigrid solution of internal flows using unstructured solution adaptive meshes
[NASA-CR-194233] 02 p0638 N94-14356
In-flight investigation of a rotating cylinder-based structural excitation system for flutter testing
[NASA-TM-4512] 03 p0867 N94-15783
Vane optimization for maximum efficiency using Design Of Experiments (DOX)
[AD-A270270] 04 p1320 N94-18907
Thermal/structural tailoring of engine blades (T/STAEBL). User's manual
[NASA-CR-194463] 07 p2839 N94-26692
Thermal/Structural Tailoring of Engine Blades (T/STAEBL): User's manual
[NASA-CR-194461] 07 p2843 N94-27776
Vortex generators for control of shock-induced separation. Part 1: Introduction and aerodynamics
[ESDU-93024-PT-1] 07 p2806 N94-28095
Thermal/structural tailoring of engine blades (T/SEAEBL). Theoretical manual
[NASA-CR-194462] 08 p3317 N94-28815
Theoretical, experimental, and computational evaluation of several vane-type slow-wave structures
[NASA-TM-106641] 10 p4041 N94-33996
Development of a HP-turbine for a small helicopter engine 10 p4003 N94-34456
Experimental measurements and analytical analysis related to gas turbine heat transfer. Part 1: Time-averaged heat-flux and surface-pressure measurements on the vanes and blades of the SSME fuel-side turbine and comparison with prediction. Part 2: Phase-resolved surface-pressure and heat-flux measurements on the first blade of the SSME fuel-side turbine
[NASA-CR-196296] 12 p4442 N94-36969

VANS
U TRUCKS

VAPOR BARRIER CLOTHING
Development of a new chemical warfare agent protective material 08 p3381 N94-28432

VAPOR DEPOSITION
NT METALORGANIC CHEMICAL VAPOR DEPOSITION
NT VACUUM DEPOSITION
Design of a CVD reactor for the deposition of diamond in a microgravity environment 01 p0109 N94-10127
Alkali metal for ultraviolet band-pass filter
[NASA-CASE-NPO-18433-1-CU] 01 p0381 N94-10657
Thermal-optical switching of a silicon based interference filter
[AD-A265152] 01 p0174 N94-11095
Damping mechanisms in chemically vapor deposited SiC fibers
[NASA-TM-106334] 01 p0066 N94-11135
Wide Band-Gap Semiconductors. 1991 Materials Research Society Symposium proceedings
[AD-A263418] 01 p0401 N94-11515
An ellipsometry investigation of nucleation and growth of electron cyclotron resonance plasma deposited silicon films
[AD-A265037] 01 p0401 N94-11651
Chemical Vapor Deposition of Refractory Metals and Ceramics 2. Materials Research Society Symposium proceedings
[AD-A265072] 01 p0092 N94-1 .66
Progress toward atomic layer epitaxy of diamond: Diamond films grown one layer at a time
[AD-A265530] 01 p0403 N94-12010
Analysis of the economics of DC arc CVD diamond
[AD-A265688] 01 p0403 N94-12339
Protective coatings for high-temperature polymer matrix composites
[NASA-TM-106276] 01 p0074 N94-12431
Deposition of crystalline boron thick layers from gas phase
[DE93-620499] 02 p0576 N94-12867
Research on chemical vapor deposition processes for advanced ceramic coatings
[NASA-CR-193613] 02 p0577 N94-13089
Scanning tunneling microscopy studies of diamond films and optoelectronic materials
[NASA-CR-194363] 02 p0578 N94-13246
Effects of growth conditions and substrate orientation on the properties of InSb
[DE93-013766] 02 p0812 N94-14344
Electrochemical planarization for microelectronic circuits
[DE93-017214] 02 p0627 N94-14870
Diamond epitaxy and diamondlike coatings
[AD-A266657] 03 p1206 N94-15747
Laser assisted CVD growth of AlN and GaN
[AD-A267150] 03 p1206 N94-15764
The corrosion protection of metals by ion vapor deposited aluminum
[NASA-TM-108425] 03 p0955 N94-15832
Method of producing a silicon carbide fiber reinforced strontium aluminosilicate glass-ceramic matrix composite
[NASA-CASE-LEW-15263-2] 03 p0934 N94-15929
A high flux radical beam diamond growth
[AD-A266754] 03 p1207 N94-15955
Continuous fabrication of SiC fiber tows by chemical vapor deposition
[AD-A266460] 03 p0936 N94-16569
Chemical vapor deposition of Ta2O5 corrosion resistant coatings
[DE93-015488] 03 p0969 N94-16889
Single crystal diamond thin films
[AD-A266457] 03 p1214 N94-17216
Anisotropic phase separation in amorphous Fe-Ge alloys
[DE93-015255] 03 p0961 N94-17251
Diamond growth on carbide surfaces using a selective etching technique
[AD-A267989] 03 p0973 N94-17413
Growth, characterization and device development in monocrystalline diamond films
[AD-A268206] 03 p1216 N94-17553

Gallium arsenide-based ternary compounds and multi-band-gap solar cell research
[DE93-010049] 04 p1467 N94-18483
Carbon/carbon composites coated with SiC by chemical vapor deposition
[AD-A269934] 04 p1341 N94-18544
Scaling laws for diamond chemical vapor deposition. 2: Atomic hydrogen transport
[AD-A269842] 04 p1371 N94-18740
Scaling laws for diamond chemical vapor deposition. Diamond surface chemistry
[AD-A269874] 04 p1599 N94-18745
Characterization of vapor plume species and deposition residues resulting from pulsed laser ablation of a graphite/epoxy composite
[AD-A270101] 04 p1343 N94-18869
Substrate temperature measurement and control during thermal plasma CVD
[DE93-040305] 04 p1433 N94-19135
The microstructural mechanism of electromigration failure in narrow interconnects of Al alloys
[DE93-018598] 04 p1365 N94-19282
Ionized-cluster beam/partially ionized beam deposition of electro-optical and nonlinear optical organic materials and device development
[AD-A270832] 04 p1604 N94-19596
Pressure and temperature effects on the kinetics and quality of diamond films
[AD-A270876] 04 p1606 N94-19771
Fabrication of stable large-area thin-film CdTe photovoltaic modules
[DE93-018204] 05 p1845 N94-20095
Plasma chemical vapor deposition of halide glasses
[AD-D015933] 05 p1701 N94-20331
Growth of zinc selenide single crystals by physical vapor transport in microgravity
[NASA-CR-194679] 05 p2017 N94-20346
Monocrystalline germanium film on sapphire
[AD-D015925] 05 p2017 N94-20348
Volatile CVD precursors based on copper alkoxides and mixed group 2A-copper alkoxides
[AD-D015930] 05 p1701 N94-20349
Analysis of cost: CVD diamond deposition
[AD-A271980] 05 p2018 N94-20616
Growth, characterization and device development in monocrystalline diamond films
[AD-A273097] 05 p2028 N94-21506
Fundamental studies of defect generation in amorphous silicon alloys grown by remote plasma-enhanced chemical-vapor deposition
[DE93-017083] 05 p2029 N94-21615
Research on polycrystalline thin-film submodules based on CuInSe2 materials
[DE93-018223] 05 p2029 N94-21617
Surface modification for corrosion resistance
[DE93-017419] 05 p1693 N94-21825
Techniques for producing free-standing thin films on frames
[DE93-041144] 05 p1708 N94-21954
Disilane LPCVD deposited silicon films: Deposition mechanisms, properties and capability of making transistors on thin films
[LAAS-93156] 06 p2252 N94-22910
Particle formation in a laser-heated aerosol reactor. Application to silicon and silicon nitride synthesis
[PB93-217982] 06 p2347 N94-22982
Ordered organic thin films self-assembled from the vapor phase 06 p2223 N94-24339
Structural characterization and thermal cycling behaviour of EB-PVD thermal barrier coating systems
[ISBN-0-315-83365-3] 06 p2257 N94-24468
Thin film cadmium telluride photovoltaic cells
[DE94-000201] 06 p2395 N94-24509
Photoinduced charge separation in solid state and molecular systems
[DE94-001727] 06 p2563 N94-24537
LPCVD of InN on GaAs(110) using HN3 and TMIn: Comparison with Si(100) results
[AD-A273555] 06 p2235 N94-24917
Intelligent control of chemical vapor deposition processes
[AD-A273356] 06 p2261 N94-24937
The reaction mechanism of W-CVD in Si
[ETN-94-95329] 06 p2261 N94-25084
Scanning probe lithography. 2: Selective chemical vapor deposition of copper into scanning tunneling microscope-defined patterns
[AD-A273304] 06 p2547 N94-25144
Investigation and application of microwave electron cyclotron resonance plasma physical vapour deposition
[DE93-613909] 06 p2555 N94-25333
The in situ observation of epitaxial diamond thin film nucleation and growth using emission electron microscopy
[AD-A273698] 06 p2263 N94-25489
Molecular beam mass spectrometry studies of the chemical vapor deposition of diamond
[DE94-003802] 07 p3049 N94-25601
Characterization of physically vapor deposited AF2400 thin films
[DE94-004019] 07 p2749 N94-25985
Buckyball microwave plasmas: Fragmentation and diamond-film growth
[DE94-003209] 07 p3053 N94-26031
The fracture behavior of a CVD crystalline Si3N4/amorphous Si3N4 composite
[DE94-002646] 07 p2750 N94-26124
The importance of vibrationally excited nitrogen in silicon nitride deposition systems
[AD-A274874] 07 p2750 N94-26167
The reactivity of lithium toward non-aqueous solvents of relevance to energy storage applications as studied by surface analytical techniques
[DE94-003483] 07 p2856 N94-26464
The deposition of boron nitride and carbon films on silica glass fibers
[DE94-004684] 07 p2751 N94-26564
Deposition of a-SiC:H using organosilanes in an argon/hydrogen plasma
[DE94-004428] 07 p2751 N94-26580
Chemical vapor deposition and characterization of tungsten boron alloy films
[DE94-002648] 07 p2738 N94-26610
Physical modelling and adaptive predictive control of diffusion/LPCVD reactors
[PB94-126398] 07 p2763 N94-26819
Growth, characterization and device development in monocrystalline diamond films
[AD-A274245] 07 p3060 N94-26839
Atomic layer epitaxy of group 4 materials: Surface processes, thin films, devices and their characterization
[AD-A274325] 07 p3061 N94-26885
Fabrication and characterization of nano-crystalline diamond films
[DE94-002202] 07 p3062 N94-26934
Vapor deposition of copper on stainless steel 304L
[DE94-001945] 07 p2740 N94-27006
Visible light emitting materials and injection devices
[AD-A274418] 07 p2786 N94-27079
Observation of stimulated emission from an MBE grown GaN film on sapphire
[DE94-003638] 07 p3068 N94-27724
High damage threshold anti-reflectors by physical vapor deposited amorphous fluoropolymer
[DE94-004865] 08 p3212 N94-28560
Analysis of cost: CVD diamond deposition and finishing --- Quarterly report
[AD-A275586] 08 p3212 N94-28725
Development of large area RF induction plasma for cost effective diamond
[AD-A275888] 08 p3504 N94-28776
Method of producing a ceramic fiber-reinforced glass-ceramic matrix composite
[NASA-CASE-LEW-15264-2] 08 p3180 N94-29508
Synthesis of diamond in a hydrogen plasma jet: Simulations of XRD patterns of diamond polytypes and boundary layer on a substrate 08 p3522 N94-29515
Preparation and structure of amorphous hydrogenated carbon film deposited with RF plasma CVD 08 p3223 N94-29518
A photoemission electron microscope investigation of chemical vapor deposition diamond films and diamond nucleation 08 p3215 N94-29745
Performance of CVD and CVR coated carbon-carbon in high temperature hydrogen
[DE94-005451] 08 p3487 N94-29841
The organometallic chemical vapor deposition of transition metal carbides: The use of homoleptic alkyls
[DE94-005577] 08 p3206 N94-30007
Plasma enhanced chemical vapor deposition of ZrO2 thin films
[DE94-006031] 08 p3218 N94-30104
The growth of InAsSb/InGaAs strained-layer superlattices by metal-organic chemical vapor deposition
[DE94-005576] 08 p3518 N94-30316
Large-area triple-junction a-Si alloy production scale up
[DE94-000249] 08 p3339 N94-30604
Fullerenes as precursors for diamond film growth without hydrogen or oxygen additions
[DE94-004582] 08 p3519 N94-30718
Surface chemistry of boron-doped SiO2 CVD: Enhanced uptake of tetraethyl orthosilicate by hydroxyl groups bonded to boron
[DE94-005428] 08 p3221 N94-30896
Thermochemical data for CVD modeling from ab initio calculations
[DE94-005269] 08 p3222 N94-30909
The development of CVR coatings for PBR fuels
[DE94-004233] 09 p3875 N94-31480
A silicon condenser microphone: Materials and technology
[ISBN-9-09-005899-0] 09 p3688 N94-31518
Chemical vapour deposition of tungsten for the application in integrated circuits
[ISBN-9-09-005151-1] 09 p3641 N94-31519
Degenerate four-wave mixing as a diagnostic of plasma chemistry
[DE94-008588] 09 p3889 N94-31766
Chemical vapor deposition of metal nitrides, phosphides, and arsenides
[DE94-008096] 09 p3654 N94-31976
Chemical vapor deposition fluid flow simulation modelling tool
[NASA-CR-189648] 09 p3707 N94-32480
Engineering scale development of the Vapor-Liquid-Solid (VLS) process for the production of silicon carbide fibrils
[DE94-007132] 09 p3659 N94-32618
Anisotropic phase separation through the metal-insulator transition in amorphous Mo-Ge and Fe-Ge alloys
[DE94-007259] 09 p3646 N94-32795
Growth, characterization, and device development in monocrystalline diamond films
[AD-A277863] 10 p4146 N94-33774
High-temperature behavior of advanced spacecraft TPS
[NASA-CR-195832] 10 p4014 N94-34063
Infrared detectors based on Si/SiGe superlattices and silicide/SiGe Schotty barriers operating beyond 12 micrometers
[AD-A277900] 10 p4147 N94-34082
Grain rims on ilmenite in the lunar regolith: Comparison to vapor deposits on regolith silicates 11 p4359 N94-35418
The optimization of interfaces in InAsSb/InGaAs strained-layer superlattices grown by metal-organic chemical vapor deposition
[DE94-010070] 11 p4340 N94-35698
Development of novel II-VI solar cells
[PB94-159415] 11 p4282 N94-35739
The growth of silicon nitride crystalline films using microwave plasma enhanced chemical vapor deposition
[AD-A278862] 11 p4340 N94-35828
Heterogeneous reaction mechanisms and kinetics relevant to the CVD of semiconductor materials
[DE94-011001] 11 p4340 N94-36032
Nonlinear optical composites of metal cluster laden polymers
[AD-D016217] 11 p4234 N94-36124
Demonstration of a high heat removal CVD diamond substrate edge-cooled multichip module
[DE94-010748] 11 p4260 N94-36245
Experiments in diamond film fabrication in table-top plasma apparatus 11 p4231 N94-36411
SCS-6 (tm) fiber reinforced titanium 12 p4400 N94-36652
Processing of titanium matrix composites 12 p4401 N94-36653
Manufacture and properties of sigma fibre reinforced titanium 12 p4401 N94-36655
Diamond deposition and defect chemistry studied via solid state NMR
[AD-A280609] 12 p4533 N94-36727
Turning soot into diamonds with microwaves
[DE94-013426] 12 p4422 N94-37068
Substrate effects on the structure and optical properties of epitaxial PbTiO3 thin films prepared by metal-organic chemical vapor deposition
[DE94-010432] 12 p4535 N94-37192
Basic solutions to carbon/carbon oxidation: Science and technology
[AD-A280447] 12 p4404 N94-37232
Numerical analysis of an impinging jet reactor for the CVD and gas-phase nucleation of titania
[NASA-TM-106619] 12 p4431 N94-37254
Low temperature atmospheric pressure chemical vapor deposition of group 14 oxide films
[DE94-013115] 12 p4425 N94-37317
Preliminary soft x ray studies of beta-SiC
[DE94-013023] 12 p4537 N94-37498
Morphological aspects of surface reactions
[DE94-011208] 12 p4413 N94-37713

VAPOR LIQUID EQUILIBRIUM

U LIQUID-VAPOR EQUILIBRIUM

VAPOR PHASE EPITAXY

Mechanical properties and crystal growth studies of semiconductor alloys
[AD-A268144] 03 p1216 N94-17454
Femtosecond carrier processes in compound semiconductors and real time signal processing
[AD-A268122] 03 p1005 N94-17519

Electric-field dependence of electroreflectance and photocurrent spectra at visible wavelengths in MOVPE-grown InAlGaP multiple strained quantum-well structures
[DE94-004692] 07 p2780 N94-25664
Observation of stimulated emission from an MBE grown GaN film on sapphire
[DE94-003638] 07 p3068 N94-27724
Innovative optoelectronic materials and structures using OMVPE
[AD-A275811] 08 p3511 N94-28773
High resistivity buffer layers by oxygen doping
[AD-A274986] 08 p3513 N94-29125
Advances in MOVPE compound semiconductor epitaxy manufacturing technology: From high throughput large area reactors to cluster tools
[DE94-006367] 09 p3901 N94-32104
New zinc-bis(dialkylamides) potentially usable as site-selective dopants for p-type ZnSe
[AD-A276947] 09 p3902 N94-32218
Research on high reliability refractory ohmic contacts for GaAs FETs and MODFETs
[AD-A276848] 09 p3897 N94-33034
High efficiency InP solar cells from low toxicity tertiarybutylphosphine
[NASA-TM-106598] 10 p4039 N94-33611
Optical spectroscopy of a nitrogen-hydrogen complex in ZnSe
[DE94-011622] 12 p4413 N94-37630

VAPOR PHASES
Laser beam deflection: A diagnostic tool for vapour growth experiments in microgravity
01 p0111 N94-10135
STARDUST: A simulation experiment of cosmic dust analogues production in microgravity conditions
01 p0113 N94-10175
Crystal growth from low temperature vapour phase
01 p0115 N94-10191
Project ARGO: Gas phase formation in simulated microgravity
[NASA-TM-104762] 01 p0125 N94-11235
Size dependence of chemical reactivity of gaseous metal clusters: A new mechanistic probe
[AD-A264690] 01 p0077 N94-11264
Characterization of gas-aerosol interaction kinetics using morphology dependent stimulated Raman scattering
[DE93-012324] 01 p0077 N94-11359
A model of elementary chemistry and fluid mechanics in the combustion of hydrogen on platinum surfaces
[DE93-012767] 01 p0077 N94-11370
CRESLAF, Version 4.0: A Fortran program for modeling laminar, chemically reacting, boundary-layer flow in cylindrical or planar channels
[DE93-012835] 01 p0152 N94-11371
Risk of decompression sickness in the presence of circulating microbubbles 01 p0312 N94-11548
Strategies and methodologies to develop techniques for computer-assisted analysis of gas phase formation during altitude decompression 01 p0312 N94-11547
Resist materials design: Base-catalyzed chemical amplification
[AD-A265286] 01 p0145 N94-11819
Graphite solubility and co-vesiculation in basalt-like melts at one-ATM 01 p0463 N94-12173
Development of a molecular beam technique to study early solar system silicon reactions
01 p0432 N94-12224
Multiphase equation of state for iron
[DE93-013956] 02 p0568 N94-12977
Research on chemical vapor deposition processes for advanced ceramic coatings
[NASA-CR-193613] 02 p0577 N94-13089
Hydrogen peroxide safety issues
[DE93-013895] 02 p0565 N94-14346
Electronic spectroscopy of the gas-phase OH-Kr van der Waals complex
[AD-A266891] 03 p0942 N94-14946
Fundamental studies of rocket combustion chemistry and combustion instability
[AD-A266248] 03 p0925 N94-16482
Sensitive detection of gas-phase nitro-containing energetic materials employing 226-nm radiation
[AD-A267633] 03 p0951 N94-17203
Ceramic fiber coatings development and demonstration
[AD-A267286] 03 p0972 N94-17242
Laser probing of the kinetics and dynamics of 3-5 semiconductor growth
[AD-A268388] 03 p1215 N94-17422
A basic principles description of liquid vapor phase transitions
[AD-A268331] 03 p1176 N94-17581
Effect of phase change in a debris cloud on a backwall structure
[DE93-017506] 04 p1358 N94-18100
Photodissociation studies of polyatomic free radicals
[AD-A270084] 04 p1350 N94-18799
Parameters affecting hydrogen chloride measurements
[AD-A271326] 05 p1851 N94-20025
Volatile loss from accreting icy protoplanets
05 p2084 N94-20793
Recondensation in the early solar system: Physical conditions and source material
05 p2085 N94-20849
Utilization of metals to improve the lubrication of ceramic load-bearing devices
[PB93-202448] 05 p1825 N94-21424
Lubricated wear of steel-ceramic and ceramic-ceramic systems
[PB93-202356] 05 p1825 N94-21450
Combustion in turbulent jets and buoyant flames
[PB93-202372] 05 p1682 N94-21452
Effect of powder characteristics on gas-pressure sintering of Si3N4 with rare earth additives
[DE94-000330] 05 p1694 N94-21945
Ultraviolet photosulfidation of III-V compound semiconductors for electronic passivation
[DE94-001417] 06 p2555 N94-22717
High-resolution soft x ray photoionization studies of selected molecules
[DE94-000568] 06 p2532 N94-23002
Vaporization behavior of non-stoichiometric refractory carbide materials and direct observations of the vapor phase using laser diagnostics
[DE93-040094] 06 p2348 N94-23203
Infrared analysis of vapor phase deposited tricresylphosphate (TCP)
[NASA-TM-106423] 06 p2253 N94-23371
Numerical modeling of physical vapor transport under microgravity conditions: Effect of thermal creep and stress 06 p2223 N94-24340
CFD simulation of coaxial injectors
06 p2342 N94-24430
Molecular beam mass spectrometry studies of the chemical vapor deposition of diamond
[DE94-003802] 07 p3049 N94-25601
Three methods to measure RH bond energies
[DE94-003795] 07 p3013 N94-25816
Gas phase thermochemistry of organogermanium compounds
[DE94-004885] 08 p3187 N94-28561
Ion-assisted tropospheric OH measurement technique
08 p3344 N94-28601
Numerical simulation of aerothermal characteristics in gas turbine combustors with complex geometries
08 p3154 N94-29255
Laboratory studies of chemical and photochemical processes relevant to stratospheric ozone
[NASA-CR-189351] 08 p3347 N94-29549
Reactions of metal ions and their clusters in the gas phase using laser ionization: Fourier transform mass spectrometry
[DE94-006208] 08 p3207 N94-30024
Investigations into ultraviolet matrix-assisted laser desorption
[DE94-005265] 08 p3296 N94-30908
Modern integral equation techniques for quantum reactive scattering theory
[DE94-007039] 09 p3857 N94-31639
Metal clusters: Dynamics and structure
[AD-A276842] 09 p3643 N94-32091
Vibrational spectroscopy at metal-solution interfaces: Some perspectives and prospects for electrochemical surface science
[AD-A276781] 09 p3644 N94-32169
New zinc-bis(dialkylamides) potentially usable as site-selective dopants for p-type ZnSe
[AD-A276947] 09 p3902 N94-32218
Formation of gas-phase peroxides in a rural atmosphere: An interpretation of the recent SOS/SERON field results
[DE94-002995] 09 p3766 N94-32692
Development of atmospheric characteristics of chlorine-free alternative fluorocarbons
[DE94-009791] 11 p4287 N94-36179
Hypobaric decompression sickness model development. Part 1: Diffusion of inert gas from a viscoelastic fluid (blood) into an expanding gas phase
[AD-A280298] 12 p4481 N94-37124
Numerical analysis of an impinging jet reactor for the CVD and gas-phase nucleation of titania
[NASA-TM-106619] 12 p4431 N94-37254
Photodissociation and spectroscopy of gas phase bimetallic clusters
[DE94-012607] 12 p4419 N94-37438

VAPOR PRESSURE
Evaluation of medical treatments to increase survival of ebullism in guinea pigs 01 p0302 N94-11548
The role of the geothermal gradient in the emplacement and replenishment of ground ice on Mars
01 p0463 N94-12169
Measuring surface fluxes in CAPE
[NASA-CR-193664] 02 p0711 N94-12788
Binary homogeneous nucleation: Temperature and relative humidity fluctuations and non-linearity
[DE93-007884] 02 p0709 N94-13911
The pressure broadening of HDO by O2, N2, H2, and He between 100 K and 600 K
[AD-A267118] 03 p0946 N94-15684
Effects of RVP, T(50), and oxygenates on hot-start and driveability performance at high and low altitude
[AD-A266382] 03 p0869 N94-16516
Method for doping GaAs with high vapor pressure elements
[AD-D015794] 03 p1210 N94-16538
Sodium-mercury excimer laser, phase 1
[AD-A267728] 03 p1042 N94-17230
Studies on gel electrolyte based on nitrile-butadiene copolymers
[AD-A269450] 04 p1370 N94-18282
Station climatic summaries: North America. Volume 1: The contiguous United States
[AD-A269567] 04 p1490 N94-18303
Station climatic summaries, North America. Volume 2: Alaska, Canada and Greenland
[AD-A269793] 04 p1493 N94-18732
Thermal behavior of natural zeolites
[DE93-040091] 05 p1699 N94-19975
Experimental and analytical study of cryogenic propellant boiloff to develop and verify alternate pressurization concepts for Space Shuttle external tank using a scaled down tank 06 p2266 N94-23657
Vapour pressures and critical points of liquids: Aliphatic and cyclic ketones
[ESDU-93009] 07 p2720 N94-28059
Condensation inside tubes: Computer program for pressure drop in straight tubes (horizontal and vertical with downflow)
[ESDU-93014] 07 p2806 N94-28064
Vapour pressures and critical points of liquids: Fused ring compounds
[ESDU-93028] 07 p2721 N94-28142
Laboratory studies of chemical and photochemical processes relevant to stratospheric ozone
[NASA-CR-189351] 08 p3347 N94-29549
Studies of interfaces and vapors with Optical Second Harmonic Generation
[DE94-006295] 08 p3476 N94-30841
New zinc-bis(dialkylamides) potentially usable as site-selective dopants for p-type ZnSe
[AD-A276947] 09 p3902 N94-32218
Unleaded AVGAS program
[AD-A278650] 11 p4247 N94-35795

VAPOR TRAILS
U CONTRAILS

VAPOR TRAPS
Spontaneous force optical traps
[AD-A280574] 12 p4514 N94-37041

VAPORIZERS
NT EVAPORATORS

VAPORIZING
NT BOILING
NT EVAPORATION
NT EVAPOTRANSPIRATION
NT FLASHING (VAPORIZING)
NT LEIDENFROST PHENOMENON
NT NUCLEATE BOILING
NT SUBLIMATION
NT TRANSPIRATION
Evaluation of medical treatments to increase survival of ebullism in guinea pigs 01 p0302 N94-11548
Vaporization by shock loading of albite, jadeite, and pyrex glass: Experimental study 01 p0097 N94-12039
The correlation of alkalis and aluminum during high-temperature volatilization of albite and nepheline
01 p0081 N94-12214
Gas-evaporation in low-gravity field (cogelation mechanism of metal vapors) (M-14)
02 p0588 N94-13746
Impact melting and vaporization in planetary regoliths
02 p0843 N94-14299
Trapping of water vapor from an atmosphere by condensed silicate matter formed by high-temperature pulse vaporization 03 p1248 N94-16180
Cryogenic spray vaporization in high-velocity helium, argon and nitrogen gasflows
[NASA-TM-106363] 03 p1035 N94-17446
On magnetodynamic effects initiated by a high-speed impact of a large cosmic body upon the Earth's surface
05 p2082 N94-20647
Stable Ni isotopes and Be-10 and Al-26 in metallic spheroids from Meteor Crater, Arizona
05 p1863 N94-20689
Liquid-phase circulation and mixing in multicomponent droplets vaporizing in a laminar convective environment
[AD-A272851] 05 p1802 N94-21193

LOX droplet vaporization in a supercritical forced convective environment 06 p2211 N94-23034
Evaporation and combustion of LOX under supercritical and subcritical conditions 06 p2211 N94-23035
Droplet turbulence interactions under subcritical and supercritical conditions 06 p2211 N94-23036
Fundamental rocket injector/spray programs at the Phillips Laboratory 06 p2211 N94-23039
Development of a computational testbed for numerical simulation of combustion instability 06 p2213 N94-23046
Vaporization behavior of non-stoichiometric refractory carbide materials and direct observations of the vapor phase using laser diagnostics [DE93-040094] 06 p2348 N94-23203
Liquid-oxygen droplet vaporization and combustion: Analysis of transcritical behavior and application to liquid-rocket combustion instability 08 p3197 N94-29592
Ultrahigh-current-density metal-ion implantation and diamondlike-hydrocarbon films for tribological applications [DE94-008958] 09 p3906 N94-32843
Characteristics of vaporizing cryogenic sprays for rocket combustion modeling [NASA-TM-106615] 10 p4055 N94-33605
Supersonic bare metal cluster beams [DE94-010790] 12 p4532 N94-36454

VAPORS
NT CESIUM VAPOR
NT METAL VAPORS
NT SODIUM VAPOR
NT WATER VAPOR
Hygroscopic absorption to falling films: The effects of the concentration level [ITN-93-85198] 01 p0148 N94-10391
Catalytic oxidation of organics in vapor streams at remediation sites [PB93-182962] 01 p0266 N94-11472
Toxicity study of dimethylethoxysilane (DMSES), the waterproofing agent for the Orbiter heat protective system 01 p0318 N94-11554
Deposition of impact-generated vapors in the lunar regolith 02 p0843 N94-14302
HyperVentilate: Decision-support software for soil vapor extraction technology application [PB93-134880] 03 p1094 N94-15136
Geometrical vapor blocker for parallel condensation tubes requiring cooling [NASA-CASE-MSC-22090-1] 03 p1022 N94-15962
Lasing dye sensor for chemical vapors [AD-D015786] 03 p1040 N94-16533
Studies of interactions between conducting polymer and organic vapors: Applications to chemical sensing [DE93-015694] 04 p1369 N94-18233
Image detection using edge extraction algorithms [AD-A272439] 05 p1911 N94-21203
Establishing the basis for validated predictions of highly non-equilibrium flows (with 9 attachments) [AD-A272918] 05 p1802 N94-21220
Atmospheric sampling glow discharge ionization and triple quadrupole tandem mass spectrometry for explosives vapor detection [DE93-040593] 05 p1852 N94-22004
Wear reduction in ceramic bearings by surface generated pyrolytic carbon continuously replenished by ethylene gas [AD-A278264] 06 p2364 N94-24090
Stress corrosion cracking and dealloying of copper-gold alloy in iodine vapor [DE93-633790] 07 p2734 N94-26264
Application of the Positron Annihilation Technique to the study of vapor absorption process in polyethylene (LDPE) and in imide polymer (6FDA-TMPD PI) [DE94-602737] 07 p2720 N94-27998
Interaction of multiple spark-generated bubbles in a compressible liquid [AD-A275037] 08 p3272 N94-29149
Empirical and semi-empirical relationships of liquid-vapor, solid-vapor, and solid-liquid surface energies [AD-A276480] 09 p3631 N94-31248
Using laser absorption spectroscopy to monitor composition and physical properties of metal vapors [DE94-001530] 09 p3716 N94-31599
Measurement of viscosity, density, and gas solubility of refrigerant blends in selected synthetic lubricants [DE94-007723] 09 p3653 N94-31917
Remote infrared vapor detection of volatile organic compounds [AD-A276982] 09 p3746 N94-31999
Final regulatory impact analysis: Refueling emission regulations for light duty vehicles and trucks and heavy duty vehicles [PB94-164027] 11 p4285 N94-35754
Solubility, viscosity and density of refrigerant/lubricant mixtures [DE94-009996] 11 p4245 N94-35771
Vapor-fortified QA/QC samples for the analysis of volatile organic compounds [AD-A278712] 11 p4229 N94-35776
Unleaded AVGAS program [AD-A278650] 11 p4247 N94-35795
A-TOUGH: A multimedia fluid-flow/energy-transport model for fully-coupled atmospheric-subsurface interactions [DE94-004304] 12 p4472 N94-36739

VARACTOR DIODES
Millimeter wave imaging technology [AD-A271257] 05 p1715 N94-19912
Non-linear analysis of the electrical properties of the active circuits of high-frequency oscillators 05 p1785 N94-22195
Planar varactor frequency multiplier devices with blocking barrier [NASA-CASE-NPO-18428-1-CU] 06 p2310 N94-23821

VARACTORS
U VARACTOR DIODES

VARIABILITY
Intraday variability and the compactness of extragalactic radio sources 01 p0135 N94-11064
Statistical analysis of environmental variability within the CELSS breadboard project's biomass production chamber [NASA-TM-109188] 01 p0315 N94-11258
Variability of wind stress, and sensible and latent heat flux in the North Atlantic during SEASAT 01 p0194 N94-11918
A preliminary study of the variability and magnitude of the flux of biogenic sulfur gases from a New Hampshire salt marsh 01 p0267 N94-12452
Mean flow and variability in the Kuroshio extension from GEOSAT altimetry data 01 p0209 N94-12650
Field research of wind wave spectrum variability 01 p0223 N94-12727
Spatial variability of throughfall chemistry in a tropical rainforest (Central Amazonia, Brazil) [INPE-5431-PRE/1765] 02 p0720 N94-13429
Polarization and variability of active galaxies and quasars 02 p0837 N94-13550
Analytical framework for modeling scale-related variabilities in remote sensing 02 p0685 N94-13592
Spatial and temporal variability of precipitation and chemistry: Case studies from the frontal boundary study [DE93-007883] 02 p0708 N94-13910
X ray emission from Wolf-Rayet stars with recurrent dust formation [NASA-CR-189321] 03 p1300 N94-15533
Reliability of autonomic responses and malaise across multiple motion sickness stimulation tests [NASA-TM-108787] 03 p1121 N94-15711
The use of General Circulation Models in detecting climate change induced by greenhouse gases [DE93-014369] 03 p1096 N94-16802
Variability of the Seyfert galaxy MKN 766 in the Rosat all sky survey [MPE-PREPRINT-221] 03 p1240 N94-17591
A survey of current approaches to modelling of hydrological time-series with respect to climate variability and change [WMO/TD-534] 04 p1463 N94-19435
Uncertainty versus interindividual variability [DE93-018105] 04 p1559 N94-19549
Large-scale circulation regimes and tropical cyclone characteristics over the western pacific ocean [AD-A273004] 05 p1867 N94-21307
Estimates of monthly mean soil moisture for 1979-1989 [NASA-TM-104571] 06 p2407 N94-23132
Convective organization in the Pacific ITCZ: Merging OLR, TOVS, and SSM/I information [NASA-CR-194850] 06 p2408 N94-23619
GEWEX Water Vapor Project (GVaP) 06 p2411 N94-24378
Two-stage versus sequential sample-size determination in regression analysis of simulation experiments [PB94-110558] 06 p2495 N94-24634
Transmittance fluctuations and non-linearity in random chains in the presence of applied electric fields [DE94-603665] 07 p2787 N94-27628
Variability of measured sonic boom signatures 07 p2651 N94-28197
The dynamics of tropical intraseasonal variability 08 p3371 N94-29741
Yield and variability optimization of integrated circuits: Principles and practical solutions 08 p3266 N94-29805
Interannual temperature variability and cyclone frequency over Eastern Canada and the New England States. A case study: Winter seasons 1931-1932 to 1984-1985 [ISBN-0-315-74841-9] 08 p3373 N94-29908
Interannual-decadal variability in tropical climate systems: Stable isotope records and general circulation model experiments 08 p3373 N94-29962
On interannual variability and climate change in the North Pacific 08 p3374 N94-29963
Satellite estimation of the global distribution and interannual variability of photosynthetically active radiation 08 p3334 N94-29970
Seed viability detection using computerized false-color radiographic image enhancement 08 p3387 N94-30461
Diagnostic studies of climate variability [DE94-003629] 09 p3767 N94-32711
Aspects of modeling uncertainty and prediction [DE94-007565] 09 p3852 N94-32744
Spatial correlation of ionospheric variability [AD-A278105] 09 p3776 N94-33041
EOF characterization of Atlantic SST fields using AVHRR data [INPE-5535-TDI/523] 10 p4093 N94-34203
Variability of the California Current System off Point Sur, California from April 1988 to December 1990 [AD-A278579] 12 p4476 N94-36985
The role of horizontal variability in air-sea interaction [AD-A280561] 12 p4476 N94-37047

VARIABLE AMPLITUDE LOADING
A simplistic look at limit stresses from random loading [NASA-TM-108427] 03 p1058 N94-15710

VARIABLE AREA WINGS
U TRAILING EDGE FLAPS

VARIABLE CYCLE ENGINES
Options for thrust augmentation for the Beta 2 two-stage-to-orbit launch vehicle [NASA-TM-106418] 05 p1649 N94-21759
Supercruiser Arrow HS-8 07 p2671 N94-25711
Tesseract supersonic business transport 07 p2671 N94-25713
Transient model applications. 2: Compressor stall modeling methods 07 p2829 N94-28049
Status of an inlet configuration trade study for the Douglas HSCT 10 p3977 N94-33506

VARIABLE GEOMETRY STRUCTURES
Real-time control of the Trussarm variable-geometry-truss manipulator utilizing machine vision [ISBN-0-315-87054-0] 09 p3830 N94-31735
Status of the variable diameter centerbody inlet program 10 p3978 N94-33509
Kinematic modeling of a double octahedral Variable Geometry Truss (VGT) as an extensible gimbal [NASA-TM-109127] 11 p4311 N94-35242

VARIABLE LIFT
U LIFT

VARIABLE PITCH PROPELLERS
Design of a controllable pitch underwater thruster system [AD-A271140] 05 p1821 N94-20021

VARIABLE STARS
NT CATACLYSMIC VARIABLES
NT CEPHEID VARIABLES
NT FLARE STARS
NT IRREGULAR VARIABLE STARS
NT MIRA VARIABLES
NT NOVAE
NT R CORONAE BOREALIS STARS
NT SUPERNOVA 1987A
NT SUPERNOVAE
NT SYMBIOTIC STARS
NT T TAURI STARS
A photometric study of massive x-ray binaries [ITN-93-85207] 02 p0829 N94-13231
Analysis of the IUE spectra of the strongly interacting binary beta Lyrae [NASA-CR-194118] 02 p0833 N94-14493

VARIABLE SWEEP WINGS
Overview of Langley systems studies 10 p3971 N94-33456

VARIABLE THRUST
Computational analysis of Variable Thrust Engine (VTE) performance [NASA-CR-193852] 03 p0928 N94-17442

VARIANCE (STATISTICS)
NT ANALYSIS OF VARIANCE
NT BIVARIATE ANALYSIS
NT COVARIANCE
NT MULTIVARIATE STATISTICAL ANALYSIS
NT REGRESSION ANALYSIS
Robust estimators and tests in one-sample location problem with particular consideration on modified maximum likelihood process [ETN-93-94391] 02 p0774 N94-14703

Bounds on inconsistent inferences for sequences of trials with varying probabilities
[AD-A267146] 03 p1172 N94-15733
Speckles statistics and decorrelation effects in complex ABCD optical systems
[AD-A267843] 03 p1193 N94-17012
An investigation of the Ground-Based High-Resolution Interferometer Sounder (GB-HIS) in a costal marine environment
[AD-A268052] 03 p1114 N94-17503
Polarimetric statistics of electromagnetic waves scattered by distributed targets
[PB93-195907] 04 p1389 N94-18951
Linear programming for standard and nonstandard Markovian control problems. A survey
[PB93-191948] 05 p1963 N94-21066
Parameter estimation with cost function of second order in output-error-problem
[DLR-FB-92-38] 05 p1964 N94-21139
Analysis of open-loop conical scan pointing error and variance estimators 06 p2291 N94-23263
Two-stage versus sequential sample-size determination in regression analysis of simulation experiments
[PB94-110558] 06 p2495 N94-24634
Correlation function estimator performance in non-Gaussian spherically invariant random processes
[AD-A273498] 06 p2496 N94-24951
Ten new checks to assess the statistical quality of Monte Carlo solutions in MCNP
[DE94-006137] 08 p3465 N94-30366
EOF characterization of Atlantic SST fields using AVHRR data
[INPE-5535-TDI/523] 10 p4093 N94-34203

VARIATION METHOD
U CALCULUS OF VARIATIONS

VARIATIONAL PRINCIPLES
Variational approach to probabilistic finite elements
[NASA-CR-187179] 02 p0674 N94-13873
Three-dimensional analysis of anisotropic spatially reinforced structures 03 p0939 N94-16863
Proof of stability of the hydrogen molecule
[PB93-221026] 05 p1977 N94-22271
A geometric weighted elliptic grid regeneration method for 3D unstructured ALE hydrodynamics
[DE94-000309] 06 p2448 N94-22980
Forced vibrations of a non-viscous drop
[MPIS-24/1992] 06 p2318 N94-23198
Application and development of the Schwinger multichannel scattering theory and the partial differential equation theory of electron-molecule scattering
[NASA-CR-194774] 06 p2536 N94-24798
Modelling the Shuttle Remote Manipulator System: Another flexible model 06 p2371 N94-25350
Cad of GeO2-SiO2 double-layer core dispersion-shifted single-mode fibre
[DE93-634325] 07 p3035 N94-26383
On the application of Allan variance method for Ring Laser Gyro performance characterization
[DE94-003880] 07 p2810 N94-26525
A relativistic quark model
[ISBN-0-315-60926-5] 07 p3025 N94-27333
Correlated mean field Ansatz for the Kondo necklace
[DE94-603671] 07 p3067 N94-27634
Dissipative quantum dynamics and nonlinear sigma-model
[DE94-606295] 08 p3523 N94-28617
Finite element analysis of time-independent superconductivity 09 p3691 N94-31905
Calculation of phase stability in Zr-Nb-Ru using LMTO and the cluster variation method
[AD-A278556] 10 p4137 N94-33896
Complex Kohn variational principle for two-nucleon bound-state and scattering with the tensor potential
[DE94-616651] 11 p4321 N94-35595
Variational method in relativistic two-body problem
[DE94-612462] 11 p4315 N94-36416

VARIATIONS
NT ANNUAL VARIATIONS
NT DIURNAL VARIATIONS
NT GEOMAGNETIC PULSATIONS
NT MAGNETIC VARIATIONS
NT NOCTURNAL VARIATIONS
NT PERIODIC VARIATIONS
NT SECULAR VARIATIONS
NT WIND VARIATIONS
Time evolution of cross-stream exchange associated with the variations in the Kuroshio 01 p0197 N94-11936
Fluctuations of the Kuroshio extension detected by the GEOSAT altimetry data 01 p0209 N94-12649
Water-levels fluctuations in a borehole at the Royal Observatory of Belgium: Effects on local gravity, Earth tidal, and barometric responses 03 p1100 N94-15812
Paired comparison models with time-varying parameters
[AD-A272016] 05 p1964 N94-21442
Surface-induced brightness temperature variations and their effects on detecting thin cirrus clouds using IR emission channels in the 8-12 micrometer region 05 p1880 N94-22341
Measurement of the volume mass by spontaneous Raman scattering. Study of turbulent fluctuations of mixing in a subsonic free jet. Measurements in supersonic wind tunnels
[ISL-R-102/92] 06 p2339 N94-25462
Autonomic nervous system and cardiovascular control: Clinical implications of the 1/f fluctuations of heart rate 07 p2932 N94-27540

VARIOMETERS
Concept report: Experimental vector magnetograph (EXVM) operational configuration balloon flight assembly
[NASA-CR-194702] 05 p1638 N94-21776

VARISTORS
Metal oxide varistor feasibility study
[DE93-012921] 02 p0620 N94-13031
Improvement of the stability of the process for synthesizing chemically prepared varistor powder
[DE94-000345] 05 p1763 N94-21654

VARNISHES
Thermal control coatings 05 p1664 N94-21400
Atomic oxygen treatment for non-contact removal of organic protective coatings from painting surfaces
[NASA-TM-106650] 12 p4421 N94-36952

VASCULAR SYSTEM
U CARDIOVASCULAR SYSTEM

VASOCONSTRICTION
Difference in skin blood flow reduction depending on activating maneuver of skin sympathetic nerve activity 07 p2929 N94-27525
Response to graded Lower Body Negative Pressure (LBNP) after space flight 10 p4096 N94-33637
Homeostatic responses to prolonged cold exposure: Human cold acclimatization
[AD-A280234] 12 p4481 N94-37136

VASOCONSTRICTOR DRUGS
NT SEROTONIN

VASODILATION
Synchronisation of cold induced vasodilation at various locations of one hand
[IZF-1992-B3] 04 p1504 N94-17966
Effect of prostaglandin E1 on the relationship between skin sympathetic nerve activity and reduction in skin blood flow 07 p2929 N94-27524
Effect of L-dopa on hemodynamic functions in humans 07 p2929 N94-27526

VASOMOTOR NERVOUS SYSTEM
U NERVOUS SYSTEM

VATOL AIRCRAFT
Design, fabrication and test of a vertical attitude takeoff and landing unmanned air vehicle
[AD-A273003] 05 p1646 N94-21283

VAX COMPUTERS
Detailed example of using ACEC release 3.0 with the DEC VAX Ada compiler
[AD-A267880] 03 p1152 N94-17014
Heavy ion nuclear physics research
[DE93-018862] 04 p1565 N94-17776
Telescope image modelling software in STSDAS 05 p1926 N94-22483
The evolution of the FIGARO data reduction system 05 p2048 N94-22528
The Ulysses spacecraft control and monitoring concepts and realities 06 p2502 N94-23862
The development of a statistical report software for computer system usages
[DE94-611061] 11 p4346 N94-35832

VCE
U VARIABLE CYCLE ENGINES

VCO
U VOLTAGE CONTROLLED OSCILLATORS

VECTOR ANALYSIS
NT VORTICITY
Multilevel computer-aided optimum design of structural systems using multiple basis vectors 01 p0187 N94-11055
Evaluation of two January - June 1992 ERS-1 AMI wind vector data sets 01 p0235 N94-11724
Characterization of measures with a convex matrix-k-range
[PB93-220655] 06 p2479 N94-23098
Note on the use of spherical vectorfields in Clifford analysis
[PB93-237667] 06 p2480 N94-23437
Polytopic vector analysis in igneous petrology: Application to lunar petrogenesis 06 p2615 N94-24368
Vcalc: A 3-space vector calculator
[AD-A274520] 07 p2965 N94-26831
Theoretical basis for state vector comparison, relative position display, and relative position/rendezvous prediction
[AD-A277216] 09 p3608 N94-32020

VECTOR CALCULUS
U VECTOR SPACES

VECTOR CONTROL
U DIRECTIONAL CONTROL

VECTOR DOMINANCE MODEL
New evaluation of hadronic contributions to the anomalous magnetic moment of charged leptons
[DE93-634394] 06 p2536 N94-24844
Heavy charged leptons in an SU(3)(sub L) x U(1)(sub N) model
[DE93-634367] 07 p3016 N94-26041
The form factors of the nucleons
[DE94-007096] 09 p3872 N94-32630

VECTOR MESONS
NT RHO-MESONS
PHENIX Conceptual Design Report
[DE93-015759] 03 p1182 N94-16161
Momentum and coordinate space three-nucleon potentials
[DE93-040868] 06 p2531 N94-22951
Gauge invariance and the electromagnetic current of composite pions
[DE93-040869] 06 p2532 N94-22952
Production of (phi) mesons in central Si + Au collisions at 14.6 AGeV/c
[DE94-003196] 07 p3012 N94-25795
Vector meson exchanges and CP asymmetry in K(sup +/-) yields pi(sup +/-)pi(sup 0)
[DE94-601605] 07 p3014 N94-25887
A dependence of exclusive vector meson production in muon-nucleus scattering
[DE94-003363] 07 p3016 N94-25957
Pi plus pi minus gamma and K+ K- production in two photon collisions at ARGUS
[ISBN-0-315-63598-3] 07 p3027 N94-27684
The form factors of the nucleons
[DE94-007096] 09 p3872 N94-32630
Low energy theorems from the effective Lagrangian with vector mesons
[DE94-611173] 11 p4322 N94-35785

VECTOR PROCESSING (COMPUTERS)
A molecular dynamics simulation code ISIS
[DE93-753187] 01 p0368 N94-11592
A path-oriented matrix-based knowledge representation system
[NASA-CR-4539] 02 p0744 N94-13065
Advanced computers and simulation
[DE93-014354] 02 p0740 N94-13286
Analysis and effects of the number of nests of DO loops during vector supercomputing
[NAL-TR-1146] 02 p0748 N94-13453
Obstacle detection by recognizing binary expansion patterns
[NASA-CR-194415] 02 p0514 N94-14495
An overview of parallel scientific visualization
[DE93-017105] 02 p0755 N94-14521
Cesar user library
[FFI-93/7021] 04 p1529 N94-19378
CVL: A C vector library manual. Version 2
[AD-A270614] 04 p1531 N94-19592
MGD1M: A parallel multigrid code with a fast vectorized ILU-relaxation
[CWI-NM-R9222] 05 p1930 N94-21077
Parallelizing a highly vectorized multigrid code with zebra relaxation
[CWI-NM-R9225] 05 p1935 N94-21610
Numerical multigrid software (MGD5M): A parallel multigrid code with a twisted ILLU-relaxation
[CWI-NM-R9226] 05 p1916 N94-21611
A low-cost vector processor boosting compute-intensive image processing operations 05 p1925 N94-22441
Algorithm on addition chains with restricted memory
[PB94-118692] 06 p2454 N94-23759
Iterative methods for the WLS state estimation on RISC, vector, and parallel computers
[DE94-004260] 07 p3000 N94-27569
Parallelization techniques for highly parallel vector computer 08 p3129 N94-28990
Performance evaluation of the NWT with parallel Fortran 08 p3129 N94-28992
A method of user interface for NWT 08 p3129 N94-28993
Information system for flow simulation based on the Navier-Stokes equations vectorization
[AD-B179293] 08 p3281 N94-30763
Parallel processing for differencing and histogramming
[AD-A277060] 09 p3826 N94-32274
A-TOUGH: A multimedia fluid-flow/energy-transport model for fully-coupled atmospheric-subsurface interactions
[DE94-004304] 12 p4472 N94-36739

VECTOR QUANTIZATION
Necessary conditions for the optimality of variable rate residual vector quantizers
[NASA-CR-193730] 01 p0326 N94-11197

Image coding using entropy-constrained residual vector quantization
[NASA-CR-193728] 02 p0744 N94-13113
Speaker independent recognition of isolated words using vector quantization and neural networks
[ETN-93-94390] 02 p0616 N94-14724
Color palette considerations for digital map displays
[AD-A269991] 04 p1462 N94-18679
Low bit rate coding of Earth science images
[NASA-CR-193729] 05 p2041 N94-20158
Data compression by using wavelet transforms and vector quantization
[AD-A272763] 05 p1738 N94-21182
Some extensions of the k-means algorithm for image segmentation and pattern classification
[AD-A271691] 05 p1913 N94-21364
Hierarchical multirate vector quantization for image coding 05 p1781 N94-22174
A constrained joint source/channel coder design and vector quantization of nonstationary sources
[NASA-CR-195145] 06 p2301 N94-24707
Speech coding at low to medium bit rates
[ISBN-0-315-84012-9] 07 p2770 N94-26630
Vector quantizer designs for joint compression and terrain categorization of multispectral imagery 07 p2947 N94-28262
Low frame rate video coding for small bandwidth realtime multimedia tele-education systems
[PB94-125531] 08 p3256 N94-30398
Applications of data compression to 3-D scalar field visualization 09 p3817 N94-32294
Combining nonlinear multiresolution system and vector quantization for still image compression
[DE94-009422] 11 p4305 N94-36017
Studies on image compression and image reconstruction
[NASA-CR-196304] 12 p4433 N94-36810

VECTOR SPACES
NT ADJOINTS
NT BANACH SPACE
NT CANONICAL FORMS
NT EIGENVALUES
NT EIGENVECTORS
NT HESSIAN MATRICES
NT HILBERT SPACE
NT MATRICES (MATHEMATICS)
NT SOBOLEV SPACE
NT STATE VECTORS
NT STIFFNESS MATRIX
NT STOKES THEOREM (VECTOR CALCULUS)
NT VECTORS (MATHEMATICS)
NT VORTICITY
The super vectorfield package for REDUCE. Version 1.0
[MEMO-1099] 01 p0321 N94-10265
The ring structure of chiral operators for minimal models coupled to 2D gravity
[DE93-613119] 01 p0409 N94-10500
Bound states of the N-dimensional Klein-Gordon equation with vector and scalar Coulomb potentials
[DE93-617650] 01 p0349 N94-10547
Exact solution of the N-dimensional generalized Dirac-Coulomb equation
[DE93-617649] 01 p0411 N94-10834
Homoclinic intermittency
[W-9302] 01 p0344 N94-10908
Numerical simulation of hypersonic flow for the design of the H-2 orbiting plane (HOPE), part 3
[NAL-TR-1168-PT-3] 02 p0499 N94-12948
On the symmetry algebra of the discrete states in d less than 2 closed string theory
[DE93-622903] 02 p0769 N94-13536
Development and comparison of advanced reduced-basis methods for the transient structural analysis of unconstrained structures
[NASA-TM-109015] 03 p1061 N94-17259
Groups on transformations in Finslerian spaces
[DE93-624765] 04 p1606 N94-17794
Content based-grid node selection for vector field visualization
[REPT-93-35] 04 p1525 N94-19155
Characterization of measures with a convex range: A generalization of Lyapounov's theorem
[PB93-220523] 06 p2523 N94-23094
The cusp horseshoe and its bifurcations in the unfolding of an inclination-flip homoclinic orbit
[W-9307] 06 p2480 N94-23141
Note on the use of spherical vectorfields in Clifford analysis
[PB93-237667] 06 p2480 N94-23437
The fundamental group of the complement of complexified real arrangements
[DE93-616847] 06 p2491 N94-25214
Deviation equations of Synge and Schild in spaces with affine connection and metric, and equations for gravitational waves detectors
[DE93-616852] 06 p2571 N94-25339
Deformation of the exterior algebra and the GL(sub q) (r, included in) algebra
[DE94-602558] 07 p2996 N94-26898
Illumination in diverse codimensions
[AD-A277602] 07 p2971 N94-27572
Homogeneous Poisson structures
[DE94-608112] 08 p3453 N94-30119
The Cameron-Martin theorem
[W-9315] 09 p3844 N94-31676
Stability and instability criteria for magnetohydrodynamics
[PB94-148475] 09 p3889 N94-31772

VECTORS (MATHEMATICS)
NT EIGENVECTORS
NT STATE VECTORS
NT VORTICITY
Evaluation of two January - June 1992 ERS-1 AMI wind vector data sets 01 p0235 N94-11724
On relations between Schmidt pairs arising in robust control
[CWI-BS-R9225] 02 p0764 N94-14000
On the Schmidt pairs of multivariable Hankel operators and robust control
[CWI-BS-R9226] 02 p0765 N94-14001
An efficient parallel algorithm for matrix-vector multiplication
[DE93-015125] 02 p0754 N94-14399
Some experiences with Krylov vectors and Lanczos vectors 02 p0677 N94-14621
A modified direct preconditioner for indefinite symmetric Toeplitz systems
[DE93-015234] 04 p1516 N94-17800
Segmented operations for sparse matrix computation on vector multiprocessors
[AD-A270601] 05 p1928 N94-19950
The quantum structure of matter grand challenge project: Large-scale 3-D solutions in relativistic quantum dynamics
[DE94-000328] 05 p1960 N94-21955
Implementation and parallelization of fast matrix multiplication for a fast Legendre transform
[DE94-002184] 06 p2478 N94-22975
Nested Krylov methods and preserving the orthogonality 06 p2483 N94-23681
Logarithm of probability measures and infinite divisibility of sub-stable random vectors
[PB94-118627] 06 p2486 N94-23758
VLUGR2: A vectorized local uniform grid refinement code for PDE's in 2D
[CWI-NM-R9306] 07 p2965 N94-26772

VEGA PROJECT
Regional geology of the Vega landing sites: Tentative results of photogeologic mapping 01 p0440 N94-12047
Comet Halley returns
[NASA-TM-109608] 03 p0885 N94-15296

VEGARD-KAPLAN BANDS
A high resolution ultraviolet Shuttle glow spectrograph 04 p1325 N94-19174

VEGETABLES
NT POTATOES

VEGETATION
NT CANOPIES (VEGETATION)
An expert system shell for inferring vegetation characteristics: Prototype help system (Task 1)
[NASA-CR-193411] 01 p0231 N94-11236
Enhancement effects in polarimetric radar returns: Phase difference statistics
[NASA-CR-193408] 01 p0231 N94-11309
The impact of vegetation on the atmospheric boundary layer and convective storms 01 p0277 N94-11480
Emissions of biogenic sulfur gases from Alaskan tundra 01 p0268 N94-12455
Emissions of sulfur gases from marine and freshwater wetlands of the Florida Everglades: Rates and extrapolation using remote sensing 01 p0269 N94-12457
Emissions of sulfur gases from wetlands 01 p0269 N94-12458
Effects of inorganic sulfur addition on fluxes of volatile sulfur compounds in Sphagnum peatlands 01 p0270 N94-12461
Information capability of NOAA-AVHRR data for monitoring oceanographic and atmospheric pollution 01 p0214 N94-12677
Wind erosion in semiarid landscapes: Predictive models and remote sensing methods for the influence of vegetation
[NASA-CR-194029] 02 p0715 N94-13956
Meteorological data, new series A monographs. Volume 6, no. 4: Modelization of heat fluxes at Earth ground with consideration of vegetation
[ETN-93-94169] 02 p0723 N94-14546
An expert system shell for inferring vegetation characteristics: Atmospheric techniques (Task G)
[NASA-CR-194570] 03 p1082 N94-15531
X-SAR: The X-band synthetic aperture radar on board the Space Shuttle 03 p0990 N94-15891
Radar response of vegetation: An overview 03 p0991 N94-15898
Application of Cloude's target decomposition theorem to polarimetric imaging radar data 03 p0991 N94-15901
Multifrequency observations 03 p0992 N94-15902
Heterogeneity and scaling land-atmospheric water and energy fluxes in climate systems 03 p1083 N94-16030
Unmixing AVIRIS data to provide a method for vegetation fraction subtraction 03 p1066 N94-16669
Mapping the spectral variability in photosynthetic and non-photosynthetic vegetation, soils, and shade using AVIRIS 03 p1068 N94-16679
Retrieval of biophysical parameters with AVIRIS and ISM: The Landes Forest, south west France 03 p1068 N94-16681
Mapping vegetation types with the multiple spectral feature mapping algorithm in both emission and absorption 03 p1069 N94-16686
MAC Europe 1991: Evaluation of AVIRIS, GER imaging spectrometry data for the land application testsite Oberpfaffenhofen 03 p1070 N94-16688
Using endmembers in AVIRIS images to estimate changes in vegetative biomass 03 p1070 N94-16689
Primary studies of trace quantities of green vegetation in Mono Lake area using 1990 AVIRIS data 03 p1071 N94-16695
Temporal variation in spectral detection thresholds of substrate and vegetation in AVIRIS images 03 p1073 N94-16706
The dynamics of hydroponic crops for simulation studies of the CELSS initial reference configurations
[NASA-CR-194654] 03 p1118 N94-17279
Surface fluxes important to cloud development
[DE93-016633] 04 p1488 N94-17715
Biophysical characterization and surface radiation balance
[NASA-CR-194659] 04 p1470 N94-17762
Modeling of interactions between biosphere and atmosphere on the global scale
[NASA-CR-193423] 05 p1837 N94-20205
An expert system shell for inferring vegetation characteristics
[NASA-CR-189318] 05 p1837 N94-20284
Classification of simple vegetation types using POLSAR image data 05 p1722 N94-20420
Application of Cloude's target decomposition theorem to polarimetric imaging radar data 05 p1724 N94-20429
Direction angle sensitivity of agricultural field backscatter with AIRSAR data 05 p1724 N94-20430
Measurement of evapotranspiration with combined reflective and thermal infrared radiance observations
[NASA-CR-194802] 05 p1837 N94-20951
The AGRHYMET data communications project 06 p2280 N94-22776
Atmospheric flow in heterogeneous vegetated regions
[W-9303] 06 p2401 N94-23175
Effect of land use change on the carbon cycle in Amazon soils
[NASA-CR-195168] 06 p2399 N94-24853
Human impacts on soil carbon dynamics of deep-rooted Amazonian forests
[NASA-CR-195127] 06 p2399 N94-24861
Landscape dynamics of northeastern forests
[NASA-CR-195272] 07 p2852 N94-28070
GCM studies of the influence of vegetation on the general circulation: The role of albedo in modulating climate change 08 p3348 N94-29749
Sensitivity and feedbacks associated with vegetation-related land surface parameters in a general circulation model 08 p3348 N94-29800
Use of satellite data to improve parameterization of spatial and temporal variations of gaseous dry deposition in regional-scale models
[DE94-005110] 08 p3334 N94-30022
A coupled approach to spatially derived parameters necessary for ecosystem modeling on the North Slope of Alaska: Appendix A
[DE94-005853] 08 p3349 N94-30046
Frequency dependence of polarization phase difference
[NASA-TM-109737] 08 p3254 N94-30094

A bottom-up evolution of terrestrial ecosystem modeling theory, and ideas toward global vegetation modeling
08 p3351 N94-30628
Development of simplified ecosystem models for applications in Earth system studies: The Century experience
08 p3352 N94-30629
Evaluating models of climate and forest vegetation
08 p3353 N94-30637
Modeling of the continental biosphere
09 p3770 N94-31011
Analysis of GER imaging spectrometry data for the identification of soil and vegetation parameters in land degradation studies
09 p3744 N94-31857
Inflight calibration, preprocessing, and data evaluatibn of GER 2 imaging spectrometry data
09 p3744 N94-31858
The effects of vegetation on the ability to map soils using GERIS data
09 p3744 N94-31860
Feasibility evaluation of new data interpretation approaches for vegetation analysis from airborne imaging spectroscopy
09 p3745 N94-31862
Monitoring fertilizer application by imaging spectrometry (Somerset Levels test site)
09 p3745 N94-31863
High resolution spectroscopy in agriculture: Results of the EISAC 1989 campaign
09 p3745 N94-31864
Extraction of agricultural parameters from imaging-spectrometry data and simulated MERIS data through red edge analysis
09 p3745 N94-31865
Use of SPOT and ERS-1 to map tropical vegetation and mangrove dynamics in Guiana
09 p3753 N94-32555
Dry deposition of PAN to grassland vegetation
[DE94-005111]
09 p3768 N94-32894
Comparison of standard multispectral and map-assisted classification methods with a new layered approach
10 p4075 N94-33422
Stratification of deforested areas by vegetation types in Amazonia, using geographic information systems: Study of case at SB20 Purus map
[INPE-5541-TDI/529]
10 p4077 N94-34230
VEG: An intelligent workbench for analysing spectral reflectance data
10 p4125 N94-35059
Response of plants and ecosystems to CO2 and climate change
[DE94-011583]
12 p4466 N94-37376
Surface-layer response over shrub-steppe canopy during springtime
[DE94-011235]
12 p4468 N94-37624

VEGETATION GROWTH
NT CROP GROWTH
Sulfur transformations in the sediments of a New Hampshire salt marsh
01 p0270 N94-12463
Elevated acetate concentrations in the rhizosphere of Spartina alterniflora and potential influences on sulfate reduction
01 p0271 N94-12468
Plant architecture, growth and radiative transfer for terrestrial and space environments
[NASA-CR-193476]
01 p0302 N94-12559
Application of remote sensing for coastal management in the north coast of Java
01 p0218 N94-12701
Biomass production chamber air analysis of wheat study (BWT931)
[NASA-TM-109192]
02 p0737 N94-13712
Driving terrestrial ecosystem models from space
03 p0991 N94-15896
Assessing impacts of climate change on forests: The state of biological modeling
[DE93-015916]
04 p1471 N94-17790
Characterization of Minnesota lunar simulant for plant growth
05 p1897 N94-20665
Microbial biofilm formation and its consequences for the CELSS program
[NASA-CR-195146]
06 p2438 N94-24706
Bioregenerative system components for microgravity
07 p2903 N94-25673
Root gravitropism in maize and Arabidopsis
[NASA-CR-195710]
07 p2903 N94-27940
Antarctic Record, Vol. 36, No. 2
[REPT-107]
07 p2883 N94-27963
Note on the structure of moss colonies composed of two species on King George Island, the South Shetland Islands
07 p2885 N94-27971
Plant-microbe interactions: Plant hormone production by phylloplane fungi
[PB94-135563]
08 p3385 N94-29189
Cellular polarity and interactions in plant gravipercepti on
[NASA-CR-195261]
08 p3385 N94-29943
Effect of microgravity on plant growth
[NASA-CR-196004]
11 p4296 N94-35257
Response of plants and ecosystems to CO2 and climate change
[DE94-011583]
12 p4466 N94-37376

VEGETATIVE INDEX
Design of a global soil moisture initialization procedure for the simple biosphere model
[NASA-TM-104590]
01 p0284 N94-10940
Assessment of ERS-1 SAR data for soil moisture estimation
01 p0249 N94-12492
Properties of spectral reflectance of crown and crown structure of mangrove species in Okinawa
01 p0218 N94-12700
Vegetation mapping of Indo-China Peninsula using MOS-1 MESSR and NOAA AVHRR
02 p0695 N94-14257
Estimation of vegetation damage due to ash fall in Mt. Pinatubo area using MOS-1 data
02 p0695 N94-14259
Change detection on land use and rainforest cover at Paragominas region, Brazilian Amazon
05 p1838 N94-20957
Linear mixing model applied to AVHRR LAC data
05 p1838 N94-20958
Analysis of hyper-spectral AVIRIS image data over a mixed-conifer forest in Maine
05 p1838 N94-20959
The 7th Brazilian Remote Sensing Symposium, volume4
05 p1840 N94-20965
Using NDVI/AVHRR data for crop monitoring and forecasting in South Italy
05 p1841 N94-20970
Session on coupled land surface/hydrological/atmospheric models
06 p2414 N94-24395
Mapping closed tropical forest cover in West Africa using NOAA/AVHRR-LAC data
07 p2850 N94-27184
Woody biomass density in the Tendelti area of the central Sudan
07 p2850 N94-27185
Study on environment monitoring over whole China using NDVI from AVHRR data and future project
07 p2875 N94-28289
Synergy of thermal infrared and microwave remote sensing for evaporation estimation
09 p3754 N94-32559
Quantitative analysis of woody vegetation in Soudano-Sahalian region. Textural approach (application to a Burkina Faso region)
09 p3757 N94-32574

VEHICLE WHEELS
NT NOSE WHEELS
Measuring methods for evaluation of dynamic tyre properties
[ETN-93-95054]
04 p1381 N94-19650
Landing gear with swivelling beam
[CA-PATENT-1323020]
06 p2176 N94-24181

VEHICLES
Automatic contact in DYNA3D for vehicle crashworthiness
[DE94-007143]
09 p3738 N94-32637

VEINS
A carbon and nitrogen isotope study of carbonaceous vein material in ureilite meteorites
05 p2083 N94-20726

VELOCITY
NT ACOUSTIC VELOCITY
NT AIRSPEED
NT ANGULAR VELOCITY
NT CRITICAL VELOCITY
NT ESCAPE VELOCITY
NT EXHAUST VELOCITY
NT FLOW VELOCITY
NT GROUP VELOCITY
NT HIGH SPEED
NT HYPERSONIC SPEED
NT LIGHT SPEED
NT LOW SPEED
NT ORBITAL VELOCITY
NT PHASE VELOCITY
NT PROPAGATION VELOCITY
NT RADIAL VELOCITY
NT RELATIVISTIC VELOCITY
NT ROTOR SPEED
NT SOLAR WIND VELOCITY
NT SUBSONIC SPEED
NT SUPERSONIC SPEED
NT TERMINAL VELOCITY
NT TIP SPEED
NT TRANSONIC SPEED
NT WIND VELOCITY
The motion of a conical shaped liner driven by explosive load
[ITN-93-85215]
02 p0585 N94-14507
The use of velocity spectra for stacking receiver functions with application to IRIS/IDA stations OBNINSK (OBN) and ARTI (ARU), Russia
[AD-A269087]
04 p1483 N94-18717
Antipodal fragment velocities for porous and weak targets at catastrophic impacts
05 p1836 N94-20891

VELOCITY DISTRIBUTION
Experimental study of axisymmetric thermocapillary flows
01 p0100 N94-10072
Marangoni and buoyant convections in zone melting of GaAs with liquid encapsulation
01 p0101 N94-10081
Comparison of hydrodynamic and semi-kinetic treatments for plasma flow along closed field lines
[NASA-CR-193589]
01 p0387 N94-10641
Examination of wall functions for a parabolized Navier-Stokes code for supersonic flow
[DE93-011590]
01 p0014 N94-11111
CRESLAF. Version 4.0: A Fortran program for modeling laminar, chemically reacting, boundary-layer flow in cylindrical or planar channels
[DE93-012835]
01 p0152 N94-11371
Dynamics and control of coherent structures in the turbulent wall layer: An overview
01 p0031 N94-11494
A four-dimensional, mesoscale, non-gaussian multispectral smoke model. Phase 1: Feasibility study
[AD-A264805]
01 p0152 N94-11519
Use of ERS-1 data at Saclant Undersea Research Centre
01 p0233 N94-11714
Parameterization of subgrid-scale stress by the velocity gradient tensor
01 p0155 N94-12286
Similarity states of homogeneous stably-stratified turbulence at infinite Froude number
01 p0156 N94-12292
Numerical simulation using vorticity-vector potential formulation
01 p0157 N94-12297
Laboratory studies on the velocity of fragments from impact disruptions
01 p0189 N94-12359
On the wake behind a high speed train
01 p0164 N94-12618
Spatial variability of the ocean underwater dynamic noise from satellite radar sensing data
01 p0225 N94-12740
On the theory of the decaying developed turbulence with spontaneous parity violation
[DE93-623190]
02 p0632 N94-13511
Cold dark matter halos
02 p0838 N94-13649
Least-squares finite element solutions for three-dimensional backward-facing step flow
[NASA-TM-106353]
02 p0770 N94-14407
The motion of a conical shaped liner driven by explosive load
[ITN-93-85215]
02 p0585 N94-14507
Vortex-induced disturbance field in a compressible shear layer
02 p0645 N94-14760
Parametric resonant triad interactions in a free shear layer
[NASA-TM-106365]
03 p1021 N94-15751
Studies of combustion reactions at the state-resolved differential cross section level
[DE93-017605]
03 p0948 N94-16462
The structure of turbulent boundary layers and shock wave boundary layer interactions
[AD-A266240]
03 p1026 N94-16929
To extend the thirteen-moment theory and its application to problems in rarefied hypersonic flow
[AD-A267384]
03 p0859 N94-17021
Experimental and computational investigation of the NASA low-speed centrifugal compressor flow field
[NASA-TM-4481]
03 p0869 N94-17386
Measurement of the velocity field and void fraction in a planar plunging jet
[AD-A268183]
03 p1030 N94-17511
Kinetic plasma processes occurring in the outer plasmasphere
[NASA-CR-193452]
03 p1300 N94-17524
Moist wind relationships
04 p1492 N94-18607
Surface wave group velocity tomography of East Asia, part 1
[AD-A270100]
04 p1484 N94-18868
Analysis of regional bodywave phases from earthquakes in western China, part 2
[AD-A270125]
04 p1485 N94-18873
PEACE: A Plasma Electron and Current Experiment
04 p1329 N94-19632
Numerical modelling of crystal growth
[AD-A271206]
04 p1605 N94-19719
Examinations of the friction behavior in nonstationary flow processes in pipes
[MITT-7]
04 p1423 N94-19730
Electrode array electromagnetic velocimeter
[AD-D015950]
05 p1806 N94-19882
Experimental and computational results from a large low-speed centrifugal impeller
[NASA-TM-106421]
05 p1636 N94-20136
Kinetic theory of runaway air-breakdown
[DE93-040731]
05 p1750 N94-20325
An experimental investigation of the drag mechanisms of a helicopter rotor in hovering flight
[AD-A270201]
05 p1636 N94-20486
Determination of cosmic bodies size-velocity distribution by observation of current impacts on Mars
05 p2082 N94-20648
Comparison of satellite-derived velocity fields in the coastal transition zone
[AD-A272565]
05 p1883 N94-21360

Low Reynolds-number turbulent boundary layers
[AD-A272011] 05 p1803 N94-21459
A study of the compressible flow through a diffusing S-duct
[NASA-TM-106411] 05 p1638 N94-21591
Direct detection of atomic ions from molecular photofragmentation during nonresonant multiphoton ionization of sputtered species
[DE93-040886] 05 p1976 N94-21951
Solar full-disk magnetic field image receiving system and observation software 05 p2079 N94-22552
Turbulent separated flows above an obstacle in an open channel 06 p2316 N94-22859
Shear coaxial injector instability mechanisms 06 p2213 N94-23047
A representation for the turbulent mass flux contribution to Reynolds-stress and two-equation closures for compressible turbulence
[NASA-CR-191569] 06 p2319 N94-23302
Measurements and modeling of flow structure in the wake of a low profile wishbone vortex generator
[NASA-TM-106468] 06 p2166 N94-23465
A random distribution reacting mixing layer model
[NASA-CR-194445] 06 p2187 N94-23552
Solution of mixed convection heat transfer from isothermal in-line fins 06 p2321 N94-23644
Evaluation of turbulence models in the PARC code for transonic diffuser flows
[NASA-TM-106391] 06 p2168 N94-24084
Vortical structure in a forced plane mixing layer 06 p2331 N94-24162
Stagnation region heat transfer: The influence of turbulence parameters, Reynolds number and body shape
[NASA-TM-106504] 06 p2334 N94-24481
A two-dimensional dispersion module for the TOUGH2 simulator
[DE94-002262] 06 p2335 N94-24655
A diagnostic model to estimate winds and small-scale drag from Mars Observer PMIRR data 06 p2617 N94-24874
The effects of profiles on supersonic jet noise
[NASA-CR-195184] 06 p2530 N94-25177
Conversion of the CLUSE model for applications over open ocean
[AD-A273750] 07 p2893 N94-26013
Predictive modeling of particle-laden, turbulent flows
[DE94-003298] 07 p2792 N94-26319
Laser Doppler velocimetry in a low speed multistage compressor
[AD-A274836] 07 p2818 N94-26498
Pump CFD code validation tests
[NASA-CR-193939] 07 p2822 N94-26597
Turbulent boundary layer inner-outer interactions
[AD-A274357] 07 p2794 N94-27059
Predictions of momentum and scalar fields in a jet in cross-flow using first and second order turbulence closures 07 p2803 N94-28025
Unified approach for direct and inverse boundary layer prediction using cubic spline collocation 07 p2653 N94-28326
Characterization of structural vibration: Field descriptors based on energy density and intensity
[PB94-132230] 08 p3316 N94-28404
Annual summary of basic research thermoacoustic heat transport, 1993
[AD-A275751] 08 p3230 N94-28644
The velocity field in the Northeast Atlantic from satellite-tracked drifting buoys
[AD-A275704] 08 p3376 N94-28690
Development and application of a thermistor current meter
[AD-A275816] 08 p3286 N94-28831
A random distribution reacting mixing layer model
[NASA-TM-106517] 08 p3150 N94-28923
Electron beam analysis for cyclotron harmonic and free-electron laser devices
[AD-A275070] 08 p3293 N94-29179
Spherical model for turbulence 08 p3274 N94-29730
Tail lobe ion composition at energies of 0.1 to 16 keV/e: Evidence for mass-dependent density gradients
[PAPER-93JA03201] 08 p3507 N94-30127
Computational analysis of high resolution unsteady airloads for rotor aeroacoustics
[NASA-CR-194894] 08 p3480 N94-30274
A single-fluid, self-consistent formulation of particle transport and fluid dynamics 08 p3280 N94-30352
Atomic oxygen interaction at defect sights in protective coatings on polymers flown on LDEF 09 p3593 N94-31024
Three-dimensional velocity measurements on a 6:1 prolate spheroid at 10 deg angle of attack
[AD-A276485] 09 p3702 N94-31476
The kinematics of dense clusters of galaxies 09 p3937 N94-32029
Scalar imaging velocimetry studies of turbulent flow structure and dynamics
[AD-A278395] 09 p3710 N94-33164
Laser measurements and analysis of flow in a radial inflow turbine inlet guide vanes and rotor 10 p3997 N94-33365
Large-scale velocity fields and small-scale magnetic fields during the maximum of solar cycle 22
[AD-A278378] 10 p4165 N94-33743
Bottom boundary layer stress measurements with BASS tripods: Data report STRESS 1988-1989
[AD-A277864] 10 p4092 N94-33775
Experimental and computational results from a large low-speed centrifugal impeller 10 p4001 N94-34446
Inverse design of radial flow impellers with prescribed velocity at hub and shroud 10 p4002 N94-34448
Forced unsteady deceleration of a turbulent boundary layer from a temporal perspective 10 p4053 N94-34983
Data reduction procedures for laser velocimeter measurements in turbomachinery rotors
[NASA-CR-195343] 10 p4057 N94-35224
Thickness of the layer of strong radial electric field in JFT-2M H-mode plasmas
[DE94-718993] 11 p4336 N94-35812
The velocity field created by a shallow bump in a boundary layer
[AD-A281064] 11 p4266 N94-35975
Doppler weather radar studies of precipitation systems
[AD-A279417] 11 p4295 N94-36262
Fast electron generation and transport in a turbulent, magnetized plasma
[DE94-012986] 12 p4531 N94-37730

VELOCITY ERRORS

Mirror velocity sampling errors in a Michelson interferometer
[AD-A273105] 05 p1809 N94-21508
Pushing the limit: Precision radial velocities, techniques, and applications 08 p3542 N94-30861

VELOCITY FIELDS

U VELOCITY DISTRIBUTION

VELOCITY MEASUREMENT

NT PARTICLE IMAGE VELOCIMETRY
NT WIND VELOCITY MEASUREMENT
Experimental analysis of Benard-convection by the combined application of liquid crystals and PIV 01 p0106 N94-10109
Particle image velocimetry technique: Calibration tests 01 p0111 N94-10137
Estimation of the direct acoustic radiation from turbulent spots using boundary layer velocity measurements 01 p0357 N94-10358
Velocity measurements in hypersonic flows: A review 01 p0005 N94-10436
Perpendicular blade vortex interaction and its implications for helicopter noise prediction: Wave-number frequency spectra in a trailing vortex for BWI noise prediction
[NASA-CR-193623] 01 p0357 N94-10752
Laser velocimeter measurements of the flow field generated by a forward-swept propfan during flutter
[NASA-TM-106195] 01 p0014 N94-10892
Wall interference correction based on interface measurements in subsonic wind tunnel testing 01 p0015 N94-11154
Measurement of the minority carrier diffusion length and edge surface-recombination velocity in InP 01 p0049 N94-11388
The subduction experiment. Cruise report, R/V Oceanus, cruise number 250 legs 1 and 2. Subduction 2 mooring deployment and recovery cruise, 25 January-26 February 1992
[AD-A264922] 01 p0289 N94-11853
The evolution of whole field optical diagnostics for external transonic testing
[ARA-MEMO-379] 01 p0383 N94-11887
Statistical study of HF ocean radar echo 01 p0139 N94-11905
An investigation of small scales of turbulence in a boundary layer at high Reynolds numbers 01 p0157 N94-12303
Probability density distribution of velocity differences at high Reynolds numbers 01 p0158 N94-12304
Development of the one-component diode-array velocimeter
[AD-A265552] 01 p0171 N94-12533
Quantitative mapping of pore fraction variations in silicon nitride using an ultrasonic contact scan technique
[NASA-TP-3377] 02 p0665 N94-13056
A three-dimensional supersonic turbulent boundary layer generated by an isentropic compression 02 p0503 N94-13556
High freestream turbulence effects on the transport of heat and momentum 02 p0633 N94-13559
Droplet-turbulence interactions in sprays exposed to supercritical environmental conditions
[NASA-CR-194408] 02 p0638 N94-14308
Calibration of a magnetic induction system for measurement of hypervelocities
[DE93-013949] 02 p0652 N94-14578
Investigation of the feasibility of optical diagnostic measurements at the exit of the SSME
[NASA-CR-193832] 02 p0553 N94-14682
Intra-blade quantitative transonic flow measurements at the DRA Pyestock Isentropic Light Piston Facility using PIV (Particle Image Velocimetry)
[RAE-TM-AERO/PROP-21] 02 p0509 N94-14706
An experimental study of ASTOVL related jet flows to produce CFD code validation data. Phase 3: Results of experiments
[TT-9203] 03 p1020 N94-15645
Evaporation from a meniscus within a capillary tube in microgravity
[NASA-CR-194593] 03 p0976 N94-15654
The shock Hugoniot of 316 SS and sound velocity measurements
[DE93-016525] 03 p1178 N94-16955
Measurement of the velocity field and void fraction in a planar plunging jet
[AD-A268183] 03 p1030 N94-17511
Laser velocimetry measurements of vortex flows on a delta wing at Mach 1.9
[AD-A268596] 03 p0861 N94-17609
Portable, solid state, fiber optic coupled Doppler interferometer system for detonation and shock diagnostics
[DE93-013917] 04 p1423 N94-17700
A mobile remote sensing laboratory for water vapor, trace gas, aerosol, and wind speed measurements
[DE93-017158] 04 p1489 N94-18132
Materials characterization of propellants using ultrasonics
[NASA-CR-193877] 04 p1378 N94-19494
Velocity measurements in a boundary layer with a density gradient
[DE93-019627] 04 p1422 N94-19515
Feasibility study for a measuring system velocity projectile
[FEL-91-A368] 04 p1434 N94-19797
Electrode array electromagnetic velocimeter
[AD-D015950] 05 p1806 N94-19882
Time-resolved shock compression of porous rutile: Wave dispersion in porous solids
[DE93-018848] 05 p1829 N94-19927
PVDF gauge characterization of hypervelocity-impact-generated debris clouds
[DE93-018831] 05 p1829 N94-19943
Coherent lidar design and performance verification
[NASA-CR-193813] 05 p1816 N94-20341
An experimental investigation of the drag mechanisms of a helicopter rotor in hovering flight
[AD-A270201] 05 p1636 N94-20486
Shipboard ADCP observations during RRS Charles Darwin Cruise 62
[IOS-298-1992] 05 p1882 N94-20531
Two-point laser Doppler velocimetry measurements of length-turbulent scales
[ECL-92-12] 05 p1801 N94-20542
Low-altitude cross-wind velocity measurements using pulsed visible fringe-type laser anemometry
[ISL-CO-216/92] 05 p1866 N94-20557
Shock compression of low-density foams
[DE93-040545] 05 p1707 N94-21546
Instantaneous velocity field imaging instrument for supersonic reacting flows
[NASA-CR-191162] 05 p1809 N94-21607
Particle image velocimetry
[DE93-040657] 05 p1804 N94-21748
Near wake measurements on a rotor model with Mie-vanes in the Delft open jet tunnel
[PB93-215382] 05 p1638 N94-22260
Breaking Kelvin-Helmholtz waves and cloud-top entrainment as revealed by K-band Doppler radar 05 p1874 N94-22310
Utilization of lasers for air data measurements 05 p1640 N94-22603
Hot wire anemometry: A versatile instrumentation used for predevelopment studies and flight testing of the Do-328 aircraft 05 p1640 N94-22604
Experimental Methods in Separated Flows
[ILR-MITT-260(1991)] 06 p2315 N94-22852
Pressure oscillation measurements in turbulent flows 06 p2316 N94-22855
SFOLDA: A semiconductor LDA for measurements in complex flows 06 p2316 N94-22856
An experimental study of characteristic combustion-driven flows for CFD validation 06 p2212 N94-23040
Studies of two phase flow
[NASA-CR-195099] 06 p2267 N94-23594

On the determination of local instantaneous averages in particulate flow measurements
06 p2325 N94-23663
Vortical structure in a forced plane mixing layer
06 p2331 N94-24162
Doppler global velocimetry: Development of a flight research instrumentation system for application to non-intrusive measurements of the flow field
[NASA-CR-191490] 06 p2344 N94-24360
Heterodyne array for measurement of target velocity
[AD-D016025] 06 p2545 N94-24722
Detection of velocity in high temperature liquid metals
06 p2247 N94-25127
Direct measurement of turbulent dissipation rate using dual laser doppler velocimeters
[AD-A273740] 06 p2340 N94-25530
Flow past a circular cylinder with a permeable wake splitter plate
[AD-A273765] 07 p2790 N94-25872
Breakwire technique for hypervelocity measurement
[AD-A274779] 07 p2809 N94-26358
Investigation of the aerodynamic environment for an advanced lightweight rotor in forward flight. Volume 4: Laser velocimeter wake data, advance ratio of 0.037
[NASA-TM-109040-VOL-4] 07 p2645 N94-26483
Investigation of the aerodynamic environment for an advanced lightweight rotor in forward flight. Volume 1: Laser velocimeter inflow data, advance ratio of 0.37, thrust coefficient of 0.0081 and hover tip speed of 603 feet/second
[NASA-TM-109040-VOL-1] 07 p2645 N94-26489
Investigation of the aerodynamic environment for an advanced lightweight rotor in forward flight. Volume 2: Laser velocimeter inflow data, advance ratio of 0.37, thrust coefficient of 0.0064 and hover tip speed of 710 feet/second
[NASA-TM-109040-VOL-2] 07 p2645 N94-26492
Investigation of the aerodynamic environment for an advanced lightweight rotor in forward flight. Volume 3: Laser velocimeter inflow data, advance ratio of 0.37, thrust coefficient of 0.0064 and hover tip speed of 603 feet/second
[NASA-TM-109040-VOL-3] 07 p2645 N94-26497
Investigation of spectral analysis techniques for randomly sampled velocimetry data
07 p3009 N94-27924
Annual summary of basic research thermoacoustic heat transport, 1993
[AD-A275751] 08 p3230 N94-28644
Development and application of a thermistor current meter
[AD-A275816] 08 p3286 N94-28831
Stereo imaging based particle velocimeter
[NASA-CR-195800] 08 p3289 N94-29742
Flow past a circular cylinder with a permeable wake splitter plate 08 p3275 N94-29764
The impact of electrically charged microspheres with planar surfaces under vacuum conditions
08 p3320 N94-29765
The effect of a wavy boundary on turbulent flow
08 p3280 N94-30272
Pushing the limit: Precision radial velocities, techniques, and applications 08 p3542 N94-30861
A preliminary investigation of high amplitude standing waves with laser Doppler anemometry
[AD-A276463] 09 p3860 N94-31242
Three-dimensional velocity measurements on a 6:1 prolate spheroid at 10 deg angle of attack
[AD-A276485] 09 p3702 N94-31476
Measuring the Hubble constant and our Virgo-infall velocity independently 09 p3926 N94-31968
Scalar imaging velocimetry studies of turbulent flow structure and dynamics
[AD-A278395] 09 p3710 N94-33164
Real-time adaptive control of mixing in a plane shear layer
[AD-A278379] 10 p4113 N94-33744
Visualization of secondary flow development in high aspect ratio channels with curvature
[NASA-TM-106658] 10 p4046 N94-33941
Time delay measurement correlator and its application
10 p4042 N94-34350
Flow quality studies of the NASA Lewis Research Center Icing Research Tunnel
[NASA-TM-106545] 10 p4010 N94-34919
Purity and cleanness of aerogel as a cosmic dust capture medium 11 p4247 N94-35469
A dynamic method for magnetic torque measurement
11 p4216 N94-35856
An automated method for Low Level Windshear Alert System (LLWAS) data quality analysis
[AD-A280313] 12 p4472 N94-37126

VELOCITY MODULATION
The A((2)pi(sub u))-X((2)pi(sub g)) system of Br2(+) studied by velocity modulation spectroscopy
[USIP-93-04] 04 p1569 N94-18847

VELOCITY PROFILES
U VELOCITY DISTRIBUTION

VENERA SATELLITES
Regional geology of the Venera landing sites: Tentative results of photogeologic mapping
01 p0440 N94-12048

VENEZIANO MODEL
One-loop quantum gravity on de Sitter space
[DE92-641349] 01 p0425 N94-11152
Q-deformations of the Veneziano model
[DE94-616769] 11 p4315 N94-36076

VENTILATION
Icing of turbine intake louvers
[AD-A265714] 01 p0029 N94-12274
Some flow properties of telescope enclosures estimated from water channel tests: Application of the flow visualization techniques
[NAL-TR-1178T] 02 p0830 N94-13452
Ventilated oscillatory boundary layers
[AD-A266226] 03 p1023 N94-16110
Indoor environment program
[DE93-018601] 04 p1513 N94-18935
Reactive trace metals as indicators of subduction and ventilation processes in the ocean
[AD-A273585] 06 p2419 N94-25164
A method for testing of HVAC automation equipment using the emulator and the application of the method
[VTT-TIED-1435] 07 p2822 N94-26306
Advanced Design of Ventilation Systems
[VKI-LS-1993-07] 08 p3231 N94-29598
Introduction to the design of ventilation systems
08 p3231 N94-29599
Human requirements to the indoor air quality and the thermal environment 08 p3232 N94-29600
Ventilation systems 08 p3232 N94-29601
Theory of age distribution 08 p3232 N94-29602
Ventilation models 08 p3232 N94-29603
Industrial ventilation 08 p3232 N94-29604
Ventilation cost and air cleaning
08 p3232 N94-29605
Computational fluid dynamics in ventilation. 1: Theory and one-dimensional test case
08 p3232 N94-29606
Computational fluid dynamics in ventilation. 2: Theory and codes 08 p3233 N94-29607
Computational fluid dynamics in ventilation. 3: The IEA annex 20 work 08 p3233 N94-29608
Computational fluid dynamics in ventilation. 4: Commercial application of CFD in ventilation
08 p3233 N94-29609
Computational fluid dynamics in ventilation. 5: New developments in CFD with relevance to ventilation
08 p3233 N94-29610
Computational fluid dynamics in ventilation: Practical approach 08 p3233 N94-29611
Control of heating, ventilation and air conditioning (HVAC) systems
[PB94-138807] 08 p3401 N94-30000
Using spacecraft trace contaminant control systems to cure sick building syndrome 08 p3354 N94-30470
Thermal performance of residential duct systems in basements
[LBL-33962] 11 p4250 N94-35364

VENTILATION FANS
Comparison of two cool vests on heat-strain reduction while wearing a firefighting ensemble in a hot/humid environment
[AD-A275103] 08 p3400 N94-28902

VENTILATORS
Determination of sound power levels of air terminal units according to ISO 5135-Nordic inter-laboratory tests, Nordtest project no. 968-91
[PB94-137411] 08 p3477 N94-29175
Advanced Design of Ventilation Systems
[VKI-LS-1993-07] 08 p3231 N94-29598
Introduction to the design of ventilation systems
08 p3231 N94-29599
Ventilation models 08 p3232 N94-29603
Ventilation cost and air cleaning
08 p3232 N94-29605

VENTING
Analysis of geophysical measurements and spacecraft interactions
[AD-A266064] 01 p0043 N94-10944
Optical properties of water released in low Earth orbit
[AD-A266197] 03 p1192 N94-16936
Experimental and numerical investigation of shock wave propagation through complex geometry, gas continuous, two-phase media
[DE94-001408] 07 p2791 N94-26121
Honeycomb sandwich structures: Vented versus unvented designs for space systems
[AD-A276713] 09 p3624 N94-32122
Cryogenic fluid management technologies for space transportation. Zero G thermodynamic vent system
[NASA-CR-193981] 12 p4430 N94-36806

VENTS
Parachute having improved vent line stacking
[NASA-CASE-MFS-28508-1] 01 p0014 N94-11021
Design of a resistojet for Space Station Freedom
[NASA-CR-195506] 06 p2221 N94-24979
Reactive trace metals as indicators of subduction and ventilation processes in the ocean
[AD-A273585] 06 p2419 N94-25164
Light in Thermal Environments (LITE) Workshop
[NASA-CR-195851] 09 p3790 N94-32981
Role of magma-water interaction in very large explosive eruptions
[DE94-002698] 11 p4291 N94-36103
Vent processes during the 1912 eruption at Novarupta, Katmai National Park, Alaska
[DE94-010740] 12 p4468 N94-36451

VENUS (PLANET)
Giant impact-induced atmospheric blow-off
01 p0435 N94-12019
Morphology of large impact craters and basins on Venus: Implications for ring formation 01 p0436 N94-12023
Venus small volcano classification and description
01 p0438 N94-12037
Estimation of age of Dali-Ganis rifting and associated volcanic activity, Venus 01 p0440 N94-12046
Regional geology of the Vega landing sites: Tentative results of photogeologic mapping
01 p0440 N94-12047
Regional geology of the Venera landing sites: Tentative results of photogeologic mapping
01 p0440 N94-12048
Global organization of tectonic deformation on Venus
01 p0444 N94-12066
Venus' center of mass - center of figure displacement and implications 01 p0444 N94-12067
Flexure and the role of inplane force around coronae on Venus 01 p0452 N94-12112
Can weak crust explain the correlation of geoid and topography on Venus? 01 p0453 N94-12118
Yana ring structure, North-Eastern Siberia: A possible counterpart of coronae on Venus
01 p0282 N94-12121
Russia's contribution to regional geologic mapping of Venus 01 p0454 N94-12122
The origin of Venusian channels: Modelling of thermal erosion by lava 01 p0456 N94-12131
Volcanism in southern Guinevere Planitia, Venus: Regional volcanic history and morphology of volcanic domes 01 p0467 N94-12190
Large volcanoes on Venus: Examples of geologic and structural characteristics from different classes
01 p0467 N94-12195
Regional mantle upwelling on Venus: The Beta-Atla-Themis anomaly and correlation with global tectonic patterns 01 p0467 N94-12196
Characteristics of arachnoids from Magellan data
01 p0469 N94-12204
Vulcanian explosive eruptions: A mechanism for localised pyroclast dispersal on Venus
01 p0477 N94-12243
Morphotectonics of Venus 01 p0478 N94-12248
Venus gravity
[NASA-CR-194077] 02 p0841 N94-12823
Regional tectonic analysis of Venus as part of the Pioneer Venus guest investigator project
[NASA-CR-194079] 02 p0842 N94-13561
Venus lightning
[NASA-TM-109644] 03 p1105 N94-15430
NASA images 13
[NASA-TM-109418] 03 p1247 N94-15512
Magellan: Principal Venus science findings
03 p0989 N94-15887
Morphometric comparison of Icelandic lava shield volcanoes versus selected Venusian edifices
03 p1248 N94-16178
Pargo Chasma and its relationship to global tectonics
03 p1249 N94-16181
The formation and evolution of Alpha and Tellus tesserae on Venus 03 p1249 N94-16183
Evolutionary implications of a steady-state water abundance on Venus 03 p1254 N94-16206
Spatially extensive uniform stress fields on Venus inferred from radial dike swarm geometries: The Aphrodite Terra example 03 p1254 N94-16207
Morphology and models for the evolution of eastern Hecate Chasma, Venus 03 p1256 N94-16215
Ishtar deformed belts: Evidence for deformation from below? 03 p1256 N94-16218
Tessera terrain on Venus: Implications of tessera flooding models and boundary characteristics for global distribution and mode of formation
03 p1258 N94-16226
Lava flow-field morphological classification and interpretation: Examples from Venus
03 p1259 N94-16230

Chemical differentiation, thermal evolution, and catastrophic overturn on Venus: Predictions and geologic observations 03 p1259 N94-16232
The three ages of Venus: A hypothesis based on the cratering record 03 p1261 N94-16239
Tessera terrain on Venus: Global characterization from Magellan data 03 p1264 N94-16262
Density of impact craters on tessera, Venus 03 p1264 N94-16263
Radar properties of several fluidized ejecta blankets on Venus 03 p1267 N94-16278
Venusian pancake domes: Insights from terrestrial voluminous silicic lavas and thermal modeling 03 p1286 N94-16381
Geophysical models of Western Aphrodite-Niobe region: Venus 03 p1286 N94-16382
Effective elastic thickness of the Venusian lithosphere with lateral viscosity variations in the mantle 03 p1293 N94-16421
Working group for planetary system nomenclature [NASA-CR-194406] 04 p1626 N94-18841
SO2 on Venus: IUE, HST and ground-based measurements, and the active volcanism connection 05 p2092 N94-20637
Geologic mapping of Northern Atla Regio on Venus: Preliminary data 05 p2095 N94-20654
Beta Regio rift system on Venus: Geologic interpretation of Magellan images 05 p2095 N94-20655
Beta Regio - Phoebe Regio on Venus: Geologic mapping with the Magellan data 05 p2096 N94-20656
Largest impact features on Venus: Non-preserved or non-recognizable? 05 p2096 N94-20657
Dynamics of large scale impacts on Venus and Earth 05 p2098 N94-20666
Formation and evolution of radial fracture systems on Venus 05 p2099 N94-20672
Mixing of a chemically buoyant layer at the top of a thermally convecting fluid: Implications for mantle dynamics with application to Venus 05 p2099 N94-20675
Venus magmatic and tectonic evolution 05 p2101 N94-20683
Studying Venus using a GIS database 05 p2105 N94-20707
Subduction on the margins of coronae on Venus: Evidence from radiothermal emissivity measurements 05 p2107 N94-20718
Comparative hypsometric analysis of both Earth and Venus topographic distributions 05 p2108 N94-20722
Named Venusian craters 05 p2109 N94-20725
Venus pancake dome formation: Morphologic effects of a cooling-induced variable viscosity during emplacement 05 p2110 N94-20732
Magellan at Venus: Summary of science findings 05 p2110 N94-20734
Venus' impact-crater database: Update to approximately 98 percent of the planet's surface 05 p2110 N94-20736
Searching for ancient Venus 05 p2111 N94-20743
Rifting at Devana Chasma, Venus: Structure and estimation of the effective thickness of the elastic lithosphere 05 p2113 N94-20754
Volcanic rises on Venus: Geology, formation, and sequence of evolution 05 p2113 N94-20755
Geoid, topography, and convection-driven crustal deformation on Venus 05 p2116 N94-20769
Venus gravity: New Magellan low altitude data 05 p2117 N94-20772
Response of the topography and gravity field on Venus to mantle upwelling beneath a chemical boundary layer 05 p2117 N94-20775
Differentiation of magma oceans and the thickness of the depleted layer on Venus 05 p2118 N94-20780
A tectonic resurfacing model for Venus 05 p2118 N94-20781
The missing impact craters on Venus 05 p2119 N94-20782
Impact basins on Venus and some interplanetary comparisons 05 p2119 N94-20785
Parga and Hecate Chasmata, Venus: Structure, volcanism and models of formation 05 p2121 N94-20796
The role of CO2 in weathering reactions and the presence of S2 on Venus: Implications for the pyrite stability field 05 p2122 N94-20799
The stability of oxyamphiboles: Existence of Ferric-bearing minerals under the reducing conditions on the surface of Venus 05 p2122 N94-20800
Parabolic features and the erosion rate on Venus 05 p2122 N94-20801
SPH modelling of energy partitioning during impacts on Venus 05 p2124 N94-20809
Elevation and igneous crater modification on Venus: Implications for magmatic volatile content 05 p2135 N94-20872
Large floor-fractured craters and isostatic crater modification: Implications for lithospheric thickness on Venus 05 p2135 N94-20873
Morphologic classes of impact basins on Venus 05 p2137 N94-20883
The connection between Venus' free obliquity and its CMB oblateness 05 p2139 N94-20896
SO2 on Venus: A final cross-calibration with Pioneer Venus [NASA-CR-195162] 06 p2599 N94-24988
Sulfur dioxide in the atmosphere of Venus 1 sounding rocket observations [NASA-CR-195224] 07 p3106 N94-26237
Some implications of large impact craters and basins on Venus for terrestrial ringed craters and planetary evolution 07 p2890 N94-28306
Venus Data Analysis Program: Directory of Research Projects (1993-1994) [NASA-CR-195742] 08 p3549 N94-29102
Analysis of crustal structure of Venus utilizing residual Line-of-Sight (LOS) gravity acceleration and surface topography data. A trial of global modeling of Venus gravity field using harmonic spline method [NASA-CR-195799] 08 p3549 N94-29737
Correlation studies of Pioneer Venus imagery obtained from PV experiments with near IR imagery obtained from ground-based observations during Venus inferior conjunction [NASA-CR-195772] 08 p3550 N94-29892
Tectonic History of the Terrestrial Planets [NASA-CR-195696] 09 p3939 N94-31105
Patterns of deformation and volcanic flows associated with lithospheric loading by large volcanoes on Venus 09 p3776 N94-31106
Geoid-to-topography ratios on Venus: A global perspective 09 p3940 N94-31110
The tectonic and volcanic evolution of Venus: Catastrophic or gradual? 09 p3940 N94-31111
Keeping that youthful look --- impact cratering of Venus 09 p3941 N94-31112
A tectonic resurfacing model for Venus 09 p3941 N94-31113
The resurfacing controversy for Venus: An overview and a mechanistic perspective 09 p3941 N94-31114
Plains tectonism on Venus: The deformation belts of Lavinia Planitia 09 p3941 N94-31115
A study of areas of low radio-thermal emissivity on Venus 09 p3942 N94-31992
The fine structure of Langmuir waves observed upstream of the bow shock at Venus [NASA-CR-196123] 11 p4354 N94-35378
Venus climate stability and volcanic resurfacing rates 11 p4358 N94-35413
Quantifying shapes of volcanoes on Venus 11 p4361 N94-35429
Volcano morphometry and volume scaling on Venus 11 p4361 N94-35431
Rheology, tectonics, and the structure of the Venus lithosphere 11 p4367 N94-35479
Atmosphere of Venus [NASA-CR-194214] 11 p4367 N94-35507
Magellan collection of radar calibration results [NASA-CR-194753] 11 p4367 N94-35509
Magellan to Venus [NASA-CR-195779] 11 p4201 N94-35510
Patterns of brittle deformation under extension on Venus 11 p4373 N94-36168

VENUS ATMOSPHERE
NT VENUS CLOUDS
Photochemical modelling of Venus clouds using Pioneer Venus data [NASA-CR-194108] 01 p0434 N94-10823
Reduction and analysis of seasons 15 and 16 (1991 - 1992) Pioneer Venus radio occultation data and correlative studies with observations of the near-infrared emission of Venus [NASA-CR-194128] 02 p0841 N94-13083
A global traveling wave on Venus [NASA-CR-194356] 03 p1246 N94-15182
Evolutionary implications of a steady-state water abundance on Venus 03 p1254 N94-16206
Principal investigators data package for Project Initiation Conference (PIC): EUVS sounding rocket no. 36.117CL. Target: Venus [NASA-CR-194663] 03 p0923 N94-17126
Magnetic effects in Venus/solar wind interaction [NASA-CR-194666] 03 p1299 N94-17281
Pioneer Venus data analysis for the retarding potential analyzer [NASA-CR-194673] 03 p1297 N94-17292
Venus lower thermosphere studies [NASA-CR-193546] 04 p1629 N94-19418
Impact disturbance of the Venus atmosphere 05 p2106 N94-20709
Searching for ancient Venus 05 p2111 N94-20743
The role of CO2 in weathering reactions and the presence of S2 on Venus: Implications for the pyrite stability field 05 p2122 N94-20799
The stability of oxyamphiboles: Existence of Ferric-bearing minerals under the reducing conditions on the surface of Venus 05 p2122 N94-20800
Parabolic features and the erosion rate on Venus 05 p2122 N94-20801
Are Plinian type eruptions possible on Venus? 05 p2123 N94-20803
Discovery Venera surface: Atmosphere geochemistry experiments mission concept 05 p2123 N94-20806
SPH modelling of energy partitioning during impacts on Venus 05 p2124 N94-20809
SO2 on Venus: A final cross-calibration with Pioneer Venus [NASA-CR-195162] 06 p2599 N94-24988
Sulfur dioxide in the atmosphere of Venus 1 sounding rocket observations [NASA-CR-195224] 07 p3106 N94-26237
Venus Data Analysis Program: Directory of Research Projects (1993-1994) [NASA-CR-195742] 08 p3549 N94-29102
Multiple scattering of polarized radiation in planetary atmospheres [ETN-94-96018] 09 p3674 N94-31551
Plasma waves in the nightside ionosphere of Venus 10 p4164 N94-33431
Venus climate stability and volcanic resurfacing rates 11 p4358 N94-35413
Atmosphere of Venus [NASA-CR-194214] 11 p4367 N94-35507

VENUS CLOUDS
Photochemical modelling of Venus clouds using Pioneer Venus data [NASA-CR-194108] 01 p0434 N94-10823
Reduction and analysis of seasons 15 and 16 (1991 - 1992) Pioneer Venus radio occultation data and correlative studies with observations of the near-infrared emission of Venus [NASA-CR-194128] 02 p0841 N94-13083
A global traveling wave on Venus [NASA-CR-194356] 03 p1246 N94-15182
Venus lightning [NASA-TM-109644] 03 p1105 N94-15430
Correlation studies of Pioneer Venus imagery obtained from PV experiments with near IR imagery obtained from ground-based observations during Venus inferior conjunction [NASA-CR-195772] 08 p3550 N94-29892
H2O-H2SO4 system in Venus' clouds and OCS, CO, and H2SO4 profiles in Venus' troposphere 11 p4370 N94-36152

VENUS PROBES
NT MAGELLAN SPACECRAFT (NASA)
NT MARINER 10 SPACE PROBE
NT VENERA SATELLITES

VENUS RADAR ECHOES
Venus mountain-top mineralogy: Misconceptions about pyrite as the high radar-reflecting phase 01 p0455 N94-12129
Resolving topographic detail on Venus by modeling complex Magellan altimetry echoes 03 p1283 N94-16368

VENUS RADAR MAPPER
U MAGELLAN SPACECRAFT (NASA)

VENUS RADAR MAPPER PROJECT
U MAGELLAN PROJECT (NASA)

VENUS SURFACE
Morphology of large impact craters and basins on Venus: Implications for ring formation 01 p0436 N94-12023
Estimation of age of Dali-Ganis rifting and associated volcanic activity, Venus 01 p0440 N94-12046
Regional geology of the Vega landing sites: Tentative results of photogeologic mapping 01 p0440 N94-12047
Global organization of tectonic deformation on Venus 01 p0444 N94-12066
Venus' center of mass - center of figure displacement and implications 01 p0444 N94-12067
Venus resurfacing rates: Constraints provided by 3-D Monte Carlo simulations 01 p0453 N94-12119
A pattern recognition system for locating small volvanoes in Magellan SAR images of Venus 01 p0455 N94-12126
Venus mountain-top mineralogy: Misconceptions about pyrite as the high radar-reflecting phase 01 p0455 N94-12129
Buoyant subduction on Venus: Implications for subduction around coronae 01 p0455 N94-12130
The origin of Venusian channels: Modelling of thermal erosion by lava 01 p0456 N94-12131
Geology and surface characteristics of Bell Regio, Venus 01 p0457 N94-12136
Lava flows on Venus: Analysis of motion and cooling 01 p0457 N94-12137

Galileo/NIMS near-infrared thermal imagery of the surface of Venus 01 p0457 N94-12139
A two-stage (turbulent-drainage) mechanism for the emplacement of impact crater outflows on Venus 01 p0458 N94-12145
Volcanism in southern Guinevere Planitia, Venus: Regional volcanic history and morphology of volcanic domes 01 p0467 N94-12190
Comparison of the distribution of large magmatic centers on Earth, Venus, and Mars 01 p0467 N94-12192
The Magellan volcanic and magmatic feature catalog 01 p0467 N94-12193
Synthesis of global thematic mapping, Venus: Geologic correlations/questions for the Magellan gravity mission 01 p0467 N94-12194
Giant radiating dyke swarms on Earth and Venus 01 p0283 N94-12236
The rate of chemical weathering of pyrite on the surface of Venus 01 p0477 N94-12246
Morphotectonics of Venus 01 p0478 N94-12248
Regional tectonic analysis of Venus as part of the Pioneer Venus guest investigator project [NASA-CR-194079] 02 p0842 N94-13561
Magellan: Principal Venus science findings 03 p0989 N94-15887
Pargo Chasma and its relationship to global tectonics 03 p1249 N94-16181
The formation and evolution of Alpha and Tellus tesserae on Venus 03 p1249 N94-16183
Spatially extensive uniform stress fields on Venus inferred from radial dike swarm geometries: The Aphrodite Terra example 03 p1254 N94-16207
Morphology and models for the evolution of eastern Hecate Chasma, Venus 03 p1256 N94-16215
Ishtar deformed belts: Evidence for deformation from below? 03 p1256 N94-16218
Tessera terrain on Venus: Implications of tessera flooding models and boundary characteristics for global distribution and mode of formation 03 p1258 N94-16226
Lava flow-field morphological classification and interpretation: Examples from Venus 03 p1259 N94-16230
Chemical differentiation, thermal evolution, and catastrophic overturn on Venus: Predictions and geologic observations 03 p1259 N94-16232
Emplacement of multiple flow units on very shallow slopes, east Kawelu Planitia flow field, Venus 03 p1260 N94-16235
The three ages of Venus: A hypothesis based on the cratering record 03 p1261 N94-16239
The depths of the largest impact craters on Venus 03 p1264 N94-16261
Tessera terrain on Venus: Global characterization from Magellan data 03 p1264 N94-16262
Density of impact craters on tessera, Venus 03 p1264 N94-16263
A first-order model for impact crater degradation on Venus 03 p1265 N94-16268
Estimates of lithospheric thickness on Venus 03 p1267 N94-16277
Radar properties of several fluidized ejecta blankets on Venus 03 p1267 N94-16278
Tectonics of Neyterkob corona on Venus 03 p1270 N94-16299
Implications of crater distributions on Venus 03 p1270 N94-16300
Megaplumes on Venus 03 p1271 N94-16301
Preliminary analysis of Dione Regio, Venus: The final Magellan regional imaging gap 03 p1271 N94-16302
The distribution of large volcanoes on Venus as a function of height and altitude 03 p1271 N94-16303
Structural mapping of Maxwell Montes 03 p1271 N94-16304
Global Magellan-image map of Venus at full resolution 03 p1274 N94-16319
The cartography of Venus with Magellan data 03 p1274 N94-16320
Meander properties of Venusian channels 03 p1275 N94-16324
Spectral study of Venus global topography and geoid from Magellan and PVO data 03 p1276 N94-16332
Sheet flow fields on Venus 03 p1278 N94-16338
Models of thermal/chemical boundary layer convection: Potential application to Venus 03 p1279 N94-16348
Resolving topographic detail on Venus by modeling complex Magellan altimetry echoes 03 p1283 N94-16368
Large-scale volcanism associated with coronae on Venus 03 p1285 N94-16376
Tectonic resurfacing of Venus 03 p1285 N94-16380
Relief of some small landforms on Venus 03 p1293 N94-16418
Working group for planetary system nomenclature [NASA-CR-194406] 04 p1626 N94-18841
SO2 on Venus: IUE, HST and ground-based measurements, and the active volcanism connection 05 p2092 N94-20637
Geologic mapping of Northern Atla Regio on Venus: Preliminary data 05 p2095 N94-20654
Beta Regio rift system on Venus: Geologic interpretation of Magellan images 05 p2095 N94-20655
Beta Regio - Phoebe Regio on Venus: Geologic mapping with the Magellan data 05 p2096 N94-20656
Largest impact features on Venus: Non-preserved or non-recognizable? 05 p2096 N94-20657
Formation and evolution of radial fracture systems on Venus 05 p2099 N94-20672
Magellan vertical polarization radar observations 05 p1744 N94-20691
Crater destruction on the Venusian highlands by tectonic processes 05 p2103 N94-20696
Some deformation trends and topographic characteristics of tesserae on Venus 05 p2105 N94-20706
Studying Venus using a GIS database 05 p2105 N94-20707
Impact disturbance of the Venus atmosphere 05 p2106 N94-20709
Chocolate tablet aspects of cytherean Meshkenet Tessera 05 p2106 N94-20710
Ridge belt-related scarps and troughs: Compressional crustal bending on Venus 05 p2106 N94-20711
Comparative hypsometric analysis of both Earth and Venus topographic distributions 05 p2108 N94-20722
Named Venusian craters 05 p2109 N94-20725
Distribution of small volcanic cones on the surface of Venus by size and elevation: Implications for differential deposition of volcanic features 05 p2110 N94-20731
Venus pancake dome formation: Morphologic effects of a cooling-induced variable viscosity during emplacement 05 p2110 N94-20732
Venus' impact-crater database: Update to approximately 98 percent of the planet's surface 05 p2110 N94-20736
Searching for ancient Venus 05 p2111 N94-20743
Rifting at Devana Chasma, Venus: Structure and estimation of the effective thickness of the elastic lithosphere 05 p2113 N94-20754
Volcanic rises on Venus: Geology, formation, and sequence of evolution 05 p2113 N94-20755
Geoid, topography, and convection-driven crustal deformation on Venus 05 p2116 N94-20769
Scattering by Venus' surface 05 p2117 N94-20771
A tectonic resurfacing model for Venus 05 p2118 N94-20781
The missing impact craters on Venus 05 p2119 N94-20782
Impact basins on Venus and some interplanetary comparisons 05 p2119 N94-20785
Earth-based measurement of lunar topography using delayed radar interferometry 05 p2119 N94-20787
The stability of oxyamphiboles: Existence of Ferric-bearing minerals under the reducing conditions on the surface of Venus 05 p2122 N94-20800
Discovery Venera surface: Atmosphere geochemistry experiments mission concept 05 p2123 N94-20806
SPH modelling of energy partitioning during impacts on Venus 05 p2124 N94-20809
Magellan Mission 05 p1652 N94-20829
Complex ridged terrain-related ridge belts on Venus: Global distribution and classification 05 p2129 N94-20835
Is there uniformitarian or catastrophic tectonics on Venus? 05 p2129 N94-20839
Arcuate and circular structures in the Tharsis region: Evidence of coronae on Mars 05 p2134 N94-20863
Geology and radiophysical properties of the Venera and Vega landing sites 05 p2135 N94-20867
Elevation and igneous crater modification on Venus: Implications for magmatic volatile content 05 p2135 N94-20872
Large floor-fractured craters and isostatic crater modification: Implications for lithospheric thickness on Venus 05 p2135 N94-20873
Morphologic classes of impact basins on Venus 05 p2137 N94-20883
SO2 on Venus: A final cross-calibration with Pioneer Venus [NASA-CR-195162] 06 p2599 N94-24988
Some implications of large impact craters and basins on Venus for terrestrial ringed craters and planetary evolution 07 p2890 N94-28306
Venus Data Analysis Program: Directory of Research Projects (1993-1994) [NASA-CR-195742] 08 p3549 N94-29102
Patterns of deformation and volcanic flows associated with lithospheric loading by large volcanoes on Venus 09 p3776 N94-31106
Geoid-to-topography ratios on Venus: A global perspective 09 p3940 N94-31110
Keeping that youthful look --- impact cratering of Venus 09 p3941 N94-31112
The resurfacing controversy for Venus: An overview and a mechanistic perspective 09 p3941 N94-31114
Plains tectonism on Venus: The deformation belts of Lavinia Planitia 09 p3941 N94-31115
A study of areas of low radio-thermal emissivity on Venus 09 p3942 N94-31992
Quantifying shapes of volcanoes on Venus 11 p4361 N94-35429
Mesoscale roughness of Venus 11 p4361 N94-35430
Volcano morphometry and volume scaling on Venus 11 p4361 N94-35431
Rheology, tectonics, and the structure of the Venus lithosphere 11 p4367 N94-35479
Formation of fold and thrust belts on Venus due to horizontal shortening of a laterally heterogeneous lithosphere 11 p4367 N94-35480

VERBAL COMMUNICATION
NT CONVERSATION
Noise levels and their effects on Shuttle crewmembers' performance: Operational concerns 01 p0314 N94-11538
Correspondence standards [NHB-1450.10B] 01 p0420 N94-11589
Complex information coordination performance: Differential changes in working memory contributions following training [AD-A267007] 03 p1132 N94-15762
ATC/pilot voice communications: A survey of the literature [DOT/FAA/AM-93/20] 05 p1738 N94-21201
The central executive component of working memory [AD-A274295] 07 p2938 N94-26683
Virtual annotation: Verbal communication in virtual reality [REPT-93-67] 09 p3674 N94-31645

VERIFICATION (PROVING)
U PROVING

VERSATILITY
Flexibility and costs in the design process: A decision support model [ISBN-9-06-814522-3] 02 p0597 N94-14808
Design patterns mixing genericity and inheritance in the development of reusable components [REPT-93-021] 09 p3808 N94-31178

VERTEBRAL COLUMN
U SPINE

VERTEBRATES
NT BABOONS
NT BIRDS
NT CATS
NT CHICKENS
NT DOLPHINS
NT FISHES
NT FROGS
NT GUINEA PIGS
NT HUMAN BEINGS
NT MAMMALS
NT MARINE MAMMALS
NT MICE
NT MONKEYS
NT PRIMATES
NT RABBITS
NT RATS
NT RODENTS
NT SCHOOLS (FISH)
NT SHEEP
NT SWINE
NT WATERFOWL
Proposed law of nature linking impacts, plume volcanism, and Milankovitch cycles to terrestrial vertebrate mass extinctions via greenhouse-embryo death coupling 07 p2876 N94-28307

VERTICAL AIR CURRENTS
Dynamics and control of coherent structures in the turbulent wall layer: An overview 01 p0031 N94-11494
Linkage of anthropogenic aerosol to clouds and climate [DE93-016434] 02 p0719 N94-13080
Modeling of biosphere-atmosphere interaction for forest and pastureland in the Amazon [INPE-5454-TDI/496] 02 p0707 N94-13330
A modeling study of the mesocyclone [AD-A274889] 07 p2893 N94-26168
On eddy accumulation with limited conditional sampling to measure air-surface exchange [DE94-005112] 08 p3368 N94-28568
On the origins of low-level tornadic circulations within the remnants of hurricane Andrews [AD-A275373] 08 p3369 N94-29011

A study of the thermospheric dynamics of the high-latitude E region using a spectral thermospheric general circulation model 08 p3362 N94-29743
Evaluation of the National Meteorological Center mesoscale model for prediction of severe convection over Central Arizona 08 p3371 N94-29744
Multiparameter radar and aircraft based studies of microphysical, kinematic, and electrical structure of convective clouds during CaPE
[AD-A278544] 10 p4085 N94-33677
A numerical study of thunderstorm electrification
[AD-A277531] 10 p4089 N94-33709
Effects of mesoscale convective organization and vertical wind shear on the cumulus-environment interaction 10 p4090 N94-34910

VERTICAL ATTITUDE TAKEOFF-LANDING AIRCRAFT
U VATOL AIRCRAFT

VERTICAL DISTRIBUTION
NT STAR DISTRIBUTION
An investigation using empirical orthogonal functions and objective analysis to analyse the vertical temperature structure of a gulf stream meander
[AD-A265116] 01 p0289 N94-11868
The acoustic arrangement for measuring vertical structure of sea current 01 p0223 N94-12729
Remote sensing of light scattering coefficient of sea water vertical distribution by the means of airborne lidar 01 p0224 N94-12736
On the vertical structure of seasonal, interannual and intraseasonal flows
[AD-A265346] 02 p0719 N94-12992
Fluxes of heat and water vapour in a convective mixed layer during EFEDA
[DLR-FB-92-21] 02 p0716 N94-14132
Meteorological data, new series A monographs. Volume 6, no. 3: Estimation of influence of high clouds in the radiation field and the climat by analysis of NOAA AVHRR data
[ETN-93-94170] 02 p0723 N94-14707
Vertical structure models of the 1990 equatorial disturbance on Saturn 03 p1277 N94-16333
Altitude profile of aerosols on Mars from measurements of its thermal radiation on limb 03 p1294 N94-16423
Second flight of the Spacelab grille spectrometer during the Atlas-1 mission
[AERONAUTICA-ACTA-A-367-1992] 03 p0923 N94-17592
A surface energy budget model modifying heat flow by foliage effects
[AD-A268598] 03 p1085 N94-17610
A one dimensional numerical model, with an application to the vertical distribution of dissolved oxygen in the ocean
[DE93-018481] 04 p1495 N94-17779
The vertical distribution of heating in the tropical atmosphere
[AD-A270452] 04 p1490 N94-18514
Using computerized tomography to determine ionospheric structures
[DE93-018904] 04 p1485 N94-19002
Meso-Beta scale numerical simulation studies of terrain-induced jet streak mass/momentum perturbations
[NASA-CR-194627] 05 p1864 N94-20138
Wrinkle ridges, reverse faulting, and the depth penetration of lithospheric stress in lunae planum, Mars 05 p2141 N94-20910
Cloud, dust, and ozone vertical profiles from solar occultation measurements: Implications for dynamics 06 p2617 N94-24877
Results from the VISA project
[AD-A273752] 06 p2406 N94-25540
Wind measurements with an incoherent lidar
[AD-A273756] 07 p2891 N94-25722
An overview of the TNO contribution to VAST 92
[AD-A273751] 07 p2893 N94-26016
Theory and observations of horizontal and vertical structure of gravity wave perturbations in the middle atmosphere 08 p3366 N94-30802
Atmospheric turbulence within and above a coniferous forest
[ISBN-0-315-75468-0] 08 p3375 N94-30870

VERTICAL FINS
U FINS

VERTICAL FLIGHT
Piloting Vertical Flight Aircraft: A Conference on Flying Qualities and Human Factors
[NASA-CP-3220] 02 p0521 N94-13294
Design criteria for integrated flight/propulsion control systems for STOVL fighter aircraft 02 p0521 N94-13297
Optimal flight guidance for aircraft in windshear
[CA-PATENT-1,307,573] 05 p1650 N94-21050
Safe heliports through design and planning
[AD-A279034] 10 p4009 N94-34104

VERTICAL LANDING
Moving-base simulation evaluation of thrust margins for vertical landing for the NASA YAV-8B Harrier aircraft
[NASA-TM-104008] 01 p0030 N94-11259
MIL-H-8501B: Application to shipboard terminal operations 02 p0521 N94-13296
Evaluation of two cockpit display concepts for civil tiltrotor instrument operations on steep approaches 02 p0517 N94-13323
Single STAGE Rocket Technology (SSRT) DC-X test program environmental assessment
[AD-A265940] 04 p1337 N94-17879
Lift and pitching moment induced on jet STOVL aircraft hovering in ground effect
[AD-A269700] 04 p1317 N94-18577
Design, fabrication and test of a vertical attitude takeoff and landing unmanned air vehicle
[AD-A273003] 05 p1646 N94-21283
Data link development for the archytas vertical takeoff and landing transitional flight unmanned aerial vehicle
[AD-A272499] 05 p1646 N94-21548
Summary of lift and lift/cruise fan powered lift concept technology
[NASA-CR-177619] 06 p2176 N94-23489
Experiments into the scaling parameters required for exhaust gas ingestion testing of vertical landing aircraft 07 p2671 N94-28017
Influence of headwind on hot gas reingestion and consideration of pressure ratio scaling 07 p2675 N94-28018

VERTICAL MOTION
The free decay of coupled heave and pitch motions of a model frigate
[DRA/TM(AWMH)92340] 03 p1146 N94-15702
New techniques for contrail forecasting
[AD-A269686] 04 p1490 N94-18573
Vertical motion in the SYNOP central array
[AD-A273593] 06 p2418 N94-24795
Three dimensional vorticity field in the California current system
[AD-A276951] 09 p3788 N94-32220
Simulation of a precipitation event in the western United States
[DE94-004835] 09 p3786 N94-32791

VERTICAL MOTION SIMULATORS
Moving-base simulation evaluation of thrust margins for vertical landing for the NASA YAV-8B Harrier aircraft
[NASA-TM-104008] 01 p0030 N94-11259
Vertical motion simulator familiarization guide
[NASA-TM-103923] 02 p0527 N94-13008
Effects of simulator motion and visual characteristics on rotorcraft handling qualities evaluations 02 p0524 N94-13317
Fidelity assessment of a UH-60A simulation on the NASA Ames vertical motion simulator
[NASA-TM-104016] 03 p0870 N94-15793
Some VTOL head-up display drive-law problems and solutions
[NASA-TM-104027] 05 p1635 N94-20035

VERTICAL STABILIZERS
U STABILIZERS (FLUID DYNAMICS)

VERTICAL TAILS
U STABILIZERS (FLUID DYNAMICS)
U TAIL ASSEMBLIES

VERTICAL TAKEOFF
Single STAGE Rocket Technology (SSRT) DC-X test program environmental assessment
[AD-A265940] 04 p1337 N94-17879
Overview of STOVL aircraft propulsion research offtakes and vertical lift systems
[NASA-TM-106387] 04 p1321 N94-19353
Summary of lift and lift/cruise fan powered lift concept technology
[NASA-CR-177619] 06 p2176 N94-23489

VERTICAL TAKEOFF AIRCRAFT
NT FLYING PLATFORMS
NT X-14 AIRCRAFT
Piloting Vertical Flight Aircraft: A Conference on Flying Qualities and Human Factors
[NASA-CP-3220] 02 p0521 N94-13294
Design, fabrication and test of a vertical attitude takeoff and landing unmanned air vehicle
[AD-A273003] 05 p1646 N94-21283
Data link development for the archytas vertical takeoff and landing transitional flight unmanned aerial vehicle
[AD-A272499] 05 p1646 N94-21548
Safe heliports through design and planning
[AD-A279034] 10 p4009 N94-34104
Tipjet 80-inch model rotor hover test: Test no. 1198
[AD-A279680] 11 p4191 N94-36261
Analysis of vertiport studies funded by the Airport Improvement Program (AIP)
[SCT-93RR-21] 12 p4390 N94-37424

VERTICAL TAKEOFF AND LANDING
U VERTICAL LANDING
U VERTICAL TAKEOFF

VERTICES
U APEXES

VERTIGO
Basic understanding of vertigo 08 p3390 N94-28855
Space and vertigo: In relation to space motion sickness 08 p3390 N94-28857
Equilibrium dysfunction in the clinical field 08 p3390 N94-28858

VERTOL MILITARY HELICOPTERS
U BOEING AIRCRAFT

VERY HIGH FREQUENCIES
NT P BAND
Groundwave HF ocean surface radar 01 p0139 N94-11906
VHF air/ground communications for air traffic control. Volume 1: A decision tree approach to system innovations
[AD-A268485] 04 p1316 N94-18384
VHF air/ground communications for air traffic control: A decision tree approach to system innovations, volume 2
[AD-A268632] 04 p1386 N94-18495
Sporadic-E observations during LoVHF transionospheric direction finder measurements
[AD-A270619] 05 p1716 N94-19951
The ORBCOMM data communications system 06 p2281 N94-22782
Radar signature related radome techniques for flush-mounted HF-, VHF- and, UHF communication antennas
[PB93-204618] 06 p2294 N94-23742
Experimental and theoretical investigation of RF absorption and reflection from preformed plasmas
[AD-A274189] 07 p3046 N94-27098
Packet radio data link applications in the NASA Langley Research Center Transport Systems Research Vehicle
[NASA-TM-109071] 07 p2665 N94-27423
Characteristics of 30-MHz interference noises observed by riometers 07 p2884 N94-27965
VHF-UHF noise surveys at Gulkana, Elmensdorf AFB, Galena AFB, Kotzebue and Cape Lisburne, Alaska and NRL, Pomonkey, Maryland
[PL-TR-93-2136] 07 p2777 N94-28211
A space-based classification system for RF transients
[DE94-003933] 08 p3240 N94-28522
VHF impedance measurement: A review
[PB94-138682] 08 p3267 N94-30115
Measurement basis of near fields in spherical coordinates in the 100 MHz to 6 GHz band
[REPT-932-430-107] 08 p3255 N94-30153
TIPC user manual
[DE94-004470] 12 p4432 N94-36443
VHF adaptive antenna development task
[AD-A280320] 12 p4434 N94-37127

VERY HIGH FREQUENCY RADIO EQUIPMENT
A compact 150 GHz SIS receiver cooled by 4 K GM refrigerator
[REPT-36] 07 p2776 N94-27340

VERY HIGH SPEED INTEGRATED CIRCUITS
U VHSIC (CIRCUITS)

VERY LARGE ARRAY (VLA)
Interferometric astronomy on the Moon 06 p2601 N94-23378
Conceptual design and architecture of hexapod robotic vehicles for the (L)OVLA project 06 p2369 N94-23405
Phasing the Very Large Array on Galileo in the presence of Jupiter's strong radio emission 08 p3164 N94-29621

VERY LARGE SCALE INTEGRATION
Design automation tools for testable VLSI circuits
[ISBN-0-315-61461-7] 02 p0621 N94-13333
NASA Space Engineering Research Center for VLSI systems design
[NASA-CR-194035] 02 p0625 N94-14325
VLSI for high-speed digital signal processing
[AD-A267709] 03 p1007 N94-14936
NASA Space Engineering Research Center for VLSI System Design
[NASA-CR-194587] 03 p1008 N94-15547
Fault handling schemes in electronic systems with specific application to radiation tolerance and VLSI design
[NASA-CR-194559] 03 p1008 N94-15640
Technology transfers and reliable oxides
[AD-A266948] 03 p1175 N94-15758
Leak detection utilizing analog binaural (VLSI) techniques
[NASA-CASE-NPO-18399-1-CU] 03 p1014 N94-17323
Fabricating binary optics: An overview of binary optics process technology 03 p1195 N94-17343
Applications of advanced diffractive optical elements 03 p1197 N94-17356

Femtosecond carrier processes in compound semiconductors and real time signal processing
[AD-A268122] 03 p1005 N94-17519
Synthesis techniques and analysis tool for on-chip fault-tolerance
[AD-A269148] 04 p1521 N94-18259
The 1991 3rd NASA Symposium on VLSI Design
[NASA-CR-194589] 04 p1397 N94-18337
New dynamic FET logic and serial memory circuits for VLSI GaAs technology 04 p1397 N94-18339
Automated ILA design for synchronous sequential circuits 04 p1397 N94-18340
Single phase dynamic CMOS PLA using charge sharing technique 04 p1397 N94-18341
Cellular logic array for computation of squares
04 p1398 N94-18343
Fault tolerant sequential circuits using sequence invariant state machines 04 p1398 N94-18344
VLSI architectures for geometrical mapping problems in high-definition image processing
04 p1398 N94-18345
Low power signal processing research at Stanford
04 p1393 N94-18351
Pulse-firing winner-take-all networks
04 p1399 N94-18353
VLSI synthesis of digital application specific neural networks 04 p1399 N94-18355
Measurement selection for parametric IC fault diagnosis 04 p1399 N94-18356
Fuzzy control of magnetic bearings
04 p1399 N94-18357
Direct kinematics solution architectures for industrial robot manipulators: Bit-serial versus parallel
04 p1399 N94-18358
Simplified microprocessor design for VLSI control applications 04 p1400 N94-18359
A modified reconfigurable data path processor
04 p1400 N94-18360
Systolic array IC for genetic computation
04 p1400 N94-18361
High-performance multiprocessor architecture for a 3-D lattice gas model 04 p1400 N94-18362
Verification of VLSI designs 04 p1400 N94-18363
A new variable testability measure
04 p1400 N94-18364
Controlling state explosion during automatic verification of delay-insensitive and delay-constrained VLSI systems using the POM verifier 04 p1400 N94-18365
Formal verification of an MMU and MMU cache
04 p1400 N94-18366
Formal hardware verification of digital circuits
04 p1401 N94-18367
A verification logic representation of indeterministic signal states 04 p1401 N94-18372
Parallel optimization algorithms and their implementation in VLSI design 04 p1401 N94-18374
Asynchronous sequential circuit design using pass transistor iterative logic arrays 04 p1402 N94-18376
Pulse mode VLSI asynchronous circuits
04 p1402 N94-18377
Improved self arbitrated VLSI asynchronous circuits
04 p1402 N94-18378
A special purpose silicon compiler for designing supercomputing VLSI systems 04 p1402 N94-18379
ARPA/CSTO rapid VLSI implementation
[AD-A269170] 04 p1403 N94-18695
VLSI for high-speed digital signal processing
[AD-A270406] 04 p1404 N94-18706
An innovative neural manufacturing concept
[DE93-017212] 04 p1527 N94-19238
FASTBUS simulation models in VHDL
[USIP-92-07] 04 p1515 N94-19295
High precision on-line standard arithmetic operators: Design and implementation
[ETN-93-95006] 04 p1552 N94-19487
Computation of large numbers and VLSI: Application to GCD, to stretched GCD and at euclidian distance
[ETN-93-95009] 04 p1552 N94-19499
Silicon compilation: From the circuit to the system
[ETN-93-95010] 04 p1406 N94-19501
VLSI implementation of neuromorphic learning networks
[AD-A270825] 04 p1407 N94-19665
Signal processing algorithms for heterogeneous architectures
[AD-A271248] 04 p1392 N94-19724
VLSI design for reliability-current density
[AD-A270719] 05 p1749 N94-20110
The Fifth NASA Symposium on VLSI Design
[NASA-CR-194644] 05 p1753 N94-21079
An adaptive, lossless data compression algorithm and VLSI implementations 05 p1753 N94-21080
Space qualified high speed Reed Solomon encoder
05 p1754 N94-21088
High performance MPEG-audio decoder IC
05 p1744 N94-21092
VLSI mixed signal processing system
05 p1744 N94-21100
Power optimization in logic isomers
05 p1756 N94-21101
Computation of signal delays in RC networks
05 p1744 N94-21102
Delay analysis of combinations of pass transistors and classical logic gates 05 p1756 N94-21103
Mixed voltage VLSI design 05 p1756 N94-21104
Bridging faults in BiCMOS circuits
05 p1756 N94-21105
Test pattern generation for ILA sequential circuits
05 p1757 N94-21107
Testing self-timed circuits using scan paths
05 p1757 N94-21109
Detection of CMOS bridging faults using minimal stuck-at fault test sets 05 p1757 N94-21110
Robust neural classifier circuits using asynchronous design 05 p1757 N94-21111
Practical issues in implementing roving spares in VLSI systolic arrays 05 p1758 N94-21114
A novel VLSI processor architecture for supercomputing arrays 05 p1758 N94-21115
Synthesis algorithm of VLSI multipliers for ASIC
05 p1758 N94-21116
Design and implementation of GaAs HBT circuits with ACME 05 p1758 N94-21117
Reliable interface design for combining asynchronous and synchronous circuits 05 p1758 N94-21119
Design methods for fault-tolerant finite state machines
05 p1758 N94-21120
A unified approach to VLSI layout automation and algorithm mapping on processor arrays
05 p1759 N94-21127
A fixed/variable bit-rate data compression architecture
05 p1759 N94-21128
High-speed Viterbi decoding with overlapping code sequences 05 p1760 N94-21130
A cost-effective methodology for the design of massively-parallel VLSI functional units
05 p1760 N94-21132
Behavioral model simulation studies of an image compressor 05 p1760 N94-21133
Polar processing project
[AD-A271583] 05 p1739 N94-21235
VLSI design for reliability-hot carrier effects
[AD-A271586] 05 p1761 N94-21256
CMU very fast range-imaging system
[AD-A272057] 05 p1761 N94-21282
The 1992 4th NASA SERC Symposium on VLSI Design
[NASA-CR-194591] 05 p1763 N94-21694
Applications of correlator chips in radio science
05 p1763 N94-21695
Single event phenomena: Testing and prediction
05 p1763 N94-21696
A 20 MHz CMOS reorder buffer for a superscalar microprocessor 05 p1764 N94-21700
Analog/digital pH meter system I.C.
05 p1764 N94-21701
On the decomposition of synchronous state mechines using sequence invariant state machines
05 p1764 N94-21703
Heuristic-based scheduling algorithm for high level synthesis 05 p1764 N94-21704
NASA SERC digital correlator projects
05 p1765 N94-21708
Fully-depleted silicon-on-sapphire and its application to advanced VLSI design 05 p1765 N94-21709
Defect-sensitivity analysis of an SEU immune CMOS logic family 05 p1765 N94-21711
A novel visual hardware behavioral language
05 p1765 N94-21715
HDL to verification logic translator
05 p1766 N94-21717
A simple modern correctness condition for a space-based high-performance multiprocessor
05 p1766 N94-21718
A mean field neural network for hierarchical module placement 05 p1766 N94-21720
Schematic driven layout of Reed Solomon encoders
05 p1766 N94-21722
Bit-systolic arithmetic arrays using dynamic differential gallium arsenide circuits 05 p1767 N94-21724
A VLSI implementation of DCT using pass transistor technology 05 p1767 N94-21725
A DRAM compiler algorithm for high performance VLSI embedded memories 05 p1767 N94-21729
Low power, CMOS digital autocorrelator spectrometer for spaceborne applications 05 p1666 N94-21733
A real time correlator architecture using distributed arithmetic principles 05 p1768 N94-21734
Low energy CMOS for space applications
05 p1768 N94-21735
Self assembly: An approach to terascale integration
[DE93-040104] 05 p1769 N94-21846
The distributed CAD system for LSI/VLSI design
05 p1923 N94-22068
VLSI architectures for the new (T,L) algorithm
05 p1745 N94-22110
VLSI design of a bit serial parallel processing 4 extender chip for M-path convolutional decoding
05 p1775 N94-22132
VLSI design of a parallel video output interface
05 p1778 N94-22153
Architectures of the free space optical interconnects
05 p1789 N94-22220
The VLBA correlator: Real-time in the distributed era
05 p2049 N94-22547
Customizable VLSI artificial neural network chips based on a novel technology
[DE94-001418] 06 p2307 N94-23008
Mixed analog-digital description and simulation: Proposition for VHDL-analogue
[RR-908-I] 06 p2450 N94-23180
Area-power-delay trade-off in logic synthesis
[ISBN-9-09-005332-8] 06 p2461 N94-25080
Real-time 3-D pose estimation using a high-speed range sensor
[AD-A273873] 07 p2809 N94-25967
A complete version of the Ada tasking coprocessor
07 p2950 N94-26721
Physical modelling and adaptive predictive control of diffusion/LPCVD reactors
[PB94-126398] 07 p2763 N94-26819
Partitioning structural VHDL circuits for parallel execution on hypercubes
[AD-A274390] 07 p2785 N94-26830
Design of a parallel discrete event simulation coprocessor
[AD-A274135] 07 p2982 N94-27123
A fast Fourier transform radix-2 complex butterfly with built-in self-test
[ISBN-0-315-84139-7] 07 p2982 N94-27649
Dry etching process development for submicron and nanometer semiconductor devices
[PB94-133196] 07 p2788 N94-28357
Construction of a connectionist network supercomputer
[AD-A275765] 08 p3405 N94-28764
Nonvolatile programmable neural network synaptic array
[NASA-CASE-NPO-18578-1-CU]
08 p3265 N94-29426
Micromanufacturing: Recent developments in this country and abroad 08 p3235 N94-29769
Self-stressing test structures used for high-frequency electromigration
[DE94-006142] 08 p3267 N94-30368
A neuron network for image classification: From algorithm to implantation
[TELECOM-93-E-005] 09 p3687 N94-31168
VLSI implementation of stray insensitive switched capacitor composite operational amplifiers
[AD-A276461] 09 p3687 N94-31240
Module generation for self-testing integrated systems
[ISBN-9-09-004570-8] 09 p3688 N94-31520
A hierarchical approach to test generation for CMOS VLSI circuits
[ISBN-9-09-005449-9] 09 p3689 N94-31535
An analysis of instruction-cached SIMD computer architecture
[AD-A276519] 09 p3806 N94-31934
Application of the modified voltage-dividing potentiometer to overlay metrology in a CMOS/bulk process
[DE94-007937] 09 p3695 N94-32700
VLSI for high-speed digital signal processing
[AD-A277617] 09 p3697 N94-32957
Research in VLSI system implementation of neuromorphic learning networks
[AD-A278247] 10 p4112 N94-33403
A CMOS VLSI IC for real-time opto-electronic two-dimensional histogram generation
[AD-A277910] 10 p4040 N94-33921
Systolic matrix inversion using a Monte Carlo method
[PB94-148798] 10 p4130 N94-34257
Theoretical and experimental studies of auditory processing
[AD-A278505] 10 p4134 N94-34293
High level modelling and design of asynchronous interface logic
[PB94-167822] 11 p4258 N94-35534

VERY LONG BASE INTERFEROMETRY

Pulsar astrometry by using VLBI (PSR0329 between Kashima 26mPhi and Usuda 64mPhi)
01 p0351 N94-10968
Propagation Effects in Space VLBI
01 p0134 N94-11060
Interstellar scattering and the selection of extragalactic radiosources with highly compact components
01 p0134 N94-11063

Intraday variability and the compactness of extragalactic radio sources 01 p0135 N94-11064
Interstellar scattering and the pulsar studies with space VLBI 01 p0135 N94-11065
VLBI and the detection of interstellar magnetohydrodynamic waves 01 p0135 N94-11066
Generalization of Dyson criterion for the amplitude-phase fluctuations case and for the system of interferometers 01 p0135 N94-11067
The possibility of image restoration under observation in a regime of strong scattering 01 p0136 N94-11068
The superresolution effect observed through a random medium 01 p0136 N94-11069
Tropospheric and ionospheric effects on differential astrometry with a ground-space based VLBI array 01 p0136 N94-11070
Elimination of the influence of the atmosphere on the accuracy of solutions to astrometric problems by means of a ground-space VLBI network 01 p0136 N94-11071
J2000.0 modelling of GEOAIM in the analysis of VLB1 data from the NASA crustal dynamics project [ISBN-0-315-59463-2] 02 p0684 N94-13368
Theory of post-block 2 VLBI observable extraction [NASA-CR-194543] 02 p0686 N94-13872
Applications of SLR 03 p0911 N94-15556
Tectonic deformation in southern California [NASA-CR-194621] 03 p1101 N94-16021
Radioastron flight operations 06 p2502 N94-23861
Navigation of space VLBI missions: Radioastron and VSOP 06 p2513 N94-23926
The 1404+286: A non-ideal calibrator for VLBI observations [PB94-104908] 06 p2599 N94-24521
LOITA: Lunar Optical/Infrared Telescope Array [NASA-CR-195532] 06 p2546 N94-24816
Constraining proposed combinations of ice history and Earth rheology using VLBI determined baseline length rates in North America 06 p2405 N94-25205
Project PARAS: Phased array radio astronomy from space 07 p3081 N94-25703
Wobble-nutation modes of the Earth [ISBN-0-315-84246-6] 07 p3102 N94-26669
Combining GPS and VLBI earth-rotation data for improved universal time 08 p3144 N94-29614
Line-of-sight tropospheric calibration from measurements in arbitrary directions 08 p3249 N94-29654
Providing hydrogen maser timing stability to orbiting VLBI radio telescope observations by post-measurement compensation of linked frequency standard imperfections 08 p3297 N94-30670
Are there two engines at the center of 3C286? [PB94-149218] 10 p4162 N94-34379
NASA Space Geodesy Program: GSFC data analysis, 1993. VLBI geodetic results 1979 - 1992 [NASA-TM-104605] 11 p4281 N94-35261
Correlator data analysis for the array feed compensation system 11 p4253 N94-35553

VERY LONG BASELINE ARRAY (VLBA)
The VLBA correlator: Real-time in the distributed era 05 p2049 N94-22547

VERY LOW FREQUENCIES
Effects of energetic particle events on VLF/LF propagation parameters/1989 [AD-A265266] 01 p0275 N94-11013
A study of the amplification of laser and VLF waves using a simple pendulum model [AD-A270857] 04 p1442 N94-19770
VLF Harold E. Holt RADHAZ measurements [AD-A272018] 05 p1737 N94-20620
Very low frequency and low frequency transmitting antenna parameter monitoring system [AD-D015989] 06 p2302 N94-25049
JARE data reports. No. 186: Upper atmosphere physics data. Syowa and Asuka Stations, 1990 [JTN-94-80594] 07 p2881 N94-27299
Memories of National Institute of Polar Research. Series A-19. Upper atmosphere physics: ELF emission in high latitudes: Ray path calculation and ground-satellite observations [JTN-94-80592] 07 p2882 N94-27342
Study of generation mechanisms of magnetospheric VLF/ELF emissions based on the direction findings 08 p3361 N94-29245
Lightning-induced coupling of the radiation belts to geomagnetically conjugate ionospheric regions 09 p3772 N94-31773
Applied Computational Electromagnetics Society Journal, volume 9, number 1, March 1994 [AD-A276753] 09 p3679 N94-32183

VERY SMALL APERTURE TERMINALS
U VSAT (NETWORK)

VESTA ASTEROID
Ejecting basaltic achondrites from Vesta: Hydrodynamical impact models 01 p0429 N94-12036
The asteroid-meteorite connection: Forging a new link to Vesta as the parent body of basaltic achondrite (HED) meteorites 01 p0429 N94-12068
Petrologic constraints on the surface processes on asteroid 4 Vesta and on excavation depths of diogenite fragments 03 p1241 N94-16208

VESTIBULAR NYSTAGMUS
Equilibrium dysfunction in the clinical field 08 p3390 N94-28858

VESTIBULAR TESTS
Motion and spatial disorientation systems: Special research capabilities [AD-A265155] 01 p0303 N94-11097
Pilot studies on object motion perception during linear self-motion after long duration centrifugation of human subjects [IZF-1993-B-3] 04 p1510 N94-19439
Equilibrium dysfunction in the clinical field 08 p3390 N94-28858
Portable Linear Sled (PLS) for biomedical research 08 p3163 N94-29648
Model-based scientific discovery: A study in space bioengineering 09 p3799 N94-31990
Visual-vestibular interaction [NASA-CR-196097] 11 p4297 N94-35379

VESTIBULES
Motion and spatial disorientation systems: Special research capabilities [AD-A265155] 01 p0303 N94-11097
Perception in flight: Shape and motion perception, space perception, spatial orientation, and visual vestibular interaction 06 p2429 N94-23979
The role of visual context in manual target localization 06 p2429 N94-25351
Effects of imaginary target on induced eye movements by linear acceleration 07 p2914 N94-27456
Basic understanding of vertigo 08 p3390 N94-28855
Posture control of goldfishes under microgravity 08 p3387 N94-29712
Relation of motion sickness susceptibility to vestibular and behavioral measures of orientation [NASA-CR-196121] 12 p4480 N94-37005
Attenuating the disorienting effects of head movement during whole-body rotation using a visual reference: Further tests of a predictive hypothesis 12 p4482 N94-37276
The use of a tactile interface to convey position and motion perceptions 12 p4486 N94-37281

VESTS
STS-29 crew bailout in WETF [NASA-TM-109548] 03 p1136 N94-15385
Comparison of two cool vests on heat-strain reduction while wearing a firefighting ensemble in a hot/humid environment [AD-A275103] 08 p3400 N94-28902

VFR (RULES)
U VISUAL FLIGHT RULES

VHDL (COMPUTERS)
U HARDWARE DESCRIPTION LANGUAGES

VHSIC (CIRCUITS)
Formal verification of digital circuits described in VHDL [ETN-94-95165] 06 p2306 N94-22883
Micro SIL-1 simulator [PB94-110889] 06 p2454 N94-23750
Japanese aerospace science and technology 1992. A bibliography with indexes [NASA-SP-7104] 06 p2631 N94-24585
Proposed Object Oriented Programming (OOP) enhancements to the Very High Speed Integrated Circuits (VHSIC) Hardware Description Language (VHDL) [AD-A274004] 07 p2957 N94-25661
Development of a MIL-STD-1750 microprocessor system for space applications 07 p2949 N94-26715
Qualified manufacturing and interoperability for space applications 07 p2949 N94-26719
Partitioning structural VHDL circuits for parallel execution on hypercubes [AD-A274390] 07 p2785 N94-26830
Formal semantics for a subset of VHDL and its use in analysis of the FTPP scoreboard circuit [NASA-CR-191577] 09 p3827 N94-32734
Rapid and accurate timing simulation of radiation-hardened digital microelectronics using VHDL [AD-A278644] 11 p4261 N94-36361

VIABILITY
Cellular and molecular level responses after radiofrequency radiation exposure, alone or in combination with x rays or chemicals [AD-A268189] 04 p1501 N94-17729
The NASA sponsored HSCT propulsion studies 10 p3974 N94-33476

VIBRATION
NT BENDING VIBRATION
NT FLUTTER
NT FORCED VIBRATION
NT FREE VIBRATION
NT LATTICE VIBRATIONS
NT LINEAR VIBRATION
NT MISSILE VIBRATION
NT RANDOM VIBRATION
NT RESONANT VIBRATION
NT SELF INDUCED VIBRATION
NT STRUCTURAL VIBRATION
NT SUBSONIC FLUTTER
NT SUPERSONIC FLUTTER
NT TORSIONAL VIBRATION
NT TRANSONIC FLUTTER
Review of SHARC 2.0 O3 kinetics and spectroscopy [AD-A265481] 01 p0274 N94-10496
On the stability of stationary regimes in a distributed autovibration system with external feedback [DE93-620979] 01 p0141 N94-10543
Dynamic tester for rotor seals and bearings [NASA-CASE-MFS-28493-1] 01 p0033 N94-10669
Sine and random vibration program evaluation on vibration control systems [DE93-011974] 01 p0188 N94-11460
Vortex-induced forces on oscillating bluff cylinders [AD-A265056] 01 p0154 N94-11865
Absorption spectrum calculations using mixed quantum-gaussian wave packet dynamics [AD-A265179] 01 p0413 N94-11877
Thermal-infrared emission spectroscopy of natural surfaces: Application to coated surfaces 01 p0081 N94-12156
A vibrational spectroscopic study of the structure of electroactive self-assembled monolayers of viologen derivatives [AD-A265705] 01 p0078 N94-12273
Vibrational overtone activation of methylcyclopropene [AD-A265588] 01 p0079 N94-12373
High resolution electron energy loss studies of surface vibrations [DE93-014441] 02 p0781 N94-13283
Predicting the vibrations of a spinning inflated membrane [DE93-010690] 02 p0676 N94-14456
Applications of computer algebra to distributed parameter systems 02 p0677 N94-14623
Free-wake computation of helicopter rotor flowfield for general flight regimes [AD-A266692] 02 p0509 N94-14781
Dynamics, stability, and control of maglev systems [DE93-015163] 03 p1047 N94-16806
In-situ electron and optical spectroscopies of translational and vibrational activated bond breaking and formation on semiconductors [AD-A268192] 03 p1015 N94-17560
Mechanical properties of interfaces and superlattices [AD-A268591] 03 p1217 N94-17606
Vibrational and electronic properties of clusters and ultrathin films [DE93-012291] 04 p1367 N94-17678
Design and test of a low jitter metal to metal contact solid dielectric switch [DE93-016957] 04 p1394 N94-17755
Wavelet transform for time-frequency analysis of the vibrational signature and its application [AD-A269928] 04 p1454 N94-18661
Unimolecular photodissociation dynamics of ketene (CH_2CO): The singlet/triplet branching ratio and experimental observation of the vibrational level thresholds of the transition-state [DE93-019252] 04 p1352 N94-19304
U.S. Tag for ISO/TC 43, acoustics, IEC/TC 29 electroacoustics, and ISO/TC 108/SC4 human exposure to mechanical vibration and shock: Minutes of the accredited standards committee on bioacoustics, S3 [AD-A273014] 05 p1897 N94-21309
Semiconductor isotope engineering [DE93-040119] 05 p2030 N94-21744
A vibration model for centrifugal contactors [DE93-040645] 05 p1833 N94-21927
Modal combination in response spectrum modal dynamic analysis [DE94-000339] 05 p1833 N94-21956
Time-frequency domain analysis of vibration signals for machinery diagnostics.(4): Interpretation using image processing techniques [OUEL-1953/92] 06 p2353 N94-23178
Energy transfer in solid explosives [DE94-001523] 06 p2265 N94-23778
US tag for ISO/TC 108 mechanical vibration and shock: Minutes of the accredited Standards Committee on Mechanical Vibration and Shock, S2 [AD-A273015] 06 p2376 N94-23789

Vibrational power transmission analysis of machinery installations in ships with the objective of noise reduction
[ISVR-TR-216] 06 p2363 N94-24076
Aeroelastic, aeromechanical and vibration problems in helicopters 06 p2154 N94-24244
Development of a nondestructive vibration technique for bond assessment of Space Shuttle tiles
[NASA-CR-195163] 06 p2201 N94-24919
A vibrating wire parallel to a type 2 superconducting slab of arbitrary thickness
[DE93-617134] 06 p2525 N94-25389
Effects of a vibrating wire carrying DC current on a moving type 2 superconducting slab of arbitrary thickness
[DE93-617136] 06 p2566 N94-25391
Remote vibration measurements at a sud aviation alouette 3 helicopter with a CW CO2-laser system
[AD-A273818] 06 p2190 N94-25516
Modeling of a large undamped space structure using time domain techniques
[AD-A273828] 06 p2206 N94-25523
Effect of longitudinal vibration on the capillary limit of a wrapped screen wick copper/water heat pipe
[AD-A273830] 06 p2571 N94-25524
High resolution fourier transform absorption spectrum of 79Br2 B3 Pi(Ou+) X1 sigma g+
[AD-A273864] 07 p2956 N94-25610
FR/GE/UK/US International Test Operations Procedure (ITOP) 1-1-050 development of laboratory vibration test schedules
[AD-A273887] 07 p2836 N94-25732
Spectroscopic and vibrational energy transfer studies in molecular bromine
[AD-A273795] 07 p3014 N94-25875
An algorithm for determination of bearing health through automated vibration monitoring
[AD-A274591] 07 p2823 N94-26986
SAG compensated vibration isolation mount
[AD-D016040] 07 p2841 N94-27110
Silence amenity engineering: Past and present 07 p3011 N94-27283
Characterization of structural vibration: Field descriptors based on energy density and intensity
[PB94-132230] 08 p3316 N94-28404
Closed loop vibrational control: Theory and applications
[AD-A275451] 08 p3154 N94-28632
Minutes: Accredited Standards Committee on Mechanical Vibration and Shock, S2. US TAG for ISO/TC 108 Mechanical Vibration and Shock
[AD-A275591] 08 p3316 N94-28726
Index of NPL acoustics publications 1981-1990
[NPL-RSA(EXT)-0044] 08 p3480 N94-30786
Rotor instability induced by dead band clearance in bearing supports 08 p3312 N94-30809
Numerical simulations of piano strings. Part 1: A physical model for a struck string using finite difference methods
[TELECOM-93-C-003] 08 p3481 N94-30972
Vibration control and design of composite cantilevers taking into account structural uncertainties and damage 09 p3733 N94-31213
Vibration dampener and method for making same
[AD-D016094] 09 p3739 N94-32733
Limiting vibration in systems with constant amplitude actuators through command preshaping
[NASA-CR-188284] 09 p3739 N94-32907
Microreflectance infrared study of electron-molecular vibrational coupling and lattice softness in BEDT-TTF salts
[DE94-008490] 09 p3907 N94-32989
Design, development, and testing of a lightweight optical sensor cover system 09 p3604 N94-33302
Intelligent control of a multi-degree-of freedom reaction compensating platform system using fuzzy logic 09 p3605 N94-33306
Vibrating hand-held machines: The applicability of vibration values measured in laboratory
[PB94-149127] 10 p4061 N94-34144
Identification of mechanical systems using probabilistic neural networks
[DE94-007555] 10 p4114 N94-34296
High temperature superconductors for magnetic suspension applications 11 p4214 N94-35843
Maneuvering and control of flexible space robots 11 p4218 N94-35867
Variations in the modal characteristics of a telescopically deploying beam 11 p4218 N94-35872
Selected topics on the active control of helicopter aeromechanical and vibration problems 11 p4200 N94-35874
Parameter estimation of the vibrational model for the SCOLE experimental facility 11 p4219 N94-35878
Analysis of achievable disturbance attenuation in a precision magnetically-suspended motion control system 11 p4225 N94-35917
Recovery of frozen flow losses in arcjets
[AD-A278739] 11 p4228 N94-36089
Dipole forbidden vibrational modes for NO and CO on Cu observed in the far IR
[DE94-003199] 12 p4408 N94-36559
Vibration signature analysis of a faulted gear transmission system
[NASA-TM-106623] 12 p4450 N94-36953

VIBRATION DAMPERS
U VIBRATION ISOLATORS

VIBRATION DAMPING
Coupled thermovibrational and thermocapillary convection in liquid bridge (floating zone system) 01 p0101 N94-10082
Vibration isolation mount with locking means
[AD-D015769] 01 p0178 N94-10381
Dynamic tester for rotor seals and bearings
[NASA-CASE-MFS-28493-1] 01 p0033 N94-10669
Momentum management in redundant manipulators for vibration suppression
[NASA-CR-194112] 01 p0180 N94-10821
Damping measurements for ultra-high carbon steel/brass laminates
[DE93-011886] 01 p0082 N94-11076
Damping mechanisms in chemically vapor deposited SiC fibers
[NASA-TM-106334] 01 p0066 N94-11135
Ground vibration and flight flutter tests of the single-seat F-16XL aircraft with a modified wing
[NASA-TM-104264] 01 p0026 N94-11233
Adaptive structures for spacecraft: A USAF perspective 01 p0045 N94-11319
Smart structures at Aastra Corporation 01 p0069 N94-11326
On the stability of shape memory materials and their properties in static and dynamic applications 01 p0069 N94-11329
Adaptive algorithms for use with digital filters in vibration control 01 p0071 N94-11338
Structural analysis and optimization of adaptive structures by use of the finite element method 01 p0071 N94-11339
Active landing gear control for improved ride quality during ground roll 01 p0027 N94-11345
Active damping augmentation of elastomechanical systems using piezoelectric sensors and actuators 01 p0072 N94-11346
Multidimensional intelligent control for superlight air vehicles 01 p0027 N94-11347
Sine and random vibration program evaluation on vibration control systems
[DE93-011974] 01 p0188 N94-11460
Microgravity vibration isolation technology: Development to demonstration
[NASA-TM-106320] 01 p0001 N94-11703
Active vibration control of adaptive flexible structures using piezoelectric smart sensors and actuators 01 p0189 N94-11823
Nonlinear damping model for flexible structures
[NASA-CR-193711] 02 p0539 N94-12790
Kinematics and constraints associated with swashplate blade pitch control
[NASA-TM-102265] 02 p0520 N94-12820
On curve veering and flutter of rotating blades
[NASA-TM-106282] 02 p0670 N94-12872
Development and application of one dimensional deployable truss 02 p0531 N94-13281
Some frequency and damping measurements of laminated beryllium beams
[DE93-015909] 02 p0676 N94-14530
Inverse dynamics: Simultaneous trajectory tracking and vibration reduction with distributed actuators 02 p0678 N94-14624
Hoph bifurcation in viscous, low speed flows about an airfoil with structural coupling
[AD-A266542] 03 p0859 N94-16798
Digital reverberation time measurement system
[AD-D015892] 03 p1177 N94-16919
A mechanical system damping measurement technique using a one-degree-of-freedom (1DOF) cylindrical gas bearing
[AD-A268402] 03 p1048 N94-17462
Generalization of optimal control theory: Linear and nonlinear structures
[PB93-188621] 04 p1540 N94-18125
The longitudinal free vibrations of a fixed-free two-phase elastic bar
[AD-A268768] 04 p1453 N94-18387
Analysis and design of robust decentralized controllers for nonlinear systems
[DE93-019224] 04 p1543 N94-19302
Study of transverse coupled bunch instabilities by using non-linear Taylor maps for the Advanced Light Source (ALS)
[DE93-040287] 05 p1979 N94-19989
Graphite/polyurethane flexible composites: Mechanical and vibration damping properties
[AD-A271608] 05 p1674 N94-20950
Vibration isolating engine mount
[CA-PATENT-1-320-710] 06 p2353 N94-23215
Low noise electric motor 06 p2315 N94-23989
Vibrational power transmission analysis of machinery installations in ships with the objective of noise reduction
[ISVR-TR-216] 06 p2363 N94-24076
Aeroelastic, aeromechanical and vibration problems in helicopters 06 p2154 N94-24244
Numerical analysis of the motion of a rigid body with an attached spring-mass-damper
[AD-A273825] 06 p2379 N94-25520
A study on piezoelectric actuators and sensors for vibration control of flexible space structures
[AD-A274925] 07 p2695 N94-26532
Identification and H(infinity)/(mu)-synthesis control of the Sandia truss
[DE94-002735] 07 p2839 N94-26810
Processing and mechanical properties of laminated metal composites of Al 6090-25 volume percent SiC(sub p) and Al 5182
[DE94-001070] 07 p2708 N94-26930
Proceedings of Damping 1993, volume 2
[AD-A274227] 07 p2840 N94-26953
Proceedings of Damping 1993, volume 3
[AD-A274228] 07 p2840 N94-27008
Finite element analysis of damped vibrations of laminated composite plates
[ISBN-0-315-84928-2] 07 p2843 N94-27585
Methods of testing for endurance of structural elements using simulated acoustic loading
[ESDU-93027] 07 p3011 N94-28141
On the use of feedback to control sound radiation from a plate excited by a turbulent boundary layer
[ISVR-TR-227] 07 p2807 N94-28175
Integrated active and passive control design methodology for the LaRC CSI evolutionary model
[NASA-CR-4580] 08 p3164 N94-28417
Closed loop vibrational control: Theory and applications
[AD-A275451] 08 p3154 N94-28632
General theory and algorithms for the non-casual inversion, slewing and control of space-based articulated structures
[AD-A275118] 08 p3167 N94-29002
Study of bridge design and technology
[PB94-137916] 08 p3121 N94-29160
Tuned mass damper for integrally bladed turbine rotor
[NASA-CASE-MFS-28697-1] 08 p3298 N94-29353
Position control of a flexible beam with active damping of vibrations
[ISBN-0-315-85841-9] 08 p3321 N94-30033
Analysis and design of inflatable aerospace structures 08 p3403 N94-30799
Second-order structural identification via state space-based system realizations 08 p3323 N94-30815
Vibration control and design of composite cantilevers taking into account structural uncertainties and damage 09 p3733 N94-31213
Transmissibility of nickel-titanium shape memory alloy springs
[AD-A276055] 09 p3640 N94-31456
Control of a flexible space robot tracking a moving target 09 p3722 N94-31469
Passive vibration damping materials: Piezoelectric ceramic composites for vibration damping applications
[AD-A276550] 09 p3653 N94-31935
The 10th International Conference on Internal Friction and Ultrasonic Attenuation in Solids (ICIFUAS)
[AD-A276849] 09 p3902 N94-32209
Vibration dampener and method for making same
[AD-D016094] 09 p3739 N94-32733
Feed-forward control of gear mesh vibration using piezoelectric actuators
[NASA-TM-106366] 09 p3728 N94-32902
Limiting vibration in systems with constant amplitude actuators through command preshaping
[NASA-CR-188284] 09 p3739 N94-32907
Structural damping studies at cryogenic temperatures
[NASA-TM-109073] 09 p3740 N94-33118
Intelligent control of a multi-degree-of freedom reaction compensating platform system using fuzzy logic 09 p3605 N94-33306
Hardware interface for isolation of vibrations in flexible manipulators: Development and applications 10 p4067 N94-34036
An analytical study of the vibration of beams fitted with neutralizers. Part 1: Assessment of the effects of neutralizer design parameters
[ISVR-TR-224-PT-1] 10 p4070 N94-34304
Real-time RMS active damping augmentation: Heavy and very light payload evaluations
[NASA-TM-109134] 10 p4015 N94-34386

Data reduction, analysis and results of LACV-30-07 air cushion vehicle tests, Fort Story, VA, August - September 1993
[AD-A278859] 11 p4190 N94-35826
High temperature superconductors for magnetic suspension applications 11 p4214 N94-35843
Measurement and characterization of force dynamics in high T(sub c) superconductors 11 p4214 N94-35844
Distributed parameter modelling of flexible spacecraft: Where's the beef? 11 p4217 N94-35866
Control of flexible structures with distributed sensing and processing 11 p4218 N94-35871
Flutter suppression digital control law design and testing for the AFW wind tunnel model 11 p4200 N94-35873
Selected topics on the active control of helicopter aeromechanical and vibration problems 11 p4200 N94-35874
Robust control design techniques for active flutter suppression 11 p4200 N94-35875
Optimal disturbance rejecting control of hyperbolic systems 11 p4220 N94-35882
Vibration suppression in flexible structures via the sliding-mode control approach 11 p4220 N94-35884
Active vibration damping using smart material 11 p4221 N94-35886
Software for continuum modeling of controls-structures interactions 11 p4223 N94-35898
Electromechanical simulation and test of rotating systems with magnetic bearing or piezoelectric actuator active vibration control 11 p4223 N94-35905
Vibration reduction in helicopter rotors using an actively controlled partial span trailing edge flap located on the blade
[NASA-CR-4611] 11 p4280 N94-36423
Correlation of analytical and experimental hot structure vibration results
[NASA-TM-104269] 12 p4386 N94-36644
A PDE-based methodology for modeling, parameter estimation and feedback control in structural and structural acoustic systems
[NASA-CR-194928] 12 p4500 N94-36924
Vibration suppression with approximate finite dimensional compensators for distributed systems: Computational methods and experimental results
[NASA-CR-194927] 12 p4500 N94-36928
Multirate flutter suppression system design for the Benchmark Active Controls Technology Wing
[NASA-CR-196112] 12 p4388 N94-36965
Modeling and control of intelligent flexible structures
[AD-A280478] 12 p4396 N94-37349

VIBRATION EFFECTS

Vibrational-thermocapillary parallel flows and stability 01 p0120 N94-10220
Comprehensive dynamic analysis of a bladed disk-turborotor-bearing system
[ISBN-0-315-73646-1] 01 p0180 N94-11155
Machinery dynamics activities in Canadian industries
[IME-MET-TR-006] 02 p0663 N94-14147
Parametric study of a finite element model of the Sidewinder missile
[AD-A267245] 03 p0865 N94-14976
Microwelding due to random vibration 06 p2359 N94-24019
Modeling of PCG fluid dynamics: Salient results 06 p2224 N94-24345
Effect of longitudinal vibration on the capillary limit of a wrapped screen wick copper/water heat pipe
[AD-A273830] 06 p2571 N94-25524
Nonequilibrium radiation and chemistry models for aerocapture vehicle flowfields
[NASA-CR-195706] 07 p2648 N94-28071
The influence of appendage vibration on the attitude dynamics of a dual-spin satellite 08 p3168 N94-29828
Dynamic structural effects and ultrafast biomolecular kinetics in photoinduced charge transfer reactions
[DE94-010421] 11 p4329 N94-36390
Characterization of spacecraft and environmental disturbances on a SmallSat
[NASA-CR-194915] 12 p4396 N94-36990

VIBRATION ISOLATORS

Vibration isolation mount with locking means
[AD-D015769] 01 p0178 N94-10381
Microgravity vibration isolation technology: Development to demonstration
[NASA-TM-106320] 01 p0001 N94-11703
Feasibility study of an orbiting laboratory for testing CSI technology
[NASA-CR-191524] 02 p0540 N94-13016
A feasibility study of a microgravity enhancement system for Space Station Freedom
[NASA-CR-191550] 03 p0886 N94-15864
Modeling and new equipment definition for the vibration isolation box equipment system
[NASA-CR-193185] 04 p1379 N94-17763
Generalization of optimal control theory: Linear and nonlinear structures
[PB93-188621] 04 p1540 N94-18125
Diagnostics and methods for real-time laser microchemistry
[AD-A270871] 05 p1680 N94-20566
Vibration isolating engine mount
[CA-PATENT-1-320-710] 06 p2353 N94-23215
Prediction of pressure drop in fluid tuned mounts using analytical and computational techniques 06 p2321 N94-23643
The low noise momentum wheel MW-X: EM design and predicted properties 06 p2360 N94-24024
Vibrational power transmission analysis of machinery installations in ships with the objective of noise reduction
[ISVR-TR-216] 06 p2363 N94-24076
Modeling of PCG fluid dynamics: Salient results 06 p2224 N94-24345
The 1991-1992 project summaries 07 p2943 N94-25698
Proceedings of Damping 1993, volume 1
[AD-A274226] 07 p2840 N94-26922
Proceedings of Damping 1993, volume 2
[AD-A274227] 07 p2840 N94-26953
Proceedings of Damping 1993, volume 3
[AD-A274228] 07 p2840 N94-27008
SAG compensated vibration isolation mount
[AD-D016040] 07 p2841 N94-27110
Tuned mass damper for integrally bladed turbine rotor
[NASA-CASE-MFS-28697-1] 08 p3298 N94-29353
Activities of Ishikawajima-Harima Heavy Industries Co. Ltd.
[PB94-137981] 08 p3555 N94-29798
Transmissibility of nickel-titanium shape memory alloy springs
[AD-A276055] 09 p3640 N94-31456
Vibration Isolation Technology (ViT) ATD project
[NASA-TM-106496] 09 p3567 N94-33064
Hardware interface for isolation of vibrations in flexible manipulators: Development and applications 10 p4067 N94-34036
Optimum design of wide frequency vibration absorbers 10 p4074 N94-34348
Microgravity isolation system design: A modern control synthesis framework 11 p4215 N94-35851
Electromagnetically levitated vibration isolation system for the manufacturing process of silicon monocrystals 11 p4223 N94-35906

VIBRATION MEASUREMENT

Transcript of workshop on machinery health monitoring
[IME-MET-TR-005] 02 p0733 N94-13847
Machinery dynamics activities in Canadian industries
[IME-MET-TR-006] 02 p0663 N94-14147
Remote tire pressure sensing technique
[NASA-CASE-LAR-14160-1] 03 p1033 N94-15884
Spacecraft vibrations due to mechanisms; measurements from Olympus on-station 06 p2207 N94-24018
The Olympus PAX, measurement of mechanism induced vibration 06 p2362 N94-24041
Remote vibration measurements at a sud aviation alouette 3 helicopter with a CW CO2-laser system
[AD-A273818] 06 p2190 N94-25516
Experimental and numerical vibration analyses of a stiffened panel
[VTT-PUBS-129] 07 p2836 N94-25650
Specialized data analysis of SSME and advanced propulsion system vibration measurements
[NASA-CR-193940] 08 p3174 N94-29868
Smart accelerometer --- vibration damage detection
[NASA-CASE-MSC-21951-1] 11 p4268 N94-35235

VIBRATION METERS

NT LUNAR SEISMOGRAPHS
NT SEISMOGRAPHS
Spacecraft vibrations due to mechanisms; measurements from Olympus on-station 06 p2207 N94-24018
The Olympus PAX, measurement of mechanism induced vibration 06 p2362 N94-24041
Smart accelerometer --- vibration damage detection
[NASA-CASE-MSC-21951-1] 11 p4268 N94-35235

VIBRATION MODE

Estimation of critical values and vibration characteristics on supersonic delta wings. Part 1: On-line time series analysis of stationary random response
[NAL-TR-1153] 01 p0002 N94-10363
NASTRAN modeling of flight test components for UH-60A airloads program test configuration
[NASA-CR-193614] 01 p0186 N94-10937
On curve veering and flutter of rotating blades
[NASA-TM-106282] 02 p0670 N94-12872
A component modes projection and assembly model reduction methodology for articulated, multi-flexible body structures 02 p0677 N94-14622
Parametric study of a finite element model of the Sidewinder missile
[AD-A267245] 03 p0865 N94-14976
A simplistic look at limit stresses from random loading
[NASA-TM-108427] 03 p1058 N94-15710
Development and comparison of advanced reduced-basis methods for the transient structural analysis of unconstrained structures
[NASA-TM-109015] 03 p1061 N94-17259
Predicted structural response of the lightweight-interceptor technology demonstration vehicle
[DE93-014676] 04 p1333 N94-17782
Comparison of the modeling solutions with the hydrogen discharge data
[DE93-015115] 04 p1565 N94-17797
Eigenvalue routines in NASTRAN: A comparison with the Block Lanczos method 04 p1450 N94-17838
System identification of the Daisy large space structure emulator
[ISBN-0-315-83533-8] 05 p1653 N94-22588
Microwelding due to random vibration 06 p2359 N94-24019
Maximum likelihood modal parameter identification and realization of stochastic systems 06 p2157 N94-24265
Development of a nondestructive vibration technique for bond assessment of Space Shuttle tiles
[NASA-CR-195163] 06 p2201 N94-24919
Space Station flexible dynamics under plume impingement 06 p2208 N94-25383
Parameter estimation by genetic algorithms
[DE94-002924] 07 p2961 N94-26146
The free vibration of plates, shallow shells and solids
[ISBN-0-315-83931-7] 07 p2838 N94-26622
Extraction of modal parameters from an operating HAWT using the Natural Excitation Technique (NExT)
[DE94-001831] 07 p2859 N94-27004
Response of structures to impact loads using elastic and plastic analysis
[ISBN-0-315-84647-X] 07 p2842 N94-27309
Understanding and development of a prediction method of transonic limit cycle oscillation characteristics of fighter aircraft
[NLR-TP-92210-U] 07 p2679 N94-27798
Stiffness-generated rigid-body mode shapes for Lanczos eigensolution with SUPORT DOF by way of a MSC/NASTRAN DMAP alter
[NASA-TM-106537] 08 p3319 N94-29406
Computation of vibration mode elastic-rigid and effective weight coefficients from finite-element computer program output 08 p3247 N94-29615
Vibrational properties of homopolar and heteropolar surfaces and interfaces of the CdTe/HgTe system
[DE94-608105] 08 p3516 N94-30069
Three-dimensional free vibration analysis of thick arbitrarily laminated, rectangular, cylindrical and spherical composite panels 08 p3184 N94-30257
Second-order structural identification via state space-based system realizations 08 p3323 N94-30815
Vibration control and design of composite cantilevers taking into account structural uncertainties and damage 09 p3733 N94-31213
Nonlinear vibration analysis of laminated plates on linear and nonlinear elastic foundations 09 p3737 N94-32079
Applying transfer matrix method to the estimation of the modal characteristics of the NASA Mini-Mass Truss 11 p4218 N94-35870
Variations in the modal characteristics of a telescopically deploying beam 11 p4218 N94-35872
Vibration suppression in flexible structures via the sliding-mode control approach 11 p4220 N94-35884
Ground vibration test of the XV-15 Tiltrotor Research Aircraft and pretest predictions 11 p4200 N94-35972
A procedure for oscillatory parameter identification
[DE94-008047] 11 p4259 N94-36054
Correlation of analytical and experimental hot structure vibration results
[NASA-TM-104269] 12 p4386 N94-36644
The dynamics of hydrogen atoms dissolved in Zr Cr2 alloy
[DE94-618756] 12 p4520 N94-37652

VIBRATION PROTECTION

U VIBRATION ISOLATORS

VIBRATION SIMULATORS

NT VERTICAL MOTION SIMULATORS
A direct digital design for a multichannel structural test system using the characteristic locus method
[MATHS-REPT-A-206] 09 p3828 N94-31161

VIBRATION TESTING MACHINES

U VIBRATION SIMULATORS

VIBRATION TESTS
Damping mechanisms in chemically vapor deposited SiC fibers
[NASA-TM-106334] 01 p0066 N94-11135
Ground vibration and flight flutter tests of the single-seat F-16XL aircraft with a modified wing
[NASA-TM-104264] 01 p0026 N94-11233
Estimation of critical values and vibration characteristics on supersonic delta wings. Part 2: Locally-stationary time series analysis of nonstationary random responses
[NAL-TR-1179] 02 p0502 N94-13345
Canadian Target Assembly (CTA) to Airborne Support Equipment (ASE) vibration test report
[IME-AMT-TR-001] 02 p0663 N94-14195
Parametric study of a finite element model of the Sidewinder missile
[AD-A267245] 03 p0865 N94-14976
The 7th International Cryocooler Conference
[AD-A268451] 04 p1379 N94-18147
The effect of delamination on the dynamic response of composite laminates as measured by embedded fiber optic Michelson sensor
[ISBN-0-315-83534-6] 05 p1677 N94-22587
Data relay system satellite: The development of an antenna pointing mechanism for the inter-orbit link antenna 06 p2359 N94-24015
Remote vibration measurements at a sud aviation alouette 3 helicopter with a CW CO2-laser system
[AD-A273818] 06 p2190 N94-25516
Effect of longitudinal vibration on the capillary limit of a wrapped screen wick copper/water heat pipe
[AD-A273830] 06 p2571 N94-25524
FR/GE/UK/US International Test Operations Procedure (ITOP) 1-1-050 development of laboratory vibration test schedules
[AD-A273887] 07 p2836 N94-25732
Baseline for a Nordtest method. Reliability stress screening of components. A guide for component users
[PB94-123775] 07 p2835 N94-27042
Report of three microgravity experiments by the drop shaft
[JTN-94-80579] 07 p2761 N94-27341
Space Station Freedom NiH2 cell testing program 07 p2861 N94-28108
Microvibrations on a GEO telecommunication satellite
[REPT-932-440-101] 08 p3168 N94-29415
A direct digital design for a multichannel structural test system using the characteristic locus method
[MATHS-REPT-A-206] 09 p3828 N94-31161
Integral testing of relays and circuit breakers
[DE94-009075] 10 p4041 N94-33937
Vibrating hand-held machines: The applicability of vibration values measured in laboratory
[PB94-149127] 10 p4061 N94-34144
Identification of mechanical systems using probabilistic neural networks
[DE94-007555] 10 p4114 N94-34296
Ground vibration test of the XV-15 Tiltrotor Research Aircraft and pretest predictions 11 p4200 N94-35972
An enhancement to the NA4 gear vibration diagnostic parameter
[NASA-TM-106553] 12 p4452 N94-37521

VIBRATIONAL FREQUENCIES (MOLECULAR)
U VIBRATIONAL SPECTRA

VIBRATIONAL FREQUENCIES (STRUCTURAL)
U RESONANT FREQUENCIES

VIBRATIONAL RELAXATION
U MOLECULAR RELAXATION

VIBRATIONAL SPECTRA
A vibrational spectroscopic study of the structure of electroactive self-assembled monolayers of viologen derivatives
[AD-A265705] 01 p0078 N94-12273
Vibrational overtone activation of methylcyclopropene
[AD-A265588] 01 p0079 N94-12373
Infrared spectroscopy of organic free radicals related to combustion processes
[DE93-017086] 02 p0562 N94-13222
First-principles studies of phase stability and the structural and dynamical properties of hydrogen-metal systems
[DE93-016129] 02 p0570 N94-13374
Dynamic Jahn-Teller effect: Calculation of fine structure spectrum, isotope shift and Zeeman behavior at deep center Ni2+ in CdS
[ETN-93-94394] 02 p0815 N94-14705
Molecular processes in comets
[NASA-CR-194148] 03 p1239 N94-15188
The quantum mass shift of the soliton in Skyrme model
[ITN-93-85219] 03 p1180 N94-15283
Effect of oxygen concentration and ordering on vanadium-oxygen alloy vibrational spectra
[DE93-627003] 04 p1355 N94-17692
An ab initio study of the weakly bonded CO-Cl2 complex
[AD-A269000] 04 p1349 N94-18395
Wavelet transform for time-frequency analysis of the vibrational signature and its application
[AD-A269928] 04 p1454 N94-18661
Rotational spectrum of a dark state in 2-fluoroethanol using microwave/radiofrequency-infrared multiple resonance
[AD-A272101] 05 p1817 N94-20583
Surface electrochemistry of metals
[AD-A272913] 05 p1691 N94-21245
Modal combination in response spectrum modal dynamic analysis
[DE94-000339] 05 p1833 N94-21956
Journal of NIRE, Vol. 2, No. 2
[JTN-94-80552] 08 p3187 N94-28675
Ab initio study of vibrational frequency shift upon the 1:1 acetone-iodine complex formation 08 p3188 N94-28681
Degenerate four-wave mixing as a diagnostic of plasma chemistry
[DE94-008588] 09 p3889 N94-31766
Vibrational spectroscopy at metal-solution interfaces: Some perspectives and prospects for electrochemical surface science
[AD-A276781] 09 p3644 N94-32169
On the effects of transforming the vibrational spectra of molecular systems under microwave radiation
[DE94-617057] 11 p4329 N94-36310
Diosmacycloalkanes as models for the formation of hydrocarbons from surface methylenes
[DE94-011211] 12 p4413 N94-37754

VIBRATIONAL STATES
Vibrational dynamics in photoinduced electron transfer
[DE93-040874] 04 p1567 N94-18533
Femtosecond Raman-induced Kerr effect study of polar solvent dynamics: Amides
[DE93-017563] 05 p1678 N94-19924
Rotational spectrum of a dark state in 2-fluoroethanol using microwave/radiofrequency-infrared multiple resonance
[AD-A272101] 05 p1817 N94-20583
Theoretical investigations of metastability and energy storage in molecular systems
[AD-A271849] 05 p1973 N94-20612
High resolution infrared spectroscopy of formamide and deuterated formamide in a molecular beam
[AD-A271986] 05 p1973 N94-20618
Semiconductor isotope engineering
[DE93-040119] 05 p2030 N94-21744
Ionization of H2(+) in intense laser fields
[DE93-019160] 05 p1818 N94-21829
Non-adiabatic effects in low-energy electron-molecule scattering
[DE93-040485] 05 p1976 N94-21968
Radiative properties of molecular nitrogen ions produced by helium Penning ionization and argon effects
[NASA-CR-195126] 06 p2534 N94-24487
Vibrational energy transfer within the B 3Pi (O(+) sub u) state of 79BR2 upon collision with N2, O2, NO, and SF6
[AD-A273905] 07 p3011 N94-25589
A study of vibrational relaxation of electronically-excited molecules
[DE93-613553] 07 p3013 N94-25827
The importance of vibrationally excited nitrogen in silicon nitride deposition systems
[AD-A274874] 07 p2750 N94-26167
Low frequency dynamics of CO/Cu-breakdown of Born-Oppenheimer approximation
[DE94-005508] 08 p3510 N94-28512
SHARC, a model for calculating atmospheric and infrared radiation under non-equilibrium conditions
[AD-A275207] 08 p3357 N94-28893
Models for vibration-dissociation coupling in high-temperature gases 08 p3273 N94-29675
Spectroscopic and dynamical studies of highly energized small polyatomic molecules
[DE94-006509] 08 p3489 N94-30061
Application of semiclassical methods to reaction rate theory
[DE94-007041] 08 p3199 N94-30266
Time-resolved infrared absorption studies applied to the study of radical plus molecule reactions
[DE94-005921] 09 p3863 N94-31202
Vibrational energy transfer of diatomic gases in hypersonic expanding flows 09 p3570 N94-31958
Electronic and nuclear factors in intramolecular charge and excitation transfer processes
[DE94-006598] 09 p3870 N94-32178
Cooling and trapping of neutral atoms
[AD-A276957] 09 p3870 N94-32360
Wave packet studies of the vibrational predissociation of three and four-atom van der Waals complexes
[DE94-007623] 09 p3871 N94-32598
Infrared spectroscopy of organic free radicals related to combustion processes
[DE94-012481] 12 p4409 N94-37168
Optical spectroscopy of a nitrogen-hydrogen complex in ZnSe
[DE94-011622] 12 p4413 N94-37630

VIBRATORY LOADS
Performance and rotor loads measurements of the Lynx XZ170 helicopter with rectangular blades
[NASA-TM-104000] 01 p0001 N94-10936
Vibro-acoustic analysis of an aircraft maintenance dock
[AD-A266778] 03 p0871 N94-14908
A parametric study of harmonic rotor hub loads
[NASA-CR-4558] 06 p2181 N94-24726

VIBROMETERS
U VIBRATION METERS

VIDEO COMMUNICATION
Studies and simulations of the DigiCipher system
[NASA-CR-193470] 01 p0321 N94-10343
New technology applied to telemedicine 01 p0306 N94-11796
Study on color video pictures transmission by digital acoustic signal 01 p0139 N94-11917
Application of modified VICAR/IBIS GIS to analysis of July 1991 Flevoland AIRSAR data 03 p1080 N94-16757
Performance evaluation of video on ethernet
[DE93-040696] 05 p1936 N94-21749
Deployable video conference table
[NASA-CASE-ARC-11950-1] 06 p2192 N94-23310
A constrained joint source/channel coder design and vector quantization of nonstationary sources
[NASA-CR-195145] 06 p2301 N94-24707
A prototype to automate the video subsystem routing for the video distribution subsystem of Space Station Freedom 06 p2306 N94-25353
The question of standards for digital interactive television
[AD-A273872] 07 p2765 N94-25725
The telemedicine spacebridge project: A joint US/Russian venture in long distance medicine via satellite
[NASA-TM-106523] 07 p2693 N94-27427
Video transmission on ATM networks
[NASA-CR-195124] 08 p3244 N94-29106
Low frame rate video coding for small bandwidth realtime multimedia tele-education systems
[PB94-125531] 08 p3256 N94-30398
Voice and video transmission using XTP and FDDI 09 p3685 N94-32468
COVICS: A covert video communications system
[DE94-007568] 09 p3682 N94-32745

VIDEO COMPRESSION
Bandwidth characteristics of multimedia data traffic on a local area network
[NASA-TM-104026] 03 p0883 N94-15648
VLSI-based video event triggering for image data compression
[NASA-TM-106500] 06 p2345 N94-25116
MPEG-2 video decoding architecture: Analysis and design
[REPT-93-069] 08 p3260 N94-30940
A visual detection model for DCT coefficient quantization 09 p3850 N94-32467
Intelligent vehicle control: Opportunities for terrestrial-space system integration 10 p4127 N94-34038
Studies on image compression and image reconstruction
[NASA-CR-196304] 12 p4433 N94-36810
Portable color multimedia training systems based on monochrome laptop computers (CBT-in-a-briefcase), with spinoff implications for video uplink and downlink in spaceflight operations
[NASA-TM-108460] 12 p4496 N94-37556

VIDEO DATA
Study on color video pictures transmission by digital acoustic signal 01 p0139 N94-11917
Massively parallel, adaptive, color image processing for autonomous road following
[AD-A266988] 03 p0864 N94-15498
Pegasus project description
[MEMO-INF-92-75] 04 p1536 N94-19159
Pegasus: Operating system support for distributed multimedia systems
[MEMO-INF-92-76] 04 p1536 N94-19160
The Amsterdam hypermedia model: Extending hypertext to support real multimedia
[CWI-CS-R9306] 05 p2045 N94-21536
Concept report: Experimental vector magnetograph (EXVM) operational configuration balloon flight assembly
[NASA-CR-194702] 05 p1638 N94-21776
Close-up analysis of inflight ice accretion
[NASA-TM-106457] 06 p2172 N94-23523

Measurement of interfacial tension by use of pendant drop video techniques
[DE93-000168] 06 p2345 N94-24831
Preliminary design of a satellite observation system for Space Station Freedom
[NASA-CR-195514] 06 p2209 N94-24840
VLSI-based video event triggering for image data compression
[NASA-TM-106500] 06 p2345 N94-25116
SHIVA: A unix-based, menu-driven, color image processing software package
[AD-A274071] 07 p2957 N94-25646
Methods for experimentally determining commercial jet aircraft landing parameters from video image data
[AD-A274207] 07 p2669 N94-27105
Video transmission on ATM networks
[NASA-CR-195124] 08 p3244 N94-29106
Automating geographically referenced digital mosaics from aerial videography with area-based feature matching 08 p3333 N94-29540
Low frame rate video coding for small bandwidth realtime multimedia tele-education systems
[PB94-125531] 08 p3256 N94-30398
Time synchronized video systems 08 p3261 N94-30675
MPEG-2 video decoding architecture: Analysis and design
[REPT-93-069] 08 p3260 N94-30940
First-wall heat-flux measurements during ELMing H-mode plasma
[DE94-008310] 09 p3888 N94-31765
Distributed Active Archive Center 10 p4157 N94-33826
Evaluation of lens distortion errors using an underwater camera system for video-based motion analysis
[NASA-TM-104795] 10 p4099 N94-33957
Controlling telerobots with video data and compensating for time-delayed video using Omniview 10 p4127 N94-34031
Evaluation of a tool for producing and presenting interactive videodisc job aids
[AD-A278599] 12 p4432 N94-36473

VIDEO EQUIPMENT
NT VIDEO TAPE RECORDERS
Video applications development platform
[AD-A266966] 03 p1163 N94-14953
Image processing as a tool in flight testing evaluation 05 p1640 N94-22606
Preliminary design of a satellite observation system for Space Station Freedom
[NASA-CR-195514] 06 p2209 N94-24840
Conceptual design of an astronaut hand anthropometry device
[NASA-CR-195490] 06 p2439 N94-24956
Development of a video fluorescence system for assessing burn depth
[AD-A278127] 09 p3798 N94-33092

VIDEO SIGNALS
GaAs sigma-delta modulator modeling for Analog to Digital Converters (ADC's)
[AD-A263419] 01 p0144 N94-11516
Observations of optical counterparts of Gamma-Ray bursts
[NASA-CR-193573] 01 p0485 N94-12589
Display system employing acousto-optic tunable filter
[NASA-CASE-NPO-18736-1-CU] 03 p1190 N94-15933
Adaptive analog video signal conditioner 05 p1744 N94-21099
Image processing for acquisition of fluid rest time in the running of an artificial heart valve 06 p2316 N94-22858
Reducing video frame rate increases remote optimal focus time
[NASA-TM-104018] 06 p2431 N94-23970
Solid state Time Base Corrector (TBC)
[AD-D015981] 06 p2312 N94-25039
Digital data, composite video multiplexer and demultiplexer boards for an IBM PC/AT compatible computer 06 p2447 N94-25377
Color head down display program
[AD-A274807] 07 p2672 N94-26340
Automated fabric inspection system
[AD-A274522] 07 p2835 N94-26833
Focal plane antenna array for millimeter waves
[AD-D016034] 07 p2774 N94-27202
An experimental compact Hi-Vision VCR using metal evaporated tape
[NHK-LABS-NOTE-423] 09 p3683 N94-33081
The iWarp display module
[AD-A278610] 11 p4260 N94-36248
Portable color multimedia training systems based on monochrome laptop computers (CBT-in-a-briefcase), with spinoff implications for video uplink and downlink in spaceflight operations
[NASA-TM-108460] 12 p4496 N94-37556

VIDEO TAPE RECORDERS
Automated fabric inspection system
[AD-A274522] 07 p2835 N94-26833
Cockpit video: A low cost BDA source
[AD-A275228] 08 p3150 N94-29389
Night vision camcorder system
[AD-A277004] 09 p3712 N94-32002
An experimental compact Hi-Vision VCR using metal evaporated tape
[NHK-LABS-NOTE-423] 09 p3683 N94-33081

VIDEO TAPES
An experimental compact Hi-Vision VCR using metal evaporated tape
[NHK-LABS-NOTE-423] 09 p3683 N94-33081
Distributed Active Archive Center 10 p4157 N94-33826

VIDICONS
The cool-star spectral catalog: A uniform collection of IUE SWP-LOs 05 p2046 N94-22446
Focal plane antenna array for millimeter waves
[AD-D016034] 07 p2774 N94-27202

VIETNAM
Shoreline change detection using remote sensing and GIS in Vietnam 01 p0196 N94-11928

VIEW EFFECTS
Synthetic image generator model; application of view angle dependent reflectivity components and performance evaluation in the visible region
[AD-A275365] 08 p3499 N94-29009

VIEWING
NT FIELD OF VIEW
Using the SPICE system to help plan and interpret space science observations 06 p2517 N94-23950
Using computer graphics to design Space Station Freedom viewing 06 p2434 N94-24191
Illumination requirements for operating a space remote manipulator 06 p2435 N94-24195
Computer visualizations in engineering applications
[DE94-003589] 07 p2822 N94-26465
Visual perception of 3-dimensional structure from different types of optical deformation
[AD-A278272] 09 p3884 N94-33141

VIGNETTING
Interferometric and optical tests of water window imaging x ray microscopes
[NASA-CR-193866] 01 p0375 N94-10506
Considerations for the use of the modified line reversal technique for gas temperature measurement
[DE93-015752] 04 p1576 N94-17857
AXAF-I ghost ray study: On orbit case
[NASA-CR-193987] 11 p4333 N94-36119

VIKING LANDER SPACECRAFT
Geologic history of central Chryse Planitia and the Viking 1 landing site, Mars 01 p0465 N94-12180
BAG: A code for predicting the performance of a gas bag impact attenuation system for the Pathfinder lander
[DE94-003688] 08 p3165 N94-28477

VIKING MARS PROGRAM
First US Mars landing
[NASA-TM-109669] 03 p0885 N94-15436
Observed climatic activity pertaining to the evolution of the northern plains 05 p2090 N94-20392
Chronology, eruption duration, and atmospheric contribution of Apollinaris Patera, Mars 05 p2108 N94-20720
GMM-1: A 50 degree and order gravitational field model for Mars 05 p2117 N94-20774
Mass spectrometer-pyrolysis experiment for atmospheric and soil sample analysis on the surface of Mars 05 p1812 N94-22435
Mars Operational Environmental Satellite (MOES): A post-Mars Observer discovery mission 06 p2620 N94-24890

VIKING SPACECRAFT
NT VIKING LANDER SPACECRAFT
A mineralized zone in Western Candor Chasma, Mars 03 p1248 N94-16179

VINEYARDS
Assisting wine growers
[NASA-TM-109812] 10 p4094 N94-33564

VINYL COPOLYMERS
Dynamics of block poly(styrene-co-vinylpyridine) (SVP) in solution and on silica
[AD-A277139] 09 p3657 N94-32364

VINYL CYANIDE
U ACRYLONITRILES

VINYL ETHYLENE
U BUTADIENE

VINYL POLYMERS
NT POLYVINYL FLUORIDE
NT VINYL COPOLYMERS
A study of relaxation transitions in the polymers under the influence of magnetic fields
[AD-A263878] 03 p0963 N94-15133
Interpenetrating polymer network acoustic damping material
[AD-D015889] 03 p0969 N94-16916
Humidity effects on soluble core mechanical and thermal properties (polyvinyl alcohol/microballoon composite) type CG extendospheres, volume 2
[NASA-CR-193893] 06 p2229 N94-24224
Object imaging accomplished with an integrated circuit robotic tactile sensor incorporating a piezoelectric polyvinylidene fluoride thin film
[AD-A274038] 07 p2780 N94-25845
Plasma treatment of polymer dielectric films to improve capacitive energy storage 08 p3223 N94-30479
PVDF pressure transducers for shock wave and explosives research
[AD-A277319] 09 p3712 N94-32051
Hydrogen peroxide electrodes based on electrical connection of redox centers of various peroxidases to electrodes through a three-dimensional electron relaying polymer network
[AD-A276543] 09 p3691 N94-32056
Electrical communication between glucose oxidase and electrodes based on poly(vinylimidazole) complex of Os(bpy)2Cl2
[AD-A276585] 09 p3635 N94-32231
Conversion of polymers of methyl- and vinylsilane to Si-C ceramics
[NASA-TM-106554] 09 p3662 N94-32945

VINYL RADICAL
Design of new polymers to improve radiation stability of plastic scintillators
[DE94-008220] 09 p3652 N94-31764

VINYLIDENE
Object imaging accomplished with an integrated circuit robotic tactile sensor incorporating a piezoelectric polyvinylidene fluoride thin film
[AD-A274038] 07 p2780 N94-25845
Plasma treatment of polymer dielectric films to improve capacitive energy storage 08 p3223 N94-30479
PVDF pressure transducers for shock wave and explosives research
[AD-A277319] 09 p3712 N94-32051

VIOLENCE
NT ATTACKING (ASSAULTING)
Criminal acts against civil aviation, fiscal year 1992
[AD-A268014] 03 p0863 N94-17586

VIRAL DISEASES
NT ACQUIRED IMMUNODEFICIENCY SYNDROME

VIRGO GALACTIC CLUSTER
Measuring the Hubble constant and our Virgo-infall velocity independently 09 p3926 N94-31968

VIRGO STAR CLUSTER
U VIRGO GALACTIC CLUSTER

VIRIAL COEFFICIENTS
Phase equilibria and volumetric properties for the system NaCl-CaCl2-H2O
[DE93-013590] 01 p0076 N94-11244
Experimental studies of equation of gases state for hydrogen and deuterium
[DE94-609877] 10 p4022 N94-34101

VIRIAL THEOREM
Quark-antiquark bound states
[DE93-613054] 07 p3013 N94-25826

VIRTUAL MEMORY SYSTEMS
Execution methods, and parallel virtual machines for distributed implementation of the LCS parallel programming language
[LAAS-93032] 02 p0761 N94-14716
Lightweight recoverable virtual memory
[AD-A270576] 05 p1898 N94-20107
Virtual data
[DE94-002718] 07 p2986 N94-26807
Virtual memory management and virtual bus overloading on multiple channel architectures
[AD-A274127] 07 p2954 N94-27152
Shared virtual memory and generalized speedup
[AD-A277573] 07 p2969 N94-27416
A comparison of distributed memory and virtual shared memory parallel programming models
[DE94-005473] 09 p3825 N94-31663
Compiler techniques for managing data motion
[AD-A276514] 09 p3918 N94-31930

VIRTUAL REALITY
Virtual sound for virtual reality
[DE93-010519] 01 p0321 N94-10291
Forecasting the impact of virtual environment technology on maintenance training 01 p0314 N94-11570
USRA/RIACS
[NASA-CR-194334] 02 p0750 N94-13932
Future of robotics
[NASA-TM-109592] 03 p1045 N94-15264
A computer-based training system combining virtual reality and multimedia
[DE93-013768] 03 p1132 N94-16819

A software architecture for the construction and management of real-time virtual worlds
[AD-A271465] 05 p1904 N94-20091
Spatial interpretation of NASA's Marshall Space Flight Center Payload Operations Control Center using virtual reality technology 06 p2198 N94-24432
World processor: An interface for textual display and manipulation in virtual reality
[PB94-118643] 06 p2592 N94-24642
A white paper: NASA virtual environment research, applications, and technology
[NASA-TM-109682] 06 p2428 N94-24855
ObjectSim: A reusable object oriented DIS visual simulation
[AD-A274030] 07 p2958 N94-25767
Weapon system sensor integration for a DIS-compatible virtual cockpit
[AD-A274088] 07 p2672 N94-26021
NPSNET-4: A real-time, 3D distributed interactive virtual world
[AD-A274942] 07 p2961 N94-26298
Utility fog: A universal physical substance 07 p2687 N94-27367
An artificial reality environment for remote factory control and monitoring 07 p2687 N94-27369
HYPER-NPSNET: Embedded multimedia in a 3D virtual world
[AD-A275063] 08 p3410 N94-29152
Virtual annotation: Verbal communication in virtual reality
[REPT-93-67] 09 p3674 N94-31645
Designing in virtual reality: Modelling Objects in a Virtual Environment (MOVE)
[REPT-93-91] 09 p3813 N94-31704
Interactive graphical model building using telepresence and virtual reality
[DE94-001421] 09 p3818 N94-32353
Virtual reality in medical education and assessment 09 p3798 N94-32471
An ethnographic object-oriented analysis of explorer presence in a volcanic terrain environment: Claims and evidence
[NASA-TM-108823] 10 p4099 N94-33608
Fusion interfaces for tactical environments: An application of virtual reality technology 10 p4100 N94-33619
Virtual reality as a human factors design analysis tool: Macro-ergonomic application validation and assessment of the Space Station Freedom payload control area 10 p4100 N94-33620
A rapid algorithm for realistic human reaching and its use in a virtual reality system 10 p4101 N94-33621
Telemedicine, virtual reality, and surgery 10 p4096 N94-33641
Quantitative 3-D imaging topogrammetry for telemedicine applications 10 p4096 N94-33645
Shared virtual environments for aerospace training 10 p4098 N94-34024
Surgery applications of virtual reality 10 p4096 N94-34025
A study of navigation in virtual space 10 p3988 N94-34026
RoboLab and virtual environments 10 p4015 N94-34027
Virtual Interfaces: Research and Applications
[AGARD-CP-541] 12 p4482 N94-37261
Profile analysis of after-effects experienced during exposure to several virtual reality environments 12 p4482 N94-37263
On the feasibility of virtual environments in medicine 12 p4483 N94-37264
Immersive virtual environments as trainer: System design from a cognitive stance 12 p4484 N94-37267
Creation of a virtual world to study human spatial perception during sustained acceleration 12 p4484 N94-37268
The DRA Virtual Cockpit Research Program 12 p4484 N94-37269
Virtual reality evolution or revolution 12 p4484 N94-37270
Manual tracking performance using a virtual hand controller: A comparison study 12 p4484 N94-37271
A comparison of two examples of magnetic tracker systems 12 p4485 N94-37275
Some side-effects of immersion virtual reality 12 p4482 N94-37277
Low cost software-based rendering and stereoscopic interfaces for teleoperation and virtual reality 12 p4486 N94-37279

VIRUSES
NT HUMAN IMMUNODEFICIENCY VIRUS
PC viruses: How do they do that?
[DE93-012581] 02 p0753 N94-14289
Recombinant protein production and insect cell culture and process
[NASA-CASE-MSC-22336-1] 12 p4478 N94-36751

VISCOELASTIC DAMPING
Computational algorithms or identification of distributed parameter systems
[AD-A265252] 01 p0331 N94-11680
Substructure synthesis methods for viscoelastic structures
[UTIAS-349] 07 p2695 N94-26712
Finite element analysis of damped vibrations of laminated composite plates
[ISBN-0-315-84928-2] 07 p2843 N94-27585
Advanced microfabrication technologies for microspacecraft 08 p3171 N94-29782
Transfer function modeling of damping mechanisms in distributed parameter models 11 p4222 N94-35895

VISCOELASTIC FLOW
U VISCOELASTICITY

VISCOELASTICITY
A method for determination of the elongational viscosity of viscoelastic fluids without body forces 01 p0124 N94-10247
Advanced model of gradual wear of viscoelastic surface film
[AD-A265130] 01 p0090 N94-11222
Stability of viscoelastic flow: Physical and numerical considerations 01 p0031 N94-11493
On temperature distribution in non-participating medium with radiation boundary condition
[DE93-619375] 01 p0153 N94-11604
Numerical simulation of the non-Newtonian mixing layer 01 p0159 N94-12314
Characterization of composite materials for aerospace structures
[ESA-TT-1260] 02 p0557 N94-13804
Predicting the vibrations of a spinning inflated membrane
[DE93-010690] 02 p0676 N94-14456
Dynamic soil pressures on rigid cylindrical vaults
[DE93-013930] 02 p0676 N94-14585
On the design of structural components using materials with time-dependent properties
[NASA-TM-108428] 03 p1059 N94-16519
An analysis of ways of determining the material constants for viscoelastic materials
[IFTR-28/91] 03 p0951 N94-17050
Electrorheological (ER) fluids: A research needs assessment
[AD-A267588] 03 p0951 N94-17210
Damage evolution in filled elastomers
[AD-A268067] 03 p1062 N94-17507
A finite strain ring dynamical model for pneumatic tires
[AD-A269286] 04 p1444 N94-18266
Wave propagation near explosive sources
[AD-A270102] 04 p1418 N94-18870
Dynamical behavior of tantalum
[DE93-017877] 04 p1362 N94-18919
Problems related to conservation laws: Phase transitions and viscoelasticity
[AD-A271429] 05 p1698 N94-19840
Nonlocal models in continuum mechanics
[DE93-040146] 06 p2316 N94-22870
Numerical simulation of non-Newtonian free shear flows 06 p2331 N94-24160
Viscoelastic analysis of seals for extended service life 06 p2371 N94-24408
Stress relaxation in dough moulding compounds
[PB94-124872] 07 p2748 N94-25894
Proceedings of Damping 1993, volume 2
[AD-A274227] 07 p2840 N94-26953
Viscous and elastic-plastic material model in the ABAQUS
[PB94-132347] 08 p3316 N94-28409
Measurement and modelling of bolted joint stress relaxation in plastics
[PB94-124849] 08 p3318 N94-28841
Effects of physical aging on long-term creep of polymers and polymer matrix composites
[NASA-TM-109081] 08 p3181 N94-29541
Analysis of pressureless densification of ceramic matrix composites 08 p3216 N94-29766
On the structure and atomic motions in liquid sodium
[DE94-608386] 08 p3490 N94-30182
Generalized Eulerian-Lagrangian formulations in free and moving boundary problems: Processing of viscoelastic polymers and fiber suspensions 08 p3283 N94-30955
State of stress, faulting, and eruption characteristics of large volcanoes on Mars 09 p3940 N94-31108
Viscoelastic fracture characterization of polymeric solids 09 p3652 N94-31745
Influence of trace components on the viscoelastic properties of a polymer solution
[AD-A277171] 09 p3656 N94-32253
Elastic as limit of viscoelastic response, in a context of self-similar viscous limits
[AD-A277043] 09 p3738 N94-32273
A thermal viscoelastic analysis for thick-walled composite cylinders
[AD-A274143] 09 p3625 N94-32604
The effects of physical aging at elevated temperatures on the viscoelastic creep on IM7/K3B
[NASA-TM-109114] 10 p4025 N94-34396
Hypobaric decompression sickness model development. Part 1: Diffusion of inert gas from a viscoelastic fluid (blood) into an expanding gas phase
[AD-A280298] 12 p4481 N94-37124
Some considerations for modeling the creep behavior of composite materials
[DE94-012112] 12 p4404 N94-37205

VISCOMETERS
Some problems in the rheological characterisation of composite rocket propellants
[AD-A268806] 04 p1376 N94-18203
Dielectric viscometer including fixed and variable cells
[AD-D016139] 09 p3639 N94-32973

VISCOMETRY
Advanced in macrostatistical hydrodynamics
[DE93-018479] 04 p1410 N94-18270

VISCOPLASTIC FLOW
U VISCOPLASTICITY

VISCOPLASTICITY
A modeling investigation of thermal and strain induced recovery and nonlinear hardening in potential based viscoplasticity
[NASA-TM-106122] 01 p0188 N94-11482
Finite element analysis of structural engineering problems using a viscoplastic model incorporating two back stresses
[NASA-TM-106046] 03 p1060 N94-16881
Inelastic deformation and damage at high temperature
[DE93-018155] 04 p1448 N94-17814
Life assessment of structural components using inelastic finite element analyses 05 p1834 N94-22614
Theory of extrusion: Advances and challenges
[PB93-201572] 06 p2241 N94-23447
A hydrostatic stress-dependent anisotropic model of viscoplasticity
[NASA-TM-106525] 07 p2711 N94-27640
An anisotropic extension of Bodner's model of viscoplasticity: Model development
[NASA-CR-195289] 08 p3318 N94-28821
Prediction of stress-strain response of SCS-6/Timetal-21S subjected to a hypersonic flight profile
[NASA-TM-109026] 08 p3177 N94-28823
Finite element analysis of axisymmetric deformations of thick thermoviscoplastic targets 08 p3320 N94-29688
Micromechanical analysis of thermo-inelastic multiphase short-fiber composites
[NASA-CR-195290] 08 p3183 N94-30178
Inelastic deformation of metal matrix composites 09 p3618 N94-31285
Micromechanics and effective properties of particulate composites and fluid suspensions 09 p3703 N94-31744
New micro- and macroscopic models of contact and friction
[AD-A277240] 09 p3726 N94-32320
A state variable material model for superplastic titanium-6 percent Al-4 percent V 09 p3644 N94-32498
Investigation of materials processing technology
[AD-A277588] 10 p4031 N94-33428
A fully associative, non-linear kinematic, unified viscoplastic model for titanium based matrices
[NASA-TM-106609] 10 p4069 N94-33958
Micromechanical modeling of damage growth in titanium based metal-matrix composites 12 p4402 N94-36664

VISCOSITY
NT EDDY VISCOSITY
NT GAS VISCOSITY
Determination of the viscous acoustic field for liquid drop positioning/forcing in an acoustic levitation chamber in microgravity 01 p0110 N94-10131
Thermophysical properties of undercooled liquid metals 01 p0086 N94-10190
A method for determination of the elongational viscosity of viscoelastic fluids without body forces 01 p0124 N94-10247
Measurement of viscosity, density and gas solubility of refrigerant blends
[DE93-014772] 01 p0089 N94-11145
Negative viscosity and generation of dissipative solitons and zonal dissipative structures by drift waves
[DE93-621656] 01 p0392 N94-11212
Viscous relaxation of the Moho under large lunar basins 01 p0452 N94-12113

Stability of oscillatory two phase Couette flow
[NASA-CR-191501] 02 p0636 N94-13817
The spectral viscosity method applied to simulation of waves in a stratified atmosphere
[FFI-92/7047] 02 p0637 N94-14040
Effects of aging time on V205 sol-gel coatings
[AD-A266824] 03 p0965 N94-15843
Physical and chemical properties of some new perfluoropolyalkylether lubricants prepared by direct fluorination
[NASA-TM-106299] 03 p0967 N94-16543
Coefficients for calculating thermodynamic and transport properties of individual species
[NASA-TM-4513] 03 p1220 N94-17624
Investigation of a matrix-model for the artificial dissipation in a cell vertex finite volume scheme for solving the Navier-Stokes equations
[DLR-FB-92-33] 04 p1409 N94-18076
Some problems in the rheological characterisation of composite rocket propellants
[AD-A268806] 04 p1376 N94-18203
Advanced in macrostatistical hydrodynamics
[DE93-018479] 04 p1410 N94-18270
Measurement of viscosity, density, and gas solubility of refrigerant blends in selected synthetic lubricants
[DE93-040221] 04 p1350 N94-18977
Viscosity in the edge of tokamak plasmas
[DE93-018039] 04 p1588 N94-18988
Polymer technology publication. Series no. 14, 1993
[PB93-195964] 04 p1372 N94-19052
Densities and viscosities of ternary ammonia/water fluids
[DE93-015966] 04 p1351 N94-19118
Locally adaptive remeshing scheme for calculating fluid instabilities
[DE93-019577] 04 p1422 N94-19568
A database of selected transport coefficients for combustion studies
[DE93-041278] 05 p1678 N94-19889
Measuring liquid properties with smooth and textured-surface resonators
[DE93-019433] 05 p1749 N94-20054
Venus pancake dome formation: Morphologic effects of a cooling-induced variable viscosity during emplacement 05 p2110 N94-20732
Experiments with a fluid deicing system for cleaning laminar wings 05 p1640 N94-22601
Measurement of the influence of deicing liquids on aircraft aerodynamics 05 p1640 N94-22602
The relaxed state and entropy production due to the electric resistivity and viscosity of plasma 05 p2010 N94-22696
Local grid refinement method for the euler equations
[PB93-223329] 06 p2317 N94-22985
Polyimide processing additives
[NASA-CASE-LAR-13669-2] 06 p2252 N94-23079
A multilevel adaptive projection method for unsteady incompressible flow 06 p2341 N94-23690
Direct simulation of isothermal-wall supersonic channel flow 06 p2172 N94-24164
Electro-rheology fluids and liquid fuel flow
[AD-A273640] 06 p2337 N94-25032
Containerless measurements on liquids at high temperatures 06 p2238 N94-25125
Measurement of viscosity, density, and gas solubility of refrigerant blends in selected synthetic lubricants
[DE94-003609] 07 p2713 N94-25934
New constitutive equation for the volume viscosity in fluids
[NASA-TM-109104] 07 p2798 N94-27867
Viscosity of liquids: Halogenated ethanes
[ESDU-93012] 07 p2720 N94-28062
Solubility, viscosity, and density of refrigerant/lubricant mixtures
[DE94-004237] 07 p2721 N94-28069
Calculation methods for steadily loaded axial groove hydrodynamic journal bearings. Low viscosity process fluid lubrication (guide to use of computer program A9306)
[ESDU-93006] 07 p2830 N94-28075
The motion of deforming bodies
[AD-A275224] 08 p3271 N94-29061
Numerical modelling of turbine combustion chambers 08 p3154 N94-29254
Electromagnetic effect on turbulent transport in liquid metals and electrolytes (bath)
[PB94-138450] 08 p3206 N94-29946
Two-phase power-law modeling of pipe flows displaying shear-thinning phenomena
[DE94-005115] 08 p3279 N94-30020
Nonlinear calculations of the time evolution of black hole accretion disks 09 p3929 N94-31127
Convective solar nebula 09 p3930 N94-31130
Rotational effects in turbulence driven by convection 09 p3930 N94-31131
Measurement of viscosity, density, and gas solubility of refrigerant blends in selected synthetic lubricants
[DE94-007723] 09 p3653 N94-31917
Status of developing a multifunctional aviation grease
[AD-A276755] 09 p3656 N94-32184
Influence of trace components on the viscoelastic properties of a polymer solution
[AD-A277171] 09 p3656 N94-32253
Dielectric viscometer including fixed and variable cells
[AD-D016139] 09 p3639 N94-32973
Determination of extensional viscosity from capillary rheometer entrance pressure drop measurements using a numerical simulation of contraction flow
[PB94-171154] 11 p4263 N94-35603
Measurement of viscosity, density, and gas solubility of refrigerant blends in selected synthetic lubricants
[DE94-010426] 11 p4244 N94-35687
Solubility, viscosity and density of refrigerant/lubricant mixtures
[DE94-009996] 11 p4245 N94-35771
Analysis of current diffusive ballooning mode
[DE94-718992] 11 p4336 N94-35811
United States Air Force Summer Research Program, 1993. Volume 6: Arnold Engineering Development Center, Frank J. Seiler Research Laboratory and Wilford Hall Medical Center
[AD-A278697] 12 p4551 N94-36982
Evaluation of the EHL film thickness and extreme pressure additives on gear surface fatigue life
[NASA-TM-106663] 12 p4451 N94-37319
Momentum-energy transport from turbulence driven by parallel flow shear
[DE94-012765] 12 p4443 N94-37362
Coupled Marangoni-Benard/Rayleigh-Benard instability with temperature dependent viscosity
[NASA-TM-106646] 12 p4444 N94-37507

VISCOUS DAMPING
NT VISCOELASTIC DAMPING
A numerical experiment of boundary layer transition at subcritical Reynolds numbers 01 p0165 N94-12625
Computational issues in optimal tuning and placement of passive dampers 02 p0681 N94-14647
Time dependent turbulence modeling and analytical theories of turbulence
[NASA-TM-106379] 03 p1029 N94-17385
A mechanical system damping measurement technique using a one-degree-of-freedom (1DOF) cylindrical gas bearing
[AD-A268402] 03 p1048 N94-17462
Time dependent identification of nonlinear structures
[ECL-92-64] 04 p1457 N94-19403
Viscous rotary damper 06 p2361 N94-24031
Low melting temperature alloy deployment mechanism and recent experiments 08 p3163 N94-29644
An investigation of angular stiffness and damping coefficients of an axial spline coupling in high-speed rotating machinery 10 p4064 N94-34192
An experimental and theoretical study of structural damping in compliant foil bearings 10 p4064 N94-34194

VISCOUS DRAG
Experimental studies of vortex flaps and vortex plates. Part 1: 0.53 m span 60 deg delta wing
[DE93-767969] 02 p0505 N94-14059
Calculation of viscous drag of two low angle of attack supercritical profiles
[FFA-TN-1984-22] 07 p2644 N94-26104

VISCOUS FLOW
NT BOUNDARY LAYER FLOW
NT BOUNDARY LAYER SEPARATION
NT COUETTE FLOW
NT REATTACHED FLOW
NT SECONDARY FLOW
NT SEPARATED FLOW
NT STOKES FLOW
Studies of hypersonic viscous flows 01 p0008 N94-10454
Calculations of viscous nonequilibrium flows in nozzles 01 p0008 N94-10455
On the accuracy and efficiency of CFD methods in real gas hypersonics 01 p0009 N94-10462
Thermal and chemical non equilibrium hypersonic flow computations 01 p0010 N94-10465
Viscous flow simulation using an upwind method for hexahedral based adaptive meshes
[AD-A265901] 01 p0148 N94-10703
High order accurate solutions of viscous problems
[NASA-TM-106267] 01 p0151 N94-11253
Viscous analysis of three-dimensional rotor flows using a multigrid method
[NASA-TM-106266] 01 p0152 N94-11481
Numerical simulation using vorticity-vector potential formulation 01 p0157 N94-12297
VIB2D: Quasi 3-D unsteady viscous flow method for blade flutter calculation
[CUED/A-TURBO/TR.129] 01 p0166 N94-12779
Non-linear effects in vortex viscous flow in superconductors-role of finite heat removal velocity
[DE93-621785] 02 p0618 N94-12856
Approaches to high aspect ratio triangulations
[NASA-TM-107684] 02 p0739 N94-12886
Integration of viscous effects into inviscid computational methods
[NASA-CR-193677] 02 p0629 N94-13007
Numerical study of the effects of icing on viscous flow over wings
[NASA-CR-193306] 02 p0500 N94-13180
A robust quasi-simultaneous interaction method for a full potential flow with a boundary layer with application to wing/body configurations
[NLR-TP-91397-U] 02 p0503 N94-13531
Numerical simulations of unsteady flows in turbomachines 02 p0633 N94-13569
Passage-averaged approximation of turbomachinery flows using vorticity-potential method
[ISBN-0-315-72716-0] 02 p0634 N94-13598
A control volume finite element method for three-dimensional, incompressible, viscous fluid flow
[ISBN-0-315-72019-0] 02 p0635 N94-13683
Hypersonic flow phenomenology 02 p0505 N94-14155
Extrapolation of ground test data to flight 02 p0507 N94-14170
Least-squares finite element solutions for three-dimensional backward-facing step flow
[NASA-TM-106353] 02 p0770 N94-14407
A vortex method for viscous unsteady flows 02 p0640 N94-14602
A finite volume method for computation of viscous flow in complex configurations 02 p0640 N94-14607
Hypersonic viscous flow computations 02 p0510 N94-14612
Development of an explicit multiblock/multigrid flow solver for viscous flows in complex geometries
[NASA-TM-106356] 02 p0642 N94-14728
Analytical description of the breakup of liquid jets in air
[NASA-CR-191503] 02 p0647 N94-14849
Proteus two-dimensional Navier-Stokes computer code, version 2.0. Volume 2: User's guide
[NASA-TM-106338-VOL-2] 03 p1019 N94-15475
Proteus two-dimensional Navier-Stokes computer code, version 2.0. Volume 1: Analysis description
[NASA-TM-106336-VOL-1] 03 p1019 N94-15485
Proteus three-dimensional Navier-Stokes computer code, version 1.0. Volume 2: User's guide
[NASA-TM-106340-VOL-2] 03 p1020 N94-15488
Proteus three-dimensional Navier-Stokes computer code, version 1.0. Volume 3: Programmer's reference
[NASA-TM-106341] 03 p1022 N94-15865
Proteus two-dimensional Navier-Stokes computer code, version 2.0. Volume 3: Programmer's reference
[NASA-TM-106339] 03 p1022 N94-15867
Effective elastic thickness of the Venusian lithosphere with lateral viscosity variations in the mantle 03 p1293 N94-16421
Proteus three-dimensional Navier-Stokes computer code, version 1.0. Volume 1: Analysis description
[NASA-TM-106337] 03 p1024 N94-16527
Hoph bifurcation in viscous, low speed flows about an airfoil with structural coupling
[AD-A266542] 03 p0859 N94-16798
Process of shaping an electrorheological solid
[AD-D015885] 03 p1012 N94-16914
An upwind multigrid method for solving viscous flows on unstructured triangular meshes
[NASA-TM-109343] 03 p1027 N94-17061
Computational aerodynamics with icing effects
[AD-A267509] 03 p0860 N94-17074
Development of iterative techniques for the solution of unsteady compressible viscous flows
[NASA-CR-194657] 03 p1027 N94-17129
Numerical solution of SUPG finite-element method for supersonic viscous flow
[AD-A267762] 03 p0860 N94-17222
Multigrid time-accurate integration of Navier-Stokes equations
[NASA-TM-106373] 03 p1028 N94-17258
Experimental and computational investigation of the NASA low-speed centrifugal compressor flow field
[NASA-TM-4481] 03 p0869 N94-17386
Vortex methods and statistics
[DE93-016974] 04 p1556 N94-17886
Efficient simulation of incompressible viscous flow over multi-element airfoils 04 p1306 N94-18421
Viscous phenomena affecting high-lift systems and suggestions for future CFD development 04 p1308 N94-18433
A fast computing method for the flow over high-lift wings 04 p1308 N94-18437
Computational techniques for high-speed flows with viscous and chemical effects 04 p1412 N94-18560

Simulation of three dimensional unsteady viscous flows in turbomachines
[ECL-92-15] 04 p1420 N94-19398
Transient response of a viscous and anchored liquid bridge to an axial pulse
[LRT-WE-9-FB-7-1992] 04 p1379 N94-19492
Numerical simulation of viscous flows in chemical nonequilibrium
[MBB-LME-211-S-PUB-506] 04 p1421 N94-19497
Theoretical examination of the flow around a cylinder with a low dimensional Galerkin process
[MPIS-25/1992] 04 p1422 N94-19525
Time-accurate Navier-Stokes calculations with multigrid acceleration 05 p1956 N94-21469
Multigrid schemes for viscous hypersonic flows 05 p1641 N94-21473
Surface path lines in plane Stokes flow driven by capillarity
[DE93-041277] 05 p1803 N94-21651
Unstructured low-Mach number viscous flow solver 05 p1919 N94-22358
Robust unstructured grid generation with VGRID 05 p1919 N94-22359
Cartesian-cell based grid generation and adaptive mesh refinement 05 p1920 N94-22364
Molecular gas dynamics applied to low-thrust propulsion 06 p2214 N94-23053
Two-dimensional Navier-Stokes computations of subsonic and supersonic flows through turbine cascades
[PB93-226223] 06 p2317 N94-23114
Transient Ejector Analysis (TEA) code user's guide
[NASA-TM-106310] 06 p2186 N94-23466
An implicit numerical scheme for the simulation of internal viscous flows on unstructured grids
[NASA-TM-106437] 06 p2481 N94-23554
A dual reciprocal boundary element formulation for viscous flows 06 p2325 N94-23666
Heat pipe vapor dynamics
[NASA-CR-194217] 06 p2327 N94-24096
Drag reduction at a plane wall 06 p2327 N94-24140
Transition to turbulence in an elliptic vortex 06 p2331 N94-24161
An analysis for high Reynolds number inviscid/viscid interactions in cascades
[NASA-CR-4519] 06 p2169 N94-24606
Carrying the mass flux terms exactly in the first and second moment equations of compressible turbulence
[AD-A276346] 06 p2335 N94-24712
Development and application of new algorithms for the simulation of viscous compressible flows with moving bodies in three dimensions
[AD-A273514] 06 p2338 N94-25157
The high Reynolds number flow through an axial-flow pump
[AD-A273844] 07 p2789 N94-25604
A numerical determination of bifurcation points for low Reynolds number conical flows
[AD-A273964] 07 p2791 N94-25991
Chemical and vibrational nonequilibrium viscous flows: Modelling, internal and external flow applications
[ESA-TT-1274] 07 p2791 N94-26316
Computation of transonic viscous flow past the NTF 65-degree Delta Wing 07 p2659 N94-27930
Viscous airfoil computations using adaptive structured grids 07 p2655 N94-28337
A study of blunt trailing edge airfoils using the Navier Stokes code: ARC2D 07 p2656 N94-28340
A new flux vector splitting scheme 07 p2657 N94-28343
Innovative processing of composites for ultra-high temperature applications, book 3
[AD-A275599] 08 p3177 N94-28731
Numerical analysis of incompressible viscous flow around a bubble 08 p3126 N94-28968
Verification of a three-dimensional viscous flow analysis for a single stage compressor 08 p3127 N94-28976
Three-dimensional external flow computations using prismatic grid 08 p3127 N94-28979
The motion of deforming bodies
[AD-A275224] 08 p3271 N94-29061
CFD analyses for advanced pump design
[NASA-CR-193969] 08 p3300 N94-29550
The h-p adaptive methods for incompressible viscous flow problems 08 p3275 N94-29836
Hopf bifurcation in viscous, low-speed flows about an airfoil with structural coupling 08 p3134 N94-30865
A solution adaptive structured-unstructured grid procedure for unsteady flows 09 p3700 N94-31217
Numerical analysis of single-vortex/free-surface interaction
[AD-A276462] 09 p3701 N94-31241
Viscous limiter functions for model convection-diffusion equations
[CRANFIELD-AERO-9103] 09 p3702 N94-31559
Finite element vorticity-based methods for the solution of the incompressible and compressible Navier-Stokes equations
[ISBN-0-315-87265-9] 09 p3703 N94-31730
Incompressible viscous flow in tubes with occlusions
[ISBN-0-315-75467-2] 09 p3704 N94-31778
Attitude dynamics of spinning rockets in space with internal mass motion 09 p3601 N94-31802
On an adaptation method for dense, 2D, C-type grids
[W-9321] 09 p3706 N94-32045
Incorporating radial mixing in axisymmetric streamline curvature through-flow analysis
[AD-A277325] 09 p3706 N94-32279
A novel potential/viscous flow coupling technique for computing helicopter flow fields
[NASA-CR-193272] 09 p3571 N94-32476
A three-dimensional multigrid technique for unsteady incompressible viscous flows 10 p4042 N94-33364
Code validation for the simulation of supersonic viscous flow about the F-16XL 10 p3981 N94-33528
Inviscid and viscous flow calculations for the F16XL configuration 10 p3981 N94-33529
Computation of unsteady flows over airfoils 10 p3986 N94-34977
Some aspects of unsteady separation 10 p3986 N94-34979
An efficient, intelligent solution for viscous flows inside solid rocket motors
[AD-A278629] 11 p4228 N94-36255
Computational Mathematics Laboratory for multiscale analysis
[AD-A278597] 11 p4315 N94-36424

VISCOUS FLUIDS
Deformation mechanisms of continuous fibre-reinforced thermoplastic composites during manufacturing: A probabilistic approach 01 p0060 N94-10030
A method for determination of the elongational viscosity of viscoelastic fluids without body forces 01 p0124 N94-10247
The physics of pattern formation of liquid interfaces
[DE93-013333] 01 p0154 N94-11814
On the motion through a viscous fluid of a spherical particle touching a plane wall: Slip boundary conditions
[DE93-012540] 02 p0628 N94-12961
Stability of oscillatory two phase Couette flow
[NASA-CR-191501] 02 p0636 N94-13817
Stability of flows in fluidized beds
[DE93-000245] 03 p1024 N94-16763
Axial response of differently excited anchored viscous liquid bridges in zero-gravity
[LRT-WE-9-FB-1-1992] 04 p1379 N94-19489
Free fall liquid column dynamics in a droptower
[LRT-WE-9-FB-6-1992] 04 p1379 N94-19491
Transient response of a viscous and anchored liquid bridge to an axial pulse
[LRT-WE-9-FB-7-1992] 04 p1379 N94-19492
Nonlinear dynamics applied to atmospheric prediction
[AD-A273437] 06 p2404 N94-24674
The hydrodynamics of a moving fluid-liquid contact line
[ETN-94-95352] 06 p2339 N94-25247
Low melting temperature alloy deployment mechanism and recent experiments 08 p3163 N94-29644
Oscillations in piston-driven shear flow of a non-Newtonian fluid
[AD-A276472] 09 p3701 N94-31245
Attitude dynamics of spinning rockets in space with internal mass motion 09 p3601 N94-31802
Design and aerodynamic performance evaluation of a high-work mixed flow turbine stage 10 p4003 N94-34459
Investigation of mechanisms for vorticity generation and flow separation on bodies in unsteady motion 10 p4051 N94-34973

VISIBILITY
NT LOW VISIBILITY
User's manual for the plume visibility model PLUVUE 2 (revised)
[PB93-188233] 01 p0265 N94-11016
On resolution of underwater stereo photogrammetry 01 p0172 N94-11966
Hardware design for the Autonomous Visibility Monitoring (AVM) observatory 02 p0533 N94-14394
Summary of conclusions and recommendations from a visibility science workshop
[DE93-012770] 02 p0710 N94-14523
Low Earth orbit constellations: Orbit control or not 03 p0875 N94-17134
Impact of launching uncertainties on the visibility of communication satellite constellations without orbit control 03 p0889 N94-17135
A comparison of ceiling and visibility observation for NWS manned observation sites and ASOS sites
[AD-A268356] 03 p1108 N94-17459
Visibility impairment assessment: Importance of using theoretically derived optical characterizations
[DE93-017147] 04 p1470 N94-17749
Station climatic summaries: North America. Volume 1: The contiguous United States
[AD-A269567] 04 p1490 N94-18303
The urban perspectives of acid rain
[DE93-018881] 04 p1474 N94-18523
Station climatic summaries, North America. Volume 2: Alaska, Canada and Greenland
[AD-A269793] 04 p1493 N94-18732
Distribution of turbidity in Australian tropical waters
[AD-A271059] 05 p1881 N94-19905
Visibility considerations in frequency sharing with low Earth orbit satellites 05 p1746 N94-22187
Validation of a second generation conspicuity meter
[IZF-1993-A-11] 06 p2542 N94-22895
A model-based approach for detection of objects in low resolution passive-millimeter wave images 06 p2442 N94-25507
Results from the VISA project
[AD-A273752] 06 p2406 N94-25540
The appearance of the Sun and Moon seen through clouds
[AD-A275338] 08 p3551 N94-29212
Optical modeling of visibility and visibility instrumentation using stratified Mie theory 08 p3348 N94-29750
Synthetic vision technology demonstration. Volume 1: Executive summary
[AD-280564] 09 p3582 N94-33076
Synthetic vision technology demonstration. Volume 2: Sensor tower testing
[DOT/FAA/RD-93/40-VOL-2] 09 p3582 N94-33077
Synthetic vision technology demonstration. Volume 3: Flight tests
[AD-A281051] 09 p3582 N94-33078
Synthetic vision technology demonstration. Volume 4: Appendices
[AD-A281052] 09 p3583 N94-33079
Vision-based aircraft guidance
[NASA-CR-195937] 10 p4007 N94-34264
The analysis of rapidly developing fog at the Kennedy Space Center
[NASA-CR-195888] 10 p4090 N94-34939
Analysis of regional visibility in the eastern United States using aerosol models
[PB94-158698] 11 p4332 N94-35584
Data requirements for ceiling and visibility products development
[AD-A278959] 11 p4293 N94-35720
Composite helicopter accident profiles: Deficient crew/aircraft performance
[SCT-90RR-46] 12 p4385 N94-37604

VISIBLE INFRARED SPIN SCAN RADIOMETER
Effects of satellite spectral resolution and atmospheric water vapor on retrieval of near-ground temperatures
[AD-A264920] 01 p0245 N94-11851
Interferometer scan unit mechanism definition 06 p2358 N94-24012

VISIBLE RADIATION
U LIGHT (VISIBLE RADIATION)

VISIBLE SPECTRUM
Continued development of an ultra-narrow bandpass filter for solar research
[NASA-CR-194169] 01 p0381 N94-10735
Compositional and textural information from the dual inversion of visible, near and thermal infrared remotely sensed data 01 p0258 N94-12097
Optical properties of CO2 ice and CO2 snow in the ultraviolet, visible, and infrared
[NASA-CR-194110] 02 p0686 N94-14081
New K type asteroids 03 p1241 N94-16195
Overview of research in progress at the Center of Excellence
[NASA-CR-194329] 04 p1618 N94-19256
Wavelength dependence of limb-darkening of Mars from visible and near-IR telescopic spectral imaging 05 p2101 N94-20685
Visible-infrared properties of controlled laboratory soils 05 p1685 N94-20689
Planetary Instrument Definition and Development Program (PIDDP). Instrument for future planetary flight missions: A visible-infrared imaging spectrometer for planetary missions
[NASA-CR-195254] 07 p3106 N94-27409
A historical perspective on fifteen years of laser damage thresholds at LLNL
[DE94-007930] 09 p3719 N94-32613
High resolution visible to short-wave near-infrared CCD spectra of Mars during 1990 11 p4356 N94-35403

VISION
NT BINOCULAR VISION
NT COLOR VISION
NT MONOCULAR VISION

NT NIGHT VISION
NT PERIPHERAL VISION
NT STEREOSCOPIC VISION

Aviation accident risk for airmen with aphakia and artificial lens implants
[DOT/FAA/AM-93/11] 01 p0303 N94-10813

Enhancing sight
[NASA-TM-109637] 03 p1221 N94-15248

Localization of figure background segregation mechanisms in primate visual cortex
[PB93-187961] 04 p1508 N94-18121

Effects of location cuing on redundant target processing
[IZF-1993-B-1] 04 p1510 N94-19443

Analysis of health status from preliminary physical examination of flight academy applicants
[AD-A267759] 05 p1889 N94-19962

Toward a neurobiological theory of visual attention
[AD-A270724] 05 p1890 N94-20112

Head-centered orientation strategies in animate vision
[TR-442] 05 p1894 N94-20520

Vision impairment and corrective considerations of civil airmen
[DOT/FAA/AM-93/21] 06 p2426 N94-23623

Image remapping strategies applied as protheses for the visually impaired 06 p2444 N94-25363

Interacting cortical filters for object recognition
[PB94-125374] 07 p2938 N94-26873

Naval aviation vision standards research at the naval aerospace medical research laboratory: The long view
[AD-A275885] 08 p3388 N94-28756

Dual use of image based tracking techniques: Laser eye surgery and low vision prosthesis 08 p3397 N94-30455

Sensory sensitivities and discriminations and their roles in aviation
[AD-A277312] 09 p3800 N94-32276

Workshop on Visual Perception: Computation and Psychophysics
[AD-A278412] 09 p3802 N94-33326

VISUAL ACCOMMODATION

Visual accommodation to virtual image displays when knowledge of object distance conflicts with optical distance 12 p4485 N94-37278

VISUAL ACUITY

Comparative night vision goggle visual acuity measurements performed in the A-10 aircraft in an operational setting
[AD-A266721] 03 p1137 N94-15820

US Army aviation epidemiology data register: Prevalence of refractive error among US aircrew members
[AD-A269550] 04 p1505 N94-18289

Psychophysical analyses of perceptual representations
[AD-A268711] 04 p1508 N94-18313

Analysis of health status from preliminary physical examination of flight academy applicants
[AD-A267759] 05 p1889 N94-19962

Evaluation of visual acuity with Gen 3 night vision goggles
[NASA-TM-108792] 06 p2431 N94-23974

Cockpit/NVG visual integration issues 06 p2432 N94-23983

An investigation of stereopsis with AN/AVS-6 night vision goggles at varying levels of illuminance and contrast
[AD-A275332] 08 p3400 N94-28918

Backscatter haze device for measurement of haze in aircraft transparencies
[AD-A275127] 08 p3146 N94-29042

VISUAL AIDS

Animating engineering science results using AVS
[DE93-011591] 01 p0325 N94-11123

Visual cueing aids for rotorcraft landings 02 p0524 N94-13313

Processes involved in the integration of pictures and discourse
[AD-A268150] 03 p1134 N94-17468

Three-dimensional cloud visualization based on satellite imagery
[AD-A269318] 04 p1490 N94-18300

The manager's guide to NASA graphics standards
[NHB-1430.2] 05 p2042 N94-20308

RIAD visual imaging branch assessment 07 p2815 N94-27895

Variable-resolution imagery for flight simulation
[AD-A276199] 09 p3586 N94-31058

VISUAL CONTROL

Compatibility of information and mode of control: The case for natural control systems 02 p0523 N94-13307

Visual information for judging temporal range 02 p0524 N94-13314

Visual cueing considerations in Nap-of-the-Earth helicopter flight head-slaved helmet-mounted displays 02 p0524 N94-13315

Primary display latency criteria based on flying qualities and performance data 02 p0525 N94-13318

Visually guided touching and manual tracking
[TR-412] 03 p1166 N94-16581

Eye-gaze control of the computer interface: Discrimination of zoom intent
[DE94-000480] 06 p2429 N94-22997

The effects of spatially displaced visual feedback on remote manipulator performance 06 p2436 N94-24201

Technology transfer of operator-in-the-loop simulation 09 p3802 N94-32472

Interactive large screen: A multi-mode dialogue tool for future cockpits 12 p4484 N94-37266

A non-intrusive way to measure point-of-gaze 12 p4484 N94-37272

Operator gaze position control interfaces: Investigation of psychophysical and operational parameters 12 p4485 N94-37273

Gaze orientation under G(z)-load. Methodological aspects: Preliminary results 12 p4485 N94-37274

A comparison of two examples of magnetic tracker systems 12 p4485 N94-37275

Night vision goggles in Emergency Medical Service (EMS) helicopters
[SCT-93RR-22] 12 p4487 N94-37742

VISUAL DISCRIMINATION

Psychophysical analyses of perceptual representations
[AD-A268711] 04 p1508 N94-18313

The 3-D Moons: The Voyager stereo atlas of the outer solar system 05 p2111 N94-20740

Quality metrics for sensor images 06 p2443 N94-25513

Function of selective attention intrinsic to the saccade system: Does the voluntary control override the stimulus driven control? 07 p2928 N94-27523

Japanese Journal of Aerospace and Environmental Medicine, vol. 30, no. 2
[JTN-94-80599] 08 p3394 N94-29863

Psychophysiological study on the effects of co-existence of lines for detecting dot target 08 p3394 N94-29867

Variable-resolution imagery for flight simulation
[AD-A276199] 09 p3586 N94-31058

Sensory sensitivities and discriminations and their roles in aviation
[AD-A277312] 09 p3800 N94-32276

A visual detection model for DCT coefficient quantization 09 p3850 N94-32467

VISUAL DISPLAYS

U DISPLAY DEVICES

VISUAL FIELDS

Visual cueing considerations in Nap-of-the-Earth helicopter flight head-slaved helmet-mounted displays 02 p0524 N94-13315

Effects of simulator motion and visual characteristics on rotorcraft handling qualities evaluations 02 p0524 N94-13317

Stochastic models of attention and search
[AD-A268622] 04 p1508 N94-18292

Endogeneous and exogenous control of visual selection: A review of the literature
[AD-A273761] 07 p2908 N94-25871

Variable-resolution imagery for flight simulation
[AD-A276199] 09 p3586 N94-31058

Anthropometric accommodation in USAF cockpits 10 p4101 N94-33630

Eye movements and visual information processing
[AD-A278364] 10 p4097 N94-33700

VISUAL FLIGHT

VMC left turn curved approaches, test results --- (visual meteorological conditions)
[AD-A269476] 04 p1316 N94-18728

Special investigation report: Safety issues related to wake vortex encounters during visual approach to landing
[PB94-917002] 07 p2660 N94-27881

VISUAL FLIGHT RULES

Federal aviation regulations. Part 91: General operating and flight rules, change 3
[PB94-159910] 10 p3987 N94-34410

VISUAL OBSERVATION

Visual Earth observation performance in the space environment. Human performance measurement 4: Flight experiments 01 p0314 N94-11539

Ultraviolet observations of clusters of Wolf-Rayet stars in the SBm3 galaxy NGC 4214 and Ultraviolet and optical observations of LINER's
[NASA-CR-194307] 04 p1622 N94-19431

Cloud fields derived from satellite and surface data during FIRE cirrus phase 2 05 p1872 N94-22302

Observational studies of the clearing phase in proto-planetary disk systems
[NASA-CR-195182] 06 p2604 N94-25265

Construction of visual representations and time-space organization of resources in astronomy
[ISBN-0-315-86694-2] 09 p3925 N94-31914

Use of Air Force cloud cover data to evaluate and improve cloud forecasts and parameterizations in mesocale meteorological models
[AD-A277384] 09 p3784 N94-32054

An integrated cloud observation and modeling investigation in support of the ARM program
[DE94-003160] 09 p3785 N94-32716

Use of cloud observations and mesoscale meteorology models to evaluate and improve cloud parameterizations
[DE94-003610] 09 p3785 N94-32717

VISUAL PERCEPTION

NT SPACE PERCEPTION
NT VISUAL DISCRIMINATION

Automaticity of processing location versus identity information in brief visual displays
[AD-A265013] 01 p0418 N94-10491

Visual encoding of spatial relations
[AD-A266049] 01 p0313 N94-10909

Computer software and hardware to determine contrast sensitivity using three methods: Tracking, limits, and constant stimuli
[AD-A265168] 01 p0324 N94-11099

Three-dimensional object recognition using an unsupervised BCM network: The usefulness of distinguishing features
[AD-A264576] 01 p0304 N94-11261

Perceptual response to visual noise and display media
[NASA-CR-193406] 01 p0313 N94-11511

Visual psychophysics of egomotion
[AD-A265253] 01 p0304 N94-11681

Comparative measurement of visual stability in Earth and cosmic space (L-4) 02 p0592 N94-13761

Validity of FAA-approved color vision tests for class 2 and class 3 aeromedical screening
[DOT/FAA/AM-93/17] 02 p0735 N94-14846

Validation of an inexpensive illuminant for aeromedical color vision screening
[DOT/FAA/AM-93/16] 02 p0736 N94-14854

YARF: An open-ended framework for robot road following
[AD-A266788] 03 p1163 N94-14910

Enhancing sight
[NASA-TM-109637] 03 p1221 N94-15248

Cooperativity and 3-D representation
[AD-A267180] 03 p1131 N94-15894

Reference frames in vision
[AD-A266174] 03 p1132 N94-16925

Localizing visual function in the brain
[AD-A267381] 03 p1133 N94-17020

ARPA unmanned ground vehicle stereo vision program at Teleos Research
[AD-A267632] 03 p1167 N94-17202

Neural basis of motion perception
[AD-A267267] 03 p1133 N94-17265

The effects of luminance boundaries on color perception
[AD-A268398] 03 p1133 N94-17397

A virtual acoustic orientation instrument
[AD-A268181] 03 p1134 N94-17510

Perception of lightness and brightness in complex patterns
[AD-A268435] 03 p1134 N94-17513

Localization of figure background segregation mechanisms in primate visual cortex
[PB93-187961] 04 p1508 N94-18121

Stochastic models of attention and search
[AD-A268622] 04 p1508 N94-18292

Visual perception of features and objects
[AD-A269879] 04 p1508 N94-18682

Interdisciplinary training in life science (FY 1991 ASSERT)
[AD-A269220] 04 p1512 N94-18886

Overview of research in progress at the Center of Excellence
[NASA-CR-194329] 04 p1618 N94-19256

Serial pattern complexity: Irregularity and hierarchy
[PB93-191914] 04 p1509 N94-19348

Stimulus-driven capture and attentional set: Selective search for color and visual abrupt onsets
[IZF-1992-B-9] 04 p1509 N94-19419

Pilot studies on object motion perception during linear self-motion after long duration centrifugation of human subjects
[IZF-1993-B-3] 04 p1510 N94-19439

On geometric and algebraic aspects of 3D affine and projective structures from perspective 2D views
[AD-A270520] 05 p1983 N94-19968

Head-centered orientation strategies in animate vision
[TR-442] 05 p1894 N94-20520

Perception/action: An holistic approach 2
[AD-A271822] 05 p1891 N94-20627

A new procedure for orbit determination based on three lines of sight: Angles only
[AD-A272937] 05 p1652 N94-21224
Two-dimensional perception based on a laser rangefinder 05 p1786 N94-22202
Validation of a second generation conspicuity meter
[IZF-1993-A-11] 06 p2542 N94-22895
A knowledge based system for scientific data visualization
[NASA-CR-194879] 06 p2452 N94-23507
Some background information on perceptual color matching pertinent to computer applications
[PB93-200327] 06 p2445 N94-23788
Visual Problems in Night Operations
[AGARD-LS-187] 06 p2431 N94-23976
Multi-sensoral approach to night flight: Perceptive and Cognitive limitations 06 p2432 N94-23981
Cockpit/NVG visual integration issues
06 p2432 N94-23983
Night vision goggle illusions and visual training
06 p2432 N94-23984
Luminance-brightness mapping: The missing decades
[ETN-94-95351] 06 p2428 N94-25298
Synthetic vision system flight test results and lessons learned 06 p2429 N94-25492
Extracting heading and temporal range from optic flow: Human performance issues 06 p2442 N94-25510
Optical information in landing scenes
06 p2442 N94-25511
Human visual system enhancement of reconstructed satellite images
[AD-A273867] 07 p2693 N94-25595
Image quality and the display modulation transfer function: Experimental findings
[AD-A274061] 07 p2679 N94-25773
Endogeneous and exogenous control of visual selection: A review of the literature
[AD-A273761] 07 p2908 N94-25871
The AFIT multielectrode array for neural recording and simulation: Design, testing, and encapsulation
[AD-A274086] 07 p2909 N94-25943
Pacing visual attention: Temporal structure effects
[AD-A273859] 07 p2937 N94-25965
Color head down display program
[AD-A274807] 07 p2672 N94-26340
Interacting cortical filters for object recognition
[PB94-125374] 07 p2938 N94-26873
Orientation competition in cortical filters
[PB94-125366] 07 p2939 N94-27001
Frequency analysis of body sway induced by optokinetic stimulation 07 p2914 N94-27455
Effects of imaginary target on induced eye movements by linear acceleration 07 p2914 N94-27456
Eye-head coordination and swinging of the visual scene when wearing visually up-down reversing mirror for 14 days 07 p2915 N94-27462
Comparative measurement of visual stability in cosmic space: Onboard experiment and pre-flight activities
07 p2916 N94-27463
Analysis of the Electrically Evoked Response (EER) of the cat 07 p2908 N94-27519
Visual surface perception: Surface reconstruction from shading and stereo
[ISBN-0-315-60974-5] 07 p2975 N94-27872
Visit to CERMA: Centre d'Etudes et de Recherches de Medecine Aerospatiale, Centre for Studies and Research in Aviation and Space Medicine, Bretigny sur Orge, France, November 16-18, 1992
[PB94-132990] 07 p2937 N94-28392
Naval aviation vision standards research at the naval aerospace medical research laboratory: The long view
[AD-A275685] 08 p3388 N94-28756
An investigation of stereopsis with AN/AVS-6 night vision goggles at varying levels of illuminance and contrast
[AD-A275332] 08 p3400 N94-28918
The appearance of the Sun and Moon seen through clouds
[AD-A275338] 08 p3551 N94-29212
Empirical studies of the value of algorithm animation in algorithm understanding
[AD-A275135] 08 p3412 N94-29287
Behavior and visual control of cyprinodonts under microgravity 08 p3387 N94-29713
Psychophysiological study on the effects of co-existence of lines for detecting dot target
08 p3394 N94-29867
Morphological directional coding of images
[ISBN-0-315-86336-6] 09 p3814 N94-31715
Analysis of pursuit tracking eye movements in pilots and nonfliers
[AD-A276597] 09 p3799 N94-32035
Algebraic functions for recognition
[AD-A276803] 09 p3846 N94-32167
Modular Simulator System (MSS). System/segment specification for the generic modular simulator system-visual module, volume 11
[AD-A276978] 09 p3589 N94-32317
Visual encoding of spatial relations
[AD-A277400] 09 p3800 N94-32344
Visual neural development and chromatic aberration
[AD-A277402] 09 p3800 N94-32345
Information theory for arm visuo-motor coordination
09 p3800 N94-32495
Mechanisms of temporal pattern discrimination by human observers
[AD-A277407] 09 p3801 N94-32577
Models of the neuronal mechanisms of target localization of the barn owl
[AD-A277332] 09 p3797 N94-32623
Visual processing of object velocity and acceleration
[AD-A277425] 09 p3801 N94-32998
Synthetic vision technology demonstration. Volume 2: Sensor tower testing
[DOT/FAA/RD-93/40-VOL-2] 09 p3582 N94-33077
Synthetic vision technology demonstration. Volume 3: Flight tests
[AD-A281051] 09 p3582 N94-33078
Visual perception of 3-dimensional structure from different types of optical deformation
[AD-A278272] 09 p3884 N94-33141
Workshop on Visual Perception: Computation and Psychophysics
[AD-A278412] 09 p3802 N94-33326
Effective declutter of complex flight displays using stereoptic 3-D cueing
[AD-A279764] 10 p3989 N94-33536
Visual motion perception and visual information processing
[AD-A278530] 10 p4096 N94-33595
Stochastic models of attention and search
[AD-A278538] 10 p4097 N94-33674
Eye movements and visual information processing
[AD-A278364] 10 p4097 N94-33700
Visual motion perception and visual information processing
[AD-A278370] 10 p4097 N94-33738
Acting to gain information: Real-time reasoning meets real-time perception 10 p4160 N94-34042
Visual-vestibular interaction
[NASA-CR-196097] 11 p4297 N94-35379
Accommodation during instrument viewing can be influenced by knowledge of object distance
[AD-A278987] 11 p4298 N94-35528
Efficient contact determination between geometric models
[AD-A280244] 12 p4494 N94-37120
Creation of a virtual world to study human spatial perception during sustained acceleration
12 p4484 N94-37268
The DRA Virtual Cockpit Research Program
12 p4484 N94-37269

VISUAL SIGNALS
Visual processing of object velocity and acceleration
[AD-A277425] 09 p3801 N94-32998
Effective declutter of complex flight displays using stereoptic 3-D cueing
[AD-A279764] 10 p3989 N94-33536

VISUAL STIMULI
Computer software and hardware to determine contrast sensitivity using three methods: Tracking, limits, and constant stimuli
[AD-A265168] 01 p0324 N94-11099
Visual information for judging temporal range
02 p0524 N94-13314
Primary display latency criteria based on flying qualities and performance data 02 p0525 N94-13318
Perception of lightness and brightness in complex patterns
[AD-A268435] 03 p1134 N94-17513
Localization of figure background segregation mechanisms in primate visual cortex
[PB93-187961] 04 p1508 N94-18121
Stimulus-driven capture and attentional set: Selective search for color and visual abrupt onsets
[IZF-1992-B-9] 04 p1509 N94-19419
Effects of location cuing on redundant target processing
[IZF-1993-B-1] 04 p1510 N94-19443
Motion sickness elicited by passive rotation in squirrel monkeys 05 p1887 N94-21905
Physical aspects of the visual stimulus
06 p2431 N94-23978
Function of selective attention intrinsic to the saccade system: Does the voluntary control override the stimulus driven control? 07 p2928 N94-27523
Visual motion perception and visual information processing
[AD-A278370] 10 p4097 N94-33738
Visual-vestibular interaction
[NASA-CR-196097] 11 p4297 N94-35379
The use of a tactile interface to convey position and motion perceptions 12 p4486 N94-37281

VISUAL TASKS
Validity of FAA-approved color vision tests for class 2 and class 3 aeromedical screening
[DOT/FAA/AM-93/17] 02 p0735 N94-14846
Enhancing sight
[NASA-TM-109637] 03 p1221 N94-15248
Perception of lightness and brightness in complex patterns
[AD-A268435] 03 p1134 N94-17513
Stimulus-driven capture and attentional set: Selective search for color and visual abrupt onsets
[IZF-1992-B-9] 04 p1509 N94-19419
Head-centered orientation strategies in animate vision
[TR-442] 05 p1894 N94-20520
Perception/action: An holistic approach 2
[AD-A271822] 05 p1891 N94-20627
Automated system function allocation and display format: Task information processing requirements
06 p2434 N94-24189
Scanning and monitoring performance: Effects of the reinforcement values of the events being monitored
[DOT/FAA/AM-94/8] 08 p3398 N94-29918
Sampling behaviour in a four instrument monitoring task: Effects of signal bandwidth and number of events per signal
[AD-B179613] 08 p3402 N94-30422
Maintaining vigilance on a simulated ATC monitoring task across repeated sessions
[DOT/FAA/AM-94/6] 08 p3143 N94-30933
Optical flow from 1D correlation: Application to a simple time-to-crash detector
[AD-A276777] 09 p3880 N94-32186
Acting to gain information: Real-time reasoning meets real-time perception 10 p4160 N94-34042
Behavioral performance in monkeys exposed to TEMPO high-peak-power microwave pulses at 3 GHz
[AD-A280551] 12 p4478 N94-37045
Assessment of night vision goggle workload: Flight test engineer's guide
[SCT-91RR-45] 12 p4487 N94-37743

VISUAL TRACKING
U OPTICAL TRACKING

VISUALIZATION OF FLOW
U FLOW VISUALIZATION

VITAMIN A
U RETINENE

VITAMIN E
U TOCOPHEROL

VITAMINS
NT RETINENE
NT TOCOPHEROL

VITERBI DECODERS
Coding performance of the Probe-Orbiter-Earth communication link 02 p0608 N94-14377
High-speed Viterbi decoding with overlapping code sequences 05 p1760 N94-21130
Design of a new squaring function for the Viterbi algorithm 05 p1764 N94-21699
Coded 64QAM using a binary convolutional code
05 p1747 N94-22223
Adaptive decoding of convolutional codes
05 p1793 N94-22246
Bidirectional algorithms for the decoding of convolutional codes over memoryless channels
05 p1793 N94-22247
On the performance of trellis coded 8PSK with Reed Solomon codes
[ISBN-0-315-84289-X] 07 p2770 N94-26626
Convolutional encoding of self-dual codes
08 p3250 N94-29662
Decoder synchronization for deep space missions
08 p3250 N94-29664
Methods of implementing the Viterbi algorithm on a massively parallel computer of the SIMD (single instruction multiple data) type
[ISBN-0-315-86783-3] 09 p3814 N94-31752
Issues in the development of a 10 MBPS K = 15 Viterbi decoder
[NASA-CR-196083] 11 p4211 N94-35357
Maximum-likelihood soft-decision decoding of block codes using the A* algorithm 11 p4254 N94-35555
Error control techniques for satellite and space communications
[NASA-CR-196302] 12 p4433 N94-36931

VITON RUBBER (TRADEMARK)
Effect of temperature and O-ring gland finish on sealing ability of Viton V747-75
[NASA-TP-3391] 04 p1368 N94-18075

VITRIFICATION
Radiation-induced aperiodicity in irradiated ceramics
[DE93-013335] 01 p0091 N94-11698

Relationship between borosilicate glass composition, structure, and durability test response (SRS)
[DE93-013578] 02 p0581 N94-14343

VLASOV EQUATIONS
Dynamics of ion acceleration in electron flux by a virtual cathode potential
[DE93-620978] 01 p0371 N94-10542
Linear stability of stationary solutions of the Vlasov-Poisson system in three dimensions
[DE93-013873] 03 p1174 N94-16820

VLBI
U VERY LONG BASE INTERFEROMETRY

VLSI
U VERY LARGE SCALE INTEGRATION

VOCODERS
Data compression by using wavelet transforms and vector quantization
[AD-A272763] 05 p1738 N94-21182
Software implementation of an adaptive digital automatic level control 05 p1773 N94-22124

VOICE
Researches of the Electrotechnical Laboratory. No. 955: Speech recognition by description of acoustic characteristic variations
[JTN-94-80604] 07 p2775 N94-27249

VOICE COMMUNICATION
NT TELEPHONY
Analysis of fundamental frequency pattern in speech 02 p0618 N94-13440
Propagation considerations in the American Mobile Satellite system design 02 p0614 N94-14668
Call sign intelligibility improvement using a spatial auditory display
[NASA-TM-104014] 03 p1177 N94-15549
A study on an experimental communication system using microsatellites 03 p0892 N94-17160
MAGSS-14: Medium Altitude Global Mobile Satellite System with enhanced regional coverage 03 p0893 N94-17164
Template based low data rate speech encoder
[AD-A270900] 04 p1392 N94-19748
A real-time spoken-language system for interactive problem-solving, combining linguistic and statistical technology for improved spoken language understanding
[AD-A270901] 04 p1392 N94-19749
Improved HF data network simulator, volume 1
[AD-A270953] 04 p1393 N94-19752
Improved HF data network simulator, software user's manual, volume 2
[AD-A270954] 04 p1393 N94-19753
Control of integrated voice/data multi-hop radio networks via reduced-load approximations
[AD-A270661] 04 p1393 N94-19779
Ground proximity warning system voice warning unit requirements study
[AD-A270541] 05 p1641 N94-19876
ATC/pilot voice communications: A survey of the literature
[DOT/FAA/AM-93/20] 05 p1738 N94-21201
Software implementation of an adaptive digital automatic level control 05 p1773 N94-22124
Proceedings of the Third International Mobile Satellite Conference (IMSC 1993)
[NASA-CR-194516] 06 p2273 N94-22735
ROCSAT-1 telecommunication experiments 06 p2279 N94-22770
Mobilesat (tm): A world first 06 p2281 N94-22783
First satellite mobile communication trials using BLQS-CDMA 06 p2284 N94-22801
A protocol for satellite access via use of spot-beams 06 p2286 N94-22811
Performance of the unique-word-reverse-modulation type demodulator for mobile satellite communications 06 p2286 N94-22813
On the quality of synthetic speech evaluation and improvements
[ETN-94-95298] 06 p2304 N94-25234
Development of satellite telecommunications during the period 1990 - 2005
[CRANFIELD-AERO-9301] 07 p2765 N94-25639
Airborne data link operational evaluation test plan
[AD-A274096] 07 p2664 N94-25788
Parametric time-scale methods in signal analysis
[AD-A274212] 07 p2773 N94-27068
NCVS, volume 5
[AD-A274975] 07 p2902 N94-27165
Virtual annotation: Verbal communication in virtual reality
[REPT-93-67] 09 p3674 N94-31645
Voice and video transmission using XTP and FDDI 09 p3685 N94-32468
An exploratory study of neuro linguistic programming and communication anxiety
[AD-A277756] 09 p3682 N94-32986
Laboratory and in-flight experiments to evaluate 3-D audio display technology 10 p4038 N94-33618
The Canadian network for the advancement of research, industry and education (CANARIE) 12 p4543 N94-37336

VOICE CONTROL
STS-41 VCS training with mission specialist Bruce Melnick and Bill Shepard
[NASA-TM-109513] 03 p1046 N94-15459
Feasibility study in linguistically motivated object-oriented conceptual design of information systems
[PB93-197754] 04 p1618 N94-19331
Representation of spoken words in a self-organizing neural net 05 p1940 N94-20243
Speech versus manual control of camera functions during a telerobotic task 06 p2436 N94-24199
Application of the wavelet transform for speech processing 09 p3600 N94-31435
Dyadic wavelet features for isolated word speaker dependent speech recognition
[AD-A278492] 10 p4034 N94-33756
Interactive large screen: A multi-mode dialogue tool for future cockpits 12 p4484 N94-37266

VOICE DATA PROCESSING
NT CEPSTRAL ANALYSIS
Necessary conditions for the optimality of variable rate residual vector quantizers
[NASA-CR-193730] 01 p0326 N94-11197
Template based low data rate speech encoder
[AD-A270900] 04 p1392 N94-19748
A real-time spoken-language system for interactive problem-solving, combining linguistic and statistical technology for improved spoken language understanding
[AD-A270901] 04 p1392 N94-19749
Ground proximity warning system voice warning unit requirements study
[AD-A270541] 05 p1641 N94-19876
Data compression by using wavelet transforms and vector quantization
[AD-A272763] 05 p1738 N94-21182
Software implementation of an adaptive digital automatic level control 05 p1773 N94-22124
A high quality voice coder with integrated echo canceller and voice activity detector for mobile satellite applications 06 p2286 N94-22812
Linear and nonlinear adaptive filtering and their application to speech intelligibility enhancement
[ISBN-9-09-005342-5] 06 p2304 N94-25292
Speech coding at low to medium bit rates
[ISBN-0-315-84012-9] 07 p2770 N94-26630
Researches of the Electrotechnical Laboratory. No. 955: Speech recognition by description of acoustic characteristic variations
[JTN-94-80604] 07 p2775 N94-27249
Application of the wavelet transform for speech processing 09 p3600 N94-31435
Spectral analysis method and sample generation for real time visualization of speech
[ETN-94-95732] 09 p3674 N94-31573
Noise reduction for speech enhancement using non-linear wavelet processing
[AD-A280469] 12 p4434 N94-37141

VOID RATIO
Characterization of voids formed during liquid impregnation of nonwoven multifilament glass networks as related to composite processing 03 p0939 N94-16858

VOIDS
A method of influence regions in the theory of vacancy swelling of metals
[DE93-620579] 01 p0083 N94-11363
Modeling void growth and movement with phase change in thermal energy storage canisters
[NASA-TM-106288] 01 p0163 N94-12576
Structure and stability of microvoids in A-Si:H
[DE93-016625] 02 p0813 N94-14413
Characterization of voids formed during liquid impregnation of nonwoven multifilament glass networks as related to composite processing 03 p0939 N94-16858
Ultrasonic wave propagation model for nondestructive evaluation of solid rocker motor propellant
[AD-A267653] 03 p0976 N94-17248
Measurement of the velocity field and void fraction in a planar plunging jet
[AD-A268183] 03 p1030 N94-17511
Evaluation of the production-grade class 4 flextensional transducer shell
[AD-A268796] 04 p1340 N94-18201
Binding of copper to nanocavity surfaces in silicon
[DE93-019073] 04 p1364 N94-19080
Shrinkage void formation and its effect on freeze and thaw processes of lithium and lithium-fluoride for space applications
[DE93-019303] 04 p1338 N94-19128
Experimental study of void formation during aluminum solidification in reduced gravity
[NASA-TM-106190] 05 p1692 N94-21604
Surface and subsurface defect detection in Si3N4 components by laser scattering
[DE93-040829] 05 p1832 N94-21772
Strength, ultrasonic and metallurgical evaluation of diffusion bonds
[DE94-000665] 05 p1697 N94-22571
Analysis of a proposed Compton backscatter imaging technique
[DE93-040537] 06 p2371 N94-22935
Analysis of Alloy 600 and X-750 stress corrosion cracks
[DE94-001578] 06 p2238 N94-22936
Microstructural development in low activation ferritic alloys irradiated to 200 dpa at 420 C
[DE94-004269] 07 p2731 N94-25803
Interfacial area and interfacial transfer in two-phase flow
[DE93-041226] 07 p2792 N94-26468
A modeling study of the effect of stress state on void linking during ductile fracture
[AD-A275505] 08 p3317 N94-28811
The influence of transmutation, void swelling, and flux/spectra uncertainties on the electrical properties of copper and copper alloys
[DE94-006213] 09 p3641 N94-31626
An experimental study of void formation during aluminum solidification in reduced gravity 09 p3667 N94-31944

VOLATILITY
Vaporization by shock loading of albite, jadeite, and pyrex glass: Experimental study 01 p0097 N94-12039
Shock induced reaction in Chicxulub target materials (CaSO4 and SiO2) and their relation to extinctions 01 p0282 N94-12149
The correlation of alkalis and aluminum during high-temperature volatilization of albite and nepheline 01 p0081 N94-12214
Regional tectonic analysis of Venus as part of the Pioneer Venus guest investigator project
[NASA-CR-194079] 02 p0842 N94-13561
On-line gas chromatographic studies of Rutherfordium (element 104), hahnium (element 105), and homologs
[DE93-013890] 03 p0948 N94-16821
Volatile CVD precursors based on copper alkoxides and mixed group 2A-copper alkoxides
[AD-D015930] 05 p1701 N94-20349
Volatility in the lunar crust: Trace element analyses of lunar minerals by PIXE proton microprobe 05 p2097 N94-20661
C-O volatiles in Apollo 15 and Apollo 17 picritic glasses 05 p1685 N94-20727
Volatile loss from accreting icy protoplanets 05 p2084 N94-20793
Impact-induced devolatilization of CaSO4 anhydrite and implications for K-T extinctions: Preliminary results 05 p2085 N94-20840
Isothiazolone volatility study of a water bottom from fuel treated with Kathon (tm) FP1.5 biocide
[AD-A273165] 06 p2266 N94-24728
Temperature dependence of static RAM volatility
[DE93-040345] 07 p2948 N94-26111
Measurement of volatile metal species at elevated temperatures
[PB94-132321] 08 p3186 N94-28407
Remote infrared vapor detection of volatile organic compounds
[AD-A276982] 09 p3746 N94-31999
Volatiles combustion in fluidized beds
[DE94-008382] 09 p3636 N94-32414
Magmatic volatiles and the weathering of Mars 09 p3946 N94-33201
Vapor-fortified QA/QC samples for the analysis of volatile organic compounds
[AD-A278712] 11 p4229 N94-35776
Alkali element constraints on Earth-Moon relations 11 p4354 N94-36169
Molecular beam surface analysis
[DE94-010773] 12 p4406 N94-36453

VOLATILIZATION
U VAPORIZING

VOLCANICS
U VOLCANOLOGY

VOLCANOES
NT MARS VOLCANOES
The Lathrop Wells Volcanic Center: Status of field and geochronology studies
[DE93-008917] 01 p0273 N94-10285
Overwater atmospheric dispersion of volcanic smokes from Mt. Sakurajima observed in NOAA-AVHRR data 01 p0205 N94-11979
Venus small volcano classification and description 01 p0438 N94-12037

Reconstruction of the dynamics of the 1800-1801 Hualalai eruption: Implications for planetary lava flows
01 p0281 N94-12041
Horizontal stresses induced by vertical processes in planetary lithospheres 01 p0281 N94-12042
Estimation of age of Dali-Ganis rifting and associated volcanic activity, Venus 01 p0440 N94-12046
Regional geology of the Vega landing sites: Tentative results of photogeologic mapping
01 p0440 N94-12047
A pattern recognition system for locating small volvanoes in Magellan SAR images of Venus
01 p0455 N94-12126
Lava flows on Venus: Analysis of motion and cooling
01 p0457 N94-12137
Graphite solubility and co-vesiculation in basalt-like melts at one-ATM 01 p0463 N94-12173
Volcanism in southern Guinevere Planitia, Venus: Regional volcanic history and morphology of volcanic domes 01 p0467 N94-12190
Comparison of the distribution of large magmatic centers on Earth, Venus, and Mars 01 p0467 N94-12192
The Magellan volcanic and magmatic feature catalog
01 p0467 N94-12193
Large volcanoes on Venus: Examples of geologic and structural characteristics from different classes
01 p0467 N94-12195
Regional mantle upwelling on Venus: The Beta-Atla-Themis anomaly and correlation with global tectonic patterns 01 p0467 N94-12196
Small volcanoes in Tempe Terra, Mars: Their detailed morphometry and inferred geologic significance
01 p0469 N94-12202
Oxidation state of the Earth's upper mantle during the last 3800 million years: Implications for the origin of life
01 p0283 N94-12210
Giant radiating dyke swarms on Earth and Venus
01 p0283 N94-12236
Estimation of vegetation damage due to ash fall in Mt. Pinatubo area using MOS-1 data
02 p0695 N94-14259
Ground truth spectrometry and imagery of eruption clouds to maximize utility of satellite imagery
[NASA-CR-194358] 03 p1081 N94-15181
Magellan: Principal Venus science findings
03 p0989 N94-15887
Morphometric comparison of Icelandic lava shield volcanoes versus selected Venusian edifices
03 p1248 N94-16178
Pargo Chasma and its relationship to global tectonics
03 p1249 N94-16181
Explosive mafic volcanism on Earth and Mars
03 p1253 N94-16204
Morphology and models for the evolution of eastern Hecate Chasma, Venus 03 p1256 N94-16215
Tessera terrain on Venus: Implications of tessera flooding models and boundary characteristics for global distribution and mode of formation
03 p1258 N94-16226
Mode of emplacement of lunar mare volcanic deposits: Graben formation due to near surface deformation accompanying dike emplacement at Rima Parry 5
03 p1258 N94-16227
Modes of formation of lunar light plains and the detection of cryptomaria deposits 03 p1259 N94-16231
Chemical differentiation, thermal evolution, and catastrophic overturn on Venus: Predictions and geologic observations 03 p1259 N94-16232
Tessera terrain on Venus: Global characterization from Magellan data 03 p1264 N94-16262
Preliminary analysis of Dione Regio, Venus: The final Magellan regional imaging gap 03 p1271 N94-16302
The distribution of large volcanoes on Venus as a function of height and altitude 03 p1271 N94-16303
Large-scale volcanism associated with coronae on Venus 03 p1285 N94-16376
A decade's overview of Io's volcanic activity
03 p1245 N94-16386
Aspects of modelling the tectonics of large volcanoes on the terrestrial planets 03 p1104 N94-16396
Relief of some small landforms on Venus
03 p1293 N94-16418
The use of TIMS data to estimate the SO2 concentrations of volcanic plumes: A case study at Mount Etna, Sicily 03 p1065 N94-16608
Volcanic thermal features observed by AVIRIS
03 p1068 N94-16680
Effects of the Mount Pinatubo eruption on solar insolation: Four case studies
[DE93-018454] 04 p1475 N94-18817
SO2 on Venus: IUE, HST and ground-based measurements, and the active volcanism connection
05 p2092 N94-20637
Geologic mapping of Northern Atla Regio on Venus: Preliminary data 05 p2095 N94-20654
Beta Regio rift system on Venus: Geologic interpretation of Magellan images 05 p2095 N94-20655
Beta Regio - Phoebe Regio on Venus: Geologic mapping with the Magellan data 05 p2096 N94-20656
Formation and evolution of radial fracture systems on Venus 05 p2099 N94-20672
Thermal and rheological controls on magma migration in dikes: Examples from the east rift zone of Kilauea volcano, Hawaii 05 p1862 N94-20673
Distribution of small volcanic cones on the surface of Venus by size and elevation: Implications for differential deposition of volcanic features 05 p2110 N94-20731
Volcanic rises on Venus: Geology, formation, and sequence of evolution 05 p2113 N94-20755
Basaltic magmatism on the Moon. A perspective from volcanic picritic glasses 05 p2114 N94-20758
Origin of the Apollo 15 very low Ti green glass. A perspective from the compositional diversity in the very low Ti glasses 05 p1685 N94-20759
Tumuli and tubes: Teaching scientific techniques
05 p2039 N94-20818
Elevation and igneous crater modification on Venus: Implications for magmatic volatile content
05 p2135 N94-20872
Formation of perched lava ponds on basaltic volcanoes: Interaction between cooling rate and flow geometry allows estimation of lava effusion rates
05 p1863 N94-20878
CO2 lidar observations of Mount Pinatubo debris: FIRE 2 and longer-term measurements
05 p1876 N94-22323
Northern hemisphere tropospheric mid-latitude circulation after violent volcanic eruptions
[MPIM-107] 06 p2403 N94-24491
Electromagnetic field changes as a precursory phenomena of earthquakes and volcanic eruptions
[REPT-157] 06 p2405 N94-24980
Volcanology and volcanic activity with a primary focus on potential hazard impacts for the Hawaii geothermal project
[DE94-001614] 07 p2879 N94-26515
Tectonic History of the Terrestrial Planets
[NASA-CR-195696] 09 p3939 N94-31105
Patterns of deformation and volcanic flows associated with lithospheric loading by large volcanoes on Venus
09 p3776 N94-31106
Aspects of modelling the tectonics of large volcanoes on the terrestrial planets 09 p3940 N94-31107
State of stress, faulting, and eruption characteristics of large volcanoes on Mars 09 p3940 N94-31108
The tectonic and volcanic evolution of Venus: Catastrophic or gradual? 09 p3940 N94-31111
Keeping that youthful look --- impact cratering of Venus 09 p3941 N94-31112
A tectonic resurfacing model for Venus
09 p3941 N94-31113
The resurfacing controversy for Venus: An overview and a mechanistic perspective 09 p3941 N94-31114
Plains tectonism on Venus: The deformation belts of Lavinia Planitia 09 p3941 N94-31115
Time-dependent behavior of Mount Pinatubo aerosol
[DE94-001877] 09 p3764 N94-31601
Concentration system performance degradation in the aftermath of Mount Pinatubo
[DE94-001879] 09 p3764 N94-31602
The use of SPOT and ERS-1 images to map the eruption of Nevado Sabancaya (Province of Arequipa, South Peru) and evaluate associated risks 09 p3751 N94-32546
Mantle melting and crustal recycling in subduction zones 10 p4084 N94-33368
Comparison of the impact of volcanic eruptions and aircraft emissions on the aerosol mass loading and sulfur budget in the stratosphere 10 p3971 N94-33460
Volcanic gas emissions and their effect on ambient air character
[DE94-005675] 10 p4081 N94-33715
Mount Rainier active cascade volcano
[NASA-CR-195893] 10 p4087 N94-33992
Quantifying shapes of volcanoes on Venus
11 p4361 N94-35429
Volcano morphometry and volume scaling on Venus
11 p4361 N94-35431
The topography of Mars: A re-evaluation of current data 11 p4364 N94-35460
Role of magma-water interaction in very large explosive eruptions
[DE94-002698] 11 p4291 N94-36103
Vent processes during the 1912 eruption at Novarupta, Katmai National Park, Alaska
[DE94-010740] 12 p4468 N94-36451

VOLCANOLOGY

Twenty-fourth Lunar and Planetary Science Conference. Part 1: A-F
[NASA-CR-193095] 01 p0435 N94-12015
Venus small volcano classification and description
01 p0438 N94-12037
Reconstruction of the dynamics of the 1800-1801 Hualalai eruption: Implications for planetary lava flows
01 p0281 N94-12041
Estimation of age of Dali-Ganis rifting and associated volcanic activity, Venus 01 p0440 N94-12046
Regional geology of the Vega landing sites: Tentative results of photogeologic mapping
01 p0440 N94-12047
Stable isotope analyses of the peralkaline volcanics Gregory Rift Valley, Kenya 01 p0281 N94-12072
Th-230 - U-238 series disequilibrium of the Olkaria basalts Gregory Rift Valley, Kenya
01 p0281 N94-12073
Th-230 - U-238 series disequilibrium of the Olkaria rhyolites Gregory Rift Valley, Kenya: Residence times
01 p0281 N94-12076
Geology and surface characteristics of Bell Regio, Venus 01 p0457 N94-12136
Volcanism in southern Guinevere Planitia, Venus: Regional volcanic history and morphology of volcanic domes 01 p0467 N94-12190
Comparison of the distribution of large magmatic centers on Earth, Venus, and Mars 01 p0467 N94-12192
Characteristics of arachnoids from Magellan data
01 p0469 N94-12204
Compositional heterogeneity within a dumbbell-shaped Apollo 15 green glass: Evidence for simultaneous eruption of different magmas 01 p0470 N94-12209
Vulcanian explosive eruptions: A mechanism for localised pyroclast dispersal on Venus
01 p0477 N94-12243
A comparison of the visible and near infrared reflectance of hydrovolcanic palagonite tuffs and Martian weathered soils 01 p0477 N94-12245
Morphometric comparison of Icelandic lava shield volcanoes versus selected Venusian edifices
03 p1248 N94-16178
Pargo Chasma and its relationship to global tectonics
03 p1249 N94-16181
The formation and evolution of Alpha and Tellus tesserae on Venus 03 p1249 N94-16183
Explosive mafic volcanism on Earth and Mars
03 p1253 N94-16204
Remote sensing studies of the northeastern portion of the lunar nearside 03 p1258 N94-16225
Mode of emplacement of lunar mare volcanic deposits: Graben formation due to near surface deformation accompanying dike emplacement at Rima Parry 5
03 p1258 N94-16227
Bubble coalescence in magmas
03 p1103 N94-16237
The history of mare volcanism in the Orientale Basin: Mare deposit ages, compositions and morphologies
03 p1269 N94-16289
The rheology and composition of cryovolcanic flows on icy satellites 03 p1243 N94-16294
Explosive volcanism and the compositions of the cores of differentiated asteroids 03 p1243 N94-16306
Martian lavas: Three complementary remote sensing techniques to derive flow properties
03 p1283 N94-16366
Venusian pancake domes: Insights from terrestrial voluminous silicic lavas and thermal modeling
03 p1286 N94-16381
Grain surface features of Apollo 17 orange and black glass 03 p1289 N94-16397
A model for the origin of Martian polygonal terrain
05 p2090 N94-20393
Twenty-Fourth Lunar and Planetary Science Conference. Part 3: N-Z
[NASA-CR-193149] 05 p2092 N94-20636
SO2 on Venus: IUE, HST and ground-based measurements, and the active volcanism connection
05 p2092 N94-20637
Largest impact features on Venus: Non-preserved or non-recognizable? 05 p2096 N94-20657
Thermal and rheological controls on magma migration in dikes: Examples from the east rift zone of Kilauea volcano, Hawaii 05 p1862 N94-20673
Mixing of a chemically buoyant layer at the top of a thermally convecting fluid: Implications for mantle dynamics with application to Venus
05 p2099 N94-20675
Spectral reflectance studies of the Humorum Basin region 05 p2101 N94-20682
Venus magmatic and tectonic evolution
05 p2101 N94-20683
A comparison of calculated and measured rheological properties of crystallising lavas in the field and in the laboratory 05 p1862 N94-20690
Eruption history of the Tharsis shield volcanoes, Mars
05 p2102 N94-20692
Geology of Biblis Patera, Ulysses Patera, and Jovis Tholus, Mars 05 p2103 N94-20693

Chronology, eruption duration, and atmospheric contribution of Apollinaris Patera, Mars
05 p2108 N94-20720
Distribution of small volcanic cones on the surface of Venus by size and elevation: Implications for differential deposition of volcanic features 05 p2110 N94-20731
Venus pancake dome formation: Morphologic effects of a cooling-induced variable viscosity during emplacement 05 p2110 N94-20732
Volcanic rises on Venus: Geology, formation, and sequence of evolution 05 p2113 N94-20755
Chronology and genesis of high-Ti mare volcanism: Melting of cogenetic depleted and enriched reservoirs
05 p2118 N94-20777
A tectonic resurfacing model for Venus
05 p2118 N94-20781
Parga and Hecate Chasmata, Venus: Structure, volcanism and models of formation
05 p2121 N94-20796
Are Plinian type eruptions possible on Venus?
05 p2123 N94-20803
Elevation and igneous crater modification on Venus: Implications for magmatic volatile content
05 p2135 N94-20872
Multispectral studies of selected crater- and basin-filling lunar Maria from Galileo Earth-Moon encounter 1
05 p2136 N94-20876
Numerical simulation of lava flows: Applications to the terrestrial planets 05 p1863 N94-20904
Basaltic Volcanism and Ancient Planetary Crusts
[NASA-CR-193151] 06 p2614 N94-24363
Lunar mare volcanism: Mixing of distinct, mantle source regions with KREEP-like component
06 p2615 N94-24370
Northern hemisphere tropospheric mid-latitude circulation after violent volcanic eruptions
[MPIM-107] 06 p2403 N94-24491
The transition from diapirism to dike intrusion: Implications for planetary volcanism
[NASA-CR-195133] 06 p2403 N94-24580
Seafloor characterization/Galapagos propagating rift
[AD-A273586] 06 p2419 N94-25165
Impacts, extinctions, volcanism, glaciations, and tectonics: Matches and mismatches
07 p2888 N94-28298
Proposed law of nature linking impacts, plume volcanism, and Milankovitch cycles to terrestrial vertebrate mass extinctions via greenhouse-embryo death coupling
07 p2876 N94-28307
Studies in Jurassic and Cretaceous North American apparent polar wander 08 p3362 N94-29940
Aspects of modelling the tectonics of large volcanoes on the terrestrial planets 09 p3940 N94-31107
State of stress, faulting, and eruption characteristics of large volcanoes on Mars 09 p3940 N94-31108
The tectonic and volcanic evolution of Venus: Catastrophic or gradual? 09 p3940 N94-31111
Keeping that youthful look --- impact cratering of Venus 09 p3941 N94-31112
A tectonic resurfacing model for Venus
09 p3941 N94-31113
The resurfacing controversy for Venus: An overview and a mechanistic perspective 09 p3941 N94-31114
Evidence for ultramafic lavas on Syrtis Major
09 p3950 N94-33229
Mount Rainier active cascade volcano
[NASA-CR-195893] 10 p4087 N94-33992
The Twenty-Fifth Lunar and Planetary Science Conference. Part 1: A-G
[NASA-CR-195743] 11 p4355 N94-35395
Volcano morphometry and volume scaling on Venus
11 p4361 N94-35431
The Twenty-Fifth Lunar and Planetary Science Conference. Part 3: P-Z
[NASA-CR-195745] 11 p4362 N94-35448
Isotopic and geochemical precursors of earthquakes and volcanic eruptions
[DE94-615824] 11 p4289 N94-35568
The Twenty-Fifth Lunar and Planetary Science Conference. Part 2: H-O
[NASA-CR-195744] 11 p4367 N94-36136

VOLT-AMPERE CHARACTERISTICS
Screening of solar cells
[NASA-TM-106298] 02 p0620 N94-13134
The 1.00 MeV proton radiation resistance studies of amorphous silicon-based alloy solar cells
02 p0703 N94-13639
Polar 2 model of the wake shield experiment
[AD-A266243] 03 p0882 N94-16468
The role of emitter states in magnetotunneling through double-barrier resonant-tunneling diodes at high magnetic fields
[REPT-A-2658] 06 p2564 N94-24959

VOLTAGE
U ELECTRIC POTENTIAL

VOLTAGE BREAKDOWN
U ELECTRICAL FAULTS

VOLTAGE CONTROLLED OSCILLATORS
An advanced communications synthesizer
[AD-A277832] 10 p4034 N94-33833

VOLTAGE CONVERTERS (AC TO AC)
Pulse transformer characterization
[PML-1992-73] 07 p2784 N94-26646

VOLTAGE CONVERTERS (DC TO DC)
Power converters for the 120 V bus supply control
[CNES-NT-134] 02 p0622 N94-13552
Operation of high power converters in parallel
[NASA-CR-191096] 02 p0622 N94-13786
Forback DC-to-DC converter
[NASA-CASE-GSC-13404-1] 03 p1010 N94-15874
High temperature co-axial winding transformers
[NASA-CR-194580] 04 p1407 N94-19643
AC to DC power converter with regulated bi-polar outputs
[AD-D016032] 07 p2786 N94-27145
A study of DC-DC converters with MCT's for arcjet power supplies
[NASA-CR-191204] 07 p2703 N94-27662
A series resonant converter in half bridge circuits with combined serial and parallel charge coupling and several output circuits
[ETN-94-95739] 09 p3687 N94-31373
Examination of fast semiconductor diodes (recovery) with respect to switching valves in PWM and resonance devices
[ETN-94-95740] 09 p3690 N94-31609
Microprocessor control of multiple peak power tracking DC/DC converters for use with solar cell arrays
[NASA-CASE-GSC-13450-2] 11 p4282 N94-35540

VOLTAGE GENERATORS
High current injector for heavy ion fusion
[DE93-019241] 05 p1979 N94-20289

VOLTAGE MEASUREMENT
U ELECTRICAL MEASUREMENT

VOLTAGE REGULATORS
Operation of high power converters in parallel
[NASA-CR-191096] 02 p0622 N94-13786
Multi-output flyback converter with ultrafast current protection
[CNES-NT-133] 02 p0625 N94-14138
Electrochemical sulfur passivation of visible (approximately 670nm) AlGaInP lasers
[DE94-002293] 06 p2350 N94-24659
Laser energized high voltage direct current power supply
[AD-D015977] 06 p2312 N94-25036
Turn-on transient overcurrent response suppressor
[AD-D016151] 10 p4039 N94-33759

VOLTAGE VARIATION INDICATORS
U VOLTMETERS

VOLTERRA EQUATIONS
Numerically solving a transient heat conduction problem with convection and radiation
[AD-A268521] 03 p1220 N94-17540
Time dependent identification of nonlinear structures
[ECL-92-64] 04 p1457 N94-19403
Modeling transonic aerodynamic response using nonlinear systems theory for use with modern control theory 06 p2164 N94-25112
Identification of 2nd and 3rd Volterra kernel of nonlinear systems 10 p4114 N94-34312
Multiquadric collocation methods in the numerical solution of Volterra integral equations with weakly singular kernels
[DE94-013000] 12 p4505 N94-37497

VOLTMETERS
An intelligent on-line failure-diagnosis card with extensive usage 10 p4068 N94-34334

VOLUME
NT BODY VOLUME (BIOLOGY)
The effect of sub-surface volume scattering on the accuracy of ice-sheet altimeter retracking algorithms
[NASA-CR-194825] 06 p2386 N94-24060
Apron heights around stepped massifs in the Cydonia Mensae region: Do they record the local paleobathymetry of Oceanus Borealis? 09 p3949 N94-33224

VOLUMETRIC ANALYSIS
Studies of critical point phenomena of fluids: Bulk fluids, fluids in pores, and at interfaces
01 p0080 N94-10228
Orthobaric densities and molar volumes of liquids: Aliphatic and cyclic ketones
[ESDU-93010] 07 p2720 N94-28060

VOMITING
Evaluation of putative neurochemical intermediaries in space/motion sickness
[NASA-CR-193607] 03 p1118 N94-17090
Susceptibility of the squirrel monkey to different motion conditions 05 , p1885 N94-21899
Reassessment of area postrema's role in motion sickness and conditioned taste aversion
05 p1886 N94-21901
Detection of emetic activity in the cat by monitoring venous pressure and audio signals
05 p1886 N94-21903
Recovery of the vomiting reflex following area postrema ablation in squirrel monkeys 05 p1886 N94-21904
Area postrema ablations in cats: Evidence for separate neural routes for motion- and xylazine-induced CTA and emesis 05 p1887 N94-21906
Immunocytochemical localization of glutamic acid decarboxylase (GAD) and substance P in neural areas mediating motion-induced emesis: Effects of vagal stimulation on GAD immunoreactivity
05 p1887 N94-21909
The effects of area postrema lesions and selective vagotomy on motion-induced conditioned taste aversion
05 p1888 N94-21910
Experimental studies of gastric dysfunction in motion sickness: The effect of gastric and vestibular stimulation on the vagal and splanchnic gastric efferents
05 p1888 N94-21911
Role of the area postrema in three putative measures of motion sickness in the rat 05 p1888 N94-21912
Profile analysis of after-effects experienced during exposure to several virtual reality environments
12 p4482 N94-37263

VON KARMAN EQUATION
Super finite elements for nonlinear static and dynamic analysis of stiffened plate structures
[ISBN-0-315-63903-2] 07 p2844 N94-27808
Finite element approximation of an optimal control problem for the von Karman equations
[NASA-CR-194955] 12 p4505 N94-37540

VON MISES THEORY
U STRESS FUNCTIONS

VORTEX ALLEVIATION
Corner vortex suppressor
[AD-D015772] 01 p0147 N94-10383
Underwing compression vortex attenuation device
[NASA-CASE-LAR-14744-1] 01 p0012 N94-10673
Prediction and control of vortex-dominated and vortex-wake flows
[NASA-CR-194722] 05 p1637 N94-21054
Controlled oscillation of forebody vortices by nozzle jet blowing
[ISBN-0-315-84134-6] 07 p2678 N94-27648
A study of the development and attenuation of wing-generated, vortical wakes
09 p3570 N94-31971

VORTEX AVOIDANCE
Optimal lateral escape maneuvers for microburst encounters during final approach
[LR-691] 02 p0511 N94-13534

VORTEX BREAKDOWN
Underwing compression vortex attenuation device
[NASA-CASE-LAR-14744-1] 01 p0012 N94-10673
Growth and breakdown of Taylor-Goertler vortices in rotating Blasius boundary layer
01 p0165 N94-12631
The effect of crossflow on Taylor vortices: A model problem
[NASA-CR-191487] 02 p0630 N94-13128
The phenomenon of vortex breakdown
02 p0510 N94-14609
Behavior of streamwise rib vortices in a three-dimensional mixing layer 02 p0644 N94-14754
The effect of the nose shape and wing location toward the wing vortex breakdown
[AD-A267724] 03 p0855 N94-14942
Adaptive Navier-Stokes calculations for vortical flow
[AD-A266236] 03 p1026 N94-16966
Experimental study of vortex and aerodynamic characteristics of stack wings with sideslip
[AD-A267722] 03 p0860 N94-17274
Navier-Stokes, dynamics and aeroelastic computations for vortical flows, buffet and flutter applications
[NASA-CR-194520] 04 p1313 N94-19621
Prediction and control of vortex-dominated and vortex-wake flows
[NASA-CR-194722] 05 p1637 N94-21054
Dynamics of tornado-like vortices
08 p3371 N94-29753
Numerical investigation into high-angle-of-attack leading-edge vortex flow
[PB94-125564] 08 p3133 N94-30388
Aspects of the modeling and numerical simulation of leading-edge vortex flow
[AD-B179108] 08 p3133 N94-30492
On the structure and stability of slender viscous vortices 09 p3700 N94-31218
Control of leading-edge vortices on a delta wing
10 p3986 N94-34971

Unsteady structure of leading-edge vortices on a delta wing
[AD-A278988] 11 p4190 N94-35529

VORTEX COLUMNS
U VORTICES

VORTEX DISTURBANCES
U VORTICES

VORTEX FILAMENTS
New vortex dynamics methods for rotor free wake analysis
[AD-A266656] 02 p0509 N94-14774
The instantaneous concentration field in the self-similar region of a high Schmidt number round jet
08 p3278 N94-29976

VORTEX FLAPS
Underwing compression vortex attenuation device
[NASA-CASE-LAR-14744-1] 01 p0012 N94-10673
Experimental studies of vortex flaps and vortex plates. Part 2: 1.15m span 60 deg delta wing
[NAL-TR-1180T-PT-2] 02 p0502 N94-13454
Experimental studies of vortex flaps and vortex plates. Part 1: 0.53 m span 60 deg delta wing
[DE93-767969] 02 p0505 N94-14059

VORTEX FLOW
U VORTICES

VORTEX GENERATION
U VORTEX GENERATORS

VORTEX GENERATORS
Generation of two-dimensional vortices in a cross-flow
01 p0160 N94-12318
Topics in pattern formation and chaotic systems
[AD-A265922] 01 p0161 N94-12342
Growth and breakdown of Taylor-Goertler vortices in rotating Blasius boundary layer
01 p0165 N94-12631
Experimental studies of vortex flaps and vortex plates. Part 2: 1.15m span 60 deg delta wing
[NAL-TR-1180T-PT-2] 02 p0502 N94-13454
Several examples where turbulence models fail in inlet flow field analysis 04 p1412 N94-18556
A method for recognition of frequency cells in a cylinder flow influenced by wall effects 06 p2316 N94-22860
Measurements and modeling of flow structure in the wake of a low profile wishbone vortex generator
[NASA-TM-106468] 06 p2166 N94-23465
Vortex generation and wave-vortex interaction over a concave plate with roughness and suction
[AD-A276839] 06 p2337 N94-24869
Improving diffusing S-duct performance by secondary flow control
[NASA-TM-106492] 06 p2170 N94-25182
Inclined air-jets used as vortex generators to suppress shock-induced separation 07 p2659 N94-28040
Vortex generators for control of shock-induced separation. Part 1: Introduction and aerodynamics
[ESDU-93024-PT-1] 07 p2806 N94-28095
Vortex generators for control of shock-induced separation. Part 3: Examples of applications of vortex generators to aircraft
[ESDU-93026-PT-3] 07 p2807 N94-28096
Evolution of the large-scale vortices in turbulent mixing-layers 08 p3273 N94-29686
Three dimensional compressible turbulent flow computations for a diffusing S-duct with/without vortex generators 08 p3281 N94-30519
Control of low-speed turbulent separated flow over a backward-facing ramp
[NASA-TM-109740] 09 p3573 N94-33071
The effects of vortex ingestion on the flow in a diffusing S-duct
[NASA-TM-106652] 10 p3998 N94-33955
Control of leading-edge separation on a cambered delta wing 10 p3992 N94-34616
Investigation of mechanisms for vorticity generation and flow separation on bodies in unsteady motion
10 p4051 N94-34973
Mars vertical axis wind machines: The design of a tornado vortex machine for use on Mars
[NASA-CR-196144] 12 p4462 N94-36823

VORTEX INJECTORS
The enhancement of compressible turbulent mixing via streamwise vorticity 08 p3280 N94-30487

VORTEX LATTICE METHOD
Computation of the loads on the AH-1/OLS model rotor in forward flight and comparison with wind tunnel tests
[ISL-CO-230/92] 06 p2176 N94-23146
LinAir: A multi-element discrete vortex Weissinger aerodynamic prediction method
[NASA-TM-108786] 06 p2167 N94-23557

VORTEX RINGS
Simulations of the creation and motion of vortex rings
[W-9319] 09 p3703 N94-31691

VORTEX SHEDDING
Perpendicular blade vortex interaction and its implications for helicopter noise prediction: Wave-number frequency spectra in a trailing vortex for BWI noise prediction
[NASA-CR-193623] 01 p0357 N94-10752
Vortex-induced forces on oscillating bluff cylinders
[AD-A265056] 01 p0154 N94-11865
On the wake behind a high speed train
01 p0164 N94-12618
Unsteady separated flows: Empirical model and control
[AD-A267282] 03 p0855 N94-14959
Active control of oscillatory lift forces on a circular cylinder
[AD-A273243] 06 p2338 N94-25140
The effects of three-dimensional imposed 3-d disturbances on bluff-body near wake flows
[AD-A274845] 07 p2791 N94-26187
Nominally 2-dimensional flow about a normal flat plate
[AD-A274472] 07 p2794 N94-27026
Research on bluff body vortex wakes
[AD-A273780] 07 p2796 N94-27319
Vibrations in engineering structures: A review of model and full-scale test of a cable-stayed bridge and a traffic sign gantry
[NLR-TP-92321-U] 07 p2843 N94-27553
Separated flow generated by a vectored jet in a crossflow 07 p2800 N94-28007
An investigation of the reacting vortex structures associated with pulse combustion
08 p3200 N94-30911
The effect of an axial flow component on a circular cylinder wake 09 p3699 N94-31209
Field studies of raindrop oscillations with applications to radar meteorology 09 p3782 N94-31743
Control of low-speed turbulent separated flow over a backward-facing ramp
[NASA-TM-109740] 09 p3573 N94-33071
Similarity in separated flow fields producing large-scale vortices 10 p3969 N94-33382
Numerical simulation of the edge tone phenomenon
[NASA-CR-4581] 10 p3982 N94-33898
Flow structure generated by perpendicular blade vortex interaction and implications for helicopter noise predictions
[NASA-CR-195824] 10 p3984 N94-34207
Yaw control by tangential forebody blowing
10 p3992 N94-34615
Unsteady flow past an airfoil pitched at constant rate
10 p3986 N94-34969
Investigation of mechanisms for vorticity generation and flow separation on bodies in unsteady motion
10 p4051 N94-34973

VORTEX SHEETS
The acoustic and instability waves of jets confined inside an acoustically lined rectangular duct
[AD-A276347] 06 p2334 N94-24602
The effects of profiles on supersonic jet noise
[NASA-CR-195184] 06 p2530 N94-25177
A study of weak solutions and their regularizations by numerical methods
[AD-A277453] 09 p3850 N94-33175

VORTEX STREETS
NT KARMAN VORTEX STREET

VORTEX TRAPS
U TRAPPED VORTICES

VORTEX TUBES
U HILSCH TUBES
U VORTICES

VORTEX-BLADE INTERACTION
U BLADE-VORTEX INTERACTION

VORTICES
NT HORSESHOE VORTICES
NT TRAPPED VORTICES
NT WING TIP VORTICES
Underwing compression vortex attenuation device
[NASA-CASE-LAR-14744-1] 01 p0012 N94-10673
Simulation study of dynamo structure in reversed field pinch
[DE93-771406] 01 p0390 N94-11128
Control of jet noise
[NASA-CR-193612] 01 p0358 N94-11176
Physics of forebody flow control
[NASA-CR-193626] 01 p0015 N94-11195
On nonlinear Tollmien-Schlichting/vortex interaction in three-dimensional boundary layers
[NASA-TM-108184] 01 p0152 N94-11377
Discrete vortex representation of magnetohydrodynamics
[DE93-012190] 01 p0393 N94-11669
Vortex-induced forces on oscillating bluff cylinders
[AD-A265056] 01 p0154 N94-11865
An investigation using empirical orthogonal functions and objective analysis to analyse the vertical temperature structure of a gulf stream meander
[AD-A265116] 01 p0289 N94-11868
Time evolution of cross-stream exchange associated with the variations in the Kuroshio
01 p0197 N94-11936
Characteristic scales and vortex features of mesoscale vortices observed by the satellites during the winter
01 p0199 N94-11943
An application of reduced gravity model to mesoscale eddies 01 p0199 N94-11945
Behavior of vortices generated by an advancing ejecta curtain in theory, in the laboratory, and on Mars
01 p0169 N94-12044
A local dynamic model for large eddy simulation
01 p0155 N94-12285
Large eddy simulations of time-dependent and buoyancy-driven channel flows
01 p0155 N94-12287
A normal stress subgrid-scale eddy viscosity model in large eddy simulation 01 p0155 N94-12288
Large eddy simulation of shock turbulence interaction
01 p0155 N94-12289
Application of a dynamic subgrid-scale model to turbulent recirculating flows 01 p0156 N94-12290
Large-eddy simulation of turbulent flow with a surface-mounted two-dimensional obstacle
01 p0156 N94-12291
Similarity states of homogeneous stably-stratified turbulence at infinite Froude number
01 p0156 N94-12292
Application of incremental unknowns to the Burgers equation 01 p0156 N94-12293
Numerical simulation using vorticity-vector potential formulation 01 p0157 N94-12297
Local isotropy in high Reynolds number turbulent shear flows 01 p0157 N94-12302
Plane mixing layer vortical structure kinematics
01 p0159 N94-12313
Generation of two-dimensional vortices in a cross-flow
01 p0160 N94-12318
Suppression of the near wall burst process of a fully developed turbulent pipe flow
[AD-A265995] 01 p0161 N94-12352
Proceedings of the 9th and 10th NAL Workshop on Investigation and Control of Boundary-Layer Transition
[NAL-SP-18] 01 p0163 N94-12611
Fluctuations of longitudinal vortices along a concave wall 01 p0016 N94-12616
On the formation process of Karman vortex street
01 p0016 N94-12621
Turbulent boundary layer interacting with spanwise periodic longitudinal vortex arrays
01 p0165 N94-12626
Observations of eddy fields in the Northwest Pacific by GEOSAT altimetry 01 p0207 N94-12639
Surface eddy fluxes from the GEOSAT satellite altimeter 01 p0208 N94-12643
Measurement of eddy structure and movement in the north-east Pacific with the GEOSAT altimeter
01 p0209 N94-12647
Fluctuations of the Kuroshio extension detected by the GEOSAT altimetry data 01 p0209 N94-12649
Aspects of applying a relaxation method to computing sea surface velocities from sea surface temperature images 01 p0214 N94-12679
Statistical features of mesoscale eddies at the Kuroshio front 01 p0215 N94-12682
The WOCE/TOGA Surface Velocity Programme (SVP)
01 p0216 N94-12691
Investigation of meso-scale fronts, eddies and upwellings in China Seas with AVHRR data
01 p0220 N94-12711
The warm eddy detection from NOAA/AVHRR thermal images using the Hough transformation
01 p0220 N94-12713
Satellite and moored buoy observations of polar frontal system over the Yamato Rise in the Japan Sea
01 p0221 N94-12715
On a nonstationary dynamics of the north-west Pacific Ocean 01 p0222 N94-12724
Mixing of drifter ensemble by mesoscale currents
01 p0228 N94-12760
Non-linear effects in vortex viscous flow in superconductors-role of finite heat removal velocity
[DE93-621785] 02 p0618 N94-12856
Sub-grid scale modeling for large eddy simulations in analysis of shock-turbulence interactions
[DE93-013425] 02 p0631 N94-13250
An experimental investigation of shock wave/vortex interaction 02 p0634 N94-13574
On the secondary instability of the most dangerous Goertler vortex
[NASA-CR-191504] 02 p0636 N94-13785

Flight validation of a pulsed smoke flow visualization system
[NASA-CR-186026] 02 p0516 N94-14106
A vortex method for viscous unsteady flows
02 p0640 N94-14602
Navier-Stokes simulation of transonic vortex flow over a delta wing 02 p0640 N94-14606
The phenomenon of vortex breakdown
02 p0510 N94-14609
Linear instability of curved free shear layers
[NASA-TM-106290] 02 p0642 N94-14729
A small-scale turbulence model
02 p0643 N94-14746
The structure of intense vorticity in homogeneous isotropic turbulence 02 p0643 N94-14747
On the local nature of the energy cascade
02 p0643 N94-14748
Behavior of streamwise rib vortices in a three-dimensional mixing layer 02 p0644 N94-14754
Direct simulation of polymer drag reduction in free shear flows and vortex dipoles 02 p0644 N94-14755
Estimation of the vortex length scale and intensity from two-dimensional samples 02 p0645 N94-14756
Vortex-induced disturbance field in a compressible shear layer 02 p0645 N94-14760
Evolution of the shock front and turbulence structures in the shock/turbulence interaction
02 p0645 N94-14761
New vortex dynamics methods for rotor free wake analysis
[AD-A266656] 02 p0509 N94-14774
Free-wake computation of helicopter rotor flowfield for general flight regimes
[AD-A266692] 02 p0509 N94-14781
Unsteady separated flows: Empirical model and control
[AD-A267282] 03 p0855 N94-14959
The turbulent wall jet
[AD-A267675] 03 p0855 N94-14963
On the receptivity problem for 0(1) wavelength Goertler vortices
[NASA-CR-191519] 03 p1016 N94-15005
Large-Eddy Simulations (LES) of flows and turbulence distribution
[AD-A267182] 03 p1016 N94-15151
Tollmien-Schlichting/vortex interactions in compressible boundary layer flows
[NASA-CR-191515] 03 p1017 N94-15183
Large eddy simulation and direct numerical simulation of high speed turbulent reacting flows
[NASA-CR-193131] 03 p1018 N94-15427
Surface and internal signatures of organized vortex motions in stratified fluid
[AD-A267015] 03 p1020 N94-15526
Aerodynamic control of NASP-type vehicles through Vortex manipulation. Volume 1: Static water tunnel tests
[NASA-CR-177626-VOL-1] 03 p0855 N94-15655
Aerodynamic control of NASP-type vehicles through Vortex manipulation. Volume 2: Static wind tunnel tests
[NASA-CR-177626-VOL-2] 03 p0856 N94-15677
Aerodynamic control of NASP-type vehicles through vortex manipulation, volume 4
[NASA-CR-177626-VOL-4] 03 p0857 N94-15720
Parametric resonant triad interactions in a free shear layer
[NASA-TM-106365] 03 p1021 N94-15751
Aerodynamic control of NASP-type vehicles through vortex manipulation. Volume 3: Wing rock experiments
[NASA-CR-177626] 03 p0857 N94-15780
Nuclear rocket plume studies
[AD-A267154] 03 p0925 N94-15837
Receptivity of boundary layers to convected gusts
[AD-A267206] 03 p1022 N94-15860
Adaptive algorithm for aircraft configuration in turbulent flow
[AD-A266188] 03 p0867 N94-16122
Search for chaos in free shear flows
[AD-A266245] 03 p1023 N94-16470
Wind tunnel investigations of forebody strakes for yaw control on F/A-18 model at subsonic and transonic speeds
[NASA-TP-3360] 03 p0859 N94-16573
Complex terrain wind model evaluation
[AD-A266467] 03 p1096 N94-16589
Adaptive Navier-Stokes calculations for vortical flow
[AD-A266236] 03 p1026 N94-16966
Structure of turbulence in three-dimensional boundary layers
[NASA-CR-194655] 03 p1027 N94-17130
Transmission of light through a turbulent mixing layer
[AD-A267266] 03 p1193 N94-17264
Experimental study of vortex and aerodynamic characteristics of stack wings with sideslip
[AD-A267722] 03 p0860 N94-17274
Time dependent turbulence modeling and analytical theories of turbulence
[NASA-TM-106379] 03 p1029 N94-17385
Laser velocimetry measurements of vortex flows on a delta wing at Mach 1.9
[AD-A268596] 03 p0861 N94-17609
Study into the limits of an Euler equation method applied to leading-edge vortex flow
[NLR-TP-91350-U] 03 p1031 N94-17627
Granular fluctuations in plasma turbulence and their role in transport
[DE93-013465] 03 p1187 N94-17674
Vortex methods and statistics
[DE93-016974] 04 p1556 N94-17886
Filamentary magnetohydrodynamic plasmas
[DE93-015616] 04 p1583 N94-17945
Wake structure and aerodynamic behavior of high lift aircraft configurations during unsteady maneuvers in ground effect 04 p1309 N94-18439
Close-coupled oscillating canard effects on post-stall lift enhancement
[AD-A268938] 04 p1321 N94-18541
Computational aero-acoustics as a branch of turbulence research 04 p1411 N94-18552
Several examples where turbulence models fail in inlet flow field analysis 04 p1412 N94-18556
Compact advection schemes on unstructured grids
04 p1413 N94-18564
Lift and pitching moment induced on jet STOVL aircraft by the ground vortex
[AD-A269816] 04 p1318 N94-18733
Interferometric investigations of compressible dynamic stall over a transiently pitching airfoil
[NASA-TM-109380] 04 p1312 N94-19119
Research and training activities of the Joint Institute for Aeronautics and Acoustics
[NASA-CR-194742] 04 p1421 N94-19493
Three dimensional network generation and Euler calculation for a wing fuselage canard configuration
[MBB-LME-211-S-PUB-511-A] 04 p1319 N94-19500
Estimation of wake vortex advection and decay using meteorological sensors and aircraft data
[AD-A270763] 04 p1316 N94-19661
Examinations of converging cylindrically symmetric second sound propagation in He2
[MPIS-9/1992] 04 p1564 N94-19715
Dynamics of vortices in superconductors
[DE93-019535] 05 p2011 N94-19808
Particle dispersion in turbulent sprays
[AD-A271314] 05 p1796 N94-19913
The fluid mechanics of vortex cutting by a blade
[AD-A270932] 05 p1636 N94-20043
A theoretical investigation of unsteady separation phenomena related to dynamic stall
[AD-A271865] 05 p1636 N94-20465
Processing of climatological data for model initialization
[AD-A271878] 05 p1865 N94-20487
Prediction and control of vortex-dominated and vortex-wake flows
[NASA-CR-194722] 05 p1637 N94-21054
Investigation of the physics of the turbulent boundary layer focusing on vortex structures
[AD-A272879] 05 p1802 N94-21155
Reaction zone models for vortex simulation of turbulent combustion
[AD-A272723] 05 p1681 N94-21213
On the stability of shear-Alfven vortices
[DE93-040912] 05 p1996 N94-21752
The effect of correlated and point defects on the vortex lattice melting Transition in single crystal YBa2Cu3O(7-delta)
[DE93-040277] 05 p2033 N94-21997
A photogrammetric solution to a particular problem
[NASA-TP-3415] 06 p2381 N94-22961
Acoustic and optical investigations of superfluid He-3
[PB93-224889] 06 p2523 N94-23101
A method to simulate viscous diffusion of vorticity by convective transport of vortices at a non-solenoidal velocity
[DE94-001777] 06 p2318 N94-23220
Measurements and modeling of flow structure in the wake of a low profile wishbone vortex generator
[NASA-TM-106468] 06 p2166 N94-23465
Feasibility of detecting aircraft wake vortices using passive microwave radiometers
[NASA-CR-191553] 06 p2343 N94-23498
Leading-edge votex-system details obtained on F-106B aircraft using a rotating vapor screen and surface techniques
[NASA-TP-3374] 06 p2166 N94-23512
LinAir: A multi-element discrete vortex Weissinger aerodynamic prediction method
[NASA-TM-108786] 06 p2167 N94-23557
Numerical analysis of a vortex controlled diffuser
06 p2324 N94-23659
Compressibility effects on dynamic stall of airfoils undergoing rapid transient pitching motion
[NASA-TM-109681] 06 p2167 N94-23975
Toward modeling wingtip vortices
06 p2171 N94-24142
Large eddy simulation of a boundary layer with concave streamwise curvature 06 p2328 N94-24146
Dynamic localization and second-order subgrid-scale models in large eddy simulations of channel flow
06 p2329 N94-24149
Toward large eddy simulation of turbulent flow over an airfoil 06 p2172 N94-24150
Unstructured grid large eddy simulation of wall bounded turbulent flows 06 p2329 N94-24151
Investigation of the asymptotic state of rotating turbulence using large-eddy simulation
06 p2330 N94-24152
A large eddy simulation scheme for turbulent reacting flows 06 p2330 N94-24154
Stretch-induced quenching in flame-vortex interactions
06 p2237 N94-24156
On streak spacing in wall-bounded turbulent flows
06 p2331 N94-24159
Numerical simulation of non-Newtonian free shear flows 06 p2331 N94-24160
Transition to turbulence in an elliptic vortex
06 p2331 N94-24161
Vortical structure in a forced plane mixing layer
06 p2331 N94-24162
Free-surface/vorticity interaction
[AD-A273263] 06 p2335 N94-24686
Vortex generation and wave-vortex interaction over a concave plate with roughness and suction
[AD-A276839] 06 p2337 N94-24869
Eddy mixing coefficient upper limit derived from the photochemical balance of O2 06 p2621 N94-24897
Simulation of the vortex motion in the high T(c) superconductors
[DE93-617138] 06 p2567 N94-25403
A nighttime structure model of atmospheric optical turbulence, c2(n), derived from thermosonde and high resolution rawinsonde measurements
[AD-A273803] 06 p2406 N94-25537
Vortex methods
[DE94-003245] 07 p2789 N94-25597
Flux flow, pinning, and resistive behavior in superconducting networks
[DE94-003400] 07 p3050 N94-25848
The effects of three-dimensional imposed 3-d disturbances on bluff-body near wake flows
[AD-A274845] 07 p2791 N94-26187
Feature isolation and quantification of evolving datasets
[NASA-CR-195230] 07 p2961 N94-26207
Vortices in curved spacetime
[DE94-601559] 07 p3072 N94-26417
A numerical study of quantized vortices in Hell
[ISBN-9-03-860232-4] 07 p2792 N94-26479
Numerical studies on the dynamics of bubble, turbulent, free shear flows: Effect of the inter-phase coupling on the global flow evolution
[AD-A274521] 07 p2794 N94-26832
Leading-edge vortex-system details obtained on F-106B aircraft using a rotating vapor screen and surface techniques
[NASA-TP-3374-VIDEO-SUPPL]
07 p2647 N94-27161
Special investigation report: Safety issues related to wake vortex encounters during visual approach to landing
[PB94-917002] 07 p2660 N94-27881
Unsteady wake structures in transverse jets
07 p2800 N94-28006
The interaction region associated with twin jets and a normal crossflow 07 p2800 N94-28009
Experimental investigation of the interaction of a thrust reverser jet with an external subsonic flow
07 p2801 N94-28011
Topological structure of a jet in a cross flow
07 p2801 N94-28014
Experiments on the ground vortex formed by an impinging jet in cross flow 07 p2802 N94-28016
Comparison of the interactions of two and three dimensional transverse jets with a hypersonic free stream 07 p2659 N94-28021
Effects, limits, and limitations of spanwise blowing
07 p2659 N94-28027
Recent developments in the simulation of steady and transient transverse jet interactions for missile, rotorcraft, and propulsive applications 07 p2804 N94-28030
Effects of free-stream turbulence on a jet in a cross flow 07 p2805 N94-28036
Inclined air-jets used as vortex generators to suppress shock-induced separation 07 p2659 N94-28040

Measurements of steady and dynamic pressure on an F/A-18 wind tunnel model at high angles of attack
07 p2653 N94-28323
Modeling turbulence in flows with a strong rotational component
[DE94-003577] 08 p3270 N94-28475
Large eddy simulations using lattice Boltzmann algorithms
[DE94-005666] 08 p3270 N94-28549
Objective analysis of a coastal ocean eddy using satellite AVHRR and in situ hydrographic data
[AD-A275715] 08 p3376 N94-28642
Boundary layers induced by three-dimensional vortex loops
[AD-A275678] 08 p3270 N94-28665
Spin-up in a rectangular cylinder
[AD-A275465] 08 p3271 N94-28738
Experimental investigation of three-dimensional vortex-airfoil interaction in a supersonic stream
[AD-A275107] 08 p3122 N94-28899
A model analysis of potential vorticity on isopycnal surfaces for the global ocean
[AD-A275047] 08 p3377 N94-29164
Long-wavelength asymptotics of unstable crossflow modes, including the effect of surface curvature
[NASA-CR-4579] 08 p3273 N94-29460
Evolution of the large-scale vortices in turbulent mixing-layers 08 p3273 N94-29686
Forced generation of solitary waves in a rotating fluid and their stability 08 p3274 N94-29689
An experimental investigation of the effect of leading edge extensions on directional stability and the effectiveness of forebody nose strakes
08 p3155 N94-29728
Dynamics of tornado-like vortices
08 p3371 N94-29753
Numerical study of the trailing vortex of a wing with wing-tip blowing
[NASA-CR-195803] 08 p3130 N94-29760
Flow past a circular cylinder with a permeable wake splitter plate 08 p3275 N94-29764
Direct and large-eddy simulations of turbulent flow in a square duct 08 p3275 N94-29809
Nominally two-dimensional flow about a normal flat plate 08 p3275 N94-29838
Large eddy simulation of subsonic mixing layers
08 p3276 N94-29851
Hydrodynamic stability analysis of swirling jets
08 p3278 N94-29974
Large eddy simulation of the upper atmospheric surface layer
[ISBN-0-315-85393-X] 08 p3365 N94-30134
Computational analysis of high resolution unsteady airloads for rotor aeroacoustics
[NASA-CR-194894] 08 p3480 N94-30274
Numerical investigation into high-angle-of-attack leading-edge vortex flow
[PB94-125564] 08 p3133 N94-30388
The enhancement of compressible turbulent mixing via streamwise vorticity 08 p3280 N94-30487
Aspects of the modeling and numerical simulation of leading-edge vortex flow
[AD-B179108] 08 p3133 N94-30492
Three dimensional compressible turbulent flow computations for a diffusing S-duct with/without vortex generators 08 p3281 N94-30519
Experiments on the aerodynamic generation of noise in centrifugal turbomachinery 08 p3480 N94-30804
Numerical simulation of leading-edge vortex flow
[AD-B175154] 08 p3134 N94-30871
An investigation of the reacting vortex structures associated with pulse combustion
08 p3200 N94-30911
Rotational effects in turbulence driven by convection
09 p3930 N94-31131
The small-scale topology of a 2:1 aspect-ratio elliptic jet 09 p3699 N94-31184
A priori tests of large eddy simulation of the compressible plane mixing layer
[MEMO-1152] 09 p3699 N94-31185
On the structure and stability of slender viscous vortices 09 p3700 N94-31218
Numerical analysis of single-vortex/free-surface interaction
[AD-A276462] 09 p3701 N94-31241
Field studies of raindrop oscillations with applications to radar meteorology 09 p3782 N94-31743
Tip effects on the vortex wake of an axisymmetric body at angle of attack 09 p3570 N94-31907
A study of the development and attenuation of wing-generated, vortical wakes
09 p3570 N94-31971
Analysis and computation for vortex dynamics and rarefied gases
[AD-A277415] 09 p3708 N94-32581
Notes on the Langevin model for turbulent diffusion of marked particles
[DE94-007847] 09 p3708 N94-32652
Quantum fluctuations of vortices in Josephson-coupled superconductors
[DE94-007609] 09 p3905 N94-32747
New advances in the modeling of high-temperature superconductors
[DE94-007649] 09 p3905 N94-32815
Active vortex control for a high performance wing
[AD-D016140] 09 p3573 N94-32974
Control of low-speed turbulent separated flow over a backward-facing ramp
[NASA-TM-109740] 09 p3573 N94-33071
Installed F/A-18 inlet flow calculations at 30 degrees angle-of-attack: A comparative study
[NASA-CR-195297] 09 p3573 N94-33119
Stationary eddies in the Mars general circulation as simulated by the NASA-Ames GCM
09 p3944 N94-33192
Eddy transport of water vapor in the Martian atmosphere 09 p3949 N94-33221
Similarity in separated flow fields producing large-scale vortices 10 p3969 N94-33382
Interaction of oblique instability waves with weak streamwise vortices
[NASA-TM-106584] 10 p4043 N94-33432
A predictor-corrector scheme for vortex identification
[AD-A279751] 10 p4043 N94-33433
The effects of vortex ingestion on the flow in a diffusing S-duct
[NASA-TM-106652] 10 p3998 N94-33955
F/A-18 forebody vortex control. Volume 2: Rotary-balance tests
[NASA-CR-4582-VOL-2] 10 p3984 N94-34430
Dynamic tests to demonstrate lateral control using forebody suction on large scale models in the DRA 24 foot wind tunnel 10 p3991 N94-34613
Yaw control by tangential forebody blowing
10 p3992 N94-34615
The effect of crossflow on Goertler vortices
[AD-280361] 10 p4049 N94-34680
Numerical simulation of two-dimensional spatially-developing mixing layers
[AD-A281683] 10 p4049 N94-34686
Unsteady flow past an airfoil pitched at constant rate
10 p3986 N94-34969
Unsteady separation process and vorticity balance on unsteady airfoils 10 p3986 N94-34970
Control of leading-edge vortices on a delta wing
10 p3986 N94-34971
Characterization of dynamic stall phenomenon using two-dimensional unsteady Navier-Stokes equations
10 p3986 N94-34974
Prediction of unsteady airfoil flows at large angles of incidence 10 p3986 N94-34978
Departure solutions of the unsteady thin-layer and full Navier-Stokes equations solved using streamline curvature based iteration techniques 10 p4052 N94-34980
Unsteady structure of leading-edge vortices on a delta wing
[AD-A278988] 11 p4190 N94-35529
Hydrodynamics of maneuvering bodies: LDRD Final Report
[DE94-009970] 11 p4265 N94-35769
F/A-18 forebody vortex control. Volume 1: Static tests
[NASA-CR-4582-VOL-1] 11 p4190 N94-35991
Vortex tubes in turbulent flows: Identification, representation, reconstruction
[AD-A280504] 11 p4267 N94-35992
On possible types of vortexes in relativistic superfluid system
[DE94-617392] 11 p4267 N94-36098
Superconducting transistors
[PB94-170743] 11 p4260 N94-36260
Influences of flame-vortex interactions on formation of oxides of nitrogen in curved methane-air diffusion flamelets
[DE94-005105] 12 p4409 N94-37221

VORTICITY

On the importance of mesoscale potential vorticity anomalies and topographic forcing during cyclone redevelopment across the Appalachians: A GALE case study 01 p0284 N94-10822
Near surface ocean processes: Acoustical observations, ambient sound, and Langmuir circulation
01 p0288 N94-11447
Unsteady flow past a NACA 0012 airfoil pitching at constant rates
[AD-A265159] 01 p0016 N94-11889
Parameterization of subgrid-scale stress by the velocity gradient tensor 01 p0155 N94-12286
The three-dimensional evolution of a plane wake
01 p0159 N94-12310
Plane mixing layer vortical structure kinematics
01 p0159 N94-12313
Passage-averaged approximation of turbomachinery flows using vorticity-potential method
[ISBN-0-315-72716-0] 02 p0634 N94-13598
A vortex method for viscous unsteady flows
02 p0640 N94-14602
A small-scale turbulence model
02 p0643 N94-14746
The structure of intense vorticity in homogeneous isotropic turbulence 02 p0643 N94-14747
Search for subgrid scale parameterization by projection pursuit regression 02 p0643 N94-14749
Isotropy of small scale turbulence
02 p0644 N94-14752
Vortex-induced disturbance field in a compressible shear layer 02 p0645 N94-14760
Evolution of the shock front and turbulence structures in the shock/turbulence interaction
02 p0645 N94-14761
Free-wake computation of helicopter rotor flowfield for general flight regimes
[AD-A266692] 02 p0509 N94-14781
Mesoscale frontogenesis: An analysis of two cold front case studies
[AD-A267950] 03 p1107 N94-17054
Granular fluctuations in plasma turbulence and their role in transport
[DE93-013465] 03 p1187 N94-17674
Vortex methods and statistics
[DE93-016974] 04 p1556 N94-17886
Filamentary magnetohydrodynamic plasmas
[DE93-015616] 04 p1583 N94-17945
Research on two equation models
04 p1411 N94-18547
Implementation of the turn function method in KIVA-F90
[DE93-018394] 04 p1419 N94-19027
Numerical modelling of crystal growth
[AD-A271206] 04 p1605 N94-19719
Direct simulation of shock-induced mixing layer
[DE93-040498] 05 p1803 N94-21531
A method to simulate viscous diffusion of vorticity by convective transport of vortices at a non-solenoidal velocity
[DE94-001777] 06 p2318 N94-23220
Measurements and modeling of flow structure in the wake of a low profile wishbone vortex generator
[NASA-TM-106468] 06 p2166 N94-23465
LinAir: A multi-element discrete vortex Weissinger aerodynamic prediction method
[NASA-TM-108786] 06 p2167 N94-23557
Effect of delta tabs on mixing and axis switching in jets from asymmetric nozzles
[NASA-TM-106450] 06 p2167 N94-23592
Diagnostic budgets of analyzed and modelled tropical plumes
[NASA-CR-194853] 06 p2409 N94-23621
Transition to turbulence in an elliptic vortex
06 p2331 N94-24161
Vortical structure in a forced plane mixing layer
06 p2331 N94-24162
Study of streamwise vorticity-stirred combustion
[NASA-CR-194450] 06 p2234 N94-24565
Nonlinear dynamics applied to atmospheric prediction
[AD-A273437] 06 p2404 N94-24674
Free-surface/vorticity interaction
[AD-A273263] 06 p2335 N94-24686
Vortex methods
[DE94-003245] 07 p2789 N94-25597
A finite wake theory for two-dimensional rotary wing unsteady aerodynamics
[AD-A274921] 07 p2645 N94-26535
Transverse vorticity measurements in the University of Houston two stream shear layer facility
[AD-A273910] 07 p2797 N94-27562
Streamwise vorticity in a turbine rotor with conical endwalls
[DLR-FB-93-13] 07 p2826 N94-27591
On the origins of low-level tornadic circulations within the remnants of hurricane Andrews
[AD-A275373] 08 p3369 N94-29011
A model analysis of potential vorticity on isopycnal surfaces for the global ocean
[AD-A275047] 08 p3377 N94-29164
Evolution of the large-scale vortices in turbulent mixing-layers 08 p3273 N94-29686
Physical processes associated with variability in successive operational model forecasts of cyclogenesis
[ISBN-0-315-74753-6] 08 p3371 N94-29751
A vorticity transport closure method for turbulent reacting flows 08 p3274 N94-29761
Numerical solution of 3-D Navier-Stokes equations in vorticity-velocity form for incompressible flows
08 p3276 N94-29843
Large eddy simulation of subsonic mixing layers
08 p3276 N94-29851

The enhancement of compressible turbulent mixing via streamwise vorticity 08 p3280 N94-30487
Convective solar nebula 09 p3930 N94-31130
The small-scale topology of a 2:1 aspect-ratio elliptic jet 09 p3699 N94-31184
The effect of an axial flow component on a circular cylinder wake 09 p3699 N94-31209
On wave interactions of rotational and irrotational flows 09 p3700 N94-31219
A study of the development and attenuation of wing-generated, vortical wakes 09 p3570 N94-31971
Three dimensional vorticity field in the California current system
[AD-A276951] 09 p3788 N94-32220
Turbulence structure associated with intercomponent and interscale energy transfer and modification by forcing
[AD-A278269] 10 p4043 N94-33414
A predictor-corrector scheme for vortex identification
[AD-A279751] 10 p4043 N94-33433
Unsteady flow past an airfoil pitched at constant rate 10 p3986 N94-34969
The unsteady pressure field and vorticity productiion at the suction surface of a pitching airfoil 10 p3986 N94-34972
Investigation of mechanisms for vorticity generation and flow separation on bodies in unsteady motion 10 p4051 N94-34973
Unsteady structure of leading-edge vortices on a delta wing
[AD-A278988] 11 p4190 N94-35529
Spatio-temporal properties of centrifugal instabilities: Abstracts of 8th Couette-Taylor Meeting
[PB94-150240] 11 p4266 N94-35981
Vortex tubes in turbulent flows: Identification, representation, reconstruction
[AD-A280504] 11 p4267 N94-35992

VORTICITY EQUATIONS
NT HELMHOLTZ VORTICITY EQUATION
Free-wake computation of helicopter rotor flowfield for general flight regimes
[AD-A266692] 02 p0509 N94-14781
Nonlinear gyrofluid models of shear Alfven instabilities in ignited and beam heated toroidal plasmas
[DE93-016235] 03 p1203 N94-16869
Cell vertex methods for steady inviscid flow 04 p1413 N94-18563
Variational approaches to CFD: Applications to potential Euler and Navier-Stokes equations 04 p1413 N94-18565
Implementation of the turn function method in KIVA-F90
[DE93-018394] 04 p1419 N94-19027
An adaptive multigrid model for hurricane track prediction 06 p2416 N94-23687
A vorticity dynamics based model for the turbulent dissipation: Model development and validation
[NASA-TM-106177] 06 p2336 N94-24713
On wave interactions of rotational and irrotational flows 09 p3700 N94-31219
Finite element vorticity-based methods for the solution of the incompressible and compressible Navier-Stokes equations
[ISBN-0-315-87265-9] 09 p3703 N94-31730

VOYAGER PROJECT
NASA images 11
[NASA-TM-109287] 02 p0842 N94-13626
NASA report to education, volume 7
[NASA-TM-109435] 03 p1247 N94-15419
NASA images 12 --- Voyager encounters
[NASA-TM-109417] 03 p1247 N94-15511
Voyager uplink planning in the interstellar mission era 06 p2305 N94-23870
Techniques and software for optimum and efficient mission science sequence development 06 p2504 N94-23872
Radio science ground data system for the Voyager-Neptune encounter, part 1 08 p3248 N94-29623
NASA report to education, volume 6
[NASA-TM-109818] 10 p4167 N94-33573
And then there was Voyager
[NASA-CR-195928] 10 p4164 N94-33587
Voyager: National Air and Space Museum
[NASA-CR-195905] 11 p4367 N94-35505
Voyager last picture show
[NASA-CR-195796] 11 p4367 N94-35506
Voyager science summary tape
[NASA-CR-195909] 11 p4367 N94-35513

VOYAGER 1 SPACECRAFT
Voyager encounter highlights
[NASA-TM-109420] 03 p1246 N94-15239
The 1980 highlights
[NASA-TM-109672] 03 p1303 N94-15509
A study of Saturn's E-ring particles using the Voyager 1 plasma wave instrument
[NASA-CR-194694] 05 p2088 N94-20048
The Jet Propulsion Laboratory space exploration: Past, present and future 06 p2153 N94-24242

VOYAGER 2 SPACECRAFT
Voyager encounter highlights
[NASA-TM-109420] 03 p1246 N94-15239
Neptune encounter highlights
[NASA-TM-109421] 03 p1246 N94-15240
Voyager encounters Uranus
[NASA-TM-109619] 03 p1247 N94-15348
Voyager 2: Neptune encounter
[NASA-TM-109423] 03 p1247 N94-15491
Mass of Saturn's A ring 03 p1263 N94-16252
Voyager's last encounter
[NASA-TM-109361] 04 p1628 N94-18957
The Jet Propulsion Laboratory space exploration: Past, present and future 06 p2153 N94-24242

VR (VIRTUAL REALITY)
U VIRTUAL REALITY

VSAT (NETWORK)
Two way time transfer results at NRL and USNO 01 p0353 N94-10983
The ACTS propagation program 03 p0995 N94-16039
NASA Lewis Meshed VSAT Workshop meeting summary
[NASA-TM-106332] 03 p0883 N94-17487
On-board packet switch architectures for communication satellites
[NASA-TM-106328] 03 p0883 N94-17488
Multichannel error correction code decoder
[NASA-TM-106331] 04 p1333 N94-19313
A European mobile satellite system concept exploiting CDMA and OBP 06 p2279 N94-22768
Modulation and synchronization technique for MF-TDMA system
[NASA-CR-194448] 06 p2304 N94-25266
Hubless satellite communications networks 09 p3600 N94-31433

VTOL
U VERTICAL LANDING
U VERTICAL TAKEOFF

VTOL AIRCRAFT
U VERTICAL TAKEOFF AIRCRAFT

VULCANIZING
Vulcanian explosive eruptions: A mechanism for localised pyroclast dispersal on Venus 01 p0477 N94-12243

VULNERABILITY
GRAFTED (GRAphical Fault Tree EDitor): A fault tree description program for target vulnerability/survivability analysis
[AD-A264078] 01 p0328 N94-11301
Current directions in the vulnerability/lethality process structure
[AD-A272836] 05 p1964 N94-21175
Vulnerability assessment using a fuzzy logic based method
[AD-A274075] 07 p2957 N94-25649
Vulnerability of manned spacecraft to crew loss from orbital debris penetration
[NASA-TM-108452] 08 p3169 N94-30161
GRAFTED - GRAphical fault tree EDitor: A fault tree description program for target vulnerability/survivability analysis. User manual
[AD-A277067] 09 p3818 N94-32390
Vulnerability assessment of a space based weapon platform electronic system exposed to a thermonuclear weapon detonation
[DE94-007229] 09 p3611 N94-32667

VYCOR
Bulletin of the Institute for Chemical Reaction Science, Tohoku University, volume 2
[JTN-94-80602] 07 p2717 N94-27385
Porous vycor glass tube joined to borosilicate glass 07 p2718 N94-27392

VZ-11 AIRCRAFT
U XV-5 AIRCRAFT

W

W STARS
U WOLF-RAYET STARS

W WINGS
U VARIABLE SWEEP WINGS

W-R STARS
U WOLF-RAYET STARS

WAFERS
RF vacuum microelectronics
[AD-A266066] 01 p0142 N94-10818
An ellipsometry investigation of nucleation and growth of electron cyclotron resonance plasma deposited silicon films
[AD-A265037] 01 p0401 N94-11651
Radiation-induced modifications of allylamino-substituted polyphosphazenes
[AD-A264914] 01 p0092 N94-11848
Analysis of the economics of DC arc CVD diamond
[AD-A265688] 01 p0403 N94-12339
Field emitter array RF amplifier development project. Phase 1: Cathode technology development
[AD-A266346] 02 p0622 N94-13776
Pseudomorphic semiconducting heterostructures from combinations of AlN, GaN and selected SiC polytypes: Theoretical advancement and its coordination with experimental studies of nucleation, growth, characterization and device deployment
[AD-A267561] 03 p1213 N94-17108
Selective electrochemical wafer thinning for silicon characterization
[DE93-015083] 04 p1592 N94-17742
RF vacuum microelectronics
[AD-A269454] 04 p1396 N94-18284
Integrated circuits: Resistless processing simplifies production and cuts costs
[DE93-018069] 04 p1405 N94-18941
Metal-glass composite field-emitting arrays
[AD-D015942] 05 p1673 N94-20064
Process for the homoepitaxial growth of single-crystal silicon carbide films on silicon carbide wafers
[NASA-CASE-LEW-15223-1] 05 p2017 N94-20381
Attenuation of epsilon(sub eff) of coplanar waveguide transmission lines on silicon substrates 05 p1733 N94-20504
Analysis of cost: CVD diamond deposition
[AD-A271980] 05 p2018 N94-20616
Study of the homogeneity of InP wafers
[AD-A273658] 07 p3055 N94-26194
A partitioning and redundancy model for wafer-scale integrated circuits 07 p2955 N94-27195
Silicon-Film (tm) photovoltaic manufacturing technology
[DE94-000258] 08 p3336 N94-28501
A sub-cm micromachined electron microscope 08 p3236 N94-29775
Epitaxial liftoff technology onto processed silicon foundry wafers
[AD-A277116] 09 p3900 N94-31985
Determination of BPSG thin-film properties using IR reflection spectroscopy of product wafers
[DE94-006591] 09 p3634 N94-32110
Silicon-Film(tm) photovoltaic manufacturing technology
[DE94-000202] 09 p3760 N94-32143
A scanning defect mapping system for semiconductor characterization 09 p3885 N94-32446
Metal-ion spin-on glasses: Novel materials for active waveguides
[DE94-007738] 09 p3882 N94-32649
Application of the modified voltage-dividing potentiometer to overlay metrology in a CMOS/bulk process
[DE94-007937] 09 p3695 N94-32700
Laser drilling of vertical vias in silicon
[DE94-009250] 11 p4270 N94-35351
Materials for efficient high-flux magnetic bearing actuators 11 p4214 N94-35845

WAKEFULNESS
Effects of methamphetamine on vigilance and tracking during extended wakefulness
[AD-A274896] 07 p2909 N94-26179

WAKES
NT AIRCRAFT WAKES
NT HELICOPTER WAKES
NT HYPERSONIC WAKES
NT LAMINAR WAKES
NT NEAR WAKES
NT PROPELLER SLIPSTREAMS
NT SLIPSTREAMS
NT SUPERSONIC WAKES
NT TURBULENT WAKES
Submarine internal waves
[MRL-GD-0049] 01 p0098 N94-11303
Topics in pattern formation and chaotic systems
[AD-A265922] 01 p0161 N94-12342
Three-dimensional structure of straight and curved plane wakes
[NASA-CR-194420] 02 p0501 N94-13266
Laboratory simulation of spacecraft charging in the plasma wake region
[FFI-93-7007] 02 p0542 N94-14107
An experimental study of a turbulent boundary layer in the trailing edge region of a curculation-control airfoil
[NASA-CR-194522] 02 p0508 N94-14541

Wake-field and space charge effects on high brightness beams calculations and measured results for the laser driven photoelectrons at BNL-ATF
[DE93-015787] 02 p0659 N94-14572
Receptivity of boundary layers to convected gusts
[AD-A267206] 03 p1022 N94-15860
Search for chaos in free shear flows
[AD-A266245] 03 p1023 N94-16470
Wake field in electron-positron plasmas
[DE93-624929] 04 p1584 N94-17955
Enhanced acceleration in a self-modulated-laser wakefield accelerator
[AD-A268452] 04 p1586 N94-18148
Wake structure and aerodynamic behavior of high lift aircraft configurations during unsteady maneuvers in ground effect 04 p1309 N94-18439
Persistent wakefields associated with waveguide damping of higher order modes
[DE93-040973] 05 p1715 N94-19874
Effects of hydrodynamics and thermal radiation in the atmosphere after comet impacts
05 p1862 N94-20649
An integro-algebraic equation for high frequency wake fields in a tube with smoothly varying radius
[DE93-040940] 05 p1741 N94-21684
Modelling stalled airfoils
[ISBN-0-315-59525-6] 05 p1639 N94-22382
Recent ONERA contributions to the development of flight test measurement techniques
05 p1641 N94-22607
Measurements and modeling of flow structure in the wake of a low profile wishbone vortex generator
[NASA-TM-106468] 06 p2166 N94-23465
Three dimensional study of an airplane wing and its wake in the subsonic regime
[ISBN-0-315-58963-9] 06 p2168 N94-24178
Free-surface/vorticity interaction
[AD-A273263] 06 p2335 N94-24686
Analysis of the effects of wake passage on heat transfer in a linear turbine cascade
[AD-A273729] 06 p2339 N94-25446
Wake passage effects on the losses in a linear turbine cascade
[AD-A273794] 07 p2790 N94-25874
A finite wake theory for two-dimensional rotary wing unsteady aerodynamics
[AD-A274921] 07 p2645 N94-26535
Direct simulation Monte-Carlo of near continuum hypersonic flow with chemical reactions
[DLR-FB-93-01] 07 p2797 N94-27588
Unsteady wake structures in transverse jets
07 p2800 N94-28006
Localized and distributed boundary-layer receptivity to convected unsteady wake in free stream
[NASA-CR-4578] 07 p2808 N94-28180
Coulomb field effect on plasma focusing and wake field acceleration
[DE94-004937] 08 p3504 N94-28564
Boundary layers induced by three-dimensional vortex loops
[AD-A275678] 08 p3270 N94-28665
A new flux-conserving numerical scheme for the steady, incompressible Navier-Stokes equations
[NASA-TM-106520] 08 p3273 N94-29471
Nominally two-dimensional flow about a normal flat plate 08 p3275 N94-29838
Three-dimensional flow characteristics downstream of a blade endwall corner 08 p3280 N94-30229
Computational analysis of high resolution unsteady airloads for rotor aeroacoustics
[NASA-CR-194894] 08 p3480 N94-30274
The effect of an axial flow component on a circular cylinder wake 09 p3699 N94-31209
Gravitational effects of cosmic strings
[ISBN-0-315-75484-2] 09 p3934 N94-31789
Tip effects on the vortex wake of an axisymmetric body at angle of attack 09 p3570 N94-31907
Ship traffic monitoring and oil spill detection using the ERS-1 SAR 09 p3751 N94-32542
Superluminous laser pulse in an active medium
[DE94-007110] 09 p3720 N94-32684
Real-time adaptive control of mixing in a plane shear layer
[AD-A278379] 10 p4113 N94-33744
Sensitivity of lag-damping correlations to structural and aerodynamic approximations of isolated experimental rotors in forward flight
[NASA-CR-195822] 10 p3983 N94-33991
Ocean magnetics
[PB94-149028] 10 p4092 N94-34142
Hydrodynamics of maneuvering bodies: LDRD Final Report
[DE94-009970] 11 p4265 N94-35769
Towards enhancing and delaying disturbances in free shear flows
[NASA-CR-194945] 12 p4445 N94-37606

WALKING
Robotic servicing on Earth orbiting satellites
01 p0045 N94-11579
Road march performance of special operations soldiers carrying various loads and load distributions
[AD-A269198] 04 p1512 N94-18882
The 1991-1992 walking robot design
07 p2833 N94-25686
The effect of platform motion on human energy expenditure during walking. An exploratory experiment
[AD-A273760] 07 p2940 N94-25724
A biologically-inspired autonomous robot
[AD-A273909] 07 p2821 N94-25782
Tripping over obstacles: Biomechanical analyses of how young and old try to avoid it 09 p3803 N94-31954

WALKING MACHINES
Simulation of tripod gaits for a hexapod underwater walking machine
[AD-A271719] 05 p1945 N94-21355
Robotic concepts for operation in barren terrain
[DE93-040539] 05 p1946 N94-21925
Walking machines for space 06 p2369 N94-23406
Design of a walking robot
[NASA-CR-195200] 06 p2367 N94-25274
The 1991-1992 walking robot design
07 p2833 N94-25686
Biologically-inspired hexapod robot design and simulation
[AIAA PAPER 94-1178-CP] 08 p3439 N94-30530
ODYSSEUS autonomous walking robot: The leg/arm design
[AIAA PAPER 94-1180-CP] 08 p3439 N94-30531

WALL FLOW
Wall interference correction based on interface measurements in subsonic wind tunnel testing
01 p0015 N94-11154
A Galilean and tensorial invariant k-epsilon model for near wall turbulence
[NASA-TM-106263] 01 p0151 N94-11192
Dynamics and control of coherent structures in the turbulent wall layer: An overview
01 p0031 N94-11494
Reynolds stress closure modeling in wall-bounded flows 01 p0157 N94-12298
Application of a Reynolds stress model to separating boundary layers 01 p0157 N94-12299
Regeneration of near-wall turbulence structures
01 p0158 N94-12308
Suppression of the near wall burst process of a fully developed turbulent pipe flow
[AD-A265995] 01 p0161 N94-12352
Fluctuations of longitudinal vortices along a concave wall 01 p0016 N94-12616
A numerical experiment of boundary layer transition at subcritical Reynolds numbers 01 p0165 N94-12625
Turbulent drag reduction of a d-type rough wall boundary layer with longitudinal ribs placed within the grooves
01 p0165 N94-12627
A wall interference assessment/correction system
[NASA-CR-194174] 02 p0500 N94-13076
An experimental study of a turbulent boundary layer in the trailing edge region of a curculation-control airfoil
[NASA-CR-194522] 02 p0508 N94-14541
Analysis, approximation, and computation of a coupled solid/fluid temperature control problem
[NASA-TM-106351] 02 p0771 N94-14731
A transport equation for eddy viscosity
02 p0646 N94-14762
DNS and modeling of the interaction between turbulent premixed flames and walls 02 p0646 N94-14763
On the receptivity problem for 0(1) wavelength Goertler vortices
[NASA-CR-191519] 03 p1016 N94-15005
Wall interference and boundary simulation in a transonic wind tunnel with a discretely slotted test section
[NASA-TP-3334] 03 p0872 N94-15794
Determination of the effect of the walls of a wind-tunnel from the parameters of flow near them
[RAE-LIB-TRANS-2201] 03 p0859 N94-16583
Transition induced by fixed and freely convecting spherical particles in laminar boundary layers
[AD-A267757] 03 p1028 N94-17276
Active turbulence control in wall bounded flows using direct numerical simulation
[AD-A267261] 03 p1028 N94-17286
Research on two equation models
04 p1411 N94-18547
Contribution to the modelling of near-wall turbulence
04 p1414 N94-18585
Relation between the fluctuating wall pressure and the turbulent structure of a boundary layer on a cylinder in axial flow
[AD-A270242] 04 p1418 N94-18906
Principles and applications of oil film interferometry for measuring wall friction fields in air flows
[ETN-93-95062] 05 p1798 N94-20147
An analysis of pressure driven cross-flow through a long slot connecting two parallel channels
[DE93-040181] 05 p1804 N94-21765
Experimental Methods in Separated Flows
[ILR-MITT-260(1991)] 06 p2315 N94-22852
A method for recognition of frequency cells in a cylinder flow influenced by wall effects 06 p2316 N94-22860
Numerical investigation of two- and three-dimensional heat transfer in expander cycle engines
06 p2213 N94-23048
Flow visualization study in high aspect ratio cooling channels for rocket engines 06 p2213 N94-23049
Computation of flows in a turn-around duct and a turbine cascade using advanced turbulence models
06 p2216 N94-23062
Development of a code for wall contour design in the transonic region of axisymmetric and square nozzles
[NASA-CR-194857] 06 p2167 N94-23625
Supersonic minimum length nozzle design for dense gases 06 p2171 N94-23656
Unstructured grid large eddy simulation of wall bounded turbulent flows 06 p2329 N94-24151
Sub-sonic flow about a slender profile in a tunnel having perforated walls
[AD-A273184] 06 p2170 N94-25137
Analytical skin friction and heat transfer formula for compressible internal flows
[NASA-CR-191185] 06 p2170 N94-25173
A numerical study of mixing and combustion in hypervelocity flows through a scramjet combustor model
07 p2808 N94-27911
Experiments on the ground vortex formed by an impinging jet in cross flow 07 p2802 N94-28016
Experimental investigations into the wall interference and sidewall boundary layer effects in the National Research Council/Inst. for Aerospace Research High Reynolds Number 2-D Test Facility
07 p2658 N94-28350
Computation of wind-tunnel side-wall interference using 3D Navier-Stokes code 07 p2658 N94-28351
A method for the modelling of porous and solid wind tunnel walls in computational fluid dynamics codes
[NASA-CR-195699] 08 p3270 N94-28724
Experimental studies of transonic flow field near a longitudinally slotted wind tunnel wall
[NASA-TP-3392] 08 p3130 N94-29545
Response of wall turbulence to high frequency streamwise and spanwise oscillations
09 p3700 N94-31211
Control of hypersonic aerodynamic forces with surface blowing 09 p3567 N94-31216
Oscillations in piston-driven shear flow of a non-Newtonian fluid
[AD-A276472] 09 p3701 N94-31245
Experimental studies of transpiration cooling with shock interaction in hypersonic flow, part B
[NASA-CR-195958] 10 p3985 N94-34965
The aerodynamic and heat transfer effects of an endwall boundary layer fence in a 90 degree turning square duct
[AD-A278903] 11 p4265 N94-35803

WALL JETS
Turbulent wall jet in blast wave precursor
[DE93-011955] 01 p0151 N94-11144
The turbulent wall jet
[AD-A267675] 03 p0855 N94-14963
Theoretical and experimental investigation of a delta wing with turbulent leading-edge jets
07 p2659 N94-28029
Experimental studies of shock-wave/wall-jet interaction in hypersonic flow
[NASA-CR-195844] 10 p4048 N94-34171
Experimental studies of shock-wave/wall-jet interaction in hypersonic flow, part A
[NASA-CR-195957] 10 p3985 N94-34964
Evolution of turbulent fields in explosions
[DE94-010405] 12 p4444 N94-37390

WALL PRESSURE
Autofrettage: Stress distribution under load and retained stresses after depressurization. A modified plane-strain case
[AD-A266320] 02 p0671 N94-13579
Wall interference and boundary simulation in a transonic wind tunnel with a discretely slotted test section
[NASA-TP-3334] 03 p0872 N94-15794
An experimental investigation of the effects of leading edge geometry on the dynamics of blunt fin-induced shock wave turbulent boundary layer interaction
[AD-A267656] 03 p0860 N94-17221
An experimental study of fluctuating wall pressures in a highly swept, sharp fin-induced, Mach 5 shock wave/turbulent boundary layer interaction
[AD-A268394] 03 p0861 N94-17461
Calculation of turbulent boundary layer wall pressure spectra
[AD-A269549] 04 p1416 N94-18642

Correlation of incoming boundary layer pitot pressure fluctuations with the unsteadiness of fin-induced shock wave turbulent boundary layer interactions
[AD-A270059] 04 p1417 N94-18796
Relation between the fluctuating wall pressure and the turbulent structure of a boundary layer on a cylinder in axial flow
[AD-A270242] 04 p1418 N94-18906
The effect of transverse curvature on the fluctuating wall pressure and structure of boundary layer turbulence
[AD-A271868] 05 p1800 N94-20466
Flowfield dynamics in blunt fin-induced shock wave/turbulent boundary layer interactions
[NASA-CR-195170] 07 p2798 N94-27802
Wall pressure events from the direct numerical simulation of a turbulent wall-bounded flow
[AD-A275890] 08 p3271 N94-28778
Wall pressure fluctuations in the reattachment region of a supersonic free shear layer
[NASA-CR-195790] 08 p3132 N94-29920
Method for making a dynamic pressure sensor and a pressure sensor made according to the method
[NASA-CASE-LAR-14029-1] 11 p4269 N94-35369

WALL TEMPERATURE
Establishing baseline data for an experimental appratus that measures heat transfer under conditions of oscillating pressure and flow
[NASA-CR-193772] 01 p0413 N94-12343
Description of cooling water calorimetry and wall thermometry diagnostic at tokamak ASDEX-Upgrade
[IPP-5/46] 03 p1200 N94-14966
Development of a multi-point two-color pyrometer for tube and wall temperature and emissivity measurement at the CFFF
[DE93-014716] 04 p1429 N94-18207
Parabolized Navier-Stokes computation of surface heat transfer characteristics for supersonic and hypersonic KE projectiles
[AD-A268858] 04 p1410 N94-18391
Correlation of incoming boundary layer pitot pressure fluctuations with the unsteadiness of fin-induced shock wave turbulent boundary layer interactions
[AD-A270059] 04 p1417 N94-18796
Finite difference program for calculating hydride bed wall temperature profiles
[DE93-019272] 04 p1523 N94-19005
Analysis of film cooling in rocket nozzles
[NASA-CR-194674] 04 p1338 N94-19438
Chemical reaction fouling model for single-phase heat transfer
[DE93-019556] 05 p1802 N94-20942
Numerical investigation of two- and three-dimensional heat transfer in expander cycle engines
06 p2213 N94-23048
Flow visualization study in high aspect ratio cooling channels for rocket engines 06 p2213 N94-23049
Development of buoyancy affected laminar flow in a heated pipe 08 p3128 N94-28988
Composite matrix experimental combustor
[AD-280344] 10 p4005 N94-34679
Compliant metal enhanced convection cooled reverse-flow annular combustor
[NASA-TM-106626] 11 p4199 N94-36379

WALLOPS ISLAND
Birds of Wallops Island, Virginia, 1970 - 1992
[NASA-TM-104589] 02 p0850 N94-13923
Operations summary for the convection and moisture experiment (CAMEX)
[NASA-TM-108445] 09 p3786 N94-33004

WALLS
NT BULKHEADS
NT NOZZLE WALLS
NT POROUS WALLS
NT THIN WALLS
NT WIND TUNNEL WALLS
Potential change in flaw geometry during pressurized-thermal-shock transients
[DE93-009709] 01 p0184 N94-10288
Application of a Reynolds stress model to separating boundary layers 01 p0157 N94-12299
On the motion through a viscous fluid of a spherical particle touching a plane wall: Slip boundary conditions
[DE93-012540] 02 p0628 N94-12961
An assessment of the potential for neck injury due to padding of aircraft interior walls for head impact protection
[DOT/FAA/AM-93/14] 02 p0738 N94-13972
Experimental investigations into the deflagration to detonation transition at TNO/PML
[AD-A266753] 03 p1021 N94-15755
Report of the 1991 Workshop on Particle-Material Interactions for Fusion Research
[DE93-788393] 04 p1573 N94-18156
Thermal analysis of coatings and substrate materials during a disruption in fusion reactors
[DE93-017688] 04 p1588 N94-18971
Pressure wall patch
[NASA-CASE-MFS-28724-1] 06 p2203 N94-23824
Methodology for first wall design
[DE94-002795] 07 p3045 N94-26861
Passive stabilization of MHD instabilities at high (beta)n in the HBT-EP tokamak
[DE94-003317] 07 p3047 N94-27735
Proceedings of Japan-US Workshop P-196 on High Heat Flux Components and Plasma Surface Interactions for Next Devices
[DE94-701164] 08 p3503 N94-28513
Wall pressure events from the direct numerical simulation of a turbulent wall-bounded flow
[AD-A275890] 08 p3271 N94-28778
The effect of a wavy boundary on turbulent flow
08 p3280 N94-30272
Operation of D3-D with all-graphite walls
[DE94-004858] 09 p3886 N94-31304
Some aspects of unsteady separation
10 p3986 N94-34979

WALSH FUNCTION
Addition of decimal numbers in optical computing architecture by Walsh coded digits
05 p1773 N94-22122

WAR GAMES
Computer model for generation of infrared images
[PB94-123551] 07 p3005 N94-27172
Optimal tactics for agile aircraft technology: A differential game methodology 10 p3994 N94-34631
The application of fuzzy logic to SAFOR in SIMNET
[AD-A279058] 11 p4312 N94-35730

WARFARE
NT ANTISUBMARINE WARFARE
NT CHEMICAL WARFARE
NT COMBAT
NT ELECTRONIC WARFARE
Aviators, air combat, and combat stress: An Air F orce commander's primer
[AD-A265083] 01 p0313 N94-11867
Sleep management user's guide for special operations personnel
[AD-A267746] 03 p1119 N94-14943
An information processing classification of beyond-visual-range air intercepts
[AD-A266927] 03 p1131 N94-15108
Not ready for the first space war. What about the second?
[AD-A266557] 03 p1174 N94-16665
Massachusetts Institute of Technology Lincoln Laboratory Journal volume 6, number 1, Spring 1993
[AD-A272273] 05 p1737 N94-20944
Night operations 06 p2431 N94-23977
Autonomous intelligent military robots: Army ants, killer bees, and cybernetic soldiers 08 p3304 N94-30276
Robotics and the battlefield of the future
08 p3304 N94-30277
DREV activities related to military vehicles robotization
08 p3305 N94-30278
Autonomous Robotic Refueling System (ARRS) for rapid aircraft turnaround 08 p3305 N94-30279
Naval Surface Warfare Center Dahlgren Division Technical Digest: Advanced materials technology
[AD-A276448] 09 p3668 N94-31364
Profile analysis of after-effects experienced during exposure to several virtual reality environments
12 p4482 N94-37263

WARHEADS
NT NUCLEAR WARHEADS
N,N'-bis(4,4,4-trinitro butyryl) hydrazine
[AD-D015897] 05 p1712 N94-20122
Design study of fiber-composite penetrator cases
[DE94-003203] 07 p2707 N94-26099

WARMING
U HEATING

WARNING
Mesoscale meteorological measurements characterizing complex flows
[DE94-002359] 07 p2895 N94-26761

WARNING DEVICES
U WARNING SYSTEMS

WARNING SIGNALS
U WARNING SYSTEMS

WARNING SYSTEMS
NT EARLY WARNING SYSTEMS
NT MINE DETECTORS
The Satellite Attack Warning and Assessment Flight Experiment (SAWAFE) 01 p0045 N94-11323
A tentative plan on China and Asian-Pacific satellite system for disaster reduction 02 p0693 N94-14247
Test plan for the evaluation of the initial capability of the National Satellite Test Bed: Phase 1D
[DOT/FAA/RD-93/20] 03 p0876 N94-16025
The use of the Air Force Academy high wind alert system in forecasting moderate intensity wind events for military bases in the Colorado Springs area
[AD-A267648] 03 p1107 N94-17245
Development of ultrasonic motor and application to silent alarm analog quartz watch 04 p1425 N94-18016
Aircraft fire sentry. Volume 1: Summary
[AD-A270087] 04 p1315 N94-18822
Aircraft fire sentry. Volume 2: Appendices A, B, C and D
[AD-A270088] 04 p1315 N94-18823
Ground proximity warning system voice warning unit requirements study
[AD-A270541] 05 p1641 N94-19876
Evaluation of head injury criteria
[NIAR-93-2] 05 p1890 N94-20190
Army aircraft fire-detection systems operation and reliability
[AD-A271327] 05 p1641 N94-20912
Windshear detection for aircraft using temperature lapse rate
[CA-PATENT-1,295,736] 05 p1641 N94-21030
Initial laboratory evaluation of color video cameras, phase 2
[DE93-040201] 05 p1809 N94-21556
Robust, wide-range hydrogen sensor for use in commercial, space, and government applications
[DE93-040902] 06 p2342 N94-22954
Lightning studies using LDAR and LLP data
06 p2416 N94-23238
Towards a new radiation protection organization
[FOA-C-40304-4.3] 06 p2437 N94-24292
The chemical detector paper as a potential alarm
[FFI-93/6007] 07 p2712 N94-25745
A feasibility study on bird classification with neural network
[AD-A273753] 07 p2659 N94-25780
System for generating, aboard an aircraft, during takeoff, of a signal capable of producing an alert or an alarm, in case of malfunction
[CA-PATENT-APPL-SN-2,018,940] 07 p2659 N94-26293
Processing of wide-angle synthetic aperture radar signals for target detection
[AD-A274225] 07 p2773 N94-27073
Ir-fibers in a laser threat warning system and robot shot warning system
[PB94-124476] 07 p3038 N94-27209
Automatic, real-time fault monitor verifying network in a microwave landing system
[CA-PATENT-1325261] 07 p2665 N94-27275
Minutes. Accredited Standards Committee on Noise, S12. US tag for ISO/TC 43/SC1 noise and ISO/TC 94/SC12 hearing protection
[AD-A275622] 08 p3477 N94-28636
Initial wave-type identification with neural networks and its contribution to automated processing in IMS version 3.0
[AD-A275058] 08 p3359 N94-29137
TacSats for NATO
[AD-A277710] 08 p3169 N94-30350
Covert channel analysis of trusted systems. A guide to understanding
[AD-A276418] 09 p3916 N94-31331
Nonlocal methods for signal detection and estimation in the dependent nonstationary environment
[AD-A278472] 10 p4033 N94-33594
Development of a machine vision fire detection system
[AD-A278208] 10 p4032 N94-34084
Terminal Doppler Weather Radar (TDWR) Low Level Wind Shear Alert System 3 (LLWAS 3) integration studies at Orlando International Airport
[AD-A278957] 11 p4294 N94-35807
An automated method for Low Level Windshear Alert System (LLWAS) data quality analysis
[AD-A280313] 12 p4472 N94-37125
Distributed detection theory and data fusion
[AD-A280410] 12 p4434 N94-37183
Terminal Doppler Weather Radar (TDWR) build 5 Test and Evaluation Master Plan (TEMP)
[AD-A280426] 12 p4434 N94-37218
Aircraft command in emergency situations prototype development users manual
[DOT/FAA/CT-94/24] 12 p4385 N94-37706

WARPAGE
Polymer infiltration studies
[NASA-CR-194521] 02 p0582 N94-14539

WASHERS (SPACERS)
Bolt and nut evaluator
[NASA-CASE-GSC-13468-1] 08 p3288 N94-29538

WASHING
A comparison of wet and dry scrubbing systems for control of metals and dioxin/furan emissions from incinerators
[DE93-017446] 04 p1474 N94-18502
Stability of reference masses 2: The effect of environment and cleaning methods on the surfaces of stainless steel and allied materials
[NPL-DMM(A)-95] 07 p2738 N94-26853

WASHINGTON
Analysis of deep seismic reflection and other data from the southern Washington Cascades
[DE94-005915] 08 p3367 N94-30883
Mount Rainier active cascade volcano
[NASA-CR-195893] 10 p4087 N94-33992
Analysis of deep seismic reflection and other data from the Southern Washington Cascades
[DE94-004075] 12 p4470 N94-37489
WASHOUT (RADIOACTIVITY)
U FALLOUT
WASPALOY
Atlas of formability: Waspaloy
[AD-A268323] 04 p1593 N94-17805
WASTE DISPOSAL
NT HAZARDOUS MATERIAL DISPOSAL (IN SPACE)
Environmental Sciences Division
[DE93-013865] 01 p0264 N94-10650
Computer models used to support cleanup decision-making at hazardous and radioactive waste sites
[PB93-183333] 01 p0274 N94-10698
Environmental awareness
[DE93-014192] 02 p0707 N94-13218
A laser-based technique to continuously monitor metal aerosol emissions
[DE93-012836] 02 p0710 N94-14183
Survey of subsurface geophysical exploration technologies adaptable to an airborne platform
[DE93-015080] 02 p0717 N94-14294
STS-35 crew trash compactor briefing
[NASA-TM-109487] 02 p0533 N94-14735
A study of hydrogen effects on fracture behavior of radioactive waste storage tanks
[DE93-018171] 02 p0574 N94-14873
Nuclear rocket plume studies
[AD-A267154] 03 p0925 N94-15837
Biomass energy: State of the technology present obstacles and future potential
[DE93-016295] 03 p1092 N94-16766
Rapid geophysical surveyor
[DE93-016637] 04 p1461 N94-17851
Research activities, Faculty of Civil Engineering, Delft University of Technology, 1990 - 1991
[PB93-195022] 04 p1380 N94-19254
Current status of environmental, health, and safety issues of nickel metal-hydride batteries for electric vehicles
[DE93-017079] 05 p1748 N94-19902
Space Station trash removal system
[NASA-CASE-MSC-21723-1] 05 p1657 N94-20367
Automating the control of robotic systems in unstructured environments
[DE93-040753] 05 p1946 N94-21929
Environmental protection using social costing
[DE94-000492] 05 p1853 N94-22569
Aqueous alkaline cleaners: An alternative to organic solvents
[AD-A273510] 06 p2260 N94-24848
Collaboration of chemical oxidation and biological treatment for removal of refractory organic substances 07 p2870 N94-28149
Treatment of refractory organic substances with combined use of chemical oxidation and biological treatment. Part 2: Biodegradability of ozonation products of chlorophenol 07 p2870 N94-28151
Novel mass spectrometric instrument for gaseous and particulate characterization and monitoring
[DE94-005896] 08 p3349 N94-30047
A modular approach for automated sample preparation and chemical analysis 08 p3354 N94-30464
Benchmarking for cost improvement
[DE94-002276] 08 p3528 N94-30824
Sandia technology engineering and science accomplishments
[DE94-008312] 09 p3668 N94-32412
The expanded role of software in a control system
[DE94-007524] 10 p4113 N94-33838
Decision and systems analysis for underground storage tank waste retrieval systems and tank waste remediation system
[SAND94-0065] 11 p4286 N94-35957
WASTE ENERGY UTILIZATION
Feasibility survey of thermoelectric conversion technology using semiconductors
[DE93-520882] 04 p1595 N94-18105
Molten carbonate fuel cell networks: Principles, analysis, and performance
[DE93-000281] 04 p1468 N94-18925
Investigating pyrolysis/incineration as a method of resource recovery from solid waste 06 p2444 N94-25375
Feasibility study on introduction of the bio-fuel power generation in tropical regions
[DE94-725203] 07 p2858 N94-26838
Feasibility study on introduction of a large methanol engine power generation plant
[DE94-732338] 08 p3224 N94-28629
Detailed design of the 2MW Demonstration Plant
[DE94-000042] 09 p3762 N94-32823
WASTE HEAT
Absorption technology for solar and waste heat utilization 07 p2854 N94-26053
WASTE TREATMENT
NT SEWAGE TREATMENT
Toxic chemical release inventory reporting Form R and instructions. Revised 1992 version. Section 313 of the Emergency Planning and Community Right-to-Know Act
[PB93-194140] 01 p0264 N94-10836
Some environmental aspects of the application of fibre reinforced plastics in structures
[LM-998] 01 p0088 N94-10877
Catalytic oxidation of organics in vapor streams at remediation sites
[PB93-182962] 01 p0266 N94-11472
An estimate of the second law thermodynamic efficiency of the various units comprising an Environmental Control and Life Support System (ECLSS) 01 p0317 N94-12369
Novel mass spectrometric instrument for gaseous and particulate characterization and monitoring
[DE93-014093] 01 p0272 N94-12783
Photocatalysis for the treatment of waste water: Applications involving the removal of metals
[DE93-011669] 02 p0561 N94-12841
A laser-based technique to continuously monitor metal aerosol emissions
[DE93-012836] 02 p0710 N94-14183
Survey of subsurface geophysical exploration technologies adaptable to an airborne platform
[DE93-015080] 02 p0717 N94-14294
Relationship between borosilicate glass composition, structure, and durability test response (SRS)
[DE93-013578] 02 p0581 N94-14343
Rapid geophysical surveyor
[DE93-016637] 04 p1461 N94-17851
Ultrasonic process for destruction of chlorinated organic compounds in aqueous solution
[DE93-015551] 04 p1348 N94-18249
Advanced Energy Projects, FY 1993
[DE94-000539] 05 p1847 N94-21755
Plasma-chemical conversion of hydrogen sulfide into hydrogen and sulfur
[DE93-041167] 05 p1682 N94-21789
Automating the control of robotic systems in unstructured environments
[DE93-040753] 05 p1946 N94-21929
Investigating pyrolysis/incineration as a method of resource recovery from solid waste 06 p2444 N94-25375
Journal of NIRE, volume 2, number 4
[JTN-94-80554] 07 p2869 N94-28147
Collaboration of chemical oxidation and biological treatment for removal of refractory organic substances 07 p2870 N94-28149
Treatment of refractory organic substances with combined use of chemical oxidation and biological treatment. Part 2: Biodegradability of ozonation products of chlorophenol 07 p2870 N94-28151
Electrochemical incineration of wastes
[NASA-CR-195262] 08 p3198 N94-29938
Novel mass spectrometric instrument for gaseous and particulate characterization and monitoring
[DE94-005896] 08 p3349 N94-30047
Benchmarking for cost improvement
[DE94-002276] 08 p3528 N94-30824
Activities of the Chemical Technology Division
[DE94-013050] 12 p4410 N94-37357
The integrated performance evaluation program quality assurance guidance in support of EM environmental sampling and analysis activities
[DE94-013043] 12 p4468 N94-37731
WASTE UTILIZATION
Some environmental aspects of the application of fibre reinforced plastics in structures
[LM-998] 01 p0088 N94-10877
Coprocessing of fossil fuels and biomass for CO2 emission reduction in the transportation sector
[PB93-194165] 01 p0267 N94-11845
First Biomass Conference of the Americas: Energy, Environment, Agriculture, and Industry, volume 2
[DE94-000435] 05 p1847 N94-21562
Current situation of development of petroleum substituting energies (Canada)
[DE94-707493] 05 p1849 N94-22014
Investigating pyrolysis/incineration as a method of resource recovery from solid waste 06 p2444 N94-25375
Journal of NIRE, volume 2, number 4
[JTN-94-80554] 07 p2869 N94-28147
Oil production from buckwheat stillage by thermochemical liquefaction 07 p2871 N94-28154
Electrochemical incineration of wastes
[NASA-CR-195262] 08 p3198 N94-29938
Publications of the NASA Controlled Ecological Life Support System (CELSS) program 1989-1992
[NASA-CR-4603] 08 p3401 N94-30122
Structural composite construction materials manufactured from municipal solid waste
[AD-A280635] 12 p4403 N94-36730
SIHTI: Energy and environmental technology
[DE94-763290] 12 p4464 N94-37007
Estimates of US biomass energy consumption 1992
[DE94-011458] 12 p4463 N94-37567
WASTE WATER
Photocatalysis for the treatment of waste water: Applications involving the removal of metals
[DE93-011669] 02 p0561 N94-12841
Multiple dataset water-quality analyses in the vicinity of an ocean wastewater plume 03 p1069 N94-16687
Ultrasonic process for destruction of chlorinated organic compounds in aqueous solution
[DE93-015551] 04 p1348 N94-18249
Growth of hydrocarbon-rich microalga Botryococcus braunii in secondarily treated sewage and its consumption of nitrate ion and phosphate ion 08 p3387 N94-29519
Catalytic methods using molecular oxygen for treatment of PMMS and ECLSS waste streams, volume 2
[NASA-CR-190299] 09 p3804 N94-32697
Characterization of spacecraft humidity condensate 10 p4102 N94-33659
WASTES
NT GARBAGE
NT HUMAN WASTES
NT INDUSTRIAL WASTES
NT RADIOACTIVE WASTES
NT SOLID WASTES
NT URINE
NT WASTE WATER
Vapor deposition of copper on stainless steel 304L
[DE94-001945] 07 p2740 N94-27006
WATCHES
U CLOCKS
WATER
NT COASTAL WATER
NT COLD WATER
NT DEEP WATER
NT FRESH WATER
NT GROUND WATER
NT HEAVY WATER
NT INLAND WATERS
NT LIGHT WATER
NT NEARSHORE WATER
NT POTABLE WATER
NT SEA WATER
NT SHALLOW WATER
NT SPRINGS (WATER)
NT SURFACE WATER
NT WASTE WATER
Atomic and molecular data for H2O, CO and CO2 relevant to edge plasma impurities
[DE93-771423] 01 p0387 N94-10662
Experimental study of multiple droplet evaporative cooling
[PB93-198463] 01 p0149 N94-10851
Structural development in ceramic precursor sols and gels
[AD-A264354] 01 p0090 N94-11281
An observational search for CO2 ice clouds on Mars 01 p0441 N94-12054
Noble gas evidence of an aqueous reservoir near the surface of Mars more recently than 1.3 Ga 01 p0473 N94-12228
Primitive SNC parent magmas and crystallization: Low PH2O experiments 01 p0433 N94-12264
Space Life Support Engineering Program
[NASA-CR-193474] 01 p0316 N94-12365
Physiological water model development 01 p0316 N94-12367
Fundamental studies of radar scattering from water surfaces: The Lake Washington experiment
[NASA-CR-194030] 01 p0139 N94-12778
Alternate cleaning methods for LCCAs
[KCP-613-5045] 02 p0624 N94-13937
Widebody cabin water spray optimization tests
[DOT/FAA/CT-TN93/29] 02 p0511 N94-14186
Room temperature degradation of YBa2Cu3O(7-x) superconductors in varying relative humidity environments
[NASA-TP-3368] 02 p0813 N94-14409
Modeling surface area to volume effects on borosilicate glass dissolution
[DE93-011891] 02 p0581 N94-14432
Moisture meter evaluation
[DE93-016581] 02 p0652 N94-14534

STS-29 crew bailout in WETF
[NASA-TM-109548] 03 p1136 N94-15385
Study of protein-H2O interactions by multidimensional NMR spectroscopy
[AD-A266955] 03 p0946 N94-15760
Global Energy and Water Cycle Experiment (GEWEX) and the Continental-scale International Project (GCIP) 03 p0994 N94-15918
Laser-liquid interactions under reduced gravity conditions 03 p0977 N94-16077
Contained liquids in microgravity, part 2 03 p0979 N94-16085
A mineralized zone in Western Candor Chasma, Mars 03 p1248 N94-16179
Evolutionary implications of a steady-state water abundance on Venus 03 p1254 N94-16206
Experimental constraints on CO2 and H2O in the Martian mantle and primary magmas 03 p1262 N94-16248
Catalytic crystallization of ices by small silicate smokes at temperatures less than 20K 03 p1219 N94-16420
Water adsorption on diamond (110) studied by multiple internal reflection infrared spectroscopy
[AD-A266415] 03 p0948 N94-16553
Optical properties of water released in low Earth orbit
[AD-A266197] 03 p1192 N94-16936
Natural convection above a horizontal heat source
[AD-A267212] 03 p1026 N94-16985
Numerical modelling of an active direct nonpotable hot water heating system making use of the energy of solar radiation
[IFTR-38/1991] 03 p1093 N94-17070
The standardized precipitation index and its use in the western contiguous United States
[AD-A267547] 03 p1107 N94-17102
Strategy for the reduction of total integrated fluid logistics to the Space Station Freedom
[NASA-TM-107744] 03 p1138 N94-17452
Continuum solvent models for computational chemistry
[DE93-016329] 03 p0953 N94-17660
Aluminum powder/water reaction ignited by electrical pulsed power
[AD-A269223] 04 p1376 N94-17840
Search for lunar water ice in cometary impact craters
[AD-A270130] 04 p1627 N94-18877
Calculation of molecular excitation rates
[NASA-CR-193782] 04 p1571 N94-19236
Encounters of H and D atoms with O2 in water: Relative diffusion and reaction rates
[DE93-018587] 05 p1970 N94-19956
Thermal behavior of natural zeolites
[DE93-040091] 05 p1699 N94-19975
Monopropellant aqueous hydroxyl ammonium nitrate/fuel
[AD-D015922] 05 p1712 N94-20061
Atmospheric moisture collection device
[AD-D015935] 05 p1865 N94-20332
Hydrological consequences of ponded water on Mars 05 p2089 N94-20383
The fate of water deposited in the low-lying northern plains 05 p2089 N94-20387
Application of the reactive flux formalism to study water hydrogen bond dynamics
[AD-A271824] 05 p1680 N94-20560
Derivation of the midinfrared (5.0-25.0 micron) optical constants of hydrous carbonate and sulfate 05 p2106 N94-20723
High D/H ratios of water in magmatic amphiboles in Chassigny: Possible constraints on the isotopic composition of magmatic water on Mars 05 p2134 N94-20862
Evaluation of pre-extraction analytical holding times for nitroaromatic and nitramine explosives in water
[AD-A271547] 05 p1712 N94-20927
The hydrologic response of Mars to the onset of a colder climate and to the thermal evolution of its early crust 05 p2143 N94-21666
The early Martian environment: Clues from the cratered highlands and the Precambrian Earth 05 p2143 N94-21667
Core formation, wet early mantle, and H2O degassing on early Mars 05 p2145 N94-21674
Wet inside and out? Constraints on water in the Martian mantle and on outgassed water, based on melt inclusions in SNC meteorites 05 p2145 N94-21678
Modeling of outgassing and matrix decomposition in carbon-phenolic composites
[NASA-CR-194741] 05 p1676 N94-21743
Plasma-chemical conversion of hydrogen sulfide into hydrogen and sulfur
[DE93-041167] 05 p1682 N94-21789
Aircraft cabin water spray disbenefits study
[NASA-CR-194750] 05 p1642 N94-21818
Water-enhanced solvation of organics
[DE93-040297] 05 p1683 N94-21947
Analysis of Alloy 600 and X-750 stress corrosion cracks
[DE94-001578] 06 p2238 N94-22936
Recent advances in SPE (tm) water electrolyzer 06 p2393 N94-23362
Extinguishment of enclosed gas fires with water sprays
[PB93-201663] 06 p2268 N94-23430
Extinguishment of combustible porous solids by water droplets
[PB93-198893] 06 p2270 N94-23740
GEWEX Continental-scale International Project (GCIP) 06 p2411 N94-24376
Water cycle research associated with the CaPE hydrometeorology project (CHymP 06 p2416 N94-24414
Impact of the CO2 and H2O clouds of the Martian polar hood on the polar energy balance 06 p2618 N94-24880
Vertical transport of water in the Martian boundary layer 06 p2622 N94-24902
Examination of the physical, electrical, and microwave evolution of water into young sea ice
[AD-A273559] 06 p2418 N94-24918
Catalog of absolutely calibrated, range normalized, wideband, electric field waveforms from triggered lightning flashes in Florida
[AD-A273793] 07 p2892 N94-25873
Macrobenthic fauna in the dutch sector of the north sea in 1991
[PB94-126414] 07 p2868 N94-27200
Why is the north polar cap on Mars different than the south polar cap? 07 p3107 N94-27889
Speciation in Water and Soil: A literature review
[PB94-132388] 08 p3341 N94-28412
Aeromedical support for casualties in extremely hot climates 08 p3382 N94-28443
Development of novel switchable protein surfaces
[AD-A275510] 08 p3384 N94-28667
Nominally two-dimensional flow about a normal flat plate 08 p3275 N94-29838
Wave generation by contaminant ions near a large spacecraft
[NASA-CR-195797] 08 p3169 N94-29917
Fatigue of carbon and low-alloy steels in LWR environments
[DE94-005116] 08 p3207 N94-30021
Regenerating using aqueous cleaners with ozone and electrolysis 08 p3240 N94-30468
Interaction of water with metal surfaces
[AD-A276260] 09 p3632 N94-31293
Development of a catalytic system for gasification of wet biomass
[DE94-006216] 09 p3759 N94-31762
Glutinous water: Protecting vertical and overhead surfaces from fire spread
[AD-A277280] 09 p3575 N94-32405
Surface probes of porous toluene/water ices: Adsorption kinetics and annealing spectra measured by second harmonic generation
[DE94-007564] 09 p3637 N94-32743
Simulation of a precipitation event in the western United States
[DE94-004835] 09 p3786 N94-32791
Thermal and hydraulic considerations regarding the fate of water discharged by the outflow channels to the Martian northern plains 09 p3946 N94-33202
Geologic controls of erosion and sedimentation on Mars 09 p3951 N94-33232
Simultaneous laboratory measurements of CO2 and H2O adsorption on palagonite: Implications for the Martian climate and volatile reservoir 09 p3952 N94-33240
Effects of elevated atmospheric CO2 concentrations and water stress on field-grown maize
[DE94-009636] 10 p4082 N94-33915
Coal-water slurry spray characteristics of an electronically-controlled accumulator fuel injection system
[DE94-008977] 10 p4060 N94-33946
Synchronized droplet size measurements for Coal-Water-Slurry (CWS) diesel sprays of an electronically-controlled fuel injection system
[DE94-008978] 10 p4061 N94-34017
Coupled ice-ocean model supporting winter navigation in the Baltic Sea. Part 1: Ice dynamics and water levels
[PB94-148780] 10 p4092 N94-34121
Application of programmable logic controller to pump regulation system for supplying water 10 p4067 N94-34344
The effects of cold exposure on wet aircraft passengers: A review
[AD-280253] 10 p4100 N94-34389
Fluvial processes in Ma'adim Vallis and the potential of Gusev crater as a high priority site 11 p4358 N94-35414
A quick look method of detecting water of hydration in small solar system bodies 11 p4352 N94-35470
Role of magma-water interaction in very large explosive eruptions
[DE94-002698] 11 p4291 N94-36103
The structural changes of water ice I during warmup 11 p4239 N94-36144
Uniqueness of a solution of a steady state photochemical problem: Applications to Mars 11 p4370 N94-36151
Equations of state valid continuously from zero to extreme pressures with H2O and CO2 as examples
[DE94-011907] 11 p4238 N94-36230
Coal-fueled diesels for modular power generation
[DE94-002960] 11 p4275 N94-36348
United States Air Force Summer Research Program, 1993. Volume 16: Arnold Engineering Development Center, Frank J. Seiler Research Laboratory and Wilford Hall Medical Center
[AD-A278658] 12 p4550 N94-36978
Investigation of ultrasonic surface wave interaction with porous saturated rocks
[DE94-013378] 12 p4469 N94-37177

WATER BALANCE

Flood monitoring in northern part of Central Java by remote sensing technique. Case study: The flooding of Semarang in January, 1990 01 p0206 N94-11989
Research into the influence of spatial variability and scale on the parameterization of hydrological processes
[NASA-CR-194610] 03 p1082 N94-16026
Evapotranspiration and runoff from large land areas: Land surface hydrology for atmospheric general circulation models 03 p1083 N94-16029
Heterogeneity and scaling land-atmospheric water and energy fluxes in climate systems 03 p1083 N94-16030
Evaluation of a distributed catchment scale water balance model
[PAPER-93WR00398] 03 p1083 N94-16031
A detailed model for simulation of catchment scale subsurface hydrologic processes
[PAPER-92WR02333] 03 p1084 N94-16032
Effects of spatial variability and scale on areal -average evapotranspiration 03 p1084 N94-16033
Scaling, soil moisture and evapotranspiration in runoff models 03 p1084 N94-16034
An investigation of current and future satellite and in-situ data for the remote sensing of the land surface energy balance
[NASA-CR-195138] 06 p2387 N94-24596
Role of remote sensing in energy, water, and carbon cycle studies over the Amazon
[INPE-5486-PRE/1786] 07 p2852 N94-27957

WATER CIRCULATION

NT COASTAL CURRENTS
NT EL NINO
NT GULF STREAM
NT OCEAN CURRENTS
NT WATER CURRENTS
Meridional circulation in the tropical north atlantic
[AD-A268222] 03 p1114 N94-17555
Ecological and environmental impacts of construction in the coastal zone
[AD-A269196] 04 p1475 N94-18881
Recent developments in the mathematical modelling and physical understanding of transport and dispersion in aquatic systems, with special reference to tidal waters
[PB94-111135] 06 p2418 N94-24600

WATER COLOR

Atmospheric correction of AVIRIS data in ocean waters
[AD-A264931] 01 p0288 N94-11287
Effects of wind-roughened sea surface on ocean color remote sensing: Noise derived from reflected light and whitecaps 01 p0191 N94-11898
Satellite-derived oceanic features 01 p0200 N94-11949
Bi-directional reflectance by oceanic waters studied via Monte-Carlo simulations 01 p0203 N94-11971
Optical characteristics in Tokyo Bay 01 p0204 N94-11972
Remote sensing for numerical modelling of radiative transfer processes in ocean environment 01 p0204 N94-11973
Seasonal variability of surface ocean color in the Omura Bay using multitemporal LANDSAT-5 TM data 01 p0218 N94-12698
Coastal zone color scanner: Nimbus 7
[NASA-TM-109590] 03 p1111 N94-15281
SeaWiFS technical report series. Volume 12, SeaWIFS technical report series cumulative index: Volumes 1-11
[NASA-TM-104566-VOL-12] 03 p1111 N94-15529
Optical properties of the Red Sea
[AD-A266466] 03 p1113 N94-16588
Optical climatology of the Northeast Pacific Ocean
[AD-A271671] 05 p1866 N94-20559

Algorithm-development activities
[NASA-CR-193225] 06 p2420 N94-23538
Factors affecting the identification of phytoplankton groups by means of remote sensing
[NASA-TM-108799] 06 p2387 N94-24403
Development of a multi-sensor in situ fiber optic fluorometer
[DE94-003399] 07 p3035 N94-26100
SeaWiFS technical report series. Volume 17: Ocean color in the 21st century. A strategy for a 20-year time series
[NASA-TM-104566-VOL-17] 10 p4093 N94-34209
Mission to Planet Earth. The living ocean: Observing ocean color from space
[NASA-PAM-554] 11 p4295 N94-35343

WATER CONSUMPTION
Optimization of two-stage hot water exchange points 03 p1029 N94-17440
Effect of carbon dioxide enrichment on radish production using Nutrient Film Technique (NFT)
[NASA-TM-107198] 07 p2902 N94-27411
Nutrition and hydration status of aircrew members consuming an improved survival ration during a simulated survival scenario 08 p3380 N94-28429

WATER CONTENT
U MOISTURE CONTENT

WATER COOLED REACTORS
NT HEAVY WATER REACTORS
NT LIGHT WATER REACTORS
NT PRESSURIZED WATER REACTORS
Facility for stress corrosion cracking test of irradiated material in high temperature water
[DE93-753189] 01 p0084 N94-11593
Test apparatus for ITER blanket cooling water distribution design
[DE93-753157] 02 p0795 N94-12944
Nuclear thermal propulsion engine based on particle bed reactor using light water steam as a propellant
[DE93-014336] 02 p0552 N94-14111

WATER COOLING
U LIQUID COOLING

WATER CURRENTS
NT COASTAL CURRENTS
NT EL NINO
NT GULF STREAM
NT OCEAN CURRENTS
Sandia ocean modeling system programmer's guide and user's manual
[DE93-007427] 01 p0287 N94-10153
Overview of physical oceanographic measurements taken during the Mount Mitchell cruise to ROPME sea area
[DE93-018460] 04 p1497 N94-18494
Method for extracting tidal and inertial motion from ARGOS ice buoys applied to the Barents Sea during CEAREX
[PB93-190213] 04 p1499 N94-19063
Time domain calculations of the second-order drift force on a floating two-dimensional object in current and waves
[REPT-93-13] 04 p1419 N94-19087
Development and application of a thermistor current meter
[AD-A275816] 08 p3286 N94-28831
Development of a simple current meter using solution 08 p3233 N94-29702
ADCIRC: An advanced three-dimensional circulation model for shelves, coasts, and estuaries. User's manual for ADCIRC-2DDI
[AD-A276150] 09 p3787 N94-31250
Characterization of tidal currents in Monterey Bay from remote and in-situ measurements
[AD-A277844] 10 p4092 N94-33767

WATER CYCLE (HYDROLOGY)
U HYDROLOGICAL CYCLE

WATER DEPRIVATION
Soil erosion rates caused by wind and saltating sand stresses in a wind tunnel
[DE93-009154] 02 p0706 N94-12905

WATER DEPTH
The extraction of bottom characteristics and mapping in Kin Bay, Okinawa Main Island, Japan, using LANDSAT-5/TM and SPOT-1/HRV data 01 p0197 N94-11931
Water-levels fluctuations in a borehole at the Royal Observatory of Belgium: Effects on local gravity, Earth tidal, and barometric responses 03 p1100 N94-15812
A laboratory model of a cooled continental shelf
[AD-A270862] 04 p1500 N94-19792
Distribution of turbidity in Australian tropical waters
[AD-A271059] 05 p1881 N94-19905
A marine sedimentary model for the evolution of the northern plains 05 p2091 N94-20395
Discharge rates in Ma'adim Vallis, Mars 05 p2128 N94-20830
Green Sheet project: Dye sheet evolution
[AD-A272019] 05 p1883 N94-21443
Scanview: A grafical program for analysis of laserbathymetry data
[PB94-124443] 07 p2900 N94-27208
Tidal atlas software development
[AD-A275251] 08 p3377 N94-29432
Storm evolution of directional seas in shallow water
[AD-A278541] 10 p4089 N94-33404
A geoacoustic model for fine-grained, unconsolidated calcareous sediments (ARSRP natural laboratory)
[AD-A277830] 10 p4092 N94-33831

WATER EROSION
Rates of fluvio-thermal erosion on Mars 01 p0435 N94-12018
Coastal scour problems and methods for prediction of maximum scour
[AD-A266658] 02 p0726 N94-14775
Sedimentation, volcanism, and ancestral lakes in the Valles Marineris: Clues from topography 03 p1283 N94-16369
Early Mars was wet but not warm: Erosion, fluvial features, liquid water habitats, and life below freezing 05 p2145 N94-21677
Fluvial processes in Ma'adim Vallis and the potential of Gusev crater as a high priority site 11 p4358 N94-35414

WATER FLOW
The flow structure around a cylindrical pier for the flow of transcritical Reynolds number 01 p0169 N94-11944
Rates of fluvio-thermal erosion on Mars 01 p0435 N94-12018
Rainfall-runoff estimation using digital radar
[AD-A265390] 01 p0286 N94-12408
Simultaneous 3D turbulent large-scale structures in a flood flow by multi-channels measuring system 01 p0165 N94-12624
Turbulence generation in the Pacific undercurrent by shear 01 p0223 N94-12730
Boundary layer flow of air over water on a flat plate
[NASA-CR-191517] 03 p1019 N94-15479
A detailed model for simulation of catchment scale subsurface hydrologic processes
[PAPER-92WR02333] 03 p1084 N94-16032
Preliminary design of a water cooled avionics cooling rack
[AD-A268826] 04 p1320 N94-18536
Ancient Martian valley genesis and paleoclimatic inference: The present as a key to the past 05 p2142 N94-21661
Performance of prefabricated geocomposite subdrainage system in an airport runway
[DOT/FAA/RD-93/23] 06 p2192 N94-23303
Transient studies of capillary-induced flow 06 p2325 N94-23662
A study on structure of benthic boundary layer in coastal waters
[REPT-4] 07 p2898 N94-25635
Calibrating/testing meters in hot water test bench VM7
[PB94-124294] 07 p2812 N94-27160
An experimental study of siphonal jets in a turbulent boundary layer crossflow 07 p2802 N94-28015
Papers in meteorology and geophysics, vol. 44, no.1
[JTN-94-80585] 08 p3324 N94-28693
The Japan Sea proper water and water circulation in the Japan Sea 08 p3324 N94-28694
Development and application of a thermistor current meter
[AD-A275816] 08 p3286 N94-28831
Fronts at the confluences of spring-fed streams with Joekulsa a Fjoellum: Possibly thermal bars?
[MATHS-REPT-A-198] 08 p3333 N94-29528
Development of a simple current meter using solution 08 p3233 N94-29702
The flow field near the body surface with thin filaments 08 p3234 N94-29706
Visualization of secondary flow development in high aspect ratio channels with curvature
[NASA-TM-106658] 10 p4046 N94-33941
Numerical simulation of nocturnal drainage flows in an idealized valley-tributary system
[DE94-011684] 12 p4472 N94-37115

WATER HAMMER
Examinations of the friction behavior in nonstationary flow processes in pipes
[MITT-7] 04 p1423 N94-19730
Fluid-structure interaction in case of water hammer with cavitation
[PB94-148277] 09 p3702 N94-31588

WATER HEATING
Department of Energy solar process heat program: FY 1991 solar process heat prefeasibility studies activity
[DE93-010010] 01 p0262 N94-10258
Development of a nonazeotropic heat pump for crew hygiene water heating
[NASA-CR-194189] 02 p0737 N94-13674
Colorado State University program for developing, testing, evaluating, and optimizing solar heating and cooling systems
[DE93-016018] 02 p0705 N94-14504
Promotion of geothermal energy development in 1991
[DE93-799061] 02 p0705 N94-14679
Numerical modelling of an active direct nonpotable hot water heating system making use of the energy of solar radiation
[IFTR-38/1991] 03 p1093 N94-17070
Optimization of two-stage hot water exchange points 03 p1029 N94-17440

WATER IMMERSION
Development and analysis of insulation constructions for aerospace wiring applications 01 p0021 N94-10791
Investigation of cracking and erratic behavior of the uranium-titanium alloy
[DE93-018591] 05 p1688 N94-19957
Transient studies of capillary-induced flow 06 p2325 N94-23662
Plasma volume shifts and exercise thermoregulation with water immersion and six-degree head-down tilt
[NASA-TM-108781] 07 p2901 N94-26093
Changes in fluid and electrolyte metabolism during water immersion at high or thermoneutral temperature 07 p2912 N94-27445
Cardiovascular function during thermoneutral head-out water immersion in the elderly 07 p2915 N94-27458
Effects of 40 C hot water immersion for an hour on thermoregulatory functions in humans: Comparison with 34 C thermoneutral immersion 07 p2915 N94-27459
Effects of bathing at 40 C on cardiovascular system in humans: Comparison with 34 C thermoneutral bathing 07 p2918 N94-27473
Effects of 41 C bathing for 20 minutes on cardiovascular and thermoregulatory functions in humans 07 p2918 N94-27474
Fuelling shivering in humans during cold water immersion 08 p3379 N94-28426
Advanced integrated cold protection for aircrew 08 p3381 N94-28436
Emergency underwater breathing aids for helicopter passengers and crew 08 p3381 N94-28437
A comparison of four methods of rewarming individuals cooled by immersion in cold water 08 p3382 N94-28442
Validation and sensitivity analysis of Texas human thermal model predictions during cold water immersion
[AD-A275240] 09 p3797 N94-32156
A model for predicting central nervous system toxicity from hyperbaric oxygen exposure in man: Effects of immersion, exercise, and old and new data
[AD-A278348] 10 p4095 N94-34005
Evaluation of flame-sprayed polymer coatings for civil works navigation structures
[AD-A280507] 12 p4422 N94-37104

WATER INJECTION
Analysis of gas turbine engines using water and oxygen injection to achieve high Mach numbers and high thrust
[NASA-TM-106270] 02 p0518 N94-13143
BOAST 2 for the IBM 3090 and RISC 6000
[DE93-000138] 02 p0638 N94-14351
Thrust expansion engine
[AD-D015896] 05 p1669 N94-20121
Thrust augmentation options for the Beta 2 two-stage-to-orbit vehicle
[NASA-TM-106448] 05 p1648 N94-21563
Options for thrust augmentation for the Beta 2 two-stage-to-orbit launch vehicle
[NASA-TM-106418] 05 p1649 N94-21759
Performance calculations and research direction for a water enhanced regenerative gas turbine cycle
[DE93-019866] 05 p1826 N94-21983

WATER JETS
U HYDRAULIC JETS

WATER LANDING
NT DITCHING (LANDING)
STS-32 bailout training in WETF
[NASA-TM-109476] 03 p1136 N94-15383

WATER LOSS
Modifications to an interactive model of the human body during exercise: With special emphasis on thermoregulation 01 p0317 N94-12368

WATER MANAGEMENT
Space Activities in the Asia Pacific Region
[JTN-93-80421] 01 p0035 N94-10676
International Space Year in China 01 p0036 N94-10680
An algorithm for the detection of mucilage (green slime) in the Adriatic Sea 01 p0191 N94-11900
High power density proton exchange membrane fuel cells 06 p2393 N94-23359

Remote sensing and GIS for the management and investigation of the Wadden Sea
[BCRS-92-20] 07 p2847 N94-26228
Bulletin of National Research Institute of Fisheries Engineering, No. 13
[JTN-94-80596] 08 p3233 N94-29701
Development of the breakwater with submerged mound for interchanging sea water 08 p3234 N94-29703
Characterization of spacecraft humidity condensate 10 p4102 N94-33659

WATER MASERS
Finnish astronomy days, 1992-1993. Proceedings of the Finnish Astronomical Society
[PB94-136892] 08 p3538 N94-29170

WATER MODERATED REACTORS
MCNP benchmark analyses of critical experiments for the Space Nuclear Thermal Propulsion program
[DE93-014046] 02 p0548 N94-12981

WATER POLLUTION
NT OIL POLLUTION
Immediate response to free product discovery
[PB93-182970] 01 p0265 N94-11015
Gulf of Mexico sales 147 and 150: Central and western planning areas. Draft environmental impact statement. Volume 1: Sections 1 through 4.C
[PB93-190304] 01 p0265 N94-11018
Gulf of Mexico sales 147 and 150: Central and western planning areas. Draft environmental impact statement. Volume 2: Sections 4.D through 9
[PB93-190312] 01 p0265 N94-11019
Biscayne bay: A bibliography of the marine environment
[PB93-184802] 01 p0266 N94-11451
An algorithm for the detection of mucilage (green slime) in the Adriatic Sea 01 p0191 N94-11900
A study of pollution courses of spilled oil floatation in the outer ocean 01 p0205 N94-11983
Remote sensing of polluting focal points and coastal disturbances in the Gulf of Arauco and adjacent bays, central Chile 01 p0217 N94-12695
Laser fluorescent monitoring of dissolved organic matter in natural water 01 p0177 N94-12755
Study of the admixture diffusion in the sea using remote techniques 01 p0228 N94-12759
Laser-induced fluorescence over optical fibers for real time in situ measurement of petroleum hydrocarbons in seawater
[AD-A265106] 02 p0790 N94-12863
Ecological and environmental impacts of construction in the coastal zone
[AD-A269196] 04 p1475 N94-18881
Manual of DRANC (release 1.1): A computer program for the Dutch risk assessment of new chemical substances
[PB93-194827] 05 p1851 N94-19998
Chemical characterization of some aerobic liquids in CELSS 06 p2422 N94-23241
Exploratory report nickel and nickel compounds
[PB93-223998] 06 p2242 N94-23496
Exploratory report antimony and antimony compounds
[PB93-224004] 06 p2397 N94-23497
Selfsimilar solutions of a nonlinear transport equation
[REPT-93-42] 07 p2865 N94-25760
Recent legal movement on water quality regulation in Japan 07 p2869 N94-28148
Determination of lead isotope ratios in seawater by purge and trap GC/MS after ethylation 07 p2870 N94-28152
Indian activities on the core programme IGAP and proposals for network activities 07 p2874 N94-28284
Changes in phytoplankton population in the Chao Phraya estuary, Thailand, during the eutrophication mechanisms studies 07 p2875 N94-28287
Focused feasibility study final field sampling plan
[AD-A277445] 09 p3769 N94-33105
Transnational environmental degradation
[AD-A278469] 10 p4080 N94-33546

WATER PRESSURE
Application of programmable logic controller to pump regulation system for supplying water 10 p4067 N94-34344

WATER PURIFICATION
U WATER TREATMENT

WATER QUALITY
Summary of implementation and demonstration projects in bays and estuaries
[PB93-194637] 01 p0265 N94-10846
Remote surface water monitoring radio based telemetry system
[DE93-009643] 01 p0041 N94-11282
Optical characteristics in Tokyo Bay 01 p0204 N94-11972
Snow cover models in operational watershed forecasting
[DE93-778332] 02 p0718 N94-12837
Activities report of the Netherlands Remote Sensing Board
[ETN-93-93880] 02 p0686 N94-14073
Educational module for the Higher Agricultural Education. Part 2: Eutrophication observed by remote sensing: An educational approach to water quality monitoring
[BCRS-92-11B] 02 p0818 N94-14462
Multiple dataset water-quality analyses in the vicinity of an ocean wastewater plume 03 p1069 N94-16687
A Geographic Information System approach to modeling nutrient and sediment transport
[DE93-013747] 03 p1097 N94-17426
Chromaticity analysis of LANDSAT multispectral scanner and thematic mapper imagery of Chilko Lake, British Columbia, using a theoretical optical water quality model
[ISBN-0-315-63832-X] 05 p1843 N94-22422
Statistical procedures for corrosion studies
[PB93-199412] 06 p2244 N94-23802
A chemical sensor and biosensor based totally automated water quality monitor for extended space flight: Step 1 06 p2443 N94-24447
Journal of NIRE, volume 2, number 4
[JTN-94-80554] 07 p2869 N94-28147
Recent legal movement on water quality regulation in Japan 07 p2869 N94-28148
Changes in phytoplankton population in the Chao Phraya estuary, Thailand, during the eutrophication mechanisms studies 07 p2875 N94-28287
Characterization of spacecraft humidity condensate 10 p4102 N94-33659
Computation of iodine species concentrations in water 10 p4102 N94-33660
Determination of copper in tap water using solid-phase spectrophotometry
[NASA-TM-106480] 12 p4408 N94-36537

WATER RECLAMATION
Microbiological test results using three urine pretreatment regimes with 316L stainless steel
[NASA-CR-192568] 01 p0299 N94-10360
Systems analysis of a closed loop ECLSS using the ASPEN simulation tool. Thermodynamic efficiency analysis of ECLSS components 01 p0316 N94-12366
Evaluation for membrane components of water recycling system
[NAL-TM-646] 02 p0737 N94-13388
An improved plating process 08 p3223 N94-30451
Catalytic methods using molecular oxygen for treatment of PMMS and ECLSS waste streams, volume 2
[NASA-CR-190299] 09 p3804 N94-32697
Characterization of spacecraft humidity condensate 10 p4102 N94-33659
Computation of iodine species concentrations in water 10 p4102 N94-33660

WATER RECOVERY
U WATER RECLAMATION

WATER RESOURCES
NT AQUIFERS
Land use/land cover mapping of central water shed of Iran area based on satellite data interpretation 01 p0219 N94-12704
Integration opportunities for computer models, methods, and GIS used in Corps planning studies
[AD-A271714] 05 p2044 N94-21354
GEWEX Continental-scale International Project (GCIP) 06 p2411 N94-24376
Snow modeling, water resources, climate change
[PB93-201770] 06 p2399 N94-24633
The HEC NexGen software development project
[AD-A273512] 06 p2460 N94-24822
Fiscal 1991 geothermal development promotion energy
[DE94-732332] 08 p3337 N94-28627
Fiscal 1990 geothermal development promotion survey
[DE94-732333] 08 p3337 N94-28628
Model-oriented data analysis with applications to lake and soil water simulation
[PB94-136942] 08 p3329 N94-29173
Glaciohydrologic and glaciohydraulic effects on runoff and sediment yield in glacierized basins
[AD-A275134] 08 p3361 N94-29286
Possible complementarity of SPOT/ERS in mapping land use: Study on agricultural land in Brittany (France) 09 p3755 N94-32563
Simulation of a precipitation event in the western United States
[DE94-004835] 09 p3786 N94-32791
Food security in the context of global environmental change
[DE94-007481] 09 p3768 N94-32812

WATER RUNOFF
On hydrologic similarity: A dimensionless flood frequency model using a generalized geomorphologic unit hydrograph and partial area runoff generation
[PAPER-89WR01579] 03 p1083 N94-16027
Similarity and scale in catchment storm response
[PAPER-89RG01615] 03 p1083 N94-16028
Evapotranspiration and runoff from large land areas: Land surface hydrology for atmospheric general circulation models 03 p1083 N94-16029
Scaling, soil moisture and evapotranspiration in runoff models 03 p1084 N94-16034
Glaciohydrologic and glaciohydraulic effects on runoff and sediment yield in glacierized basins
[AD-A275134] 08 p3361 N94-29286

WATER SPLITTING
Scenarios for multi-unit inertial fusion energy plants producing hydrogen fuel
[DE94-006614] 09 p3666 N94-32114
Multi-unit Inertial Fusion Energy (IFE) plants producing hydrogen fuel
[DE94-007241] 10 p4079 N94-34088

WATER TABLES
Water-levels fluctuations in a borehole at the Royal Observatory of Belgium: Effects on local gravity, Earth tidal, and barometric responses 03 p1100 N94-15812
Evaluation of a distributed catchment scale water balance model
[PAPER-93WR00398] 03 p1083 N94-16031
Application of ARC/INFO to regional scale hydrogeologic modeling
[DE93-015673] 04 p1461 N94-18107
Similarity solutions for gravity-dominated spreading of a lens of organic contaminant
[REPT-93-24] 04 p1420 N94-19139

WATER TEMPERATURE
NT OCEAN TEMPERATURE
NT SEA SURFACE TEMPERATURE
Temperature measurements 03 p1037 N94-15804
Efficacy of flocculating and other emergency water purification tablets
[AD-A266695] 03 p1148 N94-15840
Optimization of two-stage hot water exchange points 03 p1029 N94-17440
Early Mars was wet but not warm: Erosion, fluvial features, liquid water habitats, and life below freezing 05 p2145 N94-21677
Effectiveness of protection clothing for cold weather conditions after ejection over sea: A case report 08 p3381 N94-28435

WATER TREATMENT
Space Life Support Engineering Program
[NASA-CR-193474] 01 p0316 N94-12365
Photocatalysis for the treatment of waste water: Applications involving the removal of metals
[DE93-011669] 02 p0561 N94-12841
Evaluation for membrane components of water recycling system
[NAL-TM-646] 02 p0737 N94-13388
Survey and study on Environmental Control and Life Support (ECLS) technologies, part 2
[NASDA-CNT-930012-PT-2] 02 p0737 N94-13472
Plant research
[NASA-TM-109664] 03 p1116 N94-15235
Efficacy of flocculating and other emergency water purification tablets
[AD-A266695] 03 p1148 N94-15840
Manual of DRANC (release 1.1): A computer program for the Dutch risk assessment of new chemical substances
[PB93-194827] 05 p1851 N94-19998
Plasma-chemical conversion of hydrogen sulfide into hydrogen and sulfur
[DE93-041167] 05 p1682 N94-21789
Statistical procedures for corrosion studies
[PB93-199412] 06 p2244 N94-23802
A new material for removing heavy metals from water 08 p3354 N94-30471
Catalytic methods using molecular oxygen for treatment of PMMS and ECLSS waste streams, volume 2
[NASA-CR-190299] 09 p3804 N94-32697
Bibliography of work on the photocatalytic removal of hazardous compounds from water and air
[DE94-006906] 12 p4467 N94-37405

WATER TUNNEL TESTS
Unsteady flow past a NACA 0012 airfoil pitching at constant rates
[AD-A265159] 01 p0016 N94-11889
Some flow properties of telescope enclosures estimated from water channel tests: Application of the flow visualization techniques
[NAL-TR-1178T] 02 p0830 N94-13452
Aerodynamic control of NASP-type vehicles through Vortex manipulation. Volume 1: Static water tunnel tests
[NASA-CR-177626-VOL-1] 03 p0855 N94-15655

Aerodynamic control of NASP-type vehicles through vortex manipulation. Volume 3: Wing rock experiments
[NASA-CR-177626] 03 p0857 N94-15780
The effect of fine surface riblets on the flow around an inclined axially symmetrical body
[MPIS-105/1993] 04 p1420 N94-19356
Experimental data for CFD validation of impinging jets in crossflow with application to ASTOVL flow problems 07 p2801 N94-28010
Topological structure of a jet in a cross flow 07 p2801 N94-28014
Low-speed longitudinal aerodynamic characteristics of a flat-plate planform model of an advanced fighter configuration
[NASA-TM-109045] 08 p3130 N94-29443
Effect of initial acceleration on the development of the flow field of an airfoil pitching at constant rate 10 p3987 N94-34989

WATER VAPOR
The impact of horizontal resolution on moist processes in the ECMWF model
[DE93-011718] 01 p0276 N94-11227
Central Equatorial Pacific Experiment (CEPEX)
[DE93-011656] 01 p0190 N94-11674
Evaporation and thermal/hydrologic balance in the Pacific 01 p0195 N94-11919
Evaluation of ECMWF latent heat flux in TOGA CD-ROM 01 p0195 N94-11921
Validation of the ATSR/M microwave radiometer data 01 p0252 N94-12511
Multichannel dual angle approach for sea surface temperature retrieval in context of ERS-1 scenario 01 p0252 N94-12512
Analytical method for water vapor collection and analysis in aircraft cabin fires
[DOT/FAA/CT-TN93/33] 01 p0022 N94-12575
Worldwide map of rainfall amount over the ocean derived from passive microwave radiometer 01 p0211 N94-12663
Cloud liquid water content over the Pacific Ocean tropical zone derived from ship microwave radiometric measurement 01 p0225 N94-12743
A parameterization of cloud droplet nucleation
[DE93-007998] 02 p0718 N94-12903
DMSP F11 SSM/T-2 calibration and validation
[AD-A265817] 02 p0719 N94-12978
Binary homogeneous nucleation: Temperature and relative humidity fluctuations and non-linearity
[DE93-007884] 02 p0709 N94-13911
Water-vapour, total water and rainrate from passive microwave satellite data over ocean
[DLR-FB-92-37] 02 p0723 N94-14189
The development and implementation of an interactive retrieval/analysis/forecast algorithm 02 p0692 N94-14234
Atmospheric correction for sea surface temperature by application of microwave dual-channel technique to VTIR data 02 p0697 N94-14271
Corrosion kinetics and mechanisms for nuclear grade graphites
[DE93-015462] 03 p0947 N94-16105
Trapping of water vapor from an atmosphere by condensed silicate matter formed by high-temperature pulse vaporization 03 p1248 N94-16180
Possible sources of H2 to H2O enrichment at evaporation of parent chondritic material 03 p1244 N94-16377
A linear spectral matching technique for retrieving equivalent water thickness and biochemical constituents of green vegetation 03 p1068 N94-16678
Separation of cirrus cloud from clear surface from AVIRIS data using the 1.38 micron water vapor band 03 p1072 N94-16699
Discussion of band selection and methodologies for the estimation of precipitable water vapour from AVIRIS data 03 p1074 N94-16707
Empirical relationships among atmospheric variables from rawinsonde and field data as surrogates for AVIRIS measurements: Estimation of regional land surface evapotranspiration 03 p1074 N94-16712
Optical properties of water released in low Earth orbit
[AD-A266197] 03 p1192 N94-16936
Atmospheric propagation analysis program
[AD-A268231] 03 p1006 N94-17565
An analysis of simulated and actual DMSP SSM/T-2 brightness temperatures
[AD-A268103] 03 p1109 N94-17573
An empirical study of tropical cloud clusters using special sensor microwave imager data
[AD-A268072] 03 p1110 N94-17595
Surface fluxes important to cloud development
[DE93-016633] 04 p1488 N94-17715
A mobile remote sensing laboratory for water vapor, trace gas, aerosol, and wind speed measurements
[DE93-017158] 04 p1489 N94-18132
Analysis of satellite-derived ozone and water vapor measurements
[NASA-CR-193810] 04 p1486 N94-19237
Thermal behavior of natural zeolites
[DE93-040091] 05 p1699 N94-19975
Predicting lightning events in the KSC area: A feasibility study using single station data
[AD-A271440] 05 p1864 N94-20088
On demand, non-halon, fire extinguishing systems
[AD-D015957] 05 p1714 N94-20355
Diffusive redistribution of water vapor in the solar nebula revisited 05 p2113 N94-20751
Discovery Venera surface: Atmosphere geochemistry experiments mission concept 05 p2123 N94-20806
Analysis of the GOES 6.7 micrometer channel observations during FIRE 2 05 p1875 N94-22316
Analysis of the tropospheric water distribution during FIRE 2 05 p1876 N94-22324
A comparison of small and larger mesoscale latent heat and radiative fluxes: December 6 case study 05 p1879 N94-22335
Studies in remotely sensed geophysical parameter retrieval and analysis
[NASA-CR-193914] 05 p1842 N94-22374
Temperature/pressure and water vapor sounding with microwave spectroscopy 05 p1812 N94-22436
Implementation of a state of the art automated system for the production of cloud/water vapor motion winds from geostationary satellites
[NASA-CR-195087] 06 p2410 N94-24125
GEWEX Water Vapor Project (GVaP) 06 p2411 N94-24378
Water cycle research associated with the CaPE hydrometeorology project (CHymP 06 p2416 N94-24414
Mars Operational Environmental Satellite (MOES): A post-Mars Observer discovery mission 06 p2620 N94-24890
Mars Observer: Applications to atmospheric transport 06 p2623 N94-24904
Control of a hydrogen/oxygen steam generator
[DLR-FB-93-02] 07 p2826 N94-27589
Fire-resistant water vapour permeable buoyant insulation 08 p3380 N94-28431
Low energy ion-molecule reactions and chemiionization kinetics
[DE94-005414] 08 p3481 N94-28491
On the effect of emissions from aircraft engines on the state of the atmosphere 08 p3189 N94-29247
Propagation modeling of moist air and suspended water/ice particles at frequencies below 1000 GHz 08 p3256 N94-30497
Estimation of transmittance from satellite imagery 08 p3257 N94-30500
Atmospheric moisture fields derived by satellite observations over the tropical Pacific Ocean 08 p3375 N94-30863
High resolution properties of the marine atmospheric boundary layer
[DE94-006235] 09 p3774 N94-32736
Water vapor from sunradiometry in comparison with microwave and balloon-sonde measurements at the Southern Great Plains ARM Site
[DE94-007479] 09 p3786 N94-32759
A correlated k-distribution model of the heating rates for atmospheric mixtures of H2O, CO2, O3, CH4, and N2O in the 0-2500 cm(exp -1) wave number region at altitudes between 0 and 60 km
[DE94-005136] 09 p3775 N94-32895
Eddy transport of water vapor in the Martian atmosphere 09 p3949 N94-33221
Non-polluting gas turbine as a result of self-heating working fluid in a closed circuit 10 p4000 N94-34436
Production of long-term global water vapor and liquid water data set using ultra-fast methods to assimilate multi-satellite and radiosonde observations
[NASA-CR-196044] 11 p4292 N94-35355
Simultaneous adsorption of CO2 and H2O under Mars-like conditions and application to the evolution of the Martian climate 11 p4366 N94-35475
Production of long-term global water vapor and liquid water data set using ultra-fast methods to assimilate multi-satellite and radiosonde observations
[NASA-CR-195981] 11 p4293 N94-35499
H2O-H2SO4 system in Venus' clouds and OCS, CO, and H2SO4 profiles in Venus' troposphere 11 p4370 N94-36152
Investigation of moisture-induced embrittlement of iron aluminides
[DE94-010881] 11 p4241 N94-36196
Two-channel microwave radiometer for observations of total column precipitable water vapor and cloud liquid water path
[DE94-007480] 12 p4471 N94-36479
Measurements and modeling of the effect of convective clouds on the upper tropospheric moisture budget
[NASA-TM-109894] 12 p4473 N94-37371
Tropospheric radiative forcing of CH4
[DE94-011628] 12 p4468 N94-37631

WATER VEHICLES
NT AIRCRAFT CARRIERS
NT SHIPS
NT SUBMARINES
NT SURFACE EFFECT SHIPS
NT UNDERWATER RESEARCH LABORATORIES
NT UNDERWATER VEHICLES

WATER WAVES
NT TIDAL WAVES
Preliminary results on backscattering strength from a wind generated bubbly ocean surface
[AD-A265006] 01 p0287 N94-10490
Validation of directional wave spectra from the ERS-1 during the ESA CAL/VAL campaign 01 p0232 N94-11707
The Grand Banks ERS-1 SAR wave spectra validation experiment 01 p0232 N94-11708
Validation of ERS-1 wind and wave data by use of operational forecast models 01 p0233 N94-11710
The activity of the ERS-1 Venice (Italy) group on scatterometry 01 p0233 N94-11713
Waves and mesoscale features in the marginal ice zone 01 p0240 N94-11757
Global wave height climatologies from ERS-1 altimeter data, and comparisons with those from GEOSAT 01 p0244 N94-11781
Spatial scales of wave height 01 p0244 N94-11782
Proceedings of the PORSEC 1992 in Okinawa: Conference for Pacific Ocean Environments and Probing, volume 1
[JTN-93-80418] 01 p0191 N94-11894
Remote sensing and the air-sea boundary layers 01 p0191 N94-11896
HF ocean radar system at Okinawa Radio Observatory 01 p0139 N94-11902
Measurement of wave parameters by HF ocean radar 01 p0192 N94-11903
Statistical study of HF ocean radar echo 01 p0139 N94-11905
Groundwave HF ocean surface radar 01 p0139 N94-11906
A new expression for the production rate of sea water droplets on the sea surface 01 p0195 N94-11920
Air-sea fluxes and universal constants in weak-turbulence theory of surface gravity waves 01 p0195 N94-11922
Ocean wave detection by SAR 01 p0197 N94-11932
On the determination of the SAR ocean surface scattering patch size 01 p0197 N94-11933
The optical/computer hybrid processing of extracting ocean wave directional spectrum by airborne photograph 01 p0197 N94-11934
Ocean-ice interaction study of waves and mesoscale features 01 p0197 N94-11935
Coastal processes due to nearshore current around an upheaving island 01 p0199 N94-11942
Physical processes of microwave backscattering from laboratory wind-wave surfaces 01 p0200 N94-11952
Dependence of oceanic microwave emission on wind direction 01 p0201 N94-11957
Surface roughness variations across the Iceland-Faroes frontal region observed by the GEOSAT altimeter and NOAA AVHRR 01 p0201 N94-11958
The microwave backscattering from wind waves 01 p0201 N94-11959
Observation of wind and waves by GEOSAT altimeter 01 p0202 N94-11961
Impact of ERS-1 wind/wave/ice data on operational ocean forecasting 01 p0250 N94-12500
Real time processing wave spectra from satellite SAR 01 p0251 N94-12506
On the extraction of ocean wave spectra from ERS-1 SAR wave mode image spectra 01 p0251 N94-12509
Tide-generated nonlinear internal wave packets in the Strait of Gibraltar observed by the synthetic aperture radar aboard the ERS-1 satellite 01 p0252 N94-12510
Artificial oil pollution detection and wave observation in the sea adjacent to Japan by ERS-1 SAR 01 p0253 N94-12520
Proceedings of the PORSEC 1992 in Okinawa: Conference for Pacific Ocean Environments and Probing, volume 2
[JTN-93-80419] 01 p0207 N94-12635
Observation of wave crests by satellite remote sensed data 01 p0207 N94-12638
Field research of wind wave spectrum variability 01 p0223 N94-12727

Observations of film slicks and internal waves with Ka-band scatterometer 01 p0225 N94-12741
Wind-wave and foam dynamics from optical and radar airborne observations 01 p0226 N94-12745
Observations of surface signatures in the north-west Pacific Ocean with the spaceborne SAR 01 p0226 N94-12746
Radar observation of internal waves field in the north-west Pacific 01 p0226 N94-12747
Radar imaging of sub-mesoscale ocean phenomena [AD-A266339] 02 p0725 N94-13581
Nonlinear wave forces on large ocean structures [AD-A266820] 02 p0683 N94-14902
Arctic internal waves (CEAREX) [AD-A265822] 03 p1111 N94-15139
Ocean wave study [NASA-TM-109620] 03 p1111 N94-15349
Ventilated oscillatory boundary layers [AD-A266226] 03 p1023 N94-16110
Observations and modelling of winds and waves during the Surface Wave Dynamics Experiment. Report 1: Intensive observation period IOP-1, 20-31 October 1990 [AD-A266384] 03 p1113 N94-16517
Field observations of infragravity, sea and swell directional spectra [AD-A266439] 03 p1113 N94-16561
Preliminary estimates of frequency-direction spectra derived from the SAMSON pressure gage array, November 1990 to May 1991 [AD-A267960] 03 p1114 N94-17497
Measurement of the velocity field and void fraction in a planar plunging jet [AD-A268183] 03 p1030 N94-17511
Design of a general purpose and autonomous transmitter and receiver system for underwater acoustic experiments at sea [AD-A269268] 04 p1495 N94-17822
Wind products for use in coastal wave and surge models [AD-A269753] 04 p1497 N94-18414
Full Boltzmann discrete spectral wave model, implementation and nondimensional tests [AD-A269885] 04 p1498 N94-18685
Acoustic travel time perturbations due to an internal tide and internal wave field in the Barents Sea [AD-A270879] 04 p1499 N94-19580
SIMBAT theoretical manual [AD-A271063] 05 p1882 N94-19979
ERS-1 and Seasat scatterometer measurements of ocean winds: Model functions and the directional distribution of short waves 05 p1720 N94-20412
Analysis of Ku-band cross section at low incidence angles 05 p1720 N94-20414
Rough surface scattering from moving ocean surfaces as an indicator of scattering mechanisms 05 p1726 N94-20439
Ocean wave height transformation model using surface roller theory [AD-A272610] 05 p1883 N94-21423
VIERS-1, phase 3 [BCRS-92-24] 06 p2381 N94-23145
Investigation of passive atmospheric sounding using millimeter and submillimeter wavelength channels [NASA-CR-194858] 06 p2404 N94-24843
Nonlinear ocean waves [AD-A274651] 07 p2899 N94-26354
Topics in longshore currents [AD-A274788] 07 p2899 N94-26361
An improvement of the slender body theory for oscillating ships with finite forward speed 08 p3234 N94-29705
The dynamics of tropical intraseasonal variability 08 p3371 N94-29741
Splines and ocean wave modelling [PB94-139409] 08 p3378 N94-30002
On the nonlinear dynamics of ocean wave systems 08 p3378 N94-30790
On wave interactions of rotational and irrotational flows 09 p3700 N94-31219
Additional capabilities of the unified waves model [AD-A276114] 09 p3702 N94-31467
Observations of turbulence, internal waves and background flows: An inquiry into the relationships between scales of motion 09 p3705 N94-31988
The effects of altimeter sampling characteristics: Some Geosat examples [AD-A276899] 09 p3747 N94-32214
Index and bulk parameters for frequency-direction spectra measured at CERC Field Research Facility [AD-A277759] 09 p3791 N94-33085
Storm evolution of directional seas in shallow water [AD-A278541] 10 p4089 N94-33404
Ocean surface roughness from infrared measurements: A failure of shape from reflection [AD-A278008] 10 p4091 N94-33435
Three-parameter characterization of shallow-water directional wind wave spectra [AD-A278532] 10 p4091 N94-33671
Ocean magnetics [PB94-149028] 10 p4092 N94-34142
Observations and modelling of winds and waves during the surface wave dynamics experiment. Report 2: Intensive observation period IOP-3 [AD-A278368] 10 p4093 N94-34375
Index and bulk parameters for frequency-direction spectra measured at CERC Field Research Facility, September 1992 to August 1993 [AD-A280233] 12 p4476 N94-37135
Index and bulk parameters for frequency-direction spectra measured at CERC Field Research Facility, September 1990 to August 1991 [AD-A280423] 12 p4476 N94-37216
Index and bulk parameters for frequency-direction spectra measured at CERC Field Research Facility, September 1991 to August 1992 [AD-A280455] 12 p4477 N94-37229
Airborne ROWS data report for the high resolution experiment, June 1993 [NASA-TM-104609] 12 p4477 N94-37397

WATERFOWL
Storm evolution of directional seas in shallow water [AD-A278541] 10 p4089 N94-33404

WATERPROOFING
Toxicity study of dimethylethoxysilane (DMSES), the waterproofing agent for the Orbiter heat protective system 01 p0318 N94-11554
Mutrometre: Construction for fast water proof measurements under low pressure and air suppression 04 p1427 N94-18031
Development of a new concept diver's watch 04 p1429 N94-18041
Simulation of the effect of wind on clothing by measurements and calculations [PB94-132289] 08 p3399 N94-28406

WATERSHEDS
Energy flow in an Arctic aquatic ecosystem [DE93-013178] 01 p0267 N94-11697
Snow cover models in operational watershed forecasting [DE93-778332] 02 p0718 N94-12837
Pattern and Process in Landscape Ecology: Eighth Annual US Landscape Ecology Symposium [DE93-014032] 02 p0711 N94-14859
On hydrologic similarity: A dimensionless flood frequency model using a generalized geomorphologic unit hydrograph and partial area runoff generation [PAPER-89WR01579] 03 p1083 N94-16027
Effects of spatial variability and scale on areal -average evapotranspiration 03 p1084 N94-16033
A Geographic Information System approach to modeling nutrient and sediment transport [DE93-013747] 03 p1097 N94-17426
Urban/rural application of weather radar for flow forecasting. Proceedings of the Informal CEc -Workshop [PB93-220135] 06 p2407 N94-23129
Glaciohydrologic and glaciohydraulic effects on runoff and sediment yield in glacierized basins [AD-A275134] 08 p3361 N94-29286
Snowmelt forecasting. Further cold regions development of operational hydrological forecasting, volume 2 [AD-A278123] 09 p3757 N94-33269

WATERWAYS
NT CANALS
NT HARBORS
Overview of physical oceanographic measurements taken during the Mount Mitchell cruise to ROPME sea area [DE93-018460] 04 p1497 N94-18494
DYNLET1 model formulation and user's guide [AD-A269843] 04 p1498 N94-18723
Centrifuge modeling of explosion-induced craters in unsaturated sand [AD-A270194] 04 p1417 N94-18780
The ecological and environmental impacts of manmade marshes [AD-A269213] 04 p1475 N94-18885
Glaciohydrologic and glaciohydraulic effects on runoff and sediment yield in glacierized basins [AD-A275134] 08 p3361 N94-29286
Real-time centimeter positioning with GPS: A system developed by the US Army Corps of Engineers [AD-A278152] 09 p3577 N94-33095
Index and bulk parameters for frequency-direction spectra measured at CERC Field Research Facility, September 1990 to August 1991 [AD-A280423] 12 p4476 N94-37216
Index and bulk parameters for frequency-direction spectra measured at CERC Field Research Facility, September 1991 to August 1992 [AD-A280455] 12 p4477 N94-37229

WAVE AMPLIFICATION
A study of the amplification of laser and VLF waves using a simple pendulum model [AD-A270857] 04 p1442 N94-19770

WAVE ATTENUATION
NT ACOUSTIC ATTENUATION
NT RADAR ATTENUATION
NT RADIO ATTENUATION
Photostimulated attenuation of hypersound in superlattice [DE93-611231] 01 p0357 N94-10408
Portable acoustic wave sensor systems for real-time monitoring of volatile organic compounds [DE93-013753] 02 p0582 N94-14511
Optical attenuation mechanism upgrades, MOBLAS, and TLRS systems 03 p0922 N94-15622
Seismic studies of the geologic structure and physical properties of the seabed [AD-A270895] 04 p1500 N94-19747
Relationship of attenuation in a vegetation canopy to physical parameters of the canopy 05 p1729 N94-20450
Similarity in wave propagation under a global relaxation law [PB94-111028] 06 p2524 N94-23730
Fiber optical angular sensor: Literature study and experimental results [PB93-204345] 06 p2545 N94-24529
Temperature dependent performance of Coplanar Waveguide (CPW) on substrates of various materials [NASA-TM-106505] 06 p2313 N94-25170
Binaural room simulation [AD-A273823] 07 p3009 N94-25737
Method for cancelling expansion waves in a wave rotor [NASA-CASE-LEW-15218-2] 08 p3274 N94-29740
Strain sensing using optical fibers [NASA-CR-195807] 09 p3740 N94-32940
PSIDD: A Post-Scan Interactive Data Display system for ultrasonic scans [NASA-TM-4545] 09 p3732 N94-33038

WAVE DIFFRACTION
Diffraction of microwaves at rectangular facades of buildings with and without ground reflections (Fresnel-Kirchhoff-Approximation) [DLR-FB-92-35] 03 p0987 N94-15155
The exact solution of the problem of diffraction of an electromagnetic plane wave by a conductive half-plane situated at an interface [IFTR-3/91] 03 p1002 N94-17057
Two-dimensional acousto-optical interaction theory and experimental analysis [AD-A267761] 03 p1193 N94-17254
Review of rigorous coupled-wave analysis and of homogeneous effective medium approximations for high spatial-frequency surface-relief gratings 03 p1194 N94-17335
Nonlinear acoustics: Periodic waveguide, finite-amplitude propagation in a medium having a distribution of relaxation processes, and production of an isolated negative pulse in water [AD-A270530] 05 p1967 N94-19894
An extended UTD analysis for the scattering and diffraction from cubic polynomial strips [NASA-CR-194581] 05 p1716 N94-20139
RCS Analysis of Plate Geometries, parts 1 and 2 [NASA-CR-194173] 05 p1717 N94-20269
High-frequency techniques for RCS prediction of plate geometries 05 p1717 N94-20270
A physical optics/equivalent currents model for the RCS of trihedral corner reflectors 05 p1717 N94-20271
Electromagnetic field strength prediction in an urban environment: A useful tool for the planning of LMSS 06 p2283 N94-22795
Transient analysis of conducting half-plane problem with noncausal scattering image [PB93-225027] 06 p2524 N94-23110
Diffraction analysis of transient acoustic waves: Half-plane in a layered medium [PB94-110988] 06 p2526 N94-23726
Numerical simulation of the reignition of detonation by reflected shocks [AD-A274755] 07 p2795 N94-27252
Developments in the application of the geometrical theory of diffraction and computer graphics to aircraft inter-antenna coupling analysis [ISBN-0-315-84643-7] 07 p2776 N94-27308
Characterization of a diffraction grating as a simulant of a selective frequency antenna for radiometric applications [AD-A275793] 08 p3241 N94-28745
Numerical simulation of shock interaction with above-ground structures [AD-A278713] 11 p4279 N94-35949

Intensity of waves diffracted from symmetrical profile lamellar gratings
[DE94-611101] 12 p4433 N94-36753

WAVE DISPERSION

Nonlinear MHD-waves in a dissipative plasma with hall currents
[DE93-617844] 01 p0386 N94-10395

General renormalized statistical approach with finite cross-field correlations
[DE93-617846] 01 p0386 N94-10396

Studies of P-matrix formalism on the basis of the potential description of two-particle interaction
[DE93-617691] 01 p0362 N94-10550

On the doubling of hydrodynamic theorems in relativistic theory of superfluidity
[DE93-617895] 01 p0148 N94-10717

Wave propagation characteristics of short-period crustal phases near ARCESS and NORESS
[AD-A265959] 01 p0275 N94-11102

Dispersion of plasma waves in a finite magnetic field (omega(sub H) greater than omega(sub p))
[DE93-621654] 01 p0391 N94-11210

Negative viscosity and generation of dissipative solitons and zonal dissipative structures by drift waves
[DE93-621656] 01 p0392 N94-11212

One-dimensional calculation of high-power microwave pulse compression by the earth's ionosphere
[DE93-009517] 01 p0137 N94-11466

Electrodynamics of helical plasma structures
[DE93-620981] 02 p0797 N94-13240

Ionospheric effects on a wide-bandwidth, polarimetric, space-based, synthetic-aperture radar
[DE93-015084] 02 p0612 N94-14512

The off shell (rho)-(omega) mixing in the QCD sum rules
[DE93-014845] 02 p0786 N94-14527

On transport of energy, momentum, orbital angular momentum and self-angular momentum of electromagnetic wave in dispersal media
[DE93-624179] 02 p0617 N94-14883

Nonlinear acoustics: Periodic waveguide, scattering of sound by sound, three-layer fluid, finite amplitude sound in a medium having a distribution of relaxation processes, and production of an isolated negative pulse in water
[AD-A267145] 03 p1177 N94-15732

Magnetic effects in anomalous dispersion
[DE93-014291] 03 p1175 N94-15978

Transformation of energy and momentum due to Landau damping in space
[DE93-624921] 04 p1581 N94-17689

Phase-space description of plasma waves: Linear and nonlinear theory
[IRF-SR-211] 04 p1587 N94-18860

Time-resolved shock compression of porous rutile: Wave dispersion in porous solids
[DE93-016848] 05 p1829 N94-19927

Birefringence control and dispersion characteristics of silicon oxynitride optical waveguides, appendix 6
05 p1989 N94-21600

First principles calculations for analysis martensitic transformations
[DE94-000666] 05 p1695 N94-21964

Simulating the Euclidean time Schroedinger equations using an INTEL iPSC/860 hypercube: Application to the t-J model of high-T(sub c) superconductivity
[DE94-000489] 05 p2035 N94-22385

ASpect: A new spectrum and line analysis package for IRAF
05 p1926 N94-22485

Similarity in wave propagation under a global relaxation law
[PB94-111028] 06 p2524 N94-23730

Analysis for the computational modeling of finite cladding and lossy coating effects in fibers
[PB94-111085] 06 p2544 N94-23732

Toroidal plasma beta-FLR limit in a toroidally linked mirror system
[DE94-003119] 07 p3041 N94-25792

Kinetic resonance damping rate of the toroidal ion temperature gradient mode
[DE94-003511] 07 p3041 N94-25923

C-periodicity and the physical mass in the 3-state Potts model
[DE94-601551] 07 p3019 N94-26423

Polar optical oscillation modes in GaAs-based double heterostructures: Long wavelength limit
[DE94-601874] 07 p3062 N94-26897

Investigations of dispersion characteristics of microwave/optical guided wave structures by using transmission line matrix method
[ISBN-0-315-85856-7] 08 p3254 N94-30034

Resistive ballooning mode in a gas-dynamic trap
[DE94-608328] 08 p3508 N94-30171

Theory and observations of horizontal and vertical structure of gravity wave perturbations in the middle atmosphere 08 p3366 N94-30802

Dispersion relations for a plasma-filled helix-loaded-waveguide
[DE94-006333] 09 p3675 N94-31781

Theoretical, experimental, and computational evaluation of several vane-type slow-wave structures
[NASA-TM-106641] 10 p4041 N94-33996

Theoretical studies of the solar atmosphere and interstellar pickup ions
[NASA-CR-195846] 10 p4166 N94-34716

The energy density of fluctuative electromagnetic field near the semi-bounded plasma
[DE94-617188] 11 p4256 N94-36099

Unstable solitary-wave solutions of the generalized Benjamin-Bona-Mahony equation
[DE94-013302] 12 p4496 N94-37549

Self-sustained turbulence and L-mode confinement in toroidal plasmas
[DE94-748497] 12 p4532 N94-37734

WAVE EQUATIONS

NT DIRAC EQUATION
NT KLEIN-GORDON EQUATION
NT KORTEWEG-DEVRIES EQUATION
NT SCHROEDINGER EQUATION

Wave and pseudo-diffusion equations from squeezed states 01 p0347 N94-10607

Radar imaging of sub-mesoscale ocean phenomena
[AD-A266339] 02 p0725 N94-13581

Soliton-like structures in double stimulated Brillouin scattering 03 p1200 N94-15207

Nonlinear problems in fluid dynamics and inverse scattering
[AD-A266234] 03 p1026 N94-16927

Elastic waves in discretely continuous mechanical systems
[IFTR-21/1992] 03 p1061 N94-17091

Two-dimensional acousto-optical interaction theory and experimental analysis
[AD-A267761] 03 p1193 N94-17254

The phase mixing of shear Alfven waves
[DE93-624920] 04 p1581 N94-17688

On higher dimensional Ermakov systems: Canonical reductions
[MATHS-REPT-A-182] 04 p1548 N94-18140

Multidimensional wave decompositions for the Euler equations 04 p1413 N94-18562

Modeling of current features in Gulf Stream SAR imagery
[AD-A270734] 04 p1499 N94-19609

Variable-permittivity linear inverse problem for the H(sub z)-polarized case 05 p1719 N94-20408

Interface reflection of spherical acoustic waves in the first- and second-order rational parabolic approximations and their artifacts
[PB93-215424] 05 p1969 N94-22261

Classical scattering theory of waves from the view point of an eigenvalue problem and application to target identification
[DE94-000472] 06 p2525 N94-23206

Multigrid and cyclic reduction applied to the Helmholtz equation 06 p2304 N94-23676

Similarity in wave propagation under a global relaxation law
[PB94-111028] 06 p2524 N94-23730

Decomposition of multi-component measurements into P and S waves
[ISBN-9-09-005197-X] 06 p2405 N94-25251

The extensions of space-time. Physics in the 8-dimensional homogeneous space D is equal to SU(2,2)/K
[DE93-634336] 07 p3072 N94-26551

Numerical procedure for planetary wave solution
[DE94-004280] 07 p2879 N94-26576

Elastic wave up/down decomposition in inhomogeneous and anisotropic media: An operator approach and its approximations
[PB94-126497] 07 p2881 N94-26880

Optical characterization and guided wave loss measurements for end-capped 6F-polybenzoxazole
[AD-A274586] 07 p3036 N94-26982

Hydroacoustic wave-fields generated by different source types, a computational study
[PB94-123536] 07 p3010 N94-27037

Wave propagation in the shallow regions of the earth's crust and the borehole vicinity
[ITN-94-85237] 07 p2882 N94-27330

The (j,0) + (0,j) representation space: Majorna-like construct
[DE94-005010] 08 p3522 N94-28543

Exact spherical wave solutions to Maxwell's equations with applications 08 p3252 N94-29733

A numerical study of gravitational collapse
08 p3548 N94-30271

Numerical simulations of piano strings. Part 1: A physical model for a struck string using finite difference methods
[TELECOM-93-C-003] 08 p3481 N94-30972

Aeroacoustic sources in internal flows
[ISBN-9-03-86-0282-0] 09 p3860 N94-31653

Boundary control of scattering
09 p3861 N94-31899

Finite element solution to the Helmholtz equation with high wave number. Part 1: The h-version of the FEM
[AD-A277396] 09 p3848 N94-32341

Classical scattering theory of waves from the view point of an eigenvalue problem and application to target identification
[AD-A277886] 10 p4133 N94-33836

Application of the compound-matrix method to wave propagation in range-independent fluid-solid media
[PB94-149077] 10 p4129 N94-34105

Introduction to generalized functions with applications in aerodynamics and aeroacoustics
[NASA-TP-3428] 10 p4134 N94-34393

Goldstone pion and other mesons using a scalar confining interaction
[DE94-010016] 11 p4321 N94-35649

Theoretical studies of ultrashort phenomena
[AD-A278938] 11 p4332 N94-35664

A note on high order schemes for one dimensional wave equation
[PB94-171006] 11 p4315 N94-35821

Elimination of numerical dispersion in finite-difference modeling and migration by flux-corrected transport
[DE94-004159] 12 p4510 N94-36551

WAVE EXCITATION

NT ACOUSTIC EXCITATION
NT HARMONIC EXCITATION

Wave generation by contaminant ions
[NASA-CR-193558] 01 p0364 N94-10946

Dispersion relations for a plasma-filled helix-loaded-waveguide
[DE94-006333] 09 p3675 N94-31781

MOM3D method of moments code theory manual
[NASA-CR-189594] 09 p3682 N94-32897

Material engineering of the novel semiconductor structures
[AD-A278386] 09 p3910 N94-33355

WAVE FRONT DEFORMATION

Sodium-layer laser guide stars
[DE93-019621] 06 p2349 N94-23490

Predicted optical performance of the High-Altitude Balloon Experiment (HABE) telescope in an adverse thermal environment
[DE94-008949] 11 p4349 N94-35998

Adaptive optics for laser beamforming in the atmosphere 12 p4393 N94-36621

WAVE FRONT RECONSTRUCTION

Numerical simulation of tomographic reconstruction for the study of turbulence using optical wavefront sensor measurements
[AD-A273851] 07 p2789 N94-25587

A multi-tiered wavefront sensor using binary optics
[DE94-010393] 11 p4267 N94-36111

WAVE FRONTS

NT SHOCK FRONTS

An analytic model for calculating pump-induced wavefront distortions in laser slabs
[DE93-011953] 01 p0174 N94-11126

Multiple laser beam combining and phasing using closed-loop control
[DE93-009830] 01 p0175 N94-11283

Laser beam control and diagnostic systems for the copper-pumped dye laser system at Lawrence Livermore National Laboratory
[DE93-016529] 02 p0658 N94-14437

Wavefront sensing, control, and pointing
02 p0546 N94-14833

Fabrication techniques for very fast diffractive lenses
03 p1196 N94-17345

Test methods for acceptance testing of telescopes
[AD-A268316] 03 p1237 N94-17568

Feedback controlled optics with wavefront compensation
[NASA-CASE-NPO-18194-1-CU]
05 p1985 N94-20305

Spatiotemporal behavior and nonlinear dynamics in a phase conjugate resonator
[NASA-CR-4567] 06 p2543 N94-23529

Convective instabilities in traveling fronts of addition polymerization 06 p2226 N94-24352

Numerical simulation of tomographic reconstruction for the study of turbulence using optical wavefront sensor measurements
[AD-A273851] 07 p2789 N94-25587

Experimental verification of tomographic reconstruction of turbulent air flow structure using optical wavefront measurements
[AD-A274392] 07 p2795 N94-27129

Dynamic and kinematic P wave tracing for a three-dimensional elastic inhomogeneous media by the asymptotic ray theory and application
[ITN-94-85239] 07 p2775 N94-27244

A multi-tiered wavefront sensor using binary optics
[DE94-010393] 11 p4267 N94-36111
Wavefront simulator for evaluating RF communication array signal processors
[AD-D016281] 12 p4436 N94-37835
WAVE FUNCTIONS
NT MOLECULAR ORBITALS
Satellite structure of the xenon valence shell by electron momentum spectroscopy
[DE93-609993] 01 p0360 N94-10327
Distorted-wave calculation of He(e,2e) including core-exchange
[DE93-610072] 01 p0360 N94-10330
Electron momentum spectroscopy of atoms, molecules and solids
[DE93-610148] 01 p0360 N94-10332
Recent advances in electron momentum spectroscopy
[DE93-610149] 01 p0361 N94-10333
Wave function collapse: An unnecessary condition for the dynamical description of the Zeno and partial Zeno effect
[DE93-612970] 01 p0132 N94-10401
P-matrix description of the two-particle interaction
[DE93-617690] 01 p0361 N94-10549
Studies of P-matrix formalism on the basis of the potential description of two-particle interaction
[DE93-617691] 01 p0362 N94-10550
The uncertainty principle and quantum chaos
01 p0379 N94-10602
Wavelets and spacetime squeeze
01 p0379 N94-10604
Coherent states and uncertainty relations for the damped harmonic oscillator with time-dependent frequency
01 p0380 N94-10611
Test of a method for phase retrieval in HRTEM
[DE93-612641] 01 p0170 N94-10630
Quasi-relativistic effects in barrier-penetration processes
[DE93-617730] 01 p0410 N94-10721
On the possible unobservability of the Wu-Yang phase factor in curved space
[DE93-617645] 01 p0411 N94-10831
Exact solutions of a many-anyon problem
[DE93-617646] 01 p0411 N94-10832
Multiple Schroedinger cats from multilevel atoms
[DE93-013412] 02 p0786 N94-14526
The fractional quantum Hall effect and the spherical shell model
[DE93-014553] 02 p0818 N94-14740
Radiation perturbation theory in gravity and quantum universe as a hydrogen atom
[DE93-626621] 02 p0849 N94-14889
A hydrogen atom in the curved space: Orthogonality of radial wave functions with respect to the critical momentum
[DE93-626623] 02 p0788 N94-14891
Supersymmetry of gauge equations and geometric nonadiabatic phases
[DE93-626671] 03 p1219 N94-14935
The fractional quantum Hall effect and the rotation group
[DE93-010348] 03 p1207 N94-15972
Quark-loop effects in high energy spin-flip processes
[DE93-626692] 03 p1188 N94-17313
Continuum solvent models for computational chemistry
[DE93-016329] 03 p0953 N94-17660
A hydrogen atom in the curved space. Expansion over free solutions on the three-dimensional sphere
[DE93-629868] 04 p1549 N94-18198
An introduction to GUGA in the COLUMBUS Program System
[DE93-018994] 05 p1902 N94-19928
Qualitative and quantitative aspects of the QCD theory of elastic form factors
[DE93-040864] 05 p2038 N94-21513
Photoabsorption and Compton scattering in ionization of helium at high photon energies
[DE94-000380] 05 p1974 N94-21658
Single and double ionization of helium by high-energy photon impact
[DE94-000381] 05 p1975 N94-21785
Simulating the Euclidean time Schroedinger equations using an INTEL iPSC/860 hypercube: Application to the t-J model of high-T(sub c) superconductivity
[DE94-000489] 05 p2035 N94-22385
Calculations of Bose-Einstein correlations from Relativistic Quantum Molecular Dynamics
[DE94-000794] 06 p2569 N94-23453
Weak interactions in a bilocal chiral theory
[DE93-616887] 06 p2539 N94-25477
Weak interactions in a bilocal chiral theory
[DE93-613097] 07 p3013 N94-25836
The Dirac equation in Kerr spacetime, spheroidal coordinates and the M.I.T. bag model of hadrons
[DE94-601566] 07 p3006 N94-25886
Crystal potential retrieval in HRTEM
[DE94-601883] 07 p3055 N94-26171
How to build analogues of the Bessel-Clifford expansions for the sum of the repulsive Coulomb potential and central potential decreasing more rapidly than the centrifugal one?
[DE93-634308] 07 p3007 N94-26472
On the wave and corpuscular properties of microparticles
[DE93-634450] 07 p3020 N94-26509
Double excitation of He and H(-) by fast proton and anti-proton impact
[DE94-004581] 07 p3026 N94-27620
Stochastic space-time, confinement potential and particle propagator
[DE94-606415] 07 p3074 N94-27680
The (j,0) + (0,j) representation space: Dirac-like construct
[DE94-005011] 08 p3522 N94-28572
Miln equation for the calculation of the phases and amplitudes of wave functions for continuum spectrum of Coulomb two-center problem
[DE94-606292] 08 p3522 N94-28616
Classical interpretation of quantum mechanics
[DE94-606304] 08 p3523 N94-28719
The solving of the relativistic two-body problem with a nonlinear dependence upon a spectrum parameter
[DE94-606343] 08 p3451 N94-28783
Observation of the phase shift of the wave function of the neutron under total reflection
[DE94-608244] 08 p3489 N94-30096
Development and implementation of a full-potential ASW method
[ETN-94-95757] 09 p3858 N94-31560
The form factors of the nucleons
[DE94-007096] 09 p3872 N94-32630
Calculations on some properties of the pion in the framework of Schwinger-Dyson and Bethe-Salpeter equations
[DE94-611232] 11 p4322 N94-35786
Elastic p(4)He scattering at intermediate energies
[DE94-618544] 11 p4328 N94-36287
Solving the two-dimensional Schroedinger equation in self-consistent basis
[DE94-621535] 12 p4504 N94-37174
MCHF calculations of isotope shifts. 1: Program implementation and test runs. 2: Large-scale active space calculations
[DE94-013036] 12 p4518 N94-37313
The angular and energy distributions of ejected electrons in electron-impact ionization of helium
[DE94-618748] 12 p4519 N94-37528
WAVE GENERATION
Wave generation by contaminant ions
[NASA-CR-193558] 01 p0364 N94-10946
Investigation of plasma instabilities in the Polar cusp
[NASA-CR-194283] 02 p0796 N94-13084
Field observations of infragravity, sea and swell directional spectra
[AD-A266439] 03 p1113 N94-16561
Full Boltzmann discrete spectral wave model, implementation and nondimensional tests
[AD-A269885] 04 p1498 N94-18685
On the physics of waves in the solar atmosphere: Wave heating and wind acceleration
[NASA-CR-195197] 06 p2628 N94-25264
Investigation of plasma instabilities in the polar cusp
[NASA-CR-195212] 07 p2879 N94-26599
Forced generation of solitary waves in a rotating fluid and their stability 08 p3274 N94-29689
Wave generation by contaminant ions near a large spacecraft
[NASA-CR-195797] 08 p3169 N94-29917
Meso-beta scale numerical simulation studies of terrain-induced jet streak mass and momentum perturbations
[NASA-CR-195863] 10 p4089 N94-33752
ULF waves in the low-latitude boundary layer and their relationship to magnetospheric pulsations: A multisatellite observation
[AD-A278906] 11 p4289 N94-35587
On the physics of waves in the solar atmosphere: Wave heating and wind acceleration
[NASA-CR-194119] 11 p4375 N94-36395
WAVE INTERACTION
NT SHOCK WAVE INTERACTION
NT WAVE-PARTICLE INTERACTIONS
Evaluation of dual flow thrust vectored nozzles with exhaust stream impingement
[NASA-CR-193292] 01 p0150 N94-10912
Theoretical investigation of 3-D shock wave turbulent boundary layer interactions
[AD-A265275] 01 p0150 N94-11014
Wave structure in planetary rings
01 p0434 N94-11185
On nonlinear Tollmien-Schlichting/vortex interaction in three-dimensional boundary layers
[NASA-TM-106184] 01 p0152 N94-11377
Ultrasonic wave interaction with advanced complex materials for nondestructive evaluation applications
[AD-A265704] 01 p0074 N94-12401
MHD shocks in coronal mass ejections
[NASA-CR-193418] 02 p0828 N94-12970
A millimeter-wave tunneladder TWT
[NASA-CR-182183] 02 p0620 N94-13106
Radar imaging of sub-mesoscale ocean phenomena
[AD-A266339] 02 p0725 N94-13581
Current drive with free electron lasers in high and low temperature tokamaks 03 p1201 N94-15209
On the decay of a dipole pump wave to half-harmonics 03 p1201 N94-15211
Investigate wave-mean flow interaction and transport in the extratropical winter stratosphere
[NASA-CR-194555] 03 p1098 N94-15639
The exact solution of the problem of diffraction of an electromagnetic plane wave by a conductive half-plane situated at an interface
[IFTR-3/91] 03 p1002 N94-17057
An experimental investigation of the effects of leading edge geometry on the dynamics of blunt fin-induced shock wave turbulent boundary layer interaction
[AD-A267656] 03 p0860 N94-17221
Correlation of incoming boundary layer pitot pressure fluctuations with the unsteadiness of fin-induced shock wave turbulent boundary layer interactions
[AD-A270059] 04 p1417 N94-18796
A method for solving the KDV equation and some numerical experiments
[DE93-624726] 04 p1550 N94-19246
Asteroid collisions: Target size effects and resultant velocity distributions 05 p2083 N94-20729
Vortex generation and wave-vortex interaction over a concave plate with roughness and suction
[AD-A276839] 06 p2337 N94-24869
Extension of On-Surface Radiation Condition (OSRC) theory to full-vector electromagnetic wave scattering by three-dimensional conducting, dielectric, and coated targets
[AD-A274023] 07 p2766 N94-25757
Review of tokamak experiments on direct electron heating and current drive with fast waves
[DE94-004185] 07 p3041 N94-25801
Space Experiments with Particle Accelerators (SEPAC)
[NASA-CR-193935] 07 p2761 N94-27664
Interaction of sound with sound by novel mechanisms: Ultrasonic four-wave mixing mediated by a suspension and ultrasonic three-wave mixing at a free surface
08 p3479 N94-29988
On the nonlinear dynamics of ocean wave systems
08 p3378 N94-30790
An experimental study of nonlinear wave coupling and energy transfer characterizing the transition of a planar jet shear layer 08 p3282 N94-30953
On wave interactions of rotational and irrotational flows 09 p3700 N94-31219
Interaction of oblique instability waves with weak streamwise vortices
[NASA-TM-106584] 10 p4043 N94-33432
Analysis of random structure-acoustic interaction problems using coupled boundary element and finite element methods
[NASA-CR-195931] 10 p4134 N94-34305
Investigation of ultrasonic surface wave interaction with porous saturated rocks
[DE94-013378] 12 p4469 N94-37177
WAVE MOTION
U WAVES
WAVE OSCILLATORS
U OSCILLATORS
WAVE PACKETS
On a Lagrange-Hamilton formalism describing position and momentum uncertainties 01 p0349 N94-10583
Correlated states of a quantum oscillator acted by short pulses 01 p0380 N94-10609
Absorption spectrum calculations using mixed quantum-gaussian wave packet dynamics
[AD-A265179] 01 p0413 N94-11877
On transport of energy, momentum, orbital angular momentum and self-angular momentum of electromagnetic wave in dispersal media
[DE93-624179] 02 p0617 N94-14883
Schroedinger's hope
[AD-A270988] 04 p1581 N94-19772
About stochastization of motion of charged particles in geomagnetic field and in the field of a wave packet
[DE93-634309] 07 p2879 N94-26502
About possible types of neutrino oscillations
[DE93-634449] 07 p3020 N94-26508

Acceleration of electrons and ions by strong lower-hybrid turbulence in solar flares
[NASA-TM-109723] 07 p3111 N94-27953
Nonlinear wave packet evolution in a dispersive plasma: Application to rotational discontinuities 08 p3506 N94-29822
On determination of a momentum of Alfven wave packet
[DE94-608329] 08 p3255 N94-30172
JPRS report: Science and technology. Central Eurasia
[JPRS-UST-94-006] 11 p4249 N94-35226
Coherent states versus de Broglie-wavelets
[DE94-611075] 11 p4343 N94-36381

WAVE PROPAGATION
NT ACOUSTIC PROPAGATION
NT DIFFRACTION PROPAGATION
NT GROUND WAVE PROPAGATION
NT HALOS
NT IONOSPHERIC PROPAGATION
NT LIGHT SCATTERING
NT SCATTER PROPAGATION
NT SHOCK WAVE PROPAGATION

Nonlinear MHD-waves in a dissipative plasma with hall currents
[DE93-617844] 01 p0386 N94-10395
Wideband beamforming for a sparse nonuniform spaced sensor array
[AD-A265909] 01 p0133 N94-10660
Spatial helicon-wave echo in an inhomogeneous magnetized plasma
[DE93-617845] 01 p0389 N94-10885
Inverting ultrasonic data on solid/fluid mixtures for Biot-Gassmann parameters
[DE93-011952] 01 p0150 N94-11026
A symmetrical form for equations of a nonlinear spiral magnetic
[DE93-621350] 01 p0344 N94-11033
The influence of the propagation medium on the sensitivity and resolution of meter wavelength aperture synthesis systems 01 p0134 N94-11062
The superresolution effect observed through a random medium 01 p0136 N94-11069
Wave propagation characteristics of short-period crustal phases near ARCESS and NORESS
[AD-A265959] 01 p0275 N94-11102
Studies on the parametric decay of waves in fusion plasmas
[DE93-621659] 01 p0390 N94-11148
One-dimensional calculation of high-power microwave pulse compression by the earth's ionosphere
[DE93-009517] 01 p0137 N94-11466
Decay interaction of bulk and surface Langmuir waves
[DE93-617843] 01 p0393 N94-11477
Stability and dynamics of spatio-temporal structures
[DE93-011374] 01 p0401 N94-11610
Spaceborne SAR study: LDRD 1992
[DE93-011485] 01 p0232 N94-11623
Results from a year-long auroral-E measurement campaign
[AD-A265059] 01 p0278 N94-11871
Propagation of light pulses through a three-layer medium (cloud, pure air, and ocean water) 01 p0222 N94-12725
Trajectory curving in underwater propagation of light 01 p0226 N94-12748
Ocean acoustic processing: A model-based approach
[DE93-011902] 02 p0725 N94-12876
The 3-D massively parallel impact simulations using PCTH
[DE93-011593] 02 p0670 N94-12908
Modeling the impact behavior of AD85 ceramic under multi-axial loading
[AD-A265877] 02 p0576 N94-12932
Numerical simulations and experiments on physics of high Mach number shockwave: Turbulent flow interactions
[DE93-013424] 02 p0631 N94-13249
The propagation characteristics and instability properties of low-frequency electromagnetic waves in the Io plasma torus 02 p0601 N94-13650
Locally non-uniform finite-difference time domain with application to stealth, crosstalk, and narrow apertures
[DE93-013958] 02 p0601 N94-13696
Non-uniqueness in dynamic rate-independent non-associated plasticity
[AD-A266342] 02 p0769 N94-13731
High order hybrid numerical simulations of two dimensional detonation waves
[NASA-CR-191506] 02 p0769 N94-13792
Measurement of wave propagation for VHF/UHF and a comparison between measured and predicted values
[FFI/RAPPORT-92/7024] 02 p0605 N94-13968
Nonlinear wave predictions in ceramics
[DE93-016516] 02 p0582 N94-14436
Ionospheric effects on a wide-bandwidth, polarimetric, space-based, synthetic-aperture radar
[DE93-015084] 02 p0612 N94-14512
Atmospheric acoustic modeling
[DE93-016727] 02 p0718 N94-14518
Kinetic simulations of ultra-intense laser plasma interactions
[DE93-014419] 02 p0802 N94-14564
Proceedings of the Seventeenth NASA Propagation Experimenters Meeting (NAPEX 17) and the Advanced Communications Technology Satellite (ACTS) Propagation Studies Miniworkshop
[NASA-CR-194096] 02 p0612 N94-14654
Opening remarks: Current and future activities 02 p0612 N94-14655
New challenges in propagation research in the US 02 p0612 N94-14656
User needs for propagation data 02 p0613 N94-14657
Statistical results from the Virginia Tech propagation experiment using the Olympus 12, 20, and 30 GHz satellite beacons 02 p0613 N94-14658
Radiometric observations of atmospheric attenuation at 20.6 and 31.65 GHz: The Wave Propagation Laboratory data base 02 p0613 N94-14660
Long duration measurements of fading on a low elevation angle, 11-GHz satellite path 02 p0613 N94-14661
A database for propagation models 02 p0614 N94-14665
Propagation issues for emerging mobile and portable communications: A systems perspective 02 p0614 N94-14667
Propagation considerations in the American Mobile Satellite system design 02 p0614 N94-14668
The ACTS propagation terminal delivery and support 02 p0615 N94-14674
ACTS propagation experiment discussion: Ka-band propagation measurements using the ACTS propagation terminal and the CSU-CHILL and Space Communications Technology Center Florida propagation program 02 p0616 N94-14678
Dynamic behavior of fiber and particle reinforced composites
[AD-A266905] 03 p0930 N94-15143
Improvement of SLR accuracy, a possible new step 03 p0917 N94-15588
Pulse propagation in inhomogeneous optical waveguides
[DE93-013378] 03 p1191 N94-16007
Proceedings of the Fifteenth NASA Propagation Experimenters Meeting (NAPEX 15) and the Advanced Communications Technology Satellite (ACTS) Propagation Studies Miniworkshop
[NASA-CR-194539] 03 p0994 N94-16035
A review of OPEX activities and measurement results 03 p0994 N94-16036
Propagation measurements in Alaska using ACTS beacons 03 p0995 N94-16040
Planned LMSS propagation experiment using ACTS: Preliminary antenna pointing results during mobile operations 03 p0995 N94-16041
Propagation-related AMT design aspects and supporting experiments 03 p0995 N94-16042
A comparison of cloud attenuation models using measured cloud data 03 p0996 N94-16044
Comparison of OLYMPUS beacon and radiometric attenuation measurements at Blacksburg, Virginia 03 p0996 N94-16046
Satellite sound broadcast propagation measurements 03 p0996 N94-16047
An overview of the text propagation effects for land-mobile-satellite systems: Experimental and modeling results 03 p0996 N94-16048
Database for propagation models 03 p0996 N94-16049
A CCIR-based prediction model for Earth-Space propagation 03 p0997 N94-16050
A study of land mobile satellite service multipath effects using SATLAB software 03 p0997 N94-16051
NORSAR basic seismological research
[AD-A266193] 03 p1101 N94-16125
Acousto-optical confirmation of the localized wave phenomena
[DE93-016425] 03 p1177 N94-16448
A ray trace model for propagation loss
[AD-A266314] 03 p0997 N94-16467
Surface waves in an inhomogeneous, isotropic, elastic half-space
[IFTR-18/1991] 03 p1060 N94-17047
Ultrasonic wave propagation model for nondestructive evaluation of solid rocker motor propellant
[AD-A267653] 03 p0976 N94-17248
A search for evidence of nonlinear elasticity in the earth
[DE93-015279] 03 p1102 N94-17252
Understanding curved detonation waves
[DE93-014581] 04 p1408 N94-17728
Microwave scattering from TAE modes
[DE93-018170] 04 p1583 N94-17809
Radio wave propagation in structured ionization for satellite and radar applications
[AD-A268457] 04 p1382 N94-17844
Comments on computational underwater acoustics
[DE93-013789] 04 p1562 N94-17873
Wake field in electron-positron plasmas
[DE93-624929] 04 p1584 N94-17955
Modeling shock initiation in Composition B
[DE93-016544] 04 p1376 N94-18095
Plasma production by helicon waves
[DE93-788396] 04 p1586 N94-18213
Crystal optics of high energy gamma-beams
[DE93-630228] 04 p1577 N94-18217
On the Michelson-Morley experiment
[DE93-629908] 04 p1608 N94-18268
Acoustic intensity measurements in the presence of low Mach number flow
[AD-A269995] 04 p1562 N94-18664
Wave propagation near explosive sources
[AD-A270102] 04 p1418 N94-18870
Shock propagation in crustal rock
[AD-A270148] 04 p1485 N94-18899
Estimating the oceanic sound speed environmental for long-range acoustic propagation
[AD-A270231] 04 p1499 N94-18903
Shock-loading response of advanced materials
[DE93-018344] 04 p1455 N94-19033
Stress pulse phenomena
[DE93-019064] 04 p1456 N94-19078
Transmission of acoustic waves through strongly heterogeneous, two-dimensional velocity models
[REPT-93-09] 04 p1563 N94-19083
Liquid sound speeds at pressure from the optical analyzer technique
[DE93-018362] 04 p1563 N94-19151
Comments on computational underwater acoustics
[DE93-019880] 04 p1563 N94-19270
Acoustic propagation modeling using MATLAB
[AD-A270905] 04 p1564 N94-19750
Spatial patterns in semiconductor lasers
[DE93-040056] 05 p1814 N94-19865
Nonlinear acoustics: Periodic waveguide, finite-amplitude propagation in a medium having a distribution of relaxation processes, and production of an isolated negative pulse in water
[AD-A270530] 05 p1967 N94-19894
Proceedings of the 15th Annual Seismic Research Symposium
[AD-A271458] 05 p1855 N94-20090
High-resolution numerical methods for compressible multi-phase flow in hierarchical porous media
[DE94-000740] 05 p1799 N94-20351
The effect of dissipative inhomogeneous medium on the statistics of the wave intensity 05 p1726 N94-20440
Laser propagation in underdense plasmas: Scaling arguments
[DE93-040439] 05 p1816 N94-20480
Mathematical model and analysis of the Tactical Unmanned Ground Vehicle (TUGV) using computer simulation
[AD-A272258] 05 p1824 N94-20576
Asteroid collisions: Target size effects and resultant velocity distributions 05 p2083 N94-20729
Analysis of the effects of eurasian crustal and upper mantel structure on regional phases using broadband seismic data
[AD-A272446] 05 p1858 N94-21206
Dynamic response of multiphase porous media
[AD-A272915] 05 p1831 N94-21219
The Board on Earth sciences and resources
[DE94-000745] 05 p1859 N94-22018
Time-laplace-transform-domain analysis of wave propagation in planar waveguides
[PB93-215226] 05 p1960 N94-22096
Lidar and radar derived cirrus microphysical properties for the 26 November 1991 case study 05 p1873 N94-22305
Observations of multi-layered clouds using K-band radar 05 p1874 N94-22311
Radio wave propagation studies along an Earth-space satellite link
[ISBN-0-315-60627-4] 05 p1742 N94-22408
Theory and simulation of plasma sheath waves
[DE94-001305] 05 p1999 N94-22567
Theory of leaked auroral kilometric radiation 05 p2003 N94-22649
Enhanced absorption of p-modes on sunspot and plage regions 05 p2006 N94-22671
The characterization of reaction-convection-diffusion processes by travelling waves
[PB94-150315] 06 p2273 N94-22729

Ray and wave optics modeling of laboratory x ray lasers
[DE93-019940] 06 p2541 N94-22868
Theoretical studies of wave propagation in multilayered piezoelectric media
[DE93-040273] 06 p2371 N94-22872
Tracking sharp interface of two fluids by the CIP (Cubic-Interpolated Propagation) scheme
[DE93-508322] 06 p2319 N94-23460
Shock-induced turbulent flow in baffle systems
[DE94-001532] 06 p2319 N94-23470
Similarity in wave propagation under a global relaxation law
[PB94-111028] 06 p2524 N94-23730
Analysis of time-domain acoustic wavefields in horizontally continuously layered configurations based on the modified Cagniard method
[PB94-111044] 06 p2524 N94-23731
Generalized three-dimensional simulation of ferruled coupled-cavity traveling-wave-tube dispersion and impedance characteristics
[NASA-TP-3389] 06 p2310 N94-24056
Radio communication and wave propagation. A visit to the Netherlands in December 1992
[PB93-204360] 06 p2297 N94-24531
Near-surface seismic imaging
[PB94-119096] 06 p2404 N94-24647
Downward extrapolation of multi-component seismic data
[ISBN-9-09-005213-5] 06 p2405 N94-25229
Decomposition of multi-component measurements into P and S waves
[ISBN-9-09-005197-X] 06 p2405 N94-25251
A relativistic theory on wave propagation in inhomogeneous magnetoplasmas
[ETN-94-95322] 06 p2554 N94-25285
Arbitrary-order numerical schemes for linear hyperbolic systems
[CRANFIELD-AERO-9211] 06 p2523 N94-25480
Arbitrary-order high resolution schemes for model hyperbolic conservation laws
[CRANFIELD-AERO-9209] 07 p3005 N94-25823
Efficient modeling in transversely isotropic inhomogeneous media
[DE94-003394] 07 p2877 N94-25847
Technical description of the Vulcano software library
[FFI-93/7024] 07 p2767 N94-26105
Ionospheric modification by high power, obliquely propagated HF radio wave transmissions. Part 1: Experimental
[AD-A273746] 07 p2878 N94-26224
Cad of GeO2-SiO2 double-layer core dispersion-shifted single-mode fibre
[DE93-634325] 07 p3035 N94-26383
The effect of high frequency electric field on hypersound amplification in superlattice
[DE93-634326] 07 p3057 N94-26384
A geological and geophysical information system for Eurasia
[AD-A274818] 07 p3098 N94-26490
A preliminary shear velocity model for Central Asia
[AD-A274972] 07 p2880 N94-26752
Nonlinear hysteresis in an endochronic solid
[AD-A274594] 07 p2880 N94-26855
Hydroacoustic wave-fields generated by different source types, a computational study
[PB94-123536] 07 p3010 N94-27037
Performance statistics bulletin: High altitude meteor scatter propagation, August, September, October 1989
[AD-A274455] 07 p2773 N94-27085
Dynamic and kinematic P wave tracing for a three-dimensional elastic inhomogeneous media by the asymptotic ray theory and application
[ITN-94-85239] 07 p2775 N94-27244
Wave propagation in the shallow regions of the earth's crust and the borehole vicinity
[ITN-94-85237] 07 p2882 N94-27330
An improvement in the modified finite element procedure for underwater shock analysis
[DE94-004451] 07 p2797 N94-27617
Nonlinear transverse propagation of photons in a ultrarelativistically hot and magnetized electron-positron plasma: Coupling of Langmuir and electromagnetic solitons
[DE94-603667] 07 p3046 N94-27630
Mach reflection of spherical detonation waves
[DE93-016604] 07 p2797 N94-27705
Preliminary considerations on the diffraction (quasi-optical) grill in CASTOR tokamak
[IPPCZ-335] 07 p3048 N94-27842
Underground structure in the eastern part of Kanagawa Prefecture inferred from explosion seismic observations 07 p2886 N94-27987
Analysis of S-wave seismogram envelope of deep earthquakes and estimation of random inhomogeneities in the Kanto-Tokai area 07 p2886 N94-27988
Sonic boom propagation through turbulence: A ray theory approach 07 p2650 N94-28192
The propagation of spark-produced N waves through turbulence 07 p2650 N94-28193
On the aging of sonic booms 07 p2650 N94-28194
Plane wave propagation and polarization properties in transversely bianisotropic uniaxial medium
[PB94-132883] 07 p2778 N94-28380
Eigenwaves in the general uniaxial bianisotropic medium with symmetric parameter dyadics
[PB94-132891] 07 p2778 N94-28381
Plane wave propagation in an anisotropic chiral medium with isotropic permittivity and permeability
[PB94-133097] 07 p2778 N94-28384
Characterization of structural vibration: Field descriptors based on energy density and intensity
[PB94-132230] 08 p3316 N94-28404
Broad geoacoustic assessment of some regional areas
[AD-A275504] 08 p3356 N94-28791
Quadruplet expansion of the acoustic pressure field in a wedge shaped ocean
[AD-A275121] 08 p3477 N94-29003
Dynamic response of ceramics
[AD-A275396] 08 p3214 N94-29203
Statistical characterization of rugged propagation paths with application to Rg scattering study
[AD-A275237] 08 p3361 N94-29393
The dynamics of tropical intraseasonal variability 08 p3371 N94-29741
Nonlinear wave packet evolution in a dispersive plasma: Application to rotational discontinuities 08 p3506 N94-29822
Spectral analysis of wave propagation in connected waveguides 08 p3277 N94-29944
The effects of propagational factors on quantum wires in close parallel proximity
[ISBN-0-315-86157-6] 08 p3254 N94-30035
A relativistic solitary wave in electron positron plasma
[DE94-608107] 08 p3507 N94-30071
Extension of love wave transformation theory to laterally heterogeneous structures
[DE94-608098] 08 p3365 N94-30093
On determination of a momentum of Alfven wave packet
[DE94-608329] 08 p3255 N94-30172
Accurate finite difference methods for time-harmonic wave propagation
[AD-A279019] 08 p3454 N94-30209
Observation of the traveling component of an x ray standing wave field
[DE94-007671] 09 p3672 N94-31317
Study of wave propagation and dynamic response of laminated composite structures
[AD-A276123] 09 p3619 N94-31444
Additional capabilities of the unified waves model
[AD-A276114] 09 p3702 N94-31467
Dispersion relations for a plasma-filled helix-loaded-waveguide
[DE94-006333] 09 p3675 N94-31781
Self-consistent effects of magnetospheric hydromagnetic waves on ring current ions
[AD-A277406] 09 p3774 N94-32346
Superluminous laser pulse in an active medium
[DE94-007110] 09 p3720 N94-32684
A study of near-surface and underwater explosions by computer simulations
[DE94-009038] 09 p3708 N94-32849
Finite-element modeling of the blockage and scattering of LG propagation
[AD-A277430] 09 p3775 N94-33006
A comparison of rough surface parabolic equation models
[AD-A278090] 09 p3791 N94-33185
An approximate model for vertical polarization and surface roughness using the parabolic equation
[AD-A278091] 09 p3684 N94-33186
On the boundary integral equation methods for an extended time-harmonic Maxwell type system 10 p4128 N94-33417
Meso-beta scale numerical simulation studies of terrain-induced jet streak mass and momentum perturbations
[NASA-CR-195863] 10 p4089 N94-33752
Application of the compound-matrix method to wave propagation in range-independent fluid-solid media
[PB94-149077] 10 p4129 N94-34105
Body-wave radiation patterns and AVO in transversely isotropic media
[DE94-009214] 10 p4036 N94-34162
Vibrations of structures with cyclic symmetry: Application to the case of turbine engines 10 p4004 N94-34463
Landau damping of auroral hiss 10 p4088 N94-34950
Review of slow-wave structures
[NASA-TM-106639] 11 p4258 N94-35270
Initial perturbations and Langmuir waves in electron-positron plasma
[DE94-617190] 11 p4338 N94-36097
X ray radiographic imaging of hydrodynamic phenomena in radiation driven materials: Shock propagation and shear flow
[DE94-010891] 11 p4318 N94-36201
TSAR modeling of a TEM horn and surrounding structure
[DE94-010668] 11 p4256 N94-36301
On the physics of waves in the solar atmosphere: Wave heating and wind acceleration
[NASA-CR-194119] 11 p4375 N94-36395
Computational Mathematics Laboratory for multiscale analysis
[AD-A278597] 11 p4315 N94-36424
Propagation of radius-tailored laser pulses over extended distances in a uniform plasma
[AD-A280405] 12 p4528 N94-37182
Final report on spectral broadening by cross-phase modulation in linearly birefringent optical fibers
[DE94-010406] 12 p4524 N94-37191
Langmuir waves in the electron-positron plasma
[DE94-618779] 12 p4531 N94-37728

WAVE RADIATION

U ELECTROMAGNETIC RADIATION

WAVE REFLECTION

NT MACH REFLECTION

Preliminary results on backscattering strength from a wind generated bubbly ocean surface
[AD-A265006] 01 p0287 N94-10490
Effects of energetic particle events on VLF/LF propagation parameters/1989
[AD-A265266] 01 p0275 N94-11013
Acoustics of bubbly sediments
[AD-A263726] 01 p0288 N94-11299
Diffraction of microwaves at rectangular facades of buildings with and without ground reflections (Fresnel-Kirchhoff-Approximation)
[DLR-FB-92-35] 03 p0987 N94-15155
Nonlinear acoustics: Periodic waveguide, scattering of sound by sound, three-layer fluid, finite amplitude sound in a medium having a distribution of relaxation processes, and production of an isolated negative pulse in water
[AD-A267145] 03 p1177 N94-15732
Regular and irregular reflection of a wave from a slanting flat wall
[IFTR-13/1991] 03 p1193 N94-17049
Numerical solution of SUPG finite-element method for supersonic viscous flow
[AD-A267762] 03 p0860 N94-17222
Studies of enhanced radar backscatter
[AD-A269544] 04 p1385 N94-18288
A physical optics/equivalent currents model for the RCS of trihedral corner reflectors 05 p1717 N94-20271
Hydroacoustic wave-fields generated by different source types, a computational study
[PB94-123536] 07 p3010 N94-27037
Numerical simulation of the reignition of detonation by reflected shocks
[AD-A274755] 07 p2795 N94-27252
Mach reflection of spherical detonation waves
[DE93-016604] 07 p2797 N94-27705
Quadruplet expansion of the acoustic pressure field in a wedge shaped ocean
[AD-A275121] 08 p3477 N94-29003
Electromagnetic wave reflection from irregular plasma layers
[AD-A276727] 09 p3678 N94-32161
Green's functions for an anisotropic medium. Part 2: Two-layer case
[AD-A278788] 11 p4256 N94-35713

WAVE SCATTERING

NT ACOUSTIC SCATTERING
NT ATMOSPHERIC SCATTERING
NT ELECTROMAGNETIC SCATTERING
NT HALOS
NT LIGHT SCATTERING
NT MICROWAVE SCATTERING
NT MIE SCATTERING
NT RAMAN SPECTRA
NT RAYLEIGH SCATTERING
NT REVERBERATION
NT THOMSON SCATTERING
NT TROPOSPHERIC SCATTERING
NT X RAY SCATTERING

On the possible unobservability of the Wu-Yang phase factor in curved space
[DE93-617645] 01 p0411 N94-10831
Radiowaves propagation through inhomogeneous interstellar plasma 01 p0134 N94-11061
Sites of fine-scale electron density turbulence in the interstellar medium
[NASA-CR-193708] 02 p0839 N94-13864

Double stimulated Brillouin scattering
03 p1200 N94-15205
Dynamics of double stimulated Brillouin scattering
03 p1200 N94-15206
Soliton-like structures in double stimulated Brillouin scattering 03 p1200 N94-15207
Convergence of the multiple scattering expansion in XAFS and XANES
[DE93-011001] 03 p0948 N94-16772
Spectral inverse scattering theory for dielectric media: Application to optical devices
[AD-A268635] 03 p1199 N94-17427
Millimeter wave reflectivity measurement system
[AD-A270008] 04 p1387 N94-18601
Fast iterative solution of sparsely sampled seismic inverse problems
[REPT-93-16] 04 p1486 N94-19081
Acoustic travel time perturbations due to an internal tide and internal wave field in the Barents Sea
[AD-A270879] 04 p1499 N94-19580
RCS Analysis of Plate Geometries, parts 1 and 2
[NASA-CR-194173] 05 p1717 N94-20269
A physical optics/equivalent currents model for the RCS of trihedral corner reflectors 05 p1717 N94-20271
FD-TD modeling of 2-D dielectric waveguides for propagation and scattering of femtosecond optical solitons 05 p1719 N94-20406
Hadronic molecules and scattering amplitudes from the nonrelativistic quark model
[DE94-000377] 05 p1974 N94-21657
Continuous-time discretized-space approach to modeling short-pulse propagation and scattering
[PB93-215259] 05 p1742 N94-22347
The effect of sub-surface volume scattering on the accuracy of ice-sheet altimeter retracking algorithms
[NASA-CR-194825] 06 p2386 N94-24060
The scattering and collision of gravitational waves in Friedmann-Robertson-Walker open universes
[MATHS-REPT-A-193] 06 p2406 N94-25430
Polarimetric investigation of edge scattering by mono- and bistatic microwave imaging
[ESA-TT-1284] 07 p2768 N94-26317
Compilation of corrections for postprocessing of laser bathymetry data
[PB94-123668] 07 p2900 N94-27156
Statistical characterization of rugged propagation paths with application to Rg scattering study
[AD-A275237] 08 p3361 N94-29393
A spectral boundary integral equation method for the 2-D Helmholtz equation
[AD-A279021] 08 p3454 N94-30207
On wave interactions of rotational and irrotational flows 09 p3700 N94-31219
Electromagnetic wave reflection from irregular plasma layers
[AD-A276727] 09 p3678 N94-32161
Finite-element modeling of the blockage and scattering of LG propagation
[AD-A277430] 09 p3775 N94-33006
Classical scattering theory of waves from the view point of an eigenvalue problem and application to target identification
[AD-A277886] 10 p4133 N94-33836
Relativistic three-particle dynamical equations. 2: Theoretical development
[DE94-616654] 11 p4320 N94-35581
Scattering theory for the quantum envelope of a classical system
[DE94-008530] 12 p4539 N94-36508
Scattering cross section of sound waves by the modal element method
[NASA-TM-106667] 12 p4510 N94-37308

WAVE-PARTICLE INTERACTIONS
Nonlinear analysis of a magnicon output cavity
[AD-A265342] 01 p0145 N94-12424
Studies on equatorial shock formation during plasmaspheric refilling
[NASA-CR-194392] 02 p0715 N94-13954
Simulations of wave-particle interactions in stimulated Raman forward scattering in a magnetized plasma
[PB94-170990] 03 p1201 N94-15210
Implementation of the digital wave-processing experiment 04 p1329 N94-19628
A study of the amplification of laser and VLF waves using a simple pendulum model
[AD-A270857] 04 p1442 N94-19770
On a theory of two-beam mechanisms of charged particle acceleration in electrodynamic structures
[DE94-003482] 07 p3032 N94-26330
Gyroresonant scattering of radiation belt electrons by oblique whistler waves 10 p4166 N94-33357
Diffusion at the magnetopause: A theoretical perspective
[DE94-009356] 10 p4086 N94-33910
Studies on equatorial shock formation during plasmaspheric refilling
[NASA-CR-195864] 10 p4088 N94-34669

WAVEFORMS
NT PULSE AMPLITUDE
NT PULSE DURATION
NT SAWTOOTH WAVEFORMS
NT SQUARE WAVES
On the coupling of electromagnetic radiation into cavities
[DE93-011406] 01 p0137 N94-11621
Lower bounds on time of arrival estimation of pulse compression waveforms
[ITN-93-85189] 02 p0599 N94-13196
DATAA: Data acquisition made easy
[DE93-014683] 02 p0823 N94-13406
Center of trace algorithms for extracting digitized waveforms from two-dimensional images
[DE93-015082] 02 p0753 N94-14295
High resolution radar profiling using higher-order statistics
[AD-D015891] 03 p1000 N94-16918
An asymptotic expansion of an electromagnetic field in the velocity of a caustic in the form of simple waves
[IFTR-14/1991] 03 p1002 N94-17048
The d(exp 3)delta-a(exp 3)delta and b(exp 3)phi-a(exp 3)delta systems of ZrS, Part 2: Appendix, list of wavenumbers
[USIP-92-05] 04 p1602 N94-19293
The wideband plasma wave investigation
04 p1328 N94-19627
A study of Saturn's E-ring particles using the Voyager 1 plasma wave instrument
[NASA-CR-194694] 05 p2088 N94-20048
Optimal convolution SOR acceleration of waveform relaxation with application to semiconductor device simulation 05 p1922 N94-21475
Optimization and control of a small angle ion source using an adaptive neural network controller
[DE93-040063] 05 p1946 N94-21845
A framework of connectionist network toward speech waveform coding 05 p1746 N94-22211
Catalog of absolutely calibrated, range normalized, wideband, electric field waveforms from triggered lightning flashes in Florida
[AD-A273793] 07 p2892 N94-25873
Fast generator of program waveforms signals
[DE93-634230] 07 p2948 N94-26381
A preliminary shear velocity model for Central Asia
[AD-A274972] 07 p2880 N94-26752
Monaural and binaural processing of complex waveforms
[AD-A274209] 07 p3010 N94-27067
Scanview: A grafical program for analysis of laserbathymetry data
[PB94-124443] 07 p2900 N94-27206
Coherence and satisfiability of waveform timing specifications
[ISBN-0-315-57769-X] 07 p3009 N94-27268
Correlation between electrical activity and the size of single sinoatrial node cells 07 p2907 N94-27513
Implications for high speed research: The relationship between sonic boom signature distortion and atmospheric turbulence 07 p2650 N94-28190
Laser beam steering with semiconductor waveguide
[AD-A275775] 08 p3292 N94-28765
Design of the biosonar simulator for dolphin's clicks waveform reproduction 08 p3234 N94-29707
Numerical simulations of piano strings. Part 1: A physical model for a struck string using finite difference methods
[TELECOM-93-C-003] 08 p3481 N94-30972
Waveform generation for ultra-wideband radar system
[AD-A276352] 09 p3673 N94-31401
Performance metrics for low probability of intercept-communication system
[AD-A277346] 09 p3677 N94-32073
Development of a frequency-domain electromagnetic scattering measurement system
[AD-A276738] 09 p3678 N94-32179
Generation of the ambiguity function for ultra wideband radar waveforms
[AD-A277913] 09 p3684 N94-33261
Design and analysis of low boom concepts at Langley Research Center 10 p3973 N94-33470
Statistical and numerical study of the relation between weather and sonic boom characteristics
10 p3976 N94-33498
An analog memory integrated circuit for waveform acquisition up to 900 MHz
[DE94-009020] 10 p4041 N94-33928
Arbitrary waveform generator
[AD-D016123] 10 p4041 N94-34149
A note on windowing for the waveform relaxation
[AD-A280999] 10 p4130 N94-34922
Center for seismic studies
[AD-A278682] 11 p4290 N94-35693
Coherent states versus de Broglie-wavelets
[DE94-611075] 11 p4343 N94-36381

WAVEGUIDE ANTENNAS
NT HORN ANTENNAS
Folded waveguide designs for tokamaks
[DE93-013274] 02 p0798 N94-13577
HRMS sky survey wideband feed system design for DSS 24 beam waveguide antenna 02 p0611 N94-14397
Experimental evaluation of an adaptive focusing algorithm for a microwave planar phased-array hyperthermia system at UCSF
[AD-A267004] 03 p1121 N94-15634
Recent activities in printed Antennas at LeRC
05 p1722 N94-20422
Slot-coupled patch antenna with coplanar waveguide feed 05 p1734 N94-20506
The Telecommunications and Data Acquisition Report
[NASA-CR-194766] 06 p2290 N94-23256
Performance of the X-/Ka/KABLE-band dichroic plate in the DSS-13 beam waveguide antenna
06 p2291 N94-23261
Beam-waveguide antenna servo design issues for tracking low earth-orbiting satellites
06 p2292 N94-23268
Design of folded waveguide antenna for Alcator C-Mod
[DE94-003584] 07 p2767 N94-25924
RF modeling and design of a folded waveguide launcher for the Alcator C-Mod tokamak
[DE94-003588] 07 p3041 N94-25933
Printed circuit elements with applications to antennas, scattering, and circuits
[AD-A275512] 08 p3262 N94-28669
X-/Ka-band dichroic plate design and grating lobe study 08 p3247 N94-29616
A portable X-band front-end test package for beam-waveguide antenna performance evaluation. Part 2: Tests on the antenna 08 p3247 N94-29620
Determining noise temperatures in beam waveguide systems 08 p3249 N94-29657
Analysis of a slot coupled coplanar waveguide fed patch antenna
[NASA-TM-106567] 09 p3698 N94-33116
The electrical conductivities of candidate beam-waveguide antenna shroud materials
11 p4252 N94-35546
Thin-ribbon tapered coupler for dielectric waveguides
11 p4253 N94-35547
Design and implementation of a beam-waveguide mirror control system for vernier pointing of the DSS-13 antenna 11 p4253 N94-35548
Use of the sampling theorem to speed up near-field physical optics scattering calculations
11 p4253 N94-35549
DSS-13 S-/X-band microwave feed system
11 p4253 N94-35550

WAVEGUIDE FILTERS
A simplified method for S-parameter calculations of metal septum waveguide filters
05 p1782 N94-22180

WAVEGUIDE LASERS
Study of speckle reduction when using a CO2 waveguide laser close to its threshold state
[DSIS-93-00250] 02 p0657 N94-14067
Manufacturing and characterization of GaAs/AlGaAs multiple quantumwell ridge waveguide lasers
[EUT-92-E-265] 06 p2348 N94-23168

WAVEGUIDE WINDOWS
Experimental and theoretical investigation of broadband high-power windows for millimeter waves
[KFK-5157] 04 p1391 N94-19617

WAVEGUIDES
NT BEAM WAVEGUIDES
NT CIRCULAR WAVEGUIDES
NT EARTH-IONOSPHERE WAVEGUIDE
NT OPTICAL FIBERS
NT OPTICAL WAVEGUIDES
NT PLASMAGUIDES
NT RECTANGULAR WAVEGUIDES
NT SCINTILLATING FIBERS
Nonlinear space charge effect of bunched beam in linac
[DE93-612176] 01 p0371 N94-10409
Non classical effects in planar waveguides
01 p0376 N94-10574
About excitation of round waveguide by a point current source
[DE93-621352] 01 p0133 N94-11034
Linear antenna of an arbitrary orientation and position in cylindric screen
[DE93-621353] 01 p0134 N94-11035
Regular tensor Green functions of the round waveguide
[DE93-621354] 01 p0345 N94-11036

Asymptotic expressions for regular Green functions of a round cylindrical screen
[DE93-621356] 01 p0134 N94-11038
Dispersion of plasma waves in a finite magnetic field (omega(sub H) greater than omega(sub p))
[DE93-621654] 01 p0391 N94-11210
Non-linear dynamics of automodulation processes in coupled distributed autovibration systems with delay
[DE93-620976] 01 p0143 N94-11365
Acoustic waveguide characteristics of the Indian Ocean north of equator 01 p0193 N94-11912
Analysis and characterizations of planar transmission structures and components for superconducting and monolithic integrated circuits
[NASA-CR-193675] 02 p0619 N94-13026
A millimeter-wave tunneladder TWT
[NASA-CR-182183] 02 p0620 N94-13106
Laser CO2 beam transmission through hollow metallic waveguide coated by a thin internal dielectric layer
[ITN-93-85201] 02 p0656 N94-13571
Folded waveguide designs for tokamaks
[DE93-013274] 02 p0798 N94-13577
Prism-film coupling in anisotropic planar waveguides of epitaxial (101) rutile thin films
[DE93-012912] 02 p0811 N94-14304
Gratings and waveguides 03 p1226 N94-14987
Nonlinear acoustics: Periodic waveguide, scattering of sound by sound, three-layer fluid, finite amplitude sound in a medium having a distribution of relaxation processes, and production of an isolated negative pulse in water
[AD-A267145] 03 p1177 N94-15732
Stress sensitivity of dielectric resonators
[AD-A266767] 03 p1009 N94-15825
Comments on computational underwater acoustics
[DE93-013789] 04 p1562 N94-17873
Advances and applications of ABCI
[DE93-016971] 04 p1383 N94-18055
Waveguide and resonator perturbation techniques for measuring chirality and non-reciprocity of biisotropic materials
[PB93-187243] 04 p1384 N94-18116
Designs for a 10.6 micrometer electromagnetic wiggler Free-Electron Laser (FEL)
[AD-A269695] 04 p1439 N94-18576
Single-transverse-mode, narrow-bandwidth pulsed tunable dye laser with hollow circular intracavity dielectric waveguide
[AD-A270022] 04 p1439 N94-18614
Persistent wakefields associated with waveguide damping of higher order modes
[DE93-040973] 05 p1715 N94-19874
Process to fabricate thick coplanar microwave electrode structures
[AD-D015913] 05 p1748 N94-19892
Nonlinear acoustics: Periodic waveguide, finite-amplitude propagation in a medium having a distribution of relaxation processes, and production of an isolated negative pulse in water
[AD-A270530] 05 p1967 N94-19894
FD-TD modeling of 2-D dielectric waveguides for propagation and scattering of femtosecond optical solitons 05 p1719 N94-20406
A comprehensive theoretical and experimental study of coplanar waveguide shunt stubs
05 p1733 N94-20500
A comparative study between shielded and open coplanar waveguide discontinuities
05 p1733 N94-20501
A theoretical and experimental study of coplanar waveguide shunt stubs 05 p1733 N94-20502
Coplanar waveguide radial line stub
05 p1733 N94-20503
Attenuation of epsilon(sub eff) of coplanar waveguide transmission lines on silicon substrates
05 p1733 N94-20504
Slot-coupled patch antenna with coplanar waveguide feed 05 p1734 N94-20506
Hybrid finite element/waveguide mode analysis of passive RF devices
[AD-A273074] 05 p1740 N94-21518
Polyimide-based electrooptic materials
[DE93-019416] 05 p1706 N94-21526
Simulation of traveling-wave output structures for high power RF tubes
[DE93-041005] 05 p1763 N94-21685
On the relationship between spectral domain approach and method of lines 05 p1794 N94-22254
Generalized three-dimensional simulation of ferruled coupled-cavity traveling-wave-tube dispersion and impedance characteristics
[NASA-TP-3389] 06 p2310 N94-24056
A low noise 665 GHz SIS quasi-particle waveguide receiver
[NASA-CR-194735] 06 p2296 N94-24105
Total light loss optic spectroscopy: Progress towards a fiber optic Raman organic vapor sensor
[DE94-002545] 06 p2234 N94-24549
Temperature dependent performance of Coplanar Waveguide (CPW) on substrates of various materials
[NASA-TM-106505] 06 p2313 N94-25170
Problems in nonlinear acoustics: Rayleigh waves, pulsed sound beams, and waveguides
[AD-A274587] 07 p3010 N94-26983
Microwave coupling into a slotted cavity
[PB94-123742] 07 p2772 N94-27041
Three dimensional transient analysis of microstrip circuits in multilayered anisotropic media
[AD-A274995] 08 p3263 N94-28995
A comparison of two computer models of sound propagation for a wedge shaped ocean over a penetrable bottom
[AD-A275031] 08 p3477 N94-29117
Spectral analysis of wave propagation in connected waveguides 08 p3277 N94-29944
Investigations of dispersion characteristics of microwave/optical guided wave structures by using transmission line matrix method
[ISBN-0-315-85856-7] 08 p3254 N94-30034
Electrooptical and optical evaluation of Pb(Zr,Ti)O3 thin films using waveguide refractometry
[DE94-006374] 08 p3518 N94-30247
Manufacture of light-damage resistant, planar, single mode waveguide on lithium niobate
[DSIS-94-01503] 09 p3879 N94-31850
Applied Computational Electromagnetics Society Journal, volume 9, number 1, March 1994
[AD-A276753] 09 p3679 N94-32183
Metal-ion spin-on glasses: Novel materials for active waveguides
[DE94-007738] 09 p3882 N94-32649
Theoretical, experimental, and computational evaluation of a tunnel ladder slow-wave structure
[NASA-TM-106642] 10 p4041 N94-33945
Study on active control of waveguide with piezoceramic actuator 10 p4042 N94-34349
Thin-ribbon tapered coupler for dielectric waveguides
11 p4253 N94-35547
Characterization of lithium niobate electro-optic modulators at cryogenic temperatures
[DE94-010059] 11 p4333 N94-35697
Radially combined 30 W, 14-16 GHz amplifier
[DE94-010078] 12 p4432 N94-36471
A novel transition between rectangular waveguide and layered ridge dielectric waveguide
[NASA-TM-106661] 12 p4433 N94-36955

WAVELENGTH DIVISION MULTIPLEXING

An efficient medium access control strategy for high speed WDM multiaccess networks
[MEMO-INF-92-74] 01 p0131 N94-10165
Application of new electro-optic technology to Space Station Freedom data management system
[NASA-CR-177622] 02 p0538 N94-13257
Advanced optical fiber communication systems
[AD-A269120] 04 p1577 N94-18254
Integrated Photonics Research: Post-deadline papers
[AD-A269232] 04 p1609 N94-18908
Wide band fiber-optic communications
06 p2304 N94-23231
Advanced optical fiber communication systems
[AD-A276416] 09 p3878 N94-31330

WAVELENGTHS

Interference photocathode
[AD-D015770] 01 p0132 N94-10382
Impact of shorter wavelengths on optical quality for laws
[NASA-CR-193433] 02 p0792 N94-14473
Alternative wavelengths for laser ranging
03 p0913 N94-15564
Optimum wavelengths for two color ranging
03 p0915 N94-15580
The A((2)pi(sub u))-X((2)pi(sub g)) system of Br2(+) studied by velocity modulation spectroscopy
[USIP-93-04] 04 p1569 N94-18847
The d(exp 3)delta-a(exp 3)delta and b(exp 3)phi-a(exp 3)delta systems of ZrS, Part 2: Appendix, list of wavenumbers
[USIP-92-05] 04 p1602 N94-19293
Surface-induced brightness temperature variations and their effects on detecting thin cirrus clouds using IR emission channels in the 8-12 micrometer region
05 p1880 N94-22341

WAVELET ANALYSIS

Recursive time-varying filter banks for subband image coding
[NASA-CR-193726] 02 p0598 N94-12920
Adaptive wavelet collocation methods for initial value boundary problems of nonlinear PDE's
[NASA-CR-191507] 03 p1169 N94-15833
Nonlinear problems in fluid dynamics and inverse scattering
[AD-A266234] 03 p1026 N94-16927
Applications of the phi-transform
[AD-A266247] 03 p1170 N94-16940
Studies in turbulence and turbulence control
[AD-A266318] 03 p1026 N94-16950
Diffractive optical elements for generating arbitrary line foci 03 p1195 N94-17338
Multivariate wavelet representations and approximations
[AD-A269350] 04 p1546 N94-17825
Wavelet transform for time-frequency analysis of the vibrational signature and its application
[AD-A269928] 04 p1454 N94-18661
Introduction to wavelets
[AD-A268465] 04 p1389 N94-18801
Application of wavelet transform techniques to spread spectrum demodulation and jamming
[AD-A267389] 04 p1389 N94-19009
A non-homogeneous, spatio-temporal, wavelet multiresolution analysis and its application to the analysis of motion
[AD-A270621] 04 p1538 N94-19534
Convergence of the hermite wavelet expansion
[AD-A271435] 05 p1854 N94-19841
On the spline-based wavelet differentiation matrix
[NASA-CR-191557] 05 p1950 N94-20087
Rough surface scattering from moving ocean surfaces as an indicator of scattering mechanisms
05 p1726 N94-20439
Signal processing in the linear statistical model
[AD-A272114] 05 p1736 N94-20570
An inverse DWT for nonorthogonal wavelets
[AD-A272064] 05 p1737 N94-20582
Use of switched capacitor filters to implement the discrete wavelet transform 05 p1755 N94-21097
Data compression by using wavelet transforms and vector quantization
[AD-A272763] 05 p1738 N94-21182
A multiresolution wavelet representation in two or more dimensions 05 p1925 N94-22456
On the Daubechies-based wavelet differentiation matrix
[NASA-CR-191583] 06 p2479 N94-23090
System identification using a wavelet-based approach
[DE94-002191] 06 p2293 N94-23473
Wavelet multiresolution analyses adapted for the fast solution of boundary value ordinary differential equations
06 p2485 N94-23691
On the differentiation matrix for Daubechies-based wavelets on an interval
[AD-A276348] 06 p2487 N94-24291
Optical wavelet transform processor
[AD-A273625] 06 p2546 N94-24731
Edge detection using a complex wavelet
[AD-A273699] 06 p2493 N94-25452
Filtering, coding, and compression with Malvar wavelets
[AD-A274055] 07 p2780 N94-25770
A comparison of spectral decorrelation techniques and performance evaluation metrics for a wavelet-based, multispectral data compression algorithm
07 p2946 N94-26258
Compression of multispectral Landsat imagery using the Embedded Zerotree Wavelet (EZW) algorithm
07 p2947 N94-26261
Wavelet compression techniques for hyperspectral data 07 p2947 N94-26263
Taxonomy of gamma ray burster data using a self-organizing neural network
[DE94-006480] 08 p3553 N94-30248
The Stroemberg wavelet on the interval and the Franklin system
[TELECOM-93-C-002] 08 p3462 N94-30971
Noise reduction techniques for the restoration of musical recordings
[TELECOM-93-E-019] 08 p3291 N94-30979
Regular wavelets: Application to fixed image compression
[TELECOM-93-E-004] 09 p3858 N94-31167
On wavelet representations of differential equations
[RR-482] 09 p3842 N94-31412
Application of the wavelet transform for speech processing 09 p3600 N94-31435
Wavelet transform of fixed pattern noise in focal plane arrays
[AD-A276963] 09 p3712 N94-32393
Neural network wavelet technology: A frontier of automation 09 p3839 N94-32425
Conference on operator, wavelet and control theory
[AD-A277429] 09 p3838 N94-33174
The 2nd International Conference on Curves and Surfaces: Abstracts
[AD-A276805] 10 p4128 N94-33406

Adaptive estimation and approximation of continuously varying spectral density functions to airborne radar
[AD-A277532] 10 p4033 N94-33710
Wavelet transforms in parallel image processing
[AD-A278372] 10 p4111 N94-33740
Dyadic wavelet features for isolated word speaker dependent speech recognition
[AD-A278492] 10 p4034 N94-33756
Analysis of wavelet technology for NASA applications
[NASA-CR-195929] 10 p3985 N94-34704
Coherent states versus de Broglie-wavelets
[DE94-611075] 11 p4343 N94-36381
Computational Mathematics Laboratory for multiscale analysis
[AD-A278597] 11 p4315 N94-36424
Periodized wavelets
[DE94-010365] 11 p4316 N94-36432
Noise reduction for speech enhancement using non-linear wavelet processing
[AD-A280469] 12 p4434 N94-37141
Detection of the electrocardiogram P-wave using wavelet analysis
[DE94-010791] 12 p4481 N94-37197

WAVELET TRANSFORM
U WAVELET ANALYSIS

WAVERIDERS
Numerical investigations in three-dimensional internal flows
[NASA-CR-194143] 02 p0637 N94-13827
Optimization and performance analysis of a supersonic conical-flow waverider for a deck-launched intercept mission
[AD-A272498] 05 p1648 N94-21433
Design project: LONGBOW supersonic interceptor
[NASA-CR-195510] 06 p2180 N94-24581
Sabot high speed interceptor AE 4273 aircraft design
[NASA-CR-195495] 06 p2183 N94-24971
Advanced vehicle concepts systems and design analysis studies
[NASA-CR-195115] 08 p3147 N94-29721
Expanding the waverider design space using arbitrary generating flowfields 08 p3148 N94-30516
A new inverse method for generating high-speed aerodynamic flows with application to waverider design 09 p3569 N94-31828
Vehicle integration effects on hypersonic waveriders
[NASA-TM-109739] 10 p3990 N94-34118

WAVES
FEFF5: An ab initio multiple scattering XAFS code
[DE93-011000] 01 p0367 N94-11470

WEAK ENERGY INTERACTIONS
NT WEAK INTERACTIONS (FIELD THEORY)
A high sensitivity search for CP violating rare K(sub L) decays and precision measurement of the direct CP violation parameter (epsilon)(prime)/(epsilon) via the four K (yields) 2(pi) decay modes
[DE93-016866] 03 p1184 N94-16899
Existence of a new instanton in constrained Yang-Mills-Higgs theory
[NIKHEF-H/93-02] 03 p1186 N94-17601
Properties of nuclei in astrophysical environments: Binding energies, weak-interaction rates
[MPA-706] 03 p1240 N94-17628
Weak hadronic decays of heavy flavor mesons
[ISBN-0-315-55542-4] 07 p3026 N94-27402
Pi plus pi minus gamma and K+ K- production in two photon collisions at ARGUS
[ISBN-0-315-63598-3] 07 p3027 N94-27684

WEAK INTERACTIONS (FIELD THEORY)
Discrete space-time symmetries
[DE93-010199] 01 p0341 N94-10259
Effective action in the gauged Nambu-Jona-Lasinio model
[DE93-617654] 01 p0409 N94-10405
Future high precision experiments and new physics beyond Standard Model
[DE93-011004] 01 p0373 N94-11618
Radiative corrections in the strongly interacting limit of the standard electroweak model
[DE93-013906] 02 p0780 N94-13018
Study of electroweak interactions
[DE93-015067] 02 p0782 N94-13412
Effects of additional isoscalar vector bosons in e(sup +)e)(sup -)(yields)ff-bar processes at the TRISTAN and LEP energies
[DE93-621451] 02 p0783 N94-13506
The (mu)(+) yields e(+)gamma
[DE93-012750] 02 p0785 N94-14181
Comparing the Z(sup 0) mass and inclusive widths to the standard electroweak theory
[PREPRINT-731] 02 p0787 N94-14721
Electroweak physics from D0
[DE93-015041] 03 p1181 N94-16053
Theoretical high energy physics research at the University of Chicago
[DE93-016863] 03 p1187 N94-16116
Electroweak results from D0
[DE93-014926] 03 p1185 N94-16968
On the difference caused by CP violation in the energy spectra of pions in K(sup (+-))(yields)(pi)(+-)(pi)(+-)(pi)-+ decays
[DE93-624828] 04 p1564 N94-17687
Extraction of Z(prime) coupling data from Z(prime) (yields) jj at the LHC and SSC
[DE93-018576] 04 p1570 N94-19096
Summary of the Hadronic Weak Interaction session
[DE94-000592] 05 p1975 N94-21775
Photon-photon collisions at the next linear collider: Theory
[DE93-041025] 06 p2534 N94-23803
New evaluation of hadronic contributions to the anomalous magnetic moment of charged leptons
[DE93-634394] 06 p2536 N94-24844
Weak interactions in a bilocal chiral theory
[DE93-616887] 06 p2539 N94-25477
Weak interactions in a bilocal chiral theory
[DE93-613097] 07 p3013 N94-25836
Heavy charged leptons in an SU(3)(sub L) x U(1)(sub N) model
[DE93-634367] 07 p3016 N94-26041
Construction of a new electroweak sphaleron
[NIKHEF-H/93-09] 07 p3020 N94-26540
Constraints on singlet right-handed neutrinos coming from the Z(0)-width
[DE93-634393] 07 p3022 N94-26766
Cosmological phase transitions
[DE94-003001] 07 p3104 N94-26786
Progress in SSC Higgs physics: Report of the Higgs working group
[DE94-003224] 07 p3022 N94-26793
Electroweak and other interactions in medium-energy nuclear physics
[DE94-004161] 07 p3027 N94-27689
Topics in electroweak baryogenesis: The sphaleron and T-violation
[DE94-004886] 07 p3029 N94-27811
A measurement of the tau polarization at the resonance with the DELPHI detector at LEP
[DE94-005557] 08 p3482 N94-28520
Weak decays of charged K-mesons and charm particles
[PB94-138062] 08 p3486 N94-29143
A Tevatron collider beauty factory
[DE94-004879] 08 p3488 N94-29930
High sensitivity tests of the standard model for electroweak interactions
[DE94-005415] 08 p3490 N94-30262
Baryogenesis from a primordial lepton asymmetry
[PB94-145166] 09 p3868 N94-31921
Proceedings of the International Workshop on Low Energy Muon Science: LEMS 1993
[DE94-006495] 09 p3874 N94-32804
Spin and precision electroweak physics
[DE94-009074] 10 p4137 N94-33936
Radiatively induced electron and electron-neutrino masses
[DE94-616775] 11 p4321 N94-35582
Some consequences in weak processes of three generations mixing in the leptonic sector
[DE94-616650] 11 p4321 N94-35594

WEAPON SYSTEM MANAGEMENT
Risk analysis of the C-141 WS405 inner-to-outer wing joint 10 p3996 N94-34592

WEAPON SYSTEMS
NT GROUND OPERATIONAL SUPPORT SYSTEM
NT LASER WEAPONS
NT MISSILE SYSTEMS
Selected upper-air wind speed distributions
[AD-A264822] 01 p0284 N94-10871
Army P/M research and development overview
[AD-A266921] 03 p0954 N94-15104
RAMCAD design methodology
[AD-A267010] 03 p1145 N94-15525
Infrared spot tracker
[AD-D015778] 03 p1191 N94-16547
Preliminary validation of the task analysis/workload methodology
[AD-A267514] 03 p1138 N94-17077
Review of short-term, high-level exposure to metals: Antimony, barium, and cadmium
[AD-A268896] 04 p1505 N94-18392
Tactical laser weapons and other directed-energy weapons
[AD-A267961] 05 p1816 N94-20484
A qualified radiation hardened nonvolatile memory for space and tactical weapons applications
[DE94-001211] 06 p2559 N94-23186
Early manufacturing considerations in design 06 p2177 N94-24315
Weapon system integration for the AFIT virtual cockpit
[AD-A274058] 07 p2667 N94-25772
Weapon system sensor integration for a DIS-compatible virtual cockpit
[AD-A274088] 07 p2672 N94-26021
Smart structures, an overview
[AD-A274147] 07 p2987 N94-27093
A common Ada run-time system for avionics software 08 p3150 N94-29331
Validation and test of complex weapon systems 08 p3150 N94-29336
Testing Operational Flight Programs (OFPs) 08 p3415 N94-29337
A disciplined approach to software test and evaluation 08 p3416 N94-29339
Naval Surface Warfare Center Dahlgren Division Technical Digest: Advanced materials technology
[AD-A276448] 09 p3668 N94-31364
Unmanned Air Vehicle/Remotely Piloted Vehicle analysis for lethal UAV/RPV
[AD-A276052] 09 p3578 N94-31442
Modular Simulator System (MSS) management guide
[AD-A277098] 09 p3588 N94-32014
Getting a handle on designing for avionics software supportability and maintainability
[AD-A276362] 09 p3581 N94-32055
Analysis of Navy aircraft engine and engine component warranties
[AD-A276936] 09 p3584 N94-32238
Modular Simulator System (MSS). System/segment specification for the generic modular simulator system-weapons module, volume 7
[AD-A276974] 09 p3590 N94-32399
Vulnerability assessment of a space based weapon platform electronic system exposed to a thermonuclear weapon detonation
[DE94-007229] 09 p3611 N94-32667
Accelerated reliability testing utilizing design of experiments
[AD-A277989] 09 p3732 N94-33088
Report of the workshops: Automated generation of electronic technical manuals
[AD-A278046] 10 p4150 N94-33401
Fusion interfaces for tactical environments: An application of virtual reality technology 10 p4100 N94-33619
Operational agility
[AGARD-AR-314] 10 p3989 N94-33875

WEAPONS
NT ARTILLERY
NT FUSION WEAPONS
NT GUNS (ORDNANCE)
NT HOWITZERS
NT LASER WEAPONS
NT MINES (ORDNANCE)
NT NUCLEAR WARHEADS
NT NUCLEAR WEAPONS
NT RIFLES
NT SPACE WEAPONS
NT WARHEADS
Temperature of aircraft cargo flame exposure during accidents involving fuel spills
[DE93-019633] 04 p1381 N94-19539
Chemistry and materials science
[DE94-001449] 05 p2152 N94-21858

WEAPONS DELIVERY
Weapon system integration for the AFIT virtual cockpit
[AD-A274058] 07 p2667 N94-25772
Characterization of a diffraction grating as a simulant of a selective frequency antenna for radiometric applications
[AD-A275793] 08 p3241 N94-28745

WEAPONS DEVELOPMENT
Advanced Capability Exhaust Systems/Integrated Product Development for advanced nozzles (ACES/IPD)
[AD-A273209] 06 p2189 N94-24776
The proliferation of aerospace weapons technology: Ballistic missiles and the case of Brazil
[ISBN-0-315-84082-X] 07 p2763 N94-26634
Operational agility: An overview of AGARD Working Group 19 10 p3993 N94-34625

WEAPONS INDUSTRY
The proliferation of aerospace weapons technology: Ballistic missiles and the case of Brazil
[ISBN-0-315-84082-X] 07 p2763 N94-26634

WEAR
Report of the IAEA Consultants' Meeting on Real-Time Nondestructive Monitoring of Wear and Corrosion Using the Thin Layer Activation Technique
[DE93-617422] 01 p0183 N94-10847
Titanium alloys milling assistance by high pressure lubricoolant jet
[DE93-013302] 01 p0082 N94-11008
Advanced model of gradual wear of viscoelastic surface film
[AD-A265130] 01 p0090 N94-11222
Properties of interfacial tribo-films
[AD-A265591] 01 p0182 N94-12374

Wear-mechanism modelling
[DE93-012311] 02 p0579 N94-13974
Machining aspects of nickel-phosphorus coatings
[DE93-013037] 02 p0580 N94-14311
The friction and wear of ceramic/ceramic and ceramic/metal combinations in sliding contact
[NASA-TM-106348] 03 p0930 N94-15769
Ion implantation effects on surface-mechanical properties of metals and polymers
[DE93-014661] 03 p0958 N94-16453
Atomic-scale friction measurements using friction force microscopy. Part 1: General principles and new measurement techniques
[AD-A268391] 03 p1048 N94-17533
Continuing research on friction and wear of materials
[AD-A268291] 03 p1049 N94-17566
Interdisciplinary research on wear of materials
[AD-A268190] 04 p1443 N94-17730
Effect of temperature and O-ring gland finish on sealing ability of Viton V747-75
[NASA-TP-3391] 04 p1368 N94-18075
Studies of dynamic contact of ceramics and alloys for advanced heat engines
[DE93-016366] 04 p1368 N94-18110
MHD integrated topping cycle project
[DE93-040520] 04 p1588 N94-18978
Contribution to the tribological study of magnetic-tape head contact
[ECL-92-57] 04 p1434 N94-19414
Atomic-scale friction measurements using friction force microscopy. Part 1: General principles and new measurement techniques
[AD-A270749] 04 p1446 N94-19678
Microtribology of magnetic media
[AD-A271209] 04 p1407 N94-19722
Tribological studies of silicon for magnetic recording applications (Invited)
[AD-A270878] 04 p1447 N94-19784
Microscopic modeling of tribological and interfacial phenomena
[AD-A271864] 05 p1823 N94-20464
Development of fundamental understanding of friction and wear mechanisms by atomic-scale tribological studies of ceramic materials and multilayered thin films
[AD-A271485] 05 p1703 N94-20548
Lubricated wear of steel-ceramic and ceramic-ceramic systems
[PB93-202356] 05 p1825 N94-21450
Vapor-delivered lubrication of steel-steel and steel-ceramic systems
[PB93-202364] 05 p1825 N94-21451
Detailed study of oxidation/wear mechanism in lox turbopump bearings
[NASA-TM-108434] 05 p1825 N94-21580
Brush seal bristle flexure and hard-rub characteristics
05 p1654 N94-21791
Integrity testing of brush seal in a T-700 engine
05 p1654 N94-21792
Dynamics of face seals for high speed turbomachinery
05 p1655 N94-21796
New method for increasing machine service-life, phase 2
[PB93-200707] 06 p2354 N94-23533
A rail corrugation theory which allows for contact patch size
06 p2269 N94-23582
A linear model for corrugation and its limit of validity
06 p2269 N94-23584
Surface analysis of corrugated rail treads
06 p2270 N94-23587
Development of a theory of the wear of ceramics
[DE94-002773] 06 p2254 N94-23783
New tribocoating combination for vacuum operation
06 p2355 N94-23990
Wear reduction in ceramic bearings by surface generated pyrolytic carbon continuously replenished by ethylene gas
[AD-A278264] 06 p2364 N94-24090
Tests of highly loaded skids on a concrete runway
[NASA-TP-3435] 07 p2669 N94-26608
A non-linear mathematical model or finite, periodic rail corrugations
[REPT-93-49] 07 p2996 N94-26967
Guidelines for unlubricated sliding wear tests. Part 1: General approach
[PB94-119666] 07 p2825 N94-27322
Guidelines for unlubricated sliding wear tests. Part 2: Procedures for pin-on-disc testing
[PB94-123270] 07 p2825 N94-27324
Lubrication of space systems
[NASA-TM-106392] 08 p3214 N94-29399
Cost-effective ceramic machining: Summary of three-body wear experiments
[DE94-007757] 09 p3650 N94-31354
Continuing research on friction and wear of materials
[AD-A277690] 10 p4059 N94-33437
Multiple hollow cathode wear testing
[NASA-CR-195335] 10 p4016 N94-33975
Application of neural networks in multiple sensor fusion for on-line tool wear monitoring
10 p4119 N94-34347
Computer image analysis of wear debris with its applications to machine wear diagnosis
10 p4067 N94-34366
Durability testing of medium speed diesel engine components designed for operating on coal/water slurry fuel
[DE94-009550] 11 p4275 N94-35667

WEAR INHIBITORS

The use of screening tests in spacecraft lubricant evaluation
[AD-A272943] 05 p1705 N94-21225
Photoelectron spectroscopic studies of the electronic structure and bonding in TiC and TiN
[ATR-93(8361)-2] 07 p2746 N94-28185

WEAR RESISTANCE

NT ABRASION RESISTANCE
Processing, properties, and wear resistance of aluminides
[DE93-012186] 01 p0083 N94-11141
Weld overlay coatings for erosion control
[DE93-013592] 01 p0084 N94-11816
The effect of TiN coatings on the rolling contact fatique behavior of M50 bearing steel
[ARL-TR-40] 02 p0662 N94-13794
Vacuum plasma spraying 03 p0975 N94-16002
Wear resistant titanium material development
[AD-A266474] 03 p0959 N94-16780
Application of hard coatings to substrates at low temperatures
[NASA-CR-193867] 03 p0971 N94-17122
Joining and Adhesion of Advanced Inorganic Materials Symposium
[AD-A269748] 04 p1342 N94-18720
JBK-75 stainless steel machinability study
[DE94-002268] 06 p2242 N94-23475
Wear reduction in ceramic bearings by surface generated pyrolytic carbon continuously replenished by ethylene gas
[AD-A278264] 06 p2364 N94-24090
Development of high temperature liquid lubricants for low-heat rejection: Heavy duty diesel engines
[NASA-CR-191197] 06 p2258 N94-24753
A preliminary evaluation of the phosphazene resin PPZ
[AD-A273674] 06 p2263 N94-25410
Development of braided rope engine seals
[NASA-TM-105902] 08 p3298 N94-28838
Unscreened low tension cables scrape abrasion testing. Part 1: An interlaboratory study on scrape abrasion testing according to ISO DP 6722-1
[PB94-135605] 08 p3264 N94-29191
The effect of prolonged exposure to 750 C air on the tribological performance of PM212
[NASA-TM-106472] 09 p3617 N94-32941
Durability testing of medium speed diesel engine components designed for operating on coal/water slurry fuel
[DE94-009550] 11 p4275 N94-35667
Wear-resisting oxide films for 900 C
[DE94-010093] 11 p4246 N94-36306
Robotic weld overlay coatings for erosion control
[DE94-013477] 12 p4417 N94-37116

WEAR TESTS

Report of the IAEA Consultants' Meeting on Real-Time Nondestructive Monitoring of Wear and Corrosion Using the Thin Layer Activation Technique
[DE93-617422] 01 p0183 N94-10847
Dry film lubricant evaluation
[DE93-013114] 02 p0578 N94-13118
Surface analysis of bearings
[AD-A266800] 02 p0661 N94-13122
Wear-mechanism modelling
[DE93-012311] 02 p0579 N94-13974
Canadian Target Assembly (CTA) to Airborne Support Equipment (ASE) vibration test report
[IME-AMT-TR-001] 02 p0663 N94-14195
Wear resistant titanium material development
[AD-A266474] 03 p0959 N94-16780
Interdisciplinary research on wear of materials
[AD-A268190] 04 p1443 N94-17730
Lubricated wear of steel-ceramic and ceramic-ceramic systems
[PB93-202356] 05 p1825 N94-21450
A colour image processing algorithm to identify copper-based particles in filter debris samples
[DREP-TM-93-19] 06 p2455 N94-24122
Unscreened low tension cables scrape abrasion testing
[PB94-123767] 07 p2823 N94-26849
Guidelines for unlubricated sliding wear tests. Part 1: General approach
[PB94-119666] 07 p2825 N94-27322
Guidelines for unlubricated sliding wear tests. Part 2: Procedures for pin-on-disc testing
[PB94-123270] 07 p2825 N94-27324
Unscreened low tension cables scrape abrasion testing. Part 1: An interlaboratory study on scrape abrasion testing according to ISO DP 6722-1
[PB94-135605] 08 p3264 N94-29191
Sliding friction and wear between titanium nitride, M50 steel and silicon nitride (round 3 of VAMAS wear test program)
[IMR-TM-TR-003] 08 p3303 N94-30019
Cracking induced in small fretting: Application to the case of aeronautical aluminum alloys
[ECL-92-50] 09 p3735 N94-31870
The effect of prolonged exposure to 750 C air on the tribological performance of PM212
[NASA-TM-106472] 09 p3617 N94-32941
The preliminary evaluation of liquid lubricants for space applications by vacuum tribometry
09 p3606 N94-33313
Continuing research on friction and wear of materials
[AD-A277690] 10 p4059 N94-33437
Multiple hollow cathode wear testing
[NASA-CR-195335] 10 p4016 N94-33975
Robotic weld overlay coatings for erosion control
[DE94-013477] 12 p4417 N94-37116

WEATHER

NT COLD WEATHER
A toolkit for building Earth system models
[DE93-012147] 01 p0276 N94-11138
Development of a graphical user interface and graphics display for the WIND system
[DE93-011780] 01 p0285 N94-11614
Wind system documentation
[DE93-010381] 01 p0285 N94-11664
Preliminary meteorological results for 1992 West Coast Scotland Experiment
[DE93-014677] 02 p0720 N94-13404
Weather forecasting support for AASE-2
[NASA-CR-194342] 02 p0721 N94-13675
Venus lightning
[NASA-TM-109644] 03 p1105 N94-15430
Boundary layer structure over areas of heterogeneous heat fluxes
[DE93-010657] 03 p1110 N94-17673
New techniques for contrail forecasting
[AD-A269686] 04 p1490 N94-18573
CDIAC catalog of numeric data and computer model packages
[DE93-017675] 04 p1475 N94-18832
Eastern Europe: A climatological study
[AD-A269200] 04 p1493 N94-18883
An analysis of cloud-cover reporting in the 1977 surface observation database
[AD-A271102] 05 p1864 N94-19852
Analysis of a sandstorm weather process-translation
[AD-A272959] 05 p1867 N94-21250
Parallel runway requirement analysis study. Volume 1: The analysis
[NASA-CR-191549-VOL-1] 05 p1644 N94-22277
Cockpit weather graphics using mobile satellite communications 06 p2280 N94-22775
Aircraft accident report: In-flight engine separation. Japan Airlines, Inc., flight 46E, Boeing 747-121, N473EV, Anchorage, Alaska, 31 March 1993
[PB93-410407] 06 p2173 N94-24062
United States Weather Research Program (USWRP)
06 p2411 N94-24375
Aviation Weather Program (AWP)
06 p2411 N94-24380
ASR-9 microburst detection algorithm
[AD-A273591] 06 p2415 N94-24850
Overall analysis of meteorological information in the Daeduk nuclear complex
[DE93-632594] 07 p2894 N94-26469
Encoding approaches for data link transmission of weather graphics
[AD-A274497] 07 p2772 N94-26963
Meteorological data at the Nagaoka Institute of Snow and Ice Studies
[REPT-158] 07 p2896 N94-27169
Aircraft accident report: Runway departure following landing American Airlines flight 102, McDonnell Douglas DC-10-30, N139AA, Dallas/Fort Worth International Airport, Texas, April 14, 1993
[PB94-910402] 07 p2660 N94-27766
Catalog of Air Force weather technical publications 1992-1993
[AD-A275635] 08 p3368 N94-28638
Capabilities, products, and services of USAFETAC (USAF Environmental Technical Applications Center)
[AD-A275654] 08 p3368 N94-28652

AFGWC Dial-In Subsystem (AFDIS) software users manual, version 2.2
[AD-A275844] 08 p3371 N94-29747
Micro-sensors for in-situ meteorological measurements 08 p3236 N94-29777
Satellite direct readout: Opportunities for science education
[AD-A276257] 09 p3609 N94-31292
The evolution of jet features during the 1993 east coast white hurricane: A case study using the global spectral model
[AD-A277217] 09 p3783 N94-32021
Recommendations for meteorological data collection during physiological field studies
[AD-A276834] 09 p3901 N94-32153
Technical evaluation of the UH-60Q: Aircraft in typical aeromedical evacuation missions
[AD-A276944] 09 p3586 N94-32217
The influence of thermal inertia on Mars' seasonal pressure variation and the effect of the weather component 09 p3952 N94-33238
Impact of weather on flight operations at a major airport
[PB94-127990] 10 p4090 N94-34408

WEATHER CHARTS
U METEOROLOGICAL CHARTS

WEATHER CONDITIONS
U WEATHER

WEATHER CONTROL
U WEATHER MODIFICATION

WEATHER FORECASTING
NT LONG RANGE WEATHER FORECASTING
NT NOWCASTING
NT NUMERICAL WEATHER FORECASTING
NT STATISTICAL WEATHER FORECASTING
Updated forecast of Atlantic seasonal hurricane activity for 1993 01 p0285 N94-11194
Rainfall-runoff estimation using digital radar
[AD-A265390] 01 p0286 N94-12408
Use of ERS-1 wind and wave products in operational meteorology 01 p0250 N94-12502
Use of SAR-wave, altimeter, and wind-scatterometer data in an operational swell forecasting system 01 p0250 N94-12503
Use of ERS-1 scatterometer winds in Canadian forecast centres 01 p0250 N94-12504
The application of VAS satellite imagery to thunderstorm forecasting at Cape Canaveral
[NASA-CR-193563] 02 p0718 N94-12839
Storm prediction through barometric field analysis
[PUBL-SER-A-129] 02 p0720 N94-13587
Weather forecasting support for AASE-2
[NASA-CR-194342] 02 p0721 N94-13675
Mesoscale modeling of the atmosphere
[AD-A263236] 03 p1098 N94-15132
Short term weather forecasting in real time in a base weather station setting
[AD-A266872] 03 p1105 N94-15142
The Next Generation Weather Radar (NEXRAD)/Air Route Surveillance Radar (ARSR) operational comparison
[REPT-93W0000145] 03 p0987 N94-15439
Radar diagnostic parameters as indicators of severe weather in central Florida
[PB93-183507] 03 p1106 N94-16465
The multivariate optimum interpolation analysis of meteorological data at the Fleet Numerical Oceanography Center
[AD-A266459] 03 p1106 N94-16568
A snow wetness retrieval algorithm for SAR 03 p1075 N94-16732
The standardized precipitation index and its use in the western contiguous United States
[AD-A267547] 03 p1107 N94-17102
Solar Electro-Optical Network (SEON) upgrade/replacement program. Phase 1: Qualification operational test and evaluation plan
[AD-A266364] 03 p1237 N94-17225
Developing automated analysis methods for sea ice imagery: A status report with recommendations
[AD-A267284] 03 p1113 N94-17241
The use of the Air Force Academy high wind alert system in forecasting moderate intensity wind events for military bases in the Colorado Springs area
[AD-A267648] 03 p1107 N94-17245
Nowcasting methods for satellite imagery
[AD-A267294] 03 p1108 N94-17267
Propagation characteristics of mesoscale convective systems
[AD-A268130] 03 p1109 N94-17522
Micro- and meso-scale simulations of magnetospheric processes related to the aurora and substorm morphology
[NASA-CR-193437] 03 p1102 N94-17527
Rapid oceanic cyclogenesis studies
[AD-A269256] 04 p1490 N94-18265
Preparation of data assimilation and model evaluation experiment data sets
[AD-A269996] 04 p1498 N94-18665
Atlas of SSM/I satellite ice concentration interpolated to operational ice model domains of the Arctic for 1992
[AD-A270306] 04 p1499 N94-18727
Organized track system: Air ways above the ocean 04 p1495 N94-19702
Calamity weather: Environmental calamities and meteorology 04 p1495 N94-19703
Clouds: Their prediction and simulation
[AD-A271161] 05 p1864 N94-19900
Offshore decision support system: ERS-1 pilot project WAVEWATCH
[BCRS-92-09] 05 p1865 N94-20532
Weather tutor 1: Stability basics
[AD-A270758] 05 p1866 N94-20565
Drought early warning system for crop production 05 p1840 N94-20966
Simulated real-time intercomparison of hydrological models
[WMO-779] 05 p1867 N94-21070
Incorporation and comparative evaluation of a non-convective cloud parameterization scheme in the Naval Research Laboratory west coast mesoscale weather prediction model
[AD-A272417] 05 p1867 N94-21146
A retrieval error analysis technique for passive infrared atmospheric sounders
[AD-A272618] 05 p1867 N94-21212
Mesoscale simulations of the November 25-26 and December 5-6 cirrus cases using the RAMS model 05 p1878 N94-22331
Urban/rural application of weather radar for flow forecasting. Proceedings of the Informal CEc -Workshop
[PB93-220135] 06 p2407 N94-23129
Lightning studies using LDAR and LLP data 06 p2416 N94-23238
United States Weather Research Program (USWRP) 06 p2411 N94-24375
Aviation Weather Program (AWP) 06 p2411 N94-24380
Scientific goals of the Cooperative Multiscale Experiment (CME) 06 p2411 N94-24381
Examples of data assimilation in mesoscale models 06 p2412 N94-24384
Session on validation of coupled models 06 p2414 N94-24399
CAPE for CaPE 06 p2416 N94-24409
Modeling and data assimilation for Mars Observer 06 p2620 N94-24889
Observed and Navy operational global model climatologies of synoptic disturbances over the tropical western Pacific during winter 1991-1992
[AD-A273400] 06 p2416 N94-25071
Short-range cloud amount forecasting with model output statistics
[AD-A274769] 07 p2895 N94-26798
The NOGAPS ten year AMIP integration
[AD-A274332] 07 p2900 N94-26887
Encoding approaches for data link transmission of weather graphics
[AD-A274497] 07 p2772 N94-26963
The climate of the Mediterranean basin: Its sensitivity to global change 09 p3778 N94-30993
Estimation and analysis of climate-scale rainfall over the Tropical Pacific 09 p3783 N94-32030
Use of Air Force cloud cover data to evaluate and improve cloud forecasts and parameterizations in mesocale meteorological models
[AD-A277384] 09 p3784 N94-32054
The influence of cumulus parameterization on model forecasts of rapid oceanic cyclogenesis
[AD-A277207] 09 p3784 N94-32094
Coordination of mesoscale meteorological research between ASL and European group
[AD-A276730] 09 p3784 N94-32162
Development and testing of improved techniques for modeling the hydrologic cycle in a mesoscale weather prediction system
[AD-A277416] 09 p3786 N94-32921
Forecasters handbook for the Philippine Islands and surrounding waters
[AD-A277993] 09 p3787 N94-33089
Might it be possible to predict the onset of major Martian dust storms? 09 p3948 N94-33215
Snowmelt forecasting: Further cold regions development of operational hydrological forecasting, volume 1
[AD-A278050] 10 p4074 N94-33410
Typhoon monitoring using passive satellite observations
[AD-A277859] 10 p4089 N94-33769
The analysis of rapidly developing fog at the Kennedy Space Center
[NASA-CR-195888] 10 p4090 N94-34939
Extrapolating storm location using the Integrated Terminal Weather System (ITWS) storm motion algorithm
[AD-A278611] 11 p4295 N94-36249
Use of formal calculation to automatically obtain adjoint programs
[PB94-170701] 11 p4308 N94-36259
Doppler weather radar studies of precipitation systems
[AD-A279417] 11 p4295 N94-36262
Toward a new National Weather Service: Weather for those who fly 12 p4472 N94-36947

WEATHER FRONTS
U FRONTS (METEOROLOGY)

WEATHER MAPS
U METEOROLOGICAL CHARTS

WEATHER MODIFICATION
NT CLOUD SEEDING
NT STORM ENHANCEMENT
NOAA Federal/State Cooperative Program in Atmospheric Modification Research. Collected publication titles and abstracts
[PB93-198125] 06 p2396 N94-22913

WEATHER RADAR
U METEOROLOGICAL RADAR

WEATHER STATIONS
NT AUTOMATIC WEATHER STATIONS
CCI working group on climate data and its rapporteurs
[WCDMP-21] 02 p0723 N94-14118
Short term weather forecasting in real time in a base weather station setting
[AD-A266872] 03 p1105 N94-15142
TAFVER 2 users manual
[AD-A266850] 03 p1106 N94-15757
The multivariate optimum interpolation analysis of meteorological data at the Fleet Numerical Oceanography Center
[AD-A266459] 03 p1106 N94-16568
Report of the Experts Meeting on Reference Climatological Stations (RCS) and National Climate Data Catalogues (NCC)
[WMO-TD-535] 04 p1494 N94-19312
Cloud fields derived from satellite and surface data during FIRE cirrus phase 2 05 p1872 N94-22302
Spatial interpolation, network bias, and terrestrial air temperature variability 08 p3374 N94-30810
Selection of climate station data using clustering and triangulated irregular network techniques
[AD-A276658] 09 p3784 N94-32046
Station climatic summaries: China, the former USSR, and Mongolia
[AD-A276548] 09 p3784 N94-32057
Recommendations for meteorological data collection during physiological field studies
[AD-A276834] 09 p3901 N94-32153
Toward a new National Weather Service: Weather for those who fly 12 p4472 N94-36947

WEATHERING
Carbon in weathered ordinary chondrites from Roosevelt County 01 p0428 N94-12035
Chemical weathering on Mars: Rate of oxidation of iron dissolved in brines 01 p0455 N94-12128
The rate of chemical weathering of pyrite on the surface of Venus 01 p0477 N94-12246
Measuring and distinguishing compositional and maturity properties of lunar soils by remote VIS-NIR spectroscopy 01 p0478 N94-12251
Extrapolation of space weathering processes to other small solar system bodies 02 p0843 N94-14300
Spectral evidence of size dependent space weathering processes on asteroid surfaces 03 p1241 N94-16174
Variations in the Fe mineralogy of bright Martian soil 03 p1295 N94-16431
Lithological and textural controls on radar and diurnal thermal signatures of weathered volcanic deposits, Lunar Crater region, Nevada 03 p1080 N94-16762
Optical effects of space weathering on lunar soils and the role of the finest fraction 05 p2101 N94-20687
Local topography of Mars and its relationship to surface weathering processes 05 p2111 N94-20737
The role of CO2 in weathering reactions and the presence of S2 on Venus: Implications for the pyrite stability field 05 p2122 N94-20799
Weathering features and secondary minerals in Antarctic Shergottites ALHA77005 and LEW88516 05 p2086 N94-20869
K, U, and Th behavior in Martian environmental conditions 05 p2141 N94-20908
Oxidation of dissolved iron under warmer, wetter conditions on Mars: Transitions to present-day arid environments 05 p2143 N94-21663
An attempt to comprehend Martian weathering conditions through the analysis of terrestrial palagonite samples 05 p2143 N94-21668

Failure behaviour of high density polyethylene with an embrittled surface layer due to weathering
[PB94-126406] 07 p2840 N94-26960
An outdoor exposure testing program for optical materials used in solar thermal electric technologies
[DE94-000265] 08 p3500 N94-29799
Deposition rates of oxidized iron on Mars 09 p3945 N94-33198
Magmatic volatiles and the weathering of Mars 09 p3946 N94-33201
Antarctic weathering of the CK chondrites EET90004, 90007, and 90022: Nickel and sulfur mobility 11 p4351 N94-35451
Evaluation of flame-sprayed polymer coatings for civil works navigation structures
[AD-A280507] 12 p4422 N94-37104

WEAVING
Processing, properties and applications of composites using powder-coated epoxy towpreg technology 03 p0933 N94-15277
Research in textile composites at KU, Leuven 03 p0937 N94-16848
Weaving multi-layer fabrics for reinforcement of engineering components 03 p0937 N94-16850
Characterization and manufacture of braided composites for large commercial aircraft structures 09 p3630 N94-33137

WEBS (MEMBRANES)
U MEMBRANES

WEDGE FLOW
On the interaction between the shock wave attached to a wedge and freestream disturbances
[NASA-CR-191528] 03 p1019 N94-15478

WEDGES
Capillary surfaces in a wedge: Differing contact angles
[DE93-013903] 02 p0631 N94-13244
Translating wedge heat sink
[AD-D015814] 03 p1011 N94-16488
Quadruplet expansion of the acoustic pressure field in a wedge shaped ocean
[AD-A275121] 08 p3477 N94-29003
A comparison of two computer models of sound propagation for a wedge shaped ocean over a penetrable bottom
[AD-A275031] 08 p3477 N94-29117
Control of hypersonic aerodynamic forces with surface blowing 09 p3567 N94-31216
Penetrable wedge analysis
[AD-A277219] 09 p3845 N94-32022
Numerical simulation of the edge tone phenomenon
[NASA-CR-4581] 10 p3982 N94-33898
Wedge scattering by the method of iteration
[DE94-010404] 11 p4256 N94-36112

WEIBULL DENSITY FUNCTIONS
Selected upper-air wind speed distributions
[AD-A264822] 01 p0284 N94-10871
Constant False Alarm Rate (CFAR) detection in Weibull clutter
[ITN-93-85190] 02 p0600 N94-13537
Weibull analysis applied to the pull adhesion test and fracture of a metal-ceramic interface
[DE93-012913] 03 p1059 N94-15997
Durability evaluation of ceramic components using CARES/LIFE
[NASA-TM-106475] 06 p2258 N94-24682
Estimation and tests-of-fit for the three parameter Weibull distribution
[AD-A274827] 07 p3004 N94-26496
Simulating high-frequency wind for long durations
[DE94-002739] 07 p2682 N94-27997
Estimation of Weibull modulus from dynamic and static fatigue experiments
[PB94-138641] 08 p3322 N94-30114
Several modified goodness-of-fit tests for the cauchy distribution with unknown scale and location parameters
[AD-A278496] 10 p4130 N94-34301
Statistical characterization of rare events 12 p4454 N94-37327
Statistical scaling relationships and size effects in the strength and creep rupture of fibrous composites 12 p4460 N94-37809

WEIERSTRASS FUNCTIONS
The super Weierstrass (zeta)-function and operator product expansions in 2D-induced supergravity on the supertorus
[DE94-603664] 07 p3074 N94-27627

WEIGHT (MASS)
NT ATOMIC WEIGHTS
NT BIOMASS
NT BODY WEIGHT
NT STRUCTURAL WEIGHT
Development and application of a comprehensive, design-sensitive weight prediction method for wing structures of transport category aircraft
[LR-693] 02 p0515 N94-13687
SeaSoar and CTD sections across the Iceland-Faeroes Front and Faeroe Shetland Channel, August 1990
[IOS-295-1992] 04 p1496 N94-18064
Selection of site injecting adjuvant in chronic inflammation model 07 p2906 N94-27496
An analysis of the loads applied to a heavy Space Station rack during translation and rotation tasks
[NASA-TM-104790] 07 p2697 N94-28183

WEIGHT ANALYSIS
Development and application of a comprehensive, design-sensitive weight prediction method for wing structures of transport category aircraft
[LR-693] 02 p0515 N94-13687
Study on radiation-induced deterioration of grease at high temperature, 3
[DE93-788368] 04 p1369 N94-18220
Nonlinear aerodynamics and the design of wing tips
[NASA-CR-194732] 05 p1638 N94-21833
NASA/USRA advanced design program
[NASA-CR-195548] 06 p2180 N94-24492
Design optimization of high-speed proprotor aircraft
[NASA-TM-103988] 07 p2667 N94-26151
Aircraft weight prediction capability. Volume 1: Weight study and results
[AD-A277206] 09 p3579 N94-32062

WEIGHT FACTORS
U WEIGHT (MASS)

WEIGHT INDICATORS
NT MICROBALANCES
NT STRAIN GAGE BALANCES
A non-contacting vertical alignment system for mass properties measuring instruments
[DE94-004680] 08 p3289 N94-29927
Piggyback balance experiment: An illustration of Archimedes' principles and Newton's third law
[PB94-163060] 11 p4265 N94-35942

WEIGHT MEASUREMENT
Testing of protective coatings in hydrogen
[DE93-040326] 04 p1375 N94-19651
Mass properties measurement system dynamics 06 p2368 N94-23235
Mass properties measurement system: Dynamics and statics measurements 06 p2368 N94-23236
Innovative mechanism for measuring the mass properties of an object 09 p3604 N94-33299
Piggyback balance experiment: An illustration of Archimedes' principles and Newton's third law
[PB94-163060] 11 p4265 N94-35942

WEIGHT REDUCTION
Regenerative fuel cells for High Altitude Long Endurance Solar Powered Aircraft
[DE93-016991] 04 p1465 N94-17853
Lightweight materials for transportation: Program plan
[DE93-017381] 04 p1340 N94-18087
Nonlinear aerodynamics and the design of wing tips
[NASA-CR-194732] 05 p1638 N94-21833
NASA Lewis advanced IPV nickel-hydrogen technology 06 p2392 N94-23356
The mass of massive rover software 06 p2464 N94-23410
Bipolar Ag-Zn battery 07 p2864 N94-28135
Advanced microfabrication technologies for microspacecraft 08 p3171 N94-29782
Use of magnetic compression to support turbine engine rotors 08 p3314 N94-30484
HSCT integrated propulsion control issues 10 p3978 N94-33510
Carbon-carbon heat pipe testing and evaluation
[NASA-TM-106630] 12 p4405 N94-37318

WEIGHTING FUNCTIONS
Adaptive beamforming with imperfect arrays: Pattern effects and their partial correction
[AD-A267079] 03 p0987 N94-15541
Nonparametric statistics: Weighted rankings analysis
[AD-A266607] 03 p1173 N94-16657
Nontraditional windows in spectral analysis
[AD-A271336] 04 p1553 N94-19583
A weighted least-squares lump correction algorithm for transmission-corrected gamma ray nondestructive assay
[DE93-018474] 05 p1904 N94-20049
Smoothed-particle hydrodynamics and nonequilibrium molecular dynamics
[DE94-001059] 05 p1977 N94-22400
Optimal gains for a single polar orbiting satellite 06 p2208 N94-24873
The Casimir energy of the rigid string with massive ends
[DE93-616851] 06 p2492 N94-25338
Numeric solution of the electric field integral equation using Galerkin's method for axially symmetric cases
[ESA-TT-1264] 07 p2768 N94-28315
Method for calculating stress intensity factors for surface cracks (appendix 2/1) 07 p2841 N94-27188
Applications of the weight function method (appendix 4/1) 07 p2842 N94-27190
Track filtering by robust neural network
[DE94-606067] 08 p3434 N94-28613
Weighted and unweighted maximum clique algorithms with upper bounds from fractional coloring
[AD-A275328] 08 p3409 N94-28917
Cramer-von Mises variance estimators for simulations
[AD-A278799] 11 p4316 N94-35675

WEIGHTLESSNESS
Coupled thermovibrational and thermocapillary convection in liquid bridge (floating zone system) 01 p0101 N94-10082
Separation of gravitational effects on the flow of suspension in tubes by measurements in weightlessness 01 p0105 N94-10105
A study of the quasibinary Al-Mo-W system. Part 2: A physico-mechanical investigation of the system fabricated under the gravitylessness conditions 01 p0119 N94-10212
Use of inert immiscible liquid for crystal separation out of its feeding solution in weightlessness 01 p0124 N94-10242
Physiologic mechanisms of circulatory and body fluid losses in weightlessness identified by mathematical modeling 01 p0312 N94-11557
Proceedings of the First Joint NASA Cardiopulmonary Workshop
[NASA-CP-10068] 01 p0308 N94-11991
Pulmonary function in microgravity: KC-135 experience 01 p0309 N94-11994
Central circulatory hemodynamics as a function of gravitational stress 01 p0309 N94-11995
Spectral analysis of resting cardiovascular variables and responses to oscillatory LBNP before and after 6 degree head down bedrest 01 p0309 N94-11997
Effect of prolonged LBNP and saline ingestion on plasma volume and orthostatic responses during bed rest 01 p0310 N94-11998
Fitness, autonomic regulation and orthostatic tolerance 01 p0310 N94-11999
Hormonal regulation of fluid and electrolyte metabolism in zero-g and bedrest 01 p0311 N94-12004
Calcitonin control of calcium metabolism during weightlessness
[NASA-CR-193622] 02 p0731 N94-12960
Capillary surfaces in a wedge: Differing contact angles
[DE93-013903] 02 p0631 N94-13244
Spacelab J experiment descriptions
[NASA-TM-4517] 02 p0586 N94-13732
Drop dynamics in space and interference with acoustic field (M-15) 02 p0588 N94-13747
Study of bubble behavior in weightlessness (effects of thermal gradient and acoustic stationary wave) (M-16) 02 p0589 N94-13748
Endocrine and metabolic changes in payload specialist (L-1) 02 p0591 N94-13758
Separation of biogenic materials by electrophoresis under zero gravity (L-3) 02 p0592 N94-13760
Manual control in space research on perceptual-motor functions under zero gravity conditions (L-10) 02 p0593 N94-13767
Bone culture research 02 p0595 N94-13773
Movement in microgravity
[NASA-TM-109526] 03 p0881 N94-15389
Space research with intact organisms: The role of Space Station Freedom 04 p1502 N94-19213
Axial response of differently excited anchored viscous liquid bridges in zero-gravity
[LRT-WE-9-FB-1-1992] 04 p1379 N94-19489
Apparatus and method for measuring subject work rate on an exercise device
[NASA-CASE-MSC-21752-1] 05 p1895 N94-20194
Response of an anchored annular cylindrical liquid layer to various axial excitations in zero-gravity
[LRT-WE-9-FB-3-1992] 06 p2266 N94-23195
Liquid oscillations in a spherical system with sliding edges boundary by two conical solid surfaces in zero-gravity
[LRT-WE-9-FB-5-1992] 06 p2318 N94-23197
Artificial gravity in space flight
[AD-A273420] 06 p2427 N94-24928
Loading, electromyograph, and motion during exercise 06 p2427 N94-25359
Development of a model to assess orthostatic responses 06 p2427 N94-25376
Study on posture control and adaptation mechanism under weightlessness: Summary report of ground operations performed for carp experiment (FMPT/L-2) in Space Shuttle mission 07 p2912 N94-27447
Study on posture control and adaption mechanism under weightlessness: Differences in weight and shape of utricular otolith of carp 07 p2912 N94-27448
Workshop on Countering Space Adaptation with Exercise: Current Issues
[NASA-CP-3252] 07 p2934 N94-28361
Muscle disuse through tail-suspension: Etiology and therapeutics 09 p3796 N94-31746

An experimental testbed for a free-floating manipulator
[AD-A277350] 09 p3726 N94-32334
A large motion zero-gravity suspension system for experimental simulation of orbital construction and deployment
[NASA-CR-195881] 09 p3668 N94-33037
An overview of Space Shuttle anthropometry and biomechanics research with emphasis on STS/Mir recumbent seat system design
10 p4101 N94-33629
Modeling heat exchange characteristics of long term space operations: Role of skin wettedness and exercise
10 p4101 N94-33650

WEIGHTLESSNESS SIMULATION
NT NEUTRAL BUOYANCY SIMULATION
Exercise countermeasures for bed-rest deconditioning
[NASA-TM-103987] 01 p0300 N94-11191
Project ARGO: Gas phase formation in simulated microgravity
[NASA-TM-104762] 01 p0125 N94-11235
Physiologic mechanisms of circulatory and body fluid losses in weightlessness identified by mathematical modeling 01 p0312 N94-11557
Mechanistic studies on reduced exercise performance and cardiac deconditioning with simulated zero gravity
01 p0310 N94-12001
Fluid compartment and renal function alterations in the rat during 7 and 14 day head down tilt
01 p0310 N94-12002
Local fluid shifts and edema in humans during simulated microgravity 01 p0311 N94-12003
Gravity as a probe for understanding pattern specification
[NASA-CR-194142] 02 p0713 N94-13418
STS-30 Magellan IUS/EVA training in WETF
[NASA-TM-109300] 02 p0737 N94-13601
Circadian rhythms during simulation of the D2-spaceflight
[DLR-FB-92-27] 02 p0733 N94-14043
STS-35 EVA payload training in WETF
[NASA-TM-109492] 02 p0739 N94-14790
STS-35 Crew training: Bailout in CCT, firefighting, TAGS class and bailout in WFTF
[NASA-TM-109489] 03 p1135 N94-15195
STS-26 IUS and latch contingency training
[NASA-TM-109561] 03 p0875 N94-15331
STS-34 Chang-Diaz and E. Baker during Galileo contingency training in WFTF
[NASA-TM-109466] 03 p1135 N94-15361
STS-32 LDEF EVA training in WETF with Low and Dunbar
[NASA-TM-109473] 03 p1135 N94-15377
STS-32 crew training for lower body negative pressure unit and AFE
[NASA-TM-109475] 03 p1120 N94-15381
STS-33 Carter and Thorton during WETF activities
[NASA-TM-109471] 03 p1136 N94-15402
STS-31 Hubble space telescope contingency training in WETF with McCandless and Sullivan
[NASA-TM-109480] 03 p1136 N94-15441
STS-31 crew training inflight maintenance and bailout exercises in CCT and WFTF
[NASA-TM-109483] 03 p0876 N94-15450
Richards, Dick: Training clip
[NASA-TM-109503] 03 p0876 N94-15467
The brain electrical activity in different G situations
[AERONAUTICA-ACTA-A-372-1993]
04 p1507 N94-19523
Design and testing of a unique randomized gravity, continuous flow bioreactor 06 p2423 N94-25368
Free-floating dual-arm robots for space assembly
[AIAA PAPER 94-1195-CP] 08 p3442 N94-30546
A large motion zero-gravity suspension system for experimental simulation of orbital construction and deployment
[NASA-CR-195881] 09 p3668 N94-33037

WEINBERG-SALAM GAUGE MODEL
U ELECTROWEAK MODEL

WELD STRENGTH
Contribution to comparison of methods for determining welding procedures for the avoidance of hydrogen cracking
[VTT-PUBS-107] 02 p0674 N94-13887
The Marshall Automated Weld System (MAWS)
[TABES PAPER 93-602] 03 p1049 N94-16138
Microstructural analysis of solid-state resistance welds
[DE93-017295] 04 p1443 N94-17761
Thermal insulation of wet shielded metal arc welds
[AD-A268697] 04 p1445 N94-18465
Strength, acoustic evaluation and metallurgy of diffusion bonds
[DE94-001804] 06 p2243 N94-23717
Weldability of Accelerated-Cooled (AcC) high strength TMCP steel X80
[VTT-TIED-1413] 06 p2251 N94-25419
The study of single-pass GMA welds with different cover gas compositions on HSLA-100 steel
[AD-A274857] 07 p2822 N94-26174
The influence of weld metal alloying additions to extend the heat input range for the submerged arc welding of high strength steels
[AD-A274284] 07 p2738 N94-26679
Use of photostress and strain gages to analyze behavior of weldments
[NASA-CR-195269] 07 p2843 N94-27765
Weldability aspects in the design and fabrication of aluminium structures subjected to fatigue loads. Part 2: Weldability of aluminium alloys using advanced MIG and TIG techniques. Effect of the weld bead geometrical factors on the fatigue behavior of the welded joint
[PB94-132446] 07 p2833 N94-28375
A newly developed snow vehicle (SM100S) for Antarctica. Part 3: Low temperature toughness of the welded joints of the structural steel
08 p3364 N94-29983
Mitigation of harmful effects of welds in zirconium alloy components
[DE94-619033] 12 p4414 N94-36543

WELD TESTS
Dry film lubricant evaluation
[DE93-013114] 02 p0578 N94-13118
The Marshall Automated Weld System (MAWS)
[TABES PAPER 93-602] 03 p1049 N94-16138
Initiation and growth of microcracks in high strength steel butt welds
[AD-A268751] 04 p1454 N94-18466
Thermocapillary and arc phenomena in stainless steel welds
[DE94-000518] 05 p1821 N94-19859
Microscopic evaluation of low-temperature embrittlement in type 308 stainless steel welds
[DE93-040266] 05 p1690 N94-20282
Plasma ARC keyhole welding of aluminum
[PB93-201606] 06 p2353 N94-23449
Use of photostress to characterize the mechanical behavior of weldments
[NASA-CR-195201] 06 p2378 N94-25267
Evaluating non-chlorinated solvents for welding applications
[DE94-003332] 07 p2824 N94-27181
Use of photostress and strain gages to analyze behavior of weldments
[NASA-CR-195269] 07 p2843 N94-27765
A review of weldment failure modes and weldability testing methods
[AD-A278096] 09 p3729 N94-33251

WELDABILITY
Weldability of maraging steels
01 p0059 N94-10028
Technique to eliminate helium induced weld cracking in stainless steels
[DE93-015982] 04 p1357 N94-17859
Helium-induced weld degradation of HT-9 steel
[DE93-015981] 04 p1358 N94-17915
Weldability of Accelerated-Cooled (AcC) high strength TMCP steel X80
[VTT-TIED-1413] 06 p2251 N94-25419
Weldability of Direct-Quenched and Tempered (DQT) high strength steel HT80
[VTT-TIED-1406] 07 p2731 N94-25623
Weldability of Accelerated-Cooled (AcC) high strength TMCP steel HT50
[VTT-TIED-1410] 07 p2731 N94-25784
Weldability aspects in the design and fabrication of aluminium structures subjected to fatigue loads. Part 2: Weldability of aluminium alloys using advanced MIG and TIG techniques. Effect of the weld bead geometrical factors on the fatigue behavior of the welded joint
[PB94-132446] 07 p2833 N94-28375
Weldability aspects in the design and fabrication of aluminium structures subjected to fatigue loads. Part 1: Effect of welding on the structural integrity of joint types designed for repairing aluminium ship sections
[PB94-132487] 07 p2833 N94-28378
Casting of weldable graphite/magnesium metal matrix composites with built-in metallic inserts
08 p3186 N94-30482
A review of weldment failure modes and weldability testing methods
[AD-A278096] 09 p3729 N94-33251
Weldability of Ni-Cr-W superalloy manufactured on industrial scale
[DE94-727593] 10 p4059 N94-33873
Examination of weldability of Ni-Cr-W superalloys
[DE94-719014] 12 p4418 N94-37385
Tensile strength of simulated and welded butt joints in W-Cu composite sheet
[NASA-TM-4584] 12 p4405 N94-37460

WELDED JOINTS
NT SPOT WELDS
Heavy-section steel technology program
[DE93-009222] 01 p0184 N94-10155
Advances in low carbon, high strength ferrous alloys
[AD-A265264] 01 p0085 N94-12532
Tensile properties of LE-7 engine material with welded joint
[NAL-TR-1188] 02 p0570 N94-13460
Fatigue design curves for 6061-T6 aluminum
[DE93-011849] 02 p0571 N94-14021
Estimation of strain in 1-kW primary containment vessels by microstructural examination
[DE93-013053] 02 p0573 N94-14316
Use of photostress and strain gages to analyze behavior of weldments and use of photostress and strain gages to analyze behavior of an aft skirt test specimen
[NASA-CR-194575] 03 p1058 N94-15716
The effect of aging at 343 C on the mechanical properties and microstructure of type 308 stainless steel weldments
[DE93-015454] 03 p0957 N94-16103
The Marshall Automated Weld System (MAWS)
[TABES PAPER 93-602] 03 p1049 N94-16138
Adaptive weld control for high-integrity welding applications
[TABES PAPER 93-604] 03 p1049 N94-16140
Microstructural analysis of solid-state resistance welds
[DE93-017295] 04 p1443 N94-17761
Helium-induced weld degradation of HT-9 steel
[DE93-015981] 04 p1358 N94-17915
Development and application of specially-focused ultrasonic transducers to location and sizing of defects in 75 mm- to 127 mm-thick austenitic stainless steel weld metals
[DE93-015975] 04 p1453 N94-18108
Initiation and growth of microcracks in high strength steel butt welds
[AD-A268751] 04 p1454 N94-18466
Environmental degradation of Alloy 600 and welded filler metal EN82 in an elevated temperature aqueous environment
[DE93-018049] 04 p1363 N94-18940
Modeling of single-crystal laser-weld microstructures
[DE93-017853] 04 p1445 N94-18976
Effects of irradiation temperature on Charpy and tensile properties of high-copper, low upper-shelf, submerged-arc welds
[DE93-017858] 04 p1445 N94-19047
Ultrasonic technique for inspection of GPHS capsule girth weld integrity
[DE93-040072] 04 p1448 N94-19189
Overlay welding irradiated stainless steel
[DE93-018767] 04 p1446 N94-19334
Thermocapillary and arc phenomena in stainless steel welds
[DE94-000518] 05 p1821 N94-19859
Microscopic evaluation of low-temperature embrittlement in type 308 stainless steel welds
[DE93-040266] 05 p1690 N94-20282
Shape memory metals
[DE94-001373] 05 p1695 N94-21976
Evaluation of non-chromium-containing deoxidizers for aluminum
[DE94-001377] 05 p1695 N94-21978
Plasma ARC keyhole welding of aluminum
[PB93-201606] 06 p2353 N94-23449
Strength, acoustic evaluation and metallurgy of diffusion bonds
[DE94-001804] 06 p2243 N94-23717
Weld joint concepts for on-orbit repair of Space Station Freedom fluid system tube assemblies
06 p2371 N94-24427
Microstructural analysis of the 2195 aluminum-lithium alloy welds 06 p2251 N94-24448
Use of photostress to characterize the mechanical behavior of weldments
[NASA-CR-195201] 06 p2378 N94-25267
Weldability of Accelerated-Cooled (AcC) high strength TMCP steel X80
[VTT-TIED-1413] 06 p2251 N94-25419
Corrosion resistance at welded zones of nuclear fuel reprocessing system 07 p2722 N94-25546
Study on fatigue crack propagation characteristics around welded joint interface in complexed conditions
07 p2730 N94-25584
Weldability of Direct-Quenched and Tempered (DQT) high strength steel HT80
[VTT-TIED-1406] 07 p2731 N94-25623
The study of single-pass GMA welds with different cover gas compositions on HSLA-100 steel
[AD-A274857] 07 p2822 N94-26174
Stress analysis of a secondary-bending specimen
[AD-A274842] 07 p2838 N94-26501
The influence of weld metal alloying additions to extend the heat input range for the submerged arc welding of high strength steels
[AD-A274284] 07 p2738 N94-26679

Evaluation of crack arrest fracture toughness of parent plate, weld metal and heat affected zone of BIS 812 EMA ship plate steel
[AD-A274871] 07 p2839 N94-26859
The influence of TIG welding thermal cycles on HSLA-100 steel plate
[AD-A274248] 07 p2740 N94-27009
Evaluating non-chlorinated solvents for welding applications
[DE94-003332] 07 p2824 N94-27181
Use of photostress and strain gages to analyze behavior of weldments
[NASA-CR-195269] 07 p2843 N94-27765
Weldability aspects in the design and fabrication of aluminium structures subjected to fatigue loads. Part 2: Weldability of aluminium alloys using advanced MIG and TIG techniques. Effect of the weld bead geometrical factors on the fatigue behavior of the welded joint
[PB94-132446] 07 p2833 N94-28375
Weldability aspects in the design and fabrication of aluminium structures subjected to fatigue loads. Part 1: Effect of welding on the structural integrity of joint types designed for repairing aluminium ship sections
[PB94-132487] 07 p2833 N94-28378
Fundamental studies on the corrosion behavior of weldments in marine microbial environments
[AD-A275247] 08 p3203 N94-28900
Chamber free fusion welding root side purging method and apparatus
[NASA-CASE-MFS-28832-1] 08 p3204 N94-29380
Fusion welding with self-generated filler metal
[NASA-CASE-LEW-15671-1] 08 p3301 N94-29557
A newly developed snow vehicle (SM100S) for Antarctica. Part 3: Low temperature toughness of the welded joints of the structural steel 08 p3364 N94-29983
Nd-YAG laser welding of the fiber optic connector to the header shell on the 2SL actuator
[DE94-006104] 09 p3723 N94-31621
Acceptance criteria for weld defects in aluminium weldments
[PB94-138575] 09 p3735 N94-31841
Correlation of flux composition and inclusion characteristics with submerged arc weld metal properties in HY-100 steel
[AD-A277040] 09 p3726 N94-32261
Modeling of residual stress mitigation in austenitic stainless steel pipe girth weldment
[DE94-007184] 09 p3738 N94-32639
A review of weldment failure modes and weldability testing methods
[AD-A278096] 09 p3729 N94-33251
Laser processing of discontinuously reinforced aluminum composites
[AD-A277903] 10 p4018 N94-33593
Unique methods for on-orbit structural repair, maintenance, and assembly 10 p4102 N94-33663
On-orbit NDE: A novel approach to tube weld inspection 10 p4066 N94-33664
Mapping of residual strains of a ceramic-to-metal joint using x ray diffraction
[DE94-007421] 10 p4069 N94-33691
Use of photostress to analyze behavior of an aft skirt test specimen
[NASA-CR-195850] 10 p4069 N94-34075
Mitigation of harmful effects of welds in zirconium alloy components
[DE94-619033] 12 p4414 N94-36543
Examination of weldability of Ni-Cr-W superalloys
[DE94-719014] 12 p4418 N94-37385
Tensile strength of simulated and welded butt joints in W-Cu composite sheet
[NASA-TM-4584] 12 p4405 N94-37460
Residual stresses in a multi-pass weld in an austenitic stainless steel plate before and after thermal stress relief
[DE94-013278] 12 p4420 N94-37548

WELDED STRUCTURES
NT STEEL STRUCTURES
On-orbit NDE: A novel approach to tube weld inspection 10 p4066 N94-33664

WELDING
NT ARC WELDING
NT BRAZING
NT COLD WELDING
NT DIFFUSION WELDING
NT ELECTRIC WELDING
NT ELECTRON BEAM WELDING
NT FUSION WELDING
NT GAS TUNGSTEN ARC WELDING
NT LASER WELDING
NT PLASMA ARC WELDING
Weldability of maraging steels 01 p0059 N94-10028
Weld overlay coatings for erosion control
[DE93-013592] 01 p0084 N94-11816
Recent results from material processing studies on new generation lasers
[DE93-013841] 02 p0653 N94-12898
Krupp technical reports no. 2, English edition, October 1992
[ETN-93-94631] 03 p0984 N94-16000
Expert system for welding engineering 03 p0984 N94-16003
Automatic soldering for watch circuit components 04 p1428 N94-18037
Initiation and growth of microcracks in high strength steel butt welds
[AD-A268751] 04 p1454 N94-18466
Design considerations for remotely operated welding in space: Task definition and visual weld monitoring experiment
[AD-A268752] 04 p1445 N94-18634
New welding and finishing procedures
[DE94-602022] 06 p2352 N94-23025
Weld cladding of hard surfaces
[PB93-201598] 06 p2353 N94-23448
Microwelding due to random vibration 06 p2359 N94-24019
Weld fracture criteria for computer simulation 06 p2251 N94-24425
Microstructural analysis of the 2195 aluminum-lithium alloy welds 06 p2251 N94-24448
Welding of niobium to stainless
[DE94-003365] 06 p2365 N94-24614
The importance of properties in modeling 06 p2246 N94-25121
Digital control and data acquisition for high-value GTA welding
[DE94-000885] 07 p2821 N94-25980
Use of photostress and strain gages to analyze behavior of weldments
[NASA-CR-195269] 07 p2843 N94-27765
Upset welding process for 21-6-9 spherical vessels
[DE93-018194] 07 p2832 N94-28229
Weldability aspects in the design and fabrication of aluminium structures subjected to fatigue loads. Part 1: Effect of welding on the structural integrity of joint types designed for repairing aluminium ship sections
[PB94-132487] 07 p2833 N94-28378
On the prediction of HAZ grain size using Monte Carlo simulation
[DE94-005465] 08 p3511 N94-28535
Programmable Automated Welding System (PAWS): Control of welding through software and hardware 08 p3314 N94-30443
Metafusion: A breakthrough in metallurgy 08 p3211 N94-30446
Programmable Automated Welding System (PAWS)
[AIAA PAPER 94-1221-CP] 08 p3446 N94-30570
Effect of vibratory stress relief during welding of thick stainless steel plate
[DE94-006557] 09 p3733 N94-31312
Solid-state resistance upset welding: A process with unique advantages for advanced materials
[DE94-005941] 09 p3723 N94-31524
Pinched propagation of high-power, pulsed electron beams for welding and materials processing applications
[AD-A276925] 09 p3726 N94-32236
Empirical modeling for intelligent, real-time manufacture control 09 p3839 N94-32424
Modeling of residual stress mitigation in austenitic stainless steel pipe girth weldment
[DE94-007184] 09 p3738 N94-32639
Unique methods for on-orbit structural repair, maintenance, and assembly 10 p4102 N94-33663
Vent processes during the 1912 eruption at Novarupta, Katmai National Park, Alaska
[DE94-010740] 12 p4468 N94-36451
Examination of weldability of Ni-Cr-W superalloys
[DE94-719014] 12 p4418 N94-37385

WELDING MACHINES
Welding nozzle position manipulator
[NASA-CASE-MFS-29837-1] 03 p1047 N94-15882
Initiation and growth of microcracks in high strength steel butt welds
[AD-A268751] 04 p1454 N94-18466
Digital control and data acquisition for high-value GTA welding
[DE94-000885] 07 p2821 N94-25980
Development of an automated wire delivery system for robotic welding applications
[NASA-CR-194216] 09 p3727 N94-32479

WELLS
Promotion of geothermal energy development in 1991
[DE93-799057] 02 p0701 N94-13214
Promotion of geothermal energy development in 1991
[DE93-799058] 02 p0701 N94-13215
Penetrometer compatible, fiber-optic sensor for continuous monitoring of chlorinated hydrocarbons: Field test results
[DE93-017974] 04 p1352 N94-19266
Fiscal 1991 geothermal development promotion energy
[DE94-732332] 08 p3337 N94-28627

WENTZEL-KRAMER-BRILLOUIN METHOD
The three-dimensional ray trajectories of the WKB optical fiber modes
[AD-A267167] 03 p1189 N94-15739
Spiral Alfven instability in accretion disks 05 p2010 N94-22698
Application of semiclassical methods to reaction rate theory
[DE94-007041] 08 p3199 N94-30266

WESTERN HEMISPHERE
Research program on the Manson impact structure, Iowa 05 p1862 N94-20766

WETLANDS
Emissions of biogenic sulfur gases from Alaskan tundra 01 p0268 N94-12455
Emissions of sulfur gases from wetlands 01 p0269 N94-12458
Biogeochemical factors which regulate the formation and fate of sulfide in wetlands 01 p0270 N94-12464
DMS emissions from Sphagnum-dominated wetlands 01 p0271 N94-12466
Emissions of biogenic sulfur gases from northern bogs and fens 01 p0271 N94-12467
Factors controlling sulfur gas exchange in Sphagnum-dominated wetlands 01 p0271 N94-12469
Sulfur gas exchange in Sphagnum-dominated wetlands 01 p0271 N94-12470
Pattern and Process in Landscape Ecology: Eighth Annual US Landscape Ecology Symposium
[DE93-014032] 02 p0711 N94-14859
Characterization of wetland, forest, and agricultural ecosystems in Belize with airborne radar (AIRSAR) 03 p1076 N94-16738
Ecological and environmental impacts of construction in the coastal zone
[AD-A269196] 04 p1475 N94-18881
Methane emissions from natural wetlands
[DE93-040796] 07 p2865 N94-25790
Methane production and consumption in grassland and boreal ecosystems
[NASA-CR-196085] 11 p4284 N94-35486

WETNESS
U MOISTURE CONTENT

WETTABILITY
Determination of concentration profiles at interfaces and surfaces of partially miscible polymer blends
[DE93-013140] 01 p0089 N94-11007
Incomplete melting of the Au(100) surface
[DE93-623192] 02 p0569 N94-13227
Wetting behavior of alternative solder alloys
[DE93-016730] 04 p1359 N94-18127
Solderability perservative coatings: Electroless tin versus organic azoles
[DE93-017634] 04 p1370 N94-18477
Wettability and reaction kinetics in metal matrix composites
[AD-A270377] 04 p1342 N94-18704
Logistics for the implementation of lead-free solders on electronic assemblies
[DE94-004800] 08 p3206 N94-29936
Aging effects on the microstructure, surface characteristics and wettability of Cu pretinned with Sn-Pb solders
[DE94-007033] 09 p3641 N94-31638
Manufacturing feasibility of several lead-free solders for electronic assembly
[DE94-007732] 11 p4258 N94-35564

WETTING
Wetting effects on nylon spheres engulfment in ice 01 p0115 N94-10189
Studies of critical point phenomena of fluids: Bulk fluids, fluids in pores, and at interfaces 01 p0080 N94-10228
Determination of concentration profiles at interfaces and surfaces of partially miscible polymer blends
[DE93-013140] 01 p0089 N94-11007
Advanced soldering processes
[DE93-009856] 01 p0129 N94-11606
An analytical investigation of transient effects on rewetting of heated thin flat plates
[NASA-TM-106120] 02 p0628 N94-12968
Separation behaviour of monotectic alloys 03 p0945 N94-15170
Wetting behavior of alternative solder alloys
[DE93-016730] 04 p1359 N94-18127
Experimental study of void formation during aluminum solidification in reduced gravity
[NASA-TM-106190] 05 p1692 N94-21604
An analytic study of a two-phase laminar airfoil in simulated heavy rain 06 p2171 N94-23661
Study on interfacial reaction analysis at interfacial joining 07 p2728 N94-25574

Interfacial behaviour: Wettability in SiC(sub p) metal matrix composites
[ISBN-0-315-87206-3] 09 p3621 N94-31835
Physics of heat pipe rewetting
[NASA-CR-195902] 09 p3913 N94-33148
The effects of cold exposure on wet aircraft passengers: A review
[AD-280253] 10 p4100 N94-34389
Preliminary results of sulfide melt/silicate wetting experiments in a partially melted ordinary chondrite 11 p4353 N94-36147
Investigation of ultrasonic surface wave interaction with porous saturated rocks
[DE94-013378] 12 p4469 N94-37177

WHARVES
The flow structure around a cylindrical pier for the flow of transcritical Reynolds number 01 p0169 N94-11944
The undrained shear strength characteristics of undisturbed soil from fishing port areas 08 p3234 N94-29704

WHEAT
Paint removal using wheat starch blast media 01 p0128 N94-10627
Gordon Research Conference on Chronobiology, 1991
[AD-A266354] 02 p0728 N94-13698
Biomass production chamber air analysis of wheat study (BWT931)
[NASA-TM-109192] 02 p0737 N94-13712
Validated environmental and physiological data from the CELSS Breadboard Projects Biomass Production Chamber. BWT931 (Wheat cv. Yecora Rojo)
[NASA-TM-109191] 02 p0738 N94-13979
FT-NIR spectroscopy in quantitative and qualitative measurements of cereal products
[VTT-TIED-1331] 04 p1346 N94-17973
Chemical characterization of some aerobic liquids in CELSS 06 p2422 N94-23241

WHEATSTONE BRIDGES
The constant current loop: A new paradigm for resistance signal conditioning 09 p3685 N94-32461

WHEELCHAIRS
A robotic wheelchair
[AIAA PAPER 94-1229-CP] 08 p3447 N94-30578

WHEELS
NT FLYWHEELS
NT NOSE WHEELS
NT REACTION WHEELS
NT TURBINE WHEELS
NT VEHICLE WHEELS
Position and force control of a vehicle with two or more steerable drive wheels
[DE93-012512] 01 p0177 N94-10269
Friction drive position transducer
[AD-D015851] 04 p1424 N94-17717
A rail corrugation theory which allows for contact patch size 06 p2269 N94-23582
Surface observations of stick-slip oscillations in tightly conformal wheel/rail contacts 06 p2270 N94-23588
Aircraft wheel life assessment
[AD-A274378] 07 p2823 N94-26976

WHIP ANTENNAS
Broadband, high-power, 2-30 MHz, twin-whip antenna. Computer and 1/10-scale model design study
[AD-A277619] 09 p3682 N94-32971

WHIRL
U ROTATION

WHIRL INSTABILITY
U ROTARY STABILITY

WHIRLING
U ROTATION

WHIRLING TESTS
U SPIN TESTS

WHISKER COMPOSITES
The influence of microstructure on the mechanical behavior of silicon nitride ceramics
[DE93-015363] 03 p0966 N94-16018
Interface chemistry in ceramic matrix composites
[AD-A268629] 03 p0973 N94-17466
Bibliography on ceramic matrix composites and reinforcing whiskers, platelets, and fibers, 1970-1990
[AD-A270139] 04 p1371 N94-18750
Deformation of an alumina-zirconia-silicon carbide-whisker reinforced composite
[DE93-040244] 05 p1678 N94-21559
Fabrication of whisker-toughened alumina tubes
[DE94-001012] 05 p1677 N94-22022
Technology base enhancement program. Metal matrix composites
[AD-A275531] 08 p3178 N94-28688
Superplasticity in fine-grained ceramics
[AD-A275461] 08 p3212 N94-28733

WHISKERS (CRYSTALS)
Tin whiskers in electronic circuits
[AD-A265917] 01 p0146 N94-12565
Processing and testing of high toughness silicon nitride ceramics
[NASA-CR-191190] 02 p0582 N94-14543

WHISPERING GALLERY MODES
Full-wave simulation of the thumbtack laser
[DE93-015110] 03 p1039 N94-16054
An extended UTD analysis for the scattering and diffraction from cubic polynomial strips
[NASA-CR-194581] 05 p1716 N94-20139
Modelling short bent, graded index dielectric slab waveguides
[PB93-215283] 05 p1742 N94-22349
Mode analysis of gyrotron oscillation using a k-spectrometer
[DE94-701195] 07 p2813 N94-27703

WHISTLERS
Analysis and experiments of a whistler-wave plasma thruster
[DE94-001533] 06 p2209 N94-23012
Investigation of plasma instabilities in the polar cusp
[NASA-CR-195212] 07 p2879 N94-26599
Active electron and ion beam experiments in space
[AD-A275570] 08 p3504 N94-28828
Lightning-induced coupling of the radiation belts to geomagnetically conjugate ionospheric regions 09 p3772 N94-31773
Dispersion relations for a plasma-filled helix-loaded-waveguide
[DE94-006333] 09 p3675 N94-31781
Plasma and radio waves from Neptune: Source mechanisms and propagation
[NASA-CR-195877] 09 p3943 N94-33103
Gyroresonant scattering of radiation belt electrons by oblique whistler waves 10 p4166 N94-33357
Plasma waves in the nightside ionosphere of Venus 10 p4164 N94-33431

WHITE DWARF STARS
ROSAT guest investigator program (AO-1). On a search for coronal x ray emissions from white dwarfs
[NASA-CR-193654] 02 p0835 N94-13171
Monte Carlo simulation of the OCP freezing transition
[DE93-013039] 02 p0811 N94-14313
Eclipsing cataclysmic variables. Deep eclipses in H0928+501. YY Draconis, the whirling dervish. New x ray pulsar candidates from HEAO-1
[NASA-CR-194027] 04 p1621 N94-18855
A study of white dwarf radiative accretion shocks 08 p3544 N94-29731
Theoretical asteroseismology of white dwarf stars: The encyclopedia Seismologica 08 p3547 N94-30011
Extreme ultraviolet opacity sources in the DA white dwarf G191-B2B 09 p3924 N94-31210
Binary-binary collisions involving main-sequence stars, white dwarfs and neutron stars in globular clusters
[DE94-005086] 10 p4163 N94-33415

WHITE HOLES (ASTRONOMY)
Maximal hypersurfaces in asymptotically stationary spacetimes
[MPA-708] 04 p1621 N94-18141

WHITE NOISE
NT THERMAL NOISE
DILUTE: A code for studying beam evolution under RF noise
[DE93-011605] 01 p0133 N94-10960
The limit of frequency estimation 01 p0356 N94-11001
Analysis of temporal symmetry in non-gaussian random fields
[AD-A266496] 03 p0999 N94-16794
High order nonlinear estimation with signal processing applications
[AD-A268407] 03 p1005 N94-17463
Comparison of higher order moment spectrum estimation techniques
[AD-A272967] 05 p1967 N94-21260
A comparative robustness evaluation of feedforward neurofilters
[NASA-TM-106440] 05 p1650 N94-21742
Nonlinear smoothing for random fields
[PB94-149531] 06 p2493 N94-22728
Separable concatenated codes with iterative map decoding for Rician fading channels 06 p2286 N94-22815
Coherence lost? Not-so-fast escapes from the in-phase attractor of a set of globally coupled nonlinear oscillators
[DE94-000799] 06 p2557 N94-22940
A mixed H2/H(infinity) function for a discrete time system
[MEMO-COSOR-92-36] 06 p2480 N94-23144
Detection and analysis of unbalanced QPSK in Gaussian noise, version 1.0
[DREO-12-020.1] 06 p2296 N94-24131
Longitudinal diffusion of a proton bunch under external noise
[DE93-634022] 07 p3032 N94-26165
Three dimensional object recognition using a complex autoregressive model
[AD-A274388] 07 p2995 N94-26829
Enhanced adaptive statistical filter providing improved performance for target motion analysis noise discrimination statement of government interest
[AD-D016039] 07 p2786 N94-27109
White noise theory of robust nonlinear filtering with correlated state and observation noises
[PB94-126661] 07 p3004 N94-27211
Stability of dynamical systems in the presence of noise
[AD-A275383] 08 p3243 N94-29072
Partially coherent detection of PSK signals in Rician channels
[ISBN-0-315-85799-4] 08 p3254 N94-30031
Peak detection of Swerling type targets. Part 1: Detection probabilities in white noise
[AD-A276217] 09 p3670 N94-31062
Stochastic realization of a Gaussian stochastic control system
[CWI-BS-R9320] 09 p3852 N94-32350
The effects of a multipath channel and interference on coherent M-PSK digital communication systems
[AD-A278158] 09 p3684 N94-33254

WICKS
Effect of longitudinal vibration on the capillary limit of a wrapped screen wick copper/water heat pipe
[AD-A273830] 06 p2571 N94-25524

WIDE ANGLE LENSES
Rover imaging system for the Mars rover/sample return mission
[NASA-CR-193413] 02 p0649 N94-13464
Wide-angle imaging system with fiberoptic components providing angle-dependent virtual material stops
[NASA-CASE-NPO-18146-1-CU] 05 p1986 N94-20345
Internal camera calibration using rotation and geometric shapes
[AD-A272718] 05 p1808 N94-21167
Hubble Space Telescope Wide Field and Planetary Camera 2 Instrument handbook, version 2.0
[NASA-CR-189368] 12 p4547 N94-36918

WIDEBAND
U BROADBAND

WIDEBAND COMMUNICATION
NASA/ASEE Summer Faculty Fellowship Program
[NASA-CR-194678] 06 p2571 N94-23230
Wide band fiber-optic communications
06 p2304 N94-23231
Northern Exposure 1992: An investigation of transauroral HF radio skywave propagation
[AD-A273363] 06 p2303 N94-25089
KONRAD: Wide band digital HF receiver
[PB94-184686] 12 p4435 N94-37813

WIDMANSTATTEN STRUCTURE
Tambo Quemado: Extraordinary concentrations of REE and refractory trace elements caused by artificial heating 05 p1684 N94-20667

WIDTH
Determination of the upsilon(1s) leptonic width
[DE94-618534] 12 p4516 N94-37096

WIENER HOPF EQUATIONS
A two-dimensional kinetic model of the scrape-off layer
[DE94-001235] 05 p1999 N94-22562
Diffraction analysis of transient acoustic waves: Half-plane in a layered medium
[PB94-110988] 06 p2526 N94-23726
Wiener-Hopf factorization of rational matrix functions in terms of realizations: An alternative version
[ETN-94-95380] 06 p2491 N94-25245
NTT crosscorrelation recursive least squares procedure for on-line identification of process parameters 10 p4116 N94-34325

WIGGLER MAGNETS
Microwave generation for magnetic fusion energy applications
[DE93-013864] 02 p0654 N94-13058
Predicted performance of a dc beam driven FEM oscillator designed for fusion applications at 200-250 GHz
[DE93-013414] 02 p0655 N94-13145
Measurement of the spin of a particle using undulator radiation
[DE93-014334] 02 p0780 N94-13149
Multi-bunch beam-break-up studies for a SWFEL/TBA
[DE93-016973] 02 p0658 N94-14414
A superconducting short period undulator for a harmonic generation FEL experiment
[DE93-017581] 04 p1436 N94-17998
FEL experiment with a focusing wiggler
[DE93-788586] 04 p1438 N94-18160

Magnetic field measurements of a superconducting undulator for a Harmonic Generation FEL experiment at the NSLS
[DE93-017621] 04 p1438 N94-18504
Designs for a 10.6 micrometer electromagnetic wiggler Free-Electron Laser (FEL)
[AD-A269695] 04 p1439 N94-18576
Coherence and linewidth studies of a 4-nm high power FEL
[DE93-018533] 04 p1441 N94-19030
Compact free electron lasers for medical applications
[AD-A271272] 04 p1442 N94-19729
Measurement and correction of magnetic fields in pulsed slotted-tube microwigglers
[DE93-040100] 05 p1815 N94-20272
Demonstration of ultraviolet lasing with a low energy electron beam
[DE93-040192] 05 p1818 N94-21554
Generation of harmonic radiation using the multi-cavity free-electron laser
[DE94-001261] 05 p1820 N94-21975
Properties of the transfer matrices of deflecting magnet systems for free electron laser
[DE93-508257] 06 p2347 N94-22922
Inverse free electron laser beat-wave accelerator research
[DE94-002597] 06 p2349 N94-23702
Compact free electron lasers for medical applications
[AD-A273609] 06 p2350 N94-24934

WIGHTMAN THEORY
U FIELD THEORY (PHYSICS)
U QUANTUM THEORY
U RELATIVISTIC THEORY

WIGNER COEFFICIENT
Wigner functions for nonclassical states of a collection of two-level atoms 01 p0379 N94-10603
Wigner quantum oscillators
[DE94-601508] 07 p3073 N94-26758

WILDLIFE
Assessing impacts of climate change on forests: The state of biological modeling
[DE93-015916] 04 p1471 N94-17790
Development and implementation of a scrub habitat compensation plan for Kennedy Space Center
[NASA-TM-109202] 08 p3347 N94-29099
Sonic boom predictions using a modified Euler code 10 p3973 N94-33474
KSC wildlife show
[NASA-TM-109808] 10 p4094 N94-33770
Endangered and potentially endangered wildlife on John F. Kennedy Space Center and faunal integrity as a goal for maintaining biological diversity
[NASA-TM-109204] 11 p4288 N94-36422

WIND (METEOROLOGY)
NT GEOSTROPHIC WIND
NT GROUND WIND
NT GUSTS
NT JET STREAMS (METEOROLOGY)
NT MONSOONS
NT SEA BREEZE
NT SQUALLS
NT WINDS ALOFT
Stability model of the atmosphere 01 p0032 N94-11500
ERS-1 scatterometer data characteristics and wind retrieval skill 01 p0233 N94-11709
Validation of ERS-1 wind and wave data by use of operational forecast models 01 p0233 N94-11710
A C-band wind scatterometer model derived from the data obtained during the ERS-1 calibration/validation campaign 01 p0233 N94-11711
Availability of wind field over the North Pacific derived from data on ships-of-opportunity and analysis of long-term variabilities 01 p0202 N94-11962
Impact of ERS-1 wind/wave/ice data on operational ocean forecasting 01 p0250 N94-12500
A first assessment of the value of ERS-1 scatterometer winds for meteorological studies in the polar regions 01 p0250 N94-12501
Field research of wind wave spectrum variability 01 p0223 N94-12727
Observations of film slicks and internal waves with Ka-band scatterometer 01 p0225 N94-12741
Atmospheric soundings during the Washita 1992 campaign
[NASA-CR-194383] 02 p0712 N94-13212
Coherent Doppler lidar signal covariance including wind shear and wind turbulence
[NASA-CR-194492] 02 p0721 N94-13723
Boundary layer structure over areas of heterogeneous heat fluxes
[DE93-007887] 02 p0715 N94-13912
The nocturnal wind maximum: An interactive forecast method
[KNMI-TR-142] 02 p0722 N94-13985
The use of the Air Force Academy high wind alert system in forecasting moderate intensity wind events for military bases in the Colorado Springs area
[AD-A267648] 03 p1107 N94-17245
Boundary layer structure over areas of heterogeneous heat fluxes
[DE93-010657] 03 p1110 N94-17673
Surface fluxes important to cloud development
[DE93-016633] 04 p1488 N94-17715
A review of wind field models for atmospheric transport
[DE93-016085] 04 p1488 N94-17895
A mobile remote sensing laboratory for water vapor, trace gas, aerosol, and wind speed measurements
[DE93-017158] 04 p1489 N94-18132
Spectral analysis of synoptic time scale disturbances over the tropical eastern Pacific during summer 1989, 1990 and 1991
[AD-A268821] 04 p1490 N94-18206
SPNDL: A concept for a small satellite Doppler lidar wind sounder 04 p1327 N94-19181
Dynamics Explorer 2: Continued FPI and NACS instrument data analysis and associated scientific activity at the University of Michigan
[NASA-CR-194689] 05 p1657 N94-20173
ERS-1 and Seasat scatterometer measurements of ocean winds: Model functions and the directional distribution of short waves 05 p1720 N94-20412
Offshore decision support system: ERS-1 pilot project WAVEWATCH
[BCRS-92-09] 05 p1865 N94-20532
Imaging radar studies of atmospheric winds and waves
[AD-A271672] 05 p1866 N94-20918
The AGRHYMET data communications project 06 p2280 N94-22776
Implementation of a state of the art automated system for the production of cloud/water vapor motion winds from geostationary satellites
[NASA-CR-195087] 06 p2410 N94-24125
A diagnostic model to estimate winds and small-scale drag from Mars Observer PMIRR data 06 p2617 N94-24874
Analyzing Martian winds and tracer concentrations using Mars Observer data 06 p2619 N94-24883
Three-dimensional numerical simulation of near-surface flows over the Martian north polar cap 06 p2621 N94-24895
Wind climate and urban geometry
[ISBN-9-03-860132-8] 06 p2416 N94-25261
Machine intelligent gust front algorithm
[AD-A273695] 07 p2680 N94-26196
A preliminary analysis of the US west climatology
[DE94-003028] 07 p2894 N94-26313
A preliminary method for atmospheric soundings in real time using satellite and ground-based remotely sensed data
[AD-A274381] 07 p2880 N94-26828
On the linear stability of Verkley's modons 08 p3324 N94-28695
Radar estimations of atmospheric winds in the troposphere and lower stratosphere 08 p3370 N94-29697
On interannual variability and climate change in the North Pacific 08 p3374 N94-29963
Test of prototype liquid-water-content meter for aircraft use
[NASA-CR-189304] 08 p3374 N94-30187
A comparison of predictors for first-guess wind speed errors
[AD-A276460] 09 p3781 N94-31239
An integrated cloud observation and modeling investigation in support of the ARM program
[DE94-003160] 09 p3785 N94-32716
Evolution of diurnal surface winds and surface currents for Monterey Bay
[AD-A277649] 09 p3790 N94-33057
Observations and modelling of winds and waves during the surface wave dynamics experiment. Report 2: Intensive observation period IOP-3
[AD-A278368] 10 p4093 N94-34375

WIND CIRCULATION
U ATMOSPHERIC CIRCULATION

WIND DIRECTION
Dependence of oceanic microwave emission on wind direction 01 p0201 N94-11957
Preliminary meteorological results for 1992 West Coast Scotland Experiment
[DE93-014677] 02 p0720 N94-13404
Determination of momentum flux using a bivane and cup anemometer
[AD-A265414] 03 p1105 N94-15137
Complex terrain wind model evaluation
[AD-A266467] 03 p1096 N94-16589
Analysis of TIMS performance subjected to simulated wind blast 03 p1063 N94-16598
AN/APS-137 Forward Looking Airborne Radar (FLAR) evaluation Spring 1992 experiment
[AD-A268899] 04 p1384 N94-18228
Station climatic summaries: North America. Volume 1: The contiguous United States
[AD-A269567] 04 p1490 N94-18303
Station climatic summaries, North America. Volume 2: Alaska, Canada and Greenland
[AD-A269793] 04 p1493 N94-18732
Predicting lightning events in the KSC area: A feasibility study using single station data
[AD-A271440] 05 p1864 N94-20088
Analysis of wind observation from towers in the period 1977-1991
[KNMI-TR-148] 05 p1865 N94-20239
Comparison of remote sensing measurements with a two-scale polarimetric emission and scattering model for sea surfaces 05 p1721 N94-20415
The sea breeze convergence zone and its relationship to fair weather electricity in east central Florida
[AD-A268511] 05 p1868 N94-21502
Combined 1991 and 1992 Robinson-22B (R-22) parking test results
[AD-A273550] 06 p2193 N94-24559
Lift-curve slope for structural response calculations
[ESDU-93013] 07 p2648 N94-28063
The active titration method for measuring local hydroxyl radical concentration 08 p3345 N94-28602
Wind-speed measurements with a scanning elastic-backscatter lidar
[DE94-004974] 09 p3785 N94-32726
Mexico City ozone concentrations as a function of readily-available meteorological parameters
[DE94-007576] 09 p3768 N94-32814
Polar sediment accumulation: Role of surface winds at the two poles 09 p3951 N94-33233
Short-tower sigma(theta) measurements in the Colorado Plateaus region
[DE94-007478] 12 p4463 N94-36478

WIND EFFECTS
Effects of wind-roughened sea surface on ocean color remote sensing: Noise derived from reflected light and whitecaps 01 p0191 N94-11898
Variability of wind stress, and sensible and latent heat flux in the North Atlantic during SEASAT 01 p0194 N94-11918
A new expression for the production rate of sea water droplets on the sea surface 01 p0195 N94-11920
Field research of wind wave spectrum variability 01 p0223 N94-12727
Sand transport on Mars: Preliminary results from models 03 p1252 N94-16198
Dust-dynamic feedbacks in the Martian atmosphere: Surface dust lifting 03 p1296 N94-16434
Detecting surface roughness effects on the atmospheric boundary layer via AIRSAR data: A field experiment in Death Valley, California 03 p1078 N94-16747
Wind chill: The temperature feeling caused by the wind velocity
[KNMI-TR-103A] 05 p1890 N94-20238
CAPE for CaPE 06 p2416 N94-24409
The effects of tailwinds and control cross coupling on rotorcraft handling qualities for steep, decelerating instrument approaches and missed approaches
[IAR-AN-77] 07 p2677 N94-26710
Surface roughness lengths
[AD-A274550] 07 p2895 N94-26846
Lift-curve slope for structural response calculations
[ESDU-93013] 07 p2648 N94-28063
Simulation of the effect of wind on clothing by measurements and calculations
[PB94-132289] 08 p3399 N94-28406
Deterioration of manual performance in cold and windy climates 08 p3381 N94-28434
The effect of westerly wind bursts on a tropical ocean general circulation model
[AD-A276423] 09 p3788 N94-31448
The properties of sunflecks in a flexible plant canopy, and their relationship to turbulence 09 p3782 N94-31775
Regional sedimentological variations among dark crater floor features: Toward a model for modern eolian sand distribution on Mars 09 p3946 N94-33203
Three-parameter characterization of shallow-water directional wind wave spectra
[AD-A278532] 10 p4091 N94-33671
Ocean magnetics
[PB94-149028] 10 p4092 N94-34142
Windblown sand on Mars: The effect of saltation threshold on drift potentials derived from Mars GCM 11 p4366 N94-35474
Numerical simulation of nocturnal drainage flows in an idealized valley-tributary system
[DE94-011684] 12 p4472 N94-37115

Index and bulk parameters for frequency-direction spectra measured at CERC Field Research Facility, September 1992 to August 1993
[AD-A260233] 12 p4476 N94-37135

WIND ENERGY
U WINDPOWER UTILIZATION

WIND EROSION
Soil erosion rates caused by wind and saltating sand stresses in a wind tunnel
[DE93-009154] 02 p0706 N94-12905
Wind erosion in semiarid landscapes: Predictive models and remote sensing methods for the influence of vegetation
[NASA-CR-194029] 02 p0715 N94-13956
Geomorphic evidence for an eolian contribution to the formation of the Martian northern plains 05 p2092 N94-20402
Arid regions and wind erosion 09 p3780 N94-31005

WIND MEASUREMENT
NT WIND VELOCITY MEASUREMENT
US areal wind resource assessment
[DE93-011905] 01 p0262 N94-11051
Calibration and validation of the ERS-1 wind scatterometer 01 p0232 N94-11706
The Grand Banks ERS-1 SAR wave spectra validation experiment 01 p0232 N94-11708
ERS-1 scatterometer data characteristics and wind retrieval skill 01 p0233 N94-11709
A C-band wind scatterometer model derived from the data obtained during the ERS-1 calibration/validation campaign 01 p0233 N94-11711
The activity of the ERS-1 Venice (Italy) group on scatterometry 01 p0233 N94-11713
Wind and surface features in SAR images: The Canadian program 01 p0234 N94-11718
Preliminary analysis of circulations over the Indian Ocean and adjoining regions using ERS-1 surface winds in the NCMRWF data assimilation system 01 p0234 N94-11719
Spatial scales of wave height 01 p0244 N94-11782
Analysis of GEOSAT wind data 01 p0207 N94-12636
Observations and modelling of winds and waves during the Surface Wave Dynamics Experiment. Report 1: Intensive observation period IOP-1, 20-31 October 1990
[AD-A266384] 03 p1113 N94-16517
EOS Laser Atmosphere Wind Sounder (LAWS) investigation
[NASA-CR-193445] 03 p1109 N94-17525
Boundary layer heat budgets from wind profiler/RASS data: A feasibility study
[DE93-013187] 04 p1489 N94-18052
Some potential errors in satellite wind estimates using the geostrophic approximation and the thermal wind
[AD-A269784] 04 p1491 N94-18599
Impact of shorter wavelengths on optical quality for laws
[NASA-CR-193873] 04 p1579 N94-18858
SPNDL: A concept for a small satellite Doppler lidar wind sounder 04 p1327 N94-19181
Shape of wind gusts at a 130m tower at Wilhelmshaven (Germany)
[BER-BAND-83] 04 p1494 N94-19503
Rotorwash wind sensor evaluation
[AD-A268987] 05 p1807 N94-20203
Integrated display of multi-sensor geophysical and electromagnetic flight data 05 p1721 N94-20418
Description and availability of airborne Doppler radar data 05 p1722 N94-20419
Low-altitude cross-wind velocity measurements using pulsed visible fringe-type laser anemometry
[ISL-CO-216/92] 05 p1866 N94-20557
Presenting the Rain-Sea Interaction Facility
[NASA-RP-1322] 05 p1884 N94-21628
Vertical velocity in cirrus case obtained from wind profiler 05 p1878 N94-22330
A field evaluation of remote sensor measurements of wind, temperature, and moisture for ARM integrated sounding system research
[DE94-000565] 06 p2381 N94-23001
Wind measurements with an incoherent lidar
[AD-A273756] 07 p2691 N94-25722
Simulating high-frequency wind for long durations
[DE94-002739] 07 p2682 N94-27997
Simulation of the effect of wind on clothing by measurements and calculations
[PB94-132289] 08 p3399 N94-28406
New parameters for characterizing turbulence at a potential wind site
[DE94-004355] 08 p3368 N94-28455
Radar estimations of atmospheric winds in the troposphere and lower stratosphere 08 p3370 N94-29697
Four-dimensional data assimilation using the adjoint method 08 p3455 N94-30353
Three dimensional vorticity field in the California current system
[AD-A276951] 09 p3788 N94-32220
Wind-speed measurements with a scanning elastic-backscatter lidar
[DE94-004974] 09 p3785 N94-32726
Evolution of upwelling fronts off the coast of Portugal
[NASA-CR-195692] 09 p3790 N94-33045
Use of wind profiler data in short-range forcasting
[AD-A279482] 11 p4295 N94-36228
Doppler weather radar studies of precipitation systems
[AD-A279417] 11 p4295 N94-36262
An automated method for Low Level Windshear Alert System (LLWAS) data quality analysis
[AD-A280313] 12 p4472 N94-37126
Terminal Doppler Weather Radar (TDWR) build 5 Test and Evaluation Master Plan (TEMP)
[AD-A280426] 12 p4434 N94-37218

WIND PROFILES
HF ocean radar system at Okinawa Radio Observatory 01 p0139 N94-11902
Groundwave HF ocean surface radar 01 p0139 N94-11906
Current structures in the western equatorial Pacific during JAPACS cruises 01 p0193 N94-11911
Availability of wind field over the North Pacific derived from data on ships-of-opportunity and analysis of long-term variabilities 01 p0202 N94-11962
Wind field estimate by using one hour GMS data 01 p0202 N94-11963
The Pacific responses exhibited by an OGCM to various wind fields 01 p0202 N94-11964
On an upwelling front, propagation of upwelling and vertical velocity in the eastern Arabian Sea during monsoon, 1987 01 p0206 N94-11987
Analysis of GEOSAT wind data 01 p0207 N94-12636
SSMI wind speed variability over the Pacific Ocean 01 p0207 N94-12637
Spatial variability of the ocean underwater dynamic noise from satellite radar sensing data 01 p0225 N94-12740
Development of a global backscatter model for NASA's laser atmospheric wind sounder
[NASA-CR-192581] 02 p0718 N94-12957
On the vertical structure of seasonal, interannual and intraseasonal flows
[AD-A265346] 02 p0719 N94-12992
Investigate wave-mean flow interaction and transport in the extratropical winter stratosphere
[NASA-CR-194555] 03 p1098 N94-15639
A review of wind field models for atmospheric transport
[DE93-016085] 04 p1488 N94-17895
SPNDL: A concept for a small satellite Doppler lidar wind sounder 04 p1327 N94-19181
Empirical wind model for the middle and lower atmosphere. Part 2: Local time variations
[NASA-TM-104592] 05 p1870 N94-21862
Vertical velocity in cirrus case obtained from wind profiler 05 p1878 N94-22330
Implementation and evaluation of the new wind algorithm in NASA's 50 MHz doppler radar wind profiler
[NASA-CR-194880] 06 p2408 N94-23576
CAPE for CaPE 06 p2416 N94-24409
Analyzing Martian winds and tracer concentrations using Mars Observer data 06 p2619 N94-24883
Theoretic study of Green's modes
[INPE-5536-TDI/524] 10 p4090 N94-34202
Use of wind profiler data in short-range forcasting
[AD-A279482] 11 p4295 N94-36228

WIND SHEAR
On non-linear longitudinal stability of an aircraft in a dive in the presence of atmospheric disturbances 01 p0031 N94-11492
Flight crew interface aspects of forward-looking airborne windshear detection systems
[NASA-CR-191437] 02 p0516 N94-12829
Coherent Doppler lidar signal covariance including wind shear and wind turbulence
[NASA-CR-194492] 02 p0721 N94-13723
Windshear radar calibration, 1992 flights: Transmitter power and receiver gain stability
[NASA-TM-108997] 03 p0986 N94-15140
Wind shear and heavy rain --- effects on flight stability
[NASA-TM-109453] 03 p1105 N94-15326
Windshear detection radar signal processing studies
[NASA-CR-194615] 03 p0994 N94-16022
Windshear database for forward-looking systems certification
[NASA-TM-109012] 03 p1108 N94-17283
Coherent lidar design and performance verification
[NASA-CR-193813] 05 p1816 N94-20341
Integrated display of multi-sensor geophysical and electromagnetic flight data 05 p1721 N94-20418
Description and availability of airborne Doppler radar data 05 p1722 N94-20419
Windshear detection for aircraft using temperature lapse rate
[CA-PATENT-1,295,736] 05 p1641 N94-21030
Optimal flight guidance for aircraft in windshear
[CA-PATENT-1,307,573] 05 p1650 N94-21050
ASR-9 microburst detection algorithm
[AD-A273591] 06 p2415 N94-24850
Machine intelligent gust front algorithm
[AD-A273695] 07 p2680 N94-26196
The relationship of an integral wind shear hazard to aircraft performance limitations
[NASA-TM-109080] 07 p2677 N94-26593
Surface roughness lengths
[AD-A274550] 07 p2895 N94-26846
Nominal H(exp 2)-optimization and strong stabilization: A practical example of U-parameterization design 10 p4122 N94-34370
Effects of mesoscale convective organization and vertical wind shear on the cumulus-environment interaction 10 p4090 N94-34910
Terminal Doppler Weather Radar (TDWR) Low Level Wind Shear Alert System 3 (LLWAS 3) integration studies at Orlando International Airport
[AD-A278957] 11 p4294 N94-35807
An automated method for Low Level Windshear Alert System (LLWAS) data quality analysis
[AD-A280313] 12 p4472 N94-37126
Terminal Doppler Weather Radar (TDWR) build 5 Test and Evaluation Master Plan (TEMP)
[AD-A280426] 12 p4434 N94-37218

WIND TUNNEL APPARATUS
NT WIND TUNNEL NOZZLES
Identifying the NAL spaceplane aerodynamic model using dynamic wind tunnel tests
[NAL-TR-1171] 02 p0500 N94-12951
Control system design of a cable-mounted model used for dynamic wind tunnel testing
[NAL-TR-1161] 02 p0528 N94-13337
Monopiece strain gauge sting mounted wind tunnel balance
[CA-PATENT-1-311-626] 03 p1032 N94-15697
NASA Lewis 9- by 15-foot low-speed wind tunnel user manual
[NASA-TM-106247] 03 p0872 N94-15819
Doppler global velocimetry: Development of a flight research instrumentation system for application to non-intrusive measurements of the flow field
[NASA-CR-191490] 06 p2344 N94-24360
Shake test results of the MDHC test stand in the 40- by 80-foot wind tunnel
[NASA-TM-108801] 07 p2641 N94-26596
Installation of models in the 2 m x 3 m low speed wind tunnel
[LTR-LA-286] 07 p2681 N94-27594
Laminar Flow Supersonic Wind Tunnel primary air injector 08 p3158 N94-29649
'Real time' and the NLR aerodynamic facilities
[AD-B173626] 08 p3158 N94-30856
Langley 14- by 22-foot subsonic tunnel test engineer's data acquisition and reduction manual
[NASA-TM-4563] 11 p4189 N94-35246
Status of MSBS study at NAL 11 p4216 N94-35854
Three-dimensional force data acquisition and boundary corrections for the Walter H. Beech Memorial 7 x 10 foot low speed wind tunnel
[AR93-2] 11 p4200 N94-36437
Strength evaluation of socket joints
[NASA-CR-4608] 12 p4389 N94-37259

WIND TUNNEL BALANCES
U WEIGHT INDICATORS
U WIND TUNNEL APPARATUS

WIND TUNNEL CALIBRATION
Overview of the 1989 Wind Tunnel Calibration Workshop
[NASA-TP-3393] 01 p0034 N94-11869
Improved pressure measurement system for calibration of the NASA LeRC 10x10 supersonic wind tunnel
[NASA-TM-106470] 06 p2344 N94-24362
Experimental studies of transonic flow field near a longitudinally slotted wind tunnel wall
[NASA-TP-3392] 08 p3130 N94-29545
Flow quality studies of the NASA Lewis Research Center Icing Research Tunnel
[NASA-TM-106545] 10 p4010 N94-34919
Three-dimensional force data acquisition and boundary corrections for the Walter H. Beech Memorial 7 x 10 foot low speed wind tunnel
[AR93-2] 11 p4200 N94-36437
Experimental uncertainty and drag measurements in the national transonic facility
[NASA-CR-4600] 12 p4389 N94-36945

WIND TUNNEL MODELS
A unique facility to support cryogenic wind tunnel operations
[ARA-MEMO-377] 01 p0034 N94-12436
Results of experimental investigations to determine external tank protuberance loads using a 0.03-scale model of the Space Shuttle launch configuration (model 47-OTS) in the NASA/ARC unitary plan wind tunnel, volume 1
[NASA-CR-167690] 02 p0534 N94-12810
Propulsion simulator for magnetically-suspended wind tunnel models
[NASA-CR-189560] 02 p0527 N94-13127
Control system design of a cable-mounted model used for dynamic wind tunnel testing
[NAL-TR-1161] 02 p0528 N94-13337
Aerodynamic and aerothermal facilities 1: Hypersonic wind tunnels 02 p0506 N94-14158
NASA Lewis 9- by 15-foot low-speed wind tunnel user manual
[NASA-TM-106247] 03 p0872 N94-15819
Design of round-to-square transition section; analysis and computer code
[AD-A267173] 03 p0872 N94-15847
A wind tunnel model control surface actuator interface
[AD-A268729] 04 p1322 N94-18324
A study of the use of half-models in high-lift wind-tunnel testing 04 p1308 N94-18434
High lift systems for transport aircraft with advanced airfoils 04 p1310 N94-18446
Survey on the application of a 3D general purpose wind-tunnel research model
[LR-713] 04 p1323 N94-19372
Development and operation of the F/A-18 model control surface actuators
[AD-A271330] 05 p1645 N94-19914
Improved ceramic slip casting technique --- application to aircraft model fabrication
[NASA-CASE-LAR-14471-1] 05 p1702 N94-20377
Holographic testing of composite propfans for a cruise missile wind tunnel model
[NASA-TM-105271] 06 p2187 N94-23545
Installation of models in the 2 m x 3 m low speed wind tunnel
[LTR-LA-286] 07 p2681 N94-27594
Experimental apparatus for optimization of flap position for a three-element airfoil model 07 p2682 N94-27912
Evaluation of the buoyancy drag on automobile models in low speed wind tunnels 07 p2658 N94-28352
Variable soft sphere molecular model in the Monte Carlo simulation of air species 08 p3123 N94-28949
Rarefied gas numerical wind tunnel. Part 8: HOPE 08 p3123 N94-28950
Numerical simulation of arc heated wind tunnel flow 08 p3123 N94-28951
Numerical simulation of aerothermodynamic heating of hypersonic space transportation vehicles 08 p3124 N94-28955
Wind tunnel testing and research
[NASA-CR-188273] 08 p3156 N94-29052
Low-speed longitudinal aerodynamic characteristics of a flat-plate planform model of an advanced fighter configuration
[NASA-TM-109045] 08 p3130 N94-29443
Miniature linear-to-rotary motion actuator 08 p3163 N94-29647
Model borne data management system for wind tunnel testing, phase 2
[AD-A276296] 09 p3587 N94-31295
Status of LaRC HSCT high-lift research 10 p3979 N94-33519
Vehicle integration effects on hypersonic waveriders
[NASA-TM-109739] 10 p3990 N94-34118
A combined approach to buffet response analyses and fatigue life prediction 10 p4072 N94-34587
Dynamic tests to demonstrate lateral control using forebody suction on large scale models in the DRA 24 foot wind tunnel 10 p3991 N94-34613
Status of MSBS study at NAL 11 p4216 N94-35854
The simulation of a propulsive jet and force measurement using a magnetically suspended wind tunnel model 11 p4191 N94-35855
Flutter suppression digital control law design and testing for the AFW wind tunnel model 11 p4200 N94-35873
Three-dimensional force data acquisition and boundary corrections for the Walter H. Beech Memorial 7 x 10 foot low speed wind tunnel
[AR93-2] 11 p4200 N94-36437
NASA Lewis wind tunnel model systems criteria
[NASA-TM-106565] 12 p4390 N94-37522
Stability analysis of an F/A-18 E/F cable mount m odel
[NASA-TM-108989] 12 p4386 N94-37636

WIND TUNNEL NOZZLES
A CFD-based aerodynamic design procedure for hypersonic wind-tunnel nozzles 01 p0009 N94-10458
Method of characteristics design of a supersonic wind tunnel nozzle with square cross-section, supplement 3
[NASA-CR-194359] 02 p0527 N94-12824
Design of round-to-square transition section; analysis and computer code
[AD-A267173] 03 p0872 N94-15847
A supersonic tunnel for laser and flow-seeding techniques
[NASA-TM-106588] 11 p4265 N94-35945

WIND TUNNEL STABILITY TESTS
Estimation of critical values and vibration characteristics on supersonic delta wings. Part 2: Locally-stationary time series analysis of nonstationary random responses
[NAL-TR-1179] 02 p0502 N94-13345
Supersonic aerodynamic characteristics of a circular body Earth-to-Orbit vehicle
[NASA-TM-4533] 06 p2170 N94-24716
Aerodynamic characteristics of the National Launch System (NLS) 1 1/2 stage launch vehicle
[NASA-TP-3488] 12 p4384 N94-37577

WIND TUNNEL TESTS
An investigation on the effectiveness of the piping interference removal system for STOL aircraft wind tunnel tests
[NAL-TM-647] 01 p0002 N94-10350
Experimental results in aerodynamic stability and control of a TSTO configuration 01 p0003 N94-10424
New hypersonic test methods developed at ONERA: The R5 and F4 wind tunnels 01 p0004 N94-10429
Design and production of insulated wind tunnel models of the Hermes shuttle for heat transfer measurements at hypersonic speeds 01 p0004 N94-10431
Experimental and computational comparisons of Mach 6 high Reynolds number heat transfer and skin friction 01 p0006 N94-10443
Joint computational and experimental aerodynamic research on a hypersonic vehicle 01 p0006 N94-10445
Some experimental study and numerical simulation in wind tunnel flow 01 p0008 N94-10457
Simulated wake characteristics of tapered annular wings by a discrete vortex method
[NAL-TR-1156] 01 p0013 N94-10855
Simulated and experimental aerodynamic characteristics of tapered annular wings
[NAL-TR-1157] 01 p0013 N94-10856
An experimental investigation of the sources of propeller noise due to turbulence ingestion 01 p0358 N94-11057
A preliminary study on ice shape tracing with a laser light sheet
[NASA-TM-105964] 01 p0174 N94-11132
Supersonic airplane study and design
[NASA-CR-193219] 01 p0025 N94-11150
Boundary layer transition: Prediction and wind tunnel simulation 01 p0032 N94-11498
Modeling nonlinear aerodynamic loads for aircraft stability and control analysis 01 p0032 N94-11499
Computation of hypersonic nosetip heat transfer rates for an M829-like projectile
[AD-A263226] 01 p0016 N94-11870
Lift enhancement of a wing/strake using pneumatic blowing
[AD-A265074] 01 p0026 N94-11872
An investigation of small scales of turbulence in a boundary layer at high Reynolds numbers 01 p0157 N94-12303
Plane mixing layer vortical structure kinematics 01 p0159 N94-12313
A unique facility to support cryogenic wind tunnel operations
[ARA-MEMO-377] 01 p0034 N94-12436
Soil erosion rates caused by wind and saltating sand stresses in a wind tunnel
[DE93-009154] 02 p0706 N94-12905
Identifying the NAL spaceplane aerodynamic model using dynamic wind tunnel tests
[NAL-TR-1171] 02 p0500 N94-12951
Propulsion simulator for magnetically-suspended wind tunnel models
[NASA-CR-189560] 02 p0527 N94-13127
Aerodynamics of a sphere and an oblate spheroid for Mach numbers from 0.6 to 10.5 including some effects of test conditions
[NASA-TM-109016] 02 p0500 N94-13172
Results of wind tunnel tests of an ASRM configured 0.03 scale Space Shuttle integrated vehicle model (47-OTS) in the AEDC 16-foot Transonic wind tunnel (IA613A), volume 1
[NASA-CR-185696] 02 p0534 N94-13191
Exploratory study of in-plane streamline curvature effects on a turbulent boundary layer at a Mach number of 3
[NASA-CR-193673] 02 p0501 N94-13292
Low-speed wind tunnel tests on four types of joined-wing aircraft models
[NAL-TR-1167] 02 p0501 N94-13340
Low-speed wind tunnel tests on a joined-wing aircraft model with various upper-fin
[NAL-TR-1169] 02 p0501 N94-13341
Rolling moment control in the NAL 10 cm x 10 cm magnetic suspension and balance system
[NAL-TR-1164] 02 p0526 N94-13347
Experimental studies of vortex flaps and vortex plates. Part 2: 1.15m span 60 deg delta wing
[NAL-TR-1180T-PT-2] 02 p0502 N94-13454
Hypersonic aerodynamic characteristics of SSTO-type aerospace planes. Part 1: The NAL 0-th configuration
[NAL-TR-1186] 02 p0514 N94-13459
An experimental investigation of shock wave/vortex interaction 02 p0634 N94-13574
Measurements of wing and fin buffeting on the standard dynamics model
[IAR-AN-76] 02 p0526 N94-13859
Flow-field interference produced by an asymmetrical support strut
[IAR-AN-75] 02 p0504 N94-14031
Noise levels from a model turbofan engine with simulated noise control measures applied
[NASA-TM-106318] 02 p0518 N94-14036
Results of experimental investigations to determine external tank protuberance loads using a 0.03-scale model of the Space Shuttle launch configuration (Model 47-OTS) in the NASA/ARC unitary plan wind tunnel, volume 2
[NASA-CR-167691] 02 p0536 N94-14047
Experimental studies of vortex flaps and vortex plates. Part 1: 0.53 m span 60 deg delta wing
[DE93-767969] 02 p0505 N94-14059
Aerodynamic and aerothermal facilities 1: Hypersonic wind tunnels 02 p0506 N94-14158
Computational techniques and capabilities 02 p0506 N94-14162
An experimental study of a turbulent boundary layer in the trailing edge region of a curculation-control airfoil
[NASA-CR-194522] 02 p0508 N94-14541
Optical fibre Fabry-Perot interferometers for calorimetric heat transfer gauges
[RAE-TM-AERO/PROP-20] 02 p0653 N94-14701
An uncertainty analysis of inlet dynamic flow distortion using an analog/digital hybrid editing system
[AD-A266924] 03 p0855 N94-15105
Rotorcraft research
[NASA-TM-109452] 03 p0871 N94-15325
Spacework 16 --- Simulated Space Shuttle Program
[NASA-TM-109436] 03 p1221 N94-15420
A software interface for the ARL wind tunnel data acquisition system
[AD-A267114] 03 p1146 N94-15650
Aerodynamic control of NASP-type vehicles through Vortex manipulation. Volume 2: Static wind tunnel tests
[NASA-CR-177626-VOL-2] 03 p0856 N94-15677
Wind tunnel investigation of three axisymmetric cowls of different lengths at Mach numbers from 0.60 to 0.92
[NASA-TM-4488] 03 p0856 N94-15681
Physical properties of the benchmark models program supercritical wing
[NASA-TM-4457] 03 p0866 N94-15722
Aerodynamic control of NASP-type vehicles through vortex manipulation. Volume 3: Wing rock experiments
[NASA-CR-177626] 03 p0857 N94-15780
Wall interference and boundary simulation in a transonic wind tunnel with a discretely slotted test section
[NASA-TP-3334] 03 p0872 N94-15794
NASA Lewis 9- by 15-foot low-speed wind tunnel user manual
[NASA-TM-106247] 03 p0872 N94-15819
Wind tunnel investigation with an operational turbojet engine
[TABES PAPER 93-662] 03 p0870 N94-16157
Effects of internal yaw-vectoring devices on the static performance of a pitch-vectoring nonaxisymmetric convergent-divergent nozzle
[NASA-TP-3369] 03 p0858 N94-16572
Wind tunnel investigations of forebody strakes for yaw control on F/A-18 model at subsonic and transonic speeds
[NASA-TP-3360] 03 p0859 N94-16573
Wind-tunnel investigation of aerodynamic efficiency of three planar elliptical wings with curvature of quarter-chord line
[NASA-TP-3359] 03 p0859 N94-16574
Determining the effect of endwall boundary layer suction in a large scale subsonic compressor cascade
[AD-A267208] 03 p0859 N94-16913

An experimental investigation of the effects of leading edge geometry on the dynamics of blunt fin-induced shock wave turbulent boundary layer interaction
[AD-A267656] 03 p0860 N94-17221
Supersonic flow visualization of a nacelle in close proximity to a simulated wing
[NASA-CR-194675] 03 p0860 N94-17260
Subsonic aerodynamic characteristics of the HL-20 lifting-body configuration
[NASA-TM-4515] 03 p0861 N94-17284
User's manual for the Langley Research Center 14- by 22- foot subsonic tunnel static data acquisition system
[NASA-TM-109027] 03 p0861 N94-17639
Aerodynamic characteristics of a helicopter rotor airfoil as affected by simulated ballistic damage
[AD-A269206] 04 p1311 N94-18413
Experimental investigation of flow around a multielement airfoil 04 p1305 N94-18417
High Reynolds number configuration development of a high-lift airfoil 04 p1306 N94-18424
The GARTEUR high lift research programme 04 p1307 N94-18430
An experimental investigation of the optimum slat setting on a combat aircraft model 04 p1308 N94-18431
An experimental investigation of attachment-line transition on the slat of a combat aircraft model 04 p1308 N94-18432
A study of the use of half-models in high-lift wind-tunnel testing 04 p1308 N94-18434
High-lift design for large civil aircraft 04 p1310 N94-18445
High lift systems for transport aircraft with advanced airfoils 04 p1310 N94-18446
The world's largest wind tunnel
[NASA-TM-109371] 04 p1322 N94-18963
Development and operation of the F/A-18 model control surface actuators
[AD-A271330] 05 p1645 N94-19914
Description and assessment of a new Optical Pressure Measurement System (OPMS) demonstrated in the high speed wind tunnel in Goettingen (Germany)
[DLR-FB-92-24] 05 p1651 N94-21280
Measurement and prediction of the flow through an annular turbine cascade
[AD-A272530] 05 p1803 N94-21417
A study of the compressible flow through a diffusing S-duct
[NASA-TM-106411] 05 p1638 N94-21591
Near wake measurements on a rotor model with Mie-vanes in the Delft open jet tunnel
[PB93-215382] 05 p1638 N94-22260
Testing of a multisensor hot film technique in wind tunnel and free flight 05 p1639 N94-22599
An experimental study of the flow field surrounding a subsonic jet in a cross flow
[NASA-CR-194770] 06 p2317 N94-23072
Summary of lift and lift/cruise fan powered lift concept technology
[NASA-CR-177619] 06 p2176 N94-23489
Holographic testing of composite propfans for a cruise missile wind tunnel model
[NASA-TM-105271] 06 p2187 N94-23545
Compressibility effects on dynamic stall of airfoils undergoing rapid transient pitching motion
[NASA-TM-109681] 06 p2167 N94-23975
Lift augmentation on a delta wing via leading edge fences and the Gurney flap
[NASA-CR-194793] 06 p2168 N94-24103
Vortical structure in a forced plane mixing layer 06 p2331 N94-24162
Local isotropy in distorted turbulent boundary layers at high Reynolds number 06 p2332 N94-24166
An experimental investigation of a Mach 3.0 high-speed civil transport at supersonic speeds
[NASA-TP-3365] 06 p2169 N94-24311
Aerodynamic characteristics and pressure distributions for an executive-jet baseline airfoil section
[NASA-TM-4529] 06 p2169 N94-24586
Wind tunnel test of a variable-diameter tiltrotor (VDTR) model
[NASA-CR-177629] 06 p2181 N94-24796
Measurements of the influence of integral length scale on stagnation region heat transfer
[NASA-TM-106503] 06 p2338 N94-25183
Measurement of the volume mass by spontaneous Raman scattering. Study of turbulent fluctuations of mixing in a subsonic free jet. Measurements in supersonic wind tunnels
[ISL-R-102/92] 06 p2339 N94-25462
Off-design performance of crenulated blades in a linear compressor cascade
[AD-A273744] 06 p2340 N94-25534
Low-speed pressure distribution measurements over the aft-fuselage, fins, and stabilators of a 1/9th scale F/A-18 wind-tunnel model
[AD-A274870] 07 p2644 N94-26342
Investigation of the aerodynamic environment for an advanced lightweight rotor in forward flight. Volume 4: Laser velocimeter wake data, advance ratio of 0.037
[NASA-TM-109040-VOL-4] 07 p2645 N94-26483
Investigation of the aerodynamic environment for an advanced lightweight rotor in forward flight. Volume 1: Laser velocimeter inflow data, advance ratio of 0.37, thrust coefficient of 0.0081 and hover tip speed of 603 feet/second
[NASA-TM-109040-VOL-1] 07 p2645 N94-26489
Investigation of the aerodynamic environment for an advanced lightweight rotor in forward flight. Volume 2: Laser velocimeter inflow data, advance ratio of 0.37, thrust coefficient of 0.0064 and hover tip speed of 710 feet/second
[NASA-TM-109040-VOL-2] 07 p2645 N94-26492
Investigation of the aerodynamic environment for an advanced lightweight rotor in forward flight. Volume 3: Laser velocimeter inflow data, advance ratio of 0.37, thrust coefficient of 0.0064 and hover tip speed of 603 feet/second
[NASA-TM-109040-VOL-3] 07 p2645 N94-26497
The measurement of disturbance levels in the Langley Research Center 20-inch Mach 6 tunnel
[NASA-CR-4571] 07 p2646 N94-26548
Pressure distributions on a 0.02-scale Space Shuttle orbiter nose at Mach 21.5 in helium
[NASA-TM-4495] 07 p2646 N94-26592
Shake test results of the MDHC test stand in the 40- by 80-foot wind tunnel
[NASA-TM-108801] 07 p2641 N94-26596
Experimental investigation of advanced hub and pylon fairing configurations to reduce helicopter drag
[NASA-TM-4540] 07 p2668 N94-26604
Experimental investigation of the flow quality in the GLT20 subsonic-transonic boundary layer wind tunnel
[PB94-126539] 07 p2681 N94-26815
Wind tunnel investigation of an STOL aircraft model: An effect of engine nacelle shape
[NAL-TM-653] 07 p2647 N94-27235
Transverse vorticity measurements in the University of Houston two stream shear layer facility
[AD-A273910] 07 p2797 N94-27562
Flowfield dynamics in blunt fin-induced shock wave/turbulent boundary layer interactions
[NASA-CR-195170] 07 p2798 N94-27802
Microspheres for laser velocimetry in high temperature wind tunnel 07 p2682 N94-27903
Experimental apparatus for optimization of flap position for a three-element airfoil model 07 p2682 N94-27912
Transient flow features of a supersonic jet in a low speed cross flow 07 p2800 N94-28005
Experimental investigation of the interaction of a thrust reverser jet with an external subsonic flow 07 p2801 N94-28011
Experiments on the ground vortex formed by an impinging jet in cross flow 07 p2802 N94-28016
Experiments on interaction force of jets in hypervelocity cross-flow in a shock tunnel 07 p2659 N94-28022
Vortex generators for control of shock-induced separation. Part 1: Introduction and aerodynamics
[ESDU-93024-PT-1] 07 p2806 N94-28095
Measurements of steady and dynamic pressure on an F/A-18 wind tunnel model at high angles of attack 07 p2653 N94-28323
Infrared imaging for transition detection in a transonic blowdown wind tunnel 07 p2653 N94-28325
Experimental study on the shock wave interaction with a hypersonic boundary layer near a convex corner 07 p2654 N94-28328
Application of the influence function method using the interference distributed loads code to prediction of store aerodynamic load during separation from the CF-18 fighter aircraft 07 p2654 N94-28330
Aerodynamic performance of novel ducted-tip wings 07 p2654 N94-28331
Experimental investigations into the wall interference and sidewall boundary layer effects in the National Research Council/Inst. for Aerospace Research High Reynolds Number 2-D Test Facility 07 p2658 N94-28350
Computation of wind-tunnel side-wall interference using 3D Navier-Stokes code 07 p2658 N94-28351
Evaluation of the buoyancy drag on automobile models in low speed wind tunnels 07 p2658 N94-28352
Simulation of the effect of wind on clothing by measurements and calculations
[PB94-132289] 08 p3399 N94-28406
Design and fabrication of forward-swept counterrotation blade configuration for wind tunnel testing
[NASA-CR-191193] 08 p3155 N94-28510
Steady pressure measurements on an Aeroelastic Research Wing (ARW-2)
[NASA-TM-109046] 08 p3122 N94-28658
A method for the modelling of porous and solid wind tunnel walls in computational fluid dynamics codes
[NASA-CR-195699] 08 p3270 N94-28724
A flow visualization study of acoustically enhanced hairpin vortices
[AD-A275467] 08 p3271 N94-28809
Laser velocimeter data acquisition system for the Langley 14- by 22-foot subsonic tunnel. Software reference guide version 3.3
[NASA-CR-191606] 08 p3293 N94-28839
Wind tunnel testing and research
[NASA-CR-188273] 08 p3156 N94-29052
An experimental study of wing tip vortex in the near wake of a rectangular wing
[AD-A275389] 08 p3129 N94-29306
Experimental studies of transonic flow field near a longitudinally slotted wind tunnel wall
[NASA-TP-3392] 08 p3130 N94-29545
An experimental study of the flowfield on a semispan rectangular wing with a simulated glaze ice accretion 08 p3130 N94-29674
An experimental investigation of the effect of leading edge extensions on directional stability and the effectiveness of forebody nose strakes 08 p3155 N94-29728
Algorithm and code development for unsteady three-dimensional Navier-Stokes equations
[NASA-CR-195774] 08 p3277 N94-29942
The 3-D LDV measurements on a 30-degree swept wing with a simulated ice accretion
[NASA-CR-195327] 08 p3132 N94-30124
Computation of wind tunnel wall effects for complex models using a low-order panel method
[NASA-TM-104019] 08 p3132 N94-30151
Three-dimensional flow characteristics downstream of a blade endwall corner 08 p3280 N94-30229
The enhancement of compressible turbulent mixing via streamwise vorticity 08 p3280 N94-30487
The effect of pressure gradient on the structure of an equilibrium turbulent boundary layer 08 p3282 N94-30807
The execution of wind energy projects 1986 - 1992 between China Aerodynamics Research and Development Centre (CARDC) and The Aeronautical Research Institute of Sweden (FFA)
[FFA-TN-1993-19] 08 p3340 N94-30945
Wind tunnel tests of a 5.3 m diameter yaw controlled turbine
[FFA-TN-1993-20] 08 p3340 N94-30946
Model borne data management system for wind tunnel testing, phase 2
[AD-A276296] 09 p3587 N94-31295
Hypervelocity Tunnel 9 Mach 10/14 Calibration
[AD-A275960] 09 p3587 N94-31318
Investigation of sonic boom for the Space Shuttle: High cross-range orbiter
[NASA-TM-108238] 09 p3860 N94-31336
Investigation of sonic boom for the Space Shuttle: Low cross-range orbiter
[NASA-TM-108237] 09 p3860 N94-31337
Research in marine boundary layer intermittency
[AD-A276076] 09 p3701 N94-31460
Three-dimensional velocity measurements on a 6:1 prolate spheroid at 10 deg angle of attack
[AD-A276485] 09 p3702 N94-31476
Boundary layer study on nozzle wall at hypersonic velocities 09 p3569 N94-31882
A critical assessment of UH-60 main rotor blade airfoil data
[NASA-TM-103985] 09 p3571 N94-32063
A non-local model for prediction of the probability density function of turbulent fluctuations in boundary-layer flows 09 p3706 N94-32076
Six degree of freedom flight dynamic model of a Mk-82 store
[AD-A277065] 09 p3580 N94-32362
An experimental study of the flowfield on a semispan rectangular wing with a simulated glaze ice accretion
[NASA-CR-195301] 09 p3571 N94-32475
Aerodynamic drag of droplets in turbulent flow fields
[ISBN-0-315-75827-9] 09 p3571 N94-32491
Results for the hybrid laminar flow control experiment conducted in the NASA Langley 8-foot transonic pressure tunnel on a 7-foot chord model
[NASA-TM-107582] 09 p3601 N94-32870
Control of low-speed turbulent separated flow over a backward-facing ramp
[NASA-TM-109740] 09 p3573 N94-33071
Structural damping studies at cryogenic temperatures
[NASA-TM-109073] 09 p3740 N94-33118
Calibration and validation studies in the LENS facility
[AD-A278403] 09 p3591 N94-33167
Backward-facing step measurements at low Reynolds number, Re(sub h)=5000
[NASA-TM-108807] 09 p3711 N94-33290

Hypervelocity tunnel 9 Mach 8 Calibration
[AD-A277575] 10 p4008 N94-33424
HSCT nozzle source noise programs at Pratt and Whitney 10 p3972 N94-33465
Nacelle-wing integration 10 p3977 N94-33504
HSR high lift research program: Status and plans 10 p3980 N94-33521
Icing test results on an advanced two-dimensional high-lift multi-element airfoil
[NASA-TM-106620] 10 p3982 N94-33705
NASA Ames Fluid Mechanics Laboratory research briefs
[NASA-TM-108818] 10 p3983 N94-33997
Experimental studies of shock-wave/wall-jet interaction in hypersonic flow
[NASA-CR-195844] 10 p4048 N94-34171
Static performance investigation of a skewed-throat multiaxis thrust-vectoring nozzle concept
[NASA-TP-3411] 10 p3983 N94-34172
Semi-span model testing in the national transonic facility
[NASA-CR-195952] 10 p4048 N94-34300
F/A-18 forebody vortex control. Volume 2: Rotary-balance tests
[NASA-CR-4582-VOL-2] 10 p3984 N94-34430
Design and analysis of a highly loaded transonic compressor cascade 10 p4002 N94-34451
A combined approach to buffet response analyses and fatigue life prediction 10 p4072 N94-34587
Dynamic tests to demonstrate lateral control using forebody suction on large scale models in the DRA 24 foot wind tunnel 10 p3991 N94-34613
Flow quality studies of the NASA Lewis Research Center Icing Research Tunnel
[NASA-TM-106545] 10 p4010 N94-34919
Unsteady separation experiments on 2-D airfoils, 3-D wings, and model helicopter rotors 10 p3986 N94-34967
Mechanisms of flow control with the unsteady bleed technique 10 p3986 N94-34987
The aerodynamic and heat transfer effects of an endwall boundary layer fence in a 90 degree turning square duct
[AD-A278903] 11 p4265 N94-35803
The simulation of a propulsive jet and force measurement using a magnetically suspended wind tunnel model 11 p4191 N94-35855
Flutter suppression digital control law design and testing for the AFW wind tunnel model 11 p4200 N94-35873
Wind tunnel measurements on a full-scale F/A-18 with a tangentially blowing slot --- conducted in the Ames 80 by 120 foot wind tunnel 11 p4191 N94-35965
The velocity field created by a shallow bump in a boundary layer
[AD-A281064] 11 p4266 N94-35975
F/A-18 forebody vortex control. Volume 1: Static tests
[NASA-CR-4582-VOL-1] 11 p4190 N94-35991
A shadowgraph study of Space Transportation System (STS): The Space Shuttle Launch Vehicle (SSLV)
[NASA-RP-1341] 12 p4382 N94-36741
Experimental uncertainty and drag measurements in the national transonic facility
[NASA-CR-4600] 12 p4389 N94-36945
Pressure-sensing performance of upright cylinders in a Mach 10 boundary-layer
[NASA-TM-4633] 12 p4383 N94-37395
Subsonic aerodynamic characteristic of semispan commercial transport model with wing-mounted advanced ducted propeller operating in reverse thrust --- conducted in the Langley 14 by 22 foot subsonic wind tunnel
[NASA-TP-3427] 12 p4384 N94-37505
NASA Lewis wind tunnel model systems criteria
[NASA-TM-106565] 12 p4390 N94-37522
Aerodynamic characteristics of the National Launch System (NLS) 1 1/2 stage launch vehicle
[NASA-TP-3488] 12 p4384 N94-37577
Stability analysis of an F/A-18 E/F cable mount m odel
[NASA-TM-108989] 12 p4386 N94-37636

WIND TUNNEL WALLS

A wall interference assessment/correction system
[NASA-CR-194174] 02 p0500 N94-13076
Wall interference studies: Revisited 02 p0640 N94-14604
Wall interference and boundary simulation in a transonic wind tunnel with a discretely slotted test section
[NASA-TP-3334] 03 p0872 N94-15794
Determination of the effect of the walls of a wind-tunnel from the parameters of flow near them
[RAE-LIB-TRANS-2201] 03 p0859 N94-16583
Evaluation of the prototype dual-axis wall attitude measurement sensor
[NASA-TM-109056] 07 p2811 N94-26707
Evaluation of the buoyancy drag on automobile models in low speed wind tunnels 07 p2658 N94-28352
A method for the modelling of porous and solid wind tunnel walls in computational fluid dynamics codes
[NASA-CR-195699] 08 p3270 N94-28724
Computation of wind tunnel wall effects for complex models using a low-order panel method
[NASA-TM-104019] 08 p3132 N94-30151

WIND TUNNELS

NT BLOWDOWN WIND TUNNELS
NT CASCADE WIND TUNNELS
NT COMBUSTION WIND TUNNELS
NT CRYOGENIC WIND TUNNELS
NT HOTSHOT WIND TUNNELS
NT HYPERSONIC WIND TUNNELS
NT HYPERVELOCITY WIND TUNNELS
NT LOW SPEED WIND TUNNELS
NT SHOCK TUNNELS
NT SLOTTED WIND TUNNELS
NT SUBSONIC WIND TUNNELS
NT SUPERSONIC WIND TUNNELS
NT TRANSONIC WIND TUNNELS
Estimation of critical values and vibration characteristics on supersonic delta wings. Part 1: On-line time series analysis of stationary random response
[NAL-TR-1153] 01 p0002 N94-10363
The upgrading of the arc heated wind tunnel of the DLR (LBK) with respect to its effects on the material testing 01 p0004 N94-10432
New aerodynamic information obtained from the solution of the inverse problem for aerofoils
[NAL-TR-1172] 01 p0014 N94-10860
Numerical wind tunnel project and computational fluid dynamics at National Aerospace Laboratory, Japan
[NAL-TM-648T] 01 p0149 N94-10861
Overview of the 1989 Wind Tunnel Calibration Workshop
[NASA-TP-3393] 01 p0034 N94-11869
Superfluid turbulence 01 p0158 N94-12307
Soil erosion rates caused by wind and saltating sand stresses in a wind tunnel
[DE93-009154] 02 p0706 N94-12905
Propulsion simulator for magnetically-suspended wind tunnel models
[NASA-CR-189560] 02 p0527 N94-13127
Spacewok 16 --- Simulated Space Shuttle Program
[NASA-TM-109436] 03 p1221 N94-15420
Unitary plan wind tunnel landmark dedication and revitalization
[NASA-TM-109649] 03 p1302 N94-15434
Determination of the effect of the walls of a wind-tunnel from the parameters of flow near them
[RAE-LIB-TRANS-2201] 03 p0859 N94-16583
A wind tunnel model control surface actuator interface
[AD-A268729] 04 p1322 N94-18324
Perspective and future possibilities 04 p1431 N94-18651
Acoustic intensity measurements in the presence of low Mach number flow
[AD-A269995] 04 p1562 N94-18664
The world's largest wind tunnel
[NASA-TM-109371] 04 p1322 N94-18963
Langley's 50th year
[NASA-TM-109365] 04 p1632 N94-18980
Automatic pressure control system for the Wright Laboratory Compressor Research Facility
[AD-A273827] 06 p2194 N94-25522
Research and test facilities
[NASA-TM-109685] 07 p2681 N94-26684
Comparative analysis of different configurations of PLC-based safety systems from reliability point of view 07 p2836 N94-27925
Holographic interferometry: A user's guide
[DE94-003136] 08 p3286 N94-28466
Performance evaluation of the NWT with parallel Fortran 08 p3129 N94-28992
Application of fuzzy logic to the control of wind tunnel settling chamber temperature
[NASA-TM-109105] 08 p3157 N94-30200
The effect of pressure gradient on the structure of an equilibrium turbulent boundary layer 08 p3282 N94-30807
Icing research tunnel
[NASA-TM-109844] 10 p4009 N94-33751
Control of leading-edge separation on a cambered delta wing 10 p3992 N94-34616
National facilities study. Volume 2A: Facility Study Office on the National Wind Tunnel Complex
[NASA-TM-109856] 10 p4009 N94-34634

WIND TURBINES

NT TIP VANES
US areal wind resource assessment
[DE93-011905] 01 p0262 N94-11051
Fatigue life prediction for wind turbines: A case study on loading spectra and parameter sensitivity
[DE93-011597] 01 p0263 N94-11173
The 1992 JSEE/JWEA Joint Conference
[DE93-793955] 02 p0700 N94-12622
Inflow characteristics associated with high-blade-loading events in a wind farm
[DE93-010042] 02 p0704 N94-14423
DOE/NREL Advanced Wind Turbine Development Program
[DE93-010028] 03 p1093 N94-17668
The value of windpower: An investigation using a qualified production cost model
[DE93-010043] 04 p1465 N94-17888
FAROW: A tool for fatigue and reliability of wind turbines
[DE93-017639] 04 p1465 N94-18001
Defining the normal turbine inflow within a wind park environment
[DE93-010032] 04 p1489 N94-18046
The application of nondestructive techniques to the testing of a wind turbine blade
[DE93-016731] 04 p1447 N94-18128
Analysis of superconducting magnetic energy storage applications at a proposed wind farm site near Browning, Montana
[DE93-018793] 04 p1466 N94-18276
A rugged, low-cost advanced data acquisition system for field test projects
[DE93-010041] 04 p1615 N94-18334
Optimizing wind turbine control system parameters
[DE93-018861] 04 p1469 N94-19036
Wind energy: Program overview, FY 1992
[DE93-000056] 05 p1845 N94-19921
Derivation of a model of the exciter of a brushless synchronous machine
[EUT-92-E-258] 05 p1761 N94-21538
The FY1992 survey on multi-purpose dam and energy utilization system by the wind power generation eration
[DE94-707408] 05 p1848 N94-22012
Near wake measurements on a rotor model with Mie-vanes in the Delft open jet tunnel
[PB93-215382] 05 p1638 N94-22260
A review of the Workshop on Fatigue Life Methodologies for Wind Turbines
[DE94-002039] 06 p2394 N94-23472
Control algorithms for effective operation of variable-speed wind turbines
[DE94-002607] 06 p2394 N94-23704
The identification of inflow fluid dynamics parameters that can be used to scale fatigue loading spectra of wind turbine structural components
[DE94-000231] 07 p2791 N94-26117
An overview of DOE's wind turbine development programs
[DE93-018224] 07 p2856 N94-26513
User's guide for the frequency domain algorithms in the LIFE2 fatigue analysis code
[DE94-004678] 07 p2838 N94-26563
Analysis/test correlation using VAWT-SDS on a step-relaxation test for the rotating Sandia 34 m test bed
[DE94-002290] 07 p2857 N94-26700
Extraction of modal parameters from an operating HAWT using the Natural Excitation Technique (NExT)
[DE94-001831] 07 p2859 N94-27004
Simulating high-frequency wind for long durations
[DE94-002739] 07 p2682 N94-27997
New parameters for characterizing turbulence at a potential wind site
[DE94-004355] 08 p3368 N94-28455
International collaborative research in wind turbine rotor aerodynamics
[DE94-000244] 08 p3339 N94-30602
WISPER and WISPERX: Final definition of two standardised fatigue loading sequences for wind turbine blades
[AD-B175835] 08 p3324 N94-30872
The execution of wind energy projects 1986 - 1992 between China Aerodynamics Research and Development Centre (CARDC) and The Aeronautical Research Institute of Sweden (FFA)
[FFA-TN-1993-19] 08 p3340 N94-30945
Wind tunnel tests of a 5.3 m diameter yaw controlled turbine
[FFA-TN-1993-20] 08 p3340 N94-30946
A user's manual for the program TRES4: Random vibration analysis of vertical-axis wind turbines in turbulent winds
[DE94-009012] 10 p4079 N94-34078
Equations for estimating the strength of TV signals scattered by wind turbines
[NASA-CR-194468] 10 p4049 N94-34916
Mars vertical axis wind machines. The design of a Darreus and a Giromill for use on Mars
[NASA-CR-196143] 12 p4462 N94-36807
Mars vertical axis wind machines: The design of a tornado vortex machine for use on Mars
[NASA-CR-196144] 12 p4462 N94-36823
Fatigue case study and loading spectra for wind turbines
[DE94-010798] 12 p4457 N94-37622

WIND VANES
Preliminary meteorological results for 1992 West Coast Scotland Experiment
[DE93-014677] 02 p0720 N94-13404
Rotorwash wind sensor evaluation
[AD-A268987] 05 p1807 N94-20203
WIND VARIATIONS
Low frequency variability observed in the tropical Atlantic Ocean 09 p3778 N94-30991
WIND VELOCITY
NT SOLAR WIND VELOCITY
Preliminary results on backscattering strength from a wind generated bubbly ocean surface
[AD-A265006] 01 p0287 N94-10490
Selected upper-air wind speed distributions
[AD-A264822] 01 p0284 N94-10871
US areal wind resource assessment
[DE93-011905] 01 p0262 N94-11051
A preliminary C-band scatterometer model function for the ERS-1 AMI instrument 01 p0233 N94-11715
Wind and surface features in SAR images: The Canadian program 01 p0234 N94-11718
Evaluation of two January - June 1992 ERS-1 AMI wind vector data sets 01 p0235 N94-11724
Spatial scales of wave height 01 p0244 N94-11782
Current structures in the western equatorial Pacific during JAPACS cruises 01 p0193 N94-11911
The microwave backscattering from wind waves 01 p0201 N94-11959
On the variability of wind speeds in the North Western Pacific observed by altimeter/GEOSAT and SSM/I/DMSP 01 p0201 N94-11960
Observation of wind and waves by GEOSAT altimeter 01 p0202 N94-11961
Availability of wind field over the North Pacific derived from data on ships-of-opportunity and analysis of long-term variabilities 01 p0202 N94-11962
Analysis of GEOSAT wind data 01 p0207 N94-12636
SSMI wind speed variability over the Pacific Ocean 01 p0207 N94-12637
Theory and oceanographic applications of satellite altimeter measurements 01 p0208 N94-12641
Spatial variability of the ocean underwater dynamic noise from satellite radar sensing data 01 p0225 N94-12740
Atmospheric soundings during the Washita 1992 campaign
[NASA-CR-194383] 02 p0712 N94-13212
Preliminary meteorological results for 1992 West Coast Scotland Experiment
[DE93-014677] 02 p0720 N94-13404
Determination of momentum flux using a bivane and cup anemometer
[AD-A265414] 03 p1105 N94-15137
Complex terrain wind model evaluation
[AD-A266467] 03 p1096 N94-16589
Analysis of TIMS performance subjected to simulated wind blast 03 p1063 N94-16598
The use of the Air Force Academy high wind alert system in forecasting moderate intensity wind events for military bases in the Colorado Springs area
[AD-A267648] 03 p1107 N94-17245
Orographic microbursts in a severe winter windstorm
[AD-A267651] 03 p1108 N94-17247
On predicting the person-in-water drift for search and rescue
[AD-A268083] 03 p1055 N94-17514
Feasibility of a wind-ellipse criterion in a vortex advisory system for Schiphol Airport
[NLR-TP-91384-U] 04 p1315 N94-17733
A technique for measuring winds in the lower atmosphere using incoherent Doppler lidar
[DE93-017163] 04 p1488 N94-17758
The value of windpower: An investigation using a qualified production cost model
[DE93-010043] 04 p1465 N94-17888
A review of wind field models for atmospheric transport
[DE93-016085] 04 p1488 N94-17895
A mobile remote sensing laboratory for water vapor, trace gas, aerosol, and wind speed measurements
[DE93-017158] 04 p1489 N94-18132
AN/APS-137 Forward Looking Airborne Radar (FLAR) evaluation Spring 1992 experiment
[AD-A268899] 04 p1384 N94-18228
Some potential errors in satellite wind estimates using the geostrophic approximation and the thermal wind
[AD-A269784] 04 p1491 N94-18599
Station climatic summaries, North America. Volume 2: Alaska, Canada and Greenland
[AD-A269793] 04 p1493 N94-18732
Moments of ambient Doppler spectra
[DE93-017948] 04 p1390 N94-19114
Rotorwash wind sensor evaluation
[AD-A268987] 05 p1807 N94-20203
Wind chill: The temperature feeling caused by the wind velocity
[KNMI-TR-103A] 05 p1890 N94-20238
Analysis of wind observation from towers in the period 1977-1991
[KNMI-TR-148] 05 p1865 N94-20239
ERS-1 and Seasat scatterometer measurements of ocean winds: Model functions and the directional distribution of short waves 05 p1720 N94-20412
Ku-band ocean radar backscatter observations during SWADE 05 p1720 N94-20413
Comparison of remote sensing measurements with a two-scale polarimetric emission and scattering model for sea surfaces 05 p1721 N94-20415
Imaging radar studies of atmospheric winds and waves
[AD-A271672] 05 p1866 N94-20918
Airborne surface backscattering strength measurements in the western Atlantic Ocean
[AD-A271737] 05 p1883 N94-21358
Vertical velocity in cirrus case obtained from wind profiler 05 p1878 N94-22330
VIERS-1, phase 3
[BCRS-92-24] 06 p2381 N94-23145
Control algorithms for effective operation of variable-speed wind turbines
[DE94-002607] 06 p2394 N94-23704
Comparison between 1-minute and 15-minute averages of turbulence parameters 06 p2528 N94-24218
A nighttime structure model of atmospheric optical turbulence, c2(n), derived from thermosonde and high resolution rawinsonde measurements
[AD-A273803] 06 p2406 N94-25537
Wind measurements with an incoherent lidar
[AD-A273756] 07 p2891 N94-25722
Conversion of the CLUSE model for applications over open ocean
[AD-A273750] 07 p2893 N94-26013
Modelling atmospheric turbulence effects on ground-based telescope systems
[DE94-004211] 07 p3102 N94-26528
Simulating high-frequency wind for long durations
[DE94-002739] 07 p2682 N94-27997
Simulation of the effect of wind on clothing by measurements and calculations
[PB94-132289] 08 p3399 N94-28406
Prediction of survival times on land in a cold climate 08 p3379 N94-28423
The viability of photovoltaics on the Martian surface
[NASA-TM-106478] 08 p3338 N94-30196
Atmospheric turbulence within and above a coniferous forest
[ISBN-0-315-75468-0] 08 p3375 N94-30870
A comparison of predictors for first-guess wind speed errors
[AD-A276460] 09 p3781 N94-31239
Scatterometer wind-speed exponents: A review and SAXON 35-GHz measurements
[AD-A276568] 09 p3783 N94-31937
Recurvature dynamics of a typhoon
[AD-A276792] 09 p3784 N94-32164
Wind-speed measurements with a scanning elastic-backscatter lidar
[DE94-004974] 09 p3785 N94-32726
Mexico City ozone concentrations as a function of readily-available meteorological parameters
[DE94-007576] 09 p3768 N94-32814
Ocean magnetics
[PB94-149028] 10 p4092 N94-34142
Observations and modelling of winds and waves during the surface wave dynamics experiment. Report 2: Intensive observation period IOP-3
[AD-A278368] 10 p4093 N94-34375
Doppler weather radar studies of precipitation systems
[AD-A279417] 11 p4295 N94-36262
An automated method for Low Level Windshear Alert System (LLWAS) data quality analysis
[AD-A280313] 12 p4472 N94-37126
WIND VELOCITY MEASUREMENT
Evaluation of two January - June 1992 ERS-1 AMI wind vector data sets 01 p0235 N94-11724
Shape of wind gusts at a 130m tower at Wilhelmshaven (Germany)
[BER-BAND-B3] 04 p1494 N94-19503
Imaging radar studies of atmospheric winds and waves
[AD-A271672] 05 p1866 N94-20918
Implementation and evaluation of the new wind algorithm in NASA's 50 MHz doppler radar wind profiler
[NASA-CR-194880] 06 p2408 N94-23576
Implementation of a state of the art automated system for the production of cloud/water vapor motion winds from geostationary satellites
[NASA-CR-195087] 06 p2410 N94-24125
Micro-sensors for in-situ meteorological measurements 08 p3236 N94-29777
Scatterometer wind-speed exponents: A review and SAXON 35-GHz measurements
[AD-A276568] 09 p3783 N94-31937
WINDING
NT FILAMENT WINDING
NT HELICAL WINDINGS
NT WIRE WINDING
Tape winding of thermoplastic composites 01 p0060 N94-10035
High temperature co-axial winding transformers
[NASA-CR-194580] 04 p1407 N94-19643
Counter-balanced, multiple cable construction crane
[NASA-CASE-LAR-14565-1-CU] 05 p1822 N94-20369
Theoretical and experimental study of the winding of a thin plastic film: The role of aerodynamic effects
[ECL-93-04] 05 p1703 N94-20599
Winding numbers in homotopy theory from integers to reals
[DE94-601510] 07 p2992 N94-26367
Feasibility study of superconducting LSM rocket launcher system 11 p4225 N94-35914
WINDMILLING
U AUTOROTATION
WINDMILLS (WINDPOWERED MACHINES)
Mars vertical axis wind machines. The design of a Darreus and a Giromill for use on Mars
[NASA-CR-196143] 12 p4462 N94-36807
Mars vertical axis wind machines: The design of a tornado vortex machine for use on Mars
[NASA-CR-196144] 12 p4462 N94-36823
WINDOWS (APERTURES)
Arcjet exploratory tests of ARC optical window design for the AFE vehicle
[NASA-CR-192655] 01 p0034 N94-10930
Simulating the daylight performance of fenestration systems and spaces of arbitrary complexity: The IDC method
[DE93-015177] 02 p0704 N94-14333
WINDOW 4.0: Documentation of calculation procedures
[DE94-004935] 08 p3410 N94-29019
WINDOWS (COMPUTER PROGRAMS)
An expert system shell for inferring vegetation characteristics: Prototype help system (Task 1)
[NASA-CR-193411] 01 p0231 N94-11236
Development and implementation of a general purpose x-windows display program
[AD-A265306] 01 p0332 N94-11860
EGS (underscore) windows 2: An enhanced graphical interface to EGS
[DE93-010447] 02 p0746 N94-13382
ANNS: An X Window based version of the AFIT neural network simulator
[AD-A266540] 02 p0764 N94-13704
ORGBUG: A Windows-based combinatorial geometry debugger
[DE93-016640] 02 p0755 N94-14515
Upgrading NASA/DOSE laser ranging system control computers 03 p0918 N94-15595
Lunar laser ranging data processing in a Unix/X windows environment 03 p0918 N94-15599
Radar Analysis and Visualization Environment (RAVEN): Software for polarimetric radar analysis 03 p1080 N94-16758
Heavy ion nuclear physics research
[DE93-018862] 04 p1565 N94-17776
Why are human-computer interfaces difficult to design and implement?
[AD-A268843] 04 p1514 N94-18317
Design and implementation of a prototype PC based graphical and interactive MILSATCOM requirements database system
[AD-A272960] 05 p1658 N94-21251
Enhanced networks operations using the X Window System 05 p1932 N94-21329
Conversion and maintenance of Co-oP for Windows
[AD-A272513] 05 p1914 N94-21414
VETA x ray data acquisition and control system 05 p2047 N94-22455
Tools for the IDL widget set within the X-windows environment 05 p1927 N94-22538
XRTD: An X-Windows based, real-time radiometric display and analysis system 06 p2305 N94-23922
Interoperability through standardization: Electronic mail, and X Window systems 06 p2575 N94-24406
Horatio: Libraries for vision applications, release 2.0
[OUEL-1967/92] 06 p2593 N94-25326
Implementing a multiple criteria model base in co-op with a graphical user interface generator
[AD-A274901] 07 p3093 N94-26181
An artificial reality environment for remote factory control and monitoring 07 p2687 N94-27369

Development of Calcomp compatible interface library 'piflib' on X Window System
[DE94-701190] 07 p2973 N94-27702
Extending the X Window System
[DE94-006496] 08 p3420 N94-29844
The Views application environment
[CWI-CS-R9257] 08 p3423 N94-30341
TILDA for Windows: A system for registration of journals in the library at NDRE NBC-Defence
[PB94-149168] 10 p4158 N94-34161
Multi-window dialogue system of data processing for experimental setup VASSILISSA in PAW environment
[DE94-612439] 11 p4345 N94-35790
Netlib services and resources
[DE94-010307] 11 p4347 N94-36300

WINDOWS (INTERVALS)
NT LAUNCH WINDOWS
A note on windowing for the waveform relaxation
[AD-A280999] 10 p4130 N94-34922

WINDPOWER UTILIZATION
US areal wind resource assessment
[DE93-011905] 01 p0262 N94-11051
Renewable energy sources 1991, part 2
[DE93-605634] 01 p0263 N94-11506
The 1992 highlights
[NASA-TM-109671] 03 p1303 N94-15508
DOE/NREL Advanced Wind Turbine Development Program
[DE93-010028] 03 p1093 N94-17668
The value of windpower: An investigation using a qualified production cost model
[DE93-010043] 04 p1465 N94-17888
Analysis of superconducting magnetic energy storage applications at a proposed wind farm site near Browning, Montana
[DE93-018793] 04 p1466 N94-18276
Optimizing wind turbine control system parameters
[DE93-018861] 04 p1469 N94-19036
Seasonal variability of wind electric potential in the US
[DE93-018182] 04 p1493 N94-19051
Wind energy: Program overview, FY 1992
[DE93-000056] 05 p1845 N94-19921
The FY1992 survey on multi-purpose dam and energy utilization system by the wind power generation eration
[DE94-707408] 05 p1848 N94-22012
Current situation of development of petroleum substituting energies (Canada)
[DE94-707493] 05 p1849 N94-22014
Renewable energy systems in Mexico: Installation of a hybrid system
[DE93-013716] 07 p2853 N94-25946
NEMO 2: New energy systems and technologies
[DE94-702060] 07 p2855 N94-26240
Programme for the promotion of wind power production
[DE94-702065] 07 p2855 N94-26242
Hybrid power system for remote communications stations
[AD-A274963] 07 p2782 N94-26301
An overview of DOE's wind turbine development programs
[DE93-018224] 07 p2856 N94-26513
Applicability of digital terrain analyses to wind energy prospecting and siting
[DE94-004363] 08 p3374 N94-30587
The execution of wind energy projects 1986 - 1992 between China Aerodynamics Research and Development Centre (CARDC) and The Aeronautical Research Institute of Sweden (FFA)
[FFA-TN-1993-19] 08 p3340 N94-30945
Wind tunnel tests of a 5.3 m diameter yaw controlled turbine
[FFA-TN-1993-20] 08 p3340 N94-30946
NEMO: Advanced energy systems and technologies
[DE94-721996] 09 p3760 N94-31767
Renewable energy technology development at Sandia National Laboratories
[DE94-007734] 09 p3761 N94-32383
Equations for estimating the strength of TV signals scattered by wind turbines
[NASA-CR-194468] 10 p4049 N94-34916
Model documentation: Renewable Fuels Module of the National Energy Modeling System
[DE94-009962] 11 p4282 N94-35672
Mars vertical axis wind machines. The design of a Darreus and a Giromill for use on Mars
[NASA-CR-196143] 12 p4462 N94-36807
Mars vertical axis wind machines: The design of a tornado vortex machine for use on Mars
[NASA-CR-196144] 12 p4462 N94-36823
1993 JSES (Japan Solar Energy Society)/JWEA (Japan Wind Energy Association) Joint Conference and 1993 Japan-Korea Joint Conference on Solar Energy
[DE94-767725] 12 p4462 N94-37418
Fatigue case study and loading spectra for wind turbines
[DE94-010798] 12 p4457 N94-37622

WINDPOWERED GENERATORS
US areal wind resource assessment
[DE93-011905] 01 p0262 N94-11051
Inflow characteristics associated with high-blade-loading events in a wind farm
[DE93-010042] 02 p0704 N94-14423
The value of windpower: An investigation using a qualified production cost model
[DE93-010043] 04 p1465 N94-17888
Analysis of superconducting magnetic energy storage applications at a proposed wind farm site near Browning, Montana
[DE93-018793] 04 p1466 N94-18276
Programme for the promotion of wind power production
[DE94-702065] 07 p2855 N94-26242
Mars vertical axis wind machines. The design of a Darreus and a Giromill for use on Mars
[NASA-CR-196143] 12 p4462 N94-36807
Mars vertical axis wind machines: The design of a tornado vortex machine for use on Mars
[NASA-CR-196144] 12 p4462 N94-36823

WINDPOWERED PUMPS
Renewable energy sources 1991, part 3
[DE93-605594] 01 p0263 N94-11505
The FY1992 survey on multi-purpose dam and energy utilization system by the wind power generation eration
[DE94-707408] 05 p1848 N94-22012

WINDS ALOFT
NT GEOSTROPHIC WIND
NT JET STREAMS (METEOROLOGY)
Mesospheric and lower thermospheric winds, temperatures densities, and volume emission rates
[NASA-CR-195147] 06 p2403 N94-24486
Modeling of the coupled magnetospheric and neutral wind dynamos
[NASA-CR-195273] 07 p2883 N94-27852
Mesopause winds and OH intensities at Mid-Latitudes-Fabry-Perot interferometer observations of the OH emission at 8430 A from bear lake observatory
[AD-A275246] 08 p3361 N94-29430

WINDSCREENS
U WINDSHIELDS

WINDSHIELDS
Aircraft windscreens enhance visual search disruption produced by laser glare
[AD-A265167] 01 p0026 N94-11892
Comparative night vision goggle visual acuity measurements performed in the A-10 aircraft in an operational setting
[AD-A266721] 03 p1137 N94-15820
Definitions of terms relating to aircraft windscreens, canopies, and transparencies
[AD-A268403] 03 p0868 N94-17425
Explicit solution techniques for impact with contact constraints 04 p1459 N94-19470
Cockpit/NVG visual integration issues 06 p2432 N94-23983
Birdstrike resistant crew enclosure program
[AD-A273700] 06 p2463 N94-25453
Backscatter haze device for measurement of haze in aircraft transparencies
[AD-A275127] 08 p3146 N94-29042
Canopy breaking device
[AD-D016294] 12 p4385 N94-37767

WING CAMBER
Mission adaptive wing
[NASA-TM-109448] 03 p0865 N94-15321

WING FLAPS
NT LEADING EDGE FLAPS
NT LEADING EDGE SLATS
NT TRAILING EDGE FLAPS
NT VORTEX FLAPS
Numerical simulation of a powered-lift landing, tracking flow features using overset grids, and simulation of high lift devices on a fighter-lift-and-control wing
[NASA-CR-194260] 02 p0527 N94-14322
High-Lift System Aerodynamics
[AGARD-CP-515] 04 p1305 N94-18415
Where is high-lift today? A review of past UK research programmes 04 p1305 N94-18416
Experimental investigation of flow around a multielement airfoil 04 p1305 N94-18417
A design procedure for slotted flaps 04 p1305 N94-18418
Aircraft wing structural detail design (wing, aileron, flaps, and subsystems)
[NASA-CR-195487] 06 p2183 N94-24974

WING FLOW METHOD TESTS
Numerical simulation of a powered-lift landing 07 p2671 N94-28033

WING ICING
U AIRCRAFT ICING

WING LOADING
The reduction of takeoff ground roll by the application of a nose gear jump strut
[NASA-TM-108822] 11 p4198 N94-36380

WING NACELLE CONFIGURATIONS
Supersonic airplane study and design
[NASA-CR-193219] 01 p0025 N94-11150
Supersonic flow visualization of a nacelle in close proximity to a simulated wing
[NASA-CR-194675] 03 p0860 N94-17260
An experimental investigation of a Mach 3.0 high-speed civil transport at supersonic speeds
[NASA-TP-3365] 06 p2169 N94-24311
Aerodynamic analysis of slipstream/wing/nacelle interference for preliminary design of aircraft configurations
[AD-B173651] 08 p3135 N94-30916
Multidisciplinary optimization of high-speed civil transport configurations using variable-complexity modeling 09 p3578 N94-31881
HSCT inlet development issues 10 p3977 N94-33505

WING OSCILLATIONS
Lift enhancement device
[AD-D015868] 04 p1317 N94-17704
Understanding and development of a prediction method of transonic limit cycle oscillation characteristics of fighter aircraft
[NLR-TP-92210-U] 07 p2679 N94-27798
Development of a method to predict transonic limit cycle oscillation characteristics of fighter aircraft (continued)
[NLR-TP-92156-U] 08 p3148 N94-30342
Prospects of time-linearized unsteady calculation methods for exponentially diverging motions in aeroelasticity
[PB94-126224] 08 p3134 N94-30740
Unsteady separation experiments on 2-D airfoils, 3-D wings, and model helicopter rotors 10 p3986 N94-34967
Multirate flutter suppression system design for the Benchmark Active Controls Technology Wing
[NASA-CR-196112] 12 p4388 N94-36965

WING PANELS
Underwing compression vortex attenuation device
[NASA-CASE-LAR-14744-1] 01 p0012 N94-10673
Investigation of the bond strength of a discrete skin-stiffener interface
[NLR-TP-92183-U] 07 p2670 N94-27796
Active vortex control for a high performance wing
[AD-D016140] 09 p3573 N94-32974

WING PLANFORMS
NT DELTA WINGS
NT SWEPT FORWARD WINGS
NT SWEPTBACK WINGS
NT VARIABLE SWEEP WINGS
Ground vibration and flight flutter tests of the single-seat F-16XL aircraft with a modified wing
[NASA-TM-104264] 01 p0026 N94-11233
Static aeroelastic response of an aircraft with asymmetric wing planforms representative of combat damage
[AD-A266890] 03 p0865 N94-14951
Experimental study of vortex and aerodynamic characteristics of stack wings with sideslip
[AD-A267722] 03 p0860 N94-17274
The Triton: Design concepts and methods
[NASA-CR-195542] 06 p2184 N94-25004
Aerodynamic design of super maneuverable aircraft 10 p3992 N94-34617

WING PROFILES
NT WING SPAN
New aerodynamic information obtained from the solution of the inverse problem for aerofoils
[NAL-TR-1172] 01 p0014 N94-10860
Development and application of a comprehensive, design-sensitive weight prediction method for wing structures of transport category aircraft
[LR-693] 02 p0515 N94-13687
Development of experimental demonstration processes for laminar-turbulent flow states at wing profiles in free flight
[ILR-MITT-280(1993)] 02 p0510 N94-14800
Mission adaptive wing
[NASA-TM-109448] 03 p0865 N94-15321
The Gold Rush: A simulated commercial air transportation study
[NASA-CR-195528] 06 p2184 N94-25002
Numerical analysis of supersonic transport wings 08 p3124 N94-28959
Numerical solution of inverse problem in aerodynamics 08 p3125 N94-28965
Computation of three-dimensional compressible boundary layers to fourth-order accuracy on wings and fuselages
[NASA-CR-4269] 09 p3709 N94-32671

Status of F16XL SSLFC numerical design validation
10 p3981 N94-33527

WING SLATS
U LEADING EDGE SLATS

WING SLOTS
Fluid flow and heat convection studies for actively cooled airframes
[NASA-CR-194624] 03 p1024 N94-16491
A design procedure for slotted flaps
04 p1305 N94-18418

WING SPAN
Simulated and experimental aerodynamic characteristics of tapered annular wings
[NAL-TR-1157] 01 p0013 N94-10856
Low-speed wind tunnel tests on four types of joined-wing aircraft models
[NAL-TR-1167] 02 p0501 N94-13340

WING TANKS
Flight test certification of a 480 gallon composite fuel tank on CF-18
11 p4196 N94-36340

WING TIP VORTICES
Simulated and experimental aerodynamic characteristics of tapered annular wings
[NAL-TR-1157] 01 p0013 N94-10856
Experimental investigation of three-dimensional vortex-airfoil interaction in a supersonic stream
[AD-A275107] 08 p3122 N94-28899
An experimental study of wing tip vortex in the near wake of a rectangular wing
[AD-A275389] 08 p3129 N94-29306
Numerical modeling studies of wake vortex transport and evolution within the planetary boundary layer
[NASA-CR-196078] 11 p4192 N94-35522

WING TIPS
Nonlinear aerodynamics and the design of wing tips
[NASA-CR-194732] 05 p1638 N94-21833
Bent-tip blade for aircraft rotary-wing
[CA-PATENT-1-315-259] 06 p2176 N94-23254
Toward modeling winglip vortices
06 p2171 N94-24142
Aerodynamic performance of novel ducted-tip wings
07 p2654 N94-28331
Experimental investigation of three-dimensional vortex-airfoil interaction in a supersonic stream
[AD-A275107] 08 p3122 N94-28899

WING-FUSELAGE STORES
Application of the influence function method using the interference distributed loads code to prediction of store aerodynamic load during separation from the CF-18 fighter aircraft
07 p2654 N94-28330

WINGS
NT CAMBERED WINGS
NT CRUCIFORM WINGS
NT DELTA WINGS
NT FIXED WINGS
NT FLEXIBLE WINGS
NT JOINED WINGS
NT LIFTING ROTORS
NT LOW ASPECT RATIO WINGS
NT MISSION ADAPTIVE WINGS
NT OBLIQUE WINGS
NT RECTANGULAR WINGS
NT RING WINGS
NT ROTARY WINGS
NT SLENDER WINGS
NT SUPERCRITICAL WINGS
NT SWEPT FORWARD WINGS
NT SWEPT WINGS
NT SWEPTBACK WINGS
NT SWING WINGS
NT THIN WINGS
NT TILTING ROTORS
NT UNCAMBERED WINGS
NT UNSWEPT WINGS
NT VARIABLE SWEEP WINGS
NT X WING ROTORS
Navier-Stokes flowfield computation of wing/rotor interaction for a tilt rotor aircraft in hover
[NASA-CR-4532] 01 p0013 N94-10758
A method of predicting quasi-steady aerodynamics for flutter analysis of high speed vehicles using steady CFD calculations
[NASA-TM-109009] 02 p0514 N94-12850
Numerical study of the effects of icing on viscous flow over wings
[NASA-CR-193306] 02 p0500 N94-13180
Better airplane wings
[NASA-TM-109446] 03 p0933 N94-15345
Wind-tunnel investigation of aerodynamic efficiency of three planar elliptical wings with curvature of quarter-chord line
[NASA-TP-3359] 03 p0859 N94-16574
Adaptive Navier-Stokes calculations for vortical flow
[AD-A266236] 03 p1026 N94-16966
Supersonic flow visualization of a nacelle in close proximity to a simulated wing
[NASA-CR-194675] 03 p0860 N94-17260
Experimental study of vortex and aerodynamic characteristics of stack wings with sideslip
[AD-A267722] 03 p0860 N94-17274
Lift enhancement device
[AD-D015868] 04 p1317 N94-17704
High-Lift System Aerodynamics
[AGARD-CP-515] 04 p1305 N94-18415
Prediction of the high-lift performance of multi-element aerofoils using an unstructured Navier-Stokes solver
04 p1307 N94-18427
The GARTEUR high lift research programme
04 p1307 N94-18430
Viscous phenomena affecting high-lift systems and suggestions for future CFD development
04 p1308 N94-18433
In-flight pressure distributions and skin-friction measurements on a subsonic transport high-lift wing section
04 p1308 N94-18435
A fast computing method for the flow over high-lift wings
04 p1308 N94-18437
Calculation of multielement airfoils and wings at high lift
04 p1309 N94-18438
Forty years of high-lift R/D: An aircraft manufacturer's experience
04 p1309 N94-18441
High-lift research: Application to the design of the ATR72 flap
04 p1309 N94-18442
The aero-mechanical design of a novel Fowler flap mechanism
04 p1309 N94-18443
High lift systems for transport aircraft with advanced airfoils
04 p1310 N94-18446
Dynamic response analysis of composite structural members during missile launch
[AD-A270023] 04 p1332 N94-18760
Airflow research
[NASA-TM-109372] 04 p1312 N94-18964
Design for cyclic loading endurance of composites
[NASA-TM-106407] 04 p1457 N94-19351
Numerical investigation of the incompressible flow around a wing with a fixed spoiler
[ISL-R-109/91] 04 p1313 N94-19524
Experimental study on interference aerodynamics of close-coupled canard configuration
[AD-A267760] 05 p1636 N94-19963
Nonlinear aerodynamics and the design of wing tips
[NASA-CR-194732] 05 p1638 N94-21833
Dynamic mesh adaption for triangular and tetrahedral grids
05 p1920 N94-22363
An experimental investigation of the effect of upper surface blowing on dynamic stall
[NASA-CR-194863] 06 p2165 N94-22894
POISs3: A 3D poisson smoother of structured grids
[PB93-226231] 06 p2318 N94-23115
Leading-edge votex-system details obtained on F-106B aircraft using a rotating vapor screen and surface techniques
[NASA-TP-3374] 06 p2166 N94-23512
LinAir: A multi-element discrete vortex Weissinger aerodynamic prediction method
[NASA-TM-108786] 06 p2167 N94-23557
Aircraft wing structure detail design
[NASA-CR-195485] 06 p2180 N94-24498
Aircraft wing structural detail design (wing, aileron, flaps, and subsystems)
[NASA-CR-195487] 06 p2183 N94-24974
An investigation into the aerodynamic effects of wing patches
[ISBN-0-315-84121-4] 07 p2646 N94-26672
Automation of formation flight control
[AD-A274137] 07 p2678 N94-27132
Investigation of aerodynamic design issues with regions of separated flow
07 p2658 N94-27902
Wing design for a civil tiltrotor transport aircraft: A preliminary study
07 p2671 N94-27917
Effects, limits, and limitations of spanwise blowing
07 p2659 N94-28027
Program for calculation of maximum lift coefficient of plain aerofoils and wings at subsonic speeds
[ESDU-93015] 07 p2649 N94-28076
Wing lift increment at zero angle of attack due to deployment of single-slotted flaps at low speeds
[ESDU-93019] 07 p2649 N94-28140
Calculation of unsteady incompressible inviscid flow about wings and bodies using CANAERO-T panel model
07 p2655 N94-28334
Ice accretion on aircraft wings
07 p2657 N94-28345
Experimental investigation of three-dimensional vortex-airfoil interaction in a supersonic stream
[AD-A275107] 08 p3122 N94-28899
Numerical study of the trailing vortex of a wing with wing-tip blowing
[NASA-CR-195803] 08 p3130 N94-29760
Aerodynamic characteristics of a propeller-powered high-lift semispan wing
[NASA-TM-4541] 08 p3132 N94-29937
Sensitivity analysis of the static aeroelastic response of a wing
08 p3134 N94-30525
Grid sensitivity for aerodynamic optimization and flow analysis
09 p3568 N94-31287
Finite element analysis of MB326H Macchi wing lower spar cap fatigue cracks
[AD-A277062] 09 p3580 N94-32264
Active vortex control for a high performance wing
[AD-D016140] 09 p3573 N94-32974
Structural testing of the technology integration box beam
09 p3628 N94-33125
Resin transfer molding for advanced composite primary wing and fuselage structures 09 p3628 N94-33128
Test and analysis results for composite transport fuselage and wing structures 09 p3628 N94-33129
A new method for calculating wing along aerodynamics to angle of attack 180 deg
[AD-A277965] 09 p3574 N94-33263
Lift enhancement by trapped vortex
10 p3980 N94-33524
Risk analysis of the C-141 WS405 inner-to-outer wing joint
10 p3996 N94-34592
Design oriented structural analysis
[NASA-TM-109124] 10 p4073 N94-34722
Ground vibration test of the XV-15 Tiltrotor Research Aircraft and pretest predictions
11 p4200 N94-35972
Aeroservoelastic tailoring with piezoelectric materials: Actuator optimization studies
[AD-A278640] 11 p4199 N94-36384

WINTER
Orographic microbursts in a severe winter windstorm
[AD-A267651] 03 p1108 N94-17247
C-band radar backscatter of sea ice in the Weddell Sea, Antarctica during the austral winter of 1992
05 p1725 N94-20435
Propagation of cold air masses in East Asia and its associated planetary-scale function
[AD-A274304] 07 p2895 N94-26850
Meteorological data at the Nagaoka Institute of Snow and Ice Studies
[REPT-158] 07 p2896 N94-27169
Hydrodynamics of convection under winter polar leads
[AD-A275182] 08 p3369 N94-29067
Interannual temperature variability and cyclone frequency over Eastern Canada and the New England States. A case study: Winter seasons 1931-1932 to 1984-1985
[ISBN-0-315-74841-9] 08 p3373 N94-29908
Simulation of a precipitation event in the western United States
[DE94-004835] 09 p3786 N94-32791
Coupled ice-ocean model supporting winter navigation in the Baltic Sea. Part 1: Ice dynamics and water levels
[PB94-148780] 10 p4092 N94-34121
Cooling of the West Spitzbergen Current: Wintertime observations west of Svalbard
[AD-A280648] 12 p4475 N94-36762

WIRE
NT ELECTRIC WIRE
Casting of superconducting composite materials (M-4)
02 p0586 N94-13736
Superconductivity Technology Program for Electric Power Systems: Proceedings
[DE93-040074] 05 p2011 N94-19825
Automated HMC assembly
[DE93-040641] 05 p1749 N94-20005
Flexible heating head for induction heating
[NASA-CASE-LAR-14418-15-B]
05 p1718 N94-20368
Wire assembly for electrically conductive circuits
[AD-D015966] 05 p1761 N94-21275
Wear reduction in ceramic bearings by surface generated pyrolytic carbon continuously replenished by ethylene gas
[AD-A278264] 06 p2364 N94-24090
A vibrating wire parallel to a type 2 superconducting slab of arbitrary thickness
[DE93-617134] 06 p2525 N94-25389
Effects of a vibrating wire carrying DC current on a moving type 2 superconducting slab of arbitrary thickness
[DE93-617136] 06 p2566 N94-25391
Liquid and solid solubility of Ag in Bi2Sr2CaCu2O8
[DE94-002829] 07 p2735 N94-26273
Superconducting fibers made with yttrium and yttrium oxide interlayers and barium cuprate cover layers
[AD-D016073] 07 p3070 N94-28225
Welding wire pressure sensor assembly
[NASA-CASE-MFS-26216-1-SB]
08 p3300 N94-29506

Novel growth technologies for in situ formation of semiconductor quantum wire structures
[AD-A277188] 09 p3902 N94-32255
Development of an automated wire delivery system for robotic welding applications
[NASA-CR-194216] 09 p3727 N94-32479
Multifilamentary superconducting cable and a method of manufacturing it
[AD-D016146] 10 p4040 N94-33837

WIRE BRIDGE CIRCUITS
NT WHEATSTONE BRIDGES

WIRE CLOTH
Electrical performance of wire mesh for spacecraft deployable reflector antennas 06 p2275 N94-22744
A constitutive model for layered wire mesh and aramid cloth fabric
[DE94-003275] 07 p2708 N94-26796
Flow past a circular cylinder with a permeable wake splitter plate 08 p3275 N94-29764

WIRE MESH
U WIRE CLOTH

WIRE WINDING
Rotary actuator
[NASA-CASE-MFS-28581-1] 08 p3205 N94-29447

WIRELESS COMMUNICATION
Infra Link: A data transmission system for microgravity research 03 p0980 N94-16091
Information technology resources assessment
[DE93-015276] 04 p1613 N94-17894
Digital wireless control system
[DE93-040211] 05 p1714 N94-19946
Odyssey personal communications satellite system 06 p2282 N94-22787
Reduced cost alternatives to premise wiring using ATM and microcellular technologies 06 p2314 N94-23239
Efficient massively parallel simulation of dynamic channel assignment schemes for wireless cellular communications
[AD-A277558] 07 p2971 N94-27558
Evaluation of wireless Local Area Networks
[AD-A275133] 08 p3243 N94-29064
The 19th Convention on Radio Science: Abstracts of Papers
[PB94-136868] 08 p3244 N94-29169

WIRING
Specification and testing for power by wire aircraft
[NASA-TM-106232] 01 p0046 N94-10765
Development and analysis of insulation constructions for aerospace wiring applications 01 p0021 N94-10791
Rigid-flexible printed wiring boards
[DE93-013938] 02 p0620 N94-13094
Electronic schematics for the Donner 600 Crystal Tomograph
[DE93-015277] 02 p0625 N94-14336
Operation of digital systems in severe electromagnetic environments
[AD-A267176] 03 p0988 N94-15693
NASA/ASEE Summer Faculty Fellowship Program
[NASA-CR-194678] 06 p2571 N94-23230
Reduced cost alternatives to premise wiring using ATM and microcellular technologies 06 p2314 N94-23239
A review of wiring system safety in space power systems
[NASA-CR-194439] 06 p2203 N94-23632
Lightning tests and analyses of tunnel bond straps and shielded cables on the Space Shuttle solid rocket booster
[NASA-CR-193921] 06 p2200 N94-24801
Second NASA Workshop on Wiring for Space Applications
[NASA-CP-3244] 08 p3165 N94-28697
ESTEC wiring test programme materials related properties 08 p3165 N94-28698
NASA wiring program: Survey of NASA experiences in wiring system safety 08 p3165 N94-28700
NAVAIR aircraft wiring standardization and qualification program 08 p3166 N94-28704
Organized wiring systems 08 p3166 N94-28705
MSFC inspections of installed polyimide wire 08 p3166 N94-28707
Wiring for space applications program 08 p3166 N94-28708
Cryogenic on-orbit liquid depot storage acquisition and transfer (COLD-SAT) experiment subsystem instrumentation and wire harness design report
[NASA-CR-189172] 08 p3168 N94-29405

WIRING SYSTEMS
U WIRING

WKB APPROXIMATION
U WENTZEL-KRAMER-BRILLOUIN METHOD

WOLF-RAYET STARS
X ray emission from Wolf-Rayet stars with recurrent dust formation
[NASA-CR-189321] 03 p1300 N94-15533
Ultraviolet observations of clusters of Wolf-Rayet stars in the SBm3 galaxy NGC 4214 and Ultraviolet and optical observations of LINER's
[NASA-CR-194307] 04 p1622 N94-19431
Inhomogeneities in the wind from Wolf-Rayet stars
[ISBN-0-315-85893-1] 08 p3548 N94-30058

WOLFRAM
U TUNGSTEN

WOMEN
U FEMALES

WOOD
Moisture meter evaluation
[DE93-016581] 02 p0652 N94-14534
Biomass energy: State of the technology present obstacles and future potential
[DE93-016295] 03 p1092 N94-16766
Automated image analysis method for the detection of cracks on wood surface
[VTT-JULK-755] 03 p1056 N94-17542
Report of National Institute for Resources and Environment. No. 5: Study on direct liquefaction of woody biomass
[JTN-94-80551] 07 p2859 N94-27204
Laser applications in wood processing
[PB94-138567] 09 p3717 N94-31840
The potential impact of externalities considerations on the market for biomass power technologies
[DE94-000247] 10 p4078 N94-33726
Estimates of US biomass energy consumption 1992
[DE94-011458] 12 p4463 N94-37567

WORD PROCESSING
Smart Document System (SDS) used in managing DOE order's with electronic Engineering Procedures
[DE94-005076] 08 p3534 N94-30099

WORDS (LANGUAGE)
NT SYLLABLES
Computational Russian morphological generation on Prolog: Noun, pronoun, and adjective 02 p0747 N94-13436
Discovering sequence similarity by the algorithmic significance method
[DE93-015556] 03 p1150 N94-16659
Neural networks to classify speaker independent isolated words recorded in radio car environments
[REPT-93-013] 04 p1383 N94-17935
Feasibility study in linguistically motivated object-oriented conceptual design of information systems
[PB93-197754] 04 p1618 N94-19331
A computational theory of lexical relatedness
[TR-421] 05 p1904 N94-20067
Connectionism and Natural Language Processing
[MEMO-INF-92-64] 05 p1940 N94-20242
Representation of spoken words in a self-organizing neural net 05 p1940 N94-20243
An exploration of clause boundary effects in SRN representations 05 p1937 N94-20253
On the topological size of p-m-complete degrees
[TR-459] 05 p1965 N94-21286
Application of a back-propagation neural network to isolated-word speech recognition
[AD-A272495] 05 p1945 N94-21430
Procedural dynamic semantics, verb-phrase ellipsis, and presupposition
[CWI-CS-R9311] 05 p1914 N94-21495
Recognizing hesitation phenomena in continuous, spontaneous speech 05 p1746 N94-22210
Parallel string matching algorithms
[AD-A274502] 07 p3100 N94-27164
Researches of the Electrotechnical Laboratory. No. 955: Speech recognition by description of acoustic characteristic variations
[JTN-94-80604] 07 p2775 N94-27249
Learning new words from spontaneous speech: A project summary
[AD-A277612] 10 p4035 N94-33853
Good applications for crummy machine translation
[AD-A278689] 11 p4345 N94-35651
A graphic view of Geometric Dimensioning and Tolerancing
[DE94-011478] 12 p4435 N94-37736

WORK
NT PHYSICAL WORK

WORK CAPACITY
Glycerol-induced hyperhydration 01 p0309 N94-11996
Circadian countermeasures for shiftworkers during USMP-2: A report to mission management
[NASA-CR-195260] 08 p3402 N94-30188
Drug-related problems in the workplace
[CRANFIELD-AERO-9306] 09 p3914 N94-31538
Expanding the pilot's envelope 10 p3994 N94-34627

WORK FUNCTIONS
Squeezed states of electrons and transitions of the density of states 01 p0370 N94-10593
Low energy neutral atom imaging techniques
[DE93-012744] 02 p0779 N94-12950
High voltage conductors in spacecraft
[AD-A267268] 03 p0897 N94-17266
Engineering of systems for application of scientific computing in industry 08 p3123 N94-28947

WORK HARDENING
NT STRAIN HARDENING
The effect of oxygen, grain size, and strain rate on the mechanical behavior of forged P/M tantalum
[DE93-011251] 03 p0959 N94-16764
A review of the stages of work hardening
[DE93-016456] 04 p1359 N94-18114
Work hardening behavior in aluminum alloy 2090
[DE94-007036] 09 p3643 N94-32064

WORK-REST CYCLE
Physiological efficacy of a lightweight ambient air cooling unit for various applications
[AD-A272952] 05 p1896 N94-21247
Flight controller alertness and performance during MOD shiftwork operations 10 p4098 N94-33624
Prediction modeling of physiological responses and human performance in the heat with application to space operations 10 p4098 N94-33652

WORKING FLUIDS
Geometrical vapor blocker for parallel condensation tubes requiring cooling
[NASA-CASE-MSC-22090-1] 03 p1022 N94-15962
Malone refrigeration
[DE93-014468] 04 p1379 N94-17725
EHD enhancement of pool and in-tube boiling of alternate refrigerants
[DE94-000787] 05 p1798 N94-20101
System and method for cancelling expansion waves in a wave rotor
[NASA-CASE-LEW-15218-1] 05 p1801 N94-20588
Enhanced absorption cycle computer model
[DE94-001997] 06 p2271 N94-23793
Weld joint concepts for on-orbit repair of Space Station Freedom fluid system tube assemblies 06 p2371 N94-24427
The Lightcraft project: Flight technology for a hypersonic mass transit system 07 p2670 N94-25695
Liquid metal MHD research and development in Israel 07 p2854 N94-26055
Modelling the mass migration phenomena in partially frozen heat pipes
[DE94-002716] 07 p2797 N94-27709
ARTI Refrigerant Database
[DE94-004906] 08 p3230 N94-28563
Method for cancelling expansion waves in a wave rotor
[NASA-CASE-LEW-15218-2] 08 p3274 N94-29740
Application of natural refrigerants: A rational solution to a pressing problem
[PB94-138781] 09 p3668 N94-31073
Non-polluting gas turbine as a result of self-heating working fluid in a closed circuit 10 p4000 N94-34436
Solubility, viscosity and density of refrigerant/lubricant mixtures
[DE94-009996] 11 p4245 N94-35771
Sealed tube comparisons of the compatibility of desiccants with refrigerants and lubricants
[DE94-010002] 11 p4251 N94-36388
Refrigeration and Air-Conditioning Technology Workshop
[DE94-010813] 12 p4431 N94-37452

WORKLOADS (PSYCHOPHYSIOLOGY)
Quantitative EEG patterns of differential in-flight workload 01 p0317 N94-11528
Psychophysiological measures of cognitive workload in laboratory and flight 01 p0317 N94-11529
A perspective on the FAA approval process: Integrating rotorcraft displays, controls and workload 02 p0521 N94-13298
Functional categories for future flight deck designs
[NASA-TM-109005] 02 p0517 N94-13710
The influence of ATC message length and timing on pilot communication
[NASA-CR-177621] 02 p0512 N94-14744
Preliminary validation of the task analysis/workload methodology
[AD-A267514] 03 p1138 N94-17077
System performance modeling and analysis of a fault-tolerant, real time parallel processor
[AD-A268070] 03 p1162 N94-17551
Revision and verification of a seven-point workload estimate scale
[AD-A269194] 04 p1511 N94-18412
Integrated Terminal Weather System (ITWS)
[AD-A269884] 04 p1492 N94-18684
Cognition and the brain: A continuation of the university research initiative at New York University
[AD-A271872] 05 p1894 N94-20467

Reducing the cognitive workload: Trouble managing power systems
[NASA-TM-106413] 05 p1714 N94-21564
Investigation of time and intensity effects in operator workload and performance
[CTN-94-60927] 06 p2433 N94-24171
Pilot evaluation system 06 p2158 N94-24266
An examination of the operational error database for air route traffic control centers
[AD-A275986] 06 p2175 N94-24472
New Advances in Mission Planning and Rehearsal Systems
[AGARD-LS-192] 06 p2521 N94-25008
Human factors of mission planning systems: Theory and concepts 06 p2521 N94-25010
Multiple-camera/motion stereoscopy for range estimation in helicopter flight 06 p2441 N94-25505
Developing realistic cooperative behaviors for autonomous agents in air combat simulation
[AD-A274077] 07 p2937 N94-25774
Developing a sophisticated user interface to support domain-oriented application composition and generation systems
[AD-A274080] 07 p2960 N94-25994
A critical analysis of workload predictions generated by multiple resource theory during early crewstation design
[AD-A274804] 07 p2941 N94-26339
The use of EEG as a workload assessment tool in flight test
[AD-A274568] 07 p2910 N94-26847
Workload transition: Implications for individual and team performance
[AD-A274538] 07 p2941 N94-26964
Task demand, workload, and performance
[PB94-123627] 07 p2942 N94-27155
Effects of workload on communication processes in decision making teams
[AD-A275894] 08 p3527 N94-28796
Information presentation for expert systems in future fighter aircraft
[AD-A275126] 08 p3149 N94-29005
Stress and ergonomic design and evaluation of person-machine systems
[AD-A275156] 08 p3400 N94-29034
The use of task network simulation in workload prediction
[DCIEM-92-32] 08 p3402 N94-30132
Spectral analysis of heart rate and psychological state: A review of its validity as a workload index
[AD-B179387] 08 p3399 N94-30969
Unit specific crew rest strategies: Phase 1 evaluation of the 1/212th Aviation Battalion during shiftwork transitions
[AD-A277122] 09 p3804 N94-32379
The effects of Above Real-Time Training (ARTT) in an F-16 simulator 09 p3591 N94-32474
Flight controller alertness and performance during MOD shiftwork operations 10 p4098 N94-33624
Task network models in the prediction of workload imposed by extravehicular activities during the Hubble Space Telescope servicing mission 10 p4101 N94-33627
Expanding the pilot's envelope 10 p3994 N94-34627
Man-machine integration Design and Analysis System (MIDAS) Task Loading Model (TLM) experimental and software detailed design report
[NASA-CR-177840] 10 p4100 N94-34706
The influence of data link-provided graphical weather on pilot decision-making
[AD-A278871] 11 p4293 N94-35596
Direct reduced order mixed H2/H infinity control for the Short Take-Off and Landing/Maneuver Technology Demonstrator (STOL/MTD)
[AD-A278675] 11 p4199 N94-35796
Final-Approach Spacing Aids (FASA) evaluation for terminal-area, time-based air traffic control
[NASA-TP-3399] 11 p4192 N94-36048
Human factors for flight deck certification personnel
[AD-A280477] 12 p4487 N94-37347
Assessment of night vision goggle workload: Flight test engineer's guide
[SCT-91RR-45] 12 p4487 N94-37743

WORKSTATIONS
NT CREW WORKSTATIONS
System engineering concept demonstration, technology assessments, volume 5
[AD-A265471] 01 p0323 N94-10494
A distributed version of the NASA Engine Performance Program
[NASA-TM-106208] 01 p0327 N94-11231
RAMCAD (reliability, availability, and maintainability in computer-aided design)
[AD-A265143] 01 p0331 N94-11679
EOS workstation
[NASA-CR-191326] 02 p0736 N94-13132
Advanced computers and simulation
[DE93-014354] 02 p0740 N94-13286
A data distributed parallel algorithm for ray-traced volume rendering
[NASA-CR-191520] 02 p0749 N94-13721
Kerberos: A UNIX-TCP/IP network authentication system
[DE93-011677] 02 p0760 N94-14011
A widget based operations simulator for a planetary camera: A model for the high resolution stereo camera on Mars 94
[DLR-FB-92-30] 02 p0651 N94-14044
Oak Ridge Environmental Information System (ORIES) site workstation information packet for OREIS 6.2
[DE93-010761] 02 p0825 N94-14458
Integrating PAW, a graphical analysis interface to Sybase
[DE93-014172] 02 p0755 N94-14581
Computational Controls Workstation: Algorithms and hardware 02 p0678 N94-14626
Computational Control Workstation: Users' perspectives 02 p0681 N94-14648
HP upgrade operational streamlining 03 p0918 N94-15596
Lunar laser ranging data processing in a Unix/X windows environment 03 p0918 N94-15599
Distributed computing feasibility in a non-dedicated homogeneous distributed system
[NASA-CR-191532] 03 p1149 N94-15989
Ergonomics in the office environment 03 p1124 N94-16612
Networked workstations and parallel processing utilizing functional languages
[AD-A267464] 03 p1160 N94-17034
Advanced optical fiber communication systems
[AD-A269120] 04 p1577 N94-18254
Dialog-Based Learning (DBL) for adaptive interface agents and programming-by-demonstrations systems
[AD-A269154] 04 p1540 N94-18261
Cesar user library
[FFI-93/7021] 04 p1529 N94-19378
Multiple-fold clustered processor mesh array 05 p1757 N94-21113
Evaluation of DEC's GIGAswitch for distributed parallel computing
[DE94-001356] 05 p1936 N94-21853
Use of open systems for control, analysis, and data acquisition of the DIII-D tokamak
[DE94-001101] 05 p1998 N94-22089
Seeing the forest for the trees: Networked workstations as a parallel processing computer 05 p1938 N94-22454
The University of Hawaii Institute for Astronomy CCD camera control system 05 p1828 N94-22489
An object-oriented approach for supporting both X and terminal interfaces 05 p1926 N94-22491
CCD data acquisition systems at Lick and Keck Observatories 05 p2047 N94-22495
Deployable video conference table
[NASA-CASE-ARC-11950-1] 06 p2192 N94-23310
The Automated Instrumentation and Monitoring System (AIMS) reference manual
[NASA-TM-108795] 06 p2452 N94-23510
Customizing graphical user interface technology for spacecraft control centers 06 p2510 N94-23905
High performance, low cost, self-contained, multipurpose PC based ground systems 06 p2516 N94-23943
CADBIT 2: Computer-aided design for built-in test, volume 1
[AD-A273702] 06 p2463 N94-25455
CADBIT 2: Computer-aided design for built-in test, volume 2
[AD-A273703] 06 p2463 N94-25456
Engineering workstation: Sensor modeling 06 p2441 N94-25500
Weapon system integration for the AFIT virtual cockpit
[AD-A274058] 07 p2667 N94-25772
Object-oriented design and implementation of a parallel Ada simulation system
[AD-A274119] 07 p2979 N94-25906
Vcalc: A 3-space vector calculator
[AD-A274520] 07 p2965 N94-26831
Interactive control of a parallel simulation from a remote graphics workstation
[AD-A274217] 07 p2981 N94-27070
A graphical workstation based part-task flight simulator for preliminary rapid evaluation of advanced displays 07 p2641 N94-27286
VENI, video, VICI: The merging of computer and video technologies 07 p2686 N94-27362
The High Performance Storage System
[DE94-004350] 08 p3404 N94-28505
Data fusion and correlation techniques testbed development. Phase 1: Interim report
[SKD-1600-73-015] 08 p3405 N94-28533
ACCS Surveillance Exploratory Prototype (ASEP) 08 p3138 N94-29566
Performance of MCNP4A on seven computing platforms
[DE93-040101] 08 p3419 N94-29816
PAW using under MS DOS
[DE94-608012] 08 p3406 N94-30081
An interactive educational tool for compressible aerodynamics
[NASA-TM-106568] 08 p3422 N94-30175
Minimization of carpal tunnel syndrome
[AD-A276409] 09 p3795 N94-31363
Modular Simulator System (MSS). System/segment specification for the generic modular simulator system-instructor/operator station module, volume 12
[AD-A276979] 09 p3589 N94-32318
A high-speed linear algebra library with automatic parallelism 09 p3828 N94-32440
Gigabits to the Desktop: Installing tomorrow's networks today
[DE94-007701] 09 p3827 N94-32646
Overview of shock physics codes for armor analysis
[DE94-008948] 09 p3739 N94-32842
Design and Monte Carlo analysis of an unmanned aerial vehicle
[AD-A277648] 09 p3580 N94-33056
Implementing bright light treatment for MSFC payload operations shiftworkers 10 p4098 N94-33623
International Space Station alpha remote manipulator system workstation controls test report
[NASA-TM-104796] 11 p4274 N94-35481
North American ISDN Users' Forum agreements on Integrated Services Digital Network
[PB94-162559] 11 p4305 N94-35940
A comparison of queueing, cluster and distributed computing systems
[NASA-TM-109025-REV-1] 12 p4497 N94-36932

WORLD
U EARTH (PLANET)

WORLD METEOROLOGICAL ORGANIZATION
Manual on the global data-processing system. Volume 1: (Annex 4 to the WMO regulations) global aspects (1992 edition)
[WMO-485-VOL-1] 02 p0721 N94-13686
Manual on the global data-processing system. Volume 2: Regional aspects (1992 edition)
[WMO-485-VOL-2] 02 p0722 N94-14071

WOUND HEALING
Wound healing after laser injury to skin: The effect of occlusion and vitamin E
[AD-A266473] 03 p1128 N94-16779
Development of bioelastic material for aspects of wound repair
[AD-A267832] 05 p1673 N94-20208
Non-ionic surfactants in the treatment of third degree burns
[AD-A271582] 05 p1891 N94-21035
Enhancement of wound healing by biosynthetic growth factor
[AD-A272517] 05 p1892 N94-21415
Effect of barbiturates and hyperoxia on lipid peroxidation in hypoxic neurons
[AD-A278467] 10 p4094 N94-33545

WOVEN COMPOSITES
Micromechanical modeling of laminated composites with interfaces and woven composites using the boundary element method
[NASA-TM-106280] 02 p0670 N94-13053
Physical interpretation and development of ultrasonic nondestructive evaluation techniques applied to the quantitative characterization of textile composite materials
[NASA-CR-194549] 03 p0931 N94-15190
Processing, properties and applications of composites using powder-coated epoxy towpreg technology 03 p0933 N94-15277
Carbon-carbon grid for ion engines
[NASA-CASE-NPO-19174-1-CU] 03 p0925 N94-15876
FIBER-TEX 1992: The Sixth Conference on Advanced Engineering Fibers and Textile Structures for Composites
[NASA-CP-3211] 03 p0936 N94-16845
Research in textile composites at KU, Leuven 03 p0937 N94-16848
Weaving multi-layer fabrics for reinforcement of engineering components 03 p0937 N94-16850
Effect of tow alignment on the mechanical performance of 3D woven textile composites 03 p0937 N94-16851
An engineering approach for the application of textile composites to a structural component 03 p0938 N94-16852
New textile composite materials development, production, application 03 p0938 N94-16853

Quantification of processing artifacts in textile composites 03 p0939 N94-16860
Stochastic damage evolution in textile laminates 03 p0939 N94-16861
Three-dimensional analysis of anisotropic spatially reinforced structures 03 p0939 N94-16863
Intercalated hybrid graphite fiber composite [NASA-CASE-LEW-15241-1] 05 p1673 N94-20539
Investigation of forced and isothermal chemical vapor infiltrated SiC/SiC ceramic matrix composites [DE94-004544] 07 p2708 N94-26557
Delamination of woven E-glass fabric composites [DE94-003227] 08 p3185 N94-30827
Analysis of new composite architectures [NASA-CR-195303] 09 p3626 N94-32904
Comparison of the compressive strengths for stitched and toughened composite systems [NASA-TM-109108] 09 p3627 N94-32939
Effects of assumed tow architecture on the predicted moduli and stresses in woven composites [NASA-CR-195310] 10 p4020 N94-34258
Analysis of woven and braided fabric reinforced composites [NASA-CR-194930] 10 p4020 N94-34399
Through-the-thickness tensile strength of textile composites [NASA-TM-109115] 11 p4233 N94-35946
Development of nondestructive evaluation methods and prediction of effects of flaws on the fracture behavior of structural ceramics [DE94-012466] 12 p4425 N94-37423

WRAPAROUND CONTACT SOLAR CELLS
U SOLAR CELLS

WRENCHES
Torque application technique and apparatus [AD-D016124] 10 p4061 N94-34150

WRINKLING
The effects of processing and constituent materials on compressive strength of thick composite laminates [AD-A271912] 05 p1673 N94-20490
Theoretical and experimental study of the winding of a thin plastic film: The role of aerodynamic effects [ECL-93-04] 05 p1703 N94-20599

WRIST
Minimization of carpal tunnel syndrome [AD-A276409] 09 p3795 N94-31363

WROUGHT ALLOYS
Microstructural evolution of NARloy-Z at elevated temperatures [NASA-TM-108419] 02 p0571 N94-13715
The effect of oxygen, grain size, and strain rate on the mechanical behavior of forged P/M tantalum [DE93-011251] 03 p0959 N94-16764
Microstructural stability of wrought, laser and electron beam glazed NARloy-Z alloy at elevated temperatures [NASA-TM-108431] 05 p1689 N94-20100
Cyclic axial-torsional deformation behavior of a cobalt-base superalloy [NASA-TM-106372] 08 p3203 N94-28921

WU-2 AIRCRAFT
U U-2 AIRCRAFT

WURTZITE
Se EXAFS study of the elevated wurtzite to rock salt structural phase transition in CdSe nanocrystals [DE94-003247] 07 p3054 N94-26125
The synthesis and structural characterization of Na3WO3N [AD-A275243] 08 p3204 N94-29395
Pump-probe method for investigating laser ablation and optical damage threshold mechanisms in optical materials [DE94-008291] 09 p3720 N94-32753

X

X BAND
U SUPERHIGH FREQUENCIES

X RAY ABSORPTION
X ray absorption spectroscopy of electrochemically generated species [AD-A264749] 01 p0077 N94-11265
Apical Cu-O bond in YBa2Cu3O(7-delta) superconductors by XAFS [DE93-010861] 01 p0400 N94-11458
In situ XANES studies of the passive film on Fe and Fe-26Cr [DE93-010869] 01 p0084 N94-11459
The x ray dichroism experiments using circular polarization [DE93-013195] 02 p0568 N94-13036
Recent developments in multiple-scattering calculations of XAFS and XANES [DE93-010999] 02 p0563 N94-13477
A long-term space astrophysics research program: The evolution of the quasar continuum [NASA-CR-193714] 02 p0839 N94-14404
Ultra-soft x ray absorption spectroscopy: A bulk and surface probe of materials [DE93-014325] 02 p0566 N94-14582
In situ studies of passive film chemistry using x ray absorption spectroscopy [DE93-014023] 03 p0947 N94-16011
Dynamic behaviors of fragments ejected from the surface of carbon materials by laser ablation [DE93-788620] 04 p1438 N94-18161
Potential dependent structural changes of underpotentially deposited copper on an iodine treated platinum surface determined in situ by surface EXAFS and its polarization dependence [AD-A269890] 04 p1360 N94-18687
Magnetic circular dichroism in x ray absorption and core-level photoemission [DE93-019381] 05 p1688 N94-19986
The use of x ray techniques in the in situ study of corrosion [DE93-019845] 05 p1690 N94-20301
The x ray microprobe determination of chromium oxidation state in olivine from lunar basalt and kimberlitic diamonds 05 p1686 N94-20807
Microanalysis of iron oxidation state in iron oxides using X Ray Absorption Near Edge Structure (XANES) 05 p1686 N94-20808
Observation of x ray absorption magnetic circular dichroism in well-characterized iron-cobalt-platinum multilayers [DE94-000303] 05 p1694 N94-21944
Applications of x ray absorption fine structure to the in situ study of the effect of cobalt in nickel hydrous oxide electrodes for fuel cells and rechargeable batteries 06 p2391 N94-23347
In situ and ex situ spectroelectrochemical and x ray absorption studies on rechargeable, chemically-modified and other MnO2 materials [DE94-001387] 06 p2234 N94-24545
Morphological analysis of ionomers [DE94-003660] 07 p2749 N94-26005
X ray absorption studies of Ti/polymer and Cr/polymer interfaces [DE94-003008] 07 p2753 N94-26770
An x ray absorption fine structure study of ordering in polythiophene thin films [AD-A274235] 07 p2753 N94-26822
A novel approach to the fabrication of SiC structures of arbitrary shape [AD-A275475] 08 p3214 N94-29073
Characterization of the rare earth orthophosphates and Ce-doped LaPO4 by x ray absorption spectroscopy [DE94-006313] 09 p3898 N94-31630
The zinc electrode: Reactions and mechanisms [DE94-007977] 09 p3691 N94-31919
Near edge x ray spectroscopy theory [DE94-008179] 09 p3905 N94-32799
X ray absorption study of pulsed laser deposited boron nitride films [DE94-008295] 09 p3662 N94-32855
Dependence of x ray absorption magnetic circular dichroism on layer periodicity in iron-platinum multilayers [DE94-008786] 09 p3647 N94-32892
Evidence for symmetry breaking local distortions in thallium barium copper oxide [DE94-006149] 09 p3907 N94-32944

X RAY ANALYSIS
NT LAUE METHOD
NT X RAY SPECTROSCOPY
New x ray scanning topographic approaches to nondestructive evaluation of composites 01 p0061 N94-10039
Interferometric and optical tests of water window imaging x ray microscopes [NASA-CR-193866] 01 p0375 N94-10506
High resolution time- and 2-dimensional space-resolved x ray imaging of plasmas at NOVA [DE93-011892] 01 p0393 N94-11677
Real time radiography of Titan 4 booster [DE93-012450] 02 p0548 N94-12911
Project proposal for partial computational physics support for Survivability of Coatings program [DE93-013788] 02 p0576 N94-12939
High spatial resolution x ray microanalysis: Comparison of experiment and incoherent scattering calculations [DE93-011685] 02 p0648 N94-13044
Solution behaviour in microgravity: Considerations for protein crystal growth 03 p0982 N94-16102
X ray computed tomography for failure analysis investigations [AD-A268086] 03 p1055 N94-17515
X ray computed tomography for geometry acquisition [AD-A268085] 03 p1157 N94-17590
X ray computed tomography for casting demonstration [AD-A268084] 03 p1056 N94-17596
Analysis of HgI2 and PbI2 crystals and detectors by Particle-Induced X Ray Emission (PIXE) and Ion Backscattering Spectroscopy (IBS) [DE93-017168] 04 p1594 N94-17896
Potential dependent structural changes of underpotentially deposited copper on an iodine treated platinum surface determined in situ by surface EXAFS and its polarization dependence [AD-A269890] 04 p1360 N94-18687
Quantification of volume flaw sizes in ceramics by image processing of 3D x ray tomographic data sets [DE93-018573] 04 p1372 N94-18932
Quantitative evaluation of material composition of composites using x ray energy-dispersive NDE technique [DE93-041157] 05 p1672 N94-19888
Near atomic resolution microanalysis of interfaces by analytical electron microscopy [DE93-019437] 05 p1687 N94-19904
The use of x ray techniques in the in situ study of corrosion [DE93-019845] 05 p1690 N94-20301
Spatial organization of polymer chains in a crystallizable diblock polyethylene and polystyrene [AD-A271862] 05 p1702 N94-20463
The x ray microprobe determination of chromium oxidation state in olivine from lunar basalt and kimberlitic diamonds 05 p1686 N94-20807
X ray analysis of alpha mercuric iodide crystal structure and processing effects [DE93-017620] 05 p2027 N94-21296
X ray characterization of a three-element condenser system for soft x ray projection lithography [DE93-019916] 05 p1990 N94-21985
PROS: An IRAF based system for analysis of x ray data 05 p1925 N94-22461
Phase transformations in Cu-Zr multilayers [DE94-000393] 06 p2241 N94-23297
Evaluation of ovostatin and ovostatin assay 06 p2422 N94-24437
Inner fiber observation for metal matrix composites under the stress load condition utilizing Synchrotron Orbital Radiation (SR) by X-ray CT 07 p2724 N94-25553
In situ x ray reflectivity measurements of thin film structural evolution [DE94-002289] 07 p3051 N94-25944
Interstitially stabilized phases in the zirconium-nickel system [DE94-005561] 08 p3201 N94-28525
A novel approach to the fabrication of SiC structures of arbitrary shape [AD-A275475] 08 p3214 N94-29073
Electron microscopy: Metal alloy x ray microanalysis [REPT-932-600-101] 08 p3205 N94-29525
Element-specific magnetic hysteresis measurements, a new application of circularly polarized soft x-rays [DE94-007122] 09 p3858 N94-31397
X ray imaging and x ray source development at Lawrence Livermore National Laboratory [DE94-007077] 09 p3719 N94-32629
Simplified ultra-high resolution optic for soft x ray imaging [AD-A278424] 09 p3885 N94-33331
AEM and AES of radiation-induced segregation in proton-irradiated stainless steels [DE94-012734] 12 p4418 N94-37398
Scanning x-ray diffraction: A technique with high compositional resolution for studying phase formation in co-deposited thin films [DE94-011496] 12 p4420 N94-37516

X RAY APPARATUS
NT X RAY TUBES
Interferometric and optical tests of water window imaging x ray microscopes [NASA-CR-193866] 01 p0375 N94-10506
Characterization and possible repair of defects in soft x ray projection lithography masks [DE93-019147] 05 p1750 N94-20231

X RAY ASTRONOMY
Search for UHE point-source emission over various time scales [DE93-012718] 02 p0846 N94-12922
ROSAT guest investigator program (AO-1). On a search for coronal x ray emissions from white dwarfs [NASA-CR-193654] 02 p0835 N94-13171
ROSAT: X ray survey of compact groups [NASA-CR-193297] 02 p0829 N94-13181
X ray emission from dynamical shock models in hot-star winds [NASA-CR-194093] 02 p0847 N94-13288
Search for x ray emitting young stars outside of massive molecular clouds [NASA-CR-193609] 02 p0830 N94-13462

ROSAT observations of the binary Be-star/radio pulsar PSR1259-63
[NASA-CR-194394] 02 p0832 N94-14357
A long-term space astrophysics research program: The evolution of the quasar continuum
[NASA-CR-193714] 02 p0839 N94-14404
ROSAT observations of clusters with wide-angle tailed radio sources
[NASA-CR-193784] 02 p0833 N94-14405
The soft x ray transient Cen X-4 in quiescence
[NASA-CR-194033] 02 p0833 N94-14406
X ray microcalorimeters: Principles and performance 03 p0899 N94-15027
A new approach to optical photon detection 03 p0899 N94-15028
The imaging microstrip proportional counter: Features of a practical design 03 p0900 N94-15030
Development of x ray CCDs 03 p0900 N94-15033
The XMM pn-CCD detector system: First results 03 p0900 N94-15034
The development of back-illuminated CCD's for XMM 03 p0900 N94-15035
Microchannel plate detectors for space astronomy 03 p0901 N94-15038
Prospects for high pressure imaging gas scintillation drift chambers 03 p0901 N94-15040
Outlook for hard x ray and gamma ray astronomy 03 p0904 N94-15057
The high pressure gas scintillation proportional counter for SAX 03 p0906 N94-15076
X ray emission from Wolf-Rayet stars with recurrent dust formation
[NASA-CR-189321] 03 p1300 N94-15533
ROSAT-IUE observations of symbiotic stars. The x ray morphology of high latitude associations
[NASA-CR-194616] 03 p1236 N94-16492
Participation in the north ecliptic pole sky survey
[NASA-CR-191933] 03 p1059 N94-16815
The formation process of the He I lambda 10830 line in cool giant stars
[NASA-CR-194648] 03 p1240 N94-17094
The Einstein Observatory catalog of IPC x ray sources. Volume 4E: Right ascension range 08h 00m to 11h 59m
[NASA-TM-108401-VOL-4E] 04 p1625 N94-18612
The Einstein Observatory catalog of IPC x ray sources. Volume 5E: Right ascension range 12h 00m to 15h 59m
[NASA-TM-108401-VOL-5E] 04 p1625 N94-18613
The Einstein Observatory catalog of IPC x ray sources. Volume 6E: Right ascension range 16h 00m to 19h 59m
[NASA-TM-108401-VOL-6E] 04 p1625 N94-18615
The Einstein Observatory catalog of IPC x ray sources. Volume 7E: Right ascension range 20h 00m to 23h 59m
[NASA-TM-108401-VOL-7E] 04 p1625 N94-18618
The Einstein Observatory catalog of IPC x ray sources. Volume 1E: Documentation
[NASA-TM-108401-VOL-1E] 04 p1626 N94-18619
The Einstein Observatory catalog of IPC x ray sources. Volume 2E: Right ascension range 00h 00m to 03h 59m
[NASA-TM-108401-VOL-2E] 04 p1626 N94-18620
The Einstein Observatory catalog of IPC x ray sources. Volume 3E: Right ascension range 04h 00m to 07h 59m
[NASA-TM-108401-VOL-3E] 04 p1626 N94-18621
Related investigations on the physics of high energy emission from active galactic nuclei
[NASA-CR-193615] 04 p1630 N94-18836
Telescope for x ray and gamma ray studies in astrophysics 04 p1324 N94-19166
Rosat and optical observations of two X-ray transients: MX 0836-42 and GS 0834-430
[MPE-PREPRINT-237] 04 p1622 N94-19451
IRAS galaxies observed in the ROSAT survey: Starbursts or central activity 04 p1623 N94-19528
Particle induced background by Roentgen satellites
[MPE-242] 04 p1631 N94-19714
Stellar coronae at the end of the main sequence: A Rosat survey of the late M dwarfs
[NASA-CR-194700] 04 p1628 N94-19794
X ray, extreme and far ultraviolet optical thin films for space applications
[NASA-CR-194635] 05 p1984 N94-20128
A deep x ray survey in the Lockman hole and the soft x ray log N - log S
[NASA-CR-194698] 05 p2054 N94-20174
X ray archeology in the Coma cluster
[NASA-CR-194799] 05 p2054 N94-20175
Pre-main sequence stars in the Chamaeleon cloud and pre-main sequence stars in the Rho Ophiuchi cloud core
[NASA-CR-194713] 05 p2080 N94-20337
Studies of an x ray selected sample of cataclysmic variables
[NASA-CR-194773] 05 p2055 N94-20344
High-energy astrophysics: A theoretical analysis of thermal radiation from neutron stars
[NASA-CR-194808] 05 p2055 N94-20952
Dust content of a hydrogen rich, low surface brightness galaxy and the luminosity history of 3C273
[NASA-CR-194705] 05 p2056 N94-21779
ROSAT implementation of a proposed multi-mission x ray data format 05 p2047 N94-22462
Detection of x ray sources in PROS 05 p2062 N94-22466
SPIKE: Application for ASTRO-D mission planning 05 p1926 N94-22486
ROSAT data analysis with EXSAS 05 p2080 N94-22555
Results from ROSAT 05 p2000 N94-22630
Time variations of x rays from black hole candidates: Canonical time variations in high and low intensity states 05 p2009 N94-22690
Excitation of XUV radiation in solar flares
[NASA-CR-193703] 06 p2627 N94-24094
Shocked clouds in the Cygnus Loop
[NASA-CR-195190] 06 p2600 N94-25178
Investigation relative to the Roentgen Satellite (ROSAT)
[NASA-CR-195192] 06 p2600 N94-25269
Cosmic x ray physics
[NASA-CR-195225] 07 p3115 N94-27236
X ray studies of the Hyades cluster
[NASA-CR-189325] 08 p3538 N94-29001
Coronal temperatures of unusually active K-dwarf binary systems
[NASA-CR-189335] 08 p3545 N94-29861
Spectral and temporal behavior of low mass x ray binaries observed with the Einstein SSS and MPC, and the Broad Band X Ray Telescope 08 p3542 N94-30862
Workshop on Physics of Accretion Disks Around Compact and Young Stars
[NASA-CR-195756] 09 p3927 N94-31116
Observations of loops and prominences
[NASA-CR-195942] 10 p4166 N94-34298
SPARTAN high resolution solar studies
[NASA-CR-189340] 10 p4166 N94-34944
ROSAT/XRT-PSPC observations and the ionizing continuum of Seyfert 1 galaxy Mkn 478
[PB94-167053] 11 p4350 N94-35530
The BL LAC phenomenon: X-ray observations of transition objects and determination of the x-ray spectrum of a complete sample of flat-spectrum radio sources
[NASA-CR-195951] 12 p4546 N94-36688

X RAY ASTROPHYSICS FACILITY

The four great observatories
[NASA-TM-109311] 02 p0830 N94-13605
AXAF FITS standard for ray trace interchange
[NASA-CR-194025] 02 p0832 N94-14305
VETA x ray data acquisition and control system 05 p2047 N94-22455
Advanced X ray Astrophysics Facility-Imaging (AXAF-I) thermal analyses using Integrated Thermal Analysis System (ITAS) program 06 p2320 N94-23635
SAO mission support software and data standards, version 1.0
[NASA-CR-193906] 06 p2454 N94-24050
Space projects: Astrophysics facility program contains cost and technical risks. Report to Congressional Requesters
[GAO/NSIAD-94-80] 07 p2696 N94-27382
AXAF-I ghost ray study: On orbit case
[NASA-CR-193987] 11 p4333 N94-36119

X RAY BINARIES

A photometric study of massive x-ray binaries
[ITN-93-85207] 02 p0829 N94-13231
High time resolution studies of binary x ray pulsars
[NASA-CR-194395] 02 p0832 N94-13894
ROSAT observations of the binary Be-star/radio pulsar PSR1259-63
[NASA-CR-194394] 02 p0832 N94-14357
The soft x ray transient Cen X-4 in quiescence
[NASA-CR-194033] 02 p0833 N94-14406
Pulse-timing studies of x ray pulsars
[NASA-CR-193778] 04 p1621 N94-18611
Studies of an x ray selected sample of cataclysmic variables
[NASA-CR-194773] 05 p2055 N94-20344
Accretion disks in bright x ray binaries 05 p2002 N94-22639
Structure of accretion plasmas of x ray binary pulsars in MHD turbulence 05 p2007 N94-22679
Flux measurements using the BATSE spectroscopic detectors 06 p2580 N94-24435
ROSAT observations of the x ray binary HD 154791
[NASA-CR-195189] 06 p2600 N94-25198
A study of ultra high-energy radiation associated with Hercules X-1 08 p3552 N94-29823
Spectral and temporal behavior of low mass x ray binaries observed with the Einstein SSS and MPC, and the Broad Band X Ray Telescope 08 p3542 N94-30862
Evolution of vaporizing pulsars 09 p3929 N94-31128
Can a variable alpha induce limit cycle behavior and exponential luminosity decay in transient soft x ray sources? 09 p3929 N94-31129
A study of angular momentum loss in binaries using the free Lagrange method 09 p3931 N94-31134
A search for 100 TeV gamma ray emission from the x ray binary pulsar 4U 0115+63 using the CYGNUS extensive air-shower array 09 p3955 N94-31900
Winds from disks in compact binaries
[DE94-007452] 09 p3938 N94-32137
The evolutionary status of PSR 1259-63
[DE94-007094] 09 p3938 N94-32503
A study of low mass x-ray binaries
[NASA-CR-195813] 10 p4162 N94-34119

X RAY DENSITY MEASUREMENT

Development and application of local 3-D x ray CT reconstruction software for imaging critical regions in large ceramic turbine rotors
[DE93-015159] 04 p1369 N94-18166
Engine materials characterization and damage monitoring by using x ray technologies
[NASA-TP-3328] 06 p2372 N94-24074

X RAY DETECTORS

Metal-semiconductor, composite radiation detectors
[DE93-013313] 02 p0619 N94-12994
An x ray detector using superconducting aluminum tunnel junctions
[DE93-015103] 02 p0811 N94-14332
Absolute detection efficiency of a micro-channel plate detector to x rays in the 1-100 KeV energy range
[DE93-012592] 02 p0789 N94-14460
Outlook for hard x ray and gamma ray astronomy 03 p0904 N94-15057
Developments in extreme ultraviolet and x ray instrumentation 03 p0904 N94-15058
A new detector concept for energetic auroral x ray imaging 03 p0907 N94-15081
A multilayered approach to superconducting tunnel junction x ray detectors 03 p0908 N94-15089
Applications for large area silicon drift detectors on x ray and gamma ray astronomy 03 p0909 N94-15090
Silicon radiation sensor systems for gamma and x ray detection at SI 03 p0909 N94-15095
The epitaxial Si x ray bolometer an alternative to ion implanted devices 03 p0911 N94-15103
Quantitative evaluation of material composition of composites using x ray energy-dispersive NDE technique
[DE93-041157] 05 p1672 N94-19888
Energy-resolving x ray detectors with charge amplification due to multiple quasiparticle tunneling
[DE93-019506] 05 p2031 N94-21869
Detection of x ray sources in PROS 05 p2062 N94-22466
Characterization of CCD-based imaging x ray detectors for diffraction experiments
[DE93-041343] 06 p2556 N94-22921
Hardware design of a spherical mini-rover 07 p2833 N94-25669
A space fiber-optic x ray burst detector
[DE94-002722] 07 p2696 N94-26808
Cosmic x ray physics
[NASA-CR-195225] 07 p3115 N94-27236
The x ray holographic microscopy using the atomic-force microscope
[DE94-004003] 07 p2814 N94-27779
A high rate, low noise, x ray silicon strip detector system
[DE94-004557] 08 p3268 N94-30717
Development and application of photosensitive device systems to studies of biological and organic materials
[DE94-008503] 09 p3793 N94-32516
X-ray remote sensing and in-situ spectroscopy for planetary exploration missions and gamma-ray remote sensing and in-situ spectroscopy for planetary exploration missions
[NASA-CR-189352] 11 p4375 N94-35381

X RAY DIFFRACTION

Symmetry lowering in crystalline solid solutions: A study of cinnamamide-thienylacrylamide by x ray and neutron diffraction and solid-state photochemistry
[DE93-010871] 01 p0394 N94-10301
Tribological characteristics of hot-pressed self-lubricating composites
[NAL-TR-1160] 01 p0066 N94-10858
The x ray standing waves on surfaces
[AD-A265265] 01 p0402 N94-11682
Analysis of samples of reflector materials which are multicoated and metal samples with oxide coatings which have been exposed the space environment in LDEF testing
[NASA-CR-193647] 02 p0575 N94-12789
Crystallographic and metallurgical characterization of radiation detector grade cadmium telluride materials
[DE93-014335] 02 p0806 N94-13150

Room temperature degradation of YBa2Cu3O(7-x) superconductors in varying relative humidity environments
[NASA-TP-3368] 02 p0813 N94-14409
Is K3C60 a line phase?
[DE93-016700] 02 p0813 N94-14517
Laboratory for x ray optics
[AD-A267149] 03 p1189 N94-15735
Interfacial structure of lattice mismatched bcc(110)/bcc(110) transition metal superlattices
[DE93-015162] 03 p1208 N94-16058
Thermal stress effects in intermetallic matrix composites
[NASA-CR-191191] 03 p1054 N94-16518
Characterization of metallic multilayers using x ray diffraction analysis
[NIAR-93-13] 03 p0961 N94-17282
High pressure metallization of Mott insulators: Magnetic, structural and electronic properties
[DE93-018295] 04 p1404 N94-18805
Neutron-induced collision cascade mixing in Nb/V superlattices
[DE93-018575] 04 p1600 N94-18933
Refinement of unit cell parameters by least-squares: Comments on an old technique and the development of a new computer program
[AD-A270610] 04 p1531 N94-19590
Cooperative formation of inorganic-organic interfaces in the synthesis of silicate mesostructures
[AD-A271196] 04 p1375 N94-19742
Metastable bcc phase formation in the Nb-Cr system
[DE93-018376] 05 p2012 N94-19926
Synchrotron x ray diffraction analysis of photorefractive crystals and their gratings
[AD-A271176] 05 p2015 N94-20213
Material optimization for hard x ray Fresnel zone plates
[DE93-019569] 05 p1990 N94-21837
Characterization of CCD-based imaging x ray detectors for diffraction experiments
[DE93-041343] 06 p2556 N94-22921
Application of maximum entropy and irreducible cluster integrals to joint probability distributions for x ray structure determination
[PB93-224152] 06 p2559 N94-23109
Modifications to 8x8 dynamical theory: Polarizations redefined according to x ray diffraction convention
[DE94-001290] 06 p2560 N94-23187
Proposed additions to the SHADOW ray-tracing code for general-asymmetric perfect-crystal optics
[DE94-001291] 06 p2560 N94-23188
Demonstration of the feasibility of an integrated x ray laboratory for planetary exploration
[NASA-CR-177631] 06 p2598 N94-24832
An x ray diffraction investigation of alpha-Al2O2 addition to Yttria Stabilized Zirconia (YSZ) thermal barrier coatings subject to destabilizing vanadium pentoxide (V2O5) exposure
[AD-A273403] 06 p2261 N94-25072
X ray diffraction analysis of electrodeposited beta-tantalum
[AD-A273254] 06 p2249 N94-25142
Study on improvement in physical analysis method of metallic materials 07 p2728 N94-25577
Transition metals in highly correlated discotic phases: Designing metallomesogens with selected intermolecular organizations
[AD-A274695] 07 p2736 N94-26452
Qualitative analysis of rare earth elements contained in the phosphogypsum
[DE93-614153] 07 p2716 N94-26518
Experimental measurement of local displacement and chemical pair correlations in crystalline solid solutions
[DE94-001124] 07 p3065 N94-27251
High intensity x ray instrumentation for residual strain measurements in composites and textured materials
[ISBN-0-315-85169-4] 07 p2842 N94-27278
Multiple exposure CCD detector for high-speed laser pump, x ray probe Laue scattering
[DE94-004618] 07 p2820 N94-27781
Crystallographyic analyses of clathrate hydrates included in Vostok ice cores 07 p2885 N94-27969
Energy Dispersive X ray Diffraction (EDXD) apparatus for liquids at high temperature 07 p2721 N94-28159
Structure of ordinary ice I(sub h). Part 1: Ideal structure of ice
[AD-A275149] 08 p3486 N94-29021
Observation of the traveling component of an x ray standing wave field
[DE94-007671] 09 p3672 N94-31317
Adsorption of water to the metal/polymer interface studied by neutron and x ray reflectivity
[DE94-005578] 09 p3651 N94-31649
Group 12 thiolates: Syntheses, characterization and decomposition pathways
[AD-A277055] 09 p3900 N94-32011
The new Metals and Alloys Indexes, search manual: A phase diagram research tool
[DE94-005371] 09 p3643 N94-32098
SUNY beamline facilities at the National Synchrotron Light Source
[DE94-006343] 09 p3905 N94-32770
Deuterium absorption and material phase characteristics of SAES St198 Zr-Fe alloy
[DE94-008275] 09 p3646 N94-32781
Extended-range order in glasses
[DE94-008135] 09 p3661 N94-32798
Near edge x ray spectroscopy theory
[DE94-008179] 09 p3905 N94-32799
Dynamics of supermatrix semiconductor growth
[AD-A278380] 10 p4147 N94-34085
A mineralogical instrument for planetary applications 11 p4357 N94-35408
The growth of silicon nitride crystalline films using microwave plasma enhanced chemical vapor deposition
[AD-A278862] 11 p4340 N94-35828
In situ studies of zeolite syntheses using powder diffraction methods: Crystallization of instant zeolite A powder and CoAPO-5
[DE94-006570] 11 p4341 N94-36358
Processing, packaging, and characterization of electroceramic materials for phased array antennas
[AD-A280251] 12 p4432 N94-36743
Pair correlations in crystalline solid solutions
[DE94-012319] 12 p4535 N94-37212
X-ray diffraction studies of evaporated gold thin films deposited on aluminum nitride substates
[AD-A280454] 12 p4536 N94-37228
Scanning x-ray diffraction: A technique with high compositional resolution for studying phase formation in co-deposited thin films
[DE94-011496] 12 p4420 N94-37516

X RAY FLUORESCENCE

Remote sensing x ray fluorescence spectrometry for future lunar exploration missions 01 p0462 N94-12165
ROSAT observations of clusters with wide-angle tailed radio sources
[NASA-CR-193784] 02 p0833 N94-14405
Measurements of the spatial structure and directivity of 100 KeV photon sources in solar flares using PVO and ISEE-3 spacecraft
[NASA-CR-194080] 02 p0845 N94-14492
Comparative study of x ray and microwave emissions during solar flares
[NASA-CR-194532] 02 p0845 N94-14577
X ray emission from Wolf-Rayet stars with recurrent dust formation
[NASA-CR-189321] 03 p1300 N94-15533
Application of in situ scanning x ray fluorescence to study the concentration of metal ions in simulated pits
[DE93-014054] 03 p0956 N94-15921
Complex QSO absorbers: High-redshift clusters of galaxies?
[NASA-CR-194617] 03 p1237 N94-16833
Characterization of Ni on Si wafers: Comparison of surface analysis techniques
[DE93-016501] 03 p0953 N94-17649
In vivo animal models of body composition in aging
[DE93-012527] 04 p1501 N94-17889
X ray studies of microstructures in semiconductor and superconducting materials
[DE93-040690] 04 p1601 N94-19056
The use of x ray techniques in the in situ study of corrosion
[DE93-019845] 05 p1690 N94-20301
Wavelength dispersive analysis with the synchrotron x ray fluorescence microprobe 05 p1685 N94-20717
Combined backscatter Moessbauer spectrometer/x ray fluorescence analyzer (BaMS/XRF) for extraterrestrial surfaces 05 p1686 N94-20761
Diffraction and holography of photoelectrons and fluorescent x rays
[DE93-019240] 05 p1808 N94-21441
Demonstration of the feasibility of an integrated x ray laboratory for planetary exploration
[NASA-CR-177631] 06 p2598 N94-24832
Qualitative analysis of rare earth elements contained in the phosphogypsum
[DE93-614153] 07 p2716 N94-26518
A mineralogical instrument for planetary applications 11 p4357 N94-35408
Remote geochemical experiment package for Discovery class missions 11 p4350 N94-35420
Innovative instrumentation for mineralogical and elemental analyses of solid extraterrestrial surfaces: The Backscatter Moessbauer Spectrometer/X Ray Fluorescence analyzer (BaMS/XRF) 11 p4239 N94-35459
Continuum fluorescence of Cu in NbTi/Cu composite wires
[DE94-008940] 11 p4241 N94-36242

X RAY IMAGERY

Development of microstrip gas chamber and application to imaging gamma-ray detector
[DE93-754294] 01 p0034 N94-11041
The development of the TIMAX project: A hard x ray imaging telescope
[INPE-5474-TDI/505] 02 p0829 N94-13245
Adaptive control of interface by temperature and interface profile feedback in transparent multi-zone crystal growth furnace
[NASA-CR-194140] 02 p0762 N94-13253
The x ray lasers as sources for x ray microscopy
[DE93-013420] 02 p0655 N94-13259
X ray observations of late-type stars using the ROSAT all-sky survey
[NASA-CR-193716] 02 p0832 N94-14146
Image reconstruction for x ray holographic microscopy
[DE93-013094] 02 p0653 N94-14772
The XMM pn-CCD detector system: First results 03 p0900 N94-15034
The Rutherford Appleton Laboratory photon counting detector 03 p0910 N94-15096
Development and application of local 3-D x ray CT reconstruction software for imaging critical regions in large ceramic turbine rotors
[DE93-015159] 04 p1369 N94-18166
An assessment of COMSCAN, a Compton backscatter imaging camera, for the one-sided non-destructive inspection of aerospace components
[AD-A271331] 05 p1806 N94-19837
Pre-main sequence stars in the Chamaeleon cloud and pre-main sequence stars in the Rho Ophiuchi cloud core
[NASA-CR-194713] 05 p2080 N94-20337
High resolution, three dimensional soft x ray imaging
[DE93-018667] 05 p1989 N94-21630
Material optimization for hard x ray Fresnel zone plates
[DE93-019569] 05 p1990 N94-21837
Center for X-Ray Optics, 1992
[DE94-000726] 05 p1990 N94-21868
Some experiments on using backscattered electron and energy dispersive x ray imaging in determination of portland cement clinker phase composition 05 p1708 N94-21893
The ALEXIS data processing package: An IDL based system 05 p2047 N94-22453
Requirements for future solar-physics missions with x ray instrumentation 06 p2625 N94-22849
Imaging with x ray lasers
[DE94-002844] 07 p2816 N94-26020
A multi-frequency study of an x ray selected sample of active galactic nuclei 09 p3937 N94-31987
X ray imaging and x ray source development at Lawrence Livermore National Laboratory
[DE94-007077] 09 p3719 N94-32629
Lunar mineral feedstocks from rocks and soils: X-ray digital imaging in resource evaluation 11 p4358 N94-35415
X ray radiographic imaging of hydrodynamic phenomena in radiation driven materials: Shock propagation, material compression and shear flow
[DE94-009515] 11 p4266 N94-35982
X ray radiographic imaging of hydrodynamic phenomena in radiation driven materials: Shock propagation and shear flow
[DE94-010891] 11 p4318 N94-36201

X RAY INSPECTION

Component testing and quality assurance 03 p0932 N94-15259
An assessment of COMSCAN, a Compton backscatter imaging camera, for the one-sided non-destructive inspection of aerospace components
[AD-A271331] 05 p1806 N94-19837
Engine materials characterization and damage monitoring by using x ray technologies
[NASA-TP-3328] 06 p2372 N94-24074
An evaluation of Compton scatter imaging using COMSCAN
[DREP-TM-93-38] 06 p2372 N94-24136
The development of an in-motion radiography system for large area aircraft scanning
[DREP-TM-93-53] 07 p2670 N94-27666
Microfocus radioscopy, a high resolution means of inspecting composite materials
[REPT-932-430-109] 08 p3179 N94-29454
Characterization of interface structure in multilayers using specular x ray reflectance
[DE94-007698] 09 p3657 N94-32358

X RAY IRRADIATION

Design and testing of planar magnetic micromotors fabricated by deep x ray lithography and electroplating
[DE93-012856] 02 p0618 N94-12821
Irradiation polymerization of bismaleimide resins
[REPT-932-430-105] 08 p3215 N94-29441

Enhanced charge trapping in bipolar spacer oxides during low-dose-rate irradiation
[DE94-007863] 11 p4260 N94-36268

X RAY LASERS

High power z pinches as x ray laser photopumps
[DE93-012842] 01 p0173 N94-10746
High-order harmonic conversion efficiency in helium
[DE93-011714] 01 p0364 N94-10753
Electron temperature measurements of x ray laser plasmas
[DE93-011874] 01 p0389 N94-11074
Demonstration designs for optical-field-ionized plasma x-ray lasers
[DE93-009227] 01 p0175 N94-11266
LCLS optics: Selected technological issues and scientific opportunities
[DE93-010953] 01 p0175 N94-11468
Inexpensive capillary discharge x-ray laser driver
[AD-A265932] 01 p0176 N94-12382
Spatial coherence of soft x ray lasers
[DE93-012497] 01 p0176 N94-12590
Three dimensional time-dependent hydrodynamic and propagation modeling of x ray laser emission
[DE93-012575] 02 p0654 N94-12962
Imaging microscopy with x ray lasers at Lawrence Livermore National Laboratory
[DE93-013419] 02 p0655 N94-13258
The x ray lasers as sources for x ray microscopy
[DE93-013420] 02 p0655 N94-13259
Oscillator-amplifier experiments in neon-like yttrium
[DE93-012577] 02 p0657 N94-13976
The Livermore x ray laser program
[DE93-014118] 02 p0658 N94-14152
Selenium x ray laser line profile measurements
[DE93-012580] 02 p0658 N94-14175
Experimental measurements of selenium x-ray laser spectral line profiles
[DE93-016543] 02 p0659 N94-14595
Optimization study of x ray laser coherence in Ni-like Ta
[DE93-016419] 02 p0660 N94-14888
Time resolved measurement of electron temperatures of exploding foil x ray laser plasmas
[DE93-017161] 02 p0803 N94-14894
X ray laser program
[AD-A267075] 03 p1038 N94-15628
Analysis of neon soft x ray spectra from short-pulse laser-produced plasmas
[DE93-014420] 04 p1582 N94-17708
X-ray laser oscillator-amplifier experiments
[DE93-017165] 04 p1436 N94-17868
Production of dense vapor targets for laser-plasma interaction studies with intense, ultra-short pulses
[DE93-017175] 04 p1584 N94-17993
Development of short pulse soft x ray lasers
[DE93-017150] 04 p1437 N94-18131
Optical design for photonics. Organization of the 1993 Photonics Science Topical Meetings. Technical digest series, volume 9
[AD-A269027] 04 p1578 N94-18396
Development of robust multilayer optics for use in high-peak power radiation environments
[DE93-018557] 04 p1580 N94-18931
Legacy of the X Ray Laser Program
[DE93-019550] 04 p1442 N94-19554
PVDF gauge characterization of hypervelocity-impact-generated debris clouds
[DE93-018831] 05 p1829 N94-19943
Applications and source development for high-repetition rate x ray lasers
[DE93-019547] 05 p1815 N94-20259
Photopumped x ray laser research on Saturn
[DE93-019430] 05 p1816 N94-20298
Generation of intense ultrashort x ray pulses
[DE93-019607] 05 p1817 N94-21299
Parametric instabilities in picosecond time scales
[DE94-000384] 05 p1966 N94-21958
Characterization of germanium stripe x ray lasers
[DE93-019629] 06 p2347 N94-22867
Ray and wave optics modeling of laboratory x ray lasers
[DE93-019940] 06 p2541 N94-22868
Inertial confinement fusion
[DE94-002602] 06 p2551 N94-23703
Excitation mechanisms for XUV and x ray lasers
[DE93-617006] 06 p2351 N94-25482
Imaging with x ray lasers
[DE94-002844] 07 p2816 N94-26020
Phase conjugated lasers applied to commercial x ray lithography
[DE94-001529] 07 p2819 N94-27018
Linac Coherent Light Source (LCLS) at 2-4 nm using the SLAC linac
[DE94-005235] 08 p3292 N94-28481
Enhanced coherence x ray laser experiments and simulations
[DE94-005367] 08 p3295 N94-30060
Impact of observed hyperfine splitting on X-ray laser gain
[DE94-005822] 09 p3717 N94-32128
X ray imaging and x ray source development at Lawrence Livermore National Laboratory
[DE94-007077] 09 p3719 N94-32629
Quantum fluctuations of vortices in Josephson-coupled superconductors
[DE94-007609] 09 p3905 N94-32747
Progress in understanding and improving x ray lasers
[DE94-006048] 09 p3720 N94-32794
Ultrafast x ray sources
[AD-A277455] 09 p3721 N94-33012
Plasma physics applications to intense radiation sources, pulsed power and space physics. Short pulse ultra intense laser-plasma interaction experiment
[AD-A278440] 10 p4144 N94-33555
Ionization balance and gain calculations for neon-like selenium x-ray laser plasmas
[DE94-012590] 12 p4530 N94-37437

X RAY OPTICS

Physical optics modelling of Soft X ray Projection Lithography (SXPL) imaging experiments
[DE93-011556] 01 p0374 N94-10339
Laboratory for x ray optics
[AD-A267149] 03 p1189 N94-15735
Center for X-Ray Optics, 1992
[DE94-000726] 05 p1990 N94-21868
X ray characterization of a three-element condenser system for soft x ray projection lithography
[DE93-019916] 05 p1990 N94-21985
Ray and wave optics modeling of laboratory x ray lasers
[DE93-019940] 06 p2541 N94-22868
Theoretical investigation of variable periodicity (graded) multilayers for hard x ray applications
[NASA-CR-193913] 06 p2543 N94-23502
Germanium x ray phase plates for the production of circularly polarized x rays
[DE94-002908] 06 p2545 N94-24550
Investigate zero-stress replicated optics
[NASA-CR-193889] 06 p2545 N94-24665
Soft x ray optics by pulsed laser deposition
[NASA-CR-195139] 06 p2546 N94-24967
X ray optics for science and technology
[AD-A277369] 09 p3880 N94-32155
Diamond turning in the production of x ray optics 09 p3604 N94-33298
Simplified ultra-high resolution optic for soft x ray imaging
[AD-A278424] 09 p3885 N94-33331

X RAY SCATTERING

X-ray and neutron scattering studies of magnetic critical fluctuations in holmium
[DE93-010873] 01 p0400 N94-11467
FEFF5: An ab initio multiple scattering XAFS code
[DE93-011000] 01 p0367 N94-11470
Resonant x ray Raman scattering from atoms and molecules
[DE93-015158] 02 p0784 N94-13896
Structure and stability of microvoids in A-Si:H
[DE93-016625] 02 p0813 N94-14413
Thomson backscattered x rays from an intense laser beam
[AD-A267125] 03 p1038 N94-15686
Laboratory for x ray optics
[AD-A267149] 03 p1189 N94-15735
Magnetic effects in anomalous dispersion
[DE93-014291] 03 p1175 N94-15978
Chemical and displacement atomic pair correlations in crystalline solid solutions recovered by anomalous x ray scattering in Fe-Ni alloys
[DE93-015906] 03 p1209 N94-16171
Application of cylindrical distribution functions to anisotropic scattering from amorphous films
[DE93-015256] 03 p1183 N94-16811
Neutron and x ray scattering studies of (FeF2)(sub m)(CoF2)(sub n) multilayers
[DE93-015809] 03 p1184 N94-16838
Anisotropic phase separation in amorphous Fe-Ge alloys
[DE93-015255] 03 p0961 N94-17251
Simulation of emittance dilution in electron storage ring from Compton backscattering
[DE93-017611] 04 p1386 N94-18503
An assessment of COMSCAN, a Compton backscatter imaging camera, for the one-sided non-destructive inspection of aerospace components
[AD-A271331] 05 p1806 N94-19837
Oxidation-reduction induced roughening of platinum (111) surface
[DE93-017408] 05 p1687 N94-19922
Spatial organization of polymer chains in a crystallizable diblock polyethylene and polystyrene
[AD-A271862] 05 p1702 N94-20463
The x ray halo of Cen X-3
[NASA-CR-189309] 05 p2055 N94-21295
Laser Raman and x ray scattering studies of corrosion films on metals
[DE93-040243] 05 p1692 N94-21558
Thermal phase behavior of metal surfaces: X-ray scattering studies of Pt(001)
[DE94-002991] 06 p2245 N94-24612
Structural study of Cu/Co multilayer by anomalous small-angle x ray scattering 07 p2744 N94-28160
Experimental investigation of phonon eigenvectors using x ray interference fields
[ETN-94-95751] 09 p3865 N94-31511
Anomalous small angle x ray scattering studies of amorphous metal-germanium alloys
[DE94-007258] 09 p3900 N94-32065
X ray optics for science and technology
[AD-A277369] 09 p3880 N94-32155
Anisotropic phase separation through the metal-insulator transition in amorphous Mo-Ge and Fe-Ge alloys
[DE94-007259] 09 p3646 N94-32795
Dependence of x ray absorption magnetic circular dichroism on layer periodicity in iron-platinum multilayers
[DE94-008786] 09 p3647 N94-32892
Small-angle x ray scattering studies of microvoids in amorphous-silicon-based semiconductors
[DE94-006931] 12 p4533 N94-36745
XAFS-like structure of resonant Raman scattering
[DE94-618410] 12 p4517 N94-37171

X RAY SOURCES

NT X RAY BINARIES
NT X RAY STARS
X ray production (approximately)130 (Angstrom) from laser-produced plasmas for projection x ray lithography applications
[DE93-009256] 01 p0385 N94-10286
Physical optics modelling of Soft X ray Projection Lithography (SXPL) imaging experiments
[DE93-011556] 01 p0374 N94-10339
Wavelength considerations in soft x ray projection lithography
[DE93-014115] 01 p0381 N94-10651
Radiation hardness of Mo/Si multilayers designed for use in a soft x ray projection lithography system
[DE93-011879] 01 p0143 N94-11273
Submicrosecond, synchronizable x ray source
[AD-D015745] 01 p0176 N94-12337
HEAO-1 analysis of Low Energy Detectors (LED)
[NASA-CR-194087] 01 p0424 N94-12574
Search for UHE point-source emission over various time scales
[DE93-012718] 02 p0846 N94-12922
Studies of gas in cooling flow clusters
[NASA-CR-193597] 02 p0628 N94-12959
The x ray lasers as sources for x ray microscopy
[DE93-013420] 02 p0655 N94-13259
The onset of galactic winds in early-type galaxies
[NASA-CR-193640] 02 p0836 N94-13446
X ray observations of late-type stars using the ROSAT all-sky survey
[NASA-CR-193716] 02 p0832 N94-14146
An x ray detector using superconducting aluminum tunnel junctions
[DE93-015103] 02 p0811 N94-14332
The 8 to 11 keV x ray sources for imaging and absorption experiments
[DE93-015973] 02 p0803 N94-14865
Direct drive foil implosion experiments on Pegasus 2
[DE93-012666] 03 p1202 N94-16776
Participation in the north ecliptic pole sky survey
[NASA-CR-191933] 03 p1059 N94-16815
Resist performance in soft x ray projection lithography
[DE93-016490] 03 p1036 N94-17647
Absorption and x ray measurements from ultra-intense laser-plasma interactions
[DE93-016538] 04 p1585 N94-18115
Pulse-timing studies of x ray pulsars
[NASA-CR-193778] 04 p1621 N94-18611
The Einstein Observatory catalog of IPC x ray sources. Volume 4E: Right ascension range 08h 00m to 11h 59m
[NASA-TM-108401-VOL-4E] 04 p1625 N94-18612
The Einstein Observatory catalog of IPC x ray sources. Volume 5E: Right ascension range 12h 00m to 15h 59m
[NASA-TM-108401-VOL-5E] 04 p1625 N94-18613
The Einstein Observatory catalog of IPC x ray sources. Volume 6E: Right ascension range 16h 00m to 19h 59m
[NASA-TM-108401-VOL-6E] 04 p1625 N94-18615
The Einstein Observatory catalog of IPC x ray sources. Volume 7E: Right ascension range 20h 00m to 23h 59m
[NASA-TM-108401-VOL-7E] 04 p1625 N94-18618
The Einstein Observatory catalog of IPC x ray sources. Volume 1E: Documentation
[NASA-TM-108401-VOL-1E] 04 p1626 N94-18619

The Einstein Observatory catalog of IPC x ray sources. Volume 2E: Right ascension range 00h 00m to 03h 59m
[NASA-TM-108401-VOL-2E] 04 p1626 N94-18620
The Einstein Observatory catalog of IPC x ray sources. Volume 3E: Right ascension range 04h 00m to 07h 59m
[NASA-TM-108401-VOL-3E] 04 p1626 N94-18621
Eclipsing cataclysmic variables. Deep eclipses in H0928+501. YY Draconis, the whirling dervish. New x ray pulsar candidates from HEAO-1
[NASA-CR-194027] 04 p1621 N94-18855
Rosat and optical observations of two X-ray transients: MX 0836-42 and GS 0834-430
[MPE-PREPRINT-237] 04 p1622 N94-19451
IRAS galaxies observed in the ROSAT survey: Starbursts or central activity 04 p1623 N94-19528
The x ray halo of AM Her
[NASA-CR-189310] 05 p2054 N94-20142
Applications and source development for high-repetition rate x ray lasers
[DE93-019547] 05 p1815 N94-20259
Pre-main sequence stars in the Chamaeleon cloud and pre-main sequence stars in the Rho Ophiuchi cloud core
[NASA-CR-194713] 05 p2080 N94-20337
Studies of an x ray selected sample of cataclysmic variables
[NASA-CR-194773] 05 p2055 N94-20344
The x ray halo of Cen X-3
[NASA-CR-189309] 05 p2055 N94-21295
Generation of intense ultrashort x ray pulses
[DE93-019607] 05 p1817 N94-21299
The distribution of dark matter in the A2256 cluster
[NASA-CR-194699] 05 p2055 N94-21579
Dust content of a hydrogen rich, low surface brightness galaxy and the luminosity history of 3C273
[NASA-CR-194705] 05 p2056 N94-21779
Parametric instabilities in picosecond time scales
[DE94-000384] 05 p1966 N94-21958
CCD surface photometry of galaxies
05 p2058 N94-22445
The ALEXIS data processing package: An IDL based system 05 p2047 N94-22453
Detection of x ray sources in PROS
05 p2062 N94-22466
Spatial region filtering in IRAF/PROS
05 p1927 N94-22524
Results from ROSAT 05 p2000 N94-22630
Highlights of Yohkoh results 05 p2001 N94-22632
Thermal properties and radiation processes in astrophysical plasmas 05 p2002 N94-22640
The soft x ray halo of the spiral galaxy NGC4631
[NASA-CR-194820] 06 p2601 N94-23537
X ray simulator theory support
[AD-A273613] 06 p2553 N94-24949
Investigation relative to the Roentgen Satellite (ROSAT)
[NASA-CR-195192] 06 p2600 N94-25269
Meson spectroscopy and particle astrophysics
[DE94-001799] 07 p3115 N94-27003
Cosmic x ray physics
[NASA-CR-195225] 07 p3115 N94-27236
Correlative analysis of hard and soft x ray observations of solar flares
[NASA-CR-189329] 08 p3551 N94-29453
On observing neutron star oscillations
08 p3538 N94-29795
High redshift QSOs and the x ray background
[NASA-CR-195112] 08 p3540 N94-29957
Conceptual study of moderately coupled plasmas and experimental comparison of laboratory x ray sources
[DE94-005828] 08 p3506 N94-30045
Theoretical studies of x ray emission from clusters of galaxies 09 p3954 N94-31103
The physics of black hole x ray novae
09 p3932 N94-31143
A multi-frequency study of an x ray selected sample of active galactic nuclei 09 p3937 N94-31987
X ray imaging and x ray source development at Lawrence Livermore National Laboratory
[DE94-007077] 09 p3719 N94-32629
Near edge x ray spectroscopy theory
[DE94-008179] 09 p3905 N94-32799
Ultrafast x ray sources
[AD-A277455] 09 p3721 N94-33012
Plasma physics applications to intense radiation sources, pulsed power and space physics. Short pulse ultra intense laser-plasma interaction experiment
[AD-A278440] 10 p4144 N94-33555
Coherent multiple-foil x-ray transition radiation
[DE93-040831] 12 p4525 N94-37486

X RAY SPECTRA

Source to detector spectrum transformation and its inverse for the Pegasus Z-pinch
[DE93-012674] 01 p0334 N94-10157
X ray production (approximately)130 (Angstrom) from laser-produced plasmas for projection x ray lithography applications
[DE93-009256] 01 p0385 N94-10286
Studies of gas in cooling flow clusters
[NASA-CR-193597] 02 p0628 N94-12959
ROSAT guest investigator program (AO-1). On a search for coronal x ray emissions from white dwarfs
[NASA-CR-193654] 02 p0835 N94-13171
Selenium x ray laser line profile measurements
[DE93-012580] 02 p0658 N94-14175
A long-term space astrophysics research program: The evolution of the quasar continuum
[NASA-CR-193714] 02 p0839 N94-14404
X ray emission from Wolf-Rayet stars with recurrent dust formation
[NASA-CR-189321] 03 p1300 N94-15533
Variability of the Seyfert galaxy MKN 766 in the Rosat all sky survey
[MPE-PREPRINT-221] 03 p1240 N94-17591
Analysis of neon soft x ray spectra from short-pulse laser-produced plasmas
[DE93-014420] 04 p1582 N94-17708
X-ray laser oscillator-amplifier experiments
[DE93-017165] 04 p1436 N94-17868
Dynamic behaviors of fragments ejected from the surface of carbon materials by laser ablation
[DE93-788620] 04 p1438 N94-18161
Search for resonant electron transfer and double excitation in Kr(sup 34+) + H2 collisions
[DE93-018776] 04 p1569 N94-18999
SPIKE: Application for ASTRO-D mission planning
05 p1926 N94-22486
Pair plasmas in the central engine of active galactic nuclei 05 p2002 N94-22641
Vertical structure of accretion disks
05 p2002 N94-22645
Non-equilibrium ionization in an M class solar flare
05 p2004 N94-22653
Properties of x ray emission from x ray novae
05 p2007 N94-22676
Structure of accretion plasmas of x ray binary pulsars in MHD turbulence 05 p2007 N94-22679
Time variations of x rays from black hole candidates: Canonical time variations in high and low intensity states
05 p2009 N94-22690
Time variation of MHD accretion onto a black hole
05 p2009 N94-22692
Shock formation in magnetohydrodynamical accretion onto a black hole 05 p2010 N94-22699
High-resolution soft x ray photoionization studies of selected molecules
[DE94-000568] 06 p2532 N94-23002
1993 annual report for the Phaedrus-T RF current drive experiments
[DE94-001369] 06 p2550 N94-23192
Balloon-borne measurements of the SN1987A hard x ray continuum 07 p3115 N94-26689
Coronal abundances and their variation
[NASA-CR-195767] 08 p3551 N94-29858
A high rate, low noise, x ray silicon strip detector system
[DE94-004557] 08 p3268 N94-30717
ROSAT/XRT-PSPC observations and the ionizing continuum of Seyfert 1 galaxy Mkn 478
[PB94-167053] 11 p4350 N94-35530
The BL LAC phenomenon: X-ray observations of transition objects and determination of the x-ray spectrum of a complete sample of flat-spectrum radio sources
[NASA-CR-195951] 12 p4546 N94-36688
On the shape of x ray spectra excited by heavy ions
[DE94-618747] 12 p4519 N94-37651

X RAY SPECTROGRAPHY

U X RAY SPECTROSCOPY

X RAY SPECTROMETRY

U X RAY SPECTROSCOPY

X RAY SPECTROSCOPY

Microanalysis of directionally solidified cobalt oxide-zirconia eutectic
[DE93-013207] 01 p0088 N94-10527
X ray and gamma ray spectroscopy of solids under pressure
[DE93-014847] 01 p0076 N94-10653
Effect of surface cleanliness of bearing steel on adhesive strength and tribological properties of sputter-deposited gold films
[DE93-767974] 01 p0082 N94-10732
Tribological characteristics of hot-pressed self-lubricating composites
[NAL-TR-1160] 01 p0066 N94-10858
X ray absorption spectroscopy of electrochemically generated species
[AD-A264749] 01 p0077 N94-11265
High resolution time- and 2-dimensional space-resolved x ray imaging of plasmas at NOVA
[DE93-011892] 01 p0393 N94-11677
Remote sensing x ray fluorescence spectrometry for future lunar exploration missions
01 p0462 N94-12165
Yohkoh Bragg Crystal Spectrometer light curves for Ca XIX (3.1631-3.1912A): 1 October 1991 - 30 September 1992
[AD-A266090] 01 p0483 N94-12414
Analysis of samples of reflector materials which are multicoated and metal samples with oxide coatings which have been exposed the space environment in LDEF testing
[NASA-CR-193647] 02 p0575 N94-12789
Surface science instrumentation for the study of important catalytic and electrochemical interfaces
[DE93-015068] 02 p0563 N94-13413
Recent developments in multiple-scattering calculations of XAFS and XANES
[DE93-010999] 02 p0563 N94-13477
Many-body corrections in XAFS
[DE93-011002] 02 p0563 N94-13478
Applications of surface science to solid lubricants
[SMC-TR-93-24] 02 p0579 N94-13903
Hard x ray/microwave spectroscopy of solar flares
[NASA-CR-194399] 02 p0844 N94-13958
Ultra-soft x ray absorption spectroscopy: A bulk and surface probe of materials
[DE93-014325] 02 p0566 N94-14582
Structural and dynamical aspects of electrodeposition
[AD-A266786] 03 p0942 N94-14909
X ray microcalorimeters: Principles and performance
03 p0899 N94-15027
The imaging microstrip proportional counter: Features of a practical design 03 p0900 N94-15030
Development of x ray CCDs 03 p0900 N94-15033
The XMM pn-CCD detector system: First results
03 p0900 N94-15034
The development of back-illuminated CCD's for XMM
03 p0900 N94-15035
X-ray spectroscopy with silicon pin and avalanche photo diodes 03 p0906 N94-15072
CCD's on high resistivity bulk silicon for x ray spectroscopy on XMM 03 p0907 N94-15080
Substrate effects in superconducting tunnel junction detectors 03 p0908 N94-15083
Performance of the position-sensitive proportional counters of the Yohkoh Bragg crystal spectrometer
03 p0909 N94-15094
Application of in situ scanning x ray fluorescence to study the concentration of metal ions in simulated pits
[DE93-014054] 03 p0956 N94-15921
A sulfur segregation study of PWA 1480, NiCrAl, and NiAl alloys
[NASA-TM-106289] 03 p0956 N94-15992
In situ studies of passive film chemistry using x ray absorption spectroscopy
[DE93-014023] 03 p0947 N94-16011
Design and fabrication of a reflection far ultraviolet polarizer and retarder
[NASA-CR-194630] 03 p1191 N94-16023
The interaction of HCN(DCN) with Si(111)-7x7 studied with HREELS, UPS, and XPS
[AD-A266237] 03 p1182 N94-16111
Electron spectroscopy analysis
[NASA-CR-193591] 03 p0951 N94-17039
Characterization of nanoscale oxide and oxyhydroxide powders using EXAFS spectroscopy
[DE93-015683] 03 p0940 N94-17235
Soft x ray emission from Alexandrite laser-matter-interaction
[AD-A267905] 03 p1042 N94-17378
Guidelines for the expression of uncertainties in surface chemical analysis by Auger Electron Spectroscopy (AES) and X ray Photoelectron Spectroscopy (XPS)
[NPL-DMM(A)-99] 04 p1346 N94-17900
X ray absorption spectroscopic studies of the active sites of nickel- and copper-containing metalloproteins
[DE93-017142] 04 p1347 N94-18059
Absorption and x ray measurements from ultra-intense laser-plasma interactions
[DE93-016538] 04 p1585 N94-18115
X ray studies of microstructures in semiconductor and superconducting materials
[DE93-040690] 04 p1601 N94-19056
Legacy of the X Ray Laser Program
[DE93-019550] 04 p1442 N94-19554
Alumoxanes: Rationalization of black box materials
[AD-A272805] 05 p1704 N94-21170
Asbestos characterization using scanning electron microscopy/light element x ray spectrometry
[AD-A271611] 05 p1681 N94-21241
Center for X-Ray Optics, 1992
[DE94-000726] 05 p1990 N94-21868
Requirements for future solar-physics missions with x ray instrumentation 06 p2625 N94-22849

Imaging XUV spectroscopy of a Z-pinch plasma in the former Soviet Union
[DE93-040849] 06 p2549 N94-22949
Investigate zero-stress replicated optics
[NASA-CR-193889] 06 p2545 N94-24665
LPCVD of InN on GaAs(110) using HN3 and TMIn: Comparison with Si(100) results
[AD-A273555] 06 p2235 N94-24917
The structure and catalytic properties of supported platinum catalysts
[ETN-94-95357] 06 p2236 N94-25250
Study on analyzing method establishment for metallic material development 07 p2729 N94-25578
Se EXAFS study of the elevated wurtzite to rock salt structural phase transition in CdSe nanocrystals
[DE94-003247] 07 p3054 N94-26125
X ray absorption studies of Ti/polymer and Cr/polymer interfaces
[DE94-003008] 07 p2753 N94-26770
Structure of ordinary ice I(sub h). Part 1: Ideal structure of ice
[AD-A275149] 08 p3486 N94-29021
Miniaturization in x ray and gamma ray spectroscopy 08 p3236 N94-29773
Aggregation equilibria in arsenic doped silicon
[DE94-607269] 08 p3515 N94-30005
XPS analysis of 440C steel surfaces lubricated with perfluoropolyethers under sliding conditions in high vacuum
[NASA-TM-106548] 08 p3218 N94-30177
A low noise silicon detector preamplifier system for room temperature x ray spectroscopy
[REPT-93-058] 08 p3291 N94-30930
Spectroscopy and atomic physics in EBIT and SuperEBIT
[DE94-006050] 09 p3864 N94-31508
The Los Alamos National Laboratory precision double crystal spectrometer
[DE94-008075] 09 p3713 N94-32706
Near edge x ray spectroscopy theory
[DE94-008179] 09 p3905 N94-32799
Structural studies of photoinduced intramolecular electron transfer in cyclopentadienylnickelnitrosyl
[DE94-008467] 09 p3874 N94-32876
Evidence for symmetry breaking local distortions in thallium barium copper oxide
[DE94-006149] 09 p3907 N94-32944
Electron cyclotron resonance plasma oxidation studies of InP
[AD-A277431] 09 p3893 N94-33007
Remote geochemical experiment package for Discovery class missions 11 p4350 N94-35420
Petrographic characterization of lunar soils: Application of x ray digital-imaging to quantitative and automated analysis 11 p4368 N94-36138
Microstructure and chemistry of MgO- and CoO-doped nickel-titanate spinels
[DE94-012741] 12 p4537 N94-37382
Preliminary soft x ray studies of beta-SiC
[DE94-013023] 12 p4537 N94-37498

X RAY STARS
NT X RAY BINARIES
ROSAT guest investigator program (AO-1). On a search for coronal x ray emissions from white dwarfs
[NASA-CR-193654] 02 p0835 N94-13171
Search for x ray emitting young stars outside of massive molecular clouds
[NASA-CR-193609] 02 p0830 N94-13462
Time variations of x rays from black hole candidates: Canonical time variations in high and low intensity states 05 p2009 N94-22690
An April 1991 outburst from 4U0115+63 observed by BATSE
[DE94-007093] 07 p3116 N94-27440
Workshop on Physics of Accretion Disks Around Compact and Young Stars
[NASA-CR-195756] 09 p3927 N94-31116
Disk irradiation and light curves of x ray novae 09 p3929 N94-31124
Observational constraints on black hole accretion disks 09 p3929 N94-31126
Stellar x ray polarimeter polarizer development and calibration at LEA/LLNL
[DE94-006400] 09 p3712 N94-31783

X RAY TELESCOPES
NT X RAY ASTROPHYSICS FACILITY
The development of the TIMAX project: A hard x ray imaging telescope
[INPE-5474-TDI/505] 02 p0829 N94-13245
Telescope for x ray and gamma ray studies in astrophysics 04 p1324 N94-19166
The ALEXIS data processing package: An IDL based system 05 p2047 N94-22453
Results from ROSAT 05 p2000 N94-22630
Highlights of Yohkoh results 05 p2001 N94-22632
X ray jets in the solar corona: Observations with Yohkoh Soft X Ray Telescope 05 p2004 N94-22655
Yohkoh Gamma ray Spectral Observations (YGSO) 05 p2004 N94-22656
Large-scale structure of the solar plasma corona: An analysis of Yohkoh SXT images 05 p2004 N94-22657

X RAY TIMING EXPLORER
The H(sub infinity) optimal controller design and reduction for the inertial hold mode of the attitude control system of the XTE spacecraft
[NASA-CR-195137] 06 p2366 N94-24846

X RAY TUBES
Laser Synchrotron Source (LSS)
[AD-D015755] 01 p0173 N94-10371
Fast photoconductor CdTe detectors for synchrotron x ray studies
[DE94-001334] 07 p3054 N94-26139
Design and characterization of a pulsed x ray source for fluorescent lifetime measurements
[DE94-007495] 09 p3880 N94-32138

X RAYS
NT COSMIC X RAYS
NT SOLAR X-RAYS
X ray production (approximately)130 (Angstrom) from laser-produced plasmas for projection x ray lithography applications
[DE93-009256] 01 p0385 N94-10286
Needs for super-smooth surfaces
[DE93-012482] 01 p0382 N94-11242
The x ray standing waves on surfaces
[AD-A265265] 01 p0402 N94-11682
Two-dimensional simulations of foil implosion experiments on the Los Alamos capacitor bank
[DE93-012676] 02 p0794 N94-12814
Detection of hot muonic hydrogen atoms emitted in vacuum using x-rays
[DE93-010253] 02 p0778 N94-12860
Absolute detection efficiency of a micro-channel plate detector to x rays in the 1-100 KeV energy range
[DE93-012592] 02 p0789 N94-14460
Thomson backscattered x rays from an intense laser beam
[AD-A267125] 03 p1038 N94-15686
Direct drive foil implosion experiments on Pegasus 2
[DE93-012666] 03 p1202 N94-16776
Multi-frame x ray imaging with a large area 40ps camera
[DE93-017179] 03 p1035 N94-16960
Ultrasonic wave propagation model for nondestructive evaluation of solid rocker motor propellant
[AD-A267653] 03 p0976 N94-17248
Review of rigorous coupled-wave analysis and of homogeneous effective medium approximations for high spatial-frequency surface-relief gratings 03 p1194 N94-17335
Soft x ray emission from Alexandrite laser-matter-interaction
[AD-A267905] 03 p1042 N94-17378
Resist performance in soft x ray projection lithography
[DE93-016490] 03 p1036 N94-17647
Conical geometry for sagittal focusing as applied to x rays from synchrotrons
[DE93-017238] 04 p1593 N94-17760
PVDF measurement of soft x ray induced shock and filter debris impulse
[DE93-017633] 04 p1382 N94-17806
Characteristics and pulsed radiation response of non-ideal quartz shock stress gauges
[DE93-017628] 04 p1424 N94-17999
Tomographic mathematical ideas applied to radar detection
[AD-A268789] 04 p1384 N94-18186
Soft X Ray Projection Lithography. Organization of the 1993 photonics science optical meetings
[AD-A269159] 04 p1579 N94-18693
Development of robust multilayer optics for use in high-peak power radiation environments
[DE93-018557] 04 p1580 N94-18931
Search for resonant electron transfer and double excitation in Kr(sup 34+) + H2 collisions
[DE93-018776] 04 p1569 N94-18999
New room temperature high resolution solid-state detector (CdZnTe) for hard x rays and gamma rays 04 p1324 N94-19165
X ray, extreme and far ultraviolet optical thin films for space applications
[NASA-CR-194635] 05 p1984 N94-20128
National Synchrotron Light Source user's manual: Guide to the VUV and x ray beamlines
[DE93-019564] 05 p2015 N94-20260
Development and characterization of a time-, position- and energy-resolved x ray diagnostic for PBFA 2 target experiments
[DE93-019429] 05 p1808 N94-20297
Kinetic theory of runaway air-breakdown
[DE93-040731] 05 p1750 N94-20325
X ray reflection masks: Manufacturing, characterization and first tests
[BONN-IR-92-31] 05 p1986 N94-21043
Examination for optimization of synchrotron radiation spectrum for the x ray depth lithography
[BONN-IR-92-32] 05 p1987 N94-21148
Multifrequency data analysis software on STARLINK 05 p1925 N94-22443
VETA x ray data acquisition and control system 05 p2047 N94-22455
PROS: An IRAF based system for analysis of x ray data 05 p1925 N94-22461
ROSAT implementation of a proposed multi-mission x ray data format 05 p2047 N94-22462
Detection of x ray sources in PROS 05 p2062 N94-22466
IPP Prague Contributions to the IAEA Technical Committee Meeting on Research Using Small Tokamaks
[IPPCZ-329] 06 p2551 N94-24293
High energy collimating fine grids for HESP program
[NASA-CR-189317] 06 p2209 N94-24767
Nonequilibria in thermal emission from supernova remnants
[NIFS-264] 06 p2602 N94-24866
X ray enhancement of SN 1987A due to interaction with its ring-like nebula
[NIFS-265] 06 p2602 N94-24867
High precision x ray lithographic masks
[AD-A273342] 06 p2346 N94-25154
Excitation mechanisms for XUV and x ray lasers
[DE93-617006] 06 p2351 N94-25482
Advanced qualification techniques
[DE94-003709] 07 p2780 N94-25812
Electron energy loss spectroscopy in a crystalline environment using inner shell ionization
[DE94-601820] 07 p3018 N94-26334
Experimental measurement of local displacement and chemical pair correlations in crystalline solid solutions
[DE94-001124] 07 p3065 N94-27251
Acceleration of electrons and ions by strong lower-hybrid turbulence in solar flares
[NASA-TM-109723] 07 p3111 N94-27953
Progress in Z-Pinch Research
[IPPCZ-321] 08 p3505 N94-29074
Multichannel x ray spectral measurement of hot plasma evolution in nitrogen-puff Z-pinch
[PH-24] 08 p3505 N94-29076
X ray emission scaling and energy balance of small gas-puff Z-pinch 08 p3505 N94-29077
X ray crystal structures of ((Me3SiCH2)2InCl)2 and ((Me3SiCH2)InCl2)
[AD-A275074] 08 p3513 N94-29155
X ray standing wave studies of underpotentially deposited metal monolayers
[AD-A275409] 08 p3513 N94-29215
Correlative analysis of hard and soft x ray observations of solar flares
[NASA-CR-189329] 08 p3551 N94-29453
Microactuator production via high aspect ratio, high edge acuity metal fabrication technology 08 p3235 N94-29770
Characteristics of secondary electron emission from CsI induced by x rays with energies up to 100 keV
[DE94-608422] 08 p3395 N94-30185
Determination of photon fluence spectra from the NPL Mobaltron Co-60 unit
[PB94-149150] 08 p3492 N94-30795
Role of x ray-induced transcripts in adaptive responses following x rays
[DE94-005412] 08 p3386 N94-30895
Theoretical studies of x ray emission from clusters of galaxies 09 p3954 N94-31103
Observation of the traveling component of an x ray standing wave field
[DE94-007671] 09 p3672 N94-31317
Double photoionization of helium with synchrotron x rays: Proceedings
[DE94-006737] 09 p3866 N94-31668
X ray pulse considerations and electron flow in high voltage diodes
[AD-A277301] 09 p3868 N94-32044
X ray optics for science and technology
[AD-A277369] 09 p3880 N94-32155
Simplified ultra-high resolution optic for soft x ray imaging
[AD-A278424] 09 p3885 N94-33331
Resonant photoemission and magnetic x-ray circular dichroism in the M shell of ultrathin films of Fe
[DE94-007453] 10 p4029 N94-34120
X-ray remote sensing and in-situ spectroscopy for planetary exploration missions and gamma-ray remote sensing and in-situ spectroscopy for planetary exploration missions
[NASA-CR-189352] 11 p4375 N94-35381

AXAF-I ghost ray study: On orbit case
[NASA-CR-193987] 11 p4333 N94-36119
Activities of the optoelectronics laboratory
[PB94-171196] 11 p4334 N94-36190
Scaling laws for TEXT plasma profiles
[DE94-010832] 11 p4338 N94-36200
X ray radiographic imaging of hydrodynamic phenomena in radiation driven materials: Shock propagation and shear flow
[DE94-010891] 11 p4318 N94-36201
Kinetic theory of runaway air breakdown and the implications for lightning initiation
[DE94-001683] 11 p4295 N94-36240
Guiding hard x rays with glass polycapillary fiber
[DE94-004949] 12 p4525 N94-37258
Preliminary soft x ray studies of beta-SiC
[DE94-013023] 12 p4537 N94-37498
Advanced laser driver for soft x-ray projection lithography
[DE94-011643] 12 p4449 N94-37722

X WING ROTORS
Vibration reduction in helicopter rotors using an actively controlled partial span trailing edge flap located on the blade
[NASA-CR-4611] 11 p4280 N94-36423

X-14 AIRCRAFT
Lift-fan aircraft: Lessons learned-the pilot's perspective
[NASA-CR-177620] 03 p0867 N94-15950

X-15 AIRCRAFT
The 1966 highlights --- NASA research programs
[NASA-TM-109444] 03 p1302 N94-15343

X-29 AIRCRAFT
X-29: Longitudinal instability at high angle-of-attack
01 p0033 N94-11504
X-29: Experiment in flight
[NASA-TM-109454] 03 p0865 N94-15327
High lift and the forward swept wing
04 p1308 N94-18436
X-29: Research aircraft
[NASA-TM-109370] 04 p1318 N94-18962
X-29 flight control system: Lessons learned
[NASA-TM-4598] 10 p3984 N94-34384
Damage tolerance management of the X-29 vertical tail 10 p3996 N94-34595

X-30 VEHICLE
An environmental study of the National Aerospace Plane
[AD-A266071] 01 p0025 N94-10945
The National Aerospace Plane (NASP): Development issues for the follow-on vehicle
[AD-A278417] 09 p3581 N94-33329

X-31 AIRCRAFT
X-31 aerodynamic characteristics determined from flight data 06 p2164 N94-25109
X-31A system identification applied to post-stall flight: Aerodynamics and thrust vectoring
10 p3992 N94-34619
X-31 tactical utility: Initial results
10 p3992 N94-34620
Controlling forebody asymmetries in flight: Experience with boundary layer transition strips
[NASA-TM-4595] 12 p4383 N94-36944

XANTHINES
NT CAFFEINE
Biochemical enhancement of cold tolerance
08 p3380 N94-28427

XB-70 AIRCRAFT
U B-70 AIRCRAFT

XBQM-180A AIRCRAFT
U VATOL AIRCRAFT

XENON
NT XENON ISOTOPES
NT XENON 129
Satellite structure of the xenon valence shell by electron momentum spectroscopy
[DE93-609993] 01 p0360 N94-10327
Kinetic studies following state-selective laser excitation
[DE93-012970] 02 p0654 N94-13013
Prospects for high pressure imaging gas scintillation drift chambers 03 p0901 N94-15040
Dynamics of short-pulse excitation, ionization and harmonic conversion
[DE93-017220] 04 p1436 N94-17996
A High Resolution Liquid Xenon Imaging Telescope for 0.3-10 MeV Gamma Ray Astrophysics: Construction and Initial Balloon Flights
[NASA-CR-194709] 05 p2056 N94-22281
The polarization sensitivity of the liquid xenon imaging telescope 05 p2056 N94-22282
Contamination control and plume assessment of low-energy thrusters
[NASA-TM-104585] 06 p2218 N94-23343
Power console development for NASA's electric propulsion outreach program
[NASA-TM-106428] 06 p2218 N94-23372
Performance evaluation of the Russian SPT-100 thruster at NASA LeRC
[NASA-TM-106401] 06 p2219 N94-23630
Performance of the NASA cm ion thruster
[NASA-TM-106426] 06 p2221 N94-24770
Stationary plasma thruster plume emissions
[NASA-CR-194471] 07 p2701 N94-26209
Calculations of population transfer during intense laser pulses
[DE94-001060] 07 p2818 N94-26698
Disintegration of (C60) by Xe ion irradiation
[DE94-601913] 07 p3023 N94-26929
Damage growth in MgAl2O4 crystals by Xe ion irradiations
[DE94-005009] 07 p3069 N94-27828
Computer simulation of molecular interactions in supercritical solvents
[AD-A274977] 08 p3486 N94-29087
Remote pumping of solid state lasers with nuclear driven fluorescers
[DE94-004846] 08 p3296 N94-30614
Kinetics studies following state-selective laser excitation
[DE94-010305] 11 p4330 N94-36105
Characteristics of ions emitted from high-current hollow cathodes
[NASA-CR-195372] 12 p4398 N94-37764

XENON CHLORIDE LASERS
Microwave excitation of pulsed high pressure gas discharge lasers
[DLR-FB-93-12] 06 p2351 N94-25304
Diagnostics of high-brightness short-pulse lasers and the plasmas they generate
[DE94-006165] 09 p3716 N94-31624
Single-shot intensity and phase measurements of detuning and saturation effects in an ultrashort XeCl amplifier
[DE94-007535] 10 p4058 N94-33860
Metal-carbon nanostructures
[DE94-009177] 12 p4400 N94-36509

XENON ISOTOPES
NT XENON 129
Nitrogen and noble gases in a glass sample from LEW88516 01 p0080 N94-12051
The Xe-Q in lodranites and a hint for Xe-L. FRO90011 another lodranite? 01 p0432 N94-12239

XENON 129
Noble gases in LEW88516 shergottite: Evidence for exposure age pairing with ALH77005
01 p0080 N94-12082
Studies of the release of radiogenic Xe-129 from Bjurboele: Evidence against simple diffusion models
01 p0430 N94-12125

XI HYPERONS
Double-lambda compound nucleus and the formation of double hypernuclei
[DE93-754289] 01 p0365 N94-11040
A generalized Bethe-Weizsaecker mass formula for strange hadronic matter
[DE93-011010] 01 p0368 N94-11620

XM-6 SQUIB
U SQUIBS

XM-8 SQUIB
U SQUIBS

XV-5A AIRCRAFT
U XV-5 AIRCRAFT

XV-5 AIRCRAFT
Lift-fan aircraft: Lessons learned-the pilot's perspective
[NASA-CR-177620] 03 p0867 N94-15950

XV-15 AIRCRAFT
Determining XV-15 aeroelastic modes from flight data with frequency-domain methods
[NASA-TP-3330] 01 p0025 N94-10935
XV-15: Tiltrotor
[NASA-TM-109455] 03 p0865 N94-15328
The 1979 highlights
[NASA-TM-109443] 03 p1247 N94-15342
The 1982 highlights
[NASA-TM-109671] 03 p1303 N94-15508
Ground vibration test of the XV-15 Tiltrotor Research Aircraft and pretest predictions
11 p4200 N94-35972

Y

Y-BA-CU-O SUPERCONDUCTORS
U YBCO SUPERCONDUCTORS

YAG (GARNET)
U YTTRIUM-ALUMINUM GARNET

YAG LASERS
Nonlinear Dynamics in Optical Systems. Postdeadline papers presented at the Optical Society of America Conference
[AD-A264958] 01 p0375 N94-10486
Thermal-optical switching of a silicon based interference filter
[AD-A265152] 01 p0174 N94-11095
Short wavelength crystal fiber devices
[AD-A265716] 01 p0176 N94-12402
Tetravalent chromium (Cr(4+)) as laser-active ion for tunable solid-state lasers
[NASA-CR-194527] 02 p0659 N94-14576
Growth of new materials for solid state laser applications. The growth of ZnGeP2 by the vertical Bridgman method
[NASA-CR-194571] 03 p1038 N94-15530
An improved light source for laser ranging
03 p0913 N94-15567
Two color satellite laser ranging upgrades at Goddard's 1.2m telescope facility 03 p0915 N94-15581
Measuring atmospheric dispersion with WLRS in multiple wavelength mode 03 p0916 N94-15582
Upgrading of the Borowiec laser station
03 p0877 N94-15604
Results of the MTLRS-1 upgrade
03 p0877 N94-15610
Effects of turbulence on the geodynamic laser ranging system 03 p0921 N94-15616
Development of the Mars Observer Laser Altimeter (MOLA) 03 p0921 N94-15617
The third generation SLR station Potsdam no. 7836
03 p0877 N94-15623
Space Applications Industrial Laser System (SAILS)
04 p1325 N94-19173
Development of a lidar for integration with the Naval Postgraduate School Infrared Search and Target Designation (NPS-IRSTD) system
[AD-A271847] 05 p1817 N94-20611
Investigation of the optical and laser properties of Tm and Ho in YAG anf YLF
[REPT-94-001] 06 p2563 N94-24404
Progress toward ultra-stable lasers for use in space
[NASA-TM-109678] 06 p2349 N94-24488
The development of Cr, Tm, Ho:YAG lasers for airborne lidar
[AD-A274895] 07 p2816 N94-26178
Development of surgical CW Nd:YAG laser with optical fiber delivery system
[DE93-632902] 07 p2817 N94-26185
Development of real-time pulse shaping technology in solid-state lasers
[DE93-633438] 07 p2817 N94-26403
Development of high average power industrial Nd:YAG laser with peak power of 10 kW class
[DE93-633201] 07 p2818 N94-26520
Distributed Nd:YAG laser welding and process control in inert glove boxes
[DE94-002629] 07 p2818 N94-26605
Kinoform/lens system for injecting a high power laser beam into an optical fiber
[DE94-003226] 07 p2819 N94-27262
Laser beam steering with semiconductor waveguide
[AD-A275775] 08 p3292 N94-28765
High-power CW diode-laser-array-pumped solid-state lasers and efficient nonlinear optical frequency
[AD-A275394] 08 p3293 N94-29309
The laser approach for sequential pyrotechnic initiation systems: Envisageable chain architecture and concepts
[REPT-932-430-113] 08 p3225 N94-29414
High-power CW diode-laser-array-pumped solid-state lasers and efficient nonlinear optical frequency conversion
[AD-A276126] 09 p3714 N94-31278
Methods for SBS threshold reduction
[AD-A276554] 09 p3717 N94-31936
Backscatter and transmission of aerosol at UV through middle IR wavelengths
[AD-A277127] 09 p3718 N94-32305
High average power pulsed phase conjugate laser with birefringence correction
[DE94-006049] 09 p3719 N94-32659
900-mW average power and tunability from a diode-pumped 2.94 micron Er:YAG oscillator
[DE94-009511] 11 p4271 N94-35679
Eyesafe rare earth crystal lasers for atmosphere soudings
[AD-A279486] 11 p4273 N94-36227
Greater than 100 watt average power at 0.53 micron with 25 ns, 2.5 kHz repetition rate pulses from a single power oscillator
[DE94-011641] 12 p4447 N94-37114
High average power pulsed phase conjugate laser with birefringence correction
[DE94-012062] 12 p4447 N94-37160
Holmium quasi-two level laser
[AD-D016302] 12 p4449 N94-37772

Intracavity-pumped 2.1 micrometer Ho(3+):YAGl aser
[AD-D016308] 12 p4449 N94-37777

YAGI ANTENNAS

Modeling a Yagi array antenna for VHF radar use
[AD-A268973] 04 p1387 N94-18525

YANG-MILLS FIELDS

The Kaluza-Klein approach and gauge supersymmetry
[ISBN-0-315-86553-9] 09 p3912 N94-31911
Tensor gauge potentials in loop space formulation of Yang-Mills fields
[PB94-147147] 09 p3912 N94-31924

YANG-MILLS THEORY

Existence of a new instanton in constrained Yang-Mills-Higgs theory
[NIKHEF-H/93-02] 03 p1186 N94-17601
Derivation of the Verlinde formula from Chern-Simons theory and the G/G model
[DE93-628620] 03 p1221 N94-17632
Time evolution of the quark-gluon plasma
[DE94-000804] 05 p1998 N94-22389
On BRST quantization of constrained systems
[ETN-94-95386] 06 p2570 N94-25258
Classical solutions of Yang-Mills-Chern-Simons theory in 2+1 dimensions: A quasi-linear superposition
[DE93-634335] 07 p3006 N94-26270
C-periodicity and the physical mass in the 3-state Potts model
[DE94-601551] 07 p3019 N94-26423
Component structure of the N = 2 super-Yang-Mills theory in the harmonic superspace
[DE93-634340] 07 p3072 N94-26453
Anomaly candidates and invariants of D 4, N 1 supergravity theories
[NIKHEF-H/93-12] 07 p3072 N94-26541
Operator regularization and renormalization theory
[ISBN-0-315-49334-8] 07 p3007 N94-27264
A method for obtaining quantum doubles from the Yang-Baxter R-matrices
[DE94-606300] 07 p3001 N94-27846
Theory of fundamental interactions
[DE94-608126] 08 p3525 N94-30169
Periodic electromagnetic vacuum in the two-dimensional Yang-Mills theory with the Chern-Simons mass
[DE94-608128] 08 p3525 N94-30170
Tensor gauge potentials in loop space formulation of Yang-Mills fields
[PB94-147147] 09 p3912 N94-31924
On a connection between the Yang-Mills equations in dimension greater than four and the classical Yang-Baxter equations
[DE94-611115] 10 p4131 N94-33883

YARNS

Superconducting fibers made with yttrium and yttrium oxide interlayers and barium cuprate cover layers
[AD-D016073] 07 p3070 N94-28225
Development of braided rope engine seals
[NASA-TM-105902] 08 p3298 N94-28838

YAV-8B AIRCRAFT

U HARRIER AIRCRAFT

YAW

Static internal performance of a single expansion ramp nozzle with multiaxis thrust vectoring capability
[NASA-TM-4450] 01 p0012 N94-10675
Traveling disturbances appearing in yawed cylinder boundary layer transition 01 p0166 N94-12632
The 3D pneumatic and 2D dynamic probes: Their development and subsequent use in a transonic fan
[RAE-TM-AERO/PROP-22] 02 p0653 N94-14827
Effects of internal yaw-vectoring devices on the static performance of a pitch-vectoring nonaxisymmetric convergent-divergent nozzle
[NASA-TP-3369] 03 p0858 N94-16572
Wind tunnel investigations of forebody strakes for yaw control on F/A-18 model at subsonic and transonic speeds
[NASA-TP-3360] 03 p0859 N94-16573
Multisensor pinhole yawsonde
[AD-A271715] 05 p1808 N94-20930
The execution of wind energy projects 1986 - 1992 between China Aerodynamics Research and Development Centre (CARDC) and The Aeronautical Research Institute of Sweden (FFA)
[FFA-TN-1993-19] 08 p3340 N94-30945
Wind tunnel tests of a 5.3 m diameter yaw controlled turbine
[FFA-TN-1993-20] 08 p3340 N94-30946
Yaw control by tangential forebody blowing 10 p3992 N94-34615
Study findings on the influence of maneuverability and agility on helicopter handling qualities 10 p3993 N94-34624

YAWING MOMENTS

Contribution of body-mounted fins and tailplanes to lateral derivatives due to sideslip at subsonic speeds for general body width to height ratio
[ESDU-93007] 07 p2648 N94-28057
Yaw control by tangential forebody blowing 10 p3992 N94-34615
Wind tunnel measurements on a full-scale F/A-18 with a tangentially blowing slot --- conducted in the Ames 80 by 120 foot wind tunnel 11 p4191 N94-35965
Controlling forebody asymmetries in flight: Experience with boundary layer transition strips
[NASA-TM-4595] 12 p4383 N94-36944

YAWMETERS

U ATTITUDE INDICATORS
U YAW

YBCO SUPERCONDUCTORS

Microstructure and associated properties of YB2Cu3O(x) superconductors prepared by melt processing techniques
[DE93-010675] 01 p0398 N94-11004
Texture analysis of high Tc superconductors 01 p0399 N94-11314
Apical Cu-O bond in YBa2Cu3O(7-delta) superconductors by XAFS
[DE93-010861] 01 p0400 N94-11458
Synthesis and magnetic properties of novel La*2-x*M*x*CuO*4 equals y* compositions (La equals La, Pr, Nd, Sm, Eu, Cd; M equals Ca, Sr, Ba; O (less than or equal) x 0.2; -0.5 (less than or equal) y (less than or equal) 0.5)
[DE93-011359] 01 p0403 N94-12363
Corrosion and passivation of high temperature superconductors
[AD-A265402] 01 p0405 N94-12586
Flux-pinning related defect structures in melt-processed YBa2Cu3O(7-x)
[DE93-012759] 02 p0804 N94-12818
The study of structure-processing-property relations in copper oxide based high (Tc) superconductors
[DE93-015066] 02 p0804 N94-13003
Measurement of residual strain in composites by means of time-of-flight neutron diffraction
[DE93-012939] 02 p0555 N94-13248
Measurement of penetration depth lambda(T) in YBa2Cu3O(7-delta) thin film
[DE93-014587] 02 p0810 N94-14122
Formation of textured YBCO films by laser ablation
[DE93-013131] 02 p0581 N94-14319
Superconductivity devices: Commercial use of space
[NASA-CR-194163] 02 p0625 N94-14324
Room temperature degradation of YBa2Cu3O(7-x) superconductors in varying relative humidity environments
[NASA-TP-3368] 02 p0813 N94-14409
Quenching and annealing effects on the specific heat of YBa2Cu3O(7-delta)
[DE93-016483] 02 p0816 N94-14868
Experimental investigations of superconductivity in quasi-two-dimensional epitaxial copper oxide superlattices and trilayers
[DE93-015306] 03 p1207 N94-15829
Application of Z-contrast imaging to obtain column-by-column spectroscopic analysis of materials
[DE93-015333] 03 p0947 N94-16014
Local environment about O atoms in Pr-Y-Ba-Cu-O films studied by O K-edge XAFS
[DE93-016218] 03 p1209 N94-16447
Fast-ICCD photography and gated photon counting measurements of blackbody emission from particulates generated in the KrF-laser ablation of BN and YBC
[DE93-015491] 03 p1210 N94-16460
Powder diffraction studies using anomalous dispersion
[DE93-012531] 03 p1210 N94-16775
Diffuse scattering and image contrast of tweed in superconducting oxides: A simulation and interpretation
[DE93-016131] 03 p1212 N94-16844
Structural phase transition and superconductivity in La(2-x)Ba(x)CuO4
[DE93-015812] 03 p1212 N94-16868
A modified two-fluid model of conductivity for superconducting surface resistance calculation
[AD-A267549] 03 p1013 N94-17104
Basic optical studies of high T(c) oxide superconductors
[AD-A268148] 03 p1014 N94-17428
High temperature deformation behavior of YBa2Cu3O(6+x) superconducting ceramic materials
[AD-A268164] 03 p0973 N94-17430
Advanced thin-film deposition and physical properties of high-temperature and other novel superconducting materials
[AD-A268199] 03 p1216 N94-17561
Oxygen diffusion in YBa2Cu3O(3+delta) ceramics on heating
[DE93-629161] 03 p0974 N94-17633
Influence of the granular surface on the oxygen uptake in YBa2Cu3O(6+delta) ceramics
[DE93-629162] 03 p0974 N94-17634
Infrared detection with high-(Tc bolometers and response of Nb tunnel junctions to picosecond voltage pulses
[DE93-016963] 04 p1595 N94-17989
Mechanical properties of fiber-reinforced YBa2Cu3O(x) and Bi2Sr2CaCu2O(x) bars
[DE93-017689] 04 p1454 N94-18479
Photoemission studies of Zn, Co, and Gd substituted YBa2Cu3O(7-delta)
[DE93-017403] 04 p1597 N94-18498
High performance YBCO films
[AD-A269090] 04 p1599 N94-18719
Imaging and blackbody emission spectra of hot particulates generated during laser ablation
[DE93-015818] 04 p1439 N94-18724
High energy resolution ARPES measurements of the normal and superconducting states of Bi2Sr2CaCu2O(8 + delta)
[DE93-018294] 04 p1599 N94-18804
Superconductivity and magnetism in niobium doped YBa2Cu3O7 related high-(Tc) ceramics
[DE93-018086] 04 p1601 N94-19049
Particles on surfaces of laser ablated Y1Ba2Cu3O(7-delta) films
[DE93-040269] 05 p2013 N94-19929
Y-Ba-Cu-O superconducting/GaAs semiconducting hybrid circuits for microwave applications 05 p1735 N94-20514
Ten GHz YBa2Cu3O(7-delta) superconducting ring resonators on NdGaO3 substrates 05 p1735 N94-20515
A 10 GHz Y-Ba-Cu-O/GaAs hybrid oscillator proximity coupled to a circular microstrip patch antenna 05 p1736 N94-20517
The effect of fluctuations on the electrical transport behavior in YBa2Cu3O(7-x) 05 p1736 N94-20519
Relaxation of hysteresis loop in a single crystal of YBa2Cu4O8
[DE93-019519] 05 p2029 N94-21649
Specific heat of YBa2Cu3O7
[DE93-040640] 05 p2031 N94-21926
Spin dynamics and implications for superconductivity: Some problems with the d-wave scenario
[DE94-001183] 05 p2032 N94-21972
Melt-spin processing of high (Tc) oxide superconductors
[DE94-000696] 05 p2036 N94-22582
Anisotropic uniaxial pressure effects in YBa2Cu3O(7-delta)
[DE94-001456] 06 p2557 N94-22929
Processing of YBCO superconductors for improved levitation force
[DE94-001326] 06 p2559 N94-22994
Conductors with small Fermi energies and small gap energies
[DE93-040887] 06 p2561 N94-23432
Spectroscopic IR ellipsometry of 100 and 001 oriented YBa2Cu3O(7-delta) films
[PB93-201481] 06 p2561 N94-23445
Investigation and application of microwave electron cyclotron resonance plasma physical vapour deposition
[DE93-613909] 06 p2555 N94-25333
Critical currents in YBaCuO-ceramics
[DE93-617140] 06 p2263 N94-25404
Grain boundary degradation of YBCO superconductors sintered in CO2-containing atmospheres
[DE94-003206] 07 p3053 N94-26029
Window least squares method applied to statistical noise smoothing of positron annihilation data
[DE93-634665] 07 p3003 N94-26385
A study on the development of high T(sub c) superconducting materials
[DE93-633529] 07 p3057 N94-26404
Submillimeter residual losses in high-(Tc) superconductors
[DE94-003241] 07 p3058 N94-26516
A study on the development of high-T(c) superconducting wire
[DE93-632438] 07 p2783 N94-26546
Demonstration of monolithic co-fabrication of Y1Ba2Cu3O7-Sigma and CMOS devices on the same sapphire substrate
[AD-A274757] 07 p3059 N94-26566
Preparation and characterization of high temperature superconductor film surfaces
[AD-A274293] 07 p3059 N94-26681
Controlled heterogeneous nucleation of melt-textured YBa2Cu3O(6+x) by addition of Al2O3 particles
[AD-A274605] 07 p3062 N94-26892
Technical report of ISSP. Ser. A, no. 2681: Orbital and spin susceptibilities of the plane copper sites in YBa2Cu3O(x) system
[JTN-94-80567] 07 p3064 N94-27177
Synthesis, rheology, and forming of Y-Ba-Cu-O ceramics
[DE94-005558] 07 p2757 N94-27695

Fermi surface ridge at second and third Umklapp positron annihilations in Y Ba2Cu3O(7-delta)
[DE93-634760] 07 p3070 N94-27995
Superconducting fibers made with yttrium and yttrium oxide interlayers and barium cuprate cover layers
[AD-D016073] 07 p3070 N94-28225
Fabrication issues in optimizing YBa(2)Cu(3)O(7-x) flux transformers for low I/f noise
[DE94-005209] 08 p3261 N94-28546
Ion channeling peculiarities in YBa2Cu3 O7 monocrystal
[DE94-606885] 08 p3512 N94-28787
Atomic and magnetic structure of YBa2(Cu(1-x)Fe(x))3O(6+y) at 0.05 less than or equal to x less than or equal to 0.30, y is approximately equal to 1 and y is approximately equal to 0.5
[DE94-606852] 08 p3513 N94-29210
MuSR measurement of the magnetic penetration depth and coherence length in the high-Tc superconductor YBa2Cu3O(6.95)
[ISBN-0-315-85385-9] 08 p3517 N94-30203
Thermal conductivities, electrical resistivities, and Seebeck coefficients of YBa2Cu3O(7-x) superconductors from 80 to 300 K
[DE94-004796] 08 p3520 N94-30724
Low dispersion of the muon precession frequency in HTSC samples YBa2Cu3O(x) and EuBa2Cu3O(x)
[DE94-608388] 09 p3896 N94-31395
High performance YBCO films
[AD-A276493] 09 p3897 N94-31531
High pressure experiments on the Y-Ba-Cu-O superconductors: A major role for holes
[ETN-94-96013] 09 p3897 N94-31547
Impurities and conductivity in a D-wave superconductor
[DE94-006222] 09 p3898 N94-31628
Experimental evidence for lattice effects in high temperature superconductors
[DE94-006250] 09 p3899 N94-31633
The charging effect in high-Tc superconducting thin films
[AD-A277265] 09 p3900 N94-32040
Defect cascades produced by neutron irradiation in YBa2Cu3O(7-delta) superconductors
[DE94-007700] 09 p3903 N94-32372
Development, characterization, and applications of high temperature superconductor nanobridge Josephson junctions
[DE94-008113] 09 p3903 N94-32409
Effect of twin boundary density on the vortex melting transition in YBa2Cu3O(7-delta) single crystals
[DE94-007684] 09 p3904 N94-32601
YBCO Josephson Junction arrays
[AD-A277426] 09 p3908 N94-33005
The 20 GHz circularly polarized, high temperature superconducting microstrip antenna array
[NASA-CR-195097] 09 p3683 N94-33083
Microstructures and epitaxy in oxide superconductor thin films and devices
[AD-A278427] 09 p3910 N94-33332
Displacive transformation in ceramics
[AD-A278442] 10 p4026 N94-33539
JPRS report: Science and technology. Central Eurasia: Physics and mathematics
[JPRS-UPM-93-003] 10 p4132 N94-35118
Report on a SQUID made from high temperature superconductor
[PB94-169307] 11 p4339 N94-35598
Flux-pinning related defects in YBa2Cu3O(7-x) thin films grown on miscut LaAlO3 (001) substrates
[DE94-011463] 11 p4342 N94-36377
Activities of the Tandem Accelerator Center, University of Tsukuba
[DE94-748687] 12 p4522 N94-37237
Melt-processing of Y-Ba-Cu-O superconductors for improved levitation
[DE94-011503] 12 p4537 N94-37377
Permanent superconducting magnets for space applications
[NASA-CR-196293] 12 p4439 N94-37634

YC-14 AIRCRAFT
Design, development, and flight evaluation of the Boeing YC-14 USB powered lift aircraft
04 p1310 N94-18444

YEAST
Design and testing of a unique randomized gravity, continuous flow bioreactor 06 p2423 N94-25368
Plant-microbe interactions: Plant hormone production by phylloplane fungi
[PB94-135563] 08 p3385 N94-29189

YELLOWSTONE NATIONAL PARK (ID-MT-WY)
Saving Yellowstone
[NASA-TM-109596] 03 p1094 N94-15289
TOMS computer graphics
[NASA-TM-109597] 03 p1094 N94-15290

YF-22 AIRCRAFT
U F-22 AIRCRAFT

YHU-1 HELICOPTER
U UH-1 HELICOPTER

YIELD
Integration of ERS-1 data into the European project of agriculture statistics 01 p0248 N94-12490
Setting test limits under prescribed consumer loss
[MEMO-1107] 06 p2478 N94-22725

YIELD POINT
Damage thresholds of fluoride multilayers at 355 nm
[DE93-009523] 01 p0090 N94-11230
Absorption and damage thresholds of low defect density hafnia deposited with activated oxygen
[DE93-013853] 02 p0655 N94-13243
High damage threshold anti-reflectors by physical vapor deposited amorphous fluoropolymer
[DE94-004865] 08 p3212 N94-28560

YIELD STRENGTH
NT LOAD CARRYING CAPACITY
Collisions of small Spacewatch asteroids with the Earth 01 p0430 N94-12157
Radiation hardening and radiation-induced chromium depletion effects on intergranular stress corrosion cracking of austenitic stainless steels
[DE93-011602] 02 p0572 N94-14058
Yield properties of tungsten and tungsten heavy alloys
[AD-A266833] 02 p0575 N94-14878
The effect of irradiation on the mechanical properties of 6061-T651 aluminum
[DE93-015825] 03 p0958 N94-16168
Bulk and defect properties of ordered intermetallics: A first-principles total-energy investigation
[DE93-015492] 03 p0959 N94-16873
The Hall-Petch relationship and mechanisms of fracture in B2 compounds
[DE93-018887] 04 p1359 N94-18182
Dynamical behavior of tantalum
[DE93-017877] 04 p1362 N94-18919
Influence of peak pressure and temperature on the shock-loading response of tantalum
[DE93-018561] 04 p1457 N94-19279
Contribution to the identification of nonlinear behavior laws in material mechanics
[ECL-92-36] 04 p1458 N94-19411
Dynamic, multiaxial impact response of confined and unconfined ceramic rods
[DE93-040057] 05 p1829 N94-19824
Alloying effects on mechanical and metallurgical properties of NiAl
[DE93-040814] 05 p1694 N94-21948
Miniaturized disk-bend testing, nano-indentation, and the microstructure of ion-irradiated titanium aluminides
[DE93-040600] 05 p1697 N94-22559
Relationship of microstructure and mechanical properties for V-Cr-Ti alloys
[DE94-001431] 06 p2238 N94-22718
Effect of neutron irradiation on tensile properties of V-Cr-Ti alloys
[DE94-001433] 06 p2240 N94-23194
Use of photostress to characterize the mechanical behavior of weldments
[NASA-CR-195201] 06 p2378 N94-25267
Determination of fracture stress and effective crack tip radius from toughness (Klc) and yield strength (Y)
[AD-A274014] 07 p2836 N94-25754
Radiation hardening effects on localized deformation and stress corrosion cracking of stainless steels
[DE94-004308] 07 p2731 N94-25804
On experimental studies of yield surfaces of metals: A more general approach
[IFTR-42/1993] 07 p2739 N94-26824
Processing and mechanical properties of laminated metal composites of Al 6090-25 volume percent SiC(sub p) and Al 5182
[DE94-001070] 07 p2708 N94-26930
Fatigue propagation behaviour of short cracks (1-2 mm) in steels
[ESDU-93033] 07 p2845 N94-28145
Bolt and nut evaluator
[NASA-CASE-GSC-13468-1] 08 p3288 N94-29538
Tearing resistance of a thin shell against projectile penetration: Material property effects
[DE94-007466] 09 p3733 N94-31316
Influence of volume fraction of component materials and interlayer bond strength on fracture toughness of multi-layer Al 6090-25 volume percent SiCp and Al 5182 laminates
[DE94-007141] 09 p3626 N94-32665
Indentability of conventional and negative Poisson's ratio foams 09 p3629 N94-33131
The effect of thermomechanical processing on mechanical properties of a cast 6061 aluminum metal matrix composite
[AD-A277995] 10 p4019 N94-34220
Mechanical performance of austempered ductile iron
[AD-A280452] 12 p4420 N94-37758

YIG (GARNET)
U YTTRIUM-IRON GARNET

YJ-85 ENGINE
U J-85 ENGINE

YLF LASERS
A 1.94 micron laser apparatus, system, and method using a thulium-doped yttrium-lithium-fluoride laser crystal pumped with a diode laser
[AD-D015740] 01 p0176 N94-12321
Investigation of the optical and laser properties of Tm and Ho in YAG anf YLF
[REPT-94-001] 06 p2563 N94-24404

YO-YO DEVICES
The Solar Anomalous and Magnetospheric Particle Explorer (SAMPEX) yo-yo despin and solar array deployment mechanism 08 p3163 N94-29645

YOKES
Reconfigurable aircraft stick control
[AD-D016043] 07 p2681 N94-27113

YOUNG MODULUS
U MODULUS OF ELASTICITY

YSZ
U YTTRIA-STABILIZED ZIRCONIA

YTTERBIUM
Laser and spectroscopic properties of Yb-doped apatite crystals
[DE93-014656] 02 p0810 N94-14125
Tunable ytterbium-doped solid state laser
[AD-D015878] 04 p1440 N94-18747
Temperature dependence of 4f PES features and hole occupancy in ytterbium heavy fermions
[DE93-040131] 05 p1691 N94-20321

YTTERBIUM COMPOUNDS
Neutron-scattering studies of Yb-bearing silicate glasses
[DE93-019768] 05 p1700 N94-20265
Temperature dependence of 4f PES features and hole occupancy in ytterbium heavy fermions
[DE93-040131] 05 p1691 N94-20321
Photoemission and the electronic properties of heavy fermions: Limitations of the Kondo model
[DE93-040191] 05 p1974 N94-21553
Fibrous emissive burners selective and broad band
[PB94-128329] 07 p2859 N94-27225
Fermi surface instability at 0.4 K in a heavy-fermion YbBiPt: SDW?
[DE94-006224] 09 p3899 N94-31916

YTTRIA-STABILIZED ZIRCONIA
Combustion synthesis and engineering of nanoparticles for electronic, structural and superconductor applications
[DE94-001865] 06 p2254 N94-23720
An x ray diffraction investigation of alpha-Al2O2 addition to Yttria Stabilized Zirconia (YSZ) thermal barrier coatings subject to destabilizing vanadium pentoxide (V2O5) exposure
[AD-A273403] 06 p2261 N94-25072
Oxygen reduction at a YSZ interface with cathode materials La(1-x)(Ca or Sr)(x)MnO3(1-x)CaMnO3
[DE94-002954] 07 p3054 N94-26147
Superplasticity in fine-grained ceramics
[AD-A275461] 08 p3212 N94-28733
High-temperature deformation and fracture toughness of duplex ceramic microstructures
09 p3653 N94-31945

YTTRIUM
First-principles studies of phase stability and the structural and dynamical properties of hydrogen-metal systems
[DE93-016129] 02 p0570 N94-13374
Oscillator-amplifier experiments in neon-like yttrium
[DE93-012577] 02 p0657 N94-13976
Column chromatographic separation of Y(3+) from Sr(2+) by polymeric ionizable crown ether resins
[DE94-000935] 05 p1683 N94-22021

YTTRIUM ALLOYS
Realistic theories of heavy electron and other strongly correlated materials
[DE93-010350] 04 p1571 N94-19204
Non-Fermi-liquid and multichannel Kondo phenomena in Y(1-x)U(x)Pd3 and related alloys
[DE93-040135] 05 p2015 N94-20275
New extensions in the development of deformation processed metal-metal matrix composites
[DE94-000692] 06 p2227 N94-23004
Studies on the optimization of deformation processed metal-metal matrix composites
[DE94-006033] 08 p3185 N94-30704

YTTRIUM COMPOUNDS
NT YTTRIUM OXIDES
NT YTTRIUM-ALUMINUM GARNET
NT YTTRIUM-IRON GARNET
Small polaron conduction in Y2Ti2O7
[ITN-93-85221] 02 p0814 N94-14557

Spectroscopic studies of magnetic transitions in TbPO4
[DE94-001274] 05 p2035 N94-22565
Influences of nitrogen absorption on the magnetic properties of YFe2, YFe3 and Y6Fe23
[REPT-A-2654] 06 p2564 N94-24958
Space-R thermionic space nuclear power system: Design and technology demonstration
[DE94-001890] 07 p2699 N94-25929
Preparation, characterization, and thermal behaviour study of lanthanides (3) and yttrium (3) 4-methoxy benzylidene pyruvate in solid state
[DE94-604079] 07 p3068 N94-27697
Materials for spectral hole burning research, phase 1
[AD-A278480] 10 p4146 N94-33753

YTTRIUM LITHIUM FLUORIDE LASERS
U YLF LASERS

YTTRIUM OXIDES
Physical and structural properties of a sputtered zirconia-yttria layer used as a thermal resistance
[ONERA-NT-1992-10] 02 p0810 N94-14193
Metastability of yttrium-oxides
[DE93-016548] 02 p0813 N94-14440
Vanadium corrosion studies
[AD-A266489] 03 p0959 N94-16781
Nanostructured materials: Mind over matter
[DE93-017690] 04 p1597 N94-18480
Properties of E-beam interactive oxide films for nanometer scale structures
[AD-A272848] 05 p1675 N94-21191
Disks of YBa2Cu3O7 shocked to 10 GPa pressures
[DE94-000464] 05 p2031 N94-21931
Synthesis and characterization of charge-substituted garnets YCaLnGa5O12 (Ln = Ce, Pr, Tb)
[DE93-040227] 05 p2033 N94-21992
Processing of YBCO superconductors for improved levitation force
[DE94-001326] 06 p2559 N94-22994
An x ray diffraction investigation of alpha-Al2O2 addition to Yttria Stabilized Zirconia (YSZ) thermal barrier coatings subject to destabilizing vanadium pentoxide (V2O5) exposure
[AD-A273403] 06 p2261 N94-25072
Synthesis, rheology, and forming of Y-Ba-Cu-O ceramics
[DE94-005558] 07 p2757 N94-27695
Superconducting fibers made with yttrium and yttrium oxide interlayers and barium cuprate cover layers
[AD-D016073] 07 p3070 N94-28225
Mechanical properties of vacuum-sintered yttria ceramics
[DE94-008138] 09 p3659 N94-32617
Materials for spectral hole burning research, phase 1
[AD-A278480] 10 p4146 N94-33753

YTTRIUM-ALUMINUM GARNET
Excited state dynamics of thulium ions in yttrium aluminum garnets
[NASA-CR-195159] 06 p2564 N94-25024
Technical report of ISSP. Ser. A, no. 2682: Pressure dependence of Sm:YAG fluorescence to 50 GPa: A new calibration as a high pressure scale
[JTN-94-80568] 07 p3066 N94-27354
High-temperature deformation and fracture toughness of duplex ceramic microstructures
09 p3653 N94-31945
Development of materials for spectral hole burning applications
[AD-A278408] 09 p3909 N94-33324
Single crystal faceplate evaluation
[AD-A277922] 10 p4038 N94-33399
Growth, characterization, and device development in monocrystalline diamond films
[AD-A277863] 10 p4146 N94-33774

YTTRIUM-IRON GARNET
Nonlinear dynamics and instabilities in ferromagnetic resonance experiments: Examinations of spheres from yttrium iron garnet in coincidence area of the first Suhl instabilities
[ETN-93-95072] 04 p1604 N94-19612

YUH-1 HELICOPTER
U UH-1 HELICOPTER

YUH-60A HELICOPTER
U UH-60A HELICOPTER

YUKAWA POTENTIAL
Stitching the Yukawa quilt
[PB93-204477] 06 p2569 N94-24532
On the transverse size of a fast moving nucleon
[DE93-616891] 06 p2539 N94-25481
Stochastic space-time, confinement potential and particle propagator
[DE94-606415] 07 p3074 N94-27680
Possible explanation of the interaction cross-section growth at high energies
[DE94-606457] 08 p3494 N94-28612

YUKON TERRITORY
Minor and trace element composition and age of Yukon probable-microtektites 01 p0429 N94-12094

Z

ZEEMAN EFFECT
Dynamic Jahn-Teller effect: Calculation of fine structure spectrum, isotope shift and Zeeman behavior at deep center Ni2+ in CdS
[ETN-93-94394] 02 p0815 N94-14705
Zeeman laser interferometry for detection and chemical analysis
[DE94-003963] 07 p2719 N94-27728

ZENER DIODES
U AVALANCHE DIODES

ZENITH
Cirrus properties deduced from CO2 lidar observations of zenith-enhanced backscatter from oriented crystals
05 p1871 N94-22295

ZEOLITES
Crystallization of zeolites in the microgravity environment of space 01 p0119 N94-10210
Synthesis of molecular sieves from clear solution
01 p0124 N94-10245
Anchoring strategies for bimetallic species in zeolites
[DE93-015622] 02 p0567 N94-12834
Experimental and kinetic modeling of acid/base and redox reactions over oxide catalysts
[DE93-016203] 02 p0563 N94-13375
Mechanical properties of magnesium ammonium phosphate cements and their zeolite composites
[DE93-015155] 03 p0934 N94-16057
Conversion of ethane and of propane to higher olefin hydrocarbons
[DE93-015282] 04 p1347 N94-18194
Resonance Raman and photophysical studies of transition metal complexes in solution and entrapped in zeolites
[DE93-019892] 04 p1363 N94-19019
Thermal behavior of natural zeolites
[DE93-040091] 05 p1699 N94-19975
Embedded microclusters in zeolites and cluster beam sputtering: Simulation on parallel computers
[DE94-000741] 05 p1701 N94-20352
Use of oxygen-17 isotope in the characterization of zeolites and related structures by nuclear magnetic resonance spectroscopy
[VTT-TIED-1448] 07 p2714 N94-26251
Study of iron exchanged zeolites by Moessbauer effect and electron spin resonance spectroscopy
[DE94-605138] 08 p3514 N94-29691
Photochemistry in constrained spaces: Zeolites and layered double metal hydroxides
[DE94-004958] 08 p3200 N94-30769
Double rotation NMR studies of zeolites and aluminophosphate molecular sieves
[DE94-007032] 09 p3866 N94-31637
Studies of the fundamental nature of catalytic acidity, sites and intermediates
[DE94-006999] 09 p3646 N94-32805
NO decomposition in non-reducing atmospheres
[DE94-011157] 11 p4237 N94-36036
In situ studies of zeolite syntheses using powder diffraction methods: Crystallization of instant zeolite A powder and CoAPO-5
[DE94-006570] 11 p4341 N94-36358
Computer simulations of benzene in faujasite-type zeolites
[DE94-007533] 11 p4242 N94-36369
Direct catalytic decomposition of nitric oxide
[DE94-005025] 12 p4407 N94-36475
Thermodynamics of minerals stable near the Earth's surface
[DE94-012479] 12 p4539 N94-37094
Photochemistry without protons. Radical cation chemistry in zeolites
[DE94-012631] 12 p4412 N94-37439

ZERO ANGLE OF ATTACK
Normal force of low aspect ratio cropped-delta wings at pre-stall angles of attack and subsonic speeds
[ESDU-93034] 07 p2648 N94-27955
Wing lift increment at zero angle of attack due to deployment of single-slotted flaps at low speeds
[ESDU-93019] 07 p2649 N94-28140

ZERO CROSSINGS
U ROOTS OF EQUATIONS

ZERO GRAVITY
U WEIGHTLESSNESS

ZERO POINT ENERGY
Uncertainty relations, zero point energy and the linear canonical group 01 p0378 N94-10590

ZERO SOUND
First, second and fourth sound in relativistic superfluidity theory with account for dissipative effects
[DE94-617393] 11 p4267 N94-36314

ZETA PINCH
Source to detector spectrum transformation and its inverse for the Pegasus Z-pinch
[DE93-012674] 01 p0384 N94-10157
High power z pinches as x ray laser photopumps
[DE93-012842] 01 p0173 N94-10746
Advanced concepts theory annual report 1992
[AD-A266132] 01 p0393 N94-11474
Two-dimensional simulations of foil implosion experiments on the Los Alamos capacitor bank
[DE93-012676] 02 p0794 N94-12814
Advanced magnetic flux compression generator development issues: A comparison of coaxial and disk generators
[DE93-014025] 02 p0794 N94-12849
Instability heating of the HDZP
[DE93-012641] 02 p0798 N94-13513
Review of the Procyon explosive pulsed power system
[DE93-016562] 02 p0802 N94-14532
Direct drive foil implosion experiments on Pegasus 2
[DE93-012666] 03 p1202 N94-16776
Photopumped x ray laser research on Saturn
[DE93-019430] 05 p1816 N94-20298
Imaging XUV spectroscopy of a Z-pinch plasma in the former Soviet Union
[DE93-040849] 06 p2549 N94-22949
Computer modeling of plasma flow switches-high current switching on Procyon
[DE93-040189] 06 p2311 N94-24500
X ray simulator theory support
[AD-A273613] 06 p2553 N94-24949
Progress in Z-Pinch Research
[IPPCZ-321] 08 p3505 N94-29074
Investigation of intense XUV emission of nitrogen-puff Z-pinch with small energy input
[PH-23] 08 p3505 N94-29075
Multichannel x ray spectral measurement of hot plasma evolution in nitrogen-puff Z-pinch
[PH-24] 08 p3505 N94-29076
X ray emission scaling and energy balance of small gas-puff Z-pinch 08 p3505 N94-29077
Instability heating of solid-fiber Z pinches
[DE94-007055] 09 p3889 N94-31809
Plasma physics applications to intense radiation sources, pulsed power and space physics. Short pulse ultra intense laser-plasma interaction experiment
[AD-A278440] 10 p4144 N94-33555
D-D fusion experiments using fast z-pinches
[DE94-010090] 12 p4526 N94-36448
Preradiation studies for non-thermal Z-pinch wire load experiments on Saturn
[DE94-013459] 12 p4527 N94-37072

ZINC
Growth of new materials for solid state laser applications. The growth of ZnGeP2 by the vertical Bridgman method
[NASA-CR-194571] 03 p1038 N94-15530
Photoemission studies of Zn, Co, and Gd substituted YBa2Cu3O(7-delta)
[DE93-017403] 04 p1597 N94-18498
Photoluminescence spectroscopy of zinc germanium diphosphide (ZnGeP2)
[AD-A270705] 05 p1678 N94-19953
Integrated hydrometallurgical jarosite treatment
[PB93-217990] 06 p2232 N94-22983
Magnetic resonance study of zinc-related defects in silicon with optimized EPR spectrometer
[PB93-224640] 06 p2561 N94-23223
Evaluation of inorganic zinc-rich primers using Electrochemical Impedance Spectroscopy (EIS)
06 p2237 N94-23233
The effects of zinc borate addition on the flammability characteristics of polyester, vinyl ester, and epoxy glass reinforced plastics
[AD-A273164] 06 p2262 N94-25136
Pit initiation on passivated metal surfaces: Crystallographic orientation and environmental effects
[ISBN-0-315-85433-2] 08 p3208 N94-30138
The zinc electrode: Reactions and mechanisms
[DE94-007977] 09 p3691 N94-31919
Au/Zn contacts to Rho-InP: Electrical and metallurgical characteristics and the relationship between them
[NASA-TM-106590] 11 p4281 N94-35271
Non-alloyed, refractory metal contact optimization with shallow implantations of Zn and Mg
[DE94-010392] 11 p4240 N94-36110

ZINC ALLOYS
Crystal growth of ZnSe and related ternary compound semiconductors by physical vapor transport
[NASA-CR-193834] 02 p0807 N94-13444
Gold-copper-zinc coatings as an alternative to gold-copper-cadmium 04 p1367 N94-18012

Study of nucleation and growth in Al-Zn alloys using TEM
[DE94-006312] 08 p3211 N94-30852
Phase relationships and stability of the (mu)- and (zeta)-phases in the Ag-Al-X (X=Zn, Ga, Ge) systems
[DE94-009391] 09 p3648 N94-33270

ZINC CHLORIDES
Estimation of the concentration versus the time profile of zinc chloride particles in smoke clouds generated by the Raufoss A/S instantaneous smoke RA-90 and DM-45 HC smoke generator
[FFI-93/6001] 02 p0708 N94-13821
Zinc and titanium smoke: Chemical composition and physical characteristics
[FOA-C-40277-4.9] 05 p1680 N94-20552
Improvement of the stability of the process for synthesizing chemically prepared varistor powder
[DE94-000345] 05 p1763 N94-21654

ZINC COATINGS
Advanced zinc phosphate conversion and pre-ceramic polymetallosiloxane coatings for corrosion protection of steel and aluminum, and characteristics of polyphenyletheretherketone-based materials
[DE93-008717] 01 p0088 N94-10891
Evaluation of inorganic zinc-rich primers using Electrochemical Impedance Spectroscopy (EIS)
06 p2237 N94-23233
Cracking of textured zinc coating during forming process
[DE94-003414] 07 p2750 N94-26085

ZINC COMPOUNDS
NT WURTZITE
NT ZINC CHLORIDES
NT ZINC OXIDES
NT ZINC SELENIDES
NT ZINC SULFIDES
NT ZINC TELLURIDES
NT ZINCBLENDE
Second and third order nonlinear optical properties of crystalline inorganic/organic complexes
[DE93-011883] 01 p0173 N94-10755
Advanced zinc phosphate conversion and pre-ceramic polymetallosiloxane coatings for corrosion protection of steel and aluminum, and characteristics of polyphenyletheretherketone-based materials
[DE93-008717] 01 p0088 N94-10891
Heavy-electron behavior in large coordination compounds CeZn11 and UZn12
[REPT-A-2663] 07 p3049 N94-25614
Lightweight zinc electrode
[AD-D016181] 09 p3698 N94-33181
Polyurethane self-priming topcoats
[AD-D016160] 10 p4030 N94-34285

ZINC NICKEL BATTERIES
U NICKEL ZINC BATTERIES

ZINC OXIDES
Nanostructured materials: Mind over matter
[DE93-017690] 04 p1597 N94-18480
Pressureless densification of ceramic matrix composites
[AD-A269137] 04 p1371 N94-18691
Advanced processing technology for high-efficiency thin-film CuInSe2 solar cells
[DE93-010045] 05 p1847 N94-21614
Research on polycrystalline thin-film submodules based on CuInSe2 materials
[DE93-018223] 05 p2029 N94-21617
Zinc(2) oxide stability in alkaline sodium phosphate solutions at elevated temperatures
[DE94-003316] 07 p2715 N94-26320
Technical report of ISSP. Ser. A, no. 2677: Octa-twin model of tetrapod ZnO crystals
[JTN-94-80563] 07 p3069 N94-27756
The ZnO thin films with C-axis orientation prepared on the room temperature substrate by the ECR multipolar plasma sputtering method
[DE94-605039] 07 p2758 N94-27857
The zinc electrode: Reactions and mechanisms
[DE94-007977] 09 p3691 N94-31919

ZINC SELENIDES
Investigation of ZnSe-coated silicon substrates for GaAs solar cells 01 p0052 N94-11405
Growth of zinc selenide single crystals by physical vapor transport in microgravity
[NASA-CR-194679] 05 p2017 N94-20346
Hydrogen in compound semiconductors
[DE93-040300] 05 p2031 N94-21922
Heavy-electron behavior in large coordination compounds CeZn11 and UZn12
[REPT-A-2663] 07 p3049 N94-25614
Indium donor complexes with cation vacancies in CdTe and ZnSe
[DE94-002731] 07 p3063 N94-26958
Optical properties of cadmium sulfide, zinc selenide, and zinc manganese selenide semiconductor films
08 p3500 N94-29759
Electronic structure of Zn-based quantum wells
[DE94-608104] 08 p3516 N94-30068
The relationship of the electronic structures of semiconductor surfaces and heterostructures to crystal growth
[AD-A276465] 09 p3896 N94-31473
Investigation of polycrystalline thin-film CuInSe2 solar cells based on ZnSe windows
[DE94-006936] 12 p4462 N94-37381
Optical spectroscopy of a nitrogen-hydrogen complex in ZnSe
[DE94-011622] 12 p4413 N94-37630

ZINC SILVER BATTERIES
U SILVER ZINC BATTERIES

ZINC SILVER OXIDE BATTERIES
U SILVER ZINC BATTERIES

ZINC SULFIDES
NT WURTZITE
NT ZINCBLENDE
Optical switch evaluation support
[AD-A270948] 04 p1581 N94-19601
Characterization of ZnS-GaP naon-composites
[DE94-004888] 07 p2712 N94-27813
Formation mechanism and yield of molecules ejected from ZnS, CdS, and FeS2 during ion bombardment
[DE94-008487] 09 p3871 N94-32515
Luminescence and electroluminescence of Nd, Tm, and Yb doped GaAs and some II-VI compounds
[AD-A278413] 10 p4146 N94-33554

ZINC TELLURIDES
Laser figuring for the generation of analog micro-optics and kineform surfaces 03 p1196 N94-17346
New room temperature high resolution solid-state detector (CdZnTe) for hard x rays and gamma rays
04 p1324 N94-19165
Dual-use applications of infrared sensitive materials
[AD-A275140] 08 p3499 N94-29694
Development of novel II-VI solar cells
[PB94-159415] 11 p4282 N94-35739

ZINC-BROMIDE BATTERIES
Advanced batteries for electric vehicle applications: Nontechnical summary
[DE93-019007] 05 p1748 N94-19885

ZINCBLENDE
II-VI wide band gap semiconductors under hydrostatic pressure
[DE94-608106] 08 p3516 N94-30070

ZIRCALOYS (TRADEMARK)
Hydrogen pickup and redistribution in alpha-annealed zircaloy-4
[DE93-018050] 05 p1689 N94-20182
Consolidation of zircaloy-4 end crops by induction melting
[DE94-010031] 11 p4240 N94-35650
Thermodynamic behaviour of tellurium at high temperatures
[DE94-612823] 11 p4240 N94-35960

ZIRCONATES
Dielectric measurements of selected ceramics at microwave frequencies 11 p4232 N94-36412

ZIRCONIA
U ZIRCONIUM OXIDES

ZIRCONIUM
NT ZIRCONIUM ISOTOPES
Omega phase formation in shock-loaded zirconium
[DE93-018343] 04 p1595 N94-18162
Total hemispherical emittance of Niobium-1 percent zirconium fuel cladding for the SP-100 space reactor
[AD-A270456] 04 p1576 N94-19589
Theoretical studies of zirconium and carbon clusters with molecular dynamics simulations
[DE94-005276] 09 p3862 N94-31146
A low cost igniter utilizing an SCB and titanium sub-hydride potassium perchlorate pyrotechnic
[DE94-006467] 09 p3666 N94-31827
Study of point defect mobilities in zirconium during electron irradiation in a HVEM
[DE94-619028] 11 p4242 N94-36289
Characterization and processing of sintered products from nano-crystalline powders generated by the RTDS method
[DE94-004765] 12 p4415 N94-36553

ZIRCONIUM ALLOYS
NT ZIRCALOYS (TRADEMARK)
Structure and properties of an RS Al-Si-Ni-Mn-Zr alloy for high temperature applications
01 p0064 N94-10063
Microstructure of Zr3Al after 2 MeV proton bombardment
[DE93-015331] 03 p1211 N94-16814
Effects of processing and prolonged high temperature exposure on the microstructure of Nb-1Zr-C sheet
[NASA-TM-106370] 03 p0959 N94-16883
Using the rule of mixtures to examine the hardness of Cu/Cu-Zr multilayers
[DE94-001068] 05 p1697 N94-22402
Phase transformations in Cu-Zr multilayers
[DE94-000393] 06 p2241 N94-23297
Zr-rich corner of the Zr-Sn-O diagram
[DE93-633764] 07 p2734 N94-26161
Grain by grain study of the mechanisms of crack propagation during iodine SCC of Zry-4
[DE93-633765] 07 p2734 N94-26162
Zr-Sn-Nb alloys: Preliminary studies
[DE93-633767] 07 p2734 N94-26263
Fracture Toughness Round Robin Test International in pressure tube materials
[DE93-634140] 07 p2837 N94-26265
Eutectic transformation L in equilibrium to Zr6Fe23 + Fe(tau) in the Fe-Zr system
[DE93-633766] 07 p2735 N94-26295
Hydrothermal growth and characterization of oxides in zirconium alloys
[DE94-602981] 07 p2743 N94-27829
Differential scanning calorimetric study of solid state amorphization and crystallization in Zr/Co and Zr/Ni multilayers 07 p2745 N94-28161
The corrosion behavior of sputter-deposited magnesium-valve metal alloys 07 p2745 N94-28164
CO2 methanation catalysts prepared from amorphous Ni-valve metal alloys containing platinum group elements
07 p2745 N94-28166
Effects of thermomechanical processing on tensile and long-time creep behavior of Nb-1 percent Zr-0.1 percent C sheet
[NASA-TM-106319] 08 p3202 N94-28822
Irradiation-induced phase transformations in zirconium alloys
[DE94-008484] 09 p3648 N94-32993
Formation and stability of Fe-rich precipitates in dilute Zr(Fe) single-crystal alloys
[DE94-619027] 11 p4242 N94-36288
Mitigation of harmful effects of welds in zirconium alloy components
[DE94-619033] 12 p4414 N94-36543
Modelling irradiation creep of zirconium alloys
[DE94-619055] 12 p4414 N94-36544
Precipitation in Zr-2.5 Nb enhanced by proton irradiation
[DE94-619056] 12 p4415 N94-36563
The dynamics of hydrogen atoms dissolved in Zr Cr2 alloy
[DE94-618756] 12 p4520 N94-37652

ZIRCONIUM CARBIDES
Effects of processing and prolonged high temperature exposure on the microstructure of Nb-1Zr-C sheet
[NASA-TM-106370] 03 p0959 N94-16883
The organometallic chemical vapor deposition of transition metal carbides: The use of homoleptic alkyls
[DE94-005577] 08 p3208 N94-30007

ZIRCONIUM COMPOUNDS
NT YTTRIA-STABILIZED ZIRCONIA
NT ZIRCONATES
NT ZIRCONIUM CARBIDES
NT ZIRCONIUM HYDRIDES
NT ZIRCONIUM OXIDES
NT ZIRCONIUM TITANATES
The d(exp 3)delta-a(exp 3)delta and b(exp 3)phi-a(exp 3)delta systems of ZrS, Part 2: Appendix, list of wavenumbers
[USIP-92-05] 04 p1602 N94-19293
Advanced civil engineering materials based on inorganic polymers
[AD-A270837] 04 p1374 N94-19600
Interstitially stabilized phases in the zirconium-nickel system
[DE94-005561] 08 p3201 N94-28525
Vertical electron detachment energies for octahedral closed-shell multiply charged anions
[AD-A278835] 11 p4322 N94-35753
Metal cluster alloys and oxides: Elucidating structural and electronic effects in governing the reactivity and catalytic role of matter in finite dimensions
[DE94-010224] 11 p4328 N94-36298

ZIRCONIUM HYDRIDES
Space-R thermionic space nuclear power system: Design and technology demonstration
[DE94-001890] 07 p2699 N94-25929

ZIRCONIUM ISOTOPES
Progress in zirconium resonance ionization spectroscopy
[DE93-011881] 01 p0076 N94-11075
Influence of long-range correlations on the spectral functions and response of 48Ca and 90Zr
[ETN-94-96017] 09 p3865 N94-31537

ZIRCONIUM OXIDES
NT YTTRIA-STABILIZED ZIRCONIA
Microanalysis of directionally solidified cobalt oxide-zirconia eutectic
[DE93-013207] 01 p0088 N94-10527

Combustion synthesis and engineering of nanoparticles for electronic, structural, and superconductor applications
[DE93-016286] 02 p0809 N94-13981
Physical and structural properties of a sputtered zirconia-yttria layer used as a thermal resistance
[ONERA-NT-1992-10] 02 p0810 N94-14193
Ion mixing of thin ZrO2 films on sapphire
[DE93-015214] 03 p1206 N94-14925
Synthesis of ceramic oxide powders in a microwave plasma device
[DE93-012741] 03 p0965 N94-15920
Rheology and microstructure of concentrated zirconia-alumina suspensions for gelcasting composites
[DE93-015339] 03 p0966 N94-16016
Transformation toughening of composite ceramics
[AD-A267304] 03 p0971 N94-16980
Characterization of nanoscale oxide and oxyhydroxide powders using EXAFS spectroscopy
[DE93-015683] 03 p0940 N94-17235
Pressureless densification of ceramic matrix composites
[AD-A269137] 04 p1371 N94-18691
Optical properties of oxide coatings prepared by ion-assisted deposition
[AD-A270024] 04 p1599 N94-18711
Guanidine based vehicle/binders for use with oxides, metals, and ceramics
[NASA-CASE-LEW-15314-1] 05 p1700 N94-20195
Crystal structure and short-range oxygen defects in La- and Nd-modified ZrO2
[DE93-040229] 05 p2033 N94-21993
An x ray diffraction investigation of alpha-Al2O2 addition to Yttria Stabilized Zirconia (YSZ) thermal barrier coatings subject to destabilizing vanadium pentoxide (V2O5) exposure
[AD-A273403] 06 p2261 N94-25072
Study on film generation phenomena by particle deposition 07 p2728 N94-25575
Oxygen reduction at a YSZ interface with cathode materials La(1-x)(Ca or Sr)(x)MnO3(1-x)CaMnO3
[DE94-002954] 07 p3054 N94-26147
Stress-induced phase transformation in ZrO2 materials
[ISBN-0-315-83373-4] 07 p2752 N94-26661
Bench-scale synthesis of nanoscale materials
[DE94-004787] 07 p2742 N94-27786
Hydrothermal growth and characterization of oxides in zirconium alloys
[DE94-602981] 07 p2743 N94-27829
Interstitially stabilized phases in the zirconium-nickel system
[DE94-005561] 08 p3201 N94-28525
Pull-test adhesion measurements of diamondlike carbon films on silicon carbide, silicon nitride, aluminum oxide, and zirconium oxide
[DE94-005469] 08 p3211 N94-28536
Thick thermal barrier coatings for diesel components
[NASA-CR-187111] 08 p3537 N94-29350
Brittle composites modeling: Comparisons with MoSi2/ZrO2
[DE94-004978] 08 p3182 N94-29933
Plasma enhanced chemical vapor deposition of ZrO2 thin films
[DE94-006031] 08 p3218 N94-30104
Densification and crystallization of zirconia thin films prepared by sol-gel processing
[DE94-005573] 08 p3518 N94-30315
Sol-gel metal oxide and metal oxide/polymer multilayers applied by meniscus coating
[DE94-005813] 09 p3649 N94-31199
Cost-effective ceramic machining: Summary of three-body wear experiments
[DE94-007757] 09 p3650 N94-31354
Fatigue crack propagation and fractography of 3Y-TZP and ZTA
[ISBN-0-315-86561-X] 09 p3736 N94-31912
Ion-irradiation-induced densification of zirconia sol-gel thin films
[DE94-006248] 09 p3656 N94-32103
Sol-gel coatings for high power laser optics: Past, present, and future
[DE94-007240] 09 p3718 N94-32252
Interface engineering in oxide fiber/oxide matrix composites
[AD-A277672] 09 p3627 N94-33029
Mapping of residual strains of a ceramic-to-metal joint using x ray diffraction
[DE94-007421] 10 p4069 N94-33691
New mechanism for toughening ceramic materials
[AD-A278479] 10 p4027 N94-33747
Defect detection in multi-layered, plasma sprayed zirconia by time resolved infrared radiometry: A comparison between analytical and experimental methods
[DE94-009803] 11 p4245 N94-35779
Superacid catalysis of light hydrocarbon conversion
[DE94-011132] 12 p4411 N94-37431

ZIRCONIUM TITANATES
Preparation and properties of sol-gel derived PZT thin films for decoupling capacitor applications
[DE93-018853] 05 p2013 N94-19961

ZODIACAL DUST
Zodiacal light data investigation. Interim results for the Earthlimb Clutter Experiment
[AD-A274461] 07 p3104 N94-27265
Infrared observations of cometary dust by COBE
08 p3541 N94-29994

ZODIACAL LIGHT
Zodiacal light data investigation. Interim results for the Earthlimb Clutter Experiment
[AD-A274461] 07 p3104 N94-27265
CBSD: The celestial background scene descriptor
[AD-A275521] 08 p3538 N94-28671
Catalog of Helios 90 deg photometer events
[PL-TR-94-2040] 11 p4375 N94-36264

ZONAL CIRCULATION
U ZONAL FLOW (METEOROLOGY)

ZONAL FLOW (METEOROLOGY)
Updated forecast of Atlantic seasonal hurricane activity for 1993 01 p0285 N94-11194
Numerical simulations of thermal convection in rapidly rotating spherical fluid shells 01 p0153 N94-11635
Investigate wave-mean flow interaction and transport in the extratropical winter stratosphere
[NASA-CR-194555] 03 p1098 N94-15639
Interactions of free modes, tides, and gravity waves in the middle atmosphere
[REPT-84] 05 p1855 N94-20155
Empirical wind model for the middle and lower atmosphere. Part 2: Local time variations
[NASA-TM-104592] 05 p1870 N94-21862
Diagnostic calculations of the circulation in the Martian atmosphere 06 p2622 N94-24898
Global barotropic response to a tropical forcing
[NASA-CR-195256] 07 p2896 N94-27408
Dynamic climatology of West Africa
09 p3778 N94-30988
Theoretic study of Green's modes
[INPE-5536-TDI/524] 10 p4090 N94-34202

ZONAL HARMONICS
Implementing a 50x50 gravity field model in an orbit determination system
[AD-A267548] 03 p0888 N94-17103

ZONE MELTING
Marangoni and buoyant convections in zone melting of GaAs with liquid encapsulation
01 p0101 N94-10081
On shape of single crystals grown by FZM in microgravity 01 p0102 N94-10084
Calculation of the effects of magnetic field damping in fluid flow: Comparison of magnetohydrodynamic models of different complexity 01 p0103 N94-10089
Mission support for crystal growth experiments in Russian unmanned carriers 01 p0111 N94-10139
Crystal growth in the Zone Melting Facility (ZMF)
01 p0119 N94-10213
Growth of semiconductor compound single crystal InSb by floating zone method (M-3) 02 p0586 N94-13735

ZONE REFINING
U ZONE MELTING

ZONES
U REGIONS

ZOOM LENSES
Description of an infrared zoomcollimator
[FEL-93-A034] 04 p1580 N94-19424

ZOOPLANKTON
Automatic classification system for zooplankton
01 p0203 N94-11969
The seasonal change of phytoplankton size distribution using optical fiber sensor 01 p0210 N94-12656
Copepods collected along 33.5 deg E longitude of the Antarctic Ocean in the 1976 summer
08 p3358 N94-29082
Bioluminescence bathyphotometer
[AD-D016102] 09 p3790 N94-32959

*U.S. GOVERNMENT PRINTING OFFICE: 1995-387-253/20005

VOLUME 32 NUMBERS 1-6

Scientific and Technical Aerospace Reports

Abstracts January – June 1994

TABLE OF CONTENTS

STAR Issue	Page
1	1
2	499
3	853
4	1305
5	1635
6	2153

VOLUME 32 NUMBERS 7-12

Scientific and Technical Aerospace Reports

Abstracts July – December 1994

TABLE OF CONTENTS

STAR Issue	Page
7	2641
8	3121
9	3565
10	3969
11	4189
12	4381

FEDERAL REGIONAL DEPOSITORY LIBRARIES

ALABAMA

AUBURN UNIV. AT MONTGOMERY LIBRARY
Documents Dept.
7300 University Dr.
Montgomery, AL 36117-3596
(205) 244-3650 Fax: (205) 244-0678

UNIV. OF ALABAMA
Amelia Gayle Gorgas Library
Govt. Documents
P.O. Box 870266
Tuscaloosa, AL 35487-0266
(205) 348-6046 Fax: (205) 348-0760

ARIZONA

DEPT. OF LIBRARY, ARCHIVES, AND PUBLIC RECORDS
Research Division
Third Floor, State Capitol
1700 West Washington
Phoenix, AZ 85007
(602) 542-3701 Fax: (602) 542-4400

ARKANSAS

ARKANSAS STATE LIBRARY
State Library Service Section
Documents Service Section
One Capitol Mall
Little Rock, AR 72201-1014
(501) 682-2053 Fax: (501) 682-1529

CALIFORNIA

CALIFORNIA STATE LIBRARY
Govt. Publications Section
P.O. Box 942837 - 914 Capitol Mall
Sacramento, CA 94337-0091
(916) 654-0069 Fax: (916) 654-0241

COLORADO

UNIV. OF COLORADO - BOULDER
Libraries - Govt. Publications
Campus Box 184
Boulder, CO 80309-0184
(303) 492-8834 Fax: (303) 492-1881

DENVER PUBLIC LIBRARY
Govt. Publications Dept. BSG
1357 Broadway
Denver, CO 80203-2165
(303) 640-8846 Fax: (303) 640-8817

CONNECTICUT

CONNECTICUT STATE LIBRARY
231 Capitol Avenue
Hartford, CT 06106
(203) 566-4971 Fax: (203) 566-3322

FLORIDA

UNIV. OF FLORIDA LIBRARIES
Documents Dept.
240 Library West
Gainesville, FL 32611-2048
(904) 392-0366 Fax: (904) 392-7251

GEORGIA

UNIV. OF GEORGIA LIBRARIES
Govt. Documents Dept.
Jackson Street
Athens, GA 30602-1645
(706) 542-8949 Fax: (706) 542-4144

HAWAII

UNIV. OF HAWAII
Hamilton Library
Govt. Documents Collection
2550 The Mall
Honolulu, HI 96822
(808) 948-8230 Fax: (808) 956-5968

IDAHO

UNIV. OF IDAHO LIBRARY
Documents Section
Rayburn Street
Moscow, ID 83844-2353
(208) 885-6344 Fax: (208) 885-6817

ILLINOIS

ILLINOIS STATE LIBRARY
Federal Documents Dept.
300 South Second Street
Springfield, IL 62701-1796
(217) 782-7596 Fax: (217) 782-6437

INDIANA

INDIANA STATE LIBRARY
Serials/Documents Section
140 North Senate Avenue
Indianapolis, IN 46204-2296
(317) 232-3679 Fax: (317) 232-3728

IOWA

UNIV. OF IOWA LIBRARIES
Govt. Publications
Washington & Madison Streets
Iowa City, IA 52242-1166
(319) 335-5926 Fax: (319) 335-5900

KANSAS

UNIV. OF KANSAS
Govt. Documents & Maps Library
6001 Malott Hall
Lawrence, KS 66045-2800
(913) 864-4660 Fax: (913) 864-3855

KENTUCKY

UNIV. OF KENTUCKY
King Library South
Govt. Publications/Maps Dept.
Patterson Drive
Lexington, KY 40506-0039
(606) 257-3139 Fax: (606) 257-3139

LOUISIANA

LOUISIANA STATE UNIV.
Middleton Library
Govt. Documents Dept.
Baton Rouge, LA 70803-3312
(504) 388-2570 Fax: (504) 388-6992

LOUISIANA TECHNICAL UNIV.
Prescott Memorial Library
Govt. Documents Dept.
Ruston, LA 71272-0046
(318) 257-4962 Fax: (318) 257-2447

MAINE

UNIV. OF MAINE
Raymond H. Fogler Library
Govt. Documents Dept.
Orono, ME 04469-5729
(207) 581-1673 Fax: (207) 581-1653

MARYLAND

UNIV. OF MARYLAND - COLLEGE PARK
McKeldin Library
Govt. Documents/Maps Unit
College Park, MD 20742
(301) 405-9165 Fax: (301) 314-9416

MASSACHUSETTS

BOSTON PUBLIC LIBRARY
Govt. Documents
666 Boylston Street
Boston, MA 02117-0286
(617) 536-5400, ext. 226
Fax: (617) 536-7758

MICHIGAN

DETROIT PUBLIC LIBRARY
5201 Woodward Avenue
Detroit, MI 48202-4093
(313) 833-1025 Fax: (313) 833-0156

LIBRARY OF MICHIGAN
Govt. Documents Unit
P.O. Box 30007
717 West Allegan Street
Lansing, MI 48909
(517) 373-1300 Fax: (517) 373-3381

MINNESOTA

UNIV. OF MINNESOTA
Govt. Publications
409 Wilson Library
309 19th Avenue South
Minneapolis, MN 55455
(612) 624-5073 Fax: (612) 626-9353

MISSISSIPPI

UNIV. OF MISSISSIPPI
J.D. Williams Library
106 Old Gym Bldg.
University, MS 38677
(601) 232-5857 Fax: (601) 232-7465

MISSOURI

UNIV. OF MISSOURI - COLUMBIA
106B Ellis Library
Govt. Documents Sect.
Columbia, MO 65201-5149
(314) 882-6733 Fax: (314) 882-8044

MONTANA

UNIV. OF MONTANA
Mansfield Library
Documents Division
Missoula, MT 59812-1195
(406) 243-6700 Fax: (406) 243-2060

NEBRASKA

UNIV. OF NEBRASKA - LINCOLN
D.L. Love Memorial Library
Lincoln, NE 68588-0410
(402) 472-2562 Fax: (402) 472-5131

NEVADA

THE UNIV. OF NEVADA LIBRARIES
Business and Govt. Information Center
Reno, NV 89557-0044
(702) 784-6579 Fax: (702) 784-1751

NEW JERSEY

NEWARK PUBLIC LIBRARY
Science Div. - Public Access
P.O. Box 630
Five Washington Street
Newark, NJ 07101-7812
(201) 733-7782 Fax: (201) 733-5648

NEW MEXICO

UNIV. OF NEW MEXICO
General Library
Govt. Information Dept.
Albuquerque, NM 87131-1466
(505) 277-5441 Fax: (505) 277-6019

NEW MEXICO STATE LIBRARY
325 Don Gaspar Avenue
Santa Fe, NM 87503
(505) 827-3824 Fax: (505) 827-3888

NEW YORK

NEW YORK STATE LIBRARY
Cultural Education Center
Documents/Gift & Exchange Section
Empire State Plaza
Albany, NY 12230-0001
(518) 474-5355 Fax: (518) 474-5786

NORTH CAROLINA

UNIV. OF NORTH CAROLINA - CHAPEL HILL
Walter Royal Davis Library
CB 3912, Reference Dept.
Chapel Hill, NC 27514-8890
(919) 962-1151 Fax: (919) 962-4451

NORTH DAKOTA

NORTH DAKOTA STATE UNIV. LIB.
Documents
P.O. Box 5599
Fargo, ND 58105-5599
(701) 237-8886 Fax: (701) 237-7138

UNIV. OF NORTH DAKOTA
Chester Fritz Library
University Station
P.O. Box 9000 - Centennial and University Avenue
Grand Forks, ND 58202-9000
(701) 777-4632 Fax: (701) 777-3319

OHIO

STATE LIBRARY OF OHIO
Documents Dept.
65 South Front Street
Columbus, OH 43215-4163
(614) 644-7051 Fax: (614) 752-9178

OKLAHOMA

OKLAHOMA DEPT. OF LIBRARIES
U.S. Govt. Information Division
200 Northeast 18th Street
Oklahoma City, OK 73105-3298
(405) 521-2502, ext. 253
Fax: (405) 525-7804

OKLAHOMA STATE UNIV.
Edmon Low Library
Stillwater, OK 74078-0375
(405) 744-6546 Fax: (405) 744-5183

OREGON

PORTLAND STATE UNIV.
Branford P. Millar Library
934 Southwest Harrison
Portland, OR 97207-1151
(503) 725-4123 Fax: (503) 725-4524

PENNSYLVANIA

STATE LIBRARY OF PENN.
Govt. Publications Section
116 Walnut & Commonwealth Ave.
Harrisburg, PA 17105-1601
(717) 787-3752 Fax: (717) 783-2070

SOUTH CAROLINA

CLEMSON UNIV.
Robert Muldrow Cooper Library
Public Documents Unit
P.O. Box 343001
Clemson, SC 29634-3001
(803) 656-5174 Fax: (803) 656-3025

UNIV. OF SOUTH CAROLINA
Thomas Cooper Library
Green and Sumter Streets
Columbia, SC 29208
(803) 777-4841 Fax: (803) 777-9503

TENNESSEE

UNIV. OF MEMPHIS LIBRARIES
Govt. Publications Dept.
Memphis, TN 38152-0001
(901) 678-2206 Fax: (901) 678-2511

TEXAS

TEXAS STATE LIBRARY
United States Documents
P.O. Box 12927 - 1201 Brazos
Austin, TX 78701-0001
(512) 463-5455 Fax: (512) 463-5436

TEXAS TECH. UNIV. LIBRARIES
Documents Dept.
Lubbock, TX 79409-0002
(806) 742-2282 Fax: (806) 742-1920

UTAH

UTAH STATE UNIV.
Merrill Library Documents Dept.
Logan, UT 84322-3000
(801) 797-2678 Fax: (801) 797-2677

VIRGINIA

UNIV. OF VIRGINIA
Alderman Library
Govt. Documents
University Ave. & McCormick Rd.
Charlottesville, VA 22903-2498
(804) 824-3133 Fax: (804) 324-4337

WASHINGTON

WASHINGTON STATE LIBRARY
Govt. Publications
P.O. Box 42478
16th and Water Streets
Olympia, WA 98504-2478
(206) 753-4027 Fax: (206) 586-7575

WEST VIRGINIA

WEST VIRGINIA UNIV. LIBRARY
Govt. Documents Section
P.O. Box 6069 - 1549 University Ave.
Morgantown, WV 26506-6069
(304) 293-3051 Fax: (304) 293-6638

WISCONSIN

ST. HIST. SOC. OF WISCONSIN LIBRARY
Govt. Publication Section
816 State Street
Madison, WI 53706
(608) 264-6525 Fax: (608) 264-6520

MILWAUKEE PUBLIC LIBRARY
Documents Division
814 West Wisconsin Avenue
Milwaukee, WI 53233
(414) 286-3073 Fax: (414) 286-8074

National Aeronautics and
Space Administration
Code JT
Washington, DC 20546-0001